Y/LF-717, Rev 4
Docket No. 71-9315

Safety Analysis Report, Y-12 National Security Complex, Model ES-3100 Package with Bulk HEU Contents

Volume 1
Sections 1-2

Babcock & Wilcox Technical Services Y-12, LLC
Y-12 National Security Complex
P.O. Box 2009
Oak Ridge, Tennessee 37831

March 3, 2011

Y/LF-717, Rev. 4,
Volume 1

SAFETY ANALYSIS REPORT, Y-12 NATIONAL SECURITY COMPLEX, MODEL ES-3100 PACKAGE WITH BULK HEU CONTENTS

Prepared by
Babcock & Wilcox Technical Services Y-12, LLC
Management & Operating Contractor
for the
Y-12 National Security Complex
under Contract No. DE-AC05-00OR22800
with the
U.S. Department of Energy
National Nuclear Security Administration

March 3, 2011

APPROVALS

Y/LF-717, Rev. 4

SAFETY ANALYSIS REPORT,
Y-12 NATIONAL SECURITY COMPLEX,
MODEL ES-3100 PACKAGE WITH BULK HEU CONTENTS

Approved by:

Walter I. North
Packaging Engineering Manager

3/3/2011
Date

James C. Anderson
Safety Analysis Report for Packaging Manager

3/3/11
Date

Jeffrey G. Arbital
Transportation and Packaging Program Manager

3/3/11
Date

THIS PAGE INTENTIONALLY LEFT BLANK.

CONTENTS

Page

APPROVALS . . . iii

FIGURES . . . xi

TABLES . . . xiii

ABBREVIATIONS . . . xvii

REVISION LOG . . . xix

1. GENERAL INFORMATION . . . 1-1
   1.1 INTRODUCTION . . . 1-1
   1.2 PACKAGE DESCRIPTION . . . 1-1
      1.2.1 Packaging . . . 1-4
      1.2.2 Containment System . . . 1-7
      1.2.3 Contents . . . 1-10
      1.2.4 Operational Features . . . 1-25
   1.3 GENERAL REQUIREMENTS FOR ALL PACKAGES . . . 1-25
      1.3.1 Minimum package size . . . 1-25
      1.3.2 Tamper-indicating feature . . . 1-26
   1.4 APPENDICES . . . 1-27
      1.4.1 PACKAGE CERTIFICATION DRAWING . . . 1-29
      1.4.2 EQUIPMENT SPECIFICATION JS-YMN3-801580-A002, *ES-3100 DRUM ASSEMBLY* . . . 1-43
      1.4.3 EQUIPMENT SPECIFICATION JS-YMN3-801580-A001, *ES-3100 CONTAINMENT VESSEL* . . . 1-53
      1.4.4 EQUIPMENT SPECIFICATION, JS-YMN3-801580-A003, *MANUFACTURING PROCESS SPECIFICATION FOR CASTING KAOLITE 1600™ INTO THE ES-3100 SHIPPING PACKAGE* . . . 1-67
      1.4.5 EQUIPMENT SPECIFICATION, JS-YMN3-801580-A005, *CASTING CATALOG NO. 277-4 NEUTRON ABSORBER FOR THE ES-3100 SHIPPING PACKAGE* . . . 1-87
      1.4.6 PACKAGE CATEGORY DETERMINATION . . . 1-129
      1.4.7 HEU OXIDE MATERIAL SPECIFICATION AS PROVIDED BY Y-12 HIGHLY ENRICHED URANIUM DISPOSITION PROGRAM OFFICE . . . 1-133
      1.4.8 DETAILED ENGINEERING DRAWINGS . . . 1-137
      1.4.9 DESIGN ANALYSES AND CALCULATIONS, DAC-PKG-801624-A001, MIXING WEIGHTS AND ELEMENTAL COMPOSITION OF 277-4 NEUTRON POISON USED IN THE ES-3100 . . . 1-183
      1.4.10 PYROPHORICITY OF URANIUM METAL . . . 1-211
   SECTION 1 REFERENCES . . . 1-231

2. STRUCTURAL EVALUATION . . . 2-1
   2.1 DESCRIPTION OF STRUCTURAL DESIGN . . . 2-2
      2.1.1 Discussion . . . 2-2
      2.1.2 Design Criteria . . . 2-5
      2.1.3 Weights and Centers of Gravity . . . 2-14
      2.1.4 Identification of Codes and Standards for Package Design . . . 2-14

CONTENTS

Page

2.2 MATERIALS 2-18
2.2.1 Material Properties and Specifications 2-18
2.2.2 Chemical, Galvanic, or Other Reactions 2-18
2.2.3 Effects of Radiation on Materials 2-26
2.3 FABRICATION AND EXAMINATION 2-26
2.3.1 Fabrication 2-26
2.3.2 Examination 2-28
2.4 LIFTING AND TIE-DOWN STANDARDS FOR ALL PACKAGES 2-31
2.4.1 Lifting Devices 2-31
2.4.2 Tie-Down Devices 2-31
2.5 GENERAL CONSIDERATIONS 2-32
2.5.1 Evaluation by Test 2-32
2.5.2 Evaluation by Analysis 2-35
2.6 NORMAL CONDITIONS OF TRANSPORT 2-35
2.6.1 Heat 2-37
2.6.2 Cold 2-39
2.6.3 Reduced External Pressure 2-42
2.6.4 Increased External Pressure 2-42
2.6.5 Vibration 2-44
2.6.6 Water Spray 2-46
2.6.7 Free Drop 2-47
2.6.8 Corner Drop 2-48
2.6.9 Compression 2-48
2.6.10 Penetration 2-50
2.7 HYPOTHETICAL ACCIDENT CONDITIONS 2-51
2.7.1 Free Drop 2-54
2.7.2 Crush 2-64
2.7.3 Puncture 2-70
2.7.4 Thermal 2-71
2.7.5 Immersion—Fissile Material 2-80
2.7.6 Immersion—All Packages 2-81
2.7.7 Deep Water Immersion Test 2-81
2.7.8 Summary of Damage 2-81
2.8 ACCIDENT CONDITIONS FOR AIR TRANSPORT OF PLUTONIUM 2-96
2.9 ACCIDENT CONDITIONS FOR FISSILE MATERIAL PACKAGES FOR AIR TRANSPORT 2-96
2.9a SPECIAL FORM 2-96
2.9b FUEL RODS 2-96
2.10 APPENDICES 2-97
2.10.1 ES-3100 CONTAINMENT VESSEL ASME CODE EVALUATION 2-99
2.10.2 IMPACT ANALYSES OF ES-3100 DESIGN CONCEPTS USING BOROBOND AND CAT 277-4 NEUTRON ABSORBERS 2-157
2.10.3 KAOLITE PROPERTIES 2-463
2.10.4 CATALOG 277-4 PROPERTIES 2-535
2.10.5 BOROBOND4 PROPERTIES 2-645
2.10.6 RECOMMENDED RANDOM VIBRATION AND SHOCK TEST SPECIFICATIONS FOR CARGO TRANSPORTED ON SST AND SGT TRAILERS 2-659

CONTENTS

Page

2.10.7 TEST REPORT OF THE ES-3100 PACKAGE, VOLUME 1 - MAIN REPORT, ORNL/NTRC-013/V1, REV. 0, SEPTEMBER 10, 2004 2-677
2.10.8 THE ES-3100 TEST REPORT; VOL. 3, APPENDIX K - TU-4 DATA SHEETS 2-809
2.10.9 PACKAGING MATERIALS OUTGASSING STUDY FINAL REPORT 2-853
SECTION 2 REFERENCES 2-893

3. THERMAL EVALUATION 3-1
3.1 DISCUSSION 3-1
3.1.1 Design Features 3-3
3.1.2 Content's Decay Heat 3-4
3.1.3 Summary Tables of Temperatures 3-6
3.1.4 Summary Tables of Maximum Pressures 3-16
3.2 SUMMARY OF THERMAL PROPERTIES OF MATERIALS 3-19
3.2.1 Material properties 3-19
3.2.2 Component Specifications 3-19
3.3 GENERAL CONSIDERATIONS 3-19
3.3.1 Evaluation by Analysis 3-19
3.3.2 Evaluation by Test 3-25
3.3.3 Margins of Safety 3-28
3.4 THERMAL EVALUATION UNDER NORMAL CONDITIONS OF TRANSPORT 3-31
3.4.1 Heat and Cold 3-31
3.4.2 Maximum Normal Operating Pressure 3-33
3.4.3 Maximum Thermal Stresses 3-34
3.5 HYPOTHETICAL ACCIDENT THERMAL EVALUATION 3-35
3.5.1 Initial Conditions 3-35
3.5.2 Fire Test Conditions 3-36
3.5.3 Maximum Temperatures and Pressure 3-38
3.5.4 Accident Conditions for Fissile Material Packages for Air Transport 3-42
3.6 APPENDICES 3-43
3.6.1 THERMAL EVALUATION OF THE ES-3100 SHIPPING CONTAINER FOR NCT AND HAC (CONCEPTUAL DESIGN WITH BOROBOND4 NEUTRON ABSORBER) 3-45
3.6.2 THERMAL EVALUATION OF THE ES-3100 SHIPPING CONTAINER FOR NCT AND HAC (FINAL DESIGN WITH CATALOG 277-4 NEUTRON ABSORBER) 3-85
3.6.3 THERMAL STRESS EVALUATION OF THE ES-3100 SHIPPING CONTAINER DRUM BODY ASSEMBLY FOR NCT (FINAL DESIGN WITH CATALOG 277-4 NEUTRON ABSORBER) 3-125
3.6.4 CONTAINMENT VESSEL PRESSURE DUE TO NORMAL CONDITIONS OF TRANSPORT FOR THE PROPOSED CONTENTS 3-149
3.6.5 CONTAINMENT VESSEL PRESSURE DUE TO HYPOTHETICAL ACCIDENT CONDITIONS FOR THE PROPOSED CONTENTS 3-159
3.6.6 SILICONE RUBBER THERMAL PROPERTIES FROM THERM 1.2 DATABASE 3-167
3.6.7 ESTIMATES OF HYDROGEN BUILDUP IN THE ES-3100 PACKAGE CONTAINING HIGHLY ENRICHED URANIUM 3-169
SECTION 3 REFERENCES 3-349

CONTENTS

Page

4. CONTAINMENT 4-1
4.1 DESCRIPTION OF THE CONTAINMENT BOUNDARY 4-2
4.1.1 Containment Boundary 4-2
4.1.2 Special Requirements for Plutonium 4-4
4.2 GENERAL CONSIDERATIONS 4-4
4.2.1 Type A Fissile Packages 4-4
4.2.2 Type B Packages 4-4
4.3 CONTAINMENT UNDER NORMAL CONDITIONS OF TRANSPORT (TYPE B PACKAGES) 4-6
4.4 CONTAINMENT UNDER HYPOTHETICAL ACCIDENT CONDITIONS (TYPE B PACKAGES) 4-8
4.5 LEAKAGE RATE TESTS FOR TYPE B PACKAGES 4-10
4.6 APPENDICES 4-11
4.6.1 DETERMINATION OF A_2 FOR THE ES-3100 PACKAGE WITH HEU CONTENTS 4-13
4.6.2 CALCULATION OF THE ES-3100 CONTAINMENT VESSEL'S REGULATORY REFERENCE AIR LEAKAGE RATES 4-23
SECTION 4 REFERENCES 4-35

5. SHIELDING EVALUATION 5-1
5.1 DESCRIPTION OF SHIELDING DESIGN 5-1
5.1.1 Design Features 5-1
5.1.2 Summary Table of Maximum Radiation Levels 5-1
5.2 SOURCE SPECIFICATION 5-1
5.3 DOSE RATE ANALYSIS MODELS 5-3
5.3.1 Packaging Model Conservative Features 5-7
5.3.2 Photon model for 36-kg HEU metal content 5-9
5.3.3 Neutron model for 36-kg HEU metal content 5-11
5.3.4 Photon model for 24-kg HEU oxide content 5-11
5.3.5 Neutron model for 24-kg HEU oxide content 5-11
5.4 SHIELDING EVALUATION 5-11
5.5 APPENDICES 5-15
5.5.1 ORIGEN INPUT DATA FROM TABLE 5.3 5-17
5.5.2 CSASN AND ICE INPUT FROM TABLE 5.8 5-19
5.5.3 MORSE ROUTINES AND INPUT DATA 5-21
SECTION 5 REFERENCES 5-39

6. CRITICALITY EVALUATION 6-1
6.1 DESCRIPTION OF THE CRITICALITY DESIGN 6-1
6.1.1 Design Features 6-1
6.1.2 Summary of the Criticality Evaluation 6-2
6.1.3 Criticality Safety Index 6-32
6.2 PACKAGE CONTENTS 6-33
6.2.1 Fissile Material Contents 6-33
6.2.2 Convenience Cans, Teflon and Polyethylene Bottles, and 277-4 Canned Spacers 6-34

CONTENTS

Page

6.2.3 Packing Materials 6-35
6.2.4 Package Content Loading Restrictions 6-36
6.3 GENERAL CONSIDERATIONS 6-37
6.3.1 Model Configuration 6-38
6.3.2 Material Properties 6-55
6.3.3 Computer Codes and Cross-Section Libraries 6-57
6.3.4 Demonstration of Maximum Reactivity 6-68
6.4 SINGLE PACKAGE EVALUATION 6-70
6.4.1 Solid HEU Metal of Specified Geometric Shapes 6-71
6.4.2 HEU Solid Metal of Unspecified Geometric Shapes or HEU Broken Metal 6-79
6.4.3 HEU Oxide 6-80
6.4.4 UNH Crystals 6-82
6.5 EVALUATION OF PACKAGE ARRAYS UNDER NORMAL CONDITIONS OF TRANSPORT 6-84
6.5.1 Solid HEU Metal of Specified Geometric Shapes 6-84
6.5.2 HEU Solid Metal of Unspecified Geometric Shapes or HEU Broken Metal 6-86
6.5.3 HEU Oxide 6-89
6.5.4 UNH Crystals 6-89
6.6 EVALUATION OF PACKAGE ARRAYS UNDER HYPOTHETICAL ACCIDENT CONDITIONS 6-90
6.6.1 Solid HEU Metal of Specified Geometric Shapes 6-90
6.6.2 HEU Solid Metal of Unspecified Geometric Shapes or HEU Broken Metal 6-92
6.6.3 HEU Oxide 6-93
6.6.4 UNH Crystals 6-94
6.7 FISSILE MATERIAL PACKAGES FOR AIR TRANSPORT 6-95
6.7.1 Results for Solid HEU, One Piece per Convenience Can 6-95
6.7.2 Results for TRIGA Fuel Elements, Three Pieces per Convenience Can 6-97
6.7.3 Results for HEU Broken Metal, More Than One Piece per Convenience Can . . . 6-101
6.7.4 Conclusions 6-103
6.8 BENCHMARK EXPERIMENTS 6-103
6.8.1 Applicability of Benchmark Experiments 6-103
6.8.2 Details of Benchmark Calculations 6-104
6.8.3 Bias Determination 6-104
6.9 APPENDICES 6-105
6.9.1 FISSILE CONTENT AND PACKAGING MODELS 6-107
6.9.2 HAC PACKAGE MODEL 6-137
6.9.3 PACKAGE MATERIAL COMPOSITIONS 6-149
6.9.4 QUALIFICATION OF A NEUTRON ABSORBER MATERIAL FOR THE ES-3100 6-181
6.9.5 MISCELLANEOUS INFORMATION AND DATA 6-193
6.9.6 ABRIDGED SUMMARY TABLES OF CRITICALITY CALCULATION RESULTS 6-197
6.9.7 INPUT LISTINGS OF ES-3100 CALCULATION MODELS FOR SELECT CASES 6-353

CONTENTS

Page

6.9.8 Y/DD-896/R1, *CRITICAL EXPERIMENT BENCHMARK CALCULATIONS WITH CSAS25 FROM SCALE4.4a FOR CRITICALITY SAFETY ANALYSES ON THE HP J-5600 UNCLASSIFIED WORKSTATION (CMODB)* AND Y/DD-972R1, *DETERMINATION OF THE UPPER SUBCRITICAL LIMIT FOR CRITICALITY CALCULATIONS FOR CRITICALITY SAFETY ANALYSES* 6-577
6.9.9 CRITICALITY EVALUATION FOR INCREASING THE FISSILE LOADING LIMIT FOR HEU OXIDE IN THE ES-3100 6-717
6.9.10 Y/DD-1220, *CRITICAL EXPERIMENT BENCHMARK CALCULATIONS WITH CSAS25 FROM SCALE5 FOR CRITICALITY SAFETY ANALYSES ON THE HP zx6000 UNCLASSIFIED WORKSTATION (CMODD)* AND Y/DD-1221, *DETERMINATION OF THE UPPER SUBCRITICAL LIMIT FOR CRITICALITY CALCULATIONS FOR CRITICALITY SAFETY ANALYSES* 6-765
SECTION 6 REFERENCES 6-891

7. PACKAGE OPERATIONS 7-1
7.1 PACKAGE LOADING 7-1
7.1.1 Preparation for Loading 7-1
7.1.2 Loading of Contents 7-3
7.1.3 Preparation for Transport 7-7
7.2 PACKAGE UNLOADING 7-10
7.2.1 Receipt of Package from Carrier 7-10
7.2.2 Removal of Contents 7-11
7.3 PREPARATION OF EMPTY PACKAGE FOR TRANSPORT 7-12
7.4 OTHER OPERATIONS 7-12
SECTION 7 REFERENCES 7-13

8. ACCEPTANCE TESTS AND MAINTENANCE PROGRAM 8-1
8.1 ACCEPTANCE TESTS 8-1
8.1.1 Visual Inspections and Measurements 8-3
8.1.2 Weld Examinations 8-4
8.1.3 Structural and Pressure Tests 8-5
8.1.4 Leakage Tests 8-5
8.1.5 Component and Material Tests 8-6
8.1.6 Shielding Tests 8-6
8.1.7 Thermal Tests 8-6
8.1.8 Miscellaneous Tests 8-7
8.2 MAINTENANCE PROGRAM 8-7
8.2.1 Structural and Pressure Tests 8-7
8.2.2 Leakage Tests 8-7
8.2.3 Component and Material Tests 8-9
8.2.4 Thermal Tests 8-9
8.2.5 Miscellaneous Tests 8-9
SECTION 8 REFERENCES 8-11

FIGURES

Page

1.1. Schematic of the ES-3100 shipping package 1-2
1.2. Exploded view of the ES-3100 package with bulk HEU contents 1-3
1.3. Containment boundary of the ES-3100 shipping package 1-8
1.4. Typical shipping configurations inside the ES-3100 containment vessel 1-19
1.5. TRIGA fuel element 1-21
2.1. Containment vessel calculated stress locations 2-10
2.2. ES-3100 shipping package center of gravity locations 2-15
2.3. ES-3100 vibration testing arrangement 2-45
2.4. Water spray test arrangement for Test Unit -4 2-46
2.5. NCT free drop test on Test Unit-4 2-48
2.6. Compression test on Test Unit-4 2-49
2.7. Penetration test damage on Test Unit-4 2-50
2.8. 9-m drop test arrangement for all test units 2-54
2.9. 9-m drop test damage on Test Unit-4 2-56
2.10. Cumulative damage from 9-m drop and crush testing on Test Unit-2 2-58
2.11. Test Unit-3 damage from 1.2 and 9-m drop tests 2-59
2.12. 1.2 and 9-m drop test damage on Test Unit-1 2-61
2.13. 1.2 and 9-m drop test damage to Test Unit-5 2-63
2.14. Cumulative damage following 9-m crush on Test Unit-1 2-65
2.15. Cumulative damage following 9-m crush test on Test Unit-3 2-67
2.16. Cumulative damage from 9-m drop and crush testing on Test Unit-4 2-68
2.17. Cumulative damage from 9-m drop and crush testing on Test Unit-5 2-70
2.18. 28° oblique and horizontal puncture tests on Test Unit-1 2-72
2.19. 40° oblique puncture test on Test Unit-1 2-72
2.20. Horizontal puncture test over Test Unit-1's containment vessel flange 2-73
2.21. Horizontal CG puncture test on Test Unit-2 2-73
2.22. 24.6° oblique puncture test on Test Unit-3 2-74
2.23. Vertical puncture test on Test Unit-4 2-74
2.24. Horizontal puncture test over Test Unit-5's containment vessel flange 2-75
2.25. Visual comparison of the cumulative damage on the crush side surface after the three drop tests (from top to bottom: Test Unit-1, analytical results with BoroBond, analytical results with Cat 277-4) 2-84
2.26. Visual comparison of the cumulative damage on the rigid surface side after the four drop tests (from left to right: Test Unit-2, analytical results with BoroBond, analytical results with Cat 277-4) 2-87
2.27. Visual comparison of the cumulative damage on the crush plate side after the three drop tests (from left to right: Test Unit-2, analytical results with BoroBond, analytical results with Cat 277-4) 2-87
2.28. Visual comparison of the cumulative bottom damage after the three drop tests (from top to bottom: Test Unit-3, analytical results with BoroBond, analytical results with Cat 277-4) 2-89
2.29. Visual comparison of the cumulative lid damage after the three drop tests (from top to bottom: Test Unit-3, analytical results with BoroBond, analytical results with Cat 277-4) 2-90
2.30. Visual comparison of the cumulative damage after the three drop tests (from left to right: Test Unit-4, analytical results with BoroBond, analytical results with Cat 277-4) 2-92
2.31. Containment vessel markings at assembly (swivel hoist ring removed prior to testing) 2-95
2.32. Containment vessel marking after compliance testing 2-95
3.1. MSC.Patran axisymmetric finite element model of the ES-3100 shipping container with BoroBond 4—nodal locations of interest (elements representing air not shown for clarity). . . . 3-6
3.2. Test units preheat arrangement. 3-26
3.3. Test unit insertion into furnace. 3-26

FIGURES

Page

3.4. Test unit removal from furnace. 3-27
3.5. Test unit cool down and monitoring arrangement. 3-27
5.1. Cylindrical calculational model of the ES-3100 shipping package for NCT 5-6
5.2. ES-3100 HEU metal content radial (top view) geometric models 5-10
6.1. R/Z section view of ES-3100 single-unit packaging model 6-40
6.2. R/Z section view at bottom of ES-3100 single-unit packaging showing KENO V.a geometry units 1001–1003, and 1006 (partial) 6-41
6.3. R/Z section view at center of the ES-3100 single-unit packaging showing KENO V.a geometry units 1006 (partial), 1007, and 1008 (partial) 6-42
6.4. R/Z section view of near top of the ES-3100 single-unit packaging showing KENO V.a geometry units 1008 (partial) and 1010–1016 6-43
6.5. R/Z section view at the top of the ES-3100 single-unit packaging showing KENO V.a geometry units 1016–1019 6-44
6.6. R/Z section view of ES-3100 array packaging model with a 7% reduction in the drum's inner diameter 6-45
6.7. R/Z section view at the bottom of the ES-3100 array packaging showing KENO V.a geometry units 1001–1003, and 1006 (partial) 6-46
6.8. R/Z section view at the center of the ES-3100 array packaging showing KENO V.a geometry units 1006 (partial), 1007, and 1008 (partial) 6-47
6.9. R/Z section view of near top of the ES-3100 array packaging showing KENO V.a geometry units 1008 (partial) and 1010–1016 6-48
6.10. R/Z section view at the top of the ES-3100 array packaging showing KENO V.a geometry units 1016–1019 6-49
6.11. Model 1. 6-53
6.12. Model 2. 6-53
6.13. Model 3. 6-53
6.14. Model 4 6-54
6.15. Model 5 6-54
6.16. Model 6 6-54
6.16a. $k_{eff} + 2\sigma$ versus pitch for triangular arrangement of content in CV 6-74
6.16b. $k_{eff} + 2\sigma$ versus triangular pitch over range of CV moderation 6-75
6.16c. $k_{eff} + 2\sigma$ as a function of uranium weight fraction and moderation 6-75
6.17. K_{eff} vs. enrichment (wt % ^{235}U) for HEU ranging from 7 to 10 kg 6-96
6.18. K_{eff} vs. stainless steel shell radius (cm) for 7 kg HEU with enrichments ranging from 19 to 100 wt % ^{235}U 6-96
6.19. K_{eff} vs. Kaolite shell radius (cm) for 7 kg HEU with enrichments ranging from 19 to 100 wt % ^{235}U 6-98
6.20. K_{eff} vs. shell radius (cm) for dry and water-saturated Kaolite for 7 kg HEU at 100% enrichment 6-98
6.21. K_{eff} vs shell radius (cm) for 10.4 kg core of $UZrH_x$ with stainless steel or Kaolite shell 6-99
6.22. K_{eff} vs. core radius (cm) for homogenized core of $UZrH_x$, 500 g polyethylene, and Kaolite where the Kaolite water content ranges from the dry to the water-saturated condition 6-100
6.23. k_{eff} vs. excess water from Kaolite for fissile core blanketed with a variable thickness Kaolite shell. 6-101
6.24. K_{eff} vs. excess water from Kaolite for core of 1–7 kg enriched HEU broken metal at 100% enrichment, core blanketed with a variable thickness Kaolite shell 6-102
6.25. K_{eff} vs. excess water from Kaolite for core 20% enriched HEU broken metal (0.6–7 kg ^{235}U), core blanketed with a variable thickness Kaolite shell 6-102

TABLES

Page

1.1. Uranium concentration limits 1-10
1.2. Bounding uranium isotopic concentrations in oxide 1-11
1.3. Authorized content [a] and fissile mass loading limits [b, c] for ground transport 1-15
1.3a. Uranyl nitrate crystal content loading limits for ground transport 1-16
1.3b. Authorized content and fissile mass loading limits [a, b] for air transport 1-17
1.4. TRIGA fuel specifications 1-18
2.1. Proposed HEU contents for shipment in the ES-3100 2-2
2.2. Category designations for Type B packages 2-7
2.3. Summary of load combinations for normal and hypothetical accident conditions of transport 2-9
2.4. Containment vessel allowable stress 2-10
2.5. Allowable stress intensity (S_m) for the containment boundary materials of construction 2-11
2.6. ES-3100 containment boundary design evaluation allowable stress comparisons 2-12
2.7. ES-3100 packaging material specifications 2-13
2.8. Packaging weights for various ES-3100 shipping package arrangements 2-16
2.9. Compliance test unit weights 2-18
2.10. Calculated center of gravity for the various ES-3100 shipping arrangements 2-19
2.11. Applicable codes and standards for Category I packaging 2-20
2.12. Mechanical properties of the metallic components of the drum assembly 2-21
2.13. Mechanical properties of the lid fastening components for the drum assembly 2-22
2.14. Mechanical properties of the cast refractory insulation 2-22
2.15. Mechanical properties of containment vessel O-rings 2-22
2.16. Mechanical properties of the metallic components of the containment boundary 2-23
2.17. Mechanical properties of the cast neutron absorber 2-24
2.18. Summary of NCT – 10CFR71.71 tests for ES-3100 package 2-33
2.19. Summary of HAC – 10CFR71.73 tests for ES-3100 package 2-33
2.20. Summary of temperatures and pressures for NCT 2-37
2.21. ES-3100 containment boundary evaluation for both hot and cold conditions 2-41
2.22. NCT ES-3100 containment boundary stress compared to the allowable stress at reduced and increased external pressures 2-43
2.23. Test and analysis summary for the ES-3100 package 2-52
2.24. Recorded height damage to Test Unit-4 from 1.2-m and 9-m drop testing 2-55
2.25. Recorded diametrical damage to Test Unit-4 from 1.2-m and 9-m drop tests 2-55
2.26. Recorded diametrical damage to Test Unit-2 from NCT and HAC drop testing 2-57
2.27. Recorded flat contour damage to Test Unit-2 from NCT and HAC drop testing 2-57
2.28. Recorded height damage to Test Unit-2 from NCT and HAC drop testing 2-57
2.29. Recorded height damage to Test Unit-3 from 1.2-m and 9-m drop testing 2-59
2.30. Recorded diametrical damage to Test Unit-3 from 1.2-m and 9-m drop testing 2-59
2.31. Recorded height damage to Test Unit-1 from 1.2-m and 9-m drop testing 2-60
2.32. Recorded diametrical damage to Test Unit-1 from 1.2-m and 9-m HAC drop testing 2-60
2.33. Recorded flat contour damage to Test Unit-1 from 1.2-m and 9-m drop testing 2-61
2.34. Recorded height damage to Test Unit-5 from 1.2-m and 9-m drop testing 2-62
2.35. Recorded diametrical damage to Test Unit-5 from 1.2-m and 9-m HAC drop testing 2-62
2.36. Recorded flat contour damage to Test Unit-5 from 1.2-m and 9-m drop testing 2-63
2.37. Recorded height damage to Test Unit-1 from the 9-m crush test 2-64
2.38. Recorded diametrical damage to Test Unit-1 from the 9-m crush test 2-64
2.39. Recorded flat contour damage to Test Unit-1 from the 9-m crush test 2-65
2.40. Recorded height damage to Test Unit-3 from the 9-m crush test 2-66

TABLES

Page

2.41. Recorded flat contour damage to Test Unit-3 from the 9-m crush test 2-66
2.42. Recorded diametrical damage to Test Unit-3 from the 9-m crush test 2-66
2.43. Recorded height damage to Test Unit-4 from the 9-m crush test 2-67
2.44. Recorded diametrical damage to Test Unit-4 from the 9-m crush test 2-68
2.45. Recorded height damage to Test Unit-5 from the 9-m crush test 2-69
2.46. Recorded diametrical damage to Test Unit-5 from the 9-m crush tests 2-69
2.47. Recorded flat contour damage to Test Unit-5 from the 9-m crush test 2-69
2.48. 1-m (40-in.) puncture drop test description and results 2-70
2.49. Thermax temperature indicating patches for test units 2-75
2.50. Maximum HAC temperatures recorded on the test packages' interior surfaces 2-78
2.51. HAC ES-3100 containment boundary stress compared to the allowable stress 2-80
2.52. Diametrical damage comparison of Test Unit-1 with analytical predictions 2-83
2.53. Flat contour damage comparison of Test Unit-1 with analytical results 2-83
2.54. Cumulative analytical 12° slapdown drop tests maximum effective plastic strain results 2-85
2.55. Diametrical damage comparison of Test Unit-2 with analytical predictions 2-86
2.56. Flat contour damage comparison of Test Unit-2 with analytical predictions 2-86
2.57. Cumulative analytical side drop test maximum effective plastic strain results 2-88
2.58. Diametrical damage comparison of Test Unit-3 with analytical predictions 2-88
2.59. Cumulative analytical corner drop test maximum effective plastic strain results 2-91
2.60. Diametrical damage comparison of Test Unit-4 with analytical predictions 2-92
2.61. Cumulative analytical top drop test maximum effective plastic strain results 2-93
2.62. ES-3100 test package weights before and after 10 CFR 71.73(c)(4) HAC thermal testing 2-93
3.1. Isotopic mass and weight percent for the HEU contents 3-4
3.2. Decay heat for 35.2 kg of HEU content (watts) 3-5
3.3. Maximum "quasi steady-state" temperatures during NCT for the ES-3100 shipping container with various content heat loads—Kaolite density of 19.4 lb/ft^3 and BoroBond4 3-7
3.4. Maximum "quasi steady-state" temperatures during NCT for the ES-3100 shipping container with various content heat loads—Kaolite density of 30 lb/ft^3 and BoroBond4 3-8
3.4a. ES-3100 shipping container finite element model nodal map 3-9
3.5. ES-3100 shipping container maximum steady-state temperatures with Cat 277-4 3-10
3.6. ES-3100 shipping container maximum "quasi steady-state" temperatures during NCT with various content heat loads and Cat 277-4 3-11
3.7. ES-3100 shipping container HAC maximum temperatures 3-13
3.8. ES-3100 shipping container HAC maximum temperatures 3-14
3.9. Maximum HAC temperatures recorded on the test packages' interior surfaces 3-15
3.10. Total pressure inside the containment vessel at 87.81°C (190.06°F) 3-17
3.11. Total pressure inside the containment vessel at 123.85°C (254.93°F) 3-19
3.12. Thermal properties of the materials used in the thermal analysis 3-20
3.13. Mechanical properties of the materials used in the static stress analyses 3-21
3.14. Packaging material technical specifications 3-22
3.15. Component allowable service temperature and pressure 3-24
3.16. Summary of results of evaluation for the ES-3100 under NCT 3-29
3.17. Summary of results of evaluation under HAC for the ES-3100 shipping arrangement using bounding case parameters 3-30
3.18. ES-3100 test package weights before and after 10 CFR 71.73(c)(4) HAC thermal testing 3-38
3.19. Thermax temperature indicating patches for test units 3-39
3.20. Predicted temperature adjustments (°F) for containment vessel due to HAC 3-41
3.21. Predicted temperatures of the containment vessel due to HAC 3-41

TABLES

Page

4.1. Containment requirements of transport for Type B packages 4-1
4.2. Summary of the containment vessel design and fabrication acceptance basis 4-1
4.3. Isotopic mass and weight percent for the HEU contents 4-5
4.4. Activity, A_2 value, and number of A_2 proposed for transport 4-5
4.5. Regulatory leakage criteria for NCT 4-7
4.6. Containment vessel verification tests criteria for NCT 4-7
4.7. Regulatory leakage criteria for HAC 4-9
4.8. Containment vessel design verification tests for HAC 4-9
5.1. Calculated external dose rates for the ES-3100 package with 36 kg of HEU metal contents 5-2
5.2. Calculated external dose rates for the ES-3100 package with 24 kg of HEU oxide contents 5-2
5.3. Radioisotope specification for all ES-3100 package analysis source calculations with HEU content and other nuclides per HEU unit weight 5-3
5.4. Photon source for one gram of HEU for all contents 5-4
5.5. Neutron source for one gram of HEU for all contents 5-4
5.6. Geometric data for the shielding analysis models of the ES-3100 shipping package as shown in Fig. 5.1 for NCT 5-5
5.7. Detector locations relative to the drum for NCT and to the containment vessel for HAC 5-7
5.8. Shielding model material specifications for the ES-3100 package with HEU content 5-8
5.9. ANSI standard photon flux-to-dose-rate conversion factors 5-12
5.10. ANSI standard neutron flux-to-dose-rate conversion factors 5-13
6.1a. Summary of criticality evaluation for solid HEU metal cylinders and bars 6-5
6.1b. Summary of criticality evaluation for solid HEU metal slugs 6-9
6.1c. Summary of criticality evaluation for solid HEU metal of unspecified geometric shapes characterized as broken metal 6-14
6.1d. Summary of criticality evaluation for HEU product and skull oxide 6-21
6.1e. Summary of criticality evaluation for UNX crystals and unirradiated TRIGA reactor fuel elements 6-25
6.2a. HEU fissile material mass loading limits (case name) for surface-only modes of transportation 6-30
6.2b. HEU fissile material mass loading limits for air transport mode of transportation 6-31
6.3. Deformation of 18.37-in.-diam ES-3100 drum projected by finite element analysis Case “3100 RUN1HL Lower Bound Kaolite May 2004” 6-52
6.4. Material compositions used in the ES-3100 calculation models 6-58
7.1. Replacement parts for the ES-3100 packaging 7-2
8.1. Acceptance tests for the drum assembly 8-2
8.2. Acceptance tests for the containment vessel assembly 8-3

THIS PAGE INTENTIONALLY LEFT BLANK.

ABBREVIATIONS

ALARA	as low as reasonably achievable
AM	as-manufactured
ANC	Average Net Count
ANSI	American National Standards Institute
AS	allowable stress
ASME	American Society of Mechanical Engineers
ASTM	American Society for Testing and Materials
Cat 277-4	Thermo Electron Corporation (corporate name changed to Shieldwerx) Catalog No. 277-4™ (or Cat. No. 277-4)
CD	capacity discharge
CERCA	Compagnie pour l'Étude et la Realisation de Combustibles Atomiques
CFR	Code of Federal Regulations
CMTR	certified material test report
CoC	Certificate of Compliance
CSI	criticality safety index
CV	containment vessel
CVA	containment vessel arrangement
DOE	U.S. Department of Energy
DOT	U.S. Department of Transportation
EPDM	ethylene-propylene-diene monomer
ETP	explicit triangular pack
FEA	finite element analysis
H/X ratio	hydrogen-to-fissile isotope ratio
HAC	Hypothetical Accident Conditions
HEU	highly enriched uranium
IAEA	International Atomic Energy Agency
k_{eff}	calculated neutron multiplication factor
LOD	loss on drying
LTL	lower tolerance limit
M.S.	margin of safety
MNOP	maximum normal operating pressure
MOCFR	moisture fraction inside the containment vessel
MOIFR	moisture fraction of the package external to the containment vessel
NCT	Normal Conditions of Transport
NLF	neutron leakage fraction
NRC	U.S. Nuclear Regulatory Commission
NTRC	National Transportation Research Center
OECD	Organization for Economic Cooperation and Development
ORNL	Oak Ridge National Laboratory
PGNAA	Prompt Gamma-ray Neutron Activation Analysis
ppb	parts per billion
ppm	parts per million
QA	quality assurance
QCPI	Quality Certification and Procurement
RCSB	Rackable Can Storage Box
SAR	safety analysis report
SCALE	Standardized Computer Analysis for Licensing Evaluation
s_i	standard error

ABBREVIATIONS

SRS	Savannah River Site
SS304	type 304 stainless steel
SST/SGT	Safe-Secure Trailer/Safeguards Transporter
TGA	thermogravimetric analysis
TI	transport index
TID	tamper-indicating device
TS	test sample
UNH	uranyl nitrate hexahydrate
UNX	uranyl nitrate crystals
USL	upper subcritical limit
VF	Volume Fraction
Y-12	Y-12 National Security Complex

REVISION LOG

Date	SAR Revision No.	Description	Affected Pages
2/25/05	0	Original issue	All
8/15/05	0, Page Change 1	Page changes resulting from *Responses to Request for Additional Information* #1, Y/LF-747.	title page, iv, xxiii, 1-4, 1-145, 2-2, 2-3, 2-6, 2-31, 2-32, 2-33, 2-34, 2-57, 2-59, 2-61, 2-107, 2-125, 2-131, 2-171, 2-173, 2-181, 2-183, 2-185, 2-186, 2-189, 2-367, 2-458, 2-675, 8-8, 8-9, 8-31
2/6/06	0, Page Change 2	Page changes resulting from *Responses to Request for Additional Information #2*, Y/LF-761.	All Sections
3/20/06	0, Page Change 3	Page changes resulting from *Responses to Request for Additional Information #3*, Y/LF-764.	1.38, 1.48, Appendix 1.4.1, 2-120, Table 6.4
5/8/06	0, Page Change 4	Added polyethylene bottles and nickel alloy cans as convenience containers for authorized HEU contents. (CoC Revision 1)	Various pages in chapters 1, 2, 3 and 4.
8/21/06	0, Page Change 5	Revised equipment specifications for Kaolite and 277-4 neutron absorber. (CoC Revision 3)	Appendices 1.4.4 and 1.4.5.

REVISION LOG

Date	SAR Revision No.	Description	Affected Pages
11/15/06	1	Updated definition of pyrophoric uranium. Evaluated air transport. Revised criticality safety calculations to remove bias correct factors. Added a CSI option of 3.2. Increased mass of off-gassing material allowed in containment vessel. Increased carbon concentration in HEU contents. Increased Np-237 concentration is HEU contents. Added uranium zirconium hydride and uranium carbide as contents (TRIGA fuel). Revised equipment specifications for 277-4 neutron absorber. (CoC Revision 3)	All Sections
3/29/07	1, Page Change 1	Updated definition of TRIGA fuel for air transport and added TRIGA-related criticality safety cases.	title pages, viii, xi, xx, 1-12, 1-13, 1-20, 6-30, 6-54, 6-64, 6-66, 6-87, 6-119, 6-240 to 6-286, 6-385 to end
5/31/07	1, Page Change 2	Revised SAR in response to RAIs dated May 9, 2007 in reference to CoC Revision 4	title pages, xiii, xx, Section 1 and Section 6
6/30/07	1, Page Change 3	Revised SAR in response to RAIs dated May 9, 2007 in reference to CoC Revision 5	title pages, table of contents, Section 1, and Section 7
7/31/07	1, Page Change 4	Removed oxidation as an option for treating pyrphoric uranium metal	title pages, xx, 1-12, 1-201, 1-203, 1-212, 2-26, 7-4
8/28/07	1, Page Change 5	Modified TRIGA fuel definition to include fuel pellets with cladding	title page, xx, 1-13, 1-17, 2-4, 6-29, 6-30a, 6-66c, 6-66d, 6-73, 6-87, 6-119a

REVISION LOG

Date	SAR Revision No.	Description	Affected Pages
10/10/07	1, Page Change 6	-Revised criticality safety calculations to remove bias correction factors.	Table 6.2a and supporting calculations.
		-Added a CSI option of 3.2.	Table 6.2a and supporting calculations.
		-Increased mass of off-gassing material in containment vessel to allow Teflon bottles.	Figure 1.4, page 1-15, and Appendices 3.6.4 and 3.6.5.
		-Increased carbon and moisture concentration in HEU contents.	Pages 1-10 and 1-11, Table 6.2a and pages 6-31 and 6-52.
		-Increased Np-237 concentration is HEU contents.	Pages 5-1 to 5-4, and supporting calculations.
		-Revised equipment specifications for 277-4 neutron absorber.	Pages 1-83 and 1-97.
		-Details of alloys of uranium in contents definition.	Page 1-12.
		-More precise specification of maximum fissile mass in calculations (changed from 36 kg to 35.2 kg).	Administrative change affecting many pages. Removed round-off. No new calculations.

REVISION LOG

Date	SAR Revision No.	Description	Affected Pages
3/6/08	2	-Add the following contents for ground transport: • HEU oxides (U_3O_8-Al and UO_2-Mg) • Research reactor fuel elements or components (clad U-Al, U_3O_8-Al, UO_2, or UO_2-Mg) -Add the following contents for air transport: • HEU oxides (UO_2, UO_2-Mg, U_3O_8, and U_3O_8-Al) • Broken HEU bulk metal and uranium-aluminum alloy of unspecified geometric form • Research reactor fuel elements or components (clad U-Al, U_3O_8-Al, UO_2, or UO_2-Mg)	1-10 through 1-17, 1-20, 1-22, 2-1, 2-2, 2-4, 2-5, 2-15, 2-17, 2-18, 2-25, 2-26, 3-15 through 3-17, 3-22, 3-147, 3-149, 3-151 through 3-155, 3-157 through 3-161, 4-2, 6-1, 6-2, 6-4, 6-5, 6-30 through 6-34, 6-51, 6-56, 6-69, 6-78, 6-83, 6-87, 6-92, 6-93, 6-95, 6-119, 6-128 through 6-130, 6-168, 6-282 through 6-286, 6-303 through 6-305, and 6-488 through 6-501.
6/19/08	2, Page Change 1	Revised SAR in response to RAIs dated April 28, 2008 for review of CoC 9315, Revision 8	i, ix, x, xxii, 1-15, 3-15 through 3-17, 3-154, 3-161, 4-3, 6-1, 6-3, 6-3a, 6-3b, 6-4, 6-5, 6-9 through 6-12, 6-29, 6-30, 6-35, 6-36, 6-67, 6-69, 6-70, 6-73, 6-74, 6-80, 6-81, 6-84, 6-96, 6-97, 6-99, 6-101, 6-103, 6-103a, 6-103b, 6-104a through 6-104n, 6-167, 6-188 through 6-197, 6-316 through 6-320, 6-320a through 6-320d, 6-321 through 6-324, 6-351 through 6-354, 6-354a through 6-354b, 6-355 through 6-362, 6-503 through 6-642, and 6-644.

REVISION LOG

Date	SAR Revision No.	Description	Affected Pages
8/28/08	2, Page Change 2	Revised SAR in response to RAIs dated April 28, 2008, for review of CoC 9315, Revision 8	i, vi, viii, xii, xxiii, xxiv, 1-10, 1-14 through 1-16, 1-22, 2-1, 2-25 through 2-28, 2-894, 3-15, 3-16, 3-165 through 3-290, 4-1, 4-2, 6-1 through 6-3, 6-20 through 6-28, 6-30 6-32 through 6-34, 6-68 through 6-70, 6-70a, 6-70b, 6-75 through 6-77, 6-77a, 6-77b, 6-78, 6-81 through 6-83, 6-85, 6-86, 6-101 through 6-103, 6-103a through 6-103j, 6-104, 6-123 through 6-126, 6-167 through 6-170, 6-177, 6-177a, 6-177b, 6-218a through 6-218f, 6-219 through 6-234, 6-303 through 6-305, 6-331, 6-332, 6-332a, 6-332b, 6-333, 6-394 through 6-398, 6-501, 6-502, 6-502a through 6-502dd

REVISION LOG

Date	SAR Revision No.	Description	Affected Pages
2/26/09	2, Page Change 3	Revised SAR in response to RAIs dated January 12, 2009, for review of CoC 9315, Revision 9	i, viii, ix, xxiv, 1-7, 1-10, 1-12 through 1-16, 1-21 through 1-23, 1-29 1-31, 1-33, 1-35, 1-37, 1-39, 1-41, 1-135, 1-157, 1-177, 2-6, 2-9, 2-18, 2-36 through 2-38, 2-41 through 2-43, 2-53, 2-78, 2-80, 3-15 through 3-17, 3-27, 3-28, 3-30, 3-32, 3-39, 3-41, 3-147, 3-149 through 3-154, 3-154a, 3-154b, 3-155, 3-158 through 3-161, 3-165 through 3-174, 3-289 through 3-344, 4-2, 4-7, 4-9, 4-27 through 4-34, 6-5, 6-29, 6-30, 6-34, 6-73 through 6-86, 6-86a through 6-86d, 6-96, 6-103a through 6-103c, 6-104b, 6-104c, 6-123, 6-124, 6-168, 6-219 through 6-221, 6-221a, 6-221b, 6-222, 7-7, 7-8, 7-10

REVISION LOG

Date	SAR Revision No.	Description	Affected Pages
5/6/09	3	This revision was issued to match Amendment 9 of the COC. -Remove the following contents for ground transport that were not reviewed by NRC: • HEU oxides (U_3O_8-Al and UO_2-Mg) • Research reactor fuel elements or components (clad U-Al, U_3O_8-Al, UO_2, or UO_2-Mg) -Remove the following contents for air transport that were not reviewed by NRC: • HEU oxides (UO_2, UO_2-Mg, U_3O_8, and U_3O_8-Al) • Broken HEU bulk metal and uranium-aluminum alloy of unspecified geometric form • Research reactor fuel elements or components (clad U-Al, U_3O_8-Al, UO_2, or UO_2-Mg)	All
4/14/10	3, Page Change 1	Revised SAR to • add uranium oxide loading with a CSI value of 0.4 • remove the 8-lb minimum payload weight • add stainless-steel option for can spacers • revise allowable weight changes for drum body and top plug • revise Drawing M2E801580A005 to clarify marking requirements on drum hex nuts • allow methods other than sieving for establishing minimum content sizes for pyrophoric purposes • revise the purity of the cover gas used for pyrophoric material	i, x, xxv, 1-13, 1-16, 1-22, 1-23, 1-24, 1-27, 1-89 through 1-126, 1-126a, 1-126b, 1-135, 1-147, 1-178a, 1-178b, 1-221, 2-1, 2-14, 2-24, 6-1, 6-3, 6-4, 6-31, 6-35, 6-57, 6-67 through 6-69, 6-104, 6-105, 6-195, 6-717 through 6-892, 7-3, 7-4, 8-9, 8-10

Date	SAR Revision No.	Description	Affected Pages
		Note: The NRC performed an acceptance review of Page Change 1 and generated several Requests for Supplemental Information (RSIs). Therefore, Page Change 1 will be superceded by Page Change 2, which incorporates the responses to the RSIs.	
7/22/10	3, Page Change 2	Reissue of Page Change 1 with RSI responses incorporated	i, x, xiv, xxv, xxvi 1-13, 1-16, 1-22, 1-23, 1-24, 1-27, 1-89 through 1-126, 1-126a, 1-126b, 1-135, 1-147, 1-178a, 1-178b, 1-221, 2-1, 2-6, 2-14, 2-24, 2-26, 3-8a, 3-8b, 3-9, 3-10, 3-12, 3-13, 3-18, 3-23, 3-27, 3-27a, 3-27b, 3-100, 3-104, 3-105, 3-115, 3-116, 3-140, 6-1, 6-3, 6-4, 6-31, 6-35, 6-57, 6-67 through 6-69, 6-104, 6-105, 6-195, 6-717 through 6-892, 7-3, 7-4, 8-9, 8-10
1/27/11	3, Page Change 3	Revised SAR in response to RAIs dated October 12, 2010, for review of CoC 9315, Revision 10	i, vi, xiv, xxvi, 2-6, 2-11, 2-36, 2-37, 2-41 through 2-43, 2-53, 2-78, 2-80, 3-16 through 3-18, 3-23, 3-27, 3-27a through 3-27d, 3-28, 3-30, 3-39, 3-147, 3-153 through 3-157, 3-160 through 3-164, 4-7, 4-9, 4-23, 4-25 through 4-34, 7-2, 7-6, 7-7, 7-11
3/3/11	4	This SAR revision matches Rev. 10 of the COC. Incorporated Page Changes 1–3 and revised MNOP value in two additional locations (Sects. 1.2.3.5 and 3.5.1)	All

1. GENERAL INFORMATION

1.1 INTRODUCTION

This safety analysis report (SAR) presents the results of the safety analysis prepared in support of B&W Y-12's request for licensing of the ES-3100 package with bulk highly enriched uranium (HEU) contents and issuance of a Type B Fissile Material Certificate of Compliance. This SAR, published in the format specified in the Nuclear Regulatory Commission (NRC) draft guidance DG-7003 and using information provided in NRC Regulatory Guide 7.10, demonstrates that the Y-12 National Security Complex (Y-12) ES-3100 package with bulk HEU contents meets the applicable requirements of 10 CFR 71 and 49 CFR Pts. 100–178.

To protect the health and safety of the public, shipments of radioactive materials are made in packaging that is designed, fabricated, assembled, tested, procured, used, maintained, and repaired in accordance with the provisions cited above. Safety requirements addressed by the regulations that must be met when transporting radioactive materials are containment of radioactive materials, radiation shielding, and assurance of nuclear subcriticality.

A general description and a summary of the evaluation of the packaging are presented in this section. Subsequent sections address structural (Sect. 2) and thermal (Sect. 3) responses to Normal Conditions of Transport (NCT) and Hypothetical Accident Conditions (HAC) and the packaging's ability to contain the radioactive materials when subjected to the requirements of 10 CFR 71.71 and 71.73, respectively. A shielding evaluation was prepared to ensure adequate nuclear radiation shielding (Sect. 5). Criticality evaluations that are unique to the contents were prepared to ensure nuclear subcriticality (Sect. 6). Sections 7 and 8 discuss the operating procedures, the new packaging acceptance tests, and the maintenance program for the planned use and refurbishment of the packaging.

The ES-3100 package was subjected to verification (analysis, similarity comparisons, tests, or a combination of these) for NCT and HAC. Full-scale packages were used for design verification testing (see Sects. 2 and 3). The ES-3100 package with bulk HEU content was verified solely on the ability of the package to meet the requirements of 10 CFR 71. Transport vehicle influence on the package is not required to meet 10 CFR 71 requirements.

The packaging verification activities (Sects. 2, 3, and 4), using content test masses of between 3.6 and 50.3 kg (8 and 111 lb), show that the packaging meets the containment requirements of 10 CFR 71. The shielding evaluations (Sect. 5) show that the packaging meets the NCT requirements of 10 CFR 71.47, *External Radiation Standards for all Packages*, and the HAC requirements of 10 CFR 71.51, *Additional Requirements for Type B Packages*. Based on the results of the thermal and shielding evaluations, the ES-3100 package with bulk HEU content may be shipped as a nonexclusive use package. The criticality evaluation (Sect. 6) shows that the packaging meets the requirements of 10 CFR 71.55, *General Requirements for Fissile Material Packages*, and 10 CFR 71.59, *Standards for Arrays of Fissile Material Packages*.

1.2 PACKAGE DESCRIPTION

A schematic of the ES-3100 shipping package is shown in Fig. 1.1, and an exploded view of the packaging components is presented in Fig. 1.2. The packaging design drawings (Appendix 1.4.8) provide material lists, dimensions, safety components, welding requirements, and gasket requirements. The

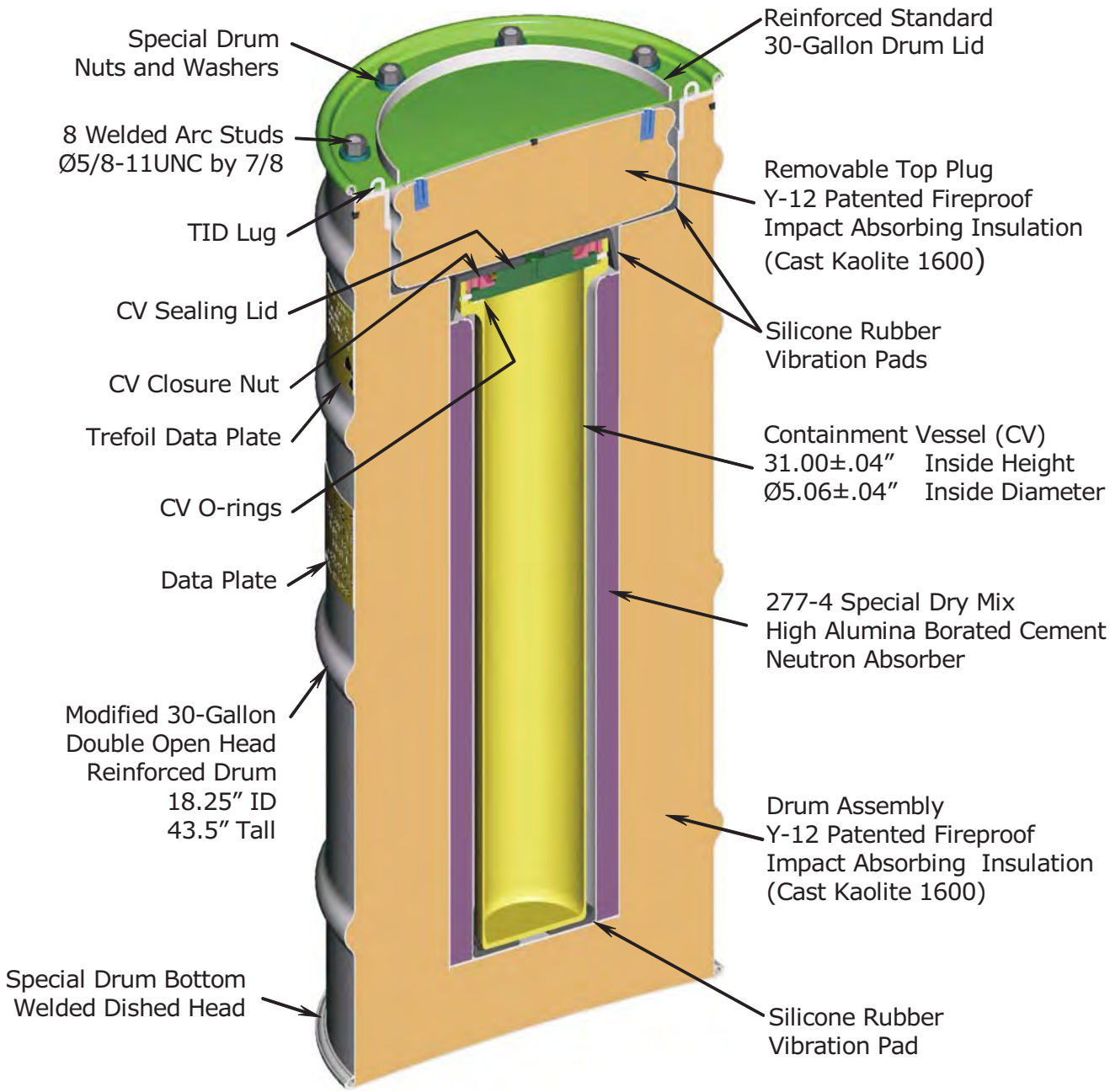

Fig. 1.1. Schematic of the ES-3100 shipping package.

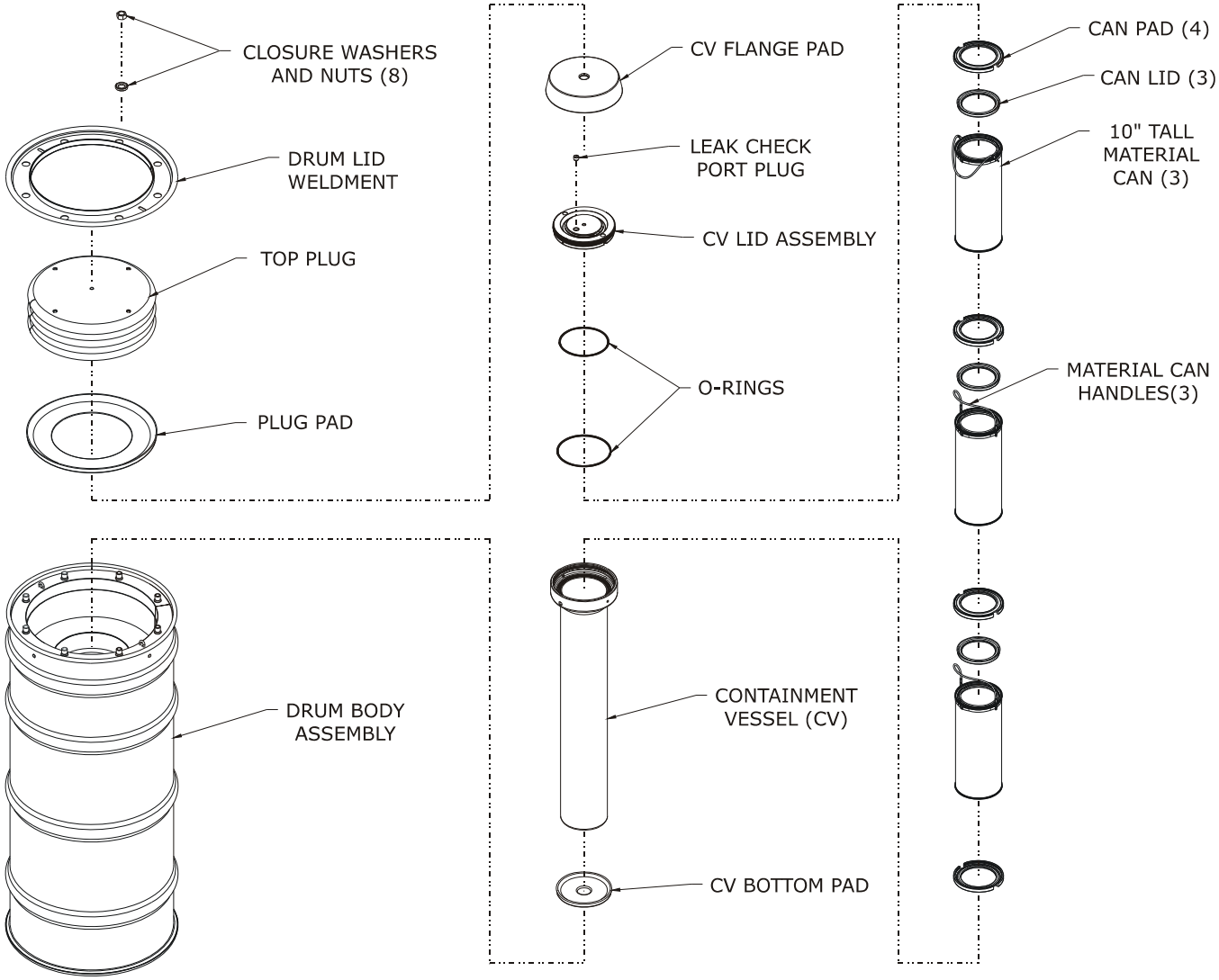

Fig. 1.2. Exploded view of the ES-3100 package with bulk HEU contents.

proposed maximum gross shipping weight of the ES-3100 package with bulk HEU content is 187.81 kg (414.05 lb). The certification drawing of the ES-3100 can be found in Appendix 1.4.1. The authorized maximum gross weight of the ES-3100 package is 190.5 kg (420 lb). The ES-3100 packaging as specified in this SAR is classified as a Category II package (see Appendix 1.4.6). However, since the ES-3100 shipping package may be used for future contents having higher A_2 values, the package has been designed and analyzed to meet the requirements of a Category I package.

1.2.1 Packaging

The main functions of the packaging are containment, shielding, and nuclear criticality safety. The bulk HEU contents create a maximum decay heat of approximately 0.4 W (Sect. 1.2.3.7 and Sect. 3.1.2); therefore, the packaging does not require any special design features such as coolant valves or continuous venting to meet the thermal requirements of 10 CFR 71.

1.2.1.1 Drum assembly

The drum assembly consists of a double open-head reinforced stainless-steel 30-gal drum, arched cover that forms the bottom, arched lid, inner liner, and top plug with cast refractory insulation (Kaolite) [see Drawing M2E801580A001, Appendix 1.4.8]. The inside diameter of the drum is 46.36 cm (18.25 in.) with an overall height of 110.49 cm (43.5 in.) including the cover and lid (Drawings M2E801580A004 and M2E801580A001, Appendix 1.4.8). The outside diameter of the drum (including the chimes) is 49.2 cm (19.37 in.). The drum and lid are made from 16-gauge [~0.152-cm (0.0598-in.)-thick] type 304 or 304L stainless steel. A 12-gauge [~0.267-cm (0.105-in.)-thick] stainless-steel arched cover (Drawing M2E801580A005, Appendix 1.4.8) is welded to the double open-head drum to create the bottom of the drum assembly. An inner liner (Drawing M2E801580A003, Appendix 1.4.8) is attached to the drum by an internal flange (angle) that is welded to both the drum and liner. The cavity created by the inner liner for placement of a containment vessel is a three-tier volume. The uppermost tier accommodates the top plug and has an inside diameter of 37.52 cm (14.77 in.) and is 13.26 cm (5.22 in.) deep (Drawing M2E801580A003, Appendix 1.4.8). The second tier, which accommodates the containment vessel flange, has a 21.84-cm (8.60-in.) inside diameter that is 5.59 cm (2.20 in.) deep (Drawing M2E801580A003, Appendix 1.4.8). The third tier, which accommodates the containment vessel body, has a 15.85-cm (6.24-in.) inside diameter that is 78.31 cm (30.83 in.) deep (Drawing M2E801580A003, Appendix 1.4.8). An additional cavity is created between the second and third tier liners. This cavity runs the full length of the third tier height [78.31 cm (30.83 in.)] and is approximately 5.99 cm (2.36 in.) thick (Drawing M2E801580A003, Appendix 1.4.8). This cavity is filled with a castable refractory (277-4 special dry mix) for neutron attenuation purposes. The additional cavities between the liner and the drum are filled with an inorganic castable refractory material (Kaolite 1600), which acts as both an impact-absorbing and thermal-insulating material.

In accordance with NUREG/CR-3854, Part 4.3 for a Category I shipping package, an acceptable specification for drums used in any of the component safety groups is U.S. Department of Transportation (DOT) Specification 17C or better. The drum used in the ES-3100 is fabricated in accordance with the dimensional requirements of MIL-D-6054F and modified as shown on Drawing M2E801580A004 (Appendix 1.4.8). Material, fabrication, and quality control criteria are generally equivalent to those imposed for a DOT Specification 17C drum. Furthermore, the drum of the ES-3100 is part of a performance-based package that has been tested and analyzed to demonstrate its ability to maintain confinement and containment of its contents under both NCT and HAC. By certifying that the outer shell of the Drum Assembly used in production meets the same specifications as those tested and analyzed, as described in subsequent sections of this SAR, the outer drum shell used for the ES-3100 is acceptable for a Category 1 shipping package.

As previously discussed, the drum has been modified by the attachment of an inner liner connected to the drum by an internal flange welded to both the drum and the liner. Weld studs are attached to the upper face of the internal flange. The body seams are welded. The following items are conducted in accordance with Sect. IX of the *American Society of Mechanical Engineers (ASME) Boiler and Pressure Vessel Code* (B&PVC, Sect. IX): welding procedures qualification and welders certification to these qualified procedures.

The drum has four circumferential hoops (chimes) formed into the body. The drum has four 0.795-cm (0.313-in.)-diam holes equally spaced around the circumference about 3.81 cm (1.50 in.) from the top rim to relieve pressure in the drum in the event of a thermal accident (Drawing M2E801580A002, Appendix 1.4.8). Plastic plugs (Nylon 6/6, Micro Plastic, Inc., Item Number 62MP0312) are placed into these holes from the outside to prevent leakage of water into the drum during NCT and storage. The drum is fabricated with a data plate, trefoil data plate, paint, and two lid TID lugs for use with tamper-indicating devices (TIDs). The two electrochemically etched data plates are affixed to the exterior of the drum body in the locations, and with the methods, indicated on Drawing M2E801580A031 (Appendix 1.4.8). The trefoil data plate (M2E8015803A010-1) provides the owner's return address, container model, container serial number, and the trefoil symbol. The other data plate (M2E801580A010-2) provides the required DOT markings—certificate number, maximum gross weight, and "Type B" designation.

The removable lid is attached to the drum body by a flange with eight silicon bronze, 5/8-11-UNC-2B hex-head nuts [C65100, American Society for Testing and Materials (ASTM) F-467] with stainless-steel washers. These nuts are tightened onto the weld studs (304 or 304L stainless steel, 5/8-11-UNC-2A, ASTM A-493 or F-593) to 40.67 ± 6.78 N·m (30 ± 5 ft-lb) of torque with no sequence specified.

The top plug is 36.5 cm (14.37 in.) in diameter and 13.41 cm (5.28 in.) in height at the center. The skin is made from 16 gauge [~0.152-cm (0.0598-in.)-thick] type 304 or 304L stainless steel and is filled with Kaolite 1600.

The drum assembly also contains three silicone rubber pads. The first pad (CV bottom pad) is placed on the bottom of the innermost liner to support the containment vessel bottom during transport. The second pad (CV flange pad) is placed on top of the containment vessel lid during transport. The third pad (plug pad) is placed on the top shelf of the mid-liner to cushion the top plug during transport. The locations of these three pads are shown on Drawing M2E801580A001 (Appendix 1.4.8), and the dimensions of the pads are shown on Drawing M2E801580A009 (Appendix 1.4.8).

The drum is designed so that lifting can be accomplished with a forklift. It can either be placed on the tines of the forklift from below, or a pincher assembly can be placed on the forklift and used to grasp the exterior of the drum assembly. Based on analytical results for a similar package (the Model ES-2100), forklift gripping forces of up to 5400 lb can be used with no detrimental effects on the package.

No tie-down devices are integral to the package, nor can any features be used for these purposes. The ES-3100 package is designed to be shipped in accordance with the safe-secure trailer/safeguards transporter (SST/SGT) requirements.

1.2.1.2 Insulation

The void area formed by the drum and the attached inner liner is filled with an inorganic castable refractory material (Kaolite 1600) made by Thermal Ceramics, Inc., which acts as both a thermal insulating and an impact limiting material. The top plug assembly, which is placed between the containment vessel and the drum lid, is also filled with Kaolite 1600. This material is a mixture of cement and vermiculite and has a nominal cured density of ~358.8 kg/m^3 (22.4 lb/ft^3). Additional information regarding the characteristics and properties of this material is presented in Appendix 2.10.3. Casting takes place while the drum is being vibrated in an inverted orientation to ensure that the castable material penetrates into all areas in the void space formed by the drum and the inner liner and that no considerable voids are formed during this process. The Kaolite material is then baked in a furnace at elevated temperatures [~260°C (500°F)] as prescribed in Manufacturing Process Specification, JS-YMN3-801580-A003, *Manufacturing Process Specification for Casting Kaolite 1600 into the ES-3100 Shipping Package,* the specification which controls manufacture of Kaolite 1600 for the ES-3100 (Appendix 1.4.4). The use of a thermal ceramic material, such as Kaolite 1600, as an impact limiting/thermal insulating material in a Type B fissile material shipping package has been previously used in other Y-12 owned and licensed packages (i.e., ES-2100 and DPP-2). The original decision to use this material was the result of considerable research. This manufacturing process is protected under U.S. Patent 6,299,950 B1 (Byington et al. 2001). The United States Government has rights in this invention pursuant to Contract No. DE-AC05-84OR21400 between DOE and B&W Y-12.

One of the design goals of Y-12's packaging development program was to build a shipping package entirely of materials that do not char, burn, or thermally decompose when exposed to the temperatures and conditions associated with HAC [800°C (1475°F)]. Cellulosic fiber board and polyurethane foams, typically used for packaging applications, undergo decomposition when exposed to these HAC thermal conditions. During thermal decomposition, these materials off-gas, producing conditions that are potentially detrimental to the performance of the package. The hot gases generated within the packaging can transfer heat to inner regions adjacent to the containment closure seals. Under severe circumstances, this process could lead to loss of containment due to overheating of containment seals. The Kaolite material is nonflammable and will not undergo chemical decomposition at temperatures below 1260°C (2300°F). When Kaolite is heated above 100°C (212°F), water vapor from free water contained within the casting will form. Pressurization of the drum and top plug is prevented by pressure relief holes (vent holes) located near the top of the drum and on the top center of the top plug (see Sect. 1.2.1.1 and Drawings M2E801580A002 and M2E801580A008, Appendix 1.4.8). The cured Kaolite 1600 material does not decompose, and thus there are no exothermic chemical reactions that could produce superheated off-gasses.

Extensive testing of Kaolite 1600 was performed by the Y-12 Development Division to determine the performance of the material for this type of application (Oakes, Appendix 2.10.3). Testing showed that Kaolite 1600 has a tremendous ability to absorb shock over a wide range of material densities, curing temperatures and times, and material temperatures. The 10 CFR 71.73 HAC testing documented in Sect. 2.7 demonstrates that Kaolite 1600 is a robust impact limiter and good thermal insulating material for Type B shipping containers. Post HAC drop testing radiographs of a similar package, the ES-2100, showed some minor cracking of the Kaolite structure in some cases. However, subsequent thermal testing of these ES-2100 packages demonstrated that these cracks were inconsequential to the package's ability to meet regulatory requirements.

Insulation thicknesses within the liner/drum volume adjacent to the side walls of the ES-3100 containment vessel are at least 4.27 cm (1.68 in.), with typical thicknesses of approximately 12.10 cm (4.77 in.). Below the containment vessel, the minimum thickness of insulation is 10.05 cm (3.96 in.), and the top plug, which is above the containment vessel, includes a 12.55-cm (4.94-in.) thickness of insulation.

1.2.1.3 Shielding

The ES-3100 packaging does not require dedicated shielding materials of specific design to control external radiation levels for the bulk HEU contents. However, the intervening packaging materials of construction (stainless steel of the drum and containment vessel, the Kaolite material, and the 277-4 material) provide some attenuation of the relatively low levels of penetrating radiation emitted by the contents. The amount of shielding modeled for the NCT analysis is represented by the thickness and density of the materials reported in Sects. 1.2.1.1, 1.2.1.2, and 1.2.2 and the packaging dimensions (Appendix 1.4.8). HAC physical testing showed that the containment vessel and insulation remain confined within the drum assembly. However, the HAC shielding evaluation conservatively assumes that only the containment vessel remains for shielding purposes (i.e., no shielding credit is taken for the drum and insulation in the HAC analysis).

1.2.1.4 Nuclear criticality safety

The packaging materials of construction in the ES-3100 provide neutron absorption (stainless steel and 277-4) and reflection (stainless steel and insulation). The 277-4 (or Cat 277-4 as it is sometimes referred) material is a noncombustible cast neutron-absorbing material. This material is cast into the innermost liner of the package adjacent to the containment vessel as shown in Fig. 1.1. The material is a high alumina borated concrete composed of aluminum, magnesium, calcium, boron, carbon, silicone, sulfur, sodium, iron, and water. The 277-4 material was manufactured specifically for the ES-3100 package by adding boron carbide to a standard material (Cat No. 277-0) and increasing the boron content from 1.56 wt % to 4.23 wt%. Additional information on the neutron-absorbing characteristics of this material is presented in Appendix 6.9.3. Properties of the 277-4 material are presented in Table 2.17 and Appendix 2.10.4. The cast material has a nominal density of 1681.9 kg/m^3 (105 lb/ft^3). The procedure for mixing this material and casting it into the ES-3100 shipping package is documented in JS-YMN3-801580-A005, *Casting Catalog No. 277-4 Neutron Absorber for the ES-3100 Shipping Package* (Appendix 1.4.5).

Although shown by tests up to HAC as not being credible, the criticality analysis considers water leakage into the containment vessel in accordance with 10 CFR 71.55(b). Depending on the content being shipped and the shipping configuration being used, criticality safety index (CSI) values for the ES-3100 package may range from 0 to 3.2 (see Sect. 1.2.3).

1.2.2 Containment System

A single containment vessel is used in the ES-3100 shipping package for the transport of bulk HEU contents. The ES-3100 containment boundary (consisting of the containment vessel body, lid assembly, and inner O-ring) is shown in Fig. 1.3.

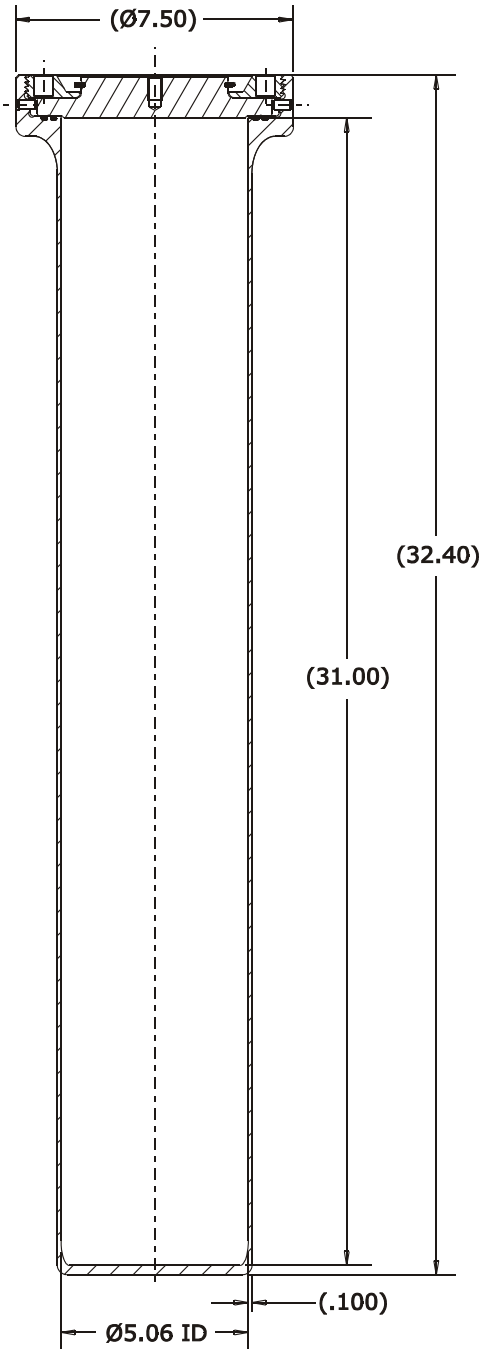

Fig. 1.3. Containment boundary of the ES-3100 shipping package.

During fabrication, all ES-3100 containment vessels will be inspected and tested to the requirements specified on the design drawings (Appendix 1.4.8) and equipment specification (Appendix 1.4.3). Certification documents received from the vendor with each component acknowledge the use of these drawings and specifications. These certifications are on file with the Y-12 Quality Organization.

The containment boundary of the ES-3100 package is a pressure vessel that is designed, fabricated, examined, and tested in accordance with the *ASME Boiler and Pressure Vessel Code,* Sect. III, Division I, Subsection NB (B&PVC, Sect. III, Div. I). The ES-3100 containment vessel body is constructed of 304L stainless steel and may be fabricated by one of two methods. The first method uses a standard 5-in., schedule 40 stainless-steel pipe (ASME SA-312 Type TP304L), a machined flat-head bottom forging (ASME SA-182 Type F304L), and a machined top flange forging (ASME SA-182 Type F304L). Each of these pieces is joined with circumferential welds as shown on Drawing M2E801580A012 (Appendix 1.4.8). The top flange is machined to provide two concentric half-dove-tailed O-ring grooves in the flat face, to provide locations for two 18-8 stainless steel dowel pins, and to provide the threaded portion for closure using the lid assembly. The second fabrication method for the ES-3100 containment vessel uses forging, flow forming, or metal spinning to create the complete body (flat bottom, cylindrical body, and flange) from a single forged billet or bar with final material properties in accordance with ASME SA-182 Type F304L. The top flange area using this fabrication technique is machined identically to that of the welded forging method.

The lid assembly, which completes the containment boundary structure, consists of a sealing lid, closure nut, and external retaining ring (Drawing M2E801580A014, Appendix 1.4.8). The containment vessel sealing lid (Drawing M2E801580A015, Appendix 1.4.8) is machined from Type 304 stainless-steel bar with final material properties in accordance with ASME SA-479. The containment vessel closure nut is machined from a Nitronic 60 stainless-steel bar with material properties in accordance with ASME SA-479. These two components are held together using a WSM-400-S02 external retaining ring made from Type 302 stainless steel. The sealing lid is further machined to accept a ⅜-16 swivel hoist ring bolt, to provide a leak-check port between the elastomeric O-rings, and notched along the perimeter to engage two dowel pins. The swivel hoist ring is only intended for use when loading and unloading the containment vessel. The swivel hoist ring will be removed for shipment. The lid assembly, with the O-rings in place on the containment vessel body, are joined together by torquing the closure nut and sealing lid assembly to 162.70 ± 6.78 N·m (120 ± 5 ft-lb). The sealing lid portion of the assembly is restrained from rotating during this torquing operation by the two dowel pins installed in the body flange.

The use of a design that includes two O-ring seals permits assembly verification leak testing of the containment vessel by measuring the leak rate from the volume between the inner and outer O-rings. An evacuation port is located between the O-rings in the containment vessel to facilitate a pressure rise or drop leakage test following assembly or 10 CFR 71 compliance testing. This port is sealed during transport using a modified VCO threaded plug. Only the inner O-ring is considered a part of the containment boundary. All O-rings on this containment vessel are fabricated to ASTM D2000, M3BA712A14B13F17.

The inner diameter of the containment vessel is 12.852 cm (5.06 in.) and the usable height inside the containment vessel is 78.74 cm (31.0 in.). The wall thickness of the body excluding the flange is 0.254 cm (0.10 in.). The maximum nominal diameter of the containment vessel body is 19.05 cm (7.50 in.). The nominal thicknesses of the containment vessel's flat bottom is 0.635 cm (0.25 in.). The overall height of the containment vessel without the swivel hoist ring is 82.296 cm (32.40 in.). The containment vessel drawing number, drawing revision, and serial number are electroetched onto the side of the containment vessel body, as well as onto the top of the sealing lid and the closure nut (Drawing M2E801580A011, Appendix 1.4.8). All outer surfaces, unless otherwise specified, are either sand- or bead-blasted, buffed, or sanded to a matte finish. No penetrations, connections, or fittings into this sealed container exist.

1.2.3 Contents

The ES-3100 shipping package will be used to ship bulk HEU in the form of oxide (UO_2, UO_3, or U_3O_8), uranium metal and alloy in the form of solid geometric shapes or broken pieces, uranyl nitrate crystals (UNX), and fuel elements from Training, Research, Isotopes, and General Atomics (TRIGA) reactors. The ES-3100 package has been designed to accommodate uranium oxide, UNX crystals, uranium metal, and uranium alloys. Actual loading limits are presented in subsequent sections of the SAR. The maximum weight of all contents (including convenience cans or bottles, can spacers, polyethylene bagging and other packing materials) shall not exceed 40.82 kg (90 lb). The maximum concentration of uranium isotopes permitted in the ES-3100 content are listed in Table 1.1. In addition to the uranium isotopes shown in Table 1.1, transuranic isotopes (with the exception of ^{237}Np) may be present in the contents at a maximum concentration of 40.0 μg/gU. The concentration of ^{237}Np is limited to 0.0250 g/gU. Unless otherwise specified, the contents described in this section pertain to ground transport only. A discussion of contents of air-transport is included in Sect. 1.2.3.1.

Table 1.1. Uranium concentration limits

Uranium isotope	Limit
^{232}U	0.040 μg/gU
^{233}U	0.006 g/gU
^{234}U	0.02 g/gU
^{235}U	1.00 g/gU
^{236}U	0.40 g/gU
^{238}U	1.00 g/gU

HEU Oxide

The HEU oxide content in the ES-3100 package includes UO_2, UO_3, and U_3O_8. Seven different oxide categories have been identified (Appendix 1.4.7). Maximum overall uranium isotopic weight percents representative of all seven oxide categories are presented in Table 1.2. The physical form of all contents is dense, loose powder which may contain clumps. Moisture content in oxide is limited to 3 wt % water (Note: loading restriction #8 in Sect. 1.2.3.8 also applies). Theoretical densities of UO_2, U_3O_8, and UO_3 are 10.96 g/cm^3, 8.30 g/cm^3, and 7.29 g/cm^3, respectively. Allowable oxide densities are 2.0 to 6.54 g/cm^3. Oxide may be shipped in tin-plated carbon steel, stainless steel, or nickel-alloy convenience cans; or polyethylene convenience bottles.

Table 1.2. Bounding uranium isotopic concentrations in oxide

Isotope	Bounding limit
^{232}U	40 ppb
^{233}U	200 ppm
^{234}U	2.0 wt %
^{235}U	97.7 wt % [a]
^{236}U	40.0 wt %
^{238}U	80.0 wt %

[a] ^{235}U must be ≥20 wt %.

For convenience, the seven oxide categories are referred to as Groups 1-7. Groups 1 to 6 are product oxides, and Group 7 is skull oxide. These groups are briefly described below.

Group 1 oxides are in the form of UO_x. Material from this group contains at least 83.0% uranium by weight and displays typical isotopic content (≤0.977 g^{235}U/gU, ≤0.014 g ^{234}U/gU, ≤0.010 g^{236}U/gU, ≤0.040 µg^{232}U/gU, ≤50.0 µg^{233}U/gU with the balance of the uranium being ^{238}U).

Group 2 oxides are in the form of UO_x. Material from this group contains at least 20.0% uranium by weight and displays typical isotopic content (≤0.977 g ^{235}U/g U, ≤0.014 g ^{234}U/g U, ≤0.010 g ^{236}U/g U, ≤0.040 µg ^{232}U/g U, ≤50.0 µg ^{233}U/g U with the balance of the uranium being ^{238}U).

Group 3 oxides are contaminated with up to 40 µg Pu/g U and are in the form of UO_x. Material from this group contains at least 83.0% uranium by weight and displays typical isotopic content for uranium (≤0.977 g ^{235}U/g U, ≤0.014 g ^{234}U/g U, ≤0.010 g ^{236}U/g U, ≤0.040 µg ^{232}U/g U, ≤50.0 µg ^{233}U/g U with the balance of the uranium being ^{238}U).

Group 4 oxides are in the form of U_3O_8. Material from this group contains at least 83.0% uranium by weight and displays typical isotopic content (≤0.977 g ^{235}U/g U, ≤0.014 g ^{234}U/g U, ≤0.010 g ^{236}U/g U, ≤0.040 µg ^{232}U/g U, ≤50.0 µg ^{233}U/g U with the balance of the uranium being ^{238}U).

Group 5 oxides are in the form of UO_x. Material from this group contains at least 20.0% uranium by weight and displays typical isotopic content (≤0.977 g ^{235}U/g U, ≤0.014 g ^{234}U/g U, ≤0.010 g ^{236}U/g U, ≤0.040 µg ^{232}U/g U, ≤50.0 µg ^{233}U/g U with the balance of the uranium being ^{238}U). This material may contain considerable activity in the form of unspecified beta emitters.

Group 6 oxides are in the form of UO_x. Material from this group contains at least 20.0% uranium by weight and may display unusually high isotopic concentrations of ^{233}U, ^{234}U, and ^{236}U (≤0.977 g ^{235}U/g U, ≤0.020 g ^{234}U/g U, ≤0.40 g ^{236}U/g U, ≤0.040 µg ^{232}U/g U, ≤200.0 µg ^{233}U/g U with the balance of the uranium being ^{238}U).

Group 7 oxides are in the form of U_3O_8. Material from this group is a mixture of graphite and U_3O_8, also referred to as skull oxides. The uranium concentration is up to 84.5% by weight and enrichment is up to 93.2% by weight. Concentrations of other uranium isotopes are ≤0.014 g ^{234}U/g U, ≤0.010 g ^{236}U/g U, ≤0.040 µg ^{232}U/g U, ≤50.0 µg ^{233}U/g U with the balance of the uranium being ^{238}U. The carbon content in these oxides is limited to 921 g per ES-3100 package.

The oxides in Groups 1, 3, 4 and 7 are high purity uranium oxide purity (the remainder is only trace impurities). Oxide Groups 2, 5, and 6 are listed to contain at least 20% uranium by weight, which allows up to 80% non-uranium material. As oxides, depending on the purity and chemical form, 3% to 17% of the total material composition will be oxygen, leaving up to 77% impurity or "filler". These three oxide groups include a range of scrap and recovered materials. For the least pure uranium oxides, the majority of the filler material is aluminum oxide (from recovered alumina traps or from oxidized uranium-aluminum alloys). Other materials that occur in appreciable quantities in some scrap materials are oxides and compounds of boron, calcium, iron, sodium, lead, zinc, magnesium, copper, molybdenum, and tungsten. These materials are essentially inert from the standpoint of criticality safety and chemical interaction with the ES-3100 convenience cans and bottles identified in this section for the shipment of oxides.

Uranium oxide shipments must be completed within 12 months after sealing the containment vessel in order to prevent the buildup of hydrogen gas beyond 5 mol %. The time period begins when the containment vessel is sealed. Hydrogen generation calculations are provided in Appendix 3.6.7.

HEU Metal and Alloy

HEU metal and alloy (alloys of uranium with aluminum, molybdenum, or zirconium) may be in the form of solid geometric shapes. Solid shapes may include the following:

1. cylinders having a diameter no larger than 4.25 in. (maximum of one cylinder per convenience can);

2. square bars having a cross section no larger than 2.29 in. × 2.29 in. (maximum of one bar per convenience can); and

3. slugs having dimensions of 1.5 in. diameter × 2 in. tall (maximum of 10 per convenience can).

HEU bulk metal and alloy contents not covered by the geometric shapes category specified above will be in the broken metal category, and will be so limited.

Alloys of uranium may include aluminum, molybdenum, or zirconium. Uranium-aluminum alloys are typically 70 to 95% aluminum. Uranium-molybdenum alloys are typically 1 to 12% molybdenum. Uranium/molybdenum alloys may be plated with, clad with, or contain traces of aluminum, gold, stainless steel, nickel and/or chromium.

HEU bulk metal and alloy contents in the broken metal category may be of unspecified geometric form. HEU bulk metal and alloy in this category may also be of a specific shape where one or more of the characteristic dimensions vary from piece to piece (i.e., the height, width, length, radius, etc.).

For pyrophoric considerations, HEU metal and alloy must meet the following restrictions:

1. Uranium metal and alloy (broken) pieces must have a surface-area-to-mass ratio of not greater than 1 cm^2/g or must not pass through a 3/8-in. mesh sieve (or equivalent size-grading method).

2. Particles and small shapes which do not pass the size restriction tests in #1, and powders, foils, turnings, and wires, are not permitted unless they are in a sealed, inerted container.

Metal and alloy may be shipped in tinned-carbon steel, stainless steel, or nickel-alloy convenience cans. The only hydrogenous packing materials that can be used inside the containment vessel when shipping broken HEU metal are those that have a hydrogen density less than or equal to water.

Uranyl Nitrate Crystals

Uranyl nitrate crystals (UNX) are formed by dissolving uranium metal or any of the uranium oxides in nitric acid. Uranyl nitrate hexahydrate (UNH) has a chemical formula of $UO_2(NO_3)_2 + 6\ H_2O$. This most reactive form is used as the bounding composition for uranyl nitrate crystals in the criticality evaluation. Therefore, for UNX contents, X must be less than or equal to 6. The theoretical density of UNH crystals is 2.79 g/cm^3; however, the working densities will be less.

The user of the ES-3100 for UNX shipments will be required to use non-metallic containers only (Teflon bottles) as the convenience container.

Shipments of UNX crystals must be completed within the times shown in Table 1.3a in order to prevent the buildup of hydrogen gas beyond 5 mol %. The time period begins when the containment vessel is sealed. Hydrogen generation calculations are provided in Appendix 3.6.7.

TRIGA Fuel Elements

Fuel pellets from Training, Research, Isotopes, and General Atomics (TRIGA) reactor elements are authorized to be shipped in the ES-3100. The fuel shall be unirradiated. The TRIGA fuel shall be in the form of uranium zirconium hydride (UZrHx), where $x \leq 2$. Fuel from three types of TRIGA fuel elements are allowed; TRIGA Standard Fuel Elements (SFE), Instrumented TRIGA Standard Fuel Elements (FTC), and TRIGA Fuel Follower Control Rods (FFCR). These fuel elements have three fuel pellets (or sections) per element. The fuel pellets from the SFEs and FTCs to be shipped are 8.5 wt% uranium and 70% enriched. Fissile loading is 45.33 g ^{235}U per pellet (136 g ^{235}U per element) and the dimensions are 5 in. in length and 1.44 in. in diameter. The fuel pellets from the FFCRs to be shipped are 8.5 wt% uranium and 70% enriched. Fissile loading is 37.33 g ^{235}U per pellet (113 g ^{235}U per element) and the dimensions are 5 in. in length and 1.31 in. in diameter. Specific TRIGA fuel element data is given in Table 1.4.

TRIGA fuel may be shipped as crimped fuel elements or as UZrHx fuel pellets (if disassembled), both of which shall be packed into convenience cans prior to shipment. Convenience cans of 4.25-in. diameter by various lengths shall be used. Fuel pellets loaded into convenience cans shall be up to 5 in. in length (full-length) and no more than three full-length pellets shall be loaded into a convenience can. Crimped fuel rods are clad fuel pellets and can be up to 15 in. in length (full-length of the fuel section from one fuel element). Cladding material is stainless steel or aluminum. Only the fuel section of the TRIGA fuel element is allowed to be shipped (Fig. 1.5); however, there may be residual cladding up to ½ in. in length at either end of the crimped fuel rod. Up to three 15-in. long crimped fuel elements shall be loaded into a single 17.5-in. long convenience can for shipping (Fig 1.4). Maximum loading of bare fuel pellets and crimped fuel elements shall be 3 fuel element equivalence per ES-3100 containment vessel. Only 70% enriched TRIGA fuel will be shipped. For SFEs and FTCs, the maximum allowable loading is 408 g ^{235}U per package, and for FFCRs, the maximum allowable loading is 339 g ^{235}U per package. No spacer cans are required.

1.2.3.1 Radioactive/fissile constituents

For the ES-3100 package with bulk HEU content, the maximum number of A_2s is 294.00 (at 70 years) and the maximum activity is 0.3243 TBq (at 10 years) [Table 4.4].

Ground Transport

Fissile material loading limits for the contents of the ES-3100, as determined by criticality analyses, structural analyses, or hydrogen gas generation evaluations, are presented in Tables 1.3 and 1.3a.

Table 1.3. Authorized content [a] and fissile mass loading limits [b, c] for ground transport

Content description		Enrichment	CSI	No spacers, ^{235}U (kg)	Basis for limit	277-4 can spacers, [d] ^{235}U (kg)	Basis for limit
Solid HEU metal or alloy (specified geometric shapes) [e]	Cylinder A	≤ 100%	0.0	15.000	Crit.	25.000	Crit.
	Cylinder B	≤ 100%	0.0	18.000	Crit.	30.000	Crit.
	Square bars	≤ 100%	0.0	30.000	Crit.	35.200 [f]	Struct.
	Slugs	≤ 95%	0.0	17.374	Crit.	-	-
	Slugs	≤ 80%	0.0	-	-	29.318	Crit.
	Slugs	> 80%, ≤ 95%	0.0	-	-	24.324	Crit.
	Slugs	> 80%, ≤ 95%	0.4	-	-	34.749	Crit.
Broken HEU metal or alloy [g]		> 95%, ≤ 100%	0.0	Spacers req'd [d]		2.774	Crit.
			0.4	Spacers req'd		5.549	Crit.
			0.8	Spacers req'd		9.248	Crit.
			2.0	Spacers req'd		13.872	Crit.
			3.2	Spacers req'd		24.969	Crit.
		> 90%, ≤ 95%	0.0	Spacers req'd		3.516	Crit.
			0.4	Spacers req'd		6.154	Crit.
			0.8	Spacers req'd		10.549	Crit.
			2.0	Spacers req'd		18.461	Crit.
			3.2	Spacers req'd		26.373	Crit.
		> 80%, ≤ 90%	0.0	Spacers req'd		3.333	Crit.
			0.4	Spacers req'd		7.500	Crit.
			0.8	Spacers req'd		12.500	Crit.
			2.0	Spacers req'd		20.000	Crit.
			3.2	Spacers req'd		28.334	Crit.
		> 70%, ≤ 80%	0.0	2.967	Crit.	4.450	Crit.
			0.4	5.192	Crit.	8.900	Crit.
			0.8	8.900	Crit.	16.317	Crit.
			2.0	17.059	Crit.	25.218	Crit.
			3.2	27.692	Crit.	28.184	Crit.
		> 60%, ≤ 70%	0.0	3.249	Crit.	5.198	Crit.
			0.4	5.848	Crit.	12.996	Crit.
			0.8	13.646	Crit.	20.793	Crit.
			2.0	21.444	Crit.	24.692	Crit.
			3.2	24.692	Crit.	24.692	Crit.
		≤ 60%	0.0	5.576 kg U	Crit.	11.154 kg U	Crit.
			0.4	14.872 kg U	Crit.	28.813 kg U	Crit.
			0.8	28.814 kg U	Crit.	35.20 kg U [f]	Struct.
			2.0	35.20 kg U [f]	Struct.	35.20 kg U [f]	Struct.
			3.2	35.20 kg U [f]	Struct.	35.20 kg U [f]	Struct.

Table 1.3. Authorized content [a] and fissile mass loading limits [b, c] for ground transport

Content description	Enrichment	CSI	No spacers, ^{235}U (kg)	Basis for limit	277-4 can spacers, [d] ^{235}U (kg)	Basis for limit
HEU oxide [h]	≤ 100%	0.0	15.13 kg oxide 9.682 kg ^{235}U 921 g carbon	Crit., H_2 gen.	Spacer not req'd	-
		0.4	15.13 kg oxide 12.323 kg ^{235}U	Crit., H_2 gen.	Spacer not req'd	-
TRIGA fuel	20 %	0.0	0.921	Crit.	Spacer not req'd	-
	70 %	0.0	0.408	Crit.	Spacer not req'd	-

[a] HEU in solution form is not permitted for shipment in the ES-3100.
[b] All limits are expressed in kg ^{235}U unless otherwise indicated.
[c] Mass loadings cannot be rounded up.
[d] 277-4 can spacers as described on Drawing No. M2E801580A026 or M2E801580A043 (Appendix 1.4.8).
[e] Geometries of solid shapes are as follows:
- Cylinder A is larger than 3.24 in. diameter but no larger than 4.25 in. diameter: maximum of 1 cylinder per can.
- Cylinder B is no larger than 3.24 in. diameter: maximum of 1 cylinder per can.
- Square bars are no larger than 2.29 in. × 2.29 in. (cross section): maximum of 1 bar per can.
- Slugs are a maximum of 1.5 in. diameter × 2.0 in. tall: a maximum of 10 per convenience can where the actual number permitted is restricted by the stated loading limit.

[f] Maximum planned content weight is 35.20 kg. Maximum analyzed for criticality safety is 35.32 kg.
[g] Mass limits for alloys (uranium with aluminum, molybdenum, or zirconium) must assume that non-uranium portion is ^{235}U.
[h] Seal time must be 12 months or less. Seal time is the length of time after the ES-3100 containment vessel is sealed that the shipment must be complete.

Table 1.3a. Uranyl nitrate crystal content loading limits for ground transport

Product [a, b]	Seal time [c] (months)	CSI	Loading limit [d, e] (kg UNX)	U content [f] (wt %)
UNX, $0 < X \leq 3$	5	0.4	11.90	$52 < U \leq 61$
	12	0.4	6.70	$52 < U \leq 61$
UNX, $X > 3$	5	0.4	9.17	$46 < U \leq 52$
	12	0.0	4.75	$46 < U \leq 52$

[a] UNX is uranyl nitrate hydrate $[UO_2(NO_3)_2 * XH_2O]$ where $0 < X \leq 6$. Uranyl nitrate solution is not allowed.
[b] Must be shipped in Teflon bottles.
[c] Seal time—length of time after the ES-3100 containment vessel is sealed that the shipment must be complete.
[d] Total mass of UNX crystals. Spacers are not required for this content type.
[e] Loading limits for uranyl nitrate crystals are based on hydrogen generation calculations presented in Appendix 3.6.7.
[f] Enrichment up to 100%.

Air Transport

Content for air transport of the ES-3100 includes HEU in the form of unirradiated TRIGA fuel pellets or crimped fuel elements. Fissile material mass loading limits for these contents, as determined by the criticality analyses, are presented in Table 1.3b for air transport. The characteristics of the air transport contents shall be similar to the ground transport contents. Fissile loading per package will be as follows:

> TRIGA fuel elements and pellets - 3 fuel element equivalence per package. Fuel shall be 70% enriched and in the form of SFEs, FTCs, and FFCRs. Maximum fissile loading for SFEs and FTCs shall be 408 g ^{235}U per package, and for FFCRs, the maximum allowable load shall be 339 g ^{235}U per package.

Table 1.3b. Authorized content and fissile mass loading limits [a, b] for air transport

Content Description	Enrichment	CSI	^{235}U (kg)
TRIGA fuel	20%	0.0	0.716
	70%	0.0	0.408

[a] All limits are expressed in kg ^{235}U unless otherwise indicated.
[b] Mass loadings cannot be rounded up.

1.2.3.2 Chemical and physical form

The fissile material contents are in solid (HEU metal, alloy, or TRIGA fuel), crystalline (UNX), or powder (HEU oxide) form. Some moisture (up to 3 wt %) may be present in the HEU oxide material, thereby making the oxide content clump together.

Table 1.4. TRIGA fuel specifications

Uranium Content/Cladding/Type	Fuel Properties						
	U (wt% of fuel)	U235 (wt% of U)	Active Fuel Length (in.)	Fuel OD (in.)	U (grams)	U235 (grams)	Hydrogen to Zirc Ratio
STANDARD ELEMENTS							
8.5 wt% aluminum clad element, 15 inch	8.5	20	15.00	1.41	189	37	1.0
8.5 wt% stainless steel clad element	8.5	20	15.00	1.44	197	39	1.6
12 wt% stainless steel, smooth clad element	12	20	15.00	1.44	285	56	1.6
12 wt% stainless steel, dimpled clad element	12	20	15.00	1.40	271	53	1.6
8.5 wt% stainless steel clad, High Enriched Uranium	8.5	70	15.00	1.44	194	136	1.6
20 wt% stainless steel clad element	20	20	15.00	1.44	503	99	1.6
30 wt% stainless steel clad element	30	20	15.00	1.44	825	163	1.6
45 wt% stainless steel clad element	45	20	15.00	1.44	1560	307	1.6
INSTRUMENTED ELEMENTS							
8.5 wt% aluminum clad element, 15 inch	8.5	20	15.00	1.41	189	37	1.6
8.5 wt% instrumented, stainless steel clad element	8.5	20	15.00	1.44	197	39	1.6
12 wt% instrumented, stainless steel, smooth clad element	12	20	15.00	1.44	285	56	1.6
12 wt% instrumented, stainless steel, dimpled clad element	12	20	15.00	1.40	271	53	1.6
8.5 wt% instrumented stainless steel clad, High Enriched Uranium	8.5	70	15.00	1.44	194	136	1.6
20 wt% instrumented, stainless steel clad element	20	20	15.00	1.44	503	99	1.6
30 wt% instrumented, stainless steel clad element	30	20	15.00	1.44	825	163	1.6
45 wt% instrumented stainless steel clad element	45	20	15.00	1.44	1560	307	1.6
FUELED FOLLOWER CONTROL RODS							
8.5 wt% stainless steel clad fueled follower control rod	8.5	20	15.00	1.31	163	32	1.6
12 wt% stainless steel, smooth clad fueled follower control rod	12	20	15.00	1.31	237	47	1.6
12 wt% stainless steel, dimpled clad fueled follower control rod	12	20	15.00	1.40	257	50	1.6
12 wt% stainless steel, dimpled clad fueled follower control rod	12	20	15.00	1.40	271	53	1.6
8.5 wt% stainless steel high enriched fueled follower control rod for a cluster rod assy	8.5	70	15.00	1.31	162	113	1.6
20 wt% stainless steel clad fueled follower control rod	20	20	15.00	1.31	418	82	1.6
30 wt% stainless steel clad fueled follower control rod	30	20	15.00	1.31	685	135	1.6
45 wt% stainless steel clad fueled follower control rod	45	20	15.00	1.31	1560	307	1.6
STANDARD RODS FOR CLUSTER ASSEMBLY							
8.5 wt% stainless steel clad cluster rod	8.5	20	15.00	1.37	166	33	1.6
12 wt% stainless steel, smooth clad cluster rod	12	20	15.00	1.37	243	58	1.6
8.5 wt% stainless steel clad, High Enriched Uranium, cluster rod	8.5	70	15.00	1.37	175	122	1.6
20 wt% stainless steel clad cluster rod	20	20	15.00	1.37	427	85	1.6
30 wt% stainless steel clad cluster rod	30	20	15.00	1.37	710	141	1.6
8.5 wt% stainless steel clad, HEU, fueled follower control rod	8.5	70	15.00	1.31	160	112	1.6
45 wt% stainless steel clad fueled follower control rod	45	20	15.00	1.37	1348	267	1.6

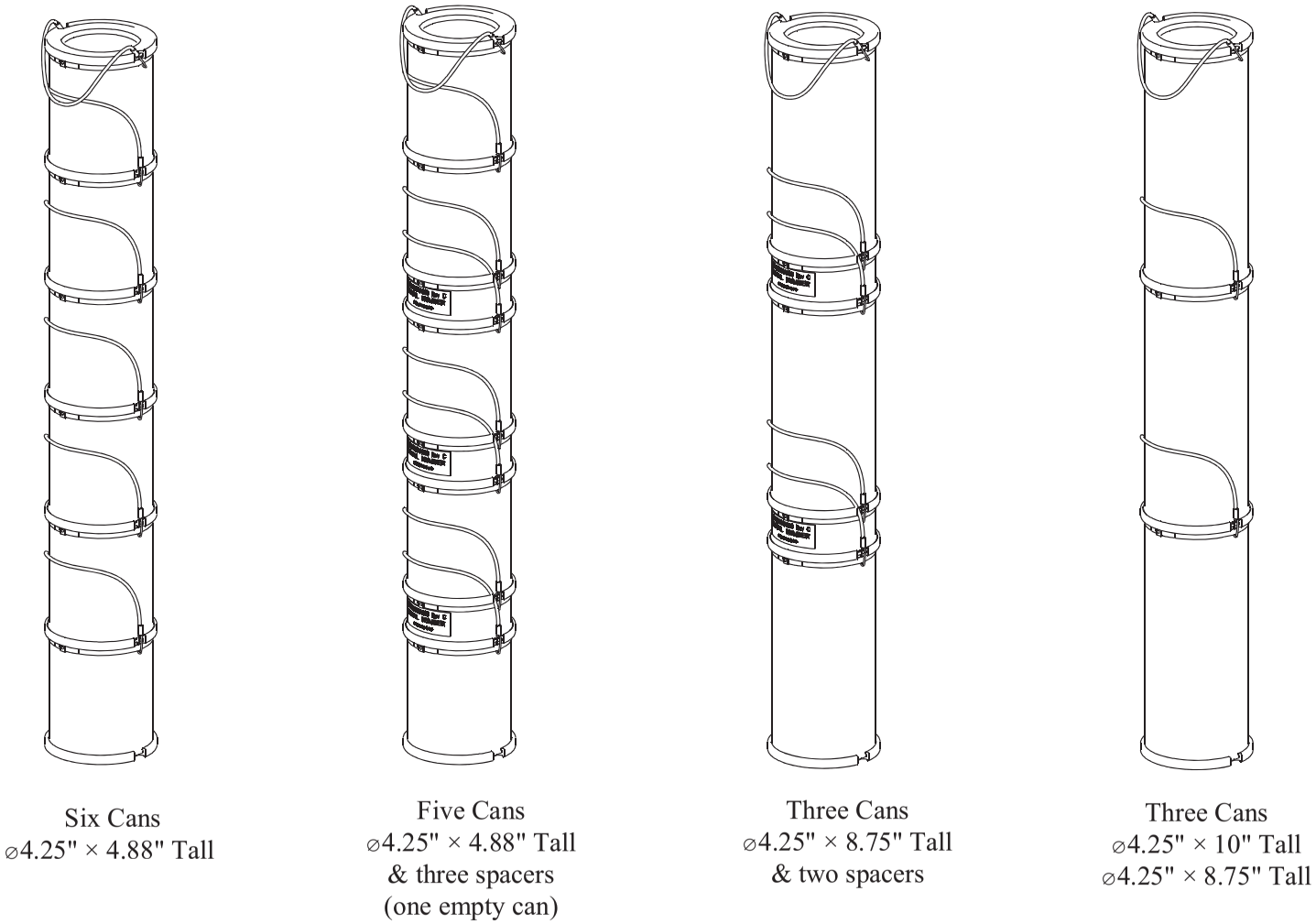

Fig. 1.4. Typical shipping configurations inside the ES-3100 containment vessel.

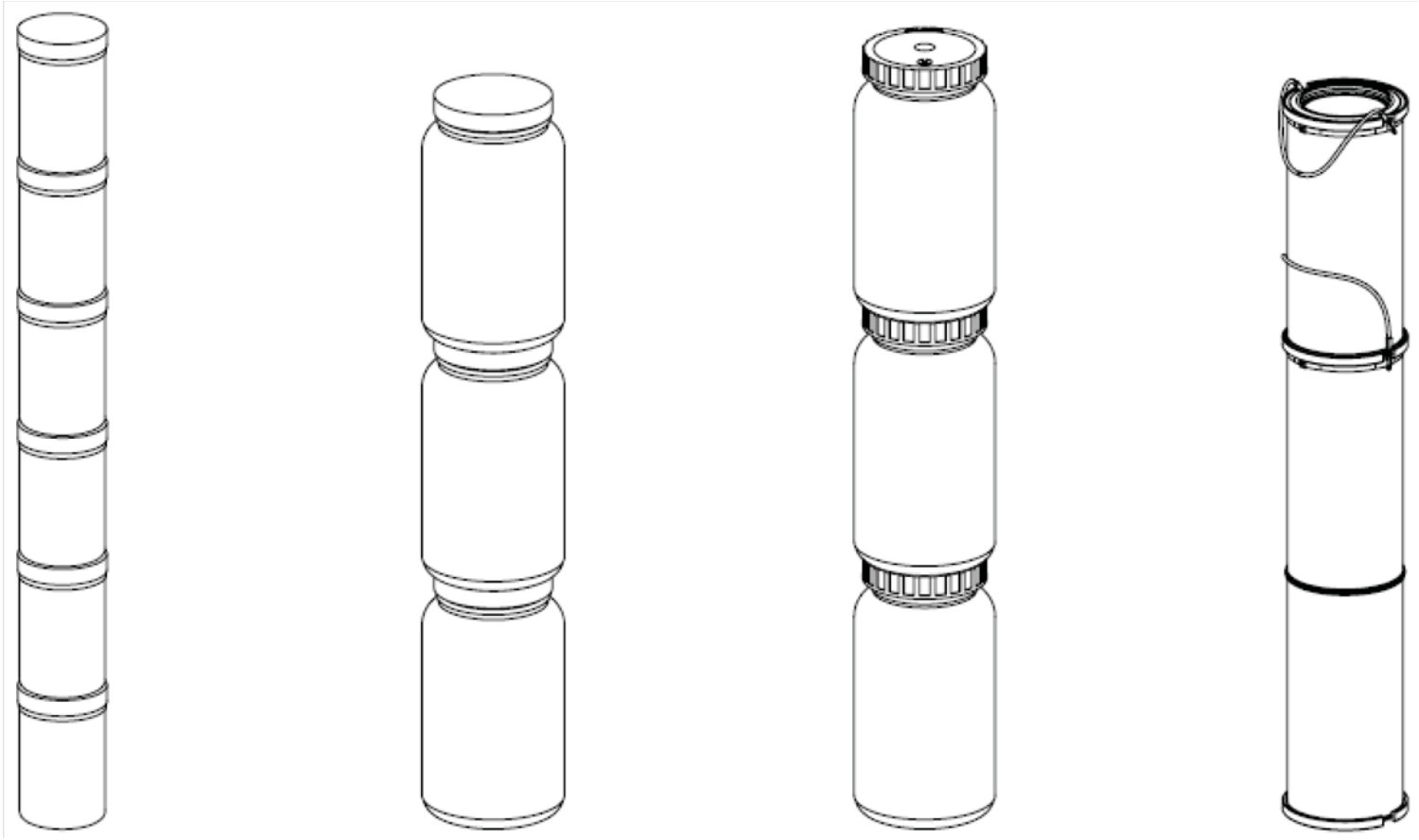

Six Nickel Cans
⌀3.0" × 4.75" Tall

Three Poly Bottles
⌀4.94" × 8.7" Tall

Three Teflon Bottles
⌀4.69" × 9.4" Tall

One Can
⌀4.25" × 17.5" Tall (two 8.75-in. cans brazed together) & one empty can

Fig. 1.4. Typical shipping configurations inside the ES-3100 containment vessel (cont.).

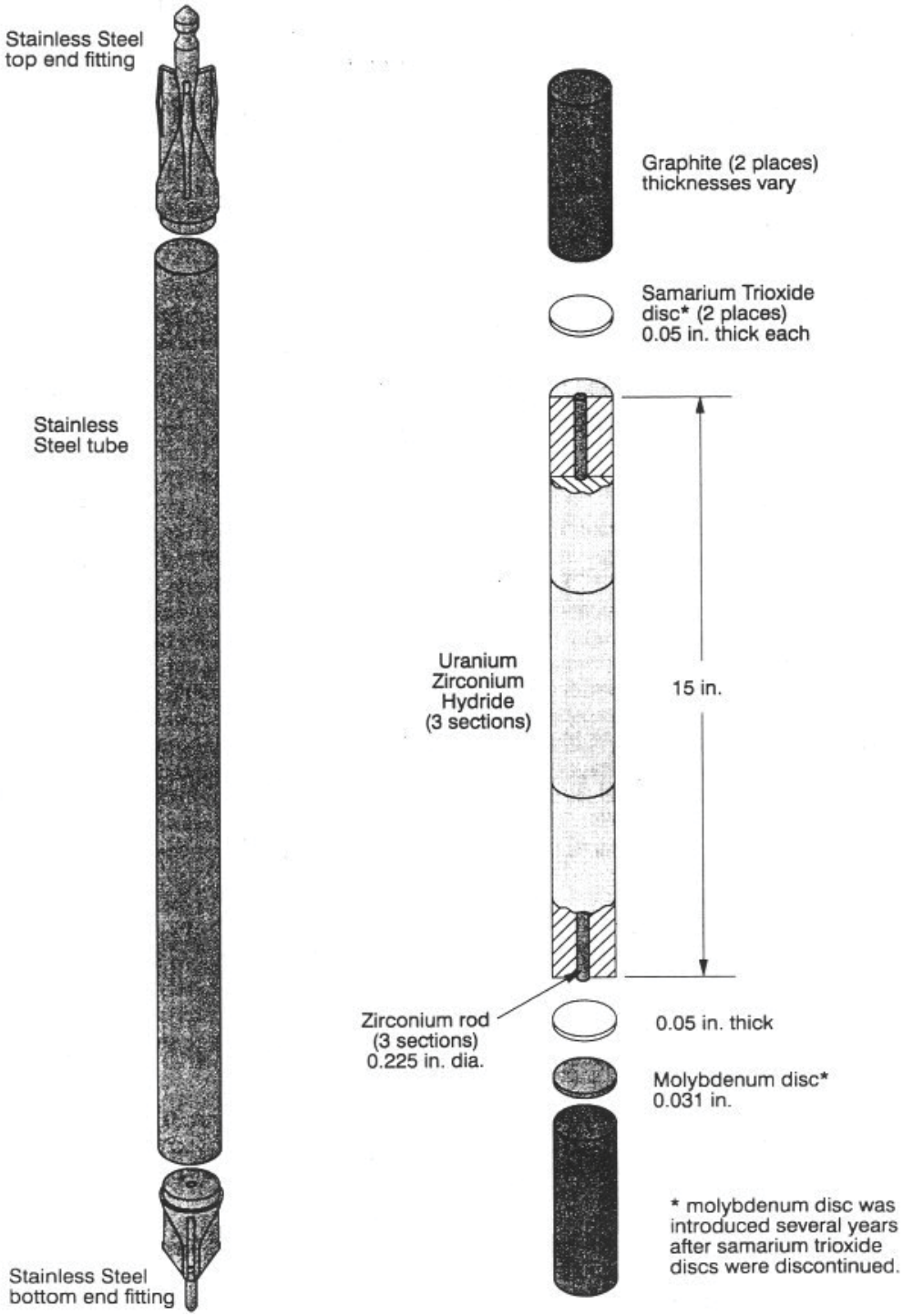

Fig 1.5. TRIGA fuel element.

1.2.3.3 Reflectors, absorbers, and moderators

The reflectors, absorbers, and moderators present in the ES-3100 package are those associated with the materials of construction. For example, the thermal insulation acts as a neutron reflector to the contents of a single package and as a neutron moderator in an array of packages. The degree of neutron moderation is a function of the hydrogen content in the Kaolite 1600 and 277-4 materials. The stainless-steel materials of the containment vessel and the drum also act as neutron reflectors to the contents of a single package but act as neutron absorbers in an array of packages. The nuclear properties of the materials of construction and of the contents are important and have been taken into account in the criticality safety evaluation (Sect. 6). In addition to the materials of construction in the ES-3100 shipping package mentioned above, the 277-4 material has been specifically added to the ES-3100 package for the purpose of enhancing the neutron absorption characteristics for safety purposes (see Sect. 6 for additional discussion of the neutron-absorbing characteristics of this material).

1.2.3.4 Shipping configurations

Authorized content convenience containers for the ES-3100 are cans constructed of stainless steel, tin-plated carbon steel, or nickel-alloy (series 200, passivated), and polyethylene and Teflon convenience bottles. These convenience containers are used to hold the HEU contents for shipment in the ES-3100 package and to assure that the inside of the containment vessel does not become contaminated with HEU under NCT. Convenience containers used in the ES-3100 package must have an outer diameter less than or equal to 12.7 cm (5 in.). The height can vary up to the full internal height of the containment vessel or 78.74 cm (31 in.). Some contents require the use of can spacers (see Table 1.3). These can spacers are thin-walled carbon steel or stainless-steel cans filled with 277-4 material (Drawing M2E801580A026 or M2E801580A043, Appendix 1.4.8). Each convenience can and spacer may be equipped with a stainless-steel band and nylon-coated wire to facilitate loading and unloading operations. Silicone rubber pads may also be used between convenience cans to dampen vibration and minimize contact between metal components. Any combination of convenience containers will be allowed in a single package, as long as the total height of the stack-up (including spacers, if required) does not exceed the inside working height of the containment vessel [78.74 cm (31 in.)]. If can spacers are required, no more than one-third of the total HEU content mass limit shown in Table 1.3 may be placed between any two spacers.

Typical configurations of authorized ES-3100 convenience containers are shown in Fig. 1.4. The shipping configurations shown in Fig. 1.4 utilize 3.00 and 4.25-in.-diameter convenience cans of various heights (such as 4.75, 4.88, 8.75, and 10 in.), 4.94 in. diameter by 8.7 in. tall polyethylene bottles, and 4.69 in. diameter by 9.4 in. tall Teflon bottles. Although any combination of the convenience cans that will fit inside the internal volume of the containment vessel may be used, content forms shall not be mixed in a single package (i.e., HEU oxides may not be packed with HEU metal). Empty cans and/or stainless-steel scrubbers may be used to fill the void space at the top of the containment vessel. If empty cans are shipped, a minimum 0.32-cm (0.125-in.)-diam hole must be placed through the lid to prevent over-pressurization of the can in the event of a thermal accident. In addition, these empty cans must be placed on top of the loaded cans. In configurations not requiring can spacers for criticality control, can spacers may be shipped for convenience if placed on top of loaded cans in the containment vessel. The HEU contents may be bagged or wrapped in polyethylene, and the convenience containers may also be wrapped in polyethylene to further reduce the possibility of contamination. If metal cans or polyethylene bottles are used as convenience containers, the total amount of offgassing material (including polyethylene bottles, polyethylene bagging, and lifting slings) is limited to 500 g per package. If Teflon bottles are used as convenience containers, the total amount of off-gassing material (including Teflon bottles, polyethylene bagging, and lifting slings) is limited to 1490 g per package (limit established by

assuming three 330-g Teflon bottles and 500-g polyethylene bagging). If closed convenience cans with an outer diameter greater than 4.25 in. are used, the containment vessel cannot contain any materials that off-gas. The only hydrogenous materials that can be present in the containment vessel when shipping HEU broken metal are those that have a hydrogen density less than or equal to water. In some shipping configurations, silicone rubber pads will be placed between the convenience cans to reduce vibration.

1.2.3.5 Maximum normal operating pressure

As defined in 10 CFR 71.4, the maximum normal operating pressure is the maximum gauge pressure that would develop in the containment system in one year under an ambient temperature of 38°C (100°F) in still air, with appropriate insolation in the absence of venting, external cooling by an ancillary system, or operational controls during transport. Under these conditions, the maximum normal operating pressure in the ES-3100 containment vessel would be 198.98 kPa (28.859 psia). In comparison, the design internal pressure of the containment vessel is 801.17 kPa (116.2 psia). The design internal pressure is a conservatively assumed value that was assigned for the purpose of the ASME code calculations in Appendix 2.10.1.

1.2.3.6 Maximum and minimum weight

The maximum gross shipping weight for the ES-3100 package is 190.5 kg (420 lb). The proposed maximum gross shipping weight of the ES-3100 package with any proposed content is 187.81 kg (414.05 lb) [Table 2.8]. The total weight of the tested ES-3100 units ranged from 157.4 to 203.7 kg (347 to 449 lb) [Table 2.9].

The weight of HEU contents in the ES-3100 shipping package is limited to 35.2 kg (77.60 lb). This limit has been established as a bounding case for the maximum structural, thermal, and containment limit for the package. Actual mass restrictions for the various contents based on the various analyses presented in the SAR are listed in Tables 1.3, 1.3a, and 1.3b. The maximum allowable payload weight of any configuration, including packing components (convenience cans and bottles, polyethylene bags, silicone pads, can spacers, etc.), is 40.82 kg (90 lb). There is no minimum payload weight requirement. ES-3100 shipping package weights are discussed in greater detail in Sect. 2 and are broken down into individual component weights in Tables 2.8 and 2.9.

The payload weight (including convenience cans, silicone rubber pads, can spacers, and the HEU mockup) used in the ES-3100 package tests ranged from a minimum of 3.6 kg (8 lb) to a maximum of 50.3 kg (111 lb).

1.2.3.7 Maximum decay heat

As shown in Sect. 3.1.2 , the conservatively calculated maximum heat generation rate of the contents is approximately 0.4 W. The ES-3100 package was designed for a maximum heat load of 20 W. Thermal analyses have been performed assuming heat sources of 0.4, 20, and 30 W in the ES-3100 containment vessel (Appendix 3.6.2).

1.2.3.8 Loading restrictions

Loading restrictions based upon the results of the criticality safety calculations presented in Sect. 6.2.4 and additional limitations on packing materials outlined in Sect. 3 are as follows:

(1) HEU fissile material to be shipped in the ES-3100 package must be placed in stainless-steel, tin-plated carbon steel or nickel alloy convenience cans, polyethylene bottles, or Teflon bottles. Convenience containers used in the ES-3100 package must have an outer diameter less than or equal to 12.7 cm (5 in.). The height can vary up to the full internal height of the containment vessel or 78.74 cm (31 in.). Any closure on the convenience can is allowed.

(2) Any combination of convenience cans is allowed in a single package, as long as the total height (including silicone rubber pads and can spacers, if required) does not exceed the inside working height of the containment vessel (approximately 31 in.).

(3) In situations where empty convenience cans are shipped in the package, they must be placed on top of the loaded cans, and a minimum 0.32-cm (0.125-in.)-diam hole must be placed through the lid to prevent over pressurization of the can.

(4) The concentration of uranium isotopes in the content is limited as shown in Table 1.1.

(5) For pyrophoric considerations, HEU metal or alloy pieces must have a specific area not greater than 1 cm^2/g or must not pass through a 3/8-in. (0.95 cm) mesh sieve (or equivalent size-grading method). Incidental small pieces that do not pass the size restriction tests, and powders, foils, turnings, and wires, may only be shipped if they are in a sealed, inerted container.

(6) The content shall not exceed "per package" fissile material mass loading limits specified in Table 1.3 based on the CSI. Where can spacers are required for a "per package" mass loading, the quantity of fissile material located in any vacancy between or adjacent to can spacers shall not exceed one-third of the mass loading limit in Table 1.3.

(7) The package content is defined as the HEU fissile material, the convenience cans and can spacers, and the associated packing materials (plastic bags, pads, tape, etc.) inside the ES-3100 containment vessel.

(8) If metal cans are used as convenience containers, the amount of polyethylene bagging and lifting slings is limited to 500 g per package. If Teflon bottles are used as convenience containers, the total amount of offgassing material (including Teflon bottles, polyethylene bagging, and lifting slings) is limited to 1490 g per package. If metal cans or polyethylene bottles are used as convenience containers, the total amount of offgassing material (including polyethylene bottles, polyethylene bagging, and lifting slings) is limited to 500 g per package (see Item 7 in Sect. 6.2.4). If closed convenience cans with an outer diameter greater than 4.25 in. are used, the containment vessel cannot contain any materials that offgas. These mass limits do not include moisture in oxide. Moisture is accounted for in criticality safety calculations (Sect. 6.1.2).

(9) The only hydrogenous packing materials that can be used in the containment vessel when shipping broken HEU metal are those that have a hydrogen density less than or equal to water.

(10) Shipments of UNX crystals must be completed in the time period noted in Table 1.3a. Shipments of uranium oxide must be completed in 12 months. This time period begins when the containment vessel is sealed.

(11) The mass of any unidentified constituents in content to be shipped in the ES-3100 must be counted against the fissile mass loading limit. Content must not contain unevaluated moderating materials.

1.2.4 Operational Features

The ES-3100 package is a Type B fissile material package designed in accordance with DOT and NRC regulations. These regulations require that the package be operated without undue risk to the public, even in the event of a severe accident, and that the dose rate and nonfixed radioactive contamination on the external surface of the package conform with 49 CFR 173.441 and 173.443, respectively. These requirements are translated into the designs for the containment, shielding, and nuclear criticality safety of the contents when subjected to NCT and HAC. Designs for containment, shielding, and nuclear subcriticality safety are supported by operational procedures for loading, unloading, and refurbishing to ensure that those design features are used and maintained in a manner commensurate with their intended function. Drop tests, crush tests, puncture tests, thermal tests, and water immersion tests (Sects. 2.6 and 2.7) show that the drum assembly maintains the insulation and the containment vessel in their intended configurations when subjected to NCT and HAC.

The decay heat generated by the contents (maximum of approximately 0.4 W) is negligible for a package of this size (Sect. 1.2.3.7 and Sect. 3.1.2).

Design features that provide shielding, containment, and nuclear criticality control perform these functions in a passive manner. No valves, connections, gauges, active coolants, or operationally pressurized parts are integral to the ES-3100 package.

1.3 GENERAL REQUIREMENTS FOR ALL PACKAGES

This section demonstrates compliance with 10 CFR 71.43(a) and (b), "General Standards for All Packages."

1.3.1 Minimum package size

Requirement. The smallest overall dimension of a package may not be less than 10 cm (4 in.).

Analysis. The drum's outside diameter (including the chimes or rolling rings) is 49.2 cm (19.37 in.), and the outside height including the lid is 110.49 cm (43.5 in.). The minimum outside diameter of the ES-3100 containment vessel is 13.36 cm (5.26 in.), and the overall height is 82.30 cm (32.4 in.). Therefore, the packaging meets this requirement.

1.3.2 Tamper-indicating feature

Requirement. The outside of a package must incorporate a feature, such as a seal, that is not readily breakable and that, while intact, provides evidence that the package has not been opened by unauthorized persons.

Analysis. The removable drum head is attached to the body by eight 5/8-11-UNC-2B silicon bronze nuts and 5/8-in. nominal washers. Two 0.51-cm (0.20-in.)-thick lugs with 0.953-cm (0.375-in.)-diam holes project through slots in the drum lid and provide attachment for wire-type TIDs. These TIDs consist of a stainless-steel cable with an aluminum crimp closure or equivalent. The requirement is satisfied by the TIDs, which are installed as specified in Sect. 7.1.2.2. The seal is only required when HEU is in the package. It is not required for empty shipments.

1.4 APPENDICES

Appendix	Description
1.4.1	PACKAGE CERTIFICATION DRAWING
1.4.2	EQUIPMENT SPECIFICATION JS-YMN3-801580-A002, *ES-3100 DRUM ASSEMBLY*
1.4.3	EQUIPMENT SPECIFICATION JS-YMN3-801580-A001, *ES-3100 CONTAINMENT VESSEL*
1.4.4	EQUIPMENT SPECIFICATION, JS-YMN3-801580-A003, *MANUFACTURING PROCESS SPECIFICATION FOR CASTING KAOLITE 1600™ INTO THE ES-3100 SHIPPING PACKAGE*
1.4.5	EQUIPMENT SPECIFICATION, JS-YMN3-801580-A005, *CASTING CATALOG NO. 277-4 NEUTRON ABSORBER FOR THE ES-3100 SHIPPING PACKAGE*
1.4.6	PACKAGE CATEGORY DETERMINATION
1.4.7	HEU OXIDE MATERIAL SPECIFICATION AS PROVIDED BY Y-12 HIGHLY ENRICHED URANIUM DISPOSITION PROGRAM OFFICE
1.4.8	PACKAGE ENGINEERING DRAWINGS
1.4.9	DESIGN ANALYSES AND CALCULATIONS, MIXING WEIGHTS AND ELEMENTAL COMPOSITION OF 277-4 NEUTRON POISON USED IN THE ES-3100
1.4.10	PYROPHORICITY OF URANIUM METAL

THIS PAGE INTENTIONALLY LEFT BLANK.

Appendix 1.4.1

PACKAGE CERTIFICATION DRAWING

Drawing No.	Rev.	Title
M2E801580A037	C	ES-3100 Shipping Container, Consolidated Assembly Drawing

THIS PAGE INTENTIONALLY LEFT BLANK.

NOTES

1. INTERPRET DIMENSIONS AND TOLERANCES PER ASME Y14.5M-1994.
2. DIMENSIONS ARE IN INCHES [mm].
3. APPROXIMATE WEIGHT: 325 LBS [147.4 Kg] FOR F/N 1 EMPTY.
4. WELDING SYMBOLS SHALL BE INTERPRETED IN ACCORDANCE WITH AWS A2.4.

[5] SEE EQUIPMENT SPECIFICATION JS-YMN3-801580-A002 ES-3100 DRUM ASSEMBLY.

[6] SEE EQUIPMENT SPECIFICATION JS-YMN3-801580-A001 ES-3100 CONTAINMENT VESSEL.

[7] SEE EQUIPMENT SPECIFICATION JS-YMN3-801580-A003 MANUFACTURING PROCESS SPECIFICATION FOR CASTING KAOLITE 1600™ INTO THE ES-3100 SHIPPING PACKAGE.

[11] SEE PROCUREMENT DOCUMENTS FOR PROPER REGISTERED USER NAME AND LOCATION.

[8] SEE EQUIPMENT SPECIFICATION JS-YMN3-801580-A005 CASTING CATALOG # 277-4 NEUTRON ABSORBER FOR THE ES-3100 SHIPPING PACKAGE.

[9] DURING INSTALLATION OF O-RINGS APPLY A THIN COAT OF SUPER-O-LUBE

[10] DURING INSTALLATION OF CONTAINER VESSEL LID ASSEMBLY, APPLY A LIGHT COAT OF KRYTOX GREASE TO THE THREADS AND UNDER THE NUT.

[11] SEE PROCUREMENT DOCUMENTS FOR PROPER REGISTERED USER NAME AND LOCATION. △C

[10]	AR	KRYTOX #240AC OR EQUAL THREAD LUBRICANT	FLUORINATED GREASE MILLER-STEPHENSON CHEMICAL CO.	NA	18
[9]	AR	SUPER-O-LUBE OR EQUAL O-RING LUBRICANT	CLEAR DIMETHYL SILOXANE POLYMER PARKER HANNIFIN CORP	NA	17
	1	MODIFIED VCO THREADED PLUG	BRASS	5	16
	1	EXTERNAL RETAINING RING	302 SST	5	15
	1	PLUG PAD	SILICONE RUBBER 22±5 SHORE A COLOR BLACK/GRAY	2	14
	1	CV FLANGE PAD		2	13
	1	CV BOTTOM PAD		2	12
	1	OUTER O-RING Ø5.859±.035 ID X Ø.139 ±.004	ETHYLENE PROPYLENE 70±5 SHORE A COLOR BLACK	2	11
	1	INNER O-RING Ø5.359±.035 ID X Ø.139±.004		2	10
[5]	1	ES3100 DATA PLATE	16 GA 304/304L SST ASTM SA240	2	9
[5]	1	ES3100 TREFOIL DATA PLATE		2	8
[6]	1	CONTAINMENT VESSEL CLOSURE NUT	NITRONIC 60 SST ASME SA-479 UNS-S21800	5	7
[6]	1	CONTAINMENT VESSEL SEALING LID	304 SST ASME SA-479	5	6
[6]	1	CONTAINMENT VESSEL BODY	304L SST	5	5
[7][5]	1	TOP PLUG WELDMENT	16 GA 304/304L SST ASTM SA240	4	4
[5]	1	DRUM LID WELDMENT		3	3
[8][7][5]	1	DRUM WELDMENT		3	2
		MAIN ASSEMBLY		2	1
		NOMENCLATURE OR DESCRIPTION	MATERIAL / SPECIFICATION	SHEET NO	FIND NO
	←	QTY REQ'D NEXT ASSEMBLY	PARTS LIST		

M2E801580A037

THIS DRAWING INCLUDES FEATURES SUPPORTING NUCLEAR CRITICALITY SAFETY. ANY REVISION TO THIS DIAGRAM REQUIRES NUCLEAR CRITICALITY SAFETY DIVISION APPROVAL.

REVISION	DATE	NCSD APPROVAL
C	09/10/08	J.F. DeCLUE

This document has been reviewed by a Y-12 DC and UCNI RO and has been determined to be UNCLASSIFIED and not UCNI. This review does not constitute clearance for public release.

Name: R.D. AIGNER Date: 9/11/08

P THIS DRAWING PRODUCED ON PRO/ENGINEER

REV	DESCRIPTION	DRW	CHKR	DE	DVR	DM	DATE	PE	DATE	PM	DATE	WE	DATE	CM/SO	DATE	AR	CV	ST	HV	EM	FP	PD	EE	IE	M	NP
C	REVISED TREFOIL DATA PLATE, F/N 8, ADDED NOTE 11	JRJ	RDA	LR	GAB	WIN	9/9/08	LR	9/9/08	JGA	9/9/08															
B	REVISED TREFOIL DATA PLATE, F/N 8	JRJ	RDA	JRJ	GAB	WIN	10/16/06	RDA for CH	10/17/06	JGA	10/17/06															
A	PAGE 1: MODIFIED GENERAL NOTES AND UPDATED FIELD NOTES ADDED TOLERANCES TO ORINGS. PAGE 3: ADDED CORRECT TOLERANCES AND REF. DIMS. PAGE 4. ADDED CORRECT INSPECTION DIMS. AND WELD SYMS. PAGE 5. ADDED CORRECT TOLERANCES AND INSPECTION DIMS. AND ADDED NOTE TO -5 ADDED SHEET 6 RN Y2003-0328	RDA	JSL	GAB	JRJ	WDS	3/22/06	RDA FOR CH	3/22/06	DBM	3/22/06															
0	RN: Y2003-0328 ORIGINAL ISSUE	JMR	GM	GAB	RBC	MLG	1/23/06	RDA	1/23/06	JGA	1/23/06															

REVISION OR ISSUE PURPOSE — REVISION APPROVALS — SQUAD CHECK

SCALE: N.T.S.

TOLERANCES UNLESS OTHERWISE SPECIFIED
FRACTIONS ±.03
XX DECIMALS ±.010
XXX DECIMALS ±0.5°
ANGLES
BREAK SHARP EDGES .03 MAX
FINISH 125 RMS

DRAWING APPROVALS		DATE
DRW	JM RAY	1/18/06
CHKR	G MCGINNIS	1/18/06
DE	GA BYINGTON	1/23/06
DVR	RB CONATSER	1/18/06
DM	ML GOINS	1/23/06
PE	RD AIGNER	1/23/06
PM	JG ARBITAL	1/23/06

BWXT Y-12 National Security Complex managed by BWXT Y-12, L.L.C. for the Department of Energy under U.S. Government contract DE-AC05-00OR22800 • Oak Ridge, Tennessee •

PROJECT NAME: ES-3100 SHIPPING PACKAGE

CONSOLIDATED ASSEMBLY DRAWING

1	48	49	50	PLANT	BLDG	FL	SH.	OF	TYPE	CLASS
6	M	L	F	Y-12	NA	NA	1	6	A	U

51	52	53		REV
CM	PKG	IN	M2E801580A037	C

THIS PAGE INTENTIONALLY LEFT BLANK.

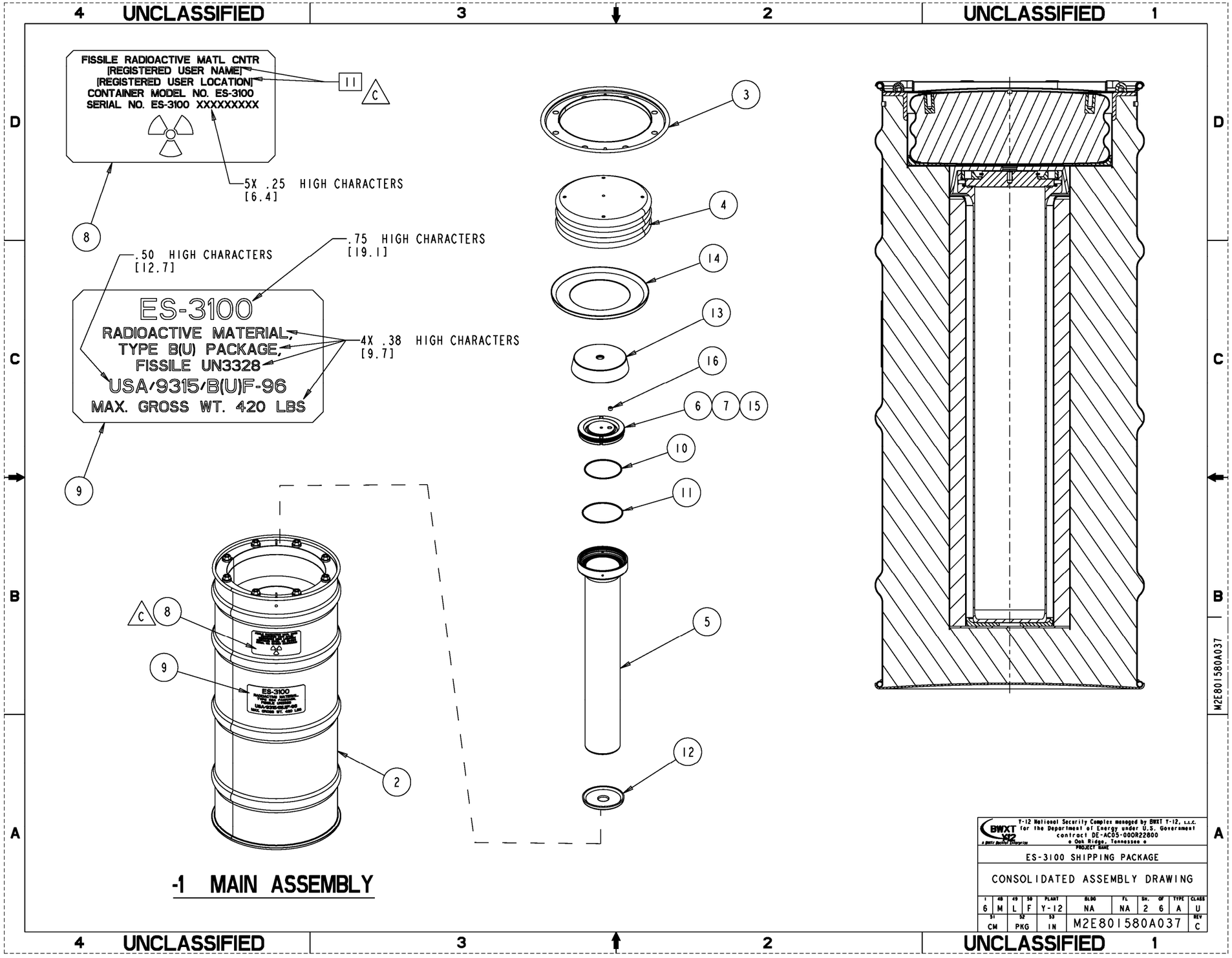
UNCLASSIFIED
UNCLASSIFIED
FISSILE RADIOACTIVE MATL CNTR
[REGISTERED USER NAME]
[REGISTERED USER LOCATION]
CONTAINER MODEL NO. ES-3100
SERIAL NO. ES-3100 XXXXXXXXX
5X .25 HIGH CHARACTERS
[6.4]
.75 HIGH CHARACTERS
[19.1]
.50 HIGH CHARACTERS
[12.7]
ES-3100
RADIOACTIVE MATERIAL,
TYPE B(U) PACKAGE,
FISSILE UN3328
USA/9315/B(U)F-96
MAX. GROSS WT. 420 LBS
4X .38 HIGH CHARACTERS
[9.7]
-1 MAIN ASSEMBLY
T-12 National Security Complex managed by BWXT Y-12, L.L.C.
for the Department of Energy under U.S. Government
contract DE-AC05-00OR22800
• Oak Ridge, Tennessee •
PROJECT NAME
ES-3100 SHIPPING PACKAGE
CONSOLIDATED ASSEMBLY DRAWING
PLANT Y-12
BLDG NA
FL NA
SH. 2 OF 6
TYPE A
CLASS U
CM
PKG
IN
M2E801580A037
REV C
M2E801580A037

THIS PAGE INTENTIONALLY LEFT BLANK.

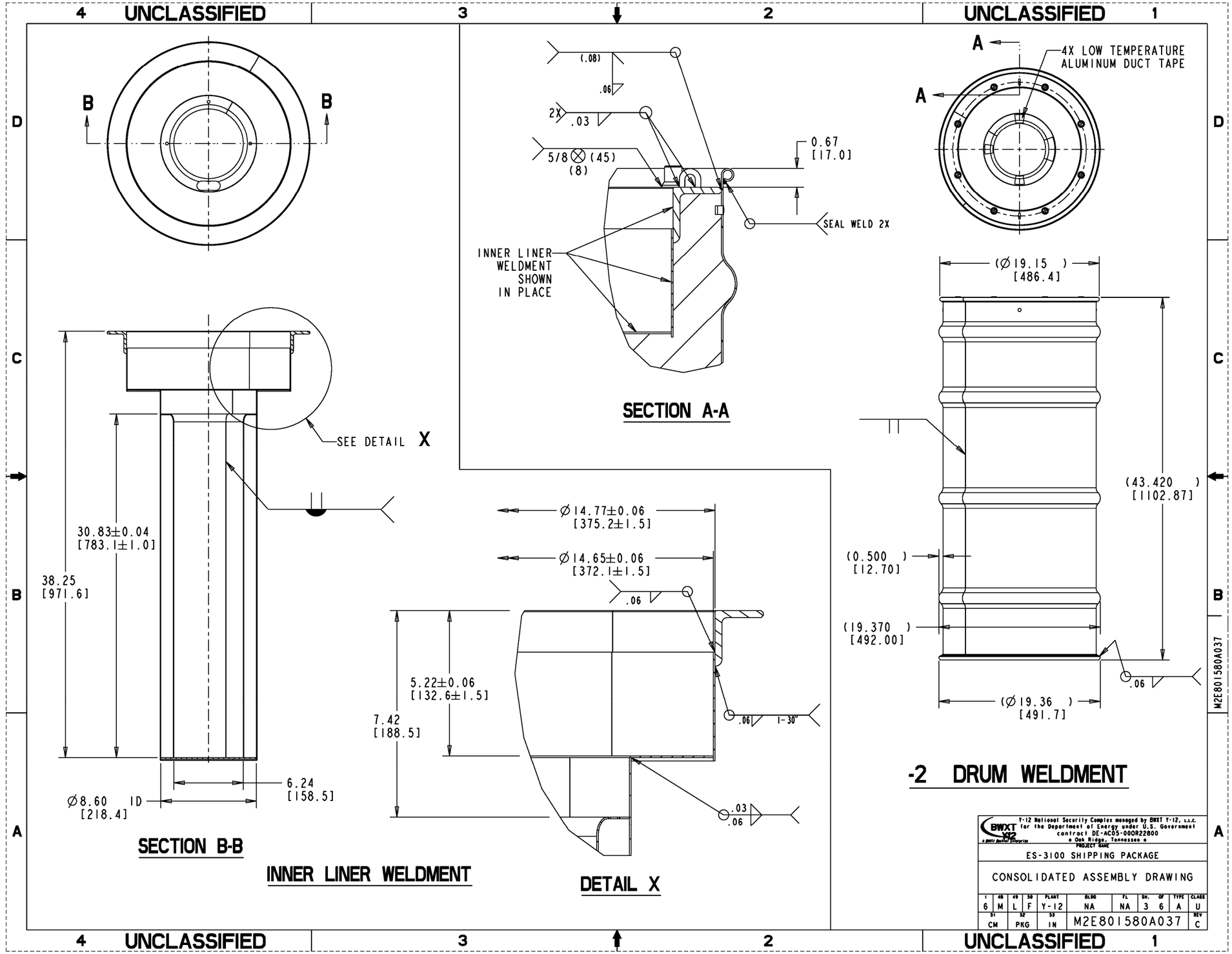
UNCLASSIFIED
UNCLASSIFIED
B
B
SEE DETAIL X
30.83±0.04
[783.1±1.0]
38.25
[971.6]
Ø8.60 ID
[218.4]
6.24
[158.5]
SECTION B-B
INNER LINER WELDMENT
(.08)
.06
2X .03
5/8 (45)
(8)
0.67
[17.0]
SEAL WELD 2X
INNER LINER WELDMENT SHOWN IN PLACE
SECTION A-A
Ø14.77±0.06
[375.2±1.5]
Ø14.65±0.06
[372.1±1.5]
.06
5.22±0.06
[132.6±1.5]
7.42
[188.5]
.06
1-30°
.03
.06
DETAIL X
A
A
4X LOW TEMPERATURE ALUMINUM DUCT TAPE
(Ø19.15)
[486.4]
(43.420)
[1102.87]
(0.500)
[12.70]
(19.370)
[492.00]
.06
(Ø19.36)
[491.7]
-2 DRUM WELDMENT
M2E801580A037
BWXT Y-12
T-12 National Security Complex managed by BWXT T-12, L.L.C. for the Department of Energy under U.S. Government contract DE-AC05-00OR22800
o Oak Ridge, Tennessee o
PROJECT NAME
ES-3100 SHIPPING PACKAGE
CONSOLIDATED ASSEMBLY DRAWING
6 M L F Y-12 NA NA 3 6 A U
CM PKG IN M2E801580A037 C

THIS PAGE INTENTIONALLY LEFT BLANK.

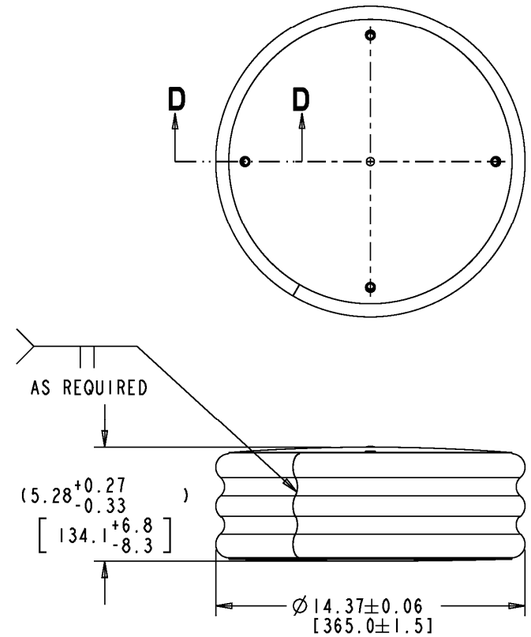

-4 TOP PLUG WELDMENT

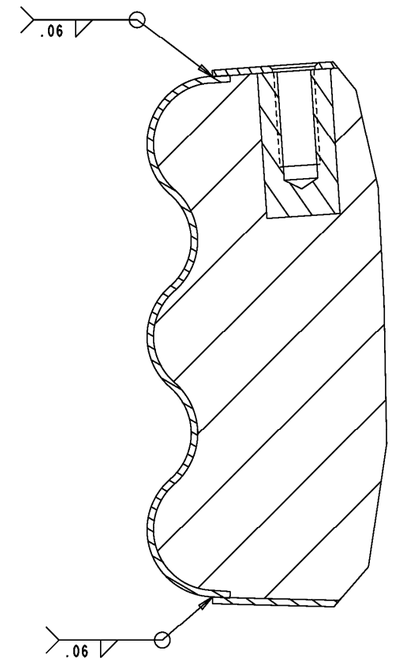

SECTION D-D

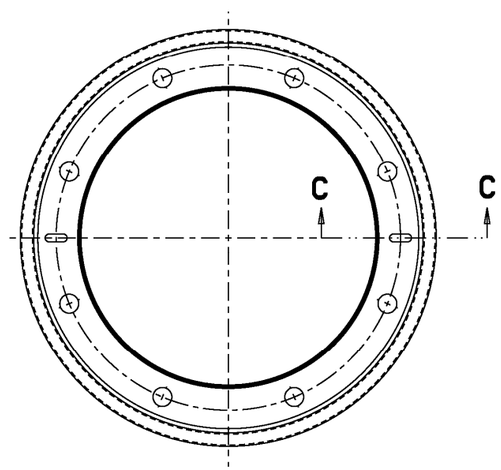

-3 DRUM LID WELDMENT

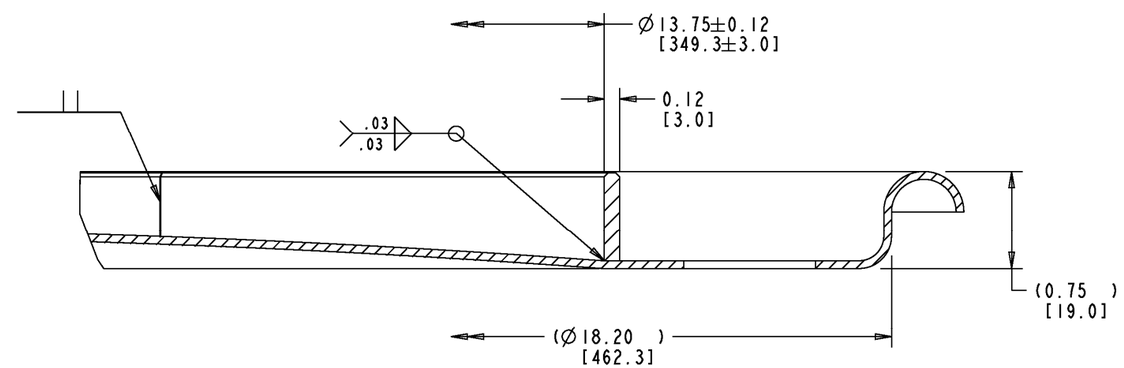

SECTION C-C

Y-12 National Security Complex managed by BWXT Y-12, L.L.C. for the Department of Energy under U.S. Government contract DE-AC05-00OR22800
o Oak Ridge, Tennessee o

PROJECT NAME
ES-3100 SHIPPING PACKAGE

CONSOLIDATED ASSEMBLY DRAWING

1	48	49	50	PLANT	BLDG	FL	SH.	OF	TYPE	CLASS
6	M	L	F	Y-12	NA	NA	4	6	A	U
51		52		53						REV
CM		PKG		IN	M2E801580A037					C

M2E801580A037

THIS PAGE INTENTIONALLY LEFT BLANK.

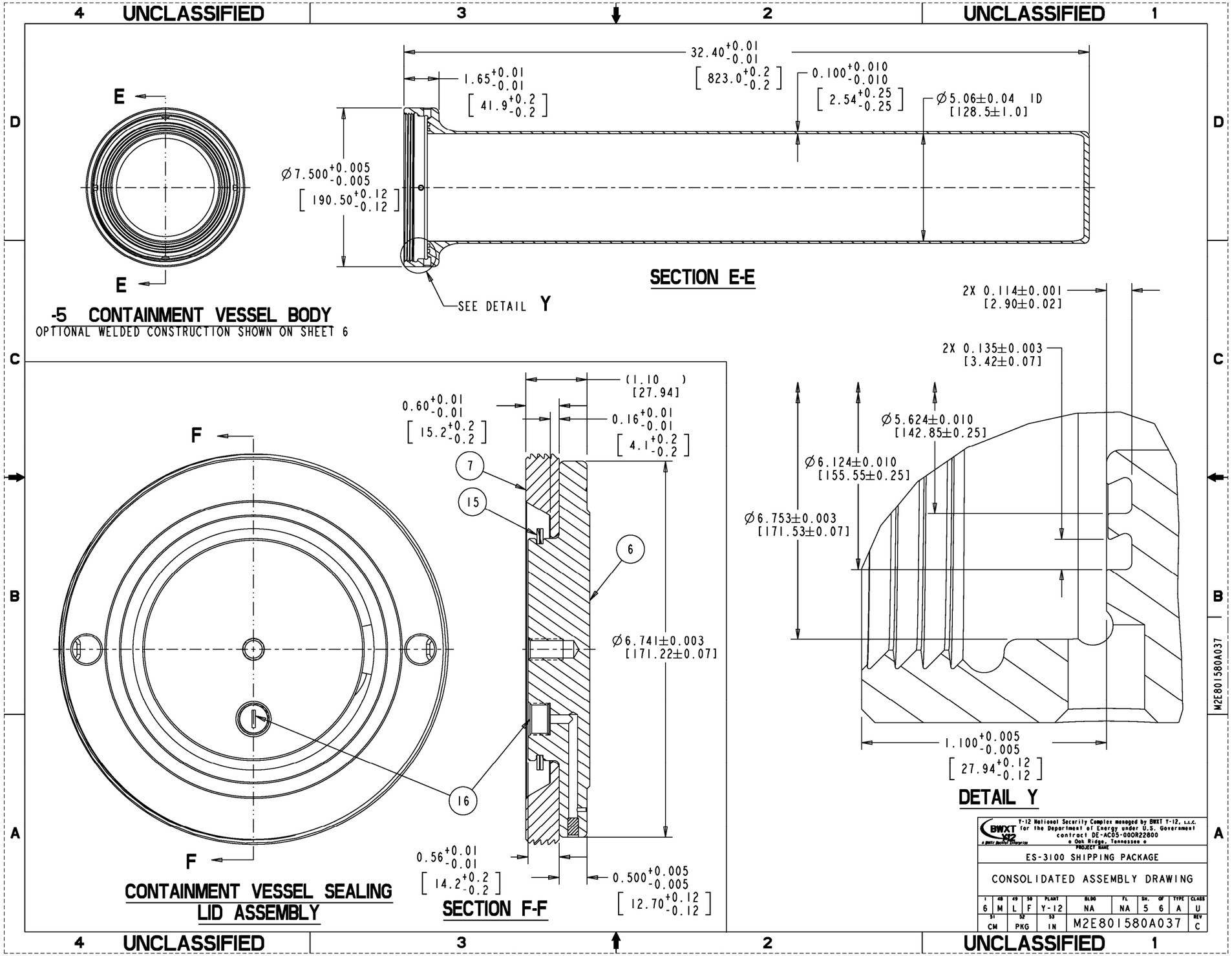
UNCLASSIFIED
UNCLASSIFIED
E
E
-5 CONTAINMENT VESSEL BODY
OPTIONAL WELDED CONSTRUCTION SHOWN ON SHEET 6
32.40 +0.01 -0.01
[823.0 +0.2 -0.2]
1.65 +0.01 -0.01
[41.9 +0.2 -0.2]
0.100 +0.010 -0.010
[2.54 +0.25 -0.25]
Ø5.06±0.04 ID
[128.5±1.0]
Ø7.500 +0.005 -0.005
[190.50 +0.12 -0.12]
SEE DETAIL Y
SECTION E-E
F
F
CONTAINMENT VESSEL SEALING
LID ASSEMBLY
(1.10)
[27.94]
0.60 +0.01 -0.01
[15.2 +0.2 -0.2]
0.16 +0.01 -0.01
[4.1 +0.2 -0.2]
7
15
6
16
Ø6.741±0.003
[171.22±0.07]
0.56 +0.01 -0.01
[14.2 +0.2 -0.2]
0.500 +0.005 -0.005
[12.70 +0.12 -0.12]
SECTION F-F
2X 0.114±0.001
[2.90±0.02]
2X 0.135±0.003
[3.42±0.07]
Ø5.624±0.010
[142.85±0.25]
Ø6.124±0.010
[155.55±0.25]
Ø6.753±0.003
[171.53±0.07]
1.100 +0.005 -0.005
[27.94 +0.12 -0.12]
DETAIL Y
T-12 National Security Complex managed by BWXT T-12, L.L.C.
for the Department of Energy under U.S. Government
contract DE-AC05-00OR22800
o Oak Ridge, Tennessee o
PROJECT NAME
ES-3100 SHIPPING PACKAGE
CONSOLIDATED ASSEMBLY DRAWING
PLANT Y-12
BLDG NA
FL NA
SH. 5 OF 6
TYPE A
CLASS U
CM
PKG
IN
M2E801580A037
REV C
M2E801580A037

THIS PAGE INTENTIONALLY LEFT BLANK.

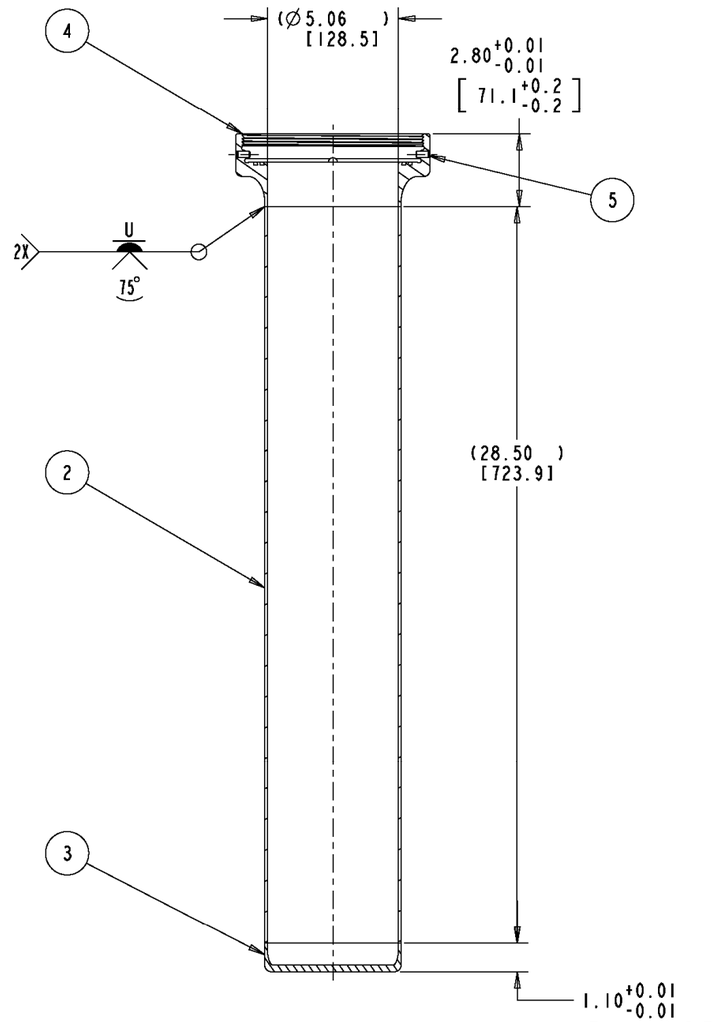

CONTAINMENT VESSEL BODY ASSEMBLY WELDED OPTION

WELD NOTES:

1. ALL WELDS ON THE CONTAINMENT VESSELS SHALL BE DONE EITHER BY THE GTAW OR GMAW PROCESS, MANUAL OR AUTOMATIC, AT THE DISCRETION OF THE SELLER UNLESS SPECIFICALLY CALLED OUT ON THE DRAWINGS. BACKING RINGS, EVEN IF REMOVED AFTER THE WELD HAS BEEN MADE, SHALL NOT BE USED. AS PREVIOUSLY STATED, WELD SYMBOLS ARE PROVIDED ON THE DRAWING INDICATING FOR EACH WELD THE TYPE OF WELD AND DIMENSIONS OF THE WELD.

2. EXCEPT AS LIMITED BY THIS SPECIFICATION, THE APPLICABLE REQUIREMENTS OF NB-4300 AND NB-4400 SHALL APPLY TO THE CONTAINMENT VESSEL.

3. PRIOR TO WELDING, ALL WELD PREPARATION AREAS AND THE SURFACES WITHIN ONE INCH OF THE WELD AREA SHALL BE EXAMINED VISUALLY AND WITH LIQUID PENETRANT. THE ACCEPTANCE CRITERIA FOR THESE EXAMINATIONS ARE THOSE STATED IN NB-5130 (A) THROUGH NB-5130 (D). THE RESULTS OF THESE SURFACE EXAMINATIONS SHALL BE REPORTED TO THE COMPANY TOGETHER WITH THE WELD EXAMINATION REPORTS, SEE SECTION 3.4 OF THIS SPECIFICATION.

4. WELDERS PERFORMING TWO OR MORE WELDS IN ONE DAY THAT ARE REJECTED BASED UPON WELDER TECHNIQUE SHALL BE SUBJECT TO BE RE-QUALIFIED TO THE APPROPRIATE WELDING PROCEDURES, SEE SECTION IX, PARAGRAPH QW-320 OF THE ASME CODE.

5. THE APPLICABLE REQUIREMENTS IN PARAGRAPHS NB-5110, NB-5120, NB-5210, NB-5220, NB-5260, AND NB-5300 SHALL APPLY TO THE CONTAINMENT VESSELS. THE PLUG WELD SHOWN ON DRAWING M2E801580A015 SHALL BE EXAMINED VISUALLY AND WITH PENETRANT. THE APPLICABLE REQUIREMENTS IN PARAGRAPHS NB-5110, AND NB-5350 SHALL APPLY TO THE PLUG WELD. NOTE THAT THE REFERENCE TO THE INSPECTOR IN NB-5112, FOR THE PURPOSES OF THIS SPECIFICATION IS EITHER THE COMPANY'S INSPECTOR OR A SUBCONTRACTOR DESIGNATED BY THE COMPANY.

6. MATERIALS USED IN THE PENETRANT EXAMINATION OF WELDS AND IN THE FINAL SURFACE EXAMINATION OF FINISHED COMPONENTS (SEE SECTION 3.7) SHALL BE SPECIFICALLY RECOMMENDED BY THEIR SUPPLIERS FOR USE WITH AUSTENITIC STAINLESS STEELS, AND COPIES OF THE CERTIFICATION OF CONTAMINANT CONTENT OF MATERIALS USED (SEE SECTION V, ARTICLE 6, T-641) SHALL BE SUPPLIED TO THE COMPANY WITH THE EXAMINATION REPORTS.

7. REPAIR WELDING SHALL MEET THE APPLICABLE REQUIREMENTS OF NB-2500.

8. CERTIFIED WRITTEN WELD EXAMINATION REPORTS TOGETHER WITH THE CORRESPONDING MATERIAL SURFACE EXAMINATION REPORTS, AND WELD MAP SHALL BE SUBMITTED TO THE COMPANY AS STATED IN THE PROCUREMENT SPECIFICATION FOR THE ES-3100 CONTAINMENT VESSEL. WELD EXAMINATION REPORTS FOR ALL WELD AND SURFACE EXAMINATION SHALL INCLUDE: THE CONTAINMENT VESSEL SERIAL NUMBER, A WELD MAP SHOWING THE LOCATION OF THE WELD AND EXAMINATION AREA, THE WELDER'S NAME, THE EXAMINER S NAME, THE TIME AND DATE OF THE WELD EXAMINATION, THE EXAMINATION PROCEDURE(S) NUMBER USED, THE WPS NUMBER, THE HEAT NUMBERS OF THE MATERIALS JOINED, THE HEAT NUMBER OF THE WELD FILLER, AND EXAMINER S REMARKS. THE EXAMINER S REMARKS SHALL INCLUDE THE RESULTS OF THE EXAMINATION AND ACCEPTANCE, OR REJECTION OF THE WELD BASED ON THE STATED CRITERIA. ONE SET OF RADIOGRAPHS SHALL BE PROVIDED TO THE COMPANY WITH RADIOGRAPHIC EXAMINATION REPORTS. IF THE WELD OR SURFACE IS REJECTED, A DESCRIPTION OF THE DEFECT AND SKETCH SHOWING THE LOCATION SHALL BE PROVIDED.

9. IF A WELD IS REJECTED, THE AREA SHALL BE WELD REPAIRED BY THE SELLER AND RE-EXAMINED. AFTER TWO UNSUCCESSFUL REPAIR ATTEMPTS, THE COMPANY SHALL BE NOTIFIED FOR APPROVAL TO PERFORM MORE REPAIR ATTEMPTS. THE COMPANY MAY, AT ITS OPTION, CHOOSE TO REJECT FURTHER REPAIR EFFORTS AND REQUIRE THAT A REPLACEMENT PART BE FABRICATED.

QTY REQ'D NEXT ASSEMBLY	PART OR IDENTIFYING NO	NOMENCLATURE OR DESCRIPTION	MATERIAL/ SPECIFICATION	FIND NO
2	-5	.2501/.2503 OD DOWEL PIN	ANSI B18.8.2 18-8-SST	5
1	-4	VESSEL FLANGE	ASME SA-182 TYPE F304L	4
1	-3	VESSEL END CAP	ASME SA-182 TYPE F304L	3
1	-2	VESSEL BODY SCH40 PIPE	ASME SA-182 TYPE F304L	2
X	-1	CONTAINMENT VESSEL WELDED ASSEMBLY		1

PARTS LIST

BWXT Y-12 — Y-12 National Security Complex managed by BWXT Y-12, L.L.C. for the Department of Energy under U.S. Government contract DE-AC05-00OR22800 • Oak Ridge, Tennessee •

PROJECT NAME: ES-3100 SHIPPING PACKAGE

CONSOLIDATED ASSEMBLY DRAWING

1	46	49	50	PLANT	BLDG	FL	SH.	OF	TYPE	CLASS
6	M	L	F	Y-12	NA	NA	6	6	A	U

51	52	53		REV
CM	PKG	IN	M2E801580A037	C

M2E801580A037

THIS PAGE INTENTIONALLY LEFT BLANK.

Appendix 1.4.2

EQUIPMENT SPECIFICATION JS-YMN3-801580-A002, *ES-3100 DRUM ASSEMBLY*

THIS PAGE INTENTIONALLY LEFT BLANK.

EQUIPMENT SPECIFICATION APPROVAL/REVISION PAGE

SPECIFICATION NO. JS-YMN3-801580-A002	REV. D	ISSUE DATE 10-15-03
PAGE i OF ii	REVISION DATE 03/15/06	
PROCURED BY BWXT L.L.C.	INSTALLED BY BWXT L.L.C.	
PROJECT TITLE ES-3100 Shipping Package	PLANT Y-12	BUILDING AREA
JOB TITLE Design Definition	W.O. OR E.S.O.. 7RCPCA5A	RECORD NUMBER 2003-0328
SPECIFICATION FOR ES-3100 DRUM ASSEMBLY		SSC IDENTIFICATION NUMBER

ENGINEERING AND PLANT APPROVALS

SIGNATURE	DATE	SIGNATURE	DATE
PREPARED BY J.L. Heck	10-21-03	PROJECT ENGINEER: M.R. Feldman	10-29-03
DISCIPLINE MANAGER J.C. Walls	10-29-03	OPERATIONS MANAGER/SYSTEM OWNER:	
DESIGN VERIFICATION Roger Aigner	10-21-03		

REVISIONS/ENGINEERING AND PLANT APPROVALS

REV. NO.	DESCRIPTION OF REVISION
A	Issue Approved
B	Change the title of drawing M2E-801580-A001 from Confinement Boundary Assembly to Drum Assembly. Change the title this specification from ES-3100 Confinement Boundary Drums to ES-3100 Drum Assembly. Deleted reference to drawing M2E-801580-A009, Pad Details. Added the reference to drawings M2E-801580-A010, Data Plates and M2E-801580-A031, Main Assembly. Changed the wording in the first paragraph of Section 3.3
C	Revised the third paragraph of Section 3.0 in accordance with REDC PE-06-058.
D	Section 3.0, paragraph 3, the phrase "certifying authority's written approval" has been revised to "regulatory authority's written approval."

SIGNATURE	DATE	SIGNATURE	DATE
PREPARED BY G. A Byington /s/	3/14/06	PROJECT ENGINEER J. Arbital /s/	3/14/06
DISCIPLINE MANAGER C. M. Amonett /s/	3/14/06	OPERATIONS MANAGER/SYSTEM OWNER:	
DESIGN VERIFICATION Roger D. Aigner /s/	3/14/06		

This document has been has been reviewed by a Y-12 ADC and UCNI RO and has been determined to be UNCLASSIFIED and not UCNI. This review does not constitute clearance for public release.

Name: Roger D. Aigner /s/ Date: 3/14/06

EXEMPT FROM IO-155

TABLE OF CONTENTS **PAGE**

1.0 SCOPE 1

2.0 APPLICABLE CODES AND STANDARDS 1

3.0 DETAILED REQUIREMENTS 2

3.1 Materials 3
3.2 Welding 3
3.3 Weld Examination 4
3.4 Cleaning and Passivation 5
3.5 Dimensional Inspection Reports 5

LIST OF COMPANY DRAWINGS

Drawing Number	Title
M2E-801580-A001	Drum Assembly
M2E-801580-A002	Body Weldment
M2E-801580-A003	Inner Liner Weldment
M2E-801580-A004	Double Open Head Reinforced Drum
M2E-801580-A005	Misc. Details
M2E-801580-A006	Drum Lid Weldment
M2E-801580-A007	Drum Lid
M2E-801580-A008	Top Plug Weldment
M2E-801580-A010	Data Plates
M2E-801580-A031	Main Assembly

1.0 SCOPE

This specification, the Procurement Specification for the ES-3100 Drum Assembly, specifications JS-YMN3-801580-A003 and JS-YMN3-801580-A005, the Company's drawings, and the referenced codes and standards in section 2.0 of this specification state the requirements for the procurement of materials and components, fabrication, inspection, examination, assembly, and testing of the Drum Assembly for the ES-3100 shipping package. If conflicting requirements appear between the Company's documents, and the standards listed in section 2.0 of this document, the Seller shall immediately notify the Company, so that these can be resolved. The Seller shall provide the number of completed assemblies specified in the purchase order.

This specification describes the applicable procedures to be followed in the fabrication, welding, examination, inspection, quality assurance, and documentation requirements for a Drum Assembly used in a Type B nuclear shipping package.

The Drum Assembly shall be manufactured in accordance with those paragraphs of the American Society of Mechanical Engineers (ASME) Boiler and Pressure Vessel Code, Section VIII, Division 1 that are specified in this document. The Drum Assemblies are not pressure vessels and are not to be hydrostatically tested, nor are they to be stamped. If the Seller does not have certificate of authorization from the ASME to apply the U stamp, the Seller shall be familiar with, and capable of meeting those requirements in Section VIII, Division 1 of the ASME Boiler and Pressure Vessel Code that are referenced in this specification.

Company specification JS-YMN3-801580-A003 gives requirements for casting Kaolite, and JS-YMN3-801580-A005 gives requirements for casting Catalog No. 277-4 in the drum as shown on the Company's drawings.

2.0 APPLICABLE CODES AND STANDARDS

The Drum Assembly shall be fabricated, inspected, and tested according to the design drawings, and the portions of the codes, standards, and regulations to the extent described herein.

- American Society of Mechanical Engineers, Boiler and Pressure Vessel Code, Section VIII, Division 1, 2001 Edition with 2002 and 2003 addenda

- American Society of Mechanical Engineers, Boiler and Pressure Vessel Code, Section II, Parts A and C, 2001 Edition and 2002 and 2003 addenda

- American Society of Mechanical Engineers, Boiler and Pressure Vessel Code, Section V, 2001 Edition and 2002 and 2003 addenda

- American Society of Mechanical Engineers, Boiler and Pressure Vessel Code, Section IX, 2001 Edition and 2002 and 2003 addenda

- American Society For Nondestructive Testing, No. SNT-TC-1A-1992, Recommended Practice for Nondestructive Testing Personnel Qualification and Certification, Dec 1992

- Military Standard, MS27683, Drum, Metal-Shipping and Storage 16 to 80 Gallons

- American Society For Testing Materials, ASTM A 380-99^{e1}, Standard Practice for Cleaning, Descaling, and Passivation of Stainless Steel Parts, Equipment and Systems.

All references to the ASME Code in this document are to the ASME Boiler and Pressure Vessel Code, the 2001 Edition with the 2002 and the 2003 addenda.

3.0 DETAILED REQUIREMENTS

Detailed dimensional requirements and the materials of construction are called out on the Company's drawings. Additional requirements for materials are given in section 3.1 of this specification. The Seller shall be responsible for determining stock sizes so that the finished machined components meet the dimensions, tolerances and surface features called out on the attached drawings.

Weld symbols are provided on the Company's drawings indicating for each weld the type of weld and dimensions of weld. Additional welding requirements are stated in section 3.2 of this specification

Any material substitution or any other deviation from the requirements shown on the Company's drawings, or stated in the Company's document is not permitted without the Seller submitting a written request for waiver or deviation, Company's written approval, and regulatory authority's written approval (see the Procurement Specification for the ES-3100 Drum Assembly).

The assembled Drum Assembly shall be marked according to the Company's drawings. The Company will assign permanent serial numbers for each Drum Assembly. Drum Assembly's records may be maintained based upon a temporary serial number assigned by the Seller. The temporary serial number for the Drum Assembly shall be cross-referenced to the Drum Assembly's permanent serial number.

The following additional requirements apply as follows:

3.1 Materials

Except for the weld studs, documented Certified Material Test Reports (CMTR's) shall be provided to the Company for all materials used in weldments for the fabrication of the Drum Assembly, including weld filler metal. The CMTR's shall be traceable to heat numbers and shall demonstrate compliance with the SA or SFA material specifications called out. For all other the materials documented Certificates of Compliance shall be provided to the Company certifying that the materials provided comply the requirements stated on the Company's drawings and specifications. See the Procurement Specification for the ES-3100 Drum Assembly for specific documentation requirements.

The markings on the weldment materials shall not be removed until after all weld examination is complete. Note that the heat numbers of base metals and weld filler are required on all weld examination reports (see section 3.3 of this specification).

The weld filler metal used in the fabrication of the Drum Assemblies shall be procured to comply with the SFA specifications of Section II, Part C of the ASME Code that are stated in the Seller's welding procedure specifications. Weld filler metal shall be procured traceable to heat numbers, and Certified Material Test Reports shall be furnished to the Company for each heat of weld wire filler. The control of weld filler by the Seller shall permit a weld examiner to be able to determine the heat number of the weld filler used in any weld on the Drum Assembly.

Prior written approval of the Company shall be obtained for any weld repair on materials, and the weld repair areas shall be noted in a sketch supplied with the CMTR for the material that was weld repaired. Note that depending on the specific defect in a specific material, the Company may or may not approve the weld repair, even if it is permitted by the material specification.

3.2 Welding

All welding shall be done in accordance with welding procedure specifications that are written and performance qualified in accordance with the ASME Code, Section IX. All welders shall be performance qualified to weld using these procedures, and their qualifications documented in accordance with the ASME Code, Section IX. The welding fabrication requirements stated in the ASME Code, Section VIII, Division 1, paragraphs UW-26 through UW-48 shall be met. The Inspector referenced in these paragraphs shall be an individual or individuals that are employed by the Company or subcontractors to the Company.

All butt welds in rolled sheet, pipe and angle joints shall be full penetration butt welds. With the exception of the seam welds in the drum body, all welds shall be done by the GTAW, GMAW, PAW or a Capacitive Discharge (CD) stud welding process.

Welders performing two or more welds in one day that are rejected shall be subject to be re-qualified to the appropriate welding procedures, see Section IX, and paragraph QW-320 of the ASME Code.

3.3 Weld Examination

A qualified weld examiner using a written weld examination procedure shall visually examine all designated welds. Weld examiners shall be qualified to perform visual weld inspection in accordance with their employer's written practice, which must be in accordance with either SNT-TC-1A (2001 Edition), "Personnel Qualification and Certification in Nondestructive Testing;" or ANSI/ASNT CP-189 (2001 Edition), "ASNT Standard for Qualification and Certification of Nondestructive Testing Personnel;" published by the American Society for Nondestructive Testing. The weld examination procedure shall meet the requirements of the ASME Code, Section V. The weld examination procedures, the weld examiners qualifications, and the weld examination reports shall be submitted to the Company.

Written weld examination reports for all weld examination shall include: the Drum Assembly serial number, a weld map showing the location of the weld, the welder's name, the examiner's name, the time and date of the weld examination, the examination procedure number used, the WPS number, the heat numbers of the materials joined, the heat number of the weld filler, and the examiner's remarks. The examiner's remarks shall include the results of the examination, and acceptance or rejection of the weld based on the stated criteria and include a description and sketch showing the location of any defects found. Weld examination reports shall be submitted to the Company as stated in the Procurement Specification for the ES-3100 Drum Assembly.

The acceptance criteria for joint fit-up and alignment, and for visual examination of welds are given in the ASME Code, Section VIII, Division 1, paragraphs UW-31 through UW-36. In addition, any visible defects such as lack of fusion, lack of penetration, linear or crack like defects, and visible porosity, shall be cause for rejection.

If a weld is rejected, the area may be weld repaired by the Seller and re-examined. After two unsuccessful repair attempts, the Company shall be notified for approval to perform more repair attempts. The Company may, at its option, choose to reject further repair efforts and require that a replacement part be fabricated.

If penetrant examination of welds or materials is performed the materials used in the examination shall be specifically recommended by their suppliers for use with austenitic stainless steels, and copies of the certification of contaminant content of materials used (see Section V, Article 6, T-641) shall be supplied to the Company with the examination reports.

3.4 Cleaning and Passivation

Cleaning procedures for the stainless steel, including weld areas, shall be submitted to the Company for approval prior to the start of fabrication, see the Procurement Specification for the ES-3100 Drum Assembly. Only non-chloride bearing chemicals shall be used for cleaning (such as trisodium phosphate detergent or acetone). Water used in cleaning shall have a maximum chlorine content of 0.5 parts per million.

Finished components awaiting assembly and assemblies shall be free of dirt, debris, foreign objects, cutting fluids, metal chips, grinding residue, and other foreign substances. The Seller shall clean, cover, and protect parts and subassemblies from becoming dirty while in storage, and to the extent practical, in the shop environment while in work.

After final machining and examination of all welds except the attachment welds for the drum bottom and the closure weld on the top plug, and prior to filling with Kaolite and Catalog No. 277-4 (see JS-YMN3-801580-A003 and JS-YMN3-801580-A005), clean and passivate all stainless steel surfaces of the Drum Assembly in accordance with ASTM A 380. After the closure weld on the top plug weldment and the attachment weld on the drum bottom are examined, clean and locally passivate the weld areas and heat affected zone areas.

3.5 Dimensional Inspection Reports

Straightening, flattening, and forming by mechanical or thermal means of some features and components after welding may be required to ensure proper assembly. The surfaces of areas of the weldment that have been worked shall be visually examined to ensure that no cracks are present or that the weldment has been degraded. Adjacent welds to these areas shall also be visually examined. The acceptance criteria are that no cracks are found. The areas worked and the visual inspections shall be noted on the dimensional inspection report. This work and examination shall be performed prior to the installation of Kaolite or Catalog No. 277-4.

After all testing, inspection and final machining, the Drum Assemblies shall be dimensionally inspected. The dimensions, and features such as flatness, runout, etc, to be inspected are indicated on the Company's drawings. A written inspection report shall be prepared, and submitted to the Company as stated in the Procurement Specification for the ES-3100 Drum Assembly.

THIS PAGE INTENTIONALLY LEFT BLANK.

Appendix 1.4.3

EQUIPMENT SPECIFICATION JS-YMN3-801580-A001, *ES-3100 CONTAINMENT VESSEL*

THIS PAGE INTENTIONALLY LEFT BLANK.

EQUIPMENT SPECIFICATION APPROVAL/REVISION PAGE

SPECIFICATION NO.	JS-YMN3-801580-A001	REV.	E
ISSUE DATE	10-15-03		
PAGE	i OF ii	REVISION DATE	03-15-06
PROCURED BY	BWXT L.L.C.	INSTALLED BY	BWXT L.L.C.
PROJECT TITLE	ES-3100 Shipping Package	PLANT	Y-12
BUILDING	AREA		
JOB TITLE	Production Design Definition	W.O. OR E.S.O.	7RCPCA5A
RECORD NUMBER	Y2003-0328		
SPECIFICATION FOR	ES-3100 CONTAINMENT VESSELS	SSC IDENTIFICATION NUMBER	

ENGINEERING AND PLANT APPROVALS

SIGNATURE	DATE	SIGNATURE	DATE
PREPARED BY J.L. Heck	10-21-03	PROJECT ENGINEER: M.R. Feldman	10-29-03
DISCIPLINE MANAGER J.C. Walls	10-29-03	OPERATIONS MANAGER/SYSTEM OWNER:	
DESIGN VERIFICATION Roger Aigner	10-21-03		

REVISIONS/ENGINEERING AND PLANT APPROVALS

REV. NO.	DESCRIPTION OF REVISION
A	Issued Approved
B	Included the requirements for a Containment Vessel that was fabricated by welding a forged bottom, a forged top flange and a cylindrical shell as shown on the revised drawing, M2E801580A012, Rev B.
C	In all locations removed the references to the Procurement Specification document number OO-PP-1210. Modified the Weld Repair reject and re-qualification requirements in Section 3.3 in the fourth paragraph. In Section 3.9, first, third, and fourth paragraphs changed the units from ref-cm^3/sec to cm^3/sec helium. Also added new Section 3.6 Welding Documentation Submittals.
D	Added two paragraphs to the end of Section 3.1 for reference to ASTM A 262 in accordance with REDC #PE-05-046-A. Added a sentence to the beginning of the first paragraph in Sect. 3.9 in accordance with REDC # PE-06-059.
E	Section 3.0, paragraph 3, the phrase "the Company's written approval" has been revised to "the Company's written approval, and regulatory authority's written approval."

SIGNATURE	DATE	SIGNATURE	DATE
PREPARED BY G. A. Byington /s/	03/15/06	PROJECT ENGINEER J. Arbital	03/15/06
DISCIPLINE MANAGER C. M. Amonett /s/	03/15/06	OPERATIONS MANAGER/SYSTEM OWNER:	
DESIGN VERIFICATION Roger D. Aigner /s/	03/15/06		

This document has been has been reviewed by a Y-12 ADC and UCNI RO and has been determined to be UNCLASSIFIED and not UCNI. This review does not constitute clearance for public release.

Name: Roger D. Aigner /s/ Date: 03/15/06

EXEMPT FROM IO-155

TABLE OF CONTENTS **PAGE**

1.0 SCOPE 1

2.0 APPLICABLE CODES AND STANDARDS 1

3.0 DETAILED REQUIREMENTS 2

3.1	Materials and Material Examinations	3
3.2	Forming, Fitting and Alignment	5
3.3	Welding and Weld Repair	5
3.4	Weld Examination	6
3.5	NDE Examiner Qualifications	7
3.6	Welding Documentation Submittals	7
3.7	Hydrostatic Testing	8
3.8	Final Examination of Finished Surfaces	8
3.9	Leak Testing	9
3.10	Cleaning, Passivation, and Bead Blasting	10
3.11	Dimensional Inspection Reports	10

LIST OF COMPANY DRAWINGS

Drawing Number	Title
M2E-801580-A011	Containment Vessel Assembly
M2E-801580-A012	Containment Vessel Body Assembly
M2E-801580-A013	Containment Vessel O-ring Details
M2E-801580-A014	Containment Vessel Lid Assembly
M2E-801580-A015	Containment Vessel Sealing Lid
M2E-801580-A016	Containment Vessel Closure Nut
M2E-801580-A021	Containment Vessel Body Test Flange Assembly
M2E-801580-A022	Containment Vessel Lid Test Flange Assembly
M2E-801580-A023	Containment Vessel Leak Test Assemblies

1.0 SCOPE

This specification, the Procurement Specification for the ES-3100 Containment Vessel, OO-PP-986, Procurement Specification For 70A Durometer Preformed Packing (O-rings), the Company's drawings, and the referenced codes and standards in section 2.0 of this specification state the requirements for the procurement of materials and components, fabrication, inspection, examination, assembly, and testing of the Containment Vessels for the ES-3100 shipping package. If conflicting requirements appear between the Company's drawings and specifications, the Seller shall immediately notify the Company, so that these can be resolved. The Seller shall provide the number of completed assemblies specified in the purchase order.

The Containment Vessel will be manufactured in accordance with the applicable requirements stated in the American Society of Mechanical Engineers (ASME) Boiler and Pressure Vessel Code, Section III, Division 1, Subsection NB for Class 1 Components as described on the Company's drawings and in this specification. If the Seller does not have certificate of authorization from the ASME to apply the N stamp, the Seller shall be familiar with, and capable of meeting those requirements in Section III, Division 1, Subsections NB and NCA of the ASME Boiler and Pressure Vessel Code that are referenced in this specification. The reference to the Inspector in any of the ASME Codes shall in this particular case be that person designated by the Company.

2.0 APPLICABLE CODES AND STANDARDS

The Containment Vessel shall be fabricated, inspected, and tested according to the design drawings and the following codes, standards, and regulations as described in this document.

- American National Standards Institute, ANSI N14.5-1997, American National Standard for Radioactive Materials – Leakage Tests on Packages for Shipment

- American Society of Mechanical Engineers, Boiler and Pressure Vessel Code, Section III, Division 1 - Subsections NB and NCA, Class 1 Components, 2001 Edition and 2002 and 2003 addenda.

- American Society of Mechanical Engineers, Boiler and Pressure Vessel Code, Section II, Parts A and C, 2001 Edition and 2002 and 2003 addenda.

- American Society of Mechanical Engineers, Boiler and Pressure Vessel Code, Section V, 2001 Edition and 2002 and 2003 addenda.

- American Society of Mechanical Engineers, Boiler and Pressure Vessel Code, Section IX, 2001 Edition and 2002 and 2003 addenda.

- American Society For Nondestructive Testing, No. SNT-TC-1A-1992, Recommended Practice for Nondestructive Testing Personnel Qualification and Certification, Dec 1992.

- American Society For Testing Materials, ASTM A 380-99^{e1}, Standard Practice for Cleaning, Descaling, and Passivation of Stainless Steel Parts, Equipment and Systems.

- Society for Protective Coatings, SSPC SP 5/NACE No. 1, White Metal Blast Cleaning

3.0 DETAILED REQUIREMENTS

Detailed dimensional requirements and the materials of construction are called out on the Company's drawings. Additional requirements for materials are given in section 3.1 of this specification. The Seller shall be responsible for determining stock sizes so that the finished machined components meet the dimensions, tolerances and surface features called out on the attached drawings.

Weld symbols are provided on the Company's drawings indicating the type of weld and dimensions for each weld. Additional welding and repair welding requirements are stated in sections 3.1 and 3.3 of this specification.

Any material substitution or other deviation from the requirements shown on the Company's drawings or stated in the Company's specifications is not permitted without the Seller submitting a written request for waiver or deviation, and Company's written approval, and regulatory authority's written approval (see the Procurement Specification for the ES-3100 Containment Vessel).

The term ASME Code in this specification refers to the ASME Boiler and Pressure Vessel Code. A paragraph referenced as NB-XXXX or NCA-XXXX, where XXXX is a specific paragraph number, is that paragraph in Section III, Subsection NB or Subsection NCA, respectively, of the ASME Code. If a given paragraph is referenced as a requirement, all the paragraphs under the stated paragraph are also to be considered as requirements. For example, if NB-2430 is referenced as a requirement, not only do the applicable requirements of NB-2430 apply, but also those of NB-2431, NB-2431.1, NB-2431.1(a), NB-2432, etc. apply. Note that the Company shall act as the Authorized Inspector, and that the Inspector referenced in the Code shall be a representative of the Company.

The assembled Containment Vessels shall be marked according to the Company's drawings. Permanent serial numbers for each Containment Vessel shall be assigned by the Company. Containment Vessel records may be maintained based upon a temporary serial number assigned by the Seller. The temporary serial number for the Containment Vessel shall be cross referenced to the Containment Vessel's permanent serial number.

The following additional requirements apply as follows:

3.1 Materials and Material Examinations

The containment vessel body (drawing M2E-801580-A012), the sealing lid, (drawing M2E-801580-A015), and the closure nut (drawing M2E-801580-A016), shall be considered pressure retaining materials as defined in paragraph NB-2110, and meet the applicable requirements of NB-2120. Documented Certified Material Test Reports (CMTR's) shall be provided to the Company for the materials used to fabricate these components in accordance with NCA-3860. The suppliers of these materials shall meet the requirements of NCA-3800. Such parts shall be traceable to each containment vessel by means of a serial number assigned by the Company. The Seller shall maintain control of materials to ensure this traceability. Other metallic materials, and the O-ring seals shall be supplied with Certificate of Compliances in accordance with NCA-3862(g) and (h).

Procured materials shall be examined in accordance with the applicable paragraphs of NB-2500, and shall meet the stated acceptance criteria. The results of these examinations shall be included with the CMTR's provided to the Company. Prior written approval of the Company shall be obtained for any weld repair on materials, and the weld repair areas shall be both surface and volumetrically examined. The repair area shall be noted in a sketch supplied with the CMTR for the material that was weld repaired and the documented results of the weld examination shall be provided to the Company. Note that depending on the specific defect in a specific material, the Company may or may not approve the weld repair, even if it is permitted by the material specification or by paragraph NB-2500.

The weld filler metal used in the fabrication and repair welding as permitted, of the Containment Vessels shall meet the applicable requirements of NB-2400. It shall be procured to comply with the SFA specifications of Section II, Part C of the ASME Code that is stated in the Seller's welding procedure specifications. Weld metal filler shall be procured traceable to heat numbers, and Certified Material Test Reports shall be furnished to the Company for each heat of weld wire filler used. The results of the delta ferrite determination shall be included in the CMTR for the weld filler metal (see NB-2433). The control of weld filler by the Seller shall permit a weld examiner to be able to determine the heat number of the weld filler used in any weld on the Containment Vessel.

The Seller shall provide the Company with certified material test reports, certified material examination reports and certificates of compliance for the materials stated above as required by the Procurement Specification for the ES-3100 Containment Vessel.

There are two containment vessel assemblies shown on drawing M2E801580A012, part number M2E801580A012-1, and M2E801580A012-4. The containment vessel assembly(s) to be fabricated will be specified in the Company's purchase order. Note that part M2E801580A012-4 is fabricated by welding a forged bottom, and forged top flange to a cylindrical shell machined from seamless pipe as shown on the drawing.

The formed containment vessel body, part number M2E801580A012-1, shall be formed from a single forged billet or bar by any process that meets the requirements stated in this specification, and shown on the Company's drawings. Such processes may include forging, flow forming, metal spinning. Special requirements for this part are given as follows.

Repair welds may be permitted depending on the nature of the defect to be weld repaired, and after receiving the written approval of the Company for such repair welds.

The formed, heat treated, and finished machined containment vessel body part number M2E801580A012-1, shall meet the applicable requirements of ASME SA 182 for Grade F304L for a forged component. After final forming, parts shall be solution annealed and quenched per the requirements of ASME SA 182 for Grade F304L. In addition, the requirements of NB-2180 shall also apply. A certified heat treatment report shall be provided stating for each furnace charge the following information: the serial numbers of the containment vessel bodies heat treated in the furnace charge, the time and date of the heat treating, the person responsible for the heat treating, the time-temperature profile of the furnace and representative parts of the furnace charge, the quench medium, and all other pertinent details of the heat treating. Such a heat treating report is required for all heat treating, both in process annealing and final heat treatment.

It shall be demonstrated that the formed, heat-treated containment vessel bodies part number M2E801580A012-1 meet the mechanical property requirements of ASME SA 182 for Grade F304L by mechanical testing of coupons. The test coupons are to be machined from the same heats of materials used to form the containment vessel bodies, and shall have the same or greater amount of cold word (plastic strain) as the containment vessels will have as a result of the forming process. The mechanical tensile testing of coupons shall be done in accordance with ASME SA 370. A minimum of six test coupons shall be tested for each final heat treatment furnace charge. The first set of three test coupons, chosen at random, shall be tested without being heat treated. The second set of three of more test coupons shall be heat treated together with the containment vessel bodies, and then tested. The heating rates and maximum temperatures of the test coupons shall be representative of the entire furnace charge. Test coupons are not required to be heat treated with intermediate processing annealing steps, but are required in the final heat treatment furnace charge.

The results of all the testing of the sample coupons shall be documented, certified and reported to the Company. The mechanical properties test report shall contain the following information: a descriptor of the furnace charge in which the test coupons are to represent; the times and dates of the heat treating and the testing; the person responsible for the testing; a statement that these coupons are prior to or after heat treatment; a description of the testing including a sketch of the tensile test specimen; the make, model, serial number, and current calibration data of the testing machine(s) used in the testing; reference to the written testing procedure used; the resulting measure yield strength, ultimate strength, % elongation and % reduction in area; and any pertinent remarks.

It is permissible to deviate from the liquid quench requirements stated in SA 182 provided that the cooling rates of the alternate quench are such that the heat treated material is not susceptible to intergranular corrosion due to chromium carbide precipitation. This is to be demonstrated by testing according to Practice E of ASTM A 262, and meeting the stated acceptance criteria. This shall be accomplished by obtaining test coupons from each furnace batch that represent the slowest cooling rates of the batch, or by following a heat treating procedure that has been qualified to ensure that the heat treated batch will not be sensitive to intergranular corrosion. In any case, the requirements of NB-2180 shall apply.

The heat treating procedure must be qualified by measuring the annealing temperatures, soak times and cooling rates of the furnace batch, and then testing heat treated specimens that represent the lowest annealing temperatures, soak times and cooling rates for that furnace batch for sensitivity to intergranular corrosion using Practice E of ASTM A 262. For subsequent annealing operations, the temperatures, soak times and cooling rates of subsequent furnace batches must be measured and compared to the qualified procedure. Other factors, such as variations of the size and arrangement of the furnace batch that can affect part temperatures and part cooling rates, and the calibration of the furnace temperature sensors must be assessed in the procedure qualification to ensure that minimum temperatures and cooling rates of production heat treating batches can be properly compared to those of the qualified procedure. Such a procedure should be requalified for each individual furnace used, and for significantly different furnace batch sizes. The procedure shall be requalified annually, or if it has not been used for a period of at least three months.

3.2 Forming, Fitting and Alignment

The forming, fitting and alignment requirements stated in paragraph NB-4200 shall be met in the fabrication of the Containment Vessels unless more stringent requirements are called out on the Company's drawings.

The roundness of cylinders, profile of formed head surfaces, and misalignment or offsets in weld joints shall be included in the dimensional inspection reports for the each Containment Vessel, see section 3.11 of this specification.

3.3 Welding and Weld Repair

All welds on the Containment Vessels shall be done either by the GTAW or GMAW process, manual or automatic, at the discretion of the Seller unless specifically called out on the drawings. Backing rings, even if removed after the weld has been made, shall not be used. As previously stated, weld symbols are provided on the drawing indicating for each weld the type of weld and dimensions of the weld.

Except as limited by this specification, the applicable requirements of NB-4300 and NB-4400 shall apply to the Containment Vessel.

Prior to welding, all weld preparation areas and the surfaces within one inch of the weld area shall be examined visually and with liquid penetrant. The acceptance criteria for these examinations are those stated in NB-5130 (a) through NB-5130 (d). The results of these surface examinations shall be reported to the Company together with the weld examination reports, see section 3.4 of this specification.

Welders performing two or more welds in one day that are rejected based upon welder technique shall be subject to be re-qualified to the appropriate welding procedures, see Section IX, paragraph QW-320 of the ASME Code.

3.4 Weld Examination

The applicable requirements in paragraphs NB-5110, NB-5120, NB-5210, NB-5220, NB-5260, and NB-5300 shall apply to the Containment Vessels. The plug weld shown on drawing M2E801580A015 shall be examined visually and with penetrant. The applicable requirements in paragraphs NB-5110, and NB-5350 shall apply to the plug weld. Note that the reference to the Inspector in NB-5112, for the purposes of this specification is either the Company's inspector or a subcontractor designated by the Company.

Materials used in the penetrant examination of welds and in the final surface examination of finished components (see section 3.7) shall be specifically recommended by their suppliers for use with austenitic stainless steels, and copies of the certification of contaminant content of materials used (see Section V, Article 6, T-641) shall be supplied to the Company with the examination reports.

Repair welding shall meet the applicable requirements of NB-2500.

Certified written weld examination reports together with the corresponding material surface examination reports, and weld map shall be submitted to the Company as stated in the Procurement Specification for the ES-3100 Containment Vessel. Weld examination reports for all weld and surface examination shall include: the Containment Vessel serial number, a weld map showing the location of the weld and examination area, the welder's name, the examiner's name, the time and date of the weld examination, the examination procedure(s) number used, the WPS number, the heat numbers of the materials joined, the heat number of the weld filler, and examiner's remarks. The examiner's remarks shall include the results of the examination and acceptance, or rejection of the weld based on the stated criteria. One set of radiographs shall be provided to the Company with radiographic examination reports. If the weld or surface is rejected, a description of the defect and sketch showing the location shall be provided.

If a weld is rejected, the area shall be weld repaired by the Seller and re-examined. After two unsuccessful repair attempts, the Company shall be notified for approval to perform more repair attempts. The Company may, at its option, choose to reject further repair efforts and require that a replacement part be fabricated.

3.5 NDE Examiner Qualifications

The qualifications of the personnel performing material or weld examination shall be those stated in paragraph NB-5500.

3.6 Welding Documentation Submittals

A. Submittal of the following are required with the bid unless the current revisions of these submittals have been previously approved by the Company. Submittals that do not demonstrate compliance with this specification will be cause for rejection of the proposal.
   1. Typical welding procedure specifications (WPS) for the applicable code.
   2. Procedure qualification records (PQR).
   3. Typical welder performance qualification (WPQ) records for the appropriate code.

B. Submittal of the following documents are required prior to welding unless the current revisions of these submittals have been previously approved by the Company.
   1. Welding Procedure Specifications (WPS).
   2. Procedure Qualification Records (PQR).
   3. Welder Performance Qualification (WPQ) records, including evidence of process usage updates.
   4. Visual examination and nondestructive examination procedures.
   5. Certification records of examination personnel.
   6. Certified Material Test Reports.

C. To facilitate prompt review by the Company of the Seller's weld program, the welding documentation required above shall be submitted electronically in Adobe pdf format either on compact disk (CD) or by email. All information submitted shall reflect the Seller's most current documentation. Upon review and approval of the documentation, the Seller will be notified.

D. If the latest revision of the Seller's welding documentation required above has been previously submitted electronically and reviewed and approved by the Company, this shall be so stated with the offer. The Seller shall submit a detailed list of the welding documentation to be used for this contract including title, revisions/dates, type components to be used on (i.e., piping, structural, sheet metal, etc.) and indicate the previous contract and approval date. The Company will then review the documentation for applicability on the new contract and approve or comment.

E. If changes have occurred since the last approval of the welding documentation, in addition to the list of welding documentation that they propose to use the Seller shall submit those documents that have changed. The Company will then review, comment and/or approve the Seller's documentation.

3.7 Hydrostatic Testing

After all machining is complete, the assembled Containment Vessel shall be hydrostatic tested by the Seller in accordance with the applicable sections of NB-6000 at a test pressure of 150 psig +/- 5 psig at ambient temperature (60°F to 90°F). Water with a maximum chlorine content of 0.5 parts per million shall be used as a test medium.

It will be necessary to hydrostatically test the Container Body Assembly separately from the Lid Assembly. It is recommended that the tooling shown on the Company's drawings M2E801580A021, M2E801580A022, and M2E801580A023 be used to pressurize the components to be tested. The use of this tooling is not mandatory, but the Seller shall provide suitable fittings to perform the hydrostatic testing.

A written hydrostatic test procedure shall be prepared by the Seller and submitted to the Company for approval prior to testing. Certified written hydrostatic test reports for each Containment Vessel shall contain the following data: serial number of the Containment Vessel; time and date of the test; name of person responsible for the hydrostatic testing; the hydrostatic test procedure number; the name, serial number and calibration date of all gages and transducers; and a sketch showing any areas of leakage or any areas where surface defects were observed after hydrostatic testing. Hydrostatic test reports shall be submitted to the Company as stated in the Procurement Specification for the ES-3100 Containment Vessel.

3.8 Final Examination of Finished Surfaces

After all finish machining, load testing and hydrostatic testing, all surfaces of the containment vessel body, drawing M2E801580A012; the containment vessel sealing lid, drawing M2E801580A015; and the containment vessel closure nut, drawing M2E801580A016, shall be examined with penetrant in accordance with NB-2546. See section 3.4 for additional requirements for the materials used in the penetrant examination. The results of the final surface examinations shall be documented in a certified examination report and provided to the Company as stated in the Procurement Specification for the ES-3100 Containment Vessel.

If a defect is found, the Company shall be notified in writing. The area may be weld repaired by the Seller only if specifically permitted by the Company in writing, and the area re-examined. After two unsuccessful repair attempts, the Company may, at its option, choose to reject further repair efforts and require that a replacement part be fabricated.

3.9 Leak Testing

There are three leak tests to be performed on the ES-3100 Containment Vessel. The leak testing is to be performed after Hydrostatic Testing. Following the hydrostatic pressure test and prior to conducting any leak test, the containment vessel and O-ring cavities must be thoroughly dried. The leak testing is to be performed in accordance with the applicable sections of ANSI N14.5-1-1997. A written leak test procedure(s) shall be prepared to perform this testing and submitted to the Company for approval, see the Procurement Specification for the ES-3100 Containment Vessel. The written test procedure(s) and leak testing report shall comply with the applicable requirements of Section V of the ASME Boiler and Pressure Vessel Code. The leak testing for the first two leak tests shall have the sensitivity to detect a leak less than or equal to 5×10^{-8} ref-cm^3/sec of air, or 9×10^{-8} cm^3/sec helium and shall use the leak test fixtures shown on the Company's drawings M2E801580A021, M2E801580A022, and M2E801580A023.

If a leak is found the Company shall be notified in writing. The leak may be weld repaired by the Seller only if specifically permitted by the Company in writing, and the leak test repeated. After two unsuccessful repair attempts, the Company may, at its option, choose to reject further repair efforts, and require that a replacement part be fabricated.

The first leak test shall be performed with the containment vessel body assembled as shown on drawing M2E801580A023-1. Note that the outer O-ring in the containment vessel body is not to be installed for this test. The leak testing acceptance criteria is that the assembly shall not have an integrated leak rate greater than 1×10^{-7} ref-cm^3/sec of air, or 1.9×10^{-7} cm^3/sec helium.

The second leak test shall be performed with the containment vessel lid assembly as shown on drawing M2E801580A023-2. The leak testing acceptance criteria is that the assembly shall not have an integrated leak rate greater than 1×10^{-7} ref-cm^3/sec of air, or 1.9×10^{-7} cm^3/sec helium.

The third leak test is to be performed with the Containment Vessel assembled as shown on drawing M2E801580A011. The sensitivity of the leak testing procedure for the third leak test shall be capable of detecting a leak rate of 1×10^{-4} ref-cm^3/sec of air, and that the acceptance criteria shall be that no leaks are detected. The third leak test shall verify that there is no detectable leakage between the two O-rings that seal the lid to the body at the detectable rate specified.

Certified written leak test reports shall be supplied to the Company that describes the leak testing and results. The test report shall identify the Containment Vessel serial number, identify all standard leaks, gauges, transducers and electronic readouts, give the date on which these instruments were certified, identify the leak detector, give the date on which the leak detector was last certified, the date of the test, time of the start and end of the test, the recorded pressures and leak rates at the start and end of the test, the name of the person conducting the test, the qualifications of the person conducting the test, identify areas of the Containment Vessel where repairs were made and any pertinent remarks. Leak testing reports shall be submitted to the Company as stated in the Procurement Specification for the ES-3100 Containment Vessel.

3.10 Cleaning, Passivation, and Bead Blasting

Cleaning procedures for the stainless steel, including weld areas, shall be submitted to the Company for approval prior to the start of fabrication. Only non-chloride bearing chemicals shall be used for cleaning (such as trisodium phosphate detergent or acetone). Water used in cleaning shall have a maximum chlorine content of 0.5 parts per million.

Finished components awaiting assembly and assemblies shall be free of dirt, debris, foreign objects, cutting fluids, metal chips, grinding residue, dye penetrant and developer, and other foreign substances. The Seller shall clean, cover, and protect parts and subassemblies from becoming dirty while in storage, and to the extent practical, in the shop environment while in work.

After final machining, and all examination of welds and surfaces, clean and passivate all stainless steel surfaces of the containment vessel in accordance with ASTM A 380. After passivating is complete, bead blast all exterior surfaces in accordance with SSPC-SP 5/NACE No. 1, White Metal Blast Cleaning with the exception of all sealing surfaces and threaded surfaces.

3.11 Dimensional Inspection Reports

After all testing, inspection and final machining, the Containment Vessels shall be dimensionally inspected. The dimensions and features to be inspected are indicated on the Company's drawings by a diamond symbol containing an "I". This dimensional inspection includes surface features such as flatness, runout, etc, as called out on the drawings. The dimensional inspection report shall also include the recorded diameter dimensions that show compliance with the requirements of paragraph NB-4200. A certified written inspection report shall prepared and submitted to the Company as stated in the Procurement Specification for the ES-3100 Containment Vessel.

Appendix 1.4.4

EQUIPMENT SPECIFICATION, JS-YMN3-801580-A003, *MANUFACTURING PROCESS SPECIFICATION FOR CASTING KAOLITE 1600™ INTO THE ES-3100 SHIPPING PACKAGE*

THIS PAGE INTENTIONALLY LEFT BLANK.

EQUIPMENT SPECIFICATION APPROVAL/REVISION PAGE

SPECIFICATION NO. JS-YMN3-801580-A003		REV. C	ISSUE DATE 11/24/03
PAGE i OF ii		REVISION DATE 6/1/06	
PROCURED BY BWXT L.L.C.		INSTALLED BY BWXT L.L.C.	
PROJECT TITLE ES-3100 SHIPPING PACKAGE	PLANT Y-12	BUILDING YAREA-00	
JOB TITLE Production Design Definition	W.O. OR E.S.O. 7RCPCA08	RECORD NUMBER 2003-0328	
SPECIFICATION FOR MANUFACTURING PROCESS SPECIFICATON FOR CASTING KAOLITE 1600™ INTO THE ES-3100 SHIPPING PACKAGE		SSC IDENTIFICATION NUMBER	

ENGINEERING AND PLANT APPROVALS

SIGNATURE	DATE	SIGNATURE	DATE
PREPARED BY R. D. Aigner	11-25-03	PROJECT ENGINEER: G. A. Byington	11-25-03
DISCIPLINE MANAGER J. C. Walls	11-25-03	OPERATIONS MANAGER/SYSTEM OWNER:	
DESIGN VERIFICATION R. D. Aigner	11-25-03		

REVISIONS/ENGINEERING AND PLANT APPROVALS

REV. NO.	DESCRIPTION OF REVISION
A	Issue for procurement
B	Removed the reference to the Prototype Procurement Specification document number OO-PP-1210. Change the equipment reference in Section 3.1.3(c) from a "large mortar mixer or plaster mixer with moving vanes or a smooth wall cement mixer with the fixed vanes removed" to "Whiteman Multiquip's WM700S-H8 plaster/mortar mixer, refereed to as WM700". In Section 3.2 changed the method and time that the water and dry mix were added into the mixer based upon the mixer qualification in Section 3.5. Added Section 3.5, added attachments E and F to determine the proper mixing time and the Mixer Qualification Castings. In section 3.3.1 and 3.3.3 added misting procedure. Section 3.3.2(b) added a circular concave of .32±.10 to the Kaolite before it is baked to match drawing M2E801580A002. Section 3.3.4(b) add a circular convex scrape of .09±.06 to the Kaolite before it is baked to match drawing M2E801580A008. Updated the attachments with general revisions. Section 3.4 has been subdivided into 3.4.1 Baking Instruction and 3.4.2 Baking Documentation and added attachment F to this section.
C	Revised patent information in scope. Added recommended "Before Baking" weights for the Body Weldment and Top Plug Weldment based upon a more refined Kaolite 1600™ product code GI80ACCUMD0027 that is produced to the lower side and a smaller range of the manufactures normal tolerance band. This Kaolite 1600™ product code requires using 1.65 times the dry weight for the water weight (instead of 1.5) and generates an acceptable wet mix density of 56.2+/− 5.8 lb/ft^3. This additional water requires between 36 to 46 hours of bake time at 500°F.

SIGNATURE	DATE	SIGNATURE	DATE
PREPARED BY G A Byington	6/1/06	PROJECT MANAGER: George Singleton	6/1/06
DISCIPLINE MANAGER C.M. Amonett for W.I. North	6/1/06	CRITICALITY SAFETY: J F DeCarl	6/1/06
DESIGN VERIFICATION Monty L Goins	6/1/06	QUALITY ASSURANCE: D.W. Eckert	6/1/06

This document has been has been reviewed by a Y-12 ADC and UNCI RO and has been determined to be UNCLASSIFIED and not UNCI. This review does not constitute clearance for public release.

Name: R. D. Aigner Date: 06/01/06

EXEMPT FROM IO-155

TABLE OF CONTENTS

		Page
1	**Scope**	3
2	**Applicable Documents**	3
3	**Kaolite 1600™ Processing Requirements**	3
3.1	**General**	3
3.1.1	Kaolite 1600™ Receiving and Storage Instructions	3
3.1.2	Cleaning Instructions	4
3.1.3	Mixing Water and Mixing Equipment Requirements	4
3.2	**Mixing of Kaolite 1600™**	4
3.3	**Vibration Casting and Curing of Kaolite 1600™ Into Assemblies**	5
3.3.1	Body Weldment Casting Instructions	5
3.3.2	Body Weldment Curing Instructions	6
3.3.3	Top Plug Assembly Casting Instructions	6
3.3.4	Top Plug Assembly Curing Instructions	7
3.4	**Baking of Assemblies Cast and Cured with Kaolite 1600™ mixture**	7
3.4.1	Baking Instructions	7
3.4.2	Baking Documentation	8
3.5	**Mixer Qualification for Kaolite 1600™ Casting Placement**	9
3.5.1	Wet Density Mixing Test	9
3.5.2	Mixer Baked Density Qualification Castings	10
4	**Quality Assurance Requirements**	10
4.1	**General**	10
4.2	**Material and Equipment Certification**	11
4.3	**Nonconformance Control**	11
4.4	**Operator and Witness Qualifications**	11
4.4.1	Kaolite 1600™ Mixing Process Qualifications	12
4.4.2	Kaolite 1600™ Vibration Casting Process Qualifications	12
4.4.3	Kaolite 1600™ Baking Process Qualifications	12

ATTACHMENTS

A	**Kaolite Mixing Control**
B	**Body Weldment**
C	**Top Plug Assembly Vibration Casting Control**
D	**Furnace and Baking Control**
E	**Wet Density Mixer Time Vibration Casting**
F	**Baked Qualification Density Sample Vibration Casting**

1 Scope

This manufacturing process specification describes the quality assurance and technical requirements that shall be met when weighing, mixing, pouring, vibrating, curing, and baking the Kaolite 1600™ for the ES-3100 shipping container Body Weldment and Top Plug Assemblies. The product produced by following this manufacturing process is protected under U.S. Patent 6,299,950. The United States Government has rights in this invention pursuant to Contract No. DE-AC05-84OR21400, between the U.S. Department of Energy and BWXT Y-12 L.L.C.

This specification describes the instructions that shall be followed for these activities. The components (Body Weldment and Top Plug Assembly) will be fabricated to the design requirements specified on the engineering drawings for the components.

Reference to the Company in this specification shall mean the package certificate holder and reference to the Seller shall mean the supplier of the fabricated Body Weldment and Top Plug Assemblies.

2 Applicable Documents

The following documents apply when Casting Kaolite 1600™ Into ES-3100 Shipping Containers.

ES-3100 Drawing Numbers
M2E801580A002, Body Weldment
M2E801580A008, Top Plug Weldment,

Procurement Specification for ES-3100 Confinement Boundary Assembly
JS-YMN3-801580-A002 Equipment Specification for the ES-3100 Drum Assembly

3 Kaolite 1600™ Processing Requirements

3.1 General

The Kaolite 1600™ material referenced with in this specification shall be provided by Thermal Ceramics, Incorporated or an authorized distributor. The material certification documentation (Certificate of Conformance) for the Kaolite 1600™ must be provided by the supplier for each manufacturer's lot of material to a product code of GI80ACCUMD0027.

3.1.1 Kaolite 1600™ Receiving and Storage Instructions

a. Damaged packages of Kaolite 1600™ shall be rejected by the Seller upon receipt. Damaged packages are those that are wet, those that are visually determined to have been wet, and packages that have been torn.

b. Packages of Kaolite 1600™ must be stored unopened in a dry location and protected from damage. Opened unused and partial used Kaolite 1600™ packages are to be discarded at the end of the work shift. The term work shift shall be defined by the Seller and approved by the Company before commencing operations.

3.1.2 Cleaning Instructions

a. Use **NO CHLORINE BLEACH** for cleaning. Potable water shall be used and if required some mild soap (tri-sodium phosphate) may be added to the water to clean all processing equipment and manufactured components before casting. Before the start of any mixing/blending operation, the mixer shall be clean from all foreign materials or previous mixing residues from the inner surface of the mixer. The mixer shall be flushed thoroughly with potable water at the completion of the final mixing operation of the work shift to remove residues. Mixing, and casting shall be performed within a temperature range of 70 (± 25) °F.

b. Fabricated assemblies must be cleaned and protected prior to the casting operation to prevent the introduction of foreign materials into the assemblies. The assemblies shall be inspected and wiped clean prior to casting to ensure no visible contaminants are present inside the casting cavity. This inspection shall be documented in the checklist.

3.1.3 Mixing Water and Mixing Equipment Requirements

a. Potable water, that has been filtered through a 20-micron filter and has a chlorine content less than 4 mg/L (4 ppm, 0.0004 percent by mass) for chlorine shall be used for the mixing of Kaolite 1600™. If the potable water is higher then 4 ppm, then use an activated charcoal filter or some other means to reduce the amount of chlorine to at or below 4 ppm. Test the water quality for chlorine weekly during casting operations. Unfiltered potable water may be used for the cleaning of equipment used to process Kaolite 1600™.

b. All weighing operations of assemblies and materials shall be conducted on certified scales with a minimum accuracy of ½ lb.

c. This specification has been developed around the Whiteman Multiquip's WM700S-H8 plaster/mortar mixer, refereed to as WM700. This steel-drum machine mixes 7-cubic feet (193 liters) of material with an 8-horsepower Honda engine running at a slow speed. Other models of plaster/mortar mixers may be used if the speeds and mix times are qualified per section 3.5 and approved by the company.

d. A Heavy Duty Drum Vibrator/Packer(like McMaster-Carr, No. 5809K11, or Company approved equal) shall be used to clamp the Body Weldment, M2E-801580-A002 or Top Plug Weldment, M2E-801580-A008 upside down for vibration casting the Kaolite 1600™ into the welded stainless steel forms.

3.2 Mixing of Kaolite 1600™

Mixing shall be performed by operators qualified in accordance with requirements in Section 4.4.

The term batch is defined as a mixture of one bag of Kaolite 1600™ with the appropriate amount of water. The required mix ratio is 1.65 pounds of filtered water per pound of Kaolite 1600™.

The mixing activity shall be recorded on Attachment A, *Kaolite Mixing Control*. Each batch shall be given a mixture control number (MCN) and recorded upon its data Attachment. (A 10-digit control number is recommended consisting of the date and the time format using a 24-hour clock. Example: 1021041515 for October 21, 2004 at 3:15 pm.)

The Kaolite 1600™ mixing shall be performed as follows:

a. Record the weight of the bag of Kaolite 1600™ on the mixing Attachment.

b. The required mix ratio is 1.65 pounds of filtered water per pound of Kaolite 1600™. For a 50 pound bag of Kaolite 1600™, weigh and record 82.5 (± ½) lbs. of filtered water generating an acceptable wet mix density of 56.2±5.8 lb/ft^3.

c. Start the mortar mixer motor and when ready to engage the moving vanes, pour the weighed filtered water, pour all of the 50-pound bag of Kaolite 1600™ over the water. Immediately start the WM700 moving vanes for 3.0 (±0.2) minutes.

3.3 Vibration Casting and Curing of Kaolite 1600™ into Assemblies

3.3.1 Body Weldment Casting Instructions

Casting operations shall be performed by operators and witnesses qualified in accordance with requirements listed in Section 4.4.

Use Attachment B, *Body Weldment Vibration Casting Control,* to record information gathered during this operation.

Complete the casting of the mixture in less than 70 minutes. This timed procedure starts when the first batch is poured into the vibrating component. The casting and vibrating procedure must be completed within 77 minutes from initial pour for each assembly.

Casting operations shall be performed as follows:

a. Weigh the Body Weldment clean and empty. Record the weight.

b. Fill the Body Weldment with potable water that has been filtered through a 20 micron filter and has a chlorine content of ≤ 4 ppm and weigh it. Record the weight.

c. Remove the water from the assembly as much as is practical.

d. Secure the assembly on the vibration table. Set the vibration table dial indicators to approximately 800 lb-force at 450 vibrations per minute (VPM). Assure that the Body Weldment is properly secured to the table and start the vibration table. The Body Weldment must be vibrated continuously throughout the casting operation.

e. The mixture shall then be poured directly into the assembly after mixing through the fill hole provided.

f. Repeat the mixing operation in Section 3.2 and continue pouring until the mixture overflows the fill hole by ½ to ¾ inch.

g. Mist the top surface of the mixture with a bottle water sprayer if necessary to get the mixture into a solution after the pouring is completed. Do not add more than 8 ounces of water.

h. Vibrate the filled assembly for 5 to 7 minutes after the casting is completed.

3.3.2 Body Weldment Curing Instructions

A designated area shall be set aside for curing the assemblies. The temperature of the curing area shall be controlled to 70°F (±25°F) and shall prevent the introduction of foreign materials into the mixture.

Curing operations shall be performed as follows:

a. Remove the Body Weldment from the vibration table and place it in the curing area. Let it rest uncovered for 2½ (±½) hours.

b. Weigh and record the Before Baking weight of the cast assembly. If the weight is outside of 330 to 386 lbs range it is recommended not to cure the casting but to clean out and recast the Kaolite. This Before Baking weight is a recommended process control for the finished baked density. The manufacture may continue with a part outside of this weight range but it has a high chance being rejected for not meeting the finished baked density.

c. After resting, scrape the excess mixture from the fill opening until the Kaolite surface has a circular concave of .32±.10 to match drawing M2E801580A002.

d. Weigh the cast assembly, and photograph the fill opening. Record the weight.

e. Cover the fill opening with plastic sheeting and let the assembly set undisturbed in the curing area for at least 24 hours.

3.3.3 Top Plug Assembly Casting Instructions

Use Attachment C, Top Plug Assembly Vibration Casting Control, to record information gathered during this operation.

Complete the casting of the mixture in less than 70 minutes. This timed procedure starts when the first batch is poured into the vibrating component. The casting and vibrating procedure must be completed within 77 minutes from initial pour for each assembly.

Casting operations shall be performed as follows:

a. Weigh the top plug assembly clean and empty. Record the weight.

b. Fill the top plug assembly with potable water that has been filtered through a 20-micron filter and has a chlorine content of ≤ 4 ppm and weigh it. Record the weight.

c. Remove the water from the assembly as much as practical.

d. Place the assembly on the vibration table. Assure that the assembly is properly secured to the table. Set the vibration table dial indicator to approximately 120 lb-force at 450 vibrations per minute and start the vibration table. The top plug assembly must be vibrated continuously throughout the casting operation.

e. The mixture shall then be poured directly into the assembly after mixing through the fill hole provided.

f. Repeat the mixing operation in Section 3.2 and continue pouring until the mixture overflows the fill hole by ½ to ¾ inch.

g. Mist the top surface of the mixture with a bottle water sprayer if necessary to get the mixture into a solution after the pouring is completed. Do not add more than 4 ounces of water.

h. Vibrate the filled assembly for 5 to 10 minutes after the casting is completed.

3.3.4 Top Plug Assembly Curing Instructions

Curing operations shall be performed as follows:

a. Remove the top plug assembly from the vibration table and place it in the curing area. Let it rest uncovered for 2½ (± ½) hours.

b. Weigh and record the Before Baking weight of the cast assembly. If the weight is outside of 29.2 to 34.2 lbs range it is recommended not to cure the casting but to clean out and recast the Kaolite. This Before Baking weight is a recommended process control for the finished baked density. The manufacture may continue with a part outside of this weight range but it has a high chance being rejected for not meeting the finished baked density.

c. After resting, scrape the excess Kaolite mixture from the fill opening until surfaces are a circular convex shape of .09±.06 before it is baked to match drawing M2E801580A008.

d. Weigh the cast assembly, and photograph the fill opening. Record the weight.

e. Cover the fill opening with plastic sheeting and let the assembly set undisturbed in the curing area for at least 24 hours.

3.4 Baking of Assemblies Cast and Cured with Kaolite 1600™ mixture

3.4.1 Baking Instructions

Several assemblies may be baked together during each furnace heating cycle. Once the furnace heating cycle has started, no additional assemblies may be inserted into the furnace. The furnace and temperature control requirements to perform the baking operation are as follows:

a. The furnace shall be a gas-fired or a forced convection fresh air circulating electric furnace.

b. The furnace heat zone shall be certified to ±25°F from the furnace set point temperature at each baking temperature process point.

c. Furnace time and temperature strip charts for each furnace heating cycle shall be provided with each completed Attachment D. Alternatively, an ASCII furnace time and temperature data file may be provided for each completed Attachment D.

3.4.2 Baking Documentation

Use Attachment D, *Furnace and Baking Control*, to record information gathered during this operation. An Attachment D identified by the Baking Control Number (BCN) shall be generated for each set of assemblies subjected to the furnace baking operations. Record the BCN from Attachment D for each assembly baked during this furnace heating cycle utilizing the proper assembly Casting Attachments B, C, and F. Qualified operators as indicated in Section 4.4 shall perform the baking of the cured assemblies. Movement of the cured assemblies before baking shall be minimized. The time and actual furnace exhaust air temperature shall be recorded at least every 15 minutes for baking control during a furnace heating cycle.

The baking furnace heating cycle shall be completed as follows:

a. Place the assemblies into the furnace.

b. Set the initial set point temperature to 200 (±10) °F.

c. Hold the temperature for 4 hours at a 200 (±10) °F steady state.

d. Increase the furnace set point temperature to 275 (±10) °F.

e. Hold the temperature for 1 hour at a 275 (±10) °F steady state.

f. Increase the furnace set point temperature to 350 (±10) °F.

g. Hold the temperature for 1 hour at a 350 (±10) °F steady state.

h. Increase the furnace set point temperature to 425 (±10) °F.

i. Hold the temperature for 1 hour at a 425 (±10) °F steady state.

j. Increase the furnace set point temperature to 500 (±10) °F.

k. Hold the temperature for 41 (±5) hours at a 500 (±10) °F steady state.

l. Remove assemblies and allow cooling in still air until they reach ambient temperature.

m. Weigh the assemblies after the baking process and record the weights upon the appropriate Attachment (Attachment B or C). Calculate the baked density of the cured mixture using the equation at the bottom of Attachment B or C and record.

Acceptance criteria:

An acceptable baking process is defined as the process in which the density of the baked mixture in an assembly is within the acceptance range of 22.4 ±3 lb/ft^3 as defined on Attachments B or C. If the density is less than the allowable value, contact the Company for disposition. If the density is greater than the allowable level, then re-bake the assembly using Section 3.4.5.a through k, with the exception of the final hold time which shall be 5 (±0.5) hours. Remove assemblies and allow cooling in still air until they reach ambient temperature. Recalculate and record the density on the appropriate Attachment. If the density still is greater than the allowable level, contact the Company for disposition.

n. Photograph the surface of the baked mixture (digital images are preferred).

o. Following the acceptable baking process, weld the cover plate onto the assemblies in accordance with the appropriate engineering drawing within 24 hours.

p. Weigh the final assembly and record on the appropriate Attachment (Attachment B or C).

3.5 Mixer Qualification for Kaolite 1600™ Casting Placement

The mixer qualification process shall verify that the mixer speed and mix time are properly set to mix the Kaolite 1600™. The end result of the mixer qualification is the as-baked density of 22.4±1 lb/ft^3 in the Baked Mixer Qualification Samples. This baked density can be estimated by monitoring the wet density. The baked density is approximately 41% of the wet density; therefore, the Target Wet Density is 56.2 lb/ft^3 for an average baked density of 22.4±1 lb/ft^3. The longer the Kaolite 1600™ is mixed the denser it becomes. The mixer qualification process shall verify the mix time required at a fixed and repeatable speed. The operators shall use the mixer to determine a repeatable speed to operate the mixer for all of the tests. Record the speed setting and assure that the speed setting is repeatable. The mixer qualification tests are a two step process: first is a Wet Density Mixer Time Vibration Casting test used to determine the range of mix time versus wet density; second is the mixer Baked Density Qualification Sample Vibration Casting. It is recommended that a 4-gallon or larger metal pail be used for the testing like the 4-1/2 gallon Tin-Plated Steel Pail (McMaster-Carr 4243T16 or equivalent), 9" Top Dia, 19-3/8" Height.

3.5.1 Wet Density Mixing Test

Use Attachment E, *Wet Density Mixer Time Vibration Casting*, to record information gathered during this operation.

Prepare the Kaolite 1600™ and water for mixing per section 3.2 except for the mix time. A digital stop watch shall be used to monitor the running mix time. The mix time shall vary per Form F from 1 to 15 minutes in 1 minute intervals. Use a quick release attachment to affix the two metal pails (at least 4 gallon) to the vibration table. Start the mixer and run it for one minute, start the vibration table and pour the Kaolite 1600™ into the two pails after filling let them vibrate for 2 minutes, stop the vibration table, scrape them flush, and remove the pails and weigh them. Record the weight, dump the Kaolite 1600™ back into the mixer and start the mixer for another minute and repeat the process.

Plot the wet mix density of the two pails versus the mix time in an Excel file. An Excel file generated by the Company can be provided for this task upon request. Curve fit the data

using a third order polynomial curve and show the equation. Plot the target density of 56.2 lb/ft^3 on a chart in Excel along with the wet mix density. Where the curves intersect the target density line is the mixer's target mix time. Consult the Company for verification of this data. Use the Company verified mix time for the Mixer Baked Density Qualification Castings in Section 3.5.2.

3.5.2 Mixer Baked Density Qualification Castings

Use Attachment F, *Baked Qualification Density Sample Vibration Casting*, to record information gathered during this operation.

Prepare the Kaolite 1600™ and water for mixing per section 3.2.1 except for the mix time. A digital stop watch shall be used to obtain the Company verified mix time. Start mixer and run it for the Company verified mix time. Start the vibration table and pour the Kaolite 1600™ into the two pails. After filling, let them vibrate for 5 to 7 minutes then stop the vibration table.

Remove the two pails from the vibration table. Place the filled two pails in the curing area, and let them sit uncovered for 2½ (±½) hours. After sitting 2½ (±½) hours, scrape the excess mixture from the fill opening until surfaces are flush. Cover the fill opening with plastic sheeting or a metal lid and let the assembly sit undisturbed in the curing area for at least 24 hours before weighing. Remove the two pails and weigh the cured qualification samples to an accuracy ±1 pounds. Record the as-cured and after-baking weights and follow the baking instructions in section 3.4.

4. Quality Assurance Requirements

4.1 General

4.1.1 The Seller shall have a quality assurance program that meets the applicable requirements of Title 10 CFR Part 71, Subpart H for packaging and transportation of radioactive material. The quality assurance plan shall be in accordance with the requirements identified in the ES-3100 procurement specification. The Seller shall submit an approved quality assurance program plan that describes the quality assurance policies and practices to be implemented in identifying, controlling and verifying quality of the Kaolite 1600™ processes (weighing, mixing, pouring, vibrating, curing, and baking).

4.1.2 The Seller shall submit a Manufacturing Plan as defined in procurement specification, and shall describe how the Seller will comply with the instructions in this specification. If subcontractors are utilized for any of the processing of the Kaolite 1600™, the Seller shall ensure that the requirements of this specification (including quality assurance requirements) are met by all suppliers and subcontractors. The subcontractor's procedures, approved by the Seller, shall be included in the procedures submitted to the Company for review and approval.

4.1.3 The Seller's quality assurance program plan shall include the requirements for the process controls for the operations, operator and witness' qualifications, and verification records. Operator qualification requirements are identified in Section 4.4.

4.1.4 The Seller shall generate the documentation necessary to show compliance with the approved quality assurance program plan. All records shall be identified based on the assembly serial numbers. The Seller shall maintain quality-related documentation in accordance with requirements in the procurement specification. The Company reserves the right to request any

such documentation and to witness all aspects of the fabrication process in accordance with this specification. The Seller shall ensure that the specified manufacturing and inspection records are generated and supplied to the Company as part of the certification package.

4.1.5 The Seller must ensure all operators are aware of and comply with the quality assurance requirements identified in this specification. The Seller must ensure all operators use and follow written procedures for the respective processes. The Seller shall ensure operators and witnesses are aware of the operational requirements for the common industrial equipment (material handling equipment, mixers, vibration tables, ovens/furnace) used for the processes.

4.2 Material and Equipment Certification

4.2.1 Material certification for the Kaolite 1600™ must be provided by the supplier as defined in Section 8.0 of the procurement specification. Bags of Kaolite 1600™ must be identified with the product name and unique lot number. The material certification will be incorporated into the quality assurance records of the certification package.

4.2.3 All weighting, mixing, casting, curing, and baking processes shall be controlled and performed by qualified personnel (see Section 4.4). Written procedures shall be utilized by the operator at each operation and shall identify process hold points where required by the Company.

4.2.4 All process equipment used for mixing, casting, and baking of the Kaolite 1600™ and water mixture must be the model type identified in this specification, and must be in good working condition. Equipment used for measurements must be certified to traceable NIST standards or similar agency. Variation from specified equipment (vibration table, mixer, and furnace) is not allowed without the written approval of the Company before implementation.

4.3 Nonconformance Control

4.3.1 The Seller shall have an approved procedure for the control of nonconformances, waivers, and deviation requests during the execution of this manufacturing specification.

4.3.2 Nonconforming components shall not be used unless it has been determined by analysis or assessment by the Company that the nonconformance does not impact the physical properties of the material.

4.2.3 The disposition of nonconforming components shall be documented. Any nonconforming component shall be clearly identified and all nonconformance reports shall be traceable to the actual component affected. Copies of all approved nonconformance reports, except for scrapped components shall be supplied by the Seller to the Company as part of the certification package.

4.4 Operator and Witness Qualifications

The Kaolite™ 1600 mixing and vibration casting qualification evaluations shall be sequential. Each operator must mix and cast at least one simulated drum. Mixing and casting operations shall be repeated as necessary to achieve fully cast mock drums. The simulated ES-3100 drums cast during qualification activities shall be baked according to procedure.

4.4.1 Kaolite 1600™ Mixing Process Qualifications

Each operator and witness performing Kaolite 1600™ mixing activities must be qualified to perform this activity. This qualification shall be documented. This qualification shall consist of the following:

a. Location and time.

b. Properly identifying a bag of Kaolite 1600™ the bag of material and associated certification data (such as lot numbers)

c. Inspection of the bag for observable damage (such as water damage)

d. Successfully weighing the bag of Kaolite 1600™ on an industrial scale

e. Successfully calculating the required amount of water to be mixed with the Kaolite 1600™ (1.65 pounds of water per pound of Kaolite 1600™)

f. Properly inspecting the mixing equipment for foreign materials (such as oil, grease, free liquids, trash, or evidence of non-Kaolite 1600™ material affixed to the inner surfaces.)

g. Successfully operating the mixing equipment while mixing a complete bag of Kaolite 1600™.

h. Successfully preparing a uniformly mixed batch of Kaolite 1600™. (Uniformly shall be defined as a thoroughly mixed material with no dry material and no free liquids remaining in the mixer.)

4.4.2 Kaolite 1600™ Vibration Casting Process Qualifications

Each operator and witness performing Kaolite 1600™ casting activities must be qualified by successfully performing a casting activity. This qualification shall consist of the following.

a. Properly inspecting the inner surfaces of an empty simulated ES-3100 drum body for residues (oil, grease, free liquids) and waste material. (A simulated ES-3100 drum body shall consist of a 55-gallon carbon steel open-head drum which has a 16-gallon carbon steel drum secured to the bottom center. The 16-gallon drum may be secured by tack welding or suitable fasteners. The lid of the 55-gallon drum must have an opening 15" in diameter through which the Kaolite 1600™ can be poured into the drum.)

b. Properly securing an empty simulated ES-3100 drum body to the vibration table.

c. Properly adjusting the vibration table controls to the specified values for drum assemblies.

d. Successfully transferring the Kaolite 1600™ from the mixer into the drum while the drum is vibrating.

4.4.3 Kaolite 1600™ Baking Process Qualifications

Each operator and witness performing Kaolite 1600™ baking operations shall review the procedure steps for calculating the as-baked density of the Kaolite 1600™ in the assemblies and perform a sample calculation.

Attachment A	Specification Number		Revision
	JS-YMN3-801580-A003-1		C
EQUIPMENT SPECIFICATION	Issue Date	Revision Date	
ES-3100 Shipping Package	11/24/03	6/1/06	
Kaolite Mixing Control	Plant	Page	of
	Y-12	1	1

Caster's Company Name			Supplier's Company Name		
Mixing Start Date	Time	Air Temp. °F	Thermal Ceramics Kaolite 1600™ Certificate of Conformance		
Kaolite 1600™ Mixing and Vibration Casting Information			Comments	Operator	Witness
50 lb. Bag ID Number					
Bag Wt.					
1.65 × Bag Wt.					
Mixing Control Number (MCN)[a]					
Water Wt. ±0.5 lbs. (1.65 times Kaolite Bag Wt.)					
Mix Finish Time					

[a] A 10-digit control number is recommended for the Mixing Control Number (MCN) consisting of the date and the time format using a 24-hour clock (i.e. 1021041515 is used for October 21, 2004 at 3:15 pm.)

EXEMPT FROM [illegible]

Attachment B	Specification Number JS-YMN3-801580-A003-2		Revision C
EQUIPMENT SPECIFICATION **ES-3100 Shipping Package** **Body Weldment**	Issue Date 11/24/03	Revision Date 6/1/06	
	Plant Y-12	Page 1	of 1

Caster's Company Name			Seller's Company Name			
Part Serial Number			Body Weldment Drawing Number M2E801580A002			
Measured Weights ±0.5 lb	Casting Information		Comments		Operator	Witness
	Weight	Date				
Clean and Empty						
Filled with Water [a]						
Before Baking [f]						
After Baking Cycle 5						
After Baking Cycle 5A [d]						
After Welding						
Water Information	Water Weight ±0.5 lb	Water Temp.	Comments		Operator	Witness
Water Conditions [a]	lb	°F				
Casting Start Date	Air Temp. °F / Vibration Settings [b] lbf	VPM				
Operation	MCN [e]	Time	Comments		Operator	Witness
Pour Start						
Pour Start						
Pour Start						
Vibration Start						
Vibration Stop						
Baking Cycle 5	Baking Control Num. [c]	Date	Time	Density [d]	Operator	Witness
Baking Cycle 5A [d]	Baking Control Num. [c]	Date	Time	Density [d]	Operator	Witness

[a] Record the water weight and water temperature within 10 minutes from completion of the weighing process.

[b] Recommended Vibration settings are at 450 VPM and twice the total vibrated weight. The total vibrated weight is the finish cast part and fixtures weight, for a setting of approximately 800 pound-force.

[c] A 10-digit Baking Control Number shall be used to define the date and the time of baking using the format with a 24-hour clock (i.e. 1021041515 is used for October 21, 2004 at 3:15 pm.)

[d] Use the above weights to calculate the Density as shown below. If the density is greater, then 25.4 lb/ft^3 then proceed with the next Baking Cycle. If the density is less then 19.4 lb/ft^3 then contact the Company for disposition.

$$\text{Density} = \frac{(AfterBaking - CleanAndEmpty)}{(WithWater - CleanAndEmpty)} \times 62.3 \text{ lb/ft}^3 \quad @\ 70°\text{F}$$

[f] Recommend Before Baking weight is to be 330 to 386 lb range.

EXEMPT FROM IQ-155

Attachment C	Specification Number JS-YMN3-801580-A003-3		Revision C
EQUIPMENT SPECIFICATION **ES-3100 Shipping Package** **Top Plug Assembly Vibration Casting Control**	Issue Date 11/24/03	Revision Date 6/1/06	
	Plant Y-12	Page 1	of 1

Caster's Company Name			Seller's Company Name		
Part Serial Number			Top Plug Assembly Drawing Number M2E801580A008		
Measured Weights ±0.5 lb	Casting Information		Comments	Operator	Witness
	Weight	Date			
Clean and Empty					
Filled with Water [a]					
Before Baking [f]					
After Baking Cycle 5					
After Baking Cycle 5A [d]					
After Welding					
Water Information	Water Weight ±0.5 lb	Water Temp.	Comments	Operator	Witness
Water Conditions [a]	lb	°F			
Casting Start Date	Air Temp. °F / Vibration Settings [b] lbf	VPM			
Operation	MCN	Time	Comments	Operator	Witness
Pour Start					
Pour Start					
Vibration Start					
Vibration Stop					
Baking Cycle 5	Baking Control Num. [c]	Date	Time / Density [d]	Operator	Witness
Baking Cycle 5A [d]	Baking Control Num. [c]	Date	Time / Density [d]	Operator	Witness

[a] Record the water weight and water temperature within 10 minutes from completion of the weighing process.

[b] Recommended Vibration settings are at 450 VPM and twice the total vibrated weight. The total vibrated weight is the finish cast part and fixtures weight, for a setting of approximately 120 pound-force.

[c] A 10-digit Baking Control Number shall be used to define the date and the time of baking using the format with a 24-hour clock (i.e. 1021041515 is used for October 21, 2004 at 3:15 pm.)

[d] Use the above weights to calculate the Density as shown below. If the density is greater than 25.4 lb/ft^3 then proceed with Baking Cycle 1A. If the density is, less then 19.4 lb/ft^3 then contact the Company for disposition.

$$\text{Density} = \frac{(AfterBaking - CleanAndEmpty)}{(WithWater - CleanAndEmpty)} \times 62.3 \text{ lb/ft}^3 \quad @\ 70°\text{F}$$

[f] Recommend Before Baking weight is to be 29.2 to 34.2 lb range.

EXEMPT FROM IQ-155

Attachment D	Specification Number JS-YMN3-801580-A003-4		Revision C
EQUIPMENT SPECIFICATION **ES-3100 Shipping Package** **Furnace and Baking Control**	Issue Date 11/24/03	Revision Date 6/1/06	
	Plant Y-12	Page 1	of 1

Baking Company Name				Seller's Company Name			
Baking Control Number [a]				Furnace Serial Number			
Bake Start Date		Air Temp. °F		Computer Data File Name [b]			
Baking Process Control	Furnace Check or NA	Start Time	Start Date	Stop Time	Stop Date	Operator	Witness
Baking Cycle (1) 200°F for 4 hrs.							
Baking Cycle (2) 275°F for 1 hrs.							
Baking Cycle (3) 350°F for 1 hrs.							
Baking Cycle (4) 425°F for 1 hrs.							
Baking Cycle (5) 500°F for 36 to 46 hrs. [c]							
Baking Cycle (1A) 200°F for 4 hrs.							
Baking Cycle (2A) 275°F for 1 hrs.							
Baking Cycle (3A) 350°F for 1 hrs.							
Baking Cycle (4A) 425°F for 1 hrs.							
Baking Cycle (5A) 500°F for 4.5 to 5.5 hrs. [c]							

[a] Record the Baking Control Number in MMDDYYTIME (with time the 24 hour format i.e. 1021041515 is used for October 21, 2004 at 3:15 pm.) on Casting Forms B, C, and F for each part baked under this furnace heating cycle.

[b] The sample baking cycle time and temperature data could be presented both in a digital and graphical form. For example, an Excel file showing the original data and time verses temperature plots shall be acceptable.

[c] Calculate the density as shown on Forms B or C following this furnace heating cycle phase. If the part density is greater than 25.4 lb/ft^3, then proceed with the remaining furnace phases.

EXEMPT FROM ID-155

Attachment E	Specification Number JS-YMN3-801580-A003-5		Revision C
EQUIPMENT SPECIFICATION **ES-3100 Shipping Package** **Wet Density Mixer Time Vibration Casting**	Issue Date 11/24/03	Revision Date 6/1/06	
	Plant Y-12	Page 1	of 1

Caster's Company Name			Seller's Company Name		
Mixer Make and Model					
Wet Mix Density Qualification Number [a]			Mix Control Number [a]		
Measured Weights ±0.5 lb	Casting Information		Comments	Operator	Witness
	Weight [c, b] (lb)	Date			
Clean and Empty					
Filled with Water [b]					
Water Information	Water Weight [c, b] ±0.5 lb	Water Temp.	Comments	Operator	Witness
Water Conditions		°F			
Casting Start Date	Air Temp. °F	Vibration Settings [c] lbf / VPM	Mixer Speed Setting		
Operation	Weight [c, b] (lb)	Time (min)	Wet Density [d] (lb/ft^3)	Operator	Witness
Wet Cast [e]		1.0			
Wet Cast [e]		2.0			
Wet Cast [e]		3.0			
Wet Cast [e]		4.0			
Wet Cast [e]		5.0			
Wet Cast [e]		6.0			
Wet Cast [e]		7.0			
Wet Cast [e]		8.0			
Wet Cast [e]		9.0			
Wet Cast [e]		10.0			
Wet Cast [e]		11.0			
Wet Cast [e]		12.0			
Wet Cast [e]		13.0			
Wet Cast [e]		14.0			
Wet Cast [e]		15.0			
Curve fit the Time required to generate the target density and contact the Company for confirmation.			Target Density 56.2 lb/ft^3		

[a] Record the Wet Mix Density Qualification Number and the Mix Control Number in MMDDYYTIME (with time the 24 hour format i.e. 1021041515 is used for October 21, 2004 at 3:15 pm.).

[b] Record water weight and water temperature within 10 minutes from completion of the weighing process.

[c] Use both steel pails to calculate the weights and density.

[d] Recommended Vibration settings are at 450 VPM and twice the total vibrated weight. The total vibrated weight is the finish cast part and fixtures weight, for a setting of approximately 120 pound-force.

[e] Use the above weights to calculate the Wet Density as shown below.

$$\text{Wet Density} = \frac{(WetCast - CleanAndEmpty)}{(WithWater - CleanAndEmpty)} \times 62.3 \text{ lb/ft}^3 \quad @\ 70°F$$

EXEMPT FROM IO-155

Attachment F	Specification Number		Revision
	JS-YMN3-801580-A003-6		C
EQUIPMENT SPECIFICATION **ES-3100 Shipping Package** **Baked Qualification Density Sample Vibration Casting**	Issue Date 11/24/03	Revision Date 6/1/06	
	Plant Y-12	Page 1	of 1

Caster's Company Name	Seller's Company Name
Mixer Make and Model	
Baked Qualification Density Number [a]	Mix Control Number [a]

Measured Weights ±0.5 lb	Casting Information		Comments	Operator	Witness
	Weight ±0.5 lb	Date			
Clean and Empty					
Filled with Water [c]					
Before Baking					
After Baking Cycle 5					

Water Information	Water Weight ±0.5 lb	Water Temp.	Comments	Operator	Witness
Water Conditions [c]		°F			

Casting Start Date	Air Temp.	Vibration Settings [b]				
	°F	lbf	VPM			

Operation	MCN	Time	Comments	Operator	Witness
Pour Start					
Vibration Start					
Vibration Stop					

	Baking Control Num.	Date	Time	Density [d]	Operator	Witness
Baking Cycle 5						

[a] Record the Baked Qualification Density Number **and the** Mix Control Number in MMDDYYTIME (with time the 24 hour format i.e. 1021041515 is used for October 21, 2004 at 3:15 pm.).

[b] Recommended Vibration settings are at 450 VPM and twice the total vibrated weight. The total vibrated weight is the finish cast part and fixtures weight, for a setting of approximately 120 pound-force.

[c] Record water weight and water temperature within 10 minutes from completion of the weighing process

[d] Use the above weights to calculate the Qualification Sample Density as shown below. If the density is greater then 23.4 lb/ft^3 or less then 21.4 lb/ft^3 contact the Company for disposition.

$$\text{Qualification Density} = \frac{(AfterBaking - CleanAndEmpty)}{(WithWater - CleanAndEmpty)} \times 62.3 \text{ lb/ft}^3 \quad @\ 70°\text{F}$$

EXEMPT FROM IQ-155

Appendix 1.4.5

EQUIPMENT SPECIFICATION, JS-YMN3-801580-A005, *CASTING CATALOG NO. 277-4 NEUTRON ABSORBER FOR THE ES-3100 SHIPPING PACKAGE*

THIS PAGE INTENTIONALLY LEFT BLANK.

EQUIPMENT SPECIFICATION APPROVAL/REVISION PAGE

SPECIFICATION NO.	REV.	ISSUE DATE
JS-YMN3-801580-A005	G	02-18-05
PAGE: i of ii	REVISION DATE: 08/31/2009	
PROCURED BY: BWXT Y-12 L.L.C.	INSTALLED BY: B&W Y-12 L.L.C.	
PROJECT TITLE: ES-3100 Shipping Package	PLANT: Y-12	BUILDING: AREA
JOB TITLE: Production Design Definition	W.O. OR E.S.O.: 7ADDEQ01	RECORD NUMBER: Y2003-0328
SPECIFICATION FOR: Casting Catalog No. 277-4 Neutron Absorber For The ES-3100 Shipping Package		SSC IDENTIFICATION NUMBER: NA

APPROVALS

SIGNATURE	DATE	SIGNATURE	DATE
PREPARED BY: G. A. Byington /s/	2/18/05	PROJECT ENGINEER: G. A. Byington /s/	2/18/05
DESIGN VERIFICATION: M. L. Goins /s/	2/18/05	CRITICALITY SAFETY: D. A. T. J. F. DeClue /s/	2/18/05
DISCIPLINE MANAGER: D. P. Sooter /s/	11 Feb 05		

REVISIONS/APPROVALS

REV. NO.	DESCRIPTION OF REVISION
A	Issued for Procurement.
B	Changed the minimum LOD from 25.3% to 30.1% at three locations on page 13 section 4.7.3 and one location on page 23 Form D.
C	General changes. Went from an off the shelf item to a two part system of boron carbide plus high alumina cement.
D	General revision. Reformatted sections and attachments. Deleted references to drawing numbers.
E	The mass limits were changed to account for volume tolerances in the 277-4 annulus. Section 3.3.8, Item l, "inner liner" was replaced with "can". A.3.1 was separated into two sections; the second part of A.3.1 became A.3.1.a with the title "Net Count Rate Time Determination". Section A.6.3 was modified by adding "Define the repeatable accuracy for" before the first sentence. JS-YMN3-801580-A005-5 was expanded to include more approval data requirements. A typo was fixed on JS-YMN3-801580-A005-6. Added Rev level to Forms and headers.
F	In Section 3.3.9.3, added maximum and minimum LOD% table based upon cured density and made reference to table on Form F.
G	Shieldwerx, supplier of 277-0 was Thermo Electron Corporation. Added Figures 9, 10, & 11 to represent design and procurement changes made to the ES-3100 Heavy Spacer Can Assembly, see drawing M2E801580A043 Rev. 0 for supplementary details. Added additional reference to M2E801580A043.

SIGNATURE	DATE	SIGNATURE	DATE
PREPARED BY: Michael Ensley /s/	09/10/09	PROJECT ENGINEER: Larry Roberson /s/	09/10/09
DESIGN VERIFICATION: Drew Winder /s/	09/10/09	CRITICALITY SAFETY: John DeClue /s/	09/10/09
DISCIPLINE MANAGER: Walter North /s/	09/10/09		

This document has been reviewed by a Y-12 DC and UCNI RO and has been determined to be UNCLASSIFIED and not UCNI. This review does not constitute clearance for public release.

Name: Roger D. Aigner /s/ Date: 09/10/09

EXEMPT FROM IO-155 (8-02)

CONTENTS

1.0 Scope 1

2.0 Applicable Documents 7

3.0 Requirements 8

4.0 Quality Assurance.....14

5.0 Preparation For Delivery 15

6.0 Manufacturer's Data 17

ATTACHMENTS

Appendix A Prompt Gamma-ray Neutron Activation Analysis Testing Setup & Tooling.....16

FORM A 277-4 Dry Blend Batch Control

FORM B 277-4 Wet Mix Control (Overcast or Special Batch)

FORM C ES-3100 Body Weldment Casting Control

FORM D ES-3100 Neutron Absorber Form Casting Control

FORM E ES-3100 Heavy Can Spacer Assembly Casting Control

FORM F ES-3100 Companion Sample Casting Control and Tests

FORM AA PGNAA Tooling Setup Control

FORM AB PGNAA Standard Setup

FORM AC PGNAA Daily Standard Setup Control

FORM AD PGNAA Measurements

Offer Apprasial Data - Subcontractor, JS-YMN3-801580-A005-1

Approval Data - Subcontractor, JS-YMN3-801580-A005-2

Certified Data - Subcontractor, JS-YMN3-801580-A005-3

Offer Apprasial Data - PGNAA Subcontractor, JS-YMN3-801580-A005-4

Approval Data - PGNAA Subcontractor, JS-YMN3-801580-A005-5

Certified Data - PGNAA Subcontractor, JS-YMN3-801580-A005-6

1.0 Scope

1.1 This specification describes the requirements for the procurement, preparation, casting, and verification of a neutron absorber material into the ES−3100 shipping package. The neutron absorber material shall be cast into ES−3100 Body Weldment (Figure 1), Neutron Absorber Form (Figures 4 and 5), Heavy Can Spacer Assembly (Figure 6 and 9), and 10 oz. double friction can (Figures 7, 8, 10 and 11) with tooling, i.e., Neutron Absorber Casting Funnel Assembly (Figure 2), and Body Weldment and Casting Funnel Assembly (Figure 3).

1.2 Definitions

277-0 - Shieldwerx Catalog No. SWX-277-0 or equivalent, Heat Resistant Shielding "Non-Borated" high alumina cement.

277-4 - A mixture of 277-0 and boron carbide (B_4C) powder to form a neutron absorber material.

Companion Sample Cans - The 10 oz. double friction cans in Figures 7 and 8 or 10 oz. crimp style cans in Figures 10 and 11 used for sampling.

Company – B&W Y-12 L.L.C.

Dry Batch - A dry mix of batch size of 277-4.

Dry Blend Batch - A thoroughly mixed Dry Batch.

Heavy Can Spacer Assembly - The 10 oz. double friction can in Figure 6 or 10 oz. crimp style can in Figure 9.

Overcast – Additional cast material required to achieve the fill requirements.

PGNAA Subcontractor – Independent testing firm that performs the Prompt Gamma-ray Neutron Analysis on the companion sample cans for the Company.

Process Procedures - Dry mixing, wet mixing, casting, sampling, and inspection procedures.

Subcontractor - The manufacturer of the ES-3100 Drum Assembly per JS-YMN3-801580-A001.

Vibration Casting – Vibration during casting to remove the air bubbles.

Wet Mix Batch - A wet mix of Dry Blend Batch and water.

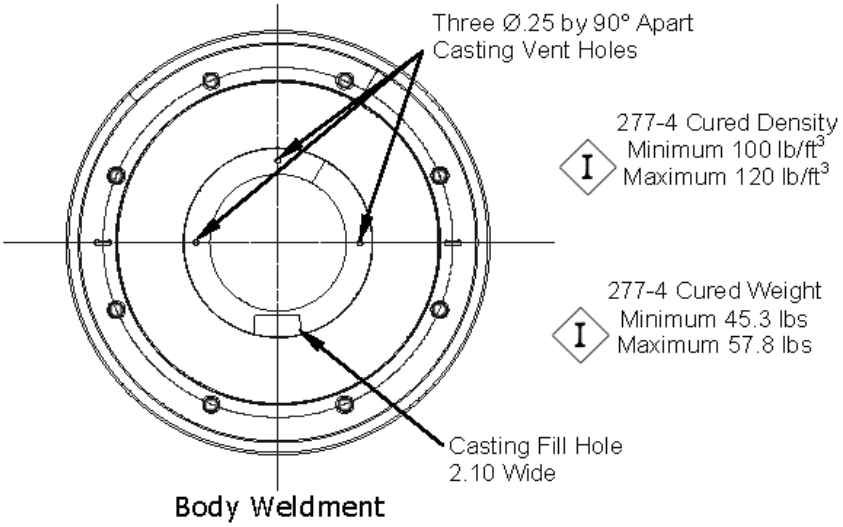

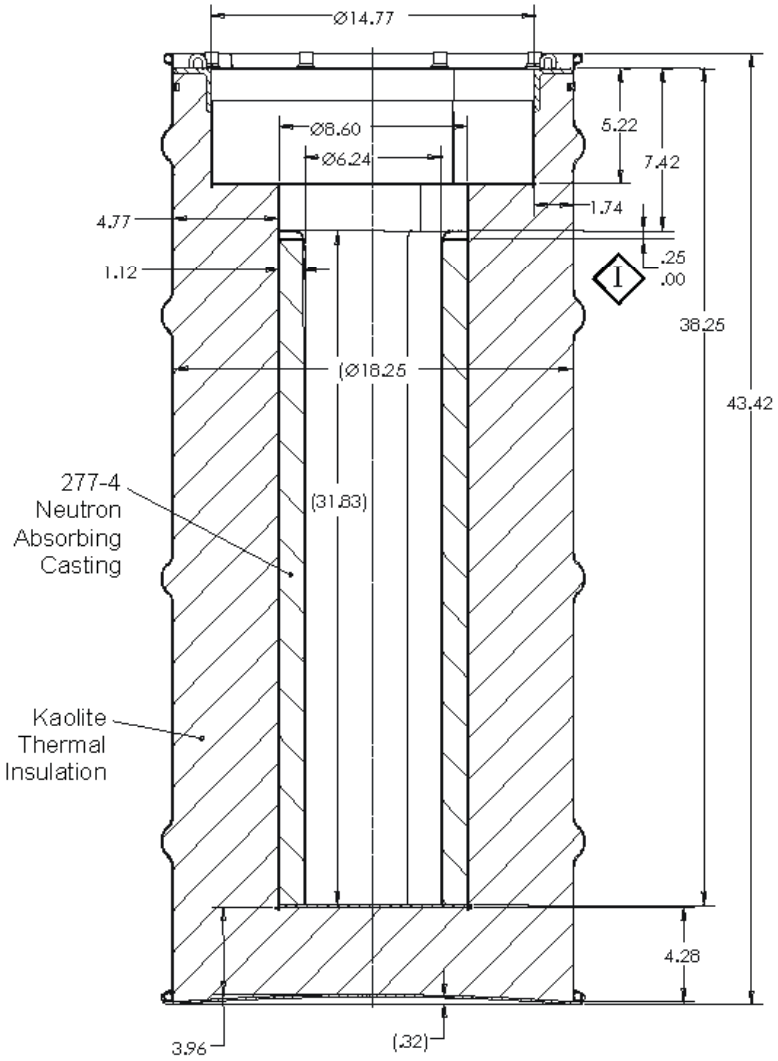

Figure 1 ES-3100 Neutron Absorbing Casting

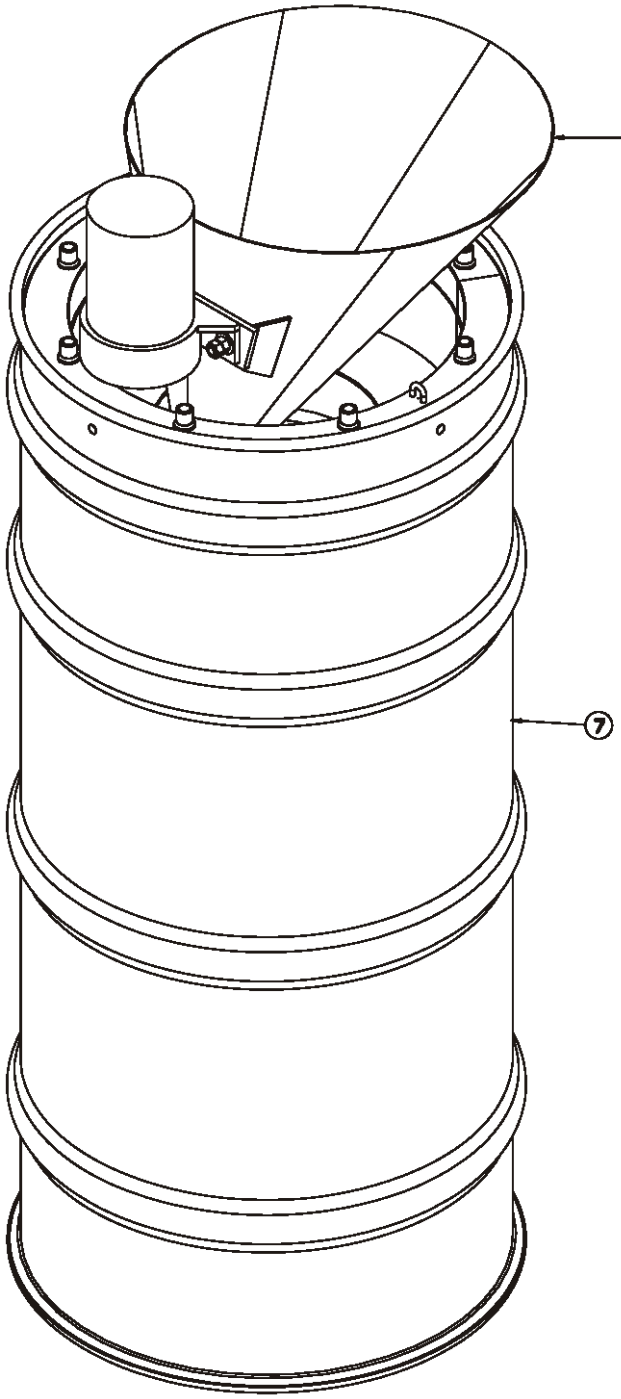

Neutron Absorber Casting Funnel Assembly

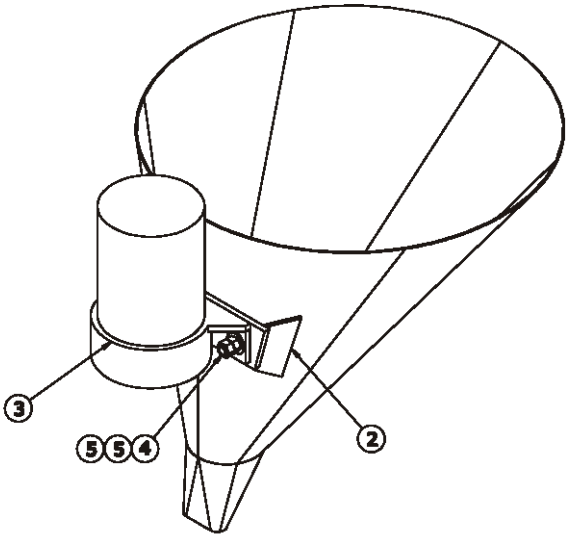

-1 NEUTRON ABSORBER CASTING FUNNEL ASSEMBLY

VIBRATOR POWERED CASTING FUNNEL

Figure 2

-6 BODY WELDMENT AND CASTING FUNNEL ASSEMBLY

Figure 3

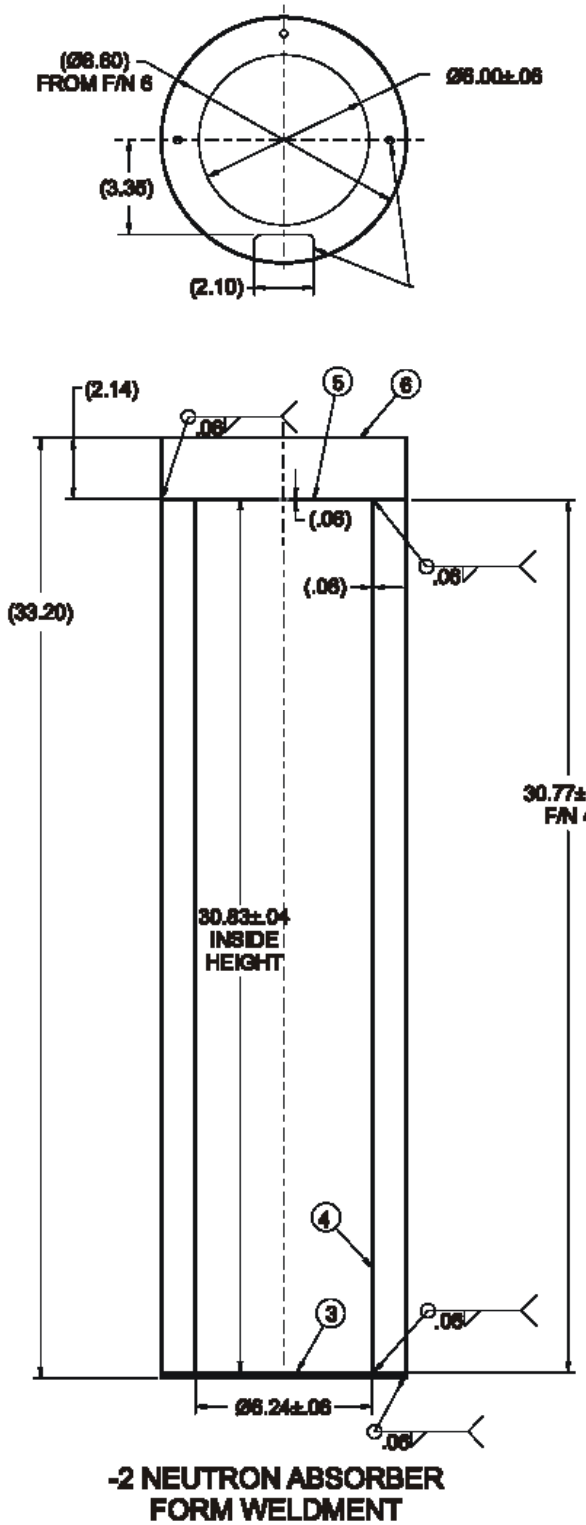

Figure 4

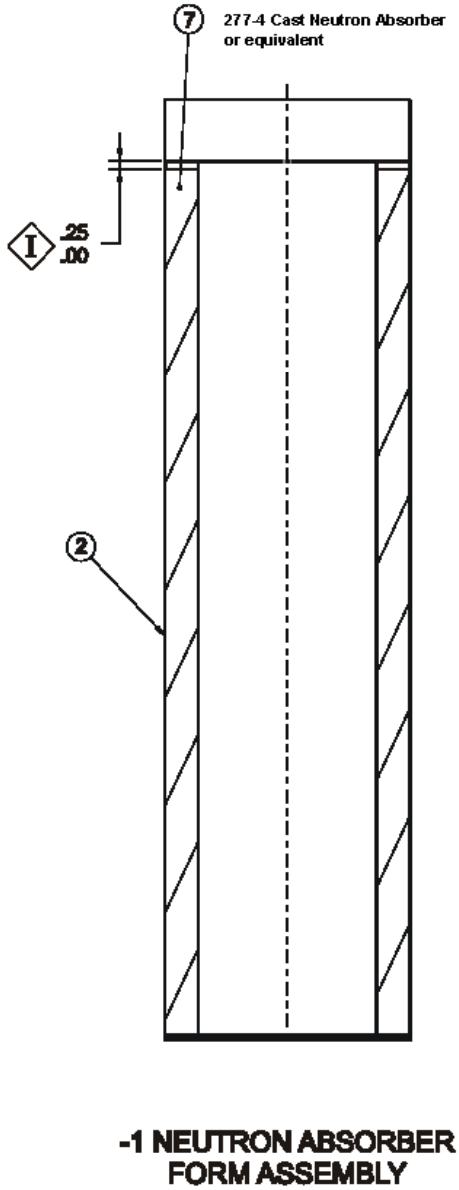

Figure 5

HEAVY CAN SPACER ASSEMBLY

10oz DOUBLE FRICTION CAN
FILLED WITH 277-4

Figure 6

Figure 7

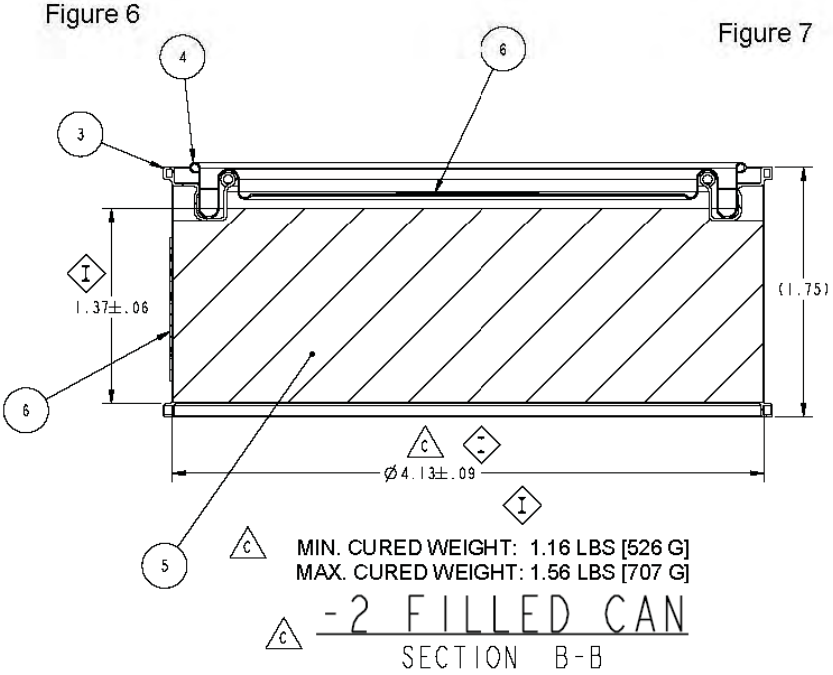

10oz DOUBLE FRICTION CAN
FILLED WITH 277-4

Figure 8

HEAVY CAN SPACER ASSEMBLY

Figure 9

10oz CRIMP STYLE CAN
FILLED WITH 277-4

Figure 10

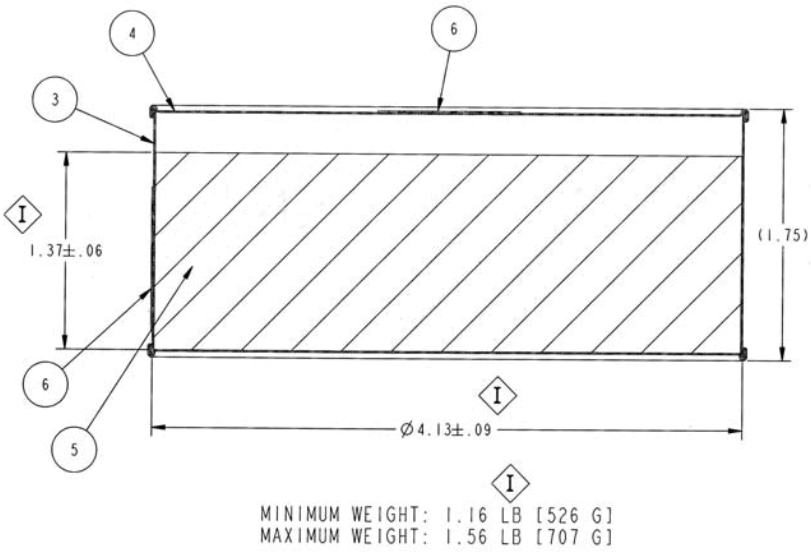

-2 FILLED CAN

SCALE 2/1

10oz CRIMP STYLE CAN
FILLED WITH 277-4

Figure 11

2.0 Applicable Documents

2.1 The following documents are a part of this specification. When there is a conflict between the specification and the applicable documents, the Subcontractor shall bring it to the attention of the Company for resolution.

2.2 Standards

ASTM A 380-99	*Standard Practice for Cleaning, Descaling, and Passivation of Stainless Steel Parts, Equipment and Systems*
ASTM C 750-03	*Specification for Nuclear-Grade Boron Carbide Powder*
ASTM C 791-04	*Test Methods for Chemical, Mass Spectrometric, and Spectrochemical Analysis of Nuclear-Grade Boron Carbide*
ASTM E 11-04	*Standard Specification for Wire Cloth and Sieves for Testing Purposes*
10 CFR 71 Subpart H	*Code of Federal Regulations - Energy - Packaging and Transportation of Radioactive Material - Quality Assurance*

2.3 Company Documents

JS-YMN3-801580-A002	*ES-3100 Drum Assembly*
JS-YMN3-801580-A003	*Manufacturing Process Specification for Casting Kaolite ™ Into the ES-3100 Shipping Package*
M2E801580A026 and M2E801580A043	*Heavy Can Spacer Assemblies*

2.4 Referenced Documents (Not Provided with Request for Proposal)

DAC-PKG-801624-A001	*Mixing Weights And Elemental Composition of 277-4 Neutron Poison used in the ES-3100*
Ltr. No. COR-NDA-04-93	Canberra Oak Ridge, LLC, January 5, 2005, *Results of Prompt Gamma-ray Neutron Activation Analysis and Neutron Transmission Measurements on Prototype Confinement Vessel Inner Liners and Spacers.*
Ltr. No.: COR-NDA-05-015	Canberra Oak Ridge, LLC November 3, 2005, *Results of Prompt Gamma-ray Neutron Activation Analysis On 20 Slip Fit Spacer Cans.*

3.0 Requirements

3.1 General Requirements

The Subcontractor shall be responsible for supplying all materials, services, facilities, and equipment to meet the requirements of this specification unless otherwise noted. Items needed to meet the requirements of this specification that are not identified in this specification shall be specified by the Subcontractor and submitted as Approval Data.

3.2 Equipment Requirements

3.2.1 Certified Scales

All weighing operations of assemblies and materials shall be conducted on certified scales with a minimum accuracy of ±1% of the required measurement or as specified by the measurement tolerance. Scale certification shall be submitted as Approval Data.

3.2.2 Dry Blending the 277-0 and B_4C

A small parts tumbler shall be used to dry blend the ingredients. The small parts tumbler shall be a Multi-Barrel Small Parts Tumbler Benchtop Base (McMaster-Carr No. 44235A11) with Multi-Barrel Small Parts Tumbler 8 Gallon Barrel, 15-3/4" Dia X 14-3/4" W (McMaster-Carr No. 44235A24) or Company approved equal.

3.2.3 Mortar or Plaster Mixer

A mortar or plaster type mixer with moving vanes to shear the wet mix shall be used. The batch volume is approximately 0.5 ft^3 (15 quarts or 3.8 gallons). Therefore, it is recommended that the mixer volume should be 1.5 to 2 times the mix volume or around 0.75 to 1.0 ft^3 (22.5 to 30 quarts, ~6 to 8 gallons). The 277-4 wet mix is thixotropic when mixed and it is recommended that a heavy duty adjustable vibrator mounted to the mixer for both mixing and pouring is used.

3.2.4 Small Plaster Mixer

A drill-powered mortar or plaster mixer and a 5-gallon plastic bucket may be used on small batches of 277-4 instead of the mortar or plaster type mixer. The 5-gallon plastic bucket shall be placed upon the Heavy Duty Drum Vibrator (see Section 3.2.6).

3.2.5 Vibration Powered Funnel Assembly

The Neutron Absorber Casting Funnel Assembly with a vibration- powered funnel (Figures 2 and 3) shall fill both the Body Weldment (Figure 1) and the Neutron Absorber Form (Figure 4). The Casting Funnel Assembly may be modified as required by the Subcontractor to get the wet mix to flow.

3.2.6 Heavy Duty Drum Vibrator

A Heavy Duty Drum Vibrator/Packer shall be used to hold the Body Weldment (Figure 1) or Neutron Absorber Form (Figure 4) for vibration casting the 277-4 into the stainless steel forms. The Heavy Duty Drum Vibrator/Packer shall be McMaster-Carr No. 5809K11, or Company approved equal.

3.2.7 Bench Vibrator

A bench vibrator shall be used during the mixing of the companion sample cans and Heavy Spacer Can Assemblies. The bench vibrator shall be Tabletop Vibration/Mixing Table 10-in. by 7-in. Platform, 10-lb Capacity Continuous Use (McMaster-Carr No. 5714K61) or Company approved equal.

3.3 277-4 Neutron Absorber

3.3.1 Raw Casting Material Requirements and Inspection

3.3.1.1 277-0

Shieldwerx Catalog No. SWX-277-0 Heat Resistant Shielding "Non-Borated" shall be procured. The manufacturer model or catalog number and expiration date shall be clearly indicated on the container. A Certificate of Conformance shall be provided with each lot or batch. The Certificate of Conformance shall include the lot or batch number and the expiration date. The 277-0 shall be sealed and stored in a dry place.

3.3.1.2 Type 1 Nuclear-Grade Boron Carbide Powder

B_4C powder shall be procured as Type 1 Nuclear-Grade Boron Carbide Powder per ASTM C 750. 100% of the powder shall pass through a No. 140 Sieve per ASTM E 11. A Certificate of Conformance and a copy of the chemical and elemental analysis purity in accordance with ASTM C 791 shall be provided.

3.3.1.3 Water

The water shall be potable, filtered through a 20-micron filter and an activated charcoal filter, have a chlorine content of less than 4 ppm, and have a temperature of 65±15°F. Unfiltered potable water may be used for the cleaning of equipment used to cast the neutron absorber system.

3.3.2 Dry Blending Process

3.3.2.1 Dry Batch

A dry batch of 277-4 shall be a mixture of 93.6 wt% 277-0 and 6.4 wt% B_4C. It shall be of sufficient quantity to fill one ES-3100 Body Weldment or Neutron Absorber Form, i.e., approximately 0.55 ft^3 poured volume and 50 lbs. of dry 277-4 weight. The batch size may be adjusted as necessary based on experience for the ES-3100 Body Weldment or Neutron Absorber Form. The tolerance for 277-0 and B_4C weighting shall be the following:

277-4 Dry Batch Size	277-0	B_4C
Equal to or greater than 30 lbs.	±.2 lbs.	±.01 lbs.
Less than 30 lbs	±.01 lbs.	±.01 lbs.

The data shall be recorded on Form A.

3.3.2.2 Blended Dry Batch

The dry batch of 277-4 shall be thoroughly blended. The data shall be recorded on Form A.

If the blended dry batch is not used immediately, the blended dry batch shall be sealed and stored in a dry place with a Blended Dry Batch control number attached to the container.

The Blended Dry Batch shall not be used if the 277-0 expiration date has expired.

3.3.3 Wet Mixing

The weight of the dry mix and water shall be to the following weight proportions of 100% dry mix and 27±1% water. The 277-4 is thixotropic when mixed. It is recommended to have a heavy duty adjustable vibrator mounted to the mixer for both mixing and pouring. Place the water in the mixer and add the dry mix into the water. Before casting, mix the dry powder and water for at least 3 minutes and less than 60 minutes. Any material in the mixer after 60 minutes shall be discarded. Mix only in a room with a temperature range of 70±25°F.

The data shall be recorded on the appropriate form, i.e., Form B for overcast, Form C for Body Weldment, Form D for Neutron Absorber Form, and Form E for Heavy Can Spacer Assembly/PGNAA Acceptance Standards.

3.3.4 Body Weldment and Neutron Absorber Form Vibration Casting

3.3.4.1 Vibration Casting Requirements for Body Weldment and Neutron Absorber Form

During the vibration casting of the 277-4, record the Body Weldment (Figure 1) casting data on Form C and the Neutron Absorber Form (Figure 5) casting data on Form D. A stainless steel vibration powered funnel (i.e., Neutron Absorber Funnel Assembly shown in Figure 3) fits inside the 2.10-in. wide slotted fill hole shown in Body Weldment and in Neutron Absorber Form.

a. Weigh and record the data on Form C or on Form D.
b. Weigh and record the water weight and temperature data when filled with water to within .25 in. of the top metal surface.
c. Remove the water.
d. Secure the part on the drum vibrator.
e. Plug the 6.24 in. diameter cavity to keep the wet mix from falling into the liner bottom.
f. Place the Neutron Absorber Funnel Assembly in the slot and secure in place. If required, additional vibrators may be added.
g. Prepare the Wet Mix per Section 3.3.3.
h. Start the drum vibrator.
i. Scoop the wet mix into the Neutron Absorber Funnel Assembly.
j. Turn on the vibrating funnel and adjust the vibration force until the wet mix flows.
k. About half way through filling the wet mix in either the Body Weldment or Neutron Absorber Form, cast two companion samples for Section 3.3.7. Record the companion sample data on Form F and either Form C or Form D.
l. Continue filling the wet mix until the part will take no more.
m. After filling is complete, vibrate the container for 45±15 seconds to remove air bubbles.

3.3.4.2 Overcast Requirements for Body Weldment and Neutron Absorber Form

A few hours after casting, the 277-4 will settle in the vertical direction and leave a layer of watery fluid on the top of the casting. Remove this fluid and overcast the top between 4 and 24 hours from the first casting. After the overcast has cured for between 4 and 24 hours inspect the depth of casting to the top metal surface and verify that it is within 0.25 in. If not within the 0.25 in., cast additional 277-4 material and perform the following:

a. Remove the water.
b. Secure the Body Weldment or Neutron Absorber Form on the drum vibrator.
c. Plug the 6.24 in. diameter cavity to keep the wet mix from falling into the liner bottom.
d. Record the Overcast Wet Mix Control Number (WMCN) on the appropriate casting data form.
e. Prepare the Wet Mix per Section 3.3.3.
f. Start the drum vibrator.
g. Scoop the wet mix into the Body Weldment or Neutron Absorber Form Assembly until the vent hole is filled.

The final shrinkage of the 277-4 shall be within 0.25 in. of the metal surface as shown in Figures 1 and 5.

3.3.4.3 Curing Requirements Body Weldment and Neutron Absorber Form

Cover the newly cast wet component with plastic or metal for 7 days. Do not store the cast 277-4 castings in temperatures below 35°F for the first 30 days after casting.

After 7 days, remove the plastic or metal cover and dehydrated using either or both vacuum and heat to create an acceptable density and weight. If heat is used, the maximum temperature of the inner liner shall not exceed 250°F.

Record the diamond I measurements shown on Figures 1 and 5 on the appropriate casting data forms. The acceptable cured height measurement shall be less than 0.25 inches. The acceptable cured casting weight shall be between 45.3 and 57.8 lbs. Cured casting weights shall be used to calculate the cured density. If the cured casting density is greater than 120 lb/ft^3, continue the dehydration process. If the cured casting density is less than 100 lb/ft^3, the casting shall be unacceptable, the appropriate form shall be completed, and a copy of the form shall be sent to the Company.

3.3.5 Heavy Can Spacer Assembly

The Heavy Can Spacer Assembly shown in Figure 6 or 9 shall be the 10-oz. double friction metal can as shown in Figures 7 and 8, or 10-oz. crimp style metal can as shown in Figures 10 and 11. The cured casting weight for each can shall be measured and the cured casting density recorded on Form E. A cured cast density of 100 to 120 lb/ft^3 and a cured weight range of 1.16 to 1.56 lbs shall be acceptable. If the cured casting density is outside the acceptable range, a copy of the form shall be sent to the Company.

Two cans from the middle of the lot on Form E, i.e., a maximum lot of 22 cans, shall be selected and identified as companion sample cans. Cans that are not from the middle of the lot on Form may be selected with Company approval.

3.3.6 PGNAA Acceptance Standards

The PGNAA Acceptance Standards shall be made with a Company representative witnessing the manufacturing processes of weighing, blending, wet mixing, and casting. The PGNAA Acceptance Standards shall be the 10-oz. double friction metal can as shown in Figures 7 and 8, or 10-oz. crimp style metal cans as shown in Figures 10 and 11. The cured casting weight for each can shall be measured and the cured casting density recorded on Form E. A cured casting density of 100 to 120 lb/ft^3 and a cured casting weight of 1.16 to 1.56 lbs shall be acceptable. If the cured casting density is outside the acceptable range, a copy of the form shall be sent to the Company.

One can from the middle of the lot on Form E, i.e., a maximum lot of 22 cans, shall be selected and identified as a companion sample can for Loss On Drying (LOD) testing. The remainder of the lot shall be sent to the PGNAA Subcontractor.

3.3.7 Companion Sample Cans

In addition to the companion sample cans selected in Sections 3.3.5 and 3.3.6, two companion sample cans shall be made half way through the casting process for the Body Weldment and the Neutron Absorber Form per Section 3.3.4.1. Companion sample can data shall be recorded on Test Form F.

a. The cured casting density of all companion sample cans shall be calculated per Section 3.3.9.2 and recorded on Form F. If the cured casting density is outside the acceptable range, a copy of the form shall be sent to the Company. A low cured casting density of a companion sample can shall not be a reason to reject the Body Weldment, Neutron Absorber Form, Heavy Can Spacer Assembly casting lot, or PGNAA Acceptance Standards casting lot.
b. The odd serial number companion sample cans for the Body Weldment, Neutron Absorber Form, Heavy Can Spacer Assembly casting lot, or PGNAA Acceptance Standards casting lot shall be LOD tested to verify the hydrogen content per Section 3.3.9.3.
c. The even serial number companion sample cans for the Body Weldment, Neutron Absorber Form, or Heavy Can Spacer Assembly casting lot shall be PGNAA tested to verify the ^{10}B content per Section 3.3.9.4.

3.3.8 Casting the 10 oz. Double Friction Metal Cans or 10 oz. Crimp Style Cans

a. Select a labeled can which has a drawing and serial number per drawings M2E801580A026 or M2E801580A043.
b. Weigh the empty labeled can and lid and record the casting can data on Forms C, D, or E. It is acceptable to weigh ten cans with ten lids for each purchase order of cans and to use the average can and lid weight on each form.
c. Weigh the water and measure the water temperature. Record this data on Form C, D, or E. Fill with water only up to the bottom of the inside rim. The can lid shall be on the scale. It is acceptable to weigh the water weight of the first ten cans with ten lids of the same lot of cans and to use the average water weight for each of the following cans if the measurements are consistent.
d. Remove the water from the cans.
e. Prepare the Wet Mix Batch following Section 3.3.3.
f. Hold the can on the bench vibrator during filling with the 277-4 wet mix. Quickly vibrate and continue to add wet mix to the can lip.
g. Once all of the cans are full of wet mix, return the first can back to the vibrator for at least 3 minute at a high frequency setting. During the 3 minutes of vibration, continue to add 277-4 wet mix until the can stays full. Repeat this process for all the cans in the casting lot.
h. Between 1 to 24 hours after casting, scrape the top of the casting to meet 1.37±0.06 dimension from bottom of can noted on Figures 8 and 11.

i. Clean the can rim around the edge per Section 3.4.2.
j. Perform an in-process measurement of the scraped casting height to ensure that the casting height parameters are met shown in Figures 8 and 11.
k. Cover the casting by placing the properly labeled can lid on the can for 7 days.
l. Remove the can lid and let the can air dry or use either or both vacuum and heat to create an acceptable density and weight. If heat is used, the maximum temperature of the can shall not exceed 250°F.
m. Measure casting height and weigh the can with lid. Record this data on Forms C, D, or E.
n. Record the final Companion Sample Can casting density, weight, or casting height measurements data on Form F.
o. Crimp lid onto crimp style can, as applicable.

3.3.9 Verification

All verification shall be completed after the casting is cured.

3.3.9.1 Cured Casting Density Verification

The density of cured casting in the Body Weldment, Neutron Absorber Form, Heavy Can Spacer Assembly, and PGNAA Acceptance Standards shall be determined by weighing the casting container before casting, while filled with water, after casting, and when cured.

Since the density of water is known, a simple relationship between the weight differences shall determine the cured casting density.

$$Density = \left(\frac{Cured - Empty}{WithWater - Empty} \right) \times 62.3 \text{ lb/ft}^3$$

3.3.9.2 Companion Sample Can Cured Casting Density Verification

The density of cured casting in each companion sample can shall be determined by weighing the can before casting, while filled with water, after casting, and when cured.

Since the density of water is known, a simple relationship between the weight differences shall determine the cured casting density.

$$Density = \left(\frac{Cured - Empty}{WithWater - Empty} \right) \times 62.3 \text{ lb/ft}^3$$

3.3.9.3 Companion Sample LOD Verification

The companion sample cans identified in Section 3.3.7.b shall be LOD tested. The acceptable LOD percent range shall be based upon the companion sample can cured casting density in Section 3.3.9.2. The Acceptable Maximum and Minimum LOD% at Density is in this table developed from data in DAC-PKG-801624-A001 Table 7, 277-4 Composition @ Extreme Densities and LOD% and compared to the average values as manufactured.

Acceptable Maximum and Minimum LOD% at Density		
Density (lb/ft^3)	Maximum LOD%	Minimum LOD%
100	31.80%	28.61%
101	32.47%	28.33%
102	33.12%	28.06%
103	33.77%	27.79%
104	34.40%	27.52%
105	35.03%	27.26%
106	35.64%	27.00%
107	36.25%	26.75%
108	36.84%	26.50%
109	37.42%	26.25%
110	37.99%	26.01%
111	38.56%	25.78%
112	39.11%	25.55%
113	39.65%	25.32%
114	40.18%	25.10%
115	40.70%	24.88%
116	41.21%	24.66%
117	41.71%	24.45%
118	42.20%	24.25%
119	42.68%	24.05%
120	43.15%	23.85%

a. The lid shall have the serial number permanently transferred by vibro etch or other method.
b. The lid shall have a small vent hole in it. It is recommended that a nail be used to punch a hole 0.12±0.06 in. diameter in the metal lid from the inside surface of the lid.
c. Match the can serial numbers and place the lid on the can.
d. The weight of the can shall be recorded on Form F.
e. The cans shall be placed in an oven at 1500±150°F (800°C) for 4 hours.
f. The weight of the can shall be recorded on Form F with the can temperature not below 100°F.
g. Calculate the LOD% using the equation below and record it on Form F. Due to can oxidizing and gaining weight during the heating cycle, a 0.024 lb correction factor is included in the following LOD% calculation.

$$\text{LOD\%} = \left[1 - \frac{(LODWeight - Empty - 0.024lb)}{(Cured\ \&\ Clean - Empty)}\right] \times 100\%$$

h. Verify that the LOD% is within the acceptable range. If water content is outside the acceptable range, a copy of the form shall be sent to the Company.

3.3.9.4 PGNAA Verification

The companion sample cans identified testing in Section 3.3.7.c shall be sent to the PGNAA Subcontractor. The PGNAA Subcontractor will test to the requirements in Appendix A and record the data on Forms AA to AD. The PGNAA Subcontractor will send copies of the completed Forms AC and AD to the Subcontractor and Company.

The PGNAA testing acceptance results on From AD shall be transferred to Form F.

3.4 Cleaning Requirements

3.4.1 Contact with Chlorides or Fluorides

The stainless steel material shall be protected from contact with chlorides in accordance with ASTM A380, paragraph 8.5, during all operations including packaging. The Material Safety Data Sheet (MSDS) for all cleaning solutions or products used on the ES-3100 shall be submitted as Approval Data to verify that no chlorides or fluorides are present.

3.4.2 Satisfactory Cleanliness

Cleaning procedures for the stainless steel per Section 3.4 of equipment specification JS-YMN3-801580-A002 shall be submitted as Approval Data. Only non-chloride-bearing chemicals shall be used for cleaning (e.g., trisodium phosphate detergent or acetone). Water used in cleaning shall have a maximum chlorine content of 4 parts per million.

After casting but prior to packaging, stainless steel components of the forms and cans shall be cleaned per the approved cleaning procedures. Satisfactory cleanliness shall be determined by visual inspection as can be observed by a person with normal visual acuity (natural or corrected) and without magnification. Light intensity of at least 100 ft-candles shall be provided on the surface to be inspected.

4.0 Quality Assurance

4.1 Quality Assurance Program

The subcontractors shall have in place and maintain a Quality Assurance (QA) Program and inspection system that meets the requirements of 10 CFR 71 Subpart H. If not previously submitted, an uncontrolled copy of the subcontractor's QA Program shall be submitted as Offer Appraisal Data.

4.2 ES−3100 Casting Quality Assurance Requirements

4.2.1 ES−3100 Documentation Package

All records shall be identified based on the ES−3100 serial numbers. The ES-3100 Documentation Package shall be provided as Certified Data with each ES-3100 casting. The ES-3100 Documentation Package shall be complete, legible, indexed, and traceable to the material supplied and include the following:

a. Material measuring, dry blending, wet mixing, casting, sampling, and inspection forms, i.e, Forms A through F.
b. A Certificate of Compliance for each lot of the 277-0 Heat Resistant Shielding "Non-Borated" dry mix documentation with the expiration date identified on each container.

c. A Certificate of Compliances for B_4C powder to Type 1 Nuclear-Grade Boron Carbide Powder per ASTM C 750, chemical and elemental analysis per ASTM C 791, and 100% of the powder passes through a No. 140 Sieve per ASTM E 11.

d. A Certificate of Compliance signed by an officer of the Subcontractor confirming that the cast neutron absorber in ES−3100 shipping package meets the subcontract requirements.

4.2.2 Batch Processes

Batch processes such as mixing, pouring, curing, sampling, inspection, etc., shall be performed in accordance with detailed written procedures. These procedures shall specifically describe the exact manner in which these processes are to be performed. All records shall be traceable to the ES−3100 Shipping Package, Neutron Absorber Form, Heavy Spacer Can Assembly, PGNAA Acceptance Stands or Companion can serial numbers.

4.2.3 Materials Traceability

A manufacturing lot or batch number shall identify material furnished to make up the neutron absorber system. Materials shall be identified by material type; applicable specification and revision number, and be traceable to their lot numbers. Traceability records shall be available for review by the Company's representative.

4.2.4 Procedures

Preparation, installation, sample collection, and inspection processes shall be controlled and performed by qualified personnel. The procedures must incorporate a mechanism to identify process step completion. Procedures shall be submitted as Approval Data. The approved procedures shall be provided as Certified Data prior to the start of casting.

4.2.5 Training and Qualification of Personnel

The Subcontractor shall provide for the training and qualification of personnel to ensure their competence in the use of process procedures and specifications. Records of personnel qualifications shall be made available to the Company upon request. Only those personnel who have been qualified to perform a specific batch process used in the casting of Kaolite per equipment specification JS-YMN3-801580-A003 shall be used to perform work in this process.

4.2.6 The Company reserves the right to request any documentation and to witness any of the processes performed in accordance with this specification.

5.0 Preparation for Delivery

After cleaning of stainless steel surfaces per Section 3.4, aluminum foil duct tape shall be applied over the fill and vent holes in the Body Weldment (Figure 1) and the Neutron Absorber Form (Figure 5).

6.0 Manufacturer's Data

6.1 Offer Appraisal Data shall be submitted with the offer. This data shall become part of the subcontract requirements.

6.2 Approval Data will be reviewed and approved by the Company. Subcontractor shall not proceed with the casting activity until Company approval is given for all the Approval Data. The Approval Data shall be transmitted to the Company by the dates agreed to by the Subcontractor and the Company Subcontractor Administrator.

6.3 Certified Data will be used by the Company as the record for the ES-3100 shipping packages. The Certified Data shall be transmitted as noted.

6.4 A request for Company approved equal shall be submitted as Approval Data. Adequate information shall be provided with the request for Company approved equal so that the Company can determine if the item is equivalent.

ATTACHMENT A -
Prompt Gamma-ray Neutron Activation Analysis Testing Setup & Tooling
(Page 1 of 4)

A.1 Prompt Gamma-ray Neutron Activation Analysis Can Testing

Prompt Gamma-ray Neutron Activation Analysis (PGNAA) of boron performs one of the acceptances of the ES-3100 277-4 casting. Specifically, ^{10}B gives rise to a 478-keV gamma-ray produced by the recoil of the lithium nucleus from the neutrons captured in ^{10}B. The gamma-ray is Doppler broadened by 10–15 keV. The PGNAA shall be performed upon a companion sample can cast made during the drum casting in accordance with JS-YMN3-801580-A005 and Body Weldment (Figure 1), Neutron Absorber Form (Figure 5), Heavy Can Spacer Assembly (Figure 6 or 9), and the cast companion samples in the same 10-oz. double friction metal can on (Figures 7 and 8), or 10-oz. crimp style metal cans as shown in (Figures 10 and 11). PGNAA is a relative measurement therefore daily baselines are required to define the acceptance values.

Canberra Industries to perform the PGNAA testing.

Canberra Industries, Inc.
Linda C. Ostrowski
1133-C Oak Ridge Turnpike Suite 260
Oak Ridge, TN 37830-6442
865-241-3963 fax 865-241-3965

A.2 PGNAA Quality Assurances

The equipment and software used in the PGNAA shall be certified to a national standard.

A.3 PGNAA Measurements Setup

A PGNAA measurement setup number shall be required for each unique setup recording the pertinent data of the setup on Form AA. A new setup is required from previous prototypical work. Several setups may be tried to determine the most efficient testing setup. These changes shall be documented using Form AA. Once the setup is defined on Form AA reference the setup number each time it is used. Measure the PGNAA acceptance standards using the defined setup to verify the setup distances are repeatable within ±0.13-in.

A.3.1 Net Count Rate Measurements

Time shall be consistently applied throughout all of the PGNAA testing. For the prototype system setup, a time of at least 15 minutes (900 seconds) for each spectrum measurement was found to be satisfactory. A net count rate (NCR) in counts per second shall be used throughout with a set target standard time limit of around 900 seconds. Record both the count and time in seconds for that count on Form AA and calculate the count rate to three decimal places (i.e., 34.245 counts/sec).

A.3.1.a Net Count Rate Time Determination

The time of the measurement shall be determined by performing the Tooling Setup on Form AA at different times like 300, 600, 900, 1800, and 72000 seconds. Determine the accuracy effect of the total counting time on the counting statistics, based upon at least a 72000 seconds (20 hour) count. The testing time shall be re-evaluated when a significant change in the source system occurs.

A.3.2 Neutron Source

A spontaneous fission neutron source similar to the 1.8-µg ^{252}Cf prototype shall be used to perform the tests. This source was rated at 4.4×10^{6} neutrons/sec on November 15, 2004. The neutron source is sealed in a 32.5-mm-long, 9.4-mm-diameter stainless steel cylinder and placed in a collimator.

ATTACHMENT A
(Page 2 of 4)

A.3.3 Collimator and Neutron Source Setup

A collimator similar to the prototype collimator shall be used to hold the source. The prototype collimator was a 3-in. cube of high-density polyethylene covered on five sides with 2 mm of cadmium as a neutron shield with at least 0.5-in. of lead on six sides as a gamma shield. The center of the sixth side of the polyethylene cube has a 9.5-mm hole into which the source was pressed. The sixth side is covered with cadmium except for a 1-in. square in the center. A 1-in. diameter hole in the cadmium at the source location shall be provided in the collimator to generate a better shaped neutron source for the sample can tests. The location of the collimator and source shall be defined in a fixture and shall be inspected to be repeatable to within ±0.13-in. to locate the collimator, can, detector, and other materials, e.g., polyethylene.

Record the setup and the results in the net detector count rate on Form AA. Record the setup source distance (SD) ±0.13-in. from the sample can lid. Move the filled sample can further away from the source, and repeat the process, increasing the distance in increments to identify the setup distance that maximizes the NCR for that source arrangement. Record the setup information on Form AA.

A.3.4 Detector

A detector system similar to the prototype shall be used. The prototype was a Canberra Model BE3825 Broad Energy Germanium (BEGe) detector, which was a gamma-ray detector, in a 2-in. thick lead shield with a Canberra Model 7935SL-7 cryostat and Canberra Model 2002CSL preamplifier to capture the gamma spectrum for the PGNAA measurements. This detector has a side lead shield but no shielding in the front to collimate the field-of-view. An Inspector 2000 along with the Genie2K gamma-ray analysis software package from Canberra was used for distinguishing the ^{10}B peak from the rest of the gamma-ray spectrum. It is recommended that a fixture be made to locate the collimator, can, and detector. Document the method used to determine the Compton boundary end points.

A.3.5 Detector Net Count Rate Determination

Use software equivalent to the Genie2K gamma-ray analysis software package from Canberra for performing the gamma-ray spectrum collection and analysis. The peak fitting routine in Genie2K does not expect a peak as broad as 10–15 keV; therefore, a region-of-interest (ROI) was set around the broad boron neutron activation peak of 478 keV. The data gathered has three components. The gross count is the total count of the gamma-rays detected with an energy that falls within the ROI. The Compton background is the portion of the gross count that is caused by scattered gamma-rays. The NCR is the portion of the total count that is from the boron in a period of time. The NCR is the difference between the gross and the Compton counts.

A.3.6 Detector Location Setup

The setup distance of the prototype detector setup was as close as possible using about 1-in. thick lead as a gamma shield to keep the detector noise signal low. This thickness was applied during the PGNAA documented in Ltr. No.: COR-NDA-05-015; Canberra Oak Ridge, LLC November 3, 2005, *Results of Prompt Gamma-ray Neutron Activation Analysis On 20 Slip Fit Spacer Cans*. Figure A.1 shows the direction this development work was heading. Document and verify that the detector setup distance (DD) from the sample can generates a maximum NCR by adjusting the detector setup distance and repeating this test. It is recommended that a fixture be made to locate the collimator, can, and detector.

ATTACHMENT A
(Page 3 of 4)

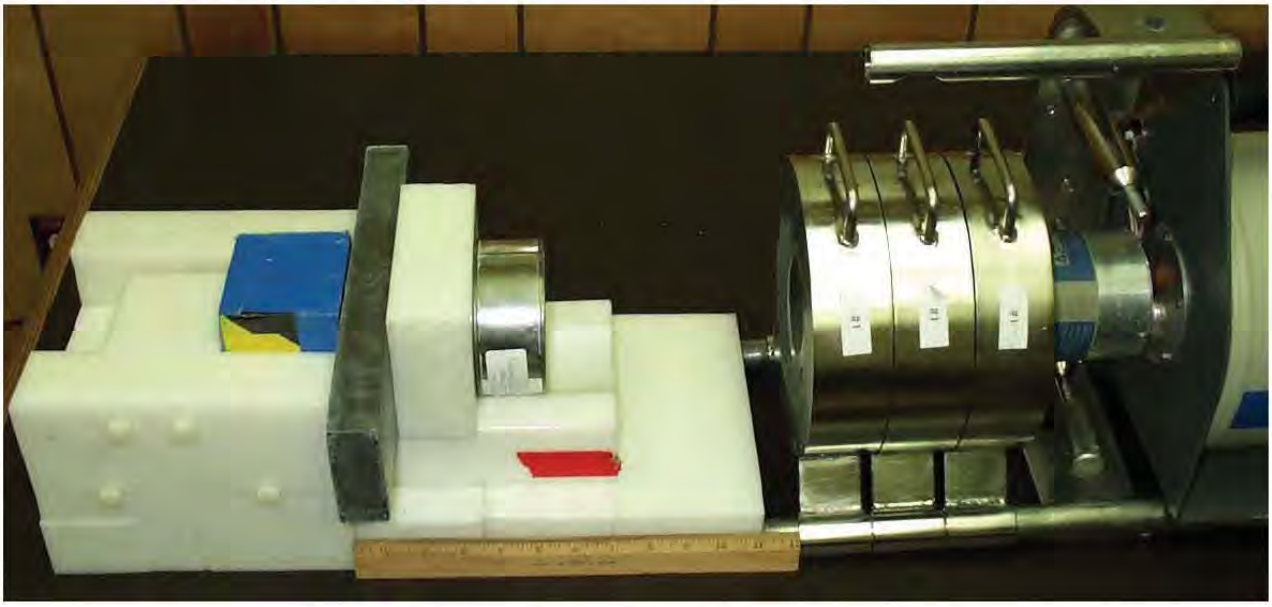

Figure A.1 Preliminary Tooling Generated for PGNAA

A.3.7 Detector Operation Setup

Set the detector setup distance (DD) ±0.13-in. and the setup source distance (SD) ±0.13-in. from the filled sample can. Record the set detector setup distance, setup source distance, 277-4 sample serial number, NCR value, and the day and time of the measurement in the setup form. Repeat this final test measurement in 30 minutes to verify the stability of the detector and this shall become the setup standard test measurement on Form AA. The repeatable measurement tolerances shall be part of the testing fixture certification inspection.

A.3.8 Net Count Rate Baseline Measurements

Once the setup is completed and the fixture dimensions are certified, Form AB shall be used to record the NCR for the twenty acceptance standards using the 10-oz. double friction metal cans or 10 oz. crimp style cans. The baseline acceptance 277-4 NCR shall be set daily using five of the twenty acceptance standards using the 10-oz. double friction metal cans or 10 oz. crimp style cans and recorded on Form AC. The twenty acceptance standards cans shall be inspected with a Company representative as a witness.

Select five PGNAA acceptance standards from Form AB as the Daily Standard Setup that generate approximately the same average and standard deviation as on Form AB. The baseline acceptance 277-4 NCR shall be set daily using five of the twenty acceptance standards using the 10-oz. double friction metal cans or 10 oz. crimp style cans and recorded on Form AC. Verify the Daily Standard cans selection with the Company. The Body Weldment (Drum), Neutron Absorber Form (From), and Heavy Can Spacer Assembly (Lot) acceptance criteria for the ^{10}B interaction is based upon this test. The Minimum acceptable standard NCR shall be set daily using the following formula.

Minimum Acceptable NCR = Can Five NCR Average − 3 × Standard Deviation Can Five NCR

ATTACHMENT A
(Page 4 of 4)

A.4 Net Count Rate Acceptance Measurements

The NCR acceptance measurement shall be made following the Daily Standard Setup using Form AC and calculating a Pass Rate. Record the PGNAA setup number, day and start time of the measurement, the associated Body Weldment, Neutron Absorber Form, Heavy Can Spacer Assembly Lot's serial number, companion sample can serial number, actual net count, acceptable net count, and testing results on the inspection form. For the testing results, if the actual NCR is equal or above the Pass Rate, then record a PASS; if less than, enter FAIL in the test Form AD. It is acceptable to group the test results for several sample cans on one form following one testing setup.

Once a 277-4 sample can NCR failure has occurred verify that the setup has not shifted by rerunning the Daily Standard Setup using Form AC and calculate a new Pass Rate. If the Pass Rate has changed more then 1% than perform a new detector operation setup and NCR baseline measurements and verify the test failure rate by retesting the failed can. If the companion sample can receives two failures in a row, the associated parts shall be rejected from service, the Company Subcontract Administrator notified, and the testing continued.

A.5 Documentation of the Acceptance or Rejection Measurements

Documentation of the acceptance or rejection NCR measurements shall be made with the Forms AA through AD plus a detailed description of the active NCR measurement hardware and software that was used.

A.6 Results

A.6.1 Equipment and Software Quality Assurances

The national standard used in the PGNAA (see Section A.2) shall be provided as Certified Data.

A.6.2 Certified Tooling Setup and Repeatable Dimensions

The final tooling setup shall be manufactured and certified that the placement of the source, detector, sample can, and tooling materials are dimensional stable and repeatable to ±0.13-in.

A.6.3 Measurement Time and Repeatable Accuracy

Define the repeatable accuracy for the Nate Rate Count time selection for the production certification inspections. The Nate Rate Count time justification (see Section A.3.1.a) shall be submitted as Approval Data.

A.6.4 Measurement Software and Methodology

For the final setup the measurement software and methodology method used to generate the net counts (see Section A.3.4) shall be documented and provided as Certified Data.

A.6.5 Forms AA through AD

Forms AA, AB, and AC shall be submitted as Approval Data.

After the process is approved, filled-in Forms AC and AD shall be provided as Certified Data to the Company and the casting company.

A.6.6 Can Disposition

After PGNAA testing is completed on a lot of companion sample can lot, the cans shall be returned to the Company. The PGNAA Acceptance Standards cans shall be stored for the life of the subcontract.

Casting Company Name	Certificate of Conformance of the 277-0 dry mix		
Blended Dry Batch Control Number [a]	Record the expiration date of the 277-0 dry mix [b]		
Certificate of Conformance of the B_4C dry mix	277-0 Heat Resistant Shielding Drum ID Number		
Planning	277-4 Weight	Units	Operator
Batch Size		lb	
Operation	Measurement	Units	Operator
277-0 Weight (Target = 277-4 Weight x 93.6 wt%)		lb	
B_4C Weight (Target = 277-4 Weight x 6.4 wt%)		lb	
Dry Blending Time		min.	
Comments			

[a] A 10-digit Blended Dry Batch Control Number shall be used to define the date and the time of mixing the casting batch using the format with a 24-hour clock (i.e. 1021041515 is used for October 21, 2004 at 3:15 pm.)

[b] Record the expiration date of the Blended Dry Batch and confirm that it is still acceptable to be cast following this specification.

Casting Company Name		Blended Dry Batch Control Number		
Wet Mix Control Number (WMCN) [a]		Record the expiration date of the Dry Blend Batch		
Water Temperature °F	Air Temperature °F	Measurement	Units	Operator
277-4 Weight			lb	
Water Weight (Target = 277-4 Weight × 27±1 wt%)			lb	
Mix Time			min.	
Mix Finish Time			min.	
Comments				

[a] A 10-digit Wet Mix Control Number (WMCN) shall be used to define the date and the time of mixing the casting batch using the format with a 24-hour clock (i.e. 1021041515 is used for October 21, 2004 at 3:15 pm.)

Casting Company Name	Body Weldment Casting Control # [a]
Part Serial Number	Drawing Number M2E801580A002

Measured Weights ±0.5 lb	Casting Information		Comments	Operator
	Weight	Date		
Clean and Empty				
Filled with Water [b]				

Water Information	Water Weight ±0.5 lb	Water Temp. [b]	Comments	Operator
Water Conditions [b]	lb	°F		
Vibration Settings [c]	lbf	VPM		

Wet Mix Control	Blended Dry Batch Control No.		Dry Blend Batch Expiration Date		
(Target Water = 277-4 Weight × 27±1 wt%)	277-4 Weight	lb	Water Weight	lb	
	Air Temperature	°F	Water Temperature	°F	
	Mix Time		Mix Finish Time		

Companion Samples [d]	−1	−2

	Time	Date	Comments	Operator
Vibration Start				
Vibration Stop				
Overcast WMCN				
After Casting	lb	Date		
After Cured and Clean	lb	Date		

Measurements ◇I◇	Height [e] (in)	Pass or Fail Height	Cured Weight (lb)	Pass or Fail Cured Weight [e]	Cured Density [f] (lb/ft^3)	Pass or Fail 100−120 (lb/ft^3)
Body Weldment						

[a] A 10-digit Body Weldment Casting Control Number shall be used to define the date and the time of mixing the casting batch using the format with a 24-hour clock (i.e., 1021041515 is used for October 21, 2004 at 3:15 pm).

[b] Record the water weight and water temperature within 10 minutes from completion of the weighing process.

[c] Recommended vibration settings are at 450 VPM and three times the total vibrated weight. The total vibrated weight is the finish cast part and fixtures weight, for a setting of approximately 800 pound-force.

[d] Use Form F, for ES-3100 Companion Sample Casting Control and Tests to control the companion sample castings.

[e] The acceptable cured height measurement is less than 0.25 inches. The Body Weldment cured casting weight shall be between 45.3 and 57.8 lbs.

[f] Use the above weights to calculate the density as shown below. $Density = \left(\frac{Cured - Empty}{WithWater - Empty}\right) \times 62.3 \text{ lb/ft}^3$

Casting Company Name	Body Weldment Casting Control # [a]
Part Serial Number	Drawing Number M2E801580A034

Measured Weights ±0.5 lb	Casting Information		Comments	Operator
	Weight	Date		
Clean and Empty				
Filled with Water [b]				

Water Information	Water Weight ±0.5 lb	Water Temp. [b]	Comments	Operator
Water Conditions [b]	lb	°F		
Vibration Settings [c]	lbf	VPM		

Wet Mix Control	Blended Dry Batch Control No.		Dry Blend Batch Expiration Date		
(Target Water = 277-4 Weight × 27±1 wt%)	277-4 Weight	lb	Water Weight	lb	
	Air Temperature	°F	Water Temperature	°F	
	Mix Time		Mix Finish Time		

Companion Samples [d]	−1	−2

	Time	Date	Comments	Operator
Vibration Start				
Vibration Stop				
Overcast WMCN				
After Casting	lb	Date		
After Cured and Clean	lb	Date		

Measurements (I)	Height [e] (in)	Pass or Fail Height	Cured Weight (lb)	Pass or Fail Cured Weight [e]	Cured Density [f] (lb/ft^3)	Pass or Fail 100−120 (lb/ft^3)
Neutron Absorber Form						

[a] A 10-digit Body Weldment Casting Control Number shall be used to define the date and the time of mixing the casting batch using the format with a 24-hour clock (i.e., 1021041515 is used for October 21, 2004 at 3:15 pm).

[b] Record the water weight and water temperature within 10 minutes from completion of the weighing process.

[c] Recommended vibration settings are at 450 VPM and three times the total vibrated weight. The total vibrated weight is the finish cast part and fixtures weight, for a setting of approximately 800 pound-force.

[d] Use Form F, for ES-3100 Companion Sample Casting Control and Tests to control the companion sample castings.

[e] The acceptable cured height measurement is less than 0.25 inches. The Neutron Absorber Form cured casting weight shall be between 45.3 and 57.8 lbs.

[f] Use the above weights to calculate the density as shown below. $Density = \left(\frac{Cured - Empty}{WithWater - Empty}\right) \times 62.3 \text{ lb/ft}^3$

Casting Company Name	Can Lot Serial Number [a]	Drawing Number M2E801580A026 or M2E801580A043
Average 10 Can and Lid **Empty** Weight	Temperature of Water Weight (°F)	Average 10 Can and Lid **Water** Weight

Wet Mix Control	Blended Dry Batch Control No.		Dry Blend Batch Expiration Date	
(Target Water = 277-4 Weight × 27±1 wt%)	277-4 Weight	lb	Water Weight	lb
	Air Temperature	°F	Water Temperature	°F
	Mix Time		Mix Finish Time	

Wet Mix Control Number (Overcast), if required

Can Serial #	After Casting Weight (lb)	Cured Weight (lb)	Pass or Fail Cured Weight [b]	Cured Height (in)	Pass or Fail Cured Height [b]	Cured Density (lb/ft^3)	Pass or Fail Cured Density [c]
Companion Samples [d]		−1				−2	

Operator	Comments

[a] A 10-digit Can Lot Serial Number shall be used to define the date and the time of setup using the format with a 24-hour clock (i.e., 1021041515 is used for October 21, 2004 at 3:15 pm).

[b] Heavy Can Spacer Assembly acceptable weight is 1.16 to 1.56 lbs and height 1.37±0.06 as shown in Figure 8.

[c] Use this equation for the; $Density = \left(\frac{Cured - Empty}{WithWater - Empty}\right) \times 62.3$ lb/ft^3. Acceptable 100 to 120(lb/ft^3).

[d] Use Form F, for ES-3100 Companion Sample Casting Control and Tests for Heavy Can Spacer Assembly companion samples..

Casting Company Name		Ave. 10 Can and Lid Empty Weight [a]		Ave. 10 Can and Lid Water Wgt. [a]		Temp. of Water Weight (°F)		Drawing Number M2E801580A026 or M2E801580A043	
Serial Numbers		Can Measurement Weights ±0.01 (lb)			For Record Only	Loss On Drying (Odd Serial Numbered Cans)		PGNAA (Even Serial Numbered Cans)	
Part # or Can Lot#	Companion Sample Can [a]	After Casting Weight	Cured Weight	LOD Weight	Cured Density (lb/ft^3)	Calculated LOD%	Pass Or Fail per Sec. 3.3.9.3	PGNAA (PMN) [c]	Pass Or Fail
Complied by					Comments				

a For the same lot of sample cans, it is acceptable to use an average weight of ten can bodies and ten can lids.

b Recommended vibration settings are at 450 VPM and three times the total vibrated weight. The total vibrated weight is the finish cast part and fixtures weight, for a setting of approximately 5 pound-force.

c Record the PGNAA Measurement Number (PMN) from Form AD for each Companion Sample Can tested.

$$Density = \left(\frac{Cured - Empty}{WithWater - Empty}\right) \times 62.3 \text{ lb/ft}^3$$

$$\text{LOD\%} = \left[1 - \frac{(LODWeight - Empty - 0.024)}{(Cured \,\&\, Clean - Empty)}\right] \times 100\%$$

EXEMPT FROM IO-155 (8-02)

FORM AA PGNAA Tooling Setup Control **Rev G Page 1 of 1**

Inspecting Company Name	Casting Company Name
PGNAA Tooling Setup Number [a]	277-4 Baseline Can Serial Number

Setup Distance [b]			Counts			Count Time (sec)	Net Count Rate (Net Counts/Sec)
#	Collimator	Detector	Gross	Compton	Net		

Describe the source and the amount of cadmium, lead and polyethylene surrounding the source for each Setup Number.

Describe the Software used and method to generate the net counts.

Operator

[a] A 10-digit PGNAA Tooling Setup Number shall be used to define the date and the time of setup using the format with a 24-hour clock (i.e., 1021041515 is used for October 21, 2004 at 3:15 pm). A –# will define the setup used for testing.

[b] The 10-oz. double friction metal lid or crimp style can lid shall face the source. The setup distances shall be measured from the can lid to the collimator face and from the can lid to the detector front face and must be documented to be repeatable to ±0.13". Also define all thickness of lead and polyethylene surrounding the source measurement to ±0.13".

[c] Use one 277-4 cast 10-oz. double friction metal can per drawing M2E801580A026 or 10-oz. crimp style can per drawing M2E801580A043 as the PGNAA reference to verify the Tooling Setup.

FORM AB PGNAA Standard Setup **Rev G Page 1 of 1**

Inspecting Company Name	Casting Company Name
PGNAA Standard Setup [a]	PGNAA Tooling Setup Number (with −#)

277-4 Standard Can Serial Numbers		Counts			Count Time (sec)	Net Count Rate (Net Counts/Sec)
		Gross	Compton	Net		
1						
2						
3						
4						
5						
6						
7						
8						
9						
10						
11						
12						
13						
14						
15						
16						
17						
18						
19						
20						
Average Values						

Comments

Operator

a A 10-digit PGNAA Standard Setup Number shall be used to define the date and the time of setup using the format with a 24-hour clock (i.e., 1021041515 is used for October 21, 2004 at 3:15 pm).

b The 10-oz. double friction metal can lid or 10-oz. crimp style can lid shall face the source following the PGNAA Standard Setup.

FORM AC PGNAA Daily Standard Setup Control **Rev G** **Page 1 of 1**

Inspecting Company Name	Casting Company Name
PGNAA Daily Standard Setup [a]	PGNAA Tooling Setup Number (with −#)

277-4 Standard Can Serial Numbers [b]		Counts			Count Time (sec)	Net Count Rate (Net Counts/Sec)
		Gross	Compton	Net		
1						
2						
3						
4						
5						
Average Values						
Standard Deviation						
3 × Standard Deviation						
(Pass Rate) Minimum Acceptable Net Count Rate = Average − 3 × Standard Deviation =						

Comments

Operator

[a] A 10-digit PGNAA Daily Standard Setup (DSS) shall be used to define the date and the time of setup using the format with a 24-hour clock (i.e., 1021041515 is used for October 21, 2004 at 3:15 pm).

[b] Select five PGNAA acceptance standards from Form AB as the Daily Standard Setup that generate approximately the same average and standard deviation as on Form AB.

FORM AD PGNAA Measurements **Rev G Page 1 of 1**

Inspecting Company Name	Casting Company Name

PGNAA Measurement Number (PMN) [a]	PGNAA Daily Standard Setup Num.	PGNAA Pass Rate (Net Cnt/Sec)

Even Serial Numbers [b]		Counts (Cnt)			Count Time (sec)	Net Cnt Rate (NetCnt/Sec)	Pass or Fail
Drum/Neutron Absorber Form/Lot#	Sample #	Gross	Compton	Net			

Comments

Operator

[a] A 10-digit PGNAA Measurement Number (PMN) shall be used to define the date and the time of setup using the format with a 24-hour clock (i.e., 1021041515 is used for October 21, 2004 at 3:15 pm).

[b] Record the Body Weldment, Neutron Absorber Form, or Heavy Can Spacer Assembly can lot with the Companion Sample Number.

EQUIPMENT SPECIFICATION	Specification Number JS-YMN3-801580-A005-1	Revision G
	Issue Date 2/17/2005	Revision Date 08/31/2009
		Page 1 of 1

MANUFACTURER'S DATA REQUIREMENTS

Item No.	Data Submittal—Purpose and Description	Specification or Reference	Number of Copies	Form[a]	
	OFFER APPRAISAL DATA - Subcontractor				
	The Offerer shall submit the following data with the offer.				
1	Subcontractor's quality assurance program manual	4.1	1	E	

[a]Indicate the following:

A—Full-size prints
B—Full-size reproducibles
C—Microfilm aperture card
D—Manual (booklet, brochure, report, etc.)
E—Other (Specify) Subcontractor's standard form
F—Other (Specify) Specimen

EQUIPMENT SPECIFICATION	Specification Number JS-YMN3-801580-A005-2	Revision G
	Issue Date 2/17/2005	Revision Date 08/31/2009
		Page 1 of 1

MANUFACTURER'S DATA REQUIREMENTS

Item No.	Data Submittal—Purpose and Description	Specification or Reference	Number of Copies	Form[a]	
	APPROVAL DATA - Subcontractor				
	The Subcontractor shall provide the following data prior to the start of production casting.				
1	Process equipment approval	3.1	1	E	
2	Scale Certifications	3.2.1	1	E	
3	Request for Company approved equal	3.2.2, 3.2.6, 3.2.7, 6.4	1	E	
4	MSDS for cleaning products	3.4.1	1	E	
5	Procedures	4.2.4	1	E	

[a]Indicate the following:

A—Full-size prints
B—Full-size reproducibles
C—Microfilm aperture card
D—Manual (booklet, brochure, report, etc.)
E—Other (Specify) Subcontractor's standard form
F—Other (Specify)
S—Sample of Workmanship

EQUIPMENT SPECIFICATION	Specification Number JS-YMN3-801580-A005-3		Revision G
	Issue Date 2/17/2005	Revision Date 08/31/2009	
		Page 1 of 1	

MANUFACTURER'S DATA REQUIREMENTS

Item No.	Data Submittal—Purpose and Description	Specification or Reference	Number of Copies	Form[a]	
	CERTIFIED DATA - Subcontractor				
	Item 1 shall be provided prior to the start of production casting.				
1	Approved procedures	4.2.4	1	E	
	Item 2 shall be provided with each ES-3100 unit.				
2	ES−3100 Documentation Package	4.2.1	1	E	

[a]Indicate the following:

A—Full-size prints
B—Full-size reproducibles
C—Microfilm aperture card
D—Manual (booklet, brochure, report, etc.)
E—Other (Specify) Subcontractor's standard form
F—Other (Specify)
S—Sample of Workmanship

EQUIPMENT SPECIFICATION	Specification Number JS-YMN3-801580-A005-4	Revision G
	Issue Date 2/17/2005	Revision Date 08/31/2009
		Page 1 of 1

MANUFACTURER'S DATA REQUIREMENTS

Item No.	Data Submittal—Purpose and Description	Specification or Reference	Number of Copies	Form[a]	
	OFFER APPRAISAL DATA – PGNAA Subcontractor				
	The Offerer shall submit the following data with the offer.				
1	Subcontractor's quality assurance program manual	4.1	1	E	

[a]Indicate the following:

A—Full-size prints
B—Full-size reproducibles
C—Microfilm aperture card
D—Manual (booklet, brochure, report, etc.)
E—Other (Specify) Subcontractor's standard form
F—Other (Specify) Specimen

EQUIPMENT SPECIFICATION	Specification Number JS-YMN3-801580-A005-5	Revision G
	Issue Date 2/17/2005	Revision Date 08/31/2009
		Page 1 of 1

MANUFACTURER'S DATA REQUIREMENTS

Item No.	Data Submittal—Purpose and Description	Specification or Reference	Number of Copies	Form[a]	
	APPROVAL DATA – PGNAA Subcontractor				
	The Subcontractor shall provide the following data prior to the start of production inspection.				
1	Source, detector, and software must be certified to a national standard.	A.6.1	1	E	
2	Final tooling setup shall be manufactured - Results of final tooling setup dimensional inspection shall be provided showing repeatability to +/- 0.13" - As built drawing of final tooling setup that was manufactured shall be provided showing setup distances and materials of construction	A.6.2	1	E	
3	Results of Net Count Rate Measurements performed on manufactured final tooling setup per section A.3.1.a of specification, based upon at least a 20 hour PGNAA measurement count and time justification.	A.6.3	1	E	
4	Software used to determine net count rate and methodology used to determine net count rate shall be identified and documented	A.6.4	1	E	
5	Completed Forms AA	A.6.5	1	E	
6	Completed Forms AB, and AC	A.6.5	1	E	

[a]Indicate the following:

A—Full-size prints
B—Full-size reproducibles
C—Microfilm aperture card
D—Manual (booklet, brochure, report, etc.)
E—Other (Specify) Subcontractor's standard form
F—Other (Specify)
S—Sample of Workmanship

EQUIPMENT SPECIFICATION	Specification Number JS-YMN3-801580-A005-6		Revision G
	Issue Date 2/17/2005	Revision Date 08/31/2009	
		Page 1 of 1	

MANUFACTURER'S DATA REQUIREMENTS

Item No.	Data Submittal—Purpose and Description	Specification or Reference	Number of Copies	Form[a]	
	CERTIFIED DATA - PGNAA Subcontractor				
	Item 1 and 2 shall be provided prior to the start of production PGNAA inspection.				
1	PGNAA national standard	A.6.1	1	E	
2	PGNAA measurement software and methodology	A.6.4	1	E	
	Item 3 shall be provided after each companion can lot is inspected.				
3	Forms AC and AD	A.6.5	2 (1 copy going to Casting Company)	E	

[a]Indicate the following:

A—Full-size prints
B—Full-size reproducibles
C—Microfilm aperture card
D—Manual (booklet, brochure, report, etc.)
E—Other (Specify) Subcontractor's standard form
F—Other (Specify)
S—Sample of Workmanship

THIS PAGE INTENTIONALLY LEFT BLANK.

Appendix 1.4.6

PACKAGE CATEGORY DETERMINATION

THIS PAGE INTENTIONALLY LEFT BLANK.

Appendix 1.4.6

PACKAGE CATEGORY DETERMINATION

The ES-3100 with HEU content package has a maximum activity of 0.3243 TBq (8.76 Ci) at 10 y after initial fabrication; the maximum number of A_2s carried is 294.00 at 70 y after initial fabrication (Table 4.4). Based on the guidance from Regulatory Guide 7.11, *Fracture Toughness Criteria of Base Material for Ferritic Steel Shipping Cask Containment Vessels with a Maximum Wall Thickness of 4 Inches (0.1 m)*, this package is classified in Table 1.1 of NUREG-1609 as a Category II package.

THIS PAGE INTENTIONALLY LEFT BLANK.

Appendix 1.4.7

HEU OXIDE MATERIAL SPECIFICATION AS PROVIDED BY Y-12 HIGHLY ENRICHED URANIUM DISPOSITION PROGRAM OFFICE

THIS PAGE INTENTIONALLY LEFT BLANK.

Uranium oxide material limits

Specified item	Units	Limit	Group 1	Group 2	Group 3	Group 4	Group 5	Group 6	Group 7
Chemical form [a]			UO_x	UO_x	UO_x	U_3O_8	UO_x	UO_x	U_3O_8
Physical form			Dense, loose powder, may contain lumps						
Uranium content									
Uranium purity	gU/gSmpl	≥	0.830	0.200	0.830	0.830	0.200	0.200	0.845
U-235	g/gU	≤	97.7%	97.7%	97.7%	97.7%	97.7%	97.7%	93.2%
U-238	g/gU	≤	80.0%	80.0%	80.0%	80.0%	80.0%	80.0%	80.0%
U-232	µg/gU	≤	0.040	0.040	0.040	0.040	0.040	0.040	0.040
U-233	µg/gU	≤	50	50	50	50	50	200	50
U-234	g/gU	≤	1.4%	1.4%	1.4%	1.4%	1.4%	2.0%	1.4%
U-236	g/gU	≤	1.0%	1.0%	1.0%	1.0%	1.0%	40.0%	1.0%
Transuranics (Np, Pu, Am, etc.)									
Concentration limit	µg/gU	≤	0.2	0.2	40.0	0.2	0.5	0.5	0.2
Activity limit	Bq/gU	≤	50	50	600,000	3,000	5,000	1,000	3,000
Unspecified beta emitters									
Activity limit	Bq/gU	≤	200	200	200	200	1,000,000[c]	10,000	200
Moisture	g/gSmpl	≤	6%	6%	6%	6%	6%	6%	6%
Carbon	µg/gU	≤	600	1,000	600	600	1,000	1,000	[d]
EBC [b]	µgEBC/gU	≤	4	10,000	4	4	10,000	10,000	4

[a] UO_x may be UO_2 or UO_3.

[b] EBC = equivalent boron content, as defined in ASTM standard C1233-98.

[c] The oxide contents of the ES-3100 were characterized with the beta emitters as an "unspecified" feature in order to establish one group limit for these nuclides rather than limits on each (of many) individual nuclides. The beta emitters are either daughter products from the decay of uranium isotopes, or activation and fission products from reprocessed material. The beta nuclides most often seen in this material are Tc-99, Sr-90, and Cs-137. Table 1.4.7-1 gives a complete list of the beta-emitting nuclides that have been observed in various oxides intended for shipment in the ES-3100. The maximum mass concentration allowable by the 1,000,000 Bq/gU activity limit is for Group 5 oxides.

[d] In this case, the total carbon allowed per ES-3100 container is 921 g.

Table 1.4.7-1

Radionuclide Reference Data - Beta Nuclides

Isotope				Specific Activity Calculation			Rad	Mass Conc at 10^6 Bq/gU
Element	Sym	At #	Iso	Mass	T½, Yr	SA, Bq/g	Type	µg/gU
Cobalt	Co	27	58	57.935755	0.194	1.177E+15	ß+	8.500E-04
Cobalt	Co	27	60	59.933819	5.271	4.187E+13	ß-	0.024
Strontium	Sr	38	90	89.907738	29.100	5.056E+12	ß-	0.198
Zirconium	Zr	40	95	94.908042	0.175	7.951E+14	ß-	0.001
Niobium	Nb	41	95	94.906835	0.096	1.456E+15	ß-	6.870E-04
Technetium	Tc	43	99	98.906254	2.130E+05	6.279E+08	ß-	1,592.656
Ruthenium	Ru	44	103	102.906323	0.108	1.196E+15	ß-	8.365E-04
Ruthenium	Ru	44	106	105.907321	1.020	1.224E+14	ß-	0.008
Antimony	Sb	51	125	124.905252	2.758	3.840E+13	ß-	0.026
Cesium	Cs	55	134	133.906696	2.065	4.784E+13	ß-	0.021
Cesium	Cs	55	137	136.907073	30.300	3.189E+12	ß-	0.314
Cerium	Ce	58	141	140.908271	0.089	1.055E+15	ß-	9.479E-04
Cerium	Ce	58	144	143.913643	0.779	1.180E+14	ß-	0.008
Europium	Eu	63	155	154.922889	4.710	1.813E+13	ß-	0.055
Thallium	Tl	81	208	207.981988	5.805E-06	1.096E+19	ß-	9.127E-08
Thallium	Tl	81	209	208.985334	4.183E-06	1.513E+19	ß-	6.609E-08
Lead	Pb	82	209	208.981065	3.708E-04	1.707E+17	ß-	5.858E-06
Lead	Pb	82	210	209.984163	22.600	2.787E+12	ß-	0.359
Lead	Pb	82	211	210.988735	6.864E-05	9.134E+17	ß-	1.095E-06
Lead	Pb	82	212	211.991871	0.001	5.141E+16	ß-	1.945E-05
Lead	Pb	82	214	213.999798	5.134E-05	1.204E+18	ß-	8.305E-07
Bismuth	Bi	83	210	209.984095	0.014	4.592E+15	ß-	2.178E-04
Bismuth	Bi	83	211	210.987255	4.069E-06	1.541E+19	ß-,a	6.490E-08
Bismuth	Bi	83	212	211.991255	1.151E-04	5.421E+17	ß-,a	1.845E-06
Bismuth	Bi	83	213	212.994359	8.670E-05	7.163E+17	ß-,a	1.396E-06
Bismuth	Bi	83	214	213.998691	3.784E-05	1.634E+18	ß-	6.121E-07
Thorium	Th	90	231	231.036298	0.003	1.967E+16	ß-	5.083E-05
Thorium	Th	90	234	234.043593	0.066	8.565E+14	ß-	0.001
Protactinium	Pa	91	234m	234.043303	2.225E-06	2.541E+19	ß-	3.936E-08

Appendix 1.4.8

DETAILED ENGINEERING DRAWINGS

Drawing No.	Rev.	Title
M2E801580A001	B	Drum Assembly
M2E801580A002	B	Body Weldment
M2E801580A003	B	Inner Liner Weldment (2 sheets)
M2E801580A004	B	Double Open Head Reinforced Drum
M2E801580A005	D	Misc. Details
M2E801580A006	B	Drum Lid Weldment
M2E801580A007	B	18.25" Diameter Drum Lid
M2E801580A008	B	Top Plug Weldment
M2E801580A009	C	Pad Details
M2E801580A010	D	Data Plate Details
M2E801580A011	C	Containment Vessel Assembly
M2E801580A012	C	Containment Vessel Body Assembly (2 sheets)
M2E801580A013	B	Containment Vessel O-ring Details
M2E801580A014	B	Containment Vessel Lid Assembly
M2E801580A015	C	Containment Vessel Sealing Lid
M2E801580A016	B	Containment Vessel Closure Nut
M2E801580A024	B	Containment Vessel Vibration Absorbing Silicone 4.25” Can Pad
M2E801580A026	C	Heavy Can Spacer Assembly
M2E801580A031	D	Main Assembly
M2E801580A043	0	Heavy Can Spacer Assembly (SST)

THIS PAGE INTENTIONALLY LEFT BLANK.

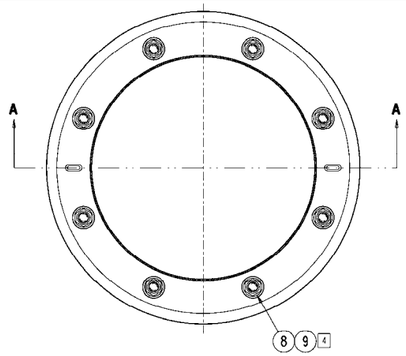

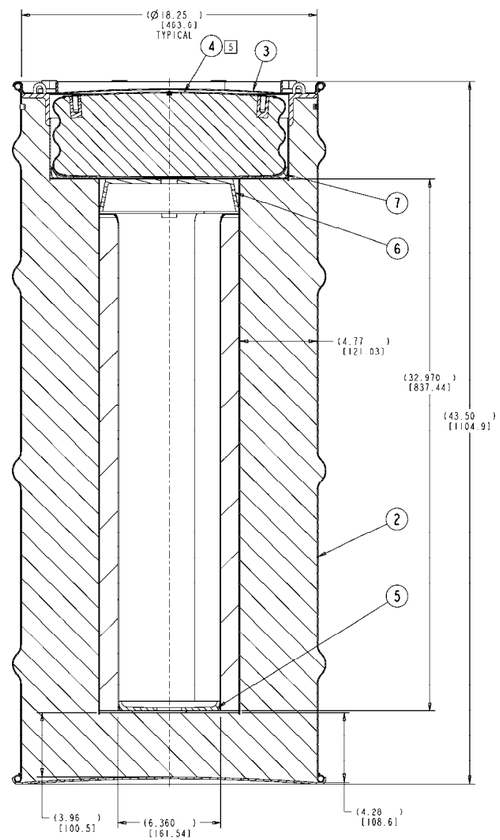

SECTION A-A

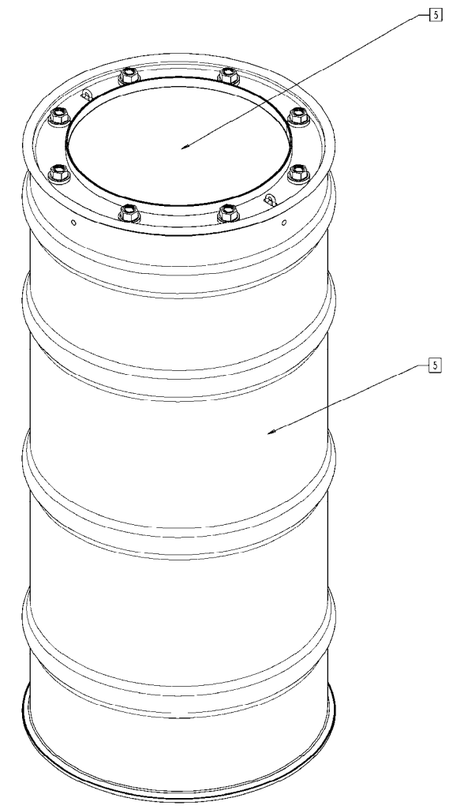

ISOMETRIC VIEW

NOTES

1 INTERPRET DRAWING PER ENGINEERING DRAFTING STANDARD ES-3.1.

2 INTERPRET DIMENSIONS AND TOLERANCES PER ASME Y14.5M-1994.

3 DIMENSIONS ARE IN INCHES [mm]. THE [mm] ARE ONLY FOR REFERENCE.

B 4 TORQUE HEX NUTS TO 30±5 ft-lb AT ASSEMBLY.

5 IN APPROXIMATE LOCATIONS SHOWN, USING BLACK ENAMEL PAINT (F/N 10), PAINT DRAWING NUMBER, REVISION LETTER AND FIVE DIGIT SERIAL NUMBER IN 1.00" HIGH CHARACTERS ON F/N 2, F/N 3, AND F/N 4.

6. FOR ADDITIONAL REQUIREMENTS SEE EQUIPMENT SPECIFICATION JS-YMN3-801580-A002.

B 7 FOR REF. ONLY APPROXIMATE WEIGHT: 289.2 LBS [131.2 Kg].

5	AR		PAINT, BLACK ENAMEL		FED SPEC 595B-17038	10
B 4	8	M2E801580A005-3	DRUM HEX NUT			9
	8	M2E801580A005-4	DRUM WASHER			8
	1	M2E801580A009-3	PLUG PAD			7
	1	M2E801580A009-2	CV FLANGE PAD			6
	1	M2E801580A009-1	CV BOTTOM PAD			5
	1	M2E801580A008-1	TOP PLUG WELDMENT			4
	1	M2E801580A006-1	DRUM LID WELDMENT			3
	1	M2E801580A002-1	BODY WELDMENT			2
AR		-1	DRUM ASSEMBLY			1
MATERIAL CODE		PART OR IDENTIFYING NO	NOMENCLATURE OR DESCRIPTION	MATERIAL	SPECIFICATION	FIND NO
		QTY REQ'D NEXT ASSEMBLY	PARTS LIST			

-1 DRUM ASSEMBLY

SCALE 3/8

THIS DRAWING INCLUDES FEATURES SUPPORTING NUCLEAR CRITICALITY SAFETY. ANY REVISION TO THIS DIAGRAM REQUIRES NUCLEAR CRITICALITY SAFETY DIVISION APPROVAL.

REVISION	DATE	NCSD APPROVAL
B	2/10/05	JF DECLUE

This document has been reviewed by a Y-12 ADC and UCNI RO and has been determined to be UNCLASSIFIED and not UCNI. This review does not constitute clearance for public release.

Name: ROGER D. AIGNER Date: 2/10/05

REV	DESCRIPTION	DRW	CHKR	DE	DVR	DM	DATE	PE	DATE	PM	DATE
B	GEN REV; TORQUE IN NOTE 4 WAS 10 +/- 1 REVISED NOTES 4 & 7; F/N 8 & 9 WAS VENDOR SUPPLIED MOVED NUT & WASHER DETAILS TO A005.	JRP	SMM	GAB	RDA	DPS	11/13/03	MRF	11/29/03	GAB	2/10/05
A	ISSUED FOR PROTOTYPE PROCUREMENT	JRJ	JSL	GAB	JLH	JCW	10/25/03	MRF	10/29/03	DBM	10/29/03

REVISION OR ISSUE PURPOSE — REVISION APPROVALS — SQUAD CHECK: AR CV ST HV EM FP FD EG IE M NP

DRAWING APPROVALS		DATE
DRW	JR JACKSON	10/29/03
CHKR	JS LOWERY	10/29/03
DE	GA BYINGTON	10/29/03
DVR	JL HECK	10/29/03
DM	JC WALLS	10/29/03
PE	MR FELDMAN	10/29/03
PM	DB MILLER	10/29/03

SCALE: NOTED

TOLERANCES UNLESS OTHERWISE SPECIFIED: FRACTIONS; XX DECIMALS; XXX DECIMALS; ANGLES; BREAK SHARP EDGES .06 MAX; FINISH

BWXT Y-12 — Y-12 National Security Complex managed by BWXT Y-12, L.L.C. for the Department of Energy under U.S. Government contract DE-AC05-00OR22800 • Oak Ridge, Tennessee •

PROJECT NAME: ES-3100 SHIPPING PACKAGE

DRUM ASSEMBLY

1	48	49	50	PLANT	BLDG	FL	SH.	OF	TYPE	CLASS
6	M	L	F	Y-12	NA	NA	1	1	A	U

A1	52	53	REV
CM	PKG	IN	M2E801580A001 B

M2E801580A001

NO REPRESENTATION OR WARRANTY, EXPRESSED OR IMPLIED, IS MADE AS TO THE ACCURACY, COMPLETENESS OR USEFULNESS OF THE INFORMATION OR STATEMENTS CONTAINED IN THESE DRAWINGS, OR THAT THE USE OR DISCLOSURE OF ANY INFORMATION, APPARATUS, METHOD, OR PROCESS DISCLOSED IN THESE DRAWINGS MAY NOT INFRINGE PRIVATE RIGHTS OF OTHERS. NO LIABILITY IS ASSUMED WITH RESPECT TO THE USE OF, OR FOR DAMAGES RESULTING FROM THE USE OF ANY INFORMATION, APPARATUS, METHOD OR PROCESS DISCLOSED IN THESE DRAWINGS. DRAWINGS MADE AVAILABLE FOR INFORMATION OR BIDDER USE ARE NOT TO BE USED FOR OTHER PURPOSES AND ARE TO BE RETURNED UPON REQUEST OF THE FORWARDING CONTRACTOR.

P THIS DRAWING PRODUCED ON PRO/ENGINEER

THIS PAGE INTENTIONALLY LEFT BLANK.

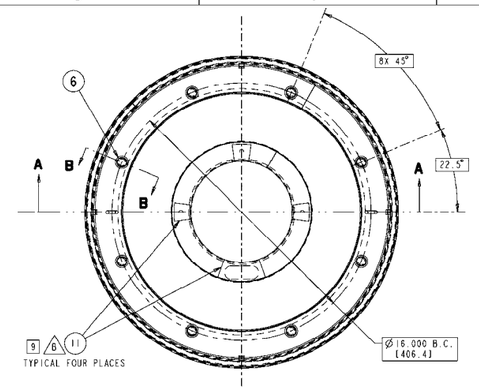

-1 BODY WELDMENT
SCALE 3/8

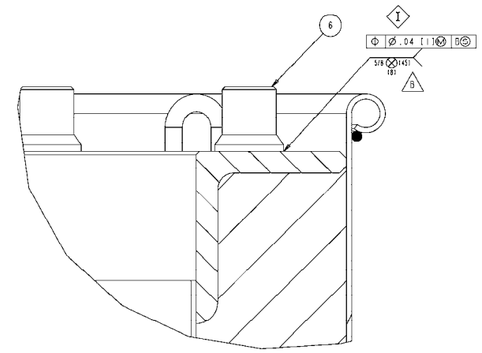

SECTION B-B
SCALE 2/1

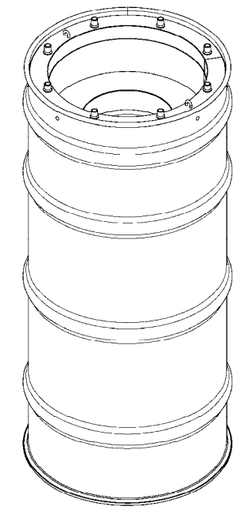

ISOMETRIC VIEW
SCALE 1/4

NOTES

1. INTERPRET DRAWING PER MECHANICAL DRAFTING STANDARD ES-3.1.
2. INTERPRET DIMENSIONS AND TOLERANCES PER ASME Y14.5M-1994.
3. DIMENSIONS ARE IN INCHES [mm].
4. OD OF ANGLE TURNED TO ID OF DRUM AT ASSEMBLY.
5. WELDING SYMBOLS SHALL BE INTERPRETED IN ACCORDANCE WITH AWS A2.4.
6. FOR ADDITIONAL REQUIREMENTS SEE EQUIPMENT SPECIFICATION JS-YMN3-801580-A002. (9)
7. DIMENSIONS AND FEATURES FLAGGED BY A (I) SYMBOL SHALL BE INSPECTED AND DOCUMENTED.
8. SEE EQUIPMENT SPECIFICATION JS-YMN3-801580-A003 FOR REQUIREMENTS OF KAOLITE PROCESSING.
9. SEE EQUIPMENT SPECIFICATION JS-YMN3-801580-A005 FOR REQUIREMENTS OF CATALOG 277-4 PROCESSING AND APPLYING THE F/N 11 OVER FILL/VENT HOLES. (8)(9)
10. FOR REFERENCE ONLY APPROXIMATE WEIGHT: 259.7 LBS [117.8 Kg] (9)

KAOLITE:
VOLUME: 4.82 CU. FT.
DENSITY: 22.4 LBS/CU. FT.
WEIGHT: 108.0 LBS [49.0 Kg]

CATALOG 277-4:
VOLUME: 0.466 CU. FT.
DENSITY: 105.0 LBS/CU. FT.
WEIGHT: 48.89 LBS [22.18 Kg]

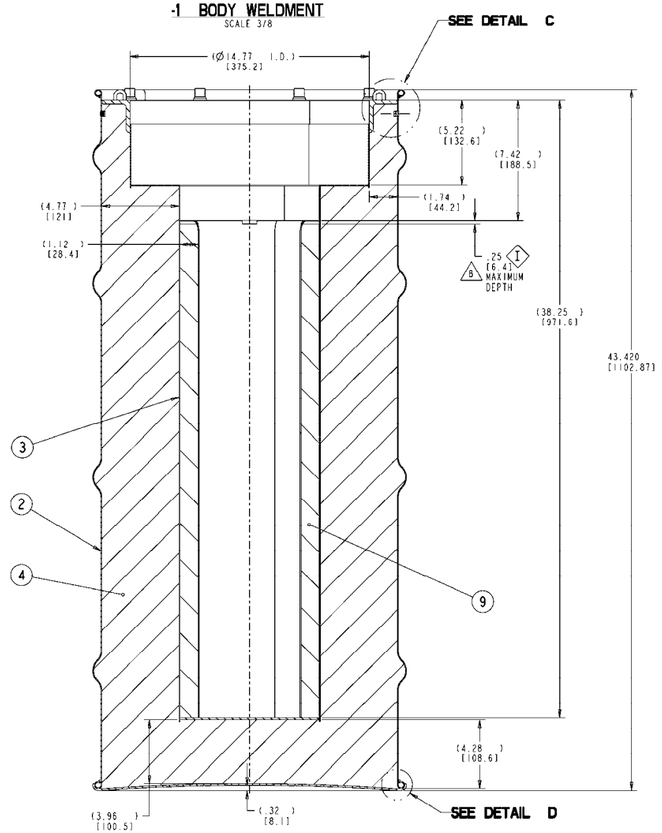

SECTION A-A
SCALE 3/8

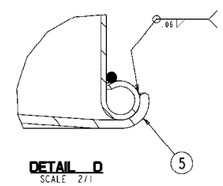

DETAIL D
SCALE 2/1

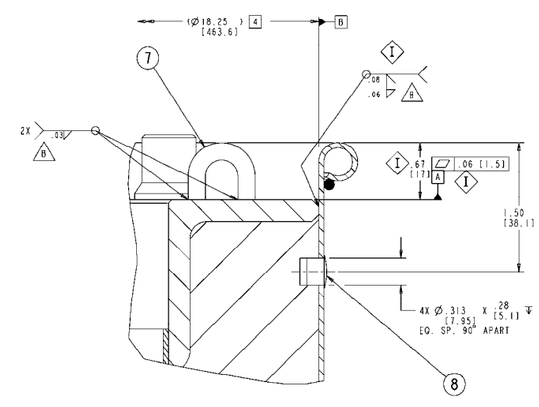

DETAIL C
SCALE 2/1

9	AR	7616A21 OR EQUAL	LOW TEMPERATURE (-40° to +250°F)	ALUMINUM FOIL DUCT TAPE 2" WIDE	McMASTER- CARR ATLANTA, GA	11
	AR		WELD FILLER METAL	PER WELD PROCEDURES		10
9	AR	-9	CATALOG NO. 277-4	THERMO ELECTRON CORP., THERMOREAX, 504 AIRPORT ROAD, SANTA FE, NM 87507 PHONE 505-428-3508, FAX 505-428-3535		9
	4	62MP0312 OR EQUAL	PLUG, NYLON 6/6	MICRO PLASTIC INC. FLIPPIN, AR 72634		8
	2	M2E801580A005-2	TID LUG			7
	8	ARC FT 5/8-11 X 7/8 LG	ARC WELD STUD	304 / 304L SST	ASTM A493 OR ASTM F593	6
	1	M2E801580A005-1	DRUM FLAT COVER			5
8	AR	-4	KAOLITE 1600 VIBRATED CAST	THERMAL CERAMICS AUGUSTA, GA 30903-0923		4
	1	M2E801580A003-1	INNER LINER WELDMENT			3
	1	M2E801580A004-1	DOUBLE OPEN HEAD REINFORCED DRUM			2
AR	X	-1	BODY WELDMENT			1
MATERIAL LIST NOTE		PART OR IDENTIFYING NO	NOMENCLATURE OR DESCRIPTION	MATERIAL	SPECIFICATION	FIND NO
		QTY REQ'D NEXT ASSEMBLY	PARTS LIST			

THIS DRAWING INCLUDES FEATURES SUPPORTING NUCLEAR CRITICALITY SAFETY. ANY REVISION TO THIS DIAGRAM REQUIRES NUCLEAR CRITICALITY SAFETY DIVISION APPROVAL.

REVISION	DATE	NCSD APPROVAL
B	2/10/05	JF DECLUE

This document has been reviewed by a Y-12 ADC and UCNI RO and has been determined to be UNCLASSIFIED and not UCNI. This review does not constitute clearance for public release.

Name: ROGER D. AIGNER Date: 2/10/05

NO REPRESENTATION OR WARRANTY, EXPRESSED OR IMPLIED, IS MADE AS TO THE ACCURACY, COMPLETENESS OR USEFULNESS OF THE INFORMATION OR STATEMENTS CONTAINED IN THESE DRAWINGS, OR THAT THE USE OR DISCLOSURE OF ANY INFORMATION, APPARATUS, METHOD, OR PROCESS DISCLOSED IN THESE DRAWINGS MAY NOT INFRINGE PRIVATE RIGHTS OF OTHERS. NO LIABILITY IS ASSUMED WITH RESPECT TO THE USE OF, OR FOR DAMAGES RESULTING FROM THE USE OF ANY INFORMATION, APPARATUS, METHOD OR PROCESS DISCLOSED IN THESE DRAWINGS. DRAWINGS MADE AVAILABLE FOR INFORMATION TO BIDDER ARE NOT TO BE USED FOR OTHER PURPOSES AND ARE TO BE RETURNED UPON REQUEST OF THE FORWARDING CONTRACTOR.

PTHIS DRAWING PRODUCED ON PRO/ENGINEER

REV	DESCRIPTION	DRW	CHKR	DE	DVR	DM	DATE	PE	DATE	PM	DATE	WE	DATE	AR	CV	ST	MV	EM	FP	PD	EE	IE	M	NP
B	GEN REV ADDED F/N 11, 5/8 WAS 1/2, F/N 9 WAS BOROBOND 4; MOD. GEN. NOTE 9; MOD. WELD SYMS. IN DET. C; MOD. WTS AND VOLS. IN NOTE 10	JRP	SMM	GAB	RDA	DPS	HEBG	GAB	2/18/05	JGA	2/18/05	DJE	2/11/05											
A	ISSUED FOR PROTOTYPE PROCUREMENT	JRJ	JSL	GAB	JLH	JCW	10/29/03	MRF	10/29/03	DBM	10/29/03													

REVISION OR ISSUE PURPOSE — REVISION APPROVALS — SQUAD CHECK

SCALE: NOTED	DRW J.R. JACKSON	10/29/03
TOLERANCES UNLESS OTHERWISE SPECIFIED	CHKR J.S. LOWERY	10/29/03
	DE G.A. BYINGTON	10/29/03
	DVR J.L. HECK	10/29/03
FRACTIONS	DM J.C. WALLS	10/29/03
XX DECIMALS ±.03	PE M.R. FELDMAN	10/29/03
XXX DECIMALS ±.005	PM D.B. MILLER	10/29/03
ANGLES ±0.5°		
BREAK SHARP EDGES .06 MAX		
FINISH 125 RMS		

DRAWING APPROVALS

BWXT Y-12 National Security Complex managed by BWXT Y-12, L.L.C. for the Department of Energy under U.S. Government contract DE-AC05-00OR22800 a BWXT Babcock & Wilcox Company, Oak Ridge, Tennessee

PROJECT NAME: ES-3100 SHIPPING PACKAGE

BODY WELDMENT

1	48	49	50	PLANT	BLDG	TL	SH.	OF	TYPE	CLASS
6	M	L	F	Y-12	NA	NA	1	1	A	U
51		52		53						REV
CM		PKG		IN	M2E801580A002					B

M2E801580A002

THIS PAGE INTENTIONALLY LEFT BLANK.

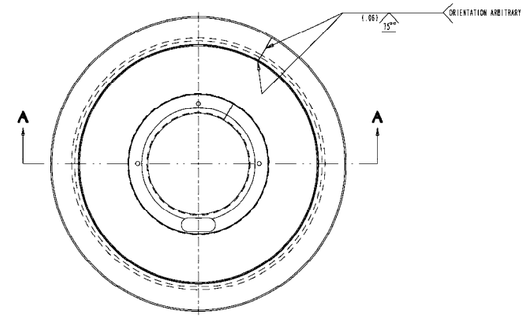

-1 INNER LINER WELDMENT

SCALE 3/8

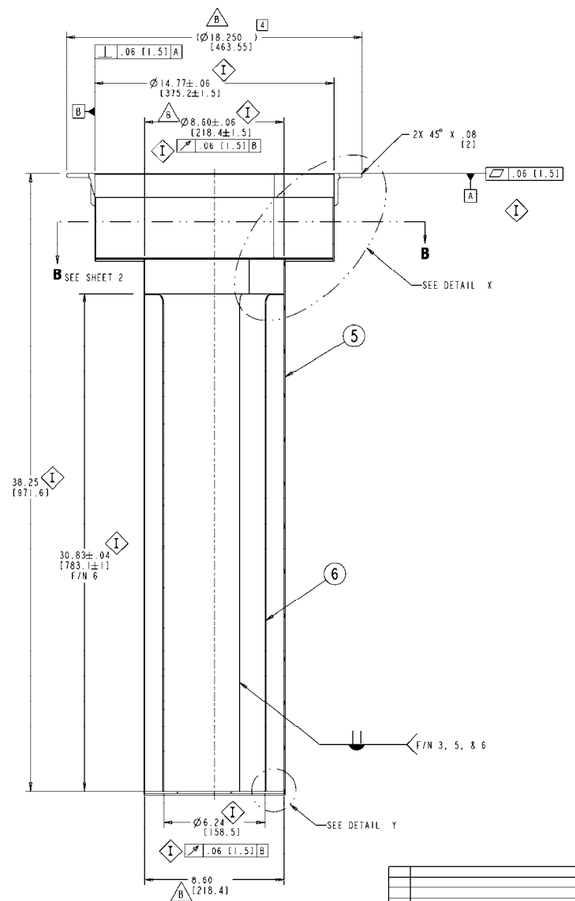

SECTION A-A

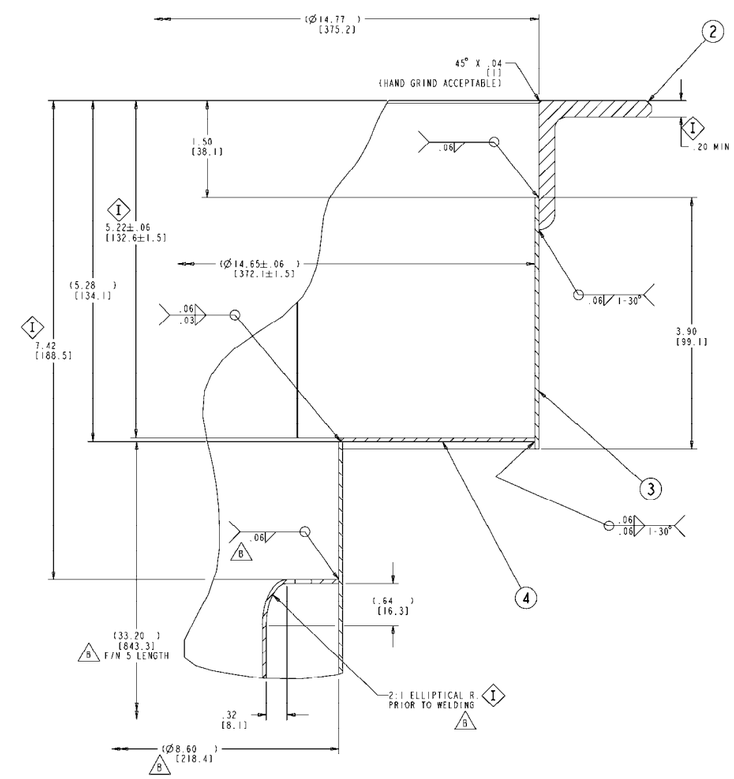

DETAIL X

SCALE 3/2

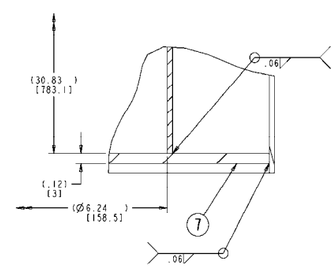

DETAIL Y

SCALE 2/1

NOTES

1. INTERPRET DRAWING PER MECHANICAL DRAFTING STANDARD ES-3.1.
2. INTERPRET DIMENSIONS AND TOLERANCES PER ASME Y14.5M-1994.
3. DIMENSIONS ARE IN INCHES [mm].
4. FINAL DIAMETER SET BY DRUM INSIDE DIAMETER, -.01 TO -.06 TOLERANCE.
5. FOR ADDITIONAL REQUIREMENTS SEE EQUIPMENT SPECIFICATION J5-YMN3-801580-A002.
6. DIMENSIONS AND FEATURES FLAGGED BY A (I) SYMBOL SHALL BE INSPECTED AND DOCUMENTED.
7. WELDING SYMBOLS SHALL BE INTERPRETED IN ACCORDANCE WITH AWS A2.4.

QTY REQ'D NEXT ASSEMBLY	PART OR IDENTIFYING NO	NOMENCLATURE OR DESCRIPTION	MATERIAL	SPECIFICATION	FIND NO
AR		WELD FILLER METAL			8
1	-7	BOTTOM PLATE	11 GAGE SHEET 304/304L SST	ASME SA240	7
1	-6	LOWER INNER RING	16 GAGE SHEET 304/304L SST		6
1	-5	LOWER OUTER RING			5
1	-4	UPPER FLOOR PLATE			4
1	-3	UPPER OUTER RING			3
1	-2	2 X 2 X 1/4 ANGLE MODIFIED	304/304L SST	ASME SA479	2
AR	-1	INNER LINER WELDMENT			1

PARTS LIST

M2E801580A003

THIS DRAWING INCLUDES FEATURES SUPPORTING NUCLEAR CRITICALITY SAFETY. ANY REVISION TO THIS DIAGRAM REQUIRES NUCLEAR CRITICALITY SAFETY DIVISION APPROVAL.

REVISION	DATE	NCSD APPROVAL
B	2/10/05	JF DECLUE

This document has been reviewed by a Y-12 ADC and UCNI RO and has been determined to be UNCLASSIFIED and not UCNI. This review does not constitute clearance for public release.

Name: ROGER D. AIGNER Date: 2/10/05

REV	DESCRIPTION	DRW	CHKR	DE	DVR	DM	DATE	PE	DATE	PM	DATE	WE	DATE
B	DELETED F/N 7, RENUMBERED F/N 8 TO 7 AND F/N 9 TO 8. CHANGED F/N 5 Ø8.80 TO Ø8.60; LENGTH 2.14 TO 33.20. F/N 6 OD WAS Ø9.13 NOW Ø8.60. REMOVED NOTE #8.	JRP	SMM	GAB	RDA	DPS	11/18/05	GAB	2/10/05	JGA	2/10/05	DJE	2/11/05
A	ISSUED FOR PROTOTYPE PROCUREMENT	JRJ	JSL	GAB	JLH	JCW	10/29/03	MRF	10/29/03	DBM	10/29/03		

REVISION OR ISSUE PURPOSE — REVISION APPROVALS

SQUAD CHECK: AR CV ST HV EM FP FD EE IE M NP

DRAWING APPROVALS

		DATE
DRW	J.R. JACKSON	10/29/03
CHKR	J.S. LOWERY	10/29/03
DE	G.A. BYINGTON	10/29/03
DVR	J.L. HECK	10/29/03
DM	J.C. WALLS	10/29/03
PE	M.R. FELDMAN	10/29/03
PM	D.B. MILLER	10/29/03

SCALE: NOTED

TOLERANCES UNLESS OTHERWISE SPECIFIED: FRACTIONS ±.03; XX DECIMALS ±.03; XXX DECIMALS ±.005; ANGLES ±0.5°; BREAK SHARP EDGES .06 MAX; FINISH 125 RMS

BWXT Y-12 — Y-12 National Security Complex managed by BWXT Y-12, L.L.C. for the Department of Energy under U.S. Government contract DE-AC05-00OR22800 • Oak Ridge, Tennessee •

PROJECT NAME: ES-3100 SHIPPING PACKAGE

INNER LINER WELDMENT

I	48	49	50	PLANT	BLDG	FL	SH.	OF	TYPE	CLASS
6	M	L	F	Y-12	NA	NA	1	2	S	U

51	52	53		REV
CM	PKG	IN	M2E801580A003	B

NO REPRESENTATION OR WARRANTY, EXPRESSED OR IMPLIED, IS MADE AS TO THE ACCURACY, COMPLETENESS OR USEFULNESS OF THE INFORMATION OR STATEMENTS CONTAINED IN THESE DRAWINGS, OR THAT THE USE OR DISCLOSURE OF ANY INFORMATION, APPARATUS, METHOD, OR PROCESS DISCLOSED IN THESE DRAWINGS MAY NOT INFRINGE PRIVATE RIGHTS OF OTHERS. NO LIABILITY IS ASSUMED WITH RESPECT TO THE USE OF, OR FOR DAMAGES RESULTING FROM THE USE OF ANY INFORMATION, APPARATUS, METHOD OR PROCESS DISCLOSED IN THESE DRAWINGS. SUBMITTAL OF THESE DRAWINGS FOR INFORMATION TO BIDDER ARE NOT TO BE USED FOR OTHER PURPOSES AND ARE TO BE RETURNED UPON REQUEST OF THE FORWARDING CONTRACTOR.

THIS DRAWING PRODUCED ON PRO/ENGINEER

THIS PAGE INTENTIONALLY LEFT BLANK.

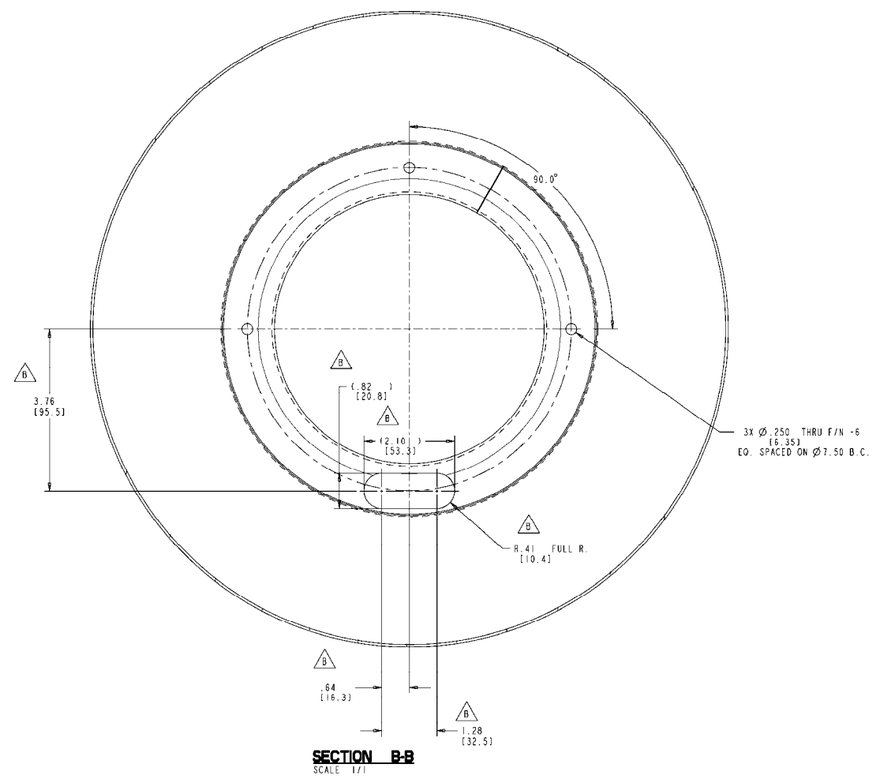

NO REPRESENTATION OR WARRANTY, EXPRESSED OR IMPLIED, IS MADE AS TO THE ACCURACY, COMPLETENESS OR USEFULNESS OF THE INFORMATION OR STATEMENTS CONTAINED IN THESE DRAWINGS, OR THAT THE USE OR DISCLOSURE OF ANY INFORMATION, APPARATUS, METHOD, OR PROCESS DISCLOSED IN THESE DRAWINGS MAY NOT INFRINGE PRIVATE RIGHTS OF OTHERS. NO LIABILITY IS ASSUMED WITH RESPECT TO THE USE OF, OR FOR DAMAGES RESULTING FROM THE USE OF ANY INFORMATION, APPARATUS, METHOD OR PROCESS DISCLOSED IN THESE DRAWINGS. DRAWINGS MADE AVAILABLE FOR INFORMATION TO BIDDER ARE NOT TO BE USED FOR OTHER PURPOSES AND ARE TO BE RETURNED UPON REQUEST OF THE FORWARDING CONTRACTOR.

THIS DRAWING PRODUCED ON PRO/ENGINEER

BWXT Y-12

Y-12 National Security Complex managed by BWXT Y-12, L.L.C. for the Department of Energy under U.S. Government contract DE-AC05-00OR22800
Oak Ridge, Tennessee

PROJECT NAME
ES-3100 SHIPPING PACKAGE

INNER LINER WELDMENT

I	AS	AS	SO	PLANT	BLDG	FL	SM	OF	TYPE	CLASS
6	M	L	F	Y-12	NA	NA	2	2	S	U
51		52		53						REV
CM		PKG		IN	M2E801580A003					B

M2E801580A003

THIS PAGE INTENTIONALLY LEFT BLANK.

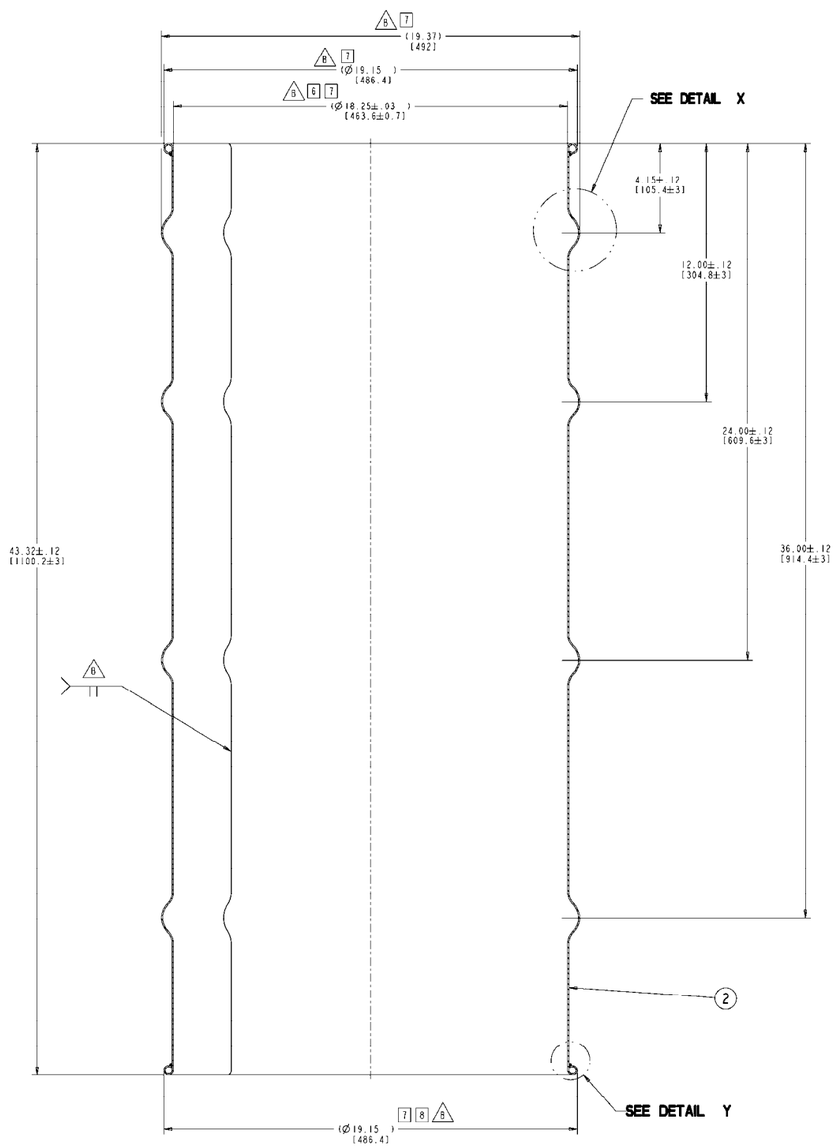

-1 DOUBLE OPEN HEAD REINFORCED DRUM

SCALE 1/2

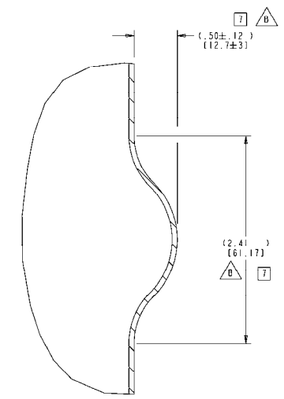

DETAIL X

SCALE 2/1
(4X)

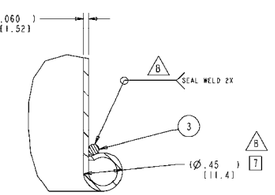

DETAIL Y

SCALE 2/1
(2 X)

NOTES

1. INTERPRET DRAWING PER MECHANICAL DRAFTING STANDARD ES-3.1.
2. INTERPRET DIMENSIONS AND TOLERANCES PER ASME Y14.5M-1994.
3. DIMENSIONS ARE IN INCHES.[mm].
4. WELDING SYMBOLS SHALL BE INTERPRETED IN ACCORDANCE WITH AWS A2.4.
5. FOR ADDITIONAL REQUIREMENTS SEE EQUIPMENT SPECIFICATION JS-YMN3-801580-A002.

6. INSPECT THE I.D. OF THE DRUM TO DETERMINE THE ACTUAL DIAMETER DIMENSION FOR FABRICATION INTERFACE WITH M2E801580A003. REFERENCE NOTE 4 ON DWG. M2E801580A002.

7. DRUM DIAMETERS, CORRUGATIONS, AND MANUFACTURING SHALL MEET THE REQUIREMENTS OF MILITARY STANDARD, MS27683-7 (DRUM, METAL SHIPPING AND STORAGE 16 TO 80 GALLS). THE SEAM WELD OF THE DOUBLE OPEN-HEAD DRUM SHALL BE TESTED BY APPLYING AN INTERNAL AIR PRESSURE TO 10 PSIG (MIL-D-6054F, PARAGRAPH 4.6.1 PROCEDURE B) AND BY CONDUCTING A ROUGH HANDLING TEST (MIL-D-6054F, PARAGRAPH 4.6.2).

8. INSPECT THE O.D. OF THE DRUM FOR INTERFACE DIMENSION WITH M2E801580A005-1, DRUM FLAT COVER. REFERENCE NOTE 5 ON DRAWING M2E801580A005.

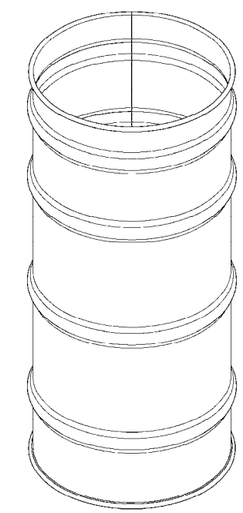

ISOMETRIC VIEW

SCALE 1/4

	AR		WELD FILLER METAL	PER WELD PROCEDURES		4
	AR	Ø1/8	WELD WIRE	ER308L	ASME SFA 5.9	3
7 8	1	-2	DRUM 16 GA (.0595)	304/304L SST	ASME SA240	2
	AR	-1	DOUBLE OPEN HEAD REINFORCED DRUM			1
M2E801580	1	PART OR IDENTIFYING NO	NOMENCLATURE OR DESCRIPTION	MATERIAL	SPECIFICATION	FIND NO
		QTY REQ'D NEXT ASSEMBLY	PARTS LIST			

M2E801580A004

THIS DRAWING INCLUDES FEATURES SUPPORTING NUCLEAR CRITICALITY SAFETY. ANY REVISION TO THIS DIAGRAM REQUIRES NUCLEAR CRITICALITY SAFETY DIVISION APPROVAL.

REVISION	DATE	NCSD APPROVAL
B	2/10/05	JF DECLUE

This document has been reviewed by a Y-12 ADC and UCNI RO and has been determined to be UNCLASSIFIED and not UCNI. This review does not constitute clearance for public release.

Name: ROGER D. AIGNER Date: 2/10/05

REV	DESCRIPTION	DRW	CHKR	DE	DVR	DM	DATE	PE	DATE	PK	DATE	WE	DATE
B	GEN REV REMOVED TOL ON 18.25 DIA. REMOVED 1 ON 19.15 DIA. REMOVED BOX 9 DIM. UPDATED NOTE NUM. 6 TO 8, REVISED NOTE 7, MOD. WELD SYMBOLS, ADDED REF DIMENSIONS IN DETAIL X	JRP	SMM	GAB	RDA	DPS	10/29/03	MRF	GAB	2/10/05	JGA	2/10/05	
A	ISSUED FOR PROTOTYPE PROCUREMENT	JRJ	JSL	GAB	JLH	JCW	10/29/03	MRF	10/29/03	DBM	10/29/03		

REVISION OR ISSUE PURPOSE — REVISION APPROVALS

SQUAD CHECK: AR CV ST HV EM FP FD EE IE M NP

DRAWING APPROVALS

		DATE
DRW	J. R. JACKSON	10/29/03
CHKR	J. S. LOWERY	10/29/03
DE	G.A. BYINGTON	10/29/03
DVR	J. L. HECK	10/29/03
DM	J. C. WALLS	10/29/03
PE	M. R. FELDMAN	10/29/03
PK	D. B. MILLER	10/29/03

SCALE: NOTED

TOLERANCES UNLESS OTHERWISE SPECIFIED
FRACTIONS ±.03
XX DECIMALS ±.03
XXX DECIMALS ±.010
ANGLES ±0.5°
BREAK SHARP EDGES .06 MAX
FINISH 125 RMS

Y-12 National Security Complex managed by BWXT Y-12, L.L.C. for the Department of Energy under U.S. Government contract DE-AC05-00OR22800
© Oak Ridge, Tennessee U.S.

PROJECT NAME: ES-3100 SHIPPING PACKAGE

DOUBLE OPEN HEAD REINFORCED DRUM

1	48	49	50	PLANT	BLDG	FL	SH.	OF	TYPE	CLASS
6	M	L	F	Y-12	NA	NA	1	1	S	U

51	52	53		REV
CM	PKG	IN	M2E801580A004	B

NO REPRESENTATION OR WARRANTY, EXPRESSED OR IMPLIED, IS MADE AS TO THE ACCURACY, COMPLETENESS OR USEFULNESS OF THE INFORMATION OR STATEMENTS CONTAINED IN THESE DRAWINGS, OR THAT THE USE OR DISCLOSURE OF ANY INFORMATION, APPARATUS, METHOD, OR PROCESS DISCLOSED IN THESE DRAWINGS MAY NOT INFRINGE PRIVATE RIGHTS OF OTHERS. NO LIABILITY IS ASSUMED WITH RESPECT TO THE USE OF, OR FOR DAMAGES RESULTING FROM THE USE OF ANY INFORMATION, APPARATUS, METHOD OR PROCESS DISCLOSED IN THESE DRAWINGS. SUBMITTAL OF THESE DRAWINGS OR INFORMATION TO BIDDER ARE NOT TO BE USED FOR OTHER PURPOSES AND ARE TO BE RETURNED UPON REQUEST OF THE FORWARDING CONTRACTOR.

THIS DRAWING PRODUCED ON PRO/ENGINEER

THIS PAGE INTENTIONALLY LEFT BLANK.

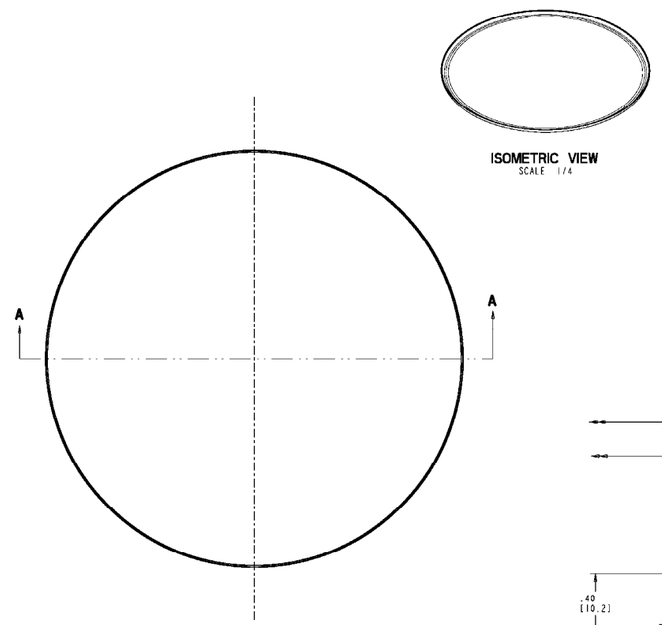

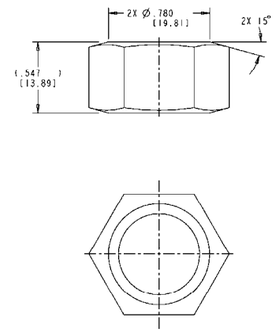

NOTES

1. INTERPRET DRAWING PER MECHANICAL DRAFTING STANDARD ES-3.1.
2. INTERPRET DIMENSIONS AND TOLERANCES PER ASME Y14.5M-1994.
3. DIMENSIONS ARE IN INCHES.[mm].
4. DIMENSIONS AND FEATURES FLAGGED BY A (I) SYMBOL SHALL BE INSPECTED AND DOCUMENTED.

5 DRUM FLAT COVER SHALL BE FABRICATED TO INTERFACE WITH DOUBLE OPEN HEAD REINFORCED DRUM DIMENSION. TOLERANCE SHALL BE -.01 TO -.04. REFERENCE NOTE 9 ON DRAWING M2E801580A004.

6. FOR ADDITIONAL REQUIREMENTS SEE EQUIPMENT SPECIFICATION JS-YMN3-801580-A002.

7 REFERENCE CONFIGURATION CONTROL EQUIPMENT DATA SHEET DS-PKG-801580-A003.

(D) 8 THE DRUM NUT MECHANICAL PROPERTY MARKING, F467K, SHALL BE FULLY VISIBLE AFTER MODIFICATION.

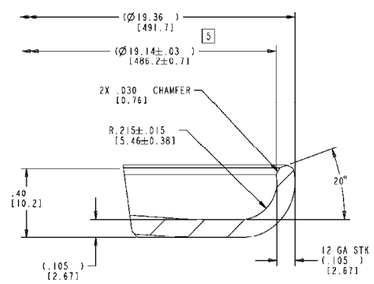

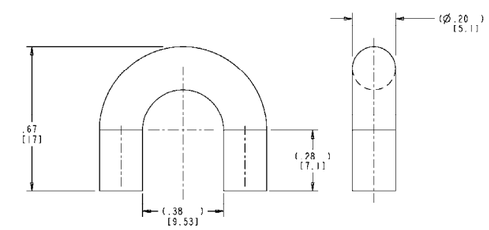

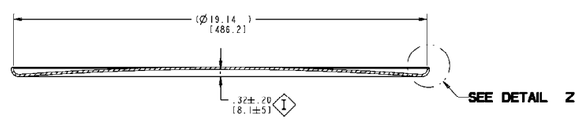

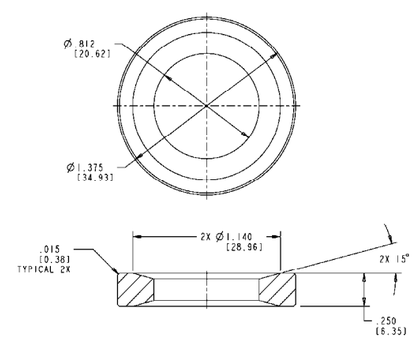

(D) 8 7

QTY REQ'D NEXT ASSEMBLY	PART OR IDENTIFYING NO	NOMENCLATURE OR DESCRIPTION	MATERIAL	SPECIFICATION	FIND NO
8	-4	DRUM WASHER	300 SERIES SST	ASTM A240 OR A276	4
8	-3	MODIFIED DRUM NUT	C65100 SILICON BRONZE	ASTM F-467 ANSI B18.2.2	3
2	MODIFIED 339215 OR EQUAL	TID LUG	304L SST CHAIN 3/16" TRADE SIZE, .20 DIA. MATERIAL, INSIDE LINK SIZE .38 WD, .95L	McMASTER-CARR SUPPLY CO. ATLANTA, GA 30374	2
1	-1	DRUM FLAT COVER	12 GA 304/304L SST	ASME SA240	1

M2E801580 M2E801580 A002

PARTS LIST

M2E801580A005

THIS DRAWING INCLUDES FEATURES SUPPORTING NUCLEAR CRITICALITY SAFETY. ANY REVISION TO THIS DIAGRAM REQUIRES NUCLEAR CRITICALITY SAFETY ANALYSIS ENGINEERING APPROVAL.

REVISION	DATE	SAE APPROVAL
D	03/17/2010	J.F. DeCLUE

This document has been reviewed by a Y-12 DC and UCNI RO and has been determined to be UNCLASSIFIED and not UCNI. This review does not constitute clearance for public release.

Name: STAN THOMAS Date: 3/17/2010

NO REPRESENTATION OR WARRANTY, EXPRESSED OR IMPLIED, IS MADE AS TO THE ACCURACY, COMPLETENESS OR USEFULNESS OF THE INFORMATION OR DATA CONTAINED IN THESE DRAWINGS, OR THAT THE USE OF ANY INFORMATION, DATA, APPARATUS, METHOD OR PROCESS DISCLOSED IN THESE DRAWINGS MAY NOT INFRINGE PRIVATE RIGHTS OF OTHERS. NO LIABILITY IS ASSUMED WITH RESPECT TO THE USE OF, OR FOR DAMAGES RESULTING FROM THE USE OF ANY INFORMATION, APPARATUS, METHOD OR PROCESS DISCLOSED IN THESE DRAWINGS. DRAWINGS MADE AVAILABLE FOR INFORMATION TO BIDDER USE ONLY. NOT TO BE USED FOR OTHER PURPOSES AND ARE TO BE RETURNED UPON REQUEST OF THE FORWARDING CONTRACTOR.

PRODUCED ON PRO/ENGINEER

REV	DESCRIPTION	DRW	CHKR	DE	DVR	DM	DATE	PE	DATE	PM	DATE
D	ADDED NOTE 8	JRJ	JRF	GAB	MLG	WIN	3/17/10	LR	3/17/10	JGA	3/17/10
C	ADDED REFERENCE NOTE 7.	MLE	JRJ	MLE	DEW	WIN	5/13/09	LR	9/10/09	JGA	9/14/09
B	REVISED F/N 2. ADDED F/N 3 & 4 REMOVED TOL FROM DETAIL Z DIM.	JRP	SMM	GAB	RDA	DPS	11/17/08	GAB	2/10/09	JGA	2/10/09
A	ISSUED FOR PROTOTYPE PROCUREMENT	JRJ	JSL	GAB	JLH	JCW	10/29/08	MRF	10/29/08	DBM	10/29/08

REVISION OR ISSUE PURPOSE — REVISION APPROVALS

SQUAD CHECK	AR	CV	ST	HV	EW	FP	PD	EC	IE	M	NP

SCALE: NOTED
TOLERANCES UNLESS OTHERWISE SPECIFIED
FRACTIONS
XX DECIMALS ±.03
XXX DECIMALS ±.010
ANGLES ±0.5°
BREAK SHARP EDGES .06 MAX
FINISH 125 RMS

DRAWING APPROVALS		
DRW	J.R. JACKSON	10/29/03
CHKR	J.S. LOWERY	10/29/03
DC	G.A. BYINGTON	10/29/03
DVR	J.L. HECK	10/29/03
DM	J.C. WALLS	10/29/03
PE	M.R. FELDMAN	10/29/03
PM	D.B. MILLER	10/29/03

BWXT Y-12 A BWXT Business Enterprise

Y-12 National Security Complex managed by BWXT Y-12, L.L.C. for the Department of Energy under U.S. Government contract DE-AC05-00OR22800 o Oak Ridge, Tennessee o

PROJECT NAME: ES-3100 SHIPPING PACKAGE

MISC. DETAILS

1	48	49	50	PLANT	BLDG	FL	SH.	OF	TYPE	CLASS
6	M	L	F	Y-12	NA	NA	1	1	S	U

51	52	53		REV
CM	PKG	IN	M2E801580A005	D

THIS PAGE INTENTIONALLY LEFT BLANK.

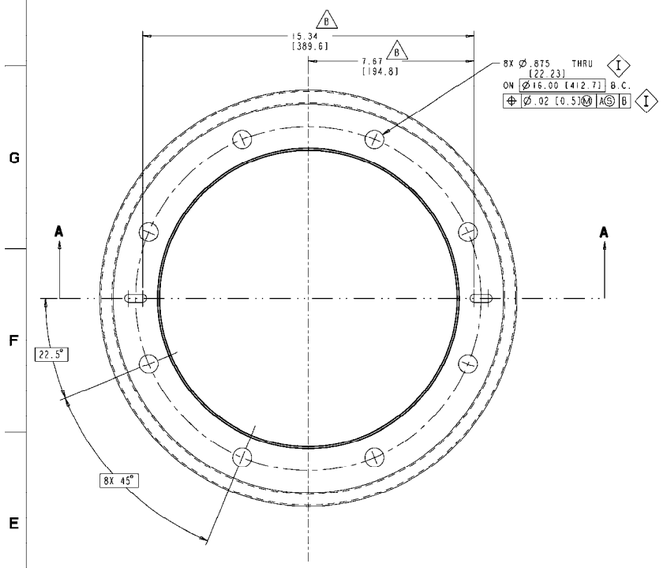

-1 DRUM LID WELDMENT
SCALE 1/2

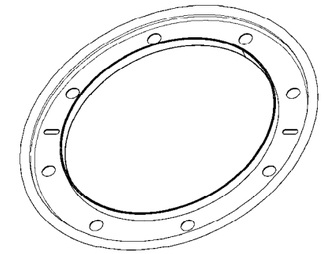

ISOMETRIC VIEW
SCALE 3/8

NOTES

1. INTERPRET DRAWING PER MECHANICAL DRAFTING STANDARD ES-3.1.
2. INTERPRET DIMENSIONS AND TOLERANCES PER ASME Y14.5M-1994.
3. DIMENSIONS ARE IN INCHES.[mm].
4. WELDING SYMBOLS SHALL BE INTERPRETED IN ACCORDANCE WITH AWS A2.4.
5. FOR ADDITIONAL REQUIREMENTS SEE EQUIPMENT SPECIFICATION JS-YMN3-801580-A002.
6. DIMENSIONS AND FEATURES FLAGGED BY A I SYMBOL SHALL BE INSPECTED AND DOCUMENTED.
7. FOR REFERENCE ONLY APPROXIMATE WEIGHT: 9.1 LBS [4.1 Kg]

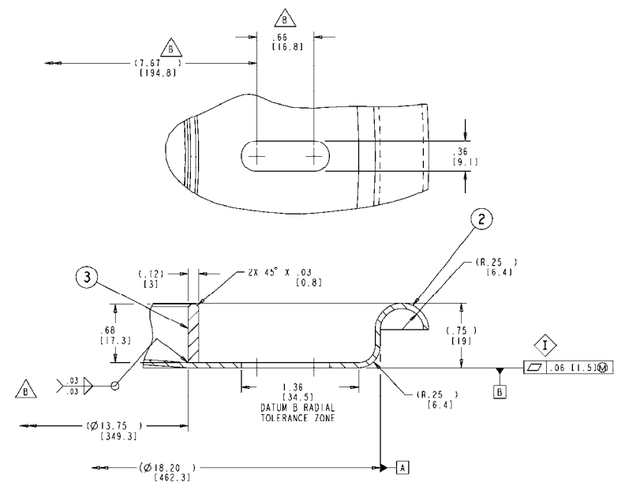

DETAIL Z
SCALE 2/1

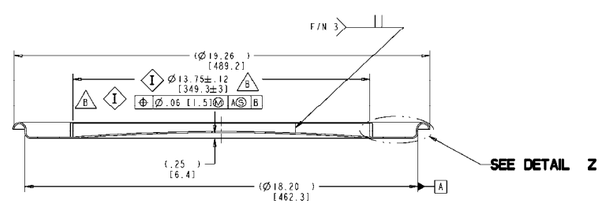

SECTION A-A

	AR		WELD FILLER METAL	PER WELD PROCEDURES	4
	1	-3	11 GA (.1197) SHEET	304/304L SST ASME SA240	3
	1	M2E801580A007-1	18.25" DIA. DRUM LID		2
AR	X	-1	DRUM LID WELDMENT		1
MATERIAL AREA		PART OR IDENTIFYING NO	NOMENCLATURE OR DESCRIPTION	MATERIAL / SPECIFICATION	FIND NO
		QTY REQ'D NEXT ASSEMBLY	PARTS LIST		

M2E801580A006

THIS DRAWING INCLUDES FEATURES SUPPORTING NUCLEAR CRITICALITY SAFETY. ANY REVISION TO THIS DIAGRAM REQUIRES NUCLEAR CRITICALITY SAFETY DIVISION APPROVAL.

REVISION	DATE	NCSD APPROVAL
B	2/10/05	JF DECLUE

This document has been reviewed by a Y-12 ADC and UCNI RO and has been determined to be UNCLASSIFIED and not UCNI. This review does not constitute clearance for public release.

Name: ROGER D. AIGNER Date: 2/10/05

NO REPRESENTATION OR WARRANTY, EXPRESSED OR IMPLIED, IS MADE AS TO THE ACCURACY, COMPLETENESS OR USEFULNESS OF THE INFORMATION OR STATEMENTS CONTAINED IN THESE DRAWINGS, OR THAT THE USE OR DISCLOSURE OF ANY INFORMATION, APPARATUS, METHOD, OR PROCESS DISCLOSED IN THESE DRAWINGS MAY NOT INFRINGE PRIVATE RIGHTS OF OTHERS. NO LIABILITY IS ASSUMED WITH RESPECT TO THE USE OF, OR FOR DAMAGES RESULTING FROM THE USE OF ANY INFORMATION, APPARATUS, METHOD OR PROCESS DISCLOSED IN THESE DRAWINGS. DRAWINGS MADE AVAILABLE FOR INFORMATION TO BIDDER ARE NOT TO BE USED FOR OTHER PURPOSES AND ARE TO BE RETURNED UPON REQUEST OF THE FORWARDING CONTRACTOR.

PTHIS DRAWING PRODUCED ON PRO/ENGINEER

REV.	DESCRIPTION	DRW	CHKR	DE	DVR	DM	DATE	PE	DATE	PM	DATE	WE	DATE
B	REPLACED HOLE WITH SLOT; ADDED TOL TO 13.75 DIM; ADDED I ;MOD WELD; GEN REV NOTE 4 WAS 5	JRP	SMM	GAB	RDA	DPS	10/29/03	GAB	2/10/05	JGA	2/10/05	DTE	2/11/05
A	ISSUED FOR PROTOTYPE PROCUREMENT	JRJ	JSL	GAB	JLH	JCW	10/29/03	MRF	10/29/03	DBM	10/29/03		

REVISION OR ISSUE PURPOSE — REVISION APPROVALS

SQUAD CHECK: AR CV ST HV EM FP PD EE IE M NP

SCALE:	NOTED
TOLERANCES UNLESS OTHERWISE SPECIFIED	
FRACTIONS	
XX DECIMALS	±.03
XXX DECIMALS	±.010
ANGLES	±0.5°
BREAK SHARP EDGES	.06 MAX
FINISH	125 RMS

DRW	J.R. JACKAON	10/29/03
CHKR	J.S. LOWERY	10/29/03
DE	G.A. BYINGTON	10/29/03
DVR	J.L. HECK	10/29/03
DM	J.C. WALLS	10/29/03
PE	M.R. FELDMAN	10/29/03
PM	D.B. MILLER	10/29/03

DRAWING APPROVALS — DATE

BWXT Y-12 — Y-12 National Security Complex managed by BWXT Y-12, L.L.C. for the Department of Energy under U.S. Government contract DE-AC05-00OR22800 • Oak Ridge, Tennessee •

PROJECT NAME: ES-3100 SHIPPING PACKAGE

DRUM LID WELDMENT

1	48	49	50	PLANT	BLDG	FL	SH.	OF	TYPE	CLASS
6	M	L	F	Y-12	NA	NA	1	1	S	U
51			52	53						REV
CM			PKG	IN	M2E801580A006					B

THIS PAGE INTENTIONALLY LEFT BLANK.

NOTES

1. INTERPRET DRAWING PER MECHANICAL DRAFTING STANDARD ES-3.1.
2. INTERPRET DIMENSIONS AND TOLERANCES PER ASME Y14.5M-1994.
3. DIMENSIONS ARE IN INCHES.[mm].
4. FOR ADDITIONAL INFORMATION SEE EQUIPMENT SPECIFICATION DS-YMN3-801580A002.
5. LID SHALL BE FABRICATED IN ACCORDANCE WITH MILITARY SPECIFICATION MS27683-61, COVER STYLE 1.

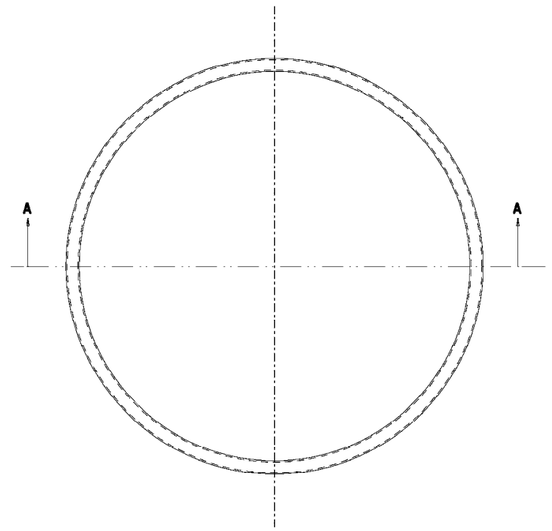

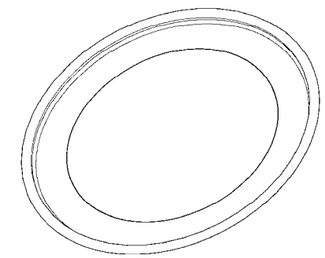

ISOMETRIC VIEW
SCALE 3/8

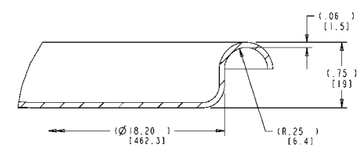

DETAIL Z
SCALE 2/1

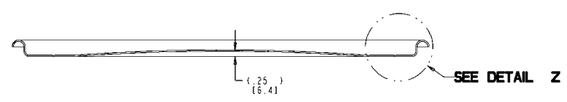

SECTION A-A

-1 18.25" DIAMETER DRUM LID
SCALE 1/2

AR	-1	18.25" DIA. DRUM LID	16 GA 304/304L SST	ASME SA240	1
REFERENCE ONLY	PART OR IDENTIFYING NO	NOMENCLATURE OR DESCRIPTION	MATERIAL	SPECIFICATION	FIND NO
	QTY REQ'D NEXT ASSEMBLY	PARTS LIST			

M2E801580A007

THIS DRAWING INCLUDES FEATURES SUPPORTING NUCLEAR CRITICALITY SAFETY. ANY REVISION TO THIS DIAGRAM REQUIRES NUCLEAR CRITICALITY SAFETY DIVISION APPROVAL.

REVISION	DATE	NCSD APPROVAL
B	2/10/05	JF DECLUE

This document has been reviewed by a Y-12 ADC and UCNI RO and has been determined to be UNCLASSIFIED and not UCNI. This review does not constitute clearance for public release.

Name: ROGER D. AIGNER Date: 2/10/05

REV	DESCRIPTION	DRW	CHKR	DE	DVR	DM	DATE	PE	DATE	PM	DATE
B	GENERAL REVISION.	JRP	SMM	GAB	RDA	DPS	11/18/03	GAB	2/10/05	JGA	2/10/05
A	ISSUED FOR PROTOTYPE PROCUREMENT	JRJ	JSL	GAB	JLH	JCW	10/25/03	MRF	10/29/03	DBM	10/29/03

REVISION OR ISSUE PURPOSE — REVISION APPROVALS

SQUAD CHECK	AR	CV	ST	HV	EM	JP	FD	EL	IC	M	NP

DRAWING APPROVALS		DATE
DRW	J.R. JACKSON	10/29/03
CHKR	J.S. LOWERY	10/29/03
DE	G.A. BYINGTON	10/29/03
DVR	J.L. HECK	10/29/03
DM	J.C. WALLS	10/29/03
PE	M.R. FELDMAN	10/29/03
PM	D.B. MILLER	10/29/03

SCALE: NOTED

TOLERANCES UNLESS OTHERWISE SPECIFIED
FRACTIONS
XX DECIMALS
XXX DECIMALS
ANGLES
BREAK SHARP EDGES MAX
FINISH

BWXT Y-12 — Y-12 National Security Complex managed by BWXT Y-12, L.L.C. for the Department of Energy under U.S. Government contract DE-AC05-00OR22800 • Oak Ridge, Tennessee •

PROJECT NAME: ES-3100 SHIPPING PACKAGE

18.25" DIAMETER DRUM LID

I	48	49	50	PLANT	BLDG	FL	SH.	OF	TYPE	CLASS
6	M	L	F	Y-12	NA	NA	1	1	S	U

A1	A2	A3	DATE
CM	PKG	IN	M2E801580A007

REV B

NO REPRESENTATION OR WARRANTY, EXPRESSED OR IMPLIED, IS MADE AS TO THE ACCURACY, COMPLETENESS OR USEFULNESS OF THE INFORMATION OR STATEMENTS CONTAINED IN THESE DRAWINGS, OR THAT THE USE OR DISCLOSURE OF ANY INFORMATION, APPARATUS, METHOD, OR PROCESS DISCLOSED IN THESE DRAWINGS MAY NOT INFRINGE PRIVATE RIGHTS OF OTHERS. NO LIABILITY IS ASSUMED WITH RESPECT TO THE USE OF, OR FOR DAMAGES RESULTING FROM THE USE OF ANY INFORMATION, APPARATUS, METHOD OR PROCESS DISCLOSED IN THESE DRAWINGS. DRAWINGS MADE AVAILABLE FOR INFORMATION TO BIDDER ARE NOT TO BE USED FOR OTHER PURPOSES AND ARE TO BE RETURNED UPON REQUEST OF THE FORWARDING CONTRACTOR.

THIS DRAWING PRODUCED ON PRO/ENGINEER

THIS PAGE INTENTIONALLY LEFT BLANK.

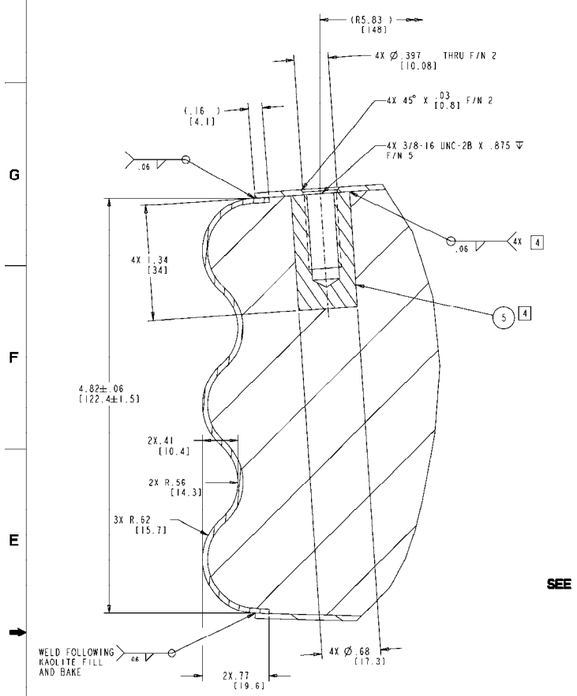

DETAIL Z
SCALE 2/1

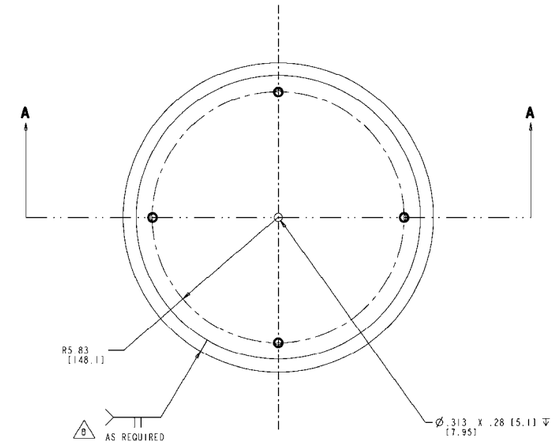

SECTION A-A

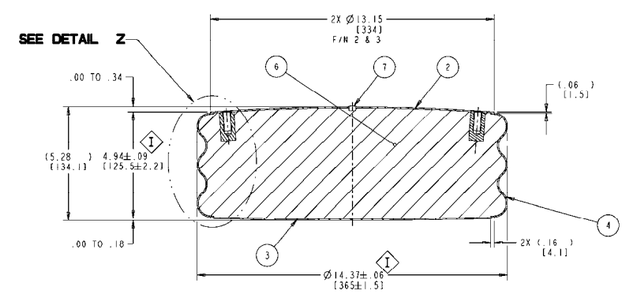

-1 TOP PLUG WELDMENT
SCALE 1/2

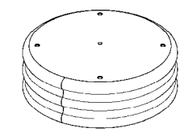

ISOMETRIC VIEW
SCALE 1/4

NOTES

1. INTERPRET DRAWING PER MECHANICAL DRAFTING STANDARD ES-3.1.
2. INTERPRET DIMENSIONS AND TOLERANCES PER ASME Y14.5M-1994.
3. DIMENSIONS ARE IN INCHES.[mm].
4. WELD LIFTING INSERTS (F/N 5) IN PLACE BEFORE FILLING WITH KAOLITE (F/N 6).
5. WELDING SYMBOLS SHALL BE INTERPRETED IN ACCORDANCE WITH AWS A2.4.
6. FOR ADDITIONAL REQUIREMENTS SEE EQUIPMENT SPECIFICATIONS JS-YMN3-801580-A002 AND A003.
7. DIMENSIONS AND FEATURES FLAGGED BY A (I) SYMBOL SHALL BE INSPECTED AND DOCUMENTED.
8. FOR REFERENCE ONLY:
   APPROXIMATE WEIGHT 19.6 LBS [8.8 Kg] WITH
   KAOLITE VOLUME 0.43 CU.FT.
   KAOLITE DENSITY 22.4 LBS/CU. FT.
   KAOLITE WEIGHT: 9.6 LBS [4.7 Kg]

	AR		WELD FILLER METAL	PER WELD PROCEDURES	8
	1	62MP0312 OR EQUAL	PLUG, NYLON 6/6	MICRO PLASTIC INC. FLIPPIN, AR 72634	7
	1	-6	KAOLITE 1600 TM VIBRATED CAST	THERMAL CERAMICS AUGUSTA, GA 30903-0923	6
	4	-5	LIFTING INSERT	11/16 ROUND 304/304L SST / ASME SA479	5
	1	-4	PLUG RIM	16 GA SHT 304/304L SST / ASME SA240	4
	1	-3	BOTTOM SHEET		3
	1	-2	TOP SHEET		2
AR	X	-1	TOP PLUG WELDMENT		1
NOTES/SUB ASSY		PART OR IDENTIFYING NO	NOMENCLATURE OR DESCRIPTION	MATERIAL / SPECIFICATION	FIND NO
		← QTY REQ'D NEXT ASSEMBLY	PARTS LIST		

M2E801580A008

THIS DRAWING INCLUDES FEATURES SUPPORTING NUCLEAR CRITICALITY SAFETY. ANY REVISION TO THIS DIAGRAM REQUIRES NUCLEAR CRITICALITY SAFETY DIVISION APPROVAL.

REVISION	DATE	NCSD APPROVAL
B	2/10/05	JF DECLUE

This document has been reviewed by a Y-12 ADC and UCNI RO and has been determined to be UNCLASSIFIED and not UCNI. This review does not constitute clearance for public release.

Name: ROGER D. AIGNER Date: 2/10/05

NO REPRESENTATION OR WARRANTY, EXPRESSED OR IMPLIED, IS MADE AS TO THE ACCURACY, COMPLETENESS OR USEFULNESS OF THE INFORMATION, STATEMENTS OR CONTENTS IN THESE DRAWINGS, OR THAT THE USE OR DISCLOSURE OF INFORMATION THEREIN WILL NOT INFRINGE PRIVATELY OWNED RIGHTS. NEITHER THE GOVERNMENT NOR THE CONTRACTOR MAKES ANY WARRANTY OR REPRESENTATION WITH RESPECT TO THE USE OF, OR FOR DAMAGES RESULTING FROM THE USE OF ANY INFORMATION, APPARATUS, METHOD OR PROCESS DISCLOSED IN THESE DRAWINGS. DRAWINGS MADE AVAILABLE FOR INFORMATION TO BIDDER ARE NOT TO BE USED FOR OTHER PURPOSES AND ARE TO BE RETURNED UPON REQUEST OF THE FORWARDING CONTRACTOR.

P THIS DRAWING PRODUCED ON PRO/ENGINEER

REV.	DESCRIPTION	DRW	CHKR	DL	DVR	DM	DATE	PE	DATE	PM	DATE	WE	DATE
B	GENERAL REVISION ADDED WELD SYMBOL	JRP	SMM	GAB	RDA	DPS	11/18/03	JGA	2/10/05	GAB	2/10/05	DJE	2/11/05
A	ISSUED FOR PROTOTYPE PROCUREMENT	JRJ	JSL	GAB	JLH	JCW	10/29/03	MRF	10/29/03	DSM	10/29/03		

REVISION OR ISSUE PURPOSE — REVISION APPROVALS

AR	CV	ST	MV	EM	FP	FD	LE	TL	M	NP

SQUAD CHECK

		DATE
SCALE:	NOTED	
TOLERANCES UNLESS OTHERWISE SPECIFIED		
FRACTIONS		
XX DECIMALS	±.03	
XXX DECIMALS	±.005	
ANGLES	±0.5°	
BREAK SHARP EDGES	.06 MAX	
FINISH	125 RMS	
DRW	J.R. JACKSON	10/29/03
CHKR	J.S. LOWERY	10/29/03
DE	G.A. BYINGTON	10/29/03
DVR	J.L. HECK	10/29/03
DM	J.C. WALLS	10/29/03
PE	M.R. FELDMAN	10/29/03
PM	D.B. MILLER	10/29/03

DRAWING APPROVALS

BWXT Y-12 A BWXT Alliance Enterprise

Y-12 National Security Complex managed by BWXT Y-12, L.L.C. for the Department of Energy under U.S. Government contract DE-AC05-00OR22800
o Oak Ridge, Tennessee o

PROJECT NAME: ES-3100 SHIPPING PACKAGE

TOP PLUG WELDMENT

46	49	50	PLANT	BLDG	FL	SH.	OF	TYPE	CLASS
6	M	L	F	Y-12	NA	NA	1	I	S	U

51	52	53		REV
CM	PKG	IN	M2E801580A008	B

THIS PAGE INTENTIONALLY LEFT BLANK.

NOTES

1. INTERPRET DRAWING PER MECHANICAL DRAFTING STANDARD ES-3.1.
2. INTERPRET DIMENSIONS AND TOLERANCES PER "RMA" RUBBER HANDBOOK (RMA-392) CLASS "A2 PRECISION."
3. DIMENSIONS ARE IN INCHES [mm].
4. MANUFACTURER/SUPPLIER TO PROVIDE CERTIFICATE OF COMPLIANCE FOR ALL FEATURES OF THESE ITEMS.
5. IN APPROXIMATE LOCATIONS SHOWN, USING WHITE SILICONE INK, (F/N 4) MARK DRAWING NUMBER AND REVISION LETTER IN 1/4" HIGH CHARACTERS.

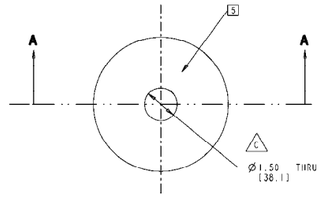

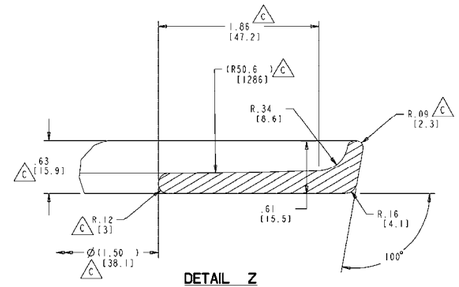

DETAIL Z
SCALE 2/1

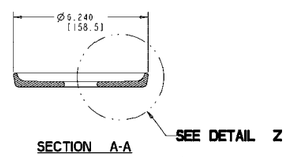

SECTION A-A
-1 CV BOTTOM PAD C
SCALE 1/2
APPROXIMATE WEIGHT- 0.37 LB

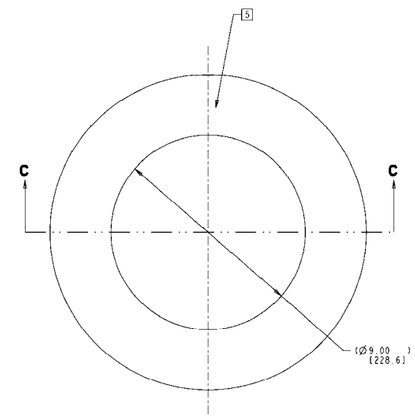

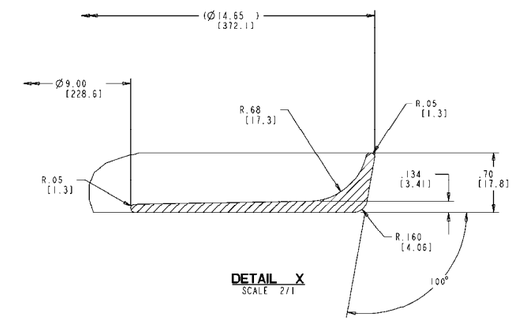

DETAIL X
SCALE 2/1

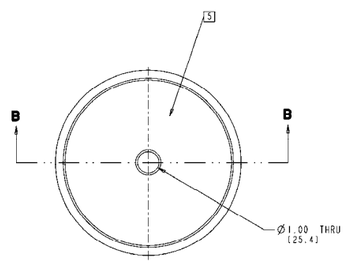

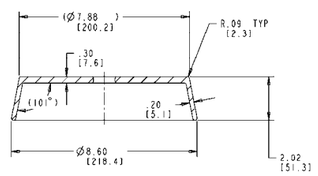

SECTION B-B
-2 CV FLANGE PAD C
SCALE 1/2
APPROXIMATE WEIGHT - 1.15 LB

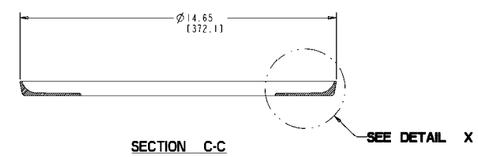

SECTION C-C

-3 PLUG PAD C
SCALE 1/2
APPROXIMATE WEIGHT 0.77 LB

AR	-4	WHITE SILICONE INK	GEM TYPE S	REISS MFG., INC. BLACKSTONE, VA 23824	4
AR	-3	PLUG PAD	SILICONE RUBBER 22±5 SHORE A COLOR BLACK/GRAY		3
AR	-2	CV FLANGE PAD			2
AR	-1	CV BOTTOM PAD			1
M2E801580A011	PART OR IDENTIFYING NO	NOMENCLATURE OR DESCRIPTION	MATERIAL	SPECIFICATION	FIND NO
	QTY REQ'D NEXT ASSEMBLY	PARTS LIST			

M2E801580A009

THIS DRAWING INCLUDES FEATURES SUPPORTING NUCLEAR CRITICALITY SAFETY. ANY REVISION TO THIS DIAGRAM REQUIRES NUCLEAR CRITICALITY SAFETY DIVISION APPROVAL.

REVISION	DATE	NCSD APPROVAL
C	2/10/05	JF DECLUE

This document has been reviewed by a Y-12 ADC and UCNI RO and has been determined to be UNCLASSIFIED and not UCNI. This review does not constitute clearance for public release.

Name: ROGER D. AIGNER Date: 2/10/05

NO REPRESENTATION OR WARRANTY, EXPRESSED OR IMPLIED, IS MADE AS TO THE ACCURACY, COMPLETENESS OR USEFULNESS OF THE INFORMATION OR STATEMENTS CONTAINED IN THESE DRAWINGS, OR THAT THE USE OR DISCLOSURE OF ANY INFORMATION, APPARATUS, METHOD, OR PROCESS DISCLOSED IN THESE DRAWINGS MAY NOT INFRINGE PRIVATE RIGHTS OF OTHERS. NO LIABILITY IS ASSUMED WITH RESPECT TO THE USE OF, OR FOR DAMAGES RESULTING FROM THE USE OF ANY INFORMATION, APPARATUS, METHOD OR PROCESS DISCLOSED IN THESE DRAWINGS. DRAWINGS MADE AVAILABLE FOR INFORMATION TO BIDDER ARE NOT TO BE USED FOR OTHER PURPOSES AND ARE TO BE RETURNED UPON REQUEST OF THE FORWARDING CONTRACTOR.

THIS DRAWING PRODUCED ON PRO/ENGINEER

REV	DESCRIPTION	DRW	CHKR	DE	DVR	DM	DATE	PE	DATE	PM	DATE
C	GEN REV: REDESIGNED F/N 1; ADDED APPROXIMATE WEIGHT TO F/N 1, 2 AND 3	JRP	SMM	GAB	RDA	DPS	11/18/03	GAB	7/16/05	JGA	7/18/05
B	MODIFIED DIMENSIONING ON -3	GAB	RA	GAB	JLH	JCW	1/22/04	GAB	1/22/04	JGA	1/22/04
A	ISSUED FOR PROTOTYPE PROCUREMENT	JRJ	JSL	GAB	JLH	JCW	10/29/03	MRF	10/29/03	DBM	10/29/03

REVISION OR ISSUE PURPOSE — REVISION APPROVALS

AR	CV	ST	HV	EM	FP	FD	EL	IC	M	NP

SQUAD CHECK

SCALE: NOTED

DRW	J.R. JACKSON	10/29/03
CHKR	J.S. LOWERY	10/29/03
DE	G.A. BYINGTON	10/29/03
DVR	J.L. HECK	10/29/03
DM	J.C. WALLS	10/29/03
PE	M.R. FELDMAN	10/29/03
PM	D.B. MILLER	10/29/03

DRAWING APPROVALS

BWXT Y-12 — Y-12 National Security Complex managed by BWXT Y-12, L.L.C. for the Department of Energy under U.S. Government contract DE-AC05-00OR22800. a BWXT Babcock & Wilcox Company. Oak Ridge, Tennessee

PROJECT NAME: ES-3100 SHIPPING PACKAGE

PAD DETAILS

1	48	49	50	PLANT	BLDG	FL	SH.	OF	TYPE	CLASS
6	M	L	F	Y-12	NA	NA	1	1	S	U

A1	A2	A3	DATE	REV
CM	PKG	IN	M2E801580A009	C

THIS PAGE INTENTIONALLY LEFT BLANK.

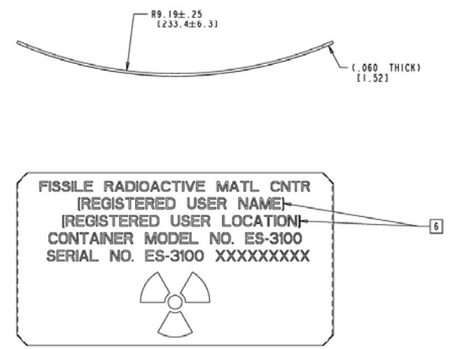

-1 ES-3100 TREFOIL DATA PLATE
FORMED

-2 ES-3100 DATA PLATE
FORMED

NOTES

1. INTERPRET DRAWING PER MECHANICAL DRAFTING STANDARD ES-3.1.
2. INTERPRET DIMENSIONS AND TOLERANCES PER ASME Y14.5M-1994.
3. DIMENSIONS ARE IN INCHES [mm].
4. CONTAINER SERIAL NUMBER SHOWN "XXXXXXXXX" IS A GENERIC REPRESENTATION, ACTUAL SERIAL NUMBERS SHALL BE SPECIFIED IN PURCHASE ORDER, OR PROCUREMENT CONTRACT.
5. ALL CHARACTERS AND SYMBOLS SHALL BE ELECTROCHEMICALLY ETCHED .003-.005 DEEP AND FILLED WITH BLACK ENAMEL PAINT (F/N 5).
6. SEE PROCUREMENT DOCUMENTS FOR PROPER REGISTERED USER NAME AND LOCATION. (D)

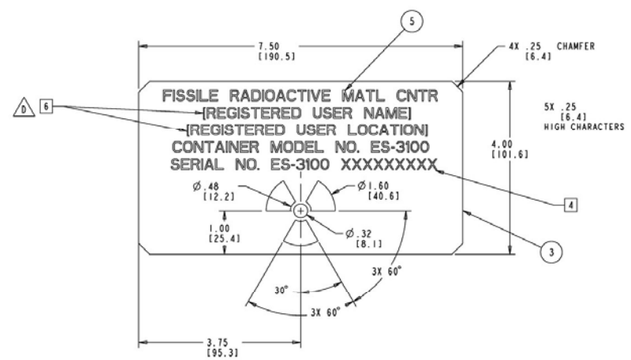

-1 ES-3100 TREFOIL DATA PLATE
SCALE 1/1
FLAT PATTERN

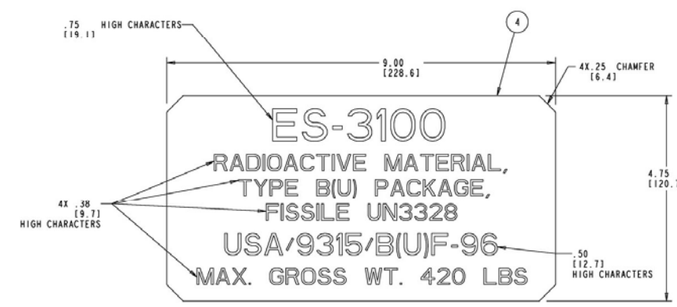

-2 ES-3100 DATA PLATE
SCALE 1/1
FLAT PATTERN

	AR	AR	-5	PAINT, BLACK ENAMEL		FED SPEC 595b-17038	5
		1	-4	16 GA, SHEET	304/304L SST	ASME SA240	4
	1		-3				3
	AR	X	-2	ES-3100 DATA PLATE			2
	AR	X	-1	ES-3100 TREFOIL DATA PLATE			1
M2E801580A010	-1	-2	PART OR IDENTIFYING NO	NOMENCLATURE OR DESCRIPTION	MATERIAL	SPECIFICATION	FIND NO
			QTY REQ'D NEXT ASSEMBLY	PARTS LIST			

THIS DRAWING INCLUDES FEATURES SUPPORTING NUCLEAR CRITICALITY SAFETY. ANY REVISION TO THIS DIAGRAM REQUIRES NUCLEAR CRITICALITY SAFETY DIVISION APPROVAL.

REVISION	DATE	NCSD APPROVAL
D	09/10/08	J.F. DeCLUE

This document has been reviewed by a Y-12 ADC and UCNI RO and has been determined to be UNCLASSIFIED and not UCNI. This review does not constitute clearance for public release.

Name: R.D. AIGNER Date: 09/11/08

NO REPRESENTATION OR WARRANTY, EXPRESSED OR IMPLIED, IS MADE AS TO THE ACCURACY, COMPLETENESS OR USEFULNESS OF THE INFORMATION OR STATEMENTS CONTAINED IN THESE DRAWINGS, OR THAT THE USE OR DISCLOSURE OF ANY INFORMATION, APPARATUS, METHOD, OR PROCESS DISCLOSED IN THESE DRAWINGS MAY NOT INFRINGE PRIVATELY OWNED RIGHTS. THE BIDDER ASSUMES ALL RISK WITH RESPECT TO THE USE OF, OR FOR DAMAGES RESULTING FROM THE USE OF ANY INFORMATION, APPARATUS, METHOD OR PROCESS DISCLOSED IN THESE DRAWINGS. DRAWINGS MADE AVAILABLE FOR INFORMATION TO BIDDER ARE NOT TO BE USED FOR OTHER PURPOSES AND ARE TO BE RETURNED UPON REQUEST OF THE FORWARDING CONTRACTOR.

THIS DRAWING PRODUCED ON PRO/ENGINEER

REV	DESCRIPTION	DRW	CHKR	DE	DVR	DM	DATE	PE	DATE	PM	DATE
D	REVISED TREFOIL DATA PLATE, F/N 1, ADDED NOTE 6	JRJ	RDA	LR	GAB	WIN	9/9/08	LR	9/9/08	JGA	9/9/08
C	REVISED TREFOIL DATA PLATE, F/N 1, AND NOTE 4	JRJ	RDA	JRJ	GAB	WIN	10/16/06	MAW	10/17/06	JGA	10/17/06
B	GEN REV: REMOVED RIVIT HOLES F/N 1 & 2; ADDED CHAMFERS F/N 1 & 2; ADDED NEW FLAT PATTERN VIEWS; REMOVED NOTE 5; CHANGED NOTE 6 TO NOTE 5; REMOVED NOTE 7; REMOVED INDEX NOTE BOX 5; CHANGED INDEX NOTE BOX 7 TO 4	JRP	SMM	GAB	RDA	DPS	11/13/05	GAB	2/16/05	JGA	2/16/05
A	ISSUED FOR PROTOTYPE PROCUREMENT	JRJ	JSL	GAB	JLH	JCW	10/26/04	MRF	10/26/04	DBM	10/26/04

REVISION OR ISSUE PURPOSE — REVISION APPROVALS

SQUAD CHECK	AR	CV	ST	HV	EM	FP	PD	EC	IE	M	NP

SCALE: NOTED
TOLERANCES UNLESS OTHERWISE SPECIFIED
FRACTIONS ±.03
XX DECIMALS ±.03
XXX DECIMALS ±.005
ANGLES ±0.5°
BREAK SHARP EDGES .06 MAX
FINISH 125 RMS

DRAWING APPROVALS		DATE
DRW	J.R. JACKSON	10/29/03
CHKR	J.S. LOWERY	10/29/03
DE	G.A. BYINGTON	10/29/03
DVR	J.L. HECK	10/29/03
DM	J.C. WALLS	10/29/03
PE	M.R. FELDMAN	10/29/03
PM	D.B. MILLER	10/29/03

BWXT Y-12 — Y-12 National Security Complex managed by BWXT Y-12, L.L.C. for the Department of Energy under U.S. Government contract DE-AC05-00OR22800 • Oak Ridge, Tennessee •

PROJECT NAME: ES-3100 SHIPPING PACKAGE

DATA PLATE DETAILS

1 48	49 50		PLANT	BLDG	FL	SH.	OF	TYPE	CLASS
6	M	L	F	Y-12	NA	NA	1	1	S	U
51	52		53						REV
CM	PKG		IN	M2E801580A010					D

M2E801580A010

THIS PAGE INTENTIONALLY LEFT BLANK.

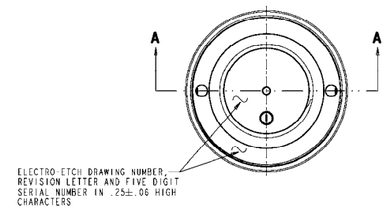

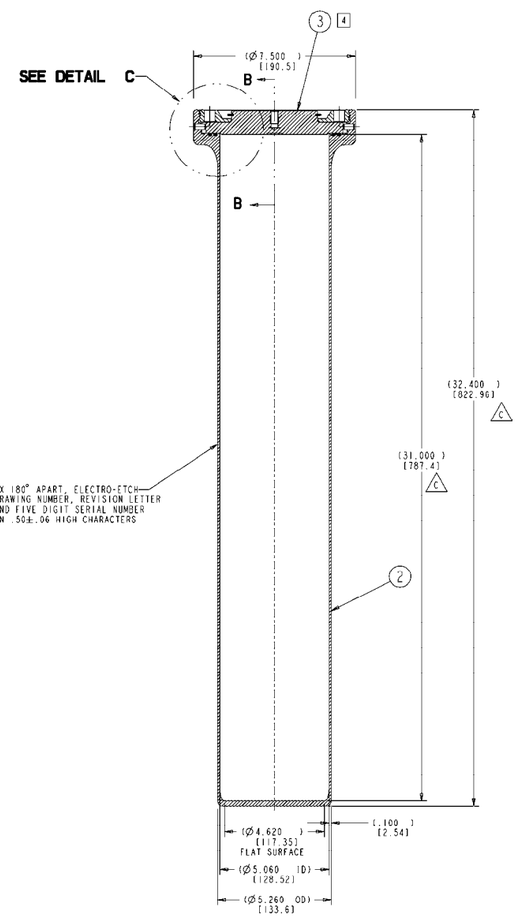

SECTION A-A

-1 CONTAINMENT VESSEL ASSEMBLY
SCALE 1/2

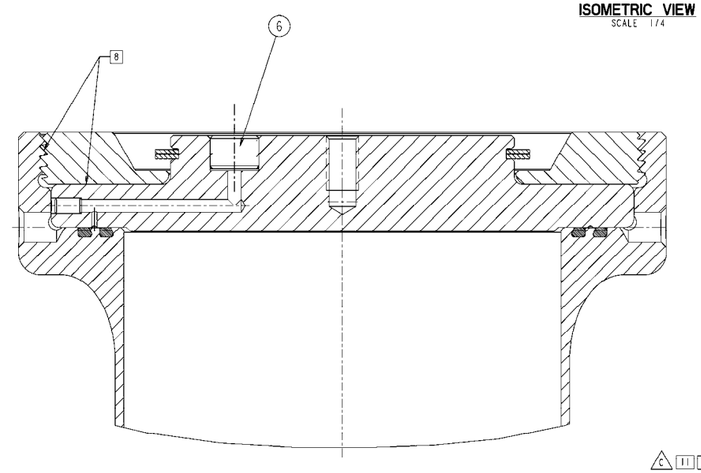

SECTION B-B
SCALE 2/1

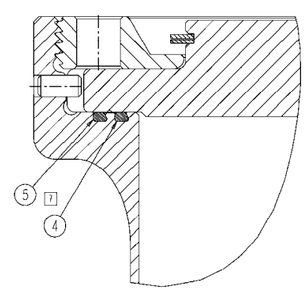

DETAIL C
SCALE 2/1

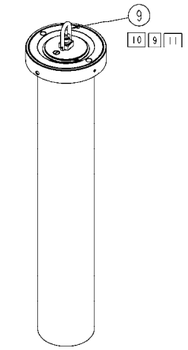

ISOMETRIC VIEW
SCALE 1/4

NOTES

1. INTERPRET DRAWING PER ENGINEERING DRAFTING STANDARD ES-3.1.
2. INTERPRET DIMENSIONS AND TOLERANCES PER ASME Y14.5M-1994. PERFECT ORIENTATION AT MMC FOR INTERRELATED FEATURES REQUIRED.
3. DIMENSIONS ARE IN INCHES [mm].
4. (C) INSTALL THE LID NUT AND TORQUE TO 120 ±5 FT-LBS AS SHOWN ON M2E801580A020-3 AND A020-4.
5. APPROXIMATE WEIGHT: 32.98 LBS. [14.96 KG].
6. FOR ADDITIONAL REQUIREMENTS SEE EQUIPMENT SPEC. DS YMN3 801580 A001.
7. DURING INSTALLATION OF O-RINGS APPLY A THIN COAT OF SUPER-O-LUBE.
8. DURING INSTALLATION OF CONTAINER VESSEL LID ASSEMBLY, APPLY A LIGHT COAT OF KRYTOX GREASE TO THE THREADS AND UNDER THE NUT.
9. SWIVEL HOIST RING FOR USE WHEN LOADING AND UNLOADING CONTAINMENT VESSEL ONLY. NOT FOR SHIPMENT.
10. TORQUE SWIVEL HOIST RING TO 12 ±1 FT.LBS. PER MFGR'S SPEC.
11. (C) THE SWIVEL HOIST RING, THREAD LUBRICANT AND O-RING LUBRICANTS ARE REQUIRED AT EACH LOADING AND MAINTENANCE STATION.

		PART OR IDENTIFYING NO	NOMENCLATURE OR DESCRIPTION	MATERIAL	SPECIFICATION	FIND NO
C 11 10 9	AR	3052T56 OR EQUAL	SWIVEL HOIST RING	ALLOY STEEL	McMASTER- CARR ATLANTA, GA	9
C 11 8	AR	KRYTOX #240AC OR EQUAL	THREAD LUBRICANT	FLUORINATED GREASE	MILLER-STEPHENSON CHEMICAL CO. DANBURY, CT 06810	8
C 11 7	AR	SUPER-O-LUBE OR EQUAL	O-RING LUBRICANT	CLEAR DIMETHYL SILOXANE POLYMER	PARKER HANNIFIN CORP. O-RING DIV,PO BOX 11751 LEXINGTON, KY 40512	7
C	1	PART # 04-2126	MODIFIED VCO THREADED PLUG	BRASS	VOLUNTEER INDUSTRIAL P. O. BOX 30371 KNOXVILLE, TN 37930 PHONE 865-660-2617	6
	1	M2E801580A013-2	O-RING, OUTER			5
	1	M2E801580A013-1	O-RING, INNER			4
	1	M2E801580A014-1	CONTAINMENT VESSEL LID ASSEMBLY			3
	1	M2E801580A012-1 OR A012-4	CONTAINMENT VESSEL BODY ASSEMBLY			2
AR	X	-1	CONTAINMENT VESSEL ASSEMBLY			1
M2E801580A011	QTY REQ'D NEXT ASSEMBLY		PARTS LIST			

THIS DRAWING INCLUDES FEATURES SUPPORTING NUCLEAR CRITICALITY SAFETY. ANY REVISION TO THIS DIAGRAM REQUIRES NUCLEAR CRITICALITY SAFETY DIVISION APPROVAL.

REVISION	DATE	NCSD APPROVAL
C	2/10/05	JF DECLUE

This document has been reviewed by a Y-12 ADC and UCNI RO and has been determined to be UNCLASSIFIED and not UCNI. This review does not constitute clearance for public release.

Name: ROGER D. AIGNER Date: 2/10/05

REV	DESCRIPTION	DRW	CHKR	DE	DVR	DM	DATE	PE	DATE	PM	DATE
C	GENERAL REVISION DELETED F/N 9; RENUMBERED F/N 10 TO NEW F/N 9; ADDED NOTE 11; NOTE 4 TORQUE WAS 100	JRP	SMM	GAB	RDA	DPS	11/18/03	GAB	11/21/03	JGA	01/16/05
B	-6 WAS A FABRICATED PART, ADDED A012-4 WELDED CV OPTION	GAB	RA	GAB	JLH	JCW	01/22/04	MG	GAB	01/22/04	JGA	01/22/04
A	ISSUED FOR PROTOTYPE PROCUREMENT	JRJ	JSL	GAB	JLH	JCW	10/29/03	MRF	10/29/03	DBM	10/29/03

REVISION OR ISSUE PURPOSE — REVISION APPROVALS

SQUAD CHECK	AR	CV	ST	HV	EM	FP	FD	EG	IE	M	NP

DRAWING APPROVALS		DATE
DRW	JRJ for D.M. SPARKS	10/29/03
CHKR	D.S. LOWERY	10/29/03
DE	G.A. BYINGTON	10/29/03
DVR	J.L. HECK	10/29/03
DM	J.C. WALLS	10/29/03
PE	M.R. FELDMAN	10/29/03
PM	D.B. MILLER	10/29/03

SCALE: NOTED
TOLERANCES UNLESS OTHERWISE SPECIFIED
FRACTIONS
XX DECIMALS ±.01
XXX DECIMALS ±.005
ANGLES ±0.5°
BREAK SHARP EDGES .06 MAX
FINISH 125 RMS

BWXT Y-12 — A BWXT Babcock & Wilcox Company
Y-12 National Security Complex managed by BWXT Y-12, L.L.C. for the Department of Energy under U.S. Government contract DE-AC05-00OR22800
a Oak Ridge, Tennessee a

PROJECT NAME: ES-3100 SHIPPING PACKAGE

CONTAINMENT VESSEL ASSEMBLY

I	48	49	50	PLANT	BLDG	FL	SH. OF	TYPE	CLASS
6	M	L	F	Y-12	NA	NA	1 / 1	A	U

A1	52	53	REV
CM	PKG	IN	C

M2E801580A011

NO REPRESENTATION OR WARRANTY, EXPRESSED OR IMPLIED, IS MADE AS TO THE ACCURACY, COMPLETENESS OR USEFULNESS OF THE INFORMATION OR STATEMENTS CONTAINED IN THESE DRAWINGS, OR THAT THE USE OR DISCLOSURE OF ANY INFORMATION, APPARATUS, METHOD, OR PROCESS DISCLOSED IN THESE DRAWINGS MAY NOT INFRINGE PRIVATE RIGHTS OF OTHERS. NO LIABILITY IS ASSUMED WITH RESPECT TO THE USE OF, OR FOR DAMAGES RESULTING FROM THE USE OF ANY INFORMATION, APPARATUS, METHOD OR PROCESS DISCLOSED IN THESE DRAWINGS. DRAWINGS MADE AVAILABLE FOR INFORMATION OR BIDDER USE NOT TO BE USED FOR OTHER PURPOSES AND ARE TO BE RETURNED UPON REQUEST OF THE FORWARDING CONTACTOR.

THIS DRAWING PRODUCED ON PRO/ENGINEER

THIS PAGE INTENTIONALLY LEFT BLANK.

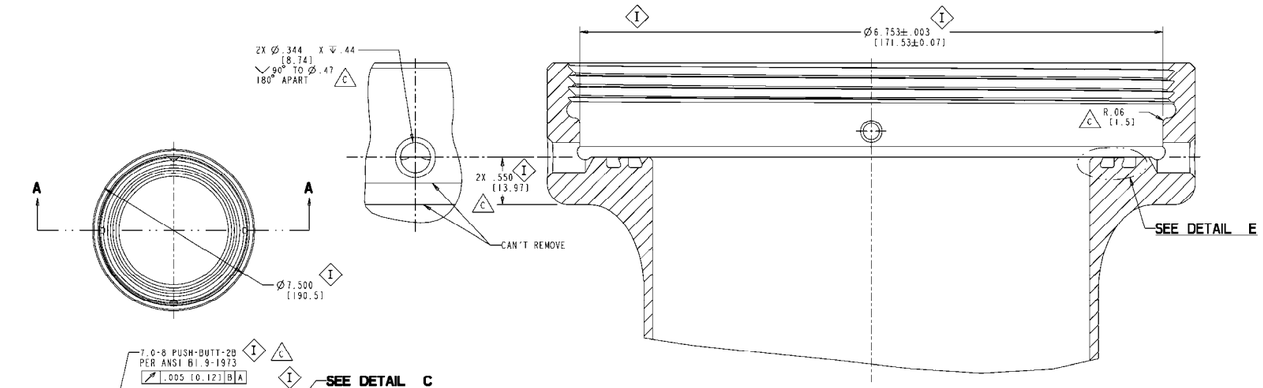

SECTION B-B
SCALE 2/1

NOTES

1 INTERPRET DRAWING PER ENGINEERING DRAFTING STANDARD ES-3.1.

2 INTERPRET DIMENSIONS AND TOLERANCES PER ASME Y14.5M-1994. PERFECT ORIENTATION AT MMC FOR INTERRELATED FEATURES REQUIRED.

3 DIMENSIONS ARE IN INCHES [mm].

4 APPROXIMATE WEIGHT: 22.44 LBS [10.18 Kg].

5 FOR ADDITIONAL REQUIREMENTS SEE JS-YMN3-801580-A001.

6 DIMENSIONS AND FEATURES FLAGGED BY A (I) SYMBOL SHALL BE INSPECTED AND DOCUMENTED.

7 VERIFY THE CONTAINMENT VESSEL INTERNAL DIAMETER BY USING THE MINIMUM CVID GAGE. THE CVID GAGE SHALL BE 10.30 +/- 0.03 LONG BY 5.020 +/- .001 EXTERNAL DIAMETER WITH A 20 DEGREE CHAMFER FROM THE CYLINDER TO A 4.52 +/- .03 DIAMETER ON THE BOTTOM. THE BOTTOM SHALL BE FINISHED WITH A .25 THICK YELLOW BRASS PLATE.

8 THE FORMED BODY CONSTRUCTION SHOWN IN PART -2 IS PREFERRED. THE ALTERNATIVE WELDED OPTION SHOWN IN PART -4 ON SHEET 2 IS ALSO ACCEPTABLE. PART -4 SHALL CONFORM TO THE PART -1 DIMENSIONS.

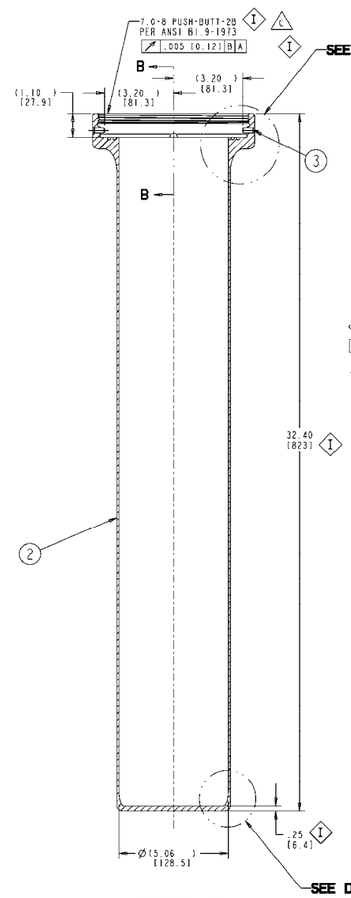

SECTION A-A

-1 CONTAINMENT VESSEL BODY ASSEMBLY

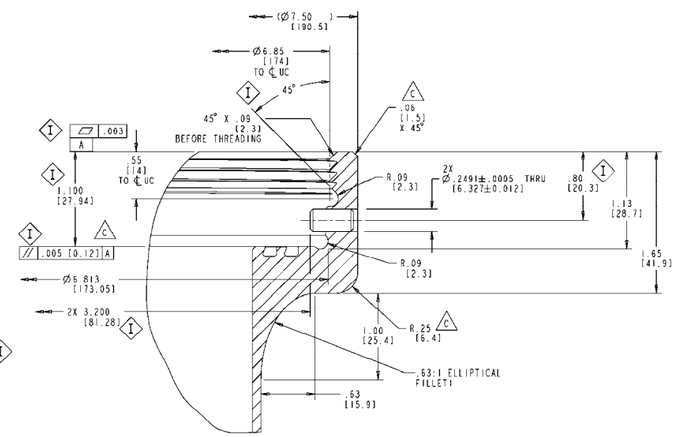

DETAIL C
SCALE 2/1

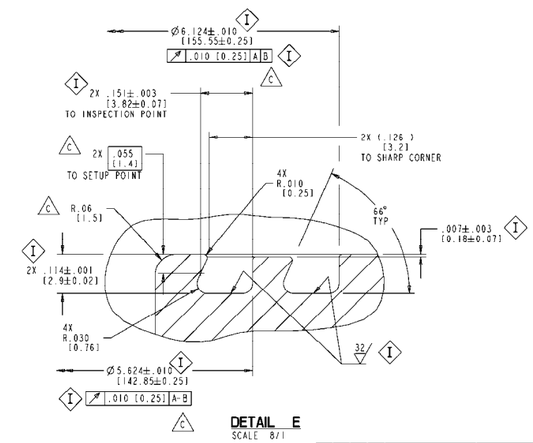

DETAIL E
SCALE 8/1

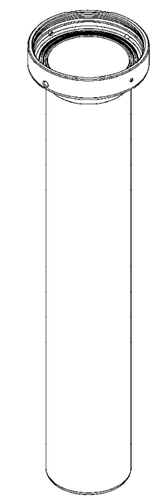

ISOMETRIC VIEW
SCALE 3/8

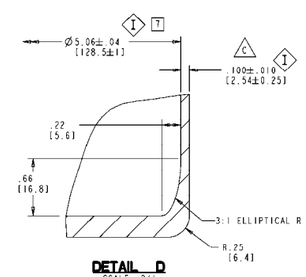

DETAIL D
SCALE 2/1

			1		-7	CONTAINMENT VESSEL END CAP	SST	ASME SA-182 TYPE F304L	7
			1		-6	CV PIPE BODY SIPS SCH40		ASME SA-312 TYPE TP304L	6
			1		-5	CONTAINMENT VESSEL FLANGE		ASME SA-182 TYPE F304L	5
7 8	AR	AR	X		-4	CONTAINMENT VESSEL BODY ASSEMBLY WELDED OPTION			4
C		2	2		-3	DOWEL PIN, .50 LONG Ø0.2501/0.2503 OD	18-8-SST	ANSI B18.8.2	3
			1		-2	CONTAINMENT VESSEL FORMED BODY	304L SST	SEE NOTE 5	2
7 8	AR	AR	X		-1	CONTAINMENT VESSEL BODY ASSEMBLY			1
				PART OR IDENTIFYING NO	NOMENCLATURE OR DESCRIPTION	MATERIAL	SPECIFICATION	FIND NO
				← QTY REQD NEXT ASSY	PARTS LIST			

THIS DRAWING INCLUDES FEATURES SUPPORTING NUCLEAR CRITICALITY SAFETY. ANY REVISION TO THIS DIAGRAM REQUIRES NUCLEAR CRITICALITY SAFETY DIVISION APPROVAL.

REVISION	DATE	NCSD APPROVAL
C	2/10/05	JF DECLUE

This document has been reviewed by a Y-12 ADC and UCNI RO and has been determined to be UNCLASSIFIED and not UCNI. This review does not constitute clearance for public release.

Name: ROGER D. AIGNER Date: 2/10/05

REV	DESCRIPTION	DRW	CHKR	DE	DVR	DM	DATE	PE	DATE	PK	DATE	WE	DATE
C	GEN REV; REMOVED ALL MMC & RFS SYMS FROM GEO TOLS; MODIFIED GEO TOLS TO PRIMARY & SECONDARY DATUM REF; ADDED VIEW ZONE G:6; ADDED .06 X 45° CHAM; ADDED TOL TO DIM IN DETAIL D; ADDED ANSI SPEC TO BOM; CHNG G TO U IN WELD SYM SHT 2	GAB	RA	GAB	JLH	JCW	01/22/04	GAB	01/22/04	JGA	01/22/04		
B	ADDED PARTS 4, 5, 6, AND 7 ON SHEET 2 ALSO, GENERAL REVISIONS TO SHEET 1.	GAB	RA	GAB	JLH	JCW	10/23/03	MRF	10/29/03	DBM	10/29/03		
A	ISSUED FOR PRODUCTION PROCUREMENT	DWS	JSL	GAB	JLH	JCW	10/23/03	MRF	10/29/03	DBM	10/29/03		

REVISION OR ISSUE PURPOSE — REVISION APPROVALS

SQUAD CHECK	AR	CV	ST	HV	EM	FP	FD	EE	IE	M	NP

DRAWING APPROVALS		DATE
DRW	JBJ for D.W. SPARKS	10/29/03
CHKR	J.S. LOWERY	10/29/03
DE	G.A. BYINGTON	10/29/03
DVR	J.L. HECK	10/29/03
DM	J.C. WALLS	10/29/03
PE	M.R. FELDMAN	10/29/03
PK	D.B. MILLER	10/29/03

SCALE: NOTED
TOLERANCES UNLESS OTHERWISE SPECIFIED
FRACTIONS ±.01
XX DECIMALS ±.01
XXX DECIMALS ±.005
ANGLES ±0.5°
BREAK SHARP EDGES .06 MAX
FINISH 125 RMS

BWXT Y-12 — Y-12 National Security Complex managed by BWXT Y-12, L.L.C. for the Department of Energy under U.S. Government contract DE-AC05-00OR22800 • Oak Ridge, Tennessee •
PROJECT NAME: ES-3100 SHIPPING PACKAGE

CONTAINMENT VESSEL BODY ASSEMBLY

SI	48	49	50	PLANT	BLDG	FL	SH.	OF	TYPE	CLASS
6	M	L	F	Y-12	NA	NA	1	2	S	U

SI	52	53		REV
CM	PKG	IN	M2E801580A012	C

M2E801580A012

NO REPRESENTATION OR WARRANTY, EXPRESSED OR IMPLIED, IS MADE AS TO THE ACCURACY, COMPLETENESS OR USEFULNESS OF THE INFORMATION OR STATEMENTS CONTAINED IN THESE DRAWINGS, OR THAT THE USE OR DISCLOSURE OF ANY INFORMATION, APPARATUS, METHOD, OR PROCESS DISCLOSED IN THESE DRAWINGS MAY NOT INFRINGE PRIVATE RIGHTS OF OTHERS. NO LIABILITY IS ASSUMED WITH RESPECT TO THE USE OF, OR FOR DAMAGES RESULTING FROM THE USE OF ANY INFORMATION, APPARATUS, METHOD OR PROCESS DISCLOSED IN THESE DRAWINGS. INFORMATION CONTAINED IN THESE DRAWINGS FOR BIDDER ARE NOT TO BE USED FOR OTHER PURPOSES AND ARE TO BE RETURNED UPON REQUEST OF THE FORWARDING CONTRACTOR.

PTHIS DRAWING PRODUCED ON PRO/ENGINEER

THIS PAGE INTENTIONALLY LEFT BLANK.

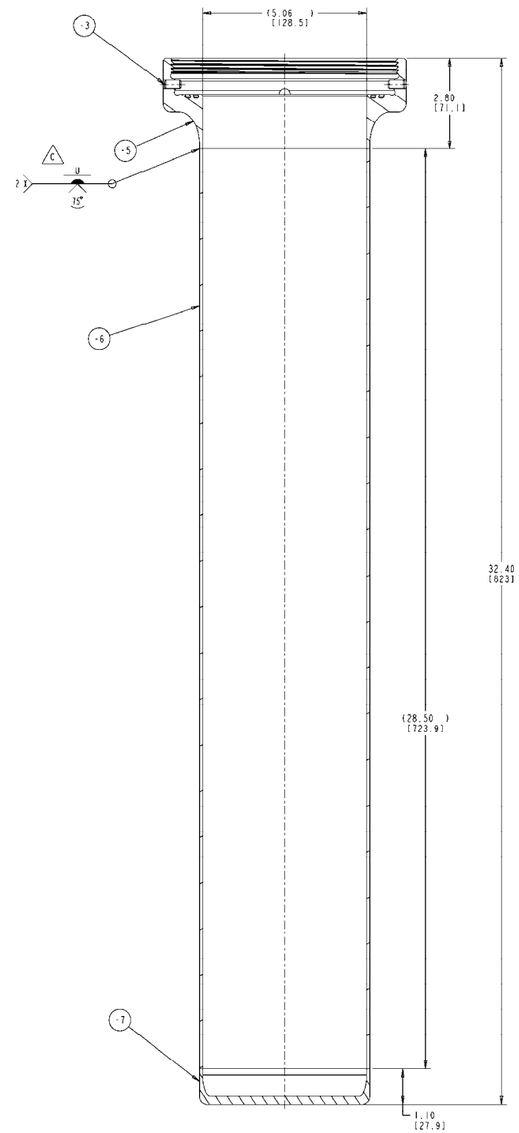

-4 CONTAINMENT VESSEL BODY ASSEMBLY WELDED OPTION

SCALE 3/4

NO REPRESENTATION OR WARRANTY, EXPRESSED OR IMPLIED, IS MADE AS TO THE ACCURACY, COMPLETENESS OR USEFULNESS OF THE INFORMATION OR STATEMENTS CONTAINED IN THESE DRAWINGS, OR THAT THE USE OR DISCLOSURE OF ANY INFORMATION, APPARATUS, METHOD, OR PROCESS DISCLOSED IN THESE DRAWINGS MAY NOT INFRINGE PRIVATE RIGHTS OF OTHERS. NO LIABILITY IS ASSUMED WITH RESPECT TO THE USE OF, OR FOR DAMAGES RESULTING FROM THE USE OF ANY INFORMATION, APPARATUS, METHOD OR PROCESS DISCLOSED IN THESE DRAWINGS. DRAWINGS MADE AVAILABLE FOR INFORMATION TO BIDDER ARE NOT TO BE USED FOR OTHER PURPOSES AND ARE TO BE RETURNED UPON REQUEST OF THE FORWARDING CONTRACTOR.

THIS DRAWING PRODUCED ON PRO/ENGINEER

BWXT Y-12 — Y-12 National Security Complex managed by BWXT Y-12, L.L.C. for the Department of Energy under U.S. Government contract DE-AC05-00OR22800 • Oak Ridge, Tennessee •

PRINCIPAL NAME: ES-3100 SHIPPING PACKAGE

CONTAINMENT VESSEL BODY ASSEMBLY

I	48	49	50	PLANT	BLDG	FL	SH	OF	TYPE	CLASS
6	M	L	F	Y-12	NA	NA	2	2	S	U

51	52	53		REV
CM	PKG	IN	M2E801580A012	C

THIS PAGE INTENTIONALLY LEFT BLANK.

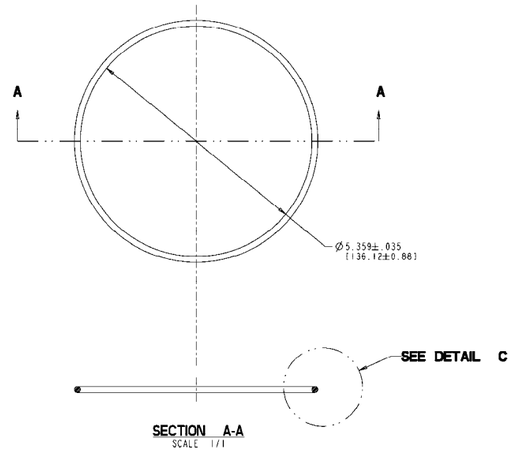

-1 INNER O-RING

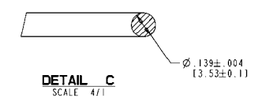

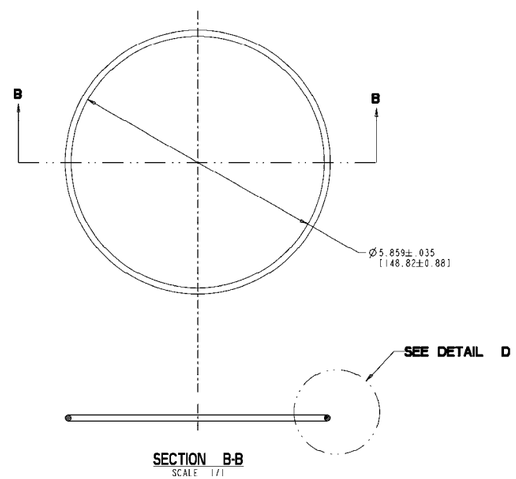

-2 OUTER O-RING
SCALE 1/2

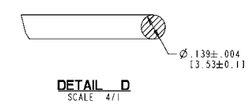

NOTES

1. INTERPRET DRAWING PER MECHANICAL DRAFTING STANDARD ES-3.1.
2. INTERPRET DIMENSIONS AND TOLERANCES PER ASME Y14.5M-1994.
3. DIMENSIONS ARE IN INCHES.[mm].
4. O-RING SHALL MEET THE FOLLOWING REQUIREMENTS IN ADDITION TO THE PROCUREMENT SPECIFICATION 00-PP-986.

TYPE OF SERVICE:	STATIC FACE SEAL
MATERIAL COMPOSITION:	ETHYLENE PROPYLENE:
COMPOUND SPECIFICATION:	ASTM D2000 M3BA712A14B13F17
B TEMPERATURE SERVICE RANGE:	302°F TO -40°F
HARDNESS:	70A +/- 5 SHORE A DUROMETER
ELONGATION %, MINIMUM:	100%
FABRICATION METHOD:	MOLDED
SURFACE CONDITION:	SMOOTH, NON POROUS, FREE OF SKIN DEFECTS
COLOR:	BLACK

FIND NO	SPECIFICATION	MATERIAL	NOMENCLATURE OR DESCRIPTION	PART OR IDENTIFYING NO	QTY REQD NEXT ASSY
2		SEE NOTE 4	OUTER O-RING	-2	AR
1		SEE NOTE 4	INNER O-RING	-1	AR

M2E801580A013 M2E801580A013 A01-1

PARTS LIST

THIS DRAWING INCLUDES FEATURES SUPPORTING NUCLEAR CRITICALITY SAFETY. ANY REVISION TO THIS DIAGRAM REQUIRES NUCLEAR CRITICALITY SAFETY DIVISION APPROVAL.

REVISION	DATE	NCSD APPROVAL
B	2/10/05	JF DECLUE

This document has been reviewed by a Y-12 ADC and UCNI RO and has been determined to be UNCLASSIFIED and not UCNI. This review does not constitute clearance for public release.

Name: ROGER D. AIGNER Date: 2/10/05

NO REPRESENTATION OR WARRANTY, EXPRESSED OR IMPLIED, IS MADE AS TO THE ACCURACY, COMPLETENESS OR USEFULNESS OF THE INFORMATION OR STATEMENTS CONTAINED IN THESE DRAWINGS, OR THAT THE USE OR DISCLOSURE OF ANY INFORMATION, APPARATUS, METHOD, OR PROCESS DISCLOSED IN THESE DRAWINGS MAY NOT INFRINGE PRIVATE RIGHTS OF OTHERS. NO LIABILITY IS ASSUMED WITH RESPECT TO THE USE OF, OR FOR DAMAGES RESULTING FROM THE USE OF ANY INFORMATION, APPARATUS, METHOD OR PROCESS DISCLOSED IN THESE DRAWINGS. DRAWINGS MADE AVAILABLE FOR INFORMATION TO BIDDER ARE NOT TO BE USED FOR OTHER PURPOSES AND ARE TO BE RETURNED UPON REQUEST OF THE FORWARDING CONTACTOR.

THIS DRAWING PRODUCED ON PRO/ENGINEER

REV	DESCRIPTION	DRW	CHKR	DE	DVR	DM	DATE	PE	DATE	PM	DATE
B	GEN REV; -1 WAS 2-253; -2 WAS 2-257,302°F WAS 300°F	JRP	SMM	GAB	RDA	DPS	11/18/03	GAB	2/10/05	JGA	2/10/05
A	ISSUED FOR PROTOTYPE PROCUREMENT	DWS	JSL	GAB	JLH	JCW	10/25/03	MRF	10/29/03	DBM	10/29/03

REVISION OR ISSUE PURPOSE — REVISION APPROVALS

SQUAD CHECK	AR	CV	ST	HV	EM	FP	FD	EE	IE	M	NP

SCALE: NOTED

DRAWING APPROVALS		DATE
DRW	JRJ for D.B. SPARKS	10/29/03
CHKR	J.S. LOWERY	10/29/03
DE	G.A. BYINGTON	10/29/03
DVR	J.L. HICKS	10/29/03
DM	J.C. WALLS	10/29/03
PE	M.R. FELDMAN	10/29/03
PM	D.B. MILLER	10/29/03

BWXT Y-12 A Babcock & Wilcox Company

Y-12 National Security Complex managed by BWXT Y-12, L.L.C. for the Department of Energy under U.S. Government contract DE-AC05-00OR22800 • Oak Ridge, Tennessee •

PROJECT NAME: ES-3100 SHIPPING PACKAGE

CONTAINMENT VESSEL O-RING DETAILS

1	48	49	50	PLANT	BLDG	FL	SH.	OF	TYPE	CLASS
6	M	L	F	Y-12	NA	NA	1	1	S	U

51	52	53		REV
CM	PKG	IN	M2E801580A013	B

M2E801580A013

THIS PAGE INTENTIONALLY LEFT BLANK.

NOTES

1. INTERPRET DRAWING PER ENGINEERING DRAFTING STANDARD ES-3.1.
2. INTERPRET DIMENSIONS AND TOLERANCES PER ASME Y14.5M-1994. PERFECT ORIENTATION AT MMC FOR INTERRELATED FEATURES REQUIRED.
3. DIMENSIONS ARE IN INCHES [mm].
4. APPROXIMATE WEIGHT: 10.54 LBS [4.78 Kg].
5. FOR ADDITIONAL REQUIREMENTS SEE JS-YMN3-801580-A001.

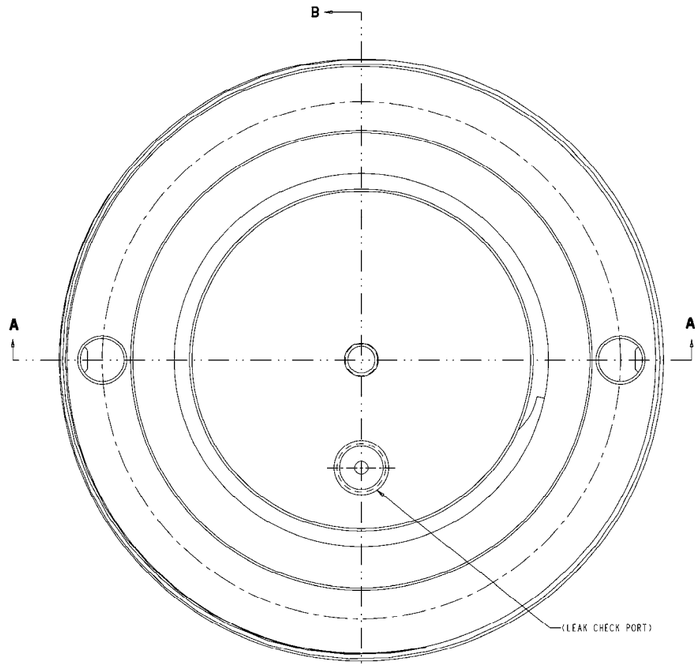

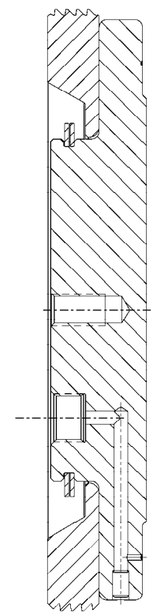

SECTION B-B

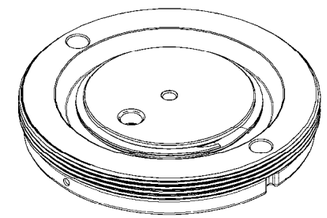

ISOMETRIC VIEW
SCALE 1/1

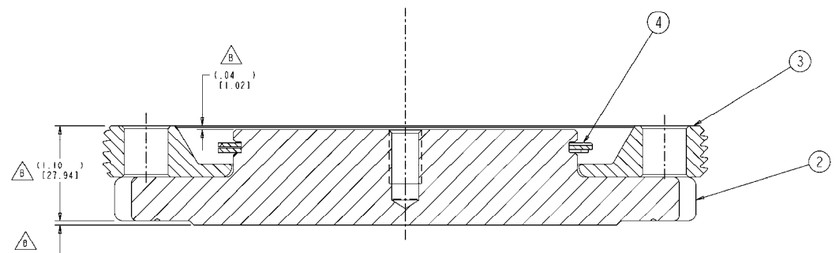

SECTION A-A
SCALE 2/1

-1 CONTAINMENT VESSEL LID ASSEMBLY

	1	WSM-400-S02	EXTERNAL RETAINING RING	SMALLEY STEEL RING CO. 385 GILMAN AVE. WHEELING, IL 60090	4
	1	M2E801580A016-1	CONTAINMENT VESSEL CLOSURE NUT		3
	1	M2E801580A015-1	CONTAINMENT VESSEL SEALING LID		2
AR	AR	1	CONTAINMENT VESSEL LID ASSEMBLY		1
WZ8A-580 A001-1 / WZ8A-580 A001-1	-	PART OR IDENTIFYING NO / QTY REQD / NEXT ASSY	NOMENCLATURE OR DESCRIPTION	MATERIAL / SPECIFICATION	FIND NO

PARTS LIST

M2E801580A014

THIS DRAWING INCLUDES FEATURES SUPPORTING NUCLEAR CRITICALITY SAFETY. ANY REVISION TO THIS DIAGRAM REQUIRES NUCLEAR CRITICALITY SAFETY DIVISION APPROVAL.

REVISION	DATE	NCSD APPROVAL
B	2/10/05	JF DECLUE

This document has been reviewed by a Y-12 ADC and UCNI RO and has been determined to be UNCLASSIFIED and not UCNI. This review does not constitute clearance for public release.

Name: ROGER D. AIGNER Date: 2/10/05

REV	DESCRIPTION	DRW	CHKR	PE	OVR	DM	DATE	PE	DATE	PM	DATE
B	GEN: REV. THREAD RELIEF IN SECTION B-B; DIMS WERE 3 PLACE	JRP	SMM	GAB	RDA	DPS	10/28/03	GAB	2/10/05	JGA	2/10/05
A	ISSUED FOR PROTOTYPE PROCUREMENT	DWS	JSL	GAB	JLH	JCW	10/28/03	MRF	10/29/03	DBM	10/29/03

REVISION OR ISSUE PURPOSE — REVISION APPROVALS

SQUAD CHECK	
AR	CV
ST	HV
EM	FP
PD	EL
IE	M
NP	

DRAWING APPROVALS

SCALE:	NOTED	DRW	JRJ for D.W. SPARKS 10/29/03
TOLERANCES UNLESS OTHERWISE SPECIFIED		CHKR	J.S. LOWERY 10/29/03
		DE	G.A. BYINGTON 10/29/03
		OVR	J.L. HECK 10/29/03
FRACTIONS		DM	J.C. WALLS 10/29/03
XX DECIMALS		PE	M.R. FELDMAN 10/29/03
XXX DECIMALS		PM	D.B. MILLER 10/29/03
ANGLES			
BREAK SHARP EDGES	MAX		
FINISH			

BWXT Y-12 — Y-12 National Security Complex managed by BWXT Y-12, L.L.C. for the Department of Energy under U.S. Government contract DE-AC05-00OR22800. a BWXT Babcock & Wilcox Enterprise. 9 Oak Ridge, Tennessee 9

PROJECT NAME: ES-3100 SHIPPING PACKAGE

CONTAINMENT VESSEL LID ASSEMBLY

1	46	49	50	PLANT	BLDG	FL	SH.	OF	TYPE	CLASS
6	M	L	F	Y-12	NA	NA	1	1	S	U

51	52	53	DATE	REV
CM	PKG	IN	M2E801580A014	B

NO REPRESENTATION OR WARRANTY, EXPRESSED OR IMPLIED, IS MADE AS TO THE ACCURACY, COMPLETENESS OR ASSENTIALNESS OF THE INFORMATION OR STATEMENTS CONTAINED IN THESE DRAWINGS, OR THAT THE USE OR DISCLOSURE OF ANY INFORMATION, APPARATUS, METHOD, OR PROCESS DISCLOSED IN THESE DRAWINGS WILL NOT INFRINGE ANY PRIVATELY OWNED RIGHTS. NO LIABILITY IS ASSUMED WITH RESPECT TO THE USE OF, OR FOR DAMAGES RESULTING FROM THE USE OF ANY INFORMATION, APPARATUS, METHOD OR PROCESS DISCLOSED IN THESE DRAWINGS. DRAWINGS MADE AVAILABLE FOR INFORMATION TO BIDDER ARE NOT TO BE USED FOR OTHER PURPOSES AND ARE TO BE RETURNED UPON REQUEST OF THE FORWARDING CONTRACTOR.

THIS DRAWING PRODUCED ON PROENGINEER

THIS PAGE INTENTIONALLY LEFT BLANK.

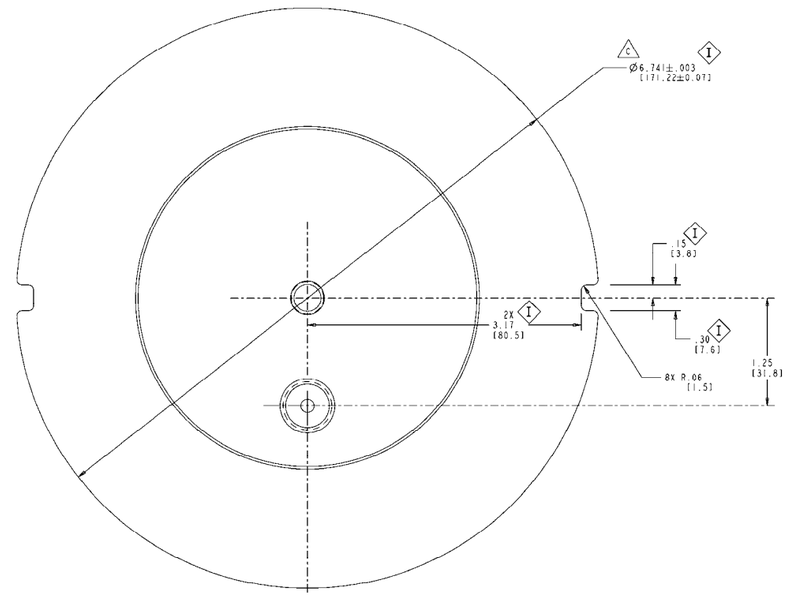

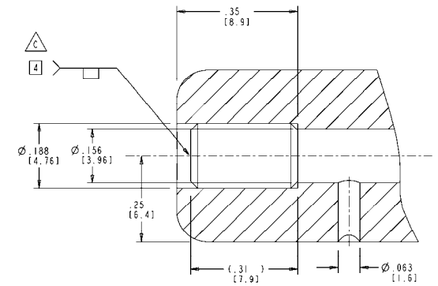

DETAIL C
SCALE 8/1

NOTES

1. INTERPRET DRAWING PER ENGINEERING DRAFTING STANDARD ES-3.1.
2. INTERPRET DIMENSIONS AND TOLERANCES PER ASME Y14.5M-1994. PERFECT ORIENTATION AT MMC FOR INTERRELATED FEATURES REQUIRED.
3. DIMENSIONS ARE IN INCHES [mm].
4. WELD BAR (F/N 3) TO CONTAINER LID (F/N 2) BEFORE FINAL MACHINING.
5. FOR ADDITIONAL REQUIREMENTS SEE JS-YWN3-801580-A001.
6. DIMENSIONS OR FEATURES FLAGGED BY A (I) SYMBOL SHALL BE INSPECTED AND DOCUMENTED.

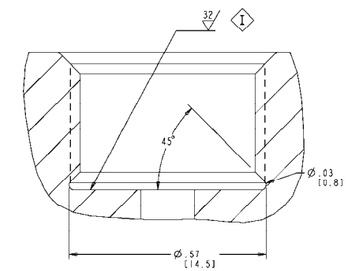

DETAIL X
SCALE 8/1

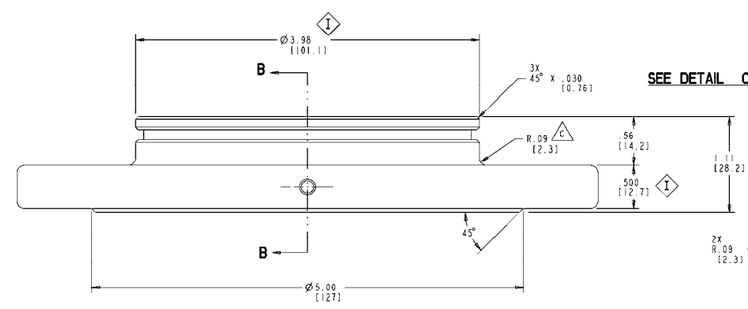

-1 CONTAINMENT VESSEL SEALING LID
SCALE 2/1

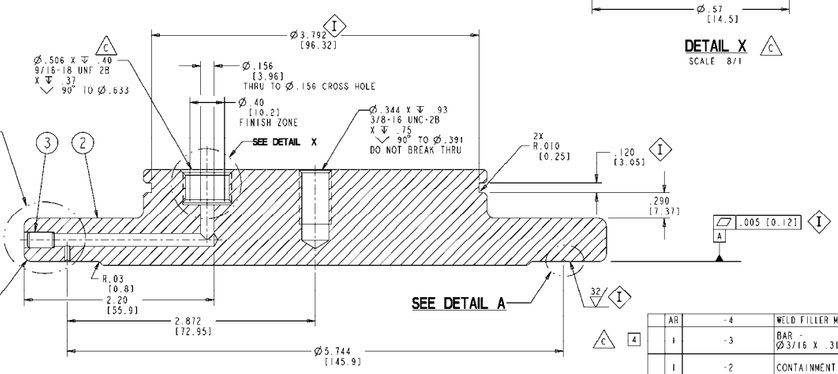

SECTION B-B

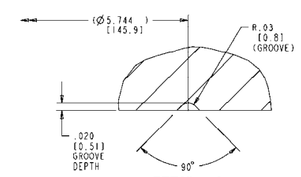

DETAIL A
SCALE 8/1

AR	-4	WELD FILLER METAL	PER WELD PROCEDURES		4
1	-3	BAR - Ø3/16 X .31 LONG	SST 304	ASME SA-479	3
1	-2	CONTAINMENT LID			2
AR	-1	CONTAINMENT VESSEL SEALING LID			1
PART OR IDENTIFYING NO / QTY REQD / NEXT ASSY	NOMENCLATURE OR DESCRIPTION	MATERIAL	SPECIFICATION	FIND NO	

PARTS LIST

M2E801580A015

THIS DRAWING INCLUDES FEATURES SUPPORTING NUCLEAR CRITICALITY SAFETY. ANY REVISION TO THIS DIAGRAM REQUIRES NUCLEAR CRITICALITY SAFETY DIVISION APPROVAL.

REVISION	DATE	NCSD APPROVAL
C	2/10/05	JF DECLUE

This document has been reviewed by a Y-12 ADC and UCNI RO and has been determined to be UNCLASSIFIED and not UCNI. This review does not constitute clearance for public release.

Name: ROGER D. AIGNER Date: 2/10/05

NO REPRESENTATION OR WARRANTY, EXPRESSED OR IMPLIED, IS MADE AS TO THE ACCURACY, COMPLETENESS OR USEFULNESS OF THE INFORMATION OR STATEMENTS CONTAINED IN THESE DRAWINGS, OR THAT THE USE OR DISCLOSURE OF ANY INFORMATION, APPARATUS, METHOD, OR PROCESS DISCLOSED IN THESE DRAWINGS MAY NOT INFRINGE PRIVATE RIGHTS OF OTHERS. NO LIABILITY IS ASSUMED WITH RESPECT TO THE USE OF, OR FOR DAMAGES RESULTING FROM THE USE OF ANY INFORMATION, APPARATUS, METHOD OR PROCESS DISCLOSED IN THESE DRAWINGS. DRAWINGS MADE AVAILABLE FOR INFORMATION OR BIDDER USE ARE NOT TO BE USED FOR OTHER PURPOSES AND ARE TO BE RETURNED UPON REQUEST OF THE FORWARDING CONTRACTOR.

PTHIS DRAWING PRODUCED ON PROENGINEER

REV	DESCRIPTION	DRW	CHKR	DE	DVR	DM	DATE	PE	DATE	PM	DATE	ML	DATE
C	MOVED Ø6.741 DIM TO ZONE H6; ZONE D6 ADDED DIM R.09; ZONE D5 CHANGED DIM .38 TO .37; ADDED DET.X MOVED 32 FINISH SYM & (I) FROM SEC B-B	JRP	SMM	GAB	RDA	DPS	10/18/05	GAB	2/10/05	JGA	2/10/05	DJE	2/11/05
B	REDUCED ORING FINISH AND LEAKCHECK DEPTH	GAB	RA	GAB	JLH	JCW	10/27/04	GAB	10/27/04	JGA	10/27/04		
A	ISSUED FOR PROTOTYPE PROCUREMENT	DWS	JSL	GAB	JLH	JCW	10/29/03	MRF	10/29/03	DBM	10/29/03		

REVISION OR ISSUE PURPOSE — REVISION APPROVALS

SQUAD CHECK	AR	CV	ST	HV	EM	FP	FD	EE	IE	M	NP

DRAWING APPROVALS		DATE
DRW	JRJ for D.R. SPARKS	10/29/03
CHKR	J.S. LOWERY	10/29/03
DE	G.A. BYINGTON	10/29/03
DVR	J.L. HECK	10/29/03
DM	J.C. WALLS	10/29/03
PE	M.R. FELDMAN	10/29/03
PM	D.B. MILLER	10/29/03

SCALE: NOTED

TOLERANCES UNLESS OTHERWISE SPECIFIED
FRACTIONS
XX DECIMALS ±.01
XXX DECIMALS ±.005
ANGLES ±0.5°
BREAK SHARP EDGES .06 MAX
FINISH 125 RMS

BWXT Y-12 — Y-12 National Security Complex managed by BWXT Y-12, L.L.C. for the Department of Energy under U.S. Government contract DE-AC05-00OR22800 a Oak Ridge, Tennessee a BWXT Babcock & Wilcox Company

PROJECT NAME: ES-3100 SHIPPING PACKAGE

CONTAINMENT VESSEL SEALING LID

1	48	49	50	PLANT	BLDG	FL	SH.	OF	TYPE	CLASS
6	M	L	F	Y-12	NA	NA	1	1	S	U

A1	A2	A3	DATE	REV
CM	PKG	IN	M2E801580A015	C

THIS PAGE INTENTIONALLY LEFT BLANK.

NOTES

1. INTERPRET DRAWING PER ENGINEERING DRAFTING STANDARD ES-3.1.
2. INTERPRET DIMENSIONS AND TOLERANCES PER ASME Y14.5M-1994. PERFECT ORIENTATION AT MMC FOR INTERRELATED FEATURES REQUIRED.
3. DIMENSIONS ARE IN INCHES [mm].
4. (C) FOR ADDITIONAL REQUIREMENTS SEE JS-YMN3-801580-A001.
5. DIMENSIONS AND FEATURES FLAGGED BY A (I) SYMBOL SHALL BE INSPECTED AND DOCUMENTED.1

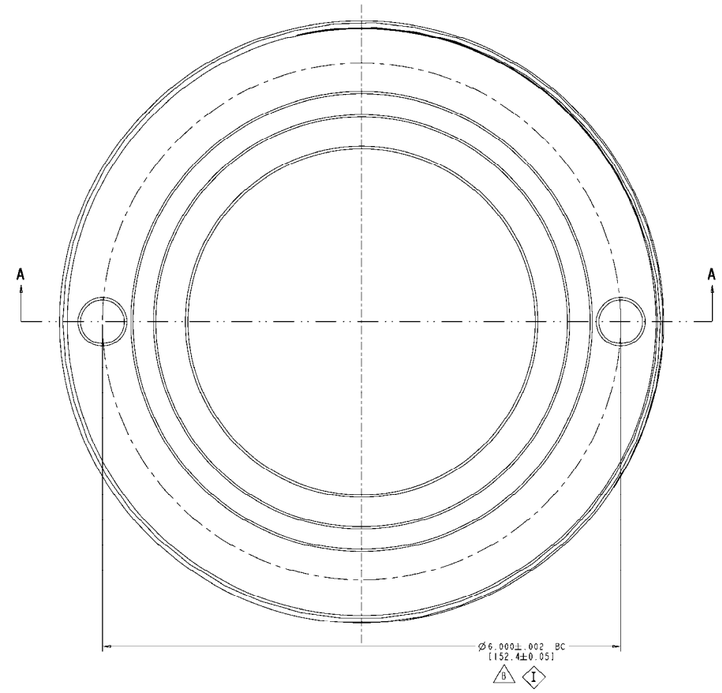

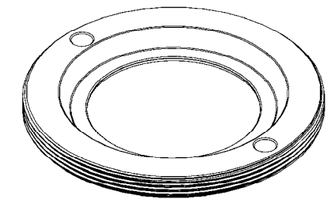

ISOMETRIC VIEW
SCALE 1/1

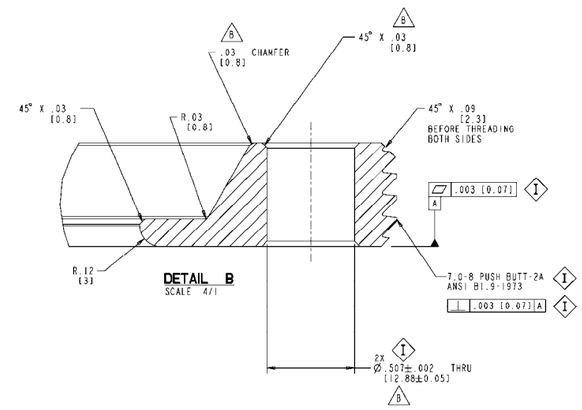

DETAIL B
SCALE 4/1

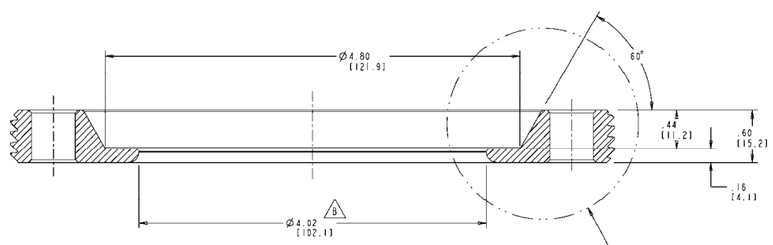

SECTION A-A
SCALE 2/1

-1 CONTAINMENT VESSEL CLOSURE NUT

AR	AR	-1	CONTAINMENT VESSEL CLOSURE NUT	NITRONIC 60 SST	ASME SA-479 UNS-S21800	1
M2E801580 A001-1	M2E801580 A001-1	PART OR IDENTIFYING NO	NOMENCLATURE OR DESCRIPTION	MATERIAL	SPECIFICATION	FIND NO
		← QTY REQD NEXT ASSY	PARTS LIST			

M2E801580A016

THIS DRAWING INCLUDES FEATURES SUPPORTING NUCLEAR CRITICALITY SAFETY. ANY REVISION TO THIS DIAGRAM REQUIRES NUCLEAR CRITICALITY SAFETY DIVISION APPROVAL.

REVISION	DATE	NCSD APPROVAL
B	2/10/05	JF DECLUE

This document has been reviewed by a Y-12 ADC and UCNI RO and has been determined to be UNCLASSIFIED and not UCNI. This review does not constitute clearance for public release.

Name: ROGER D. AIGNER Date: 2/10/05

REV	DESCRIPTION	DRW	CHKR	DE	DVR	DM	DATE	PE	DATE	PM	DATE
B	ADDED CHAMFER IN DETAIL B; MOD. HOLE TOL REMOVED NOTE 4;RENUMBERED NOTES IN GEN NOTES	JRP	SMM	GAB	RDA	DPS	11/18/03	GAB	2/10/05	JGA	2/10/05
A	ISSUED FOR PROTOTYPE PROCUREMENT	DWS	JSL	GAB	JLH	JCW	10/29/03	MRF	10/29/03	DBM	10/29/03

REVISION OR ISSUE PURPOSE — REVISION APPROVALS

AR	CV	ST	HV	EM	FP	FD	EL	IC	M	NP

SQUAD CHECK

DRW	JRJ (or D.W. SPARKS)	10/29/03
CHKR	J.S. LOWERY	10/29/03
DE	G.A. BYINGTON	10/29/03
DVR	J.L. HECK	10/29/03
DM	J.C. WALLS	10/29/03
PE	M.R. FELDMAN	10/29/03
PM	D.B. MILLER	10/29/03

DRAWING APPROVALS

SCALE: NOTED

TOLERANCES UNLESS OTHERWISE SPECIFIED
FRACTIONS
XX DECIMALS ±.01
XXX DECIMALS ±.005
ANGLES ±0.5°
BREAK SHARP EDGES .06 MAX
FINISH 125 RMS

BWXT Y-12 — Y-12 National Security Complex managed by BWXT Y-12, L.L.C. for the Department of Energy under U.S. Government contract DE-AC05-00OR22800 in Oak Ridge, Tennessee

PROJECT NAME: ES-3100 SHIPPING PACKAGE

CONTAINMENT VESSEL CLOSURE NUT

DATE	1	48	49	50	PLANT	BLDG	FL	SH.	OF	TYPE	CLASS
	6	M	L	F	Y-12	NA	NA	1	1	S	U
	51 CM		52 PKG		53 IN	M2E801580A016					REV B

NO REPRESENTATION OR WARRANTY, EXPRESSED OR IMPLIED, IS MADE AS TO THE ACCURACY, COMPLETENESS OR USEFULNESS OF THE INFORMATION OR STATEMENTS CONTAINED IN THESE DRAWINGS, OR THAT THE USE OR DISCLOSURE OF ANY INFORMATION, APPARATUS, METHOD, OR PROCESS DISCLOSED IN THESE DRAWINGS MAY NOT INFRINGE PRIVATE RIGHTS OF OTHERS. NO LIABILITY IS ASSUMED WITH RESPECT TO THE USE OF, OR FOR DAMAGES RESULTING FROM THE USE OF ANY INFORMATION, APPARATUS, METHOD OR PROCESS DISCLOSED IN THESE DRAWINGS. DRAWINGS MADE AVAILABLE FOR INFORMATION TO BIDDER ARE NOT TO BE USED FOR OTHER PURPOSES AND ARE TO BE RETURNED UPON REQUEST OF THE FORWARDING CONTRACTOR.

THIS DRAWING PRODUCED ON PRO/ENGINEER

THIS PAGE INTENTIONALLY LEFT BLANK.

NOTES

1 INTERPRET DRAWING PER MECHANICAL DRAFTING STANDARD ES-3.1.

2 INTERPRET DIMENSIONS AND TOLERANCES PER "RMA" RUBBER HANDBOOK (RMA-392) CLASS "A2 PRECISION."

3 DIMENSIONS ARE IN INCHES [mm].

4 MANUFACTURER/SUPPLIER TO PROVIDE CERTIFICATE OF COMPLIANCE FOR ALL FEATURES OF THESE ITEMS.

5 IN APPROXIMATE LOCATION SHOWN, USING WHITE SILICONE INK, MARK DRAWING NUMBER AND REVISION LETTER IN 1/4" HIGH CHARACTERS.

6 MANUFACTURED BY:
REISS MANUFACTURING, INC.
1 POLYMER PLACE
BLACKSTONE VA, 23824-0060

7 FOR REFERENCE ONLY:
WEIGHT: 0.0588 LBS (26.7 g)

B

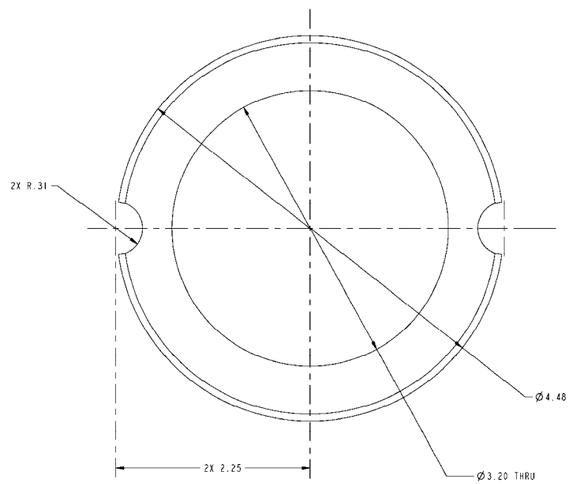

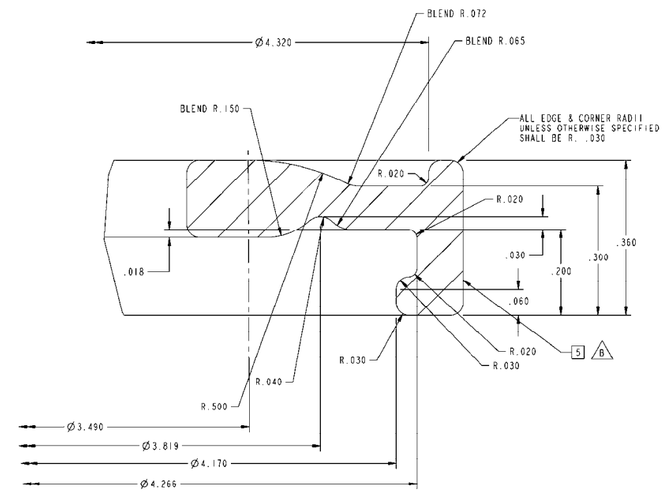

DETAIL B
SCALE 10/1

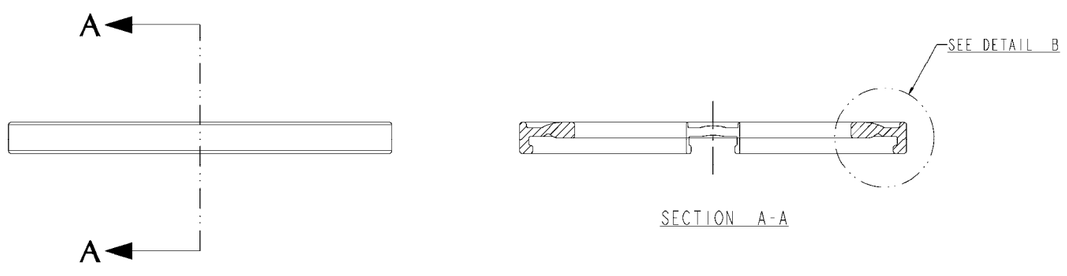

SECTION A-A

-1 CONTAINMENT VESSEL VIBRATION ABSORBING SILICONE 4.25" CAN PAD
SCALE 2/1

4	AR	AR	AR	AR			-1	CONTAINMENT VESSEL VIBRATION ABSORBING SILICONE 4.25" CAN PAD	SILICONE RUBBER A50-83B, SILICA FILLED, LOW HYDROGEN AND LOW VOLATILE VAPORS, POST CURED HARDNESS 75+/- 5 SHORE A		1
B	M2E801580 A024	M2E801580 A023	M2E801580 A022	M2E801580 A021	M2E801580 A020	1					
						CAGE CODE	PART OR IDENTIFYING NO	NOMENCLATURE OR DESCRIPTION	MATERIAL	SPECIFICATION	FIND NO

NEXT ASSEMBLY

PARTS LIST

M2E801580A021

THIS DRAWING INCLUDES FEATURES SUPPORTING NUCLEAR CRITICALITY SAFETY. ANY REVISION TO THIS DIAGRAM REQUIRES NUCLEAR CRITICALITY SAFETY DIVISION APPROVAL.

REVISION	DATE	NCSD APPROVAL
B	2/10/05	JF DECLUE

This document has been reviewed by a Y-12 ADC and UCNI RO and has been determined to be UNCLASSIFIED and not UCNI. This review does not constitute clearance for public release.

Name: ROGER D. AIGNER Date: 2/10/05

NO REPRESENTATION OR WARRANTY, EXPRESSED OR IMPLIED, IS MADE AS TO THE ACCURACY, COMPLETENESS OR USEFULNESS OF THE INFORMATION OR STATEMENTS CONTAINED IN THESE DRAWINGS, OR THAT THE USE OR DISCLOSURE OF ANY INFORMATION, APPARATUS, METHOD, OR PROCESS DISCLOSED IN THESE DRAWINGS MAY NOT INFRINGE PRIVATE RIGHTS OF OTHERS. NO LIABILITY IS ASSUMED WITH RESPECT TO THE USE OF, OR FOR DAMAGES RESULTING FROM THE USE OF ANY INFORMATION, APPARATUS, METHOD OR PROCESS DISCLOSED IN THESE DRAWINGS. DRAWINGS MADE AVAILABLE FOR INFORMATION TO BIDDER ARE NOT TO BE USED FOR OTHER PURPOSES AND ARE TO BE RETURNED UPON REQUEST OF THE FORWARDING CONTRACTOR.

THIS DRAWING PRODUCED ON PRO/ENGINEER

REV	DESCRIPTION	DRW	CHKR	DE	DVR	DM	DATE	PE	DATE	PM	DATE	AR	CV	ST	HV	EM	JP	PD	EL	IC	M	NP
B	DELETED NOTE 8; ADDED NEXT ASS'Y TO BOM CHNG LOCATION OF INDEX NOTE 5 TO DET. B	JRP	SMM	GAB	RDA	DPS	11/30/05	GAB	2/10/05	JGA	2/10/05											
A	ISSUED FOR DESIGN REVIEW	RDA	JSL	GAB	JLH	JCW	11/30/05	GAB	11/30/05	GBS	11/30/05											

REVISION OR ISSUE PURPOSE — REVISION APPROVALS — SQUAD CHECK

SCALE: NOTED
TOLERANCES UNLESS OTHERWISE SPECIFIED

DRW	R.D. AIGNER	11/26/03
CHKR	J.S. LOWERY	11/26/03
DE	G.A. BYINGTON	11/26/03
DVR	J.L. HECK	11/26/03
DM	J.C. WALLS	11/26/03
PE	G.A. BYINGTON	11/26/03
PM	G.B. SINGLETON	11/26/03

DRAWING APPROVALS

BWXT Y-12 — Y-12 National Security Complex managed by BWXT Y-12, L.L.C. for the Department of Energy under U.S. Government contract DE-AC05-00OR22800 a BWXT Babcock & Wilcox Company — Oak Ridge, Tennessee

PROJECT NAME: ES-3100 SHIPPING PACKAGE

CONTAINMENT VESSEL VIBRATION ABSORBING SILICONE 4.25" CAN PAD

DATE	1 46	49 50	51 52	PLANT	BLDG	FL	SH.	OF	TYPE	CLASS
	6 M	L F	Y-12		NA	NA	1	1	S	U
	CM	PKG	IN		M2E801580A024					REV B

THIS PAGE INTENTIONALLY LEFT BLANK.

NOTES:

1. INTERPRET DRAWING PER MECHANICAL DRAFTING STANDARD ES-3.1.
2. INTERPRET DIMENSIONS AND TOLERANCES PER ASME Y14.5M-1994.
3. DIMENSIONS ARE IN INCHES.
4. FOR FURTHER INFORMATION, SEE EQUIPMENT SPECIFICATION DS-YMN3-801580-A005, CASTING CATALOG NO. 277-4 NEUTRON ABSORBER.
5. FOR PURCHASE OF F/N 8, SEE DOCUMENT #DS-YMN3-801580-A001.
6. USE THE BAND-IT TIE-LOCK II HAND TOOL "A920" TO ATTACH THE STAINLESS STEEL BANDS AND CABLE ASSEMBLIES TO THE MATERIAL CANS. THE TOOL'S TENSION SETTING SHALL BE SET BETWEEN 4 AND 8.
7. REFERENCE DOCUMENT #DAC-YMN3-801580-A001.
8. FOR REFERENCE ONLY (FIND NO. 1). NOMINAL WEIGHT: 1.38 LBS (0.626 KG)
9. DIMENSIONS AND FEATURES FLAGGED BY SYMBOL (I) SHALL BE INSPECTED AND DOCUMENTED. THESE DIMENSIONS ARE OF CRITICALITY SAFETY CONCERNS AND SHALL NOT BE DEVIATED WITHOUT PRIOR APPROVAL.
10. MARK WITH PERMANENT LABELS F/N 6 DRAWING NUMBER, REVISION LETTER AND SIX DIGIT SERIAL NUMBER IN .16±.03 HIGH CHARACTERS.

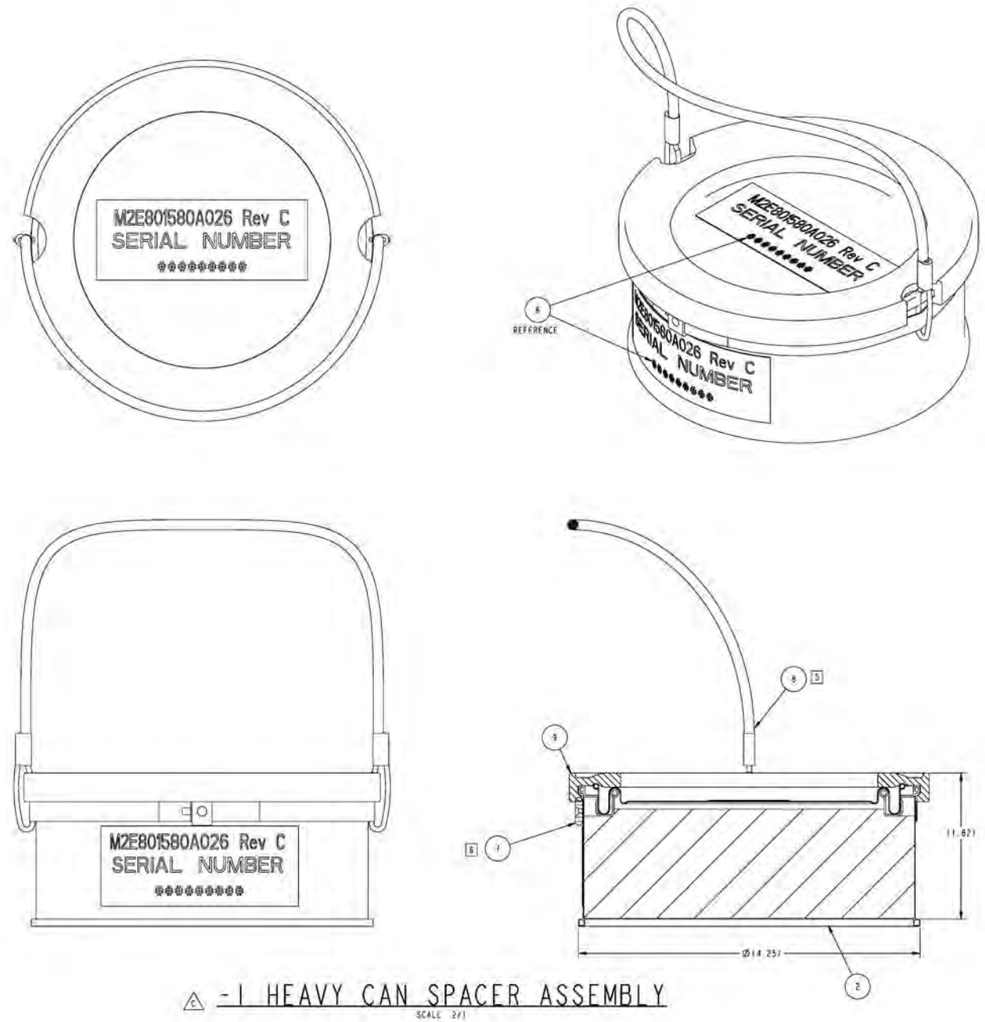

△C -1 HEAVY CAN SPACER ASSEMBLY
SCALE 2/1

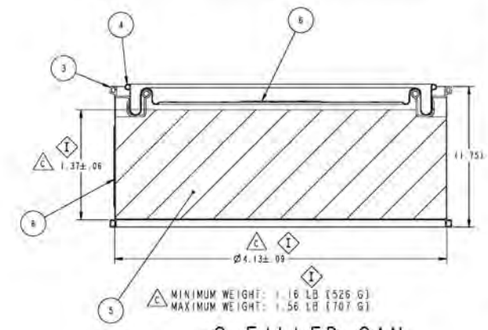

△C -2 FILLED CAN
SECTION B-B
SCALE 2/1

			1	M2E801580A024-1	VIBRATION ABSORBING SILICONE 4.25" CAN PAD				9
5			1	-8	CABLE LANYARD	REFERENCE NOTE 5			8
6			1	AS213	BAND CLAMP	304 SST	BAND-IT-IDEX, INC DENVER, CO 80216		7
10			2	WL-OLB750J OR EQUAL	2.625" BY 1" VINYL COATED WEATHERPROOF WHITE PRINTER LABELS		WORLDLABEL.COM 330 CONVENT AVE,STE 2A NEW YORK NY 10031 SALES (866) 726-0669		6
4			1	-5	277-4 FILLER		JS-YMN3-801580-A005		5
△C			1	-4	CAN LID	10 oz. (4-1/4" X (-3/4")	TRUMBO CONTAINER 1535 S. CENTRAL AVE		4
△C			1	-3	CAN BASE	DOUBLE-FRICTION CAN STOCK NUMBER 3051 OR EQUAL	ALSIP, IL 60803 PHONE: 800.363.9822		3
△C		X	1	-2	FILLED CAN				2
AR	AR	X		-1	HEAVY CAN SPACER ASSEMBLY				1
M2E801580A026 M2E801581A026	-2	-1		PART OR IDENTIFYING NO.	NOMENCLATURE OR DESCRIPTION	MATERIAL	SPECIFICATION		FIND NO
				QTY REQ'D NEXT ASSEMBLY	PARTS LIST				

M2E801580A026

THIS DRAWING INCLUDES FEATURES SUPPORTING NUCLEAR CRITICALITY SAFETY. ANY REVISION TO THIS DIAGRAM REQUIRES NUCLEAR CRITICALITY SAFETY DIVISION APPROVAL.

REVISION	DATE	NCSD APPROVAL
S	1/26/2006	J. T. DeClue

This document has been reviewed by a Y-12 ADC and UCNI RO and has been determined to be UNCLASSIFIED and not UCNI. This review does not constitute clearance for public release.

Name: Roger D. Aigner Date: 01/26/06

REV	DESCRIPTION	DRW	CHKR	DE	DVR	DM	DATE	PE	DATE	PM	DATE
C	CHANGED CAN SIZE FROM 8 OZ TO 10 OZ	GAB	HM	JGAB	RDA	MLG	11/06/03	GAB	11/06/03		
B	REDESIGNED, ADDED NEW ASSEMBLY F/N 2 AND MODIFIED PARTS LISTS AND NOTES	JRP	SMM	GAB	RDA	DPS	11/13/03	GAB	11/14/03	JGA	11/14/03
A	ISSUED FOR PROTOTYPE PROCUREMENT	RDA	JSL	GAB	JLH	JCW	11/06/03	GAB	11/06/03	GBS	11/06/03

REVISION OR ISSUE PURPOSE

REVISION APPROVALS: AR CV ST HV EM TP FD EE IE W MP

SQUAD CHECK

DRAWING APPROVALS

		DATE
DRW	R. D. AIGNER	11/26/03
CHKR	J. S. LOWERY	11/26/03
DE	G. A. STINGTON	11/26/03
DVR	J. L. HECK	11/26/03
DM	J. C. WALLS	11/26/03
PE	G. A. STINGTON	11/26/03
PM	G. B. SINGLETON	11/26/03

SCALE: NOTED

TOLERANCES UNLESS OTHERWISE SPECIFIED: FRACTIONS ±; XX DECIMALS ±; XXX DECIMALS ±; ANGLES ±; BREAK SHARP EDGES .010; FIN 125

Y-12 National Security Complex managed by BWXT Y-12, LLC for the Department of Energy under U.S. Government Contract DE-AC05-00OR22800

PROJECT NAME: ES-3100 SHIPPING PACKAGE

HEAVY CAN SPACER ASSEMBLY

I	AS	AS	SD	PLANT	SCHE	FL	SH	OF	TYPE	CLASS
6	M	L	F	Y-12	NA	NA	1	1	S	U

SIZE	SD	UNIT	REV
CM	PKG	IN	C

M2E801580A026

THIS DRAWING PRODUCED ON PROVENGINEER

NO REPRESENTATION OR WARRANTY, EXPRESSED OR IMPLIED, IS MADE AS TO THE ACCURACY, COMPLETENESS OR USEFULNESS OF THE INFORMATION OR STATEMENTS CONTAINED IN THESE DRAWINGS, OR THAT THE USE OF DISCLOSURE IN THESE DRAWINGS MAY NOT INFRINGE ON THE RIGHTS OF OTHERS. NO LIABILITY IS ASSUMED WITH RESPECT TO THE USE OF, OR FOR DAMAGES RESULTING FROM THE USE OF ANY INFORMATION, APPARATUS, METHOD OR PROCESS DISCLOSED IN THESE DRAWINGS. DRAWINGS MADE AVAILABLE FOR INFORMATION TO BIDDERS ARE NOT TO BE USED FOR OTHER PURPOSES AND ARE TO BE RETURNED UPON REQUEST OF THE FORWARDING CONTRACTOR.

THIS PAGE INTENTIONALLY LEFT BLANK.

NOTES

1. INTERPRET DRAWING PER MECHANICAL DRAFTING STANDARD ES-3.1.
2. INTERPRET DIMENSIONS AND TOLERANCES PER ASME Y14.5M-1994.
3. DIMENSIONS ARE IN INCHES [mm].
4. APPROXIMATE WEIGHT: 323.8 LBS [146.9 Kg]
5. FOR ADDITIONAL REQUIREMENTS SEE EQUIPMENT SPECIFICATION JS-YMN3-801580-A002.
6. WELDING SYMBOLS SHALL BE INTERPRETED IN ACCORDANCE WITH AWS A2.4.

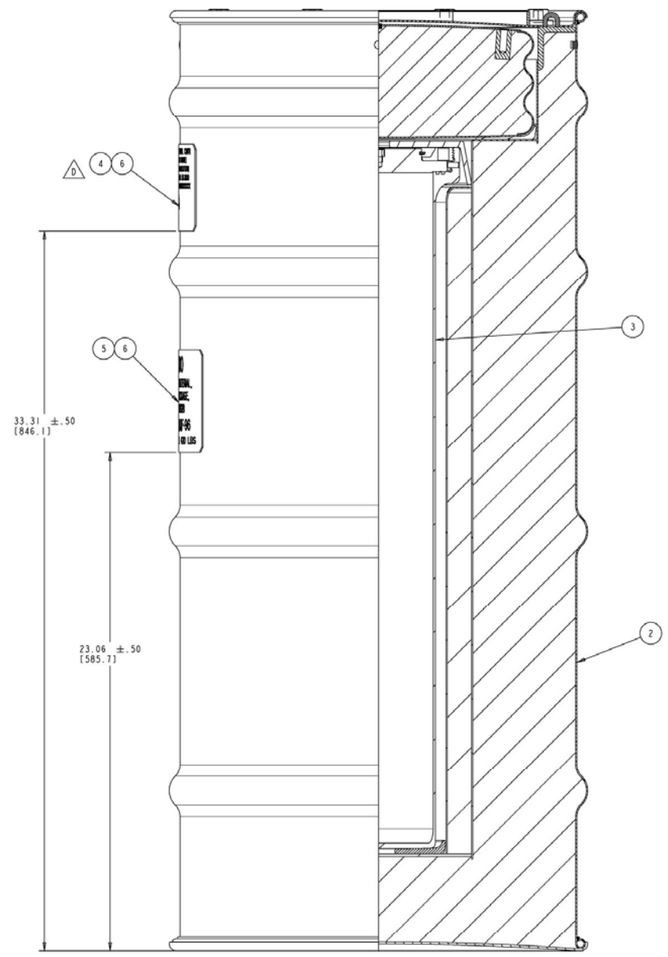

-1 MAIN ASSEMBLY
SCALE 1/2

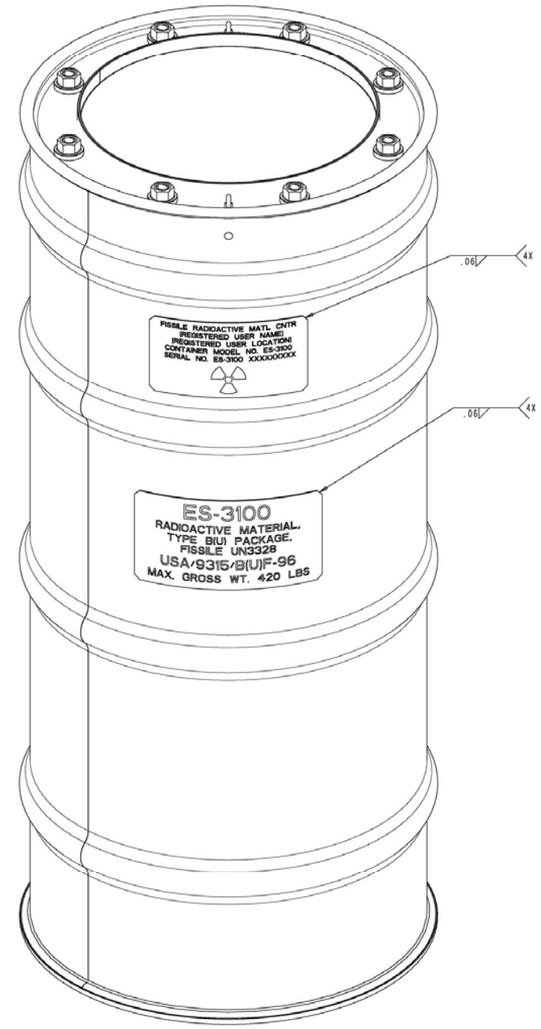

ISOMETRIC VIEW
SCALE 1/2

AR					
	-6	WELD FILLER METAL			6
1	M2E801580A010-2	ES-3100 DATA PLATE			5
1	M2E801580A010-1	ES-3100 TREFOIL DATA PLATE			4
1	M2E801580A011-1	CONTAINMENT VESSEL ASSEMBLY			3
1	M2E801580A001-1	DRUM ASSEMBLY			2
	-1	MAIN ASSEMBLY			1
	PART OR IDENTIFYING NO	NOMENCLATURE OR DESCRIPTION	MATERIAL	SPECIFICATION	FIND NO
	QTY. REQ'D NEXT ASSEMBLY	PARTS LIST			

THIS DRAWING INCLUDES FEATURES SUPPORTING NUCLEAR CRITICALITY SAFETY. ANY REVISION TO THIS DIAGRAM REQUIRES NUCLEAR CRITICALITY SAFETY DIVISION APPROVAL.

REVISION	DATE	NCSD APPROVAL
D	09/10/08	J.F. DeCLUE

This document has been reviewed by a Y-12 ADC and UCNI RO and has been determined to be UNCLASSIFIED and not UCNI. This review does not constitute clearance for public release.

Name: R.D. AIGNER Date: 09/11/08

NO REPRESENTATION OR WARRANTY, EXPRESSED OR IMPLIED, IS MADE AS TO THE ACCURACY, COMPLETENESS OR USEFULNESS OF THE INFORMATION OR STATEMENTS CONTAINED IN THESE DRAWINGS, OR THAT THE USE OR DISCLOSURE OF ANY INFORMATION, APPARATUS, METHOD, OR PROCESS DISCLOSED IN THESE DRAWINGS MAY NOT INFRINGE PRIVATE RIGHTS OF OTHERS. NO LIABILITY IS ASSUMED WITH RESPECT TO THE USE OF OR FOR DAMAGES RESULTING FROM THE USE OF ANY INFORMATION, APPARATUS, METHOD OR PROCESS DISCLOSED IN THESE DRAWINGS. DRAWINGS MADE AVAILABLE FOR INFORMATION TO BIDDER ARE NOT TO BE USED FOR OTHER PURPOSES AND ARE TO BE RETURNED UPON REQUEST OF THE FORWARDING CONTRACTOR.

P THIS DRAWING PRODUCED ON PRO/ENGINEER

REV	DESCRIPTION	DRW	CHKR	DC	DVR	DM	DATE	PE	DATE	PM	DATE	NE	DATE	AR	CV	ST	HV	EM	FP	PD	EC	IE	M	NP
D	REVISED TREFOIL DATA PLATE	JRJ	RDA	LR	GAB	WIN	9/9/08	LR	9/9/08	JGA	9/9/08	NA	NA											
C	REVISED TREFOIL DATA PLATE	JRJ	RDA	JRJ	GAB	WIN	08/16/06	DJW	08/17/06	JGA	08/22/06	NA	NA											
B	GEN REV;CHG. NOTE 4;ADDED NOTES 5 & 6; CHG. F/N 6 WAS BLIND RIVIT,WEIGHTS & VOLS IN NOTE 10 UPDATED TO REFLECT NEW MAT'L.	JRP	SMM	GAB	RDA	DPS	11/13/05	GAB	2/10/05	JGA	2/10/05	DJE	2/11/05											
A	ISSUED FOR PROTOTYPE PROCUREMENT	JRJ	JSL	GAB	JLH	JCW	02/25/05	MRF	02/25/05	DBM	02/25/05													

REVISION OR ISSUE PURPOSE — REVISION APPROVALS — SQUAD CHECK

SCALE: NOTED	DRW J.R. JACKSON	10/29/03
TOLERANCES UNLESS OTHERWISE SPECIFIED	CHKR J.S. LOWERY	10/29/03
	DC G.A. BYINGTON	10/29/03
	DVR J.L. HECK	10/29/03
FRACTIONS	DM J.C. WALLS	10/29/03
XX DECIMALS ±.29	PE M.R. FELDMAN	10/29/03
XXX DECIMALS	PM D.B. MILLER	10/29/03
ANGLES		
BREAK SHARP EDGES MAX		
FINISH		
DRAWING APPROVALS		

BWXT Y-12 — T-12 National Security Complex managed by BWXT Y-12, L.L.C. for the Department of Energy under D.O. Government contract DE-AC05-00OR22800 • Oak Ridge, Tennessee •

PROJECT NAME: ES-3100 SHIPPING PACKAGE

MAIN ASSEMBLY

1	48	49	50	PLANT	BLDG	FL	SH.	OF	TYPE	CLASS
6	M	L	F	Y-12	NA	NA	1	1	A	U

51	52	53		REV
CM	PKG	IN	M2E801580A031	D

M2E801580A031

THIS PAGE INTENTIONALLY LEFT BLANK.

NOTES

1 INTERPRET DRAWING PER MECHANICAL DRAFTING STANDARD ES-3.1.

2 INTERPRET DIMENSIONS AND TOLERANCES PER ASME Y14.5M-1994.

3 DIMENSIONS ARE IN INCHES.

4 FOR FURTHER INFORMATION, SEE EQUIPMENT SPECIFICATION JS-YMN3-801580-A005, CASTING CATALOG NO. 277-4 NEUTRON ABSORBER.

5 FOR PURCHASE OF F/N 8, SEE DOCUMENT #DS-YMN3-801580-A001.

6 USE THE BAND-IT TIE-LOCK II HAND TOOL "A920" TO ATTACH THE STAINLESS STEEL BANDS AND CABLE ASSEMBLIES TO THE MATERIAL CANS. THE TOOL'S TENSION SETTING SHALL BE SET BETWEEN 4 AND 8.

7 REFERENCE DOCUMENT #DAC-YMN3-801580-A001.

8 FOR REFERENCE ONLY FIND NO 1; NOMINAL WEIGHT: 1.38 LBS [0.626 KG]

9 DIMENSIONS AND FEATURES FLAGGED BY SYMBOL (I) SHALL BE INSPECTED AND DOCUMENTED. THESE DIMENSIONS ARE OF CRITICALITY SAFETY CONCERNS AND SHALL NOT BE DEVIATED WITHOUT PRIOR APPROVAL.

10 MARK WITH PERMANENT LABELS F/N 6 DRAWING NUMBER, REVISION LETTER AND SIX DIGIT SERIAL NUMBER IN .16±.03 HIGH CHARACTERS.

11 REFERENCE CONFIGURATION CONTROL EQUIPMENT DATA SHEET DS-PKG-801580-A004.

12 SUPPLIED BY COMPANY.

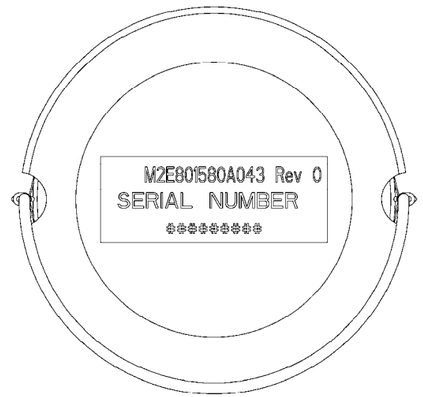

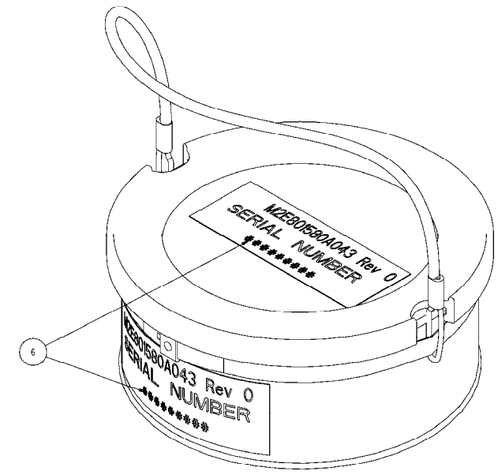

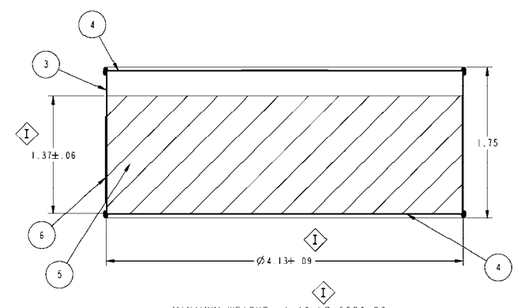

MINIMUM WEIGHT: 1.16 LB [526 G]
MAXIMUM WEIGHT: 1.56 LB [707 G]

-2 FILLED CAN

SCALE 2/1

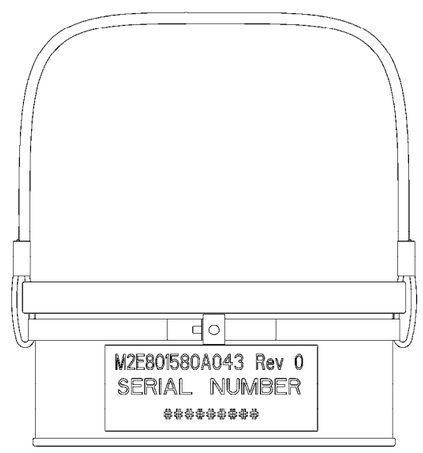

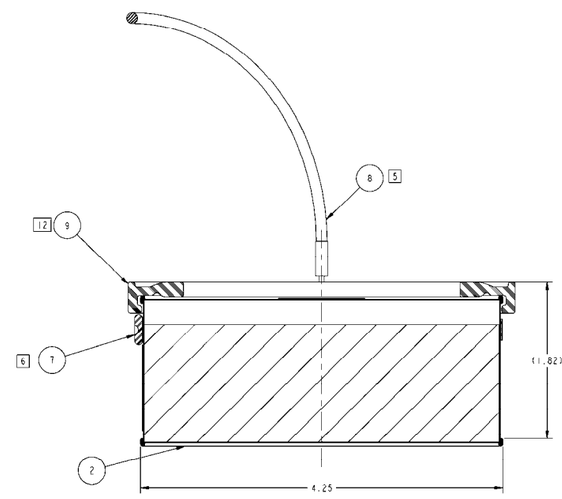

-1 HEAVY CAN SPACER ASSEMBLY (SST)

SCALE 2/1

12	1	M2E801580A024-1	VIBRATION ABSORBING SILICONE 4.25" CAN PAD			9
5	1	-8	CABLE LANYARD	REFERENCE NOTE 5		8
6	1	AS213	BAND CLAMP	304 SST	BAND-IT-IDEX, INC. DENVER, CO 80216	7
10	2	WL-OLB75WJ OR EQUAL	2.625" BY 1" VINYL COATED WEATHERPROOF WHITE PRINTER LABELS		WORLDLABEL.COM 335 CONVENT AVE.,STE 2A NEW YORK NY 10031 SALES (866) 226-8669	6
4	AR	-5	277-4 FILLER		JS-YMN3-801580-A005	5
	2	-4	CAN END COVER	304/304L STAINLESS STEEL 30 GA. (0.012)	ASTM A240	4
	1	-3	CAN BODY			3
	1	-2	FILLED CAN			2
11		-1	HEAVY CAN SPACER ASSEMBLY (SST)			1
-2	-1	PART OR IDENTIFYING NO.	NOMENCLATURE OR DESCRIPTION	MATERIAL	SPECIFICATION	FIND NO
		QTY REQ'D NEXT ASSEMBLY	PARTS LIST			

THIS DRAWING INCLUDES FEATURES SUPPORTING NUCLEAR CRITICALITY SAFETY. ANY REVISION TO THIS DIAGRAM REQUIRES NUCLEAR CRITICALITY SAFETY ANALYSIS ENGINEERING APPROVAL.

REVISION	DATE	SAE APPROVAL
0	09/10/09	J.E. DECLUE

This document has been reviewed by a Y-12 DC and UCNI RO and has been determined to be UNCLASSIFIED and not UCNI. This review does not constitute clearance for public release.

Name: R.D. AIGNER Date: 09/10/09

NO REPRESENTATION OR WARRANTY, EXPRESSED OR IMPLIED, IS MADE AS TO THE ACCURACY, COMPLETENESS OR USEFULNESS OF THE INFORMATION OR STATEMENTS CONTAINED IN THESE DRAWINGS, OR THAT THE USE OR DISCLOSURE OF ANY INFORMATION, APPARATUS, METHOD, OR PROCESS DISCLOSED IN THESE DRAWINGS MAY NOT INFRINGE PRIVATE RIGHTS OF OTHERS. NO LIABILITY IS ASSUMED WITH RESPECT TO THE USE OF, OR FOR DAMAGES RESULTING FROM THE USE OF ANY INFORMATION, APPARATUS, METHOD OR PROCESS DISCLOSED IN THESE DRAWINGS. DRAWINGS MADE AVAILABLE FOR INFORMATION TO BIDDERS ARE NOT TO BE USED FOR OTHER PURPOSES AND ARE TO BE RETURNED UPON REQUEST OF THE FORWARDING CONTRACTOR.

PTHIS DRAWING PRODUCED ON PRO/ENGINEER

REV	DESCRIPTION	DRW	CHKR	DE	DVR	DN	DATE	PE	DATE	PM	DATE	AR	CV	ST	MV	EM	FP	FD	EL	IE	M	NP
0	ORIGINAL ISSUE.	MLE	JRJ	MLE	DEW	WIN	9/10/09	LR	9/10/09	JGA	9/14/09											

REVISION OR ISSUE PURPOSE — REVISION APPROVALS — SQUAD CHECK

SCALE: NOTED	DRW M.L. ENSLEY	09/02/09
TOLERANCES UNLESS OTHERWISE SPECIFIED	CHKR JR JACKSON	09/03/09
	DE M.L. ENSLEY	09/03/09
	DVR D.E. WINDER	09/10/09
FRACTIONS	DN W.I. NORTH	09/10/09
XX DECIMALS ±.01	PE L. ROBERSON	09/10/09
XXX DECIMALS ±.005	PM J.G. ARDITAL	09/14/09
ANGLES ±0.5°		
BREAK SHARP EDGES .06 MAX		
FINISH 125 RMS		

DRAWING APPROVALS

BWXT Y-12 National Security Complex managed by BWXT Y-12, L.L.C. for the Department of Energy under U.S. Government contract DE-AC05-00OR22800
a BWXT Babcock & Wilcox Enterprise
Oak Ridge, Tennessee

PROJECT NAME: ES-3100 SHIPPING PACKAGE

HEAVY CAN SPACER ASSEMBLY (SST)

DATE	1	48	49	50	PLANT	BLDG	FL	SH.	OF	TYPE	CLASS
	6	M	L	F	Y-12	NA	NA	1	1	S	U
	51		52		53						REV
CM			PKG		IN	M2E801580A043					0

M2E801580A043

THIS PAGE INTENTIONALLY LEFT BLANK.

Appendix 1.4.9

DESIGN ANALYSES AND CALCULATIONS, DAC-PKG-801624-A001, MIXING WEIGHTS AND ELEMENTAL COMPOSITION OF 277-4 NEUTRON POISON USED IN THE ES-3100

THIS PAGE INTENTIONALLY LEFT BLANK.

Design Analyses and Calculations

Title Page

Calculation No.:	DAC-PKG-801624-A001
Calculation Title:	Mixing Weights And Elemental Composition Of 277-4 Neutron Poison used in the ES-3100
Preparer's Organization:	Packaging Engineering
Project/Task Name:	ES-3100 Shipping Package
Record Number:	Y2003-0328
Rev.:	B

Comments/Purpose: The purpose of this DAC is to enable a tight quality control on the amount of neutron poison materials used in each shipping package.

Printed Name and Signature

Prepared By:	G. A. Byington /s/	Date:	10/11/06
Checked/Verified By:	John F DeClue /s/	Date:	10/17/06
Checked/Verified By:	James H. Clinton /s/	Date:	10/23/2006
Discipline Manager Approval:	W. I. North /s/	Date:	10/23/06

This document has been reviewed by a Y-12 DC / UCNI RO and has been determined to be UNCLASSIFIED and contains no UCNI. This review does not constitute clearance for Public Release.

Name: Roger D. Aigner /s/ Date: 11/8/06

Prepared by: G. A. Byington
Checked/Verified by: J. Clinton & J. DeClue

Revision Log

Rev	Date	Description	Total Pages	Affected Pages
0	January 18, 2006	Initial issue	Front matter, 1-3 Body 4-21 Appendix 1, 22-24 Appendix 2, 24	All
A	January 20, 2006	Removed Report references and Updated Tables 10, 11, 12, and 13.	Front matter, 1-3 Body 4-21 Appendix 1, 22-24 Appendix 2, 24	4, 10, 18, 19, 20
B	October 12, 2006	Updated Table 7, 277-4 Composition @ Extreme Densities and LOD%. Updated DAC format to new log. New DAC format applied.	Front matter, 1-3 Body 4-22 Appendix 1, 23-24 Appendix 2, 25	1, 2, 14

Table of Contents

1. Objective ..... 4 of 25
2. Purpose ..... 4 of 25
3. References ..... 4 of 25
4. Materials to Mix ..... 4 of 25
5. Scope of Calculations ..... 5 of 25
6. Base Material Elemental Volumetric Concentrations ..... 6 of 25
7. Calculations ..... 9 of 25
8. Conclusion ..... 22 of 25

1. Objective

The purpose of this DAC is to define the amounts of materials to mix and manufacture the borated cement neutron poison used in the ES-3100 Shipping Container as one batch per shipping container. The exact amount of B_4C added to be the mixture shall be calculated in this design analysis to be greater than 7.61×10^{20} atoms/cc of ^{10}B at the minimum density and maximum hydration. This elemental analysis of the minimum value of ^{10}B was used in the ES-3100 SAR Criticality Safety calculations.

2. Purpose

By adding the proper amount of boron carbide in each ES-3100 Shipping Container mass balanced, assuming thorough mixing, macro homogeneity is obtained. This will enable a tight quality control on the amount of neutron poison materials used in each shipping package.

3. References

The ES-3100 Shipping Container is placed in BWXT Y-12 National Security Complex drawing M2E801580A002 following Equipment Specification JS-YMN3-8015580-A005. Two sample cans are taken during each shipping package pouring of the casting into drawing M2E801580A026-2.

4. Materials to Mix

4.1. B_4C

Boron carbide (B_4C) powder shall be procured as Type 1 Nuclear-Grade Boron Carbide Powder per ASTM C 750-03 shipped in sealed steel containers. An approximate partial size of 106 micrometers (0.0041 inches) is generated by having 100% of the grit pass through a No. 140 Sieve per ASTM E 11. A copy of the chemical and elemental analysis purity shall be in accordance with ASTM C 791.

4.2. 277-0

Thermo Electron's proprietary Catalog No. 277 – Heat Resistant Shielding (with no Boron), is a type of high alumina cement and will be referred to as 277-0. The manufactures information can be found in Appendix 1 & 2. This dry powder shall be shipped in sealed open head steel drums and has no shelf life limitations if keep dry and free flowing. Once the container is opened it shall be discarded if clumps or lumps are observed in the material greater than 0.5 inches.

4.3. Water

The water shall be potable, filtered through a 20-micron filter, and have a chlorine content of less than 4 ppm. If the potable water's chlorine content is higher then 4 ppm, use an activated charcoal filter or some other means to reduce the amount of chlorine below 4 ppm.

5. Scope of Calculations

The bounding elemental calculations shall be completed at the minimum ^{10}B level for the compositional purity, isotopic atomic percentage, and scale measurements.

5.1. Amount of B_4C in 277-4 Borated High Alumina Cement

Define the method for mixing 277-4 as a two part method of 277-0 and B_4C and calculate the volumetric atomic concentrations.

5.2. 277-4 Borated High Alumina Cement at Extreme Conditions

Calculate the minimum amount of B_4C to add to the 277-4 mixture to generate a volumetric atomic concentration greater than 7.61×10^{20} atoms/cc of ^{10}B at the minimum density and maximum hydration.

5.3. ^{10}B Areal Density at Minimum ^{10}B Content and Density

Calculate the ^{10}B Areal Density between the fissile mass loads in two adjacent shipping packages.

5.4. Volumetric Atomic Concentrations at Average Density and LOD%

Calculate the average density and hydration volumetric atomic concentrations.

5.5. Extreme Densities and LOD% Volumetric Atomic Concentrations

Calculate the extreme density and hydration volumetric atomic concentrations.

5.6. Define the Masses Needed To Mix a Batch of 277-4 For a ES-3100

Calculate the mass weights used to mix a batch used in one ES-3100.

5.7. Define the Volumetric Atomic Concentrations at NCT and HAC

At higher temperatures especially above 212°F the chemically unbound or free water will leave the cast cement. Using the minimum boron mixer weights calculated in Section 7.2 define the NCT and HAC volumetric atomic concentrations at a minimum manufactured density, hydration for the calculated temperatures.

5.8. Define the Nominal Volumetric Atomic Concentrations

Using nominal mixer weights from Section 7.6 calculate the nominal ^{10}B content.

6. Base Material Elemental Volumetric Concentrations

6.1. Boron Carbide Powder B_4C

The elemental composition weight percents of B_4C must be defined per ASTM C 750-03, using Type 1 Nuclear-Grade Boron Carbide Powder as noted in Table 1 from ASTM C 750-03.

TABLE 1 Chemical Requirements

Constituent	Composition, Weight %[A]		
	Type 1	Type 2	Type 3
Total boron[B]	81.0 max 76.5 min	81.0 max 73.0 min	81.0 max 70.0 min
HNO_3-soluble boron	0.5 max	0.6 max	not determined
Water soluble boron	0.2 max	0.2 max	1.0 max
Fluoride	25 µg/g max	25 µg/g max	not determined
Chloride	75 µg/g max	75 µg/g max	not determined
Calcium	0.3 max	0.3 max	not determined
Iron	1.0 max	1.0 max	2.0 max
Total boron plus total carbon	98.0 min	97.0 min	94.0 min

[A]Unless otherwise indicated (percentages based on a dry weight of boron carbide).
[B]Unless otherwise specified, the ^{10}B isotopic content in the boron shall be 19.90 ± 0.3 atom % for Types 1 and 2 and 19.90 ± 0.5 atom % for Type 3.

Find the minimum ^{10}B weight percents using ASTM C 750-03 Type 1 at ^{10}B equal to 19.9±0.3 atom % of natural boron (NatB).

At the minimum 19.6 atom % of ^{10}B the ^{11}B would be 100-19.6 = 80.4 atom %.

Using the molecular weights of ^{10}B the ^{11}B:
B10 = 10.0129370×19.6% = 1.962535652 (g/mol)
B11 = 11.0093055×80.4% = 8.851481622 (g/mol)
NatB = B10 + B11 = 1.962535652 + 8.851481622 (g/mol)
NatB = 10.81401727% (g/mol) Min per ASTM C 750-03 Type 1

B10 wt% = B10 / NatB = 1.962535652 / 10.81401727
B10 wt% = 18.14807211 wt% Min per ASTM C 750-03 Type 1

Using the minimum total natural boron of 76.5 wt% the following weight percentages are calculated.

B10 wt% = 76.5% × 18.148 wt%
B10 wt% = 13.883 wt%

B11 wt% = 76.5 − 13.883 wt%
B11 wt% = 62.617 wt%

One of the largest B_4C impurities in Table 1 is the nitric acid (HNO_3). As shown in Table 4 the 277-4 neutron poison solid requires hydrogen and contains a large amount of oxygen. Therefore, a conservative approximation shall be to change the balance of the weight percents from 0.5 to 0.7 wt% and make up the difference with nitrous trioxide (NO_3) removing the hydrogen from this impurity.

Determine the weight percents of nitrous trioxide (NO_3)
NO_3 = MW(N) + 3×MW(O) (g/mol)
NO_3 = 14.0067 + 3×15.9949 (g/mol)
NO_3 = 61.9914 (g/mol)

N wt% = 14.0067 / 61.9914
N wt% = 0.225946 wt%

For 0.7 wt% NO_3
N wt% = 0.225946 % ×0.7 wt%
N wt% = 0.158 wt%

O wt% = NO_3 wt% − N wt%
O wt% = 0.7 − 0.158 wt%
O wt% = 0.542 wt%

Table 2, Nuclear-Grade Boron Carbide Powder Elemental Composition Weight Percents

Element	At.wt (g/mol)	B_4C (wt%)
Hydrogen	1.0078	
B Nat	10.8140	
^{10}B	10.0129	13.883%
^{11}B	11.0093	62.617%
Carbon	12.0000	21.500%
Nitrogen	14.0067	0.158%
Oxygen	15.9949	0.542%
Sodium	22.9895	
Magnesium	24.3051	
Aluminum	26.9818	
Silicon	28.0853	
Sulfur	32.0636	
Calcium	40.0803	0.300%
Iron	55.8447	1.000%
Sum		100.000%

6.2. Catalog No. 277 – Heat Resistant Shielding With no Boron (277-0)

Verify the hydrogen elemental composition weight percent of Thermo Electron's proprietary Catalog No. 277 – Heat Resistant Shielding using the density of 1.61 g/cc (100.509 lb/ft^3), also called 277-0. Used the published weight percents for No. 277 – Heat Resistant Shielding with no boron and calculate the hydrogen atoms per cc. According to Appendix 2; Thermo Electron Corp. Heat Resistant Shielding Catalog No. 277 Typical Elemental Analysis Without Boron, EA-277, May 1988.

Table 3, Catalog No. 277 – Heat Resistant Shielding Elemental Composition for one ft^3

Element	At.wt (g/mol)	(wt%)	(lb/ft^3)	N_e (Atoms/cc)
Hydrogen	1.0078	3.730%	3.749	3.588E+22
B Nat	10.8140			
^{10}B	10.0129			
^{11}B	11.0093			
Carbon	12.0000			
Nitrogen	14.0067			
Oxygen	15.9949	59.140%	59.441	3.585E+22
Sodium	22.9895	0.080%	0.080	3.374E+19
Magnesium	24.3051	0.230%	0.231	9.175E+19
Aluminum	26.9818	26.590%	26.725	9.555E+21
Silicon	28.0853	1.680%	1.689	5.800E+20
Sulfur	32.0636	0.210%	0.211	6.350E+19
Calcium	40.0803	8.040%	8.081	1.945E+21
Iron	55.8447	0.300%	0.302	5.209E+19
Sum		100.00%	100.509	

The calculated value of hydrogen atoms per cc matched the recorded value in the typical elemental analysis of Catalog No. 277 – Heat Resistant Shielding. The following calculations use the molecular weights; Hydrogen 1.0078 g/mol, Oxygen 15.9994 g/mol, and water 18.0153 g/mol.

One must now determine how much water is in this solid casting. Water within the cast solid is defined in a water weight "Loss On Drying" (LOD) test in a weight percent of the initial density. The LOD% is calculated based upon the amount of hydrogen.

LOD% = H wt% × (MW H_2O) / (MW H_2)
LOD% = 3.730% × (18.0150 / (2× 1.0078)
LOD% = 33.338% as defined by the manufacture

$$H\ (lb/ft^3) = \frac{277\ \text{cast density}(lb/ft^3) \times \text{LOD wt\%} \times (2 \times \text{H Mw (g/mol)})}{\text{Water Mw (g/mol)}}$$

$$H\ (lb/ft^3) = \frac{277\ \text{cast density}(lb/ft^3) \times \text{LOD wt\%} \times (2 \times 1.0078\ \text{(g/mol)})}{18.0153\ \text{(g/mol)}}$$

$$H\ (lb/ft^3) = 277\ \text{cast density}(lb/ft^3) \times \text{LOD wt\%} \times 0.1118826775$$

The volumetric atomic concentrations are calculated below.

$$\text{H atoms/cc} = \frac{((\text{H density(lb/ft}^3)) \times (N_A \text{ atoms/mol}))}{(\text{H Mw (g/mol)} \times (62.42796 \text{ (lb/ft}^3)/(\text{g/cc}))}$$

$$\text{H atoms/cc} = \frac{((\text{H density(lb/ft}^3)) \times (6.0221415\times10^{23} \text{ atoms/mol}))}{(1.0078 \text{ (g/mol)} \times (62.42796 \text{ (lb/ft}^3)/(\text{g/cc}))}$$

$$\text{H atoms/cc} = ((\text{H density(lb/ft}^3)) \times 9.571884693\times10^{21}(\text{H atoms/cc})/(\text{lb/ft}^3)$$

$$\text{H atoms/cc} = (277 \text{ cast den (lb/ft}^3) \times \text{LOD wt\%}\times0.1118826775) \times 9.571884693\times10^{21}(\text{H atoms/cc})/(\text{lb/ft}^3)$$

$$\text{H atoms/cc} = (277 \text{ cast density (lb/ft}^3) \times \text{LOD wt\%})\times 1.070928088\times10^{21}(\text{H atoms/cc})/(\text{lb/ft}^3)$$

$$\text{H atoms/cc} = (100.509 \text{ (lb/ft}^3) \times 33.338 \text{ wt\%})\times 1.070928088\times10^{21}(\text{H atoms/cc})/(\text{lb/ft}^3)$$
$$\text{H atoms/cc} = 3.588432683\times10^{22} \text{ atoms/cc}$$

This calculated hydrogen elemental composition compares well to the documented value found in Appendix 2.

Using the hydrogen density the volume of water in the casting may be calculated as a fraction of Specific Gravity.
@ H = 3.749 (lb/ft^3)

SGF = H (lb/ft^3) × Water Mw (g/mol) / ((2 × H Mw (g/mol) × Water density (lb/ft^3))
SGF = H (lb/ft^3) × 18.0153 (g/mol) / ((2 × 1.0078 (g/mol)) × 62.42796 (lb/ft^3))
SGF = H (lb/ft^3) × 0.143172
SGF = 3.749 (lb/ft^3) × 0.143172 (1/(lb/ft^3))
SGF = 0.53675
Or the casting is 53.67% water by volume

7. Calculations

7.1. Amount of B_4C in 277-4 Borated High Alumina Cement

The boron carbide powder and Catalog No. 277 – Heat Resistant Shielding materials must now be combined to generate our neutron poison called 277-4 borated high alumina cement. An iterative solution was used to calculate the density of the 277-4 using the single component weight percents. First the mass amount of boron carbide powder must be selected and volume calculated. The B_4C volume is subtracted from one cubic foot to determine the volume of 277-0 cement. From the 277-0 cement volume the mass is calculated and all of the components' masses. As more boron carbide powder is added to the mixture it gets heavier and reduces the amount of relative hydrogen available to the neutron poison system in the cement.

Select or guess a mass of 5.88 lbs of B_4C for one cubic foot of casting with a theoretical density of 2.52 g/cc (157.318 lb/ft^3), found in the CRC Handbook of Chemistry and Physics, 55th Ed., page B-74. Verify this amount of B_4C needed in Section 7.2.

Calculate the volume of B_4C;
B4C vol = Mass (lb) / Den (lb/ft^3)
B4C vol = 5.88 lb / 157.318 lb/ft^3
B4C vol = 0.03738 ft^3

Calculate the volume and mass of the 277-0 material using the density of 1.61 g/cc (100.509 lb/ft^3).

277-0 vol = 1 - 0.03738 ft^3
277-0 vol = 0.96262 ft^3

277-0 mass = 0.96262 ft^3×100.509 lb/ft^3
277-0 mass = 96.7523 lb

Table 4, 277-4 Borated High Alumina Cement Elemental Composition for one ft^3

Element	At.wt (g/mol)	277-0 (lb/ft^3)	B_4C (lb/ft^3)	277-4 (lb/ft^3)
Hydrogen	1.0078	3.6089	0.0000	3.6089
B Nat	10.8140			
^{10}B	10.0129	0.0000	0.8163	0.8163
^{11}B	11.0093	0.0000	3.6819	3.6819
Carbon	12.0000	0.0000	1.2642	1.2642
Nitrogen	14.0067	0.0000	0.0093	0.0093
Oxygen	15.9949	57.2193	0.0319	57.2512
Sodium	22.9895	0.0774	0.0000	0.0774
Magnesium	24.3051	0.2225	0.0000	0.2225
Aluminum	26.9818	25.7264	0.0000	25.7264
Silicon	28.0853	1.6254	0.0000	1.6254
Sulfur	32.0636	0.2032	0.0000	0.2032
Calcium	40.0803	7.7789	0.0176	7.7965
Iron	55.8447	0.2903	0.0588	0.3491
Sum		96.7523	5.8800	102.6323

Calculate the as-defined by the manufacture and mixed to this ratio LOD%.
H wt% = H lb/ft^3 / Total Mass lb/ft^3
H wt% = 3.6089 / 102.6323
H wt% = 3.5163 wt%

LOD% = H wt% × (MW H_2O) / (MW H_2)
LOD% = 3.5163 wt% × (18.0150 / (2× 1.0078)
LOD% = 31.4279 wt%

7.2. 277-4 Borated High Alumina Cement at Extreme Conditions

The casting process overloads the mixture with water to allow the wet mix to flow. Dependent upon the amount of surface area and curing conditions of the casting the water content varies. As the water content varies both oxygen and hydrogen elemental masses change while the other solid masses stay fixed from in the matrix shown in Table 4. The left most density column in Table 5 shows the adjusted hydrogen and oxygen masses to a LOD% of 31.8%, while keeping all the other elemental concentrations the same. At this calculated LOD% the weight percent is calculated. Due to the possibility of small air bubbles the density could also vary. Therefore the calculated LOD% weight percents can now be multiplied by a density to generate the elemental volumetric concentrations at any LOD%. From the elemental volumetric concentration the atomic concentrations are calculated at the selected LOD% and density. Testing has shown that 99.7% of the 277-4 companion sample can castings will have an LOD% of 30.2%±1.6% and density of 105±5 lb/ft^3. Although, the ES-3100 drum has a larger casting with small percentage of the surface open to the air. The small open surface to volume ratio keep the 277-4 casting hydrated. Three castings that have been stored in an office environment for over a year had a density of 123 lb/ft^3. The difference being water content measured by the LOD% testing. This extra water make the 277-4 work better. Therefore, we would not want to overly reduce the extra moisture. An acceptable density range for this material shall be 105 −5+15 lb/ft^3 has been selected.

To calculate the elemental weight percents at a different LOD% like 31.8% another iterative calculation is required to adjust the volumetric concentrations of water. Assume a LOD% for Table 4 was 31.9735%

Delta LOD% = 31.9735% − 31.4279%
Delta LOD% = 0.5456%

Therefore for one cubic foot the water loss or gain from the definition in Table 4 is;
Del WW = Delta LOD% × Tab4Den × Volume
Del WW = 0.5456% × 102.6323 (lb/ft^3) × 1 (ft^3)
Del WW = 0.5599 lb

The amount of hydrogen weight change in a cubic foot is;
Del H = Del WW × (MW H_2) / MW H_2O
Del H = 0.5599 × (2×1.0078) / 18.0150
Del H = 0.0626 lb

Del O = Del WW − Del H
Del O = 0.5599 − 0.0626
Del O = 0.4973 lb

All values in the left column of Table 5 are same as the 277-4 masses in Table 4 except that the Hydrogen has gained 0.0626 lb and the Oxygen has gain 0.4973 lb. Using the new Table 5 elemental volumetric concentrations the weight percents are calculated. The elemental weight percents are multiplied by a desired density. The minimum acceptable density based upon testing is 100 lb/ft^3.

Table 5, 277-4 Elemental Composition @ 100 lb/ft^3 & 31.8% LOD as manufactured

Element	@LOD% (lb/ft^3)	@LOD% (wt%)	@Den & LOD% (lb/ft^3)	N_e (Atoms/cc)
Hydrogen	3.6715	3.5579%	3.5579	3.406E+22
B Nat				
^{10}B	0.8163	0.7911%	0.7911	7.621E+20
^{11}B	3.6819	3.5680%	3.5680	3.126E+21
Carbon	1.2642	1.2251%	1.2251	9.848E+20
Nitrogen	0.0093	0.0090%	0.0090	6.207E+18
Oxygen	57.7485	55.9620%	55.9620	3.375E+22
Sodium	0.0774	0.0750%	0.0750	3.147E+19
Magnesium	0.2225	0.2156%	0.2156	8.559E+19
Aluminum	25.7264	24.9306%	24.9306	8.913E+21
Silicon	1.6254	1.5752%	1.5752	5.410E+20
Sulfur	0.2032	0.1969%	0.1969	5.924E+19
Calcium	7.7965	7.5553%	7.5553	1.818E+21
Iron	0.3491	0.3383%	0.3383	5.843E+19
Sum	103.1923	100.0000%	100.0000	8.419E+22

B Nat	4.4982	4.3590%	4.3590	3.888E+21

The minimum amount of B_4C added to be the mixture shall be calculated to be greater than 7.61×10^{20} atoms/cc of ^{10}B at the minimum density and maximum hydration as defined in Section 5.1.

7.3. Calculate the ^{10}B Areal Density at Minimum ^{10}B Content and Density

The ^{10}B Areal Density for one cylinder casting thickness of 1.12 inches (2.8448 cm)
B10 Areal Density = (B10 atoms/cc × Thickness cm) × (B10 Mw g/mol / N_A atoms/mol)

$$\text{B10 Areal Den} = \frac{7.621\times10^{20}\ (\text{B10 atoms/cc}) \times (2.8448\ \text{cm}) \times (10.0129370\ \text{g/mol})}{6.0221415 \times 10^{23}\ \text{atoms/mol}}$$

B10 Areal Den = 0.0360474235 g/cm^2 for one thickness

Between two packages next to each other in the most reactive arrangement the fissile mass loads are separated by two cast neutron poison cylinders.
B10 Areal Den = 0.0360474235 × 2
B10 Areal Den = 0.072094847 g/cm^2
B10 Areal Den = 72.09 mg/cm^2

7.4. Volumetric Atomic Concentrations at Average Density and LOD%

Using the same methodology shown in Section 7.1 the volumetric atomic concentrations shall be calculated at the average density and LOD%. The average LOD% of 30.2% and density should be 105 −5+15 lb/ft^3 shall be used and shown in Table 6.

Table 6, 277-4 Elemental Composition @ 105 lb/ft^3 & 30.2% LOD as manufactured

Element	@LOD% (lb/ft^3)	@LOD% (wt%)	@Den & LOD% (lb/ft^3)	N_e (Atoms/cc)
Hydrogen	3.4068	3.3789%	3.5479	3.396E+22
B Nat				
^{10}B	0.8163	0.8096%	0.8501	8.190E+20
^{11}B	3.6819	3.6517%	3.8343	3.360E+21
Carbon	1.2642	1.2538%	1.3165	1.058E+21
Nitrogen	0.0093	0.0092%	0.0097	6.670E+18
Oxygen	55.6477	55.1913%	57.9509	3.495E+22
Sodium	0.0774	0.0768%	0.0806	3.382E+19
Magnesium	0.2225	0.2207%	0.2317	9.198E+19
Aluminum	25.7264	25.5155%	26.7913	9.578E+21
Silicon	1.6254	1.6121%	1.6927	5.814E+20
Sulfur	0.2032	0.2015%	0.2116	6.366E+19
Calcium	7.7965	7.7326%	8.1192	1.954E+21
Iron	0.3491	0.3462%	0.3635	6.279E+19
Sum	100.8268	100.0000%	105.0000	8.652E+22

B Nat	4.4982	4.4613%	4.6844	4.179E+21

7.5. Extreme Densities and LOD% Volumetric Atomic Concentrations

The high density is base upon both the hydration and compaction or the amount of entrapped air, if any. The ES-3100 shipping package 277-4 neutron poison cylinder castings hold the moisture well. This moisture is a key part of how the 277-4 neutron poison works. Therefore, it has been decided to accept the 277-4 neutron poison casting up to 120 lb/ft^3 making the density range 100 to 120 lb/ft^3. Most of the companion sample cans will have a density close to 105 lb/ft^3 while the cylinders are expected to be dried to just below the 120 lb/ft^3 limit, therefore density should be 105 −5+15 lb/ft^3. Using the calculation method in Section 7.1 the extreme densities and hydration levels atomic concentrations were calculated (Table 7).

Table 7, 277-4 Composition @ Extreme Densities and LOD% and compared to the average values as manufactured

Den (lb/ft^3)	^{10}B (wt%)	^{10}B (atoms/cc)	B Nat (wt%)	B Nat (atoms/cc)	LOD (wt%)	H (wt%)	H (atoms/cc)
100.0	0.7911%	7.621E+20	4.359%	3.888E+21	31.80%	3.5579%	3.406E+22
105.0	0.7534%	7.621E+20	4.152%	3.888E+21	35.05%	3.9212%	3.941E+22
110.0	0.7192%	7.621E+20	3.963%	3.888E+21	38.00%	4.2516%	4.477E+22
115.0	0.6879%	7.621E+20	3.791%	3.888E+21	40.69%	4.5531%	5.012E+22
120.0	0.6592%	7.621E+20	3.633%	3.888E+21	43.17%	4.8296%	5.547E+22
105.0	0.8096%	8.190E+20	4.461%	4.179E+21	30.20%	3.3789%	3.396E+22
100.0	0.8282%	7.979E+20	4.564%	4.071E+21	28.60%	3.1999%	3.063E+22
105.0	0.8440%	8.538E+20	4.651%	4.356E+21	27.24%	3.0475%	3.063E+22
110.0	0.8584%	9.096E+20	4.730%	4.641E+21	26.00%	2.9090%	3.063E+22
115.0	0.8715%	9.655E+20	4.802%	4.926E+21	24.87%	2.7825%	3.063E+22
120.0	0.8835%	1.021E+21	4.868%	5.211E+21	23.83%	2.6666%	3.063E+22

7.6. Mass of Materials Needed To Mix a Batch of 277-4 For One ES-3100

The as define 277-4 mixture shown in Table 4 shall be the bases for the two part dry mixing recipe. The amount of B_4C added to be the mixture shall be calculated to be greater than 7.61×10^{20} atoms/cc of ^{10}B at the minimum density and maximum hydration as shown in Section 7.2. Now the amount of water, B_4C and Thermo Electron's proprietary Catalog No. 277 – Heat Resistant Shielding (277-0) dry powder must be calculated per shipping container.

According to Appendix 1; Thermo Electron Corp. Heat Resistant Shielding Catalog No. 277 product information sheet 277-103:

96 lbs of dry mix is required to obtain one cubic foot.
Required water is 27±1% of the total dry powder weight.

From Section 7.1 for one cubic foot the volume and mass of B_4C is 0.03738 ft^3, 5.88 lb at a density of 157.318 lb/ft^3. The 277-0 materials volume and mass is 0.96262 ft^3, 96.7523 lb a density of 100.509 lb/ft^3. Together this mixture generated a total density of 102.6323 lb/ft^3.

For one cubic foot Cast Volume
277-4 Vol = Vol B_4C + Vol 277-0
277-4 Vol = 0.03738 + 0.96262 ft^3
277-4 Vol = 1.00000 ft^3

For one cubic foot Cast Mass for one cubic foot
277-4 Mass = Mass B_4C + Mass 277-0
277-4 Mass = 5.88 + 96.7523 lb
277-4 Mass = 102.6323 lb for one cubic foot

Using the 96 lbs of dry mix required to obtain 1 ft^3 calculate the mass of 277-0 dry mix required for this casting.
277-0 Dry Mix Mass = Vol 277-0 × Dry Mix Density
277-0 Dry Mix Mass = 0.96262 ft^3 × (96 lb/ft^3)
277-0 Dry Mix Mass = 0.96262 ft^3 × (96 lb/ft^3)
277-0 Dry Mix Mass = 92.4115 lb

The 277-0 dry mix plus the B_4C mass required for one cubic foot casting is;
277-4 Dry Mix Mass = 277-0 Dry Mix Mass × Mass B_4C
277-4 Dry Mix Mass = 92.4115 + 5.88 lb
277-4 Dry Mix Mass = 98.2915 lb

Defining the calculated mass as percent weight one gets;
Dry Mix B_4C wt% = Mass B_4C / 277-4 Dry Mix Mass
Dry Mix B_4C wt% = 5.88 / 98.2915 × 100%
Dry Mix B_4C wt% = 5.9822%

277-0 Dry Mix wt% = 100% − Dry Mix B_4C wt%
277-0 Dry Mix wt% = 100% − 5.9822%
277-0 Dry Mix wt% = 94.0178%

For a 50 lb 277-4 Dry Mix Mass calculate the weights of 277-0 Dry Mix, B_4C, and water;
Dry Mix B_4C = 5.9822% × 50 lb
Dry Mix B_4C = 2.9911 lb

277-0 Dry Mix = 94.0178%× 50 lb
277-0 Dry Mix = 47.0089 lb

The divisions on the scale used to weigh the 277-0 Dry Mix are every 0.2 lbs. I will assume that the tolerance on the measurement is 0.1%.
Therefore, the maximum scale error could be;
Max Scale Error = Mass × 0.001 + 0.1
Max Scale Error = 47.0089× 0.001 + 0.1
Max Scale Error = 0.147 lb

To assure the minimum amount of ^{10}B the maximum amount of cement must be controlled. Therefore the Maximum 277-0 Dry Mix mass should be;
Max 277-0 Dry Mix = 277-0 Dry Mix − Max Scale Error
Max 277-0 Dry Mix = 47.0089 − 0.147 lb
Max 277-0 Dry Mix = 46.8619 lb

Since the scales divisions are every 0.2 lbs the maximum 277-0 mass is;
Max 277-0 Dry Mix = 46.80 lb (for the scales)
Should be weigh on a small scale with divisions of at least 0.20 lb

The Dry Mix B_4C for a 50 lb 277-4 Dry Mix Mass would be;
Dry Mix B_4C = 50.00 − 46.80 lb
Dry Mix B_4C = 3.20 lb
Should be weigh on a small scale with divisions of at least 0.01 lb

Defining the scale mass as percent weight one gets;
Dry Mix B_4C wt% = Mass B_4C / 277-4 (Dry Mix Mass)
Dry Mix B_4C wt% = 3.20 / 50 × 100%
Dry Mix B_4C wt% = 6.40%

277-0 Dry Mix wt% = 100% − 6.40%
277-0 Dry Mix wt% = 93.60%

Mixing water required for the 50 lb dry mix bag at 27±1% dry mix weight.
Water Mix Weight = 277-4 Dry Mix Mass × 27%
Water Mix Weight = 50.0 × 27%
Water Mix Weight = 13.50 lb

Table 8, 277-4 Dry Mixing weights for one ES-3100

277-0 Dry Mix wt		Dry Mix B_4C		277-4 Dry Mix Mass		Water Mix Weight	
Mass	Scale Div	Mass	Scale Div	Mass	Scale Div	Mass	Scale Div
46.80	0.20	3.20	0.01	50.00	NA	13.50	0.2

Using the maximum total natural boron of 76.5 wt% calculate the weight percentage of natural boron in the dry powder mix.

NatB = B_4C wt% × 76.5 wt%
NatB = 6.4% × 76.5 wt%
NatB = 4.896 wt%

7.7. Define the Volumetric Atomic Concentrations at NCT and HAC

Testing of cast 277-4 shows that our sample cans will be dehydrated at elevated temperatures. Twenty five sample cans were tested at 250°F for 168 hours for the Normal Conditions of Transport (NCT). Then after weighing them they were heated to 320°F for 4 hours for the Hypothetical Accidental Conditions (HAC). Then after weighing them they were heated to 1475°F for 4 hours to totally dehydrate them. This test information has defined the change in hydration from the "as manufactured" to a worst case NCT and the worst case HAC. As the water was removed the cast solids density was also reduced.

Specific Gravity Fraction of water
SGF = H (lb/ft^3) × 0.143172 (1/(lb/ft^3))
SGF = 3.531 (lb/ft^3) × 0.143172 (1/(lb/ft^3))
SGF = 0.5055
On the average the castings are 50.55% water by volume.

Inversely the hydrogen weight concentration is calculated by;
H (lb/ft^3) = SGF / 0.143172

The as manufactured 277-4 casting has an amount of water that was measured with "Lost On Drying" (LOD) tests. Sample cans were placed in an oven at 250°F for 168 hours the weights were measured and after an additional heating to 320°F for 4 hours the weights were measured again. From those weights the amount of water was calculated and presented in Table 9 as a fractional specific gravity of hydration levels generated at different conditions were calculated to be;

Table 9, 277-4 Average Affects Of Temperature Conditions on 25 Tested Cans

	As Manufactured	NCT (250°F @ 168 hours)	HAC (NCT+320°F @ 4 hours)
SG	0.5055	0.4445	0.4435
H (lb/ft^3)	3.531	3.105	3.098
H (wt%)	3.378%	3.083%	3.078%
Percent H (%)	100%	87.93%	87.73%
Ave Density (lb/ft^3)	104.51	100.70	100.64

Therefore, the 277-4 cast solid material at NCT values has 87.93% the hydrogen of the as manufactured material and at HAC values has 87.73% the hydrogen of the as manufactured material. The reduction in hydrogen of water weight affect both the hydrogen and oxygen content in the 277-4 cast solid material. The as manufactured data in Table 6 277-4 Elemental Composition @ 105 lb/ft^3 & 30.2% LOD matches the average hydrogen weight percent in Table 9. In order to generate the minimum density and minimum hydrogen calculation the calculation method in section 7.4 must be modified.

The minimum as manufactured density is 100 lb/ft^3. Only the water weight in the form of hydrogen and oxygen is reduced by leaving the casting matrix. The hydrogen weight percent should also be reduced from the minimum manufactured value of 100% to 87.93% for NCT and 87.73% for HAC. This water mass reduction must be applied at the minimum density and hydrogen content. Table 7 has two different extreme values for ^{10}B and hydrogen. The affects of extended temperature extremes must be evaluated for both conditions. The conservation of mass shall be used for these calculations keeping the lb/ft^3 of the minerals the same while the weight percents change as the hydration level does.

The minimum hydrogen of 3.1999% occurs at a 28.60% LOD and 100 lb/ft^3 density shown in Tables 7 and 10. Therefore, using the data from Table 9 the hydrogen concentration would be reduced by the percentage;
Minimum Manufactured H wt%= 3.1999% Table 10

NCT Hydrogen wt% = 3.1999% × 87.93%
NCT Hydrogen wt% = 2.8137% Table 11

HAC Hydrogen wt% = 3.1999% × 87.73%
HAC Hydrogen wt% = 2.8073% Table 12

The minimum ^{10}B mixture has hydrogen at 3.5579%, and it occurs at a 31.80% LOD and 100 lb/ft^3 density. Therefore, using the data from Table 9 the hydrogen concentration would be reduced by the percentage;

Minimum Manufactured H wt%= 3.5579% Table 5

NCT Hydrogen wt% = 3.5579% × 87.93%
NCT Hydrogen wt% = 3.1284% Table 13

HAC Hydrogen wt% = 3.5579% × 87.73%
HAC Hydrogen wt% = 3.1213% Table 14

Table 10, 277-4 Manufactured Minimum Density @ Minimum Hydrogen
277-4 Elemental Composition @ 100 lb/ft^3 & 28.6% LOD

Element	@LOD% (lb/ft^3)	@LOD% (wt%)	@Den & LOD% (lb/ft^3)	N_e (Atoms/cc)
Hydrogen	3.1541	3.1999%	3.1999	3.063E+22
B Nat				
^{10}B	0.8163	0.8282%	0.8282	7.979E+20
^{11}B	3.6819	3.7354%	3.7354	3.273E+21
Carbon	1.2642	1.2826%	1.2826	1.031E+21
Nitrogen	0.0093	0.0094%	0.0094	6.498E+18
Oxygen	53.6410	54.4207%	54.4207	3.282E+22
Sodium	0.0774	0.0785%	0.0785	3.295E+19
Magnesium	0.2225	0.2258%	0.2258	8.960E+19
Aluminum	25.7264	26.1004%	26.1004	9.331E+21
Silicon	1.6254	1.6491%	1.6491	5.664E+20
Sulfur	0.2032	0.2061%	0.2061	6.202E+19
Calcium	7.7965	7.9098%	7.9098	1.904E+21
Iron	0.3491	0.3541%	0.3541	6.117E+19
Sum	98.5673	100.0000%	100.0000	8.061E+22

B Nat	4.4982	4.5636%	4.5636	4.071E+21

Table 11, 277-4 Reduce for NCT Minimum Density @ Minimum Hydrogen 277-4 Elemental Composition @ 95.39 lb/ft^3 & 25.15% LOD after 250°F for 168 hours

Element	@LOD% (wt%)	@Den & LOD% (lb/ft^3)	N_e (Atoms/cc)
Hydrogen	2.8137%	2.6840	2.569E+22
B Nat			
^{10}B	0.8682%	0.8282	7.979E+20
^{11}B	3.9160%	3.7354	3.273E+21
Carbon	1.3446%	1.2826	1.031E+21
Nitrogen	0.0099%	0.0094	6.498E+18
Oxygen	52.7581%	50.3252	3.035E+22
Sodium	0.0823%	0.0785	3.295E+19
Magnesium	0.2367%	0.2258	8.960E+19
Aluminum	27.3622%	26.1004	9.331E+21
Silicon	1.7288%	1.6491	5.664E+20
Sulfur	0.2161%	0.2061	6.202E+19
Calcium	8.2922%	7.9098	1.904E+21
Iron	0.3713%	0.3541	6.117E+19
Sum	100.0000%	95.3886	7.320E+22

B Nat	4.7842%	4.5636	4.071E+21

Table 12, 277-4 Reduce for HAC Minimum Density @ Minimum Hydrogen 277-4 Elemental Composition @ 95.32 lb/ft^3 & 25.09% LOD after NCT & 320°F for 4 hours

Element	@LOD% (wt%)	@Den & LOD% (lb/ft^3)	N_e (Atoms/cc)
Hydrogen	2.8073%	2.6758	2.561E+22
B Nat			
^{10}B	0.8689%	0.8282	7.979E+20
^{11}B	3.9190%	3.7354	3.273E+21
Carbon	1.3456%	1.2826	1.031E+21
Nitrogen	0.0099%	0.0094	6.498E+18
Oxygen	52.7305%	50.2605	3.031E+22
Sodium	0.0824%	0.0785	3.295E+19
Magnesium	0.2369%	0.2258	8.960E+19
Aluminum	27.3831%	26.1004	9.331E+21
Silicon	1.7301%	1.6491	5.664E+20
Sulfur	0.2163%	0.2061	6.202E+19
Calcium	8.2986%	7.9098	1.904E+21
Iron	0.3715%	0.3541	6.117E+19
Sum	100.0000%	95.3158	7.308E+22

B Nat	4.7879%	4.5636	4.071E+21

Table 13, 277-4 Reduce for NCT Minimum Density @ Minimum Boron 277-4
Elemental Composition @ 94.67 lb/ft^3 & 27.96% LOD after 250°F for 168 hours

Element	@LOD% (wt%)	@Den & LOD% (lb/ft^3)	N_e (Atoms/cc)
Hydrogen	3.1284%	2.9617	2.835E+22
B Nat			
^{10}B	0.8356%	0.7911	7.621E+20
^{11}B	3.7688%	3.5680	3.126E+21
Carbon	1.2941%	1.2251	9.848E+20
Nitrogen	0.0095%	0.0090	6.207E+18
Oxygen	54.1129%	51.2291	3.090E+22
Sodium	0.0792%	0.0750	3.147E+19
Magnesium	0.2278%	0.2156	8.559E+19
Aluminum	26.3340%	24.9306	8.913E+21
Silicon	1.6638%	1.5752	5.410E+20
Sulfur	0.2080%	0.1969	5.924E+19
Calcium	7.9806%	7.5553	1.818E+21
Iron	0.3573%	0.3383	5.843E+19
Sum	100.0000%	94.6709	7.563E+22

B Nat	4.6044%	4.3590	3.888E+21

Table 14, 277-4 Reduce for HAC Minimum Density @ Minimum Boron 277-4
Elemental Composition @ 94.59 lb/ft^3 & 27.90% LOD after NCT & 320°F for 4 hours

Element	@LOD% (wt%)	@Den & LOD% (lb/ft^3)	N_e (Atoms/cc)
Hydrogen	3.1213%	2.9524	2.826E+22
B Nat			
^{10}B	0.8363%	0.7911	7.621E+20
^{11}B	3.7721%	3.5680	3.126E+21
Carbon	1.2952%	1.2251	9.848E+20
Nitrogen	0.0095%	0.0090	6.207E+18
Oxygen	54.0823%	51.1551	3.085E+22
Sodium	0.0793%	0.0750	3.147E+19
Magnesium	0.2280%	0.2156	8.559E+19
Aluminum	26.3572%	24.9306	8.913E+21
Silicon	1.6653%	1.5752	5.410E+20
Sulfur	0.2082%	0.1969	5.924E+19
Calcium	7.9877%	7.5553	1.818E+21
Iron	0.3576%	0.3383	5.843E+19
Sum	100.0000%	94.5876	7.550E+22

B Nat	4.6085%	4.3590	3.888E+21

7.8. Define the Nominal Volumetric Atomic Concentrations

Using nominal mixer weights from Table 8 in Section 7.6 calculate the nominal ^{10}B content at the nominal density and hydration. The following tolerances were taken at the minimum ^{10}B values in ASTM C 750-03 Type 1 at ^{10}B is 19.9±.3 atom% of NatB, Total Boron 81.0 to 76.5, and the mixing weights of 5.88 lb of B_4C to a 102.6323 lb/ft^3 total as shown in Table 4. When these minimum tolerances values are brought to the nominal values one the following differences are found.

NomF ≈Change Atom% × Boron Percentage × Mixer weight changes
NomF ≈ (19.9/19.6) × (78.75/76.5) × (6.4/5.88)
NomF ≈ 1.138

Approximately 13.8% more ^{10}B on the average comparing the values to an exact calculated value is confirmed by comparing the nominal ^{10}B data shown in Table 15 to the data in Table 6.

NomF = Table 15 ^{10}B / Table 6 ^{10}B
NomF = 9.388E+20 / 8.190E+20
NomF = 1.146

On the average 14.6% more ^{10}B is found in the nominal elemental composition.

Table 15, 277-4 At Nominal Density, Boron%, and Mixer Weights
Elemental Composition @ 105 lb/ft^3 & 30.2% LOD

Element	@LOD% (lb/ft^3)	@LOD% (wt%)	@Den & LOD% (lb/ft^3)	N_e (Atoms/cc)
Hydrogen	3.4264	3.3789%	3.5479	3.396E+22
B Nat				
^{10}B	0.9411	0.9280%	0.9744	9.388E+20
^{11}B	4.2445	4.1856%	4.3949	3.851E+21
Carbon	1.2802	1.2624%	1.3255	1.066E+21
Nitrogen	0.0094	0.0093%	0.0098	6.716E+18
Oxygen	55.6706	54.8984%	57.6434	3.476E+22
Sodium	0.0770	0.0760%	0.0798	3.347E+19
Magnesium	0.2215	0.2184%	0.2293	9.103E+19
Aluminum	25.6067	25.2515%	26.5141	9.479E+21
Silicon	1.6179	1.5954%	1.6752	5.754E+20
Sulfur	0.2022	0.1994%	0.2094	6.300E+19
Calcium	7.7605	7.6529%	8.0356	1.934E+21
Iron	0.3484	0.3436%	0.3608	6.232E+19
Sum	101.4065	100.0000%	105.0000	8.682E+22

B Nat	5.1855	5.1136%	5.3693	4.790E+21

8. Conclusion

The dry mix ratios are shown in Table 8 and for 100% dry mix weight and are the following 93.6±0.43% 277-0 Heat Resistant Shielding and 6.4±0.32% Boron Carbide Powder. Once thoroughly dry blended, 27±1% water shall be added to the dry mix weight. Follow the casting specification for final instructions.

The elemental compositional calculations are performed at the minimum ^{10}B level for the compositional purity, isotopic atomic percentage, and scale measurements. The probability of each of these ^{10}B levels being at the minimum limits at the same time is quite remote. As shown in Section 7.8 the minimum limits are over 13 to 14% conservative from the nominal values.

The minimum acceptable casting density at the minimum hydration and ^{10}B levels were subsequently taken at and dehydrated to a worst Normal Conditions of Transport (NCT) and the Hypothetical Accidental Conditions (HAC) temperatures. The thermal stability of the cast 277-4 neutron poison shows little differences between the NCT and the HAC elemental compositions. Therefore, I recommend using the worst case HAC elemental composition for the final Nuclear Criticality Safety Calculations. The largest difference seen is dependent upon the input data. In order to determine the most criticality reactive HAC elemental composition Tables 12 and 14 should both be used to run an infinite array nuclear criticality safety calculation. Upon completion of these calculations the most reactive HAC elemental compositions shall be used for both NCT and HAC calculations.

Appendix 1; Thermo Electron Corp. Heat Resistant Shielding
Catalog No. 277 product information sheet 277-103, page 1 of 2

Heat Resistant Shielding
Catalog No. 277

Radiation Measurement & Protection

Thermo ELECTRON CORPORATION

Well suited to attenuate the neutron flux from power reactors by the inclusion of hydrogen and boron in the form of temperature-resistant additives. It incorporates approximately three times as much hydrogen as ordinary concrete, making the material far superior for neutron shielding applications.

- **Low cost material is completely non-combustible**
- **Rugged and easily cast in the field**

General

High temperature resistance is a frequent requirement for power reactor shielding. Type 277 Heat Resistant Shielding is a refractory material designed to retain a significant portion of its shielding properties at temperatures up to 450° F (230° C) . This material will maintain its physical integrity at temperatures up to 1900° F (1038° C). In addition, this low-cost rugged material is completely non-combustible and can be easily cast in the field. Its compressive strength is 1000 psi (90 BAR).

Type 277 is well suited to attenuate the neutron flux from power reactors by the inclusion of hydrogen and boron in the form of temperature-resistant additives. It incorporates approximately three times as much hydrogen as ordinary concrete, making the material far superior for neutron shielding applications. The refractory matrix also provides good resistance to heat.

Type 277 Heat Resistant material has a boron content of 1.56 %. The hydrogen concentration (which moderates fast neutrons) is approximately one-half that of water. For additional technical information on Type 277, including temperature resistance, refer to TD-277-1002.

Type 277 is offered in the form of a dry mix for casting in place, but can also be supplied in pre-cast shapes.It is readily shaped with ordinary tools (e.g., band-saws or drills). Type 277 Dry Mix is available in 100-lb (45.5kg) or larger containers. Approximately 96-lbs. of dry mix are required to obtain one-cubic ft. of cast material. (1.54 kg of dry mix will give one liter). Detailed mixing instructions are provided with each order. Recommended shelf-life under dry storage conditions is six months.

Catalog No. 277 Heat Resistant Shielding is a refractory material designed to retain a significant portion of its shielding properties at temperatures up to 450° F (230° C). This material will maintain its physical integrity at temperatures of up to 1900° F (1038° C).

In addition Catalog No. 277 is a low cost rugged material which is completely non-combustible and can easily be cast in the field. Its compressive strength is 1000 psi (90 BAR).

Catalog No. 277 is well suited to attenuate neutron flux from power reactors by the inclusion of hydrogen and boron (natural isotope distribution) in the form of temperature resistant additives. It incorporates approximately three times as much hydrogen as ordinary concrete, making the material far superior for neutron shielding applications. The refractory matrix also provides good resistance to heat.

For Contact Information visit www.thermo.com/rmp

Appendix 1; Thermo Electron Corp. Heat Resistant Shielding
Catalog No. 277 product information sheet 277-103, page 2 of 2

SPECIFICATIONS

Products Available

Catalog No. 277 is offered in the form of dry mix for casting in place, but can also be supplied in pre-cast shapes and blocks.It is readily shaped with ordinary power tools (e.g. band-saws or drills).

Catalog No. 277 Dry Mix is available in 300-lb (136 kg) containers. Approximately 96-lbs of dry mix are required to obtain one-cubic foot of cast material (1.54 kg of dry mix will give one liter). Water 27 PPH, parts of dry mix (by weight).

Recommended shelf life for Catalog No. 277 under dry-storage conditions is 6 months.

Composition Data

Active Components:

Hydrogen atom density / cm^3:	3.4×10^{22}/cc
Natural isotope distribution:	99.98% $_1H$
Boron atom density / cm^3:	1.43×10^{21}
Natural isotope distribution:	19.6% $_{10}B$ and 80.4% $_{11}B$
Weight percent of all isotopes of boron:	1.56%
Total Density:	1.68 g / cc

Radiation Properties

Macroscopic thermal neutron cross section:	1.1 cm^{-1}
Gamma resistance:	1×10^{11} rads
Neutron resistance:	5×10^{19} n / cm^2

Physical Properties

Appearance and Odor:

State	Powder
Color	Light Gray
Odor	no odor

Mechanical Properties

Machining of 277:	Fair, can be saw cut and drilled
Hardness:	N/A
Tensile Strength (ASTM D368):	100 psi (kg/m^2)
Compressive Strength:	1000 psi (kg/m^2)

Thermal Properties

Recommended Temperature Limit:	350°F
Melting Point:	N/A
Boiling Point:	N/A
Coefficient of Thermal Conductivity:	1.24×10^{-3} cal-cm/sec cm^2 ° C = 0.3 BTU - ft/hr ft^2 ° F
Heat Capacity:	0.22 cal/g ° C
Cubical Coefficient of Expansion:	8×10^{-6} cm^3/cm^3 ° C = 1.4×10^{-5} in^3/in^3 ° F
Linear Coefficient of Expansion	N/A
Vapor Pressure (mm Hg):	N/A
Vapor Density (Air = 1):	N/A
Evaporation Rate (ether=1):	N/A
Percent Volatile by Volume:	N/A
Specific Gravity (H_2O = 1):	1.68 g/cm^3

Chemical Properties

Chemical Name & Synonyms:	Borated Hydrogenated Casting Mix
Trade Name & Synonyms:	Catalog No. 277
Chemical Family:	Calcium salts, boron, and hydrogen containing compounds
Formula:	Proprietary
Solubility in Water:	Negligible

Reactivity Data

Reactive Materials	
Reactive Acids:	N/A
Reactive Bases:	N/A
Reactive Metals and Metal Compounds:	N/A
Reactive Oxidizing Agents:	N/A
Reactive Reducing Agents:	N/A

Material Incompatibility

Materials to Avoid: :	N/A
Hazardous Decomposition Products:	
Solid	None
Liquid	None
Gas	None
Hazardous Polymerization:	Will Not Occur

For more information see: TD-277-001

277-103

Radiation Measurement & Protection

Thermo ELECTRON CORPORATION

Appendix 2; Thermo Electron Corp. Heat Resistant Shielding Catalog No. 277 Typical Elemental Analysis Without Boron, EA-277, May 1988.

EA-277
Without Boron
May, 1988

TYPICAL ELEMENTAL ANALYSIS

CATALOG NO. 277 - HEAT RESISTANT SHIELDING

Element	Weight Percent
O	59.14%
Al	26.59
Ca	8.04
H	3.73
Si	1.68
Fe	0.30
Mg	0.23
S	0.21
Na	0.08
Total	100.00%

PROPERTIES

Density = 1.61 g/cc (101 lbs/cu ft)

Hydrogen Atoms per cc = 3.59×10^{22}

Macroscopic Thermal Neutron Cross Section: $\Sigma = 0.01 cm^{-1}$

Recommended Temperature Limit = 350°F (177°C)

Machinability: Fair; can be saw-cut and drilled

Thermal Conductivity, K = 1.24×10^{-3} cal-cm/(sec)(cm)²(°C)

Specific Heat = 0.22 cal/gpC

Coefficient of Theraml Expansion = 1.4×10^{-5}cm per cm per °C

Compressive Strength = 1400 psi

Tensile Strength = 95 psi

Radiation Resistance, gammas: 1×10^{11} Rads

Radiation Resistance, neutrons: 1×10^{21} n/cm²

THERMAL TESTS AND CHARACTERISTICS

These tests have not been performed on this Type 277 without boron. We have examined each test separately, and we feel confident that the results of all these tests and that the characteristics of the material would be essentially the same as for Type 277 with boron.

THIS PAGE INTENATIONALLY LEFT BLANK.

Appendix 1.4.10

PYROPHORICITY OF URANIUM METAL

Prepared by: Russell W. Schmidt
BWXT Y-12, L.L.C.
November 2006
Revised June 2007

Reviewed by: Sanford G. Bloom
BWXT Y-12, L.L.C.
November 2006
Re-reviewed June 2007

THIS PAGE INTENTIONALLY LEFT BLANK.

Appendix 1.4.10

PYROPHORICITY OF URANIUM METAL

I. Introduction

The ES-3100 is a new shipping container designed for safe and efficient transportation of highly enriched uranium in a wide range of material forms. The ES-3100 has been certified for use with a variety of contents, including enriched uranium metal and alloy. However, the current size limitations on uranium contents in the form of broken metal are unnecessarily restrictive. The size limits exist because under certain conditions uranium metal and some uranium alloys are pyrophoric – they have the potential to spontaneously ignite. The size restrictions are intended to eliminate the possibility of spontaneous ignition during transport.

The purpose of this analysis is to evaluate the potential for uranium metal pieces to spontaneously ignite under the conditions expected for shipment in the ES-3100 shipping container, and to identify limits on the uranium metal content that will prevent spontaneous ignition during transport, while still allowing a high degree of flexibility and utility.

It is important to remember that the content limits developed for the ES-3100 must be implemented in the field. Therefore the criteria derived from this evaluation must be simple, robust, and readily applied in all of the facilities using this package.

This evaluation does not include new laboratory tests of uranium metal ignition parameters. Such tests have been performed and well documented in the past. This evaluation draws on the extensive body of existing data and proven storage and transport practice to identify the bounds within which uranium metal and alloys can be safely transported in the ES-3100 shipping container.

II. Proposed Definition of Pyrophoricity

The Certificate of Compliance (CoC), gives the definition of broken metal in paragraph 5.(b)(1)(ii), as follows:

> *For metal or alloy defined as broken metal, mass limits are specified in Table 2. Uranium metal and alloy pieces must have a surface-area-to-mass ratio of not greater than 1 cm^2/g or must have a mass not less than 50 g, whichever is most restrictive. Powders, foils, turnings, wires, and incidental small particles are not permitted, unless they are restricted to not more than 1 percent by weight of the content per convenience can, and they are either in a sealed, inerted container or are stabilized to an oxide prior to shipment.*

It is suggested that the definition of broken metal in paragraph 5.(b)(1)(ii) be revised to the following:

> *For metal and alloy defined as broken metal, mass limits are specified in Table 2. Uranium metal and alloy pieces must have a surface-area-to-mass ratio of not greater than 1 cm^2/g or must not pass freely through a 3/8-inch (0.0095m) mesh sieve. Particles and small shapes that do not pass this size restriction, as well as powders, foils, turnings, and wires, are not permitted, unless they are either in a sealed container under an inert cover gas.*

III. Rational for Proposed Changes

The proposed text makes the following changes:

- The 50 g minimum piece size is eliminated;
- A 3/8-in. mesh limit is added;
- The phrase "whichever is most restrictive" is deleted;
- Remove oxidation as a treatment for pyrophoric uranium, in this context
- The 1% limit on inerted material is eliminated.

The 1 cm^2/g maximum specific surface area limit is the most significant limit in the original text, and that limit is retained unchanged. Specific surface area is the most significant parameter in determining if a given piece of uranium is at risk of spontaneous ignition under a given set of conditions, and therefore it is appropriate that this restriction should control any other restrictions to the package contents. The discussion section below will demonstrate that the 1 cm^2/g maximum allowable specific surface area is adequate to prevent spontaneous ignition in the ES-3100.

The 50 g minimum piece size is overly restrictive and is inconsistent with the 1 cm^2/g upper limit on specific surface area. Smooth uranium metal pieces can have a mass of less than 0.5 g and still have a specific surface area less than 1 cm^2/g (see example 1). This makes the 50 g limit two orders of magnitude too large. The 50 g limit is nearly an order of magnitude too large even considering metal pieces with the rough surface of broken metal instead of a smooth cast or polished surface.

Example 1.
Consider a smooth uranium metal sphere with a diameter of 0.32 cm (0.126 in.).
The radius of the sphere is 0.16 cm. The density of uranium metal is 19 g/cm^3.
The volume is $V = (4/3) \cdot Pi \cdot r^3 = (4/3) \cdot Pi \cdot (0.16)^3 = 0.01716\ cm^3$
The mass is $M = Density \cdot V = 19\ g/cm^3 \cdot 0.01716\ cm^3 = 0.3260\ g$
The surface area is $A = 4 \cdot Pi \cdot r^2 = 4 \cdot Pi \cdot (0.16)^2 = 0.3217\ cm^2$
The specific surface area is $SA = A/M = 0.3217\ cm^2 / 0.3260\ g = 0.9868\ cm^2/g$
This specific surface area is just within the 1 cm^2/g upper limit.

If instead of a smooth surface the sphere has a rough surface characteristic of broken uranium metal, a larger size is needed to ensure that the 1 cm^2/g limit is maintained. For a roughness factor of three (meaning that the rough surface has an actual surface area that is three times the surface area calculated from the radius), the radius would need to be three times the above example to give the same specific area. In this case:
$r = 3*0.16\ cm = 0.48\ cm$; $V = (4/3) \cdot Pi \cdot (0.48)^3 = 0.463\ cm^3$;
$M = 19\ g/cm^3 \cdot 0.463\ cm^3 = 8.802\ g$; $A = 4 \cdot Pi \cdot (0.48)^2 \cdot 3$ (roughness factor) $= 8.686\ cm^2$
And so the specific surface area is $8.686\ cm^2/8.802g = 0.9868\ cm^2/g$ as above.

Depending on the surface roughness, a sphere with a mass between 0.33 and 8.8 grams will meet the 1 cm^2/g specific surface area limit

The 1 cm^2/g specific surface area limit controls the parameter that is most important in terms of preventing spontaneous ignition, but it is not easy to measure or to use in the field. A mass limit (similar to the 50 g limit in the existing certificate, but more consistent with the 1 cm^2/g specific area limit) could be used, but it is very time-consuming to weigh every piece of metal in a package. An approach that is both effective at enforcing the 1 cm^2/g specific surface area limit and quick and easy to use in the field is

to separate large pieces from small ones in a sieve. The recommended text stipulates a 3/8-in. mesh sieve to quickly remove small particles (with a large specific surface area) from large particles which have a small specific surface area.

As demonstrated in example 1, rough-surfaced spheres 3/8 in. (0.95 cm) in diameter meet the 1 cm^2/g specific surface area limit (a smooth-surfaced sphere of this size has a specific surface area of 0.33 cm^2/g). Therefore, a sphere which does not pass freely through the 3/8-in. mesh sieve will meet the 1 cm^2/g specific surface area limit. Other simple shapes such as cubes and rods are also effectively controlled by the 3/8-in. sieve. Foils, turnings, and wires are explicitly forbidden in both the current and proposed text, unless they are packed in an inert atmosphere.

The phrase "whichever is most restrictive" has been deleted from the proposed text since the sieve test has been sized to effectively enforce the 1 cm^2/g specific surface area limit.

The option of converting pyrophoric uranium to an oxide is removed, since metals need to be shipped as metals for maximum usefulness at the receiver site. In addition, if oxides are produced, packing limits for oxides have been explicitly given in the certificate of compliance.

The final change in the proposed text is to eliminate the 1% of content weight limit on inerted material. This limit is unnecessary for uranium metal sealed in a container containing an inert atmosphere. If the metal has been sealed in a container containing an inert atmosphere, there is no oxygen available to the metal and therefore no chance of combustion.

Uranium metal packaged for transport in the ES-3100 is first placed inside a convenience can or other container. These cans are then placed into the ES-3100 containment vessel (CV). The convenience cans will displace most of the oxygen from the containment vessel, leaving only enough to react with a few grams of metal. If a sealed container containing an inert atmosphere somehow came open in transport (an unlikely scenario given the very limited amount of movement possible inside a properly loaded containment vessel), this small amount of oxygen is not enough to support spontaneous ignition. The containment vessel has been shown to retain its structural integrity and remain leak tight under hypothetical accident conditions, so no additional oxygen can enter.

IV. Discussion

In his 1995 review,[1] Terry Totemeier explains pyrophoricity this way: "Pyrophoricity refers to the tendency of certain metals to ignite and burn in a self-sustaining oxidation reaction. The pyrophoric nature of metals is usually defined in terms of an ignition temperature, which is the temperature at which a metal will ignite and burn in a self-sustained fashion for a given set of conditions." ASTM C-1454[2] defines pyrophoric as "capable of igniting spontaneously under temperature, chemical, or physical/mechanical conditions specific to the storage, handling, or transportation environment".

This evaluation will demonstrate that uranium metal with a specific surface area of 1 cm^2/g will not spontaneously ignite under the conditions existing in the ES-3100 during packaging and transport.

The primary factors determining if the conditions for spontaneous ignition exist are specific surface area and temperature. Totemeier explains, "Because oxidation is a surface reaction, the amount of area available for reaction is a critical factor in the determination of the heat generated in oxidation. Specific area is the best parameter to describe the effect of area, as it also accounts for the amount of material not reacting which can serve as a heat sink." Temperature is critical because the amount of heat generated by the reaction is a function of the reaction rate, which is in turn a function of the temperature. Higher temperatures give higher reaction rates.

An additional safety factor in the case of the ES-3100 is the small amount of oxygen available in the sealed inner containment vessel. This serves to limit the total amount of uranium that can oxidize, and therefore prevents any potential heat build-up from reaching the ignition point of uranium metal.

Ignition Temperature and Transport Conditions

In figures 4 and 5 of his review, Totemeier plots two separate tests of uranium ignition temperatures as a function of specific surface area. For a specific surface area of 1 cm^2/g these two plots give values of 390°C (663 K)[a] and 340°C (613 K), respectively. Using the lower value and rounding down gives a conservative value of 600 K for the ignition temperature of uranium metal in the ES-3100.

The ES-3100 thermal analysis determined that the temperature at the containment vessel wall would not exceed 190°F (361 K) for normal conditions of transport (NCT) and 255°F (397 K) for hypothetical accident conditions (HAC). These values, particularly the HAC temperature, are very conservative. The actual results from six separate package tests showed that the CV wall temperature was typically around 210 °F (372 K), with the highest recorded value of 241 °F (389 K). Note that all of these temperatures are well below the 600 K ignition temperature of the uranium metal contents.

Maximum Temperature from Oxidation – Basic Equations

Uranium metal readily reacts with oxygen to form uranium dioxide (UO_2). This reaction is exothermic. The heat released by the reaction warms the uranium metal, increasing the reaction rate. Under normal conditions for storage and transport, the reaction rate is slow enough that the small amount of heat generated by the reaction is lost to the environment, and a stable steady-state is achieved. If the reaction rate is fast enough, and the metal is relatively well insulated, the temperature of the uranium metal can build, slowly at first but at an increasing rate, until the ignition temperature is reached and the metal ignites and burns.

The task at hand is to evaluate the balance between heat generation and heat loss in the ES-3100 under hypothetical accident conditions to verify that a stable steady state is reached, and that the steady-state condition is safely below the ignition point of uranium metal. A recent paper by Epstein, Malinovic, and Plys[3] lays out a useful approach, which will be followed here without the approximations used in their paper.

---

[a] The curve in Totemeier figure 4 is discontinuous, with a transition from a lower curve to an upper curve shown at a specific surface area of 6 cm^2/g. At a specific surface area of 1 cm^2/g the upper curve would give an ignition temperature of 550ºC, while extrapolation of the lower curve gives 390ºC. The original reference from which Totemeier drew figure 4 explains that the transition from the lower curve to the upper curve is influenced by many factors, including the metallurgy of the uranium, any alloying metals or impurities, and the oxygen content of the gas involved. Therefore this analysis uses the lower curve value of 390ºC.

For uranium metal packed in cylindrical cans, the generation of heat throughout the can and the associated transfer of heat to the can wall is mathematically identical to the generation of heat within a wire due to electrical resistance. In their text "Transport Phenomena"[4] Bird, Stewart & Lightfoot develop the desired relation (equation 9.2-14):

$$Tcenter - Twall = (S \cdot R^2) / (4 \cdot Kth) \qquad \text{(Equation 1)}$$

where

Tcenter is the temperature at the center of the can (K)
Twall is the temperature at the can wall (K)
S is the heat production per unit volume (W/cm^3)
R is the radius of the can (cm)
Kth is the thermal conductivity of the uranium contents (W/cm K)

The heat production per unit volume is a function of the reaction rate and the heat of reaction. Since the oxidation reaction occurs at the surface of the uranium, the reaction rate is typically stated as a mass reacted per second per unit area. The specific surface area, the uranium metal density, and the packing density are applied to convert the rate per unit uranium surface area to a rate per unit can volume. The result is:

$$S = Rho \cdot Phi \cdot SArea \cdot dHrxn \cdot RxnRate \qquad \text{(Equation 2)}$$

where

Rho is the density of the uranium metal (g/cm^3)
Phi is the packing density of the uranium in the can (cm^3 U/cm^3 can volume)
SArea is the specific surface area of the uranium (cm^2/g)
dHrxn is the heat of reaction (J/g uranium)
RxnRate is the reaction rate (g uranium / (s • cm^2))

The reaction rate of uranium metal with oxygen has been evaluated by many researchers over the years. The general form of the rate equation used is:

$$RxnRate = K0 \cdot P^n \cdot e^{(-Te/T)} \qquad \text{(Equation 3)}$$

where

K0 is the reaction rate coefficient (g uranium / (s • cm^2))
P is the partial pressure of water vapor (kPa)
n is the exponential coefficient on the partial pressure of water vapor
Te is the activation energy (K)
T is the temperature of the reactants (K)

For the case at hand, the temperature of the reactants is the highest at the can center (Tcenter) and the lowest at the can wall (Twall). The average temperature of the reactants is midway between these two values. For conservatism the reaction rate of the entire contents is evaluated at the maximum temperature, which occurs at the center of the can (Tcenter). This analysis considers heat transfer only through the can walls, and ignores heat transfer through the top and bottom of the can. This is also a conservative assumption.

Equations 1, 2, and 3 are combined to yield:

$$Tcenter - Twall = (R^2 \cdot Rho \cdot Phi \cdot SArea \cdot dHrxn \cdot K0 \cdot P^n \cdot e^{(-Te/Tcenter)}) / (4 \cdot Kth) \quad \text{(Equation 4)}$$

Note that Kth is a property of the can contents (that is, for the bed of uranium metal particles with air in between), and not a property of solid uranium metal. The thermal conductivity of uranium metal is much higher than the thermal conductivity of a bed of uranium metal pieces.

P is the partial pressure of H_2O present in the containment vessel at the center-line temperature. This value is calculated by assuming that the ES-3100 was loaded at ambient conditions of T0 and 100% relative humidity, which yields a water vapor pressure of P0. When the temperature in the containment vessel increases the partial pressure of water vapor increases according to the ideal gas law, which in this case reduces to:

$$P = P0 \cdot (Tcenter/T0) \quad \text{(Equation 5)}$$

In this evaluation, the maximum possible rate of heat generation due to the oxidation of the uranium metal is also of interest since this heat must be carried away by the package, even at HAC. The maximum rate of heat generation is the heat generated by the oxidation of uranium metal at the highest temperature reached during HAC, assuming the maximum allowable load of uranium metal. This is:

$$Qmax = Mmax \cdot SArea \cdot dHrxn \cdot K0 \cdot P^n \cdot e^{(-Te/Tcenter)} \quad \text{(Equation 6)}$$

where

Qmax = the maximum rate of heat generation (W)
Mmax = the maximum uranium metal loading (g)

Evaluation of Thermal Stability

Equation 4 provides the means to evaluate the maximum temperature reached in the uranium metal. It does not by itself validate the stability of the system. This system does present a simple means to evaluate stability – both numerical stability and more importantly physical stability (meaning that the temperature cannot build to spontaneous ignition).

Solving equation 4 for Twall over a range of Tcenter values and plotting the results produces figure 1:

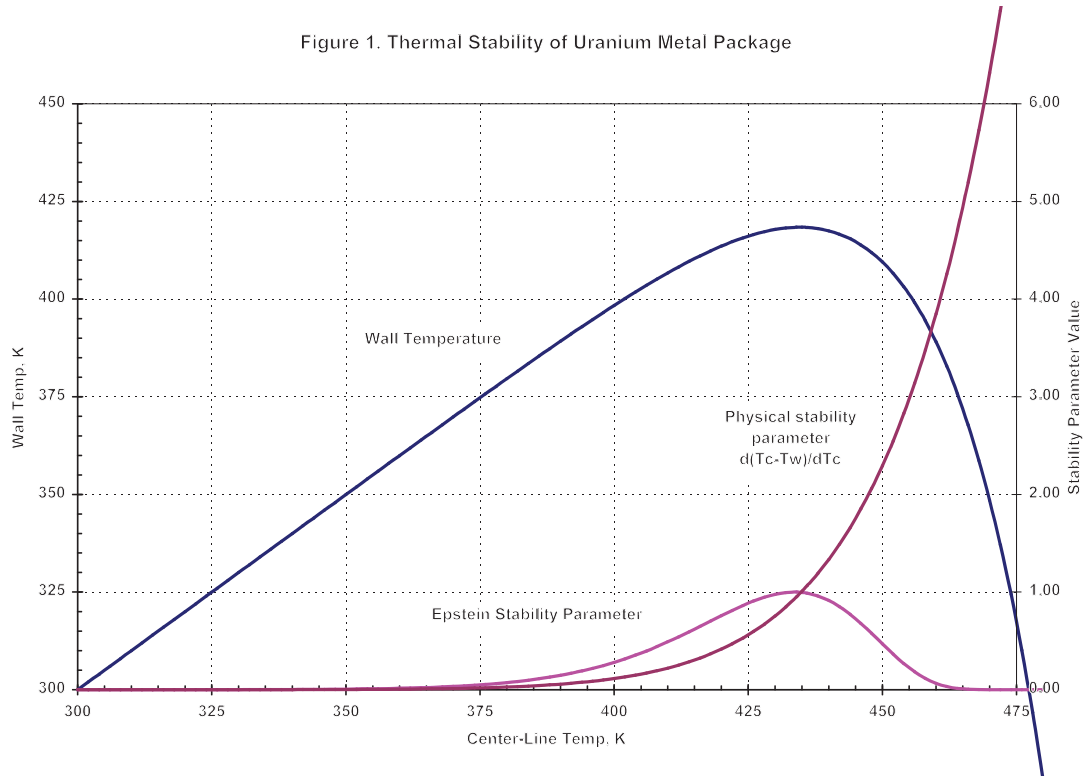

The wall temperature calculated from equation 4 and plotted here is the temperature needed in order to provide enough heat transfer to maintain the given center-line temperature. The wall temperature initially tracks the center-line temperature – the rate of heat generation is low, so a very small temperature difference is sufficient to remove that heat. As the center-line temperature (and therefore the amount of heat generated) increases, the temperature difference needed to keep the center-line temperature steady at the given value increases exponentially. At some point (about 435 K in figure 1) the required temperature difference gets so large that the wall temperature would have to decrease in order to maintain a stable center-line temperature. In an actual package there is no cooling mechanism to do this, and once the center-line temperature exceeds this point the amount of heat generated will exceed the ability to carry off that heat, and the center-line temperature will increase until either the reaction runs out of oxygen or the ignition point is reached. The point at which the required wall temperature stops increasing, marks the maximum stable center-line temperature for the package. The required wall temperature stops increasing at the point where the rate of increase in the needed temperature difference (d(Tcenter-Twall)) equals the rate of increase of the center-line temperature (dTcenter). Stated mathematically, when d(Tcenter-Twall)/dTcenter is less than 1 the required Twall increases along with Tcenter, and stability is maintained. When d(Tcenter-Twall)/dTcenter is greater than 1 Twall would have to drop to maintain stability as Tcenter increases. Since this is not possible in a real package, the temperature in the package would steadily increase to either ignition or consumption of all available oxygen. The value of d(Tcenter-Twall)/dTcenter = 1 marks the maximum stable point for a given package.

Equation 4 is

$$Tcenter - Twall = (R^2 \bullet Rho \bullet Phi \bullet SArea \bullet dHrxn \bullet K0 \bullet P^n \bullet e^{(-Te/Tcenter)}) / (4 \bullet Kth)$$

Taking the first derivative of this equation with respect to Tcenter yields an equation for the stability parameter derived above:

$$d(Tcenter-Twall)/dTcenter = (Tcenter-Twall) \bullet Te/Tcenter^2 \qquad \text{(Equation 7)}$$

The thermal stability of the system is maintained as long as $(Tcenter-Twall) \bullet Te/Tcenter^2 \leq 1$. This parameter is equivalent to the stability parameter "B" developed in Epstein et al, without the simplifying assumptions made in that paper. The value of d(Tcenter-Twall)/dTcenter is plotted in Figure 1, along with the Epstein "B" parameter.

Input Parameters

The key values used to evaluate equations 4, 5, 6, and 7 are shown in Table 1.

Table 1. Key input parameters

Parameter	Value	Units
R	5.27	cm
Rho	19	g/cm^3
Phi	0.26	cm^3/cm^3
SArea	1	cm^2/g
dHrxn	4559	J/g Uranium
K0	76086	$gU/(s \bullet cm^2)$
P0	3.53	kPa
T0	300	K
n	0.3	
Te	11490	K
Kth	0	$W/(cm \bullet K)$

The sources of these parameters are:

R is the inside radius of a convenience can. The typical can used has an outside diameter of 4.25 in., and an inside diameter of 4.15 in. (10.54 cm).

Rho is the density of uranium metal.

Phi is the packing density of uranium metal when packed into the convenience cans. Operator experience at Y-12 is that a maximum of 5 kg U of broken metal will fit into a 4.25-in. OD by 4.875-in. high can, which has an internal volume of 1000 cm^3. This yields a packing density of 0.26 cm^3/cm^3. The effects of variations on this value are discussed below.

SArea is the specific surface area, which is limited by the package certification to 1 cm^2/g.

dHrxn is the heat of reaction, on a uranium basis. This value came from Totemeier, page 17 (1089 cal/gU = 4559 J/gU).

K0, n, and Te are parameters for the reaction rate equation. As noted above, a number of researchers have analyzed the reaction rate of uranium metal with various combinations of oxygen and water vapor. Numerous models have been developed from this data. This analysis used the published model that best fit the conditions present. Many of the published rate models are only valid up to 100 to 130°C. This evaluation requires evaluation beyond 140°C. Many of the models are for either pure oxygen or pure water vapor. McGillivray[5] notes that the reaction rate at a given temperature varies with both the oxygen concentration and the partial pressure of water vapor. The published model that best matches the conditions of this evaluation (reaction in air at temperatures exceeding 140°C, with a small water vapor partial pressure) is the Pearce model (Pearce, < 100% RH, in Air, T < 192°C) as reported in the Epstein paper.

P0 and T0 are used to calculate P, the partial pressure of H_2O vapor present in the containment vessel at the center-line temperature. This value is calculated by assuming that the ES-3100 was loaded at ambient conditions of T0 = 300 K (80°F) and 100% relative humidity. P0 is therefore the vapor pressure of water at 300K, which is P0 = 3.53 kPa. When the temperature in the containment vessel increases, the partial pressure of water vapor increases according to equation 5.

Kth is the thermal conductivity of the uranium particle bed. The value here was taken from Epstein et al, page 6. Because of the air-filled void spaces, the bed thermal conductivity is much lower than the uranium metal value of 0.3 W/(cm • K).

Results

The set of equations (4, 5, 6, and 7) was evaluated using a commercial software package named Tk!Solver, which has the advantage of being able to automatically iterate to solutions as needed. This is necessary when solving equation 4 for a fixed wall temperature to determine Tcenter. Attachment 1 shows the rules, input and output for the TK!Solver model for the HAC and NCT cases.

The hypothetical accident condition evaluation gave a maximum containment vessel (CV) temperature (Twall) of 255°F (397 K). Evaluating equations 4 through 7 for these conditions yields a Tcenter of 398.4 K (257.5°F), with a maximum heat output (assuming a full load of 36 kgU) of 5.9 Watts, and a stability parameter d(Tcenter-Twall)/dTcenter of 0.102, well below the critical value of 1.0.

The 255°F HAC temperature was based on a uranium heat generation of 0.4 W. The 5.9 W maximum heat generated from the oxidation reaction under those conditions would heat the CV wall above that temperature. The thermal analysis evaluated the HAC for heat generation rates of 20 W and 30 W as well as the 0.4 W standard value. Table 3.7 in the thermal analysis shows that for an assumed 20 W heat generation in the uranium metal contents, the peak CV wall temperature is 277 °F (409.3 K). Using this value ensures that the heat transfer from the uranium contents to the CV wall and to the rest of the package is conservatively addressed.

For the revised HAC wall temperature of 277 °F (409.3 K), equations 4 through 7 yield the following results:

Tcenter = 413.3 K (284.4 °F) (well below the ignition temperature of 600 K)
MaxQ = 17.0 Watts (below the 20W assumption)
d(Tcenter-Twall)/dTcenter = 0.272 (well below the critical value of 1.0)

At the NCT wall temperature of 190°F (360.9 K) the results are:

Tcenter = 361.0 K (190.1 °F) (well below the ignition temperature of 600 K)
MaxQ = 0.289 Watts (below the 0.4W assumption)
d(Tcenter-Twall)/dTcenter = 0.006 (well below the critical value of 1.0)

These values clearly show that uranium metal with a specific surface area of no more than 1 cm^2/g will not spontaneously ignite under any anticipated transport conditions.

Variation in Input Packing Density

The density with which uranium metal is packed into the convenience cans limits the surface area available to oxidize. Operator experience at Y-12 is that a maximum of 5 kg U of broken metal will fit into a 4.25-in. OD by 4.875-in. high can, which has an internal volume of 1000 cm^3. This yields a packing density of 0.26 cm^3/cm^3.

A search of the literature on packing densities reveals a lot of work on smooth spheres, and very little on anything else. Scott and Kilgour[6] experimented with packing smooth steel spheres in cylinders, and reported a maximum packing density of 0.6366 after extensive vibration to compact the steel spheres as much as possible. The steel balls used in this experiment had a coefficient of friction of 0.2, well below the value for smooth uranium metal of 1.0. Subsequent analysis by Kong and Lannutti[7] considering the effects of friction between particles gives packing fractions in the range of 0.41 to 0.46, with higher friction coefficients producing lower packing fractions.

The broken metal routinely packed at Y-12 consists of large, rough, irregular pieces. The reported packing density of 0.26 for this material is consistent with the literature reviewed, particularly Kong and Lannutti. Therefore the value of 0.26 was used as the base value in the analyses reported above.

To bound the metal contents of the ES-3100 two additional cases have been analyzed under hypothetical accident conditions: rough broken metal at a packing density of 0.46 (the upper end of the range reported by Kong & Lannutti); and smooth cast spheres at a packing density of 0.64 (consistent with Scott & Kilgour).

For rough broken metal at a packing density of 0.46 the maximum center temperature at HAC was 422 K, well below the ignition temperature of 600 K. For smooth cast 3/8” spheres at a packing density of 0.64 the maximum center temperature at HAC was 412 K, well below the ignition temperature of 600 K.

Oxygen Limitation in the Containment Vessel

The analysis above placed no restriction on the amount of oxygen available to react with the uranium metal contents. In reality, the ES-3100 containment vessel has a finite volume, which restricts the amount of oxygen available for reaction.

The CV is a cylinder with inside dimensions of 31.00 in. (78.74 cm) tall and 5.06 in. (12.85 cm) in diameter. This produces a volume of 10,215 cm^3, or 10.215 liters. At ambient conditions of 300 K (80.3°F) and 100% relative humidity, 10.215 liters of humid air contains 2.78 g of oxygen from the air, and another 0.23 grams of oxygen in the H_2O. These 3.01 grams of oxygen can react with 22.40 g of uranium metal. This is 0.06% of the ES-3100’s capacity.

A mass of 22.4 g of U metal when reacted with 3.01 g of oxygen will produce a maximum total heat output of 102 kJ (96.8 BTU), spread out over the time required for the reaction to take place. This total amount of oxygen could sustain the NCT maximum heat output of 0.289 W for 4.1 days, or the HAC peak heat output for 1.7 hours. If somehow released all at once, the 102 kJ would only raise the temperature of 36 kg of uranium by 24.5 K. More realistically, as shown by the calculations above, any reaction will be slow, with enough time for the heat generated to flow to the CV and the rest of the package.

The ES-3100 CV is 15.1 kg of stainless steel, with a heat capacity of 0.515 J/(g •K). The 102 kJ maximum produced by the oxidation reaction could only raise the temperature of the CV (ignoring contents) by 13.1 K. This heat sink, plus the heat sinks offered by the CV contents, ensures that the oxidation reaction will not be able to build to the 600 K ignition temperature required for spontaneous ignition.

In practice there will less than 3 g of oxygen available to react with the uranium metal inside the closed CV. A full load of uranium will, by itself, displace nearly 20% of the air in the CV. The convenience cans, spacer cans, and other packing materials will displace even more air, further reducing the amount of uranium that could possibly react. Also, the uranium metal is packed inside closed convenience cans. These cans limit the oxygen available to react with the contents to the oxygen in the convenience can itself. Finally, part of the available oxygen will react with the uranium before the peak HAC conditions are reached. Figure 22b in section 3 shows that it will take about 4 hours for the CV wall to reach the maximum temperature in the HAC fire. During this four-hour temperature ramp-up 0.9 grams of oxygen would be consumed by reaction with the uranium, leaving only 2.1 grams available to react once the HAC temperature was reached. Even if the uranium surface area was uncontrolled, lack of oxygen would snuff out any increase in the uranium reaction rate before it could reach the ignition point.

Specific Surface Area Implementation via Sieve

As noted above, the 1 cm^2/g specific surface area limit is not easy to measure or to use in the field. A screening method that is simple and easy to use in the field will reduce the potential for packaging mistakes. The recommended approach is to separate large pieces from small ones in a sieve. The recommended text stipulates a 3/8-in. mesh sieve to quickly remove small particles (with a large specific surface area) from large particles which have a small specific surface area.

Example 1 above showed that the minimum size of a metal sphere meeting the 1 cm^2/g specific surface area limit varies with the degree of surface roughness. In example 1 a smooth sphere 1/8 inch in diameter and a rough sphere 3/8 inch in diameter both had specific surface areas just below the 1 cm^2/g limit. The 3/8-in. mesh is stipulated in the recommended text in order to accommodate both smooth and rough metal.

The actual metal contents of the ES-3100 will include both smooth-surfaced and rough-surfaced metal. The smooth-surfaced items include a variety of cast and machined shapes. The rough-surfaced items are “broken metal” – large castings that have been fractured into smaller pieces. These broken metal pieces will typically have two or three cast surfaces with the remaining 3 or 4 surfaces of fractured metal.

The 3/8-inch mesh recommendation is based on a surface roughness factor of three, meaning that the rough surface has an actual surface area available to react with oxygen that is three times that of a smooth-surface of the same gross dimensions. This roughness factor of three was derived from an evaluation of fracture surfaces for cast uranium metal. Roughness factors ranged from 1.1 to 2.7, with a mean value of 2.0. A roughness factor of three was selected to bound the highest value observed. The 3/8 inch mesh screening is therefore suitable for metal that is fractured on all surfaces. Since as noted

above even broken metal will have several smooth faces the 3/8-inch mesh screening should be quite conservative.

As demonstrated above, a rough-surfaced sphere which does not pass freely through the 3/8-in. mesh sieve will meet the 1 cm^2/g specific surface area limit. Other simple shapes such as cubes and rods are also effectively controlled by the 3/8-in. sieve. Foils, turnings, and wires are explicitly forbidden in both the current and proposed text, unless they are packaged in an inert atmosphere. Attachment 2 shows the dimensions of a variety of shapes that have a specific surface area of 1 cm^2/g. All of these items will fall through a 3/8-in. sieve, demonstrating that the sieve will effectively enforce the 1 cm^2/g specific surface area limit.

Most foils and wires will not fall through a sieve of any reasonable size. The current 50 g test would likewise not reliably exclude these materials, which is why foils, turnings, and wires are explicitly forbidden in both the current and proposed text, unless they are packed in an inert atmosphere. Operator training will be required under either the current or the proposed text to ensure that these items are properly packaged.

Operator Training

As part of the transition to using the new shipping container, training materials are being prepared to instruct the field operations personnel on the proper way to use the ES-3100. As noted above, the training for the operators packing uranium metal into the convenience cans for shipment in the ES-3100 will be important in ensuring that potentially pyrophoric materials are properly categorized and inerted as necessary. This training will cover the following points:

- All metal pieces must be evaluated to ensure that their smallest dimension is larger than the 3/8 inch mesh size.
  - Single solid-metal pieces that are clearly larger than the 3/8-inch mesh in every dimension do not require sieving.
  - Items which are obviously unacceptable, such as foils, wires, and turnings, may be removed before the sieving
  - Any item that is not obviously larger than the 3/8-inch mesh in every dimension and which has not been rejected must be sieved.
  - Any item that falls through the sieve must be rejected.

- Operators need to be alert to items which may not fall through the sieve but which are too small:
  - Long, thin shapes such as wires and turnings may not fall through the sieve when shaken. If the wire or turning could be picked up and poked through the mesh it must be rejected, even if it did not fall through unassisted.
  - Wires or turnings may form a tangled ball which will not fall through. The above criterion applies: if the wire or turning could be separated and poked through the mesh it must be rejected.
  - No distinction is made between wires and rods – if the item could be picked up and poked through the mesh it must be rejected.
  - Foils, thin chips or shards - any item less than 1/8 inch thick – must be rejected.
  - Metal showing visible moisture or signs of having been stored in water must be rejected.

- Rejected items must be separated for proper handling:
  - Rejected items can be shipped if packed under an inert cover gas.
  - An acceptable cover gas must be high-purity (≥ 99%) and dry (≤ 5 ppm moisture).

V. Conclusion

The evaluations performed show that uranium metal conforming to the 1 cm^2/g limit on specific surface area will not spontaneously ignite under any anticipated transport conditions. Spontaneous ignition is independently prevented by both the 1 cm^2/g limit on the uranium metal and by the limited amount of oxygen available in the sealed ES-3100 containment vessel.

The 3/8-in. sieve specified in the revised text effectively applies the 1 cm^2/g specific surface area limit to broken uranium metal in a manner that is quick and easy to use in the field.

THIS PAGE INTENTIONALLY LEFT BLANK.

Attachment 1 TK!Solver Model and Results

Rules

Tcenter-Twall=((R^2*rho*phi*SArea*dHrxn*K0*P^n)/(4*Kth))*exp(-Te/Tcenter)
P=P0*(Tcenter/T0)
Deriv=(Tcenter-Twall)*Te/Tcenter^2
HRate=SArea*dHrxn*K0*P^n*exp(-Te/Tcenter)
MaxQ=HRate*MaxM
RRate=SArea*MaxM*K0*P^n*exp(-Te/Tcenter)
ORate=RRate*32/238
OTime=MaxO/ORate

HAC - 277 °F Wall Temperature

Input	Name	Output	Unit	Comment
	Tcenter	413.348	K	Temperature at the center of the can
409.3	Twall		K	Temp at the can wall
	HRate	.000472	W/gU	Rate of heat production (w/unlimited O2)
	MaxQ	16.9945	W	Maximum heat production (from max KgU)
36000	MaxM		gU	Maximum ES-3100 contents
3.01	MaxO		gO	Maximum ES-3100 Oxygen Content
	RRate	.003728	gU/s	Reaction Rate at given Conditions
	ORate	.000501	gO/s	Oxygen Use rate at given conditions
	OTime	1.66822	hr	Oxygen time to run-out
5.27	R		cm	Can radius
1	SArea		cm^2/gU	Specific Surface Area of U particles
	Deriv	.272221		d(Tcenter-Twall)/dTcenter
19	rho		gU/cm^3	Density of uranium
.26	phi			
				Packing density, U cm^3 / Can cm^3
4559	dHrxn		J/gU	Heat of Reaction
76086	K0		gU/(s*cm^2)	Reaction rate coefficient - Pearce <100%
11490	Te		K	Reaction rate coefficient - Pearce <100%
.3	n			
				Reaction rate coefficient - Pearce <100%
3.53	P0		kPa	Vapor pressure of water at T0
300	T0		K	Temperature for P0
	P	4.86373	kPa	Vapor Pressure of Water at Tcenter
.004	Kth		W/cm*K	Thermal Conductivity of U particle bed

NCT - 190 °F Wall Temperature

Input	Name	Output	Unit	Comment
	Tcenter	360.969	K	Temperature at the center of the can
360.9	Twall		K	Temp at the can wall
	HRate	8.03E-6	W/gU	Rate of heat production (w/unlimited O2)
	MaxQ	.288991	W	Maximum heat production (from max KgU)
36000	MaxM		gU	Maximum ES-3100 contents
3.01	MaxO		gO	Maximum ES-3100 Oxygen Content
	RRate	6.34E-5	gU/s	Reaction Rate at given Conditions
	ORate	8.52E-6	gO/s	Oxygen Use rate at given conditions
	OTime	98.1015	hr	Oxygen time to run-out
5.27	R		cm	Can radius
1	SArea		cm^2/gU	Specific Surface Area of U particles
	Deriv	.00607		d(Tcenter-Twall)/dTcenter
19	rho		gU/cm^3	Density of uranium
.26	phi			Packing density, U cm^3 / Can cm^3
4559	dHrxn		J/gU	Heat of Reaction
76086	K0		gU/(s*cm^2)	Reaction rate coefficient - Pearce <100%
11490	Te		K	Reaction rate coefficient - Pearce <100%
.3	n			Reaction rate coefficient - Pearce <100%
3.53	P0		kPa	Vapor pressure of water at T0
300	T0		K	Temperature for P0
	P	4.2474	kPa	Vapor Pressure of Water at Tcenter
.004	Kth		W/cm*K	Thermal Conductivity of U particle bed

Attachment 2. Pyrophoric Size Limits on Small Uranium Metal Pieces

Specific Surface Area:		1.0	cm^2/g					
Uranium Metal Density:		19.0	g/cm^3					
Surface Area Multiplier:		3.0						
	The surface area multiplier is the ratio of the actual surface area							
	divided by the simple geometeric surface area.							
Spheres - Minimum Safe Diameter								
Limiting diameter		0.9474	cm	or	0.3730	in	8.459	grams
Rods - Minimum Safe Diameter								
	Length	**Diameter**						
	0.9 cm	0.9474	cm	or	0.3730	in	12.688	grams
	1.0 cm	0.9231	cm	or	0.3634	in	12.715	grams
	1.5 cm	0.8000	cm	or	0.3150	in	14.326	grams
	2.0 cm	0.7500	cm	or	0.2953	in	16.788	grams
	2.5 cm	0.7229	cm	or	0.2846	in	19.495	grams
	Infinite	0.6316	cm	or	0.2487	in		
Cubes - Minimum Safe Side Length								
Limiting side length		0.9474	cm	or	0.3730	in	16.155	grams
Square Cross-Section Rods - Minimum Safe Side Length								
	Length	**Side**						
	0.9 cm	0.9474	cm	or	0.3730	in	16.155	grams
	1.0 cm	0.9231	cm	or	0.3634	in	16.189	grams
	1.5 cm	0.8000	cm	or	0.3150	in	18.240	grams
	2.0 cm	0.7500	cm	or	0.2953	in	21.375	grams
	2.5 cm	0.7229	cm	or	0.2846	in	24.822	grams
	Infinite	0.6316	cm	or	0.2487	in		
Chips & Shards - Minimum Safe Thickness								
Length	**Width**	**Thickness**						
1.0 cm	0.5 cm	6.0000	cm	or	2.3622	in	57.000	grams
1.5 cm	0.5 cm	2.0000	cm	or	0.7874	in	28.500	grams
2.0 cm	0.5 cm	1.5000	cm	or	0.5906	in	28.500	grams
2.5 cm	0.5 cm	1.3043	cm	or	0.5135	in	30.978	grams
3.0 cm	0.5 cm	1.2000	cm	or	0.4724	in	34.200	grams
Infinite	0.5 cm	0.8571	cm	or	0.3375	in		
1.0 cm	0.6 cm	2.0000	cm	or	0.7874	in	22.800	grams
1.5 cm	0.6 cm	1.2000	cm	or	0.4724	in	20.520	grams
2.0 cm	0.6 cm	1.0000	cm	or	0.3937	in	22.800	grams
2.5 cm	0.6 cm	0.9091	cm	or	0.3579	in	25.909	grams
3.0 cm	0.6 cm	0.8571	cm	or	0.3375	in	29.314	grams
Infinite	0.6 cm	0.6667	cm	or	0.2625	in		
Infinite	Infinite	0.3158	cm	or	0.1243	in		

VI. References

1. Totemeier, Terry C. ANL/ED/95-2 "A Review of the Corrosion and Pyrophoricity Behavior of Uranium and Plutonium", June 1995, Argonne National Lab-West.

2. ASTM C-1454-00, "Standard Guide for Pyrophoricity/Combustibility Testing in Support of Pyrophoricity Analyses of Metallic Uranium Spent Nuclear Fuel", January 10, 2000, ASTM International.

3. M. Epstein, B. Malinovic, M. G. Plys, SNF-6192-FP, "Uranium Pyrophoricity Phenomena and Prediction", April 2000, Fluor Hanford, Richland Washington.

4. R. Byron Bird, Warren E. Stewart, Edwin N. Lightfoot, "Transport Phenomena", 1960, John Wiley & Sons.

5. G. W. McGillivray, D. A. Geeson, R. C. Greenwood, "Studies of the Kinetics and Mechanism of the Oxidation of Uranium by Dry and Moist Air – A Model for Determining the Oxidation Rate Over a Wide Range of Temperatures and Water Vapor Pressures", June 1993, Journal of Nuclear Materials # 208 (1994) pg 81-97.

6. G. D. Scott, D. M. Kilgour, "The Density of Random Close Packing of Spheres", February 1969, British Journal of Applied Physics, Series 2, Volume 2, pp 863 - 866.

7. C. M. Kong, J. J. Lannutti, "Effect of Agglomerate Size Distributions on Loose Packing Fraction", March 2000, Journal of the American Ceramic Society, Volume 83, pp 2183 – 2188.

SECTION 1 REFERENCES

10 CFR 71, *Packaging and Transportation of Radioactive Material*, Jan. 1, 2007.

49 CFR, *Transportation*, Oct. 1, 2007.

ASME Boiler and Pressure Vessel Code, An American National Standard, Rules for Construction of Nuclear Facility Components, Sect. III, Div. 1, Subsection NB, American Society of Mechanical Engineers, New York, 2001 ed. with 2002 and 2003 addenda.

ASTM D-2000, *Standard Classification System for Rubber Products in Automotive Applications*, American Society for Testing and Materials, Philadelphia, current revision.

Byington, G. A. et al., "Fireproof Impact Limiter Aggregate Package Inside Shipping Container," U.S. patent 6,299,950 B1, Oct. 9, 2001.

DG-7003 (Proposed Revision 2 of Regulatory Guide 7.9), *Standard Format and Content of Part 71 Applications for Approval of Packaging for Radioactive Material*, U.S. NRC, December 2003.

MIL-D-6054F, *Drum, Metal—Shipping and Storage*, June 30, 1989.

NUREG/CR-3854, *Fabrication Criteria for Shipping Containers*, Lawrence Livermore Natl. Lab., March 1985.

Regulatory Guide 7.10, rev. 1, *Establishing Quality Assurance Programs for Packaging Used in the Transport of Radioactive Material*, U.S. NRC, June 1986.

Regulatory Guide 7.11, *Fracture Toughness Criteria of Base Material for Ferritic Steel Shipping Cask Containment Vessels with a Maximum Wall Thickness of 4 Inches (0.1 m)*, U. S. NRC, June 1991.

NUREG-1609, *Standard Review Plan for Transportation Packages for Radioactive Material*, U. S. NRC, March 1999.

THIS PAGE INTENTIONALLY LEFT BLANK.

2. STRUCTURAL EVALUATION

The ES-3100 package is used to ship highly enriched uranium (HEU) in the following forms: oxide; bulk and broken metal shapes; and uranyl nitrate crystals. Content will be packed in various size convenience cans made of stainless, tin-plated carbon steel, or nickel alloy, and polyethylene, or Teflon FEP bottles. The cans shall have a diameter of ≤12.7 cm (5 in.) and heights of ≤25.4 cm (10 in.). Containment vessel arrangements that utilize closed metal cans with a diameter greater than 10.8 cm (4.25 in.) will not contain any materials that off gas at the temperatures associated with Normal Conditions of Transport (NCT) or Hypothetical Accident Conditions (HAC). Any combination of these cans shall be allowed in a single package, as long as the total length of the can stack (with spacers when required) does not exceed the inside working height of the containment vessel. Any closure on the convenience can is allowed. When space is available inside the containment vessel, stainless-steel metal scrubbers will be placed on the top and bottom of this partially canned assembly or an empty convenience can will be placed on top of this assembly inside the containment vessel. Polyethylene bags may be used inside or outside any convenience can as long as the loading restrictions in Sect. 1.2.3.8 are met. The amount of polyethylene bagging and lifting slings used inside the ES-3100 containment vessel is limited to 500 g. For the structural evaluation, the maximum payload inside the containment vessel will be as follows and as shown in Table 2.1: (1) 24 kg oxide or compounds (up to 100% enrichment in ^{235}U); (2) HEU oxide shall be in the form of UO_2, UO_3, or U_3O_8; (3) 24 kg of uranyl nitrate crystals; (4) 35.2 kg of uranium metal and alloy (up to 100% enrichment in ^{235}U); (5) HEU metal and alloy may be in the form of broken pieces, ingots, buttons, or small castings; and (6) the maximum weight of all contents, including nuclear material, convenience containers, polyethylene bags, spacers, slings, etc., shall not exceed 40.82 kg (90 lb). There is no minimum payload weight requirement. Uranium and transuranic isotopic allowances are defined in Sect. 4. Mass limits and total weights for each shipping arrangement are defined and described in Sect. 2.1.3. The 40.82-kg (90-lb) maximum containment vessel content weight and 35.2-kg (77.60-lb) HEU content weight limits have been established as a bounding case for the maximum structural, thermal, and containment limit for the shipping package. The above content masses and forms used for the proposed content do not take into consideration limits based on shielding and subcriticality.

As described in the following sections, design analysis, similarity, drop simulations, and the full-scale testing documented herein demonstrates that the ES-3100 package is in compliance with the requirements of Title 10 Code of Federal Regulations (CFR) 71 and Title 49 CFR 100–178 when it is used to ship contents described above. The maximum bounding activity of the contents (35.2 kg of HEU) is 3.2328×10^{-1} TBq (8.737 Ci) when the maximum activity-to-A_2 value is reached at ~70 years from material fabrication. The corresponding maximum number of A_2s carried is 293.99. This information is further discussed in Sect. 4.

Table 2.1. Proposed HEU contents for shipment in the ES-3100

Form	Chemical or physical description	Total weight of HEU contents kg (lb)
HEU oxide	UO_2, UO_3, U_3O_8	24 (52.91)
Uranyl nitrate crystals	$UO_2(NO_3)_2 + 6H_2O$	24 (52.91)
HEU metal and alloy	Specific geometric shapes (spheres, cylinders, square bars or slugs) or broken metal pieces	35.2 (77.60)

2.1 DESCRIPTION OF STRUCTURAL DESIGN

2.1.1 Discussion

The principal structural members of the shipping package consist of the following: the drum assembly, the containment boundary, packaging material, and the contents. Each of these will be described and discussed in the following sections.

2.1.1.1 Drum assembly

The drum assembly of the shipping package is defined as the structure that maintains the position of and provides protection to the impact and thermal barrier surrounding the containment boundary. Preserving the location of the containment boundary within the packaging prevents reduction of the shielding and subcriticality effectiveness. The drum assembly for the ES-3100 consists of an internally flanged Type 304L stainless-steel 30-gal modified drum with two type 304L stainless-steel inner liners, one filled with noncombustible cast refractory insulation and impact limiter (Kaolite) and one filled with noncombustible cast neutron absorber (Cat 277-4), a stainless-steel top plug with cast refractory insulation, silicone rubber pads, silicon bronze hex-head nuts, and a stainless-steel lid and bottom (Drawing M2E801580A031, Appendix 1.4.8). The nominal weight of these components is 131.89 kg (290.76 lb).

The drum's diameters (inner diameter of 18.25 in.) and corrugations meet the requirements of Military Standard MS27683-7. All other dimensions are controlled by Drawing M2E801580A004 (Appendix 1.4.8). Modifications to the drum from MS27683-7 include the following: (1) the overall height was increased; (2) the drum was fabricated with two false wire open ends; and (3) a 0.27-cm (12-gauge, 0.1046-in.)–thick concave cover was welded to the bottom false wire opening (Drawing M2E801580A005, Appendix 1.4.8). Four 0.795-cm (0.313-in.)–diameter equally spaced holes are drilled in the top external sidewall to prevent a pressure buildup between the drum and inner liner. The holes are sealed with a plastic plug to provide a moisture barrier for the cast refractory insulation during Normal Conditions of Transport (NCT). The cavity created by the inner liners is a three-tiered volume with a 37.52-cm (14.77-in.) inside diameter 13.26 cm (5.22 in.) deep, a 21.84-cm (8.60-in.) inside diameter 5.59 cm (2.20 in) deep, and an additional 15.85-cm (6.24-in.) inside diameter 78.31-cm (30.83 in.) deep. The volume between the mid liner and the drum and the top plug's internal volume is completely filled with the noncombustible cast refractory insulation called Kaolite 1600 from Thermal Ceramics, Inc. Kaolite properties, such as mechanical, thermal conductivity, and impact, are presented in Appendix 2.10.3. The volume between the most inward liner and the mid liner wall is completely filled with a noncombustible neutron absorber (poison) from Thermo Electronic Corp. called Cat 277-4. Cat 277-4 properties, such as thermophysical, mechanical, and neutron activation, are

presented in Appendix 2.10.4. BoroBond4, another noncombustible neutron absorber, was used only in prototype test packages instead of Cat 277-4. The drum body, inner liners, and lid are fabricated from 0.15-cm (16-gauge, 0.0598-in.) thick Type 304/304L stainless-steel sheet. A rolled stainless-steel flange with a 5.08 × 5.08 × 0.64-cm (2 × 2 × 0.25-in.) thick modified stainless-steel structural angle is welded around the top of the mid inner liner. The mid inner liner is then welded to the inside surface of the drum along this flange. Eight ⅝-11-UNC-2A studs welded to the drum and silicon bronze nuts provide the structural attachment for the drum lid, and are torqued to 40.67 ± 6.78 N·m (30 ± 5 ft-lb) at assembly. The drum lid's diameter and shape meet the requirements of Military Standard MS27683-61. All other dimensions are controlled by Drawings M2E801580A006 and A007, Appendix 1.4.8. The welded angle ring (Find Number 3 on Drawing M2E801580A006, Appendix 1.4.8) provides the lid with an inner flange. The welded angle ring was incorporated in the ES-3100 package for use during handling and transport to protect the lid closure studs and nuts. During transport, the welded angle ring helps position drum tie-down adapters that are used for tie-down of a single unit configuration in Safe-Secure Trailers/Safeguards Transporters (SSTs/SGTs) in accordance with U.S. Department of Energy (DOE) Order 5610.14. The drum is marked by two stainless-steel data plates. The data plate lettering and mounting requirements on the drum are shown on Drawings M2E801580A010 and M2E801508A031 (Appendix 1.4.8), respectively. Painting and marking requirements for the drum are shown on Drawing M2E801508A001 (Appendix 1.4.8). Two lugs are welded to the mid inner liner and project through the drum lid at assembly. Each lug has a 0.953-cm (0.38-in.)–diameter hole through which a tamper-indicating device (TID) can be threaded.

The volume between the drum and mid-liner is filled with a lightweight noncombustible cast refractory material called Kaolite 1600. The top plug is also filled with this material and represents the thermal insulation and impact limiting barrier. The material is composed of portland cement, water, and vermiculite and has an average density of 358.8 kg/m^3 (22.4 lb/ft^3). The procedure for manufacturing and documenting the installation of this material, JS-YMN3-801580-A003 (Appendix 1.4.4), is referenced on Drawings M2E801580A002 and M2E801580A008 (Appendix 1.4.8) for the drum assembly weldment and top plug weldment, respectively. The insulation has a maximum continuous service temperature limit of 871°C (1600°F) due to the presence of the vermiculite and portland cement.

The volume between the most internal liner and the mid-liner is filled with a noncombustible cast neutron absorber (poison) material from Thermo Electronic Corp. called Cat 277-4. The material is a high alumina borated concrete composed of aluminum, magnesium, calcium, boron, carbon, silicon, sulfur, sodium, iron and water. The final mixture has an average density of 1681.9 kg/m^3 (105 lb/ft^3). The procedure for manufacturing and documenting the installation of this material, JS-YMN3-801580-A005 (Appendix 1.4.5), is referenced on Drawing M2E801580A002 (Appendix 1.4.8). This neutron absorber material has a maximum continuous service temperature limit of 150°C (302°F) in order to retain the bound mass of water in the final cured mixture for subcriticality control.

The top plug is fabricated in accordance with Drawing M2E801580A008 with an overall diameter of 36.50 cm (14.37 in.) and a height of 13.41 cm (5.28 in.). The plug's rim, bottom sheet, and top sheet are fabricated from 0.15-cm (16-gauge, 0.0598-in.) thick Type 304/304L stainless-steel sheet per ASME SA240. Four lifting inserts are welded into the top sheet for loading and unloading operations. The internal volume of the top plug is filled with Kaolite 1600 in accordance with JS-YMN3-801580-A003, Appendix 1.4.4.

Three silicone rubber pads complete the drum assembly. One pad is placed on the bottom of the most internal liner to support the containment vessel during transport. Another pad is placed on the top shelf of the mid-liner to support the top plug during transport. The final plug is placed over the top of the containment vessel during transport. The pads are molded to the shapes as defined on Drawing M2E801580A009 (Appendix 1.4.8). The material is silicone rubber with a Shore A durometer reading of 22 ±5.

2.1.1.2 Containment boundary

The containment vessel's body, lid assembly, and inner O-ring provide the containment boundary (Fig. 1.3). Two methods of fabrication may be used to fabricate the containment vessel body of the ES-3100 package as shown on Drawing M2E801580A012 (Appendix 1.4.8). The first method uses a standard 5-in., schedule 40 stainless-steel pipe per ASME SA-312 Type TP304L, a machined flat-head bottom forging per ASME SA-182 Type F304L, and a machined top flange forging per ASME SA-182 Type F304L. The nominal outside diameter of the 5-in schedule 40 pipe is machined to match the nominal wall thickness of 0.100 in. Each of these pieces is joined with circumferential welds as shown on sheet 2 of Drawing M2E801580A012 (Appendix 1.4.8). The top flange is machined to match the schedule 5-in. pipe, to provide two concentric half-dove tailed O-ring grooves in the flat face, to provide locations for two 18-8 stainless-steel dowel pins, and to provide the threaded portion for closure using the lid assembly. The second method of fabrication uses forging, flow forming, or metal spinning to create the complete body (flat bottom, cylindrical body, and flange) from a single forged billet or bar with final material properties in accordance with ASME SA-182 Type F304L. The top flange area using this fabrication technique is machined identically to that of the welded forging method. The lid assembly, which completes the containment boundary structure, consists of a sealing lid, closure nut, and external retaining ring (Drawing M2E801580A014, Appendix 1.4.8). The containment vessel sealing lid (Drawing M2E801580A015, Appendix 1.4.8) is machined from Type 304 stainless-steel bar with final material properties in accordance with ASME SA-479. The containment vessel closure nut (Drawing M2E801580A016, Appendix 1.4.8) is machined from a Nitronic 60 stainless-steel bar with material properties in accordance with ASME SA-479. These two components are held together using a WSM-400-S02 external retaining ring made from Type 302 stainless steel. The sealing lid is further machined to accept a ⅜-16 swivel hoist ring bolt to facilitate loading and unloading, to provide a leak-check port between the elastomeric O-rings, and notched along the perimeter to engage two dowel pins. The lid assembly, with the O-rings in place on the body, are joined together by torquing the closure nut and sealing lid assembly to 162.70 ± 6.78 N·m (120 ± 5 ft-lb). The sealing lid portion of the assembly is restrained from rotating during this torquing operation by the two dowel pins installed in the body flange. An evacuation port is located between the O-rings in the containment vessel to facilitate a pressure rise or drop leakage test following assembly or 10 CFR 71 compliance testing. This port is sealed during transport using a modified VCO threaded plug. Only the inner O-ring is considered a part of the containment boundary.

There are no penetrations of, connections to, or fittings for the sealed containment boundary. To meet the requirements for package certification, the containment boundary must remain intact during all conditions of transport. This integrity must be demonstrated by test or other acceptable methodology for NCT and Hypothetical Accident Conditions (HAC) as described in 10 CFR 71.

2.1.1.3 Packaging materials

Contents will be packed in various size convenience cans made of stainless steel, tin-plated carbon steel, or nickel-alloy, and polyethylene bottles or Teflon FEP bottles. The cans shall have a diameter of ≤12.7 cm (5 in.) and heights of ≤44.5 cm (17.5 in.). Any combination of these cans shall be allowed in a single package, as long as the total length of the can stack (with spacers and pads as

required) does not exceed the inside working height of the containment vessel (~31 in.). Any closure on the convenience can is allowed. Multiple short cans may be tack brazed together. Containment vessel arrangements that utilize closed metal cans with a diameter greater than 10.8 cm (4.25 in.) will not contain any materials that off gas at the temperatures associated with NCT or HAC. When space is available inside the containment vessel, stainless-steel metal scrubbers will be placed on the top and bottom of this partially canned assembly or an empty convenience can will be placed on top of this assembly inside the containment vessel. The polyethylene bottles have a diameter of ~12.54 cm (4.94 in.) and a height of ~22.1 cm (8.7 in.). A total of three polyethylene bottles may be loaded into the containment vessel. The Teflon FEP bottles have a diameter of ~ 11.91 cm (4.69 in.) and a height of ~23.88 cm (9.4 in.). A total of three Teflon FEP bottles may be loaded into the containment vessel. Polyethylene bags may be used inside or outside any convenience can or bottle. In some packing arrangements, silicone rubber pads will be used between convenience cans. Also, some arrangements will require spacers between cans. These spacers are thin stainless-steel cans filled with the noncombustible cast neutron poison. Each convenience can and spacer is equipped with a stainless-steel band clamp and nylon coated wire for loading and unloading operations. The spacers are ~10.11 cm (3.98-in.) in diameter by 4.45 cm (1.75 in.) in height and a maximum weight ~0.58 kg (1.27 lb). In order to minimize displacement of convenience containers during transport, stainless-steel scrubbers or polyethylene bags may be added on top of the last can or bottle in the containment vessel. If partial loading configurations are employed and empty cans or bottles are used, these empty cans or bottles will be loaded last and will require a minimum 0.32 cm (⅛ in.) diameter hole to be placed through the lid.

2.1.2 Design Criteria

2.1.2.1 General standards for all packages

The general design standards for all packages in accordance with 10 CFR 71.43(a) through (e), (g) and (h) are addressed in the following paragraphs.

10 CFR 71.43(a)

Requirement: The smallest overall dimension of a package shall not be <10 cm (4 in.).

Compliance: The drums' outside diameter over the rolled rings is 49.20 cm (19.37 in.), and the outside height including the lid is 110.49 cm (43.50 in.). The minimum outside diameter of the ES-3100 containment vessel is 13.36 cm (5.26 in.), and the overall height is 82.30 cm (32.40 in.). Therefore, the packaging meets this requirement.

10 CFR 71.43(b)

Requirement: The outside of the package must incorporate a feature, such as a seal, that is not readily breakable and that, while intact, would be evidence that the package has not been opened by unauthorized persons.

Compliance: The removable drum head is attached to the body by eight ⅝-11-UNC-2B silicon bronze nuts and ⅝-in. nominal washers. Two 0.51-cm (0.20-in.)-thick lugs with 0.953-cm (0.38-in.)-diam holes (Drawing M2E801580A005, Appendix 1.4.8) project through slots in the drum lid and provide attachment for tamper-indicating devices (TIDs). These TIDs consist of a stainless-steel cable with an aluminum crimp closure or equivalent. The requirement is satisfied by the TIDs, which are installed as specified in Sect. 7.1.2.2. The TID is only required when the containment vessel has HEU in the package. It is not required for empty shipments.

10 CFR 71.43(c)

Requirement: Each package must include a containment system securely closed by a positive fastening device that cannot be opened unintentionally or by pressure that may arise within the package.

Compliance: The fastened lid on the drum with tamper-indicating features provides assurance that the drum assembly will not be unintentionally breached. The containment boundary is sealed using the lid assembly and closure nut to ensure that this boundary will be breached only through a deliberate effort, and then only after the drum assembly is breached. The design of the containment boundary is analyzed in Appendix 2.10.1 for a differential pressure of 699.82 kPa (101.5 psi) internal and 150 kPa (21.7 psi) external. The internal design pressure exceeds the maximum differential pressure of 173.98 kPa (25.233 psi) and 494.64 kPa (71.741 psi) attained during NCT (Sect. 2.6.2) and HAC (Sect. 3.5.3), respectively. In addition, calculation results are provided in Sects. 2.6.1 and 2.7.4.3 to demonstrate that the stresses in the containment boundary and closure nut threads do not exceed the stress limits established by the ASME code for NCT and HAC. Therefore, the containment boundary will not be breached during any mode of transport due to pressurization of the containment boundary.

10 CFR 71.43(d)

Requirements: A package must be made of materials and construction that assure that there will be no significant chemical, galvanic, or other reaction among the packaging components, among package contents, or between the packaging components and the package contents including possible reaction resulting from inleakage of water, to the maximum credible extent. Account must be taken of the behavior of materials under irradiation.

Compliance: Compliance with the regulatory requirements are discussed in Sect. 2.2.2.

10 CFR 71.43(e)

Requirement: A package valve or other device, the failure of which would allow radioactive contents to escape, must be protected against unauthorized operation and, except for a pressure relief device, must be provided with an enclosure to retain any leakage.

Compliance: No penetrations, connections, or fittings into the containment vessels exist; therefore, the requirements of 10 CFR 71.43(e) are not applicable.

10 CFR 71.43(g)

Requirement: A package must be designed, constructed, and prepared for transport so that in still air at 38°C (100°F) and in the shade, no accessible surface of a package would have a temperature exceeding 50°C (122°F) in a nonexclusive use shipment or 85°C (185°F) in an exclusive use shipment.

Compliance: Since the components to be shipped have a calculated maximum decay heat load of 0.4 W, thermal analyses were conducted for the ES-3100 package; results are summarized in Appendix 3.6.2. The predicted temperatures, while the package is stored at 38°C (100°F) in the shade, for the drum lid center, and the containment vessel flange, are approximately 38.3°C (101°F). The analysis shows that no accessible surface of the package would have a temperature exceeding 50°C (122°F). Therefore, the requirement of 10 CFR 71.43(g) would be satisfied for either transportation mode (exclusive or nonexclusive use).

10 CFR 71.43(h)

Requirement. A package must not incorporate a feature intended to allow continuous venting during transport.

Compliance. No penetrations, connections, or fittings into the containment vessel exist that would allow venting during transport. The materials of package construction do not provide any pressure buildup during transportation. Four vent holes through the drum are covered with a plastic plug during NCT. Therefore, the requirements of 10 CFR 71.43(h) are satisfied.

2.1.2.2 Component design criteria

The ES-3100 packaging/content combination addressed in this safety analysis report is intended to ship contents with a maximum activity of 3.2328×10^{-1} TBq (8.737 Ci) at 70 years from initial fabrication; the maximum number of A_2s carried is 293.99 at 70 years following initial fabrication (Table 4.4). Based on the guidance from Regulatory Guide 7.11, *Fracture Toughness Criteria of Base Material for Ferritic Steel Shipping Cask Containment Vessels with a Maximum Wall Thickness of 4 Inches (0.1 m)*, this package is classified in NUREG-1609 (Table 1.1) and Table 2.2 as a Category II shipping package. However, since the ES-3100 may be used for future contents that exceed 3000 A_2 (under a different SAR and certificate), this package has been classified as a Category I shipping package. Therefore, the containment vessel is designed (using nominal dimensions for each component), fabricated, and inspected in accordance with the American Society of Mechanical Engineers (ASME) *Boiler and Pressure Vessel Code*, Sect. III, Division I, Subsection NB. The design and subsequent verification comply with the requirements of 10 CFR 71. The structural requirements for the packaging under NCT are addressed in Sect. 2.6. The structural requirements for the packaging under HAC are addressed in Sect. 2.7.

Table 2.2. Category designations for Type B packages

Contents Form/ Category	Category I	Category II	Category III
Special Form	Greater than 3,000 A_1 or greater than 1.11 PBq (30,000 Ci)	Between 3,000 A_1 and 30 A_1, and not greater than 1.11 PBq (30,000 Ci)	Less than 30 A_1 and less than 1.11 PBq (30,000 Ci)
Normal Form	Greater than 3,000 A_2 or greater than 1.11 PBq (30,000 Ci)	Between 3,000 A_2 and 30 A_2, and not greater than 1.11 PBq (30,000 Ci)	Less than 30 A_2 and less than 1.11 PBq (30,000 Ci)

The drum assembly of the shipping package is defined as the structure that maintains the position of and provides protection to the impact , thermal barrier, and neutron poison surrounding the containment boundary. Because the location of the containment boundary within the packaging is stable, the shielding and subcriticality effectiveness of the package is not reduced. The drum assembly for the ES-3100 consists of an internally flanged Type 304L stainless-steel 30-gallon modified drum with two Type 304L stainless-steel inner liners, one filled with noncombustible cast refractory insulation and impact limiter and one filled with noncombustible cast neutron absorber; a stainless-steel top plug with cast refractory insulation, silicone rubber pads, silicon bronze hex-head nuts, and a stainless-steel lid and bottom (Drawing M2E801580A001, Appendix 1.4.8). The drum assembly is maintained when there are no breaches in the drum surface, the lid remains attached, the relative position of the containment

boundary is not altered significantly, and no substantial amount of insulation is exposed following testing stipulated in 10 CFR 71.71 and 73. The drum assembly's design requirements for compliance testing are as follows:

1. The drum lid shall remain attached to the drum under all loading conditions.

2. No opening in the drum shall occur large enough to pass a 10-cm cube [10 CFR 71.43(a)].

3. The outer drum's effective diameter shall exceed requirements to maintain subcriticality and shielding effectiveness.

4. The drum assembly shall provide the structural and thermal protection needed to ensure the containment vessel meets the test leakage criteria for both NCT and HAC of $\leq 1.0 \times 10^{-7}$ ref-cm^3/s.

5. Neutron poison remains in place and retains the amount of water needed to maintain subcriticality.

In accordance with NUREG/CR-3854, Part 4.3, for a Category I shipping package, an acceptable specification for a drum used in any of the component safety groups is U.S. Department of Transportation (DOT) Specification 17C or better. The drum used in the ES-3100 is fabricated in accordance with the dimensional requirements of MS27683-7 (MIL-D-6054F) and modified as shown on Drawing M2E801508A004 (Appendix 1.4.8). Material, fabrication, and quality control criteria are generally equivalent to those imposed for a DOT Specification 17C drum. The drum weld seam is pressure tested to 68.95 kPa (10 psi) gauge and a rough handling test in accordance with MIL-D-6054F is conducted. As discussed in Sect. 1.2.1.1, the drum used for the ES-3100 is equivalent to or better than that stipulated by NUREG/CR-3854 for a Category I shipping package. In accordance with DOE, a performance-based package is an approved, quality-controlled, hazardous material container that has been tested or analyzed to demonstrate its ability to maintain confinement and/or containment of its contents under both normal use and credible accident conditions as stipulated in 10 CFR 71. The drum assembly and containment boundary have been maintained for the ES-3100 shipping package as demonstrated by test results documented in the test report (Appendix 2.10.7) and the analytical comparisons discussed in Sects. 2.6 and 2.7.

The codes and standards used for design, analysis, and fabrication of the containment vessel's components are satisfied by complying with the appropriate paragraphs in Sect. III, Div. 1, Subsection NB, and Sect. IX of the *ASME Boiler and Pressure Vessel Code*. Nominal dimensions, not minimum dimensions, were used in the design analysis of the containment vessel components. Though not explicitly expressed, the load combinations and tests stated in Regulatory Guide 7.8, *Load Combinations for the Structural Analysis of Shipping Casks* are used in the structural evaluation of the containment vessel for both NCT and HAC as depicted in Table 2.3. Acceptance criteria for the containment vessel stresses are shown in Table 2.4 and locations are depicted in Fig. 2.1.

The design internal pressure of 699.82 kPa (101.5 psi) gauge for the containment boundary was generated based on its stress capability before the *ASME Boiler and Pressure Vessel Code* evaluation shown in Appendix 2.10.1 was started. The containment vessel is tested with an internal pressure of 1034.21 kPa (150 psi) gauge or 1.48 times the design pressure, which exceeds the requirement stipulated in Sect. III, Paragraph NB-6221 (a minimum hydrostatic test pressure of 1.25 times the design pressure) and the regulatory requirement of 10 CFR 71.85(b) (1.5 times the

Table 2.3. Summary of load combinations for normal and hypothetical accident conditions of transport

Normal or accident condition	Applicable initial condition									SAR reference
	Ambient temperature		Insolation		Decay heat		Internal pressure		Fabrication stresses	
	38°C	-29°C	Max	0	Max	0	Max	Min		
Normal conditions (analyze separately)										
Hot environment (38°C ambient temperature)			X		X		X		X	Sect. 2.6.1
Cold environment (−40°C ambient temperature)				X		X		X	X	Sect. 2.6.2
Increased external pressure (20 psia)		X		X		X		X	X	Sect. 2.6.4
Minimum external pressure (3.5 psia)	X		X		X		X		X	Sect. 2.6.3
Vibration and shock:	X		X		X		X		X	Sect. 2.6.5[a]
Normally incident to the mode of transport		X		X		X		X	X	
Free drop:	X		X		X		X		X	Sect. 2.6.7[b]
1.2-m drop		X		X		X		X	X	
Compression test	X		X		X		X		X	Sect. 2.6.9[a]
		X		X		X		X	X	
Penetration test	X		X		X		X		X	Sect. 2.6.10[a]
		X		X		X		X	X	
Accident conditions (apply sequentially)										
Free drop: 9-m drop	X		X		X		X		X	Sect. 2.7.1[c]
		X		X		X		X	X	
Crush: 9-m drop	X		X		X		X		X	Sect. 2.7.2[c]
		X		X		X		X	X	
Puncture: 1-m drop onto bar	X		X		X		X		X	Sect. 2.7.3[c]
		X		X		X		X	X	
Thermal: fire accident	X		X		X		X		X	Sect. 2.7.4

[a] This condition was conducted at room temperature with atmospheric pressure inside the containment vessel.
[b] This condition was conducted at ambient temperature at the time of the test except for Test Unit-2. The containment vessel was at atmospheric pressure except for Test Unit-2. Justification for compliance with the environmental requirements of Reg. Guide 7.8 is provided in Sect. 2.6.
[c] This condition was conducted at ambient temperature at the time of the test except for Test Unit-2. The containment vessel was at atmospheric pressure except for Test Unit-2. Justification for compliance with the environmental requirements of Reg. Guide 7.8 is provided in Sect. 2.7.

Table 2.4. Containment vessel allowable stress

Stress Category	Maximum allowable stress	
	Level A (NCT)	**Level D (HAC)**
Primary membrane stress intensity	S_m	Lesser of 2.4 S_m and 0.7 S_u
Primary membrane + primary bending stress intensity	1.5 S_m	Lesser of 3.6 S_m and S_u
Range of primary + secondary stress intensity	3.0 S_m	Not applicable
Fatigue stress range	S_a @ 10^6 cycles	2 S_a @ 10^6 cycles
Buckling	No buckling	No buckling

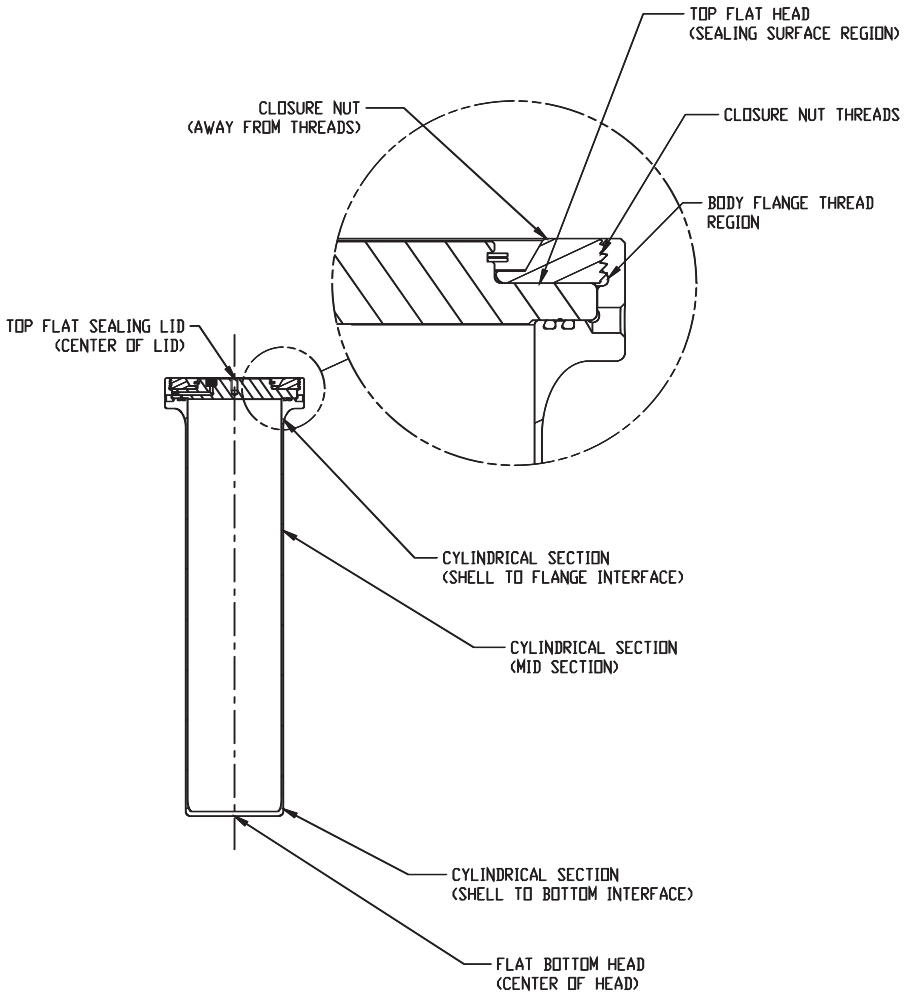

Fig. 2.1. Containment vessel calculated stress locations.

maximum normal operating pressure). As shown in Table 2.6, the containment vessel design stresses are well below the allowable stresses (see Fig. 2.1 for stress locations). Therefore, this ES-3100 containment vessel is capable of shipping at a higher internal pressure. The external pressure requirement from 10 CFR 71.73(c)(6) is 150 kPa (21.7 psi) gauge. These design and operating pressures were used to calculate the stresses (Appendix 2.10.1) in all components of the containment boundary, which are well below the allowable limits at all operating conditions. The maximum normal operating pressure calculated for NCT in accordance with 10 CFR 71.4 and 10 CFR 71.71(c)(1) for the bounding load case is 198.98 kPa (28.859 psia). The maximum internal gauge pressure calculated for NCT is 173.98 kPa (25.233 psi), which is the maximum normal operating pressure minus the reduced external pressure condition of 10 CFR 71.71(c)(3) [198.98 – 25.00 kPa (28.859 – 3.626 psia)] (Sect. 2.6.3). A summary of the package's design, NCT, and HAC pressures and temperatures is presented in Appendices 3.6.4 and 3.6.5. Allowable stress intensity limits and calculated stresses at the design evaluation conditions for the containment vessel are summarized in Tables 2.4 through 2.6. The stresses used in the design of all metal containment vessel components are in the elastic range of the material properties.

For conditions addressed by analysis, the margin of safety is calculated. The margin of safety (M.S.) is defined as:

Margin of Safety = Allowable Stress/ Actual Stress – 1.

In Regulatory Guide 7.11, below Table 1, the following quote is found: "Although NUREG/CR-1815 (Ref. 2) addresses the use of ferritic steels only, it does not preclude the use of austenitic stainless steels. Since austenitic stainless steels are not susceptible to brittle failure at temperatures encountered in transport, their use in containment vessels is acceptable to the staff and no tests are needed to demonstrate resistance to brittle failure." According to Regulatory Guide 7.11, because the containment vessel is manufactured from type 304L stainless steel (which is an austenitic stainless steel), "no tests are needed to demonstrate resistance to brittle failure." Therefore, brittle or fatigue failures are not anticipated under any design, transport, accident, or storage condition (Sects. 2.6 and 2.7). Material specifications for the ES-3100 packaging components are listed in Table 2.7.

Table 2.5. Allowable stress intensity (S_m) for the containment boundary materials of construction [a]

Description	Specification	S_m
Pipe body (Method 1)	ASME SA-312 welded or seamless pipe, type TP304L stainless steel	8.825×10^4 kPa (12,800 psi)[b]
Formed body, end cap and flange (Method 2)	ASME SA-182, F304L stainless steel	8.825×10^4 kPa (12,800 psi)[b]
Flange and end cap (Method 1)	ASME SA-182 Forging, F304L stainless steel	8.825×10^4 kPa (12,800 psi)[b]
Containment vessel sealing lid	ASME SA-479, stainless steel 304	8.825×10^4 kPa (12,800 psi)[b]
Containment vessel closure nut	ASME SA-479, UNS-S21800, Nitronic 60 SST	1.524×10^5 kPa (22,100 psi)

[a] *ASME Boiler and Pressure Vessel Code*, Sect. II, Part D, Table 2A at 148.89°C (300°F).
[b] Lower of two allowable values was chosen to limit deflection of the flange and lid attachment in accordance with note G7 in Table 2A of Part D.

Table 2.6. ES-3100 containment boundary design evaluation allowable stress comparisons [a]

Stress locations shown in Fig. 2.1	Internal pressure design evaluation containment boundary stress @ 699.82 kPa (101.5 psi) gauge		External pressure design evaluation containment boundary stress @ −149.62 kPa (−21.7 psi) gauge		Allowable stress or shear capacity (AS)
	kPa (psi) or kg (lb)	M.S.	kPa (psi) or kg (lb)	M.S.	kPa (psi) or kg (lb)
Top flat portion of sealing lid (center of lid)	6.895×10^3 (1000)	18.2	1.474×10^3 (213.8)	88.8	1.727×10^5 (19,200)[b]
Closure nut ring (Away from threaded portion)	8.621×10^4 (12,504)	4.3	4.246×10^4 [f] (6158)	9.8	4.571×10^5 (66,300)[c]
Top flat head (sealing surface region)	2.717×10^4 (3941)	8.74	1.665×10^4 [f] (2415)	14.9	1.324×10^5 (38,400)[c]
Cylindrical section (middle)	1.999×10^4 (2899)	3.41	4.273×10^3 (619.8)	19.7	8.825×10^4 (12,800)[d]
Cylindrical section (shell to flange interface)	3.016×10^4 (4374)	7.78	1.236×10^4 (1793)	20.4	1.324×10^5 (38,400)[c]
Cylindrical section (shell to bottom interface)	5.127×10^4 (7436)	4.16	1.096×10^4 (1589.8)	23.2	1.324×10^5 (38,400)[c]
Body flange threads load, kg (lb)	2.051×10^3 (4521)	9.01	9.072×10^2 [f] (2000)	21.6	2.053×10^4 (45266)[e]
Body flange thread region (under cut region)	5.926×10^4 (8595)	3.47	2.397×10^4 [f] (3476)	10	2.648×10^5 (38,400)[c]
Flat bottom head (center)	4.826×10^4 (7000)	1.74	1.032×104 (1496.6)	11.8	1.727×10^5 (19,200)[b]
Closure nut thread load, kg (lb)	2.051×10^3 (4521)	16.29	9.072×10^2 [f] (2000)	38.1	3.545×10^4 (78154)[e]

[a] Stresses are calculated using pressures, gasket and closure nut preload, and nominal dimensions for all containment boundary components in Appendix 2.10.1. Calculated stresses for external pressure were determined by multiplying the stress at the design conditions by a factor equal to the ratio of external pressure to design pressure and adding in contribution from preload. Allowable stress values are taken from Table 2.5.

[b] Stress interpreted as the sum of $P_l + P_b$; allowable stress intensity value is $1.5 \times S_m$.

[c] Stress interpreted as the sum of $P_l + P_b + Q$; allowable stress intensity value is $3.0 \times S_m$.

[d] Stress interpreted as the primary membrane stress (P_m); allowable stress intensity value is S_m.

[e] Allowable shear capacity is defined as $0.6 \times S_m \times$ thread shear area. Thread shear area = 38.026 cm^2 (5.894 $in.^2$).

[f] Stress and shear load in these areas are dominated by the 162.7 ± 6.8 N·m (120 ± 5 ft-lb) preload.

Table 2.7. ES-3100 packaging material specifications

Component	Specifications
	Drum assembly
Drum washers	1.375 OD × 0.812 ID × 0.25 in. thick, 300 Series stainless steel
Drum threaded weld studs	5/8-11 × 7/8 Lg, ARC FT, type 304/304L stainless-steel studs
Drum hex nuts	⅝-11 UNC-2B, silicon bronze C65100
Drum lid weldment	Modified 30-gal, 16-gauge (MS27683-61) lid, type 304 or 304L stainless steel; and a 11-gauge thick sheet, type 304 or 304L stainless steel, ASME SA-240
Drum weldment	Modified 30-gal, 16-gauge (MS27683-7), type 304 or 304L stainless steel, ASME SA-240, manufactured per Drawing M2E801580A004 (Appendix 1.4.8)
Drum plugs	Nylon plastic plug, Micro Plastic, Inc.
	Impact limiter, insulation enclosure, neutron absorber, and drum packing material
Insulation and impact limiter (not removable)	Lightweight cast refractory insulation, Kaolite 1600, 358.8 ±48.1 kg/m^3 (22.4 ±3 lb/ft^3) density, cast in stainless-steel shells in the drum and top plug
Neutron absorber	Cat 277-4, 1681.9 +240.3/−80.1 kg/m^3 (105 +15/−5 lb/ft^3) density
Top plug (removable)	Type 304 or 304L stainless steel, ASME SA-240 (body), ASME SA-479 (lifting inserts)
Inner liners	Type 304 or 304L stainless steel, ASME SA-240 (body), ASME SA-479 (modified angle)
Silicone pads	Silicone rubber, 22 ±5 Shore A, color black/gray
Aluminum foil duct tape	McMaster Carr Part # 7616A21, temperature range −40 to 121°C (−40 to 250°F)
	Containment boundary
Containment vessel plug	Part # 04-2126, Modified VCO threaded plug, brass
Containment vessel hoist ring	3052T56, Swivel hoist ring, alloy steel (not used for shipment)
Containment vessel	Method 1: Type TP304L stainless steel ASME SA-312 (welded or seamless pipe body); type F304L, stainless steel, ASME SA-182 (flange, and end cap); type 304, stainless steel, ASME SA-479 (sealing lid), Nitronic 60 SST per ASME SA-479, UNS-S21800 (closure nut)
	Method 2: Type F304L stainless ASME SA-182 (body, flange, and end cap); type 304, stainless steel, ASME SA-479 (sealing lid), Nitronic 60 SST per ASME SA-479, UNS-S21800 (closure nut)
	All components per *ASME Boiler and Pressure Vessel Code*, Sect. II, Part D, Table 2A
Containment vessel O-rings	Elastomer, ethylene propylene, normal service temperature range of −40 to 150°C, Specification M 3BA712A14B13F17 in ASTM D-2000, per OO-PP-986
Containment vessel lid assembly retaining ring	Part # WSM-400-S02, type 302 stainless steel

Table 2.7. ES-3100 packaging material specifications (cont.)

Component	Specifications
Containment vessel O-ring lubricant	Clear dimethyl siloxane polymer
Containment vessel closure nut lubricant	Krytox #240AC
Containment vessel body dowel pins	0.2501/0.2503 OD × 0.50 long, 18-8 stainless steel
Containment vessel packing material	
Convenience cans	Stainless steel or tinned carbon steel with stainless-steel can handles and nylon-coated stainless-steel wire; nickel-alloy (200 series, passivated) in nylon mesh bag
Convenience bottles	Polyethylene or Teflon FEP
Silicone rubber pads	Silicone rubber, 22 ±5 Shore A, color black/gray
Can spacers	Carbon steel or stainless-steel can filled with Cat 277-4
Bagging	Polyethylene
Metal scouring scrubbers	Stainless steel, McMaster Carr Part # 7361T13

2.1.3 Weights and Centers of Gravity

The weights of the packaging components for the actual proposed contents ready for shipment and the test units are provided in Tables 2.8 and 2.9. The values listed for the test weights are the actual data recorded during compliance testing. The remaining weights listed for the shipping package are calculated weights. Nominal dimensions and densities were used in the calculations. Miscellaneous parts (nuts, and washers) are included.

The range of the centers of gravity for the ES-3100 shipping package with the various HEU arrangements and the test packages is shown in Fig. 2.2. A summary of the calculations are provided in Table 2.10.

2.1.4 Identification of Codes and Standards for Package Design

Based on the discussion in Sect. 2.1.2.2, the shipping package has been designed, analyzed, and will be fabricated, tested and maintained to the requirements of a Category I package. In accordance with the references from NUREG/CR-1815, Table 2.11 describes the appropriate codes and standards that are and will be used to comply with Category I packaging. These requirements have been extracted from NUREG/CR-3854 and NUREG/CR-3019.

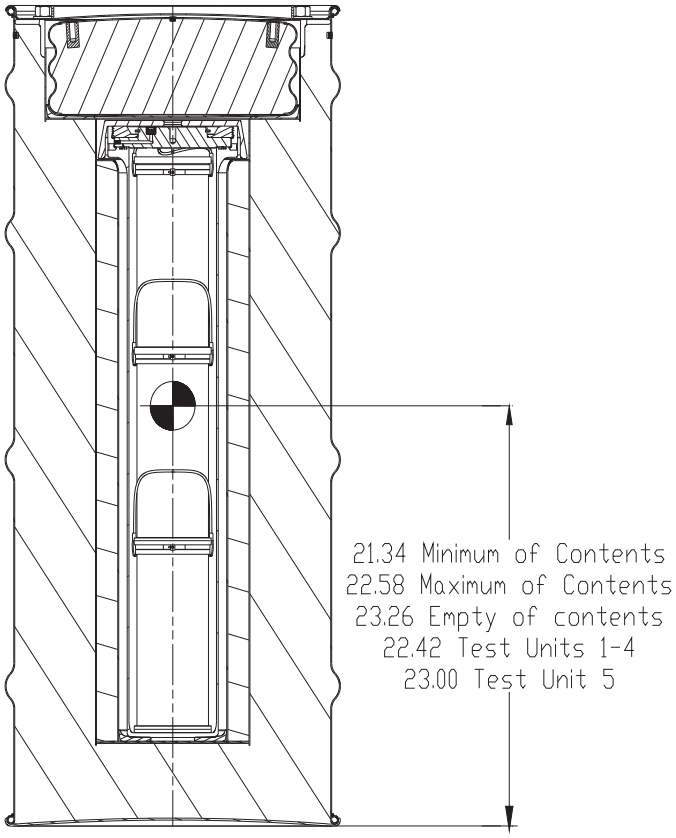

Note: Dimensions are in inches.

Fig. 2.2. ES-3100 shipping package center of gravity locations.

Table 2.8. Packaging weights for various ES-3100 shipping package arrangements [a]

Item	ES-3100 Three 10" tall can configuration kg (lb)	ES-3100 Six 4.875" tall can configuration kg (lb)	ES-3100 Five 4.875" tall can configuration kg (lb)	ES-3100 Six 4.75" tall can configuration kg (lb)	ES-3100 Three 8.75" tall can configuration kg (lb) [c]
			Drum assembly		
Drum assembly (drum body, lid, bottom, mid liner, inner liner, cast refractory insulation, cast neutron absorber, nuts, washers, and data plates) [b]	121.96 (268.87)	121.96 (268.87)	121.96 (268.87)	121.96 (268.87)	121.96 (268.87)
Top plug	8.9 (19.6)	8.9 (19.6)	8.9 (19.6)	8.9 (19.6)	8.9 (19.6)
Silicone support pads	1.04 (2.29)	1.04 (2.29)	1.04 (2.29)	1.04 (2.29)	1.04 (2.29)
Total drum assembly weight	**131.89 (290.76)**	**131.89 (290.76)**	**131.89 (290.76)**	**131.89 (290.76)**	**131.89 (290.76)**
			Containment Vessel		
Containment vessel (flange, dowel pins, cylindrical body, and end cap)	10.18 (22.44)	10.18 (22.44)	10.18 (22.44)	10.18 (22.44)	10.18 (22.44)
Lid assembly (sealing lid, VCO plug, retaining ring, closure nut and O-rings)	4.92 (10.85)	4.92 (10.85)	4.92 (10.85)	4.92 (10.85)	4.92 (10.85)
Total containment vessel weight	**15.10 (33.29)**	**15.10 (33.29)**	**15.10 (33.29)**	**15.10 (33.29)**	**15.10 (33.29)**
			Contents		
Convenience cans with handles	0.72 (1.59)	1.0 (2.22)	0.84 (1.85)	--	0.67 (1.47)
Silicone vibration pads	0.11 (0.23)	0.l8 (0.41)	0.16 (0.353)	--	0.11 (0.23)
Nickel cans	--	--	--	1.84 (4.07)	--
Polyethylene bottles	--	--	--	--	--
Teflon FEP bottles	--	--	--	--	--
Spacers with handles	--	--	1.88 (4.14)	--	1.25 (2.76)
Polyethylene bagging or lifting sling	0.5 (1.10)	0.5 (1.10)	0.5 (1.10)	0.5 (1.10)	0.5 (1.10)
Metal scouring pads	--	--	--	--	0.14 (0.30)
HEU or HEU/Alloy content	35.2 (77.60)	35.2 (77.60)	35.2 (77.60)	24 (52.91)	35.2 (77.60)
Total proposed content weight	**36.52 (80.52)**	**36.89 (81.33)**	**38.57 (85.04)**	**26.34 (58.08)**	**37.86 (83.46)**
Total shipping package weight	**183.51 (404.57)**	**183.88 (405.38)**	**185.56 (409.09)**	**173.33 (382.13)**	**184.84 (407.51)**

Table 2.8. Packaging weights for various ES-3100 shipping package arrangements [a]

Item	ES-3100 Three 8.7" tall bottle configuration kg (lb)	ES-3100 Three 9.4" tall bottle configuration kg (lb)	ES-3100 Empty CV configuration kg (lb)	ES-3100 with maximum weight contents kg (lb)
	Drum assembly			
Drum assembly (drum body, lid, bottom, mid liner, inner liner, cast refractory insulation, cast neutron absorber, nuts, washers, and data plates)	121.96 (268.87)	121.96 (268.87)	121.84 (268.61)[b]	121.96 (268.87)
Top plug	8.9 (19.6)	8.9 (19.6)	8.9 (19.6)	8.9 (19.6)
Silicone support pads	1.04 (2.29)	1.04 (2.29)	1.04 (2.29)	1.04 (2.29)
Total drum assembly weight	**131.89 (290.76)**	**131.89 (290.76)**	**131.78 (290.50)**	**131.89 (290.76)**
	Containment Vessel			
Containment vessel (flange, dowel pins, cylindrical body, and end cap)	10.18 (22.44)	10.18 (22.44)	10.18 (22.44)	10.18 (22.44)
Lid assembly (sealing lid, VCO plug, retaining ring, closure nut and O-rings)	4.92 (10.85)	4.92 (10.85)	4.92 (10.85)	4.92 (10.85)
Total containment vessel weight	**15.10 (33.29)**	**15.10 (33.29)**	**15.10 (33.29)**	**15.10 (33.29)**
	Contents			
Convenience cans with handles	--	--	--	--
Silicone vibration pads	--	--	--	--
Nickel can	--	--	--	--
Polyethylene bottles	0.345 (0.76)	--	--	--
Teflon FEP bottles	--	0.99 (2.18)	--	--
Spacers with handles	--	--	--	--
Polyethylene bagging or lifting sling	0.155 (0.34)	0.50 (1.10)	--	--
Metal scouring pads	--	--	--	--
HEU content	24.0 (52.91)	24.0 (52.91)	--	--
Total proposed content weight	**24.50 (54.01)**	**25.49 (56.19)**	**0**	**40.82 (90)**
Total shipping package weight	**171.49 (378.07)**	**172.47 (380.24)**	**146.88 (323.79)**	**187.81 (414.05)**

[a] Calculated weight using Pro/ENGINEER software with nominal dimensions and densities (Pro/ENGINEER Version 20).
[b] Weight excluding tamper indicating device.
[c] The weight of this configuration bounds the weight of the two 22.2 cm (8.75 in.) high cans that are brazed together containing the TRIGA fuel elements.

Table 2.9. Compliance test unit weights [a]

Item	Test Unit kg (lb)					
	1	2	3	4	5	6
Drum body assembly [b]	126.6 (279)	127.9 (282)	127.9 (282)	127.9 (282)	128.8 (284)	--
Top plug	9.5 (21)	9.5 (21)	9.53 (21)	8.6 (19)	9.5 (21)	--
Drum silicone support pads	0.9 (2)	0.9 (2)	0.9 (2)	0.5 (1)	0.9 (2)	--
Containment boundary [c]	15.4 (34)	15.0 (33)	15.0 (33)	14.5 (32)	15.0 (33)	15.0 (33)
Mock-up test contents [d]	49.9 (110)	49.9 (110)	50.3 (111)	49.9 (110)	3.6 (8)	
Contents [e]						6.3 (14)
Total test unit weight	202.3 (446)	202.8 (447)	203.7 (449)	201.8 (445)	157.4 (347)	21.3 (47)

[a] Total weight may be different from sum of individual component weights due to scale tolerance of ±0.45 kg (1 lb).
[b] This weight includes the drum, mid liner, inner liner, cast refractory, cast neutron absorber, bottom, lid, washers and nuts.
[c] This weight includes containment vessel cylindrical body, end cap, flanged top, and lid assembly.
[d] This weight includes convenience cans, silicone rubber pads, can handles, spacers (if required), and HEU mockup.
[e] This weight was added to reduce buoyancy of containment vessel during 15-m (50 ft) immersion test.

2.2 MATERIALS

2.2.1 Material Properties and Specifications

The mechanical properties and specifications of the packaging materials are presented in Tables 2.12–2.17. See the drawings in Appendix 1.4.8 for details of all components. Design temperature ranges are listed where they are required to establish the allowable stresses used in the design calculations for the containment boundary (Appendix 2.10.1). Service temperature ranges for the remaining shipping container components were obtained from the references shown in Tables 2.12–2.17.

Appendix 2.10.3 contains the Kaolite 1600 property values presented in Table 2.14, as well as additional Kaolite property and source information. Appendix 2.10.4 contains the Cat 277-4 property and source information. Appendix 2.10.5 contains *Compressive Strength and Coefficient of Thermal Expansion of BoroBond4*. (BoroBond4 was used in the prototype test units, but it is not used in the package to be certified.)

2.2.2 Chemical, Galvanic, or Other Reactions

Requirement. A package must be of materials and construction that assure that there will be no significant chemical, galvanic, or other reaction among the packaging components, among package contents, or between the packaging components and the package contents, including a possible reaction resulting from inleakage of water, to the maximum credible extent. Account must be taken for the behavior of materials under irradiation.

Table 2.10. Calculated center of gravity for the various ES-3100 shipping arrangements

Content description	Distance from drum's bottom (in.)
Cylinders, bars, slugs, broken metal - 35,200 g (77.60 lb) max - no can spacers	
3 full 4.88" cans + 3 empty 4.88" can	21.139
2 full 4.88" cans + 4 empty 4.88" cans	21.405
1 full 4.88" cans + 5 empty 4.88" cans	22.066
3 full 10" cans	22.071
2 full 10" cans + 1 empty 10" can	21.762
1 full 10"can + 2 empty 10" cans	22.075
3 full 8.75" cans	21.875
2 full 8.75" cans + 1 empty 8.75" can	21.662
1 full 8.75"can - 2 empty 8.75" cans	22.060
Cylinders, bars, slugs, broken metal - 35,200 g (77.60 lb) max - with can spacers	
3 full 8.75" cans + 2 spacers	22.245
2 full 8.75" cans + 1 empty 8.75" can + 2 spacers	21.802
1 full 8.75" can + 2 empty 8.75" cans + 2 spacers	22.072
3 full 4.88" cans + 2 empty 4.88" cans + 3 spacers	21.471
2 full 4.88" cans + 3 empty 4.88" cans + 3 spacers	21.500
1 full 4.88" cans + 4 empty 4.88" cans + 3 spacers	22.028
UNX crystals 24,000 g (52.910 lb) max - with no spacers	
3 full 8.94" high Teflon FEP bottles + bagging	22.674
2 full 8.94" high Teflon FEP bottles + 1 empty 8.94" high Teflon FEP bottle + bagging	22.383
1 full 8.94" high Teflon FEP bottle + 2 empty 8.94" high Teflon FEP bottles + bagging	22.543
Oxide - 24,000 g (52.910 lb) max - with no spacers	
6 full 4.75" high Nickel cans + bagging	22.631
5 full 4.75" high Nickel cans + 1 empty 4.75" high Nickel can + bagging	22.434
4 full 4.75" high Nickel cans + 2 empty 4.75" high Nickel can + bagging	22.343
3 full 4.75" high Nickel cans + 3 empty 4.75" high Nickel can + bagging	22.366
2 full 4.75" high Nickel cans + 4 empty 4.75" high Nickel can + bagging	22.511
1 full 4.75" high Nickel cans + 5 empty 4.75" high Nickel can + bagging	22.787
Oxide - 24,000 g (52.910 lb) max - with no spacers	
3 full 8.7" high polyethylene bottles + bagging	22.372
2 full 8.7" high polyethylene bottles + 1 empty 8.7" high polyethylene bottle + bagging	22.210
1 full 8.7" high polyethylene bottle + 2 empty 8.7" high polyethylene bottles + bagging	22.480

Table 2.11. Applicable codes and standards for Category I packaging

	Containment ASME Boiler and Pressure Vessel Code, Sect. III, Subsection NB	**Criticality** [a]
Materials		Cat 277-4[a]
Base materials	NB-2000 (except NB-2300) and NB-4100	
Welding materials	NB-2400	
Fabrication		
Forming, fitting, aligning, and joint preparation	NB-4200	
Welding	NB-4400	
Qualification of procedures and personnel	NB-4300	
Examination	NB-5000	[b]
Acceptance testing	NB-6000	[c]
Quality assurance	Subpart H in Title 10, CFR, Part 71	

[a] NUREG/CR-3854 states "The designer may specify a neutron absorber material by a commercial trade name or as a mixture of elements or common compounds. When appropriate, qualification data should be included to demonstrate that the material functions as specified. When special absorber materials are used to control criticality, an acceptance test should be performed for each container to ensure that the absorber material has been properly installed."

[b] NUREG/CR-3854 states "Packages designed to transport fissile material which contain neutron absorber material should be tested to demonstrate the presence of the neutron absorber material. The test description should include information similar to that requested for gamma shield testing 3.2.1. Fabrication records of the absorber material and its installation and testing should be maintained."

[c] NUREG/CR-3854 states "Gamma scanning or probing may be used to demonstrate the soundness of the neutron absorber. Alternatively, ultrasonic testing may be used. Whatever method is used, the following information should be provided in the test procedure:
(1) Description of the measuring technique including the electronics;
(2) The source type and strength used to measure the neutron absorber effectiveness;
(3) The standards and methods use to calibrate the source, sensors, and other pertinent equipment;
(4) The grid pattern used to check the neutron absorber;
(5) The type of gamma sensor used to measure the neutron absorber effectiveness;
(6) The specific test requirements and measurements;
(7) The acceptance criteria."

Table 2.12. Mechanical properties of the metallic components of the drum assembly [a]

Drum, bottom cover and lid	ASME SA-240 type 304 or 304L, stainless-steel plate	
Inner liners	ASME SA-240 type 304 or 304L, stainless-steel plate	
Top plug weldment	ASME SA-240 type 304 or 304L, stainless-steel plate	
Materials of construction	ASME SA-240 type 304	ASME SA-240 type 304L
Design stress intensity, MPa (ksi) at:		
−40°C (−40°F)	137.9 (20)	115.1 (16.7)
37.78°C (100°F)	137.9 (20)	115.1 (16.7)
93.33°C (200°F)	137.9 (20)	115.1 (16.7)
148.89°C (300°F)	137.9 (20)	115.1 (16.7)
Ultimate strength, MPa (ksi) at:		
−40°C (−40°F)	517.1 (75)	482.6 (70)
37.78°C (100°F)	517.1 (75)	482.6 (70)
93.33°C (200°F)	489.5 (71)	455.7 (66.1)
148.89°C (300°F)	456.4 (66.2)	422.0 (61.2)
Yield strength, MPa (ksi) at:		
−40°C (−40°F)	206.8 (30)	172.4 (25)
37.78°C (100°F)	206.8 (30)	172.4 (25)
93.33°C (200°F)	172.4 (25)	147.5 (21.4)
148.89°C (300°F)	154.4 (22.4)	132.4 (19.2)
Elongation in 5.08 cm (2 in.) (%)	40 [b]	40 [b]
Coefficient of thermal expansion, cm/cm/°C (in./in./°F) at:		
−40°C (−40°F) [c]	0.00001476 (0.0000082) [c]	0.00001476 (0.0000082) [c]
37.78°C (100°F)	0.00001548 (0.0000086)	0.00001548 (0.0000086)
93.33°C (200°F)	0.00001602 (0.0000089)	0.00001602 (0.0000089)
148.89°C (300°F)	0.00001656 (0.0000092)	0.00001656 (0.0000092)
Modulus of elasticity, GPa (Mpsi) at:		
−40°C (−40°F)	197.2 (28.6)	197.2 (28.6)
37.78°C (100°F)	194.0 (28.14)	194.0 (28.14)
93.33°C (200°F)	190.3 (27.6)	190.3 (27.6)
148.89°C (300°F)	186.2 (27.0)	186.2 (27.0)

[a] *ASME Boiler and Pressure Vessel Code*, Sect. II, Part D, Subpart 1, Tables 2A, U, and Y-1; and Subpart 2, Tables TE-1, B column, and TM-1.
[b] *ASME Boiler and Pressure Vessel Code*, Sect. II, Part A for ASME SA-240 material.
[c] MIL-HDBK-5H.

Table 2.13. Mechanical properties of the lid fastening components for the drum assembly

Drum weld studs	Specification
Material	ASTM A-493 Type 304/304L stainless steel
Fabrication standard	ASTM F593
Service temperature range, °C (°F)	−40 to 816 (−40 to 1500) [a]
Maximum allowable stress, S, MPa (ksi) at temperatures [a]	
−29°C to 38°C (−20 to 100°F)	129.6 (18.8)
93.3°C (200°F)	115.1 (16.7)
148.9°C (300°F)	103.4 (15.0)
Coefficient of thermal expansion, cm/cm/°C (in./in./°F) [a]	
21.1°C (70°F)	1.53×10^{-5} (8.5×10^{-6})
93.3°C (200°F)	1.60×10^{-5} (8.9×10^{-6})
148.9°C (300°F)	1.66×10^{-5} (9.2×10^{-6})
Drum hex-head nuts	**Specification**
Material	silicon bronze
Fabrication standard	ASTM F-467
UNS designation	C65100 [b]
Minimum proof stress, MPa (ksi)	485 (70) [b]
Drum washer	**Specification**
Drum	1.375 OD × 0.812 ID × 0.25 in. thick, Series 300 stainless steel

[a] *ASME Boiler and Pressure Vessel Code*, Sect. II, Part D, Subpart 1, Table 3; and Subpart 2, Table TE-1, group 3, B value.
[b] ASTM F-467M.

Table 2.14. Mechanical properties of the cast refractory insulation

Material composition:	Cast Refractory, Kaolite 1600
Flexural tensile strength, kPa (psi)	133 (19.4) [a]
Standard deviation	32 (4.7)
Average coefficient of thermal expansion, cm/cm/°C (in./in./°F)	9.07×10^{-6} (5.04×10^{-6}) [b]
Average modulus of rupture per ASTM C133-84, kPa (psi)	258.6 (37.5) [c]
Normal operating temperature, °C (°F)	−40 to 871 (−40 to 1600) [c]
Density after curing, kg/m^3 (lb/ft^3)	358.8 (22.4) [c]
Force/deflection curves	Smith, Appendix 2.10.3

[a] *Mechanical Properties of a Low-Density Concrete for the New ES-2 Shipping/Storage Container Insulation, Impact Mitigation Media and Neutron Absorber* (Appendix 2.10.3).
[b] Fax from J. Street, Thermal Ceramics, Inc. (Appendix 2.10.3).
[c] *Product Information, Refractory Castables and Monolithics* (Appendix 2.10.3).

Table 2.15. Mechanical properties of containment vessel O-rings

Material composition:	Ethylene propylene, Specification—M3BA712A14B13F17 [a, b]
Normal service temperature range, °C (°F)	−40 to 150 (−40 to 302) [c]
Permissible exposure time at 150°C (302°F), h	1000 [c]
Hardness durometer, Shore A	70 ± 5 [a]
Minimum elongation, %	100 [a]
Fabrication method	Molded [a]

[a] ASTM D-2000.
[b] Per Specification OO-PP-986.
[c] Parker O-ring Handbook, Sect. 2.13.2 and Fig. 2-24, p. 2-30.

Table 2.16. Mechanical properties of the metallic components of the containment boundary

Containment vessel: body; flange; and seal lid	Specifications
Material of construction: stainless steel, type 304L	ASME SA-312 (pipe); ASME SA-182 (flange, formed body, or end cap); ASME SA-479 (seal lid)
Design temperature range, °C (°F)	−40 to 176.67 (−40 to 350)
Minimum ultimate strength, MPa (ksi)	482.6 (70) [a]
Yield strength, 0.2% offset, MPa (ksi) at temperatures,	
37.8°C (100°F)	172 (25) [a]
149°C (300°F)	132 (19.2) [b]
176.67°C (350°F)	126.52 (18.35) [b]
Elongation in 5.08 cm (2 in.), %	57 [c]
Modulus of elasticity, GPa (Mpsi) at temperature [b]	
−40°C (−40°F)	197.2 (28.60)
37.78°C (100°F)	194.0 (28.14)
93.33°C (200°F)	190.3 (27.60)
121.11°C (250°F)	188.2 (27.30)
148.89°C (300°F)	186.2 (27.00)
176.67°C (350°F)	184.4 (26.75)
Allowable stresses (S_m)[d] at 149°C (300°F)	
Welded pipe, MPa (ksi)	
149°C (300°F)	115.14 (16.7)
176.67°C (350°F)	112.03 (16.25)
Forged flanges, lids, end caps, MPa (ksi)	
at 149°C (300°F)	115.14 (16.7)
176.67°C (350°F)	112.03 (16.25)
Coefficient of thermal expansion, cm/cm/°C (in./in./°F) at temperatures [e]	
−40°C (−40°F)	0.00001476 (0.00000820)
37.78°C (100°F)	0.00001548 (0.00000860)
93.33°C (200°F)	0.00001602 (0.00000890)
121.11°C (250°F)	0.00001638 (0.00000910)
148.89°C (300°F)	0.00001656 (0.00000920)
176.67°C (350°F)	0.00001674 (0.00000930)
Containment vessel closure nut	**Specification**
Material of construction:	Nitronic 60, UNS-S21800
Elongation, %	10–12 [f]
Design temperature range, °C (°F)	−40 to 176.67 (−40 to 350)
Ultimate strength, MPa (ksi), room temperature	1655–1813 (240–263) [f]
Yield strength, 0.2% offset, MPa (ksi), room temperature	1344–1496 (195 – 217) [f]
Coefficient of thermal expansion, cm/cm/°C (in./in./°F) at temperatures [e]	
93.33°C (200°F)	0.0000158 (0.0000088)
204.40°C (400°F)	0.00001660 (0.0000092)

[a] Listed in the appropriate material specification identified under materials of construction.
[b] *ASME Boiler and Pressure Vessel Code,* Sect. II, Part D, Tables Y-1 and TM-1.
[c] Value presented in THERM 1.2, thermal properties database by R. A. Bailey.
[d] *ASME Boiler and Pressure Vessel Code,* Sect. II, Part D, Table 2A.
[e] *ASME Boiler and Pressure Vessel Code*, Sect. II, Part D, Subpart 2, Table TE-1, Column B, except that −40°C is from MIL-HDBK-5H, Table 2.7.1.0.
[f] Value presented in ARMCO NITRONIC 60 Stainless Steel Product Data Bulletin, S-56b.

Table 2.17. Mechanical properties of the cast neutron absorber

Material	Cat 277-4
Service temperature range, °C (°F)	−40 to 150 (−40 to 302)
Modulus of elasticity in tension, GPa (Mpsi) at temperatures [a]	
−40°C (−40°F)	13.72 (1.991)
21.11°C (70°F)	4.72 (0.684)
37.78°C (100°F)	2.78 (0.403)
Coefficient of thermal expansion, cm/cm/°C (in./in./°F) at temperatures [b]	
−40°C (−40°F)	12.700×10^{-6} (7.056×10^{-6})
−20°C (−4°F)	13.000×10^{-6} (7.222×10^{-6})
0°C (32°F)	13.000×10^{-6} (7.222×10^{-6})
40°C (104°F)	12.600×10^{-6} (7.000×10^{-6})
60°C (140°F)	11.599×10^{-6} (6.444×10^{-6})
80°C (176°F)	10.400×10^{-6} (5.778×10^{-6})
100°C (212°F)	9.700×10^{-6} (5.389×10^{-6})
120°C (248°F)	9.101×10^{-6} (5.056×10^{-6})
Poisson Ratio	
−40°C (−40°F)	0.33 [a]
21.11°C (70°F)	0.28
37.78°C (100°F)	0.25
Density, g/cm^3 (lb/in.^{3})	1.682 (0.0608)

[a] *Mechanical Properties of 277-4* (Appendix 2.10.4).
[b] *Thermophysical Properties of Heat Resistant Shielding Material* (Appendix 2.10.4).

Analysis. Starting with the outer components, the packaging consists of the drum (austenitic type 304 stainless steel), weld studs (austenitic stainless steel), nuts (silicon bronze), insulation (cast refractory), neutron absorber (Cat 277-4), silicone support pads, containment vessel (austenitic type 304L stainless steel), closure nut (Nitronic 60), silicone support pads, can spacers (carbon or stainless steel and Cat 277-4), stainless-steel scrubbers, convenience cans (stainless steel, tin-plated carbon steel, or nickel-alloy [series 200, passivated]), polyethylene or Teflon FEP bottles, polyethylene bags, and the HEU contents.

The cast refractory insulation (Kaolite) is contained between the drum and mid liner and within the top plug assembly's stainless-steel sheet metal. Due to the alkaline nature of this material, greater permanence of the surrounding structure is assured. Also, this material has been used successfully for years as an insulation heat treatment liner adjacent to metal surfaces of furnaces.

The cast neutron absorber (Cat 277-4) is contained between the inner liner and mid liner. During the casting process, the chlorine content is limited to 100 parts per million. The small quantity of chlorine will not affect the stainless-steel liners.

The nuts used to attach the drum to the lid are silicon bronze. All other metal components of the packaging are either stainless steel, Nitronic 60, or tinned steel. All stainless-steel components are passivated per ASTM A380, Paragraph 6.4, and Table A2.1, Part II. Prior to assembly, the packaging will be kept inside a building or transported between buildings in an enclosed truck. The assembled components are protected from the weather and inspected at the time of packaging; therefore, the package will not contain any free water at the time it is loaded for transport. Under NCT, the only moisture present will be the relative humidity or moisture absorbed by the cast refractory or neutron absorber materials. When the package is subjected to a water-spray type environment, some water may leak into the cavity formed by the inner liner and occupied by the containment vessel. To minimize the possibility of any potentially corrosive situation, a visual examination of the interior surface of the inner

liner and the exterior surface of the containment vessel shall be conducted prior to packing and following transport of the shipping package (see Sect. 7). Any free water present and any corrosion discovered shall be promptly removed.

During immersion under HAC, water can enter the holes at the top of the drum, be absorbed into the cast refractory material, and fill all void spaces within the drum and inner liner. The insulating value of the insulation material may be decreased, and an overall weight increase would occur. The most important consideration is that the containment boundary remain intact and leaktight. This situation has been evaluated by completely immersing the containment vessel in a tank simulating 0.9-m and 15-m (3- and 50-ft) immersion depths. The containment vessel remained intact and water tight, as demonstrated by the analysis and testing discussed in Sect. 2.7.

All physical contact between the convenience cans and the containment vessel wall, bottom, or top is minimized through the use of the silicone support pads. The polyethylene or Teflon FEP bottles may be in contact with the stainless steel of the containment vessel, but will not react. All cans and bottles will provide the necessary separation of the HEU contents from the containment vessel walls. When space is available inside the containment vessel, stainless-steel metal scrubbers will be placed on the top and bottom of this partially canned assembly or an empty convenience can will be placed on top of this assembly inside the containment vessel. The passivated Nickel-alloy cans are galvanically similar to the stainless steel of the containment vessel and thus will not react. Additionally, polyethylene bagging may be used around the convenience container (in some cases the HEU is bagged inside the convenience container) as required by packaging personnel. Therefore, galvanic corrosion between the containment vessel wall and convenience containers is highly unlikely. In addition, the environment inside the containment vessel is free of electrolytic solutions, further assuring there will be no galvanic reactions occurring inside the containment vessel.

The material testing documented in Y/DZ-2720 (Appendix 2.10.9) does not identify the composition of the volatiles or gases generated during testing. Since Teflon fluorinated ethylene propylene (FEP), a fluorine-containing polymer, is used to transport uranyl nitrate crystals, the possible development of a corrosive environment inside the containment vessel is investigated. Based on the following literature, FEP is notable among addition polymers for its high thermal stability. It decomposes at temperatures above ~260°C (500°F). In air or in oxygen, FEP decomposes in one way at lower temperatures and in another at higher temperatures. In this discussion, "oxygen" implies oxygen at a pressure of 300 torr. In air, the partial pressure of oxygen is near 150 torr. Below about 525°C, the decomposition of FEP is first order, and the main decomposition product is hexafluoropropylene (C_3F_6), although tetrafluoroethylene (C_2F_4) is a near second in abundance. (Leidecker, Teflon thermal decomposition) The carbon-fluorine compound is one of the strongest compounds found in organic chemistry (its dissociation energy is 460 kJ/mol). The carbon chain is nearly completely covered by fluorine atoms, and is therefore protected against external influences. This results in the exceptionally high chemical resistance of FEP. (Daikin America) Based on the preceding statements, it is reasonable to conclude that most, if not all, of the gas coming from any decomposition of the Teflon FEP bottles would be hexafluoropropylene and tetrafluoroethylene rather than fluorine gas. The maximum temperature predicted (NCT or HAC) inside the ES-3100 containment vessel at the location near the Teflon FEP bottles is 123.85°C (254.93°F). This temperature is considerably below the lower limit of the FEP decomposition temperature [260°C (500°F)]. Due to the difference between the decomposition temperature of FEP [260°C (500°F)] and the maximum predicted temperature from testing [123.85°C (254.93°F)], essentially no C_3F_6 or C_2F_4 and no fluorine is expected to form during transport. Therefore, a corrosive environment with fluorine as the base is not anticipated. It should be noted that the offgassing rate and quantity used for Teflon FEP at lower temperatures in Appendices 3.6.4 and 3.6.5 are very conservative estimates. The actual values shown for the Teflon bottle sample in Y/DZ-2720

(Appendix 2.10.9) may have resulted from the cumulative tolerance in the testing setup and data recording, and not from actual offgassing.

For pyrophoric considerations, broken metal and alloy pieces shall be of a size that: a) the specific surface area does not exceed 1 cm^2/g or b) will not pass freely through a mesh size of 3/8 in. (0.95 cm) as discussed in Sect. 1.2.3, Appendix 1.4.10, and Sect. 7.1.2. Incidental small particles which do not pass the size restriction tests, and powders, foils, turnings, and wires may only be shipped if they are in a sealed, inerted container.

The containment boundary remains intact even when the drum and inner liner are filled with water; therefore, the package is acceptable to the maximum credible extent from the standpoint of chemical, galvanic, or other reactions.

2.2.3 Effects of Radiation on Materials

The HEU material is not irradiated. The neutron and photon dose rates (Sect. 5) are well below those required to damage any of the package materials by radiolytic interactions. However, NUREG-1609, Sect. 4.5.2.3, requires the applicant to demonstrate that any combustible gases generated in the package during a period of one year do not exceed 5% (by volume) of the free gas volume in any confined region of the package. No credit should be taken for getters, catalysts, or other recombination devices. Appendix 3.6.7 evaluates the various packaging arrangements for the generation of hydrogen gas due to the radiolysis of water vapor, free water, interstitial water, polyurethane bags, and polyurethane or Teflon bottles. When the content mass and the material composition are limited as shown in Appendix 3.6.7, the combustible gas concentration limit stated in NUREG-1609 is not exceeded. Getters, catalysts, or other recombination devices are not employed in any of the containment vessel packaging arrangements.

2.3 FABRICATION AND EXAMINATION

2.3.1 Fabrication

2.3.1.1 Drum assembly fabrication

The drum assembly is fabricated in accordance with equipment specifications JS-YMN3-801580-A002 (Appendix 1.4.2), JS-YMN3-801580-A003 (Appendix 1.4.4), and JS-YMN3-801580-A005 (Appendix 1.4.5). The later two specifications control the casting of the Kaolite 1600 and Cat 277-4 materials inside the liners, spacer cans and the top plug as appropriate.

The drum assembly and top plug are fabricated according to the design drawings (Appendix 1.4.8), and the portions of the codes, standards, and regulations to the extent described below:

1. *ASME, Boiler and Pressure Vessel Code*, Sect. VIII, Division 1, 2004 edition;

2. *ASME, Boiler and Pressure Vessel Code*, Sect. II, Parts A and C, 2004 edition;

3. *ASME, Boiler and Pressure Vessel Code*, Sect. IX, 2004 edition;

4. Military Standard, MS27683, *Drum, Metal-Shipping and Storage 16 to 80 Gallons*; and

5. ASTM A 380-99e1, *Standard Practice for Cleaning, Descaling, and Passivation of Stainless Steel Parts, Equipment and Systems*.

Detailed dimensional requirements, and the materials of construction are called out on the drawings in Appendix 1.4.8. Except for the weld studs, documented Certified Material Test Reports (CMTRs) are provided for all materials used in weldments for the fabrication of the drum, including weld filler metal. The CMTRs are traceable to heat numbers and demonstrate compliance with the SA or SFA material specifications called out. For all other materials, documented Certificates of Compliance (CoC) are provided certifying that the materials provided comply with the requirements stated on the drawings and specifications. All welding is done in accordance with welding procedure specifications that are written and performance qualified in accordance with the ASME B&PV Code, Section IX. All welders are performance qualified to weld using these procedures, and their qualifications documented in accordance with the ASME Code, Section IX. The welding fabrication requirements stated in the ASME Code, Section VIII, Division 1, paragraphs UW-26 through UW-48 are met. All butt welds in rolled sheet, pipe and angle joints are full penetration butt welds. With the exception of the seam welds in the drum body, all welds shall be done by the GTAW, GMAW, PAW or a Capacitive Discharge (CD) stud welding process. The weld filler metal used in the fabrication of the drum assembly is procured to comply with the SFA specifications of Section II, Part C of the ASME Code that are stated in the welding procedure specifications. Weld filler metal is procured traceable to heat numbers, and CMTRs are furnished for each heat of weld wire filler. The control of weld filler permits a weld examiner to be able to determine the heat number of the weld filler used in any weld on the drum assembly. Weld symbols are provided on the drawings indicating for each weld the type of weld and dimensions of weld. These weld symbols are interpreted in accordance with the American Welding Society, Section A2.4.

2.3.1.2 Containment boundary fabrication

The containment boundary consists of the containment vessel, lid assembly and inner O-ring. The containment vessel is manufactured in accordance with the applicable requirements stated in the ASME Boiler and Pressure Vessel Code, Section III, Division 1, Subsection NB for Class 1 Components as described on the drawings in Appendix 1.4.8 and equipment specification JS-YMN3-801580-A001 (Appendix 1.4.3). The containment vessel is fabricated according to the design drawings and the following codes, standards, and regulations as described in JS-YMN3-801580-A001.

1. *ASME, Boiler and Pressure Vessel Code*, Sect. III, Division 1 Subsections NB and NCA, Class 1 Components, 2004 edition;

2. *ASME, Boiler and Pressure Vessel Code*, Sect. II, Parts A and C, 2004 edition;

3. *ASME, Boiler and Pressure Vessel Code*, Sect. IX, 2004 edition; and

4. ASTM A 380-99e1, *Standard Practice for Cleaning, Descaling, and Passivation of Stainless Steel Parts, Equipment and Systems*.

Detailed dimensional requirements, and the materials of construction are called out on the drawings in Appendix 1.4.8. CMTRs are provided for the materials used to fabricate these components in accordance with NCA-3860. The suppliers of these materials will meet the requirements of NCA-3800. Such parts are traceable to each containment vessel by means of a serial number. The fabricator maintains control of materials to ensure this traceability. Other metallic materials, and the O-ring seals are supplied with CoCs in accordance with NCA-3862(g) and (h). The weld filler metal used in the fabrication, and repair welding as permitted, of the containment vessels meets the applicable requirements of NB-2400. It is procured to comply with the SFA specifications of Section II, Part C of the ASME B&PV Code that is stated in the fabricator's welding procedure specifications. Weld metal is procured traceable to heat numbers, and CMTRs are furnished for each heat of weld wire filler used. The results of the delta ferrite determination is included in the CMTR for the weld filler metal (see NB-2433). There are two

containment vessel assemblies shown on drawing M2E801580A012 (Appendix 1.4.8), part number M2E801580A012-1, and M2E801580A012-4. Part number M2E801580A012-4 is fabricated by welding a forged bottom and forged top flange to a cylindrical shell machined from seamless pipe as shown on the drawing. All welds on the containment vessels are accomplished by either the GTAW or GMAW process, manual or automatic, at the discretion of the fabricator unless specifically called out on the drawings. Backing rings, even if removed after the weld has been made, are not be used. As previously stated, weld symbols are provided on the drawing indicating the type of weld and dimensions of the weld. These weld symbols are interpreted in accordance with the American Welding Society, section A2.4. The forming, fitting and alignment requirements stated in paragraph NB-4200 are met in the fabrication of the containment vessels unless more stringent requirements are called out on the design drawings.

The preferred fabrication method for the containment vessel body (part number M2E801580A012-1), is from a single forged billet or bar by any process that meets the requirements stated in JS-YMN3-801580-A001 (Appendix 1.4.3), and shown on the design drawings. Such processes may include forging, flow forming, or metal spinning. The formed, heat treated, and finished machined containment vessel body shall meet the applicable requirements of ASME SA 182 for Grade F304L for a forged component. After final forming, parts are solution annealed and quenched per the requirements of ASME SA 182 for Grade F304L. A certified heat treatment report is provided stating the following information for each furnace charge: the serial numbers of the containment vessel bodies heat treated in the furnace charge, the time and date of the heat treating, the person responsible for the heat treating, the time-temperature profile of the furnace and representative parts of the furnace charge, the quench medium, and all other pertinent details of the heat treating. Such a heat treating report is required for all heat treating, both in process annealing and final heat treatment.

2.3.2 Examination

2.3.2.1 Examination of the drum assembly fabrication

The drum and top plug assemblies are examined and tested according to the design drawings, and the portions of the codes, standards, and regulations to the extent described below:

1. *ASME, Boiler and Pressure Vessel Code*, Sect. VIII, Division 1, 2004 edition;

2. *ASME, Boiler and Pressure Vessel Code*, Sect. V, 2004 edition; and

3. SNT-TC-1A-1992, *Recommended Practice for Nondestructive Testing Personnel Qualification and Certification*, American Society For Nondestructive Testing, December 1992.

All welded or weld-repair surfaces shall be visually examined by a qualified weld examiner for indications of inclusions, cracks, or porosity using a written weld examination procedure. Weld examiners are qualified to perform visual weld inspections in accordance with SNT-TC-1A (2001 Edition), "Personnel Qualification and Certification in Nondestructive Testing;" or ANSI/ASNT CP-189 (2001 Edition), "ASNT Standard for Qualification and Certification of Nondestructive Testing Personnel;" published by the American Society for Nondestructive Testing. ASME Boiler and Pressure Vessel Code, Section IX is to be employed as the applicable requirement. Section VIII of the ASME B&PVC Code is invoked for acceptance criteria for Code specified examinations which are to be performed in accordance with the provisions of ASME B&PVC Section V. Any indication of inclusions, cracks, or porosity in the welds is cause for rejection. The item may be reworked to meet the specifications. The weld examination procedures, the weld examiners qualifications, and the weld examination reports are submitted to B&W Y-12 for records. The acceptance criteria for joint fit-up and alignment, and for visual examination of welds are given in the ASME B&PV Code, Section VIII,

Division 1, paragraphs UW-31 through UW-36. In addition, any visible defects such as lack of fusion, lack of penetration, linear or crack-like defects, and visible porosity, are cause for rejection. Straightening, flattening, and forming by mechanical or thermal means of some features and components after welding may be required to ensure proper assembly. The surfaces of areas of the weldment that have been worked are visually examined to ensure that no cracks are present or that the weldment has not been degraded. Adjacent welds to these areas are also visually examined. The acceptance criteria is that no cracks are found. The areas worked and the visual inspections are noted on the dimensional inspection report. The external seam weld of the drum assembly is pressure tested by attaching removable lids on both the top and bottom false wire locations and injecting water and air inside the assembly up to the final pressure of 149.61 kPa (21.7 psia). After all testing, inspection and final machining, the drum assembly and top plug are dimensionally inspected. The dimensions, and features such as flatness, run-out, etc, to be inspected are indicated on the design drawings. A written inspection report is prepared, submitted and maintained for each ES-3100 drum assembly.

The above examination criteria address the stainless-steel components. However, the drum assembly also consists of the Kaolite 1600 material and the Cat 277-4 neutron poison. Acceptance criteria for the installation of the Kaolite 1600 material are addressed by specification JS-YMN3-801580-A003 (Appendix 1.4.4). This specification controls and documents the raw materials used for mixing, casting and vibration methodology, and the baking of the material inside the drum assembly. The final acceptance criterion is achieved by producing a cast Kaolite 1600 material density of 358.8 ± 48 kg/m^3 (22.4 ± 3 lb/ft^3). Acceptance criteria for the installation of Cat 277-4 neutron poison are addressed in specification JS-YMN3-801580-A005 (Appendix 1.4.5). This specification also controls and documents the raw materials used for mixing, casting and vibration methodology, and the final density of the casting [1682 +240/-80 kg/m^3 (105 +15/-5 lb/ft^3)]. Further examination criteria to verify the concentration and homogeneity of the Cat 277-4 in each drum assembly are also provided in specification JS-YMN3-801580-A005. The various parameters specified in NUREG/CR-3854 and in Table 2.11 for a neutron poison are addressed in detail in this specification.

2.3.2.2 Examination of the containment vessel fabrication

The containment vessel is examined and tested according to the design drawings and the following codes, standards, and regulations as described below:

1. *ASME, Boiler and Pressure Vessel Code*, Sect. III, Division 1 Subsections NB and NCA, Class 1 Components, 2004 edition;

2. ANSI N14.5-1997, *American National Standard for Radioactive Materials – Leakage Tests on Packages for Shipment*; *ASME, Boiler and Pressure Vessel Code*, Sect. V, 2001 edition and 2002 and 2003 addenda;

3. ASME, B & PVC, Section V, 2001 edition and 2003 addenda; and,

4. NT-TC-1A-1992, *Recommended Practice for Nondestructive Testing Personnel Qualification and Certification*, American Society For Nondestructive Testing, December 1992.

Procured materials are examined in accordance with the applicable paragraphs of NB-2500, and meet the stated acceptance criteria. The results of these examinations are be included with the CMTRs provided to B&W Y-12. All welded or weld-repair surfaces shall be visually examined by a qualified weld examiner for indications of inclusions, cracks, or porosity. ASME Boiler and Pressure Vessel Code, Section IX is to be employed as the applicable requirements. Section III of the ASME B&PVC Code is invoked for acceptance criteria for Code specified examinations which are to be performed in accordance with the

provisions of ASME B&PVC Section V. Prior written approval is obtained for any weld repair on materials, and the weld repair areas are both surface and volumetrically examined. The repair area is noted in a sketch supplied with the CMTR for the material that was weld repaired and the documented results of the weld examination are provided to B&W Y-12. The markings on the weldment materials are not removed until after all weld examination is complete. The heat numbers of base metals and weld filler are required on all weld examination reports. Control of weld filler by the fabricator permits a weld examiner to be able to determine the heat number of the weld filler used in any weld on the containment vessel.

As previously stated, the containment vessel body may be fabricated by two different methods shown on drawing M2E801580A012 (Appendix 1.4.8). Part number M2E801580A012-4 is fabricated by welding a forged bottom, and forged top flange to a cylindrical shell machined from seamless pipe as shown on the drawing. Prior to welding these components, all weld preparation areas and the surfaces within one inch of the weld are examined visually and with liquid penetrant. The acceptance criteria for these examination are those stated in NB-5130(a) through NB-5130(d). The applicable requirements in paragraphs NB-5110, NB-5120, NB-5210, NB-5220, NB-5260, and NB-5300 apply to the containment vessels. The plug weld shown on Drawing M2E801580A015 (Appendix 1.4.8) shall be examined visually and with penetrant. The applicable requirements in paragraphs NB-5110, and NB-5350 shall apply to the plug weld. Materials used in the penetrant examination of welds and in the final surface examination of finished components (see Section 3.7) shall be specifically recommended by their suppliers for use with austenitic stainless steels, and copies of the certification of contaminant content of materials used (see ASME, Section V, Article 6, T-641) shall be supplied with the examination reports. Repair welding shall meet the applicable requirements of NB-2500. Certified written weld examination reports together with the corresponding material surface examination reports, and weld map shall be submitted as stated in the procurement specification for the containment vessel. Weld examination reports for all weld and surface examination shall include: the containment vessel serial number, a weld map showing the location of the weld and examination area, the welder's name, the examiner's name, the time and date of the weld examination, the examination procedure(s) number used, the WPS number, the heat numbers of the materials joined, the heat number of the weld filler, and examiner's remarks. The examiner's remarks shall include the results of the examination and acceptance, or rejection of the weld based on the stated criteria. One set of radiographs shall be provided with radiographic examination reports. If the weld or surface is rejected, a description of the defect and sketch showing the location shall be provided.

The nonwelded containment vessel body, part number M2E801580A012-1, shall be formed from a single forged billet or bar by any process that meets the requirements stated in JS-YMN3-801580-A001 (Appendix 1.4.3), and shown on the design drawings (Appendix 1.4.8). Such processes may include forging, flow forming, or metal spinning. The formed, heat treated, and finished machined containment vessel body shall meet the applicable requirements of ASME SA 182 for Grade F304L for a forged component. Mechanical properties are verified by testing of coupons. The test coupons are to be machined from the same heats of materials used to form the containment vessel bodies, and shall have the same or greater amount of cold work (plastic strain) as the containment vessels will have as a result of the forming process. The mechanical tensile testing of coupons shall be done in accordance with ASME SA-370. A minimum of six test coupons shall be tested for each final heat treatment furnace charge. The first set of three test coupons, chosen at random, shall be tested without being heat treated. The second set of three or more test coupons shall be heat treated together with the containment vessel bodies, and then tested. The heating rates and maximum temperatures of the test coupons shall be representative of the entire furnace charge. Test coupons are not required to be heat treated with intermediate processing annealing steps, but are required in the final heat treatment furnace charge. The results of all the testing of the sample coupons shall be documented, certified and reported to B&W Y-12. The mechanical properties test report shall contain the following information: a descriptor

of the furnace charge in which the test coupons are to represent; the times and dates of the heat treating and the testing; the person responsible for the testing; a statement that these coupons are prior to or after heat treatment; a description of the testing including a sketch of the tensile test specimen; the make, model, serial number, and current calibration data of the testing machine(s) used in the testing; reference to the written testing procedure used; the resulting measure yield strength, ultimate strength, % elongation and % reduction in area; and any pertinent remarks.

2.4 LIFTING AND TIE-DOWN STANDARDS FOR ALL PACKAGES

This section addresses the requirements of 10 CFR 71.45, "Lifting and Tie-Down Standards for All Packages."

2.4.1 Lifting Devices

Requirement. Any lifting attachment that is a structural part of a package must be designed with a minimum safety factor of three against yielding when used to lift the package in the intended manner, and it must be designed so that failure of any lifting device under excessive load would not impair the ability of the package to meet other requirements of 10 CFR 71, Subpart E. Any other structural part of the package that could be used to lift the package must be capable of being rendered inoperable for lifting the package during transport, or must be designed with strength equivalent to that required for lifting attachments.

Analysis. The ES-3100 packages, as delivered for transport, have no lifting devices or structural parts that can be used for lifting. Therefore, the lifting devices requirements of 10 CFR 71.45 are not applicable.

2.4.2 Tie-Down Devices

Requirement. If there is a system of tie-down devices that is a structural part of the package, the system must be capable of withstanding, without generating stress in any material of the package in excess of its yield strength, a static force applied to the center of gravity of the package having a vertical component of two times the weight of the package with its contents, a horizontal component along the direction in which the vehicle travels of ten times the weight of the package with its contents, and a horizontal component in the transverse direction of five times the weight of the package with its contents. Any other structural part of the package that could be used to tie down the package must be capable of being rendered inoperable for tying down the package during transport, or must be designed with strength equivalent to that required for tie-down devices. Each tie-down device that is a structural part of a package must be designed so that failure of the device under excessive load would not impair the ability of the package to meet other requirements of this part.

Analysis. The ES-3100 package, as delivered for transport, has no tie-down devices that are structural parts of the package. Therefore, the tie-down requirements of 10 CFR 71.45 are not applicable. Safe tie down and transport of the package is accomplished by methods explained in the Sandia National Laboratories (SNL) Tie-Down Manual [*Tie-down Procedures for Type B Containers Shipped in Safe-Secure Trailer/Safeguards Transporter (SST/SGT*)]. For single-unit tie-down, a drum tie-down adapter is positioned on top of the drum and two chains, passing through the adapter, are attached to equipment positioned on the floor of the transport vehicle. The welded ring on the drum lid helps to initially position this drum tie-down adapter as well as prevent inadvertent assembly damage to the studs and nuts. Another method of securing the ES-3100 package is by the use of the Cargo-Restraint Transporter (CRT) or Cargo Pallet Assembly (CPA). In these methods, a frame is positioned around the

base and top of either five or six packages. These frames are then chained or locked to the floor as depicted in SNL Tie-Down Manual. Tension is applied to the chains to eliminate any slack. The downward load resulting from the chain tensioning is insignificant when compared to the compression loading as specified in 10 CFR 71.71(c)(9).

2.5 GENERAL CONSIDERATIONS

Package structural evaluation is performed by the combination of full scale testing, similarity, and analysis as described in the following sections.

2.5.1 Evaluation by Test

The ES-3100 package was tested in accordance with a test plan developed by the National Transportation Research Center (NTRC) at the Oak Ridge National Laboratory (ORNL) (Appendix 2.10.8). Testing of ES-3100 prototype units was performed at the NTRC facility, except as noted below. Five full-scale test units were assembled with content weights ranging from 3.6 kg (8 lb) to 50.3 kg (111 lb). One of these test units (TU-4) was subjected to the tests specified in 10 CFR 71.71(c)(5) through (c)(10) excluding (c)(8) prior to the HAC sequential tests stipulated in 10 CFR 71.73 and shown in Table 2.18. Test Unit 2 was chilled prior to being subjected to any structural testing (i.e., 1.2-m NCT drop, 9-m HAC drop, HAC crush, and HAC puncture tests). This unit was chilled to a nominal temperature of −40°C (−40°F). This was accomplished by placing the unit in an environmental chamber in Bldg. 5800 at the Oak Ridge National Laboratory (ORNL) with initially setting of the chamber at ~ −57°C (−70°F) for 24 h. After this initial period, the control on the environmental chamber was set to ~ −43°C (−45°F) for another 48 h. Prior to the initiation of structural testing of this unit, it was removed from the environmental chamber and placed in an insulated box. Once transported to the NTRC, sequential structural testing, as shown in Table 2.19 was performed as quickly as possible. The other test units were first subjected to the free drop from 1.2 m (4 ft) test prior to the HAC testing of 10 CFR 71.73. These additional tests were conducted to show that the NCT testing would not reduce the effectiveness of the package to withstand HAC testing. Tables 2.18 and 2.19 summarize the testing procedure and the drop orientations for each ES-3100 test unit.

The essentially unyielding surface used for the 1.2-m (4 ft) drop test was the indoor drop test pad at the NTRC. All 9-m (30-ft) drop and crush tests were conducted at the outside drop pad at the NTRC. The indoor pad consists of a 5.08-cm (2-in.)-thick steel plate embedded inside a reinforced concrete pad ~127 cm (50 in.) thick. The outside drop pad consists of a 10.16-cm (4-in.)-thick steel plate embedded inside a reinforced concrete pad ~167.6 cm (66 in.) thick. An article has been prepared by the NTRC staff to describe the integrity of these test pads (Shappert 1991).

Table 2.18. Summary of NCT – 10CFR71.71 tests for ES-3100 package [a]

Test	TU-1 (heavy) 12° Slap-down	TU-2 (heavy) Side Drop	TU-3 (heavy) CG over Top Corner	TU-4 (heavy) Top Down	TU-5 (light) 12° Slap-down
Operational Leak Test (CALT5)	1	1	1	1	1
NCT – 10CFR71.71 (c)(5) Vibration				5	
NCT – 10CFR71.71 (c)(6) Water Spray				2	
NCT – 10CFR71.71 (c)(7) 1.2 m (4 ft) Free Drop	2	2	2	3	2
NCT – 10CFR71.71 (c)(9) Compression				6	
NCT – 10CFR71.71 (c)(10) Penetration				4	

[a] The numbers 1 through 6 indicate the sequence of the tests.

Table 2.19. Summary of HAC – 10CFR71.73 tests for ES-3100 package [a]

Test	TU-1 (heavy) 12° Slap-down	TU-2 (heavy) Side Drop	TU-3 (heavy) CG over Top Corner	TU-4 (heavy) Top Down	TU-5 (light) 12° Slap-down	TU-6 [b] 15m Immersion
10CFR71.73 (c) (1) Free Drop 9m (30 ft.)	1	1	1	1	1	
10CFR71.73 (c) (2) Crush 9m (30 ft.)	2	2	2	2	2	
10CFR71.73 (c) (3) Puncture 1m (40 in.)	3456	3	3	3	3	
Preheat to above 38 °C (100 °F) before Thermal test	7	4	4	4	4	
10CFR71.73 (c) (4) Thermal 800°C (1475°F)	8	5	5	5	5	
Operational Leak Test of CV (CALT5)	9	6	6	6	6	1
Full Containment Boundary Leak Test (He Leak Test)	10	7	7	7	7	
10CFR71.73 (c) (5) Immersion Test Fissile materials – 0.9 m (3 ft.)	11	8	8	8	8	
10CFR71.73 (c) (6) Immersion Test –All Packages 15 m (50 ft.)						2

[a] The numbers 1 through 11 indicate the sequence of the tests.
[b] TU-6 is only a containment vessel with ballast to ensure non-buoyancy.

Thermal testing of the five test units was conducted at the No. 3 furnace at Timken Steel Company in Latrobe, Pennsylvania. Prior to the testing, the furnace was characterized for temperature and heat recovery times. Oxygen content in stack gases of the furnace was not monitored because it was not anticipated that any of the package's materials of construction were combustible. There was some burning of the silicone pads which are placed between the inner liners and the top plugs of the packages. However, it should be noted that this furnace employs "pulsed" fire burners. This type of burner is unique in that the natural gas flow rate is varied based on furnace controller demands, but the flow of air through the burners is constant, even when no gas is flowing, thereby ensuring a very rich furnace atmosphere capable of supporting any combustion of package materials of construction. The support stand was welded to a large steel plate which had been placed on the floor of the furnace prior to heating. This steel plate acted as the radiating surface at the bottom of the furnace as well as providing the ability to hold the test stand rigidly in place. Before heating the furnace, workers practiced loading and unloading test packages from the cold furnace to assure that the furnace door would not remain open >90 s during each loading. In fact, the maximum time the door was open during any loading was 64 s.

Damage resulting from physical testing is quantitatively described including photographs in Sect. 2.7. The full-scale test units were fabricated in accordance with drawings created for production hardware. During the procurement process for the full-scale test units, several small changes were suggested by the manufacturer to improve the efficiency and to reduce the cost of fabrication. These changes were incorporated and tested. However, following compliance testing the following changes have been made to the proposed production hardware. First, a change in the neutron poison from BoroBond4 to Cat 277-4 has been adopted; second, the mid liner design has been changed to a continuous shell by reducing the diameter of the step in the inner liner for the CV flange from 22.35 cm (8.8 in.) to 21.84 cm (8.6 in.); and third, the silicone rubber pad thickness on the drum assembly bottom liner was increased by ~0.15 cm (0.06 in.). The second change increased the amount of Kaolite 1600 around the CV flange, increased the final volume of the neutron poison, and slightly decreased the volume of the Kaolite 1600 adjacent to the neutron poison. The third change was made to stiffen the rubber pad so it would remain in place during vibration normally incurred during transport. In order to evaluate the impact of these changes, analytical drop simulations were conducted and documented in Appendix 2.10.2. The drop simulations were conducted in the same attitude and temperature regime as those conducted during the compliance testing phase for certification. The results of the structural deformation from compliance testing, drop simulation using BoroBond4 and drop simulations using Cat 277-4 material are presented in Sect. 2.7.8. The analytical structural deformation results shown in Tables 2.52 through 2.61 are nearly identical between the two neutron poisons. The analytical results are also well representative of the results recorded during compliance testing. Analytical strain prediction in the structural components are also compared. Although there are minor differences between simulations, the overall magnitude of the strains are very similar. The thermal aspects of these changes are addressed in Sect. 3. NCT and HAC results predicted for an undamaged package show that the change in neutron poison actually reduces the final temperature of the containment vessel components. Therefore, the substitution of Cat 277-4 material and the minor changes in the inner and mid liners for production hardware should not reduce the effectiveness of the packaging when subjected to the regulatory requirements of 10 CFR 71 and the results of compliance testing would be analogous.

The contents used as surrogate payloads for the test units are shown on drawings M2E801580A029, and M2E801580A027. In the light-weight configuration, the contents consist of three 25.4 cm (10 in.) high convenience cans with handles, and 4 silicone rubber pads. These convenience cans, handles and silicone rubber pads are identical to those proposed for transport. The bottom convenience can was filled with tungsten grit until the convenience can and grit assembly weighed ~3 kg (6.6 lb). The actual weight of the tungsten grit was 2.77 kg (6.11 lb). The total content weight for the light- weight content configuration including the convenience cans, silicone rubber pads, can handles, and tungsten grit was ~3.6 kg (8 lb). In the heavy-weight configurations, the surrogate

payload consists of three steel cylindrical shaped components with handles, two can spacers filled with BoroBond4 and handles, and 6 silicone rubber pads. The can spacers, handles and silicone rubber pads are identical to those proposed for transport. These components weighed a total of approximately 50 kg (110.2 lb). These different weight assemblies bound the range of possible content configurations and structural deformation resulting from compliance testing. Since the decay heat of the proposed contents is ~0.4 W, little or no impact on the pressure or temperature of the package components will result during NCT. Differences in thermal capacitance of these surrogate payloads from the proposed HEU contents during HAC thermal testing are evaluated in Sect. 3.5.3.

2.5.2 Evaluation by Analysis

Although physical testing of the ES-3100 containers was performed generally at or near room temperature except for Test Unit-2, the effectiveness of the Kaolite insulating material at various temperature extremes was examined through the use of laboratory testing and structural analysis of a similar package, the ES-2LM (Handy 1997). For low-temperature service, Kaolite specimens were tested at −28.89 and −40°C (−20 and −40°F). These tests showed little change in the response of the material as compared to room temperature. Furthermore, structural analyses for bounding soft and stiff material cases were run. The Kaolite 1600 data used in these bounding analyses were from laboratory experiments that used a heavily cured sample (stiff) and a sample to which borax had been added (soft) [Oaks 1997]. Following the production run for the ES-2100 and DPP-2 shipping containers, new casting specimens were available for compression testing. In order to reduce the total cost of Kaolite testing, specimens were tested to approximately −40°C (−40°F) to cover both the cold conditions stipulated in 10 CFR 71.71(c)(2) and the −29°C (−20°F) temperature stipulated in 10 CFR 71.71(b)(1) and at 38°C (100°F). The results of Kaolite specimen testing are documented in Y/DW-1890 (Smith and Byington, Appendix 2.10.3) and Y/DW-1972 (Smith, Appendix 2.10.3). Upon further review of the data, the new test data was somewhat stiffer in the cold/high-density specimens than the data previously used in Y/DW-1972 (Smith, Appendix 2.10.3). Therefore, in order to encompass the extremes of all existing data, an additional drop simulation sequence using the new bounding curves has been conducted on the ES-3100 package as documented in Appendix 2.10.2. In addition to the analytical effort, the ES-3100 Test Unit-2 was pre-chilled to a nominal temperature of −40°C (−40°F). This was accomplished by placing the unit in an environmental chamber in Bldg. 5800 at ORNL and initially setting the chamber control to −56.7°C (−70°F) for 24 hours. After this initial period, the control on the environmental chamber was set to −42.8°C (−45° F) for at least 48 hours. Prior to the initiation of structural testing of this unit, it was removed from the environmental chamber and placed in an insulated box and transported to the NTRC. High-temperature [up to 38°C (100°F)] behavior was not addressed. However, in light of the fact that the insulation material is typically used as a cast refractory insulation in furnace applications, and that structural tests were performed in the range of 20.8 to 30.6°C (69.4 to 87°F) or just 7.4 to 17.2°C (13 to 30°F) below the high-temperature limit, it is not anticipated that any decline in impact absorption would be detrimental at 38°C (100°F).

2.6 NORMAL CONDITIONS OF TRANSPORT

This section demonstrates compliance with 10 CFR 71.43(f) and with 10 CFR 71.51(a)(1) and (b) following the tests and NCT conditions stipulated in 10 CFR 71.71. It is shown that the package will not experience any loss in shielding effectiveness or spacing and will not release any radioactive content or undergo leakage of water into the containment vessel during exposure to NCT. The four tests (water spray, free drop, compression, and penetration) made on Test Unit-4 were conducted in the 20.8 to 22.4°C (69.4 to 72.4°F) range, with the 1.2-m drop test conducted at 22.4°C (72.4°F). The maximum regulatory reference air leakage rate is $\leq 2.2976 \times 10^{-3}$ ref-cm^3/s. Compliance with this permitted activity

release limit is not dependent on filters or mechanical cooling systems. Following NCT compliance testing, the package was subjected to the sequential HAC test battery.

Title 10 CFR 71.71(b) specifies that the tests for NCT be conducted at the most unfavorable ambient temperature within the range of −28.89 to 38°C (−20 to 100°F). The drum is fabricated from type 304 stainless steel, and the containment boundary is fabricated from type 304L stainless steel, which is particularly suitable for low-temperature service. The Izod impact strength for the stainless steel used in the package components remains constant over a large range [specifically, from 21.11 to −195.5°C (70 to −320°F)] (*Stainless Steel Handbook*). Tensile strength increases from a minimum of 4.826×10^5 to 1.696×10^6 kPa (70,000 to 246,000 psi), and the yield strength increases about 10% over the same temperature range. The O-rings in the containment vessel have a normal service temperature range of −40 to 150°C [−40 to 302°F (Table 2.15)]. The normal service temperature range of the drum and containment vessel is −40 to 426.7°C (−40 to 800°F) [ASME, B&PV Code, Sect. II, Part D]. At −28.89°C (−20°F), the impact limiting material has been shown by tests to be stiffer than at 22.4°C (72.4°F). This condition has been evaluated by the compliance testing conducted on Test Unit-2. The reduction in tensile strength of the stainless steel from 22.4 to 38°C (73 to 100°F) is only approximately 2%, and the impact-limiting material test trends show that the impact-limiting material may become slightly softer. However, these slight reductions in tensile strength and absorption characteristics should not affect the results significantly compared to those conducted at 38°C (100°F).

Title 10 CFR 71.71(b) also states that the initial internal pressure within the containment system during NCT drop testing shall be considered as the maximum normal operating pressure. The maximum normal operating pressure is defined in 10 CFR 71.4 as the maximum gauge pressure that would develop in the containment system in a period of 1 year under the heat conditions specified in 10 CFR 71.71(c)(1). The internal pressure developed under these conditions in the ES-3100 containment vessel is calculated in Appendix 3.6.4 and discussed in Sects. 2.6.1.1 and 3.4.2. As noted in these sections, the internal pressure is calculated to be 198.98 kPa (28.859 psia). As shown in Appendix 2.10.1, the design absolute pressure of the containment vessel is 801.17 kPa (116.2 psia), and the hydrostatic test pressure stipulated in JS-YMN3-801580-A001 is 1135.57 kPa (164.7 psia). Thus, increasing the internal pressure of the containment vessel to a maximum of 198.98 kPa (28.859 psia) during NCT would have no detrimental effect. Table 2.20 provides a summary of the pressures and temperatures in the various shipping configurations. As discussed in Sect. 2.6.1.4, the containment vessel and the closure nut stresses for this pressure condition are well below the allowable stress values.

Title 10 CFR 71.71(c) specifies that the package service temperature must extend from −40 to 38°C (−40 to 100°F) with solar insolation. As shown in Sect. 3.4.1 and calculated in Appendix 3.6.2, the upper service temperature with solar insolation is calculated to be 87.81°C (190.06°F) for an empty ES-3100 containment vessel. Thermal cycling of the packages over the above temperature range from −40°C (−40°F) is considered an unlikely event, and the change would occur over a long period of time. In any event, the 127.81°C (230.06°F) thermal cycle would not result in brittle fracture or fatigue failure in the packaging. The acceptability of the packaging against brittle fracture is discussed in Sect. 2.6.2. The only concern for fatigue or endurance failure is related to the containment boundary cyclic pressure changes as the temperature varies from low to high. A 25°C (77°F) ambient temperature normally exists for the containment boundary during assembly. The containment boundary is sealed at an absolute pressure of ~101.35 kPa (14.70 psi). The internal absolute pressure at an average gas temperature of 87.81°C (190.06°F) is 198.98 kPa (28.859 psi) for the ES-3100 containment vessel (Table 2.20). The absolute internal pressure at −40°C or −40°F is 76.74 kPa (11.13 psi) for the containment vessel. Therefore, the maximum cyclic pressure differential for the containment vessel from low to high

temperatures is (198.98 – 76.74) kPa or 122.24 kPa (17.729 psi). This cyclic pressure is insignificant when considering the integrity of the containment boundary as shown by the stress levels discussed in Sect. 2.6.1.3.

The ES-3100 package has been tested to determine the effectiveness of the package following a sequential NCT 1.2-m (4-ft) drop test and an HAC test battery. Testing conducted on Test Unit-4 showed that there would be no loss or dispersal of radioactive contents and no significant increase in external surface radiation levels if the actual contents had been subjected to these tests, and no substantial reduction in the effectiveness of the packaging to survive the HAC testing. Thus, the requirements of 10 CFR 71.43(f) are satisfied.

Table 2.20. Summary of temperatures and pressures for NCT

Average gas evaluation temperature °C (°F)	Containment vessel absolute internal pressure kPa (psia)
−40 (−40) [a]	76.74 (11.13)
25.0 (77) [b]	101.35 (14.70)
87.81 (190.06) [c]	198.98 (28.859)

[a] Analysis conducted with no decay heat load in accordance with 10 CFR 71.71(c)(2).
[b] Assembly temperature and pressure.
[c] Due to the lack of measurable off-gassing, all ES-3100 containment vessel configurations with solar insolation, and 0.4 W decay heat produce the same internal pressure (Appendix 3.6.4).

2.6.1 Heat

Requirement. Exposure to an ambient temperature of 38°C (100°F) in still air and insolation as stated in 10 CFR 71.71(c)(1).

Analysis. An increase in ambient temperature to 38°C (100°F) with insolation will have no effect on the ability of the containment boundary to provide containment.

The maximum normal operating pressure is defined in 10 CFR 71.4 as the maximum gauge pressure that would develop in the containment system in a period of 1 year under the heat conditions specified in 10 CFR 71.71(c)(1). The internal pressure developed under these conditions in the ES-3100 containment vessel is calculated in Appendix 3.6.4 and discussed in Sects. 2.6.1.1 and 3.4.2. As noted in these sections, the internal pressure varies with temperature. Based on the isotopic determination of the proposed contents, a decay heat of 0.4W was calculated and used for the maximum internal heat load in evaluating the package for NCT (Sect. 3.1.2). The maximum calculated internal absolute pressure in the containment vessel with solar insolation and using the bounding case parameters is 198.98 kPa (28.859 psia). The design absolute pressure of the containment vessel is 801.17 kPa (116.20 psia), and the hydrostatic test pressure is 113.55 kPa (164.7 psia). Thus, increasing the internal pressure of the containment vessel to a maximum of 198.98 kPa (28.859 psia) during NCT would have no detrimental effect. Table 2.20 provides a summary of the pressures and temperatures for the various shipping configurations. As discussed in Sect. 2.6.1.4, the containment vessel and closure nut stresses for these pressure conditions are well below the allowable stress values. If the package is exposed to solar radiation at 38°C (100°F) in still air, the conservatively calculated temperatures at the top of the drum, on the surface of the containment vessel, and on the containment vessel near the O-ring sealing surfaces

are 117.72°C (243.89°F), 87.81°C (190.06°F), and 87.72°C (189.9°F), respectively (Sect. 3.4.1). Nevertheless, these temperatures are within the service limits of all packaging components, including the O-rings. The normal service temperature range of the O-rings used in the containment boundary is −40 to 150°C (−40 to 302°F) as shown in Table 2.15.

2.6.1.1 Summary of pressures and temperatures

An ambient temperature of 25°C (77°F) is assumed for the packaging at assembly. Since there are four ventilation holes near the top of the drum, and holes in the liner encapsulating the neutron poison material that are not hermetically sealed, the drum assembly will not become pressurized as the temperature increases. The containment boundary is sealed; thus, the internal pressure will change with temperature. Maximum calculated pressures at various temperatures (Sect. 3.4.1) are listed in Table 2.20.

2.6.1.2 Differential thermal expansion

The drum, inner liners, and containment vessel are all constructed of type 304 or 304L stainless steel. Radial and vertical expansion among these components will not cause any interferences or thermally induced stresses due to design clearances at assembly. Due to similarities of the coefficient of thermal expansion between type 304/304L and the containment vessel closure nut material (ASME SA-479), the compression of the O-rings does not change appreciably during the temperature excursion from 25°C (77°F) to the maximum temperature of 87.81°C (190.06°F).

The Kaolite 1600 insulation and Cat 277-4 material is poured and cast in place during the fabrication of the drum weldment (Drawing M2E801508A002, Appendix 1.4.8). Although some contraction of these materials may occur during curing, it is assumed for analysis purpose that a zero gap will exist between the Kaolite and the bounding drum and mid liner and a zero gap exists between the Cat 277-4 and the two liners. Due to differences in coefficients of thermal expansion, some radial and axial interferences are expected due to thermal growth of the inner liners. These radial and axial interferences and induced stresses are calculated in Appendix 3.6.3. A maximum von Mises stress of 6.693×10^4 kPa (9708 psi) was calculated for the inner liners. This stress value is well below the allowable yield strength of 1.324×10^5 kPa (19200 psi) at 148.9°C (300°F). A maximum von Mises stress of 1.379×10^3 kPa (200 psi) and 1.034×10^3 kPa (150 psi) occurs in the Cat 277-4 and Kaolite 1600 materials, respectively. Based on tabulated data and curves presented in Y/DW-1987 (Smith and Byington, Appendix 2.10.4) and the curves presented in Y/DW-1972 (Smith, Appendix 2.10.3) at 38°C (100°F), these compressive stresses are well below the failure limit of ~4.826×10^3 kPa (700 psi) and 5.171×10^3 kPa (750 psi) for the Cat 277-4 and Kaolite 1600 materials, respectively. Therefore, these thermally induced stresses will not reduce the effectiveness of the drum assembly.

The effects of differences in coefficient of thermal expansion between the HEU contents and their associated convenience cans, polyethylene or Teflon FEP bottles are not addressed. No credit is taken for the ability of the convenience can or bottle to maintain it structural integrity during transport. Section 4 of this document assumes the HEU content is in the form of an aerosol and all is available for release; therefore, no credit for the convenience can or bottle is taken. Based on assembly clearances and the flexibility of the polyethylene or Teflon FEP bottles, no radial or vertical interferences will develop during NCT. Based on assembly clearances and insignificant differences in the coefficient of thermal expansion between the stainless-steel, tin-plated carbon steel, or nickel-alloy convenience cans and the stainless-steel containment vessel, no radial or vertical interferences will develop during NCT testing.

2.6.1.3 Stress calculations

During normal conditions, stresses are only imposed by changes in internal pressure of the containment boundary as the temperature varies slowly over the operating range as shown in Table 2.20. Stress levels imposed on the package during NCT are insignificant, as shown in Tables 2.21, and 2.22. These tabulated stresses were determined by multiplying the stress at the design conditions (Appendix 2.10.1 and Table 2.6) by a factor equal to the ratio of operating pressures to design pressures and adding any contribution from the closure nut preload. This methodology is based on linear elastic material behavior. As shown in Sect. 2.6.1.4, all stresses in the containment boundary components are well below the *ASME Boiler and Pressure Vessel Code* allowable stress intensity limits.

2.6.1.4 Comparison with allowable stresses

NCT containment vessel stresses are calculated in accordance with the load combinations listed in Table 2.3 and their values are shown in Tables 2.21 and 2.22. The hot environment, cold environment, minimum external pressure, increased external pressure condition, and vibration normally incident to transport are addressed in Sects. 2.6.1, 2.6.2, 2.6.3 , 2.6.4, and 2.6.5, respectively. The fatigue or endurance limits for austenitic stainless steel are normally assumed to be about one-half the ultimate tensile strength (*Design Guidelines for Selection of Stainless Steel*, pp. 17–18). For type 304 stainless steel, one-half the ultimate tensile strength is 2.4×10^5 kPa (35,000 psi). Tensile and compressive hoop stresses of the magnitude shown in Tables 2.21 and 2.22 are insignificant compared to the endurance limit of 2.4×10^5 kPa (35,000 psi). As shown in Tables 2.21 and 2.22, the containment vessel stresses during NCT are insignificant. Even at the maximum test temperature and internal pressure (Sect. 3.5.3), the stresses in the containment boundaries were insignificant when compared with the allowable stress intensities shown in Tables 2.4 and 2.5. Corresponding calculated stress regions are shown in Fig. 2.1. Thermal expansion or contraction issues are addressed in Sects. 2.6.1.2 and 2.6.2.

2.6.2 Cold

Requirement. An ambient temperature of −40°C (−40°F) in still air and shade, as required by 10 CFR 71.71(c)(2).

Analysis. The drum is fabricated from type 304 stainless-steel sheet (Table 2.7). As discussed in Sect. 2.6, stainless steel is excellent for low-temperature service, particularly regarding tensile and impact strength. The thermal insulation (Kaolite) is a lightweight noncombustible cast refractory made from portland cement and vermiculite. The only moisture available for freezing at −40°C (−40°F) would be moisture that had not been removed during the curing and cool-down phase of fabrication. Because there will be no free water present for freezing and the insulation is a bonded mass of random fibers and cement, the properties of the insulation will not change appreciably. The matrix may become less flexible when subjected to the cold temperature, but the inner liner will remain in the position in which it was placed at the time of fabrication. The Kaolite 1600 insulation and Cat 277-4 materials are poured and cast in place during the fabrication of the drum weldment (Drawing M2E801508A002, Appendix 1.4.8). Although some contraction of these material may occur during curing, it is assumed for analysis purposes that a zero gap will exist between the Kaolite and the bounding drum and mid liner and a zero gap exists between the Cat 277-4 and the two liners. Due to differences in the coefficient of thermal expansion, some radial and axial interference is expected due to contraction of the outer drum and inner liners. These radial and axial interferences and induced stresses are calculated in Appendix 3.6.3. A maximum von Mises stress of 6.115×10^4 kPa (8869 psi) was calculated for the inner liners. This stress value is well below the allowable yield strength of 1.724×10^5 kPa (25000 psi) at −40°C (−40°F). A maximum von Mises stress of 979 kPa (142 psi) and 510 kPa (74 psi) occurs in the Cat 277-4 and Kaolite 1600 materials, respectively. Based on tabulated data and curves presented in Y/DW-1987 (Smith and

Byington, Appendix 2.10.4) and the curves presented Y/DW-1972 (Smith, Appendix 2.10.3) at −40°C (−40°F), these compressive stresses are well below the failure limit of ~ 6.895×10^3 kPa (1000 psi) and 5.308×10^3 kPa (770 psi) for the Cat 277-4 and Kaolite 1600 materials, respectively. Therefore, these thermally induced stresses will not reduce the effectiveness of the drum assembly.

The containment boundary is fabricated from type 304L stainless steel, which is suitable for low-temperature service, particularly regarding impact resistance. This material does not show a transition from ductile to brittle failure at this temperature. The *ASME Boiler and Pressure Vessel Code*, Sect. III, Subsection NB-2311, exempts impact testing of type 304L stainless steels. The Izod impact strength for type 304 stainless steel is 149.14 N·m (110 ft-lb) from 21.11 to −195.5°C (70 to −320°F). The tensile strength increases from ~4.826×10^5 to 1.696×10^6 kPa (70,000 to 246,000 psi) between 21.11 and −195.5°C (70 and −320°F), and the yield strength increases about 10% over the same range. NRC Regulatory Guide 7.6, Part B, states, "these designs were made of austenitic stainless steel which is ductile even at low temperatures. Thus, this guide does not consider brittle fracture." The drum, inner liner, top plug, and containment boundary are made from austenitic stainless steel. Similarly, the containment boundary closure nut material is a galling and wear resistant austenitic stainless steel. Therefore, brittle fracture of these structural materials at −40°C (−40°F) is not possible.

The specified O-rings used in the containment boundary have a continuous service temperature range of −40 to 150°C (−40 to 302°F) as shown in Table 2.15. The low temperature extreme has been verified by compliance testing of Test Unit-2 (Sect. 2.7.1.2). Test Unit-2 was pre-chilled to a nominal temperature of −40°C (−40°F). This was accomplished by placing the unit in an environmental chamber in Bldg. 5800 at ORNL and initially setting the chamber control to −56.7°C (−70°F) for 24 hours. After this initial period, the control on the environmental chamber was set to −42.8°C (−45°F) for at least 48 hours. Prior to the initiation of structural testing of this unit, it was removed from the environmental chamber and placed in an insulated box and transported to NTRC for testing.

As previously noted, the containment vessels will be assembled for shipment in a temperature environment of ~25°C (77°F). If the package should be exposed to −40°C (−40°F) for an extended period, all components will equalize near this low temperature. The absolute internal pressure inside the containment boundary would decrease to a pressure of 76.74 kPa (11.13 psi), assuming no decay heating (Table 2.20). Therefore, the pressure differential across the containment vessel at −40°C (−40°F) is −24.61 kPa (−3.57 psia) [76.739 − 101.35 kPa] (11.13 − 14.7 psia). Due to similarities of the coefficient of thermal expansion between type 304/304L and the containment vessel closure nut material (Nitronic 60, ASME SA-479), the compression of the O-rings does not change appreciably during the temperature excursion from 25°C (77°F) to −40°C (−40°F). The calculated stresses shown in Table 2.21 were determined by multiplying the stress at the design conditions (Appendix 2.10.1 and Table 2.6) by a factor equal to the ratio of operating pressure to design pressure and adding any contribution from the closure nut preload. This methodology is based on linear elastic material behavior. As shown in Sect. 2.6.1.4, all stresses in the containment boundary components are well below the *ASME Boiler and Pressure Vessel Code* allowable stress intensity limits. As demonstrated by the information presented above, the packaging is acceptable for NCT at −40°C (−40°F).

Table 2.21. ES-3100 containment boundary evaluation for both hot and cold conditions [a]

Stress locations shown in Fig. 2.1	Hot conditions [10 CFR 71.71(c)(1)] containment boundary stress @ 97.62 kPa 14.159 psi) gauge		Cold conditions [10 CFR 71(c)(2)] containment boundary stress @ −24.61 kPa (−3.57 psi) gauge		Allowable stress or shear capacity (AS)
	kPa (psi) or kg (lb)	M.S.	kPa (psi) or kg (lb)	M.S.	kPa (psi) or kg (lb)
Top flat portion of sealing lid (center of lid)	9.618×10^2 (139.5)	137	2.425×10^2 (35.17)	545	1.324×10^5 (19,200) [b]
Closure nut ring (away from threaded portion)	5.031×10^4 (7,297)	8.1	4.246×10^4 [f] (6,158)	9.8	4.571×10^5 (66,300) [c]
Top flat head (sealing surface region)	1.899×10^4 (2,754.4)	12.9	1.665×10^4 [f] (2,415)	14.9	2.648×10^5 (38,400) [c]
Cylindrical section (middle)	2.788×10^3 (404.4)	30.7	7.030×10^2 (102)	124.5	8.825×10^4 (12,800) [d]
Cylindrical section (shell to flange interface)	1.056×10^4 (1,532)	24.1	8.034×10^3 (1,165.2)	32	2.648×10^5 (38,400) [c]
Cylindrical section (shell to bottom interface)	7.152×10^3 (1,037.3)	36.0	1.803×10^3 (261.5)	145.8	2.648×10^5 (38,400) [c]
Body flange threads load, kg (lb)	1.067×10^3 (2,351.7)	18.2	9.072×10^2 [f] (2,000)	21.6	2.053×10^4 (45,266) [e]
Body flange thread region (under cut region)	2.954×10^4 (4,284.9)	8	2.256×10^4 [f] (3,272)	10	2.648×10^5 (38,400) [c]
Flat bottom head (center)	6.733×10^3 (976.5)	18.7	1.698×10^3 (246.2)	77	1.324×10^5 (19,200) [b]
Closure nut thread load, kg (lb)	2.351×10^3 (1,066.7)	32.2	9.072×10^2 [f] (2,000)	38.1	3.545×10^4 (78,154) [e]

[a] Calculated stresses were determined by multiplying the stress at the design conditions (Appendix 2.10.1) by a factor equal to the ratio of operating pressures to design pressures (independent of pressure direction) plus contribution from preload. Allowable stress values are taken from Table 2.5.

[b] Stress interpreted as the sum of $P_l + P_b$; allowable stress intensity value is $1.5 \times S_m$.

[c] Stress interpreted as the sum of $P_l + P_b + Q$; allowable stress intensity value is $3.0 \times S_m$.

[d] Stress interpreted as the primary membrane stress (P_m); allowable stress intensity value is S_m.

[e] Allowable shear capacity is defined as $0.6 \times S_m \times$ thread shear area. Thread shear area = 38.026 cm^2 (5.894 $in.^2$).

[f] Stress and shear load in these areas are dominated by the 162.7 ± 6.8 N·m (120 ± 5 ft-lb) preload.

2.6.3 Reduced External Pressure

Requirement. An absolute external pressure of 25 kPa (3.5 psi) is required by 10 CFR 71.71(c)(3).

Analysis. Reducing the absolute external pressure from ambient pressure to 25 kPa (3.626 psi) will have no effect on the drum assembly because the plastic plugs and aluminum tape covering the ventilation holes for the Cat 277-4 will allow the internal pressure of the drum assembly to equalize. This reduced pressure and a maximum internal pressure produces the maximum pressure differential across the containment boundary of 173.98 kPa (25.233 psi) [198.98 – 25 (28.859 – 3.626)]. The containment boundary is designed and fabricated in accordance with Sects. III and IX of the *ASME Boiler and Pressure Vessel Code* for an internal pressure differential of 699.82 kPa (101.5 psi) as shown in Appendix 2.10.1. A summary of the resulting stress intensities at various locations identified in Fig. 2.1 on the containment vessel in comparison with the ASME code allowable limits for this condition is shown in Table 2.22. These tabulated stresses were determined by multiplying the stress at the design conditions (Appendix 2.10.1 and Table 2.6) by a factor equal to the ratio of operating pressures to design pressures and adding any contribution from the closure nut preload. This methodology is based on linear elastic material behavior. As shown in Table 2.22, all stresses in the containment boundary components are well below the *ASME Boiler and Pressure Vessel Code* allowable stress intensity limits. Therefore, the ES-3100 packaging is acceptable for NCT at an absolute external pressure of 25 kPa (3.626 psi).

2.6.4 Increased External Pressure

Requirement. An absolute external pressure of 140 kPa (20 psi) is required by 10 CFR 71.71(c)(4).

Analysis. Increasing the absolute external pressure from ambient pressure to 140 kPa (20.31 psi) would have no effect on the drum assembly because the plastic plugs and aluminum tape covering the ventilation holes for the Cat 277-4 will allow the internal pressure of the drum assembly to equalize. At this increased external pressure, the maximum pressure differential across the containment boundary would be –63.26 kPa (–9.18 psi) [76.74 – 140 (11.13 – 20.31)], assuming the vessel's absolute pressure and temperature to be 76.74 kPa (11.13 psi) and –40°C (–40°F), respectively. Each containment boundary is designed and fabricated in accordance with Sects. III and IX of the *ASME Boiler and Pressure Vessel Code* for a minimum external pressure of 150 kPa (21.7 psi) gauge. A comparison of the resulting stress intensities at various locations on the containment vessel (Fig. 2.1) with the ASME code allowable limits for this condition is shown in Table 2.22. These tabulated stresses were determined by multiplying the stress at the design conditions (Appendix 2.10.1 and Table 2.6) by a factor equal to the ratio of operating pressures to design pressures and adding any contribution from the closure nut preload. This methodology is based on linear elastic material behavior. As shown in Table 2.22, all stresses in the containment boundary components are well below the *ASME Boiler and Pressure Vessel Code* allowable stress intensity limits. Therefore, the ES-3100 packaging is acceptable for NCT at an external absolute pressure of 140 kPa (20.31 psi).

Table 2.22. NCT ES-3100 containment boundary stress compared to the allowable stress at reduced and increased external pressures [a]

Stress locations shown in Fig. 2.1	Reduced external pressure [10 CFR 71.71(c)(3)] containment boundary stress @ 173.98 kPa (25.233 psi) gauge kPa (psi)		Increased external pressure [10 CFR 71.71(c)(4)] containment boundary stress @ −63.26 kPa (−9.18 psi) gauge kPa (psi)		Allowable stress or shear capacity (AS)
	kPa (psi) or kg (lb)	M.S.	kPa (psi) or kg (lb)	M.S.	kPa (psi) or kg (lb)
Top flat portion of sealing lid (center of lid)	1.714×10^3 (248.6)	76.2	6.236×10^2 (90.4)	211.3	1.324×10^5 (19,200) [b]
Closure nut ring (away from threaded region)	5.526×10^4 (8,014.1)	7.3	4.246×10^4 [f] (6,158)	9.8	4.571×10^5 (66,300) [c]
Top flat head (sealing surface region)	2.019×10^4 (2,928.9)	12.1	1.665×10^4 [f] (2415)	14.9	2.648×10^5 (38,400) [c]
Cylindrical section (middle)	4.969×10^3 (720.7)	16.8	1.808×10^3 (262.2)	47.8	8.825×10^4 (12,800) [d]
Cylindrical section (shell-to-flange interface)	1.321×10^4 (1,915.5)	19.0	9.374×10^3 (1,359.6)	27.2	2.648×10^5 (38,400) [c]
Cylindrical section (shell-to-bottom interface)	1.275×10^4 (1,848.6)	19.8	4.637×10^3 (672.5)	56.1	2.648×10^5 (38,400) [c]
Body flange threads load, kg (lb)	1.192×10^3 (2,626.7)	16.2	9.072×10^2 [f] (2,000)	21.6	2.053×10^4 (45,266)
Body flange thread region (under cut region)	3.348×10^4 (4,856)	6.9	2.397×10^4 [f] (3,476)	10	2.648×10^5 (38,400) [c]
Flat bottom head (center)	1.200×10^4 (1,740.2)	10	4.365×10^3 (633)	29.3	1.324×10^5 (19,200) [b]
Closure nut thread load, kg (lb)	1.192×10^3 (2,626.7)	28.8	9.072×10^2 [f] (2,000)	38.1	3.545×10^4 [e] (78,154)

[a] Calculated stresses were determined by multiplying the stress at the design conditions (Appendix 2.10.1) by a factor equal to the ratio of operating pressures to design pressures (independent of pressure direction) plus contribution from preload. Allowable stress values are taken from Table 2.5.

[b] Stress interpreted as the sum of $P_l + P_b$; allowable stress intensity value is $1.5 \times S_m$.

[c] Stress interpreted as the sum of $P_l + P_b + Q$; allowable stress intensity value is $3.0 \times S_m$.

[d] Stress interpreted as the primary membrane stress (P_m); allowable stress intensity value is S_m.

[e] Allowable shear capacity is defined as $0.6 \times S_m \times$ thread shear area. Thread shear area = 38.026 cm^2 (5.894 $in.^2$).

[f] Stress and shear load in these areas are dominated by the 162.7 ± 6.8 N·m (120 ± 5 ft-lb) preload.

2.6.5 Vibration

Requirement. Vibration normally incident to transportation is required by 10 CFR 71.71(c)(5).

Analysis. Vibration testing on a prototypical ES-3100 package (Test Unit-4) was conducted in accordance with the ES-3100 test plan (Appendix 2.10.8) and documented in the test report (Appendix 2.10.7). Testing was conducted with the package restrained as shown in Fig. 2.3. The containment vessel was assembled with the mock-up content weighing 49.90 kg (110 lb). The total weight of the test unit was 201.8 kg (445 lb). The unit was subjected to an endurance test with random vibrations modeled after the power spectral density plot for the Safe-Secure Trailer/Safeguards Transporter (SST/SGT) vibration envelope in the vertical axis (Cap, Appendix 2.10.6). At this level of vibration intensity, the test unit compares with MIL-STD-810F. MIL-STD-810F is a standard random vibration test for basic transportation vibrations generated by a large truck or tractor-trailer combination. MIL-STD-810F defines 60 min of testing as equal to 1609 km (1000 miles) of common carrier transportation. Assuming that the two random vibration tests are similar in intensity, Test Unit-4 had about 6436 km (4000 miles) of simulated random vibration testing. Based on a nominal shipping distance of 3218 km (2000 miles), Test Unit-4 was subjected to a test that was approximately two times more severe than that required by 10 CFR 71.71(c)(5). As shown by the following paragraphs, containment, shielding effectiveness, and subcriticality were maintained even when the package was subjected to such an arduous environment.

The test was run at ~22.8°C (73°F) rather than at the high or low temperatures specified for NCT. This was reasonable because the thermal coefficients of expansion of the flange and closure nut materials are very close. Therefore, the temperature extremes would not have a significant effect on the closure tightness.

Summarizing 10 CFR 71.43(f), the tests and conditions of NCT shall not substantially reduce the effectiveness of the packaging to withstand HAC sequential testing. The effectiveness of the ES-3100 to withstand HAC sequential testing is not diminished through application of the tests and conditions stipulated in 10 CFR 71.71. The justification for this statement is provided by physical testing of both the ES-2M (Byington 1997) and ES-3100 test packages. Due to the similarities in design, fabrication, and construction materials of the ES-2M and the ES-3100 packages, the physical characteristics of the Kaolite 1600 will hold true for both designs. The integrity of the Kaolite 1600 is not significantly affected by the NCT vibration and 1.2-m drop tests. Prior to testing the ES-2M design, each test unit was radiographed to determine the integrity of the Kaolite 1600 impact and insulation material. Following casting of the material inside the drum, some three-dimensional curving cracks were seen in some packages near the thinner top sections from the bottom of the liner to the bottom drum edge. After vibration testing, radiography of the ES-2M Test Unit-4 showed that the lower half of the impact limiter was broken into small pieces. In order to evaluate these findings, Test Unit-4 was reassembled and subjected to HAC sequential testing. After vibration and impact testing, many three-dimensional curving cracks were seen around the impact areas, and the inner liner was visibly deformed. Nevertheless, Test Unit-4 maintained the adequate spacing required for shielding effectiveness and subcriticality. Temperatures at the containment boundary were also similar to other packages not subjected to vibration testing prior to HAC testing. No inleakage of water was recorded following immersion. Additionally, Test Unit-4 of the ES-3100 test series was subjected to tests and conditions stipulated in 10 CFR 71.71(c)(5) through (c)(10), excluding (c)(8). Following completion of both the NCT and HAC tests, the containment vessel was removed, and a full-body helium leak test was conducted to the leaktight criterion ($\leq 2 \times 10^{-7}$ cm^3/s) in accordance with ANSI N14.5-1997.

Fig. 2.3. ES-3100 vibration testing arrangement.
(MD-1 test unit removed during actual testing.)

Following compliance testing of the ES-3100 shipping package, minor changes were incorporated into the proposed design as described in Sect. 2.5.1. During the vibration test, the shipping package is restrained from movement in the vertical direction with a tie-down arrangement similar to that used on a SST/SGT for a single package. Based on the acceleration spectral density presented in Appendix 2.10.6, the largest contributor to shipping package motion is in the vertical direction. Since the containment vessel and contents are not restrained within the inner liner cavity, the containment vessel is free to bounce up and down. In the vertical direction, the top plug and the bottom of the inner liner restrict the movement of this vessel. Since the inner liner contour has not changed with respect to the containment vessel, and the fact that there are clearances between the containment vessel flange and the inner liner in the vertical direction, the cast neutron poison and inner liner are not directly impacted by the movement of the containment vessel. Therefore, changes in the neutron poison and minor radial dimension changes in the mid liner will not affect the outcome from vibration testing. Based on the success of the previously tested units and the fact that these proposed changes will have little or no effect on testing, vibration normally incident to transport does not reduce the effectiveness of the packaging during HAC testing. Thus, the requirements of 10 CFR 71.43(f) are satisfied.

Procedures will be followed to ensure that the packaging is assembled as specified (Sect. 7). The drum, lid, and fasteners are refurbished as required before each use. The ⅝-in.–diam flange nuts on the drum are torqued to 40.67 N·m (30 ft-lb) nominal. The closure nut on the containment boundary is

torqued to 162.7 N·m (120 ft-lb) nominal. The package is acceptable for vibration normally incident to transport in an SST/SGT.

2.6.6 Water Spray

Requirement. A water spray that simulates exposure to rainfall of ~5.08 cm (2 in.) per hour for at least 1 h is required by 10 CFR 71.71(c)(6).

Analysis. A water spray of 5.08 cm (2 in.) per hour was directed from above and around the periphery of the ES-3100 Test Unit-4 for a minimum of 1 h as shown in Fig. 2.4. The drum had four plastic plug-sealed ventilation holes near the top which prevents water from entering the insulation cavity. Aluminum duct tape, covering the installation holes in the mid liner, prevents water from entering the neutron poison cavity. There was evidence of water leakage into the volume between the containment boundary and the inner liner at the conclusion of the test. Water entered this cavity through the holes provided in the lid for the TID lugs, but none penetrated the containment boundary. The criticality analysis shown in Sect. 6 was conducted with moderation by water to the most reactive credible extent and close full reflection of the containment system by water on all sides. Because the package remained subcritical under these conditions, the ES-3100 package is acceptable for use under the water spray conditions of NCT.

Fig. 2.4. Water spray test arrangement for Test Unit -4.

2.6.7 Free Drop

Requirement. A free drop of 1 m (4 ft) onto a flat, essentially unyielding, horizontal surface in a position for which maximum damage is expected is required by 10 CFR 71.71(c)(10). This test shall be made between 1½ and 2½ h after the conclusion of the water spray test (Sect. 2.6.6).

Analysis. The ES-3100 test package, Test Unit-4, previously sprayed with water (Sect. 2.6.6) with a measured gross weight of 201.85 kg (445 lb) and containing a content weight of 49.90 kg (110 lb) was tested in accordance with 10 CFR 71.71(c)(7). The temperature and pressure at the time of the drop test was 22.8°C (73°F) and ~101.35 kPa (14.70 psi), respectively. As discussed in Sect. 2.6, the response of the test package would not have been significantly different if it had been tested at the extremes of the temperature range dictated by 10 CFR 71.71(b) with the containment vessel at the maximum normal operating pressure.

The essentially unyielding surface used for this test was the indoor drop test pad at the NTRC. All 9-m (30-ft) drop and crush tests were conducted at the outside drop pad at the NTRC. The indoor pad consists of a 5.08-cm (2-in.) thick steel plate embedded inside a reinforced concrete pad ~127-cm (50-in.) thick. The outside drop pad consists of a 10.16-cm (4-in.) thick steel plate embedded inside a reinforced concrete pad ~167.6-cm (66-in.) thick. An article has been prepared by the NTRC staff to describe the integrity of these test pads (Shappert 1991).

Test Unit-4 was dropped from 1.2 m (4 ft) in a vertical position, with the drum's top initially striking the unyielding surface (Fig. 2.5). This attitude was assumed to be the most vulnerable orientation for producing damage to the sealing surfaces of the containment vessel and for introducing buckling into the cylindrical portion of the containment vessel body. The long axis of the drum was 0° from vertical. The test package made a free fall, with initial contact on the drum's lid. Damage consisted of shortening the drum height from 110.81 cm (43⅝ in.) to 110.49 cm (43½ in.) There were no breaks in the drum assembly. Additional details and sketches can be obtained from the test report (Appendix 2.10.7). Based on the HAC analytical structural deformation results shown in Sect. 2.7.8, the drop test damage would be nearly identical had this test been conducted on the proposed configuration using the Cat 277-4 neutron absorber. On this basis, the ES-3100 package meets the requirements of 10 CFR 71.71(c)(7).

In addition to the tests conducted on Test Unit-4, all test units (except Test Unit-6) were initially subjected to a free drop of 1.2-m (4 ft) onto a flat, essentially unyielding horizontal surface. As shown in Table 2.18, the orientations for these drops were two drops bottom to lid slapdown with the long axis of the drum ~ 12° from parallel to the drop pad; one drop with the long axis of the test unit parallel to the drop pad; one drop with the center of gravity drop over the drum/lid interface with the long axis of the drop rotated ~24.6° from perpendicular to the drop pad; and one with the long axis of the drum perpendicular to the drop pad. Package description, damage from testing, and drop orientation concerns are discussed in Sect. 2.7.1 for each test unit. Following the 1.2-m (4-ft) drop, each of these test units was subjected to the full HAC sequential test battery. The robustness of the ES-3100 containment vessel was demonstrated through whole boundary helium leak testing to $\leq 2.0 \times 10^{-7}$ cm^3/s (leaktight). This helium leak test eclipses the required criteria for both NCT and HAC based on the bounding case contents. Visual inspection of the containment boundaries showed no distortion or deformation from testing. Therefore, based on the various drop orientations, the severity of the HAC test sequence, and the testing conducted on Test Unit-4, the ES-3100 shipping package has been shown to meet the requirements of 10 CFR 71.43, 71.51(a)(1), and 71.71(c)(7).

Fig. 2.5. NCT free drop test on Test Unit-4.

2.6.8 Corner Drop

Requirement. 10 CFR 71.71(c)(8) requires a free drop onto each corner of the package in succession, or in the case of a cylindrical package, onto each quarter of each rim, from a height of 0.3 m (1 ft) onto a flat, essentially unyielding, horizontal surface. This test applies only to fiberboard, wood, or fissile material rectangular packages not exceeding 50 kg (110 lb) and fiberboard, wood, or fissile material cylindrical packages not exceeding 100 kg (220 lb).

Analysis. This test is not applicable because the range of package weights for the ES-3100 [146.88 kg (323.79 lb) to 187.81 kg (414.05 lb)] exceed the above-weight restrictions for fissile material cylindrical packages.

2.6.9 Compression

Requirement. Title 10 CFR 71.71(c)(9) requires that packages weighing up to 5000 kg (11,000 lb) must be subjected for a period of 24 h to a compressive load applied uniformly to the top and bottom of the package in the position in which the package would normally be transported. The compressive load must be the greater of the following:

1. the equivalent of five times the weight of the package; or,
2. the equivalent of 13 kPa (2.0 psi) multiplied by the vertically projected area of the package.

Analysis. The proposed maximum weight of the ES-3100 shipping package is calculated to be 187.81 kg (414.05 lb) [Table 2.8]. As shown on Drawing M2E801580A010 (Appendix 1.4.8), the data plate states that the maximum gross weight of the ES-3100 shipping package is 190.51 kg (420 lb). In accordance with Item 1 above, the minimum compressive load would be 5 × 190.51 kg or 952.55 kg (2100 lb). The vertically projected area of the package is 1891 cm^2 (293.16 $in.^2$) or the area of the lid weldment. Based on Item 2 above, the minimum compressive load would be 13 kPa × 1891 cm^2 or 250.72 kg (552.75 lb). Therefore, the approach stipulated in Item 1 above represents the greatest compressive load for this configuration. A conservative 1043 kg (2300 lb) compressive load was uniformly applied to the top and bottom of Test Unit-4 for at least 24 h (Fig. 2.6). The test package had been sprayed with water as noted in Sect. 2.6.6. No change in height or diameter of the test unit resulted from the test.

Fig. 2.6. Compression test on Test Unit-4.

Due to the design of the ES-3100 drum lid, the applied compressive load was distributed equally around the lid and supported primarily through the outer drum contour and Kaolite 1600 substrate. Little or no load is transferred to the neutron poison (BoroBond4 in the test units) and internal liners. Therefore, the changes in the design of the liners and neutron poison proposed for this shipping package should not impact the outcome resulting from compression testing. Based on the results of compliance testing of Test Unit-4 and the insignificant changes in the design, the ES-3100 package meets the requirements of 10 CFR 71.71(c)(9).

2.6.10 Penetration

Requirement. Impact of the hemispherical end of a vertical steel cylinder of 3.2 cm (1.25 in.) diameter and 6 kg (13 lb) mass dropped from a height of 1 m (40 in.) onto the exposed package surface that is expected to be most vulnerable to puncture is required by 10 CFR 71.71(c)(10). The long axis of the cylinder must be perpendicular to the package surface.

Analysis. A 6-kg (13-lb) steel cylinder was dropped from 1 m (40 in.) onto the surface of Test Unit-4, which was previously subjected to water spray, free drop, vibration and compression tests. The penetration bar impacted the side of the drum at the welded seam near the package's center of gravity. The bar did not penetrate the drum, but an indentation 0.64-cm (0.25-in.) deep was recorded at the drum seam weld as shown in Fig. 2.7. The magnitude of this indentation is insignificant. Based on the HAC analytical structural deformation results shown in Sect. 2.7.8, the magnitude of indentation would be nearly identical had this test been conducted on the proposed configuration using the Cat 277-4 neutron absorber. On this basis, the ES-3100 package meets the requirements of 10 CFR 71(c)(10).

Fig. 2.7. Penetration test damage on Test Unit-4.

2.7 HYPOTHETICAL ACCIDENT CONDITIONS

This section demonstrates compliance with 10 CFR 71.73, "Hypothetical Accident Conditions." It shows that the package will experience no loss in shielding effectiveness or spacing and no release of radioactive content or leakage of water into the containment boundary during HAC. A summary of the tests and analyses conducted on the ES-3100 configuration is shown in Table 2.23.

Title 10 CFR 71.51 requires that the ES-3100 package satisfy the standards under HAC specified in 10 CFR 71.73. For the tests specified in 10 CFR 71.73, five test packages were subjected to the five sequential tests: free drop, crush, puncture, thermal, and immersion. The configuration for Test Units-1 through -4 used full-scale shipping packages with steel mock-ups similar to the maximum contents to be shipped in the ES-3100 configuration. Test Unit-5, also a full-scale shipping package, was dropped with a mock-up of the lightest component proposed for shipping. All test units were first subjected to the NCT free drop from 1.2 m (4 ft). In addition to the 1.2-m (4-ft) drop, Test Unit-4 was also subjected to the full battery of tests in accordance with applicable paragraphs of 10 CFR 71.71(c)(5) through (c)(10) except (c)(8). These preliminary tests were conducted to provide evidence that the ES-3100's ability to withstand HAC testing was not degraded through NCT testing. Demonstration of the ES-3100 package's ability to satisfy the requirements of HAC is provided in the following sections. A summary of the test results is provided in each area of Sect. 2.7; details are documented in the test report (Appendix 2.10.7).

Extensive computer impact simulation and analysis was conducted using LS-Dyna software. (LS-Dyna 2002) The results are documented in Appendix 2.10.2. Early in the design phase, the simulation was used to determine areas of large structural deformation and stress concentrations. Prior to the compliance testing in accordance with 10 CFR 71.71, the simulation was used to determine the drop orientation that would cause the most structural damage to the drum assembly and thereby propose a worst-case scenario for potential breeching of the containment boundary. Prior drop test programs have shown the slapdown orientation to cause the most structural degradation of a drum-style container. Computer software LS-DYNA-3D was used to simulate a 9-m (30-ft) drop orientation at a slapdown angle of 12° with a friction factor of $\mu = 0.0$ as calculated using the computer code Slapdown, Version 05.20.93. Slapdown calculated that no matter what friction factor was assumed, the tail-end velocity peaked at approximately 14° (Handy 1997, Appendix 6.10). The maximum tail-end velocity versus slapdown angle is presented in Fig. 6.10.4 in Handy 1997, and the logic for the development of this figure is explained in Appendix 6.10 in Handy 1997. Due to the mitigating effects of the length to diameter ratios and the relative closeness of the 12° increase in velocity to the maximums (shown in Fig. 6.10.4 in Handy 1997), the 12°slapdown is considered to be representative of the worst-case slapdown. Based on the correlation of data obtained from preliminary drop tests of the similar ES-2M configuration and computer-simulated drops, several orientations were eliminated from the drop test matrix (Table 2.23). Several other impact simulations have been conducted using a wide range of material properties for the impact limiter material (Kaolite 1600) to determine the variance in structural deformation. Results of these simulations are documented in Sect. 5.6 in Handy (1997). Although the analysis shows some variance, the magnitude of difference was not large enough to degrade the performance of the drum assembly and containment boundary. Due to the similarities in design, fabrication, and material used in construction of the shipping packages, these same results would hold true for the ES-3100 package.

Table 2.23. Test and analysis summary for the ES-3100 package [a]

Container	NCT water spray, compression, penetration, vibration	1.2-m (4 ft) drop	9-m (30 ft) drop and crush test				1.2-m (4-ft) puncture drop	Preheat over 38°C (100°F)	HAC thermal burn test	O-ring cavity leak check (operational)	Full-body helium leak test [b]	0.9-m (3-ft) immer. test	15-m (50-ft) immer. test
			Top drop	CG over lid corner	Bottom to lid slapdown	Side drop							
TU-1		1—YES			12° 2—YES		3—YES [c]	4—YES	5—YES	6–YES $\leq 1.0 \times 10^{-4}$ ref. cm^3/s	7—YES 1.6×10^{-7} cm^3/s	8—YES	
TU-2		1—YES				2—YES	3—YES	4—YES	5—YES	6–YES $\leq 1.0 \times 10^{-4}$ ref. cm^3/s	7—YES Pulsing between 1.0×10^{-9} to 1.4×10^{-6} cm^3/s	8—YES	
TU-3		1—YES		24.6° 2—YES			3—YES	4—YES	5—YES	6–YES $\leq 1.0 \times 10^{-4}$ ref. cm^3/s	7—YES 1.0×10^{-7} cm^3/s	8—YES	
TU-4	Yes	1—YES	2—YES				3—YES	4—YES	5—YES	6–YES $\leq 1.0 \times 10^{-4}$ ref. cm^3/s	7—YES 2.0×10^{-7} cm^3/s	8—YES	
TU-5		1—YES			12° 2—YES		3—YES	4—YES	5—YES	6–YES $\leq 1.0 \times 10^{-4}$ ref. cm^3/s	7—YES 3.1×10^{-8} cm^3/s	8—YES	
TU-6										1–YES $\leq 1.0 \times 10^{-4}$ ref. cm^3/s			2—YES
Impact Analysis		YES	YES	YES	YES	YES							
Thermal Analysis	YES [d]							YES	YES [d]				

[a] Numbering refers to sequence of activities.
[b] Full-body helium leak test conducted following HAC testing. Leakage value recorded after 20 minutes of the test period.
[c] Test Unit-1 was puncture tested in four different orientations.
[d] Thermal analysis was conducted to determine time for cooling to -40°C and to evaluate the application of decay heating and insolation during the cool-down phase.

Title 10 CFR 71.73(b) requires that the HAC tests, except for the water immersion tests, be conducted at the most unfavorable ambient temperature within the range of −29 to 38°C (−20 to 100°F). This requirement was previously discussed in Sect. 2.6 for NCT, in which it was concluded that the tests performed at 70 to 90°F ambient temperatures should provide essentially the same results, except for thermal, as those made at any ambient temperature between −29 to 38°C (−20 to 100°F). Buckling failures are not anticipated for this package design. This assumption is based on the fact that no evidence of buckling occurred when the package was subjected to the compression test in accordance with 10 CFR 71.71(c)(9); the water immersion tests in accordance with 10 CFR 71.73(c)(5) and 71.73(c)(6); and the 1.2-m and 9-m drop test conducted on Test Unit-4. Code calculations further substantiate that buckling failures of the containment vessel are not anticipated for this package design (Appendix 2.10.1).

Title 10 CFR 71.73(b) states that the HAC initial pressure within the containment boundary vessel during testing shall be considered as the maximum internal normal operating pressure. The internal pressures in the ES-3100 containment vessel at various temperatures for NCT are discussed in Sects. 3.4.1 and 3.4.2 and tabulated in Table 2.20. The maximum normal absolute operating pressure due to insolation and the bounding case parameters is 198.98 kPa (28.859 psia) for the containment vessel. This pressure is well below the design internal gauge pressure of 699.82 kPa (101.5 psi). Increasing the internal pressure in the containment boundary to the value noted above before a free drop (Sect. 2.7.1), crush (Sect. 2.7.2), puncture (Sect. 2.7.3), or water immersion (Sect. 2.7.5) testing would have no detrimental effect on the containment boundary's structural integrity due to the low stresses shown in Table 2.21. Temperature and pressure increases in the containment boundary due to the compliance thermal tests are discussed and evaluated in Sects. 2.7.4 and 3.5.3. A summary of these pressures is presented in Appendix 3.6.5.

Summarizing 10 CFR 71.43(f) and 71.55(d)(4), the tests and conditions of NCT will not substantially reduce the effectiveness of the packaging to withstand HAC sequential testing. The effectiveness of the ES-3100 to withstand HAC sequential testing is not diminished through application of the tests and conditions stipulated in 10 CFR 71.71. The justification for this statement is provided by physical testing of both the ES-2M and ES-3100 test packages, and the analytical structural deformation predicted in Appendix 2.10.2 (summarized in Sect. 2.7.8). Due to the similarities in design, fabrication, and material used in construction of both the ES-2M and the ES-3100 package, the physical characteristics of the Kaolite 1600 will hold true for both designs. The integrity of the Kaolite 1600 is not significantly affected by the NCT vibration and 1.2-m (4-ft) drop tests. Prior to testing the ES-2M design, each test unit was radiographed to determine the integrity of the Kaolite 1600 impact and insulation material. Following casting of the material inside the drum, some three-dimensional curving cracks were seen in some packages near the thinner top sections from the bottom of the liner to the bottom drum edge. After vibration testing, radiography of the ES-2M Test Unit-4 showed that the lower half of the impact limiter was broken into small pieces. In order to evaluate these findings, Test Unit-4 was reassembled and subjected to HAC sequential testing. After vibration and impact testing, many three-dimensional curving cracks were seen around the impact areas, and the inner liner was visibly deformed. Nevertheless, the ES-2M Test Unit-4 maintained the adequate spacing required for shielding effectiveness and subcriticality. Temperatures at the containment boundary were also similar to other packages not subjected to vibration testing prior to HAC testing. No inleakage of water was recorded following immersion. Additionally, Test Unit-4 of the ES-3100 test series was subjected to tests and conditions stipulated in 10 CFR 71.71(c)(5) through (c)(10), excluding (c)(8). Following completion of these NCT tests, the test unit was subjected to the full HAC test battery. Following these tests, the containment vessel was removed and subjected to a full-body helium leak test. Criteria for a leaktight condition was achieved. Based on the success of these units, vibration normally incident to transport does not reduce the effectiveness of the packaging during HAC testing. Thus, the requirements of 10 CFR 71.43(f) and 71.55(d)(4) are satisfied.

2.7.1 Free Drop

Requirement. A free drop of 9 m (30 ft) onto a flat, unyielding, horizontal surface, striking the surface in a position for which maximum damage is expected is required by 10 CFR 71.73(c)(1).

Analysis. Five test packages were drop tested from 9 m (30 ft) in accordance with 10 CFR 71.73(c)(1) with the set up as shown in Fig. 2.8. A description of the drop pad is presented in Sect. 2.6.7. Four different drop positions were used in the testing based on the analytical results from LS-Dyna drop simulations. The ES-3100 test units were designated as Test Units-1, through -5. Test Unit-4 was subjected to the full NCT testing (water spray, 1.2-m (4-ft) drop, compression, penetration, and vibration) prior to HAC testing. The gross weight of the ES-3100 test units varied between 157.4 kg (347 lb) and 203.7 kg (449 lb). Mock-up components weighing between 3.6 kg (8 lb) [Test Unit-5] to 50.3 kg (111 lb) [Test Unit-3] were used during testing. Discussion of the damage to each test package resulting from the 9-m (30 ft) drop is given in subsequent paragraphs. Rationale for the four drop positions is included in the discussion for each test unit. Minor changes to the mid liner and the substitution of the neutron poison from BoroBond4 to Cat 277-4 are further evaluated in Sect. 2.7.8.

Fig. 2.8. 9-m drop test arrangement for all test units.

2.7.1.1 End drop

Test Unit-4, weighing 201.8 kg (445 lb), was dropped from 9-m (30 ft) with the long axis of the drum perpendicular to the impact surface within 0.2°. The mock-up components are shown on Drawing M2E801580A027. The concern for this drop orientation was that the containment boundary assembly would crush, buckle or compress the insulation to a thickness that would result in excessive O-ring temperatures during the thermal testing cycle. Following initial impact, the package bounced very little before landing on its side. The damage to the drum consisted of reducing the overall height from 43.5 in. [following the 1.2 m (4 ft) drop] to a minimum 42.63 in. The diameter of the drum was measured at six locations along the long axis of the package and at two radial locations. The measurements and pictorials of the damage are recorded on Test Form 1 of procedure TTG-PRF-08 shown in the test report data sheets (Appendix 2.10.7) and are summarized in Tables 2.24 and 2.25 and Fig. 2.9.

Table 2.24. Recorded height damage to Test Unit-4 from 1.2-m and 9-m drop testing

	0°	90°	180°	270°
Pre-drop height (in.)	43.50	43.50	43.63	43.63
Post 1.2-m drop height (in.)	43.50	43.50	43.50	43.50
Post 9-m drop height (in.)	43.00	43.13	42.88	42.63

Table 2.25. Recorded diametrical damage to Test Unit-4 from 1.2-m and 9-m drop tests [Diameter (in.)]

Axial measurement location	0 to 180°			90 to 270°		
	Pre drop test	Post 1.2-m drop test	Post 9-m drop test	Pre drop test	Post 1.2-m drop test	Post 9-m drop test
Top false wire	19.25	19.25	19.25	19.38	19.38	19.38
Top rolling hoop	19.25	19.25	19.13	19.25	19.25	19.88
CG & top rolling hoop	19.25	19.25	19.81	19.25	19.25	19.38
CG rolling hoop	19.13	19.13	19.13	19.25	19.25	19.25
Bottom rolling hoop	19.13	19.13	19.25	19.25	19.25	19.25
Bottom false wire	19.38	19.38	19.25	19.25	19.25	19.25

Fig. 2.9. 9-m drop test damage on Test Unit-4.

2.7.1.2 Side drop

Test Unit-2, weighing 202.8 kg (447 lb) was chilled to −40°C (−40°F) prior to conducting the drop tests. This unit was sequentially dropped from 1.2 m (4 ft), 9 m (30 ft), crushed from 9 m (30 ft), and puncture tested with the long axis of the drum parallel to the impact surface. The mock-up component used in Test Unit-2 is shown on Drawing M2E801580A027 and weighed 49.9 kg (110 lb). There were two concerns for this drop orientation. The primary concern was that the containment boundary assembly would crush or compress the insulation to a thickness that would result in excessive O-ring temperatures during the thermal testing cycle. Another concern was that the cold temperatures might cause excessive loads and deformation in the containment vessel body during impact. This, in turn, might cause leaking above the regulatory limit to occur. The test package made a free fall with initial contact occurring between the rolling hoops of the drum and the impact surface with the ambient temperature at 24.2°C (75°F). Since it was important to evaluate the package at the regulatory minimum temperature, individual results of each test were not recorded. Time required to measure the package between drops would have allowed the package to further increase in temperature. Cumulative results of damage to Test Unit-2 from drop testing is shown in Tables 2.26, 2.27, and 2.28 and Fig. 2.10.

Table 2.26. Recorded diametrical damage to Test Unit-2 from NCT and HAC drop testing [Diameter (in.)]

Axial measurement location	0 to 180°		90 to 270°	
	Pre drop test	Post drop test [a]	Pre drop test	Post drop test [a]
Top false wire	19.25	17.63	19.25	19.81
Top rolling hoop	19.25	17.38	19.25	19.75
CG & top rolling hoop	19.25	17.00	19.25	20.00
CG rolling hoop	19.25	16.00	19.25	20.25
Bottom rolling hoop	19.25	15.50	19.25	20.13
Bottom false wire	19.25	18.00	19.25	19.38

[a] Includes cumulative damage from 1.2-m drop, 9-m drop, and crush test.

Table 2.27. Recorded flat contour damage to Test Unit-2 from NCT and HAC drop testing

Axial measurement location	Flat width @ 0° (in.)	Flat width @ 180° (in.)
Top false wire	8	6.25
Top rolling hoop	9	8.88
CG & top rolling hoop	10.13	9.63
CG rolling hoop	9.88	12.00
Bottom rolling hoop	9.88	14.88
Bottom false wire	9.38	0
Crease (see Fig. 2.10 for location)		15.25

Table 2.28. Recorded height damage to Test Unit-2 from NCT and HAC drop testing

	0°	90°	180°	270°
Pre-drop height (in.)	43.50	43.50	43.50	43.50
Post-drop height (in.)[a]	44.75	43.75	42.75	43.63

[a] Includes cumulative damage from 1.2-m drop, 9-m drop, and crush test.

Fig. 2.10. Cumulative damage from 9-m drop and crush testing on Test Unit-2.

2.7.1.3 Corner drop

Test Unit-3, weighing 203.7 kg (449 lb), was dropped from 9 m (30 ft), with the long axis of the drum at an oblique angle of 24.8° (desired angle was 24.6°) from the impact surface. The mock-up component used in Test Unit-3 is shown on Drawing M2E801580A027 and weighed 50.3 kg (111 lb). The primary concern for this drop orientation was that the combination of plastic deformation at impact on the corner of the drum and the crushing or compacting of the adjacent insulation by the containment vessel flange would result in excessive O-ring temperatures during thermal testing. Another concern was that the mock-up contents would be forced against the containment boundary lid at impact. This, in turn, might yield the flange or closure nut, resulting in loss of containment. The test package made a free fall, with initial contact occurring between the top rim of the drum and the impact surface with the ambient temperature at 28°C (82.4°F). A secondary contact occurred between the bottom drum rim and the impact surface. No drum studs, nuts, or washers were lost due to the impact. The lid was still firmly attached to the drum assembly, with no visible separations or rips; thus, the position of the containment vessel inside the drum (and therefore the contents of the shipping container) was maintained. A general description of damage to Test Unit-3 is summarized in Tables 2.29 and 2.30. Pictorials of damage are shown on Fig. 2.11.

Table 2.29. Recorded height damage to Test Unit-3 from 1.2-m and 9-m drop testing

	0°	90°	180°	270°
Pre-drop height (in.)	43.50	43.50	43.50	43.50
Post 1.2-m drop height (in.)	43.00	43.50	43.63	43.50
Post 9-m drop height (in.)	40.63	43.25	43.75	43.38

Table 2.30. Recorded diametrical damage to Test Unit-3 from 1.2-m and 9-m drop testing [Diameter (in.)]

Axial measurement location	0 to 180°			90 to 270°		
	Pre drop test	Post 1.2-m drop test	Post 9-m drop test	Pre drop test	Post 1.2-m drop test	Post 9-m drop test
Top false wire	19.25	19.25	19.25	19.13	19.38	19.19
Top rolling hoop	19.13	19.13	18.63	19.13	19.25	19.88
CG & top rolling hoop	19.13	19.13	19.13	19.13	19.25	19.38
CG rolling hoop	19.13	19.13	19.13	19.13	19.25	19.38
Bottom rolling hoop	19.13	19.13	19.13	19.13	19.25	19.38
Bottom false wire	19.13	19.13	19.13	19.13	19.25	19.25

Fig. 2.11. Test Unit-3 damage from 1.2 and 9-m drop tests.

2.7.1.4 Oblique drops

Two oblique (slapdown) drops were conducted in the same attitude with maximum and minimum content weights to determine the structural response on the package in accordance with Regulatory Guide 7.8. Paraphrasing Regulatory Position 1.6, a local structural response might be greater during an impact test if the weight of the contents were less than the maximum. Therefore, Test Units-1 and -5 contained the maximum and minimum weight configurations, respectively.

2.7.1.4.1 Test Unit-1 slapdown

Test Unit-1, weighing 202.3 kg (446 lb) was dropped from 9-m (30 ft) with the long axis of the unit at an oblique angle of 12.2° (desired angle was 12°) to the essentially unyielding surface. The mock-up component used in Test Unit-1 is shown on Drawing M2E801580A027 and weighed 49.90 kg (110 lb). Based on Sect. 3.1 of Regulatory Guide 7.8, the structural performance of the package must be evaluated for the minimum and maximum weight of the contents. Therefore, this unit was tested above the maximum proposed content weight to see if the containment vessel would react differently from the much lighter mock-up used in Test Unit-5 in a similar drop orientation. The primary concern was that the orientation would cause greater angular acceleration of the contents near the package top. This in turn would cause the containment boundary to crush or compress the insulation to a thickness that would result in excessive O-ring temperatures during the thermal testing cycle. The test package made a free fall with initial contact occurring between the rolling hoops of the drum and the impact surface with the ambient temperature at 28°C (82.4°F). No drum studs, nuts, or washers were lost due to the impact. The lid was still firmly attached to the drum assembly, with no visible separations or rips; thus, the position of the containment vessel inside the drum (and therefore the contents of the shipping container) was maintained. A general description of damage is provided in Tables 2.31, 2.32, and 2.33 and Fig. 2.12.

Table 2.31. Recorded height damage to Test Unit-1 from 1.2-m and 9-m drop testing

	0°	90°	180°	270°
Pre-drop height (in.)	43.50	43.50	43.50	43.50
Post 1.2-m drop height (in.)	43.50	43.50	43.50	43.50
Post 9-m drop height (in.)	42.63	43.38	43.25	43.38
Buckle (in.)	44.50			

Table 2.32. Recorded diametrical damage to Test Unit-1 from 1.2-m and 9-m HAC drop testing [Diameter (in.)]

Axial measurement location	0 to 180°			90 to 270°		
	Pre drop test	Post 1.2-m drop test	Post 9-m drop test	Pre drop test	Post 1.2-m drop test	Post 9-m drop test
Top false wire	19.25	19.13	18.50	19.25	19.25	19.38
Top rolling hoop	19.25	19.00	18.50	19.25	19.25	19.38
CG & top rolling hoop	19.25	19.13	18.50	19.25	19.25	19.38
CG rolling hoop	19.25	19.13	18.63	19.25	19.25	19.38
Bottom rolling hoop	19.25	19.00	18.63	19.25	19.25	19.25
Bottom false wire	19.25	19.00	17.81	19.25	19.25	19.38

Table 2.33. Recorded flat contour damage to Test Unit-1 from 1.2-m and 9-m drop testing

Axial measurement location	Flats width maximum post 1.2-m drop (in.)	Flats width maximum post 9-m drop (in.)
Top false wire	5.25	8.00
Top rolling hoop	4.38	7.38
CG & top rolling hoop	4.50	7.13
CG rolling hoop	3.00	6.38
Bottom rolling hoop	4.00	6.75
Bottom false wire	4.63	10

Fig. 2.12. 1.2 and 9-m drop test damage on Test Unit-1.

2.7.1.4.2 Test Unit-5 slapdown

Test Unit-5, weighing 157.4 kg (347 lb), was dropped from 9-m (30 ft), with the long axis of the drum at an oblique angle of 12.5° (desired angle was 12°) from the impact surface. The mock-up component (Drawing M2E801580A029), weighing 3.6 kg (8 lb), was the hardware with the majority of the mass located near the bottom of the containment vessel (Sect. 2.5.1). Based on Sect. 3.1 of Regulatory Guide 7.8, the structural performance of the package must be evaluated for the minimum and maximum weight of the contents. Therefore, this unit was tested at the minimum proposed weight to see if the containment vessel would react differently from the much heavier mock-up used in Test Unit-1 in a similar drop orientation. The test package made a free fall with initial contact occurring between the bottom rim of the drum and the impact surface with the ambient temperature at 30.6°C (87°F). A secondary contact occurred between the top drum lid and the impact surface. No drum studs, nuts, or washers were lost during this impact test. The lid was still firmly attached to the drum assembly, with no visible separations or rips; thus, the position of the containment vessel inside the drum (and therefore the contents of the shipping container) was maintained. A general description of damage is provided in Tables 2.34, 2.35, and 2.36 and Fig. 2.13.

Table 2.34. Recorded height damage to Test Unit-5 from 1.2-m and 9-m drop testing

	0°	90°	180°	270°
Pre-drop height (in.)	43.50	43.50	43.50	43.50
Post 1.2-m drop height (in.)	43.88	43.50	43.50	43.50
Post 9-m drop height (in.)	44.50	43.50	43.38	43.50

Table 2.35. Recorded diametrical damage to Test Unit-5 from 1.2-m and 9-m HAC drop testing [Diameter (in.)]

Axial measurement location	0 to 180°			90 to 270°		
	Pre drop test	Post 1.2-m drop test	Post 9-m drop test	Pre drop test	Post 1.2-m drop test	Post 9-m drop test
Top false wire	19.25	18.88	18.75	19.38	19.38	19.38
Top rolling hoop	19.25	19.00	18.75	19.25	19.25	19.38
CG & top rolling hoop	19.25	19.13	18.75	19.25	19.25	19.38
CG rolling hoop	19.25	19.13	18.75	19.25	19.25	19.25
Bottom rolling hoop	19.25	19.13	18.75	19.25	19.25	19.25
Bottom false wire	19.25	19.13	18.44	19.25	19.25	19.31

Table 2.36. Recorded flat contour damage to Test Unit-5 from 1.2-m and 9-m drop testing

Axial measurement location	Flats width maximum post 1.2-m drop (in.)	Flats width maximum post 9-m drop (in.)
Top false wire	5.38	8.38
Top rolling hoop	4.25	8.38
CG & top rolling hoop	3.88	7.63
CG rolling hoop	2.50	7.50
Bottom rolling hoop	3.25	8.25
Bottom false wire	5.00	9.25

Fig. 2.13. 1.2 and 9-m drop test damage to Test Unit-5.

2.7.2 Crush

Requirement. Title 10 CFR 71.73(c)(2) requires that the specimen be subjected to a dynamic crush test in which the specimen is placed on a flat, essentially unyielding, horizontal surface so as to suffer maximum damage by the drop of a 500-kg (1100-lb) mass from 9 m (30 ft) onto the specimen. The mass must consist of a solid mild steel plate 1 m (40 in.) by 1 m (40 in.) and must fall in a horizontal attitude. The crush test is required only when the specimen has a mass ≤500 kg (1100 lb), an overall density ≤1000 kg/m^3 (62.4 lb/ft^3) based on external dimensions, and radioactive contents >1000 A_2 not as special form radioactive material. For packages containing fissile material, the radioactive contents greater than 1000 A_2 criterion does not apply.

Analysis. Five test packages were subjected to the dynamic crush test from 9 m (30 ft) in accordance with 10 CFR 71.73(c)(2). The previously drop-tested packages (described in Sect. 2.7.1) were restrained in the orientation used for drop testing. Discussion of the damage to each test package that resulted from the crush test is given in subsequent paragraphs, with details given in the test report. (Appendix 2.10.7) Rationale for the three drop positions is included in Sect. 2.7.1 for each test unit. The impact of the steel plate only increased the overall concern for each orientation.

Test Unit-1, weighing 202.3 kg (446 lb), was positioned in a horizontal attitude with the damaged portion of the test unit, resulting from prior drop tests, placed on the drop pad (0° mark facing down on test pad). The 500-kg (1100-lb) crush plate was centered over the sealing lid location on the containment vessel and dropped from 9 m (30 ft) and squarely contacted the top false wire of the drum at an ambient temperature of 29°C (84.2°F). Following initial impact, the package bounced very little before landing on its side. No drum studs, nuts, or washers were lost due to the impact. The lid was still firmly attached to the drum, with no visible separation or rips; thus, the position of the thermal barrier and neutron poison was maintained. A summary of the resulting damage is shown in Tables 2.37, 2.38, and 2.39. Since the length of the crush plate did not encompass the entire length of the test package, a crush edge indentation is recorded in Table 2.39. Additional pictorials of damage are shown on Fig. 2.14.

Table 2.37. Recorded height damage to Test Unit-1 from the 9-m crush test

	0°	90°	180°	270°
Pre-crush height (in.)	44.50	43.38	43.25	43.38
Post 9-m crust test height (in.)	44.88	43.38	44.00	43.63

Table 2.38. Recorded diametrical damage to Test Unit-1 from the 9-m crush test [Diameter (in.)]

Axial measurement location	0 to 180°		90 to 270°	
	Pre crush test	Post 9-m crush test	Pre crush test	Post 9-m crush test
Top false wire	18.50	15.63	19.38	20.63
Top rolling hoop	18.50	16.00	19.38	20.43
CG & top rolling hoop	18.50	16.25	19.38	20.25
CG rolling hoop	18.63	16.50	19.38	19.88
Bottom rolling hoop	18.63	18.25	19.25	19.50
Bottom false wire	17.81	17.81	19.38	19.25

Table 2.39. Recorded flat contour damage to Test Unit-1 from the 9-m crush test

Axial measurement location	Flats width maximum @ 0° (in.)	Flats width maximum@ 180° (in.)
Top false wire	9.00	8.50
Top rolling hoop	10.00	10.00
CG & top rolling hoop	10.00	10.13
CG rolling hoop	9.00	10.63
Bottom rolling hoop	8.25	--
Bottom false wire	9.75	--
Dent where edge of plate struck test unit	--	9.13

Fig. 2.14. Cumulative damage following 9-m crush on Test Unit-1.

Test Unit-2 (chilled package), weighing 202.8 kg (447 lb), was positioned in an horizontal attitude with the long axis of the drum parallel with respect to the drop pad. The damaged portion of the test unit, resulting from prior drop tests, was placed nearest the drop pad (0° mark facing down on pad). The 500-kg (1100-lb) crush plate was centered over the test unit's center of gravity and dropped from 9 m (30 ft) squarely onto the top false wire of the drum at an ambient temperature of 26.8°C (80.4°F). Following initial impact, the package bounced very little before landing on its side. No drum studs, nuts, or washers were lost due to the impact. The lid was still firmly attached to the drum, with no visible separation or rips; thus, the position of the thermal barrier and neutron poison was maintained. A summary of the cumulative damage is shown in Tables 2.26, 2.27, and 2.28 in Sect. 2.7.1.2. Additional pictorials of damage are shown on Fig. 2.10.

Test Unit-3, weighing 203.7 kg (449 lb), was positioned in the same oblique attitude as previously drop tested from 9 m (30 ft). The long axis of the drum was at an oblique angle of 24.7° (desired angle was 24.6°) from the impact surface with the damaged portion of the lid in contact with the drop pad (0° mark in contact with pad). The 500-kg (1100-lb) crush plate was dropped from 9 m (30 ft) with the center of gravity of both the plate and test unit in line at an ambient temperature of 30.5°C (86.9°F). The initial impact of the plate was with the edge of the drum bottom. A secondary contact occurred between the bottom drum rim and the impact surface. One drum stud was sheared from the test unit; however, the lid was still firmly attached to the drum, with no visible separation or rips. Therefore, the thermal barrier and neutron poison was maintained in position. Tables 2.40, 2.41, and 2.42 describe the measured damage which is recorded on Test Form 3 (Appendix 2.10.8). A photograph of the damage to Test Unit-3 is shown in Fig. 2.15.

Table 2.40. Recorded height damage to Test Unit-3 from the 9-m crush test

	0°	90°	180°	270°
Pre-crush height (in.)	40.63	43.25	43.75	43.38
Post 9-m crust test height (in.)	39.38	42.43	39.13	42.50

Table 2.41. Recorded flat contour damage to Test Unit-3 from the 9-m crush test

Axial measurement location	Flats width maximum pre crush (in.)	Flats width maximum post crush (in.)
Top of test unit	14.00	18.38
Bottom of test unit	0.00	17.88

Table 2.42. Recorded diametrical damage to Test Unit-3 from the 9-m crush test [Diameter (in.)]

Axial measurement location	0 to 180°		90 to 270°	
	Pre crush test	Post 9-m crush test	Pre crush test	Post 9-m crush test
Top false wire	19.25	19.25	19.19	19.06
Top rolling hoop	18.63	18.75	19.88	20.25
CG & top rolling hoop	19.13	19.25	19.38	19.75
CG rolling hoop	19.13	19.13	19.38	19.25
Bottom rolling hoop	19.13	19.13	19.38	19.75
Bottom false wire	19.13	18.00	19.25	19.38

Fig. 2.15. Cumulative damage following 9-m crush test on Test Unit-3.

Test Unit-4, weighing 201.8 kg (445 lb), was positioned vertically with the previously damaged drum top in contact with the drop pad. The 500-kg (1100-lb) crush plate was dropped from 9 m (30 ft) and squarely contacted the bottom of the test unit. The center of the 500-kg (1100-lb) crush plate was positioned over the radial test unit's center of gravity, in this case over the center of the drum's bottom at an ambient temperature of 29.8°C (85.6°F). Following initial impact, the package bounced very little before landing on its side. No drum studs, nuts, or washers were lost due to the impact. The lid was still firmly attached to the drum, with no visible separation or rips; thus, the position of the thermal barrier and neutron poison was maintained. A summary of the resulting damage is shown in Tables 2.43 and 2.44 and a photograph is shown in Fig. 2.16.

Table 2.43. Recorded height damage to Test Unit-4 from the 9-m crush test

	0°	**90°**	**180°**	**270°**
Pre-crush height (in.)	43.00	43.13	42.88	42.63
Post 9-m crust test height (in.)	39.38	40.38	40.63	39.75

Table 2.44. Recorded diametrical damage to Test Unit-4 from the 9-m crush test [Diameter (in.)]

Axial measurement location	0 to 180°		90 to 270°	
	Pre crush test	Post 9-m crush test	Pre crush test	Post 9-m crush test
Top false wire	19.25	19.25	19.38	19.38
Top rolling hoop	19.13	20.00	19.88	20.13
CG & top rolling hoop	19.81	20.00	19.38	20.06
CG rolling hoop	19.13	19.43	19.25	19.50
Bottom rolling hoop	19.25	19.94	19.25	20.00
Bottom false wire	19.25	19.25	19.25	19.25

Fig. 2.16. Cumulative damage from 9-m drop and crush testing on Test Unit-4.

Test Unit-5, weighing 157.4 kg (347 lb), was positioned in a horizontal attitude with the damaged portion of the test unit, resulting from prior drop tests, placed on the drop pad (0° mark facing down on test pad). The 500-kg (1100-lb) crush plate was centered over the test unit's center of gravity and dropped from 9 m (30 ft) squarely onto the top false wire of the drum at an ambient temperature of 29.6°C (85.3°F). Following initial impact, the package bounced very little before landing on its side. No drum studs, nuts, or washers were lost due to the impact. The lid was still firmly attached to the drum, with no visible separation or rips; thus, the position of the thermal barrier and neutron poison was maintained. A summary of the resulting damage is shown in Tables 2.45, 2.46, and 2.47. Additional pictorials of damage are shown on Fig. 2.17. Since the length of the crush plate did not encompass the entire length of the test package, additional indentations are recorded on Test Form 3.

Table 2.45. Recorded height damage to Test Unit-5 from the 9-m crush test

	0°	90°	180°	270°
Pre-crush height (in.)	44.50	43.50	43.38	43.50
Post 9-m crust test height (in.)	45.00	43.50	43.75	43.88

Table 2.46. Recorded diametrical damage to Test Unit-5 from the 9-m crush tests [Diameter (in.)]

Axial measurement location	0 to 180°		90 to 270°	
	Pre crush test	Post 9-m crush test	Pre crush test	Post 9-m crush test
Top false wire	18.75	18.69	19.38	19.38
Top rolling hoop	18.75	17.13	19.38	19.63
CG & top rolling hoop	18.75	17	19.38	20
CG rolling hoop	18.75	16.75	19.25	20
Bottom rolling hoop	18.75	16.50	19.25	19.75
Bottom false wire	18.44	17.00	19.31	19.38

Table 2.47. Recorded flat contour damage to Test Unit-5 from the 9-m crush test

Axial measurement location	Flats width maximum @ 0° (in.)	Flats width maximum @ 180° (in.)
Top false wire	8.88	0.00
Top rolling hoop	8.50	12.50
CG & top rolling hoop	8.00	12.00
CG rolling hoop	8.75	11.38
Bottom rolling hoop	10.25	11.38
Bottom false wire	11.38	10.50

Fig. 2.17. Cumulative damage from 9-m drop and crush testing on Test Unit-5.

Conclusion. As noted in the discussion above, plastic deformation of the drum occurred in all test packages at the impacted areas. However, the position of the impact limiting material (Kaolite) and neutron poison material (BoroBond in the test packages) was maintained in all test packages. The maximum areal deformation along the side of the test packages was a flat measuring 31.75 cm (12.50 in.) wide at the drum's top rolling hoop and ending with a width of 26.67 cm (10.50 in.) at the drum bottom in Test Unit-5.

2.7.3 Puncture

Requirement. A free drop of 1 m (40 in.) from a position to obtain maximum damage onto the upper end of a solid, vertical, cylindrical, 15-cm (6-in.)–diameter mild steel bar mounted on an unyielding horizontal surface, is required by 10 CFR 71.73(c)(3). The bar must be ≥20 cm (8 in.) long with the top end rounded to 6-mm (0.25-in.) maximum radius. The long axis of the bar must be vertical.

Analysis. The five units previously dropped and crushed from 9-m (30 ft) [Sects. 2.7.1 and 2.7.2] were dropped from 1 m (40 in.) in accordance with 10 CFR 71.73(c)(3). The puncture bar was bolted to the steel plate of the inside drop pad surface at NTRC (see Sect. 2.6.7 regarding the indoor drop test pad). A description of the drop orientations and results are shown in Table 2.48. Figures 2.18 through 2.24 show the results of puncture testing.

Table 2.48. 1-m (40-in.) puncture drop test description and results

Test Unit	Test unit's long axis drop orientation	Axial and radial location from drum lid [a]	Recorded damage (indentation depth - in.)[b]	Photograph
1	Horizontal	Test Unit's CG (0° mark)	0.63	Fig. 2.18
1	Horizontal	8 in. down (180° mark)	0.38	Fig. 2.20
1	28° oblique from vertical	Drum lid's edge (90° mark)	three impact locations 1. 0.63 2. 0.38 3. 0.13	Fig. 2.18
1	40° oblique from vertical	In line with test unit's CG (270° mark)	two impact locations 1. 0.75 2. 0.13	Fig. 2.19
2	Horizontal	Test Unit's CG (0° mark)	0.13	Fig. 2.21
3	24.6° oblique from vertical	In line with test unit's CG (270° mark)	two impact locations 1. Additional flattening of lid 2. 0.88	Fig. 2.22
4	Vertical	Center of drum's lid & CG	0.13	Fig. 2.23
5	Horizontal	8 in. down (0° mark)	0.13	Fig. 2.24

[a] See detailed description of test units in Sect. 5.4.3 of ORNL/NTRC-013.
[b] For detailed description of damaged locations, see Test Form 4 for Test Units 1, 3, 4, and 5 and Test Form 3 for Test Unit-2.

Conclusion. Although all test units were deformed by this puncture test, no drum surfaces were breached, thereby maintaining the integrity of the thermal barrier and neutron poison.

2.7.4 Thermal

Requirement. Exposure of the specimen fully engulfed, except for a simple support system, in a hydrocarbon fuel/air fire of sufficient extent and in sufficiently quiescent ambient conditions to provide an average emissivity coefficient of at least 0.9, with an average flame temperature of at least 800°C (1475°F) for a period of 30 min, or any other thermal test that provides the equivalent total heat input to the package and that provides a time-averaged environmental temperature of 800°C (1475°F). The fuel source must extend horizontally at least 1 m (40 in.) but may not extend more than 3 m (10 ft) beyond any external surface of the specimen, and the specimen must be positioned 1 m (40 in.) above the surface of the fuel source. For purposes of calculation, the surface absorptivity must be either that value which the package may be expected to possess if exposed to the fire specified or 0.8, whichever is greater; and the convective coefficient must be that value which may be demonstrated to exist if the package were exposed to the fire specified. Artificial cooling may not be applied after cessation of external heat input, and any combustion of materials of construction must be allowed to proceed until it terminates naturally.

Analysis. The five test units previously subjected to both NCT and HAC drop testing were thermal tested in accordance with 10 CFR 71.73(c)(4). To determine the maximum temperatures reached during thermal testing, temperature indicating patches were placed at various locations throughout the test packages at assembly. The temperature range for each patch used is identified in Table 2.49. When the temperature of an indicator was reached, the color would change to black (i.e., blackout temperature). The range of possible blackout temperatures of the patches was from 51.67 to 260°C (125 to 500°F). For Test Units-1 through -5, Table 2.49 defines the number and location of the temperature indicating patches.

Fig. 2.18. 28° oblique and horizontal puncture tests on Test Unit-1.

Fig. 2.19. 40° oblique puncture test on Test Unit-1.

Fig. 2.20. Horizontal puncture test over Test Unit-1's containment vessel flange.

Fig. 2.21. Horizontal CG puncture test on Test Unit-2.

Fig. 2.22. 24.6° oblique puncture test on Test Unit-3.

Fig. 2.23. Vertical puncture test on Test Unit-4.

Fig. 2.24. Horizontal puncture test over Test Unit-5's containment vessel flange.

Table 2.49. Thermax temperature indicating patches for test units

Patch Location	Internal surface	External surface	Temperature range °C (°F)	Test report figure (ORNL/NTRC-013)
Inner liner of drum assembly		8 (Full Range) 10 (5B & 5C)	52 to 260 (125 to 500) "B" 77 - 127 (171-261) "C" 132 - 182 (270-360)	5.3
Top plug weldment		4 (Full Range)	52 to 260 (125 to 500)	5.31
Containment vessel body flange	8 (4B & 4C)	8 (4B & 4C)	"B" 77 - 127 (171-261) "C" 132 - 182 (270-360)	5.28
Containment vessel body (end cap and cylinder)		5 (B)	"B" 77 - 127 (171-261)	5.28
Containment vessel sealing lid	4 (B)	4 (B)	"B" 77 - 127 (171-261)	5.29
Test mock-up components		6 (B)	"B" 77 - 127 (171-261)	5.26 & 5.27

Prior to the beginning of the thermal test, the No. 3 furnace at Timken Steel Company in Latrobe, Pennsylvania, was characterized for temperature and heat recovery times. Oxygen content in stack gases of the furnace was not monitored because it was not anticipated that any of the package's materials of construction were combustible. There was some burning of the silicone pads which are placed between the inner liners and the top plugs of the packages. However, it should be noted that this furnace employs "pulsed" fire burners. This type of burner is unique in that the natural gas flow rate is varied based on

furnace controller demands, but the flow of air through the burners is constant, even when no gas is flowing, thereby ensuring a very rich furnace atmosphere capable of supporting any combustion of package materials of construction. The support stand was welded to a large steel plate which had been placed on the floor of the furnace prior to heating. This steel plate acted as the radiating surface at the bottom of the furnace as well as providing the ability to hold the test stand rigidly in place. Before heating the furnace, workers practiced loading and unloading test packages from the cold furnace to assure that the furnace door would not remain open >90 s during each loading. In fact, the maximum time the door was open during any loading was 64 s.

A total of 18 thermocouples was installed on the furnace surfaces and on the test package support stand. (Appendix 2.10.7) All units were tested in a horizontal attitude with the end of the package facing the right and left side walls of the furnace. The test units were thermally tested with the 0° mark on the drum facing the floor of the furnace.

Each test unit was preheated to over 37.78°C (100°F) by placing the packages in an environmental chamber. The environmental chamber was heated by a torpedo-type kerosene space heater controlled by a mechanical bulb thermostat with a control range of 100°F to 200°F. The environmental chamber is a welded steel frame with fiberglass insulation panels. It was heated from the bottom with four floor register vents located around the perimeter and an 8 in. manual dampened center venting stove pipe. The setpoint temperature of the environmental chamber was monitored and adjusted for the duration of the preheat cycle. Initially, the thermostat was set to 66°C (150°F) for ~23 h. The thermostat set point was then reduced to ≥43°C (110°F) for the remainder of the preheat cycle. All packages were preheated for at least 47 h.

Six thermocouples were attached to the exterior surface of each test package after preheating. Metal retainer clips were welded to the drum to hold the thermocouples in place. The thermocouple tips were inserted underneath the metal clips and the wire was wrapped around the metal clip. To eliminate any radiant heat exchange between the thermocouples and the furnace walls, the tips and metal clips were covered with a ceramic coating.

No test package was loaded into the furnace until all functioning thermocouples on the furnace walls and support stand had a reading of 800°C (1475°F) or higher. All packages were placed in the preheated furnace on the support stand positioned with the long axis horizontal, the package lid facing toward a furnace side wall and oriented as described above. These packages were exposed to the radiation environment for a minimum of 30 min after all functioning furnace thermocouples, and at least five of the six test package exterior surface thermocouples reached a temperature of 800°C (1475°F). During the testing, the thermocouple temperature data were recorded every 15 s.

A minimum of 24 h prior to the beginning of all testing, the furnace was turned on with a set-point temperature of 871°C (1600°F). After each test, the furnace was allowed to reheat for a minimum of 45 min after obtaining the setpoint temperature before testing the next unit. The furnace control temperature data recorder ran continuously for the duration of the preheat. No test package was loaded into the furnace until all functioning thermocouples on the furnace walls and support stand had a reading of 800°C (1475°F) or higher.

Each test package was removed from the furnace and placed in an area where it was not exposed to artificial cooling. As the furnace door was opened for each test unit, smoking or flaming was visible from the TID lug hole at 0°. Flaming continued on some packages for 22 minutes and smoking continued up to one hour on others. All of the packages were allowed to cool naturally to room temperature. The post-thermal test weights of each unit were recorded on Test Form 1 of the test report.

(Appendix 2.10.8) The drums were disassembled, and the damage was photographed. The post-thermal test weight of each loaded containment vessel was also recorded. Each package was visually inspected, and the condition of the package and any observations were recorded.

After the containment vessels were removed from Test Units 1 through 5, two different leak tests were performed on each containment vessel. An operational leak test was conducted between the O-rings using a CALT5 leak tester. Following this operational leak test, a full body helium leak test was conducted. Details of these leak tests are provided in the test report (Appendix 2.10.7) and the results are summarized in Table 2.23. All five containment vessels were then removed from the drum assembly and immersed under a head of water of at least 0.9 m (3 ft) in a horizontal position for a period of ≥8 h. Following the immersion test of 10 CFR 71.73(c)(6), the containment boundary of Test Units-1 through -5 were opened to remove the contents, gather available data and look for signs of water in-leakage. No water in-leakage was detected in any of the units.

The blackout temperatures on the surface of all five containment boundaries, inner liners, and mock-up components used in the test packages are given in the test report (Test Form 5 for each test unit). Maximum blackout temperatures recorded on the surface of all test units are tabulated in Table 2.50. These values and temperature adjustments are discussed in Sect. 3.5.3.

Conclusion. All five test packages were intact following the 30-min exposure to the high-temperature thermal environment as required in 10 CFR 71.73(c)(4). Examination during disassembly showed that the containment boundary surfaces, flanges, fasteners, sealing surfaces, and O-rings were not damaged by the thermal testing. All five containment boundary assemblies met the subsequent 0.9-m (3-ft) water immersion test and maintained a full-body helium leak rate $\leq 2.0 \times 10^{-7}$ cm^3/s. Following compliance testing, minor changes were made to the mid liner, and the neutron poison was changed from BoroBond4 to Cat 277-4. In order to evaluate the impact of these changes, extensive analytical drop simulations were utilized. A detailed description of the models, material properties, and drop orientations evaluated is shown in Appendix 2.10.2. Results comparing structural deformation and maximum strains in the various material of construction are shown in Sect. 2.7.8. Based on the HAC analytical structural deformation results shown in Sect. 2.7.8, similar compliance test results would be expected had testing been conducted on packages employing the new proposed Cat 277-4 neutron poison. Therefore, the requirements of 10 CFR 71.73(c)(4) were satisfied, and containment was maintained.

2.7.4.1 Summary of pressures and temperatures

The ES-3100 shipping packages will typically be loaded at an ambient temperature and absolute pressure of ~25°C (77°F) and 101.35 kPa (14.70 psi), respectively. If the temperature of the package increases during shipment due to external temperature or solar insolation, the drum will not pressurize because four ventilation holes are drilled near the top of the drum, and the drum is not sealed at the drum lid–flange interface. The containment boundary is sealed at assembly. The internal pressure will increase due to transport temperatures, solar insolation (Sect. 3.4.1), decay heating, and the temperatures during HAC (Sect. 3.5.3). Temperature and pressures are summarized in Tables 3.21 and 3.11.

Table 2.50. Maximum HAC temperatures recorded on the test packages' interior surfaces

Temperature patch location [a]	ES-3100 Test Unit				
	1	2	3	4	5
	°C (°F)	°C (°F)	°C (°F)	°C (°F)	°C (°F)
Top plug bottom	149 (300)	163 (325)	177 (350)	177 (350)	177 (350)
Inner liner					
Flange step wall	135 (275)	163 (325)	135 (275)	135 (275)	135 (275)
BoroBond4 step	107 (225)	135 (275)	107 (225)	177 (350)[b]	121 (250)
CV body wall high	99 (210)	99 (210)	99 (210)	99 (210)	104 (219)
CV body wall middle	99 (210)	93 (199)	116 (241)[b]	93 (199)	99 (210)
Bottom flat portion	104 (219)	99 (210)	99 (210)	127 (261)	110 (230)
Containment boundary					
Lid (external top)	116 (241)	110 (230)	116 (241)	127 (261)	127 (261)
Lid (internal)	104 (219)	104 (219)	110 (230)	110 (230)	116 (241)
Flange (external)	116 (241)	110 (230)	110 (230)	116 (241)	121 (250)
Flange (internal)	104 (219)	99 (210)	116 (241)[b]	104 (219)	116 (241)
Body wall mid height	99 (210)	88 (190)	99 (210)	82 (180)	93 (199)
Bottom end cap (center)	99 (210)	99 (210)	88 (190)	110 (230)	99 (210)
Mock-up					
Side top	82 (180)	77 (171)	77 (171)	77 (171)	99 (210)
Side middle	77 (171)	77 (171)	77 (171)	77 (171)	93 (199)
Side bottom	77 (171)	77 (171)	77 (171)	77 (171)	88 (190)

[a] Refer to figures for exact locations and to Test Form 5 in the test report for recorded values. (ORNL/NTRC-013)
[b] Temperature indicating patch may have been damaged due to impact with surrounding structure. See Test Form 5 in ORNL/NTRC-013 for additional information.

The maximum HAC internal absolute pressure in the containment boundary of the ES-3100 has been calculated to be 595.99 kPa (86.441 psia). This predicted pressure is based on a conservative maximum adjusted average gas temperature of 123.85°C (254.93°F) as shown in Sect. 3.5.3 and Appendix 3.6.5.

2.7.4.2 Differential thermal expansion

The drum, inner liner, and containment vessel are all constructed of type 304 or 304L stainless steel. Because of design clearances used during assembly, radial and vertical expansion among these components will not cause any interferences or thermally induced stresses. Due to similarities of the coefficient of thermal expansion between type 304/304L and the containment vessel closure nut (ASTM A-479 and ARMCO Nitronic 60), the compression of the O-rings and the closure nut and containment vessel thread load do not change appreciably during the temperature excursion from 25°C (77°F) to the maximum adjusted containment vessel temperature of 152.22°C (306.0°F) [Sect. 3.5.3].

The Kaolite 1600 insulation and Cat 277-4 neutron poison are poured and cast in place during the fabrication of the drum assembly weldment (Drawing M2E801580A002, Appendix 1.4.8). This process produces a zero gap between the insulation and the bounding drum and inner liner and zero gap between the neutron poison and the mid and inner liners. Because of differences in coefficients of thermal expansion, some radial and axial interferences are expected from thermal growth of the liners. These radial and axial interferences have been addressed by the HAC thermal test. The results show that the stresses induced are minimal and do not reduce the effectiveness of the drum assembly.

Since there are ample clearances between the various size convenience containers and HEU contents, no induced thermal stresses from differences in coefficient of thermal will exist.

2.7.4.3 Stress calculations

The temperature gradient on the containment boundary was essentially uniform from top to bottom during the thermal tests (Table 2.50). The gradient around the periphery of the six test units was also essentially uniform and similar to the vertical gradient. As noted in the ES-3100 test report, the temperatures recorded on the containment vessels of all the test units were fairly uniform, both vertically and circumferentially. The maximum temperature variation on the containment vessels was ~50°F (from the test temperatures reported in Table 2.50). No damage would be expected on the containment vessel from thermal stresses resulting from a temperature differential of this magnitude. This conclusion is based on the guidelines given in the *ASME Boiler and Pressure Vessel Code*, Sect. III, Div. 1. Thermal stress is defined as a self-balancing stress produced by a nonuniform distribution of temperature (ASME B&PVC, Sect. III, Paragraph NB-3213.13). This paragraph further states that there are two types of thermal stresses: general thermal stress and local thermal stress. An example of a general stress is that produced by an axial temperature distribution in a cylindrical shell (ASME B&PVC, Paragraph NB-3213.9). This general stress is further classified (Paragraph NB-3213.9) as a secondary stress (that is, a normal stress or a shear stress developed by the constraint of adjacent materials or by self-constraint of the structure) [ASME B&PVC, Paragraph NB-3213.9]. Paragraph NB-3213.9 further states that the basic characteristic of a secondary stress is that it is self-limiting. Local yielding and minor distortions can satisfy the conditions that cause the stress to occur, and failure from a single application would not be expected. An example of a local thermal stress is a small hot spot in the wall of a pressure vessel (ASME B&PVC, Paragraph NB-3213.13). Local thermal stress is associated with almost complete suppression of the differential expansion and thus produces no significant distortion. Such stresses are considered only from a fatigue standpoint. Fatigue will not result from a one-time cyclic event such as an accidental fire.

The principal effect of the elevated temperature on stress levels is caused by the increase in the internal pressure. The calculated stresses as shown in Table 2.51 were determined by multiplying the stress at the design conditions (Appendix 2.10.1) by a factor equal to the ratio of operating pressures to design pressures and adding any contribution from the closure nut preload. This methodology is based on the application of linear elastic material behavior. As shown in Sect. 2.7.4.4, all stresses in the containment boundary components (based on nominal dimensions for the components) are well below the *ASME Boiler and Pressure Vessel Code* allowable stress intensity limits.

2.7.4.4 Comparison with allowable stresses

As noted in Sect. 2.7.4.3, the differential stresses resulting from temperatures recorded during HAC are negligible. Also, as shown in Table 2.51, stresses of this low magnitude do not affect the adequacy of the packaging. Corresponding calculated stress regions are shown in Fig. 2.1.

Table 2.51. HAC ES-3100 containment boundary stress compared to the allowable stress [a]

Stress locations shown in Fig. 2.1	Thermal condition 10 CFR 71.73 (c)(4) containment boundary stress @494.64 kPa (71.741 psi) gauge & 123.85°C (254.93°F) kPa (psi)		Immersion condition 10 CFR 71.73 (c)(6) containment boundary stress @−150 kPa (−21.76 psi) gauge & −2.22°C (28°F) kPa (psi)		Allowable stress (AS)
	kPa (psi)	M.S.	kPa (psi)	M.S.	kPa (psi)
Top flat portion of sealing lid (center of head)	4.873×10^3 (706.8)	26.2	1.478×10^3 (214.4)	88.6	1.324×10^5 (19,200) [b]
Closure nut ring (away from threaded portion)	7.603×10^4 (11,027)	5.0	4.246×10^4 [f] (6,158)	9.8	4.571×10^5 (66,300) [c]
Top flat head (sealing surface region)	2.525×10^4 (3,661.8)	9.5	1.665×10^4 [f] (2,415)	14.9	2.648×10^5 (38,400) [c]
Cylindrical section (middle)	1.413×10^4 (2,049)	5.2	4.285×10^3 (621.5)	19.6	8.825×10^4 (12,800) [d]
Cylindrical section (shell-to-flange interface)	2.431×10^4 (3,526.5)	9.9	1.238×10^4 (1,795.3)	20.4	2.648×10^5 (38,400) [c]
Cylindrical section (shell-to-bottom interface)	3.624×10^4 (5,255.8)	6.3	1.099×10^4 (1,594.2)	23.1	2.648×10^5 (38,400) [c]
Body flange threads load, kg (lb)	1.715×10^3 (3,781.9)	11	9.072×10^2 [f] (2,000)	21.6	2.053×10^4 (45,266) [e]
Body flange thread region (under cut region)	5.002×10^4 (7,254.7)	4.3	2.397×10^4 [f] (3,476)	10	2.648×10^5 (38,400) [c]
Flat bottom head (center)	3.411×10^4 (4,947.7)	2.9	1.035×10^4 (1,500.7)	11.8	1.324×10^5 (19,200) [b]
Closure nut thread load, kg (lb)	1.715×10^3 (3,781.9)	19.7	9.072×10^2 [f] (2,000)	38.1	3.545×10^4 (78,154) [e]

[a] Calculated stresses were determined by multiplying the stress at the design conditions (Appendix 2.10.1) by a factor equal to the ratio of operating pressures to design pressures (independent of pressure direction) plus contribution from preload. Allowable stress values are taken from Table 2.5.
[b] Stress interpreted as the sum of $P_l + P_b$; allowable stress intensity value is $1.5 \times S_m$.
[c] Stress interpreted as the sum of $P_l + P_b + Q$; allowable stress intensity value is $3.0 \times S_m$.
[d] Stress interpreted as the primary membrane stress (P_m); allowable stress intensity value is S_m.
[e] Allowable shear capacity is defined as $0.6 \times S_m \times$ thread shear area. Thread shear area = 38.026 cm^2 (5.894 $in.^2$).
[f] Stress and shear load in these areas are dominated by the 162.7 ± 6.8 N·m (120 ± 5 ft-lb) preload.

2.7.5 Immersion—Fissile Material

Requirement. In those cases for which water leakage into the containment boundary has not been assumed for criticality analysis, the specimen must be immersed under a 0.9-m (3-ft) head of water in an attitude for which maximum leakage is expected, as required by 10 CFR 71.73(c)(5).

Analysis. The containment vessels for the ES-3100 test packages (Units-1 through -5) were removed from their respective drum assemblies following the thermal tests described in Sect. 2.7.4.

After examination for damage (distortion, warpage, heating), the volume between the O-rings was pressurized, and the O-ring seals were leak checked in accordance with the CALT5 manufacturer's instructions manual using the CALT5 leak tester. Following the O-ring cavity check, the containment vessel lids were drilled and tapped for a full-body helium leak check. The seals remained functional on all vessels, and the integrity of the containment vessel structure was maintained (indicated by a helium leak rate $\leq 2.0 \times 10^{-7}$ cm^3/s). Following these leak tests, each unit was then submerged under a 0.9-m (3-ft) head of water for at least 8 h. No water leakage into the vessel was seen in any of the test units. The results of this test for each unit are recorded on the data sheet of Procedure TTG-PRF-14 shown in the test report. (Appendix 2.10.8) It should be noted that the criticality analysis does assume water leakage into the ES-3100 containment vessel; however, the 0.9-m (3-ft) immersion tests were performed anyway.

2.7.6 Immersion—All Packages

Requirement. A separate, undamaged specimen must be immersed under water at a pressure equivalent to a 15-m (50-ft) head of water, as required by 10 CFR 71.73(c)(6). This requirement may be satisfied by an external pressure of 150 kPa (21.7 psi) gauge.

Analysis. Immersion under a 15-m (50-ft) head of water would result in water entering the drum because the plastic plugs covering the four ventilation holes could fail, and the drum/lid flange is not gasketed. The ES-3100 containment boundary has been designed and tested for an external pressure of 150 kPa (21.7 psi) gauge and an internal gauge pressure of 699.82 kPa (101.5 psi), using nominal dimensions for all boundary components. Each containment vessel design incorporates an O-ring seal of verified integrity to provide assurance that no water will penetrate the containment boundary. The containment boundary of Test Unit-6 was subjected to this 15-m (50-ft) water immersion test. No visual signs of water leakage into the containment boundary were recorded.

2.7.7 Deep Water Immersion Test (for Type B Packages Containing More than 10^5 A_2)

The amount of A_2s proposed for transport is ~293.99. Therefore, the deep water immersion test is not applicable.

2.7.8 Summary of Damage

After testing five full scale ES-3100 test packages under HAC, the drum, drum lid, and top plug were damaged as expected. The containment boundary flange, O-ring grooves, and closure nut were not damaged. Plastic deformation occurred in the five drum assemblies in the impact areas from the 1.2-m and 9-m (30-ft) drop, crush and subsequent puncture tests. No breaks were noted in the drum assembly, and no insulation was exposed. The resultant damage did not reduce the effective center-to-center package spacing to a point of criticality concern (Sect. 6).

The full scale test units were fabricated in accordance with drawings created for production hardware. During the procurement process for the full scale test units, several small changes were suggested by the manufacturer to improve the efficiency and to reduce the cost of fabrication. These changes were incorporated and tested. However, following compliance testing, the following changes have been made to the proposed production hardware. First, a change in the neutron poison from BoroBond4 to Cat 277-4 has been adopted; second, the mid liner design has been changed to a continuous shell by reducing the diameter of the step in the inner liner for the containment vessel flange

from 22.35 cm (8.8 in.) to 21.84 cm (8.6 in.); and third, the silicone rubber pad thickness on the drum assembly bottom liner was increased by ~0.15 cm (0.06 in.). The second change increased the amount of Kaolite 1600 around the containment vessel flange, increased the final volume of the neutron poison, and slightly decreased the volume of the Kaolite 1600 adjacent to the neutron poison. The third change was made to stiffen the rubber pad so it would remain in place during vibration normally incurred during transport. In order to evaluate the impact of these changes, analytical drop simulations were conducted and documented in Appendix 2.10.2. The drop simulations were conducted in the same attitude and temperature regime as those conducted during the compliance testing phase for certification. Temperature dependent material properties were used in the analysis. The results of the structural deformation from compliance testing, drop simulation using BoroBond4 and drop simulations using Cat 277-4 material are presented in the following tables and figures. The analytical structural deformation results shown in Tables 2.52 through 2.61 are nearly identical for the two neutron poisons. The analytical results are also well representative of the results recorded during compliance testing as depicted in Figs. 2.25 through 2.30. Analytical strain prediction in the structural components are also compared for the two neutron poisons. Although there are minor differences between the compliance testing and drop simulations, the overall magnitude of the strains is very similar. The thermal aspects of these changes are addressed in Sect. 3. NCT and HAC results predicted for an undamaged package show that the change in neutron poison actually reduces the final temperature of the containment vessel components. Therefore, the substitution of Cat 277-4 material and the minor changes in the inner and mid liners for production hardware should not reduce the effectiveness of the packaging when subjected to the regulatory requirements of 10 CFR 71.71 and 71.73, and the results of compliance testing would be analogous. Some of the test units lost approximately 0.45 kg (1 lb) of their gross weight due to boiling off of the water trapped in the refractory and BoroBond4 materials (Table 2.62).

Assuming all water loss is from the neutron poison, the BoroBond4 material lost ~ 9.4% of its water content. Using the temperature data recorded during HAC testing shown in Table 2.50 and applying the temperature adjustments discussed in Sect. 3.5.3, the average temperature of the neutron poison would be ~150°C (302°F). Since the ES-3100 test units were not fabricated packages with Cat 277-4, thermogravimetric analysis (TGA) was used to compare the neutron poison's propensity to lose water. The results of this analysis are shown in Appendix 2.10.4 (Thompson, *Summary of TGA Testing*). Samples of both BoroBond4 and Cat 277-4 were TGA tested, and the results were compared at 150°C (302°F). The BoroBond4 samples lost ~ 61.6% of their original water content. The dry Cat 277-4 lost a maximum of only 6.61%. The BoroBond4 TGA samples lost ~6.5 times the amount of water lost by the ES-3100 test units during HAC compliance testing. Assuming comparable results would be expected for the Cat 277-4 material due to similarity in the structural configuration, installation methodology, and LS-Dyna drop simulation structural deformation results, the Cat 277-4 water loss would be only 1.02%. Criticality safety analysis assumes a greater percent loss; therefore, additional conservatism is being applied in this SAR.

The maximum blackout temperature recorded adjacent to the O-rings during testing was 127.22°C (241°F) [Table 2.50]. Using the adjustments discussed in Sect. 3.5.3, the maximum adjusted temperature at the containment boundary O-rings during shipment under HAC was calculated to be 141.22°C (286.2°F). The normal operating temperature for these O-rings is −40 to 150°C (−40 to 302°F) as shown in Table 2.15. Therefore, containment will be maintained during HAC.

Table 2.52. Diametrical damage comparison of Test Unit-1 with analytical predictions [Diameter (in.)]

	0 to 180°			90 to 270°		
Axial measurement location	**Test results**	**Analytical results with BoroBond**	**Analytical results with Cat 277-4**	**Test results**	**Analytical results with BoroBond**	**Analytical results with Cat 277-4**
Top false wire	15.63	15	14.9	20.63	20.7	20.7
Top rolling hoop	16	15.3	15.1	20.44	20.8	20.8
CG & top rolling hoop	16.25	15.9	15.7	20.25	20.6	20.7
CG rolling hoop	16.5	16.4	16.2	19.88	20.1	20.4
Bottom rolling hoop	18.25	18.3	18.1	19.5	19.6	19.8
Bottom false wire	17.81	18.1	18	19.25	19.4	19.4

Table 2.53. Flat contour damage comparison of Test Unit-1 with analytical results

Axial measurement location	**Flats width @ 0° (in.)**			**Flats width @ 180° (in.)**		
	Test results	**Analytical results with BoroBond**	**Analytical results with Cat 277-4**	**Test results**	**Analytical results with BoroBond**	**Analytical results with Cat 277-4**
Top false wire	9	10.5	10.5	8.5	10.5	10.9
Top rolling hoop	10	11	11	10	11	11
CG & top rolling hoop	10	10.1	10.1	10.13	10.1	10.1
CG rolling hoop	9	8.4	8.4	10.63	10.1	10.1
Bottom rolling hoop	8.25	7.6	7.6	---	0	0
Bottom false wire	9.88	10.1	10.1	---	0	0

Fig. 2.25. Visual comparison of the cumulative damage on the crush side surface after the three drop tests (from top to bottom: Test Unit-1, analytical results with BoroBond, analytical results with Cat 277-4).

Table 2.54. Cumulative analytical 12° slapdown drop tests maximum effective plastic strain results

Component	Component material	Effective plastic strain (in./in.)			
		Offset crush		Centered crush	
		Model with BoroBond	Model with Cat 277-4	Model with BoroBond	Model with Cat 277-4
CV body	Type 304L stainless steel	0.0457	0.0564	0.0741	0.0643
CV lid	Type 304L stainless steel	0.0005	0.0013	0.0006	0.0018
CV closure nut	A-479 nitronic 60	0.0000	0.0001	0.0003	0.0000
Angle	Type 304 stainless steel	0.1045	0.1070	0.0917	0.0944
Drum	Type 304 stainless steel	0.3972	0.3920	0.3537	0.3443
Drum bottom	Type 304 stainless steel	0.2877	0.2879	0.2919	0.3000
Liner	Type 304 stainless steel	0.2702	0.2060	0.2363	0.2846
Lid	Type 304 stainless steel	1.0797	0.9689	1.0795	0.5828
Lid stiffener	Type 304 stainless steel	0.0838	0.0894	0.0303	0.0288
Drum lid studs	Type 304 stainless steel	>0.57	0.4018	0.3174	0.2390
Lid hex nut	Silicon bronze - C65100	0.0086	0.0028	0.0000	0.0000
Drum washer	300 series stainless steel	0.1003	0.0790	0.0597	0.0775
Top plug weldment	Type 304 stainless steel	0.2715	0.2665	0.1636	0.1644

Table 2.55. Diametrical damage comparison of Test Unit-2 with analytical predictions [Diameter (in.)]

Axial measurement location	0 to 180°			90 to 270°		
	Test results	Analytical results with BoroBond	Analytical results with Cat 277-4	Test results	Analytical results with BoroBond	Analytical results with Cat 277-4
Top false wire	17.63	18.1	18	19.81	19.6	19.6
Top rolling hoop	17.38	16.6	16.6	19.75	19.75	20.1
CG & top rolling hoop	17	16.5	16.5	20	20	20.4
CG rolling hoop	16	16.3	16.3	20.25	20.25	20.5
Bottom rolling hoop	15.5	16.1	16.1	20.13	20.13	20
Bottom false wire	18	17.6	17.6	19.25	19.38	19.4

Table 2.56. Flat contour damage comparison of Test Unit-2 with analytical predictions

Axial measurement location	Flats width @ 0° (in.)			Flats width @ 180° (in.)		
	Test results	Analytical results with BoroBond	Analytical results with Cat 277-4	Test results	Analytical results with BoroBond	Analytical results with Cat 277-4
Top false wire	8	9.2	9.2	6.25	0	0
Top rolling hoop	9	8.4	9.3	8.88	10.1	10.1
CG & top rolling hoop	10.13	8.4	8.4	9.63	8.4	9.3
CG rolling hoop	9.88	9.3	9.3	12	9.3	9.3
Bottom rolling hoop	9.88	9.3	9.3	14.88	10.1	10.1
Bottom false wire	9.38	10.1	10.1	0	0	0

Fig. 2.26. Visual comparison of the cumulative damage on the rigid surface side after the four drop tests (from left to right: Test Unit-2, analytical results with BoroBond, analytical results with Cat 277-4).

Fig. 2.27. Visual comparison of the cumulative damage on the crush plate side after the three drop tests (from left to right: Test Unit-2, analytical results with BoroBond, analytical results with Cat 277-4).

Table 2.57. Cumulative analytical side drop test maximum effective plastic strain results

Component	Component material	Effective plastic strain (in./in.)	
		Model with BoroBond	Model with Cat 277-4
CV body	Type 304L stainless steel	0.0462	0.0525
CV lid	Type 304L stainless steel	0.0004	0.0004
CV closure nut	A-479 nitronic 60	0.0000	0.0005
Angle	Type 304 stainless steel	0.0816	0.0845
Drum	Type 304 stainless steel	0.2623	0.2814
Drum bottom	Type 304 stainless steel	0.2807	0.2827
Liner	Type 304 stainless steel	0.2005	0.2022
Lid	Type 304 stainless steel	0.6411	0.6413
Lid stiffener	Type 304 stainless steel	0.0217	0.0171
Drum studs	Type 304 stainless steel	0.1753	0.2364
Drum hex nut	Silicon bronze - C65100	0.0000	0.0018
Drum washer	300 series stainless steel	0.1034	0.0439
Top plug weldment	Type 304 stainless steel	0.1258	0.1286

Table 2.58. Diametrical damage comparison of Test Unit-3 with analytical predictions [Diameter (in.)]

Axial measurement location	0 to 180°			90 to 270°		
	Test results	Analytical results with BoroBond	Analytical results with Cat 277-4	Test results	Analytical results with BoroBond	Analytical results with Cat 277-4
Top false wire	19.25	19	19	19.06	19	19
Top rolling hoop	18.75	18.9	18.9	20.25	20.6	20.6
CG & top rolling hoop	19.25	19.4	19.4	19.75	19.9	19.8
CG rolling hoop	19.13	19.3	19.3	19.25	19.4	19.4
Bottom rolling hoop	19.13	19.3	19.3	19.75	20.4	20.4
Bottom false wire	18	18.6	18.6	19.38	19.4	19.4

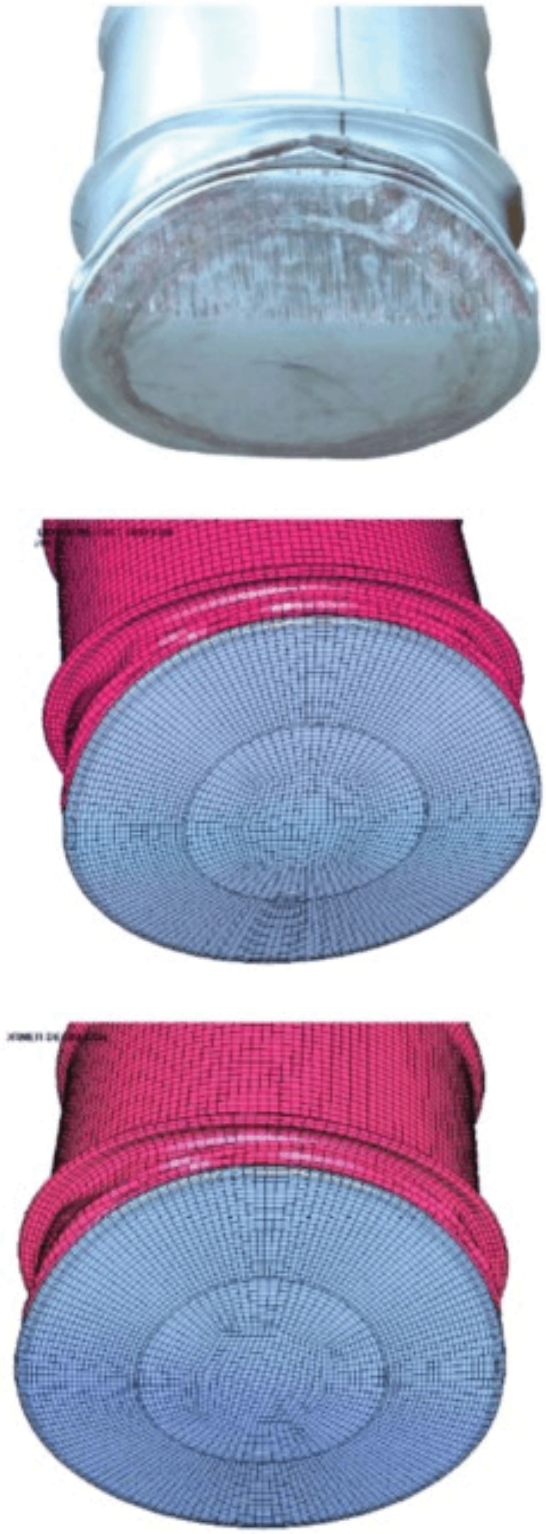

Fig. 2.28. Visual comparison of the cumulative bottom damage after the three drop tests (from top to bottom: Test Unit-3, analytical results with BoroBond, analytical results with Cat 277-4).

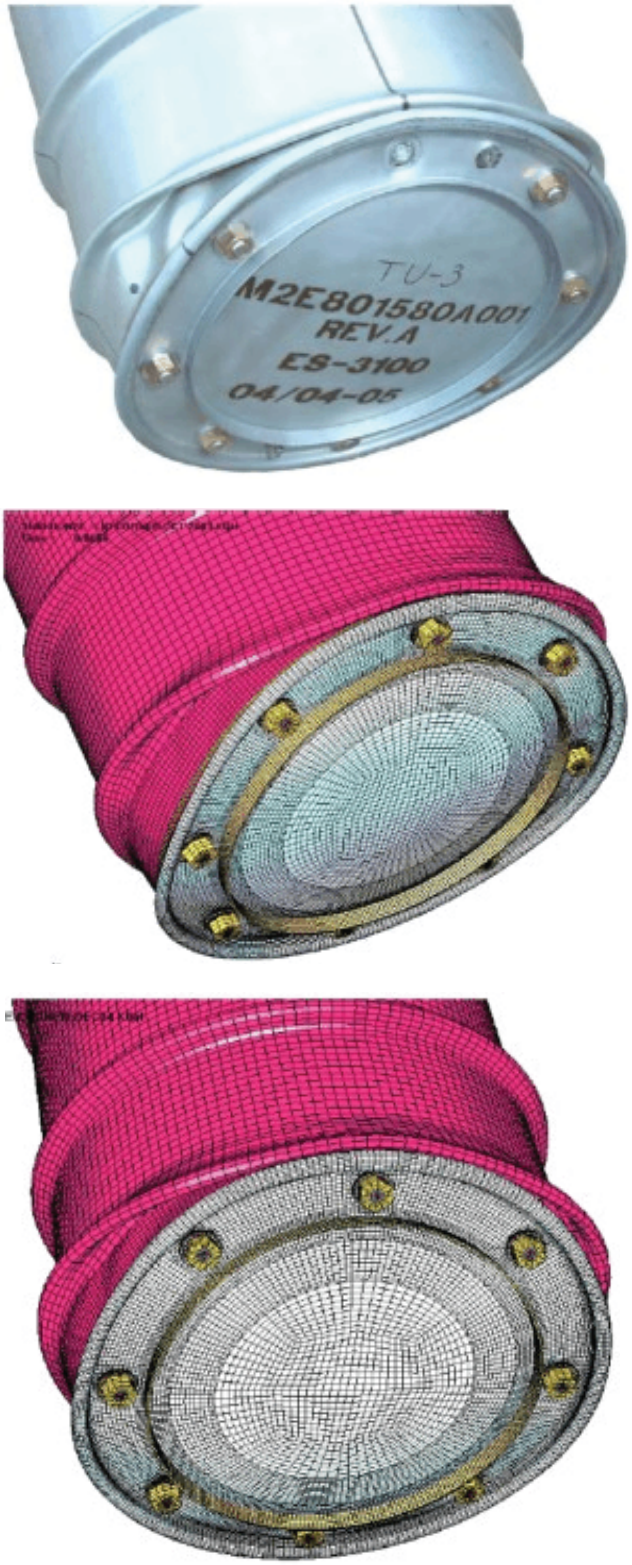

Fig. 2.29. Visual comparison of the cumulative lid damage after the three drop tests (from top to bottom: Test Unit-3, analytical results with BoroBond, analytical results with Cat 277-4).

Table 2.59. Cumulative analytical corner drop test maximum effective plastic strain results

Component	Component material	Effective plastic strain (in./in.)	
		Model with BoroBond	Model with Cat 277-4
CV body	Type 304L stainless steel	0.0364	0.0371
CV lid	Type 304L stainless steel	0.0024	0.0051
CV closure nut	A-479 nitronic 60	0.0000	0.0002
Angle	Type 304 stainless steel	0.0464	0.0462
Drum	Type 304 stainless steel	0.3787	0.3830
Drum bottom	Type 304 stainless steel	0.0731	0.0761
Liner	Type 304 stainless steel	0.5507	0.5254
Lid	Type 304 stainless steel	0.3579	0.3622
Lid stiffener	Type 304 stainless steel	0.0272	0.0272
Drum studs	Type 304 stainless steel	0.5578	0.5598
Drum hex nut	Silicon bronze - C65100	0.2258	0.2266
Drum washer	300 series stainless steel	0.1111	0.1528
Top plug weldment	Type 304 stainless steel	0.1170	0.1166

Table 2.60. Diametrical damage comparison of Test Unit-4 with analytical predictions [Diameter (in.)]

Axial measurement location	0 to 180°			90 to 270°		
	Test results	Analytical results with BoroBond	Analytical results with Cat 277-4	Test results	Analytical results with BoroBond	Analytical results with Cat 277-4
Top false wire	19.25	19.3	19.3	19.38	19.3	19.3
Top rolling hoop	20.00	20.2	20.1	20.13	20.2	20.1
CG & top rolling hoop	20.00	20.2	20.2	20.06	20.2	20.2
CG rolling hoop	19.44	20.1	20.1	19.5	20.1	20.1
Bottom rolling hoop	19.94	20.5	20.5	20	20.5	20.5
Bottom false wire	19.25	19.4	19.4	19.25	19.4	19.4

Fig. 2.30. Visual comparison of the cumulative damage after the three drop tests (from left to right: Test Unit-4, analytical results with BoroBond, analytical results with Cat 277-4).

Table 2.61. Cumulative analytical top drop test maximum effective plastic strain results

Component	Component material	Effective plastic strain (in./in.)	
		Model with BoroBond	Model with Cat 277-4
CV body	Type 304L stainless steel	0.0053	0.0083
CV lid	Type 304L stainless steel	0.0034	0.0072
CV closure nut	A-479 nitronic 60	0.0000	0.0011
Angle	Type 304 stainless steel	0.0304	0.0308
Drum	Type 304 stainless steel	0.1258	0.1237
Drum bottom	Type 304 stainless steel	0.0312	0.0267
Liner	Type 304 stainless steel	0.3585	0.3812
Lid	Type 304 stainless steel	0.1415	0.1389
Lid stiffener	Type 304 stainless steel	0.0098	0.0100
Drum studs	Type 304 stainless steel	0.1541	0.1535
Drum hex nuts	Silicon bronze - C65100	0.0170	0.0173
Drum washer	300 series stainless steel	0.0510	0.0506
Top plug weldment	Type 304 stainless steel	0.0944	0.0960

Table 2.62. ES-3100 test package weights before and after 10 CFR 71.73(c)(4) HAC thermal testing

Test Unit	Pre-test [a] weight kg (lb)	Post-test [a] weight kg (lb)	Thermal test weight loss kg (lb)	BoroBond4 original weight [b] kg (lb)	Water weight in BoroBond4[c] kg (lb)	Water loss percent [d] (%)
1	202.3 (446)	202.3 (446)	0.0 (0)	20.7 (45.64)	4.91 (10.82)	0.00
2	202.8 (447)	202.8 (447)	0.0 (0)	20.5 (45.19)	4.86 (10.72)	0
3	203.7 (449)	203.2 (448)	0.45 (1)	20.5 (45.19)	4.87 (10.74)	9.31
4	201.8 (445)	201.4 (444)	0.45 (1)	20.4 (44.97)	4.84 (10.66)	9.38
5	157.4 (347)	156.9 (346)	0.45 (1)	20.6 (45.42)	4.89 (10.77)	9.29

[a] Data from the test report. (Appendix 2.10.7)
[b] Weight of BoroBond4 and water obtained from casting data. (ES-3100 Weldments)
[c] This weight is based on TGA measurements and calculation showing that the minimum water percent is 23.71%.
[d] All weight loss attributed to loss of water in BoroBond4.

Following the thermal test, all five containment boundaries were subjected to leak testing of the O-ring cavity as well as the full-body helium leak check. To verify the entire containment boundary, all test units were drilled and tapped for a helium leak check using the procedure documented in the test report. (Appendix 2.10.7) The procedure consisted of creating a near vacuum inside the containment vessel and supplying a helium environment around the exterior of the assembly. The maximum recorded helium leak rate for any of these containment vessels was 2.0×10^{-7} cm^3/s as documented after 20 min of leak checking. This procedure measures leakage in the opposite direction to leakage from the vessel. It could be postulated that the additional pressure differential (ambient on the exterior and a near vacuum inside) would help to further compress the O-rings during this test. However, since the containment vessel closure nut is screwed down, the additional pressure does not compress the O-ring more than a few ten thousands of an inch based on mismatch between the internal and external threaded joint. Only rotation of the closure nut will alter O-ring compression significantly. Pictures taken of all containment vessel tops following testing showed that the closure nut had rotated a maximum of 0.15 cm (0.060 in.) [Fig. 2.31] from its original radial position obtained during assembly (Fig. 2.32) except for Test Unit-4, which showed no rotation. Based on the pitch of the closure nut, this rotation translates into only 0.0009 cm (0.00035 in.) decompression of the O-rings. This compares to the original nominal compression of 0.064 cm (0.025 in.). According to the *Parker O-Ring Handbook*, the minimum squeeze for all seals, regardless of cross section should be about 0.018 cm (0.007 in.). Using the nominal compression of 0.064 cm (0.025 in.) and subtracting the decompression from rotation and the minimal pressure differential compression, there is ample O-ring compression. Therefore, the leak test in either direction for this containment vessel arrangement is valid. As required in 10 CFR 71.73(c)(5), the containment vessels were submerged under a 0.9-m (3-ft) head of water following the leakage tests, with no water in-leakage permitted. Following this immersion test, the containment vessels were opened. The lid assembly, with the O-rings in place on the body, are joined together by torquing the closure nut and sealing lid assembly to 162.7 ± 6.8 N·m (120 ± 5 ft-lb). The lowest break-loose torque value of 40.7 N·m (30 ft-lb) was recorded for Test Unit-4. Visual inspection following the testing indicated that neither the vessel bodies, the O-rings, the seal areas, nor the vessel lid assemblies were damaged during the tests. In Test Unit-5, the convenience cans had buckled from the pressure differential caused during the leak testing operation. However, the containment vessel wall showed little or no signs of impact. Therefore, based on the success of these six test units (including the containment vessel of Test Unit-6) and the analytical drop simulation effort, the structural integrity of the ES-3100 package, with the previously mentioned modifications, meets all the applicable requirements of 10 CFR 71.73 for transport of the proposed contents.

Fig. 2.31. Containment vessel markings at assembly (swivel hoist ring removed prior to testing).

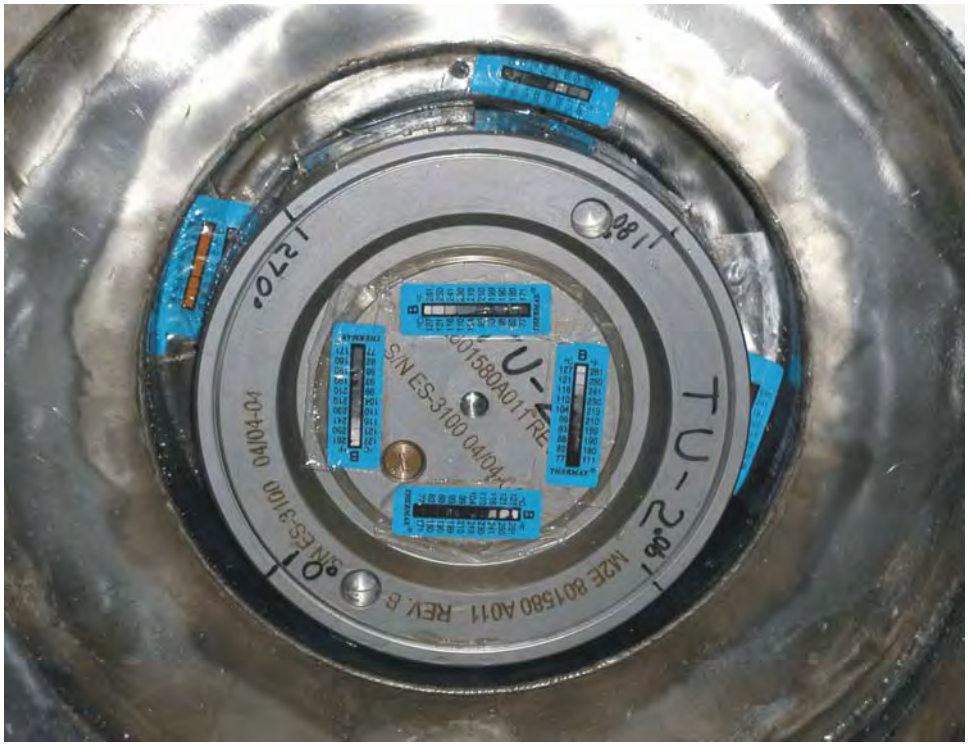

Fig. 2.32. Containment vessel marking after compliance testing.

2.8 ACCIDENT CONDITIONS FOR AIR TRANSPORT OF PLUTONIUM

The proposed contents are not shipped by air; therefore, this section is not applicable.

2.9 ACCIDENT CONDITIONS FOR FISSILE MATERIAL PACKAGES FOR AIR TRANSPORT

The expanded tests specified in 10 CFR 71.55(f)(1), (2), or (3) for fissile material package designs for air transportation were not conducted. The issue of subcriticality is addressed in Section 6 with content mass limits as addressed in Section 1.2.3 for air transport.

2.9a SPECIAL FORM

The package does not include any special form of radioactive material. Hence, the requirements of 10 CFR 71.75 and 71.77 are not applicable.

2.9b FUEL RODS

The contents do not utilize cladding for the containment of radioactive materials. Therefore, this requirement is not applicable.

2.10 APPENDICES

Appendix	Description
2.10.1	ES-3100 CONTAINMENT VESSEL ASME CODE EVALUATION (DAC-EA-900000-A006 and DAC-EA-900000-A007)
2.10.2	IMPACT ANALYSES OF ES-3100 DESIGN CONCEPTS USING BOROBOND AND CAT 277-4 NEUTRON ABSORBERS
2.10.3	KAOLITE PROPERTIES
2.10.4	CATALOG 277-4 PROPERTIES
2.10.5	BOROBOND4 PROPERTIES
2.10.6	RECOMMENDED RANDOM VIBRATION AND SHOCK TEST SPECIFICATIONS FOR CARGO TRANSPORTED ON SST AND SGT TRAILERS
2.10.7	TEST REPORT OF THE ES-3100 PACKAGE; VOL 1 - MAIN REPORT, ORNL/NTRC-013/V1; SEPT. 10, 2004
2.10.8	THE ES-3100 TEST REPORT; VOL. 3, APPENDIX K - TU-4 DATA SHEETS
2.10.9	PACKAGING MATERIALS OUTGASSING STUDY FINAL REPORT

THIS PAGE INTENTIONALLY LEFT BLANK.

Appendix 2.10.1

ES-3100 CONTAINMENT VESSEL ASME CODE EVALUATION (DAC-EA-900000-A006 and DAC-EA-900000-A007)

THIS PAGE INTENTIONALLY LEFT BLANK.

GENERAL DESIGN AND COMPUTATION SHEET

JOB ASME Code Subsection NB Stress Analysis of ES-3100 Containment Vessel		DATE 14 December 2006	SHEET 1 of 26
DAC NO. DAC-EA-900000-A006	REVISION NO. 2	COMPUTED C. R. Hammond	CHECKED BY R. M. Jessee

TABLE OF CONTENTS

OBJECTIVE…… 2

EVALUATION INPUT (CRITERIA) AND SOURCE…… 2

REFERENCES USED …… 2

ASSUMPTIONS MADE …… 3

IDENTIFICATION OF COMPUTER CALCULATION …… 3

METHODS TO BE USED…… 3

ANALYSES AND/OR CALCULATIONS ……...…… 3

DESIGN CONDITIONS…… 3

ALLOWABLE STRESS INTENSITIES …… 4

NB-3133 COMPONENTS UNDER EXTERNAL PRESSURE …… 4

NB-3200 DESIGN BY ANALYSIS …… 5

NB-3230 STRESS LIMITS FOR BOLTS ……... 9

CONCLUSIONS ……..……10

ATTACHMENT A – O-RING SPRING CONSTANT……22

ATTACHMENT B –RESULTS FOR O-RING ELEMENTS FROM FINITE ELEMENT ANALYSIS OF CONTAINMENT VESSEL……23

ATTACHMENT C – O-RING INTERFACE LOADS……25

ATTACHMENT D – INTERFACE LOADS ON NUT ……26

DESIGN PROCESS CHECKLIST

OBJECTIVE

The design for the ES-3100 Containment Vessel is evaluated for compliance with ASME Code, Section III structural design rules using bounding loads taken from the U. S. Code of Federal Register and International Atomic Energy Agency Requirements.

EVALUATION INPUT (CRITERIA) AND SOURCE

REFERENCES USED

BWXT Y-12 drawings (Project: ES-3100 Shipping Package, all dated 10/29/03):

M2E801580A011, Rev. C, "Containment Vessel Assembly"

M2E801580A012, Rev. C, "Containment Vessel Body Assembly"

M2E801580A013, Rev. B, "Containment Vessel O-ring Details"

M2E801580A014, Rev. B, "Containment Vessel Lid Assembly"

M2E801580A015, Rev. C, "Containment Vessel Sealing Lid"

M2E801580A016, Rev. B, "Containment Vessel Closure Nut"

Texts

(B1.1) *Unified Inch Screw Threads*, ASME B1.1-1989, The American Society of Mechanical Engineers, 1989.

(B1.9) *Buttress Inch Screw Threads*, ANSI B1.9 – 1973, The American Society of Mechanical Engineers, 1973.

(CFR) *Packaging and Transportation of Radioactive Material*, 10CFR71, Code of Federal Regulations, the Nuclear Regulatory Commission, 2004.

(Code) *Class 1 Components, Section III, Rules for Construction of Nuclear Power Plant Components*, Division 1, 2001 Edition with 2003 Addenda, The American Society of Mechanical Engineers, 2003.

(IAEA) *Regulations for the Safe Transport of Radioactive Material, Requirements*, 1996 Edition (Revised), No. TS-R-1 (ST-1, Revised), International Atomic Energy Agency, 2000.

(Parker) *Parker O-Ring Handbook*, 2001 Edition, Catalog ORD 5700A/US, Parker Seals, 2001.

(Roark) R. J. Roark and W. C. Young, *Formulas for Stress and Strain*, 5th Ed., McGraw-Hill Book Company, 1975, p. 363.

(Section II) *Section II, Materials*, Part D – Properties, 2001 Edition with 2003 Addenda, The American Society of Mechanical Engineers, 2003.

ASSUMPTIONS MADE

Calculations are based on geometry and specifications from referenced drawings.

Results are rounded to significant figures although more digits may be retained in intermediate calculations.

IDENTIFICATION OF COMPUTER CALCULATION

Computer Type: Dell PC x86 Family processor Family 6 Model 8 Stepping 1 using the Microsoft Windows 2000 operating system level 5.00.2195 with Service Pack 4.

Computer Program Name, Revision, Verification, Applicability: Programs used were Algor (R) Linear Static Stress Version 12.26-WIN 28-OCT-2002, ALG.DLL VERSION:13180000 and FEMPRO Version 13.26-WIN 22-NOV-2002. Verification was by running example programs with known solutions on the same computer used for final calculations. The expected results were produced exactly. Hand calculations are used here to confirm results. The program is applicable to linear elastic solutions for bodies of revolution as needed here.

METHODS TO BE USED

The Finite Element Method is used to determine the response of the CV components to internal pressure and gasket seating loads. External pressure resistance of the cylindrical shell is evaluated following Code rules. The finite element results also serve to demonstrate the external pressure resistance of the lid and bottom of the CV. Buttress threads used to restrain the lid are evaluated by a method derived from an accepted way of determining the strength of standard threads.

ANALYSES AND/OR CALCULATIONS

DESIGN CONDITIONS

Internal Pressure: 101.5 psig at 300 F. per IAEA.

External Pressure: 21.7 psig at 300 F. per 10CFR71.73.

ALLOWABLE STRESS INTENSITIES

From Section II.

PART	SPECIFICATION	ALLOWABLESTRESS INTENSITY, PSI
Containment vessel	ASME SA-182, Type F304L forging or bar (<5 in. thick)	12,800 @ 300 F.*
Containment lid	ASME SA-479, 304 bar	12,800 @ 300 F.*
Closure nut	ASME SA-479, UNS-S21800 bar	22,100 @ 300 F.

* The lower of two allowable values was chosen to limit deflection of the flange.

NB-3133 COMPONENTS UNDER EXTERNAL PRESSURE

The design internal pressure is higher than the external pressure across the bottom of the vessel and the lid. Since stability or buckling was not an issue, these flat heads were evaluated for resistance to internal pressure only. They can resist the external pressure by linearity.

NB-3133.3 Cylindrical Shells and Tubular Products

Data: Outside diameter of cylindrical shell, D_o = 5.04” + 2(0.100”) = 5.24”

Shell thickness, T = 0.100”

Total length, L = 32.40” – (0.25”)/2 – 1.10” = 31.18”

$D_o/T = 52.4$

$L/D_o = 5.95$

From ASME Section II, Fig. G, A = 0.00053

From ASME Section II, Fig. HA-3, conservatively using the 400 F. curve, B(400 F.) = 4900.

The maximum acceptable external pressure in this case is $P_a = 4B/3(D_o/T)$ = 125 psig.

This allowable value exceeds the design external pressure and the shell is acceptable.

NB-3133.6 Cylinders Under Axial Compression

Data: Inside radius, R = 5.04”/2 = 2.52”

$A = 0.125/(R/T) = 0.0050$

From ASME Section II, Fig. HA-3, conservatively using the 400 F. curve, B(400 F.) = 7100.

This is the maximum acceptable compressive stress limited by axial buckling. The maximum external pressure applied to the axial cross section of the cylinder at 400 F. can be derived using nominal values from:

$$7100\ psi = \frac{p_e \frac{\pi}{4}(5.24\,in.)^2}{\frac{\pi}{4}\left[(5.24\,in.)^2 - (5.04\,in.)^2\right]}$$

p_e = 532 psi. This is less than the design external pressure and the shell is still acceptable.

NB-3200 DESIGN BY ANALYSIS

Individual axisymmetric finite element models were constructed of the CV body, the lid, and the closure nut and identified es5100, es3100lid, and es3100nut, respectively. Two loading conditions were applied to each model per Section III requirements: internal pressure and gasket seating. Load Case 1 is internal pressure including gasket load and Load Case 2 is gasket load alone.

The material properties at 300 F. obtained from Section II are as follows:

MATERIAL	MODULUS OF ELASTICITY	POISSON'S RATIO*
304 or 304L stainless steel	27,000,000 psi	0.3
UNS-S21800 stainless steel	27,000,000 psi**	0.3

* Typical values. Stress distributions are not sensitive to Poisson's ratios near 0.3 .

** Not in Tables. Based on principal constituents same as 304 stainless (18% Cr, 8% Ni).

Gasket load

Two concentric O-rings are specified to provide a redundant and testable seal. Per normal ASME practice, the O-ring grooves were not included in the finite element model. Elements reasonably close to the actual O-ring locations were chosen and elements representing the O-rings were added to the model of the CV. The gasket force was applied by displacing the top surface by 0.139 in. – 0.114 in. = 0.025 in. This way a reduction in gasket load will be caused by deformation of the CV from application of pressure.

Each O-ring has a 0.139 inch cross section diameter and is specified to have a 70 +/- 5 Shore A durometer reading. The O-ring manufacturer's catalog (Parker, P. 2-15) gives ranges of distributed force required to compress O-rings. The O-ring grooves cut into the flange surface are specified to be 0.114 inch deep. The lid is expected to be pressed down so contact is metal-to-metal. Then the O-rings will be compressed

$$\frac{0.025\,in.}{0.139\,in.} \times 100\ ^\circ/_\circ = 18.0\ ^\circ/_\circ$$

This is equivalent to a strain of 0.18 in./in.

Attachment A shows the effective distributed compression force for different amounts of compression based on values of distributed force averaged between high and low values for the highest allowed durometer reading, 75. The distributed force for 18% compression was about 20 lb/in. The stress-strain relationship for a thin annular shell t thick of average radius r loaded axially by the force F=20 lb/in(2πr) and an elastic modulus E is approximately

$$\frac{20\,lb/in\,(2\pi r)}{2\pi r t} = E\,\varepsilon = E\,(0.18\,in/in)\,.\ \text{So}$$

$$E = \frac{20\,lb/in}{0.18\,t}\,.$$

For the outer O-ring, the thickness is 3.04584 in. – 2.96172 in. and E_o = 1321 psi. For the inner O-ring, the thickness is 2.817 in. – 2.718 in. and E_i = 1122 psi.

These moduli were applied to the respective O-ring elements in the CV model.

Pressure was applied over the inner surface of the CV model up to the outer edge of the inner O-ring groove per Code rules. Two nodal forces had to be applied at the inner corner of the flange area since the program could not apply pressure to two faces of one element. The pressure and gasket seating forces were resisted by stiff elastic boundary elements canted 7 degrees out from the axis of symmetry to simulate the effect of the 7 degree surface on the threads to meet Code rules to consider radial forces and resulting hoop stress at the threads.

Results from the O-ring elements and the boundary element restraint are collected in Attachment B. The local 2-axes of the O-ring elements are parallel to the CV axis of symmetry, the global Z-axis. The values from load case 2 are -237.1 psi for the first set of elements representing the outer O-ring and -201.3 psi for the inner O-ring. These stresses were achieved by applying a displacement of 0.025 inches. The equivalent distributed loads in the O-ring elements are -237.1 psi (3.04584 in. – 2.96172 in.) = -19.94 lb/in. and -201.3 psi (2.817 in. – 2.718 in.) = -19.93 lb/in. which are within 1% of the target, 20 lb/in.

The gasket reaction forces and internal pressure were applied to a model of the lid. The nodal forces are shown in Attachment C. The lid was restrained by a portion of the surface under the nut. The contact area was moved radially inward until there was no tension developed during Load Case 1. The dimensions of the contact area may not be exact but the Code requirement to maintain equilibrium of forces and moments is met. One of the contact nodes for Load Case 2 was in tension but equilibrium of force and moment were still maintained by the force distribution applied to the model of the nut. Also Load Case 2 produces such low stresses that optimizing the model for it is unnecessary.

The interface forces were applied to a model of the nut. The force magnitude and moment of the distributed forces was maintained using small added nodal forces as shown in Attachment D.

The distribution of stress intensity is shown on Figs. 1 – 10. Stress intensities are very low relative to the basic allowable stress for the material. Code compliance is trivial since the Code tests subdivide the computer results but the sum is less than the allowable for any of the subsets. By the numbers.

NB-3221.1 General Primary Membrane Stress Intensity

General primary membrane stress intensity is limited to the basic allowable stress intensity at temperature. That is 12,800 psi in the CV. The general primary membrane stress intensity is based on stresses averaged across the thickness of a section. The highest calculated stress intensities (called 2 times Tresca Stress by the program) were 7436 psi for Load Case 1 and 1203 psi for Load Case 2. Average stress is always less than peak stress so the CV is acceptable.

Fig. 4 is a close look at the cylindrical section. The stress intensity away from thickened sections appears to be less than 3000 psi. As a check the average elastic stresses in the middle of the cylindrical side of the vessel are easily calculated from equilibrium. Section III of the ASME Code provides values in Nonmandatory Appendix A. The tolerance on critical dimensions is ±0.01 in. and is taken into consideration to calculate maximum values of stress intensity.

A-2221 General Primary Membrane Stress Intensity

$$S = (p\,R/t) + (p/2) = 101.5\,psig\left(\frac{5.04\,in. + 0.01\,in.}{2\,(0.10\,in. - 0.01\,in.)}\right) + \frac{101.5\,psig}{2} = 2898\,psi.$$

A-2222 Maximum Value of Primary Plus Secondary Stress Intensity

$$S = 2\,pY^2/(Y^2 - 1) = \frac{2\,(101.5\,psig)\left(\dfrac{5.04\,in. + 0.01\,in.}{5.04\,in. + 0.01\,in. - 2\,(0.10\,in. - 0.01\,in.)}\right)^2}{\left(\dfrac{5.04\,in. + 0.01\,in.}{5.04\,in. + 0.01\,in. - 2\,(0.10\,in. - 0.01\,in.)}\right)^2 - 1} = 2899\,psi.$$

This confirms the computer solution for the cylindrical section.

There is a small radial membrane stress in the CV bottom but there is no need to calculate it since the sum of all order stresses is less than the allowable for the membrane stress.

The highest calculated stress intensity in the lid was 2398 psi for Load Case 1 and 872 psi for Load Case 2. The general primary membrane radial stress in the lid is zero from equilibrium so the highest average membrane stress is p/2 = 200 psi/2 = 100 psi. The allowable stress intensity is also 12,800 psi so the lid is acceptable.

NB-3221.2 Local Membrane Stress Intensity

Local membrane stress intensity is the average stress across the thickness of a cross section at the junction between the side and bottom of the CV. The allowable value of this stress component is 1.5 times the basic allowable stress. Figs. 4 and 5 show that the peak values of stress at this junction are below the basic allowable so the average must also be below the allowable and the CV is acceptable.

NB-3221.3 Primary Membrane plus Primary Bending Stress Intensity

Primary membrane plus primary bending stress intensity in the CV bottom and the lid.

Fig. 3 shows the stress intensity at the center of the CV bottom. The distribution is primarily due to bending and the peak value is less than 1.5 times the basic allowable stress intensity.

The stress in the bottom cover is complicated by attachment to the side but bending stress at the center can be checked by bounding stress by assuming both simple support and fixed support around the outside edge. From the Code Appendix:

A-5212 Radial bending stress at center (r = 0) and outside surface (x = t/2)

$$\sigma_r = p\frac{3(x)}{4t^3}\left[(3+\nu)(R^2-r^2)\right] = 101.5\ psig\ \frac{3(t/2)}{4t^3}\left[(3+0.3)\left(\frac{5.04\,in.}{2}\right)^2\right]$$

$$= 101.5\ psig\ \frac{3}{8(0.25\,in.)^2}\left[3.3(2.52\,in.)^2\right] = 12{,}762\ psi.$$

This equation is based on a simply supported outer edge. For a fixed edge, the stress at the same point using Roark (Table 24, Case 10b) is:

$$\sigma_r = p\frac{6}{16(0.25\,in.)^2}\left[(1+\nu)R^2\right] = 101.5\ psig\ \frac{3}{8(0.25\,in.)^2}\left[1.3(2.52\,in.)^2\right] = 5{,}028\ psi\ .$$

From Fig. 3 it is seen that the peak stress intensity at the center of the CV bottom is about 7,000 psi. This value is between the bending stresses for the simply supported and fixed edge cases as expected.

The pattern of stress intensity in the lid is also primarily bending of the relatively thin outboard edge with bearing under the restraining nut and some intensification at a fillet. The bending stress appears to be less than 300 psi which is far below the allowable.

<u>NB-3222.3 Expansion Stress Intensity</u>

Expansion stress intensity is undefined but can be bounded. The largest temperature range possible for the CV is between -40 F. which is the minimum temperature specified in 10CFR71 and 300 F. defined here. Suppose a tendril maintains a temperature of -14 F. while the surrounding material is heated to 300 F. The result is a 340 F. temperature difference across a sharp boundary – an infinite gradient. The stress in the tendril would be $\sigma = E\,\alpha_{(-40)-300}\ 340^\circ$. E is the cold modulus of elasticity – 28,800,000 psi by interpolation from Table TM-1 in Section II. The temperature at the midpoint of the range is 170 F. and the instantaneous α at that temperature is 9.1×10^{-6} in/in/º F. from Table TE-1 in Section II. The bounding expansion stress is 89,000 psi. This is a fictitious elastic stress per the Code. Add to this the highest stress from the CV and lid models multiplied by an intensification factor of 2 since the finite element program may extrapolate to the surface too simplistically. That is 89,000 psi + 2 (7436 psi) = 100,000 psi. The alternating stress is half this value or 50,000 psi. The allowable number of cycles for this stress per Fig. I-9.2.1 in Code Mandatory Appendix I is 30,000. The vessel should acceptable for a few hundred years although a severe transportation accident should be counted as two cycles, one for impact and one for fire.

NB-3230 STRESS LIMITS FOR BOLTS

NB-3232.1 Average Stress

Average stress across a bolt cross section has a different allowable value. Since the CV is threaded to retain the lid special consideration is given to the neck above the lid. Allowable stress on bolts per Appendix III, Article III-2000, of Section III is one-third of the minimum specified yield strength of the material. This is half of the basic allowable but the service stress may be twice the allowable so we are back to an allowable service stress of 12,800 psi. Fig. 5 shows that the peak stress intensity in the neck region is under 6000 psi and the average service stress is much less so the CV is acceptable.

NB-3232.2 Maximum Stress

Maximum service stress in a bolt including bending stress may be three times the basic allowable bolt stress and since the bending component is included in the calculated stress the CV is clearly acceptable.

NB-3227.2 Pure Shear

Pure shear across threads on CV and Closure Nut. These threads are 7.0 inch 8 threads per inch push buttress threads Class 2A fit per ANSI B1.9-1973. The 7 degree slope of the mating surface was accounted for in the finite element models. The threads were not modeled in detail and they are evaluated using a traditional method (B1.1). Internal threads are limiting because the allowable stress for the CV material is about half the allowable stress for the nut material. The appropriate shear area on internal threads is the cylindrical area at the tip of the external thread with minimum height. That is the area at the minimum major diameter of the external thread called *MIN* D_s in B1.9. *MIN* D_s is the nominal D_s, $D - G$, where D is the nominal diameter and G is the allowance for easy assembly minus the tolerance on D. The minimum width of the internal thread at this radius, say t_e, is a function of the theoretical sharp thread form, H, defined as $0.89064p$ where p is the thread pitch, the crest truncation, f ($=0.14532p$), and the sum of radial allowance and tolerances (the *gap*). The *gap* based on thread tolerances is half the tolerance on the pitch diameter and half the tolerance on the major diameter of the thread. The gap should also include any outward radial deformation of the threads. Fig. 11 shows that due to rotation of the flange, the threads in the CV actually move inward and do not increase the gap. In any case the calculated displacements are smaller than the thread tolerances. So, limited to thread properties

$$gap = \frac{PD\,tol}{2} + \frac{G}{2} + \frac{D\,tol}{2} = \frac{0.0101\,in.}{2} + \frac{0.0067}{2} + \frac{0.0101\,in.}{2} = 0.0134\,in.$$

$$\begin{aligned} t_e &= \left(0.89064\,p - 0.14532\,p - gap\right)\left(\tan(7^\circ) + \tan(45^\circ)\right) \\ &= \left((0.89064 - 0.14532)(0.125\,in.) - 0.0134\,in.\right)\left(1.1228\right) \\ &= 0.08956\,in. \end{aligned}$$

$$MIN\,D_s = 7\,in. - 0.0067 - 0.0101\,in. = 6.9832\,\text{in.}$$

Three threads are fully engaged so the shear area is at least

$$A_{s,i} = 3(0.08956\,in.)\pi(6.9832\,in.) = 5.894\,in^2.$$

The shear capacity given the Code limit on shear stress of 0.6 S_m is 0.6 (12,800 psi)(5.894 in.^{2}) = 45,300 lb.

The load due to pressure to the outer edge of the inner O-ring groove is

$$W_{m1} = \underline{\pi}\frac{101.5\,psi\,(5.624\,in.)^2}{4} = 2521\ lb.$$

The force due to gasket seating is

$$W_{m2} = 20\,lb./in.\pi\left[(5.359\,in. + 0.139\,in.) + (5.859\,in. + 0.139\,in.)\right] = 722.3\,lb.$$

The combined force is 3244 lb. This is much less than the shear capacity so the threads are acceptable for shear.

<u>NB-3232.3 Fatigue Analysis of Bolts</u>

Fatigue analysis of bolts is contained in Section 2 of the Safety Analysis Report for Packaging

CONCLUSIONS

The ES-3100 Containment Vessel meets ASME Code, Section III, requirements for structural design except for fatigue analysis of the threaded closure which was not evaluated. Fatigue analysis of the threaded closure is contained in Section 2 of the Safety Analysis Report for Packaging.

.

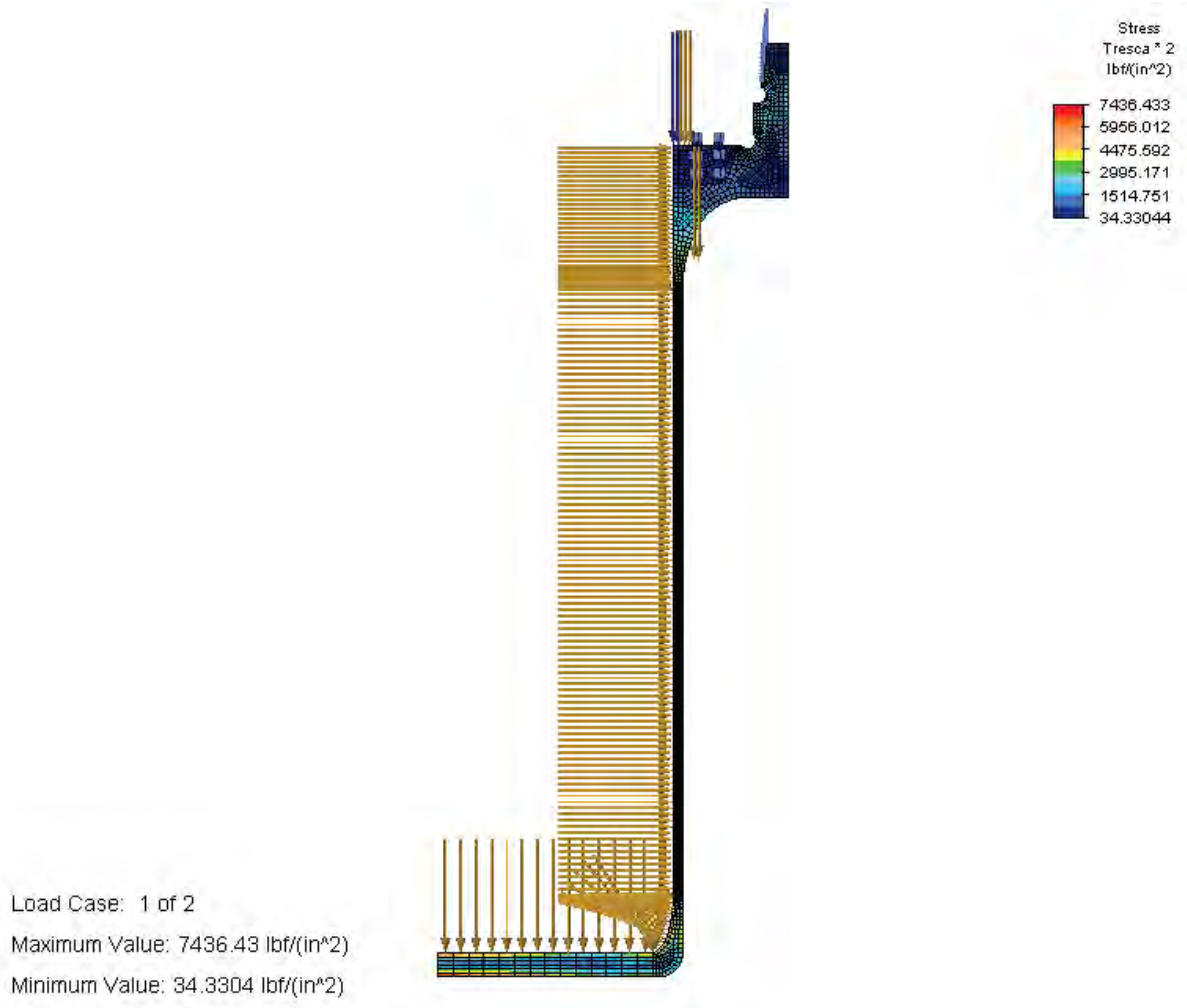

Fig. 1 – Stress Intensity in Containment Vessel due to Load Case 1

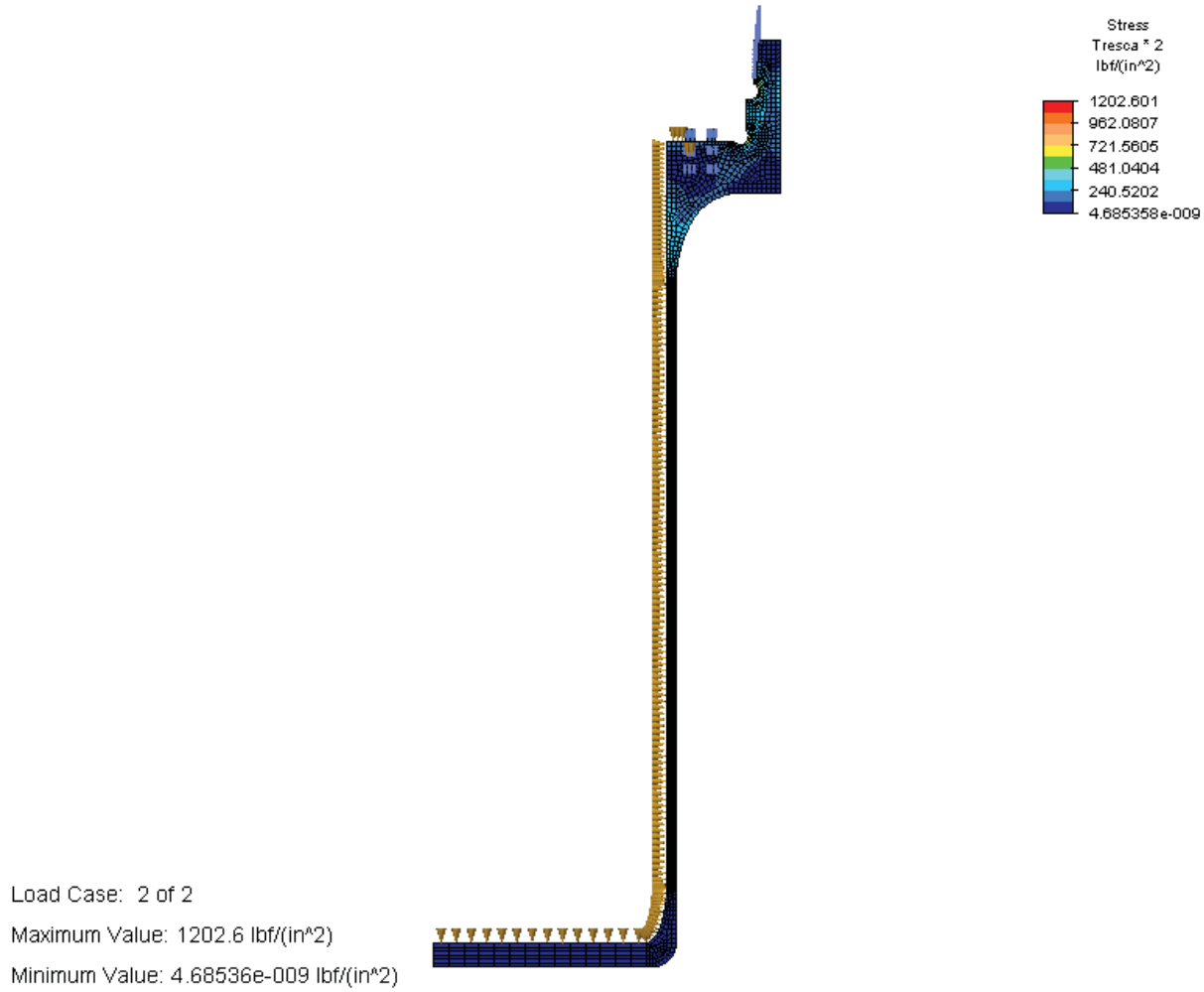

Fig. 2 – Stress Intensity in Containment Vessel due to Load Case 2

.

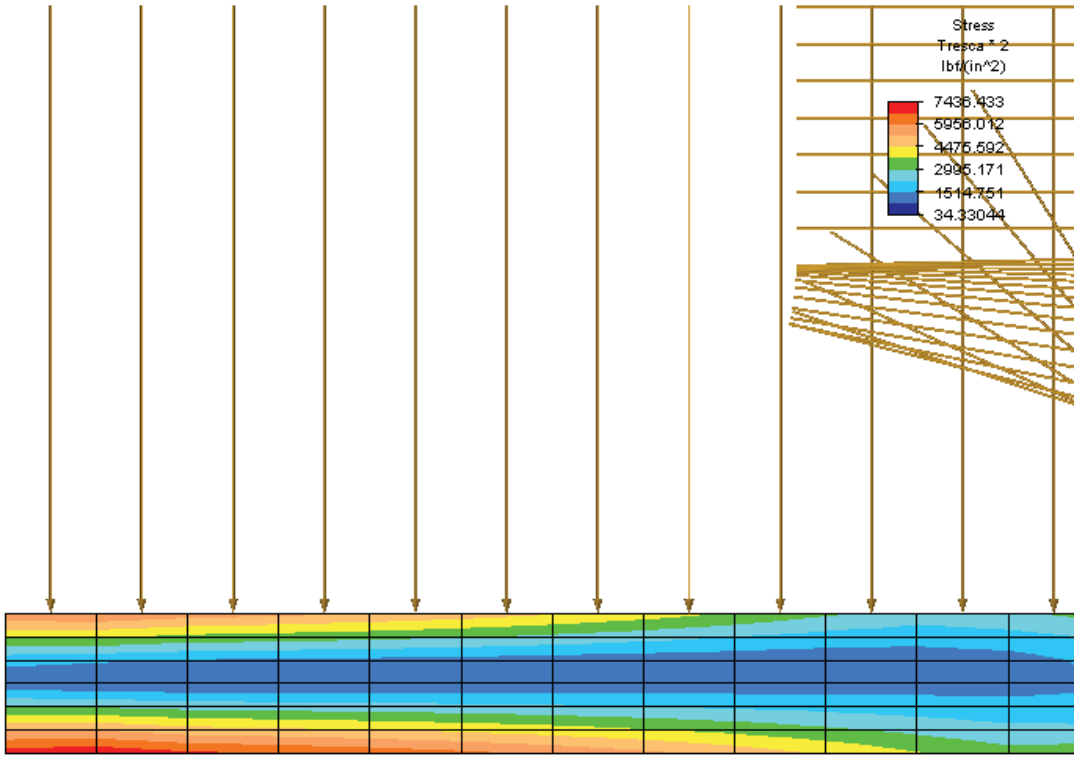

Load Case: 1 of 2

Maximum Value: 7436.43 lbf/(in^2)

Minimum Value: 34.3304 lbf/(in^2)

Fig. 3 – Stress Intensity in the Bottom of the Containment Vessel due to Load Case 1

.

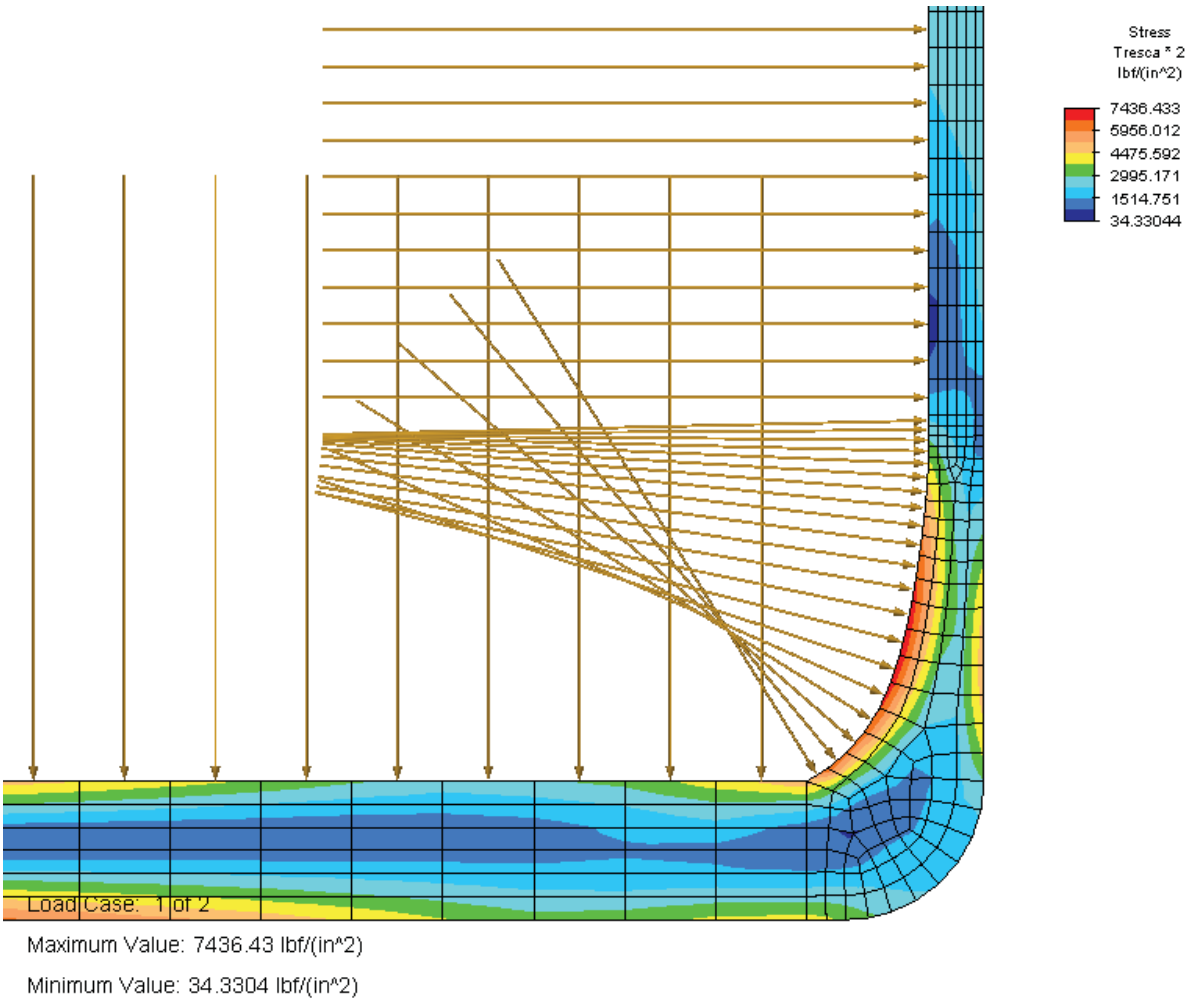

. **Fig. 4 – Stress Intensity at Junction of Bottom and Side of Containment Vessel due to Load Case 1**

.

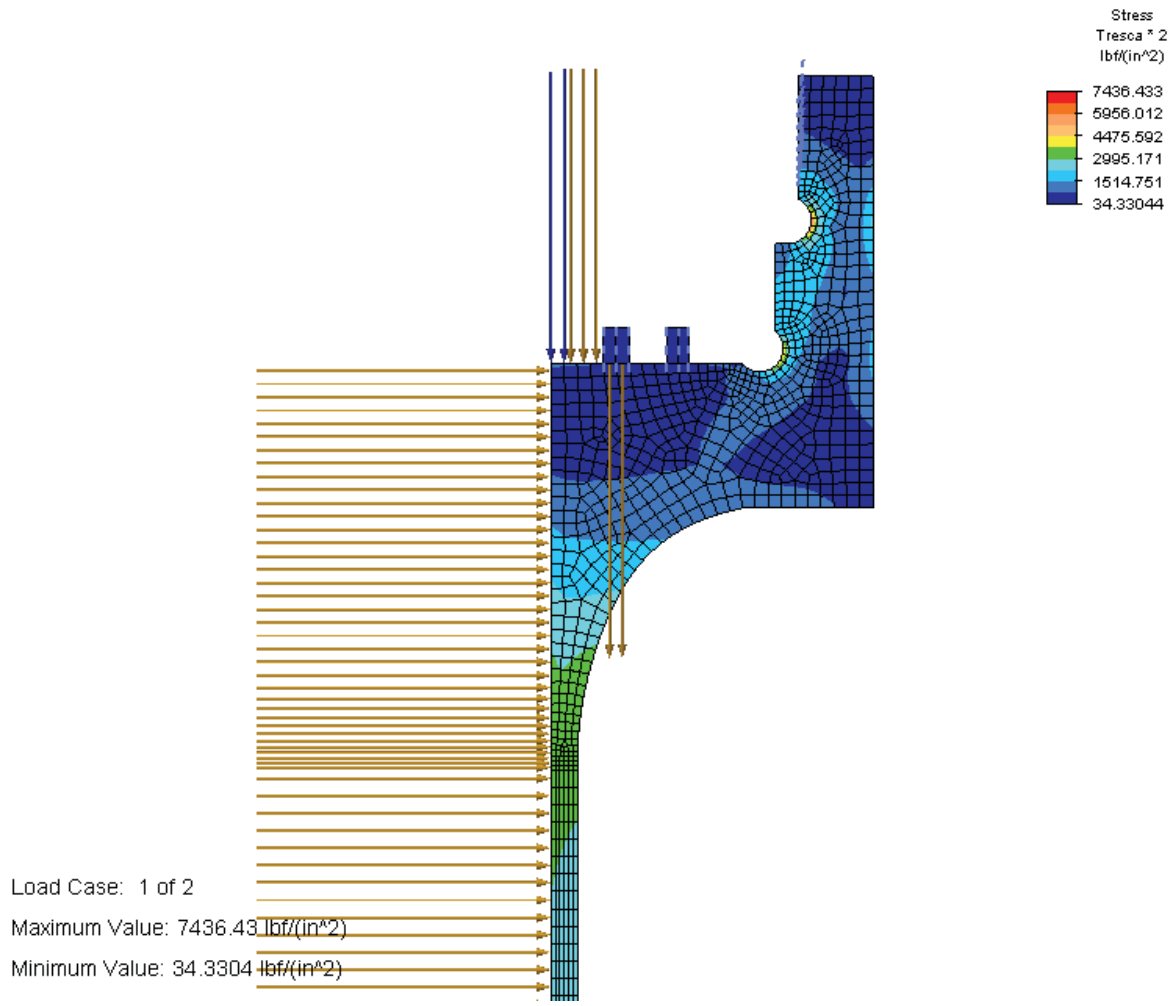

Fig. 5 – Stress Intensity in Flange Region of Containment Vessel due to Load Case 1

.

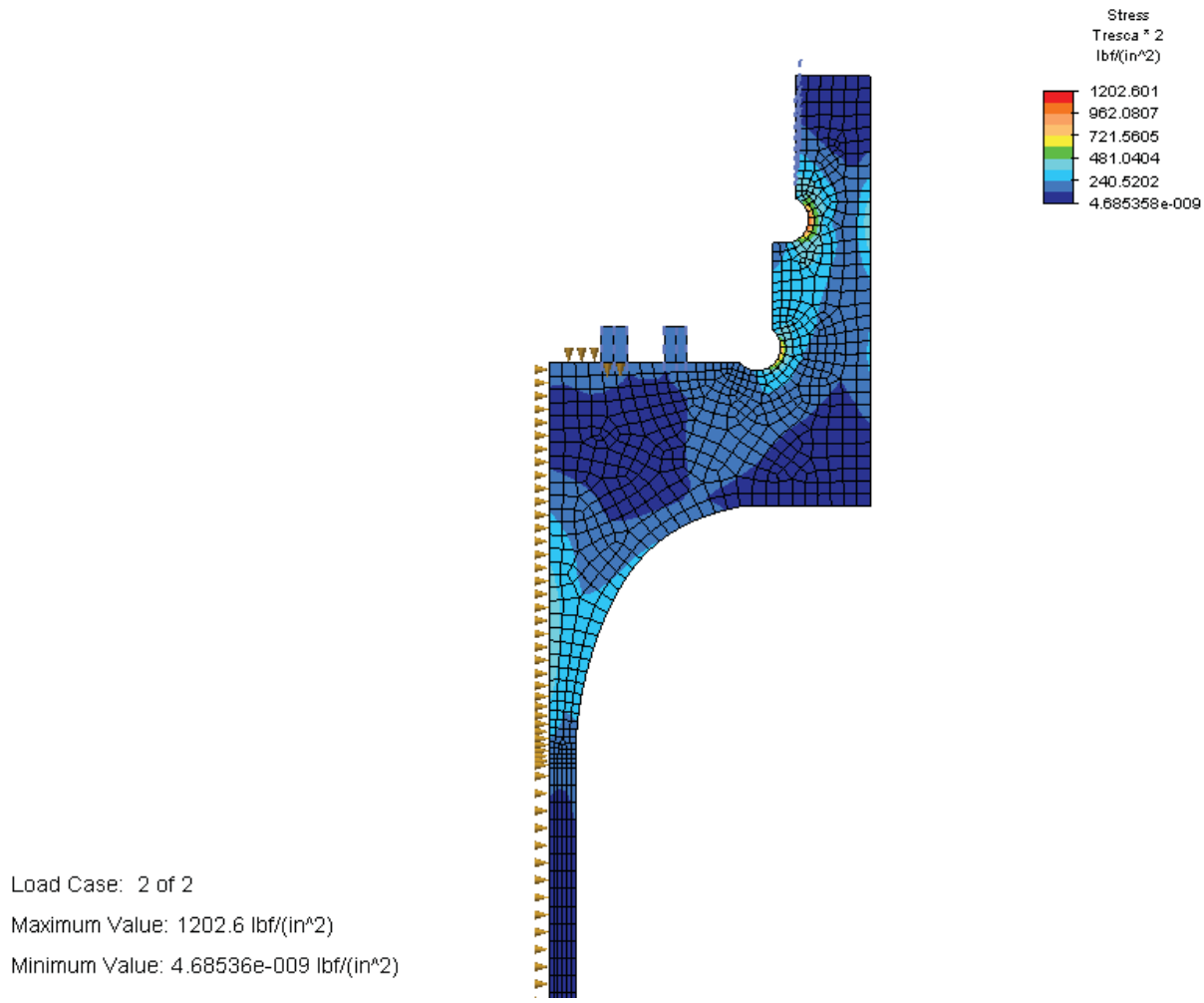

Fig. 6 – Stress Intensity in Flange Region of Containment Vessel due to Load Case 2

.

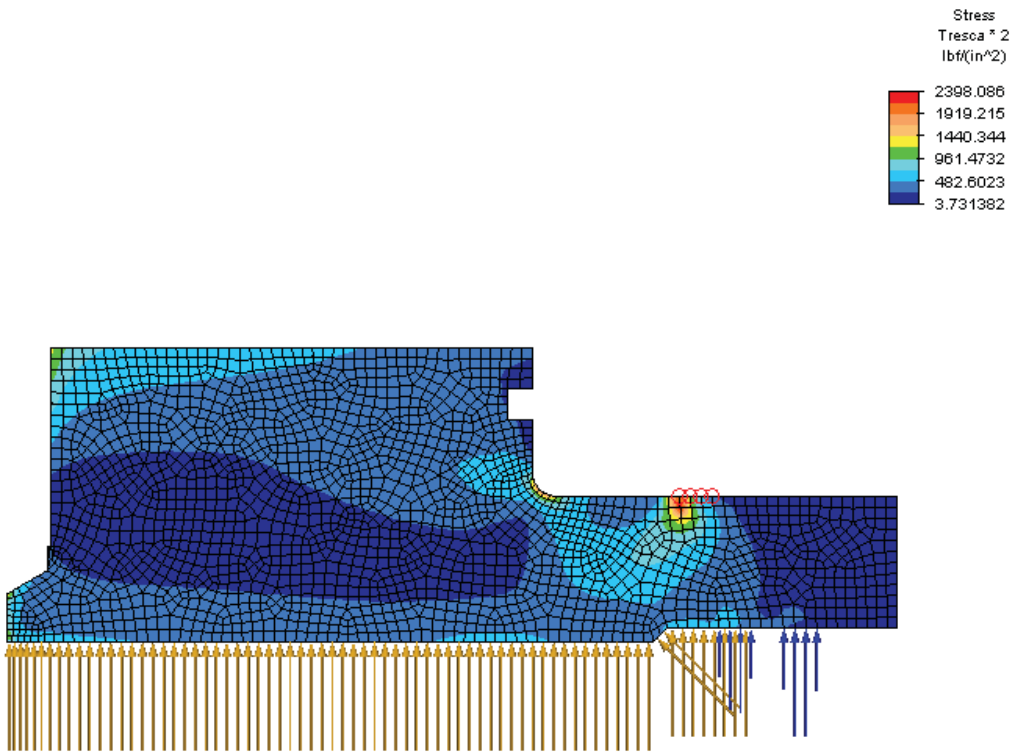

Load Case: 1 of 2

Maximum Value: 2398.09 lbf/(in^2)

Minimum Value: 3.73138 lbf/(in^2)

Fig. 7 – Stress Intensity in CV Lid due to Load Case 1

.

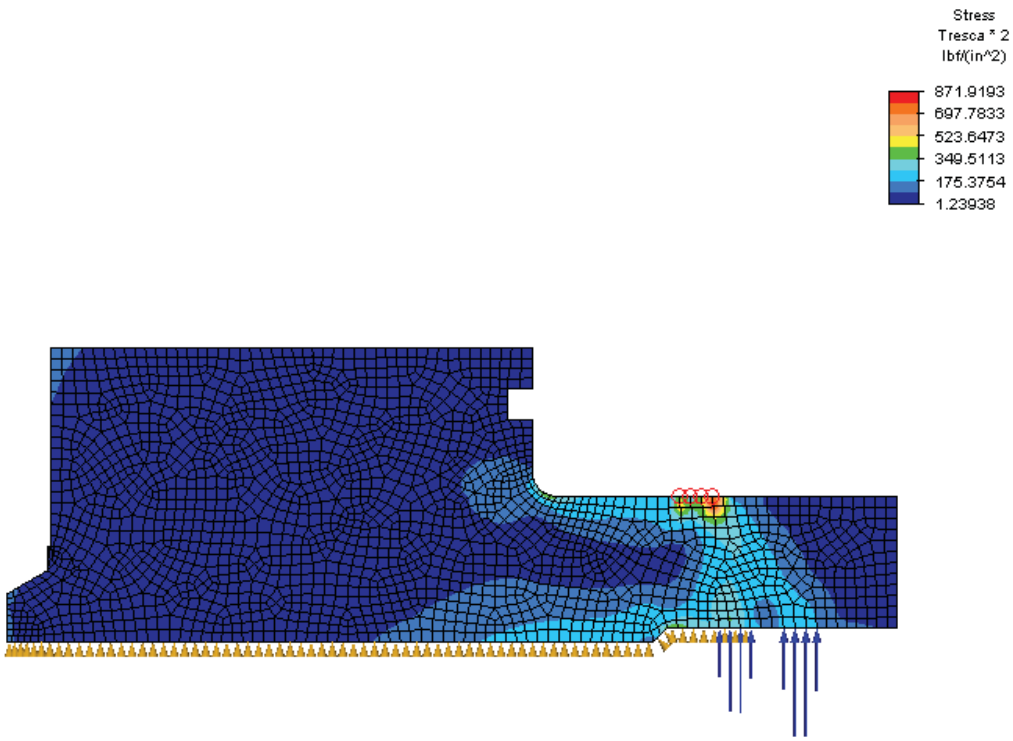

Load Case: 2 of 2

Maximum Value: 871.919 lbf/(in^2)

Minimum Value: 1.23938 lbf/(in^2)

Fig. 8 – Stress Intensity in CV Lid due to Load Case 2

.

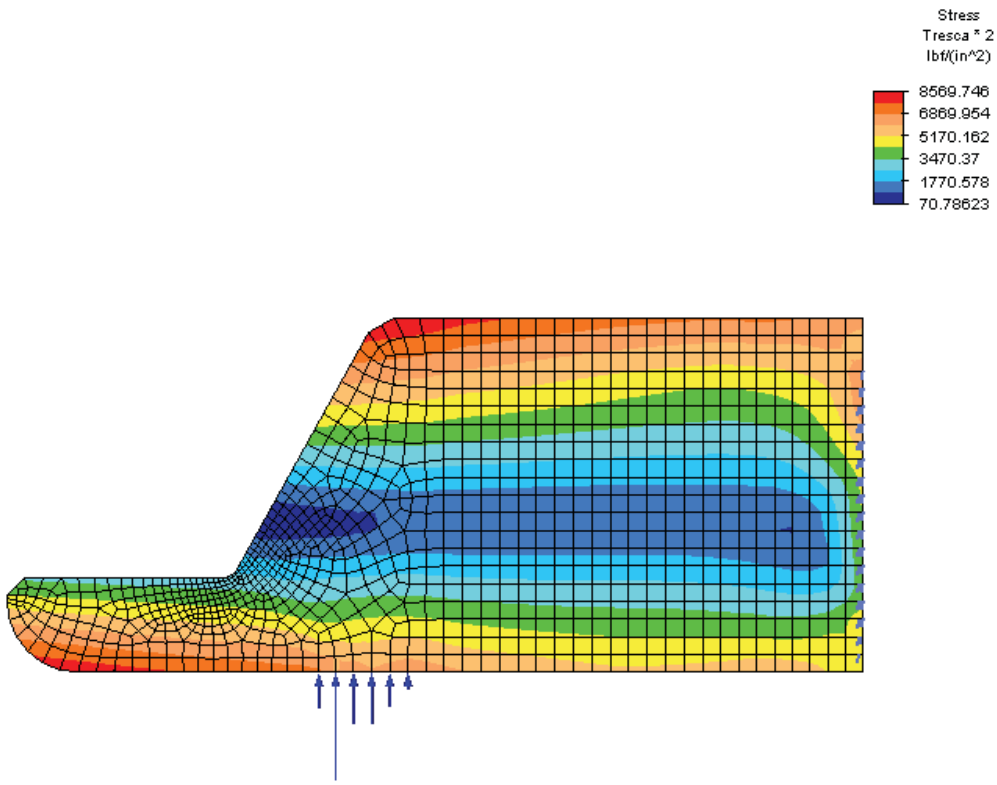

Load Case: 1 of 2

Maximum Value: 8569.75 lbf/(in^2)

Minimum Value: 70.7862 lbf/(in^2)

Fig. 9 – Stress Intensity in Nut due to Load Case 1

.

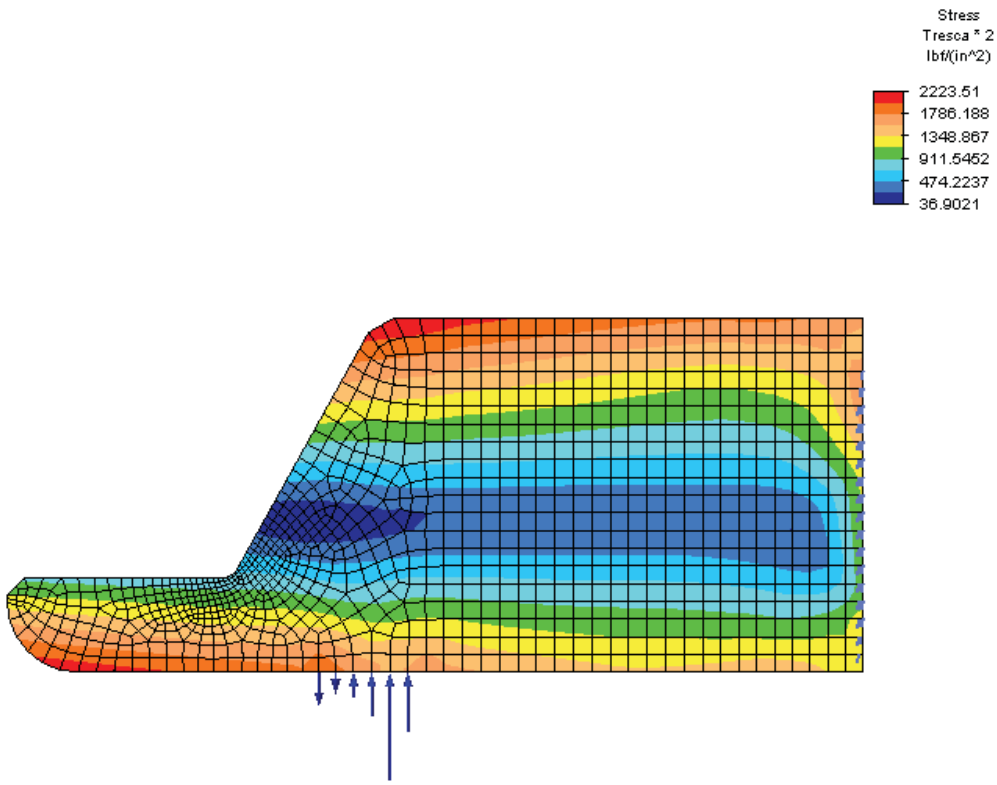

Load Case: 2 of 2

Maximum Value: 2223.51 lbf/(in^2)

Minimum Value: 36.9021 lbf/(in^2)

Fig. 10 – Stress Intensity in Nut due to Load Case 2

.

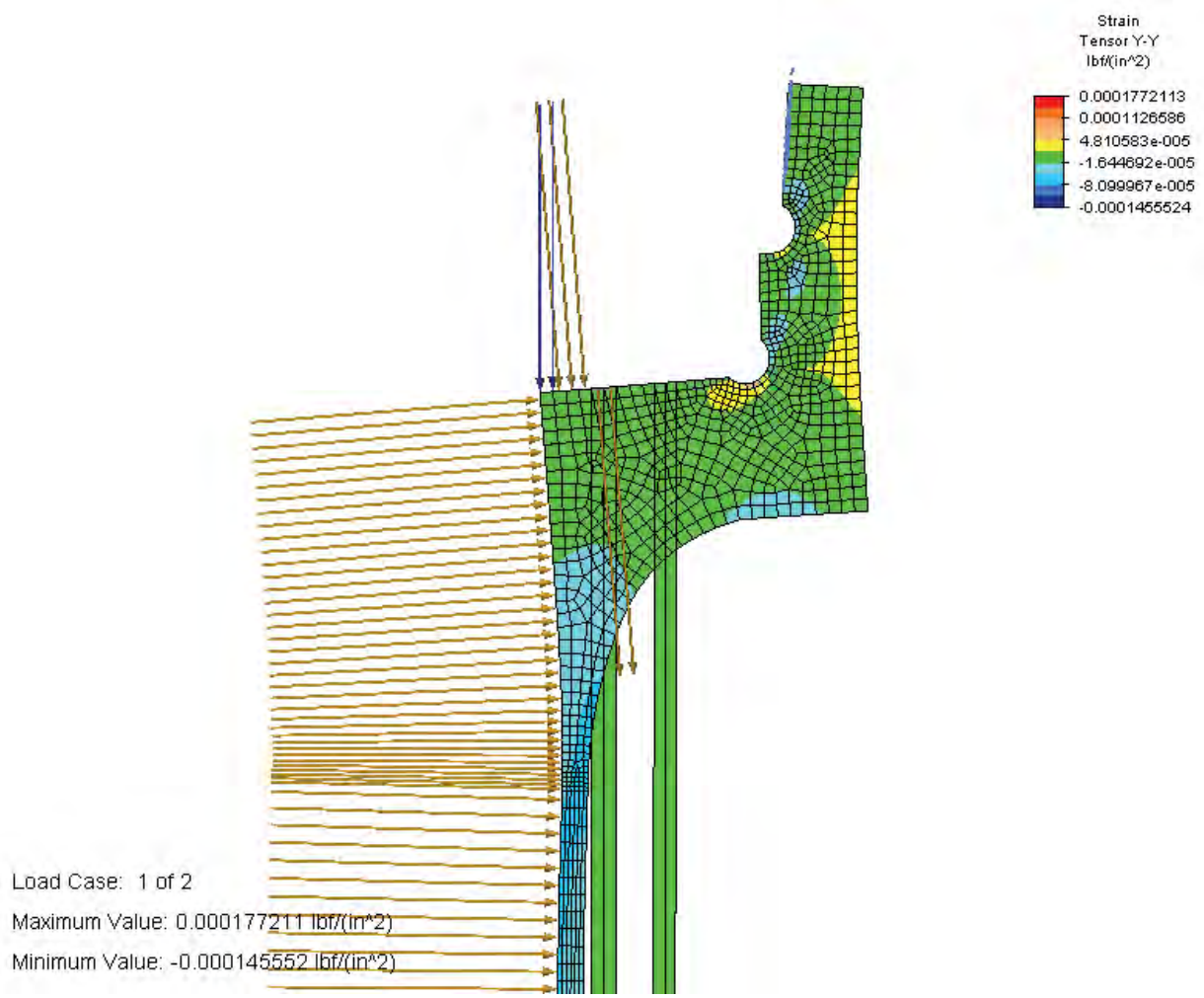

Fig. 11 – Radial Strain in the Flange Region of the Containment Vessel due to Load Case 1 (Distortion is Exaggerated)

ATTACHMENT A – O-RING SPRING CONSTANT

Compression of 0.139 in. dia. O-ring (Parker Seals, "O-Ring Handbook," ORD-5700A/US, 2001) [a]

Diameter = 0.139 D = 70 D = 80

% compression		Force Min	Max			Ave	Del	K
5	0.00695	0.93	6.1	2.5	10	4.8825	0.00695	702.518
10	0.0139	2	14	4.5	20	10.125	0.0139	728.4173
20	0.0278	4.5	30	9	45	22.125	0.0278	795.8633
30	0.0417	11	72	20	90	48.25	0.0417	1157.074
40	0.0556	19	160	40	180	99.75	0.0556	1794.065

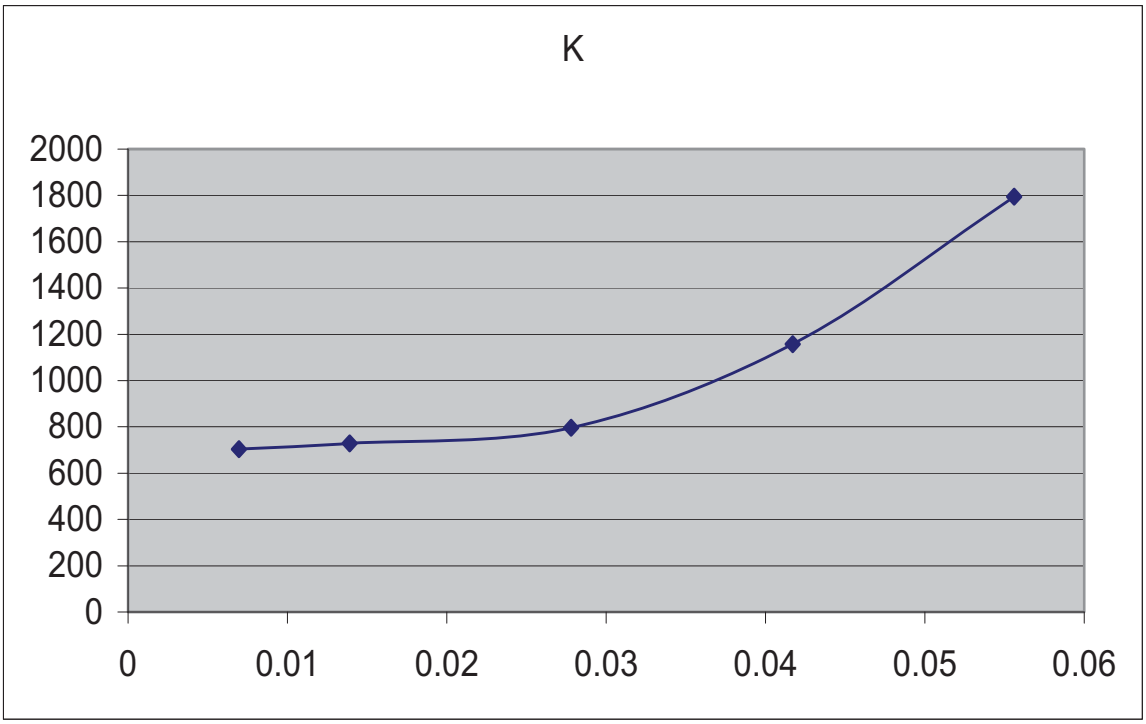

a. Page 2-15 in the O-ring Handbook.

ATTACHMENT B –RESULTS FOR O-RING ELEMENTS FROM FINITE ELEMENT ANALYSIS OF CONTAINMENT VESSEL

```
**** Nodal stresses for 2-D elasticity elements:

 El. #  LC ND  Sigma-11   Sigma-22   Sigma-33    Tau-12    Sigma-Max  Sigma-Min
                Sigma-Int
 ----- --- -- ---------- ---------- ---------- ---------- ---------- ----------
     1   1  I  7.151E-03 -2.347E+02 -3.629E-02  1.115E-02  7.152E-03 -2.347E+02
               -3.629E-02
     1   1  J  6.460E-03 -2.348E+02 -3.564E-02  1.099E-02  6.460E-03 -2.348E+02
               -3.564E-02
     1   1  K  7.565E-04 -2.348E+02 -4.589E-02  9.078E-03  7.568E-04 -2.348E+02
               -4.589E-02
     1   1  L  1.448E-03 -2.347E+02 -4.662E-02  9.233E-03  1.448E-03 -2.347E+02
               -4.662E-02
     1   2  I -3.586E-03 -2.371E+02 -6.498E-03  8.397E-03 -3.586E-03 -2.371E+02
               -6.498E-03
     1   2  J -3.713E-03 -2.371E+02 -6.454E-03  8.271E-03 -3.713E-03 -2.371E+02
               -6.454E-03
     1   2  K  5.712E-03 -2.371E+02 -7.804E-03  7.936E-03  5.712E-03 -2.371E+02
               -7.804E-03
     1   2  L  5.839E-03 -2.371E+02 -8.014E-03  8.062E-03  5.839E-03 -2.371E+02
               -8.014E-03

     2   1  I  8.755E-03 -2.348E+02 -3.608E-02 -8.886E-03  8.756E-03 -2.348E+02
               -3.608E-02
     2   1  J  8.182E-03 -2.350E+02 -3.552E-02 -8.763E-03  8.183E-03 -2.350E+02
               -3.552E-02
     2   1  K -7.855E-05 -2.350E+02 -4.575E-02 -1.064E-02 -7.807E-05 -2.350E+02
               -4.575E-02
     2   1  L  4.944E-04 -2.348E+02 -4.633E-02 -1.077E-02  4.949E-04 -2.348E+02
               -4.633E-02
     2   2  I -3.637E-03 -2.371E+02 -6.900E-03 -9.129E-03 -3.636E-03 -2.371E+02
               -6.900E-03
     2   2  J -3.745E-03 -2.371E+02 -6.860E-03 -9.012E-03 -3.745E-03 -2.371E+02
               -6.860E-03
     2   2  K  5.687E-03 -2.371E+02 -8.074E-03 -9.358E-03  5.687E-03 -2.371E+02
               -8.074E-03
     2   2  L  5.795E-03 -2.371E+02 -8.250E-03 -9.475E-03  5.796E-03 -2.371E+02
               -8.250E-03


 **** 2-D Elasticity elements:

      Number of elements       =     2
      Number of materials      =    5
      Maximum temperature pts  =    1
      Analysis code            =    0
        0 : axisymmetric
        1 : plane strain
        2 : plane stress
      Incompatible modes        =    0
        0 : included
        1 : not included

 **** Nodal stresses for 2-D elasticity elements:

 El. #  LC ND  Sigma-11   Sigma-22   Sigma-33    Tau-12    Sigma-Max  Sigma-Min
                Sigma-Int
 ----- --- -- ---------- ---------- ---------- ---------- ---------- ----------
     1   1  I  1.838E-03 -1.987E+02 -3.397E-02  7.582E-03  1.838E-03 -1.987E+02
               -3.397E-02
     1   1  J  1.110E-03 -1.988E+02 -3.334E-02  7.464E-03  1.111E-03 -1.988E+02
               -3.334E-02
```

```
1   1  K  1.855E-03 -1.988E+02 -4.282E-02  5.515E-03  1.856E-03 -1.988E+02
         -4.282E-02
1   1  L  2.583E-03 -1.987E+02 -4.364E-02  5.634E-03  2.583E-03 -1.987E+02
         -4.364E-02
1   2  I -1.419E-03 -2.013E+02 -5.945E-03  6.027E-03 -1.419E-03 -2.013E+02
         -5.945E-03
1   2  J -1.558E-03 -2.013E+02 -5.865E-03  5.923E-03 -1.558E-03 -2.013E+02
         -5.865E-03
1   2  K  3.687E-03 -2.013E+02 -7.071E-03  5.591E-03  3.687E-03 -2.013E+02
         -7.071E-03
1   2  L  3.825E-03 -2.013E+02 -7.268E-03  5.696E-03  3.825E-03 -2.013E+02
         -7.268E-03

2   1  I  1.931E-03 -1.988E+02 -3.367E-02 -3.542E-03  1.931E-03 -1.988E+02
         -3.367E-02
2   1  J  1.223E-03 -1.990E+02 -3.305E-02 -3.463E-03  1.223E-03 -1.990E+02
         -3.305E-02
2   1  K  1.761E-03 -1.990E+02 -4.236E-02 -5.358E-03  1.762E-03 -1.990E+02
         -4.236E-02
2   1  L  2.469E-03 -1.988E+02 -4.316E-02 -5.436E-03  2.469E-03 -1.988E+02
         -4.316E-02
2   2  I -1.833E-03 -2.013E+02 -6.185E-03 -5.247E-03 -1.833E-03 -2.013E+02
         -6.185E-03
2   2  J -1.970E-03 -2.013E+02 -6.110E-03 -5.152E-03 -1.969E-03 -2.013E+02
         -6.110E-03
2   2  K  3.840E-03 -2.013E+02 -7.192E-03 -5.486E-03  3.841E-03 -2.013E+02
         -7.192E-03
2   2  L  3.977E-03 -2.013E+02 -7.391E-03 -5.581E-03  3.978E-03 -2.013E+02
         -7.391E-03
```

ATTACHMENT C – O-RING INTERFACE LOADS

Axisymmetric nodal forces on lid from O-ring pressure

Inner O-ring

Node number	Node radius	Mean radius	Force/pressure factor	Load case 1 Pressure	Load case 1 Force	Load case 2 Pressure	Load case 2 Force
143	2.69812		0.053659565	198.825	10.66886299	201.3	10.80167042
		2.717935					
144	2.73775		0.108483245	198.825	21.56918112	201.3	21.83767716
		2.75756					
145	2.77737		0.110053385	198.825	21.88136433	201.3	22.15374646
		2.797185					
146	2.817		0.055622538	198.825	11.0591511	201.3	11.19681688

Outer O-ring

149	2.942		0.061513619	234.825	14.44493549	237.1	14.58487897
		2.962835					
150	2.98367		0.124314506	234.825	29.19215396	237.1	29.47496946
		3.0045					
151	3.02533		0.126050479	234.825	29.59980364	237.1	29.88656848
		3.046165					
152	3.067		0.063683896	234.825	14.95457097	237.1	15.09945183

ATTACHMENT D – INTERFACE LOADS ON NUT

Matching interface pressure loads
Load Case 1

	Side 1					Side 2			
Index	Radius	Szz	FORCEz	Force/Rad	Index	Radius	Szz	FORCEz	Force/Rad
0	2.50507	0				2.50964	0		
1	2.54629	-3300.16	-136.0161	-346.3364		2.53798	-800	-22.668	-57.53093
2	2.5875	-1230.75	-50.71921	-131.2359		2.56631	-3300.16	-97.27222	-249.6307
3	2.62871	-662.77	-27.31275	-71.7973		2.59693	-1230.75	-37.67941	-97.85079
4	2.66992	-65.6015	-2.703438	-7.217963		2.62754	-1230.75	-37.67941	-99.00416
5	2.71113	0				2.65816	-662.77	-20.2907	-53.93594
Sum			-216.7515	-556.5876		2.68877	-65.6015	-2.00839	-5.400099
						2.71939	0		
					Sum			-217.5981	-563.3526

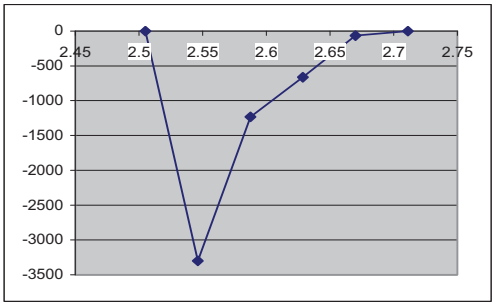

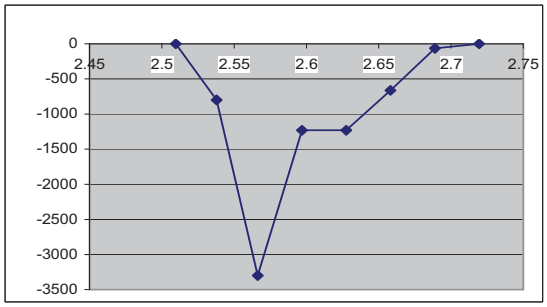

Load Case 2

	Side 1					Side 2			
Index	Radius	Szz	FORCEz	Force/Rad	Index	Radius	Szz	FORCEz	Force/Rad
0	2.50507	0				2.50964	0		
1	2.54629	301.824	12.43968	31.67502		2.53798	301.824	8.552183	21.70527
2	2.5875	-132.484	-5.459666	-14.12688		2.56631	100	2.9475	7.564199
3	2.62871	-398.673	-16.42931	-43.1879		2.59693	-132.484	-4.055998	-10.53314
4	2.66992	-1240.54	-51.12265	-136.4934		2.62754	-398.673	-12.20537	-32.07011
5	2.71113	0				2.65816	-1240.54	-37.97913	-100.9546
Sum			-60.57196	-162.1332		2.68877	-600	-18.369	-49.39002
						2.71939	0		
					Sum			-61.10982	-163.6784

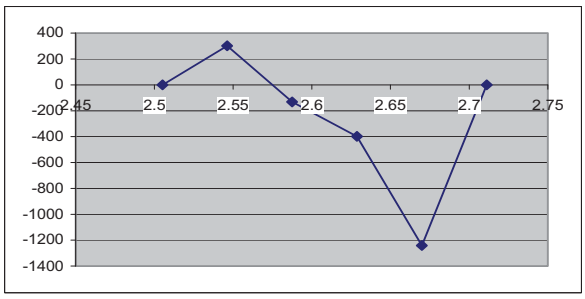

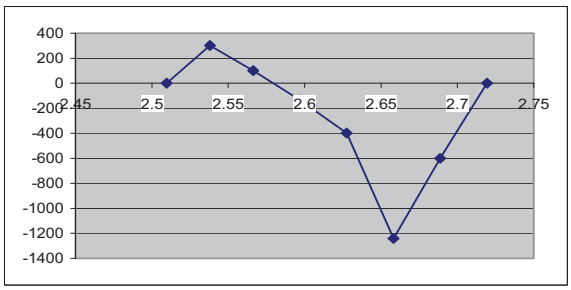

GENERAL DESIGN AND COMPUTATION SHEET

JOB Fatigue Analysis of ES-3100 CV Threads under Normal Conditions of Use		DATE 16 February 2005	SHEET 1 of 30
DAC NO. DAC-EA-900000-A007	REVISION NO. 0	COMPUTED C. R. Hammond	CHECKED BY M. L. Goins

1.0 TABLE OF CONTENTS

1.0 TABLE OF CONTENTS 1
2.0 OBJECTIVE 2
3.0 EVALUATION INPUT (CRITERIA) AND SOURCE 2
3.1 REFERENCES USED 2
3.2 DESIGN CONDITIONS 2
3.3 METHODS TO BE USED 2
4.0 ANALYSES AND/OR CALCULATIONS 3
4.1 TIGHTENING TORQUE 3
4.2 DIFFERENTIAL THERMAL EXPANSION 6
4.3 TRANSPORTATION LOADS 7
4.4 FATIGUE ANALYSIS 7
5.0 CONCLUSIONS 8
Appendix 1 – Axial Stresses across Neck of ES-3100 due to Torque 13
Appendix 2 - Finite Element Data 21

2.0 OBJECTIVE

The 7º/45º Buttress threads, specified per ANSI B1.9-1973 7.0-8 Push, used to secure the lid of the ES-3100 Containment Vessel are evaluated for fatigue resistance under normal conditions of use. The evaluation is based on rules in NB-3232.3 from ASME B&PV Code, Section III.

3.0 EVALUATION INPUT (CRITERIA) AND SOURCE

3.1 REFERENCES USED

(B1.9) *Buttress Inch Screw Threads*, ANSI B1.9 – 1973, The American Society of Mechanical Engineers, 1973.

(Code) *Class 1 Components, Section III, Rules for Construction of Nuclear Power Plant Components*, Division 1, 2001 Edition with 2003 Addenda, The American Society of Mechanical Engineers, 2003.

(Drawing) "Containment Vessel Assembly," M2E801580A011, Rev. A, BWXT Y-12, 2003.

(Hammond) "ASME Code Subsection NB Stress Analysis of ES-3100 Containment Vessel," DAC-EA-900000-A006, Rev. 1, BWXT Y-12, 2004.

(Laughner & Hargan) *Handbook of Fastening and Joining of Metal Parts*, McGraw-Hill Book Company, 1956, pp. 167-168.

(Section II) *Section II, Materials*, Part D – Properties, 2001 Edition with 2003 Addenda, The American Society of Mechanical Engineers, 2003.

(SST/SGT) J. S. Cap, "Recommended Random Vibration and Shock Test Specifications for Cargo Transported on SST and SGT Trailers," letter to distribution, Sandia National Laboratory, Albuquerque, New Mexico, 2002.

3.2 DESIGN CONDITIONS

Hot NCT: Internal pressure of 17.786 psia at 190.06º F.

Cold NCT: Internal pressure of 11.13 psia at -40º F.

3.3 METHODS TO BE USED

A finite element model described in DAC-EA-900000-A006 by Hammond was used. The program was verified by running problems with known solutions. The file name for the model is ES3100CV1. Properties used in the model are shown in Appendix 2.

4.0 ANALYSES AND/OR CALCULATIONS

The previous analysis (Hammond) followed ASME Code rules to validate the vessel design under a bounding internal pressure of 101.5 psi. The design margin of the vessel, including the vessel body, the lid, and the retaining nut but not including threads on the nut or vessel body, was limited by stress intensity calculated at the side wall to bottom transition of the vessel. The actual maximum expected internal pressure is 17.786 psia or 17.786 psia – 14.7 psia = 3.1 psig. Away from the contact region between the lid and vessel body, stresses are proportional to pressure so the stress in the body and at the center of the lid will be reduced to 3.1 psi/101.5 psi = 0.0305 or 3.05% of values calculated previously. The design margin in the vessel becomes limited by stresses in the clamping region primarily due to gasket seating load or the load produced by tightening the nut. These calculations determine the load from torquing the nut and their effects on stress in the vessel components in the contact or clamping region.

4.1 TIGHTENING TORQUE

The specified nut torque is 120 +/- 5 ft.-lb. From Laughtner & Hargan, the ratio of axial force, P (lb.), to torque, T (in.-lb.) is

$$P/T = 2/(D\nu + d_p\, m), \text{ where}$$

D = mean bearing diameter of nut (in.),

dp = pitch diameter of screw thread (in.),

ν = coefficient of friction between nut and bearing surface,

$$m = \frac{\tan(\beta + \phi)}{\cos\alpha}, \text{ where}$$

α = one-half of thread profile angle (degrees),

β = helix angle (degrees), and

ϕ = friction angle the tangent of which is the friction coefficient.

The threads are 7 inch nominal diameter with 8 threads per inch or having a pitch of 0.125 in. From B1.9 the pitch diameter is

$$d_p = 7\,\text{in.} - 0.6\,(0.125\,\text{in.}) = 6.93\,\text{in}.$$

The helix angle on the pitch diameter is

$$\beta = \arctan\frac{0.125\,\text{in.}}{\pi\,(6.93\,\text{in.})} = 0.329^\circ.$$

The thread profile angle at the mating surfaces is 7º so $\alpha = 3.5^\circ$.

The mean effective bearing diameter of the nut is about 5.8 inches. That is D = 5.8 in.

The referenced drawing has the note: "During installation of container vessel lid assembly, apply a light coat of Krytox grease to the threads and under the nut." A typical value for coefficient of friction for lubricated threads is 0.11. In this case

$\phi = \arctan(0.11) = 6.3$.

$$m = \frac{\tan(0.329^\circ + 6.3^\circ)}{\cos(3.5^\circ)} = 0.12 .$$

$$P/T = 2/\left(5.8\,\text{in.}(0.11) + 6.93\,\text{in.}(0.12)\right) = 1.36 .$$

The maximum and the minimum force, assuming that the friction coefficient 0.11 is correct are

Pmax = 1.36 T = 1.36 (125 ft.-lb)(12 in./ft.) = 2,000 lb., rounding to 2 significant figures, and

Pmin = 1.36 (115 ft.-lb.)(12 in./ft.) = 1,900 lb.

According to Hammond the force required to seat the gaskets is
$W_{m2} = 20\,\text{lb./in.}\,\pi\left[(5.359\,\text{in.} + 0.139\,\text{in.}) + (5.859\,\text{in.} + 0.139\,\text{in.})\right] = 722.3\,\text{lb}$ and

the load due to the maximum allowable pressure, 101.5 psig, to the outer edge of the inner O-ring groove is

$$W_{m1} = \pi \frac{101.5\,\text{psig}\,(5.624\,\text{in.})^2}{4} = 2521\,\text{lb} .$$

The sum of gasket seating and pressure forces is 3,244 lb. so the specified torque is not adequate for the bounding pressure. However, the highest expected internal pressure is 17.786 psia which is (17.786 psia – 14.7 psia =) 3.1 psig so

$$W_{m1} = \pi \frac{3.1\,\text{psig}\,(5.624\,\text{in.})^2}{4} = 77\,\text{lb} .$$

The sum of gasket seating force and actual pressure force is 799 lb and there is a large margin on torque required to maintain a tight gasket and consequently the required torque is not sensitive to the coefficient of friction.

The minimum cross section area of the CV subject to the axial force from torquing the nut is at the undercut just below the threads. The inside diameter at the undercut is 6.85 in. +2(0.09 in.) = 7.03 in. The outside diameter in the same plane is 7.50 in. The minimum cross section area considering the tolerances listed on the drawing is $\pi((7.50\,\text{in.} - 0.01\,\text{in.})^2 - (7.03\,\text{in.} + 0.01\,\text{in.})^2))/4 = 5.14\,\text{in}^2$.

The average axial stress due to the force due to maximum torque at this section is

$\bar{\sigma}_{torque}$ = 2,000 lb. / 5.14 in^2 = 389 psi.

The maximum diameter at the root of a thread on the CV is 7.04 in. That is called the maximum major diameter of the internal thread which per B1.9 is D – h + PDtol. + 0.80803 p, where D is the major diameter (7 in.), h is the basic height of thread engagement (0.6 p), PDtol. is tolerance on pitch diameter (0.0101 in.), and p is pitch (0.125 in.). The cross section area at the root of the thread is thus the same as the minimum area at the undercut (i.e. 7.03 in. + 0.01 in. including tolerance) and the average stress is the same.

The finite element model used by Hammond to evaluate pressure resistance was modified to simulate the effect of the axial force due to torquing the nut. The section of the vessel between the flange surface and the threads was forced to shrink in the axial direction by applying an artificial temperature drop of 100º F. and manipulating the axial coefficient of thermal expansion to produce an axial force of 2,000 lb. Fig. 1 shows the effected region of the vessel with dots at the locations where axial stresses were recorded. The O-ring elements were removed and the entire flange surface was held in place by stiff axial spring elements. Nodal axial stresses were obtained across the two horizontal sections. There were two stresses calculated at each point, one above and one below the section boundary. The stress in the section without the temperature-dependent properties was recorded to avoid including thermal strain in the stress calculation. The results from the final run are shown on the spreadsheet along with the axial stress calculated at each point across the two sections in Appendix 1.

The net axial forces across each section were calculated by multiplying the axial stress over the tributary area. There was a slight but acceptable difference (4%) between the upper and lower sections attributed to model coarseness. The net force across the section with the highest axial stress was about 2% greater than 2000 lb.

The plot of axial stress shown in Appendix 1 clearly indicates that the peak stress at the left edge is higher than an extrapolated equivalent linear bending stress. The value of peak stress due to preload from torque, 3,476 psi, is so low that we can substitute this peak stress for the sum of membrane and bending stress in combination with axial stress from other loads.

The gasket seating force between the lid and CV body is the sum of gasket seating forces at both O-rings or 722.3 lb. total. The pressure force due to the 101.5 psig from the earlier calculation over the area to the back side of the inner O-ring groove is

$$F_P = 101.5\,\text{psi}\,\pi\left(2.817\,\text{in.}\right)^2 = 2530\,\text{lb.}$$

In general, stress intensities are not linear functions of applied force but in our case of the axial force due to torque on the nut alone, stress intensities will increase by the ratio 2000 lb./722.3 lb. = 2.77 . The calculated peak stress intensity due to gasket seating load alone (Load Case 2) were highest near points of high compression that would be affected by the applied torque. The peak values were 872 psi in the lid and 2224 psi in the nut (Hammond, pp. 18, 20). The stresses in these components due to torque would be 2.77(872 psi) = 2415 psi in the lid and 2.77(2224 psi) = 6158 psi in the nut.

Bending or radial stress near the center of the lid and stresses in the vessel body away from the contact region will be reduced to about 3.05% of previously calculated values.

The effect of an internal 3.1 psig pressure plus the torque is shown in Fig. 3. Maximum stress intensity is 3501 psi. This is in the same location as for the pressure plus gasket seat case, in the transition between the side and bottom of the vessel. The axial stress in this region due to 3.1 psi pressure and torque is shown on Fig. 4. The peak axial stress is 3714 psi. The slight pressure causes just a slight increase in stress over the case with torque alone. The stress intensities in the clamping regions of the lid and nut will become about (3714 psi/3476 psi) 2415 psi = 2580 psi and (3714 psi/3476 psi) 6158 psi = 6580 psi, respectively.

4.2 DIFFERENTIAL THERMAL EXPANSION

The range of temperatures to which the CV may be exposed is -40º F. to 190.06º F. The average thermal expansion coefficient for the 304 material of the CV between 70 and 200 F. is 8.9 10^{-6} in./in./º F. and greater for higher upper temperatures per Section II. From the HP Alloys web site the average thermal expansion coefficient of the Nitronic 60 material of the nut between 75 and 200 F. is 8.8 10^{-6} in./in./º F. and greater for higher upper temperatures. Since the temperatures on opposite sides of the thread mating surface are expected to be the same an upper bound on the stress due to differential thermal expansion is

$\sigma_t = E_c \, \Delta T \left(\alpha_{CV} - \alpha_N\right)$, where E_c is the cold elastic modulus of either part, T is temperature, and α is average thermal expansion coefficient.

In the CV the stress, using a modulus interpolated from Table TM-1 in Section II, is

$$\sigma_{tCV} = 28.8 \times 10^6 \text{ psi} (190.06^\circ - (-40^\circ))(8.9 \times 10^{-6} \text{ in./in./}\circ - 8.8 \times 10^{-6} \text{ in./in/}\circ)$$
$$= 663 \text{ psi}.$$

The nut material has a slightly lower modulus listed so the stress in the nut will be slightly less. The room temperature modulus of the nut material is 26.2×10^6 psi per the HP Alloy website. The cold temperature modulus is not available but an approximation is obtained by comparing the modulus of Nitronic 60 at room temperature with the modulus of 304 at room temperature. From Table TM-1, the modulus of 304 at 70F. is 28.3×106 psi. Stress in the nut at the threads is about

$$\sigma_{tN} = \frac{26.2 \times 10^6 \text{ psi}}{28.3 \times 10^6 \text{ psi}} 663 \text{ psi} = 613 \text{ psi}.$$

The CV material has the higher thermal expansion coefficient so the effect of temperature increase is to reduce preload on the lid. Consider the mid-height of the threads to be fixed. The fixed plane is 1.100 in. – 0.55 in. / 2 = 0.825 in. above the mating plane. The lid is 0.5 in. thick under the nut and the lid will grow the same amount as the CV. The nut has 0.325 in. of material below the fixed plane and the difference in growth between the CV and the nut is

$$0.325 \text{ in.} (190.06^\circ - (-40^\circ))(8.9 \times 10^{-6} \text{ in./in./}\circ - 8.8 \times 10^{-6} \text{ in./in./}\circ)$$
$$= 0.0000075 \text{ in}.$$

Even if the torque load in the metal is ignored, the O-rings are compressed at least

Comp. = (0.139 in.-0.004 in.) – (0.114 in.+0.001 in.) = 0.020 in.

and a reduction in compression of 0.004% due to temperature change is insufficient to unload the O-rings enough to allow leakage.

4.3 TRANSPORTATION LOADS

The highest shock acceleration expected during transport is 11g in the vertical direction compared to a maximum horizontal acceleration of 5g per SST/SGT. The contents of the CV are specified to not exceed 90 lbs. The lid can be viewed as three disks, the volumes of which are:

Disk	Volume Formula	Volume, in^3
Top	$\pi(3.98\,\text{in.})^2\,(0.56\,\text{in.})/4$	6.97
Middle	$\pi(6.741\,\text{in.})^2\,(0.500\,\text{in.})/4$	17.84
Bottom	$\pi(5.00\,\text{in.})^2\,(0.05\,\text{in.})/4$	0.98
Sum		25.8

The weight density of the lid material is about 0.29 lb./cu. in. so the weight of the lid is about 7.5 lb. Assume the threads must restrain 100 lbs. as the package is transported. Assuming the CV is upright, gravity provides 1g downward acceleration so the nut must restrain at most a net of 100 lbm. (11g – 1g) = 1,000 lbf. The average stress at the minimum cross section due to shock load is 1,000 lb. / 5.14 in^2 = 195 psi.

4.4 FATIGUE ANALYSIS

For each use of the vessel, the part of the CV equivalent to a bolt is loaded in tension by a torque producing a maximum axial load of 2,000 lb., an average stress of 389 psi and a peak stress (including bending) of 3,563 psi. When the vessel is pressurized to 3.1 psi the peak axial stress is 3,714 psi. This is the peak stress at the undercut which has a stress concentration factor of about 3. Per the Code, paragraph NB-3232.3 (c), the fatigue strength reduction factor for the threads shall not be less than 4 so the fatigue stress on the threads is 3,714 psi (4/3) = 4,952 psi.

Conservatively ignoring the interplay between the CV and the nut and lid, the stress due to impact during transportation is added to produce a maximum tensile stress of 4,952 psi + 195 psi = 5,147 psi. The thermal expansion reduces the preload so it will not extend the stress range. The range is zero to 5,147 psi and the alternating stress is half of the range or 5,147 psi / 2 = 2,574 psi.

The threads are evaluated for cyclic service by comparison with the design Curve A on Table I—9.2.2. For alternating stresses below 23,700 psi the allowable number of cycles exceeds 10^{11}. In every case the stress in the nut has been less than in the CV and since the nut material is also austenitic it does not limit fatigue design.

5.0 CONCLUSIONS

Force due to torquing the nut on the vessel was determined. The actual maximum expected internal pressure is low so the torque load produces much higher stresses in the vessel than pressure but the combined effect of torque and actual pressure was less than the conditions including bounding pressure used in the previous evaluation of the vessel design.

Thermal loads were evaluated relative to gasket compression it was shown that gaskets would remain seated through the maximum expected temperature change.

The threaded components of the ES-3100 Containment Vessel were evaluated per ASME Section III requirements and were found to have an allowable fatigue life in excess of 10^{11} cycles. Since the allowable life of the vessel is limited to a mere 30,000 cycles, the threads do not limit the life of the vessel.

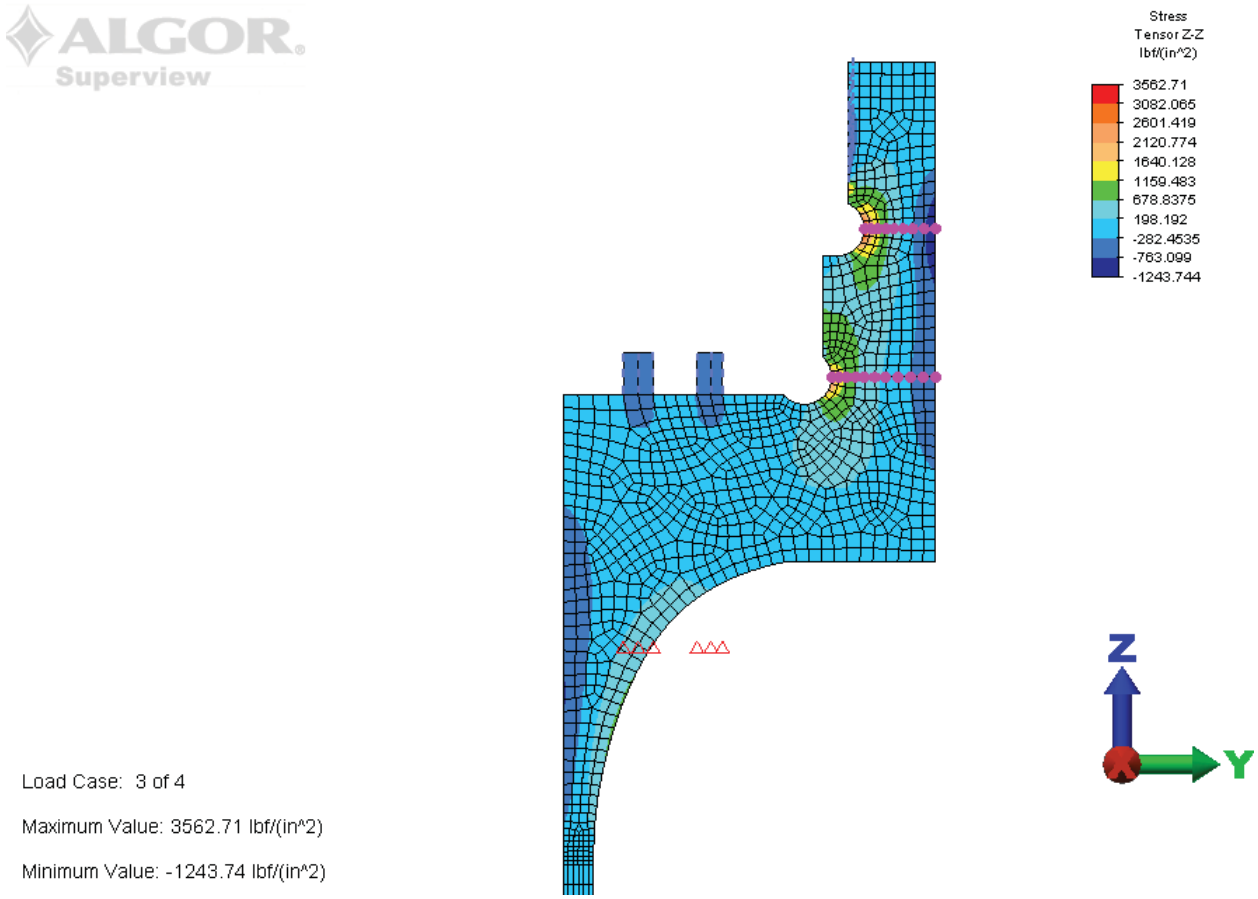

Fig. 1 – Axial Stress Due to Torque Load in Containment Vessel Neck

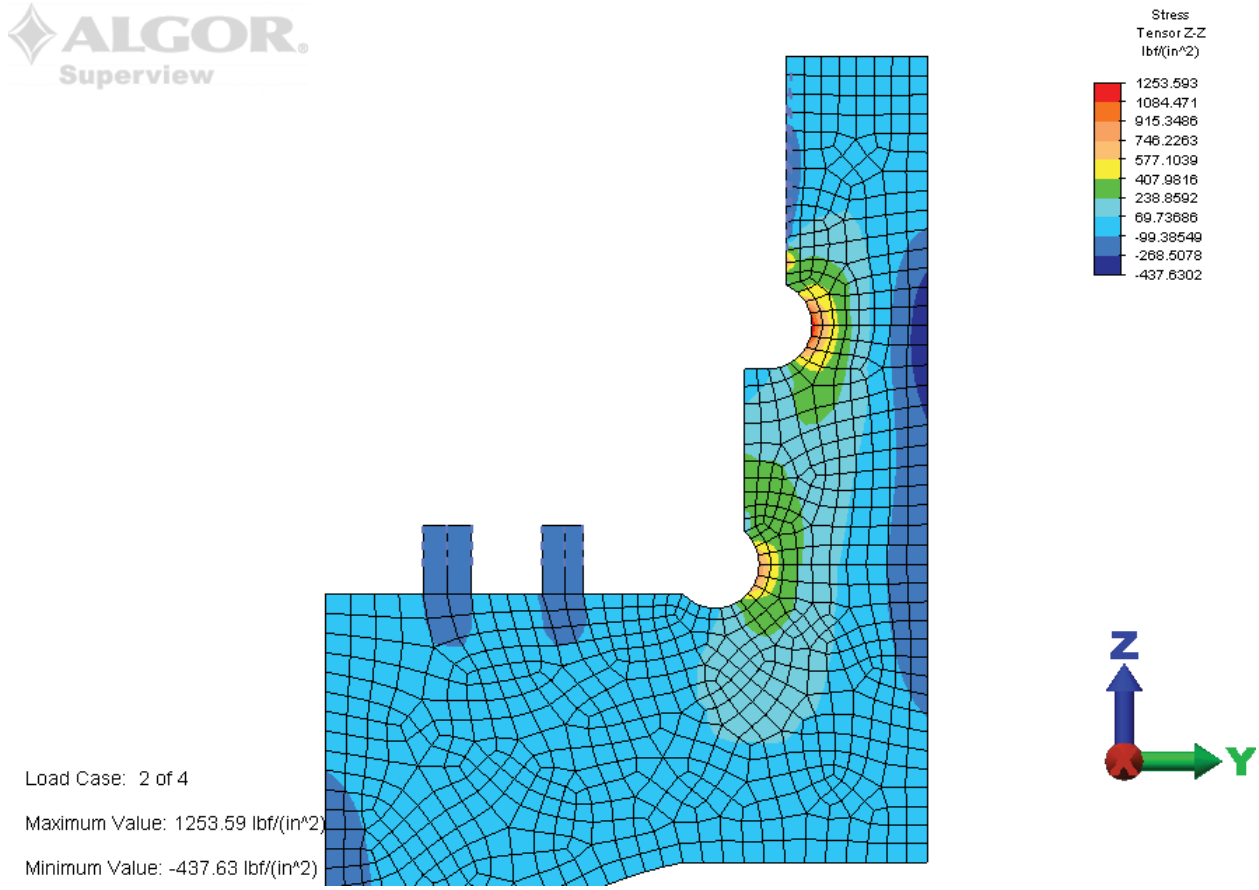

Fig. 2 – Axial Stress below the Threads in the Containment Vessel due to Gasket Seating Load

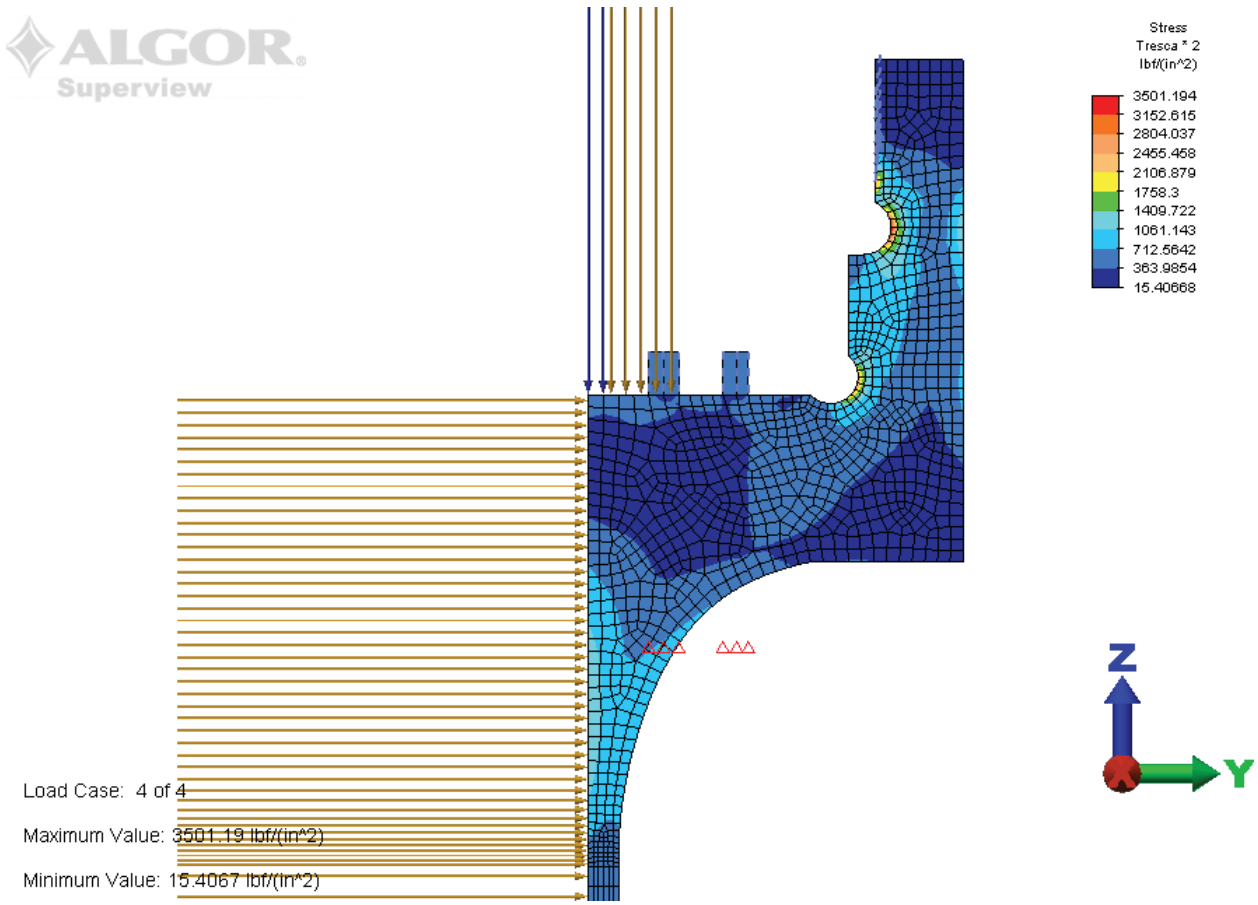

Fig. 3 –Stress Intensity below the Threads in the Containment Vessel due to 3.1 psi Pressure and Torque Loads

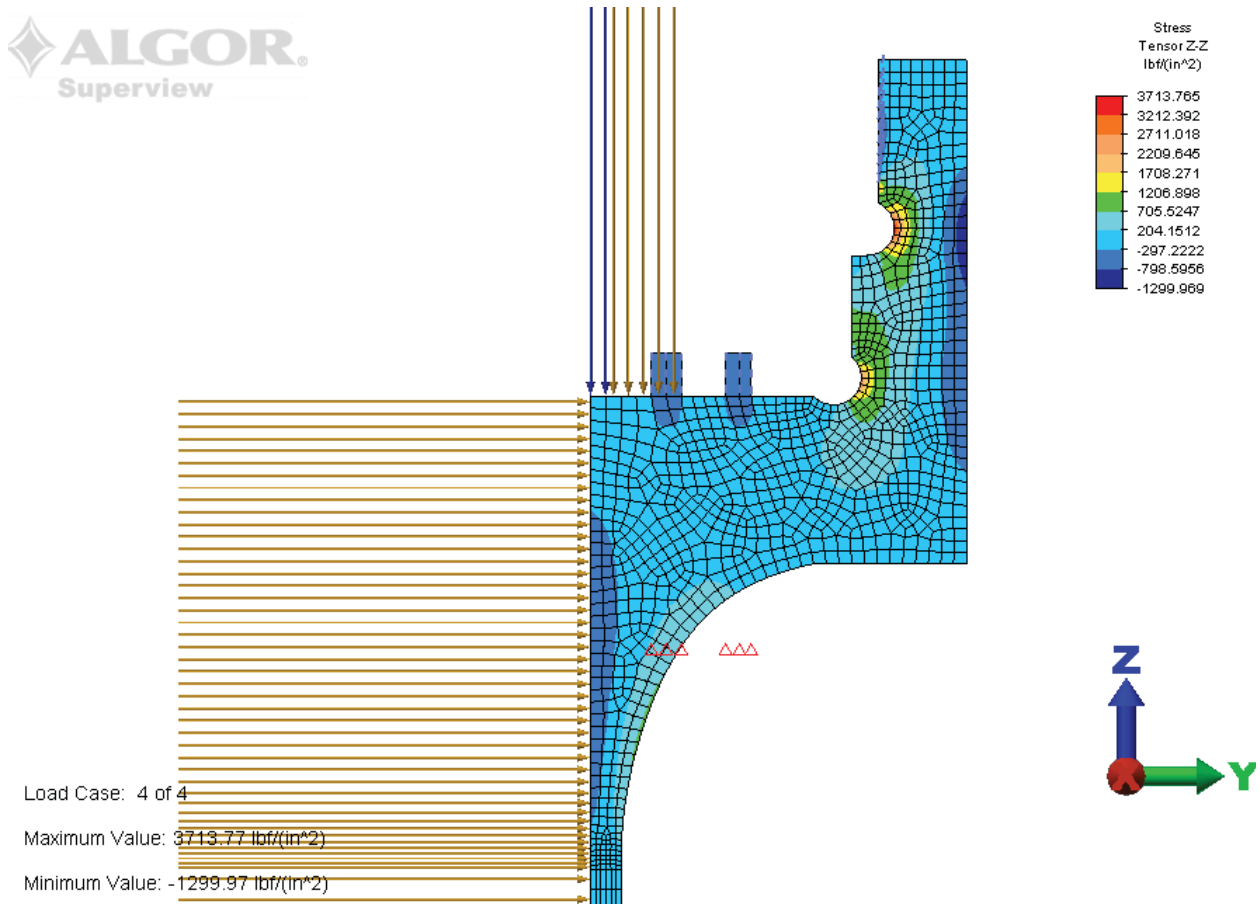

Fig. 4 – Axial Stress in Containment Vessel Due to 3.1 psi Pressure and Torque

Appendix 1 – Axial Stresses across Neck of ES-3100 due to Torque

Top Section

```
Current Load Case = 3

Node # 1894 ( X = 0, Y = 3.515, Z = 9.45 )

    Displaced Position : X = 0, Y = 3.51496, Z = 9.44997

    Displacement = DX: 0, DY: -4.55757e-005, DZ: -2.7064e-005, Magnitude: 5.30057e-005

    appears in 2 Elements

    Part: 8    Element: 1

    Current Result Value: 3476.397428 lbf/(in^2)

    Part: 6    Element: 152

    Current Result Value: 3562.710297 lbf/(in^2)

Node # 1895 ( X = 0, Y = 3.53702, Z = 9.45 )

    Displaced Position : X = 0, Y = 3.53697, Z = 9.44998

    Displacement = DX: 0, DY: -4.64674e-005, DZ: -1.54912e-005, Magnitude: 4.89816e-005

    appears in 4 Elements

    Part: 8    Element: 1

    Part: 8    Element: 2

    Current Result Value: 2076.571725 lbf/(in^2)

    Part: 6    Element: 151

    Part: 6    Element: 152

    Current Result Value: 2150.404851 lbf/(in^2)

Node # 1896 ( X = 0, Y = 3.55903, Z = 9.45 )

    Displaced Position : X = 0, Y = 3.55898, Z = 9.44998

    Displacement = DX: 0, DY: -4.70825e-005, DZ: -1.69066e-005, Magnitude: 5.0026e-005

    appears in 4 Elements

    Part: 8    Element: 2

    Part: 8    Element: 3

    Current Result Value: 1338.334401 lbf/(in^2)
```

```
    Part: 6    Element: 150

    Part: 6    Element: 151

    Current Result Value: 1388.726762 lbf/(in^2)

Node # 1897 ( X = 0, Y = 3.58545, Z = 9.45 )

    Displaced Position : X = 0, Y = 3.5854, Z = 9.44998

    Displacement = DX: 0, DY: -4.7175e-005, DZ: -1.82265e-005, Magnitude: 5.05735e-005

    appears in 4 Elements

    Part: 8    Element: 3

    Part: 8    Element: 4

    Current Result Value: 815.1134205 lbf/(in^2)

    Part: 6    Element: 149

    Part: 6    Element: 150

    Current Result Value: 856.9278605 lbf/(in^2)

Node # 1898 ( X = 0, Y = 3.61186, Z = 9.45 )

    Displaced Position : X = 0, Y = 3.61182, Z = 9.44998

    Displacement = DX: 0, DY: -4.7039e-005, DZ: -1.97662e-005, Magnitude: 5.10232e-005

    appears in 4 Elements

    Part: 8    Element: 4

    Part: 8    Element: 5

    Current Result Value: 422.3549006 lbf/(in^2)

    Part: 6    Element: 148

    Part: 6    Element: 149

    Current Result Value: 454.1958936 lbf/(in^2)

Node # 1899 ( X = 0, Y = 3.64356, Z = 9.45 )

    Displaced Position : X = 0, Y = 3.64352, Z = 9.44998

    Displacement = DX: 0, DY: -4.6803e-005, DZ: -2.12778e-005, Magnitude: 5.14127e-005

    appears in 4 Elements

    Part: 8    Element: 5
```

```
    Part: 8    Element: 6

    Current Result Value: 60.92361234 lbf/(in^2)

    Part: 6    Element: 147

    Part: 6    Element: 148

    Current Result Value: 92.87579812 lbf/(in^2)

Node # 1900 ( X = 0, Y = 3.67526, Z = 9.45 )

    Displaced Position : X = 0, Y = 3.67522, Z = 9.44998

    Displacement = DX: 0, DY: -4.64719e-005, DZ: -2.30637e-005, Magnitude: 5.18804e-005

    appears in 4 Elements

    Part: 6    Element: 145

    Part: 6    Element: 147

    Current Result Value: -276.2872177 lbf/(in^2)

    Part: 8    Element: 6

    Part: 8    Element: 7

    Current Result Value: -291.8618414 lbf/(in^2)

Node # 1901 ( X = 0, Y = 3.71263, Z = 9.45 )

    Displaced Position : X = 0, Y = 3.71258, Z = 9.44997

    Displacement = DX: 0, DY: -4.6099e-005, DZ: -2.48703e-005, Magnitude: 5.23798e-005

    appears in 4 Elements

    Part: 8    Element: 7

    Part: 8    Element: 8

    Current Result Value: -690.1878235 lbf/(in^2)

    Part: 6    Element: 145

    Part: 6    Element: 146

    Current Result Value: -699.5449043 lbf/(in^2)

Node # 1902 ( X = 0, Y = 3.75, Z = 9.45 )

    Displaced Position : X = 0, Y = 3.74996, Z = 9.44997

    Displacement = DX: 0, DY: -4.48856e-005, DZ: -2.93433e-005, Magnitude: 5.3626e-005
```

```
    appears in 2 Elements

    Part: 8    Element: 8

    Current Result Value: -1189.038154 lbf/(in^2)

    Part: 6    Element: 146

    Current Result Value: -1243.744425 lbf/(in^2)
```

Lower Section

```
Current Load Case = 3


Node # 1718 ( X = 0, Y = 3.4065, Z = 8.96 )

    Displaced Position : X = 0, Y = 3.40646, Z = 9.03102

    Displacement = DX: 0, DY: -3.86154e-005, DZ: 0.0710243, Magnitude: 0.0710243

    appears in 2 Elements

    Part: 6    Element: 1

    Current Result Value: 2381.970074 lbf/(in^2)

    Part: 3    Element: 713

    Current Result Value: 2573.760605 lbf/(in^2)

Node # 1719 ( X = 0, Y = 3.43091, Z = 8.96 )

    Displaced Position : X = 0, Y = 3.43087, Z = 9.03103

    Displacement = DX: 0, DY: -3.82805e-005, DZ: 0.071027, Magnitude: 0.071027

    appears in 4 Elements

    Part: 6    Element: 1

    Part: 6    Element: 2

    Current Result Value: 1429.725908 lbf/(in^2)

    Part: 3    Element: 712

    Part: 3    Element: 713

    Current Result Value: 1507.238598 lbf/(in^2)
```

```
Node # 1720 ( X = 0, Y = 3.45532, Z = 8.96 )

    Displaced Position : X = 0, Y = 3.45529, Z = 9.03102

    Displacement = DX: 0, DY: -3.93058e-005, DZ: 0.0710167, Magnitude: 0.0710167

    appears in 4 Elements

    Part: 3    Element: 711

    Part: 3    Element: 712

    Current Result Value: 1015.779644 lbf/(in^2)

    Part: 6    Element: 2

    Part: 6    Element: 3

    Current Result Value: 1035.108104 lbf/(in^2)

Node # 1721 ( X = 0, Y = 3.48462, Z = 8.96 )

    Displaced Position : X = 0, Y = 3.48458, Z = 9.03103

    Displacement = DX: 0, DY: -3.78762e-005, DZ: 0.0710297, Magnitude: 0.0710297

    appears in 4 Elements

    Part: 3    Element: 710

    Part: 3    Element: 711

    Current Result Value: 699.5787633 lbf/(in^2)

    Part: 6    Element: 3

    Part: 6    Element: 4

    Current Result Value: 752.6151572 lbf/(in^2)

Node # 1722 ( X = 0, Y = 3.51391, Z = 8.96 )

    Displaced Position : X = 0, Y = 3.51388, Z = 9.03103

    Displacement = DX: 0, DY: -3.73704e-005, DZ: 0.0710323, Magnitude: 0.0710323

    appears in 4 Elements

    Part: 3    Element: 707

    Part: 3    Element: 710

    Current Result Value: 479.8616501 lbf/(in^2)

    Part: 6    Element: 4
```

```
    Part: 6    Element: 5

    Current Result Value: 524.8054716 lbf/(in^2)

Node # 1723 ( X = 0, Y = 3.54907, Z = 8.96 )

    Displaced Position : X = 0, Y = 3.54903, Z = 9.03101

    Displacement = DX: 0, DY: -3.89625e-005, DZ: 0.0710096, Magnitude: 0.0710096

    appears in 4 Elements

    Part: 3    Element: 704

    Part: 3    Element: 707

    Current Result Value: 286.7099034 lbf/(in^2)

    Part: 6    Element: 5

    Part: 6    Element: 6

    Current Result Value: 319.4018001 lbf/(in^2)

Node # 1724 ( X = 0, Y = 3.58422, Z = 8.96 )

    Displaced Position : X = 0, Y = 3.58418, Z = 9.03101

    Displacement = DX: 0, DY: -3.94127e-005, DZ: 0.071011, Magnitude: 0.071011

    appears in 4 Elements

    Part: 3    Element: 704

    Part: 3    Element: 705

    Current Result Value: 104.2072763 lbf/(in^2)

    Part: 6    Element: 6

    Part: 6    Element: 7

    Current Result Value: 126.0936862 lbf/(in^2)

Node # 1725 ( X = 0, Y = 3.62567, Z = 8.96 )

    Displaced Position : X = 0, Y = 3.62563, Z = 9.03101

    Displacement = DX: 0, DY: -3.94951e-005, DZ: 0.0710126, Magnitude: 0.0710126

    appears in 4 Elements

    Part: 6    Element: 7

    Part: 6    Element: 8
```

```
    Current Result Value: -69.65167919 lbf/(in^2)

    Part: 3    Element: 705

    Part: 3    Element: 706

    Current Result Value: -87.34285327 lbf/(in^2)

Node # 1726 ( X = 0, Y = 3.66711, Z = 8.96 )

    Displaced Position : X = 0, Y = 3.66707, Z = 9.03101

    Displacement = DX: 0, DY: -3.94338e-005, DZ: 0.0710146, Magnitude: 0.0710146

    appears in 4 Elements

    Part: 6    Element: 8

    Part: 6    Element: 9

    Current Result Value: -274.1379622 lbf/(in^2)

    Part: 3    Element: 706

    Part: 3    Element: 708

    Current Result Value: -286.8211743 lbf/(in^2)

Node # 1727 ( X = 0, Y = 3.70856, Z = 8.96 )

    Displaced Position : X = 0, Y = 3.70852, Z = 9.03102

    Displacement = DX: 0, DY: -3.91153e-005, DZ: 0.0710191, Magnitude: 0.0710191

    appears in 4 Elements

    Part: 6    Element: 9

    Part: 6    Element: 10

    Current Result Value: -489.6421277 lbf/(in^2)

    Part: 3    Element: 708

    Part: 3    Element: 709

    Current Result Value: -498.9915546 lbf/(in^2)

Node # 1728 ( X = 0, Y = 3.75, Z = 8.96 )

    Displaced Position : X = 0, Y = 3.74996, Z = 9.03102

    Displacement = DX: 0, DY: -3.89012e-005, DZ: 0.0710215, Magnitude: 0.0710215

    appears in 2 Elements
```

Part: 6 Element: 10

Current Result Value: -726.5076374 lbf/(in^2)

Part: 3 Element: 709

Current Result Value: -737.209287 lbf/(in^2)

Appendix 1 - Axial stress across neck of ES-3100 CV due to torque

Top section - Part 8

Y, in.	Sigma ZZ, psi	Delta R, in.	Force, lb.	Force (hard way), lb.
3.515	3476.397428	0.01101	845.3215421	846.6454383
3.53702	2076.571725	0.022015	1015.974973	1015.974255
3.55903	1338.334401	0.024215	724.7039558	724.9284512
3.58545	815.1134205	0.026415	485.0563535	485.0560153
3.61186	422.3549006	0.029055	278.4897363	278.5917067
3.64356	60.92361234	0.0317	44.21307309	44.21307309
3.67526	-291.8618414	0.034535	-232.7580525	-232.8478243
3.71263	-690.1878235	0.03737	-601.6610939	-601.6610939
3.75	-1189.038154	0.018685	-523.4799217	-522.1757588
		Sum	2035.860566	2038.724263
Lower section - Part 3				
3.4065	2573.760605	0.012205	672.3481194	673.5525828
3.43091	1507.238598	0.02441	793.1201445	793.1201445
3.45532	1015.779644	0.026855	592.2332744	592.4428079
3.48462	699.5787633	0.029295	448.7096535	448.7093316
3.51391	479.8616501	0.032225	341.4125422	341.5551249
3.54907	286.7099034	0.035155	224.7626947	224.7625364
3.58422	104.2072763	0.0383	89.88171407	89.92121045
3.62567	-87.34285327	0.041445	-82.46461971	-82.46456285
3.66711	-286.8211743	0.041445	-273.8969268	-273.8971135
3.70856	-498.9915546	0.041445	-481.8928886	-481.8925638
3.75	-737.209287	0.02072	-359.9081529	-358.9138467
		Sum	1964.305555	1966.895652

Section difference = 0.036518771

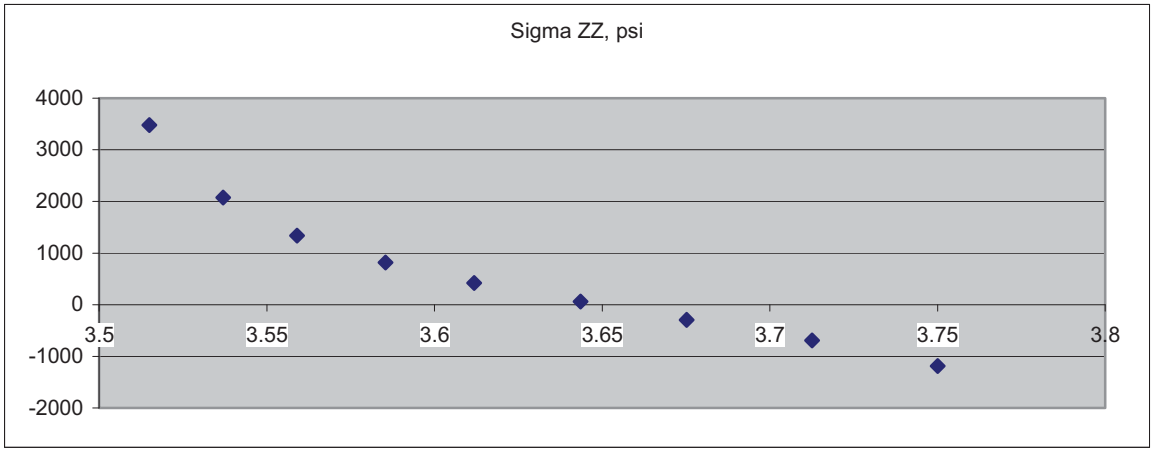

Appendix 2 – Finite Element Data

Summary

Description

Thread Analysis

Model Information

Analysis Type - Static Stress with Linear Material Models
Units - English (in) - (lbf, in, s, deg F, deg R, V, ohm, A, in*lbf)
Model location - C:\ALGOR12\es3100CV1

Analysis Parameters Information

Load Case Multipliers

Static Stress with Linear Material Models may have multiple load cases. This allows a model to be analyzed with multiple loads while solving the equations a single time. The following is a list of load case multipliers that were analyzed with this model.

Load Case	Pressure/ Surface Forces	Acceleration/ Gravity	Displaced Boundary	Thermal	Voltage
1	1	0	1	0	0
2	0	0	1	0	0
3	0	0	0	1	0
4	0.0305	0	0	1	0

Multiphysics Information

Default Nodal Temperature	70°F
Source of Nodal Temperature	None
Time step from Heat Transfer Analysis	Last

Processor Information

Type of Solver	Sparse
Disable Calculation and Output of Strains	No
Calculate Reaction Forces	Yes
Invoke Banded Solver	Yes
Avoid Bandwidth Minimization	No
Stop After Stiffness Calculations	No
Displacement Data in Output File	No
Stress Data in Output File	No
Equation Numbers Data in Output File	No
Element Input Data in Output File	No
Nodal Input Data in Output File	No
Centrifugal Load Data in Output File	No

Part Information

Part ID	Part Name	Element Type	Material Name
1	Plate & shell	2-D	[Customer Defined] (Part 1)
2	Bottom corner	2-D	[Customer Defined] (Part 2)
3	Top transition	2-D	[Customer Defined] (Part 3)
4	Outer O-ring	2-D	[Customer Defined] (Part 4)
5	Inner O-ring	2-D	[Customer Defined] (Part 5)
6	Top flange neck	2-D	[Customer Defined] (Part 6)
8	Thread region	2-D	[Customer Defined] (Part 8)

Element Properties used for:

- Plate & shell
- Bottom corner
- Top transition
- Thread region

Element Type	2-D
Geometry Type	Axisymmetric
Material Model	Isotropic
Thickness	1 in
Stress Free Reference Temperature	70°F
Principle Axes Transformational Angle	0°
Nodal Order Method	Default
Nodal Order Y Coordinate	0 in
Nodal Order Z Coordinate	0 in

Element Properties used for:

- Outer O-ring
- Inner O-ring

Element Type	2-D
Geometry Type	Axisymmetric
Material Model	Isotropic
Thickness	1 in
Stress Free Reference Temperature	0°F
Principle Axes Transformational Angle	0°
Nodal Order Method	Default
Nodal Order Y Coordinate	0 in
Nodal Order Z Coordinate	0 in

Element Properties used for:

- Top flange neck

Element Type	2-D
Geometry Type	Axisymmetric
Material Model	Orthotropic
Thickness	1 in
Stress Free Reference Temperature	170°F
Principle Axes Transformational Angle	0°
Nodal Order Method	Default
Nodal Order Y Coordinate	0 in
Nodal Order Z Coordinate	0 in

Material Information

[Customer Defined] (Part 1) - 2-D

Material Model	Standard
Material Source	Not Applicable
Material Source File	
Date Last Updated	2004/09/28-14:35:06
Material Description	Customer defined material properties
Mass Density	7.50e-4 lbf*s^2/in/in³
Modulus of Elasticity	27e6 lbf/in²
Poisson's Ratio	0.3
Thermal Coefficient of Expansion	9.2e-6 1/°F
Shear Modulus of Elasticity	10384615 lbf/in²

[Customer Defined] (Part 2) - 2-D

Material Model	Standard
Material Source	Not Applicable
Material Source File	
Date Last Updated	2004/09/28-14:36:43
Material Description	Customer defined material properties
Mass Density	7.50e-4 lbf*s^2/in/in³
Modulus of Elasticity	27e6 lbf/in²
Poisson's Ratio	0.3
Thermal Coefficient of Expansion	9.2e-6 1/°F
Shear Modulus of Elasticity	10384615 lbf/in²

[Customer Defined] (Part 3) - 2-D

Material Model	Standard
Material Source	Not Applicable
Material Source File	
Date Last Updated	2004/09/28-14:38:39
Material Description	Customer defined material properties
Mass Density	7.50e-4 lbf*s^2/in/in³
Modulus of Elasticity	27e6 lbf/in²
Poisson's Ratio	0.30
Thermal Coefficient of Expansion	9.2e-6 1/°F
Shear Modulus of Elasticity	10384615 lbf/in²

[Customer Defined] (Part 4) - 2-D

Material Model	Standard
Material Source	Not Applicable
Material Source File	
Date Last Updated	2004/09/28-14:39:52
Material Description	Customer defined material properties
Mass Density	0 lbf*s^2/in/in³
Modulus of Elasticity	1321 lbf/in²
Poisson's Ratio	0
Thermal Coefficient of Expansion	0 1/°F
Shear Modulus of Elasticity	660.5 /²

[Customer Defined] (Part 5) - 2-D

Material Model	Standard
Material Source	Not Applicable
Material Source File	
Date Last Updated	2004/09/28-14:40:41
Material Description	Customer defined material properties
Mass Density	0 lbf*s^2/in/in³
Modulus of Elasticity	1122 lbf/in²
Poisson's Ratio	0
Thermal Coefficient of Expansion	0 1/°F
Shear Modulus of Elasticity	561. /²

[Customer Defined] (Part 6) - 2-D

Material Model	OrthotropicTempDep
Material Source	Not Applicable
Material Source File	
Date Last Updated	2004/10/14-14:27:16
Material Description	Customer defined material properties
Mass Density	7.50e-4 lbf*s^2/in/in³
Index 1 - Temperature	170 °F
Index 1 - E1	27e6 lbf/in²
Index 1 - E2	27e6 lbf/in²
Index 1 - E3	27e6 lbf/in²
Index 1 - V12	.3
Index 1 - V13	.3
Index 1 - V23	.3
Index 1 - G12	10384615 lbf/in²
Index 1 - G13	10384615 lbf/in²
Index 1 - G23	10384615 lbf/in²
Index 1 - Alpha 1	0 1/°F
Index 1 - Alpha 2	1.45e-3 1/°F
Index 1 - Alpha 3	0 1/°F

[Customer Defined] (Part 8) - 2-D

Material Model	Standard
Material Source	Not Applicable
Material Source File	
Date Last Updated	2004/09/28-14:43:25
Material Description	Customer defined material properties
Mass Density	7.50e-4 lbf*s^2/in/in³
Modulus of Elasticity	27e6 lbf/in²
Poisson's Ratio	0.30
Thermal Coefficient of Expansion	9.2e-6 1/°F
Shear Modulus of Elasticity	10384615 lbf/in²

Processor Output

Processor Summary

```
ALGOR (R) Static Stress with Linear Material Models
Version 16.00-WIN 29-SEP-2004
Copyright (c) 1984-2004 ALGOR, Inc. All rights reserved.

--------------------------------------------------
                       DATE: FEBRUARY 16, 2005
                       TIME: 07:55 AM
                INPUT MODEL: C:\ALGOR12\es3100CV1

            PROGRAM VERSION: 16000001
            ALG.DLL VERSION: 13240000
      AlgConfig.DLL VERSION: 15000000
       agsdb_ar.DLL VERSION: 14000004
       amgsolve.DLL VERSION: 03220000
--------------------------------------------------

      Linear Stress

1**** CONTROL INFORMATION

      number of node points          (NUMNP)   =          2061
      number of element types        (NELTYP)  =             8
      number of load cases           (LL)      =             4
```

```
      number of frequencies          (NF)      =             0
      analysis type code             (NDYN)    =             0
      equations per block            (KEQB)    =             0
      bandwidth minimization flag    (MINBND)  =             0
      gravitational constant         (GRAV)    =    3.8640E+02
      number of equations            (NEQ)     =          4092

 **** PRINT OF NODAL DATA SUPPRESSED
 **** PRINT OF EQUATION NUMBERS SUPPRESSED
 **** PRINT OF TYPE-4 ELEMENT DATA SUPPRESSED
 **** PRINT OF TYPE-4 ELEMENT DATA SUPPRESSED
 **** PRINT OF TYPE-4 ELEMENT DATA SUPPRESSED
 **** PRINT OF TYPE-4 ELEMENT DATA SUPPRESSED
 **** PRINT OF TYPE-4 ELEMENT DATA SUPPRESSED
 **** PRINT OF TYPE-4 ELEMENT DATA SUPPRESSED
 **** PRINT OF TYPE-4 ELEMENT DATA SUPPRESSED
 **** PRINT OF TYPE-7 ELEMENT DATA SUPPRESSED
 **** Hard disk file size information for processor:

      Available hard disk space on current drive =   3849.848 megabytes

1**** NODAL LOADS (STATIC) OR MASSES (DYNAMIC)

   NODE  LOAD     X-AXIS     Y-AXIS     Z-AXIS     X-AXIS     Y-AXIS     Z-AXIS
  NUMBER CASE      FORCE      FORCE      FORCE     MOMENT     MOMENT     MOMENT

    1685    1  0.000E+00  0.000E+00 -6.362E+00  0.000E+00  0.000E+00  0.000E+00
    1685    4  0.000E+00  0.000E+00 -1.943E-01  0.000E+00  0.000E+00  0.000E+00
    1686    1  0.000E+00  0.000E+00 -6.424E+00  0.000E+00  0.000E+00  0.000E+00
    1686    4  0.000E+00  0.000E+00 -1.962E-01  0.000E+00  0.000E+00  0.000E+00

1**** ELEMENT LOAD MULTIPLIERS

      load case      case A     case B     case C     case D     case E
      ---------    ---------- ---------- ---------- ---------- ----------

          1         1.000E+00  0.000E+00  1.000E+00  0.000E+00  0.000E+00
          2         0.000E+00  0.000E+00  1.000E+00  0.000E+00  0.000E+00
          3         0.000E+00  0.000E+00  0.000E+00  1.000E+00  0.000E+00
          4         3.050E-02  0.000E+00  0.000E+00  1.000E+00  0.000E+00
```

Appendix 2.10.2

IMPACT ANALYSES OF ES-3100 DESIGN CONCEPTS USING BOROBOND AND CAT 277-4 NEUTRON ABSORBERS

THIS PAGE INTENTIONALLY LEFT BLANK.

Index

1.0 Problem Statement 3

Part A - Initial Design with Borobond Cylinder

2.0 Analytical Model 7
2.1 Model Description - Detailed Model 7
2.2 Model Description - Simplified Model 18
2.3 Material Models 23

3.0 Solution Results 38
3.1 Run1g - Side 41
3.2 Run1ga - Side 71
3.3 Run1hl - Side 87
3.4 Run1hh - Side 108
3.5 Run2e - Corner 128
3.6 Run3b - End 138
3.7 Run4g - Slapdown 147
3.8 Run4ga - Slapdown 156
3.9 Run4h - Slapdown 162
3.10 Run4ha - Slapdown 170
3.11 Punch Runs 175
3.12 Comparison of Test vs Analysis 179

4.0 Summary and Conclusions 197

5.0 References 201

Part B - Design with HABC Cylinder

6.0 Analytical Model 202
6.1 Model Description 202
6.2 Material Models 210

7.0 Analysis Results 216
7.1 HABC-run1hl - Lower Bounding Side 216

Part B - Design with HABC Cylinder (continued)

7.2 HABC-run1hh - Upper Bounding Side 231
7.3 HABC-run2e - Corner 243
7.4 HABC-run3b - End 255
7.5 HABC-run4g - Slapdown 262
7.6 HABC-run4ga - Slapdown 275
7.7 Comparison of Test vs Analysis 283
8.0 Summary 300

9.0 Comparison of Borobond Cylinder and HABC Cylinder Models 302

1.0 Problem Statement

This calculation summarizes the impact simulation computer runs made in support of the ES-3100 shipping package design effort. From the summer of 2003 through the spring of 2004 the design impact simulations were run with borobond as the neutron absorber. During the summer of 2004, the ES-3100 with the borobond neutron absorber was tested to the 10CFR71 impact requirements. In August 2004 a decision was made to change the neutron absorber material to a high alumina borated cement (HABC). The HABC material is also known as "Catalog 277-4" or just "277-4", but the HABC notation is used in this report. The August 2004 absorber change also involved some minor design changes to the configuration of the package liners surrounding the HABC material. Material testing on the HABC material occurred during the Fall of 2004. The simulation impacts were run in the late Fall of 2004.

This calculation is presented in two parts, Part A and Part B. Part A summarizes the impact simulations made for the initial borobond design. Part B summarizes the impact analyses made with the HABC design. A beginning section, Section 1.0 and an ending section, Section 9.0, address both designs. The Part A borobond design simulations are documented in Sections 2 through 5. The Part B, HABC simulations are documented in Sections 6 through 8. A detailed explanation of changes to the Part A, borobond models to develop the Part B HABC models is given in Part B, Section 6.1.

A qualitative, cross sectional view of a ES-3100 package with the initial design borobond neutron absorber (presented in Part A) is shown in Figure 1.1. The ES-3100 shipping package is a stainless steel drum with kaolite insulation material. The overall dimensions of the overpack are a height of about 44 inches and a diameter of about 19.4 inches. At the top of the overpack is a bolted lid restrained by eight, 5/8 inch welded studs. The lid restrains a removable plug filled with the kaolite material. The plug covers a cavity in which the stainless steel containment vessel (CV) is placed. The CV is about 32.9 inches tall with a 5.4 inch inside diameter and a body wall thickness of 0.1 inches. The CV closure is a flat plate constrained by a threaded ring. In the shipping package, and immediately surrounding the CV cavity is a 0.90 inch thick layer of borobond, a neutron absorbing cast material. All the kaolite and borobond materials are wrapped by stainless steel liners. In this model, there is a slight indentation (about 0.32 in) of the liner near the CV flange region into the kaolite, as can be seen in Figure 1.1.

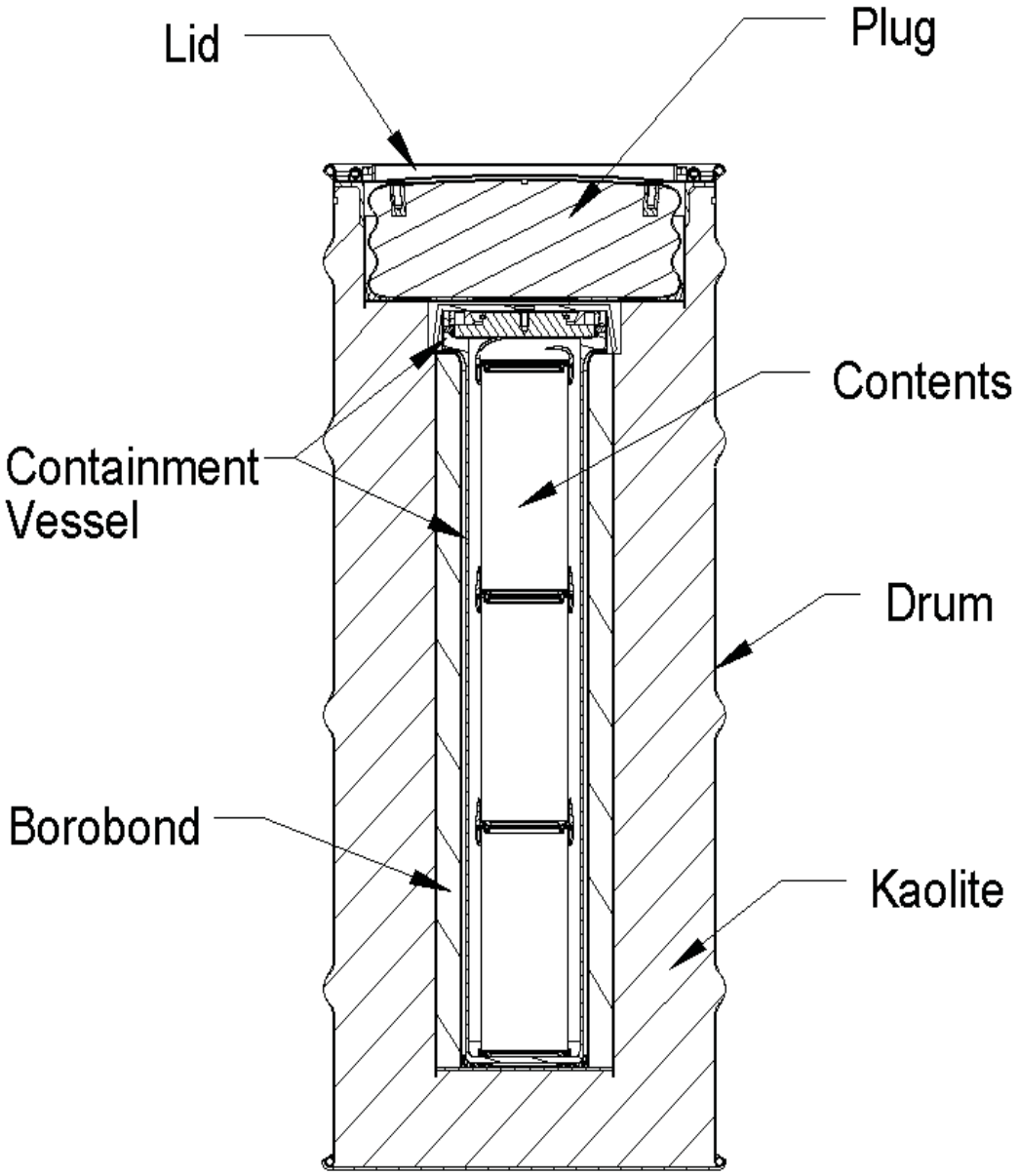

Figure 1.1 - Configuration of the Initial, Borobond Neutron Absorber ES-3100 Package, Presented in Part A

The redesigned package with the HABC (Part B) is shown in Figure 1.2. As can be qualitatively seen in the figure, the liner between the HABC and the kaolite is moved out slightly and there is no indentation into the kaolite near the CV flange. The HABC design changes are minor as shown by qualitatively comparing Figures 1.1 and 1.2. The detailed differences between the Part A borobond model and the Part B, HABC model are presented in Part B, Section 6.

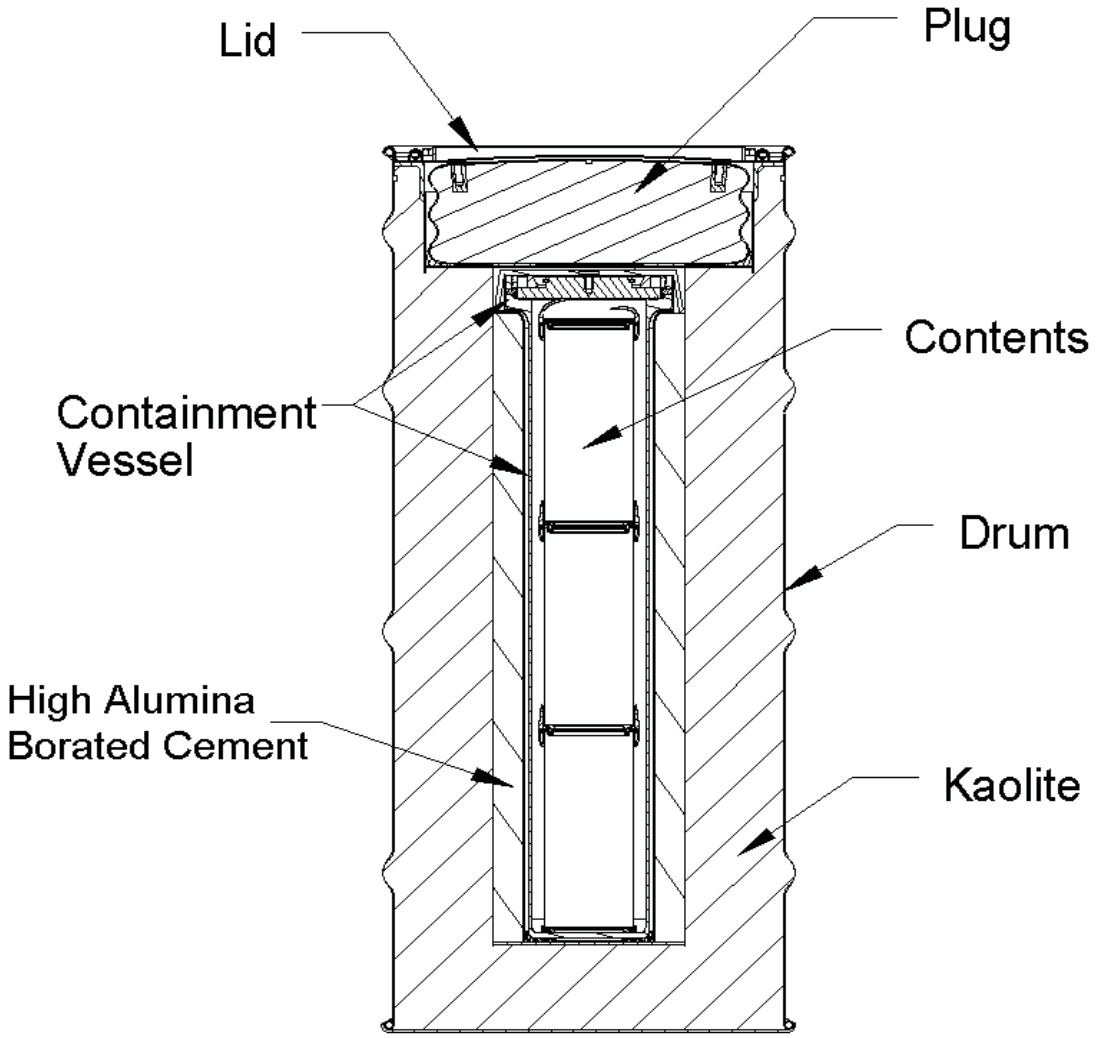

Figure 1.2 - Configuration of the Redesigned ES-3100 with the HABC as the Neutron Absorber, Presented in Part B

The Part A and Part B impact simulations were modeled with the pre-processor software TrueGrid (reference 5.1), solved with the software LS-Dyna (reference 5.2), and results obtained with the post-processor LS-Post (reference 5.3). The computers used for these simulations were Dell dual processor machines (Y12 machines ep0134, ep0141 and ep0142). TrueGrid was run on a Silicon Graphics Workstation (Y12 machine ew204). Typical solution times for one impact ranged from 1 to 4 days.

The impact simulations of the ES3100 package are driven by the 10CFR71, subpart F, sections 71.71 and 71.73 impact requirements. LS-Dyna allows successive restarts to be made which enables cumulative damage to be obtained in the shipping package model. Part A, Section 2.1, describes the specific impact simulations performed for the initial borobond design. Part B, Section 6.1, describes the simulations performed for the HABC design. Sections 3.12 and 7.7 compare the respective model results to physical test results.

2.0 Analytical Model

Two models were used in the dynamic impact runs for the borobond design of the ES-3100 shipping container; a detailed model and a simplified model. A detailed model included the drum closure details, CV details and generally a finer element mesh. The detailed model was used for all the runs, except the study which evaluated the response of the drum to various punch angles. A simplified model was used to investigate the variation in punch angles. The detailed model is discussed in Section 2.1 and the simplified model is discussed in Section 2.2.

Design drawings were used to develop the ES-3100 analytical models. The reference 5.5 AutoSketch software was used as an aid in the creation of the TrueGrid input file. The running of TrueGrid created the bulk of the LS-Dyna input file (e.g., the nodal data, element data, contact surfaces, etc). The LS-Dyna command lines and material properties were created in a separate file and edited into the TrueGrid created LS-Dyna input file. The resulting file was a complete LS-Dyna input file which was then submitted for execution.

2.1 Model Description - Detailed Model

Figure 2.1.1 shows the typical detailed model assembly for the ES-3100. All of the entities shown (rigid surface, crush plate, shipping package and punch) exist in the model, however, only the entities of concern in an impact were active in that impact. In the 4-foot impact and 30-foot impact only the shipping package and the rigid plate were in contact. The crush plate and the punch existed in the model, however, there was no contact between them and the shipping package. During the crush impact, the crush plate contacts the shipping package, which then contacts the rigid plate. During the crush impact, the punch exists, but is not contacted. During the punch impact, the crush plate and the rigid surface are deleted from the model, allowing contact to be made between the shipping package and the punch.

Figure 2.1.2 shows the components of the detailed model in an exploded view. The element mesh is not included in Figure 2.1.1, nor in Figure 2.1.2 for clarity. Representative element meshes for the detailed model are shown in Figures 2.1.3 and 2.1.4.

Various impact configurations of the ES-3100 detailed model are documented in this calculation. Figure 2.1.5 shows icons representing the impact configurations run for the design effort. The 4-foot impact and the punch impact are not as structurally demanding as is the 30-foot free fall impact, nor the 30-foot crush impact. Therefore, only the 30-foot impact and the crush impact were performed in the design effort runs. Figure 2.1.6

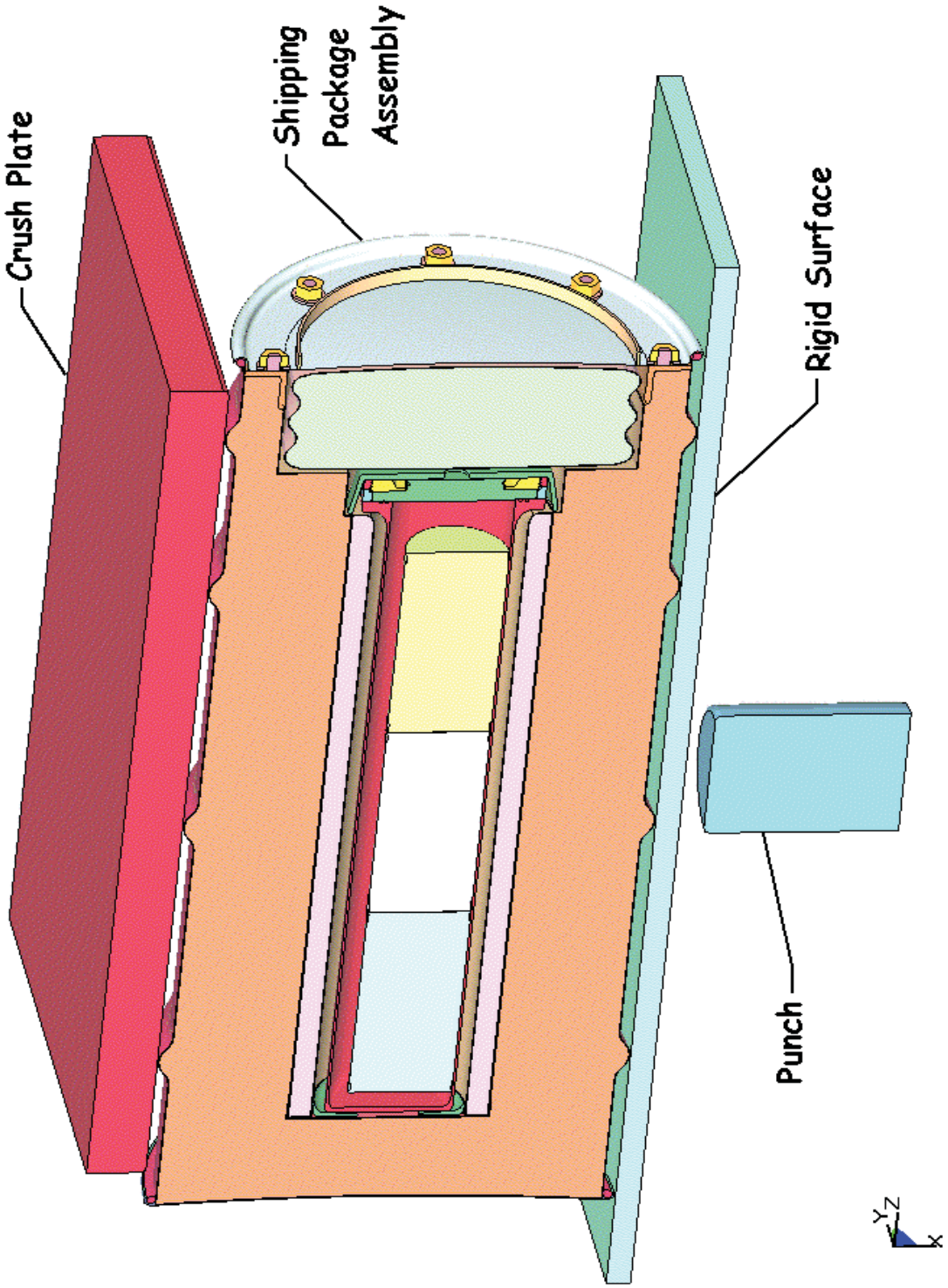

Figure 2.1.1 - Typical ES-3100 Detailed Model Assembly

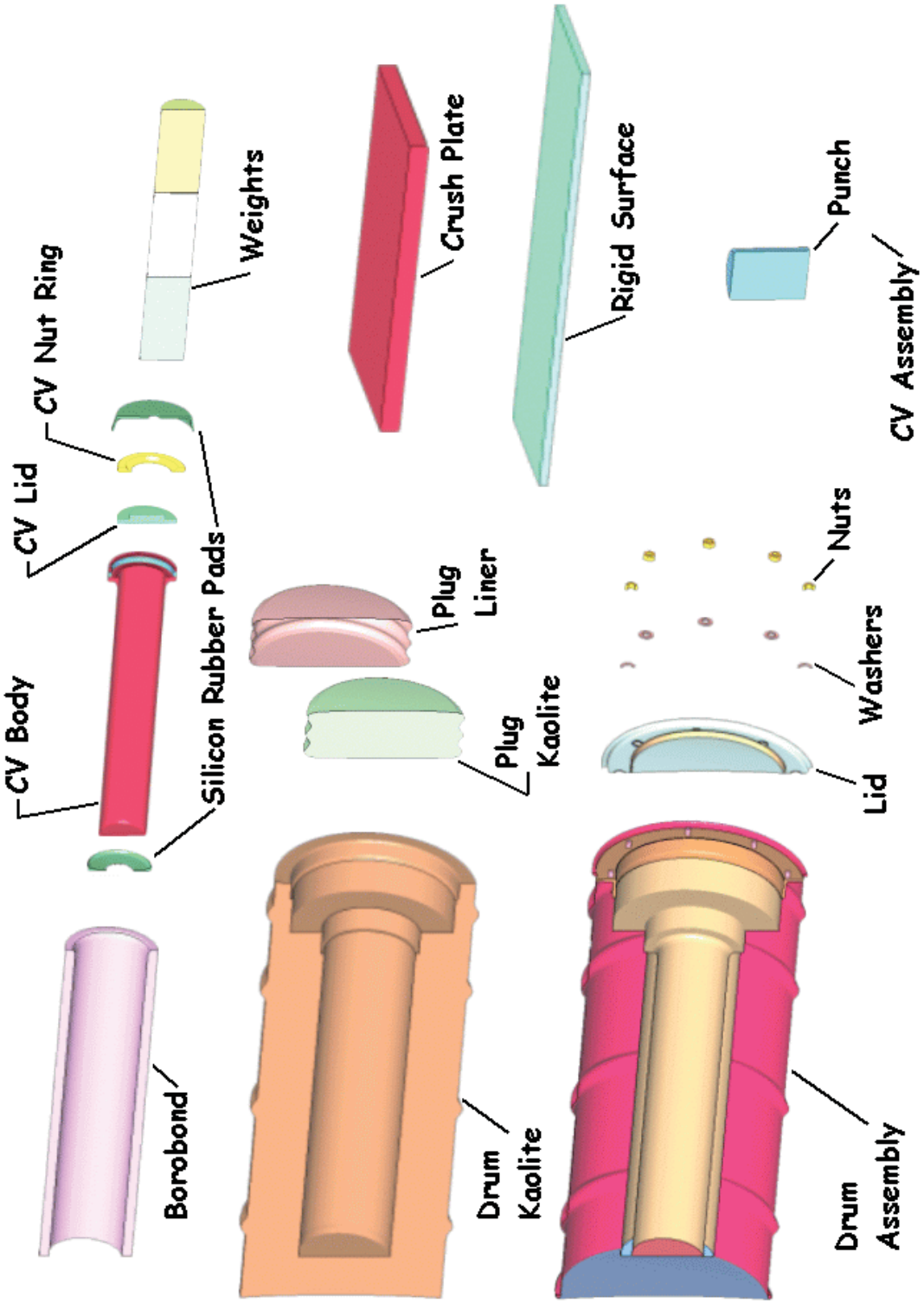

Figure 2.1.2 - ES-3100 Detailed Model Components

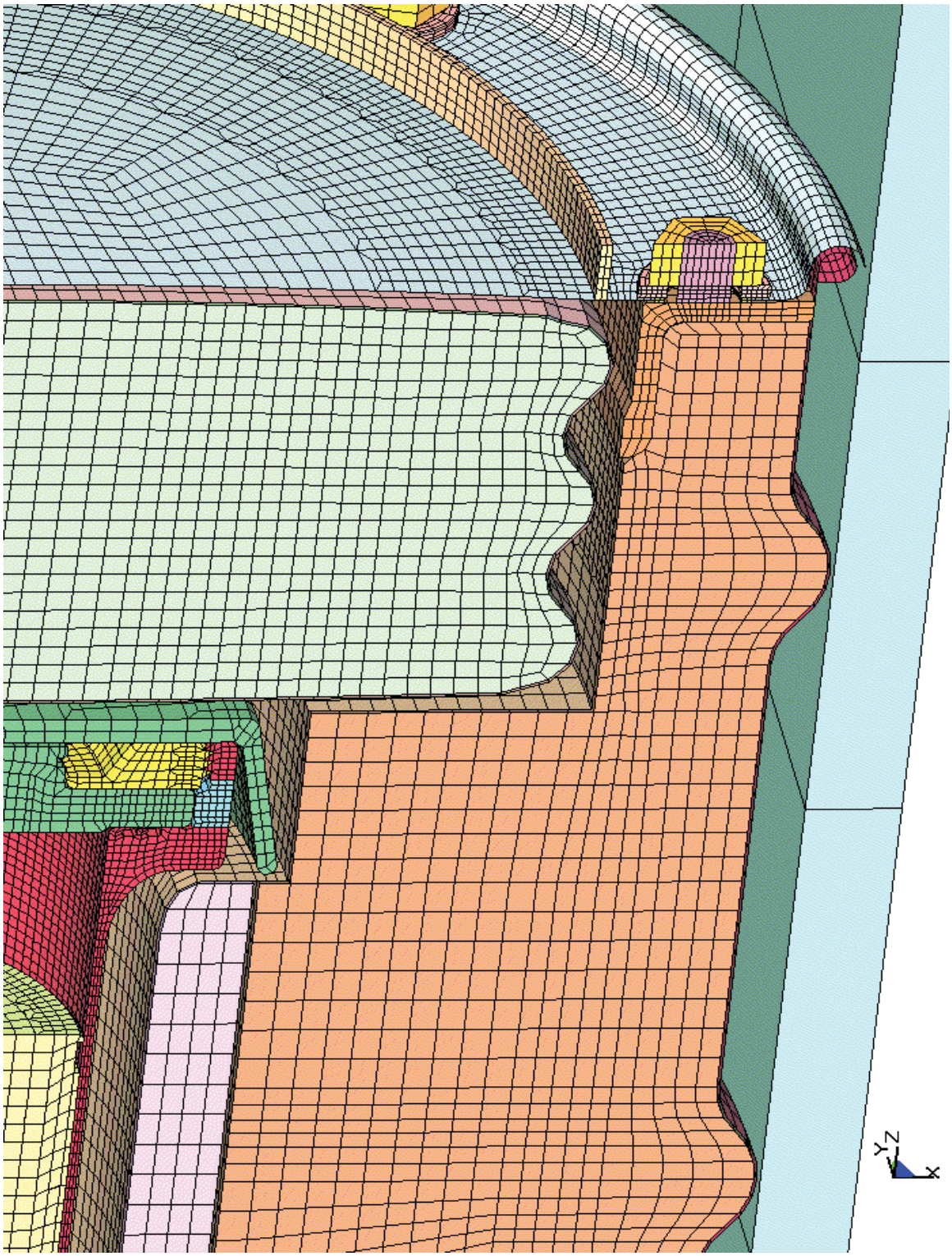

Figure 2.1.3 - Typical Element Mesh in the Upper Container Region of the Detailed Model

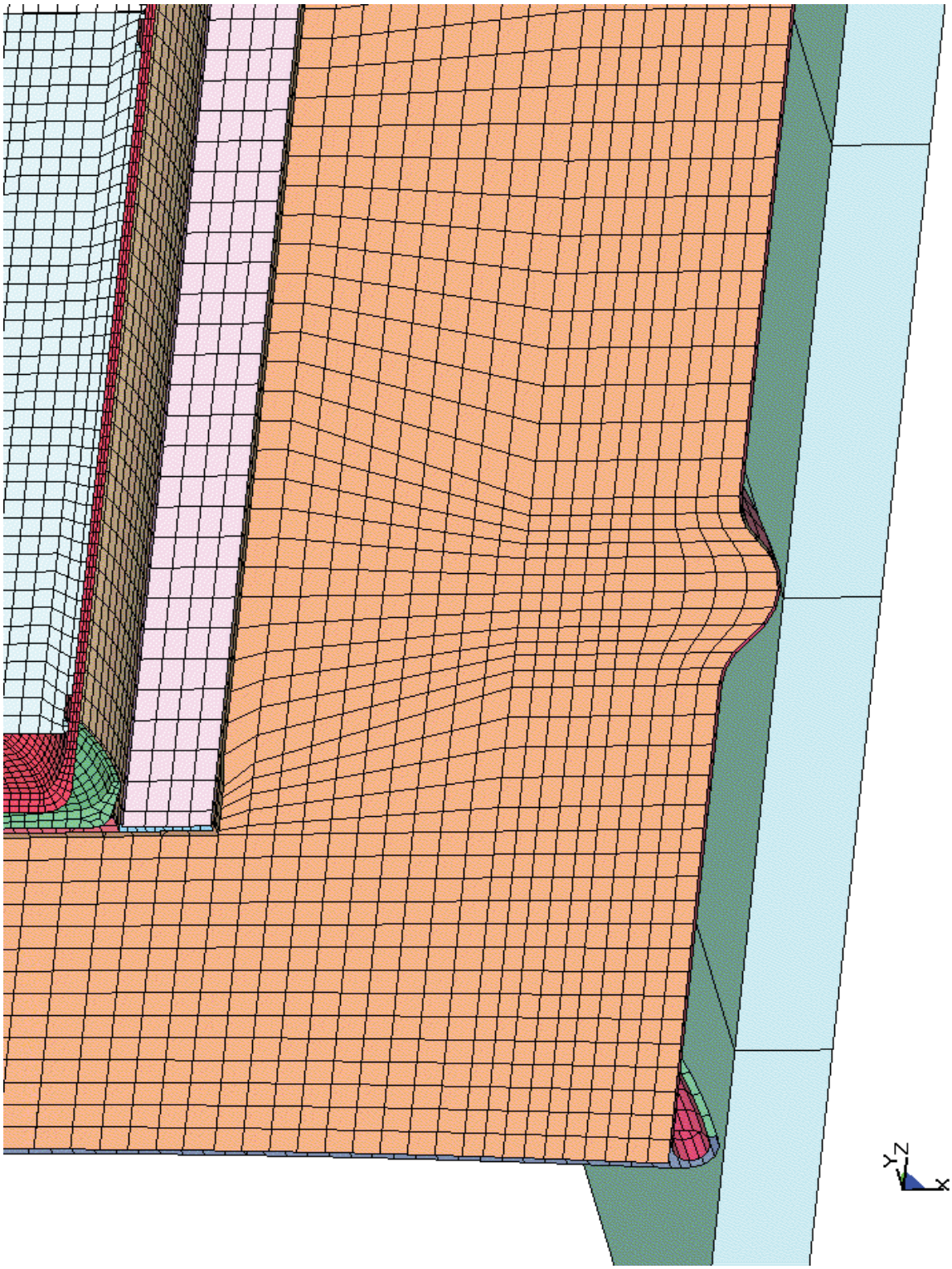

Figure 2.1.4 - Typical Element Mesh in the Lower Container Region of the Detailed Model

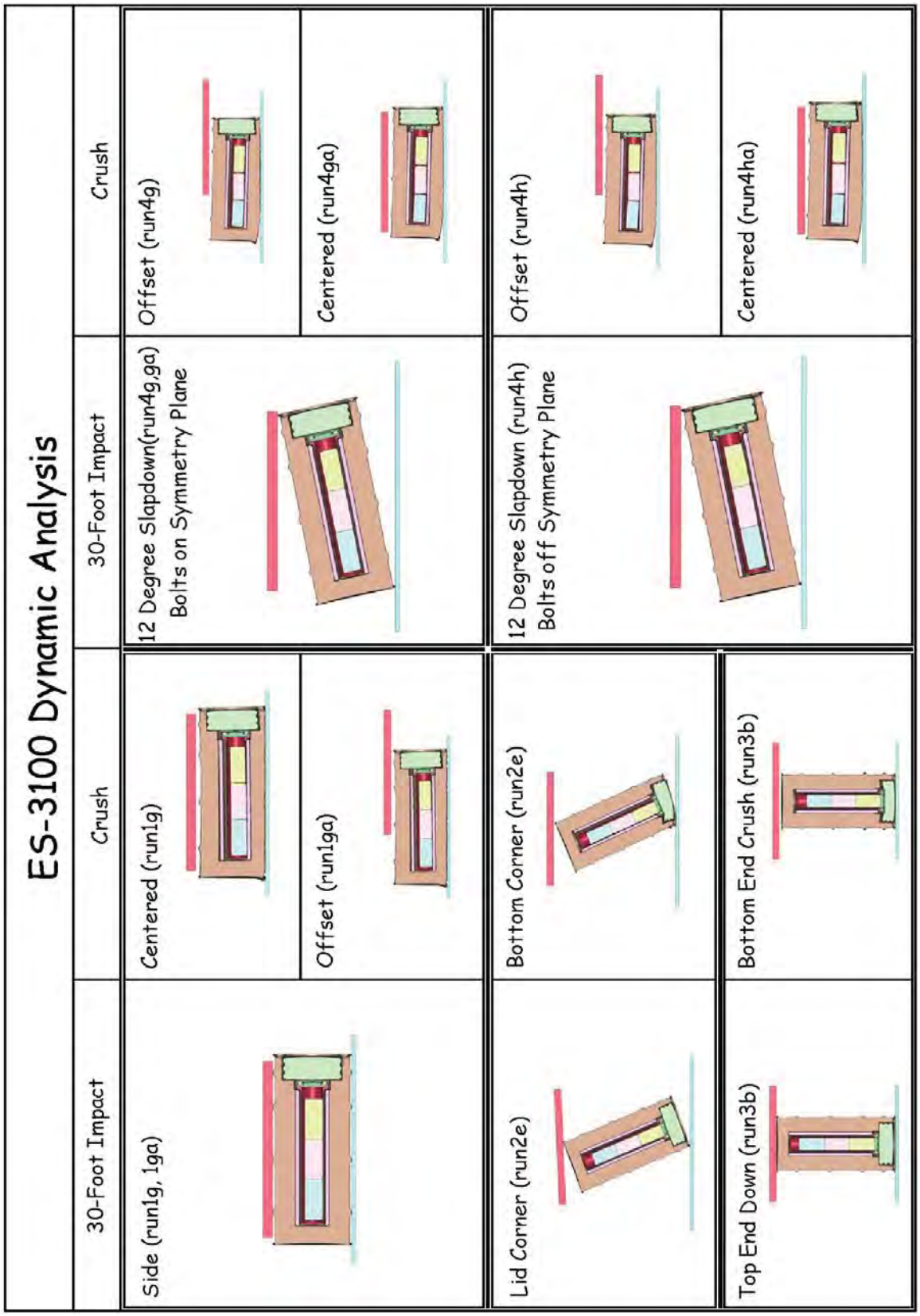

Figure 2.1.5 - LS-Dyna Design Runs for Successive 30-Foot and 30-Foot Crush Impacts

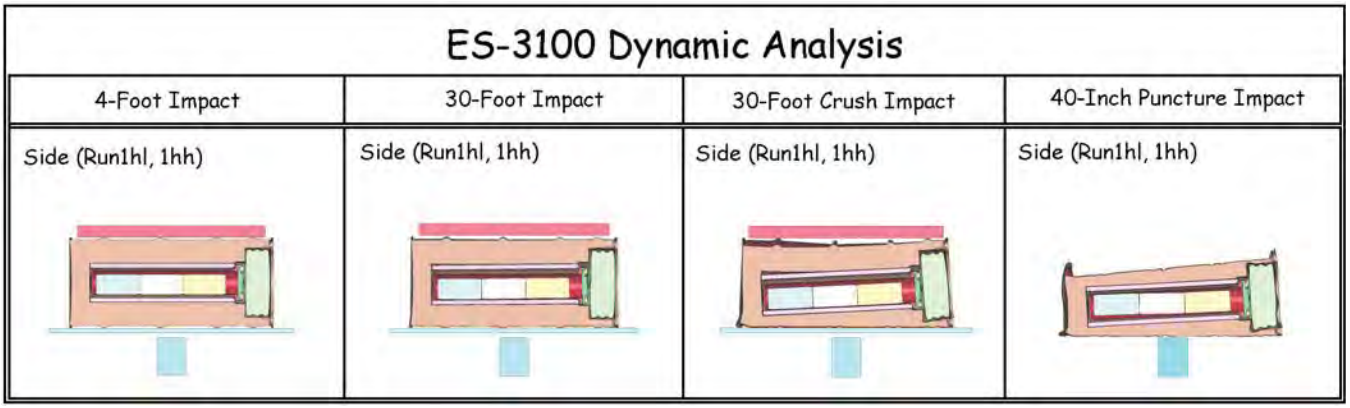

Figure 2.1.6 - Four Successive Impacts with the ES-3100 Bounding Kaolite Stiffness Models

shows icons representing the configurations run for the successive 4-foot + 30-foot + 30-foot crush + 40-inch punch impacts. The Figure 2.1.6 impacts were performed with the upper (-40°F, run1hh) and lower bound (100°F, run1hl) kaolite properties (see Section 2.3.5). The Figure 2.1.5 design runs were made with averaged kaolite properties (see Section 2.3.5). The run numbers (e.g., run1g, etc) are listed in Table 2.1.1 along with a verbal description of the impacts. Table 2.1.1 also identifies the Kaolite material model used for each run (see Section 2.3.5 for definition of the material properties).

Cumulative damage to the shipping package is obtained through successive impact restart solutions of LS-Dyna. At the beginning of the first impact, the initial velocity is assigned to the appropriate model nodes for the first impact. The solution is initiated and is considered over, when the kinetic energy reaches a constant value (after a minimum is reached) and when the rebound velocity reaches a constant value. Consideration was also given to the motion of the masses internal to the CV with regard to a primary impacts against the CV wall. When a run is considered over, the solution is halted and a restart file is written by LS-Dyna. The restart file captures the state of the container assembly at that point in the execution (including nodal velocities and element strains). A restart input file (text file) is then created which defines changes to be made to the model. The restart input file is used to redefine the velocity for the nodes of interest in a successive impact, or delete materials (components) if desired. The redefined velocity becomes the initial velocity, for the successive impact. The successive impact solution is then initiated with the restart file written by the halting of the previous impact and the restart input file. The velocities used in this analysis are: 193 in/sec for the 4-foot impact; 528 in/sec for the 30-foot impact; and 176 in/sec for the 40-inch punch impact.

Table 2.1.1 - Description of the ES-3100 Impacts Using the Detailed Model		
Run ID	Description	Kaolite Model†
Run1g	30-foot side impact + 30-foot crush with plate centered on drum	Average stiffness, 22.4 lb/0ft^3
Run1ga	30-foot side impact + 30-foot crush with plate centered on CV flange	Average stiffness, 22.4 lb/ft^3
Run1hl	4-foot side impact + 30-foot side impact + 30-foot crush impact + 40-inch punch impact	Lower bound stiffness, 27 lb/ft^3
Run1hh	4-foot side impact + 30-foot side impact + 30-foot crush impact + 40-inch punch impact	Upper bound stiffness, 27 lb/ft^3
Run2e	30-foot CG over lid corner impact + 30-foot crush on bottom corner	Average stiffness, 22.4 lb/ft^3
Run3b	30-foot top end impact + 30-foot bottom end crush	Average stiffness, 22.4 lb/ft^3
Run4g	30-foot, 12° slapdown with lid studs on plane of symmetry + 30-foot crush with plate centered on CV flange	Average stiffness, 22.4 lb/ft^3
Run4ga	30-foot, 12° slapdown with lid studs on plane of symmetry + 30-foot crush with plate centered on drum	Average stiffness, 22.4 lb/ft^3
Run4h	30-foot, 12° slapdown with lid studs off plane of symmetry + 30-foot crush with plate centered on the CV flange	Average stiffness, 22.4 lb/ft^3
Run4ha	30-foot, 12° slapdown with lid studs off plane of symmetry + 30-foot crush with plate centered on the drum	Average stiffness, 22.4 lb/ft^3
† - Defined in Section 2.3.5		

In the successive design impacts (Figure 2.15), a 30-foot impact was followed by a 30-foot crush impact. For these runs, the initial velocities of the shipping package assembly nodes were all defined as 528 in/sec in a direction normal and toward the rigid surface. When the initial impact was over, the run was halted and the velocities of the shipping package assembly nodes were all re-defined as 0.0 in/sec in the restart input file. This file also defined the velocity of the crush plate nodes as 528 in/sec in a direction towards the shipping package.

For the bounding kaolite stiffness runs (Figure 2.1.6), the impacts were successive 4-foot, 30-foot, 30-foot crush and 40-inch punch impacts. The 4-foot, 30-foot and 30-foot crush impacts were carried out as defined previously. The successive punch impact was initiated with the restart input file deleting the crush plate and the rigid plate from the model. The restart input file also redefined the velocity of the shipping package nodes to be towards the punch. This allowed the shipping package to pass through the original position of the rigid surface and impact the punch.

Table 2.1.2 gives the shipping package component masses and weights used in the detailed model analyses. Summations for assembly weights are also listed along with a total assembly weight. As discussed in the Section 2.3 on material models, an initial mass based on preliminary information supplied by the designer is adjusted to match expected hardware weights. This adjustment is required due to the faceted element faces on the inner and outer radius surfaces and the fact that small details are not explicitly modeled (holes, notches, etc). The total weight (full model) of the model is about 427.85 pounds, with 22.4 lb/ft^3 kaolite. The mass moment of inertia for the package is 90.84 $in*lb*sec^2$ about the global Y axis and the CG is located at Z = 22.4 inches.

Contact surfaces are used to allow adjacent components to separate, bear and/or slide along an adjacent surface. The contact used between the metal components of the model is a LS-Dyna single surface contact. Each node is reactive against every other element in the defined set. The contact between the borobond and its stainless steel liners; and the kaolite and its stainless steel liners is a surface to surface contact. All package nodes are defined as reactive to the rigid surface.

Table 2.1.2 - Analysis Weights for ES-3100

Material Number	Component Description	Run1g-Side		Run1hl-Side		Run1hh-Side		Run2e-Lid Corner		Run3b-Lid End		Run4g-Slapdown		Run4h-Slapdown	
		mass *	weight **	mass*	weight**	mass*	weight**	mass *	weight **	mass *	weight **	mass *	weight **	mass *	weight **
m 1	CV body	2.73E-02	21.10	2.73E-02	21.10	2.73E-02	21.10	2.73E-02	21.10	2.73E-02	21.10	2.73E-02	21.10	2.73E-02	21.10
m 2	CV body at flange	1.73E-03	1.34	1.73E-03	1.34	1.73E-03	1.34	1.73E-03	1.34	1.73E-03	1.34	1.73E-03	1.34	1.73E-03	1.34
m 3	CV lid	9.57E-03	7.39	9.57E-03	7.39	9.57E-03	7.39	9.57E-03	7.39	9.57E-03	7.39	9.57E-03	7.39	9.57E-03	7.39
m 4	CV screw ring	4.27E-03	3.30	4.27E-03	3.30	4.27E-03	3.30	4.27E-03	3.30	4.27E-03	3.30	4.27E-03	3.30	4.27E-03	3.30
m 5	angle	1.69E-02	13.02	1.69E-02	13.02	1.69E-02	13.02	1.69E-02	13.02	1.69E-02	13.02	1.69E-02	13.02	1.69E-02	13.02
m 6	drum	6.02E-02	46.50	6.02E-02	46.50	6.02E-02	46.50	6.02E-02	46.50	6.02E-02	46.50	6.02E-02	46.50	6.02E-02	46.50
m 7	drum bottom head	1.22E-02	9.42	1.22E-02	9.42	1.22E-02	9.42	1.22E-02	9.42	1.22E-02	9.42	1.22E-02	9.42	1.22E-02	9.42
m 8	weld drum to drum bottom head	1.18E-04	0.09	1.18E-04	0.09	1.18E-04	0.09	1.18E-04	0.09	1.18E-04	0.09	1.18E-04	0.09	1.18E-04	0.09
m 9	liner overlap to angle (0.03)	1.36E-04	0.11	1.36E-04	0.11	1.36E-04	0.11	1.36E-04	0.11	1.36E-04	0.11	1.36E-04	0.11	1.36E-04	0.11
m 10	liner (0.06)	3.95E-02	30.51	3.95E-02	30.51	3.95E-02	30.51	3.95E-02	30.51	3.95E-02	30.51	3.95E-02	30.51	3.95E-02	30.51
m 11	liner bottom (0.120) (see m 27 for	1.40E-03	1.08	1.40E-03	1.08	1.40E-03	1.08	1.40E-03	1.08	1.40E-03	1.08	1.40E-03	1.08	1.40E-03	1.08
m 12	lid shells (0.06)	7.25E-03	5.59	7.25E-03	5.59	7.25E-03	5.59	7.25E-03	5.59	7.25E-03	5.59	7.25E-03	5.59	7.25E-03	5.59
m 13	thin lid shell at bolts	1.37E-05	0.01	1.37E-05	0.01	1.37E-05	0.01	1.37E-05	0.01	1.37E-05	0.01	1.37E-05	0.01	1.37E-05	0.01
m 14	lid solids at the lid bolts	5.03E-05	0.04	5.03E-05	0.04	5.03E-05	0.04	5.03E-05	0.04	5.03E-05	0.04	5.03E-05	0.04	5.03E-05	0.04
m 15	lid stiffener	1.39E-03	1.07	1.39E-03	1.07	1.39E-03	1.07	1.39E-03	1.07	1.39E-03	1.07	1.39E-03	1.07	1.39E-03	1.07
m 16	drum bolts	5.06E-04	0.39	5.06E-04	0.39	5.06E-04	0.39	5.06E-04	0.39	5.06E-04	0.39	5.06E-04	0.39	5.06E-04	0.39
m 17	drum bolt nuts	1.20E-03	0.93	1.20E-03	0.93	1.20E-03	0.93	1.20E-03	0.93	1.20E-03	0.93	1.20E-03	0.93	1.20E-03	0.93
m 18	drum bolt washers	4.71E-04	0.36	4.71E-04	0.36	4.71E-04	0.36	4.71E-04	0.36	4.71E-04	0.36	4.71E-04	0.36	4.71E-04	0.36
m 19	plug liner	1.29E-02	10.00	1.29E-02	10.00	1.29E-02	10.00	1.29E-02	10.00	1.29E-02	10.00	1.29E-02	10.00	1.29E-02	10.00
m 20	plug kaolite	1.26E-02	9.70	1.52E-02	11.70	1.52E-02	11.70	1.26E-02	9.70	1.26E-02	9.70	1.26E-02	9.70	1.26E-02	9.70
m 21	drum kaolite	1.43E-01	110.08	1.72E-01	133.03	1.72E-01	133.03	1.43E-01	110.08	1.43E-01	110.08	1.43E-01	110.08	1.43E-01	110.08
m 22	drum borobond	5.66E-02	43.70	5.66E-02	43.70	5.66E-02	43.70	5.66E-02	43.70	5.66E-02	43.70	5.66E-02	43.70	5.66E-02	43.70
m 24	lower internal cv mass	4.75E-02	36.69	4.75E-02	36.69	4.75E-02	36.69	4.75E-02	36.69	4.75E-02	36.69	4.75E-02	36.69	4.75E-02	36.69
m 25	middle internal cv mass	4.75E-02	36.69	4.75E-02	36.69	4.75E-02	36.69	4.75E-02	36.69	4.75E-02	36.69	4.75E-02	36.69	4.75E-02	36.69
m 26	upper internal cv mass	4.75E-02	36.69	4.75E-02	36.69	4.75E-02	36.69	4.75E-02	36.69	4.75E-02	36.69	4.75E-02	36.69	4.75E-02	36.69
m 27	liner bottom solids	9.87E-04	0.76	9.87E-04	0.76	9.87E-04	0.76	9.87E-04	0.76	9.87E-04	0.76	9.87E-04	0.76	9.87E-04	0.76
m 29	visual rigid plane	7.80E-04	0.60	7.80E-04	0.60	7.80E-04	0.60	9.00E-04	0.69	8.00E-04	0.62	9.00E-04	0.69	9.00E-04	0.69
m 30	crush plate	1.42E+00	1099.99	1.42E+00	1099.99	1.42E+00	1099.99	1.42E+00	1099.99	1.42E+00	1099.99	1.42E+00	1099.99	1.42E+00	1099.99
m 31	punch	8.24E-02	63.62	8.24E-02	63.62	8.24E-02	63.62	8.24E-02	63.62	8.24E-02	63.62	8.24E-02	63.62	8.24E-02	63.62
m32	silicon rubber	1.65E-03	1.27	1.65E-03	1.27	1.65E-03	1.27	1.65E-03	1.27	1.65E-03	1.27	1.65E-03	1.27	1.65E-03	1.27
	dyna total model weight	2.06E+00	1592.05	2.09E+00	1617.00	2.09E+00	1617.00	2.06E+00	1592.15	2.06E+00	1592.07	2.06E+00	1592.15	2.06E+00	1592.15
	CV lid and nut ring		10.68		10.68		10.68		10.68		10.68		10.68		10.68
	CV body wt		22.44		22.44		22.44		22.44		22.44		22.44		22.44
	CV total wt		33.12		33.12		33.12		33.12		33.12		33.12		33.12
	plug liner and kaolite		19.70		21.69		21.69		19.70		19.70		19.70		19.70
	liner + angle		45.49		45.49		45.49		45.49		45.49		45.49		45.49
	drum body + kaolite + borobond4		256.94		279.90		279.90		256.94		256.94		256.94		256.94
	drum + lid + plug + kaolite + borobond4		284.65		309.60		309.60		284.65		284.65		284.65		284.65
	internal cv masses		110.08		110.08		110.08		110.08		110.08		110.08		110.08
	Total Package Weight		427.85		452.79		452.79		427.85		427.85		427.85		427.85
	Crush Plate Weight		1099.99		1099.99		1099.99		1099.99		1099.99		1099.99		1099.99
	Punch Weight		63.62		63.62		63.62		63.62		63.62		63.62		63.62
	Visual Rigid Plane		0.60		0.60		0.60		0.69		0.62		0.69		0.69
	Total Model Weight		1592.05		1617.00		1617.00		1592.15		1592.07		1592.15		1592.15

* - Mass is for the 1/2 model and is units of (pound * second^2) / inch

** - Weight is for the total package (2 x model weight) and is in units of pounds.

Friction factors are used in the contact surfaces of the models. Generally speaking, a static coefficient of 0.3 and a dynamic value of 0.2 is used. For the silicon rubber parts, a static coefficient of 0.6 and a dynamic value of 0.5 is assumed. The general factors of 0.3 (static) and 0.2 (dynamic) are also used for the shipping package contact with the rigid surface.

The design of the ES-3100 and the impact configurations are symmetrical. An analytical half model is used with conditions of symmetry defined for all nodes initially on the plane of symmetry. The drum bolting and the CV nut ring are modeled with surfaces initially in contact, but not pre-loaded. The CV is not pressurized. Gravity is included in the models.

The model typically used for a drum welded stud which secures the lid is shown in Figure 2.1.7. The mesh footprint in the stud is mirrored in the angle such that there is a one-to-one match of the stud nodes to angle nodes on the mating surface. The lower nodes on the studs are allowed to merge with the angle nodes. This is structurally conservative at the stud/angle intersection due to the fact that in the stud arc welding process a shoulder boss (area greater than the nominal stud area) is formed. The radius of the modeled studs is such that the faceted area of the stud model equates to the tensile stress area of the studs. Similarly to the stud/angle nodes, the nut/stud nodes are positioned and allowed to merge. The lid is modeled with shell elements, however, at the radius around each stud a transition to brick elements is made. This allows frictional bearing of the lid thickness onto the stud shank to be modeled. This modeling approach has been used and accepted for NNSA-licensed shipping packages that were subject to independent review and verification analysis (i.e., DPP-2 and ES-2100).

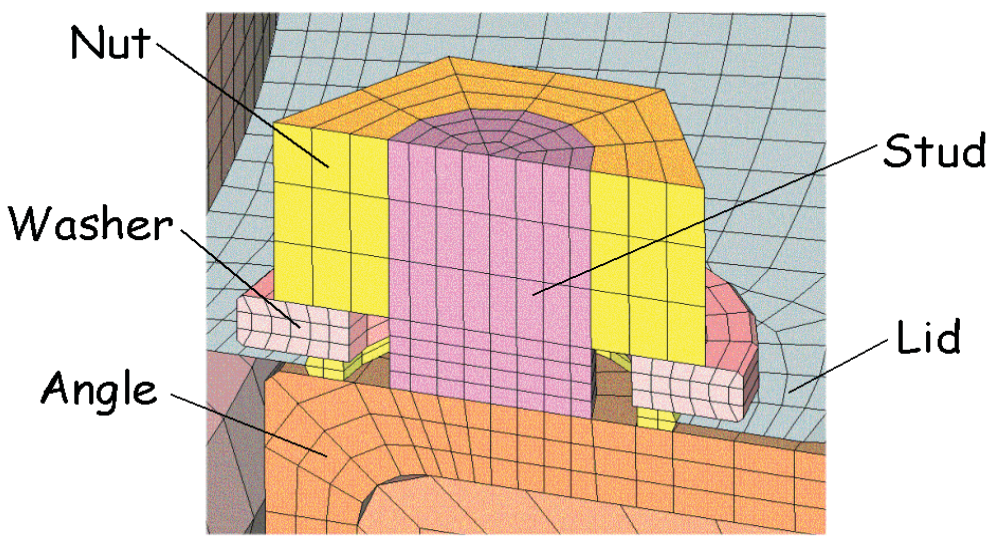

Figure 2.1.7 - Localized Model of a Stud

2.2 Model Description - Simplified Model

A series of punch impact runs were made on a simple model of the ES-3100 shipping container by varying the angle between the container liner and the punch, see Figure 2.2.1. In Figure 2.2.1, the position of the punch relative to the drum is shown with the angles in degrees. The purpose of the punch runs was to determine the response of the stainless steel drum liner due to the angled punch impacts. A series of eight, angled drops as shown in Figure 2.2.2 and described in Table 2.2.1 were made. In Figure 2.2.2, the punch is held stationary and the drum is positioned relative to the punch. The center of gravity of the shipping package was located directly above the side of the punch as shown in Figure 2.2.1. The initial velocity of the container is parallel to the axis of the punch as shown in Figure 2.2.2.

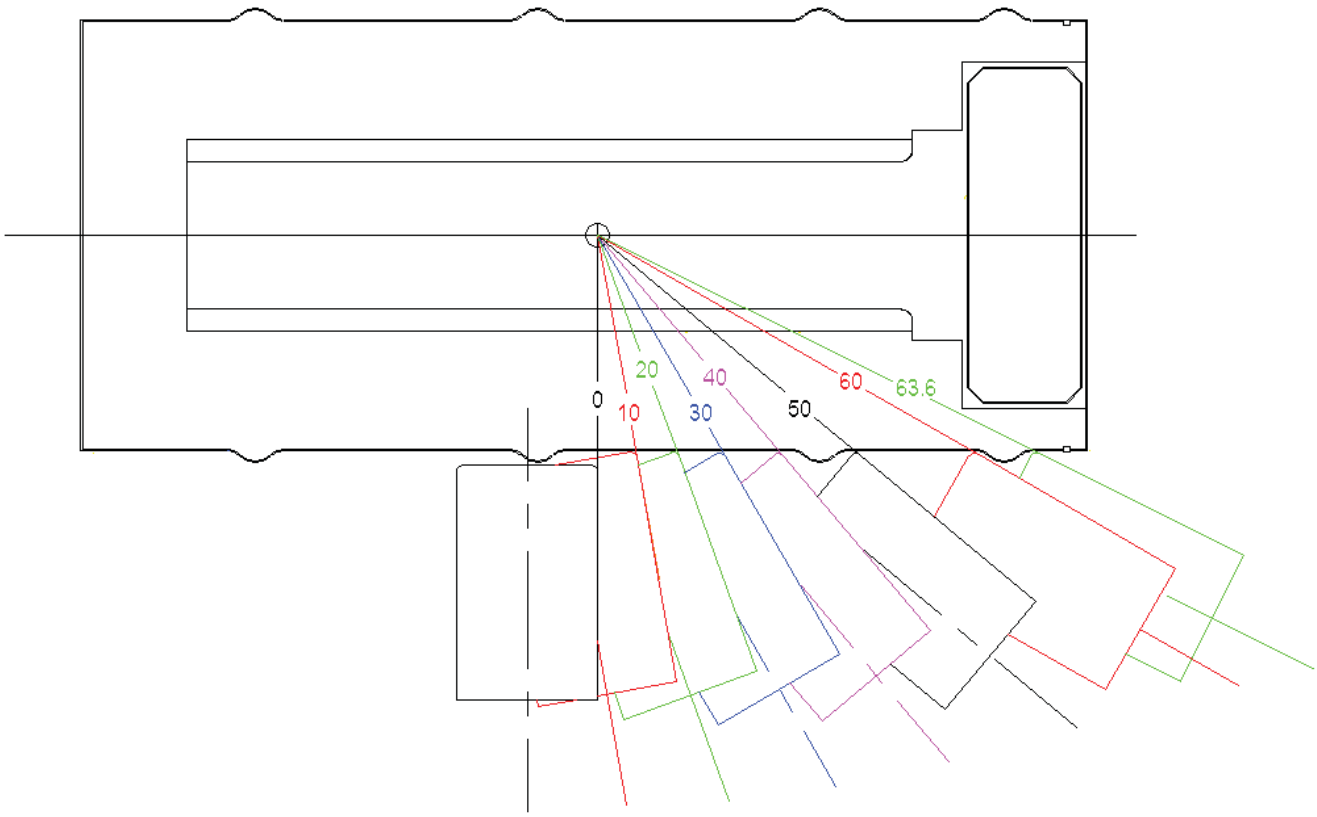

Figure 2.2.1 - Punch Angles on the Drum Liner

A simplified model of the ES-3100 was derived from the more detailed model (described in Section 2.1) for this series of runs. The model detail needed in the 4-foot, 30-foot, crush, and successive punch impact is not needed for the series of punch impacts. The purpose of the series of punch impacts is to evaluate the response of the drum skin to various punch angles.

The detailed model (section 2.1) was simplified (see below) to form the simple model. The detailed model was simplified except for the drum skin and the drum kaolite mesh nearest the punch impact. Figure 2.2.3 shows the simplified shipping package model used for the series of punch impacts. Figure 2.2.4 shows an exploded view of the simple model components.

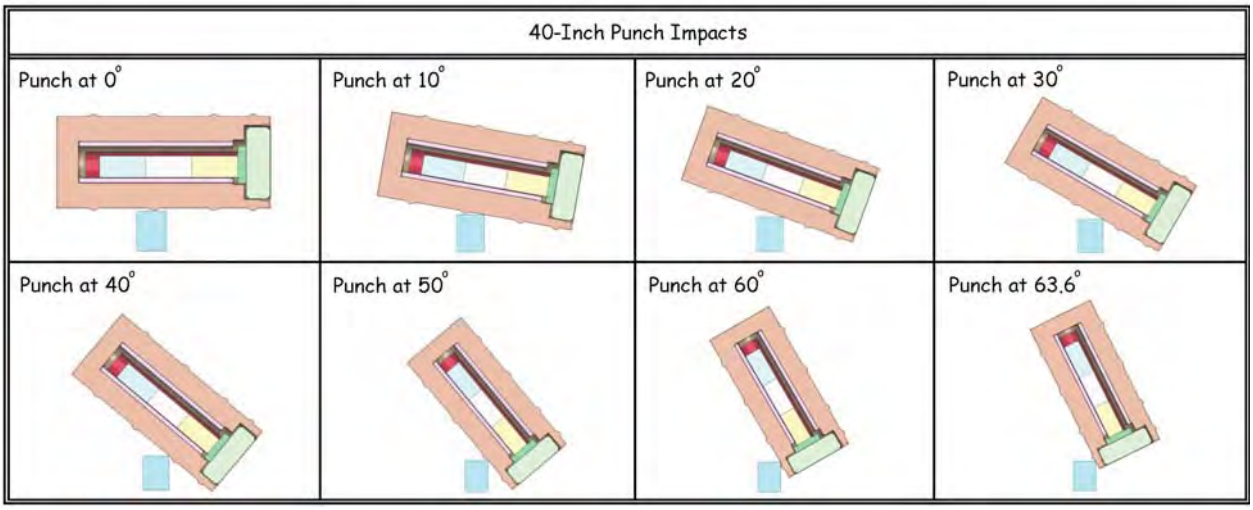

Figure 2.2.2 - ES-3100 Punch Configurations for the Series of Punch Impacts

Table 2.2.1 - Description of the ES-3100 Impacts with the Simplified Model Summarized in this DAC		
Run ID †	Description †	Kaolite Model
Punch at 0°	40-inch punch impact at 0°	Average stiffness, 22.4 lb/ft^3 (note the density is altered slightly so that the punch model weights approximate the full model runs)
Punch at 10°	40-inch punch impact at 10°	
Punch at 20°	40-inch punch impact at 20°	
Punch at 30°	40-inch punch impact at 30°	
Punch at 40°	40-inch punch impact at 40°	
Punch at 50°	40-inch punch impact at 50°	
Punch at 60°	40-inch punch impact at 60°	
Punch at 63.6°	40-inch punch impact at 63.6°	
† - Angles in degrees, measured from a perpendicular to the drum axis as shown in Figure 2.2.1		

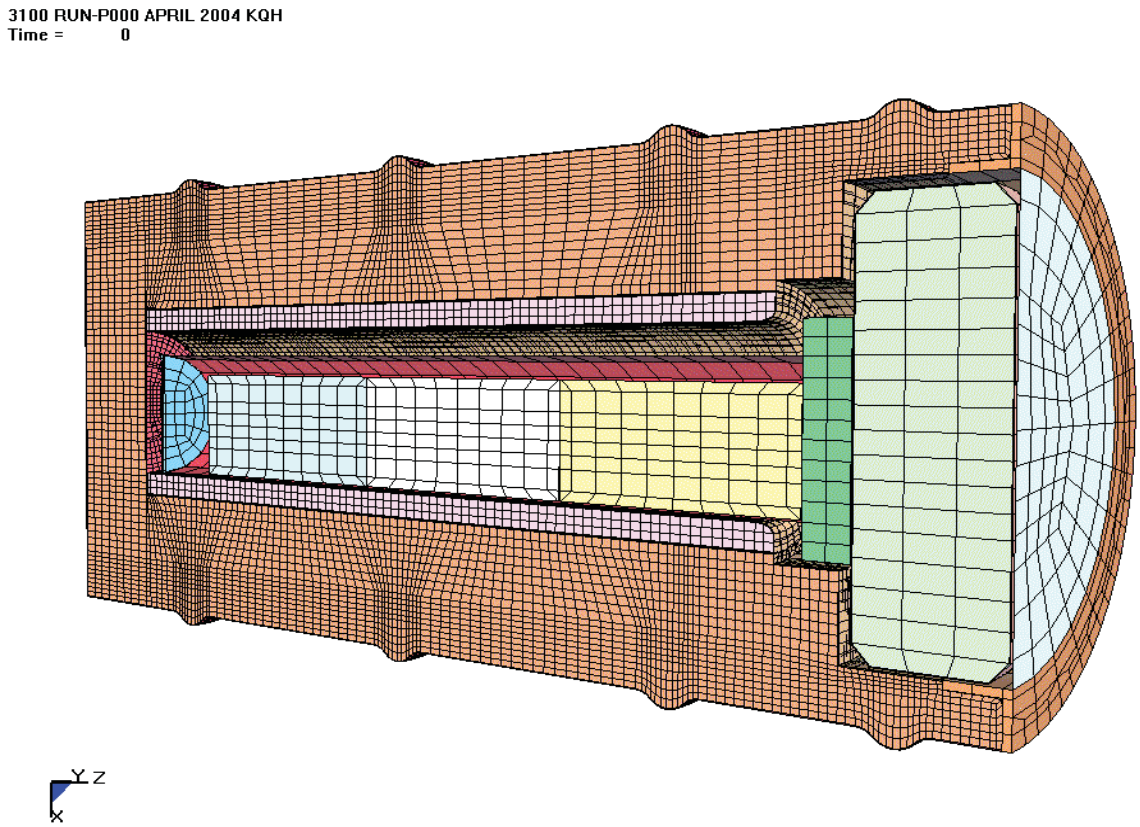

Figure 2.2.3 - Simplified ES-3100 Shipping Package Model for the Series of Punch Impacts

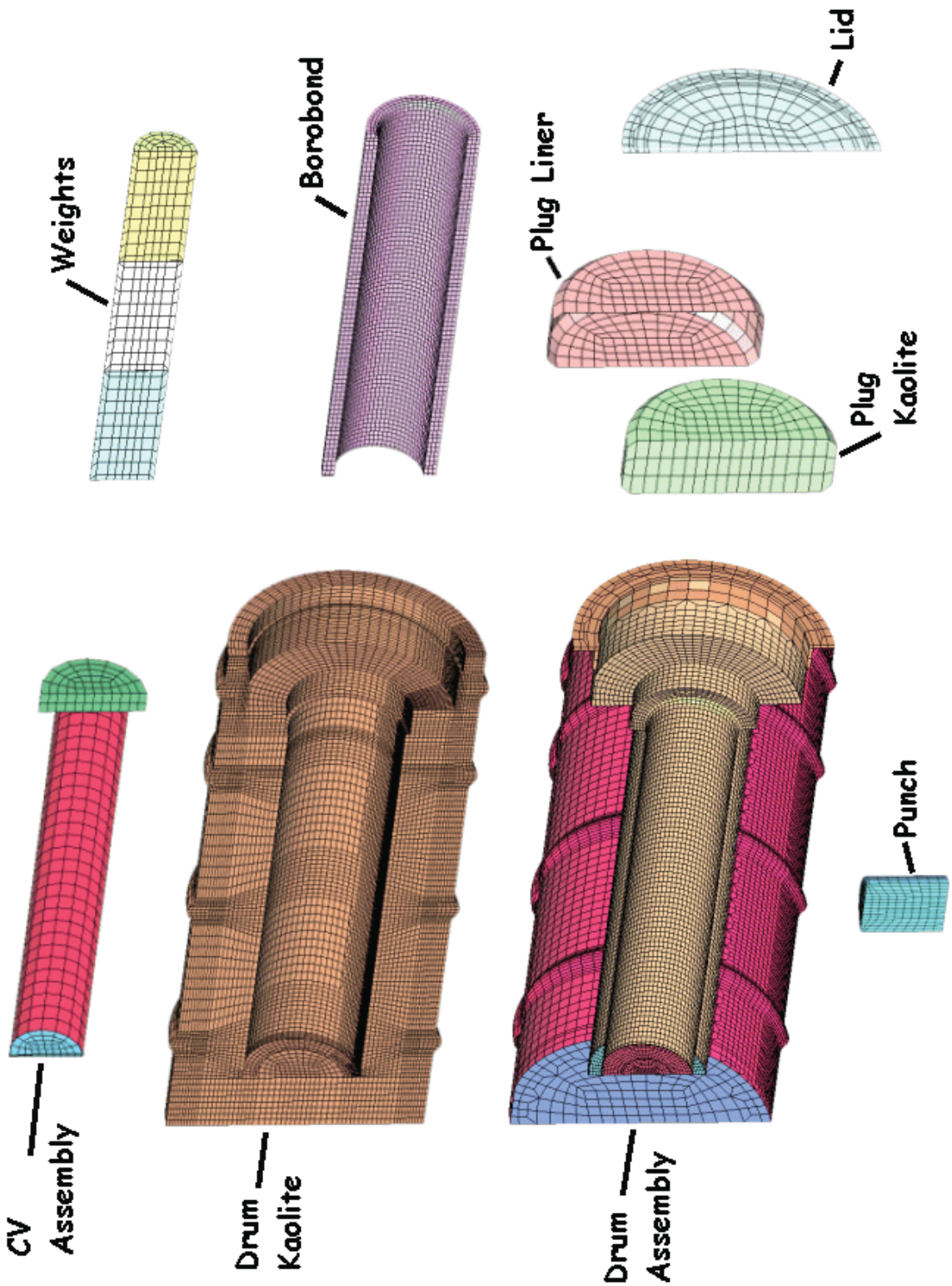

Figure 2.2.4 - Exploded View of the ES-3100 Simple Model

Since the concern is the response of the drum skin to the punch, detail in the shipping container components remote from this concern is not warranted and only the mass/stiffness effects on the region of concern become important. In general, there is a simplification of the element mesh (coarser element mesh) away from the punch impact location. Items such as the CV, the plug and the drum lid retention details were greatly simplified in modeling detail (compare Figures 2.2.3 and 2.2.4 verses Figures 2.1.1 through 2.1.4). The CV was simplified to a simple cylinder (shell elements) with a simple solid lid. The drum lid attachment details were replaced by a simple flat lid whose nodes were allowed to merge with the angle nodes. The container plug was also simplified to a simple disk with chamfered corners. This simple model allowed a savings on computer run time and storage allotment without sacrificing the item of concern, the response of the drum liner due to the angled punch.

An effort was made in the geometrical/mesh simplification to maintain the mass distribution of the container as close as is reasonable to the detailed model. Table 2.2.2 shows the weights for all the punch impacts. The total weight for the simple model package assembly was 427.91 pounds with the 22.4 lb/ft^3 kaolite. The mass inertia about the global Y axis for the simple model is 89.64 in*lb*sec^2 and the CG is located at Z= 23.0 inches.

Table 2.2.2 - Analysis Weights for Punch Runs

Material Number	Component Description	mass*	weight**
1	CV Body	2.6336E-02	20.33
2	CV Bottom Head	2.7398E-03	2.12
3	CV Flange/Lid	1.5492E-02	11.96
4	removed for punch runs	0.0000E+00	0.00
5	Angle	1.9249E-02	14.86
6	Drum	6.0236E-02	46.50
7	Drum Bottom	1.2318E-02	9.51
8	removed for punch runs	0.0000E+00	0.00
9	removed for punch runs	0.0000E+00	0.00
10	Liner	3.9641E-02	30.60
11	Liner Bottom	1.3361E-03	1.03
12	Lid	8.6358E-03	6.67
13	removed for punch runs	0.0000E+00	0.00
14	removed for punch runs	0.0000E+00	0.00
15	removed for punch runs	0.0000E+00	0.00
16	removed for punch runs	0.0000E+00	0.00
17	removed for punch runs	0.0000E+00	0.00
18	removed for punch runs	0.0000E+00	0.00
19	Plug Liner	1.2949E-02	10.00
20	Plug Kaolite	1.2573E-02	9.71
21	Drum Kaolite	1.4265E-01	110.13
22	Borobond	5.6607E-02	43.70
24	CV Lower Inner Weight	4.7530E-02	36.69
25	CV Middle Inner Weight	4.7530E-02	36.69
26	CV Upper Inner Weight	4.7530E-02	36.69
27	Liner Kaolite Cavity Bottom	9.3847E-04	0.72
28	removed for punch runs	0.0000E+00	0.00
29	removed for punch runs	0.0000E+00	0.00
30	removed for punch runs	0.0000E+00	0.00
31	Punch	8.2405E-02	63.62
32	removed for punch runs	0.0000E+00	0.00
pkg			427.91
punch			63.62
total		6.3670E-01	491.53

* - Mass is for the 1/2 model and is units of (pound * second^2) / inch

** - Weight is for the total package (2 x model weight) and is in units of pounds.

2.3 Material Models

The LS-Dyna material models used in the ES-3100 analytical model are shown in the Table 2.3.1 index. Note that the designation 304L (capital L) is used for clarity.

Table 2.3.1 - Material Model Index for the ES-3100 LS-Dyna Model

LS-Dyna Part #	Part Description	Material Description	Described in DAC Section
1	CV Body	304L	2.3.1
2	CV Body Neck	304L	2.3.1
3	CV Lid	304L	2.3.1
4	CV Nut Ring	A-479 Nitronic-60	2.3.2
5	Angle	304	2.3.3
6	Drum	304	2.3.3
7	Bottom Head	304	2.3.3
8	Attachment Shell Elements	304	2.3.3
9	Attachment Shell Elements	304	2.3.3
10	Liner	304	2.3.3
11	Liner Bottom	304	2.3.3
12	Lid Shell Elements	304	2.3.3
13	Attachment Shell Elements	304	2.3.3
14	Lid Solid Elements	304	2.3.3
15	Lid Stiffener	304	2.3.3
16	Studs	304	2.3.3†
17	Stud Nuts	Bronze	2.3.4
18	Stud Washers	304	2.3.3
19	Plug Liner	304	2.3.3
20	Plug Kaolite	Kaolite 1600	2.3.5
21	Drum Kaolite	Kaolite 1600	2.3.5
22	Borobond	Borobond 4	2.3.6
23	Not Used	Not Used	Not Used
24	Lower Internal CV Mass	Mild Steel	2.3.7
25	Middle Internal CV Mass	Mild Steel	2.3.7
26	Upper Internal CV Mass	Mild Steel	2.3.7
27	Liner Bottom	304	2.3.3
28	Not Used	Not Used	Not Used
29	Visual Rigid Plane	Rigid	2.3.8
30	Crush Plate	Mild Steel	2.3.7
31	Punch	Mild Steel	2.3.7
32	Silicon Rubber Pads	Silicon Rubber	2.3.9

† - An elastic/plastic model with material failure is used for the studs as explained in the noted section.

Density values listed in Section 2.3 were used as initial values for the material weights. Once the model was completed and initial runs made, the initial density was then ratioed such that the preliminary weights obtained from the designer were matched by the analysis results. Table 2.1.2 shows the resulting component and assembly weights for the detailed model.

The material presented in this section is for room temperature (about 70°) unless otherwise stated. Section 2.3.5 presents Kaolite data at room temperature in section 2.3.5.1, 100°F in section 2.3.5.2 and -40°F in section 2.3.5.3.

2.3.1 304L Stainless Steel

The material 304L is used for the CV components except the nut ring. A software database obtained from Lawrence Livermore National Lab personnel is used to obtain the 304L material data which is reproduced below.

```
Material density . . . . . .      0.28600   lb/in**3
Young's Modulus. . . . . . .      2.800E+07 psi
Shear Modulus. . . . . . . .      1.085E+07 psi
Bulk Modulus . . . . . . . .      2.222E+07 psi
Poisson's ratio. . . . . . .      0.2900
Yield stress at offset . . .  32000.0       psi
Engineering ultimate stress.  85000.0       psi
Elongation at failure. . . .     57.00      %
Yield offset . . . . . . . .      0.20000   %
---------- Calculated values ----------------------
Strain Hardening equation      s  = s0 e**m
Equation constants             s0 = 160455    m  = 0.27916
Yield point                    sy =  21735    ey = 0.00078
Ultimate (Engineering)         Su =  85000    Nu = 0.32202
Ultimate (True)                sut= 112372    eut= 0.27916
Failure  (True)                sft= 168989    eft= 1.20397
Energy to ultimate                   24605 in-lb/in**3
```

The LS-Dyna power law plasticity model (*MAT_POWER_LAW_PLASTICITY) is used for 304L. The material model is:

$$\sigma = K\varepsilon^m$$

were, K = strength coefficient = 160455 (psi)
m = hardening exponent = 0.27916

The density listed in the reference was an initial density (0.286 lb/in^3) and equates to an initial mass density of 7.4093e-4 lb*sec^2/in^4.

2.3.2 A-479 Nitronic-60

The CV nut ring is modeled with A-479 Nitronic-60 properties. The Reference 5.4 was used to obtain the following material data for the S21800 material.

Tensile Strength	95 ksi
Yield Strength	50 ksi
Elongation	35%

The modulus of elasticity is assumed to be 26.2e6 psi.

From this data the following tangent modulus was calculated for the LS-Dyna, *MAT_PLASTIC_KINEMATIC material model.

$$\varepsilon = \frac{\sigma}{E} = \frac{50000psi}{26.2e6psi} = 0.00192in/in$$

$$E_{\tan} = \frac{95000psi - 50000psi}{0.35 - 0.00192} \approx 129000psi$$

A poisson's ratio of 0.298 was used. A density of 0.2754 lb/in^3 was initially used. This equates to an initial mass density of 7.1347 lb*sec^2/in^4.

2.3.3 304 Stainless Steel

The general shipping container components were modeled as 304 stainless steel. The LS-Dyna material model *MAT_POWER_LAW_PLASTICITY was used for the general container components. The 304 material data was obtained from a software database obtained from Lawrence Livermore National Lab personnel and is reproduced below.

```
Material density . . . . . .      0.29000   lb/in**3
Young's Modulus. . . . . . .      2.810E+07 psi
Shear Modulus. . . . . . . .      1.089E+07 psi
Bulk Modulus . . . . . . . .      2.230E+07 psi
Poisson's ratio. . . . . . .      0.2900
Yield stress at offset . . .  34000.0       psi
Engineering ultimate stress.  87000.0       psi
Elongation at failure. . . .     57.00      %
---------- Calculated values ----------------------
Strain Hardening equation      s  = s0 e**m
Equation constants             s0 = 162738    m  = 0.27208
Yield point                    sy =  23729    ey = 0.00084
Ultimate (Engineering)         Su =  87000    Nu = 0.31269
Ultimate (True)                sut= 114204    eut= 0.27208
Failure  (True)                sft= 167370    eft= 1.10866
```

Similar to section 2.3.1, the power law coefficients for the 304 model used for the general shipping container components were:

K = strength coefficient = 162738 (psi)
m = hardening exponent = 0.27208

The 0.290 lb/in^3 density equates to 7.513 e-4 lb*sec^2/in^4 for the initial mass density.

The drum studs were modeled using the *MAT_PLASTIC_KINEMATIC material model in LS-Dyna using the following 304 material properties. This material model allowed material failure to be used for the studs. With material failure, LS-Dyna removes elements which reach the defined failure strain. The following elastic-plastic model was derived from the above material properties.

Modulus of Elasticity = 2.81e7 psi†
Poisson's Ratio = 0.29
Yield = 34000 psi
Plastic Modulus = 93180 psi
Failure Strain = 0.57 in/in

The modeling of the drum studs with engineering stress/strain data curve is conservative from a design standpoint. This approach has been used and accepted for NNSA-licensed shipping packages that were subject to independent review and verification analysis (i.e., DT-22 and DT-23).

† - Note: the value of 2.9e7 psi (vs 2.81e7 psi) was inadvertently used in the analysis for the modulus of elasticity. This is seen to cause minimal concern due to the minimal energy absorption in the elastic range.

2.3.4 Bronze

The drum lid nuts are made of bronze. A software database obtained from Lawrence Livermore National Lab personnel was used to obtain the material data which is reproduced below.

```
Material . . . .bronze commercial cu.9 zn.1 ½ hard
Material density . . . . . .      0.31800   lb/in**3
Young's Modulus. . . . . . .      1.700E+07 psi
Shear Modulus. . . . . . . .      6.391E+06 psi
Bulk Modulus . . . . . . . .      1.667E+07 psi
Poisson's ratio. . . . . . .      0.3300
Yield stress at offset . . .  45000.0       psi
Engineering ultimate stress.  52000.0       psi
Elongation at failure. . . .     15.00      %
---------- Calculated values ----------------------
Strain Hardening equation      s  = s0 e**m
Equation constants             s0 =  70989    m  = 0.09191
Yield point                    sy =  40775    ey = 0.00240
Ultimate (Engineering)         Su =  52000    Nu = 0.09626
Ultimate (True)                sut=  57006    eut= 0.09191
```

The LS-Dyna power law model was used for the bronze material. The coefficients used were:

K = strength coefficient = 70989(psi)
m = hardening exponent= 0.09191

The density of 0.318 lb/in^3, or 8.2371e-4 lb*sec^2/in^4 was the initial mass density.

2.3.5 Kaolite 1600

Kaolite 1600 properties were used to model the drum and plug kaolite. The LS-DYNA honeycomb material model (*MAT_HONEYCOMB) used for the ES-3100 has been shown to be a good representation of the Kaolite material and approved for NNSA-licensed shipping packages that were subject to independent review and verification analysis (i.e., DPP-2 and ES-2100). There have been several testing programs to determine the structural properties of Kaolite since 1995. Each time new data is obtained, it is compared to the old data to maintain enveloping upper and lower bound stiffness curves. The lower stress/strain portion of the curves presented in this section is shown in Figure 2.3.5.1 below. Each curve shown in Figure 2.3.5.1 is documented in the following sub-sections. The Kaolite test data was obtained from constrained test specimens. For the constrained Kaolite test data, the material data is the same for uniaxial and volumetric strain.

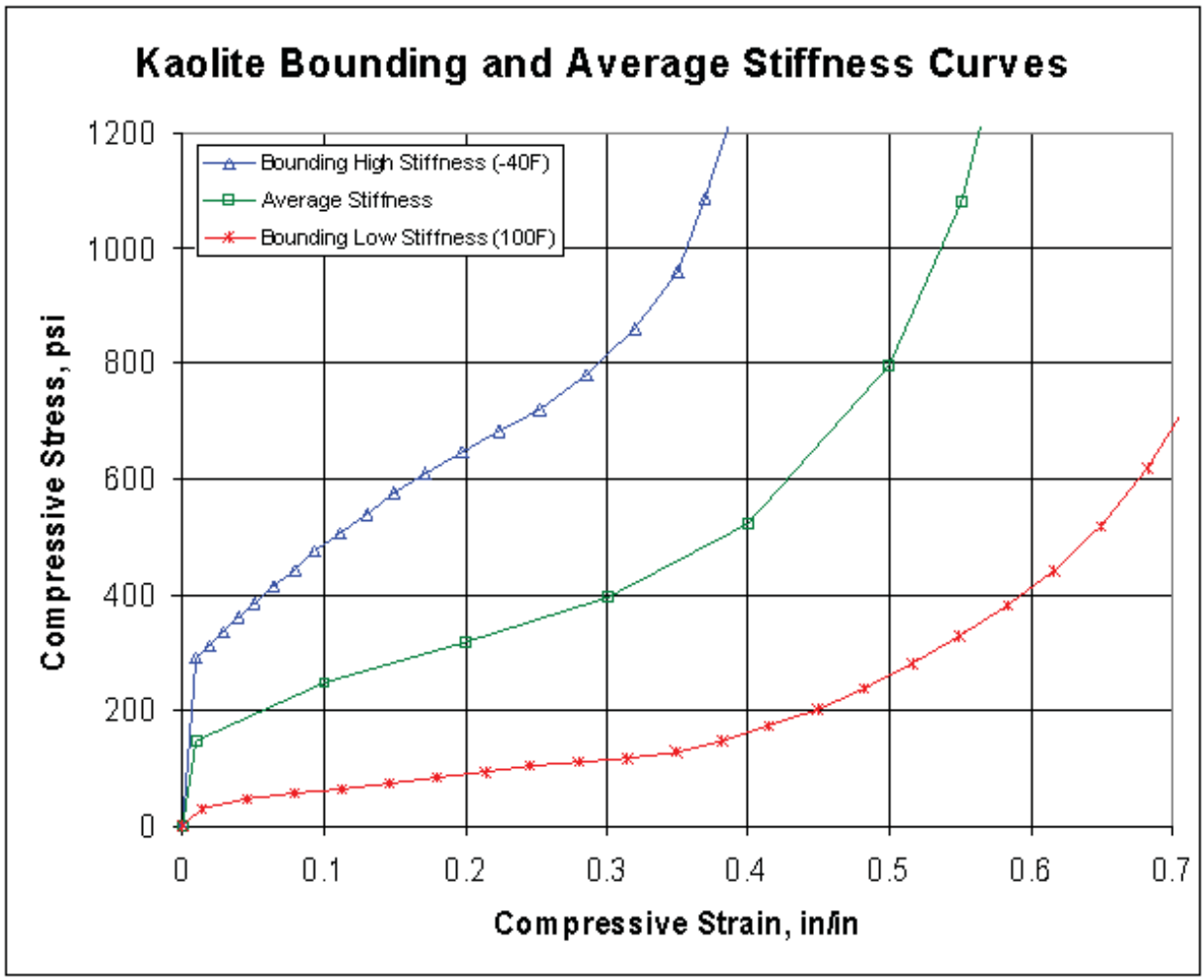

Figure 2.3.5.1 - Bounding Kaolite and Average Stiffness Curves

2.3.5.1 Kaolite 1600 - Averaged Stiffness

A Y12 report gives test data for constrained Kaolite 1600 material at 100°F and -40°F. The maximum peaks from the -40°F high density samples defined an upper bound load deflection curve. The minimum peaks to the 100°F low density samples defined a lower bound load deflection curve. The upper and lower curves were averaged to obtain the average stiffness results. The averaged results up to about 60% strain are then derived from test results for the LS-DYNA material model. The curve is extrapolated above 60% strain, to give a "lock-up" region (collapsing of voids). LS-Dyna does not extrapolate data curves, therefore, the curves must envelope all expected values and assumed values extend the curve well into the lock-up range. Figure 2.3.5.1 shows the lower portion of the averaged stiffness curve. The digital values for the points defined in the LS-DYNA material model are given below in Table 2.3.5.1.1.

Table 2.3.5.1.1 - Digital Load Curve for Kaolite 1600

Strain, in/in	Stress, psi	Strain, in/in	Stress, psi	Strain, in/in	Stress, psi
0.00	0.0	0.40	523.	0.70	5000. †
0.01	148.	0.50	797.	0.75	10000. †
0.10	248.	0.55	1079.	0.775	20000. †
0.20	317.	0.60	1553.	0.79	30000. †
0.30	396.	0.65	2500. †	0.8	40000. †

† - Assumed values to obtain lockup

The Young's Modulus for the compacted kaolite material is taken as the slope of the last two data points.

$$\frac{40000psi - 30000psi}{0.79\,in/in - 0.80\,in/in} = 1.0e6psi$$

The initial slope is taken as the uncompressed modulus of elasticity.

$$E_{uncompressed} = \frac{148.11psi - 0.0psi}{0.01 - 0.0} = 14811psi$$

Assuming a low poisson's ratio (0.01), the shear modulus is,

$$G = \frac{E}{2(1+\nu)} = \frac{14811psi}{2(1+0.01)} \approx \frac{14811psi}{2} = 7405\ psi$$

Full compaction is also assumed at a relative volume of 0.20 (this corresponds with the 80% strain assumed data point). The mass density used for the nominal kaolite runs in the analysis is 3.3583e-5 lb*sec^2/in^4, which equates to 22.4lb/ft^3.

2.3.5.2 Kaolite 1600 - Lower Bound Stiffness

The kaolite lower bounding stiffness model shown in Figure 2.3.5.1, originated in the ES2LM shipping container calculation and is associated with 100°F. The digital values for the points which define in the LS-Dyna lower bound stiffness curve are given in Table 2.3.5.2.1.

Table 2.3.5.2.1 - Digital Load Curve for Kaolite 1600, Lower Bound

Strain, in/in	Stress, psi	Origin
0.00	0.0	Test Data and ES2LM Shipping Container Calculation
0.0132	29.	
0.0456	48.	
0.0792	56.	
0.1128	64.	
0.1464	75.	
0.1800	83.	
0.2136	93.	
0.2460	105.	
0.2796	109.	
0.3144	117.	
0.3480	127.	
0.3816	148.	
0.4140	174.	
0.4488	202.	
0.4824	237.	
0.5160	281.	
0.5496	330.	
0.5832	381.	
0.6168	443.	
0.6492	520.	
0.6828	619.	
0.7140	744.	
0.7476	896.	
0.7800	1099.	
0.7944	1205.	
0.8200	3000.	Assumed†
0.8700	10000.	Assumed†
0.9000	40000.	Assumed†

† - Assumed to provide "lock-up"

The Young's Modulus for the compacted kaolite material is taken as the slope of the last two data points.

$$\frac{40000psi - 10000psi}{0.90in/in - 0.87in/in} = 1.0e6psi$$

The initial slope is taken as the uncompressed modulus of elasticity.

$$E_{uncompressed} = \frac{29.psi - 0.0psi}{0.0132 - 0.0} = 2197psi$$

Assuming a low poisson's ratio, the shear modulus is,

$$G \approx \frac{E}{2} = 1099\ psi$$

A low poisson's ratio is assumed, 0.01. Full compaction is also assumed at a relative volume of 0.10. The density used is 27 lb/ft^3, or 4.0479e-5 lb*sec^2/in^4.

2.3.5.3 Kaolite 1600 Upper Bound Stiffness

The upper bound stiffness of the kaolite 1600 material is an enveloping curve obtained from two sets of material test data. Table 2.3.5.3.1 shows the digital values of the curve.

The Young's Modulus for the compacted kaolite material is taken as the slope of the last two data points.

$$\frac{40000psi - 22000psi}{0.88in/in - 0.85in/in} = 6.0e5\ psi$$

The initial slope is taken as the uncompressed modulus of elasticity.

$$E_{uncompressed} = \frac{292.1psi - 0.0psi}{0.01 - 0.0} = 29210psi$$

Assuming a low poisson's ratio, the shear modulus is,

$$G \approx \frac{E}{2} = 14605\ psi$$

A density of 27 lb/ft^3 is used as in the low stiffness run. A low poisson's ratio is assumed, 0.01. Full compaction is also assumed at a relative volume of 0.12.

Table 2.3.5.3.1 - Upper Bounding Kaolite Curve		
Strain, in/in	Stress, psi	Origin
0	292.1	Summer 2004 Material Testing
0.01	292.1	
0.019	313.3	
0.029	336.1	
0.04	360.5	
0.051	386.6	
0.064	414.3	
0.079	443.6	
0.094	474.5	
0.111	506.9	
0.13	540.7	
0.15	575.7	
0.172	611.6	
0.197	647.9	
0.224	684.1	
0.253	719.6	
0.285	780	assumed for smooth transition†
0.32	860	
0.3504	958	DPP2 Shipping Container Calculation
0.3696	1086	
0.3888	1231	
0.45	2000	assumed for lock-up †
0.5	3000	
0.6	6000	
0.7	10000	
0.8	16000	
0.85	22000	
0.88	40000	
† - Assumed values for transition and lock-up		

2.3.6 Borobond 4 Casting Material

The following soil and foam model is used for the borobond 4 casting material. The model is obtained from work done on the Y12, HEU storage pallet and the subsequent physical testing.

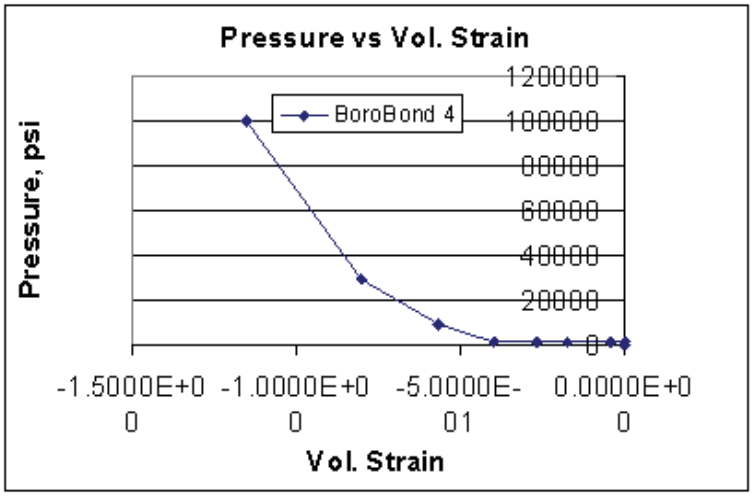

Figure 2.2.3 - Pressure vs Volumetric Strain

The following material data was used for the model of the Borobond 4 casting material.

LS-Dyna Material Model	*MAT_SOIL_AND_FOAM
Density	1.7991e-4 lb-sec^2/in^4 (120 lb/ft^3)
Shear Modulus	1.019e6 psi
Bulk Modulus	2.491e6 psi
A_0	1.008e7 (psi)^2
A_1	0
A_2	0
Tensile Cutoff	309.3 psi

Pressure vs Volumetric Strain Data:

Pressure, psi	Volumetric Strain, in^3/in^3
0	0
1833.3	-7.387e-4
1850	-4.2363e-2
1866	-1.7334e-1
1883	-2.6993e-1
1900	-3.9631e-1
10000	-5.6503e-1
30000	-7.9972e-1
100000	-1.1536

2.3.7 Mild Steel

AISI 1020 carbon steel was used to obtain properties for a typical or nominal low carbon steel. A software database obtained from Lawrence Livermore National Lab personnel was used to obtain the material data for AISI 1020 and is reproduced below.

```
Material . . . .steel carbon AISI 1020 plate bar sheet strip to 18 in.
Young's Modulus. . . . . . .      3.000E+07 psi
Shear Modulus. . . . . . . .      1.163E+07 psi
Bulk Modulus . . . . . . . .      2.381E+07 psi
Poisson's ratio. . . . . . .      0.2900
Yield stress at offset . . .  30000.0       psi
Engineering ultimate stress.  55000.0       psi
Elongation at failure. . . .     25.00      %
```

A modulus of elasticity of 2.9e7 (vs 3.0e7 psi) was inadvertently used in the analysis for this material. This material model was used for the inner CV weights, the crush plate and the punch. This is seen to be of minimal concern due to the fact that the components which use this modulus are not of concern themselves, it is their effect on the package/CV that is of concern.

A density of about 490 lb/ft^3 is also initially assumed, which equates to a mass density of 7.35 lb-sec^2/in^4. This initial mass value was then adjusted based on the expected component weight.

Using the ultimate (55000 psi) and yield (30000 psi); the failure strain of 0.25 and assuming a 2% offset, a simple bi-linear tangent modulus of 1.0e5 is assumed.

$$E_{\tan} = \frac{55000psi - 30000psi}{0.25 - 0.002} \approx 1.0e5psi$$

2.3.8 Rigid Plane

The following properties were assigned to the rigid plane (for contact surface concerns):

Modulus of Elasticity = 28e6 psi
Poisson's Ratio = 0.29

A relatively low value of density was also specified for the rigid plane, 1e-6 lb*sec^2/in^4. Each node of the rigid plane was restrained from rotation and translation in the material definition.

2.3.9 Silicon Rubber

The pads outboard of the CV bottom and top are used to isolate the CV with regards to a transportation vibration concern. The following properties were assumed for the silicon rubber pads:

$E \approx 150000$ psi
Density = 0.0446 lb/in^3 = 1.1554 e-4 lb*sec^2/in^4

A modulus of elasticity for the silicon rubber of about 150 psi can be obtained from Figure 35.13 of reference 5.6 (relative magnitude can be mimicked by various sources on the internet). However, this low E value will not allow a stable solution of LS-Dyna. The value of E = 150000 psi results in a stable solution. The silicon rubber piece at the CV lid/flange and the piece at the base of the CV offer only bearing to the CV. A stiffer silicon material would tend to minimize the bearing footprint on the CV, hence force higher stresses/strains in the CV. Initial runs show this to be the case, up to the point that the softer (E = 150 psi) solution fails. Therefore, the value of E = 150000 psi is used due to the fact that it tends to be conservative with respect to the CV and it allows a stable solution of LS-Dyna.

The density shown above is assumed and was found by averaging several nominal silicon rubber values obtained from the internet.

The shear modulus was calculated as:

$$G = \frac{E}{2(1+\nu)} = \frac{150000psi}{2(1+0.463)} = 51260psi$$

The LS-Dyna *MAT_BLATZ-KO_RUBBER was used to model the silicon rubber components. The model defines the poisson's ratio as 0.463.

3.0 Solution Results

In this section, the results of the different analyses are presented. A voluminous amount of data can be obtained for each and every run presented in this DAC. An attempt is made to present the response story of each impact, yet not to overburden the reader, nor the expense of this report with similar images/data. Components of relatively low strain, or whose strain contour patterns are similar to other impacts which have been presented, may be presented digitally in a table (maximum) and not visually in an image. In the bounding kaolite runs, an effort was made to present the same images for comparison purposes.

Results from run1g are presented in detail as are results from the crush impact of run1ga. An effort is made to abbreviate the results of the other runs due to repetition. Only configuration and strain results of note, or uniqueness due to the configuration are included in the other runs. For ease of reading, the plots in sub-sections of Section 3.0 will be shown after the discussion in each section. Time is generally given in seconds, displacements in inches and velocity in inches/seconds.

The kinetic energy and velocity time history plots are nodal averages for the set of nodes that make up the body of concern (e.g., the shipping package for 4-foot impacts or the crush plate for crush impacts). Therefore, the plots are an averaged value to represent the body of concern.

The element mesh is generally not included on package assembly views such as Figure 3.0.1. The element mesh is generally quite small and its inclusion would make it more difficult to observe the components. In close up images, the element mesh is generally included.

The effective plastic strain level contour plots in the shell elements are surface strains (bending/peak strains) unless otherwise noted. Maximum, or in effect, bending strain is the default in LS-Post fringe plotting of shell elements. The maximum value for the plotted elements is given in the title block in the upper left corner of each fringe plot. The maximum fringe value (shown in the upper right hand corner of each fringe plot) may be redefined by the analyst and may or may not reflect the maximum value shown in the left, title block corner. In some fringe plots, the range may be adjusted to show regions in excess of a specific level. Note that shell elements are modeled at the centerline of the thickness. Therefore, in time history plots, one-half the shell thickness needs to be added/subtracted to obtain the desired metal surface for each node.

The nodes on the plane of symmetry and near the rigid plane are termed at "0°". The nodes initially on the Y plane are termed at "90°". And the nodes on the plane of symmetry

and typically nearer the crush plate are termed "180°". This terminology is typically used only in the side and slapdown impacts and denotes the circumferential positions.

The global coordinate system is the default system in LS-Dyna and is the coordinate system of default in this calculation. The global system is centered on the package centerline, at the bottom of the package as shown in Figure 3.0.1 (if the package were sitting on a flat floor, the surface of the floor would define Z = 0.0). The global XZ axes define the plane of symmetry. The global coordinate system triad icon is shown on most images in this section; offset by default in LS-Post for visual purposes. A local coordinate system was defined for the CV assembly due to lid/body flange separation concerns. The local system used is shown in Figure 3.0.2 and moves with the three defining nodes on the CV body and lid. The local X direction is in the direction of CV lid separation at the O-ring location in the flange. The local CV coordinate system is used in the lid separation time history plots in the results sections.

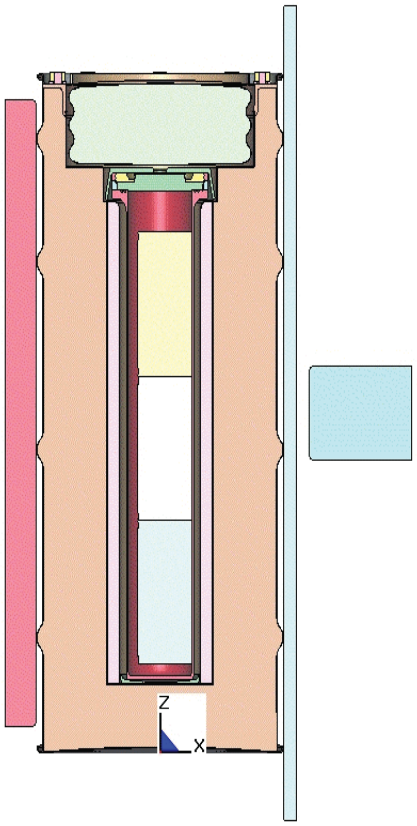

Figure 3.0.1 - Global Coordinate System

Figure 3.02 - CV Local Coordinate System

A study of the slapdown angle was performed using a computer code obtained from Los Alamos National Lab. The code considers a simplified, deformable body whose slapdown angle can be varied through multiple runs. The response of interest was the velocity of the secondary impacting end as it strikes the rigid surface.

To obtain all the input constants needed by the slapdown code, trial runs of the ES-3100 model were made. From the trial run, the load on the rigid surface and the deflection of the ES-3100 package ends were used to obtain the simple spring constants. The overall body dimensions, center of gravity location, mass moment of inertia and container mass were also input to the slapdown code. Figure 2.1.7 shows the results of the slapdown study. The friction factor between the rigid surface and the container was varied between 0.0 and 0.3. An angle of 12° was found to maximize the secondary impact and was chosen for the slapdown angle for the ES-3100.

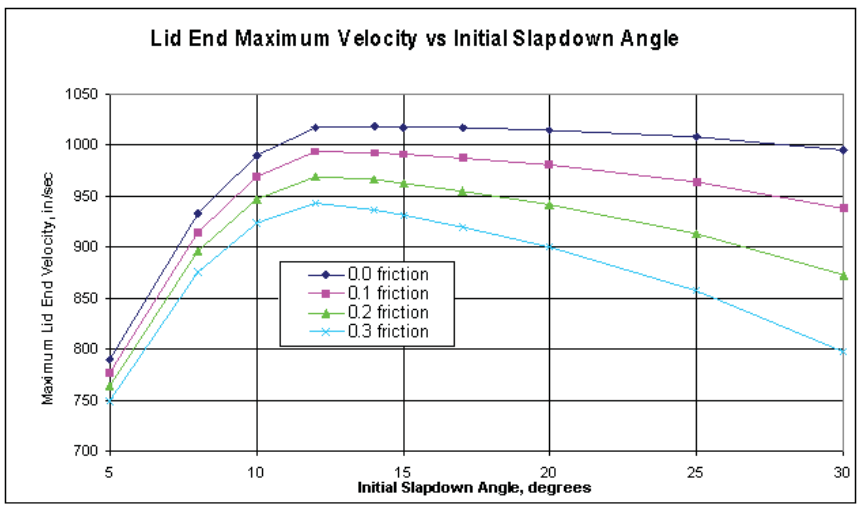

Figure 2.1.7 - Secondary Velocity Maximum from the Slapdown Study

3.1 Run1g - Side

Run1g is a design run with a 30-foot side impact (run time from 0 to about 0.0085 seconds) followed by a 30-foot, centered crush impact (from about 0.0085 to 0.025 seconds). Figure 3.1.1 shows the initial configuration of the model. Note that the punch was in the model, but a punch impact was not included in this run. Figure 3.1.2 shows the configuration of the model after the 30-foot impact. Figure 3.1.3 shows the lid region of the model after the 30-foot impact. Figure 3.1.4 shows the final configuration in the bottom region of the drum nearest the 30-foot impact with the rigid plane.

The effective plastic strain in the CV body at the end of the 30-foot impact is shown in Figure 3.1.5 to be a maximum of 0.0346 in/in. The maximum effective plastic strain occurs near the bottom head as shown in one of the enlarged views in the figure. Figure 3.1.6 shows the maximum effective plastic strain in the CV lid to be 0.0002 in/in for the 30-foot impact. The nut ring remained elastic during the 30-foot impact and is not shown in an image.

The effective plastic strain in the drum angle for the 30-foot impact is shown in Figure 3.1.7. The maximum strain is found to be 0.0682 in/in nearest the rigid plane. Figure 3.1.8 shows the maximum effective plastic strain in the drum to be 0.2218 in/in near the location of the angle and rigid plane. Figure 3.1.9 shows the effective plastic strain in the drum bottom head to be a maximum of 0.2444 in/in. The maximum effective plastic strain in the liner is 0.1189 in/in as given in Figure 3.1.10. The maximum is localized at the junction of the borobond/kaolite liner, near the CV flange, opposite the impact (180°). Figure 3.1.11 shows the maximum effective plastic strain in the drum lid to be 0.3580 in/in and occurs near the stud nearest the impact (0°). The maximum effective plastic strain in the lid stiffener is 0.0060 in/in and is not shown in a Figure. The maximum effective plastic strain in the drum studs is shown in Figure 3.1.12 to be 0.1171 in/in. The maximum effective plastic strain in the drum stud nuts is 0.0005 in/in and in the washers is 0.1628 in/in. The maximum effective plastic strain in the plug liner is 0.08260 in/in. Figures for the nuts, washers and plug liner are not shown.

The time history for the kinetic energy of the package assembly in the 30-foot impact is shown in Figure 3.1.13. Figure 3.1.14 shows the assembly X velocity time history. A constant rebound velocity was obtained at 0.0085 seconds, so the solution was halted at that point. The abrupt response near 0.0085 seconds in both figures is a precipitate of the successive impact restarts (redefining the velocities for the successive impact).

A restart of the LS-Dyna solution is used to create the crush impact. The state of the shipping package at time = 0.0085 seconds was written to a restart file at the end of the 30-foot impact. A second file, the restart input file (user defined) was used to extend the solution to 0.025 seconds, redefine the shipping container nodal velocity to 0.0 in/sec, and

redefine the crush plate nodal velocity to 528 in/sec. With the restart file and the restart input file, the crush impact solution was initiated on the 30-foot damaged container.

The initial configuration of the crush impact was the final configuration of the 30-foot impact as shown in Figure 3.1.2. The final configuration for the crush impact is shown in Figure 3.1.15. Figure 3.1.16 shows a view of the lid region near the rigid plane after the crush impact (0°). Figure 3.1.17 shows the upper lid region (180°). Figure 3.1.18 shows the lower bottom region (0°) and Figure 3.1.19 shows the upper bottom region after the crush impact (180°).

Figure 3.1 20 shows the maximum effective plastic strain in the CV body after the crush impact to be 0.0348 in/in. This is approximately the value after the 30-foot impact. The internal weights bare on the CV side wall forcing the local elevated strain region. Figure 3.1.21 shows the effective plastic strain in the CV lid to be a maximum of 0.0002 in/in. The CV nut ring remains elastic during the crush impact.

Figure 3.1.22 shows the maximum effective plastic strain in the drum angle due to the crush impact to be 0.0945 in/in. The maximum effective plastic strain in the drum is 0.3028 in/in as shown in Figure 3.1.23. Elevated regions of plastic strain occur in localized crimped regions at each end of the crush plate and at the attachment of the angle to the drum near the rigid surface (0°). Figure 3.1.24 shows the effective plastic strain in the drum bottom head. The maximum in the bottom head is 0.2945 in/in. The maximum effective plastic strain in the liner is 0.2063 in/in as shown in Figure 3.1.25. The maximum value occurs at the borobond/kaolite liner junction at 180°, as in the initial 30-foot impact.

The maximum effective plastic strain in the lid due to the crush impact occurs at the base of the hole for the upper stud (180°), near the crush plate. The maximum is 0.6430 in/in as shown in Figure 3.1.26. The membrane strain maximum is 0.4475 in/in and is very localized to the upper stud hole (similar to the bending shown in Figure 3.1.26). If failure were to occur it would be very localized to the lower region of the upper stud hole (near the crush plate - possible surface cracking). There is a lack of a general region of high strain in the lid which would promote an extended tear, or ripping of the lid.

Figure 3.1.27 shows the drum studs with a maximum effective plastic strain of 0.1937 in/in due to the crush impact. Not shown in figures: the maximum effective plastic strain in the lid stiffener is 0.0303 in/in; the maximum effective plastic strain in the drum stud nuts is 0.0005 in/in; the maximum effective plastic strain in the drum stud washers is 0.1628 in/in and the maximum effective plastic strain in the plug liner is 0.1212 in/in.

Figure 3.1.28 shows the kinetic energy time history for the crush plate. Figure 3.1.29

shows the X velocity time history for the plate.

The location of the nodes chosen to investigate the separation of the CV lid and the body flange at the O-rings are shown in Figure 3.1.30. The nodes are at 45° positions around the half model. The nodes are at the inside radius of the inner O-ring groove on the body and are at comparable positions on the opposite, lid surface. Figure 3.1.31 shows the separation time history for the node pairs. A positive value in the plot indicates separation (gap). The plot is quite noisy with ringing (contact chatter) of the node pair separations, but its purpose is to show relative magnitudes of separation in the model. From the figure, it can be seen that a gap spike of almost 0.004 in is obtained in the 30-foot impact just before 0.005 seconds. In the crush impact, spikes of almost 0.005 in in gap separation are seen. When the solution was halted, spikes on the order of 0.004 in are evident (there is no damping in the model other than friction). The ringing maximum is approximately 0.004 in and its minimum is about 0.00 in at the end of the solution (sinusoidal in nature). The ringing would then be about a mid-point value of 0.002 in. An implicit solution, or relaxed state is not obtained. In a relaxed state, if a permanent set were obtained in the flange region, then the average gap would be about 0.002 in, or less would be expected.

Figure 3.1.32 shows the kaolite nodes on the plane of symmetry chosen to obtain the kaolite thickness response to the impacts. Figure 3.1.33 shows the time history thickness at the nodal pairs shown. The thickness is obtained by subtracting one node X-coordinate time history from another nodes. The time in Figure 3.1.33 is in seconds and the X coordinate is the relative value in inches. For example, curve "A" represents the kaolite thickness on the plane of symmetry between the angle and the drum, nearest the crush plate. From Figure 3.1.33 it can be seen that the curve "A" thickness initially is about 1.75 inches and remains at that value for the 30-foot impact. The crush impact is seen to reduce the kaolite thickness to just under 1.0 inches for curve "A". The correlation of nodes, Figure 3.1.33 curve letter and a description of the location is given in Table 3.1.1.

Table 3.1.1 - Location of Kaolite Thickness Measurements			
Model Direction	Description	Figure 3.1.33 Curve	Figure 3.1.32 Nodes
-X	Liner at Base of Angle / Drum	A	191112 / 206004
	Liner at Base of Plug Cavity / Drum	B	188411 / 200529
	Liner at Top of CV Cavity / Drum	C	224181 / 200522
	Liner at Second Drum Roll from the Lid / Drum Roll Extreme	D	222721 / 361713
	Liner at Second Drum Roll from the Bottom / Drum Roll Extreme	E	218049 / 350033
	Liner at First Drum Roll from the Bottom / Drum Roll Extreme	F	213377 / 338353
	Liner at Base of CV Cavity / Drum	G	210749 / 334338
+X	Liner at Base of CV Cavity / Drum	H	333258 / 209669
	Liner at First Drum Roll from the Bottom / Drum Roll Extreme	I	338281 / 213305
	Liner at Second Drum Roll from the Bottom / Drum Roll Extreme	J	349961 / 217977
	Liner at Second Drum Roll from the Lid / Drum Roll Extreme	K	361641 / 222649
	Liner at Top of CV Cavity / Drum	L	199946 / 223677
	Liner at Base of Plug Cavity / Drum	M	199953 / 187835
	Liner at Base of Angle / Drum	N	205932 / 191040

Figure 3.1.34 shows nodes in the drum, drum bottom and drum lid which will be used to define the diameter changes in the outer surfaces of the shipping package. Figure 3.1.35 gives the relative X coordinate values (diameter changes) for the nodes on the plane of symmetry. From the plot it is seen that the minimum diameter reaches approximately 14.5 inches and then rebounds slightly. This minimum is at the lower barrel roll in the drum. From Figure 3.1.35 it is seen that the barrel roll diameters decrease from top to bottom. The greater deflection of the crush plate nearer the bottom of the package is evident in the Figure 3.1.15 final configuration plot. Figure 3.1.36 gives the Y coordinate time history response of the nodes at the Y extreme of the shipping package (see Figure 3.1.34). The values in Figure 3.1.36 are relative to the plane of symmetry and therefore need to be doubled to obtain the diameter changes. The correlation of nodes, curve numbers and a description of the location are given in Table 3.1.2. The ovalization of the package is also evident in comparing Figures 3.1.35 and 3.1.36.

Table 3.1.2 - Nodal Locations for Drum Diameter Time Histories				
Description	Diameter (X Direction)		Radius (Y Direction)	
	Figure 3.1.35 Curve	Figure 3.1.34 Nodes	Figure 3.1.36 Curve	Figure 3.1.34 Nodes
Lid Roll	A	133634 / 133778	A	133706
First Drum Roll Below Lid	B	98158 / 98230	B	98194
Second Drum Roll Below Lid	C	100202 / 100274	C	100238
Second Drum Roll Above Bottom	D	102976 / 103048	D	103012
First Drum Roll Above Bottom	E	105750 / 105822	E	105786
Bottom Attachment Roll to Drum	F	108889 / 108961	F	108925

Figure 3.1.37 shows nodes chosen to obtain liner diameter time histories. Figure 3.1.38 shows the diameter time histories for the node pairs. Table 3.1.3 shows the location of the nodal pairs along the length of the liner.

Table 3.1.3 - Nodal Locations for Liner Diameter Time Histories		
Curve	Node Pairs	Distance Above Base of Liner (in)
A	122522 / 122666	0.0
B	123259 / 129667	5.0
C	123276 / 129684	10.3
D	123292 / 129700	15.3
E	123309 / 129717	20.6
F	123324 / 129732	25.2
G	123340 / 129748	30.2

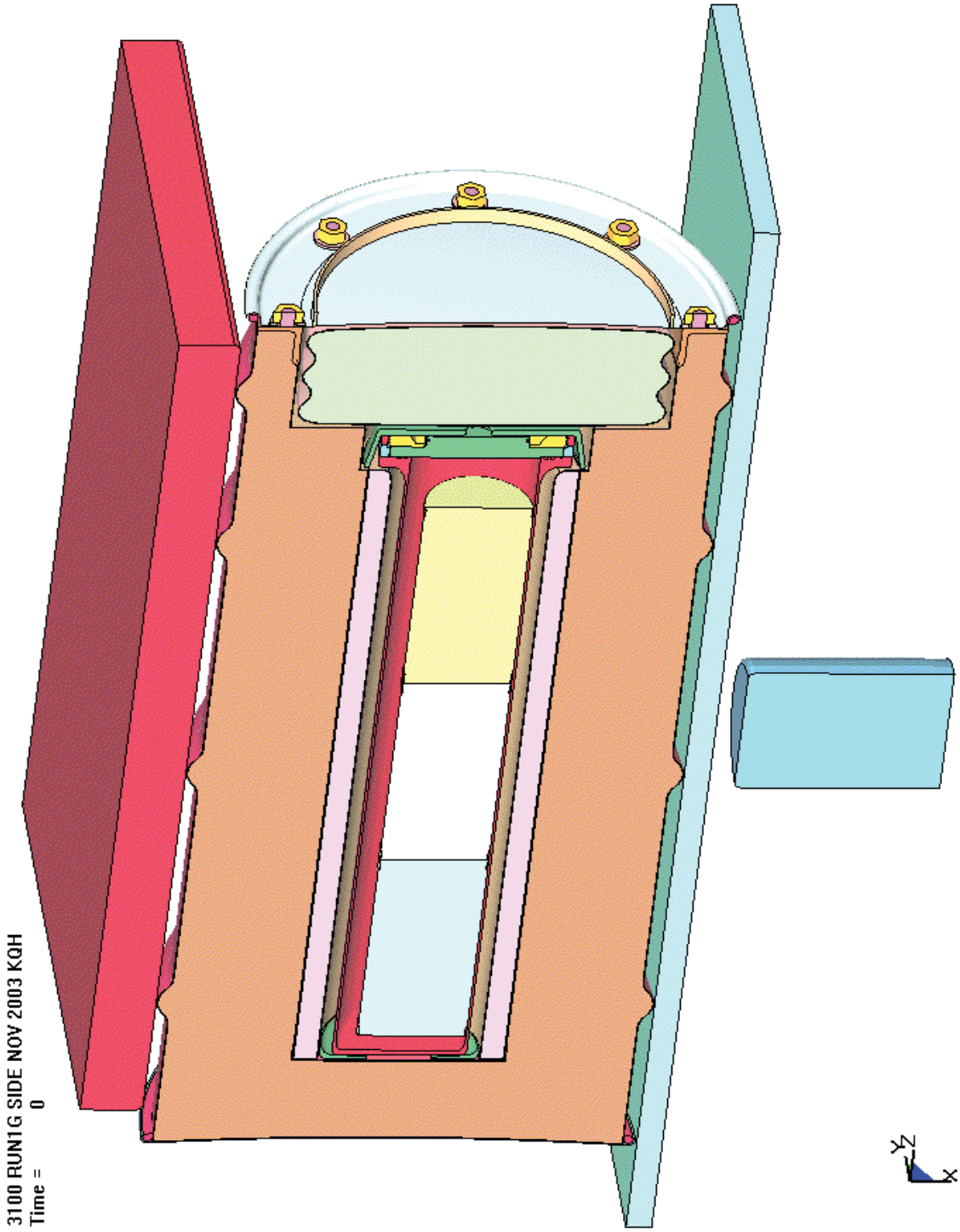

Figure 3.1.1 - Run1g, Initial Configuration

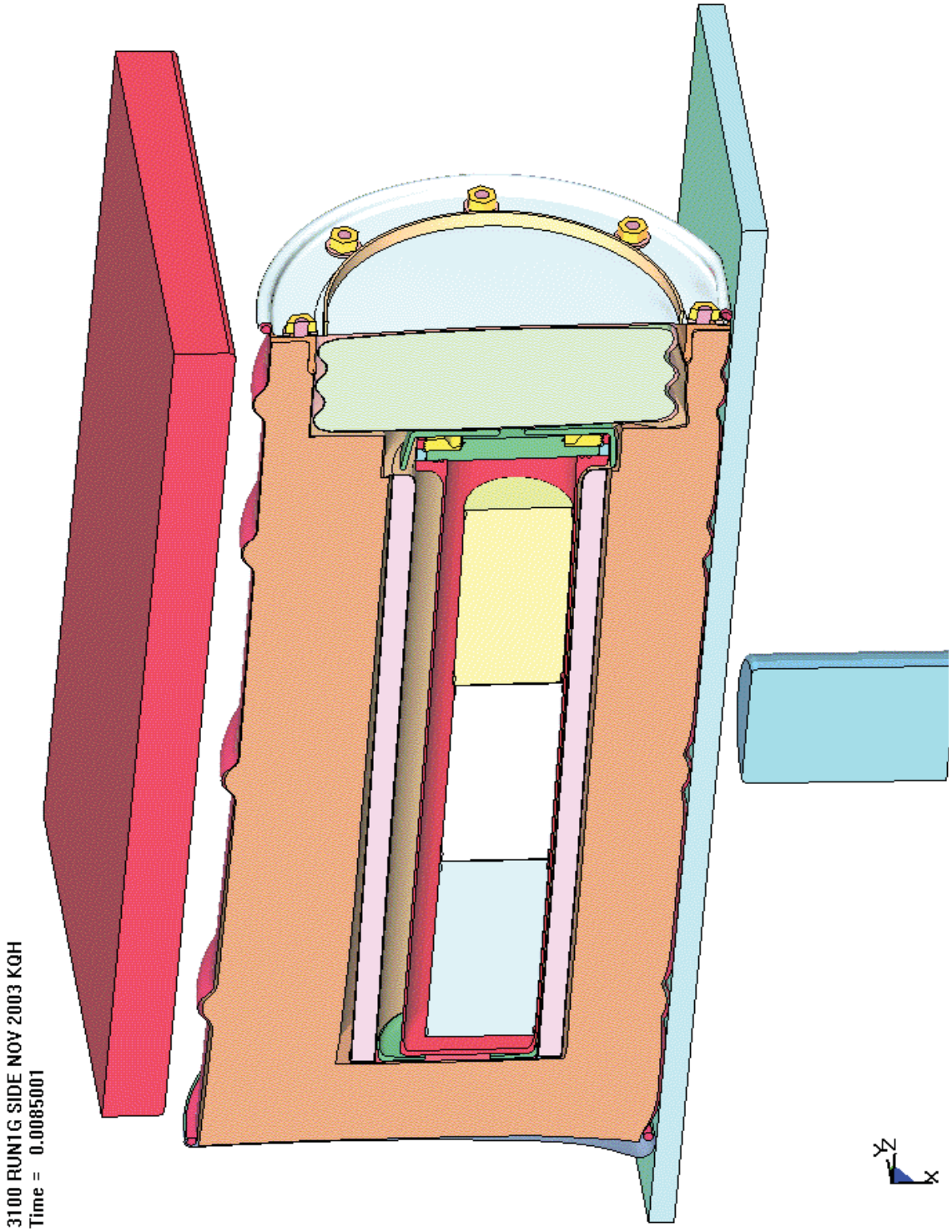

Figure 3.1.2 - Run1g, 30-Foot Impact, Final Configuration

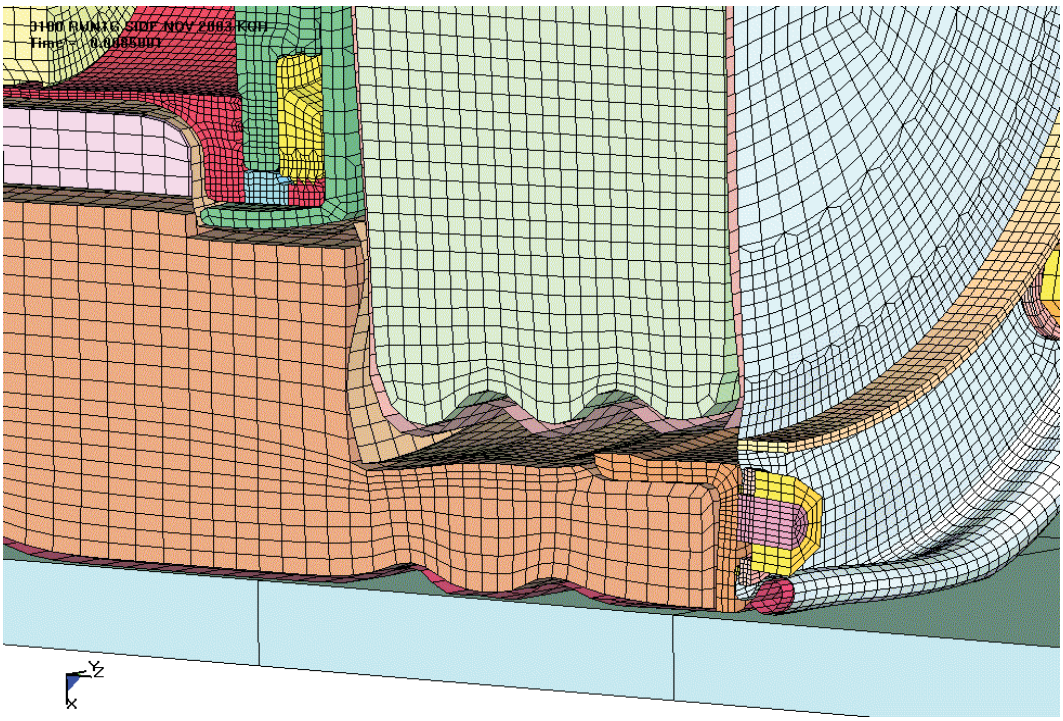

Figure 3.1.3 - Run1g, 30-Foot Impact, Configuration of the Drum Bolted Region

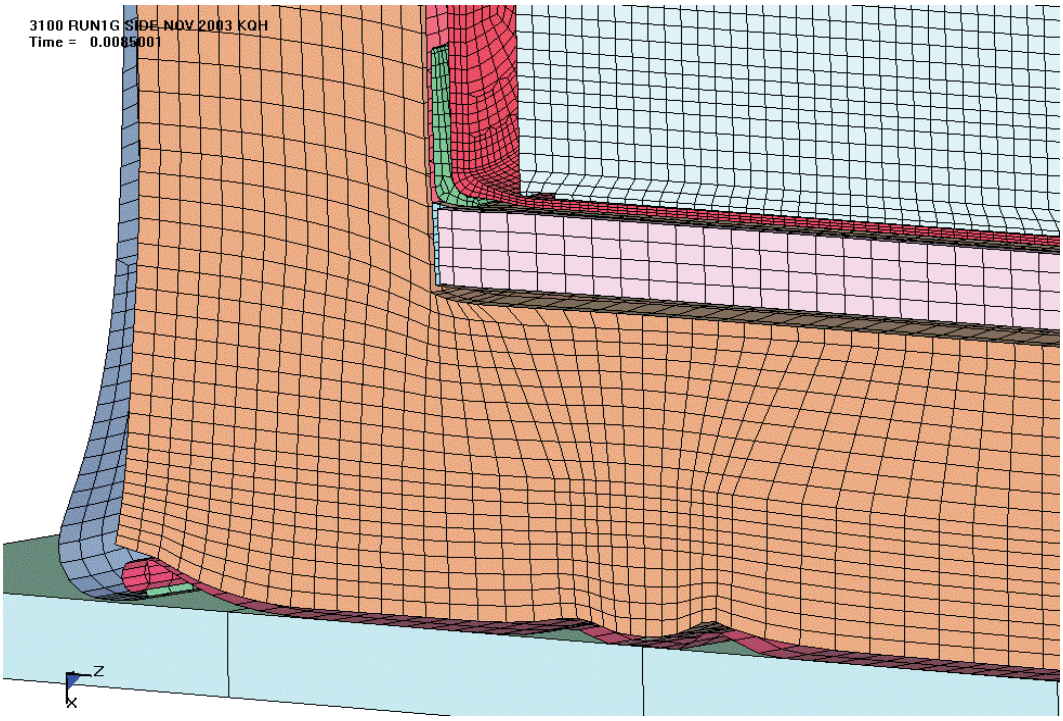

Figure 3.1.4 - Run1g, 30-Foot Impact, Configuration of the Bottom Drum Corner

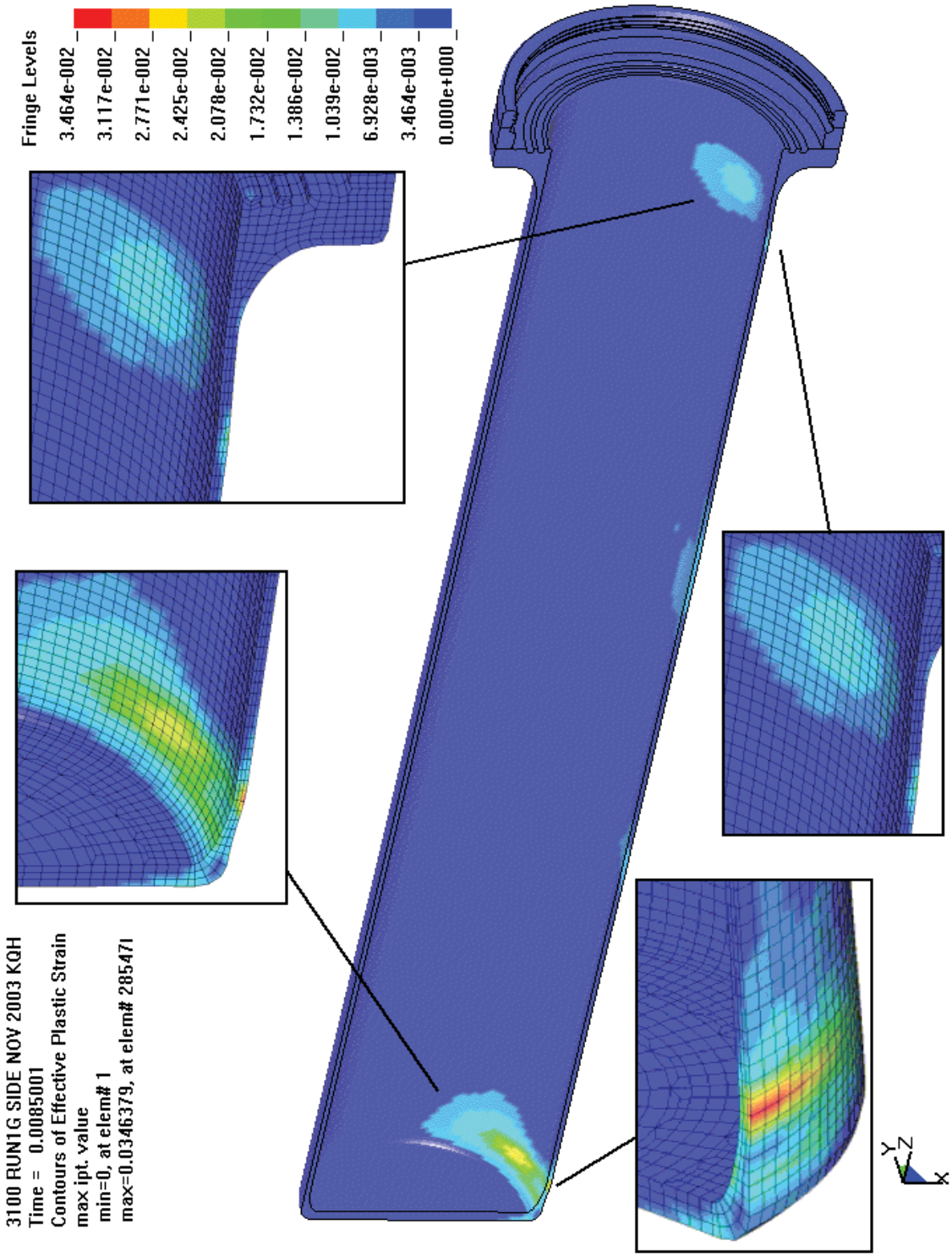

Figure 3.1.5 - Run1g, 30-Foot Impact, Effective Plastic Strain in the CV Body

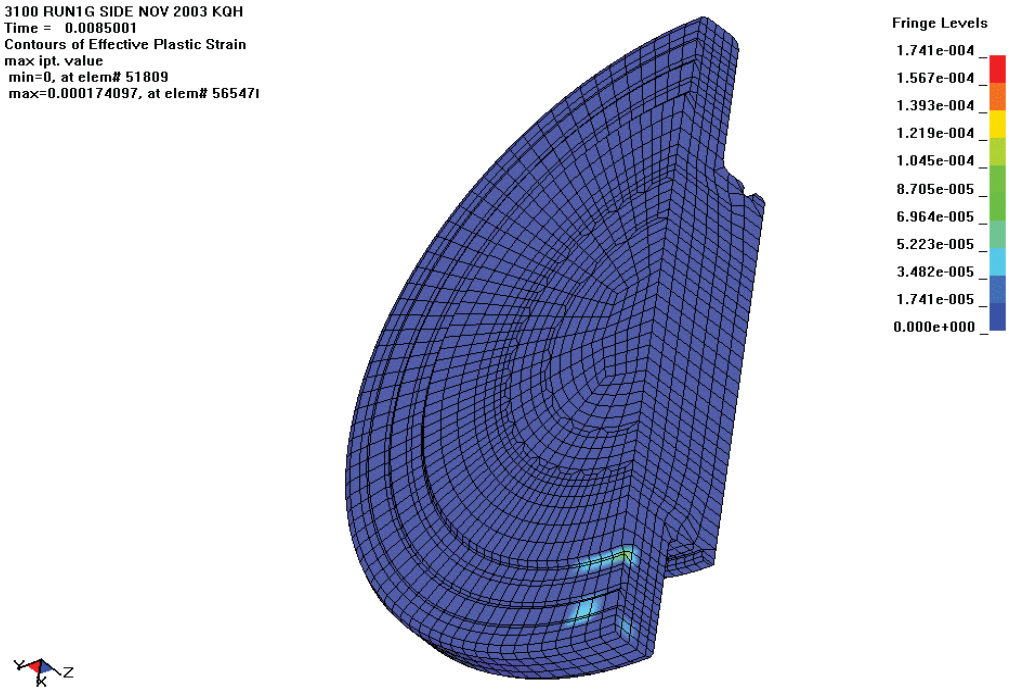

Figure 3.1.6 - Run1g, 30-Foot Impact, Effective Plastic Strain in the CV Lid

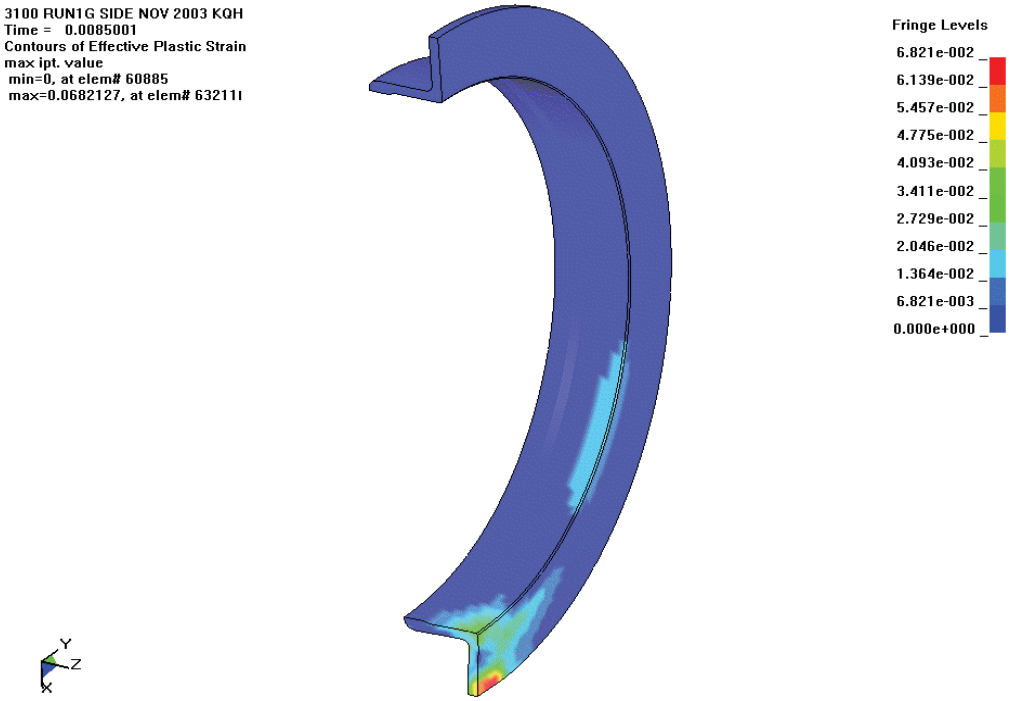

Figure 3.1.7 - Run1g, 30-Foot Impact, Effective Plastic Strain in the Drum Angle

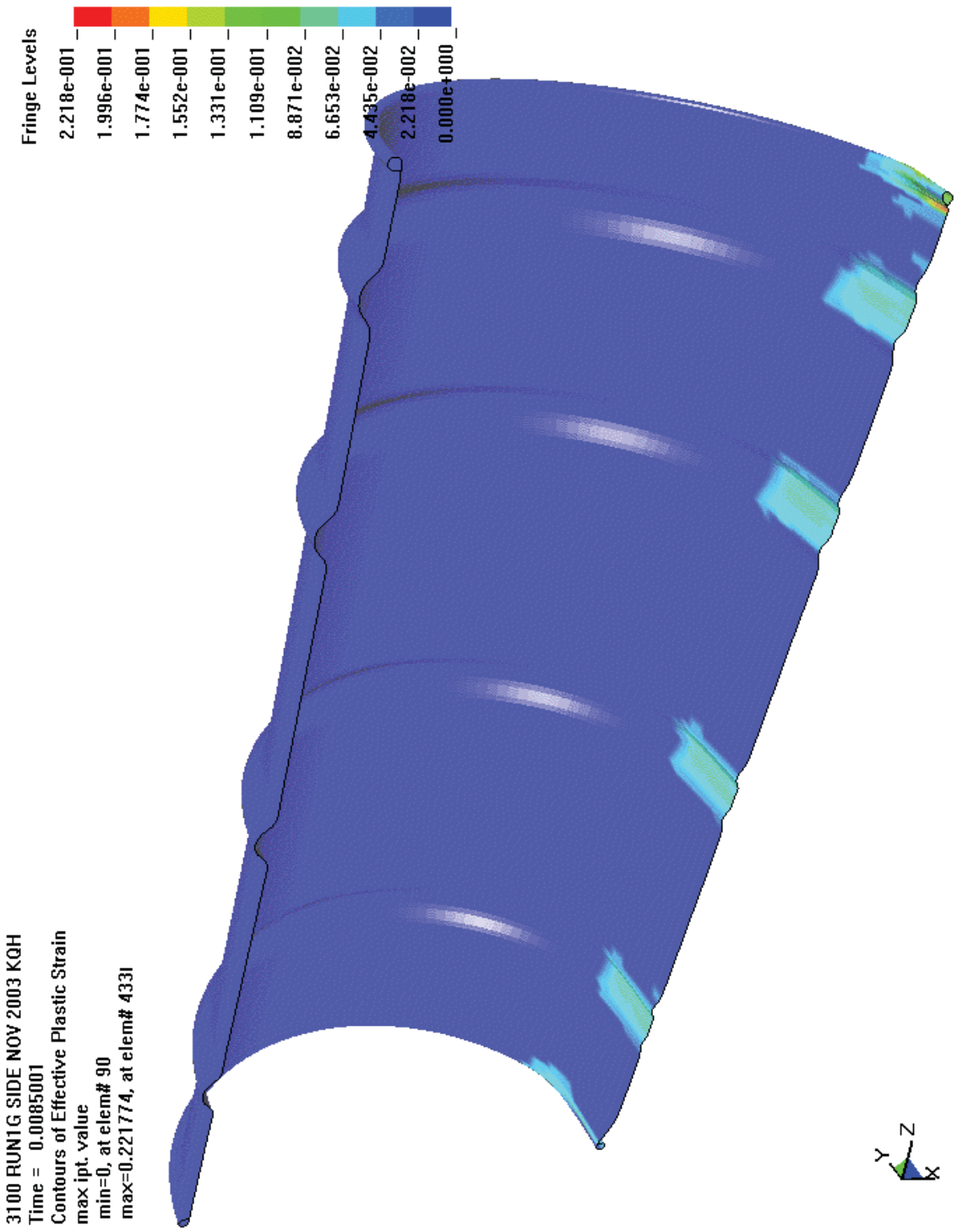

Figure 3.1.8 - Run1g, 30-Foot Impact, Effective Plastic Strain in the Drum Outer Liner

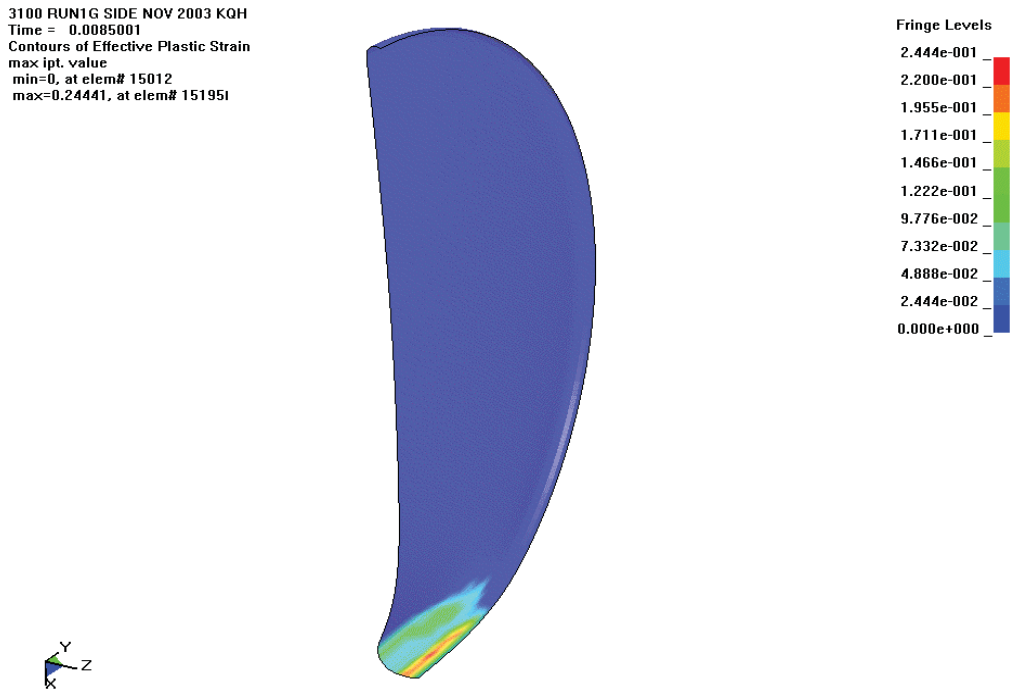

Figure 3.1.9 - Run1g, 30-Foot Impact, Effective Plastic Strain in the Drum Bottom Head

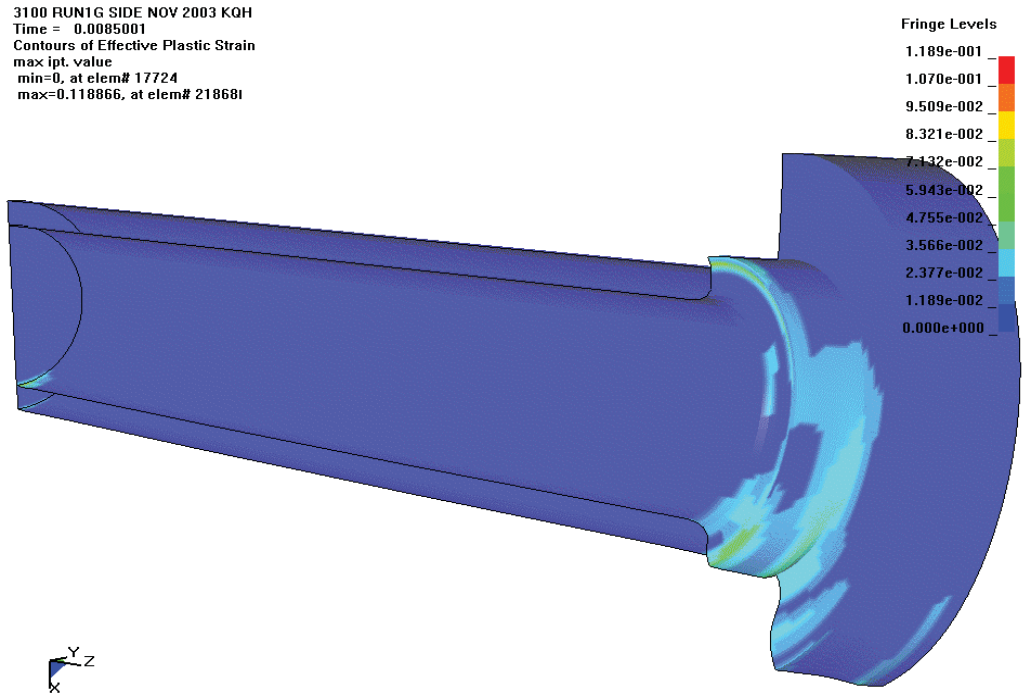

Figure 3.1.10 - Run1g, 30-Foot Impact, Effective Plastic Strain in the Liner

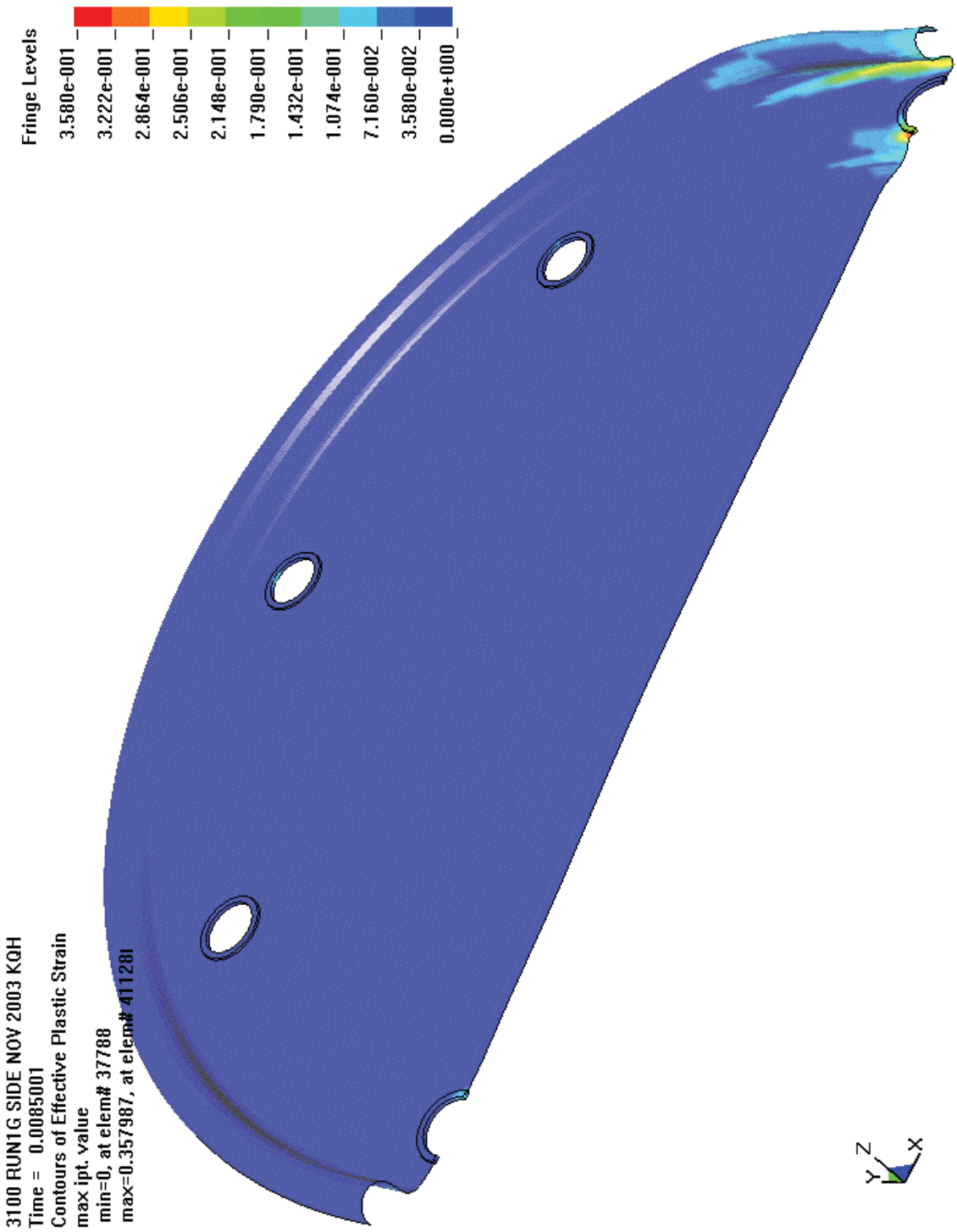

Figure 3.1.11 - Run1g, 30-Foot Impact, Effective Plastic Strain in the Drum Lid

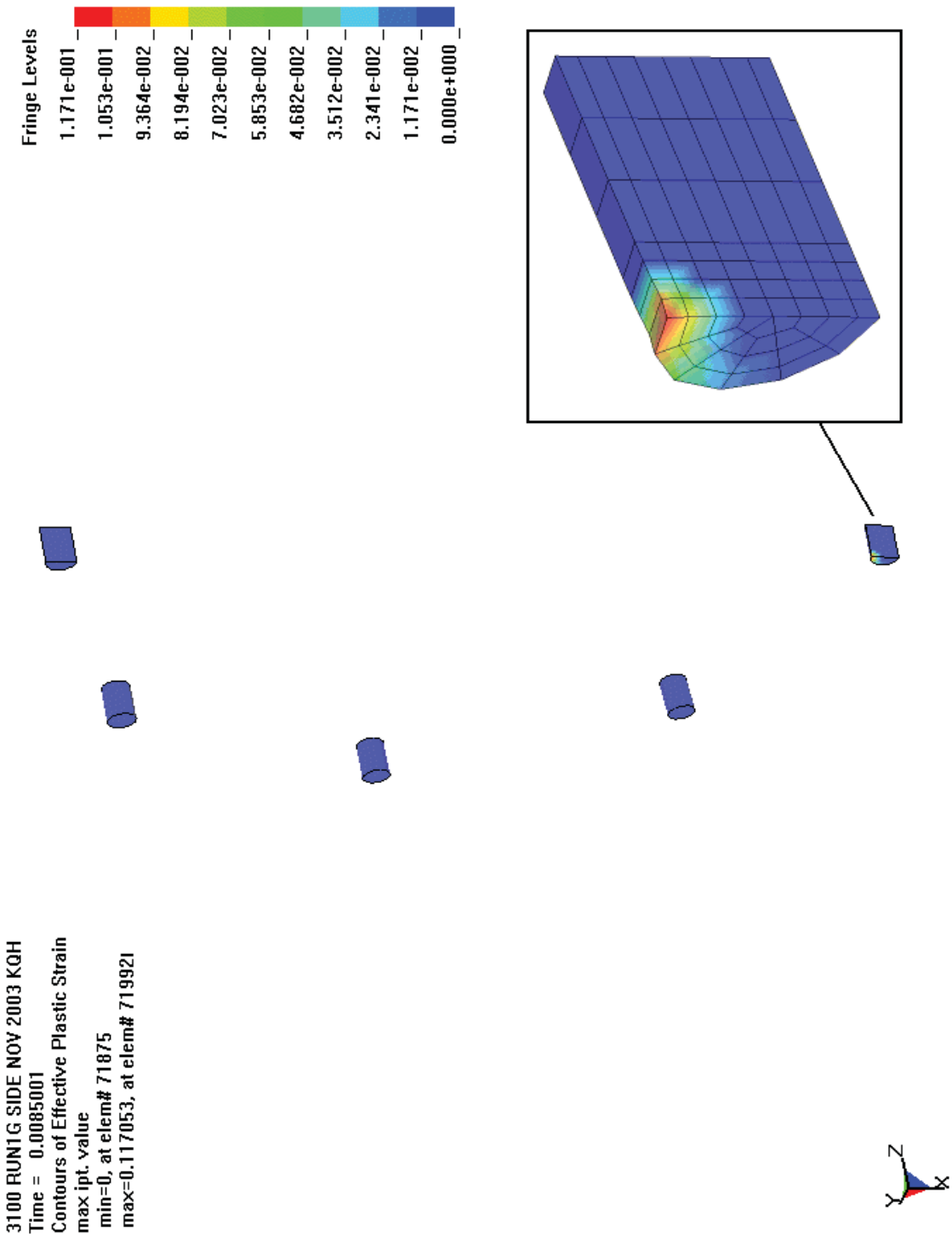

Figure 3.1.12 - Run1g, 30-Foot Impact, Effective Plastic Strain in the Drum Studs

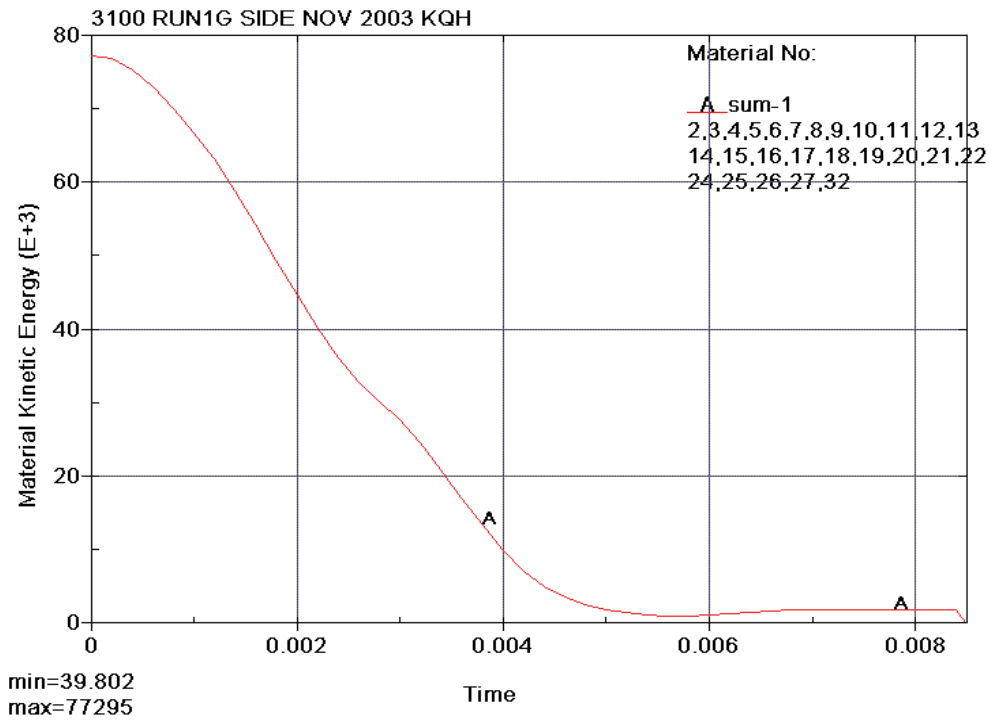

Figure 3.1.13 - Run1g, 30-Foot Impact, Kinetic Energy Time History

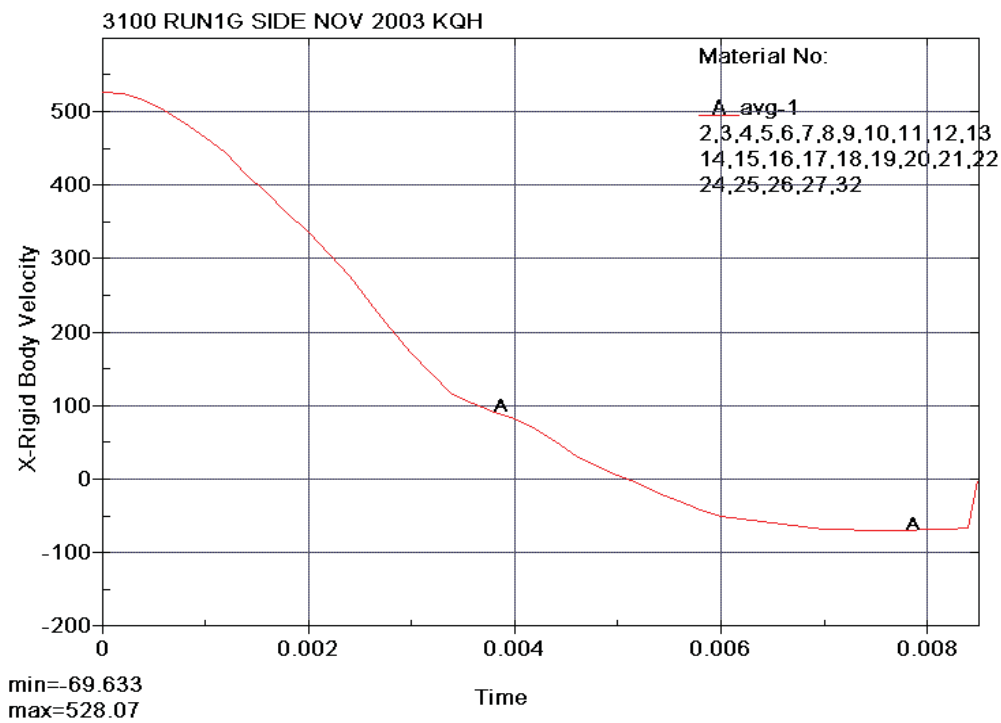

Figure 3.1.14 - Run1g, 30-Foot Impact, X Velocity Time History

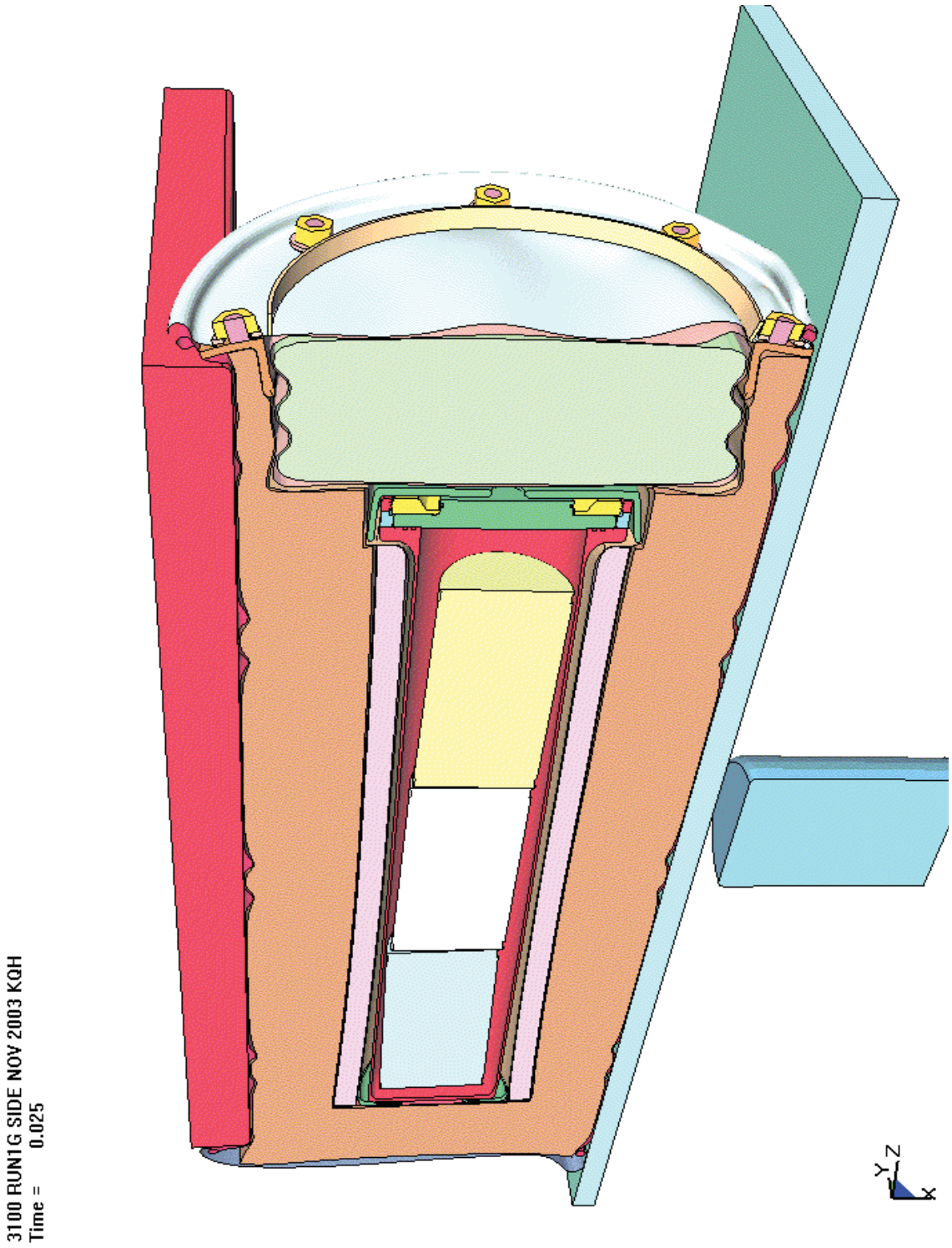

Figure 3.1.15 - Run1g, Crush Impact, Final Configuration

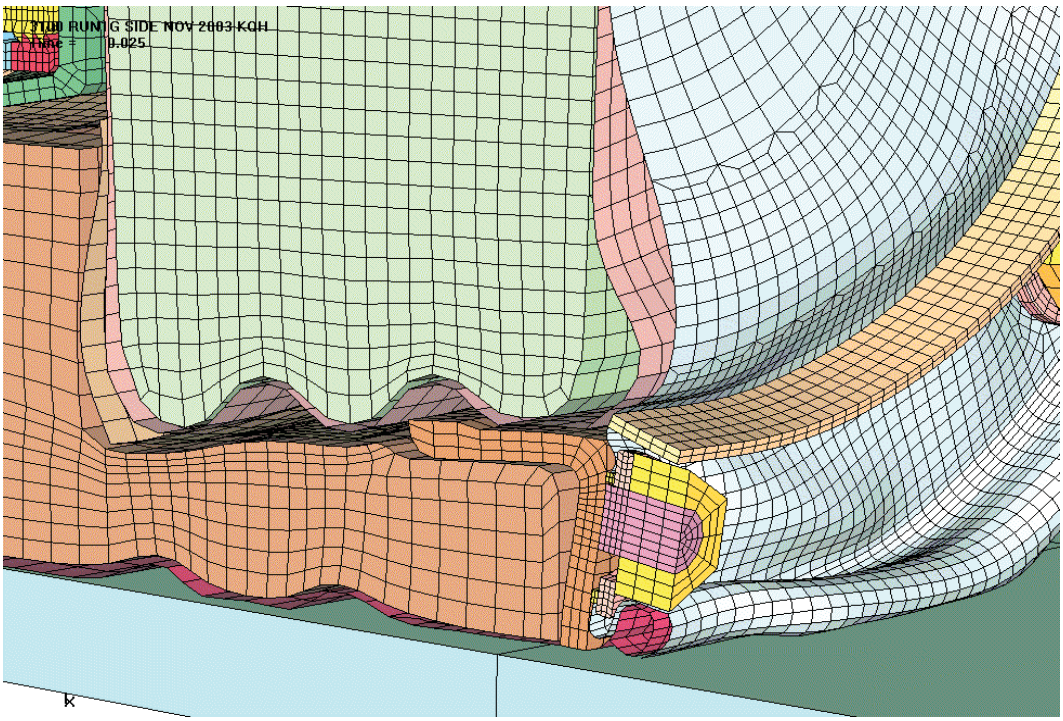

Figure 3.1.16 - Run1g, Crush Impact, Configuration of the Lower Lid Region

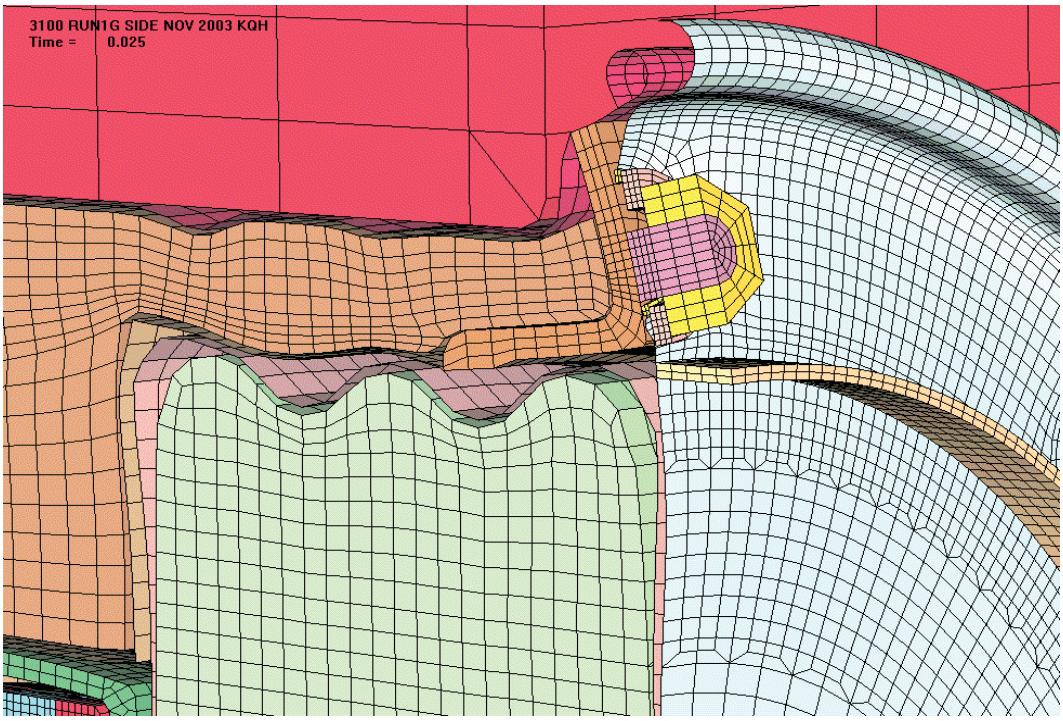

Figure 3.1.17 - Run1g, Crush Impact, Configuration of the Upper Lid Region

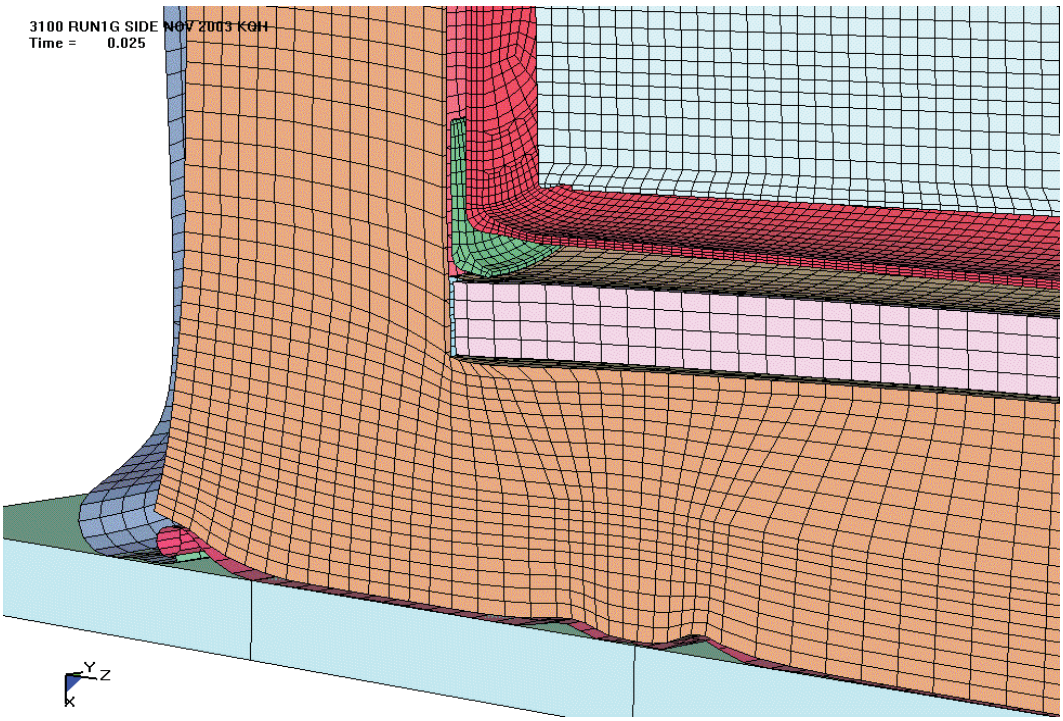

Figure 3.1.18 - Run1g, Crush Impact, Configuration of the Lower Bottom Region

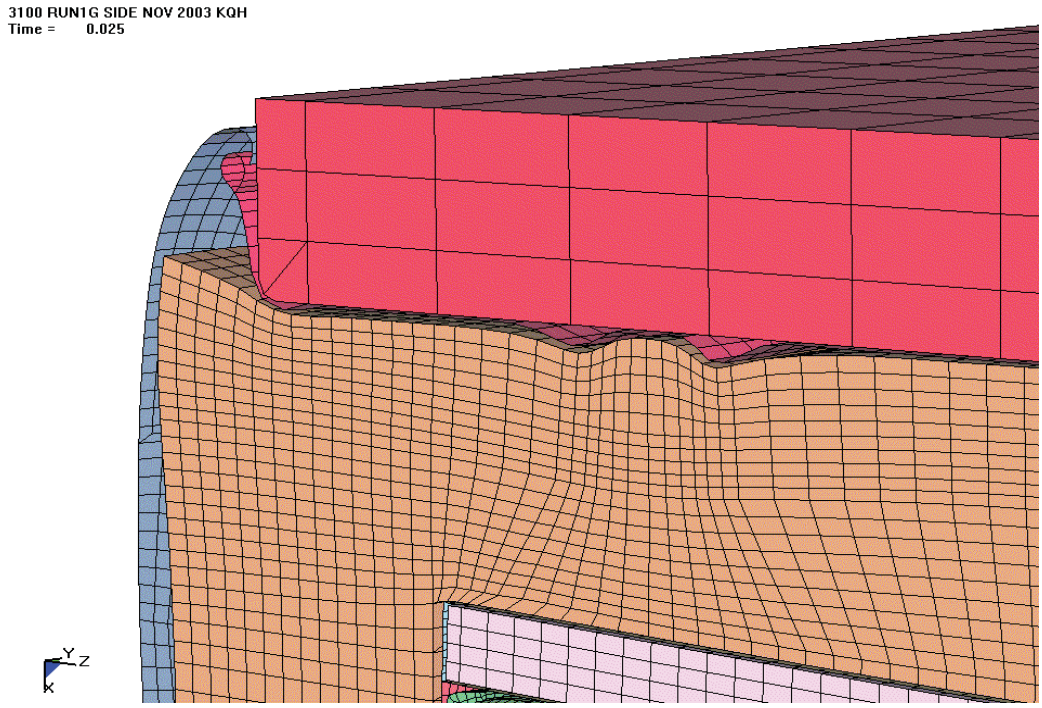

Figure 3.1.19 - Run1g, Crush Impact, Configuration of the Upper Bottom Region

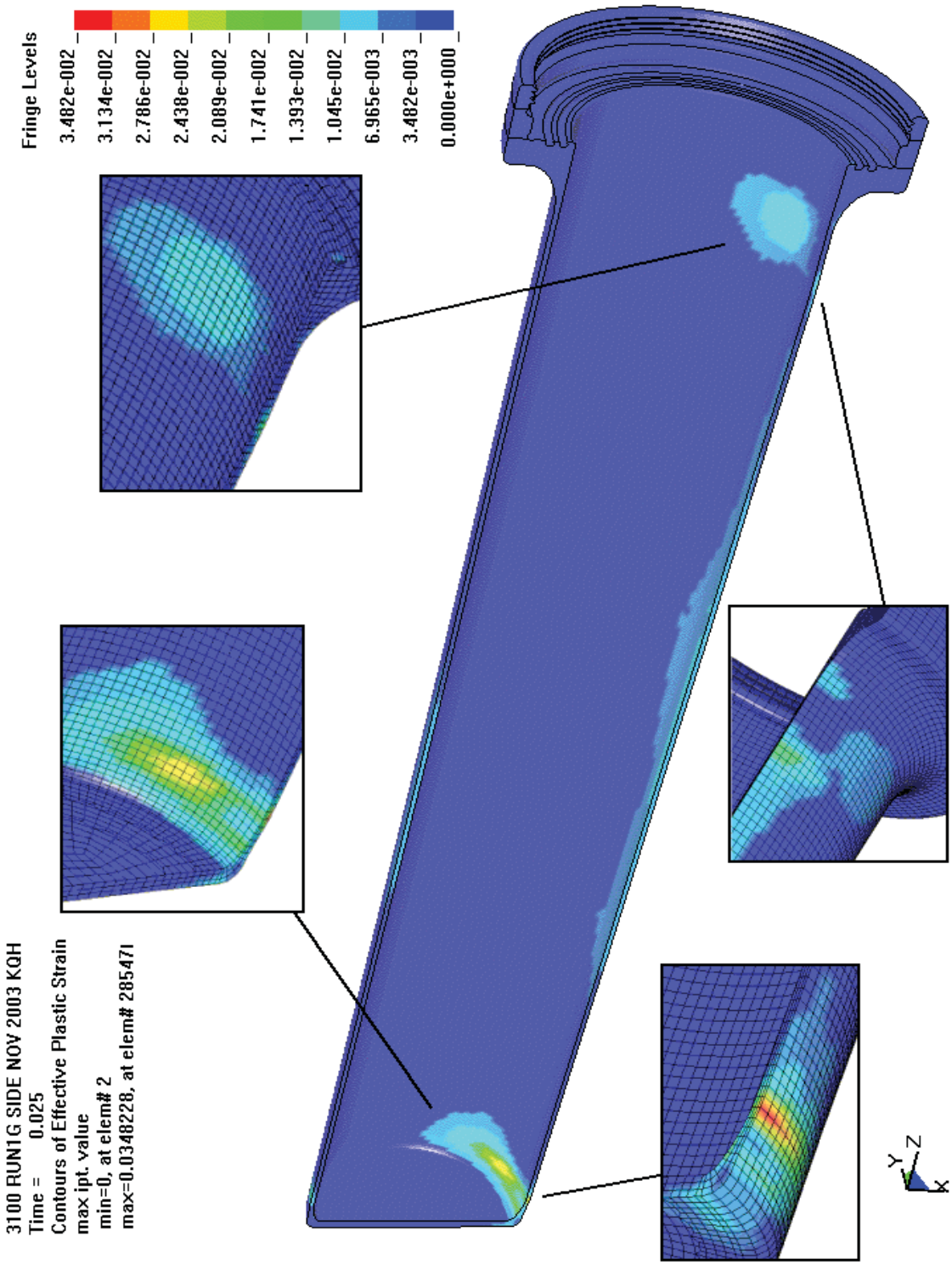

Figure 3.1.20 - Run1g, Crush Impact, Effective Plastic Strain in the CV Body

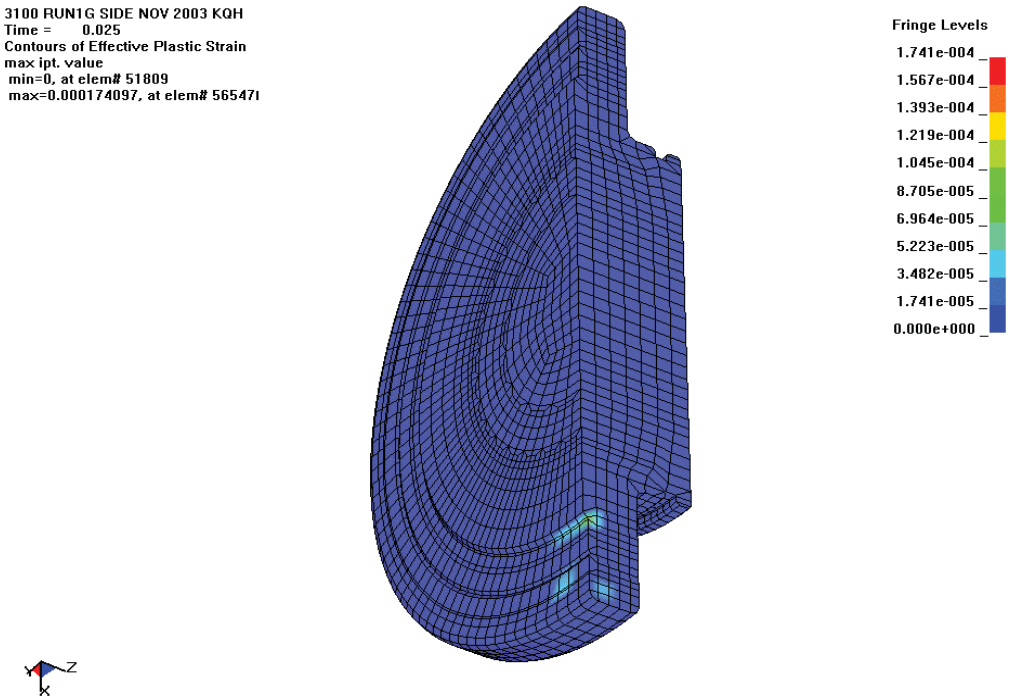

Figure 3.1.21 - Run1g, Crush Impact, Effective Plastic Strain in the CV Lid

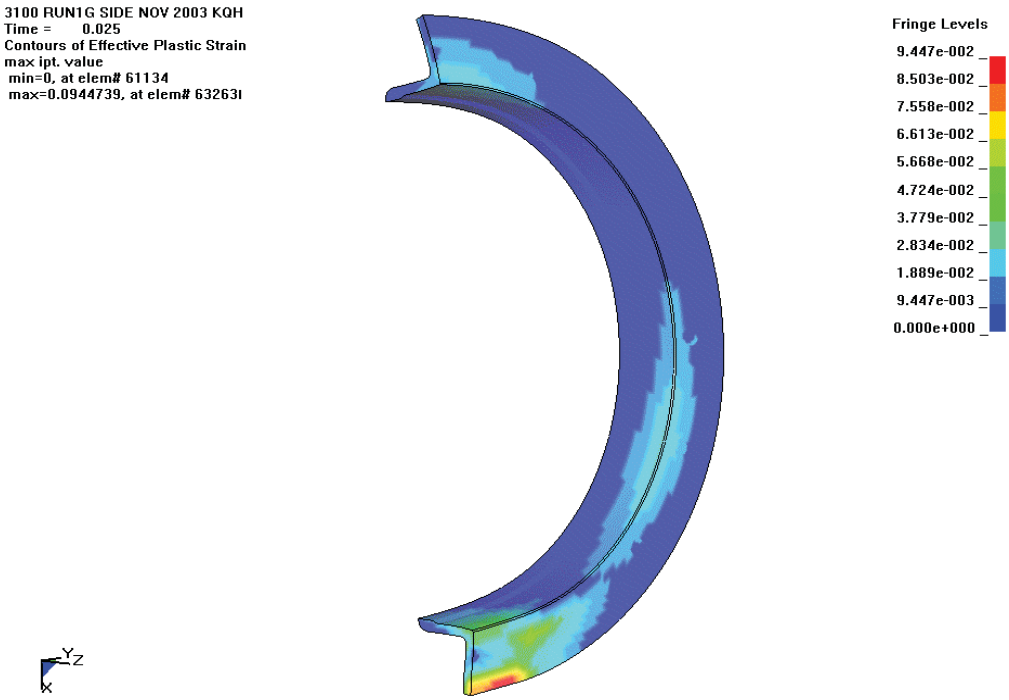

Figure 3.1.22 - Run1g, Crush Impact, Effective Plastic Strain in the Drum Angle

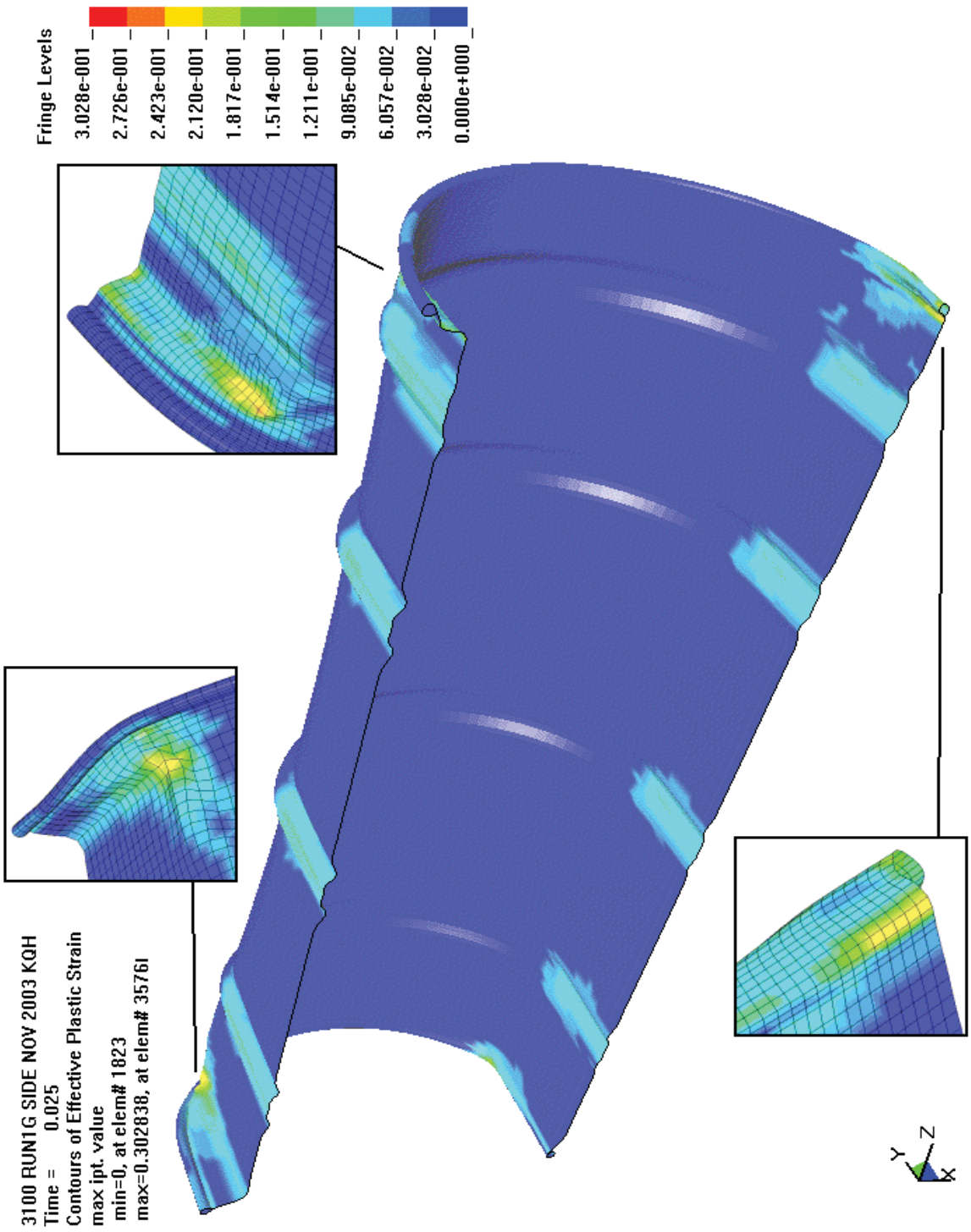

Figure 3.1.23 - Run1g, Crush Impact, Effective Plastic Strain in the Drum

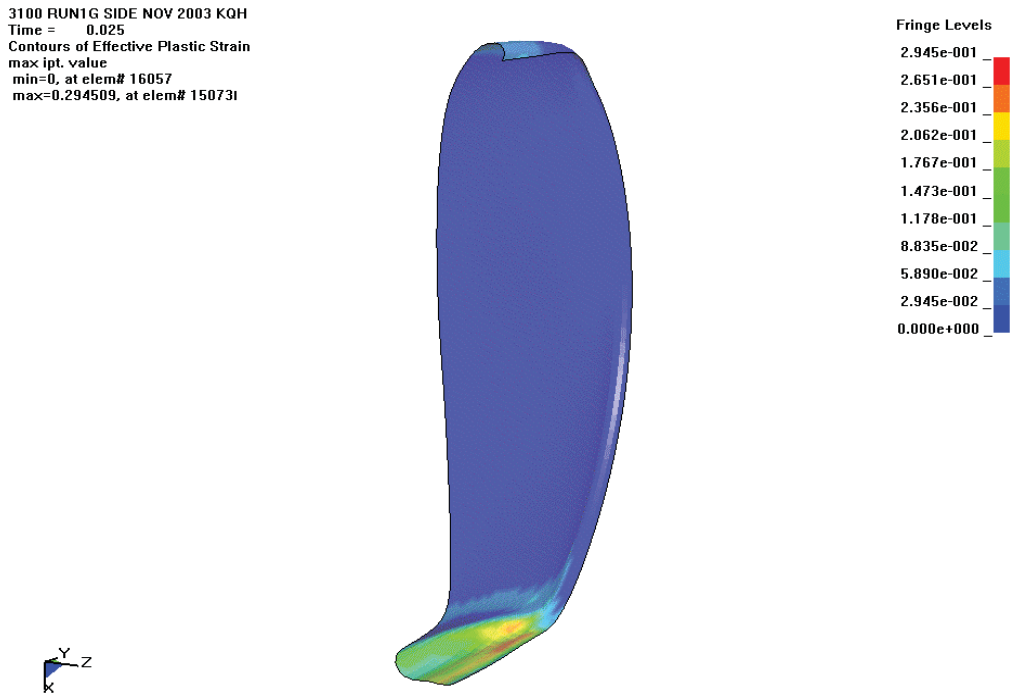

Figure 3.1.24 - Run1g, Crush Impact, Effective Plastic Strain in the Drum Bottom Head

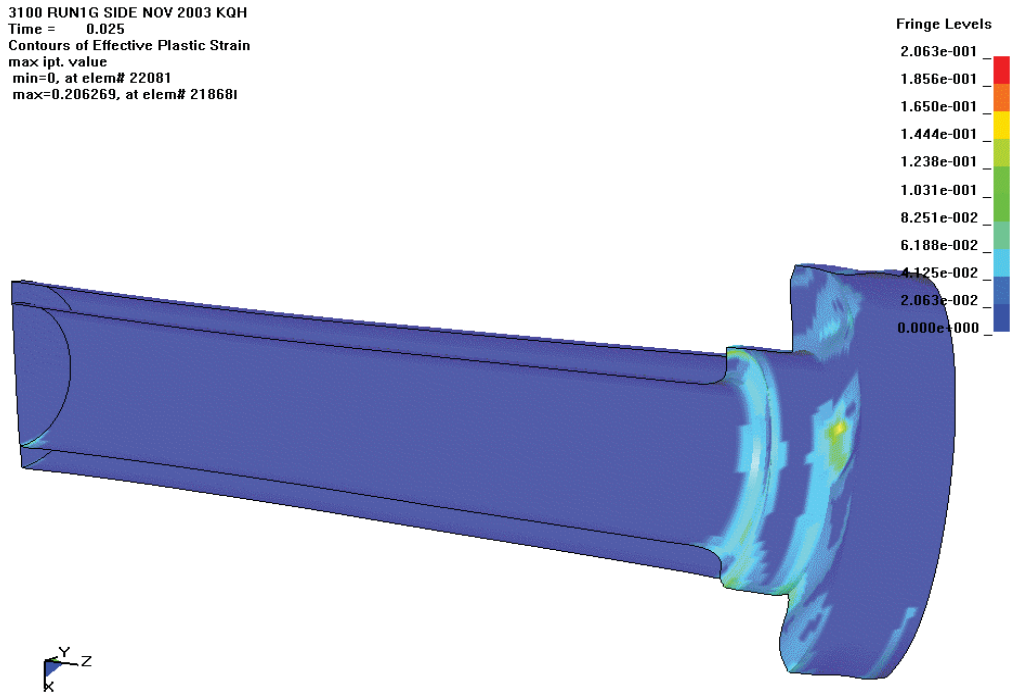

Figure 3.1.25 - Run1g, Crush Impact, Effective Plastic Strain in the Drum Inner Liner

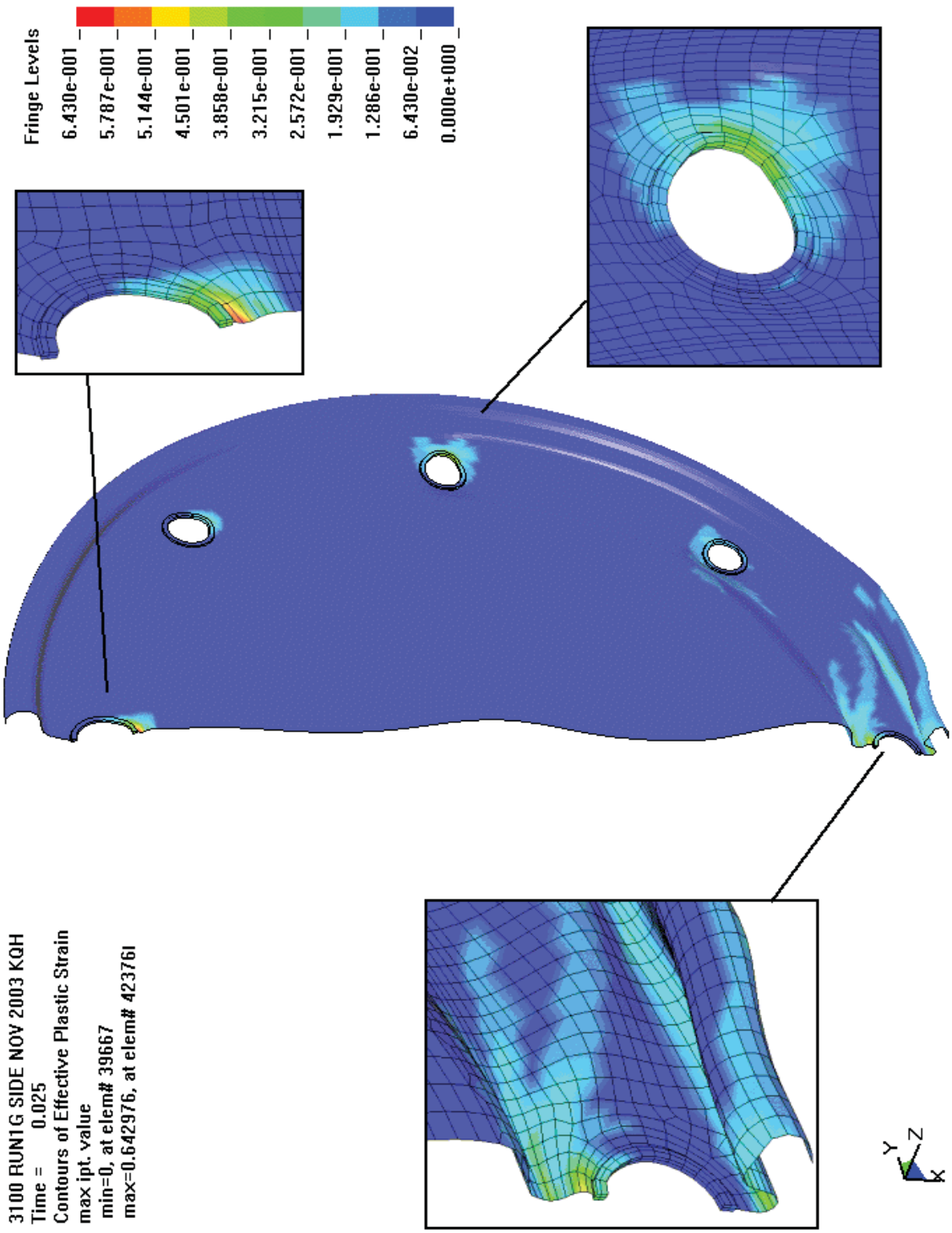

Figure 3.1.26 - Run1g, Crush Impact, Effective Plastic Strain in the Drum Lid

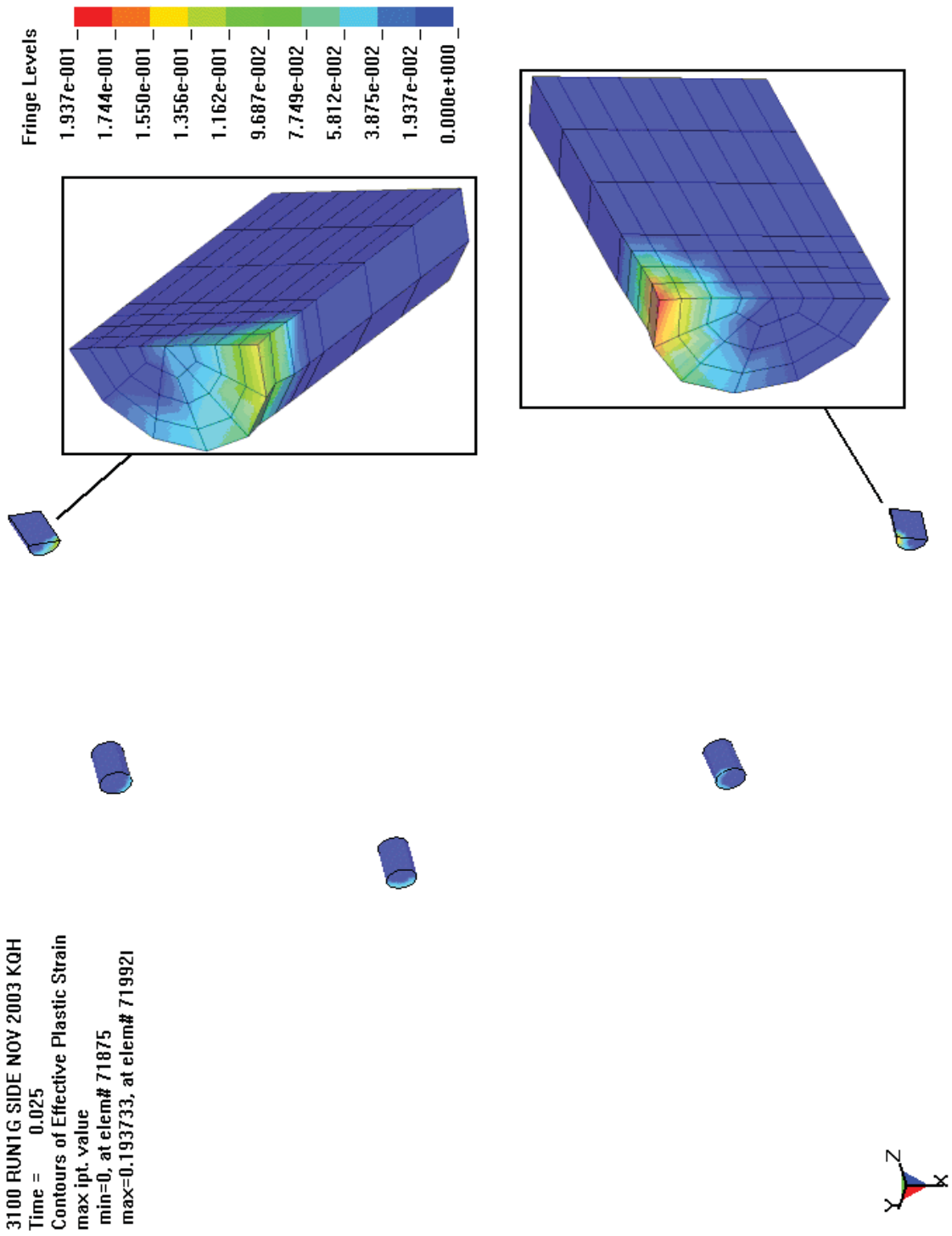

Figure 3.1.27 - Run1g, Crush Impact, Effective Plastic Strain in the Drum Studs

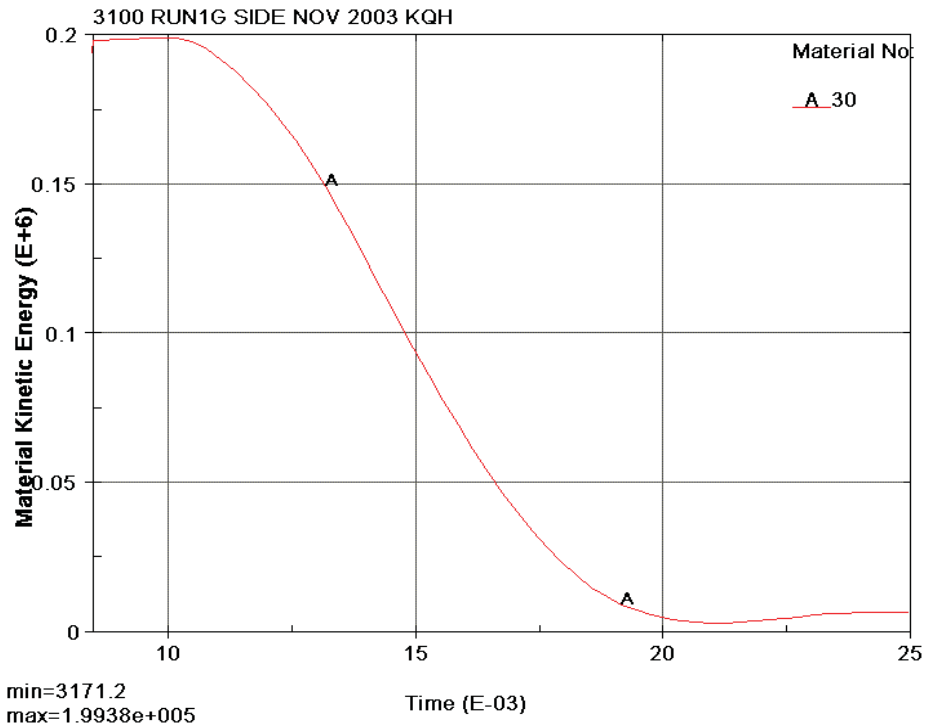

Figure 3.1.28 - Run1g, Crush Impact, Kinetic Energy Time History of the Crush Plate

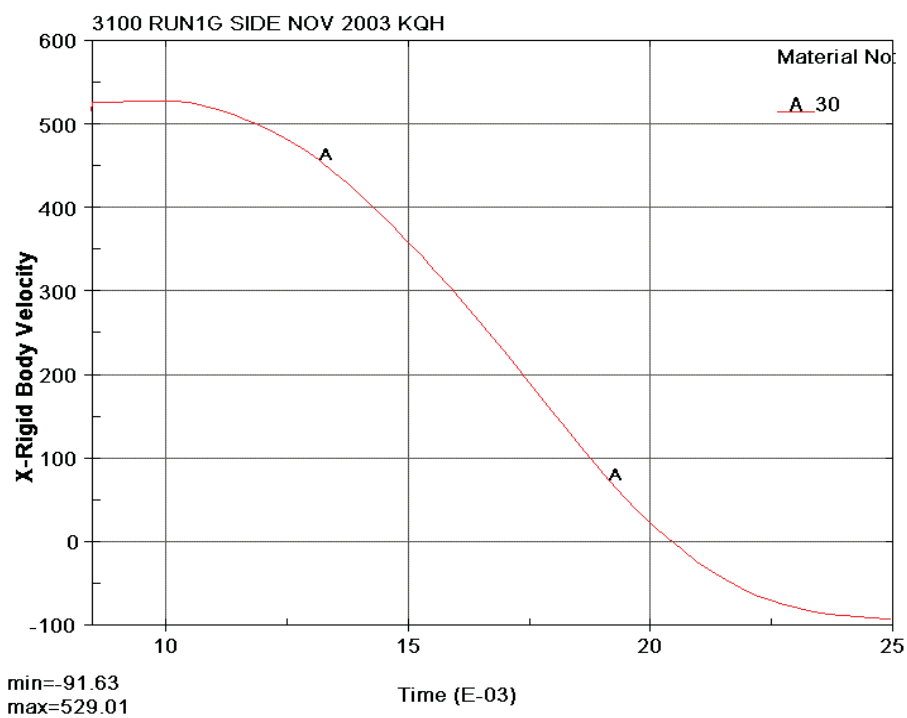

Figure 3.1.29 - Run1g, Crush Impact, X Velocity Time History of the Crush Plate

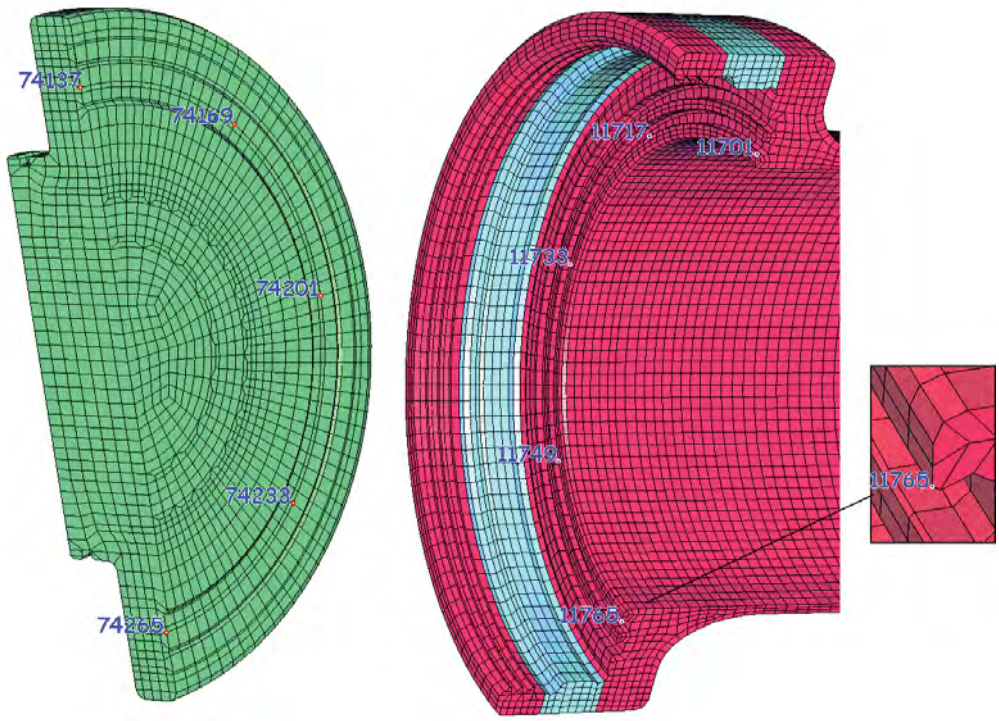

Figure 3.1.30 - Run1g, Nodes on CV Lid and Body Flange for Separation Time History

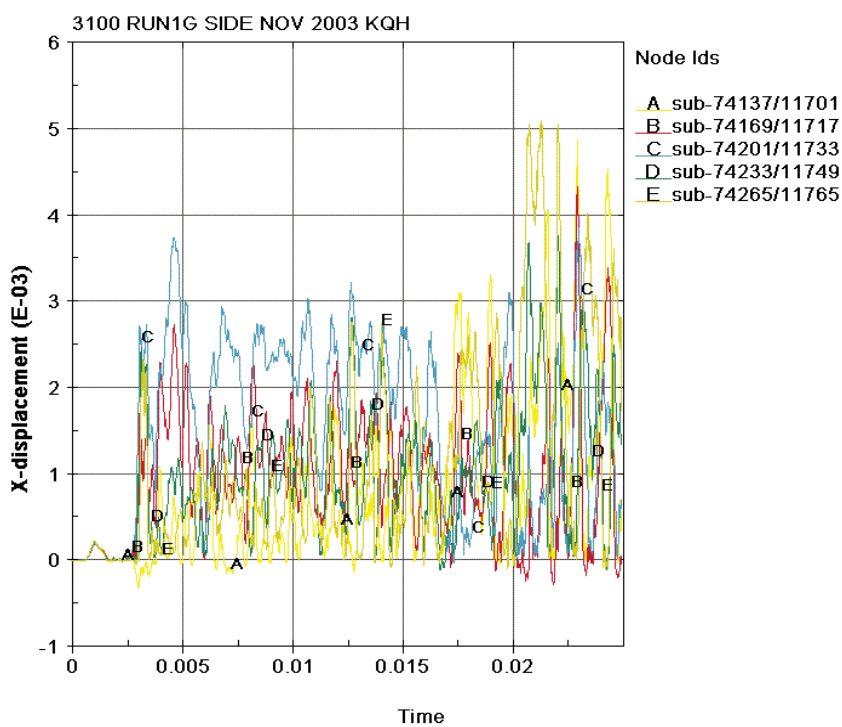

Figure 3.1.31 - Run1g, CV Flange Separation Time History

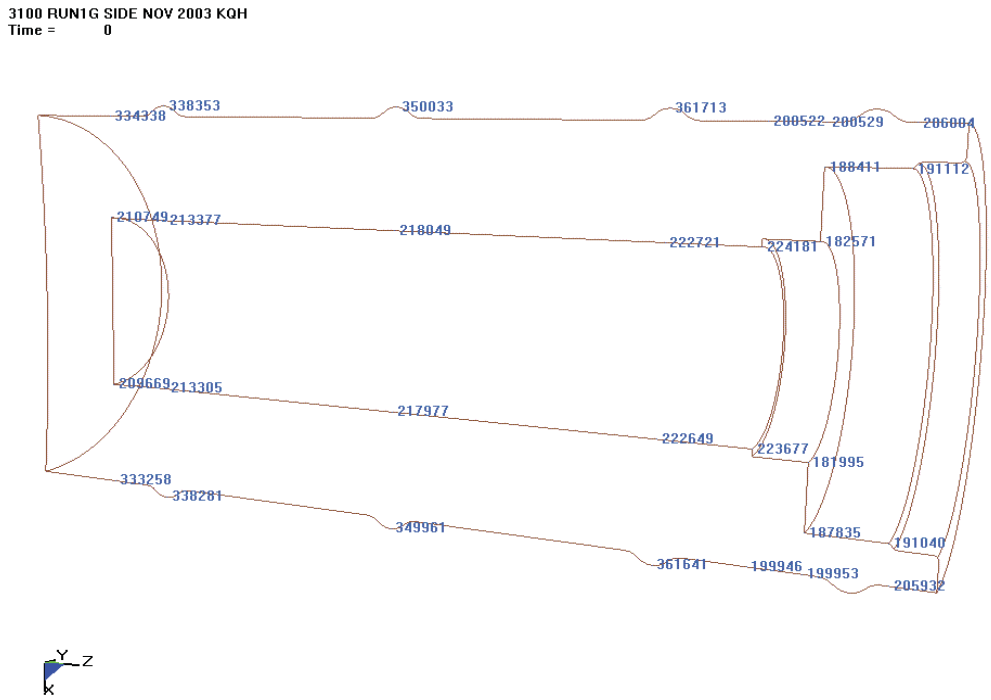

Figure 3.1.32 - Run1g, Drum Kaolite Nodes Used for Thickness Time Histories

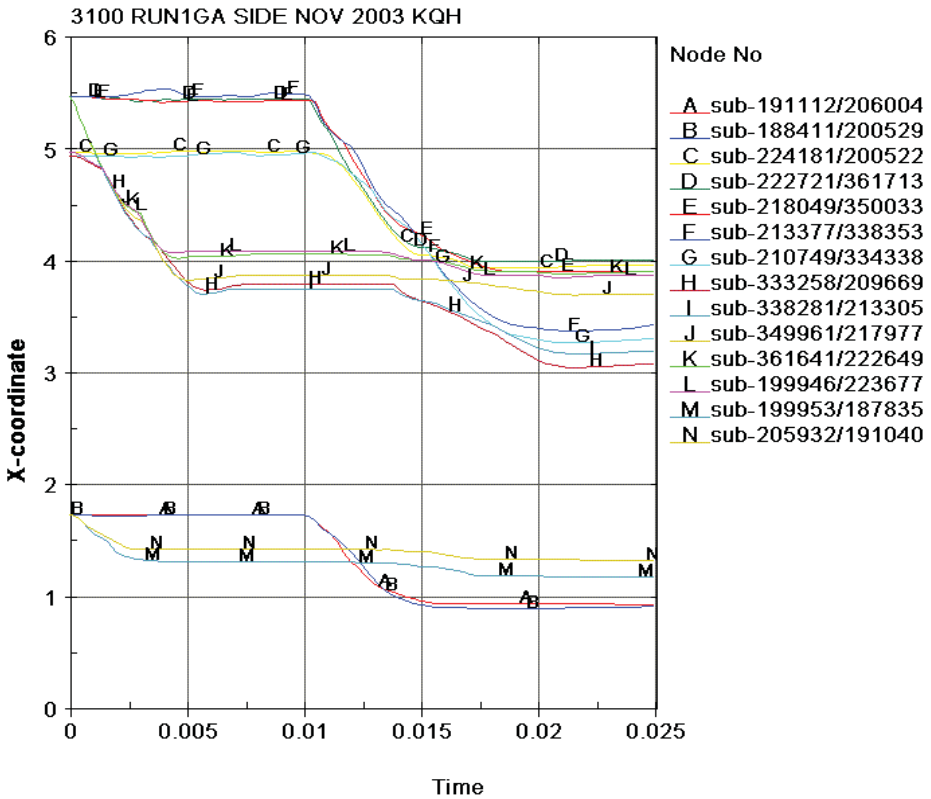

Figure 3.1.33 - Run1g, Drum Kaolite Thickness Time History

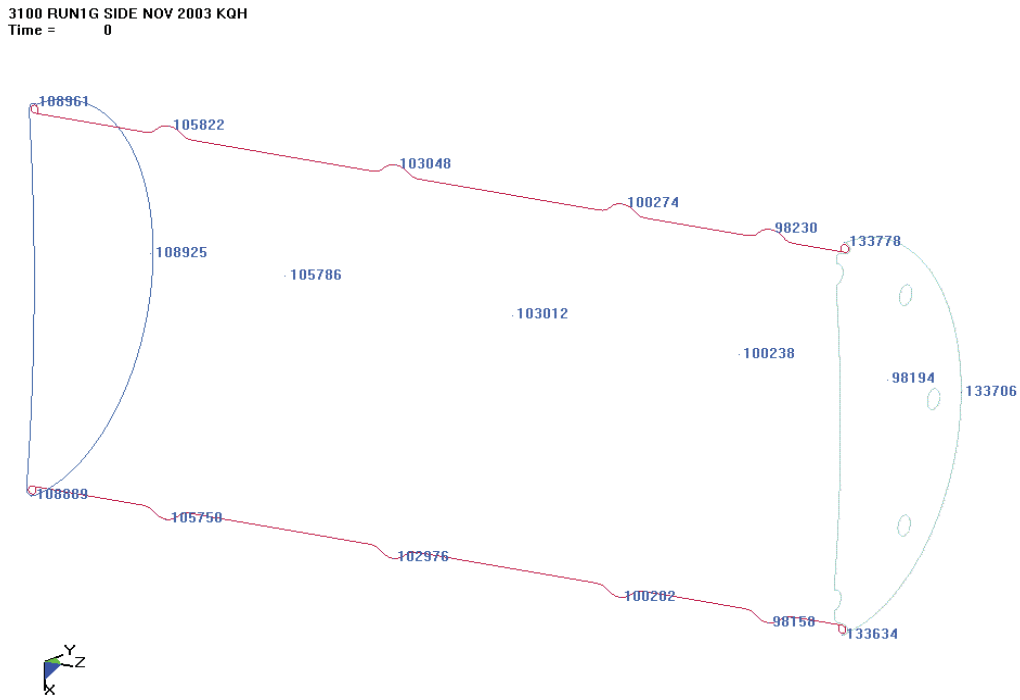

Figure 3.1.34 - Run1g, Drum Nodes Used to Measure Deformation Time Histories

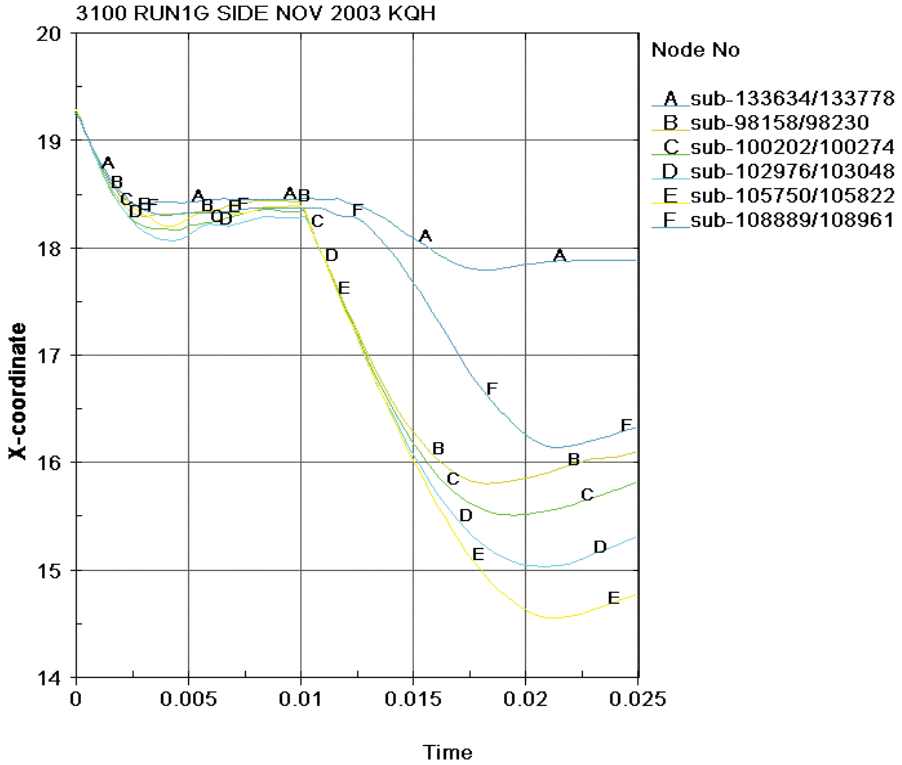

Figure 3.1.35 - Run1g, Drum Measurement Time History in the X-Direction

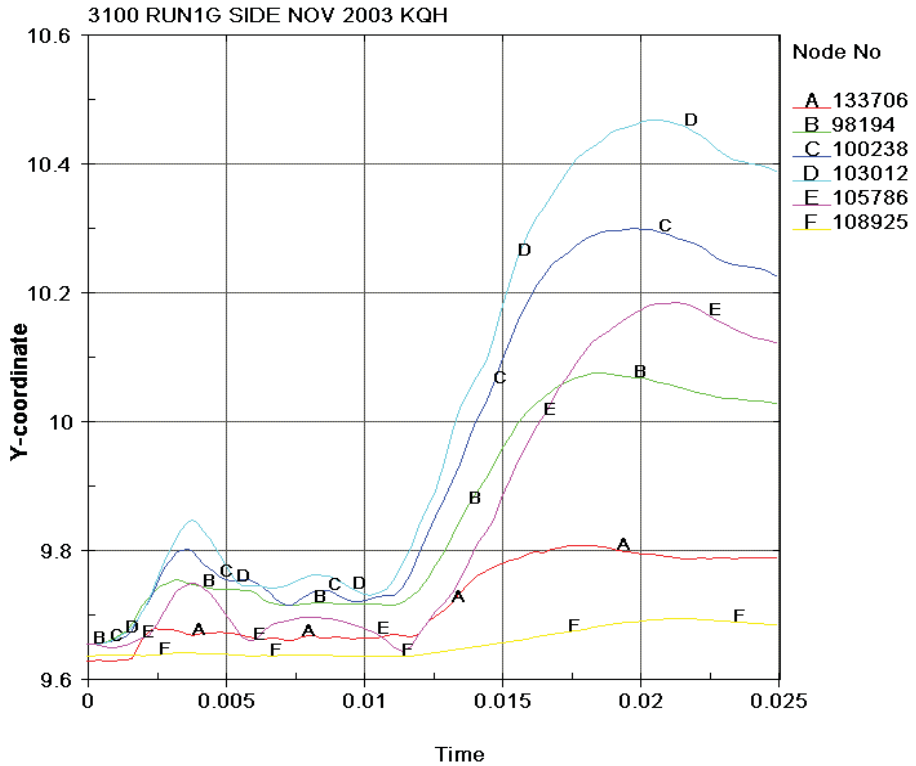

Figure 3.1.36 - Run1g, Drum Measurement Time History in the Y-Direction

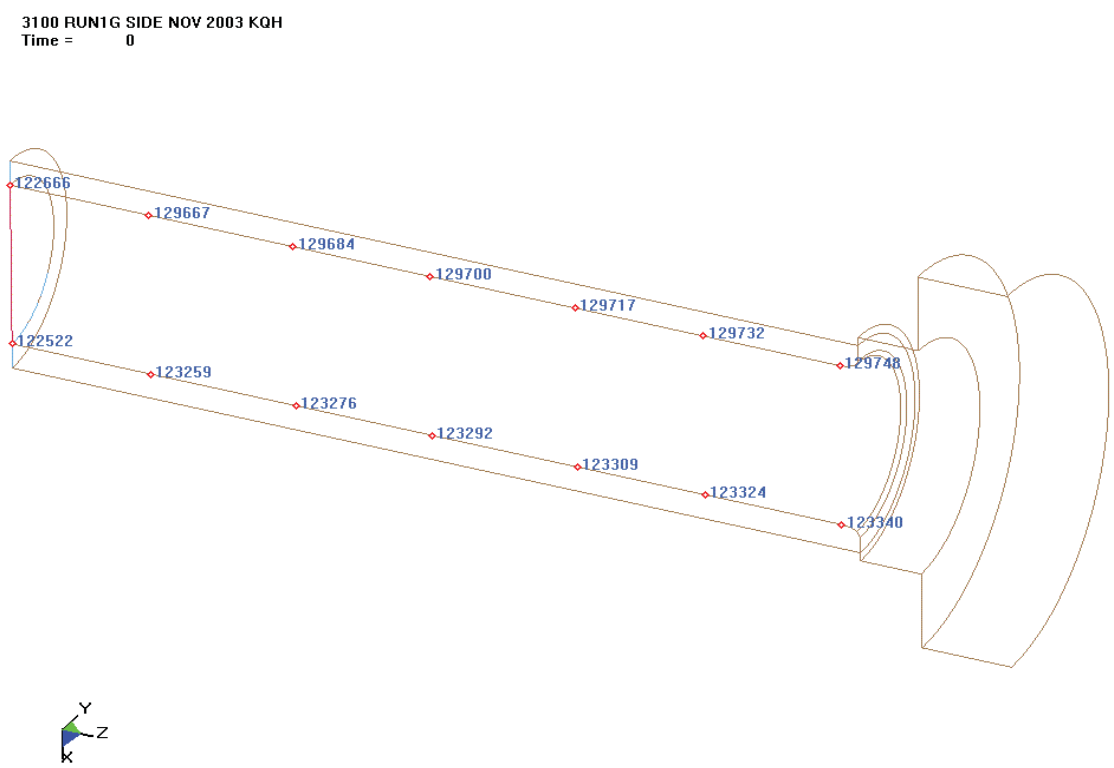

Figure 3.1.37 - Run1g, Position of Inner Liner Nodes Used for Diameter Time History

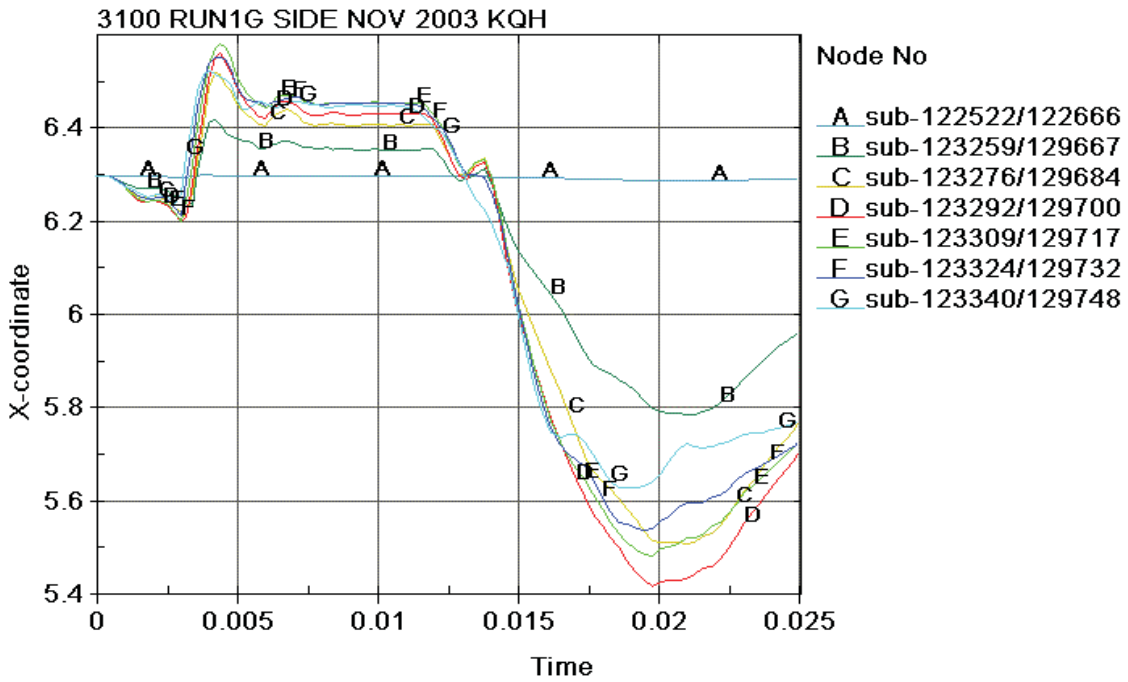

Figure 3.1.38 - Run1g, Inner Liner Diameter Time History

3.2 Run1ga - Side

The run1ga is a 30-foot impact followed by a crush impact, with the crush plate centered above the CV flange. The run1g 30-foot impact restart file was used and the crush plate was moved during the restart phase so that its centerline was approximately above the CV flange. The 30-foot impact was from time 0.0 to 0.0085 sec. The crush plate translation to center it above the CV flange was from time 0.0085 sec to 0.0086 sec. The run1ga crush occurred from 0.0086 sec to 0.027 sec. Therefore, the 30-foot impact results for this run would be the Section 3.1, 30-foot results for run1g, and the crush results for run 1ga (offset crush) are presented in this section.

Figure 3.2.1 shows the configuration of the model after the crush plate was moved above the CV flange (time = 0.0086 sec). Figure 3.2.2 shows the model configuration after the run1ga crush impact. Figure 3.2.3 through Figure 3.2.6 show enlarged views in the lid and bottom regions of the package assembly.

Figure 3.2.7 shows that the maximum strain in the CV body for the run1ga crush impact is 0.0348 in/in. The effective plastic strain in the CV lid is 0.0002 in/in and is shown in Figure 3.2.8. The CV nut ring remains elastic for the crush impact of run1ga.

The maximum effective plastic strain in the drum angle is shown in Figure 3.2.9 to be 0.1058 in/in. The maximum effective plastic strain in the drum is 0.3818 in/in and occurs in the top drum roll near the crush plate (Figure 3.2.10).

Figure 3.2.11 gives the maximum effective plastic strain in the lid to be 1.1345 in/in. This is a relatively high strain level and the maximum occurs near the stud hole at the 90° position (initially along Y axis). Another high region of strain is near the upper stud nearest the crush plate. The solid elements (used for contact bearing on the studs) around the stud holes show effective plastic strain maximum of 0.8745 in/in. The membrane effective plastic strain in the shell elements is a maximum of 0.8057 in/in and is highly localized near the stud hole at the 90° position. Some tearing of the lid could occur in the lid hole at the 90° position and at the lid hole nearest the crush plate (180°).

Figure 3.2.12 shows the effective plastic strain levels in the drum studs. The maximum is shown to be 0.5207 in/in and occurs in the stud at the 90° position. From Figure 3.2.12 it is seen that the elevated strain occurs near the outer extreme of the stud, and that the through thickness strain levels between 0.3170 and 0.3802 in/in exist.

A study of the timing of the elevated effective plastic strain levels in the lid and the drum studs shows that the lid reaches failure magnitudes before the studs. At the stud hole in the drum lid nearest the crush plate (180°), the bending strain crosses the 0.57 in/in

strain at about 0.0122 seconds in the crush impact. The membrane strain in the lid elements at 180° reaches a maximum of .5295 in/in. The stud at 180° does not experience elevated strain levels (final maximum in this stud is 0.17 in/in). So at the 180° position, only the lid experiences relatively high levels of effective plastic strain.

At the 90° position in the lid, the membrane effective plastic strain exceeds the 0.57 in/in level near 0.0164 seconds in the crush impact. The surface maximum effective plastic strain exceeds 0.57 in/in at about 0.0161 seconds, slightly ahead of the membrane. At time 0.0164 seconds, the effective plastic strain levels in the stud at 90° is about 0.35 in/in maximum, with the through thickness levels between 0.104 in/in to 0.136 in/in. Therefore, at the 90° position, the lid reaches the failure level of 0.57 in/in before the stud.

From this timing data, it is shown that the lid would reach failure levels in bending and membrane before the stud effective plastic strain levels become relatively high. Therefore, it would be expected that the lid would locally tear before the bolting reached elevated effective plastic strain levels, thus possibly reducing the loadings on the studs. Due to the extent of the relatively high levels of effective plastic strain in the drum lid, it would be expected that any lid tearing would be localized and that the large washers would restrain the drum lid.

The effective plastic strain contour patterns for the other components are not shown in figures. The maximum effective plastic strain in the drum bottom is 0.2444 in/in; in the liner it is 0.2853 in/in; in the lid stiffener it is 0.1116 in/in; in the drum stud nuts it is 0.0103 in/in; in the drum stud washers it is 0.1685 in/in and in the plug liner it is 0.2181 in/in.

The kinetic energy time history for the crush plate impact is shown in Figure 3.2.13. The X velocity time history is shown in Figure 3.2.14.

The lid separation time history is shown in Figure 3.2.15 (nodes defined in Figure 3.1.30). From Figure 3.2.15 it is seen that the spike separation of just under 0.004 inches can occur with a final nominal separation of less than 0.002 inches expected.

The kaolite thickness time histories for the nodes defined in Figure 3.1.32 are given in Figure 3.2.16 for run1ga. The drum diameter time histories are given in Figures 3.2.17 and 3.2.18. The nodes defining this response are shown in Figure 3.1.34. As shown in Figure 3.2.17, the bottom head and the bottom drum roll remain at, or near 30-foot impact diameters for the crush impact. This response is expected as qualitatively shown in Figure 3.2.2. The response in the Y-direction is shown in Figure 3.2.18.

Figure 3.2.19 shows the diameter time history for various locations along the liner length. Figure 3.1.37 and Table 3.1.3 define the locations at which the diameters are obtained.

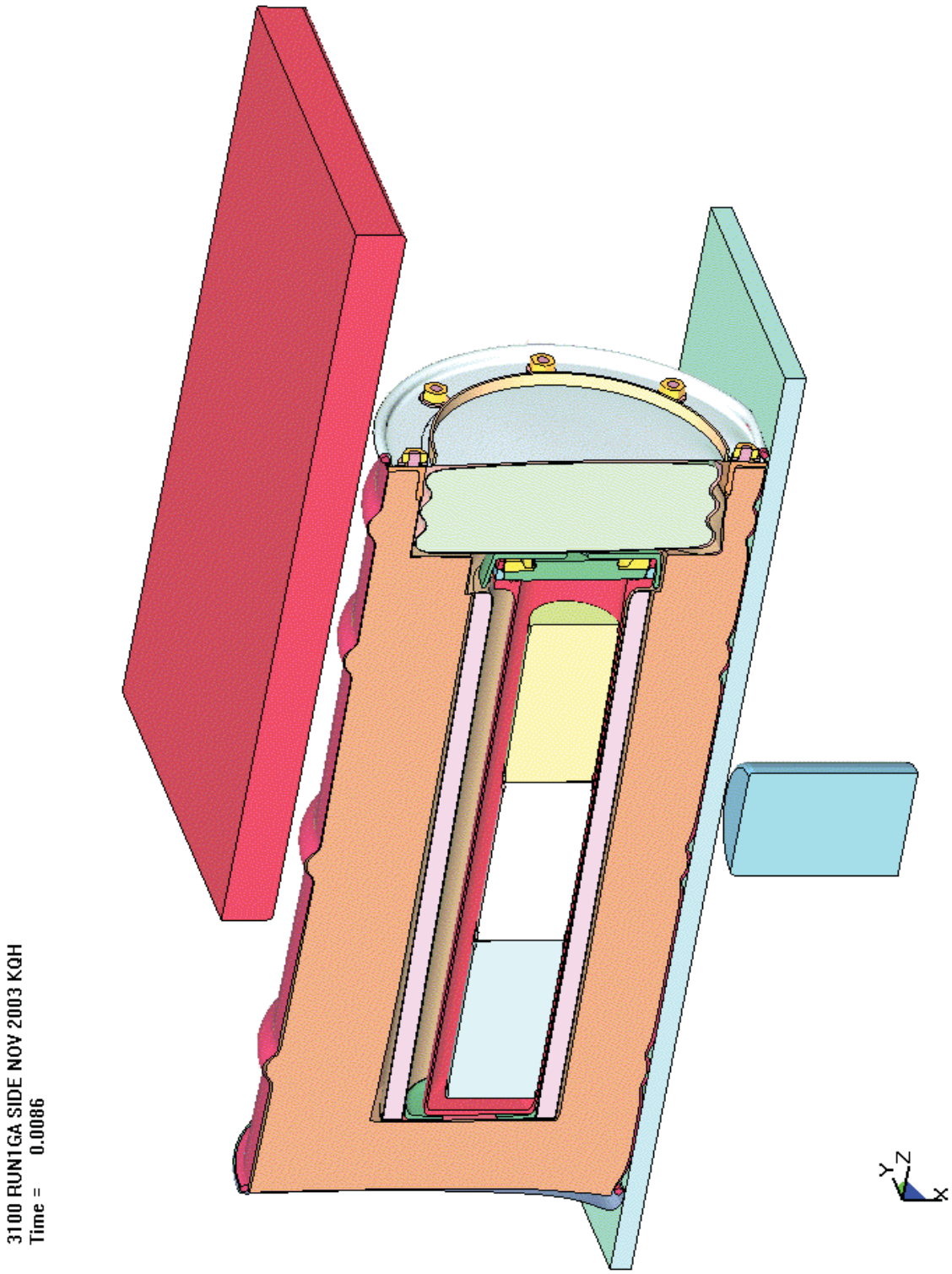

Figure 3.2.1 - Run1ga, Crush Impact, Initial Configuration for the Crush Impact

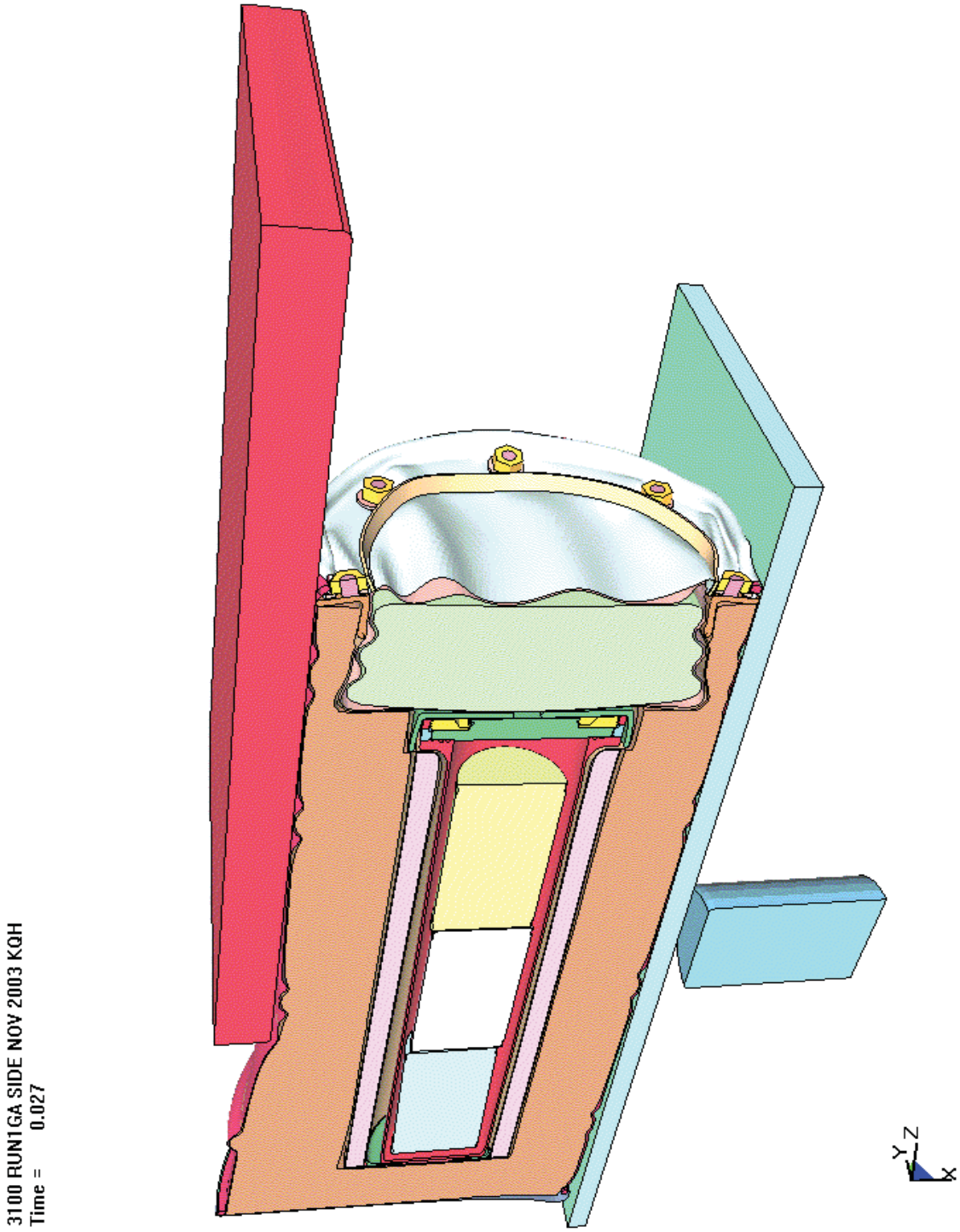

Figure 3.2.2 - Run1ga, Crush Impact, Configuration of the ES-3100 After the Crush Impact

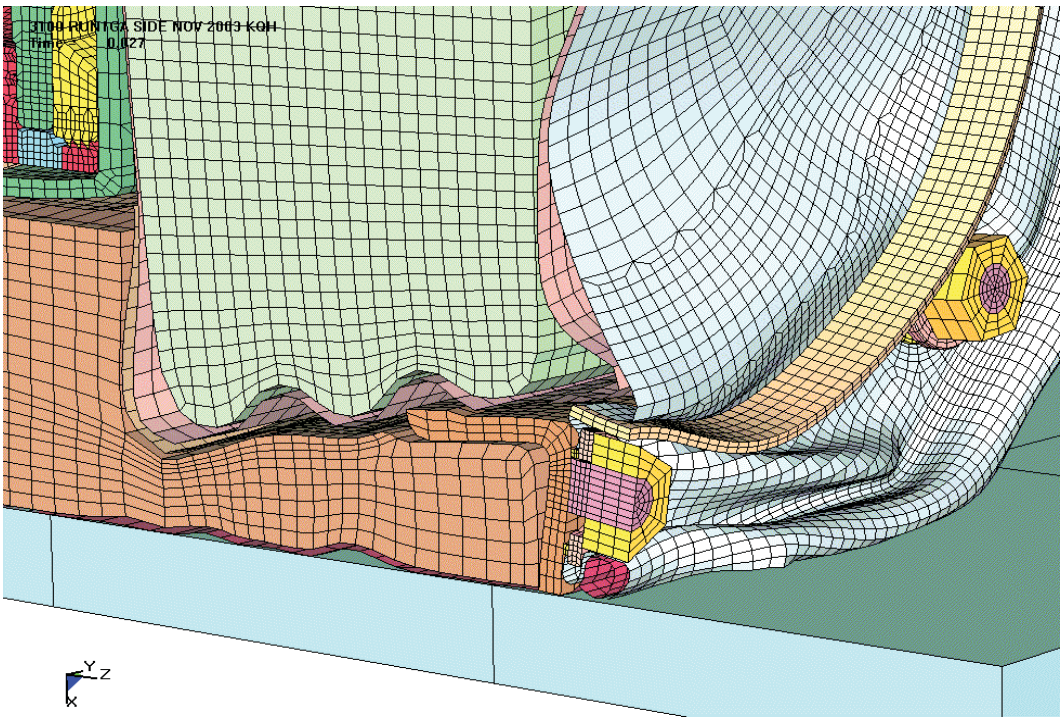

Figure 3.2.3 - Run1ga, Crush Impact, Configuration of the Lid Region Near the Rigid Plane

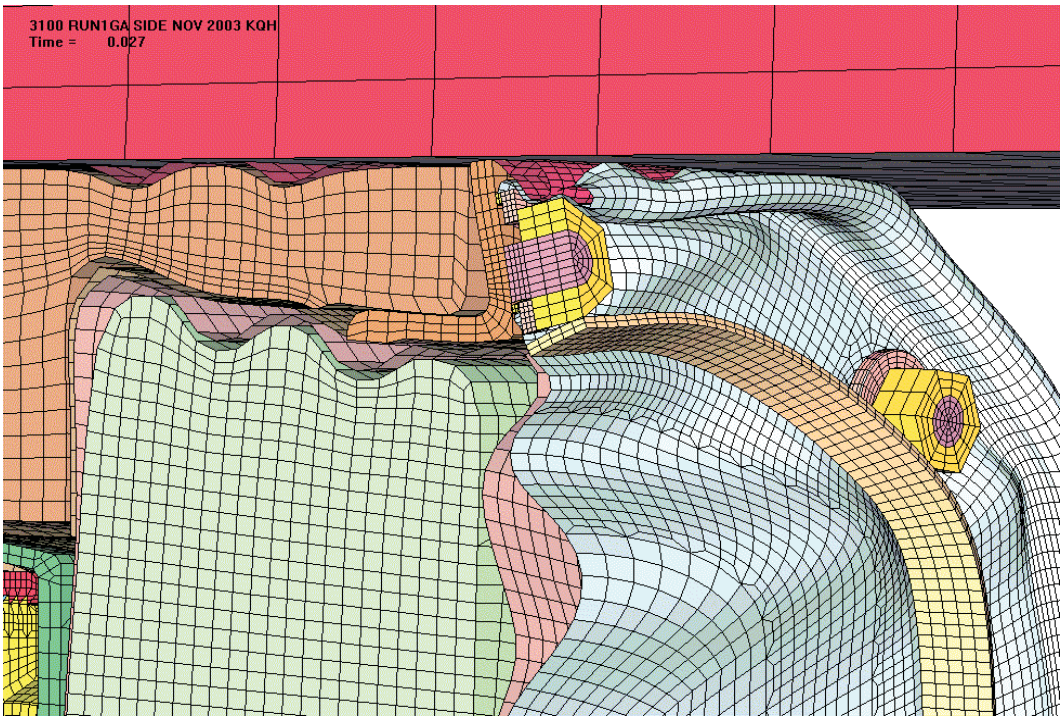

Figure 3.2.4 - Run1ga, Crush Impact, Configuration of the Lid Region Near the Crush Plate

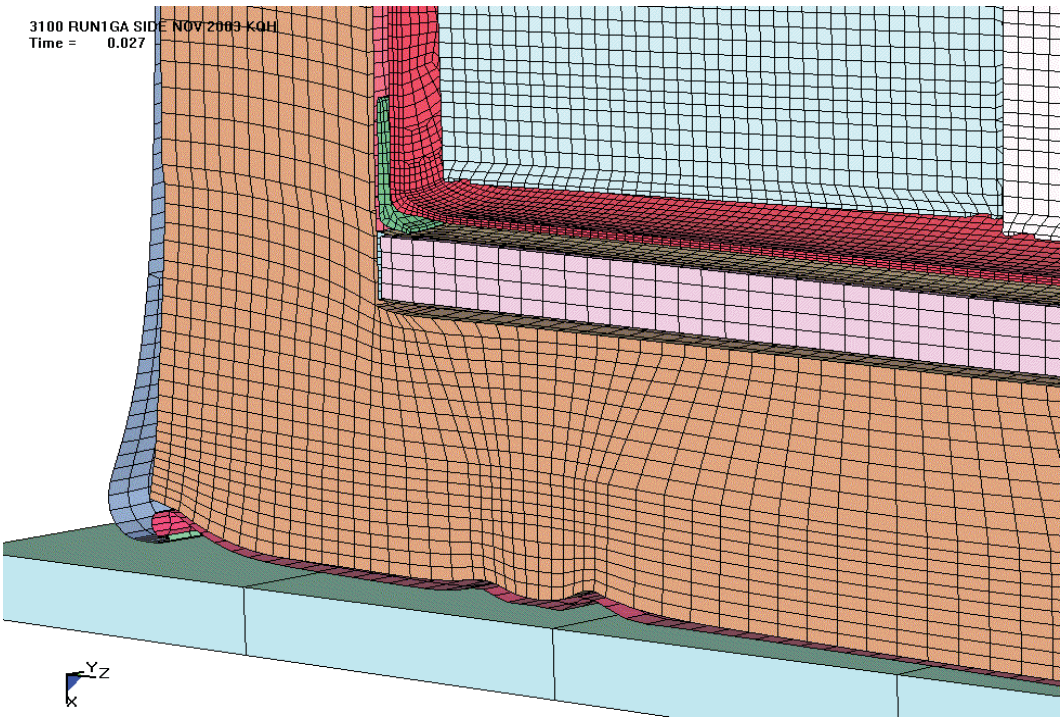

Figure 3.2.5 - Run1ga, Crush Impact, Configuration of the Bottom Near the Rigid Plate

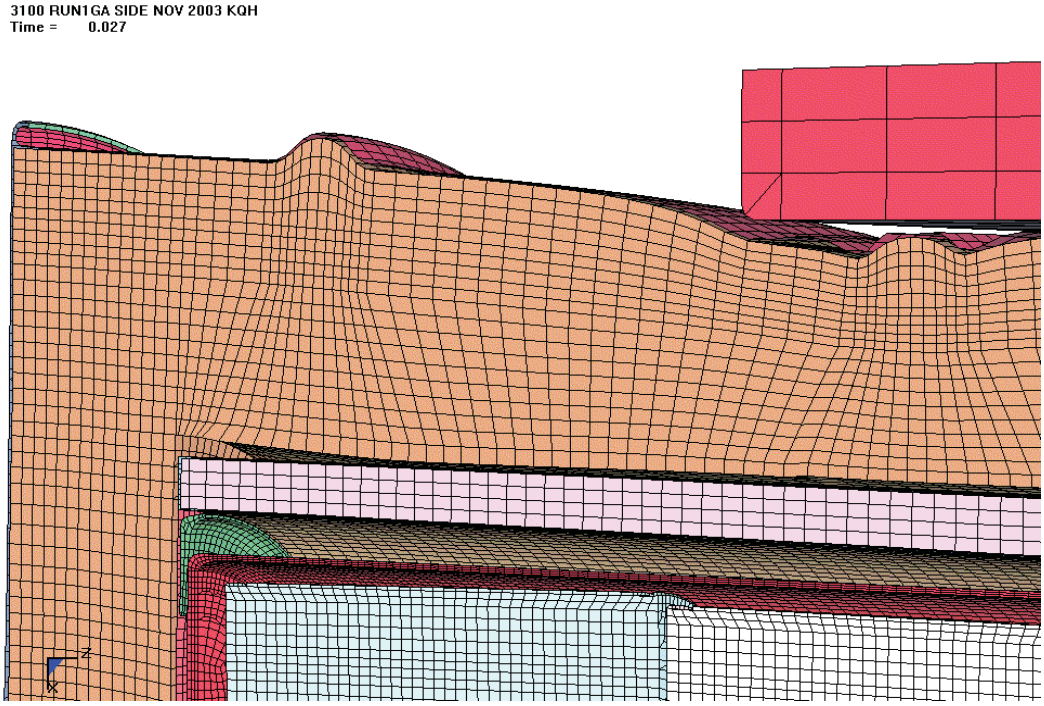

Figure 3.2.6 - Run1ga, Crush Impact, Configuration of the Bottom Near the Crush Plate

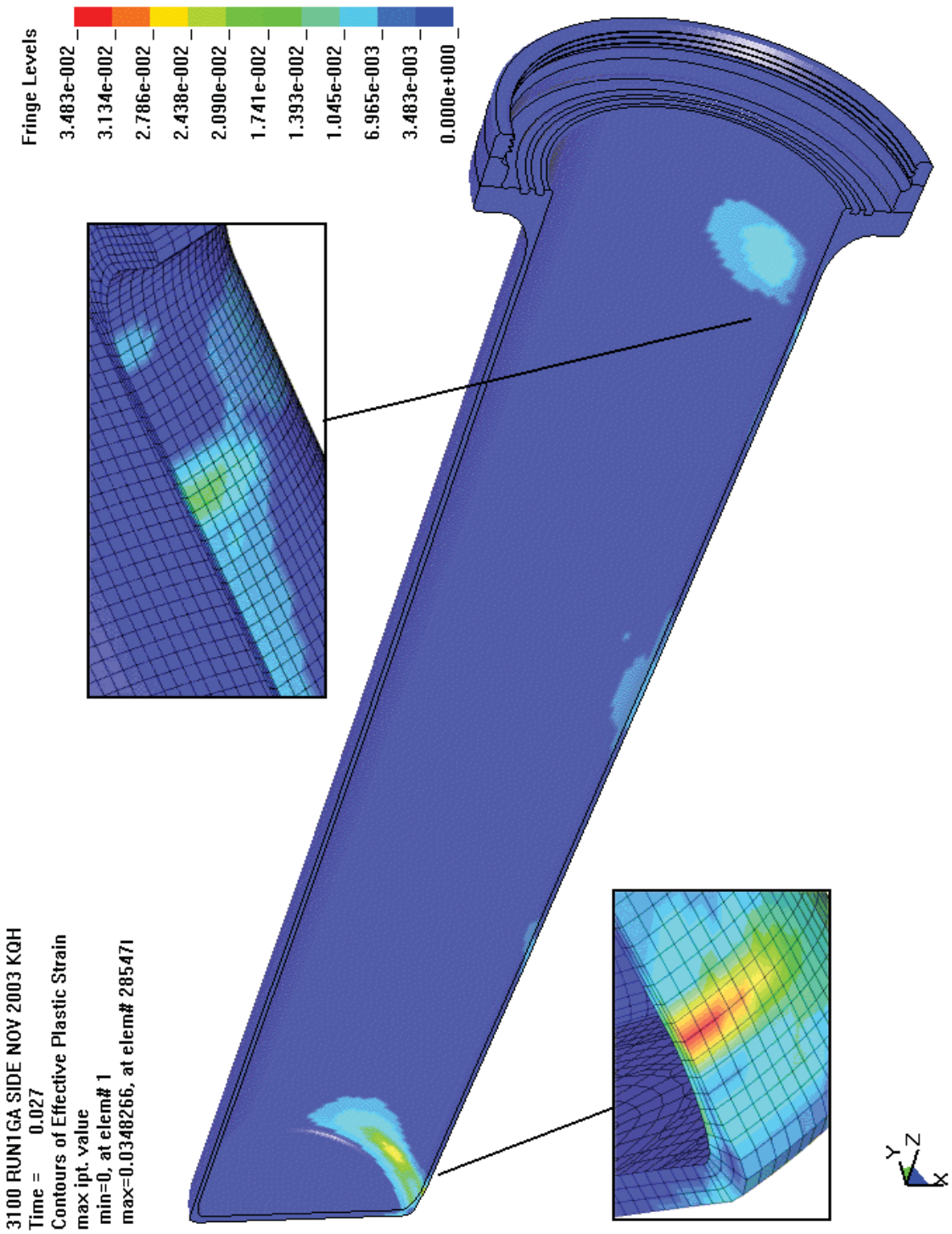

Figure 3.2.7 - Run1ga, Crush Impact, Effective Plastic Strain in the CV Body

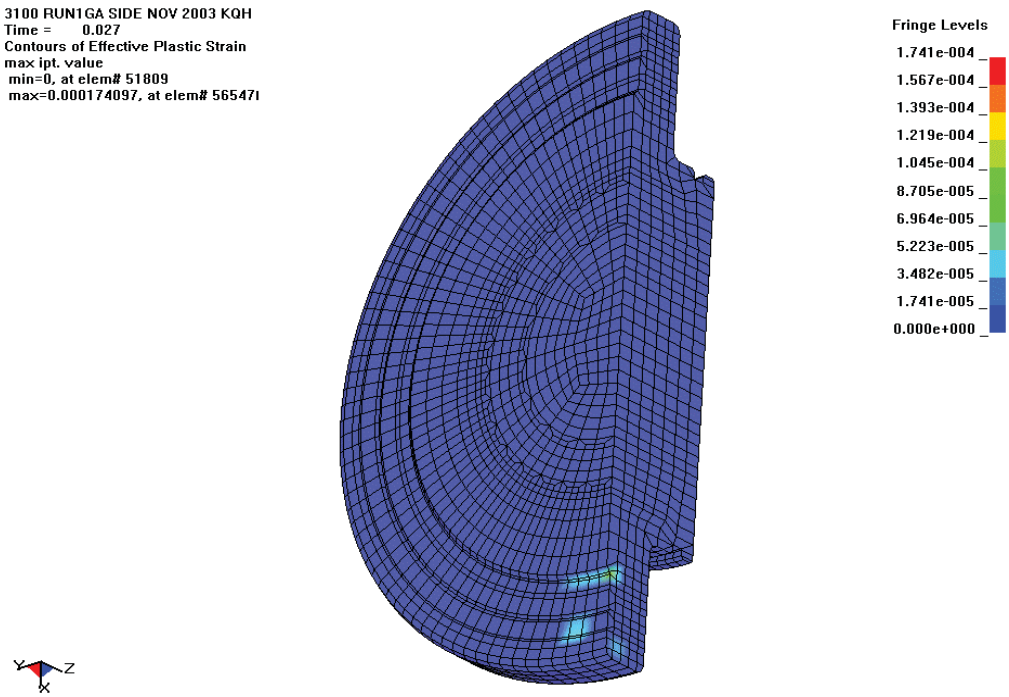

Figure 3.2.8 - Run1ga, Crush Impact, Effective Plastic Strain in the CV Lid

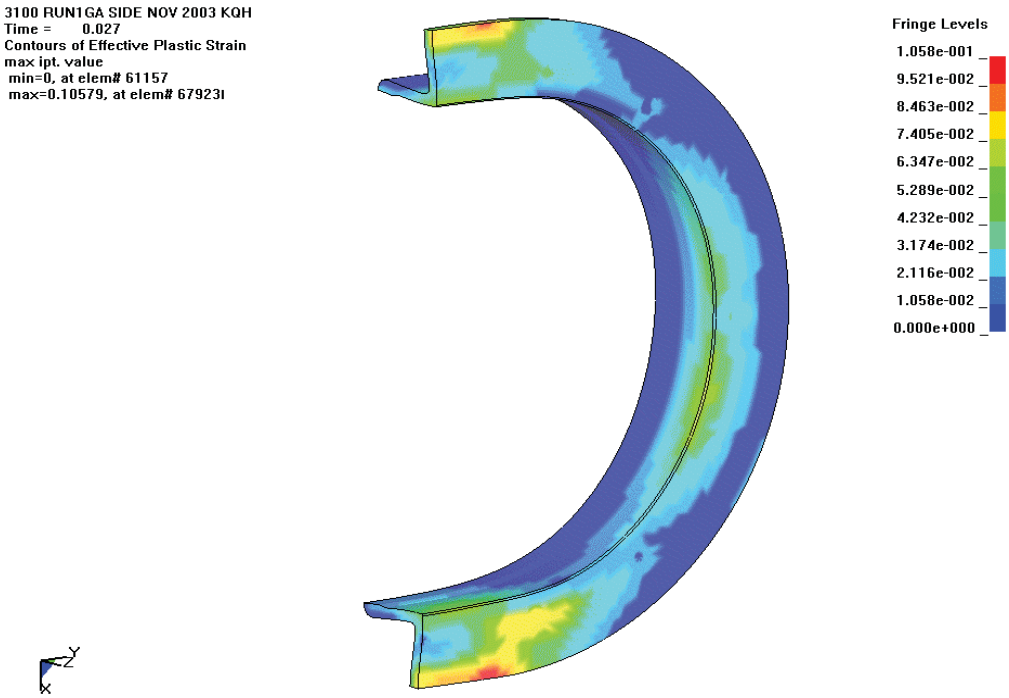

Figure 3.2.9 - Run1ga, Crush Impact, Effective Plastic Strain in the Drum Angle

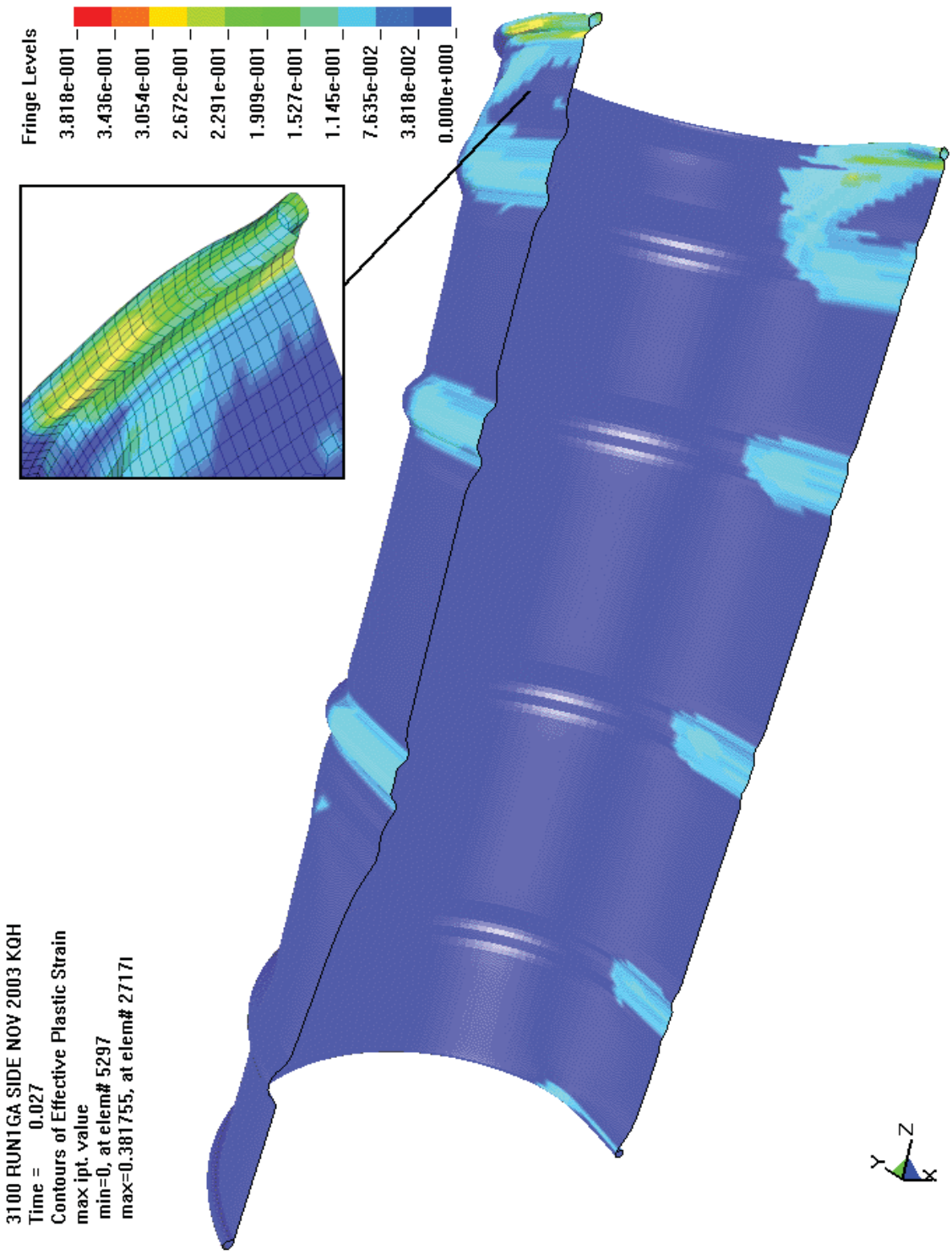

Figure 3.2.10 - Run1ga, Crush Impact, Effective Plastic Strain in the Drum

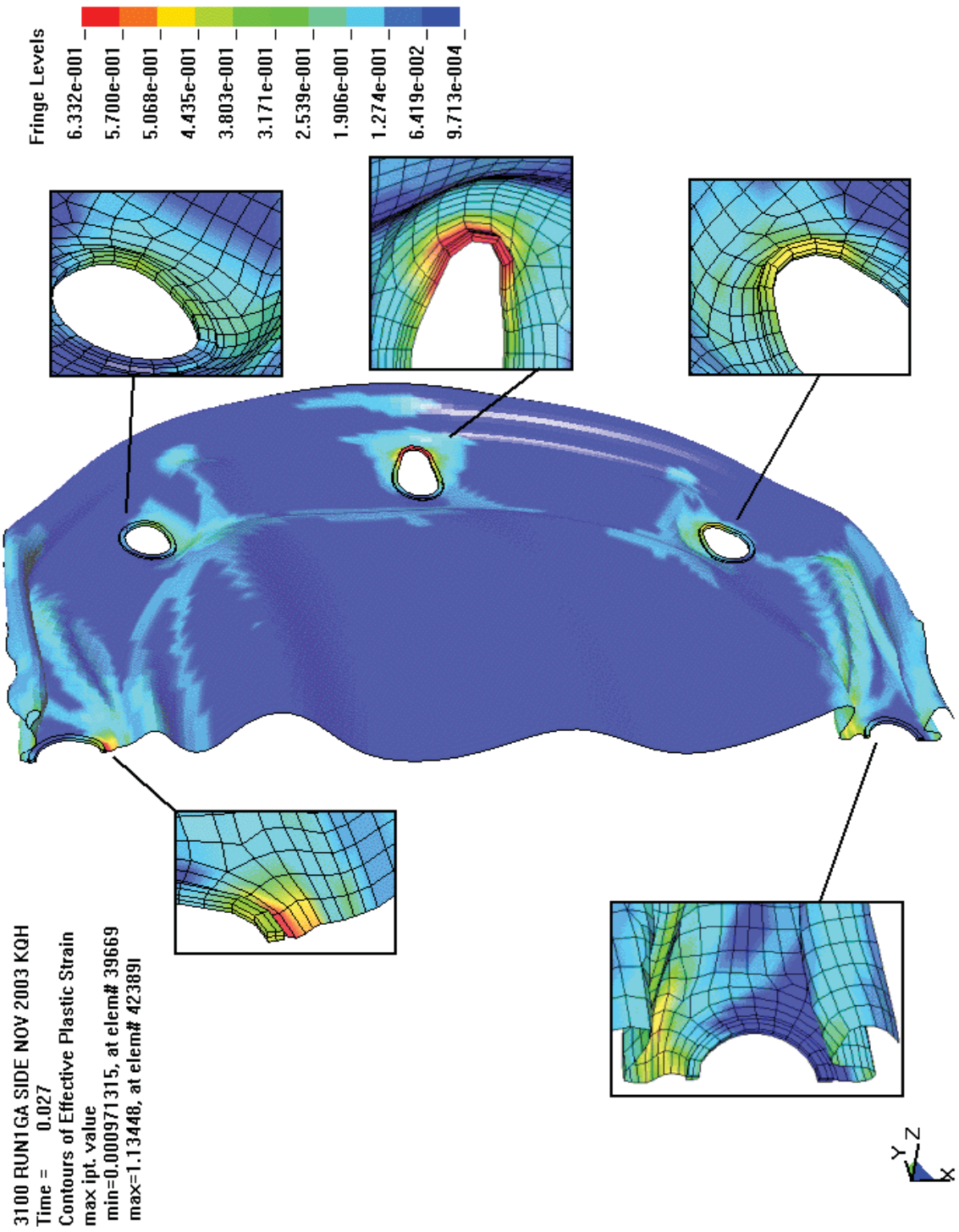

Figure 3.2.11 - Run1ga, Crush Impact, Effective Plastic Strain in the Lid

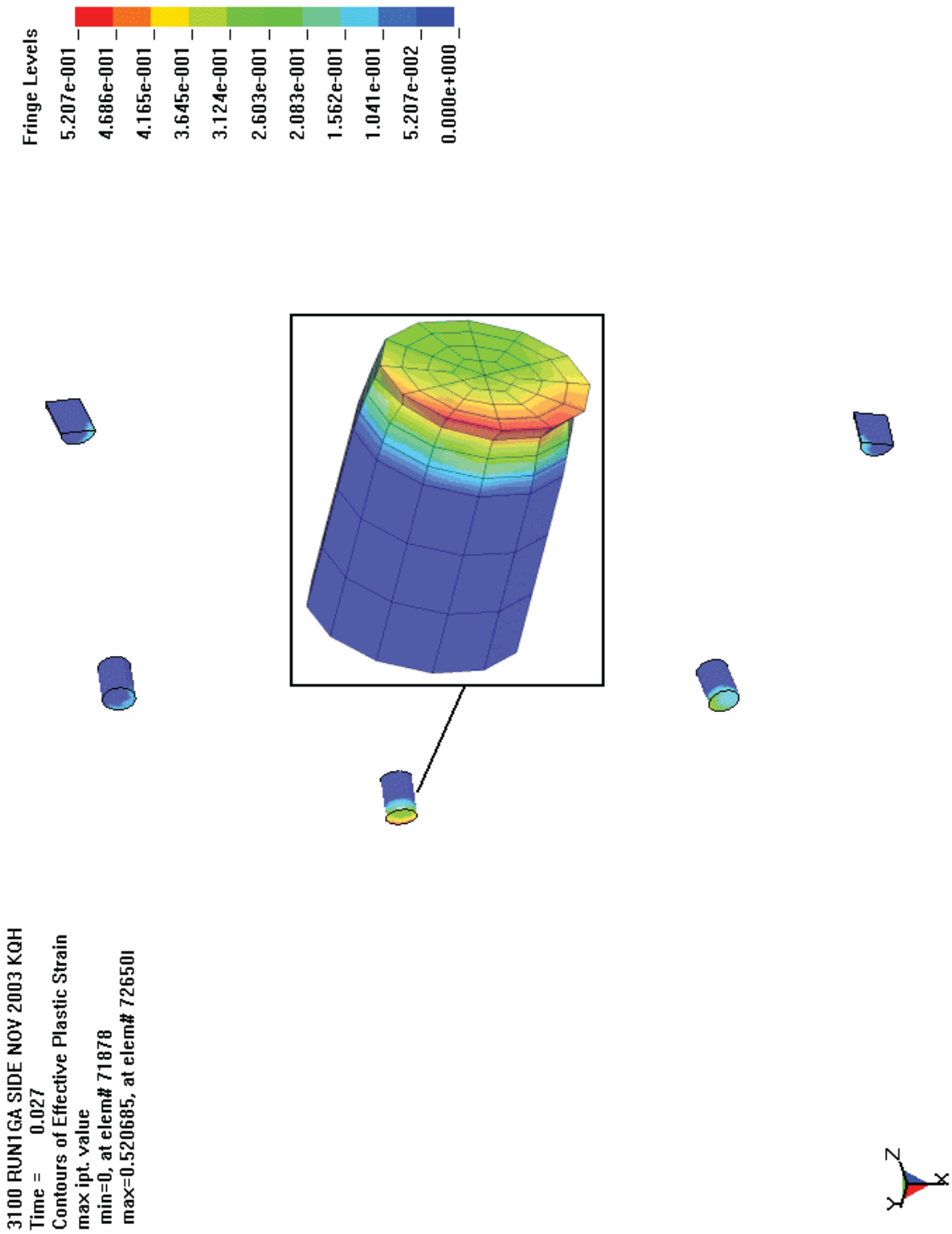

Figure 3.2.12 - Run1ga, Crush Impact, Effective Plastic Strain in the Drum Studs

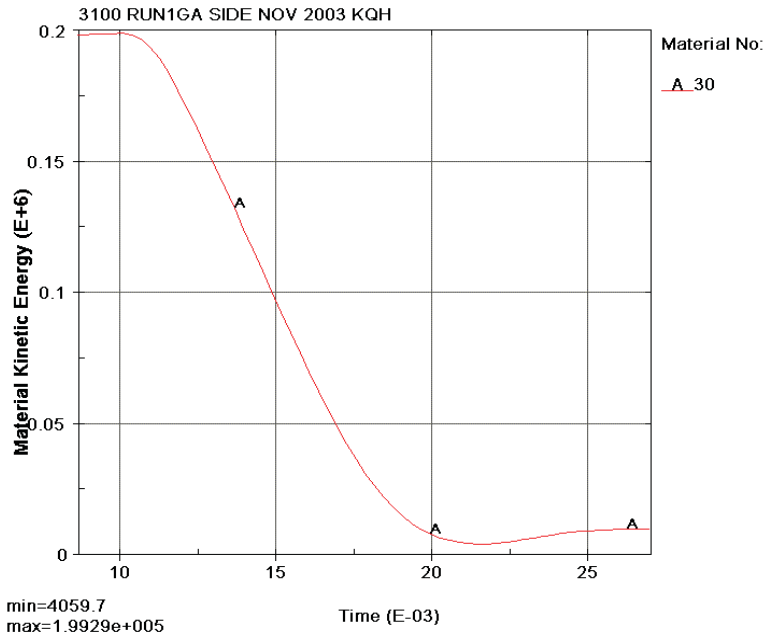

Figure 3.2.13 - Run1ga, Crush Impact, Kinetic Energy Time History

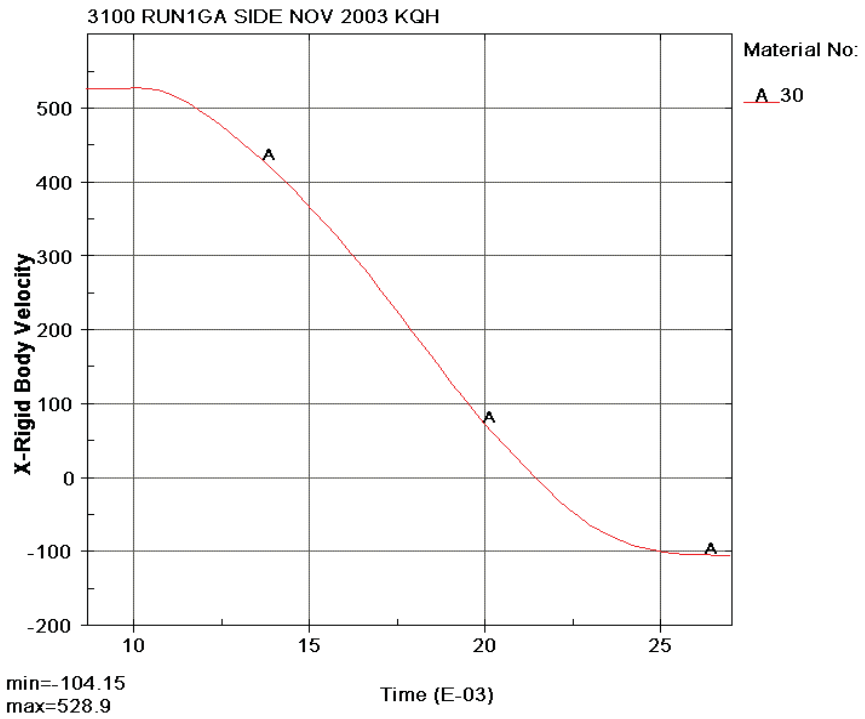

Figure 3.2.14 - Run1ga, Crush Impact, X Velocity Time History

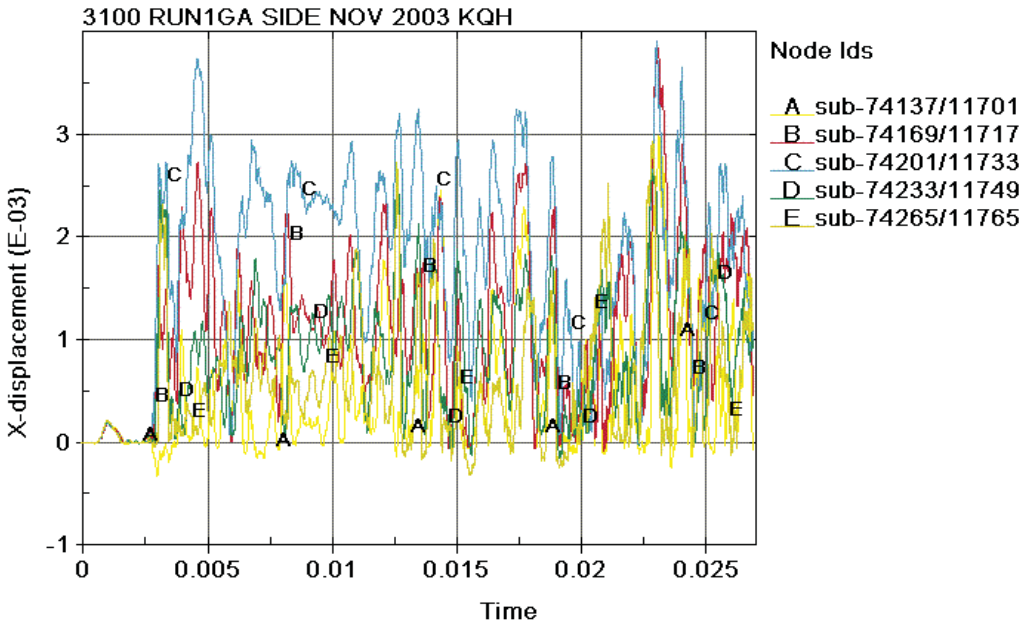

Figure 3.2.15 - Run1ga, Lid Separation Time History

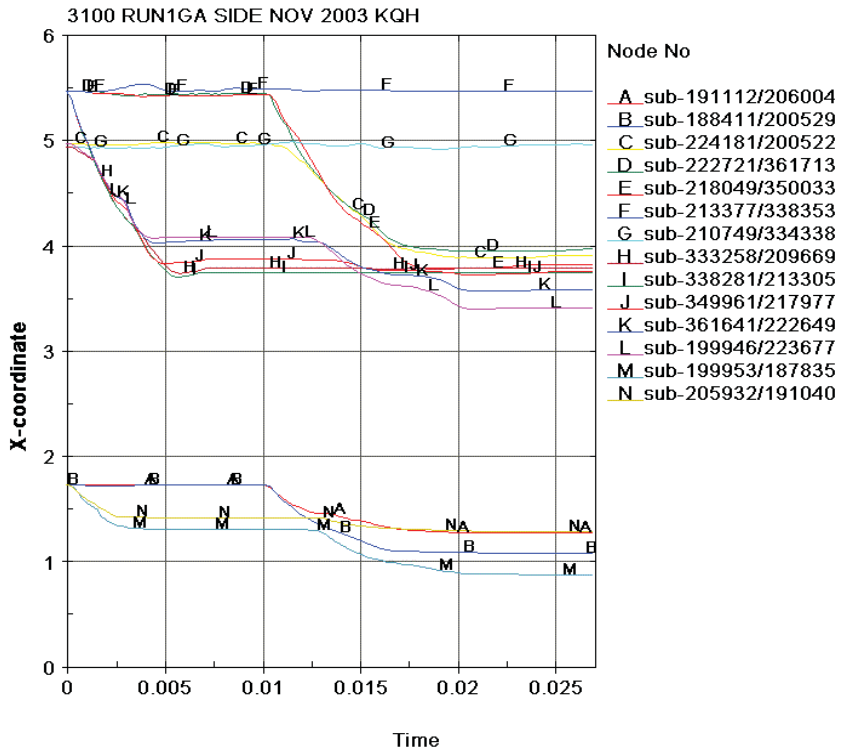

Figure 3.2.16 - Run1ga, Drum Kaolite Thickness Time Histories

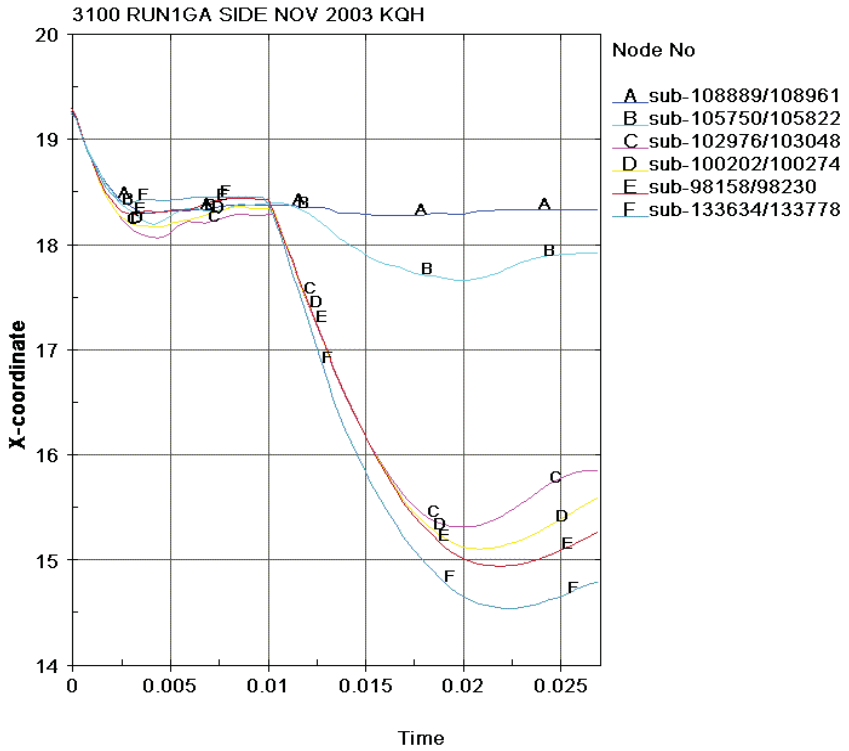

Figure 3.2.17 - Run1ga, Drum Dimension Time History in the X-Direction

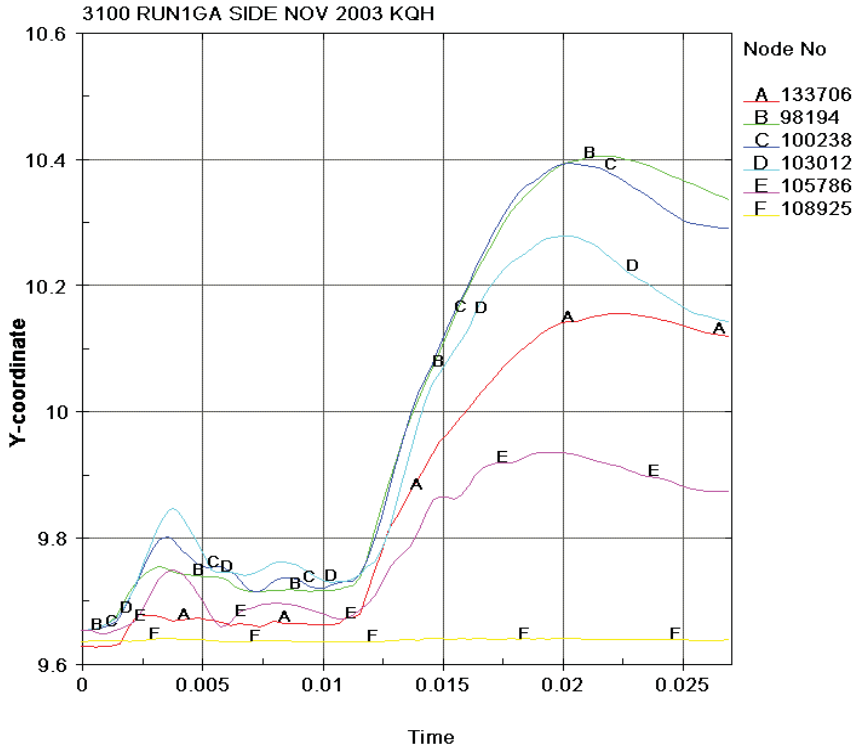

Figure 3.2.18 - Run1ga, Drum Dimension Time History in the Y-Direction

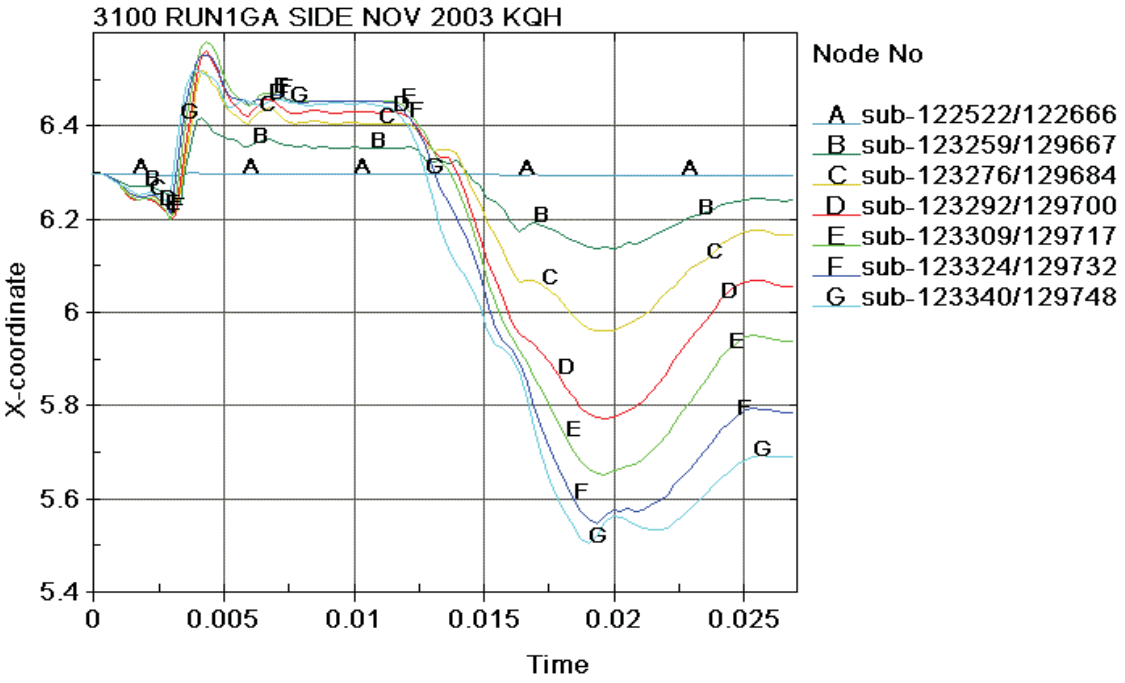

Figure 3.2.19 - Run1ga, Liner Diameter Time History

3.3 Run1hl - Side

Run1hl is the lower bounding kaolite run (100°F). It is basically the run1g model, but with kaolite properties of section 2.3.5.2. It is a run with a 4-foot impact (time = 0 to 0.01 seconds), followed by a 30-foot impact (0.01 to 0.02 seconds), followed by a 30-foot crush impact (0.02 to 0.04 seconds), finally followed by a 40-inch punch impact (0.04 to 0.055 seconds). The initial configuration of run1hl is similar to Figure 3.1.1. The configuration after the 4-foot impact is shown in Figure 3.3.1. Figure 3.3.2 and 3.3.3 show the configuration at the extremes of the package.

The CV body undergoes plastic deformation in the 4-foot impact. The effective plastic strain in the CV body is shown in Figure 3.3.4 to have a maximum of 0.0263 in/in. The elevated plastic strain levels are near the CV bottom head. The CV lid and nut ring remain elastic during the 4-foot impact. The plastic strain in other components for the 4-foot impact are given in Table 3.3.1.

Table 3.3.1 - Run1hl, 4-Foot Impact, Effective Plastic Strain Levels in Some Components

Component	Effective Plastic Strain, in/in
Angle	0.0054
Drum	0.1561
Drum Bottom Head	0.0991
Liner	0.0537
Lid	0.1320
Lid Stiffener	0.0001
Lid Studs	0.0000
Lid Stud Nuts	0.0000
Lid Stud Washers	0.0011
Plug Liner	0.0022

Figure 3.3.5 shows the final configuration for the run1hl 30-foot impact. Figures 3.3.6 and 3.3.7 show the configurations for the package extremes.

The maximum effective plastic strain due to the 30-foot impact in the CV body is 0.0287 in/in as shown in Figure 3.3.8. The maximum effective plastic strain in the drum lid

is shown to be 0.5180 in/in in Figure 3.3.9. The maximum lid strain is a surface strain at the stud hole nearest the rigid surface (0°). The membrane effective plastic strain component is 0.4026 in/in in the localized region near the stud hole. Effective plastic strain levels in other components for the 30-foot impact are given in Table 3.3.2.

Table 3.3.2 - Run1hl, 30-Foot Impact, Effective Plastic Strain Levels in Some Components

Component	Effective Plastic Strain, in/in
CV Lid	0.0001
CV Nut Ring	0.0000
Angle	0.0777
Drum	0.2250
Drum Bottom Head	0.2125
Liner	0.1800
Lid Stiffener	0.0118
Lid Studs	0.1098
Lid Stud Nuts	0.0000
Lid Stud Washers	0.0225
Plug Liner	0.0956

The final configuration for the crush impact is shown in Figure 3.3.10. The configuration at the package extremes are shown in Figure 3.3.11. The maximum effective plastic strain in the CV body is 0.0287 in/in as shown in Figure 3.3.12. The maximum effective plastic strain in the drum for the crush impact is 0.5309 in/in (surface strain). The maximum in the drum occurs near the angle on the crush plate side of the drum as shown in Figure 3.3.13. The maximum membrane effective plastic strain at this location is 0.3616 in/in.

The maximum effective plastic strain in the lid is 1.2969 in/in (surface strain) and occurs just below the upper stud hole (hole nearest the crush plate, 180°) as shown in Figure 3.3.14. The maximum membrane effective plastic strain in this region of the lid is 0.8995 in/in. A time line investigation during the crush impact shows that the lid exceeds 0.57 in/in strain in bending at about 0.0228 seconds at the 180° stud hole. The crush impact started at about 0.0200 seconds, so the lid reaches failure level near the start of the crush impact. The membrane levels in the lid reach 0.57 in/in at about 0.0236 seconds.

The elevated effective plastic strain levels in the lid are localized in the region just inboard of the upper stud.

The effective plastic strain in the drum studs is 0.4159 in/in and occurs in the upper stud at the bearing of the lid onto the stud (180°). The elevated strains in the stud are localized on the inner surface. Effective plastic strain levels throughout the thickness of the stud are generally 0.25 in/in or less.

Considering the strain levels in the lid and the studs, some tearing in the lid at the 180° stud hole would be expected. But the tearing would be localized to the stud hole due to the extent of the strain patterns. Failure of the stud to restrain the lid due to this tearing is not expected. The lid stiffener would limit any tearing from the stud at 180° and the large washer would be expected to restrain the lid.

The effective plastic strain in other components due to the crush impact are listed in Table 3.3.3.

Table 3.3.3 - Run1hl, Crush Impact, Effective Plastic Strain Levels in Some Components

Component	Effective Plastic Strain, in/in
CV Lid	0.0003
CV Nut Ring	0.0000
Angle	0.1178
Drum Bottom Head	0.3342
Liner	0.2637
Lid Stiffener	0.0530
Lid Stud Nuts	0.0007
Lid Stud Washers	0.0832
Plug Liner	0.1255

The final configuration after the punch impact is shown in Figure 3.3.16. The effective plastic strain level in the CV body is shown in Figure 3.3.6. The maximum strain is 0.0299 in/in and is located near the bottom head. The effective plastic strain level in the drum after the punch impact remains at 0.5309 in/in as shown in Figure 3.3.18. The maximum effective plastic strain in the other package components for the punch impact are listed in Table 3.3.4.

Table 3.3.4 - Run1hl, Punch Impact, Effective Plastic Strain Levels in Some Components	
Component	Effective Plastic Strain, in/in
CV Lid	0.0006
CV Nut Ring	0.0000
Angle	0.1178
Drum Bottom Head	0.3345
Liner	0.2637
Lid	1.2971
Lid Stiffener	0.0530
Lid Studs	0.4221
Lid Stud Nuts	0.0007
Lid Stud Washers	0.0844
Plug Liner	0.1255

Figure 3.3.19 shows the lid separation time history for all the impacts. The CV lid separation shows a maximum spike separation of about 0.006 inches occurs during the punch. The spike is a response to the rebounding impact of the CV/weights. An average value of .003 in or less is demonstrated in the response when the solution is stopped.

Figure 3.3.20 shows the time history for the kaolite thicknesses. The nodal locations for nodes shown in Figure 3.3.20 are shown in Figure 3.1.32.

Figure 3.3.21 shows the diameter changes in the drum in the model X direction.
Figure 3.3.22 shows the radial changes in the Y direction (normal to the impact directions). The nodes are defined in Figure 3.1.34.

Figure 3.3.23 shows the liner diameter time history. The node pair locations are shown in Figure 3.1.37 and Table 3.1.3.

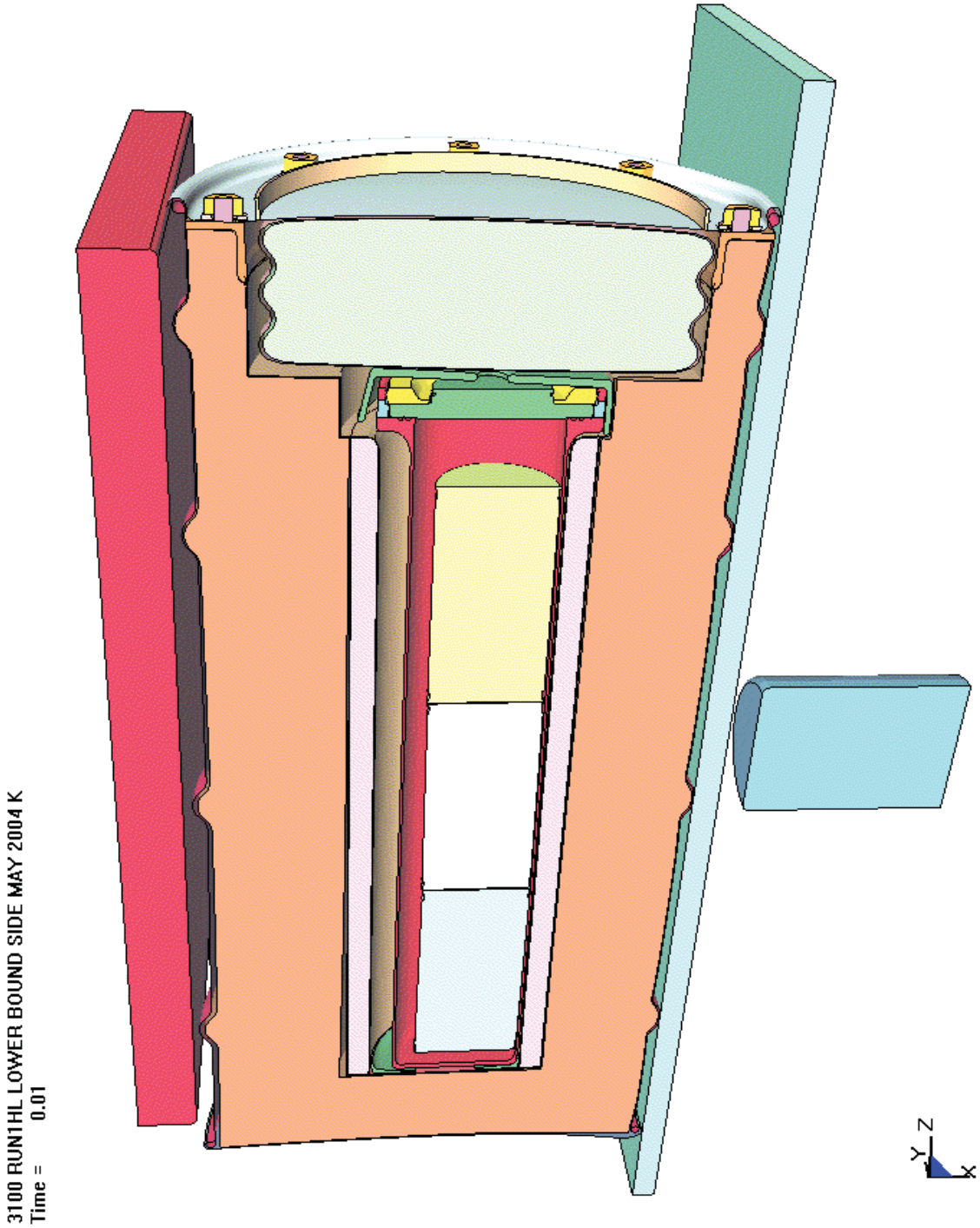

Figure 3.3.1 - Run1hl, 4-Foot Impact, Final Configuration

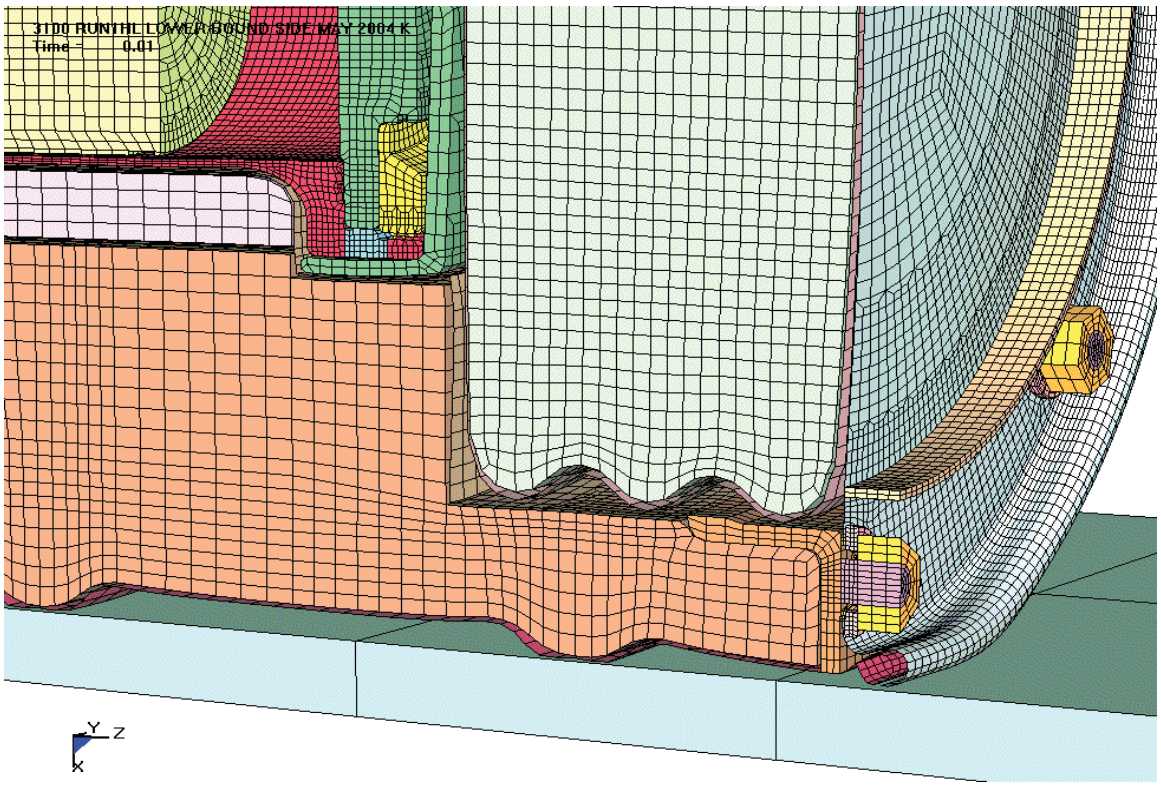

Figure 3.3.2 - Run1hl, 4-Foot Impact, Configuration in the Lid

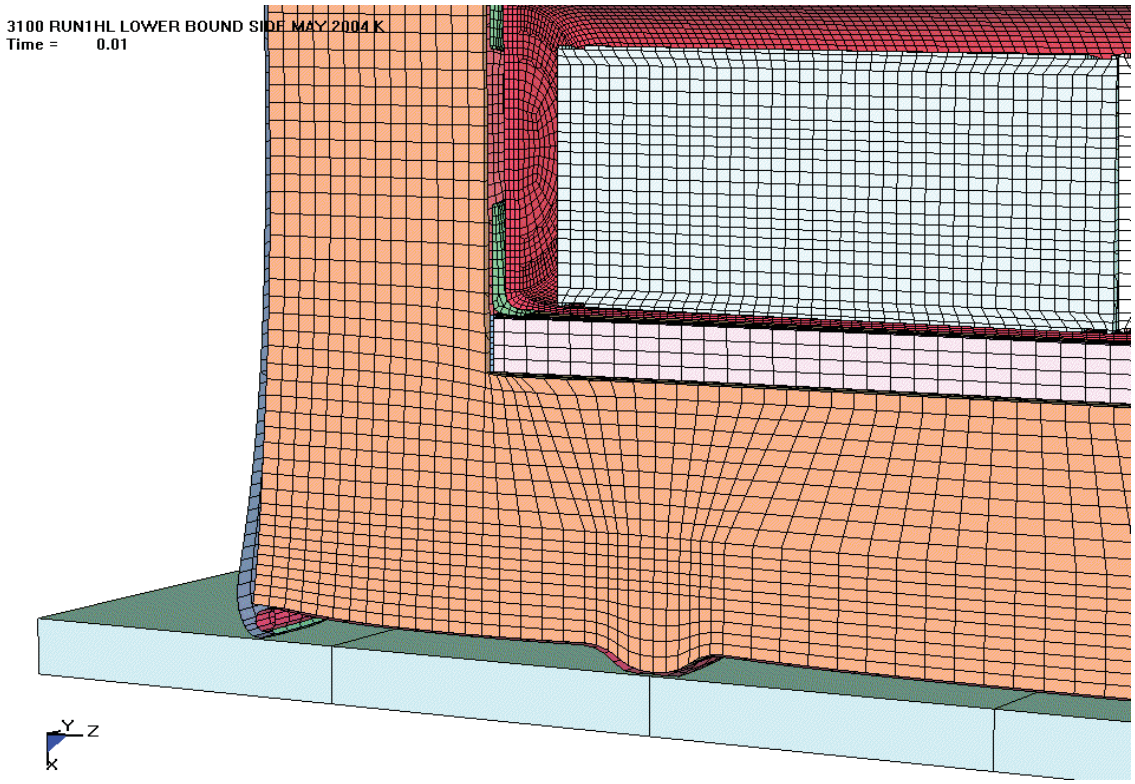

Figure 3.3.3 - Run1hl, 4-Foot Impact, Configuration in the Bottom

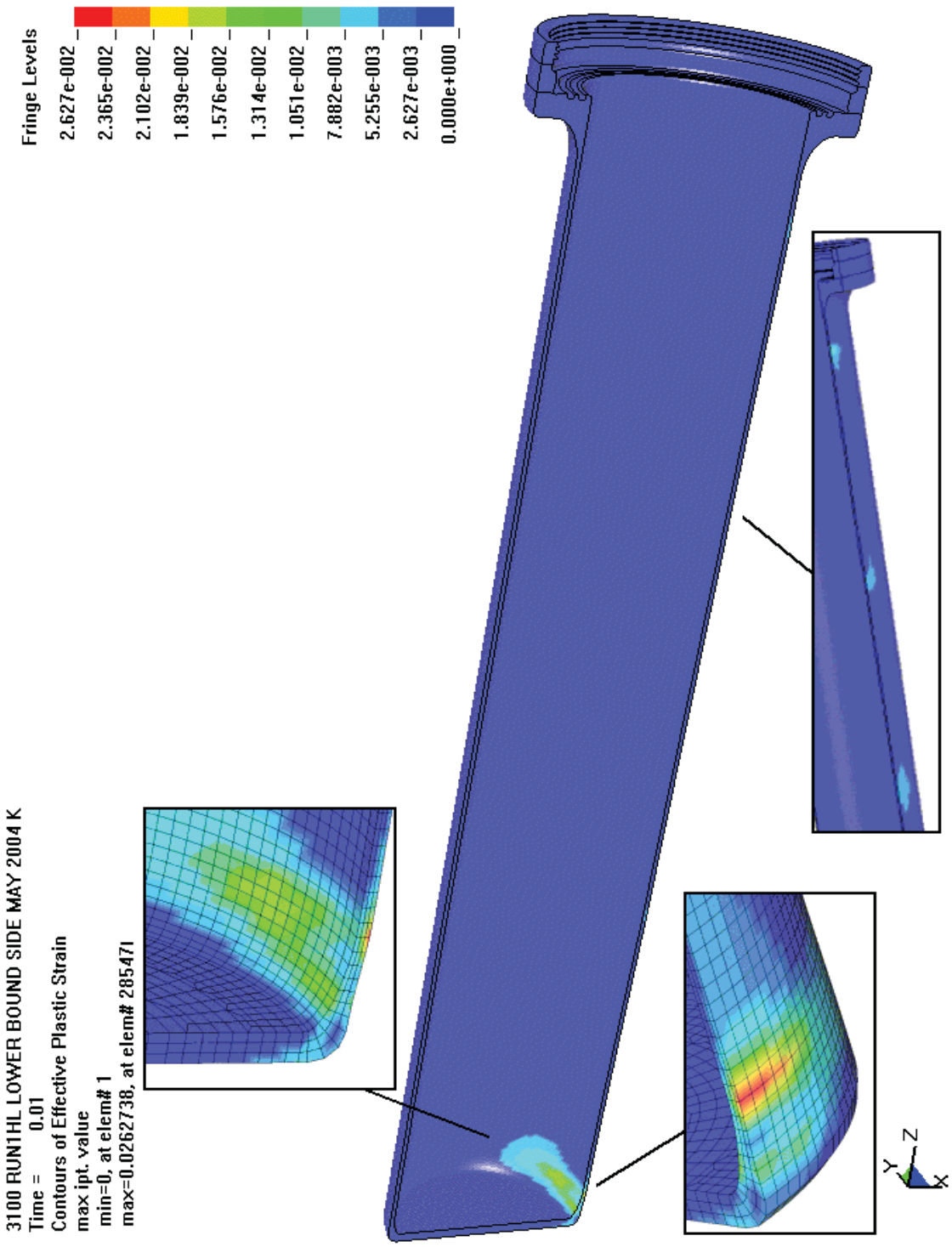

Figure 3.3.4 - Run1hl, 4-Foot Impact, Effective Plastic Strain in the CV Body

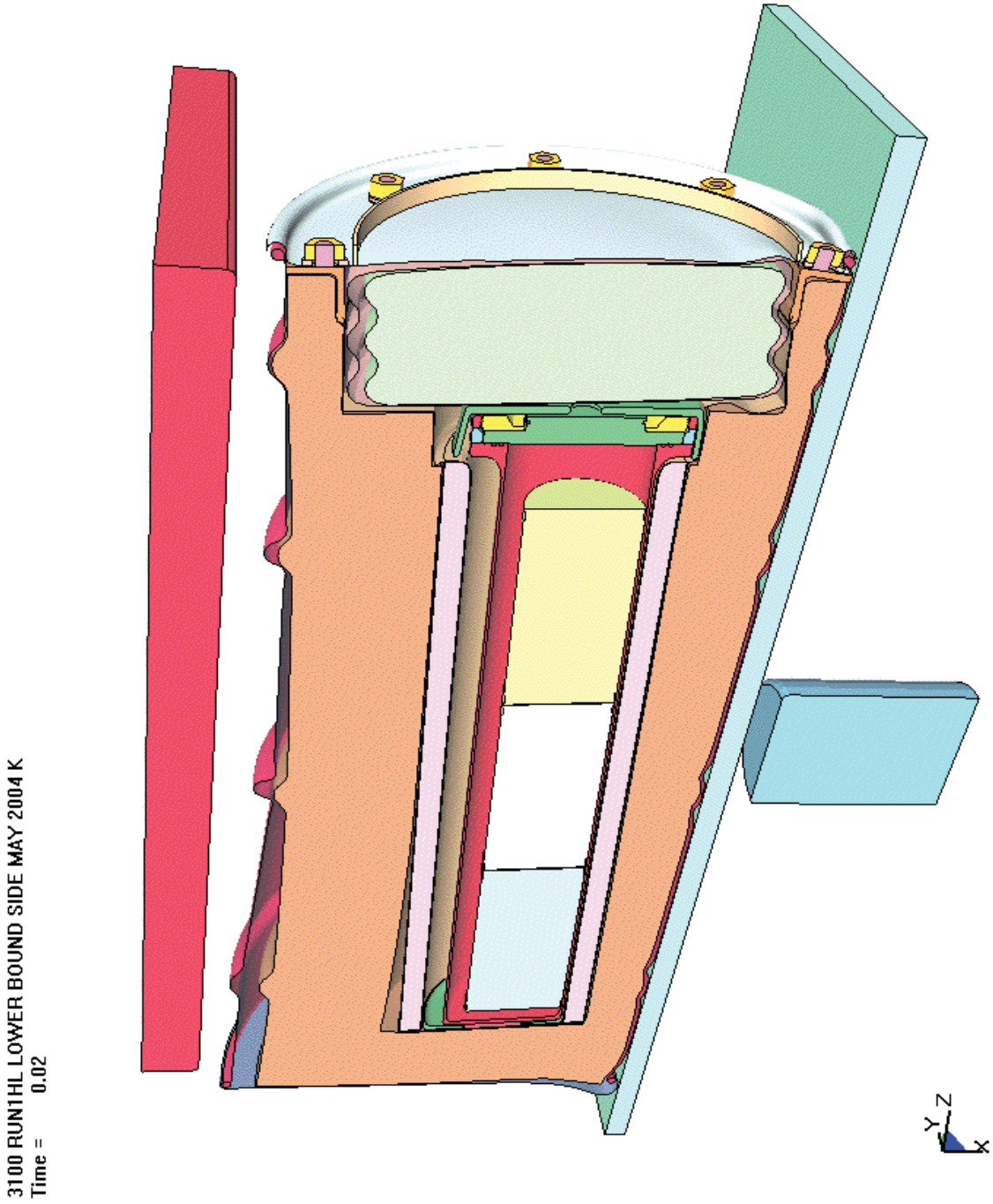

Figure 3.3.5 - Run1hl, 30-Foot Impact, Final Configuration

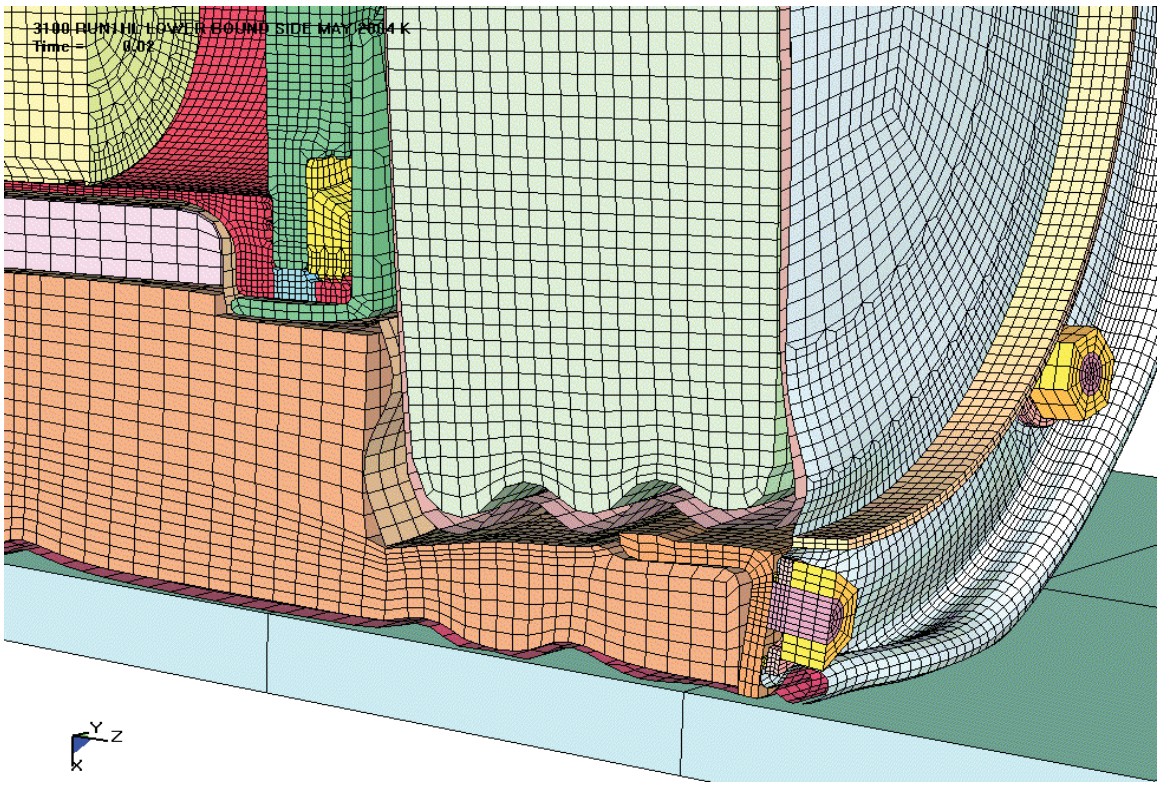

Figure 3.3.6 - Run1hl, 30-Foot Impact, Configuration of the Lid

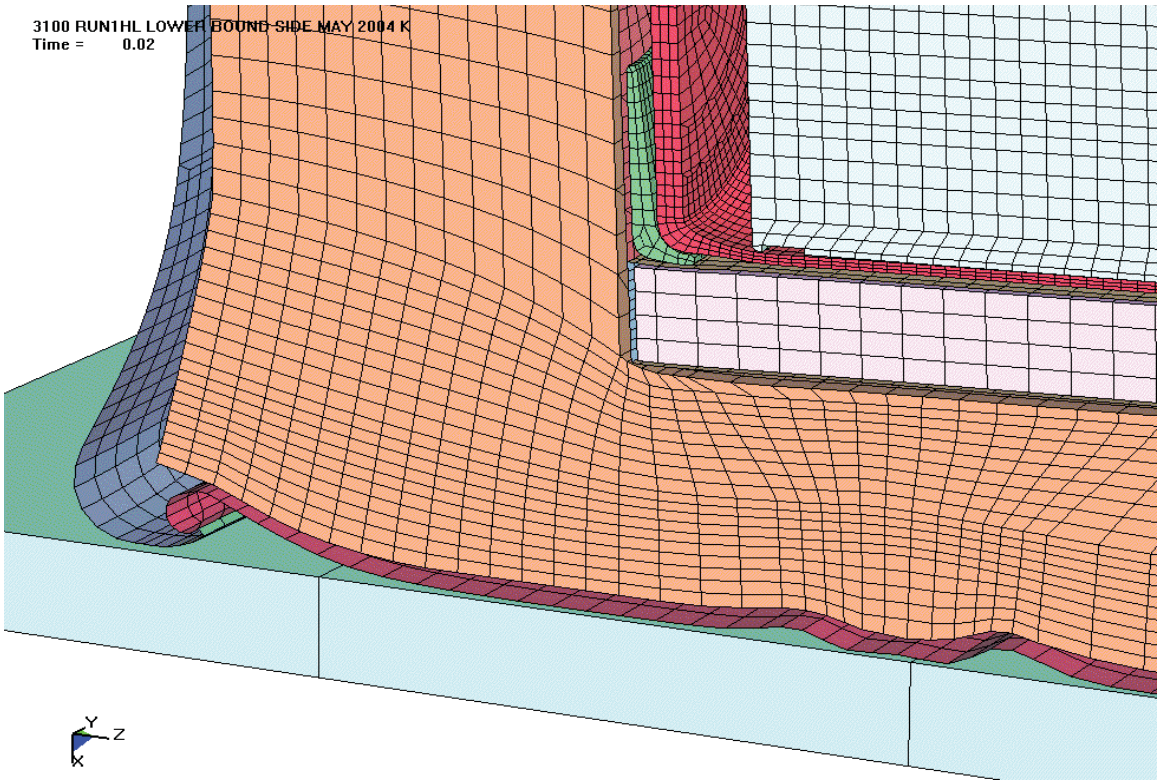

Figure 3.3.7 - Run1hl, 30-Foot Impact, Configuration of the Bottom

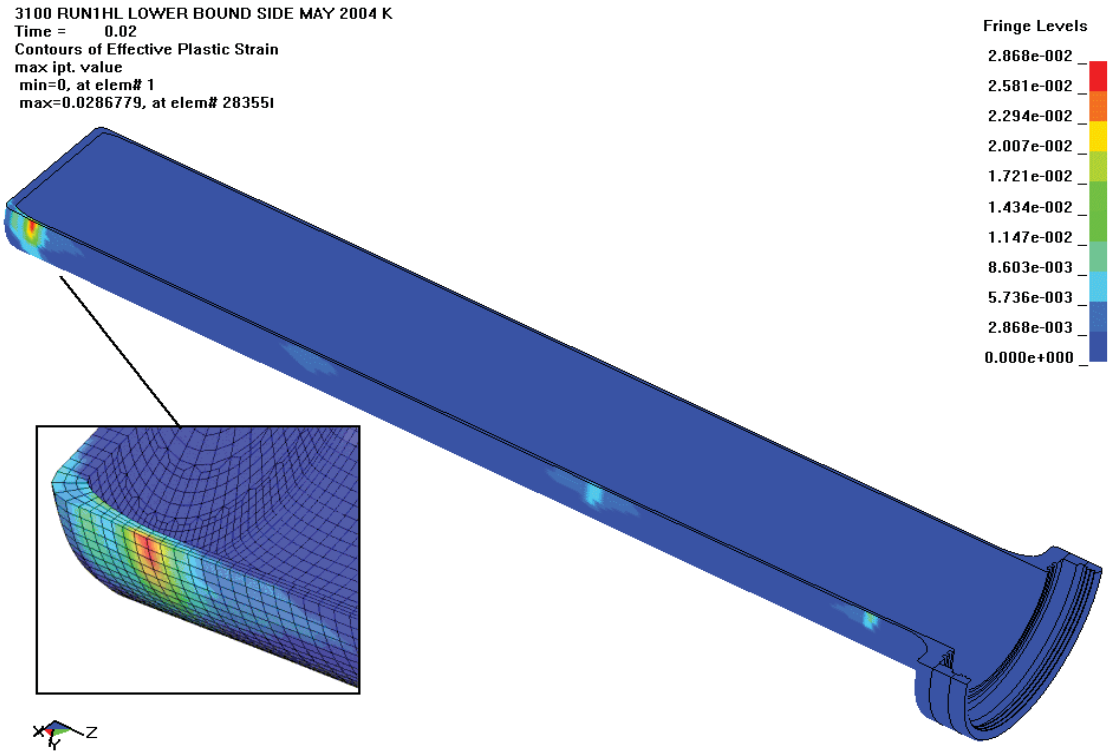

Figure 3.3.8 - Run1hl, 30-Foot Impact, Effective Plastic Strain in the CV

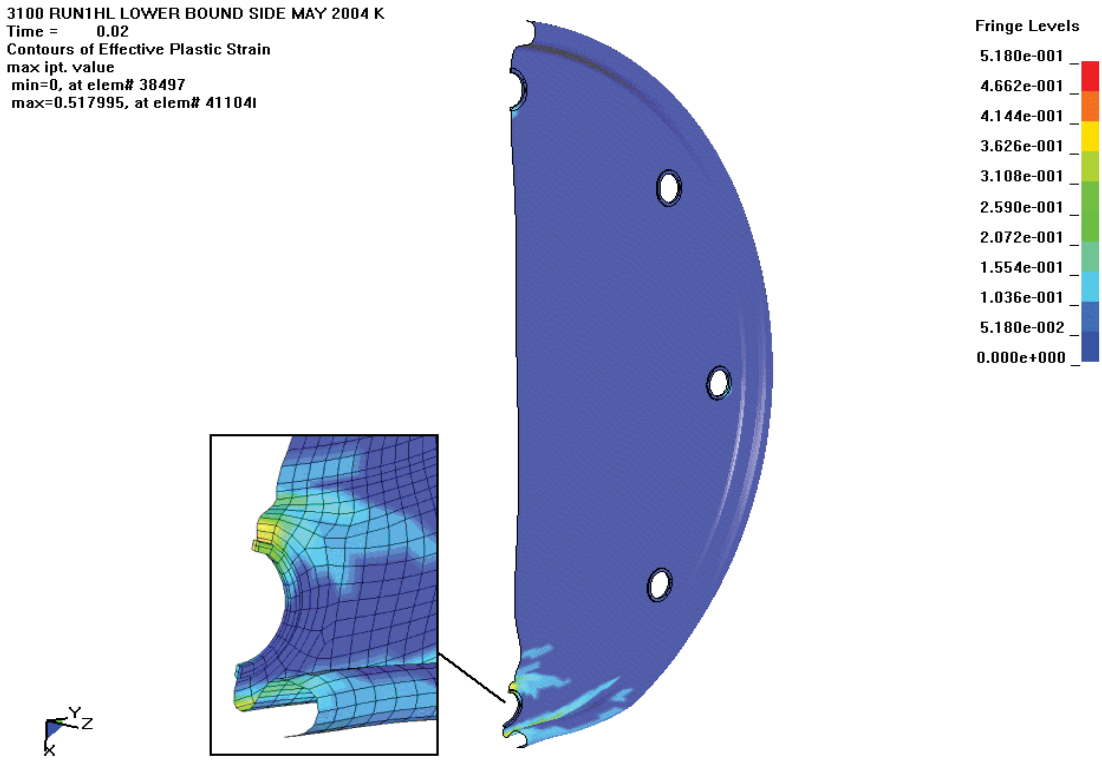

Figure 3.3.9 - Run1hl, 30-Foot Impact, Effective Plastic Strain in the Lid

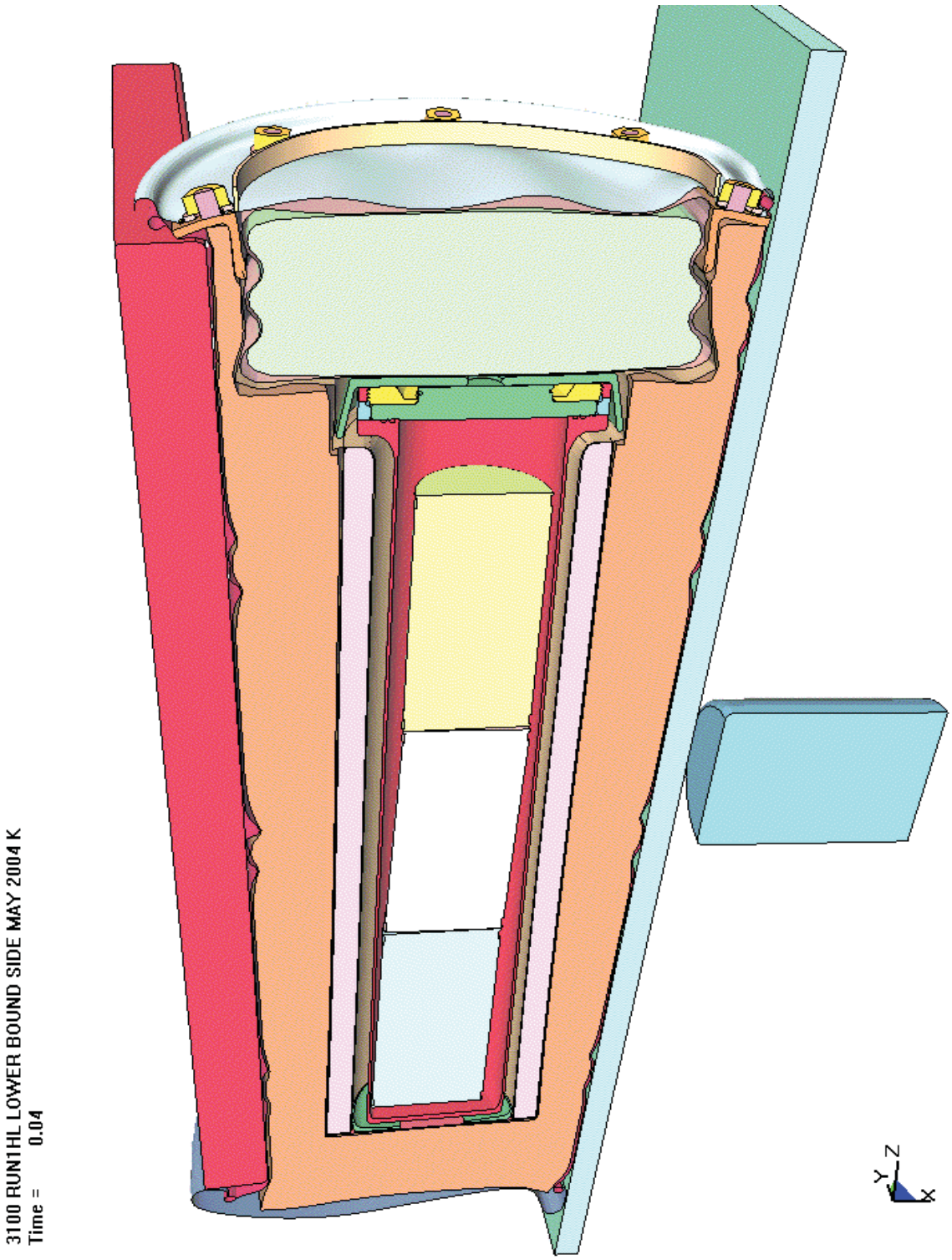

Figure 3.3.10 - Run1hl, Crush Impact, Final Configuration

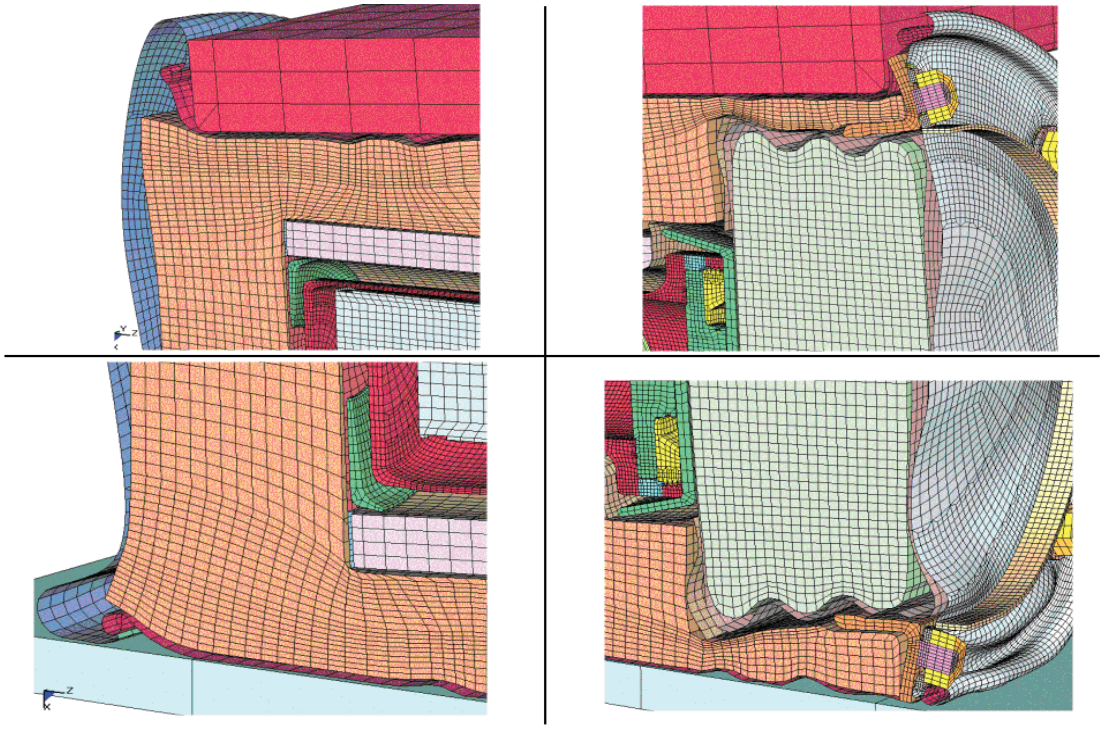

Figure 3.3.11 - Run1hl, Crush Impact, Configuration at the Package Corners

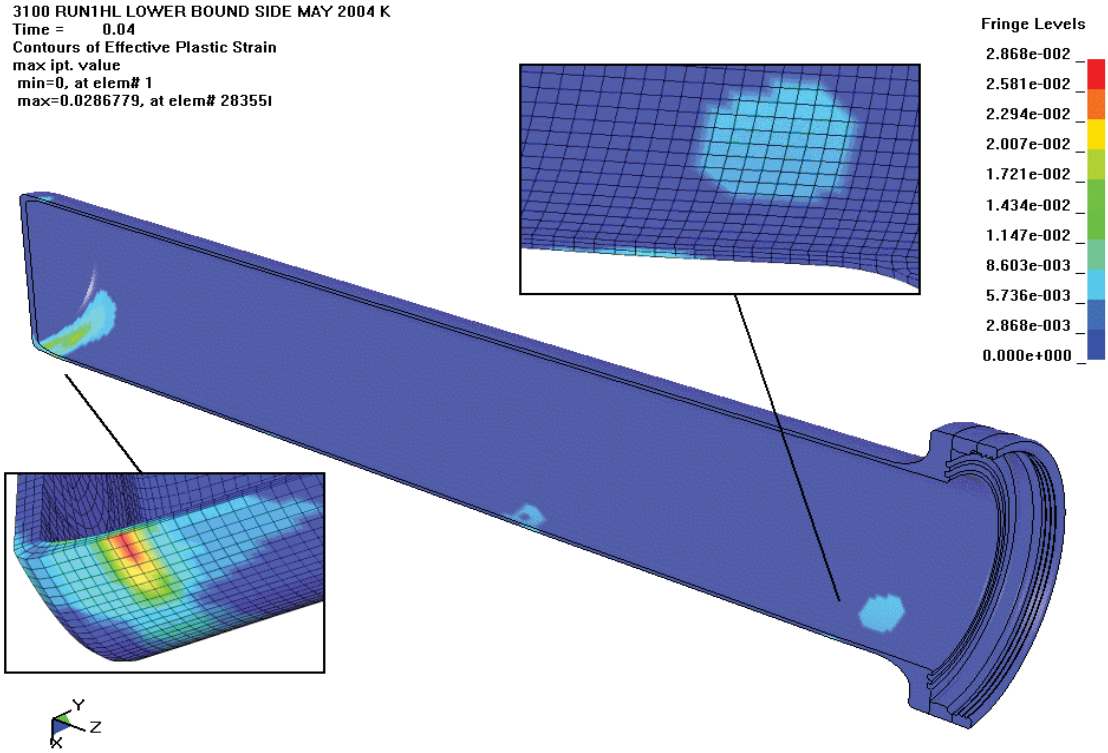

Figure 3.3.12 - Run1hl, Crush Impact, Effective Plastic Strain in the CV Body

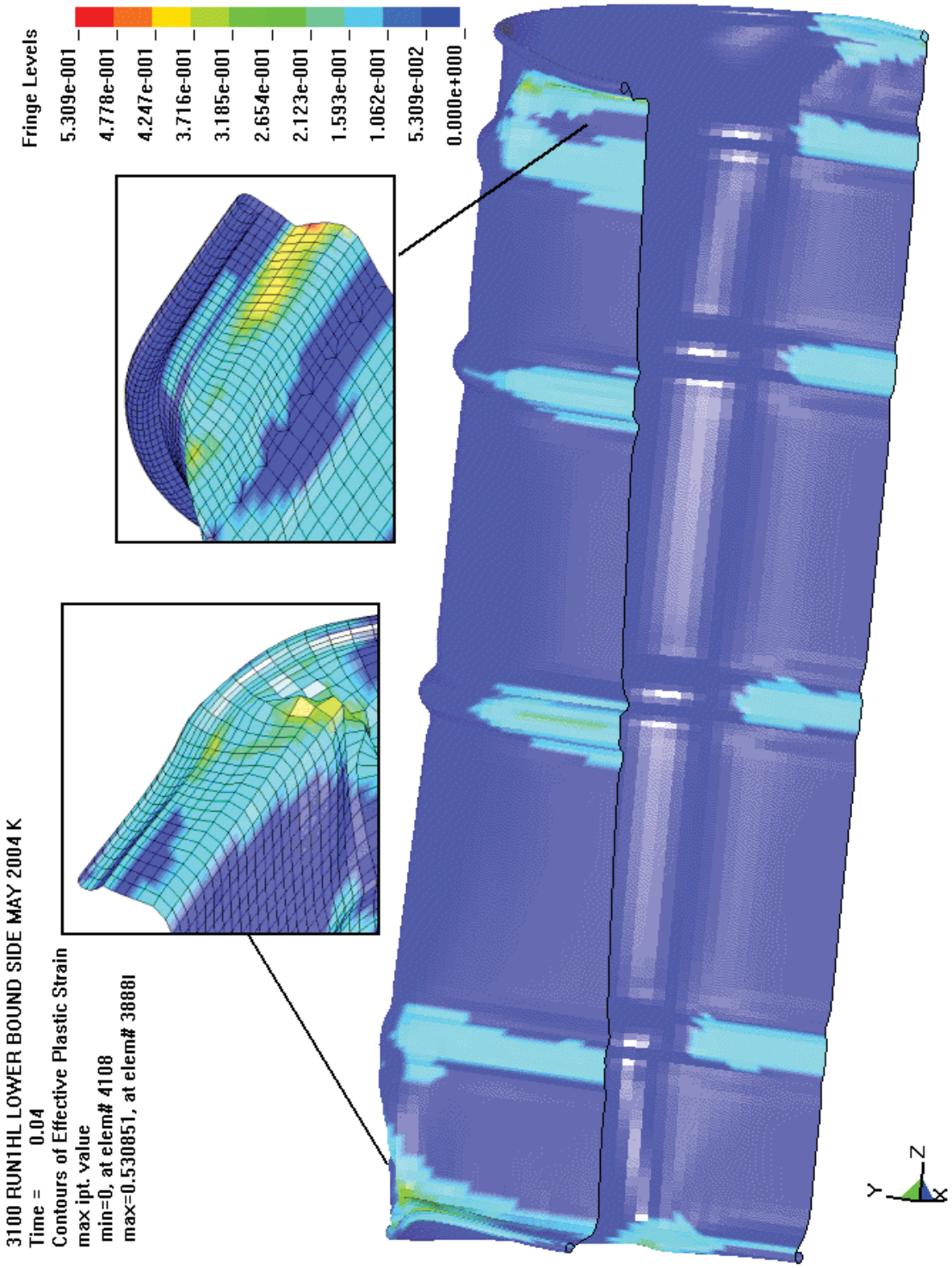

Figure 3.3.13 - Run1hl, Crush Impact, Effective Plastic Strain in the Drum

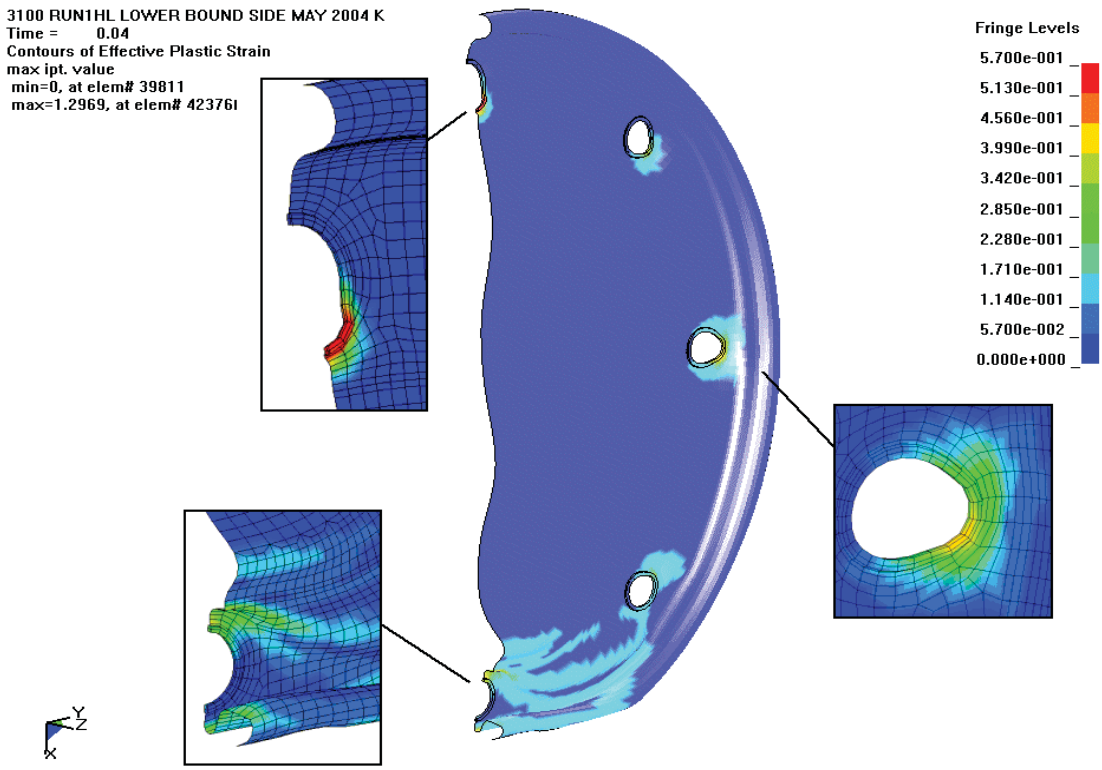

Figure 3.3.14 - Run1hl, Crush Impact, Effective Plastic Strain in the Lid

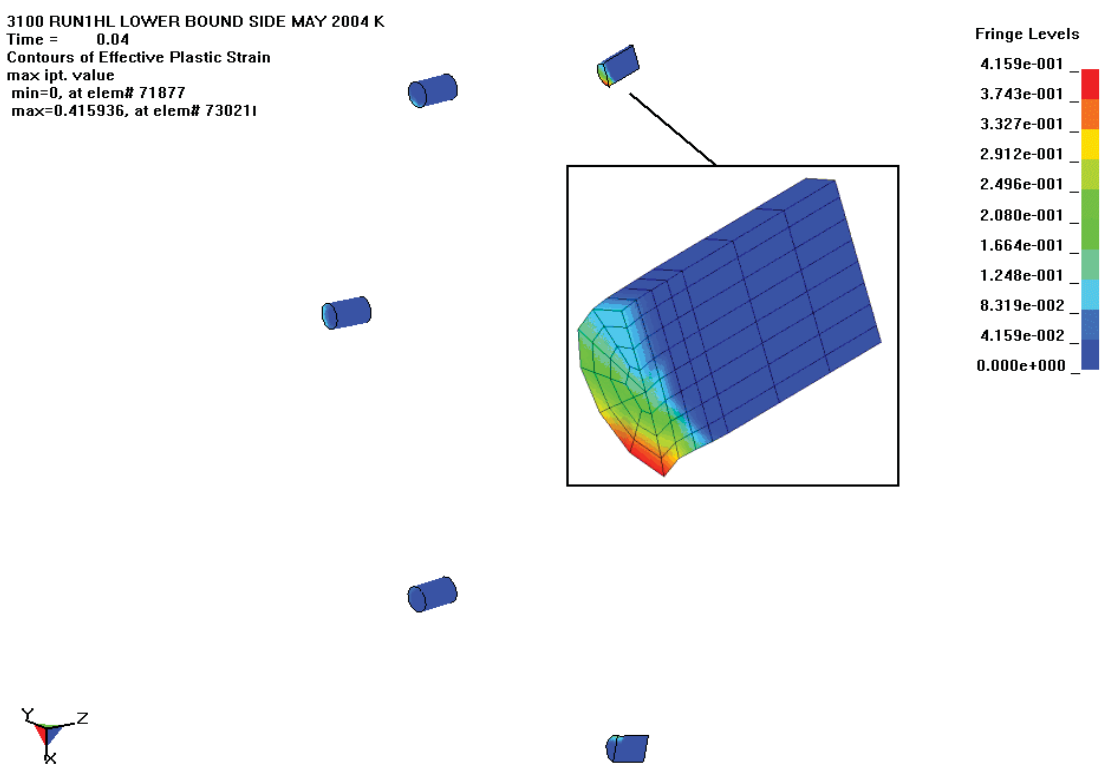

Figure 3.3.15 - Run1hl, Crush Impact, Effective Plastic Strain in the Studs

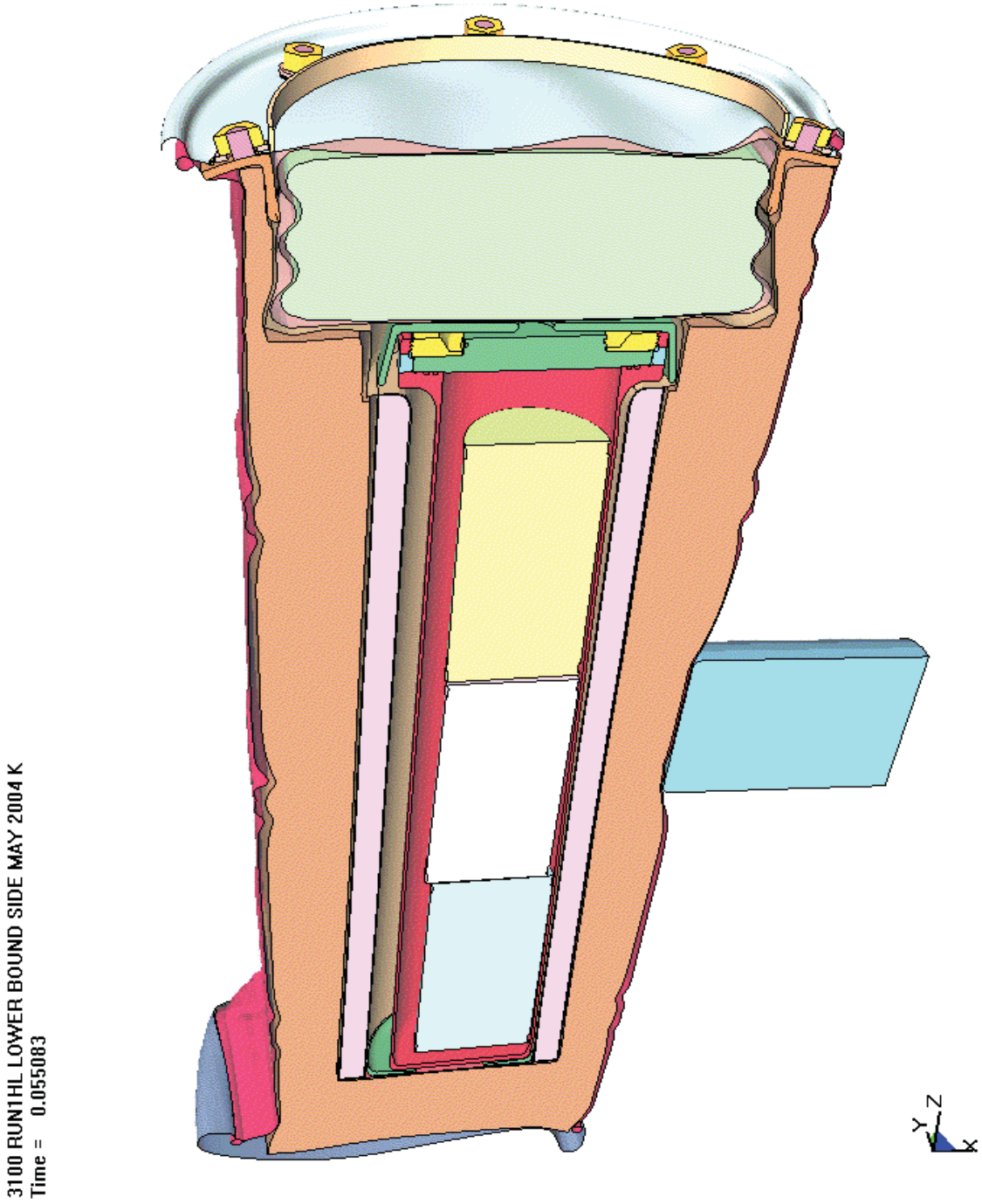

Figure 3.3.16 - Run1hl, Punch Impact, Final Configuration

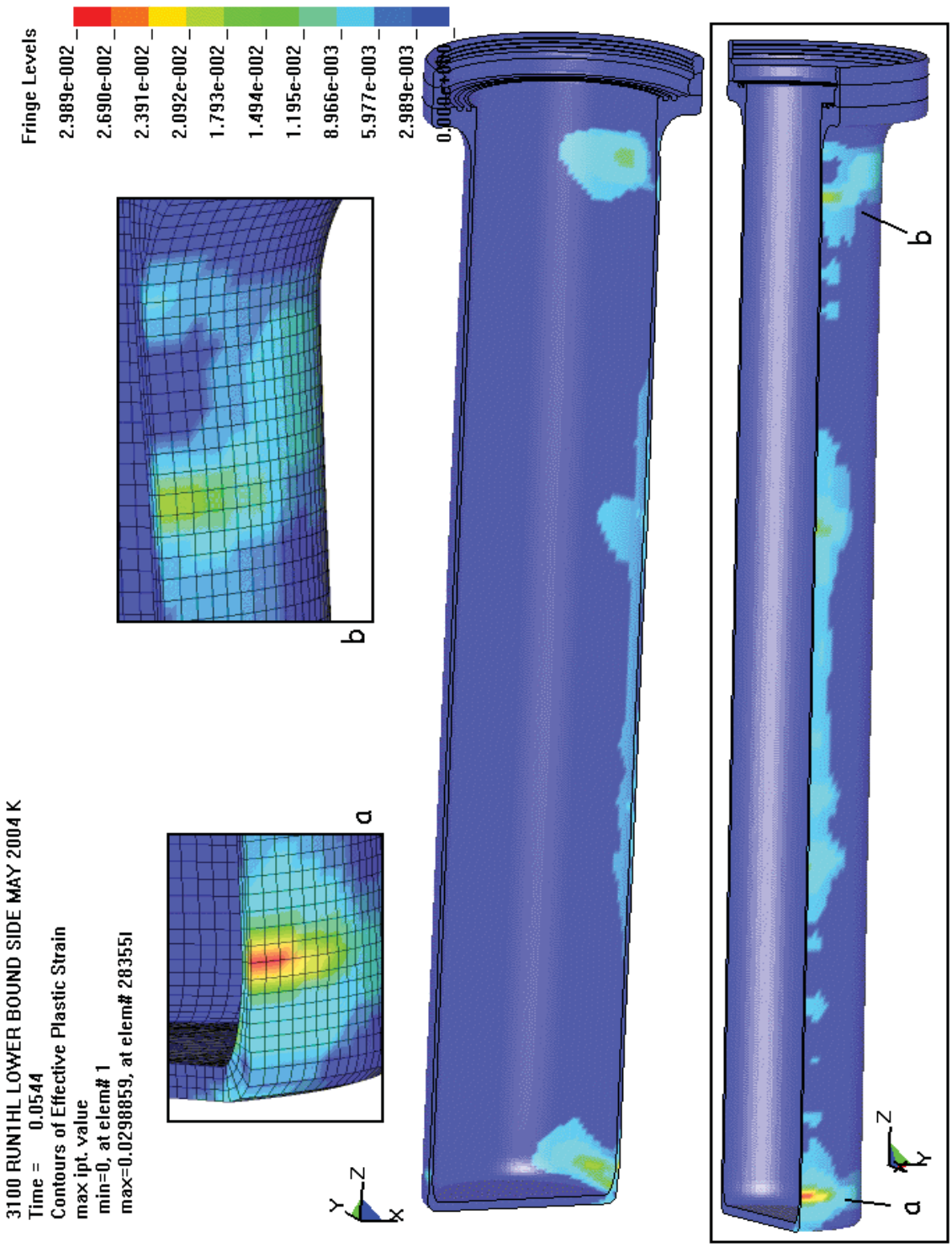

Figure 3.3.17 - Run1hl, Punch Impact, CV Effective Plastic Strain

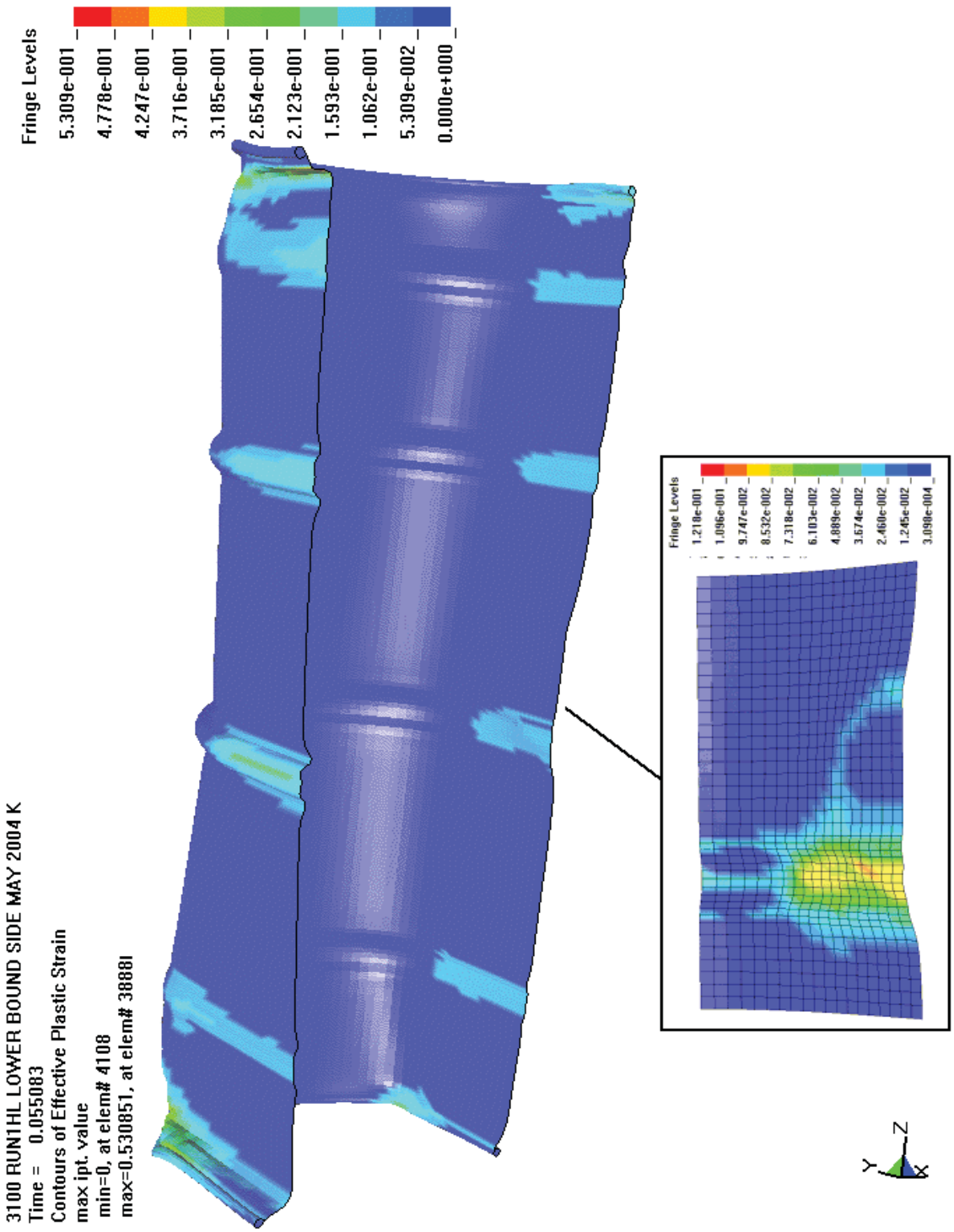

Figure 3.3.18 - Run1hl, Punch Impact, Effective Plastic Strain in the Drum

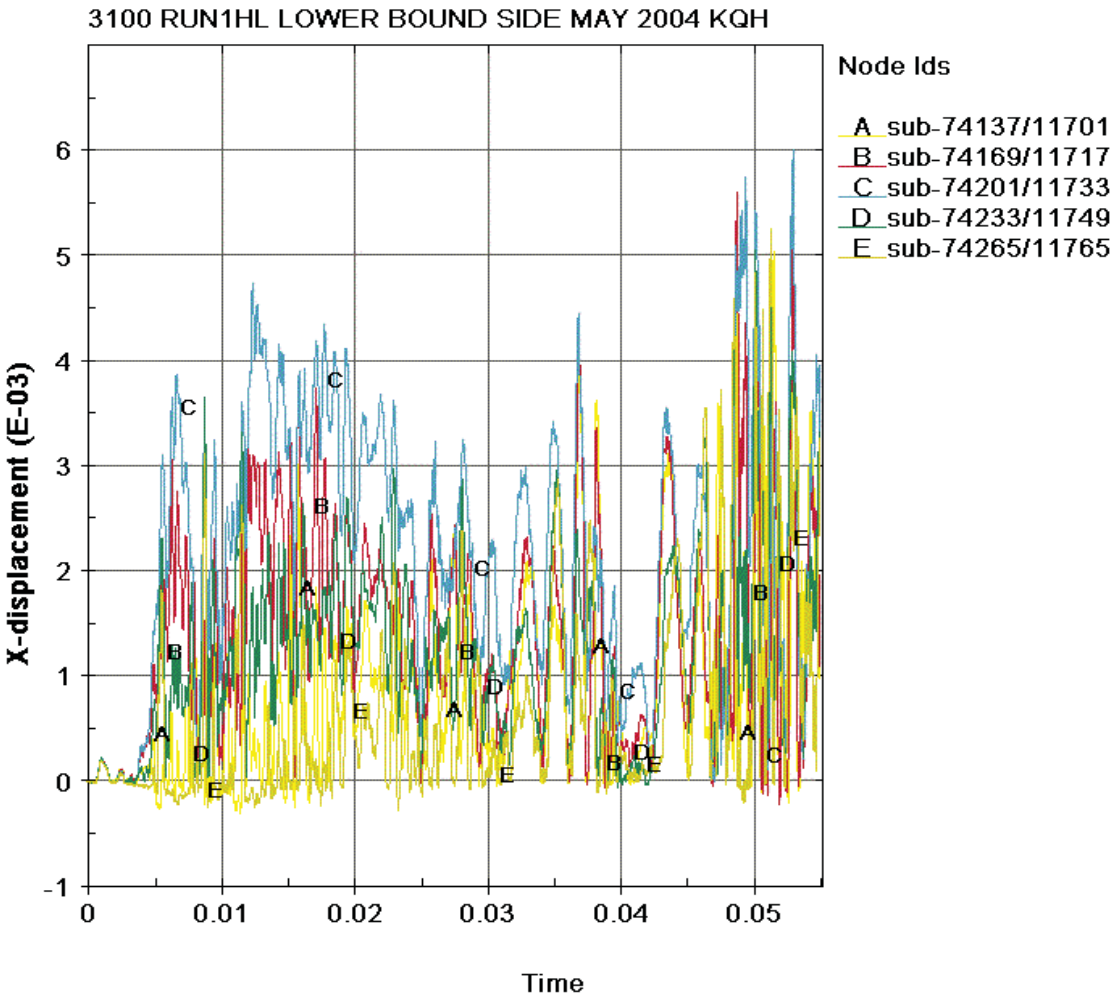

Figure 3.3.19 - Run1hl, CV Lid Separation Time History

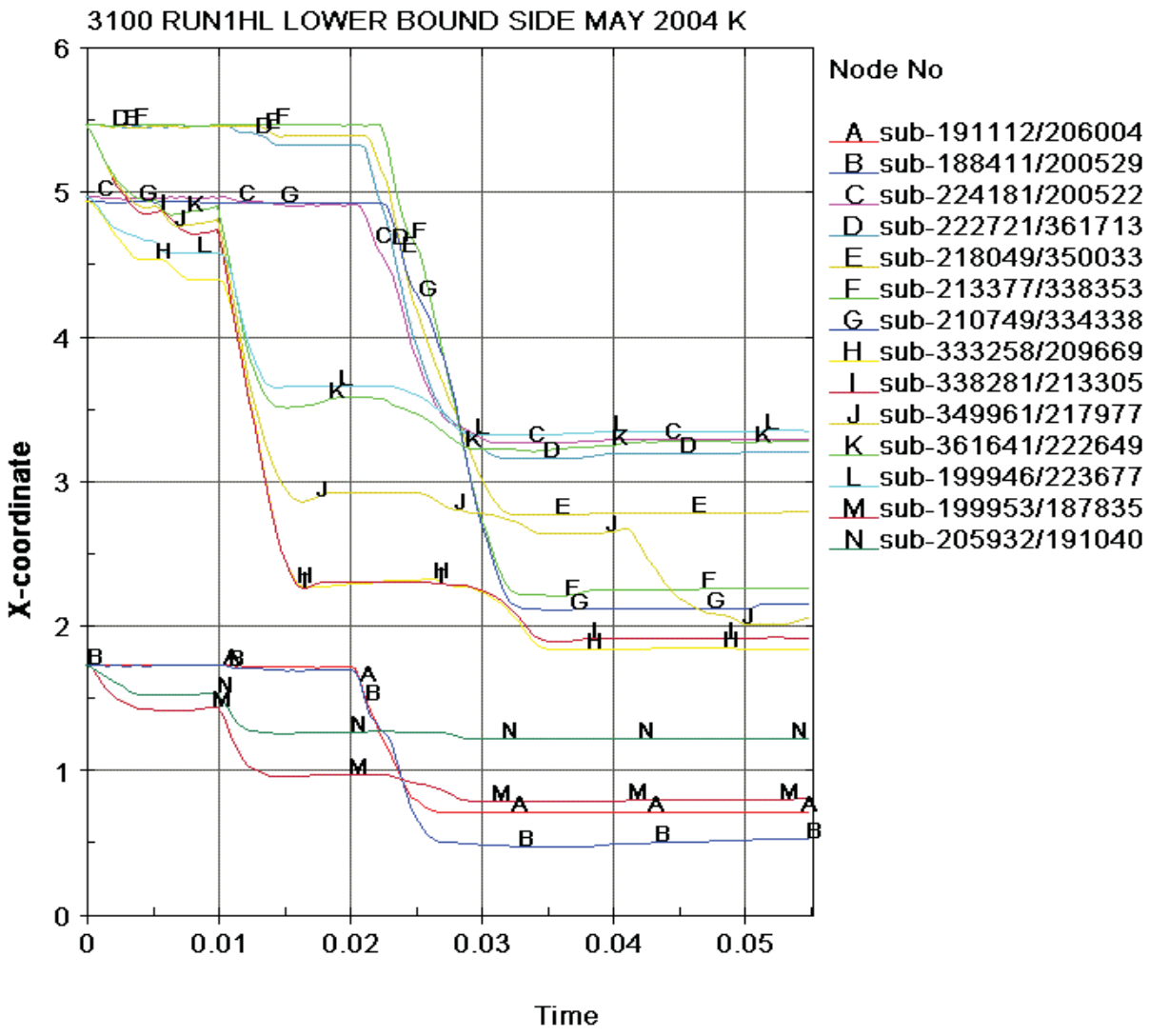

Figure 3.3.20- Run1hl, Kaolite Thickness Time History

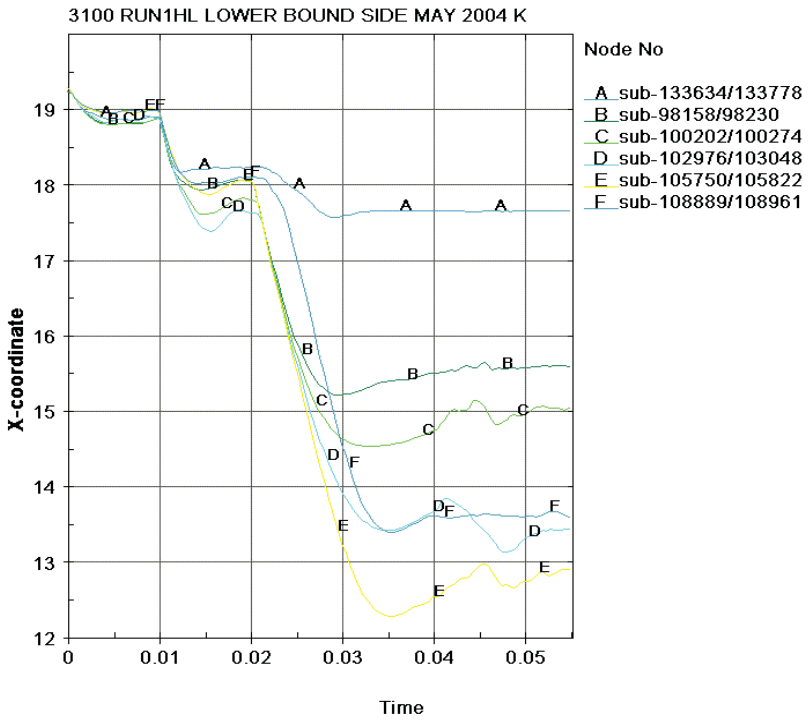

Figure 3.3.21 - Run1hl, Drum Dimension Time History in the X-Direction

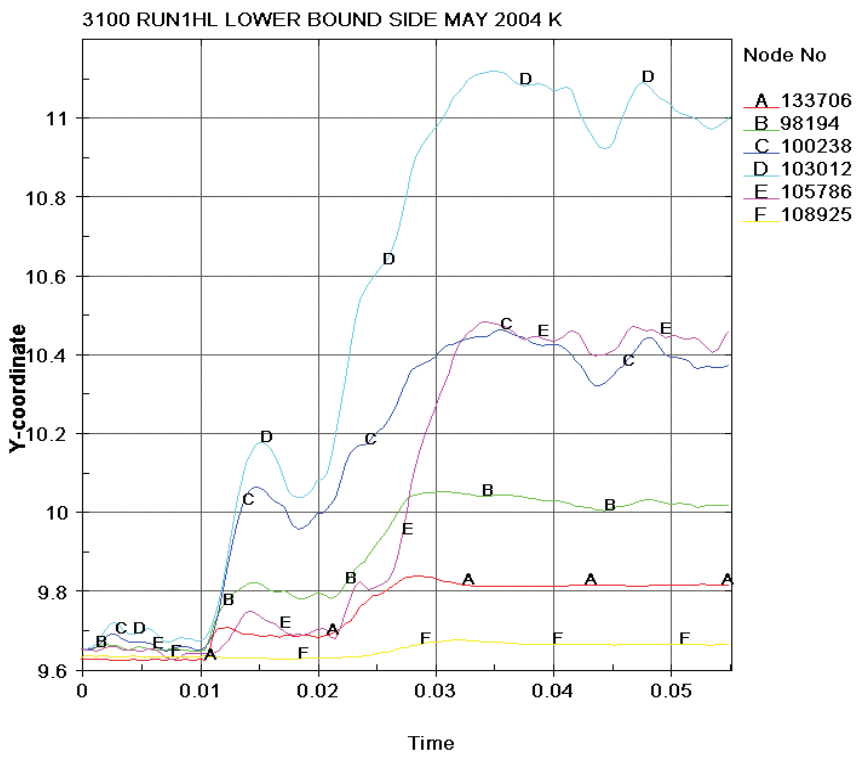

Figure 3.3.22- Run1hl, Drum Dimension Time History in the Y-Direction

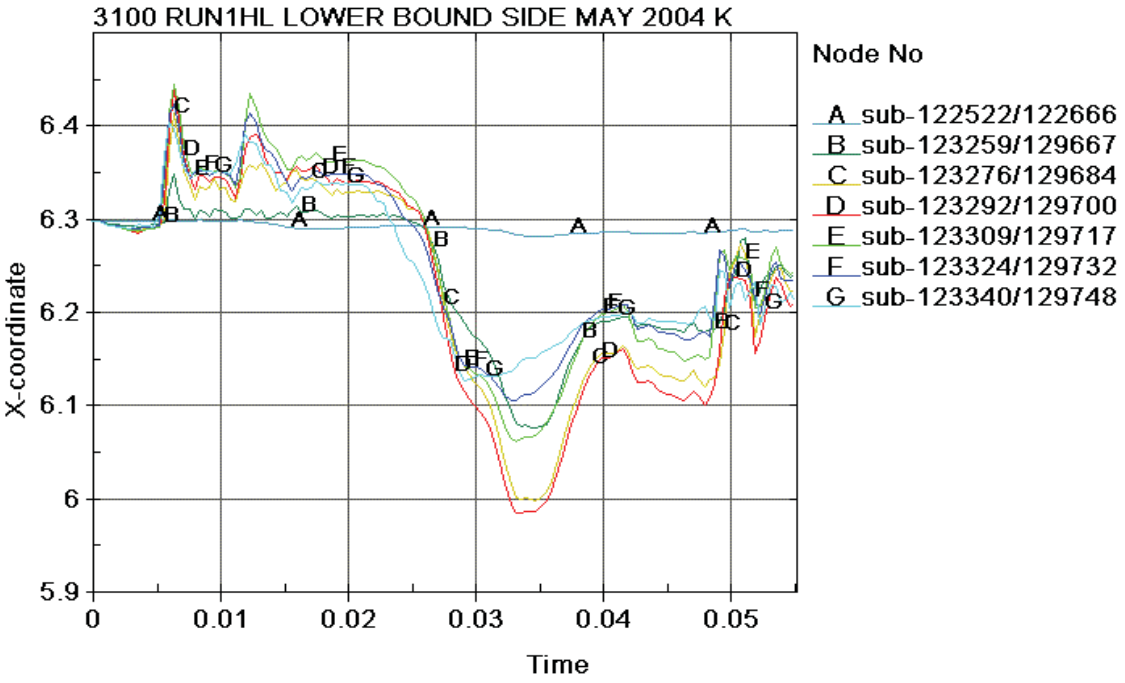

Figure 3.3.23 - Run1hl, Liner Diameter Time History

3.4 Run1hh - Side

Run1hh is the upper bounding kaolite run(-40°). It is basically the run1g model, but with the upper bound kaolite properties of section 2.3.5.3. It is a run with a 4-foot impact (time = 0 to 0.01 seconds), followed by a 30-foot impact (0.01 to 0.0188 seconds), followed by a 30-foot crush impact (0.0188 to 0.04 seconds), finally followed by a 40-inch punch impact (0.04 to 0.052 seconds).

The final configuration for the 4-foot impact is shown in Figure 3.4.1. Figures 3.4.2 and 3.4.3 show the configuration at the corners of the shipping package. The effective plastic strain in the CV body for the 4-foot impact is shown in Figure 3.4.4. The maximum effective plastic strain is shown to be 0.0298 in/in near the bottom head. The effective plastic strain in other package components for the 4-foot impact are listed in Table 3.4.1.

Table 3.4.1 - Run1hh, 4-Foot Impact, Effective Plastic Strain Levels in Some Components

Component	Effective Plastic Strain, in/in
CV Lid	0.0000
CV Nut Ring	0.0000
Angle	0.0059
Drum	0.1170
Drum Bottom Head	0.1215
Liner	0.0598
Lid	0.0860
Lid Stiffener	0.0000
Lid Studs	0.0000
Lid Stud Nuts	0.0000
Lid Stud Washers	0.0310
Plug Liner	0.0046

The final configuration for the 30-foot impact is shown in Figure 3.4.5. Figures 3.4.6 and 3.4.7 show the configuration at the corners of the package. The maximum effective plastic strain for the 30-foot impact in the CV Body is 0.0386 in/in near the bottom head. The maximum effective plastic strain in the drum lid is 0.4073 in/in near the rigid plane.

The effective plastic strain in other components for the 30-foot impact are given in Table 3.4.2.

Table 3.4.2 - Run1hh, 30-Foot Impact, Effective Plastic Strain Levels in Some Components	
Component	Effective Plastic Strain, in/in
CV Lid	0.0000
CV Nut Ring	0.0000
Angle	0.0622
Drum	0.2259
Drum Bottom Head	0.2528
Liner	0.0970
Lid Stiffener	0.0069
Lid Studs	0.1226
Lid Stud Nuts	0.0000
Lid Stud Washers	0.0951
Plug Liner	0.0995

The final configuration for the crush impact is shown in Figure 3.4.10. The configuration at the extremes of the package are shown in Figure 3.4.11. The maximum effective plastic strain for the crush impact in the CV body is 0.0462 in/in, on the crush plate side near the lid end of the top inner weight as shown in Figure 3.4.12. The maximum effective plastic strain in the drum is 0.2623 in/in near the angle and the rigid plane (Figure 3.4.13). The maximum effective plastic strain in the drum lid is 0.6411 in/in (surface strain), Figure 3.4.14. The maximum occurs at the lid hole for the stud closest to the crush plate(180°). The membrane effective plastic strain is 0.4922 in/in at this location. The effective plastic strain in the studs is 0.1753 in/in as shown in Figure 3.4.15. The effective plastic strain in other components are listed in Table 3.4.3 for the crush impact.

Table 3.4.3 - Run1hh, Crush Impact, Effective Plastic Strain Levels in Some Components	
Component	Effective Plastic Strain, in/in
CV Lid	0.0004
CV Nut Ring	0.0000
Angle	0.0816
Drum Bottom Head	0.2807
Liner	0.2005
Lid Stiffener	0.0217
Lid Stud Nuts	0.0000
Lid Stud Washers	0.1034
Plug Liner	0.1258

The final configuration for the punch impact is shown in Figure 3.4.16. The maximum effective plastic strain in the CV body after the punch impact is shown to be 0.0599 in/in in Figure 3.4.17. The maximum effective plastic strain in the drum is 0.2623 in/in (surface strain) and is located near the angle at the rigid surface. The maximum effective plastic strain in elements local to the punch impact is 0.1382 in/in (surface strain) as shown in the insert in Figure 3.4.18. The maximum effective plastic strain for the lid and other package components at the end of the punch impact are listed in Table 3.4.4.

Table 3.4.4 - Run1hh, Punch Impact, Effective Plastic Strain Levels in Some Components	
Component	Effective Plastic Strain, in/in
CV Lid	0.0004
CV Nut Ring	0.0000
Angle	0.0816
Drum Bottom Head	0.2807
Liner	0.2027
Lid	0.6411
Lid Stiffener	0.0217
Lid Studs	0.1761
Lid Stud Nuts	0.0000
Lid Stud Washers	0.1034
Plug Liner	0.1258

Figure 3.4.19 shows the CV lid separation for all the impacts. A maximum spike for the lid separation of less than 0.008 inches is found. At the end of the impacts, the maximum separation is on the order of 0.006 in, with the response being oscillatory in nature. Average separation of 0.003 inches or less is shown to be expected after the successive impacts.

Figure 3.4.20 shows the drum diameter time history response to the impacts in the X direction (direction of the impacts). Figure 3.4.21 shows the Y direction radial response (normal to the impact direction). The drum nodes are defined in Figure 3.1.34.

The Figure 3.4.22 shows the kaolite thickness time history for the four impacts. Figure 3.1.32 shows the nodal locations.

Figure 3.4.23 shows the liner diameter time history along its length. The nodal pairs are defined in Figure 3.1.37 and Table 3.1.3.

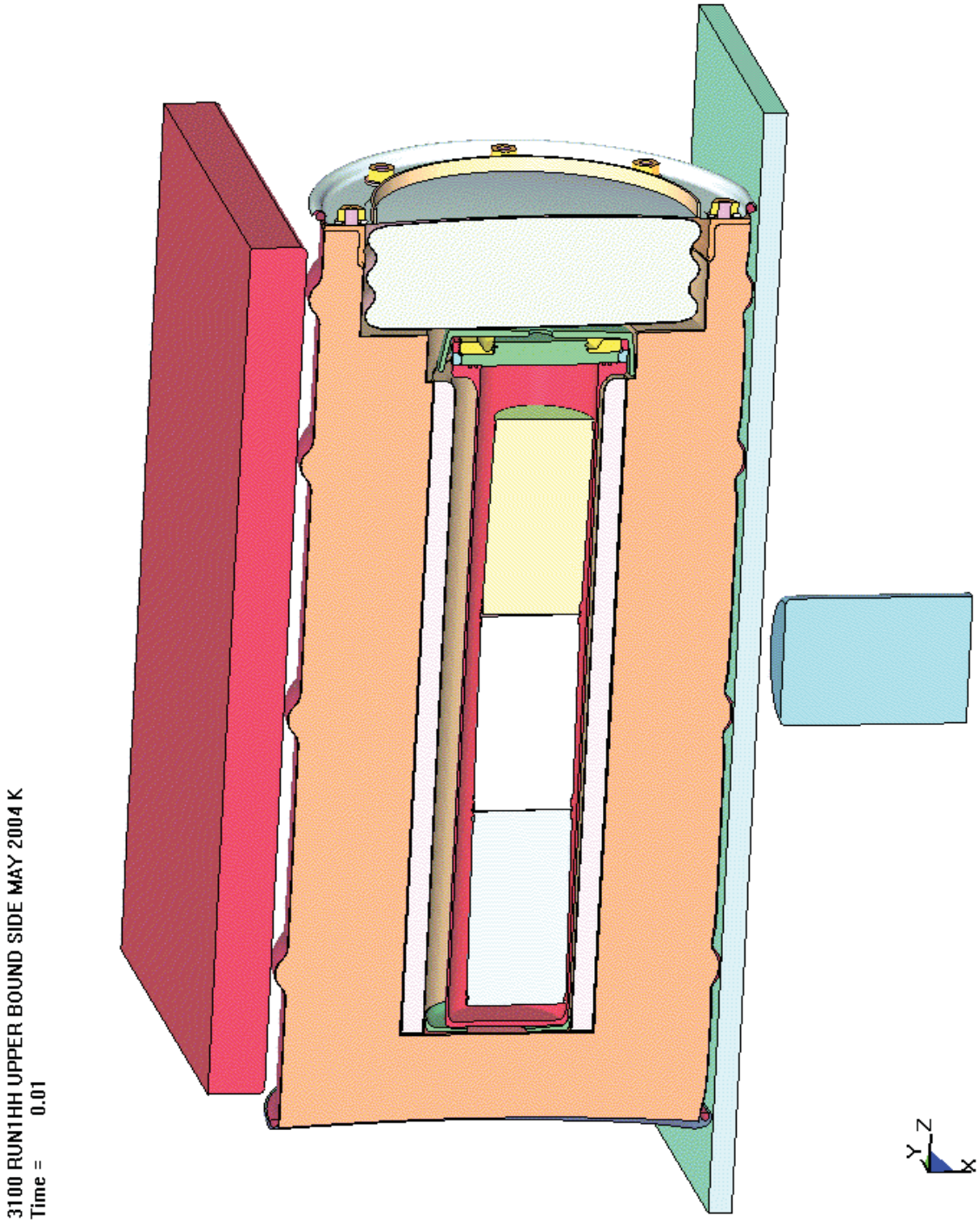

Figure 3.4.1 - Run1hh, 4-Foot Impact, Final Configuration

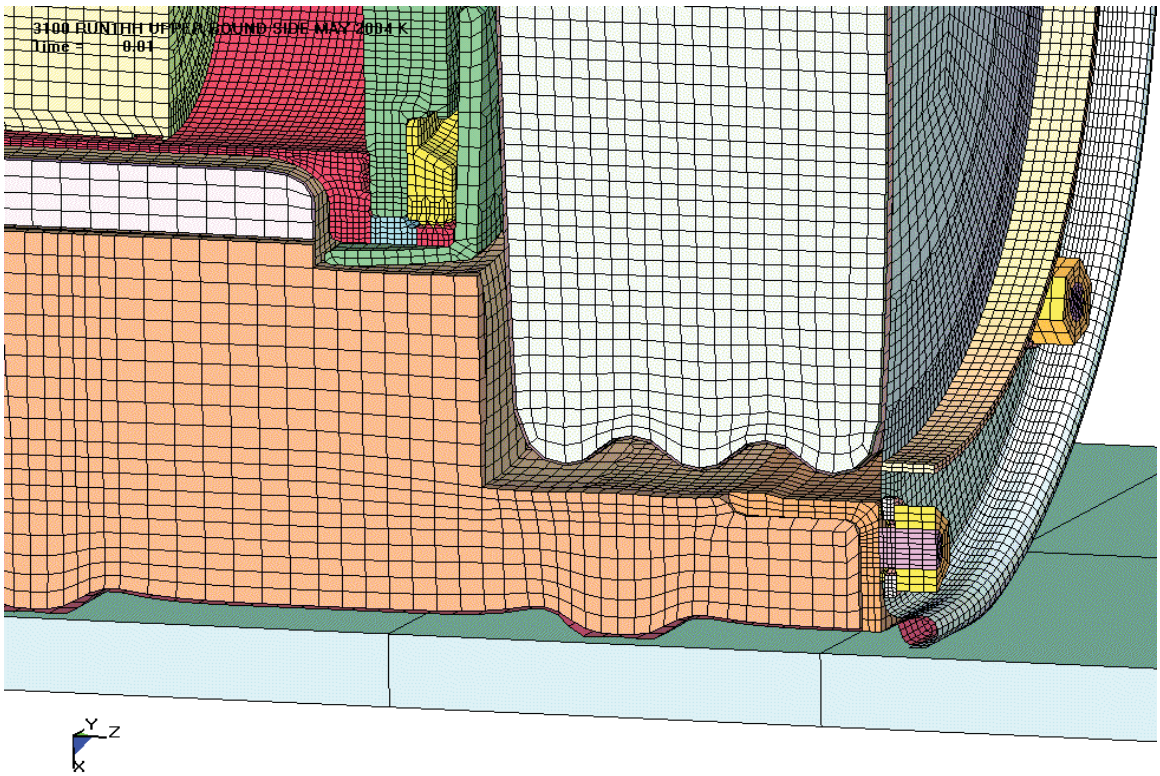

Figure 3.4.2 - Run1hh, 4-Foot Impact,

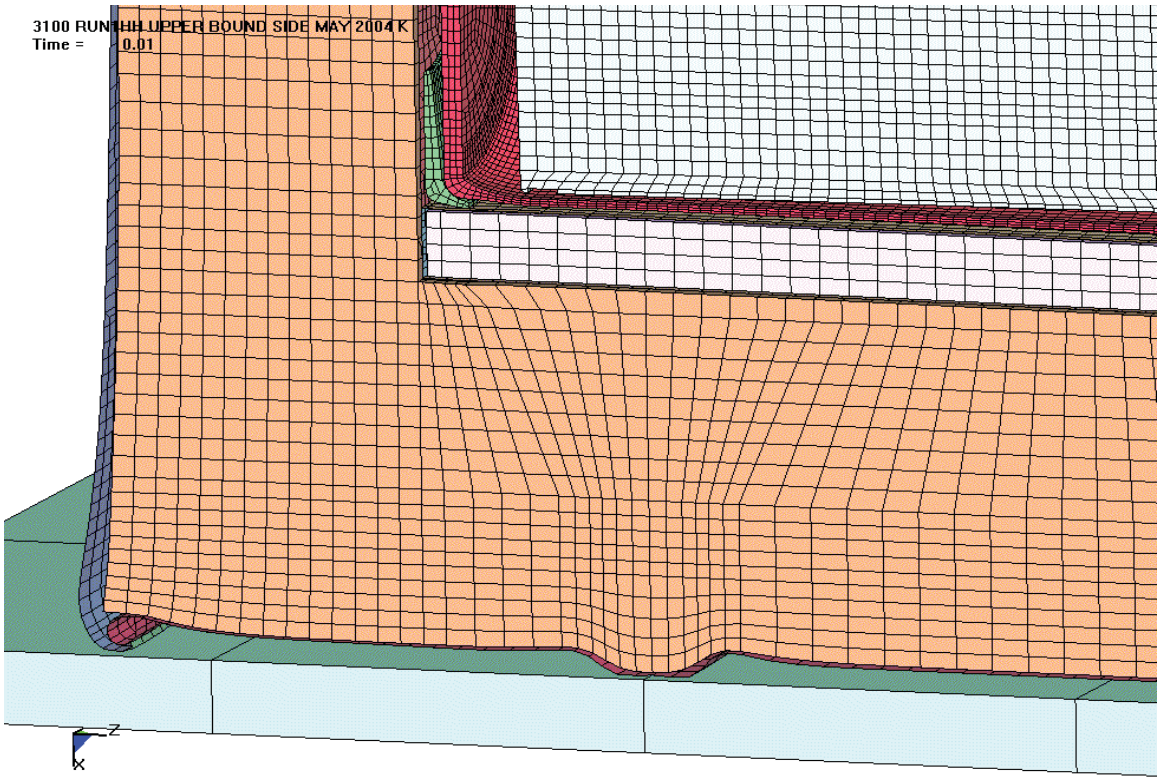

Figure 3.4.3 - Run1hh, 4-Foot Impact,

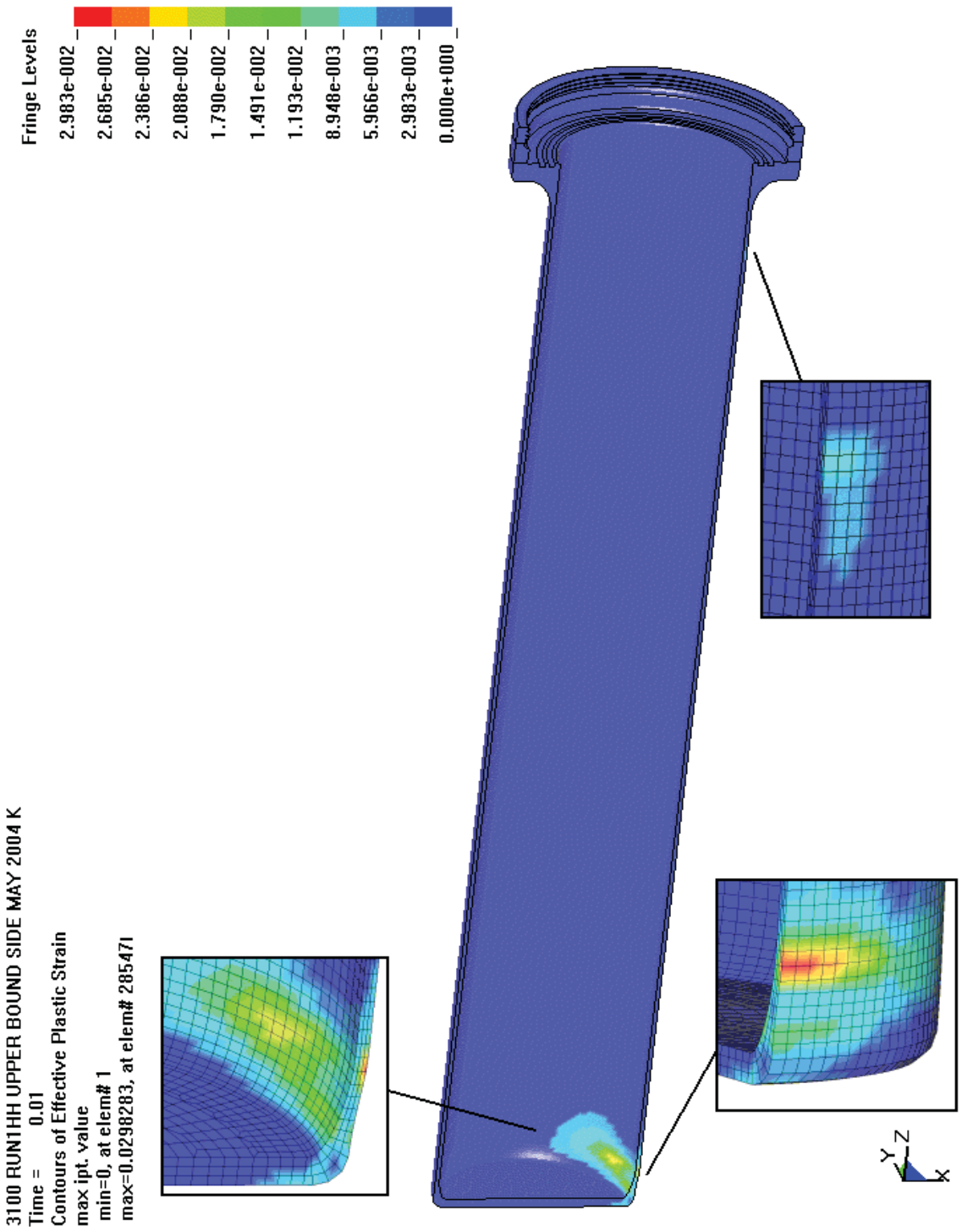

Figure 3.4.4 - Run1hh, 4-Foot Impact, Effective Plastic Strain in the CV Body

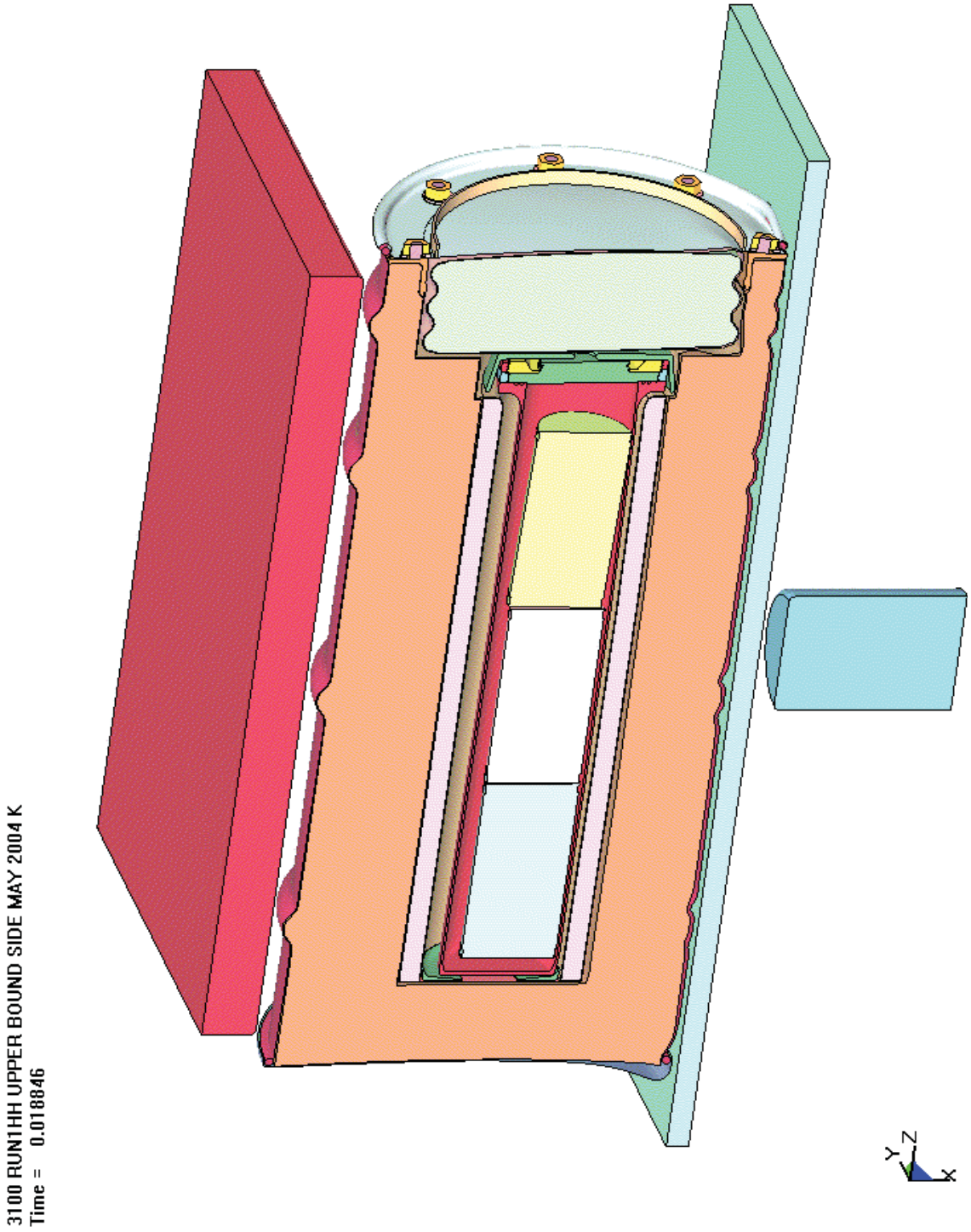

Figure 3.4.5 - Run1hh, 30-Foot Impact, Final Configuration

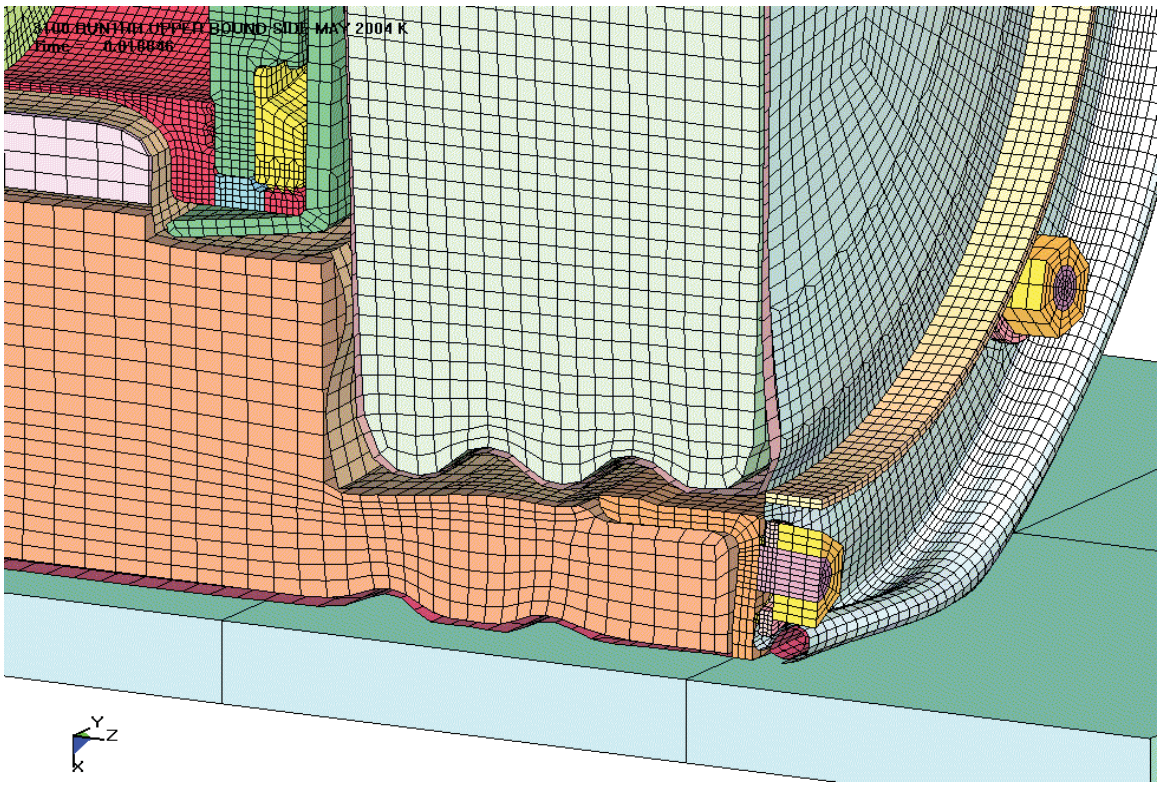

Figure 3.4.6 - Run1hh, 30-Foot Impact, Configuration in the Lid

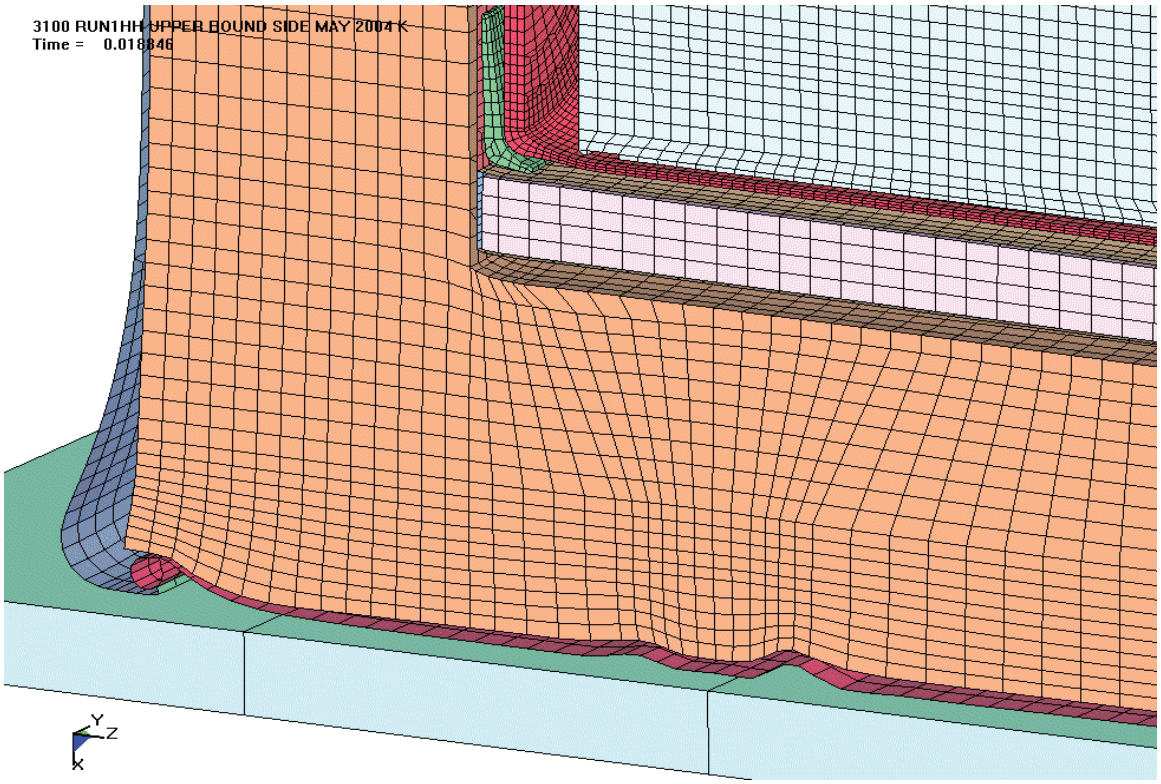

Figure 3.4.7 - Run1hh, 30-Foot Impact, Configuration in the Bottom

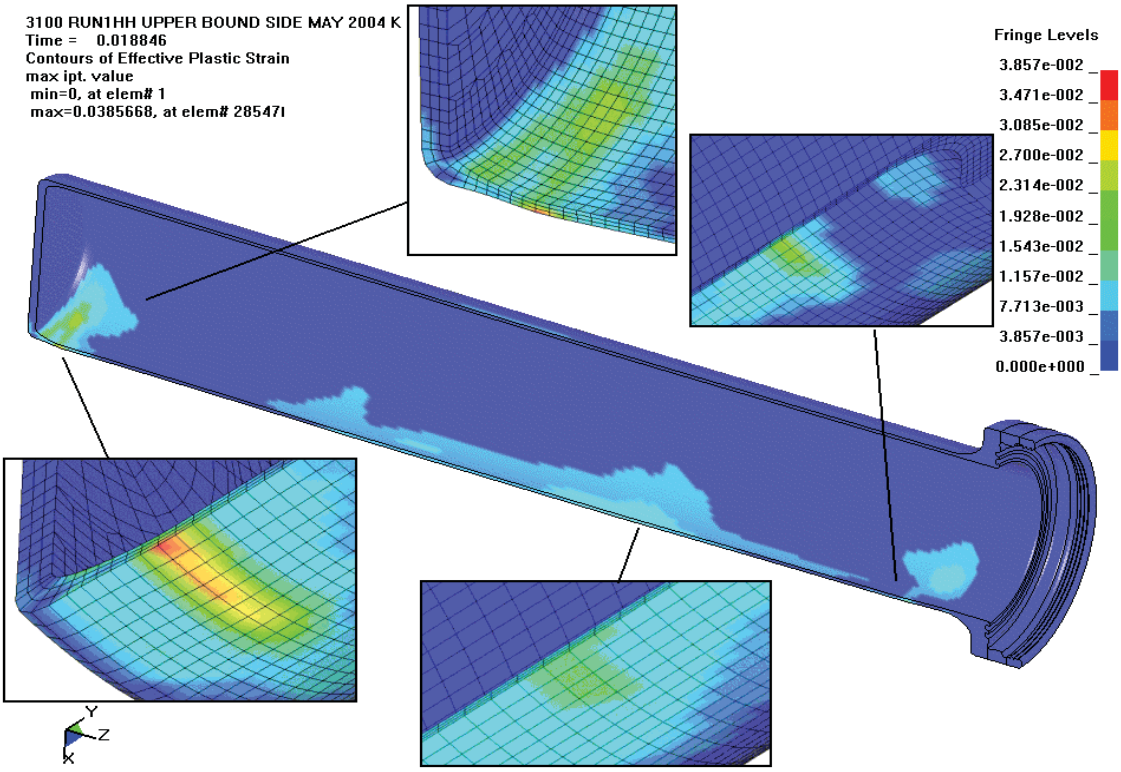

Figure 3.4.8 - Run1hh, 30-Foot Impact, Effective Plastic Strain in the CV Body

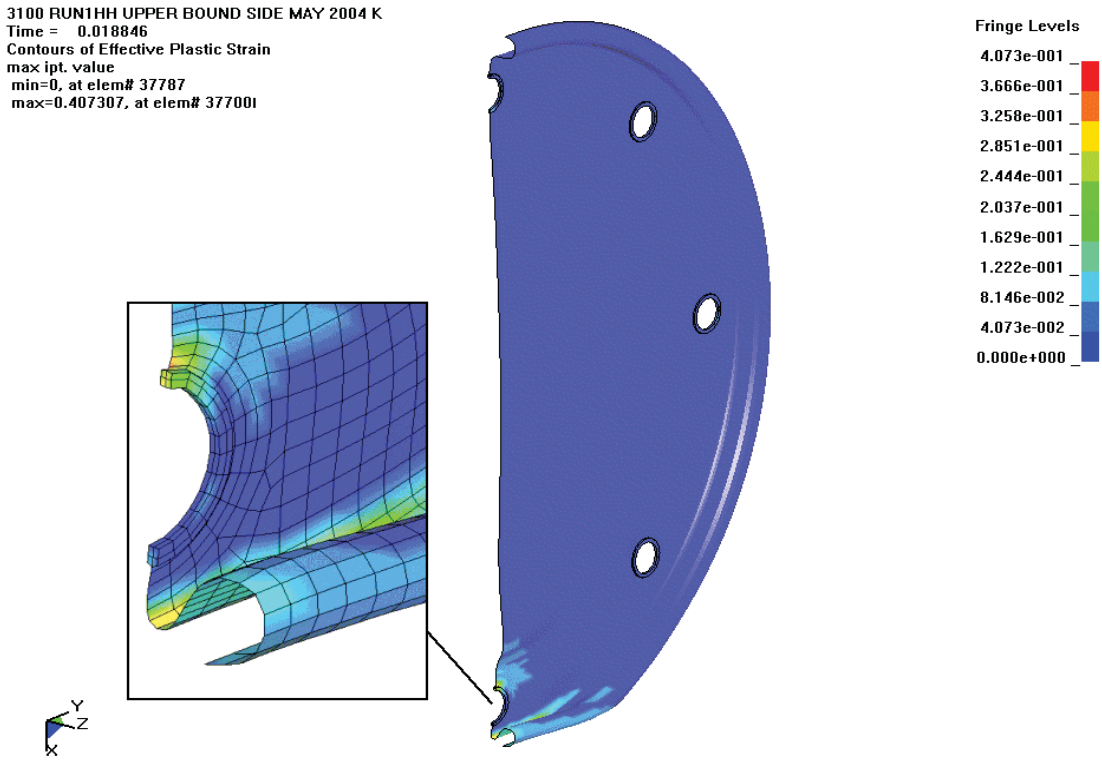

Figure 3.4.9 - Run1hh, 30-Foot Impact, Effective Plastic Strain in the Lid

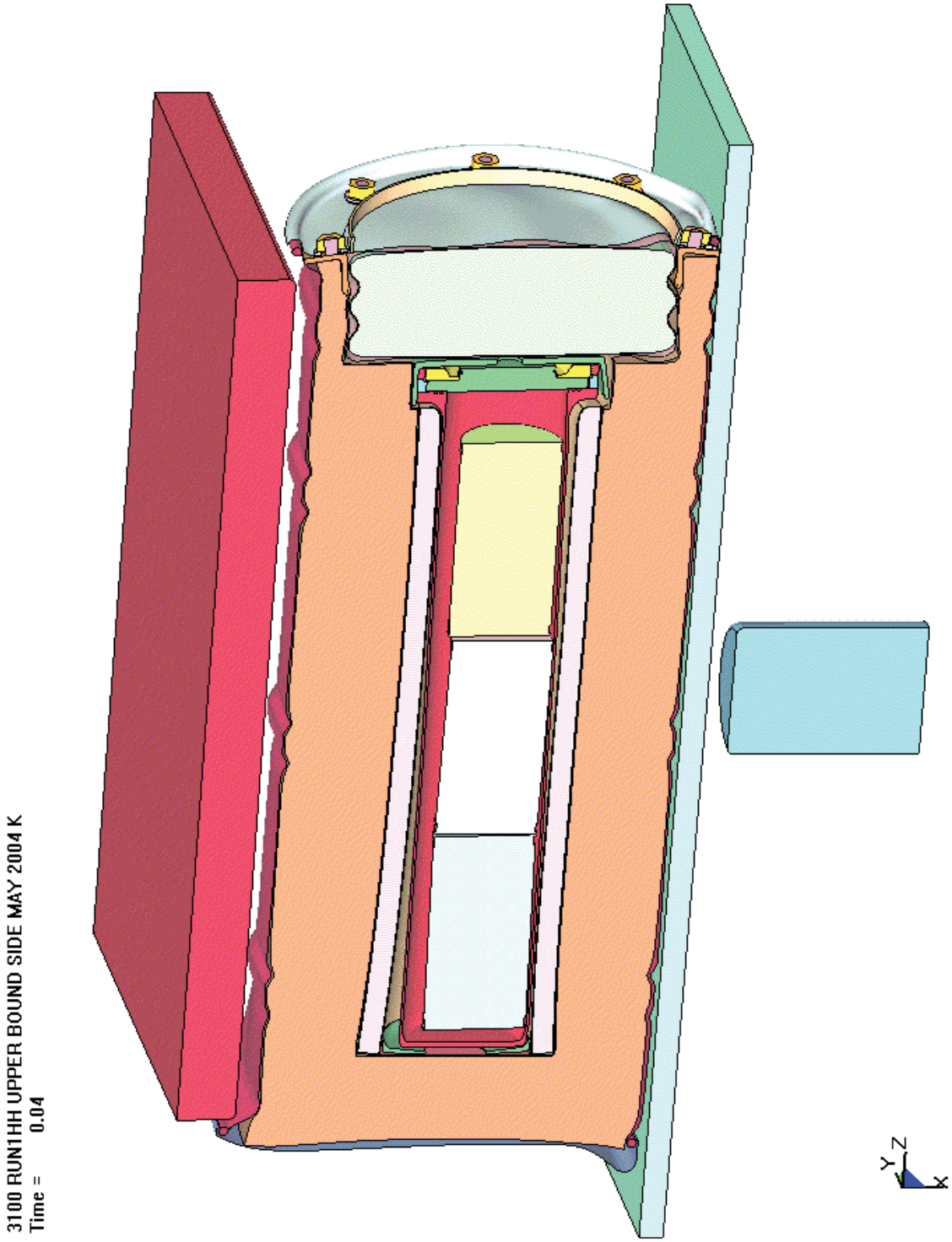

Figure 3.4.10 - Run1hh, Crush Impact, Final Configuration

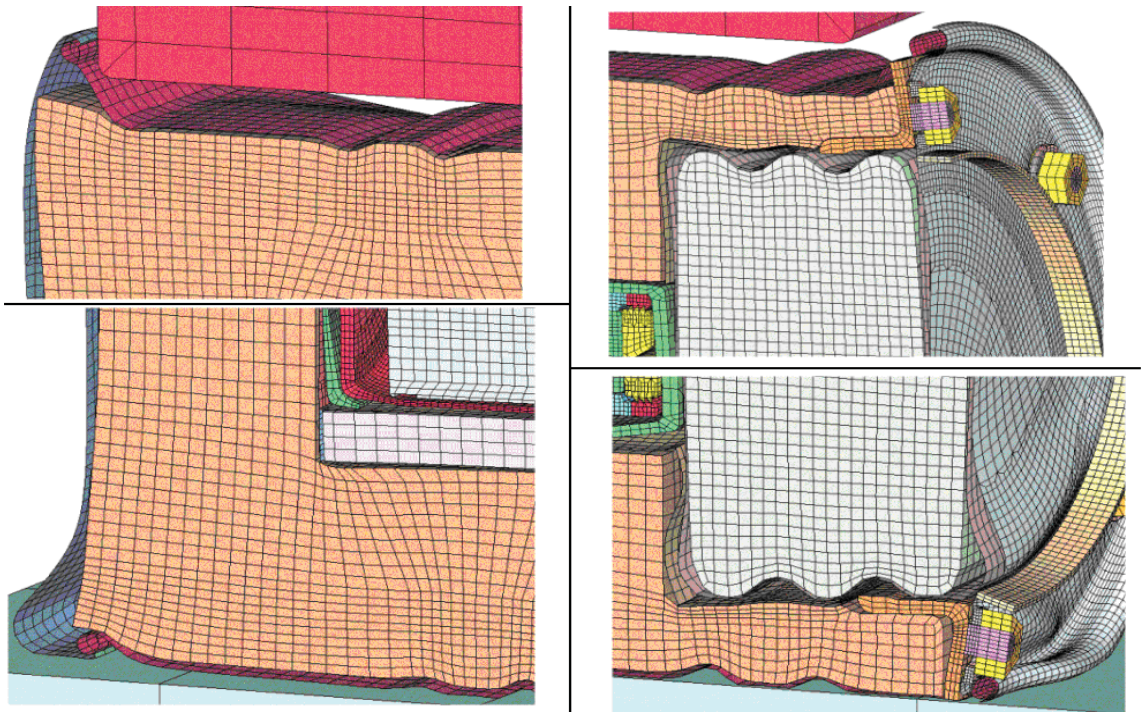

Figure 3.4.11 - Run1hh, Crush Impact, Configuration of the Package Corners

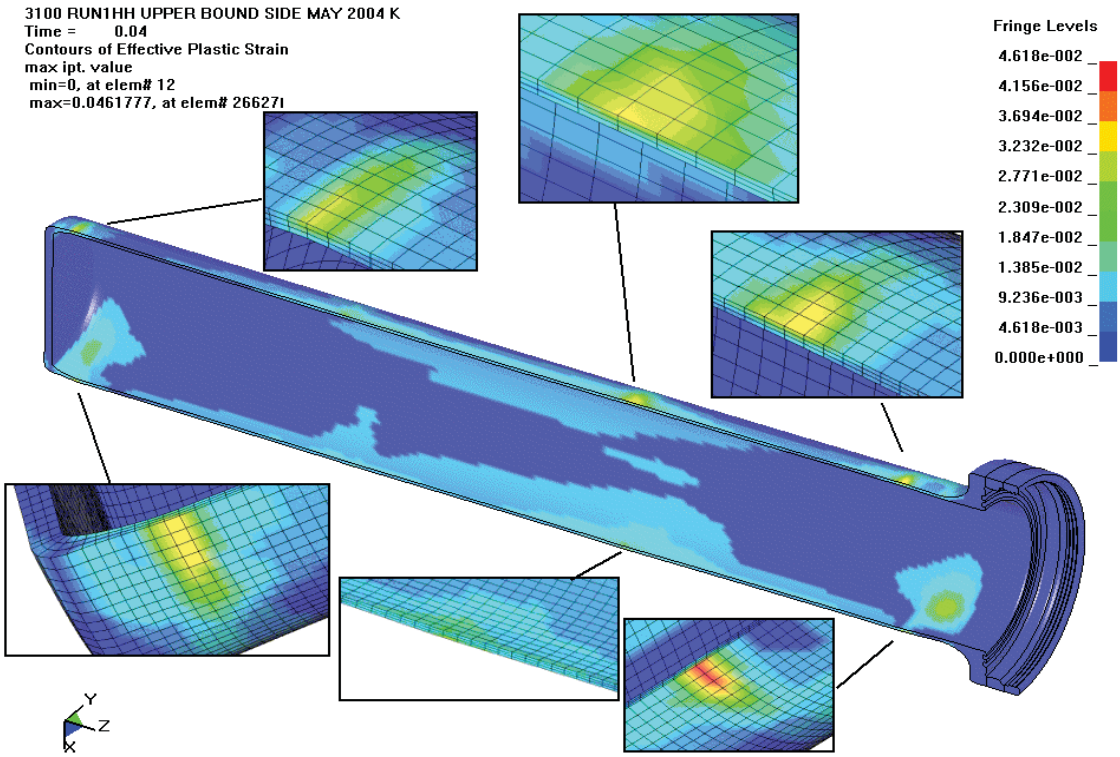

Figure 3.4.12 - Run1hh, Crush Impact, Effective Plastic Strain in the CV Body

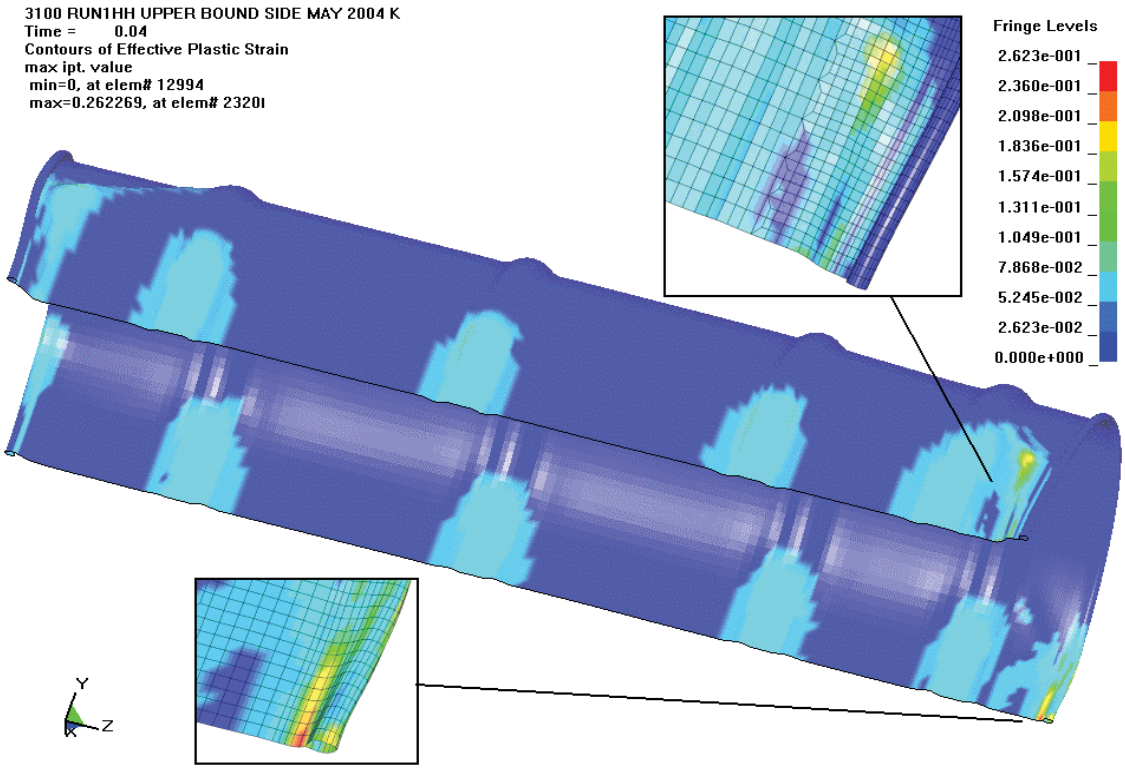

Figure 3.4.13 - Run1hh, Crush Impact, Effective Plastic Strain in the Drum

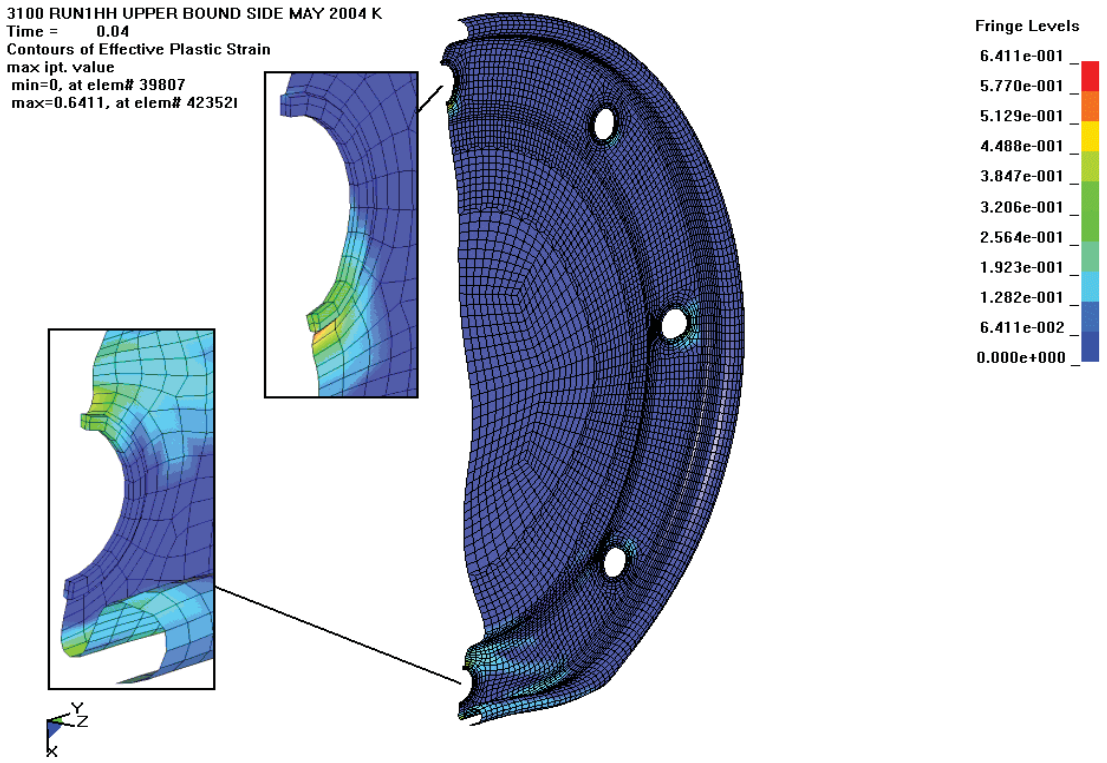

Figure 3.4.14 - Run1hh, Crush Impact, Effective Plastic Strain in the Lid

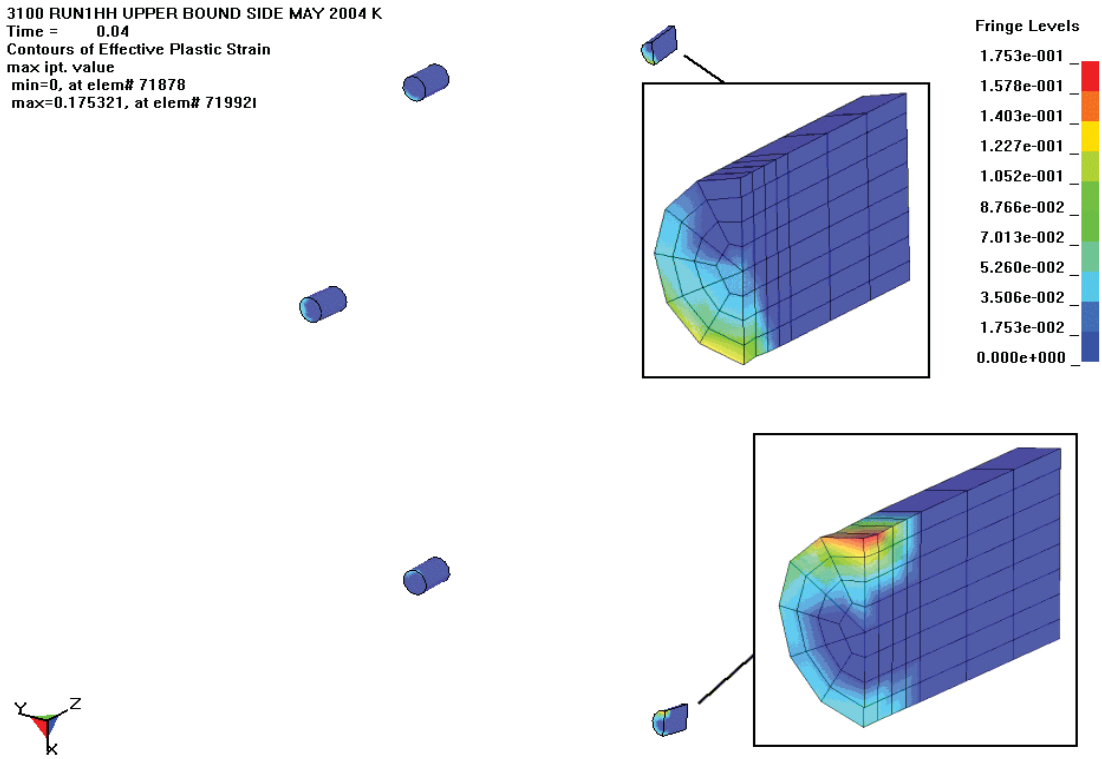

Figure 3.4.15 - Run1hh, Crush Impact, Effective Plastic Strain in the Studs

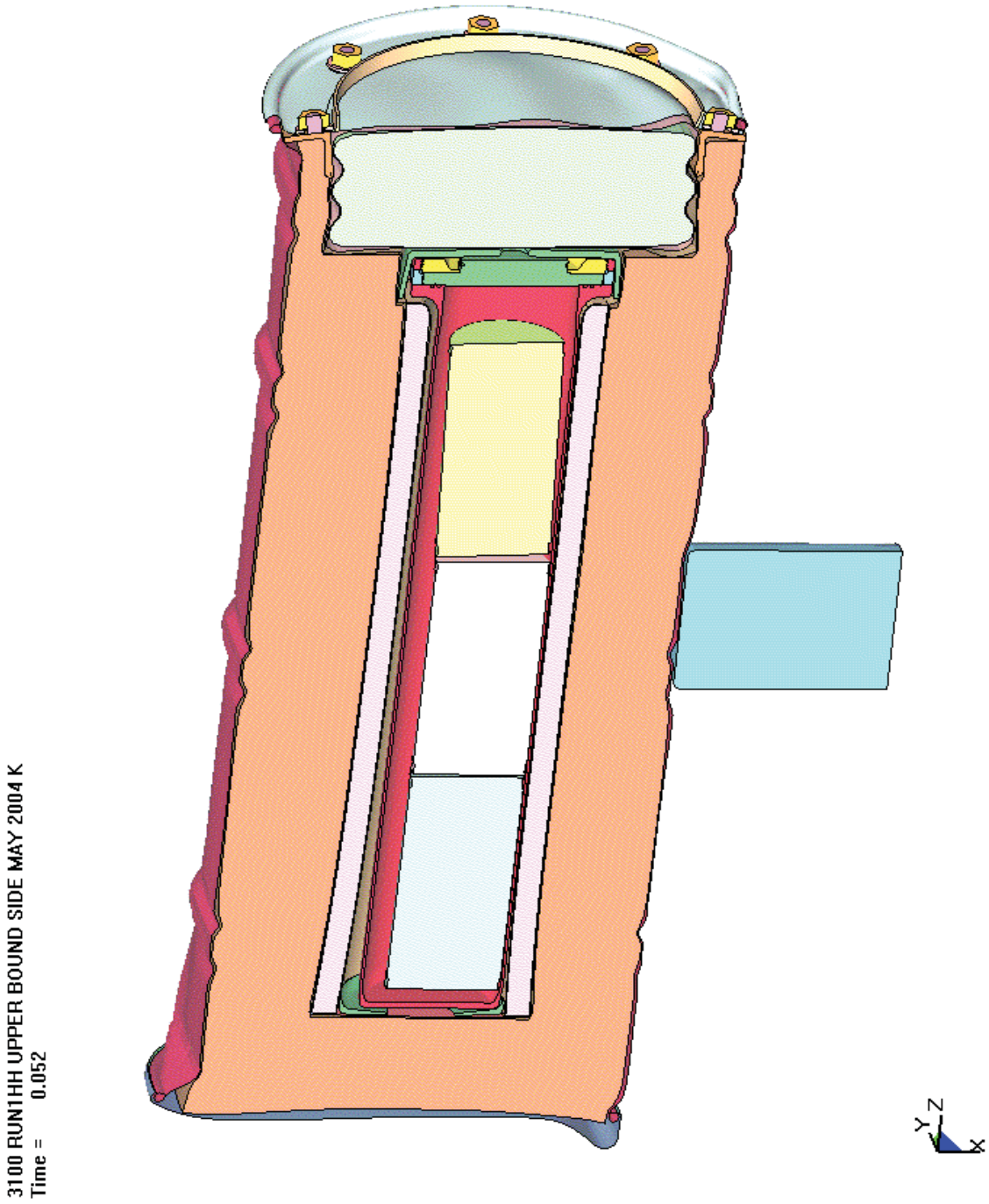

Figure 3.4.16 - Run1hh, Punch Impact, Final Configuration

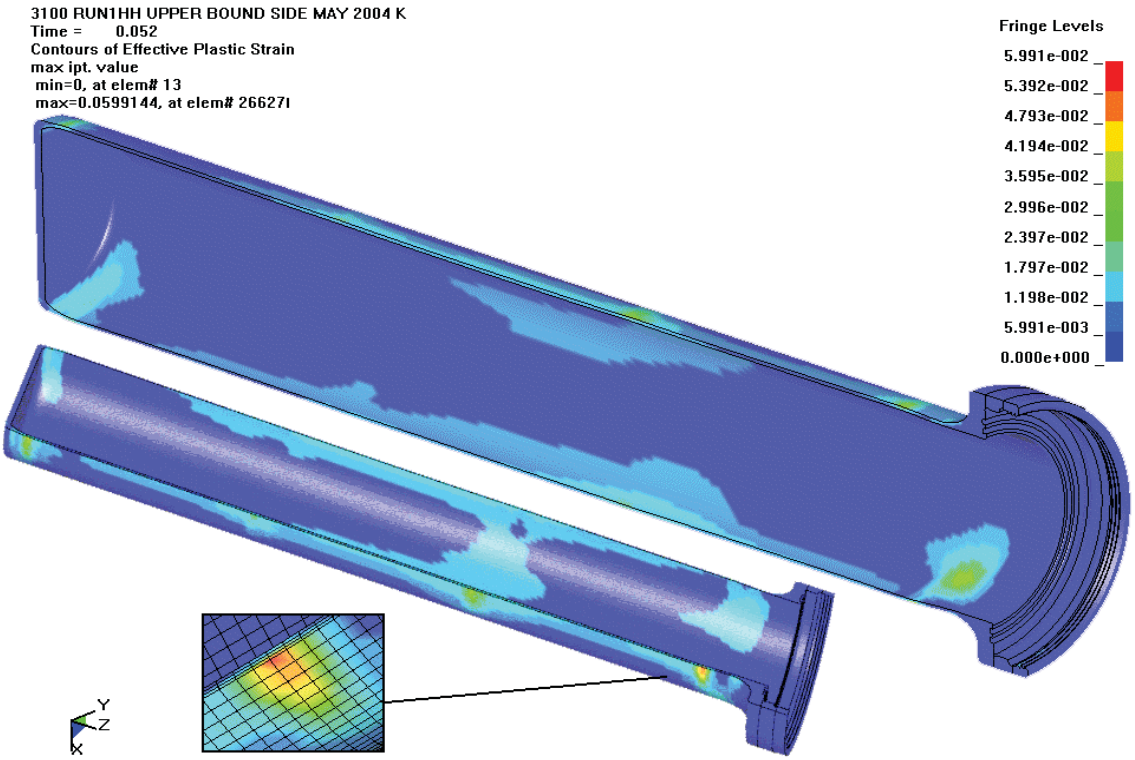

Figure 3.4.17 - Run1hh, Punch Impact, Effective Plastic Strain in the CV Body

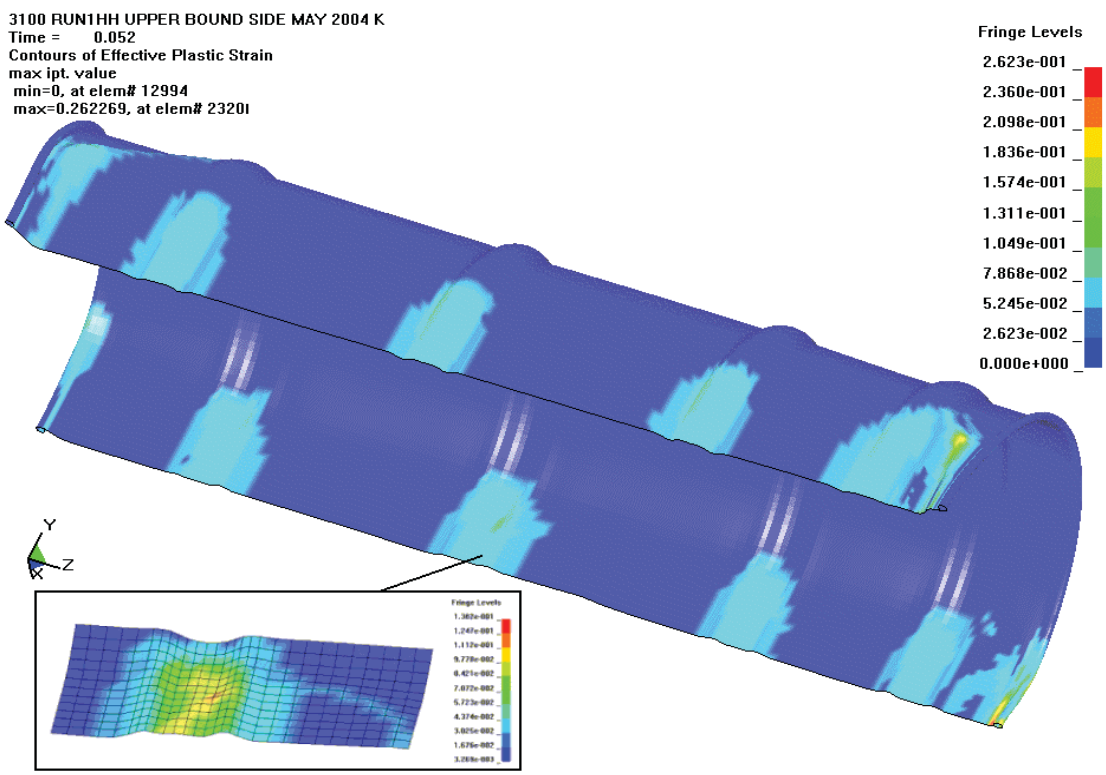

Figure 3.4.18 - Run1hh, Punch Impact, Effective Plastic Strain in the Drum

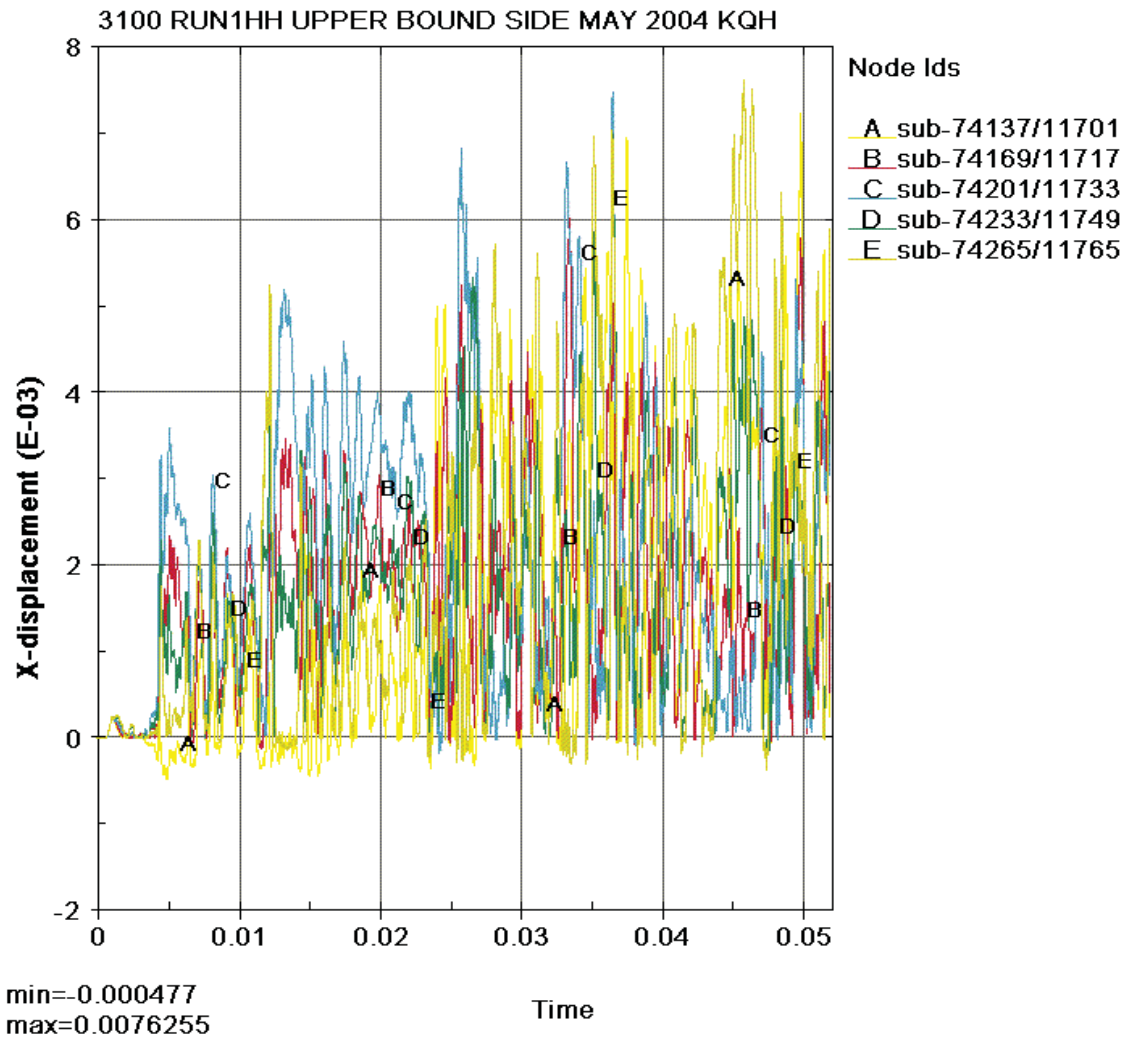

Figure 3.4.19 - Run1hh, CV Lid Separation Time History

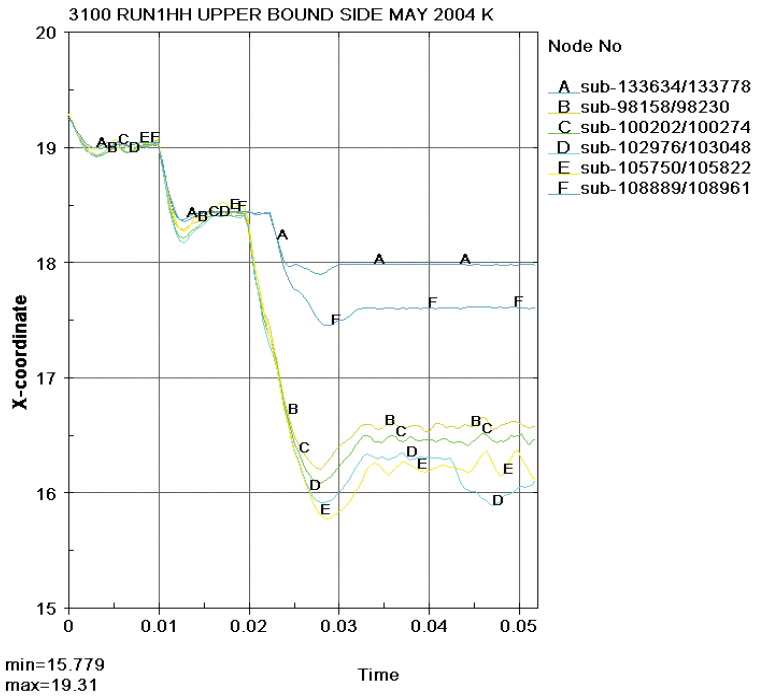

Figure 3.4.20 - Run1hh, Diameter of the Drum in the Direction of the Impacts

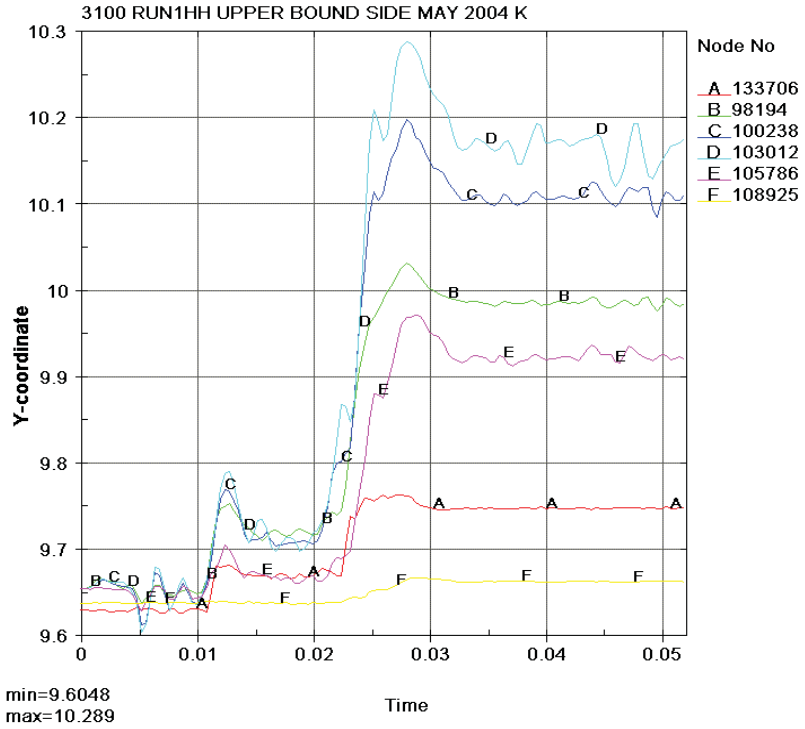

Figure 3.4.21 - Run1hh, Radius of the Drum in the Direction Normal to the Impacts

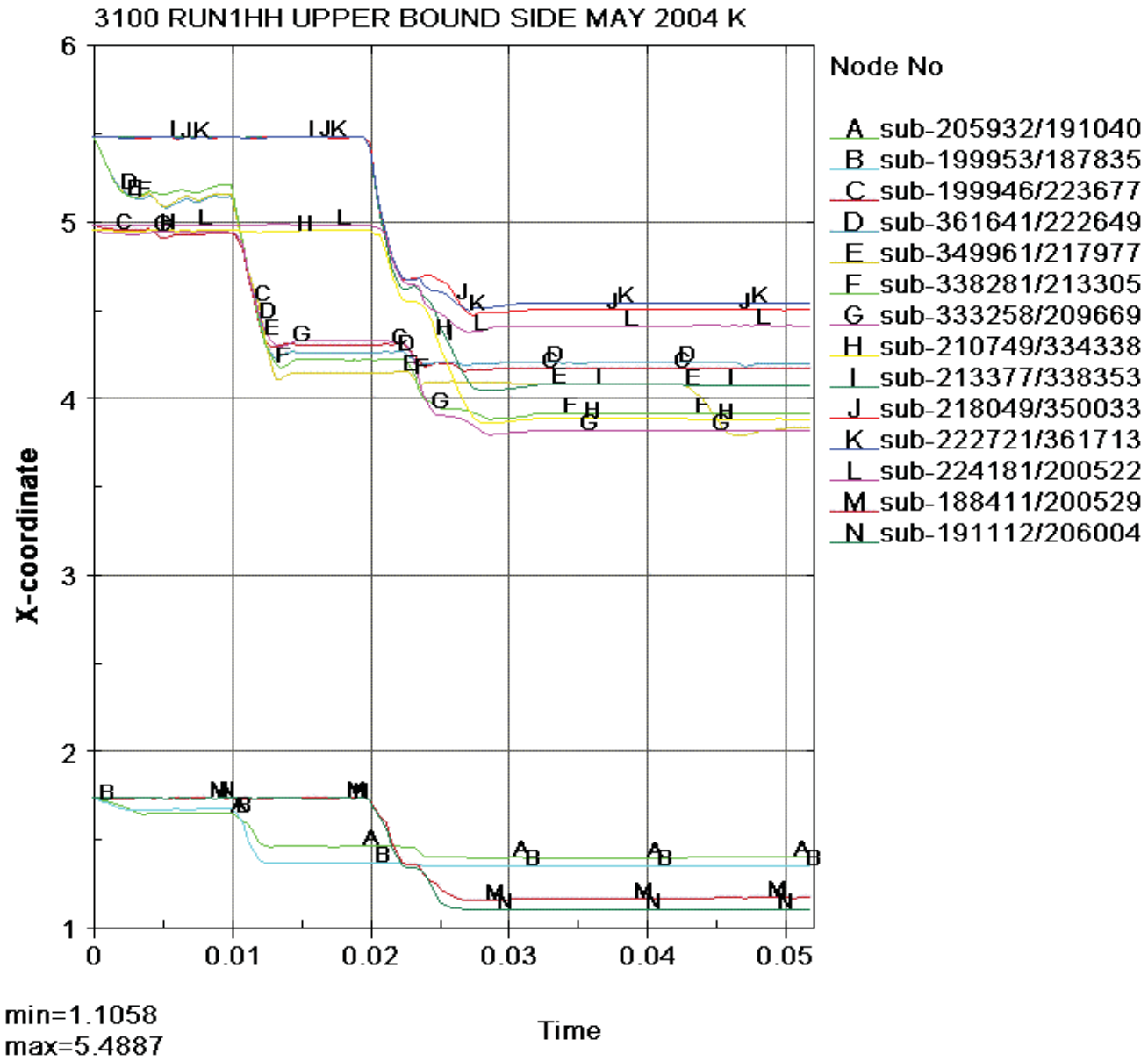

Figure 3.4.22 - Run1hh, Thickness Time History of the Drum Kaolite

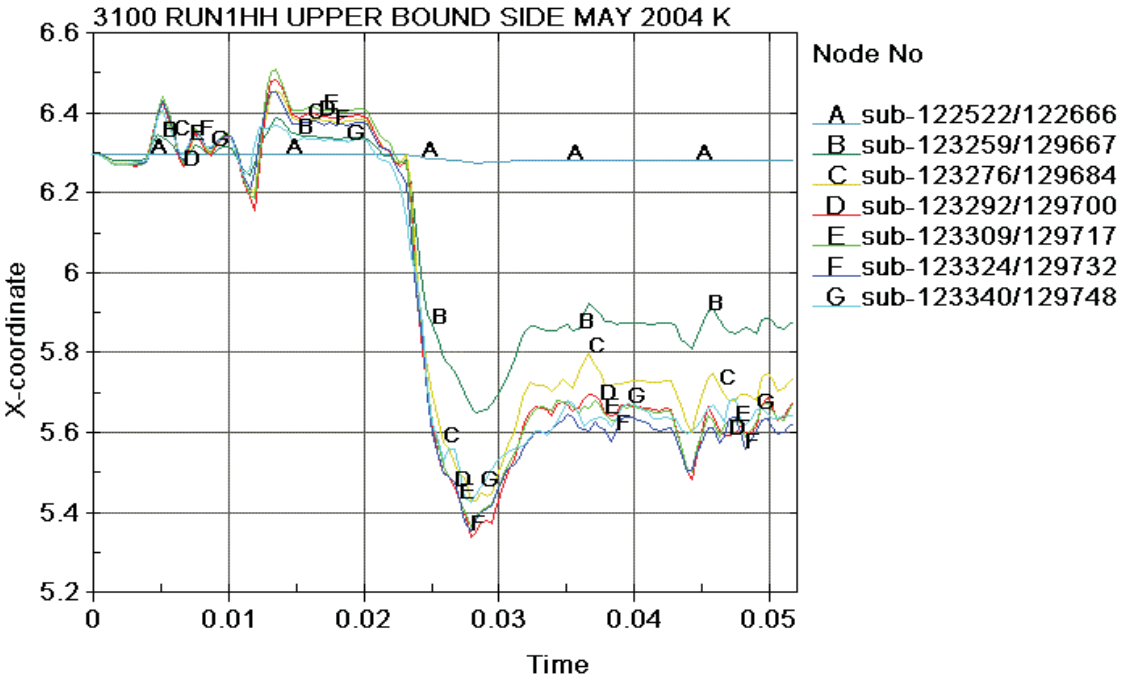

Figure 3.4.23 - Run1hh, Liner Diameter Time Histories

3.5 Run2e - Corner

Run2e is a package CG over corner impact with a 30-foot impact (time = 0 to 0.015 seconds)followed by a crush impact (0.015 to 0.05 seconds).

The configuration after the 30-foot impact is shown in Figure 3.5.1. The maximum effective plastic strain in the lid studs is in the stud at the impact with the rigid plane (0°) and is 0.5197 in/in as shown in Figure 3.5.2. It can be seen from the insert in Figure 3.5.2, that strains near the maximum exist across the thickness of the stud. Therefore, it should be noted that slight differences between the modeled length and actual length of the stud could be significant relative to possible failure of the stud. Other differences such as friction and local flexibility in the test pad armored plate (stud "digging in") could also significantly effect this stud and cause failure. The maximum effective plastic strain of other components for this impact are listed in Table 3.5.1.

Table 3.5.1 - Run2e, 30-Foot Impact, Effective Plastic Strain Levels in Some Components

Component	Effective Plastic Strain, in/in
CV Body	0.0142
CV Lid	0.0024
CV Nut Ring	0.0000
Angle	0.0393
Drum	0.3238
Drum Bottom Head	0.0000
Liner	0.3797
Lid	0.2968
Lid Stiffener	0.0271
Lid Stud Nuts	0.2252
Lid Stud Washers	0.0907
Plug Liner	0.1131

Figure 3.5.3 shows the final configuration for the crush impact. In Figure 3.5.4 the maximum effective plastic strain in the CV lid is shown to remain at 0.0024 in/in. Figure 3.5.5 shows the effective plastic strain in the liner to be a maximum of 0.5507 in/in. The maximum effective plastic strain in the drum is in the crimping as shown in Figure 3.5.6 and is a maximum of 0.3787 in/in. The maximum effective plastic strain in the drum studs

is shown to be 0.5578 in/in in Figure 3.5.7. As explained in the 30-foot impact results, slight variances in the length/configuration in this vicinity could prove significant in the test due to the relatively high level of strain through the thickness of the stud. There is a crimping of the lid and the drum roll in this local region, hence, even if the stud did shear, the lid would be held captive by the drum roll.

Table 3.5.2 - Run2e, Crush Impact, Effective Plastic Strain Levels in Some Components

Component	Effective Plastic Strain, in/in
CV Body	0.0364
CV Nut Ring	0.0000
Angle	0.0464
Drum Bottom Head	0.0731
Lid	0.3579
Lid Stiffener	0.0272
Lid Stud Nuts	0.2258
Lid Stud Washers	0.1111
Plug Liner	0.1170

The lid separation time history is given in Figure 3.5.8. A spike separation occurs in the crush impact with a maximum gap of about 0.010 inches. The run2e was extended to about 0.06 seconds so that the ringing associated with the gap at 0.05 seconds could relax. From the figure it is seen that an average value of gap would be 0.002 inches, or less due to the oscillatory nature of the gap response.

Figure 3.5.9 shows the location of the nodes used to obtain the minimum koalite thickness in the package bottom. The time history thickness is shown in Figure 3.5.10 for the bottom kaolite. A minimum thickness of about 1.8 inches is shown.

Figure 3.5.11 shows the location of the nodes used to obtain the minimum kaolite thickness in the plug. Figure 3.5.12 shows the distance time history with the minimum being about 2.8 inches.

Figure 3.5.13 shows the nodes used to obtain overall drum dimensions for the impacts. The final lengths from the bottom head to the lid are used to describe the deformations. Curve A in Figure 3.5.14 gives the length response of the crush corner to the lid. It has a

final length of about 38.2 inches. Curve B in Figure 3.5.14 gives the length response from the initial 30-foot impact corner on the rigid surface to the bottom of the drum. This length has a final value of about 38.75 inches.

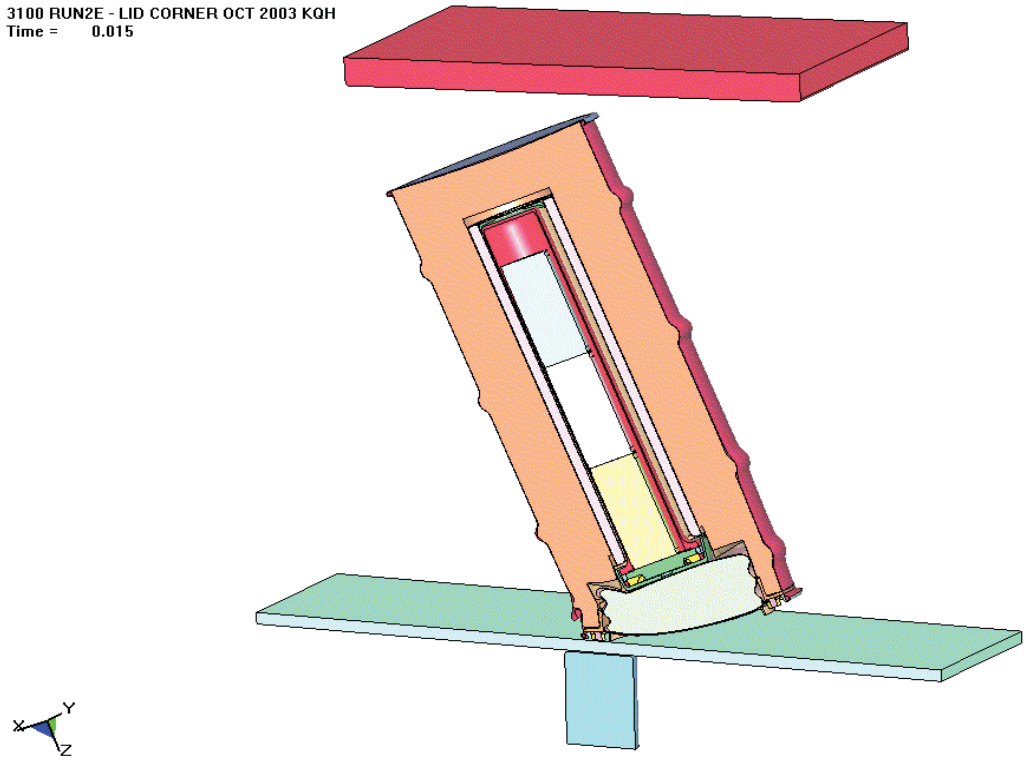

Figure 3.5.1 - Run2e, 30-Foot Impact, Final Configuration

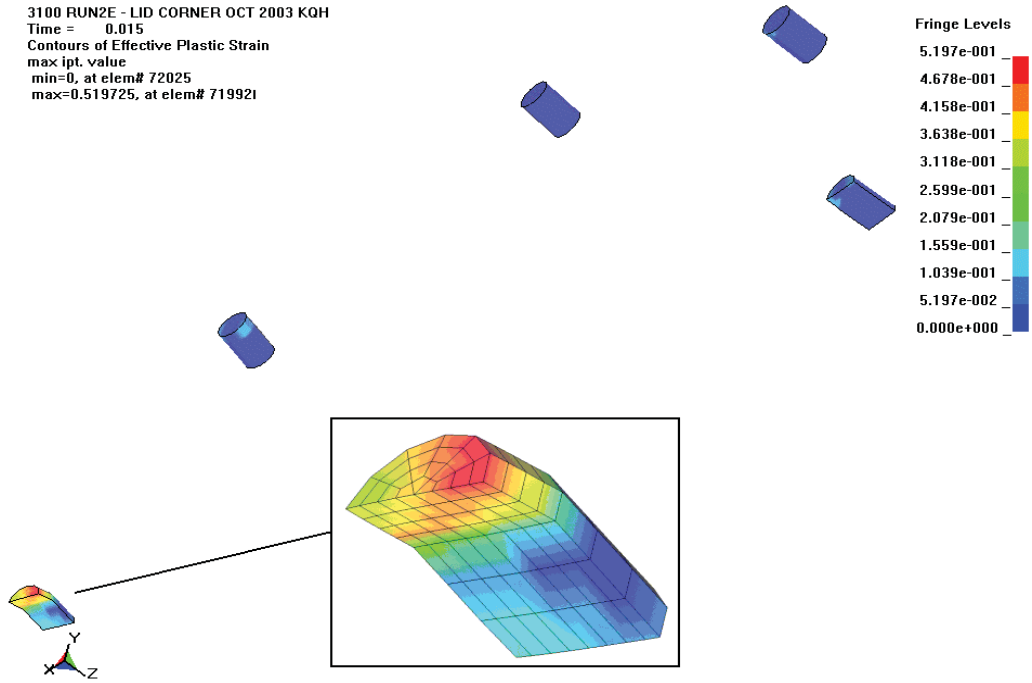

Figure 3.5.2 - Run2e, 30-Foot Impact, Effective Plastic Strain in the Drum Studs

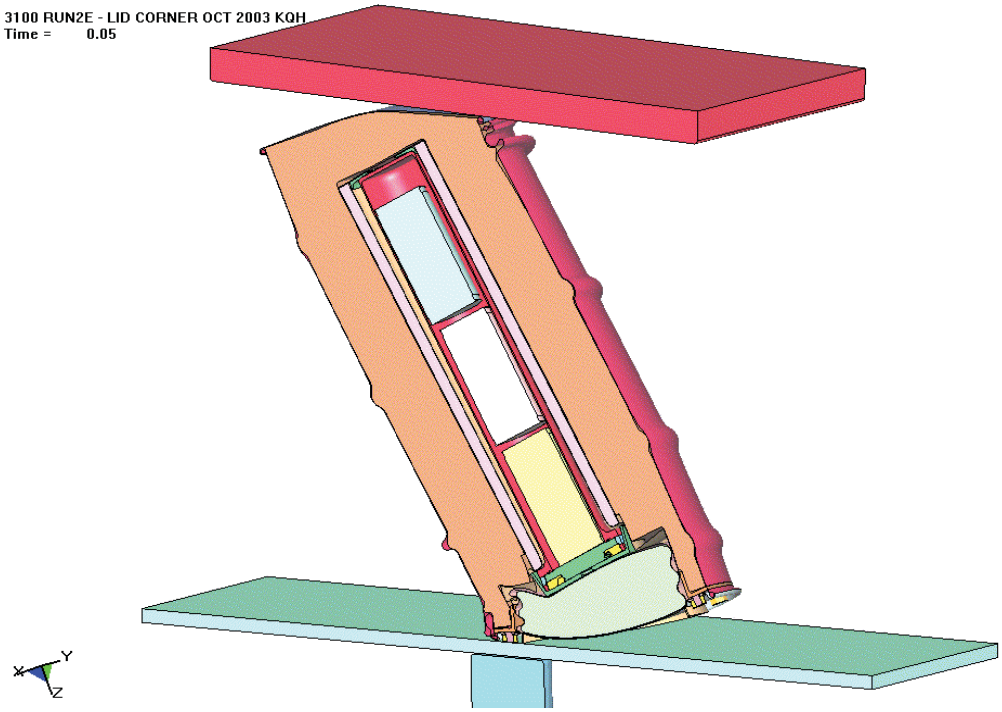

Figure 3.5.3 - Run2e, Crush Impact, Final Configuration

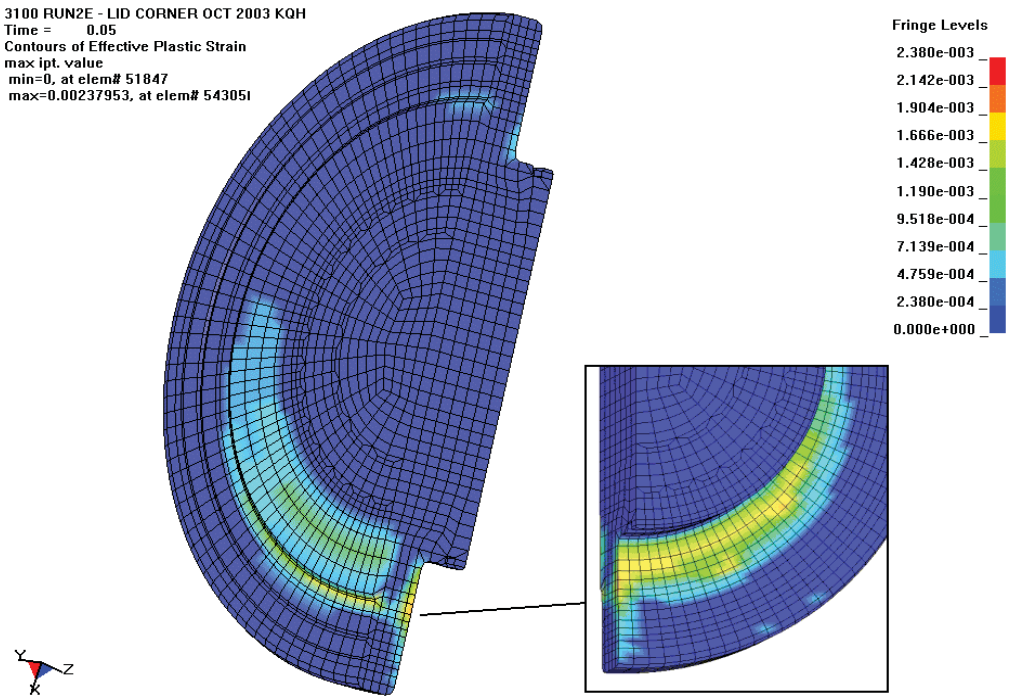

Figure 3.5.4 - Run2e, Crush Impact, Effective Plastic Strain in the CV Lid

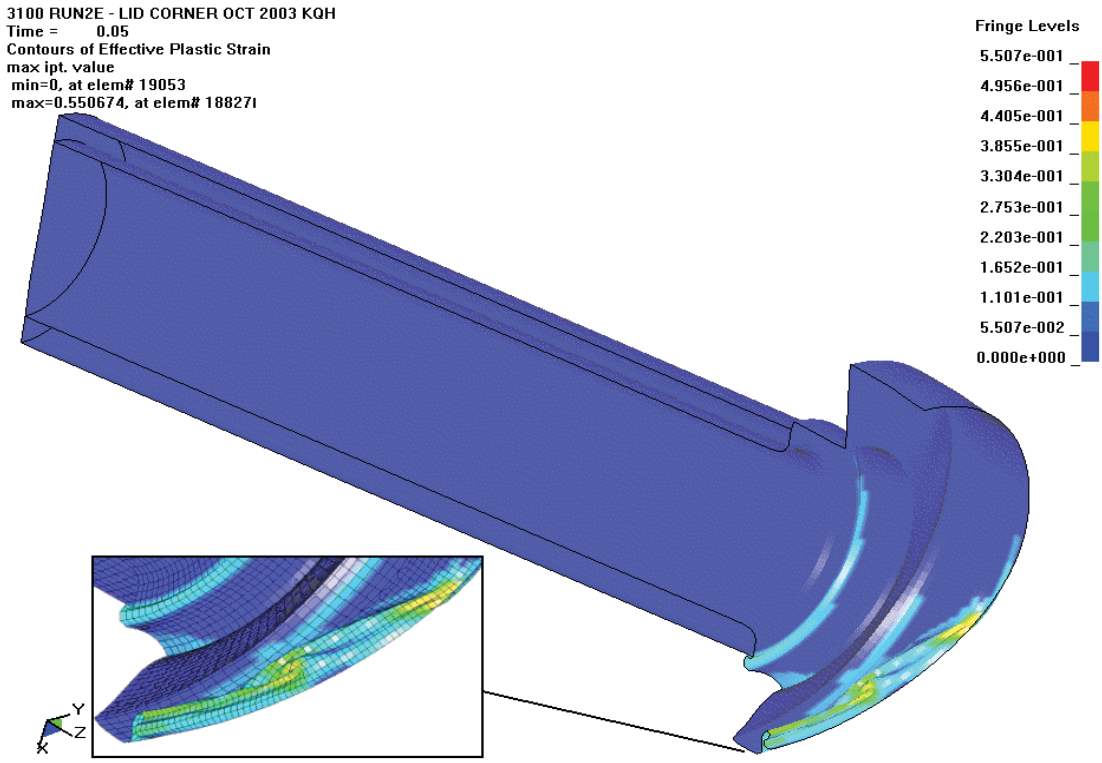

Figure 3.5.5 - Run2e, Crush Impact, Effective Plastic Strain in the Liner

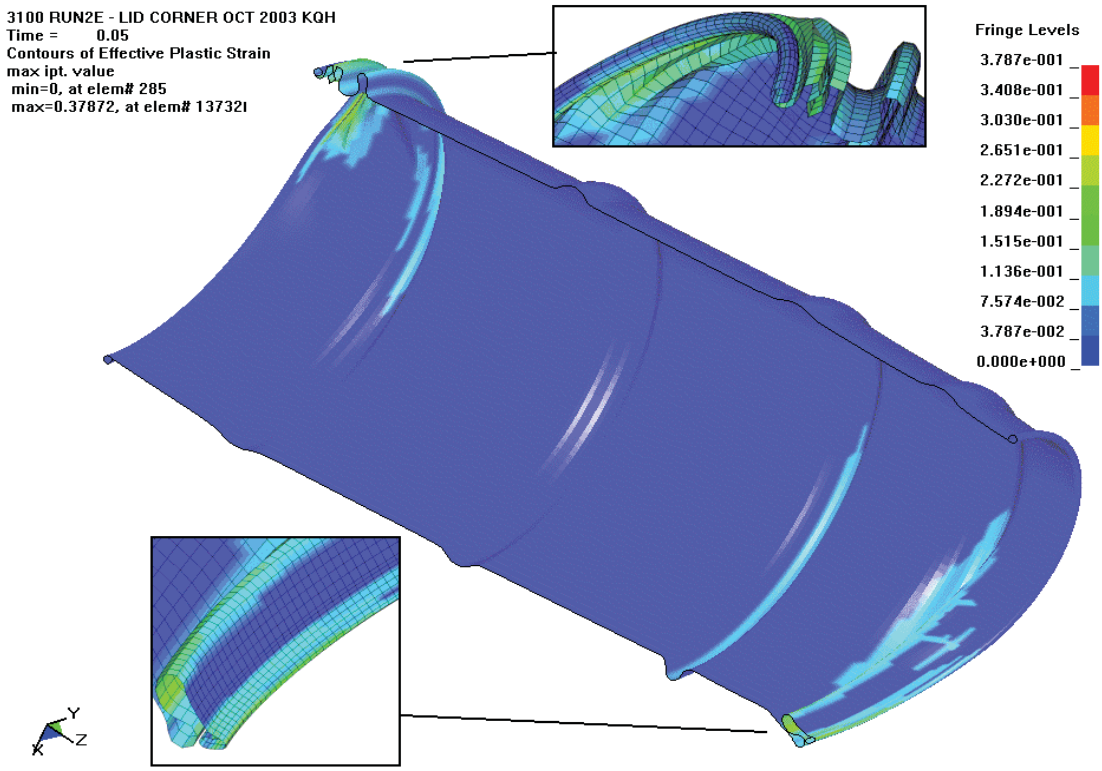

Figure 3.5.6 - Run2e, Crush Impact, Effective Plastic Strain in the Drum

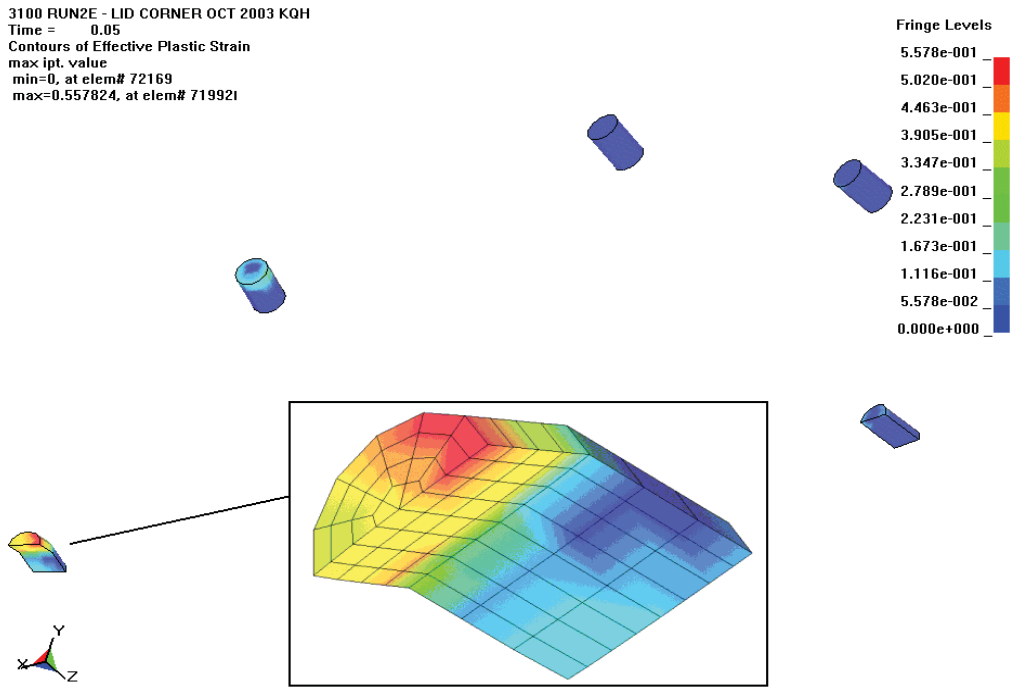

Figure 3.5.7 - Run2e, Crush Impact, Effective Plastic Strain in the Drum Studs

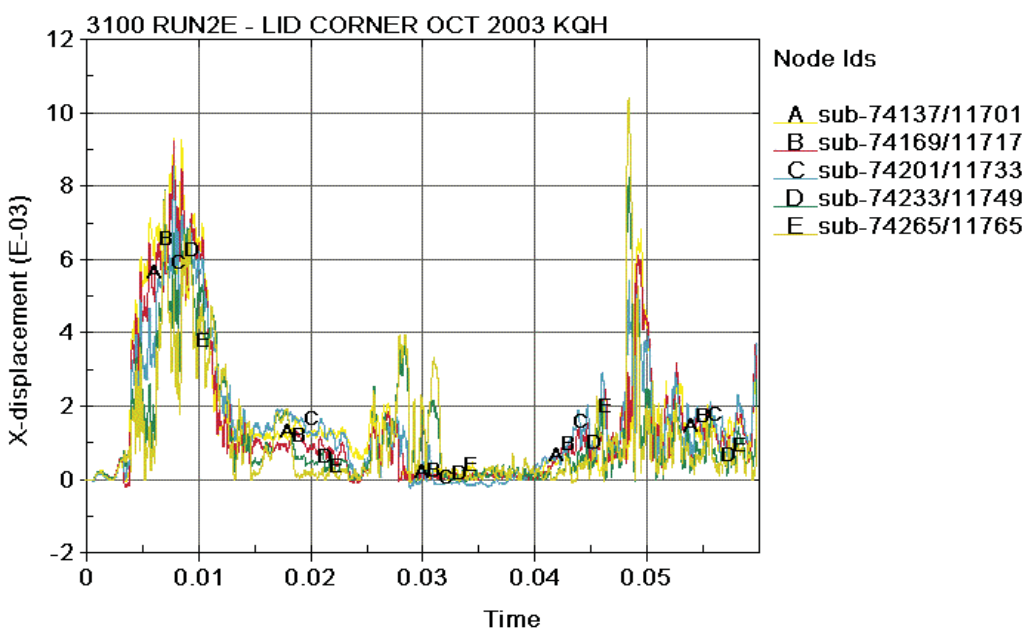

Figure 3.5.8 - Run2e, CV Lid/Body Separation Time History

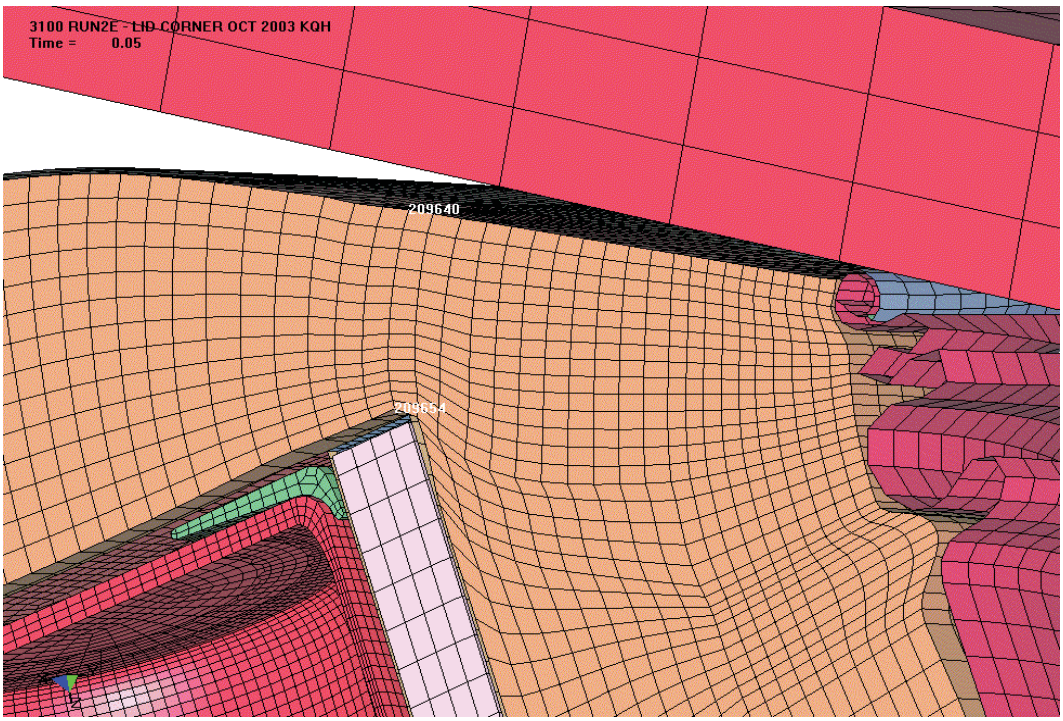

Figure 3.5.9 - Run2e, Location of Kaolite Nodes at the Bottom for Thickness Evaluation

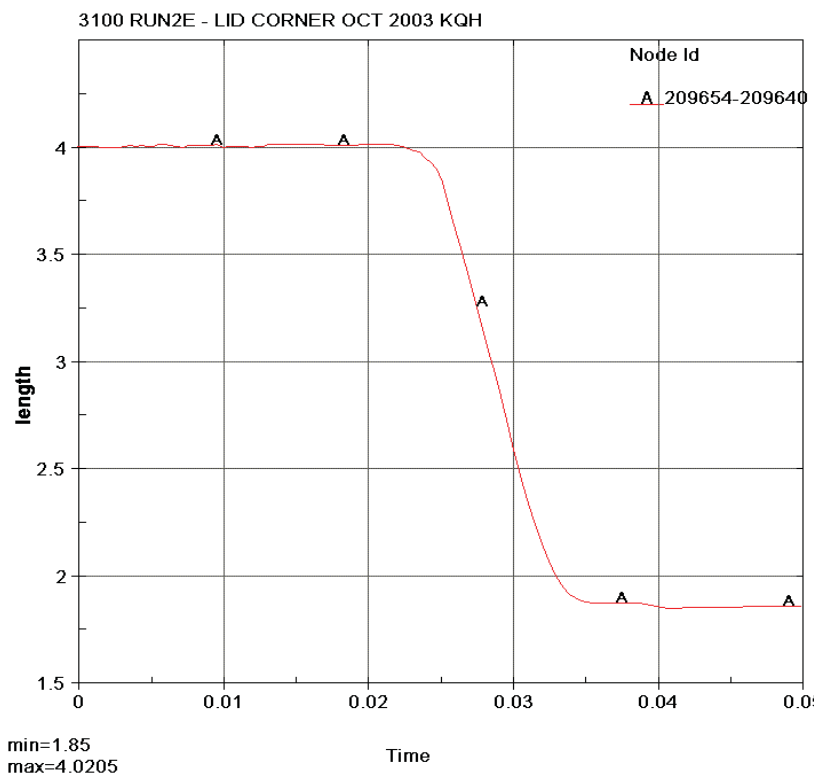

Figure 3.5.10 - Run2e, Minimum Thickness Time History for the Bottom Kaolite

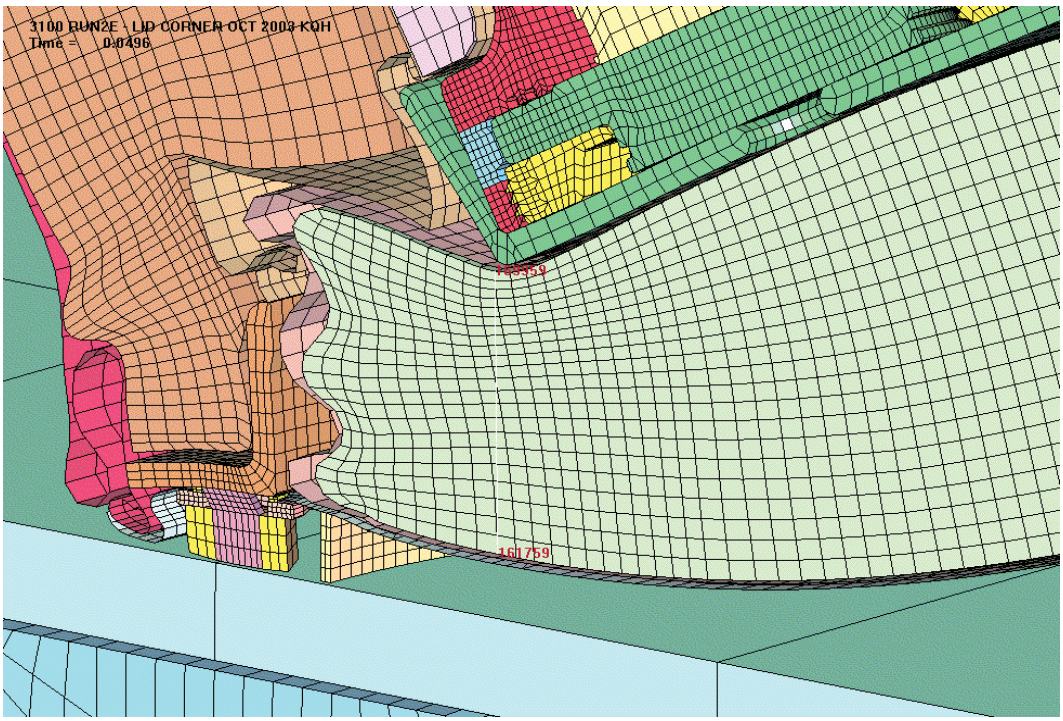

Figure 3.5.11 - Run2e, Location of Kaolite Nodes in the Plug for Thickness Evaluation

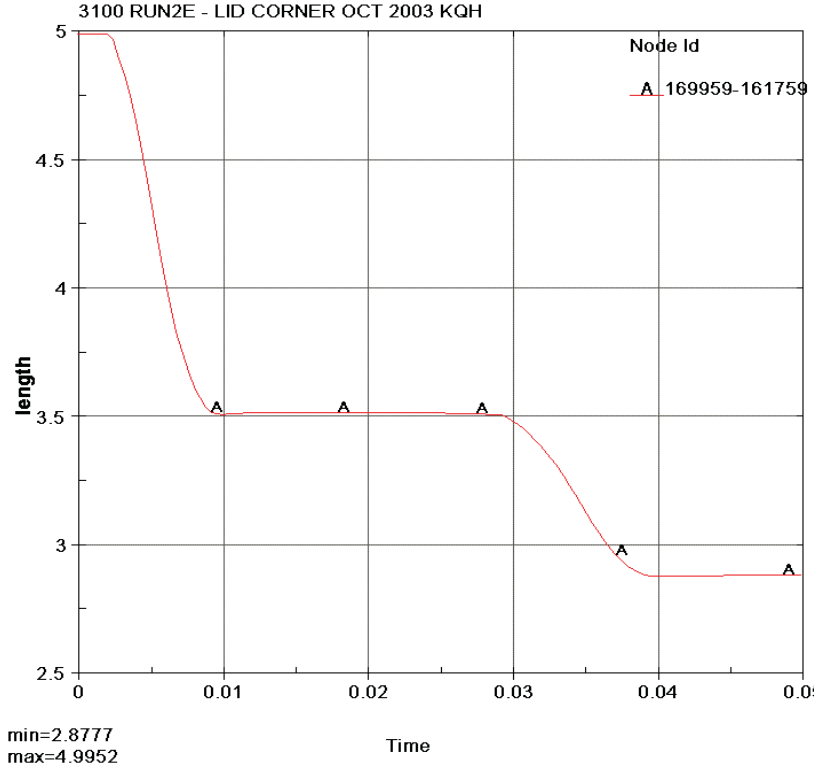

Figure 3.5.12 - Run2e, Minimum Thickness Time History for the Plug Kaolite

Figure 3.5.13 - Run2e, Length Dimensions in the Drum

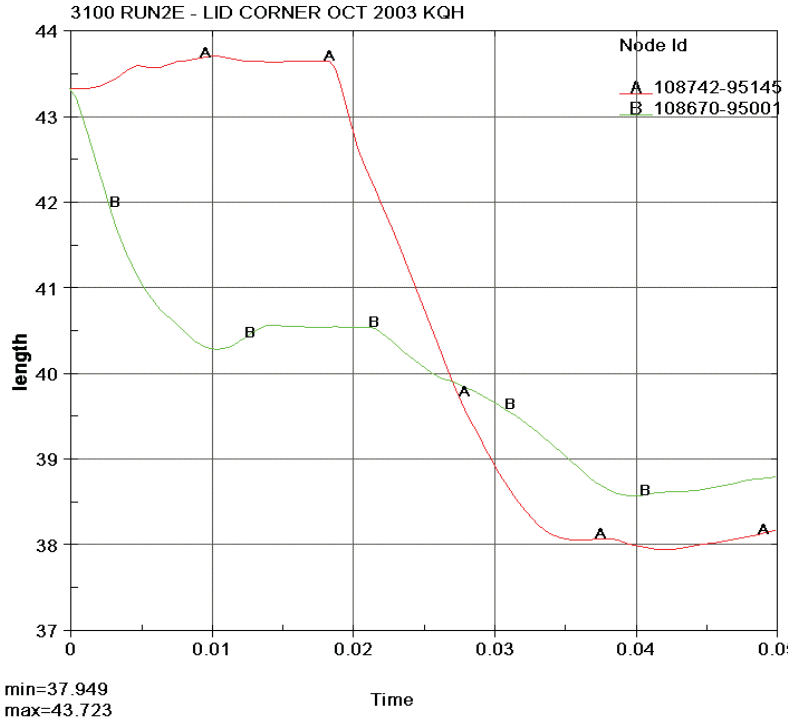

Figure 3.5.14 - Run2e, Time History of Length Dimensions in the Drum

3.6 Run3b - End

Run3b is a 30-foot lid end impact (time = 0 to 0.010 seconds) followed by a crush impact onto the package bottom (0.010 to 0.028 seconds). Figure 3.6.1 shows the final configuration for the 30-foot impact. Because of the relatively low demand placed on the components, no strain plots are presented for the 30-foot impact. Table 3.6.1 summarizes the maximum effective plastic strains in the package components.

Table 3.6.1 - Run3b, 30-Foot Impact, Effective Plastic Strain Levels in Some Components

Component	Effective Plastic Strain, in/in
CV Body	0.0012
CV Lid	0.0031
CV Nut Ring	0.0000
Angle	0.0287
Drum	0.0565
Drum Bottom Head	0.0024
Liner	0.1665
Lid	0.1094
Lid Stiffener	0.0068
Lid Studs	0.0962
Lid Stud Nuts	0.0162
Lid Stud Washers	0.0510
Plug Liner	0.0636

Figure 3.6.2 shows the final configuration for the 30-foot impact and the successive crush impact. Figure 3.6.3 shows that the maximum effective plastic strain in the CV body is 0.0053 in/in. The maximum occurs in the bearing of the body flange onto the lid (at the O-ring seals). The magnitude of effective plastic strain is questioned due to the fact that the elevated strains occur at single nodes and are not symmetric (see the insert in Figure 3.6.3). The maximum effective plastic strain in the bottom region of the CV body is found to be 0.0035 in/in and does exhibit a symmetric characteristic as is shown in Figure 3.6.3.

The CV lid effective plastic strain fringes are shown from both sides in a split image in Figure 3.6.4. The maximum effective plastic strain in the lid is shown to be 0.0034 in/in in the figure. The other components are summarized in Table 3.6.2.

Table 3.6.2 - Run3b, Crush Impact, Effective Plastic Strain Levels in Some Components

Component	Effective Plastic Strain, in/in
CV Nut Ring	0.0000
Angle	0.0304
Drum	0.1258
Drum Bottom Head	0.0312
Liner	0.3585
Lid	0.1415
Lid Stiffener	0.0098
Lid Studs	0.1541
Lid Stud Nuts	0.0170
Lid Stud Washers	0.0510
Plug Liner	0.0944

The CV lid separation time history is shown in Figure 3.6.5. The response during the 30-foot impact is a spike separation of about 0.012 inches, which relaxes to a maximum value of 0.003 inches for the remainder of the 30-foot impact. During the crush impact it is seen that separation is spikes to a maximum of about 0.004 inches, but the average remains at about 0.002 inches or less at the end of the impact.

Figure 3.6.6 shows the nodes chosen to obtain the drum height and kaolite thickness time history data. Figure 3.6.7 shows the drum height time history. From the figure it is seen that the overall height would be approximately 39 inches. Figure 3.6.8 shows the thickness time histories in the kaolite for the plug and the bottom. The curve A in the figure is for the bottom kaolite thickness, and it reaches about 2.2 inches as a final value. Curve B, is for the plug and it reaches about 3.4 inches for the final kaolite thickness.

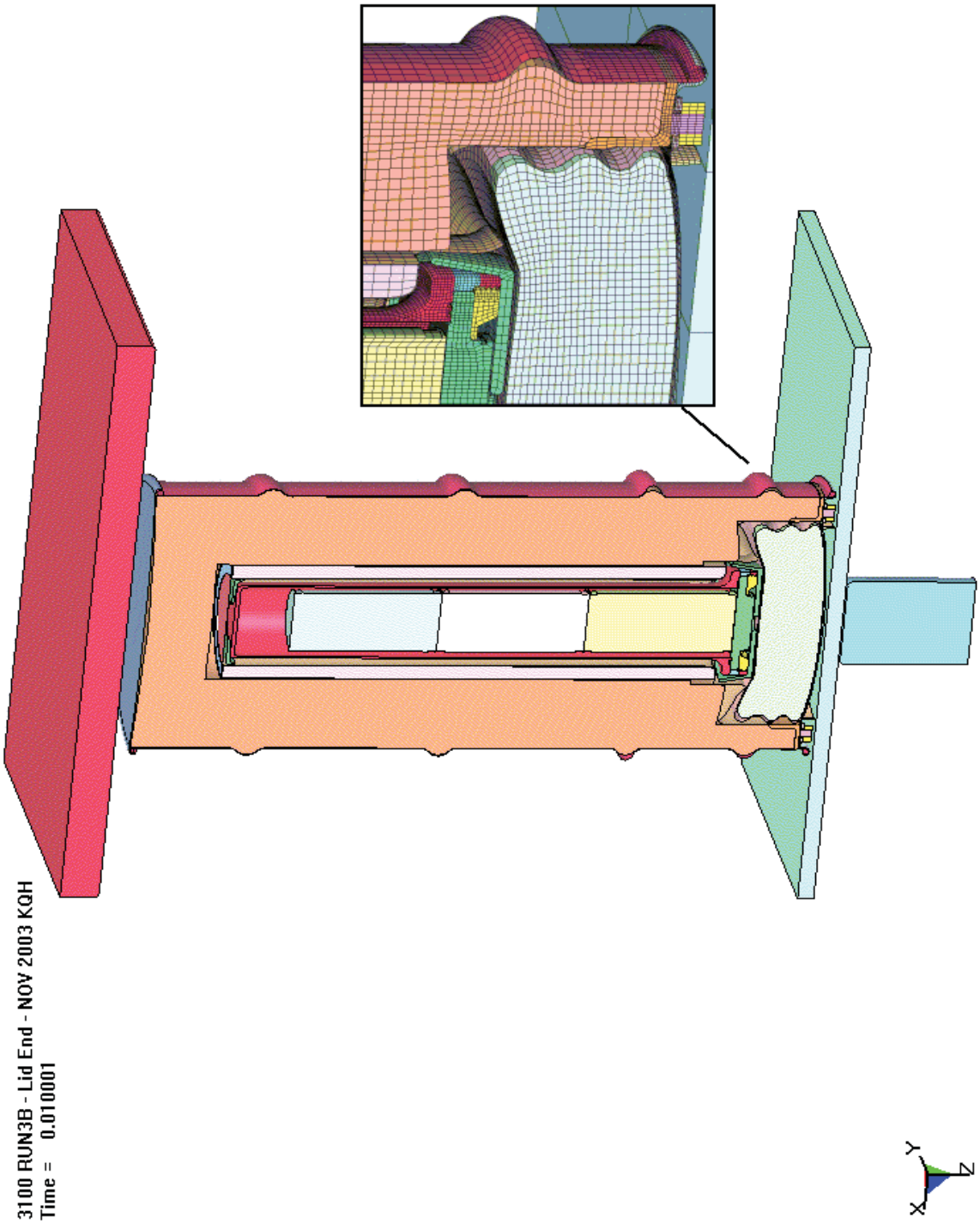

Figure 3.6.1 - Run3b, Configuration After the 30-Foot Impact

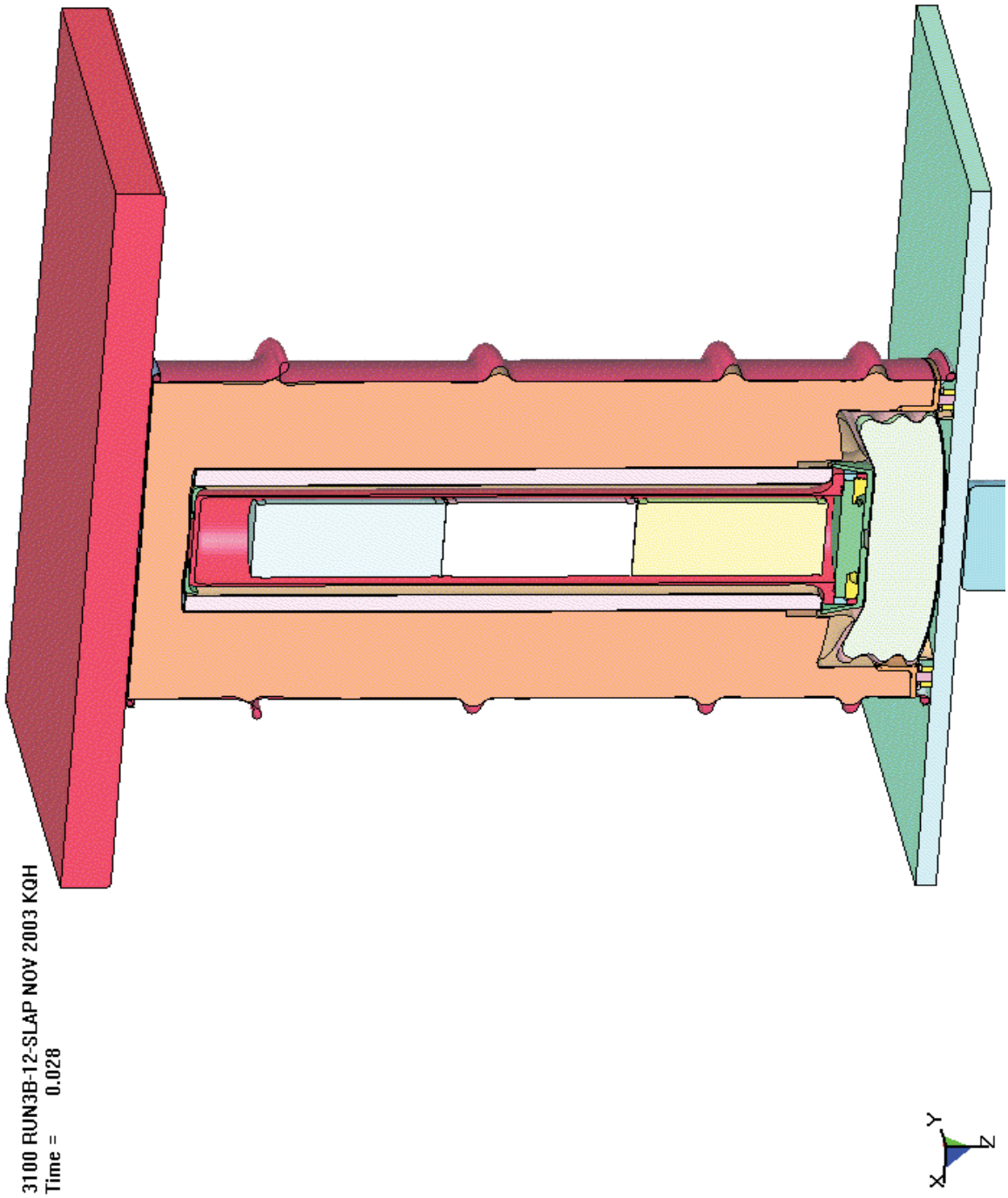

Figure 3.6.2 - Run3b, Crush Impact, Final Configuration

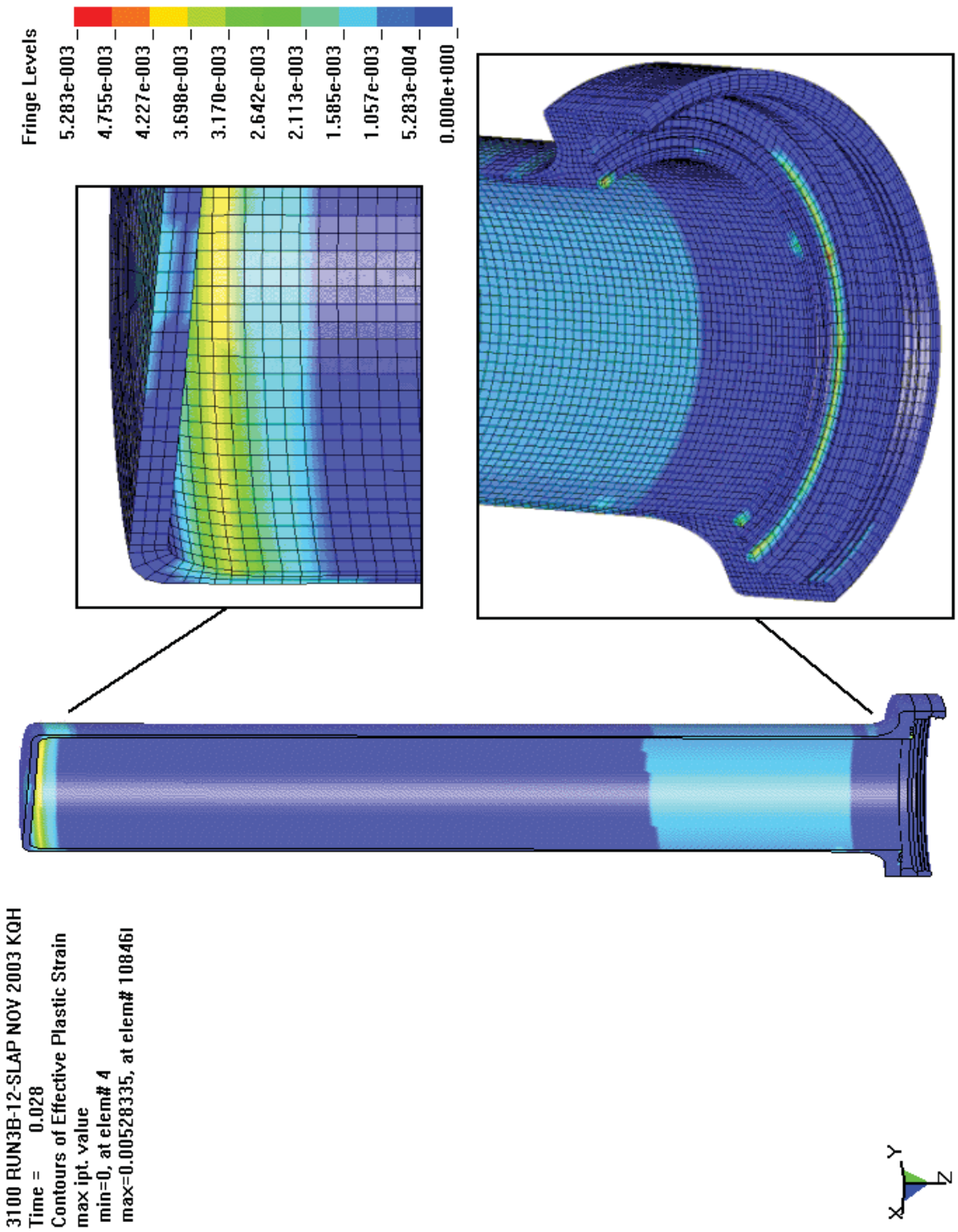

Figure 3.6.3 - Run3b, Crush Impact, Effective Plastic Strain in the CV Body

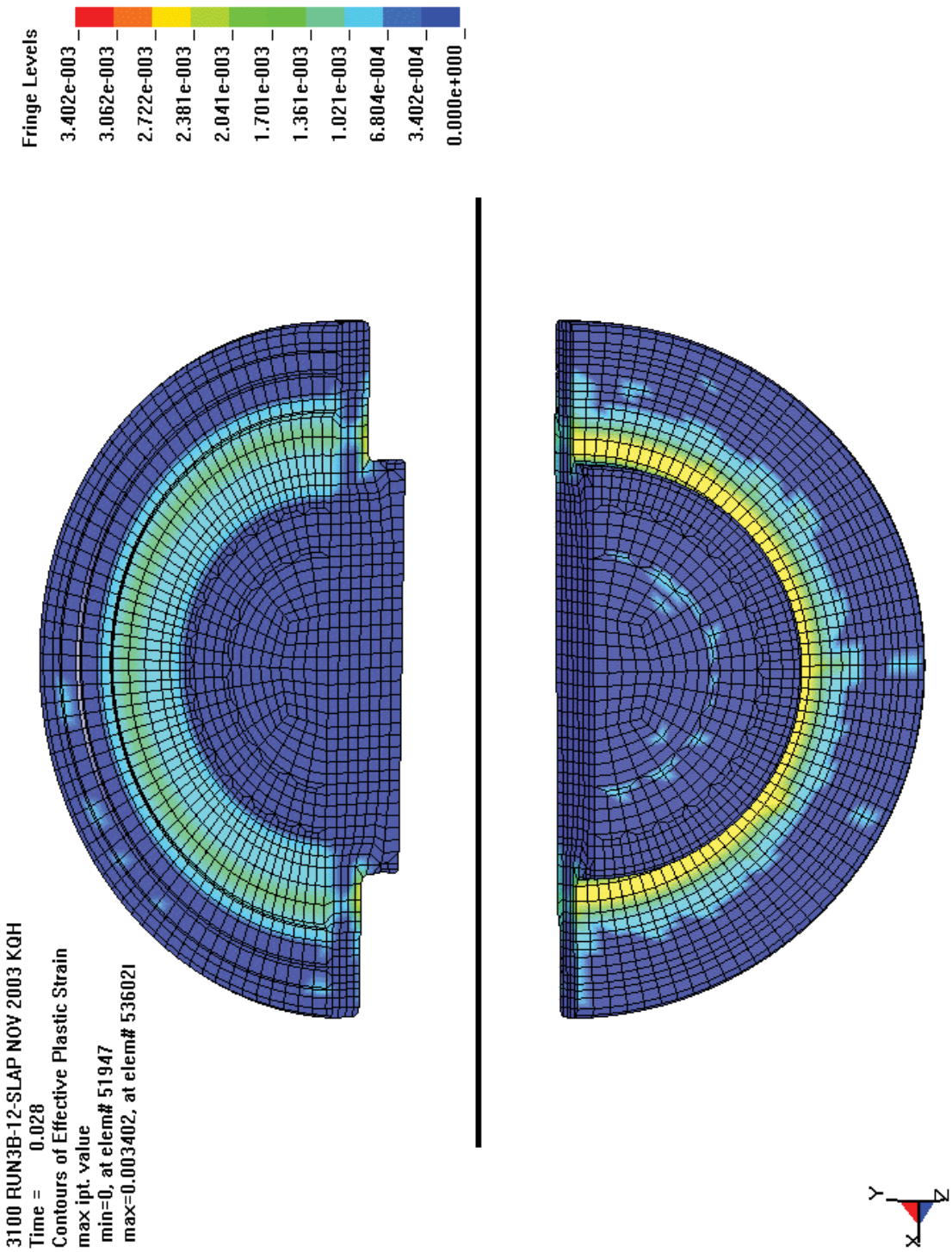

Figure 3.6.4 - Run3b, Crush Impact, Effective Plastic Strain in the CV Lid

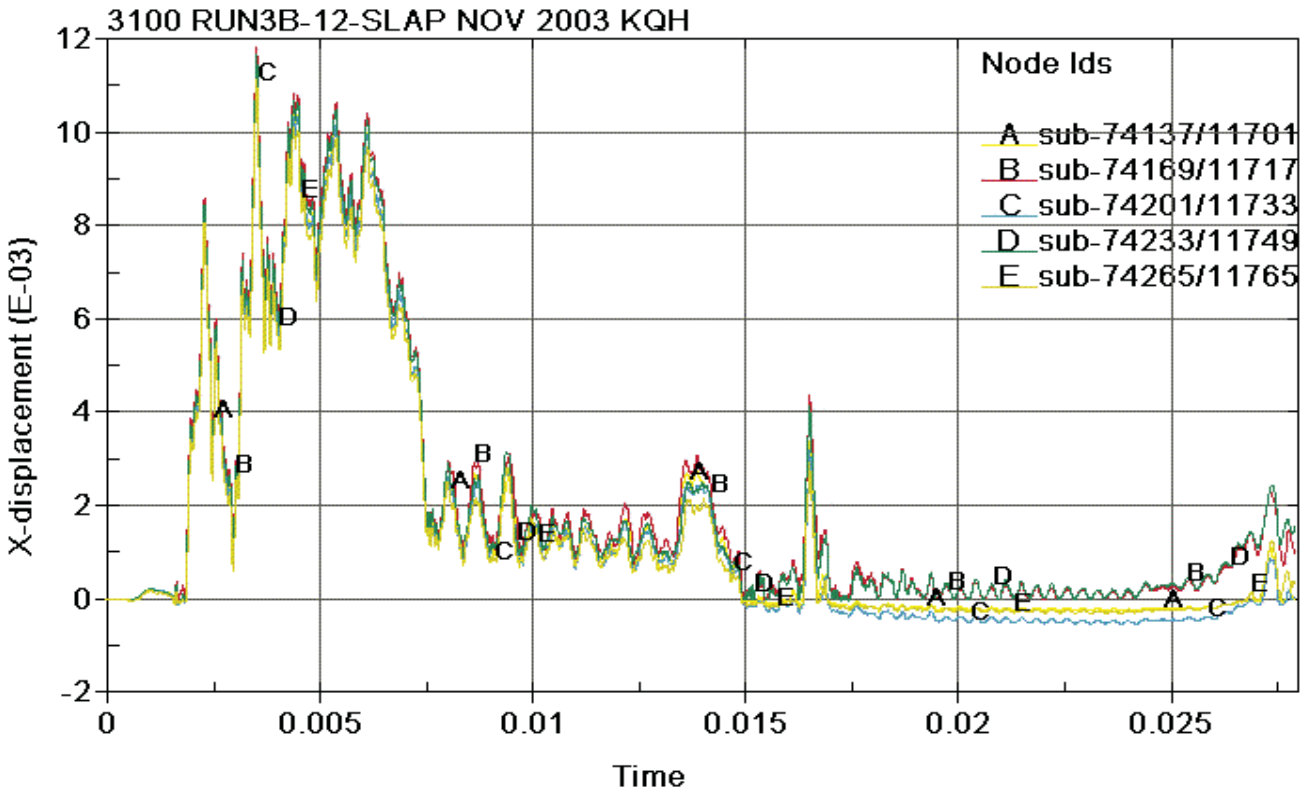

Figure 3.6.5 - Run3b, CV Lid Separation Time History

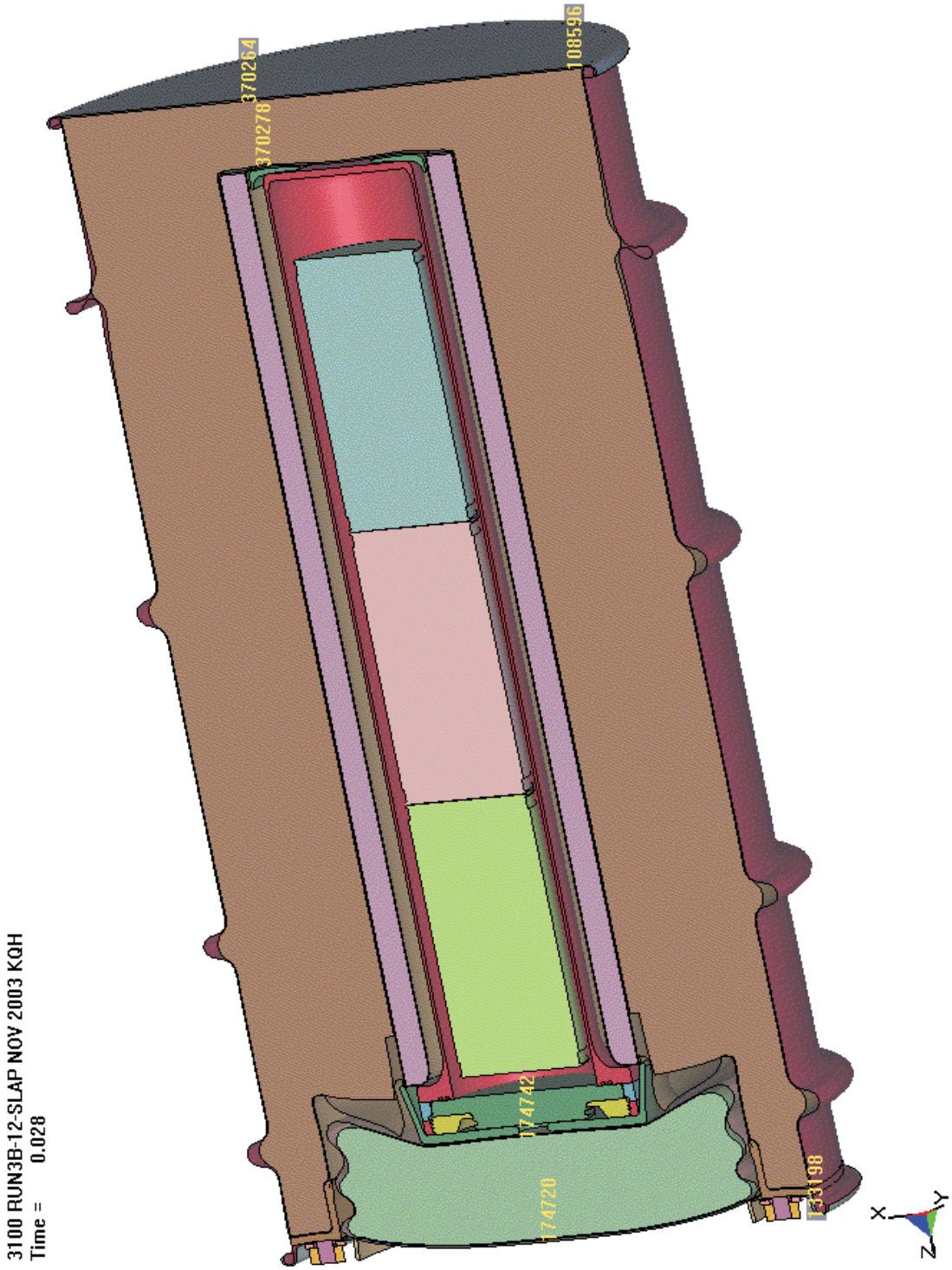

Figure 3.6.6 - Run3b, Nodes Chosen for Displacement Time Histories

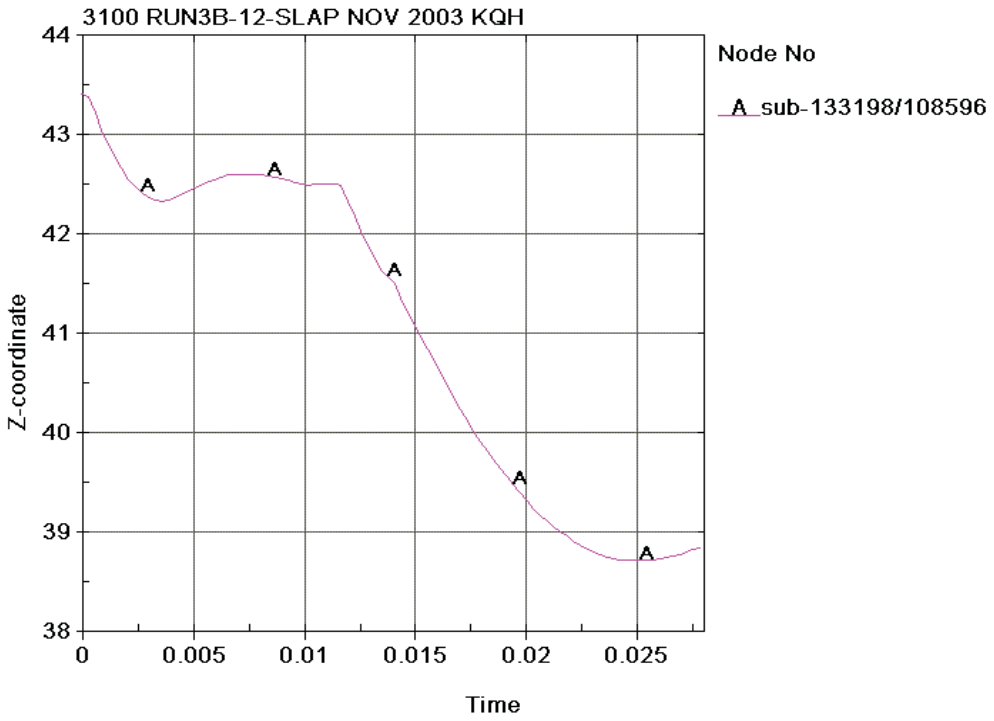

Figure 3.6.7 - Run3b, Drum Height Time History

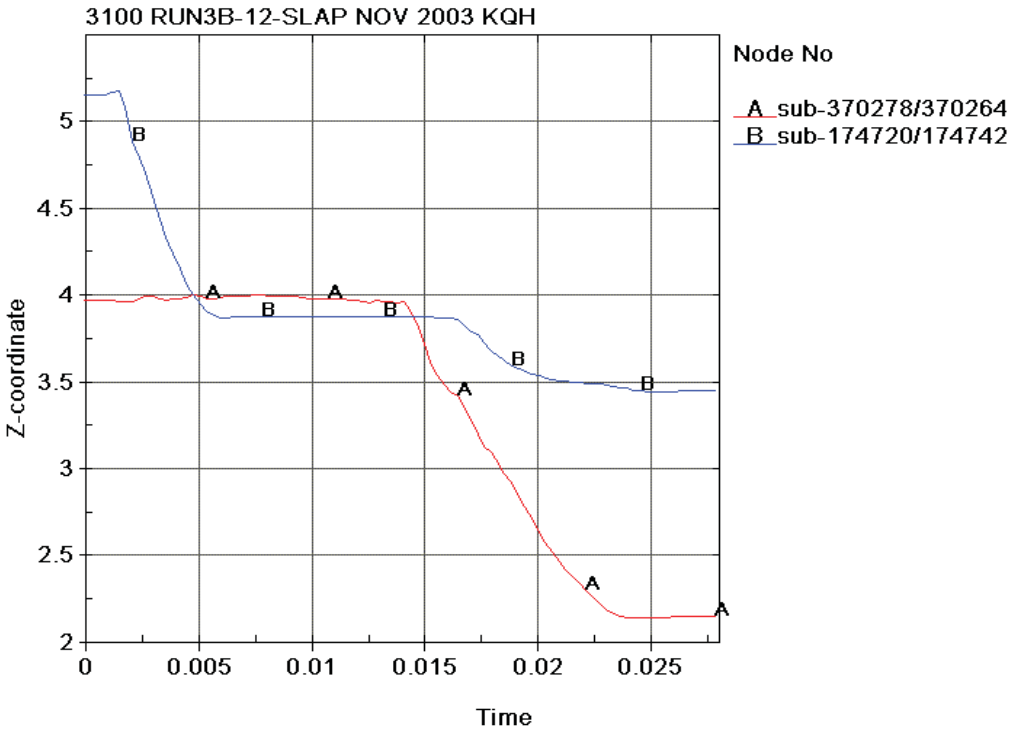

Figure 3.6.8 - Run3b, Kaolite Thickness Time History

3.7 Run4g - Slapdown

Run4g is a 12° slapdown, 30-foot impact (time 0 to 0.02 seconds) followed by a crush with the crush plate CG over the CV flange (0.02 to 0.04 seconds). A drum stud is located on the line of impact (0°) in this model.

The deflected shape of the package after the 30-foot impact is shown in Figure 3.7.1. The maximum effective plastic strain in the CV body for the 30-foot impact is 0.0445 in/in as shown in Figure 3.7.2 and occurs near the bottom head. The maximum effective plastic strain in other components for the 30-foot impact are listed in Table 3.7.1.

Table 3.7.1 - Run4g, 30-Foot Impact, Effective Plastic Strain Levels in Some Components

Component	Effective Plastic Strain, in/in
CV Lid	0.0003
CV Nut Ring	0.0000
Angle	0.0881
Drum	0.3017
Drum Bottom Head	0.2877
Liner	0.1234
Lid	0.5537
Lid Stiffener	0.0232
Lid Studs	0.1737
Lid Stud Nuts	0.0000
Lid Stud Washers	0.0597
Plug Liner	0.1290

Figure 3.7.3 shows the final configuration for the crush impact for run4g. The maximum effective plastic strain in the CV body is 0.0457 in/in as shown in Figure 3.7.4. The maximum effective plastic strain in the drum lid is 1.0797 in/in (surface strain) as shown in Figure 3.7.5. The maximum occurs near the stud at 90°, or initially along the Y axis. This high strain is caused by lid/stud reacting the ovalization response of the package due to the crush plate impact. The fringe range has been set such that the strain levels above 0.57 in/in are colored in red in Figure 3.7.5. The maximum membrane strain in the lid at

the same location (as the surface strain) is 0.8920 in/in. The region of elevated strain is localized to the hole at 90°, therefore any tearing of the lid would be localized. The large washers would restrain the lid.

Figure 3.7.6 shows the effective plastic strain in the drum studs. At the time shown the stud at the 90° position has failed (evident by removed element row at the base of the stud). All of the elements on the cross section reached the prescribed failure strain of 0.57 in/in and were deleted by LS-Dyna during the impact. Only one stud, the one at 90°, was shown to reach elevated strain levels and be severed for the crush impact. The plastic-kinematic model used for the studs allows a failure value to be used (0.57 in/in). The stud elements reach failure and elements begin to be deleted at about solution time = 0.0312 seconds. By 0.0332 seconds, all the elements on the cross section have been deleted by LS-Dyna.

The lid uses a power law model, which does not allow material failure in the model. Investigation shows that the lid reaches 0.57 in/in at about 0.0272 seconds, a time at which the stud maximum strain is about 0.28 in/in. This demonstrates that the lid reaches failure levels before the stud and at that time, the stud effective plastic strain is relatively low. Therefore, it would be expected that the lid would tear before the stud reaches failure. Due to the extent of the effective plastic strain fringe patterns in the lid plus the conservative modeling of the stud due to lid shear (Section 2.1 discussion), it is believed that the tearing would be local and that the lid (and by default the plug) would be restrained by the large washers. Table 3.7.2 shows the maximum effective plastic strain in the remainder of the package components for the crush impact.

Table 3.7.2 - Run4g, Crush Impact, Effective Plastic Strain Levels in Some Components

Component	Effective Plastic Strain, in/in
CV Body	0.0457
CV Lid	0.0005
CV Nut Ring	0.0000
Angle	0.1045
Drum	0.3972
Drum Bottom Head	0.2877
Liner	0.2702
Lid Stiffener	0.0838
Lid Stud Nuts	0.0086
Lid Stud Washers	0.1003
Plug Liner	0.2715

Figure 3.7.7 shows the lid separation time history for the nodal pairs shown in Figure 3.1.30. There are several spikes up to about 0.007 inches evident in the lid separation time history. However, most of the noise level is about 0.004 inches or less and is oscillatory in nature. Therefore, an average of 0.002 inches or less would be expected.

Figure 3.7.8 shows the drum diameter deformation in the X-direction. The nodes are those defined in Figure 3.1.34. Curve A in the figure shows that the final distance in at the lid, between the two flattened regions is about 13.5 inches. Figure 3.7.9 gives the radial deformation time history in the Y-direction.

Figure 3.7.10 gives the kaolite thickness time histories. The nodes are those defined in Figure 3.1.32.

Figure 3.7.11 shows the liner diameter time history at various locations along its length. Figure 3.1.37 and Table 3.1.3 show the locations of the nodal pairs along the liner.

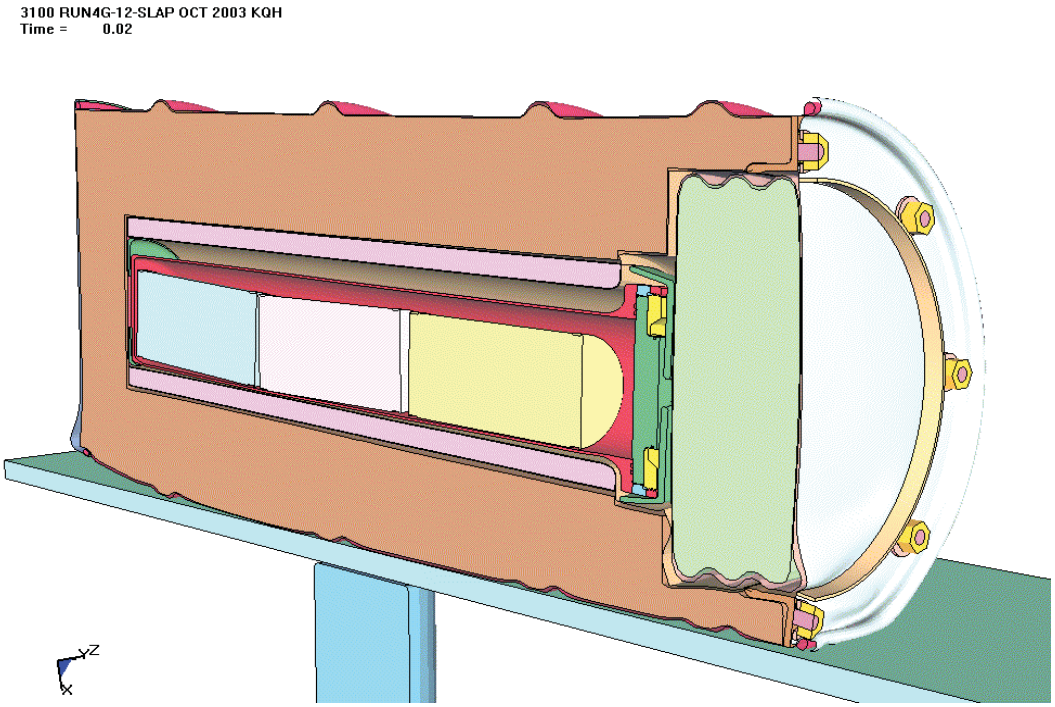

Figure 3.7.1 - Run4g, Slapdown Impact, Final Configuration

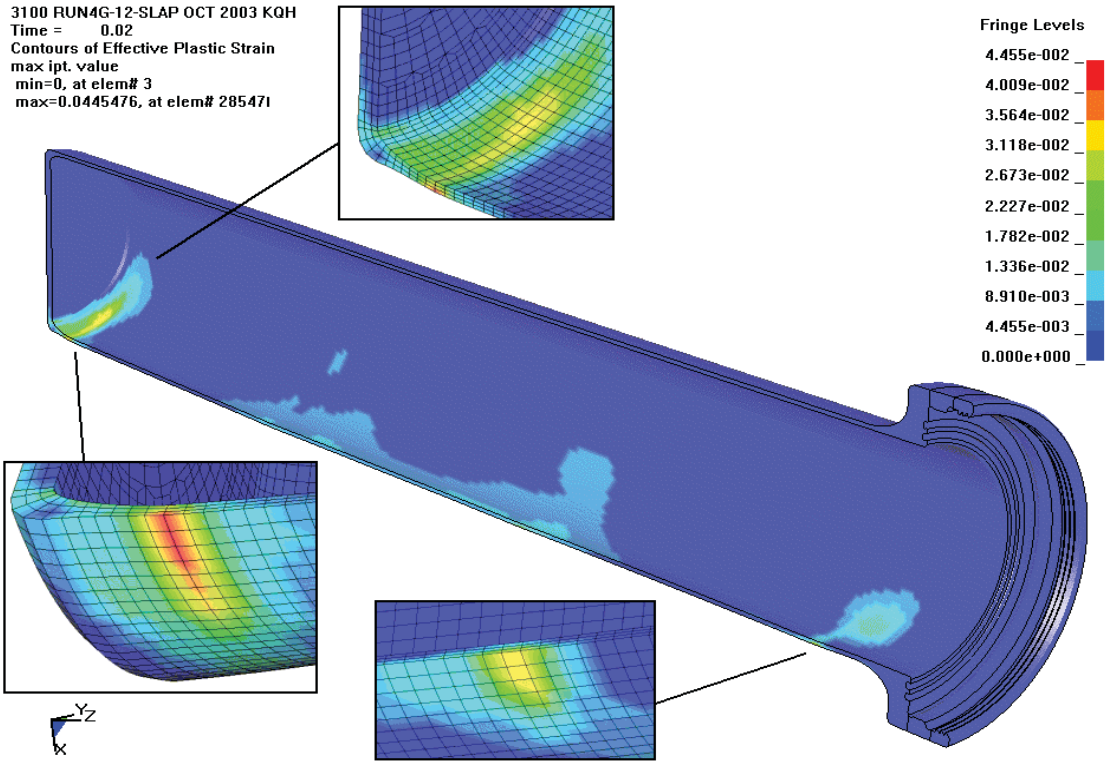

Figure 3.7.2 - Run4g, Slapdown Impact, Effective Plastic Strain in the CV Body

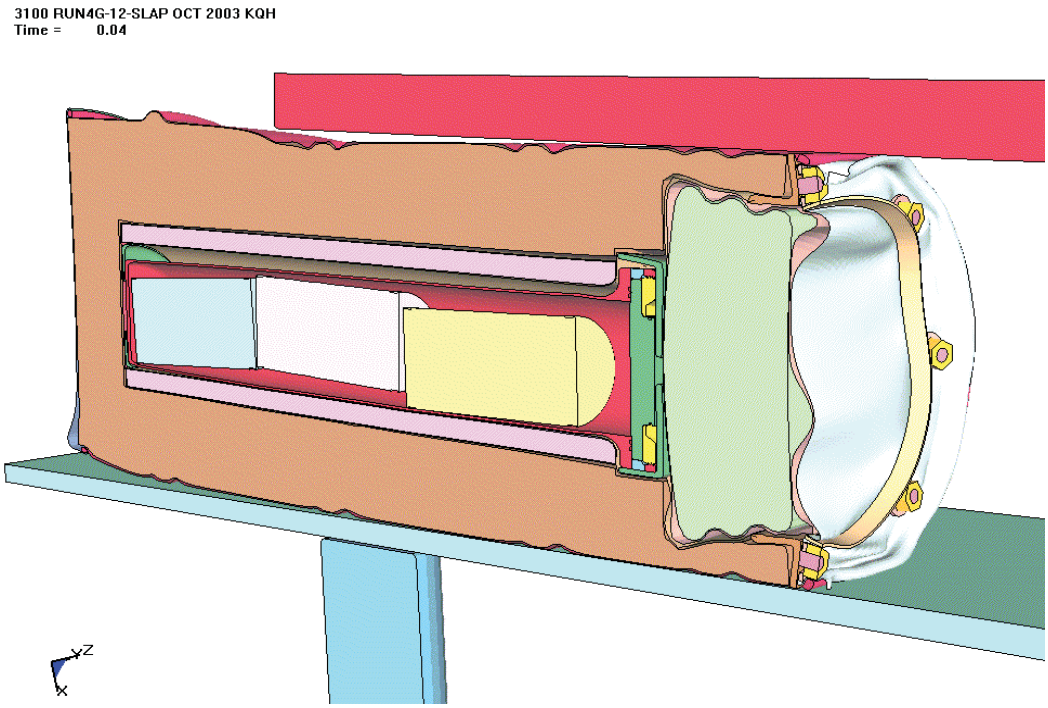

Figure 3.7.3 - Run4g, Crush Impact, Final Configuration

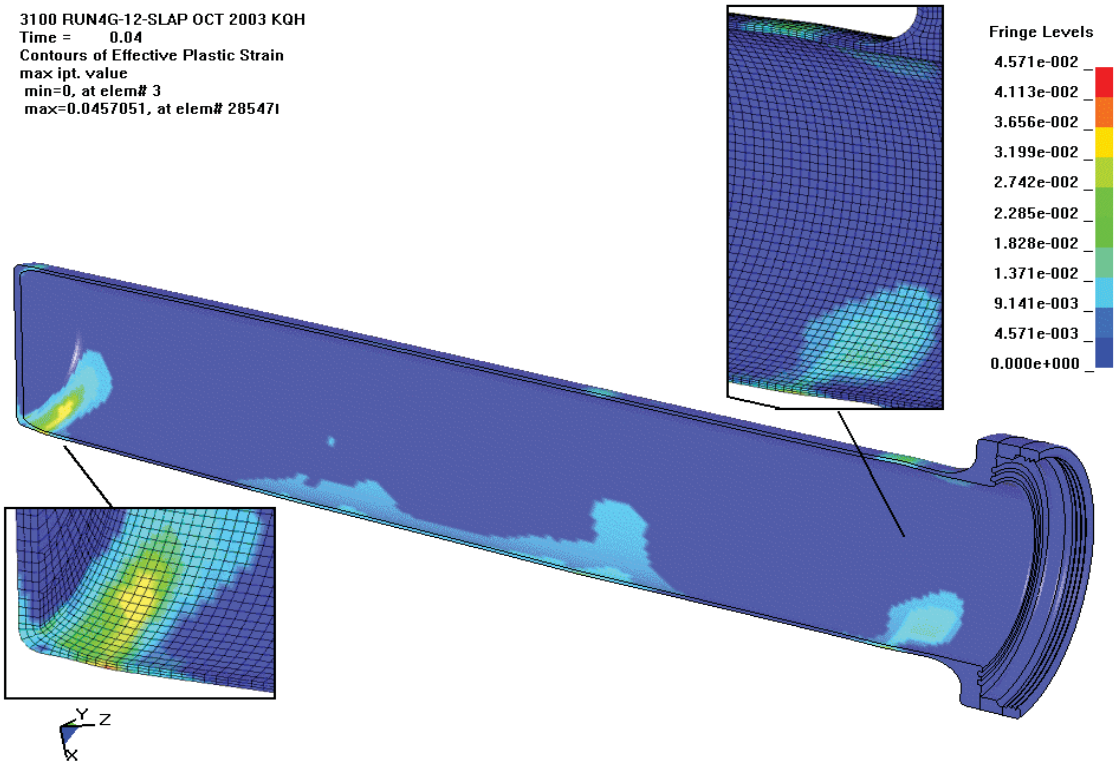

Figure 3.7.4 - Run4g, Crush Impact, Effective Plastic Strain in the CV Body

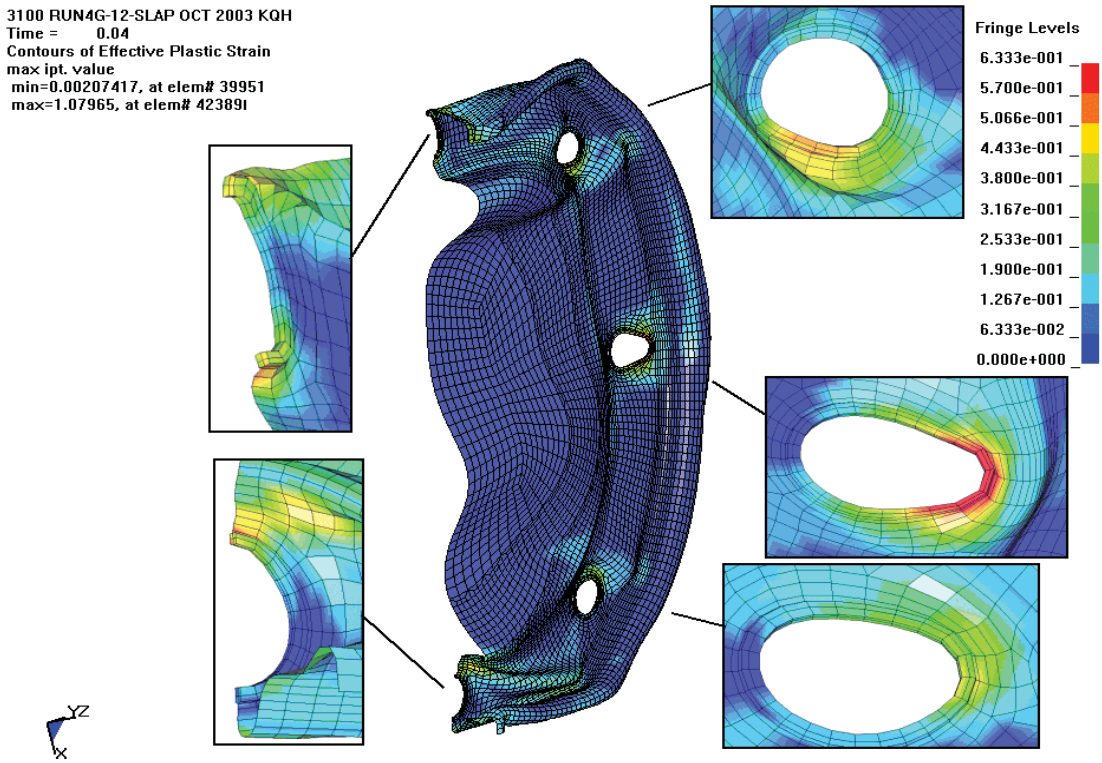

Figure 3.7.5 - Run4g, Crush Impact, Effective Plastic Strain in the Lid

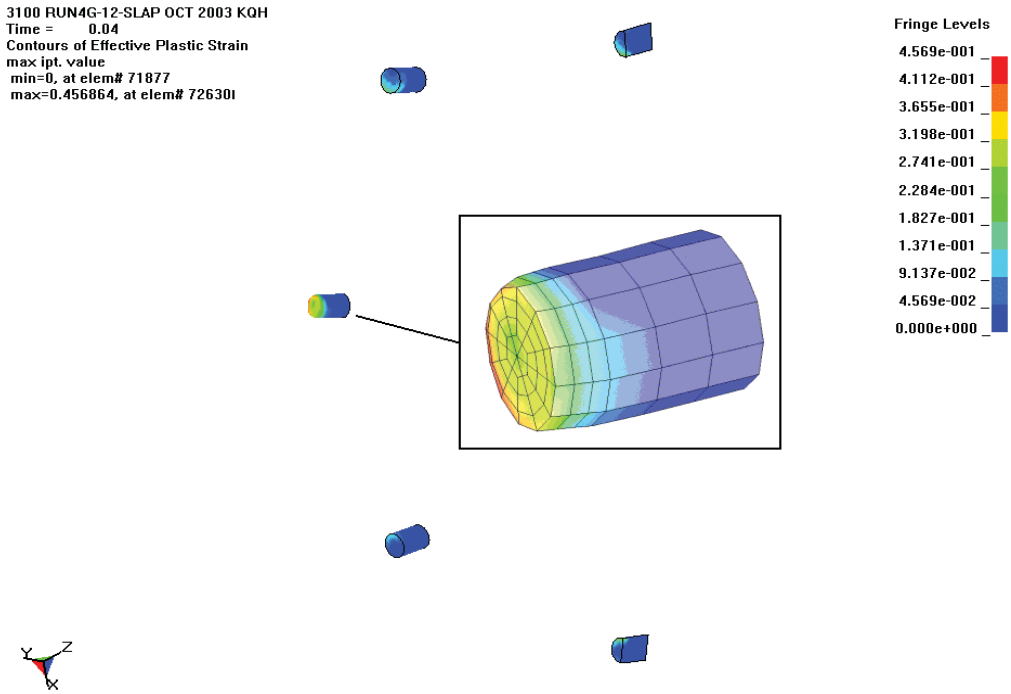

Figure 3.7.6 - Run4g, Crush Impact, Effective Plastic Strain in the Drum Studs

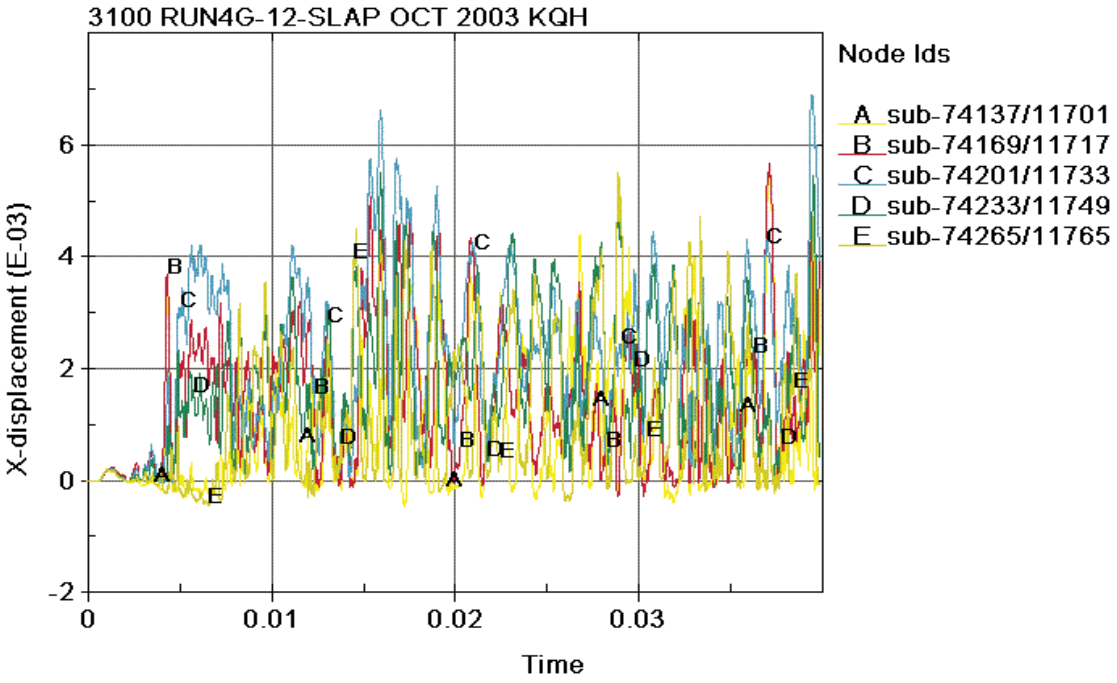

Figure 3.7.7 - Run4g, Lid Separation Time History

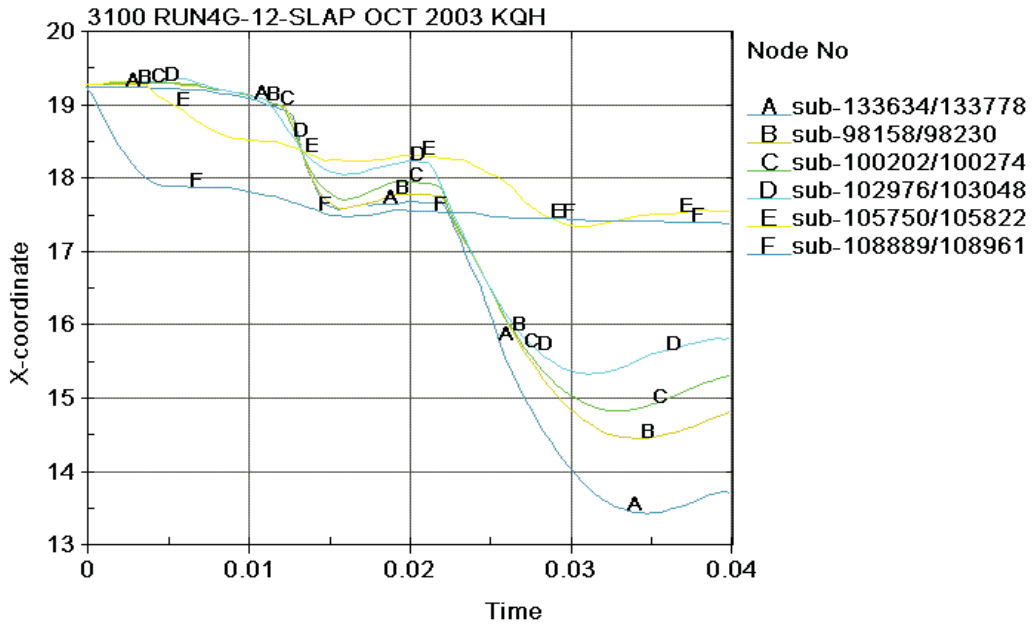

Figure 3.7.8 - Run4g, Drum Deformation in the Direction of the Impacts

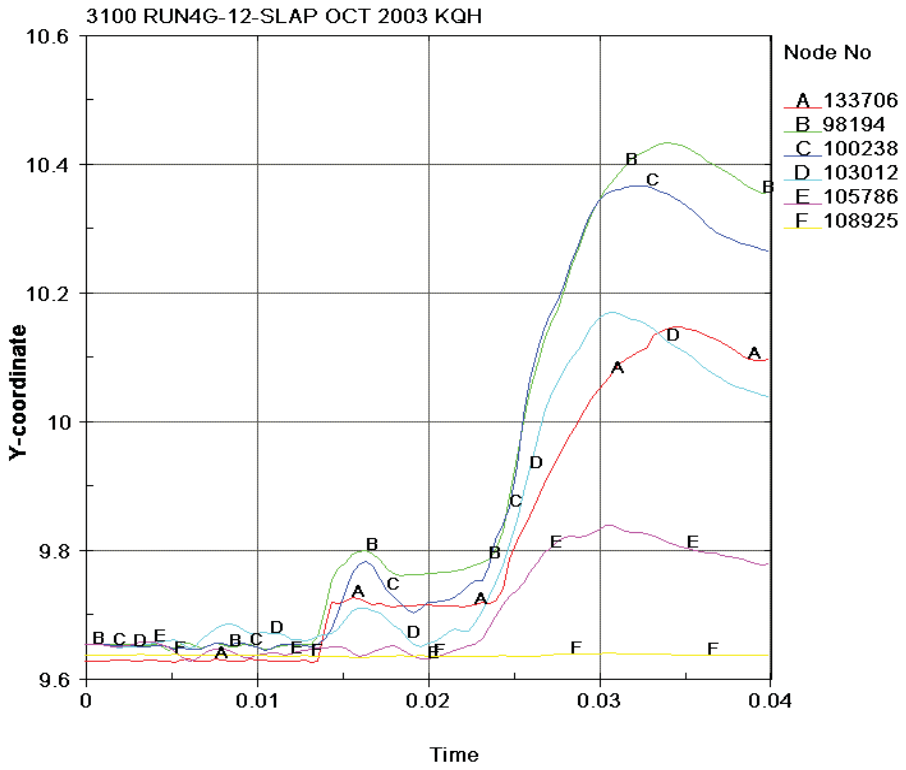

Figure 3.7.9 - Run4g, Drum Deformation Normal to the Impacts

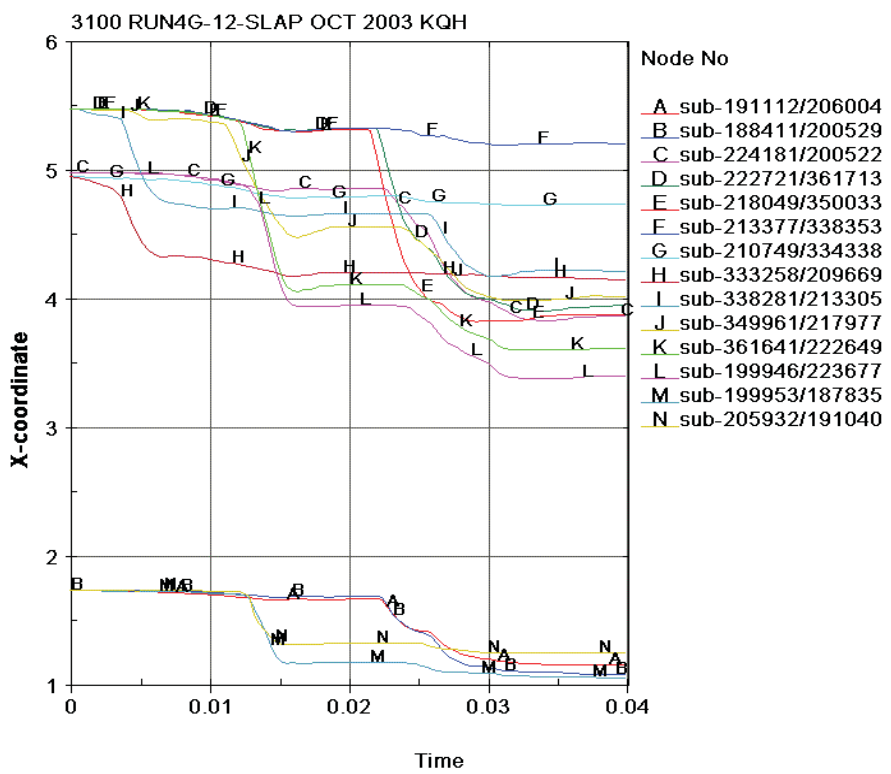

Figure 3.7.10 - Run4g, Kaolite Thickness Time Histories for the Impacts

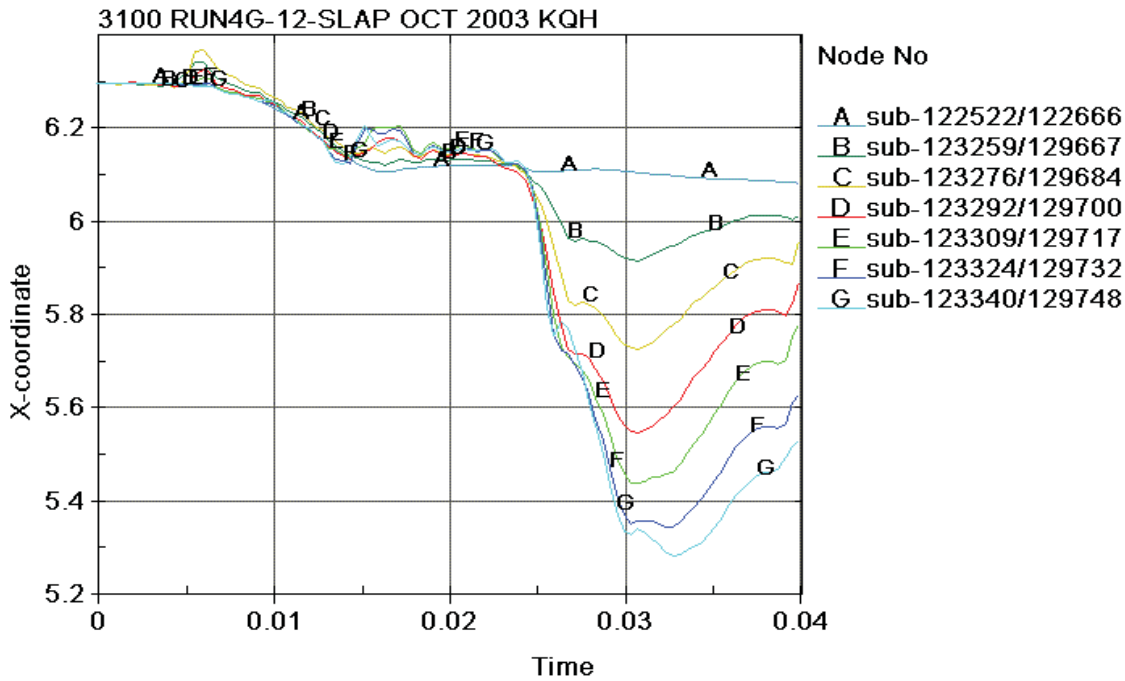

Figure 3.7.11 - Run4g, Liner Diameter Time History

3.8 Run4ga - Slapdown

Run4ga is a 30-foot, 12° slapdown impact (time - 0 to 0.02 seconds) followed by a crush impact with the crush plate centered on the drum (0.0201 to 0.04 seconds). The run4g 30-foot impact restart file was taken and the crush plate was moved by specifying nodal velocities so that it was centered on the drum. The translation occurred from time 0.02 to 0.0201 sec. Once the crush plate was centered, the run was halted and the crush impact was initiated. Therefore, the run4ga 30-foot impact is the run4g 30-foot impact. The 30-foot impact results for run1ga are presented in section 3.7 for run4g. The run4ga crush results are presented in this section.

The final configuration for the run4ga crush impact is shown in Figure 3.8.1. The maximum effective plastic strain in the CV body is 0.0741 in/in in the upper wall near the bottom head as shown in Figure 3.8.2.

The maximum effective plastic strain in the drum lid is 1.0795 in/in as shown in Figure 3.8.3. The regions of elevated strain are quite localized at the upper and lower stud holes in the lid. The value of 1.0795 in/in is a surface strain. The value of membrane strain is 0.6005 in/in. Due to the relatively localized regions of high effective plastic strain, some localized tearing may occur. Extended tearing or failure of the lid is not predicted due to the localized elevated fringe ranges of effective plastic strain. The large washers would provide restraint of the lid. Table 3.8.1 presents the maximum effective plastic strain in other shipping package components for the run4ga crush impact.

Table 3.8.1 - Run4ga, Crush Impact, Effective Plastic Strain Levels in Some Components	
Component	Effective Plastic Strain, in/in
CV Lid	0.0006
CV Nut Ring	0.0003
Angle	0.0917
Drum	0.3537
Drum Bottom Head	0.2919
Liner	0.2363
Lid Stiffener	0.0303
Lid Studs	0.3174
Lid Stud Nuts	0.0000
Lid Stud Washers	0.0597
Plug Liner	0.1636

The CV lid separation time history is shown in Figure 3.8.4. A maximum spike of about 0.009 inches is shown for the nodal pairs shown in Figure 3.1.30. The average value at the end of the impact is about 0.002 inches or less.

The time history of the drum diameter in the direction of the impacts is shown in Figure 3.8.5. Figure 3.8.6 shows the radial changes in the direction normal to the impacts. The location of the nodes is shown in Figure 3.1.34.

Figure 3.8.7 shows the kaolite thickness time histories for the run4ga crush impact. The nodes are shown in Figure 3.1.32.

Figure 3.8.8 shows the diameter time history at various locations along the liner. Figure 3.1.37 and Table 3.1.3 show the locations of the nodal pairs.

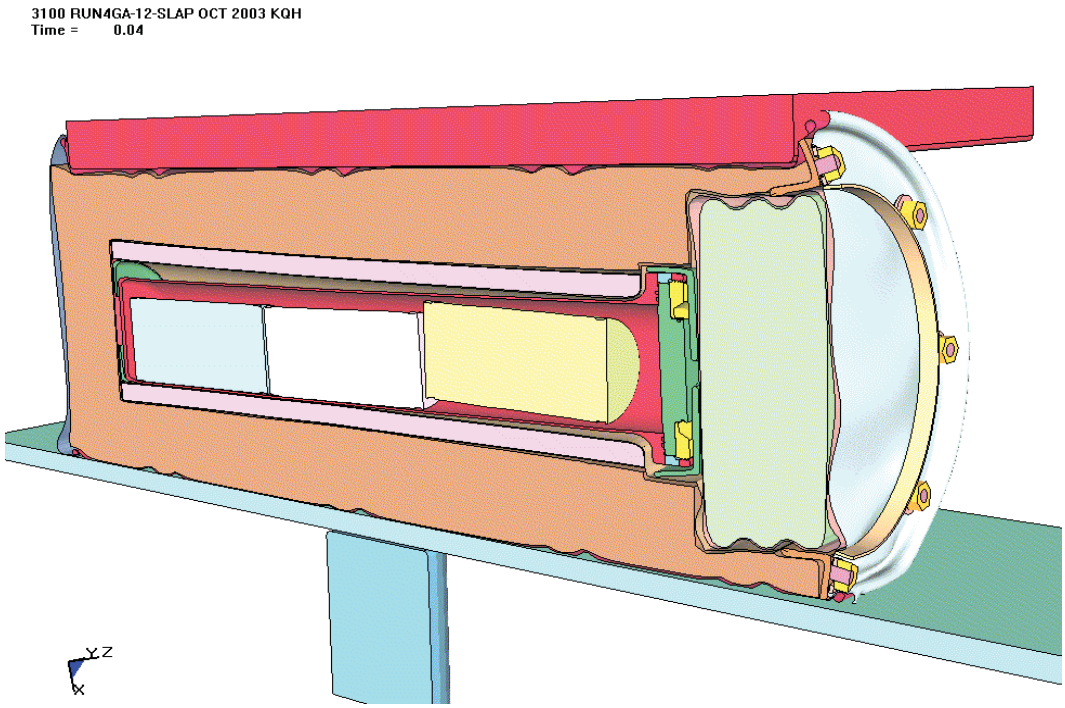

Figure 3.8.1 - Run4ga, Crush Impact, Final Configuration

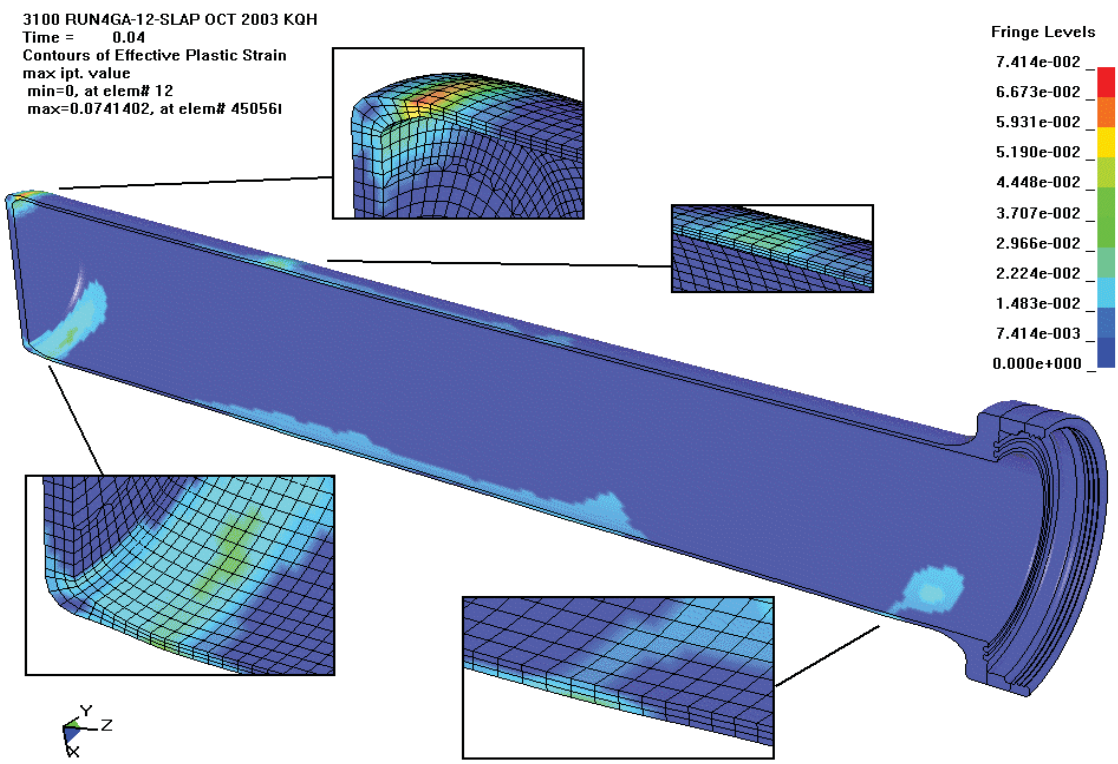

Figure 3.8.2 - Run4ga, Crush Impact, Effective Plastic Strain in the CV Body

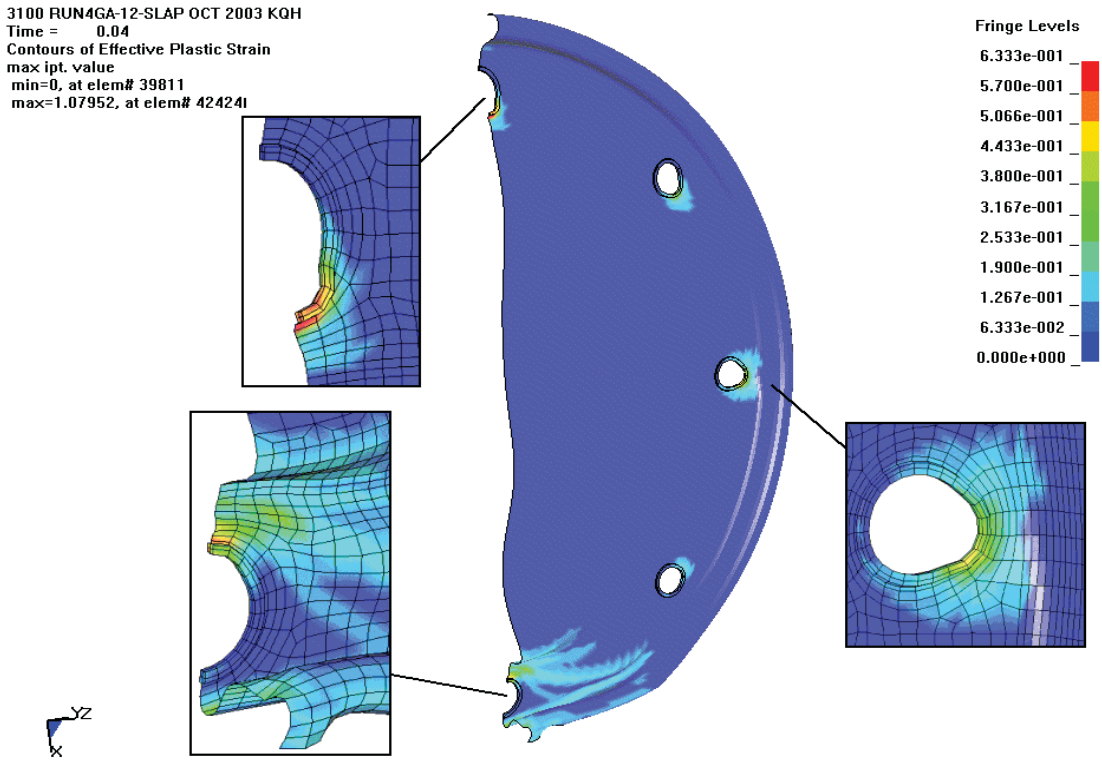

Figure 3.8.3 - Run4ga, Crush Impact, Effective Plastic Strain in the Lid

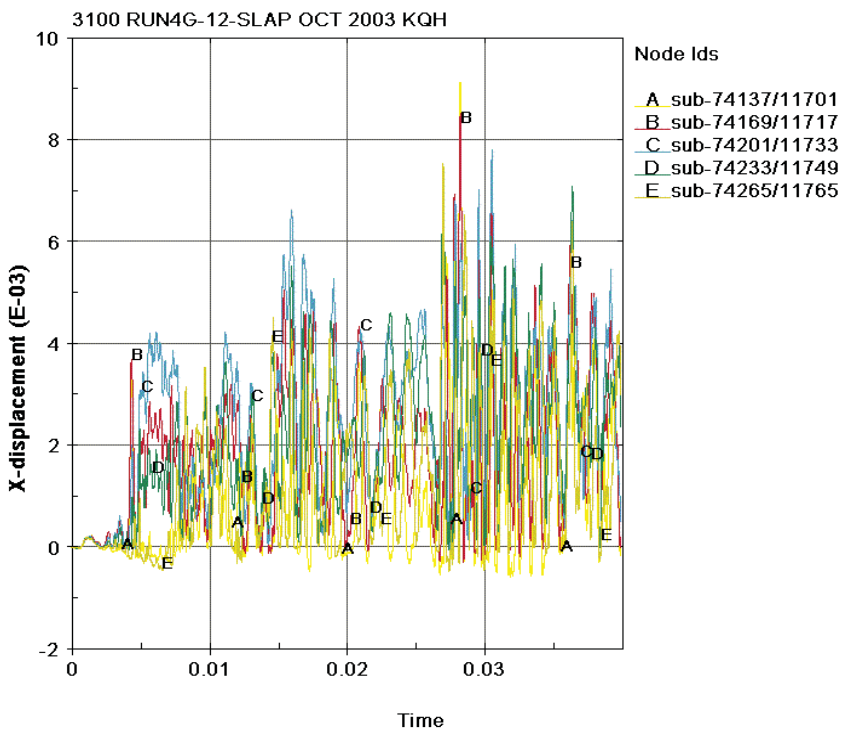

Figure 3.8.4 - Run4ga, Crush Impact, Lid Separation Time History

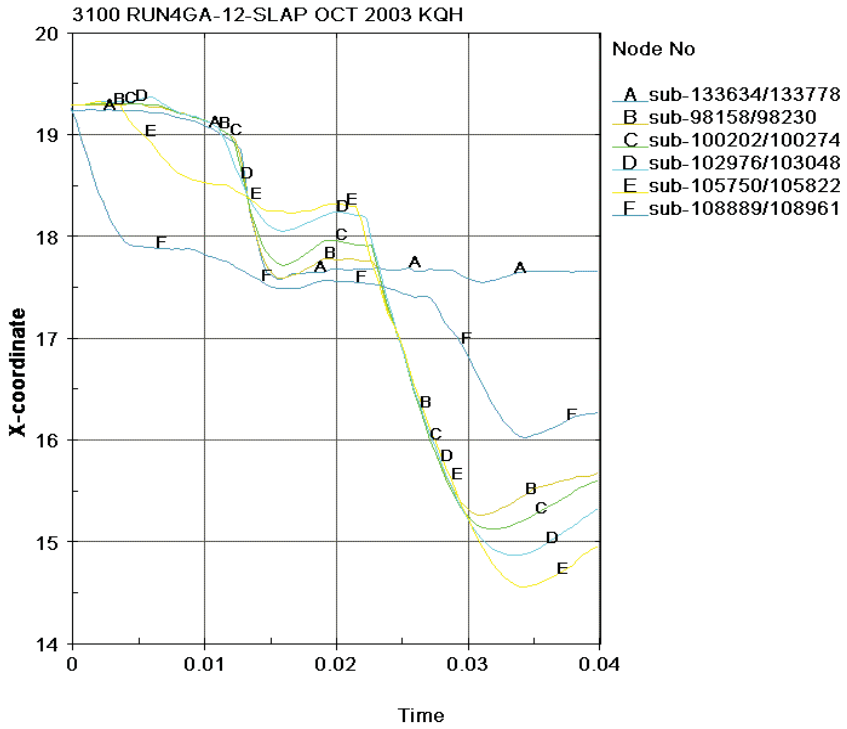

Figure 3.8.5 - Run4ga, Drum Deformation in the Direction of the Impacts

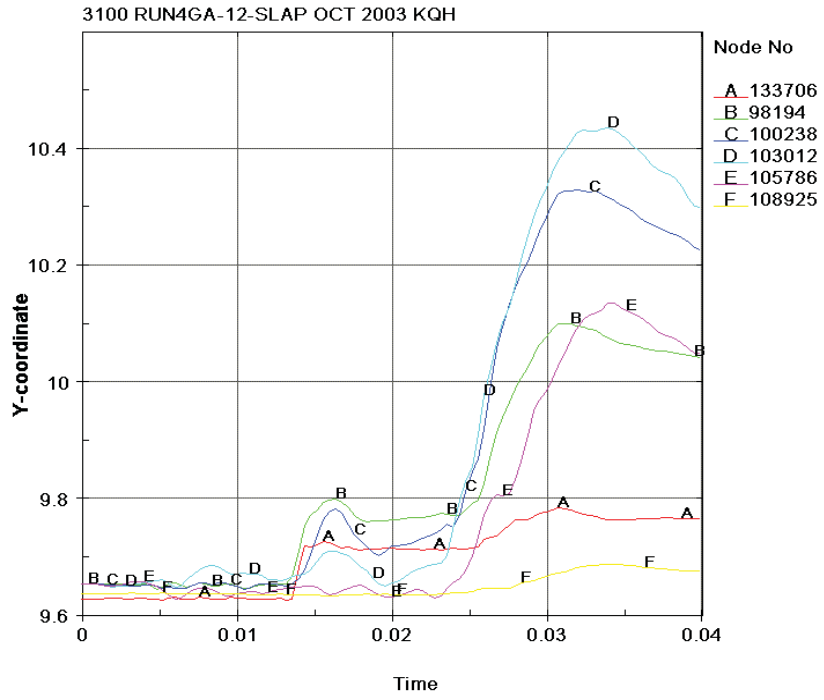

Figure 3.8.6 - Run4ga, Drum Deformation Time History in the Y-Direction

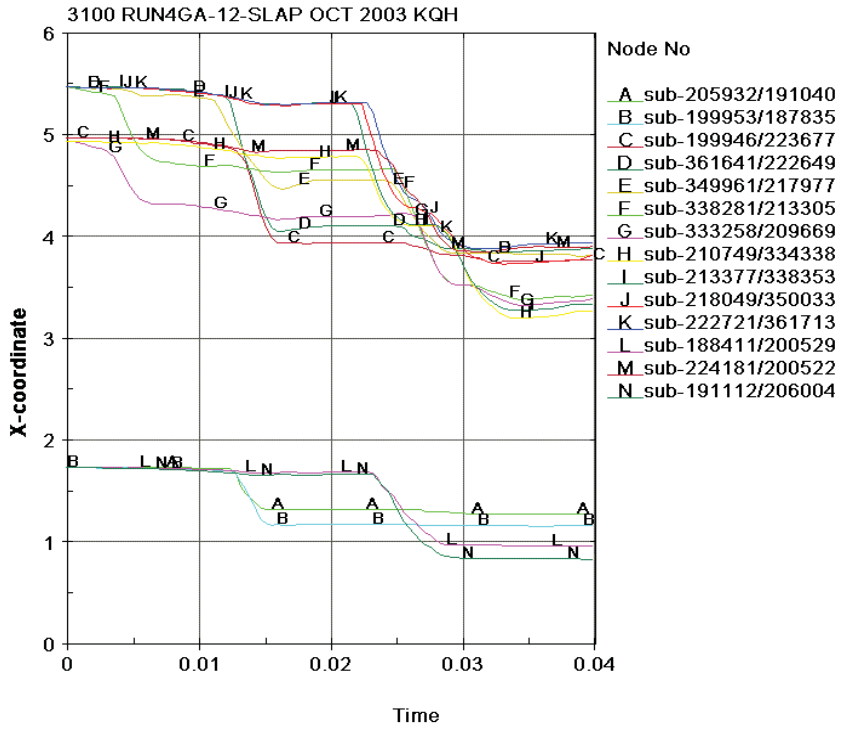

Figure 3.8.7 - Run4ga, Thickness in the Drum Kaolite in the Direction of the Impacts

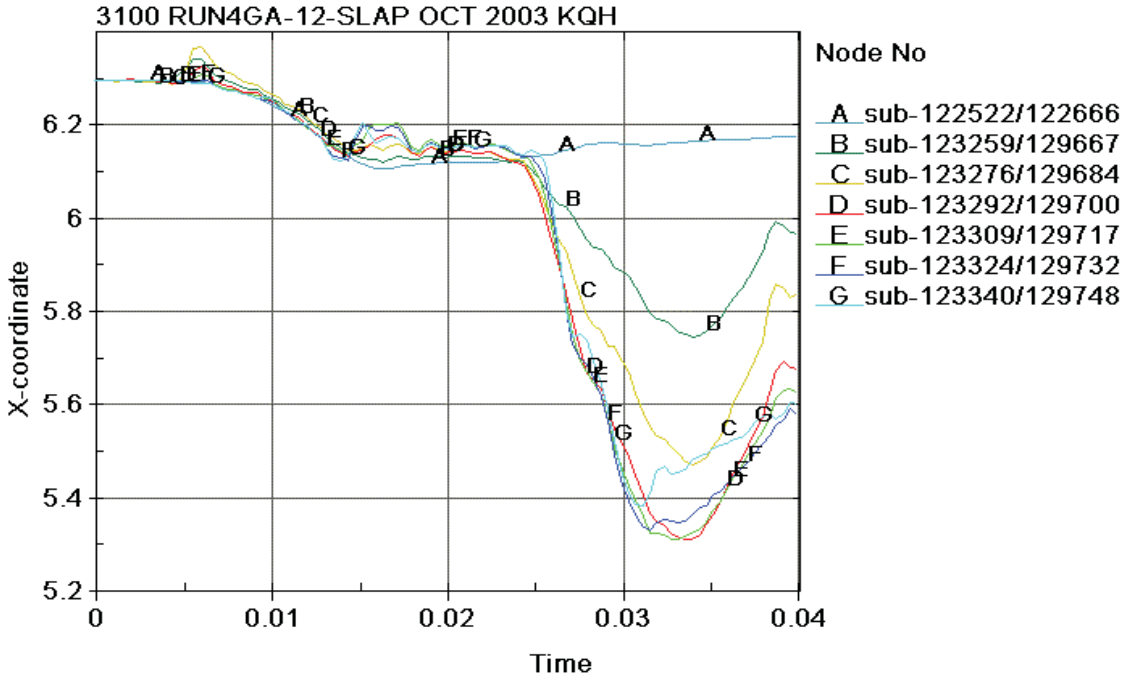

Figure 3.8.8 - Run1ga, Liner Diameter Time History

3.9 Run4h - Slapdown

Due to the minimal number of studs securing the lid, a model with the impact centered between the studs is made. Run4h is similar to run4g, except that the drum studs are rotated, such that the plane of symmetry is centered between two studs. Run4h is a 30-foot, 12° slapdown impact (time = 0 to 0.02 seconds) followed by a crush impact with the crush plate centered over the CV flange (0.02 to 0.04 seconds).

Figure 3.9.1 shows the final configuration for the 30-foot impact. Figure 3.9.2 shows the configuration in the lid region near the rigid plate. The effective plastic strain contours in the package components for the 30-foot impact are similar to strain patterns already presented. Therefore, no strain contour plots are presented for the 30-foot impact and the maximum strains are listed in Table 3.9.1.

Table 3.9.1 - Run4h, 30-Foot Impact, Effective Plastic Strain Levels in Some Components

Component	Effective Plastic Strain, in/in
CV Body	0.0450
CV Lid	0.0000
CV Nut Ring	0.0000
Angle	0.0861
Drum	0.3017
Drum Bottom Head	0.2877
Liner	0.1181
Lid	0.3831
Lid Stiffener	0.0184
Lid Studs	0.0891
Lid Stud Nuts	0.0000
Lid Stud Washers	0.0782
Plug Liner	0.1592

The final configuration for the run4h crush is shown in Figure 3.9.3. Figure 3.9.4 shows the lid configuration for the crush impact. The maximum effective plastic strain in the drum lid is 0.9830 in/in, which is a surface strain. The maximum membrane strain is 0.7225 in/in and is localized around the stud holes in the lid at the 67.5° and the 112.5° positions. The regions of high strain are localized at all the stud holes in the lid,

therefore extended tearing is not predicted. Some localized tearing of the lid may be experienced, but the lid will be retained by the large washers.

The maximum effective plastic strain in the studs is 0.5364 in/in and occurs at the outer radius of the stud. The nominal effective plastic strain through the stud shank is about 0.300 in/in. Therefore, the studs would not be expected to fail. The maximum effective plastic strain in other components are listed in Table 3.9.2.

Table 3.9.2 - Run4h, Crush Impact, Effective Plastic Strain Levels in Some Components

Component	Effective Plastic Strain, in/in
CV Body	0.0461
CV Lid	0.0004
CV Nut Ring	0.0000
Angle	0.1071
Drum	0.3881
Drum Bottom Head	0.2877
Liner	0.2475
Lid Stiffener	0.1083
Lid Stud Nuts	0.0052
Lid Stud Washers	0.0885
Plug Liner	0.2719

The lid separation time history is similar to those presented in Sections 3.7 and 3.8. A maximum lid separation spike of approximately 0.007 inches is reached during the impacts and is oscillatory in nature. An average value of 0.003 inches or less is shown at the end of the crush impact.

Figure 3.9.7 shows the X-diameter time history for drum nodes shown in Figure 3.1.34. Figure 3.9.8 shows the radial time history for nodes normal to the direction of impact.

Due to the rotation of the studs on the lid, the nodes for the kaolite changed for the run4h model. The nodes used to obtain the kaolite thickness time histories for run4h are shown in Figure 3.9.9. The time histories for the kaolite thickness on the plane of symmetry is shown in Figure 3.9.10. Figure 3.9.11 shows the liner diameter time history at location shown in Figure 3.1.37 and Table 3.1.3.

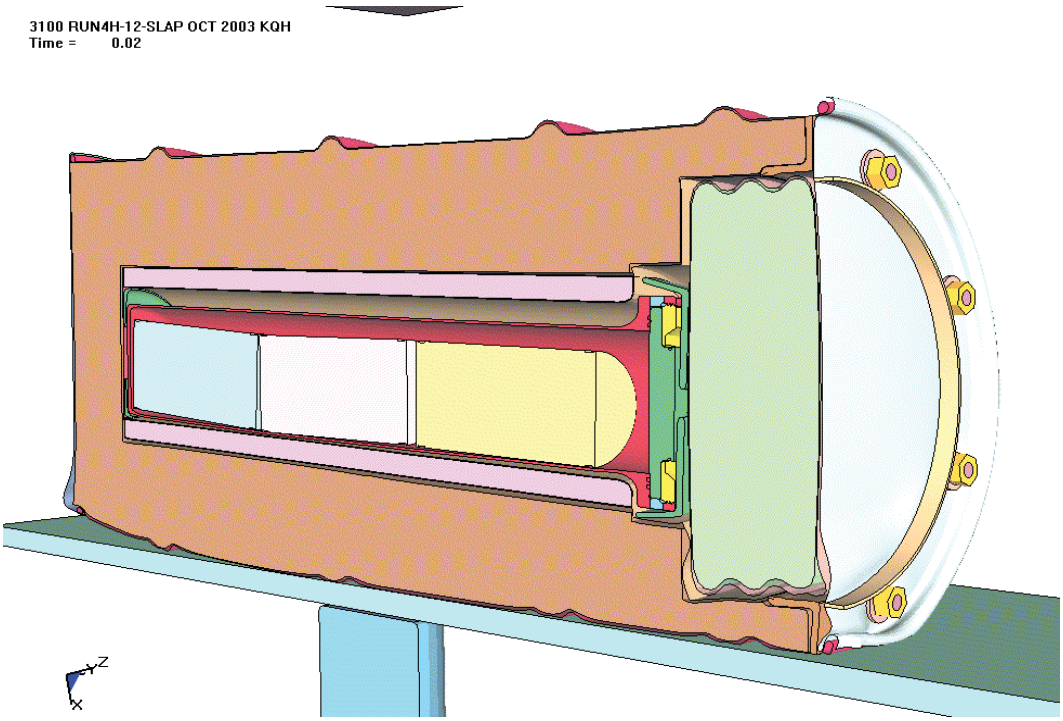

Figure 3.9.1 - Run4h, 30-Foot Impact, Final Configuration

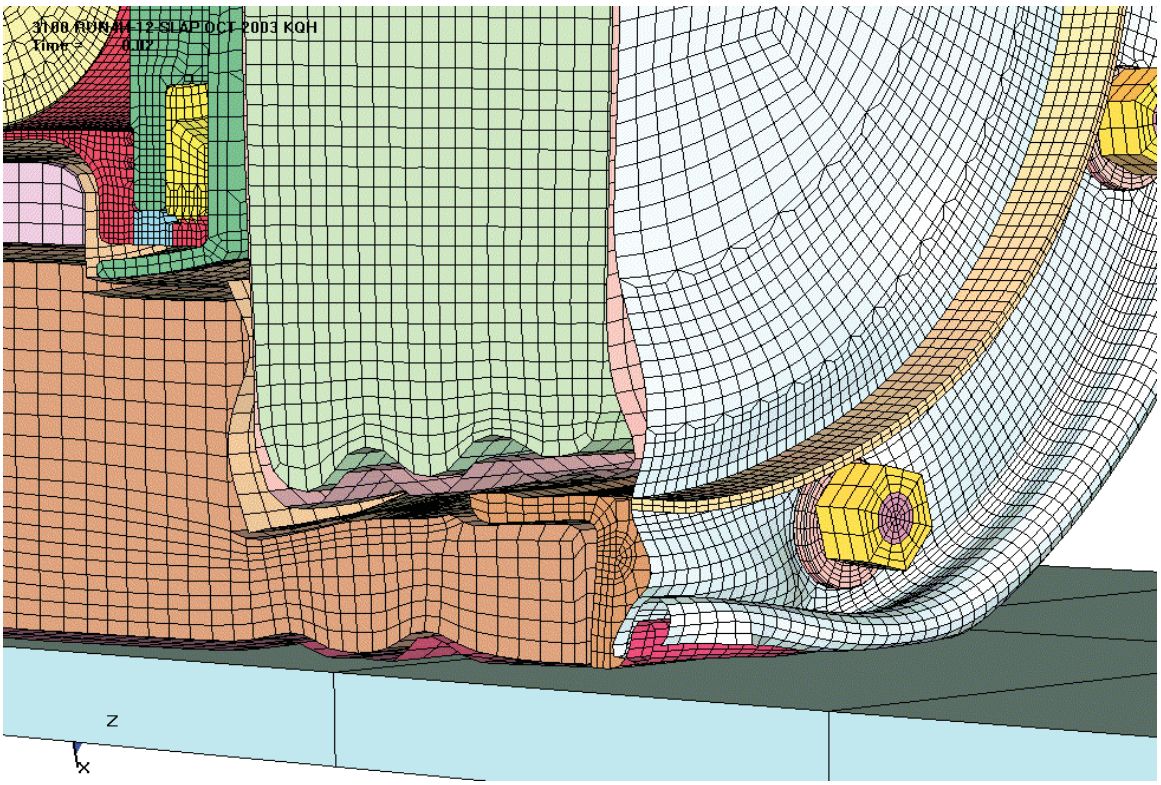

Figure 3.9.2 - Run4h, 30-Foot Impact, Configuration in the Lid

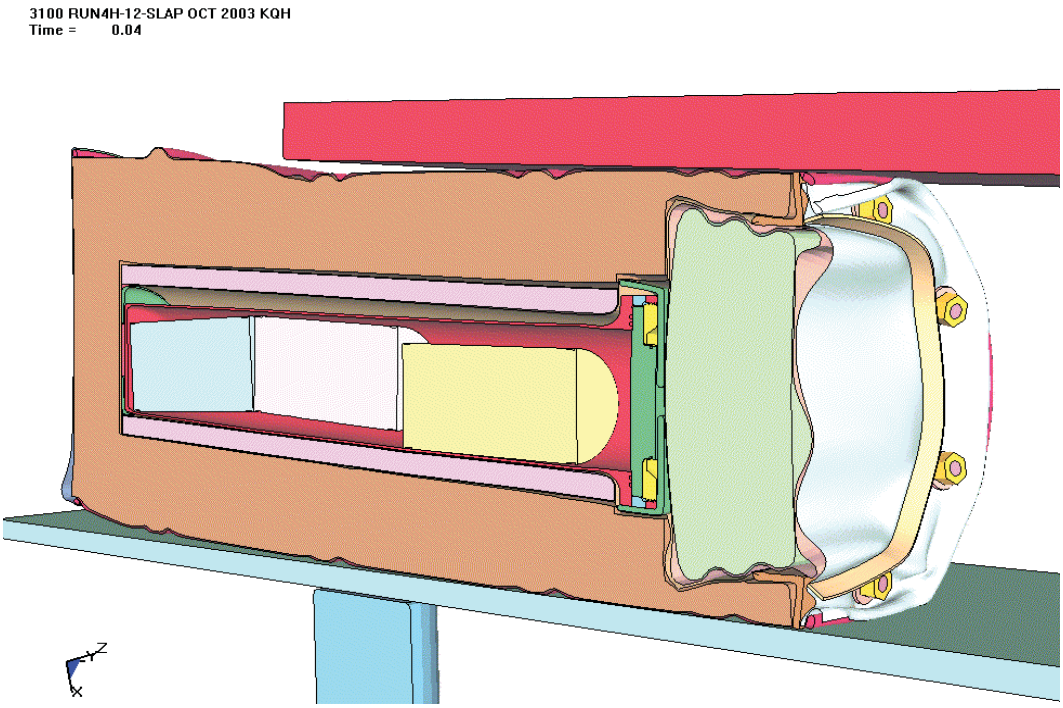

Figure 3.9.3 - Run4h, Crush Impact, Final Configuration

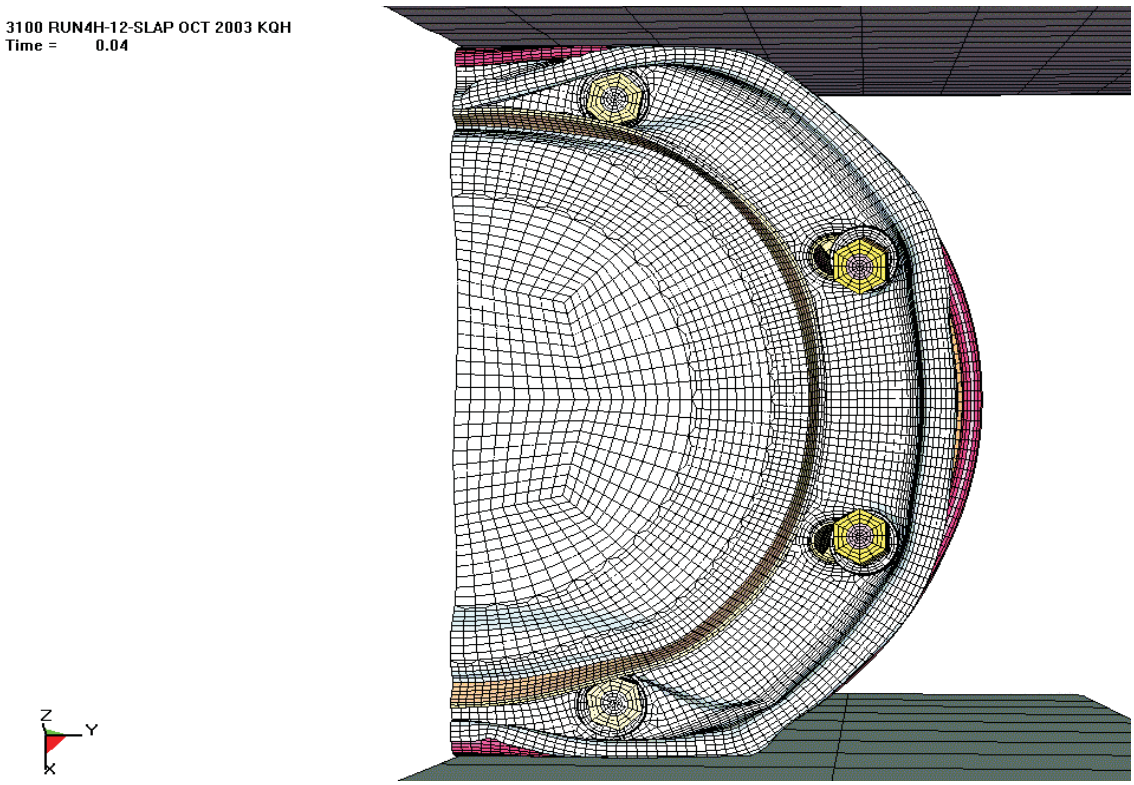

Figure 3.9.4 - Run4h, Crush Impact, Configuration of the Lid

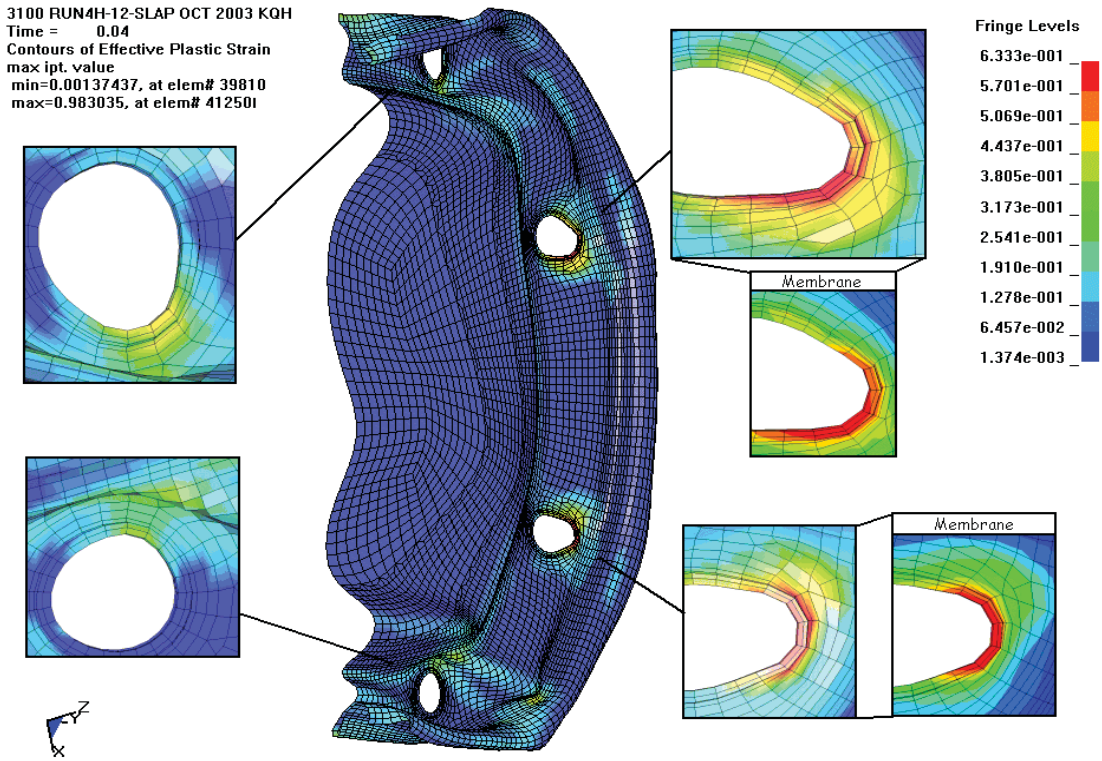

Figure 3.9.5 - Run4h, Crush Impact, Effective Plastic Strain in the Lid

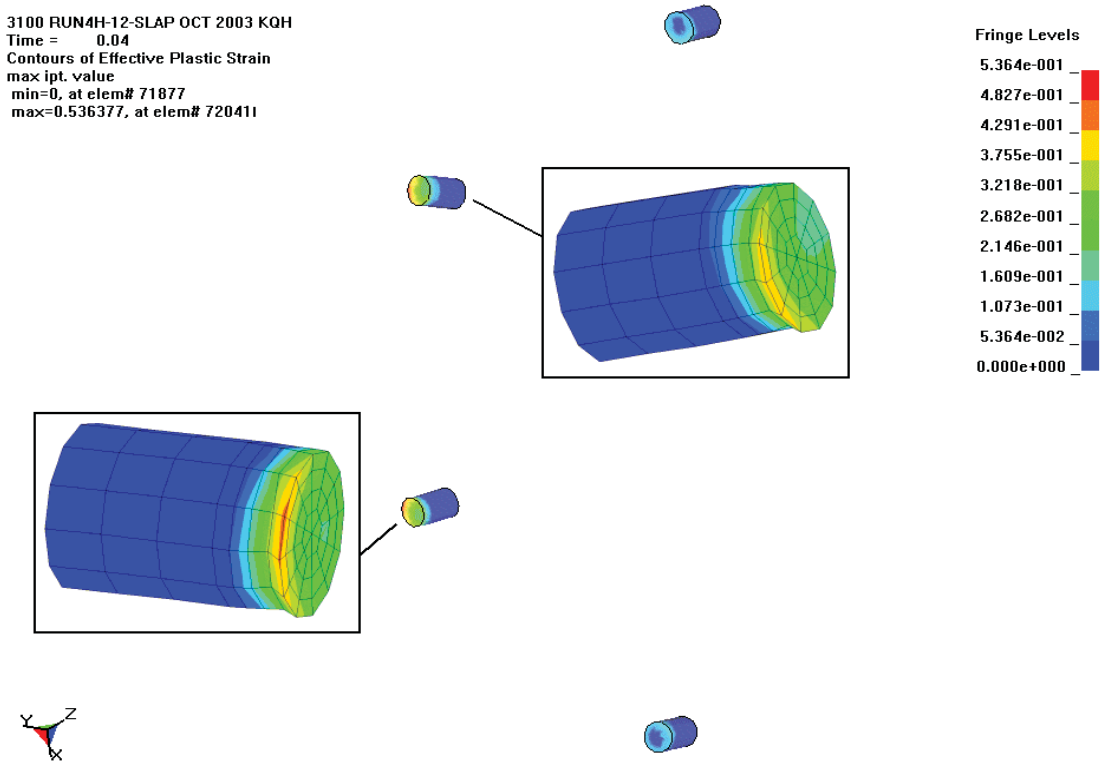

Figure 3.9.6 - Run4h, Crush Impact, Effective Plastic Strain in the Studs

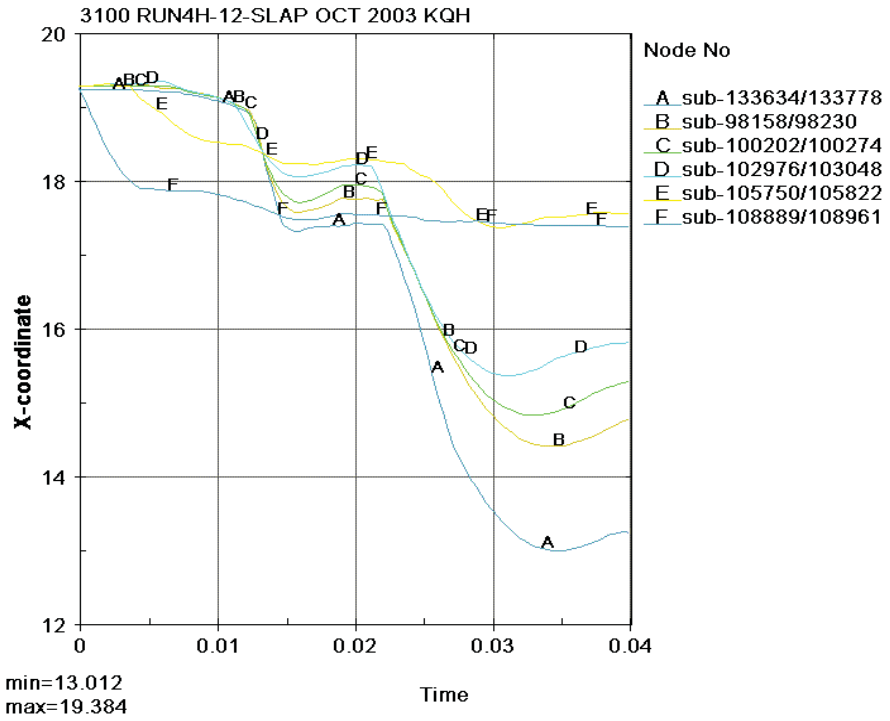

Figure 3.9.7 - Run4h, Drum Diameter in the Direction of the Impacts

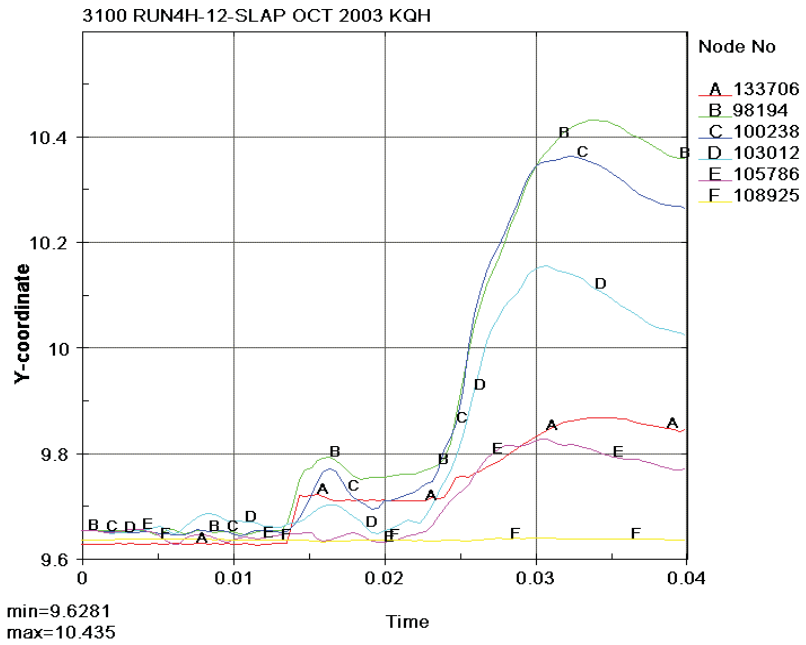

Figure 3.9.8 - Run4h, Drum Radius Normal to the Direction of the Impacts

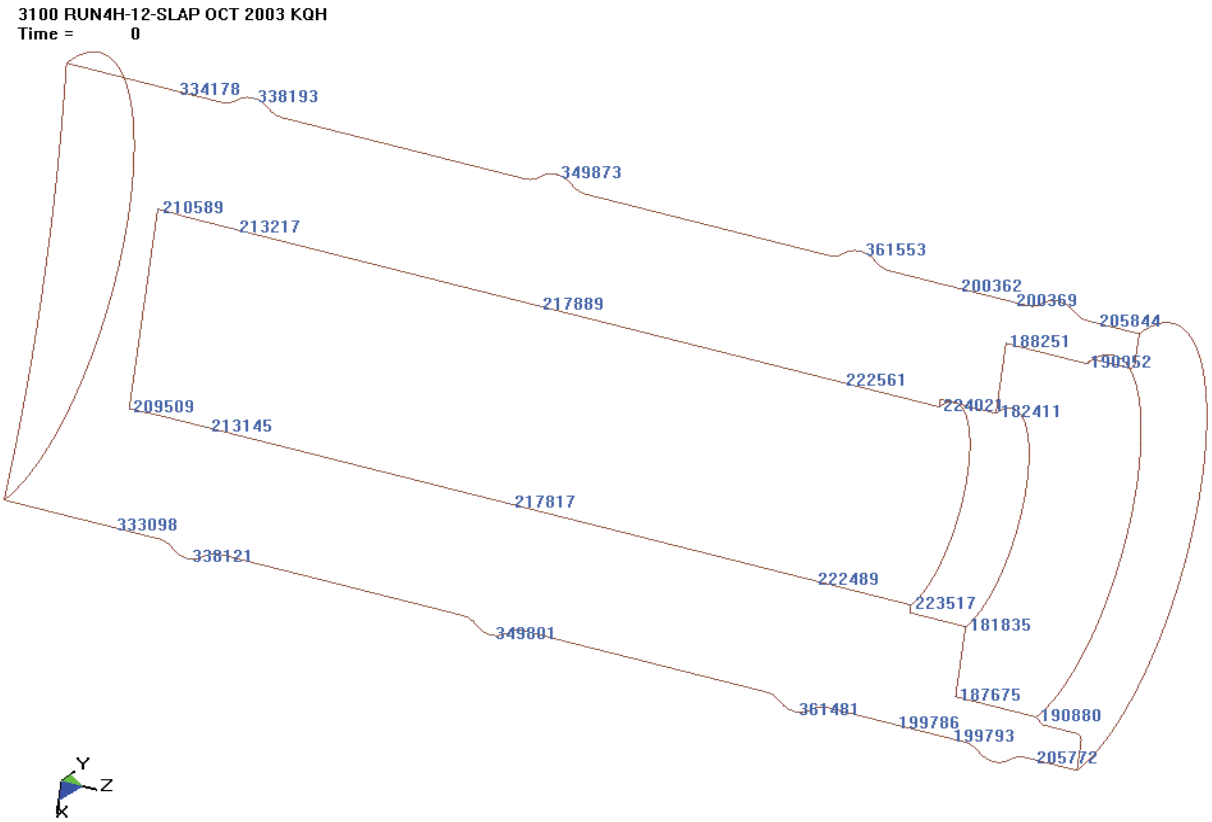

Figure 3.9.9 - Run4h, Drum Kaolite Nodes

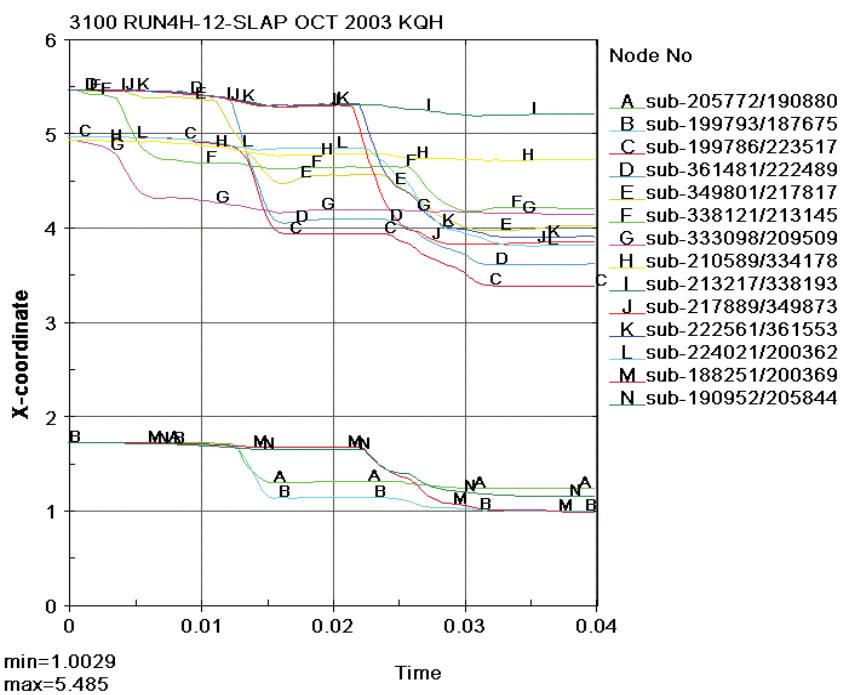

Figure 3.9.10 - Run4h, Thickness of the Drum Kaolite in the Direction of the Impacts

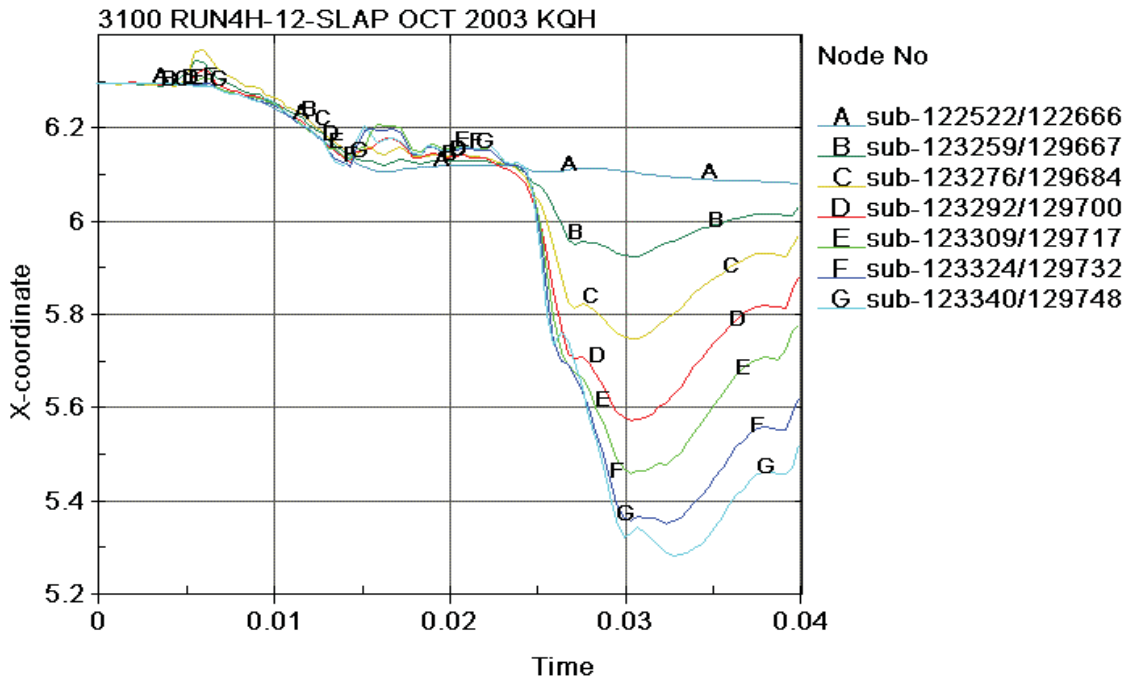

Figure 3.9.11 - Run4h, Liner Diameter Time History

3.10 Run4ha - Slapdown

Run4ha is similar to run4h except that the crush impact is with the crush plate centered on the drum. For run4ha, the restart file at the end of the run4h, 30-foot impact is used to initiate a run which moves of the crush plate such that it is centered on the drum (crush impact from 0.0201 to 0.04 seconds). The translation of the crush plate occurs at the end of the 30-foot impact, or time = 0.02 sec and lasts till 0.0201 sec. The restart file written at the end of the translation of the crush plate, becomes the restart file used to initiate the run4ha crush impact. Therefore, the 30-foot impact results from run4ha are presented in the run4h results. The results presented in this section are those of the centered crush impact for run4ha.

The final configuration for the crush impact is shown in Figure 3.10.1. The maximum effective plastic strain in the drum lid is 0.6335 in/in as shown in Figure 3.10.2. The maximum membrane strain is 0.5249 in/in and is highly localized at the stud hole nearest the crush plate (157.5°). If failure were to occur in the lid, it would be localized and the large washers would restrain the lid. The effective plastic strain in other components is shown in Table 3.10.1.

Table 3.10.1 - Run4ha, Crush Impact, Effective Plastic Strain Levels in Some Components

Component	Effective Plastic Strain, in/in
CV Body	0.0839
CV Lid	0.0013
CV Nut Ring	0.0000
Angle	0.0881
Drum	0.3848
Drum Bottom Head	0.2922
Liner	0.2633
Lid Stiffener	0.0338
Lid Studs	0.1705
Lid Stud Nuts	0.0000
Lid Stud Washers	0.0782
Plug Liner	0.1832

The lid separation time history is similar to that shown in Section 3.8. A maximum spike of 0.009 inches is shown to occur for the CV lid separation. The average separation at the end of the crush impact is 0.002 inches or less due to the oscillatory nature of the gap response.

Figure 3.10.3 gives the diameter time history in the X-direction for drum nodes shown in Figure 3.1.34. Figure 3.10.4 shows the radial time history in the Y-direction for the nodes normal to the direction of the impact.

Figure 3.9.9 shows the nodes used to obtain the kaolite thickness time history for the impact. Figure 3.10.5 shows the thickness time history for the kaolite.

Figure 3.10.6 show the liner diameter time histories in the liner. Figure 3.1.37 and Table 3.1.3 give the locations of the nodal pairs along the length of the liner.

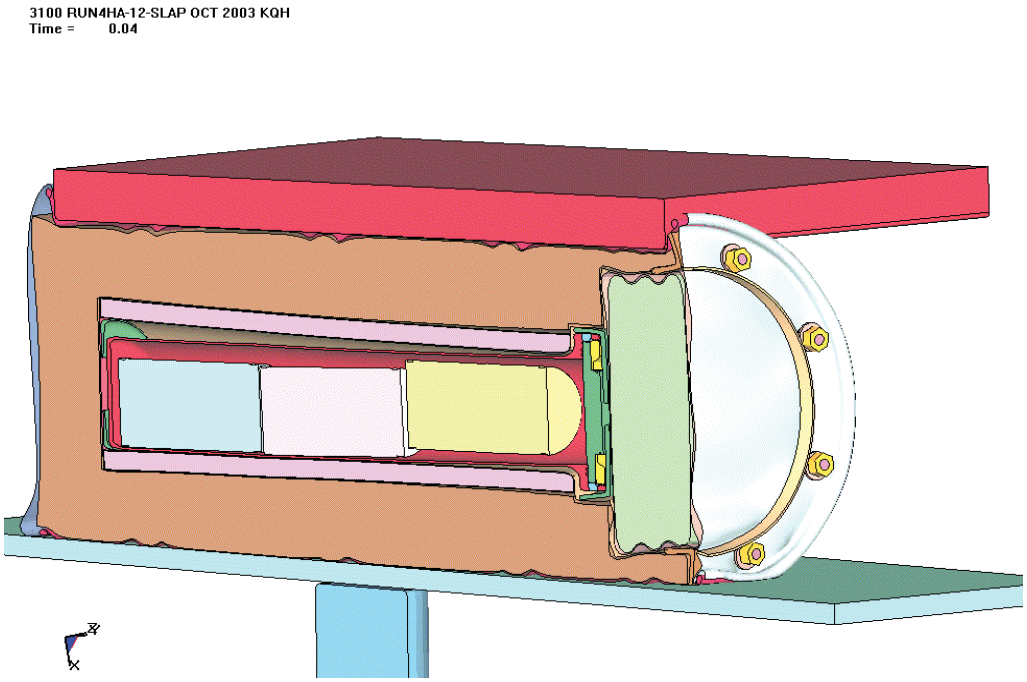

Figure 3.10.1 - Run4ha, Crush Impact, Final Configuration

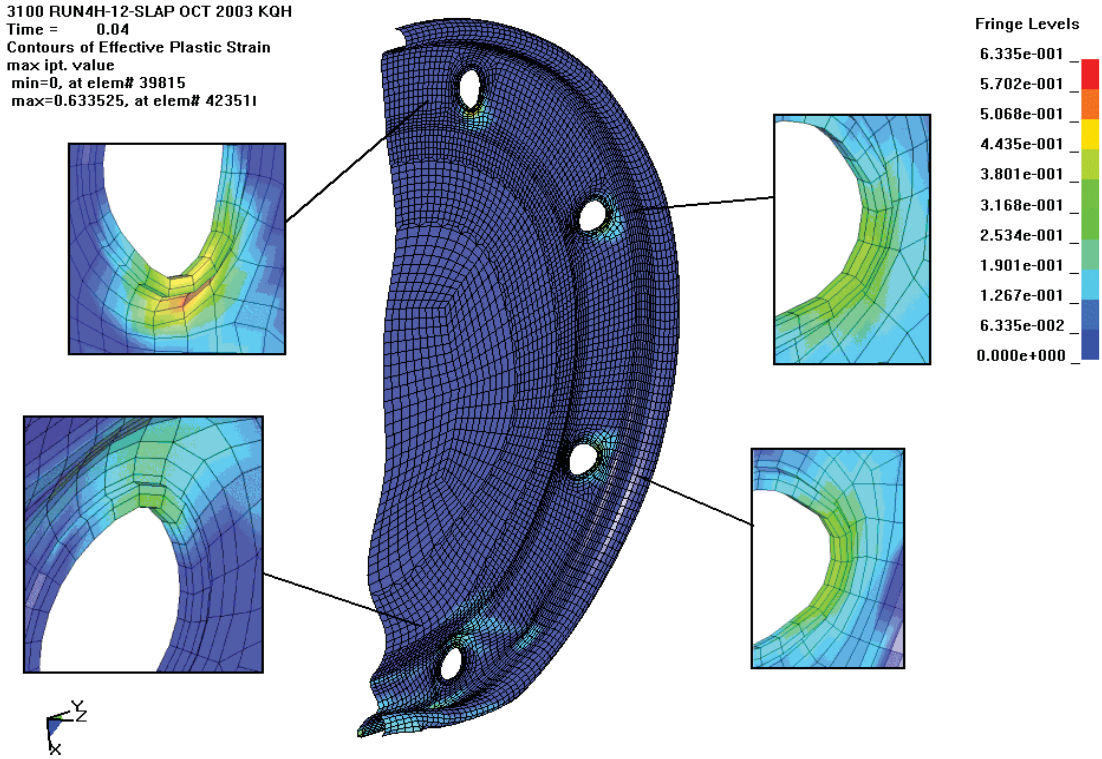

Figure 3.10.2 - Run4ha, Crush Impact, Effective Plastic Strain in the Lid

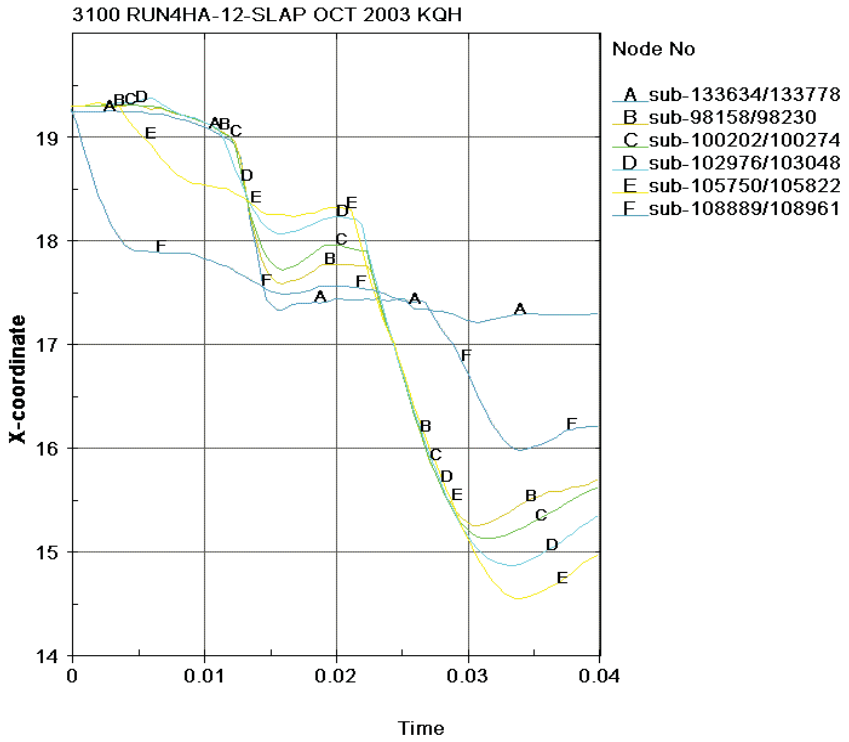

Figure 3.10.3 - Run4ha, Drum Diameter Time History in the Direction of the Impacts

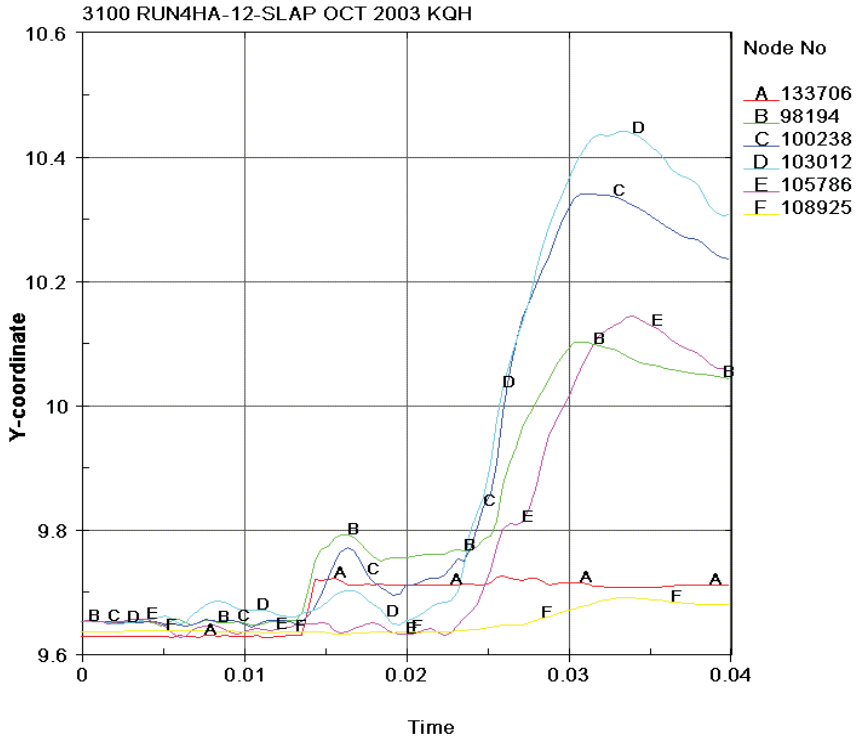

Figure 3.10.4 - Run4ha, Drum Radius Time History Normal to the Direction of the Impacts

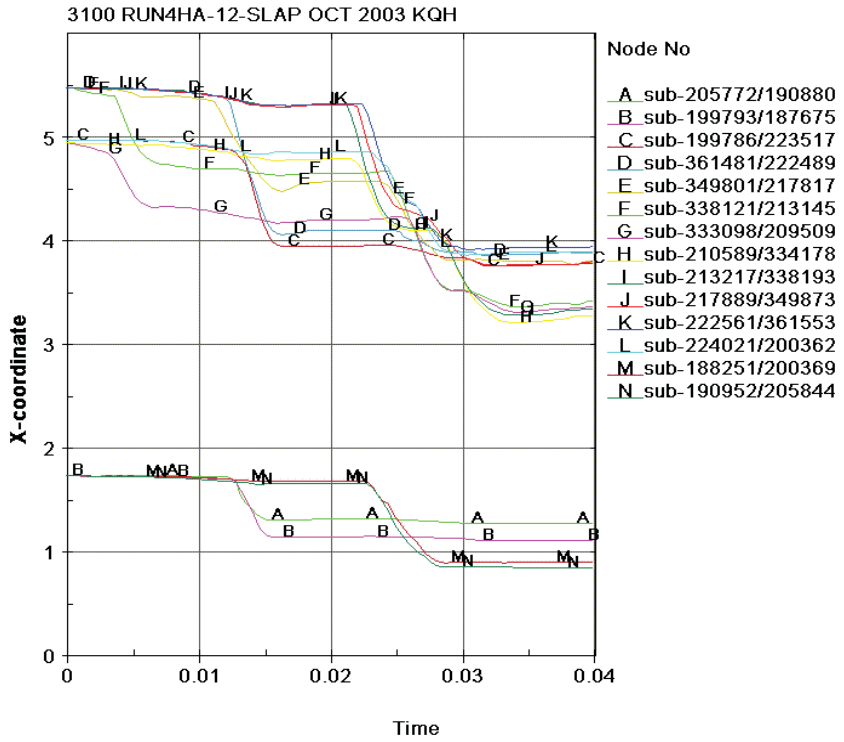

Figure 3.10.5 - Run4ha, Drum Kaolite Thickness in the Direction of the Impacts

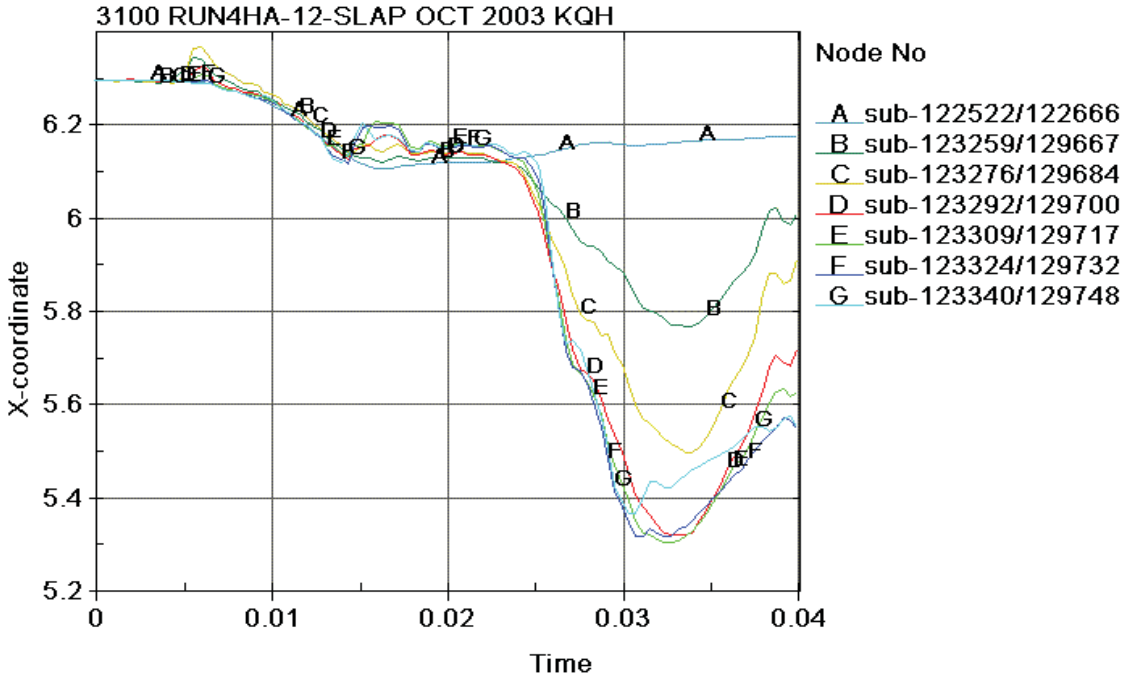

Figure 3.10.6 - Run4ha, Liner Diameter Time History

3.11 Punch Runs

The punch impacts were made with the simple model described in Section 2.2. The final configuration for the punch at 0° is shown in Figure 3.11.1. The surface effective plastic strain in the drum is shown in Figure 3.11.2 to be a maximum of 0.2030 in/in. The maximum membrane strain fringe plot is not shown, but is a maximum of 0.1385 in/in with a contour pattern similar to the surface strain.

Fringe plots of effective plastic surface strain for punch impacts at 40, 50, 60 and 63.6 are shown in Figures 3.11.3 through 3.11.6. Table 3.11.1 summarizes the maximum surface and membrane strain for all the punch impacts.

Table 3.11.1 - ES-3100 Summary of Punch Impacts

Punch Angle (degrees)	Maximum Effective Plastic Strain in the Drum (in/in)	
	Surface	Membrane
0	0.2030	0.1385
10	0.1204	0.0633
20	0.1100	0.0529
30	0.1551	0.0951
40	0.1632	0.1115
50	0.3340	0.1238
60	0.1844	0.0646
63.6	0.3895	0.1858

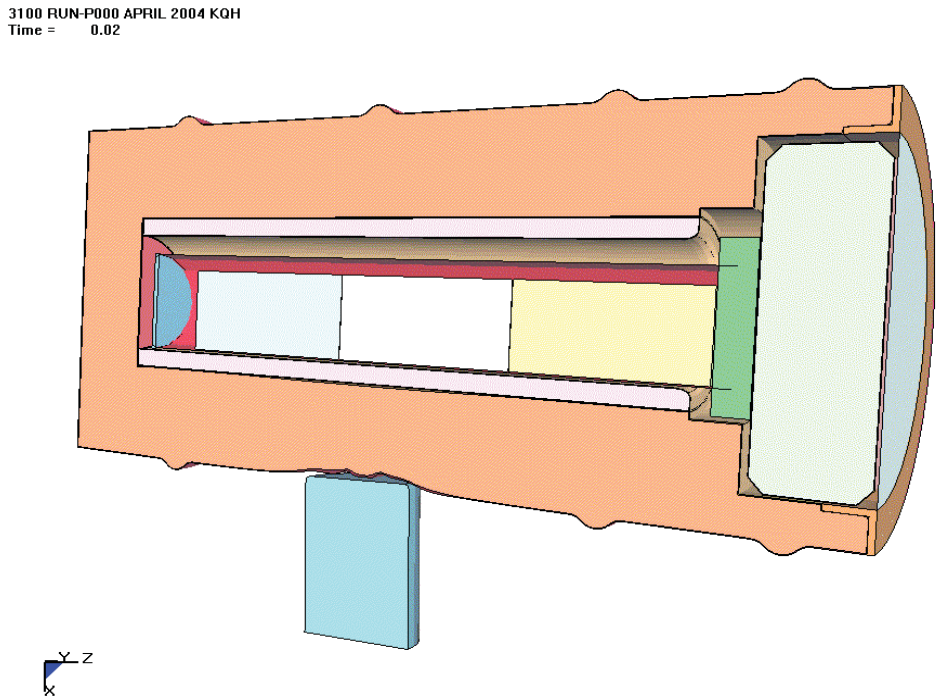

Figure 3.11.1 - Punch at 0°, Final Configuration

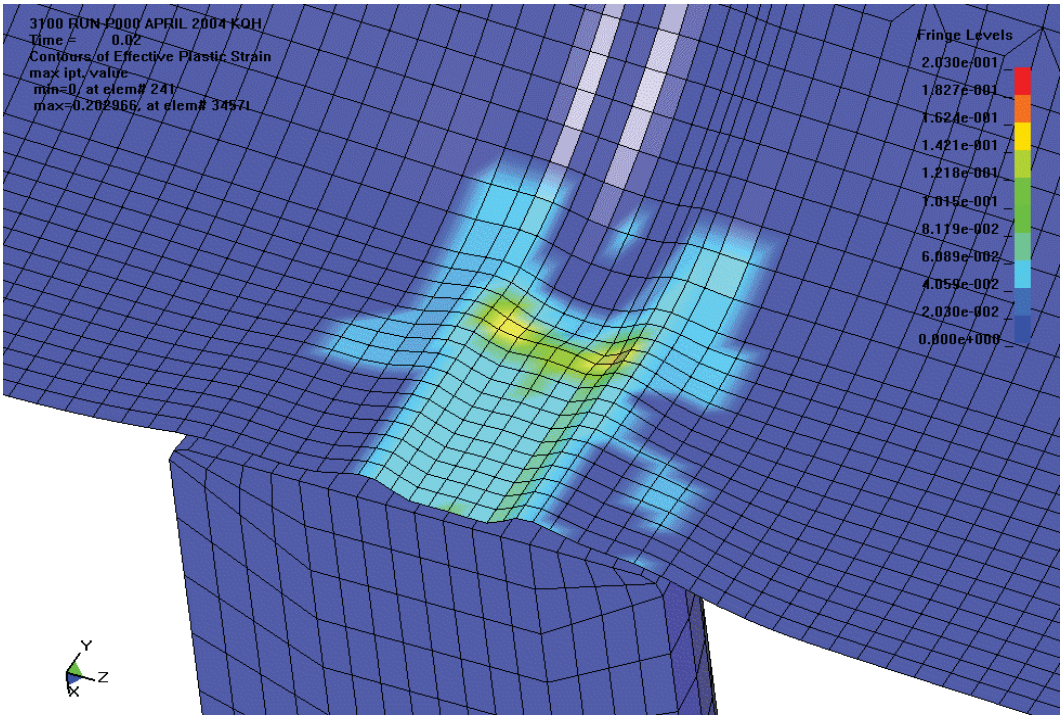

Figure 3.11.2 - Punch at 0°, Surface Strain in the Drum Liner

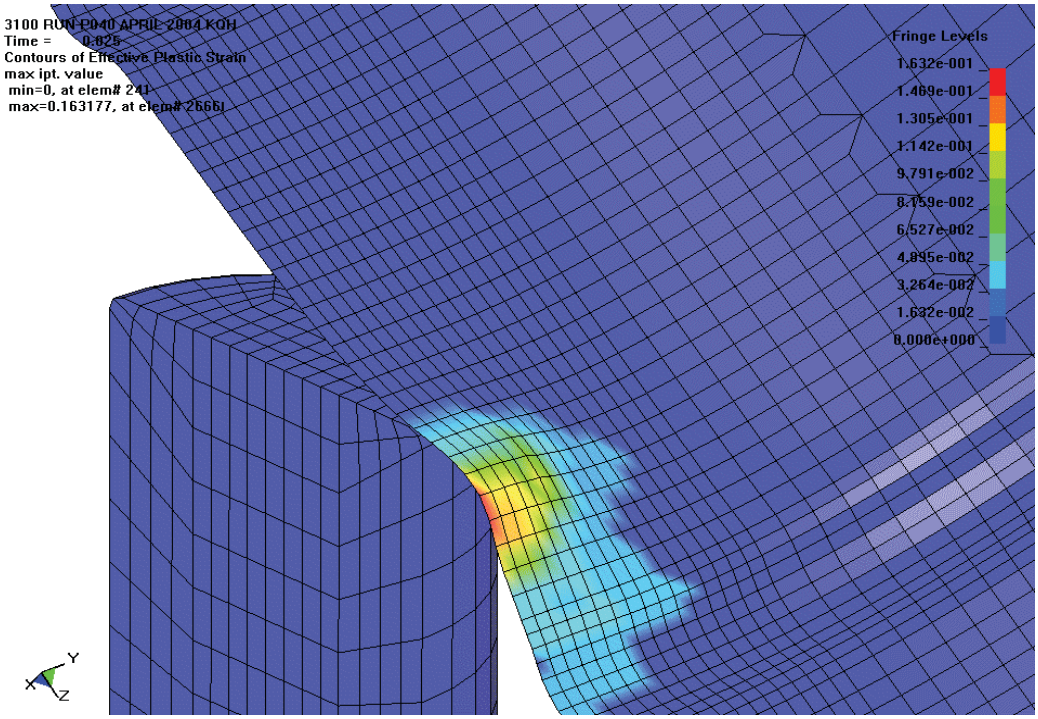

Figure 3.11.3 - Punch at 40°, Surface Strain in the Drum Liner

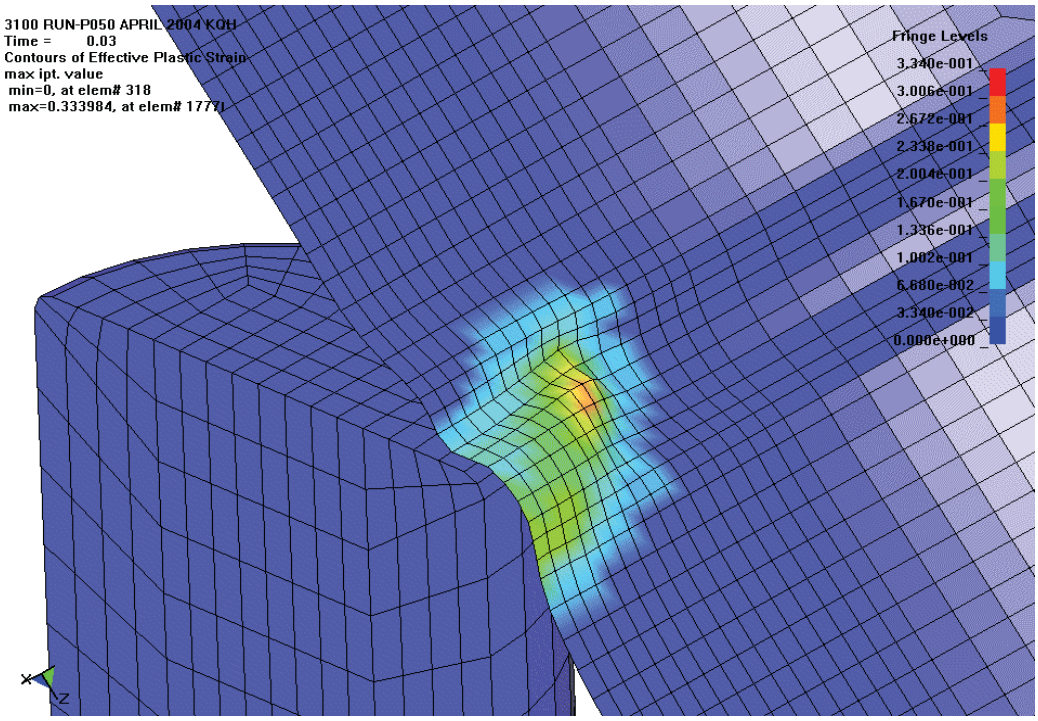

Figure 3.11.4 - Punch at 50°, Surface Strain in the Drum Liner

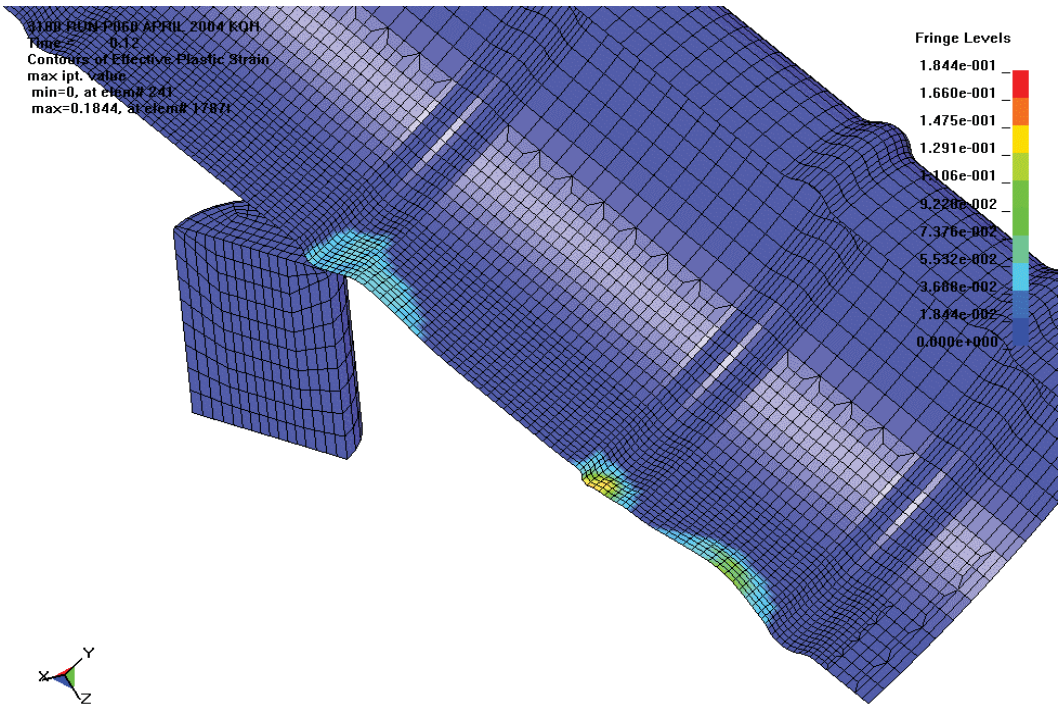

Figure 3.11.5 - Punch at 60°, Surface Strain in the Drum Liner

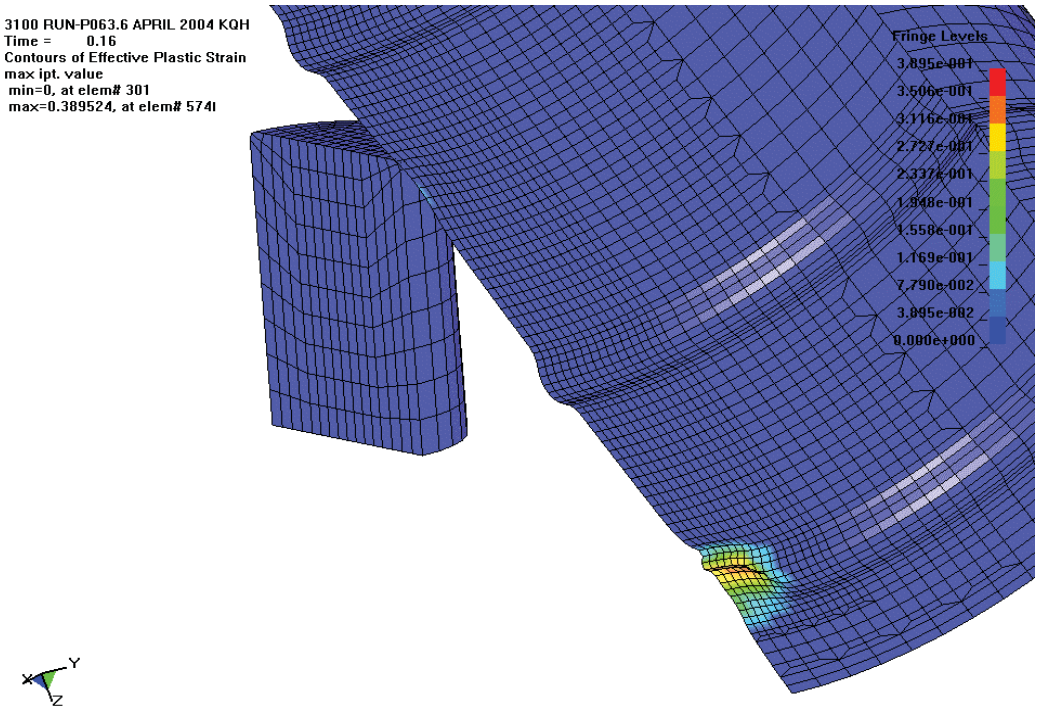

Figure 3.11.6 - Punch at 63.6°, Surface Strain in the Drum Liner

3.12 Comparison of Test vs Analysis

Physical testing of the ES-3100 shipping container to the 4-foot, 30-foot, 30-foot crush and 40-inch punch impacts were carried out in late May, 2004 at the Oak Ridge National Lab (ORNL), National Transportation Research Center (NTRC) facility in Oak Ridge.

The test specimen were subject to the entire series of impacts (4-foot, 30-foot, crush and punch), however the analytical impacts were not all subject to the entire series. Typically, the analysis was a design run which was subjected to a 30-foot impact followed by a crush impact. So the 30-foot analysis comparison was made to a test specimen that had experienced a 4-foot and a 30-foot impact. And likewise for the crush impact comparisons, the analysis results are lacking the initial 4-foot impact.

The comparisons are made for TU1 (Test Unit #1), TU2, TU3 and TU4. TU1 is the 12° slapdown, TU2 is the cold package side impact, TU3 is the corner impact and TU4 is the end impact. The nodes in the analysis model shell elements lie on the thickness centerline. Therefore, where appropriate, half thickness dimensions are included to render surface to surface comparisons with the test data. Figure 3.12.1 shows locations for which test diameters were obtained.

Dimensions in the tables are inches, unless otherwise noted. The analysis model was reflected with the post processor so that it appears as a full model. This was done to aid in the visual comparison between the test specimen and the model results. The background in the test photos has been erased, also to aid visual comparisons.

The "flats" is the region of relative flatness in the drum liner due to the impact. The analysis flats dimensions are obtained by knowing the element width (whole widths used) and judging which elements are dominantly in a relatively flat plane. The test flat dimensions are taken by visually judging when the drum deviates from a permanent, relatively flat region.

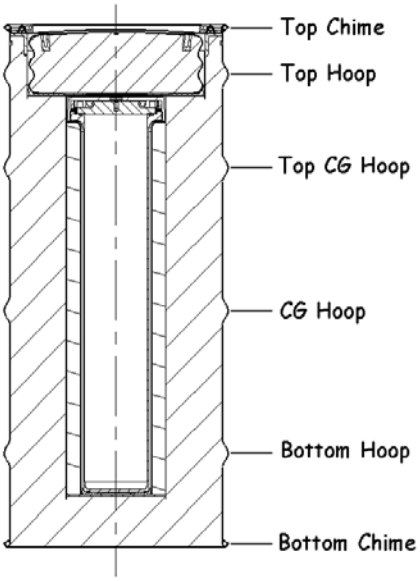

Figure 3.12.1 - Locations of Test Diameter Measurements

3.12.1 Comparison of Run4g to TU1

Run4g is a 30-foot, 12° slapdown impact followed by an offset crush (crush plate centered over the CV flange). TU1 is a 12° slapdown with a 4-foot impact, 30-foot impact, offset crush, and punch test specimen. The following Table 3.12.1.1 shows the initial diameter comparisons (pre-impact) using test data compared to the analysis results.

Table 3.12.1.1 - Run4g vs TU1, Comparison of Initial Diameters (Pre-Impact)				
Location	0°- 180°		90°-270°	
	Test	Analysis	Test	Analysis
Top Chime	19.25	19.32	19.25	19.32
Top Hoop	19.25	19.37	19.25	19.37
Top CG Hoop	19.25	19.37	19.25	19.37
CG Hoop	19.25	19.37	19.25	19.37
Bottom Hoop	19.25	19.37	19.25	19.37
Bottom Chime	19.25	19.38	19.25	19.38

The Table 3.12.1.2 shows the digital results of the 30-foot impact. The test diameters are after the 4 and 30-foot impacts, while the analysis is after the 30-foot impact.

Table 3.12.1.2 - Run4g vs TU1, Diameter Results After the 30-Foot Impact				
	0°-180°		90°-270°	
	Test	Analysis	Test	Analysis
Top Chime	18-1/2	18.1	19-3/8	19.5
Top Hoop	18-1/2	18.2	19-3/8	19.6
Top CG Hoop	18-1/2	18.5	19-3/8	19.5
CG Hoop	18-5/8	18.8	19-3/8	19.4
Bottom Hoop	18-5/8	18.9	19-1/4	19.3
Bottom Chime	17-13/16	18.1	19-3/8	19.4

Figure 3.12.1.1 shows the final configuration of the test specimen after the 4 and 30-foot impacts. Figure 3.12.1.2 shows the analytical model configuration after the 30-foot impact.

Figure 3.12.1.1 - TU1, Results of 30-Foot Impact

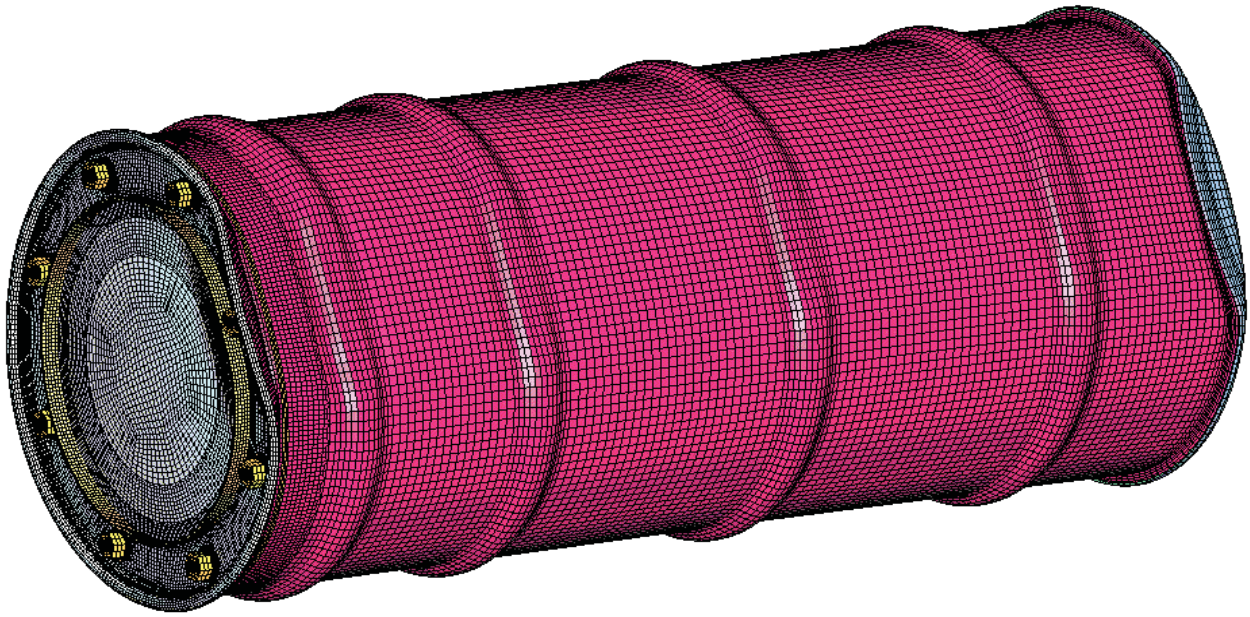

Figure 3.12.1.2 - Run4g, Results of the 30-Foot Impact

Table 3.12.1.3 shows the comparison of the digital results of the crush impact. The test data is for the cumulative effects of a 4-foot, 30-foot, and crush impact. The analysis data is for a cumulative 30-foot impact and crush impact.

Table 3.12.1.3 - Run4g vs TU1, Diameter Results After the Crush Impact				
	0°-180°		90°-270°	
	Test	Analysis	Test	Analysis
Top Chime	15-5/8	15.0	20-5/8	20.7
Top Hoop	16	15.3	20-7/16	20.8
Top CG Hoop	16-1/4	15.9	20-1/4	20.6
CG Hoop	16-1/2	16.4	19-7/8	20.1
Bottom Hoop	18-1/4	18.3	19-1/2	19.6
Bottom Chime	17-13/16	18.1	19-1/4	19.4

Figure 3.12.1.3 shows an isometric view of the test specimen with the crush side up. Figure 3.12.1.4 shows a similar view for the analysis results.

Figure 3.12.1.3 - TU1, View of Crush Damage with the Crush Side Up

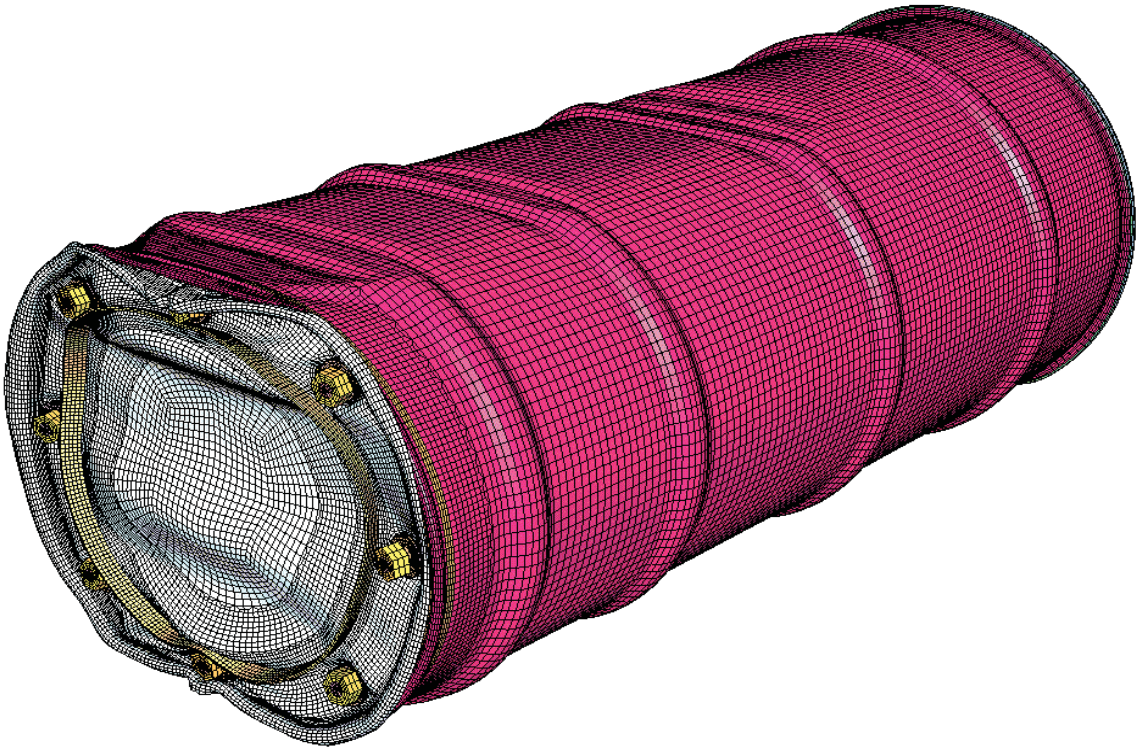

Figure 3.12.1.4 - Run4g, View of the Crush Damage With the Crush Side Up

Table 3.12.1.4 shows the results of a comparison of the "flats" measurements on the drum for the 30-foot impact and Table 3.12.1.5 compares the crush impact test measurements and analysis results.

Table 3.12.1.4 - Run4g vs TU1, Comparison of Flats for the 30-Foot Impact		
	Test	Analysis
Top Chime	8	8.8
Top Hoop	7-3/8	8.4
Top CG Hoop	7-1/8	7.6
CG Hoop	6-3/8	5.9
Bottom Hoop	6-3/4	5.9
Bottom Chime	10	10.1

Table 3.12.1.5 - Run4g vs TU1, Comparison of Flats for the Crush Impact				
Location	Rigid Surface Side		Crush Plate Side	
	Test	Analysis	Test	Analysis
Top Chime	9	10.5	8-1/2	10.5
Top Hoop	10	11.0	10	11.0
Top CG Hoop	10	10.1	10-1/8	10.1
CG Hoop	9	8.4	10-5/8	10.1
Bottom Hoop	8-1/4	7.6	- - -	0.0
Bottom Chime	9-7/8	10.1	- - -	0.0

The stud at the 90° position was severed in the model (reference Section 3.7, Figure 3.7.6), however arguments were made that the lid would tear first, relieving the loading on the stud. This was verified in the test results where tears were noted at both stud holes at 90° to the impacts/crush.

3.12.2 Comparison of Run2e vs TU3

Run2e is a CG over lid corner 30-foot impact, followed by a bottom corner crush. TU3 is a similar impact configuration with a 4-foot impact and 30-foot impact on the lid corner, then a crush impact on the bottom corner followed by a punch.

Test measurements show that there is 1.125 inches between the top chime and the top hoop in the test. Similar measurements in the analysis show that the distance is about 1.7 inches. This would be a somewhat judgmental comparison due to points chosen for measurement on the test specimen might not be the same as those chosen in the analysis. The analysis measurement is from the top of the crimped drum roll to the center of the flattened region in the lid roll, on the plane of symmetry. Actual point locations chosen in the test measurements are not known.

Table 3.12.2.1 shows the comparison of the TU3 test unit and the computer run2e diameter changes after the 30-foot impact.

Table 3.12.2.1 - Run2e vs TU3, Diameter Results After the 30-Foot Impact

	0°-180°		90°-270°	
	Test	Analysis	Test	Analysis
Top Chime	19-1/4	19.0	19-3/16	19.1
Top Hoop	18-5/8	19.1	19-7/8	20.0
Top CG Hoop	19-1/8	19.4	19-3/8	19.5
CG Hoop	19-1/8	19.4	19-3/8	19.4
Bottom Hoop	19-1/8	19.4	19-1/4	19.4
Bottom Chime	19-1/8	19.3	19-3/8	19.4

Figure 3.12.2.1 is an image of the damage after the 30-foot impact of TU3. The test photo shows the cumulative damage from the 4-foot and 30-foot impacts. Figure 3.12.2.2 shows the analysis damage from only the 30-foot impact.

Figure 3.12.2.1 - TU3, Deformed Shape After the 30-Foot Impact

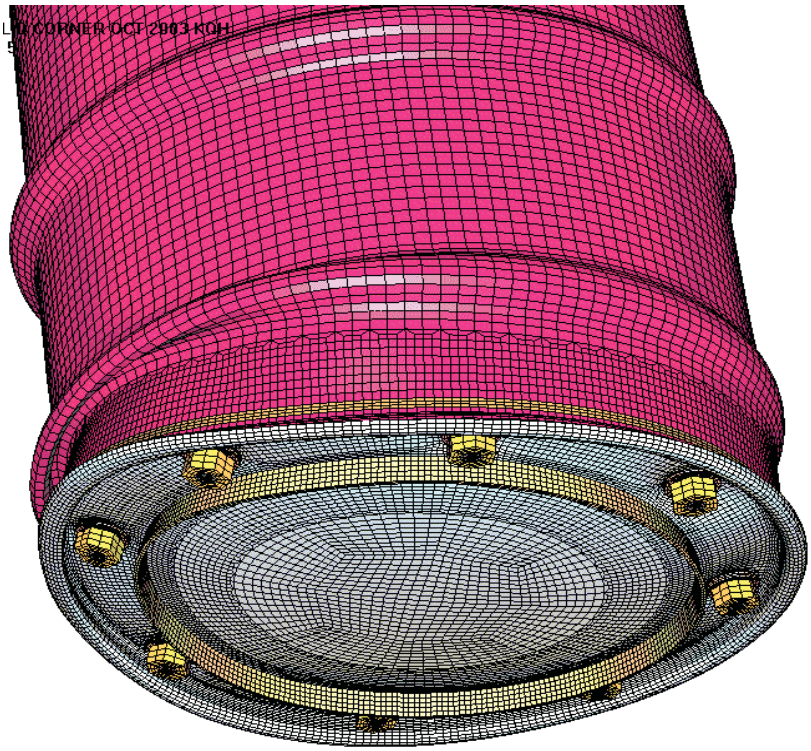

Figure 3.12.2.2 - Run2e, Deformed Shape After the 30-Foot Impact

The package diameters after the crush impact are compared in Table 3.12.2.2.

Table 3.12.2.2 - Run2e vs TU3, Diameter Results After the Crush Impact				
	0°-180°		90°-270°	
	Test	Analysis	Test	Analysis
Top Chime	19-1/4	19.0	19-1/16	19.0
Top Hoop	18-3/4	18.9	20-1/4	20.6
Top CG Hoop	19-1/4	19.4	19-3/4	19.9
CG Hoop	19-1/8	19.3	19-1/4	19.4
Bottom Hoop	19-1/8	19.3	19-3/4	20.4
Bottom Chime	18	18.6	19-3/8	19.4

The final images after the crush impact are shown for the test and the analysis. Figure 3.12.2.3 shows the final shape of the crushed bottom on the test specimen (4ft + 30ft + crush impacts) and Figure 3.12.2.4 shows a similar view of the analysis (30ft + crush impacts).

Figure 3.12.2.3 - TU3, Damage to the Bottom Head in the Crush Impact

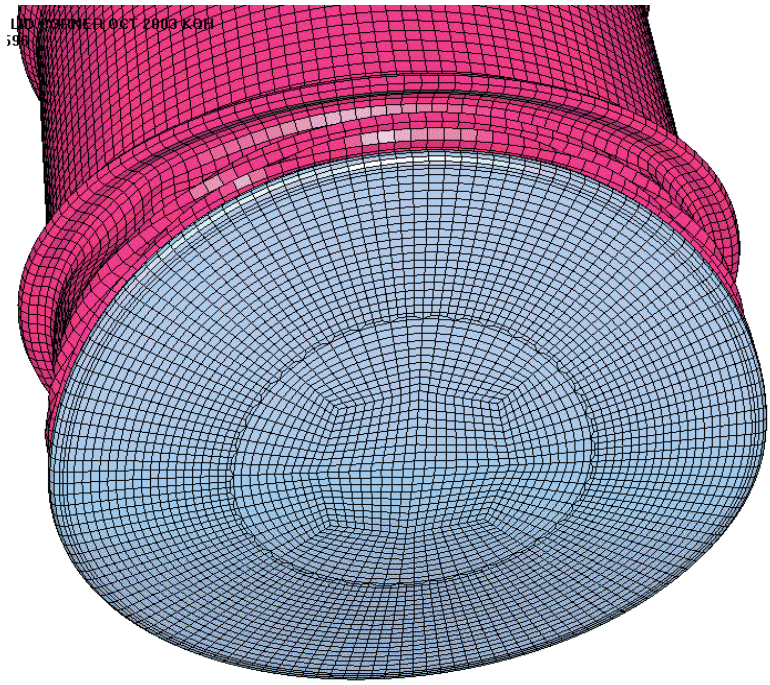

Figure 3.12.2.4 - Run2e, Damage to the Bottom Head in the Crush Impact

The damage to the lid region at the end of the crush impact is shown in Figure 3.12.2.5 for the TU3. The damage to the lid region in the analysis run2e is shown in Figure 3.12.2.6. Note that the stud at the initial 30-foot impact onto the rigid surface has failed in the test. Elevated plastic strains throughout the stud shank are noted in Section 3.5 along with discussion about the stud.

Figure 3.12.2.5 - TU3, Lid Damage from the Crush Impact

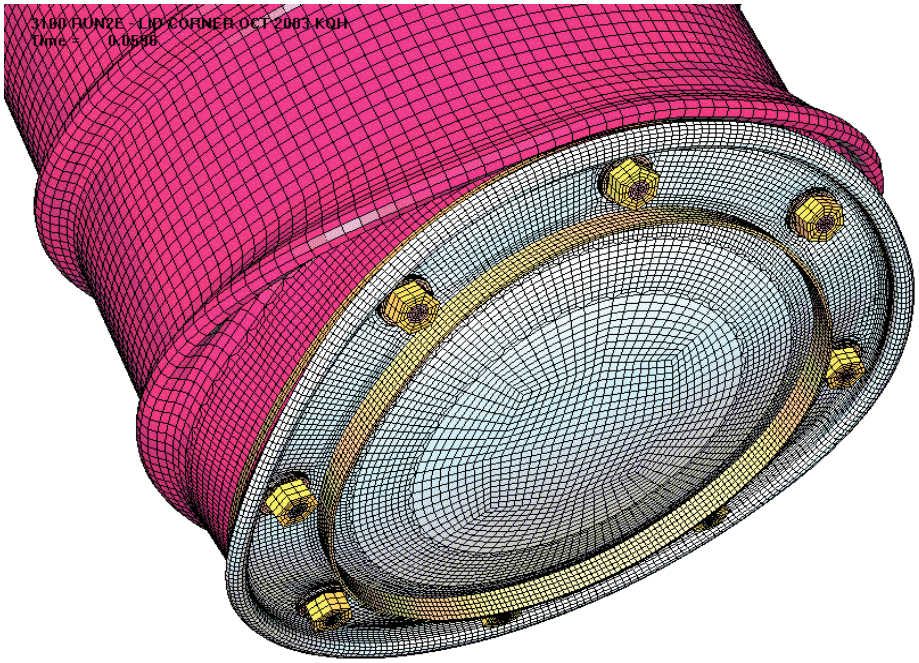

Figure 3.12.2.6 - Run2e, Lid Damage from the Crush Impact

3.12.3 Comparison of Run3b vs TU4

The run3b is a 30-foot lid end down impact onto the rigid surface, followed by a crush impact onto the container bottom. TU4 is a test unit subjected to a 4- and 30-foot impact onto the lid end, followed by a crush impact onto the bottom.

The diameter measurements after the 30-foot impact are given in Table 3.12.3.1.

Table 3.12.3.1 - Run3b vs TU4, Diameter Results After the 30-Foot Impact				
	0°-180°		90°-270°	
	Test	Analysis	Test	Analysis
Top Chime	19-1/4	19.3	19-3/8	19.3
Top Hoop	19-1/8	19.7	19-7/8	19.7
Top CG Hoop	19-13/16	20.0	19-3/8	20.0
CG Hoop	19-1/8	19.5	19-1/4	19.5
Bottom Hoop	19-1/4	19.4	19-1/4	19.4
Bottom Chime	19-1/4	19.4	19-1/4	19.4

The overall height measurements of the drum are compared. The 30-foot impact test results vary around the circumference: 43.0 inches at 0°, 43.125 inches at 90°, 42.875 inches at 180° and 42.625 inches at 270°. The analysis is symmetrical, and the height from the top of the lid drum roll to the bottom head surface after the 30-foot impact is about 42.6 inches.

Figure 3.12.3.1 shows the configuration of the TU4 after the 30-foot impact (4ft + 30ft). Figure 3.12.3.2 shows the analysis model configuration after the 30-foot impact in a similar orientation to the test unit.

Figure 3.12.3.1 - TU4, 30-Foot Impact Damage

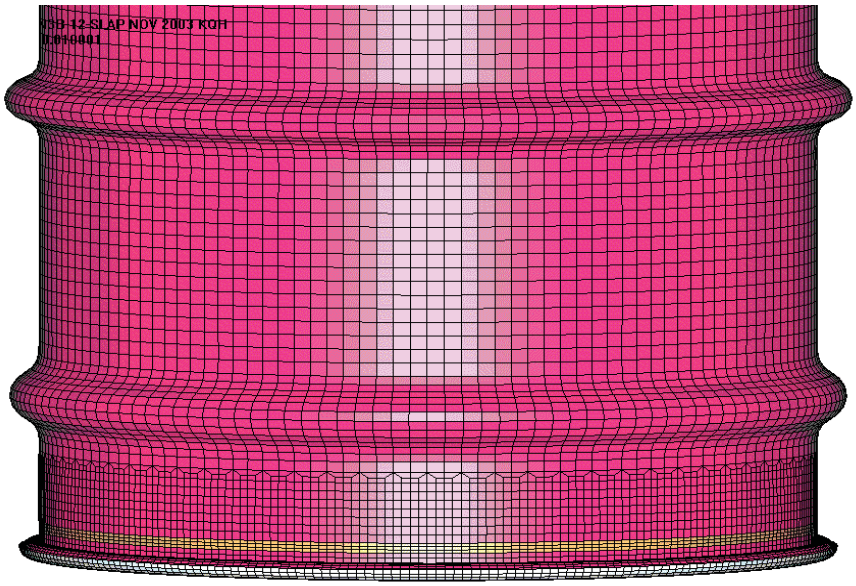

Figure 3.12.3.2 - Run3b, 30-Foot Impact

The height measurement of TU4 after the crush impact is 39.375 inches at 0°, 40.375 inches at 90°, 40.625 inches at 180°, and 39.75 inches at-270°. The analytical value for the height is about 38.9 inches.

The diameters after the crush impact are compared in Table 3.12.3.2.

Table 3.12.3.2 - Run3b vs TU4, Diameter Results After the Crush Impact				
	0°-180°		90°-270°	
	Test	Analysis	Test	Analysis
Top Chime	19-1/4	19.3	19-3/8	19.3
Top Hoop	20	20.2	20-1/8	20.2
Top CG Hoop	20	20.2	20-1/16	20.2
CG Hoop	19-7/16	20.1	19-1/2	20.1
Bottom Hoop	19-15/16	20.5	20	20.5
Bottom Chime	19-1/4	19.4	19-1/4	19.4

Figure 3.12.3.3 shows the TU4 at the end of the crush impact (4ft + 30ft + crush), while Figure 3.12.3.4 shows the configuration of the run3b model (30ft + crush).

Figure 3.12.3.3 - TU4, Crush Damage

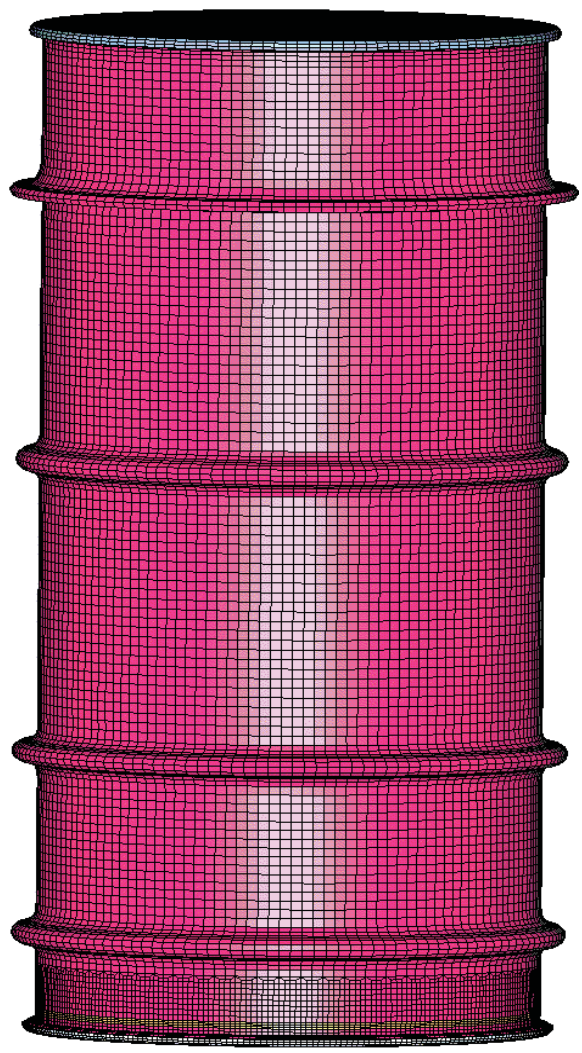

Figure 3.12.3.4 - Run3b, Crush Damage

3.12.4 Comparison of Run1hh vs TU2

Run1hh was the upper bounding kaolite (-40°F) run which included a 4-ft, 30-foot, crush, and punch impacts. The test results are for the cumulative damage from all four impacts, therefore, only one set of data is compared. The table 3.12.4.1 shows the results for the diameter changes due to all four impacts for the test and the analysis.

Table 3.12.4.1 - Run1hh vs TU2, Cumulative Diameter Results After the Punch Impact				
	0°-180°		90°-270°	
	Test	Analysis	Test	Analysis
Top Chime	17-5/8	18.1	19-13/16	19.5
Top Hoop	17-3/8	16.7	19-3/4	20.0
Top CG Hoop	17	16.5	20	20.3
CG Hoop	16	16.4	20-1/4	20.4
Bottom Hoop	15-1/2	16.3	20-1/8	19.9
Bottom Chime	18	17.7	19-3/8	19.4

Table 3.12.4.2 shows the comparison of the "flats" dimensions for the test and the analysis.

Table 3.12.4.2 - Run1hh vs TU2, Cumulative Flats Results After the Punch Impact				
	180° - Crush Plate Side		0° - Rigid Surface Side	
	Test‡	Analysis	Test	Analysis
Top Chime	6-1/4	0	8.0	9.2
Top Hoop	8-7/8	10.1	9.0	8.4
Top CG Hoop	9-5/8	8.4	10-1/8	8.4
CG Hoop	12	9.3	9-7/8	9.3
Bottom Hoop	14-7/8	10.1	9-7/8	9.3
Bottom Chime	0	0	9-3/8	10.1
‡ - Note - The crush plate edge was 4.75 inches from bottom of package, therefore the top chime was engaged with the crush plate in the test.				

A visual comparison of the cumulative damage on the rigid surface side after the four impacts is shown in Figures 3.12.4.1 (test) and Figure 3.12.4.2 (analysis).

Figure 3.12.4.1 - TU2, Cumulative Damage After the Punch Impact, Rigid Surface Side

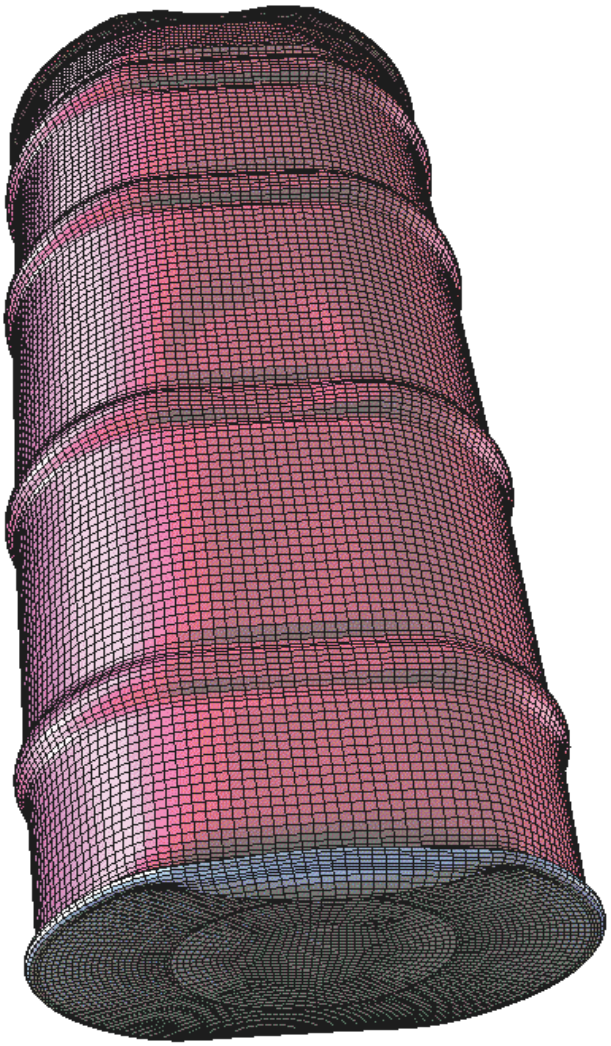

Figure 3.12.4.2 - Run1hh, Cumulative Damage After the Punch Impact, Rigid Surface Side

A visual comparison of the cumulative damage on the crush side after the four impacts is shown in Figures 3.12.4.3 (test) and Figures 3.12.4.4 (analysis).

Figure 3.12.4.3 - TU2, Cumulative Damage After the Punch Impact, Crush Plate Side

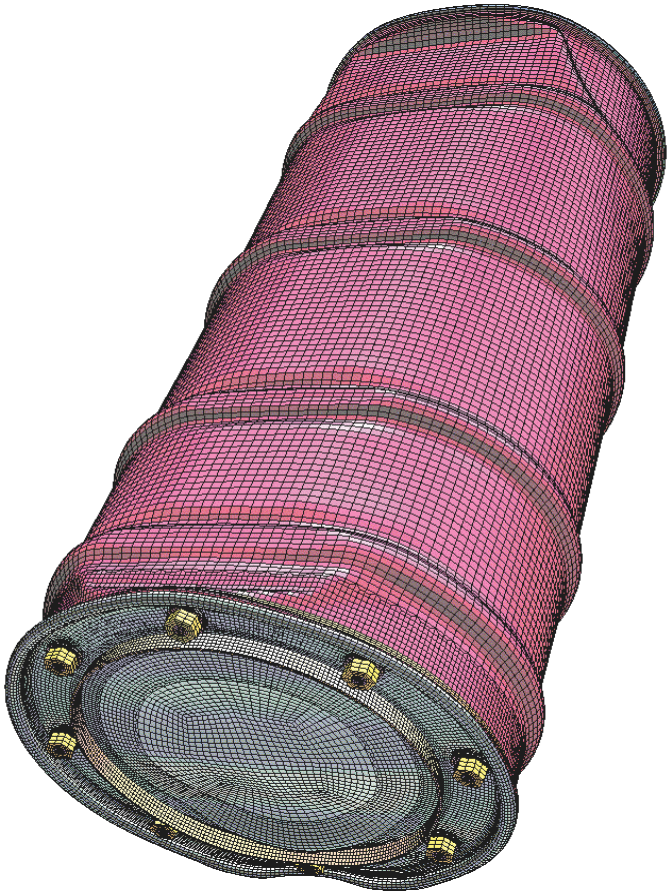

Figure 3.12.4.4 - Run1hh, Cumulative Damage After the Punch Impact, Crush Plate Side

4.0 Summary and Conclusions

The response of the ES-3100 shipping container to various 10CFR71 required impacts is presented in Sections 3.1 to 3.10. The maximum effective plastic strain for each component in the Section 3.1 to 3.10 impacts is summarized in Table 4.0.1. The effective plastic strain for shell elements in Table 4.0.1 is maximum surface strain. Section 3.11 presents the response of the drum to various punch angles. The maximum effective plastic strain for the drum in each punch angle orientation of Section 3.11 is summarized in Table 4.0.2. Section 3.12 compares the analytical results to physical test results.

Maximum strains in excess of 0.5 in/in are near the 304L strain limit of 0.57 in/in and are highlighted in red in Table 4.0.1. The components which are highlighted include the drum, lid, studs and liner.

From Table 4.0.1, the fact that is apparent is the high demand placed on the drum lid and studs. During the design phase of the ES-3100, an effort was made to minimize the number of fasteners in the drum lid. The relatively high lid/stud strains are therefore a precipitate of that effort. The side and slapdown impacts place a high demand on the lid/stud components.

In the side crushes (run1g, run1ga, run1hl, run1hh, run4g, run4ga, run4h and run4ha) a large demand is placed on the lid and the studs. In all the runs the impact of concern is the crush impact and the demand it places on the lid and studs. In all the runs, the relatively high levels of effective plastic strain (surface and membrane) are shown to exist over localized regions of stud/lid interaction in the lid. Investigations revealed that the elevated plastic strains in the lid occurred before the studs experienced elevated strain levels. Therefore, it would be expected that the lid would tear and relieve loading on the studs, before the studs would fail. Some tearing of the lid may take place, but catastrophic tearing or ripping of the lid is not predicted. The large washer would restrain the lid, even if the crimping of the lid/drum roll didn't pin the lid in place. This was verified in the TU1 test specimen with local tearing at the stud holes at 90° and 270° without the loss of a stud.

Table 4.0.1 - ES-3100 Shipping Package Summary of Componenet Maximum Effective Plastic Strains (in/in)

Material	Description	Run1g		Run1ga		Run1hl				Run1hh			
		Side (Section 3.1)		Side (Section 3.2)		Side - Lower Bound Kaolite (Section 3.3)				Side - Upper Bound Kaolite (Section 3.4)			
		Impact	Centered Crush	Impact	Offset Crush	4-foot	30-foot	Centered Crush	Punch	4-foot	30-foot	Centered Crush	Punch
1	CV Body	0.0346	0.0348	Same as Run1g Impact Results	0.0348	0.0263	0.0287	0.0287	0.0299	0.0298	0.0386	0.0462	0.0599
3	CV Lid	0.0002	0.0002		0.0002	0.0000	0.0001	0.0003	0.0006	0.0000	0.0000	0.0004	0.0004
4	CV Nut Ring	0.0000	0.0000		0.0000	0.0000	0.0000	0.0000	0.0000	0.0000	0.0000	0.0000	0.0000
5	Angle	0.0682	0.0945		0.1058	0.0054	0.0777	0.1178	0.1178	0.0059	0.0622	0.0816	0.0816
6	Drum	0.2218	0.3028		0.3818	0.1561	0.2250	0.5309	0.5309	0.1170	0.2259	0.2623	0.2623
7	Drum Bottom	0.2444	0.2945		0.2444	0.0991	0.2125	0.3342	0.3345	0.1215	0.2528	0.2807	0.2807
10	Liner	0.1189	0.2063		0.2853	0.0537	0.1800	0.2637	0.2637	0.0598	0.0970	0.2005	0.2027
12	Lid	0.3580	0.6430		1.1345	0.1320	0.5180	1.2969	1.2971	0.0860	0.4073	0.6411	0.6411
15	Lid Stiffener	0.0060	0.0303		0.1116	0.0001	0.0118	0.0530	0.0530	0.0000	0.0069	0.0217	0.0217
16	Lid Studs	0.1171	0.1937		0.5207	0.0000	0.1098	0.4159	0.4221	0.0000	0.1226	0.1753	0.1761
17	Lid Stud Nuts	0.0005	0.0005		0.0103	0.0000	0.0000	0.0007	0.0007	0.0000	0.0000	0.0000	0.0000
18	Lid Stud Washer	0.1628	0.1628		0.1685	0.0011	0.0225	0.0832	0.0844	0.0310	0.0951	0.1034	0.1034
19	Plug Liner	0.0826	0.1212		0.2181	0.0022	0.0956	0.1255	0.1255	0.0046	0.0995	0.1258	0.1258

Material	Description	Run2e		Run3b		Run4g		Run4ga		Run4h		Run4ha	
		Corner (Section 3.5)		End (Section 3.6)		Slapdown (Section 3.7)		Slapdown (Section 3.8)		Slapdown (Section 3.9)		Slapdown (Section 3.10)	
		Impact	Crush	Impact	Crush	Impact	Offset Crush	Impact	Centered Crush	Impact	Offset Crush	Impact	Centered Crush
1	CV Body	0.0142	0.0364	0.0012	0.0053	0.0445	0.0457	Same as Run4g Impact Results	0.0741	0.0450	0.0461	Same as Run4h Impact Results	0.0839
3	CV Lid	0.0024	0.0024	0.0031	0.0034	0.0003	0.0005		0.0006	0.0000	0.0004		0.0013
4	CV Nut Ring	0.0000	0.0000	0.0000	0.0000	0.0000	0.0000		0.0003	0.0000	0.0000		0.0000
5	Angle	0.0393	0.0464	0.0287	0.0304	0.0881	0.1045		0.0917	0.0861	0.1071		0.0881
6	Drum	0.3238	0.3787	0.0565	0.1258	0.3017	0.3972		0.3537	0.3017	0.3881		0.3848
7	Drum Bottom	0.0000	0.0731	0.0024	0.0312	0.2877	0.2877		0.2919	0.2877	0.2877		0.2922
10	Liner	0.3797	0.5507	0.1665	0.3585	0.1234	0.2702		0.2363	0.1181	0.2475		0.2633
12	Lid	0.2968	0.3579	0.1094	0.1415	0.5537	1.0797		1.0795	0.3831	0.9830		0.6335
15	Lid Stiffener	0.0271	0.0272	0.0068	0.0098	0.0232	0.0838		0.0303	0.0184	0.1083		0.0338
16	Lid Studs	0.5197	0.5578	0.0962	0.1541	0.1737	>0.57		0.3174	0.0891	0.5364		0.1705
17	Lid Stud Nuts	0.2252	0.2258	0.0162	0.0170	0.0000	0.0086		0.0000	0.0000	0.0052		0.0000
18	Lid Stud Washer	0.0907	0.1111	0.0510	0.0510	0.0597	0.1003		0.0597	0.0782	0.0885		0.0782
19	Plug Liner	0.1131	0.1170	0.0636	0.0944	0.1290	0.2715		0.1636	0.1592	0.2719		0.1832

Table 4.0.2 - ES-3100 Punch Angle Variation		
Punch Angle	Maximum Effective Plastic Strain in the Drum (in/in)	
	Surface	Membrane
0	0.2030	0.1385
10	0.1204	0.0633
20	0.1100	0.0529
30	0.1551	0.0951
40	0.1632	0.1115
50	0.3340	0.1238
60	0.1844	0.0646
63.6	0.3895	0.1858

The drum in run1hl (lower bounding kaolite impacts) is shown to experience a high demand during the centered crush impact. The regions of high effective plastic strain are in the drum at each edge of the crush plate. The lid end of the drum experiences the highest strain (about 0.53 in/in), but its magnitude is below the failure limit of 0.57 in/in in bending and less than (about 0.36 in/in) in membrane. Therefore, tearing of the drum is not expected.

The liner in run2e (corner impact) also experiences relatively high effective plastic strain in its crush impact (about 0.55 in/in). This is in a region of localized crimping and the membrane stain is found to be about 0.25 in/in. Therefore, tearing of the liner is not expected.

The run2e corner impact shows high effective plastic strain in the drum stud at the 0° position (at the initial impact point with the rigid surface). The region of high strain exists across the diameter of the stud, near its attachment to the angle. High strain levels are shown in the 30-foot impact (about 0.52 in/in) and higher in the crush impact (about 0.56 in/in). Two factors direct concern to this stud. One factor is that this stud is right at the rigid surface and, therefore, experiences direct loading between the shipping package and the rigid surface. The second factor is that effective plastic strain quickly (about 0.003 seconds into the 30-foot impact) reaches a significant value (about 0.5 in/in) throughout the stud shank. Slight changes in configuration in the stud from the modeled configuration (e.g. length, end configuration and boundary conditions) could quickly elevate the strains past failure. Boundary conditions such as changes in the friction factor could also prove detrimental for the stud. This was verified in the test

with the failure of the stud at 0°.

The CV lid/body flange separation is reported as time history nodal separation data. The data is from a transient analysis and therefore contains analytical ringing or contact chatter. The maximum gap spike value is about 0.012 inches in run3b. The largest elevated value of gap is also for run3b and is between 0.008 inches and 0.010 inches for about 0.005 seconds. The gap response is oscillatory in nature and reaches an average value of 0.003 inches or less.

In conclusion, review of the results of the ES-3100 borobond design runs presented in this calculation predict:

1) The lid is predicted to locally tear at the stud holes in the side and slapdown crush impacts. Extensive tearing is not predicted. The studs are predicted to remain in place to secure the lid in the side and slapdown impacts.
2) The single stud at the point of contact in the corner impact could easily fail. The remainder of the studs in the corner impact experience relatively low demand and are predicted to restrain the lid/plug. The failure of the single stud, would not result in shielding or thermal protection concerns for the CV.
3) The maximum CV lid/body flange separation spikes to about 0.012 inches briefly, and between 0.008 to 0.010 inches for about 0.005 seconds. The maximum relaxed value of the gap would be expected to be 0.003 inches or less.
4) The remaining kaolite thickness is shown in time history plots in each analysis results in summarized in Section 3(e.g., Figure 3.1.33).

5.0 References

5.1 The software "TrueGrid", by XYZ Scientific Applications, Inc, Version 2.1.5.

5.2 Livermore Software Technology Corporation (LSTC), "LS-Dyna", A Program for Nonlinear Dynamic Analysis of Structures in Three Dimensions, Version 960, Revision 1106, dated 01/28/2002.

5.3 LSTC, "LS-Post", version 2.0, revision 1622, dated July 17, 2002.

5.4 Standard Specification for Stainless Steel Bars and Shapes for Use in Boilers and Other Pressure Vessels, ASTM A479/A 479M -03.

5.5 The software "AutoSketch", by Autodesk, Inc, Release 2.1, October 5, 1995.

5.6 Harris, C. M, and Crede, C. E., "Shock and Vibration Handbook", Second Edition, McGraw Hill.

6.0 Analytical Model

The differences between the initial, detailed borobond model (described in Section 2.1) and the redesigned ES-3100 package are described in detail in Section 6.1. The material properties for the HABC are described in Section 6.2. Other than the geometric differences described in Section 6.1 and the material models described in Section 6.2, the detailed analytical models are the same as those presented in Part A, Section 2.1.

6.1 Model Description

The redesign configuration details to incorporate the HABC will be described as changes to the initial model. Figures 6.1 and 6.2 show the design configuration changes that were made in the analytical models. In the two figures, the black color indicates the initial design and the red (magenta) color indicates the redesign configuration.

The changes to the configuration of the analytical model were:

1. The internal radius of the liner between the neutron absorbing material and the kaolite was increased from 4.08 in to 4.30 in (Figure 6.1 and 6.2).

2. The internal radius of the liner above the neutron absorbing material and near the CV flange was decreased from 4.40 in to 4.30 in (Figure 6.1).

3. The radius of the CV bottom pad at its inner most part radius was increased from 0.05 in to 0.11 in. This effectively slightly thickens the pad at the footprint of the CV bottom head and therefore the CV was raised by about 0.068 in (Figure 6.1 and 6.2).

As a precipitate of the above configuration changes, some changes were made to the contact surfaces between the neutron absorber material, the kaolite and the stainless steel (SS) liners. The contact type remained the same as in the Part A computer runs (SURFACE_TO_SURFACE).

Figures 6.1.3 and 6.1.4 show the element mesh configurations near the CV flange and the CV bottom. These figures can be compared to Figures 2.1.3 and 2.1.4 to show the differences between the two design configurations.

The runs chosen to be made with the HABC modifications and compared to the original borobond model are shown in Figure 6.1.5. To differentiate the runs, yet show similarity,

the "HABC" is added to the borobond run identification to identify the redesign runs. For example, the Part A, borobond "run2e" impact configuration is known as "HABC-run2e" for the Part B, HABC runs.

Table 6.1.1 describes the impact configurations for the HABC computer runs. Note that the bounding stiffness runs (1hh and 1hl) do not include the punch impact following the crush impact. The Part A, 1hh and 1hl impacts and the punch study demonstrate the integrity of the drum/kaolite. The drum/kaolite remained the same for the Part B HABC runs, therefore the punch impacts were not included in the HABC runs. Table 6.1.1 also gives the kaolite and HABC models used in each run.

Table 6.1.2 shows the component mass/weight for the HABC models. The total weight for the fully loaded models is about 432 pounds with the 22.4 lb/ft^3 kaolite. The mass inertia about the global Y axis is 90.98 $in*lb*sec^2$ and the CG is located at Z=22.41 inches above the bottom surface of the container.

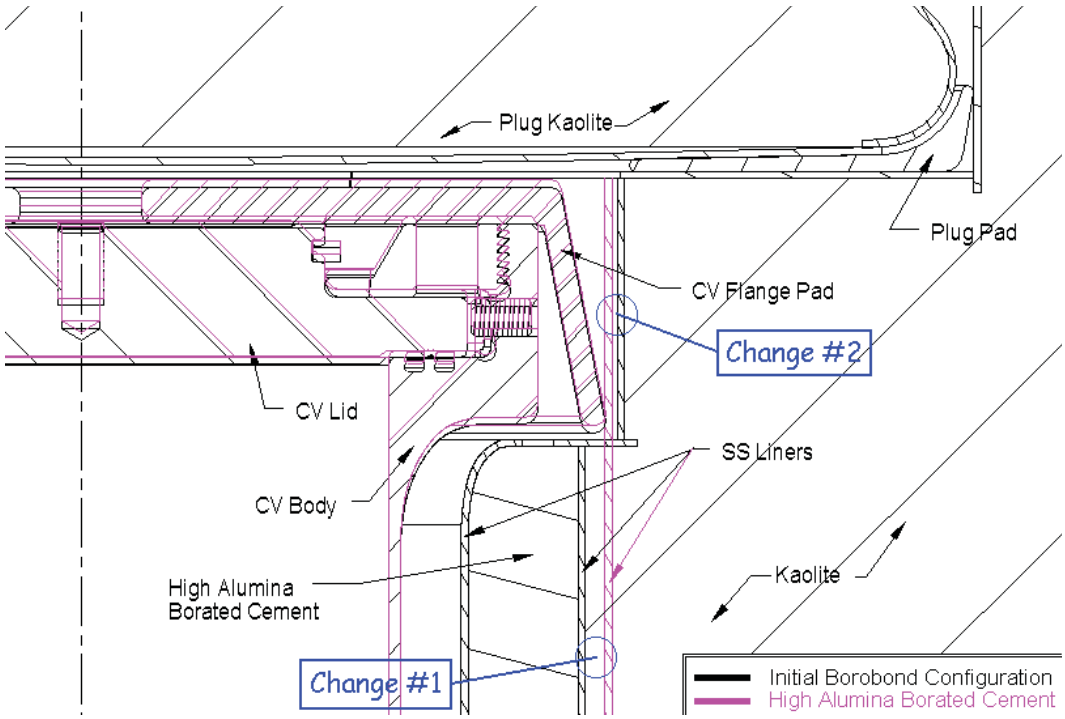

Figure 6.1.1 - Configuration Changes for the HABC, Compared to the Borobond Model Near the CV Flange

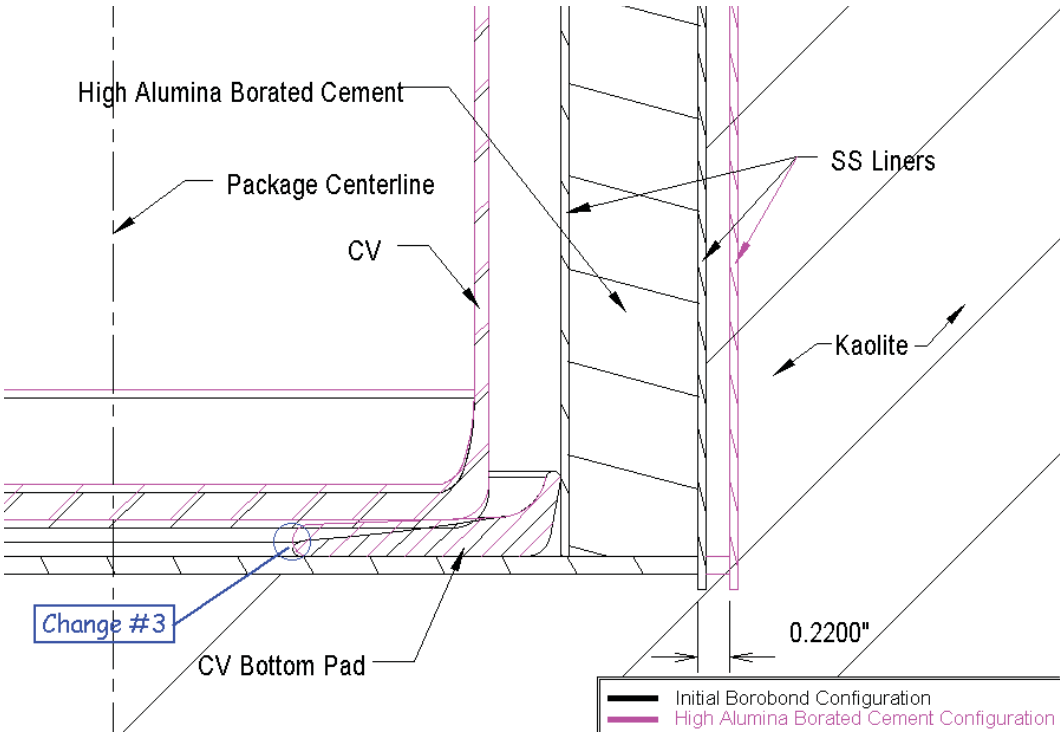

Figure 6.1.2 - Configuration Changes for the HABC, Compared to the Borobond Model Near the Bottom of the CV Body

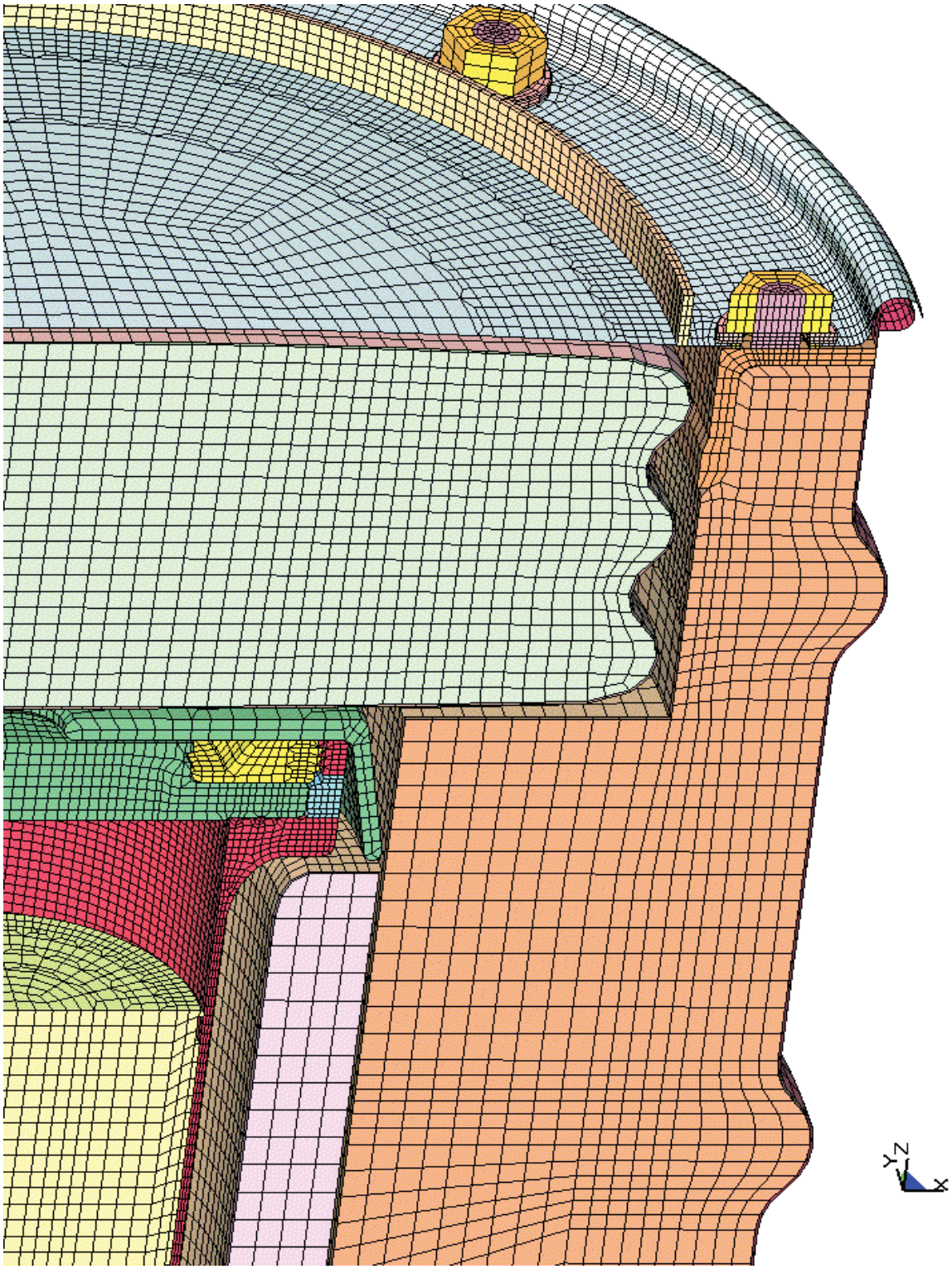

Figure 6.1.3 - Configuration of the HABC Analytical Model Near the Package Top

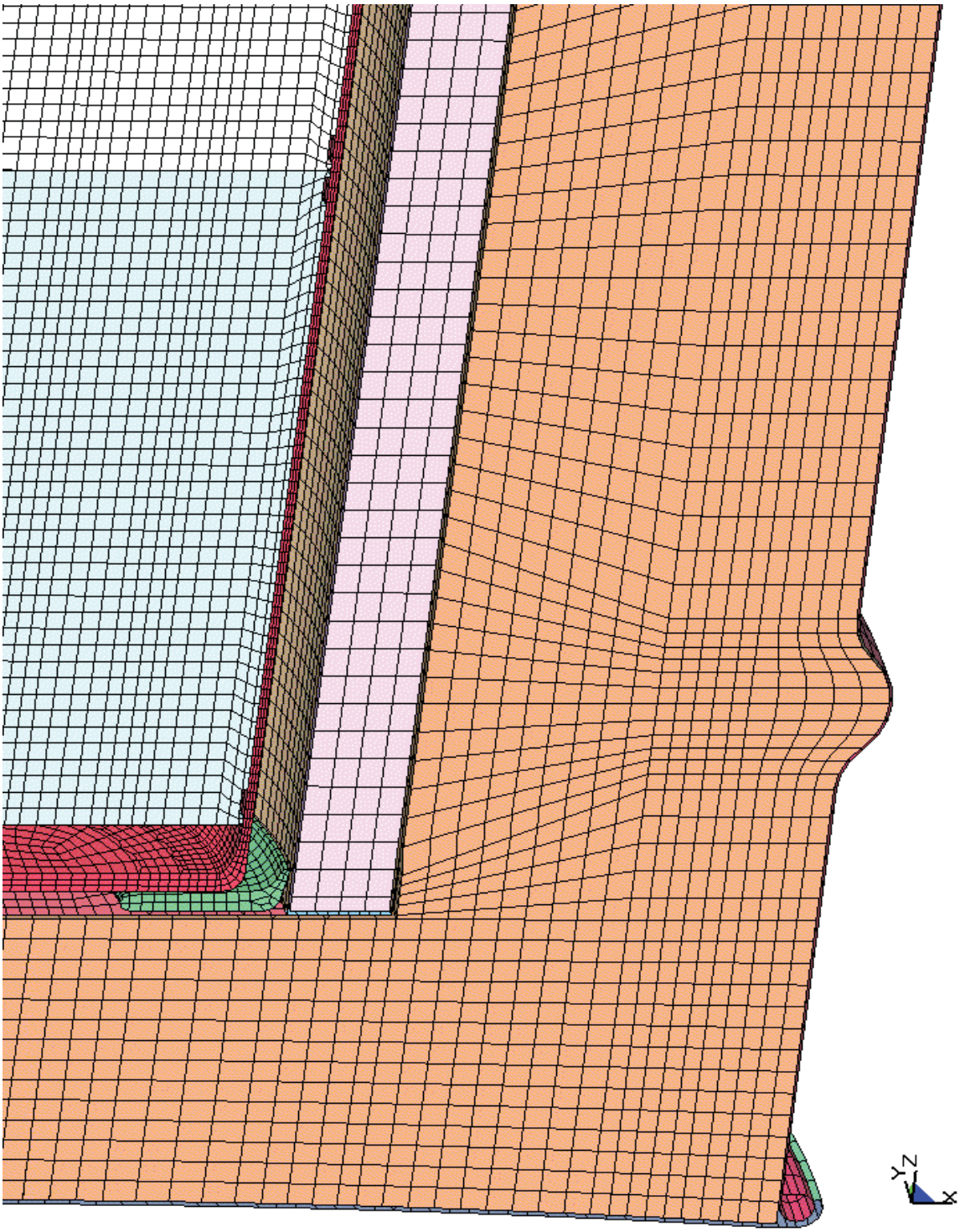

Figure 6.1.4 - Configuration of the HABC Analytical Model Near the Package Bottom

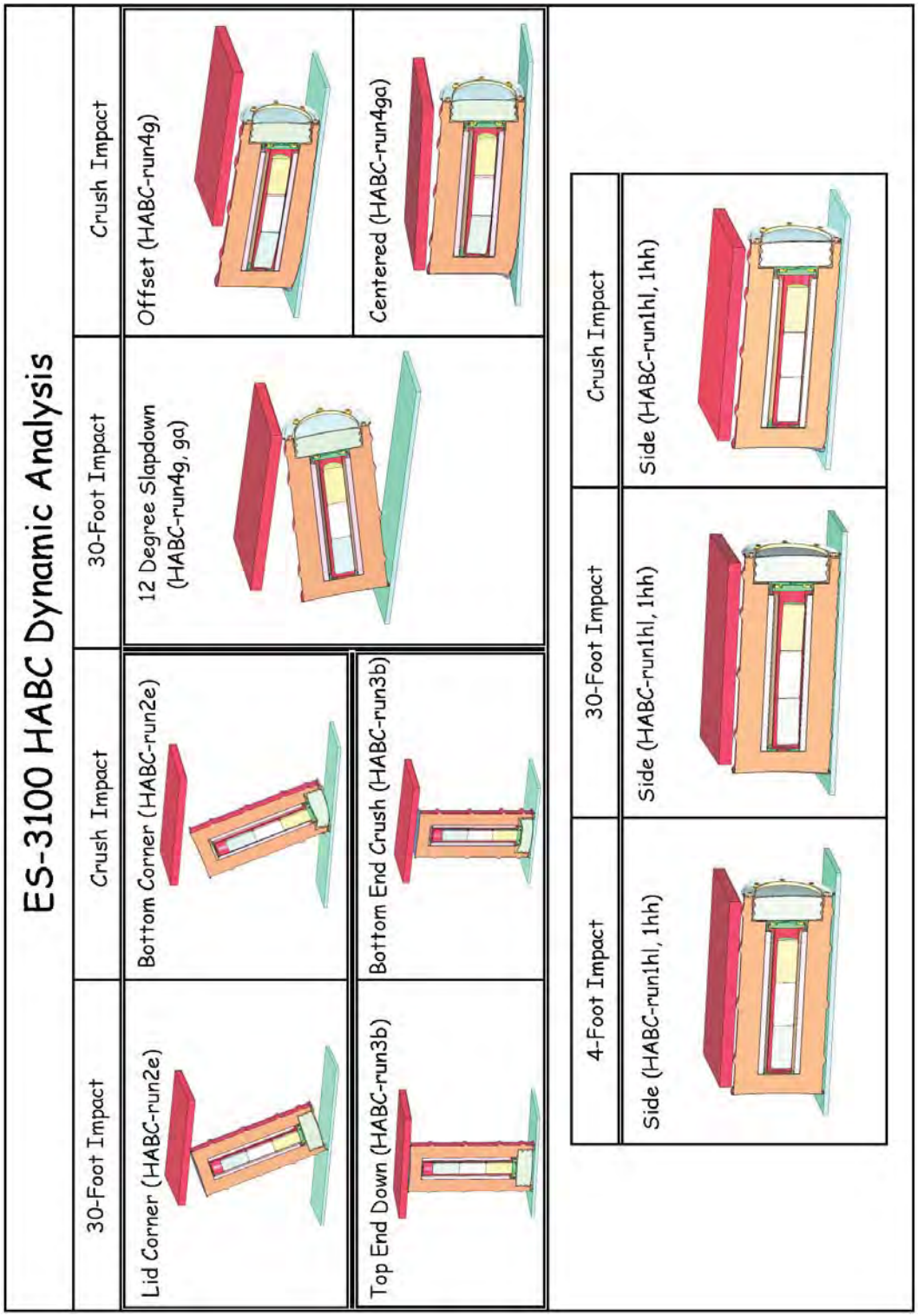

Figure 6.1.5 - LS-Dyna Impact Configurations for the HABC Model

Table 6.1.1 - Description of the ES-3100 HABC Impacts			
Run ID	Impact Description	Kaolite Model	HABC Model
HABC-run1hl	4-foot side impact + 30-foot side impact + 30-foot crush impact	Lower bound stiffness, Section 3.2.5.2	100°F, Section 6.2.3
HABC-run1hh	4-foot side impact + 30-foot side impact + 30-foot crush impact	Upper bound stiffness, Section 3.2.5.3	-40°F, Section 6.2.1
HABC-run2e	30-foot CG over lid corner impact + 30-foot crush on bottom corner	Average stiffness, Section 3.2.5.1	70°F, Section 6.2.2
HABC-run3b	30-foot top end impact + 30-foot bottom end crush	Average stiffness, Section 3.2.5.1	70°F, Section 6.2.2
HABC-run4g	30-foot, 12° slapdown with lid studs on plane of symmetry + 30-foot crush with plate centered on CV flange	Average stiffness, Section 3.2.5.1	70°F, Section 6.2.2
HABC-run4ga	30-foot, 12° slapdown with lid studs on plane of symmetry + 30-foot crush with plate centered on drum	Average stiffness, Section 3.2.5.1	70°F, Section 6.2.2

Table 6.1.2 - Analysis Weights for the ES-3100 HABC Models

Material Number	Component Description	HABC-run2e			HABC-run1hh			HABC-run1hl			HABC-run3b			HABC-run4g		
		mass *	weight **	change***	mass	weight	change***	mass	weight	change***	mass	weight	change***	mass	weight	change***
m 1	CV body	2.73E-02	21.10	0.00	2.73E-02	21.10	0.00	2.73E-02	21.10	0.00	2.73E-02	21.10	0.00	2.73E-02	21.10	0.00
m 2	CV body at flange	1.73E-03	1.34	0.00	1.73E-03	1.34	0.00	1.73E-03	1.34	0.00	1.73E-03	1.34	0.00	1.73E-03	1.34	0.00
m 3	CV lid	9.57E-03	7.39	0.00	9.57E-03	7.39	0.00	9.57E-03	7.39	0.00	9.57E-03	7.39	0.00	9.57E-03	7.39	0.00
m 4	CV screw ring	4.27E-03	3.30	0.00	4.27E-03	3.30	0.00	4.27E-03	3.30	0.00	4.27E-03	3.30	0.00	4.27E-03	3.30	0.00
m 5	angle	1.69E-02	13.02	0.00	1.69E-02	13.02	0.00	1.69E-02	13.02	0.00	1.69E-02	13.02	0.00	1.69E-02	13.02	0.00
m 6	drum	6.02E-02	46.50	0.00	6.02E-02	46.50	0.00	6.02E-02	46.50	0.00	6.02E-02	46.50	0.00	6.02E-02	46.50	0.00
m 7	drum bottom head	1.22E-02	9.42	0.00	1.22E-02	9.42	0.00	1.22E-02	9.42	0.00	1.22E-02	9.42	0.00	1.22E-02	9.42	0.00
m 8	weld drum to drum bottom head	1.18E-04	0.09	0.00	1.18E-04	0.09	0.00	1.18E-04	0.09	0.00	1.18E-04	0.09	0.00	1.18E-04	0.09	0.00
m 9	liner overlap to angle (0.03)	1.36E-04	0.11	0.00	1.36E-04	0.11	0.00	1.36E-04	0.11	0.00	1.36E-04	0.11	0.00	1.36E-04	0.11	0.00
m 10	liner (0.06)	4.05E-02	31.23	0.71	4.05E-02	31.23	0.71	4.05E-02	31.23	0.71	4.05E-02	31.23	0.71	4.05E-02	31.23	0.71
m 11	liner bottom (0.120) (see m 27 for solids)	1.40E-03	1.08	0.00	1.40E-03	1.08	0.00	1.40E-03	1.08	0.00	1.40E-03	1.08	0.00	1.40E-03	1.08	0.00
m 12	lid shells (0.06)	7.25E-03	5.59	0.00	7.25E-03	5.59	0.00	7.25E-03	5.59	0.00	7.25E-03	5.59	0.00	7.25E-03	5.59	0.00
m 13	thin lid shell at bolts	1.37E-05	0.01	0.00	1.37E-05	0.01	0.00	1.37E-05	0.01	0.00	1.37E-05	0.01	0.00	1.37E-05	0.01	0.00
m 14	lid solids at the lid bolts	5.03E-05	0.04	0.00	5.03E-05	0.04	0.00	5.03E-05	0.04	0.00	5.03E-05	0.04	0.00	5.03E-05	0.04	0.00
m 15	lid stiffener	1.39E-03	1.07	0.00	1.39E-03	1.07	0.00	1.39E-03	1.07	0.00	1.39E-03	1.07	0.00	1.39E-03	1.07	0.00
m 16	drum bolts	5.06E-04	0.39	0.00	5.06E-04	0.39	0.00	5.06E-04	0.39	0.00	5.06E-04	0.39	0.00	5.06E-04	0.39	0.00
m 17	drum bolt nuts	1.20E-03	0.93	0.00	1.20E-03	0.93	0.00	1.20E-03	0.93	0.00	1.20E-03	0.93	0.00	1.20E-03	0.93	0.00
m 18	drum bolt washers	4.71E-04	0.36	0.00	4.71E-04	0.36	0.00	4.71E-04	0.36	0.00	4.71E-04	0.36	0.00	4.71E-04	0.36	0.00
m 19	plug liner	1.29E-02	10.00	0.00	1.29E-02	10.00	0.00	1.29E-02	10.00	0.00	1.29E-02	10.00	0.00	1.29E-02	10.00	0.00
m 20	plug kaolite	1.26E-02	9.70	0.00	1.52E-02	11.70	0.00	1.52E-02	11.70	0.00	1.26E-02	9.70	0.00	1.26E-02	9.70	0.00
m 21	drum kaolite	1.40E-01	107.88	-2.20	1.69E-01	130.43	-2.60	1.69E-01	130.43	-2.60	1.40E-01	107.88	-2.20	1.40E-01	107.88	-2.20
m 22	drum HABC	6.36E-02	49.08	5.38	6.36E-02	49.08	5.38	6.36E-02	49.08	5.38	6.36E-02	49.08	5.38	6.36E-02	49.08	5.38
m 24	lower internal cv mass	4.75E-02	36.69	0.00	4.75E-02	36.69	0.00	4.75E-02	36.69	0.00	4.75E-02	36.69	0.00	4.75E-02	36.69	0.00
m 25	middle internal cv mass	4.75E-02	36.69	0.00	4.75E-02	36.69	0.00	4.75E-02	36.69	0.00	4.75E-02	36.69	0.00	4.75E-02	36.69	0.00
m 26	upper internal cv mass	4.75E-02	36.69	0.00	4.75E-02	36.69	0.00	4.75E-02	36.69	0.00	4.75E-02	36.69	0.00	4.75E-02	36.69	0.00
m 27	liner bottom solids	1.25E-03	0.96	0.20	1.25E-03	0.96	0.20	1.25E-03	0.96	0.20	1.25E-03	0.96	0.20	1.25E-03	0.96	0.20
m 29	visual rigid plane	8.00E-04	0.62	-0.08	7.80E-04	0.60	0.00	7.80E-04	0.60	0.00	8.00E-04	0.62	0.00	9.00E-04	0.69	0.00
m 30	crush plate	1.42E+00	1099.99	0.00	1.42E+00	1099.99	0.00	1.42E+00	1099.99	0.00	1.42E+00	1099.99	0.00	1.42E+00	1099.99	0.00
m 31	punch	8.24E-02	63.62	0.00	8.24E-02	63.62	0.00	8.24E-02	63.62	0.00	8.24E-02	63.62	0.00	8.24E-02	63.62	0.00
m32	silicon rubber	1.74E-03	1.34	0.07	1.74E-03	1.34	0.07	1.74E-03	1.34	0.07	1.74E-03	1.34	0.07	1.74E-03	1.34	0.07
	dyna total model weight	2.07E+00	1596.23	4.09	2.10E+00	1620.77	3.77	2.10E+00	1620.77	3.77	2.07E+00	1596.23	4.16	2.07E+00	1596.31	4.16
	CV lid and nut ring		10.68			10.68			10.68			10.68			10.68	
	CV body wt		22.44			22.44			22.44			22.44			22.44	
	CV total wt		33.12			33.12			33.12			33.12			33.12	
	plug liner and kaolite		19.70			21.69			21.69			19.70			19.70	
	liner + angle		46.41			46.41			46.41			46.41			46.41	
	drum body + kaolite + borobond4		261.10			283.66			283.66			261.10			261.10	
	drum + lid + plug + kaolite + borobond4		288.81			313.36			313.36			288.81			288.81	
	internal cv masses		110.08			110.08			110.08			110.08			110.08	
	Total Package Weight		432.01			456.56			456.56			432.01			432.01	
	Crush Plate Weight		1099.99			1099.99			1099.99			1099.99			1099.99	
	Punch Weight		63.62			63.62			63.62			63.62			63.62	
	Visual Rigid Plane		0.62			0.60			0.60			0.62			0.69	
	Total Model Weight		1596.23			1620.77			1620.77			1596.23			1596.31	

* - Mass is for the 1/2 model and is the units of (pound* second^2)/inch

**- Weight is for the total package (2 * model weight) and is in units of pounds

*** - Change is the difference between the HABC run and the Table 2.1.2 results

6.2 Material Models

The material models used in the Part B HABC runs are those described in the Part A, Section 2.3 except for the Section 2.3.6 which covered the Borobond material. As in the initial borobond models the stud material was defined with a material failure at the 0.57 in/in strain level.

The borobond material was replaced with the catalog 277-4 high alumina borated cement material which is described in this section and sub-sections. The LS-Dyna material model used for the HABC material is the *MAT_SOIL_AND_FOAM model. The material data was obtained from testing performed at Y12 in the Fall of 2004. Figure 6.2.1 shows the stress vs strain curves obtained in the test.

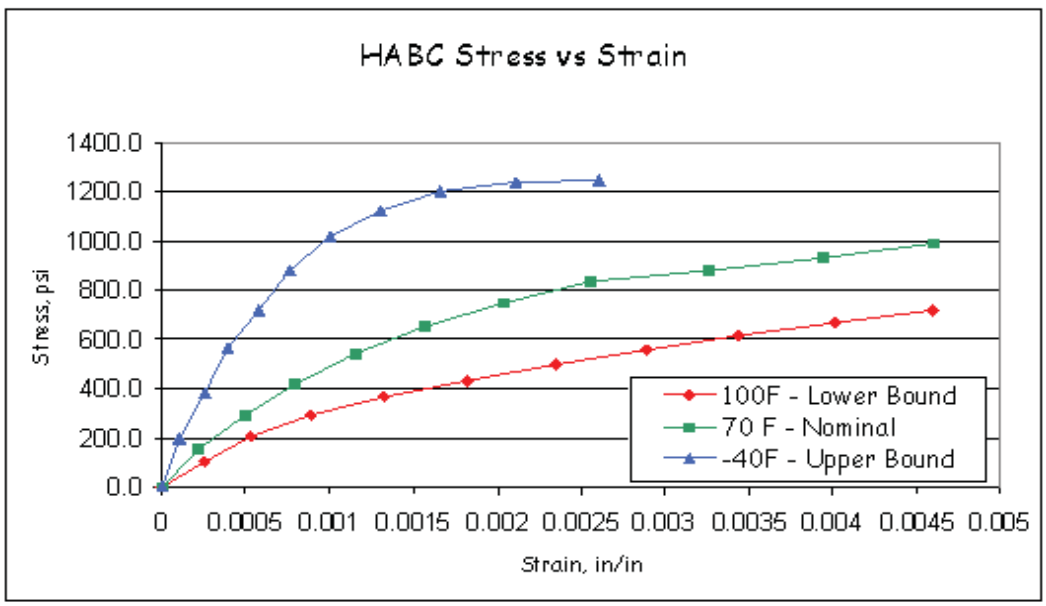

Figure 6.2.1 - HABC Stress vs Strain Curves

6.2.1 HABC at -40° F

Poisson's ratio is given as 0.33 by the testing results. The modulus of elasticity was taken to be the slope of the load deflection curve for the first data point.

$$E = \frac{\sigma}{\varepsilon} = \frac{201.3psi - 0psi}{(101.1e-6) - 0} = 1.991e6psi$$

The shear modulus is then calculated as:

$$ShearModulus = \frac{E}{2(1+\nu)} = \frac{1.991e6\ psi}{2(1+0.33)} = 7.485e5psi$$

The bulk modulus is calculated as:

$$BulkModulus = \frac{E}{3(1-2\nu)} = \frac{1.991e6\ psi}{3(1+2(0.33))} = 1.952e6\ psi$$

Volumetric response data for the HABC material is lacking. A volumetric response will be derived from the one dimensional compressive test data. The HABC material is assumed to behave as a homogeneous, isotropic material.

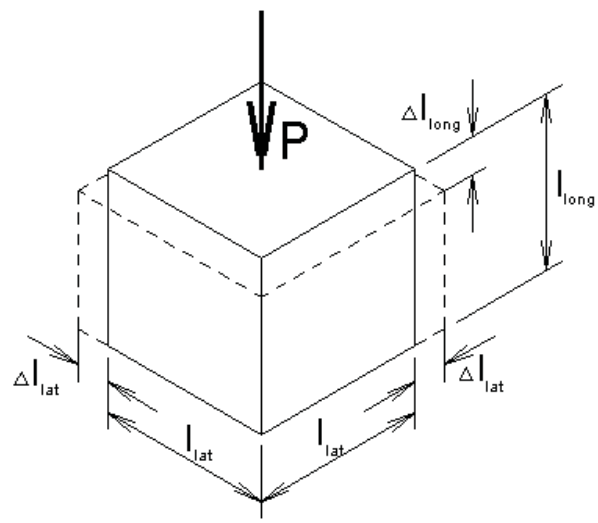

Figure 6.2.1.1 - Assumed Response of a Unit Cube

Using Figure 6.2.1.1 and noting the following definitions,

$$\varepsilon_{long} = \frac{\Delta l_{long}}{l_{long}} \quad ; \quad \varepsilon_{lat} = \frac{\Delta l_{lat}}{l_{lat}} \quad ; \quad \nu = \frac{\varepsilon_{lat}}{\varepsilon_{long}}$$

$$\varepsilon_{lat} = \nu\ \varepsilon_{long}$$

$$l_{lat} = l_{long} = l$$

The initial volume is, l^3, and the final volume is:

$$final\ volume = (l - \Delta l_{long})(l + \Delta l_{lat})(l + \Delta l_{lat})$$

Substituting the above definitions into this equation and simplifying results in the following expression for the final volume.

$$final\ volume = l^3(1 - \varepsilon_{long})(1 + \nu\varepsilon_{long})^2$$

The relative volume then is,

$$V = \frac{current\ volume}{initial\ volume} = (1 - \varepsilon_{long})(1 + \nu\varepsilon_{long})^2$$

The volumetric strain then is:

$$volumetric\ strain = ln\ V$$

Using this and P = σ/3, a pressure vs volumetric strain curve is derived. The pressure cut off for tension is derived from the tensile failure of 234.7 psi. The pressure cut off for the material model is: $P = \frac{\sigma}{3} = \frac{234.7\ psi}{3} = 78.2\ psi$.

The constants a_0, a_1, and a_2 are yield function constants defined in the material model. To eliminate the pressure dependence of the yield strength, $a_1 = a_2 = 0$ and $a_0 = \sigma^2_y/3 = (1165.8\ psi)^2/3 = 4.530e5\ psi^2$. The following material model was used for the upper stiffness bound of the HABC material (-40°).

LS-Dyna Material Model	*MAT_SOIL_AND_FOAM
Density	1.5742e-4 lb-sec^2/in^4 (105 lb/ft^3)
Shear Modulus	7.485e5 psi
Bulk Modulus	1.952e6 psi
A_0	4.530e5 (psi)^2
A_1	0
A_2	0
Tensile Cutoff	78.2 psi

Volumetric Strain Data vs Pressure:

Volumetric Strain, in^3/in^3	Pressure, psi
0	0
-3.4380E-05	67.100
-1.3300E-04	187.300
-2.5971E-04	294.367
-4.4481E-04	374.067
-8.8812E-04	416.567
-3.4612E-03†	433.333†
-1.6787E-01†	566.667†
-5.5498E-01†	1000.000†
-1.1409E+00†	100000.000†

† - assumed values to achieve numerical lock-up.

6.2.2 HABC at 70° F

Poisson's ratio is given as 0.28 by the testing. The modulus of elasticity was taken to be the slope of the load deflection curve for the first data point.

$$E = \frac{\sigma}{\varepsilon} = \frac{150.3psi - 0psi}{(219.8e-6) - 0} = 6.838e5psi$$

The shear modulus is then calculated as:

$$ShearModulus = \frac{E}{2(1+\nu)} = \frac{6.838e5\ psi}{2(1+0.28)} = 2.671e5psi$$

The bulk modulus is calculated as:

$$BulkModulus = \frac{E}{3(1-2\nu)} = \frac{6.838e5\ psi}{3(1+2(0.28))} = 5.180e5\ psi$$

The pressure cut off is calculated as P=184 psi / 3 = 61.3 psi and the constants a_0 is calculated as (983psi)^2/3 = 3.221e5 psi^2. The following material model was used for the 70°F runs of the HABC material.

LS-Dyna Material Model	*MAT_SOIL_AND_FOAM
Density	1.5742e-4 lb-sec^2/in^4 (105 lb/ft^3)
Shear Modulus	2.671e5 psi
Bulk Modulus	5.180e5 psi
A_0	3.221e5 (psi)^2
A_1	0
A_2	0
Tensile Cutoff	61.3 psi

Volumetric Strain Data vs Pressure:

Volumetric Strain, in^3/in^3	Pressure, psi
0.0000E+00	0.000
-9.6740E-05	50.100
-3.5131E-04	140.400
-6.9019E-04	217.100
-1.1268E-03	278.133
-2.0363E-03	329.067
-1.9536E-01†	500.000†
-6.0570E-01†	1000.000†
-8.4601E-01†	10000.000†
-1.2052E+00†	100000.000†

† - assumed values to achieve numerical lock-up.

6.2.3 HABC at 100° F

Poisson's ratio is given as 0.25. The modulus of elasticity was taken to be the slope of the load deflection curve for the first data point.

$$E = \frac{\sigma}{\varepsilon} = \frac{103.7psi - 0psi}{(257.5e-6) - 0} = 4.027e5psi$$

The shear modulus is then calculated as:

$$ShearModulus = \frac{E}{2(1+\nu)} = \frac{4.027e5\ psi}{2(1+0.25)} = 1.6108e5psi$$

The bulk modulus is calculated as:

$$BulkModulus = \frac{E}{3(1-2\nu)} = \frac{4.027e5\ psi}{3(1+2(0.25))} = 2.6847e5\ psi$$

The pressure cut off is calculated as P=209.7 psi/3 = 69.9 psi and the constants a_0 is calculated as (833.7 psi)^2/3 = 2.317e5 psi^2. The following material model was used for the lower bound, 100°F runs of the HABC material.

LS-Dyna Material Model	*MAT_SOIL_AND_FOAM
Density	1.5742e-4 lb-sec^2/in^4 (105 lb/ft^3)
Shear Modulus	1.6108e5 psi
Bulk Modulus	2.6847e5 psi
A_0	2.317e5 (psi)^2
A_1	0
A_2	0
Tensile Cutoff	69.9 psi

Volumetric Strain Data vs Pressure:

Volumetric Strain, in^3/in^3	Pressure, psi
0.0000E+00	0.0
-1.2879E-04	34.567
-6.6103E-04	123.133
-1.1769E-03	165.533
-1.7225E-03	204.967
-2.3119E-03	240.0
-5.5975E-02†	333.333†
-4.5758E-01†	500.0†
-6.3677E-01†	1000.0†
-1.2448E+00†	100000.0†

† - assumed values to achieve numerical lock-up.

The volumetric strain vs pressure curves used by the analytical models are plotted in Figure 6.2.3.1 for the lower values.

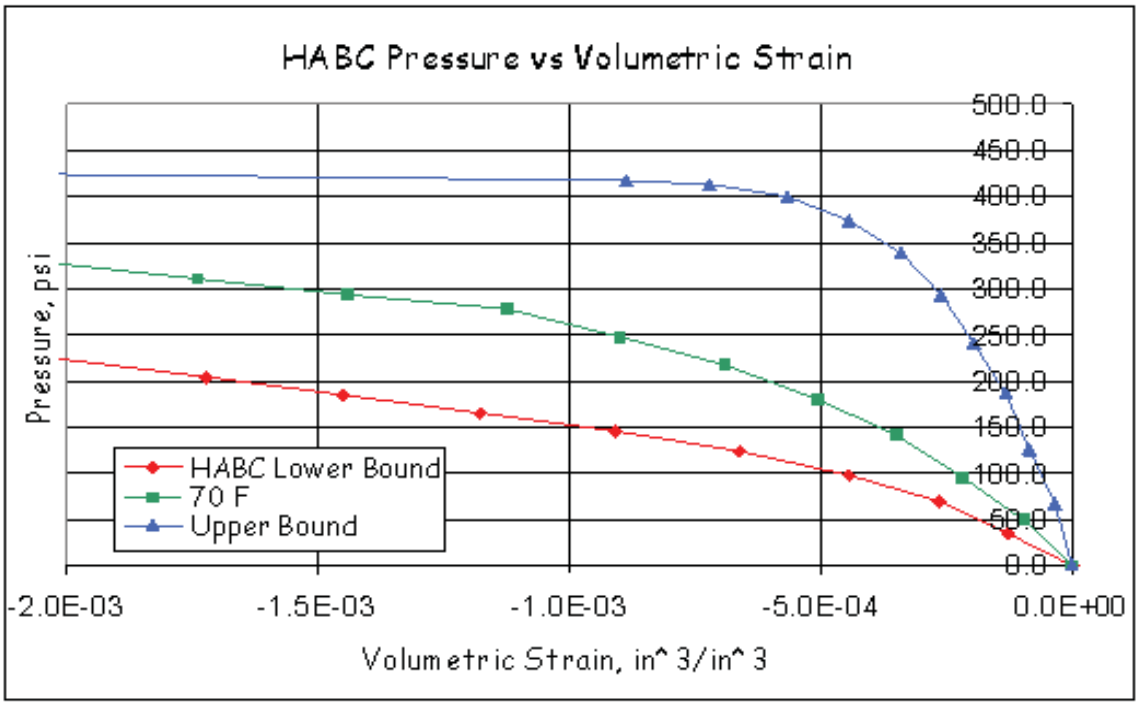

Figure 6.2.3.1 - Volumetric Strain vs Pressure Curves for the HABC Material

7.0 Analysis Results

The figures presented in Section 7 may show the punch, however, no punch impacts were made on the HABC model as discussed in Section 6.1.

7.1 HABC-run1hl - Lower Bounding Side

HABC-run1hl are the runs with the lower bounding material properties for the kaolite and the HABC materials. The 4-foot impact occurs from time = 0.0 to 0.01 seconds; the 30-foot impact occurs from 0.01 to 0.02 seconds; and the crush impact occurs from 0.02 to 0.04 seconds.

The initial configuration for HABC-run1hl is shown in Figure 7.1.1. The configuration after the 4-foot impact is shown in Figure 7.1.2. Enlargement of the lid and bottom regions after the 4-foot impact is shown in Figure 7.1.3.

The effective plastic strain in the CV body after the 4-foot impact is shown in Figure 7.1.4. The maximum is 0.0185 in/in and occurs near the bottom head of the CV body. The plastic strain in other components for the 4-foot impact are given in Table 7.1.1.

Table 7.1.1 - HABC-run1hl, 4-Foot Impact, Effective Plastic Strain Levels in Some Components

Component	Effective Plastic Strain, in/in
CV Lid	0.0001
CV Nut Ring	0.0000
Angle	0.0055
Drum	0.1599
Drum Bottom Head	0.1033
Liner	0.1045
Lid	0.1393
Lid Stiffener	0.0004
Lid Studs	0.0000
Lid Stud Nuts	0.0000
Lid Stud Washers	0.0194
Plug Liner	0.0022

Figure 7.1.5 shows the final configuration for the HABC-run1hl 30-foot impact. Figure 7.1.6 shows the lid and bottom regions after the 30-foot impact.

The maximum effective plastic strain due to the 30-foot impact in the CV body is 0.0195 in/in as shown in Figure 7.1.7. The maximum effective plastic strain in the drum lid is shown to be 0.5790 in/in in Figure 7.1.8. The maximum lid strain is a surface strain at the stud hole nearest the rigid surface. The membrane effective plastic strain component is 0.4416 in/in in the localized region near the stud hole. Effective plastic strain levels in other components for the 30-foot impact are given in Table 7.1.2.

Table 7.1.2 - HABC-run1hl, 30-Foot Impact, Effective Plastic Strain Levels in Some Components

Component	Effective Plastic Strain, in/in
CV Lid	0.0002
CV Nut Ring	0.0000
Angle	0.0780
Drum	0.2251
Drum Bottom Head	0.2126
Liner	0.1078
Lid Stiffener	0.0093
Lid Studs	0.1140
Lid Stud Nuts	0.0000
Lid Stud Washers	0.0194
Plug Liner	0.0958

The final configuration for the crush impact is shown in Figure 7.1.9. Figure 7.1.10 shows the configuration at the bottom and lid regions after the crush impact.

Figure 7.1.11 shows the effective plastic strains in the CV body. The maximum is shown to be 0.0206 in/in and occurs below the flange region due to the upper internal weight.

The maximum effective plastic strain in the drum for the crush impact is 0.5139 in/in (surface strain) as shown in Figure 7.1.12. The maximum in the drum occurs near the angle on the crush plate side of the drum. The maximum membrane effective plastic strain at this location is 0.3551 in/in.

Figure 7.1.13 shows that the maximum effective plastic strain in the lid is 1.2580 in/in (surface strain) and occurs just below the upper stud hole (hole nearest the crush plate, 180°). The maximum membrane effective plastic strain in this region of the lid is 0.7746 in/in. A time line investigation during the crush impact shows that the lid exceeds 0.57 in/in strain in bending at about 0.0248 seconds at the 180° stud hole. The crush impact started at about 0.0200 seconds, so the lid reaches failure level near the start of the crush impact. The membrane levels in the lid reach 0.57 in/in at about 0.0264 seconds. The elevated effective plastic strain levels in the lid are localized in the region just inboard of the upper stud.

Figure 7.1.14 shows that the effective plastic strain in the drum studs is 0.5121 in/in and occurs in the upper stud at the bearing of the lid onto the stud. The elevated strains in the stud are localized on the inner surface (bearing of the lid on the stud). Effective plastic strain levels throughout the thickness of the stud are generally 0.25 in/in or less. At time 0.0264 sec, the lid has reached 0.57 in/in strain in membrane, and the maximum strain in the drum studs is about 0.2870 in/in.

Considering the strain levels in the lid and the studs, some tearing at the 180° stud hole would be expected. But the tearing would be localized to the stud hole due to the extent of the strain patterns. Failure of the stud to restrain the lid due to this tearing is not expected. The lid stiffener would limit any tearing from the stud at 180° and the large washer would be expected to restrain the lid. The effective plastic strain in other components due to the crush impact are listed in Table 7.1.3.

Table 7.1.3 - HABC-run1hl, Crush Impact, Effective Plastic Strain Levels in Some Components

Component	Effective Plastic Strain, in/in
CV Lid	0.0002
CV Nut Ring	0.0000
Angle	0.1142
Drum Bottom Head	0.3562
Liner	0.1593
Lid Stiffener	0.0515
Lid Stud Nuts	0.0005
Lid Stud Washers	0.0693
Plug Liner	0.1220

The lid separation time history is shown in Figure 7.1.15. The nodes used in Figure 7.1.15 are shown in Figure 3.1.30. From the time history plot it can be seen that a lid separation of 0.005 in or less would be expected.

Figure 7.1.16 shows kaolite nodes used to find the kaolite thickness time history. Figure 7.1.17 shows the remaining thickness time histories for the nodal pairs shown.

Figure 7.1.18 and 7.1.19 show the diameter and radial time histories for the drum. The nodes are defined in Figure 3.1.34.

Figure 7.1.20 shows the diameter time history for nodal pairs along the length of the liner. Figure 3.1.37 shows the nodes and Table 3.1.3 gives the location of the nodes.

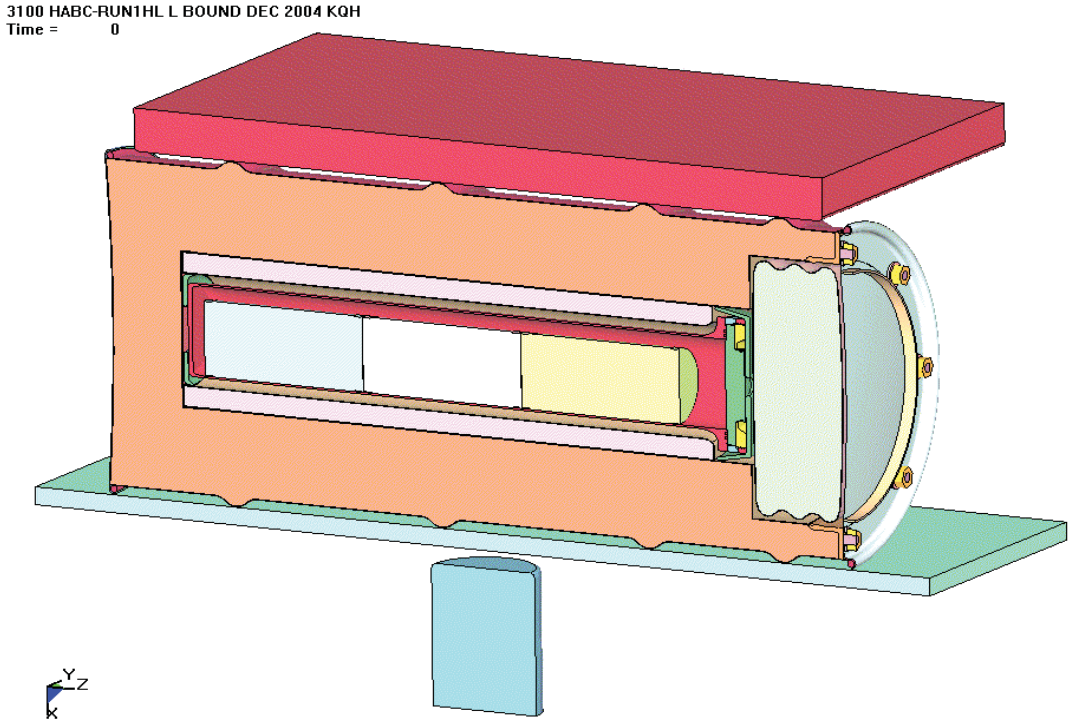

Figure 7.1.1 - HABC-run1hl, Initial Configuration

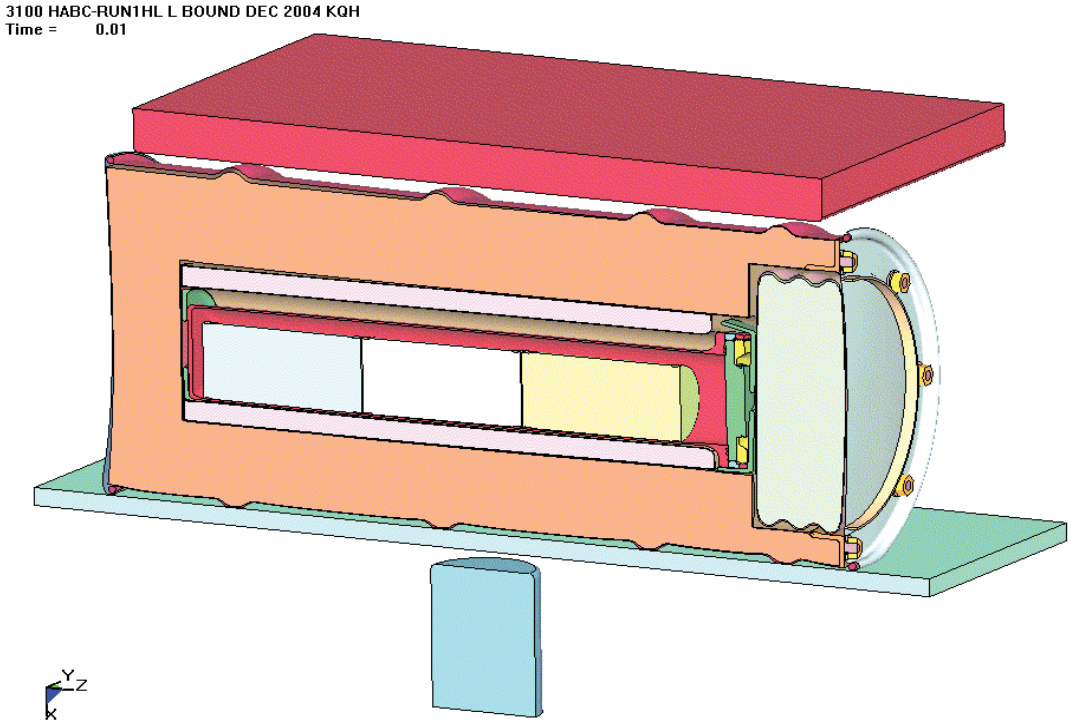

Figure 7.1.2 - HABC-run1hl, Configuration After the 4-Foot Impact

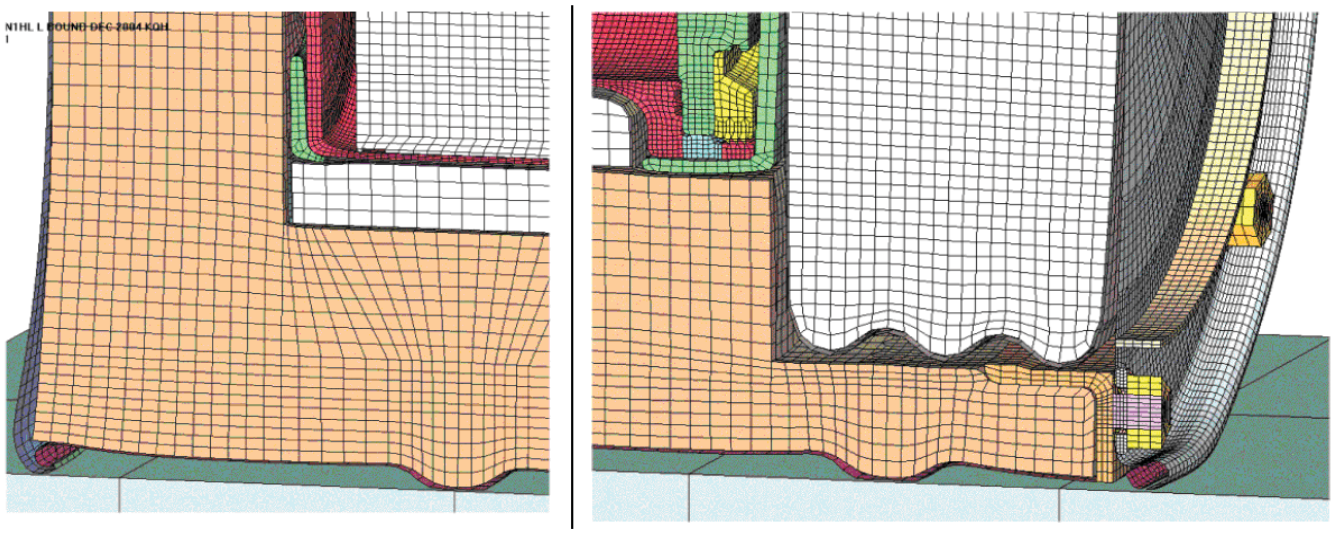

Figure 7.1.3 - HABC-run1hl, 4-Foot Impact, Configuration in the Lid and Bottom

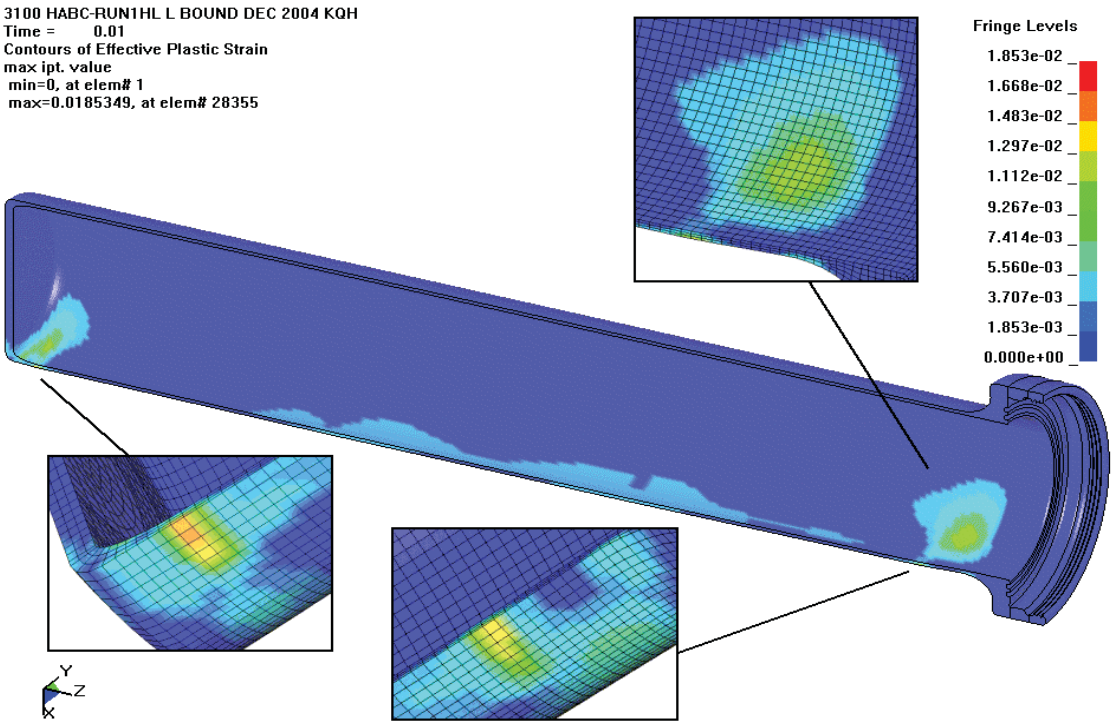

Figure 7.1.4 - HABC-run1hl, 4-Foot Impact, Effective Plastic Strain in the CV Body

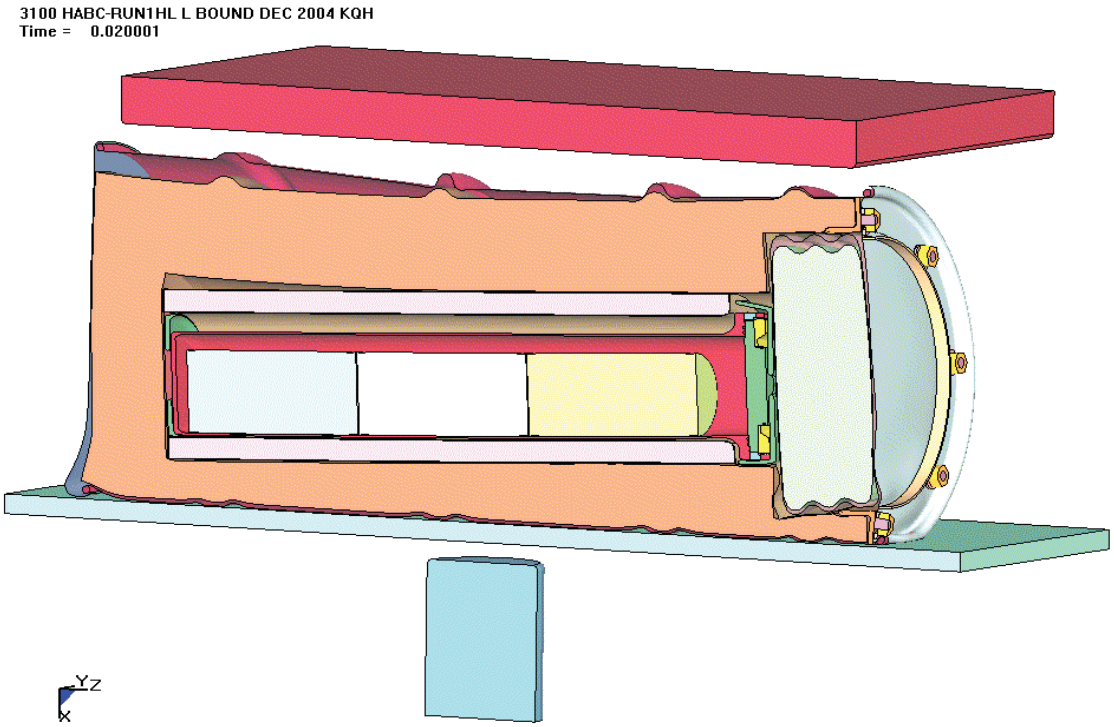

Figure 7.1.5 - HABC-run1hl, 30-Foot Impact, Final Configuration

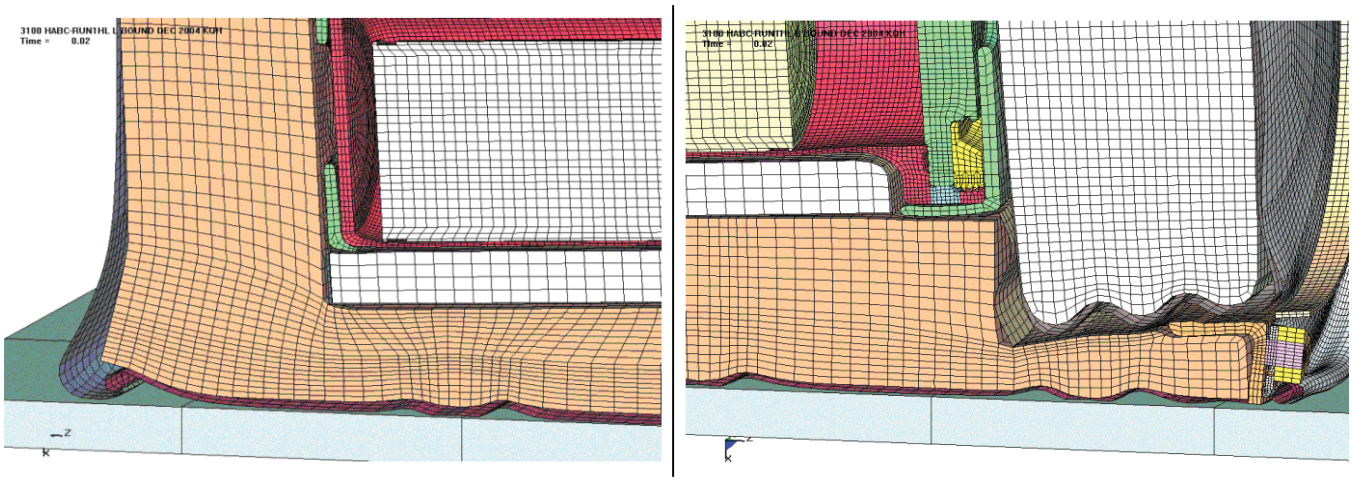

Figure 7.1.6 - HABC-run1hl, 30-Foot Impact, Configuration of the Lid and Bottom

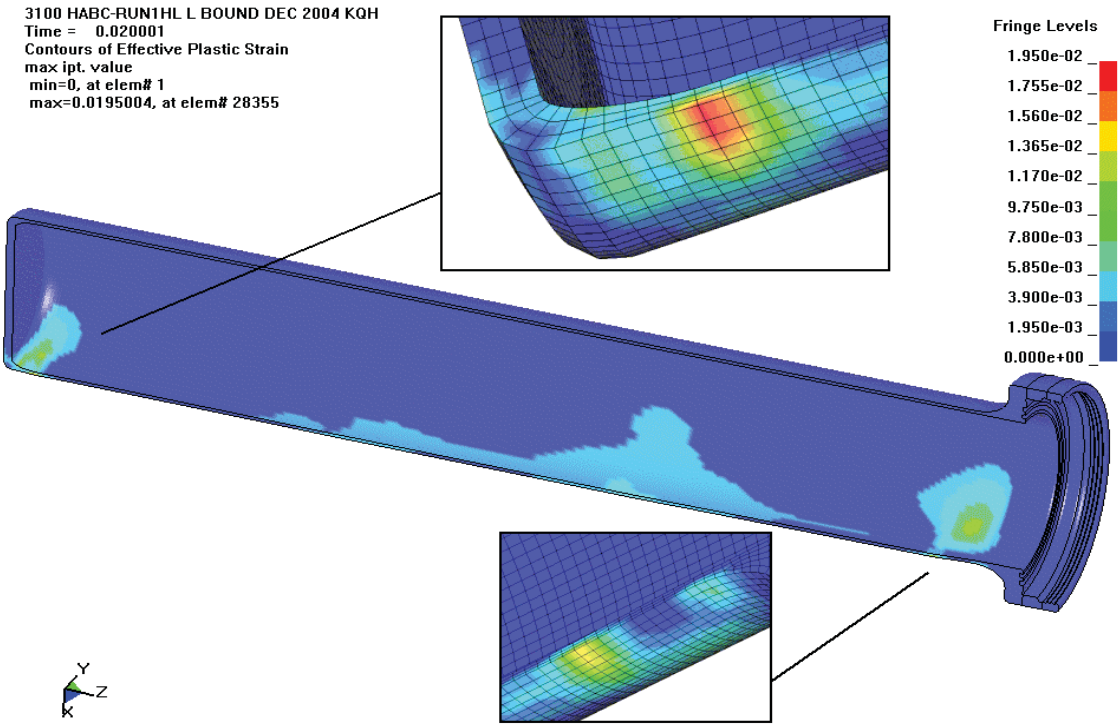

Figure 7.1.7 - HABC-run1hl, 30-Foot Impact, Effective Plastic Strain in the CV Body

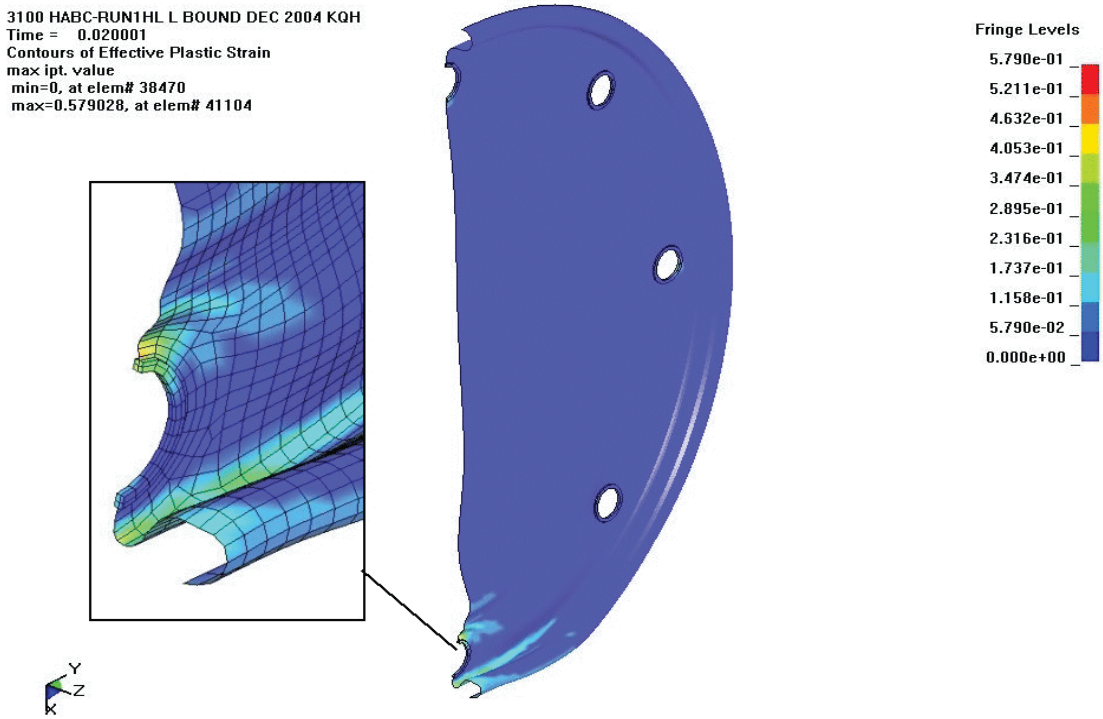

Figure 7.1.8 - HABC-run1hl, 30-Foot Impact, Effective Plastic Strain in the Lid

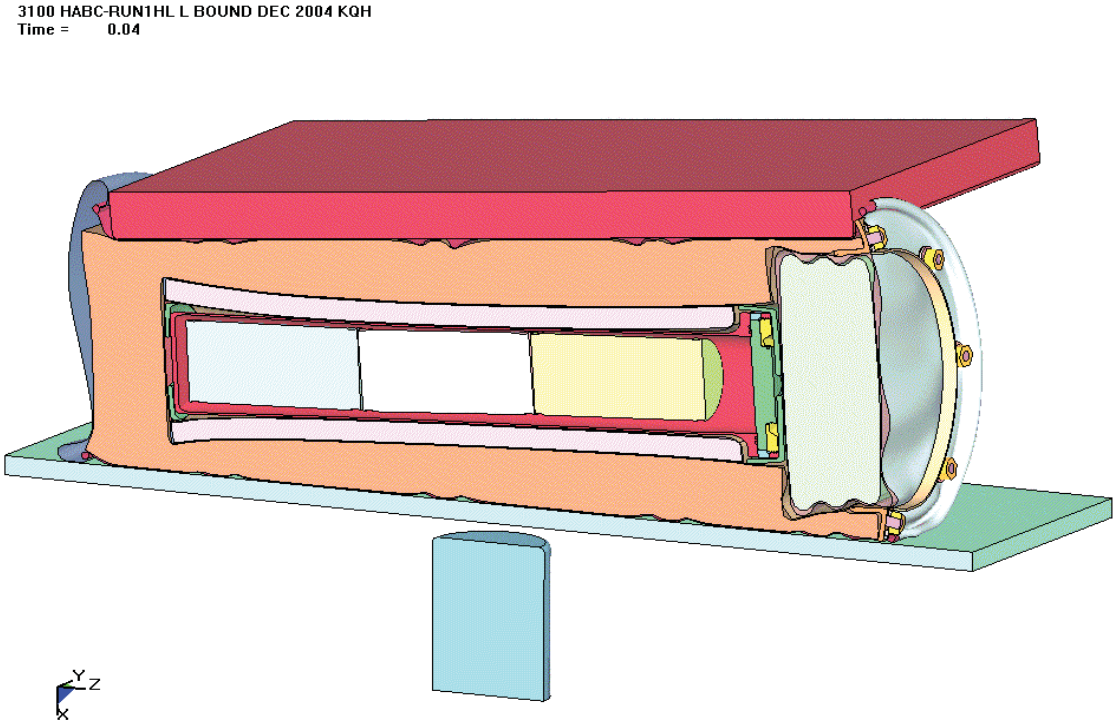

Figure 7.1.9 - HABC-run1hl, Crush Impact, Final Configuration

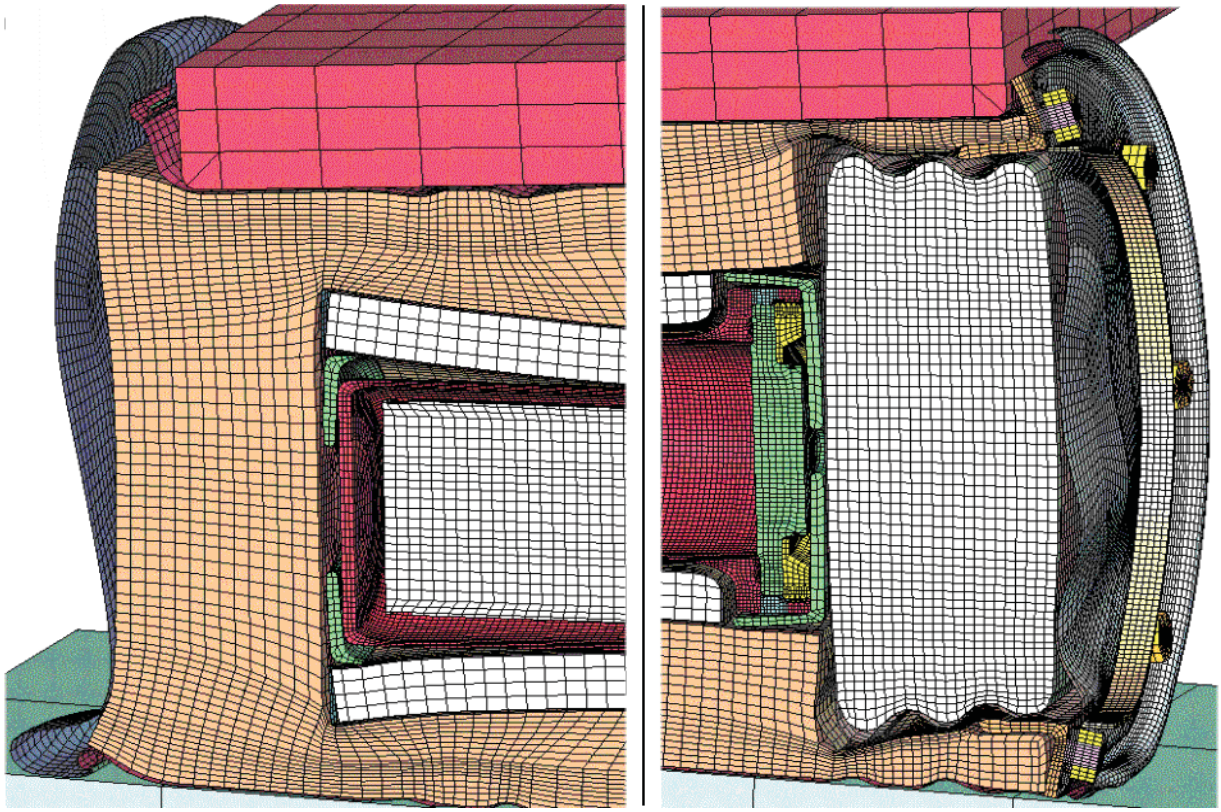

Figure 7.1.10 - HABC-run1hl, Crush Impact, Configuration of the Lid and Bottom

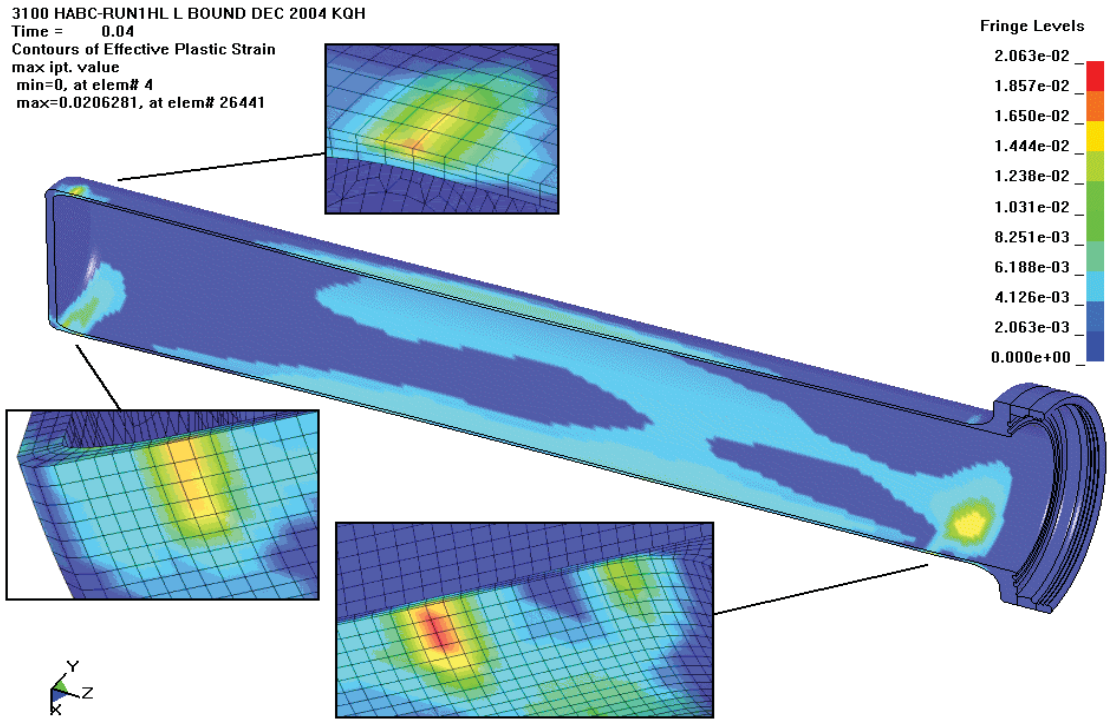

Figure 7.1.11 - HABC-run1hl, Crush Impact, Effective Plastic Strain in the CV Body

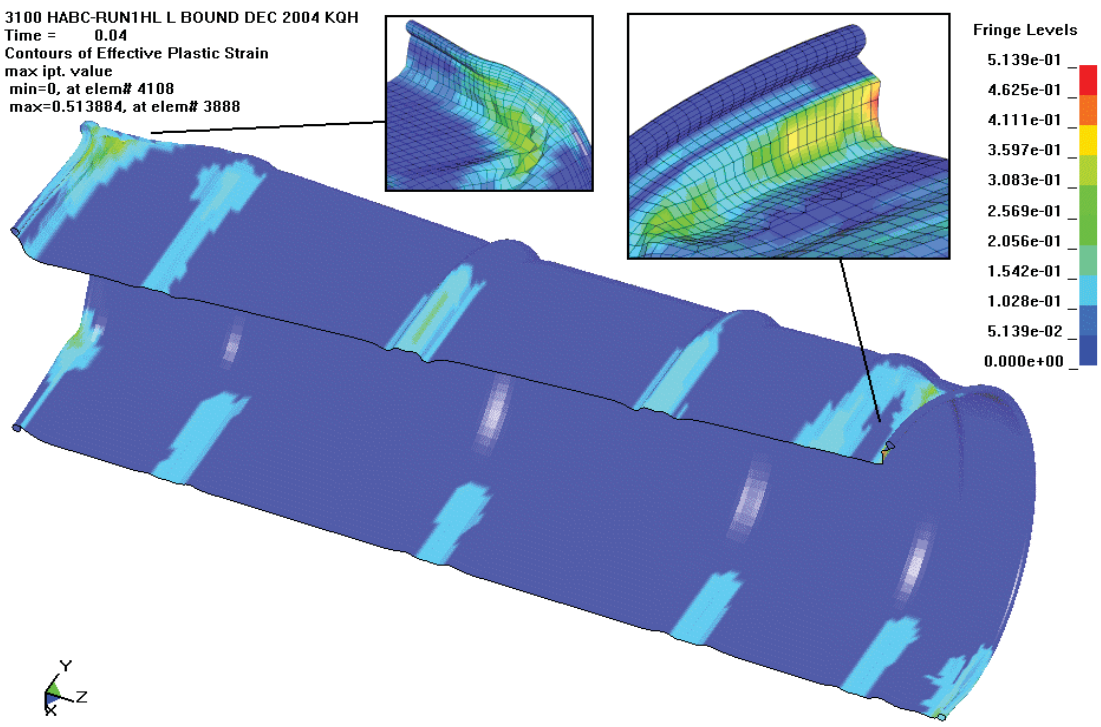

Figure 7.1.12 - HABC-run1hl, Crush Impact, Effective Plastic Strain in the Drum

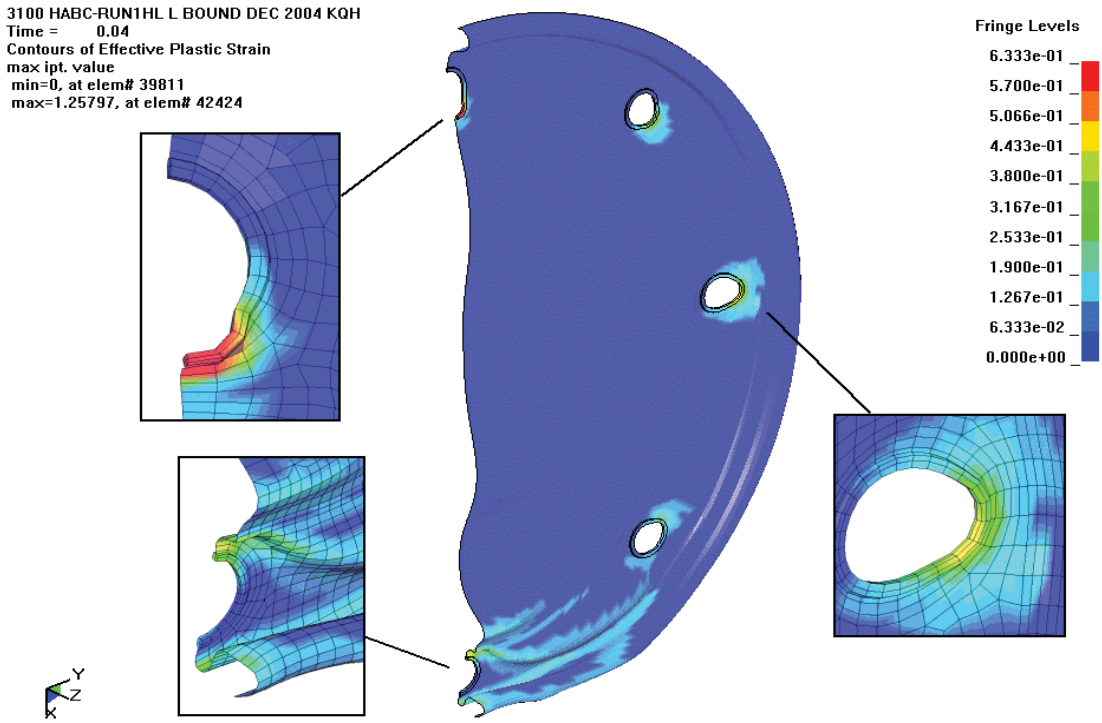

Figure 7.1.13 - HABC-run1hl, Crush Impact, Effective Plastic Strain in the Lid

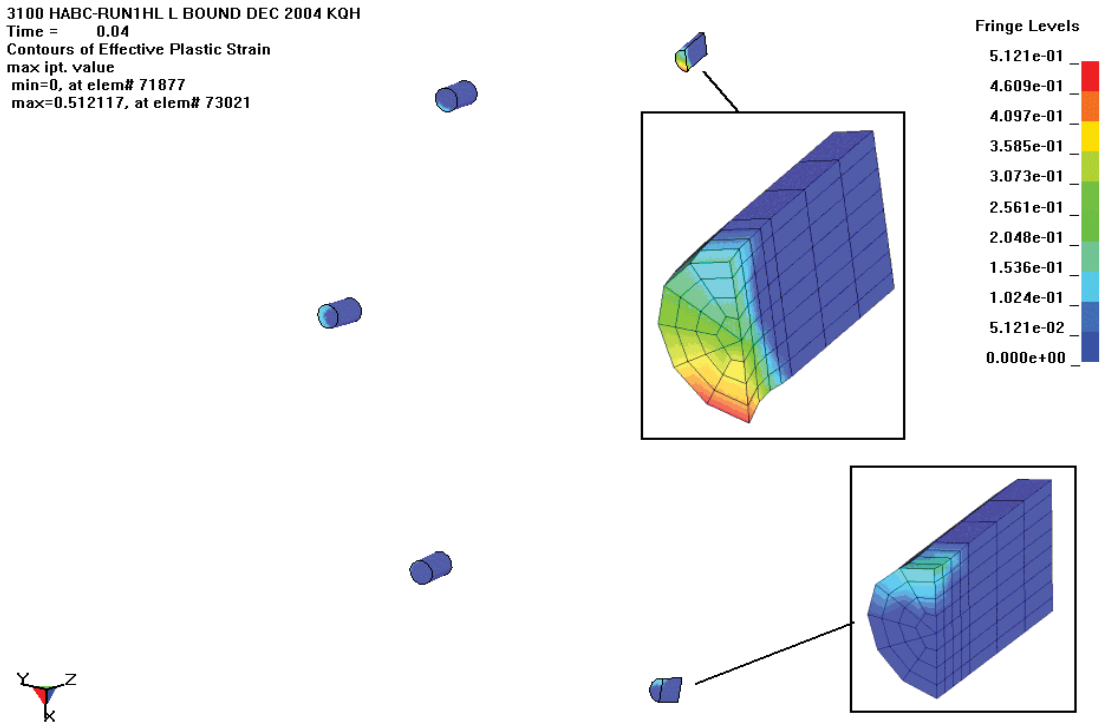

Figure 7.1.14 - HABC-run1hl, Crush Impact, Effective Plastic Strain in the Studs

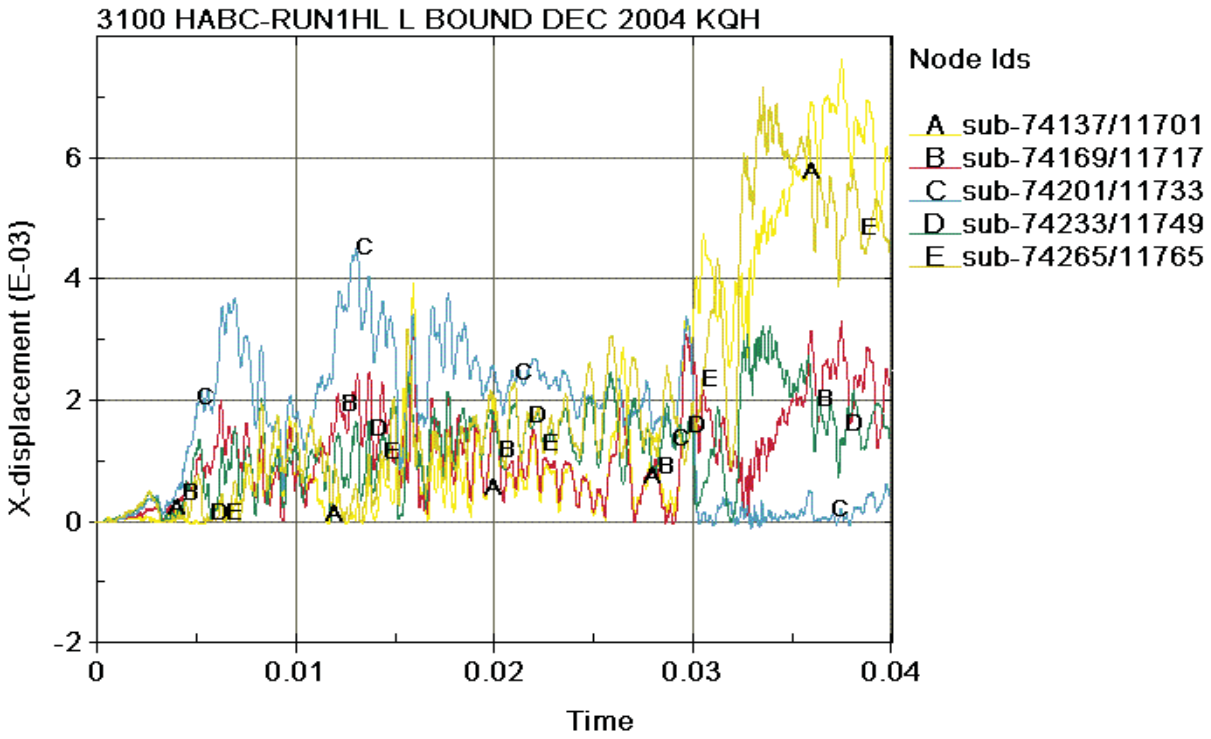

Figure 7.1.15 - HABC-run1hl, CV Lid Separation Time History

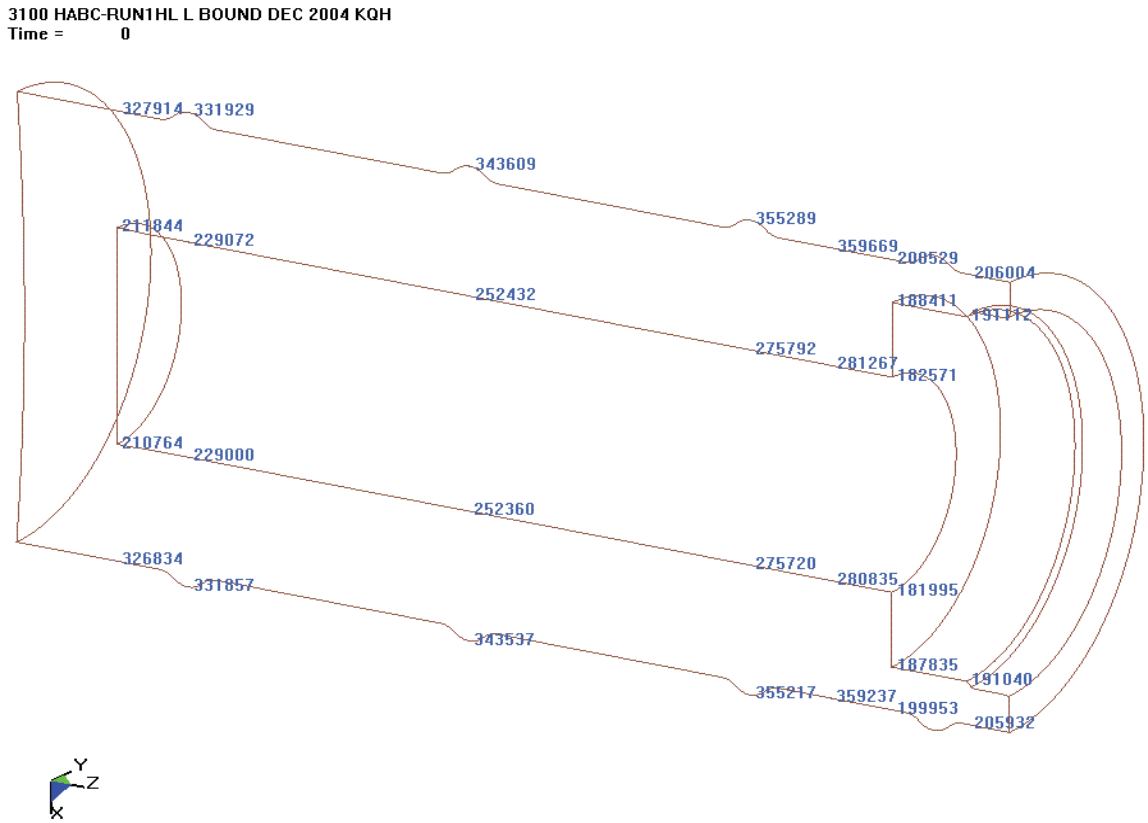

Figure 7.1.16 - HABC-run1hl, Kaolite Nodes

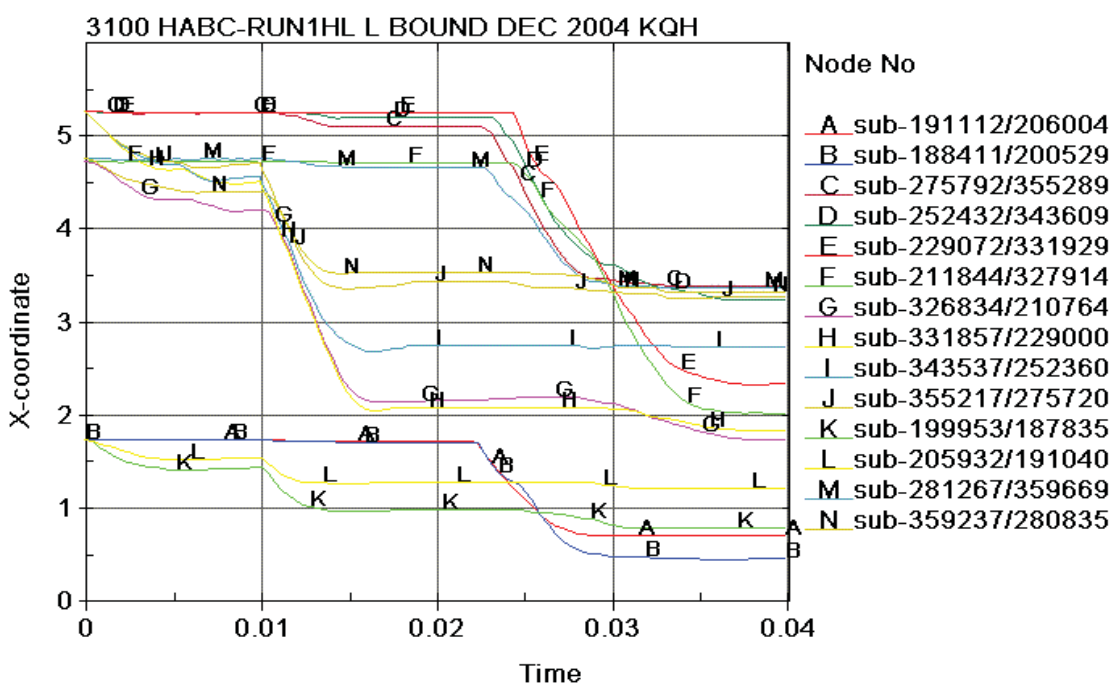

Figure 7.1.17 - HABC-run1hl, Kaolite Thickness Time History

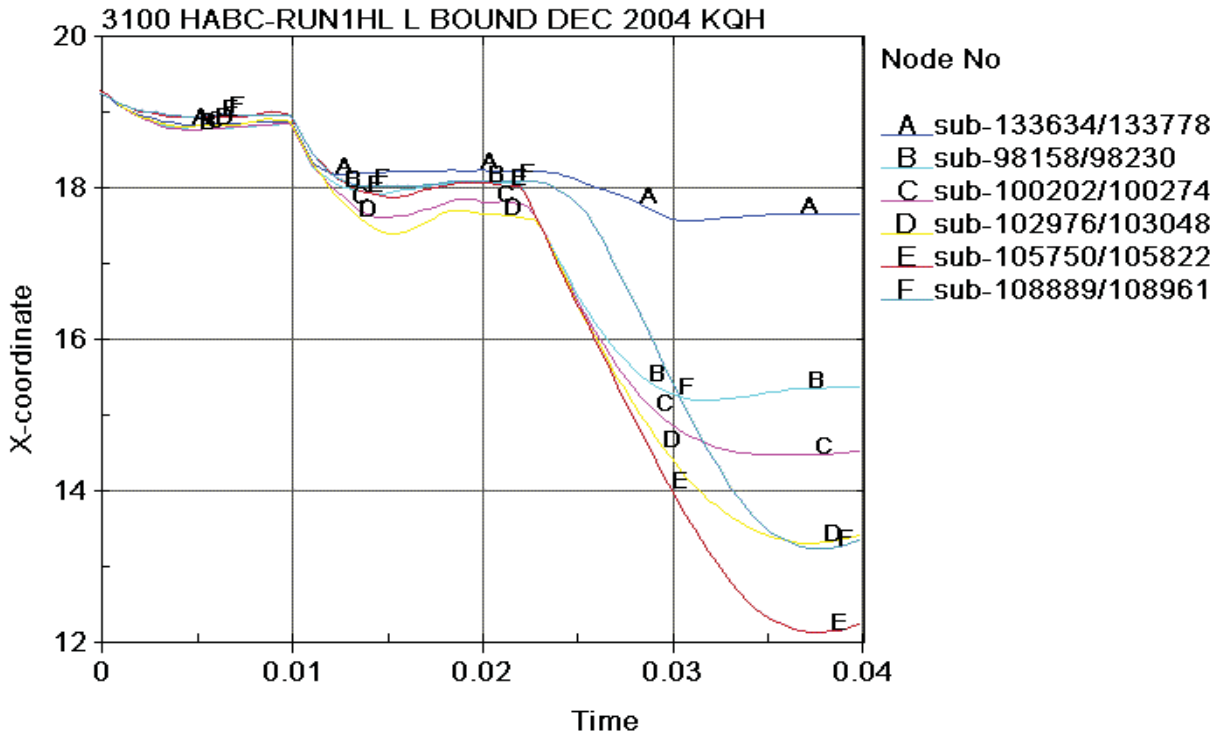

Figure 7.1.18 - HABC-run1hl, Drum Diameter Time History in the X Direction

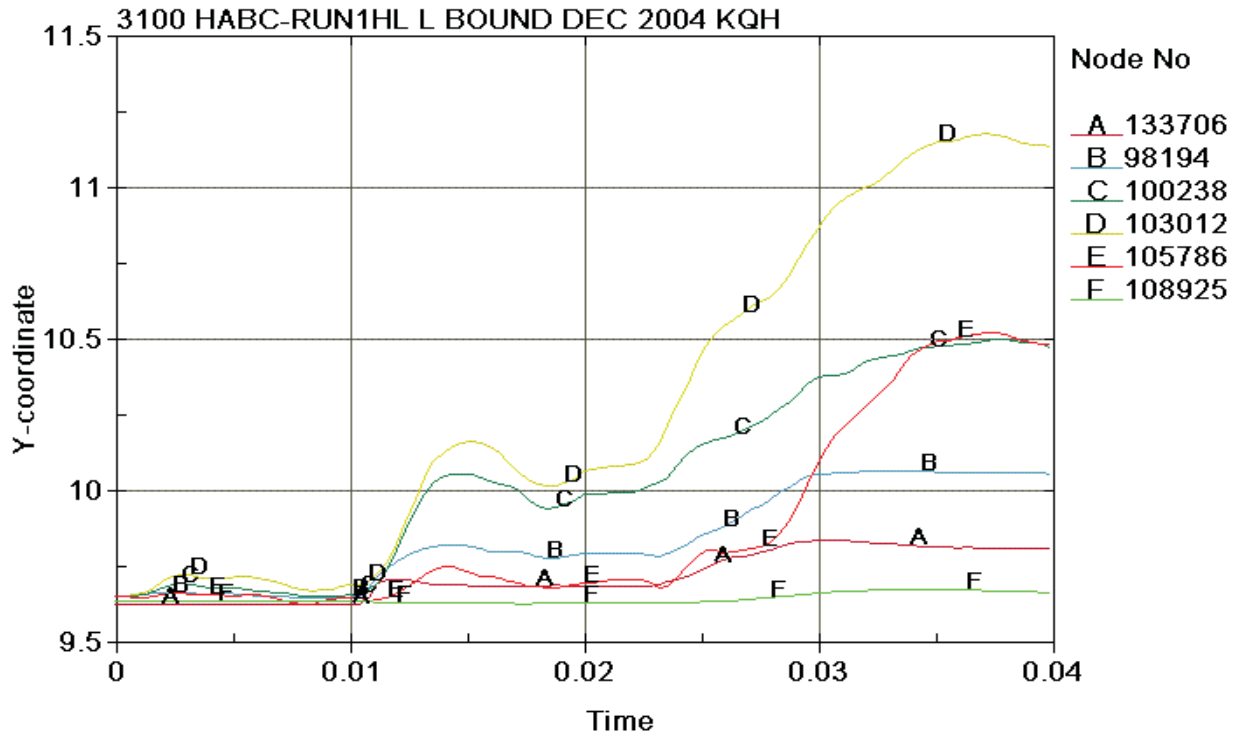

Figure 7.1.19 - HABC-run1hl, Drum Diameter Time History in the Y Direction

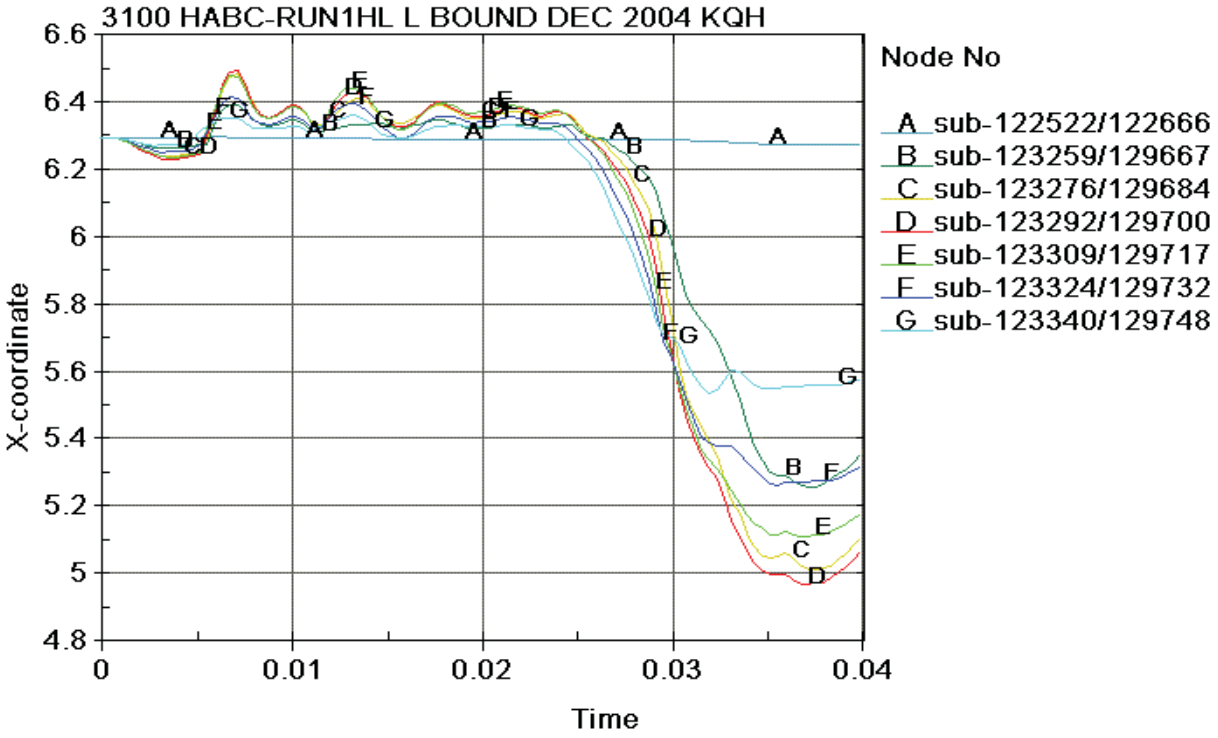

Figure 7.1.20 - HABC-run1hl, Diameter Changes in the Inner Liner

7.2 HABC-run1hh - Upper Bounding Side

HABC-run1hh are the runs with the lower bounding material properties for the kaolite and the HABC materials. The 4-foot impact occurs from time = 0.0 to 0.01 seconds; the 30-foot impact occurs from 0.01 to 0.0188 seconds; and the crush impact occurs from 0.0188 to 0.04 seconds.

The final configuration for the 4-foot impact is shown in Figure 7.2.1. The configuration at the ends of the package are shown in Figure 7.2.2. The effective plastic strain in the CV body for the 4-foot impact is shown in Figure 7.2.3 to be a maximum of 0.0238 in/in. The effective plastic strains in other package components for the 4-foot impact are listed in Table 7.2.1.

Table 7.2.1 - Run1hh, 4-Foot Impact, Effective Plastic Strain Levels in Some Components

Component	Effective Plastic Strain, in/in
CV Lid	0.0000
CV Nut Ring	0.0000
Angle	0.0061
Drum	0.1207
Drum Bottom Head	0.1252
Liner	0.0991
Lid	0.1604
Lid Stiffener	0.0006
Lid Studs	0.0000
Lid Stud Nuts	0.0000
Lid Stud Washers	0.0411
Plug Liner	0.0045

The final configuration for the 30-foot impact is shown in Figure 7.2.4. The configuration at the ends of the package are shown in Figure 7.2.5. The maximum effective plastic strain for the 30-foot impact in the CV Body is 0.0347 in/in near the bottom head (Figure 7.2.6). The maximum effective plastic strain in the drum lid is 0.4063 in/in at the stud near the rigid plane as shown in Figure 7.2.7. The effective plastic strain in other components for the 30-foot impact are given in Table 7.2.2.

Table 7.2.2 - HABC-run1hh, 30-Foot Impact, Effective Plastic Strain Levels in Some Components	
Component	Effective Plastic Strain, in/in
CV Lid	0.0001
CV Nut Ring	0.0000
Angle	0.0632
Drum	0.2296
Drum Bottom Head	0.2517
Liner	0.1184
Lid Stiffener	0.0076
Lid Studs	0.1306
Lid Stud Nuts	0.0004
Lid Stud Washers	0.0424
Plug Liner	0.1072

The configuration after the crush impact is shown in Figure 7.2.8. The configuration at the ends of the package are shown in Figure 7.2.9. The maximum effective plastic strain for the crush impact in the CV body is 0.0525 in/in, on the crush plate side near the lid end of the top inner weight (Figure 7.2.10). The maximum effective plastic strain in the drum is 0.2814 in/in near the angle and the rigid plane (Figure 7.2.11). The maximum effective plastic strain in the drum lid is 0.6413 in/in (surface strain) a shown in Figure 7.2.12. The maximum occurs at the lid hole for the stud closest to the crush plate (180°). The membrane effective plastic strain is 0.4907 in/in at this location in the lid. Figure 7.2.13 shows that the maximum effective plastic strain in the studs is 0.2364 in/in. The effective plastic strain in other components are listed in Table 7.2.3 for the crush impact.

Table 7.2.3 - Run1hh, Crush Impact, Effective Plastic Strain Levels in Some Components	
Component	Effective Plastic Strain, in/in
CV Lid	0.0004
CV Nut Ring	0.0005
Angle	0.0845
Drum Bottom Head	0.2827
Liner	0.2022
Lid Stiffener	0.0171
Lid Stud Nuts	0.0018
Lid Stud Washers	0.0439
Plug Liner	0.1286

The lid separation time history is shown in Figure 7.2.14. The nodes are shown in Figure 3.1.30. The response is oscillatory with peak gap separation on the order of 0.010 in. At the end of the impact, the peaks are on the order of 0.006 in with an average gap on the order of 0.003 in or less.

The kaolite thickness time history is shown in Figure 7.2.15. The nodal pairs are shown in Figure 7.1.16.

Figure 7.2.16 and 7.2.17 show the drum diameter and radial time histories. The nodes are defined in Figure 3.1.34.

Figure 7.2.18 shows the diameter response of the liner. Figure 3.1.37 and Table 3.1.3 define the liner nodes used in Figure 7.2.18.

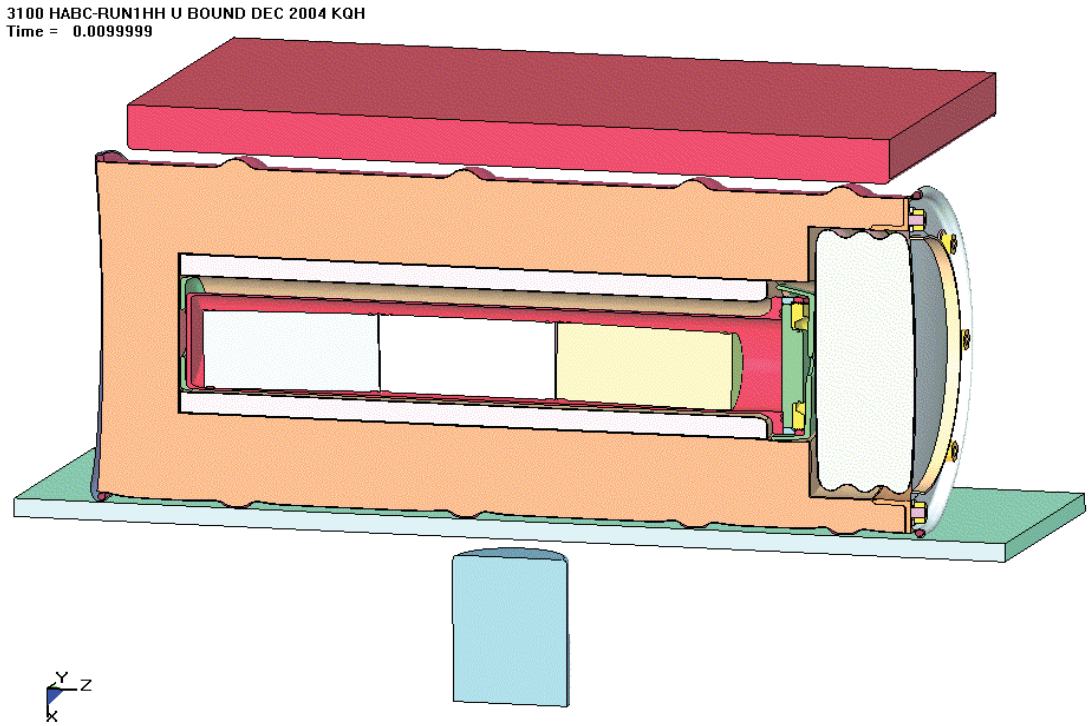

Figure 7.2.1 - HABC-run1hh, Configuration After the 4-Foot Impact

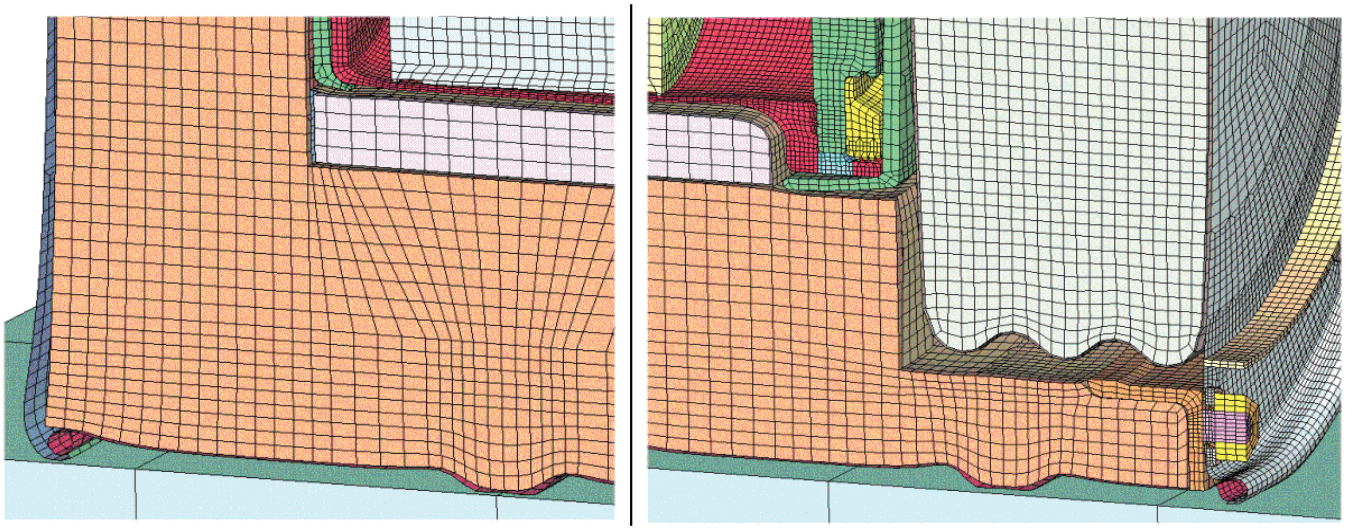

Figure 7.2.2 - HABC-run1hh, 4-Foot Impact, Configuration of the Lid and Bottom

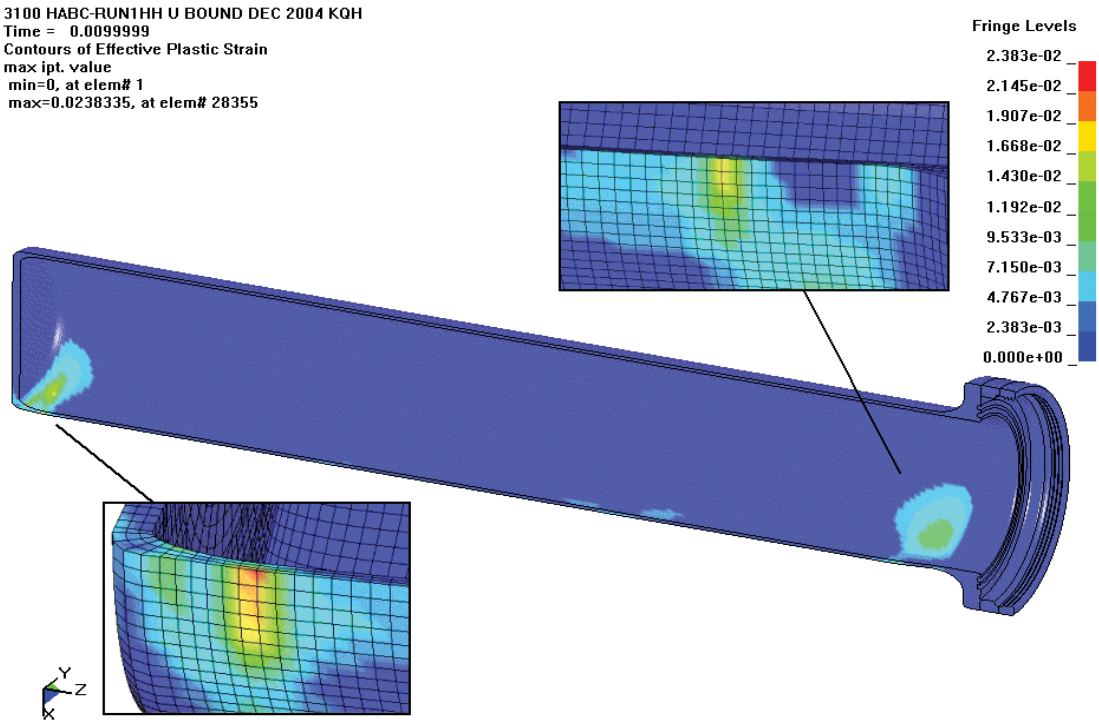

Figure 7.2.3 - HABC-run1hh, 4-Foot Impact, Effective Plastic Strain in the CV Body

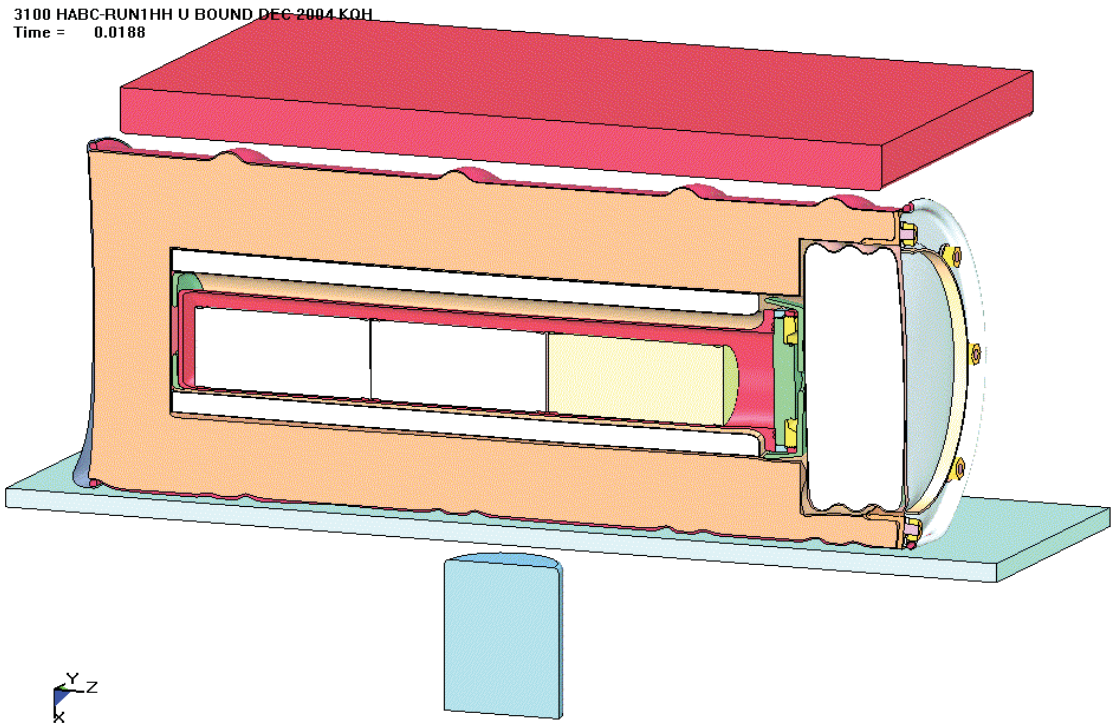

Figure 7.2.4 - HABC-run1hh, Configuration After the 30-Foot Impact

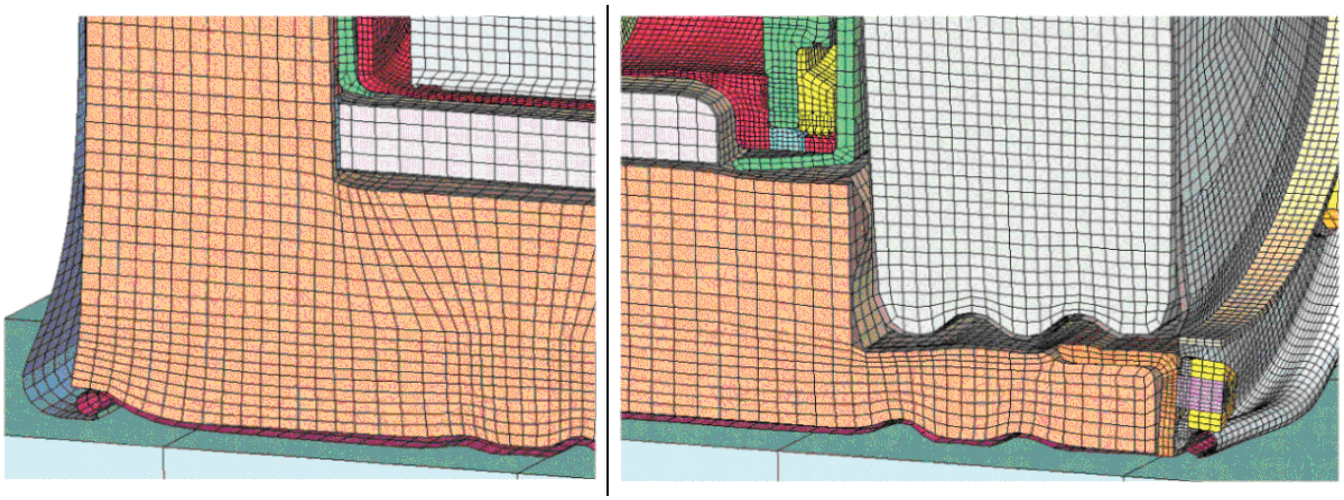

Figure 7.2.5 - HABC-run1hh, 30-Foot Impact, Configuration of the Lid and Bottom

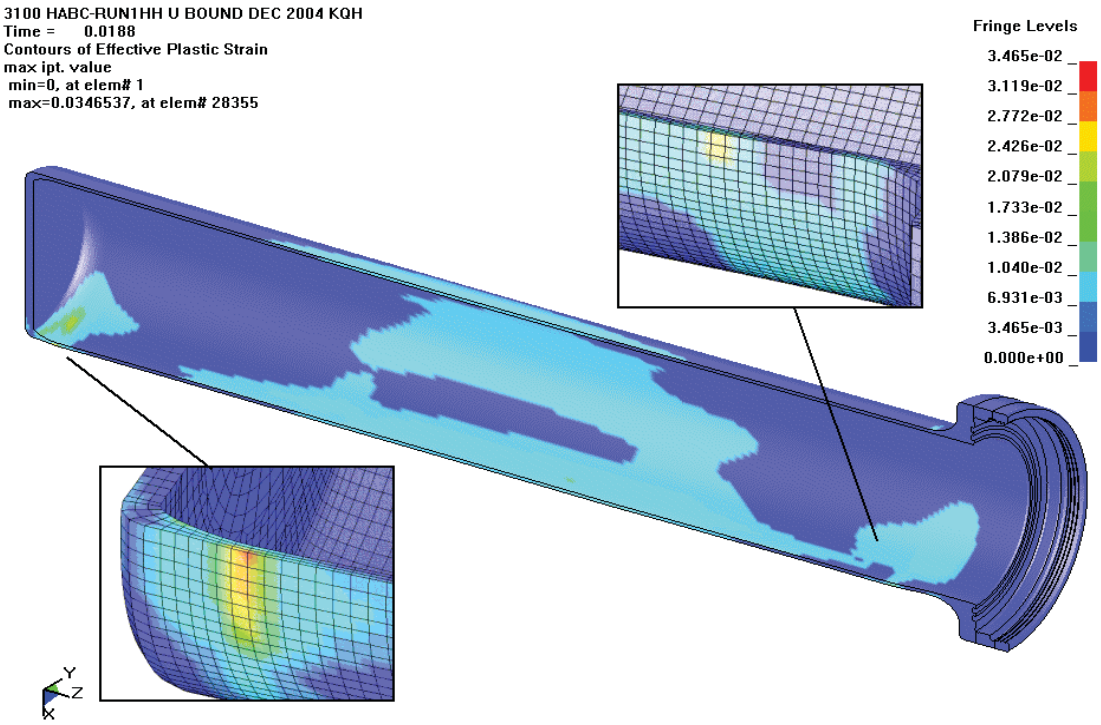

Figure 7.2.6 - HABC-run1hh,30-Foot Impact, Effective Plastic Strain in the CV Body

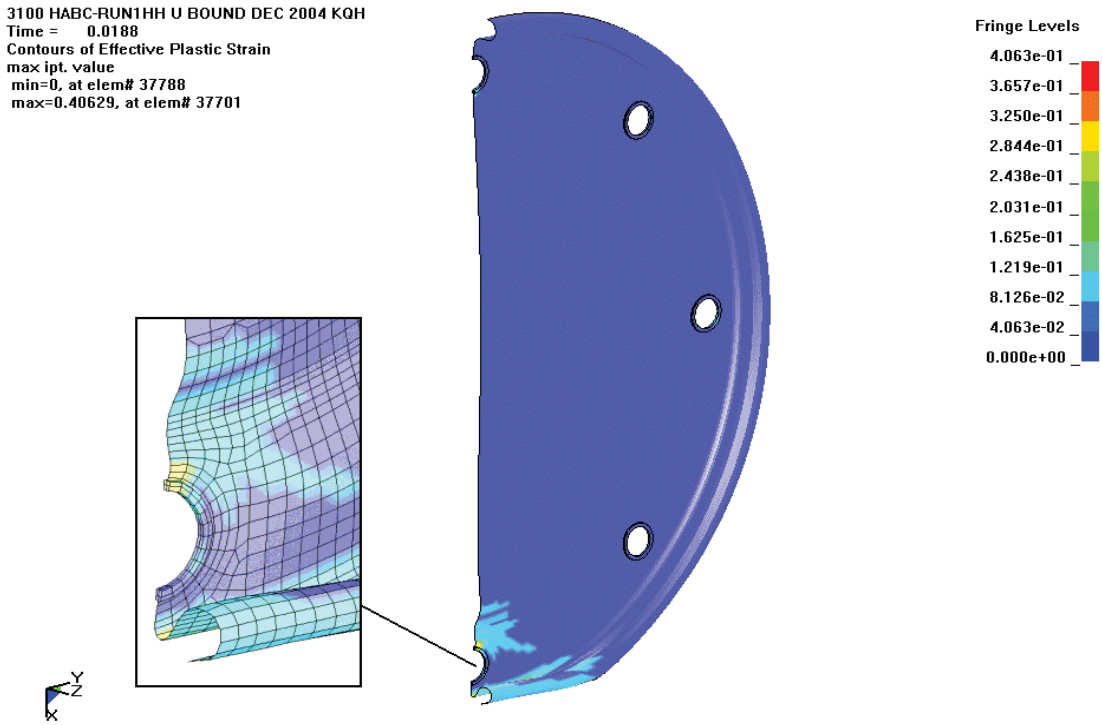

Figure 7.2.7 - HABC-run1hh, 30-Foot Impact, Effective Plastic Strain in the Lid

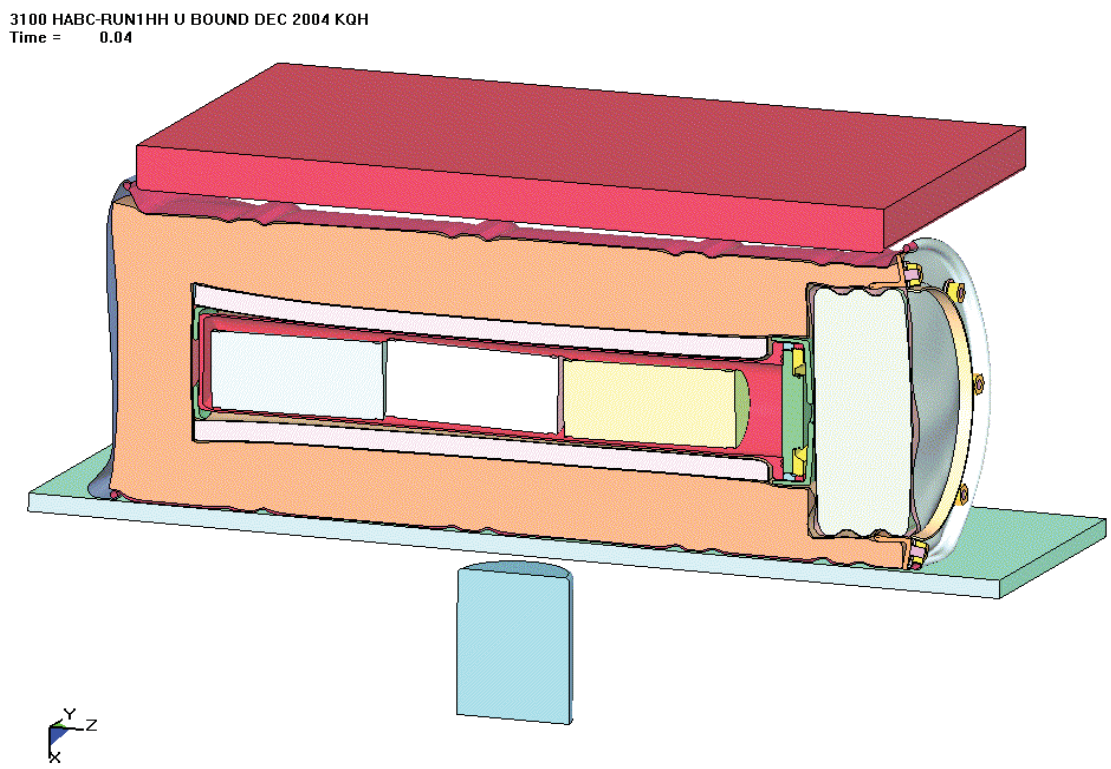

Figure 7.2.8 - HABC-run1hh, Configuration After the Crush Impact

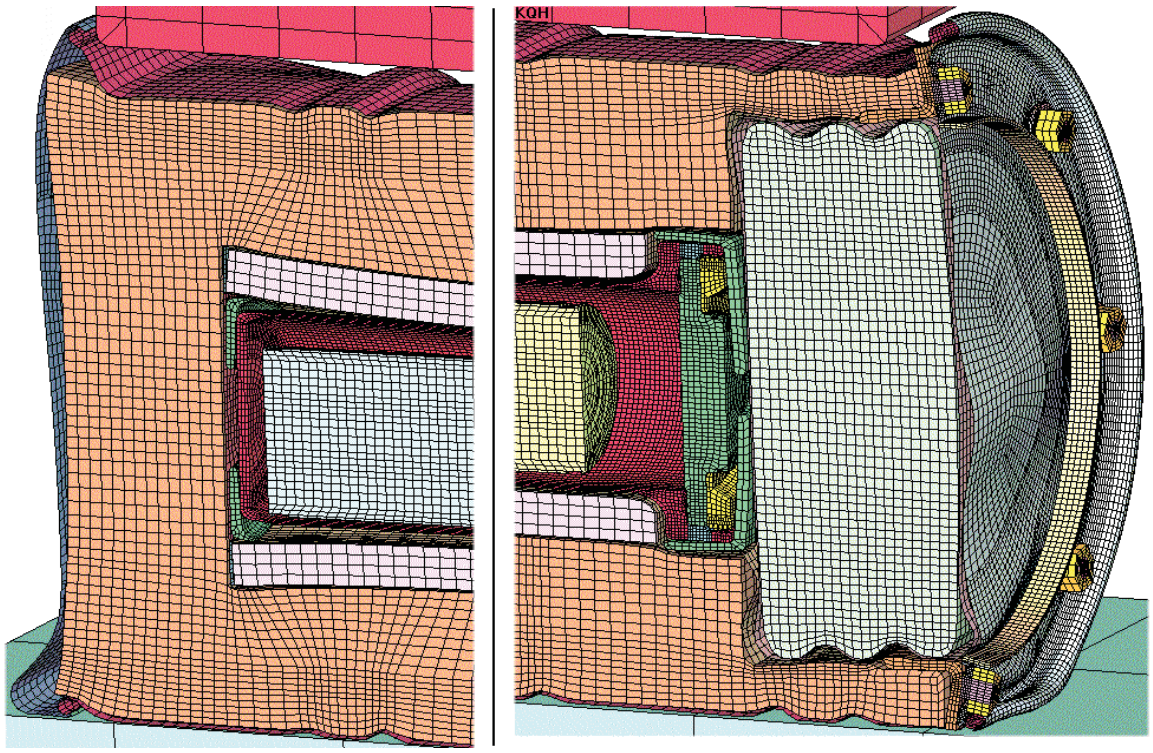

Figure 7.2.9 - HABC-run1hh, Crush Impact, Configuration of the Lid and Bottom

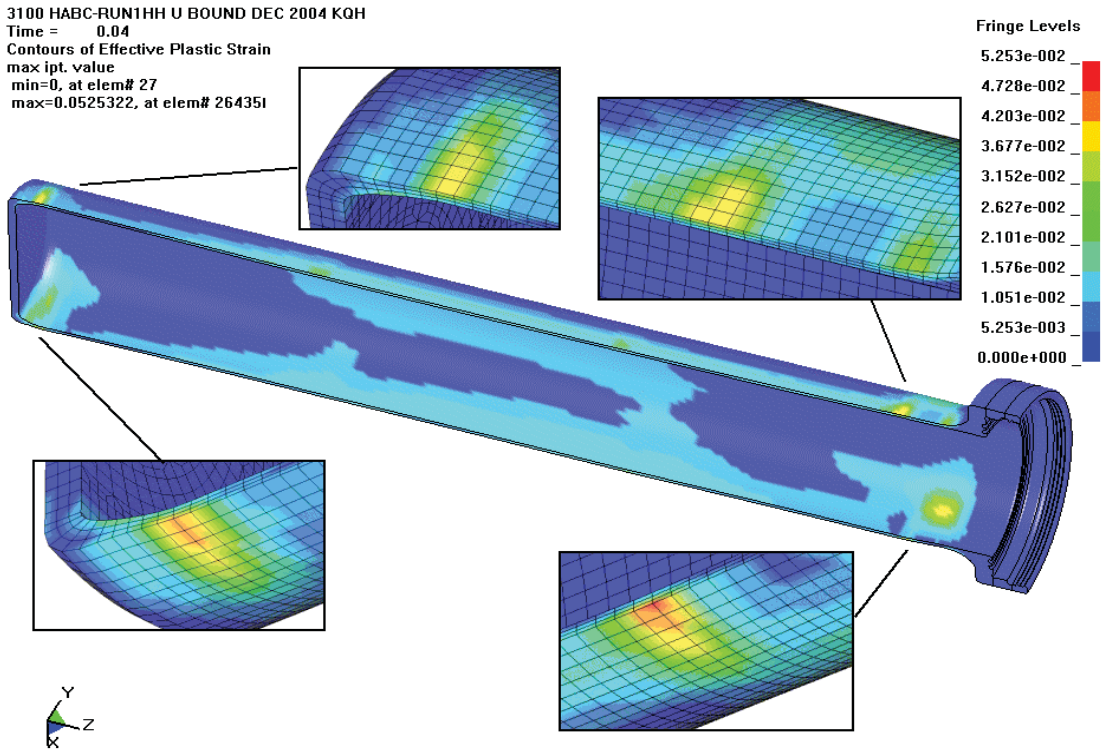

Figure 7.2.10 - HABC-run1hh, Crush Impact, Effective Plastic Strain in the CV Body

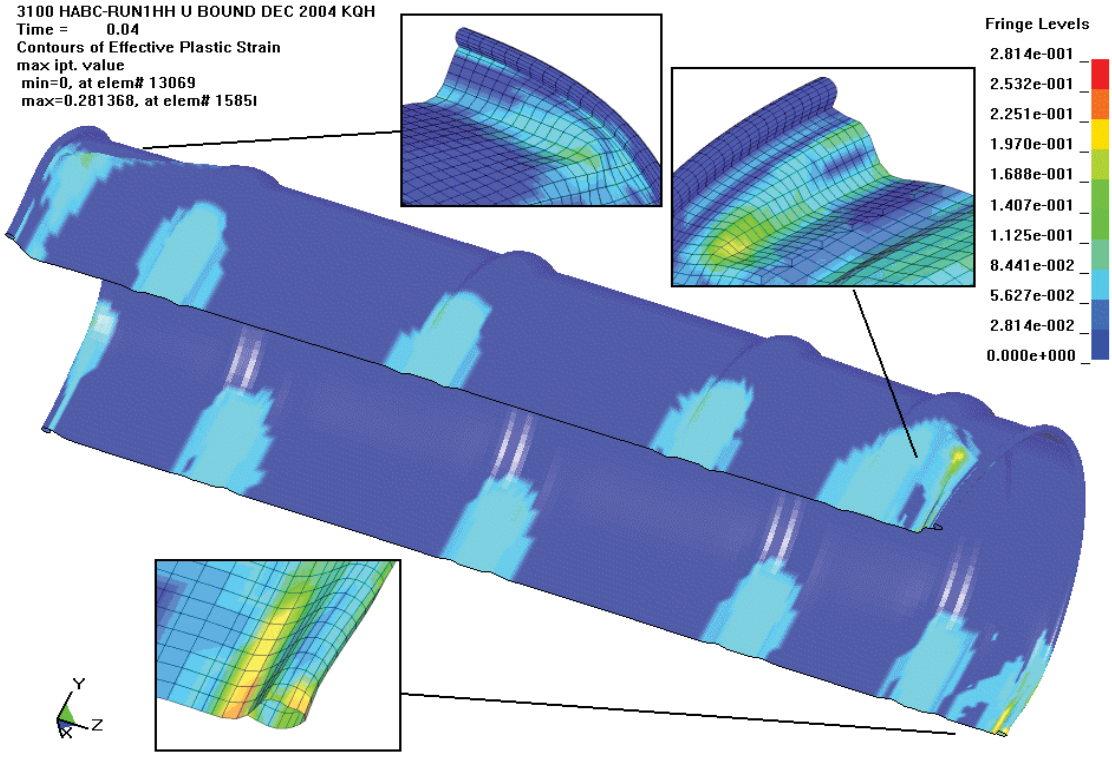

Figure 7.2.11 - HABC-run1hh, Crush Impact, Effective Plastic Strain in the Drum

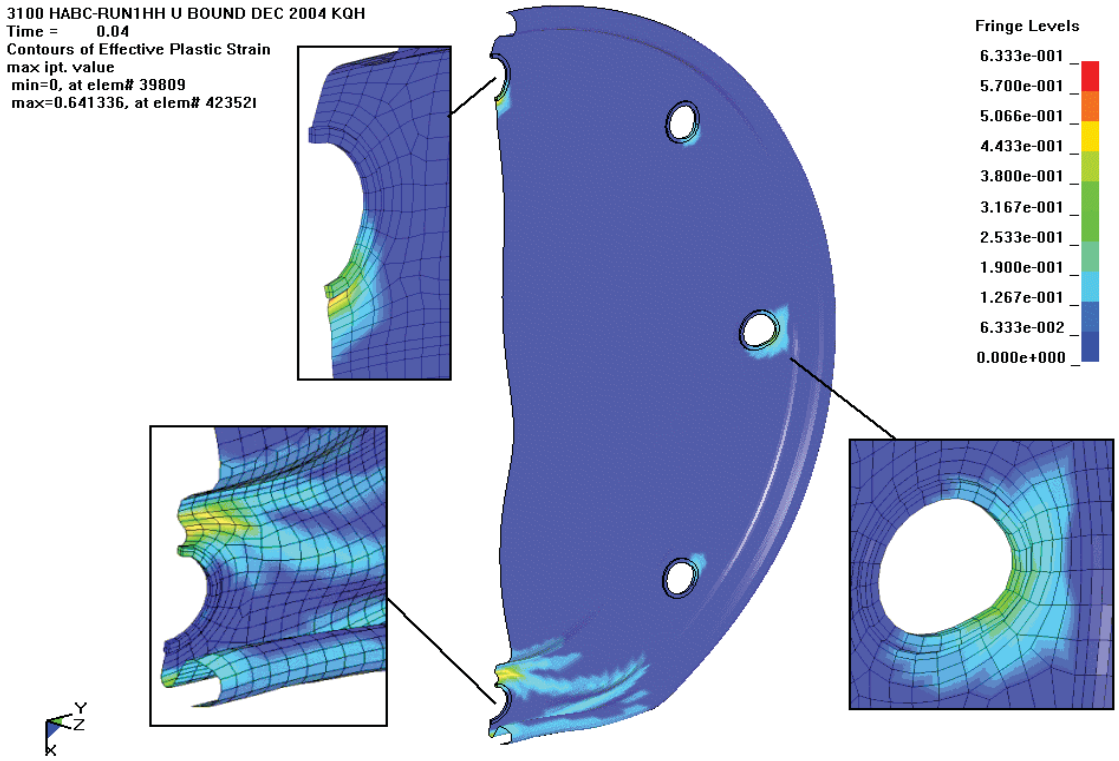

Figure 7.2.12 - HABC-run1hh, Crush Impact, Effective Plastic Strain in the Lid

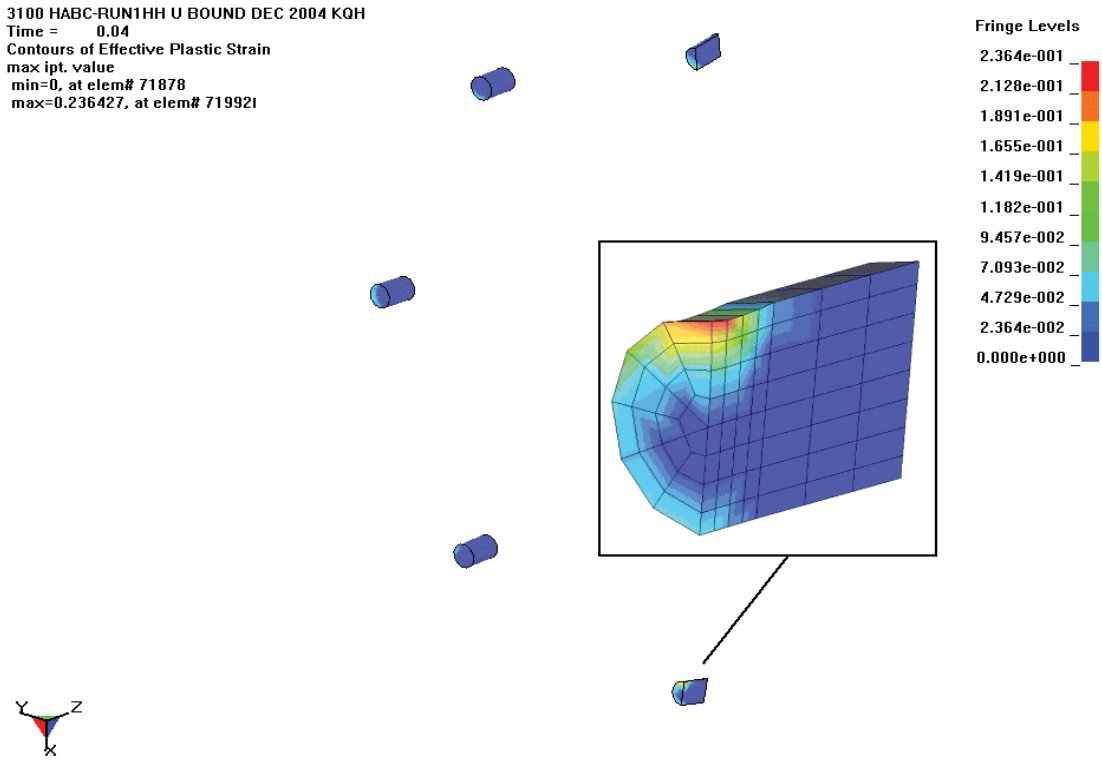

Figure 7.2.13 - HABC-run1hh, Crush Impact, Effective Plastic Strain in the Studs

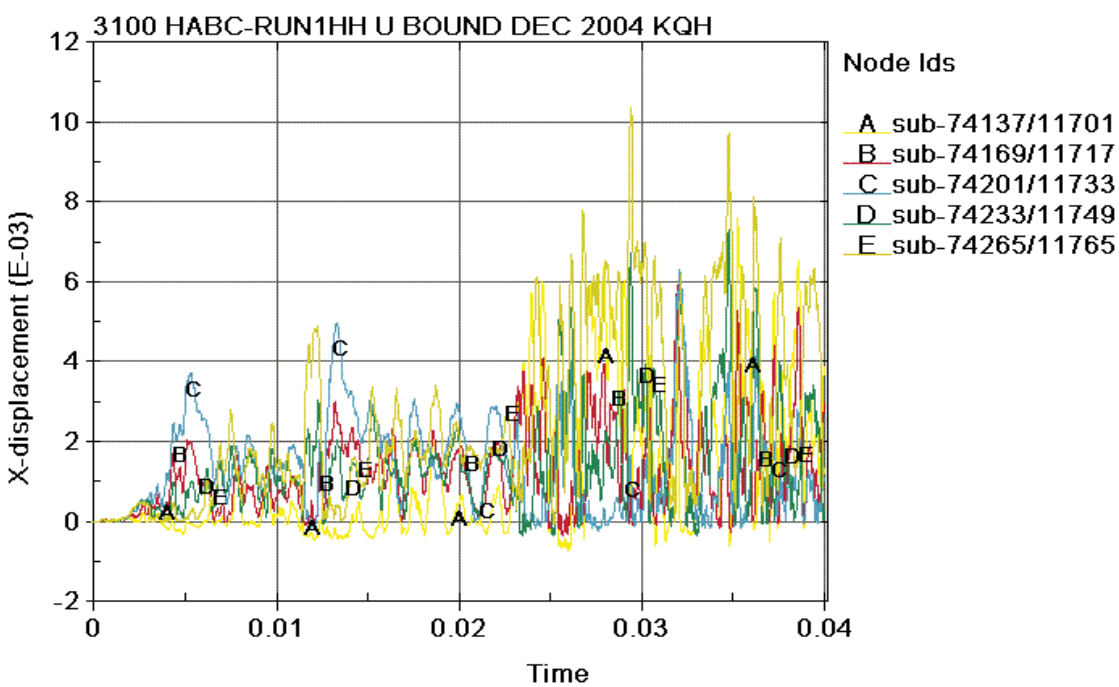

Figure 7.2.14 - HABC-run1hh, CV Lid Separation Time History

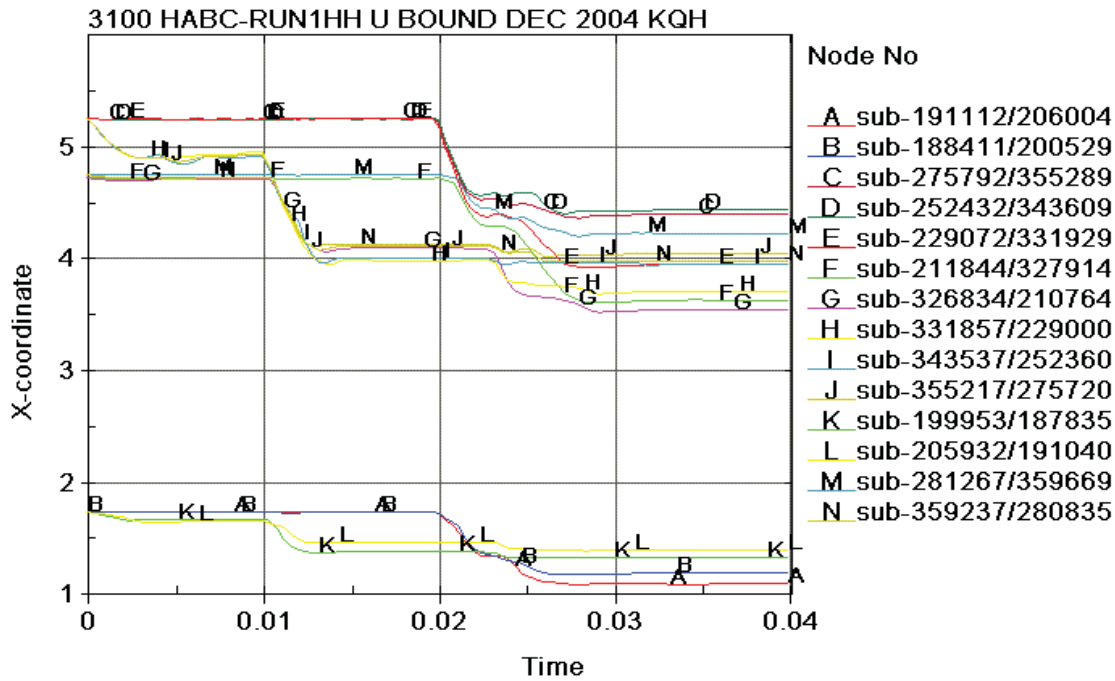

Figure 7.2.15 - HABC-run1hh, Kaolite Thickness Time History

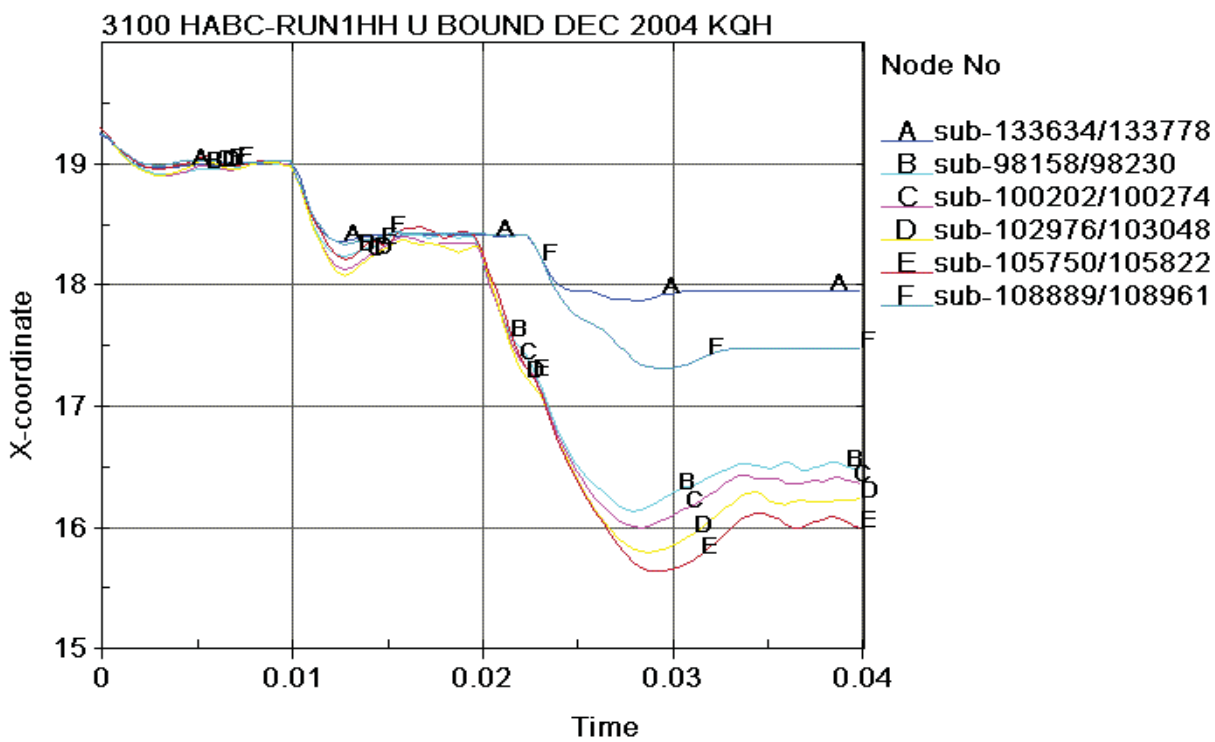

Figure 7.2.16 - HABC-run1hh, Drum Diameter Time History in the X Direction

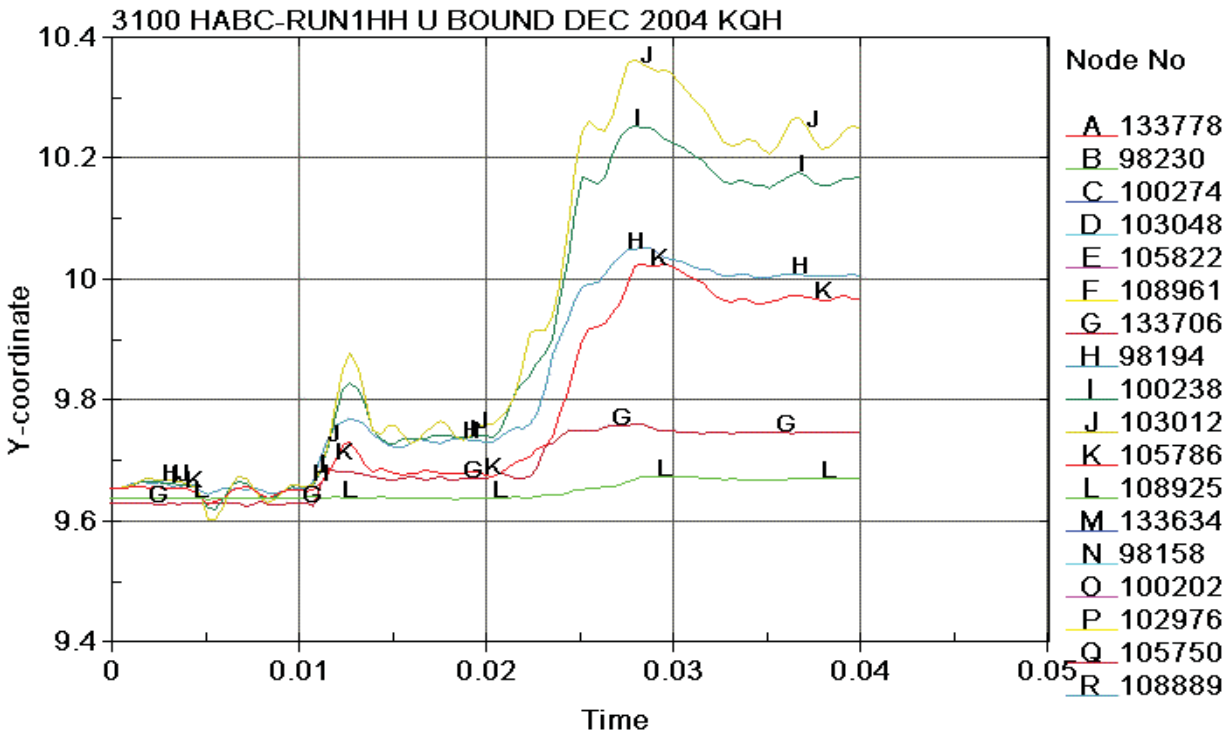

Figure 7.2.17 - HABC-run1hh, Drum Diameter Time History in the Y Direction

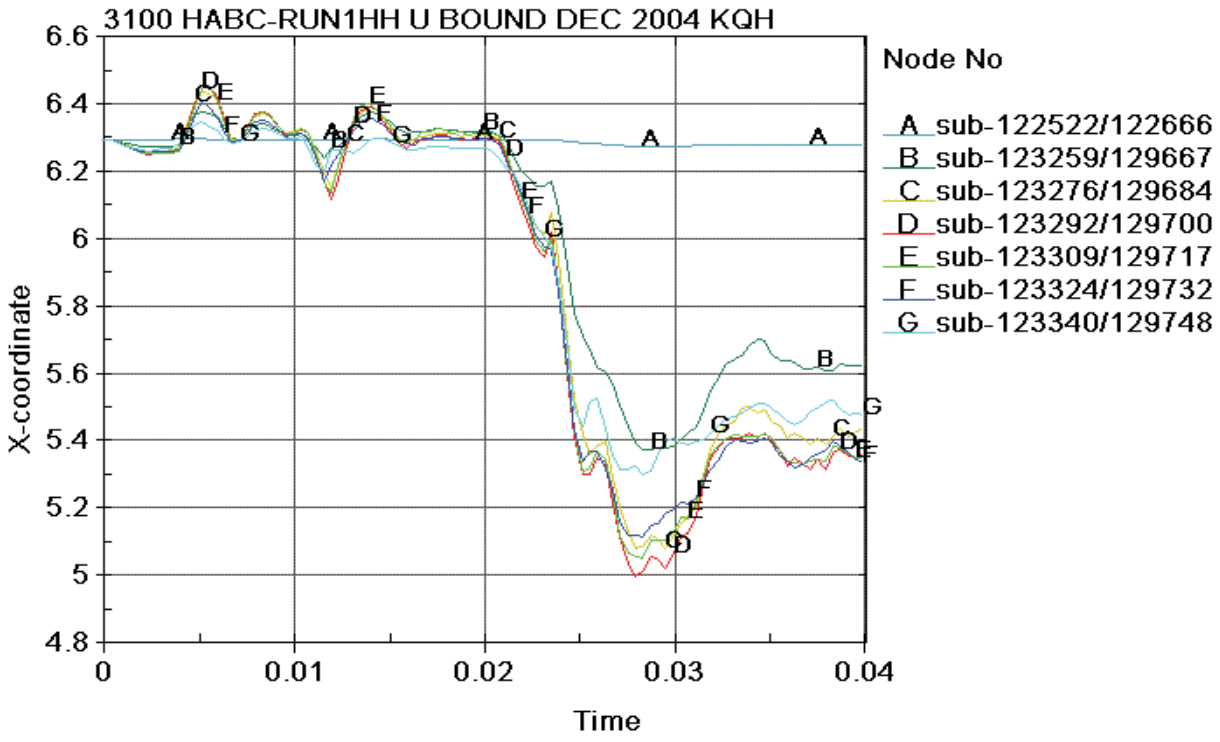

Figure 7.2.18 - HABC-run1hh, Diameter Changes in the Inner Liner

7.3 HABC-run2e - Corner

HABC-run2e is a package CG over corner impact with a 30-foot impact (time = 0 to 0.015 seconds) followed by a crush impact (0.015 to 0.05 seconds).

The configuration after the 30-foot impact is shown in Figure 7.3.1. The maximum effective plastic strain in the CV body is 0.0371 in/in as shown in Figure 7.3.2. Figure 7.3.3 shows that the maximum effective plastic strain in the CV lid is 0.0051 in/in near the outer radius of the center boss.

The maximum effective plastic strain in the lid studs is in the stud at the impact with the rigid plane (0° position) and is 0.5233 in/in. It can be seen from the insert in Figure 7.3.4, that strains near the maximum exist across the thickness of the stud. Therefore, it should be noted that slight differences between the modeled length and actual length of the stud could be significant relative to possible failure of the stud. Other differences such as friction and local flexibility in the test pad armored plate could also significantly effect this stud and cause failure. The maximum effective plastic strains of other components for this impact are listed in Table 7.3.1.

Table 7.3.1 - HABC-run2e, 30-Foot Impact, Effective Plastic Strain Levels in Some Components

Component	Effective Plastic Strain, in/in
CV Nut Ring	0.0002
Angle	0.0394
Drum	0.3247
Drum Bottom Head	0.0000
Liner	0.3983
Lid	0.2791
Lid Stiffener	0.0272
Lid Stud Nuts	0.2260
Lid Stud Washers	0.1528
Plug Liner	0.1152

Figure 7.3.5 shows the final configuration for the crush impact. Figure 7.3.6 shows that the maximum effective plastic strain in the CV body due to the crush impact is 0.0371 in/in.

Figure 7.3.7 shows the effective plastic strain in the CV lid maximum to be 0.0051 in/in. The maximum occurs near the outer radius of the center boss, nearest the impact.

The maximum effective plastic strain in the drum studs is shown to be 0.5598 in/in in Figure 7.3.8. The elevated values of plastic strain occur through out the cross section of the stud. As explained in the 30-foot impact results, slight variances in the length/configuration in this vicinity could prove detrimental for the stud in the test due to the relatively high level of strain through the thickness of the stud.

The maximum effective plastic strain in the liner is 0.5254 in/in as shown in Figure 7.3.9. The maximum is a surface strain and occurs in the folding at about the 80° position at the attachment of the liner to the angle. Investigation shows that the membrane maximum strain is 0.2205 in/in and occurs at the same location.

Table 7.3.2 - HABC-run2e, Crush Impact, Effective Plastic Strain Levels in Some Components

Component	Effective Plastic Strain, in/in
CV Nut Ring	0.0002
Angle	0.0462
Drum	0.3830
Drum Bottom Head	0.0761
Liner	0.5254
Lid	0.3622
Lid Stiffener	0.0272
Lid Stud Nuts	0.2266
Lid Stud Washers	0.1528
Plug Liner	0.1166

The CV lid separation time histories for the nodes shown in Figure 3.1.30 are given in Figure 7.3.10 for the HABC-run2e. Spike separation occurs (about 0.013 in) during the 30-foot impact with the general separation of about 0.008 in. The general separation lasts about 0.01 seconds, then settles to 0.003 in or less. The general separation due to the crush impact is 0.005 in or less, with some spiking to about 0.010 in noted. Nominal separation of 0.003 in or less would be expected.

Figure 7.3.11 shows the location of the nodes used to obtain the minimum kaolite thickness in the plug. Figure 7.3.12 shows the minimum plug thickness time history. A minimum

thickness of about 3.5 inches is reached in the 30-foot impact, and about 3.0 inches is reached in the successive crush impact.

Figure 7.3.13 shows the location of the nodes used to obtain the minimum koalite thickness in the package bottom. The time history thickness is shown in Figure 7.3.14 for the bottom kaolite. A minimum thickness of about 1.75 inches is shown.

Figure 7.3.15 shows the nodes used to obtain overall drum heights for the impacts. The final lengths from the bottom head to the lid are used to describe the deformations. Curve A in Figure 7.3.16 gives the length response of the 30-foot impacted lid corner to the drum bottom. The length after the 30-foot lid impact is about 40.5 in and goes to about 39 in after the crush impact. The Curve B in Figure 7.3.16 shows that the length from the crushed corner of the bottom to the lid reaches about 38 in in length.

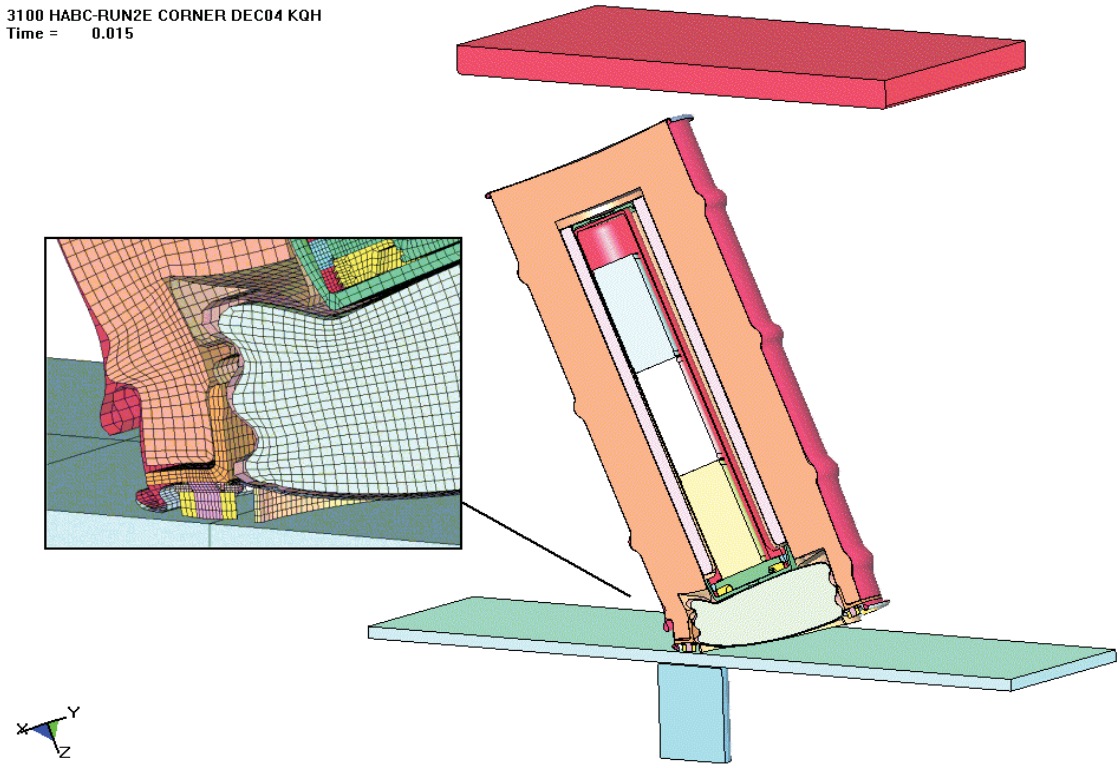

Figure 7.3.1 - HABC-run2e, Configuration of the ES-3100 After the 30-Foot Impact

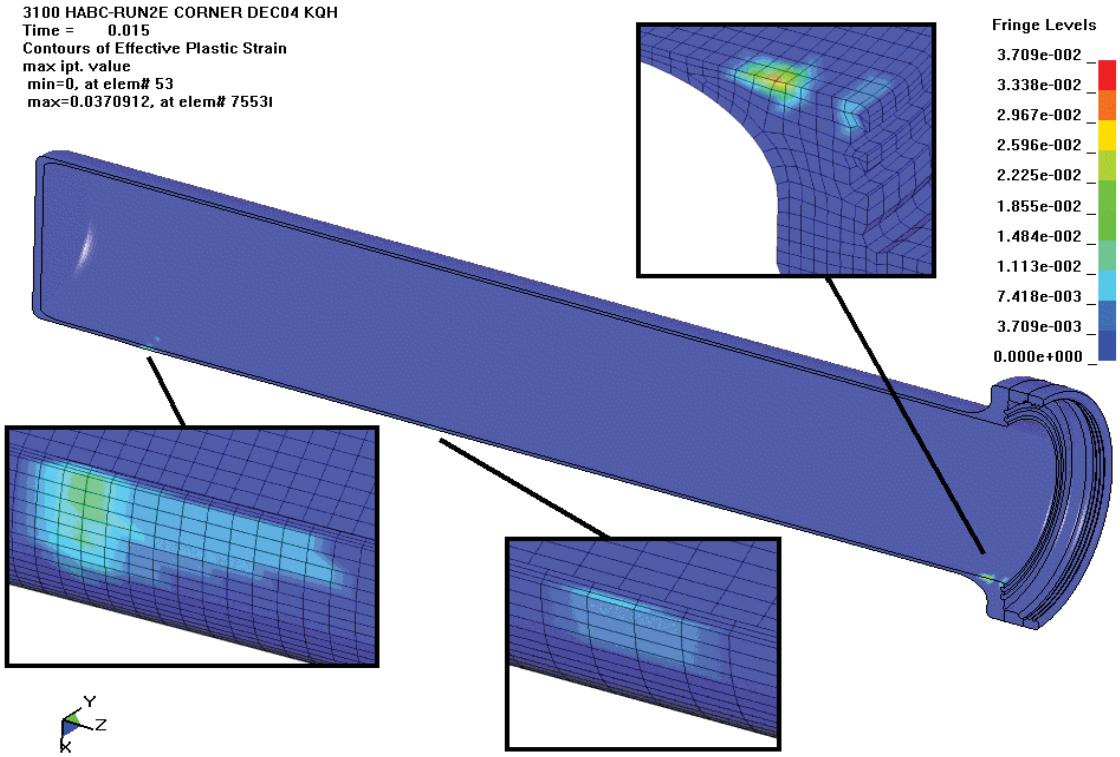

Figure 7.3.2 - HABC-run2e, 30-Foot Impact, Effective Plastic Strains in the CV Body

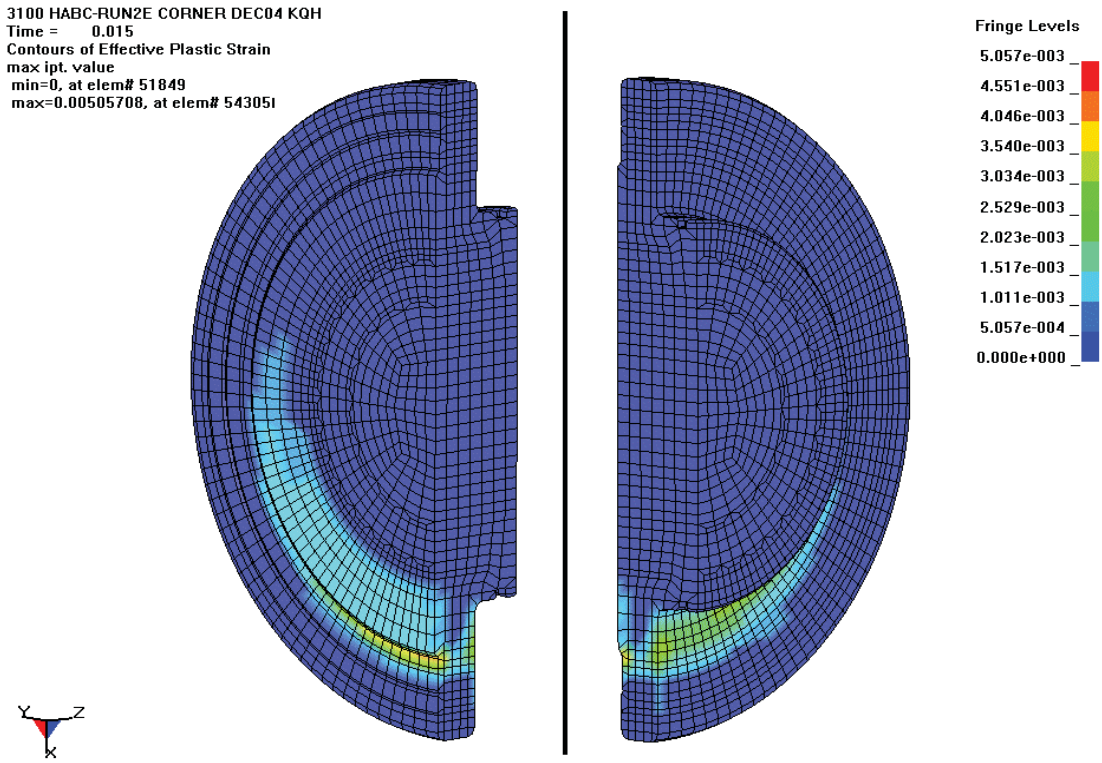

Figure 7.3.3 - HABC-run2e, 30-Foot Impact, Effective Plastic Strain in the CV Body

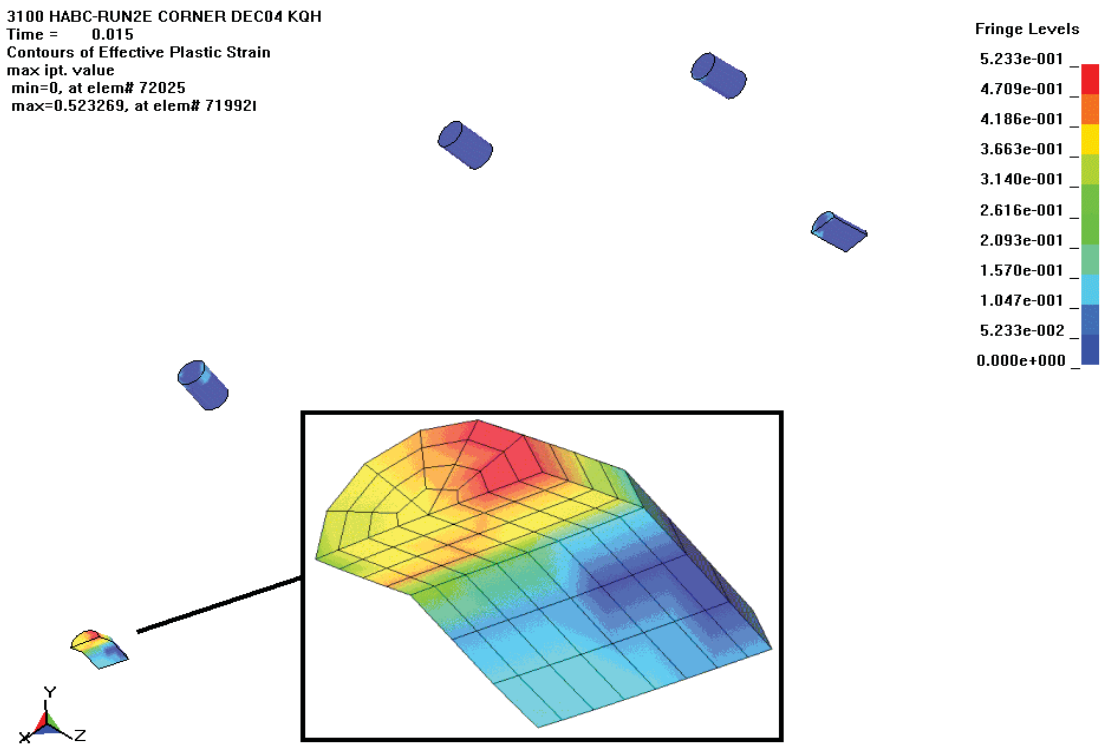

Figure 7.3.4 - HABC-run2e, 30-Foot Impact, Effective Plastic Strain in the Studs

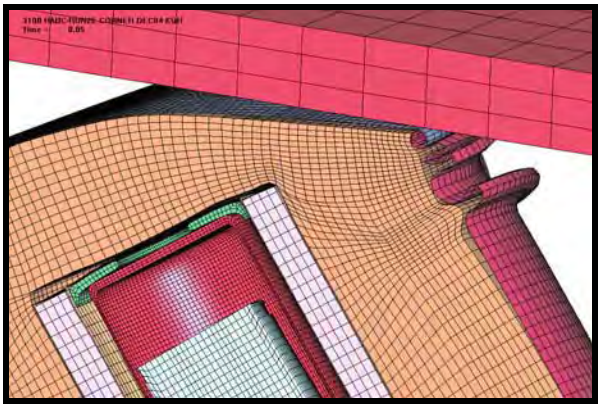

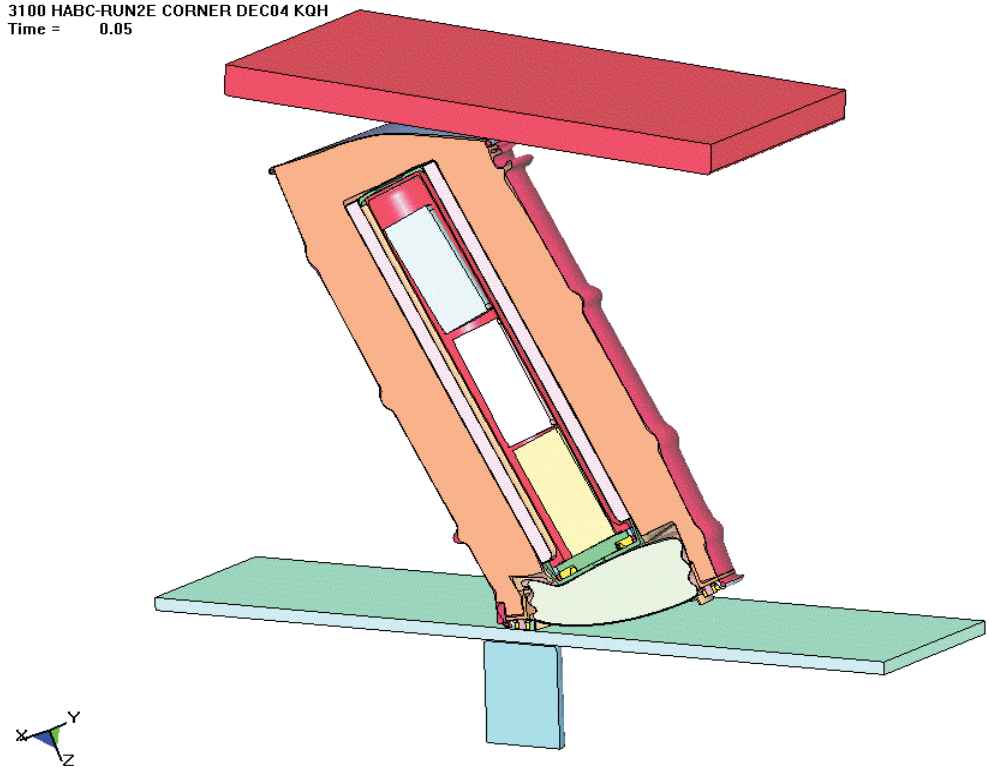

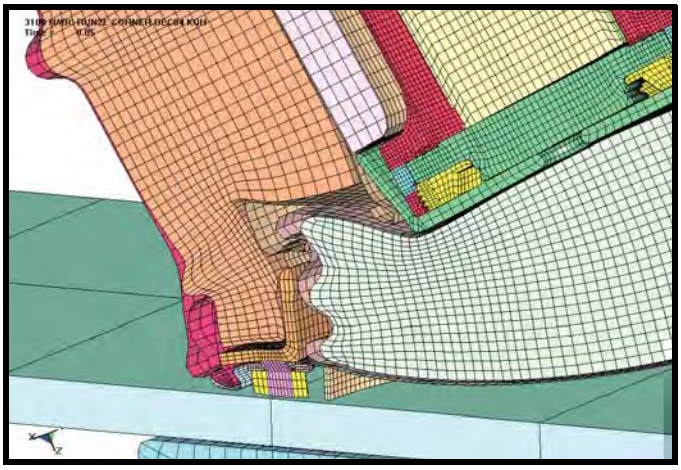

Figure 7.3.5 - HABC-run2e, Configuration After the Crush Impact

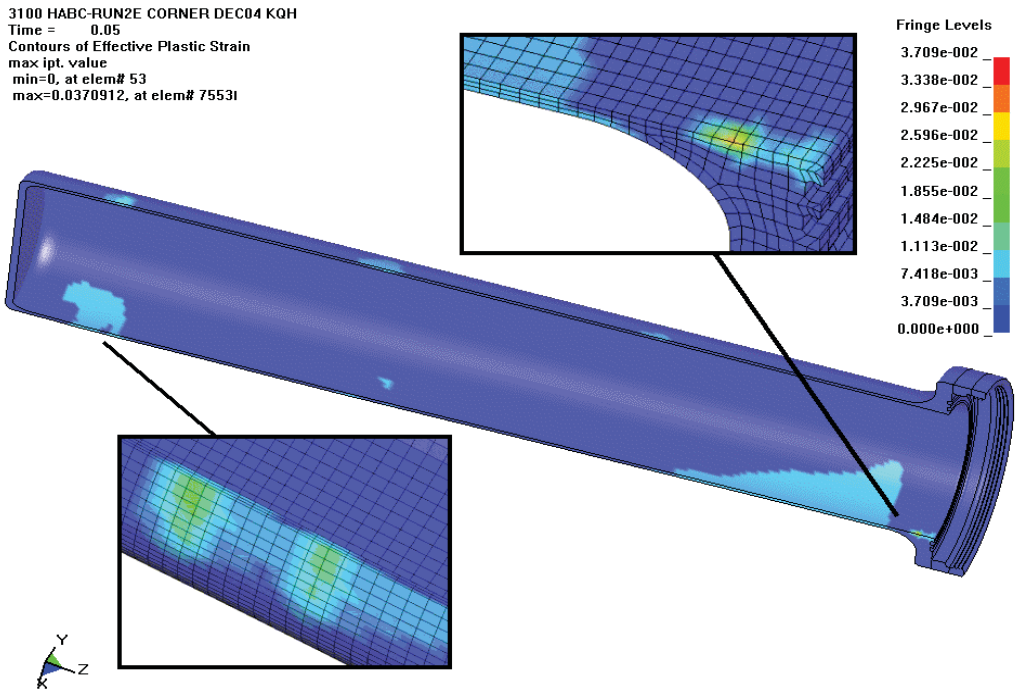

Figure 7.3.6 - HABC-run2e, Crush Impact, Effective Plastic Strain in the CV Body

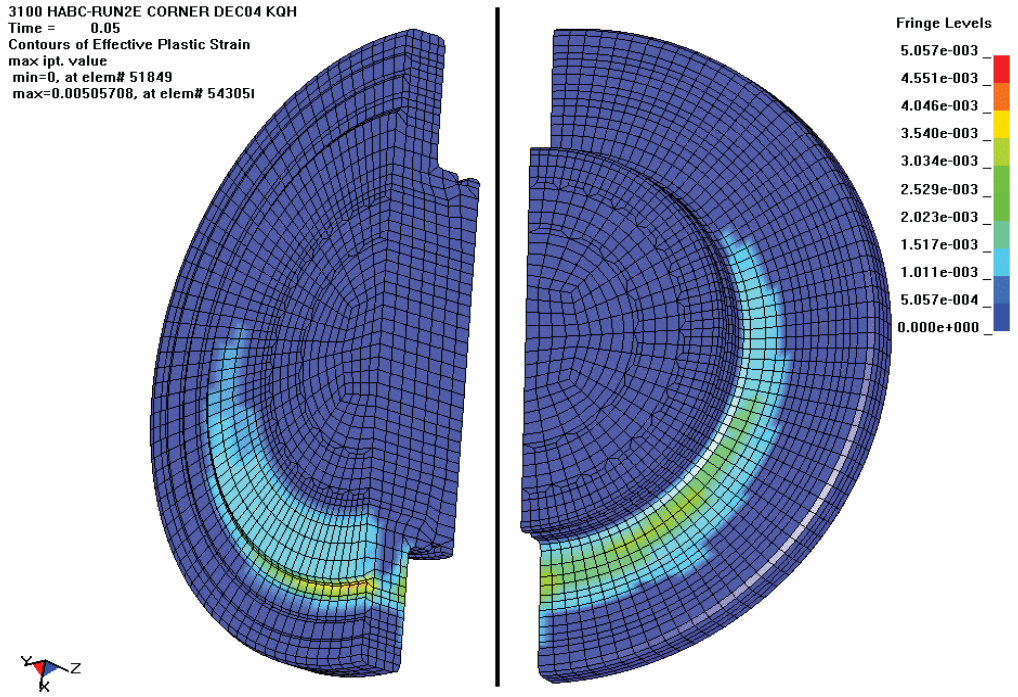

Figure 7.3.7 - HABC-run2e, Crush Impact, Effective Plastic Strain in the CV Lid

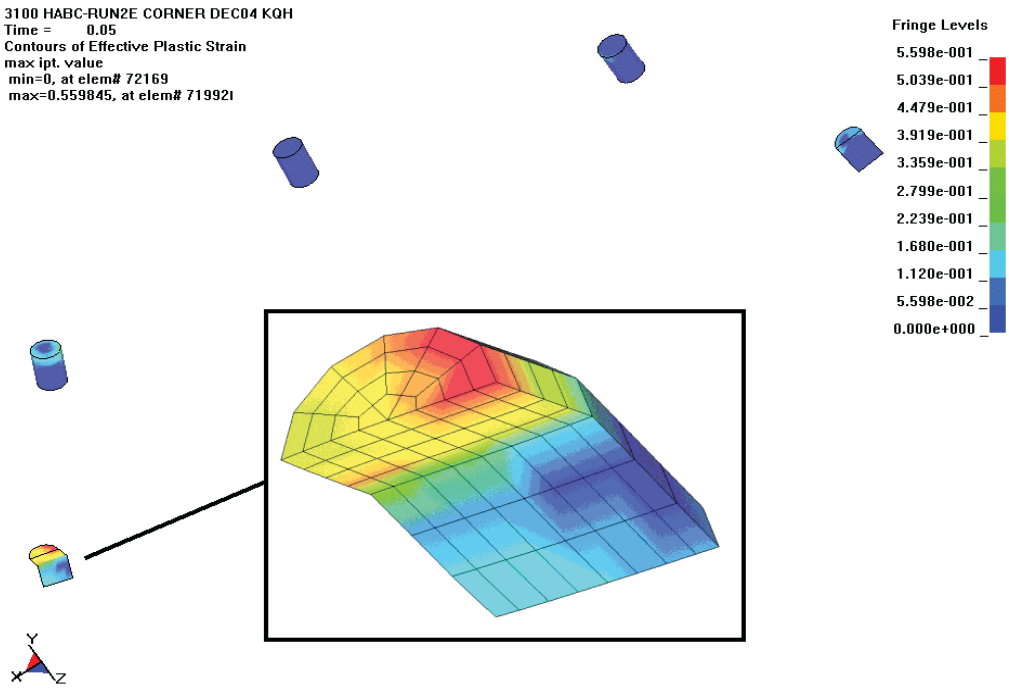

Figure 7.3.8 - HABC-run2e, Crush Impact, Effective Plastic Strain in the Studs

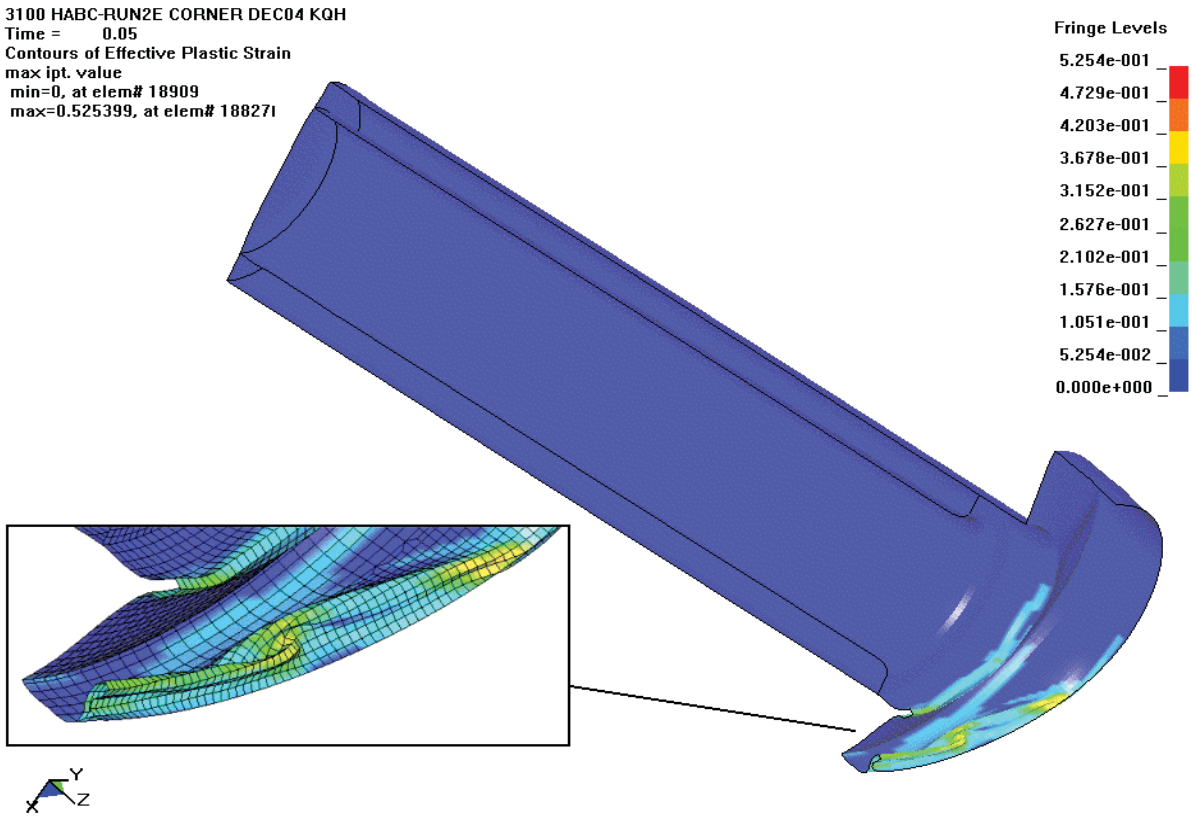

Figure 7.3.9 - HABC-run2e, Crush Impact, Effective Plastic Strain in the Liner

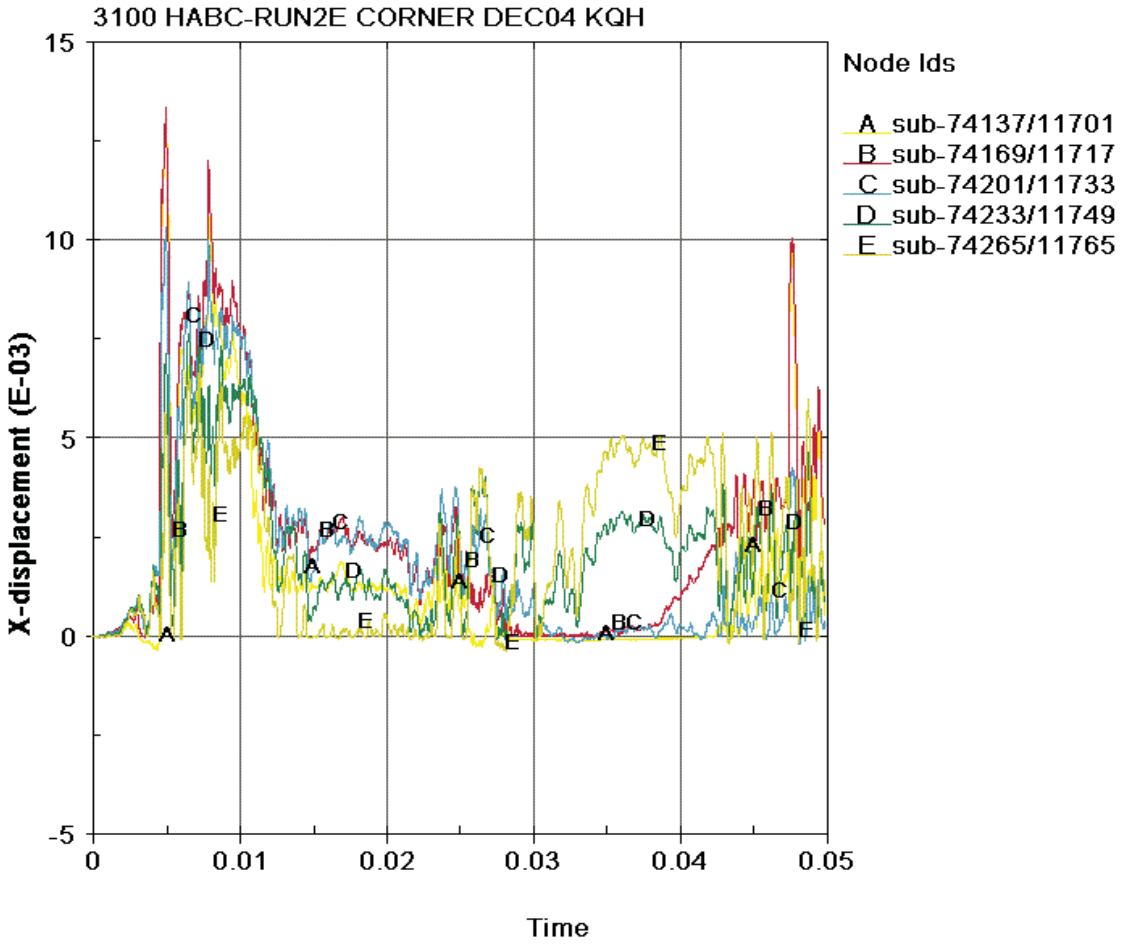

Figure 7.3.10 - HABC-run2e, Crush Impact, CV Lid/Body Separation Time History

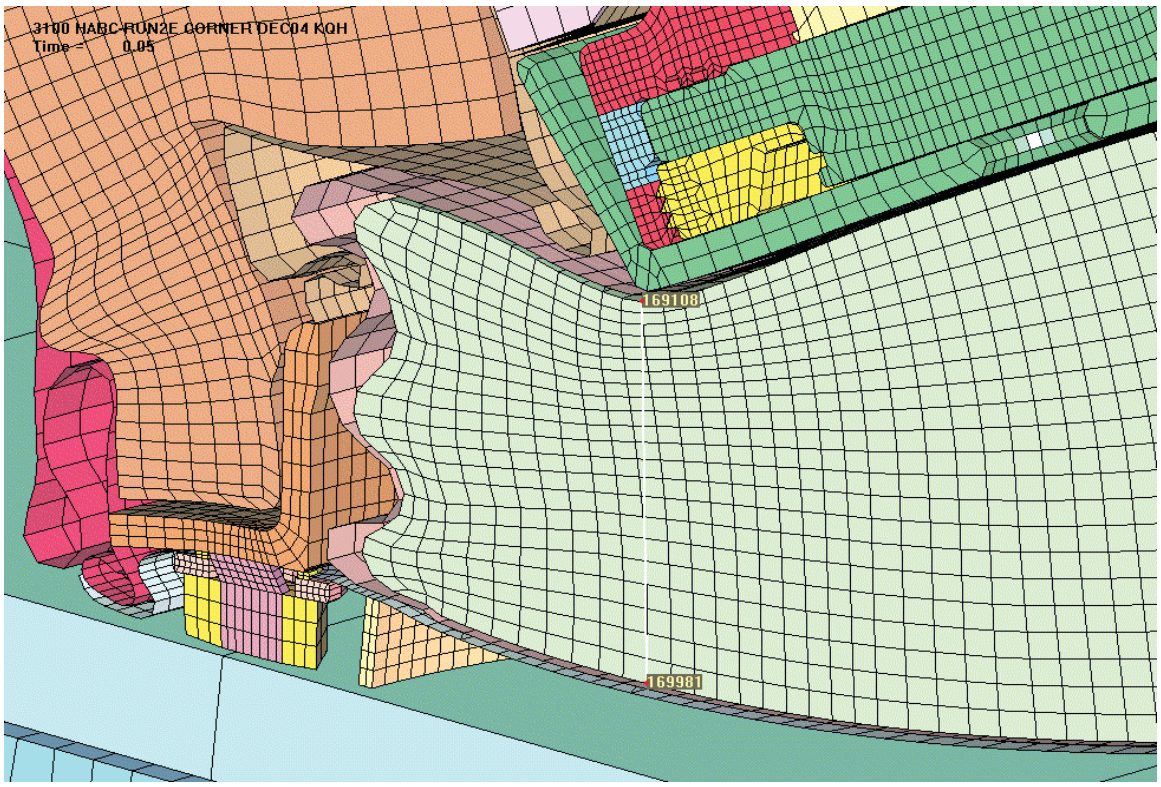

Figure 7.3.11 - HABC-run2e, Plug Thickness After the Crush Impact

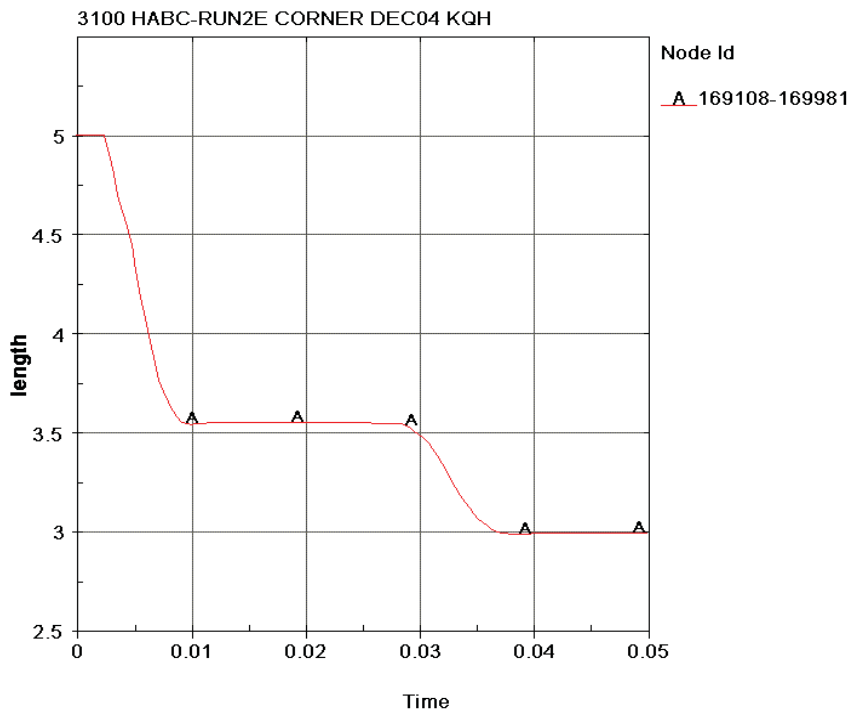

Figure 7.3.12 - HABC-run2e, Plug Thickness Time History

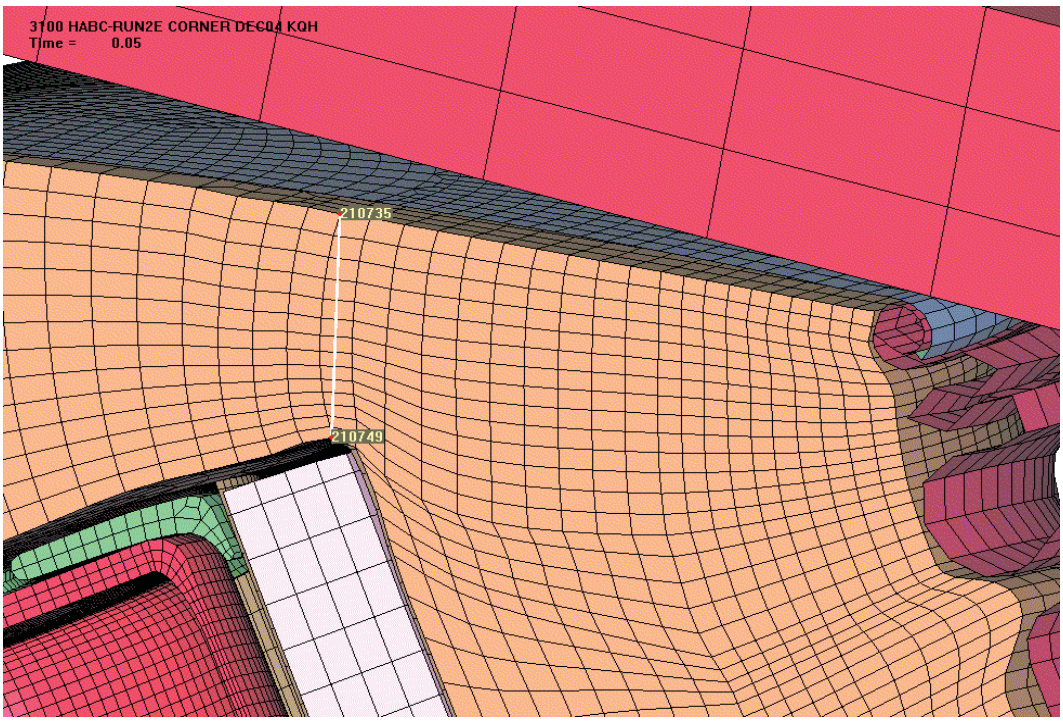

Figure 7.3.13 - HABC-run2e, Bottom Kaolite Thickness After the Crush Impact

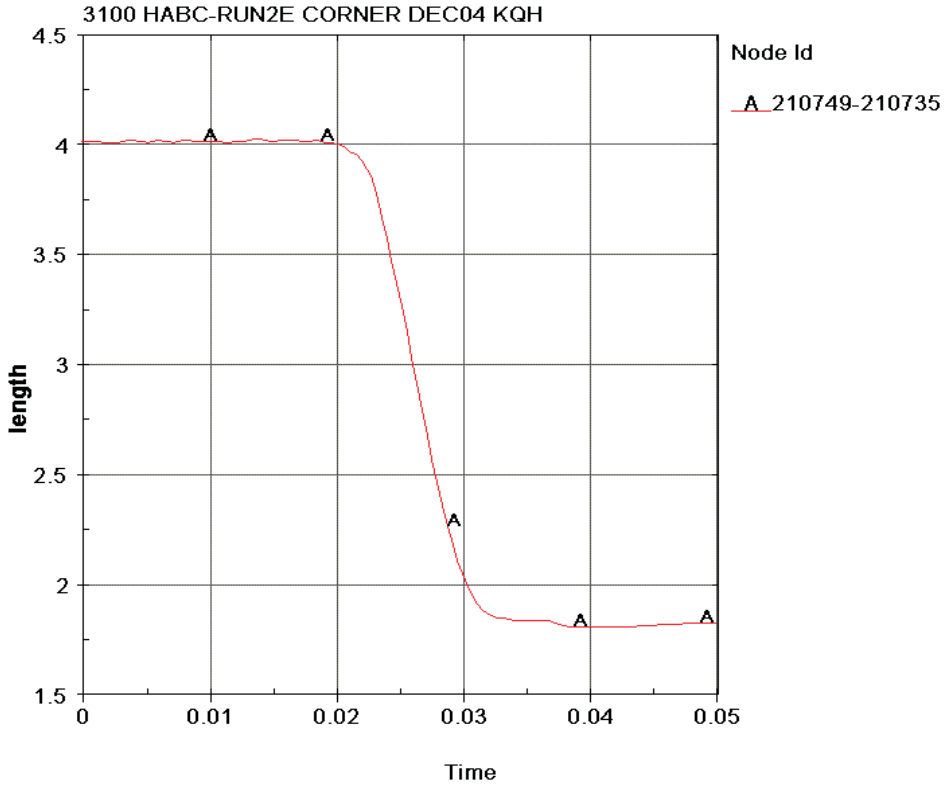

Figure 7.3.14 - HABC-run2e, Bottom Kaolite Thickness Time History

Figure 7.3.15 - HABC-run2e, Length Dimensions in the Drum

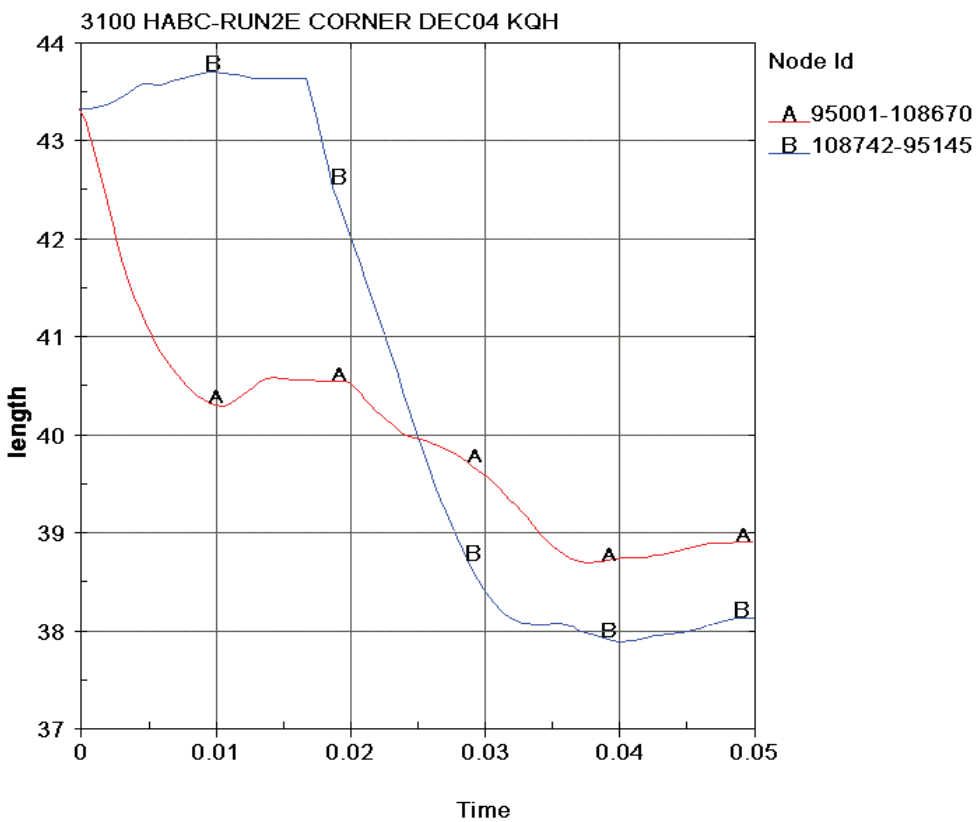

Figure 7.3.16 - HABC-run2e, Drum Length Time History

7.4 HABC-run3b - End

HABC-run3b is a 30-foot lid end impact (time = 0 to 0.010 seconds) followed by a crush impact onto the package bottom (0.010 to 0.028 seconds). Figure 7.4.1 shows the configuration of the container at the end of the 30-foot impact. Figure 7.4.2 shows that the maximum effective plastic strain in the CV body is 0.0028 in/in. The maximum plastic strain occurs in the bottom head. Figure 7.4.3 shows the CV lid. The maximum effective plastic strain is found to be 0.0072 in/in and occurs just outboard of the center boss on the outer surface.

The maximum effective plastic strain in the nut ring is shown to be 0.0011 in/in in Figure 7.4.4. It is believed this plastic strain is an anomaly with the contact surface because: 1) the fringes of plastic strain are not symmetrical, 2) the maximum value of plastic strain occurs at single nodes on an edge of the component and 3) the nut ring bares on the relatively soft silicone pad. Table 7.4.1 summarizes the maximum effective plastic strains in the other package components.

Table 7.4.1 - HABC-run3b, 30-Foot Impact, Effective Plastic Strain Levels in Some Components

Component	Effective Plastic Strain, in/in
Angle	0.0287
Drum	0.0557
Drum Bottom Head	0.0031
Liner	0.0607
Lid	0.1082
Lid Stiffener	0.0069
Lid Studs	0.0962
Lid Stud Nuts	0.0166
Lid Stud Washers	0.0506
Plug Liner	0.0670

Figure 7.4.5 shows the final configuration for the successive crush impact. Figure 7.4.6 shows that the maximum effective plastic strain in the CV body is 0.0083 in/in. The ring of plastic deformation in the sidewall at the bottom head is due to the bending of the bottom head. The other components are summarized in Table 7.4.2.

Table 7.4.2 - HABCrun3b, Crush Impact, Effective Plastic Strain Levels in Some Components	
Component	Effective Plastic Strain, in/in
CV Lid	0.0072
CV Nut Ring	0.0011
Angle	0.0308
Drum	0.1237
Drum Bottom Head	0.0267
Liner	0.3812
Lid	0.1389
Lid Stiffener	0.0100
Lid Studs	0.1535
Lid Stud Nuts	0.0173
Lid Stud Washers	0.0506
Plug Liner	0.0960

The CV lid separation time history is shown in Figure 7.4.7. The response during the 30-foot impact are separation spikes up to about 0.018 in with a general separation of about 0.012 in. The spikes occur for about 0.001 sec, while the general separation occurs for about 0.005 sec. During the crush impact, the gap response oscillates about values of general separation. The general separation remains below a gap of about 0.005 in.

Figure 7.4.8 shows the nodes chosen to observe the plug and bottom kaolite thicknesses and the overall drum height. Figure 7.4.9 shows the time history of the drum height. After the 30-foot impact and the successive crush impact, the drum height is found to be about 39 inches. Figure 7.4.10 shows the minimum plug thickness time history with Curve B. The minimum plug thickness after the 30-foot impact is about 3.75 in. The minimum plug thickness after the successive crush impact is about 3.4 in. Curve A shows the bottom kaolite minimum thickness is about 2.2 in after the crush impact.

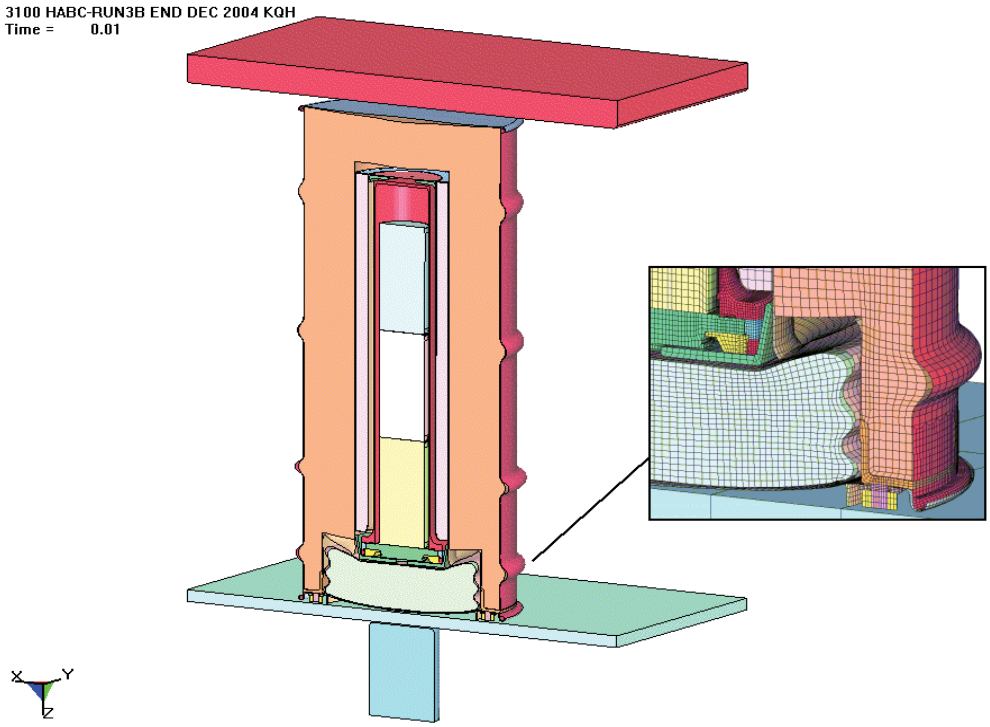

Figure 7.4.1 - HABC-run3b, Configuration After the 30-Foot Impact

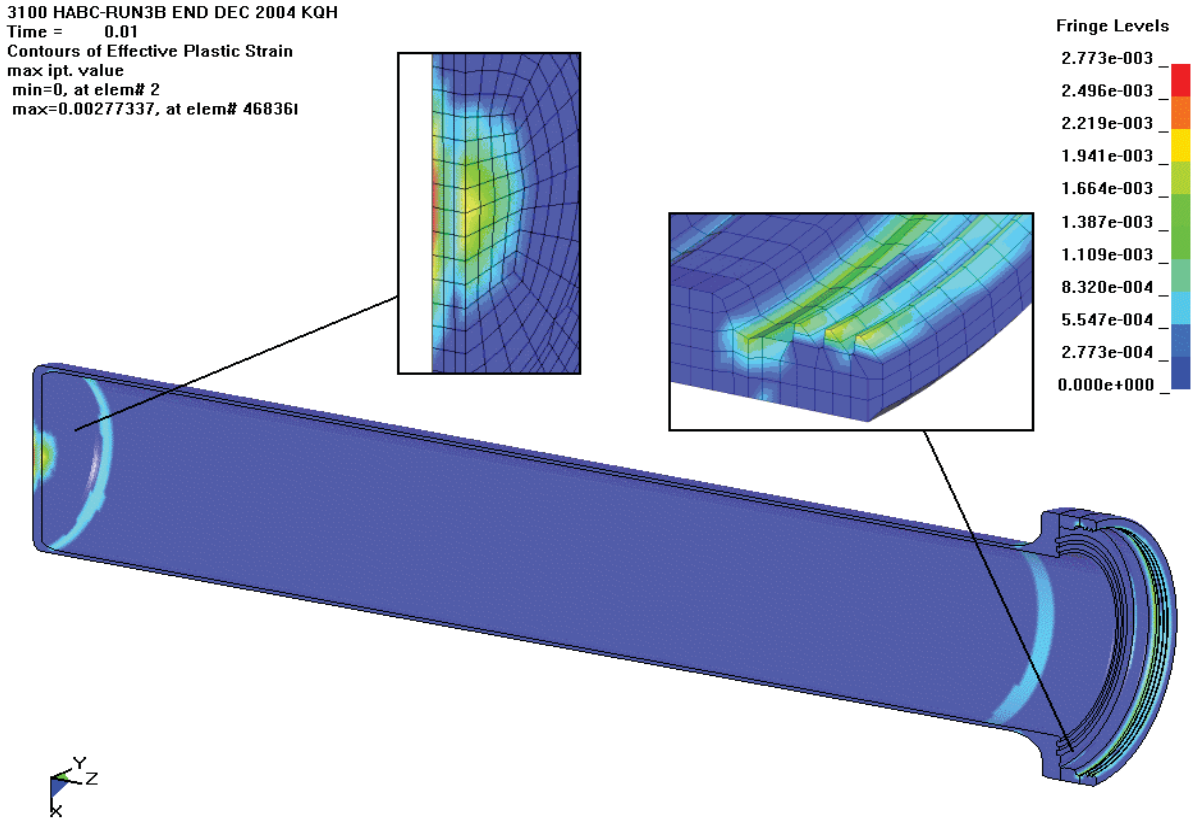

Figure 7.4.2 - HABC-run3b, 30-Foot Impact, Effective Plastic Strain in the CV Body

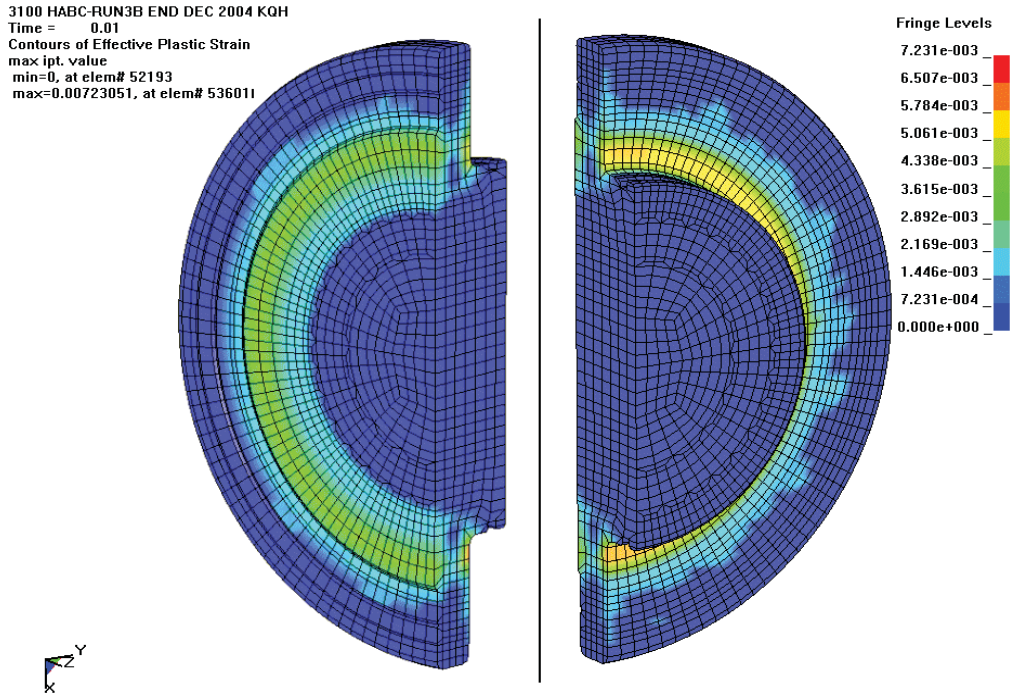

Figure 7.4.3 - HABC-run3b, 30-Foot Impact, Effective Plastic Strain in the CV Lid

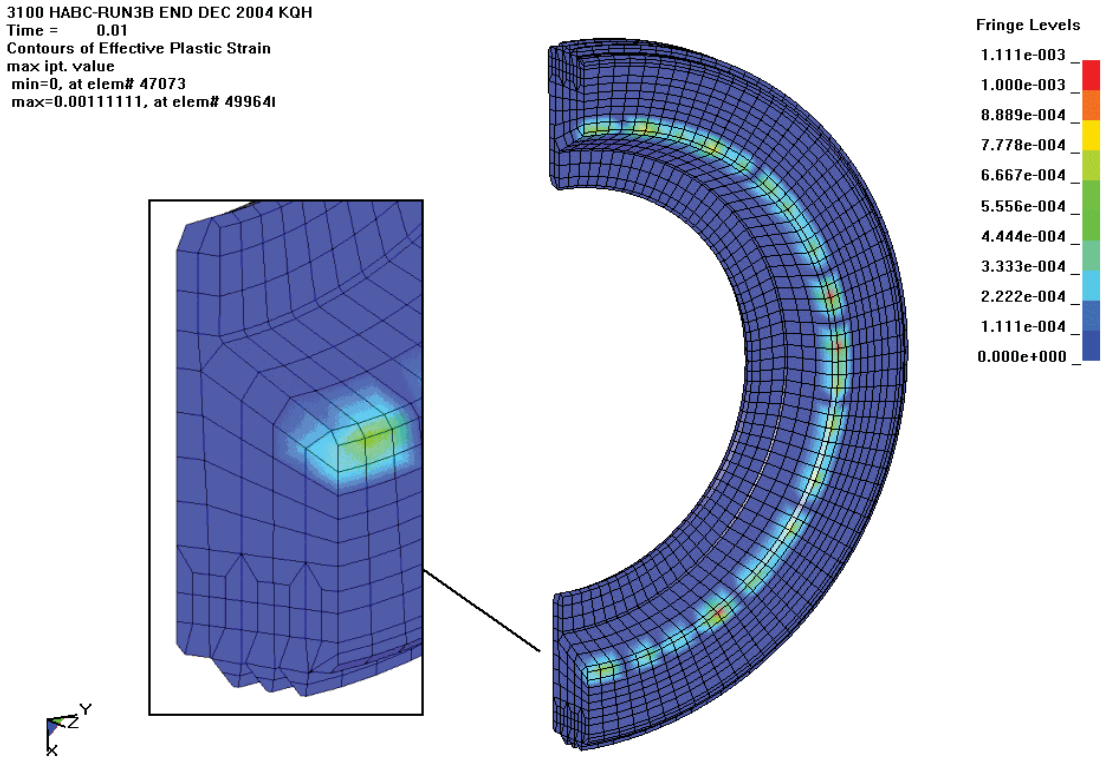

Figure 7.4.4 - HABC-run3b, 30-Foot Impact, Effective Plastic Strain in the CV Nut Ring

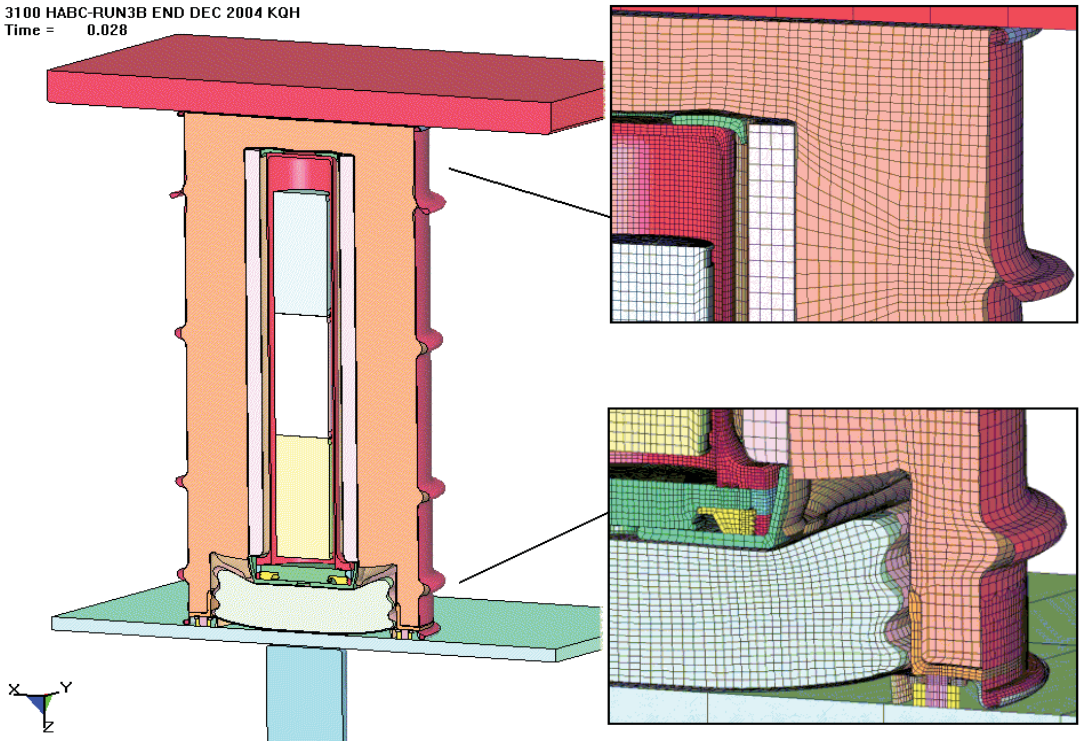

Figure 7.4.5 - HABC-run3b, Configuration After the Crush Impact

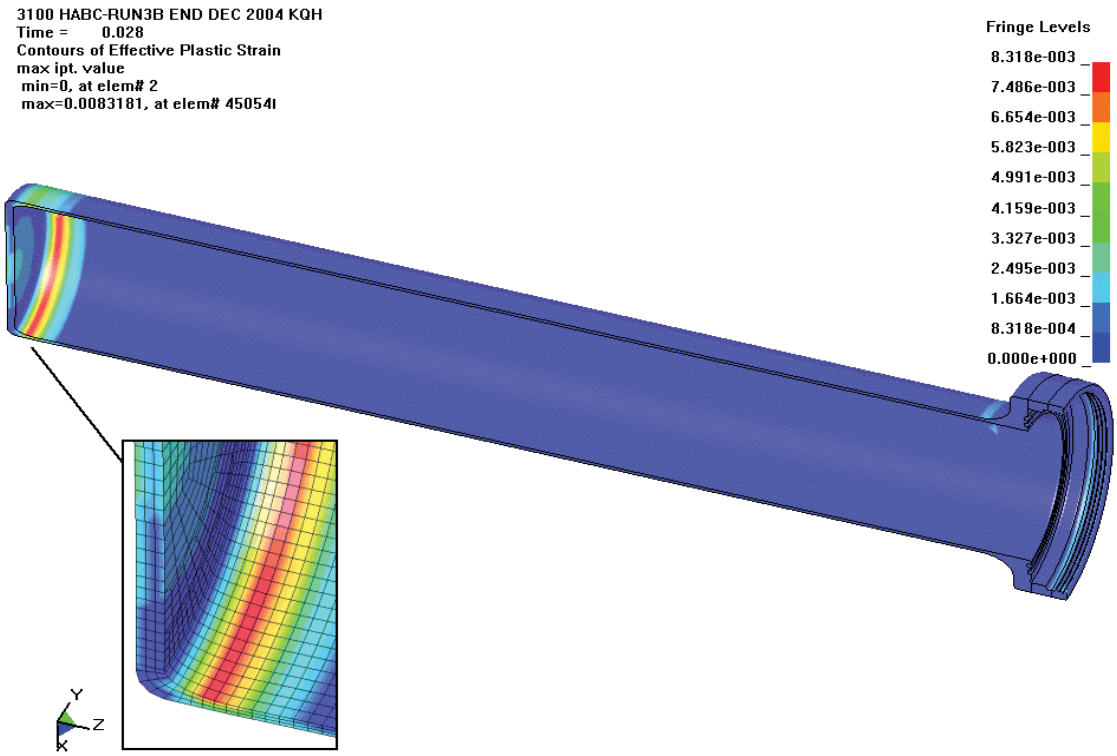

Figure 7.4.6 - HABC-run3b, Crush Impact, Effective Plastic Strain in the CV Body

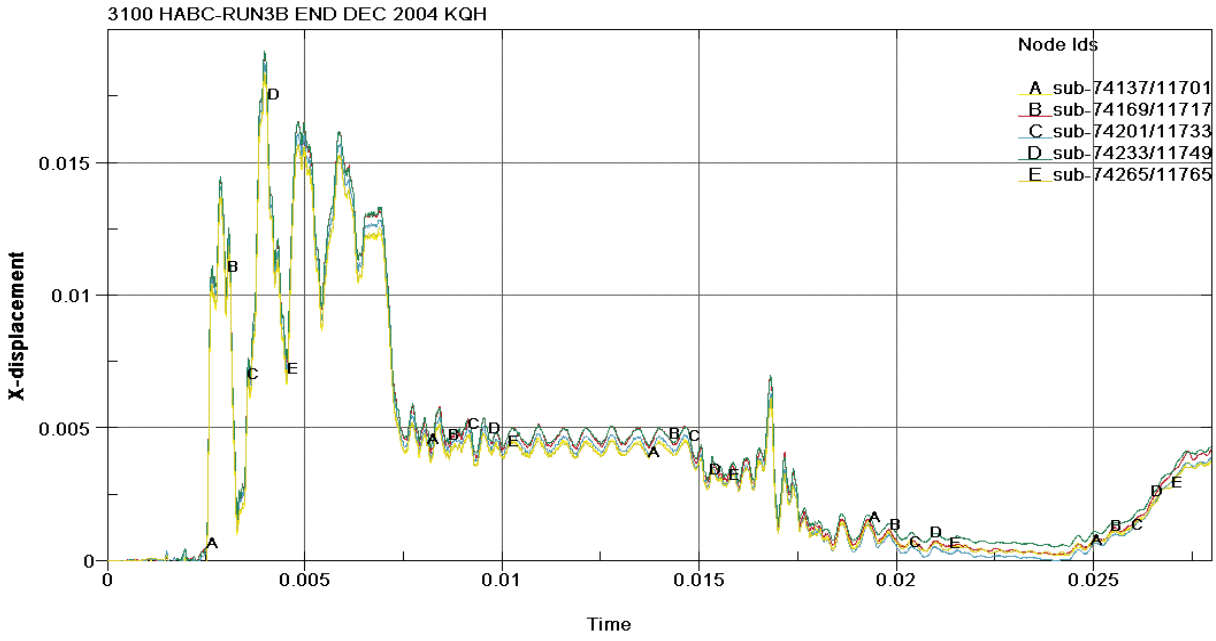

Figure 7.4.7 - HABC-run3b, CV Lid Separation Time History

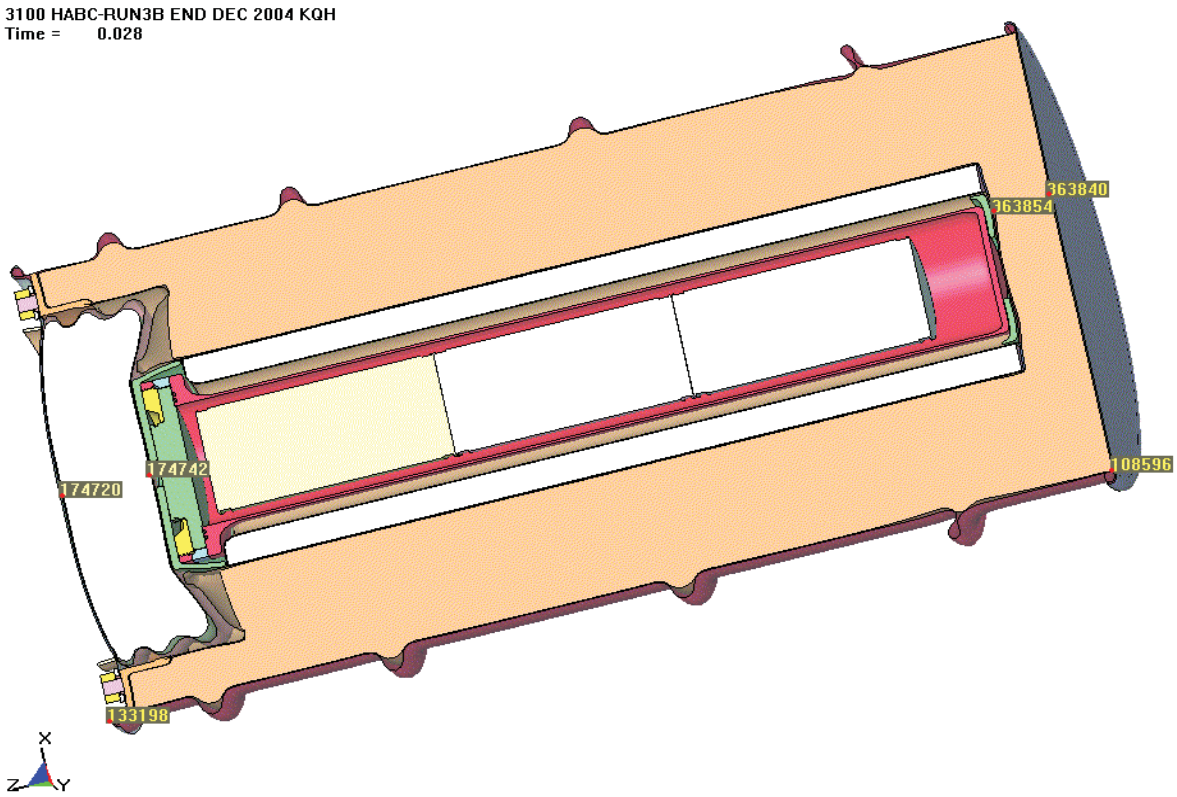

Figure 7.4.8 - HABC-run3b, Nodes to Determine Drum/Kaolite Heights

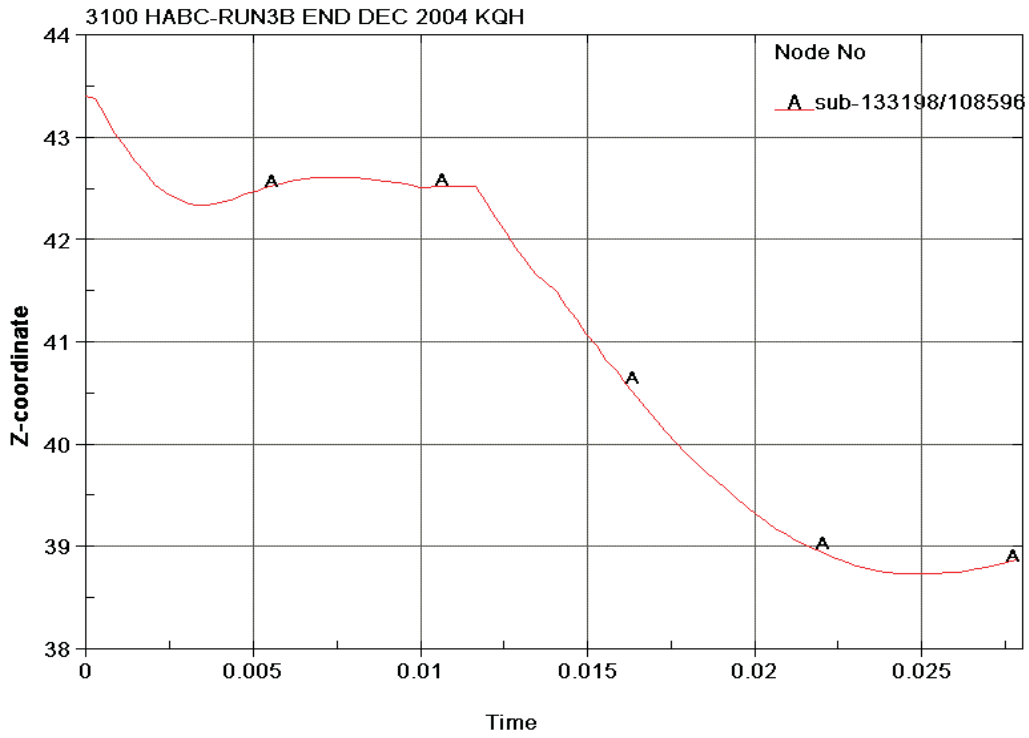

Figure 7.4.9 - HABC-run3b, Drum Height Time History

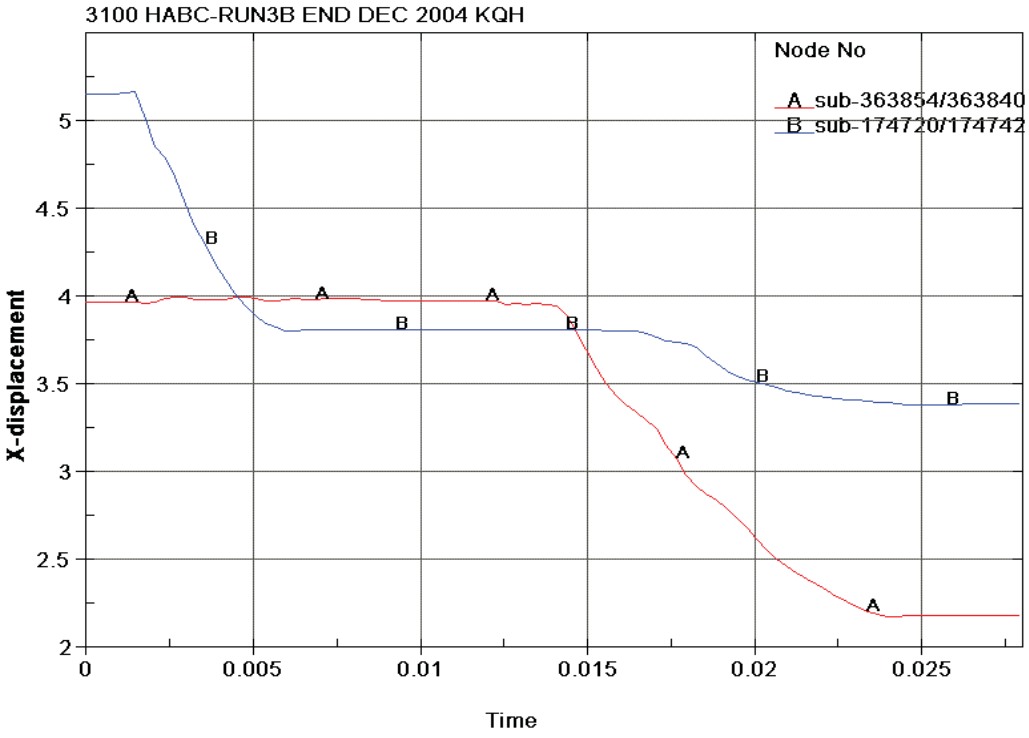

Figure 7.4.10 - HABC-run3b, Kaolite Thickness Time Histories

7.5 HABC-run4g - Slapdown

HABC-run4g is a 12° slapdown, 30-foot impact (time 0 to 0.02 seconds) followed by an offset crush with the crush plate CG over the CV flange (0.0202 to 0.04 seconds). From 0.0200 to 0.0202 sec, the crush plate is moved (via nodal velocities) such that its geometric center is approximately in line with the CV flange.

The initial configuration of the model is shown in Figure 7.5.1. The deflected shape of the package after the 30-foot impact is shown in Figure 7.5.2. Figure 7.5.3 shows enlargements of the corners of the package due to the 30-foot slapdown impact. The maximum effective plastic strain in the CV body for the 30-foot impact is 0.0376 in/in and occurs below the flange and nearest the impacted rigid surface as shown in Figure 7.5.4. Figure 7.5.5 shows that the maximum effective plastic strain in the drum is 0.3018 in/in. The maximum occurs at the bottom drum roll attachment to the drum, as is shown by the element number in the enlargement of the base region of the drum. Figure 7.5.5 does not show this by color fringes due to the nodal averaging of adjacent elements by the plot routine. The maximum strain is a highly localized bending strain in the bottom drum roll. The maximum effective plastic strain in the lid is 0.5278 in/in as shown in Figure 7.5.6. The maximum occurs due to the bearing of the lid onto the stud at the 0° position. The maximum effective plastic strains in other components for the 30-foot impact are listed in Table 7.5.1.

Table 7.5.1 - HABC-run4g, 30-Foot Impact, Effective Plastic Strain Levels in Some Components

Component	Effective Plastic Strain, in/in
CV Lid	0.0004
CV Nut Ring	0.0000
Angle	0.0900
Drum Bottom Head	0.2879
Liner	0.1458
Lid Stiffener	0.0213
Lid Studs	0.1892
Lid Stud Nuts	0.0000
Lid Stud Washers	0.0724
Plug Liner	0.1258

Figure 7.5.7 shows the initial configuration for the offset impact. Figure 3.5.8 shows the final configuration for the crush impact for run4g. Figure 3.5.9 shows enlargements of the package corners after the crush.

The maximum effective plastic strain in the CV body is 0.0564 in/in as shown in Figure 7.5.10. Figure 7.5.11 shows the maximum effective plastic strain in the drum to be 0.3920 in/in, and it occurs on the crush plate side of the drum at the attachment of the angle. Figure 7.5.12 shows the lid after the offset crush impact. The maximum bending effective plastic strain is 0.9689 in/in and occurs at the 90° stud hole. The fringe range in Figure 7.5.12 has been defined to show all values near 0.57 in/in in the color red. The maximum membrane strain is 0.8935 in/in and also occurs at the 90° stud hole. This extremely high level of plastic strain is the lid response to the package trying to ovalize due to the crush impact. Due to the extreme level of effective plastic strain (>0.57 in/in), some localized tearing of the lid would be expected.

Figure 7.5.13 shows the effective plastic strain in the drum studs at the end of the crush impact, 0.4018 in/in. The stud at the 90° position has failed (evident by removed element row at the base of the stud). All of the elements on the cross section at the stud base attachment to the angle reached the prescribed failure strain of 0.57 in/in and were deleted by LS-Dyna. Therefore, the 0.4108 in/in is the plastic strain of the remaining elements. The stud elements reach failure and elements begin to be deleted at about time = 0.0311 seconds. By 0.0319 seconds, all the elements on the stud cross section have been deleted by LS-Dyna.

The lid uses a power law material model, which does not allow material failure in the model. Investigation shows that the lid reaches 0.57 in/in in membrane at about 0.0272 seconds, a time at which the stud strain is about 0.2451 in/in. This demonstrates that the lid reaches failure levels before the stud and at a time which the stud effective plastic strain is relatively low. Therefore, it would be expected that the lid would tear before the stud reaches failure. Due to the extent of the effective plastic strain fringe patterns in the lid plus the conservative modeling of the stud relative to lid shear (Section 2.1 discussion), it is believed that the tearing would be local and that the lid (and by default the plug) would be restrained by the large washers. Table 7.5.2 shows the maximum effective plastic strain in the remainder of the package components for the crush impact.

Table 7.5.2 - HABC-run4g, Crush Impact, Effective Plastic Strain Levels in Some Components	
Component	Effective Plastic Strain, in/in
CV Lid	0.0013
CV Nut Ring	0.0001
Angle	0.1070
Drum	0.3920
Drum Bottom Head	0.2879
Liner	0.2060
Lid Stiffener	0.0894
Lid Stud Nuts	0.0028
Lid Stud Washers	0.0790
Plug Liner	0.2665

Figure 7.5.14 shows the CV lid separation time history. During the 30-foot impact, the maximum spikes reach the 0.0065 in range with a general gap of about 0.005 in reached. During the crush impact, the spikes in gap reach about 0.009 in, while the general separation is about 0.007 in. At the end of the crush impact, the separations appear oscillatory from 0.0 in to about 0.006 in, therefore if a permanent gap were to exist, the maximum separation would be about 0.003 in.

Figure 7.5.15 gives the kaolite thickness time history for chosen kaolite nodes. The nodes are given in Figure 7.1.16.

The nodes on the drum chosen to investigate the diameter/radius changes during the impact are shown in Figure 3.1.34. Figure 7.5.16 shows the drum diameter time histories in the X direction. Figure 7.5.17 shows the drum radial changes in the Y direction.

Figure 7.5.18 shows the diameter time history for the inner liner. The position of the nodes is shown in Figure 3.1.37 and Table 3.1.3.

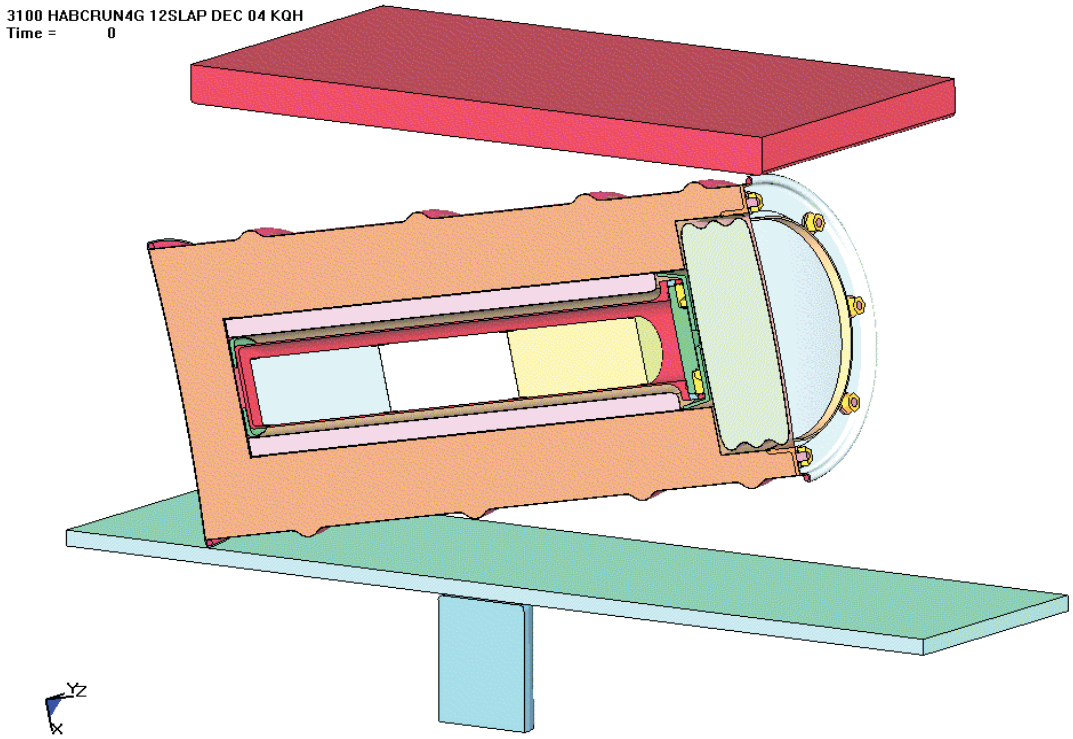

Figure 7.5.1 - HABC-run4g, 12 Degree Slapdown Initial Configuration

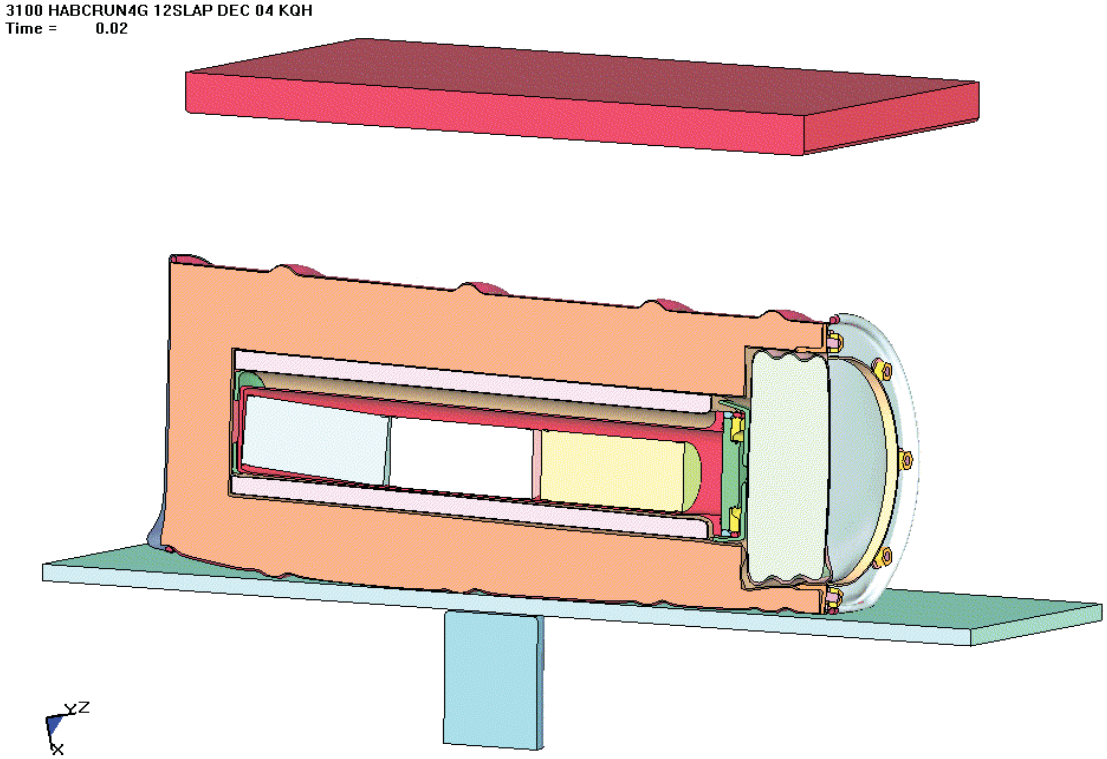

7.5.2 - HABC-run4g, Configuration After the 30-Foot Impact

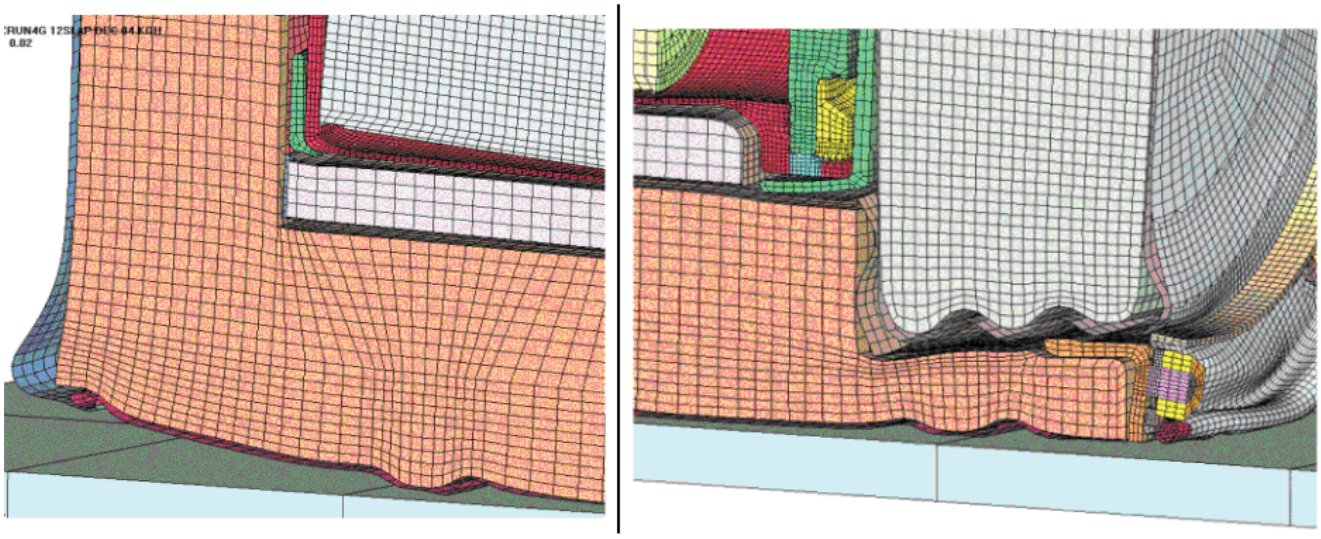

Figure 7.5.3 - HABC-run4g, 30-Foot Impact, Bottom and Lid Configurations

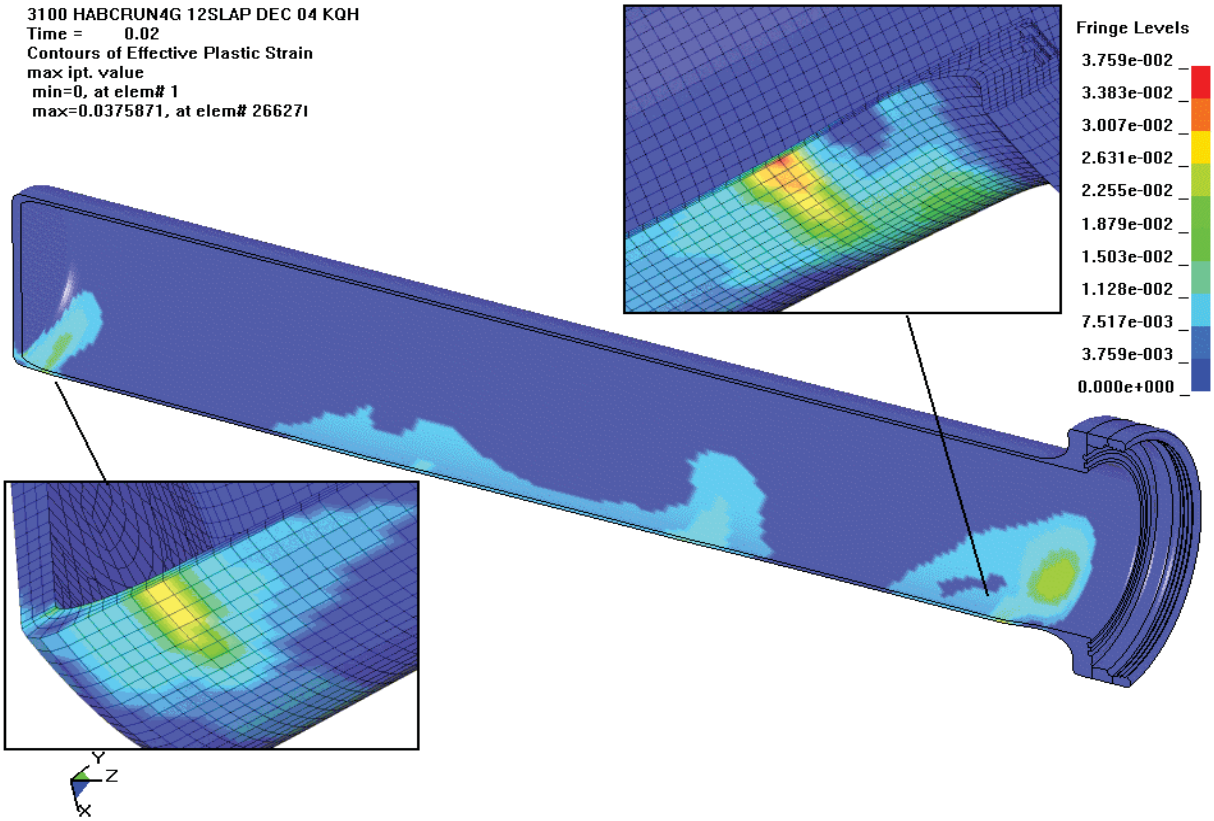

Figure 7.5.4 - HABC-run4g, 30-Foot Impact, Effective Plastic Strain in the CV Body

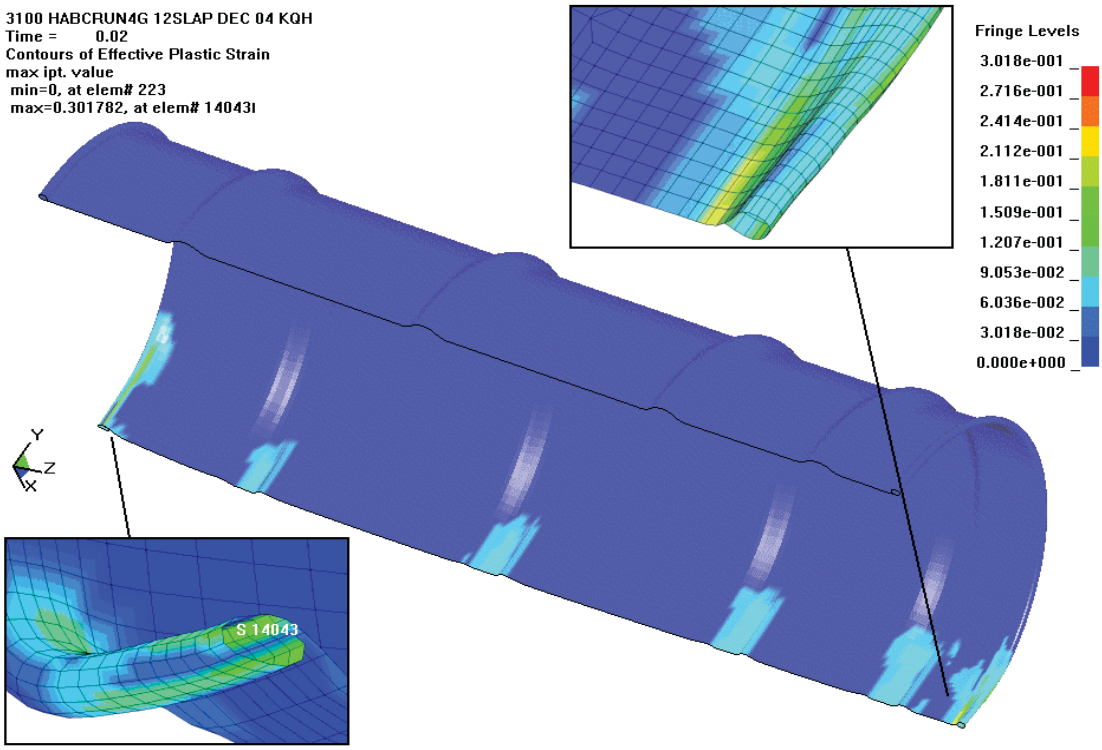

Figure 7.5.5 - HABC-run4g, 30-Foot Impact, Effective Plastic Strain in the Drum

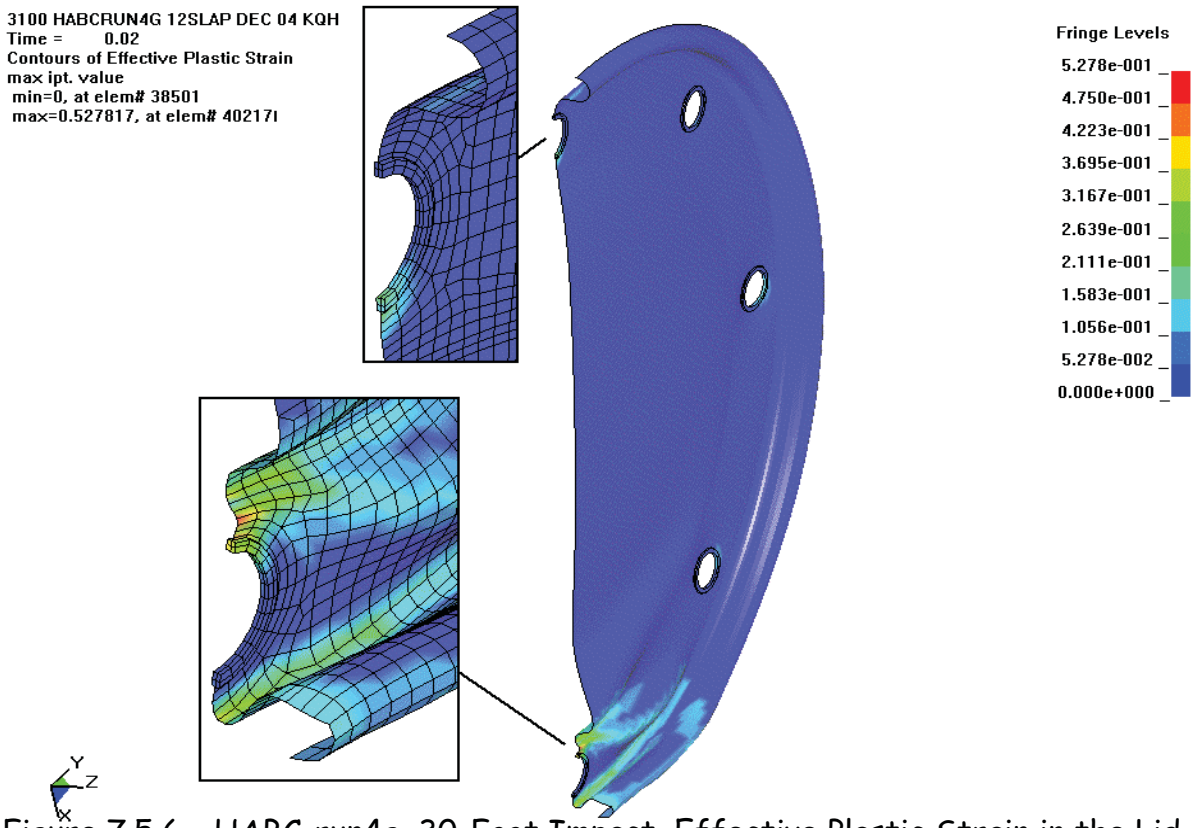

Figure 7.5.6 - HABC-run4g, 30-Foot Impact, Effective Plastic Strain in the Lid

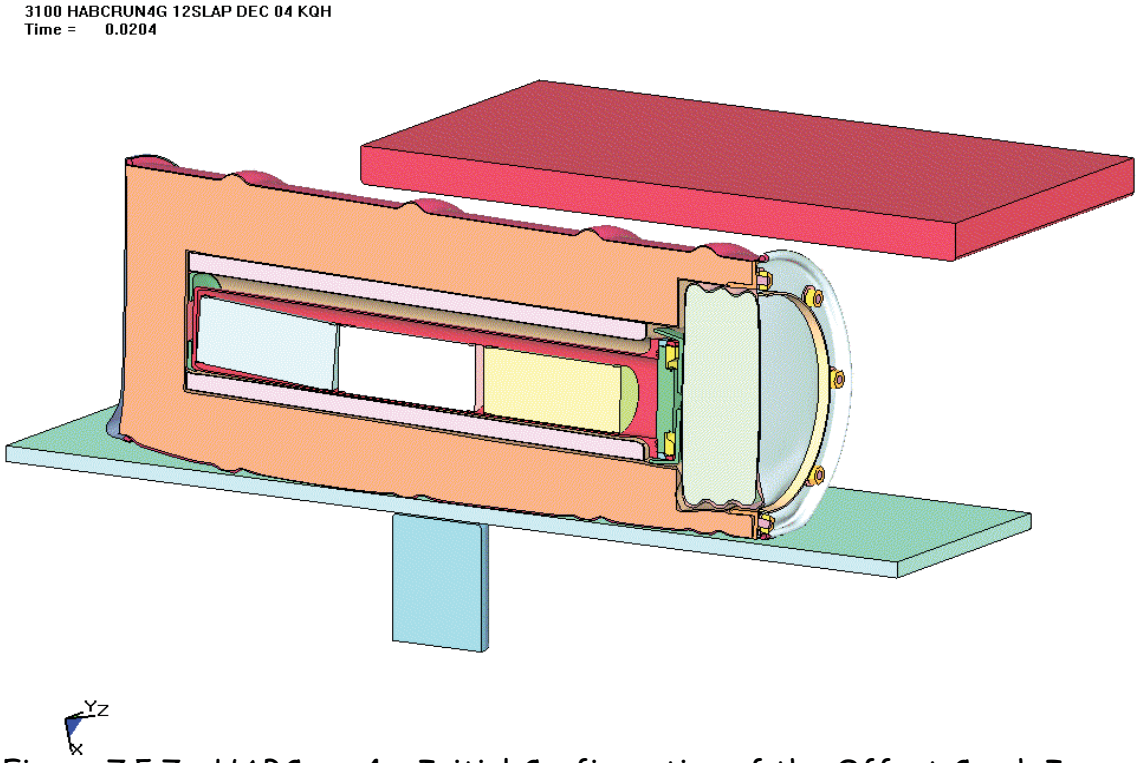

Figure 7.5.7 - HABC-run4g, Initial Configuration of the Offset Crush Impact

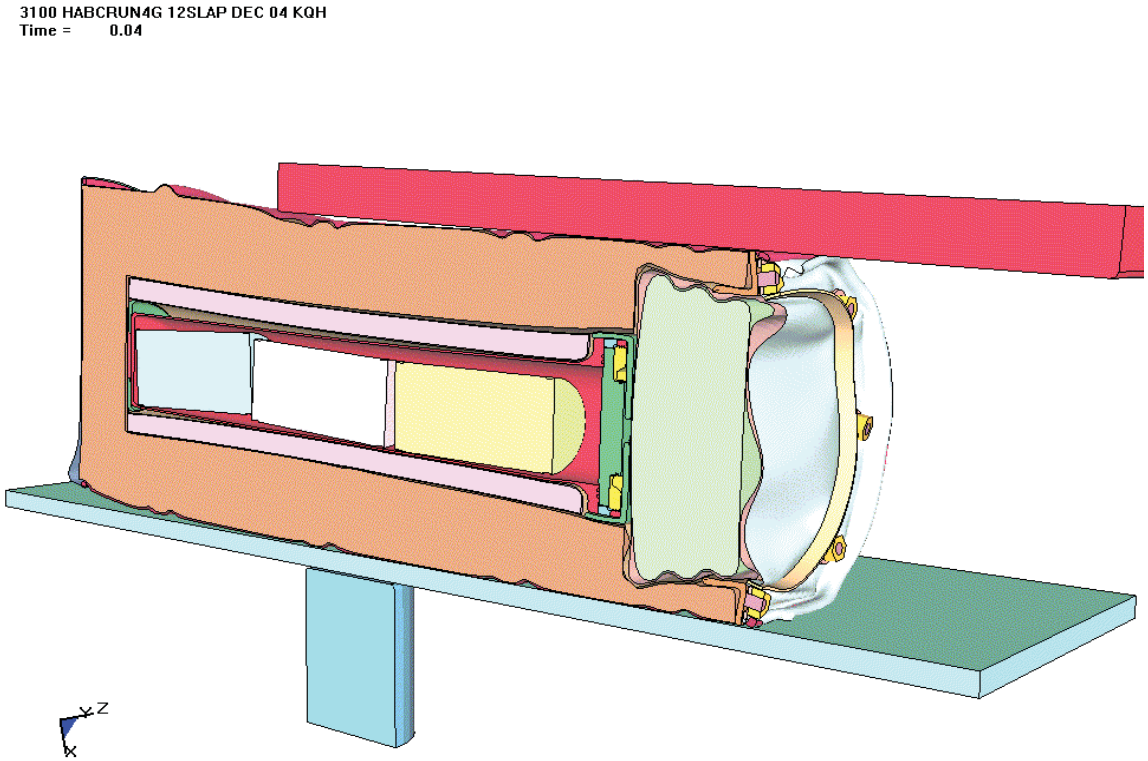

Figure 7.5.8 - HABC-run4g, Final Configuration After the Offset Crush Impact

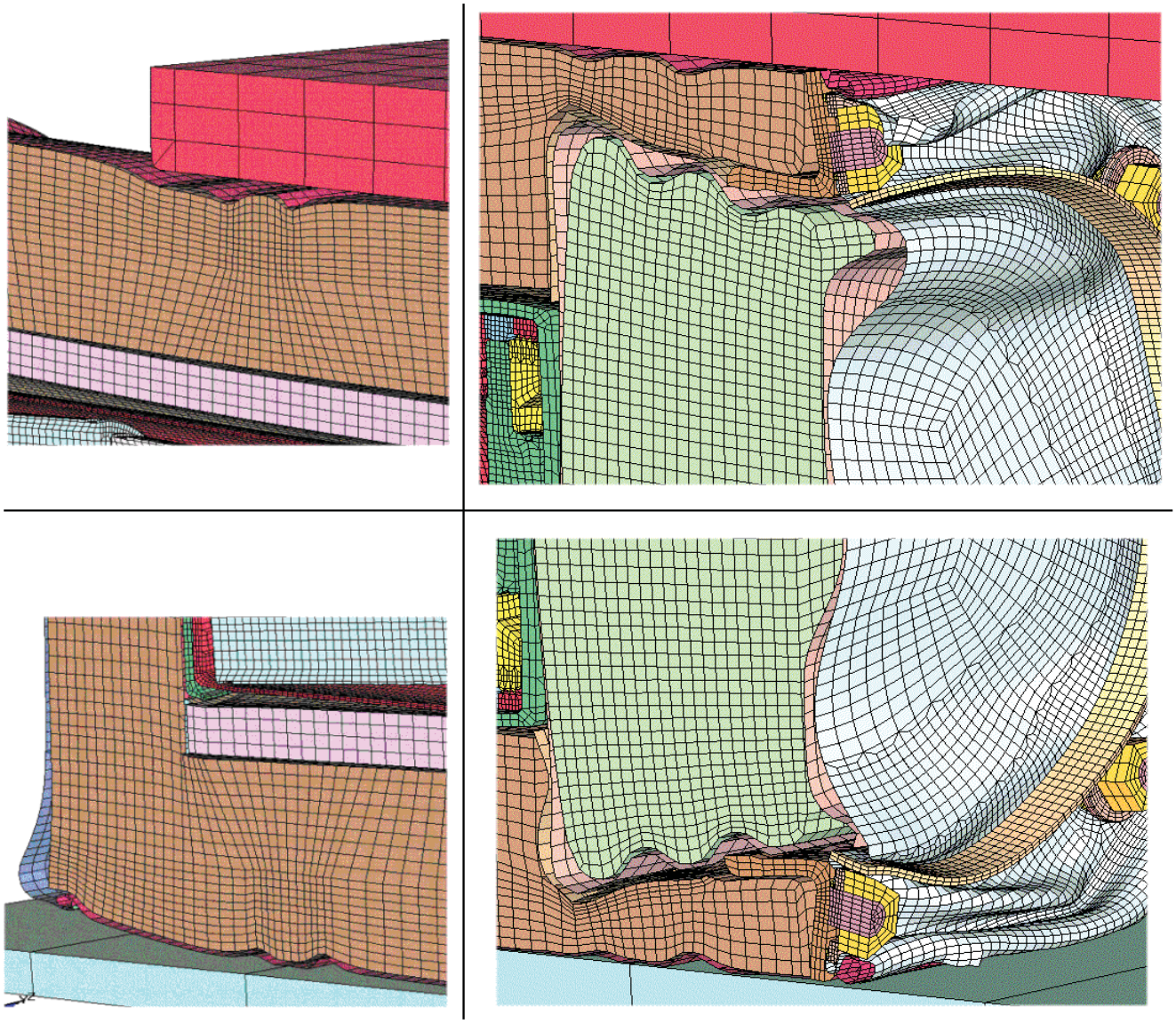

Figure 7.5.9 - HABC-run4g, Crush Impact, Enlarged Views of the Resulting Configuration

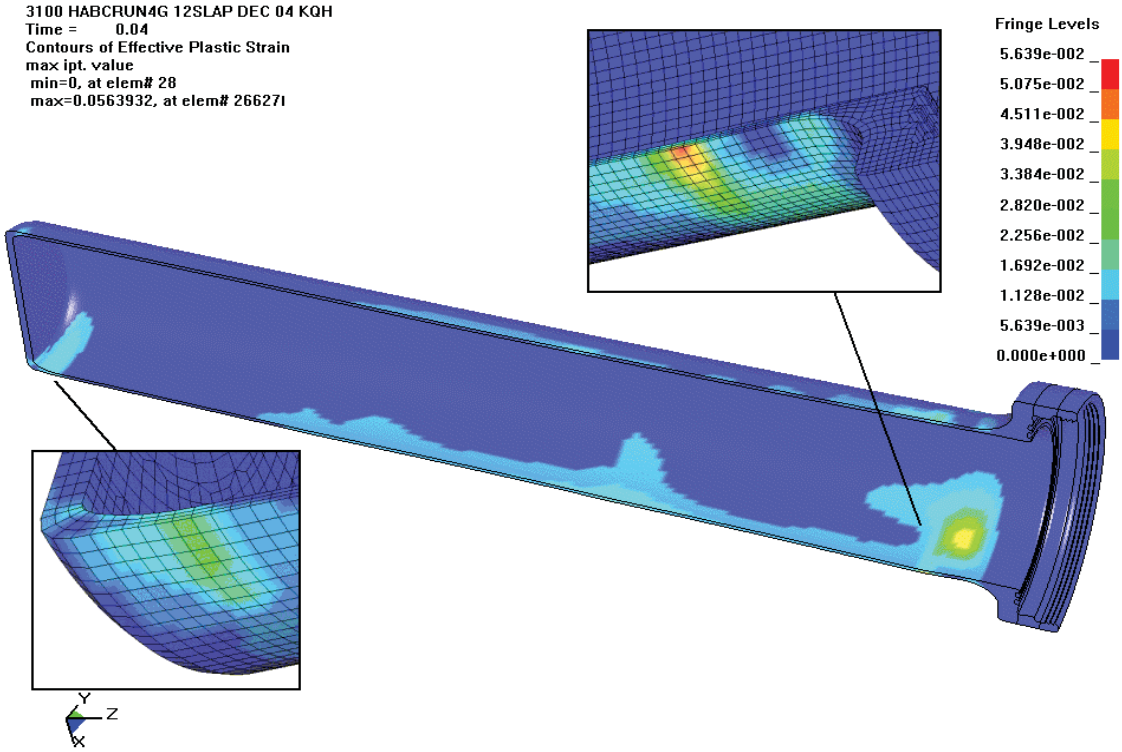

Figure 7.5.10 - HABC-run4g, Crush Impact, Effective Plastic Strain in the CV Body

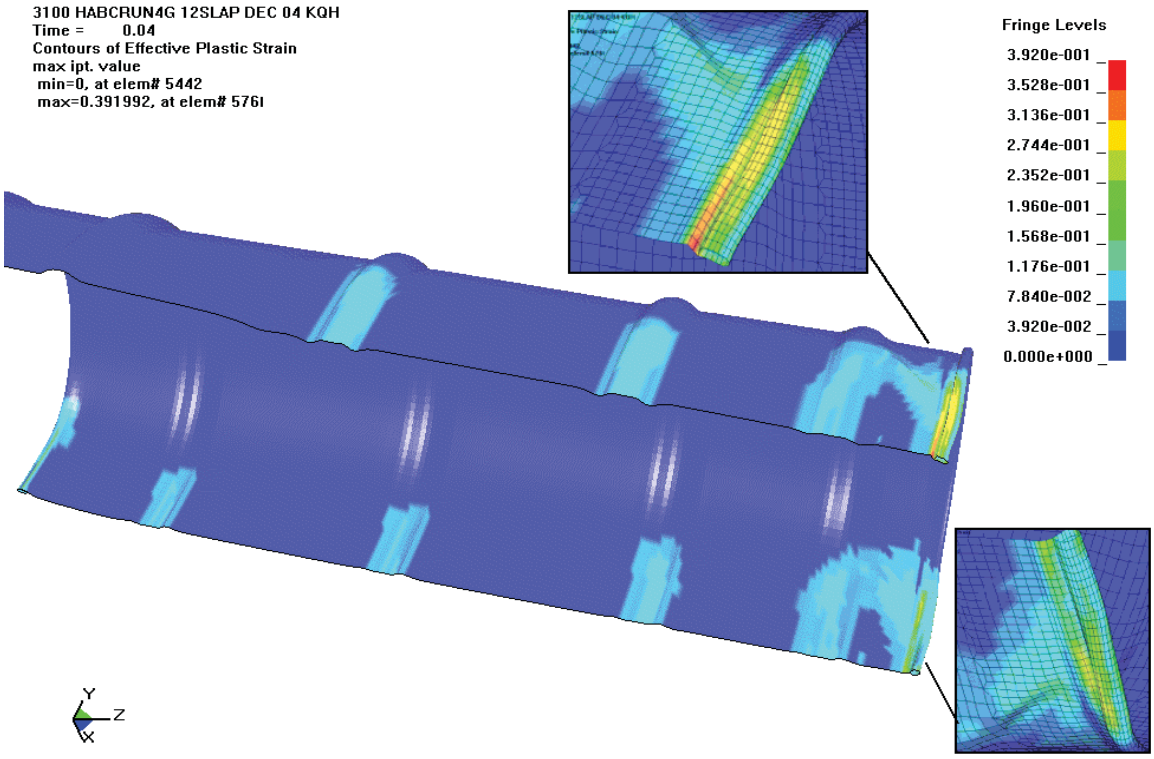

Figure 7.5.11 - HABC-run4g, Crush Impact, Effective Plastic Strain in the Drum

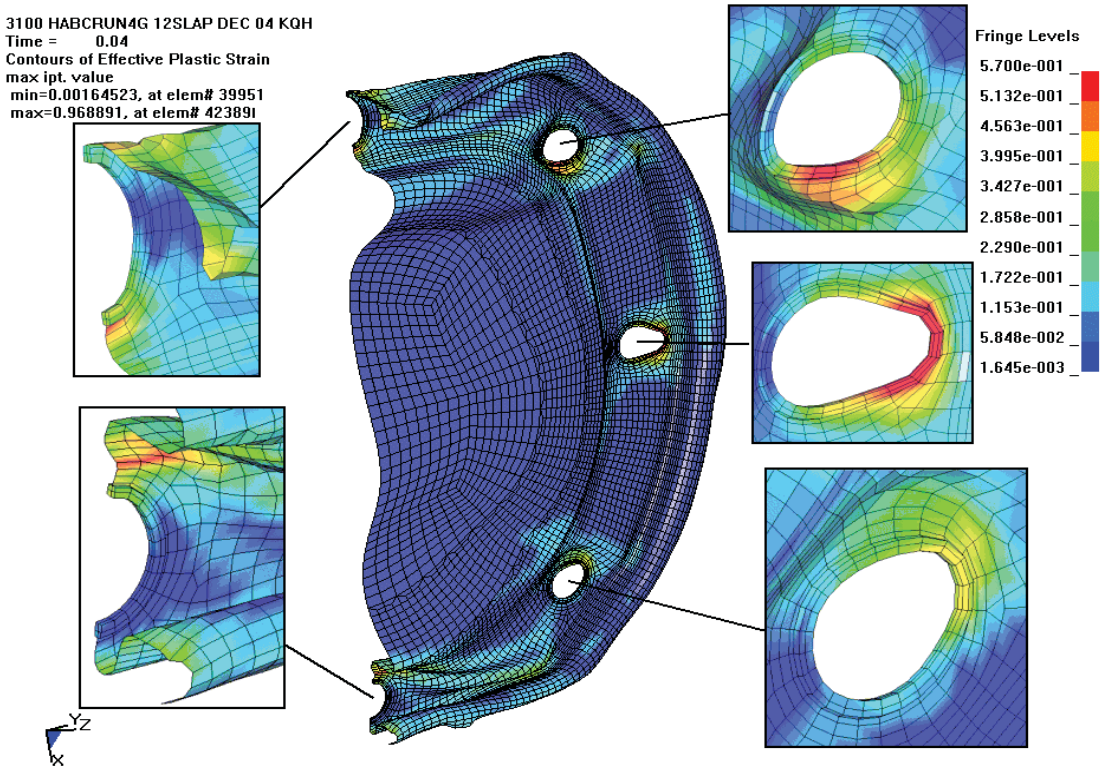

Figure 7.5.12 - HABC-run4g, Crush Impact, Effective Plastic Strain in the Lid

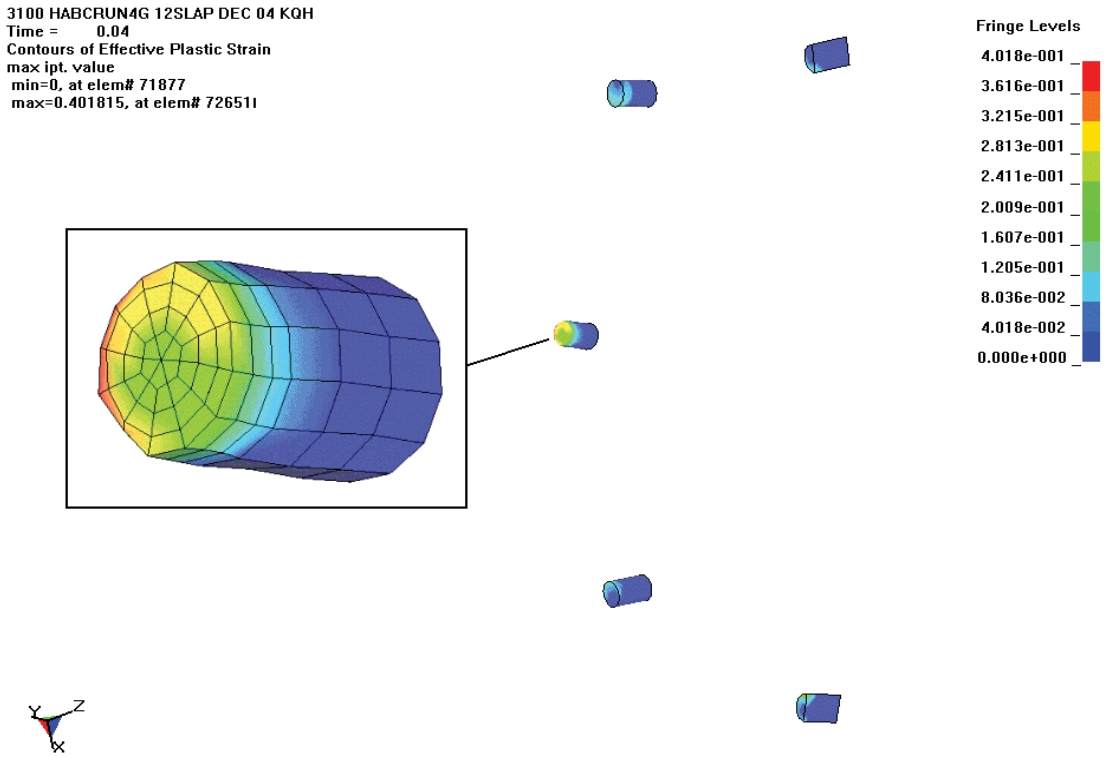

Figure 7.5.13 - HABC-run4g, Crush Impact, Effective Plastic Strain in the Studs

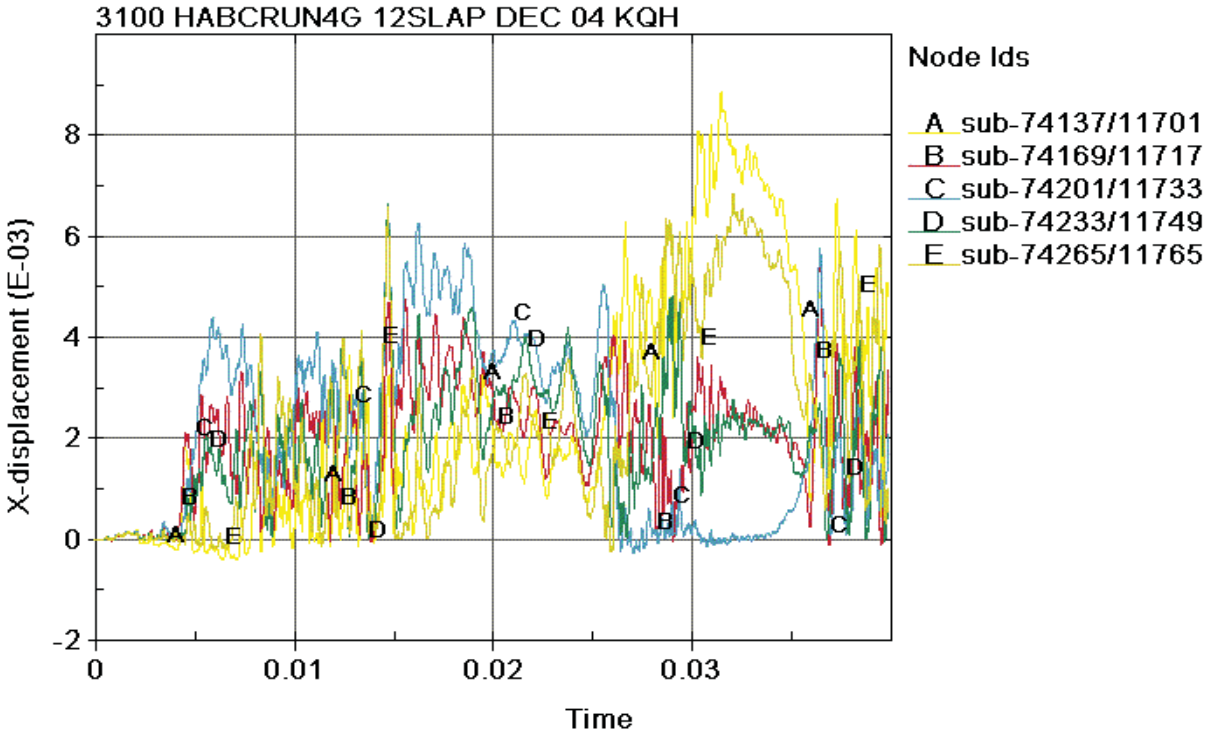

Figure 7.5.14 - HABC-run4g, CV Lid/Body Separation Time History

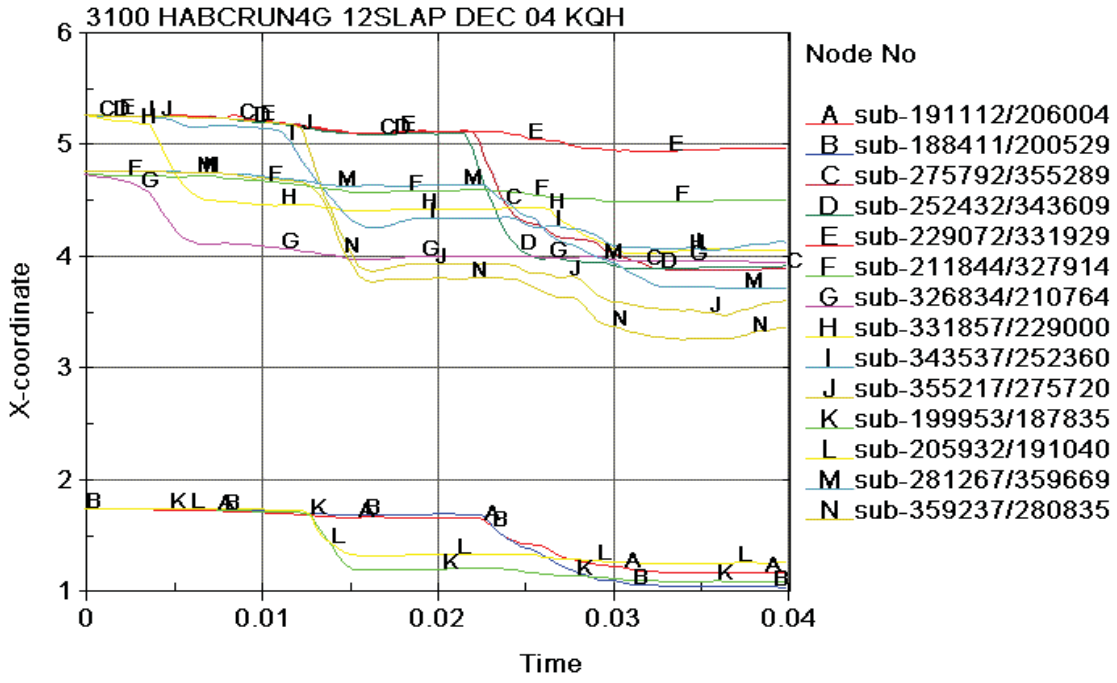

Figure 7.5.15 - HABC-run4g, Kaolite Thickness Time History

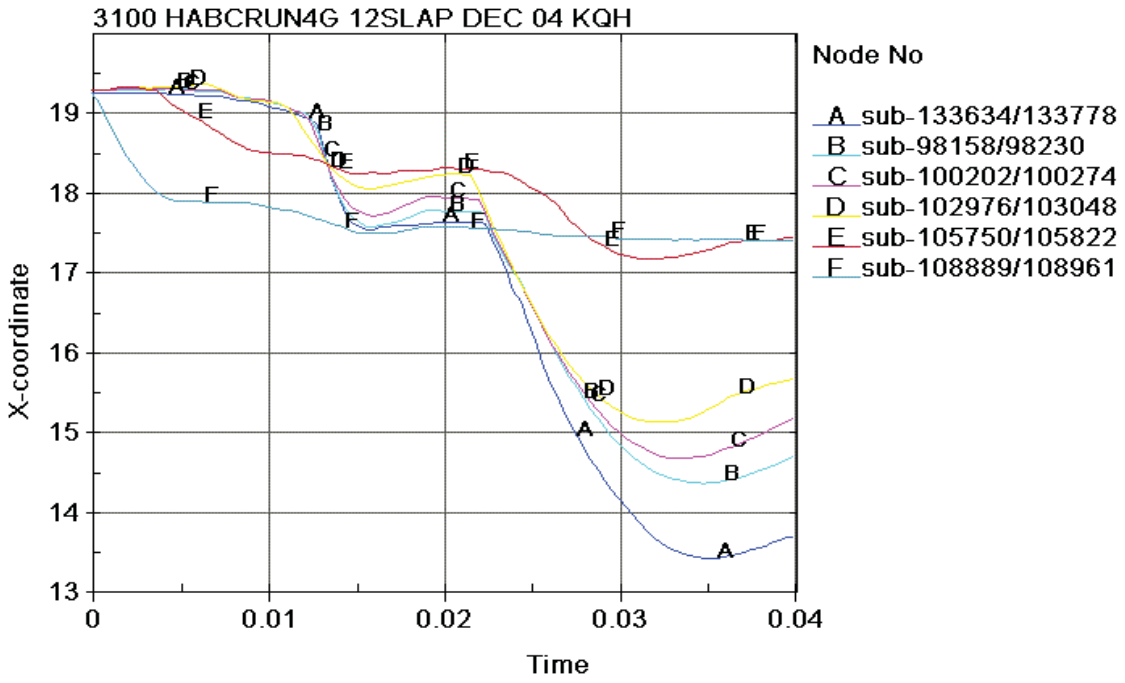

Figure 7.5.16 - HABC-run4g, Diameter Time History for the Drum in the X Direction

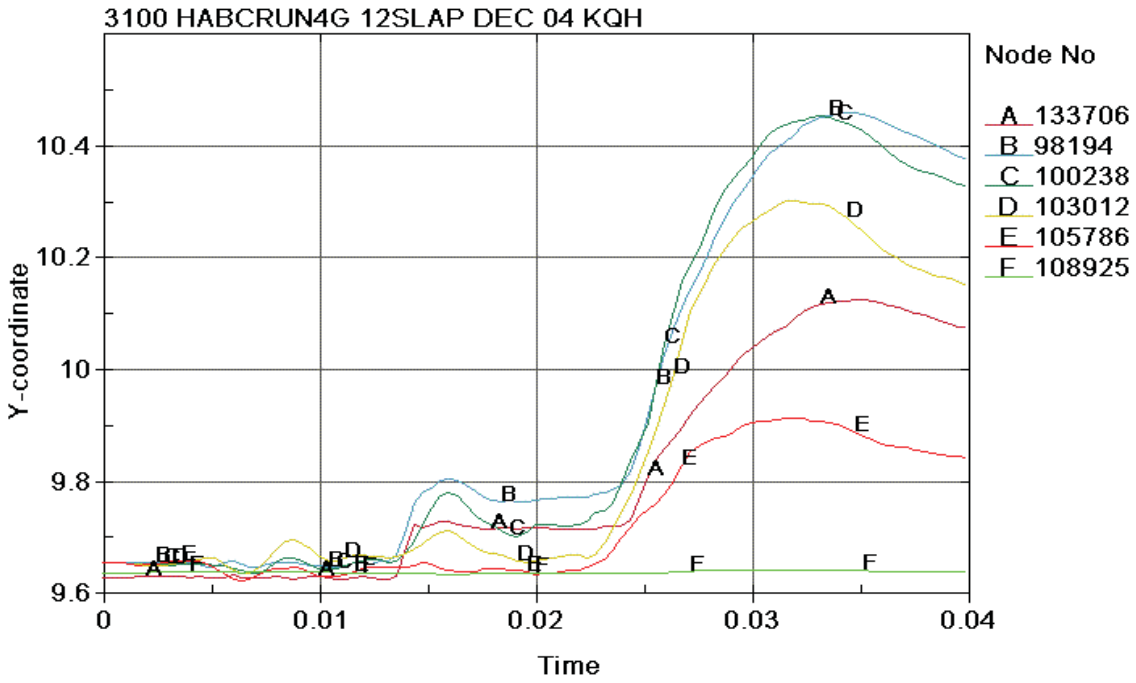

Figure 7.5.17 - HABC-run4g, Radius Time History for the Drum in the Y Direction

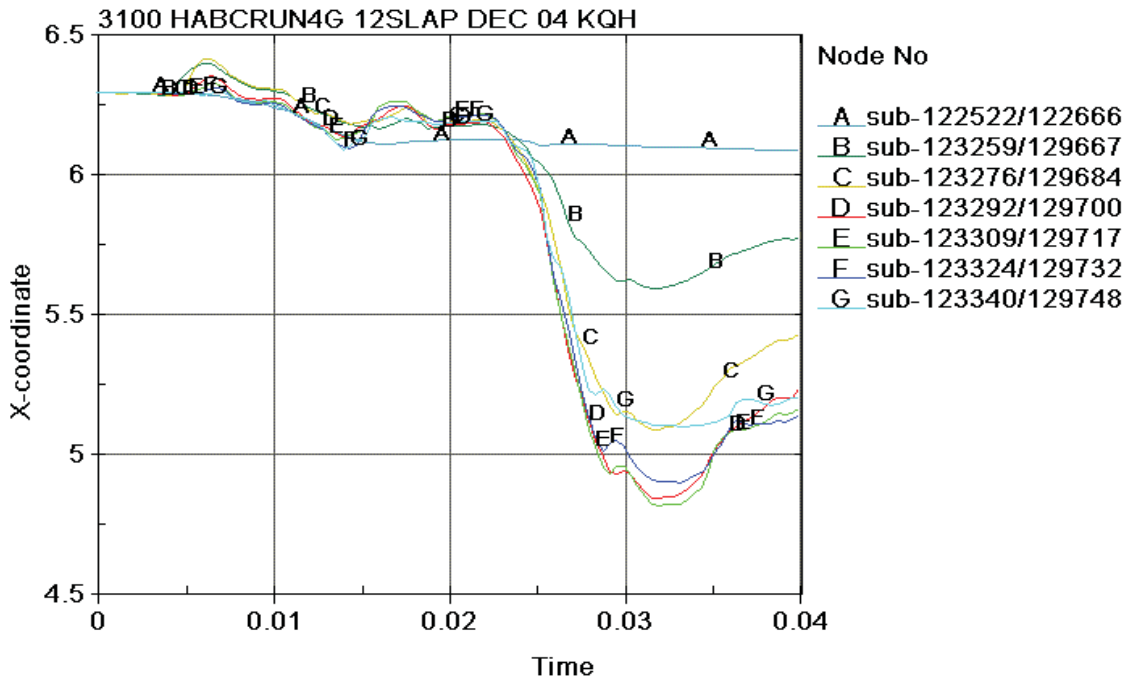

Figure 7.5.18 - HABC-run4g, Diameter Time History for the Inner Liner

7.6 HABC-run4ga - Slapdown

HABC-run4ga is a 30-foot, 12° slapdown impact (time - 0 to 0.02 sec) followed by a crush impact with the crush plate centered on the drum (0.0201 to 0.0400 sec). The HABC-run4g, 30-foot impact is the 30-foot impact for both the HABC-run4g offset crush and this HABC-run4ga centered crush. The difference between the 4g and 4ga impacts is the location to which the crush plate is moved by way of specifying velocities for specific times. In HABC-run4ga, the translation of the crush plate occurs from 0.02 to 0.0201 sec. Therefore, the 30-foot impact results are presented in Section 7.5 and the centered crush results are presented in this section (7.6).

The initial configuration for the start of the centered crush is shown in Figure 7.6.1. The final configuration for the HABC-run4ga crush impact is shown in Figure 7.6.2. Figure 7.6.3 shows the configuration at each end of the package following the centered crush impact.

The maximum effective plastic strain in the CV body is shown to be 0.0643 in/in in Figure 7.6.4. The maximum occurs in the body side wall, on the side nearest the crush plate. Figure 7.6.5 shows the fringes of effective plastic strain in the drum. The maximum strain in the drum is 0.3443 in/in and occurs near the lid in the crimped region shown in the enlarged view. Figure 7.6.6 shows that the maximum effective plastic strain in the lid is 0.5828 in/in. The maximum occurs at the 180° stud hole, and is localized. This value is a surface, or bending strain, the membrane strain is 0.4736 in/in. Therefore, the bending strain is above the failure limit of 0.57 in/in, however the membrane strain is below the limit. Some cracking may occur, but tearing of the lid is not expected. The large washers would provide restraint of the lid.

Table 7.6.1 presents the maximum effective plastic strain in other shipping package components for the run4ga crush impact.

Table 3.6.1 - Run4ga, Crush Impact, Effective Plastic Strain Levels in Some Components	
Component	Effective Plastic Strain, in/in
CV Lid	0.0018
CV Nut Ring	0.0000
Angle	0.0944
Drum Bottom Head	0.3000
Liner	0.2846
Lid Stiffener	0.0288
Lid Studs	0.2390
Lid Stud Nuts	0.0000
Lid Stud Washers	0.0775
Plug Liner	0.1644

The CV lid separation time history is shown in Figure 7.6.7. For the crush impact (0.0201 to 0.0400 sec) the spikes in the gap reach just over 0.01 in. The general gap during the impact reaches about 0.009 in. At the time the impact was halted, the maximum separation was on the order of 0.006 in.

Figure 7.6.8 shows the kaolite thickness time history. The nodes chosen are shown in Figure 7.1.16

Figure 7.6.9 shows the X direction diameter changes in the drum. Figure 7.6.10 shows the Y direction radial changes in the drum. Figure 3.1.34 shows the location of the nodes in the Figure 7.6.9 and 7.6.10 time histories.

Figure 7.6.11 shows the diameter time history for the inner liner. The position of the nodes are shown in Figure 3.1.37 and Table 3.1.3.

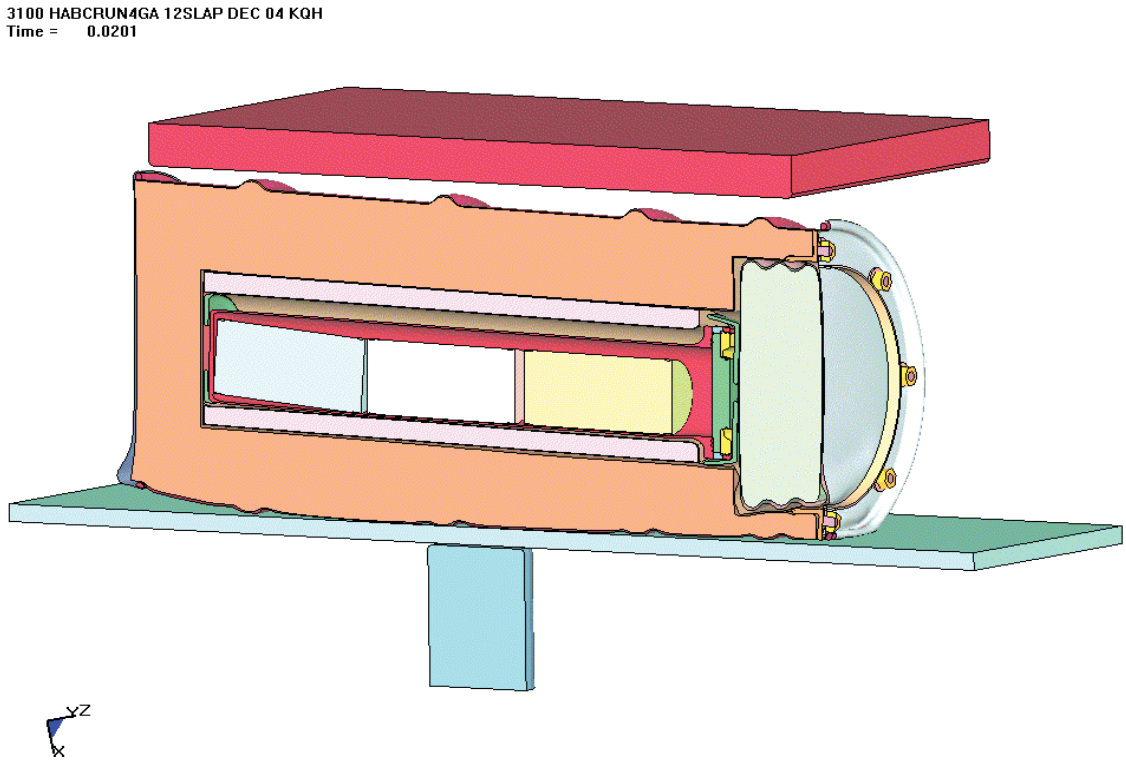

Figure 7.6.1 - HABC-run4ga, Initial Configuration for the Centered Crush Impact

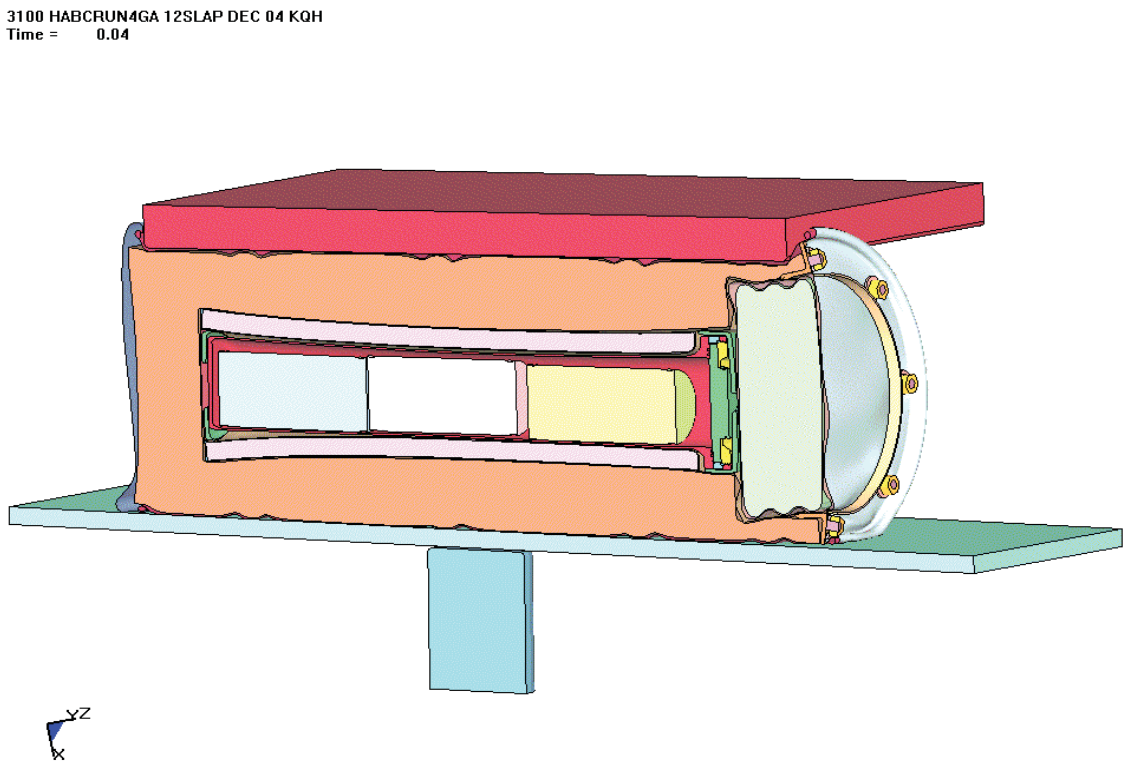

Figure 7.6.2 - HABC-run4ga, Final Configuration of the Centered Crush Impact

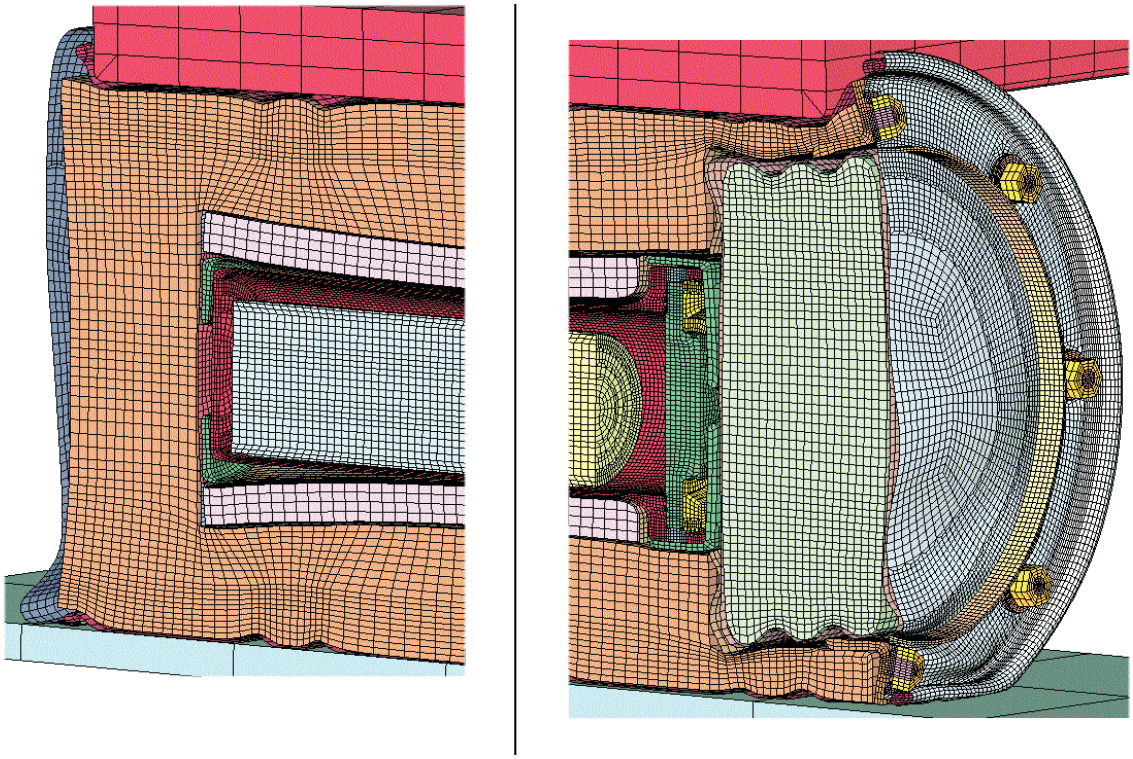

Figure 7.6.3 - HABC-run4ga, Crush Impact, Configurations at the Package Ends

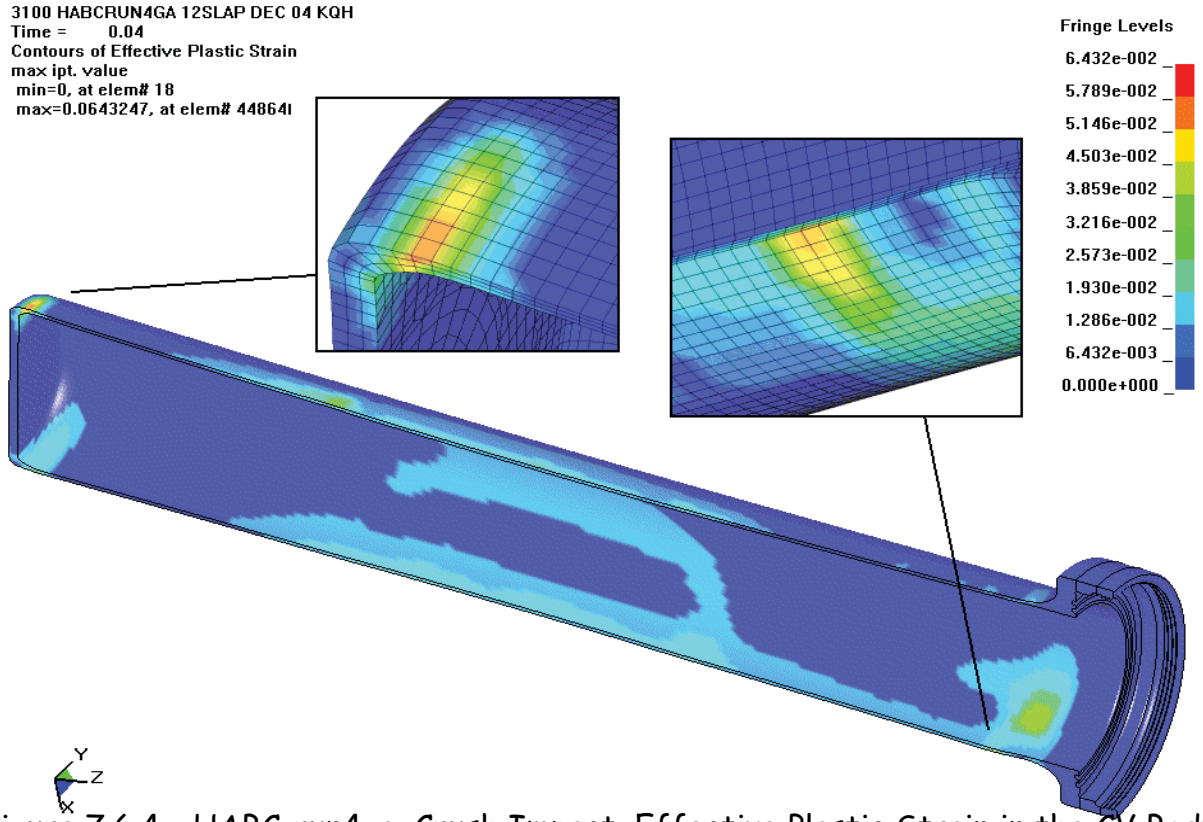

Figure 7.6.4 - HABC-run4ga, Crush Impact, Effective Plastic Strain in the CV Body

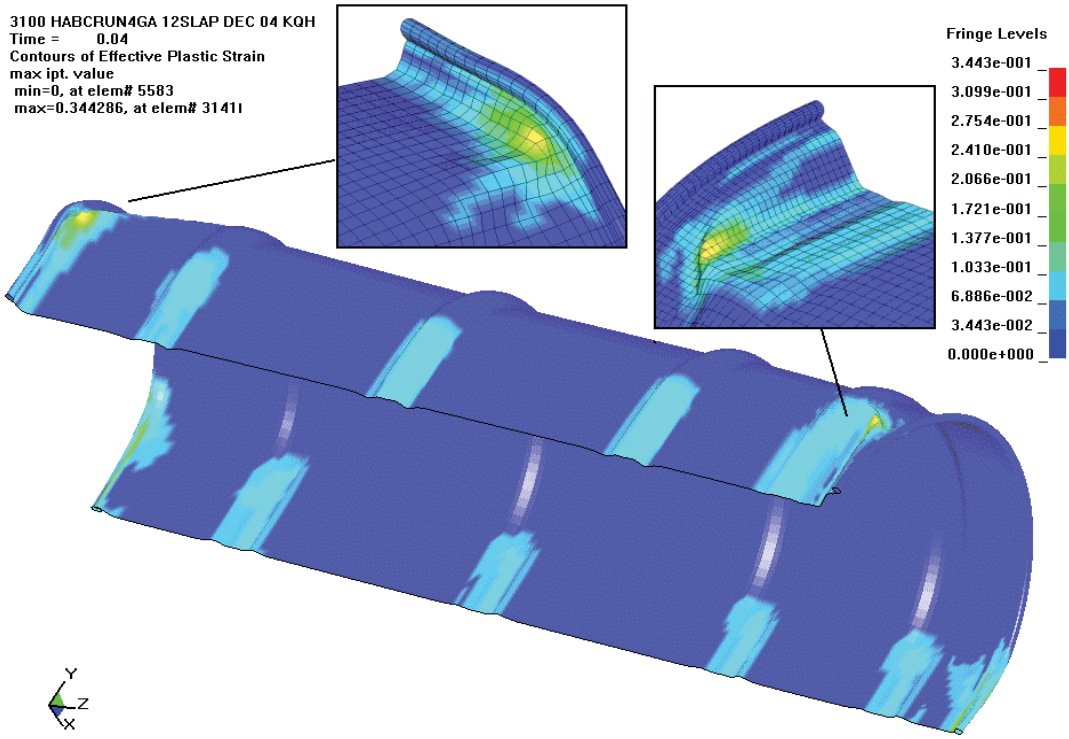

Figure 7.6.5 - HABC-run4ga, Crush Impact, Effective Plastic Strain in the Drum

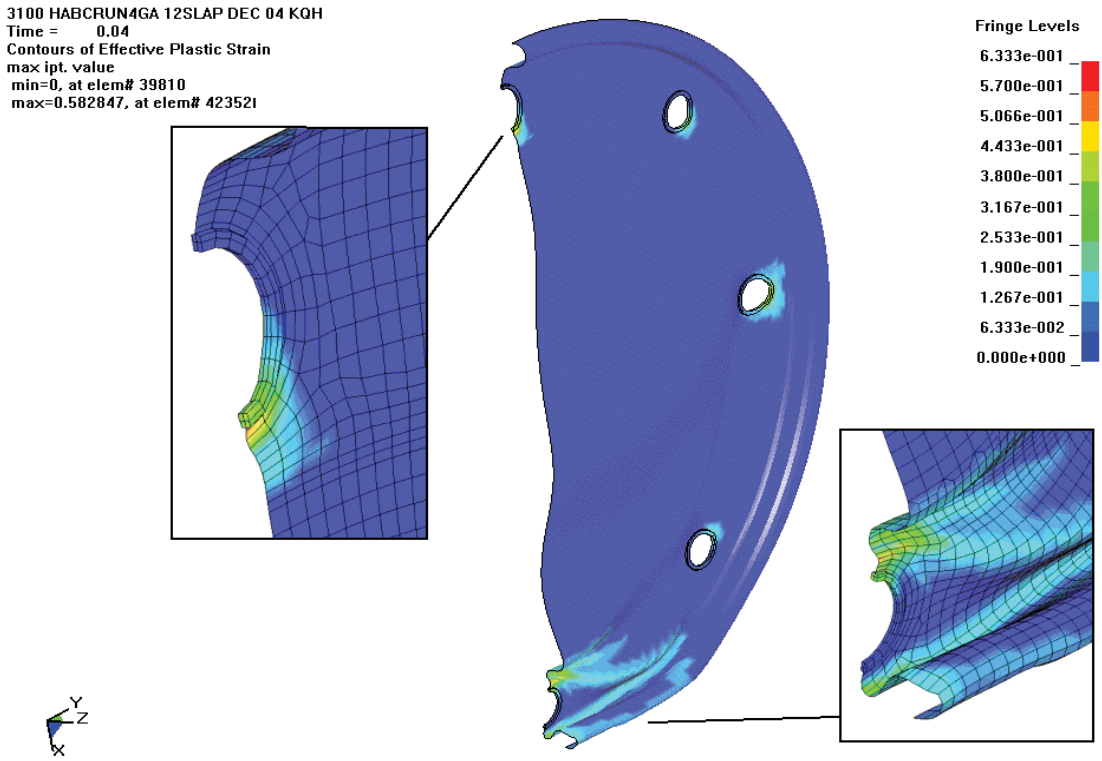

Figure 7.6.6 - HABC-run4ga, Crush Impact, Effective Plastic Strain in the Lid

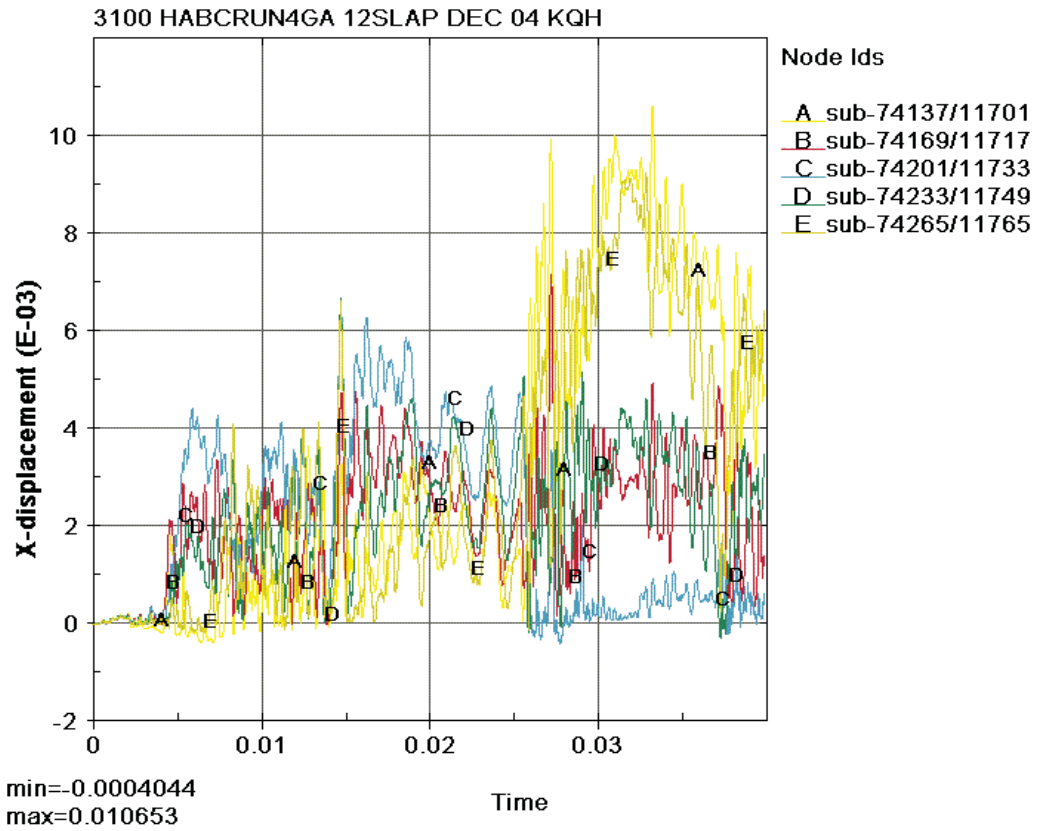

Figure 7.6.7 - HABC-run4ga, CV Lid Separation Time History

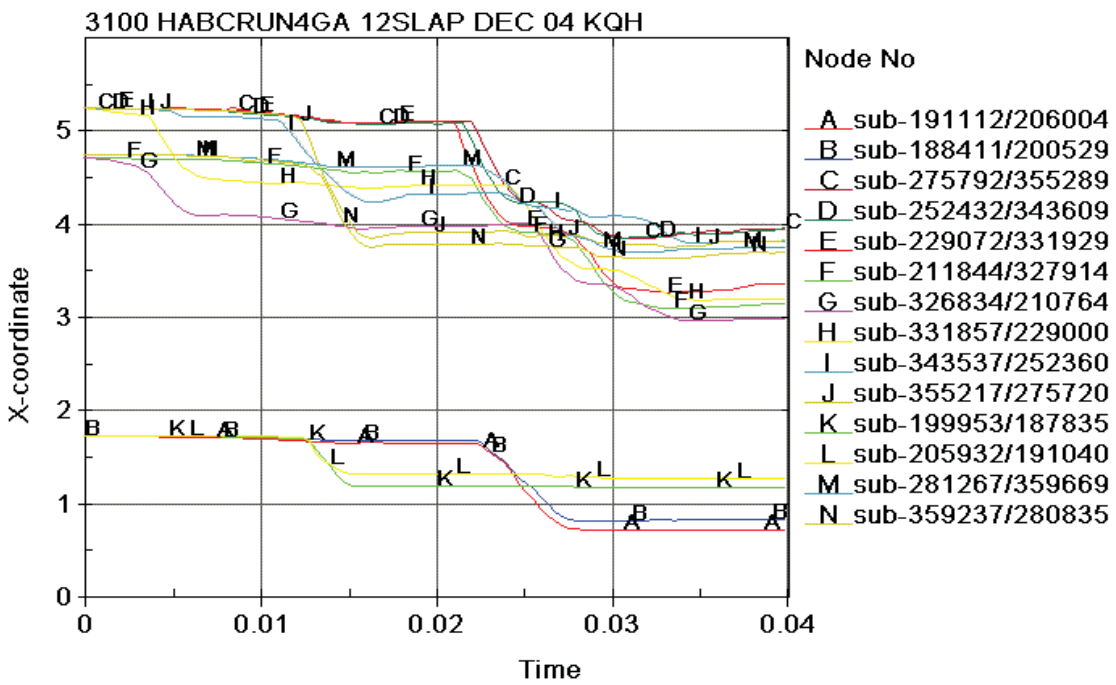

Figure 7.6.8 - HABC-run4ga, Kaolite Thickness Time History

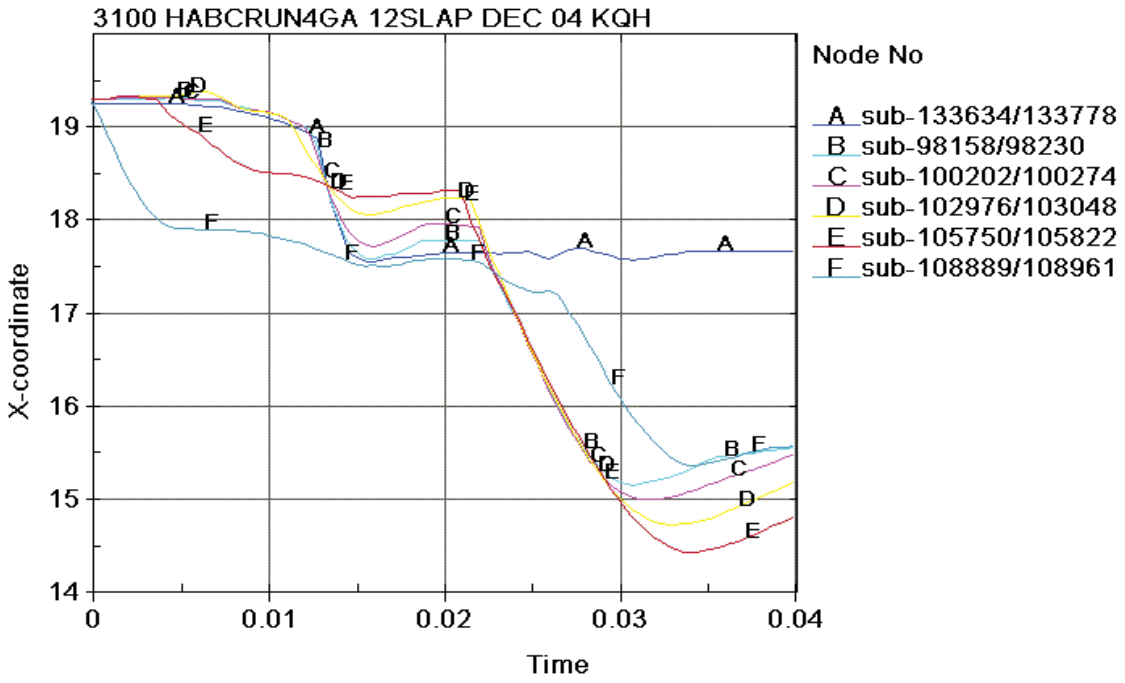

Figure 7.6.9 - HABC-run4ga, Diameter Time History for the Drum in the X Direction

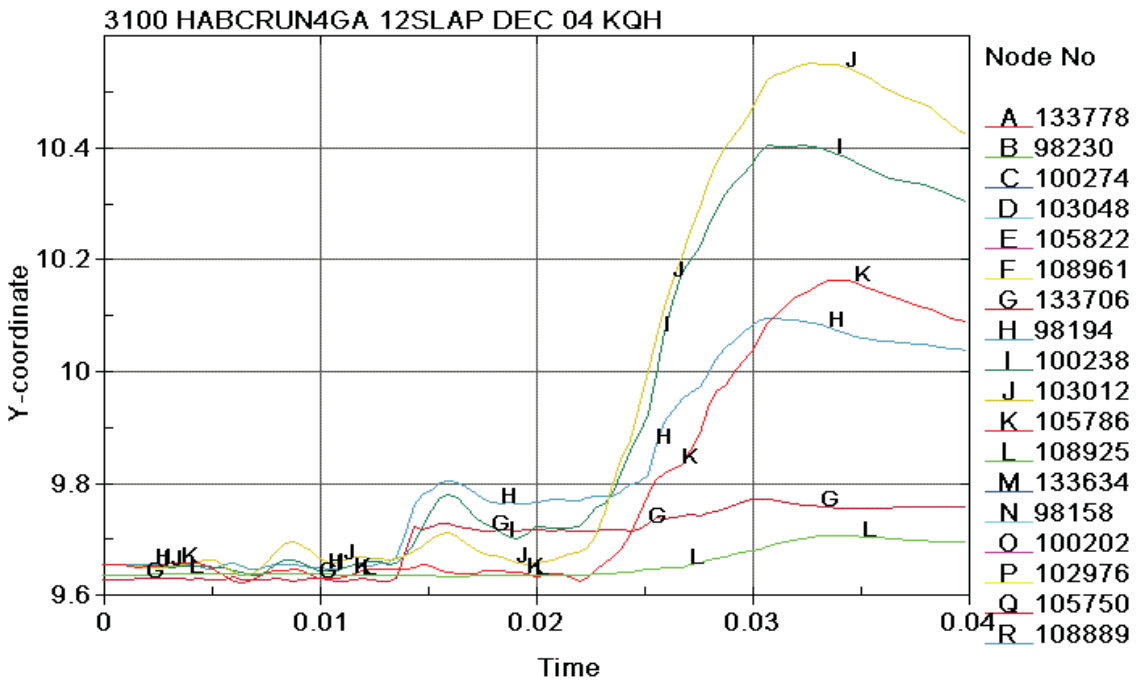

Figure 7.6.10 - HABC-run4ga, Radius Time History for the Drum in the Y Direction

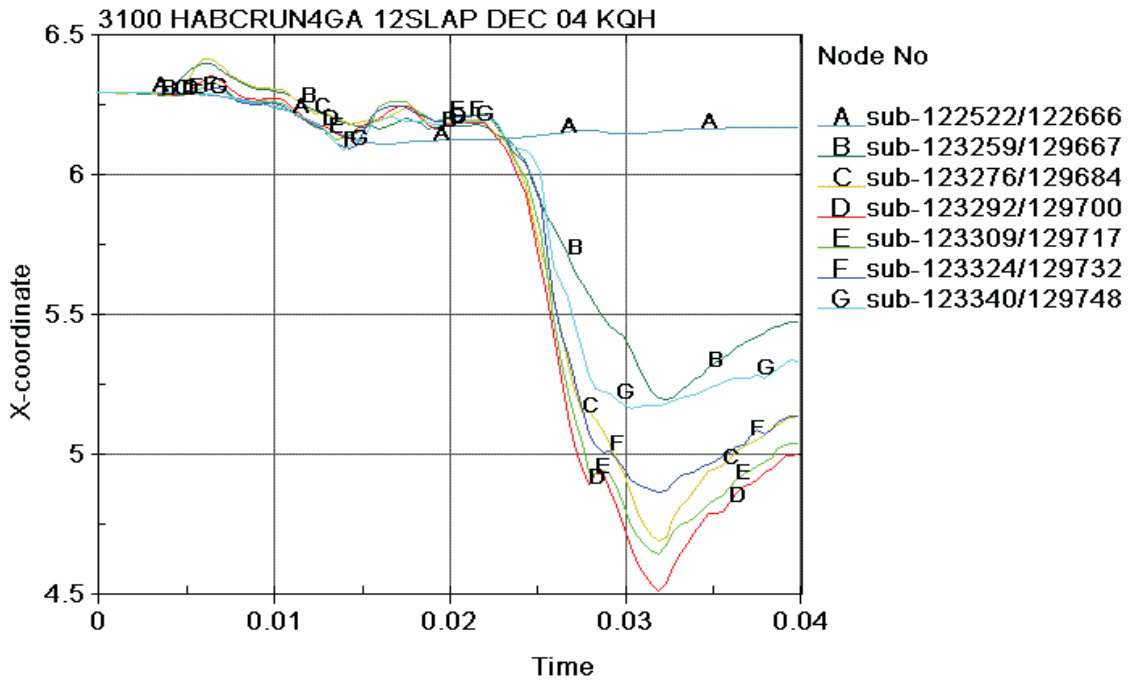

Figure 7.6.11 - HABC-run4ga, Diameter Time History for the Inner Liner

7.7 Comparison of Test vs Analysis

The HABC analysis runs are compared to the test results similar to that performed in Section 3.12 for the initial design using borobond. It should be noted that the testing was with specimen of the borobond neutron absorber design, whereas the analysis models in this section are of the HABC design.

7.7.1 Comparison of HABC Run4g to TU1

The HABC-run4g is a 30-foot, 12° slapdown impact followed by an offset crush (crush plate centered over the CV flange). TU1 is a 12° slapdown with a 4-foot impact, 30-foot impact, offset crush, and punch test specimen. The following Table 7.7.1.1 shows the initial diameter comparisons (pre-impact) using the test data compared to the analysis results.

Table 7.7.1.1 - HABC-run4g vs TU1, Comparison of Initial Diameters (Pre-Impact)				
Location	0°- 180°		90°-270°	
	Test	Analysis	Test	Analysis
Top Chime	19.25	19.32	19.25	19.32
Top Hoop	19.25	19.37	19.25	19.37
Top CG Hoop	19.25	19.37	19.25	19.37
CG Hoop	19.25	19.37	19.25	19.37
Bottom Hoop	19.25	19.37	19.25	19.37
Bottom Chime	19.25	19.38	19.25	19.38

The Table 7.7.1.2 shows the results of the 30-foot test and analysis impacts. The test diameters are after the 4 and 30-foot impacts, while the analysis is after the 30-foot impact.

Table 7.7.1.2 - HABC-run4g vs TU1, Diameter Results After the 30-Foot Impact				
	0°-180°		90°-270°	
	Test	Analysis	Test	Analysis
Top Chime	18-1/2	18.1	19-3/8	19.5
Top Hoop	18-1/2	18.2	19-3/8	19.6
Top CG Hoop	18-1/2	18.4	19-3/8	19.5
CG Hoop	18-5/8	18.8	19-3/8	19.4
Bottom Hoop	18-5/8	18.9	19-1/4	19.3
Bottom Chime	17-13/16	18.1	19-3/8	19.4

Figure 7.7.1.1 shows the final configuration of the test specimen after the 4-foot and 30-foot impacts. Figure 7.7.1.2 shows the analytical model configuration after the 30-foot impact.

Figure 7.7.1.1 - TU1, Results of 30-Foot Impact

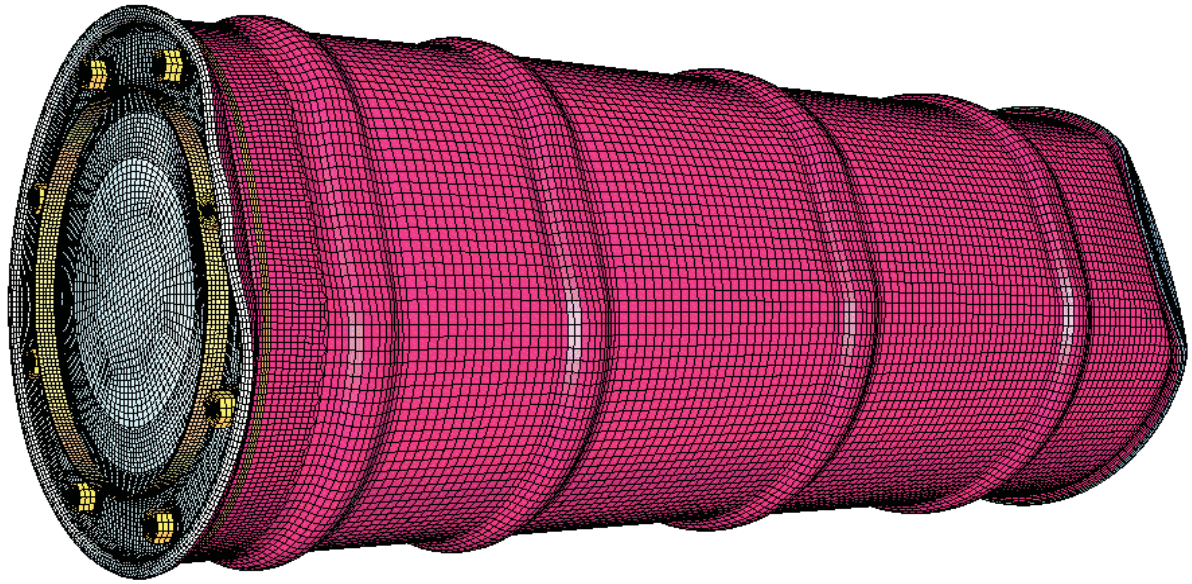

Figure 7.7.1.2 - HABC-run4g, Results of the 30-Foot Impact

Table 7.7.1.3 shows the comparison of the results of the crush impacts. The test data is for the cumulative effects of a 4-foot, 30-foot, and crush impact. The analysis data is for a cumulative 30-foot impact and crush impact.

Table 7.7.1.3 - Run4g vs TU1, Diameter Results After the Crush Impact				
	0°-180°		90°-270°	
	Test	Analysis	Test	Analysis
Top Chime	15-5/8	14.9	20-5/8	20.7
Top Hoop	16	15.1	20-7/16	20.8
Top CG Hoop	16-1/4	15.7	20-1/4	20.7
CG Hoop	16-1/2	16.2	19-7/8	20.4
Bottom Hoop	18-1/4	18.1	19-1/2	19.8
Bottom Chime	17-13/16	18.0	19-1/4	19.4

Figure 7.7.1.3 shows an isometric view of the test specimen with the crush side up. Figure 7.7.1.4 shows a similar view for the analysis results.

Figure 7.7.1.3 - TU1, View of Crush Damage with the Crush Side Up

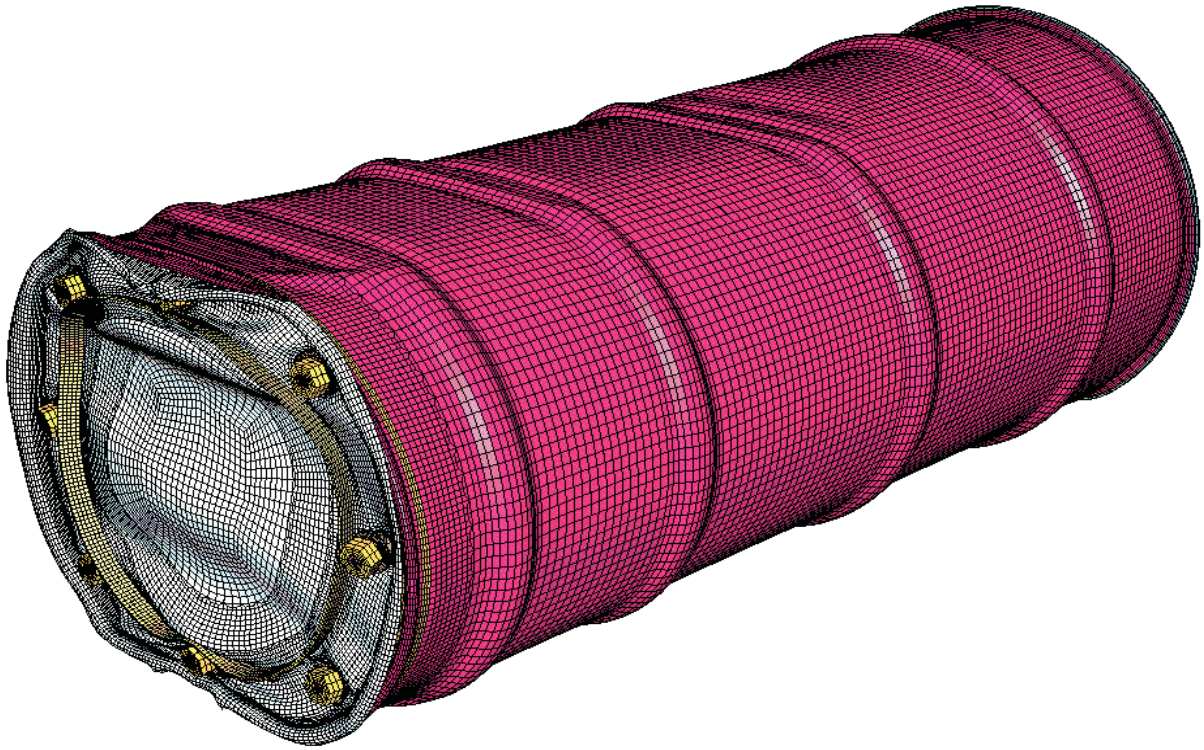

Figure 7.7.1.4 - HABC-run4g, View of the Crush Damage, Crush Side Up

Table 7.7.1.4 shows the results of a comparison of the "flats" measurements from the test after the 30-foot impacts and Table 3.12.1.5 compares the crush impact results.

Table 7.7.1.4 - HABC-run4g vs TU1, Comparison of Flats for the 30-Foot Impact		
	Test	Analysis
Top Chime	8	8.8
Top Hoop	7-3/8	8.4
Top CG Hoop	7-1/8	7.6
CG Hoop	6-3/8	5.9
Bottom Hoop	6-3/4	5.9
Bottom Chime	10	10.1

Table 7.7.1.5 - HABC-run4g vs TU1, Comparison of Flats for the Crush Impact				
Location	Rigid Surface Side		Crush Plate Side	
	Test	Analysis	Test	Analysis
Top Chime	9	10.5	8-1/2	10.9
Top Hoop	10	11.0	10	11.0
Top CG Hoop	10	10.1	10-1/8	10.1
CG Hoop	9	8.4	10-5/8	10.1
Bottom Hoop	8-1/4	7.6	- - -	0.0
Bottom Chime	9-7/8	10.1	- - -	0.0

7.7.2 Comparison of HABC Run2e vs TU3

The HABC-run2e is a CG over lid corner 30-foot impact, followed by a bottom corner crush. TU3 is a similar test impact configuration with a 4-foot impact, 30-foot impact on the lid corner, then a crush impact on the bottom corner followed by a punch.

The test results show that there is 1.125 inches between the top chime and the top hoop in the test. Similar measurements in the analysis show that the distance is about 1.7 inches. This would be a somewhat judgmental comparison due to points chosen for measurement on the test specimen might not be the same as those chosen in the analysis. The analysis measurement is from the top of the crimped drum roll to the center of the flattened region in the lid roll, on the plane of symmetry.

Table 7.7.2.1 shows the comparison of the TU3 test unit and the computer run2e drum diameter changes after the 30-foot impact.

Table 7.7.2.1 - Run2e vs TU3, Diameter Results After the 30-Foot Impact

	0°-180°		90°-270°	
	Test	Analysis	Test	Analysis
Top Chime	19-1/4	19.0	19-3/16	19.2
Top Hoop	18-5/8	19.1	19-7/8	20.0
Top CG Hoop	19-1/8	19.3	19-3/8	19.5
CG Hoop	19-1/8	19.4	19-3/8	19.4
Bottom Hoop	19-1/8	19.4	19-1/4	19.4
Bottom Chime	19-1/8	19.4	19-3/8	19.4

Figure 7.7.2.1 is an image of the damage after the 30-foot impact of TU3. The test photo shows the cumulative damage from the 4-foot and 30-foot impacts. Figure 7.7.2.2 shows a similar view after the 30-foot impact in run2e. The analysis image is the damage from only the 30-foot impact.

Figure 7.7.2.1 - TU3, Deformed Shape After the 30-Foot Impact

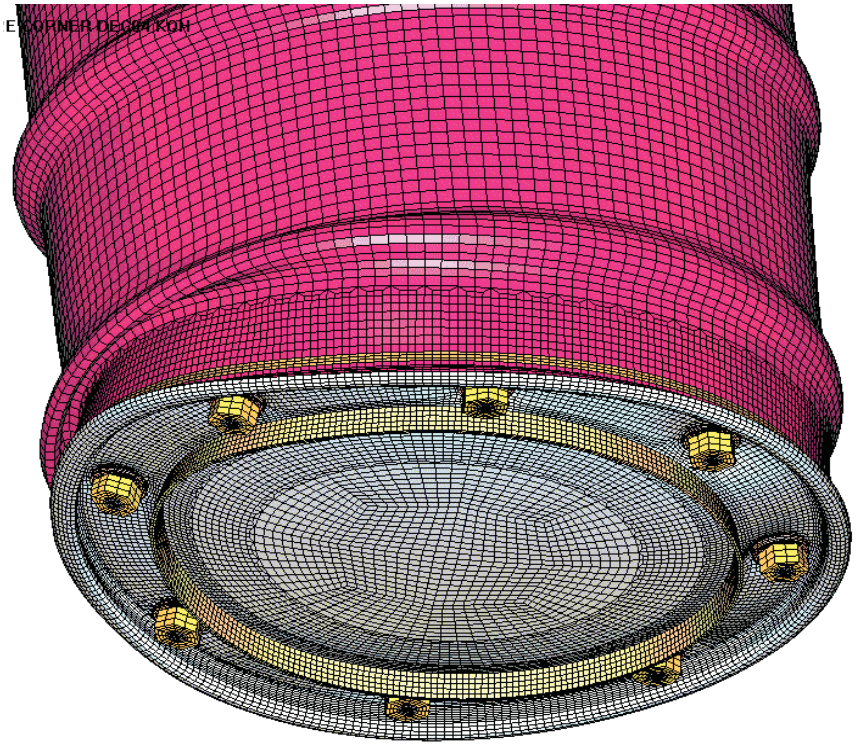

Figure 7.7.2.2 - HABC-run2e, Deformed Shape After the 30-foot Impact

The package drum diameters after the crush impact are compared in Table 7.7.2.2.

Table 7.7.2.2 - Run2e vs TU3, Diameter Results After the Crush Impact				
	0°-180°		90°-270°	
	Test	Analysis	Test	Analysis
Top Chime	19-1/4	19.0	19-1/16	19.0
Top Hoop	18-3/4	18.9	20-1/4	20.6
Top CG Hoop	19-1/4	19.4	19-3/4	19.8
CG Hoop	19-1/8	19.3	19-1/4	19.4
Bottom Hoop	19-1/8	19.3	19-3/4	20.4
Bottom Chime	18	18.6	19-3/8	19.4

The final images after the crush impact are shown for the test and the analysis. Figure 7.7.2.3 shows the final shape of the crushed bottom on the test specimen (4ft + 30ft + crush) and Figure 7.7.2.4 shows a similar view of the analysis (30ft + crush).

Figure 7.7.2.3 - TU3, Damage to the Bottom Head in the Crush Impact

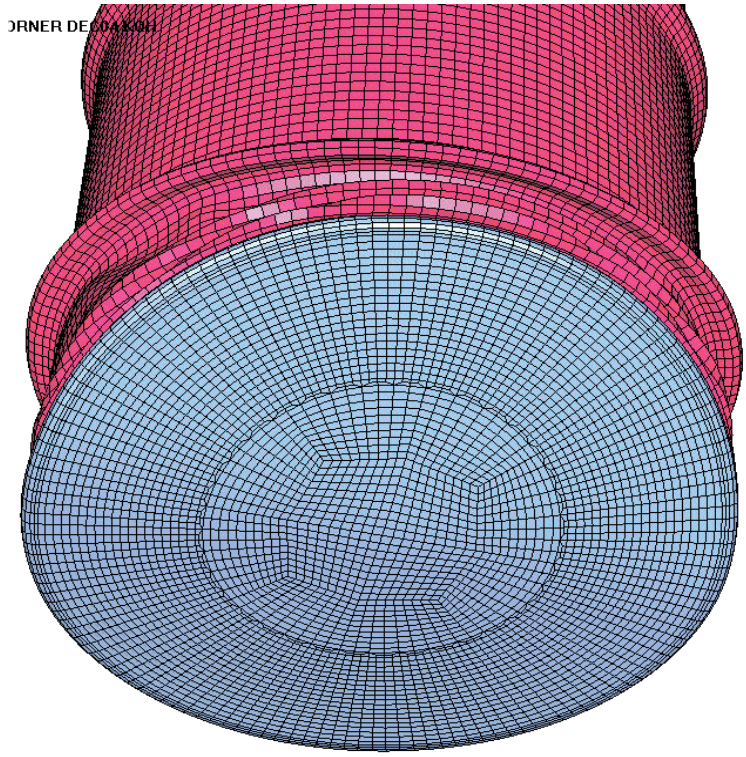

Figure 7.7.2.4 - HABC-run2e, Damage to the Bottom Head in the Crush Impact

The damage to the lid region at the end of the crush impact is shown in Figure 7.7.2.5 for the TU3. The damage to the lid region in the analysis run2e is shown in Figure 7.7.2.6.

Figure 7.7.2.5 - TU3, Lid Damage from the Crush Impact

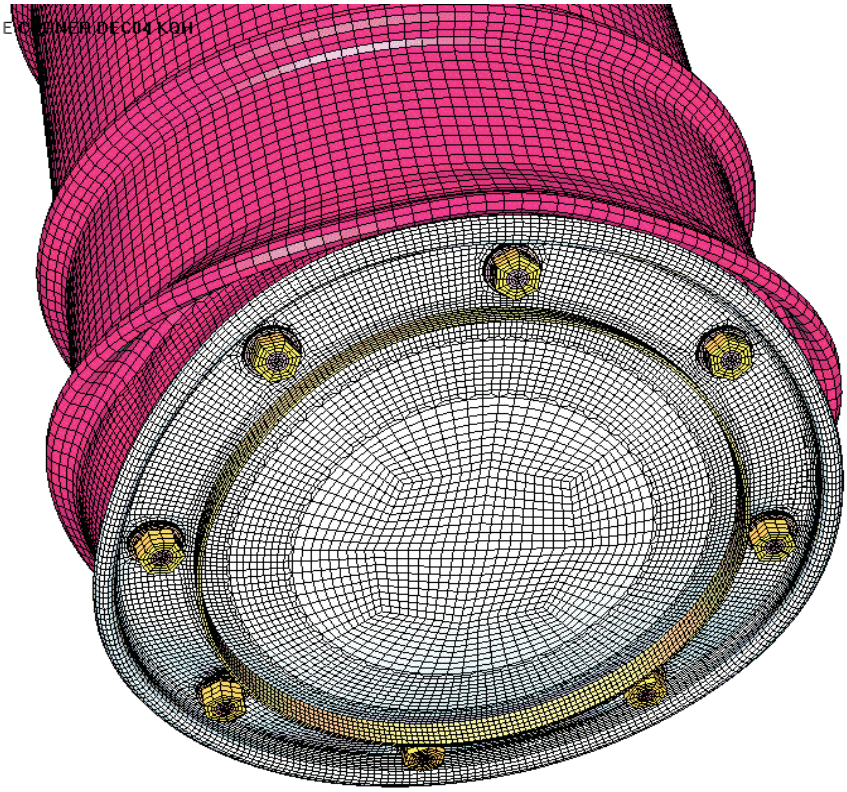

Figure 7.7.2.6 - HABC-run2e, Damage to the Bottom Head from the Crush Impact

7.7.3 Comparison of HABC-Run3b vs TU4

The HABC-run3b is a 30-foot lid down impact onto the rigid surface, followed by a crush impact onto the container bottom. The diameter measurements after the 30-foot impact are given in Table 7.7.3.1.

Table 7.7.3.1 - HABC Run3b vs TU4, Diameter Results After the 30-Foot Impact				
	0°-180°		90°-270°	
	Test	Analysis	Test	Analysis
Top Chime	19-1/4	19.3	19-3/8	19.3
Top Hoop	19-1/8	19.7	19-7/8	19.7
Top CG Hoop	19-13/16	20.0	19-3/8	20.0
CG Hoop	19-1/8	19.5	19-1/4	19.5
Bottom Hoop	19-1/4	19.4	19-1/4	19.4
Bottom Chime	19-1/4	19.4	19-1/4	19.4

The overall height measurements were compared between the test and the analysis. For the 30-foot impact, the test results vary around the circumference: 43.0 inches at 0°, 43.125 inches at 90°, 42.875 inches at 180° and 42.625 inches at 270°. The analysis is symmetrical, and the height from the top of the lid drum roll to the bottom head surface after the 30-foot impact is about 42.6 inches.

Figure 7.7.3.1 shows the configuration of the TU4 after the 30-foot impact (4ft + 30ft). Figure 7.7.3.2 shows the analysis model configuration after the 30-foot impact in a similar orientation to the test unit.

Figure 7.7.3.1 - TU4, 4-Foot + 30-Foot Impact Damage

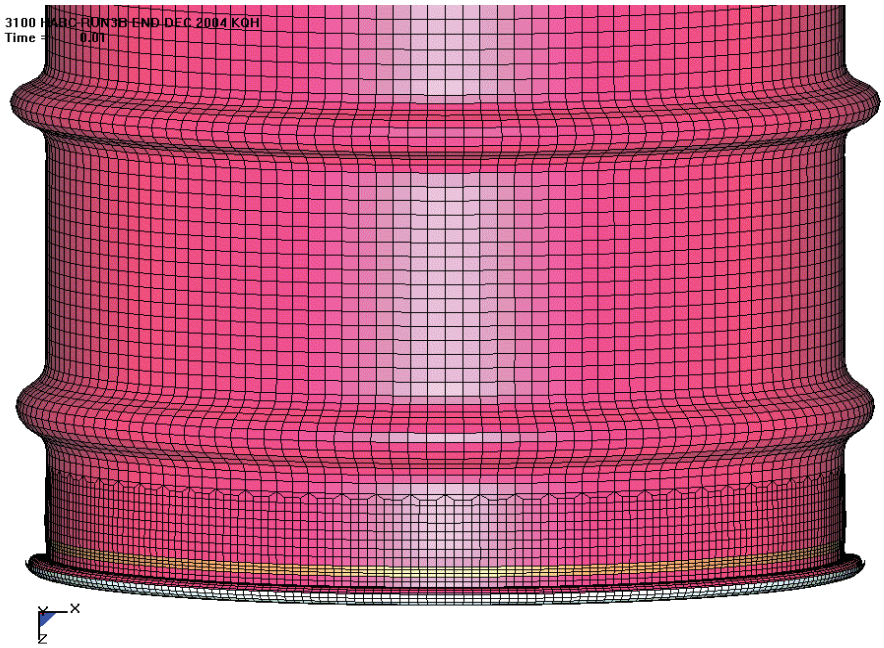

Figure 7.7.3.2 - HABC-Run3b, 30-Foot Impact Damage

The drum height measurement after the test crush impact is 39-3/8 inches at 0°, 40-3/8 inches at 90°, 40-5/8 inches at 180°, and 39-3/4 inches at-270°. The analytical value for the height is about 39.0 inches.

The drum diameters after the crush impact are compared in Table 7.7.3.2.

Table 7.7.3.2 - HABC Run3b vs TU4, Diameter Results After the Crush Impact

	0°-180°		90°-270°	
	Test	Analysis	Test	Analysis
Top Chime	19-1/4	19.3	19-3/8	19.3
Top Hoop	20	20.1	20-1/8	20.1
Top CG Hoop	20	20.2	20-1/16	20.2
CG Hoop	19-7/16	20.1	19-1/2	20.1
Bottom Hoop	19-15/16	20.5	20	20.5
Bottom Chime	19-1/4	19.4	19-1/4	19.4

Figure 7.7.3.3 shows the TU4 at the end of the crush impact (4ft + 30ft + crush), while Figure 7.7.3.4 shows the configuration of the HABC-run3b model (30ft + crush).

Figure 7.7.3.3 - TU4, Crush Damage

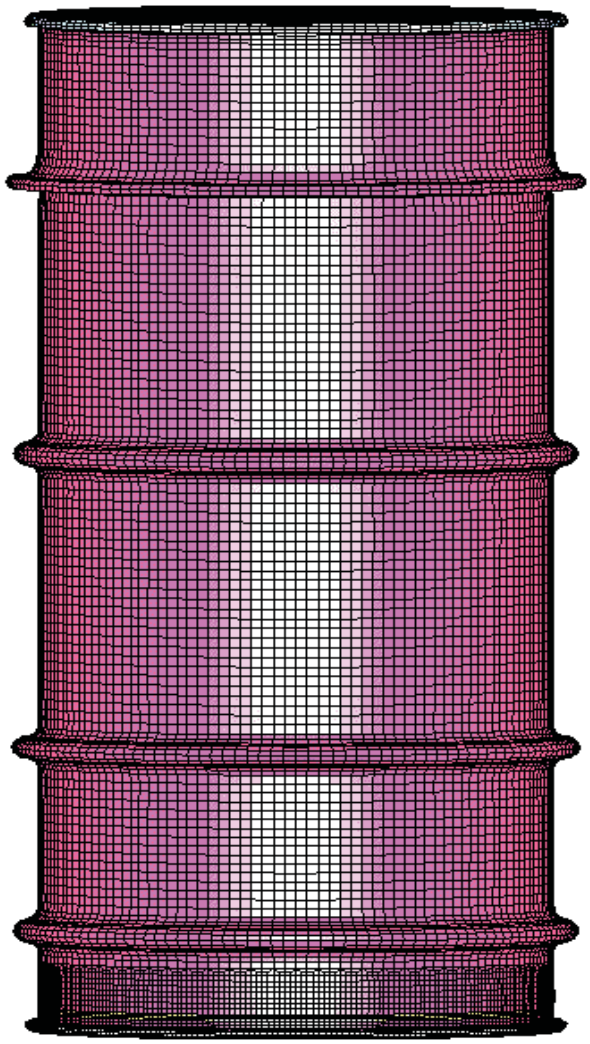

Figure 7.7.3.4 - HABC Run3b, Crush Damage

7.7.4 Comparison of HABC Run1hh vs TU2

HABC-run1hh was the upper bounding kaolite run which included a 4-ft, 30-foot and crush impacts. The test results are for the cumulative damage from the 4-ft, 30ft, crush and punch impacts. The table 7.7.4.1 shows the results for the diameter changes due to all the impacts for the test and the analysis.

Table 7.7.4.1 - Run1hh vs TU2, Cumulative Diameter Results				
	0°-180°		90°-270°	
	Test	Analysis	Test	Analysis
Top Chime	17-5/8	18.0	19-13/16	19.6
Top Hoop	17-3/8	16.6	19-3/4	20.1
Top CG Hoop	17	16.5	20	20.4
CG Hoop	16	16.3	20-1/4	20.5
Bottom Hoop	15-1/2	16.1	20-1/8	20.0
Bottom Chime	18	17.6	19-3/8	19.4

Table 7.7.4.2 shows the comparison of the "flats" dimensions for the test and the analysis.

Table 7.7.4.2 - Run1hh vs TU2, Cumulative Flats Results†				
	180° - Crush Plate Side		0° - Rigid Surface Side	
	Test‡	Analysis	Test	Analysis
Top Chime	6-1/4	0	8.0	9.2
Top Hoop	8-7/8	10.1	9.0	9.3
Top CG Hoop	9-5/8	9.3	10-1/8	8.4
CG Hoop	12	9.3	9-7/8	9.3
Bottom Hoop	14-7/8	10.1	9-7/8	9.3
Bottom Chime	0	0	9-3/8	10.1

† - Note - The reported test results for the 0 and the 180 sides are reversed in the test report (evidence Figure 7.7.4.3 below).
‡ - Note - The crush plate edge was 4.75 inches from bottom of package.

A visual comparison of the cumulative damage on the rigid surface side after the impacts is shown in Figures 7.7.4.1 (test) and Figure 7.7.4.2 (analysis).

Figure 7.7.4.1 - TU2, Cumulative Damage After the Punch Impact, Rigid Surface Side

Figure 7.7.4.2 - HABC-run1hh, Cumulative Damage, Rigid Surface Side

A visual comparison of the cumulative damage on the crush side after the four impacts is shown in Figures 7.7.4.3 (test) and Figures 7.7.4.4 (analysis).

Figure 7.7.4.3 - TU2, Cumulative Damage After the Punch Impact, Crush Plate Side

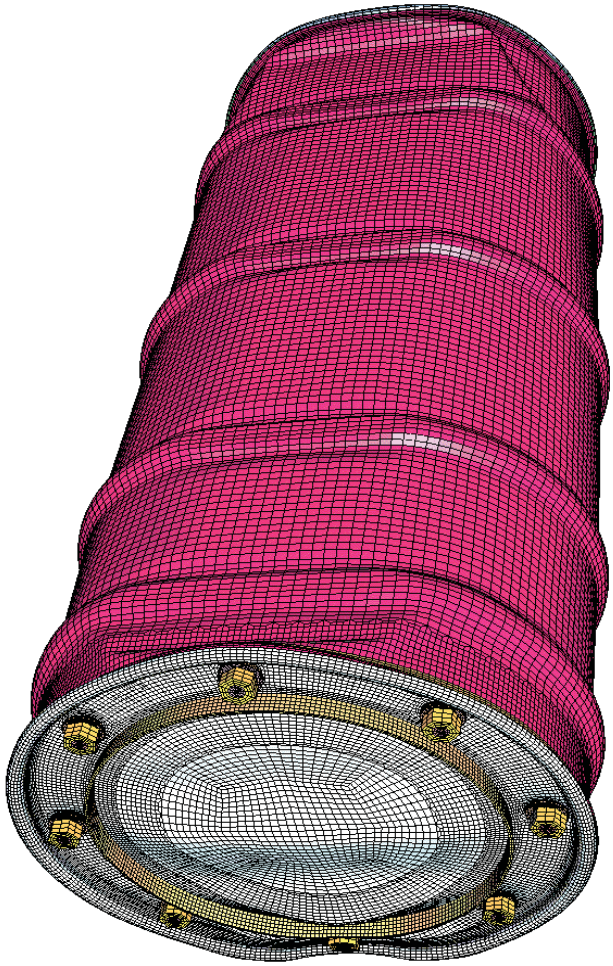

Figure 7.7.4.4 - HABC-run1hh, Cumulative Damage, Crush Plate Side

8.0 Summary

The computer simulation impacts for the HABC re-design of the ES-3100 shipping container are presented in Sections 7.1 to 7.6. The comparison of the HABC re-design container to the physical tests is presented in Section 7.7. The effective plastic strain for the components are summarized in Table 8.0.1. The punch impact is not included in the HABC runs, due to the fact that the drum shell capability is demonstrated in the initial borobond models, and the tested specimen.

Maximum strains in excess of 0.5 in/in are near the 304L strain limit of 0.57 in/in and are highlighted in red in Table 8.0.1. The components which are highlighted included the drum , lid, studs and liner. Evidence from looking at the Table 8.0.1 summary, a high demand is placed on the lid and the studs in the side and slapdown impacts.

In runs HABC-runs1hl, 1hh, 4g and 4ga a high demand is placed on the lid/studs. In runs 1hh, 1hl, 4g and 4ga, the region of plastic strain is very localized at the stud holes. Runs 1hl and 4g also have relatively high demands placed on the studs. In runs1hl and 4g, it is shown that the times at which the lid strains become excessive in membrane, the stud strains are relatively low. Hence, it is predicted that the lid will locally tear, thereby relieving loading on the studs. The tearing associated with the lid is expected to be local due to the localized fringes of extreme strain shown in the Section 7 fringe plots. The large washers provided on the packages would restrain the lid.

In runs HABC-run1hl, 2e and 4g, the studs reach high levels of effective plastic strain. In HABC-run1hl, the lid was shown to tear before the studs reached an elevated level of plastic strain.

HABC-run2e shows that the stud at the impact reaches extreme levels of plastic strain near the 0.57 in/in failure strain in the 30-foot impact and the subsequent crush impact. The level of high strain is throughout the cross section of the stud in HABC-run2e. Due to this high level of strain and the direct load path between the shipping package and the rigid surface, any slight changes in length, friction, localized deformations (stud "digging" into the relatively rigid plate in the test) could cause the stud to fail.

In HABC-run4g, the stud reached its failure strain and the cross section row of elements failed (removed by LS-Dyna). A time study shows that the lid reaches its levels of elevated strain in membrane before the stud. Therefore, the lid is expected to tear before the stud fails, thus relieving loading on the stud. However, the model does show the shipping container response if the lid were not to tear, and the stud were to fail.

The relatively high level of plastic strain in the HABC-run2e liner is a surface strain. Investigation shows that the membrane strain is about 0.2205 in/in, or well below the expected failure level. The deformation/fringe plot shows that the region of high strain is relatively local at the attachment of the liner to the angle. The plot also shows that it is the result of crimping or folding of the liner due to the relatively stiffer angle. Any tearing that might take place would be limited, evidence the local concentration of fringe levels.

Table 8.0.1 - ES-3100 HABC Shipping Package Summary of Component Maximum Effective Plastic Strain (in/in)

Material	Description	HABC-run1hl			HABC-run1hh		
		Side - Lower Bound Kaolite (Section 7.1)			Side - Upper Bound Kaolite (Section 7.2)		
		4-foot	30-foot	Centered Crush	4-foot	30-foot	Centered Crush
1	CV Body	0.0185	0.0195	0.0206	0.0238	0.0347	0.0525
3	CV Lid	0.0001	0.0002	0.0002	0.0000	0.0001	0.0004
4	CV Nut Ring	0.0000	0.0000	0.0000	0.0000	0.0000	0.0005
5	Angle	0.0055	0.0780	0.1142	0.0061	0.0632	0.0845
6	Drum	0.1599	0.2251	0.5139	0.1207	0.2296	0.2814
7	Drum Bottom	0.1033	0.2126	0.3562	0.1252	0.2517	0.2827
10	Liner	0.1045	0.1078	0.1593	0.0991	0.1184	0.2022
12	Lid	0.1393	0.5790	1.2580	0.1604	0.4063	0.6413
15	Lid Stiffener	0.0004	0.0093	0.0515	0.0006	0.0076	0.0171
16	Lid Studs	0.0000	0.1140	0.5121	0.0000	0.1306	0.2364
17	Lid Stud Nuts	0.0000	0.0000	0.0005	0.0000	0.0004	0.0018
18	Lid Stud Washe	0.0194	0.0194	0.0693	0.0411	0.0424	0.0439
19	Plug Liner	0.0022	0.0958	0.1220	0.0045	0.1072	0.1286

Material	Description	HABC-run2e		HABC-run3b		HABC-run4g		HABC-run4ga	
		Corner (Section 7.3)		End (Section 7.4)		Slapdown (Section 7.5)		Slapdown (Section 7.6)	
		Impact	Crush	Impact	Crush	Impact	Offset Crush	Impact	Centered Crush
1	CV Body	0.0371	0.0371	0.0028	0.0083	0.0376	0.0564	Same as HABC-Run4g Impact Results	0.0643
3	CV Lid	0.0051	0.0051	0.0072	0.0072	0.0004	0.0013		0.0018
4	CV Nut Ring	0.0002	0.0002	0.0011	0.0011	0.0000	0.0001		0.0000
5	Angle	0.0394	0.0462	0.0287	0.0308	0.0900	0.1070		0.0944
6	Drum	0.3247	0.3830	0.0557	0.1237	0.3018	0.3920		0.3443
7	Drum Bottom	0.0000	0.0761	0.0031	0.0267	0.2879	0.2879		0.3000
10	Liner	0.3983	0.5254	0.0607	0.3812	0.1458	0.2060		0.2846
12	Lid	0.2791	0.3622	0.1082	0.1389	0.5278	0.9689		0.5828
15	Lid Stiffener	0.0272	0.0272	0.0069	0.0100	0.0213	0.0894		0.0288
16	Lid Studs	0.5233	0.5598	0.0962	0.1535	0.1892	0.4018		0.2390
17	Lid Stud Nuts	0.2260	0.2266	0.0166	0.0173	0.0000	0.0028		0.0000
18	Lid Stud Washe	0.1528	0.1528	0.0506	0.0506	0.0724	0.0790		0.0775
19	Plug Liner	0.1152	0.1166	0.0670	0.0960	0.1258	0.2665		0.1644

9.0 Comparison of Borobond Cylinder and HABC Cylinder Models

Part A of this calculation (Sections 2 through 5) apply to the initial, borobond neutron absorber model. Section 3.12 compared the borobond model results to the physical tested specimen. Part B (Sections 6 through 8) apply to the HABC redesigned neutron absorber model. Section 7.7 compares the HABC model to the physical tested specimen. The HABC model was derived from the initial borobond model, with changes detailed in Section 6. Section 6.1 gives the configuration changes and Section 6.2 gives the material model derivation for the HABC neutron absorber.

The borobond and the HABC materials are similar in nature in that they are castable, cement type materials. The LS-Dyna material model used in both analytical simulations was the *MAT_SOIL_AND_FOAM model. Similar approaches were taken for both the borobond and the HABC to match the material test results to the needed material properties in the analytical model. The approach is shown explicitly for the HABC material model in Section 6.2. The borobond model used in the Part A models, was also used in the Highly Enriched Uranium Materials Facility (HEUMF) storage pallet modeling, testing and qualification.

The CV body cylinder has an outside diameter of about 5.6 in. A minimum liner diameter of about 5.3 inches was found to occur in the borobond slapdown runs (4g, 4ga, 4h and 4ha). This minimum occurred at several locations along the liner length, and also near the CV flange. A somewhat similar response is noted for the HABC models, but with more deflection near the mid-height of the CV cavity. A minimum liner diameter of about 5.2 inches near the CV flange is noted in slapdowns HABC-run4g and 4ga. However, a minimum diameter of about 4.5 in is noted in HABC-run4ga near the mid-height of the CV body. This region of the CV body is remote from the bottom head or the flange and plastic strains in the body are relatively low (compare Figures 3.8.2 and Figure 7.6.4). The region of concern, near the CV flange, experiences about the same deformation (5.3 in vs 5.2 in).

A significant demand is placed on the lid and the studs in both the borobond and the HABC model side and slapdown impacts. This is a precipitate of the design attempt to minimize the number of studs securing the lid. The lid power law material model does not allow for element failure, whereas the model used for the studs (elastic-plastic) did allow element failure to be modeled. The effective plastic strain in bending and membrane reach significantly high levels (about 1.0 strain) in the lid. The regions of elevated plastic strain in the lid are shown to be localized at the stud holes. The studs also reached elevated levels of plastic strain. Investigation into the time history of the demand placed on the lid and the studs reveals that the lid reaches the elevated levels earlier in the impact, and therefore tearing of the lid would be expected. The tearing of the lid is expected to relieve the

loading on the studs, such that the integrity of the studs would be maintained. The large washers will restrain the lid. This fact was verified in the test with some tearing at the 90°and 270° position stud holes and no loss of a stud.

Both models compared favorably with the test results and with each other. This can be seen in the tables in Section 3.12 for the borobond and 7.7 for the HABC material.

THIS PAGE INTENTIONALLY LEFT BLANK.

Appendix 2.10.3

KAOLITE PROPERTIES

Kaolite SuperLightweight Insulating Castables, Thermal Ceramics, Augusta, Ga., September 1999.

Material Safety Data Sheet, *Refractory Castable, Silicate Product, Kaolite*, Thermal Ceramics, Augusta, Ga., September 1999.

R. E. Oakes, Jr., *Mechanical Properties of a Low Density Concrete for the New ES-2 Shipping/Storage Container Insulation, Impact Mitigation Media and Neutron Absorber*, Y/DW-1661, Lockheed Martin Energy Systems, Inc., Oak Ridge Y-12 Plant, Apr. 10, 1997.

H. Wang, *Thermal Conductivity Measurements of Kaolite*, ORNL-TM-2003/49, UT-Battelle, Oak Ridge Natl. Lab., n.d.

B. F. Smith and G. A. Byington, *Water Content and Temperature-Dependent Impact Properties of an Inorganic Cast Refractory Material*, Y/DW-1890, BWXT Y-12, Y-12 Natl. Security Complex, Feb. 14, 2003.

B. F. Smith, *Low Temperature Impact Properties of an Inorganic Cast Refractory Material*, Y/DW-1972, BWXT Y-12, Y-12 Natl. Security Complex, Sept. 14, 2003.

Advantages of Using a Fireproof Inorganic Cast Refractory Material in Hazardous Content Shipping Packages, Y/LF-565, Lockheed Martin Energy Systems, Inc., Oak Ridge Y-12 Plant, Nov. 10, 1998.

K. Moody, Thermal Ceramics, Augusta, Ga., *RE: Coefficient of thermal expansion for Kaolite 1600*, email to P. A. Bales, BWXT Y-12, Oak Ridge, Tenn., Dec. 9, 2004.

THIS PAGE INTENTIONALLY LEFT BLANK.

KAOLITE SUPER LIGHTWEIGHT INSULATING CASTABLES

Super lightweight Kaolite castables reduce both the quantity of heat storage and heat transfer through the lining producing significant savings in furnace fuel consumption. The lower densities of these vermiculite based Kaolite castables reduce the amount of supporting furnace steel work required and provide more insulation with a thinner lining. These products can be cast, poured, or gunited.

Kaolite 1600 is a super lightweight, low thermal conductivity vermiculite based castable designed for backup insulation up to 1600°F. Kaolite 1600 contains portland cement which limits use temperature to 1600°F; however, this makes it an economical product based on cost per cubic foot.

Kaolite 1800 is a super lightweight, low thermal conductivity vermiculite castable designed for both backup insulation and hot face applications up to 1800°F. Kaolite 1800 contains a calcium-aluminate cement which gives it better high-temperature stability when compared to Kaolite 1600. Typical applications would be low-temperature lining for ovens and ductwork lining.

Kaolite 2000 is a super lightweight, low thermal conductivity castable designed for backup insulation and hot face applications up to 2000°F. Typical applications would be low-temperature lining for ovens and ductwork lining.

Instructions For Using

Casting

Highest strength is obtained with castable refractory by using the least amount of clean mixing water. This will allow thorough working of material into place by lightly vibrating or rodding. A mechanical mixer is required for proper placement (paddle-type mortar mixers are best suited). After achieving a ball-in-hand consistency, mix for 6 minutes. Place material within 20 minutes after mixing.

Gunning

Use suitable gunite equipment. Material should be predampened uniformly with approximately 10 - 12% by weight of clean water in mechanical mixer before placing into gun. This will reduce rebound and dust. Add required water at nozzle for effective placement. Suggested air pressure at the nozzle is between 15 and 25 psi.

Precautions

Store bagged castables in a dry place, off the ground and, when possible, with the original shrink wrapping intact.

Watertight forms must be used when placing material. All porous surfaces that will come into contact with the material must be waterproofed with a suitable coating or membrane. For maximum strength, cure 24 hours under damp conditions before initial heat-up. Keep freshly placed castable warm during cold weather, ideally between 70°F and 80°F. New castable installations must be heated slowly the first time.

Freshly placed lightweight castables are prone to a deteriorating condition called alkali hydrolysis when they are kept in a non-dried state for a sustained period of time in a warm, humid environment. Under these conditions, the castables should be force dried soon after placement or coated with Kao-Seal™ to resist the possible deterioration effects.

For mor information on castable placement, consult your Thermal Ceramics representative or call 1-800-329-7444 to receive faced instruction manuals.

Kaolite	**1600**	**1800**	**2000**
Specifications	cast, gunned	cast, gunned	cast, gunned
Recommended use limit, °F	1600	1800	2000
Melting point, °F,	2300	2400	2400
Average lb required to place one cubic ft[1]	23, 36*	23, 35*	25, 35*
Nominal density, pcf, fired	20 - 25, 31 - 39	20 - 25, 29 - 38	21 - 26, 29 - 35
Pounds per bag	50	50	50
Method of installation[2]	C,G,P	C,G,P	C,G,P
Recommended water ranges, % by weight			
Casting (by vibrating)	120 - 145	145 - 165	155 - 180
Pouring	150 - 180	175 - 190	175 - 190

*Note: For overhead gunning applications, pounds required to place one ft³ should be increased to 40-50 pcf. Does not include rebound loss.

Physical Properties[3]			
Modulus of rupture, psi (ASTM C 133)	cast, gunned	cast, gunned	cast, gunned
Dried 18-24 hrs. @ 220°F	45 - 75, 70 - 120	25 - 40, 50 - 100	18 - 26, 50 - 100
Fired 5 hrs. @ 1500°F	25 - 40, 35 - 55	30 - 50, 40 - 60	28 - 36, 40 - 65
Fired 5 hrs. @ use limit	25 - 40, 35 - 50	25 - 40, 35 - 55	–
Cold Crushing strength			
Dried 18-24 hrs. @ 220°F	80 - 120, 125 - 175	35 - 50, 70 - 120	55 - 64, 75 - 85
Fired 5 hrs. @ 1500°F	50 - 70, 90 - 120	50 - 80, 80 - 110	70 - 120, 80 - 110
Fired 5 hrs. @ use limit	50 - 70, 90 - 120	40 - 60, 60 - 80	–
Perm. linear change, % (ASTM C 113)[4]			
Fired 5 hrs. @ 1500°F	-1.0 to -2.0	-0.5 to -1.5	-0.5 to -1.5
Fired 5 hrs. @ use limit	-1.5 to -2.5	-1.5 to -2.5	-1.5 to -3.0

Chemical Analysis (Nominal, %)			
Alumina, Al_2O_3	11	29	34
Silica, SiO_2	33	32	26
Ferric oxide, Fe_2O_3	7.9.	7.0	7.0
Titanium oxide, TiO_2	1.4	2.3	1.0
Calcium oxide , CaO	30	14	17
Magnesium oxide, MgO	12.1	12	10
Alkalies, as, Na_2O	3.7	3.5	2.5

Thermal Conductivity, Btu•in./hr•ft²•°F (ASTM C 417)			
Mean temperature			
@ 500°F	0.87, 1.03	0.79, 0.93	0.79, 0.93
@ 1000°F	1.02, 1.11	0.95, 1.06	0.95, 1.06
@ 1500°F	1.19, 1.20	1.11, 1.26	1.11, 1.27
@ 2000°F	–	–	1.28, 1.49

1. Gunite installation may require 10-30% overage due to rebound and on-site loss.
2. Installation key: C-cast, G-gun, P-pour
3. Properties indicated are for vibratory cast materials unless specified otherwise.
4. Fired linear change values reflect samples taken from a dried to fired state.

Consult Thermal Ceramics for specific curing and heat-up recommendations.

Data are average results of tests conducted under standard procedures and are subject to variation. Results should not be used for specification purposes.

Refer to the Material Safety Data Sheet (MSDS) for recommended work practices and other product safety information.

For further information, contact your nearest Thermal Ceramics technical sales office or your local Thermal Ceramics authorized distributor. You may also fax us toll-free at 1-800-KAOWOOL or write to Thermal Ceramics, P. O. Box 923, Dept. 140, Augusta, GA 30903.

AUGUSTA, GA
(800) 338-9284
Fax: (706) 796-4324

CHICAGO, IL
(888) 649-2442
Fax: (630) 527-0285

DETROIT, MI
(800) 590-4338
Fax: (734) 459-7860

LOS ANGELES, CA
(800) 990-5264
Fax: (714) 521-4662

INTERNATIONAL
(706) 796-4216
Fax: (706) 796-4262

BATON ROUGE, LA
(877) 722-2866
Fax: (504) 292-4082

CLEVELAND, OH
(877) 787-3385
Fax: (216) 831-4485

HOUSTON, TX
(800) 824-6878
Fax: (713) 680-9070

TRANSPORTATION
(888) 205-2358
Fax: (219) 296-3585

THERMAL CERAMICS
BURLINGTON, ONTARIO, CANADA
(905) 335-3414
Fax: (905) 335-5145

Thermal Ceramics

MATERIAL SAFETY DATA SHEET

MSDS No: 154	Date Prepared: 09/06/1993	Current Date: 2/3/2003 Last Revised: (01/16/2003)

1. PRODUCT AND COMPANY IDENTIFICATION

Product Group: **REFRACTORY CASTABLE**
Chemical Name: Silicate Product
Intended Use: High Temperature Thermal Insulation
Trade Names: Kaolite® 1600; Kaolite® 1600 RFT; Kaolite® 1800; Kaolite® 1800 RFT; Kaolite® 2000; Therm-O-Flake Coating

Manufacturer/Supplier:

Thermal Ceramics Inc.
P. O. Box 923; Dept. 300
Augusta, GA 30903-0923

For Product Stewardship and Emergency Information -
Hotline: 1-800-722-5681
Fax: 706-560-4054

For additional MSDSs and to confirm this is the most current MSDS for the product, visit our web page [*www.thermalceramics.com*] or call our automated FaxBack: 1-800-329-7444

2. COMPOSITION/INFORMATION ON INGREDIENTS

INGREDIENT & CAS NUMBER	% BY WEIGHT	OSHA PEL	ACGIH TLV
Vermiculite 01318-00-9	52 - 78	15 mg/m^3 (total dust); 5 mg/m^3 (respirable dust)	10 mg/m^3 (inhalable dust) 3 mg/m^3 (respirable dust)
Cement, alumina, chemicals 65997-16-2	15 - 50	15 mg/m^3 (total dust); 5 mg/m^3 (respirable dust)	10 mg/m^3 (inhalable dust) 3 mg/m^3 (respirable dust)
Crystalline silica 14808-60-7 or 14464-46-1	0.5 - 7	See notes[1]	0.05 mg/m^3 (respirable dust)

NOTES:

[1] Depending on the percentage and type(s) of silica in the mineral, the OSHA Permissible Exposure Limit (PEL) for respirable dust containing crystalline silica (8 HR TWA) is based on the formula listed in 29 CFR 1910.1000, "Air Contaminants" under Table Z-3, "Mineral Dust". For quartz containing mineral dust, the PEL = 10 mg/m^3 / (% of silica + 2); for cristobalite or tridymite, the PEL = 5 mg/m^3/ (% of silica + 2); for mixtures, the PEL = 10 mg/m^3 / (% of quartz + 2 (% of cristobalite) + 2 (% of tridymite) + 2).

(See Section 8 "Exposure Controls / Personal Protection" for exposure guidelines.)

MATERIAL SAFETY DATA SHEET

MSDS No: 154	Date Prepared: 09/06/1993	Current Date: 2/3/2003 Last Revised: (01/16/2003)

3. HAZARDS IDENTIFICATION

EMERGENCY OVERVIEW

WARNING!
Respirable dust from these products may contain crystalline silica, which is known to cause respiratory disease.
(See Section 11 for more information)

POSSIBLE HEALTH EFFECTS

Target Organs:	Eyes, skin, nose and/or throat
Primary Entry Route:	Inhalation
Acute effects:	May cause temporary, mild mechanical irritation to the eyes, skin, nose and/or throat. Pre-existing skin and respiratory conditions may be aggravated by exposure.
Chronic effects:	Prolonged/repeated inhalation of respirable crystalline silica may cause delayed lung injury (e.g.: silicosis, lung cancer).

HAZARD CLASSIFICATION

Dust samples from these products have not been tested for their specific toxicity, but may contain more than 0.1% crystalline silica, for which the following apply:

The **International Agency for Research on Cancer (IARC)** has classified crystalline silica inhaled in the form of quartz or cristobalite from occupational sources as carcinogenic to humans (Group 1).

The Ninth Annual Report on Carcinogens (2000), prepared by the **National Toxicology Program (NTP),** classified silica, crystalline (respirable size), as a substance known to be a human carcinogen.

The **American Conference of Governmental Industrial Hygienists (ACGIH)** has classified crystalline silica (quartz) as "A2-Suspected Human Carcinogen."

The **State of California,** pursuant to Proposition 65, The Safe Drinking Water and Toxic Enforcement Act of 1986, has listed "silica, crystalline (airborne particles of respirable size)" as a chemical known to the State of California to cause cancer.

The **Canadian Workplace Hazardous Materials Information System (WHMIS) –** Crystalline silica [quartz and cristobalite] is classified as Class D2A - Materials Causing Other Toxic Effects.

The **Hazardous Materials Identification System (HMIS) –**
Health: 1* Flammability: 0 Reactivity: 0 Personal Protection Index: X (Employer determined)
(* denotes potential for chronic effects)

4. FIRST AID MEASURES

EYE IRRITATION:
Flush with large amounts of water for at least 15 minutes. Do not rub eyes.

SKIN IRRITATION:
Wash affected area gently with soap and water. Skin cream or lotion after washing may be helpful.

INGESTION:
Unlikely route of exposure.

MATERIAL SAFETY DATA SHEET

MSDS No: 154	Date Prepared: 09/06/1993	Current Date: 2/3/2003 Last Revised: (01/16/2003)

INHALATION:
Remove affected person to dust free location. See Section 8 for additional measures to reduce or eliminate exposure.

- If symptoms persist, seek medical attention. -

5. FIRE FIGHTING MEASURES

NFPA CODES: **Flammability: 0 , Health: 1 , Reactivity: 0 , Special: 0**

NFPA Unusual Hazards:	None
Flash Point:	None
Extinguishing Media:	Use extinguishing media suitable for type of surrounding fire.
Explosion Hazards:	None
Hazardous Decomposition Products:	None

6. ACCIDENTAL RELEASE MEASURES

SPILL/LEAK PROCEDURES:
Avoid creating airborne dust. Follow routine housekeeping procedures. Vacuum only with HEPA filtered equipment. If sweeping is necessary, use a dust suppressant and place material in closed containers. Do not use compressed air for clean-up. Personnel should wear gloves, goggles and approved respirator.

7. HANDLING AND STORAGE

HANDLING
Limit the use of power tools unless in conjunction with local exhaust. Use hand tools whenever possible. Frequently clean the work area with HEPA filtered vacuum or wet sweeping to minimize the accumulation of debris. Do not use compressed air for clean-up.

STORAGE
Store in original factory container in a dry area. Keep container closed when not in use.

EMPTY CONTAINERS
Product packaging may contain residue. Do not reuse.

8. EXPOSURE CONTROLS/PERSONAL PROTECTION

ENGINEERING CONTROLS
Use engineering controls, such as ventilation and dust collection devices, to reduce airborne particulate concentrations to the lowest attainable level.

RESPIRATORY PROTECTION
When it is not possible or feasible to reduce airborne crystalline silica or particulate levels below the PEL through engineering controls, or until they are installed, employees are encouraged to use good work practices together with respiratory protection. Before providing respirators to employees (especially negative pressure type), employers should **1)** monitor for airborne crystalline silica and/or dust concentrations using appropriate NIOSH analytical methods and select respiratory protection based upon the results of that monitoring , **2)** have the workers evaluated by a physician to determine the workers' ability to wear respirators, and **3)** implement respiratory protection training programs. Use NIOSH-certified particulate respirators (42 CFR 84), in compliance with OSHA Respiratory Protection Standard 29 CFR 1910.134 and 29 CFR 1926.103, for the particular hazard or airborne concentrations to be encountered in the work environment. For the most current information on respirator selection, contact your supplier.

MATERIAL SAFETY DATA SHEET

MSDS No: 154	Date Prepared: 09/06/1993	Current Date: 2/3/2003 Last Revised: (01/16/2003)

PROTECTIVE CLOTHING

Wear full body clothing, gloves, hat, and eye protection as necessary to prevent skin irritation. Washable or disposable clothing may be used. If possible, do not take unwashed work clothing home. If soiled work clothing must be taken home, employers should ensure employees are trained on the best practices to minimize or avoid non-work dust exposure (e.g., vacuum clothes before leaving the work area, wash work clothing separately, rinse washer before washing other household clothes, etc.).

EYE PROTECTION

Wear safety glasses with side shields or other forms of eye protection in compliance with appropriate OSHA standards to prevent eye irritation. The use of contact lenses is not recommended, unless used in conjunction with appropriate eye protection. Do not touch eyes with soiled body parts or materials. If possible, have eye-washing facilities readily available where eye irritation can occur.

9. PHYSICAL AND CHEMICAL PROPERTIES

ODOR AND APPEARANCE:	Coarse brown powder.
CHEMICAL FAMILY:	Silicate
BOILING POINT:	Not applicable
WATER SOLUBILITY (%):	Slight
MELTING POINT:	> 2300°F
SPECIFIC GRAVITY:	Not applicable
VAPOR PRESSURE:	Not applicable
pH:	Not applicable
VAPOR DENSITY:	Not applicable
VOLATILE BY VOLUME (%):	Not applicable
MOLECULAR FORMULA:	Not Applicable

10. STABILITY AND REACTIVITY

HAZARDOUS POLYMERIZATION:	Will not occur
CHEMICAL INCOMPATIBILITIES:	Powerful oxidizers; fluorine, manganese trioxide, oxygen disulfide
HAZARDOUS DECOMPOSITION PRODUCTS:	None

11. TOXICOLOGICAL INFORMATION

TOXICOLOGY

Dust samples from these products have not been tested. They may contain respirable crystalline silica.

Crystalline silica

Some samples of crystalline silica administered to rats by inhalation and intratracheal instillation have caused fibrosis and lung cancer. Mice and hamsters, similarly exposed, develop inflammatory disease including fibrosis but no lung cancer.

Vermiculite

This product contains vermiculite. Some vermiculite deposits may contain other naturally occurring substances such as crystalline silica or asbestiform materials. Thermal Ceramics has relied upon supplier MSDSs to conclude that crystalline silica or asbestiform materials are not present, in regulated quantities, in the vermiculite used in this product.

EPIDEMIOLOGY

No studies have been undertaken on humans exposed to these products in occupational environments.

Crystalline silica

Exposure to crystalline silica can cause silicosis, and exacerbate pulmonary tuberculosis and bronchitis. IARC (Monograph vol. 68, 1997) concluded that "crystalline silica from occupational sources inhaled in the form of quartz or cristobalite is carcinogenic to humans (Group 1)", and noted that "carcinogenicity in humans was not detected in all industrial circumstances studied" and "may be dependent on inherent characteristics of the crystalline silica or on external factors affecting its biological activity".

12. ECOLOGICAL INFORMATION

Adverse effects of this material on the environment are not anticipated.

13. DISPOSAL INFORMATION

WASTE MANAGEMENT

To prevent waste materials becoming airborne during waste storage, transportation and disposal, a covered container or plastic bagging is recommended. Comply with federal, state and local regulations.

DISPOSAL

If discarded in its purchased form, this product would not be a hazardous waste under Federal regulations (40 CFR 261) Any processing, use, alteration or chemical additions to the product, as purchased, may alter the disposal requirements. Under Federal regulations, it is the waste generator's responsibility to properly characterize a waste material, to determine if it is a hazardous waste. Check local, regional, state or provincial regulations to identify all applicable disposal requirements.

14. TRANSPORT INFORMATION

U.S. DEPARTMENT OF TRANSPORTATION (DOT)

Hazard Class:	Not Regulated	United Nations (UN) Number:	Not Applicable
Labels:	Not Applicable	North America (NA) Number:	Not Applicable
Placards:	Not Applicable	Bill of Lading:	Product Name

INTERNATIONAL

Canadian TDG Hazard Class & PIN: Not regulated
Not classified as dangerous goods under ADR (road), RID (train) or IMDG (ship).

15. REGULATORY INFORMATION

UNITED STATES REGULATIONS

SARA Title III:	This product does not contain any substances reportable under Sections 302, 304, 313 (40 CFR 372). Sections 311 and 312 apply.
OSHA:	Comply with Hazard Communication Standards 29 CFR 1910.1200 and 29 CFR 1926.59 and Respiratory Protection Standards 29 CFR 1910.134 and 29 CFR 1926.103.
TSCA:	All substances contained in this product are listed in the TSCA Chemical Inventory
California:	"Silica, crystalline (airborne particles of respirable size)" is listed in Proposition 65, The Safe Drinking Water and Toxic Enforcement Act of 1986 as a chemical known to the State of California to cause cancer.

MATERIAL SAFETY DATA SHEET

MSDS No: 154	Date Prepared: 09/06/1993	Current Date: 2/3/2003 Last Revised: (01/16/2003)

Other States: Crystalline silica products are not known to be regulated by states other than California; however, state and local OSHA and EPA regulations may apply to these products. Contact your local agency if in doubt.

INTERNATIONAL REGULATIONS

Canadian WHMIS: Class D-2A Materials Causing Other Toxic Effects
Canadian EPA: All substances in this product are listed, as required, on the Domestic Substance List (DSL).

16. OTHER INFORMATION

SARA TITLE III HAZARD CATEGORIES

Acute Health:	No	**Pressure Hazard:**	No
Chronic Health:	Yes	**Reactivity Hazard:**	No
Fire Hazard:	No		

MATERIAL SAFETY DATA SHEET

MSDS No: 154	Date Prepared: 09/06/1993	Current Date: 2/3/2003 Last Revised: (01/16/2003)

DEFINITIONS:

ACGIH:	American Conference of Governmental Industrial Hygienists
ADR:	Carriage of Dangerous Goods by Road (International Regulation)
CAA:	Clean Air Act
CAS:	Chemical Abstracts Service Registry Number
CERCLA:	Comprehensive Environmental Response, Compensation and Liability Act
EPA:	Environmental Protection Agency
EU:	European Union
f/cc:	Fibers per cubic centimeter
HEPA:	High Efficiency Particulate Air
HMIS:	Hazardous Materials Identification System
IARC:	International Agency for Research on Cancer
IATA:	International Air Transport Association
IMDG:	International Maritime Dangerous Goods Code
mg/m^3 :	Milligrams per cubic meter of air
mppcf:	Million particles per cubic meter
MSHA:	Mine Safety and Health Administration
NFPA:	National Fire Protection Association
NIOSH:	National Institute for Occupational Safety and Health
OSHA:	Occupational Safety and Health Administration
PEL:	Permissible Exposure Limit
PNOC:	Particulates Not Otherwise Classified
PNOR:	Particulates Not Otherwise Regulated
RCRA:	Resource Conservation and Recovery Act
RID:	Carriage of Dangerous Goods by Rail (International Regulation)
SARA:	Superfund Amendments and Reauthorization Act
Title III:	Emergency Planning and Community Right to Know Act
...Section 302:	Extremely Hazardous Substances
...Section 304:	Emergency Release
...Section 311:	MSDS/List of Chemicals
...Section 312:	Emergency and Hazardous Inventory
...Section 313:	Toxic Chemicals Release Reporting
STEL:	Short-Term Exposure Limit
TCLP:	Toxicity Characteristics Leaching Procedures (EPA)
TLV:	Threshold Limit Values (ACGIH)
TSCA:	Toxic Substance Control Act
WHMIS:	Workplace Hazardous Materials Information System (Canada)
29 CFR 1910.134 & 1926.103:	OSHA Respiratory Protection Standards
29 CFR 1910.1200 & 1926.59:	OSHA Hazard Communication Standards

Revision Summary:

1) MSDS revised in its entity with updated information.
2) Product "Therm-O-Flake Coating" added (see Section 1).

MSDS Prepared By: THERMAL CERAMICS ENVIRONMENTAL, HEALTH & SAFETY DEPARTMENT

DISCLAIMER

The information presented herein is presented in good faith and believed to be accurate as of the effective date of this Material Safety Data Sheet. Employers may use this MSDS to supplement other information gathered by them in their efforts to assure the health and safety of their employees and the proper use of the product. This summary of the relevant data reflects professional judgment; employers should note that information perceived to be less relevant has not been included in this MSDS. Therefore, given the summary nature of this document, Thermal Ceramics does not extend any warranty (expressed or implied), assume any responsibility, or make any representation regarding the completeness of this information or its suitability for the purposes envisioned by the user.

THIS PAGE INTENTIONALLY LEFT BLANK.

Y/DW-1661

Y-12

OAK RIDGE
Y-12
PLANT

LOCKHEED MARTIN

MECHANICAL PROPERTIES OF A LOW DENSITY CONCRETE FOR THE NEW ES-2 SHIPPING/STORAGE CONTAINER INSULATION, IMPACT MITIGATION MEDIA AND NEUTRON ABSORBER

Raymon E. Oakes, Jr.
Development Division
Oak Ridge Y-12 Plant

April 10, 1997

LOCKHEED MARTIN

Prepared by the
Oak Ridge Y-12 Plant
Oak Ridge, Tennessee 37831
managed by
LOCKHEED MARTIN ENERGY SYSTEMS, INC.,
for the
U.S. DEPARTMENT OF ENERGY
Under contract DE-AC05-84OR21400

MANAGED BY
LOCKHEED MARTIN ENERGY SYSTEMS, INC.
FOR THE UNITED STATES
DEPARTMENT OF ENERGY

UCN-13672 (2 11-97)

INTRODUCTION

The design, analysis and testing of new Shipping/Storage container design for enriched uranium, labeled ES-2, is underway at the Oak Ridge Y-12 Plant. To assure greater containment during an accidental impact or fire, a better insulating/energy-absorbing material is being sought for the outermost filler. A replacement for the presently used Celotex(R), a low density wood product, and plywood is desirable. A more fire retardant material with otherwise equal or better impact energy and neutron absorption is being sought.

Kaolite(R) 1600, a castable Portland cement-based product by Thermal Ceramics, contains vermiculite (expanded mica) instead of gravel or other high density aggregates. It is a low density, high temperature insulating material with non-recoverable impact energy absorption capabilities. The major components of Kaolite 1600 according to the manufacturers Product Information sheet are:

Alumina	Al_2O_3	9.6%
Silica	SiO_2	31.5%
Ferric Oxide	Fe_2O_3	6.7%
Titanium Oxide	TiO_2	1.0%
Calcium Oxide	CaO	29.8%
Magnesium Oxide	MgO	11.9%
Alkalies,as	Na_2O	1.8%

The purpose of this work is to quantify the mechanical properties of this product for a variety of thermal cures, test temperatures and neutron absorbing additives in a form useable for data input for finite element analysis of a variety of potential accident scenarios.

EXPERIMENTAL WORK

Test Types_ Four properties tests are conducted on the Kaolite 1600 material, Flexural Tensile Strength, Unconstrained Compressive Strength, Constrained Compressive Strength and Density.

All specimens are cast in containers the shape of the desired specimen. The vendors wet mix ratio of water/Kaolite, 36 quarts water to 50 lb Kaolite 1600 is used exclusively (473 cc water/315 g Kaolite used in laboratory size specimens). After mixing and packing in the molds, mild impacts from a plastic hammer against the mold sides are made until air bubbles ceased to rise to the top.

An electrically heated, liquid nitrogen cooled convection oven with +/-2EF control is used for elevated temperature cures and testing.

Tensile Strength_ Nine tensile strength values are obtained from cast and tested quarter-point, four-point bend specimens, 1 in wide x 1 in high x 8 in long. Each are tested over a 6-in support span and 3-in compression span, having the following very low outer fiber tensile strength and density:

average tensile strength = 19.4 psi, standard deviation 4.7 psi, and
average density = 21.2 lb/ft^3, standard deviation 1.0 lb/ft^3.

Low tensile strengths should not be detrimental in this application where the predominate failure mode is constrained compression.

Cure for the tensile specimens is 24 hr at 72EF plus 24 hr at 220EF, high enough to drive off free water but retain the water of hydration. Water of hydration is loosely bound to a number of cement components and can be driven off at elevated temperatures either by using elevated temperature curing or could occur in a hypothetical long term fire environment.

Unconstrained Compressive Strength_ Unconstrained or uniaxial compression test specimens are molded, cured and tested in 3-in diam polyurethane coated paper mailing tubes cut to 6-in heights with one end sealed. The cure is 24 hr at 72EF + 24 hr at 220EF. The tubes are thin and weak enough to add little strength to the specimen. Figure 1 shows the stress-strain curves and initial densities for three tests each at different test rates, including impact conditions (200 in/s). The increased strength values of the two highest test rates probably result from air entrapment in the cells. Also shown is the minor strength contribution of an empty paper mold.

Three deformation stages are associated with compression of low density materials containing voids (vermiculite is considered to be a void as well as any remaining air entrapments). First, the matrix surrounding the voids buckles, shown as the steep initial portion of the curves in Figure 1. The buckling stage is followed by a large strain region of compaction with minor stiffness increase. In the unconstrained compression tests large-scale shear failures occur across

the sample prior to full compaction. Specimen buckling and gross shear failures forced the tests to be terminated. Constrained compression tests will show the steeper rise of more densified material.

Figure 2 is the integrated area under each of the three stress-strain curves of Figure 1, the cumulative work or energy per unit volume absorbed by the material as a function of strain.

Constrained, Hydrostatic Compression Tests_ Constrained compression tests simulate the deformation mode of accident conditions in the material as it is used in the ES-2 container. The material is constrained by filling the outer stainless steel drum. In the event of an accident the inner container and its contents must remain intact. In the absence of vacant volume compaction or hydrostatic compression is the only deformation mode available. Laboratory simulations require compressing a specimen in a rigid, tight closed-ended cylinder with a tight fitting piston. A 20k pound testing machine loads the piston. The cylinders are four-inch ID thick-walled pipe and the specimens are cast, cured and tested in the cylinder. The specimen height is 4.5 in.

This test is used to provide primary input to the Finite Element Analysis as well as a relevant means to evaluate repeatability, cures , test temperature and additive effects on properties.

Note that percent compressive strain and percent volume change values are equivalent for all constrained compression tests.

Repeatability_The five stress-strain curves of Figure 3 represent material cured for 24 hr at 72EF + 24 hr at 220EF + 48 hr at 500EF. Each specimen is individually mixed and cast. Initial measured densities are shown for each specimen. Repeatability of density and the stress-strain curves are good for this type material. Note the three stages of deformation, cell buckling , densification and the beginning of compression of densified material are present. Load limitations of the test machine prevent reaching full compaction, a near vertical rise in the curve.

Cure Effects_Both cure time and temperature have major effects on the constrained compressive properties of Kaolite 1600, Figures 4 and 5. Cures at higher temperatures and/or longer cure times remove the most water as noted by decreasing density. Material strength increases in proportion to the degree of water loss. Cure time/temperature would be volume dependent so these cures may only represent the limiting cure for the much larger ES-2 container.

Test Temperature Effects_Decreasing test temperature in well cured specimens, Figures 6 and 7, lowers both strength and energy absorption only slightly.

Neutron Absorbing Additives_Residual water, free or as hydrates, is the primary neutron absorber in Kaolite. Adequate water or other neutron absorber must be present before, during and after all ES-2 container accident scenarios. The 500EF cure should eliminate most of the free water and part of the water of hydration, at least in specimen sized lots where equilibrium

temperatures are reached throughout the material. Higher temperatures are required to release all the water of hydration of two of the basic Portland cement components:

$$Fe_2O_3 \cdot xH_2O \quad (660\text{-}750^0F)$$
$$CaO_2 \cdot 8H_2O \quad (400^0F).$$

These hydrates during curing actually form very complex and unique hydrates. The disassociation temperatures for these complex hydrates are unique for each cement formulation and are unknown for Kaolite 1600. One requirement for the ES-2 container is survival in a fire environment of 1470EF for 0.5 hr without loss of seal of the inner container. Certainly loss of criticality protection must be assured in the same scenario.

Measured Kaolite densities cast and cured in ES-2 containers is about 29 lb/ft^3 when cured at 200EF for 48 hr. followed by 500EF for 48 hr. This is much higher than 21-22 lb/ft^3 in similarly cured laboratory samples, indicating either considerable residual water is retained in the ES-2 containers or large differences in compaction exist or both. Under long term fire conditions the amount of residual water and its distribution throughout the container is unknown.

Boron is a nonvolatile neutron absorber available in numerous chemical forms. Two forms, borax ($Na_2B_4O_7.10H_2O$) and boron carbide (B_4C), are investigated as potential neutron absorbers. The required amount according to criticality calculations is 2.5% natural boron. Weight percentages of 11.3% borax or 3.0% boron carbide meet this requirement. Note that natural boron implies the isotopic ratio found in nature. Not all boron in the market meets this criteria.

Figure 8 and 9 show that borax degrades both the strength and energy absorption an unacceptable amount. Due to the high molecular weight of borax the amount of material needed to provide adequate boron is excessive.

Unlike borax, boron carbide is predominately boron and Figures 8 and 9 show that the needed amount and even double the needed amount does not degrade the Kaolite and would be an acceptable, nonvolatile neutron absorbing additive.

Bibliography

(1) *Handbook of Chemistry and Physics*, 60th Edition, Robert C. Weast, ed., CRC Press, Inc., Boca Raton, Florida 33431.

(2) *Concrete Admixtures Handbook, Properties, Science , and Technology*, V. S. Ramachandran, ed., Noyes Publications, Park Ridge, New Jersey.

Ka16fig1.xlc

Figure 1_Kaolite 1600 Compressive Stress-Strain vs Strain Rate

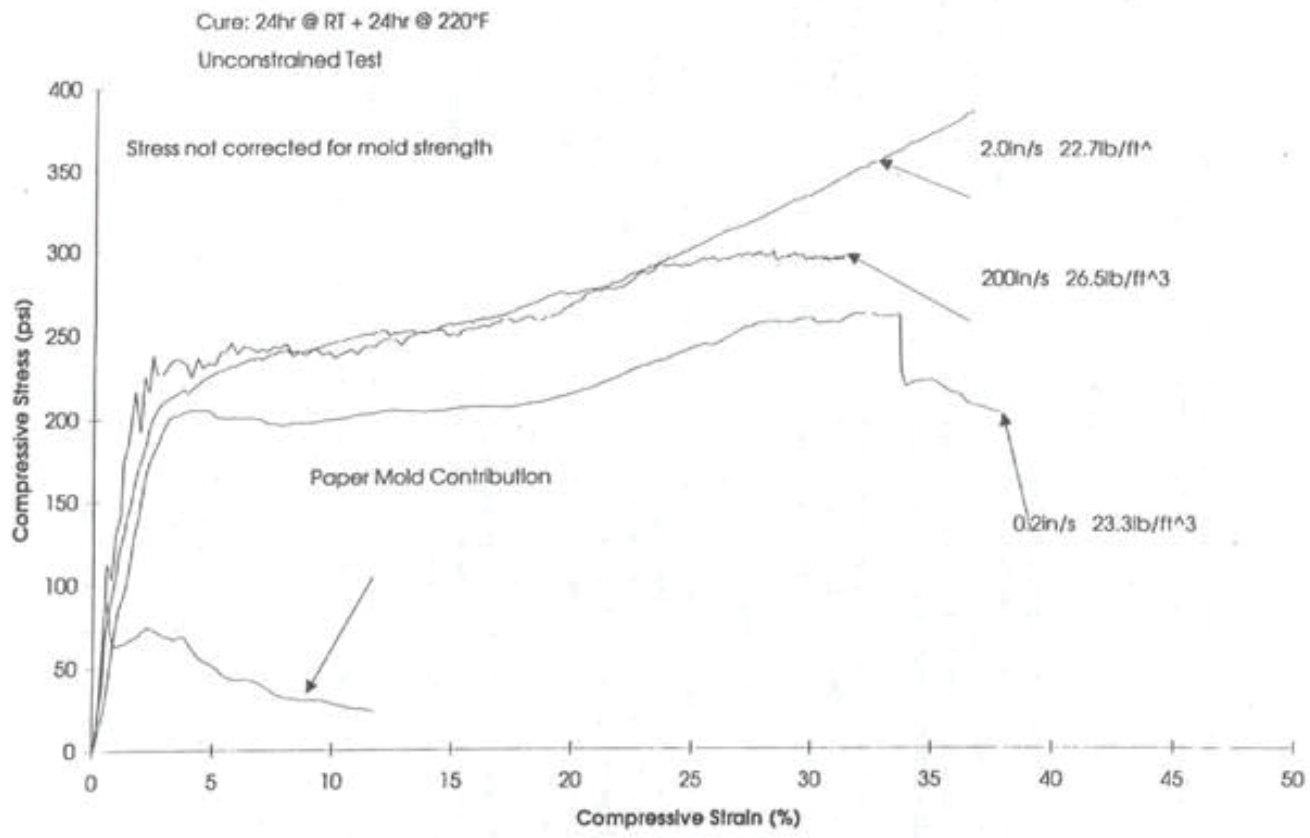

Ka16fig2.xlc

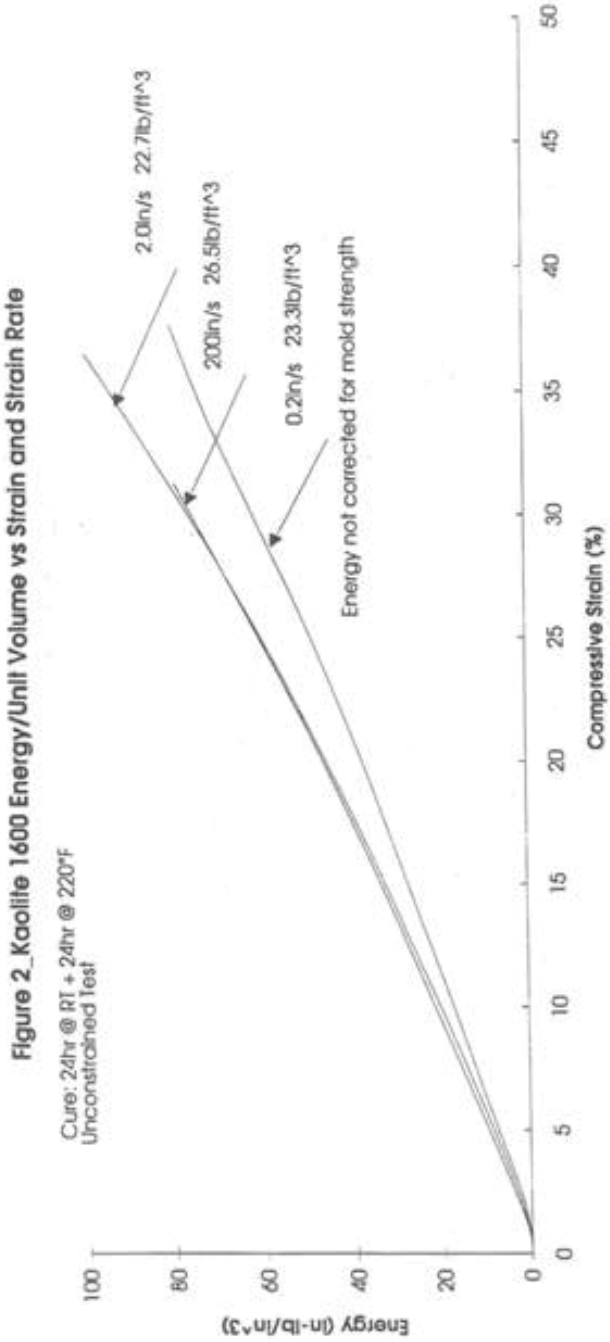

Ka16fig3.xlc

Figure 3_Kaolite 1600 Stress-Strain Curves, Repeatability Tests

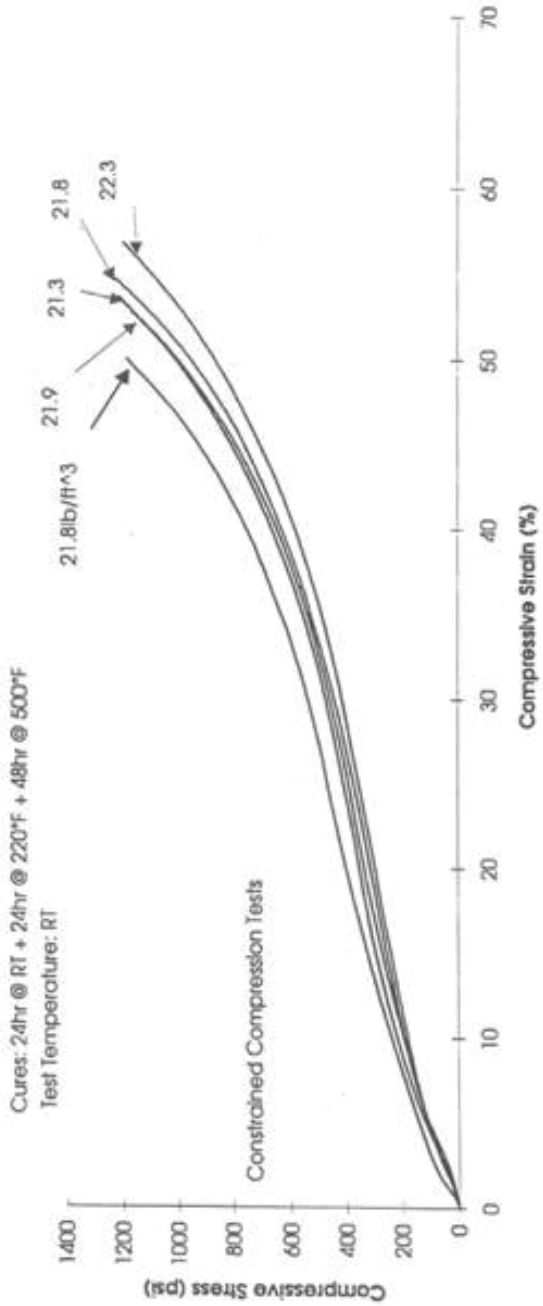

Figure 4_Kaolite 1600 Stress-Strain Curves for Different Cures

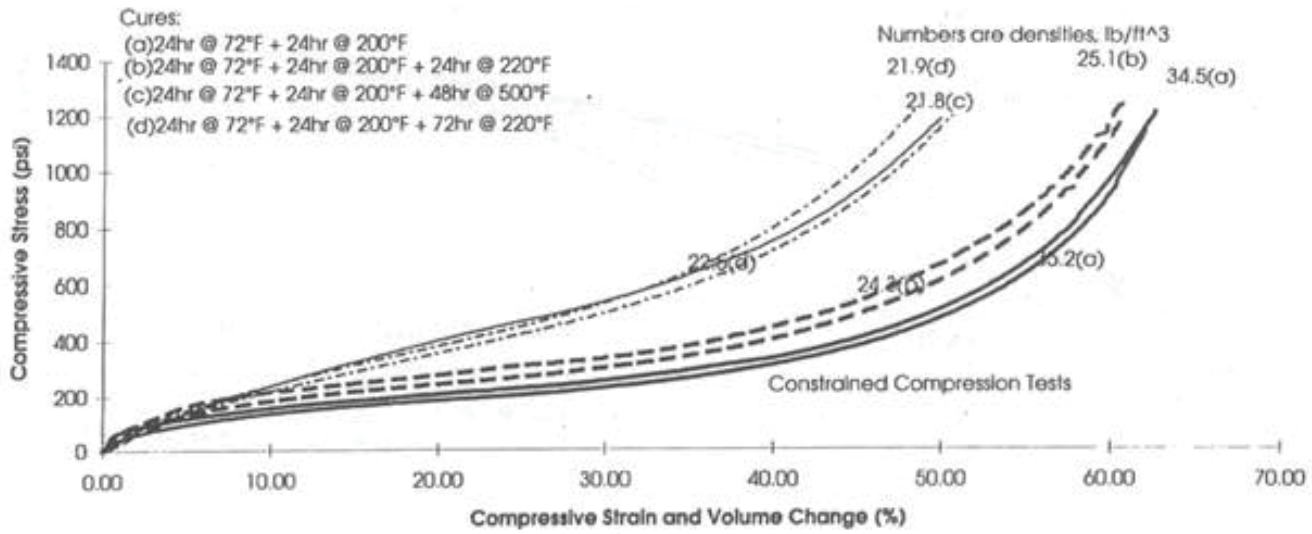

Ka16fig5.xls

Figure 5_Kaolite 1600 Energy-Strain Curves for Different Cures

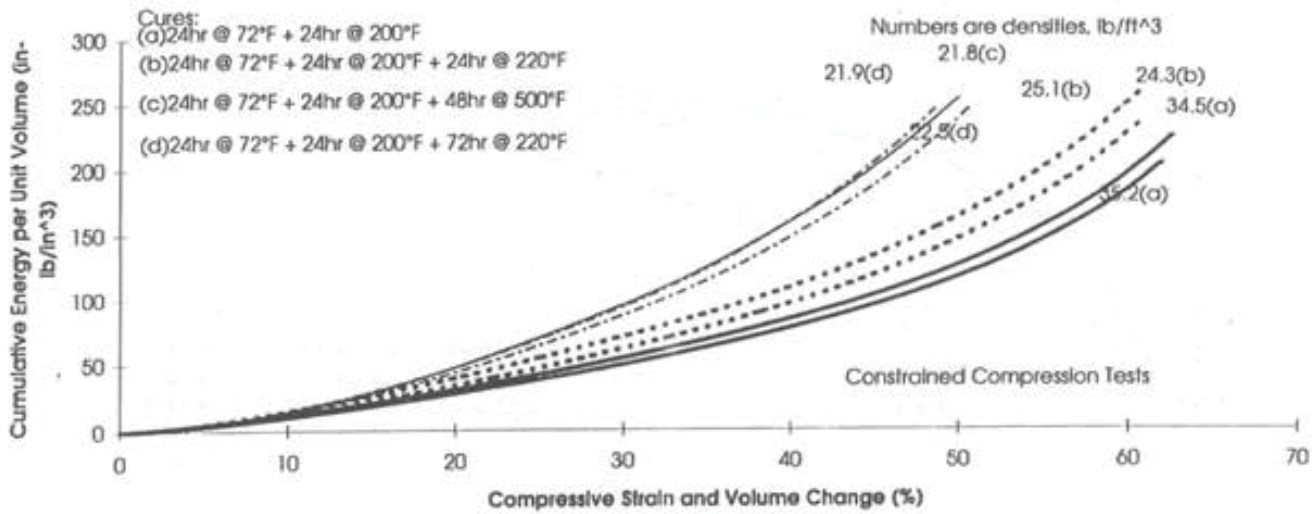

Ka1fig6.xls

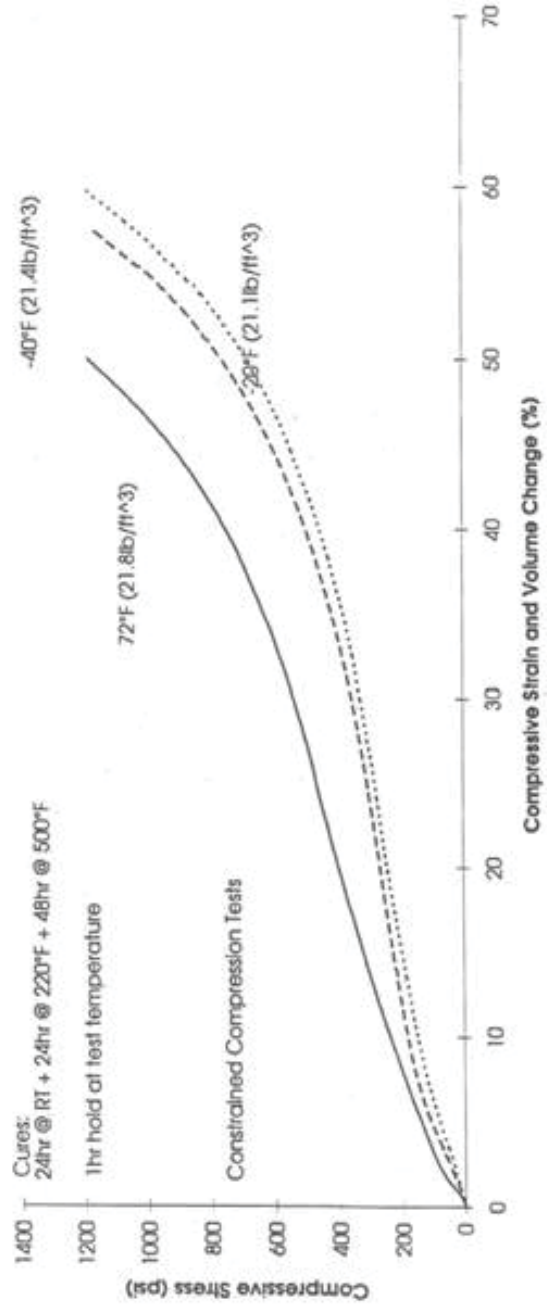
Figure 6_Kaolite 1600 Stress-Strain Curves for Different Test Temperatures
Cures:
24hr @ RT + 24hr @ 220°F + 48hr @ 500°F
1hr hold at test temperature
Constrained Compression Tests
-40°F (21.4lb/ft^3)
72°F (21.8lb/ft^3)
28°F (21.1lb/ft^3)
Compressive Stress (psi)
1400
1200
1000
800
600
400
200
0
0
10
20
30
40
50
60
70
Compressive Strain and Volume Change (%)

Figure 7_Kaolite 1600 Energy-Strain Curves for Different Test Temperatures

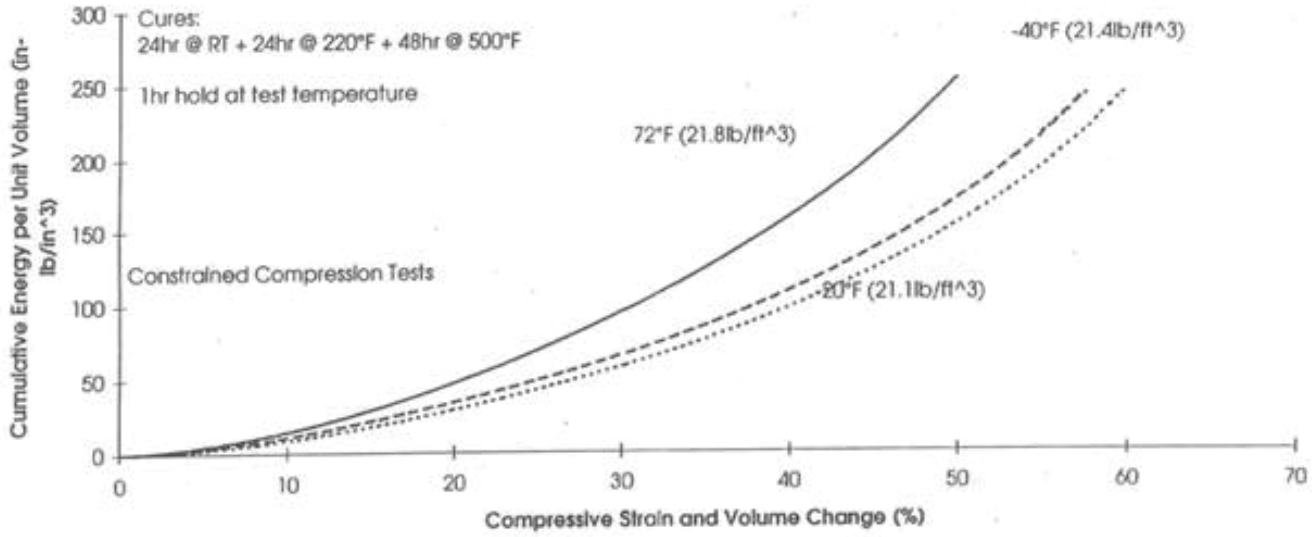

ORNL-TM-2003/49

Thermal Conductivity Measurements of Kaolite

Hsin Wang

Prepared by the
Thermophysical Properties User Center
High Temperature Material Laboratory
Metal and Ceramics Division

Oak Ridge National Laboartory
Oak Ridge, TN 37831-6064
Managed by UT-BATTELLE LLC.
For the
U.S. DEPARTMENT OF ENERGY
Under contract DE-AC05-00OR22725

Introduction

Testing was performed to determine the thermal conductivity of Kaolite 1600, which primarily consists of Portland cement and vermiculite. The material was made by Thermal Ceramics for refractory applications. Its combination of light weight, low density, low cost, and noncombustibility made it an attractive alternative to the materials currently used in ES-2 container for radioactive materials.

Mechanical properties and energy absorption tests of the Kaolite have been conducted at the Y-12 complex. Heat transfer is also an important factor for the application of the material. The Kaolite samples are porous and trap moisture after extended storage. Thermal conductivity changes as a function of moisture content below 100° C. Thermal conductivity of the Kaolite at high temperatures (up to 700° C) are not available in the literature. There are no standard thermal conductivity values for Kaolite because each sample is somewhat different. Therefore, it is necessary to measure thermal conductivity of each type of Kaolite. Thermal conductivity measurements will help the modeling and calculation of temperatures of the ES-2 containers. This report focuses on the thermal conductivity testing effort at ORNL.

Experimental

Thermal conductivity of the Kaolite was measured using a Hot Disk Thermal Constants Analyzer. A picture of the system is shown in Figure 1. A box furnace, with

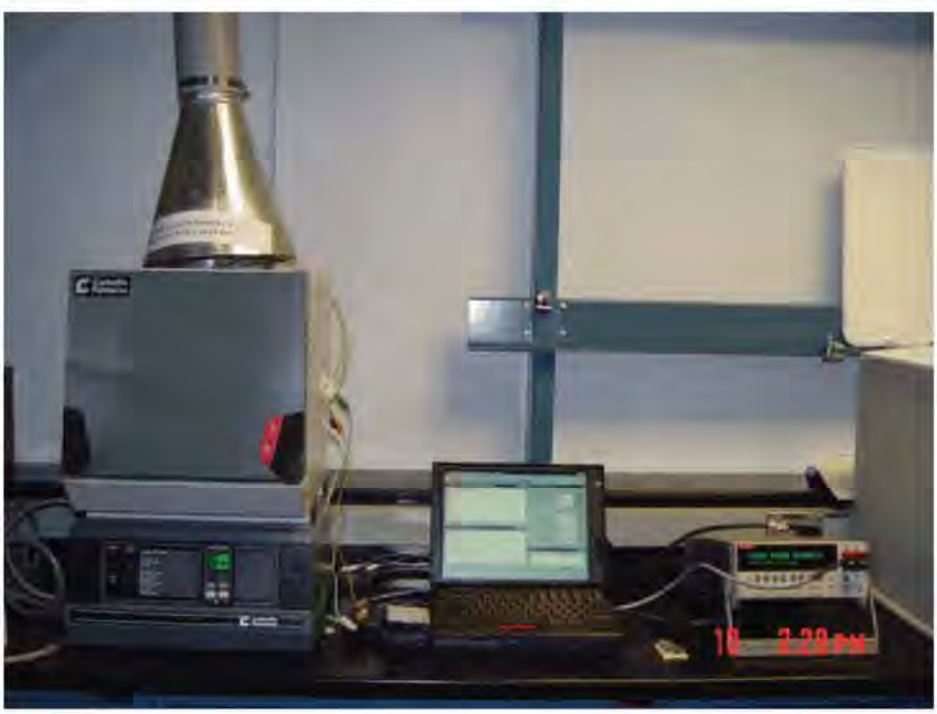

Figure 1. Experimental set up for thermal conductivity measurements.

maximum temperature of 1050° C, was used for high temperature tests. The Hot Disk sensor is a flat, thin, double-spiral nickel wire sandwiched between two mica sheets. The sensor is placed between two identical hockey-puck Kaolite samples (2" in diameter and 1" thick). During the measurement, the mica sensor acts as both a heater and a temperature sensor.

A typical test for Kaolite uses 0.05-watt constant-power heating for 80 seconds. The sensor temperature is recorded as a function of time. Thermal conductivity is then calculated directly from the experimental data. Detailed theory and experimental descriptions of the Hot Disk technique can be found in the references [1-3].

In order to perform high temperature measurements, special contacts were made from stainless steel. Four high temperature wires with insulation were connected to the mica sensor with the wires being fed through an opening on top of the furnace. A rectangular mica sheet with four screw holes was used as the support for the sensors. The four wires were connected to the contacts as shown in Figure 2. The mica sensor can be delaminated due to high temperature exposure, therefore, the sensor has to be replaced after a 600° C measurement. A heavy alloy block was placed on top of the sample to ensure good contact at the interface.

Figure 2. Kaolite samples and mica sensor used for high temperature testing.

Results and Discussion:

Thermal conductivities of six Kaolite samples were tested using the mica sensor. Since high temperature tests can destroy the sensor and only one set of samples was tested in the furnace, all the samples were tested at room temperature and then at 100° C. but only one sample was tested up to 600° C.

At room temperature and 100° C, the thermal conductivity values of the 6 Kaolite samples are similar, although the densities of the samples are grouped in 3 pairs at high, medium and low. The test results are shown in Table 1 for room temperature and Table 2 for 100° C. During the tests the humidity was not controlled in the laboratory or in the furnace. The samples did not have the same thermal history. For example, one set of sample was heated up from room temperature to 100° C, but the other 5 sets of samples had to wait outside the furnace. In addition, the local density of the sampling volume, i.e. ¾" diameter semi sphere, can also vary due the existence of large pores and

Table 1. Thermal conductivity of six Kaolite at 20° C (unit: W/mK)

Density (lb/ft3)	H 23.690	H 23.541	M 22.055	M 22.011	L 20.407	L 20.281
Test 1	0.188	0.183	0.152	0.198	0.165	0.172
Test 2	0.188	0.185	0.157	0.182	0.168	0.192
Test 3	0.191	0.181	0.167	0.198	0.169	0.181
Average	**0.189**	**0.183**	**0.158**	**0.192**	**0.167**	**0.181**
	High Density	**0.186**	**Medium Density**	**0.176**	**Low Density**	**0.175**

Table 2. Thermal conductivity of six Kaolite at 100° C (unit: W/mK)

Density ρ (lb/ft3)	H 23.690	H 23.541	M 22.055	M 22.011	L 20.407	L 20.281
Test 1	0.165	0.172	0.157	0.179	0.163	0.177
Test 2	0.152	0.172	0.157	0.191	0.163	0.179
Test 3	0.161	0.179	0.156	0.194	0.152	0.178
Average	**0.159**	**0.174**	**0.156**	**0.188**	**0.159**	**0.178**
	High Density	**0.166**	**Medium Density**	**0.172**	**Low Density**	**0.168**

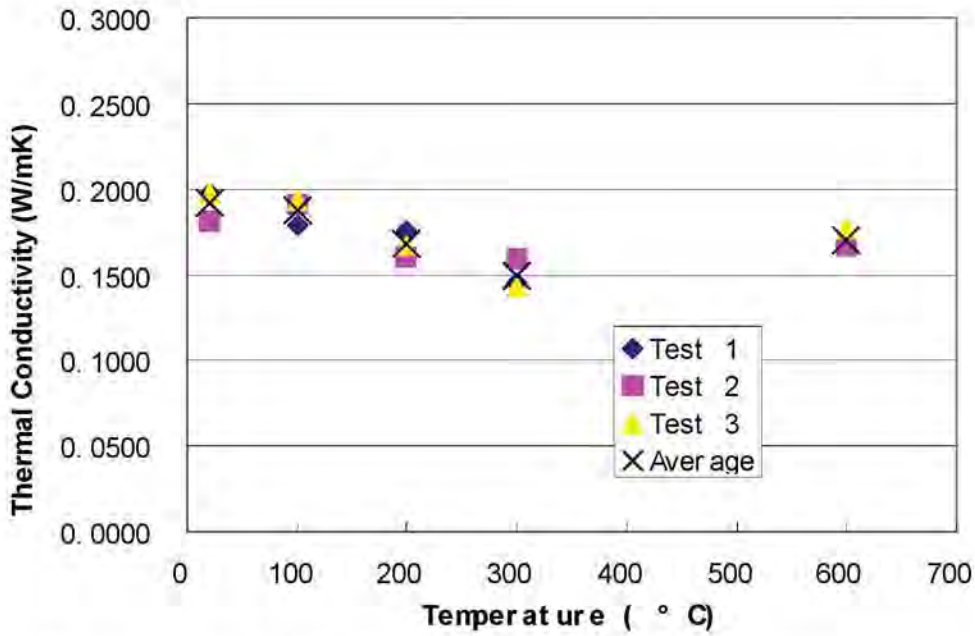

Figure 3. Thermal conductivity of Kaolite from room temperature to 600° C

Table 3. High Temperature Thermal Conductivity of Kaolite (unit: W/mK)

No. 323011258	Test 1	Test 2	Test 3	Average
20	0.1978	0.1815	0.1976	0.1923
100	0.1792	0.1913	0.1936	0.1880
200	0.1758	0.1601	0.1673	0.1677
300	0.1452	0.1592	0.1427	0.1490
600	0.1676	0.1665	0.1771	0.1704

density variation. Thermal conductivity results showed some scatter at these two temperatures.

The high temperature tests were performed on one medium density Kaolite sample. The thermal conductivity data are shown in Table 3. As shown in Figure 3, thermal conductivity values decreased as a function of temperature up to 300° C. This trend is consistent with ceramics and other insulating materials. At 600° C, thermal conductivity started to increase. This is also consistent with the fact that thermal radiation effect takes place in this temperature range. As temperature goes up, thermal conductivity of most insulating materials also goes up.

References:

[1] S.E. Gustafsson, E. Karawacki and M.N., Khan, *J. Phys.D.: Appl. Phys*, **1979**, 12, 1411.
[2] S.E. Gustafsson, *Rev. Sci. Instrum*., **1991**, 62, 797
[3] V. Bohac, M.K. Gustavsson, L. Kubicar and S.E. Gustafsson, *Rev. Sci. Instrum*., **2000**, 71, 2452

Distribution List:

Name	Bldg.	Mail Stop	#
C. N. Heatherly	9113	8206	1
J. L. Heck	9111	8201	1
S. T. Holder	9113	8206	1
G. A. Byington	9111	8201	1
M. R. Feldman	9113	8206	1
M. L. Goins	9112	8201	1
S. E. McClanahan	9113	8206	2
J.C. Walls	9201-2	8073	1
K. H. Luk	9201-2	8073	1
K. D. Handy	9201-2	8073	1
J. C. Anderson	9113	8206	1
J. H. Doyle	9113	8206	1
Jacob Y. Neal	9201-2	8073	1

Y/DW-1890

BWXT Y-12
A BWXT/Bechtel Enterprise

Water Content and Temperature-Dependent Impact Properties of an Inorganic Cast Refractory Material

B. F. Smith
Technology Development

G. A. Byington
Mechanical, Manufacturing, and
Specialty Engineering

February 14, 2003

LIMITED DISTRIBUTION

Y-12
NATIONAL
SECURITY
COMPLEX

MANAGED BY
BWXT Y-12, L.L.C.
FOR THE UNITED STATES
DEPARTMENT OF ENERGY

UCN-13672 (10-00)

DISCLAIMER

This report was prepared as an account of work sponsored by an agency of the United States Government. Neither the United States Government nor any agency thereof, nor any of their employees, makes any warranty, express or implied, or assumes any legal liability or responsibility for the accuracy, completeness, or usefulness of any information, apparatus, product, or process disclosed, or represents that its use would not infringe privately owned rights. Reference herein to any specific commercial product, process, or service by trade name, trademark, manufacturer, or otherwise, does not necessarily constitute or imply its endorsement, recommendation, or favoring by the United States Government or any agency thereof. The views and opinions of authors expressed herein do not necessarily state or reflect those of the United States Government or any agency thereof.

Y/DW-1890

WATER CONTENT AND TEMPERATURE-DEPENDENT IMPACT PROPERTIES OF AN INORGANIC CAST REFRACTORY MATERIAL

B. F. Smith
Technology Development

G. A. Byington
Mechanical, Manufacturing, and
Specialty Engineering

Date of Issue: February 14, 2003

LIMITED DISTRIBUTION

Prepared by the
Y-12 National Security Complex
P.O. Box 2009
Oak Ridge, Tennessee, 37831-8169
Managed by BWXT Y-12, L.L.C.
for the
U.S. DEPARTMENT OF ENERGY
under contract DE-AC05-00OR22800

THIS PAGE INTENTIONALLY LEFT BLANK.

CONTENTS

FIGURES iv

TABLES iv

INTRODUCTION 1

EXPERIMENTAL PROCEDURE 2
  IMPACT TESTING 2
  DEHYDRATION TESTING 4

RESULTS 4
  IMPACT TESTING 4
  DEHYDRATION TESTING 9

DISCUSSION 10
  IMPACT TESTING 10
  DEHYDRATION TESTING 11

REFERENCES 11

FIGURES

Figure Page

1. Impact testing apparatus 3
2. Average stress-strain curves for Kaolite specimens tested at 100°F 5
3. Average stress-strain curves for Kaolite specimens tested at –40°F 6
4. Average stress-strain curves, upper and lower bounding curves, and average of upper and lower bounding curves 7
5. Upper and lower bounding curves, average of upper and lower bounding curves, all extrapolated to 100% compressive strain 8

TABLES

Table Page

1. Test conditions for Kaolite specimens tested at 100°F 3
2. Test conditions for Kaolite specimens tested at –40°F 4
3. Coefficients to upper and lower bounding equations 9
4. High-density dehydration data 9
5. Medium-density dehydration data 10
6. Low-density dehydration data 10

INTRODUCTION

Impact-absorbing media used in radioactive material packaging systems have historically left much to be desired. Common materials included woods, papers, cardboards, foams, and other hydrocarbons. While relatively easy to install, these types of materials generate toxic gases, are flammable, and are prone to rupture the container in an overheating scenario.[1]

Kaolite 1600 primarily consists of portland cement and vermiculite.[2] This ceramic was originally intended for use in refractory applications by its manufacturer, Thermal Ceramics. Its combination of light weight, low density, low cost, and noncombustibility made Kaolite an attractive alternative to the materials mentioned above for use in shipping packages.[3] A variety of mechanical property tests were performed in the past on Kaolite specimens to gage its selection and effectiveness as an impact absorber in the ES-2 shipping package container. The mechanical properties included tensile strength, unconstrained compressive strength, and constrained compressive strength. Since the ES-2 will primarily contain radioactive materials, the neutron-absorbing properties of Kaolite are important. Since boron is a good neutron absorber, the addition of boron-containing compounds to Kaolite was proposed, but their effect on the mechanical properties of Kaolite had to be measured. For this reason, the strength and energy absorption of Kaolite that contained borax and boron carbide were also measured. If boron-containing compounds are not mixed with standard Kaolite, the only compound present that can absorb neutrons is the water of hydration.[4]

The ES-2 shipping package design was modified and renamed the ES-2100. During the production of 100 ES-2100 shipping containers, 280 insulation samples were taken. An insulation sample was taken for each 50-lb bag of material mixed. These constrained compressive production-run test samples were cast approximately 4 in. tall in a 4-in. schedule 40 steel pipe 6.5 in. long.

All of the samples were statically evaluated on the basis of their density. The upper and lower densities were statically rejected based upon the normal distribution probability of 90%, which rejected 11 high- and 13 low-density specimens. Three small groups' high, middle, and low densities containing eight samples each were made from the remaining samples. Each of the density groups was divided into three testing sets. Two of the test sets of four specimens were used for temperature-dependent constrained compressive testing and for dehydration testing. The third sample set of two specimens was used for temperature-dependent thermal conductivity testing performed at Oak Ridge National Laboratory.

This work follows up on the mechanical property testing previously performed on Kaolite but concentrates on constrained compression testing and measuring the water of hydration and latent water reabsorbed from air. No further tensile tests or unconstrained compression tests were performed. No investigations into the effects of boron-containing compounds were done, either. Previous mechanical testing was performed on specimens that were mixed in very small batches in a laboratory environment. The main purpose of this work is to ensure that Kaolite mixed according to Manufacturing Process Specification No. Y/EN-5984[5] in a production environment is as strong as that mixed in a lab.

EXPERIMENTAL PROCEDURE

It was determined that 24 Kaolite 1600 specimens would be impact tested; 12 tested at 100°F and 12 tested at –40°F. Each set would contain four each of high-, medium-, and low-density specimens. All specimens would be subsequently heated to 1600°F to drive off the water of hydration and the latent water reabsorbed from air. The difference between the initial weight and the final weight would be the water of hydration and reabsorbed from air weight. Densities were calculated for each specimen and compared to the manufacturer's calculated values.

IMPACT TESTING

Each specimen consisted of a Kaolite plug, measuring 4-in. in diameter by 4 in. tall, inside a 6.5-in.-long, 4-in. schedule 40 steel pipe. One end of the plug was flush with the end of the pipe. The steel pipe of each specimen was engraved with its mix control number (MCN). A 4-in. schedule 40 pipe was specified in order to withstand the anticipated pressure generated during a constrained compression test. All impact testing was to be performed at the fastest readily obtainable speed. The machine that met this requirement was a 20,000-lb_f-capacity servohydraulic load frame with an actuator (hydraulic piston) that can reach 200 in./s. Compression platens of 3⅞-in. diameter were used. Test fixtures were designed and fabricated. The standard load cell used during slow-speed tests could not be used with high-speed tests, so a Kistler quartz force transducer was used in its place. The test fixtures were designed such that each specimen would be compressed to 50% strain. Typically, the deformation of a specimen is measured with an external sensor such as an extensometer, strain gage, or external linear variable differential transformer (LVDT). Measurements of extension or compression can be taken using the LVDT that is inside the hydraulic actuator, but this is not usually done since it introduces the overall deflection of the load frame into the deflection reading of the specimen. The maximum deflection of the load frame is about 0.040 in., which is negligible compared to the 2-in. deflection of the specimen. Thus, the LVDT internal to the actuator would be used to measure the compression of the specimen. Figure 1 shows that several extenders had to be used to allow for the height of the environmental chamber in which all tests were performed. Calculations showed that the extenders would buckle under a load of approximately 74,000 lb_f, which is significantly more than the 20,000-lb_f maximum capacity of the load frame. Since testing would be done at elevated and lowered temperatures, each specimen would need to soak until the interior of the specimen reached its test temperature. Rough calculations showed that a soak time of 39 h would get the specimen to within 10% of the test temperature. All specimens were soaked significantly longer than 39 h. The 100°F specimens were soaked for approximately 100 h, and the –40°F specimens were soaked for approximately 300 h. Tables 1 and 2 summarize these testing conditions.

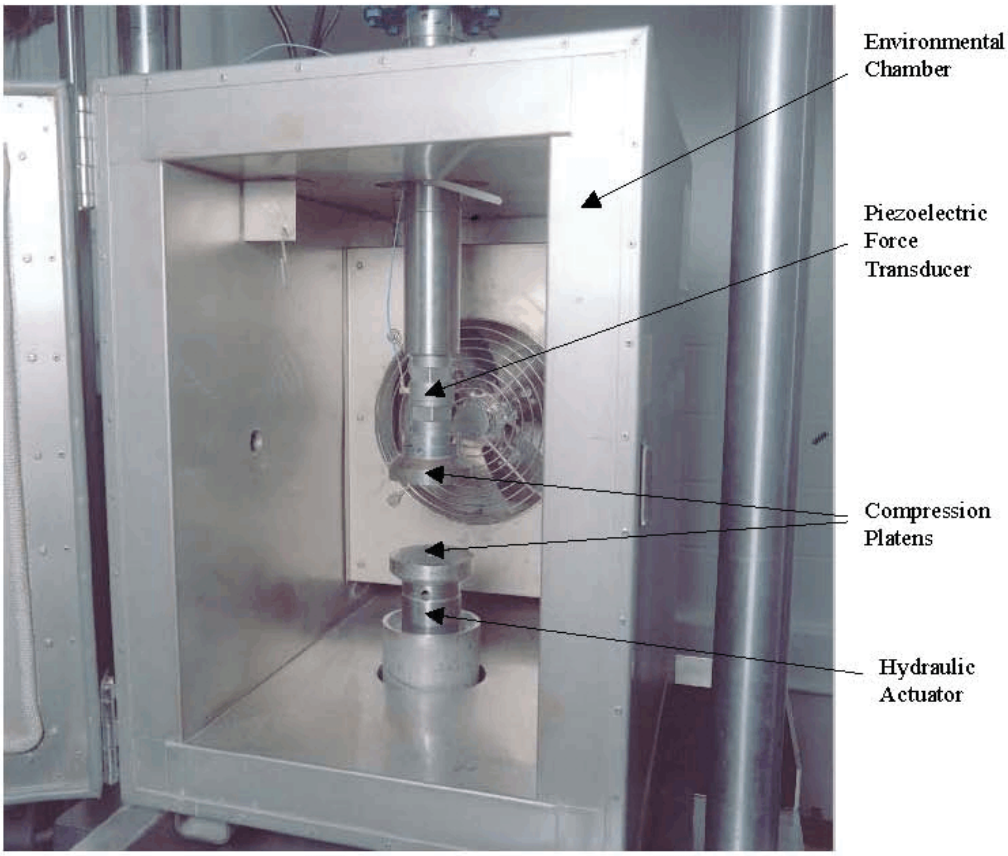

Fig. 1. Impact testing apparatus.

Table 1. Test conditions for Kaolite specimens tested at 100°F

MCNID	Heating time (h)	Density group	Documented density (lb/ft^3)	Density gain[a] (lb/ft^3)	Density before heating (lb/ft^3)	Heating density change (lb/ft^3)	Density after heating (lb/ft^3)	Average test velocity (in./s)
411011216	101.25	Low	20.27	1.43	21.70	–0.15	21.55	192.9
402011246	120.42	Low	20.35	1.82	22.17	–0.20	21.97	190.6
419011046	93.92	Low	20.42	2.74	23.16	–0.08	23.08	189.7
406011219	98.80	Low	20.47	3.07	23.54	–0.06	23.48	194.6
222011053	100.85	Mid	21.98	1.46	23.44	–0.17	23.27	191.7
309011000	102.25	Mid	22.06	1.04	23.10	–0.16	22.94	192.3
406011232	93.67	Mid	22.06	2.44	24.50	–0.09	24.41	192.6
425011101	96.90	Mid	22.06	2.34	24.40	–0.09	24.31	195.3
316011054	94.40	High	23.49	-0.78	22.71	–0.07	22.64	186.8
425011046	93.00	High	23.53	3.44	26.97	–0.10	26.87	183.5
118010847	101.65	High	23.68	1.48	25.16	–0.16	25.00	185.1
425011329	53.72	High	23.71	3.17	26.88	–0.25	26.63	

[a] It is assumed that the change in density is latent water.

Table 2. Test conditions for Kaolite specimens tested at –40°F

MCNID	Cooling time (h)	Density group	Documented density (lb/ft^3)	Density gain[a] (lb/ft^3)	Density before cooling (lb/ft^3)	Cooling density change (lb/ft^3)	Density after cooling (lb/ft^3)	Average test velocity (in./s)
508010845	338.48	Low	20.28	2.64	22.92	0.08	23.00	192.3
316011150	362.03	Low	20.40	1.71	22.11	0.09	22.20	187.7
425010912	340.38	Low	20.41	2.33	22.74	0.09	22.83	191.7
508010830	364.87	Low	20.47	2.65	23.12	0.11	23.23	192.4
326011220	337.45	Mid	21.99	1.78	23.77	0.11	23.88	185.6
301010815	361.40	Mid	22.06	2.20	24.26	0.10	24.36	188.7
326011239	339.62	Mid	22.06	2.20	24.26	0.10	24.36	185.8
426011155	364.23	Mid	22.06	1.88	23.94	0.09	24.03	185.7
425011235	339.02	High	23.53	3.16	26.69	0.11	26.80	182.0
425010941	363.58	High	23.53	2.71	26.24	0.07	26.31	183.7
323010953	360.85	High	23.56	1.93	25.49	0.08	25.57	174.6
425011007	337.13	High	23.71	3.57	27.28	0.09	27.37	189.9

[a] It is assumed that the change in density is latent water.

DEHYDRATION TESTING

The water content of Kaolite determines the neutron-absorbing properties. Properly cured Kaolite should have very little latent water, but may have a significant amount of water of hydration. This water of hydration can be driven off by heating the specimens above a critical temperature, 1600°F. Each specimen was heated at this temperature until consecutive measurements differed by <0.1%. Each plug was removed from its metal sleeve using a larger, 200,000-lb_f capacity load frame. This load frame was used instead of the 20,000-lb_f capacity machine since its larger actuator area and load cell area simplified setting up fixturing. During heating, each compacted Kaolite plug was placed into an Inconel crucible, which was placed in a small lab furnace. A metal crucible had to be used because ceramic ones would not withstand the thermal shock associated with repeated removal from the furnace into cool, room-temperature air.

RESULTS

IMPACT TESTING

Figure 2 shows average compressive stress-strain curves for specimens tested at 100°F. Each curve is the average of the specimens in a density group, high, medium, or low. Using the average density group values dampened some of the noise in the gathered data. The average density of the high-density group was documented as 23.6 lb/ft^3. The average density of the medium density group was documented as 22.0 lb/ft^3. The average density of the low-density group was documented as 20.4 lb/ft^3. These curves were generated by averaging the stresses at discrete strain points at intervals of 1% strain. Figure 3 shows the average compressive stress-strain curves for specimens tested at –40°F. Figure 4 repeats the average compressive stress-strain curves shown in Figs. 2 and 3 and adds to them upper, lower, and average bounding curves.

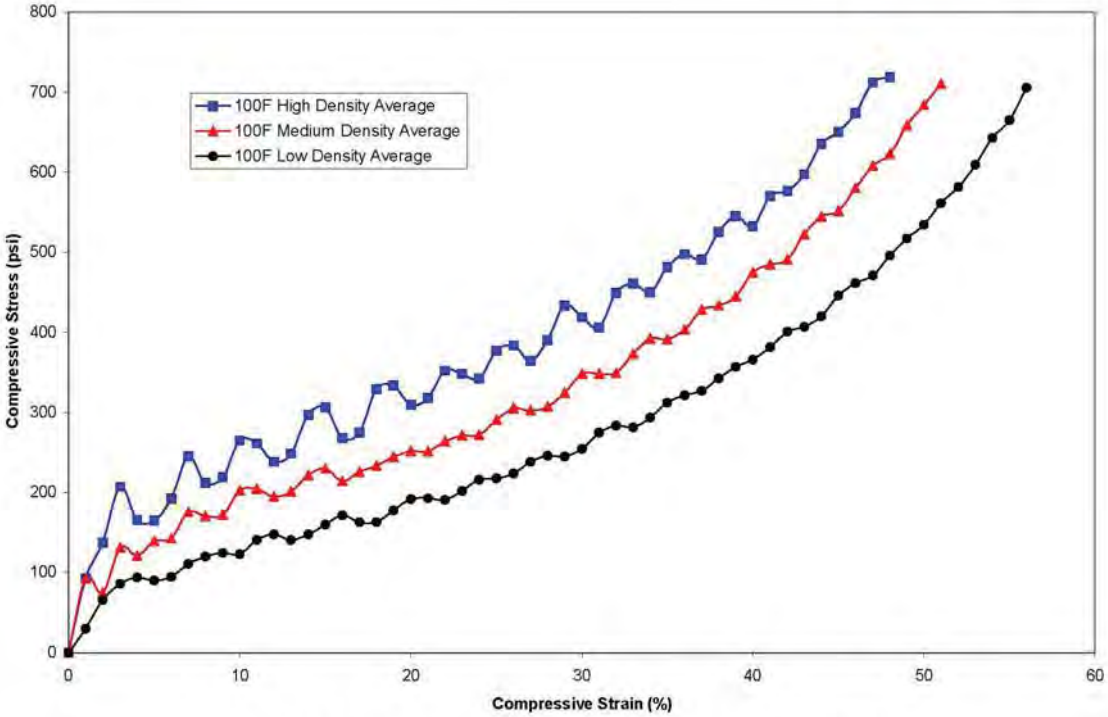

Fig. 2. Average stress-strain curves for Kaolite specimens tested at 100°F.

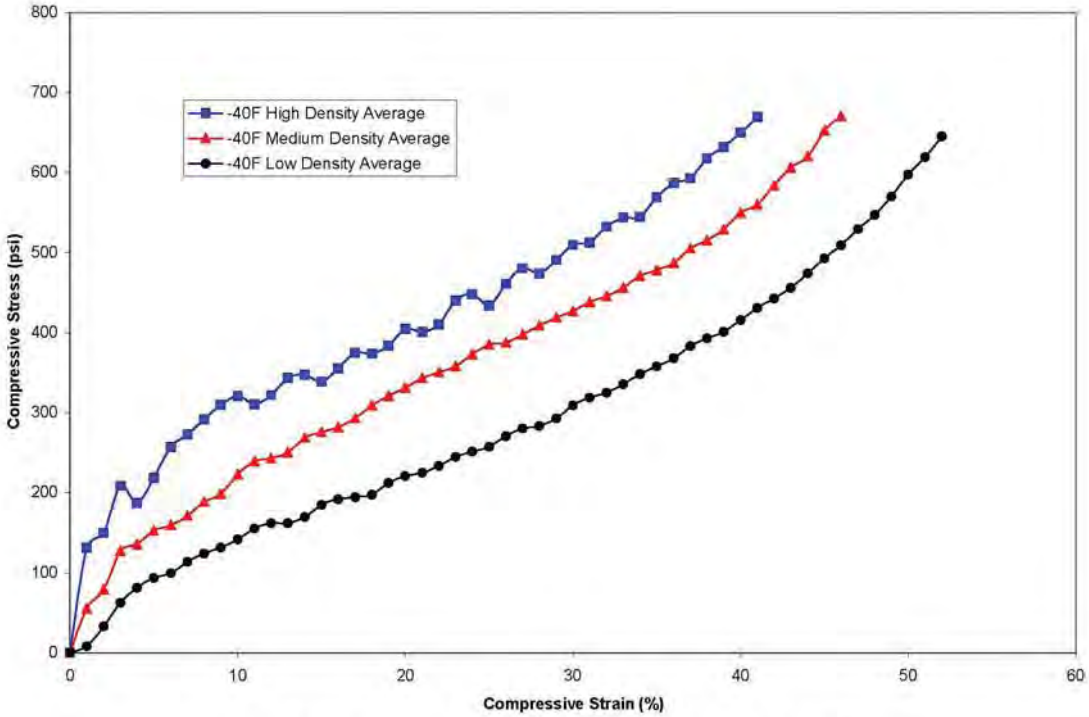

Fig. 3. Average stress-strain curves for Kaolite specimens tested at -40°F.

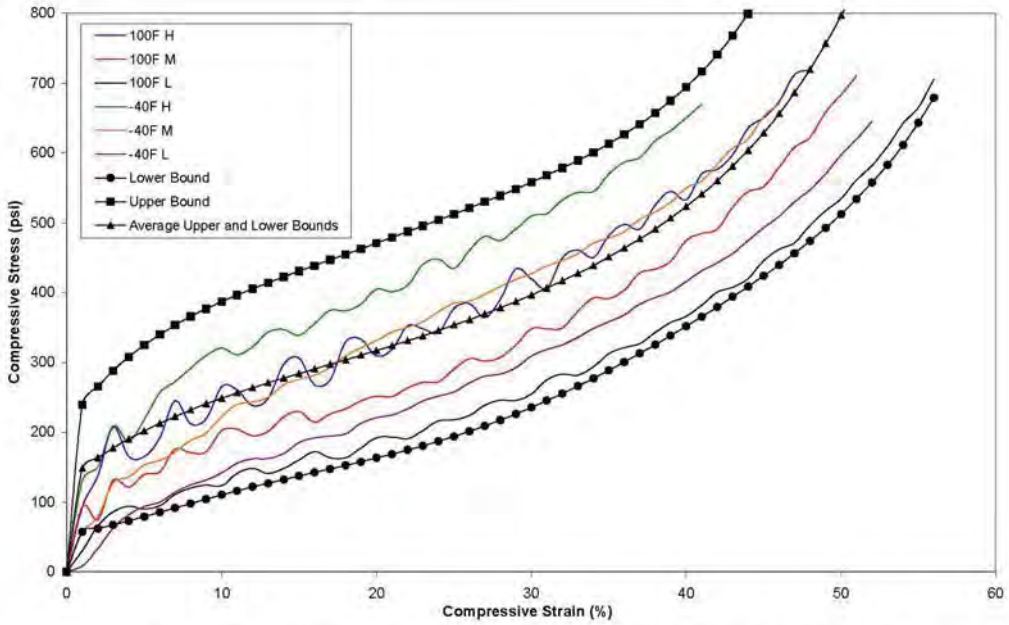

Fig. 4. Average stress-strain curves, upper and lower bounding curves, and average of upper and lower bounding curves.

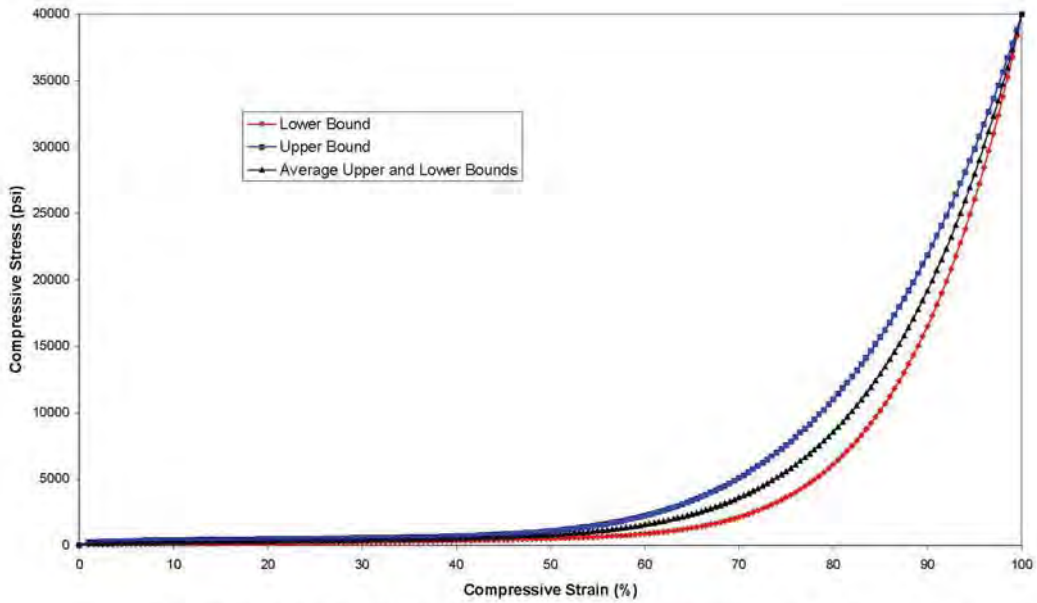

Fig. 5. Upper and lower bounding curves, average of upper and lower bounding curves, all extrapolated to 100% compressive strain.

The bounding curves were generated at the extreme noise peaks. The strongest material created the upper bound, and it was the –40°F high-density group. The weakest material generated the lower bounding curve, and it was the 100°F low-density group. Table 3 shows the coefficients for the equations of the bounding curves between 1 and 100% strain. A value of 40,000 psi at 100% strain was used with the collected data to create a smooth curve beyond the tested values for computer drop test simulations. A straight line is assumed to be from zero stress and strain to the curve value at 1% strain.

Table 3. Coefficients to upper and lower bounding equations

$\sigma = a + b\varepsilon + c\varepsilon^2 + d\varepsilon^3 + e\varepsilon^4 + f\varepsilon^5 + g\varepsilon^6$							
	a	**b**	**c**	**d**	**e**	**f**	**g**
Upper	209.2	31.96	–2.244	0.1050	–0.00253	2.78×10^{-5}	7.06×10^{-8}
Average	131.5	17.29	–0.7443	0.01878	4.31×10^{-5}	-8.36×10^{-6}	1.06×10^{-7}
Lower	53.86	2.613	0.7550	–0.06748	0.002618	-4.45×10^{-5}	2.83×10^{-7}

DEHYDRATION TESTING

Tables 4, 5, and 6 show the initial weight of each specimen and total water loss after heating at 1600°F. The percent of the initial weight of water is given in the third column. No data are included for MCNIDs 0425011007 and 0425011329 since their initial weights were mistakenly not measured. Without the initial weight, it is impossible to know how much water was lost through heating.

Table 4. High-density dehydration data

MCNID	Initial weight (lb)	Water loss (lb)	Initial weight (%)	Documented density (lb/ft^3)	Density before dehyd (lb/ft^3)	Dehyd water lost (lb/ft^3)	Water gained (lb/ft^3)	Initial water (lb/ft^3)
0316011054	0.6189	0.0842	13.60	23.49	22.64	3.08	-0.85	3.93
0425010941	0.7098	0.0982	13.83	23.53	26.31	3.64	2.78	0.86
0425011046	0.7135	0.0934	13.09	23.53	26.87	3.52	3.34	0.18
0425011235	0.7190	0.0961	13.37	23.53	26.80	3.58	3.27	0.31
0323010953	0.7250	0.0996	13.74	23.56	25.57	3.51	2.01	1.50
0118010847	0.7022	0.0946	13.47	23.68	26.63	3.59	2.95	0.64
0425011007								
0425011329								
Average	0.6981	0.0944	13.52	23.55	25.80	3.49	2.25	1.24

Table 5. Medium-density dehydration data

MCNID	Initial weight (lb)	Water loss (lb)	Initial weight (%)	Documented density (lb/ft^3)	Density before dehyd (lb/ft^3)	Dehyd water lost (lb/ft^3)	Water gained (lb/ft^3)	Initial water (lb/ft^3)
0222011053	0.6104	0.0844	13.83	21.98	23.27	3.22	1.29	1.93
0326011220	0.6851	0.0928	13.55	21.99	23.88	3.24	1.89	1.35
0309011000	0.6612	0.0879	13.29	22.06	22.94	3.05	0.88	2.17
0301010815	0.6800	0.0978	14.38	22.06	24.36	3.50	2.30	1.20
0326011239	0.6849	0.0945	13.80	22.06	24.36	3.36	2.30	1.06
0406011232	0.6586	0.0879	13.35	22.06	24.41	3.26	2.35	0.91
0426011155	0.6651	0.0876	13.17	22.06	24.03	3.16	1.97	1.19
0425011101	0.6772	0.0950	14.03	22.06	24.31	3.41	2.25	1.16
Average	0.6653	0.0910	13.68	22.04	23.95	3.28	1.90	1.37

Table 6. Low-density dehydration data

MCNID	Initial weight (lb)	Water loss (lb)	Initial weight (%)	Documented density (lb/ft^3)	Density before dehyd (lb/ft^3)	Dehyd water lost (lb/ft^3)	Water gained (lb/ft^3)	Initial water (lb/ft^3)
0411011216	0.5180	0.0710	13.71	20.27	21.55	2.95	1.28	1.67
0508010845	0.6320	0.0897	14.19	20.28	23.00	3.26	2.72	0.54
0402011246	0.6025	0.0825	13.69	20.35	21.97	3.01	1.62	1.39
0316011150	0.6348	0.0876	13.80	20.40	22.20	3.06	1.80	1.26
0425010912	0.6299	0.0888	14.10	20.41	22.83	3.22	2.42	0.80
0419011046	0.6391	0.0909	14.22	20.42	23.08	3.28	2.66	0.62
0508010830	0.6404	0.0912	14.24	20.47	23.23	3.31	2.76	0.55
0406011219	0.6418	0.0825	12.85	20.47	23.48	3.02	3.01	0.01
Average	0.6173	0.0855	13.85	20.38	22.67	3.14	2.28	0.86

Additional evaluations of the water loss and density changes need to be examined further. On the average the samples gained about 1.9 lb/ft^3 in density after manufacturing and lost 3.28 lb/ft^3 during the dehydration testing. The difference between these average density values is assumed to be water, and the as-cast manufactured water content is 1.37 lb/ft^3. Therefore, the cast insulation Kaolite specimens used for this testing tends to absorb water from the air if it is available.

DISCUSSION

IMPACT TESTING

Generally, the constrained compressive strength of Kaolite is proportional to its density and inversely proportional to its temperature. For each temperature group and for each strain point, the stress in the specimen was higher at the next higher density group. Also, for a given density group, the specimens tested at low temperatures displayed higher stress levels than those tested at high temperatures. (Refer to Figs. 2 and 3.)

DEHYDRATION TESTING

During heating at 1600°F, the Kaolite specimens lost between 12.85% and 14.38% of their initial weight as water. The high-density group lost an average of 13.52% of its initial weight as water. The medium-density lost an average of 13.67% and the low-density group lost an average of 13.85%. In general, the percentage of water loss by weight is inversely proportional to the density. The less dense specimens lost a larger percentage of their starting weight as water.

REFERENCES

1. *Advantages of Using a Fireproof Inorganic Cast Refractory Material in Hazardous Content Shipping Packages*, Y/LF-565, compiled by Y-12 Nuclear Package Systems, Lockheed Martin Engineering Systems, Inc., Manufacturing Engineering, Engineering Analysis, Lockheed Martin Energy Systems, Inc., Oak Ridge Y-12 Plant, Oak Ridge, Tennessee, November 1998.

2. Thermal Ceramics, *Kaolite Super Lightweight Insulating Castables*, Augusta, Georgia, http:/www.thermalceramics.com.

3. Byington et al., "Fireproof Impact Limiter Aggregate Packaging Inside Shipping Containers," U.S. Patent No. US 6,299,850 B1, October 9, 2001.

4. Oakes, R., *Mechanical Properties of a Low Density Concrete for the New ES-2 Shipping/Storage Container Insulation, Impact Mitigation Media and Neutron Absorber*, Y/DW-1661, Lockheed Martin Energy Systems, Inc., Oak Ridge Y-12 Plant, Oak Ridge, Tennessee, April 1997.

5. *For Casting Kaolite 1600™ into ES Shipping Containers*, Manufacturing Process Specification No., Y/EN-5984, Rev. A, February 11, 2000.

DISTRIBUTION

Y-12 National Security Complex

Anderson, J. C., 9113, MS-8206
Byington, G. A., 9111, MS-8201 (2)
Doyle, J. H., 9113, MS-8206
Feldman, M. R., 9113, MS-8206
Goins, M. L., 9112, 8201
Handy, K. D., 9201-2, MS-8073 (2)
Heatherly, C. N., 9113, MS-8206
Heck, J. L., 9111, MS-8201
Holder, S. T., 9113, MS-8206
Kitzke, K. A., 9203, MS-8084
Luk, K. H., 9201-2, MS-8073
McClanahan, S. E., 9113, MS-8206 (2)
Neal, J. Y., 9201-2, MS-8073
Smith, B. F., 9203, MS-8084
Walls, J.C., 9201-2, MS-8073
Y-12 Plant Records—RC

Y/DW-1972

Low Temperature Impact Properties of an Inorganic Cast Refractory Material

B. F. Smith
Technology Development

September 14, 2004

Prepared by the
Y-12 National Security Complex
P.O. Box 2009
Oak Ridge, Tennessee, 37831-8169
Managed by BWXT Y-12, L.L.C.
for the
U.S. DEPARTMENT OF ENERGY
under contract DE-AC05-00OR22800

Y/DW-1972

LOW TEMPERATURE IMPACT PROPERTIES OF AN INORGANIC CAST REFRACTORY MATERIAL

B. F. Smith
Technology Development

Date of Issue: September 14, 2004

Prepared by the
Y-12 National Security Complex
P.O. Box 2009
Oak Ridge, Tennessee, 37831-8169
Managed by BWXT Y-12, L.L.C.
for the
U.S. DEPARTMENT OF ENERGY
under contract DE-AC05-00OR22800

CONTENTS

FIGURES iv
TABLES iv

FIGURES

Figure Page

1. Average Stress-Strain Curves for Kaolite Specimens Tested at -40°F 3
2. Average Stress-Strain Curves, Upper and Lower Bounding Curves, and Average of Upper and Lower Bounding Curves 4
3. Comparison of Upper Bounding Curves 5

TABLES

Table Page

1. Test Conditions for Kaolite Specimens 2
2. Coefficients to Upper and Lower Bounding Equations 6

INTRODUCTION

Several Y-12 shipping containers such as the ES-2100, DPP-2, MD-1, and ES-3100 now use Kaolite 1600 as an impact-absorbing medium. For quality and design control reasons, procedures for mixing, curing, and baking Kaolite were written specifically for each container. The first certified shipping container to use Kaolite was the ES-2100. The procedures for mixing Kaolite for use in this container are documented in manufacturing process specification number Y/EN-5984.[1] This document requires the final, dry density of mixed Kaolite to be 22.4 lb/ft^3, but densities between 19.4 lb/ft^3 and 25.4 lb/ft^3 are acceptable. The manufacturer of the containers followed the mixing specification and switched from a low power mixer to a high volume, high power mortar mixer. This new mortar mixer reduced the labor required to manufacture the casting by over two-thirds. However, there was an unforeseen consequence. During the prototype shipping container production runs, the density has been consistently too high, averaging 26.7 lb/ft^3 in ES-3100 containers and 25.2 lb/ft^3 in MD-1 containers. The dynamic response of the ES-3100 container was modeled using data from previous testing on within-spec Kaolite which is documented in Y/DW-1890, "Water Content and Temperature-Dependent Impact Properties of an Inorganic Cast Refractory Material."[2] It was unknown how the higher-density material would affect the response of the container. Thus, the purpose of this study was to measure the impact properties of the higher-density Kaolite as it was produced for the prototype shipping containers. The mixing procedure was modified such that the densities of the production run castings were controlled close to the nominal density. Engineering now has the opportunity to design a container with a Kaolite density over a range of 21 to 31 lb/ft^3 and adjust the strength accordingly.

EXPERIMENTAL PROCEDURE

This procedure duplicates the one described in Y/DW-1890, with a few exceptions. Only impact testing was performed, no dehydration was done. All 12 impact tests were at -40°F, none were at 100°F. It was expected that more dense material would result in higher stress for a given strain. In order to prevent overloading the load cell, the total displacement or strain of the specimen would have to be reduced. This was done by lengthening the test stand one inch. This was achieved by cutting a one inch section of schedule 40 pipe from an old Kaolite test specimen and attaching it onto the end of the existing fixture.

It was hypothesized that the mechanism by which Kaolite density came out too high was due to the mixing procedure. It was speculated that mixing for extended periods effectively pulverized the vermiculite aggregate used in Kaolite, resulting in finer particles, more surface area to absorb water, and higher densities. Regardless of the exact mechanism, the density of the material is proportional to the length of mixing time. Six pairs of specimens were produced. Each pair was taken from batches mixed for specific lengths of time. The mixing times were 4, 5, 7.5, 10, 12, and 14 min. Each specimen was named using its mixing time and an arbitrary "1" or "2."

The densities of 12 specimens were measured prior to being placed in a heat pump cycle environmental chamber. Here they soaked for approximately 140 h at -40°F. Six specimens were then placed in an expanded polystyrene container and transferred to the Mechanical Properties Laboratory where impact testing would commence. Unfortunately, multiple equipment problems appeared during the first test and no data was taken. The specimens remained there for 168 h during which time the temperature gradually rose to -13°F. Eleven specimens were then transferred to a liquid nitrogen-cooled environmental chamber in the Mechanical Properties Laboratory where they soaked for 13 h at -40°F. Impact tests were then performed inside this chamber.

RESULTS

Impact testing was successful on nine specimens. No data was taken on specimens 5-2, 7.5-1, and 7.5-2. The remaining specimens were divided into high, medium, and low density groups. Table 1 summarizes the test conditions for each specimen. Figure 1 shows the average stress-strain curves for each of these density groups at maximum actuator speeds. Figure 2 adds to these the upper and lower bounding curves as determined by sixth order polynomial curve fits. A sixth order fit was determined to be the lowest order that would result in acceptable low errors. An average curve of the upper and lower bounds is also included in Fig. 2. Figure 3 compares the upper bound of the higher density material of this study with the upper bound of the material as determined in Y/DW-1890. Finally, Table 2 gives the coefficients of the equations of the upper and lower bounding curves. Note that these curves are not to be extrapolated beyond the strains shown in Fig. 2.

Table 1. Test Conditions for Kaolite Specimens

Specimen ID	Density (lb/ft^3)	Density Group	Approx. Cooling Time (h)	Average Test Velocity (in/s)
4-1	24.23	Low	323.0	159.1
4-2	24.05	Low	323.5	159.2
5-1	23.45	Low	325.8	162.1
5-2	23.71	N/A		
7.5-1	26.40	N/A		
7.5-2	24.91	N/A		
10-1	27.39	Medium	329.2	178.2
10-2	27.32	Medium	330.0	176.3
12-1	27.83	Medium	327.6	170.6
12-2	27.68	Medium	329.5	173.0
14-1	33.55	High	324.3	172.3
14-2	33.21	High	326.7	169.9

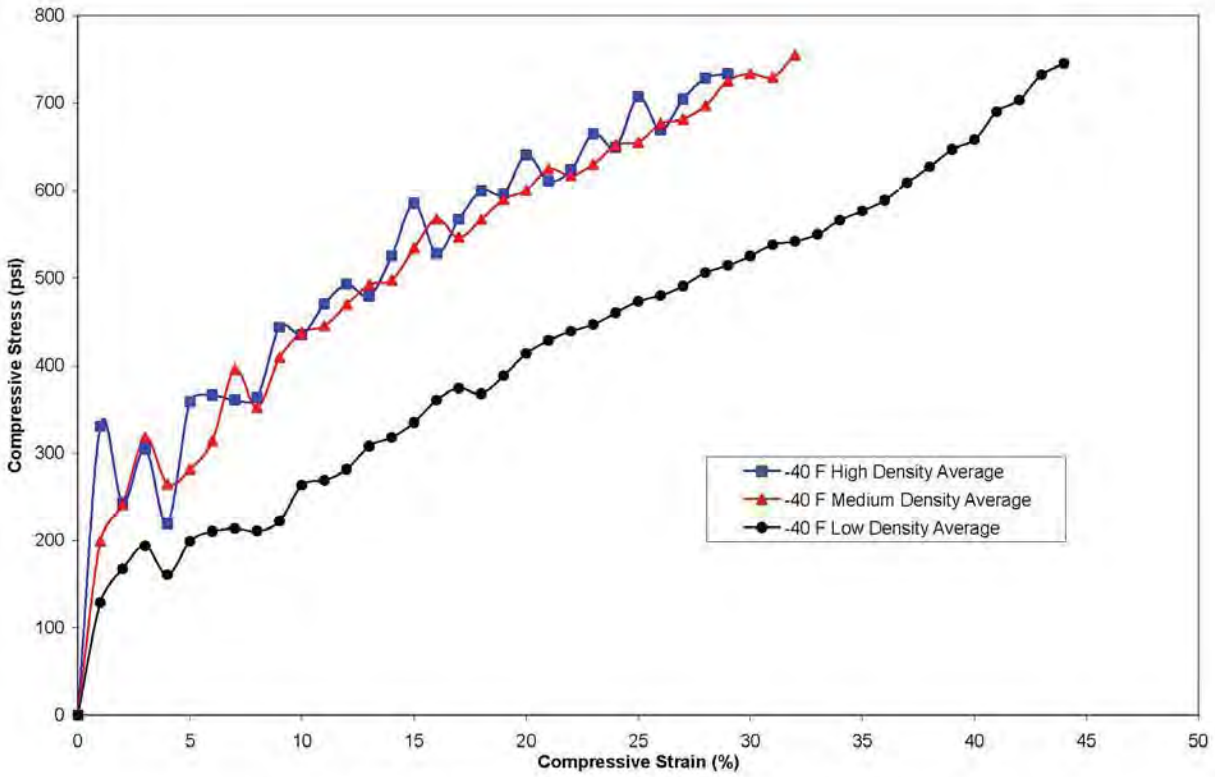

Fig. 1. Average Stress-Strain Curves for Kaolite Specimens Tested at -40°F

3

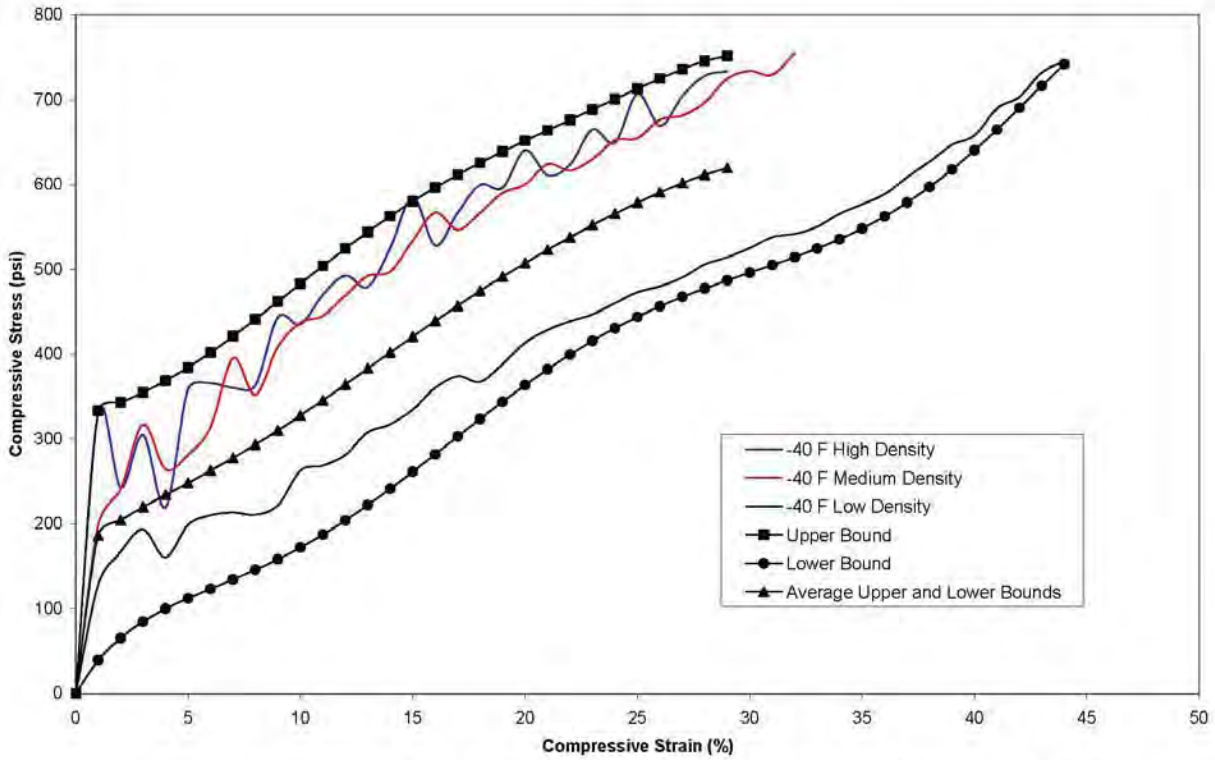

Fig. 2. Average Stress-Strain Curves, Upper and Lower Bounding Curves, and Average of Upper and Lower Bounding Curves

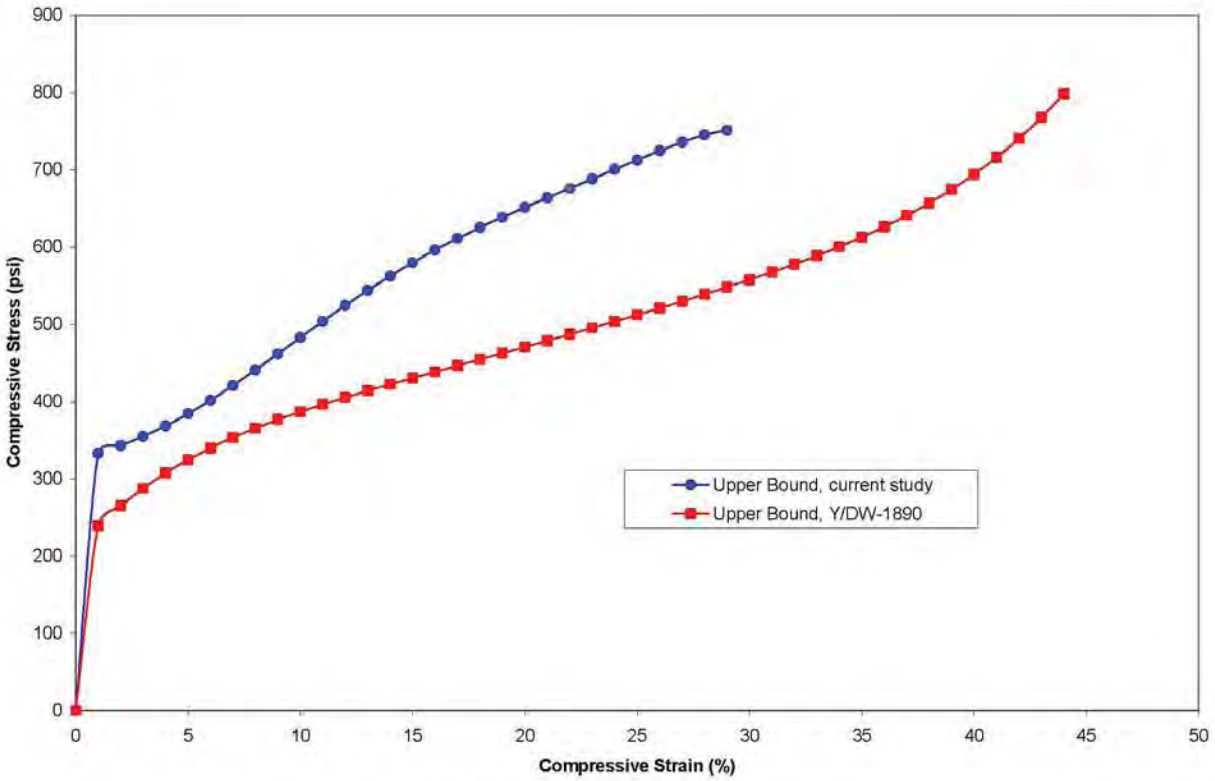

Fig. 3. Comparison of Upper Bounding Curves

5

Table 2. Coefficients to Upper and Lower Bounding Equations

$\sigma = a + b\varepsilon + c\varepsilon^2 + d\varepsilon^3 + e\varepsilon^4 + f\varepsilon^5 + g\varepsilon^6$							
	a	**b**	**c**	**d**	**e**	**f**	**g**
Upper	3.25×10^{2}	8.24	2.22×10^{-1}	1.80×10^{-1}	-1.82×10^{-2}	6.39×10^{-4}	-7.75×10^{-6}
Lower	4.23	4.06×10^{1}	-6.07	5.59×10^{-1}	-2.31×10^{-2}	4.34×10^{-4}	-3.03×10^{-6}

DISCUSSION

As expected, the high density Kaolite is significantly stronger than the Kaolite tested in Y/DW-1890. Upon comparing upper bounding curves, the high density material averaged 32% higher stress over the strain range of 1% to 29%.

REFERENCES

1. *For Casting Kaolite 1600™ into ES Shipping Containers*, Manufacturing Process Specification No., Y/EN-5984, Rev. A, February 11, 2000.

2. Smith, B.F., Byington, G.A., *Water Content and Temperature-Dependent Impact Properties of an Inorganic Cast Refractory Material,* Y/DW-1890, BWXT Y-12, L.L.C., Y-12 National Security Complex, Oak Ridge, Tennessee, February, 2003.

DISTRIBUTION

Y-12 National Security Complex

Anderson, J. C.
Arbital, J. G.
Baker, M. L./Kitzke, K. A.
Bales, P. A.
Byington, G. A. (2)
DeClue, J. F. (2)
Doyle, J. H.
Goins, M. L.
Hammond, C. R.
Handy, K. D. (2)
Heatherly, C. N.
Miller, D. B.
Neal, J. Y.
Smith, B. F.
Sooter, D. P.
Y-12 Plant Records - RC

Y/LF-565

Y-12

OAK RIDGE Y-12 PLANT

LOCKHEED MARTIN

Advantages of Using a Fireproof Inorganic Cast Refractory Material in Hazardous Content Shipping Packages

Y-12 Nuclear Packaging Systems
Lockheed Martin Energy Systems, Inc.

November 10, 1998

Fireproof Inorganic Cast Refractory

Flammable Organic Hydrocarbons

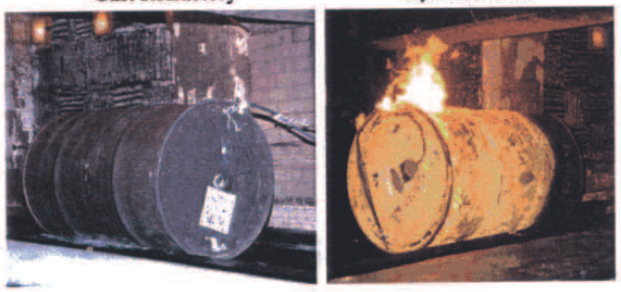

Thermal insulating impact limiters being removed from furnace after more than a 30-minute burn time in excess of 1475°F

This procedure has been reviewed by an Authorized Derivative Classifier and has been determined to be UNCLASSIFIED. This review does not constitute clearance for public release.

Steve M. Schneider
Name & Date

Nov. 11, 1998
Effective Date

MANAGED BY
LOCKHEED MARTIN ENERGY SYSTEMS, INC.
FOR THE UNITED STATES
DEPARTMENT OF ENERGY

UCN-13872 (26 6-95)

Advantages of Using a Fireproof Inorganic Cast Refractory Material in Hazardous Content Shipping Packages

Compiled by

Y-12 Nuclear Packaging Systems
LMES Manufacturing Engineering
Engineering Analysis

Prepared by the
Oak Ridge Y-12 Plant
Oak Ridge, Tennessee 37831
managed by
Lockheed Martin Energy Systems, Inc.
for the
U.S. Department of Energy
under contract DE-AC05-84OR21400

Advantages of Using a Fireproof Inorganic Cast Refractory Material in Hazardous Content Shipping Packages

1.0 Introduction

Lockheed Martin Energy Systems, Inc. (Energy Systems) has developed a superior design for hazardous material shipping packages. The use of a fireproof castable refractory material for impact absorption and thermal insulation allows these shipping packages to outperform similar shipping packages of conventional design when subjected to a series of hypothetical accident condition (HAC) tests. This material also has the advantages of reducing the risk of human exposure to inhalation of toxic smoke and material release due to high temperatures, and the material does not burn under these accident conditions. During normal conditions of transport (NCTs), personal safety is also improved. These improvements can be achieved using packaging designs that are competitively priced when compared to similar packages of conventional design.

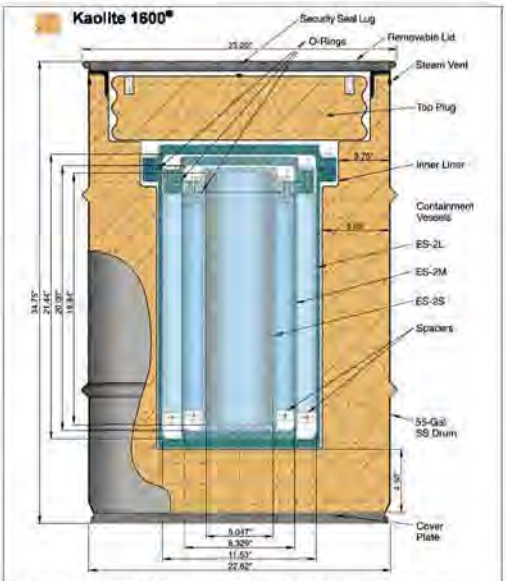

Figure 1. ES-2 shipping package with small, medium and large containment vessels.

The newly designed ES-2 shipping package, a Type-B radioactive material shipping package,[1] includes an inorganic castable refractory material which acts as an impact limiter and a thermal insulator[2] (see Figure 1). Kaolite 1600®, a castable Portland cement and vermiculite (expanded mica)-based aggregate produced by Thermal Ceramics was chosen for this application.[3] This material replaces the flammable organic hydrocarbon material (e.g., cane fiberboard, polyurethane foams, wood, cork, cardboard, paper or plastics) typically used in many shipping packages. This new material is ideal for crush and impact protection and is fireproof with a maximum continuous service temperature of 870°C (1600°F). The ES-2 shipping package has passed certification testing for a Type-B shipping package as outlined in the U.S. Code of Federal Regulations (CFR) Part 10 Section 71, *Packaging and Transportation of Radioactive Material.*

This paper details the advantages of using a castable refractory material for hazardous material shipping packages when compared to commonly used materials. The improvements listed above and the performance of the package during HAC and NCT testing are discussed in detail.

2.0 Comparison of Kaolite 1600® to Other Materials

2.1 Thermal Insulating, Energy Absorbing Impact Limiters

Type-B radioactive material shipping packages are subjected to a series of HAC tests prior to certification for use. These tests include a 30-foot free-fall drop onto an essentially unyielding surface, a puncture drop onto a 6-inch diameter pin from a height of 4 feet, a thermal exposure of 30 minutes at 800°C (1475°F), and a water immersion test. Packages must maintain containment during and after testing to satisfy 10 CFR §71.

2.1.1 Hydrocarbon materials. The hydrocarbon materials typically used for these types of packages perform very well during structural drop and puncture tests. However, these materials undergo severe degradation during thermal testing. While conditions during thermal testing can be energy absorbing (i.e., endothermic), the byproducts (ash, toxic smoke, soot and tars) can cause problems. Most significantly, offgasses from decomposing hydrocarbons[4] in the vapor phase may get into the interior portions of the package and condense. Heat transfer from the hot vapors to the containment vessel can lead to temperatures at the inner container which are considerably higher than would be predicted using conventional conduction heat transfer models. It can also lead to hot spots at the inner container, resulting in high local temperatures. If a hot spot is near a sealed closure such as an O-ring, package performance may be compromised.

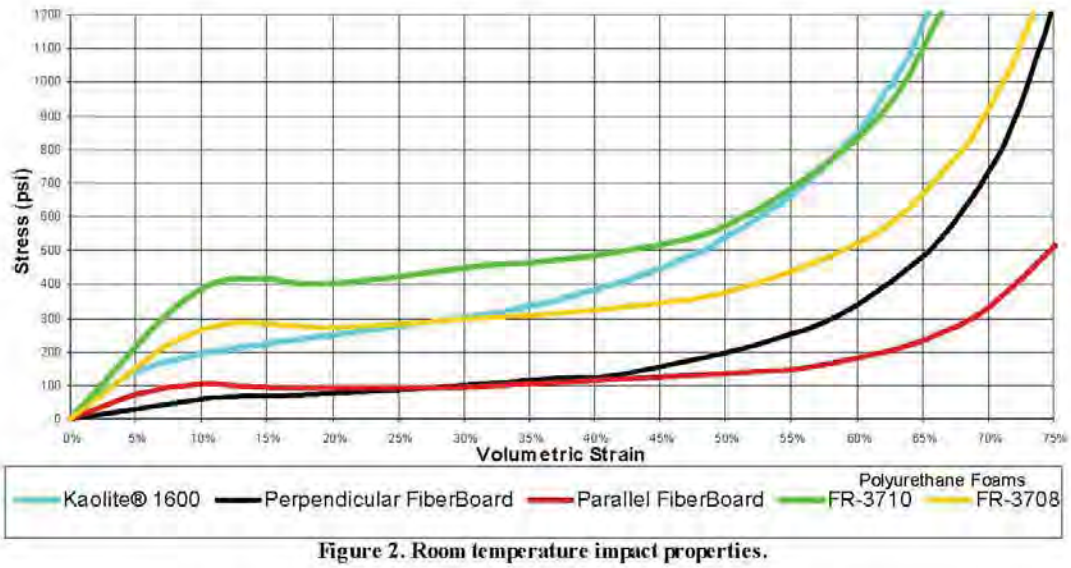

Figure 2. Room temperature impact properties.

2.1.2 Inorganic Materials. Cast refractory materials can be used to perform the same duties as the organic hydrocarbon materials discussed above with better results. Specifically, Kaolite 1600® has been used in the ES-2 shipping package. When this cast refractory material is used in a constrained configuration, its impact-absorbing properties are similar to those of the organic materials discussed in section 2.1.1. Unconstrained cast refractory materials tend to crack and fall apart or explode into dust during impact, but when a constrained system is used, these effects are greatly decreased. To the extent that cracking does occur, the damaged material is held in place by the constraints. Therefore, the cast refractory material is poured or cast into the void area formed by the confinement vessel (stainless steel drum) and the inner liner which is welded to the drum.

Extensive structural testing of lab-scale constrained specimens of Kaolite 1600® has been performed.[5] Figure 2 compares results from these tests with results of tests on other organic materials.[6] Kaolite 1600® compares favorably with polyurethane foams FR-3710 and FR-3708.[7] If required, other lightweight refractories can be mixed with Kaolite 1600® to customize its stress-strain response curve. A discussion of the mechanics of impact absorption of Kaolite 1600® is included in section 3.1.1.

This cast refractory material is preferable to hydrocarbon-based materials for this use due to its response to high temperature exposures. At the elevated temperatures for HAC testing of these materials (800°C or 1475°F), there is no decomposition of the Kaolite 1600®. This material has a recommended continuous service temperature of 870° C (1600°F), although no discernable degradation processes take place up to about 1260°C (2300°F). Some steam is generated during the exposure to an 800°C (1475°F) environment, and it is possible for the steam to travel through cracks in the Kaolite 1600® which were created during structural testing to the inner liner. However, this steam is typically at or near atmospheric pressure, which means that the temperature of the condensation is at or near 100°C (212°F). This is much more acceptable than the various tars which transport in a similar manner through organic materials but typically condense at much higher temperatures.

2.2 Elimination of Ancillary Health Hazards

2.2.1 Health Hazards Associated with Typical Use

One method to improve the performance of organically based materials is to use one or two layers of ceramic fiber products between the organic material and the confinement drum. Like cast refractory materials, these ceramic fiber products do not degrade during exposure to HAC temperatures. This thin layer of protection can offer greatly increased performance in organic material-based shipping packages. However, during loading, unloading and refurbishment, abrading of these materials may occur, thus leading to the creation of

airborne ceramic fibers. Chronic personnel exposure to ceramic fibers can lead to eye, skin and lung problems. While there are no known health or irritation problems associated with Kaolite 1600®, when the material is fully constrained inside a stainless steel casing, personnel cannot be exposed to any such airborne particles. This assures that ancillary health hazards are not an issue for this application.

2.2.2 Health Hazards Associated with Accident Conditions

During accident conditions involving a fire, packages with organically based materials can become fuel for the fire. However, Kaolite 1600® is fireproof at these temperatures. Kaolite 1600® maintains its impact-absorbing attributes after exposure to high temperatures. When hydrocarbon thermal insulating materials reach temperatures greater that 204°C (400°F), toxic smoke is present. Between 260 and 575°C (500 and 1070°F), flames are generated.[8] At temperatures over 575°C (1070°F), more than 90% of the insulation weight is consumed,[9] leaving behind a solid char which has little or no impact-absorbing qualities. If a thermally damaged package were to experience a subsequent fall of any significant distance, damage to the inner container could occur. Because Kaolite 1600® is designed to be used at these elevated temperatures, there is no degradation of the impact-absorbing properties of the material. Furthermore, emergency personnel and others would not be exposed to hot toxic smoke generated by hydrocarbon materials or to flaming gas jets which may extend two feet or more from the shipping package. The stainless steel liner ensures that hot vapors cannot reach the containment vessel, thus moving heat out of exterior gas vent holes. The water released as steam helps to decrease heating of the containment vessel. These determinations were based on data from HAC free-fall drop and thermal testing.[10]

2.3 Cost Factors

Many factors must be considered to determine the overall cost of any material, organic or inorganic, over the lifetime of a package. However, such a determination is beyond the scope of this paper. It can be stated that the raw material cost for a cast refractory material such as Kaolite 1600® (about $80 for a 55-gallon drum application) is substantially less than that of a typical organic material such as cane fiberboard (about $300 for a typical 55-gallon drum application). However, much of these savings may be offset by additional costs such as design and installation of the inner liner, manpower costs to pour the material, and oven curing of the material.

The true cost advantage would be realized with long-term use of the package. Typical cane fiberboard package designs require extensive inspection and often this material must frequently be repaired or replaced. However, the Kaolite 1600® material has been shown to have no reduction in either structural or thermal protection properties after being transported 40,000 miles in a standard flatbed semi-trailer. When the shock-absorbing effects of the Safe Secure Transport method are considered, the range is probably extended to 300,000 to 400,000 miles.[11] This essentially ensures that the initial casting of Kaolite 1600® material in a package will not need to be replaced for the life of the package.

3.0 <u>In-Situ Performance of Cast Refractory Material Kaolite 1600®</u>

The ES-2 shipping package was designed using Kaolite 1600® as the primary thermal insulator and structural absorber. This package has been tested to the standards of 10 CFR §71 and is currently in the process of being certified for use.

3.1 HAC Testing

Several prototype units of both single containment and double containment configurations of the ES-2 shipping package were sequentially exposed to the tests outlined in 10 CFR §71.73, including drop, puncture, thermal, and immersion tests. Before and after structural testing, real-time radiography techniques were used to determine the condition of the Kaolite 1600®. The performance of these units is detailed below.

One ES-2M unit was specially equipped with 20 internal thermocouples and was exposed to the thermal portion of the HAC tests. However, this unit was not structurally tested. This unit was identified as a baseline unit since its testing provided insight into the thermal response of an undamaged package and allowed for determination of the effect on the performance of Kaolite 1600® due to structural testing.

3.1.1 Structural Testing. The structural tests required in 10 CFR §71.73 for this package include a 9-m (30-ft) drop test and a 1-m (40-in) puncture test. Several prototype units of both the ES-2M (medium inner

container) and ES-2LM (large and medium inner containers) configurations were subjected to each of these tests.[10, 12] The puncture test is conducted to determine the ability of the package's outer shell to resist tearing and has little bearing on the impact-absorbing material. This discussion focuses on the results of the 9-m drop test.

When fissile material packages (the smallest of the Type B shipping packages) are subjected to the 9-m drop test, there is substantial damage to the package. Localized crushing of the impact-absorbing material often results in reductions of thickness of this material by as much as 50%. In turn, this damage can have great effects on the ability of the package to withstand subsequent thermal testing. The ES-2 shipping packages were significantly damaged by the 9-m drop test, with localized crushing of the material resulting in thickness reductions of up to 45%.

To the naked eye, the damage caused to these packages was similar to that which has been seen in similar fissile material shipping packages using conventional materials. However, closer inspection of these packages using real-time radiography revealed that damage to the internal structure of the package was quite unique. The Kaolite 1600® did crack during testing, particularly near the impact zone. However, the cracks were not long and straight; instead they tended to be relatively short with curved ends. This type of cracking indicates that no direct thermal radiation paths exist from the drum shell through to the inner liner, which is a very important factor in the package's reaction to subsequent thermal testing.

3.1.2 Thermal Testing. Each package which was subjected to the HAC structural tests (as well as the baseline unit) was subjected to thermal testing as specified in 10 CFR §71.73 (c) (4).[10, 12] This test requires exposure of the package to an 800°C (1475°F) environment for thirty minutes. The test was performed inside of a specially equipped furnace. Prior to testing, each of the packages was preheated in a small oven so that temperatures throughout the packages were at least 38°C (100°F). After testing, the packages were allowed to cool naturally. Maximum internal temperatures of packages other than the baseline unit were determined using temp-labels which indicate the highest temperature attained between 38° and 260°C (100° and 500°F).

Performance of the ES-2 shipping packages was outstanding when exposed to these thermal conditions. Temperatures at the inner container, including temperatures near the O-ring seal, were significantly lower than those which have been recorded for packages using hydrocarbon-based materials.

More importantly, temperatures peaks were much more evenly distributed in the packages with the cast refractory, so hot spots did not occur due to offgasses reaching the inner container. As discussed in section 2, hot spots are a significant problem if they occur near the O-ring seal since they can lead to loss of containment. These high peak temperatures tend to occur randomly in conventional packages, which makes it difficult to determine if such a hot spot could occur near an O-ring seal on a specific package design.

Figure 3 compares the burning characteristics of several conventional materials to those of Kaolite 1600®. As can be seen, foams, fiberboards and wood all add significant

For 6 ft^3 of Insulation Used in a 55-gal Drum	Density (lb/ft^3)	Weight (lb)	Heating Values (Btu/lb)	Available Fuel Energy [d] (Btu)	Gasoline for the Fire [e] (gal)
PolyurethaneFoam [a]	10	60	10,910	654,600	5.1
Cane Fiberboard [b]	17	102	8,390	855,780	6.7
Redwood or Maple [c]	27	162	7,875	1,275,750	10.0
Kaolite 1600®	25 to 29	150 to 174	0	0	0.0

[a] Average heat of combustion, pages 5-121, Arthur E. Cote, *Fire Protection Handbook*
[b] For Bagasse, dried sugarcane scrap, pages 7-13, *Mark's Handbook*, 8th edition
[c] Available energy in 10% moisture for wood, pages 7-13, *Mark's Handbook*, 8th edition
[d] Not all of the available fuel will convert to heat, but all is shown for comparison
[e] Gasoline @ 127,654 Btu/gal, pages 7-14, *Mark's Handbook*, 8th edition

Figure 3. Comparison of Burning Characterisitics of Hydrocarbon Insulation and Kaolite ® 1600

equivalent quantities of gasoline to such a fire situation. In contrast, the fireproof Kaolite 1600® adds no additional equivalent fuel to the fire.
The advantage of using a cast refractory material for such an application is very clear when two of its thermal characteristics are considered: (1) the only offgassing taking place is the evolution of steam which occurs at 100°C (212°F), and (2) no cracks which extend through the thickness of the material are formed. These characteristics result in the package's superior performance when it is exposed to thermal conditions. The steam is generated at 100°C (212°F), but it is possible for the steam to then be superheated. Most of the superheating would occur near the drum wall. Four vent holes near the top of the drum allow most of the steam (and virtually all of the superheated steam) to be released outside the package. Each package lost an average of 9 lbs of water/steam during thermal testing. Because there is a large amount of steam generated and there are only four vent holes, some pressurization of the drum/inner liner cavity does occur. This pressure is the driving force to push steam toward the inner liner. However, there are no direct paths from the point of steam generation (near the drum wall) to the inner liner due to the lack of long continuous cracks through the Kaolite 1600® casting. The baseline unit, which was instrumented with internal thermocouples, showed that some steam reached the inner liner, as some thermocouple readings rose to 100°C (212°F) much more quickly than standard conduction through the cast material would account for. However, these temperatures remained within a couple of degrees of 100°C throughout the duration of the test and into the cool-down phase, indicting that superheated steam was not able to reach the inner liner.

While the Kaolite 1600® has a thermal conductivity which is about twice that of some conventional materials, temperatures at the inner container are considerably cooler. This is proof that the primary mode of heat transfer during such a test is not heat conduction, but is rather a mixture of mass transfer and heat conduction. Since the only mass being transferred within a Kaolite 1600®-containing package is steam (not various hydrocarbons with various condensation temperatures) the temperatures at internal surfaces remain substantially lower than they would in a conventionally designed package. This higher thermal conductivity allows the Kaolite 1600®-containing package to be used in conjunction with higher heatload-producing contents than conventional packages, as conduction is the primary form of heat transfer at the lower temperatures associated with NCT.

As the ES-2 shipping packages were being removed from the furnace after the test, the fireproof nature of the Kaolite 1600® was very evident. When conventionally designed packages are removed from such a test, flames are typically seen shooting 2 to 3 feet out of the vent holes. Flames are also usually emanating from the drum flange/drum lid interface region. When the ES-2 packages were removed from the furnace, there were no flames. Close inspection revealed jets of steam emitting from the vent holes; this observation is evidence that the Kaolite 1600® does not add additional fuel to the thermal environment and thereby does not increase the package's maximum internal temperatures.

Another significant finding was that peak temperatures for units which were damaged from structural testing prior to thermal testing were very close to those of the baseline unit which was not damaged prior to the thermal test. This means that localized crushing of the Kaolite 1600® material did not have a significant impact on the package's overall thermal response, which has typically not been the case for conventionally designed packages. It also indicates that thermal analytical modeling may be a very valuable tool for certification of packages since it is very difficult to conduct a thermal analysis on a damaged package. Since the damage does not affect the thermal response of the package, thermal analyses models of undamaged packages can be applied to structurally damaged packages. Analytical modeling of HACs is discussed in further detail below.

3.1.3 Analytical Modeling of Accident Conditions. Analytical modeling of structural and thermal tests is often used in the design of Type B shipping packages. Federal regulations also allow the use of these models to substitute for actual physical testing of packages when tested to 10 CFR §71.73 specifications. Tests are rarely performed in this manner because thermal analytical models to date are not capable of modeling all decomposition processes which occur in a conventional package design. Using an analytical method to perform testing reduces in cost, particularly if a model has already been constructed during the design phase.

During the design phase of the ES-2 shipping container, analytical modeling (structural and thermal) was used extensively. Structural modeling was performed using the LS-DYNA3D[13] computer code, while thermal modeling was performed using the PATRAN P-

Thermal[14] computer code.

Comparison of the results of actual structural testing of the ES-2 shipping packages with the analytical models shows remarkable agreement.[15] Not only is the external damage (flattening of the drum body in the impact zone) correctly predicted, but the internal damage (bending of the inner liner and the lack of plastic deformation to the inner container) is also correctly predicted.

Thermal modeling of the ES-2 shipping container under accident conditions was also performed, though the results were not as outstanding.[16] The HAC thermal analysis predicted peak testing temperatures higher than the actual measured temperatures.[17] The simple heat conduction thermal model was initially constructed for over- predicted maximum internal temperatures because the energy absorption of the water vaporization process was not taken into account. As mentioned earlier, tested packages lost an average of 9 lbs of water weight due to the evolution of steam, which constitutes a considerable amount of energy. While this simple modeling technique does not agree with experimental results, it provides an upper bound on the temperatures which may be reached in the internal portions of the package. Additional modeling has been performed which considers the energy loss due to steam generation exit. This model slightly under-predicts peak temperatures because the effects of mass transfer (i.e., steam which does not exit the package, but rather works its way toward the inner liner) are not taken into account. If future improvements of this modeling are successful, it may be possible to greatly reduce the number of packages tested, or it could eliminate the need for physical testing altogether.

3.2 Normal Conditions

3.2.1 Normal Conditions and Sequential Tests. As specified in 10 CFR §71.71, a series of NCT tests must be performed. One ES-2LM unit was subjected to each of the NCT tests except for the vibration test. A single ES-2M unit was subjected to a severe vibration test followed by HAC testing described above. Results from these tests are described below.

3.2.2 Normal Conditions of Transport Tests (Excluding Vibration). The sequential NCT tests specified in 10 CFR §71.71 include heat, cold, reduced external pressure, increased external pressure, water spray, 1.2-m (4-ft) free drop, 0.3-m (1-ft) corner drop, compression, and penetration. These tests are generally innocuous for a well-designed package. Some superficial damage may result from the 1.2-m drop test, but overall, most packages are expected to survive these tests with no damage. As mentioned above, one ES-2LM unit was exposed to each of these tests either physically or analytically. No ES-2M unit underwent these tests because the greater weight of the ES-2LM unit gave conclusive bounding evidence that either of the units could withstand the tests.

The ES-2 easily survived all of the NCT tests. There was no discernable damage to the package from any of these tests. Research has indicated that it would require a pressure of about 56 psig to cause a dent in the package. This high level of tolerance assures that the ES-2 can not only withstand the NCT 1.2-m drop test, but also that it will hold up very well in daily use when rough handling and incidental drops may occur.

3.2.3 Vibration Testing. One ES-2M prototype unit was exposed to severe vibration testing at Wyle Laboratories in Huntsville, Alabama. The two vibration tests performed included a scan of individual frequencies to determine resonant frequencies for the shipping package, as well as a 40-hour white noise endurance test.[11] For these tests, accelerometers were mounted on the drum lid on the inner container lid. The individual scan of frequencies found several resonant frequencies for the package, all of which were below 200 hz. The white noise endurance test included the package receiving random frequencies between 10 and 500 hz for 40 hours. This test has been estimated to equal about 40,000 miles on a standard flat-bed tractor trailer truck and at least 200,000 miles on the Safe Secure Trailer vehicle for which its use is intended.[18] At the conclusion of the test, the unit was thoroughly examined. Tapping by hand on the inner liner (directly below where the containment vessel had been sitting) revealed a hollow sound, indicating that some damage to the Kaolite 1600® had occurred. Subsequent real time radiographs of the package showed that about 2 inches of the Kaolite 1600® directly below the containment vessel had been pulverized. However, no void spaces were visible in the area between the drum and the inner liner. Since the indications of damage to the Kaolite 1600® casting were not clear, a decision was made to subject the unit to the test associated with HACs (see section 3.1).

The vibrated unit was side dropped from 9-m (30-ft), side-puncture tested from 1-m (40-in), and then thermally tested in a furnace. Maximum temperatures

reached within the package were comparable to those for other units that had been similarly tested. This indicated that while some destruction of the Kaolite 1600® material occurred during vibration and will occur during normal use, this type of damage does not significantly affect the package's ability to protect the contents during subsequent accident conditions.

4.0 Use of Kaolite® 1600

Kaolite 1600® is relatively easy to use. Because the cast material is fully enclosed, there is no costly refurbishment involving removal, inspection and replacement of worn materials as is common with most hydrocarbon-based materials. The only special processes required for the use of this material are the casting and curing during package manufacture. Each of these processes is discussed below.

4.1 Casting Kaolite 1600® in ES-2 Shipping Packages

A small portable cement mixer was used to mix two parts Kaolite 1600® with three parts water. When thoroughly mixed, the material was poured into the cavity formed by the drum and the inner liner through a hole in the bottom of the drum. Several top plugs (see Figure 1) were also poured. During pouring, each part was attached to a vibrating table to ensure that no voids were formed.

Small amounts of dry material and water were mixed thoroughly and poured into the vibrating drum until it was full. It took two workers about one hour to complete this process for one drum. When a drum was filled slightly past full, it was removed from the vibrating table and set aside. The material expanded during the initial part of the setting process, pushing it up through the fill hole. As this occurred, the material was scraped flush with the drum's edge. This method formed wet pours which contained approximately 25 lbs/ft^3 of dry Kaolite 1600®.

4.2 Curing Kaolite 1600® in ES-2 Shipping Packages

The curing process was initiated by allowing the drums and top plugs to set for at least 24 hours as recommended by the manufacturer. A small electric furnace was then used to speed the curing of the Kaolite 1600®. The furnace temperature was held at about 500°F for about 48 hours. At completion of this process, the material had hardened considerably but was still flush with the edge of the drum and the majority of the water in the initial pour had evaporated.

4.3 Considerations for Using Kaolite 1600 ® in Other Packages

The processes described in sections 4.1 and 4.2 were successfully employed during small scale production of prototype units (in lots of about 4). For production runs of 50 to 100 or more, the process could be optimized using specialized equipment to cut production costs (e.g., a larger cement mixer to quickly pour several drums, or a larger furnace to heat treat a larger quantity of packages). It should be noted that during the mixing phase, additives could be introduced in order to obtain specially desired properties from the cast refractory material.[5]

5.0 Hazardous Material Packaging Solutions

Hazardous material packaging performance has been significantly improved with this new design. The cast refractory material has been subjected to many tests and has achieved excellent results. The ES-2 shipping package withstands the damage from crushing or dropping, as well as thermal testing at maximum temperatures. When compared to the conventional materials, this improved performance has been accomplished at an overall reduced cost. Furthermore, the safety of hazardous material storage, shipping, and handling has been improved by removing several risks.

For radioactive material packaging solutions, contact:

Ed Stumpfl
Nuclear Packaging Systems
Lockheed Martin Energy Systems, Inc.
P.O. Box 2009, MS-8206
Oak Ridge, Tennessee 37831-8206

Phone: (423) 574-2547
Fax: (423) 574-3514
E-mail: eus@ornl.gov

6.0 References

1. *ES-2 Safety Analysis Report for Packaging (SARP)*, Y/LF-511, Lockheed Martin Energy Systems, Inc.,Y-12 Plant, Oak Ridge, Tennessee 37831.

2. *Fireproof Impact Limiter Aggregate Packaging Inside Shipping Containers*, U.S. Patent Application, ESID 1919-Y, September 30, 1997.

3. Kaolite 1600® is a registered trademark of Thermal Ceramics. Thermal Ceramics, P.O. Box 923, Augusta, Georgia 30903-0923.

4. Williams, W. Reid and James C. Anderson, *Assessing Post-Fire Combustion of Polyurethane*, 1994 U.S. Department of Energy Defense Workshop Proceedings, Martin Marietta Energy Systems, Inc., Oak Ridge, Tennessee 37831-6322.

5. Oaks, Raymon, *Mechanical Properties of a Low Density Concrete for the New ES-2 Shipping/Storage Container Insulation, Impact Mitigation Media and Neutron Absorber*, Y/DW-1661, Lockheed Martin Energy Systems, Inc., Y-12 Plant, Oak Ridge, Tennessee, April 1997.

6. Walker, M.S., *Packaging Materials Properties Data*, Martin Marietta Energy Systems, Inc., Y/EN-4120, Y-12 Plant, Oak Ridge, Tennessee, January 1991.

7. *General Plastics Last-A-Foam® FR-3700 for Crash & Fire Protection of Nuclear Material Shipping Containers*, General Plastics Manufacturing Company, 4910 Burlington Way, P.O. Box 9097, Tocoma, Washington 98409, December 1993.

8. Cote, Arther E., *Fire Protection Handbook*, 16th Ed., National Fire Protection Handbook, Quincy, Massachusetts, 1986.

9. General Plastics Manufacturing Company, *Thermal Decomposition of Last-A-Foam FR-3700*, FPH-1/31/91, 4910 Burlington Way, P.O. Box 9097, Tocoma, Washington 98409.

10. Byington, G.A., *Certification Test Report of the ES-2LM Shipping Package*, GAB 0297, Lockheed Martin Energy Systems, Inc., Y-12 Plant, Oak Ridge, Tennessee, April 1997.

11. Byington, G.A., *Vibration Test Report of the ES-2M Shipping Package*, GAB 1296-2, Lockheed Martin Energy Systems, Inc., Y-12 Plant, Oak Ridge, Tennessee, April 1997.

12. Byington, G.A., *Test Report of the ES-2M Shipping Package*, GAB 0796-2, Lockheed Martin Energy Systems, Inc., Y-12 Plant, Oak Ridge, Tennessee, April 1997.

13. LS-DYNA3D software version 936.02, Livermore Software Technology Corporation, December 20, 1995.

14. P/Thermal Version 7.5, MacNeil-Schwendler Corp., Los Angeles, California, April 1997.

15. Handy, K.D., *Drop Simulation of the ES-2M Shipping Container*, DAC-EA-9000000-A001, X-10 Plant, Oak Ridge, Tennessee, April 1997.

16. Anderson, J.C., *Thermal Analysis of the ES-2M Shipping Package for Normal Conditions of Transport*, DAC-EA-801208-A001, Oak Ridge National Laboratory, Oak Ridge, Tennessee, December 1996.

17. Romesburg, L.E., et. al., TRUPACT-1, *Unit 0, Test Data Analysis*, SAND-85-0943, Sandia National Laboratories, Albuquerque, New Mexico, September 1985.

18. Magnuson, C.F., *Manufacture-to-Stockpile Sequence*, SAND83-0480, Figure 3.30, "SST Transport Vibration Envelope."

Bales, Paul A (B6P)

From: Moody, Ken [kmoody@thermalceramics.com]
Sent: Thursday, December 09, 2004 12:31 PM
To: 'mailto:balespa@y12.doe.gov'
Subject: RE: Coefficient of thermal expansion for Kaolite 1600

Paul,

The Thermal Expansion for Kaolite 1600 is 5.04 X10-6 in/in/oF which is what was quoted to you earlier.

If you need additional help please contact me by email

Regards,

Ken

-----Original Message-----
From: Bales, Paul A (B6P) [mailto:balespa@y12.doe.gov]
Sent: Thursday, December 09, 2004 9:11 AM
To: 'tceramics@thermalceramics.com'
Subject: Coefficient of thermal expansion for Kaolite 1600

Dear Sir/Madam:

I am an engineer at BWXT Y-12 (Y-12 National Security Complex) in Oak Ridge, TN. We use Kaolite 1600 in several shipping package applications (for impact limiting and thermal protection). I am in need of a material property (linear coefficient of thermal expansion) that is not included in your material data sheet available online.

One of our engineers (R. E. Oaks) here at Y-12 received a fax from someone (J. Street) of Thermal Ceramics, Inc. dated 1/12/97 that stated that the average coefficient of thermal expansion for Kaolite 1600 is 5.039e-6 in/in/°F. This fax has been referenced in several calculations generated here at Y-12; however, I have been unable to locate an actual copy of this fax.

Could an engineer from Thermal Ceramics send me a fax or e-mail with this (or an updated) value for the linear coefficient of thermal expansion for Kaolite 1600 as well as a reference temperature? If temperature-dependent information is available, please provide.

Thank you for your help.

Paul A. Bales
Packaging Engineering
BWXT Y-12
b6p@y12.doe.gov
(865)576-4209
(865)574-3514 (FAX)
Bldg. 9113, Room 153, MS 8206

Appendix 2.10.4

CATALOG 277-4 PROPERTIES

W. D. Porter and H. Wang, *Thermophysical Properties of Heat Resistant Shielding Material*, ORNL/TM-2004/290, UT-Battelle, Oak Ridge Natl. Lab., Dec. 2004.

B. F. Smith and G. A. Byington, *Mechanical Properties of 277-4*, Y/DW-1987, BWXT Y-12, Y-12 Natl. Security Complex, Jan. 19, 2005.

R. A. Smith, *Volatile Components from Packing Materials*, Y/DZ-2585, rev. 2, BWXT Y-12, Y-12 Natl. Security Complex, Dec. 22, 2004.

R. W. Brandenburg, Canberra Oak Ridge, letter to D. B. Miller, BWXT Y-12, *Results of Prompt Gamma-ray Neutron Activation Analysis and Neutron Transmission Measurements on Prototype Confinement Vessel Inner Liners and Spacers*, Jan. 5, 2005.

L. M. Thompson, *Summary of TGA Testing of Borated Concrete and Adhesive-Backed Silicone Foam*, Y/DV-1914, BWXT Y-12, Y-12 Natl. Security Complex, Jan. 2005.

THIS PAGE INTENTIONALLY LEFT BLANK.

OAK RIDGE
NATIONAL LABORATORY

MANAGED BY UT-BATTELLE
FOR THE DEPARTMENT OF ENERGY

ORNL/TM-2004/290

Thermophysical Properties of Heat Resistant Shielding Material

December 2004

W. D. Porter
H. Wang

UT-BATTELLE

DOCUMENT AVAILABILITY

Reports produced after January 1, 1996, are generally available free via the U.S. Department of Energy (DOE) Information Bridge:

Web site: http://www.osti.gov/bridge

Reports produced before January 1, 1996, may be purchased by members of the public from the following source:

National Technical Information Service
5285 Port Royal Road
Springfield, VA 22161
Telephone: 703-605-6000 (1-800-553-6847)
TDD: 703-487-4639
Fax: 703-605-6900
E-mail: info@ntis.fedworld.gov
Web site: http://www.ntis.gov/support/ordernowabout.htm

Reports are available to DOE employees, DOE contractors, Energy Technology Data Exchange (ETDE) representatives, and International Nuclear Information System (INIS) representatives from the following source:

Office of Scientific and Technical Information
P.O. Box 62
Oak Ridge, TN 37831
Telephone: 865-576-8401
Fax: 865-576-5728
E-mail: reports@adonis.osti.gov
Web site: http://www.osti.gov/contact.html

This report was prepared as an account of work sponsored by an agency of the United States Government. Neither the United States government nor any agency thereof, nor any of their employees, makes any warranty, express or implied, or assumes any legal liability or responsibility for the accuracy, completeness, or usefulness of any information, apparatus, product, or process disclosed, or represents that its use would not infringe privately owned rights. Reference herein to any specific commercial product, process, or service by trade name, trademark, manufacturer, or otherwise, does not necessarily constitute or imply its endorsement, recommendation, or favoring by the United States Government or any agency thereof. The views and opinions of authors expressed herein do not necessarily state or reflect those of the United States Government or any agency thereof.

ORNL/TM-2004/290

Metals and Ceramics Division

THERMOPHYSICAL PROPERTIES OF HEAT RESISTANT SHIELDING MATERIAL

W. D. Porter and H. Wang

Date Published: December 2004

Prepared by
OAK RIDGE NATIONAL LABORATORY
Oak Ridge, TN 37831-6285
managed by
UT-BATTELLE LLC
for the
U.S. DEPARTMENT OF ENERGY
under contract DE-AC05-00OR22725

THIS PAGE INTENTIONALLY LEFT BLANK.

CONTENTS

	Page
LIST OF FIGURES	v
LIST OF TABLES	vii
1. INTRODUCTION	1
2. EXPERIMENTAL	1
2.1 THERMAL CONDUCTIVITY AND VOLUMETRIC SPECIFIC HEAT	1
2.2 THERMAL EXPANSION	2
3. RESULTS	2
3.1 THERMAL CONDUCTIVITY AND VOLUMETRIC SPECIFIC HEAT	2
3.2 THERMAL EXPANSION	6
4. SUMMARY	13
REFERENCES	13

THIS PAGE INTENTIONALLY LEFT BLANK.

LIST OF FIGURES

Figure		Page
1.	Hot Disk System.	1
2.	Thermal conductivity of Thermo Electron RM&P Catalog No. 277-4.	3
3.	Volumetric specific heat vs. temperature.	4
4.	Average thermal conductivity of Thermo Electron RM&P No. 277-4.	5
5.	Average volumetric specific heat of Thermo Electron RM&P Catalog No. 277-4.	6
6.	Thermal expansion of Type 277-4 cement material as a function of temperature.	7
7.	Comparison of smoothed data and cubic spline fit of smoothed data to raw pooled experimental data for thermal expansion of Type 277-4 cement material as a function of temperature.	10
8.	Relative residuals of cubic spline fit used to estimate expansion values tabulated in Table 5.	10
9.	Comparison of MCTE calculated from estimated expansion with MCTE calculated from smoothed expansion data and raw pooled MCTE values.	11
10.	Relative residuals of the 9th order polynomial fit of the estimated MCTE values using 8 significant digits for the coefficients as shown in Equation 2.	12

THIS PAGE INTENTIONALLY LEFT BLANK.

LIST OF TABLES

Table		Page
1.	Thermal conductivity (W/m•K)	3
2.	Volumetric Specific Heat (MJ/m^3•K)	4
3.	Average values of k and Cp	5
4.	Measured thermal expansion values and Mean CTE for Type 277-4 specimens	7
5.	Expansion values at even intervals estimated from cubic spline fit of pooled, sorted and smoothed data from Runs 2, 3, and 5	8
6.	Weight loss (%) behavior during testing	12
7.	Initial density (10^6 g/m^3) of specimens tested	13

THIS PAGE INTENTIONALLY LEFT BLANK.

1. INTRODUCTION

This project was aimed at determining thermal conductivity, specific heat and thermal expansion of a heat resistant shielding material for neutron absorption applications. These data are critical in predicting the structural integrity of the shielding under thermal cycling and mechanical load. The measurements of thermal conductivity and specific heat were conducted in air at five different temperatures (-31°F, 73.4°F, 140°F, 212°F and 302°F). The transient plane source (TPS) method was used in the tests. Thermal expansion tests were conducted using push rod dilatometry over the continuous range from -40°F (-40°C) to 302°F (150°C).

2. EXPERIMENTAL

2.1 THERMAL CONDUCTIVITY AND VOLUMETRIC SPECIFIC HEAT

The Hot Disk Thermal Constants Analyzer was used to measure both thermal conductivity and specific heat of the samples.[1-3] The recently upgraded system (Fig. 1) uses a bridge to balance out changes in heater resistance at different temperatures. Two samples are needed for the measurement. A Kapton sensor/heater is sandwiched between the two samples. For the heat resistant shielding material, each measurement took 80 s during which the interface was heated up by a constant power output of 0.05 W. The overall temperature rise was kept under 5°C. Thermal conductivity and volumetric specific heat can be calculated from the interface temperature vs. time plot using the Hot Disk® software.

Six heat resistant shielding samples, Thermo Electron RM&P Catalog No. 277-4, were provided and were paired up in random. Each pair was measured at room temperature at HTML. The system was then taken to Building 4508 where a freezer (at -31°F) was available. After the freezer test, the specimens were tested in a box furnace at three elevated temperatures. To reach thermal equilibrium, the specimens were left in the freezer or furnace for at least 2.5 hr before measurements were started.

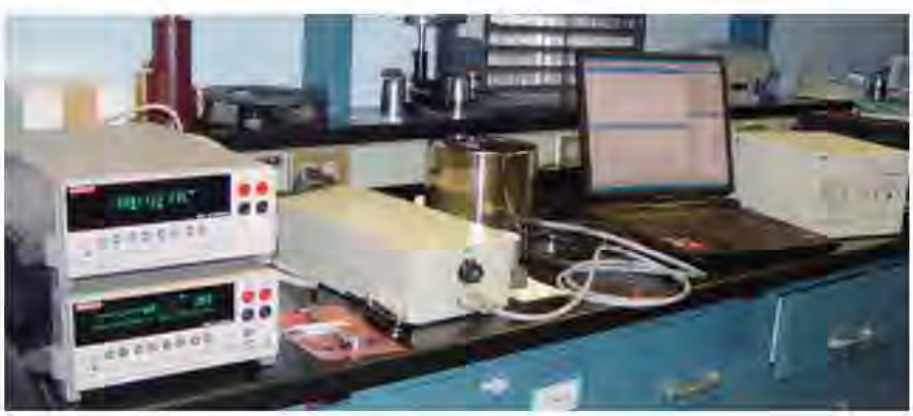

Fig. 1. Hot Disk System.

2.2 THERMAL EXPANSION

Specimens of cast Type 277-4 cement were received and tested by staff of the High Temperature Materials Laboratory at ORNL. The specimens were received in two shipments and consisted of three separate pours (lots) of the material. Lot 1 contained one specimen, poured in a one-piece mold, and having a diameter of ~5.5 mm. Lot 2 contained 7 specimens, poured in a split two-piece mold, also with a diameter of ~5.5 mm. Lot 3 had 5 specimens with a diameter of ~12.5 mm. No specimens from Lot 3 were used for measurements. The nominal length of all specimens was 25 mm.

Thermal expansion measurements were conducted using a Theta Industries dual push rod dilatometer. The testing followed the constant ramping procedure of ASTM E-228 for "Linear Thermal Expansion of Solid Materials with a Vitreous Silica Dilatometer."[4] A cryogenic furnace, cooled with helium gas bubbled through liquid nitrogen and heated by nichrome wires, was used with a silica specimen holder and push rods. A type K thermocouple in direct contact with the specimen was used to measure the specimen temperature. NIST Tungsten SRM 737 was used for the reference standard in the differential measurements. The specimens were tested over the range of -40°C to 150°C using heating rates of 3°C/min. The reference temperature for all expansion calculations was 20°C. A 5 cc/min flowrate of helium was used inside the specimen enclosure during the tests. This was a separate stream of helium from that used for cooling the cryogenic furnace. The displacements of the specimen and reference rods were determined by an LVDT housed in a constant temperature enclosure which also contained the RTD used for cold junction compensation of the specimen thermocouple signal.

The temperature schedule for the measurement tests was as follows:

1. Cool specimen to ~15°C prior to starting test using cooled helium.
2. Start data collection and heat specimen to 40°C. (Expansion is automatically zeroed as the specimen temperature goes through the 20°C reference temperature.)
3. Cool to -40°C at a nominal rate of 3°C/min.
4. Heat to 150°C.
5. Cool to -40°C at a nominal rate of 3°C/min.
6. Heat to 25°C and end test.

The schedule used allowed any hysteresis of the specimen expansion behavior to be noted.

3. RESULTS

3.1 THERMAL CONDUCTIVITY AND VOLUMETRIC SPECIFIC HEAT

Thermal conductivity values of the three pairs of samples are shown in Table 1 and the Thermal Conductivity vs. Temperature plot is shown in Fig. 2. Three measurements were taken at each temperature for each pair of samples. There is some scatter among the pairs (<5% between 3 measurements at the same temperature, 3-10% among the pairs) but they all showed similar changes over the temperature range. Since the specimens had to be taken out several times at each temperature, their exposure to air and thermal cycles was not controlled.

Table 1. Thermal conductivity (W/m•K)

Temperature (F)	Pair A	Pair B	Pair C
-31	0.96	0.97	0.92
73.4	1.00	0.97	1.05
140	0.87	0.75	0.87
212	0.64	0.62	0.58
302	0.67	0.59	0.64

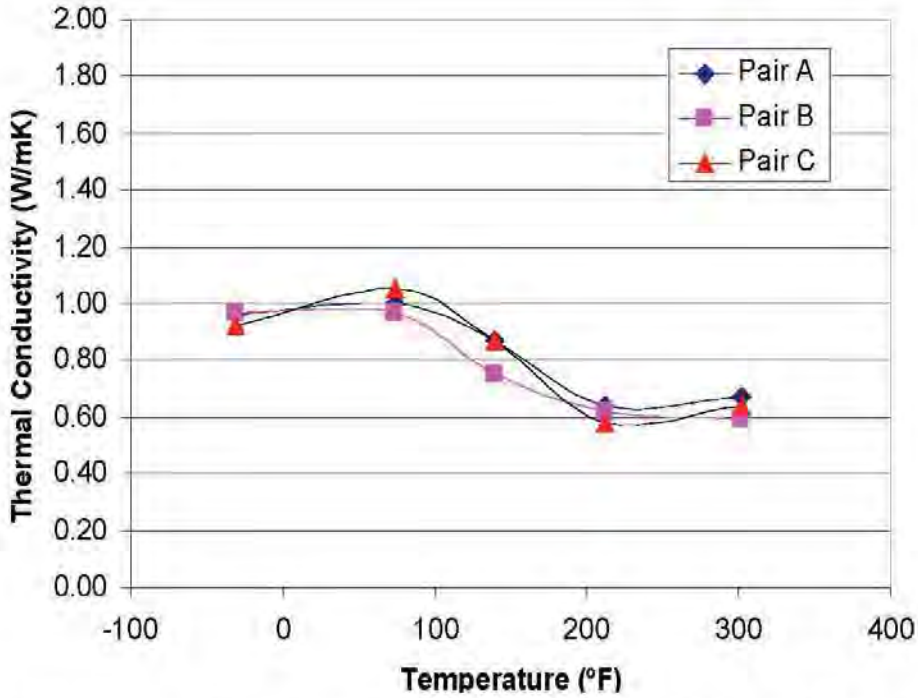

Fig 2. Thermal conductivity of Thermo Electron RM&P Catalog No. 277-4.

The volumetric specific heats were also obtained in the calculation. The value is a product of specific heat and density with the unit of $10^6 J/m^3 \cdot K$, as shown in Table 2 and Fig. 3. Since the weight of the samples exceeded the limit of the balance in the lab we were not able to measure the density of the specimens accurately. If the density is known ($1.68 * 10^6 g/m^3$ from product literature), the specific heat values can be calculated simply by dividing the current experimental value by density.

Table 2. Volumetric Specific Heat (MJ/m³•K)

Temperature (F)	Pair A	Pair B	Pair C
-31	0.92	0.80	0.92
73.4	1.33	1.27	1.32
140	1.71	1.68	1.65
212	1.72	1.67	1.72
302	1.99	2.14	2.01

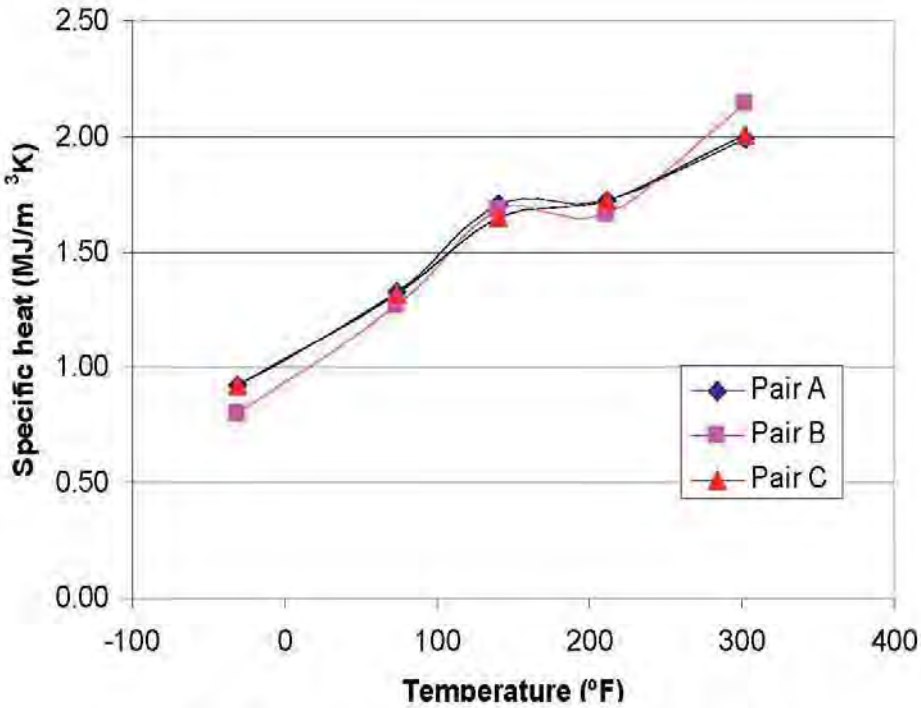

Fig. 3. Volumetric specific heat vs. temperature.

Since the three pairs of specimens were randomly grouped, we averaged the results to show the material properties. The values are shown in Table 3 and the plots are shown in Figures 4-5.

Table 3. Average values of k and Cp

Temperature (°F)	Average k (W/m•K)	Average Cp (MJ/m^3•K)
-31	0.95	0.88
73.4	1.01	1.31
140	0.83	1.68
212	0.61	1.70
302	0.63	2.05

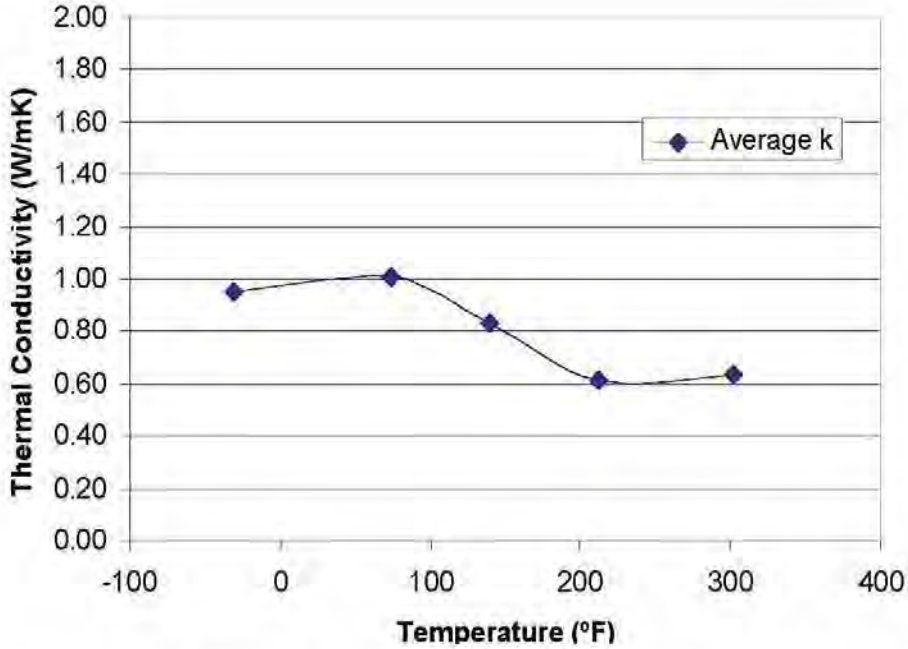

Fig. 4. Average thermal conductivity of Thermo Electron RM&P No. 277-4.

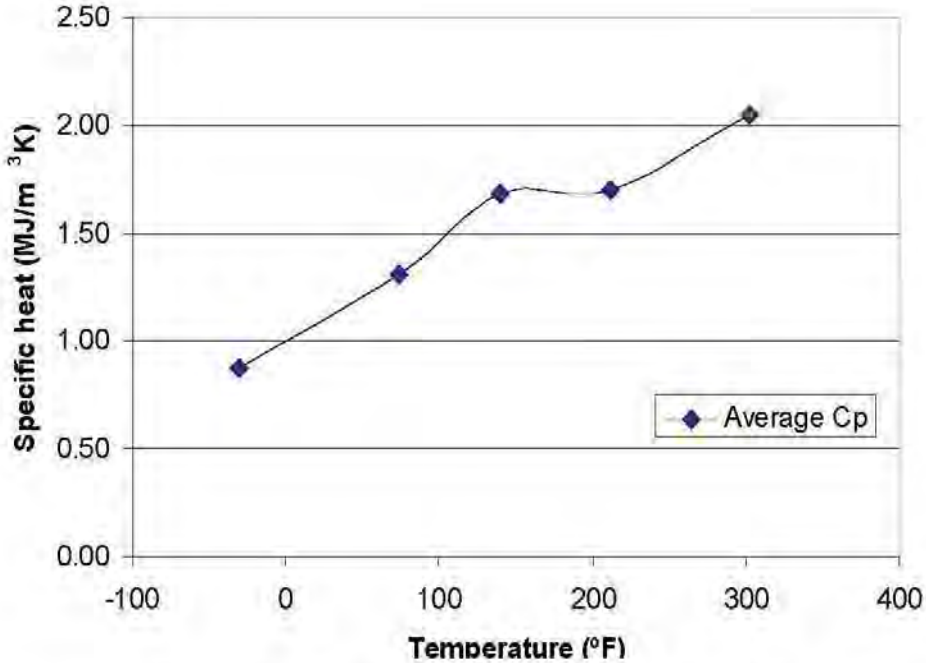

Fig. 5. Average volumetric specific heat of Thermo Electron RM&P Catalog No. 277-4.

3.2 THERMAL EXPANSION

One specimen from Lot 1 and four specimens from Lot 2 were tested. The thermal expansion results of the five specimens are shown in Fig. 6. Three Lot 2 specimen results grouped almost on top of each other. The fourth Lot 2 specimen deviated from the other three at temperatures greater than about 100°C. The single specimen from Lot 1 behaved markedly different than the Lot 2 specimens when heated above 50°C. The expansion behavior during cooling was very similar for all five specimens tested. All specimens tested exhibited a permanent strain (shrinkage) as a result of heating above 50°C. Measured data for the expansion of the five specimens taken from the initial heating from -40°C to 150°C can be found in Table 4. Also shown in Table 4 are values for the Mean Coefficient of Thermal Expansion (MCTE) calculated from 20°C. MCTE is defined as:

$$\text{MCTE} = (\text{expansion @ T}) / (\text{T} - 20) \qquad (1)$$

where T is the temperature in °C.

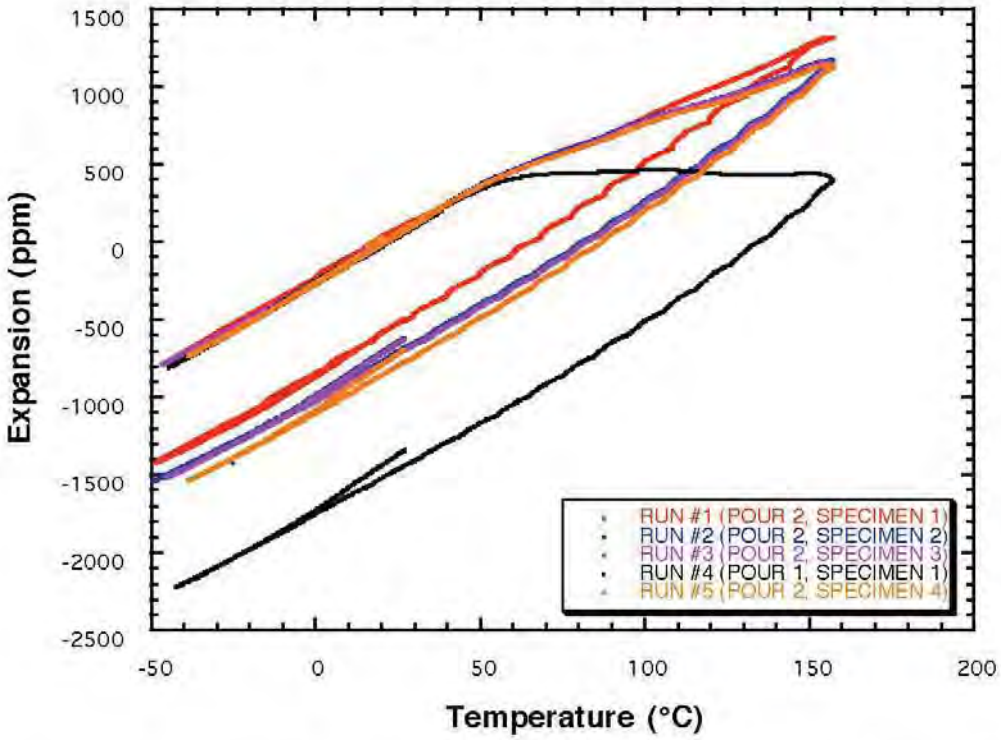

Fig. 6. Thermal expansion of Type 277-4 cement material as a function of temperature.

Table 4. Measured thermal expansion values and Mean CTE for Type 277-4 specimens

Temperature, °C	Run #1		Run #2		Run #3		Run #4		Run #5	
	exp, ppm	MCTE, ppm/°C	exp, ppm	MCTE, ppm/°C	exp, ppm	MCTE, ppm/°C	exp, ppm	MCTE, ppm/°C	exp, ppm	MCTE, ppm/°C
-40	-741	12.4	-727	12.1	-725	12.1	-759	12.6	-753	12.6
-20	-517	12.9	-500	12.5	-498	12.4	-519	13.0	-520	13.0
0	-266	13.3	-251	12.6	-247	12.3	-251	12.5	-260	13.0
20	0		0		0		0		0	
40	239	12.0	252	12.6	245	12.3	240	12.0	248	12.4
60	463	11.6	466	11.6	455	11.4	410	10.2	458	11.5
80	628	10.5	622	10.4	611	10.2	448	7.5	605	10.1
100	797	10.0	778	9.7	772	9.7	465	5.8	757	9.5
120	983	9.8	907	9.1	905	9.1	447	4.5	882	8.8
140	1166	9.7	1050	8.8	1042	8.7	434	3.6	1019	8.5
150	1271	9.8	1136	8.7	1126	8.7	449	3.4	1108	8.5

The expansion data in the interval -40 to 150°C for 3 of the Lot 2 specimens (Run #2, #3 and #5) were pooled and then sorted in ascending order by temperature. A moving average smoothing routine with a 31-point window (corresponds to less than 1°C temperature interval) was used to smooth both the temperature and expansion data. A cubic spline fit through this pooled, sorted and smoothed data set was then used to generate values for the expansion at increments of 1°C as shown in Table 5. The spline fit indicated an expansion of 1.6 ppm at 20°C. Since by definition the expansion is zero at the 20°C reference temperature, the values of Table 5 have been offset by this amount.

Table 5. Expansion values at even intervals estimated from cubic spline fit of pooled, sorted and smoothed data from Runs 2, 3, and 5.

TEMPERATURE, °C	ESTIMATED EXPANSION, ppm	ESTIMATED MCTE, ppm/°C	TEMPERATURE, °C	ESTIMATED EXPANSION, ppm	ESTIMATED MCTE, ppm/°C
-37	-706	12.4	5	-190	12.7
-36	-695	12.4	6	-177	12.7
-35	-683	12.4	7	-165	12.7
-34	-671	12.4	8	-152	12.7
-33	-661	12.5	9	-139	12.7
-32	-649	12.5	10	-126	12.7
-31	-638	12.5	11	-114	12.7
-30	-625	12.5	12	-101	12.7
-29	-614	12.5	13	-88	12.7
-28	-603	12.6	14	-76	12.7
-27	-591	12.6	15	-63	12.6
-26	-578	12.6	16	-50	12.6
-25	-567	12.6	17	-37	12.6
-24	-555	12.6	18	-25	12.6
-23	-544	12.7	19	-12	12.6
-22	-532	12.7	20	0	12.6
-21	-519	12.7	21	12	12.6
-20	-508	12.7	22	25	12.6
-19	-496	12.7	23	38	12.7
-18	-484	12.7	24	50	12.6
-17	-470	12.7	25	63	12.6
-16	-458	12.7	26	75	12.6
-15	-446	12.8	27	88	12.6
-14	-433	12.8	28	100	12.6
-13	-420	12.8	29	113	12.6
-12	-408	12.8	30	125	12.5
-11	-395	12.7	31	137	12.5
-10	-382	12.8	32	150	12.5
-9	-369	12.7	33	162	12.5
-8	-356	12.7	34	174	12.5
-7	-344	12.7	35	186	12.4
-6	-331	12.7	36	198	12.4
-5	-317	12.7	37	210	12.4
-4	-304	12.7	38	222	12.4
-3	-292	12.7	39	235	12.4
-2	-279	12.7	40	246	12.3
-1	-267	12.7	41	258	12.3
0	-254	12.7	42	270	12.3
1	-241	12.7	43	281	12.3
2	-228	12.7	44	293	12.2
3	-216	12.7	45	305	12.2
4	-203	12.7	46	316	12.2

Table 5. (Continued)

TEMPERATURE, °C	ESTIMATED EXPANSION, ppm	ESTIMATED MCTE, ppm/°C	TEMPERATURE, °C	ESTIMATED EXPANSION, ppm	ESTIMATED MCTE, ppm/°C
47	327	12.1	99	759	9.62
48	338	12.1	100	767	9.60
49	349	12.1	101	776	9.58
50	360	12.0	102	783	9.55
51	371	12.0	103	790	9.53
52	381	11.9	104	797	9.50
53	392	11.9	105	804	9.46
54	402	11.8	106	812	9.44
55	412	11.8	107	818	9.40
56	421	11.7	108	825	9.38
57	431	11.7	109	831	9.34
58	440	11.6	110	837	9.31
59	449	11.5	111	844	9.28
60	458	11.5	112	850	9.25
61	466	11.4	113	856	9.21
62	475	11.3	114	862	9.18
63	483	11.3	115	867	9.13
64	492	11.2	116	873	9.10
65	500	11.1	117	879	9.06
66	508	11.0	118	885	9.03
67	515	11.0	119	890	8.99
68	523	10.9	120	897	8.97
69	530	10.8	121	902	8.94
70	538	10.8	122	908	8.91
71	545	10.7	123	914	8.88
72	552	10.6	124	920	8.85
73	559	10.6	125	926	8.82
74	566	10.5	126	933	8.81
75	573	10.4	127	939	8.78
76	581	10.4	128	946	8.76
77	588	10.3	129	953	8.74
78	596	10.3	130	959	8.72
79	603	10.2	131	966	8.71
80	611	10.2	132	974	8.70
81	619	10.1	133	980	8.68
82	626	10.1	134	987	8.67
83	634	10.1	135	996	8.66
84	642	10.0	136	1003	8.65
85	650	10.0	137	1011	8.64
86	658	9.98	138	1019	8.64
87	666	9.94	139	1026	8.63
88	673	9.91	140	1034	8.62
89	681	9.88	141	1043	8.62
90	689	9.86	142	1051	8.62
91	697	9.83	143	1059	8.62
92	705	9.79	144	1068	8.62
93	713	9.78	145	1076	8.62
94	720	9.74	146	1085	8.62
95	728	9.72	147	1094	8.62
96	736	9.69	148	1104	8.63
97	744	9.67	149	1113	8.64
98	752	9.64	150	1122	8.63

Figure 7 compares the pooled experimental expansion data with the smoothed data and the cubic spline fit. The relative residuals of the spline fit are shown in Fig. 8. It can be seen that the estimated expansion values from the spline fit are within 0.2% of the smoothed data.

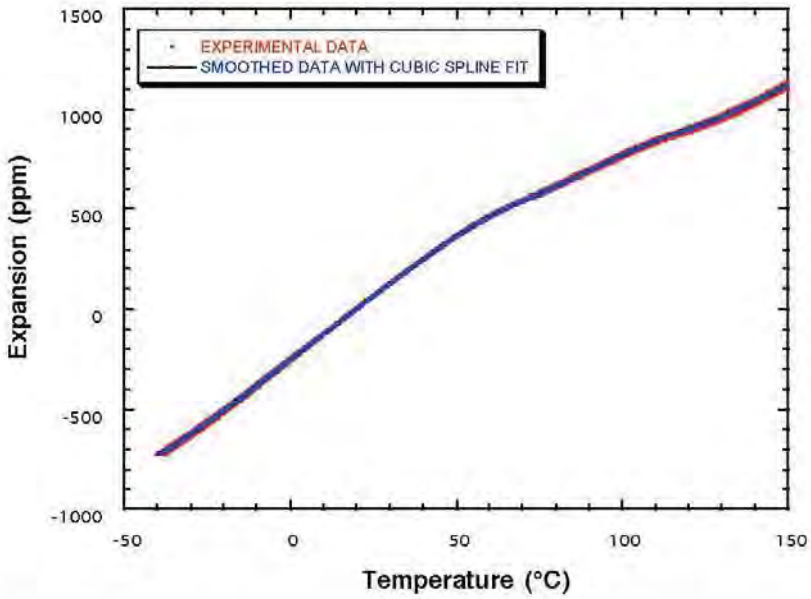

Fig. 7. Comparison of smoothed data and cubic spline fit of smoothed data to raw pooled experimental data for thermal expansion of Type 277-4 cement material as a function of temperature.

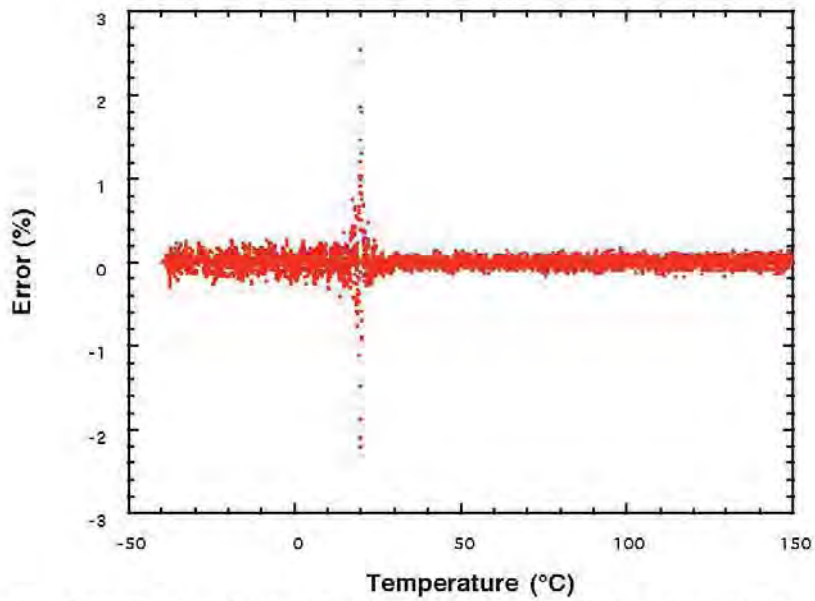

Fig. 8. Relative residuals of cubic spline fit used to estimate expansion values tabulated in Table 5.

The estimated expansion at the 1°C increments was used to calculate the MCTE values shown in Table 5. The value of MCTE at 20°C cannot be calculated because of a division by zero condition; therefore, the average of the 19 and 21°C MCTE values is listed in Table 5. Figure 9 shows a plot of the MCTE values from Table 5 along with a 9th order polynomial used to fit the values. The MCTE at any temperature in the range -37 to 150°C can be calculated using

$$\begin{aligned}\text{MCTE (ppm/°C)} = {} & 12.699164 - 0.0073715235*T + 0.00018778752*T^2 \\ & + 1.517514e\text{-}05*T^3 - 6.6945913e\text{-}07*T^4 - 2.4414824e\text{-}09*T^5 \\ & + 2.7529257*T^6 - 3.4686036e\text{-}12*T^7 + 1.7626873e\text{-}14*T^8 \\ & - 3.2800845e\text{-}17*T^9 \end{aligned} \quad (2)$$

It is strongly cautioned that Eq. (2) cannot be used to extrapolate MCTE values outside the measured range and describes the behavior only during an initial heating. Figure 10 shows the relative residuals for Eq. (2) using 8 significant digits for the polynomial coefficients compared to the MCTE values from Table 5. It can be seen that Eq. (2) generates the MCTE values of Table 5 to within better than 1% over the temperature range measured in this study.

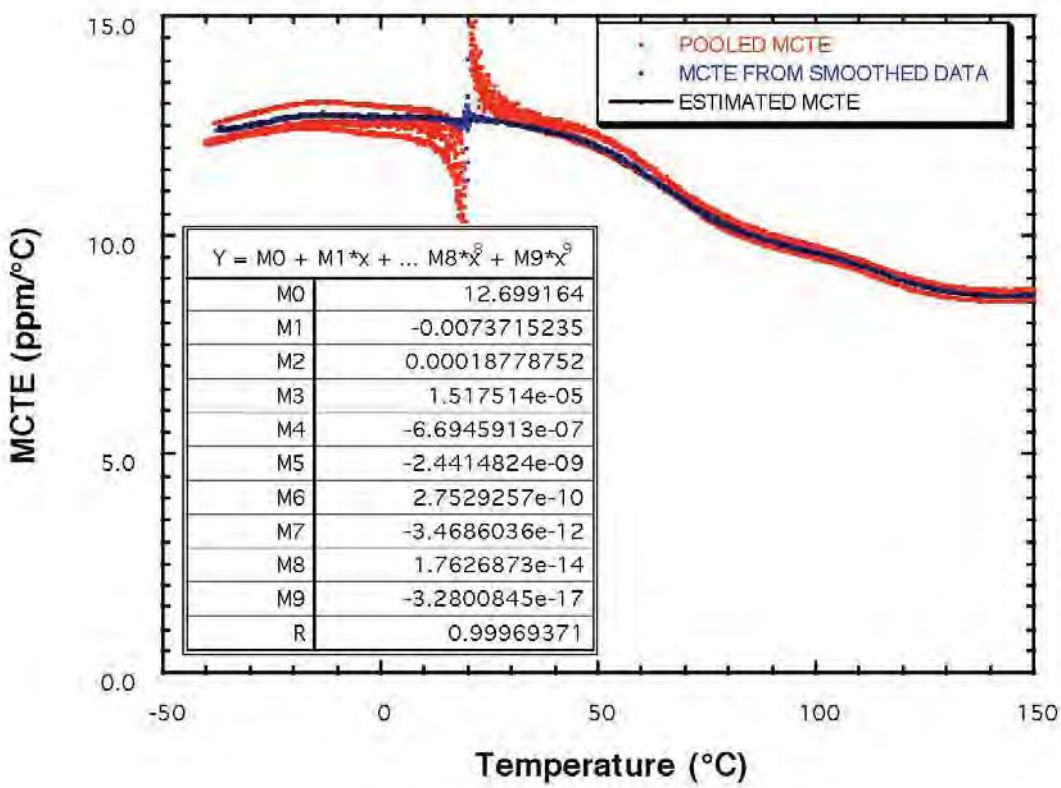

Y = M0 + M1*x + ... M8*x^8 + M9*x^9	
M0	12.699164
M1	-0.0073715235
M2	0.00018778752
M3	1.517514e-05
M4	-6.6945913e-07
M5	-2.4414824e-09
M6	2.7529257e-10
M7	-3.4686036e-12
M8	1.7626873e-14
M9	-3.2800845e-17
R	0.99969371

Fig. 9. Comparison of MCTE calculated from estimated expansion with MCTE calculated from smoothed expansion data and raw pooled MCTE values. Also shown is a 9th order polynomial fit of the MCTE calculated from the estimated expansion values of Table 5.

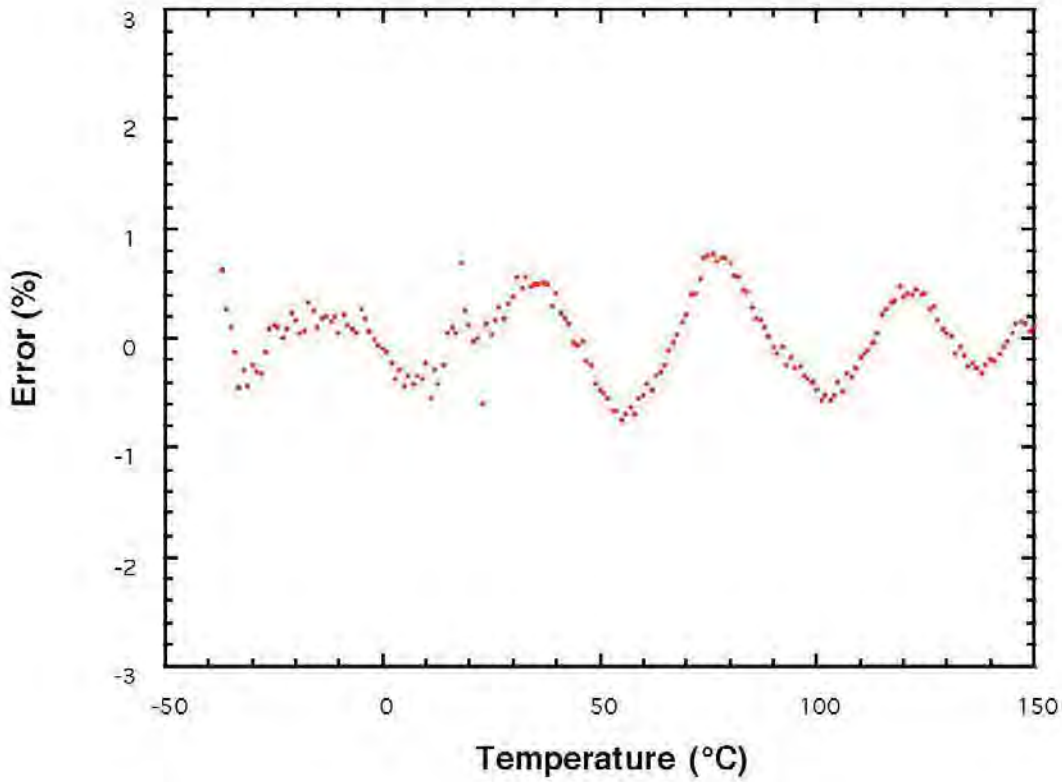

Fig. 10. Relative residuals of the 9th order polynomial fit of the estimated MCTE values using 8 significant digits for the coefficients as shown in Eq. (2).

After non-reversible behavior was demonstrated by the first specimen tested, the remaining four specimens were weighed before and after the expansion testing to determine any changes in mass resulting from heating the specimens. All specimens exhibited a weight loss of ~1.3% with individual results shown in Table 6. The initial density for the specimens tested is listed in Table 7. The Lot 1 specimen (Run #4) appeared to have a higher density than the Lot 2 specimens.

Table 6. Weight loss (%) behavior during testing

Run #1 (Lot 2, Specimen 1)	Not measured
Run #2 (Lot 2, Specimen 2)	-1.39
Run #3 (Lot 2, Specimen 3)	-1.24
Run #4 (Lot 1, Specimen 1)	-1.29
Run #5 (Lot 2, Specimen 4)	-1.34

Table 7. Initial density (10^6 g/m^3) of specimens tested

Run #1 (Lot 2, Specimen 1)	Not measured
Run #2 (Lot 2, Specimen 2)	1.47
Run #3 (Lot 2, Specimen 3)	1.50
Run #4 (Lot 1, Specimen 1)	1.60
Run #5 (Lot 2, Specimen 4)	1.48

4. SUMMARY

Two thermophysical properties, thermal conductivity and volumetric specific heat, were measured using the Hot Disk® method. The results among three random pairs of samples are consistent. All the specimens exhibited the same variations as a function of temperature.

The thermal expansion behavior was determined using a push rod dilatometer. Two specimens were considered to be outliers. Data from the remaining 3 specimens were pooled and the MCTE was described by a 9th order polynomial equation to within 1%.

All specimens lost about 1.3% during the expansion testing. Measured density of the specimens was found to be about $1.50*10^6$ g/m^3 for Lot 2 and about $1.60*10^6$ g/m^3 for Lot 1.

Since the material tested in this study undergoes irreversible changes the first time it is heated above 50°C, the data reported is valid only for the first time the material is heated above 50°C and must not be used to describe subsequent heating cycles.

REFERENCES

1. S.E. Gustafsson, E. Karawacki and M.N., Khan, *J. Phys. D.: Appl. Phys.* **12**, 1411(1979).
2. S.E. Gustafsson, *Rev. Sci. Instrum.* **62**, 797(1991).
3. V. Bohac, M.K. Gustavsson, L. Kubicar and S.E. Gustafsson, *Rev. Sci. Instrum.* **71**, 2452(2000).
4. ASTM E-228-95, "Standard Test Method for Linear Thermal Expansion of Solid Materials With a Vitreous Silica Dilatometer," *Annual Book of Standards* **Vol. 14.02**, ASTM International, West Conshohocken, PA(2003).

THIS PAGE INTENTIONALLY LEFT BLANK.

INTERNAL DISTRIBUTION

1. C. M. Amonett, 9111, MS8201
2. J. C. Anderson, 9113, MS8208
3. J. G. Arbital, 9113, MS8206
4. P. A. Bales, 9113, MS8206
5. E. E. Bloom

6-7. G. A. Byington, 9111, MS8201

8. S. N Cramer, 9113, MS8208
9. M. D. Crenshaw, 9110, MS8238
10. J. F. DeClue, 9110, MS8238
11. R. B. Dinwiddie
12. G. W. Eckert, 9119, MS8234

13-14. M. L. Goins, 9112, MS8201

15. K. D. Handy, 9201-2, MS8073
16. C. N. Heatherly, 9113, MS8208
17. S. T. Holder, 9113, MS8208
18. C. R. Hubbard
19. D. T. Johnson, 9110, MS8238
20. D. B. Miller, 9113, MS8206
21. A. E. Pasto
22. R. G. Perkins, 9113, MS8208

23-27. W. D. Porter

28. G. B. Singleton, 9113, MS8206
29. R. H. Smith, 9110, MS8238
30. D. P. Sooter, 9111, MS8201
31. S. K. Thomas, 9201-2, MS8073
32. D. A. Tollefson, 9110, MS8238
33. S. B. Turner, 9110, MS8238

34-38. H. Wang

39. T. L. Warren, 9113, MS8206
40. Central Research Library
41. ORNL Laboratory Records-RC

42-43. ORNL Laboratory Records-OSTI

THIS PAGE INTENTIONALLY LEFT BLANK.

Y/DW-1987

BWXT Y12
A BWXT/Bechtel Enterprise

Y-12 NATIONAL SECURITY COMPLEX

Mechanical Properties of 277-4

B. F. Smith
Technology Development

G. A. Byington
Mechanical and Manufacturing Engineering

January 19, 2005

Prepared by the
Y-12 National Security Complex
P.O. Box 2009
Oak Ridge, Tennessee, 37831-8169
Managed by BWXT Y-12, L.L.C.
for the
U.S. DEPARTMENT OF ENERGY
under contract DE-AC05-00OR22800

MANAGED BY
BWXT Y-12, L.L.C.
FOR THE UNITED STATES
DEPARTMENT OF ENERGY

UCN-13672 (10-00)

DISCLAIMER

This report was prepared as an account of work sponsored by an agency of the United States Government. Neither the United States Government nor any agency thereof, nor any of their employees, makes any warranty, express or implied, or assumes any legal liability or responsibility for the accuracy, completeness, or usefulness of any information, apparatus, product, or process disclosed, or represents that its use would not infringe privately owned rights. Reference herein to any specific commercial product, process, or service by trade name, trademark, manufacturer, or otherwise, does not necessarily constitute or imply its endorsement, recommendation, or favoring by the United States Government or any agency thereof. The views and opinions of authors expressed herein do not necessarily state or reflect those of the United States Government or any agency thereof.

Y/DW-1987

MECHANICAL PROPERTIES OF 277-4

B. F. Smith
Technology Development

G. A. Byington
Mechanical and Manufacturing Engineering

Date of Issue: January 19, 2005

Prepared by the
Y-12 National Security Complex
P.O. Box 2009
Oak Ridge, Tennessee, 37831-8169
Managed by BWXT Y-12, L.L.C.
for the
U.S. DEPARTMENT OF ENERGY
under contract DE-AC05-00OR22800

CONTENTS

LIST OF FIGURES iv

LIST OF TABLES iv

INTRODUCTION 1

EXPERIMENTAL PROCEDURE 1

RESULTS 2

DISCUSSION 9

REFERENCES 10

APPENDIX 11

LIST OF FIGURES

Figure 1. Tensile specimen 2
Figure 2. Boundary and average stress-strain curves 7
Figure 3. All specimen and boundary curves 8

LIST OF TABLES

Table 1. Compressive strengths of 277-4 at 100°F 2
Table 2. Compressive strengths of 277-4 at 70°F 3
Table 3. Compressive strengths of 277-4 at -40°F 3
Table 4. Tensile strengths of 277-4 at 100°F 3
Table 5. Tensile strengths of 277-4 at 70°F 3
Table 6. Tensile strengths of 277-4 at -40°F 4
Table 7. Ten-point stress-strain curve summary, lower bound 5
Table 8. Ten-point stress-strain curve summary, 70°F average 5
Table 9. Ten-point stress-strain curve summary, upper bound 6
Table 10. Young's modulus values 6
Table 11. Poisson's ratio of 277-4 at three temperatures 6

INTRODUCTION

It was desired to reduce the costs associated with a shipping container by replacing Eagle Picher BoroBond4 with a lighter, less expensive material. Thermo Electron Corporation Catalog 277-4 material met both of these requirements. At 105 lb/ft^3, 277-4 is significantly less dense than BoroBond4, which has a density of 123 lb/ft^3. Before the container could be certified, a number of tests had to be performed on the material. These included measuring coefficient of thermal expansion, thermal conductivity, and specific heat. Other tests included thermogravimetric analysis, neutron transmission, and outgassing. Several mechanical properties were needed, including compressive strength, tensile strength, modulus of elasticity, and Poisson's ratio. This study focuses on the mechanical properties of 277-4 at three temperatures: -40°F, 70°F, and 100°F.

EXPERIMENTAL PROCEDURE

The procedure for measuring the compressive strength was based on ASTM C109-02, *Standard Test Method for Compressive Strength of Hydraulic Cement Mortars (Using 2-in. or [50-mm] Cube Specimens)*.[1] Two batches of cubes were cast on October 4 and October 11. Tensile specimens were cast at the same time; they will be described below. Eighteen cubes were delivered to the mechanical testing lab on November 1. The density of each cube was measured using a scale and calipers. Each cube was assigned a number according to the following system:

[Compression or Tension][Date of cast][Mix time in minutes]-[Arbitrary number]

Thus, specimen C1043-1 is a compression specimen that was cast on October 4. It was mixed for three minutes prior to pouring. In addition to providing compressive strength values, these cube specimens were used for measuring the modulus of elasticity and Poisson's ratio of the material. Stress-strain curves were needed for calculating the modulus. Also, accurate measurements of transverse strain were required for Poisson's ratio. Measuring stress is relatively straightforward, but measuring strain of cement is more complex. It was decided to use 90° tee rosette strain gages to measure axial strain and transverse strain simultaneously. Originally, two rosettes were to be adhered to each specimen on opposite faces, however, time constraints prohibited this. Only one rosette was attached to each cube. During strain gage application, each cube experienced the same thermal treatment while curing the precoat and gage adhesive. See the Appendix for detailed application procedures. Six cubes were tested at -40°F, six were tested at 70°F (room temperature), and six were tested at 100°F. Prior to testing, each specimen had to soak at the appropriate temperature long enough to ensure the center was at the test temperature. The -40°F cubes were thermally "shocked" at -50°F for approximately 23 h. Three of the 100°F cubes were heated at 110°F for 3.5 h. The other three 100°F cubes were heated at 120°F for 45 min.

The tensile test was based on ASTM C307-03, *Standard Test Method for Tensile Strength of Chemical-Resistant Mortar, Grouts, and Monolithic Surfacings*.[2] The briquet specimen described in this method has a "dogbone" shape and is approximately three inches long and has a reduced section of one inch wide by one inch thick. A photograph of one is shown in Figure 1. These specimens were cast and delivered at the same time as the compression cubes. These specimens have a discontinuous cross-section, so generating stress-strain curves from them would be difficult. For this reason, strain gages were not attached to them. The tensile test was used only for determining tensile strength. Six briquets were tested at -40°F, six were tested at 70°F (room temperature), and six were tested at 100°F. All briquets were soaked for the same lengths of time and at the same temperatures as the cubes, even though calculations for thermal equilibrium were based on the cube geometry. The only exception to this was that none of the 100°F briquets were soaked at 120°F.

Fig. 1. Tensile specimen

RESULTS

Tables 1 through 3 give room temperature densities and compressive strength values at the three temperatures being considered. Tables 4 through 6 give tensile strength values at the same three temperatures.

Table 1. Compressive strengths of 277-4 at 100°F

Cube ID	Density @ Room Temp (lb/ft^3)	Compressive Strength (psi)
C10043-2	99.76	746.2
C10043-5	99.96	854.4
C10113-9	100.65	1185.2
C10043-6	101.01	777.3
C10043-3	101.24	711.3
C10043-4	101.32	727.9
Average	100.66	833.7

Table 2. Compressive strengths of 277-4 at 70°F

Cube ID	Density @ Room Temp (lb/ft^3)	Compressive Strength (psi)
C10043-1	101.37	757.5
C10113-8	101.80	1073.0
C10113-2	101.95	977.9
C10113-3	102.22	1043.4
C10113-4	102.32	1041.8
C10113-7	102.65	1004.3
Average	102.05	983.0

Table 3. Compressive strengths of 277-4 at -40°F

Cube ID	Density @ Room Temp (lb/ft^3)	Compressive Strength (psi)
C10113-6	103.67	1250.7
C10113-5	104.36	1253.8
C10113-1	104.55	1227.4
C10043-7	108.97	1013.4
C10043-9	109.80	1176.9
C10043-8	109.91	1072.8
Average	106.88	1165.8

Table 4. Tensile strengths of 277-4 at 100°F

Briquet ID	Location of Fracture	Tensile Strength (psi)
T10113-4	Grip	255.9
T10113-5	Grip	232.6
T10113-6	Middle	238.5
T10043-4	Middle	161.4
T10043-5	Grip	144.5
T10043-6	Grip	225.1
Average		209.7

Table 5. Tensile strengths of 277-4 at 70°F

Briquet ID	Location of Fracture	Tensile Strength (psi)
T10113-1	Grip	170.1
T10113-2	Middle	129.1
T10113-3	Grip	145.2
T10043-1	Middle	226.0
T10043-2	Middle	241.2
T10043-3	Grip	192.1
Average		184.0

Table 6. Tensile strengths of 277-4 at -40°F

Briquet ID	Location of Fracture	Tensile Strength (psi)
T10113-7	Middle	341.1
T10113-8	Middle	286.7
T10113-9	Grip	206.7
T10043-7	Middle	201.7
T10043-8	Grip	180.7
T10043-9	Grip	191.2
Average		234.7

The stress-strain curves for several of the specimens turn back when fracture begins. However, the stress continues to increase as the strain decreases, generating a "hook" at the top of the curve. ASTM C 109 defines the strength as the maximum stress achieved during the test, regardless of the strain behavior. In order to simplify modulus calculations, the turned back portion of the stress-strain curve was cut out. The strength was still calculated using the maximum stress reading, per C 109. In order to evaluate each of the data curves, a straight line interpolation was used to generate points at discrete strain levels. An increment of 100 microstrain was used up to 400 microstrain. Beyond 400 microstrain, an increment of 200 microstrain was used until the end of the curve. Dividing each curve in this manner resulted in uniform strain curves ranging from 16 to 26 points, depending on the total compression of the specimen. This data decimation technique reduces the number of data points from approximately 200 and allows a simple average to be computed for each sample group at the same strain levels. The simple average curves had large discontinuities where each constituent curve in that group ended. An upper bounding curve was generated by taking the maximum stress value for each strain value of the -40°F sample. Similarly, a lower bounding curve was generated by taking the minimum stress value of the 100°F sample for each strain value.

To unify the data handling and for input into modeling software, composite 10 point curves were generated for the minimum and maximum bounding curves and for the 70°F average curve . An approximated arclength parameterization technique was used for interpolating between the data points. This approximation was generated by calculating delta arclength parameter (ΔS) segments. The delta arclength parameter segments were calculated by adding the fractional change in strain with the corresponding fractional change in stress and dividing the sum by 2. See equation 1. This parameterization approximation technique works best on functions. The plotting scale has no effect on the results because the delta arclength parameter segments are the percent differences or fractional changes between each of the strain and stress data points. Summing all of the fractional changes of the strain will generate a value of 1. Summing all of the fractional changes of the stress will also generate a value of 1.

$$\Delta S = \left(\frac{\Delta strain}{totalstrain} + \frac{\Delta stress}{totalstress} \right) \Big/ 2 \qquad (1)$$

By iteratively summing the delta arclength parameter (ΔS) segments the fractional arclength parameter (S) was calculated according to equation 2.

$$S = \sum_{0}^{n} \Delta S \qquad (2)$$

The fractional arclength parameter indicates the location along the curve, such that at the origin S equals zero and at the end of the curve S equals one. Now one can use a straight line interpolation to map the arclength parameter S to both strain and stress. At every 10 percent of the arclength parameter, both strain and stress were calculated using a straight line interpolation. This method was applied to the upper and lower bounding curves and the 70°F average curve. Tables 7 through 9 give the numerical values, while Figure 2 shows them graphically. In addition to the boundary curves, Figure 3 shows the decimated stress-strain curves for all specimens used in calculations. Several specimens were rejected due to abnormally shaped curves. It is possible these anomalous curves were due to imperfect strain gage application. Often, after seemingly adequate surface preparation, small peaks would be apparent underneath the gage. These peaks could have caused the strange readings in the rejected specimens.

Table 7. Ten-point stress-strain curve summary, lower bound

Strain (microstrain)	Stress (psi)
0.0	0.0
257.5	103.7
527.0	205.5
885.0	293.5
1320.1	369.4
1814.8	436.0
2347.5	496.6
2887.8	556.0
3431.8	614.9
4003.7	669.3
4600.0	720.0

Table 8. Ten-point stress-strain curve summary, 70°F average

Strain (microstrain)	Stress (psi)
0.0	0.0
219.8	150.3
490.0	289.7
797.6	421.2
1155.4	541.8
1565.4	651.3
2042.0	746.5
2552.4	834.4
3262.3	879.4
3935.3	932.4
4600.0	987.2

Table 9. Ten-point stress-strain curve summary, upper bound

Strain (microstrain)	Stress (psi)
0.0	0.0
101.1	201.3
251.8	378.8
390.9	561.9
579.6	721.1
762.8	883.1
1002.9	1017.6
1305.2	1122.2
1663.2	1200.1
2108.4	1236.1
2600.0	1249.7

Values of Young's modulus for each temperature were calculated using the first nonzero data point and the origin. The modulus is reported in Table 10. Poisson's ratio was determined from the plot of transverse strain versus axial strain. Poisson's ratio is the slope of the linear portion of this plot. Table 11 gives Poisson's ratio at each temperature.

Table 10. Young's modulus values

Temperature	Modulus (Mpsi)
100°F	0.4027
70°F	0.6838
-40°F	1.991

Table 11. Poisson's ratio of 277-4 at three temperatures

Temperature	Poisson's Ratio	Standard Deviation
100°F	0.25	0.045
70°F	0.28	0.105
-40°F	0.33	0.088

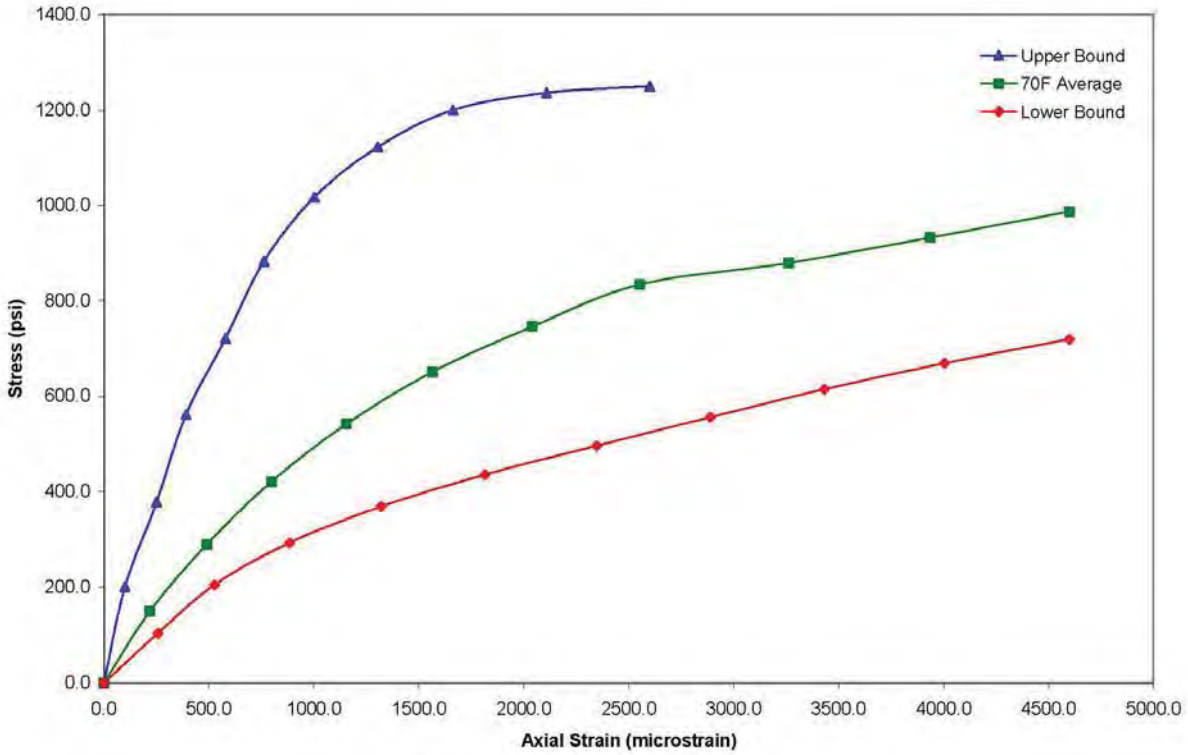

Fig. 2. Boundary and average stress-strain curves.

7

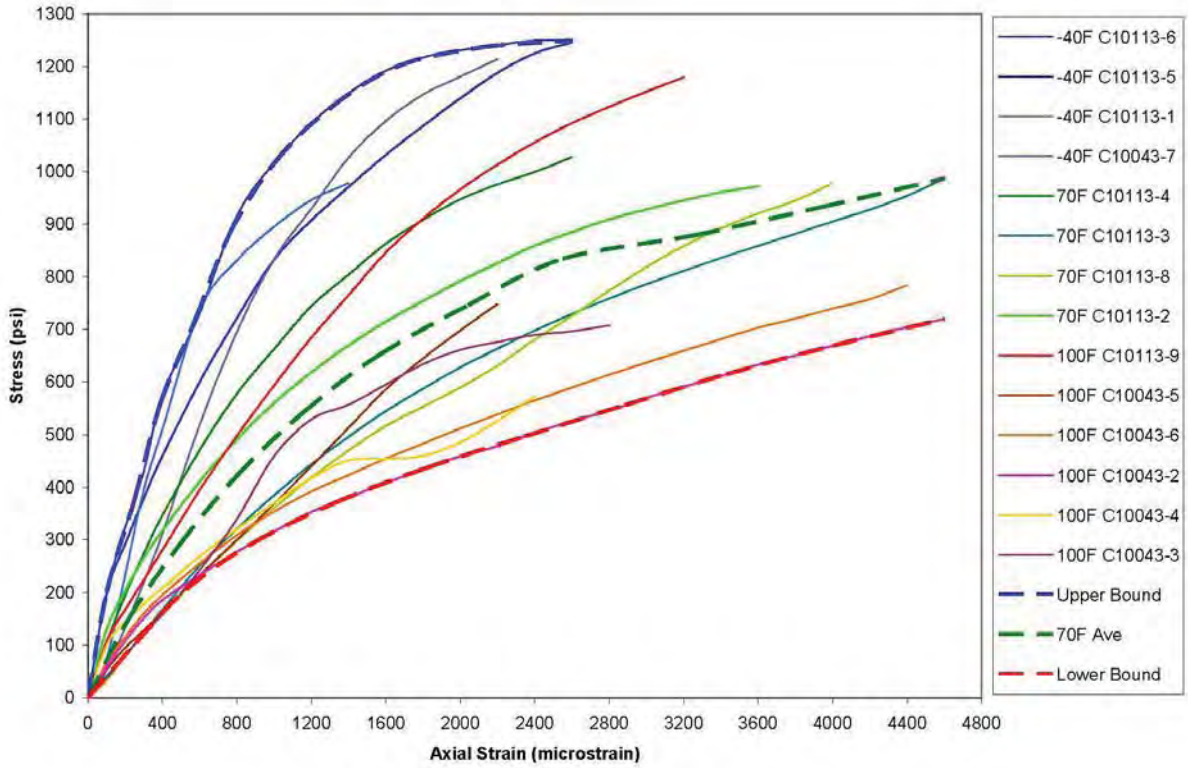

Fig. 3. All specimen and boundary curves.

DISCUSSION

Tables 1 through 3 give compressive strength values in order of increasing density, under the assumption there would be a strong correlation between the two. However, a better predictor of strength is the casting date. Cubes cast on October 11 were generally stronger than those cast on October 4. This contradicts the generalization that cements increase in strength with age. Except for the specimens tested at 70°F, the tensile specimens cast on October 11 were generally stronger than the ones cast on October 4. Without information on the casting procedure or steps taken to control extraneous variables (ambient temperature, humidity, etc.) it is impossible to determine the reason for the difference in strengths.

Tables 4 through 6 give the location of the tensile specimen fracture, either at the narrow middle portion, or at the wider section that contacts the cylindrical grip. This test was loosely based on ASTM C 307, which states that "jawbreaks should be rejected" in paragraph 11.2. This requirement is understandable due to localized deformation and stress concentrations at the grips, which have the potential of introducing fracture toughness as a variable. Only a few aspects of C 307 were used for this study, such as the specimen shape, grip shape, and testing speed. Thus, the information on break location is included for the reader's information only.

REFERENCES

1. ASTM International. *Standard Test Method for Compressive Strength of Hydraulic Cement Mortars (Using 2-in. or [50-mm] Cube Specimens).* ASTM Standard C 109/C 109M-02.

2. ASTM International. *Standard Test Method for Tensile Strength of Chemical-Resistant Mortar, Grouts, and Monolithic Surfacings.* ASTM Standard C 307-03.

APPENDIX

SURFACE PREPARATION AND STRAIN GAGE APPLICATION

Note: All cleaners and adhesives were purchased from Vishay Intertechnology, Inc.

1. Partially coat one face of 18 cubes with M-Bond AE-10 epoxy adhesive. Cure for 3 h at 125°F.

2. Nine cubes still tacky three days later. These were given a second coat of adhesive. All 18 cubes heated at 80°F for 2 h.

3. Smooth coating as much as practical by abrading with silicon-carbide paper.

4. Degrease coating with M-Line GC-6 Isopropyl Alcohol.

5. Wet-abrade coating with 400-grit silicon-carbide paper and M-Prep Conditioner A phosphoric acid solution. Wipe off residue with cotton gauze sponge.

6. Apply gage location layout lines.

7. Scrub with M-Prep Conditioner A using cotton swabs. Wipe off solution with cotton gauze sponge.

8. Scrub with M-Prep Neutralizer 5A ammonia solution. Wipe off solution with cotton gauze sponge.

9. Temporarily tape strain gage to cube and line up with layout lines.

10. Apply a small amount of M-Bond AE-10 epoxy adhesive to prepared face of cube and gage.

11. Clamp assembly together and cure overnight.

12. With clamp still on, cure adhesive for 1 h at 145°F.

13. Remove clamp and tape and solder on leadwires. Use M-Flux AR to aid soldering.

14. Thoroughly clean off flux with rosin solvent (toluene/isopropanol mix) and let dry.

15. Apply M-Coat A polyurethane protective coating. Let dry overnight.

DISTRIBUTION

Y-12 National Security Complex

1. C. M. Amonett
2. J. C. Anderson
3. J. G. Arbital
4. M. L. Baker
5. P. A. Bales
6. W. D. Brosey
7. G. A. Byington (2)
8. S. N. Cramer
9. M. D. Crenshaw
10. J. F. DeClue
11. G. W. Eckert
12. M. L. Goins (2)
13. K. D. Handy
14. C. N. Heatherly
15. S. T. Holder
16. D. T. Johnson
17. D. B. Miller
18. G. Perkins
19. G. B. Singleton
20. B. F. Smith
21. R. H. Smith
22. D. P. Sooter
23. S. K. Thomas
24. D. A. Tollefson
25. S. B. Turner
26. T. L. Warren
27. Y-12 Central Files (RC)

THIS PAGE INTENTIONALLY LEFT BLANK.

Y/DZ-2585

Volatile Components from Packing Materials, Rev.2

R. A. Smith

Compatibility & Surveillance
Technology Development

December 22, 2004

Prepared by the
Y-12 National Security Complex
Oak Ridge, TN 37831-8169
Managed by
BWXT Y-12, L.L.C.
for the
U. S. DEPARTMENT OF ENERGY
under contract DE-AC05-00OR22800

MANAGED BY
BWXT Y-12, L.L.C.
FOR THE UNITED STATES
DEPARTMENT OF ENERGY

UCN-13872 (10-00)

DISCLAIMER

This report was prepared as an account of work sponsored by an agency of the United States Government. Neither the United States Government nor any agency thereof, nor any of their employees, makes any warranty, express or implied, or assumes any legal liability or responsibility for the accuracy, completeness, or usefulness of any information, apparatus, product, or process disclosed, or represents that its use would not infringe privately owned rights. Reference herein to any specific commercial product, process, or service by trade name, trademark, manufacturer, or otherwise, does not necessarily constitute or imply its endorsement, recommendation, or favoring by the United States Government or any agency thereof. The views and opinions of authors expressed herein do not necessarily state or reflect those of the United States Government or any agency thereof.

Y/DZ-2585

Volatile Components from Packing Materials, Rev.2

R. A. Smith

Compatibility & Surveillance
Technology Development

December 22, 2004

Prepared by the
Y-12 National Security Complex
Oak Ridge, TN 37831-8169
Managed by
BWXT Y-12, L.L.C.
for the
U. S. DEPARTMENT OF ENERGY
under contract DE-AC05-00OR22800

TABLE OF CONTENTS

LIST OF FIGURES AND TABLES ii

SUMMARY 1

INTRODUCTION 1

Experimental 1
Experimental Procedures 2
Data and Results 2

CONCLUSIONS 2

FIGURES 3

TABLES 8

LIST OF FIGURES

Figure 1. Outgassing of two polyethylene film specimens at 338 degrees F. 3

Figure 2. Outgassing of two silicone foam specimens at 338 degrees F. 4

Figure 3. Outgassing of two silicone elastomer specimens at 338 degrees F. 5

Figure 4. Outgassing of a Borobond4 concrete at 338 degrees F. 6

Figure 5. Outgassing of a 277-4 Borated concrete at 338 degrees F. 7

LIST OF TABLES

Table 1. Outgassing at 180°F at standard temperature (298K) and pressure (1 atm) 8

Table 2. Weight Changes in grams after Experiment #1 (338°F or 170°C) 8

Table 3. Material Information Summary 9

SUMMARY

An outgassing study was conducted on five packing materials, comprising two experiments. These materials comprised 277-4 borated concrete, Borobond4 concrete, polyethylene bags, silica-filled silicone rubber seals, and silicone foam padding. The purpose was to measure the volume of gases which diffuse from packaging materials when sealed in containers. Two heating profiles were used to study the offgassing quantities in a set of accelerated aging tests. It was determined that the concretes contain a large quantity of water. The plastic materials hold much less moisture, with the silicone materials even consuming water, possibly due to the presence of silica filler. Polyethylene tends to degrade as the temperature is elevated and the foam stiffens.

INTRODUCTION

A variety of materials are required for safely packaging items for transport or storage. These materials must physically protect components while not causing damage by virtue of their own compositions. According to de Premare, "Sensitive products can begin to deteriorate at just 30% relative humidity (RH). Many products require a constant RH of 10-15% or less for stability and an extended shelf life."

The current study utilizes small samples of ceramic and polymeric packaging materials contained in measured volumes within stainless steel containers. Each container is then attached to a capacitance manometer or "baratron" for on-going measurement of the internal container pressure as the temperature is increased. This method allows determination of the volatiles quantity within the materials, which is most likely moisture but also decomposition products of the some materials. While such moisture is not immediately apparent under ambient conditions, the water contained in packaging is available to diffuse out over long time frames, such as years. To this extent, the maximum or "worst-case" amount can be calculated.

Two heating profiles were used and data calculated in terms of volume of gas at standard temperature and pressure, per material mass, a unit called "specific volume." This quantity was plotted versus time, as was the temperature profile. Visual observation of aged materials was conducted to ascertain obvious changes.

Experimental

Standard vacuum hardware is used to seal randomly sized specimens of each material (from 0.2 to 5 g) in air after they are weighed on a calibrated scale. In most cases, the experiment was repeated, but time limitations made this difficult. Additionally a "blank" container was tested under each experimental condition. Each container comprised a 5-inch height stainless steel retort of 1.3" diameter, in which was placed 3.75 – 4.0 inch heights of stainless steel block cylinders. This "filler" provided a smaller open volume of which the pressure was measured. This volume could be theoretically estimated, but was experimentally measured by expanding air from each unit into a known volume and measuring the resulting pressures. For experiments, each unit was attached to a pressure measurement system comprising a) and MKS Instruments Type 690A14TRB 10,000 torr baratron; b) MKS 670 signal conditioner electronics for data collection through an Omega datalogger; and c) a computer for data download and storage. The heating steps were conducted in a Despatch LAC 1-67-6 programmable laboratory oven which uses a Protocol Plus microprocessor control. A thermocouple was used to independently track and download the oven temperature to the aforementioned datalogger in concurrence with the pressure data. Upon experiment completion, containers remained sealed until disassembly. Material specimens were re-weighed and stored in labeled plastic bags.

Experimental Procedures:

I. A thermocouple is incorporated with the baratron such that the pressure is measured as the temperature is increased in a stepwise manner, from ambient to 300°F (23 – 150°C). Use 50°F increments and hold for 120 minutes before each rise. The outgassing pressure in torr is tracked for reporting in specific volume units of cm^3(STP)/g as a function of time and temperature. The planned 300°F upper limit was actually recorded at 338°F.

II. Perform another set of experiments where test materials are held at 180°F for two hours; measure pressure over that time frame. Present total offgassing quantity for each material (two specimens each) in specific volume units of cm^3(STP)/g.

Data and Results

The data was collected by Omega Hyperware, then downloaded and analyzed using Microsoft Excel. For all materials, charts were produced giving outgassing volume in cm^3(STP)/g and temperature in °F from ambient to 338°F, as a function of time; a text table for outgassing quantity at 180°F is provided. The outgassing curves are adjusted for linear rise in background outgassing from the container and filler materials which was measured at a total 19.2 cm^3 (STP). A similar background quantity of 4.0 cm^3 (STP) is subtracted from the 180°F outgas volumes.

I. Experiment 1 (Use 50°F increments and hold for 120 minutes before each rise up to 338°F). Figures 1 through 5 are provided for polyethylene, foam, elastomer, Borobond4, and 277-4 Borated concrete. Table 2 provides typical weight changes in specimens before and after the 13-hour heating experiments to 338°F were conducted.

II. Experiment 2 (Reach 180°F and hold for two hours; measure pressure over that time). Table 1 summarizes the total quantity of outgassing in this test. Several materials render negative results, indicating an overall reduction in gas due to absorption or reaction with the material at this temperature. The silicone foam and elastomer contain silica filler (SiO_2) which is known for its reactivity with water. The polyethylene is most likely reacting with the oxygen as its chains fragment and degrade. This material was the most obviously physically changed from this test – the originally flexible and clear film became brittle and slightly cloudy.

CONCLUSIONS

The concrete materials demonstrate the most massive degree of water content, outgassing under each experimental condition. The Borobond4 did not change much in appearance, although it was slightly darker in color after heating. However the 277-4 Borated concrete became extremely friable and more sandy than its original texture. It also turned a very light gray color.

The polyethylene film was least likely to hold moisture, but did degrade in each case. This material became glassy and yellowed due to heating, with outgassing observed in the longer duration 338°F test. This may result from degradation products, rather than water.

The silicone foam did retain some moisture content over a longer period of time and outgassed at higher temperatures. The silicone elastomer outgas quantity was very small.

Further information about gas composition could be obtained from headspace gas analysis of the captured outgassing products.

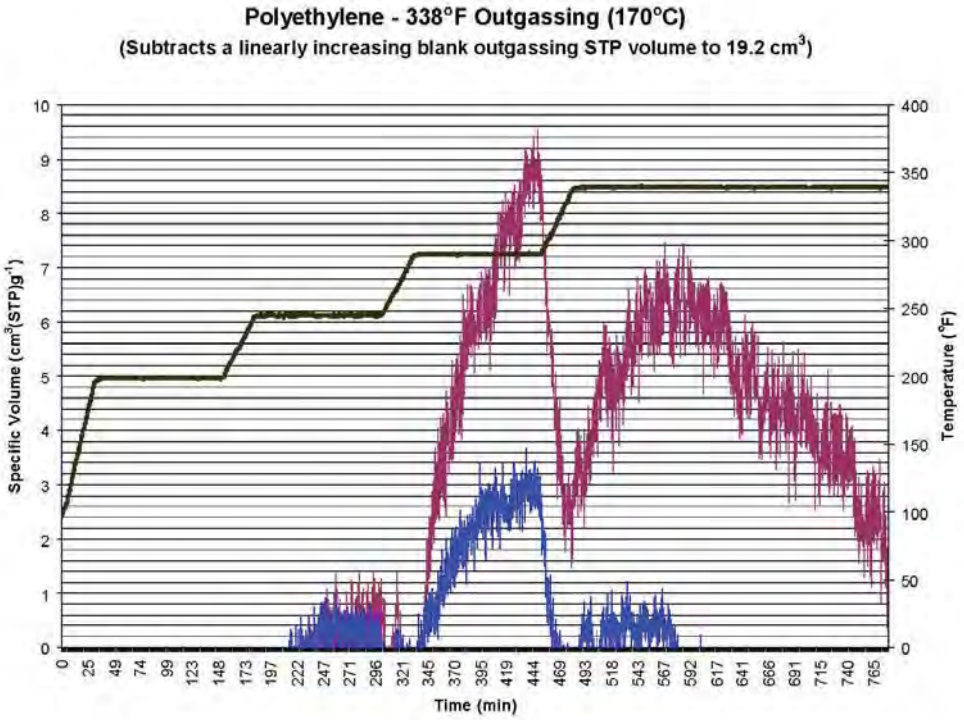

Figure 1. Outgassing of two polyethylene film specimens at 338 degrees F.

3

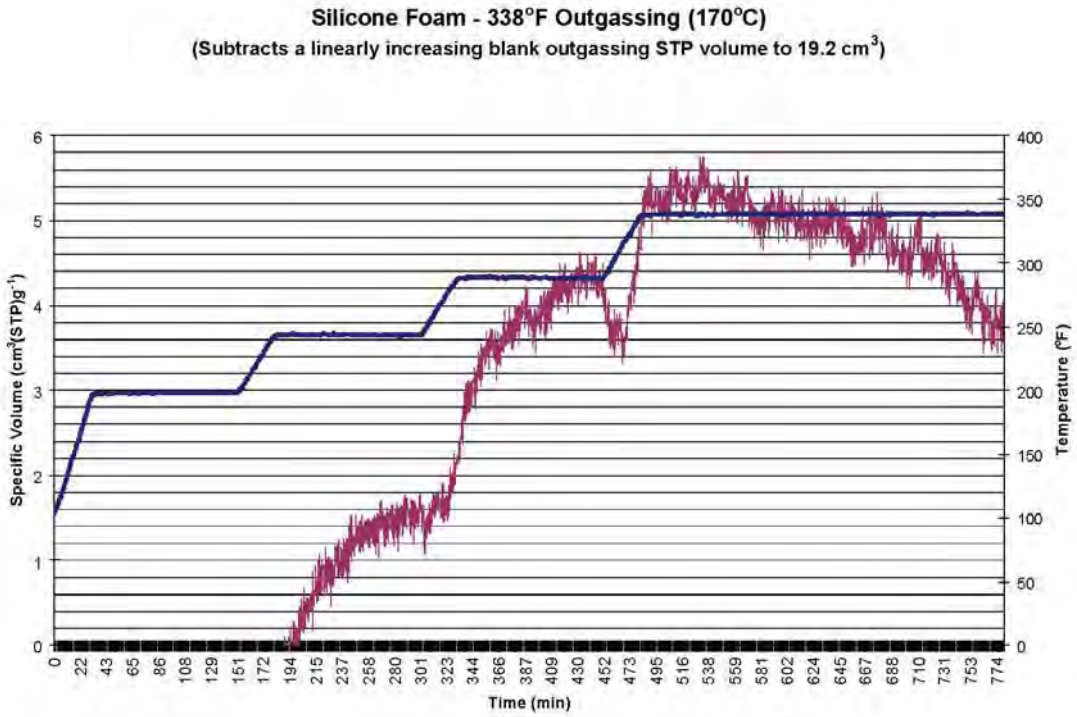

Figure 2. Outgassing of two silicone foam specimens at 338 degrees F.

4

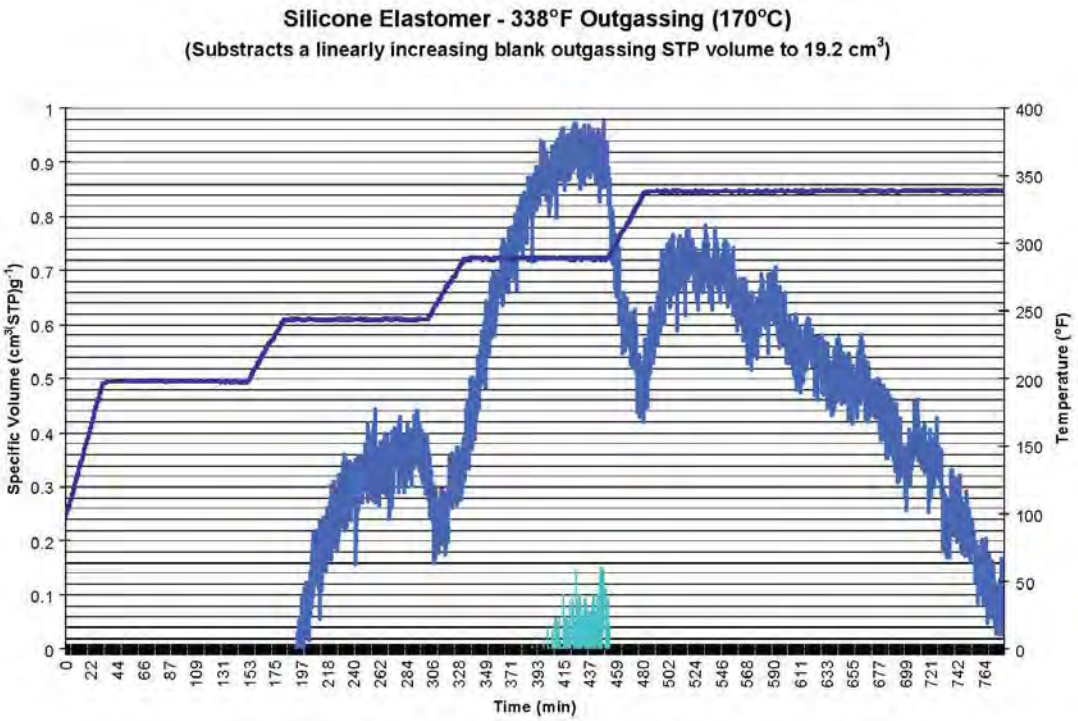

Figure 3. Outgassing of two silicone elastomer specimens at 338 degrees F.

5

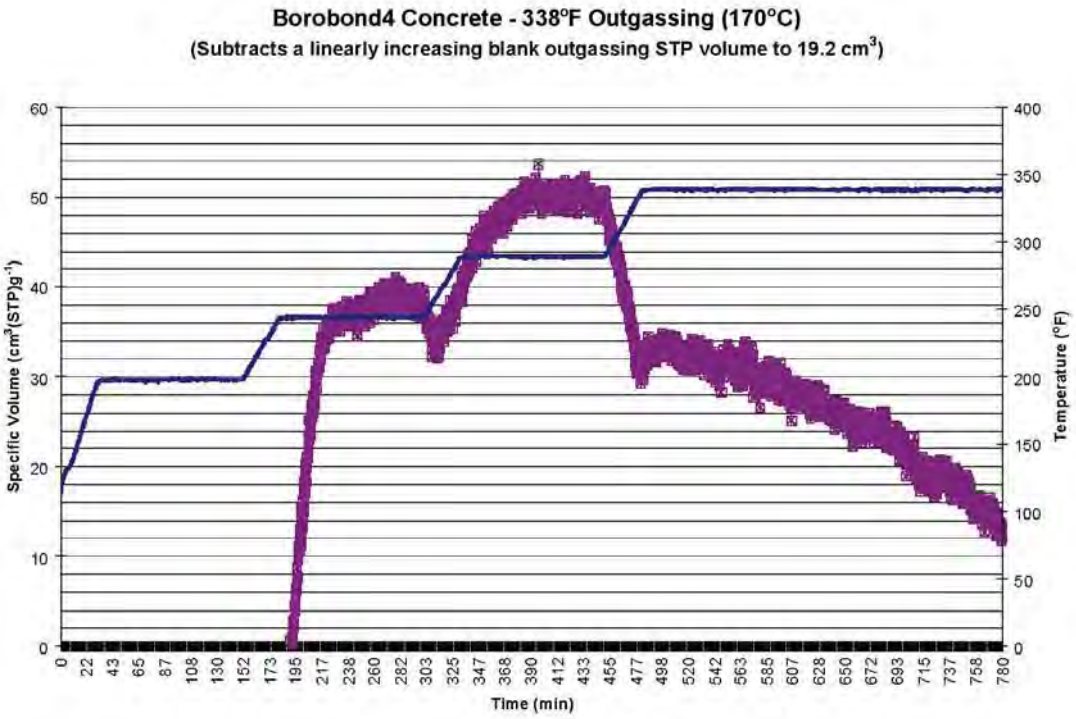

Figure 4. Outgassing of a Borobond4 concrete at 338 degrees F.

6

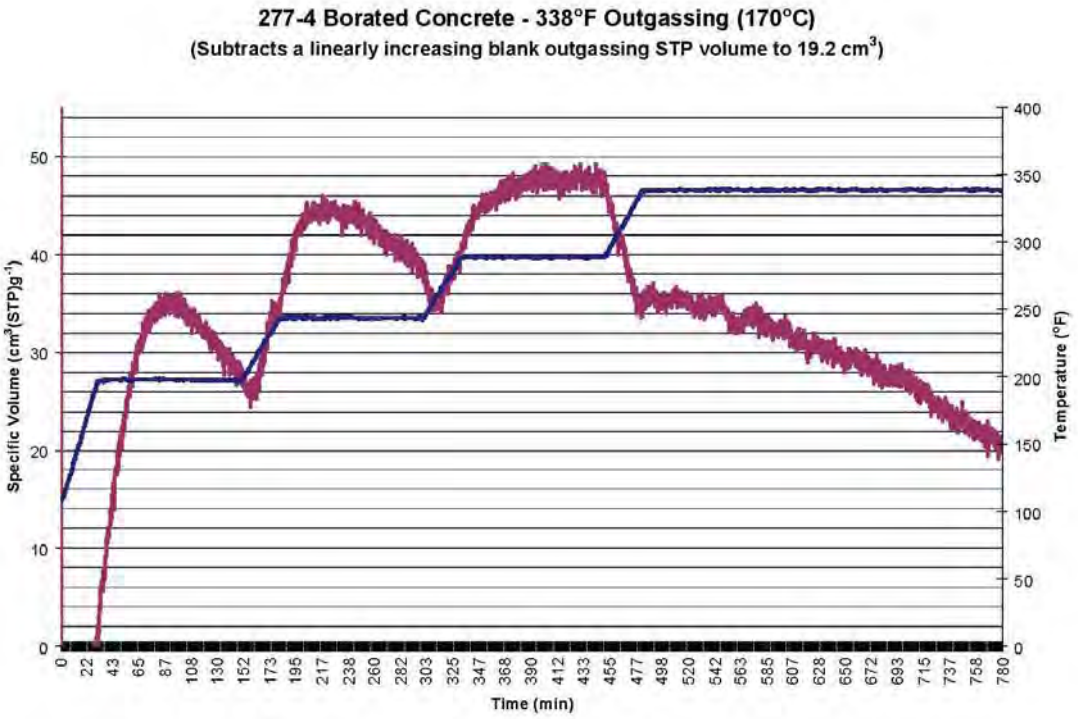

Figure 5. Outgassing of a 277-4 Borated concrete at 338 degrees F.

7

Table 1. Outgassing at 180°F at standard temperature (298K) and pressure (1 atm).

Specimen	Quantity (in units cm^{-3}(STP)/g)
Polyethylene – 1	0
Polyethylene – 2	0
Silicone Foam – 1	0
Silicone Foam – 2	0
Silicone Elastomer – 1	0
Silicone Elastomer – 2	0
Borobond4 – 1	29.3
Borobond4 – 2	32.0
277-4 Borated Concrete – 1	20.3
277-4 Borated Concrete - 2	46.9

Table 2. Weight Changes in grams after Experiment #1 (338°F or 170°C).

Material	Before	After	Weight Δ	Fractional Loss	mol H_2O*
borobond4	4.04	3.35	0.69	0.17	0.038
borobond4	1.99	1.69	0.3	0.15	0.017
elastomer	2.38	2.38	0	0.00	0.000
elastomer	1.45	1.45	0	0.00	0.000
277 borated	4.7	3.93	0.77	0.16	0.043
277 borated	2.82	2.34	0.48	0.17	0.027
polyethylene	0.26	0.26	0	0.00	0.000
polyethylene	0.19	0.2	-0.01	(0.05)	(0.001)
foam	0.72	0.75	-0.03	(0.04)	(0.002)

*Assumed outgas identity - should be verified with headspace gas analysis.

8

Table 3. Material Information Summary.

Material / Property	277-4 borated concrete	Borobond4	Polyethylene	Silica-filled polysiloxane elastomer	Fire-Retardant Polysiloxane foam
Composition	Hi-alumina cement	Phosphated cement	LDPE	Polysiloxane compression molded jar seal	Polysiloxane foam with carbon black
Application	Spacers between HEU parts for shipping (inside tin cans)	RT cure and neutron absorber. This is baseline material	Storage	Cap for cans; fits on top of paint cans used to ship broken pieces	Liner materials to cushion impact
Density**	120 lb/ft^3(1.93 g/cm^3)	120 lb/ft^3(1.93 g/cm^3)	~0.92 g/cm^3	1.16 g/cm^3	10 lb/ft^3 (0.16 g/cm^3)
Appearance	2"x2" block of gray ceramic-looking solid. Porous appearance	2"x2" block of dark gray metallic-looking solid. Very hard	Clear plastic bags as in "zip-loc"	Dark gray elastomeric pliable ring	Medium gray smooth skinned small-celled foam, soft with adhesive backed paper
Temperature of interest and durations	300°F (150°C) ramp in 50°F (10°C) increments – "Experiment 1" (Oven Profile 2) 180°F (82°C) for 2 hrs – "Experiment 2" (Oven Profile 3)				
Amount received	203.30 g	259.36 g	2 bags = 32.95 g	38.37 g	5.95 g

**Density data not measured – for reference only.

DISTRIBUTION

1. Amonett, C. M.
2. Anderson, J. C.
3. Arbital, J. G.
4. Baker, M. L.
5. Bales, P. A.
6. Byington, G. A.
7. Cramer, N.
8. Crenshaw, M. D.
9. DeClue, J. F.
10. Eckert, G. W.
11. Goins, M. L.
12. Handy, K. D.
13. Heatherly, C. N.
14. Holder, S. T.
15. Johnson, D. T.
16. Leckey, J. H.
17. McKenzie, P. E.
18. Miller, D. B.
19. Perkins, G.
20. Singleton, G. B.
21. Smith, R. A.
22. Smith, R. H.
23. Sooter, D. P.
24. Thomas, S. K.
25. Tollefson, D. A.
26. Turner, S. B.
27. Warren, T. L.
28. Y-12 Central Files – RC

THIS PAGE INTENTIONALLY LEFT BLANK.

CANBERRA

Canberra Oak Ridge, LLC
1133-C Oak Ridge Turnpike, Suite 260
Oak Ridge, TN 37830-6442

Ltr. No.: COR-NDA-04-93

Date: January 5, 2005

To: D. B. Miller

c: G. A. Byington, J. F. DeClue, L. C. Ostrowski, D. A. Tollefson, File

From: R. W. Brandenburg

Ref: BWXT-4300038751

Subject: **Results of Prompt Gamma-ray Neutron Activation Analysis and Neutron Transmission Measurements on Prototype Confinement Vessel Inner Liners and Spacers**

INTRODUCTION

Canberra was contracted by BWXT to perform prompt gamma-ray neutron activation analysis (PGNAA) on confinement vessel inner liners (CVIL) for the ES-3100 prototype replacement for the 6M shipping container and spacers to be used in the containers. Neutron transmission measurements on the CVILs are also part of the project. The CVILs are cylinders with an inside diameter of 6.5 in. and outer diameter of 8.5 in. The shell of the CVIL is made of 304L stainless steel and the annulus is filled with high alumina-content cement. For test purposes Canberra was supplied with three CVILs and ten spacers. The cement in two of the test CVILs contains boron in the form of 4 wt% boron carbide (B_4C). The third CVIL contains no boron. The portion of the CVIL filled with the cement is approximately 31 in. tall. The spacers are in 4-in. diameter tin coated steel cans that are 1.25 in. thick. Four of the ten spacers contain 4 wt% boron carbide while the other six contain no boron. Some of the cement mixture from each pour is used to make spacers as well as fill the annulus of the cylinder.

The measurements for the project had three parts:

1. Twelve PGNAA measurements using a BEGe gamma-ray detector were made at 30° increments around each CVIL at the center height of the CVIL.

2. Two PGNAA measurements using a BEGe gamma-ray detector were made on each spacer with a 180° rotation of the spacer between the measurements.

3. Sixty neutron transmission measurements were made on each CVIL using a BF_3 neutron detector. The measurements were made at 30° increments around each CVIL at five heights starting at five inches from the bottom of the CVIL and at five inch increments up the CVIL.

NEUTRON SOURCE CONFIGURATION

A 1.8-µg ^{252}Cf spontaneous fission neutron source was purchased from AEA Technology to be the neutron source for the tests. The source was rated at $4.4 * 10^6$ neutrons/sec. The source is sealed in a 32.5 mm long, 9.4 mm diameter stainless steel cylinder (Fig. 1).

X.224 - stainless steel capsule

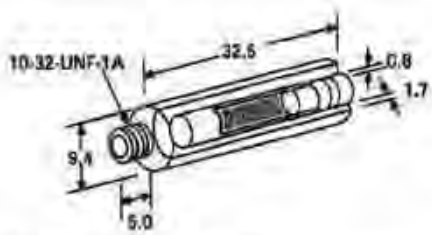

Safety performance testing

ANSI/ISO classification	IAEA special form	Model no.
C64545	GB/204/S	CVN.CY6

Fig. 1. Neutron Source Capsule

Fig. 2. Neutron Source Holder

A collimator was fabricated from high density polyethylene to hold the source. The collimator is a 3-in. cube of polyethylene covered on five sides with 2 mm of cadmium. The sixth side is covered with cadmium except for a 1-in. square in the center. A 9.5-mm hole in the center of the 1-in. square is the source location (Fig. 2). The collimator, which is suspended from a rod attached to the ceiling, is small enough to fit down the center of the CVILs. The source in the collimator is approximately 54 in. from the concrete floor. The detectors were placed on a Genie lift and centered on the source. The CVIL was placed on a second Genie lift and centered within ± 1/16 in. under the collimator. The lift was used to raise the CVIL to the designated height within ± 1/16 in. for the measurements. The spacers were clamped in a small vise and placed on the second lift and centered 1/2 ± 1/16 in. in front of the source. For the gamma-ray measurements, the detector to CVIL distance was 30 ± 1/8 in. and the detector to spacer distance was 20 ± 1/8 in. The neutron detector to CVIL distance was 4 ± 1/8 in.

GAMMA-RAY METHOD

The gamma-ray detector was a BEGe detector from Canberra in a 2-in thick lead shield. The shield covered the sides of the detector but did not collimate the field-of-view of the detector (Fig. 3). Quality assurance (QA) measurements for the gamma-ray detector were made using the QA software that is part of the Genie2K gamma-ray analysis software package from Canberra. Three small sources (^{137}Cs, ^{60}Co, and ^{109}Cd) were

attached to the face of the detector and counted for 60 seconds. One gamma-ray peak from each of the sources was analyzed for peak area and width (FWHM) and compared with previous measurements.

Prompt neutron activation of boron (specifically ^{10}B) gives rise to a 478 keV gamma ray produced by the recoil of the lithium nucleus from the neutrons captured in ^{10}B. The gamma ray is Doppler broadened by 10-15 keV. Gamma-ray spectrum collection and analysis was performed using the Genie2K gamma-ray analysis software package from Canberra. The peak fitting routine in Genie2K does not expect a peak as broad as 10-15 keV, therefore a region-of-interest (ROI) was set around the broad boron neutron activation peak. The data has three components. The gross count is the total count of the gamma rays detected with an energy that falls within the ROI. The Compton background is the portion of the gross count that is caused by scattered gamma rays. The net count is the portion of the total count that is from the boron. The net count is the difference between the gross and Compton counts.

Fig. 3. BEGe Gamma-Ray Detector and Collimator

GAMMA-RAY RESULTS

The two CVILs containing boron were labeled 277-4-C1 and 277-4-C2. The CVIL containing no boron was labeled 277-0. CVIL 277-4-C1 was filled with three pours. CVILs 177-4-C2 and 277-0 were each filled with one continuous pour. Each CVIL in-turn was centered under the source collimator on the turntable on the Genie lift. The CVIL was raised to position the center of the CVIL at the level of the source for the twelve measurements (Fig. 4). Each measurement consisted of collecting a spectrum for 10 minutes. The spectrum was saved and counts in the ROI were recorded. Table 1 contains the results of the PGNAA measurements on the three CVILs. Chart 1 is a plot of the results. The average net counts for the two boron containing CVILs, agree very well. The net count for the non-boron containing CVIL is small and probably due to some minor activation of other materials in or near the CVIL. In all cases, CVILs and spacers, the standard deviation of the net counts and gross counts was less than or close to the standard deviation that would be expected based on counting statistics. The Compton background for all three CVILs agrees well, implying that there are no major effects from other materials.

Fig. 4 BEGe Detector and CVIL Positioned for PGNAA Measurement

CVIL	277-4-C1			277-4-C2			277-0		
Angle	Gross Counts	Compton	Net Counts	Gross Counts	Compton	Net Counts	Gross Counts	Compton	Net Counts
0	39,002	20,658	18,344	39,403	20,816	18,587	21,552	20,066	1,486
30	39,038	21,152	17,886	39,681	21,211	18,470	21,394	20,392	1,002
60	39,378	21,429	17,949	39,110	20,925	18,185	21,145	20,184	961
90	39,306	20,036	19,270	39,890	21,732	18,158	21,347	21,123	224
120	39,287	20,421	18,866	39,407	21,123	18,284	21,463	19,661	1,802
150	39,126	20,895	18,231	39,573	20,905	18,668	21,367	20,500	867
180	39,218	21,241	17,977	39,696	21,093	18,603	21,327	19,977	1,350
210	39,356	21,468	17,888	39,693	20,856	18,837	21,547	19,682	1,865
240	39,258	20,570	18,688	39,565	20,965	18,600	21,317	20,382	935
270	39,351	20,658	18,693	39,762	21,300	18,462	21,424	19,918	1,506
300	39,281	20,431	18,850	39,470	20,955	18,515	21,576	20,155	1,421
330	39,406	21,034	18,372	39,574	20,708	18,866	21,460	20,984	476
Average	39,251	20,833	18,418	39,569	21,049	18,520	21,410	20,252	1,158
Std. Dev.	132	444	456	204	274	227	122	457	503
Rel SD	0.3%	2.1%	2.5%	0.5%	1.3%	1.2%	0.6%	2.3%	43.4%

Table 1. Results of PGNAA on CVILs

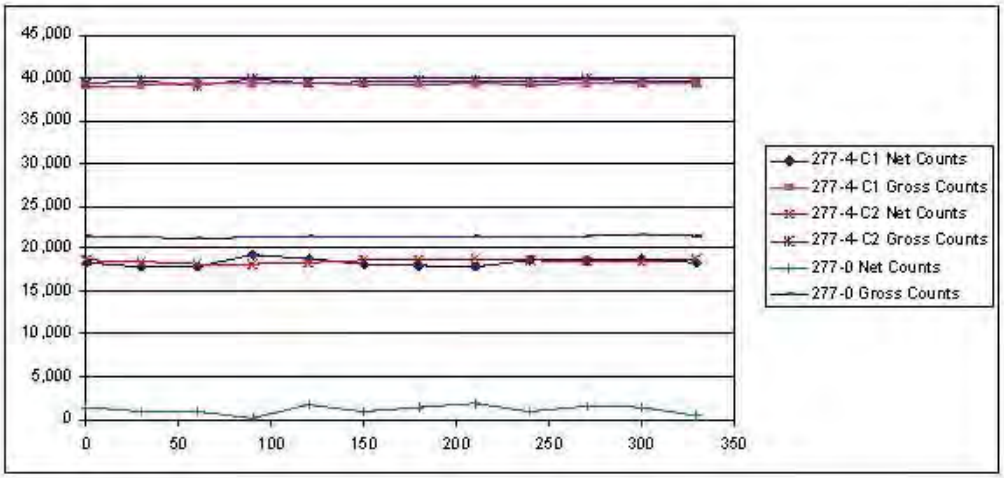

Chart 1: Results of PGNAA on CVILs

The spacers were measured by centering them vertically in front of the source (Fig. 5).

Fig. 5. Spacer Positioned for PGNAA Measurement

A 15-minute spectrum was collected then the spacer was rotated 180° and a second 15-minute spectrum collected. Each spectrum was saved and the counts in the ROI were recorded. The spacers with no boron were labeled 277-0-S1 through –S6 and the boron containing spacers were labeled 277-4-S1 through –S4. Side A is with the cover of the can facing the detector and side B is with the cover facing the source. Table 2 contains the results from the measurements of the ten spacers. Chart 2 is a plot of the results.

Spacer Number	Gross Count	Compton	Net Count
277-4-S1-A	72,749	61,156	11,593
277-4-S1-B	71,471	59,605	11,866
277-4-S2-A	74,181	62,844	11,337
277-4-S2-B	73,478	60,761	12,717
277-4-S3-A	75,877	62,548	13,329
277-4-S3-B	73,651	60,415	13,236
277-4-S4-A	75,194	61,778	13,416
277-4-S4-B	72,634	59,833	12,801
Average	73,654	61,118	12,537
Std Dev	1,427	1,197	826
Rel SD	1.9%	2.0%	6.6%

Spacer Number	Gross Count	Compton	Net Count
277-0-S1-A	65,385	61,738	3,647
277-0-S1-B	63,964	59,280	4,684
277-0-S2-A	63,861	59,744	4,117
277-0-S2-B	62,261	56,850	5,411
277-0-S3-A	64,510	59,526	4,984
277-0-S3-B	63,653	59,684	3,969
277-0-S4-A	64,952	60,544	4,408
277-0-S4-B	62,865	59,961	2,904
277-0-S5-A	65,635	60,188	5,447
277-0-S5-B	63,881	59,161	4,720
277-0-S6-A	64,041	59,921	4,120
277-0-S6-B	64,154	60,366	3,788
Average	64,211	59,919	4,293
Std Dev	839	455	786
Rel SD	1.3%	0.8%	18.3%

Table 2. Results of PGNAA on Spacers

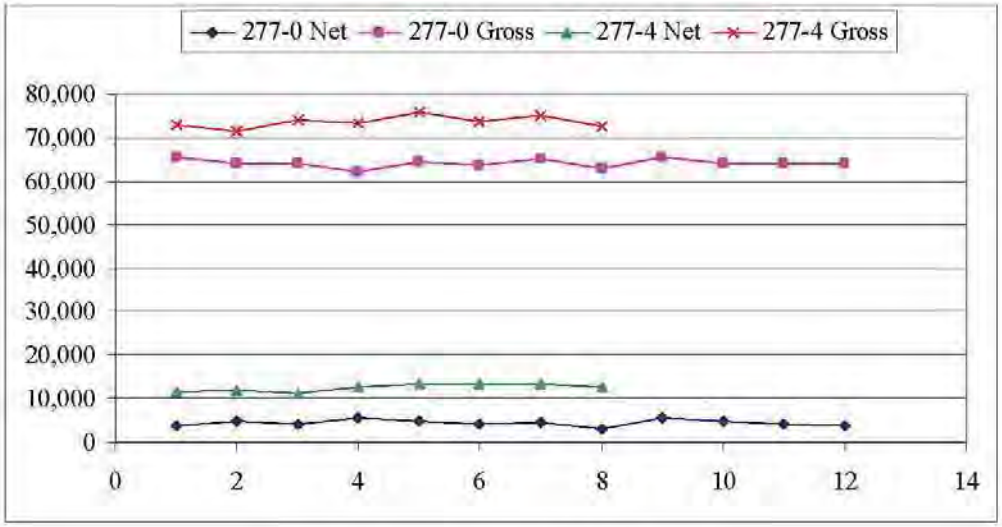

Chart 2. Results of PGNAA on Spacers

The results for the spacers show less difference between the spacers with and without boron than the CVILs. The variation among the measurements is larger for the spacers. Direct comparison between the CVIL results and the spacer results is difficult because the source to sample distance, the detector to sample distance, the area of the sample exposed to the source, and the count times are all different.

NEUTRON METHOD

The neutron detector was a 1-in.diameter BF_3 tube surrounded by a cylindrical block of polyethylene. The polyethylene is inside an aluminum case lined with a sheet of cadmium. The cadmium liner is intended to stop thermal neutrons from the surroundings and allow only fast neutrons from the source through to be moderated by the polyethylene and detected by the BF_3 tube. There was no additional shielding around the detector (Fig. 6). The detector assembly and 2241-7 handheld electronics package were from Ludlum Measurements, Inc. Quality assurance (QA) measurements were made by counting the neutron source with no CVIL in the beam of neutrons. The measurement results were entered into the Measurement Control software used by Canberra at ETTP.

The CVIL was positioned as in the gamma-ray measurements. Measurements were made at 60 points on each CVIL. As with the gamma-ray measurements, 12 measurements were made at 30^0 increments around the CVIL but these measurements were made at five different heights on the CVIL. The measurements were made at heights of 5, 10, 15, 20, and 25 inches from the bottom of the CVIL. The neutrons were counted for five minutes at each position then the CVIL was rotated to the next measurement position. The zero degree starting positioned was remeasured after the full rotation. The CVIL was the moved to the next height and the process repeated.

NEUTRON RESULTS

For all three CVILs, the standard deviation of the counts at any level on the CVILs was about 1.5 times the standard deviation expected from counting statistics. This indicates that there is little true variation in the neutron transmission around the circumference of the CVILs. The variation of the counts with height was larger. The standard deviation of the counts at different heights was 3 to 4 times the standard deviation expected from counting statistics for CVILs 277-4-C1 and 277-0, the three pour CVILs, but only 1.7 for 277-4-C2, the one pour CVIL. For both of the CVILs containing boron, the measurements 5 inches from the bottom yielded the highest transmission and the measurement at 25 inches from the bottom yielded the lowest transmission. This effect is presumed to be due to neutron scattering from the floor. The floor was more exposed to the neutron source when the CVIL was at maximum height (the 5-in position) than when the CVIL was down further and provided some shielding. The average transmission when compared to the measurement of the source with no CVIL is 81.4% for 277-4-C1, 83.6% for 277-4-C2, and 85.3% for 277-0. One interesting point is on 277-4-C1 at 150° and 25 inches. The results for that point were 4.4% higher that the average at the 25-in. level (Chart 3). The measurement was repeated with similar results. No clear cause of this anomaly could be determined without further investigation. Tables 3, 4, and 5 and Charts 3, 4, and 5 show the results of the neutron measurements on the three CVILs.

Fig. 6. Neutron Detector and CVIL Positioned for Transmission Measurements

Angle (°)	Height (in)	Counts	Height (in)	Counts	Height (in)	Counts	Height (in)	Counts	Height (in)	Counts	Mean	Std Dev
0	5	20,954	10	20,249	15	20,142	20	20,041	25	19,544	20,186	507
30		21,072		20,319		20,463		20,329		19,533	20,343	548
60		21,387		20,600		20,739		20,260		19,655	20,528	637
90		21,310		20,371		20,398		19,889		19,620	20,318	645
120		21,168		20,834		20,500		20,500		19,425	20,485	654
150		21,288		20,665		20,741		20,434		20,398	20,705	357
180		21,185		20,675		20,840		20,282		19,624	20,521	598
210		21,237		20,581		20,162		20,025		19,361	20,273	695
240		20,980		20,593		20,273		20,046		19,300	20,238	631
270		20,933		20,342		20,189		19,966		19,287	20,143	598
300		21,126		20,754		20,404		20,064		19,586	20,387	597
330		20,909		20,345		20,295		20,086		19,707	20,268	437
360		20,831		20,220		20,490		20,111		19,725	20,275	415
Mean		21,106		20,504		20,434		20,156		19,597	20,359	
Std Dev		175		204		229		187		282	538	

Table 3. Results of Neutron Transmission Measurements on CVIL 277-4-C1

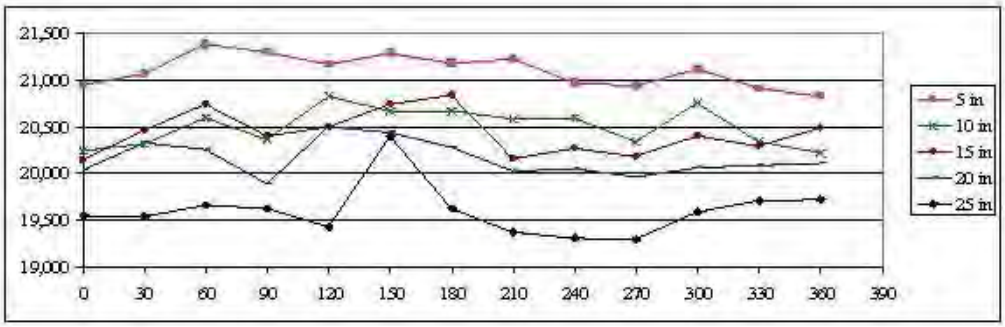

Chart 3. Results of Neutron Transmission Measurements on CVIL 277-4-C1

Angle (°)	Height (in)	Counts	Height (in)	Counts	Height (in)	Counts	Height (in)	Counts	Height (in)	Counts	Mean	Std Dev
0	5	21,451	10	20,985	15	20,857	20	20,916	25	20,188	20,879	452
30		21,444		21,094		20,998		21,028		20,259	20,965	433
60		21,382		20,974		20,714		20,674		19,978	20,744	513
90		21,563		20,960		20,819		20,655		20,230	20,845	486
120		21,280		21,172		20,926		20,839		20,334	20,910	368
150		21,416		20,998		21,149		20,697		20,371	20,926	405
180		21,420		20,947		20,802		20,782		19,874	20,765	768
210		21,737		21,140		20,833		20,598		19,915	20,845	737
240		22,032		21,211		20,904		20,911		20,250	21,062	460
270		21,925		21,252		21,269		21,105		20,415	21,193	389
300		21,484		21,243		20,886		20,952		20,417	20,996	377
330		21,391		21,010		20,600		21,085		19,990	20,815	581
360		21,394		20,957		20,609		20,858		20,341	20,832	395
Mean		21,532		21,073		20,874		20,854		20,197	20,906	
Std Dev		226		117		190		166		193	468	

Table 4. Results of Neutron Transmission Measurements on CVIL 277-4-C2

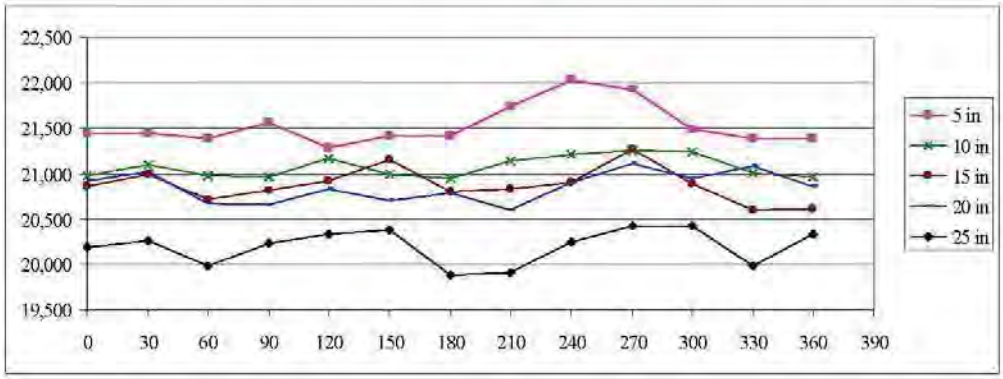

Chart 4. Results of Neutron Transmission Measurements on CVIL 277-4-C2

Angle (°)	Height (in)	Counts	Height (in)	Counts	Height (in)	Counts	Height (in)	Counts	Height (in)	Counts	Mean	Std Dev
0	5	21,752	10	21,329	15	21,377	20	20,946	25	20,624	21,206	433
30		21,376		21,848		21,084		21,243		20,576	21,225	462
60		21,129		21,518		21,172		21,085		20,378	21,056	416
90		21,437		21,482		21,472		21,138		20,588	21,223	383
120		21,743		21,685		21,765		21,265		20,679	21,427	465
150		21,550		21,867		21,535		21,298		20,637	21,377	461
180		21,359		21,939		21,385		21,009		20,524	21,243	522
210		21,456		21,898		21,434		21,346		20,616	21,350	463
240		21,043		21,888		21,754		21,319		20,640	21,329	512
270		21,415		21,954		21,446		21,132		20,682	21,326	466
300		21,495		22,037		21,674		21,411		20,898	21,503	415
330		21,443		22,399		21,847		21,828		20,894	21,682	557
360		21,259		21,542		21,864		21,511		21,022	21,440	317
Mean		21,420		21,799		21,524		21,272		20,674	21,338	
Std Dev		204		283		246		231		172	438	

Table 5. Results of Neutron Transmission Measurements on CVIL 277-0

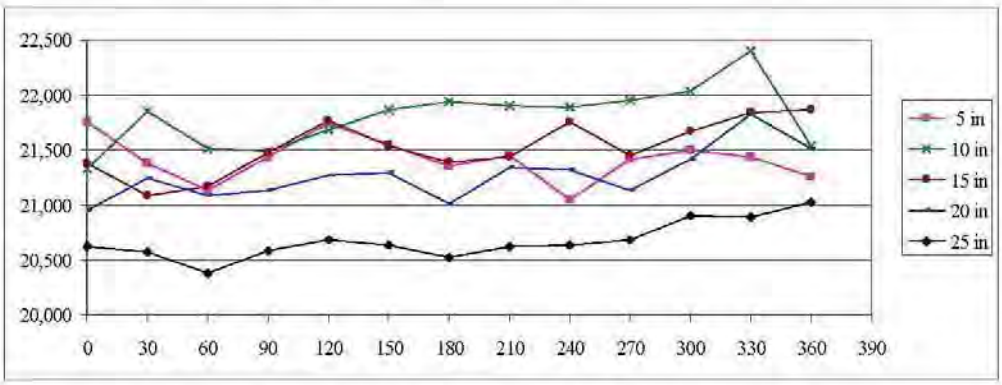

Chart 5. Results of Neutron Transmission Measurements on CVIL 277-0

SUMMARY AND CONCLUSIONS

For the measurement of gamma rays resulting from the prompt neutron activation of ^{10}B, the average net counts for the two boron containing CVILs, agreed very well. The net count for the non-boron containing CVIL is small and probably due to some minor activation of other materials in or near the CVIL. In all cases, CVILs and spacers, the standard deviation of the net counts and gross counts were less than or close to the standard deviation that would be expected based on counting statistics. The Compton background for all three CVILs agreed well, implying that there are no major effects from other materials.

The results for the spacers showed less difference between the spacers with and without boron than the CVILs. The variation among the measurements was larger for the spacers. Direct comparison between the CVIL results and the spacer results is difficult because the source to sample distance, the detector to sample distance, the area of the sample exposed to the source, and the count times were all different.

In the neutron transmission measurements for all three CVILs, the standard deviation of the counts at any level on the CVILs was about 1.5 times the standard deviation expected from counting statistics. This indicates that there was little true variation in the neutron transmission around the circumference of the CVILs. The variation of the counts with height was larger. The standard deviation of the counts at different heights was 3 to 4 times the standard deviation expected from counting statistics for CVILs 277-4-C1 and 277-0, the three pour CVILs, but only 1.7 for 277-4-C2, the one pour CVIL. The result for the measurement on 277-4-C1 at 150° and 25 inches is 4.4% higher that the average at the 25-in. level (Chart 3), but this anomalous result does not lead to any different conclusions than those derived from the other CVIL measurements.

For both of the CVILs containing boron, the measurements 5 inches from the bottom yielded the highest transmission and the measurement at 25 inches from the bottom yielded the lowest transmission. The average transmission when compared to the measurement of the source with no CVIL was in the range from 81.4 to 85.3%.

THIS PAGE INTENTIONALLY LEFT BLANK.

Y/DV-1914

BWXT Y12
A BWXT/Bechtel Enterprise

Summary of TGA Testing of Borated Concrete and Adhesive-Backed Silicone Foam

L. M. Thompson
J. D. Brown

Technology Development

Y-12 NATIONAL SECURITY COMPLEX

January 2005

MANAGED BY
BWXT Y-12, L.L.C.
FOR THE UNITED STATES
DEPARTMENT OF ENERGY

UCN-13672 (10-00)

SUMMARY

A request was made by personnel in Engineering to conduct thermogravimetric analysis (TGA) on three different materials being evaluated for use. Two of the materials were boron loaded concrete: borated concrete 277-4 and Borobond 4. The third material was an adhesive-backed silicone foam. The samples were heated to 800°C at a ramp rate of 10°C/min. The borated concrete 277-4 showed some variability in the results. The variability was thought to be due to varying amounts of moisture that was coming off of the material initially. The experiment was repeated using borated concrete that had been allowed to air dry for approximately 1 month. Much more consistent results were obtained on these samples. There also appears to be up to 5 different types of decomposition occurring in the material over this temperature range. The Borobond 4 and the adhesive-backed silicone foam were much more consistent. The Borobond 4 had only one type of decomposition occurring over the temperature range. The amount of residue from this material was approximately 76%. The adhesive-backed silicone foam had three different areas of decomposition. These were thought to be due to the adhesive, the silicone and possibly a filler or wetting agent. The amount of residue from this material was approximately 29%.

INTRODUCTION

A request was made by personnel in Engineering to conduct thermogravimetric analysis (TGA) on three different materials that may be used in the new Highly Enriched Uranium (HEU) storage facility. The materials included two boron-loaded concretes: borated concrete 277-4 and Borobond 4. The third material was an adhesive-backed silicone foam. Initially, three tests were conducted on each material type using a TA Instruments TGA 2950. An additional three tests were conducted on the borated concrete 277-4 due to the variability seen in the initial set of samples. These still showed some variability so another three tests were conducted on material that had been allowed to air dry for one month. The material was tested using a temperature sweep with a ramp rate of 10°C/min from room temperature to 800°C.

RESULTS

Borated Concrete 277-4

An overlay of the results obtained on the initial six samples of borated concrete 277-4 is shown in Fig.1.

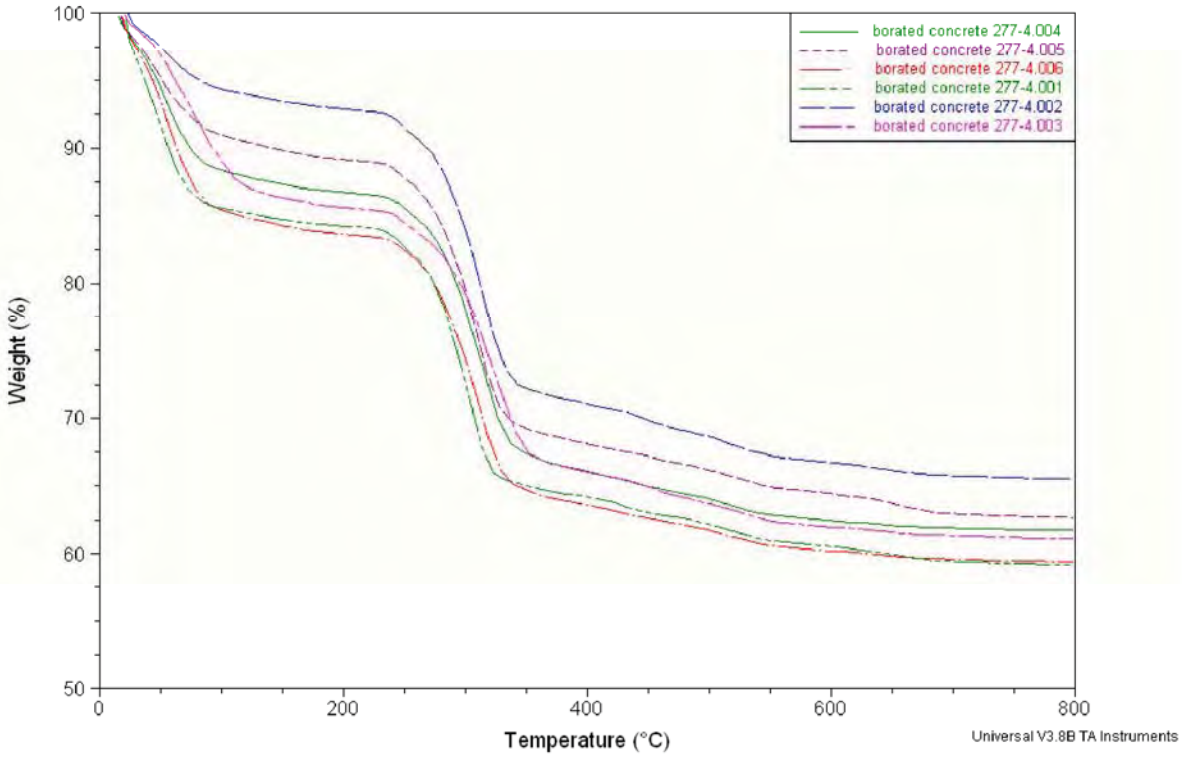

Fig. 1. Overlay of TGA results obtained on several samples of borated concrete 277-4.

The initial weight loss is thought to be due to water. The onset of decomposition occurred at approximately 265°C. The residue from the material varied from 59.2 to 65.6%. Table One summarizes the results obtained on the six samples. By taking a derivative of the weight percent curve as a function of temperature, four separate areas of decomposition were noted for the curves with the exception of the curve for samples 3, 4 and 6 which had five separate areas. Graphs of the results for each sample are contained in Appendix A.

Table 1. Results of TGA Testing of Borated Concrete 277-4

Sample Number	Weight Loss prior to Decomposition (%)	Onset of Decomposition (°C)	Residue (%)	Peaks on Derivative Curve for Weight Loss (°C)
1	14.74	269	59.22	302.74, 432.96, 523.12, 653.27
2	6.974	262.42	65.56	312.84, 442.98, 523.12, 653.27
3	14.28	267	61.13	70.49, 321.11, 451.24, 531.35, 651.5
4	13.74	257.49	61.73	56.76, 306.46, 436.7, 526.84, 636.97
5	11.33	250.21	62.7	48.98, 307.88, 518.2, 658.36
6	16.94	270.91	59.4	59.04, 309.01, 429.2, 519.34, 649.5

This material had been stored in a plastic bag and was still visibly damp. Because of this variability that was thought to be due to water, another three samples were run using material that had been air dried. The material was removed from the plastic bag and allowed to dry at room temperature for approximately 1 month. An overlay of the results obtained on these samples is shown in Fig. 2.

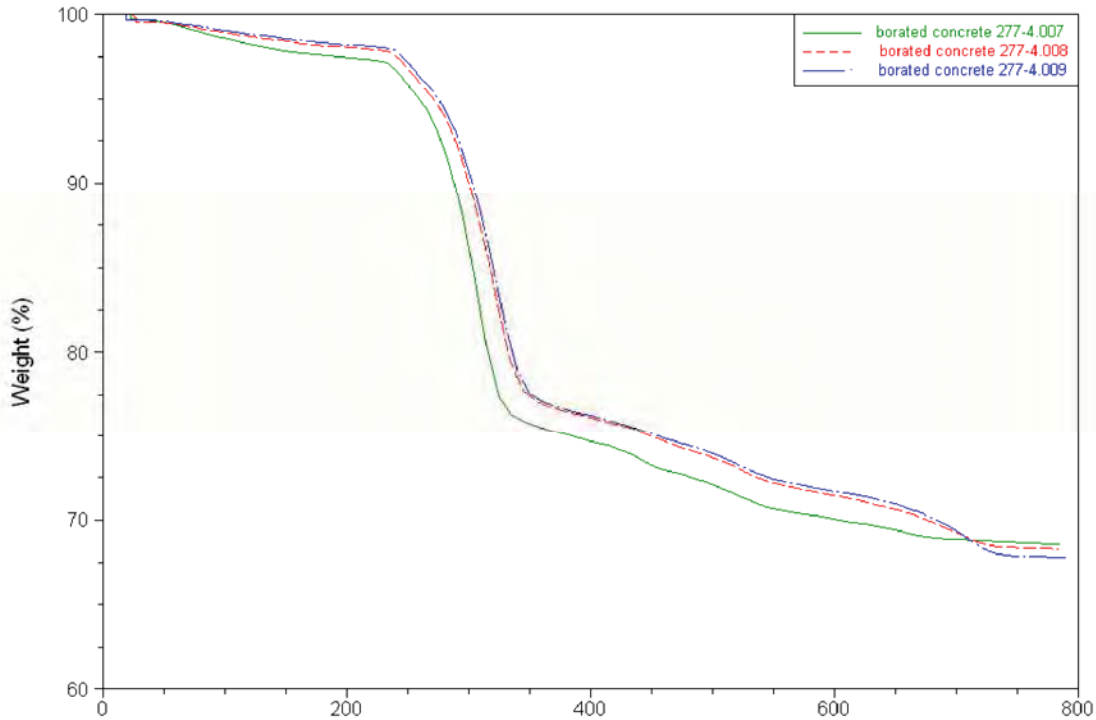

Fig. 2. Overlay of TGA results obtained on samples of borated concrete 277-4 that had been air dried for approximately 1 month.

These results were more repeatable than the previous samples. However, we still see an initial weight loss. A summary of the results are shown in Table Two. The individual graphs for each sample are contained in Appendix B.

Table 2. TGA Results Obtained on "Dried" Borated Concrete 277-4

Sample Number	Weight Loss prior to Decomposition (%)	Onset of Decomposition (°C)	Residue (%)	Peaks on Derivative Curve for Weight Loss (°C)
7	2.78	235.16	68.57	73.03, 303.91, 434.11, 514.24, 654.39
8	2.53	269.75	68.32	313.42, 453.63, 523.72, 693.9
9	2.00	239.35	67.8	319.65, 449.8, 519.9, 710.09

A Balzers mass spectrometer was run in conjunction with the TGA on these samples to determine the elements present in the sample offgas. The mass spectrometer was baked out prior to use in order to minimize gases from materials in the lines and instrument. Continuous scans were generated from masses 1 to 100 with an argon carrier gas. Initially, water (masses 16, 17 and 18) and air are the main gases that are coming off. A small amount of an alcohol (mass 30) and CxHy (mass 41) are also present in the offgases. During the first decomposition that occurs, water, hydrogen (masses 1 and 2) and CxHy (masses 41 and 30) are the main offgases with water again being the dominant material. As the material reaches approximately 440°C, water and

carbon dioxide (masses 44 and 12) appear to be the main offgases. Figure 3 is a graph of the mass spec data obtained on one of the samples. Only the masses that exhibited some changes are shown in this graph.

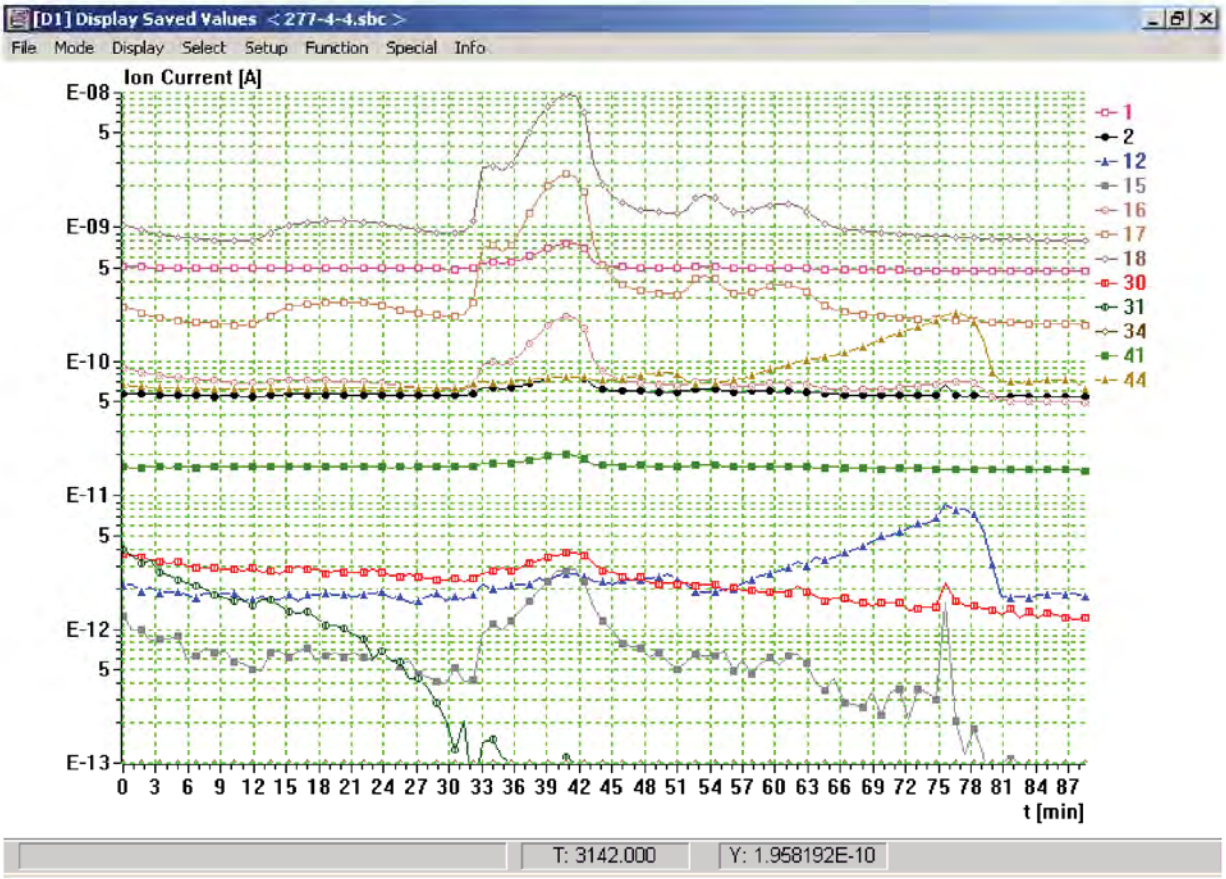

Fig. 3. Mass spectrum obtained from TGA testing of borated concrete 277-4.

A request was also made to obtain a density on this material. The density was calculated using three different techniques. The density was initially determined by weighing the material and dividing this by a calculated volume of the material obtained by measuring the cylindrical piece of the material. The density obtained using this technique was 1.51 g/cc (94.3 lb/ft^3). The second technique was to weigh a piece of the material. This piece was then submerged in a graduated cylinder of liquid and the volume determined by the amount of water displaced. The density obtained using this technique was 2.65 g/cc (165.4 lb/ft^3). The material does have some open pores so the volume obtained from this technique would be affected by these pores. The third technique used to obtain the density is to weigh the sample dry, weigh the sample submerged in water and calculate the density based upon the buoyancy of the material. The density obtained using this technique was 2.05 g/cc (128.0 lb/ft^3).

Borobond 4

Results for the sample of Borobond 4 are shown in Fig. 4.

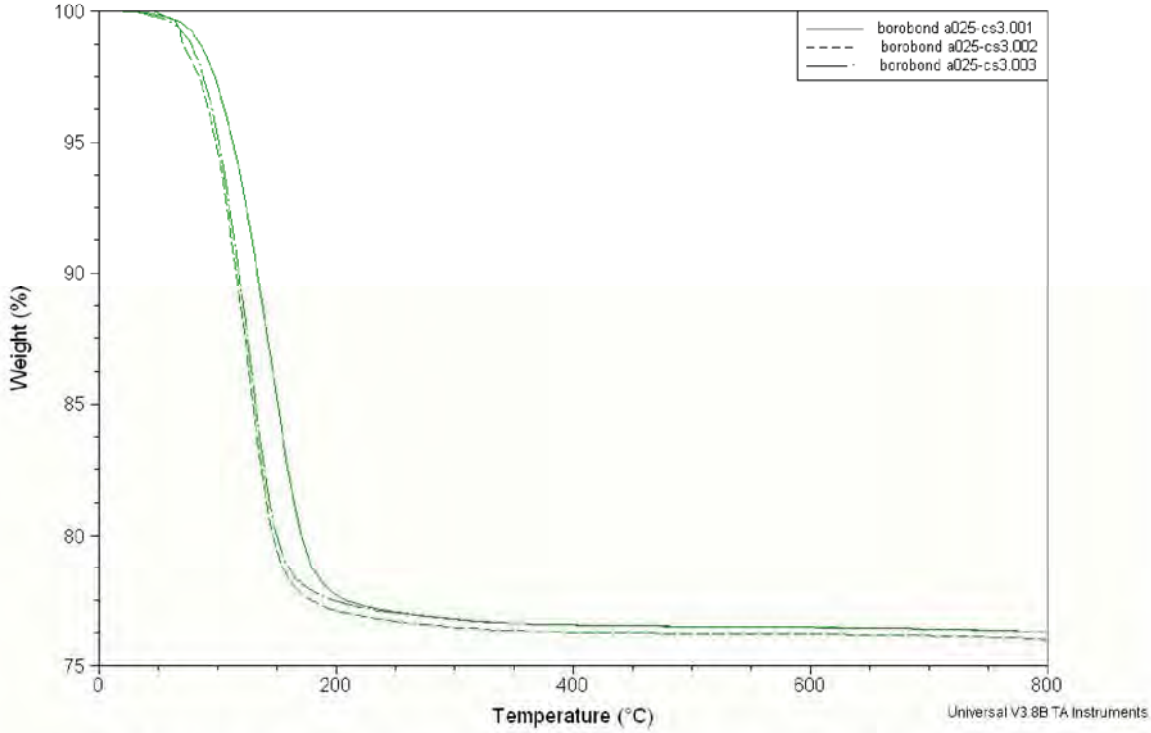

Fig. 4. Overlay of TGA Results Obtained on Three Samples of Borobond 4

The onset of decomposition occurred at approximately 70°C. The amount of residue was very similar for the three samples and averaged 76.2%. Table Three summarizes the results obtained on each sample. When the derivative of the weight loss curve as a function of temperature was taken, only one area of decomposition was noted for this material. Graphs of the results for each sample are contained in Appendix C.

Table 3. TGA Results for Borobond 4

Sample Number	Onset of Decomposition (°C)	Residue (%)	Peak on Derivative Curve (°C)
1	70.58	76.29	138.64
2	67.03	76.02	123.32
3	69.46	76.28	125.34

Adhesive Backed Silicone Foam

The third material tested was an adhesive backed silicone foam rubber. The material is part number 85925K541 from McMaster Carr. The foam was gray in color indicating some type of filler. The adhesive backing is acrylic per the material description. An overlay of the TGA results is shown in Fig. 5.

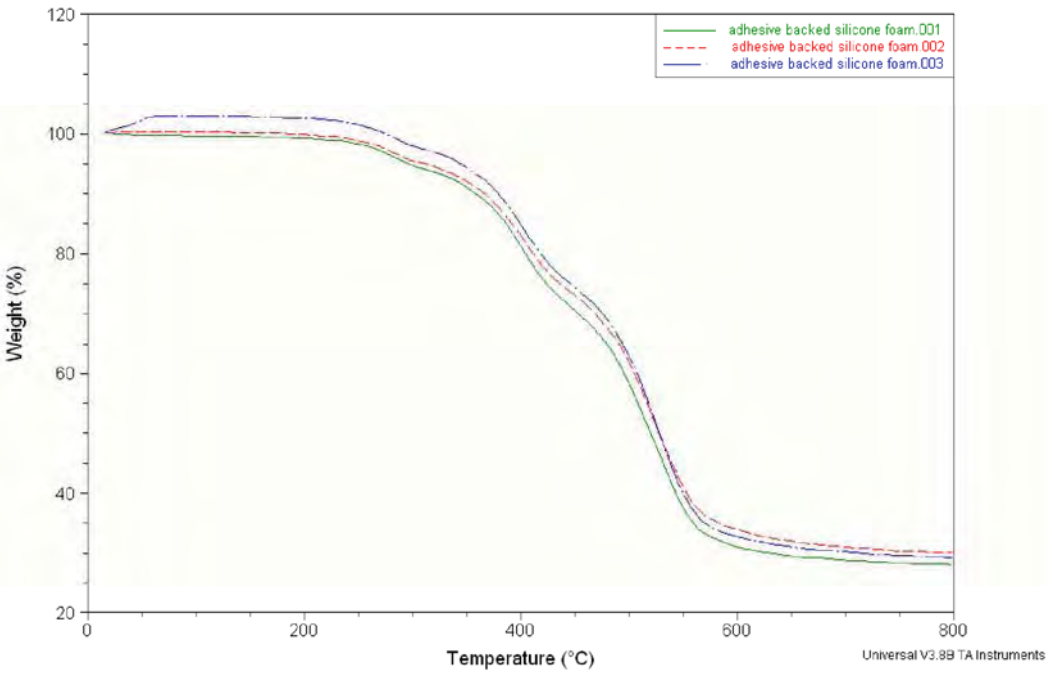

Fig. 5. Overlay of TGA results obtained on three samples of adhesive-backed silicone foam.

Three areas of decomposition are noted on these results. They are probably due to the adhesive, the silicone foam and either the filler or some type of wetting agent associated with the filler. Table Four summarizes the results obtained on these samples. Graphs for the results for each sample are located in Appendix D.

Table 4. Results of TGA Conducted on Adhesive-backed Silicone Foam

Sample Number	First Onset of Decomposition (°C)	Second Onset of Decomposition (°C)	Third Onset of Decomposition (°C)	Residue (%)	Peaks on Derivative Curve (°C)
1	254.5	361.38	487.26	28.06	283.91, 414.18 and 524.37
2	255.42	368.69	478.07	30.07	278.48, 398.78, and 528.98
3	243.96	367.94	496.69	29.26	276.11, 396.41, and 526.63

CONCLUSIONS

TGA was conducted on three different materials types: borated concrete 277-4, Borobond 4 and an adhesive-backed silicone foam The Borobond 4 and adhesive-backed silicone foam had very repeatable results. Initial results from the borated concrete 277-4 had some variability from sample to sample. The variability was thought to be due to the evolution of water from the samples. Four to five different areas of decomposition appeared to occur over the temperature range of room temperature to 800°C for the borated concrete 277-4. Tests were repeated on a sample of borated concrete 277-4 that had been allowed to dry in open air for approximately 1 month. These results were more repeatable although there was some still initial weight loss that was thought to be due to water. The Borobond 4 had only one incident of decomposition with an onset at approximately 70°C. The adhesive-backed silicone foam appeared to have three different areas of decomposition. These were thought to be due to the adhesive, the foam and possibly a filler or additive.

THIS PAGE INTENTIONALLY LEFT BLANK.

Appendix A
TGA Results for Borated Concrete 277-4

THIS PAGE INTENTIONALLY LEFT BLANK.

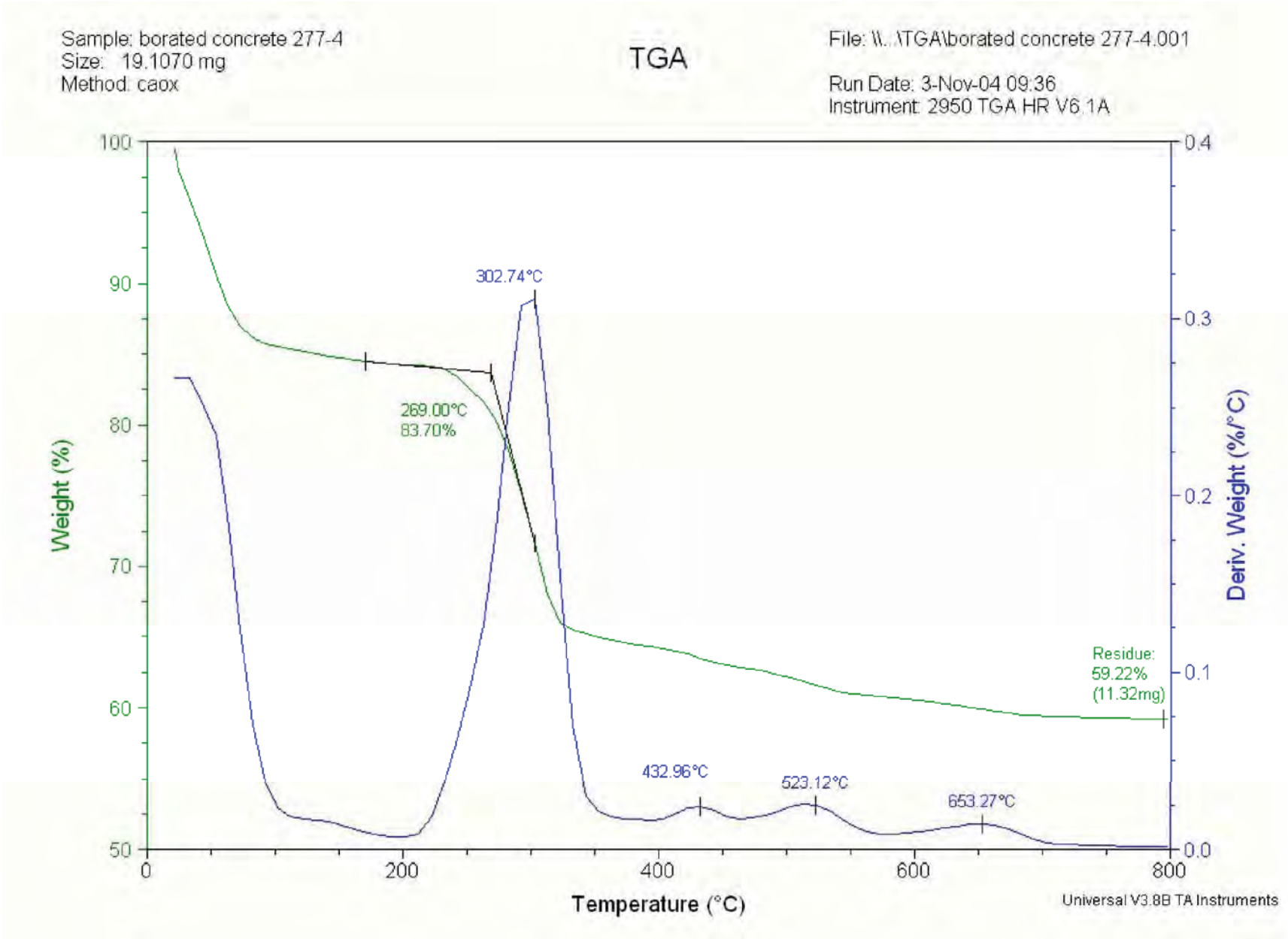
Sample: borated concrete 277-4
Size: 19.1070 mg
Method: caox
TGA
File: \\..\TGA\borated concrete 277-4.001
Run Date: 3-Nov-04 09:36
Instrument: 2950 TGA HR V6.1A
302.74°C
269.00°C
83.70%
Residue:
59.22%
(11.32mg)
432.96°C
523.12°C
653.27°C
Weight (%)
Deriv. Weight (%/°C)
Temperature (°C)
Universal V3.8B TA Instruments

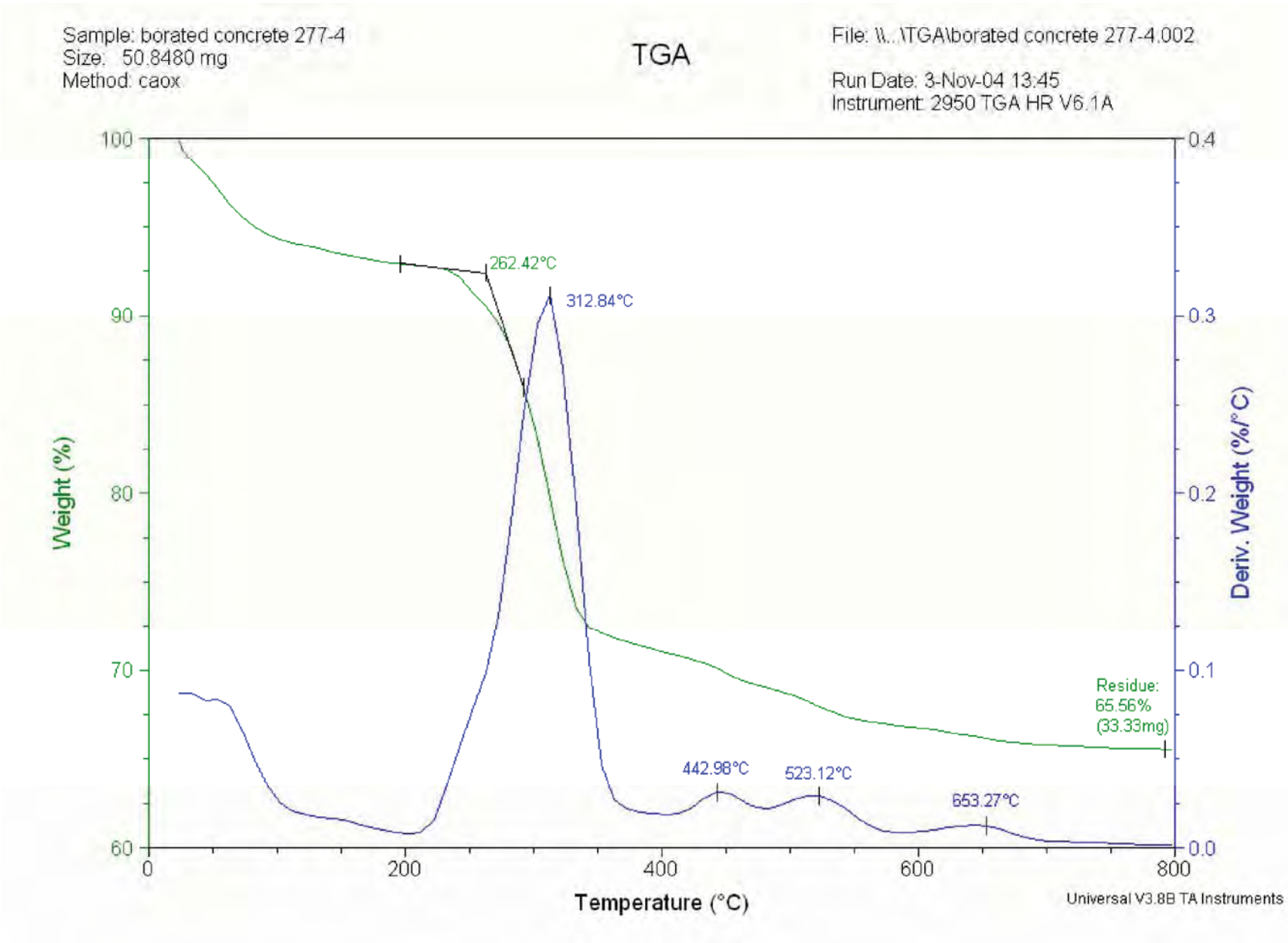
Sample: borated concrete 277-4
Size: 50.8480 mg
Method: caox
TGA
File: \\...\TGA\borated concrete 277-4.002
Run Date: 3-Nov-04 13:45
Instrument: 2950 TGA HR V6.1A
262.42°C
312.84°C
442.98°C
523.12°C
653.27°C
Residue:
65.56%
(33.33mg)
Weight (%)
Deriv. Weight (%/°C)
Temperature (°C)
Universal V3.8B TA Instruments

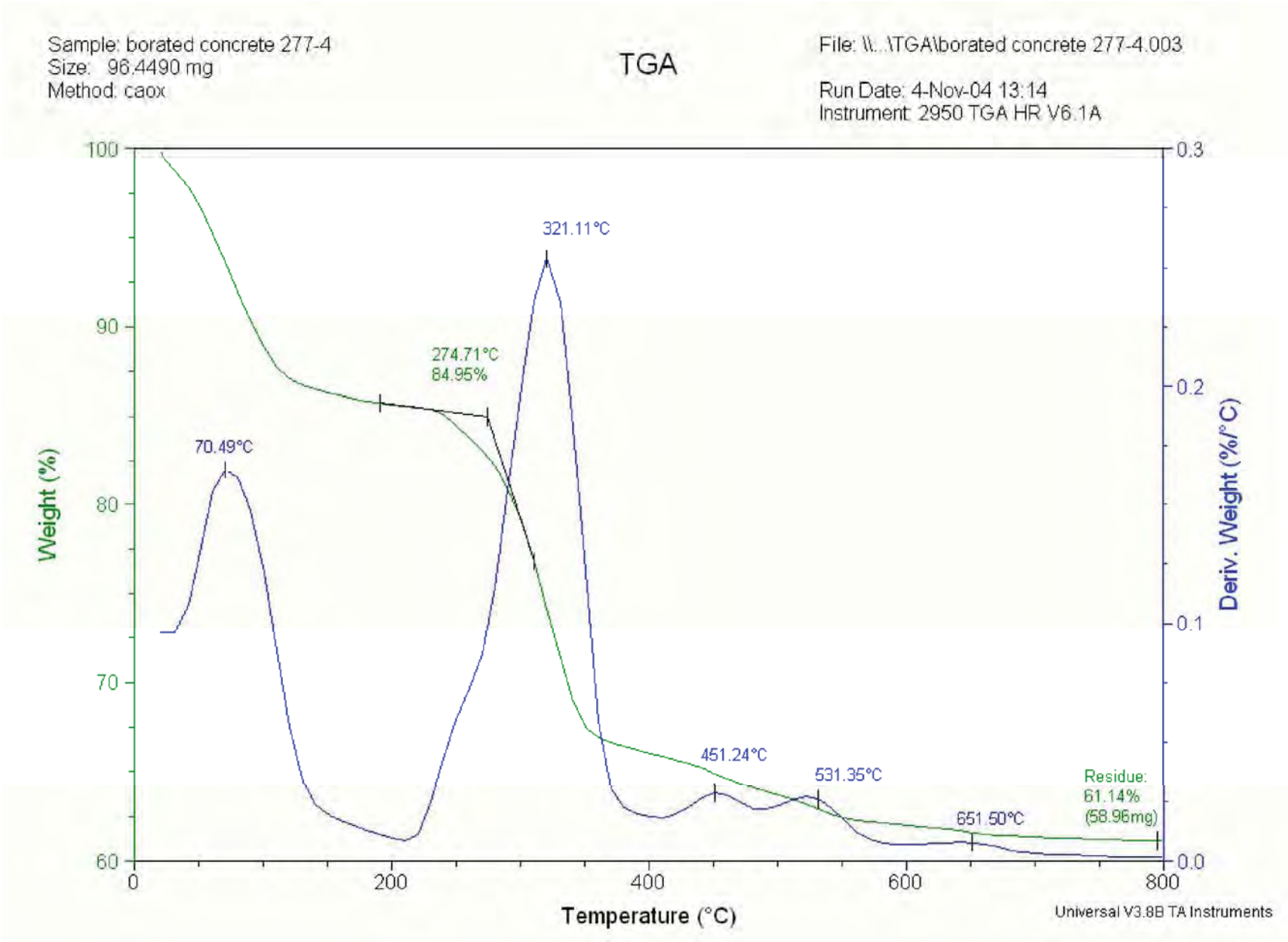
Sample: borated concrete 277-4
Size: 96.4490 mg
Method: caox
TGA
File: \\...\TGA\borated concrete 277-4.003
Run Date: 4-Nov-04 13:14
Instrument: 2950 TGA HR V6.1A
321.11°C
274.71°C
84.95%
70.49°C
451.24°C
531.35°C
651.50°C
Residue:
61.14%
(58.96mg)
Weight (%)
Deriv. Weight (%/°C)
Temperature (°C)
Universal V3.8B TA Instruments

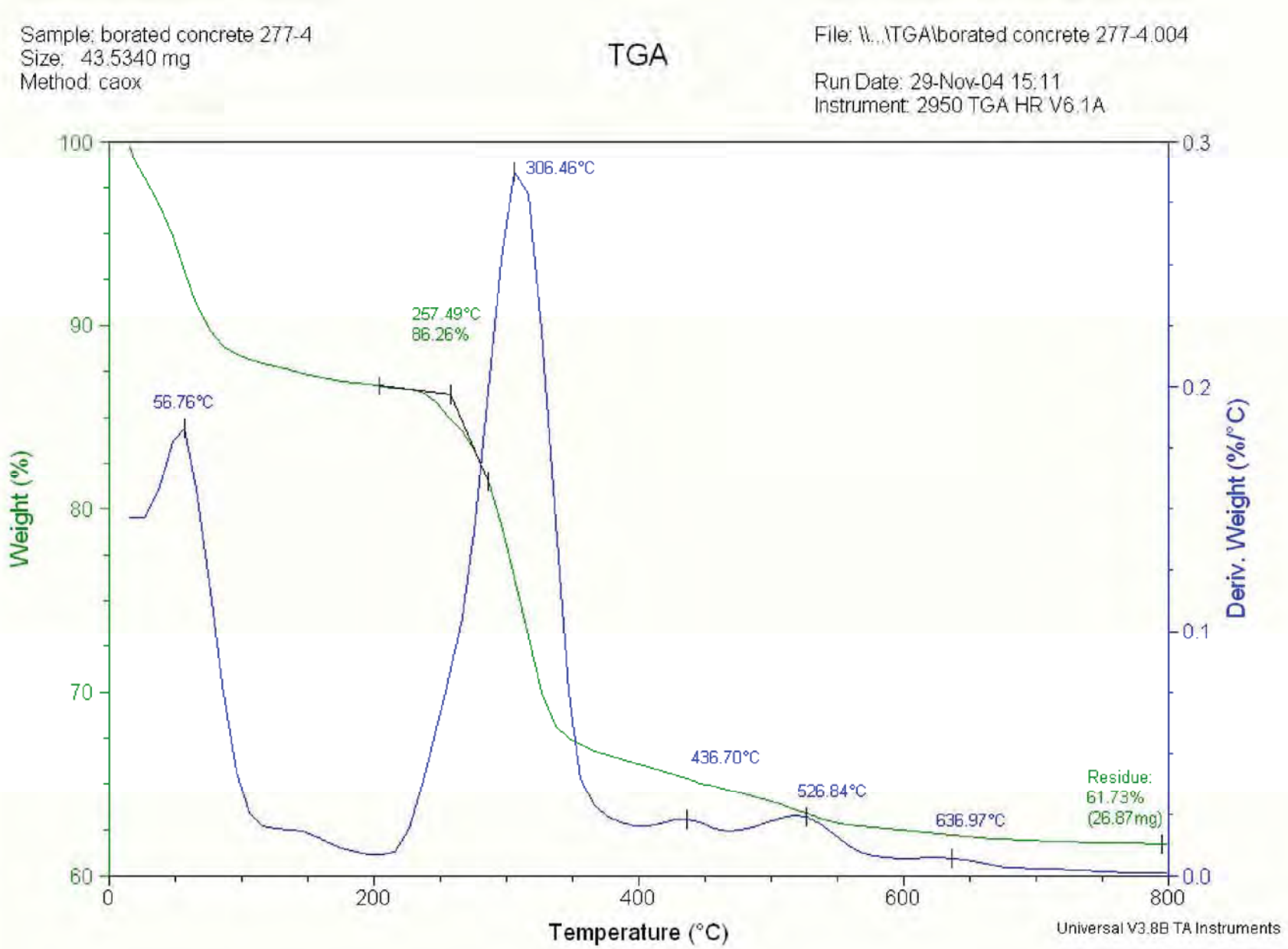
Sample: borated concrete 277-4
Size: 43.5340 mg
Method: caox
TGA
File: \\..\TGA\borated concrete 277-4.004
Run Date: 29-Nov-04 15:11
Instrument: 2950 TGA HR V6.1A
306.46°C
257.49°C
86.26%
56.76°C
436.70°C
526.84°C
636.97°C
Residue:
61.73%
(26.87mg)
Weight (%)
Deriv. Weight (%/°C)
Temperature (°C)
Universal V3.8B TA Instruments

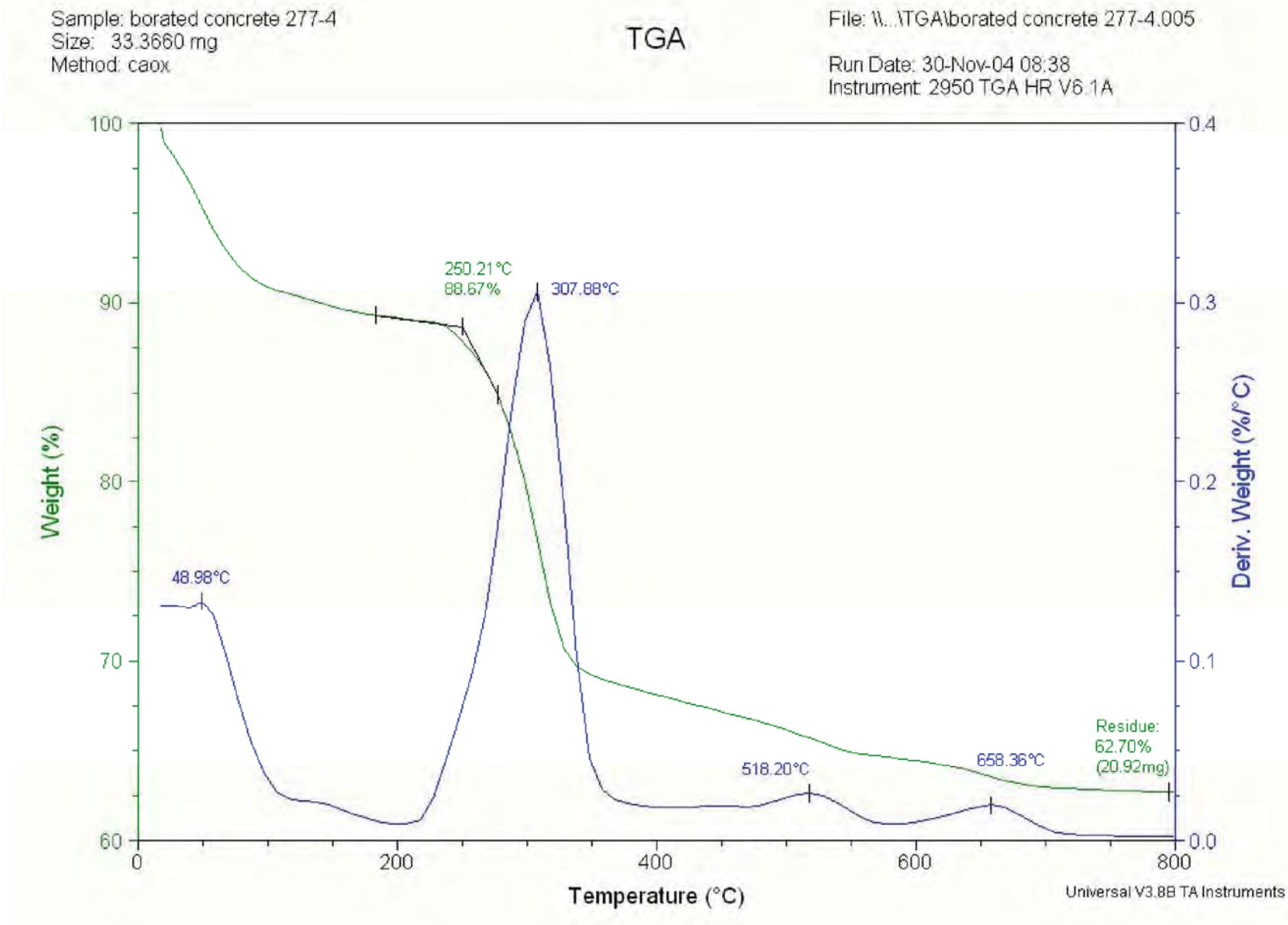
Sample: borated concrete 277-4
Size: 33.3660 mg
Method: caox
TGA
File: \\...\TGA\borated concrete 277-4.005
Run Date: 30-Nov-04 08:38
Instrument: 2950 TGA HR V6.1A
250.21°C
88.67%
307.88°C
48.98°C
518.20°C
658.36°C
Residue:
62.70%
(20.92mg)
Weight (%)
Deriv. Weight (%/°C)
Temperature (°C)
Universal V3.8B TA Instruments

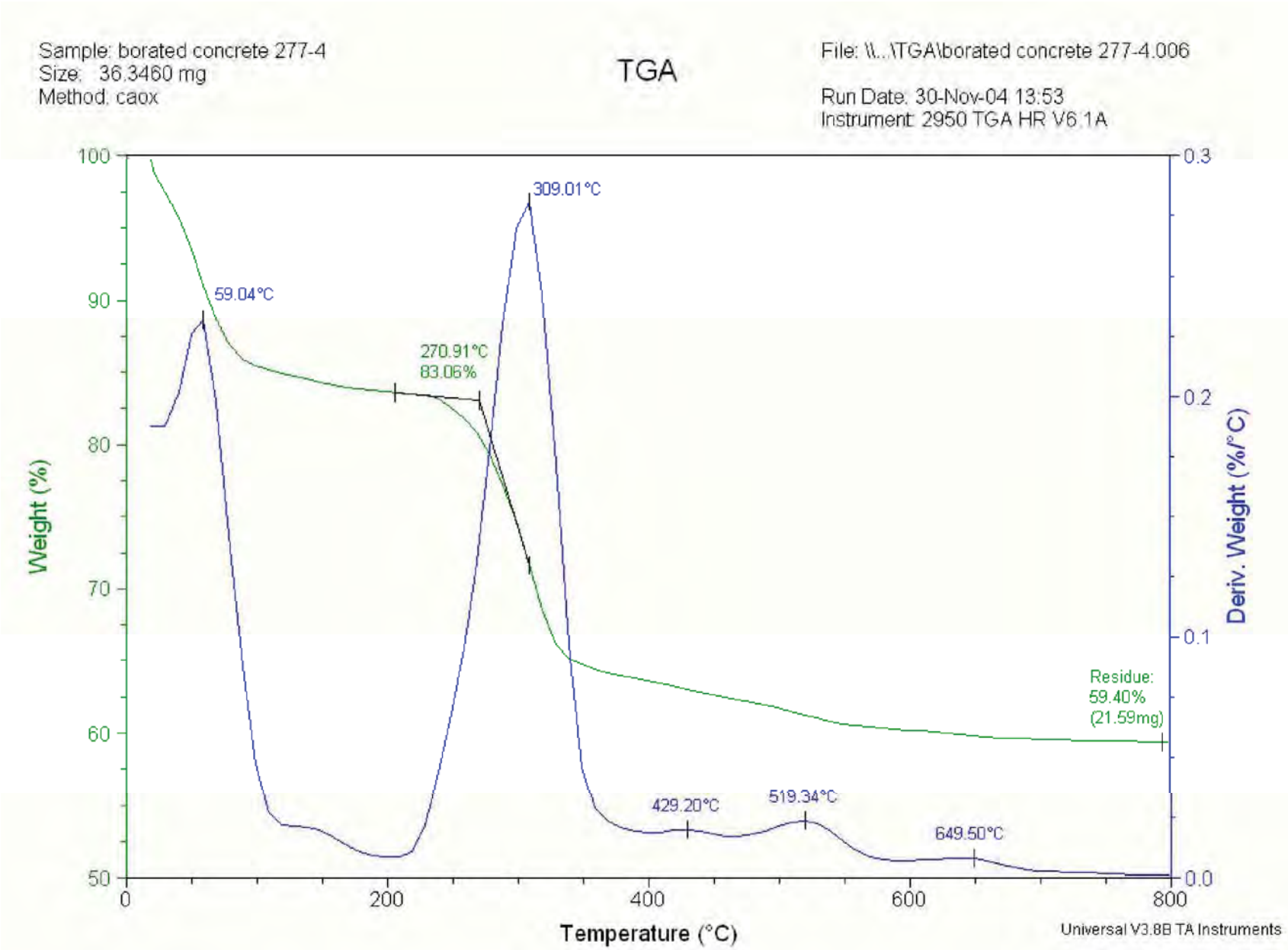
Sample: borated concrete 277-4
Size: 36.3460 mg
Method: caox
TGA
File: \\...\TGA\borated concrete 277-4.006
Run Date: 30-Nov-04 13:53
Instrument: 2950 TGA HR V6.1A
309.01°C
59.04°C
270.91°C
83.06%
Residue:
59.40%
(21.59mg)
429.20°C
519.34°C
649.50°C
Weight (%)
Deriv. Weight (%/°C)
Temperature (°C)
Universal V3.8B TA Instruments

Appendix B
TGA Results Obtained on "Dried" Borated Concrete 277-4

THIS PAGE INTENTIONALLY LEFT BLANK.

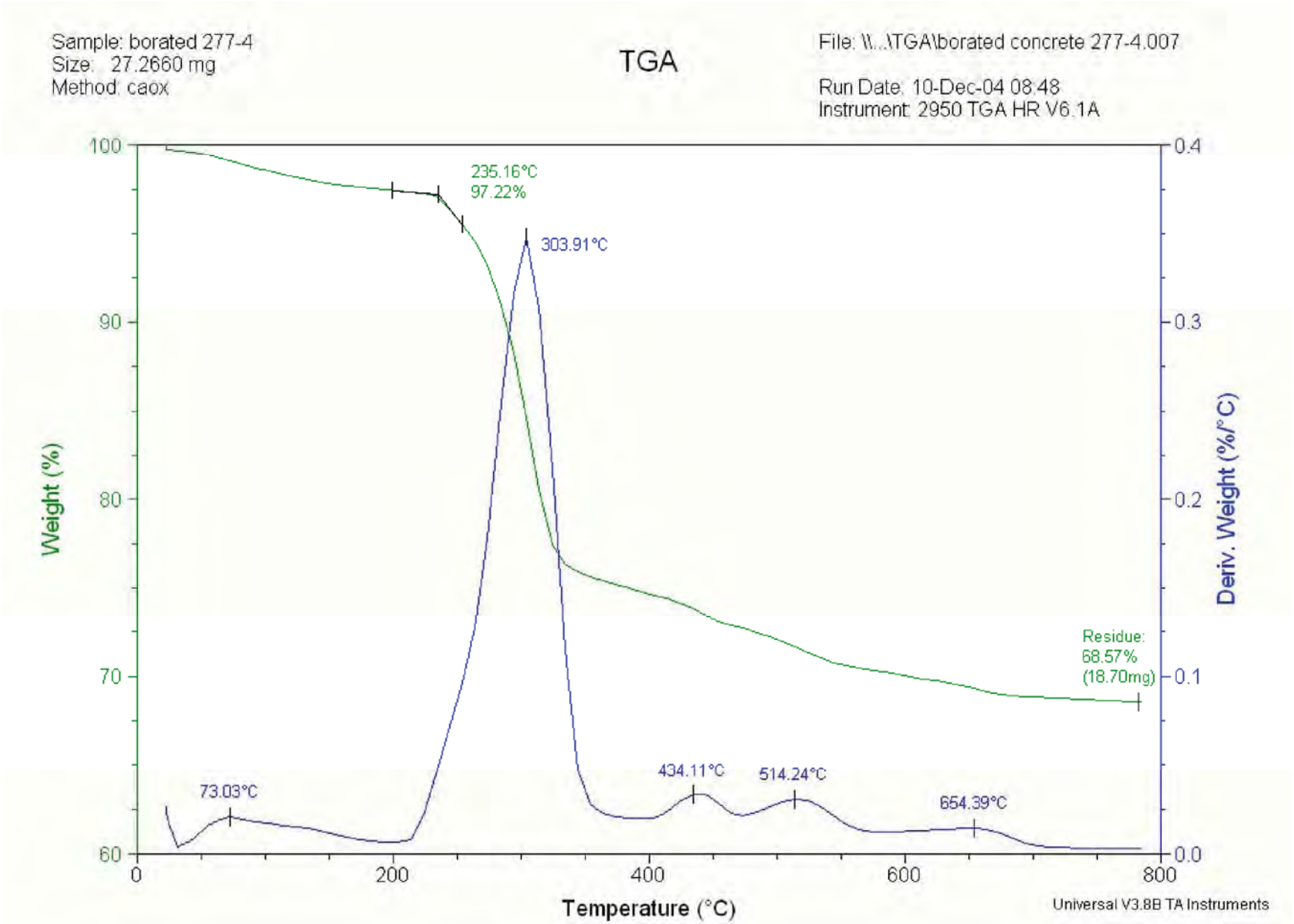
Sample: borated 277-4
Size: 27.2660 mg
Method: caox
TGA
File: \\...\TGA\borated concrete 277-4.007
Run Date: 10-Dec-04 08:48
Instrument: 2950 TGA HR V6.1A
235.16°C
97.22%
303.91°C
Residue:
68.57%
(18.70mg)
73.03°C
434.11°C
514.24°C
654.39°C
Weight (%)
Deriv. Weight (%/°C)
Temperature (°C)
Universal V3.8B TA Instruments

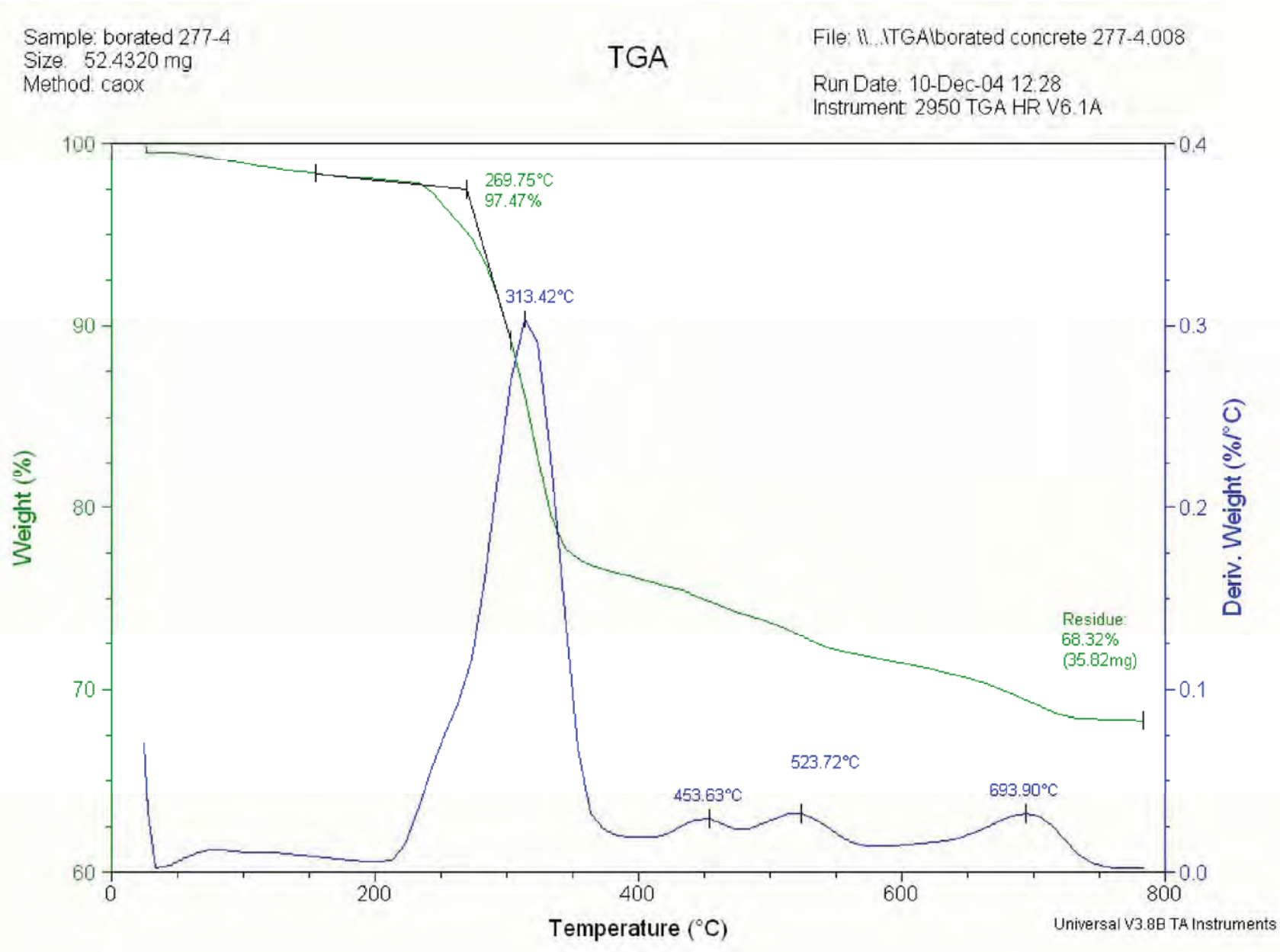
Sample: borated 277-4
Size: 52.4320 mg
Method: caox
TGA
File: \\..\TGA\borated concrete 277-4.008
Run Date: 10-Dec-04 12:28
Instrument: 2950 TGA HR V6.1A
269.75°C
97.47%
313.42°C
Residue:
68.32%
(35.82mg)
453.63°C
523.72°C
693.90°C
Weight (%)
Deriv. Weight (%/°C)
Temperature (°C)
Universal V3.8B TA Instruments

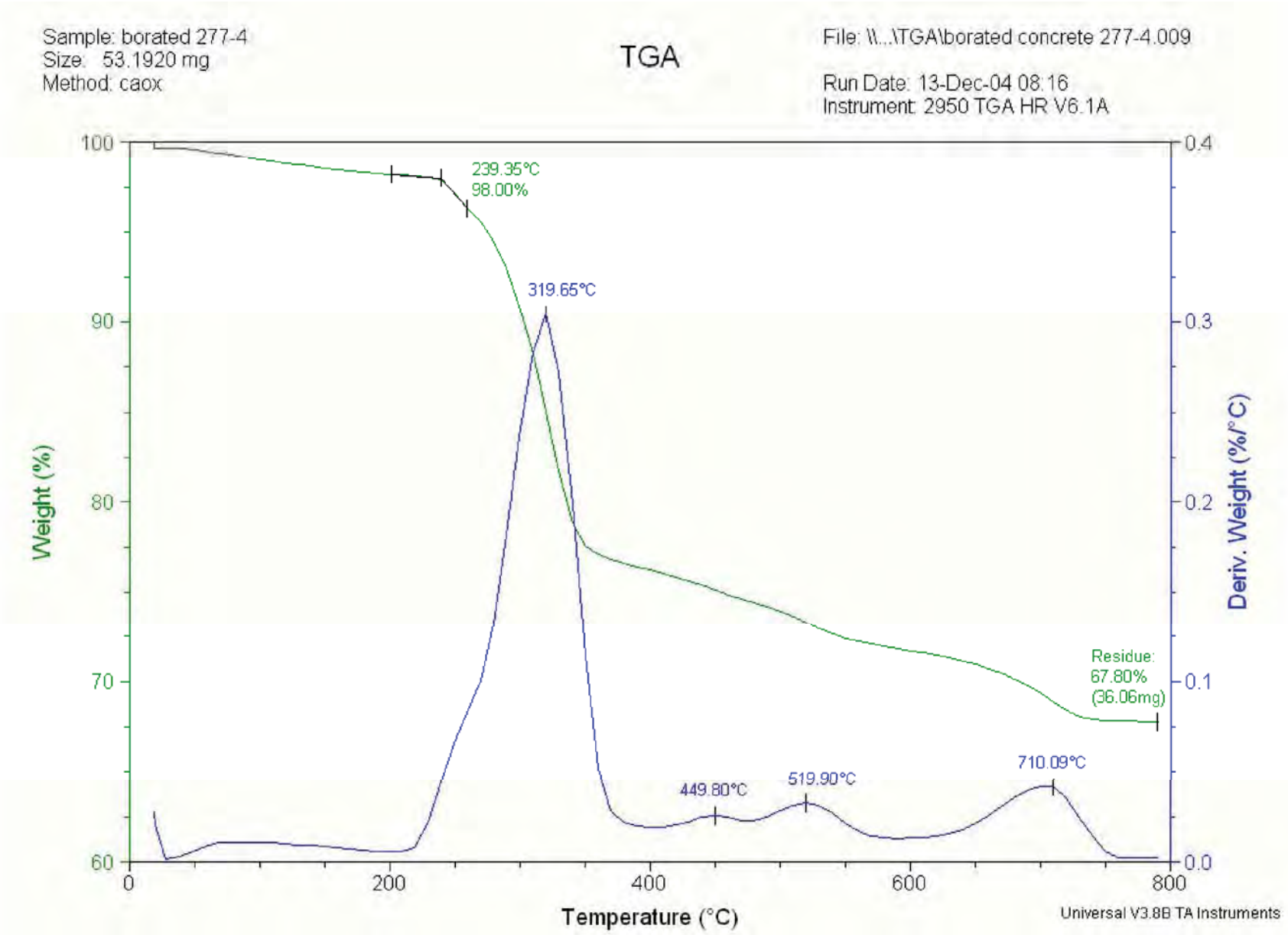
Sample: borated 277-4
Size: 53.1920 mg
Method: caox
TGA
File: \\...\TGA\borated concrete 277-4.009
Run Date: 13-Dec-04 08:16
Instrument: 2950 TGA HR V6.1A
239.35°C
98.00%
319.65°C
Residue:
67.80%
(36.06mg)
449.80°C
519.90°C
710.09°C
Weight (%)
Deriv. Weight (%/°C)
Temperature (°C)
Universal V3.8B TA Instruments

THIS PAGE INTENTIONALLY LEFT BLANK.

Appendix C -
TGA Results Obtained on Borobond 4

THIS PAGE INTENTIONALLY LEFT BLANK.

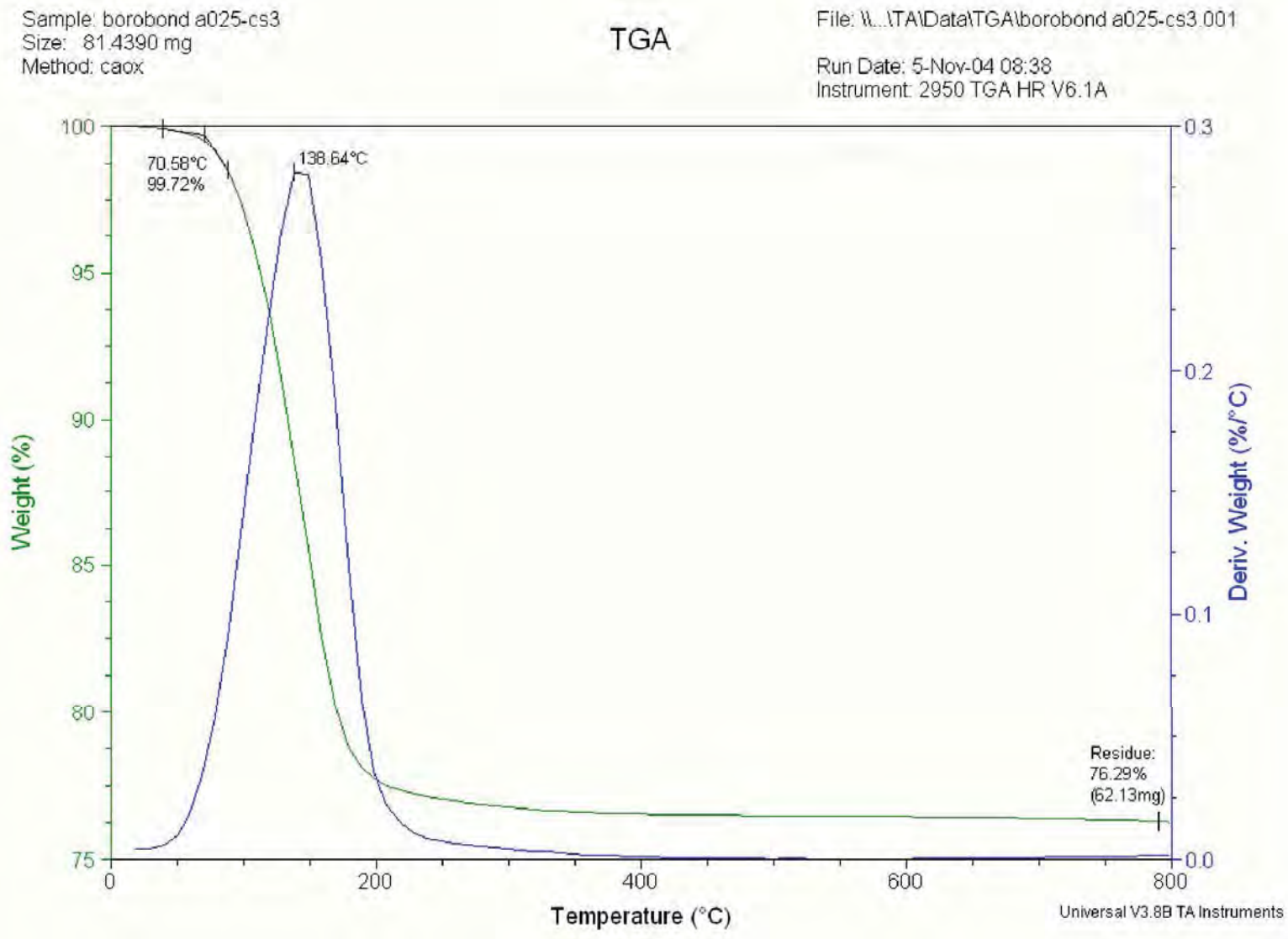
Sample: borobond a025-cs3
Size: 81.4390 mg
Method: caox
TGA
File: \\...\TA\Data\TGA\borobond a025-cs3.001
Run Date: 5-Nov-04 08:38
Instrument: 2950 TGA HR V6.1A
70.58°C
99.72%
138.64°C
Residue:
76.29%
(62.13mg)
Weight (%)
Deriv. Weight (%/°C)
Temperature (°C)
Universal V3.8B TA Instruments

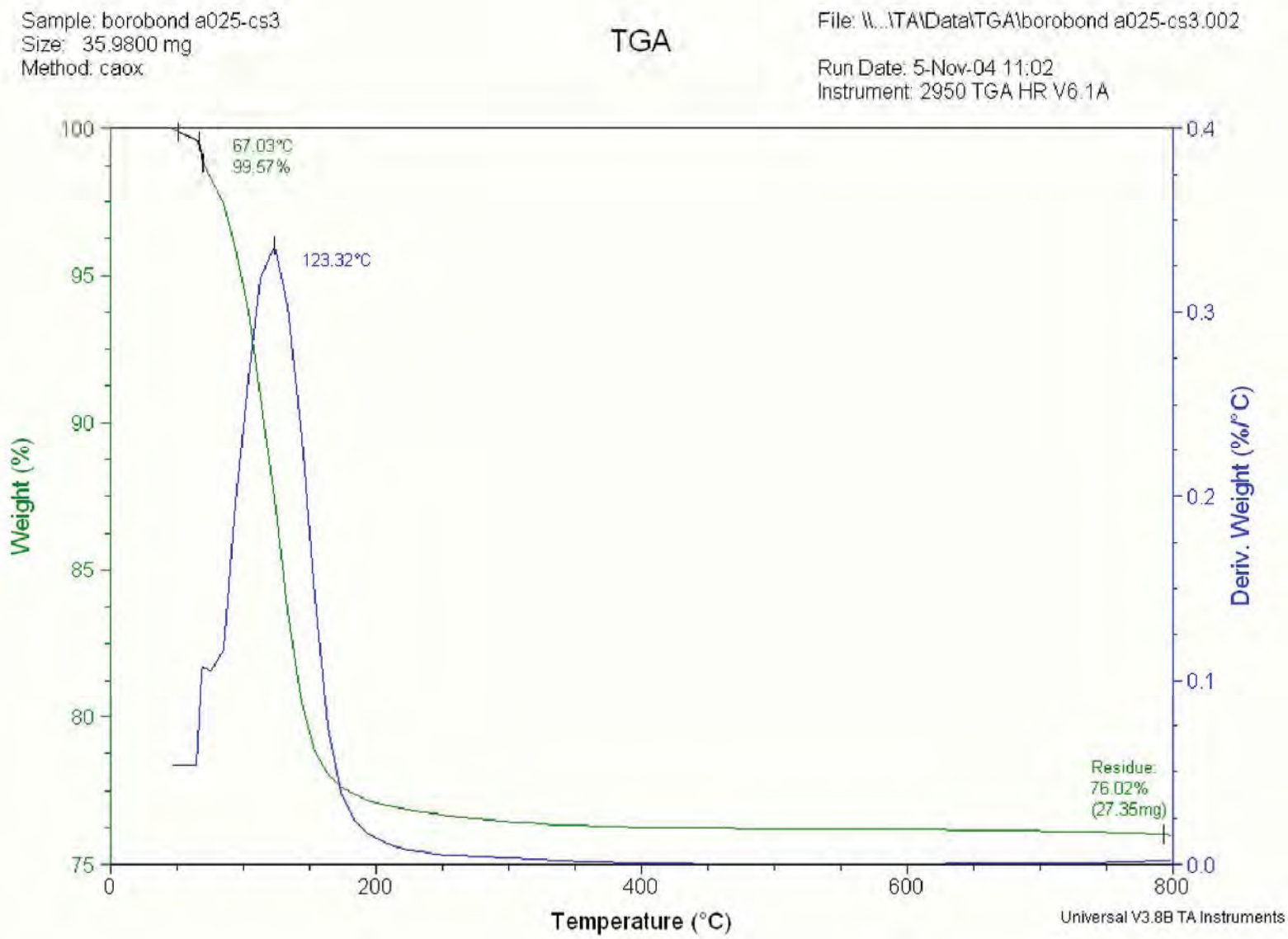
Sample: borobond a025-cs3
Size: 35.9800 mg
Method: caox
TGA
File: \\...\TA\Data\TGA\borobond a025-cs3.002
Run Date: 5-Nov-04 11:02
Instrument: 2950 TGA HR V6.1A
67.03°C
99.57%
123.32°C
Residue:
76.02%
(27.35mg)
Weight (%)
Deriv. Weight (%/°C)
Temperature (°C)
Universal V3.8B TA Instruments

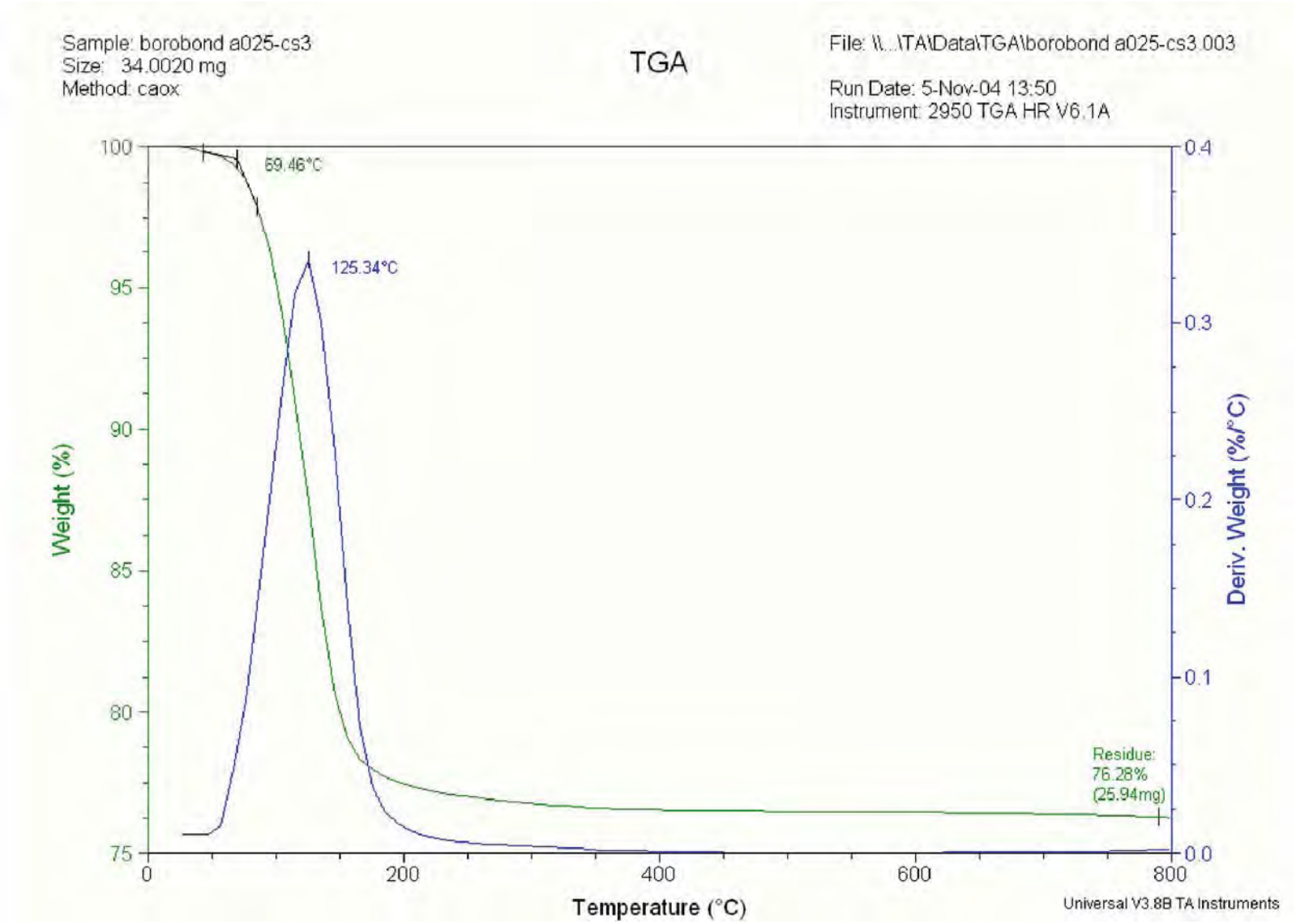
Sample: borobond a025-cs3
Size: 34.0020 mg
Method: caox
TGA
File: \\...\TA\Data\TGA\borobond a025-cs3.003
Run Date: 5-Nov-04 13:50
Instrument: 2950 TGA HR V6.1A
69.46°C
125.34°C
Residue:
76.28%
(25.94mg)
Weight (%)
Deriv. Weight (%/°C)
Temperature (°C)
Universal V3.8B TA Instruments

Appendix D
TGA Results for Adhesive Backed Silicone Foam

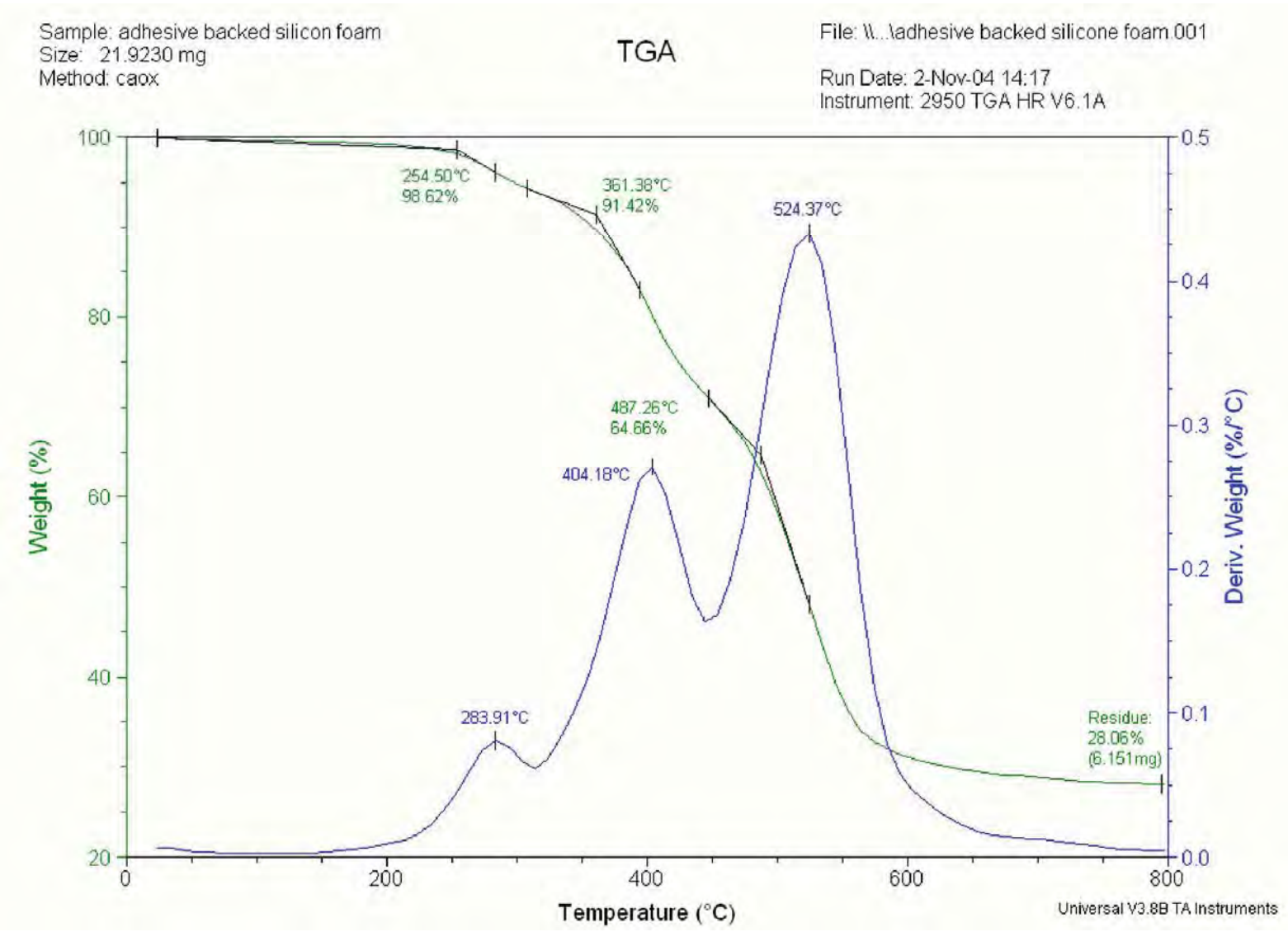
Sample: adhesive backed silicon foam
Size: 21.9230 mg
Method: caox
TGA
File: \\...\adhesive backed silicone foam.001
Run Date: 2-Nov-04 14:17
Instrument: 2950 TGA HR V6.1A
254.50°C
98.62%
361.38°C
91.42%
524.37°C
487.26°C
64.66%
404.18°C
283.91°C
Residue:
28.06%
(6.151mg)
Weight (%)
Deriv. Weight (%/°C)
Temperature (°C)
Universal V3.8B TA Instruments

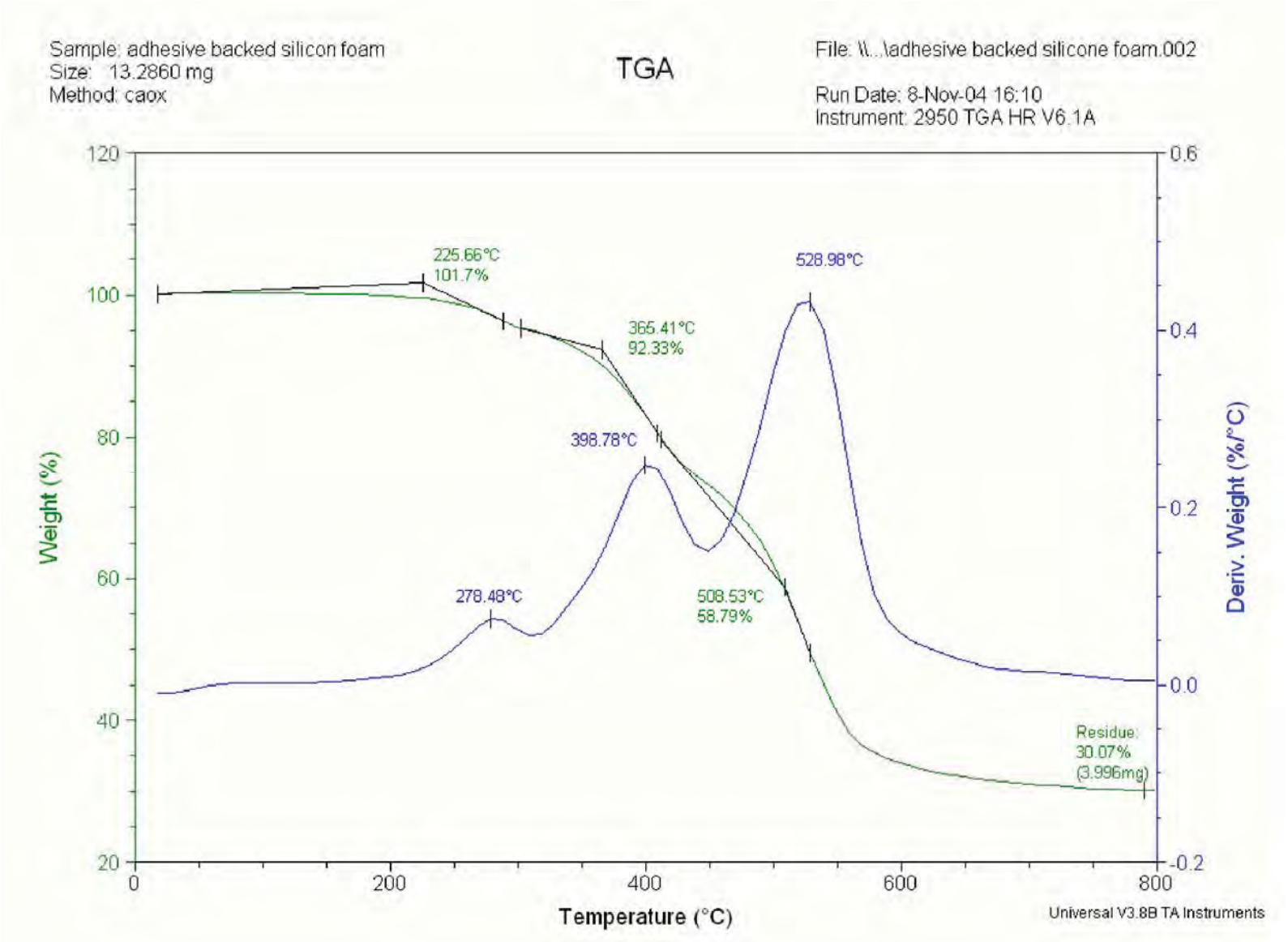
Sample: adhesive backed silicon foam
Size: 13.2860 mg
Method: caox
TGA
File: \\...\adhesive backed silicone foam.002
Run Date: 8-Nov-04 16:10
Instrument: 2950 TGA HR V6.1A
225.66°C
101.7%
365.41°C
92.33%
398.78°C
278.48°C
508.53°C
58.79%
528.98°C
Residue:
30.07%
(3.996mg)
Weight (%)
Deriv. Weight (%/°C)
Temperature (°C)
Universal V3.8B TA Instruments

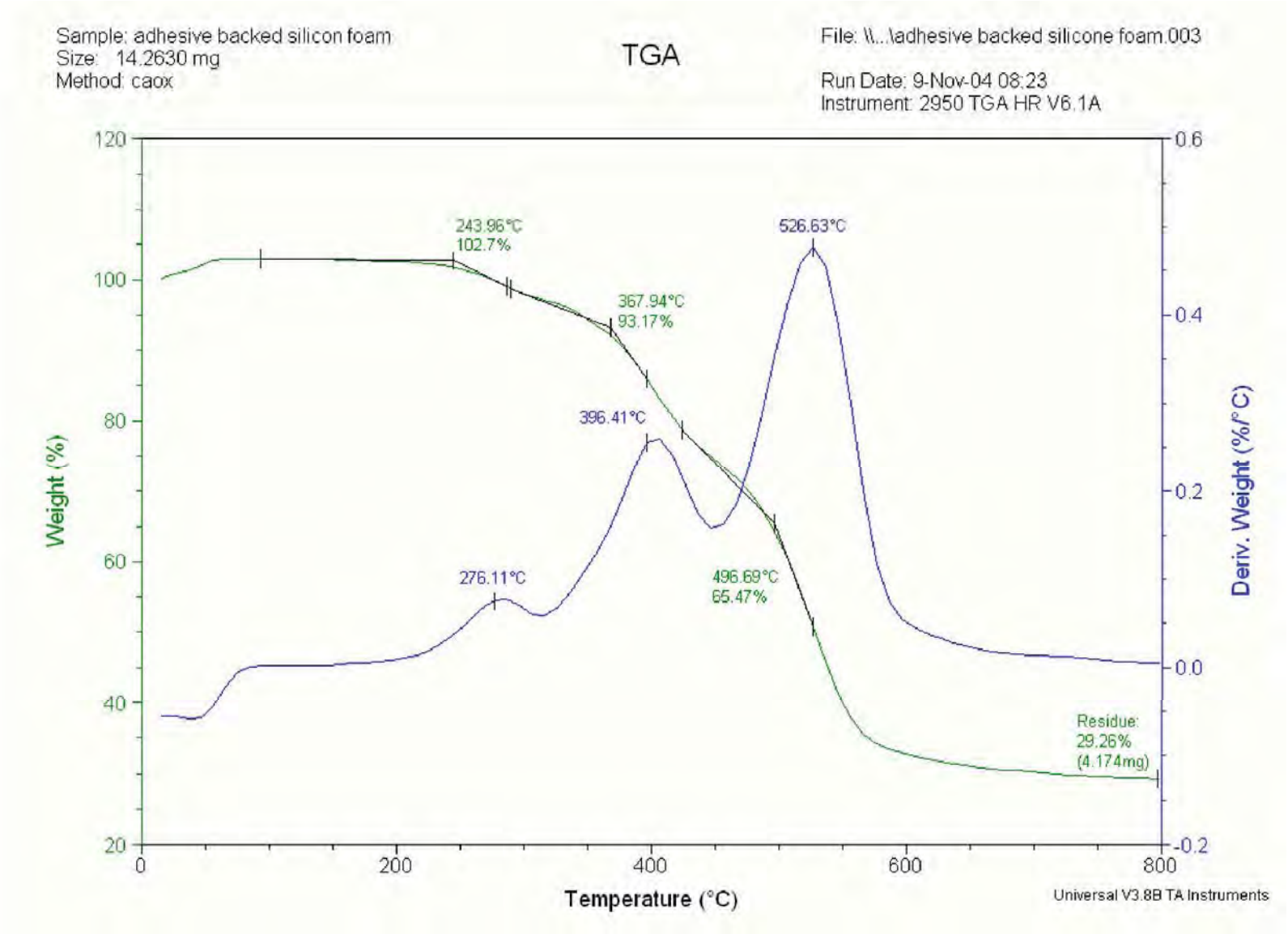
Sample: adhesive backed silicon foam
Size: 14.2630 mg
Method: caox
TGA
File: \\...\adhesive backed silicone foam.003
Run Date: 9-Nov-04 08:23
Instrument: 2950 TGA HR V6.1A
243.96°C
102.7%
367.94°C
93.17%
396.41°C
276.11°C
526.63°C
496.69°C
65.47%
Residue:
29.26%
(4.174mg)
Weight (%)
Deriv. Weight (%/°C)
Temperature (°C)
Universal V3.8B TA Instruments

Distribution:

Amonett, C. M.
Anderson, J. C.
Arbital, J. G.
Bales, P. A.
Byington, G. A.
Cramer, Noel
Crenshaw, M. D.
DeClue, J. F.
Eckert, G. W.
Goins, M. L.
Handy, K. D.
Heatherly, C. N.
Holder, S. T.
Johnson, D. T.
Miller, D. B.
Perkins, G.
Singleton, G. B.
Smith, R. H.
Sooter, D. P.
Thomas, S. K.
Tollefson, D. A.
Turner, S. B.
Warren, T. L.
Y-12 Central Files

Appendix 2.10.5

BOROBOND4 PROPERTIES

B. F. Smith, *Compressive Strength and Coefficient of Thermal Expansion of BoroBond4*, Y/DW-1968, BWXT Y-12, Y-12 Natl. Security Complex, Jan. 19, 2005.

Note: For BoroBond4 outgassing properties, see Appendix 2.10.4: R. A. Smith, *Volatile Components from Packing Materials*, Y/DZ-2585, rev. 2, BWXT Y-12, Y-12 Natl. Security Complex, Dec. 22, 2004.

THIS PAGE INTENTIONALLY LEFT BLANK.

Y/DW-1968

Compressive Strength and Coefficient of Thermal Expansion of BoroBond4

B. F. Smith
Characterization and Analysis Technology
Technology Development

August 11, 2004

Prepared by the
Y-12 National Security Complex
P.O. Box 2009
Oak Ridge, Tennessee, 37831-8169
Managed by BWXT Y-12, L.L.C.
for the
U.S. DEPARTMENT OF ENERGY
under contract DE-AC05-00OR22800

MANAGED BY
BWXT Y-12, L.L.C.
FOR THE UNITED STATES
DEPARTMENT OF ENERGY

UCN-13672 (10-00)

DISCLAIMER

This report was prepared as an account of work sponsored by an agency of the United States Government. Neither the United States Government nor any agency thereof, nor any of their employees, makes any warranty, express or implied, or assumes any legal liability or responsibility for the accuracy, completeness, or usefulness of any information, apparatus, product, or process disclosed, or represents that its use would not infringe privately owned rights. Reference herein to any specific commercial product, process, or service by trade name, trademark, manufacturer, or otherwise, does not necessarily constitute or imply its endorsement, recommendation, or favoring by the United States Government or any agency thereof. The views and opinions of authors expressed herein do not necessarily state or reflect those of the United States Government or any agency thereof.

Y/DW-1968

COMPRESSIVE STRENGTH AND COEFFICIENT OF THERMAL EXPANSION OF BOROBOND4

B. F. Smith
Characterization and Analysis Technology
Technology Development

Date of Issue: August 11, 2004

Prepared by the
Y-12 National Security Complex
P.O. Box 2009
Oak Ridge, Tennessee, 37831-8169
Managed by BWXT Y-12, L.L.C.
for the
U.S. DEPARTMENT OF ENERGY
under contract DE-AC05-00OR22800

CONTENTS

FIGURES iv
TABLES iv

FIGURES

Figure Page

1. Coefficient of Thermal Expansion vs. Average Temperature....4

TABLES

Table Page

1. Compressive Strengths of BoroBond4 at 100°F....2
2. Compressive Strengths of BoroBond4 at 70°F....2
3. Compressive Strengths of BoroBond4 at -40°F....2
4. Coefficients of Thermal Expansion of BoroBond4 at 200°F....2
5. Coefficients of Thermal Expansion of BoroBond4 at 100°F....3
6. Coefficients of Thermal Expansion of BoroBond4 at -40°F....3
7. Changes in CTE Specimens....5

INTRODUCTION

BoroBond4 is used as a neutron absorber in the ES-3100 packaging system. Mechanical and Manufacturing Engineering requested that Technology Development provide measurements of the compressive strength and rough estimates of the coefficient of thermal expansion (CTE) of BoroBond4 for use in simulations. The compressive strength measurements were to be done at room temperature (approximately 70°F), at -40°F, and at 100°F. Estimates of CTEs were to be done at -40°F, 100°F, and 200°F.

EXPERIMENTAL PROCEDURE

ASTM C 109[1] was used as a guide in measuring the compressive strength of BoroBond4. This standard provides an outline for measuring the maximum stress a two inch cube will experience before fracture. Fifty-six two inch cube specimens were provided by Eagle Picher. The density of each specimen was measured to determine the temperature distribution during compression testing. Six were tested at room temperature, six were tested at -40°F, and five were tested at 100°F. Rudimentary CTE measurements were taken on the specimens that were later compression tested at -40°F. A different group of six specimens were used only for CTE estimation at 100°F and 200°F.

As recommended by ASTM C 109, each cube was placed between two platens and loaded at a rate of 200 lb/s. The upper platen was spherically seated and the bottom platen was fixed. A 200,000 lb capacity servohydraulic load frame was used with a load cell set to the +/-50,000 lb range. Each specimen was brought to its test temperature by thermally "shocking" it, whereby it was placed in an environmental chamber at a more extreme temperature than it would be tested at. The 100°F compression specimens soaked at 110°F for 75 min, after which the chamber temperature was brought down to 100°F until testing began 6.5 h later. Similarly, the -40°F compression specimens soaked at -50°F for 15.5 h, after which the chamber temperature was raised to -40°F and testing began with little delay.

In estimating the CTE of BoroBond4, no formal standard was used and a method had to be improvised due to the lack of proper specimens and equipment. Thus, the CTE values reported here are only very rough ones and are by no means certified. The same type of two inch cubes were used for estimating CTEs that were used for the compressive strength measurements. The general procedure was to place the cube against a datum while at room temperature and measure lengths along two axes by butting a set of calipers against the top of the datum. The datum would ensure the same place on the cube was being measured before and after being brought to the appropriate temperature. A vise with faces 1.315 in. tall was used as the datum. Since the datum would result in measurements not on the center of the cube face, it was critical to keep the orientation of the cube consistent. After soaking for an adequate amount of time, the axis lengths were measured as close as possible to the original location. The CTE of BoroBond4 was then calculated using these two measurements.

RESULTS

Tables 1 through 3 summarize the BoroBond4 compressive strengths and test conditions. Tables 4 through 6 summarize the CTEs of BoroBond4.

Table 1. Compressive Strengths of BoroBond4 at 100°F

Cube ID	Density @ Room Temp (lb/ft^3)	Compressive Strength (psi)
AO19-CS1	121.84	7711.5
AO17-CS3	121.94	7508.9
AO17-CS1	122.05	7422.8
AO20-CS2	122.08	7280.8
AO15-CS3	122.18	7440.6
Average Strength		7472.9

Table 2. Compressive Strengths of BoroBond4 at 70°F

Cube ID	Density @ Room Temp (lb/ft^3)	Compressive Strength (psi)
AO22-CS2	122.69	9061.3
AO18-CS1	122.70	7697.5
AO25-CS2	122.70	9587.4
AO26-CS2	122.72	9651.4
AO20-CS1	122.75	7494.5
AO21-CS4	122.76	8263.0
Average Strength		8625.9

Table 3. Compressive Strengths of BoroBond4 at -40°F

Cube ID	Density @ Room Temp (lb/ft^3)	Compressive Strength (psi)
AO24-CS3	123.10	9197.1
AO23-CS3	123.10	10347.7
AO25-CS4	123.12	11180.8
AO16-CS3	123.18	8232.8
AO16-CS1	123.19	9167.8
AO16-CS2	123.57	7081.7
Average Strength		9201.3

Table 4. Coefficients of Thermal Expansion of BoroBond4 at 200°F

Cube ID	Density @ Room Temp (lb/ft^3)	CTE @ 0° Face (in/in-°F)	CTE @ 90° Face (in/in-°F)
AO21-CS1	122.27	-1.50E-05	-2.99E-05
AO21-CS2	122.30	-9.99E-06	-5.00E-06
AO22-CS4	122.70	-9.99E-06	-1.99E-05
AO16-CS4	122.81	0	-2.50E-05
AO25-CS1	123.08	-1.50E-05	-2.99E-05
AO23-CS4	123.09	-1.49E-05	-2.98E-05
Average CTEs		-1.08E-05	-2.32E-05

Table 5. Coefficients of Thermal Expansion of BoroBond4 at 100°F

Cube ID	Density @ Room Temp (lb/ft^3)	CTE @ 0° Face (in/in-°F)	CTE @ 90° Face (in/in-°F)
AO21-CS1	122.27	0	-9.22E-06
AO21-CS2	122.30	0	-1.85E-05
AO22-CS4	122.70	0	-1.84E-05
AO16-CS4	122.81	-1.84E-05	-2.77E-05
AO25-CS1	123.08	1.85E-05	-9.22E-06
AO23-CS4	123.09	0	0
Average CTEs		1.07E-08	-1.38E-05

Table 6. Coefficients of Thermal Expansion of BoroBond4 at -40°F

Cube ID	Density @ Room Temp (lb/ft^3)	CTE @ 0° Face (in/in-°F)	CTE @ 90° Face (in/in-°F)
AO24-CS3	123.10	9.02E-06	9.05E-06
AO23-CS3	123.10	4.53E-06	4.51E-06
AO25-CS4	123.12	9.07E-06	1.36E-05
AO16-CS3	123.18	0	4.53E-06
AO16-CS1	123.19	2.26E-06	2.27E-06
AO16-CS2	123.57	9.06E-06	4.53E-06
Average CTEs		5.66E-06	6.41E-06

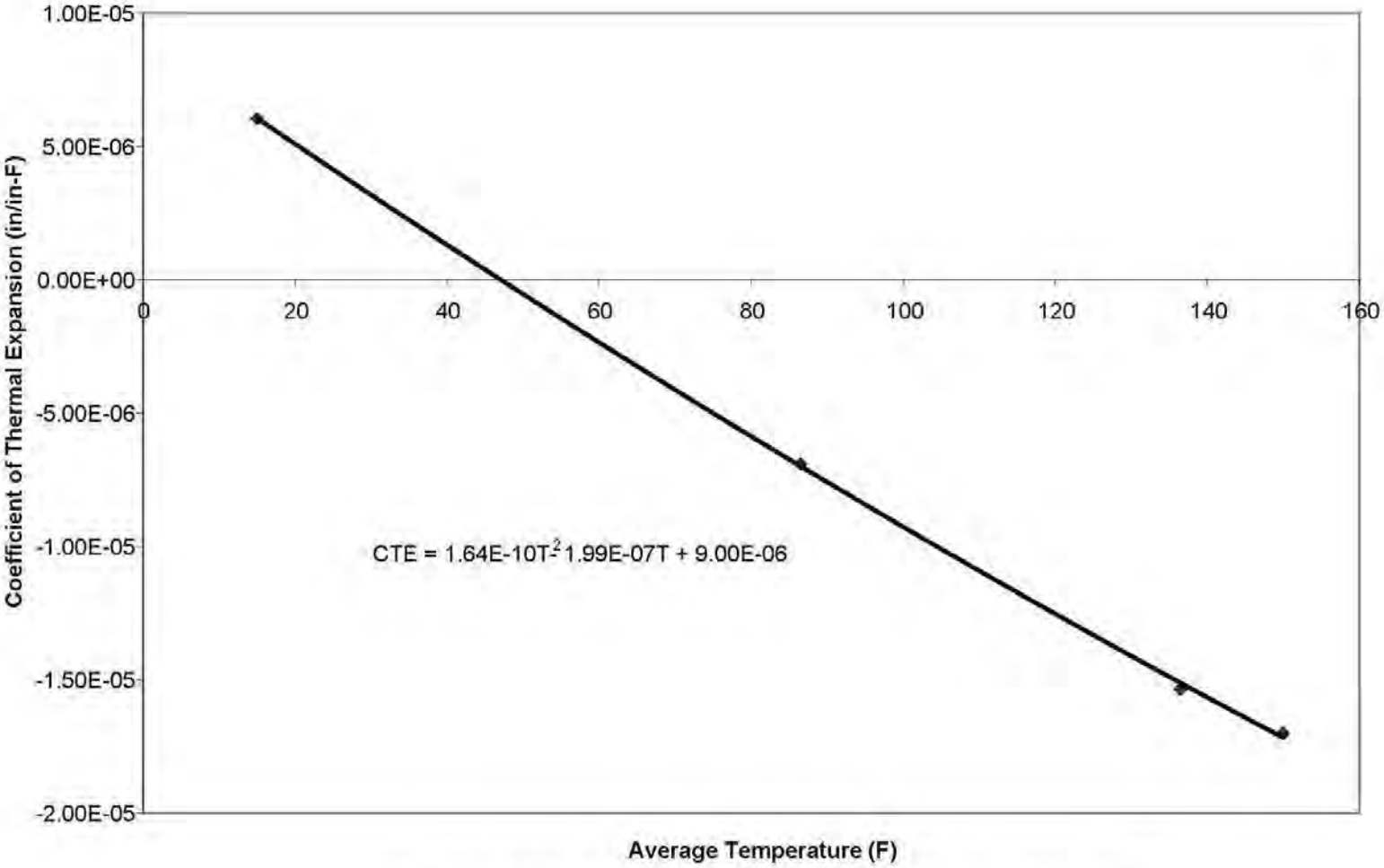

Fig. 1. Coefficient of Thermal Expansion vs. Average Temperature

DISCUSSION

As expected, the strength of BoroBond4 is inversely proportional to its temperature. The average strength increased from 7472.9 psi at 100°F to 9201.3 psi at -40°F.

As illustrated in Fig. 1, the coefficient of thermal expansion of BoroBond4 tends to decrease as the average temperature increases. The variation in CTE within temperature groups was very wide. The sense of the coefficient was not consistent. For example, the CTE estimated at 100°F showed that the 0° face expanded while the 90° face contracted. This may be negligible, however, since the change in temperature of only 27°F was relatively small.

The mechanism of thermal expansion or contraction is apparently due to dehydration. After measuring CTEs at 200°F and allowing the specimens to cool to room temperature, it was noted that all cubes were significantly lighter in color. Measurements showed that the cubes had not returned to their original dimensions and their masses had decreased. This could only be due to dehydration since each cube was in good condition and had not lost any noticeable mass due to chipping or rough handling. Table 7 summarizes the changes in dimensions, all taken at room temperature. All of these cubes had soaked at 110°F for 3 h followed by soaking at 100°F for 92.5 h, which was followed by a soaking at 220°F for a period of 3 h. The excessive length of time the specimens were at 100°F may explain the water loss.

Table 7. Changes in CTE Specimens

Cube ID	ΔL, 0° Face (in)	ΔL 90° Face (in)	Δ mass (g)
AO21-CS1	-0.004	-0.0055	-27.14
AO21-CS2	-0.005	-0.007	-29.295
AO22-CS4	-0.004	-0.007	-25.44
AO16-CS4	-0.006	-0.0075	-28.625
AO25-CS1	-0.004	-0.0075	-25.565
AO23-CS4	-0.001	-0.007	-27.74

REFERENCES

1. ASTM International. *Standard Test Method for Compressive Strength of Hydraulic Cement Mortars (Using 2-in. or [50-mm] Cube Specimens).* ASTM Standard C 109/C 109M-02.

DISTRIBUTION

Y-12 National Security Complex

Anderson, J. C.
Arbital, J. G.
Bales, P. A.
Byington, G. A. (2)
DeClue, J. F. (2)
Doyle, J. H.
Goins, M. L.
Hammond, C. R.
Handy, K. D. (2)
Heatherly, C. N.
Kitzke, K. A.
Miller, D. B.
Neal, J. Y.
Smith, B. F.
Sooter, D. P.
Y-12 Plant Records - RC

THIS PAGE INTENTIONALLY LEFT BLANK.

Appendix 2.10.6

RECOMMENDED RANDOM VIBRATION AND SHOCK TEST SPECIFICATIONS FOR CARGO TRANSPORTED ON SST AND SGT TRAILERS

THIS PAGE INTENTIONALLY LEFT BLANK.

Sandia National Laboratories
Operated for the U.S. Department of Energy by
Sandia Corporation
Albuquerque, New Mexico 87185

date: April 19, 2002

to: Distribution

from: J. S. Cap, 9125

subject: Recommended Random Vibration and Shock Test Specifications for Cargo Transported on SST and SGT Trailers

References

[1] UNC document from J. S. Cap, 9735; to G. W. Crowder, 5512; dated 5/1/97; "Maximum Expected Mechanical Shock and Vibration Environments and Test Requirements for Cargo Transported on SSTs & SGTs."
[2] UNC Document MIL-STD-810E; "Environmental Test Methods and Engineering Guidelines."

Introduction

The primary goal of this document is to provide a set of random vibration test specifications and a set of shock test specifications for cargo being transported on the Safe-Secure Trailers (SST2/82 and SST2/90) and the Safeguards Transporter (SGT). An earlier study [1] established that the random vibration and shock profiles measured during road tests for each trailer indeed represented the Maximum Expected Environments (MEE) (i.e., statistically conservative upper bounds). That study also established the appropriate random vibration test durations for producing the equivalent fatigue damage as a function of trip distance.

copy to:

Dept	MS	Name	Dept	MS	Name
5851	0790	G. W. Crowder	8234	9035	K. E. Carbiener
5851	0790	J. K. Deuel	8234	9035	T. Harrison
8242	9014	W. R. Delameter	8727	9042	J. J. Lauffer
8242	9014	D. M. Kwon	9125	0557	T. J. Baca
8242	9014	A. H. Leung	9125	0557	File(EE6.7)
8242	9014	A. A. Ver Berkmoes			Steve Jensen (LLNL)

The raw Acceleration Spectral Densities (ASDs) and the raw Shock Response Spectra (SRS) that define the MEE for random vibration and shock respectively are not practical for use as laboratory test specifications. Therefore, reference [1] also provided a set of straight-line segment ASDs and SRS that envelop the raw MEE spectra and are suitable for use in the laboratory. However, those straight-line segment ASDs and SRS were deemed to be less than ideal, so a slightly improved set is presented in this document.

Random Vibration Test Duration

For purposes of estimation, we have identified a generic 2000-mile cross-country road trip that will last 45 hours. Of course, the cargo will not be subjected to the MEE vibration levels for the entire time, but instead will experience a distribution of input levels that is by definition at or below the MEE levels. Using the distribution of input levels for the entire road trip identified in reference [1], it is possible using fatigue theory to define a laboratory test that produces the same amount of fatigue damage in a few hours that the cargo would experience during the 2000-mile trip. The most logical initial (baseline) choice for the laboratory test specifications is the MEE ASDs (and hence the corresponding straight-line segment ASDs).

Table 1, which is taken verbatim from [1], identifies the amount of time spent on each of the different type roads during the generic 2000-mile road trip and the corresponding laboratory test durations for different types of cargo (the definition of which are explained in the table notes).

Table 1: Accelerated Laboratory Test Times for a 2000-Mile Road Trip

Road Type	Trip Time	Lab Scale Factors and Test Times (1,2,3)		
		1 dB/decade	3 dB/decade	4 dB/decade
Interstate	37 Hrs	0.23 Hrs/Axis	0.41 Hrs/Axis	0.8 Hrs/Axis
Rural Highways	6 Hrs	0.07 Hrs/Axis	0.09 Hrs/Axis	0.2 Hrs/Axis
Urban Streets & Unpaved Roads (4)	2 Hrs	1.5 Hrs/Axis	1.5 Hrs/Axis	1.5 Hrs/Axis
Total Test Times	45 Hrs	1.8 Hrs/Axis	2.0 Hrs/Axis	2.5 Hrs/Axis

Notes for Table 1:

1) Some of the laboratory test times identified in this table have been rounded up for simplicity.
2) The amount of time compression to be achieved for a given increase in test level will depend on the materials and assembly techniques present in the item being tested. The literature identifies a range of compression factors (defined in terms of the dB increase in test level per decade of time compression) that vary from 1 dB/decade for brittle materials exposed to coulomb friction (such as for un-potted bolted assemblies) to 4 dB/decade for ductile materials supported in viscoelastic media (as for encapsulated assemblies). Table 1 identifies the compressed test times for several compression factors of interest.
3) If the specifics of a system design are not known, or contain a range of materials, it is recommended that the time compression be performed using a 3 dB/decade compression factor.

4) The environmental levels for urban streets and unpaved roads were so close in magnitude to the MEE levels that minimal time compression was possible.

It is interesting to note that the resulting test time for the 3 dB/decade compression factor (2 hours/axis for a 2000-mile trip) agrees exactly with the recommended ratio of test duration versus trip distance identified in MIL-STD-810E [2] for truck-transport.

If the total laboratory test-duration is still too long after the initial time compression has been applied (usually true for components that must make many trips on one of the trailers), then additional time compression can be achieved by increasing the test specifications by a specified number of dB to achieve additional time compression. The user is cautioned that there are risks associated with testing one's hardware to levels that are higher than they would ever expect to see in the field. However, since the absolute magnitude of the SST/SGT MEE test levels are relatively low compared with other truck transport inputs (such as MIL-STD-810E), an increase of 3-6 dB should not significantly increase the risk of a component failure, while permitting an additional time compression factor of 10-100 (assuming the 3 dB/decade compression factor).

Random Vibration Test Specifications

Figure 1 presents the recommended straight-line segment ASD random vibration test specifications for transport of cargo on SST and SGT trailers. The axes identified in the figure (LONG, LAT, and VERT) refer to the trailer coordinate system.

However, there may be instances where the orientation of the cargo relative to the longitudinal and lateral trailer axis is not unique. In such cases it is recommended that the cargo be tested in two mutually perpendicular horizontal axes using to the "HORIZ" test specifications identified in Figure 2 (the "VERT" test specification, which has been reproduced in Figure 2 for convenience, must still be applied in that axis).

These ASDs should be applied to the cargo at a point that is in intimate contact with the shaker table. Assuming that the 3 dB/decade compression factor is chosen and no additional scaling is done, the test specifications presented in Figure 1 should be applied for 1 Hr/axis for each 1000 miles of road transport.

The test specifications presented in these figures have been defined down to 1 Hz for completeness. However, the cargo need only be tested down to a frequency that is equal to one-half of its lowest resonant mode, or 10 Hz, whichever is lower. The ASDs identified in Figures 1 and 2 would be truncated accordingly.

Appendix A compares the straight-line ASD test specifications against the underlying MEE ASDs.

Figure 1: SST/SGT Random Vibration Test Specifications
Input to Base of Cargo

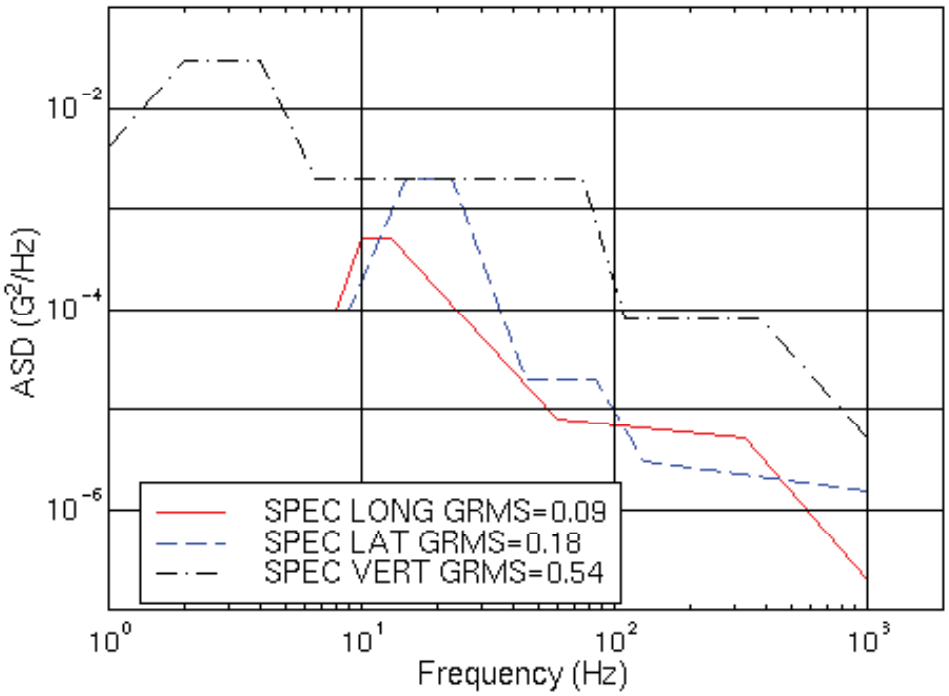

LONG		LAT		VERT	
Freq (Hz)	G^2/Hz	Freq (Hz)	G^2/Hz	Freq (Hz)	G^2/Hz
1.0	1.0e-4	1.0	1.0e-4	1.0	4.0e-3
8.0	1.0e-4	9.0	1.0e-4	2.0	3.0e-2
10.0	5.0e-4	15.0	2.0e-3	4.0	3.0e-2
13.0	5.0e-4	23.0	2.0e-3	6.5	2.0e-3
60.0	8.0e-6	45.0	2.0e-5	75.0	2.0e-3
330.0	5.0e-6	85.0	2.0e-5	110.0	8.0e-5
1000.0	2.0e-7	130.0	3.0e-6	380.0	8.0e-5
		1000.0	1.5e-6	1000.0	5.0e-6

Figure 2: SST/SGT Random Vibration Test Specifications
Alternative Test Specifications for Cargo with a Non-Unique Horizontal Orientation
Input to Base of Cargo

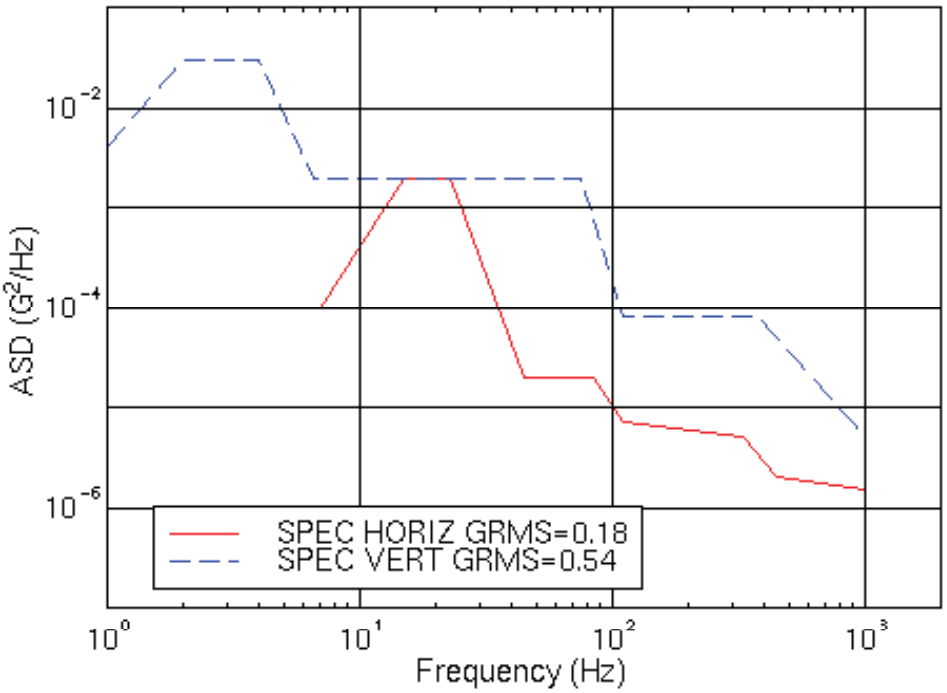

HORIZ		VERT	
Freq (Hz)	G^2/Hz	Freq (Hz)	G^2/Hz
1.0	1.0e-4	1.0	4.0e-3
7.0	1.0e-4	2.0	3.0e-2
15.0	2.0e-3	4.0	3.0e-2
23.0	2.0e-3	6.5	2.0e-3
45.0	2.0e-5	75.0	2.0e-3
85.0	2.0e-5	110.0	8.0e-5
110.0	7.0e-6	380.0	8.0e-5
330.0	5.0e-6	1000.0	5.0e-6
450.0	2.0e-6		
1000.0	1.5e-6		

Shock Test Specifications

Figure 3 presents the recommended straight-line segment SRS shock test specifications for transport of cargo on SST and SGT trailers. All of the SRS presented in this document were calculated using a Maxi-Max Absolute Acceleration (MMAA) algorithm with a 3% critical damping ratio. The axes identified in the figure (LONG, LAT, and VERT) refer to the trailer coordinate system.

However, there may be instances where the orientation of the cargo relative to the longitudinal and lateral trailer axis is not unique. In such cases it is recommended that the cargo be tested in two mutually perpendicular horizontal axes using to the "HORIZ" test specifications identified in Figure 4 (the "VERT" test specification, which has been reproduced in Figure 4 for convenience, must still be applied in that axis).

These SRS should be applied to the cargo at a point that is in intimate contact with the shaker table. It is recommended that the cargo be subjected to 5 hits/axis for every 1000 miles of trip distance (this number of hits is admittedly somewhat arbitrary and has been defined to match the guidelines in similar specifications).

The preferred method for simulating the SRS identified in these figures is with an oscillatory pulse (such as the sum of decayed sinusoids or wavelets) on a shaker table. Such a pulse is an acceptable representation of the test specification if its SRS matches the specified SRS within some tolerance range defined by the project group (typically ±3dB).

The test specifications presented in these figures have been defined down to 1 Hz for completeness. However, the cargo need only be tested down to a frequency that is equal to one-half of its lowest resonant mode, or 10 Hz, whichever is lower. The SRS identified in Figures 3 and 4 would be truncated accordingly.

Appendix B compares the straight-line SRS test specifications against the underlying MEE SRS.

Figure 3: SST/SGT Shock Test Specifications
Input to Base of Cargo
3% Damped MMAA SRS

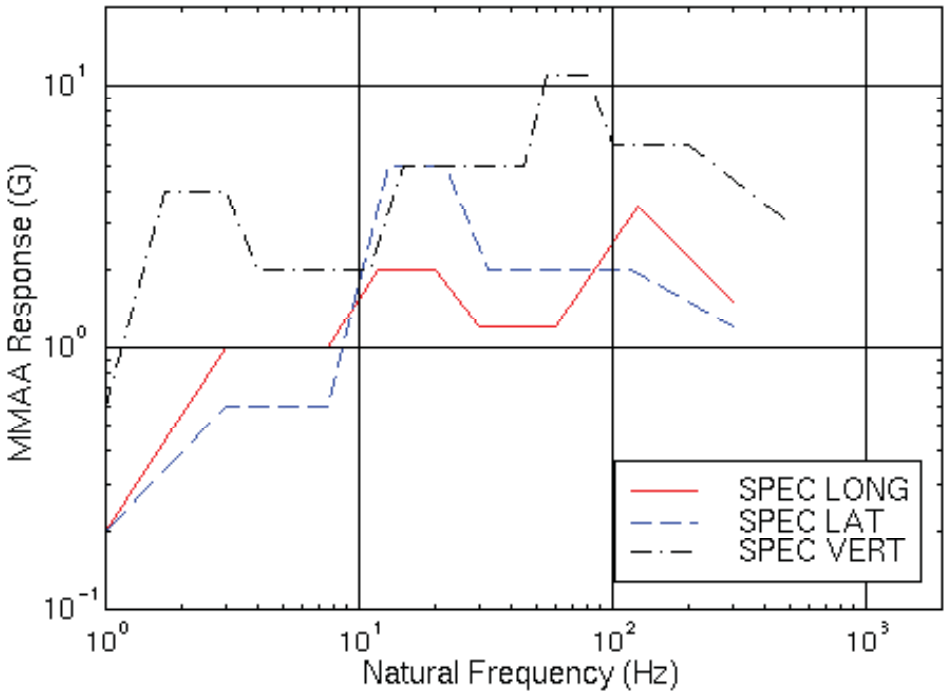

LONG		LAT		VERT	
Freq (Hz)	G^2/Hz	Freq (Hz)	G^2/Hz	Freq (Hz)	G^2/Hz
1.0	0.2	1.0	0.2	1.0	0.6
3.0	1.0	3.0	0.6	1.7	4.0
7.5	1.0	7.5	0.6	3.0	4.0
12.0	2.0	13.0	5.0	4.0	2.0
20.0	2.0	22.0	5.0	11.0	2.0
30.0	1.2	32.0	2.0	15.0	5.0
60.0	1.2	120.0	2.0	45.0	5.0
125.0	3.5	300.0	1.2	55.0	11.0
300.0	1.5			80.0	11.0
				100.0	6.0
				200.0	6.0
				500.0	3.0

Figure 4: SST/SGT Shock Test Specifications
Alternative Test Specifications for Cargo with Non-Unique Horizontal Axes
Input to Base of Cargo
3% Damped MMAA SRS

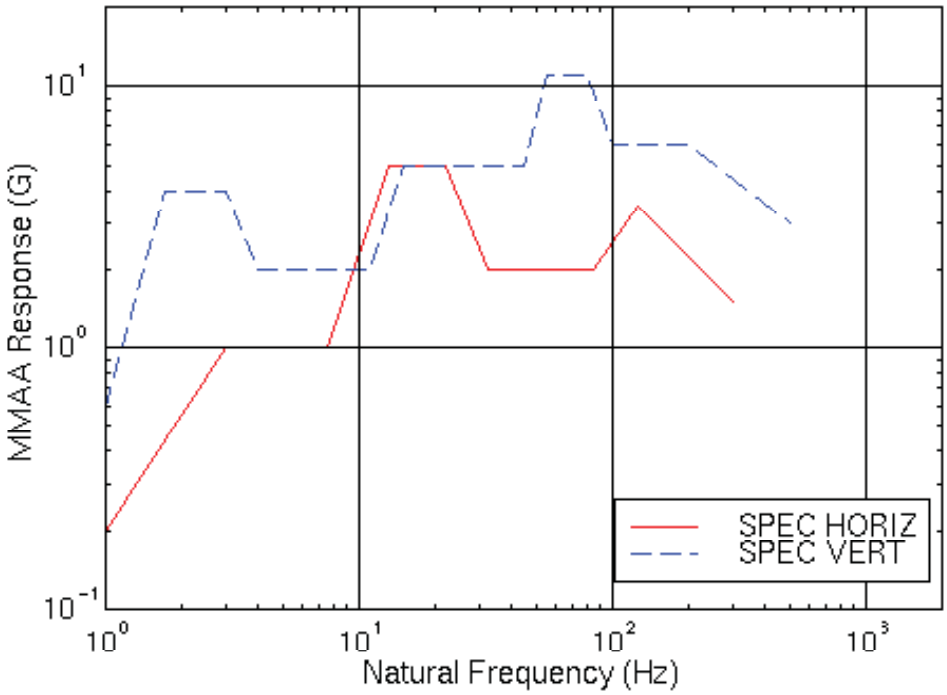

HORIZ		VERT	
Freq (Hz)	G^2/Hz	Freq (Hz)	G^2/Hz
1.0	0.2	1.0	0.6
3.0	1.0	1.7	4.0
7.5	1.0	3.0	4.0
13.0	5.0	4.0	2.0
22.0	5.0	11.0	2.0
32.0	2.0	15.0	5.0
85.0	2.0	45.0	5.0
125.0	3.5	55.0	11.0
300.0	1.5	80.0	11.0
		100.0	6.0
		200.0	6.0
		500.0	3.0

APPENDIX A
COMPARISON OF TEST SPECIFICATIONS AGAINST UNDERLYING MEE RESPONSE SPECTRA FOR RANDOM VIBRATION

Figures A-1, A-3, and A-5 present comparisons of the recommended test specifications identified in the main section of this document (denoted SPEC…) against the envelopes of the MEE response spectra for the individual trailers (denoted ALL…). Figures A-2, A–4, and A-6 present the MEE spectra for the individual trailers (denoted 282, 290, and SGT for the SST2/82, SST2/90, and SGT respectively).

Figure A-1: SST/SGT Random Vibration Environment
Comparison of Recommended Test Specification Versus MEE Response (All Trailers)
Trailer Floor – Longitudinal Axis

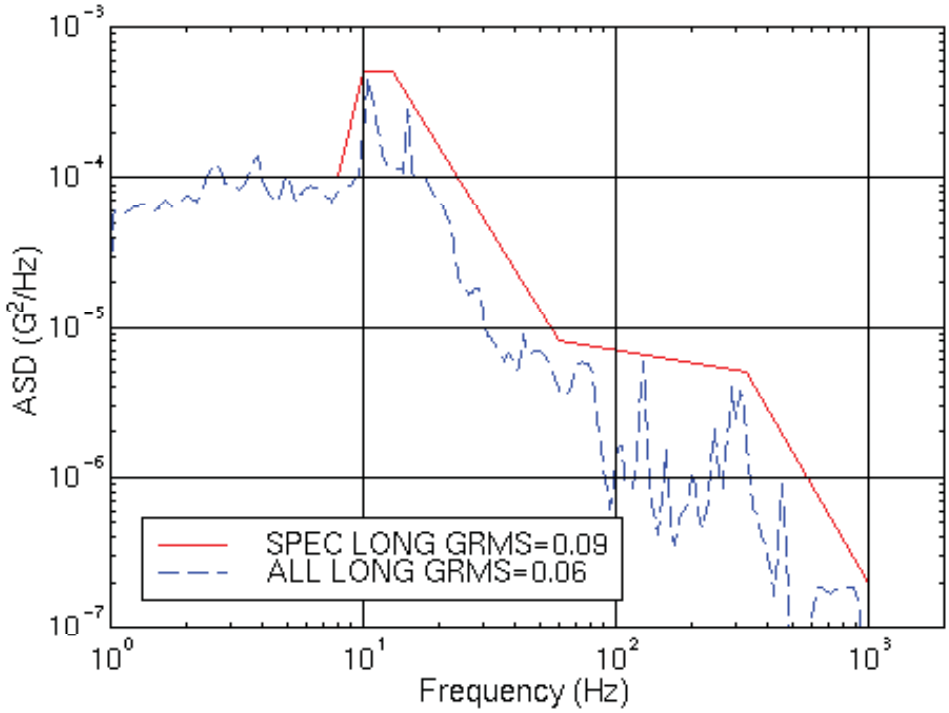

Figure A-2: SST/SGT Random Vibration Environment
Comparison of MEE Responses for SST2/82, SST2/90, and SGT
Trailer Floor – Longitudinal Axis

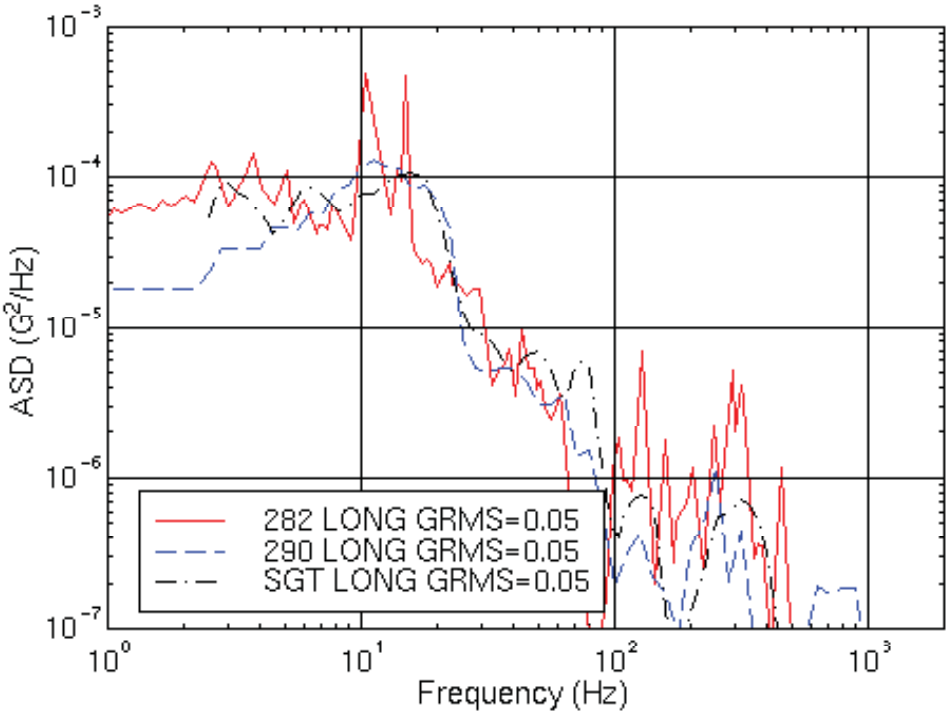

Figure A-3: SST/SGT Random Vibration Environment
Comparison of Recommended Test Specification Versus MEE Response (All Trailers)
Trailer Floor – Lateral Axis

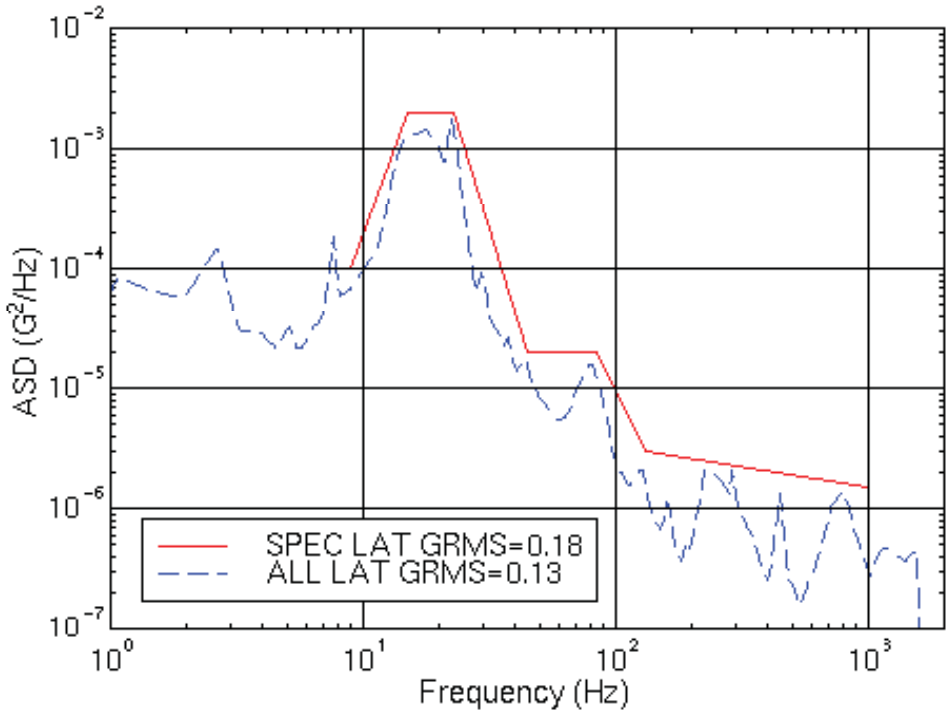

Figure A-4: SST/SGT Random Vibration Environment
Comparison of MEE Responses for SST2/82, SST2/90, and SGT
Trailer Floor – Lateral Axis

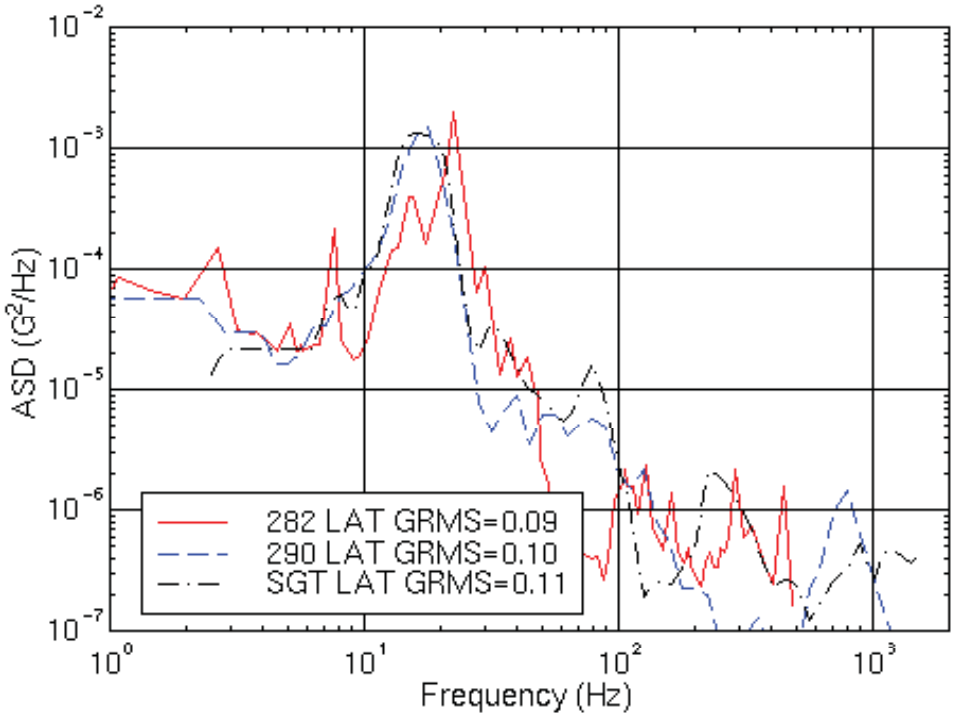

Figure A-5: SST/SGT Random Vibration Environment
Comparison of Recommended Test Specification Versus MEE Response (All Trailers)
Trailer Floor – Vertical Axis

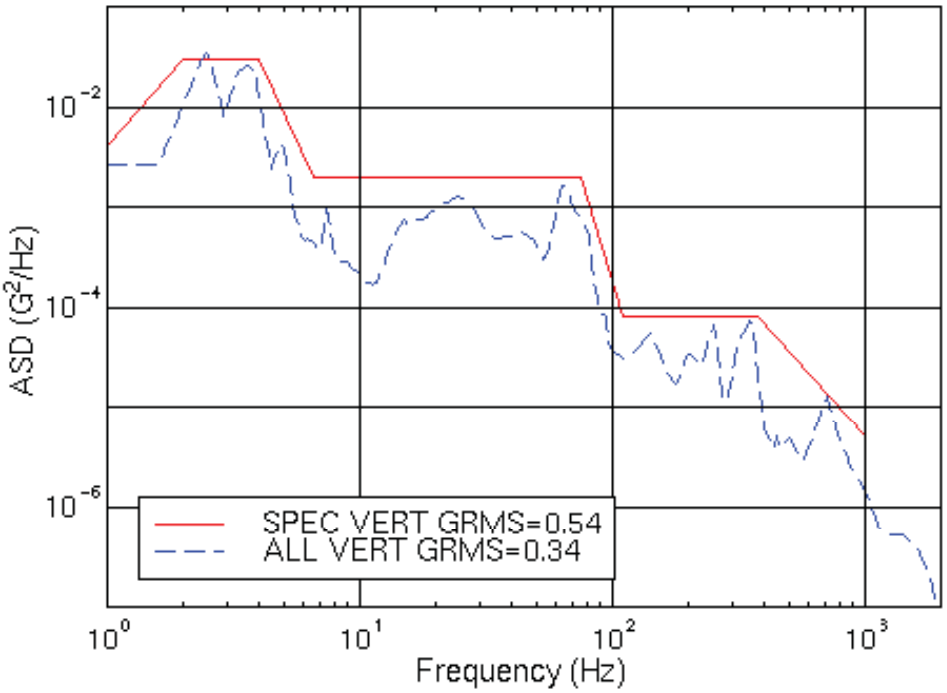

Figure A-6: SST/SGT Random Vibration Environment
Comparison of MEE Responses for SST2/82, SST2/90, and SGT
Trailer Floor – Vertical Axis

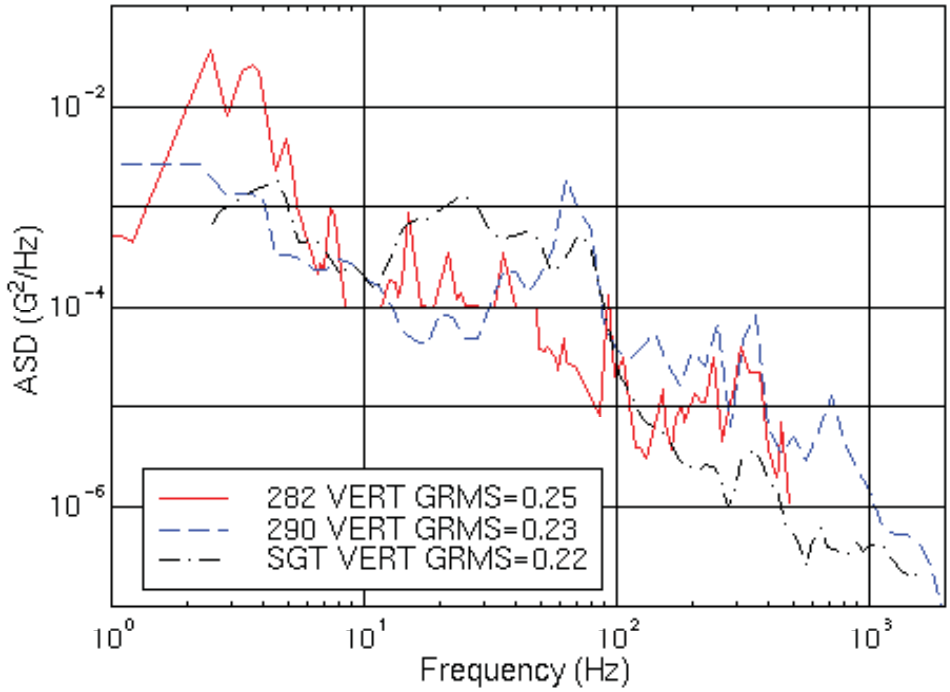

APPENDIX B
COMPARISON OF TEST SPECIFICATIONS AGAINST UNDERLYING MEE RESPONSE SPECTRA FOR SHOCK

Figures B-1, B-3, and B-5 present comparisons of the recommended test specifications identified in the main section of this document (denoted SPEC…) against the envelopes of the MEE response spectra for the individual trailers (denoted ALL…). Figures B-2, B-4, and B-6 present the MEE spectra for the individual trailers (denoted 282, 290, and SGT for the SST2/82, SST2/90, and SGT respectively).

Figure B-1: SST/SGT Shock Environment
Comparison of Recommended Test Specification Versus MEE Response (All Trailers)
Trailer Floor – Longitudinal Axis - 3% Damped MMAA SRS

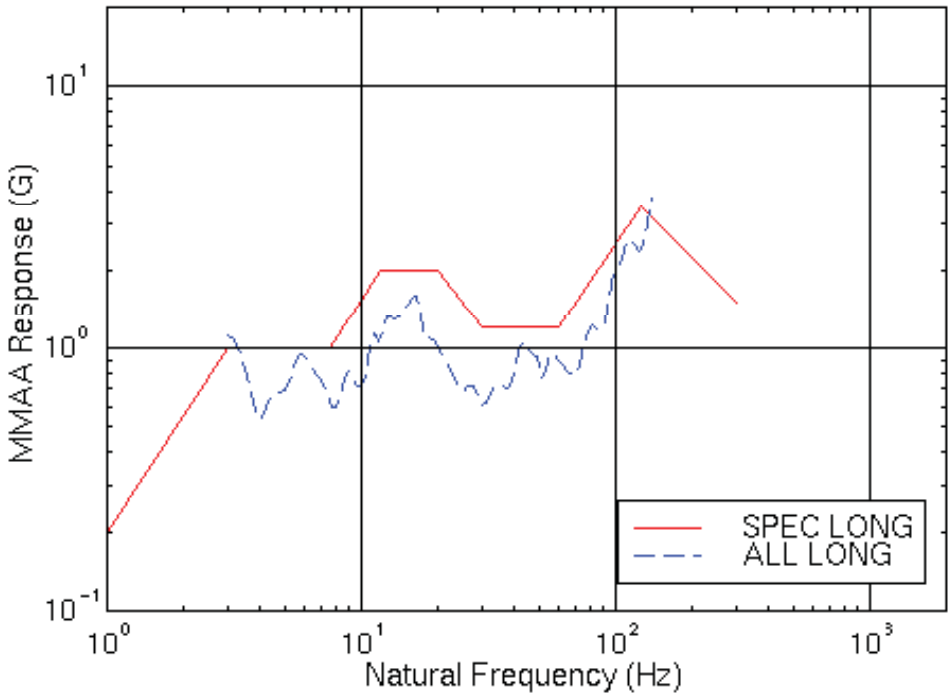

Figure B-2: SST/SGT Shock Environment
Comparison of MEE Responses for SST2/82, SST2/90, and SGT
Trailer Floor – Longitudinal Axis - 3% Damped MMAA SRS

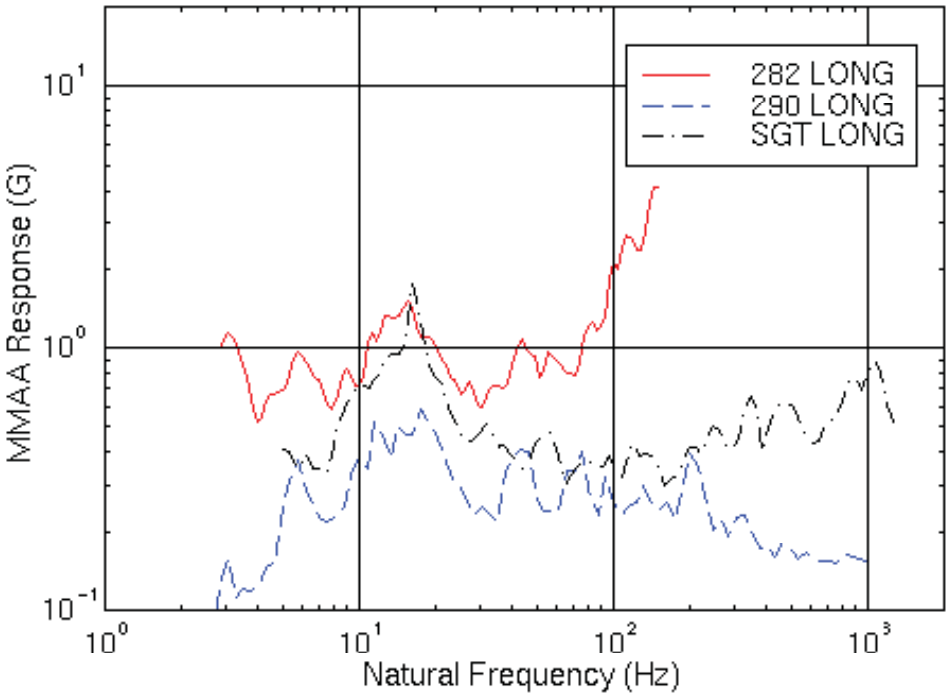

Figure B-3: SST/SGT Shock Environment
Comparison of Recommended Test Specification Versus MEE Response (All Trailers)
Trailer Floor – Lateral Axis - 3% Damped MMAA SRS

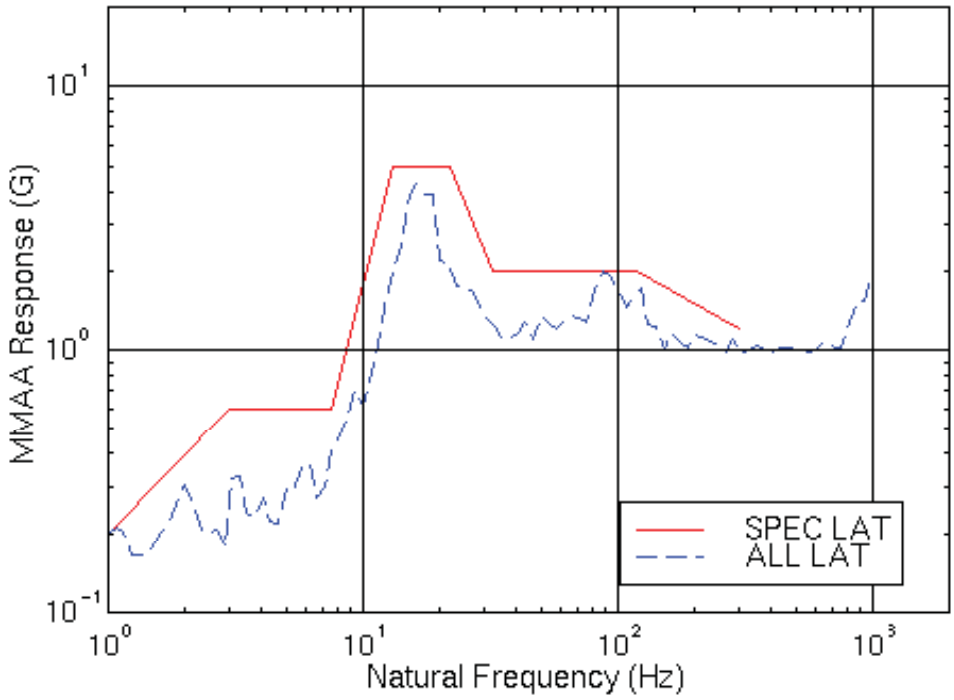

Figure B-4: SST/SGT Shock Environment
Comparison of MEE Responses for SST2/82, SST2/90, and SGT
Trailer Floor – Lateral Axis - 3% Damped MMAA SRS

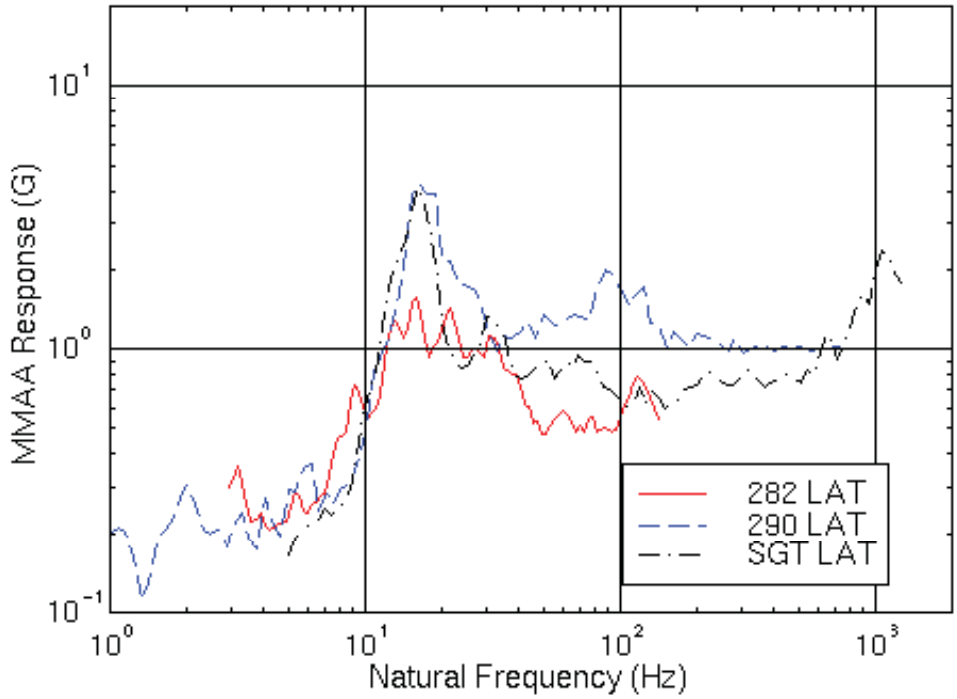

Figure B-5: SST/SGT Shock Environment
Comparison of Recommended Test Specification Versus MEE Response (All Trailers)
Trailer Floor – Vertical Axis - 3% Damped MMAA SRS

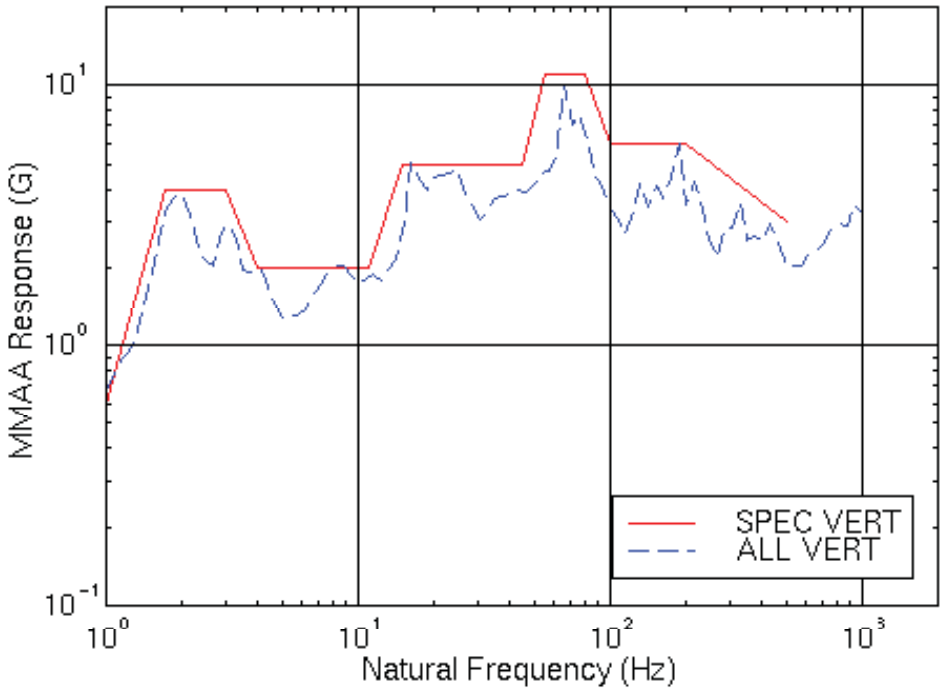

Figure B-6: SST/SGT Shock Environment
Comparison of MEE Responses for SST2/82, SST2/90, and SGT
Trailer Floor – Vertical Axis - 3% Damped MMAA SRS

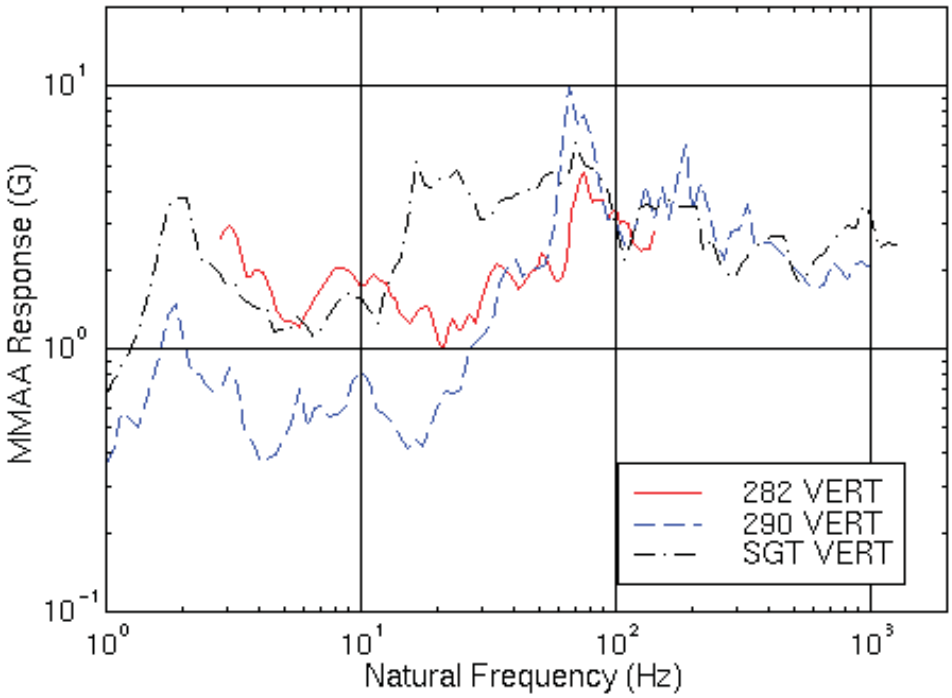

Appendix 2.10.7

TEST REPORT OF THE ES-3100 PACKAGE, VOLUME 1 - MAIN REPORT, ORNL/NTRC-013/V1, REV. 0, SEPTEMBER 10, 2004

THIS PAGE INTENTIONALLY LEFT BLANK.

OAK RIDGE
NATIONAL LABORATORY

MANAGED BY UT-BATTELLE
FOR THE DEPARTMENT OF ENERGY

ORNL/NTRC-013/V1
Rev. 0

TEST REPORT OF THE ES-3100 PACKAGE

Volume 1- Main Report

Revision 0
September 10, 2004

ornl

NTRC
NATIONAL TRANSPORTATION RESEARCH CENTER

UT-BATTELLE
ORNL-27 (4-00)

ORNL/NTRC-013/V1
Rev. 0

Nuclear Science and Technology Division

Test Report of the ES-3100 Package
Volume 1 – Main Report

L. S. Dickerson
M. R. Feldman
R. D. Michelhaugh

September 10, 2004

Prepared for the
Y-12 National Security Complex
Highly Enriched Uranium Disposition Program Office

Prepared by
OAK RIDGE NATIONAL LABORATORY
P.O. Box 2008
Oak Ridge, Tennessee 37831-6285
Managed by UT-Battelle, LLC
For the
U.S. DEPARTMENT OF ENERGY
Under contract DE-AC05-00OR22725

Test Report of the ES-3100 Package
Volume 1 – Main Report

Prepared for the
Y-12 National Security Complex
Highly Enriched Uranium Disposition Program Office

Prepared by
L. S. Dickerson
M. R. Feldman
R. D. Michelhaugh

Oak Ridge National Laboratory
Nuclear Science and Technology Division
National Transportation Research Center

APPROVALS

Name	Position	Date
R.D. Michelhaugh	Test Director	9-9-04
M. R. Feldman, PE	Program Manager	9/9/04
S. B. Ludwig	TTG Leader	9-9-04

TABLE OF CONTENTS

ABSTRACT 1
1 INTRODUCTION 3
1.1 Description of the ES-3100 Shipping Package 3
1.2 ES-3100 Test Matrix 5
1.3 Test Data Records 7
2 PRE-TESTING ACTIVITIES 9
2.1 Description of Test Units 9
2.2 Application of Temperature Labels 13
2.3 Package Assembly 15
2.4 Pre-test Operational Leak Test 15
2.5 Chilling of TU-2 17
3 NCT TESTS 19
3.1 Full NCT Test Series (TU-4 Only) 19
3.1.1 Water Spray Test 19
3.1.2 Penetration Test 19
3.1.3 Compression Test 21
3.1.4 Vibration Test 23
3.2 Free Drop Test (Test Units 1 through 5) 25
4 HAC TESTS 31
4.1 HAC 9-m (30 ft) Drop Test 31
4.2 HAC Dynamic Crush Test 35
4.3 HAC Puncture Test 41
4.4 Summary of Cumulative Damage from Impact Tests 49
4.5 HAC Thermal Test 53
4.5.1 Furnace Description 53
4.5.2 Furnace Setup 55
4.5.3 Test Unit Setup and Preparation 59
4.5.4 Thermal Testing 61
4.5.5 Thermal Test Data 63
5 POST-HAC DISASSEMBLY AND INSPECTION 79
5.1 Drum Disassembly Observations 79
5.2 Post-test Leak Tests 87
5.2.1 Post-test Operational Leak Test 87
5.2.2 Post-test Helium Leak Test 87
5.3 0.9-m (3 ft) Immersion Test 93
5.4 15-m (50 ft) Immersion Test on TU-6 95
5.5 CV Disassembly Observations 97
5.6 Temperature-indicating Label Results 103

TABLE OF APPENDICES

Volume 2

Appendix A – TU-1 Photos
Appendix B – TU-2 Photos
Appendix C – TU-3 Photos
Appendix D – TU-4 Photos
Appendix E – TU-5 Photos
Appendix F – TU-6 Photos
Appendix G – Pre-thermal Test Activity Photos

Volume 3

Appendix H – TU-1 Data Forms
Appendix I – TU-2 Data Forms
Appendix J – TU-3 Data Forms
Appendix K – TU-4 Data Forms
Appendix L – TU-5 Data Forms
Appendix M– TU-6 Data Forms
Appendix N – Field Marked ES-3100 Test Plan

LIST OF FIGURES

Page
Figure 1.1 Cut-away view of the ES-3100 4
Figure 2.1 Surrogate payload for TU-1 through TU-4 9
Figure 2.2 Temperature-indicating labels affixed to inner liner of TU-3 11
Figure 2.3 Vertical and CG markings on TU-1 and TU2 11
Figure 2.4 Temperature labels applied to outer CV 13
Figure 3.1 TU-4 undergoing the water spray test 20
Figure 3.2 TU-4 penetration test setup 20
Figure 3.3 TU-4 damage from penetration test 21
Figure 3.4 TU-4 in Compression Tester. 22
Figure 3.5 Test units staged for vibration testing 24
Figure 3.6 TU-1 positioned for the 12.1° NCT side drop test 26
Figure 3.7 TU-2 being dropped horizontally while still cold 26
Figure 3.8 TU-3 being angled 24.6° so that 0° corner contacts the drop pad first 27
Figure 3.9 Damage to TU-3 after NCT drop 27
Figure 3.10 TU-4 being positioned head-down for the NCT vertical drop test 28
Figure 3.11 Flattening of top false wire of TU-5 29
Figure 4.1 Test setup for the HAC 9-m free drop of TU-3 32
Figure 4.2 Results of the HAC drop of TU-3 32
Figure 4.3 TU-1 and TU-5 HAC 9-m drop test setup 33
Figure 4.4 TU-2 HAC 9-m drop test setup 33
Figure 4.5 TU-3 HAC 9-m drop test setup 33
Figure 4.6 TU-4 HAC 9-m drop test setup 33
Figure 4.7 Results of the dynamic crush test of TU-1. 35
Figure 4.8 TU-3 dynamic crush test set-up, ready to raise crush plate 36
Figure 4.9 Damaged bottom of TU-3 after the dynamic crush test 36
Figure 4.10 Damaged top of TU-3 after the dynamic crush test 37
Figure 4.11 HAC crush test setup for TU-1 38
Figure 4.12 HAC crush test setup for TU-2 and TU-5 38
Figure 4.13 HAC crush test setup for TU-3 38
Figure 4.14 HAC crush test setup for TU-4 38
Figure 4.15 Test setup for the puncture test of TU-1 42
Figure 4.16 Damage from puncture test of TU-1 43
Figure 4.17 Initial TU-1 puncture test setup 44
Figure 4.18 Orientation for third TU-1 HAC 1m puncture test 44
Figure 4.19 Second TU-1 puncture test setup 44
Figure 4.20 Orientation for fourth TU-1 HAC 1m puncture test 44
Figure 4.21 TU-2 puncture test setup 45
Figure 4.22 TU-3 puncture test setup 45
Figure 4.23 TU-3 second puncture test setup 45
Figure 4.24 TU-4 puncture test setup 45
Figure 4.25 TU-5 puncture test setup 46
Figure 4.26 Locations where measurements were made on test unit exteriors 50
Figure 4.27 Interior of furnace #3 54
Figure 4.28 Approximate location of 3 thermocouples in left wall of furnace 56
Figure 4.29 Approximate location of 3 thermocouples in right wall of furnace 56

Figure 4.30 Approximate location of thermocouples in door (O) and back wall (X) 57
Figure 4.31 Furnace #3 left wall thermocouple layout 57
Figure 4.32 Furnace #3 right wall thermocouple layout. 58
Figure 4.33 Furnace #3 back wall thermocouple layout (Note: flue in center of picture)58
Figure 4.34 Test units in preheat chamber 59
Figure 4.35 TU-1 wired with thermocouples, ready for loading 60
Figure 4.36 Fork truck and modified fork used for test unit insertion and extraction..... 62
Figure 4.37 Ambient Temperature 66
Figure 4.38 Preheat Chamber Temperature 67
Figure 4.39 TU-1 Thermal test, Furnace thermocouples 68
Figure 4.40 TU-1 Thermal test, Package thermocouples 69
Figure 4.41 TU-2 Thermal test, Furnace thermocouples 70
Figure 4.42 TU-2 Thermal test, Package thermocouples 71
Figure 4.43 TU-3 Thermal test, Furnace thermocouples 72
Figure 4.44 TU-3 Thermal test, Package thermocouples 73
Figure 4.45 TU-4 Thermal test, Furnace thermocouples 74
Figure 4.46 TU-4 Thermal test, Package thermocouples 75
Figure 4.47 TU-5 Thermal test, Furnace thermocouples 76
Figure 4.48 TU-5 Thermal test, Package thermocouples 77
Figure 5.1 The compression table being used to assist with top plug removal 80
Figure 5.2 TU-1 with top plug removed 80
Figure 5.3 TU-1 - Purplish liquid from decomposition of cushion 81
Figure 5.4 TU-2 disassembly using compression 82
Figure 5.5 The lid of TU-3 being prepared for cutting 82
Figure 5.6 Top plug and kaolite from TU-3 83
Figure 5.7 Convex appearance of inner liner of TU-4 drum 84
Figure 5.8 Top view of inner liner of TU-4 84
Figure 5.9 Silicone cushion skirting the CV of TU-4 85
Figure 5.10 Deterioration of TU-5's silicone cushion 85
Figure 5.11 TU-4 undergoing the containment boundary helium leak test 88
Figure 5.12 TU-1 helium leak (in cc/sec) rate for full boundary leak check 90
Figure 5.13 TU-2 helium leak rate (in cc/sec) for full boundary leak check 90
Figure 5.14 TU-3 helium leak rate (in cc/sec) for full boundary leak check 90
Figure 5.15 TU-4 helium leak rate (in cc/sec) for full boundary leak check 90
Figure 5.16 Test #1 - TU-5 helium leak rate (in cc/sec) for full boundary leak check.... 91
Figure 5.17 Test # 4 - TU-5 helium leak rate (in cc/sec) for full boundary leak check... 91
Figure 5.18 TU-1, -2, and -5 inside immersion tank 93
Figure 5.19 Disintegration of spacer cushion of surrogate load 98
Figure 5.20 TU-1 surrogate load showing rust 98
Figure 5.21 Broken cable lanyard of TU-2 99
Figure 5.22 Surrogate payloads of TU-3 99
Figure 5.23 Blemishing of temperature labels on flange of CV 100
Figure 5.24 Silicone cushion skirting TU-4 101
Figure 5.25 Crushed surrogate payloads due to vacuum during helium leak test 101
Figure 5.26 Surrogate payload temperature label locations (TU-1, TU-2, TU-3, and TU-4) 104
Figure 5.27 Light-weight test assembly temperature-indicating label locations 105

Figure 5.28 CV body temperature-indicating label locations 106
Figure 5.29 CV lid temperature-indicating label locations 107
Figure 5.30 Inner liner temperature label indicating locations 108
Figure 5.31 Top Plug temperature-indicating label locations 109

LIST OF TABLES

Page

Table 1.1 Drum and CV serial numbers for each Test Unit 5
Table 1.2 Summary of NCT – 10CFR71.71 Tests performed on ES-3100 Package..... 6
Table 1.3 Summary of HAC – 10CFR71.73 Tests performed on ES-3100 Packages..... 6
Table 1.4 Listing of appendices for photos and data sheets by test unit..... 7
Table 2.1 Surrogate payload vs. Test Unit..... 10
Table 2.2 Total weight of each test unit pre- and post-testing..... 15
Table 2.3 Pre-test leak rate for the test unit CV..... 16
Table 3.1 Vertical Power Spectrum Density (PSD)..... 23
Table 3.2 Planned vs. measured package orientation for NCT drop tests 25
Table 4.1 HAC 9-m drop test desired package orientation vs. measured orientation 31
Table 4.2 Package orientations for HAC puncture test..... 41
Table 4.3 Summary of total height change of each test unit after all impact testing (units = inches)..... 51
Table 4.4 Measurement of the width of "flats" after HAC crush test for side impact units (TU-1, TU-2 and TU-5) (units = inches) 51
Table 4.5 Changes in diameter after all impact testing (units = inches)..... 52
Table 4.6 Mapping of furnace thermocouple location to thermal recorder channel number 64
Table 4.7 Mapping of test unit thermocouple location to thermal recorder channel number 65
Table 5.1 Post-test leak rate for the test unit CV lids 87
Table 5.2 CV Lid removal torque..... 97
Table 5.3 Temperature-indicating Labels reading for TU-1..... 110
Table 5.4 Temperature-indicating Labels reading for TU-2..... 111
Table 5.5 Temperature-indicating Labels reading for TU-3..... 112
Table 5.6 Temperature-indicating Labels reading for TU-4..... 113
Table 5.7 Temperature-indicating Labels reading for TU-5..... 114

Test Report of the ES-3100 Package

ABSTRACT

The Y-12 Highly Enriched Uranium Disposition Program Office (HDPO) is developing a new package design designated the ES-3100. Between May 2004 and July 2004, the Oak Ridge National Laboratory (ORNL) National Transportation Research Center (NTRC) tested six ES-3100 prototype units to the Type B performance tests prescribed in Part 71 of Title 10 Code of Federal Regulations (10 CFR). This test report documents test unit preparation, pre-test condition of each test unit, the Normal Conditions of Transport (NCT) and Hypothetical Accident Condition (HAC) testing, and the post-test measurements and observations of the damage resulting from these tests.

1 INTRODUCTION

The Y-12 Highly Enriched Uranium Disposition Program Office (HDPO) is developing a new package designated the ES-3100. In order to support the certification of the ES-3100 package design, Y-12 contracted the ORNL Transportation Technologies Group (TTG) to perform independent testing of the ES-3100 to the requirements of 10 CFR Part 71. TTG conducted the tests according to a test plan (ORNL/NTRC-011, May 17, 2004) approved by the Y-12 Packaging Engineering and HDPO organizations and reports the testing and test results in this document. The test results will be used in the preparation of the ES-3100 package Safety Analysis Report (SAR).

Six ES-3100 packages were tested to demonstrate compliance with the requirements of Title 10, Code of Federal Regulations (CFR), Part 71.71, *Normal Conditions of Transport* (NCT), and Title 10, CFR, Part 71.73, *Hypothetical Accident Conditions* (HAC). (A seventh package was available just in case additional testing was necessary.) The packages were identified by sequential designation numbers: TU-1-05/04, TU-2-05/04, TU-3-05/04, TU-4-05/04, TU-5-05/04, and TU-6-05/04. The undamaged containment vessel of TU-6-05/04 was used for the 15-m immersion test. Hereafter in this report, the test units are identified simply by their "TU-*X*" designation.

All the NCT tests were performed on TU-4 while the NCT free drop test was performed on test units TU-1 through TU-5. All HAC drop and thermal tests were performed on TU-1 through TU-5. TU-6 (which was comprised of a CV only) was only subjected to the HAC 15-m (50-ft) immersion test. Test matrices are presented in Section 1.2.

Section 2 describes the pre-testing activities. Section 3 describes the NCT tests performed and results. Section 4 describes the HAC tests and results, and Section 5 describes the disassembly, the subsequent leak and immersion tests, and inspection and post-test measurements.

1.1 Description of the ES-3100 Shipping Package

The ES-3100 package consists of an outer drum and a containment vessel (CV) (Figure 1.1). The exterior of the package is a drum that is about 19 inches in diameter and about 44 inches in height, and is fabricated from 16-gauge, 304 stainless steel. The package has an integral annular liner that is filled with Kaolite 1600™, a mixture of Portland cement and expanded vermiculite which is cast in place. An inch thick layer of Borobond4 is located along the inner walls of the CV cavity to provide neutron absorption.

The test units will be made of drum assemblies and CV assemblies with specific serial numbers. Table 1.1 below indicates the specific serial numbers of the drums and CVs to be combined to assemble each complete test unit.

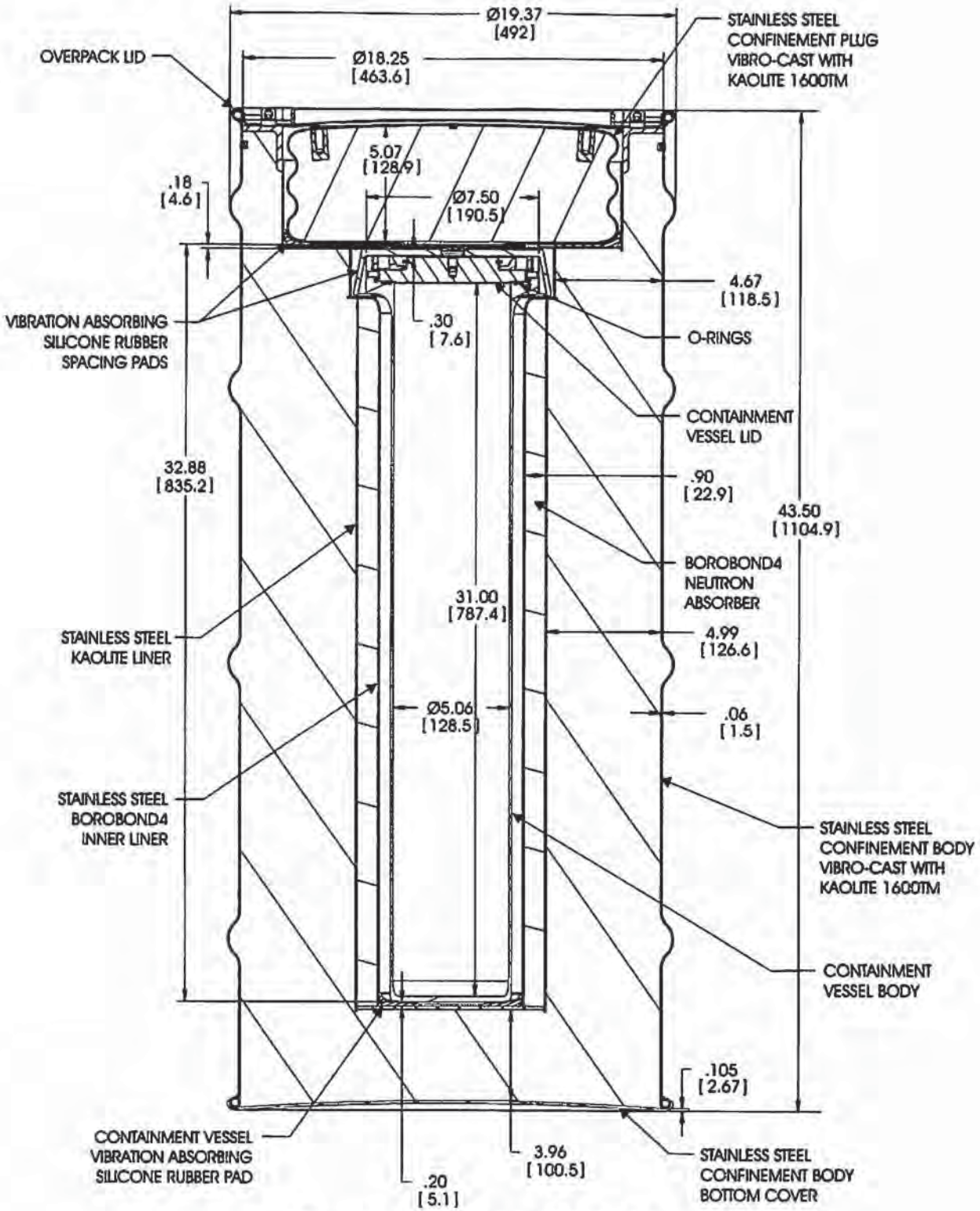

Figure 1.1 Cut-away view of the ES-3100.

.

Table 1.1 Drum and CV serial numbers for each Test Unit

Test Unit	Drum Serial Number	CV Serial Number
TU-1	2	2
TU-2	4	4
TU-3	5	5
TU-4	9	9
TU-5	11	11
TU-6	N/A	1
TU-7	6	6

The test units were configured with simulated payloads in the containment vessels. For TU-1 through TU-4, the simulated payloads consisted of three product can-size test weights with a band clamp, cable lanyard and silicone vibration absorbing pad on the top of each can. The bottom test weight also had a silicone vibration absorbing pad. These test units had a "full" payload consisting of a total mass of 110 lb. BoroBond4 spacers were used between the top test weight and the middle test weight and also between the middle test weight and the bottom test weight. Test Unit 5 had a light weight test assembly which consisted of three product cans stacked together. The lower can was filled with ballast such that its total weight was 6.6 lb, and the other two cans were empty. No BoroBond4 spacers were used between the cans. TU-6 was a containment vessel (CV) with approximately 15 pounds of steel shot in a plastic bag serving as ballast weight to ensure that it would sink for the immersion test. TU-6 weighed 47 pounds.

1.2 ES-3100 Test Matrix

Table 1.2 and Table 1.3 summarize the order of the tests performed on each individual test unit along with the general orientation of each test unit when it was drop tested and crush tested. The cells containing numbers indicate that the designated test was performed on the test unit. The number in the cell indicates the sequence that the test was performed on the test unit. The NCT tests preceded the HAC tests.

TU-4 underwent the full battery of NCT tests. For the impact tests, a variety of package orientations were used to ensure that one or more test units would be subjected to impacts in "the most damaging orientation." As can be seen by reviewing Table 1.3, TU-1 through TU-5 were subjected to the full battery of HAC tests. TU-6 was an "undamaged" CV only and was only subjected to the HAC 15-m (50-ft) immersion test.

Table 1.2 Summary of NCT – 10CFR71.71 Tests performed on ES-3100 Package

Test	TU-1 (heavy) 12° Slap-down	TU-2 (heavy) Side Drop	TU-3 (heavy) CG over Top Corner	TU-4 (heavy) Top Down	TU-5 (light) 12° Slap-down
Operational Leak Test (CALT5)	1	1	1	1	1
NCT – 10CFR71.71 (c)(6) Water Spray				2	
NCT – 10CFR71.71 (c)(7) Free Drop	2	2**	2	3	2
NCT – 10CFR71.71 (c)(10) Penetration				4	
NCT – 10CFR71.71 (c)(9) Compression				5	
NCT – 10CFR71.71 (c)(5) Vibration				6	

*- TU-6 is only a containment vessel (CV)
** - TU-2 was chilled to below -40°F for this test
Note: Numbers in table indicate testing sequence

Table 1.3 Summary of HAC – 10CFR71.73 Tests performed on ES-3100 Packages

Test	TU-1 (heavy) 12° Slap-down	TU-2 (heavy) Side Drop	TU-3 (heavy) CG over Top Corner	TU-4 (heavy) Top Down	TU-5 (light) 12° Slap-down	TU-6* 15m Immerse (CV only)
HAC – 10CFR71.73 (c) (1) Free Drop – 9-m (30 ft.)	1	1**	1	1	1	
HAC – 10CFR71.73 (c) (2) Crush – 9-m (30 ft.)	2	2**	2	2	2	
HAC – 10CFR71.73 (c) (3) Puncture – 1m (40 in.)	3,4,5,6	3**	3,4†	3	3	
Preheat to above 38 °C (100 °F) before Thermal test	7	4	5	4	4	
HAC – 10CFR71.73 (c) (4) Thermal – 800°C (1475°F)	8	5	6	5	5	
Operational Leak Test of CV (CALT5)	9	6	7	6	6	1
Full Containment Boundary Leak Test (He Leak Test)	10	7	8	7	7	
HAC – 10CFR71.73 (c) (5) Immersion Test – Fissile materials – 0.9-m (3 ft.)	11	8	9	8	8	
HAC – 10CFR71.73 (c) (6) Immersion Test – All Packages – 15-m (50 ft.)						2

*- TU-6 is only a containment vessel (CV)
** - TU-2 was chilled to below -40°F for these tests
†This differs from original test plan.
Note: Numbers in table indicate testing sequence.

1.3 Test Data Records

This report (Volumes 1, 2, and 3) documents the tests performed and measurements observed from the ES-3100 testing. The general data types for these tests are:

- manually derived measurements and observations,
- automatically recorded temperatures from the thermal testing,
- digital still photography, and
- video and high-speed motion photography of drop tests.

The primary recording media for each of the general types of data are:

- Procedure Checklists and Data Sheets for data, measurements, and observations,
- Computer files (Excel spreadsheets) for the temperature records,
- Computer files (JPG format) for the digital photography, and
- VHS and DVD video media for the video and motion photography.

The completed Data Sheets and Procedure Checklists have been scanned into a digital format. The still photography, scanned data sheets and the field marked test plan are attached to this document as appendices in separate volumes (Volumes 2 and 3). There is an appendix of photographs and an appendix of completed Data Sheets and Procedure Checklists for each test unit. Additionally, Appendix G, *Pre-Thermal Test Activities Photos*, contains the collection of digital photos related to preparation of the ES-3100 packages and thermal test facility for the thermal testing and Appendix N contains the as field-marked version of the test plan. Table 1.4 provides a listing of appendices and subject matter.

Table 1.4 Listing of appendices for photos and data sheets by test unit

Test Unit	Photo Appendix (Volume 2)	Data Sheet and Procedure Checklist Appendix (Vol. 3)
TU-1	A	H
TU-2	B	I
TU-3	C	J
TU-4	D	K
TU-5	E	L
TU-6	F	M
ALL	G	N

Appendix G contains digital photos related to preparation of the ES-3100 packages for the thermal testing
Appendix N contains the field marked version of the test plan

2 PRE-TESTING ACTIVITIES

Several activities were required to prepare the test units for testing. These activities focused on documenting the initial condition of each test unit, installing data acquisition devices (temperature-indicating labels) in various locations on the test units, and assembling each test unit per operational procedures developed by the package design team.

2.1 Description of Test Units

The test units were full-scale ES-3100 packages equipped with surrogate payloads in the containment vessels. For TU-1 Through TU-4, the simulated payloads consisted of three product can size test weights with a band clamp, cable lanyard and silicone vibration absorbing pad on the top of each can. The bottom test weight also had a silicone vibration absorbing pad on its bottom. These units had a "full" payload consisting of a total mass of 110 lb. BoroBond4 spacers were used between the test weights in these four units. Figure 2.1 shows the surrogate payloads for TU-1 through TU-4.

Figure 2.1 Surrogate payload for TU-1 through TU-4

The picture shows the three solid cylindrical masses that are stacked on top of each other when put inside the containment vessel, the vibration-absorbing pads placed on top of the three cans, and the BoroBond4 spacers (to the left of the picture). The rubber silicone

cushions used to reduce metal-to-metal contact and jarring are shown between the top plug and the cans.

Test Unit 5 had a light weight test assembly which consisted of three product cans stacked together. The lower can was filled with a plastic bag of steel shot to add ballast such that its total weight was 6.6 lb, and the other two cans were empty. The cans in TU-5 had band clamps, cable lanyards and silicone vibration absorbing pads on the top of each can. The bottom can also had a silicone vibration absorbing pad on its bottom; however, no BoroBond4 spacers were used. TU-6 was only a containment vessel (CV) with 13 lbs. of steel shot ballast added, which Y-12 engineers calculated would be enough to ensure that it did not float during the immersion test. With the ballast, TU-6 weighed a total of 47 pounds.

As stated above, the test units were loaded with two different configurations of surrogate payloads. As a result the location of the center of gravity (CG) for TU-5 varied from the other test units. Table 2.1 shows the test weight configuration inside each CV and identifies the location of the CG for each test unit. The CG locations were provided by Y-12 Packaging Engineering and were not measured or independently verified by ORNL-TTG personnel.

Table 2.1 Surrogate payload vs. Test Unit

	TU-1	TU-2	TU-3	TU-4	TU-5	TU-6
Payload (heavy) M2E801580A028	X	X	X	X		
Payload (light) M2E801580A030					X	
CV + ballast (M2E801580A011)						X
Location of CG (from base of outside drum)	22.42 in.	22.42 in.	22.42 in.	22.42 in.	23.00 in.	N/A CV only

Test Units 1 through 5 had temperature-indicating labels affixed to the surrogate payload, the outside of the CV, the inside surface of the drum liner, and the top plug prior to assembly. Figure 2.2 shows the temperature labels on the inside of the outer drum for TU-3.

The vertical seam of the outside drum of TU-1 through TU-5 was marked with a 0º vertical reference line and the other three quadrants were marked with a vertical line at 90º, 180º, and 270º as measured around the top perimeter of the package in a counterclockwise direction looking down onto the top of the package. A horizontal line was also marked around the circumference of each outer drum, which designated the center-of-gravity plane of each package. The intersection of the vertical lines and the circumferential line provided CG "targets" on each quarter of the outer drum surface. Figure 2.3 shows the markings on a typical test unit.

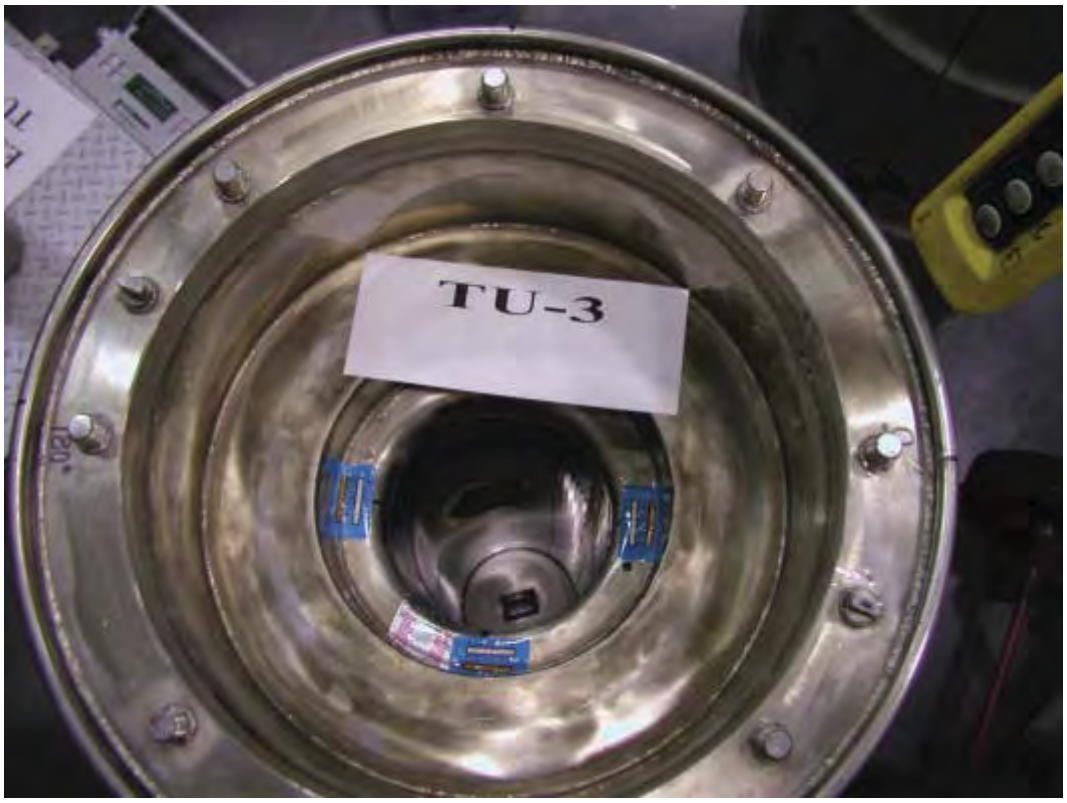

Figure 2.2 Temperature-indicating labels affixed to inner liner of TU-3

Figure 2.3 Vertical and CG markings on TU-1 and TU2

2.2 Application of Temperature Labels

Prior to assembly, an array of temperature-indicating labels was applied to the components of the test units. Type B labels (171 °F to 261 °F) were affixed to opposite sides of each surrogate payload can; 17 total temperature labels of a combination of Type B and Type C labels (270 °F to 360 °F) were placed on each CV; and an additional 18 labels were affixed to the inner surface liner of each drum. The B range labels were used on the inner wall of the drum, as specified by the test plan. A mistake was made during assembly and B range labels were used on the CV lid instead of the 125 ºF to 300 ºF labels specified in the test plan. The full range labels are designed with 16 indicating spots that range from 125 ºF to 500 ºF, in 25 º increments. Also, full-range temperature labels were applied at the 0°, 90°, 180°, and 270° positions on the underside of the top plug. General placement of the temperature labels inside the drum can be seen in the previous Figure 2.2. Figure 2.4 shows some of the temperature labels applied to the outside of the containment vessel. Each label was affixed at a specific location and an additional strip of Teflon™ tape was placed over the label to ensure that it would remain in place during the thermal test. Details of temperature-indicating label locations are in Section 5.6.

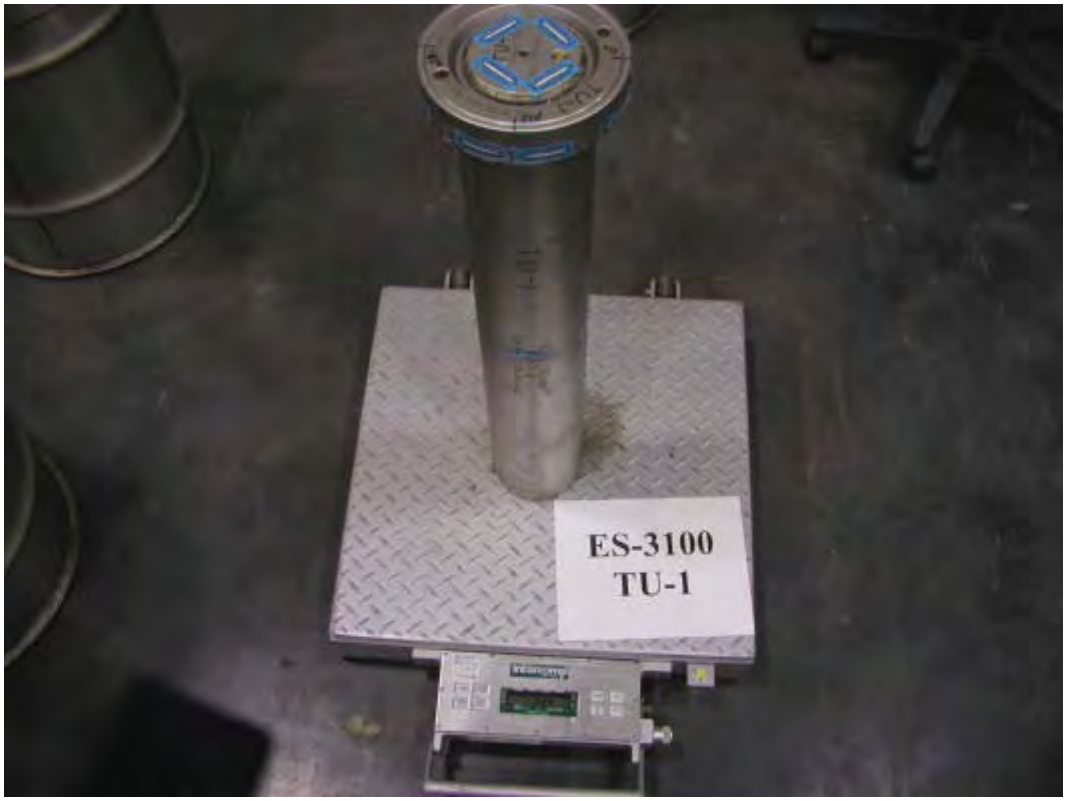

Figure 2.4 Temperature labels applied to outer CV

In addition to the use of temperature labels, after the structural testing and just prior to the thermal testing, thermocouples were also placed on the surface of the test units by fitting them underneath welded tabs. Six thermocouples were placed on the exterior of each test unit along the 0°-, 90°-, 180°-, and 270°-line, and the bottom and top of the drums.

2.3 Package Assembly

Before assembly of each test unit, the components of each CV were given a visual inspection and weighed. The weights of the various components making up the package were measured and recorded on TEST FORM 1. The assembly process for each test unit was documented on TEST FORM 2. TEST FORM 3 describes assembly of the test package: placement of the CV, drum lid installation, weighing, etc. The total weight of each package is given in Table 2.2. The slight weight loss shown in the last row, *Change in weight*, could be a factor of the accuracy of the weighing scale, water loss from Kaolite, or combustion of silicone gaskets. In the table, TU-5 weighs roughly 100 lbs less than the other test units (except TU-6, of which only the weight of its CV and included ballast is shown) because its containment vessel had only a light-weight test assembly installed.

Table 2.2 Total weight of each test unit pre- and post-testing

Item	TU-1	TU-2	TU-3	TU-4	TU-5	TU-6
Pre-test total weight (lb)	446	447	449	445	347	47
Post-test total weight	446	447	448	444	346	47
Change in weight	0	0	-1	-1	-1	0

2.4 Pre-test Operational Leak Test

Prior to the initiation of testing, the O-ring seals of the CV assembly of TU-1 through TU-6 were leak tested using a CALT5 leak check system manufactured by Croft and Associates. The leak check was conducted in accordance with ANSI N14.5-1997 using a CALT5 Leak Detector and following the manufacturer's leak testing procedure. If a CV successfully passed this test (1×10^{-4} ref-cc/sec), it showed that the O-rings were installed and functioning properly.

The CALT5 pressurizes the volume between the O-rings and then uses a very precise pressure transducer to measure the pressure drop over the test period. The CALT5 will compute a leak rate; however, the ES-3100 package operating procedures call for the computation of the leak rate based on the ANSI N14.5-1997 algorithm, using data from the CALT5 as inputs for *Vcm3 (interstitial volume), M(length of test),* P_1*atm (initial pressure),* P_2*atm (ending pressure),* T_1 K, and T_2 K:

$$Lr = \frac{Vcm3 * 298K}{3600 * \frac{M\ \min}{60\ \min} * 1atm}\left(\frac{P_1atm}{T_1K} - \frac{P_2atm}{T_2K}\right) ref - cc/\sec$$

The instrument was set to a test sensitivity of 5×10^{-5}ref-cc/sec. A summary of the leak rates is given in Table 2.3. All leakage rate data and calculations resulting from the tests are documented in Appendices H, I, J, K, L and M.

Table 2.3 Pre-test leak rate for the test unit CV

Drum ID	TU-1	TU-2	TU-3	TU-4	TU-5	TU-6
Leak Rate, std-cc/sec	2.760E-5	2.102E-5	2.381E-5	2.967E-5	2.116E-5	4.772E-5

2.5 Chilling of TU-2

TU-2 was chilled before the structural tests were conducted. TU-2 was placed in an environmental chamber at ORNL and chilled to -70 ºF for 24 hours and then -45 ºF for 72 hours. TU-2 was then placed in an insulated box and transported to the NTRC test site. The four structural tests, NCT 1.2-m drop test, HAC 9-m drop test, HAC crush test, and the HAC puncture test, were conducted as quickly as possible after its removal from the environmental chamber. The package was removed from the environmental chamber at 8:28 a.m. The NCT drop test was conducted on it at 9:30 and the HAC drop took place 8 minutes later. The remaining crush and puncture tests concluded before 10:33 a.m. Therefore, all of the structural tests were performed within 125 minutes of removal of the test unit from the environmental chamber.

3 NCT TESTS

The applicable Normal Conditions of Transport (NCT) test sequence as specified in 10 CFR 71.71 includes a water spray test, a static compression test, a vibration test, a penetration test, and a 1.2 m (4 ft) drop test. Table 1.2 lists the NCT tests that were performed on the test units and the sequence in which they were conducted. Because the full battery of NCT tests were conducted only on TU-4, this unit will be used to guide discussion of the NCT test application.

3.1 Full NCT Test Series (TU-4 Only)

As noted above, TU-4 was the only test unit to be subjected to all of the applicable NCT tests. This section discusses only the NCT testing performed on TU-4. Drop testing will be discussed in the following Section 3.2, since it was applied to all the test units.

3.1.1 Water Spray Test

The water spray test was performed using a four-nozzle spray manifold with the four nozzles directed to spray the top as well as the four quadrants of TU-4. The water spray was conducted on the package within two hours of the subsequent tests and is noted on the test forms for the subsequent tests. The water spray test was conducted prior the free-drop, penetration, and compression testing. Figure 3.1 shows TU-4 undergoing the water spray test. (Using a rain gauge, which is positioned near the bottom of the package in Fig. 3.1, the flow rate was measured to be ~91 cm/h.) Water accumulated in the drum between the inner liner and the CV. The water drained out during the setup for the drop test.

3.1.2 Penetration Test

TU-4 was placed on its side on the center of the indoor drop pad with the 0° (drum seam) line facing upward. TU-4 was chocked to keep it from moving during the test. The 6-kg penetration bar was raised to 1 m (40 in.) above the contact point. The contact point was the "X" marking placed at the 0° line to indicate the location of the internal CV flange. Figure 3.2 shows the test setup. The bar struck the package slightly left of center and formed a ~1/4 inch deep dent in the side of the package (Figure 3.3). See the data sheets in Appendix K for results of the test.

Figure 3.1 TU-4 undergoing the water spray test

Figure 3.2 TU-4 penetration test setup

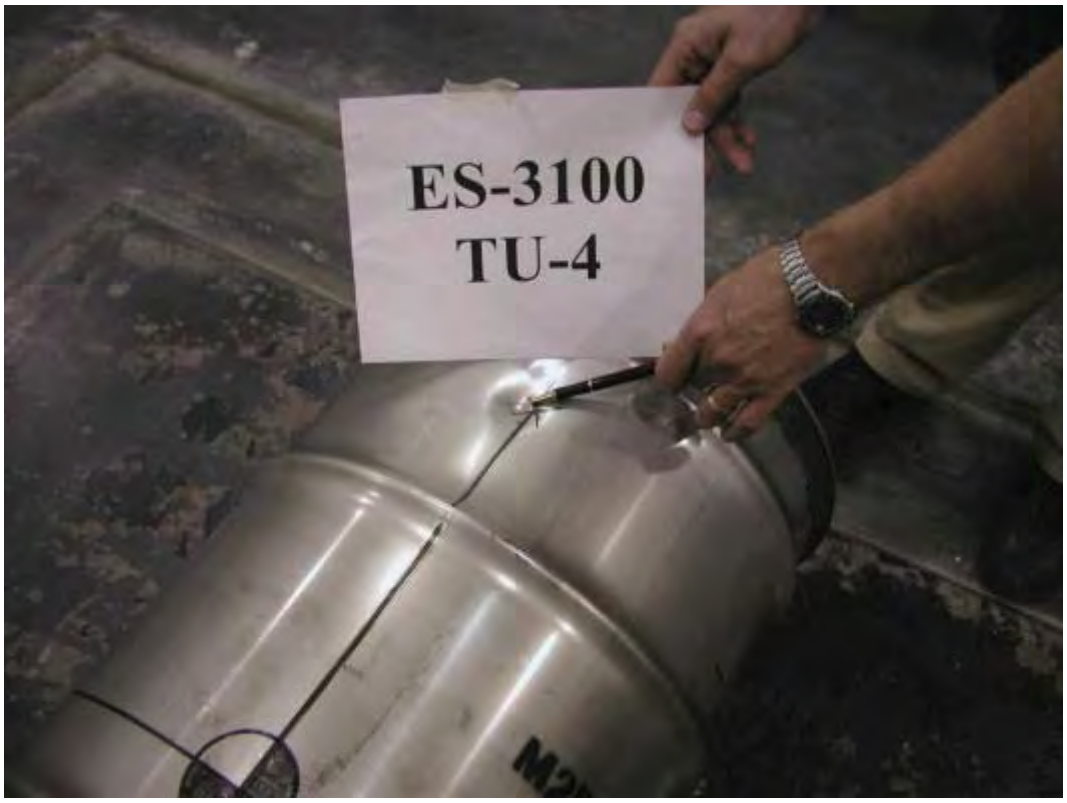

Figure 3.3 TU-4 damage from penetration test

3.1.3 Compression Test

The static compression test was performed on TU-4 using a Lansmont model 152-30K compression tester (Figure 3.4.). In accordance with 10 CFR 71.71(c)(9), 1.9 psi times the projected vertical area of the package was shown to be only 1,008 pounds; hence the more restrictive load of 5 times the maximum package weight or 2,500 pounds was applied to the package. (A maximum package weight of 500 lbs was assumed; actual maximum package weight may be lower.) After being compressed for 24 hours and 1 minute, there were no measurable effects on the package. See the data sheet in Appendix K.

Figure 3.4 TU-4 in Compression Tester.

3.1.4 Vibration Test

The vibration test for the ES-3100 package is designed to simulate the environmental effects of the vibration regime that the ES-3100 will experience during use. A Lansmont model 10000-10 vibration table was used to perform the testing. A vibration spectrum simulating the Safe-Secure Trailer/Safeguards Transporter (SST/SGT) was used. The test duration was based on the longest trip that the package is likely to endure, namely one hour per 1000 trip-miles. Hence, the 4-h test duration used was conservative and should encompass any conceivable trip that the ES-3100 might undergo. The vibration controller was programmed to the power spectrum density shown in Table 3.1.

After having undergone the water spray test, free drop, penetration test, and the compression test, TU-4 was securely strapped to the vibration table with a nylon tie-down strap (as specified in the test plan) to begin the 4-hour test (Figure 3.5).

Table 3.1 Vertical Power Spectrum Density (PSD)

Freq (Hz)	G^2/Hz
1.0	4.0e-3
2.0	3.0e-2
4.0	3.0e-2
6.5	2.0e-3
75.0	2.0e-3
110.0	8.0e-5
380.0	8.0e-5
1000.0	5.0e-6

Figure 3.5 Test units staged for vibration testing

After the vibration test there was no apparent damage to the exterior of the package. The package was not opened to inspect the internal condition. However, upon later opening the package, there was an effect observed that was attributed to the vibration test. See Section 5.1, Drum Disassembly Observations.

3.2 Free Drop Test (Test Units 1 through 5)

TU-1 through TU-5 were subjected to the 1.2 m (4 ft) NCT drop test. As shown in Table 3.2, these units were dropped in various orientations. Deformation of each test unit from the NCT drop test is described in this section. Total deformation, cumulative for all impact tests, for each package, is reported in tabular form in Section 4.4. The details of the NCT free drop test, including data on damage, measurements, and damage sketches for each package, are reported in Appendices H-L for test units TU-1 through TU-5, respectively.

The drop tests on TU-1, TU-3, TU-4, and TU-5 were carried out at the NTRC indoor drop pad, located in Room L110. This provided the essentially unyielding surface for the NCT free drop tests (Ref: ORNL/NTRC-001 *Design and Certification of Targets for Drop Testing at the NTRC Package Research Facility*, Rev. 0) Table 3.2 shows the desired package orientation for each drop test and the orientation of each package achieved for the test. TU-2, the chilled unit, was drop tested on the outdoor drop pad just before the HAC drop tests were conducted.

Figure 3.6 shows a typical test set-up being performed. The measuring bar is used to determine the proper drop height and assist in aligning the package to the center of the drop pad. The figure shows TU-1 suspended for the drop test and is also representative of the TU-5 slap-down drop at an angle of 12°. Figure 3.7 shows the chilled TU-2 being dropped on the outdoor drop pad. Figure 3.8 shows how TU-3 was angled so that it would drop on the 0° marking with package CG over the impacting edge. Figure 3.9 shows the damage that occurred to TU-3 after it was dropped. Finally, Figure 3.10 shows the orientation of TU-4 for its top-down drop test.

Table 3.2 Planned vs. measured package orientation for NCT drop tests

Test Unit	Desired Orientation	Measured Orientation
TU-1	Axis of package 12° angle to horizontal; 0° marking should contact drop pad first	Axis of package 12.1° from horizontal
TU-2	Axis of package horizontal; 0° marking should contact drop pad first	Axis of package 0.1° from horizontal
TU-3	Axis of package rotated downward 24.6° from horizontal; 0° marking should contact first	Axis of package 25° from horizontal
TU-4	Axis of package vertical; drum lid should contact drop pad first	Axis of package 0.1° from vertical
TU-5	Axis of package 12° angle to horizontal; 0° marking should contact drop pad first	Axis of package 12.1° from horizontal

Figure 3.6 TU-1 positioned for the 12.1° NCT side drop test

Figure 3.7 TU-2 being dropped horizontally while still cold

Figure 3.8 TU-3 being angled 24.6° so that 0° corner contacts the drop pad first

Figure 3.9 Damage to TU-3 after NCT drop

Figure 3.10 TU-4 being positioned head-down for the NCT vertical drop test

TU-1 had a measured angle of 12.1° from horizontal for the NCT drop along its 0° line with the bottom of the package lower. (To view this positioning, refer back to Fig. 3.6.) It experienced slight flattening at the top and bottom false wires and on the hoops along the 0° line. Use of a caliper determined that its diameter from 0° to 180° at both the top and bottom false wires decreased by 1/8 in and 1/4 in, respectively. The top false wire, where the impact occurred, had a flattened region 4-3/8 in long. The bottom false wire also had a flattened region of 4-5/8 in length. The flats of the top and bottom hoop were 4-1/2 in and 4 in, respectively.

TU-2 was dropped horizontally along its 0° line, deviating only 0.1° from the horizontal. It experienced a modest decrease in diameter and showed only slight flattening of its rolling hoops. Its top false wire flattened about 4 in, but the bottom false wire showed only a small dimple.

TU-3 was dropped at a 25° angle (desired was 24.6°) along its 0° line with the lid end impacting first. Because of the sharpness of the angle, the top false wire absorbed most of the damage and bent outward but did not flatten. See Figure 3.9 for an illustration of this damage. The height of the package decreased by 0.5 in along the 0° line but increased along the 180° line by 1/8 in. The diameters of the hoops and false wires remained constant.

TU-4 had a measured angle of 0.1° from vertical (Figure 3.10) and was dropped squarely on its top. In fact, it rested on its top after the drop. There was no visible damage

to the top false wire, and it did not have a measurable change in diameter. The drum did show a modest 1/8-in decrease in height at the 180° and 270° lines.

TU-5 deviated only 0.1° from the intended 12° angle to horizontal and was dropped on the 0° line of the package. The top false wire absorbed most of the impact and showed the most damage resulting from 1.2-m NCT drop. Figure 3.11 shows the extent of the flattening that occurred. It lost 0.5 in diameter along the 0° to 180° width and had a flat of 5-3/8 in. Also, the washer at about 270° was movable, though the nut remained more than finger tight. The diameters of the rolling hoops uniformly decreased by 1/8 in, and the diameter of the bottom false wire decreased by 1/4 in. The bottom false wire also had a flat of 5 in.

Figure 3.11 Flattening of top false wire of TU-5.

4 HAC TESTS

The 10 CFR 71.73 *Hypothetical Accident Conditions* (HAC) compliance testing sequence was performed on test units TU-1 through TU-5. TU-2 was chilled to below -40 °C (-40 °F) before the structural tests. TU-1 through TU-5 were subjected to the 9-m (30-ft) free fall drop test followed by the 9-m (30-ft) dynamic crush test. For the 9-m (30-ft) dynamic crush test, the portion of the package damaged in the previous tests was placed in contact with the drop pad and the 1 m × 1 m 500 kg (1102 lb) crush plate was dropped to impact on the opposite (i.e., the undamaged) side. Next, all five test units were subjected to the HAC puncture test. Then all 5 test unit were subjected to the thermal test. Separately, an undamaged CV, TU-6, was subjected to the 15-m (50-ft) immersion test. Following each of the tests on TU-1, TU-3, TU-4, and TU-5, dimensional measurements were made to document the damage and are presented in Appendices H - L. Dimensional measurements were not taken between the tests on TU-2, so that it could remain as cold as possible for the tests. A summary of the cumulative damage measurements are presented in Section 4.4.

4.1 HAC 9-m (30 ft) Drop Test

Following the NCT drops, the test units were subjected to the 9-m (30-ft) HAC drop test. The HAC drop testing was performed at the NTRC outdoor drop pad. This pad provided the essentially unyielding surface required by the regulations. The construction of the drop pad is described in ORNL/NTRC-001 *Design and Certification of Targets for Drop Testing at the NTRC Package Research Facility*, Rev. 0.

The packages were dropped in the orientations shown in Table 4.1. All test units were dropped with the 0° side or edge contacting the drop pad first. Table 4.1 shows the desired package orientation for the HAC 9-m drop tests and the measured package orientations achieved for those tests.

Table 4.1 HAC 9-m drop test desired package orientation vs. measured orientation

Test Unit	Desired Orientation	Measured Orientation
TU-1	Axis of package 12° from horizontal, lid up, 0° side down	Axis of package 12.2° from horizontal
TU-2	Axis of package horizontal, 0° side down	Axis of package 0.1° from horizontal
TU-3	Axis of package 24.6° from vertical, lid down, 0° side down	Axis of package 24.8° from vertical
TU-4	Axis of package vertical, lid down	Axis of package 0.2° from vertical
TU-5	Axis of package 12° from horizontal, lid up, 0° side down	Axis of package 12.5° from horizontal

Following this test, a variety of dimensional measurements were made to document the damage. The measurements taken after this test for each of the test units are presented in Appendices H - L. Figure 4.1 and Figure 4.2 show setup and results, respectively, for the HAC drop test of TU-3. Figure 4.3 through Figure 4.6 diagram the HAC drop test setup for each test unit.

Figure 4.1 Test setup for the HAC 9-m free drop of TU-3

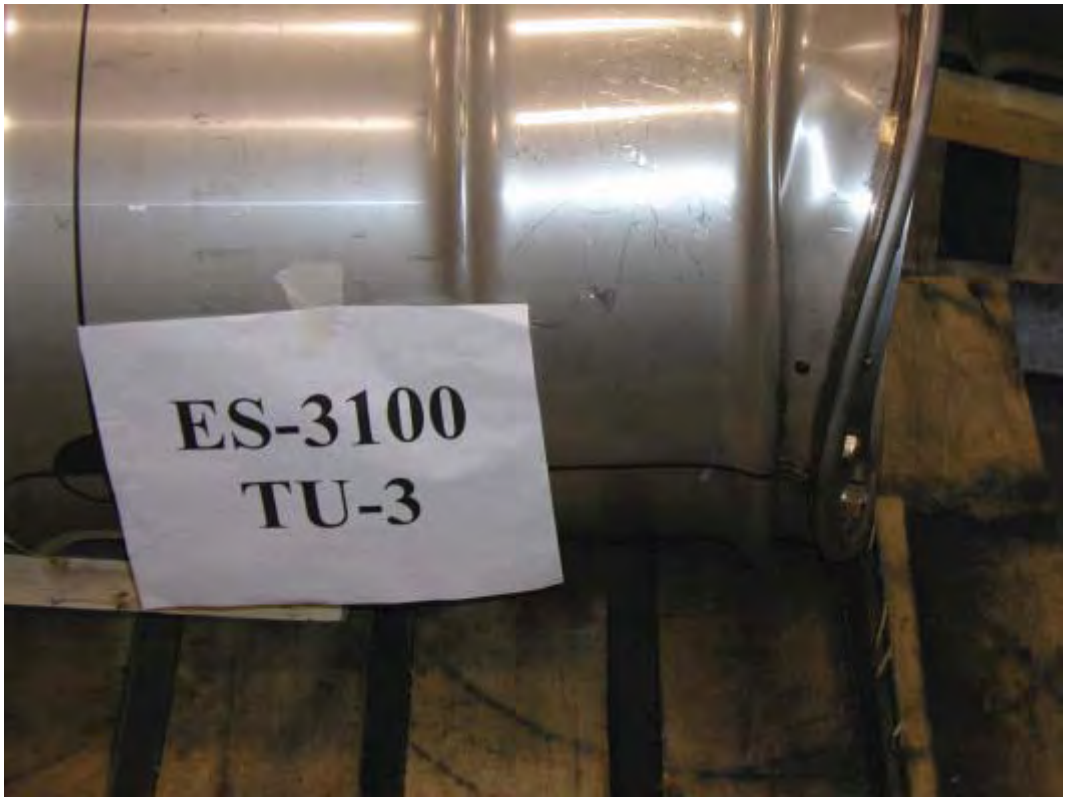

Figure 4.2 Results of the HAC drop of TU-3

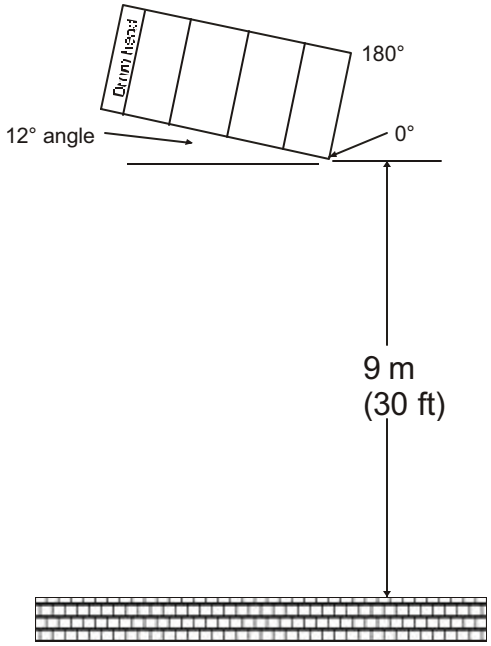

Figure 4.3 TU-1 and TU-5 HAC 9-m drop test setup

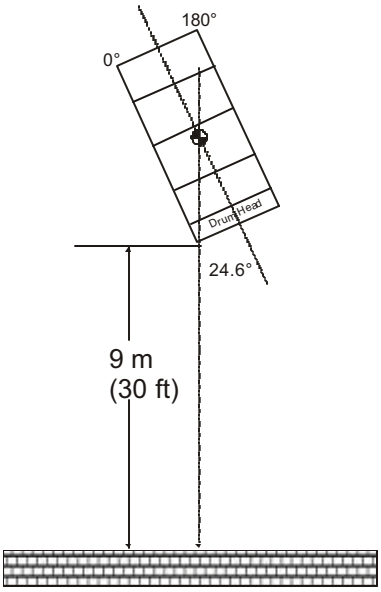

Figure 4.5 TU-3 HAC 9-m drop test setup

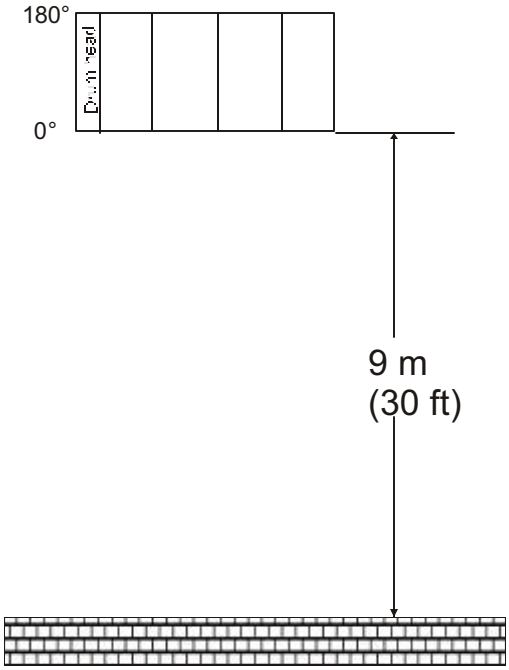

Figure 4.4 TU-2 HAC 9-m drop test setup

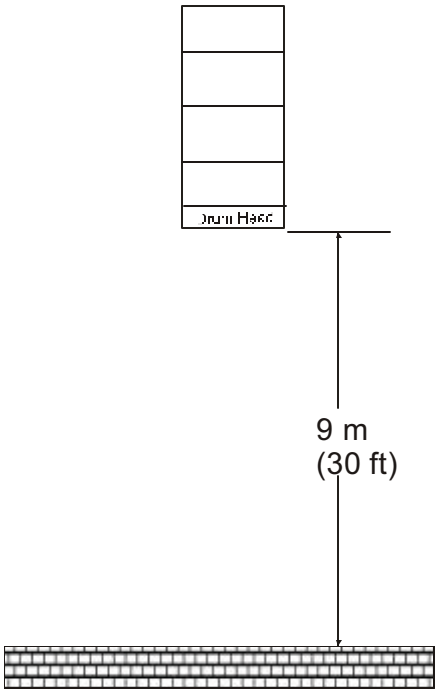

Figure 4.6 TU-4 HAC 9-m drop test setup

TU-1 was dropped with the axis of the package at an angle of 12.2° from horizontal with the lid up, on its 0° side from a distance of 9 m. The drum's side was flattened, generating a flat of 8 inches at the top false wire and 10 inches at the bottom false wire. The diameter of the drum along the direction of impact was reduced by 5/8 inch at the top false wire and by 1-3/16 inch at the bottom false wire. No nuts were loosened. See the datasheet in the Appendix H for more details. See Appendix A for photographs of damage.

TU-2 was dropped with the axis of the package at an angle of 0.4° from horizontal on its 180° side from a distance of 9 m. The package had been cooled to below -40 °C prior to testing. In order to test the package while it was as cold as possible, the NCT drop, HAC drop, HAC crush, and puncture tests were conducted promptly one after the other. Physical measurement of the intermediate damage was not taken. Only the cumulative damage at the end of these tests was taken. The cumulative damage is described in Section 4.3. No nuts were loosened. See the datasheet in the Appendix I for more details. See Appendix B for photographs of damage.

TU-3 was dropped with the CG over the edge of the lid, at an angle of 24.8° from vertical, with its 0° side impacting first from a distance of 9 m. The drum's top false wire was forced down 1-1/8 inches at the point of impact, creating a flat 16 inches long. No nuts were loosened. See the datasheet in the Appendix J for more details. See Appendix C for photographs of damage.

TU-4 was dropped with the lid impacting first from a distance of 9 m at an angle of 0.2° from vertical. The drum's lid was flattened slightly. The overall height of the package was reduced about 3/8 inch on the 90° side to 7/8 inch on the 270° side. No nuts were loosened. See the datasheet in the Appendix K for more details. See Appendix D for photographs of damage.

TU-5 was dropped with the axis of the package at an angle of 12.5° from horizontal with lid up, on its 0° side from a distance of 9 m. The drum's side was flattened, generating a flat of 8-3/8 inches at the top false wire and 9-1/4 inches at the bottom false wire. The diameter of the drum along the direction of impact was reduced by 1/8 inch at the top false wire and 5/8 inch at the bottom false wire. No nuts were loosened. See the datasheet in the Appendix L for more details. See Appendix E for photographs of damage.

4.2 HAC Dynamic Crush Test

When a fissile material, Type B package weighs less than 500 kg and has an overall density less than 1000kg/m^3 (62.4 lb/ft^3) 10 CFR 71.73 stipulates that the dynamic crush test follows the 9-m free drop test. Therefore, the test units were subjected to the dynamic crush test after being subjected to the 9-m free drop test.

Test Units 1 through 5 were subjected to the dynamic crush test. This test consisted of placing the test units on the unyielding impact pad and dropping a 1 m × 1 m square 500 kg (1102 lb) steel plate onto the package from a 9-m (30-ft) drop height. Figure 4.7 shows the results of the dynamic crush test of TU-1.

Figure 4.7 Results of the dynamic crush test of TU-1.

Figure 4.8 shows the test setup for TU-3 after the package had been balanced and prior to the raising of the 500 kg steel plate. Figure 4.9 and Figure 4.10 show the damage resulting from the crush test of TU-3. Figure 4.11 through Figure 4.14 show the setup for each of the crush tests performed.

Figure 4.8 TU-3 dynamic crush test set-up, ready to raise crush plate

Figure 4.9 Damaged bottom of TU-3 after the dynamic crush test

Figure 4.10 Damaged top of TU-3 after the dynamic crush test

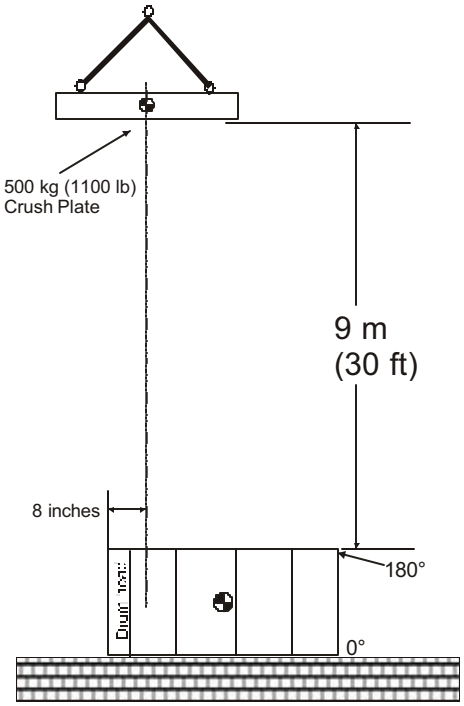

Figure 4.11 HAC crush test setup for TU-1

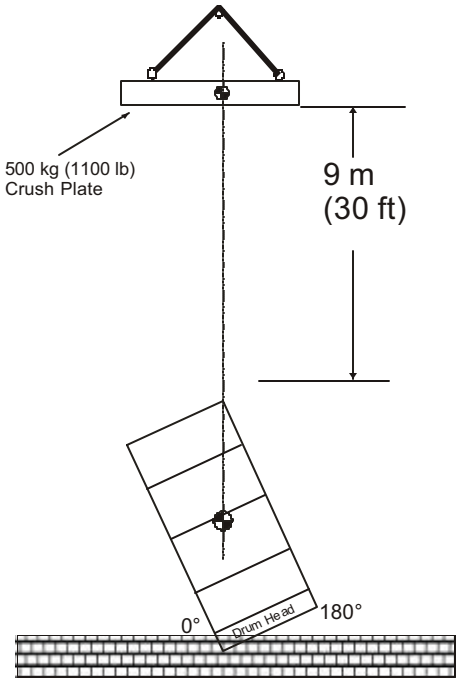

Figure 4.13 HAC crush test setup for TU-3

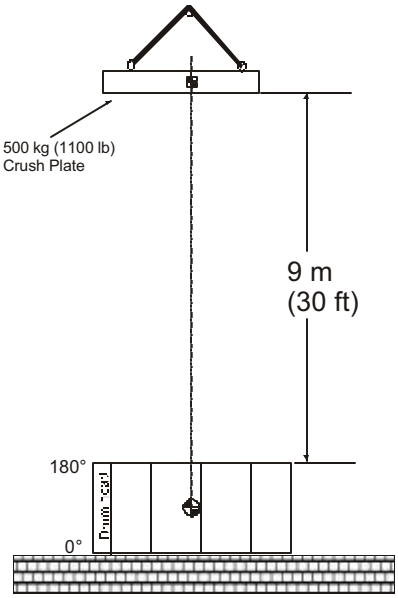

Figure 4.12 HAC crush test setup for TU-2 and TU-5

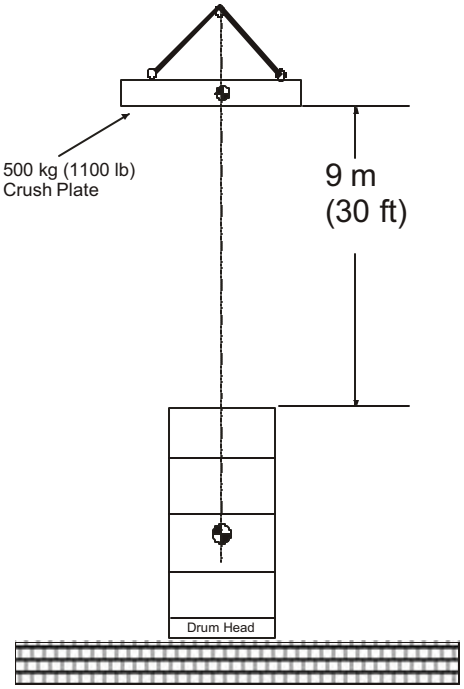

Figure 4.14 HAC crush test setup for TU-4

TU-1 was set horizontally on the impact pad with the previously damaged 0° side down and the crush plate was centered over the approximate location of the CV flange, about 8 inches from the top of the package. The impact flattened the 180° side above the bottom hoop, generating a flat of 8-1/2 inches at the top false wire and 10-5/8 inches just above the bottom hoop. The impact also increased the flattening of the 0° side, generating a flat of 10 inches at the CG hoop to 9 inches at the top false wire. The diameter of the drum along the direction of impact was reduced by 2-7/8 inch at the top false wire and about 2-3/8 inch just above the bottom hoop. No nuts were loosened. See the datasheet in the Appendix H for more details. See Appendix A for photographs of damage.

TU-2, the chilled unit, was set horizontally on the impact pad with the previously damaged 0° side down and the crush plate was centered over the CG of the package. The package's 0° side was flattened, generating a flat of 6-1/4 inches at the top hoop and 14-7/8 inches at the bottom hoop. The diameter of the drum along the direction of impact was reduced by 1-5/8 inch at the top false wire and 3-3/4 inch at the bottom hoop. The package's 180° side was flattened, generating a flat of 8 inches at the top false wire to 10-1/8 inches at the CG + top hoop. The diameter of the drum along the direction of impact was reduced by 1-5/8 inch at the top false wire and 3-3/4 inch at the bottom hoop. No nuts were loosened. See the datasheet in the Appendix I for more details. See Appendix B for photographs of damage.

TU-3 was tested by orienting the package on the impact pad in the same CG-over-corner attitude that was used when it was previously dropped from 9 m. To do this the package had to be balanced with its damaged edge on the impact pad and the bottom of the package in an upward position. To hold the package in position, two thin nylon cords were anchored to the impact pad and attached around the diameter of the package. These cords were adjusted in length to properly balance the package at the desired angle. The bottom false wire of the package on the 180° side was flattened. The bottom false wire was crushed down about 6 inches and the damaged top false wire was crushed down about 5 inches. The stud and its nut nearest the 0° position was sheared off. See the datasheet in the Appendix J for more details. See Appendix C for photographs of damage.

TU-4 was set vertically, top down on the drop pad, and the crush plate was centered over the bottom of the drum. The height of the package was reduced by 3-5/8 at 0° to about 2-1/4 at 180°. No nuts were loosened. See the datasheet in the Appendix K for more details. See Appendix D for photographs of damage.

TU-5 was set horizontally on the drop pad with previously damaged, 0° side down. The crush plate was aligned so that the edge of the crush plate would impact the top hoop rather than over the CG. This was a field change from the Test Plan. The actual impact created a crease about 3 inches from the top and 1 inch from the bottom. The impact flattened the 180° side below the top, generating a flat of 8-5/8 inches at the top crease and 11 inches at the bottom crease. The impact increased the flattening of the 0° side, generating a flat of 8-7/8 inches at the top to 11-3/8 inches at the bottom hoop. The diameter of the drum along the direction of impact was reduced by 1-3/4 inches at the CG + top hoop (3) and 1-7/16 inch at the bottom false wire. No nuts were loosened. See the datasheet in the Appendix L for more details. See Appendix E for photographs of damage.

4.3 HAC Puncture Test

TU-1 through TU-5 were each subjected to at least one HAC puncture test. Each package was raised to a height of 1 m (40 inches) above a 15-cm (6-inch) diameter steel puncture bar that had been bolted to the steel impacting surface of the drop pad. TU-1 was subjected to four puncture tests. In the first test the punch impacted the CG on the 0° line. Then the area of the CV flange on the 180° line was impacted. Afterwards, the third test was designed to impact at 28° from vertical through the CG on the 90° line.

After completion of these first three tests, it was then noticed the drawings in the test plan were not in agreement with the text of the test plan. The angles specified in the text were from horizontal rather than from vertical as shown in the drawings. After conferring with Y-12 personnel, the fourth test was changed to impact at 40° from horizontal on the 270° line instead of 40° from vertical as shown in the drawing. Also, an additional puncture test was conducted on TU-3 at an angle of 28° from horizontal, impacting the 270° side.

Figure 4.15 shows the TU-1 set-up process for the HAC puncture test. The set-up process was essentially the same for each test unit. The 1-m bar was used to both determine the correct drop height and to assist in aligning the impact point with the center of the puncture bar.

The prior damage caused by both the HAC 9-m (30 ft) drop and HAC crush test misaligned the test unit surfaces from the horizontal axis of the package. Therefore, TU-1, TU-2, and TU-5 were rigged to be dropped so that the impacted surface was parallel to the puncture bar face. To accomplish this, prior to lifting, the angle of the upper surface of the package was measured while the package was lying flat on the floor. Once the package was raised, the rigging was adjusted to reproduce the same reading on the level. Table 4.2 shows the desired package orientation and the orientation that was achieved for each puncture test. The orientation readings recorded on the data sheets for each test unit is the difference between the level reading with the test unit on the drop pad and with it suspended and ready to drop. Figure 4.17 through Figure 4.25 diagram the HAC puncture test set-up for each of the test units.

Table 4.2 Package orientations for HAC puncture test

Test Unit	Desired Orientation	Measured Orientation
TU-1	Axis of package horizontal	Axis of package 0.0° from horizontal
TU-1	Axis of package horizontal	Axis of package 0.0° from horizontal
TU-1	Axis of package 28° from vertical	Axis of package 27.9° from vertical
TU-1	Axis of package 40° from horizontal	Axis of package 40.1° from horizontal
TU-2	Axis of package horizontal	Axis of package 0.8° from horizontal
TU-3	Axis of package 24.6° from vertical	Axis of package 25.2° from vertical
TU-3	Axis of package 28° from horizontal	Axis of package 28.4° from horizontal
TU-4	Axis of package vertical	Axis of package 0.3° from vertical
TU-5	Axis of package horizontal	Axis of package 0.1° from horizontal

The resulting impacts produced indentations in the surface of the outer drums, but did not puncture the drum surfaces (Figure 4.16). Typically, damage was observed to cover a circular-shaped area approximately 6 inches in diameter or a crescent shaped dent. The dent depths ranged from a slight indentation to 7/8-in deep. The detailed dimensional data for this test was recorded on data sheets in Appendices H- L.

Figure 4.15 Test setup for the puncture test of TU-1

Figure 4.16 Damage from puncture test of TU-1

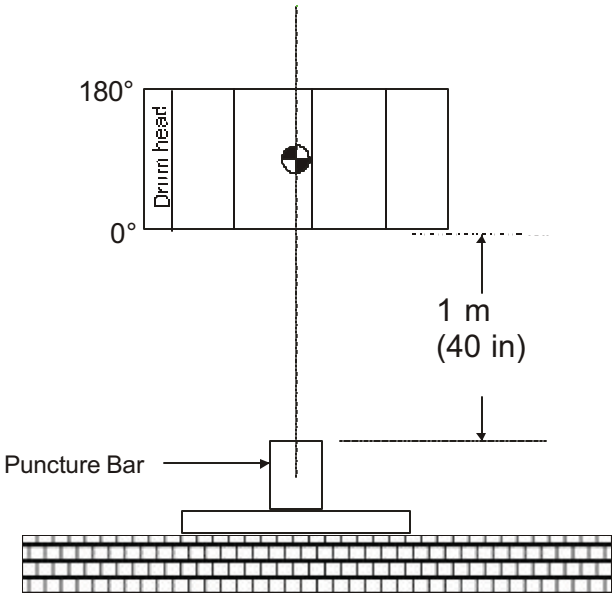

Figure 4.17 Initial TU-1 puncture test setup

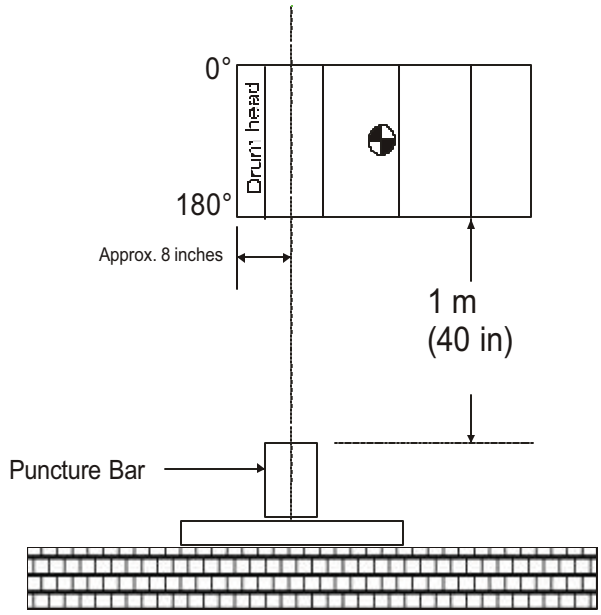

Figure 4.19 Second TU-1 puncture test setup

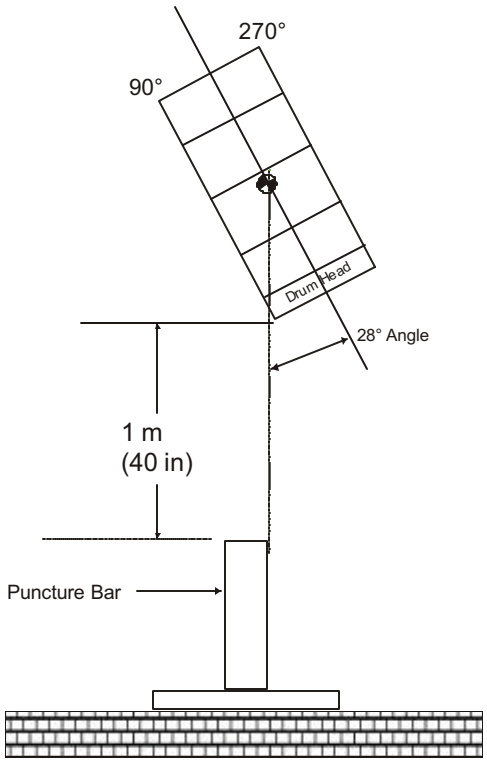

Figure 4.18 Orientation for third TU-1 HAC 1m puncture test

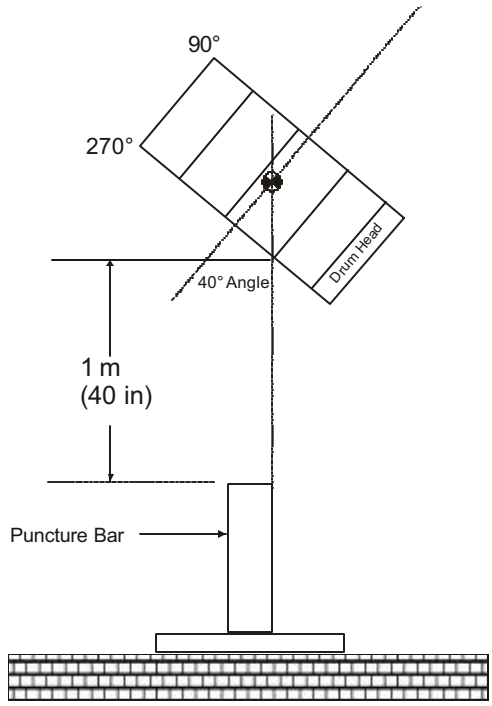

Figure 4.20 Orientation for fourth TU-1 HAC 1m puncture test

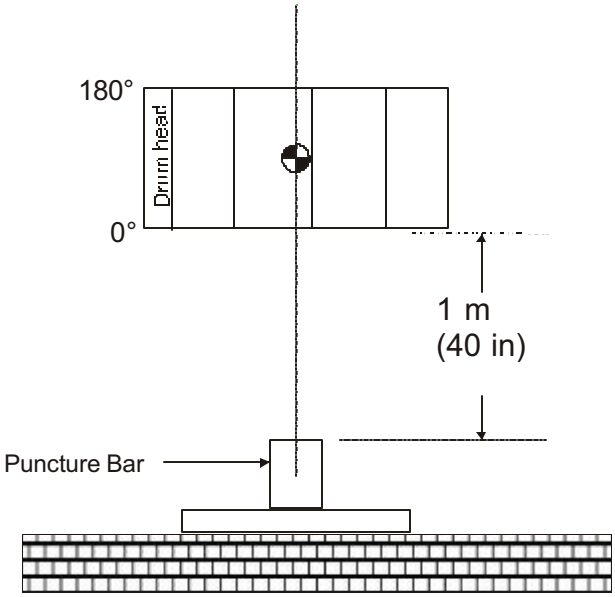

Figure 4.21 TU-2 puncture test setup

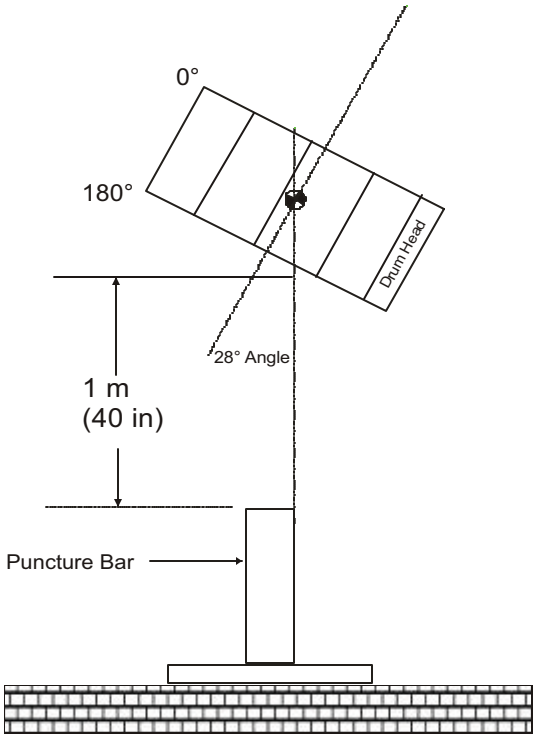

Figure 4.23 TU-3 second puncture test setup

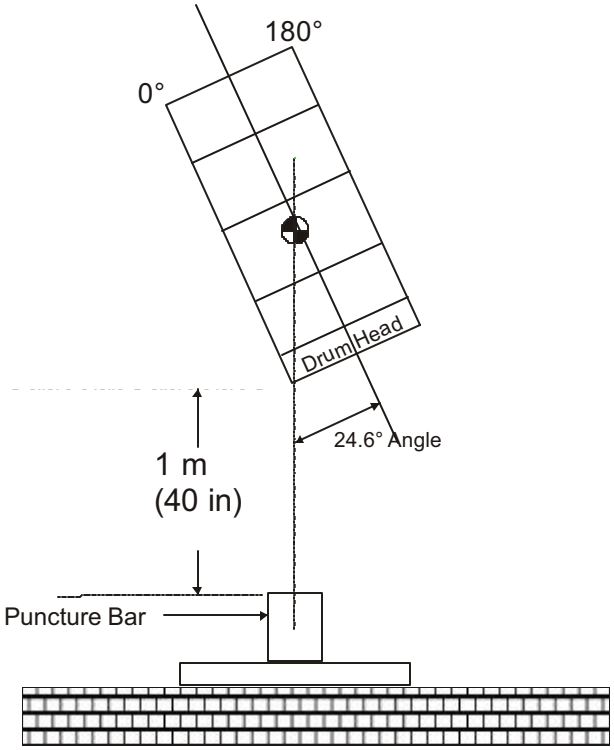

Figure 4.22 TU-3 puncture test setup

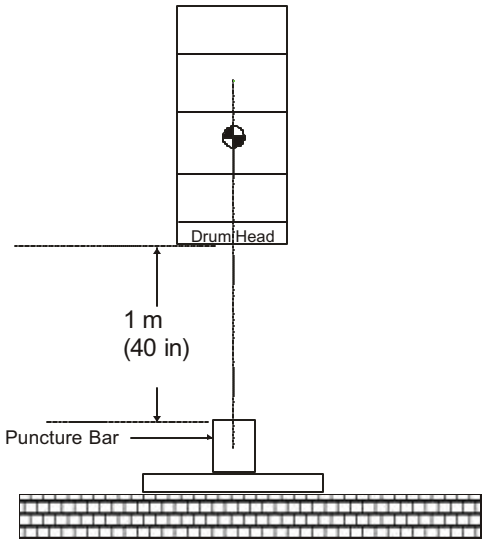

Figure 4.24 TU-4 puncture test setup

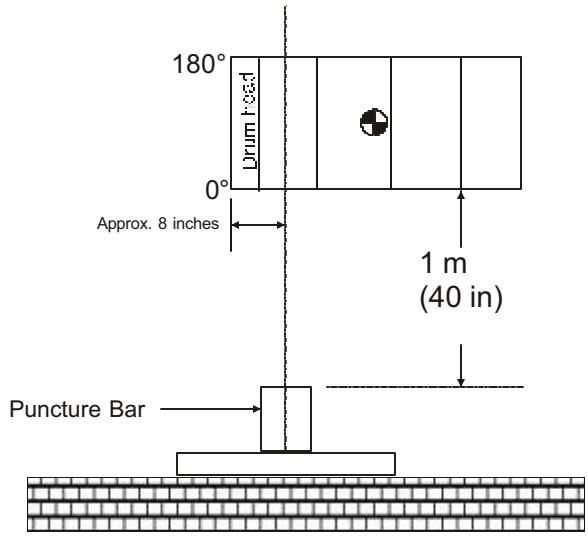

Figure 4.25 TU-5 puncture test setup

TU-1 was puncture tested in four different orientations. TU-1 was dropped with the package horizontal on its 0° side from a distance of 1 m at an angle of 0.0° from horizontal onto the puncture bar which was located under the CG of the package. For the second test, TU-1 was dropped with the package horizontal on its 180° side from a distance of 1 m at an angle of 0.0° from horizontal onto the puncture bar which was located under the CV flange, about 8 inches from the top of the drum. These impacts produced circular dents with a depth of about 5/8 and 3/8 of an inch. TU-1 was dropped a third time with the lower side of the package on its 90° side from a distance of 1 m at an angle of 27.9° from vertical. The puncture bar was located under the CG of the drum. The impact produced crescent shaped dents along the side of the package with the deepest dent having a depth of about 5/8 of an inch. TU-1 was dropped a fourth time with the lower side of the package on its 270° side from a distance of 1 m at an angle of 40.1° from horizontal. The puncture bar was located under the CG of the drum. The impact produced crescent shaped dents along the side of the package with the deepest dent having a depth of about 3/4 of an inch. No nuts were loosened. See the datasheet in the Appendix H for more details. See Appendix A for photographs of damage.

TU-2 was puncture tested with the lower side of the package horizontal on its 0° side from a distance of 1 m at an angle of 0.8° from horizontal. The puncture bar was located under the CG of the package. The impact produced a circular dent with a depth of about 1/8 of an inch. No nuts were loosened. See the datasheet in the Appendix I for more details. See Appendix B for photographs of damage.

TU-3 was puncture tested in the CG over edge orientation from a distance of 1 m with the axis of the package at 25.2° from vertical. The puncture bar was position to impact the damaged 0° edge of the lid. The impact produced a shallow crescent-shaped dent in the reinforcing rim with a depth of about 1/16 of an inch. TU-3 was dropped a second time with the lower side of the package on its 270° side from a distance of 1 m at an

angle of 28.4° from horizontal. The puncture bar was located under the CG of the drum. The impact produced a crescent-shaped dent in the side of the drum with a depth of about 7/8 of an inch. No nuts were loosened. See the datasheet in the Appendix J for more details. See Appendix C for photographs of damage.

TU-4 was puncture tested with the axis of the package vertical onto its top from a distance of 1 m at an angle of 0.3° from vertical. The puncture bar was located under the center of the top of the drum. The impact produced a circular dent with a depth of about 1/8 of an inch. The package stood balanced on top of the puncture bar after the test. No nuts were loosened. See the datasheet in the Appendix K for more details. See Appendix D for photographs of damage.

TU-5 was puncture tested with the lower side of the package horizontal on its 0° side from a distance of 1 m at an angle of 0.1° from horizontal. The puncture bar was located under the CV flange, about 8 inches from the top of the drum. The impact produced a circular dent with a depth of about 1/8 of an inch. No nuts were loosened. See the datasheet in the Appendix L for more details. See Appendix E for photographs of damage.

4.4 Summary of Cumulative Damage from Impact Tests

To quantify the damage from the drop testing, the diameters of the outer drums were measured across the 0° – 180° plane and the 90° – 270° plane at six locations on each test unit. Figure 4.26 shows the six locations along the side of each test unit where deformation measurements were taken. The height of each test unit was measured at the 0°, 90°, 180°, and 270° locations. The width of flattening from impact and crush was measured at six locations along the package on the impacted sides for the cumulative drop and crush damage. Total damage from all drop tests is summarized in Table 4.3 through Table 4.5 .

Some measurements were taken on some test units and not the others because damage was not incurred on some test units due to the various orientations the packages were tested in. For instance, side flattening did not exist for TU-4 as the test unit was subjected exclusively to end impacts. The damage produced on TU-3 by the CG over corner impacts is difficult to summarize; the reader is referred to the data sheets in Appendix J to understand both the shape and dimensions of the damage resulting from this testing.

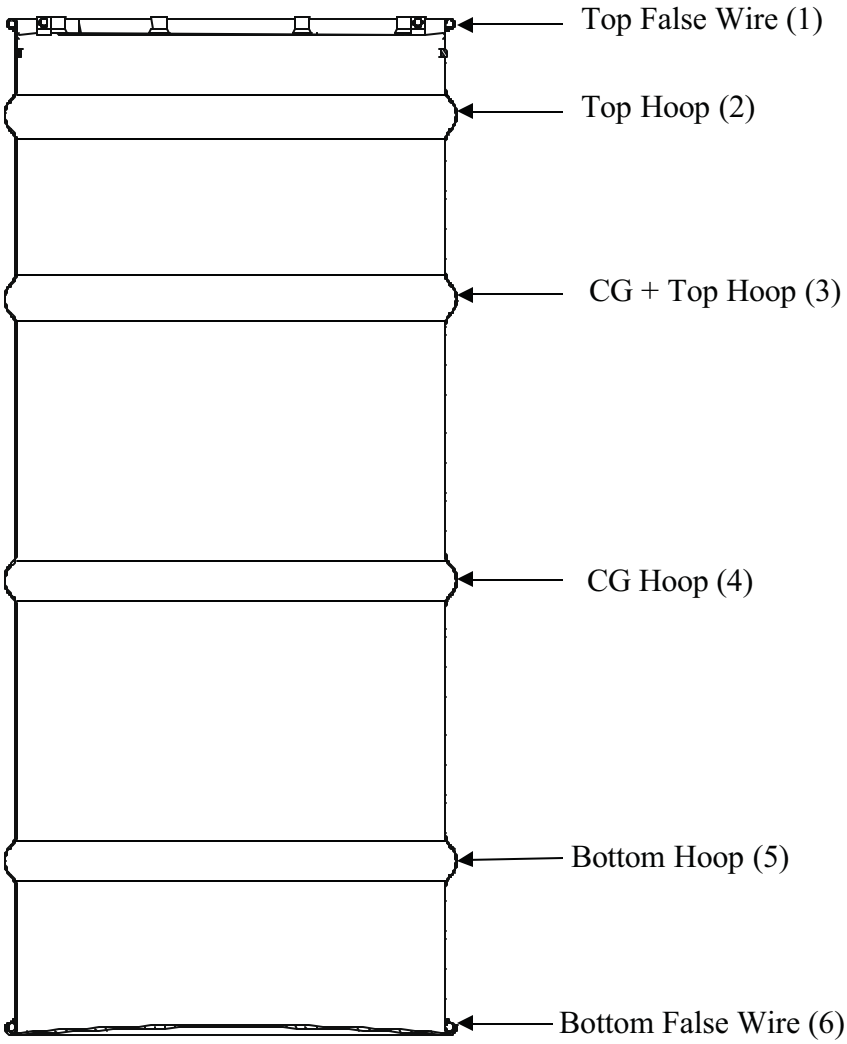

Figure 4.26 Locations where measurements were made on test unit exteriors

Table 4.3 Summary of total height change of each test unit after all impact testing (units = inches)

Test Unit	Initial Height 0°	Final Height 0°	Change in Height 0°	Initial Height 90°	Final Height 90°	Change in Height 90°	Initial Height 180°	Final Height 180°	Change in Height 180°	Initial Height 270°	Final Height 270°	Change in Height 270°
TU-1	43 1/2	44 7/8	+ 1 3/8	43 1/2	43 3/8	- 1/8	43 1/2	44	+ 1/2	43 1/2	43 5/8	+ 1/8
TU-2	43 1/2	44 3/4	+ 1 1/4	43 1/2	43 3/4	+ 1/4	43 1/2	42 3/4	- 3/4	43 1/2	43 5/8	+ 1/8
TU-3	43 1/2	39 3/8	- 1 1/8	43 1/2	42 7/16	- 1/16	43 1/2	39 1/8	- 4 3/8	43 1/2	42 1/2	- 1
TU-4	43 1/2	39 3/8	- 1 1/8	43 1/2	40 3/8	- 3 1/8	43 5/8	40 5/8	- 3	43 5/8	39 3/4	- 3 7/8
TU-5	43 1/2	45	+ 1 1/2	43 1/2	43 1/2	0	43 1/2	43 3/4	+ 1/4	43 1/2	43 7/8	+ 3/8

Table 4.4 Measurement of the width of "flats" after HAC crush test for side impact units (TU-1, TU-2 and TU-5) (units = inches)

Test Unit	Top false wire (1) 0°	Top hoop (2) 0°	CG + Top Hoop (3) 0°	CG Hoop(4) 0°	Bottom hoop (5) 0°	Bottom false wire (6) 0°	Top false wire (1) 180°	Top hoop (2) 180°	CG + Top Hoop (3) 180°	CG Hoop(4) 180°	Bottom hoop (5) 180°	Bottom false wire (6) 180°
TU-1	8 7/8	8 1/2	8	8 3/4	10 1/4	11 3/8	0	12 1/2	12	11 3/8	11 3/8	10 1/2
TU-2	6 1/4	8 7/8	9 5/8	12	14 7/8	0	8	9	10 1/8	9 7/8	9 7/8	9 3/8
TU-5	8 7/8	8 1/2	8	8 3/4	10 1/4	11 3/8	0	12 1/2	12	11 3/8	11 3/8	10 1/2

Table 4.5 Changes in diameter after all impact testing (units = inches)

Test Unit		Top false wire (1)	Top hoop (2)	CG + Top Hoop (3)	CG Hoop (4)	Bottom hoop (5)	Bottom false wire (6)
TU-1	Initial Diameter 0° - 180°	19 1/4	19 1/4	19 1/4	19 1/4	19 1/4	19 1/4
	Final Diameter 0° - 180°	15 5/8	16	16 1/4	16 1/2	18 1/4	17 13/16
	Change in Diameter 0° - 180°	- 3 5/8	- 3 1/4	- 3	- 2 3/4	- 1	- 1 9/16
	Initial Diameter 90° - 270°	19 1/4	19 1/4	19 1/4	19 1/4	19 1/4	19 1/4
	Final Diameter 90° - 270°	20 5/8	20 7/16	19 7/8	19 1/2	19 1/4	20 1/4
	Change in Diameter 90° - 270°	+ 1 3/8	+ 1 3/16	+ 5/8	+ 1/4	0	+ 1
TU-2	Initial Diameter 0° - 180°	19 1/4	19 1/4	19 1/4	19 1/4	19 1/4	19 1/4
	Final Diameter 0° - 180°	17 5/8	17 3/8	17	16	15 1/2	18
	Change in Diameter 0° - 180°	- 1 5/8	- 1 7/8	- 2 1/4	- 3 1/4	- 3 3/4	- 1 1/4
	Initial Diameter 90° - 270°	19 1/4	19 1/4	19 1/4	19 1/4	19 1/4	19 1/4
	Final Diameter 90° - 270°	19 13/16	19 3/4	20	20 1/4	20 1/8	19 3/8
	Change in Diameter 90° - 270°	+ 9/16	+ 1/2	+ 3/4	+ 1	+ 7/8	+ 1/8
TU-3	Initial Diameter 0° - 180°	19 1/4	19 1/8	19 1/8	19 1/8	19 1/8	19 1/8
	Final Diameter 0° - 180°	19 1/4	19 3/4	19 1/4	19 1/8	19 1/8	18
	Change in Diameter 0° - 180°	0	+ 5/8	+ 1/8	0	0	- 1 1/8
	Initial Diameter 90° - 270°	19 1/8	19 1/8	19 1/8	19 1/8	19 1/8	19 1/8
	Final Diameter 90° - 270°	19 1/16	20 1/4	19 3/4	19 1/4	19 3/4	19 3/8
	Change in Diameter 90° - 270°	- 1/16	+ 1 1/8	+ 5/8	+ 1/8	+ 5/8	+ 1/4
TU-4	Initial Diameter 0° - 180°	19 1/4	19 1/4	19 1/4	19 1/4	19 1/4	19 3/8
	Final Diameter 0° - 180°	19 1/4	20	20	19 7/16	19 15/16	19 1/4
	Change in Diameter 0° - 180°	0	+ 3/4	+ 3/4	+ 3/16	+ 11/16	- 1/8
	Initial Diameter 90° - 270°	19 3/8	19 1/4	19 1/4	19 1/4	19 1/4	19 1/4
	Final Diameter 90° - 270°	19 3/8	20 1/8	20 1/16	19 1/2	20	19 1/4
	Change in Diameter 90° - 270°	0	+ 7/8	+ 11/16	+ 1/4	+ 3/4	0
TU-5	Initial Diameter 0° - 180°	19 3/8	19 1/4	19 1/4	19 1/4	19 1/4	19 1/4
	Final Diameter 0° - 180°	19 3/8	19 3/8	19 3/8	19 1/4	19 1/4	19 5/16
	Change in Diameter 0° - 180°	0	+ 1/8	+ 1/8	0	0	+ 1/16
	Initial Diameter 90° - 270°	19 3/8	19 1/4	19 1/4	19 1/4	19 1/4	19 1/4
	Final Diameter 90° - 270°	19 3/8	19 5/8	20	20	19 3/4	19 3/8
	Change in Diameter 90° - 270°	0	+ 3/8	+ 3/4	+ 3/4	+ 1/2	+1/8

4.5 HAC Thermal Test

The HAC thermal test requirements are given in 10 CFR 71.73(c)(4). For the ES-3100 test units, a furnace located at the Timken Precision Forging Facility in Latrobe, PA was used for the HAC thermal testing. The test method used was based upon and closely followed ASTM E2230 *Standard Practice for Thermal Qualification of Type B Packages for Radioactive Material*.

4.5.1 Furnace Description

The thermal testing of the ES-3100 test units was performed in the gas-fired Furnace #3 in the Precision Forging Facility at Timken Steel Company in Latrobe, PA. Timken Steel maintains and operates this furnace as an AMS2750 certified Class 1A furnace. The furnace is an open-fired natural gas fueled box furnace with a 20 ft x 12 ft x 8 ft work zone and a guillotine door. The furnace has been in service since the mid 1980s. The furnace is normally used as a billet reheat furnace for the forging of billets and round bars. The estimated heating design load is 10 tons within a range of 1400°F to 2100°F.

The heating system consists of six North American high-velocity pulse-fired burners with a total heating capacity 10M to 12M BTU. Pulse-fired burners operate with air being blown through them continuously with natural gas being pulsed into the burners when the control system calls for additional heat. The burners are crown mounted with two zone controls. A single flue is located 24 inches above the hearth line in the center of the back wall. The flue is rear-chambered for a power damper (disconnected) with an external vented stack. The furnace insulation consists of a cast hearth floor refractory brick curb 12-in w x 24-in high on the wall with the remaining height of the walls and the ceiling lined with ceramic fiber pyro-block. Figure 4.27 shows the interior of Furnace #3.

The control system consists of a Honeywell UDC3300 controller, DOR2500 multipoint recorder, Vista Interface software, and UDC3300 over-temperature controller. Control and over-temperature thermocouples are type S 20ga. The control thermocouple junctions are mounted flush at the wall. The thermocouples are located 12 inches to the left and down of burner #1 for zone 1 and 12 inches to the left and down of burner #6. The over-temperature thermocouples are mounted in the roof at the center of each zone. The over-temperature thermocouple junctions are 4 inches below the ceiling.

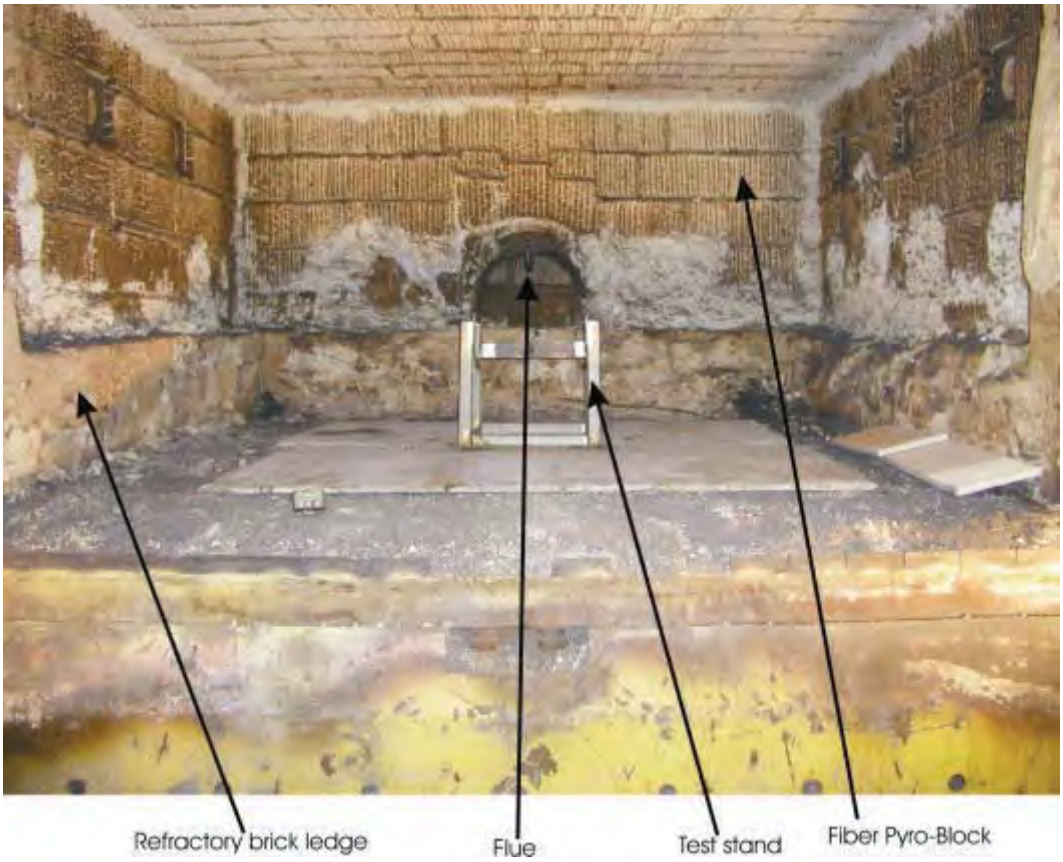

Figure 4.27 Interior of furnace #3

4.5.2 Furnace Setup

Furnaces used for performing the HAC thermal testing are required to operate in very tight temperature ranges with relatively light loads. In addition, a thorough understanding of the thermal environment surrounding the test unit is required. Commercial furnaces, like the Timken furnace #3, usually require that the operating parameters of the furnace be changed considerably from the normal settings to meet the desired thermal regime for HAC testing. In addition, considerable additional instrumentation must be installed for monitoring during testing. Furnace #3 was no exception, and in order to perform the ES-3100 testing several temporary additions and modifications were made to Furnace #3.

In the area of physical modifications, two 4 ft x 8 ft x 1 in thick plates of steel were placed on the floor to provide a secure and flat surface to which the test stand was mounted. The test stand was centered in the furnace then tack-welded to the steel plates.

A computer-based thermal monitoring system, developed by ORNL, was used to monitor the furnace environment and the test units during these tests. This system provides 72 data channels that are continuously logged to a data file. During the test runs the system was set to log data every 15 seconds from each data channel. The thermocouples used for the ES-3100 thermal testing were calibrated .063-inch and .037-inch diameter Type K thermocouples. These lightweight thermocouples provide a very rapid response to changes in temperature which provides a very accurate picture of the furnace and test unit thermal behavior.

In order to monitor the furnace environment during testing, a total of 18 thermocouples were installed on the furnace surfaces and the test stand. Figure 4.28 diagrams the location of the thermocouples in the left wall, Figure 4.29 diagrams the location of thermocouples on the right wall, and Figure 4.30 diagrams the location of thermocouples on the back wall and front door (locations in the furnace are referenced from a position looking into the furnace from the door). Figure 4.31 through Figure 4.32 show the thermocouples installed on the left, back, and right walls. The wall thermocouples were fastened to the both the refractory brick or pyro-block with 3/8 in x 2 in lag screw anchors and the tip of each thermocouple was covered with refractory cement. Three thermocouples were installed on the steel floor plate. These thermocouples were aligned along the axis of the test unit as it sits on the test stand. Finally, three thermocouples were attached to the test stand — one on the inward facing surface of each side member and the back member. The floor plate and test stand thermocouples were attached with metal clips tack-welded to the surface and the thermocouple tips were covered with refractory cement. See Appendix G for additional photographs of thermal test activities.

Once furnace preparations were completed, several practice loadings were performed on the cold furnace to ensure that the test units could be loaded onto the test stand and rapidly unloaded from the furnace to minimize the cooling of the furnace due to the door being open. After the cold load/unload practice was completed, the furnace was fired. Once fired, the furnace was allowed to heat soak for more than at 24 h before testing was initiated.

A number of changes to the furnace and its control system were made to produce an acceptable thermal regime. To compensate for the furnace over-firing, the fuel supply to burners

#2 and #5 was shut down after TU-3 was tested. Because the air supply for burners #2 and #5 ran continuously, excess oxygen needed to support combustion of material in the test unit was ensured. After these changes were performed, furnace control thermocouple cycles were controlled to +/-15°F of set point of the furnace controller thermocouple. A set point temperature of 1600°F was needed to consistently keep all additional furnace thermocouples above 1475°F.

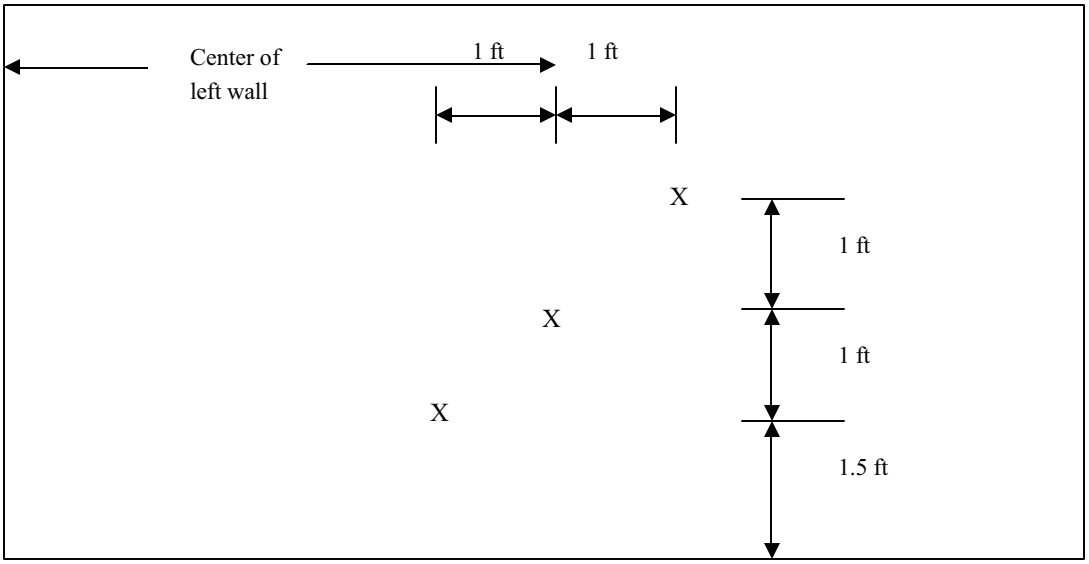

Figure 4.28 Approximate location of 3 thermocouples in left wall of furnace

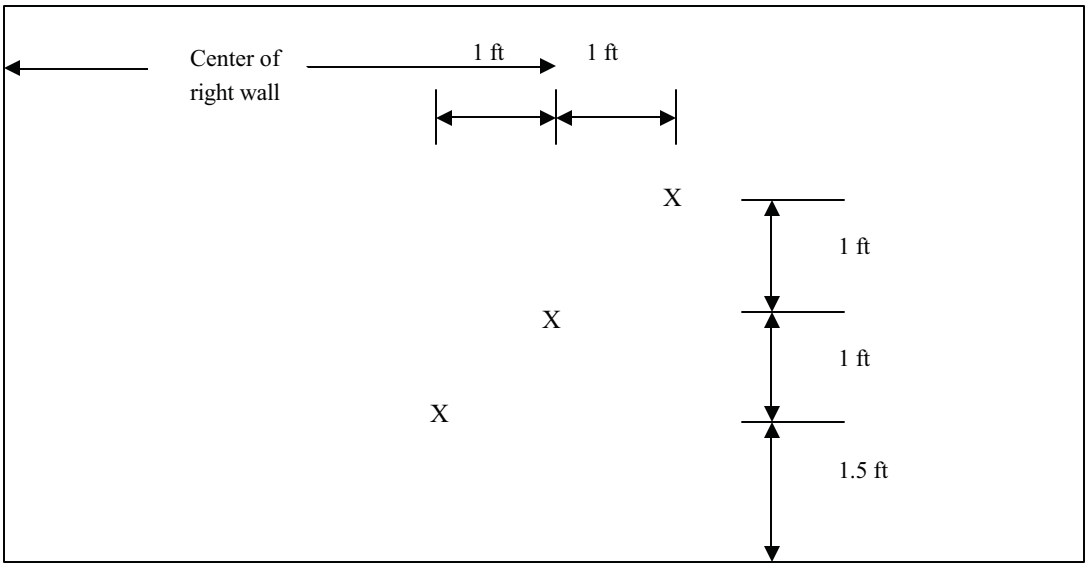

Figure 4.29 Approximate location of 3 thermocouples in right wall of furnace

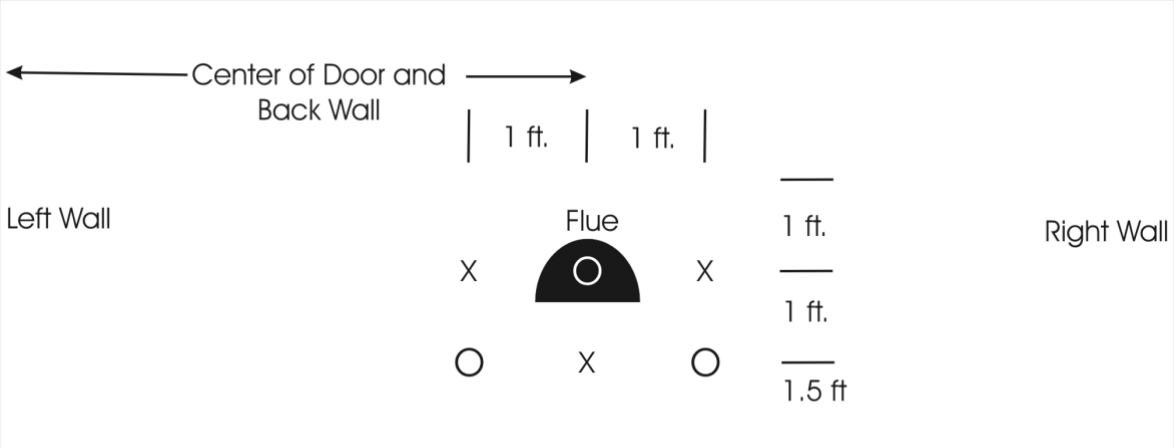

Figure 4.30 Approximate location of thermocouples in door (O) and back wall (X)

Figure 4.31 Furnace #3 left wall thermocouple layout

Figure 4.32 Furnace #3 right wall thermocouple layout.

Figure 4.33 Furnace #3 back wall thermocouple layout (Note: flue in center of picture)

4.5.3 Test Unit Setup and Preparation

All of the test units were preheated to raise the internal temperature to above 38°C (100°F) by placing them in a 6 ft x 6 ft x 6 ft environmental chamber. Figure 4.34 shows the preheat chamber with some of the test units loaded. The environment chamber was heated by a torpedo-type kerosene space heater which is controlled by a mechanical bulb thermostat with a control range of 100°F to 200°F. In accord with the stipulations and procedures referenced in the Test Plan for pre-heating, the temperature in the environmental chamber was set at 66°C (150°F) at 09:24 on 06/14/2004 for approximately 23 hours and then set to 43°C (110°F) at 08:19 on 06/15/2004 for the next ~24 hours. The Thermal Data Acquisition System was set up and connected to the preheat chamber when the preheat chamber was loaded and turned on. The data channel F-35 is the exhaust temperature from the preheat chamber while channel F-36 is the skin temperature of one of the test units in the preheat chamber. Channel F-34 is the ambient temperature of the room.

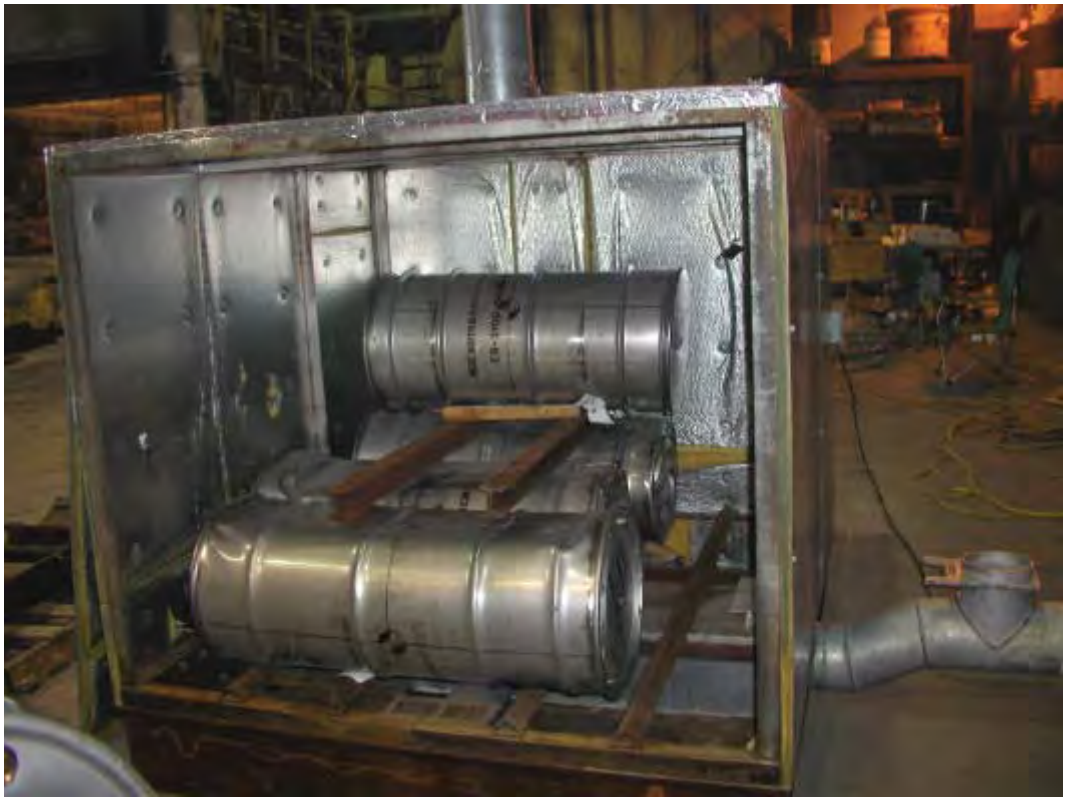

Figure 4.34 Test units in preheat chamber

After preheating and just prior to loading a test unit into the furnace, six .063-inch diameter thermocouples were attached to the exterior surface of each package. Metal retainer clips had previously been tack-welded to the drums to hold the thermocouples in place. The thermocouple tips were inserted underneath the metal clips, and then wrapped around the metal clips. In order to eliminate any radiant viewing factor between the thermocouples and the furnace walls, the tips and metal clips were covered with a ceramic coating. After installation and just prior to insertion of the test unit into the furnace, the functionality of each thermocouple was tested using a propane torch.

Figure 4.35 TU-1 wired with thermocouples, ready for loading

4.5.4 Thermal Testing

The HAC thermal test requires that the package be exposed to an 800°C (1475°F) or greater thermal source for a minimum of 30 minutes. The recovery time between test runs was reduced from 60 minutes to 45 minutes because the furnace demonstrated that it would become thermally stable in that length of time.

Packages were loaded into the furnace using a fork truck with an extended arm that had a cradle used to stabilize the package at the end of the arm (Figure 4.36). The chronological order of the thermal tests was TU-3, TU-4, TU-1, TU-5, and TU-2.

The 30-minute thermal test for each test unit did not begin until the furnace thermocouples recovered to a temperature above 800 °C (1475 °F) and five of the six external thermocouples on the test unit had reached 800 °C (1475 °F). Thermocouple readings were recorded every 15 seconds. The test units required 7 to 13 minutes to reach the test temperature threshold. This meant that each test unit was actually in the furnace environment for a total of 37 to 43 minutes.

Upon completion of the 30-minute test, each test package was removed from the furnace and placed on a stand where it was permitted to cool naturally. All loading and unloading cycles were videotaped and are available on the DVD or VHS tape of the ES-3100 testing. See the data sheets in Appendices H-L for additional details. See Appendices A-E and G for photographs of the thermal testing.

Figure 4.36 Fork truck and modified fork used for test unit insertion and extraction

4.5.5 Thermal Test Data

TU-1 was preheated to above 100 °F for more than 48 hours. After preheating, the test unit was removed from the preheat chamber and the 6 external thermocouples were installed. The unit was oriented horizontally, top to the right, with 0° down. The unit was loaded into the furnace and door closed in 64 seconds. The 30-minute test began 7 minutes after loading. There was some difficulty removing the test unit from the furnace, causing the test unit to be inside the furnace with the door opened for approximately an additional minute. Upon removal, small flames coming from the TID hole at 0° were noted. The unit was placed on a cooling stand. The flames quit after about 22 minutes, turned to smoke and the package smoked lightly for about one hour.

TU-2 was preheated to above 100 °F for more than 48 hours. After preheating, the test unit was removed from the preheat chamber and the 6 external thermocouples were installed. The unit was oriented horizontally, top to the right, with 0° down. The unit was loaded into the furnace and door closed in 61 seconds. The 30-minute test began 10 minutes after loading. Upon removal, smoke was coming from the TID hole at 180°. The unit was placed on a cooling stand. The package smoked lightly for about 40 minutes.

TU-3 was preheated to above 100 °F for approximately 47 hours. After preheating, the test unit was removed from the preheat chamber and the 6 external thermocouples were installed. The unit was oriented horizontally, top to the right, with 0° down. The unit was loaded into the furnace and door closed in 59 seconds. The 30-minute test began 13 minutes after loading. Upon removal, smoke coming from the TID holes was noted. The unit was placed on a cooling stand. The package smoked lightly for about 35 minutes. All six burners were on for this test only.

TU-4 was preheated to above 100 °F for more than 48 hours. After preheating, the test unit was removed from the preheat chamber and the 6 external thermocouples were installed. The unit was oriented horizontally, top to the right, with 0° down. The unit was loaded into the furnace and door closed in 50 seconds. The 30-minute test began 9 minutes after loading. Upon removal, small flames coming from the TID hole at 0° were noted. The unit was placed on a cooling stand. The flames quit in less than a minute. The package smoked lightly for about 12 minutes.

TU-5 was preheated to above 100 °F for more than 48 hours. After preheating, the test unit was removed from the preheat chamber and the 6 external thermocouples were installed. The unit was oriented horizontally, top to the right, with 0° down. The unit was loaded into the furnace and door closed in 64 seconds. The 30-minute test began 10 minutes after loading. Upon removal, no flame, only smoke was noted. The unit was placed on a cooling stand. The package smoked lightly for about 1/2 hour.

Data from all of the thermocouples were recorded at 15-second intervals. There are two graphs for each test unit. On each graph there is a horizontal line indicating the 800 °C (1475 °F) minimum temperature of the HAC test criteria. The first graph for each test unit shows the furnace thermocouples from opening the furnace door to inserting the test unit until after the test

unit was extracted. For the plots of furnace temperatures, the temperature scale has been limited to 1400 °F to 1700°F to increase the visibility of the details of the plot. The time axis of each plot is relative to the opening of the door for loading. The second graph shows the test unit's external thermocouple readings. For the plots of external package temperatures, the scale has been set to 1400 °F to 1700 °F.

To minimize clutter in the legend of the graphs, the thermal recorder channel designations are used. Table 4.6 shows the thermocouple locations and the channel identification for the furnace thermocouples, and Table 4.7 provides this information for the thermocouples of the test units. The graphs are presented in Figure 4.37 through Figure 4.48.

Table 4.6 Mapping of furnace thermocouple location to thermal recorder channel number

FURNACE THERMOCOUPLE LOCATION	CHANNEL IDENTIFICATION
Left wall upper	F-1
Left wall center	F-2
Left wall lower	F-3
Back wall left	F-4
Back wall center	F-5
Back wall right	F-6
Right wall upper	F-7
Right wall center	F-8
Right wall lower	F-9
Floor plate left	F-10
Floor plate center	F-11
Floor plate right	F-12
Stand left	F-13
Stand center (back)	F-14
Stand right	F-15
Door left	F-16
Door center	F-17
Door right	F-18
Preheat Chamber Exhaust	F-35
Package Surface in Preheat Chamber	F-36
Ambient Temperature	F-34

Table 4.7 Mapping of test unit thermocouple location to thermal recorder channel number

	THERMOCOUPLE LOCATION	CHANNEL IDENTIFICATION
TU-1	TU-1 Lid	P-1-1
	TU-1 0°	P-1-2
	TU-1 90°	P-1-3
	TU-1 180°	P-1-4
	TU-1 270°	P-1-5
	TU-1 Bottom	P-1-6
TU-2	TU-2 Lid	P-2-1
	TU-2 0°	P-2-2
	TU-2 90°	P-2-3
	TU-2 180°	P-2-4
	TU-2 270°	P-2-5
	TU-2 Bottom	P-2-6
TU-3	TU-3 Lid	P-3-1
	TU-3 0°	P-3-2
	TU-3 90°	P-3-3
	TU-3 180°	P-3-4
	TU-3 270°	P-3-5
	TU-3 Bottom	P-3-6
TU-4	TU-4 Lid	P-4-1
	TU-4 0°	P-4-2
	TU-4 90°	P-4-3
	TU-4 180°	P-4-4
	TU-4 270°	P-4-5
	TU-4 Bottom	P-4-6
TU-5	TU-5 Lid	P-4-7
	TU-5 0°	P-4-8
	TU-5 90°	P-4-9
	TU-5 180°	P-4-10
	TU-5 270°	P-4-11
	TU-5 Bottom	P-4-12

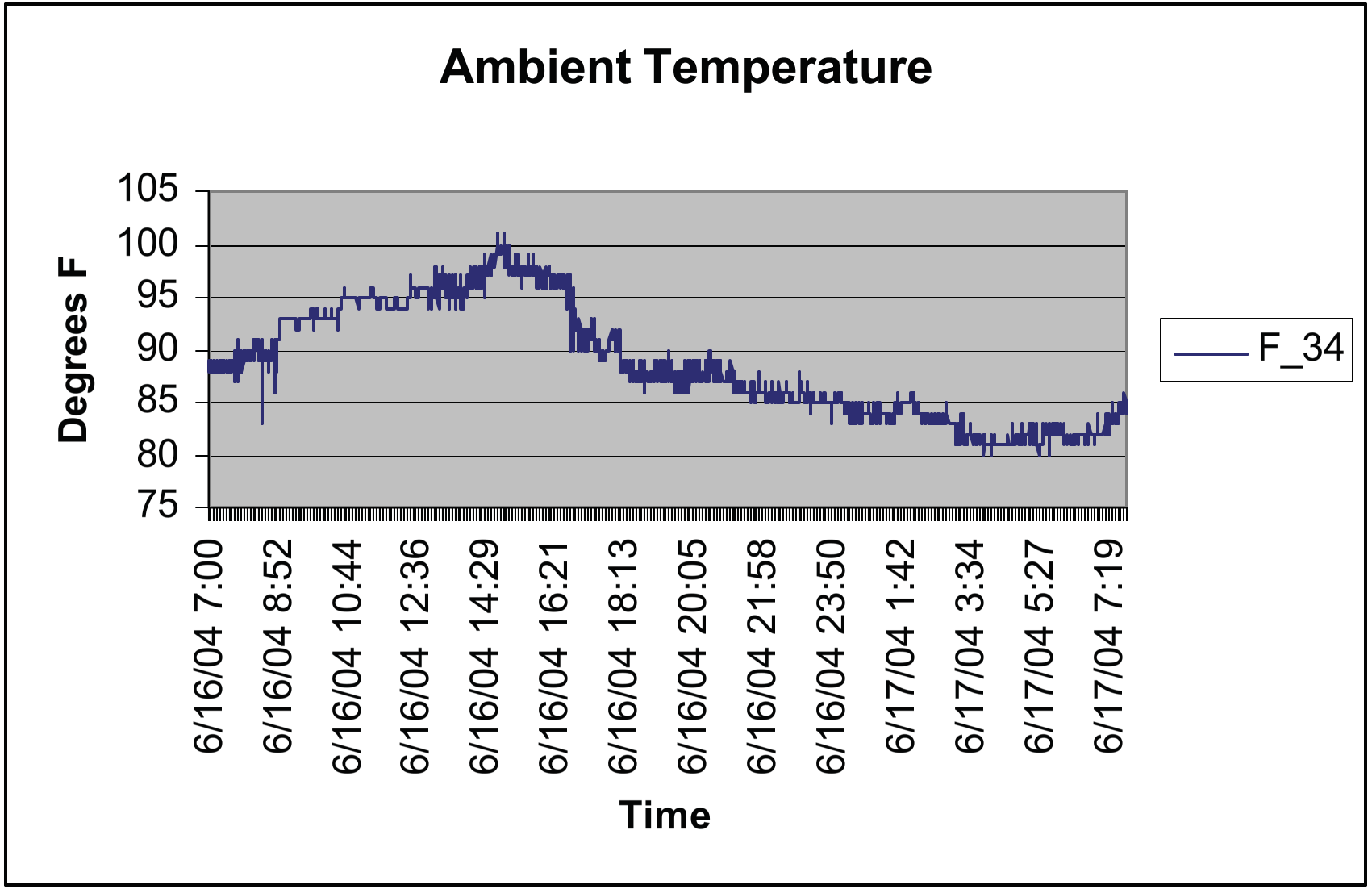

Figure 4.37 Ambient Temperature

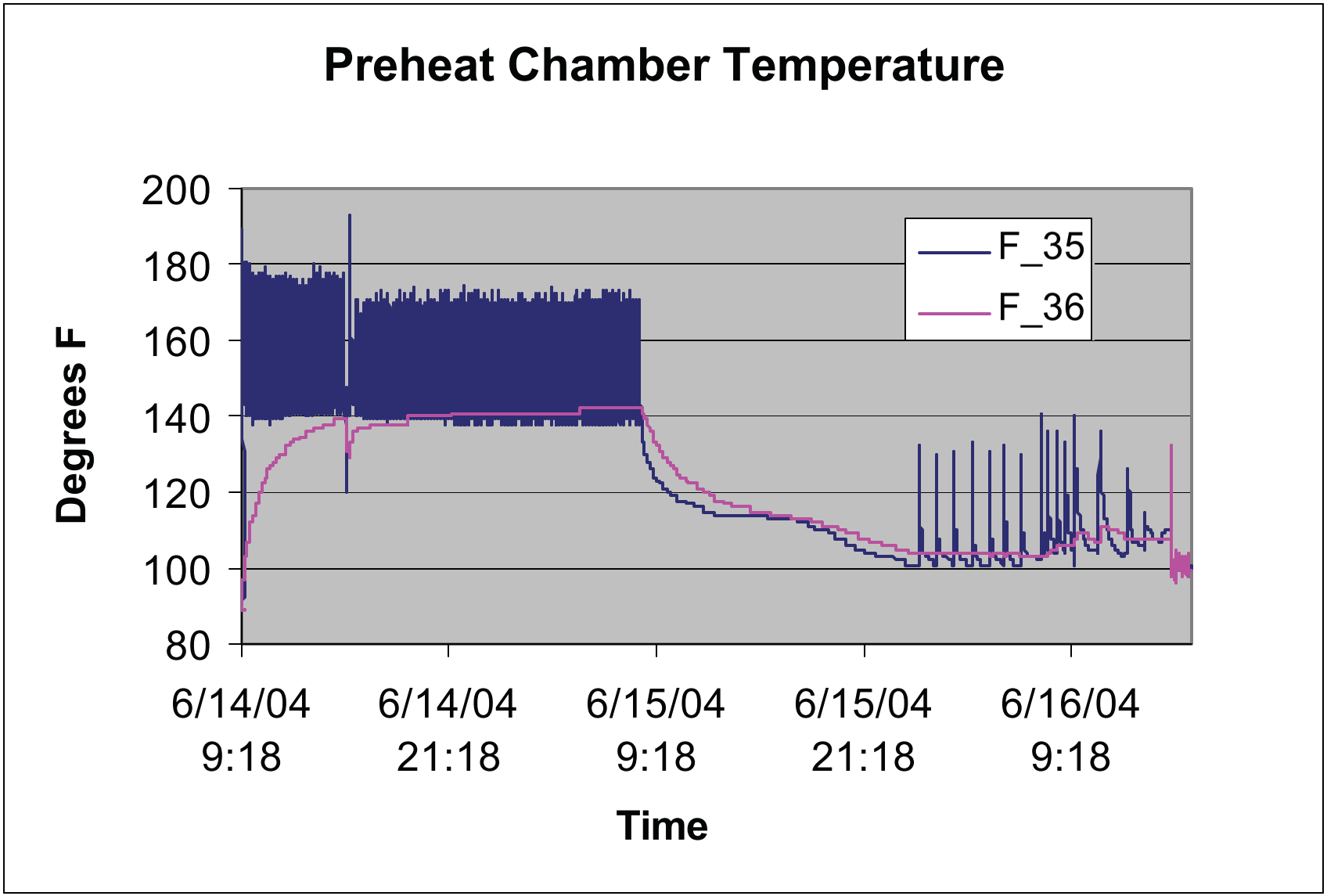

Figure 4.38 Preheat Chamber Temperature

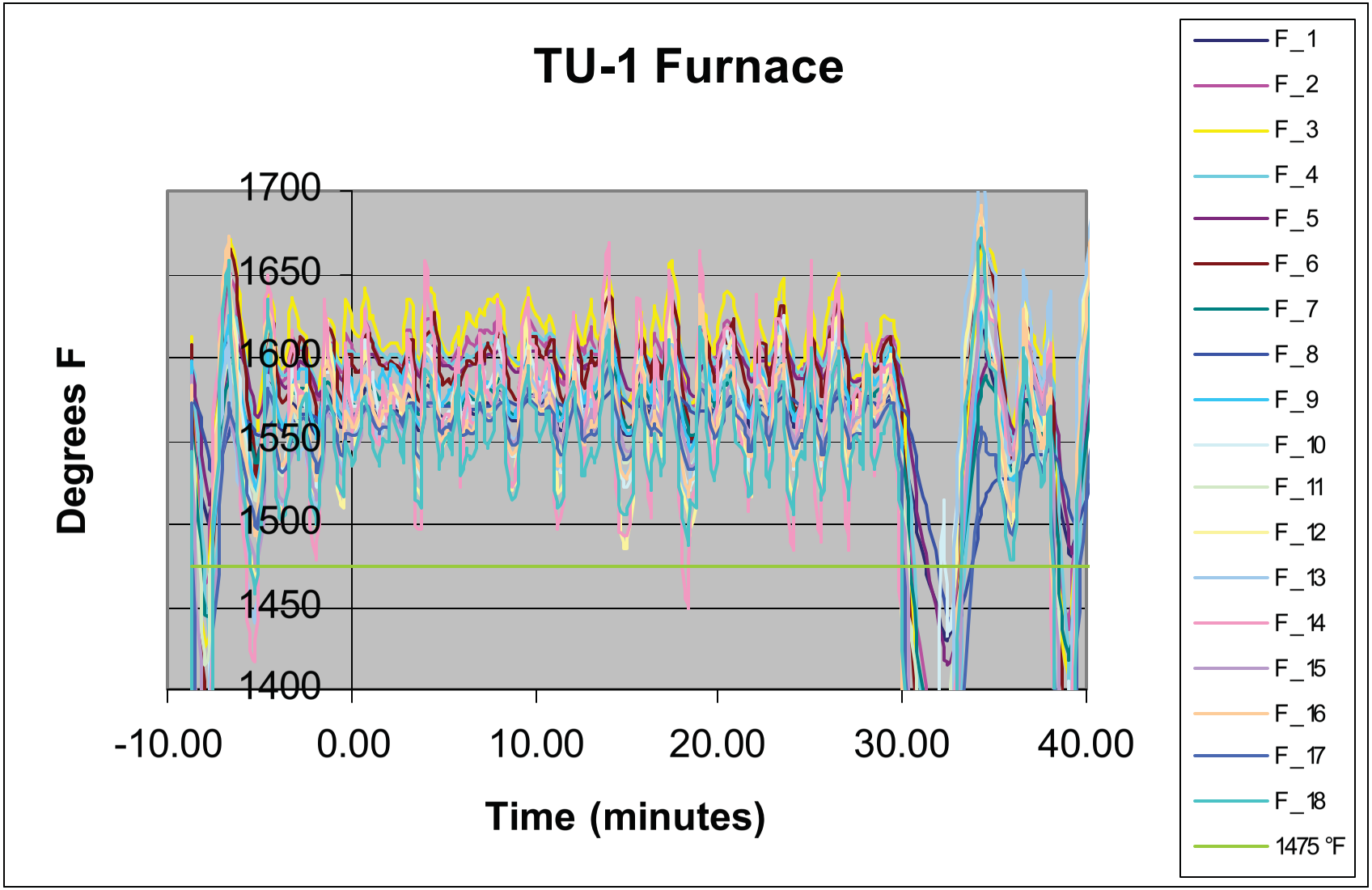

Figure 4.39 TU-1 Thermal test, Furnace thermocouples

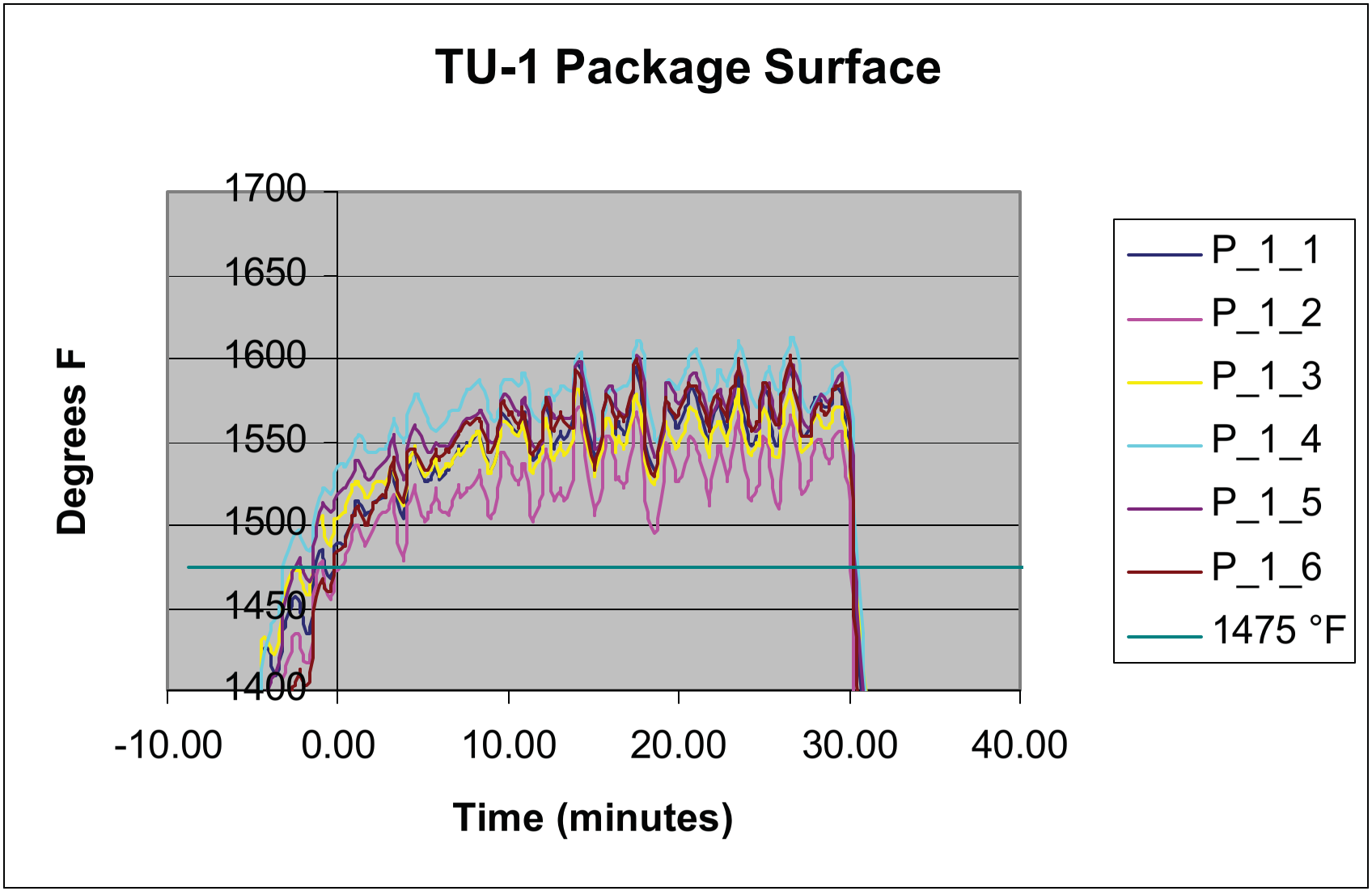

Figure 4.40 TU-1 Thermal test, Package thermocouples

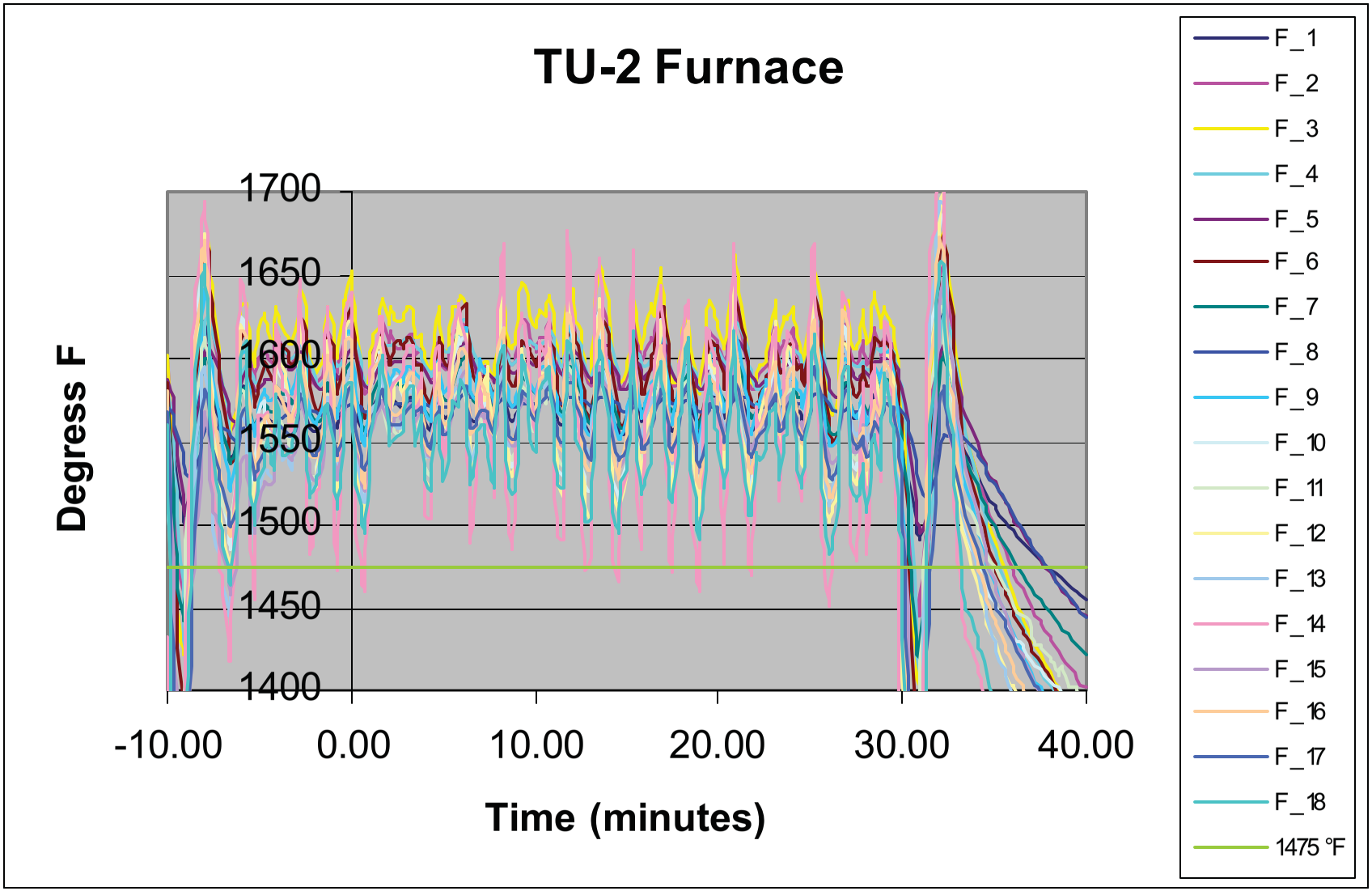

Figure 4.41 TU-2 Thermal test, Furnace thermocouples

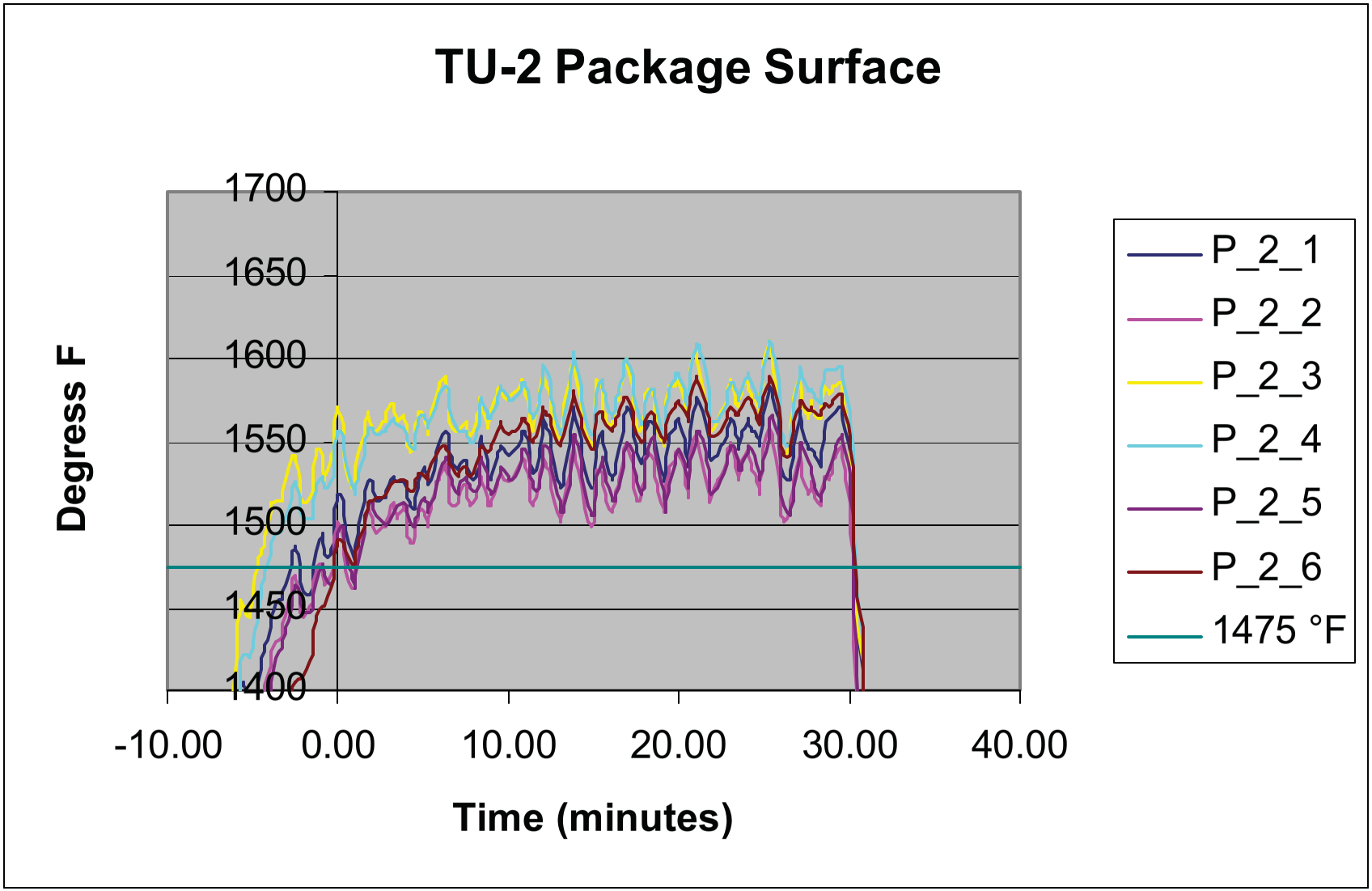

Figure 4.42 TU-2 Thermal test, Package thermocouples

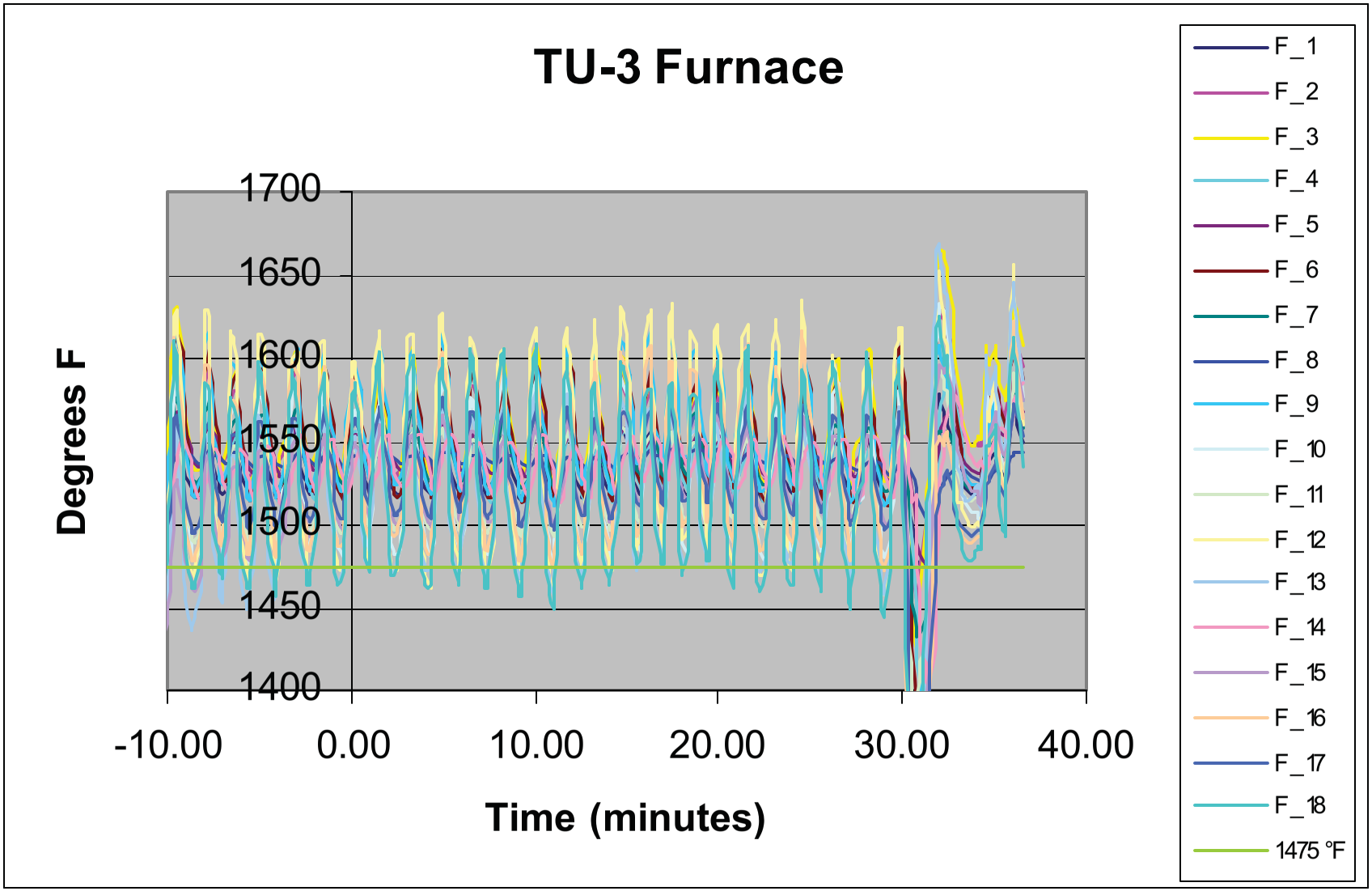

Figure 4.43 TU-3 Thermal test, Furnace thermocouples

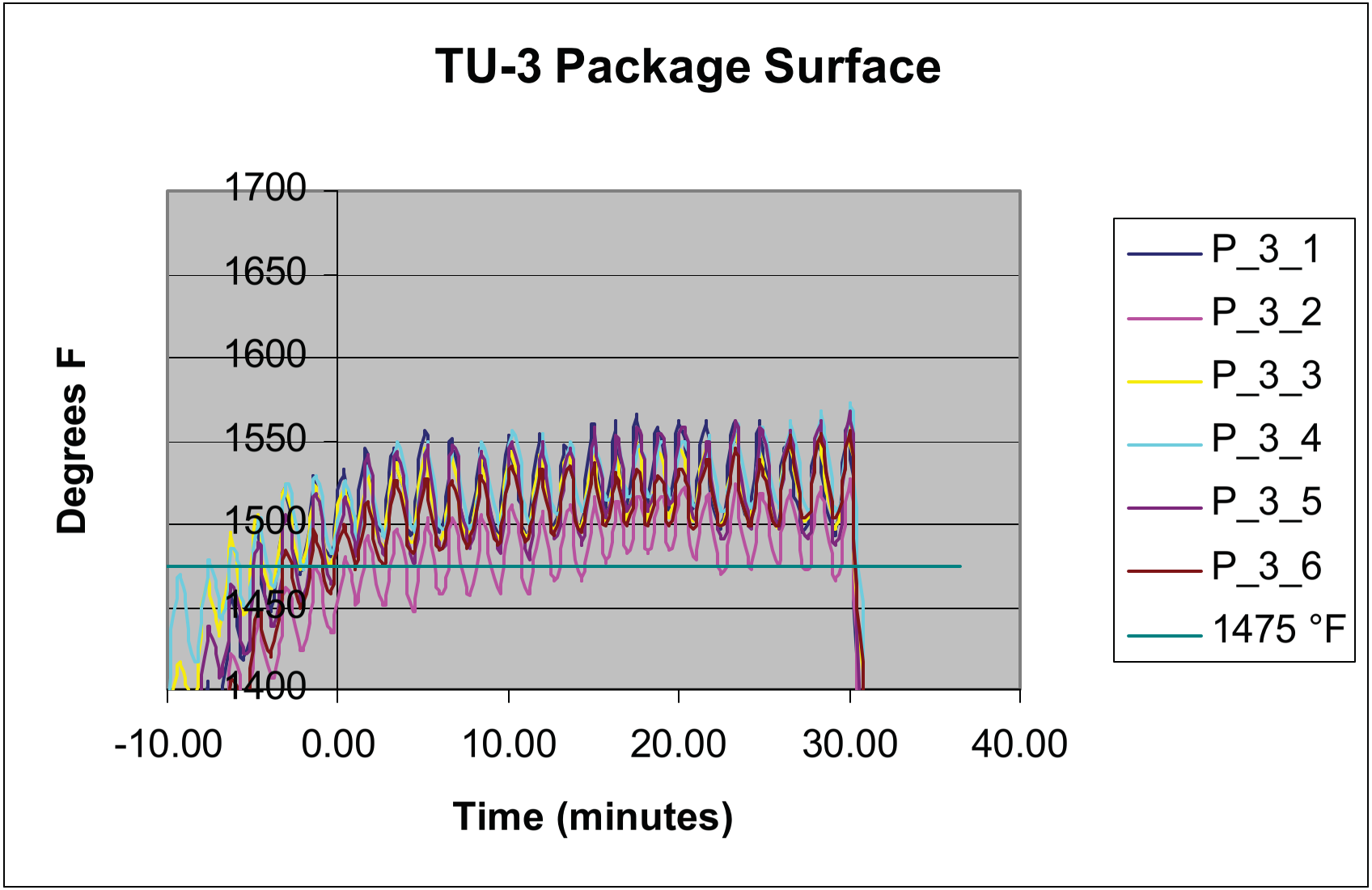

Figure 4.44 TU-3 Thermal test, Package thermocouples

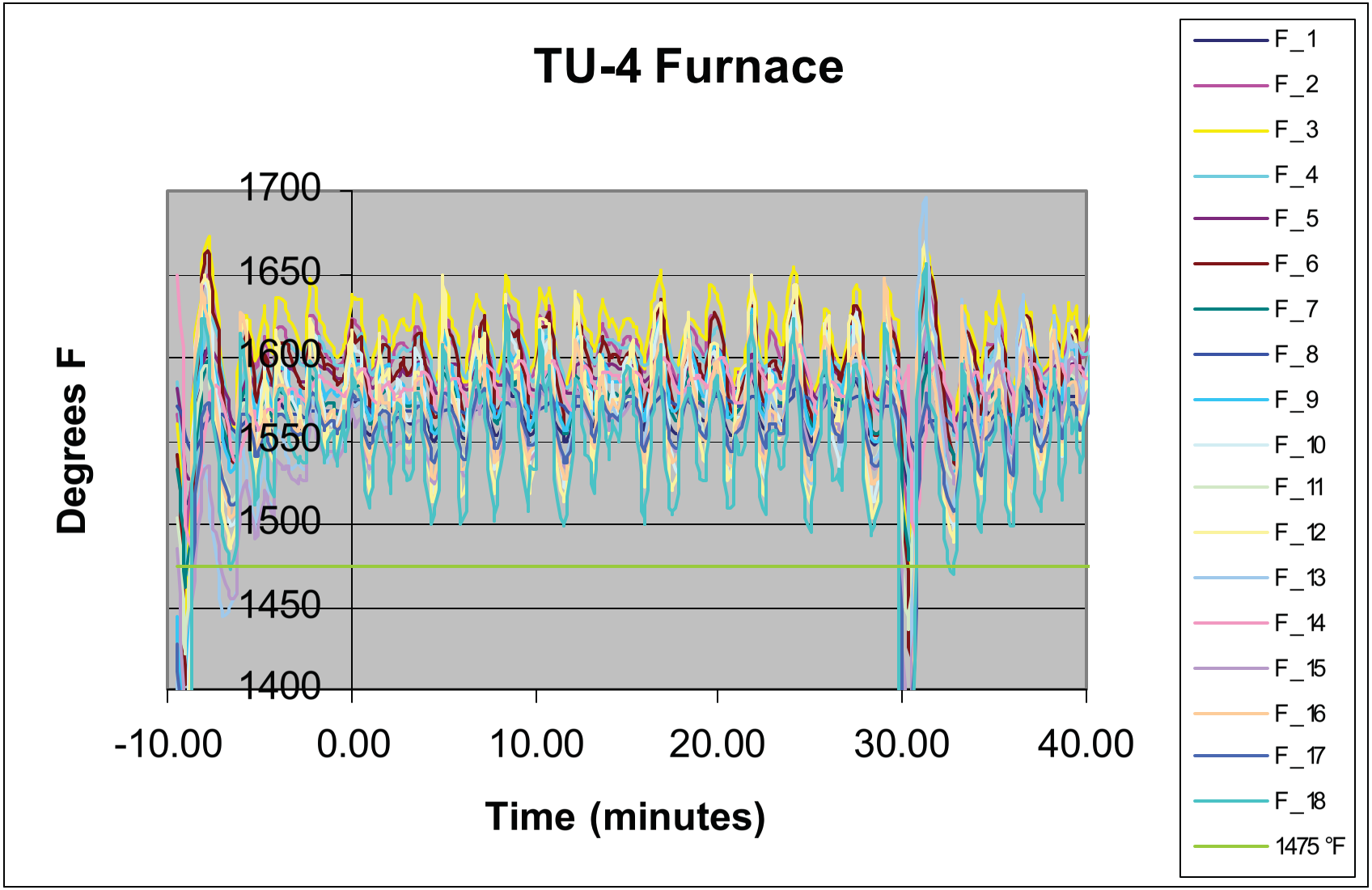

Figure 4.45 TU-4 Thermal test, Furnace thermocouples

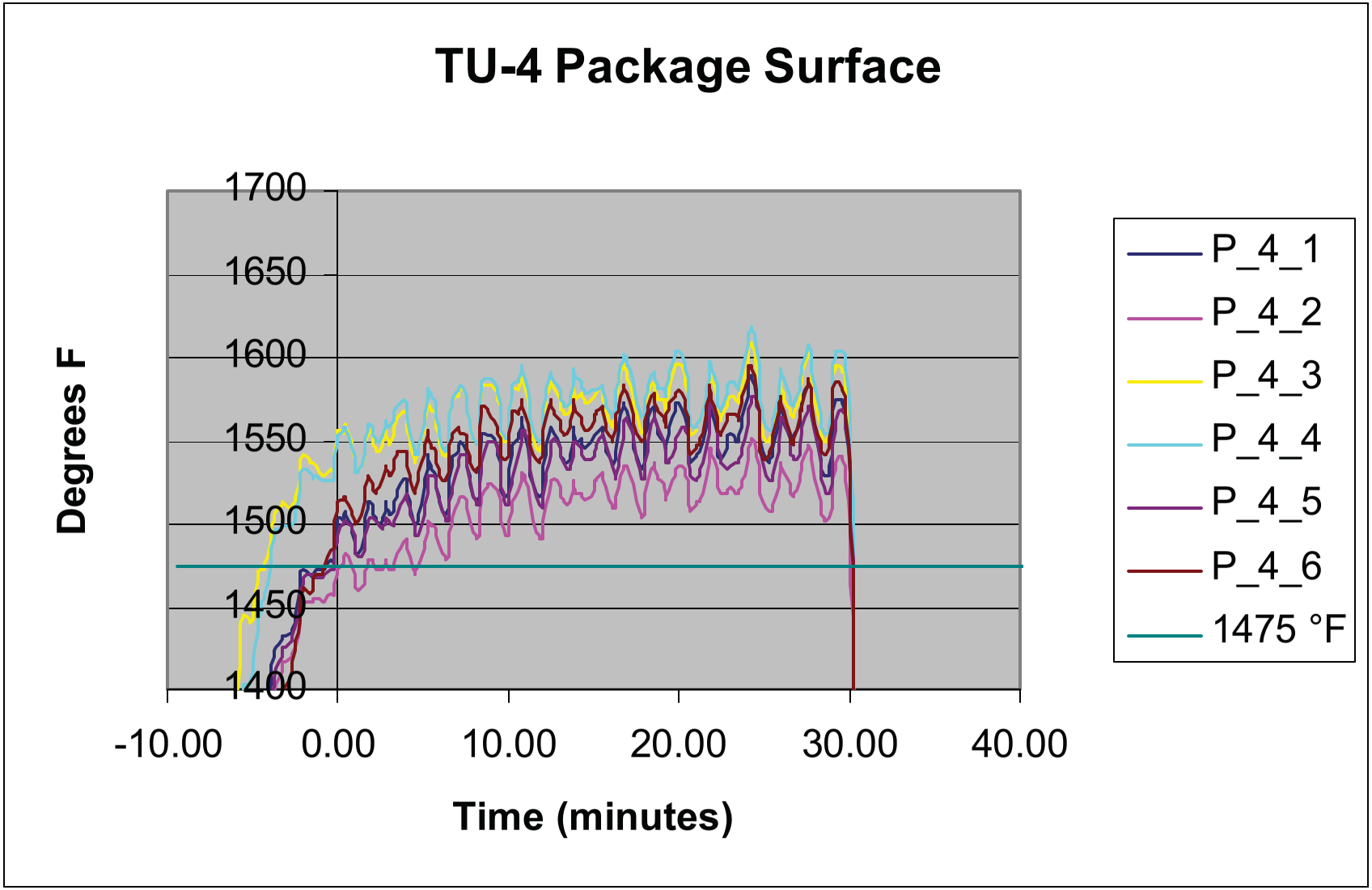

Figure 4.46 TU-4 Thermal test, Package thermocouples

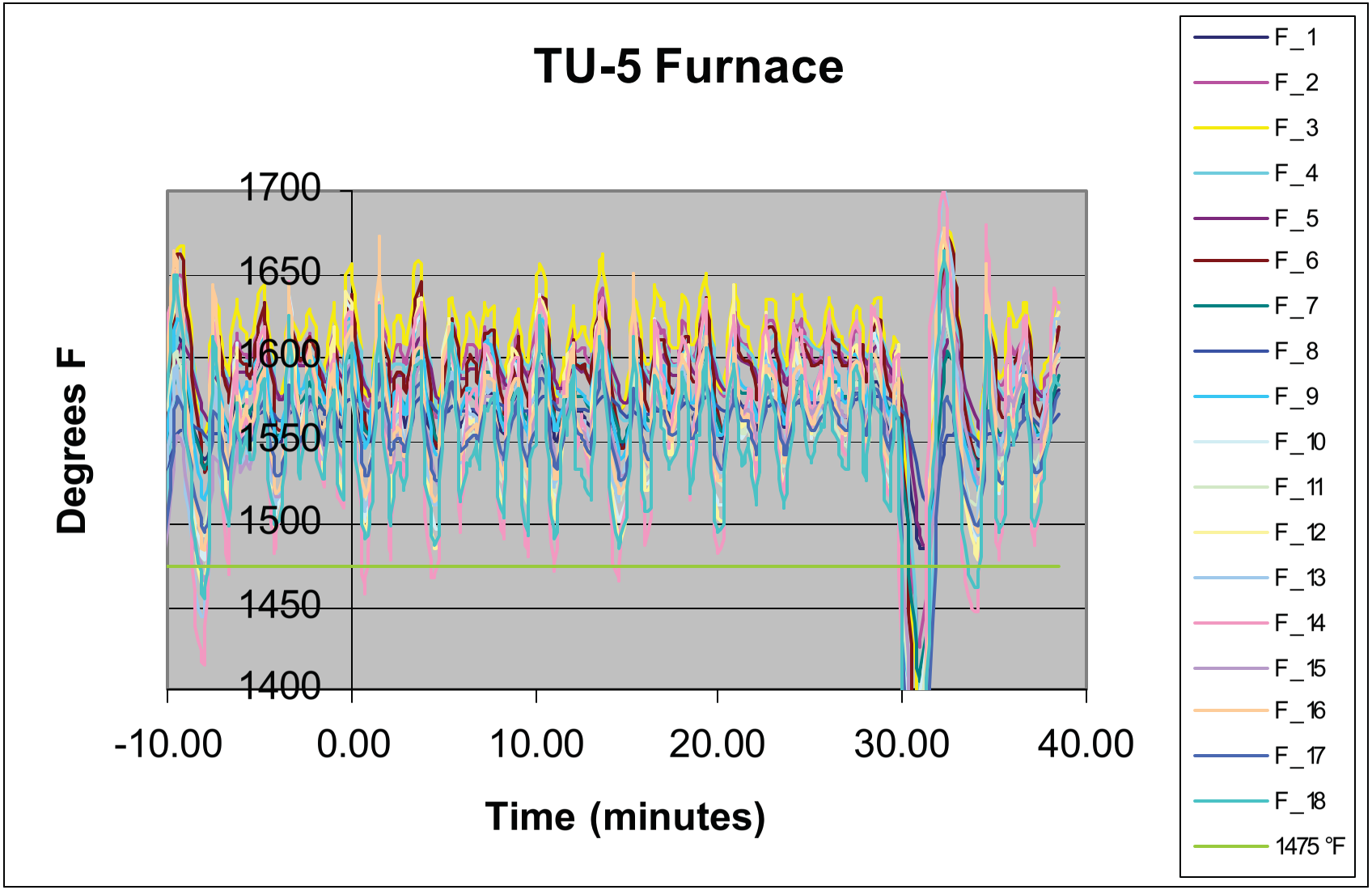

Figure 4.47 TU-5 Thermal test, Furnace thermocouples

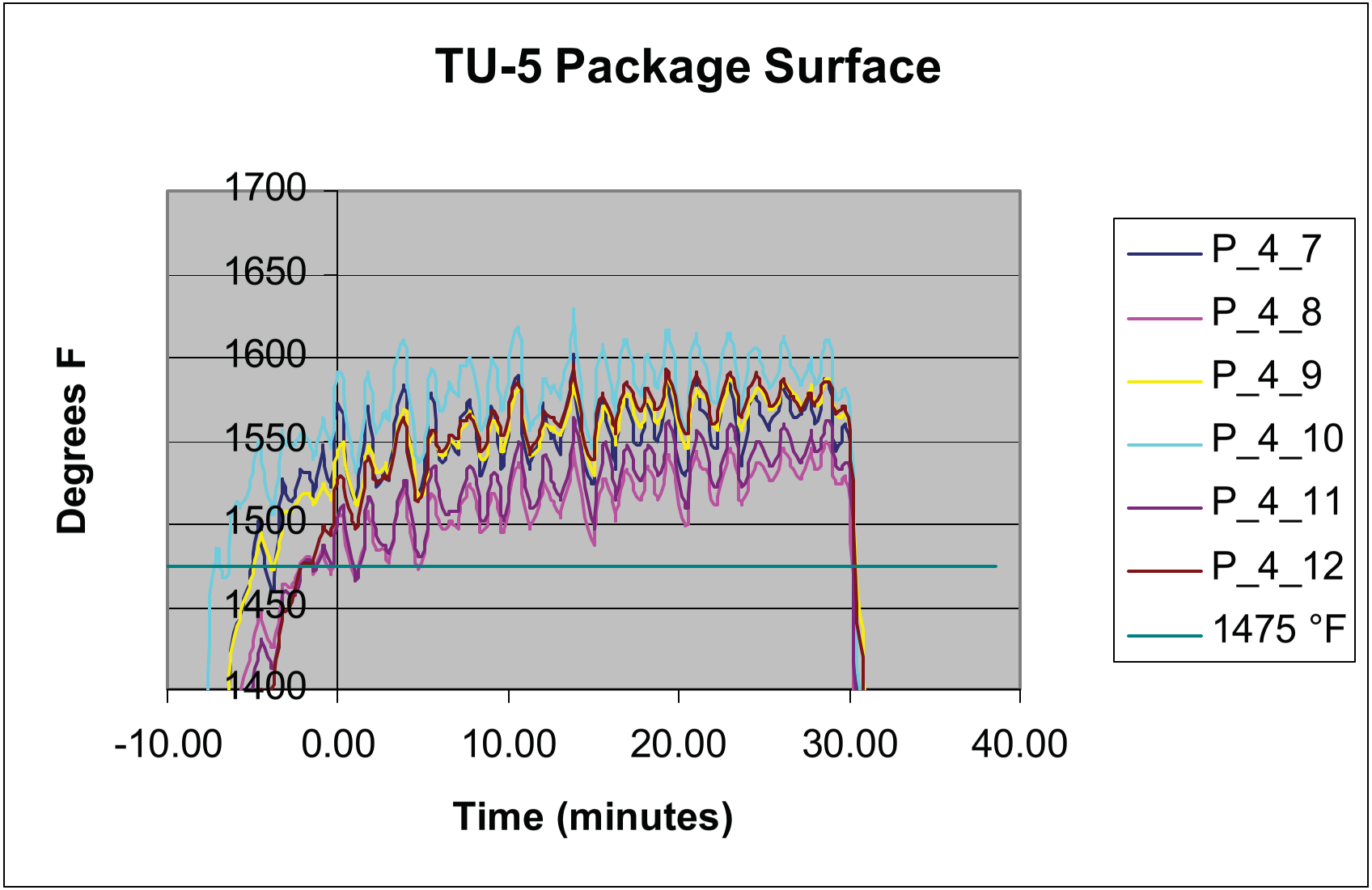

Figure 4.48 TU-5 Thermal test, Package thermocouples

5 POST-HAC DISASSEMBLY AND INSPECTION

After being returned to the NTRC from the thermal test facility, the test units were disassembled and inspected. The post-thermal weights of each test unit, top plug, and containment vessel were recorded on TEST FORM 4. The drums were disassembled and photographic records of the process were taken. Each test unit was visually inspected, and the condition of the package and any observations were recorded on the test forms. Photographs were taken of the disassembly process and any conditions that deserved documenting.

The drum lids, top plugs and CVs from each test unit (TU-1 through TU-5) were removed from the drum. Removal of the lids and top plugs was the most difficult part of the disassembly process. Once the lids and top plugs were removed, all of the CVs were easily removed without the need of any force. Then post-test leak testing and immersion testing was performed on each CV. Next, disassembly of the CVs was performed. This section describes all of the disassembly processes. Subsequently, post-test leak testing and immersion testing of these units are discussed in Sections 5.2 and 5.3, respectively.

5.1 Drum Disassembly Observations

TU-1 had experienced both a 1.2-m drop and a 9-m drop on its 0° side and a crush test along its 180° side. Therefore the package was so pinched that it made the top plug difficult to extract. First, it was necessary to use a crowbar to remove the lid because of the severe pinch on the lid, mainly due to the crush test. Figure 4.7 shows how the lid had crinkled and folded after the tests, and the flattening along the 0° and 180° sides gave warning that the disassembly process would be difficult. The lid came off easily enough once a crowbar was applied to it, but the top plug resisted removal. In order to facilitate disassembly, the compression tester was employed to squeeze the drum and restore some roundness to it before the top plug could be extracted (Figure 5.1). Even after compressing the drum with up to 29,000 lbs of force, the top plug could not be extracted easily. Further compression on alternate sides and levering with a crowbar finally succeeded in freeing the top plug. The CV then slid out easily from the drum.

Figure 5.2 shows how the silicone cushion that fits between the top plug and inner liner had partially disintegrated, but the cushion at the top of the CV had remained intact. The gray char on the floor at the lip of the drum resulted from the dark gray silicone cushion turning whitish upon charring and depositing a residue. Another effect that was attributed to the charring of the silicone cushion was the presence of a few drops of purplish fluid. (See Figure 5.3) This was also seen in other units where the silicone cushion had burned and is likely a by-product of decomposition.

Figure 5.1 The compression table being used to assist with top plug removal

Figure 5.2 TU-1 with top plug removed

Figure 5.3 TU-1 - Purplish liquid from decomposition of cushion

TU-2 had experienced two horizontal drops onto its 0° side and the 1,100 lb crush plate dropping flat onto its 180° side. Therefore, the test unit was somewhat oblong from being flattened on both sides. The compression tester was used to restore some roundness to it, and the top plug was removed without too much difficulty. Figure 5.4 illustrates that the components of TU-2 were in good condition after being disassembled. The white residue on the side of the top plug indicates that part of the silicone cushion was degraded.

Having experienced a drop on the lid edge, CG over corner and the impact of the crush plate on its opposite corner, the drum of TU-3 could not stand upright because the bottom and top of it had been considerably deformed. The lid of TU-3 had to be pried off with considerable effort, and the top plug was extremely difficult to remove. In fact, it was necessary to cut the top plug with a pneumatic cutting shear and remove the exposed Kaolite so that the top plug shell could be collapsed enough to allow it to be removed from the drum (Figure 5.5). After a section of the top of the plug had been removed, the Kaolite was scooped out and the plug was then cut, folded away from the pinch-point of the drum, and removed with a crowbar. The Kaolite was retained in a plastic bag for weighing or material balance. Figure 5.6 shows a view of the top plug after removal. After the top plug was removed, the CV was easily removed.

Figure 5.4 TU-2 disassembly using compression

Figure 5.5 The lid of TU-3 being prepared for cutting

Figure 5.6 Top plug and kaolite from TU-3

TU-4 had experienced both a 4 ft and a 30-ft drop onto its drum head and the crush plate had been dropped on its bottom. Thus, most of the apparent damage was to the lid area. The lid and top plug were removed with crowbars. The uppermost vertical section of the inner liner was protruding upward. Figure 5.7 shows how the uppermost vertical section of the inner liner protrudes upward. Figure 5.8 is a top view of this phenomenon.

Another oddity, which was not seen in any of the other test units, was that the lower containment vessel's silicone cushion expanded around the sides of the CV vessel and worked its way upward. Figure 5.9 shows the silicone cushion wrapped around the body of the CV and another undamaged silicone cushion being displayed for comparison. Because no other test units displayed this phenomenon, it is believed to have occurred during the vibration test.

TU-5 was in relatively good shape after the tests and was easily disassembled. Most of the silicone cushion underneath the top plug withstood the thermal test. So not much char was present but the silicone itself was gooey and sticky. Figure 5.10 gives an indication of the degraded state of the silicone cushion.

Figure 5.7 Convex appearance of inner liner of TU-4 drum

Figure 5.8 Top view of inner liner of TU-4

Figure 5.9 Silicone cushion skirting the CV of TU-4

Figure 5.10 Deterioration of TU-5's silicone cushion

5.2 Post-test Leak Tests

After the CVs were removed from TU-1 through TU-5, two different leak tests were performed on each CV:

- an operational leak test of the CV O-rings,
- a full containment boundary leak test with helium

5.2.1 Post-test Operational Leak Test

The O-rings of the CV were leak tested using a CALT5 leak tester. Additional details regarding the CALT5 leak tests can be found in Section 2.4. The sensitivity of the leak check was 5×10^{-5} cc/sec. Using the algorithm referenced in Section 2.4, all of the test units had leak rates less than 1×10^{-4} ref-cc/sec (Table 5.1).

Table 5.1 Post-test leak rate for the test unit CV lids

Drum ID	TU-1	TU-2	TU-3	TU-4	TU-5
Lid Leak Rate, ref-cc/sec	4.1432E-5	3.2361E-5	2.5899E-5	2.4773E-5	2.3829E-5

5.2.2 Post-test Helium Leak Test

The main body of the each CV was leak checked to a sensitivity of 1×10^{-7} cc/sec using the Varian Model 959 helium leak test system and was performed to the TTG Procedure TTG-PRF-02, Rev. 0, dated 1-30-04. Each CV was prepared for the test by drilling a hole in the CV lid and tapping for a ¼-inch NPT tapered pipe thread. A K-flange adapter was screwed into the hole with fast setting epoxy on the threads to seal them. After the epoxy hardened, the mass spectrometer helium leak tester was connected to the adapter. The vacuum pump was then engaged and the volume of the CV was evacuated to < 100 milliTorr. The CV was enclosed in a plastic bag and evacuated with a shop vacuum to reduce the ambient air in the bag. A constant flow of helium gas was introduced into the bag to ensure that the CV would remain bathed in helium during the test. The helium atmosphere was maintained for at least 20 minutes. Figure 5.11 shows one of the test units being subjected to the full containment boundary leak test. Complete data from these tests are given on Appendices H – L. Photos of the various leak tests are shown in Appendices A – E.

Figure 5.11 TU-4 undergoing the containment boundary helium leak test

TU-1 was tested twice. The first test indicated no helium detected at all. It was discovered that the test port plug had not been removed; thus the helium was not against the inner O-ring. The plug was removed and the CV evacuated and leak tested again. The second test indicated no leaks, just typical diffusion through the polymer O-ring. See Figure 5.12 for details of the leak rate curve.

TU-2 remained at 0.0E-9 cc/sec for most of the 20 minute test period but displayed an unusual pulsing. Because of these unusual readings it was re-tested 3 days later. Due to the unusual pulsing of the leak-rate reading the data was taken differently during the second test. The start time, amplitude, and duration of the pulses were recorded rather than the leak-rate readings at regular time intervals. The second test showed pulsing that initiated at roughly 1-minute intervals and had a duration 10 s, 10s, 13, 15, 15, 20, 21.5, 23, 24.3, and 30 seconds respectively. The leak rate pulses ranged from less than 1E-8 to 1.4E-6. The readings between pulses were <1E-9. See Figure 5.13 for details of the leak rate curve. The peak amplitude changed after adding helium in a manner expected for diffusion through the O-rings rather than a rise immediately following the addition of helium that would indicate a leak to the outside of the CV. This indicated that there were no leaks.

TU-3 was leak tested and there were no indicated leaks, just typical diffusion through the polymer O-ring. See Figure 5.14 for details of the leak rate curve.

TU-4 was leak tested and there were no indicated leaks, just typical diffusion through the polymer O-ring. See Figure 5.15 for details of the leak rate curve.

TU-5 was tested 4 times because of unusual pulsing of the leak rate reading. During the first test it was discovered that the brass plug had not been removed. The plug was removed and the test restarted. The first test showed a typical diffusion curve with 5 short duration pulses occurring during the test. These pulses occurred between the readings taken every 2 minutes. See Figure 5.16.

TU-5 had three product cans as the surrogate payload. As the CV was evacuated, the lids of the can popped loose allowing the air inside to escape. It was speculated that the lids remained against the sealing surface and allowed the remaining air in the cans to slowly and intermittently leak out thus giving an indicated leak rate on the leak detector. TU-5 was tested a second time with similar results. The pulses in the leak rate reading occurred even when there was no helium being added to the bag. This indicated that the 'leak' was internally from the cans rather than from the containment boundary. The third test was an attempt to test the inner O-ring. The intent was to connect the leak tester to the leak test port and add helium to the inside of the CV through the hole drilled for the first leak test. This attempt was aborted because a tight seal between the leak tester adapter and the leak test port could not be made. The fourth test, setup as in the normal manner, was allowed to pump down over the weekend. This test showed a typical diffusion curve with only three unusual pulses. The peak amplitude changed after adding helium in a manner expected for diffusion through the O-rings rather than a rise immediately following the addition of helium that would indicate a leak to the outside of the CV. The CV is considered to be leak tight. The fourth test is charted in Figure 5.17.

Although some units had unusual spikes in the leak rate readings, all five test units show leak rate curves typical of diffusion through the O-rings and did not show a typical sustained jump in the leak rate readings. Therefore, all of these test units are considered to be leak-tight.

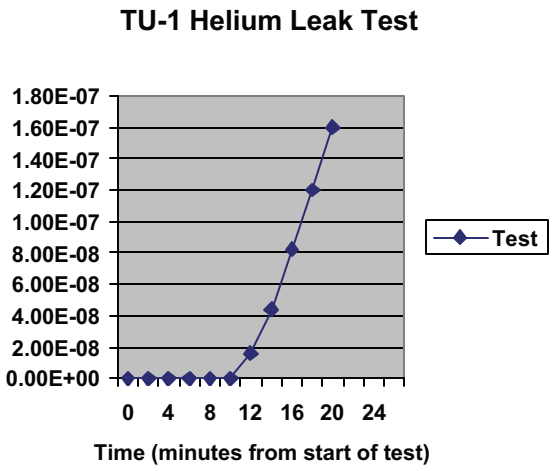

Figure 5.12 TU-1 helium leak (in cc/sec) rate for full boundary leak check

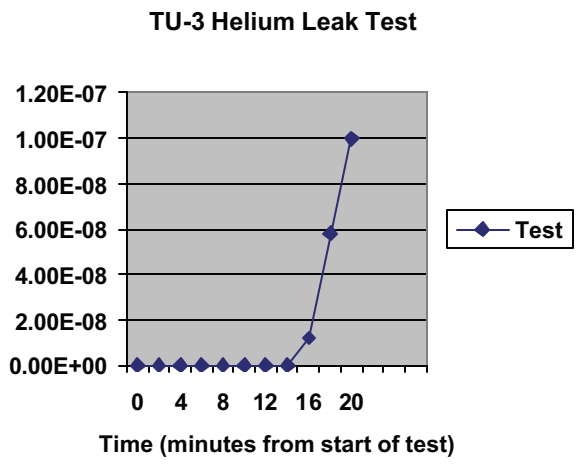

Figure 5.14 TU-3 helium leak rate (in cc/sec) for full boundary leak check

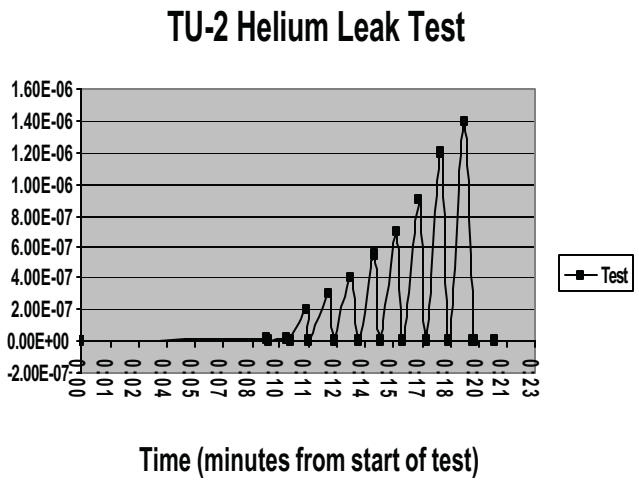

Figure 5.13 TU-2 helium leak rate (in cc/sec) for full boundary leak check

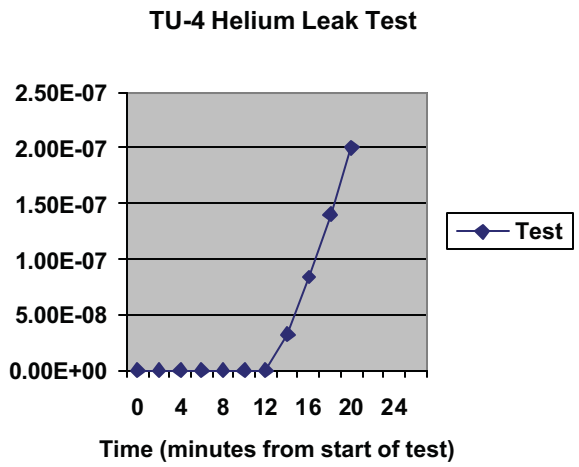

Figure 5.15 TU-4 helium leak rate (in cc/sec) for full boundary leak check

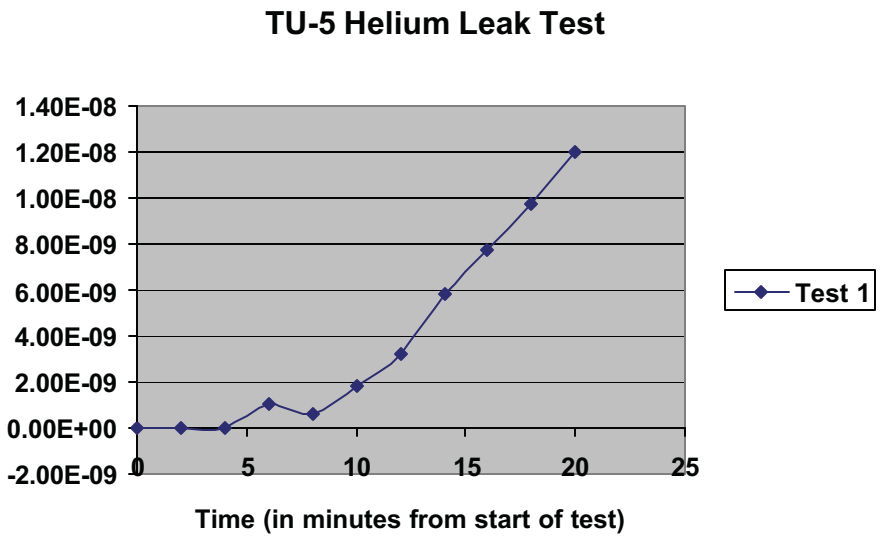

Figure 5.16 Test #1 - TU-5 helium leak rate (in cc/sec) for full boundary leak check

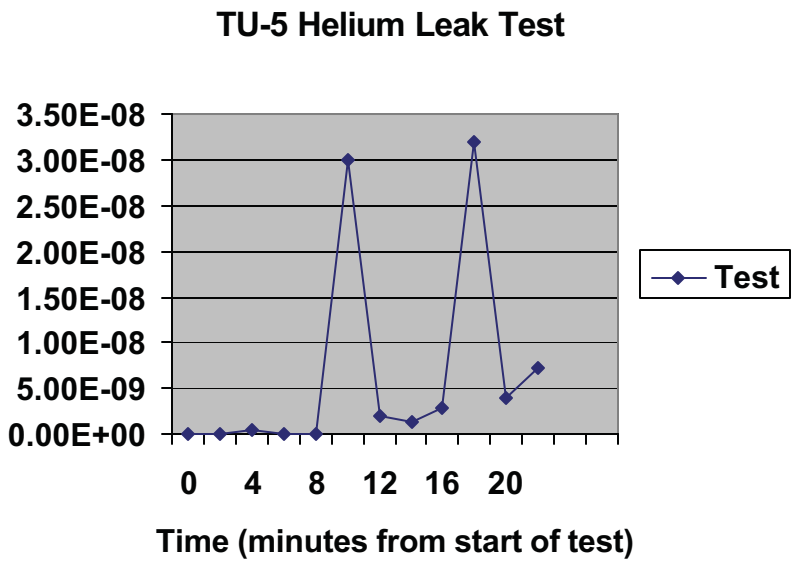

Figure 5.17 Test # 4 - TU-5 helium leak rate (in cc/sec) for full boundary leak check

5.3 0.9-m (3 ft) Immersion Test

After the operational leak tests were performed, the test units were subjected to the required 0.9 m (3 ft) water immersion test. The CVs from TU-1 through TU-5 were immersed under a head of water of at least 0.9 m (3 ft) for over 8 hours. Figure 5.18 shows three of the units undergoing testing and a tape measure being used to assure that the water depth was greater than 0.9 m.

Once the immersion tests had been completed, the CVs were opened to remove the contents, gather available data and look for signs of water in-leakage. No water in-leakage was detected in any of the units.

Figure 5.18 TU-1, -2, and -5 inside immersion tank

5.4 15-m (50 ft) Immersion Test on TU-6

10 CFR 71 requires that a "separate undamaged specimen must be subjected to a water pressure equivalent to immersion under a head of water of at least 15 m (50 ft)." The CV from TU-6 was used as the undamaged specimen. This CV was tested in the Y-12 Immersion Test Tank. The test tank is a vertical axis cylinder about 30 inches in diameter and 6 ft in height with a lid on the top secured by bolts.

Because this test was conducted at the hydro-testing facility in the secure area of Y-12, no photographs could be taken. The tank was filled with water and TU-6 was placed in it so that it sat upright on the bottom of the tank. The lid was then installed onto the tank. The tank was pressurized to 21.7 psig [the equivalent of 15.26 m (50.05 ft.) of water] and held at that pressure for 8 hours. At the end of the test run, TU-6 was removed from the tank and allowed to drip dry. Data forms from this test can be found in Appendix M.

The CV was opened and inspected for water in-leakage and physical damage to the test unit. There was no sign of water in-leakage or physical damage. Some small drops of water were noticed on the outside of the O-rings when the top of the CV was removed. Water on the outside of the O-ring is a normal occurrence.

5.5 CV Disassembly Observations

Once the top plug was removed from the units, the CVs were easily removed from the drums. During the disassembly of the CVs the torque required to remove the lid was measured and recorded. (The nuts of the lid were initially torqued to 115 ± 5 ft-lbs.) Table 5.2 shows the torque required to loosen the CV lid nut. The surrogate payloads of TU-1, TU-2, TU-3, and TU-4 had rust on their surface, which is likely a result of oils and moisture transferred from fingerprints during handling. Often the cable lanyards of the lower two sections of the surrogate load were flattened because the cable had been squeezed between the test weights and the CV wall. The Borobond4 spacers functioned well and withstood the tests with little visible damage, whereas the silicone vibration absorbing pad on the top of each surrogate test weight often showed signs of shredding if not outright disintegration. Because the temperature labels can be blemished by impact or abrasion, some of the labels inside the units were unreadable.

Table 5.2 CV Lid removal torque

	TU-1	**TU-2**	**TU-3**	**TU-4**	**TU-5**	**TU-6**
Torque (ft-lbs)	105	45	60	30	60	100

More specific details of the disassembly of the test units are presented below, and temperatures of the temperature-indicating labels attached to both the inside and outside of the units can be found in Section 5.6.

Inside the CV of TU-1, the spacer cushion on the top surrogate load had partially disintegrated (see Figure 5.19) because of the pounding it experienced, and the temperature labels attached just below the flange were scraped and marred due to movement of the surrogate load. The lifting cables attached to the loads were flattened, and the loads had rust spots that were believed to have been caused by handprints from assembling the CV and the leak check procedure pulling moisture from the Borobond4 spacers. (See Figure 5.20.) The spacer cushions on the lower two surrogate load units survived the testing intact. The protective silicone cushion placed on the CV floor was in very good condition, remaining partially stuck to the bottom of the CV after the surrogate load was removed.

The surrogate payloads of TU-2 were also easily removed from the CV and showed nothing remarkable. The Borobond4 spacers were in excellent condition with the upper one being dented only slightly. The cable lanyards attached to the load showed some damage. Referring to Figure 5.21, the cable attached to the load to the left actually broke, and the cable of the next load showed damage. None of the cables of the other test units broke.

The surrogate payloads of TU-3 displayed more rust than most of the other units. Also, the silicone pads on top of the metallic payloads were beginning to unravel and fray. In Figure 5.22, note particularly how the cushion of the top load (further left in the picture) had stripped. On the other hand, the Borobond4 spacers were in excellent condition. Figure 5.23 is an illustration of how the temperature labels were abraded and marred by the movement of the load inside the CV.

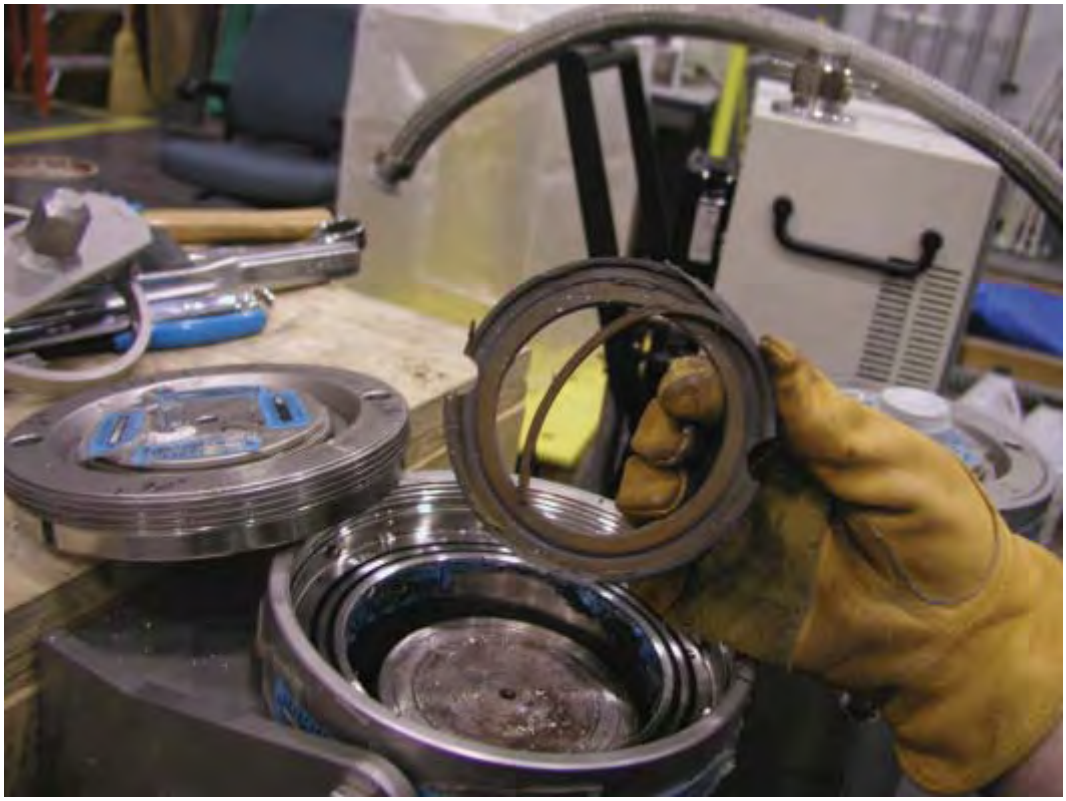

Figure 5.19 Disintegration of spacer cushion of surrogate load

Figure 5.20 TU-1 surrogate load showing rust

Figure 5.21 Broken cable lanyard of TU-2

Figure 5.22 Surrogate payloads of TU-3

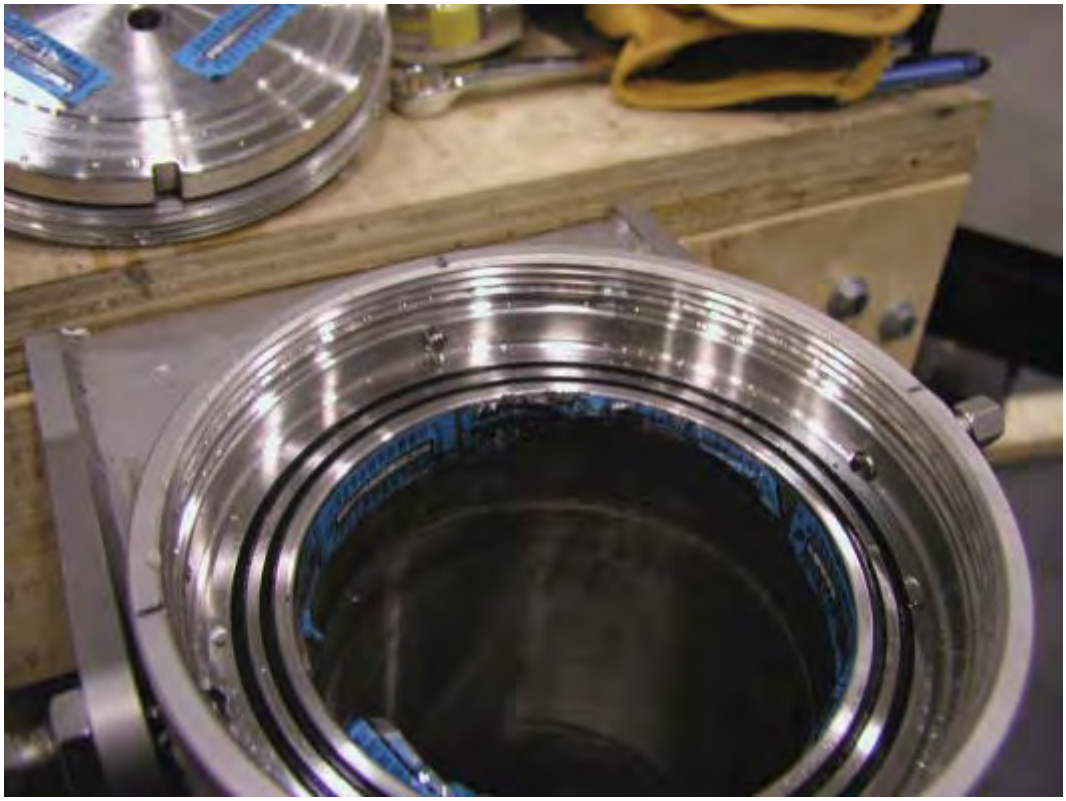

Figure 5.23 Blemishing of temperature labels on flange of CV

TU-4 was disassembled with no difficulties. Some temperature-indicating labels around the flange of TU-4 were blemished by the movement of the surrogate load. In this case, though, the bottom half of the horizontally-placed labels appeared to be more chewed up than blackened. As usual, the silicone pad of the top load showed damage. An oddity that was not seen in any of the other test units was that the lower containment vessel's silicone cushion, which was designed to absorb vibration and shock, expanded around the outside of the CV vessel and worked its way upward. Figure 5.24 shows the silicone cushion wrapped around the body of the CV and another undamaged silicone cushion being displayed for comparison. It is believed that the silicone cushion became "impaled" on the CV during the vibration test, though it may have occurred during either the top-down drop test or top crush test.

TU-5 had lightweight surrogate payloads. The placement of empty cans into the unit to simulate a lightweight load had an unexpected effect. A vacuum was placed on the unit to conduct the post-helium leak test. Later when the vacuum in the CV was being vented, after the initial helium leak check, the lids of the cans were apparently re-sealed and hence collapsed by atmospheric pressure. Figure 5.25 shows how the surrogate payloads were crushed by the pressure of the atmosphere after the cans retained a vacuum. The silicone cushioning was in good condition.

Figure 5.24 Silicone cushion skirting TU-4

Figure 5.25 Crushed surrogate payloads due to vacuum during helium leak test

5.6 Temperature-indicating Label Results

Each test unit had 48 temperature-indicating label locations installed during the assembly of the test unit. Upon disassembly the temperature-indicating labels were read and the highest indicated temperatures recorded. The locations of the temperature labels are shown in Figure 5.26 through Figure 5.31. When applying the temperature labels to the CV lids the B range labels (171°F-261°F) were mistakenly used in place of the 125°F-300°F label specified in the Test Plan.

In general, none of the labels were burned and the temperatures of the CV flanges were less than 300°F. The labels on the top of the CV and on the Borobond4 step of the outer drum of TU-4 were almost completely black. These temperature labels are impact sensitive as well as temperature sensitive. These labels on TU-4 were directly impacted since this unit was subjected to multiple axial impacts. As noted on the data form, the labels on the top of the Borobond4 liner are inconsistent and are likely blacked-out from the impact of the CV rather than temperature. The same is true for the CV top of TU-4 where the CV impacted the top plug. Impact damage is probable because some temperature-indicating spots show part of the spot black while part is still white. Also several labels were lost due to physical damage especially the ones on the inside of the CV flange. The readings of the temperature labels for each test unit are presented in Table 5.3 through Table 5.7.

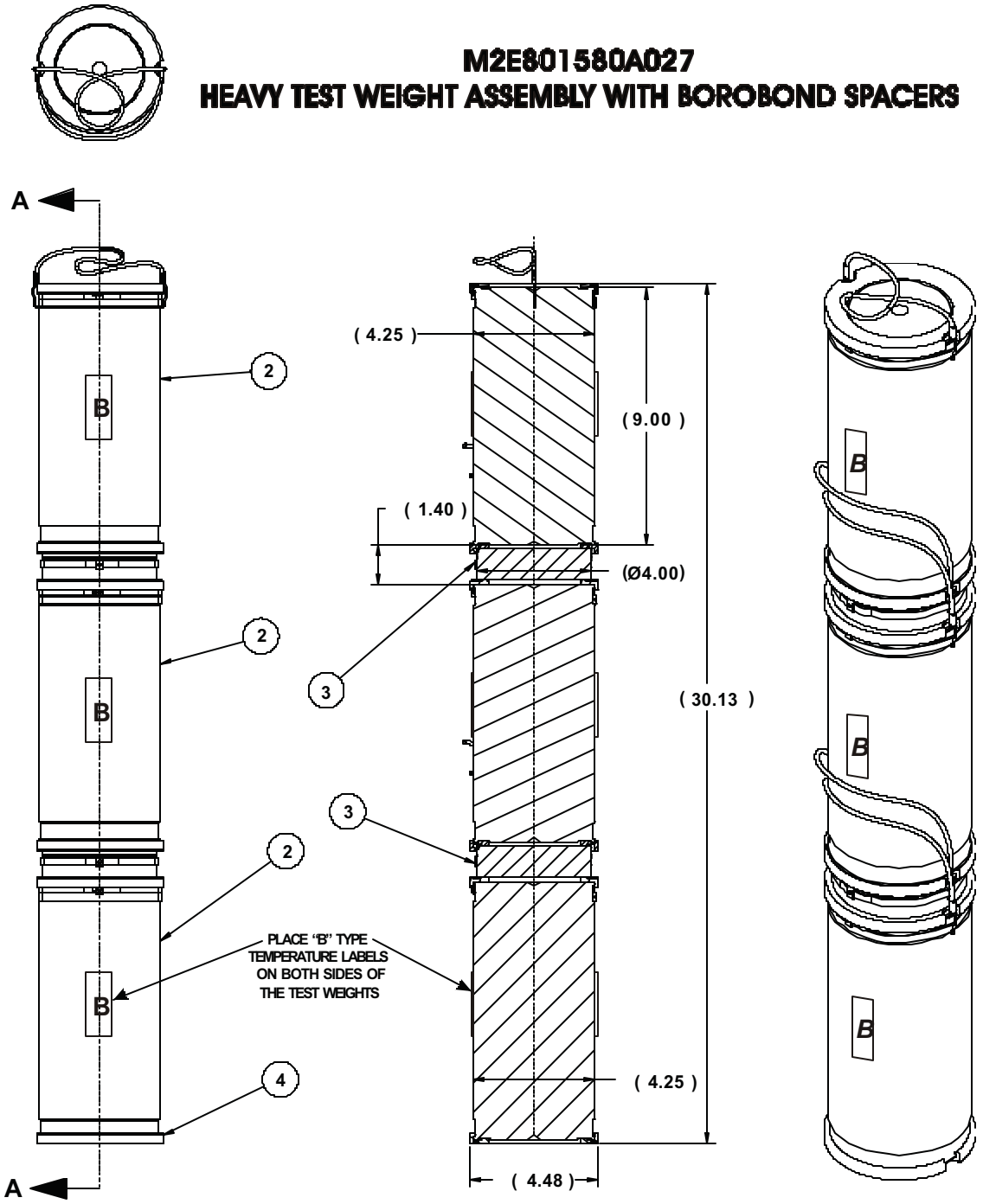

Figure 5.26 Surrogate payload temperature label locations (TU-1, TU-2, TU-3, and TU-4)

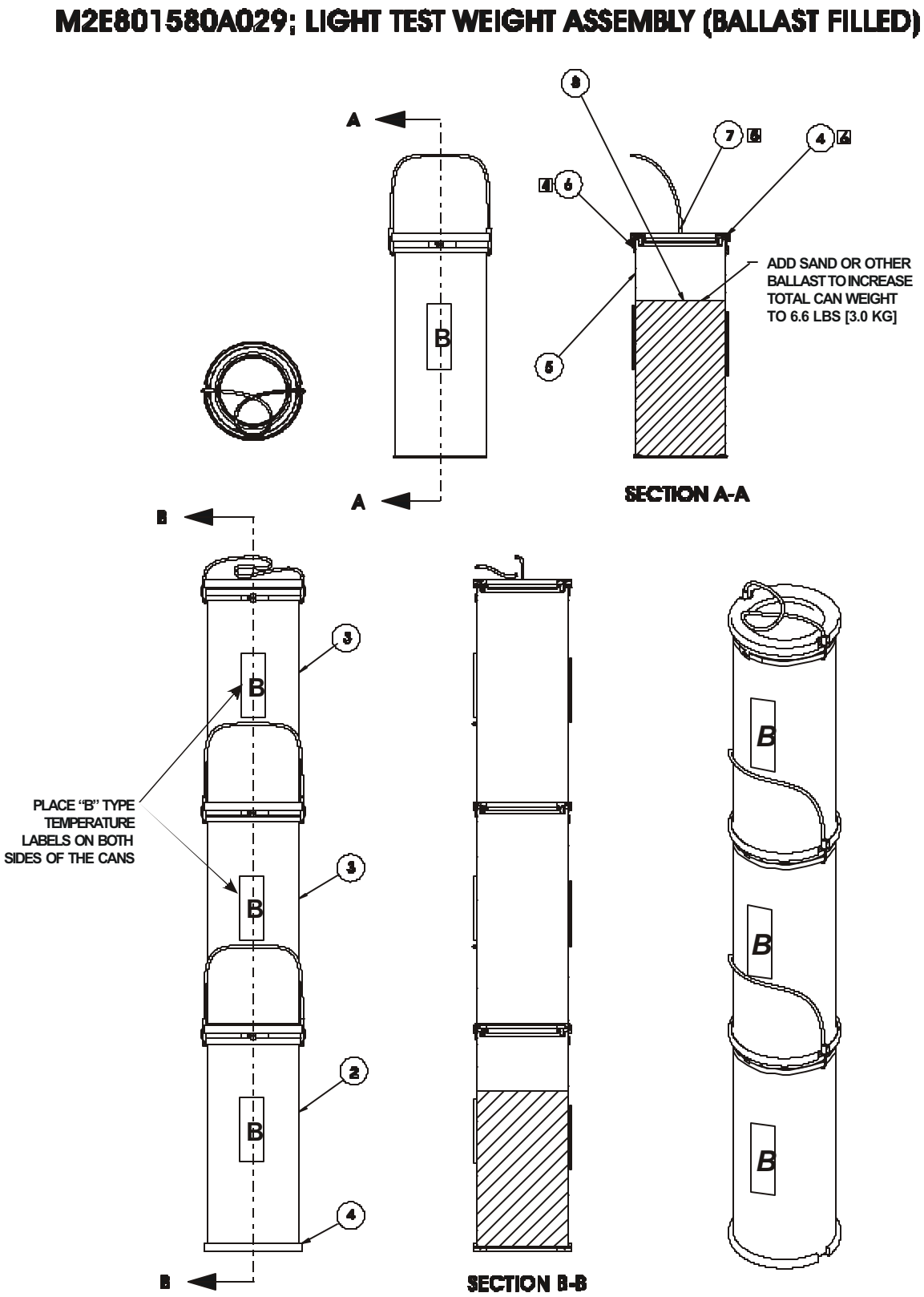

Figure 5.27 Light-weight test assembly temperature-indicating label locations

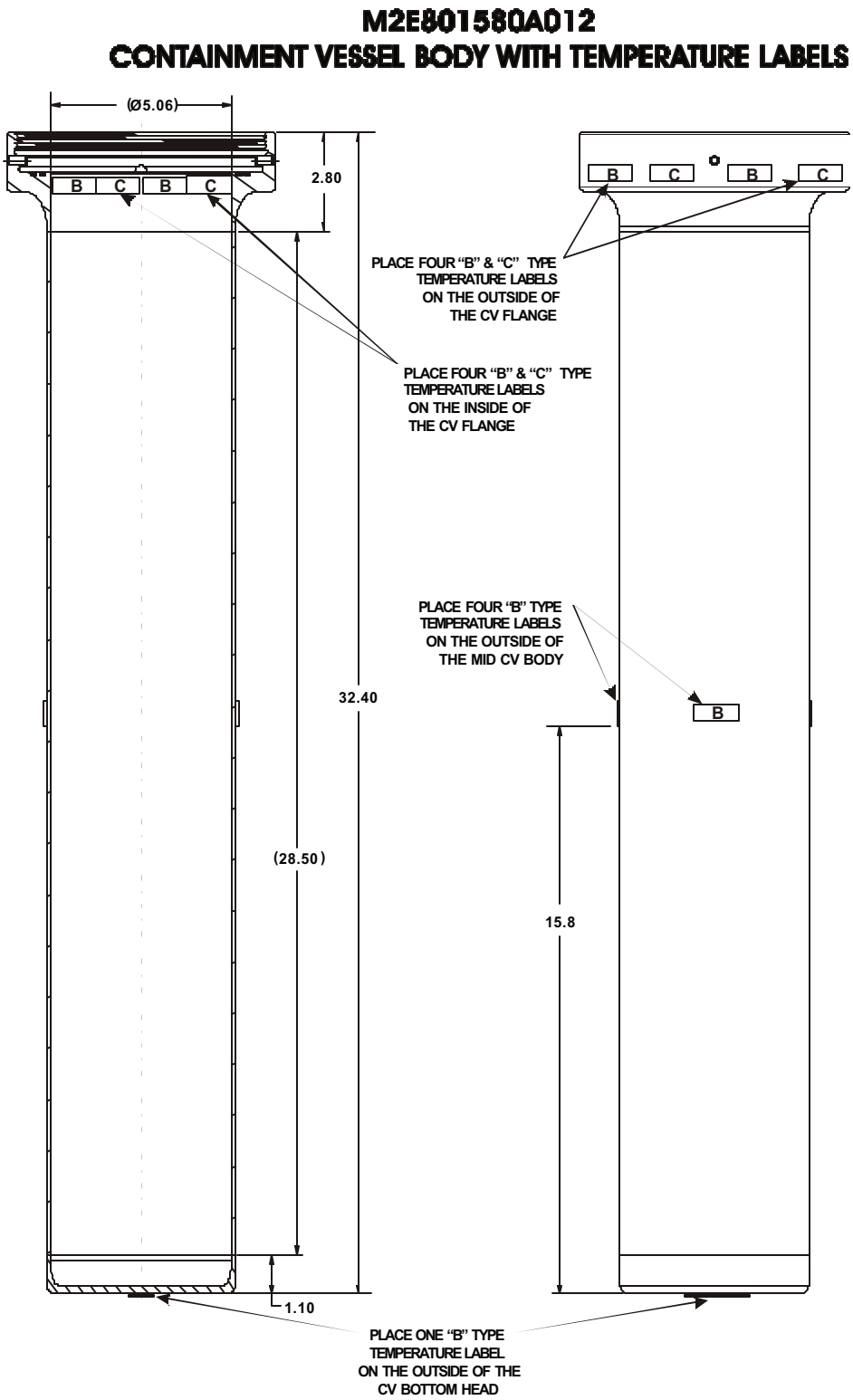

Figure 5.28 CV body temperature-indicating label locations

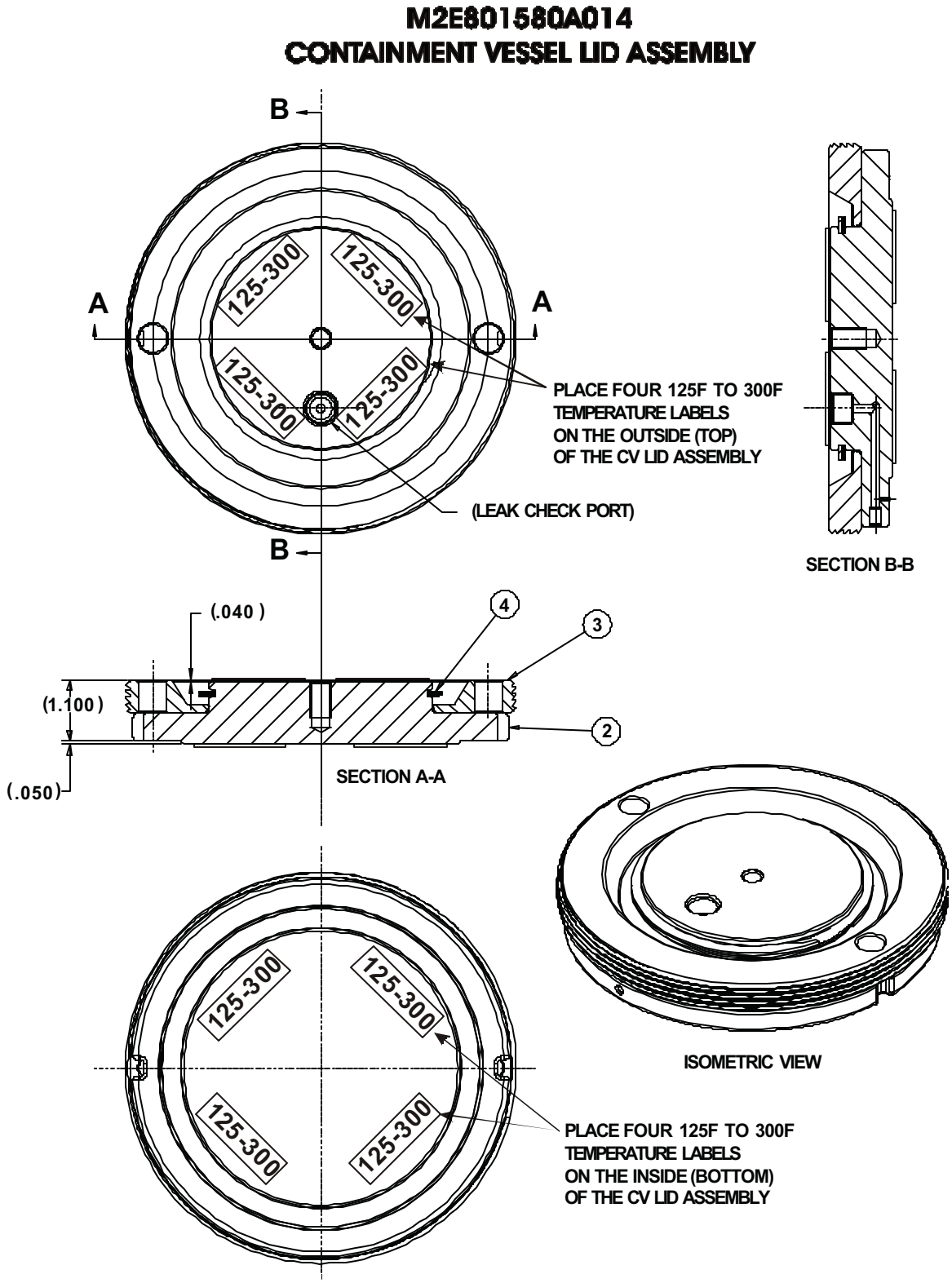

Figure 5.29 CV lid temperature-indicating label locations

(Note: B range labels were mistakenly used on the CV lid instead of the 125-300°F range labels.)

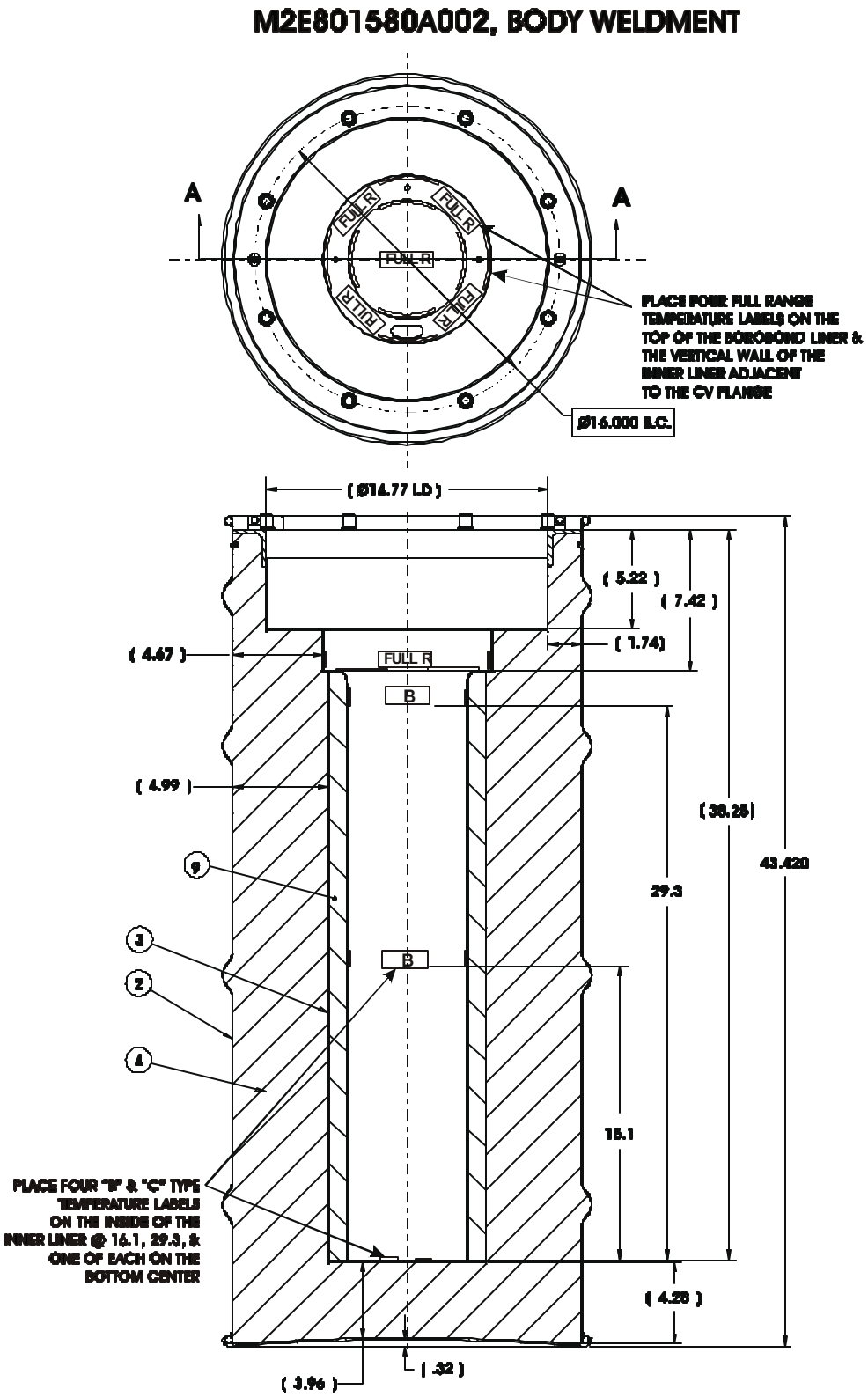

Figure 5.30 Inner liner temperature label indicating locations

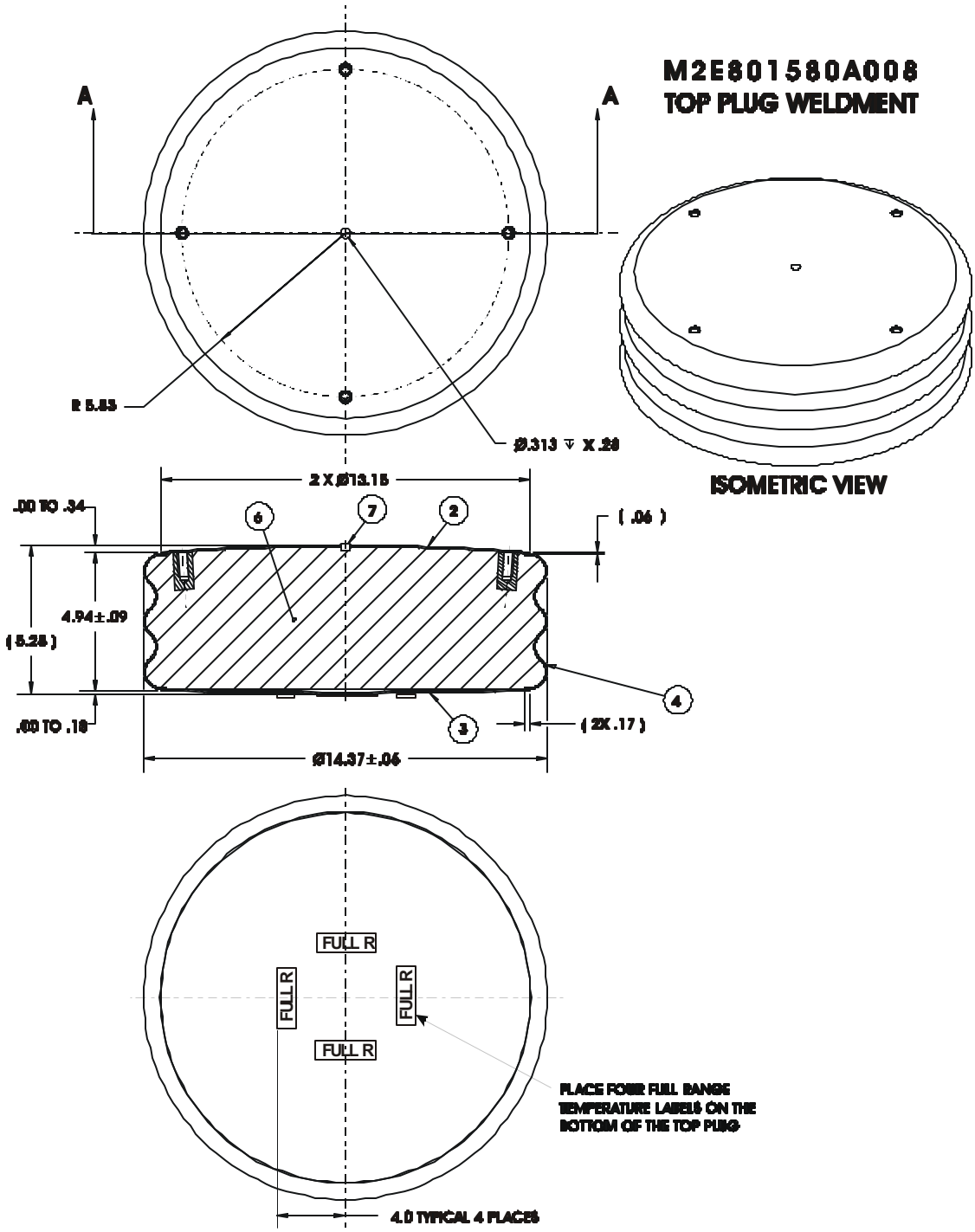

Figure 5.31 Top Plug temperature-indicating label locations

Table 5.3 Temperature-indicating Labels reading for TU-1

TEMPERATURE INDICATOR NUMBER LOCATION CHART												
ON THE SURROGATE PAYLOAD												
Location	**0°**						**180°**					
Side Top	1	B 180	°F				4	B 180	°F			
Side Middle	2	B 171	°F				5	B 171	°F			
Side Bottom	3	B 171	°F				6	B 171	°F			
ON THE CV												
Location	**0°**			**90°**			**180°**			**270°**		
CV Lid Top (outside)	7	B 230	°F	8	B 241	°F	9	B 241	°F	10	B 230	°F
CV Lid Bottom (inside)	11	B 210	°F	12	B 210	°F	13	B 210	°F	14	B 219	°F
Flange (outside)	15	B 230 C ----	°F	16	B 230 C ----	°F	17	B 241 C ----	°F	18	B 230 C ----	°F
Flange (inside)	19	B-Destroyed C- Destroyed	°F	20	B 210 C-Damaged	°F	21	B 210 C ----	°F	22	B 219 C ----	°F
Body Mid Height (outside)	23	B 210	°F	24	B 171	°F	25	B 171	°F	26	B 180	°F
CV Base (outside)	27	B 210	°F	Note: Temp label centered on bottom								
ON THE INNER LINER AND TOP PLUG												
Location	**0°**			**90°**			**180°**			**270°**		
Top Plug Bottom	28	300	°F	29	300	°F	30	300	°F	31	300	°F
Flange Step Wall	32	275	°F	33	200	°F	34	250	°F	35	275	°F
BoroBond4 Step	36	225	°F	37	200	°F	38	225	°F	39	225	°F
CV Body Wall High	40	B 210	°F	41	C ----	°F	42	B 210	°F	43	C ----	°F
CV Body Wall Middle	44	B 210	°F	45	C ----	°F	46	B 190	°F	47	C ----	°F
Liner Bottom	48	B 219	°F	Note: Temp label centered on bottom								

Note: B and C indicate range type of label.
Note: ---- indicates no spots were blacked-out.

Table 5.4 Temperature-indicating Labels reading for TU-2

TEMPERATURE INDICATOR NUMBER LOCATION CHART												
ON THE SURROGATE PAYLOAD												
Location	**0°**						**180°**					
Side Top	1	B 171	°F				4	B 171	°F			
Side Middle	2	B 171	°F				5	B 171	°F			
Side Bottom	3	B 171	°F				6	B 171	°F			
ON THE CV												
Location	**0°**			**90°**			**180°**			**270°**		
CV Lid Top (outside)	7	B 230	°F	8	B 230	°F	9	B 230	°F	10	B 230	°F
CV Lid Bottom (inside)	11	B 190	°F	12	B 219	°F	13	B 210	°F	14	B 219	°F
Flange (outside)	15	B 210 C ----	°F	16	B 230 C ----	°F	17	B 230 C ----	°F	18	B 230 C ----	°F
Flange (inside)	19	B-Destroyed C- Destroyed	°F	20	B 210 C ----	°F	21	B-Destroyed C- Destroyed	°F	22	B-Destroyed C- Destroyed	°F
Body Mid Height (outside)	23	B 180	°F	24	B 180	°F	25	B 190	°F	26	B 180	°F
CV Base (outside)	27	B 210	°F	Note: Temp label centered on bottom								
ON THE INNER LINER AND TOP PLUG												
Location	**0°**			**90°**			**180°**			**270°**		
Top Plug Bottom	28	325	°F	29	325	°F	30	300	°F	31	300	°F
Flange Step Wall	32	Destroyed	°F	33	250	°F	34	325	°F	35	275	°F
BoroBond4 Step	36	225	°F	37	225	°F	38	275	°F	39	225	°F
CV Body Wall High	40	B 210	°F	41	C ----	°F	42	B 210	°F	43	C ----	°F
CV Body Wall Middle	44	B 171	°F	45	C ----	°F	46	B 199	°F	47	C ----	°F
Liner Bottom	48	B 210	°F	Note: Temp label centered on bottom								

Note: B and C indicate range type of label.
Note: ---- indicates no spots were blacked-out.

Table 5.5 Temperature-indicating Labels reading for TU-3

TEMPERATURE INDICATOR NUMBER LOCATION CHART						
ON THE SURROGATE PAYLOAD						
Location	**0°**			**180°**		
Side Top	1	B 171	°F	4	B 171	°F
Side Middle	2	B 171	°F	5	B 171	°F
Side Bottom	3	B 171	°F	6	B 171	°F

ON THE CV												
Location	**0°**			**90°**			**180°**			**270°**		
CV Lid Top (outside)	7	B 230	°F	8	B 230	°F	9	B 241	°F	10	B 241	°F
CV Lid Bottom (inside)	11	B 230	°F	12	B 230	°F	13	B 230	°F	14	B 230	°F
Flange (outside)	15	B 230 C ----	°F	16	B 230 C ----	°F	17	B 230 C ----	°F	18	B 230 C ----	°F
Flange (inside)	19	B 210 C ----	°F	20	B-Destroyed C- Destroyed	°F	21	B 230 C ----	°F	22	B-Destroyed C- Destroyed	°F
Body Mid Height (outside)	23	B 210	°F	24	B 180	°F	25	B 180	°F	26	B 171	°F
CV Base (outside)	27	B 190	°F	Note: Temp label centered on bottom								

ON THE INNER LINER AND TOP PLUG												
Location	**0°**			**90°**			**180°**			**270°**		
Top Plug Bottom	28	275	°F	29	300	°F	30	350	°F	31	300	°F
Flange Step Wall	32	225	°F	33	275	°F	34	275	°F	35	275	°F
BoroBond4 Step	36	200	°F	37	225	°F	38	225	°F	39	225	°F
CV Body Wall High	40	B 210	°F	41	C ----	°F	42	B 210	°F	43	C ----	°F
CV Body Wall Middle	44	B 241	°F	45	C ----	°F	46	B 199	°F	47	C ----	°F
Liner Bottom	48	B 210	°F	Note: Temp label centered on bottom								

Note: B and C indicate range type of label.
Note: ---- indicates no spots were blacked-out.

Table 5.6 Temperature-indicating Labels reading for TU-4

TEMPERATURE INDICATOR NUMBER LOCATION CHART												
ON THE SURROGATE PAYLOAD												
Location	**0°**						**180°**					
Side Top	1	B 171		°F			4	B 171		°F		
Side Middle	2	B 171		°F			5	B 171		°F		
Side Bottom	3	B 171		°F			6	B 171		°F		
ON THE CV												
Location	**0°**			**90°**			**180°**			**270°**		
CV Lid Top (outside)	7	B 261	°F	8	B 261	°F	9	B 261	°F	10	B 261	°F
CV Lid Bottom (inside)	11	B 230	°F	12	B 230	°F	13	B 230	°F	14	B 230	°F
Flange (outside)	15	B 241 C ----	°F	16	B 241 C ----	°F	17	B 241 C ----	°F	18	B 241 C ----	°F
Flange (inside)	19	B 219 C ----	°F	20	B-Destroyed C- Destroyed	°F	21	B-Destroyed C- Destroyed	°F	22	B 219 C ----	°F
Body Mid Height (outside)	23	B 180	°F	24	B 180	°F	25	B 180	°F	26	B 180	°F
CV Base (outside)	27	B 230	°F	Note: Temp label centered on bottom								
ON THE INNER LINER AND TOP PLUG												
Location	**0°**			**90°**			**180°**			**270°**		
Top Plug Bottom	28	350	°F	29	350	°F	30	350	°F	31	350	°F
Flange Step Wall	32	275	°F	33	275	°F	34	275	°F	35	275	°F
BoroBond4 Step	36	350	°F	37	350	°F	38	300	°F	39	350	°F
CV Body Wall High	40	B 210	°F	41	C ----	°F	42	B 210	°F	43	C ----	°F
CV Body Wall Middle	44	B 190	°F	45	C ----	°F	46	B 199	°F	47	C ----	°F
Liner Bottom	48	B 261	°F	Note: Temp label centered on bottom								

Note: B and C indicate range type of label.
Note: ---- indicates no spots were blacked-out.

Table 5.7 Temperature-indicating Labels reading for TU-5

TEMPERATURE INDICATOR NUMBER LOCATION CHART												
ON THE SURROGATE PAYLOAD												
Location	**0°**						**180°**					
Side Top	1	B 210	°F				4	B 210	°F			
Side Middle	2	B 199	°F				5	B 199	°F			
Side Bottom	3	B 190	°F				6	B 190	°F			
ON THE CV												
Location	**0°**			**90°**			**180°**			**270°**		
CV Lid Top (outside)	7	B 250	°F	8	B 261	°F	9	B 261	°F	10	B 250	°F
CV Lid Bottom (inside)	11	B 241	°F	12	B 241	°F	13	B 241	°F	14	B 241	°F
Flange (outside)	15	B 250 C ----	°F	16	B 241 C ----	°F	17	B 250 C ----	°F	18	B 241 C ----	°F
Flange (inside)	19	B 230 C ----	°F	20	B 241 C ----	°F	21	B 241 C ----	°F	22	B 230 C ----	°F
Body Mid Height (outside)	23	B 199	°F	24	B 199	°F	25	B 199	°F	26	B 199	°F
CV Base (outside)	27	B 210	°F	Note: Temp label centered on bottom								
ON THE INNER LINER AND TOP PLUG												
Location	**0°**			**90°**			**180°**			**270°**		
Top Plug Bottom	28	325	°F	29	300	°F	30	325	°F	31	350	°F
Flange Step Wall	32	250	°F	33	250	°F	34	275	°F	35	275	°F
BoroBond4 Step	36	225	°F	37	225	°F	38	250	°F	39	250	°F
CV Body Wall High	40	B 210	°F	41	C ----	°F	42	B 219	°F	43	C ----	°F
CV Body Wall Middle	44	B 210	°F	45	C ----	°F	46	B 210	°F	47	C ----	°F
Liner Bottom	48	B 230	°F	Note: Temp label centered on bottom								

Note: B and C indicate range type of label.
Note: ---- indicates no spots were blacked-out.

Appendix 2.10.8

THE ES-3100 TEST REPORT; VOL. 3, APPENDIX K - TU-4 DATA SHEETS

THIS PAGE INTENTIONALLY LEFT BLANK.

Appendix K – TU-4 Data Sheets

TEST FORM 1 - COMPONENT WEIGHTS

Test Plan ES-3100

Test Unit 4

PRE-DROP TEST WEIGHTS			POST THERMAL TEST WEIGHTS		
PART NAME	**WEIGHT**	**UNITS**	**PART NAME**	**WEIGHT**	**UNITS**
CV (lid assem. & body)	32	*lbs.*			*lbs.*
CV surrogate payload,	110	*lbs.*			*lbs.*
CV assembly	143	*lbs.*	CV assembly	143	*lbs.*
Drum Silicone inserts	1	*lbs.*	Drum Silicone inserts	2	*lbs.*
Drum Top Plug	19	*lbs.*	Drum Top Plug	18	*lbs.*
Drum Body Assy	282	*lbs.*	Drum Body Assy	281	*lbs.*
Test package Assy	445	*lbs.*	Test package Assy	444	*lbs.*

EQUIPMENT

Scale: X-502322 Expiration Date: 10-28-04

Accuracy: ± 1 lb

Comments: Drum plug was weighed twice to verify its lighter weight (2 lbs less than other units)

I certify that the above tasks have been performed and that the observations and comments are correct.

Leonard Dickerson — Testing Technician — 5-19-04 Date — Witness — 5-19-04 Date

*All photographs/movies will be uniquely identified with test unit, date and time to ensure that the proper sequence can be reconstructed

TEST FORM 2 - **ASSEMBLY OF THE CV**

Test Plan ES-3100

Test Unit 4

VERIFIED	TASK
✓	CV test unit serial number: ES-3100 04/04-09
✓	All containment vessel (CV) components have been visually inspected to ensure they are present and in good condition.
✓	Temperature indicators have been affixed to the surface of the CV and on Surrogate payload as indicated on Figure 5.1 through Figure 5.6.
✓	None of the temperature indicators indicate exposure to a temperature in the measured range.
✓	The container and lid have been clearly marked as "TU- 4".
✓	The CV O-rings and sealing surfaces have been inspected for defects and found acceptable.
✓	Clean all surfaces with isopropyl alcohol and air dry.
N/A	The CV O-rings have been lubricated and installed. Use new O-rings.
✓	The surrogate payload # N/A, weighing 110 pounds was aligned and installed in the CV.
✓	The nut ring has been lubricated with Krytox grease per Y-12 Drawing M2E801580A011.
✓	The lid has been installed on the container and the previously applied markings align. This lid has had a torque of 115±5 ft-lb applied. Ambient temperature at closure is 21 °C (72 °F).
	Torque wrench # 2-020040628A2 Calibration Expiration Date 5/14/05
✓	Mark the top of the CV lid with 0°, 90°, 180° and 270° locations with a permanent marker. 0° is on the centerline of the leak test port and the axis of the package
✓	The CV assembly has been weighed and the weight has been recorded on TEST FORM 1.
✓	The CV assembly has been leak tested with the CALT5 per the Manufacturer's Instructions Manual.
✓	Install modified VCO plug (Y-12 will supply) in leak test port and hex plug in lifting ring hole. *
✓	Photographs of the assembly have been taken*.

Comments: * approved the hexplug to be left out

certify that the above tasks have been performed and that the observations and comments are correct.

Testing Technician	Date	Witness	Date
[signature]	5-19-04	Leonard Dickerson	5-19-04

*All photographs/movies will be uniquely identified with test unit, date and time to ensure that the proper sequence can be reconstructed

TEST FORM 3 - ASSEMBLY OF TEST PACKAGE

Test Plan ES-3100

Test Unit 4

VERIFIED	TASK
✓	Verify operational leak test is complete and form completed and modified VCO plug is installed.
✓	The exterior of the drum has been clearly marked "TU-4".
✓	Record the drum serial number: ES-3100 04/04-09
✓	The center-of-gravity markings have been applied to the drum.
✓	Mark the 0°, 90°, 180°, 270° locations on the Drum Lid, Top Plug, and the inner and outside walls of the drum with a permanent marker. The 0° location is the vertical, outside-wall seam of the drum.
✓	The silicone CV Bottom Pad has been installed at the bottom of the inner liner.
✓	The silicone Plug Pad has been installed on the horizontal portion of the top plug step of the inner liner.
✓	The CV assembly has been loaded into the drum with the 0° rotated and aligned with the 0° location on the drum.
✓	The silicone CV Flange Pad has been installed over the CV lid.
✓	The Drum Top Plug was weighed and the weight has been recorded on TEST FORM 1
✓	The Drum Top Plug has been loaded into the drum with the 0° rotated and aligned with the 0° location on the drum.
✓	The Drum Lid has been installed with the 0° mark aligned with the 0° mark on the drum.
✓	The drum lid washers are placed over the lugs and the drum lid nuts were initially installed and a torque of 30 ± 1 ft.-lb applied. The nuts were then tightened a second time with a torque of 30 ± 1 ft-lbs again applied No torque sequence is required to be followed. Torque wrench # 4010282626 Calibration Expiration Date 10-27-04
✓	The test package assembly has been weighed and the weight recorded on TEST FORM
✓	Photographs of the assembly have been taken*.

Comments.

I certify that the above tasks have been performed and that the observations and comments are correct.

Leonard Dickerson	5-19-04	[illegible]	5-19-04
Testing Technician	Date	Witness	Date

*All photographs/movies will be uniquely identified with test unit, date and time to ensure that the proper sequence can be reconstructed

Procedure Checklist

Test Plan: ORNL/~~TTG~~- NTRC-011 ES-3100

Test Unit: TU-4

VERIFIED	TASK
✓	Have a photographer's clapboard with package name and test unit number.
✓	A photograph of the leak tester connections has been taken.
✓	Both CALT5 Leak Tester and CVs have been in the same ambient conditions for 24 hours.
✓	Determine the interstitial volume of the test unit. Print out results.
✓	Determine the length of test from CALT5 Instruction Manual Table according to volume and accuracy needed.
✓	Program the info into the CALT5 tester.
✓	Run the CALT5 leak test. Print out results.
✓	Enter the data from CALT5 printout onto Data Sheet.
✓	Calculate the leak rate and enter on Data Sheet.

Comments:

I certify that the above tasks have been performed and that the observations and comments are correct.

Testing Technician — Date: 5/19/04

Date: 5-19-04

5. Data Sheet

Test Plan: ORNL/NTRC-011 ES-3100

Test Unit: 4

VERIFIED	TASK	
✓	Assembly Leak Test	Post Testing Leak Test
✓		
✓	A leak test in accordance with the CALT5 Manufacturer's Instructions Manual was performed on the CV assembly. Both CALT5 Leak Tester and CVs have been in the same ambient conditions for 24 hours.	
✓	Ambient temperature: 21 °C (__ °F)	

Leak Tester Cert. # M287134 Expiration Date: 3/3/2005

Measuring device TTG Fluke

Attach CALT5 Printout Here

$$Lr = \frac{3.84\ cm3 * 4.96667}{9\ \min}\left(\frac{\frac{1969.06\ mBar}{1013.25\ mBar/atm}}{(21\ °C + 273)°K} - \frac{\frac{1964.89\ mBar}{1013.25\ mBar/atm}}{(21\ °C + 273)°K}\right) ref - cc/\sec$$

$$Lr = \frac{3.84\ cm3 * 4.96667}{9\ \min}\left(\frac{____\ atm}{294\ °K} - \frac{____\ atm}{294\ °K}\right) ref - cc/\sec$$

$$Lr = 2.1191 * 1.39982 \times 10^{-5} = 2.96638 \times 10^{-5}\ ref - cc/\sec$$

Comments:

I certify that the above tasks have been performed and that the observations and comments are correct.

Testing Technician	Date	Checked by	Date
[signature]	5/19/04	[signature]	5-19-04

System Date WED 19 MAY 2004 00:51:29
CALT No: 0052 Transducer No: 835279
Days since last calibration: 8

ORNL
CALT5 - Version U1.43

****MEASURE VOLUME****

Reference Volume: 2 cc
Reference Volume No: ISN026
Test Reference No: TTGPRF01
Design/Serial Nos: ES-3100/TU-4
Number of Readings: 2
Comment: cv lid

Pressure mbar			Volume
Atmos	Start	Final	(cc)
977.74	1915.88	1588.91	3.84
977.96	1981.90	1632.77	3.84

Average Volume: 3.84 cc

Sig: [signature] Date: 5/19/04
(Tested by)

Sig: [signature] Date: 5-19-04
(Supervisor)

System Date WED 19 MAY 2004 00:56:18
CALT No: 0052 Transducer No: 835279
Days since last calibration: 8

ORNL
CALT5 - Version U1.43

Pressure Drop
*** LEAKAGE TEST ***

Test Reference No: TTGPRF01
Design/Serial Nos: ES-3100/TU-4
Comment: cv lid
Interspace Volume: 3.84 cc
Settling Time: 3 mins
Test Duration: 9 mins
Temperature: 21°C
Temperature ratio: 1.014

Sig: _____
(Tested by)

Sig: _____ Date: 5-19-04
(Supervisor)

System Date WED 19 MAY 2004 00:56:18
CALT No: 0052 Transducer No: 835279
Days since last calibration: 8

ORNL
CALT5 - Version U1.43

Pressure Drop
***** LEAKAGE TEST *****

Test Reference No: TTGPRF01
Design/Serial Nos: ES-3100/TU-4
Comment: cv lid
Interspace Volume: 3.84 cc
Settling Time: 3 mins
Test Duration: 9 mins
Temperature: 21°C
Temperature ratio: 1.014
μ ratio: 0.991
Pass Rate (SLR): 1.0E-04 bar cc/sec
Allowable δP : -40 mbar

******* RESULTS *******
Pressure mbar Date/Time

Atmos: 977.85
Start: 1969.06 19 MAY 2004 01:01:46
Final: 1964.89 19 MAY 2004 01:10:45

Leakage Rate: 1.0E-05 bar cc/sec

PASS

Standard conditions:
Temperature: 25°C
Up stream pressure: 1013 mbar
Down stream pressure: 0 mbar

Sig: _____ Date: 5/19/04
(Tested by)

Sig: _____ Date: 5-19-04

5. Procedure Checklist

Test Plan: ES-3100

Test Unit: 4

VERIFIED	TASK
✓	Water Spray apparatus has been assembled (§4.2).
✓	Photographer's clapboard with package name and test unit number recorded (§4.2).
✓	Test Unit placed properly in the water spray zone and spray function verified (§4.3).
✓	Photograph of the test arrangement taken, documenting test unit identification (§4.3).
✓	Place the rain gauge upright on the ground adjacent to the test specimen (§4.4).
✓	Water spray has been started is spraying on the top and 4 sides, with a minimum rate of 2 in/hr (5 cm/hr) (§4.5). 9:10 a.m. — 1 p.m.
✓	Water spray has been stopped after 1 hour, rain gauge reading has been recorded and any damage noted (§4.5).
✓	Photographs of the resulting damage (if any) were taken (§4.5).

Comments Rain gage used to measure flowrate; four readings of 10 to 15 min duration were taken from different sides to give an average 15 in/h (nominally 0.16 in/min)

I certify that the above tasks have been performed and that the observations and comments are correct.

Leonard Dickerson — Testing Technician — 5-20-04 Date

Richard D Weyler — Checked by — 5-20-04 Date

6. Data Sheet

Test Plan: ES-3100

Test Unit: 4

VERIFIED	TASK	
✓	Start Date and Time of Water Spray Test:	5-20-04 9:10 a.m. (§4.5)
✓	End Date and Time of Water Spray Test:	5-20-04 13:00 (§4.6)
✓	Rain Gauge Reading:	15 in/h (§4.6)
✓	Ambient temperature:	°C (69.4 F) Measuring device: Fluke 52 K/J Thermometer

Testing Damage Observations: _____

Comments: after test, unit was lowered to its side and inverted by crane to drain water

I certify that the above tasks have been performed and that the observations and comments are correct.

Leonard Dickerson	5-20-04	Richard D Hugh	5-20-04
Testing Technician	Date	Checked by	Date

5. Procedure Checklist

Test Plan: ES-3100

Test Unit: 4

VERIFIED	TASK
✓	Water Spray Test (TTG-PRF-05) has been completed within 2 hours before Drop Test. (§4.3)
✓	Have a photographer's clapboard with package name and test unit number. (§4.4)
✓	Attitude of the rigged and raised test unit is set. (§4.5)
✓	Photograph of the rigging arrangements has been taken. (§4.5)
✓	Photograph of the measured drop angle has been taken. (§4.5)
✓	The test unit has been raised designated drop height. (§4.6)
✓	Photograph of the height measurement has been taken. (§4.6)
✓	Video camera(s) are setup and running to take video of the drop. (§4.7)
✓	The release mechanism has been plugged into power outlet. (§4.7)
✓	Countdown, Release the test unit, unplug release mechanism. (§4.7)
✓	Videos camera stopped. (§4.8)
✓	Photographs of the resulting damage were taken. (§4.9)
✓	Ambient temperature recorded. (§4.10)
✓	Date and time of test recorded. (§4.10)

Comments:

I certify that the above tasks have been performed and that the observations and comments are correct.

Testing Technician: [signature] Date: 5-20-04

Checked by: Leonard Dickerson Date: 5-20-04

6. Data Sheet

Test Plan: ES-3100

Test Unit: 4

VERIFIED	TASK
✓	Water Spray Test (TTG-PRF-05) Time completed: 13:00. (§4.3)
✓	Intended attitude and angle of the test unit 0. Tolerance ± 2. (§4.2)
✓	Attitude Description: Head down (§4.2)
✓	Measured attitude and angle of the test unit 0.1 degrees. (§4.2)
✓	Level number 311-024-501 Calibration Exp. Date 6-04 (§4.2)
✓	Height above the drop pad 4 ft Measuring device TTG Rod (§4.6)
✓	Date and Time of Drop Test: 14:10 (§4.10)
✓	Ambient temperature: 22.4°C (72.4°F) Measuring device Fluke 52 (§4.10)

Testing Damage Observations:

Comments:

I certify that the above tasks have been performed and that the observations and comments are correct

Testing Technician — Date: 5-20-04 — Checked by: Leonard Dickerson — Date: 5-20-04

TEST FORM 1 – **Post 1.2m (4 ft) FREE FALL DROP TEST**

Test Plan - ES-3100

DAMAGE MEASUREMENTS

Test Unit TU4

Height	0	90	180	270
Pre	43 1/2	43 1/2	43 5/8	43 5/8
Post	43 1/2	43 1/2	43 1/2	43 1/2

DIAMETER	0 to 180		90 to 270	
	Pre	Post	Pre	Post
Top Chime	19 1/4	19 1/4	19 3/8	19 3/8
Top Hoop	19 1/4	19 1/4	19 1/4	19 1/4
CG Hoop	19 1/8	19 1/8	19 1/4	19 1/4
Bottom Hoop	19 1/8	19 1/8	19 1/4	19 1/4
Bottom Chime	19 3/8	19 3/8	19 1/4	19 1/4
CG+Top Hoop	19 1/4	19 1/4	19 1/4	19 1/4

Sketch Drop Setup Here

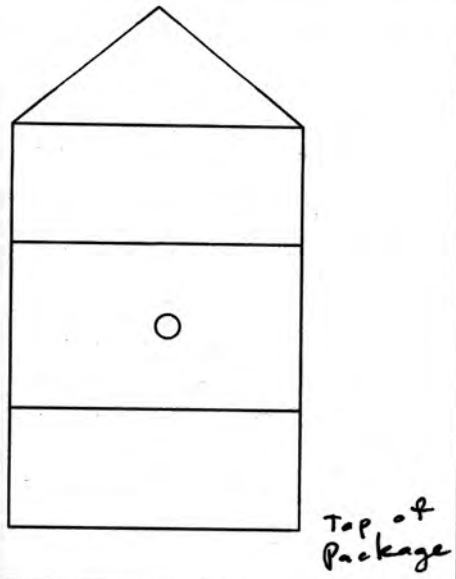

Sketch Package Damage Here

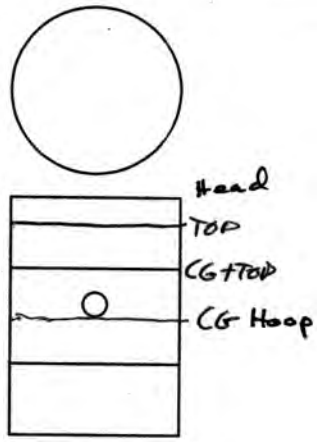

Comments:

I certify that the above tasks have been performed and that the observations and comments are correct.

Testing Technician — Date: 5-28-04

Verified By: Leonard Dickerson — Date: 5-28-04

5. Procedure Checklist

Test Plan: ES-3100

Test Unit: 4

VERIFIED	TASK
✓	Water Spray Test (TIN-03) has been completed within 2 hours before Drop Test. (§4.2)
✓	Have a photographer's clapboard with package name and test unit number. (§4.3)
✓	Penetration Bar Serial Number: NTRC - 001
✓	The package has been placed on the drop pad and blocked to keep from moving during test. (§4.4)
✓	The penetration bar has been suspended above and aligned to the target point on the package. (§4.5)
✓	Photograph of the target alignment has been taken. (§4.5)
✓	The penetration bar has been raised to the specified drop height above the target point. (§4.5)
✓	Photograph of the height measurement has been taken. (§4.5)
✓	Video camera(s) are setup and running to take video of the drop. (§4.6)
✓	The release mechanism has been plugged into power outlet. (§4.6)
✓	Countdown; release the test unit; unplug release mechanism. (§4.6)
✓	The penetration bar has impacted the package at the target point. (§4.6)
✓	Videos camera stopped. (§4.7)
✓	Date and Time of test recorded. (§4.8)
✓	Ambient temperature recorded. (§4.9)
✓	Photographs of the resulting damage were taken. (§4.10)

Comments:

I certify that the above tasks have been performed and that the observations and comments are correct.

Testing Technician	Date	Checked by	Date
[signature]	5-20-04	Leonard Dickerson	5-20-04

6. Data Sheet

Test Plan: ES-3100

Test Unit: 4

VERIFIED	TASK
✓	Water Spray Test (TTG-PRF-05) Time completed: 13:00 (§4.2)
✓	Description of the target point: 7½ from top on 0° line (§4.5)
✓	Height above the package: 1 m Measuring device: 1m Stick (§4.5)
✓	Date and Time of Penetration Test: 13:30 (§4.8)
✓	Ambient temperature: 21.6°C (___°F) Measuring device TTG Fluke (§4.9)

Testing Damage Observations: _____

Comments: _____

I certify that the above tasks have been performed and that the observations and comments are correct.

Testing Technician	Date	Checked by	Date
[signature]	5-20-04	Leonard Dickerson	5-20-04

5. Procedure Checklist

Test Plan: ES-3100

Test Unit: 4

VERIFIED	TASK
✓	Determine load to be applied. (§4)
✓	Water Spray Test (TTG-PRF-05) completed within 2 hours prior to Compression Test. (§4.3)
✓	Excess water from the Water Spray Test permitted to drain from test specimen. (§4.3)
✓	Photographer's clapboard with package name and test unit number prepared. (§4.4)
✓	Package placed in the center of the compression tester base and upper platen lowered onto package top. Alternatively, package placed on sturdy horizontal surface for stacking test, and initial dead weight placed on top. (§4.5)
✓	Photograph of the test specimen test setup taken. (§4.6)
✓	Record height measurement of the package prior to loading. (§4.6)
✓	Photograph of the height measurement taken. (§4.6)
	Program the compression tester to apply the required force and duration per Procedure TTG-PRF-17 and start the test. Alternatively, stack the remaining required dead weight onto the package top, completing the stack. (§4.7)
✓	Compression tester has successfully completed per program. Alternatively, carefully remove the dead weight from the test specimen. (§4.8)
✓	Record final height measurement of the test specimen (post-test). (§4.8)
✓	Photograph of the post test height measurement taken. (§4.8)
✓	Photographs of any other resulting damage taken. (§4.9)

Comments:

I certify that the above tasks have been performed and that the observations and comments are correct.

Robert D Mackey Jr — Testing Technician — 5-21-04 Date

[illegible] — [illegible] — 5/21/04 Date

6. Data Sheet

Test Plan: ES-3100

Test Unit: 4

VERIFIED	TASK
✓	Calculate and record the greater of 5 times the weight of the package OR 1.9 psi times the projected vertical area of the package. (§4) 5 × 450 = 2,250 lbs => 2,300 lbs applied
	1.9 psi × projected vertical area N/A = _____ lbs.
✓	Load to be applied to package 2,300 lbs. (§4)
✓	Water Spray Test (TIN-03) Time completed: 1 P.M. (§4.3)
✓	Height Measurements: 0°: 43.5 in; 90°: 43.5 in; 270°: 43 5/8; 43 5/8 (§4.6)
✓	Start Date and Time: May 20, 2004 ; 2:55 p.m. (§4.7)
✓	Finish Date and Time: 5-21-04, 8:00 (§4.8)
	Height Measurements: 0° → 43.5, 90° → 43.5, 180° → 43 5/8, 270° 43 5/8 (§4.8)
✓	Ambient temperature: 21.4 °C (70.6 °F) Measuring device: Fluke 52 (§4.9)

Testing Damage Observations: No observable damage

Comments.

I certify that the above tasks have been performed and that the observations and comments are correct.

Testing Technician	Date	Checked by	Date
[signature]	5-21-04	[signature]	5/21/04

Procedure Checklist

Test Plan: ES-3100

Test Unit: 4

VERIFIED	TASK
✓	Prepare photographer's clapboard with package name and test unit number (§4.2).
✓	Package has been placed in the center of the vibration table (§4.3).
✓	Package has been secured to the vibration table, if required (§4.3).
✓	Photograph of the package in place has been taken (§4.4).
✓	Vibration table controller has been programmed for applied vibration and duration per Procedure TTG-PRF-16, using specifications outlined in the Test Plan (§4.5).
✓	Vibration test initiated per program (§4.6).
✓	Record vibration test information on Data Sheet (§4.7).
✓	Vibration test successfully completed per program, results printed (§4.8).
✓	Test specimen removed from vibration table and examined for damage (§4.9).
✓	Photographs of any observed damage completed, and recorded on Data Sheet (§4.9).

Comments: No observable damage externally. Not disassembled

I certify that the above tasks have been performed and that the observations and comments are correct.

Testing Technician: [signature] Date: 5-28-04

Checked by: Leonard Dickerson Date: 6-2-04

Data Sheet

Test Plan: ES-3100

Test Unit: TU-4

VERIFIED	TASK
✓	Ambient temperature: 20.6 °C (___ °F) (§4.6)
✓	Start Date and Time: 5-22-04 08:15 (§4.6)
N/A	The DOT Bounce test has been performed for one hour. (§4.8)
OR ✓	The random vibration test has been performed for 4 hour(s). (§4.8) The PSD for this test was as follows:
✓	End Date and Time: 5-22-04 | 12:20 (§4.8)
	Vibration controller test printout attached: Y/N (§4.8)

Testing Damage Observations: None Not disassembled

Comments:

I certify that the above tasks have been performed and that the observations and comments are correct.

Testing Technician	Date	Checked by	Date
[signature]	5-23-04	Leonard Dickerson	6-2-04

5. Procedure Checklist

Test Plan: ORNL/NTRL-011 Test Unit: 4

VERIFIED	TASK
✓	Have a photographer's clapboard with package name and test unit number. (§4.3)
✓	The ambient temperature has been recorded. (§4.4)
✓	Attitude of the rigged test unit is set. (§4.5)
✓	Photograph of the rigging arrangements has been taken. (§4.5)
✓	Photograph of the measured drop angle has been taken. (§4.5)
✓	The test unit has been raised to the designated drop height. (§4.7)
✓	Photograph of the height measurement has been taken. (§4.7)
✓	Video camera(s) are setup and running to take video of the drop. (§4.8)
✓	The release mechanism has been plugged into power outlet. (§4.8)
✓	Countdown, Release the test unit, unplug release mechanism. (§4.8)
✓	Videos camera stopped. (§4.9)
✓	Date and time of test were recorded. (§4.10)
✓	Photographs of the resulting damage were taken. (§4.11)
✓	Remove plumbob from Test piece
✓	Hold release mechanism in hand and ensure it is in hand until after drop is completed.

rwf 5/25/04

Comments:

I certify that the above tasks have been performed and that the observations and comments are correct.

Testing Technician — Date: 5-25-04

Checked by: Leonard Dickerson — Date: 5-25-04

6. Data Sheet

Test Plan: PRNL/NTRC-011 Test Unit: 4

VERIFIED	TASK
✓	Intended attitude of the test unit 0°. Tolerance ± 2 (§4.2)
✓	Measured attitude of the test unit 0.2° degrees. (§4.5)
✓	Level number 311-006-501 Calibration Exp. Date 6/04 (§4.5)
✓	Height above the drop pad 9 m Measuring device TTG string (§4.7)
✓	Date and Time of Drop Test: 5/25/04 11:54 (§4.10)
✓	Ambient temperature: 27.3 °C (___ °F) Measuring device TTG Fluke (§4.4)

Testing Damage Observations: _____

Comments. _____

I certify that the above tasks have been performed and that the observations and comments are correct.

Testing Technician	Date	Checked by	Date
[signature]	5-25-04	Leonard Dickerson	5-25-04

TEST FORM 2 – **Post 9m (30 ft) FREE FALL DROP TEST** Test Plan - ES-3100

DAMAGE MEASUREMENTS ES 3100 Test Unit 4

Height	0	90	180	270
Pre	43 1/2	43 1/2	43 1/2	43 1/2
Post	43	43 1/8	42 7/8	42 5/8

DIAMETER	0 to 180		90 to 270	
	Pre	Post	Pre	Post
Top Chime	19 1/4	19 1/4	19 7/8	19 3/8
Top Hoop	19 1/4	19 1/8	19 1/4	19 7/8
CG Hoop	19 1/8	19 1/8	19 1/4	19 1/4
Bottom Hoop	19 1/8	19 1/4	19 1/4	19 1/4
Bottom Chime	19 3/8	19 1/4	19 1/4	19 1/4
CG+Top Hoop	19 1/4	19 13/16	19 1/4	19 3/8

Sketch Drop Setup Here

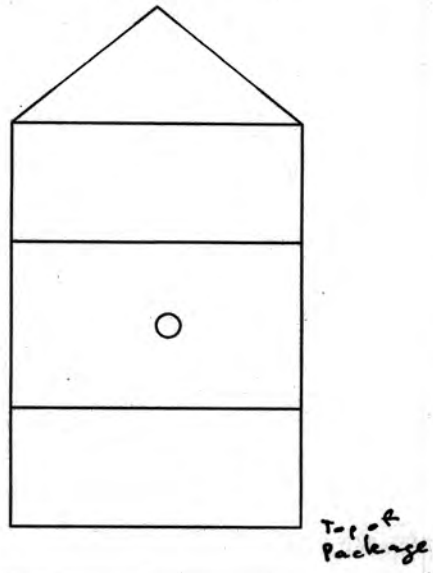

Sketch Package Damage Here

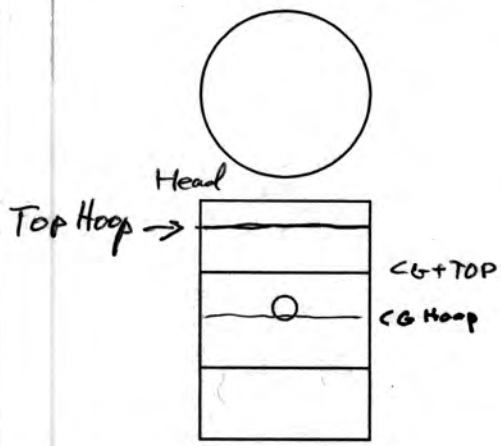

Comments: No Flats noted.

Concavity on bottom evenly distributed from edge, maximum depth is 3/8 inch.

Top Hoop narrowed – no value recorded.

I certify that the above tasks have been performed and that the observations and comments are correct.

Leonard Dickerson — Testing Technician — 5-25-04 Date

[illegible] — Verified By — 5-25-04 Date

5. Procedure Checklist

Test Plan: ES-3100 | Test Unit: 4

VERIFIED	TASK
✓	Have a photographer's clapboard with package name and test unit number. (§4.3)
✓	The ambient temperature has been recorded. (§4.4)
✓	Attitude of the test unit is set. (§4.5)
✓	Photograph of the attitude has been taken. (§4.5)
N/A	Photograph of the measured angle has been taken. (§4.5)
✓	The crush plate has been raised to the designated drop height and located over the target point. (§4.7)
✓	Photograph of the set position has been taken. (§4.7)
✓	Video camera(s) are setup and running to take video of the drop. (§4.8)
✓	The release mechanism has been plugged into power outlet. (§4.8)
✓	Countdown, Release the crush plate, unplug release mechanism. (§4.8)
✓	Videos camera stopped. (§4.9)
✓	Date and time of test recorded. (§4.10)
✓	Photographs of the resulting damage were taken. (§4.11)
✓	Remove plumbob from ~~Test~~ ~~piece~~ crush plate.
✓	Hold release mechanism in hand and ensure it is in hand until after drop is completed

uff 5/25/04

Comments:

I certify that the above tasks have been performed and that the observations and comments are correct.

[signature]	5-25-04	Leonard Dickerson	5-25-04
Testing Technician	Date	Checked by	Date

6. Data Sheet

Test Plan: ES-3100

Test Unit: 4

VERIFIED	TASK
✓	Intended attitude of the test unit ~~Horizontal~~ Vert. Tolerance ± ____ (§4.5)
N/A	Measured attitude of the test unit degrees. (§4.5)
N/A	Level number _____ Calibration Exp. Date _____ (§4.5)
✓	Height above the target: 30 feet Measuring device TTG String (§4.7)
✓	Date and Time of Crush Test: 5/25/04 2:18p (§4.10)
✓	Ambient temperature: 29.8 °C (____ °F) Measuring device TT2 Fluke (§4.11)

Testing Damage Observations: _____

Comments: _____

I certify that the above tasks have been performed and that the observations and comments are correct.

Testing Technician	Date	Checked by	Date
[signature]	5-25-04	Leonard Dickerson	5-25-04

TEST FORM 3 – **Post 9m (30 ft) DYNAMIC CRUSH TEST**

Test Plan - ES-3100

DAMAGE MEASUREMENTS

Test Unit 4

Height	0	90	180	270
Pre	43	43 1/8	42 7/8	42 5/8
Post	39 3/8	40 7/8	40 5/8	39 3/4

	DIAMETER	0 to 180		90 to 270	
		Pre	Post	Pre	Post
1	~~Top Chime~~	19 1/4	19 1/4	19 3/8	19 3/8
2	~~Top Hoop~~	19 1/8	20	19 7/8	20 1/8
3	~~CG~~	19 13/16	20	19 3/8	20 1/16
4	~~Bottom Hoop~~	19 1/8	19 7/16	19 1/4	19 1/2
5	~~Bottom Chime~~	19 1/4	19 15/16	19 1/4	20
6		19 1/4	19 1/4	19 1/4	19 1/4

Sketch Drop Setup Here

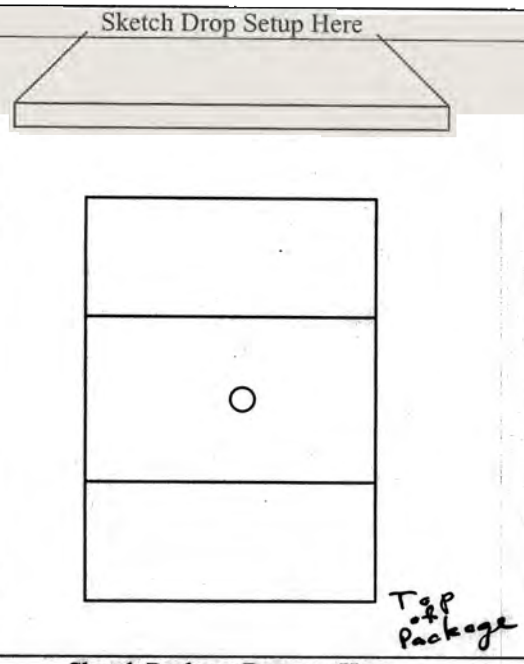

Sketch Package Damage Here

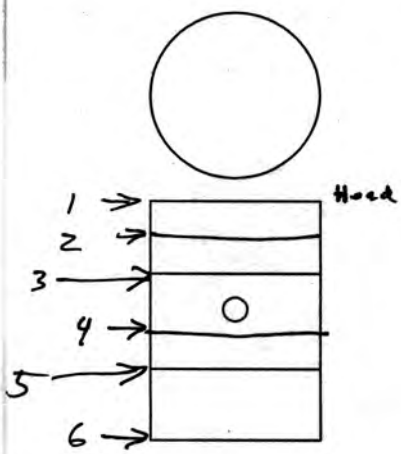

Comments:

I certify that the above tasks have been performed and that the observations and comments are correct.

Testing Technician — Date: 5-26-04 — Verified By: Leonard Dickerson — Date: 5-26-04

5. Procedure Checklist

Test Plan: ES-3100

Test Unit: 4

VERIFIED	TASK
✓	Have a photographer's clapboard with package name and test unit number. (§4.3)
✓	Attitude of the rigged test unit is set. (§4.4)
✓	Photograph of the rigging arrangements has been taken. (§4.4)
✓	Photograph of the measured drop angle has been taken. (§4.4)
✓	The test unit has been raised to the designated drop height. (§4.5)
✓	Photograph of the height measurement has been taken. (§4.5)
✓	Video camera(s) are setup and running to take video of the drop. (§4.6)
✓	The release mechanism has been plugged into power outlet. (§4.6)
✓	Countdown, Release the test unit, unplug release mechanism. (§4.6)
✓	Videos camera stopped. (§4.7)
✓	The ambient temperature has been recorded. (§4.8)
✓	Date and time of test recorded. (§4.9)
✓	Photographs of the resulting damage were taken. (§4.10)

Comments:

I certify that the above tasks have been performed and that the observations and comments are correct.

[illegible]	5-27-04	Leonard Dickerson	5-27-04
Testing Technician	Date	Checked by	Date

6. Data Sheet

Test Plan: ES-3100

Test Unit: 4

VERIFIED	TASK
✓	Intended attitude of the test unit 90° Vertical head down. Tolerance ± 2 (§4.4)
✓	Measured attitude of the test unit 89.7 degrees. (§4.4)
✓	Level number 381-006-501 Calibration Exp. Date 6-04 (§4.4)
✓	Height above the punch 1m Measuring device TTG 1m Rod (§4.5)
✓	Date and Time of Drop Test: 5-27-04 1315 (§4.8)
✓	Ambient temperature: 22 °C (71.4°F) Measuring device TTG Fluke (§4.9)

Testing Damage Observations: _____

Comments: Package stood on punch after impact.

I certify that the above tasks have been performed and that the observations and comments are correct.

R P Mey — Technician — 5-27-04 Date — Leonard Dickerson — Checked by — 5-27-04 Date

TEST FORM 4 – **Post 1 m (40 in) PUNCTURE DROP TEST** Test Plan - ES-3100

DAMAGE MEASUREMENTS

Test Unit 4

Sketch Drop Setup Here

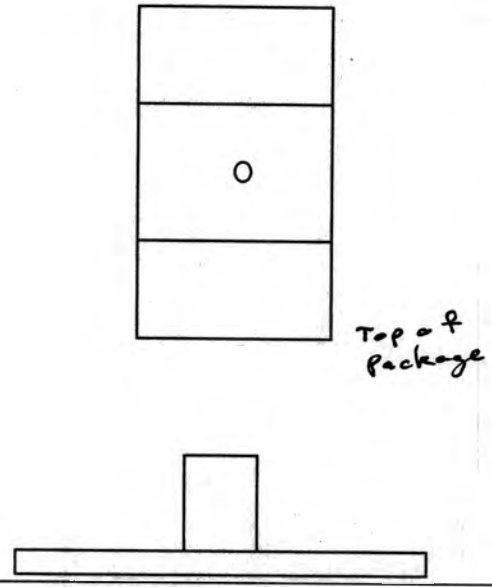

Sketch Package Damage Here

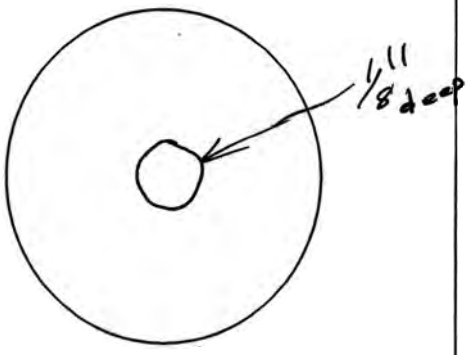

Comments: Slight indent ≈ 1/8" deep

I certify that the above tasks have been performed and that the observations and comments are correct.

Testing Technician — Date: 6-2-04 — Verified By — Date: 6/2/04

5. Procedure Checklist

Test Plan: ES-3100 ORNL/NTRC-011

Test Unit: TU-4

VERIFIED	TASK
✓	All thermocouples channels on the data acquisition system have been tested. (§4.2a)
✓	All thermocouples have been installed in the furnace, connected to Data Acquisition System (DAS), labeled and tested. (§4.3c)
✓	The test unit has been preheated to over 38 °C (100 °F). (§4.2b)
✓	Furnace has reached the minimum soak point temperature of 800 °C (1475 °F), and has soaked at this temperature for a minimum of 24 hours. (§4.3c)
✓	The thermal data acquisition system is set to read every 30 seconds or less. (§4.3c) 15 s
✓	All thermocouples have been installed on the exterior of drum, in accordance with the Test Plan, attached to DAS , labeled and tested. (§4.2c)
✓	Photographs and/or video of the test setup have been taken. (§4.3c)
✓	The unit has been placed in the furnace, on the support stand, with the 0° point down or as specified in the test plan. (§4.4c)
✓	The 30 minute timed test begins when 5 out of 6 test unit thermocouples and 15 of 18 furnace thermocouples reached the test temperature of 800 °C (1475 °F), as specified in this procedure. (§4.4d)
✓	Immediately following the timed test (minimum of 30 minutes at 800 °C) the test unit was taken out of the furnace and allowed to cool naturally. (§4.4e)
✓	Notes regarding smoke and/or flames emanating from the test specimen are recorded. (§4.4e)

Comments:

I certify that the above tasks have been performed and that the observations and comments are correct.

[signature]	6/16/04	Leonard Dickerson	6-16-04
Testing Technician	Date	Checked by	Date

6. Data Sheet

Test Plan: ES-3100 ORNL/NTRC-011

Test Unit: TU-4

VERIFIED	TASK
✓	The test unit has been preheated to over 38 °C (100 °F). Measuring device: TTG DATA Acq Calibration expiration date: N/A (§4.2b)
✓	The furnace has reached the minimum soak point temperature of 800 °C (1475 °F), and has soaked at this temperature for a minimum of 8 hours. The furnace set point temperature has been adjusted to _____ °C (1600 °F) at least ~~one hour~~ 45 min prior to each test (§4.3c) Date: 6/16 Time: 8:55 am/pm MK CAB
✓	The test unit has been placed in the furnace, on the support stand, at: (§4.4c) Time: 9:53 am/pm Open furnace door time: 50 seconds
✓	The 30 minute timed test began when 5 out of 6 test unit thermocouples and 15 of 18 furnace thermocouples reached the test temperature of 800 °C (1475 °F): (§4.4d) Time: 10:02 am/pm
✓	The test unit was removed from the furnace and allowed to cool naturally. (§4.4e) Time: 10:32 am/pm Ambient Temperature _____ °C (95 °F)
✓	The unit stopped outgassing (flames) at _____; outgassing/burnout elapsed time was _____ minutes. (§4.4e)

Testing Damage Observations: Flaming from TID when removed. Flaming ceased in less than 1 minute. Smoking continued. Outgassing (smoking) stopped at 10:44 (42 min ~~into~~ after run).

Comments:

I certify that the above [illegible] performed and that the observations and comments are correct.

[illegible]	6/16/04	Leonard Dickerson	6/16/04
Testing Technician	Date	Checked by	Date

Procedure Checklist

Test Plan: ES-3100

Test Unit: 4

VERIFIED	TASK
✓	Have a photographer's clapboard with package name and test unit number.
✓	A photograph of the leak tester connections has been taken.
✓	Both CALT5 Leak Tester and CVs have been in the same ambient conditions for 24 hours.
✓	Determine the interstitial volume of the test unit. Print out results.
✓	Determine the length of test from CALT5 Instruction Manual Table according to volume and accuracy needed.
✓	Program the info into the CALT5 tester.
✓	Run the CALT5 leak test. Print out results.
✓	Enter the data from CALT5 printout onto Data Sheet.
✓	Calculate the leak rate and enter on Data Sheet.

Comments:

I certify that the above tasks have been performed and that the observations and comments are correct.

Testing Technician — Date: 6-30-04 — Checked by: Leonard Dickerson — Date: 6-30-04

5. Data Sheet

Test Plan: ES-3100

Test Unit: 4

VERIFIED	TASK
✓	Assembly Leak Test Post Testing Leak Test X
✓	Length of test from CALT5 Instruction Manual Table according to volume and accuracy needed. Test Time: 9 min.
✓	A leak test in accordance with the CALT5 Manufacturer's Instructions Manual was performed on the CV assembly. Both CALT5 Leak Tester and CVs have been in the same ambient conditions for 24 hours. Leak Tester Cert. # M287139 Expiration Date: 3/3/05
✓	Ambient temperature: 21.1 °C (___ °F) Measuring device TTG Fluke

Attach CALT5 Printout Here

$$Lr = \frac{3.772\ cm3 * 4.96667}{9\ \text{min}} \left(\frac{\frac{2131.16\ mBar}{1013.25\ mBar/atm}}{(21.1\ °C + 273)°K} - \frac{\frac{2127.63\ mBar}{1013.25\ mBar/atm}}{(21.1\ °C + 273)°K} \right) ref - cc/\text{sec}$$

$$Lr = \frac{3.772\ cm3 * 4.96667}{9\ \text{min}} \left(\frac{2.1033\ atm}{294.1\ °K} - \frac{2.0998\ atm}{294.1\ °K} \right) ref - cc/\text{sec}$$

$$Lr = 2.0816 * .00001190 = 2.4773 \times 10^{-5}\ ref - cc/\text{sec}$$

Comments:

I certify that the above tasks have been performed and that the observations and comments are correct.

Testing Technician	Date	Checked by	Date
[signature]	6-30-04	Leonard Dickerson	6-30-04

System Date WED 30 JUN 2004 04:29:44
CALT No: 0052 Transducer No: 835279
Days since last calibration: 50

ORNL
CALT5 - Version U1.43

******MEASURE VOLUME******

Reference Volume: 2 cc
Reference Volume No: ISN026
Test Reference No: TTGPRF01
Design/Serial Nos: ES-3100/TU-4
Number of Readings: 2
Comment: cv lid

Pressure mbar			Volume
Atmos	Start	Final	(cc)
977.00	2107.94	1709.49	3.76
976.57	2121.53	1719.55	3.78

Average Volume: 3.772 cc

Sig: Richard D Hey Jr Date: 6-30-04
(Tested by)

Sig: Leonard Dickerson Date: 6-30-04
(Supervisor)

System Date WED 30 JUN 2004 04:34:23
CALT No: 0052 Transducer No: 835279
Days since last calibration: 50

ORNL
CALT5 - Version U1.43

Pressure Drop
***** LEAKAGE TEST *****

Test Reference No: TTGPRF01
Design/Serial Nos: ES-3100/TU-4
Comment: cv lid
Interspace Volume: 3.772 cc
Settling Time: 3 mins
Test Duration: 9 mins
Temperature: 21.1°C
Temperature ratio: 1.013
μ ratio: 0.992
Pass Rate (SLR): 1.0E-04 bar cc/sec
Allowable ΔP : -50 mbar

****** RESULTS ******

	Pressure mbar	Date/Time
Atmos:	976.46	
Start:	2131.16	30 JUN 2004 04:38:38
Final:	2127.63	30 JUN 2004 04:47:38

Leakage Rate: 7.1E-06 bar cc/sec

PASS

Standard conditions:
Temperature: 25°C
Up stream pressure: 1013 mbar
Down stream pressure: 0 mbar

Sig: Richard D Hey Jr Date: 6-30-04
(Tested by)

Sig: Leonard Dickerson Date: 6-30-04
(Supervisor)

5. Procedure Checklist

a. Prepare Test Unit

Test Plan: ES-3100

Test Unit: 4

VERIFIED	TASK
✓	Area around where the package will be penetrated cleared of any tape, paint, loose labels, etc. (§4a.1)
✓	¼ in NPT threaded hole drilled and tapped. (§4a.2)
✓	Test weight bag penetrated (if necessary). (§4a.3)
✓	Threaded hole and surrounding surface cleaned with a wiping cloth or tissue soaked in isopropyl alcohol or a wet Vacu-Solve swab. (§4a.4)
✓	Solvent has evaporated. (§4a.5)
✓	Epoxy mixed and applied to the thread of a ¼ in NPT to K-Flange adaptor taking care to not obstruct the hole in the adaptor with epoxy. (§4a.6)
✓	Adapter threaded into the ¼ in NPT hole in the package ensuring that there is a continuous filet of epoxy between the adaptor stem and the surface of the Test Unit (if necessary, add epoxy to create a filet). (§4a.7)
✓	Epoxy has hardened at least 4 hours. (§4a.8)
✓	Mixing tools properly disposed of. (§4a.9)

Comments:

I certify that the above tasks have been performed and that the observations and comments are correct.

Testing Technician	Date	Checked by	Date
[illegible]	7-21-04	Leonard Dickerson	7-30-04

b. Check List for Test Unit Pump-out

Test Plan: ES-3100

Test Unit: 4

VERIFIED	TASK
✓	Test unit placed on a plastic bag that is large enough to envelop the test unit. (§4b.1)
✓	Varian 959 Turbo Leak Detector positioned so that it can be attached to the test unit without further movement. (§4b.2)
✓	Varian 959 Turbo Leak Detector started. (CAUTION: Once the leak detector is started DO NOT move the leak detector until it is fully shutdown and the internal turbo-pump has come to a complete stop. Movement of the leak detector with a spinning turbo-pump will damage or destroy the pump.) (§4b.3)
✓	Varian 959 Turbo Leak Detector calibrated and zeroed per the calibration procedure provided in the leak detector manual. (§4b.4)
✓	Calibration leak rate, serial number, and calibration expiration date recorded. (§4b.5)
✓	Leak detector attached to the test unit. (§4b.6)
✓	Test unit pump-out initiated (record date and time). (§4b.7)
N/A	¼ in. flexible plastic tubing used for vent attached hear the bottom of the test unit. (§4b.8)
✓	¼ in. flexible plastic tubing used for He fill attached at the top of the test unit. (§4b.9)
✓	Test unit enveloped in the plastic bag and bag secured with a reasonably tight seal. Note: Do not envelop the K-Flange adaptor or the point where the adaptor enters the test unit. (§4b.10)
✓	Slit for evacuating bag cut into bag. (§4b.11)
✓	He regulator attached to the He cylinder and the ¼ in. plastic tubing that is attached to the top of the test unit. (§4b.12)
✓	Picture taken of test unit connected to leak check system, including photo clapboard. (§4b.13)

Comments

I certify that the above tasks have been performed and that the observations and comments are correct.

Testing Technician: [signature] Date: 7-23-04

Checked by: Leonard Dickerson Date: 7-30-04

c. Check List for Leak Check of Test Unit

Test Plan: ES-3100

Test Unit: 4

VERIFIED	TASK
✓	Vacuum in test unit less than 100 milliTorr (preferably less than 50 milliTorr). Record date and time. (§4c.1)
✓	Leak detector range switch set to the 10^{-9} position. (§4c.2)
✓	Plastic bag surrounding test unit evacuated using shop-vac. (§4c.3)
✓	Inflate bag with He. Record the time (hour:minute:second ± 5 sec) and leak rate reading from the leak detector display. (§4c.4)
✓	He leak rate recorded every 2 minutes (±5 sec) and the time that the range switch is changed to the next higher decade (e.g. from 10^{-9} to the 10^{-8} range). (§4c.5)
✓	Final reading taken at 20 minutes (± 5 sec) elapsed time and He supply turned off. (§4c.7)
✓	Leak detector placed in Vent mode. (§4c.8)
✓	Plastic bag and tubes removed from the test unit. (§4c.9)
✓	Leak Detector detached from test unit. (§4c.10)
✓	Close out test unit data sheet with signatures and date. (§4c.11)
NA	IF another test unit is to be leak checked THEN bring the next test unit into position for checking. (CAUTION: Once the leak detector is started DO NOT move the leak detector until it is fully shutdown and the internal turbo-pump has come to a complete stop. Movement of the leak detector with a spinning turbo-pump will damage or destroy the pump.) (§4c.12)
✓	IF this is the last test unit THEN completely shutdown the leak detector. Allow all components to come to a full stop prior to moving the leak detector. (§4c.13)

I certify that the above tasks have been performed and that the observations and comments are correct.

Testing Technician	Date	Checked by	Date
[signature]	7-23-04	Leonard Dickerson	7-30-04

6. Data Sheet

Test Plan: ES-3100

Test Unit: 4

VERIFIED	TASK
✓	He calibration leak identification: Leak rate He cc/sec 7.2 *10 - 8 (§4b.5) Calibration expiration date mm 8 /dd 29 /yyyy 2004
✓	Test unit pump-out started Date and time mm 7 /dd 21 /yyyy 2004 hh 16 :mm 35 (§4b.7)
✓	Test unit vacuum at or below 100 milliTorr. Pressure in milliTorr 60 (§4c.4) Date and time mm 7 /dd 23 /yyyy 2004 hh 11 :mm 04
✓	He Leak Rate Table (§4c.4 - 6)

Clock Time hr:min:sec	He Leak Rate
11:04	0×10^{-9}
11:06	0×10^{-9}
11:08	0×10^{-9}
11:10	0×10^{-9}
11:12	0×10^{-9}
11:14	0×10^{-9}
11:16	0×10^{-9}
11:18	3.2×10^{-8}
11:20	8.4×10^{-8}
11:22	1.4×10^{-7}
11:24	2.0×10^{-7}

✓ Ambient temperature during test: 21.8°C Measuring device TTG Fluke (§4c.7)

Comments:

I certify that the above tasks have been performed and that the observations and comments are correct.

Testing Technician	Date	Checked by	Date
[signature]	7-23-04	Leonard Dickerson	7-30-04

TEST FORM 4 - **POST-THERMAL TESTING INSPECTION**

Test Plan ES-3100

Test Unit 4

VERIFIED	TASK
✓	Following the thermal test and after cooling, the test package was weighed, and the weight recorded on TEST FORM 1 .
✓	The drum, lid, nuts, and studs have been visually examined to determine the extent of the testing damage. Observations:
✓	The camera(s) are set up to take photographs* and/or videotape of the damage due to testing.
✓	The drum lid has been removed and the condition of the exposed parts have been visually examined for damage and the condition has been recorded. Observations:
✓	The Top Plug Assembly has been removed and visually inspected to determine the extent of impact and thermal damage. Record the exposed temperature indicator blackout reading on TEST FORM 5 . Observations:
✓	The CV assembly has been removed and visually examined for damage. Record the exposed temperature indicator blackout readings on TEST FORM 5 . Observations:
✓	The CV assembly has been weighed and the weight recorded on TEST FORM 1
✓	Use TTG-PRF-01 for the CV post-test operational leak check, TTG-PRF-02 for the full containment boundary leak check and TTG-PRF-14 for the 3 ft. immersion test.
✓	Disassemble the CV. Record torque value needed to loosen CV lid. 30 ft-lb.
✓	Read the temperature indicators from the surrogate payload. Record the temperature indicators' blackout readings on TEST FORM 5 .
✓	All loose parts will be placed in separate polyethylene bags, marked with test unit identification, tape closed, and prepared for storage with the test package.
✓	Mark and reassemble the test package to the extent possible for shipment.
✓	*Photographs and/or video of the damage resulting from the testing have been taken.

Comments: Borobond cans in tact

I certify that the above tasks have been performed and that the observations and comments are correct.

Testing Technician	Date	Witness	Date
[illegible]	7-27-04	Leonard Dickerson	7-30-04

TTG/TP/ES-3100 - May 17, 2004

5. Procedure Checklist

Test Plan: ES-3100

Test Unit: 4

VERIFIED	TASK
✓	Have a photographer's clapboard with package name and test unit number. (§4.2)
✓	The test unit has been lowered to the bottom of the tank in designated orientation. (§4.5)
✓	The depth to the highest point of the test unit has been measured and is at least 0.9m (3 ft.). (§4.5)
✓	Photograph of the depth measurement has been taken. (§4.5)
✓	Start date and time has been noted. (§4.6)
✓	Test time has expired. (§4.7)
✓	Test unit has been removed from the tank. (§4.7)
✓	End date and time has been noted. (§4.7)
✓	Open the test unit and record breaking torque values during removal, if required. (§4.8)
✓	Inspect for water in-leakage or structural damage. (§4.8)
✓	Photographs of any resulting damage or lack thereof were taken. (§4.8)

Comments:

I certify that the above tasks have been performed and that the observations and comments are correct.

Testing Technician — Date: 7-26-04

Checked by: Leonard Dickerson — Date: 7-30-04

6. Data Sheet

Test Plan: ES-3100

Test Unit: 4

VERIFIED	TASK	
✓	Intended attitude of the test unit in tank (e.g. on side) on side	(§4.3)
✓	Depth of water above the test unit 39" Measuring device Tape Measure	(§4.5)
✓	Start Date and Time of Immersion Test: 7-26-04 10:40	(§4.6)
✓	Water temperature: 22.1 °C (___ °F) Measuring device TTG Fluke	(§4.6)
✓	End Date and Time of Immersion Test: 7-27-04 08:30	(§4.7)
✓	Water temperature: 21.1 °C (69.8 °F) Measuring device TTG Fluke	(§4.7)
✓	Detected in-leakage of water: (YES/NO)	(§4.7)
✓	Detected structural damage: (YES/NO)	(§4.7)

Testing Damage Observations: _____

Comments: _____

I certify that the above tasks have been performed and that the observations and comments are correct.

Testing Technician: [signature] · Date: 7-26-04 · Checked by: Lemuel Dickerson · Date: 7-30-04

TEST FORM 5 - TEMPERATURE INDICATOR READINGS

Test Plan ES-3100

Test Unit 4

A visual inspection of each temperature indicator on the package consisting of those indicators inside the CV, outside the CV, and on the drum liner will be made. The values of the blackouts that occurred will be recorded below.

RECORD BLACKOUT TEMPERATURES AT THESE LOCATIONS:

TEMPERATURE INDICATOR NUMBER LOCATION CHART

ON THE SURROGATE PAYLOAD

Location	0°		180°	
Side Top	1 B 171 °F		2 B 171 °F	
Side Middle	3 B 171 °F		4 B 171 °F	
Side Bottom	5 B 171 °F		6 B 171 °F	

ON THE CV

Location	0°	90°	180°	270°
CV Lid Top (outside)	7 B 261 °F	8 B 261 °F	9 B 261 °F	10 B 261 °F
CV Lid Bottom (inside)	11 B 230 °F	12 B 230 °F	13 B 230 °F	14 B 230 °F
Flange (outside)	15 B 241 °F	16 B 241 °F	17 B 241 °F	18 B 241 °F
Flange (inside)	19 B 219 °F	20 B Destroyed	21 B Destroyed °F	22 B 219 °F
Body Mid Height (outside)	23 B 180 °F	24 B 180 °F	25 B 180 °F	26 B 180 °F
CV Base (outside)	27 B 230 °F	Note: Temp label centered on bottom		

ON THE INNER LINER AND TOP PLUG

Location	0°	90°	180°	270°
Top Plug Bottom	28 350 °F	29 350 °F	30 350 °F	31 350 °F
Flange Step Wall	32 275 °F	33 275 °F	34 275 °F	35 275 °F
BoroBond4 Step	36 350 °F	37 350 °F	38 300 °F	39 350 °F
CV Body Wall High	40 B 210 °F	41 C — °F	42 B 210 °F	43 C — °F
CV Body Wall Middle	44 B 190 °F	45 C — °F	46 B 199 °F	47 C — °F
Liner Bottom	48 B 261 °F	Note: Temp label centered on bottom Impact damage on Liner Bottom Label		

Comments: Borobond4 Step temperature are higher than Flange Step wall, these labels may be blacked from impact damage. Labels on CV lid maxed out - inconsistent - may be black from impact damage.

I certify that the above tasks have been performed and that the observations and comments are correct.

Testing Technician [signature] Date 7-27-04

Witness Leonard Dickerson Date 7-30-04

*All photographs/movies will be uniquely identified with test unit, date and time to ensure that the proper sequence can be reconstructed

Appendix 2.10.9

PACKAGING MATERIALS OUTGASSING STUDY FINAL REPORT

THIS PAGE INTENTIONALLY LEFT BLANK.

Y/DZ-2720

Packaging Materials Outgassing Study Final Report

R. A. Smith
Compatibility and Surveillance
Technology Development

Issue Date: September 26, 2006

Prepared by the
Y-12 National Security Complex
Oak Ridge, TN 37831
Managed by
BWXT Y-12, L.L.C.
for the
U. S. DEPARTMENT OF ENERGY
under contract DE-AC05-00OR22800

MANAGED BY
BWXT Y-12, L.L.C.
FOR THE UNITED STATES
DEPARTMENT OF ENERGY

UCN-13672 (11-03)

DISCLAIMER

This work of authorship and those incorporated herein were prepared by Contractor as accounts of work sponsored by an agency of the United States Government. Neither the United States Government nor any agency thereof, nor Contractor, nor any of their employees, makes any warranty, express or implied, or assumes any legal liability or responsibility for the accuracy, completeness, use made, or usefulness of any information, apparatus, product, or process disclosed, or represents that its use would not infringe privately owned rights. Reference herein to any specific commercial product, process, or service by trade name, trademark, manufacturer, or otherwise, does not necessarily constitute or imply its endorsement, recommendation, or favoring by the United States Government or any agency or Contractor thereof. The views and opinions of authors expressed herein do not necessarily state or reflect those of the United States Government or any agency or Contractor thereof.

Y/DZ-2720

PACKAGING MATERIALS OUTGASSING STUDY FINAL REPORT

R. A. Smith
Compatibility and Surveillance
Technology Development
Building 9202, MS 8097, 576-0615

Issue Date: September 26, 2006

Prepared by the
Y-12 National Security Complex
Oak Ridge, TN 37831
Managed by
BWXT Y-12, L.L.C.
for the
U. S. DEPARTMENT OF ENERGY
under contract DE-AC05-00OR22800

TABLE OF CONTENTS

LIST OF FIGURES v

LIST OF TABLES v

ABBREVIATIONS, ACRONYMS, AND INITIALISMS vii

ABSTRACT ix

INTRODUCTION 1

DIFFERENTIAL SCANNING CALORIMETRY 2

THERMOGRAVIMETRIC ANALYSIS 2

OUTGASSING STUDIES 3
- EXPERIMENTAL 3
  - Materials 3
  - Equipment and Procedure 3

DATA AND RESULTS 5
- BLANK OUTGASSING RESULTS 6
- FOAM OUTGASSING RESULTS 6
- TEFLON AND POLYETHYLENE OUTGASSING RESULTS 6

OUTGASSING COMPARISONS 7

CONCLUSIONS 7

REFERENCES 22

APPENDIX 1: DATA ANALYSIS 23

LIST OF FIGURES

Figure **Page**

1. Stainless steel vacuum container or *retort* 4
2. Red PU thermogram showing thermal transitions at 200°C and 490°C 8
3. White PU thermogram showing thermal transitions at 325°C and 560°C 9
4. Red PU foam showing three regions of thermal decomposition 10
5. White PU foam showing two regions of decomposition 11
6. Variation in heating profile from oven may lead to variation in outgassing results 12
7. Outgassing pressures from two stainless steel retorts 13
8. Outgassing of two red PU foam specimens (8.88 g and 2.98 g) 14
9. Outgassing of an 11.06-g specimen of white PU foam 15
10. Outgassing of two polytetrafluoroethylene (Teflon) specimens (8.14 g and 12.41 g) competes with measurement noise 16
11. Outgassing of an 8.18-g specimen of polyethylene bottle is at noise level and decreases rapidly upon cooling 17
12. Outgassing of an 8.3-g specimen of an HDPE bottle lid 18
13. Outgassing of an 8.90-g specimen of a black plastic bottle lid, possibly polyethylene 19
14. Relative outgassing by polymer types examined 20
15. Polyurethane molecular structure 21
16. Polyethylene molecular structure 21
17. Polytetrafluoroethylene (Teflon) molecular structure 21

LIST OF TABLES

1. Characteristic values for polymer resins and PU foam in this study (Fried, Gibson, and MatWeb 1
2. Heating and cooling profile (Profile 5) for outgassing tests 4

ABBREVIATIONS, ACRONYMS, AND INITIALISMS

PE	polyethylene
PTFE	polytetrafluoroethylene
HAC	Hypothetical Accident Conditions
HDPE	high-density polyethylene
NCS	Normal Condition for Storage
PU	polyurethane
DSC	differential scanning calorimetry
TGA	thermogravimetric analysis
ppm	parts per million
STP	standard temperature and pressure
NRC	Nuclear Regulatory Commission

ABSTRACT

An outgassing study was conducted on two polyurethane packaging foams, two polymer bottles (polytetrafluoroethylene and polyethylene), and two polymer lids. The purpose was to measure the volume of gases that diffuse from these packaging materials at a maximum of 400°F when stored in ambient air within sealed containers. A specific heating profile was used to measure the offgassing quantities in a set of accelerated aging tests. This set of experiments was designed to duplicate an earlier study conducted in 1991. Thermogravimetric analysis and differential scanning calorimetry tests were conducted to obtain basic information about the polyurethane foams. The polyurethane foams demonstrated the largest degree of outgassing per mass; specifically, the white foam outgassed 50% less than the red foam. The polytetrafluoroethylene and polyethylene materials provided relatively small amounts of outgassing. The polyethylene materials appeared to react further upon cooling, leading to negative outgassing values due to consumption of gas in the container.

INTRODUCTION

Various materials are required for safely packaging items for transport or storage. Polymeric foams are a common means of protecting items from impact damage. The use of the foams in this study has the added requirement of minimal outgassing such that the closed container is not breeched if exposed to fire. The experiments completed here provide measurements of the gases per polymer mass that would be released at elevated temperatures. It is assumed that the major constituent of such gases is water, as polymers have a tendency to adsorb water, particularly if a filler is compounded into the polymeric matrix. Fillers, processing aids, colorants, stabilizers, and other additives are typically added to polymers for mechanical property enhancement (Fried). Little information is available about the composition of the materials in this study.

Another packaging application for polymers includes plastic bottles, used to contain liquids and solid powders. The current study measures outgassing from a Teflon (polytetrafluoroethylene or PTFE) and a polyethylene (PE) bottle, as well as their respective lids. The latter are unknown polymer types, although one is assumed to be high-density polyethylene by its manufacturer's stamp. Table 1 lists some characteristic average values for the polymer resins under study. The polyurethane (PU) foam, also listed in this table, has a significantly low moisture absorption level due to its probable closed cell configuration (MatWeb). PU resin properties vary widely according to the formulation and processing.

Table 1. Characteristic values for polymer resins and PU foam in this study (Fried, Gibson, and MatWeb

Polymer	T_g (°C)	T_m (°C)	Density (g/cm^3)	Water absorption (%)
Polytetrafluoroethylene	−73 (−99°F)	327 (621°F)	2.1	0.01
Polyethylene	−120 (−184°F)	98–135 (208–275°F)	1.0	0.03
Polyurethane	−70 (−94°F)	177 (350°F)	1.2	1.0–38.0
Polyurethane foam	−70 (−94°F)	177 (350°F)	0.45	1.0–5.0

The objective of this project is to heat plastic materials in ramped stages up to 400°F (204°C) and measure outgassing quantities within sealed containers. The goal is to reproduce test results from similar tests done in 1991, as reported in a letter authored by earlier researchers (Tinnel). Data from that document were used in safety documentation submitted in 1991 as characterization for the scenarios called Hypothetical Accident Conditions (HAC) and Normal Condition for Storage (NCS). Starting with the assumption that an item being shipped is contained in a polyethylene bag, it is then cushioned in PU foam. The foam is sealed in a can that is insulated by a lightweight concrete. The concrete is packaged in an outer steel drum that is vented. According to standards set forth by the U. S. Nuclear Regulatory Commission,

- In the HAC scenario, the drum is assumed to burn in a fire for 30 min, and the foam reaches a 300°F (149°C) temperature.
- In the NCS situation, a drum is assumed to sit out in the sun for several days and nights, which means that it is subject to continual temperature excursions between cool and 180°F (82°C).

In both cases, the PU foam will outgas over a short or long time, and it is required not to exceed a pressure that will damage the shipping container and cause the container to be breeched. It is assumed that moisture is the major offgassed constituent from this polymer structure, which only degrades beyond temperatures higher than 250°C (Hobbs).

PU foams are typically formulated from a polyol and an isocyanate component, adding a gas or blowing agent to one of these components to achieve the cellular structure. As stated earlier, additional constituents may be among the starting materials, as required in various applications. The original PU foam is a reddish-orange polyurethane formulated from Dow Chemicals components and was used for shipping protection until Dow decided to no longer manufacture this material. A white PU foam is now being considered to replace the earlier type and has components produced by BJB Enterprises, Inc. Both PU foams are tough and rigid and feature a nonporous skin where the foam apparently contacted the mold walls. There was random variability between the ratio of foam to skin in the specimens cut initially; smaller samples tended to have a larger fraction of skin. Care was taken to cut specimens from the mass of the foam, as the skin can demonstrate different properties; these foams are essentially composite materials (Broos). The density of the red foam specimens ranged from 0.45 to 0.50 g/cm^3 in the experiments discussed here. The density of the white foam material ranged from 0.27 to 0.49 g/cm^3. The polyethylene bottle is an opaque white material and has a density typically similar to water (1.0 g/cm^3). Teflon material typically has a density of 2.1 g/cm^3; this bottle has a smooth waxy texture.

Preliminary examination of the two foams was done using differential scanning calorimetry (DSC) and thermogravimetric analysis (TGA) in order to characterize some thermal properties. Figures 2 through 5 present the data. Figures 6 through 13 provide the outgassing data in this study. Figures 14, 15, and 16 comprise the basic molecular structures of these polymers.

DIFFERENTIAL SCANNING CALORIMETRY

DSC is an analytical method that measures the quantity of heat flow required to maintain a reference and sample at a particular temperature. The specific heat of the sample is then determined over a temperature range, giving information about phase transitions, kinetic processes, and other thermal attributes (Kämpf). The PU foams undergo some type of transition, cell softening or a glass transition, near 200°F (93°C); however, the presence of additives such as flame retardants, catalysts, or antioxidants could also have an effect on the DSC output. The red foams and white foams begin melting at 480°F and 560°F, respectively (250°C and 293°C).

THERMOGRAVIMETRIC ANALYSIS

TGA was run on each polymer, and weight loss was tracked as a function of temperature. The structure of PUs typically begins degradation between 250 and 350°C (480–660°F). The red PU demonstrates three regions of decomposition at 480°F, 553°F, and 696°F. The white PU only gives evidence of two decomposition processes, at 562°F and 689°F. The 550–560°F temperature is where polymer bridges begin to break and re-form into a secondary polymer structure; over 600°F, the secondary polymer structure breaks down as well. In the case of the red PU, the early decomposition is possibly loss of some additive. In both cases, the initial 1–2% weight loss corresponds well with the loss of moisture.

OUTGASSING STUDIES

During the outgassing study, samples of polymeric packaging materials were placed in vacuum-sealed stainless steel containers (retorts). Each retort was then attached to a capacitance manometer or "baratron" for direct measurement of the internal container pressure as the temperature was increased. This method allows tracking of the volatiles emitted from the materials, which are thought to mainly comprise moisture but also decomposition products at sufficiently high temperatures. While absorbed moisture is not immediately apparent under ambient conditions, the water contained in packaging is available to diffuse out over long time frames, such as years. Controlled heating provides a method to ascertain the maximum amount of outgassing from a material mass. This study provides information about the outgassing of volatiles in the situation combining elevated temperatures with the presence of air.

After the polymer specimens were loaded into retorts, the open or "free" volume within the containers was calculated. This study was initiated in the presence of atmospheric moisture and air pressure with a single absolute pressure gauge established to monitor the pressure as the temperature was ramped to a 204°C (400°F) maximum. Outgassing pressures are the sum of those gases emitted from the polymer specimen and retort, in addition to the air trapped inside the retort. The pressure gauge used has a maximum measurement range of 10,000 torr and was located outside the oven. The actual measurement volume included the retort headspace and the 24-in. flexible stainless steel hose used to connect the sample retort in the oven to the measurement device. An additional 1000-torr baratron was used as a reference to provide a measurement of the ambient pressure in the laboratory.

EXPERIMENTAL

Materials

The Packaging Engineering group provided the following test items for this study:

1. orange/dark red polyurethane foam in blocks (111.58 g)—this material had been formulated using components from Dow Chemical;
2. off-white polyurethane foam in blocks (168.8 g)—this material was formulated with components known as BJB280;
3. a clear/translucent Teflon (polytetrafluoroethylene) bottle capped with a white plastic lid labeled "Nalgene," possibly made of high-density polyethylene; and
4. an opaque polyethylene bottle capped with a black plastic lid, probably polyethylene.

Samples of random sizes and weights were cut using a blade or large scissors. Care was taken to exclude the skin from the foam materials being tested. Specimens were cut and weighed immediately before being sealed into a vacuum container. The total weight of pieces placed into a particular container was recorded in grams.

Equipment and Procedure

Standard vacuum hardware was used to seal randomly sized specimens of each material (weighing from 8 to 12 g) in air after these were weighed on a calibrated scale. (For the two PU foams, the experiment had been repeated with smaller masses.) Additionally a "blank" container was tested over the temperature range. This blank served to provide a baseline outgassing level for the container. The oven was programmed to heat to specific temperature plateaus and hold for a specified time period

before ramping linearly to the next temperature. The temperature profile, named "Profile 5," is described in Table 2. Despite the programming of the oven to cool to 50°F, its minimum temperature after heating was about 110°F; to cool the oven to room temperature the oven door was opened, which allowed free circulation of air into the heating zone.

Table 2. Heating and cooling profile (Profile 5) for outgassing tests

Temperature setting		Duration of ramp or hold
77–150°F	25–65°C	1-h ramp
150°F	65°C	2-h hold
150–200°F	65–93°C	1-h ramp
200°F	93°C	2-h hold
200–250°F	93–121°C	1-h ramp
250°F	121°C	2-h hold
250–300°F	121–149°C	1-h ramp
300°F	149°C	4-h hold
300–350°F	149–177°C	1-h ramp
350°F	177°C	4-h hold
350–400°F	177–204°C	1-h ramp
400°F	204°C	4-h hold
400–111°F	204–44°C	2-h ramp
111°F	44°C	Lower oven limit
77°F	25°C	Oven opened to lab

It should be noted that during the test period the test laboratory experienced continual temperature swings between 56 and 80°F (13–27°C). This range is typical for this laboratory and can cause random noise in the data under collection. For example, according to its specifications, the Despatch oven control stability is ±0.5°C per 5°C change in ambient temperature. The signal conditioner and display have linearity and accuracies in the parts per million (ppm) range per degree °C, but the combination of these small variations provides a visible noise level at extremely small outgassing levels.

The containers were constructed of stainless steel and bolted with the use of a copper gasket between 2.75-in. conflat flanges (Fig. 1). The assembly was completed with ¼-in. VCR® fittings and Swagelok or Nupro valves, using silver-plated nickel gaskets to seal interfaces.

Fig. 1. Stainless steel vacuum container or *retort.*

Pressure measurements were conducted using an MKS Instruments Type 690A14TRB 10,000-torr baratron providing output to an MKS 670 signal conditioner electronics unit. The baratron had an accuracy of 0.12% of reading and operates with a 59–104°F (15–40°C) ambient temperature span. The signal outputs were processed using a program called "Generic Application for Reading Pressure Gages for Import into Excel," and data were collected using LabView software on a laboratory computer. Data were downloaded from this computer for storage and analysis on an office personal computer.

The heating procedure displayed in Table 2 was conducted in a Despatch LAC 1-67-6 programmable laboratory oven that uses a Protocol Plus microprocessor control. A thermocouple was used to separately track and write the oven temperature to the aforementioned LabView program.

Experimental Steps

- Clean stainless steel retorts using isopropanol and wipe dry. Allow to air dry for 24 h.
- Cut and weigh polymer samples in atmosphere.
- Document material type, sample name, and weight.
- Place polymer pieces in stainless steel retort; label retort with sample name.
- Bolt container to conflat flange using a copper gasket and six bolts.
- Store retorts near Despatch oven until testing could be conducted.
- Select random retort for test; use nickel gasket to connect container to flexible tubing inside oven.
- Record pressures from baratrons measuring ambient and experimental pressures; these should be equivalent before test.
- Open National Instruments program and establish data collection mode and sampling rate (in data points per minute).
- Check data readout from signal conditioner and thermocouple.
- Check data download to personal computer via Labview program using Excel.
- Open sample retort valve.
- Turn oven on and load Profile 5; select Run.
- Periodically check system to ensure that data are being collected as planned.
- At end of test, record pressures according to both ambient and experimental baratrons; note oven temperature.
- Turn off oven and open oven door.
- Allow pressure to reach a new "ambient" equilibrium, and again record pressures.
- Close sample retort valve.
- Unbolt sample retort, and reserve for possible headspace gas analysis.
- Download data immediately in Excel *.csv format.
- Stop data collection program.

DATA AND RESULTS

The data were collected, then downloaded and analyzed using Microsoft Excel. The raw data were recorded as pressure in units torr as a function of time; temperature in degrees centigrade was also tracked as a function of time. For all materials, charts were later calculated to provide outgassing volume in cm^3(STP)/g and temperature in degrees Fahrenheit from ambient to 400°F, as a function of elapsed time (duration in hours). Blank data were used to calculate the moles of outgassed species

contributed by the sample container and other system components. Appendix 1, *Data Analysis*, provides additional detail on data processing.

BLANK OUTGASSING RESULTS

Two empty containers (blanks 1 and 3) were subjected to the same temperature profile in separate tests. Outgassing patterns shown in Figs. 6 and 7 provide a guide to the variation in (a) oven runs at different times and (b) blank outgassing under identical temperature profiles. The oven temperature was observed to vary as much as 5% at the same temperature setting. In concert with this, the blank outgassing pressures varied from each other by −0.25 to 4.2% in these tests. An analysis shows a 0.58 correlation of pressure to temperature variation between these two experiments. The other significant variable that can cause variation in outgassing between the two seemingly identical blanks is dimensional variations. The container volume difference (observed to be <2%) will lead to pressure discrepancies for identical gas quantities. In the current tests, molar quantities were calculated using container data developed through successive gas expansions to measure their volumes.

FOAM OUTGASSING RESULTS

The results from two red foam specimens are averaged in Fig. 8, where the specific volume of outgassing from each specimen is plotted with the temperature in degrees Fahrenheit. This normalized value is cited as specific volume at standard temperature and pressure (STP), providing the volume per specimen mass at standard temperature (273 K) and pressure (1 atm); the specific volume = $V/g = (nRT/p)g^{-1}$. It can be noted that the magnitude of outgassing is comparable to the 1991 data, but perhaps slightly less due to the material outgassing over time in storage. The experiment described here increases the temperature range and time of outgassing, so larger ultimate values than those of 1991 are observed. As well, the ramping and hold times were longer in the current experiment. The white foam outgassing quantities are shown in Fig. 7, and while on the same order of magnitude as the red PU, this material appears to produce only half the overall quantity of outgassed species. Both materials had continually increasing outgassing of volatiles at the highest test temperature, indicating that decomposition has started rather than outgassing has been seen at lower temperatures. The molecular structure of polyurethane includes an ester linkage that is subject to hydrolysis. Although some PU has a large moisture content, rigid foams typically have no more than 5% moisture. In this study, the red PU demonstrates about 1.2 wt % and the white foam 0.5 wt % moisture.

TEFLON AND POLYETHYLENE OUTGASSING RESULTS

The polytetrafluoroethylene and polyethylene materials outgassed relatively little, making it difficult to detect outgassing due to the heated container and that arising from the polymer alone. In other words, the final plots (Figs. 11–13) show a great deal of noise. It could be concluded that these materials would not present a large consideration for their outgassing potential in a heated situation. Their polyolefin structure does not attract moisture to the degree of the ester group in the PU structure. An interesting feature of the polyethylene materials is observable as the test vessel is cooled to room temperature. These experiments actually went into a negative pressure status, indicating that a reaction was taking place that consumed the gas phase inside the container. It is recognized that polyolefins degrade in air by oxidative reactions (Boenig). A mechanism for pressure decrease occurs if oxygen present in the original headspace reacts with the polymer and suppresses outgassing, even

during the heating cycle. Polymers also degrade by fragmentation, producing free radicals, which can then continue to react with one another (cross-linking). During a cooling of this system, these moieties would have reduced mobility, thereby increasing the probability of reaction with the gas phase. An analysis of the headspace would provide a means to study the remaining constituents.

OUTGASSING COMPARISONS

Figure 14 sets forth a straightforward comparison of outgassing quantities. The maximum and minimum amounts of gas are calculated for various samples after the background quantities are subtracted. These were weighted by the specimen mass and plotted on a bar chart as moles per gram of polymer specimen. The PUs demonstratedly have a larger outgassing of volatile species per mass, in comparison to PE and PTFE. Again, it is interesting to note the negative outgassing values in the case of PE minimums.

CONCLUSIONS

The next experimental procedure would be to conduct a gas analysis of the headspace on each container. The Y-12 National Security Complex Plant Laboratory is the best resource to complete this task. This would pinpoint the identity of outgassed species and provide a guide to ascertaining chemical reactions taking place in the solid–gas interface. This certainly would verify that reactions between the oxygen and polymer fragments have occurred.

Another stage would be to clearly identify the identity and manufacturer of each material, including the age, ingredients, and processing steps. Processing information for each polymer would assist in explaining the DSC and TGA output, if such an effort is desired. The response of a polymer to its environment involves its constituents, processing history, and treatment in storage. The large range of polymer properties, including outgassing, is due to these variables.

It can be concluded that PU foams absorb and outgas moisture to a larger extent than the polyolefins, as expected according to their respective molecular structures. This is also reflected in the literature absorption values. The white PU outgassing is no more likely to cause a shipping container breech than the red PU outgassing in the Nuclear Regulatory Commission (NRC) scenarios. The red PU outgassed a specific volume per mass similar to that quantity derived in the 1991 study.

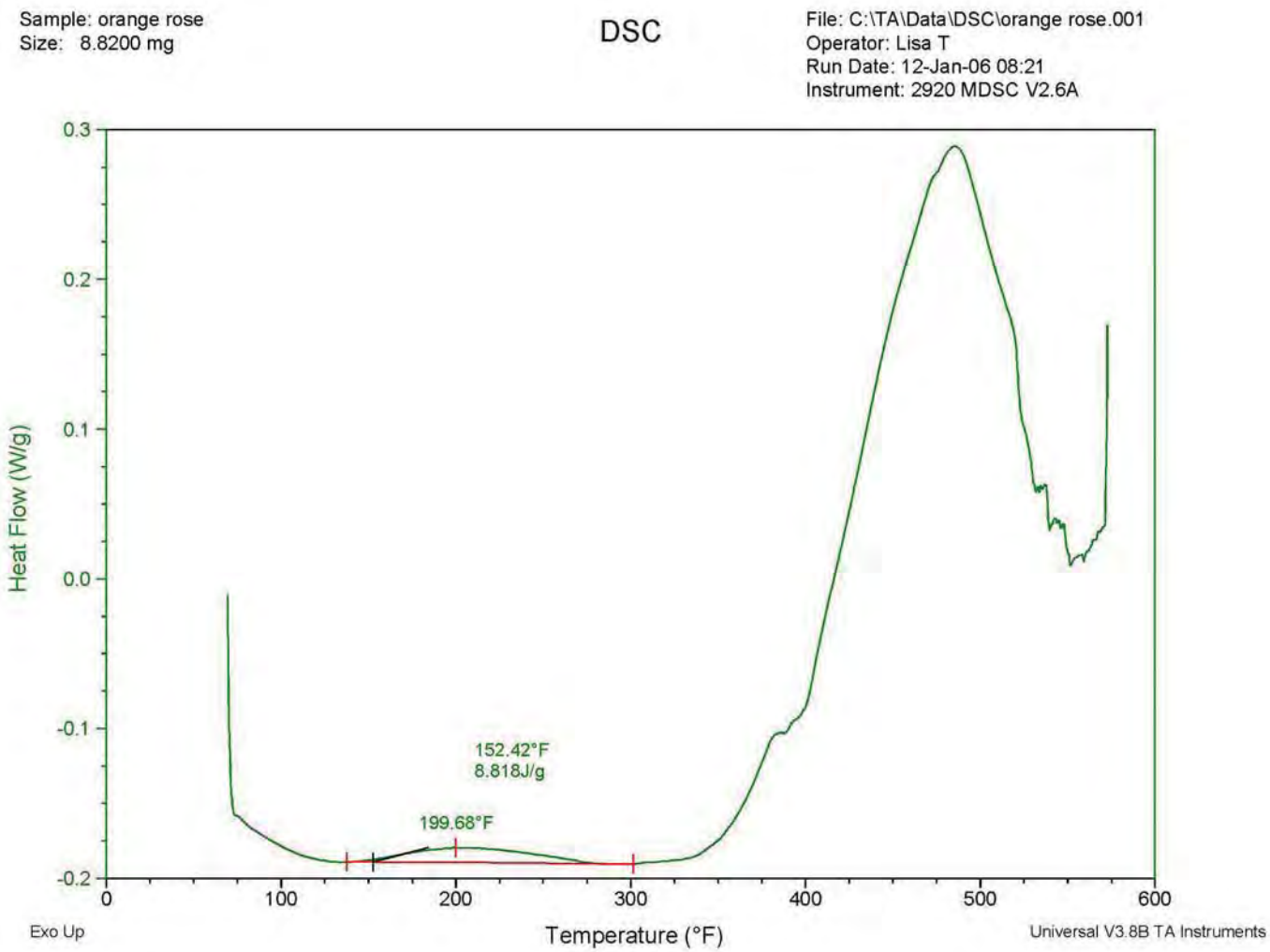

Fig. 2. Red PU thermogram showing thermal transitions at 200°C and 490°C.

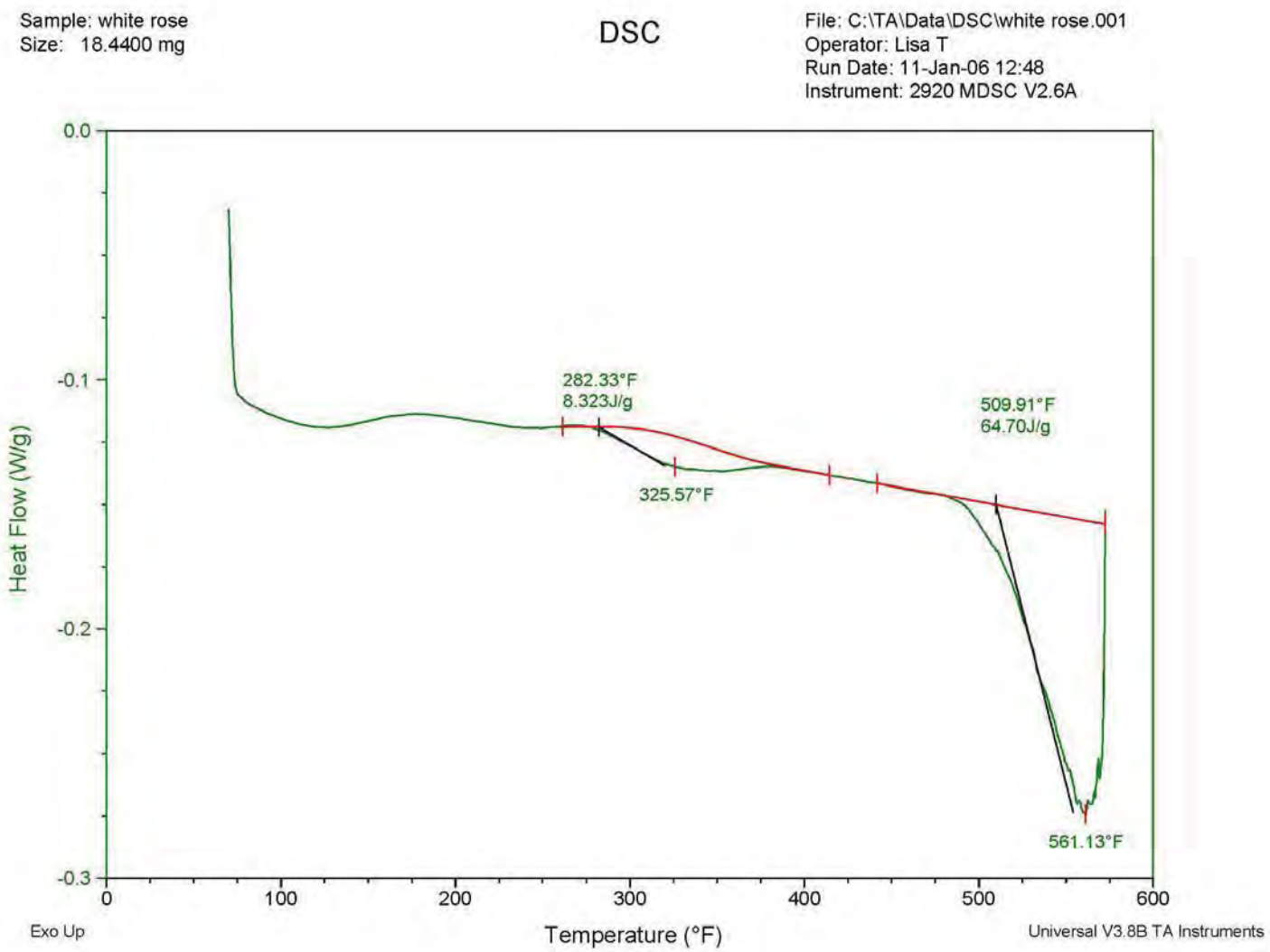

Fig. 3. White PU thermogram showing thermal transitions at 325°C and 560°C.

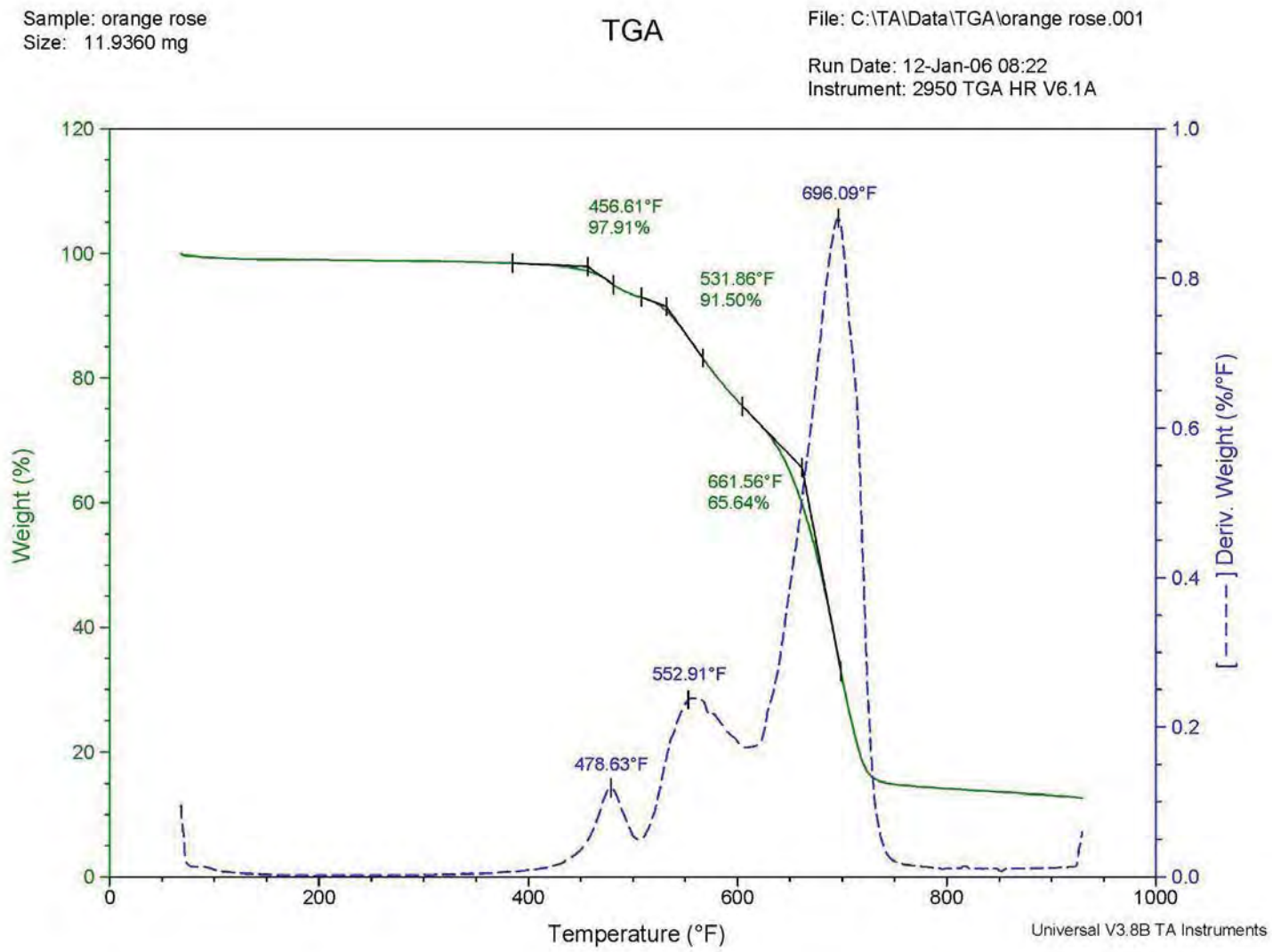

Fig. 4. Red PU foam showing three regions of thermal decomposition.

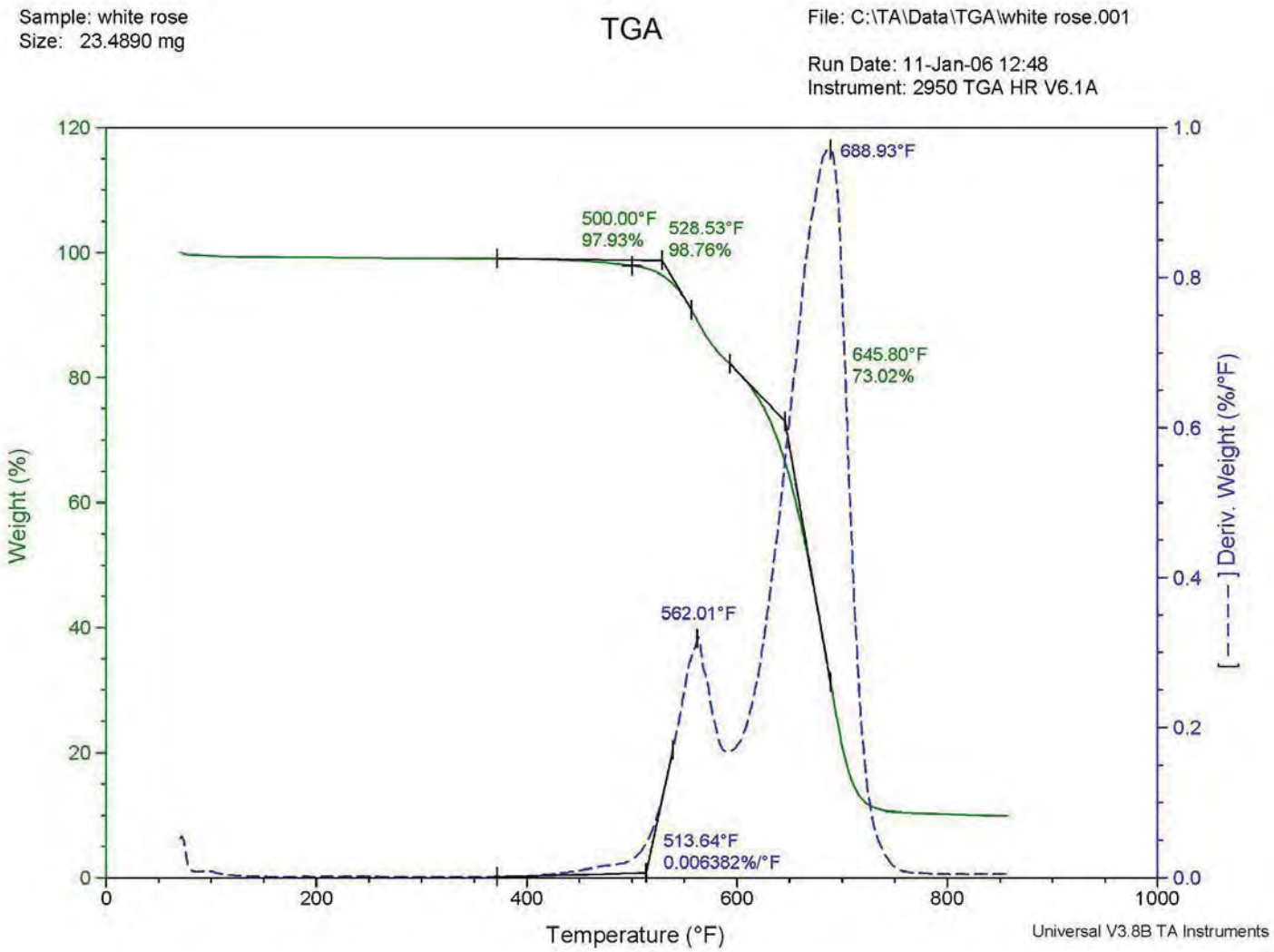

Fig. 5. White PU foam showing two regions of decomposition.

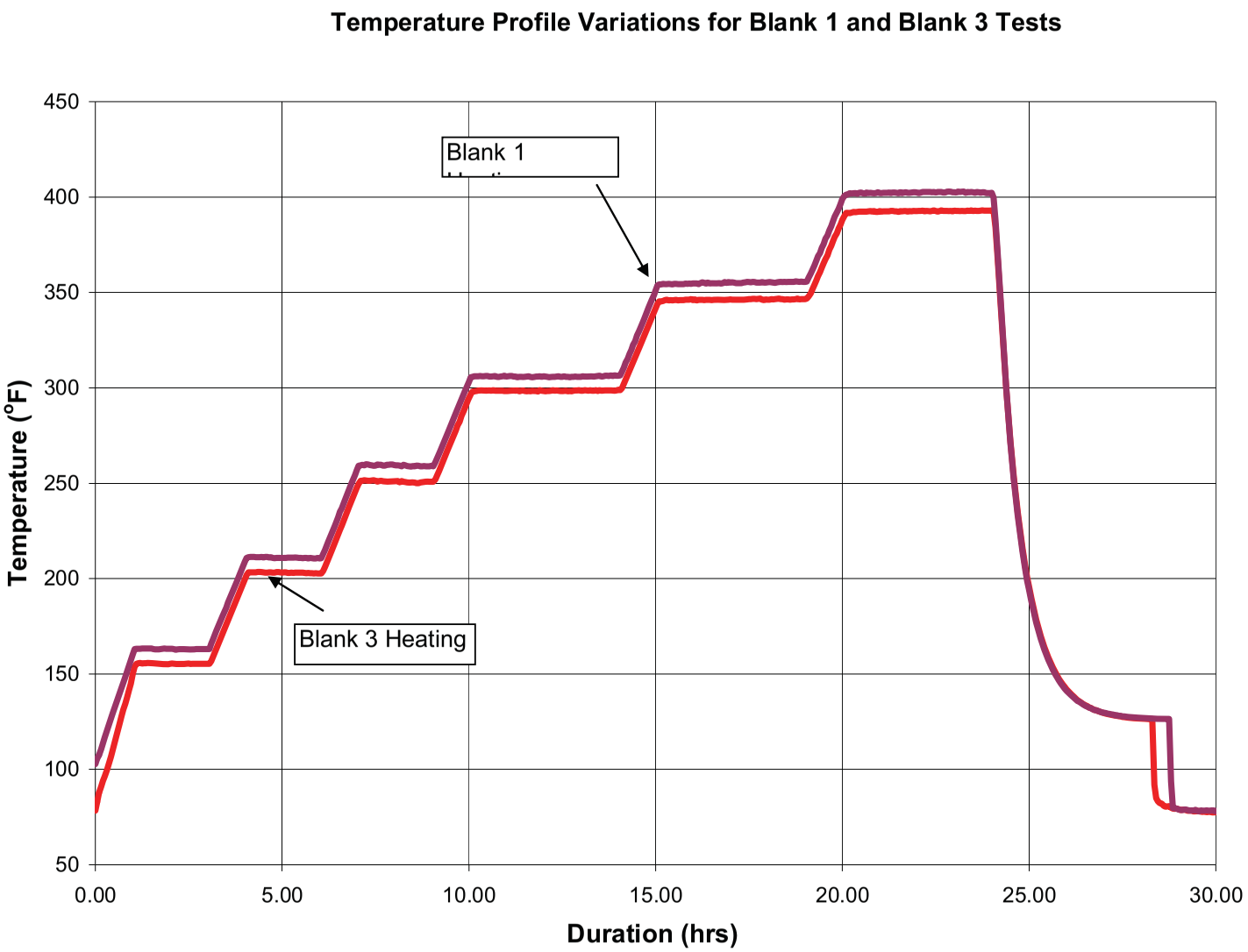

Fig 6. Variation in heating profile from oven may lead to variation in outgassing results.

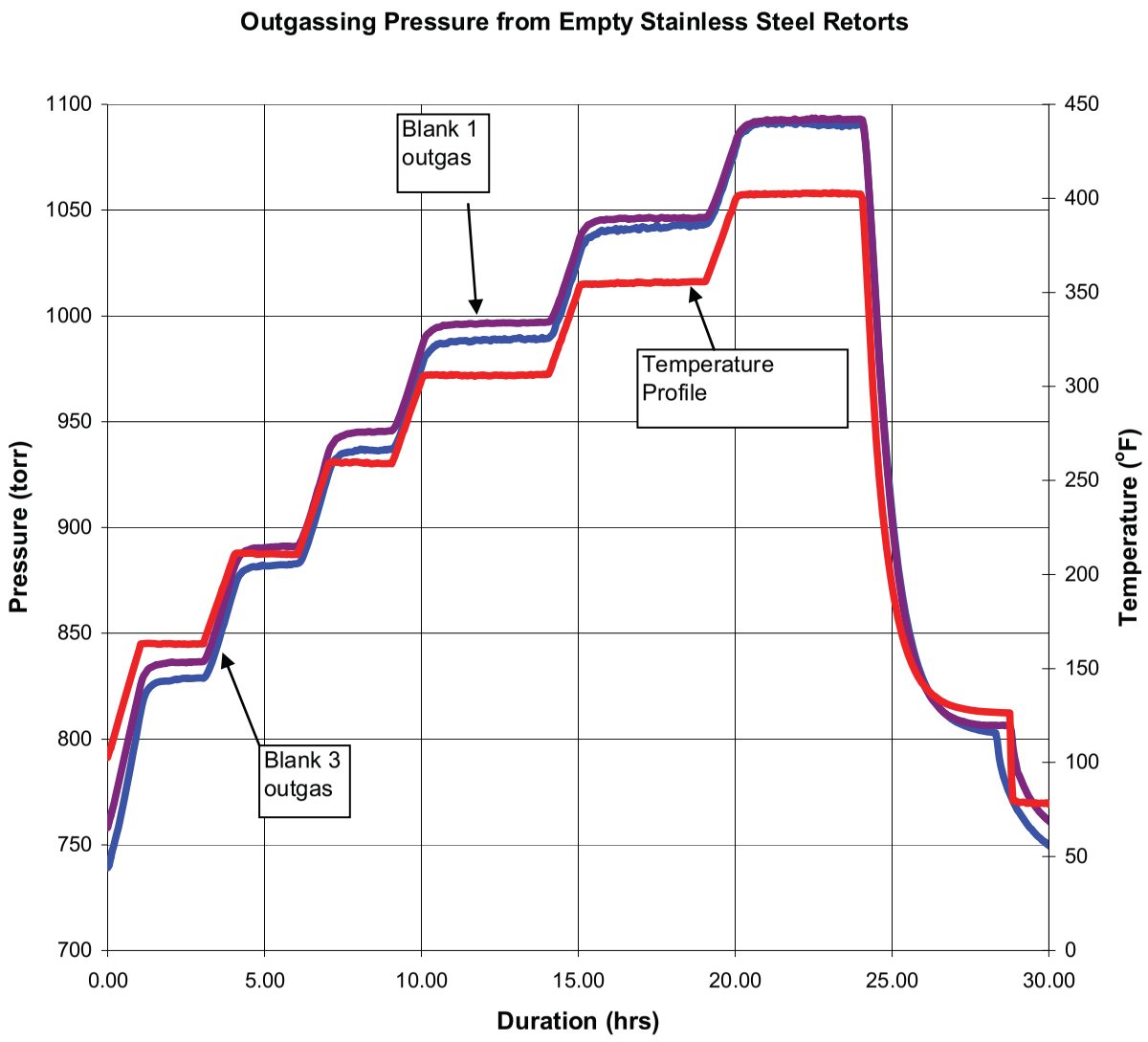

Fig. 7. Outgassing pressures from two stainless steel retorts.

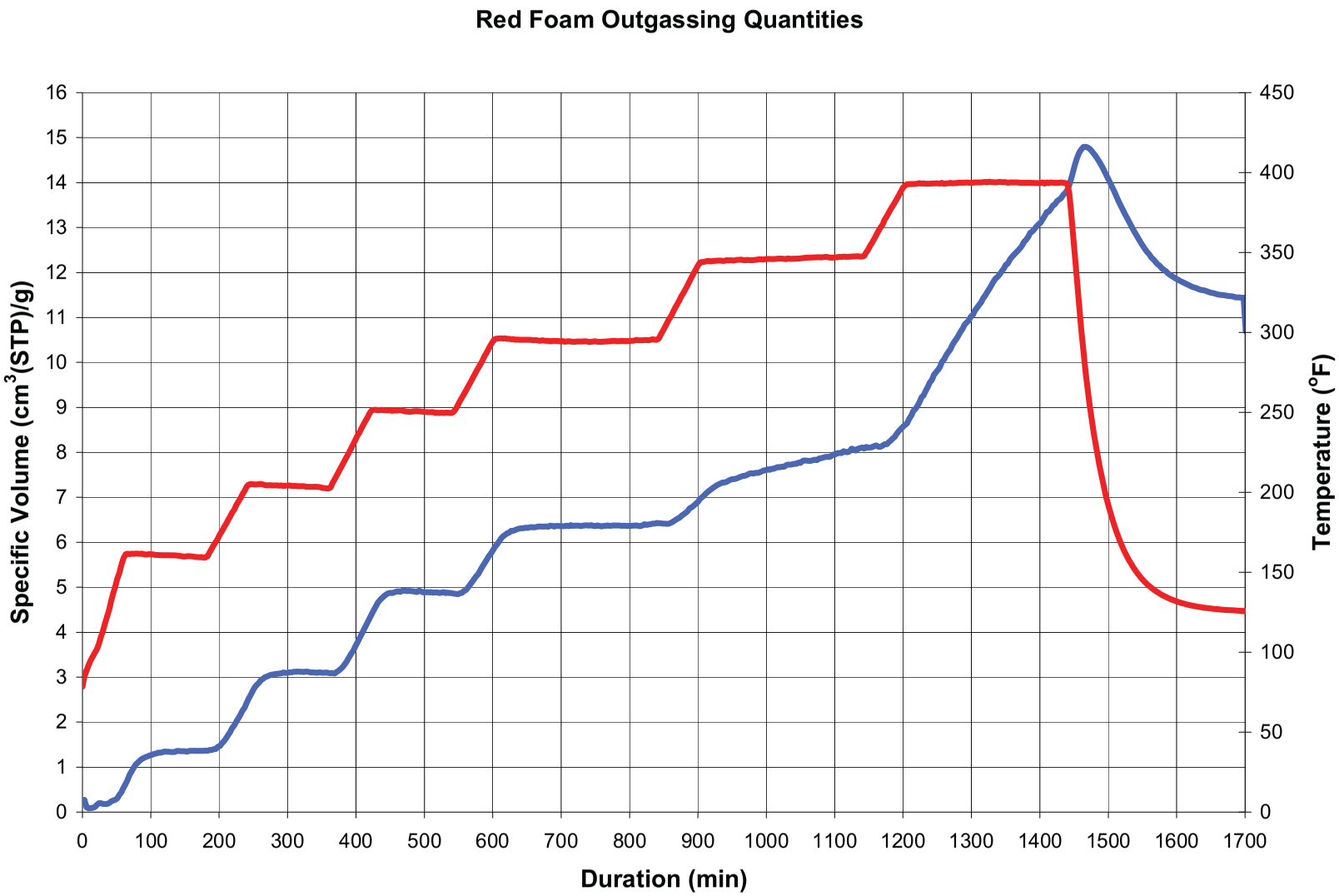

Fig. 8. Outgassing of two red PU foam specimens (8.88 g and 2.98 g).

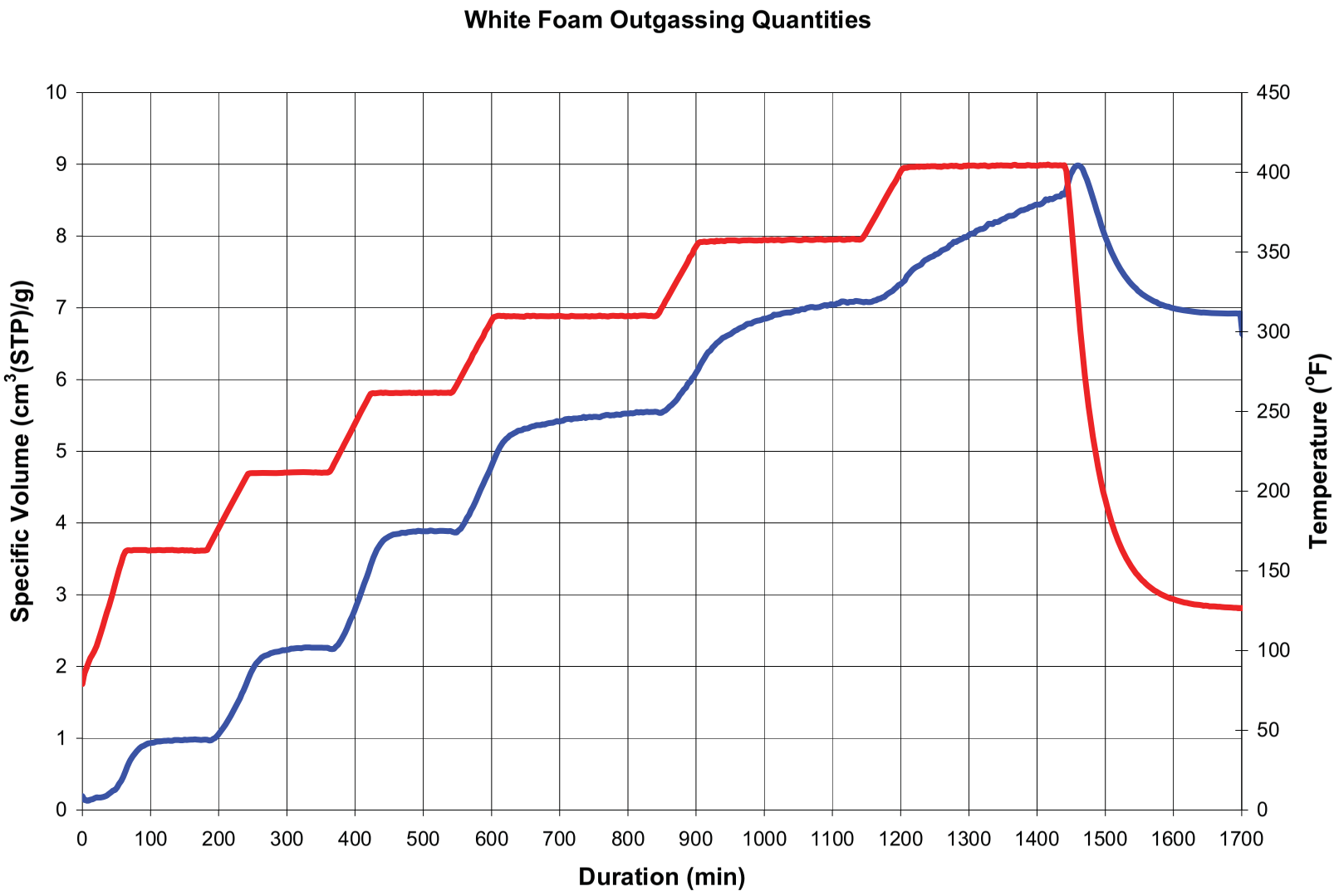

Fig. 9. Outgassing of an 11.06-g specimen of white PU foam.

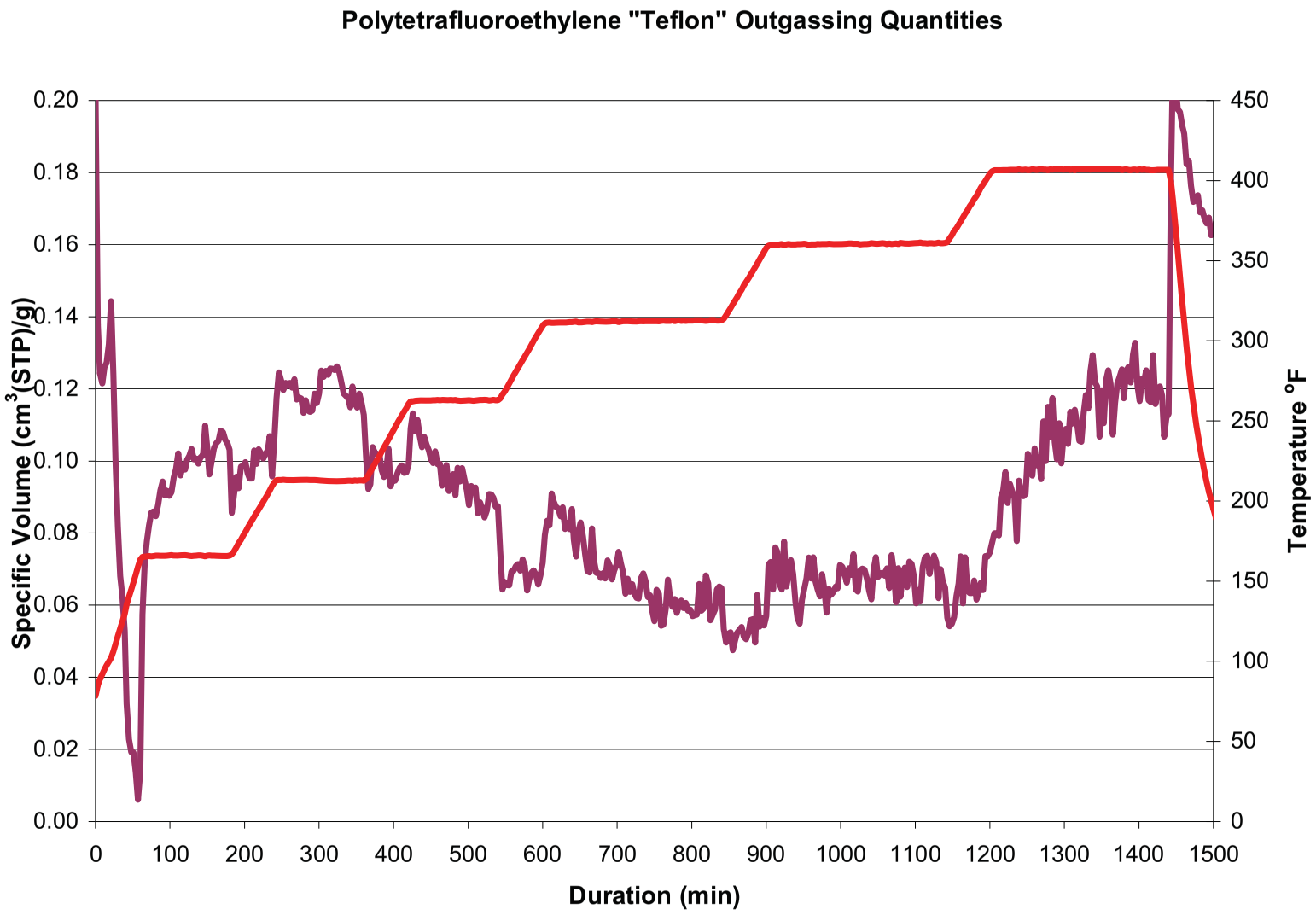

Fig 10. Outgassing of two polytetrafluoroethylene (Teflon) specimens (8.14 g and 12.41 g) competes with measurement noise.

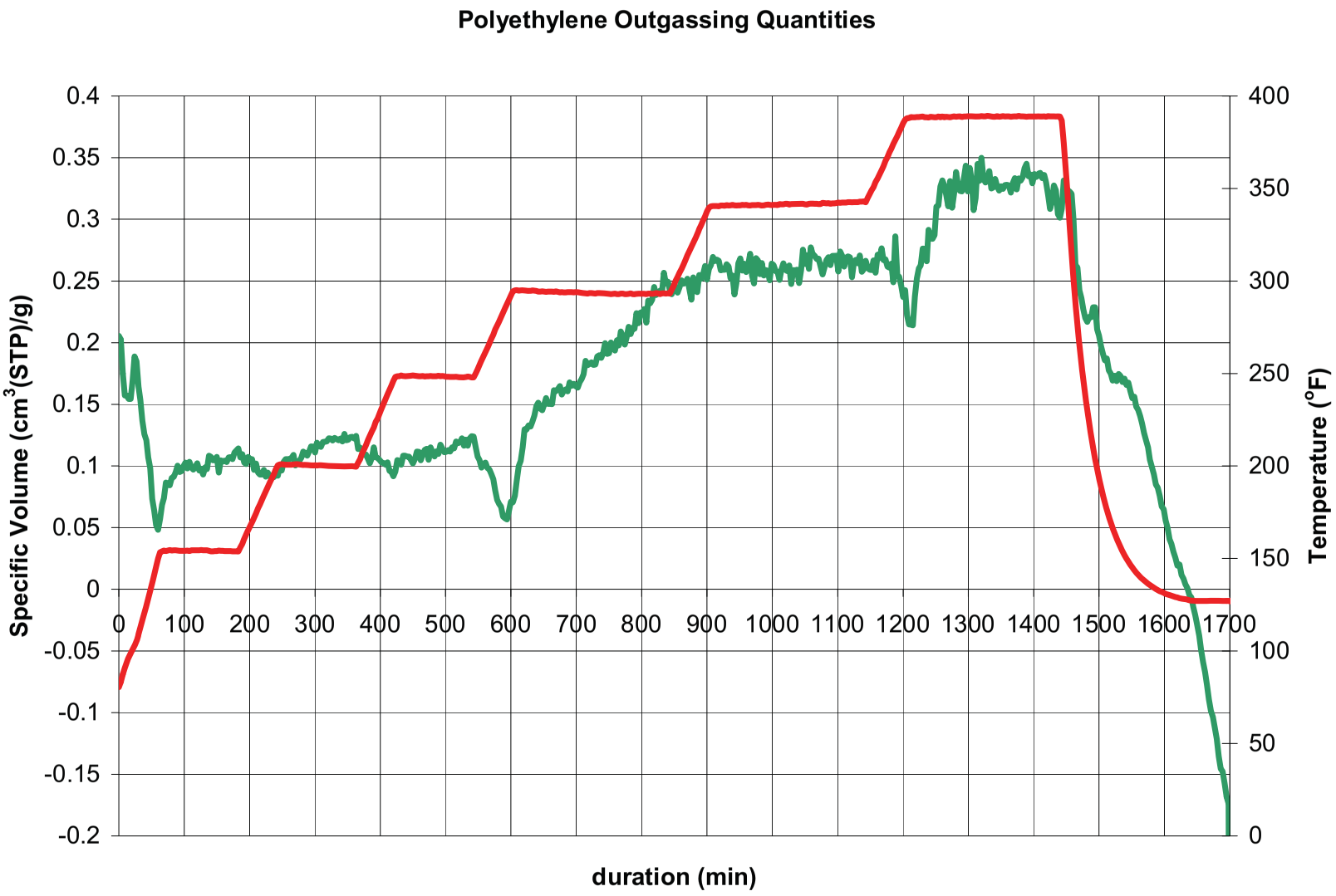

Fig. 11. Outgassing of an 8.18-g specimen of polyethylene bottle is at noise level and decreases rapidly upon cooling.

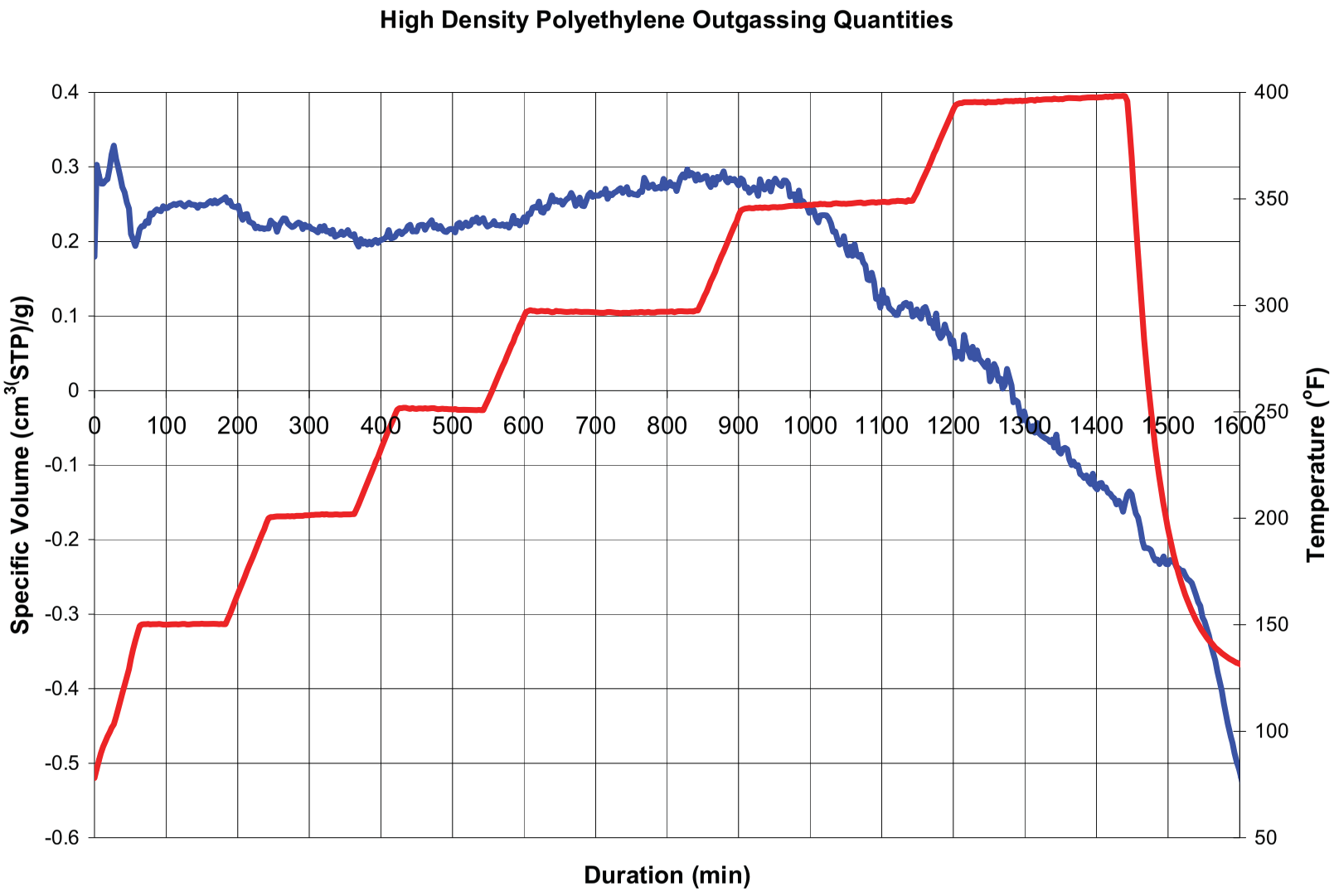

Fig. 12. Outgassing of an 8.3-g specimen of an HDPE bottle lid.

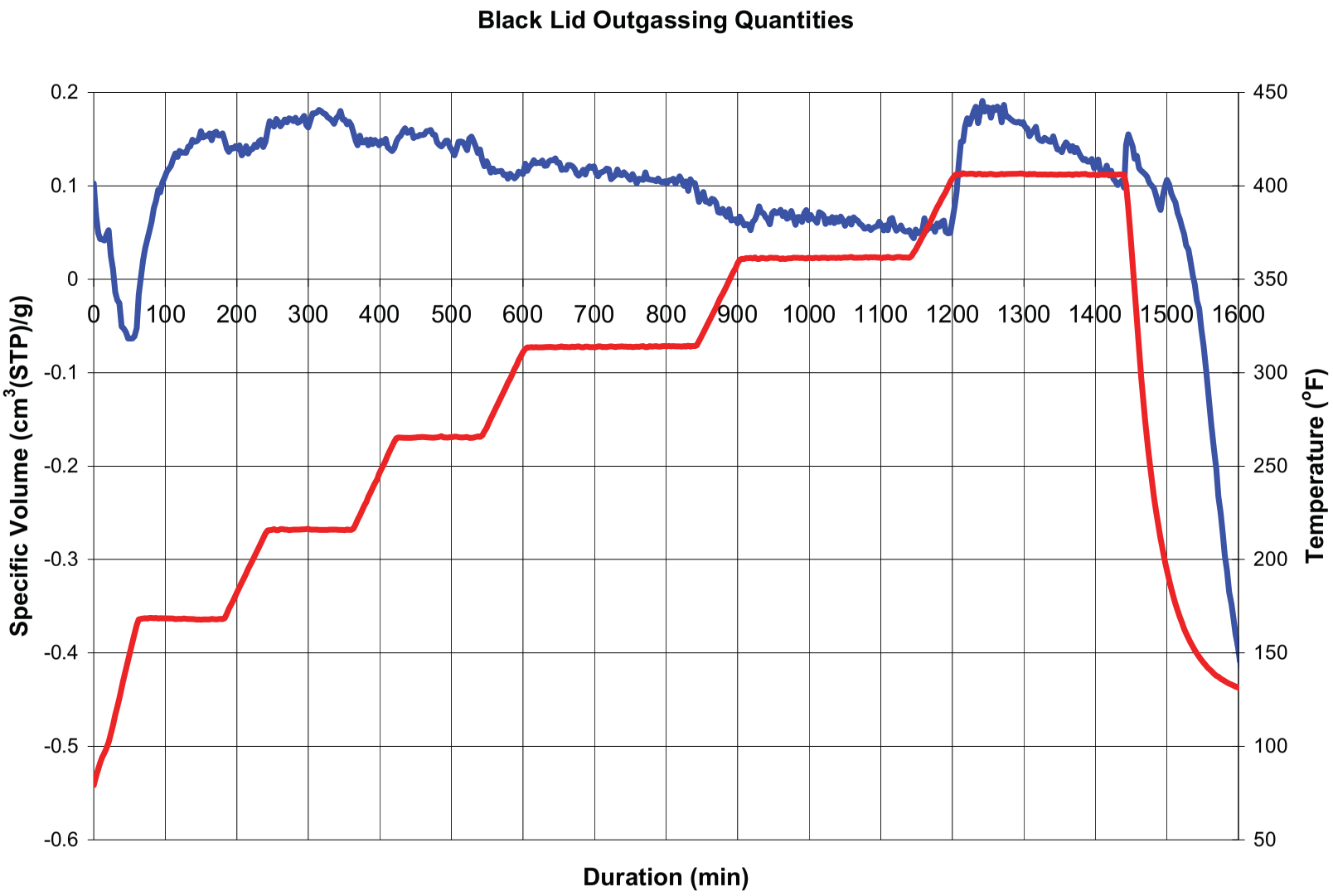

Fig. 13. Outgassing of an 8.90-g specimen of a black plastic bottle lid, possibly polyethylene.

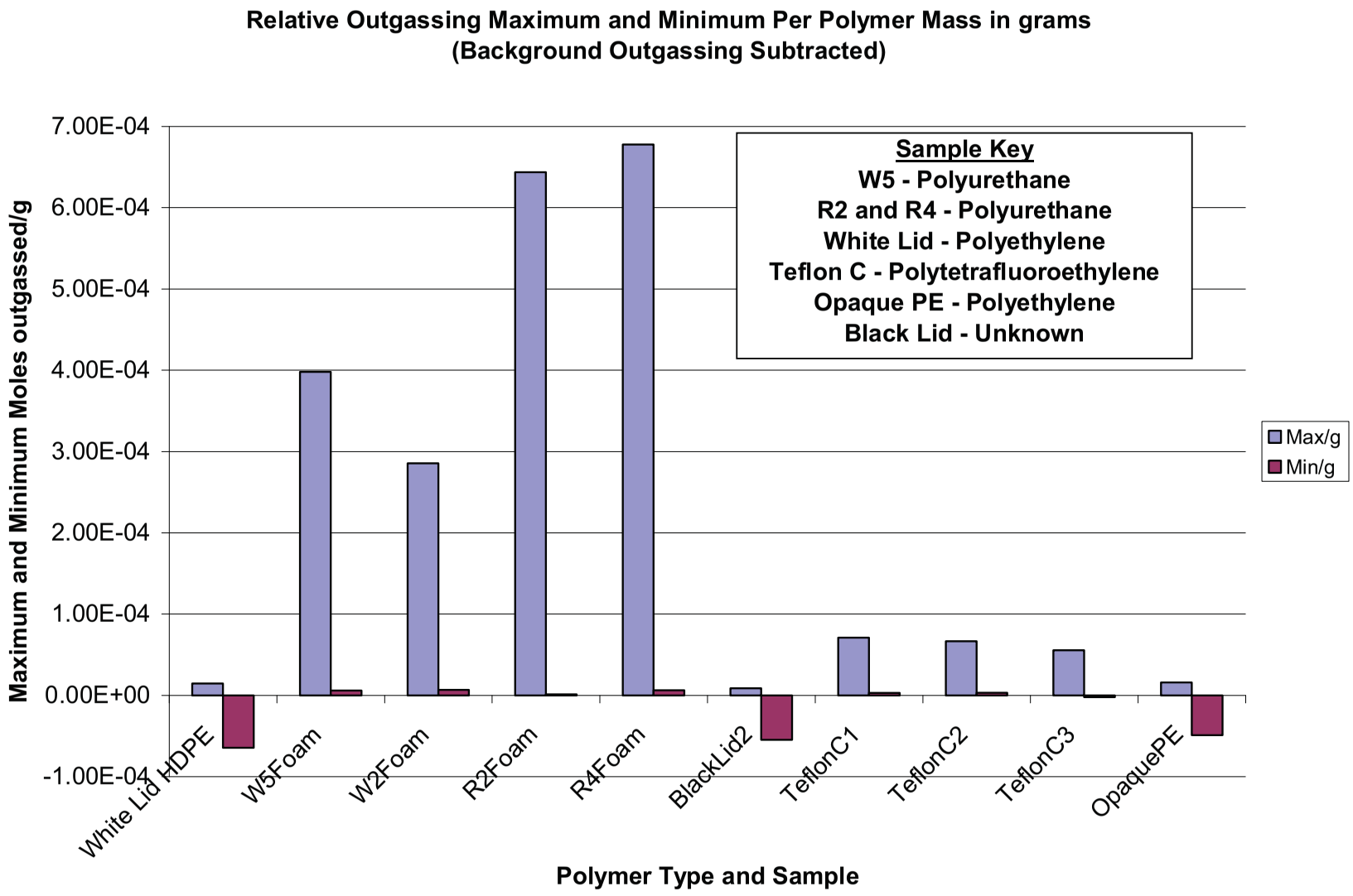

Fig. 14. Relative outgassing by polymer types examined.

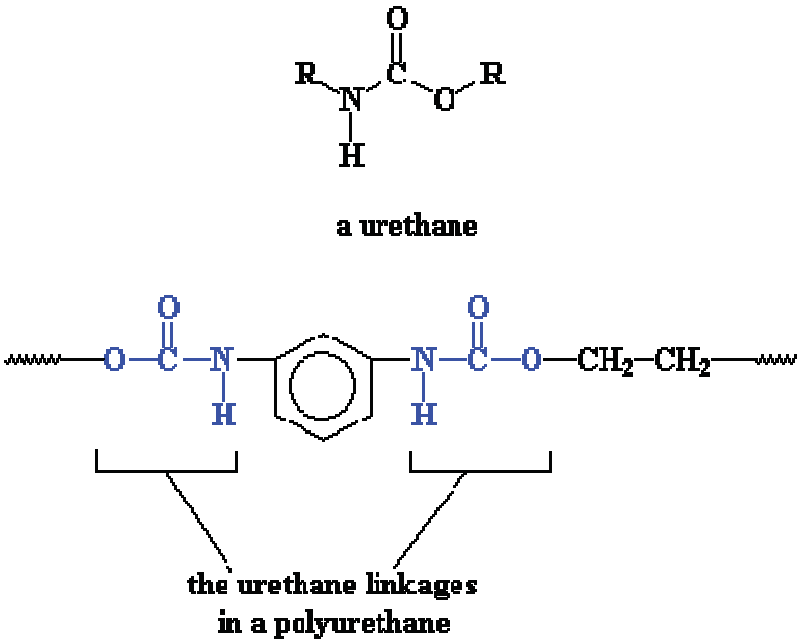

Fig. 15. Polyurethane molecular structure.

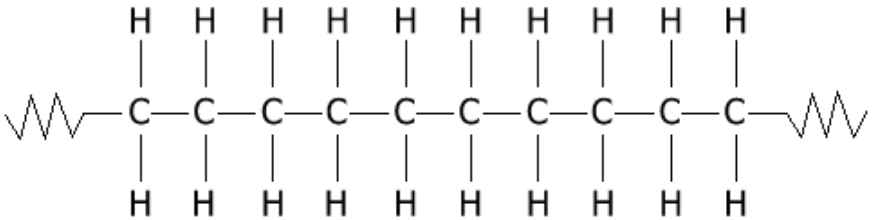

Fig. 16. Polyethylene molecular structure.

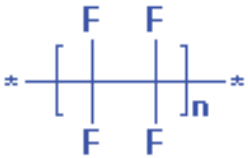

Fig. 17. Polytetrafluoroethylene (Teflon) molecular structure.

REFERENCES

BJB Enterprises, Inc., *Technical Datasheet for TC-280 A/B 8 Lb. Self Skinning Flexible Foam*, August 26, 2004.

H. V. Boenig, *Polyolefins: Structure and Properties*, pp. 234–235, Elsevier Publishing Co., Amsterdam, 1966.

R. Broos, J.-M Sonney, H. P. Thanh, and F. M. Casati, "Polyurethane Foam Molding Technologies for Improving Total Passenger Compartment Comfort," p. 348, from http://www.polyurethane.org/conferences/expo/2004/proceedings/2000/contents.pdf.

J. R. Fried, *Polymer Science and Technology*, pp. 252–263, 473, Prentice Hall PTR, New Jersey, 1995.

L. J. Gibson and M. F. Ashby, *Cellular Solids—Structure and Properties*, pp. 56–57, 2nd ed., Cambridge University Press, Cambridge, 1997.

M. L. Hobbs, K. L. Erickson, , and T. Y. Chu, *Modeling Decomposition of Unconfined Rigid Polyurethane Foam*, Sandia Report SAND99-2758, Sandia National Laboratories, Albuquerque, New Mexico, November 1999.

P. I. Tinnel and J. H. Leckey, internal correspondence to distribution, entitled "Rate of Generation of Volatile Components," February 25, 1991.

G. Kämpf, *Characterization of Plastics by Physical Methods*, pp. 175–196, Hanser Publishers, Munich, 1986.

MatWeb, The Online Materials Database, http://www.matweb.com.

U. S. Nuclear Regulatory Commission, "Hypothetical Accident Conditions," U.S. NRC 10 CFR 71.73(c)(1-3) from www.nrc.gov/reading-rm/doc-collections/cfr/part071/part071-0073.html.

APPENDIX 1: DATA ANALYSIS

This is a description of steps taken in Excel software to process data downloaded in the form of *.csv spreadsheets from National Instruments software. In general, new columns are set up for each calculation.

1. Open file
2. Data columns appear including Date and Time, Temperature, Pressure (torr)
3. Input sample name and weight (in grams) above pressure column
4. Insert column for duration—units can include days, hours, or minutes
5. Use CONVERT function to establish column of Fahrenheit temperatures
6. Input values for *R* (gas constant) and *V* (volume of container and flex hose) into cells on top of spreadsheet
7. Set up column to calculate the number of moles according to the Ideal Gas Law:
    a. N = {p(torr)V(cm^3)/[R (82.057 atm-cm^3/K-mol)*T (T°C + 273)K]} * (1 atm/760 torr) using cell addresses for *p*, *V*, *R*, and *T* values
8. Paste column of blank outgassed moles
9. Subtract column of blank moles outgassed from specimen moles outgassed; this eliminates initial air and system outgassing
10. Calculate the volume of outgassed species at standard temperature and pressure (273 K and 1 atm) or by assuming an ideal gas that will have a volume of 22.4 liters per mole
11. Divide V_{STP} by specimen weight in grams; this column is Specific Volume
12. Plot T (°F) and Specific Volume vs Time (min), created separate axes for temperature and volume variables
13. Apply appropriate titles and formatting.

DISTRIBUTION*

Y-12 National Security Complex

C. M. Cecala *cm6*
J. H. Clinton *cjh*
C. Heatherly *cqh*
M. L. Goins *mlg*
J. H. Leckey *lec*
J. S. Morrell *jkr*
W. I. North *wno*
M. W. Richey *mwr*
R. A. Smith *rox*
Technology Development Archives
T. L. Warren *wte*
Y-12 Central Files—RC (hard copy only)

* Electronic copy unless otherwise noted.

SECTION 2 REFERENCES

10 CFR 71, *Packaging and Transportation of Radioactive Material*, Jan. 1, 2007.

49 CFR, *Transportation*, Oct. 1, 2007.

ARMCO NITRONIC 60 Stainless Steel Product Data Bulletin, S-56b.

ASME Boiler and Pressure Vessel Code, An American National Standard, Rules for Construction of Nuclear Power Plant Components, Parts A and C, American Society of Mechanical Engineers, New York, 2004 ed.

ASME Boiler and Pressure Vessel Code, An American National Standard, Sect. II, *Materials,* Part A, *Ferrous Material Specifications*, American Society of Mechanical Engineers, New York, latest edition.

ASME Boiler and Pressure Vessel Code, An American National Standard, Materials, Sect. II, *Materials,* Div. 1, Part D, American Society of Mechanical Engineers, New York, 2001 ed. with 2002 and 2003 addenda.

ASME Boiler and Pressure Vessel Code, An American National Standard, Rules for Construction of Nuclear Facility Components, Sect. III, Div. 1, Subsection NB, American Society of Mechanical Engineers, New York, 2001 ed. with 2002 and 2003 addenda.

ASME Boiler and Pressure Vessel Code, An American National Standard, Rules for Construction of Nuclear Facility Components, Sect. III, Div. 1, Subsection NCA, American Society of Mechanical Engineers, New York, 2004 ed.

ASME Boiler and Pressure Vessel Code, An American National Standard, Nondestructive Evaluation, Sect. V, American Society of Mechanical Engineers, New York, 2001 ed. with 2002 and 2003 addenda.

ASME Boiler and Pressure Vessel Code, An American National Standard, Nondestructive Evaluation, Sect. V, American Society of Mechanical Engineers, New York, 2004 ed.

ASME Boiler and Pressure Vessel Code, An American National Standard, Welding and Brazing Qualifications, Sect. IX, American Society of Mechanical Engineers, New York, 2001 ed. with 2002 and 2003 addenda.

ASME Boiler and Pressure Vessel Code, An American National Standard, Welding and Brazing Qualifications, Sect. IX, American Society of Mechanical Engineers, New York, 2004 ed.

ANSI N14.5-1997, *Radioactive Materials—Leakage Tests on Packages for Shipment,* American Natl. Standards Institute, Feb. 5, 1998.

ASTM A 380-99e1, *Standard Practice for Cleaning, Descaling, and Passivation of Stainless Steel Parts, Equipment and Systems*, American Society for Testing and Materials, Philadelphia, current revision.

ASTM D-2000, *Standard Classification System for Rubber Products in Automotive Applications*, American Society for Testing and Materials, Philadelphia, current revision.
Bailey, R. A., *THERM 1.2, A Thermal Properties DataBase for the IBM PC*, Lawrence Livermore Natl. Lab., Nov. 18, 1987.

Byington, G. A., *Vibration Test Report of the ES-2M Shipping Package*, GAB1296-2, Lockheed Martin Energy Systems, Inc., Oak Ridge Y-12 Plant, Sept. 3, 1997.

Daikin America, Inc., Neoflon™ FEP Fact Sheet, http://www.daikin.cc/Products/ProductLines/default.aspx?productlineid=1.

Design Guidelines for the Selection and Use of Stainless Steel, American Iron and Steel Institute, Washington, D.C., 1977.

DOE Order 5610.14, *Transportation Safeguards System Program Operations*, May 1993.

Drawing M2E801580A027, rev. A, *Containment Vessel Heavy Test Weight Assembly*, BWXT Y-12, Y-12 Natl. Security Complex, Oct. 29, 2003.

Drawing M2E801580A029, rev. A, *Light Test Weight Confirmation Assembly*, BWXT Y-12, Y-12 Natl. Security Complex, Oct. 29, 2003.

ES-3100 Weldments P.O. 203-102-029, Document package from EaglePicher Technologies, Boron Dept., Quapaw, Okla., May 21, 2004.

Handy, K. D., *Drop Simulation of the ES-2LM Shipping Container,* DAC-EA-900000-A002, Lockheed Martin Energy Systems, Inc., Oak Ridge Natl. Lab., April 1997.

Leidecker, Henning, "The thermal decomposition of Teflon," http://misspiggy.gsfc.nasa.gov/tva/issfoc/iss/docs/HenningFEP.doc.

LS-Dyna, A Program for Nonlinear Dynamic Analysis of Structures in Three Dimensions, Livermore Software Technology Corporation (LSTC), Version 960, rev. 1106, Jan. 28, 2002.

MIL-D-6054F, *Drum, Metal—Shipping and Storage*, June 30, 1989.

MIL-HDBK-5H, *Metallic Materials and Elements for Aerospace Vehicle Structures*, Dec. 1, 1998.

MIL-STD-810F, *Test Method Standard for Environmental Engineering Considerations and Laboratory Tests,* Jan. 1, 2000.

MS27683, *Drum, Metal—Shipping and Storage 16 to 80 Gallons.*

NUREG-1609, *Standard Review Plan for Transportation Packages for Radioactive Material*, U.S. NRC, Mar. 31, 1999.

NUREG/CR-3019, *Recommended Welding Criteria for Use in the Fabrication of Shipping Containers for Radioactive Materials*.

NUREG/CR-3854, *Fabrication Criteria for Shipping Containers*, Lawrence Livermore Natl. Lab., March 1985.

NUREG/CR-1815, *Recommendations for Protecting Against Failure by Brittle Fracture in Ferritic Steel Shipping Containers up to Four Inches Thick.*

OO-PP-986, rev. D, *Procurement Specification for 70A Durometer Preformed Packing (O-rings)*, Lockheed Martin Energy Systems, Inc., Oak Ridge Y-12 Plant, Jan. 26, 1999.

OO-PP-1210, *Procurement Specification for the MD-1 Containment Vessel*.

Parker O-ring Handbook, Catalog ORD 5700A/US, Parker Hannifin Corp., O-Ring Div., Lexington, Ky., 2001.

Pro/ENGINEER™, Wildfire release, Parametric Technology Corp., Needham, Mass., date code 2003490.

Regulatory Guide 7.6, rev. 1, *Design Criteria for the Structural Analysis of Shipping Cask Containment Vessels*, U.S. NRC, March 1978.

Regulatory Guide 7.8, *Load Combinations for the Structural Analysis of Shipping Casks*, U.S. NRC, May 1977.

Regulatory Guide 7.11, *Fracture Toughness Criteria of Base Material for Ferritic Steel Shipping Cask Containment Vessels with a Maximum Wall Thickness of 4 Inches (0.1 m)*, U.S. NRC, June 1991.

Shappert, L. B., "Test Facilities for Radioactive Material Transport Packages (Oak Ridge National Laboratory, USA)," RAMSTRANS, 2 (4/5), 73–79, Nuclear Technol., 1991.

Slapdown: A Rigid Body Dynamics Code, Version 05.20.93, Sandia Natl. Lab.

SNT-TC-1A-1992, *Recommended Practice for Nondestructive Testing Personnel Qualification and Certification*, American Society for Nondestructive Testing, December 1992.

Stainless Steel Handbook, Allegheny Ludlum Steel Corp., Pittsburgh, Penn, February 20, 2005.

THIS PAGE INTENTIONALLY LEFT BLANK.

Y/LF-717, Rev 4
Docket No. 71-9315

Safety Analysis Report, Y-12 National Security Complex, Model ES-3100 Package with Bulk HEU Contents

Volume 2
Sections 3-8

Babcock & Wilcox Technical Services Y-12, LLC
Y-12 National Security Complex
P.O. Box 2009
Oak Ridge, Tennessee 37831

March 3, 2011

Y/LF-717, Rev. 4,
Volume 2

SAFETY ANALYSIS REPORT, Y-12 NATIONAL SECURITY COMPLEX, MODEL ES-3100 PACKAGE WITH BULK HEU CONTENTS

Prepared by
Babcock & Wilcox Technical Services Y-12, LLC
Management & Operating Contractor
for the
Y-12 National Security Complex
under Contract No. DE-AC05-00OR22800
with the
U.S. Department of Energy
National Nuclear Security Administration

March 3, 2011

APPROVALS

Y/LF-717, Rev. 4

SAFETY ANALYSIS REPORT,
Y-12 NATIONAL SECURITY COMPLEX,
MODEL ES-3100 PACKAGE WITH BULK HEU CONTENTS

Approved by:

Walter I. North
Packaging Engineering Manager

3/3/2011
Date

James C. Anderson
Safety Analysis Report for Packaging Manager

3/3/11
Date

Jeffrey G. Arbital
Transportation and Packaging Program Manager

3/3/11
Date

THIS PAGE INTENTIONALLY LEFT BLANK.

CONTENTS

Page

APPROVALS iii

FIGURES xi

TABLES xiii

ABBREVIATIONS xvii

REVISION LOG xix

1. GENERAL INFORMATION 1-1
   1.1 INTRODUCTION 1-1
   1.2 PACKAGE DESCRIPTION 1-1
      1.2.1 Packaging 1-4
      1.2.2 Containment System 1-7
      1.2.3 Contents 1-10
      1.2.4 Operational Features 1-25
   1.3 GENERAL REQUIREMENTS FOR ALL PACKAGES 1-25
      1.3.1 Minimum package size 1-25
      1.3.2 Tamper-indicating feature 1-26
   1.4 APPENDICES 1-27
      1.4.1 PACKAGE CERTIFICATION DRAWING 1-29
      1.4.2 EQUIPMENT SPECIFICATION JS-YMN3-801580-A002, *ES-3100 DRUM ASSEMBLY* 1-43
      1.4.3 EQUIPMENT SPECIFICATION JS-YMN3-801580-A001, *ES-3100 CONTAINMENT VESSEL* 1-53
      1.4.4 EQUIPMENT SPECIFICATION, JS-YMN3-801580-A003, *MANUFACTURING PROCESS SPECIFICATION FOR CASTING KAOLITE 1600™ INTO THE ES-3100 SHIPPING PACKAGE* 1-67
      1.4.5 EQUIPMENT SPECIFICATION, JS-YMN3-801580-A005, *CASTING CATALOG NO. 277-4 NEUTRON ABSORBER FOR THE ES-3100 SHIPPING PACKAGE* 1-87
      1.4.6 PACKAGE CATEGORY DETERMINATION 1-129
      1.4.7 HEU OXIDE MATERIAL SPECIFICATION AS PROVIDED BY Y-12 HIGHLY ENRICHED URANIUM DISPOSITION PROGRAM OFFICE 1-133
      1.4.8 DETAILED ENGINEERING DRAWINGS 1-137
      1.4.9 DESIGN ANALYSES AND CALCULATIONS, DAC-PKG-801624-A001, MIXING WEIGHTS AND ELEMENTAL COMPOSITION OF 277-4 NEUTRON POISON USED IN THE ES-3100 1-183
      1.4.10 PYROPHORICITY OF URANIUM METAL 1-211
   SECTION 1 REFERENCES 1-231

2. STRUCTURAL EVALUATION 2-1
   2.1 DESCRIPTION OF STRUCTURAL DESIGN 2-2
      2.1.1 Discussion 2-2
      2.1.2 Design Criteria 2-5
      2.1.3 Weights and Centers of Gravity 2-14
      2.1.4 Identification of Codes and Standards for Package Design 2-14

CONTENTS

Page

2.2 MATERIALS 2-18
2.2.1 Material Properties and Specifications 2-18
2.2.2 Chemical, Galvanic, or Other Reactions 2-18
2.2.3 Effects of Radiation on Materials 2-26
2.3 FABRICATION AND EXAMINATION 2-26
2.3.1 Fabrication 2-26
2.3.2 Examination 2-28
2.4 LIFTING AND TIE-DOWN STANDARDS FOR ALL PACKAGES 2-31
2.4.1 Lifting Devices 2-31
2.4.2 Tie-Down Devices 2-31
2.5 GENERAL CONSIDERATIONS 2-32
2.5.1 Evaluation by Test 2-32
2.5.2 Evaluation by Analysis 2-35
2.6 NORMAL CONDITIONS OF TRANSPORT 2-35
2.6.1 Heat 2-37
2.6.2 Cold 2-39
2.6.3 Reduced External Pressure 2-42
2.6.4 Increased External Pressure 2-42
2.6.5 Vibration 2-44
2.6.6 Water Spray 2-46
2.6.7 Free Drop 2-47
2.6.8 Corner Drop 2-48
2.6.9 Compression 2-48
2.6.10 Penetration 2-50
2.7 HYPOTHETICAL ACCIDENT CONDITIONS 2-51
2.7.1 Free Drop 2-54
2.7.2 Crush 2-64
2.7.3 Puncture 2-70
2.7.4 Thermal 2-71
2.7.5 Immersion—Fissile Material 2-80
2.7.6 Immersion—All Packages 2-81
2.7.7 Deep Water Immersion Test 2-81
2.7.8 Summary of Damage 2-81
2.8 ACCIDENT CONDITIONS FOR AIR TRANSPORT OF PLUTONIUM 2-96
2.9 ACCIDENT CONDITIONS FOR FISSILE MATERIAL PACKAGES FOR AIR TRANSPORT 2-96
2.9a SPECIAL FORM 2-96
2.9b FUEL RODS 2-96
2.10 APPENDICES 2-97
2.10.1 ES-3100 CONTAINMENT VESSEL ASME CODE EVALUATION 2-99
2.10.2 IMPACT ANALYSES OF ES-3100 DESIGN CONCEPTS USING BOROBOND AND CAT 277-4 NEUTRON ABSORBERS 2-157
2.10.3 KAOLITE PROPERTIES 2-463
2.10.4 CATALOG 277-4 PROPERTIES 2-535
2.10.5 BOROBOND4 PROPERTIES 2-645
2.10.6 RECOMMENDED RANDOM VIBRATION AND SHOCK TEST SPECIFICATIONS FOR CARGO TRANSPORTED ON SST AND SGT TRAILERS 2-659

CONTENTS

Page

2.10.7 TEST REPORT OF THE ES-3100 PACKAGE, VOLUME 1 - MAIN REPORT, ORNL/NTRC-013/V1, REV. 0, SEPTEMBER 10, 2004 2-677
2.10.8 THE ES-3100 TEST REPORT; VOL. 3, APPENDIX K - TU-4 DATA SHEETS 2-809
2.10.9 PACKAGING MATERIALS OUTGASSING STUDY FINAL REPORT 2-853
SECTION 2 REFERENCES 2-893

3. THERMAL EVALUATION 3-1
3.1 DISCUSSION 3-1
3.1.1 Design Features 3-3
3.1.2 Content's Decay Heat 3-4
3.1.3 Summary Tables of Temperatures 3-6
3.1.4 Summary Tables of Maximum Pressures 3-16
3.2 SUMMARY OF THERMAL PROPERTIES OF MATERIALS 3-19
3.2.1 Material properties 3-19
3.2.2 Component Specifications 3-19
3.3 GENERAL CONSIDERATIONS 3-19
3.3.1 Evaluation by Analysis 3-19
3.3.2 Evaluation by Test 3-25
3.3.3 Margins of Safety 3-28
3.4 THERMAL EVALUATION UNDER NORMAL CONDITIONS OF TRANSPORT 3-31
3.4.1 Heat and Cold 3-31
3.4.2 Maximum Normal Operating Pressure 3-33
3.4.3 Maximum Thermal Stresses 3-34
3.5 HYPOTHETICAL ACCIDENT THERMAL EVALUATION 3-35
3.5.1 Initial Conditions 3-35
3.5.2 Fire Test Conditions 3-36
3.5.3 Maximum Temperatures and Pressure 3-38
3.5.4 Accident Conditions for Fissile Material Packages for Air Transport 3-42
3.6 APPENDICES 3-43
3.6.1 THERMAL EVALUATION OF THE ES-3100 SHIPPING CONTAINER FOR NCT AND HAC (CONCEPTUAL DESIGN WITH BOROBOND4 NEUTRON ABSORBER) 3-45
3.6.2 THERMAL EVALUATION OF THE ES-3100 SHIPPING CONTAINER FOR NCT AND HAC (FINAL DESIGN WITH CATALOG 277-4 NEUTRON ABSORBER) 3-85
3.6.3 THERMAL STRESS EVALUATION OF THE ES-3100 SHIPPING CONTAINER DRUM BODY ASSEMBLY FOR NCT (FINAL DESIGN WITH CATALOG 277-4 NEUTRON ABSORBER) 3-125
3.6.4 CONTAINMENT VESSEL PRESSURE DUE TO NORMAL CONDITIONS OF TRANSPORT FOR THE PROPOSED CONTENTS 3-149
3.6.5 CONTAINMENT VESSEL PRESSURE DUE TO HYPOTHETICAL ACCIDENT CONDITIONS FOR THE PROPOSED CONTENTS 3-159
3.6.6 SILICONE RUBBER THERMAL PROPERTIES FROM THERM 1.2 DATABASE 3-167
3.6.7 ESTIMATES OF HYDROGEN BUILDUP IN THE ES-3100 PACKAGE CONTAINING HIGHLY ENRICHED URANIUM 3-169
SECTION 3 REFERENCES 3-349

CONTENTS

Page

4. CONTAINMENT 4-1
4.1 DESCRIPTION OF THE CONTAINMENT BOUNDARY 4-2
4.1.1 Containment Boundary 4-2
4.1.2 Special Requirements for Plutonium 4-4
4.2 GENERAL CONSIDERATIONS 4-4
4.2.1 Type A Fissile Packages 4-4
4.2.2 Type B Packages 4-4
4.3 CONTAINMENT UNDER NORMAL CONDITIONS OF TRANSPORT (TYPE B PACKAGES) 4-6
4.4 CONTAINMENT UNDER HYPOTHETICAL ACCIDENT CONDITIONS (TYPE B PACKAGES) 4-8
4.5 LEAKAGE RATE TESTS FOR TYPE B PACKAGES 4-10
4.6 APPENDICES 4-11
4.6.1 DETERMINATION OF A_2 FOR THE ES-3100 PACKAGE WITH HEU CONTENTS 4-13
4.6.2 CALCULATION OF THE ES-3100 CONTAINMENT VESSEL'S REGULATORY REFERENCE AIR LEAKAGE RATES 4-23
SECTION 4 REFERENCES 4-35

5. SHIELDING EVALUATION 5-1
5.1 DESCRIPTION OF SHIELDING DESIGN 5-1
5.1.1 Design Features 5-1
5.1.2 Summary Table of Maximum Radiation Levels 5-1
5.2 SOURCE SPECIFICATION 5-1
5.3 DOSE RATE ANALYSIS MODELS 5-3
5.3.1 Packaging Model Conservative Features 5-7
5.3.2 Photon model for 36-kg HEU metal content 5-9
5.3.3 Neutron model for 36-kg HEU metal content 5-11
5.3.4 Photon model for 24-kg HEU oxide content 5-11
5.3.5 Neutron model for 24-kg HEU oxide content 5-11
5.4 SHIELDING EVALUATION 5-11
5.5 APPENDICES 5-15
5.5.1 ORIGEN INPUT DATA FROM TABLE 5.3 5-17
5.5.2 CSASN AND ICE INPUT FROM TABLE 5.8 5-19
5.5.3 MORSE ROUTINES AND INPUT DATA 5-21
SECTION 5 REFERENCES 5-39

6. CRITICALITY EVALUATION 6-1
6.1 DESCRIPTION OF THE CRITICALITY DESIGN 6-1
6.1.1 Design Features 6-1
6.1.2 Summary of the Criticality Evaluation 6-2
6.1.3 Criticality Safety Index 6-32
6.2 PACKAGE CONTENTS 6-33
6.2.1 Fissile Material Contents 6-33
6.2.2 Convenience Cans, Teflon and Polyethylene Bottles, and 277-4 Canned Spacers 6-34

CONTENTS

Page

6.2.3 Packing Materials 6-35
6.2.4 Package Content Loading Restrictions 6-36
6.3 GENERAL CONSIDERATIONS 6-37
6.3.1 Model Configuration 6-38
6.3.2 Material Properties 6-55
6.3.3 Computer Codes and Cross-Section Libraries 6-57
6.3.4 Demonstration of Maximum Reactivity 6-68
6.4 SINGLE PACKAGE EVALUATION 6-70
6.4.1 Solid HEU Metal of Specified Geometric Shapes 6-71
6.4.2 HEU Solid Metal of Unspecified Geometric Shapes or HEU Broken Metal 6-79
6.4.3 HEU Oxide 6-80
6.4.4 UNH Crystals 6-82
6.5 EVALUATION OF PACKAGE ARRAYS UNDER NORMAL CONDITIONS OF TRANSPORT 6-84
6.5.1 Solid HEU Metal of Specified Geometric Shapes 6-84
6.5.2 HEU Solid Metal of Unspecified Geometric Shapes or HEU Broken Metal 6-86
6.5.3 HEU Oxide 6-89
6.5.4 UNH Crystals 6-89
6.6 EVALUATION OF PACKAGE ARRAYS UNDER HYPOTHETICAL ACCIDENT CONDITIONS 6-90
6.6.1 Solid HEU Metal of Specified Geometric Shapes 6-90
6.6.2 HEU Solid Metal of Unspecified Geometric Shapes or HEU Broken Metal 6-92
6.6.3 HEU Oxide 6-93
6.6.4 UNH Crystals 6-94
6.7 FISSILE MATERIAL PACKAGES FOR AIR TRANSPORT 6-95
6.7.1 Results for Solid HEU, One Piece per Convenience Can 6-95
6.7.2 Results for TRIGA Fuel Elements, Three Pieces per Convenience Can 6-97
6.7.3 Results for HEU Broken Metal, More Than One Piece per Convenience Can . . . 6-101
6.7.4 Conclusions 6-103
6.8 BENCHMARK EXPERIMENTS 6-103
6.8.1 Applicability of Benchmark Experiments 6-103
6.8.2 Details of Benchmark Calculations 6-104
6.8.3 Bias Determination 6-104
6.9 APPENDICES 6-105
6.9.1 FISSILE CONTENT AND PACKAGING MODELS 6-107
6.9.2 HAC PACKAGE MODEL 6-137
6.9.3 PACKAGE MATERIAL COMPOSITIONS 6-149
6.9.4 QUALIFICATION OF A NEUTRON ABSORBER MATERIAL FOR THE ES-3100 6-181
6.9.5 MISCELLANEOUS INFORMATION AND DATA 6-193
6.9.6 ABRIDGED SUMMARY TABLES OF CRITICALITY CALCULATION RESULTS 6-197
6.9.7 INPUT LISTINGS OF ES-3100 CALCULATION MODELS FOR SELECT CASES 6-353

CONTENTS

Page

6.9.8 Y/DD-896/R1, *CRITICAL EXPERIMENT BENCHMARK CALCULATIONS WITH CSAS25 FROM SCALE4.4a FOR CRITICALITY SAFETY ANALYSES ON THE HP J-5600 UNCLASSIFIED WORKSTATION (CMODB)* AND Y/DD-972R1, *DETERMINATION OF THE UPPER SUBCRITICAL LIMIT FOR CRITICALITY CALCULATIONS FOR CRITICALITY SAFETY ANALYSES* 6-577
6.9.9 CRITICALITY EVALUATION FOR INCREASING THE FISSILE LOADING LIMIT FOR HEU OXIDE IN THE ES-3100 6-717
6.9.10 Y/DD-1220, *CRITICAL EXPERIMENT BENCHMARK CALCULATIONS WITH CSAS25 FROM SCALE5 FOR CRITICALITY SAFETY ANALYSES ON THE HP zx6000 UNCLASSIFIED WORKSTATION (CMODD)* AND Y/DD-1221, *DETERMINATION OF THE UPPER SUBCRITICAL LIMIT FOR CRITICALITY CALCULATIONS FOR CRITICALITY SAFETY ANALYSES* 6-765
SECTION 6 REFERENCES 6-891

7. PACKAGE OPERATIONS 7-1
7.1 PACKAGE LOADING 7-1
7.1.1 Preparation for Loading 7-1
7.1.2 Loading of Contents 7-3
7.1.3 Preparation for Transport 7-7
7.2 PACKAGE UNLOADING 7-10
7.2.1 Receipt of Package from Carrier 7-10
7.2.2 Removal of Contents 7-11
7.3 PREPARATION OF EMPTY PACKAGE FOR TRANSPORT 7-12
7.4 OTHER OPERATIONS 7-12
SECTION 7 REFERENCES 7-13

8. ACCEPTANCE TESTS AND MAINTENANCE PROGRAM 8-1
8.1 ACCEPTANCE TESTS 8-1
8.1.1 Visual Inspections and Measurements 8-3
8.1.2 Weld Examinations 8-4
8.1.3 Structural and Pressure Tests 8-5
8.1.4 Leakage Tests 8-5
8.1.5 Component and Material Tests 8-6
8.1.6 Shielding Tests 8-6
8.1.7 Thermal Tests 8-6
8.1.8 Miscellaneous Tests 8-7
8.2 MAINTENANCE PROGRAM 8-7
8.2.1 Structural and Pressure Tests 8-7
8.2.2 Leakage Tests 8-7
8.2.3 Component and Material Tests 8-9
8.2.4 Thermal Tests 8-9
8.2.5 Miscellaneous Tests 8-9
SECTION 8 REFERENCES 8-11

FIGURES

Page

1.1. Schematic of the ES-3100 shipping package 1-2
1.2. Exploded view of the ES-3100 package with bulk HEU contents 1-3
1.3. Containment boundary of the ES-3100 shipping package 1-8
1.4. Typical shipping configurations inside the ES-3100 containment vessel 1-19
1.5. TRIGA fuel element 1-21
2.1. Containment vessel calculated stress locations 2-10
2.2. ES-3100 shipping package center of gravity locations 2-15
2.3. ES-3100 vibration testing arrangement 2-45
2.4. Water spray test arrangement for Test Unit -4 2-46
2.5. NCT free drop test on Test Unit-4 2-48
2.6. Compression test on Test Unit-4 2-49
2.7. Penetration test damage on Test Unit-4 2-50
2.8. 9-m drop test arrangement for all test units 2-54
2.9. 9-m drop test damage on Test Unit-4 2-56
2.10. Cumulative damage from 9-m drop and crush testing on Test Unit-2 2-58
2.11. Test Unit-3 damage from 1.2 and 9-m drop tests 2-59
2.12. 1.2 and 9-m drop test damage on Test Unit-1 2-61
2.13. 1.2 and 9-m drop test damage to Test Unit-5 2-63
2.14. Cumulative damage following 9-m crush on Test Unit-1 2-65
2.15. Cumulative damage following 9-m crush test on Test Unit-3 2-67
2.16. Cumulative damage from 9-m drop and crush testing on Test Unit-4 2-68
2.17. Cumulative damage from 9-m drop and crush testing on Test Unit-5 2-70
2.18. 28° oblique and horizontal puncture tests on Test Unit-1 2-72
2.19. 40° oblique puncture test on Test Unit-1 2-72
2.20. Horizontal puncture test over Test Unit-1's containment vessel flange 2-73
2.21. Horizontal CG puncture test on Test Unit-2 2-73
2.22. 24.6° oblique puncture test on Test Unit-3 2-74
2.23. Vertical puncture test on Test Unit-4 2-74
2.24. Horizontal puncture test over Test Unit-5's containment vessel flange 2-75
2.25. Visual comparison of the cumulative damage on the crush side surface after the three drop tests (from top to bottom: Test Unit-1, analytical results with BoroBond, analytical results with Cat 277-4) 2-84
2.26. Visual comparison of the cumulative damage on the rigid surface side after the four drop tests (from left to right: Test Unit-2, analytical results with BoroBond, analytical results with Cat 277-4) 2-87
2.27. Visual comparison of the cumulative damage on the crush plate side after the three drop tests (from left to right: Test Unit-2, analytical results with BoroBond, analytical results with Cat 277-4) 2-87
2.28. Visual comparison of the cumulative bottom damage after the three drop tests (from top to bottom: Test Unit-3, analytical results with BoroBond, analytical results with Cat 277-4) 2-89
2.29. Visual comparison of the cumulative lid damage after the three drop tests (from top to bottom: Test Unit-3, analytical results with BoroBond, analytical results with Cat 277-4) 2-90
2.30. Visual comparison of the cumulative damage after the three drop tests (from left to right: Test Unit-4, analytical results with BoroBond, analytical results with Cat 277-4) 2-92
2.31. Containment vessel markings at assembly (swivel hoist ring removed prior to testing) 2-95
2.32. Containment vessel marking after compliance testing 2-95
3.1. MSC.Patran axisymmetric finite element model of the ES-3100 shipping container with BoroBond 4—nodal locations of interest (elements representing air not shown for clarity). . . . 3-6
3.2. Test units preheat arrangement. 3-26
3.3. Test unit insertion into furnace. 3-26

FIGURES

Page

3.4. Test unit removal from furnace. 3-27
3.5. Test unit cool down and monitoring arrangement. 3-27
5.1. Cylindrical calculational model of the ES-3100 shipping package for NCT 5-6
5.2. ES-3100 HEU metal content radial (top view) geometric models 5-10
6.1. R/Z section view of ES-3100 single-unit packaging model 6-40
6.2. R/Z section view at bottom of ES-3100 single-unit packaging showing KENO V.a geometry units 1001–1003, and 1006 (partial) 6-41
6.3. R/Z section view at center of the ES-3100 single-unit packaging showing KENO V.a geometry units 1006 (partial), 1007, and 1008 (partial) 6-42
6.4. R/Z section view of near top of the ES-3100 single-unit packaging showing KENO V.a geometry units 1008 (partial) and 1010–1016 6-43
6.5. R/Z section view at the top of the ES-3100 single-unit packaging showing KENO V.a geometry units 1016–1019 6-44
6.6. R/Z section view of ES-3100 array packaging model with a 7% reduction in the drum's inner diameter 6-45
6.7. R/Z section view at the bottom of the ES-3100 array packaging showing KENO V.a geometry units 1001–1003, and 1006 (partial) 6-46
6.8. R/Z section view at the center of the ES-3100 array packaging showing KENO V.a geometry units 1006 (partial), 1007, and 1008 (partial) 6-47
6.9. R/Z section view of near top of the ES-3100 array packaging showing KENO V.a geometry units 1008 (partial) and 1010–1016 6-48
6.10. R/Z section view at the top of the ES-3100 array packaging showing KENO V.a geometry units 1016–1019 6-49
6.11. Model 1. 6-53
6.12. Model 2. 6-53
6.13. Model 3. 6-53
6.14. Model 4 6-54
6.15. Model 5 6-54
6.16. Model 6 6-54
6.16a. $k_{eff} + 2\sigma$ versus pitch for triangular arrangement of content in CV 6-74
6.16b. $k_{eff} + 2\sigma$ versus triangular pitch over range of CV moderation 6-75
6.16c. $k_{eff} + 2\sigma$ as a function of uranium weight fraction and moderation 6-75
6.17. K_{eff} vs. enrichment (wt % ^{235}U) for HEU ranging from 7 to 10 kg 6-96
6.18. K_{eff} vs. stainless steel shell radius (cm) for 7 kg HEU with enrichments ranging from 19 to 100 wt % ^{235}U 6-96
6.19. K_{eff} vs. Kaolite shell radius (cm) for 7 kg HEU with enrichments ranging from 19 to 100 wt % ^{235}U 6-98
6.20. K_{eff} vs. shell radius (cm) for dry and water-saturated Kaolite for 7 kg HEU at 100% enrichment 6-98
6.21. K_{eff} vs shell radius (cm) for 10.4 kg core of $UZrH_x$ with stainless steel or Kaolite shell 6-99
6.22. K_{eff} vs. core radius (cm) for homogenized core of $UZrH_x$, 500 g polyethylene, and Kaolite where the Kaolite water content ranges from the dry to the water-saturated condition 6-100
6.23. k_{eff} vs. excess water from Kaolite for fissile core blanketed with a variable thickness Kaolite shell. 6-101
6.24. K_{eff} vs. excess water from Kaolite for core of 1–7 kg enriched HEU broken metal at 100% enrichment, core blanketed with a variable thickness Kaolite shell 6-102
6.25. K_{eff} vs. excess water from Kaolite for core 20% enriched HEU broken metal (0.6–7 kg ^{235}U), core blanketed with a variable thickness Kaolite shell 6-102

TABLES

Page

1.1. Uranium concentration limits 1-10
1.2. Bounding uranium isotopic concentrations in oxide 1-11
1.3. Authorized content [a] and fissile mass loading limits [b, c] for ground transport 1-15
1.3a. Uranyl nitrate crystal content loading limits for ground transport 1-16
1.3b. Authorized content and fissile mass loading limits [a, b] for air transport 1-17
1.4. TRIGA fuel specifications 1-18
2.1. Proposed HEU contents for shipment in the ES-3100 2-2
2.2. Category designations for Type B packages 2-7
2.3. Summary of load combinations for normal and hypothetical accident conditions of transport 2-9
2.4. Containment vessel allowable stress 2-10
2.5. Allowable stress intensity (S_m) for the containment boundary materials of construction 2-11
2.6. ES-3100 containment boundary design evaluation allowable stress comparisons 2-12
2.7. ES-3100 packaging material specifications 2-13
2.8. Packaging weights for various ES-3100 shipping package arrangements 2-16
2.9. Compliance test unit weights 2-18
2.10. Calculated center of gravity for the various ES-3100 shipping arrangements 2-19
2.11. Applicable codes and standards for Category I packaging 2-20
2.12. Mechanical properties of the metallic components of the drum assembly 2-21
2.13. Mechanical properties of the lid fastening components for the drum assembly 2-22
2.14. Mechanical properties of the cast refractory insulation 2-22
2.15. Mechanical properties of containment vessel O-rings 2-22
2.16. Mechanical properties of the metallic components of the containment boundary 2-23
2.17. Mechanical properties of the cast neutron absorber 2-24
2.18. Summary of NCT – 10CFR71.71 tests for ES-3100 package 2-33
2.19. Summary of HAC – 10CFR71.73 tests for ES-3100 package 2-33
2.20. Summary of temperatures and pressures for NCT 2-37
2.21. ES-3100 containment boundary evaluation for both hot and cold conditions 2-41
2.22. NCT ES-3100 containment boundary stress compared to the allowable stress at reduced and increased external pressures 2-43
2.23. Test and analysis summary for the ES-3100 package 2-52
2.24. Recorded height damage to Test Unit-4 from 1.2-m and 9-m drop testing 2-55
2.25. Recorded diametrical damage to Test Unit-4 from 1.2-m and 9-m drop tests 2-55
2.26. Recorded diametrical damage to Test Unit-2 from NCT and HAC drop testing 2-57
2.27. Recorded flat contour damage to Test Unit-2 from NCT and HAC drop testing 2-57
2.28. Recorded height damage to Test Unit-2 from NCT and HAC drop testing 2-57
2.29. Recorded height damage to Test Unit-3 from 1.2-m and 9-m drop testing 2-59
2.30. Recorded diametrical damage to Test Unit-3 from 1.2-m and 9-m drop testing 2-59
2.31. Recorded height damage to Test Unit-1 from 1.2-m and 9-m drop testing 2-60
2.32. Recorded diametrical damage to Test Unit-1 from 1.2-m and 9-m HAC drop testing 2-60
2.33. Recorded flat contour damage to Test Unit-1 from 1.2-m and 9-m drop testing 2-61
2.34. Recorded height damage to Test Unit-5 from 1.2-m and 9-m drop testing 2-62
2.35. Recorded diametrical damage to Test Unit-5 from 1.2-m and 9-m HAC drop testing 2-62
2.36. Recorded flat contour damage to Test Unit-5 from 1.2-m and 9-m drop testing 2-63
2.37. Recorded height damage to Test Unit-1 from the 9-m crush test 2-64
2.38. Recorded diametrical damage to Test Unit-1 from the 9-m crush test 2-64
2.39. Recorded flat contour damage to Test Unit-1 from the 9-m crush test 2-65
2.40. Recorded height damage to Test Unit-3 from the 9-m crush test 2-66

TABLES

Page

2.41. Recorded flat contour damage to Test Unit-3 from the 9-m crush test 2-66
2.42. Recorded diametrical damage to Test Unit-3 from the 9-m crush test 2-66
2.43. Recorded height damage to Test Unit-4 from the 9-m crush test 2-67
2.44. Recorded diametrical damage to Test Unit-4 from the 9-m crush test 2-68
2.45. Recorded height damage to Test Unit-5 from the 9-m crush test 2-69
2.46. Recorded diametrical damage to Test Unit-5 from the 9-m crush tests 2-69
2.47. Recorded flat contour damage to Test Unit-5 from the 9-m crush test 2-69
2.48. 1-m (40-in.) puncture drop test description and results 2-70
2.49. Thermax temperature indicating patches for test units 2-75
2.50. Maximum HAC temperatures recorded on the test packages' interior surfaces 2-78
2.51. HAC ES-3100 containment boundary stress compared to the allowable stress 2-80
2.52. Diametrical damage comparison of Test Unit-1 with analytical predictions 2-83
2.53. Flat contour damage comparison of Test Unit-1 with analytical results 2-83
2.54. Cumulative analytical 12° slapdown drop tests maximum effective plastic strain results 2-85
2.55. Diametrical damage comparison of Test Unit-2 with analytical predictions 2-86
2.56. Flat contour damage comparison of Test Unit-2 with analytical predictions 2-86
2.57. Cumulative analytical side drop test maximum effective plastic strain results 2-88
2.58. Diametrical damage comparison of Test Unit-3 with analytical predictions 2-88
2.59. Cumulative analytical corner drop test maximum effective plastic strain results 2-91
2.60. Diametrical damage comparison of Test Unit-4 with analytical predictions 2-92
2.61. Cumulative analytical top drop test maximum effective plastic strain results 2-93
2.62. ES-3100 test package weights before and after 10 CFR 71.73(c)(4) HAC thermal testing 2-93
3.1. Isotopic mass and weight percent for the HEU contents 3-4
3.2. Decay heat for 35.2 kg of HEU content (watts) 3-5
3.3. Maximum "quasi steady-state" temperatures during NCT for the ES-3100 shipping container with various content heat loads—Kaolite density of 19.4 lb/ft^3 and BoroBond4 3-7
3.4. Maximum "quasi steady-state" temperatures during NCT for the ES-3100 shipping container with various content heat loads—Kaolite density of 30 lb/ft^3 and BoroBond4 3-8
3.4a. ES-3100 shipping container finite element model nodal map 3-9
3.5. ES-3100 shipping container maximum steady-state temperatures with Cat 277-4 3-10
3.6. ES-3100 shipping container maximum "quasi steady-state" temperatures during NCT with various content heat loads and Cat 277-4 3-11
3.7. ES-3100 shipping container HAC maximum temperatures 3-13
3.8. ES-3100 shipping container HAC maximum temperatures 3-14
3.9. Maximum HAC temperatures recorded on the test packages' interior surfaces 3-15
3.10. Total pressure inside the containment vessel at 87.81°C (190.06°F) 3-17
3.11. Total pressure inside the containment vessel at 123.85°C (254.93°F) 3-19
3.12. Thermal properties of the materials used in the thermal analysis 3-20
3.13. Mechanical properties of the materials used in the static stress analyses 3-21
3.14. Packaging material technical specifications 3-22
3.15. Component allowable service temperature and pressure 3-24
3.16. Summary of results of evaluation for the ES-3100 under NCT 3-29
3.17. Summary of results of evaluation under HAC for the ES-3100 shipping arrangement using bounding case parameters 3-30
3.18. ES-3100 test package weights before and after 10 CFR 71.73(c)(4) HAC thermal testing 3-38
3.19. Thermax temperature indicating patches for test units 3-39
3.20. Predicted temperature adjustments (°F) for containment vessel due to HAC 3-41
3.21. Predicted temperatures of the containment vessel due to HAC 3-41

TABLES

Page

4.1. Containment requirements of transport for Type B packages 4-1
4.2. Summary of the containment vessel design and fabrication acceptance basis 4-1
4.3. Isotopic mass and weight percent for the HEU contents 4-5
4.4. Activity, A_2 value, and number of A_2 proposed for transport 4-5
4.5. Regulatory leakage criteria for NCT 4-7
4.6. Containment vessel verification tests criteria for NCT 4-7
4.7. Regulatory leakage criteria for HAC 4-9
4.8. Containment vessel design verification tests for HAC 4-9
5.1. Calculated external dose rates for the ES-3100 package with 36 kg of HEU metal contents 5-2
5.2. Calculated external dose rates for the ES-3100 package with 24 kg of HEU oxide contents 5-2
5.3. Radioisotope specification for all ES-3100 package analysis source calculations with HEU content and other nuclides per HEU unit weight 5-3
5.4. Photon source for one gram of HEU for all contents 5-4
5.5. Neutron source for one gram of HEU for all contents 5-4
5.6. Geometric data for the shielding analysis models of the ES-3100 shipping package as shown in Fig. 5.1 for NCT 5-5
5.7. Detector locations relative to the drum for NCT and to the containment vessel for HAC 5-7
5.8. Shielding model material specifications for the ES-3100 package with HEU content 5-8
5.9. ANSI standard photon flux-to-dose-rate conversion factors 5-12
5.10. ANSI standard neutron flux-to-dose-rate conversion factors 5-13
6.1a. Summary of criticality evaluation for solid HEU metal cylinders and bars 6-5
6.1b. Summary of criticality evaluation for solid HEU metal slugs 6-9
6.1c. Summary of criticality evaluation for solid HEU metal of unspecified geometric shapes characterized as broken metal 6-14
6.1d. Summary of criticality evaluation for HEU product and skull oxide 6-21
6.1e. Summary of criticality evaluation for UNX crystals and unirradiated TRIGA reactor fuel elements 6-25
6.2a. HEU fissile material mass loading limits (case name) for surface-only modes of transportation 6-30
6.2b. HEU fissile material mass loading limits for air transport mode of transportation 6-31
6.3. Deformation of 18.37-in.-diam ES-3100 drum projected by finite element analysis Case “3100 RUN1HL Lower Bound Kaolite May 2004” 6-52
6.4. Material compositions used in the ES-3100 calculation models 6-58
7.1. Replacement parts for the ES-3100 packaging 7-2
8.1. Acceptance tests for the drum assembly 8-2
8.2. Acceptance tests for the containment vessel assembly 8-3

THIS PAGE INTENTIONALLY LEFT BLANK.

ABBREVIATIONS

ALARA	as low as reasonably achievable
AM	as-manufactured
ANC	Average Net Count
ANSI	American National Standards Institute
AS	allowable stress
ASME	American Society of Mechanical Engineers
ASTM	American Society for Testing and Materials
Cat 277-4	Thermo Electron Corporation (corporate name changed to Shieldwerx) Catalog No. 277-4™ (or Cat. No. 277-4)
CD	capacity discharge
CERCA	Compagnie pour l'Étude et la Realisation de Combustibles Atomiques
CFR	Code of Federal Regulations
CMTR	certified material test report
CoC	Certificate of Compliance
CSI	criticality safety index
CV	containment vessel
CVA	containment vessel arrangement
DOE	U.S. Department of Energy
DOT	U.S. Department of Transportation
EPDM	ethylene-propylene-diene monomer
ETP	explicit triangular pack
FEA	finite element analysis
H/X ratio	hydrogen-to-fissile isotope ratio
HAC	Hypothetical Accident Conditions
HEU	highly enriched uranium
IAEA	International Atomic Energy Agency
k_{eff}	calculated neutron multiplication factor
LOD	loss on drying
LTL	lower tolerance limit
M.S.	margin of safety
MNOP	maximum normal operating pressure
MOCFR	moisture fraction inside the containment vessel
MOIFR	moisture fraction of the package external to the containment vessel
NCT	Normal Conditions of Transport
NLF	neutron leakage fraction
NRC	U.S. Nuclear Regulatory Commission
NTRC	National Transportation Research Center
OECD	Organization for Economic Cooperation and Development
ORNL	Oak Ridge National Laboratory
PGNAA	Prompt Gamma-ray Neutron Activation Analysis
ppb	parts per billion
ppm	parts per million
QA	quality assurance
QCPI	Quality Certification and Procurement
RCSB	Rackable Can Storage Box
SAR	safety analysis report
SCALE	Standardized Computer Analysis for Licensing Evaluation
s_i	standard error

ABBREVIATIONS

SRS	Savannah River Site
SS304	type 304 stainless steel
SST/SGT	Safe-Secure Trailer/Safeguards Transporter
TGA	thermogravimetric analysis
TI	transport index
TID	tamper-indicating device
TS	test sample
UNH	uranyl nitrate hexahydrate
UNX	uranyl nitrate crystals
USL	upper subcritical limit
VF	Volume Fraction
Y-12	Y-12 National Security Complex

REVISION LOG

Date	SAR Revision No.	Description	Affected Pages
2/25/05	0	Original issue	All
8/15/05	0, Page Change 1	Page changes resulting from *Responses to Request for Additional Information* #1, Y/LF-747.	title page, iv, xxiii, 1-4, 1-145, 2-2, 2-3, 2-6, 2-31, 2-32, 2-33, 2-34, 2-57, 2-59, 2-61, 2-107, 2-125, 2-131, 2-171, 2-173, 2-181, 2-183, 2-185, 2-186, 2-189, 2-367, 2-458, 2-675, 8-8, 8-9, 8-31
2/6/06	0, Page Change 2	Page changes resulting from *Responses to Request for Additional Information #2*, Y/LF-761.	All Sections
3/20/06	0, Page Change 3	Page changes resulting from *Responses to Request for Additional Information #3*, Y/LF-764.	1.38, 1.48, Appendix 1.4.1, 2-120, Table 6.4
5/8/06	0, Page Change 4	Added polyethylene bottles and nickel alloy cans as convenience containers for authorized HEU contents. (CoC Revision 1)	Various pages in chapters 1, 2, 3 and 4.
8/21/06	0, Page Change 5	Revised equipment specifications for Kaolite and 277-4 neutron absorber. (CoC Revision 3)	Appendices 1.4.4 and 1.4.5.

REVISION LOG

Date	SAR Revision No.	Description	Affected Pages
11/15/06	1	Updated definition of pyrophoric uranium. Evaluated air transport. Revised criticality safety calculations to remove bias correct factors. Added a CSI option of 3.2. Increased mass of off-gassing material allowed in containment vessel. Increased carbon concentration in HEU contents. Increased Np-237 concentration is HEU contents. Added uranium zirconium hydride and uranium carbide as contents (TRIGA fuel). Revised equipment specifications for 277-4 neutron absorber. (CoC Revision 3)	All Sections
3/29/07	1, Page Change 1	Updated definition of TRIGA fuel for air transport and added TRIGA-related criticality safety cases.	title pages, viii, xi, xx, 1-12, 1-13, 1-20, 6-30, 6-54, 6-64, 6-66, 6-87, 6-119, 6-240 to 6-286, 6-385 to end
5/31/07	1, Page Change 2	Revised SAR in response to RAIs dated May 9, 2007 in reference to CoC Revision 4	title pages, xiii, xx, Section 1 and Section 6
6/30/07	1, Page Change 3	Revised SAR in response to RAIs dated May 9, 2007 in reference to CoC Revision 5	title pages, table of contents, Section 1, and Section 7
7/31/07	1, Page Change 4	Removed oxidation as an option for treating pyrphoric uranium metal	title pages, xx, 1-12, 1-201, 1-203, 1-212, 2-26, 7-4
8/28/07	1, Page Change 5	Modified TRIGA fuel definition to include fuel pellets with cladding	title page, xx, 1-13, 1-17, 2-4, 6-29, 6-30a, 6-66c, 6-66d, 6-73, 6-87, 6-119a

REVISION LOG

Date	SAR Revision No.	Description	Affected Pages
10/10/07	1, Page Change 6	-Revised criticality safety calculations to remove bias correction factors.	Table 6.2a and supporting calculations.
		-Added a CSI option of 3.2.	Table 6.2a and supporting calculations.
		-Increased mass of off-gassing material in containment vessel to allow Teflon bottles.	Figure 1.4, page 1-15, and Appendices 3.6.4 and 3.6.5.
		-Increased carbon and moisture concentration in HEU contents.	Pages 1-10 and 1-11, Table 6.2a and pages 6-31 and 6-52.
		-Increased Np-237 concentration is HEU contents.	Pages 5-1 to 5-4, and supporting calculations.
		-Revised equipment specifications for 277-4 neutron absorber.	Pages 1-83 and 1-97.
		-Details of alloys of uranium in contents definition.	Page 1-12.
		-More precise specification of maximum fissile mass in calculations (changed from 36 kg to 35.2 kg).	Administrative change affecting many pages. Removed round-off. No new calculations.

REVISION LOG

Date	SAR Revision No.	Description	Affected Pages
3/6/08	2	-Add the following contents for ground transport: • HEU oxides (U_3O_8-Al and UO_2-Mg) • Research reactor fuel elements or components (clad U-Al, U_3O_8-Al, UO_2, or UO_2-Mg) -Add the following contents for air transport: • HEU oxides (UO_2, UO_2-Mg, U_3O_8, and U_3O_8-Al) • Broken HEU bulk metal and uranium-aluminum alloy of unspecified geometric form • Research reactor fuel elements or components (clad U-Al, U_3O_8-Al, UO_2, or UO_2-Mg)	1-10 through 1-17, 1-20, 1-22, 2-1, 2-2, 2-4, 2-5, 2-15, 2-17, 2-18, 2-25, 2-26, 3-15 through 3-17, 3-22, 3-147, 3-149, 3-151 through 3-155, 3-157 through 3-161, 4-2, 6-1, 6-2, 6-4, 6-5, 6-30 through 6-34, 6-51, 6-56, 6-69, 6-78, 6-83, 6-87, 6-92, 6-93, 6-95, 6-119, 6-128 through 6-130, 6-168, 6-282 through 6-286, 6-303 through 6-305, and 6-488 through 6-501.
6/19/08	2, Page Change 1	Revised SAR in response to RAIs dated April 28, 2008 for review of CoC 9315, Revision 8	i, ix, x, xxii, 1-15, 3-15 through 3-17, 3-154, 3-161, 4-3, 6-1, 6-3, 6-3a, 6-3b, 6-4, 6-5, 6-9 through 6-12, 6-29, 6-30, 6-35, 6-36, 6-67, 6-69, 6-70, 6-73, 6-74, 6-80, 6-81, 6-84, 6-96, 6-97, 6-99, 6-101, 6-103, 6-103a, 6-103b, 6-104a through 6-104n, 6-167, 6-188 through 6-197, 6-316 through 6-320, 6-320a through 6-320d, 6-321 through 6-324, 6-351 through 6-354, 6-354a through 6-354b, 6-355 through 6-362, 6-503 through 6-642, and 6-644.

REVISION LOG

Date	SAR Revision No.	Description	Affected Pages
8/28/08	2, Page Change 2	Revised SAR in response to RAIs dated April 28, 2008, for review of CoC 9315, Revision 8	i, vi, viii, xii, xxiii, xxiv, 1-10, 1-14 through 1-16, 1-22, 2-1, 2-25 through 2-28, 2-894, 3-15, 3-16, 3-165 through 3-290, 4-1, 4-2, 6-1 through 6-3, 6-20 through 6-28, 6-30 6-32 through 6-34, 6-68 through 6-70, 6-70a, 6-70b, 6-75 through 6-77, 6-77a, 6-77b, 6-78, 6-81 through 6-83, 6-85, 6-86, 6-101 through 6-103, 6-103a through 6-103j, 6-104, 6-123 through 6-126, 6-167 through 6-170, 6-177, 6-177a, 6-177b, 6-218a through 6-218f, 6-219 through 6-234, 6-303 through 6-305, 6-331, 6-332, 6-332a, 6-332b, 6-333, 6-394 through 6-398, 6-501, 6-502, 6-502a through 6-502dd

REVISION LOG

Date	SAR Revision No.	Description	Affected Pages
2/26/09	2, Page Change 3	Revised SAR in response to RAIs dated January 12, 2009, for review of CoC 9315, Revision 9	i, viii, ix, xxiv, 1-7, 1-10, 1-12 through 1-16, 1-21 through 1-23, 1-29 1-31, 1-33, 1-35, 1-37, 1-39, 1-41, 1-135, 1-157, 1-177, 2-6, 2-9, 2-18, 2-36 through 2-38, 2-41 through 2-43, 2-53, 2-78, 2-80, 3-15 through 3-17, 3-27, 3-28, 3-30, 3-32, 3-39, 3-41, 3-147, 3-149 through 3-154, 3-154a, 3-154b, 3-155, 3-158 through 3-161, 3-165 through 3-174, 3-289 through 3-344, 4-2, 4-7, 4-9, 4-27 through 4-34, 6-5, 6-29, 6-30, 6-34, 6-73 through 6-86, 6-86a through 6-86d, 6-96, 6-103a through 6-103c, 6-104b, 6-104c, 6-123, 6-124, 6-168, 6-219 through 6-221, 6-221a, 6-221b, 6-222, 7-7, 7-8, 7-10

REVISION LOG

Date	**SAR Revision No.**	**Description**	**Affected Pages**
5/6/09	3	This revision was issued to match Amendment 9 of the COC. -Remove the following contents for ground transport that were not reviewed by NRC: • HEU oxides (U_3O_8-Al and UO_2-Mg) • Research reactor fuel elements or components (clad U-Al, U_3O_8-Al, UO_2, or UO_2-Mg) -Remove the following contents for air transport that were not reviewed by NRC: • HEU oxides (UO_2, UO_2-Mg, U_3O_8, and U_3O_8-Al) • Broken HEU bulk metal and uranium-aluminum alloy of unspecified geometric form • Research reactor fuel elements or components (clad U-Al, U_3O_8-Al, UO_2, or UO_2-Mg)	All
4/14/10	3, Page Change 1	Revised SAR to • add uranium oxide loading with a CSI value of 0.4 • remove the 8-lb minimum payload weight • add stainless-steel option for can spacers • revise allowable weight changes for drum body and top plug • revise Drawing M2E801580A005 to clarify marking requirements on drum hex nuts • allow methods other than sieving for establishing minimum content sizes for pyrophoric purposes • revise the purity of the cover gas used for pyrophoric material	i, x, xxv, 1-13, 1-16, 1-22, 1-23, 1-24, 1-27, 1-89 through 1-126, 1-126a, 1-126b, 1-135, 1-147, 1-178a, 1-178b, 1-221, 2-1, 2-14, 2-24, 6-1, 6-3, 6-4, 6-31, 6-35, 6-57, 6-67 through 6-69, 6-104, 6-105, 6-195, 6-717 through 6-892, 7-3, 7-4, 8-9, 8-10

REVISION LOG

Date	SAR Revision No.	Description	Affected Pages
		Note: The NRC performed an acceptance review of Page Change 1 and generated several Requests for Supplemental Information (RSIs). Therefore, Page Change 1 will be superceded by Page Change 2, which incorporates the responses to the RSIs.	
7/22/10	3, Page Change 2	Reissue of Page Change 1 with RSI responses incorporated	i, x, xiv, xxv, xxvi 1-13, 1-16, 1-22, 1-23, 1-24, 1-27, 1-89 through 1-126, 1-126a, 1-126b, 1-135, 1-147, 1-178a, 1-178b, 1-221, 2-1, 2-6, 2-14, 2-24, 2-26, 3-8a, 3-8b, 3-9, 3-10, 3-12, 3-13, 3-18, 3-23, 3-27, 3-27a, 3-27b, 3-100, 3-104, 3-105, 3-115, 3-116, 3-140, 6-1, 6-3, 6-4, 6-31, 6-35, 6-57, 6-67 through 6-69, 6-104, 6-105, 6-195, 6-717 through 6-892, 7-3, 7-4, 8-9, 8-10
1/27/11	3, Page Change 3	Revised SAR in response to RAIs dated October 12, 2010, for review of CoC 9315, Revision 10	i, vi, xiv, xxvi, 2-6, 2-11, 2-36, 2-37, 2-41 through 2-43, 2-53, 2-78, 2-80, 3-16 through 3-18, 3-23, 3-27, 3-27a through 3-27d, 3-28, 3-30, 3-39, 3-147, 3-153 through 3-157, 3-160 through 3-164, 4-7, 4-9, 4-23, 4-25 through 4-34, 7-2, 7-6, 7-7, 7-11
3/3/11	4	This SAR revision matches Rev. 10 of the COC. Incorporated Page Changes 1–3 and revised MNOP value in two additional locations (Sects. 1.2.3.5 and 3.5.1)	All

3. THERMAL EVALUATION

Design analysis, similarity, and full-scale testing (see Sect. 2) have demonstrated that the ES-3100 shipping package is in compliance with the applicable requirements of Title 10 Code of Federal Regulations (CFR) 71 (10 CFR 71) when used to ship highly enriched uranium (HEU) having a maximum gross weight up to 35.2 kg (77.60 lb). The ES-3100 has a nominal gross shipping weight that ranges from 146.88 kg (323.79 lb) to 187.81 kg (414.05 lb) for the empty and maximum weight containment vessel configurations shown in Table 2.8, respectively.

3.1 DISCUSSION

The drum assembly of the shipping package is defined as the structure that maintains the position of and provides the impact and thermal barrier surrounding the containment boundary. Preserving the location of the containment boundary within the packaging prevents reduction of the shielding and subcriticality effectiveness. The drum assembly for the ES-3100 consists of an internally flanged Type 304L stainless-steel 30-gal modified drum with two Type 304L stainless-steel inner liners, one filled with noncombustible cast refractory insulation and impact limiter and one filled with noncombustible cast neutron poison; a stainless-steel top plug with noncombustible cast refractory insulation; silicone rubber pads; silicon bronze hex-head nuts; and a stainless-steel lid and bottom (Drawing M2E801580A031, Appendix 1.4.8). The nominal weight of these components is 131.89 kg (290.76 lb).

The drum's diameters (inner diameter of 18.25 in.) and corrugations meet the requirements of Military Standard, MS27683-7. All other dimensions are controlled by Drawing M2E801580A004 (Appendix 1.4.8). Modifications to the drum from MS27683-7 include the following: (1) the overall height was increased; (2) the drum was fabricated with two false wire open ends; and (3) a 0.27-cm (12-gauge, 0.1046-in.)-thick concave cover was welded to the bottom false wire opening (Drawing M2E801508A005, Appendix 1.4.8). Four 0.795-cm (0.313-in.)-diam equally spaced holes are drilled in the top external sidewall to prevent a pressure buildup between the drum and inner liner. The holes are filled with a plastic plug to provide a moisture barrier for the cast refractory insulation during Normal Conditions of Transport (NCT). The cavity created by the inner liners is a three-tiered volume with a 37.52-cm (14.77-in.) inside diameter 13.26 cm (5.22 in.) deep, a 21.84-cm (8.60-in.) inside diameter 5.59 cm (2.20 in) deep, and an additional 15.85-cm (6.24-in.) inside diameter 78.31-cm (30.83 in.) deep. The volume between the drum and mid liner is filled with a lightweight noncombustible cast refractory material called Kaolite 1600 (Thermal Ceramics, Appendix 2.10.3). The material is composed of portland cement, water, and vermiculite and has an average density of 358.8 kg/m^3 (22.4 lb/ft^3). The procedure for manufacturing and documenting the insulation, JS-YMN3-801580-A003 (Appendix 1.4.4), is referenced on Drawings M2E801580A002 and M2E801580A008 (Appendix 1.4.8) for the drum body weldment and top plug weldment, respectively. The insulation has a maximum continuous service temperature limit of 871°C (1600°F) due to the presence of the vermiculite and portland cement. The volume between the most internal liner and the mid liner is filled with a noncombustible cast neutron poison (absorber) material called Cat 277-4 from Thermo Electron Corporation. The material is composed of aluminum, magnesium, calcium, boron, carbon, silicone, sulfur, sodium, iron, and water. The final mixture will have an average density of 1681.9 kg/m^3 (105 lb/ft^3). The procedure for manufacturing and documenting this material, JS-YMN3-801580-A005 (Appendix 1.4.5), is referenced on Drawing M2E801580A002 (Appendix 1.4.8). This neutron poison material has a maximum continuous service temperature limit of 150.0°C (302°F). At this temperature,

the moisture inside the Cat 277-4 material remains an integral part of the composite material, and moisture content loss is negligible.

The top plug is fabricated in accordance with Drawing M2E801580A008 (Appendix 1.4.8), with an overall diameter of 36.50 cm (14.37 in.) and a height of 13.41 cm (5.28 in.). The plug's rim, bottom sheet, and top sheet are fabricated from 0.15-cm (16-gauge, 0.0598-in.)-thick Type 304/304L stainless-steel sheet per ASME SA240. Four lifting inserts are welded into the top sheet for loading and unloading operations. The internal volume of the top plug assembly is filled with Kaolite 1600 in accordance with JS-YMN3-801580-A003 (Appendix 1.4.4).

Three silicone rubber pads complete the drum assembly. One pad is placed on the bottom of the most inward liner to support the containment vessel during transport. Another pad is placed on the top shelf of the mid liner to support the top plug during transport. The final plug is placed over the top of the containment vessel lid and closure nut interface. The pads are molded to the shapes as defined on Drawing M2E801580A009 (Appendix 1.4.8). The material is silicone rubber with a Shore A durometer reading of 22 ±5.

The ES-3100 package is evaluated for a maximum heat source of 0.4 W (Sect. 1.2.3.7); however, no active cooling systems or specific thermal design features are required. A lightweight cast refractory insulation between the inner liner and the drum provides thermal protection of the contents from external heat sources.

Thermal criteria are applied to the package in accordance with 10 CFR 71 for NCT and Hypothetical Accident Conditions (HAC). These requirements specify that each package design provide containment, shielding, and criticality safety at temperatures ranging from −40 to 38°C (−40 to 100°F) with full insolation. Also, in accordance with *Packaging and Transportation of Radioactive Material* [10 CFR 71.43(g)], a package must be designed, constructed, and prepared for transport so that in still air at 38°C (100°F) and in the shade no accessible surface of a package would have a temperature exceeding 50°C (122°F) in a nonexclusive use shipment, or 85°C (185°F) in an exclusive use shipment. In addition, each package will experience no significant reduction in effectiveness as the result of being exposed to a thermal radiation environment of 800°C (1475°F) for 30 min with an emissivity coefficient of at least 0.9.

The maximum internal pressures and thermal stresses for both NCT and HAC are discussed and calculated (Sects. 3.4.2, 3.4.3, and 3.5.3) for use in the structural evaluation. The calculated pressures are well below the design pressures of the package components, and the effect of thermal stresses on the package is negligible (Sects. 2.6.1.2 and 2.7.4.2).

Compliance with the NCT thermal requirements is shown by analysis (Sect. 3.3.1). Since the components to be shipped have a maximum decay heat load of 0.4 W, a thermal analysis was conducted for the ES-3100 package (Appendix 3.6.2). Since the decay heat load is so meager, the maximum predicted temperature of the entire package, while stored at 38°C (100°F) in the shade, is 38.52°C (101.33°F) [Table 3.5]. The analysis shows that no accessible surface of the package would have a temperature exceeding 50°C (122°F). Therefore, the requirement of 10 CFR 71.43(g) would be satisfied. If the package is exposed to solar radiation at 38°C (100°F) in still air, the conservatively calculated temperatures at the top of the drum, center of containment vessel lid, and on the containment vessel near the O-ring sealing surfaces are 117.72°C (243.89°F), 87.81°C (190.06°F), and 87.72°C (189.90°F), respectively (Sect. 3.4.2 and Table 3.6). For conservatism, the O-ring sealing surface temperature will be assumed to be 87.81°C (190.06°F). At the low-temperature range and neglecting

decay heating, the package components would stabilize at −40°C (−40°F), which is within normal operating limits of the packaging materials (Sect. 2.2).

Five full-scale packages were subjected to the HAC thermal test following the drop, crush and puncture tests (Sects. 2.7.1 through 2.7.3). All of these test packages were exposed to a thermal radiation environment of >800°C (>1475°F) for well over 30 min in a furnace. Other temperature conditions before and during the thermal testing are given in *Test Report of the ES-3100 Package* for the furnace, test packages, and package supports. The maximum temperature recorded during the tests on the external surface of any of the containment vessels was 127.2°C (261°F). This containment vessel maximum temperature reading is the highest value shown in Table 3.9. This temperature was recorded on Test Units-4 and -5 on the containment vessel sealing lid. The maximum internal temperature adjacent to the O-rings was 116°C (241°F). Temperature adjustments are then added to the containment vessel's maximum recorded temperature to correct for measuring accuracy, internal decay heating, insolation heating during cool down, location of crush plate damage, neutron poison substitution, thermal capacitance difference between mockups and actual contents, and material density variations. Detailed discussion of each temperature adjustment is provided in Sect. 3.5.3. Since Test Unit-5 was tested with a mock-up that represented the lightest proposed content, no temperature correction was needed for mass differences. The containment vessel's recorded temperature values were lower on all other test units, which consisted of much heavier mock-up contents.

3.1.1 Design Features

The drum assembly for the ES-3100 consists of an internally flanged Type 304L stainless-steel 30-gal modified drum with two Type 304L stainless-steel inner liners, one filled with noncombustible cast refractory insulation and impact limiter and one filled with noncombustible cast neutron poison; a stainless-steel top plug with noncombustible cast refractory insulation, silicone rubber pads, silicon bronze hex-head nuts, and a stainless-steel lid and bottom (Drawing M2E801580A031, Appendix 1.4.8). The drum's diameter (inner diameter of 18.25 in.) and corrugations meet the requirements of Military Standard, MS27683-7. All other dimensions are controlled by Drawing M2E801580A004 (Appendix 1.4.8). Modifications to the drum from MS27683-7 include the following: (1) the overall height was increased; (2) the drum was fabricated with two false wire open ends; and (3) a 0.27-cm (12-gauge, 0.1046-in.)-thick concave cover was welded to the bottom false wire opening (Drawing M2E801508A005, Appendix 1.4.8). Four 0.795-cm (0.313-in.)-diam equally spaced holes are drilled in the top external sidewall to prevent a pressure buildup between the drum and inner liner. The cavity created by the inner liners is a three-tiered volume with a 37.52-cm (14.77-in.) inside diameter 13.26 cm (5.22 in.) deep, a 21.84-cm (8.60-in.) inside diameter 5.59 cm (2.20 in) deep, and an additional 15.85-cm (6.24-in.) inside diameter 78.31 cm (30.83 in.) deep. Drum and inner liner wall thickness is 0.15 cm (16 gauge, 0.0598 in.).

The volume between the drum and mid liner is filled with a lightweight noncombustible cast refractory material called Kaolite 1600 (Thermal Ceramics, Appendix 2.10.3). The material is composed of portland cement, water, and vermiculite and has an average density of 358.8 kg/m^3 (22.4 lb/ft^3). The procedure for manufacturing and documenting the insulation, JS-YMN3-801580-A003 (Appendix 1.4.4), is referenced on Drawings M2E801580A002 and M2E801580A008 (Appendix 1.4.8) for the drum body weldment and top plug weldment, respectively.

The volume between the most internal liner and the mid liner is filled with a noncombustible cast neutron poison material from Thermo Electron Corporation (Cat 277-4). The material is composed of aluminum, magnesium, calcium, boron, carbon, silicone, sulfur, sodium, iron, and water. This mixture will have an average density of 1681.9 kg/m^3 (105 lb/ft^3). The procedure for manufacturing and documenting this material, JS-YMN3-801580-A005 (Appendix 1.4.5), is referenced on Drawing M2E801580A002 (Appendix 1.4.8).

Three silicone rubber pads complete the drum assembly. One pad is placed on the bottom of the most inward liner to support the containment vessel during transport. Another pad is placed on the top shelf of the mid liner to support the top plug during transport. The final plug is placed over the top of the containment vessel lid and closure nut assembly. Pads are molded to the shapes as defined on Drawing M2E801580A009 (Appendix 1.4.8) using silicone rubber with a Shore A durometer reading of 22 ± 5.

3.1.2 Content's Decay Heat

The maximum decay heat and radioactivity of the contents (Sect. 4) are based on a maximum of 35.2 kg of HEU in the isotopic and mass distribution at fabrication as shown in Table 3.1.

Table 3.1. Isotopic mass and weight percent for the HEU contents [a]

Nuclide	Weight percent	Mass (g)
^{232}U	0.000004	0.001408
^{233}U	0.600000	211.200000
^{234}U	2.000000	704.000000
^{235}U	54.895996	19,323.390592
^{236}U	40.000000	14,080.000000
^{238}U	0.000000	0.000000
Transuranic	0.004000	1.408000
^{237}Np	2.500000	880.000000
Total	100.000000	35,200.000000

[a] Weight percent values of individual isotopes are those that generate the largest activity within the allowable ranges presented in Sect. 1.2.3.

Using the ORIGEN-S program for determining decay heat values and predicting the isotopic decay patterns from 0 to 70 years from original fabrication, the following decay heat loads are predicted and shown in Table 3.2. Isotopic mass distribution has been calculated in Sect. 4 and shown in Table 2 of Appendix 4.6.1. The maximum decay heat load is rounded up from 0.3954 to 0.4 W, and 0.4 W is used in subsequent analyses for temperature predictions. Contributions from the transuranics and ^{237}NP at the bottom of Table 3.2 remain constant for the time period evaluated. The decay heat per gram value used for the transuranic isotopes was an average of the decay heat values for ^{238}Pu, ^{239}Pu, ^{240}Pu, ^{241}Pu, ^{242}Pu and ^{241}Am.

Table 3.2. Decay heat for 35.2 kg of HEU content (watts)

Decay Heat (Watts per gram)	Isotope	DECAY TIME								
		0 years	5 years	10 years	20 years	30 years	40 years	50 years	60 years	70 years
1.7920E-02	Pb-210	0.0000E+00	2.5360E-12	1.9556E-11	1.4635E-10	4.5799E-10	1.0156E-09	1.8547E-09	3.0280E-09	4.5294E-09
2.6280E+03	Pb-212	0.0000E+00	4.7733E-05	5.3284E-05	4.9583E-05	4.4773E-05	4.0703E-05	3.6781E-05	3.3302E-05	3.0157E-05
2.8650E+02	Bi-210	0.0000E+00	2.5008E-11	1.9280E-10	1.4339E-09	4.5175E-09	1.0003E-08	1.8312E-08	2.9848E-08	4.4570E-08
2.4500E+05	Bi-212	0.0000E+00	4.2147E-04	4.6984E-04	4.3875E-04	3.9729E-04	3.5929E-04	3.2578E-04	2.9503E-04	2.6705E-04
1.4420E+02	Po-210	0.0000E+00	3.4726E-10	2.6806E-09	1.9902E-08	6.2751E-08	1.3911E-07	2.5486E-07	4.1327E-07	6.1939E-07
5.1130E+03	Rn-222	0.0000E+00	7.2355E-09	2.8942E-08	1.1555E-07	2.5990E-07	4.6077E-07	7.1995E-07	1.0331E-06	1.4075E-06
1.8230E+03	Ra-223	0.0000E+00	1.1907E-08	4.5091E-08	1.6416E-07	3.3642E-07	5.4602E-07	7.8557E-07	1.0463E-06	1.3210E-06
5.4700E+03	Ra-224	0.0000E+00	8.6260E-04	9.6272E-04	9.0111E-04	8.1639E-04	7.3783E-04	6.6774E-04	6.0459E-04	5.4760E-04
2.8380E+01	Ra-225	0.0000E+00	5.9942E-07	1.2947E-06	2.5895E-06	3.8842E-06	5.1730E-06	6.4737E-06	7.7325E-06	9.0512E-06
2.8600E-02	Ra-226	0.0000E+00	6.3026E-09	2.5170E-08	1.0068E-07	2.2553E-07	4.0071E-07	6.2624E-07	9.0009E-07	1.2243E-06
1.5200E-02	Ra-228	0.0000E+00	3.1241E-15	1.0485E-14	3.1241E-14	5.4992E-14	7.9599E-14	1.0442E-13	1.2946E-13	1.5449E-13
2.0290E+03	Ac-225	0.0000E+00	3.4282E-05	6.2564E-05	1.2513E-04	1.8769E-04	2.4983E-04	3.1239E-04	3.7453E-04	4.3709E-04
3.5000E-02	Ac-227	0.0000E+00	1.6165E-10	6.1483E-10	2.2253E-09	4.5656E-09	7.4402E-09	1.0687E-08	1.4204E-08	1.7924E-08
1.7460E+04	Ac-228	0.0000E+00	4.3760E-13	1.4701E-12	4.3760E-12	7.6949E-12	1.1161E-11	1.4652E-11	1.8143E-11	2.1659E-11
1.1250E+03	Th-227	0.0000E+00	1.2065E-08	4.5869E-08	1.6630E-07	3.4130E-07	5.5434E-07	7.9781E-07	1.0609E-06	1.3413E-06
2.6850E+01	Th-228	0.0000E+00	8.2427E-04	9.1879E-04	8.5830E-04	7.7889E-04	7.0327E-04	6.3900E-04	5.7850E-04	5.2178E-04
6.0870E-03	Th-229	0.0000E+00	3.8569E-05	5.5025E-05	1.0992E-04	1.6456E-04	2.1984E-04	2.7384E-04	3.2912E-04	3.8440E-04
5.8220E-04	Th-230	0.0000E+00	5.6970E-06	1.1353E-05	2.2747E-05	3.4100E-05	4.5494E-05	5.6970E-05	6.8037E-05	7.9513E-05
5.7940E+02	Th-231	0.0000E+00	4.5568E-05	4.5568E-05	4.5568E-05	4.5568E-05	4.5568E-05	4.5568E-05	4.5568E-05	4.5568E-05
2.6590E-09	Th-232	0.0000E+00	5.4281E-12	1.0894E-11	2.1787E-11	3.2681E-11	4.3425E-11	5.4281E-11	6.5512E-11	7.6368E-11
9.5900E+00	Th-234	0.0000E+00	0.0000E+00	0.0000E+00	0.0000E+00	0.0000E+00	0.0000E+00	0.0000E+00	0.0000E+00	0.0000E+00
1.4390E-03	Pa-231	0.0000E+00	1.3457E-07	2.6942E-07	5.3940E-07	8.0910E-07	1.0760E-06	1.3457E-06	1.6154E-06	1.8823E-06
5.2710E+01	Pa-233	0.0000E+00	0.0000E+00	0.0000E+00	0.0000E+00	0.0000E+00	0.0000E+00	0.0000E+00	0.0000E+00	0.0000E+00
7.0800E-01	U-232	9.9686E-04	9.4702E-04	9.0216E-04	8.1743E-04	7.3967E-04	6.6989E-04	6.0709E-04	5.4927E-04	4.9744E-04
2.8070E-04	U-233	5.9280E-02	5.9278E-02	5.9278E-02	5.9275E-02	5.9273E-02	5.9270E-02	5.9268E-02	5.9265E-02	5.9263E-02
1.7910E-04	U-234	1.2609E-01	1.2609E-01	1.2609E-01	1.2609E-01	1.2608E-01	1.2608E-01	1.2608E-01	1.2607E-01	1.2607E-01
6.0000E-08	U-235	1.1594E-03	1.1594E-03	1.1594E-03	1.1594E-03	1.1594E-03	1.1594E-03	1.1594E-03	1.1594E-03	1.1594E-03
2.0000E-06	U-236	2.4656E-02	2.4656E-02	2.4656E-02	2.4656E-02	2.4656E-02	2.4656E-02	2.4656E-02	2.4656E-02	2.4656E-02
8.5111E-09	U-238	0.0000E+00	0.0000E+00	0.0000E+00	0.0000E+00	0.0000E+00	0.0000E+00	0.0000E+00	0.0000E+00	0.0000E+00
1.1580E-01	transuranic	1.6306E-01	1.6306E-01	1.6306E-01	1.6306E-01	1.6306E-01	1.6306E-01	1.6306E-01	1.6306E-01	1.6306E-01
2.0100E-05	Np-237	1.7688E-02	1.7688E-02	1.7688E-02	1.7688E-02	1.7688E-02	1.7688E-02	1.7688E-02	1.7688E-02	1.7688E-02
	Total watts	3.9293E-01	3.9517E-01	3.9542E-01	3.9530E-01	3.9514E-01	3.9500E-01	3.9489E-01	3.9480E-01	3.9473E-01

3.1.3 Summary Tables of Temperatures

3.1.3.1 NCT summary tables

The ES-3100 shipping container has been conservatively evaluated empty of all containment vessel internal components for NCT. Prior to the change of neutron absorber from BoroBond4 to Cat 277-4, parameters, such as Kaolite 1600 density, BoroBond4 thermal conductivity, and decay heat loads, were varied to encompass the range of potential variations in material properties. The available thermal conductivity information on BoroBond4 was limited to moderate temperatures in the range of −3.89°C (25°F) to 40°C (104°F) [Eagle-Picher presentation excerpts sent to Gerry Byington via e-mail from Jim Hall on March 12, 2004]. Using the available thermal conductivity data for BoroBond4, thermal analyses for NCT and HAC have been performed and are documented in DAC-PKG-801699-A001 (summarized in Appendix 3.6.1). Nodal locations for temperatures presented are shown in Fig. 3.1. Based on the results reported in the above document and shown in Tables 3.3 and 3.4, it was determined that the higher temperatures occurred when the lowest density of the Kaolite 1600 was used. Therefore, subsequent analysis using the proposed Cat 277-4 neutron absorber during NCT uses a Kaolite 1600 density of 19.4 lb/ft^3. The results for the steady state condition at 38°C (100°F) in the shade, and the transient condition of applying solar insolation are shown in Tables 3.5 and 3.6 for the proposed configuration (package with Cat 277-4 neutron absorber).

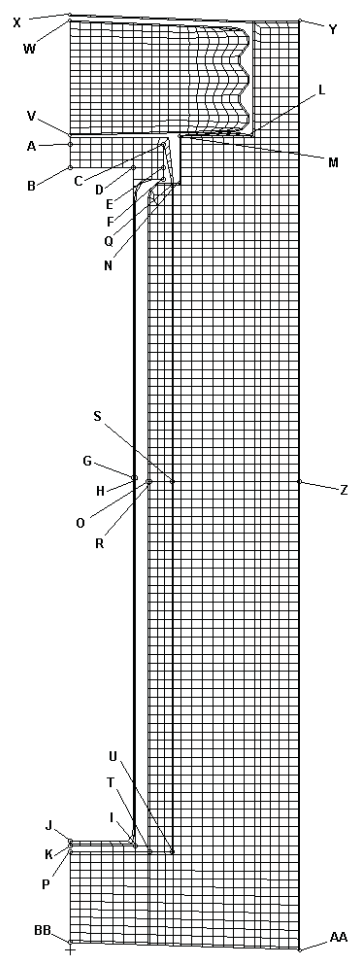

Fig. 3.1. MSC.Patran axisymmetric finite element model of the ES-3100 shipping container with BoroBond 4—nodal locations of interest (elements representing air not shown for clarity).

Table 3.3. Maximum "quasi steady-state" temperatures during NCT for the ES-3100 shipping container with various content heat loads—Kaolite density of 19.4 lb/ft^3 and BoroBond4

Node [a]	Location	Maximum "quasi steady-state" temperature, °C (°F)			
		0 W	0.4 W	20 W	30 W
A	CV lid, top, center	88.30 (190.95)	88.62 (191.52)	103.84 (218.91)	111.35 (232.42)
B	CV lid, bottom, center	88.28 (190.90)	88.60 (191.48)	103.90 (219.03)	111.45 (232.62)
C	CV lid, top, outer	88.32 (190.97)	88.63 (191.54)	103.61 (218.50)	111.00(231.80)
D	CV flange at interface, inner [b]	88.24 (190.83)	88.56 (191.41)	103.87 (218.96)	111.42 (232.55)
E	CV flange at interface, outer [b]	88.25 (190.84)	88.56 (191.41)	103.77 (218.78)	111.27 (232.28)
F	CV flange, bottom, outer	88.24 (190.82)	88.55 (191.39)	103.75 (218.75)	111.25 (232.24)
G	CV shell, mid-height, inner	83.04 (181.47)	83.61 (182.50)	110.50 (230.89)	123.46 (254.23)
H	CV shell, mid-height, outer	83.04 (181.47)	83.61 (182.50)	110.49 (230.88)	123.45 (254.21)
I	CV bottom, outer	83.36 (182.04)	83.75 (182.74)	102.58 (216.64)	111.99 (233.59)
J	CV bottom, center, inner	88.37 (182.07)	83.76 (182.77)	102.70 (216.86)	112.17 (233.91)
K	CV bottom, center, outer	88.37 (181.07)	83.76 (182.77)	102.69 (216.84)	112.15 (233.87)
L	Drum liner, plug cavity, outer	98.72 (209.70)	98.80 (209.85)	102.63 (216.73)	104.58 (220.24)
M	Drum liner, plug cavity, inner	94.43 (201.97)	94.58 (202.24)	101.92 (215.46)	105.65 (222.16)
N	Drum liner, CV flange cavity, outer	89.43 (192.97)	89.63 (193.34)	99.83 (211.70)	105.01 (221.02)
O	Drum liner, CV cavity, mid-height, inner	83.12 (181.62)	83.43 (182.18)	98.63 (209.54)	106.40 (223.52)
P	Drum liner, CV cavity, bottom, inner	83.62 (182.52)	83.96 (183.13)	100.36 (212.65)	108.60 (227.48)
Q	Borobond4, top, outer	88.82 (191.88)	89.04 (192.27)	99.65 (211.38)	105.04 (221.07)
R	Borobond4, mid-height, inner	83.12 (181.62)	83.43 (182.18)	98.63 (209.53)	106.39 (223.51)
S	Borobond4, mid-height, outer	83.03 (181.46)	83.33 (182.00)	97.91 (208.23)	105.36 (221.65)
T	Borobond4, bottom, inner	83.55 (182.39)	83.85 (182.93)	98.58 (209.45)	106.03 (222.86)
U	Borobond4, bottom, outer	83.51 (182.31)	83.80 (182.83)	97.82 (208.07)	104.90 (238.82)
V	Drum plug liner, bottom, center	112.01 (233.62)	112.05 (233.69)	113.95 (237.11)	114.90 (238.82)
W	Drum plug liner, top, center	92.09 (197.77)	92.31 (198.16)	102.93 (217.27)	108.26 (226.87)
X	Drum lid, top, center	118.01 (244.42)	118.03 (244.45)	118.77 (245.79)	119.15 (246.47)
Y	Drum lid, top, outer	107.33 (225.19)	107.34 (225.22)	108.22 (226.80)	108.67 (227.60)
Z	Drum, mid-height, outer	92.27 (198.08)	92.30 (198.14)	93.81 (200.86)	94.58 (202.24)
AA	Drum bottom, outer	91.70 (197.06)	91.74 (197.13)	93.61 (200.49)	94.54 (202.18)
BB	Drum bottom, center	88.82 (191.88)	88.93 (192.07)	93.84 (200.91)	96.30 (205.35)

[a] See Fig. 3.1.
[b] Approximate location of the CV O-rings.

Table 3.4. Maximum "quasi steady-state" temperatures during NCT for the ES-3100 shipping container with various content heat loads—Kaolite density of 30 lb/ft^3 and BoroBond4

Node [a]	Location	Maximum "quasi steady-state" temperature, °C (°F)			
		0 W	0.4 W	20 W	30 W
A	CV lid, top, center	86.56 (187.81)	86.88 (188.38)	102.98 (215.74)	109.59 (229.26)
B	CV lid, bottom, center	86.56 (187.80)	86.88 (188.38)	102.16 (215.90)	109.71 (229.47)
C	CV lid, top, outer	86.54 (187.78)	86.86 (188.34)	101.89 (215.41)	109.31 (228.75)
D	CV flange at interface, inner [b]	86.47 (187.64)	86.79 (188.21)	102.09 (215.77)	109.67 (229.40)
E	CV flange at interface, outer [b]	86.44 (187.59)	86.76 (188.16)	102.00 (215.61)	109.53 (229.15)
F	CV flange, bottom, outer	86.42 (187.56)	86.74 (188.13)	101.99 (215.58)	109.51 (229.12)
G	CV shell, mid-height, inner	81.52 (178.74)	82.09 (179.76)	109.01 (228.21)	121.98 (251.57)
H	CV shell, mid-height, outer	81.52 (178.74)	82.09 (179.76)	109.00 (228.19)	121.97 (251.55)
I	CV bottom, outer	81.32 (178.37)	81.71 (179.08)	100.57 (213.02)	109.99 (229.99)
J	CV bottom, center, inner	81.37 (178.47)	81.77 (179.18)	100.73 (213.31)	110.21 (230.38)
K	CV bottom, center, outer	81.37 (178.47)	81.77 (179.18)	100.72 (213.29)	110.19 (230.34)
L	Drum liner, plug cavity, outer	97.74 (207.93)	97.82 (208.07)	101.65 (214.96)	103.59 (218.47)
M	Drum liner, plug cavity, inner	92.91 (199.23)	93.06 (199.50)	100.40 (212.72)	104.13 (219.43)
N	Drum liner, CV flange cavity, outer	87.69 (189.84)	87.90 (190.21)	98.09 (208.57)	103.27 (217.43)
O	Drum liner, CV cavity, mid-height, inner	81.30 (178.35)	81.61 (178.90)	96.82 (206.27)	104.13 (219.43)
P	Drum liner, CV cavity, bottom, inner	81.52 (178.74)	81.86 (179.35)	98.30 (208.94)	106.56 (223.80)
Q	Borobond4, top, outer	87.36 (189.25)	87.58 (189.64)	98.19 (208.74)	103.57 (218.43)
R	Borobond4, mid-height, inner	81.30 (178.35)	81.61 (178.90)	98.81 (206.26)	104.58 (220.24)
S	Borobond4, mid-height, outer	81.37 (178.46)	81.66 (178.99)	96.24 (205.23)	103.69 (218.64)
T	Borobond4, bottom, inner	81.67 (179.01)	81.98 (179.56)	96.73 (206.12)	104.19 (219.55)
U	Borobond4, bottom, outer	81.78 (179.21)	82.07 (179.72)	96.11 (205.00)	103.23 (217.81)
V	Drum plug liner, bottom, center	111.30 (232.35)	111.34 (232.42)	113.25 (235.85)	114.21 (237.57)
W	Drum plug liner, top, center	90.70 (195.26)	90.92 (195.66)	101.53 (214.76)	106.87 (224.36)
X	Drum lid, top, center	117.74 (243.93)	117.75 (243.96)	118.50 (245.30)	118.88 (245.98)
Y	Drum lid, top, outer	107.04 (224.68)	107.06 (224.71)	107.94 (226.29)	108.39 (227.10)
Z	Drum, mid-height, outer	91.86 (197.36)	91.90 (197.41)	93.42 (200.15)	94.18 (201.53)
AA	Drum bottom, outer	91.00 (195.79)	91.04 (195.86)	92.92 (199.26)	93.87 (200.96)
BB	Drum bottom, center	87.21 (188.97)	87.31 (189.15)	92.26 (198.07)	94.74 (202.54)

[a] See Fig. 3.1.
[b] Approximate location of the CV O-rings.

Table 3.4a. ES-3100 shipping container finite element model nodal map

Node map[a]

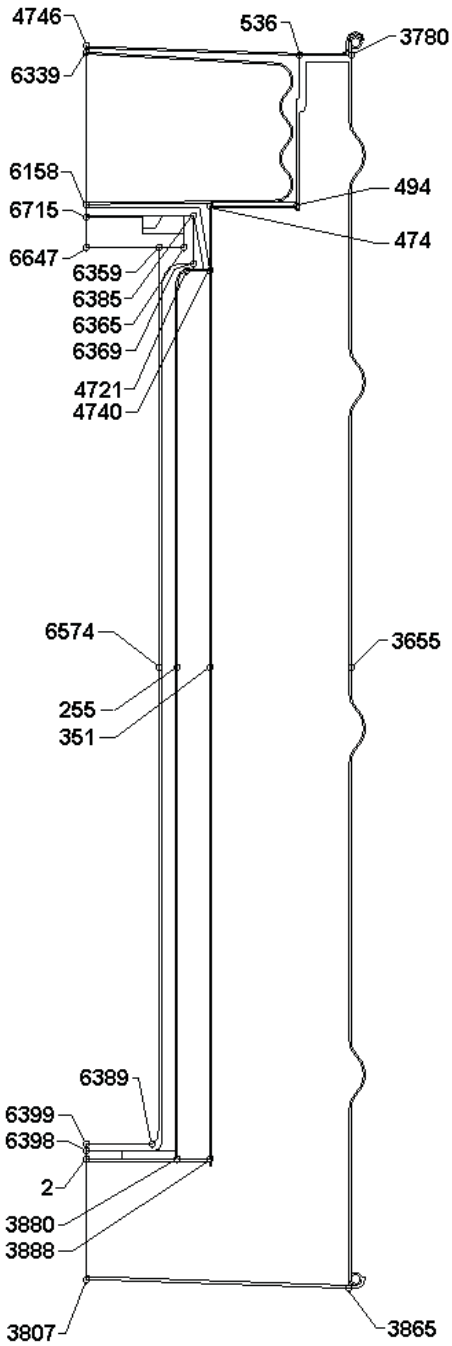

Node location and coordinates (in.)			
No.	Location description	r	z
2	Drum liner, CV cavity, bottom, inner	0.000	4.505
255	Drum liner, CV cavity, mid-height, outer	3.180	21.528
351	Cat. 277-4, mid-height, outer	4.300	21.528
474	Drum liner, plug cavity, inner	4.300	37.535
494	Drum liner, plug cavity, outer	7.325	37.525
536	Drum liner, flange, inner	7.385	42.755
3655[c]	Drum, mid-height, outer	9.185	21.528
3780[c]	Drum lid, top, outer	9.185	42.755
3807[c]	Drum, bottom, center, outer	0.000	0.320
3865[c]	Drum, bottom, edge, outer	9.185	0.008
3880	Cat. 277-4, bottom, inner	3.178	4.505
3888	Cat. 277-4, bottom, outer	4.300	4.505
4721	Cat. 277-4, top, inner	3.500	35.275
4740	Cat. 277-4, top, outer	4.300	35.275
4746[c]	Drum lid, top, center, outer	0.000	43.065
6158	Top plug liner, bottom, center, outer	0.000	37.579
6339	Top plug liner, top, center, outer	0.000	42.859
6359[b]	CV flange at lid interface, inner	2.530	36.075
6365[b]	CV flange at lid interface, outer	3.425	36.075
6369	CV flange, bottom, outer	3.750	35.525
6385	CV lid, top, outer	3.750	37.175
6389	CV bottom edge, inner	2.310	5.025
6398	CV bottom, center, outer	0.000	4.775
6399	CV bottom, center, inner	0.000	5.025
6574	CV shell, mid-height, inner	2.530	21.528
6647	CV lid, bottom, center	0.000	36.075
6715	CV lid, top, center	0.000	37.135

[a] See Figs. 8 through 11 in Appendix 3.6.2 for details of node locations.
[b] Approximate location of the CV O-ring.
[c] These nodes are at the accessible surfaces of the package (i.e., the drum, drum lid, and drum bottom plate).

Table 3.5. ES-3100 shipping container maximum steady-state temperatures with Cat 277-4 (100°F ambient temperature, no insolation)

Node map[a]	Node coordinates (in.)			Maximum "quasi steady-state" temperature (°F)		
	No.	r	z	0.4 W	20 W	30 W
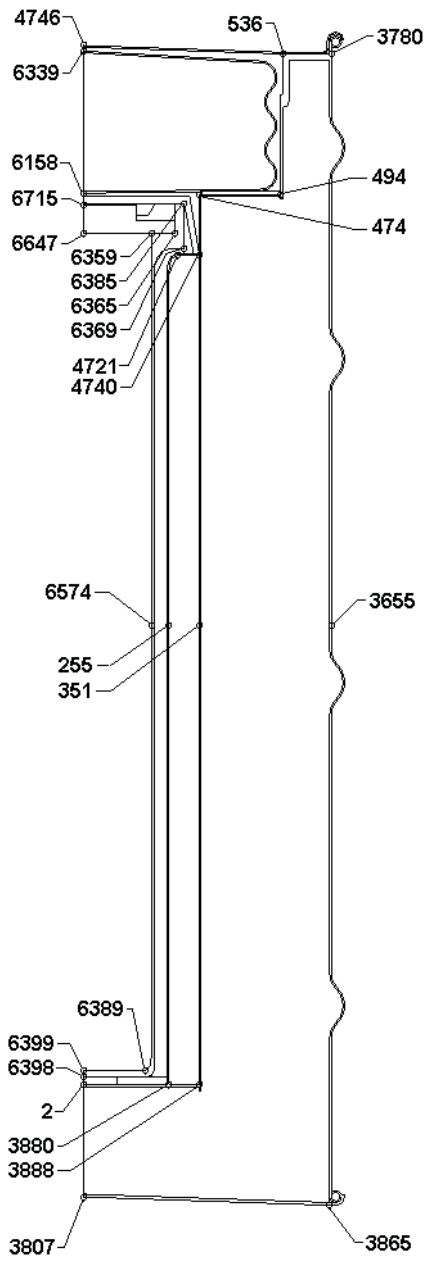	2	0.000	4.505	100.83	134.54	150.15
	255	3.180	21.528	100.75	131.57	146.21
	351	4.300	21.528	100.71	129.45	142.87
	474	4.300	37.535	100.46	117.90	125.67
	494	7.325	37.525	100.32	110.87	115.19
	536	7.385	42.755	100.21	105.50	107.19
	3655[c]	9.185	21.528	100.28	107.58	109.92
	3780[c]	9.185	42.755	100.21	105.29	106.89
	3807[c]	0.000	0.320	100.43	114.39	120.08
	3865[c]	9.185	0.008	100.32	108.97	111.97
	3880	3.178	4.505	100.74	130.48	144.23
	3888	4.300	4.505	100.71	128.60	141.42
	4721	3.500	35.275	100.59	124.08	134.90
	4740	4.300	35.275	100.57	122.92	133.15
	4746[c]	0.000	43.065	100.20	104.99	106.43
	6158	0.000	37.579	100.57	123.14	133.42
	6339	0.000	42.859	100.25	107.42	110.04
	6359[b]	2.530	36.075	100.80	133.51	148.56
	6365[b]	3.425	36.075	100.79	133.33	148.28
	6369	3.750	35.525	100.79	133.27	148.20
	6385	3.750	37.175	100.78	132.85	147.58
	6389	2.310	5.025	100.97	141.27	160.06
	6398	0.000	4.775	100.96	140.91	159.55
	6399	0.000	5.025	100.96	140.94	159.60
	6574	2.530	21.528	101.33	157.70	183.56
	6647	0.000	36.075	100.80	133.56	148.63
	6715	0.000	37.135	100.79	133.40	148.40

[a] See Table 3.4a and Figs. 8–11 in Appendix 3.6.2 for details of node locations.
[b] Approximate location of the CV O-ring.
[c] These nodes are at the accessible surfaces of the package (i.e., the drum, drum lid, and drum bottom plate).

Table 3.6. ES-3100 shipping container maximum "quasi steady-state" temperatures during NCT with various content heat loads and Cat 277-4 (100°F ambient temperature, with insolation)

Node map [a]	Node coordinates (in.)			Maximum "quasi steady-state" temperature (°F)			
	No.	r	z	0 W	0.4 W	20 W	30 W
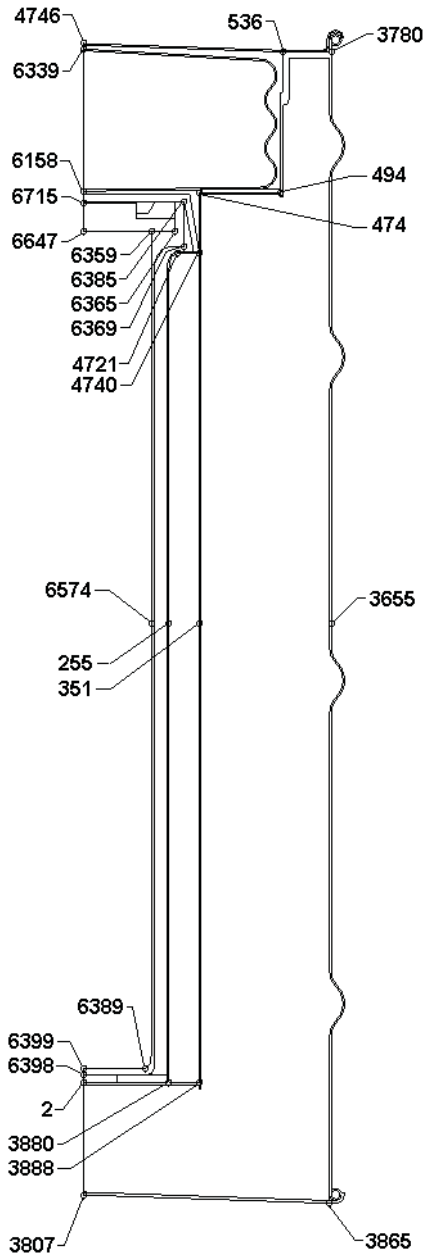	2	0.000	4.505	180.59	181.23	210.15	224.69
	255	3.180	21.528	179.33	179.93	207.32	221.43
	351	4.300	21.53	179.59	180.14	204.73	217.27
	474	4.300	37.54	198.88	199.20	212.72	219.58
	494	7.325	37.53	207.40	207.56	214.4	217.87
	536	7.385	42.76	226.44	226.49	228.31	229.24
	3655	9.185	21.528	198.09	198.15	200.81	202.16
	3780	9.185	42.755	223.47	223.51	225.13	225.95
	3807	0.000	0.320	190.48	190.70	199.84	204.43
	3865	9.185	0.008	195.87	195.97	199.91	201.90
	3880	3.178	4.505	180.72	181.28	206.65	219.52
	3888	4.300	4.505	181.03	181.55	205.08	217.01
	4721	3.500	35.275	189.45	189.90	209.53	219.47
	4740	4.300	35.275	190.56	190.98	209.37	218.68
	4746	0.000	43.065	243.86	243.89	245.32	246.03
	6158	0.000	37.579	198.42	198.84	217.12	226.32
	6339	0.000	42.859	233.98	234.06	237.32	238.95
	6359 [b]	2.530	36.075	189.28	189.90	217.07	230.51
	6365 [b]	3.425	36.075	189.27	189.88	216.88	230.23
	6369	3.750	35.525	189.23	189.85	216.79	230.12
	6385	3.750	37.175	189.39	190.00	216.57	229.72
	6389	2.310	5.025	179.94	180.70	215.75	233.27
	6398	0.000	4.775	179.99	180.76	215.52	232.92
	6399	0.000	5.025	179.99	180.76	215.55	232.96
	6574	2.530	21.528	179.27	180.35	229.19	252.87
	6647	0.000	36.075	189.40	190.02	217.24	230.72
	6715	0.000	37.14	189.44	190.06	217.14	230.54

[a] See Table 3.4a and Figs. 8–11 in Appendix 3.6.2 for details of node locations.
[b] Approximate location of the CV O-ring.

3.1.3.2 HAC temperature summary tables

In order to predict the maximum temperature for the packaging components during HAC, a transient thermal analyses was performed on the finite element model of the ES-3100 shipping container (undamaged configuration) to simulate HAC as prescribed by 10 CFR 71.73(c)(4). A 30-min fire of 800°C (1475°F) was simulated by applying natural convection and radiant exchange boundary conditions to all external surfaces of the drum (assuming the drum is in a horizontal orientation) with content heat loads of 0, 0.4, 20, and 30 W. There are no heat flux boundary conditions simulating insolation applied to the model before and during the 30-minute fire. The initial temperature distribution within the package having content heat loads of 0.4, 20, and 30 W is obtained from their respective steady-state analyses (Table 3.5). The initial temperature distribution within the package having no content heat load (0 W) is assumed to be at a uniform temperature equal to the ambient temperature of 38°C (100°F). The content heat load is simulated by applying a uniform heat flux to the internal surfaces of the elements representing the containment vessel.

Following the 30-min fire transient analyses, 48-h cool-down transient thermal analyses are performed using the temperature distribution at the end of the fire as the initial temperature distribution. During post-fire cool-down, natural convection and radiant exchange boundary conditions are applied to all external surfaces of the drum (assuming the drum is in a horizontal orientation). Additionally, cases are analyzed in which insolation is included during the post-fire cool-down. For the cases in which insolation is applied to the model during cool-down, insolation is applied during the first 12-h period following the 30-min fire, and then alternated (off, then on) as was done for NCT.

Based on the previous analysis of the ES-3100 package using BoroBond4 (Appendix 3.6.1), it was noted that using the low-end density of Kaolite 1600 results in higher containment vessel temperatures than using the high-end density of Kaolite 1600. For this reason, the NCT and HAC thermal analyses were run using a density of 19.4 lb/ft^3. Similarly, the low-end density of the Cat 277-4 material (100 lb/ft^3) was also used in these analyses. However, while using these low-end densities will result in higher temperatures to the containment vessel, using the high-end densities for these two materials will result in higher temperature differences from the baseline case. Thus, HAC runs are also made for heat loads of 0, 0.4, 20, and 30 W using a Kaolite 1600 density of 30 lb/ft^3 and a Cat 277-4 density of 110 lb/ft^3.

The maximum temperatures calculated for the ES-3100 shipping container for HAC are summarized in Table 3.7 for the analyses using a Kaolite 1600 density of 19.4 lb/ft^3 and a Cat 277-4 density of 100 lb/ft^3. The maximum temperatures calculated for the ES-3100 shipping container for HAC are summarized in Table 3.8 for the analyses using a Kaolite 1600 density of 30 lb/ft^3 and a Cat 277-4 density of 110 lb/ft^3. The thermal analyses that use the low-end density values for Kaolite 1600 and Cat 277-4 achieve the higher package temperatures (see Table 3.7).

Table 3.7. ES-3100 shipping container HAC maximum temperatures (Kaolite 1600 density of 19.4 lb/ft^3 and Cat 277-4 density of 100 lb/ft^3)

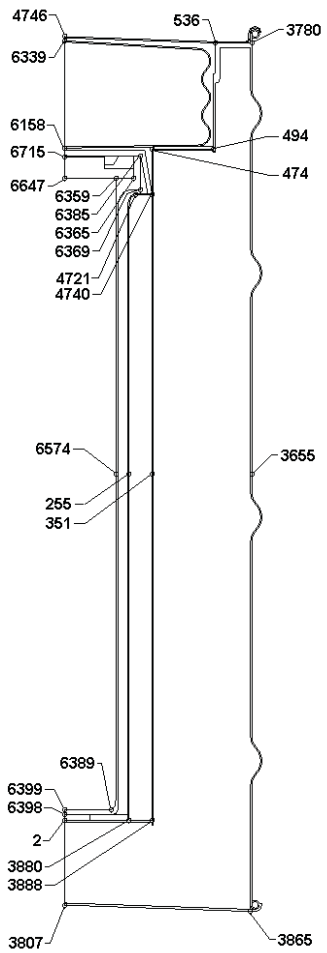

Node map [a]	Node coordinates (in.)			HAC maximum temperature (°F)							
				0 W		0.4 W		20 W		30 W	
	No.	r	z	Insolation during cool-down?		Insolation during cool-down?		Insolation during cool-down?		Insolation during cool-down?	
				No [b]	Yes	No	Yes	No	Yes	No	Yes
	2	0.000	4.505	225.5	232.1	226.2	232.8	255.5	261.7	269.5	275.7
	255	3.180	21.528	194.5	212.5	195.2	213.2	223.8	241.3	237.8	255.3
	351	4.300	21.528	195.8	211.9	196.4	212.5	222.3	237.8	234.8	250.3
	474	4.300	37.535	392.9	395.0	393.2	395.4	407.6	409.7	414.2	416.3
	494	7.325	37.525	671.2	672.0	671.4	672.3	679.1	680.0	682.5	683.3
	536	7.385	42.755	1380.4	1380.4	1380.4	1380.4	1380.9	1380.9	1381.1	1381.1
	3655	9.185	21.528	1457.8	1457.8	1457.8	1457.8	1458.0	1458.0	1458.1	1458.1
	3780	9.185	42.755	1427.8	1427.8	1427.9	1427.9	1428.1	1428.1	1428.2	1428.2
	3807	0.000	0.320	1454.5	1454.5	1454.5	1454.5	1454.9	1454.9	1455.0	1455.0
	3865	9.185	0.008	1470.1	1470.1	1470.1	1470.1	1470.1	1470.1	1470.2	1470.2
	3880	3.178	4.505	230.6	236.4	231.2	237.0	257.1	262.5	269.4	274.8
	3888	4.300	4.505	236.9	241.7	237.5	242.3	261.5	266.1	272.9	277.5
	4721	3.500	35.275	245.7	252.8	246.2	253.3	266.8	273.8	276.6	283.6
	4740	4.300	35.275	258.4	263.5	258.8	264.0	278.1	283.1	287.1	292.1
	4746	0.000	43.065	1448.0	1448.0	1448.0	1448.0	1448.2	1448.2	1448.3	1448.3
	6158	0.000	37.579	308.7	311.6	309.1	312.0	328.3	331.2	337.3	340.2
	6339	0.000	42.859	1335.1	1335.1	1335.2	1335.2	1336.4	1336.4	1336.9	1336.9
	6359 [c]	2.530	36.075	236.7	247.6	237.3	248.3	266.2	276.6	279.8	289.9
	6365 [c]	3.425	36.075	236.6	247.6	237.3	248.3	266.0	276.4	279.5	289.7
	6369	3.750	35.525	236.5	247.6	237.2	248.2	265.8	276.2	279.3	289.5
	6385	3.750	37.175	237.3	248.2	237.9	248.8	266.1	276.4	279.4	289.5
	6389	2.310	5.025	219.0	227.4	219.9	228.2	255.3	263.1	272.2	279.9
	6398	0.000	4.775	219.7	227.9	220.5	228.7	255.6	263.3	272.5	280.0
	6399	0.000	5.025	219.7	227.9	220.5	228.7	255.6	263.3	272.5	280.0
	6574	2.530	21.528	196.1	214.9	197.3	216.0	246.7	263.8	269.9	286.5
	6647	0.000	36.075	237.2	248.0	237.9	248.6	266.8	277.0	280.4	290.4
	6715	0.000	37.135	237.4	248.1	238.0	248.8	266.8	277.0	280.4	290.4

[a] See Table 3.4a and Figs. 8–11 in Appendix 3.6.2 for details of node locations.
[b] Baseline case for ΔT comparisons.
[c] Approximate location of the CV O-ring.

Table 3.8. ES-3100 shipping container HAC maximum temperatures (Kaolite 1600 density of 30 lb/ft^3 and Cat 277-4 density of 110 lb/ft^3)

Node map [a]	Node coordinates (in.)			HAC maximum temperature (°F)							
				0 W		0.4 W		20 W		30 W	
	No.	r	z	Insolation during cool-down?		Insolation during cool-down?		Insolation during cool-down?		Insolation during cool-down?	
				No [b]	Yes	No	Yes	No	Yes	No	Yes
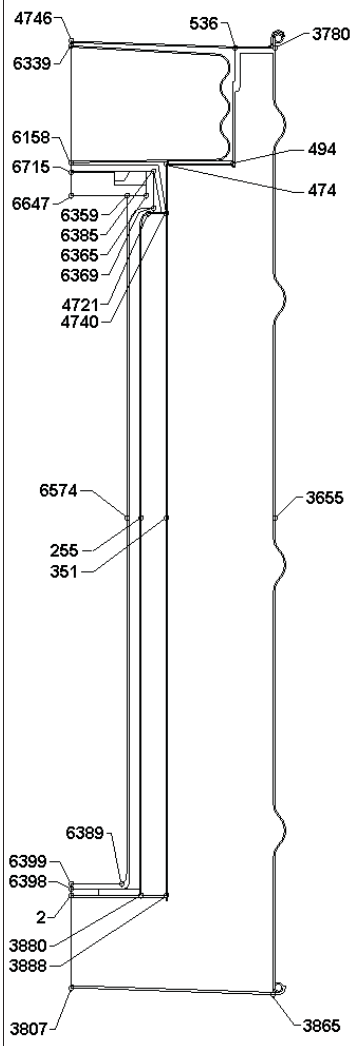	2	0.000	4.505	209.9	218.9	210.6	219.6	240.4	248.8	254.6	262.8
	255	3.180	21.528	185.5	207.7	186.1	208.4	215.1	236.6	229.3	250.6
	351	4.300	21.528	185.6	207.4	186.2	208.0	212.3	233.3	225.0	245.9
	474	4.300	37.535	342.9	345.5	343.3	345.9	358.1	360.7	365.0	367.5
	494	7.325	37.525	596.3	597.4	596.5	597.6	604.7	605.8	608.3	609.4
	536	7.385	42.755	1366.8	1366.8	1366.8	1366.8	1367.4	1367.4	1367.6	1367.6
	3655	9.185	21.528	1452.8	1452.8	1452.8	1452.8	1453.0	1453.0	1453.1	1453.1
	3780	9.185	42.755	1420.8	1420.8	1420.8	1420.8	1421.0	1421.0	1421.2	1421.2
	3807	0.000	0.320	1449.4	1449.4	1449.4	1449.4	1449.8	1449.8	1449.9	1449.9
	3865	9.185	0.008	1467.3	1467.3	1467.3	1467.3	1467.4	1467.4	1467.4	1467.4
	3880	3.178	4.505	213.1	221.4	213.7	222.0	240.0	247.9	252.5	260.3
	3888	4.300	4.505	217.0	224.4	217.6	225.0	242.1	249.1	253.8	260.7
	4721	3.500	35.275	228.0	237.5	228.5	238.0	249.7	259.0	259.7	269.0
	4740	4.300	35.275	236.5	243.8	236.9	244.3	256.7	263.9	266.0	273.2
	4746	0.000	43.065	1441.8	1441.8	1441.8	1441.8	1442.0	1442.0	1442.1	1442.1
	6158	0.000	37.579	277.3	281.8	277.8	282.3	297.5	302.0	306.7	311.2
	6339	0.000	42.859	1299.5	1299.5	1299.6	1299.6	1301.1	1301.1	1301.7	1301.7
	6359 [c]	2.530	36.075	225.1	237.3	225.8	237.9	254.7	266.1	268.3	279.6
	6365 [c]	3.425	36.075	225.0	237.3	225.7	237.9	254.5	266.0	268.1	279.3
	6369	3.750	35.525	224.9	237.2	225.6	237.8	254.3	265.8	267.9	279.2
	6385	3.750	37.175	225.5	237.6	226.2	238.3	254.6	266.1	268.0	279.2
	6389	2.310	5.025	205.3	215.9	206.2	216.8	242.0	251.9	259.2	268.9
	6398	0.000	4.775	205.8	216.3	206.7	217.1	242.2	252.0	259.2	268.8
	6399	0.000	5.025	205.8	216.3	206.7	217.1	242.2	252.0	259.3	268.8
	6574	2.530	21.528	187.8	209.1	189.0	210.2	238.9	258.4	262.4	281.3
	6647	0.000	36.075	225.6	237.7	226.3	238.3	255.2	266.5	268.9	280.0
	6715	0.000	37.135	225.8	237.8	226.4	238.4	255.2	266.5	268.9	280.0

[a] See Table 3.4a and Figs. 8–11 in Appendix 3.6.2 for details of node locations.
[b] Baseline case for ΔT comparisons.
[c] Approximate location of the CV O-ring.

Table 3.9. Maximum HAC temperatures recorded on the test packages' interior surfaces

Temperature patch location [a]	ES-3100 Test Unit				
	1	2	3	4	5
	°C (°F)	°C (°F)	°C (°F)	°C (°F)	°C (°F)
Top plug bottom	149 (300)	163 (325)	177 (350)	177 (350)	177 (350)
Inner liner					
Flange step wall	135 (275)	163 (325)	135 (275)	135 (275)	135 (275)
BoroBond4 step	107 (225)	135 (275)	107 (225)	177 (350)[b]	121 (250)
Adjacent to CV body wall high	99 (210)	99 (210)	99 (210)	99 (210)	104 (219)
Adjacent to CV body wall middle	99 (210)	93 (199)	116 (241)	93 (199)	99 (210)
Bottom flat portion	104 (219)	99 (210)	99 (210)	127 (261)	110 (230)
Containment boundary					
Lid (external top)	116 (241)	110 (230)	116 (241)	127 (261)	127 (261)
Lid (internal)	104 (219)	104 (219)	110 (230)	110 (230)	116 (241)
Flange (external)	116 (241)	110 (230)	110 (230)	116 (241)	121 (250)
Flange (internal)	104 (219)	99 (210)	116 (241)[b]	104 (219)	116 (241)
Body wall mid height	99 (210)	88 (190)	99 (210)	82 (180)	93 (199)
Bottom end cap (center)	99 (210)	99 (210)	88 (190)	110 (230)	99 (210)
Mock-up					
Side top	82 (180)	77 (171)	77 (171)	77 (171)	99 (210)
Side middle	77 (171)	77 (171)	77 (171)	77 (171)	93 (199)
Side bottom	77 (171)	77 (171)	77 (171)	77 (171)	88 (190)

[a] Refer to figures for exact locations and to Tables 5.3 through 5.7 in ORNL/NTRC-013, Vol. 1 for recorded values.
[b] Temperature indicating patch may have been damaged due to impact with surrounding structure.

3.1.4 Summary Tables of Maximum Pressures

3.1.4.1 Maximum NCT pressures

Table 3.10 summarizes the results from Appendix 3.6.4 in which the pressure of the containment vessel when subjected to the tests and conditions of NCT per 10 CFR 71.71 has been determined for the most restrictive containment vessel arrangements (CVAs) shipped in the ES-3100. The most restrictive CVAs are those in which the void volume inside the containment vessel is minimized based on content volumes and those CVAs that carry the largest mass of items that offgas at the predicted temperatures during NCT. Several convenience container heights are proposed for shipment (Fig. 1.4). Shipping configurations will use these containers in any configuration as long as it does not exceed the HEU weight limit and form and does not exceed the height constraint of the containment vessel. However, in order to determine the worst-case shipping configuration, the arrangements that minimize the void volume inside the containment vessel are analyzed as follows:

1. one shipment will contain six cans with external dimensions of 10.8 cm (4.25 in.) diameter by 12.38 cm (4.875 in.) high cans;

2. one shipment will contain five cans with external dimensions of 10.8 cm (4.25 in.) diameter by 12.38 cm (4.875 in.) high cans and three can spacers;

3. one shipment will contain three cans with external dimensions of 10.8 cm (4.25 in.) diameter by 22.23 cm (8.75 in.) high and two can spacers;

4. one shipment will contain three cans with external dimensions of 10.8 cm (4.25 in.) diameter by 25.4 cm (10 in.) high;

5. one shipment will contain six nickel cans with external dimensions of 7.62 cm (3.00 in.) diameter by 12.07 cm (4.75 in.) high;

6. one shipment will contain three polyethylene bottles with external dimensions of 12.54 cm (4.94 in.) diameter by 22.1 cm (8.7 in.) high; and

7. one shipment will contain three teflon bottles with external dimensions of 11.91 cm (4.69 in.) diameter by 23.88 cm (9.4 in.) high.

Table 3.10. Total pressure inside the containment vessel at 87.81°C (190.06°F) [a]

CVA	n_a [b] (lb-mole)	n_v [b] (lb-mole)	n_{po} [b] (lb-mole)	n_{bo} [b] (lb-mole)	n_{tf} [b] (lb-mole)	n_{H2} [b] (lb-mole)	n_{O2} [b] (lb-mole)	n_T [b] (lb-mole)	P_T (psia)
2	5.7148E-04	1.8626E-05	0.0000E+00	0.0000E+00	0.0000E+00	3.1895E-05	1.5948E-05	6.3795E-04	19.238
7	4.5793E-04	2.4829E-04	0.0000E+00	0.0000E+00	2.2296E-05	2.5558E-05	1.2779E-05	7.6685E-04	28.859

[a] This assumes that the internal convenience cans, polyethylene or Teflon FEP bottles, and Cat 277-4 spacer cans are not sealed.

[b] n_a –molar quantity of dry air in the gas mixture;
n_v –molar quantity of water vapor in the gas mixture due primarily from efflorescence;
n_{po} –molar quantity of gas due to offgassing of the silicone rubber pads;
n_{bo} –molar quantity of gas due to offgassing of the polyethylene bags, bottles, and lifting sling;
n_{tf} –molar quantity of gas due to offgassing of the Teflon bottles;
n_{H2} –molar quantity of hydrogen gas due to radiolysis of water;
n_{O2} –molar quantity of oxygen gas due to radiolysis of water;
n_T –total molar quantity in the gas mixture.

These arrangements are shown in Fig. 1.4. To determine the ES-3100's maximum normal operating pressure, the following assumptions have been used in the calculations:

1. The HEU contents are loaded into convenience cans, and convenience cans are placed inside the containment vessel at standard temperature (T_{amb}) and pressure (P_t) [25°C (77°F) and 101.35 kPa (14.7 psia)] with air at a maximum relative humidity of 100%;

2. The convenience cans and bottles are assumed to not be sealed to maximize the void volume inside the containment vessel;

3. Convenience can and bottle geometry does not change during pressure increase inside containment vessel;

4. If metal convenience cans are used, the total amount of polyethylene bagging and lifting slings is limited to 500 g per containment vessel shipping arrangement;

5. The mass of offgassing material (polyethylene bagging or bottles, Teflon bottles, silicone pads, lifting slings) is assumed to be 1490 g for the offgassing evaluation of containment vessel arrangement #7 and 500 g for containment vessel arrangement #6; and

6. Containment vessel arrangements that utilize closed convenience cans with a diameter greater than 10.8 cm (4.25 in.) will not contain any materials that off gas at the temperatures associated with Normal Conditions of Transport (NCT).

The offgassing material limits identified in assumptions 4 and 5 have been established based on the needs of shippers. All configurations are limited to 500 g of polyethylene in the form of bags, slings, and/or bottles. When the requirement to ship material in Teflon bottles arose, the upper limit of 1490 g of offgassing material was established. This limit is a combination of three Teflon bottles (330 g per bottle) and the original 500 g allowance for polyethylene material. These offgassing material limits have been used in calculations pertaining to containment vessel pressure, radioactive material leakage criteria, and criticality control. Therefore, portion of the safety basis of this shipping package has been based on these material limits.

NUREG-1609, Sect. 4.5.2.3, requires the applicant to demonstrate that any combustible gases generated in the package during a period of one year do not exceed 5% (by volume) of the free gas volume in any confined region of the package. No credit should be taken for getters, catalysts, or other recombination devices. The analysis conducted in Appendix 3.6.7 evaluates the different packaging arrangements for the generation of hydrogen gas due to the radiolysis of water vapor, free water, interstitial water, polyurethane bags, and polyurethane or Teflon bottles. By limiting the mass and the material composition as shown in Appendix 3.6.7, the combustible gas concentration limit stated in NUREG-1609 is not exceeded. These limits are further discussed and shown in Tables 1.3 and 1.3a. Getters, catalysts, or other recombination devices are not employed in any of the containment vessel packaging arrangements. The analysis conducted in Appendix 3.6.4 predicts the maximum normal operating pressure inside the containment vessel for the various packaging arrangements and masses discussed previously. This appendix also includes the hydrogen gas generation predicted by Appendix 3.6.7.

3.1.4.2 Maximum HAC pressures

Table 3.11 summarizes the results from Appendix 3.6.5 in which the pressure of the containment vessel when subjected to the tests and conditions of HAC per 10 CFR 71.73 has been determined for the most restrictive CVAs shipped in the ES-3100. The shipping configurations discussed in Sect. 3.1.4.1 are evaluated for HAC. To determine the maximum pressure generated inside the ES-3100's containment vessel due to HAC conditions, the following assumptions have been used in the calculations:

1. The initial pressure inside the containment vessel is the maximum normal operating pressure shown in Table 3.10 for each CVA at standard temperature [25°C (77°F)];

2. The convenience cans and bottles are assumed to not be sealed in order to maximize the void volume inside the containment vessel;

3. Convenience can and bottle geometry does not change during pressure increase inside containment vessel or because of damage from compliance testing;

4. If metal convenience cans are used, the total amount of polyethylene bagging and lifting slings is limited to 500 g per containment vessel shipping arrangement;

5. The mass of offgassing material (polyethylene bagging or bottles, Teflon bottles, silicone pads, lifting slings) is assumed to be 1490 g for the offgassing evaluation of containment vessel arrangement #7 and 500 g for containment vessel arrangement #6; and

6. Containment vessel arrangements that utilize closed convenience cans with a diameter greater than 10.8 cm (4.25 in.) will not contain any materials that off gas at the temperatures associated with Hypothetical Accident Conditions (HAC).

Table 3.11. Total pressure inside the containment vessel at 123.85°C (254.93°F) [a]

CVA	n_{MNOP} [b] (lb-mole)	n_{po} [b] (lb-mole)	n_{bo} [b] (lb-mole)	n_{tf} [b] (lb-mole)	n_{r-H2} (lb-mole)	n_{r-O2} (lb-mole)	n_{wv} [b] (lb-mole)	n_T [b] (lb-mole)	P_T (psia)
2	7.7228E-04	1.7302E-05	3.1529E-04	0.0000E+00	3.1895E-05	1.5948E-05	0.0000E+00	1.1527E-03	38.236
7	9.2831E-04	0.0000E+00	3.1529E-04	2.2296E-05	2.5558E-05	1.2779E-05	7.8428E-04	2.0885E-03	86.441

[a] This assumes that the internal convenience cans, polyethylene or Teflon FEP bottles, and Cat 277-4 spacer cans are not sealed.

[b] n_{MNOP} –molar quantity of the gas mixture at maximum normal operating pressure at standard temperature [25°C (77°F)];
n_{po} –molar quantity of gas due to offgassing of the silicone rubber pads;
n_{bo} –molar quantity of gas due to offgassing of the polyethylene bags, bottles, and lifting sling;
n_{tf} –molar quantity of gas due to offgassing of the Teflon bottles;
n_{r-H2} –molar quantity of hydrogen gas due to radiolysis of water;
n_{r-O2} –molar quantity of oxygen gas due to radiolysis of water;
n_{wv} –molar quantity of water vapor due to efflorescence of UNX crystals; and
n_T –total molar quantity in the gas mixture.

The offgassing material limits identified in assumptions 4 and 5 have been established based on the needs of shippers. All configurations are limited to 500 g of polyethylene in the form of bags, slings, and/or bottles. When the requirement to ship material in Teflon bottles arose, the upper limit of 1490 g of offgassing material was established. This limit is a combination of three Teflon bottles (330 g per bottle) and the original 500 g allowance for polyethylene material. These offgassing material limits have been used in calculations pertaining to containment vessel pressure, radioactive material leakage criteria, and criticality control. Therefore, portion of the safety basis of this shipping package has been based on these material limits.

3.2 SUMMARY OF THERMAL PROPERTIES OF MATERIALS

3.2.1 Material properties

Thermal properties at various temperatures for the stainless steel used in the fabrication of the drum, noncombustible cast refractory (Kaolite 1600), noncombustible neutron poison (BoroBond 4 or Cat 277-4), silicone rubber pads, and air are listed in Table 3.12. Properties used to evaluate thermal stresses due to differences in coefficient of thermal expansion are listed in Table 3.13.

3.2.2 Component Specifications

Component specifications are listed in Tables 3.14 and 3.15.

3.3 GENERAL CONSIDERATIONS

Thermal evaluation of the package design for NCT was performed by analysis. Evaluation of the package design for HAC was performed by a combination of testing and analysis.

3.3.1 Evaluation by Analysis

A description of the method and calculations used to perform the thermal and thermal stress analyses of the package for NCT and HAC is presented in detail in Appendices 3.6.1, 3.6.2 and 3.6.3.

Table 3.12. Thermal properties of the materials used in the thermal analysis

Material	Temperature (°F)	Thermal conductivity (Btu/h-in.-°F)	Density (lbm/in.³)	Specific heat (Btu/lbm-°F)	Emissivity
Stainless steel	−279.67	0.443 [a]	0.285 [a]	0.065 [a]	0.22 [a]
	−99.67	0.607	–	0.096	–
	260.33	0.799	–	0.123	–
	620.33	0.953	–	0.133	–
	980.33	1.088	–	0.139	–
	1340.33	1.223	–	0.146	–
	1700.33	1.348	–	0.153	–
	2240.33	1.526	–	0.163	–
Kaolite 1600	68	0.0093 [b]	0.011 [c]	0.2 [d]	–
	212	0.0091	–	–	–
	392	0.0081	–	–	–
	572	0.0072	–	–	–
	1112	0.0082	–	–	–
Neutron poison (Cat 277-4)	−31	0.0457 [e]	0.0579 [f]	0.125 [e]	–
	73.4	0.0485	–	0.186	–
	140	0.04	–	0.239	–
	212	0.0295	–	0.242	–
	302	0.0305	–	0.291	–
Neutron poison (BoroBond4)	25	0.0450 [g]	0.0683 [g]	0.2160 [g]	-
	77	0.0576	-	-	-
	100	0.0632	-	-	-
	104	0.0642	-	-	-
Silicone rubber	–	0.0161 [h]	0.047 [h]	0.300 [h]	1.0 [i]
Air	−9.67	1.074×10^{-3} [a]	$4.064 \times 10-5$ [a, j]	0.240 [a]	–
	80.33	1.266×10^{-3}	–	0.241	–
	170.33	1.445×10^{-3}	–	0.241	–
	260.33	1.628×10^{-3}	–	0.242	–
	350.33	1.796×10^{-3}	–	0.244	–
	440.33	1.960×10^{-3}	–	0.246	–
	530.33	2.114×10^{-3}	–	0.248	–
	620.33	2.258×10^{-3}	–	0.251	–
	710.33	2.393×10^{-3}	–	0.254	–
	800.33	2.523×10^{-3}	–	0.257	–
	890.33	2.644×10^{-3}	–	0.260	–
	980.33	2.759×10^{-3}	–	0.263	–
	1070.33	2.870×10^{-3}	–	0.265	–
	1160.33	2.985×10^{-3}	–	0.268	–
	1250.33	3.096×10^{-3}	–	0.270	–
	1340.33	3.212×10^{-3}	–	0.273	–
	1520.33	3.443×10^{-3}	–	0.277	–

[a] F. P. Incropera and D. P. DeWitt, *Fundamentals of Heat and Mass Transfer*, 2nd edition, John Wiley & Sons, New York, 1985.
[b] Hsin Wang, *Thermal Conductivity Measurements of Kaolite*, ORNL/TM-2003/49 (Appendix 2.10.3).
[c] Based on a baked density of 19.4 lbm/ft^3 (0.011 lbm/in^3). Specification JS-YMN3-801580-A003 (Appendix 1.4.4) requires a baked density of 22.4 ± 3 lbm/ft^3. Using a lower value for the Kaolite density results in higher temperatures on the containment vessel because the heat capacity of the Kaolite is minimized-allowing more heat to flow to the containment vessel; therefore, the thermal analyses are performed using a low-end density of 19.4 lbm/ft^3. The HAC analyses also consider a high-end density of 30 lbm/ft^3.
[d] FAX communication from J. W. Breuer of Thermal Ceramics, Engineering Department, August 11, 1995.
[e] Hsin Wang, *Thermophysical Properties of Heat Resistant Shielding Material*, ORNL/TM-2004/290 (Appendix 2.10.4). Specific heat values are presented in MJ/m^3-K in ORNL/TM-2004/290-converted to mass-based units using a density of 105 lbm/ft^3.
[f] Based on a cured density of density of 100 lbm/ft^3 (0.0579 lbm/in^3). B. F. Smith and G. A. Byington, *Mechanical Properties of 277-4*, Y/DW-1987, January 19, 2005 (Appendix 2.10.4), presents a range of measured densities between approximately 100 and 110 lbm/ft^3 for Catalog No. 277-4. Therefore, in order to minimize the heat capacity of the material and allow more heat to be transferred to the containment vessel, the lower-bound value is used. The HAC analyses also consider a high-end density of 110 lbm/ft^3.
[g] E-mail communication with presentation attachment, Jim Hall (Eagle-Picher) to Jerry Byington (BWXT Y-12), 3/12/2004.
[h] THERM 1.2, thermal properties database by R. A. Bailey.
[i] Conservatively modeled as 1.0.
[j] Constant density value evaluated at 100°F.

Table 3.13. Mechanical properties of the materials used in the static stress analyses

Material	Temperature (°F)	Modulus of Elasticity (psi)	Poisson's Ratio	Density (lbm/in.^{3})	Coefficient of thermal expansion (in./in./°F)
Stainless steel	−40	28.6×10^6 [a]	0.29 [b]	0.285 [d]	8.2×10^{-6} [e]
	100	28.14×10^6	—	—	8.6×10^{-6}
	200	27.6×10^6	—	—	8.9×10^{-6}
	300	27.0×10^6	—	—	9.2×10^{-6}
Kaolite	—	29,210 [c]	0.01 [c]	0.013 [f]	5.04×10^{-6} [g]
Neutron absorber (Cat 277-4)	−40	1.991×10^6 [h]	0.33 [h]	0.0608 [h]	7.056×10^{-6} [i]
	−4	—	—	—	7.222×10^{-6}
	32	—	—	—	7.222×10^{-6}
	70	0.984×10^6	0.28	—	—
	100	0.403×10^6	0.25	—	—
	104	—	—	—	7.000×10^{-6}
	140	—	—	—	6.444×10^{-6}
	176	—	—	—	5.778×10^{-6}
	212	—	—	—	5.389×10^{-6}
	248	—	—	—	5.056×10^{-6}
	284	—	—	—	4.889×10^{-6}
	302	—	—	—	4.833×10^{-6}

[a] *ASME Boiler and Pressure Vessel Code*, Sect. II, Part D, Subpart 2, Tables TE-1, B column, and TM-1.
[b] R. A. Bailey, *Strain - A Material Database*, Lawrence Livermore National Laboratory, 1989.
[c] The Poisson's Ratio of Kaolite is assumed to be a small value of 0.01 (Appendix 2.10.2).
[d] F. P. Incropera and D. P. DeWitt, *Fundamentals of Heat and Mass Transfer*, 2nd edition, John Wiley & Sons, New York, 1985.
[e] *Metallic Materials and Elements for Aerospace Vehicle Structures*, MIL-HDBK-5H, May 1986.
[f] Specification JS-YMN3-801580-A003 (Appendix 1.4.4) requires a baked density of 22.4 ± 3 lbm/ft^3.
[g] E-mail communication, Ken Moody (Thermal Ceramics, Inc.) to Paul Bales (BWXT Y-12), December 9, 2004.
[h] B. F. Smith and G. A. Byington, *Mechanical Properties of 277-4*, Y/DW-1987, January 19, 2005 (Appendix 2.10.4).
[i] W. D. Porter and H. Wang, *Thermophysical Properties of Heat Resistant Shielding Material*, ORNL/TM-2004/290, Oak Ridge National Laboratory, Oak Ridge, Tenn., December 2004 (Appendix 2.10.4). Coefficient of thermal expansion at each temperature taken as the maximum of values for Runs #2, #3, and #5.

Table 3.14. Packaging material technical specifications

Component	Specifications
	Drum assembly
Drum washers	1.375 OD × 0.812 ID × 0.25-in. thick, 300 Series stainless steel
Drum threaded weld studs	⅝-11 × ⅞ long, fabricated per ASME SA-193, using Type 304/304L stainless-steel per ASME 479
Drum hex nuts	⅝-11 UNC-2B, silicon bronze C65100, ASTM F-467
Drum lid weldment	Modified 30-gal, 16-gauge (MS27683-61) lid, type 304 or 304L stainless steel; and a 11-gauge thick sheet, type 304 or 304L stainless steel, ASME SA-240
Drum weldment	Modified 30-gal, 16-gauge (MS27683-7), type 304 or 304L stainless steel, ASME SA-240, manufactured per Drawing M2E801580A004 (Appendix 1.4.8)
Drum plugs	Nylon plastic plug, Micro Plastic, Inc.
	Impact limiter, insulation enclosure, neutron absorber, and drum packing material
Insulation and impact limiter (not removable)	Lightweight cast refractory insulation, Kaolite 1600, 358.8 kg/m^3 (22.4 lb/ft^3) density, cast in stainless-steel shells in the drum and top plug
Neutron absorber	Cat 277-4, 1681.9 +240/-80 kg/m^3 (105 +15/- 5 lb/ft^3) density
Top plug (removable)	Type 304 or 304L stainless steel, ASME SA-240 (body), ASME SA-79 (lifting inserts),
Inner liners	Type 304 or 304L stainless steel, ASME SA-240 (body), ASME SA-79 (modified angle)
Aluminum tape	
Silicone pads	Silicone rubber, 22 ± 5 Shore A, color black/gray
	Containment boundary
Containment vessel plug	Part # 04-2126, Modified VCO threaded plug, brass
Containment vessel swivel hoist ring	3052T56, Swivel hoist ring, alloy steel (not used for shipment)

Table 3.14. Packaging material technical specifications

Component	Specifications
Containment vessel	Method 1: Type TP304L stainless steel ASME SA-312 (welded or seamless pipe body); type F304L, stainless steel, ASME SA-182 (flange, and end cap); type 304, stainless steel, ASME SA-479 (sealing lid), Nitronic 60 SST per ASME SA-479, UNS-S21800 (closure nut) Method 2: Type F304L stainless ASME SA-182 (body, flange, and end cap); type 304, stainless steel, ASME SA-479 (sealing lid), Nitronic 60 SST per ASME SA-479, UNS-S21800 (closure nut) All components per *ASME Boiler and Pressure Vessel Code*, Sect. II, Part D, Table 2A
Containment vessel O-rings	Elastomer, ethylene propylene, normal service temperature range of −40 to 150°C, Specification M 3BA712A14B13F17 in ASTM D-2000, per OO-PP-986, Rev. D
Containment vessel lid assembly retaining ring	Part # WSM-400-S02, type 302 stainless steel
Containment vessel O-ring lubricant	Clear dimethyl siloxane polymer
Containment vessel closure nut lubricant	Krytox #240AC
Containment vessel body dowel pins	0.2501/0.2503 OD × 0.50 long, 18-8 stainless steel
	Containment vessel packing material
Convenience cans	Stainless steel or tin plated carbon steel with stainless-steel can handles and nylon coated stainless-steel wire, or passivated nickel
Silicone rubber pads	Silicone rubber, 22 ±5 Shore A, color black/gray
Spacers	Stainless-steel can filled with Cat 277-4
Bottles	Polyethylene or Teflon FEP
Bagging	Polyethylene
Metal scrubbers	Stainless steel, McMaster Carr Part # 7361T13

Table 3.15. Component allowable service temperature and pressure

Component	Allowable service temperature range °C (°F)	Allowable pressure range kPa (psi) gauge
Drum assembly		
Stainless-steel drum and lid	−40 to 871 (−40 to 1600) [a]	48.3 (7)
Silicon bronze nuts	−40 to 871 (−40 to 1600) [a]	N/A
Stainless-steel washers	−40 to 871 (−40 to 1600) [a]	N/A
Stainless-steel mid liner	−40 to 871 (−40 to 1600) [a]	N/A
Stainless-steel inner liner	−40 to 871 (−40 to 1600) [e]	N/A
Stainless-steel top plug weldment	−40 to 871 (−40 to 1600) [a]	
Kaolite 1600	−40 to 871 (−40 to 1600) [a]	N/A
Cat 277-4	−40 to 150 (−40 to 302) [b] −40 to 161 (−40 to 320) [g]	N/A
Silicone rubber pads	−40 to 232 (−40 to 450) [f]	N/A
Containment vessel		
Stainless-steel body and sealing lid	−40 to 427 (−40 to 800) [c]	149.62 (21.7) external 699.82 (101.5) internal
Nitronic 60 closure nut	−40 to 427 (−40 to 800) [c]	149.62 (21.7) external 699.82 (101.5) internal
Stainless-steel retaining ring	−40 to 427 (−40 to 800) [c]	N/A
Dowel pins	−40 to 427 (−40 to 800) [c]	N/A
Brass VCO fitting (Viton O-rings)	−40 to 204 (−40 to 400) [d]	N/A
Ethylene propylene O-rings	−40 to 150 (−40 to 302) [d]	5.52×10^3 (800) with no backing rings
Containment vessel silicone pads	−40 to 232 (−40 to 450) [f]	N/A

[a] In accordance with *Kaolite SuperLightweight Insulating Castables* (Appendix 2.10.3), the recommended use limit temperature for Kaolite 1600 material is 871 °C (1600 °F). This temperature is the established limit for material in immediate contact with the Kaolite 1600 material and is based on continuous service.
[b] This limit is established based on criticality limits of moisture loss for NCT. It is based on continuous service.
[c] This limit is established by the *ASME Boiler and Pressure Vessel Code*.
[d] This limit is provided by the *Parker O-Ring Handbook* for each material's continuous service limit.
[e] This limit is established based on the fact that the inner liner material is identical to the drum material.
[f] This represents the allowable service temperature limit listed in the McMaster-Carr catalog description for this material.
[g] This limit is established based on criticality limits of moisture loss for HAC. It is based on four hours at this temperature.

3.3.2 Evaluation by Test

Full-scale testing of five ES-3100 test units was conducted in accordance with 10 CFR 71.73 for HAC. A single full-scale ES-3100 (TU-4) was assembled and subjected to both NCT testing and the sequential tests specified in 10 CFR 71.73(c). The furnace used for thermal testing was the No. 3 furnace at Timken Steel Company in Latrobe, Penn., which is a gas-fired furnace. This furnace employs "pulsed" fire burners, in which the natural gas flow rate is varied based on furnace controller demands, but the flow of air through the burners is constant, even when no gas is flowing. This ensures a very rich furnace atmosphere capable of supporting any combustion of package materials of construction.

Oxygen content was not monitored in stack gases of the furnace because it was not anticipated that any of the package's materials of construction were combustible. There was some burning of the silicone pads which are placed between the inner liner and the top plug of the package.

The most significant change to the definition of the HAC thermal test in the current 10 CFR 71 is the requirement for calculation purposes to base convective heat input on "that value which may be demonstrated to exist if the package was exposed to the fire specified." This is not especially significant for this package because it was tested in the gas-fired furnace with burners placed in an attitude which produced a strong convective swirl. Careful examination of the thermal test data indicates that the total heat imparted to the packages was significantly greater than the required total heat specified in 10 CFR 71.73(c)(4).

Compliance with ASTM E-2230-02, *Standard Practice for Thermal Qualification of Type B Packages for Radioactive Materials* (ASTM E-2230-02), was accomplished by the method described in Sect. 7.3 of this standard. This standard is in general agreement with Paragraph 2.2.1 ("Steady-state Method of Compliance") of SG 140.1 entitled *Combination Test Analysis/ Method Used to Demonstrate Compliance to DOE Type B Packaging Thermal Test Requirements (30 Minute Fire Test)*. The data from each of the thermal tests, as shown in the test report, show that five of the six thermocouple-instrumented exterior surfaces of each package reached temperatures well in excess of 800°C (1475°F) during the 30-min thermal testing. Similarly, all other surfaces of the furnace, including the support stand, exceeded 800°C (1475°F) during the timed portion of the thermal test. For the test specified in the regulations, regardless of the amount of heat input by convection, radiation, or conduction, the maximum temperature the skin of the package could reach would be 800°C (1475°F). That is, the source of the heat in the regulatory-specified test is at 800°C (1475°F). Heat can only be transferred from a hotter source to a colder source. Thus, regardless of the mode of heat transfer, the greatest temperature a specimen exposed to the 10 CFR 71.73,(c)(4) thermal test can attain is 800°C (1475°F). The thermal performance of the packaging components as an assembled unit has been demonstrated through full-scale tests. Actual tests and procedures followed are described in Sect. 4.5 of ORNL/NTRC-013, Vol. 1. Figures 3.2 through 3.5 show the general testing arrangements.

Since full-scale testing in accordance with 10 CFR 71.73 for HAC was conducted on prototypical packages. No analyses were conducted to show compliance with the HAC thermal test. However, to determine the thermal impacts of (1) an internal heat source, (2) application of insolation during cool down, (3) thermal capacitance differences between test mock-ups and actual contents, and (4) the change in neutron absorbing material, analyses were conducted and are summarized in Appendices 3.6.1 and 3.6.2. Further discussion of these issues is found in Sect. 3.5.3.

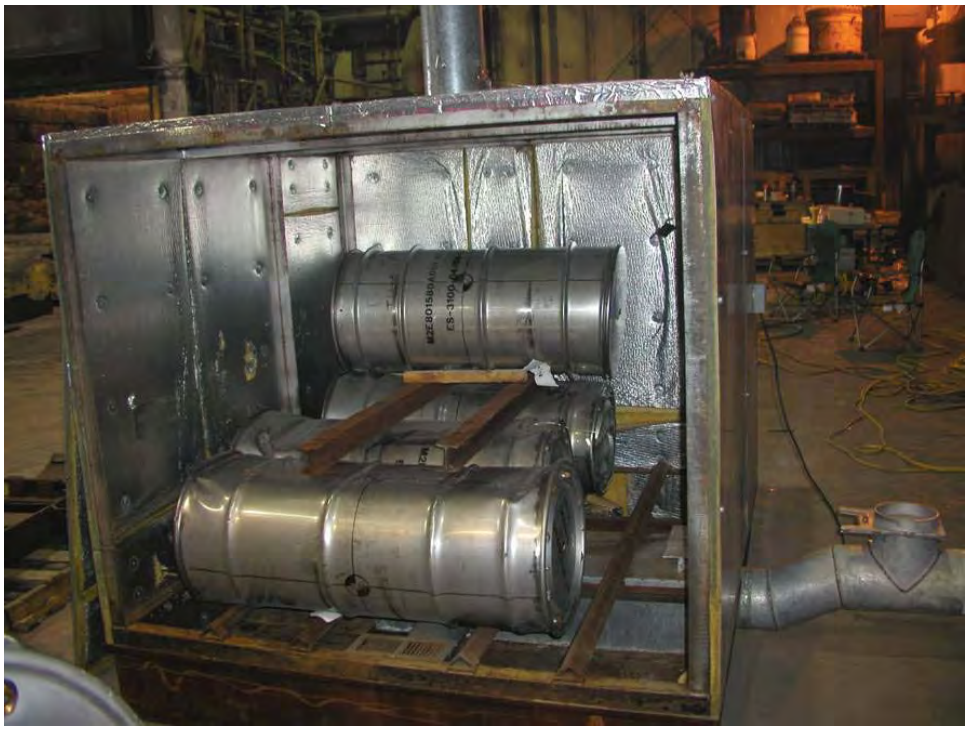

Fig. 3.2. Test units preheat arrangement.

Fig. 3.3. Test unit insertion into furnace.

Fig. 3.4. Test unit removal from furnace.

Fig. 3.5. Test unit cool down and monitoring arrangement.

3.3.3 Margins of Safety

Tables 3.16 and 3.17 summarize the results of thermal analysis and testing in accordance with NCT and HAC regulatory requirements. Margins of safety have not been calculated. However, the predicted or calculated results of individual components are compared with their allowable continuous service limit for NCT in Table 3.16 and for HAC in Table 3.17. For all components, the values calculated during NCT (Table 3.16) do not approach their allowable limits stated in Table 3.15. The temperature values predicted or calculated for the Kaolite 1600 material, the top plug stainless steel, the silicon bronze nuts, and the Cat 277-4 neutron poison do approach and/or exceed their allowable continuous service limits during HAC thermal testing. However, short-term excursions above these allowable limits as shown in ORNL/NTRC-013/V1 do not reduce the ability of the packaging components to provide their safety functions during HAC. Justification of this statement is provided by the following information:

1. As discussed in Sect. 3.5.2, the thermal tests were conducted in compliance with ASTM E 2230-02 and SG 140.1 using the steady state environmental method to comply with 10 CFR 71.73(c)(4). In order to maintain a 800°C thermal environment at all locations inside the furnace and on all external surfaces of the shipping package, the set point of the furnace had to be adjusted upward to 871°C (1600°F). A direct result of this action was that some of the external thermocouples on the package surface exceeded 871°C (1600°F) for short periods of time during the timed thermal test.

2. In accordance with National Bronze & Metals, Inc., the silicon bronze nuts remain solid or crystalline in nature up to a temperature of 1032°C (1890°F). Their only safety function during and following the thermal test is to keep the lid attached to the drum assembly. By remaining solid during and following HAC testing, the silicon bronze nuts performed their safety function. All lids remained attached to the drum assembly following HAC thermal testing.

3. In accordance with ASM Aerospace Specification Metals Inc., Type 304/304L stainless steel has a continuous service temperature of 927°C (1700°F). During the thermal test, the safety function of the stainless steel in the top plug is to encapsulate the Kaolite 1600 insulating material. As shown in ORNL/NTRC-013/V1, the external temperature does intermittently exceed the continuous service limit of the Kaolite 1600 material. However, these short-term temperature excursions do not diminish the ability of the stainless steel to maintain the boundary around the insulating material. The solidus temperature for stainless steel is ~1399°C (2550°F); therefore, there is a significant thermal margin of safety in the stainless steel. All top plugs were intact following HAC thermal testing.

4. As documented in Appendix 2.10.3, the recommended use limit temperature for Kaolite 1600 is 871°C (1600°F) and the melting point is 1260°C (2300°F). This use limit temperature is also the established limit for material in immediate contact with the Kaolite 1600 material and is based on continuous service at this temperature. As previously stated, the external temperature does intermittently exceed the continuous service limit of the Kaolite 1600 material during the thermal test, but it remains well below its melting point. The safety function of the Kaolite 1600 material is to keep the containment vessel as cool as possible and to meet the leaktight criteria established in ANSI N14.5-1997. Based on temperature and pressure calculations, the containment vessel maintains containment during and after thermal testing to the above criteria. Therefore, short-term temperature excursions above 871°C do not diminish the ability of the Kaolite 1600 material to perform its safety function.

Table 3.16. Summary of results of evaluation for the ES-3100 under NCT

Conditions	Calculated results	Allowable limit	SARP reference
Minimum package temperature, °C (°F)	−40 (−40)	−40 (−40)	Sect. 3.4.1
Maximum drum assembly stress due to cold conditions per 10 CFR 71.71(c)(2), kPa (psia)	61,150 (8,869)	132,379 (19,200)	Appendix 3.6.3
Minimum containment vessel pressure, kPa (psia)	76.74 (11.13)	0.0 (0.0)	Sect. 3.4.1
Maximum drum temperature with insolation, °C (°F)	117.72 (243.89) [a]	N/A	Appendix 3.6.2 Sect. 3.4.1
Maximum drum assembly stress due to hot conditions per 10 CFR 71.71(c)(1), kPa (psia)	66,934 (9,708)	132,379 (19,200)	Appendix 3.6.3
Containment vessel temperature with insolation, °C (°F)	87.81 (190.06) [a]	427 (800) [b]	Appendix 3.6.2 Sect. 3.4.1
Maximum ethylene propylene O-ring temperature, °C (°F)	87.81 (190.06)	150 (302) [c]	Appendix 3.6.2 Sect. 3.4.1
Maximum containment vessel pressure, kPa (psia)	198.98 (28.859) [d]	801.2 (116.2) [e]	Appendix 3.6.4 Sect. 3.4.2
Maximum silicone bronze nut temperature with insolation, °C (°F) [Node 536]	~108.05 (226.49)	871 (1600) [f]	Sect. 3.1.3.1 Table 3.6
Maximum stainless-steel washer temperature with insolation, °C (°F) [Node 536]	~108.05 (226.49)	871 (1600) [f]	Sect. 3.1.3.1 Table 3.6
Maximum stainless-steel mid liner temperature with insolation, °C (°F) [Node 474]	92.89 (199.20)	871 (1600) [f]	Sect. 3.1.3.1 Table 3.6
Maximum stainless-steel inner liner temperature with insolation, °C (°F) [Node 4721]	87.72 (189.90)	871 (1600) [f]	Sect. 3.1.3.1 Table 3.6
Maximum top plug temperature with insolation, °C (°F) [Node 6339]	112.26 (234.06)	871 (1600) [f]	Sect. 3.1.3.1 Table 3.6
Maximum Kaolite 1600 temperature with insolation, °C (°F) [Node 6339]	112.26 (234.06)	871 (1600) [f]	Sect. 3.1.3.1 Table 3.6
Maximum Cat 277-4 temperature with insolation, °C (°F) [Node 4740]	88.32 (190.98)	150 (302) [f]	Sect. 3.1.3.1 Table 3.6
Maximum silicone rubber pad temperature with insolation, °C (°F) [Node 494]	97.53 (207.56)	232 (450) [f]	Sect. 3.1.3.1 Table 3.6
Maximum Viton O-ring temperature with insolation, °C (°F) [Node 6715]	~87.81 (190.06)	204 (400) [f]	Sect. 3.1.3.1 Table 3.6
Maximum brass VCO fitting temperature with insolation, °C (°F) [Node 6715]	~87.81 (190.06)	204 (400) [f]	Sect. 3.1.3.1 Table 3.6

[a] Appendix 3.6.2.
[b] *ASME Boiler and Pressure Code*, Sect. II, Part D, maximum allowable temperature for Sect. III, Div. 1, Subsection NB vessel.
[c] Maximum O-ring seal life up to 150°C (302°F) for continuous service (*Parker O-ring Handbook,* Fig. 2-24).
[d] Appendix 3.6.4.
[e] Appendix 2.10.1 allowable limit.
[f] See Table 3.15.

Table 3.17. Summary of results of evaluation under HAC for the ES-3100 shipping arrangement using bounding case parameters

Condition with HAC temperature adjustments	Calculated results	Allowable limit	SARP references
Maximum adjusted containment vessel temperature during testing, °C (°F)	152.22 (306.00)	426.67 (800) [a]	Sect. 3.5.3
Maximum containment vessel pressure during testing, kPa (psia)	595.99 (86.441) [b]	801.2 (116.2) [c]	Appendix 3.6.5 Sect. 3.5.3
Maximum adjusted ethylene propylene O-ring temperature, °C (°F)	141.22 (286.20)	150 (302) [d]	Sect. 3.5.3
Maximum silicone bronze nut temperature, °C (°F) [Node 536]	<871 (<1600)	871 (1600) [e]	Sect. 3.1.3.2 Figures 4.40, 4.42, 4.44, 4.46, and 4.48 of ORNL/NTRC-013/V1
Maximum stainless-steel drum washer temperature, °C (°F) [Node 536]	<871 (<1600)	871 (1600) [e]	Sect. 3.1.3.2 Figures 4.40, 4.42, 4.44, 4.46, and 4.48 of ORNL/NTRC-013/V1
Maximum stainless-steel mid liner temperature, °C (°F) [Node 474]	~204 (400) [f]	871 (1600) [e]	Sect. 3.1.3.2 Tables 3.6, 3.7, 3.8, and 3.9
Maximum stainless-steel inner liner temperature, °C (°F) [Node 4721]	~203 (397) [g]	871 (1600) [e]	Sect. 3.1.3.2 Tables 3.6, 3.7, 3.8, and 3.9
Maximum top plug temperature, °C (°F) [Node 6339]	<871 (<1600)	871 (1600) [e]	Sect. 3.1.3.2 Figures 4.40, 4.42, 4.44, 4.46, and 4.48 of ORNL/NTRC-013/V1
Maximum Kaolite 1600 temperature, °C (°F)	>871 (>1600)	871 (1600) [e]	Sect. 3.1.3.2 Figures 4.40, 4.42, 4.44, 4.46, and 4.48 of ORNL/NTRC-013/V1
Maximum Cat 277-4 temperature, °C (°F) [Node 4721]	~161 (320) [g]	161 (320) [e]	Sect. 3.1.3.2 Table 3.6, 3.7, 3.8, and 3.9
Maximum silicone rubber pad temperature, °C (°F) [Node 494]	>232 (450)	NSS [h]	Sect. 3.1.3.2 Figure 5.4 of ORNL/NTRC-013/V1
Maximum Viton O-ring temperature, °C (°F) [Node 6715]	~152 (306)	204 (400) [e]	Sect. 3.1.3.2 Tables 3.20 and 3.21
Maximum brass VCO fitting temperature, °C (°F) [Node 6715]	~152 (306)	204 (400) [e]	Sect. 3.1.3.2 Tables 3.20 and 3.21

[a] *ASME Boiler and Pressure Code*, Sect. II, Part D, max allowable temperature for Sect. III, Div. 1, Subsection NB vessel.
[b] Appendix 3.6.5.
[c] Appendix 2.10.1 at 148.89°C (300°F).
[d] Maximum O-ring seal life up to 150°C (302°F) for continuous service (*Parker O-ring Handbook,* Fig. 2-24).
[e] See Table 3.15.
[f] Maximum HAC temperature adjustments for this location are 6.1°C for blackout readings, 6.1°C for crush plate location differences, 1.4°C for decay heat and insolation after thermal test, and 27.8°C for variation in Kaolite 1600 and Cat. 277-4 densities.
[g] Maximum HAC temperature adjustments for this location are 6.1°C for blackout readings, 6.1°C for crush plate location differences, 4.2°C for decay heat and insolation after thermal test, and 9.8°C for variation in Kaolite 1600 and Cat. 277-4 densities.
[h] Considered a non-safety significant (NSS) component. Therefore, maximum allowable temperature limit during HAC is unknown.

5. By using the appropriate temperature adjustments shown in Table 3.20, the maximum recorded HAC temperature shown in Table 3.9, and the data for Node 4740 in Fig. 21 of Appendix 3.6.2, the 277-4 material reaches its peak temperature (~320°F) ~2 h following the thermal test. Figure 21 in Appendix 3.6.2 also shows that this peak temperature drops ~15°F ~4 h after furnace removal and continuously drops thereafter. The maximum temperature in the 277-4 material occurs at the top of neutron absorber cavity (Node 4740 in the analytical models). As shown in Tables 3.7 and 3.8, the temperature in other regions of the 277-4 (e.g., Nodes 351 and 3888) is well below this maximum temperature for the entire length of time associated with the thermal test and cool-down period. For HAC criticality safety analysis, the entire mass of the 277-4 material is conservatively assumed to have the properties resulting from exposure to 320°F for 4 h.

Based on these results, the ES-3100 components will perform their safety functions during both NCT and HAC.

3.4 THERMAL EVALUATION UNDER NORMAL CONDITIONS OF TRANSPORT

3.4.1 Heat and Cold

The ambient temperature requirement for NCT is 38°C (100°F). The 35.2 kg of HEU shipped in the ES-3100 package generates a maximum bounding heat load of 0.4 W. The insolation heat flux stipulated in 10 CFR 71.71(c)(1) was used in the calculations. If the package is exposed to solar radiation at 38°C (100°F) in still air, the conservatively calculated temperatures at the top of the drum, on the top surface of the containment vessel, and on the containment vessel near the O-ring sealing surfaces, are 117.72, 87.81, and 87.72°C (243.89, 190.06, 189.90°F), respectively, for the ES-3100. Nevertheless, these temperatures are within the service limits of all packaging components, including the O-rings. The normal service temperature range of the O-rings used in the containment boundary is −40 to 150°C (−40 to 302°F), in accordance with B&PVC, Sect. III; thus, the seal will not be affected by this maximum normal operating temperature.

Using the temperatures calculated for the conditions of 10 CFR 71.71(c)(1), Appendix 3.6.4 predicts that the maximum normal operating pressure inside the containment vessel will be 198.98 kPa (28.859 psia). The design absolute pressure of the containment vessel is 801.17 kPa (116.2 psia), and the hydrostatic test pressure is 1135.57 kPa (164.7 psia). Thus, increasing the internal pressure of the containment vessel to a maximum of 198.98 kPa (28.859 psia) during NCT would have no detrimental effect. Stresses generated in the containment vessel at this pressure are insignificant compared to the materials of construction allowable stress. Table 2.20 provides a summary of the pressure and temperature for the various shipping configurations. As discussed in Sect. 2.6.1.4, the containment vessel and vessel closure nut stresses for these pressure conditions are below the allowable stress values.

Summarizing 10 CFR 71.43(f), the tests and conditions of NCT shall not substantially reduce the effectiveness of the packaging to withstand HAC sequential testing. The effectiveness of the ES-3100 to withstand HAC sequential testing is not diminished through application of the tests and conditions stipulated in 10 CFR 71.71. The justification for this statement is provided by physical testing of both the ES-2M and ES-3100 test packages. Due to the similarities in design, fabrication, and material used in construction of both the ES-2M and the ES-3100 package, the Kaolite 1600 physical characteristics will hold true for both designs. The integrity of the Kaolite 1600 is not significantly affected by the NCT vibration and 1.2-m (4-ft) drop tests.

Prior to testing the ES-2M design (a similarly constructed shipping package), each test unit was radiographed to determine the integrity of the Kaolite 1600 impact and insulation material. Following

casting of the material inside the drum, some three-dimensional curving cracks were seen in some packages near the top thinner sections from the bottom of the liner to the bottom drum edge. After vibration testing, radiography of the ES-2M Test Unit-4 showed that the lower half of the impact limiter was broken into small pieces (Byington 1997). To evaluate these findings, Test Unit-4 was reassembled and subjected to HAC sequential testing (Byington 1997). After vibration and impact testing, many three-dimensional curving cracks were seen around the impact areas, and the inner liner was also visibly deformed. Nevertheless, temperatures at the containment boundary were also similar to other packages not subjected to vibration testing prior to HAC testing. No inleakage of water was recorded following immersion. Also, Test Unit-4 of the ES-3100 shipping package was subjected to the full NCT test battery including vibration.

Following these tests, the containment vessel of the ES-2M Test Unit-4 was removed, and a full body helium leak check was performed. The test unit passed the leak-tight criteria in accordance with ANSI N14.5-1997. The containment vessel was then reassembled into the previously tested drum assembly and subjected to the complete HAC testing. Based on the success of this unit and the similar design of the ES-2M, it can be concluded that vibration normally incident to transport does not reduce the effectiveness of the ES-3100 packaging during HAC testing. The ES-3100 has been tested to determine the effectiveness of the package following a sequential NCT 1.2-m (4-ft) drop test and HAC test battery. Throughout all of the vibration and structural testing, the effectiveness of the Kaolite 1600 material as an impact limiter and thermal insulation was not substantially reduced.

Since the components to be shipped have an assumed decay heat load of 0.4 W, a thermal analysis was conducted for the ES-3100 package with and without full solar insolation. The package was analyzed using the ABAQUS/Standard computer code, and the finite element geometry was constructed for each model using MSC.Patran 2004. The predicted temperature, while stored at 38°C (100°F) in the shade, for the drum lid center and the containment vessel flange near the inner O-ring, is 37.89°C (100.20°F) and 38.22°C (100.80°F), respectively. The analysis shows that no accessible surface of the package would have a temperature exceeding 50°C (122°F). Therefore, the requirement of 10 CFR 71.43(g) would be satisfied for either transportation mode (exclusive use or nonexclusive use).

Also, in accordance with 10 CFR 71.71(c)(2), the containment vessel pressure must be calculated at −40°C (−40°F). Given the initial conditions of temperature, relative humidity, no silicone rubber or polyethylene bag offgassing, the pressure is calculated as follows:

$$P_1 \text{ @ } 25°C = P_a + P_v + P_{fo},$$

where,

P_a	=	98.15 kPa (14.236 psia)	(Appendix 3.6.4)
P_v	=	3.20 kPa (0.464 psia)	(Appendix 3.6.4)
P_{fo}	=	0	(no offgassing, Appendix 3.6.4)

At −40°C (−40°F), the partial pressure of the water vapor is conservatively assumed to be zero. Therefore, the final pressure of the mixture at −40°C (−40°F) is calculated according to the ideal gas law based solely on the partial pressure of the air.

$$\frac{P_1 V_1}{T_1} = \frac{P_2 V_2}{T_2}$$

where,

P_1	=	98.15 kPa (14.236 psia)
T_1	=	25°C (298.15 K)

$$T_2 = -40°C\ (233.15\ K)$$
$$V_1 = V_2$$

rearranging and solving for P_2,

$$P_2 = P_1\ (T_2/T_1)$$
$$= (98.15)(233.15/298.15)$$
$$P_2 = 76.76\ kPa\ (11.13\ psia).$$

The cold condition for NCT specified in 10 CFR 71.71 is an ambient temperature in still air and shade of −40°C (−40°F). The 35.2 kg (77.60 lb) of HEU contents in the ES-3100 package generates a maximum bounding decay heat load of 0.4 W. However, in accordance with Regulatory Guide 7.8, the thermal effects of this internal heat source are neglected during evaluation of the package performance at −40°C (−40°F). When exposed to this condition, the package component temperatures will stabilize over time at a temperature approaching −40°C (−40°F). The package has been examined for use at −40°C (−40°F) (Sect. 2.6.2). No detrimental effects on the package structure or sealing capability result from this minimum temperature requirement. The normal service temperature range of the O-rings used in the containment boundary is −40 to 150°C (−40 to 302°F), in accordance with the *Parker O-ring Handbook*; thus, the seal will not be affected by this minimum package temperature in accordance with 10 CFR 71.71(c)(2). Leak testing conducted on Test Unit-2 to the leak tight criteria stipulated by ANSI N14.5-1997 following compliance testing provides justification of the above statements.

3.4.2 Maximum Normal Operating Pressure

The stainless-steel drum and cast refractory system will not pressurize as a result of temperature increases because of four ventilation holes (0.795 cm [0.313 in.] in diameter) drilled in the drum side wall 3.81 cm (1.5 in.) from the flanged top and equally spaced around the drum. The holes are filled with nylon plugs, but they are not hermetically sealed. The inner liner encapsulating the noncombustible neutron poison (Cat 277-4) will not pressurize as a result of temperature increases because of three ventilation holes (0.635 cm [0.25 in.] in diameter) and a slot (1.63 cm [0.64 in.] in width and 4.17 cm [1.64 in.] in length) drilled into this inner liner. These features are covered during transport with aluminum tape to prevent contamination of the neutron poison. This tape does not represent a hermetic seal.

The maximum normal operating pressure is defined in 10 CFR 71.4 as the maximum gauge pressure that would develop in the containment system in a period of one year under the heat conditions specified in 10 CFR 71.71(c)(1). The internal pressure developed under these conditions in the ES-3100 containment vessel is calculated in Appendix 3.6.4 for the most restrictive containment vessel configurations. For conservatism, the decay heat of 0.4 W was used for the maximum internal heat load in evaluating the package for NCT. The maximum calculated internal absolute pressure in the containment vessel with solar insolation and the bounding case parameters is 198.98 kPa (28.859 psia). This pressure incorporates offgassing of the silicone rubber pads, polyethylene bottles, Teflon bottles, and polyethylene bagging and hydrogen gas generation from the radiolysis of water and/or other packing materials. The initial environment inside the containment vessel when assembled is at ambient temperature and pressure with 100% relative humidity. The heat-transfer capability of the packaging is not degraded due to gap creation caused by differences in the fabrication material's coefficient of thermal expansion. Modeling assumed nominal gaps and position based on the engineering drawings of Appendix 1.4.8.

3.4.3 Maximum Thermal Stresses

The temperature of the package under NCT will vary from a low of −40°C (−40°F) throughout the package to a maximum of 117.72 and 87.81°C (243.89 and 190.06°F) (Appendix 3.6.2) on the surface of the drum and the containment vessel, respectively (Sect. 3.4.1). The slow temperature increase or decrease experienced in normal conditions between these limits will result in an essentially uniform temperature change throughout the package. All materials of construction are within this operating temperature range (Table 3.15). Thermal stresses due to differences in thermal expansion are insignificant, as discussed in Sects. 2.6.1.2 and 2.6.2.

Most of the components of the packaging are completely unrestrained. Therefore, any thermal stresses in the packaging components as the temperature varies between the extremes listed above will have no effect on the ability of the packaging to maintain containment, shielding integrity, and nuclear subcriticality. The maximum stresses due to pressure under NCT for the containment vessel are given in Tables 2.21 and 2.22. These values are significantly below the allowable stresses for the packaging components. The Kaolite 1600 insulation and Cat 277-4 materials are poured and cast in place during the fabrication of the drum weldment (Drawing M2E801508A002, Appendix 1.4.8). This situation produces a zero gap between the these materials and the bounding drum and inner liners. Due to differences in coefficients of thermal expansion, some radial and axial interference is expected due to thermal growth or contraction of the inner liners. These radial and axial interferences and induced stresses are calculated in Appendix 3.6.3. The results show that the stresses induced are minimal and do not reduce the effectiveness of the drum assembly.

The containment vessel, which is Type 304L austenitic (iron-nickel-chromium) stainless steel, is designed and fabricated in accordance with Sects. III SubSect. NB and IX of the *ASME Boiler and Pressure Vessel Code* (B&PVC Sect. III and B&PVC Sect. IX). The two sealing surfaces of each containment boundary are joined together by torquing the closure nut inside the containment vessel body to 162.7 ±6.8 N·m (120 ±5 lbf-ft). The O-ring material is ethylene-propylene elastomer.

The design temperature range of the containment vessel is −29 to 148.89°C (−20 to 300°F) (Appendix 2.10.1). However, the package has been evaluated to −40°C (−40°F) (Sect. 2.6.2). The thermal properties of the stainless-steel container body, lid, and closure nut are not critical at these temperatures. The O-ring seal is important for the containment properties of the containment vessel. The normal service temperature range for the elastomer O-ring is −40 to 150°C (−40 to 302°F) for continuous service and up to 165°C (329°F) for 72 h (*Parker O-ring Handbook*). The maximum adjusted HAC temperature of the ES-3100 containment vessel was based upon the thermal testing results in the vicinity of the O-rings. The maximum temperature recorded in the vicinity of the ES-3100 O-rings (241°F) is shown in Table 3.9. As shown in Sect. 3.5.3, the maximum temperature for the containment vessel at the O-ring location was adjusted for the ES-3100 package to 141.22°C (286.20°F). Hence, no damage would be expected to the O-rings during HAC.

The test packages were all preheated to above 38°C (100°F) prior to being placed in the furnace, which was heated to over 800°C (1475°F). As noted in the test report (Appendix 2.10.7), the temperatures recorded on the containment vessels of all the test units were fairly uniform, both vertically and circumferentially. The maximum temperature variation on the containment vessels was ~50°F (from the test temperatures reported in Table 3.9). No damage would be expected on the containment vessel from thermal stresses resulting from a temperature differential of this magnitude. This conclusion is based on the guidelines given in B&PVC, Sect. III. Thermal stress is defined as a self-balancing stress produced by a nonuniform distribution of temperature (Paragraph NB-3213.13 of B&PVC, Sect. III). This paragraph further states that there are two types of thermal stresses: general thermal stress and local thermal stress. An example of a general stress is that produced by an axial temperature distribution in a

cylindrical shell (Paragraph NB-3213.9). This general stress is further classified (Paragraph NB-3213.9) as a secondary stress (that is, a normal stress or a shear stress developed by the constraint of adjacent materials or by self-constraint of the structure). Paragraph NB-3213.9 further states that the basic characteristic of a secondary stress is that it is self-limiting. Local yielding and minor distortions can satisfy the conditions that cause the stress to occur, and failure from a single application would not be expected. An example of a local thermal stress is a small hot spot in the wall of a pressure vessel (Paragraph NB-3213.13). Local thermal stress is associated with almost complete suppression of the differential expansion and thus produces no significant distortion. Such stresses are considered only from a fatigue standpoint. Fatigue will not result from a one-time cyclic event such as an accidental fire.

Following the thermal test, the volume between the O-rings on the five containment vessels (Sect. 2.7.4) was then leak tested and met the air leak-rate criterion of 10^{-4} ref-cm^3/s. Following the O-ring leak check, the five containment vessels were drilled and tapped for full body helium leak testing. All five containment vessels passed the leak rate criteria for leaktightness per ANSI N14.5-1997. The containment vessels were then submerged under a pressure equivalent to 0.9 m (3 ft) of water for 8 h, with no leakage noted. (Sect. 2.7.5). Visual inspection following testing and disassembly also indicated that no distortion or damage occurred in the containment vessel wall, sealing lid, closure nut, O-rings, or sealing surfaces. These tests and observations demonstrate that thermal stresses produced during testing did not affect the containment capability of the containment vessel.

3.5 HYPOTHETICAL ACCIDENT THERMAL EVALUATION

3.5.1 Initial Conditions

Five full-scale packages were tested in the sequence shown in Table 2.19. Each ES-3100 test package was subjected to the 1.2-m (4-ft) drop test in accordance with 10 CFR 71.71(c)(5) prior to the sequential HAC tests in accordance with 10 CFR 71.73 (free drop, crush, puncture, thermal, and immersion tests). One of these units (Test Unit-4) had previously completed the tests and conditions stipulated in 10 CFR 71.71(c)(5) through (c)(10), excluding (c)(8). Two different mock-up configurations were used to represent the minimum and maximum proposed shipping weight and to simulate various center of gravity locations. The structural and thermal interface between the mock-up component and the containment vessel was designed to match that of the actual hardware proposed for transport. Based on LS-DYNA-3D drop simulations (Appendix 2.10.2) the five test units with their associated test weights represent the worst drop orientations for the ES-3100 package. Test Unit-5 used a near replicate of the lightest weight contents for its mock-up component. NCT free-drop, 9 m (30 ft) free drop, 9 m (30 ft) crush and puncture tests were made as specified in 10 CFR 71.71(c)(1), and 73(c)(1) through (c)(3) on all five full-scale test packages prior to thermal testing. The results of this testing are discussed in Sects. 2.7.1, 2.7.2, and 2.7.3. The 1.2-m (4-ft), 9-m (30-ft) drop and crush test orientations were as follows: two tests with the long axis of drum at an oblique angle of 12° to impact surface; a center of gravity over the corner of the drum lid; a drop with the long axis of drum parallel with the impact surface; and a vertical drop on to the drum's lid. The subsequent 40-in. puncture drops were made at various orientations as shown in Table 2.19.

Prior to the thermal test, each test unit was preheated to the maximum temperature extreme in accordance with 10 CFR 71.73(b)(1). Since the containment vessels were initially assembled at ~101.35 kPa (14.7 psia) at 25°C (77°F), the initial internal containment vessel pressure was ~105.70 kPa (15.33 psia) at 38°C (100°F) using the ideal gas law. In accordance with 10 CFR 71.73(b)(1), the internal pressure should be that calculated for the maximum normal operating pressure or 198.98 kPa (28.859 psia). This slight pressure differential has little or no effect on the thermal test results. The maximum decay heat load of the contents is calculated to be 0.4 W based on 35.2 kg of HEU. Analysis

of the ES-3100 package after thermal HAC tests both with and without the decay heat load has been performed. The maximum projected temperature differential between the two packages following furnace exposure, as calculated in Appendix 3.6.2, would be 0.4°C (0.7°F) at the top center of the containment vessel lid , 0.4°C (0.7°F) at the containment vessel flange near the O-rings, 0.45°C (0.8°F) at the containment vessel bottom center, and 0.6°C (1.1°F) at the containment vessel mid body. These temperature differentials are representative for both the Kaolite 1600 densities evaluated.

3.5.2 Fire Test Conditions

Full-scale testing in accordance with 10 CFR 71.73 for HAC was conducted on prototypical packages. Therefore, no analyses were conducted to show compliance with the HAC thermal test. However, analyses were conducted and are discussed in Sect. 3.5.3 to determine the thermal impacts of an internal heat source, application of insolation during cool down, location of crush plate impact on test unit, and thermal capacitance differences between test hardware and proposed shipping hardware.

Full-scale testing of five ES-3100 test units was conducted in accordance with 10 CFR 71.73(c)(4) for HAC. A single full-scale ES-3100 test unit (TU-4) was assembled and subjected to both NCT and to the sequential tests specified in 10 CFR 71.73(c). The furnace used for thermal testing was the No. 3 Furnace at Timken Steel Company in Latrobe, Penn., which is a gas-fired furnace. Oxygen content in stack gases from the furnace were not monitored because it was not anticipated that any of the package's materials of construction were combustible. There was some burning of the silicone pads which are placed between the inner liners and the top plugs of the packages. However, it should be noted that this furnace employs "pulsed" fire burners. This type of burner is unique in that the natural gas flow rate is varied based on furnace controller demands, but the flow of air through the burners is constant, even when no gas is flowing, thereby ensuring a very rich furnace atmosphere capable of supporting any combustion of package materials of construction.

The most significant change to the definition of the HAC thermal test in the current 10 CFR 71 is the requirement for calculation purposes to base convective heat input on "that value which may be demonstrated to exist if the package was exposed to the fire specified." This is not especially significant for this package because it was tested in the gas-fired furnace with burners placed in an attitude which produced a strong convective swirl. Careful examination of the thermal test data indicates that the total heat imparted to the packages was significantly greater than the required total heat specified in 10 CFR 71.73(c)(4). Compliance with ASTM E-2230-02, *Standard Practice for Thermal Qualification of Type B Packages for Radioactive Materials*, was accomplished by the method described in Sect. 7.3 of this standard. This standard is in general agreement with Paragraph 2.2.1 ("Steady-state Method of Compliance") of SG 140.1 entitled *Combination Test Analysis/ Method Used to Demonstrate Compliance to DOE Type B Packaging Thermal Test Requirements (30 Minute Fire Test).*

Prior to the beginning of the thermal test, the furnace was characterized for temperature and heat recovery times. The support stand was welded to a large steel plate which had been placed on the floor of the furnace prior to heating. This steel plate acted as the radiating surface at the bottom of the furnace, as well as providing the ability to hold the test stand rigidly in place. Before heating the furnace, workers practiced loading and unloading test packages from the cold furnace to ensure that the furnace door would not remain open >90 s during each loading. In fact, the maximum time the door was open during any loading was 64 s. As discussed in *Test Report of the ES-3100 Package* (Appendix 2.10.7), six thermocouples were affixed to the drum assembly's exterior surface. Metal retainer clips were welded to the exterior surface to hold the thermocouples in place. The thermocouple tips were inserted underneath the metal clips, and the wire was wrapped around the metal clip. To eliminate any radiant heat exchange between the thermocouples and the furnace walls, the tips and metal clips were covered with a ceramic

coating. Three thermocouples were mounted on each of the walls of the furnace, as well as on the furnace floor, on the furnace door, and three thermocouples were mounted on the test stand.

A minimum of 24 h prior to the beginning of all testing, the furnace was turned on with a set-point temperature of 871°C (1600°F). Following each test, the furnace set point was adjusted to 871°C (1600°F) for at least 45 min prior to the beginning of the next test. The furnace control data recorder ran continuously for the entire duration of the preheat cycle test. Each test unit was preheated to over 38°C (100°F) by placing the packages in an environmental chamber. The environmental chamber was heated by a torpedo-type kerosene space heater controlled by a mechanical bulb thermostat with a control range of 38 to 93°C (100 to 200°F). The environmental chamber is a welded steel frame with fiberglass insulation panels. It was heated from the bottom with four floor register vents located around the perimeter and a 20.32-cm (8-in.)-diam manual dampened center venting stove pipe.

The set point temperature of the environmental chamber was monitored and adjusted for the duration of the preheat cycle. Initially, the thermostat was set to 66°C (150°F) for ~23 h. The thermostat set point was then reduced to 43°C (110°F) for the remainder of the preheat cycle (24 h). All packages were preheated for at least 47 h. No test package was loaded into the furnace until 15 of the 18 thermocouples monitoring the furnace had a reading of 800°C (1475°F) or higher. All packages were placed in the preheated furnace on the support stand with the long axis positioned horizontally, and the package lid facing toward a furnace side wall. During the testing of each package, the thermocouple temperature data recorder was set to record every 15 s.

These packages were exposed to the radiation environment for a minimum of 30 min after all functioning furnace thermocouples and at least five of the six test package exterior surface thermocouples reached a temperature of 800°C (1475°F). During the testing, the package thermocouple temperature data were recorded every 15 s.

After each test, the furnace was allowed to reheat for a minimum of 45 min after obtaining the set point temperature before testing the next unit. The furnace control temperature data recorder ran continuously for the duration of the preheat. No test package was loaded into the furnace until all functioning thermocouples on the furnace walls and support stand had again reached a temperature of 800°C (1475°F) or higher.

All units were tested in a horizontal attitude with the top end of the package facing to the right side wall of the furnace and the 0° mark on the drum facing the floor of the furnace. The data from each of the thermal tests, as shown in the test report, show that at least four of the six external drum thermocouples reached temperatures well in excess of 800°C (1475°F) and remained above 800°C (1475°F) during the 30-min thermal testing. Similarly, all other surfaces of the furnace, including the support stand, exceeded 800°C (1475°F) during the timed portion of the thermal test. For the test specified in the regulations, regardless of the amount of heat input by convection, radiation, or conduction, the maximum temperature the skin of the package could reach would be 800°C (1475°F). That is, the source of the heat in the regulatory specified test is at 800°C (1475°F). Heat can only be transferred from a hotter source to a colder source. Thus, regardless of the mode of heat transfer, the greatest temperature a specimen exposed to the 10 CFR 71.73,(c)(4) thermal test can attain is 800°C (1475°F). Therefore, the fact that these test packages attained temperatures well in excess of 800°C (1475°F) is an excellent indication that the thermal tests performed not only met the requirements of 10 CFR 71.73(c)(4) but actually exceeded them markedly. The results of these tests are provided in the test report (Appendix 2.10.7).

Each test package was removed from the furnace and placed in an area where it was not exposed to artificial cooling. As the furnace door was opened for each test unit, flaming or smoking was visible at

the tamper indicating device (TID) holes in the drum/lid interface. Flaming continued on some of the packages for a short duration; the longest flame duration was 22 min after removal from the furnace. Smoke was also visible from each of the packages and continued after flames were no longer visible. The packages continued to smoke between 12 and 60 min after removal from the furnace. All the packages were allowed to cool naturally to room temperature. The post-thermal testing weights of each unit are summarized in Table 3.18. The drums were disassembled, and the damage was photographed. Each package was visually inspected, and the condition of the package and any observations were recorded.

Table 3.18. ES-3100 test package weights before and after 10 CFR 71.73(c)(4) HAC thermal testing

Test Unit	Pre-test [a] weight kg (lb)	Post-test [a] weight kg (lb)	Thermal test weight loss kg (lb)	BoroBond4 original weight [b] kg (lb)	Water weight in BoroBond4 [c] kg (lb)	Water loss percent [d] (%)
1	202.3 (446)	202.3 (446)	0.0 (0)	20.7 (45.64)	4.91 (10.82)	0.00
2	202.8 (447)	202.8 (447)	0.0 (0)	20.5 (45.19)	4.86 (10.72)	0.00
3	203.7 (449)	203.2 (448)	0.45 (1)	20.5 (45.19)	4.87 (10.74)	9.31
4	201.8 (445)	201.4 (444)	0.45 (1)	20.4 (44.97)	4.84 (10.66)	9.38
5	157.4 (347)	156.9 (346)	0.45 (1)	20.6 (45.42)	4.89 (10.77)	9.29

[a] Data from ORNL/NTRC-013.
[b] Weight of BoroBond4 and water obtained from casting data. (ES-3100 Weldments 2004)
[c] This weight is based on TGA measurements and calculation showing that the minimum water percent is 23.71%.
[d] All weight loss attributed to loss of water in BoroBond4.

3.5.3 Maximum Temperatures and Pressure

The five test unit's previously subjected to both NCT and HAC drop testing were thermal tested in accordance with 10 CFR 71.73(c)(4). To determine the maximum temperatures reached during thermal testing, temperature indicating patches were placed at various locations throughout the test package at assembly. The temperature range for each patch used is identified in Table 3.19. When the temperature of an indicator was reached, the color would change to black (i.e., blackout temperature). The range of possible blackout temperatures of the patches was from 51.67 to 260°C (125 to 500°F). For Test Units-1 through -5, Table 3.19 defines the number and location of the temperature indicating patches.

Since the structural and thermal interface between the various mock-ups and containment vessels is the same as the actual hardware, the use of steel mock-ups to simulate the contents is not expected to affect the results of the thermal test significantly. The total maximum weight of the test packages ranged from 157.4 kg (347 lb) to 203.7 kg (449 lb). The ES-3100 package has a nominal gross shipping weight that ranges from 146.88 kg (323.79 lb) to 187.81 kg (414.05 lb) for the minimum and maximum weight containment vessel configurations shown in Table 2.8, respectively. However, the effect on temperature is evaluated in the following paragraphs due to thermal capacitance differences between the mock-up and the actual contents.

Table 3.19. Thermax temperature indicating patches for test units

Patch Location	Internal surface	External surface	Temperature range °C (°F)	Test report figure [a]
Inner liner of drum assembly		17 (Full Range)	52–260 (125–500)	5.30
Top plug weldment		4 (Full Range)	52–260 (125–500)	5.31
Containment vessel body flange	8 (4B & 4C)	8 (4B & 4C)	"B" 77–127 (171–261) "C" 132–182 (270–360)	5.28
Containment vessel body (end cap and cylinder)		5 (B)	"B" 77–127 (171–261)	5.28
Containment vessel sealing lid	4 (B)	4 (B)	"B" 77–127 (171–261)	5.29
Test mock-up components		6 (B)	"B" 77–127 (171–261)	5.26 & 5.27

[a] ORNL/NTRC-013, Volume 1.

As previously stated, temperature indicators (patches) were placed on the surface of each containment vessel, inner liner, and mock-up component. The blackout temperatures that occurred during thermal testing are recorded for each test unit; the maximum blackout temperatures are listed in Table 3.9. A maximum blackout temperature of 116°C (241°F) was recorded in the vicinity of the O-rings on the containment vessel of Test Unit-5. As discussed below, this temperature will be conservatively adjusted to correlate the test conditions to shipping conditions with decay heat and solar insolation. The blackout temperatures are increased to account for (1) the temperature interval between blackout dots; (2) the ambient temperature of the package prior to insertion into the furnace; (3) the temperature increase due to the effects of applying solar insolation during post-HAC thermal test cool down; (4) the temperature increase due to the decay heat load of the actual contents being shipped; (5) effects of crushing at different locations along the body of the shipping package; (6) thermal capacitance difference in the proposed contents and hardware used during testing; (7) temperature difference occurring when using Borobond4 and Cat 277-4; and (8) temperature difference resulting from variations in Kaolite 1600 and Cat 277-4 material densities.

The initial adjustment for the blackout reading is an increase of 6.11°C (11.0°F) from the patch that blacked out. The highest blackout reading indicates that the actual temperature is somewhere between the highest temperature indicated and the next higher temperature.

The second adjustment compensates for thermal testing at package soak temperatures less than the maximum temperature of 38°C (100°F). In the case of the ES-3100 package, each test unit was thermally soaked to over 38°C (100°F) prior to insertion into the furnace. Therefore, there is no temperature adjustment required.

The third adjustment is a temperature increase to represent the effect of insolation heat flux on the package immediately following the conclusion of the thermal HAC test. Analyses of the ES-3100 package after thermal HAC tests both with and without insolation have been performed. Results from these analyses indicate an increase of ~5.94°C (10.7°F) at the containment vessel top (node 6715), ~6.06°C (10.9°F) at the containment vessel O-ring (node 6359), ~10.44°C (18.8°F) at the containment vessel mid body (Node 6574), and ~4.56°C (8.2°F) at the containment vessel bottom (node 6399), as a result of applying insolation following HAC thermal testing. These increases are extracted from Tables 3.7 and 3.8. The most pronounced effect of applying the insolation heat flux was that it increased the time required to cool the package to NCT type conditions. Nevertheless, the influence of insolation is included in the adjustments to the blackout temperatures.

The fourth temperature adjustment considered is the temperature increase due to the decay heat load of the actual contents being shipped. A maximum decay heat load of 0.4 W is calculated as the bounding case for 35.2 kg of HEU. HAC analysis of the ES-3100 package both with and without the decay heat load has been performed, with the results shown in Tables 3.7 and 3.8. The maximum projected temperature increase during HAC due to a 0.4-W heat source, as calculated in Appendix 3.6.2, would be ~0.39°C (0.7°F) at the containment vessel's top (node 6715), ~0.39°C (0.7°F) at the containment vessel's O-ring (node 6359), ~0.6°C (1.1°F) at the containment vessel's mid body (node 6574), and ~0.45°C (0.8°F) at the containment vessel bottom (node 6399).

The fifth temperature adjustment considered is the temperature increase to the containment vessel based on the location of impact from the 500 kg (1100 lb) crush plate. Based on the differences in location of the crush plate between Test Units-1 and -2, crushing the shipping package with the center of gravity of the plate directly above the containment vessel flange increases the containment vessel temperature on average ~6.11°C (11°F).

The sixth adjustment compensates for the shipment of only 3 kg of HEU rather than the steel mock-ups. The higher content weight was used for testing to cover the possibility of shipping larger components without retesting. The larger content weight gave conservative structural deformation test results to the drum assembly than would the actual shipping weight. One effect, however, of using the larger test mass could be to reduce the containment vessel's temperature rise during the thermal test because the mock-up acts like a heat sink. In order to eliminate this temperature adjustment, a mock-up of the lightest proposed shipment was used in Test Unit-5. The structural and thermal interface between the mock-up components and the containment vessel was designed to match that of the actual shipping hardware, thereby providing the same conductive heat path for thermal testing. As shown by the test results, both the containment vessel and mock-up components of Test Unit-5 recorded higher temperatures than the other test units. This supports the theory that the heavier mock-ups act as heat sinks for the containment vessel. Therefore, by testing the 3.6-kg (8-lb) mock-up representing the lightest assembly to be shipped, a more accurate prediction of actual temperatures reached during thermal testing was achieved. No further temperature adjustments due to differences in mock-up weight are needed.

The seventh temperature adjustment compensates for conducting the HAC compliance tests with BoroBond4 and substituting Cat 277-4 for the production shipping containers. This adjustment is determined by using an undamaged package and subjecting it to a thermal environment representative of that required by 10 CFR 71.73(c)(4). Based on the analytical results shown in Appendix 3.6.2, the containment vessel in a package using Cat 277-4 would be from 2.5°F to 8.°F cooler than a package with BoroBond4. Conservatively, the temperatures will not be adjusted due to the neutron poison change.

The eighth and final temperature adjustment compensates for material density variation in the Kaolite 1600 and Cat 277-4 material during HAC compliance tests. Again, this temperature adjustment was predicted for an undamaged package using the finite element method. Based on the analytical results shown in Appendix 3.6.2 (Tables 3.7 and 3.8), the containment vessel temperature was predicted to be ~6.4°C (11.6°F) higher at the containment vessel's top (node 6715), ~6.4°C (11.6°F) higher at the containment vessel's O-ring (node 6359), ~4.6°C (8.3°F) higher at the containment vessel's mid body, and ~7.72°C (13.9°F) at the containment vessel's bottom (node 6399) when the lower density values for Kaolite 1600 and the neutron poison were used. Since actual compliance testing was conducted with these densities on the high side, the above adjustments must be added to the containment vessel temperatures.

Table 3.20 summarizes the numerous temperature adjustments needed for the containment vessel.

Table 3.20. Predicted temperature adjustments (°F) for containment vessel due to HAC

Node [a]	Analytical Temperature Adjustments								Total Temp Adjustment
	1	2	3	4	5	6	7	8	
6715	11.00	0.00	10.70	0.70	11.00	0.00	0.00	11.60	45.00
6359	11.00	0.00	10.90	0.70	11.00	0.00	0.00	11.60	45.20
6574	11.00	0.00	18.80	1.10	11.00	0.00	0.00	8.30	50.20
6399	11.00	0.00	8.20	0.80	11.00	0.00	0.00	13.90	44.90

[a] See Figs. 8 through 11 in Appendix 3.6.2 for details of node locations.

Table 3.21 shows the results of adding the eight temperature adjustments previously discussed to the black-out temperatures for the containment vessel with the 3.6-kg (8-lb) mock-up (Test Unit-5). These adjusted temperatures would not adversely affect the stainless-steel components or the O-ring materials of the containment vessel.

Table 3.21. Predicted temperatures of the containment vessel due to HAC (°F)

Node [a]	Analytical temperature adjustments (°F)	Maximum blackout temperature on Test Unit-5 (°F)	Final predicted CV temperature (°F)
6715	45.00	261	306.00
6359	45.20	241	286.20
6574	50.20	199	249.20
6399	44.90	210	254.90

[a] See Figs. 8 through 11 in Appendix 3.6.2 for details of node locations.

To determine the maximum pressure inside the containment vessel as a result of thermal testing, the average adjusted gas temperature must be calculated based on the above results. The approach used is to divide the containment vessel volume into three distinct equal regions and then average the three together. The first volume is represented by the gas adjacent to the containment vessel lid and flange region and the top convenience can. Based on the temperature recorded near the O-rings [116.11°C (241°F)] and the temperature recorded on the external surface of the convenience can [98.89°C (210°F)], the average temperature of the gas in this region is 107.50°C (225.50°F). Using the temperature adjustment of 25.11°C (45.20°F) for this region, the adjusted average temperature in the first region is 132.61°C (270.70°F). The second volume is represented by the gas adjacent to the second convenience can from the top. Based on the temperature recorded on the containment vessel wall and convenience can [92.78°C (199°F)], the average temperature of gas in this region is 92.78°C (199°F). Using the temperature adjustment of 27.89°C (50.20°F) for this region, the adjusted average temperature in the second region is 120.67°C (249.20°F). The third and final volume is represented by the gas adjacent to the bottom convenience can. Again based on the convenience can temperature [87.78°C (190°F)] and the containment vessel end cap temperature [98.89°C (210°F)], the average temperature of gas in this region is 93.33°C (200°F). Using the temperature adjustment of 24.94°C (44.90°F) for this region, the adjusted average temperature in the third region is 118.28°C (244.90°F). Averaging these

three temperatures, an average adjusted gas temperature of 123.85°C (254.93°F) is determined for the containment vessel.

As shown in Appendix 3.6.5, the maximum adjusted average gas temperature and pressure in the containment vessel during accident conditions was calculated to be 123.85°C (254.93°F) and 595.99 kPa (86.441 psia), respectively.

The maximum adjusted temperature on the surface of the containment vessel, adjacent to the O-rings, was 141.22°C (286.20°F). This is well within the design range for the packaging. The full body helium leak test on all test units following thermal testing meets the "leaktight" criteria in accordance with ANSI N14.5-1997. Visual inspection following testing and unloading indicated that no distortion or damage occurred in the containment vessel wall, sealing lid, closure nut, O-rings, or sealing surfaces. No water was visible inside the containment vessel following the 0.9-m (3-ft) water immersion test or the 15-m (50-ft) water immersion test on Test Unit-6.

The ES-3100 package satisfies the requirements of 10 CFR 71.73 for transport of the 35.2-kg (77.60-lb) arrangements shown in Table 2.8. Section 2.7 has additional details to support this conclusion.

3.5.4 Accident Conditions for Fissile Material Packages for Air Transport

The expanded fire test conditions specified in 10 CFR 71.55(f)(1)(iv) for fissile material package designs for air transportation was not conducted. The issue of subcriticality is addressed in Section 6 with content mass limits as addressed in Section 1 for air transport.

3.6 APPENDICES

Appendix	Description
3.6.1	THERMAL EVALUATION OF THE ES-3100 SHIPPING CONTAINER FOR NCT AND HAC (CONCEPTUAL DESIGN WITH BOROBOND4 NEUTRON ABSORBER)
3.6.2	THERMAL EVALUATION OF THE ES-3100 SHIPPING CONTAINER FOR NCT AND HAC (FINAL DESIGN WITH CATALOG 277-4 NEUTRON ABSORBER)
3.6.3	THERMAL STRESS EVALUATION OF THE ES-3100 SHIPPING CONTAINER DRUM BODY ASSEMBLY FOR NCT (FINAL DESIGN WITH CATALOG 277-4 NEUTRON ABSORBER)
3.6.4	CONTAINMENT VESSEL PRESSURE DUE TO NORMAL CONDITIONS OF TRANSPORT FOR THE PROPOSED CONTENTS
3.6.5	CONTAINMENT VESSEL PRESSURE DUE TO HYPOTHETICAL ACCIDENT CONDITIONS FOR THE PROPOSED CONTENTS
3.6.6	SILICONE RUBBER THERMAL PROPERTIES FROM THERM 1.2 DATABASE
3.6.7	ESTIMATES OF HYDROGEN BUILDUP IN THE ES-3100 PACKAGE CONTAINING HIGHLY ENRICHED URANIUM

THIS PAGE INTENTIONALLY LEFT BLANK.

Appendix 3.6.1

THERMAL EVALUATION OF THE ES-3100 SHIPPING CONTAINER FOR NCT AND HAC (CONCEPTUAL DESIGN WITH BOROBOND4 NEUTRON ABSORBER)

THIS PAGE INTENTIONALLY LEFT BLANK.

Appendix 3.6.1

THERMAL EVALUATION OF THE ES-3100 SHIPPING CONTAINER FOR NCT AND HAC (CONCEPTUAL DESIGN WITH BORBOND4 NEUTRON ABSORBER)

INTRODUCTION

Thermal analyses of the ES-3100 shipping container are performed to determine the temperature distribution within the packaging during Normal Conditions of Transport (NCT) as specified in 10 CFR 71.71(c)(1).[1] Transient thermal analyses are performed by treating the problem as a cyclic transient with the incident heat flux due to solar radiation applied and not applied in alternating 12-hour periods.

Additionally, thermal analyses of the ES-3100 shipping container are performed to determine the thermal response of the packaging to Hypothetical Accident Conditions (HAC) as specified in 10 CFR 71.73(c)(4).[1] Since physical testing of the ES-3100 shipping container will be conducted with no internal heat source or insolation during cool-down, temperature increases due to internal heat loads of 0.4, 20, and 30 W as well as temperature increases due to the application of insolation during cool-down following the HAC fire are calculated. Although earlier revisions of 10 CFR 71 specifically state that insolation does not need to be evaluated before, during, or after HAC, the current version of 10 CFR 71 and associated guidance are unclear regarding the need for consideration following HAC testing. Since the Nuclear Regulatory Commission (NRC) has taken the position that insolation must be considered and evaluated following fire testing, analyses are conducted to determine the effect of insolation following the HAC fire on the ES-3100 shipping container. The predicted temperature increases may be used to adjust physical test data for those loads not included in the tests.

FINITE ELEMENT MODEL DESCRIPTION

A two-dimensional axisymmetric (r-z) finite element model of the ES-3100 shipping container is constructed using MSC.Patran (2004, Version 12.0.044)[2] for evaluation for NCT. The actual contents of the ES-3100 shipping container are not specifically modeled—instead, the content source heat load (if desired) is modeled by applying a uniform heat flux to the inner surfaces of the containment vessel. This is a conservative approach in that package temperatures will not be reduced in a transient analysis by the heat capacity of the contents. A schematic of the finite element model is presented in Figure 1. The model consists of five materials: stainless steel (drum, liners, and containment vessel), Kaolite, Borobond4, silicone rubber, and air in the gaps between the drum liner and containment vessel and between the drum liner and top plug. Thermal properties of the materials used in the analysis are presented in Table 1.

Heat is transferred to the model from the contents (i.e., decay heat of the contents) via heat flux boundary conditions applied to the inner surface of the elements representing the containment vessel. Additionally, solar heat fluxes are applied to the model during NCT and HAC post-fire cool-down via heat flux boundary conditions. The heat applied to the model via the boundary conditions is transferred through the model via conduction and thermal radiation. Heat is rejected from the external surfaces of the model via natural convection and thermal radiation boundary conditions.

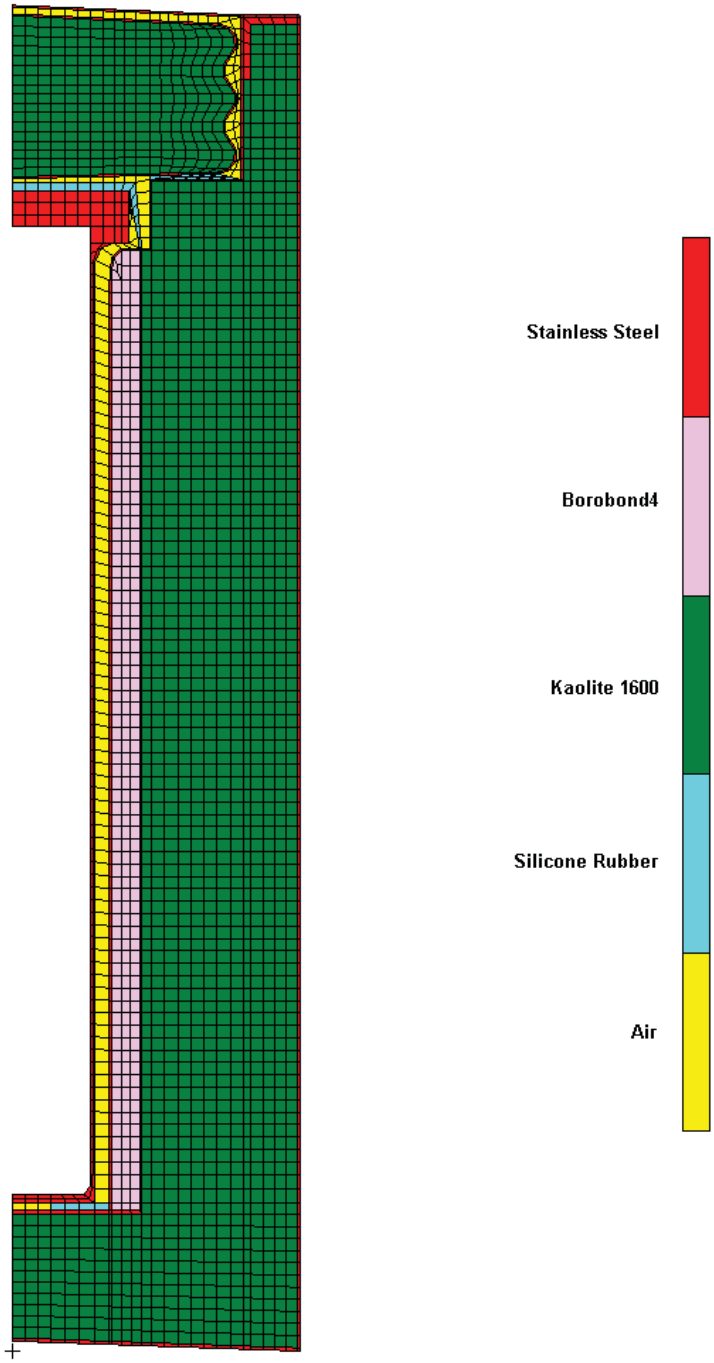

Figure 1. MSC.Patran axisymmetric finite element model of the ES-3100 shipping container.

Table 1. Thermal properties of the materials used in the thermal analysis.

Material	Temperature (°F)	Thermal conductivity (Btu/h-in.-°F)	Density (lbm/in.³)	Specific heat (Btu/lbm-°F)	Emissivity
Stainless steel	-279.67	0.443[a]	0.285[a]	0.065[a]	0.22[a]
	-99.67	0.607	–	0.096	–
	260.33	0.799	–	0.123	–
	620.33	0.953	–	0.133	–
	980.33	1.088	–	0.139	–
	1340.33	1.223	–	0.146	–
	1700.33	1.348	–	0.153	–
	2240.33	1.526	–	0.163	–
Kaolite 1600	68	0.0093[b]	0.011[c]	0.2[d]	–
	212	0.0091	–	–	–
	392	0.0081	–	–	–
	572	0.0072	–	–	–
	1112	0.0082	–	–	–
Borobond4	25	0.0450[e]	0.0683[e]	0.2160[e]	–
	77	0.0576	–	–	–
	100	0.0632	–	–	–
	104	0.0642	–	–	–
Silicone rubber	–	0.0161[f]	0.047[f]	0.300[f]	1.0[g]
Air	-9.67	1.074×10^{-3}[a]	4.064×10^{-5}[a],[h]	0.240[a]	–
	80.33	1.266×10^{-3}	–	0.241	–
	170.33	1.445×10^{-3}	–	0.241	–
	260.33	1.628×10^{-3}	–	0.242	–
	350.33	1.796×10^{-3}	–	0.244	–
	440.33	1.960×10^{-3}	–	0.246	–
	530.33	2.114×10^{-3}	–	0.248	–
	620.33	2.258×10^{-3}	–	0.251	–
	710.33	2.393×10^{-3}	–	0.254	–
	800.33	2.523×10^{-3}	–	0.257	–
	890.33	2.644×10^{-3}	–	0.260	–
	980.33	2.759×10^{-3}	–	0.263	–
	1070.33	2.870×10^{-3}	–	0.265	–
	1160.33	2.985×10^{-3}	–	0.268	–
	1250.33	3.096×10^{-3}	–	0.270	–
	1340.33	3.212×10^{-3}	–	0.273	–
	1520.33	3.443×10^{-3}	–	0.277	–

Notes:
(a) F. P. Incropera and D. P. DeWitt, *Fundamentals of Heat and Mass Transfer*, 2nd edition, John Wiley & Sons, New York, 1985.
(b) Hsin Wang, *Thermal Conductivity Measurements of Kaolite*, ORNL/TM-2003/49.
(c) Based on a baked density of 19.4 lbm/ft^3 (0.011 lbm/in^3). Specification JS-YMN3-801580-A003 requires a baked density of 22.4 ± 3 lbm/ft^3. Using a lower value for the Kaolite density results in higher temperatures on the containment vessel because the heat capacity of the Kaolite is minimized—allowing more heat to flow to the containment vessel; therefore, the thermal analyses are performed using a low-end density of 19.4 lbm/ft^3. The HAC analyses also consider a high-end density of 30 lbm/ft^3.
(d) FAX communication from J. W. Breuer of Thermal Ceramics, Engineering Department, August 11, 1995.
(e) Data via email from Jim Hall (Eagle-Picher) to Jerry Byington (BWXT Y-12), March 12, 2004.
(f) THERM 1.2, thermal properties database by R. A. Bailey.
(g) Conservatively modeled as 1.0.
(h) Constant density value evaluated at 100°F.

.

MODELED HEAT TRANSFER MECHANISMS

The heat transfer mechanisms included in the thermal model such as thermal radiation, natural convection, and insolation (solar heat flux) are described in detail in the following sections.

Heat Transfer Between Package Exterior and Ambient

The heat transfer between the exterior of the package and the ambient (or fire) is modeled as a combination of radiant heat transfer and natural convection. The heat transfer due to radiant exchange with the environment is calculated as:[3]

$$q''_{rad} = \sigma F_e \left(T_s^{\,4} - T_a^{\,4} \right), \tag{1}$$

where σ = Stefan-Boltzmann constant,
F_e = overall exchange factor,
T_s = container outer surface temperature (absolute), and
T_a = ambient or fire temperature (absolute).

The overall interchange factor is calculated as:[3]

$$F_e = \left[\frac{1}{\dfrac{1}{\varepsilon_p} + \dfrac{A_p}{A_s}\left(\dfrac{1}{\varepsilon_s} - 1 \right)} \right], \tag{2}$$

where ε_p = emissivity of package surface,
A_p = surface area of the package,
A_s = surface area of the surroundings, and
ε_s = emissivity of surroundings.

For NCT and the cool-down period following the HAC fire, the area of the surroundings is assumed to be much larger than the surface area of the package; therefore, Eq. 2 reduces to:

$$F_e \approx \varepsilon_p \,. \tag{3}$$

An emissivity value of 0.22,[4] which is typical of clean stainless steel, is assumed for the outer surfaces of the drum during NCT and during the cool-down period following the HAC fire. In reality, the outer surfaces of the drum will have a much higher emissivity following the HAC fire; therefore, this assumption is conservative.

During the HAC fire, the area of the surroundings is assumed to be approximately equal to the surface area of the drum; therefore, Eq. 2 reduces to:

$$F_e = \left[\frac{1}{\frac{1}{\varepsilon_p} + \frac{1}{\varepsilon_s} - 1} \right]. \tag{4}$$

During the HAC 30-minute fire, an emissivity of 0.8 is assumed for the drum, and an emissivity of 0.9 is assumed for the fire per the guidance of 10 CFR 71.74(c)(4).[1] This results in an overall exchange factor of 0.7347 during the HAC fire using Eq. 4.

The natural convection heat transfer from the package surface to the ambient air is calculated as:

$$q''_{convection} = h\left(T_s - T_a\right). \tag{5}$$

where, h = natural convection heat transfer coefficient,
T_s = container outer surface temperature, and
T_a = ambient or fire temperature.

During the NCT transient thermal analyses and the steady-state thermal analyses (used to obtain the starting temperature distribution in the package for NCT and HAC when a content heat load is present), the shipping container is assumed to be in an upright (vertical) orientation. The top of the drum is modeled as a heated horizontal flat plate facing up using the following correlation:[5]

$$h = \left(\frac{k}{L}\right) C_1 \, Ra^{C_2}, \tag{6}$$

where, k = thermal conductivity of air,
L = characteristic length (= D/4 per Ref. 5),
D = diameter of the package,
Ra = Rayleigh number,
C_1 = constant (see Table 2), and
C_2 = constant (see Table 2).

The Rayleigh number in Eq. 6 is defined as:

$$Ra = \frac{g \beta \Delta T L^3}{\nu \alpha}, \tag{7}$$

where, g = acceleration of gravity,
β = coefficient of thermal expansion,
ΔT = temperature difference,
ν = kinematic viscosity [μ/ρ],
μ = absolute viscosity,
α = thermal diffusivity [$k/(\rho C_p)$],
ρ = density of air, and
C_p = specific heat of air.

The properties of air used in the natural convection calculations are presented in Table 3.

Table 2. Coefficients for natural convection correlations.

Coefficient	Rayleigh Number Range	Value
C_1	$2.6\times10^4 < Ra < 1.0\times10^7$ $1.0\times10^7 < Ra < 3.0\times10^{10}$	0.54 0.15
C_2	$2.6\times10^4 < Ra < 1.0\times10^7$ $1.0\times10^7 < Ra < 3.0\times10^{10}$	0.25 1/3
C_3	$Ra < 1.0\times10^9$ $Ra > 1.0\times10^9$	0.680 0.825
C_4	$Ra < 1.0\times10^9$ $Ra > 1.0\times10^9$	0.670 0.387
C_5	$Ra < 1.0\times10^9$ $Ra > 1.0\times10^9$	0.25 1/6
C_6	$Ra < 1.0\times10^9$ $Ra > 1.0\times10^9$	4/9 8/27
C_7	$Ra < 1.0\times10^9$ $Ra > 1.0\times10^9$	1 2
C_8	$1.0\times10^4 < Ra < 1.0\times10^9$ $1.0\times10^9 < Ra < 1.0\times10^{12}$	0.53 0.13
C_9	$1.0\times10^4 < Ra < 1.0\times10^9$ $1.0\times10^9 < Ra < 1.0\times10^{12}$	0.25 1/3

Source: *MSC.Patran Thermal User's Guide, Volume 1: Thermal/Hydraulic Analysis*, MSC.Software Corporation,Santa Ana, CA 92702, 2003.

Table 3. Properties of air used in natural convection calculations.

Temperature (K)	Thermal Conductivity (W/m-K)	Density (kg/m^3)	Specific heat (J/kg-K)	Absolute viscocity (N-s/m²)	Coefficient of thermal expansion (K^{-1})
250	22.3×10^{-3}	1.3947	1006	159.6×10^{-7}	4.00×10^{-3}
300	26.3×10^{-3}	1.1614	1007	184.6×10^{-7}	3.33×10^{-3}
350	30.0×10^{-3}	0.9950	1009	208.2×10^{-7}	2.86×10^{-3}
400	33.8×10^{-3}	0.8711	1014	230.1×10^{-7}	2.50×10^{-3}
450	37.3×10^{-3}	0.7740	1021	250.7×10^{-7}	2.22×10^{-3}
500	40.7×10^{-3}	0.6964	1030	270.1×10^{-7}	2.00×10^{-3}
550	43.9×10^{-3}	0.6329	1040	288.4×10^{-7}	1.82×10^{-3}
600	46.9×10^{-3}	0.5804	1051	305.8×10^{-7}	1.67×10^{-3}
650	49.7×10^{-3}	0.5356	1063	322.5×10^{-7}	1.54×10^{-3}
700	52.4×10^{-3}	0.4975	1075	338.8×10^{-7}	1.43×10^{-3}
750	54.9×10^{-3}	0.4643	1087	354.6×10^{-7}	1.33×10^{-3}
800	57.3×10^{-3}	0.4354	1099	369.8×10^{-7}	1.25×10^{-3}
850	59.6×10^{-3}	0.4097	1110	384.3×10^{-7}	1.18×10^{-3}
900	62.0×10^{-3}	0.3868	1121	398.1×10^{-7}	1.11×10^{-3}
950	64.3×10^{-3}	0.3666	1131	411.3×10^{-7}	1.05×10^{-3}
1000	66.7×10^{-3}	0.3482	1141	424.4×10^{-7}	1.00×10^{-3}
1100	71.5×10^{-3}	0.3166	1159	449.0×10^{-7}	9.09×10^{-4}

Source: F. P. Incropera and D. P. DeWitt, *Fundamentals of Heat and Mass Transfer*, 2nd ed., John Wiley & Sons, New York, 1985.

During the NCT transient thermal analyses and the steady-state thermal analyses, the sides of the drum are modeled as a vertical flat plate using the following correlation:[5]

$$h = \left(\frac{k}{L}\right)\left[C_3 + \frac{C_4\,Ra^{C_5}}{\left(1+\left[\frac{0.492}{Pr}\right]^{9/16}\right)^{C_6}}\right]^{C_7}, \tag{8}$$

where L = characteristic length = the drum height,
C_3 = constant (see Table 2),
C_4 = constant (see Table 2),
C_5 = constant (see Table 2),
C_6 = constant (see Table 2),
C_7 = constant (see Table 2), and
Pr = Prandtl number $[(C_p \times \mu)/k]$.

The bottom of the drum is conservatively modeled as adiabatic during the NCT transient analyses and the steady-state analyses.

During the HAC 30-minute fire and the post-fire cool-down, the shipping container is assumed to be in a horizontal orientation (as it is during furnace testing). As such, the top and bottom of the drum are modeled as vertical flat plates using Eq. 8 having a characteristic length, L, equivalent to the drum diameter, and the sides of the drum are modeled as a horizontal cylinder using the following correlation:[5]

$$h = \left(\frac{k}{D}\right) C_8\,Ra^{C_9}, \tag{9}$$

where D = diameter of the package,
C_8 = constant (see Table 2), and
C_9 = constant (see Table 2).

Insolation

The following insolation (incident solar radiation) data is required for NCT per 10 CFR 71.71(c)(1):[1]

Form and location of surface	Total insolation for a 12-hour period (cal/cm²)
Flat surfaces transported horizontally	
Base	None
Other surfaces	800
Flat surfaces not transported horizontally	200
Curved surfaces	400

The total insolation values specified in the previous table are for a 12-hour period. For analytical purposes, these values are "time-averaged" over the entire 12-hour period (i.e., divided by 12).

Therefore, the incident solar heat fluxes ($q''_{solar,\,i}$) used in the analyses for NCT and cool-down following the HAC fire are as follows:

During NCT, the drum is in an upright (vertical) orientation; therefore, the following heat fluxes are applied to the external surfaces of the drum to represent insolation:

Top $$q''_{solar,i} = 775.3\,W/m^2\,, \tag{10}$$

Sides $$q''_{solar,i} = 387.7\,W/m^2\,, \tag{11}$$

Bottom $$q''_{solar,i} = 0\,. \tag{12}$$

During the cool-down period following the HAC 30-minute fire, the drum is assumed to be in a horizontal orientation; therefore, the following heat fluxes are applied to the external surfaces of the drum to represent insolation:

Top $$q''_{solar,i} = 193.83\,W/m^2\,, \tag{13}$$

Sides $$q''_{solar,i} = 387.7\,W/m^2\,, \tag{14}$$

Bottom $$q''_{solar,i} = 193.83\,W/m^2\,. \tag{15}$$

The insolation is applied as a square-wave function (i.e., alternating on and off in 12-hour periods) in the thermal analysis. The heat flux values presented in Eqs. 10–15 represent the insolation absorbed by the package surface since a drum absorptivity of 1.0 was conservatively assumed. An analytical study has been performed on a similar shipping package that investigated three methods of applying the insolation.[6] The three methods consisted of 1) performing a steady-state analysis assuming the insolation is applied continuously by distributing the heat flux evenly throughout a 24-hour period, 2) performing a transient analysis assuming the insolation is represented by a step function (i.e., applied and then not applied in 12-hour cycles, and 3) performing a transient analysis where the incident insolation is represented by a sinusoidal function that varies throughout the day. The results of the study indicate that the method used in applying the insolation has a significant effect on the temperatures of the outermost portions of the package. However, since the total insolation over any 24-hour period is the same for all cases, internal package temperatures are relatively unaffected by the way in which the insolation is applied. Since containment vessel O-ring temperatures are of primary concern in this report, the step function method for applying the insolation is suitable.

Heat Transfer Across Gaps in the Package

Heat transfer across all gaps in the package is modeled by a combination of radiant exchange and conduction. Natural convection heat transfer is not included across the gaps in the model. Scoping studies performed for a similar shipping package indicate that the heat transfer due to natural convection in relatively small gaps is approximately a factor of 6 times less than the heat transfer due to radiant exchange.[6] These calculations assumed a temperature difference of 5°C across the gap. Based on these previous calculations, the effect of neglecting the natural convection in the gap regions is minimal. P/VIEWFACTOR[7] was used to calculate the view factors in all enclosures.

Content Heat Load

In order to simulate the decay heat generated by the ES-3100 shipping container contents, a uniform heat flux is applied to the inner surfaces of the elements representing the containment vessel in the model. Content heat loads of 0.4, 20, and 30 W as well as no content heat load are investigated in this report. The uniform heat flux (q''_{source}) for a given content heat load is calculated using the following equation:

$$q''_{source} = \frac{Q}{2\left(\frac{\pi D_i^2}{4}\right) + \pi(D_i)(H)}, \tag{16}$$

where Q = content heat load,
D_i = inside diameter of the containment vessel (0.12802 m),
H = height of the containment vessel cavity (0.78867 m).

Using Eq. 16, a content heat load of 0.4 W results in a uniform heat flux of 1.1664 W/m², a content heat load of 20 W results in a uniform heat flux of 58.32 W/m², and a content heat load of 30 W results in a uniform heat flux of 87.48 W/m².

DISCUSSION OF ANALYTICAL RESULTS

All thermal analyses discussed in this report were performed using MSC.Patran Thermal (2004 Version 12.0.044)[8] on an Intel Pentium 4–based Microsoft Windows 2000 computer. Temperatures are monitored at selected locations in the model as shown in Figure 2.

Steady-state Conditions Analyses Results

Steady-state thermal analyses are performed on the finite element model of the ES-3100 shipping container for three cases having content heat loads of 0.4, 20, and 30 W. The temperature distribution results from these analyses are used as the starting temperature distribution within the model when performing the transient thermal analyses for NCT and the HAC 30-minute fire. The boundary conditions for these steady-state analyses include a combination of thermal radiation exchange and natural convection applied to the top and sides of the drum using an ambient temperature of 37.8°C (100°F). The bottom of the drum is modeled as an adiabatic surface (i.e., no heat transfer). Additionally, the content heat load is simulated by applying a uniform heat flux to the internal surfaces of the elements representing the containment vessel. The calculated steady-state temperature distribution with the model of the ES-3100 shipping container for content heat loads of 0.4, 20, and 30 W is presented in Table 4.

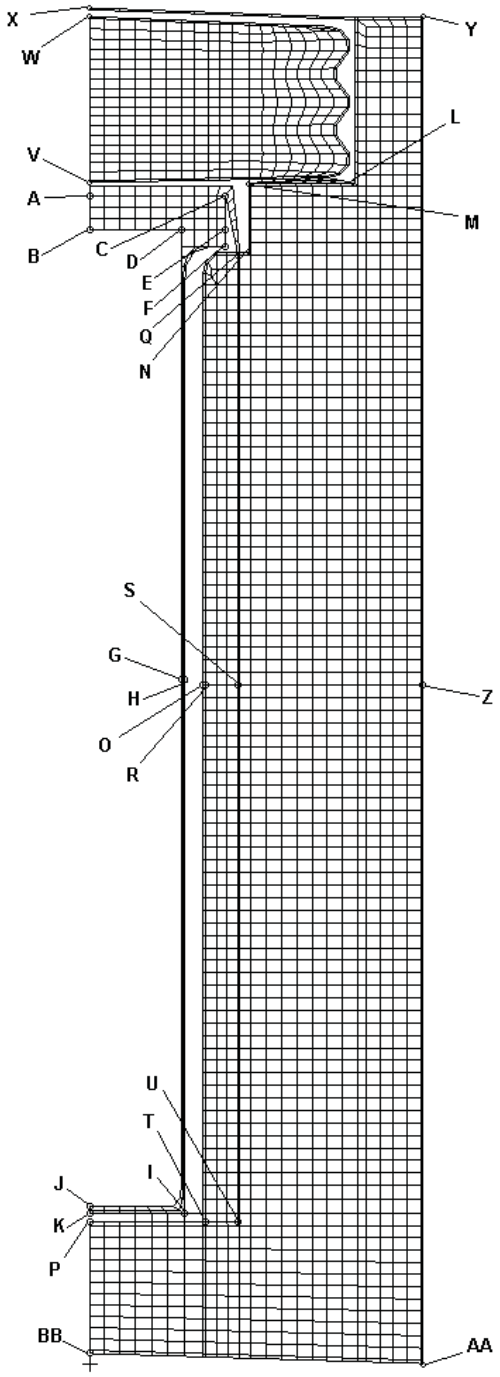

Figure 2. MSC.Patran axisymmetric finite element model of the ES-3100 shipping container—nodal locations of interest (elements representing air not shown for clarity).

Table 4. ES-3100 shipping container steady-state temperatures (37.8°C ambient temperature, no insolation).

Node[a]	Location	Steady-state temperature, °C (°F)		
		0.4 W	20 W	30 W
A	CV lid, top, center	38.09 (100.56)	56.06 (132.90)	64.65 (148.37)
B	CV lid, bottom, center	38.09 (100.56)	56.16 (133.08)	64.79 (148.63)
C	CV lid, top, outer	38.09 (100.55)	55.82 (132.47)	64.30 (147.73)
D	CV flange at interface, inner[b]	38.09 (100.57)	56.17 (133.10)	64.81 (148.66)
E	CV flange at interface, outer[b]	38.09 (100.56)	56.06 (132.90)	64.65 (148.37)
F	CV flange, bottom, outer	38.09 (100.56)	56.05 (132.88)	64.63 (148.34)
G	CV shell, mid-height, inner	38.36 (101.04)	69.36 (156.85)	83.91 (183.04)
H	CV shell, mid-height, outer	38.36 (101.04)	69.35 (156.83)	83.90 (183.01)
I	CV bottom, outer	38.18 (100.72)	59.56 (139.20)	69.97 (157.94)
J	CV bottom, center, inner	38.18 (100.72)	59.65 (139.38)	70.11 (158.20)
K	CV bottom, center, outer	38.18 (100.72)	59.64 (139.35)	70.09 (158.17)
L	Drum liner, plug cavity, outer	37.85 (100.13)	43.26 (109.87)	45.81 (114.46)
M	Drum liner, plug cavity, inner	37.91 (100.25)	46.93 (116.47)	51.29 (124.33)
N	Drum liner, CV flange cavity, outer	37.97 (100.34)	49.87 (121.77)	55.70 (132.26)
O	Drum liner, CV cavity, mid-height, inner	38.07 (100.52)	55.08 (131.15)	63.53 (146.36)
P	Drum liner, CV cavity, bottom, inner	38.12 (100.62)	56.87 (134.37)	66.02 (150.83)
Q	Borobond4, top, outer	37.97 (100.35)	50.31 (122.55)	56.35 (133.43)
R	Borobond4, mid-height, inner	38.07 (100.52)	55.08 (131.14)	63.53 (146.35)
S	Borobond4, mid-height, outer	38.12 (100.50)	54.45 (130.02)	62.59 (144.66)
T	Borobond4, bottom, inner	38.08 (100.55)	54.95 (130.91)	63.21 (145.79)
U	Borobond4, bottom, outer	38.07 (100.52)	54.16 (129.48)	62.05 (143.69)
V	Drum plug liner, bottom, center	37.82 (100.07)	41.36 (106.46)	42.96 (109.34)
W	Drum plug liner, top, center	37.98 (100.37)	50.51 (122.93)	56.59 (133.87)
X	Drum lid, top, center	37.79 (100.03)	39.82 (103.67)	40.67 (105.20)
Y	Drum lid, top, outer	37.79 (100.03)	40.08 (104.14)	41.06 (105.90)
Z	Drum, mid-height, outer	37.84 (100.11)	41.60 (106.88)	43.26 (109.86)
AA	Drum bottom, outer	37.85 (100.13)	41.94 (107.50)	43.76 (110.76)
BB	Drum bottom, center	37.91 (100.23)	45.14 (113.25)	48.51 (119.33)

Notes: (a) See Figure 2.
(b) Approximate location of the CV O-ring.

Normal Conditions of Transport Analyses Results

Transient thermal analyses are performed on the finite element model of the ES-3100 shipping container to simulate NCT with content heat loads of 0, 0.4, 20, and 30 W. The insolation required for NCT per 10 CFR 71.71(c)(1)[1] is applied to the top and sides of the drum in alternating 12-hour periods (i.e., 12 hours on and 12 hours off) with the drum bottom remaining adiabatic during the transient thermal analysis. An ambient temperature of 37.8°C (100°F) as stipulated in 10 CFR 71 is used in the NCT analysis. The initial temperature distribution within the package for the NCT transients was determined from steady-state analyses (with radiation and natural convection boundary conditions applied to the top and sides of the drum) for each internal heat load. For the case with no internal heat source (0 W), the initial temperature distribution within the package was assumed to be at a uniform 37.8°C (100°F).

The transient thermal analyses simulate a five-day period of cyclic solar loading with 12 hours of insolation being applied at the beginning of each day (i.e., onset of sunrise) followed by 12 hours in which there is no insolation to end the day (i.e., onset of sunset). This five-day period allows for "quasi

steady-state" conditions to be reached. While the temperature of a particular node within the model changes with respect to time in the transient analyses, the maximum temperature that node reaches from day-to-day does not change once a "quasi steady-state" condition is reached. In particular, the maximum temperature of the key location on the containment vessel (i.e., at the O-ring) on day 5 is within 0.01°C of the maximum temperature of the same location on day 4.

The maximum temperatures of several locations within the model are summarized in Table 5 and Table 6 for content heat loads of 0, 0.4, 20, and 30 W and Kaolite densities of 30 (maximum density) and 19.4 lbm/ft^3 (minimum density), respectively. The maximum temperatures reported in Table 5 and Table 6 represent "quasi steady-state." Temperature-history plots of several locations within the model are also depicted graphically in Figure 3 through Figure 10 for various content heat loads and Kaolite density. Additionally, temperature contours of the model at sunrise (0 hours) and sunset (12 hours) for day 5 of the transient are presented in Figure 11 through Figure 18 for various content heat loads and Kaolite density. The elements representing the air between the drum liner and containment vessel and between the drum liner and top plug liner are not shown in the temperature contours presented in these figures so that the containment vessel temperature contours can be more easily viewed.

The maximum temperature in the model occurs at the top center of the drum lid. This maximum temperature is 118.01°C (244.42°F), 118.03°C (244.45°F), 118.77°C (245.79°F), and 119.15°C (246.47°F) for content heat loads of 0, 0.4, 20, and 30 W, respectively, and occurs at sunset in each case (see Table 6, Kaolite density of 19.4 lbm/ft^3). The maximum temperature at the containment vessel O-ring is 88.25°C (190.84°F), 88.56°C (191.41°F), 103.87°C (218.96°F), and 111.42°C (232.55°F) for content heat loads of 0, 0.4, 20, and 30 W, respectively, and occurs at approximately 1 hour after sunset in each case (see Table 6, Kaolite density of 19.4 lbm/ft^3).

Table 5. Maximum "quasi steady-state" temperatures during NCT for the ES-3100 shipping container with various content heat loads (see Figure 2 for node locations)—Kaolite density of 30 lbm/ft^3.

Node[a]	Location	Maximum "quasi steady-state" temperature, °C (°F)			
		0 W	0.4 W	20 W	30 W
A	CV lid, top, center	86.56 (187.81)	86.88 (188.38)	102.98 (215.74)	109.59 (229.26)
B	CV lid, bottom, center	86.56 (187.80)	86.88 (188.38)	102.16 (215.90)	109.71 (229.47)
C	CV lid, top, outer	86.54 (187.78)	86.86 (188.34)	101.89 (215.41)	109.31 (228.75)
D	CV flange at interface, inner[b]	86.47 (187.64)	86.79 (188.21)	102.09 (215.77)	109.67 (229.40)
E	CV flange at interface, outer[b]	86.44 (187.59)	86.76 (188.16)	102.00 (215.61)	109.53 (229.15)
F	CV flange, bottom, outer	86.42 (187.56)	86.74 (188.13)	101.99 (215.58)	109.51 (229.12)
G	CV shell, mid-height, inner	81.52 (178.74)	82.09 (179.76)	109.01 (228.21)	121.98 (251.57)
H	CV shell, mid-height, outer	81.52 (178.74)	82.09 (179.76)	109.00 (228.19)	121.97 (251.55)
I	CV bottom, outer	81.32 (178.37)	81.71 (179.08)	100.57 (213.02)	109.99 (229.99)
J	CV bottom, center, inner	81.37 (178.47)	81.77 (179.18)	100.73 (213.31)	110.21 (230.38)
K	CV bottom, center, outer	81.37 (178.47)	81.77 (179.18)	100.72 (213.29	110.19 (230.34)
L	Drum liner, plug cavity, outer	97.74 (207.93)	97.82 (208.07)	101.65 (214.96)	103.59 (218.47)
M	Drum liner, plug cavity, inner	92.91 (199.23)	93.06 (199.50)	100.40 (212.72)	104.13 (219.43)
N	Drum liner, CV flange cavity, outer	87.69 (189.84)	87.90 (190.21)	98.09 (208.57)	103.27 (217.43)
O	Drum liner, CV cavity, mid-height, inner	81.30 (178.35)	81.61 (178.90)	96.82 (206.27)	104.13 (219.43)
P	Drum liner, CV cavity, bottom, inner	81.52 (178.74)	81.86 (179.35)	98.30 (208.94)	106.56 (223.80)
Q	Borobond4, top, outer	87.36 (189.25)	87.58 (189.64)	98.19 (208.74)	103.57 (218.43)
R	Borobond4, mid-height, inner	81.30 (178.35)	81.61 (178.90)	98.81 (206.26)	104.58 (220.24)
S	Borobond4, mid-height, outer	81.37 (178.46)	81.66 (178.99)	96.24 (205.23)	103.69 (218.64)
T	Borobond4, bottom, inner	81.67 (179.01)	81.98 (179.56)	96.73 (206.12)	104.19 (219.55)
U	Borobond4, bottom, outer	81.78 (179.21)	82.07 (179.72)	96.11 (205.00)	103.23 (217.81)
V	Drum plug liner, bottom, center	111.30 (232.35)	111.34 (232.42)	113.25 (235.85)	114.21 (237.57)
W	Drum plug liner, top, center	90.70 (195.26)	90.92 (195.66)	101.53 (214.76)	106.87 (224.36)
X	Drum lid, top, center	117.74 (243.93)	117.75 (243.96)	118.50 (245.30)	118.88 (245.98)
Y	Drum lid, top, outer	107.04 (224.68)	107.06 (224.71)	107.94 (226.29)	108.39 (227.10)
Z	Drum, mid-height, outer	91.86 (197.36)	91.90 (197.41)	93.42 (200.15)	94.18 (201.53)
AA	Drum bottom, outer	91.00 (195.79)	91.04 (195.86)	92.92 (199.26)	93.87 (200.96)
BB	Drum bottom, center	87.21 (188.97)	87.31 (189.15)	92.26 (198.07)	94.74 (202.54)

Notes: (a) See Figure 2.
(b) Approximate location of the CV O-ring.

Table 6. Maximum "quasi steady-state" temperatures during NCT for the ES-3100 shipping container with various content heat loads (see Figure 2 for node locations)—Kaolite density of 19.4 lbm/ft^3.

Node[(a)]	Location	Maximum "quasi steady-state" temperature, °C (°F)			
		0 W	0.4 W	20 W	30 W
A	CV lid, top, center	88.30 (190.95)	88.62 (191.52)	103.84 (218.91)	111.35 (232.42)
B	CV lid, bottom, center	88.28 (190.90)	88.60 (191.48)	103.90 (219.03)	111.45 (232.62)
C	CV lid, top, outer	88.32 (190.97)	88.63 (191.54)	103.61 (218.50)	111.00(231.80)
D	CV flange at interface, inner[(b)]	88.24 (190.83)	88.56 (191.41)	103.87 (218.96)	111.42 (232.55)
E	CV flange at interface, outer[(b)]	88.25 (190.84)	88.56 (191.41)	103.77 (218.78)	111.27 (232.28)
F	CV flange, bottom, outer	88.24 (190.82)	88.55 (191.39)	103.75 (218.75)	111.25 (232.24)
G	CV shell, mid-height, inner	83.04 (181.47)	83.61 (182.50)	110.50 (230.89)	123.46 (254.23)
H	CV shell, mid-height, outer	83.04 (181.47)	83.61 (182.50)	110.49 (230.88)	123.45 (254.21)
I	CV bottom, outer	83.36 (182.04)	83.75 (182.74)	102.58 (216.64)	111.99 (233.59)
J	CV bottom, center, inner	88.37 (182.07)	83.76 (182.77)	102.70 (216.86)	112.17 (233.91)
K	CV bottom, center, outer	88.37 (181.07)	83.76 (182.77)	102.69 (216.84)	112.15 (233.87)
L	Drum liner, plug cavity, outer	98.72 (209.70)	98.80 (209.85)	102.63 (216.73)	104.58 (220.24)
M	Drum liner, plug cavity, inner	94.43 (201.97)	94.58 (202.24)	101.92 (215.46)	105.65 (222.16)
N	Drum liner, CV flange cavity, outer	89.43 (192.97)	89.63 (193.34)	99.83 (211.70)	105.01 (221.02)
O	Drum liner, CV cavity, mid-height, inner	83.12 (181.62)	83.43 (182.18)	98.63 (209.54)	106.40 (223.52)
P	Drum liner, CV cavity, bottom, inner	83.62 (182.52)	83.96 (183.13)	100.36 (212.65)	108.60 (227.48)
Q	Borobond4, top, outer	88.82 (191.88)	89.04 (192.27)	99.65 (211.38)	105.04 (221.07)
R	Borobond4, mid-height, inner	83.12 (181.62)	83.43 (182.18)	98.63 (209.53)	106.39 (223.51)
S	Borobond4, mid-height, outer	83.03 (181.46)	83.33 (182.00)	97.91 (208.23)	105.36 (221.65)
T	Borobond4, bottom, inner	83.55 (182.39)	83.85 (182.93)	98.58 (209.45)	106.03 (222.86)
U	Borobond4, bottom, outer	83.51 (182.31)	83.80 (182.83)	97.82 (208.07)	104.90 (238.82)
V	Drum plug liner, bottom, center	112.01 (233.62)	112.05 (233.69)	113.95 (237.11)	114.90 (238.82)
W	Drum plug liner, top, center	92.09 (197.77)	92.31 (198.16)	102.93 (217.27)	108.26 (226.87)
X	Drum lid, top, center	118.01 (244.42)	118.03 (244.45)	118.77 (245.79)	119.15 (246.47)
Y	Drum lid, top, outer	107.33 (225.19)	107.34 (225.22)	108.22 (226.80)	108.67 (227.60)
Z	Drum, mid-height, outer	92.27 (198.08)	92.30 (198.14)	93.81 (200.86)	94.58 (202.24)
AA	Drum bottom, outer	91.70 (197.06)	91.74 (197.13)	93.61 (200.49)	94.54 (202.18)
BB	Drum bottom, center	88.82 (191.88)	88.93 (192.07)	93.84 (200.91)	96.30 (205.35)

Notes: (a) See Figure 2.
(b) Approximate location of the CV O-ring.

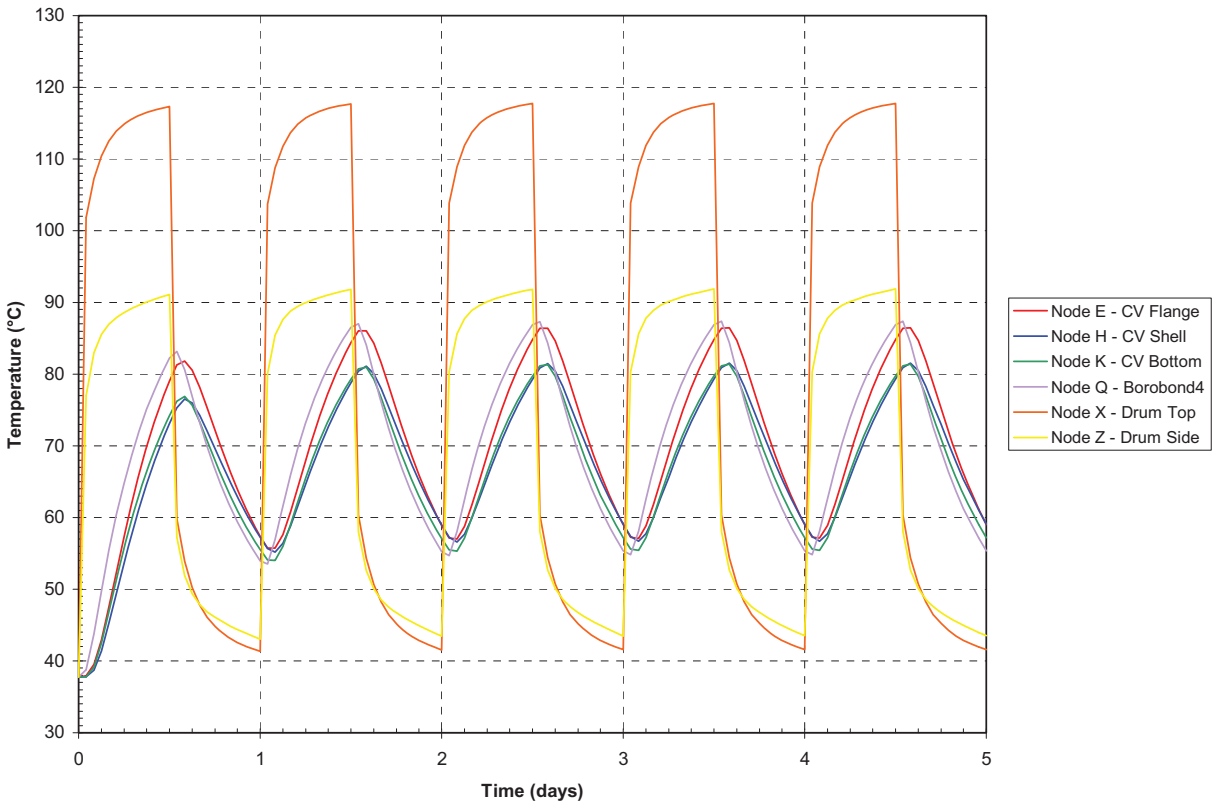

Figure 3. Transient temperatures of the ES-3100 shipping container for NCT (no content heat load) Kaolite density of 30 lbm/ft^3 (see Figure 2 for node locations).

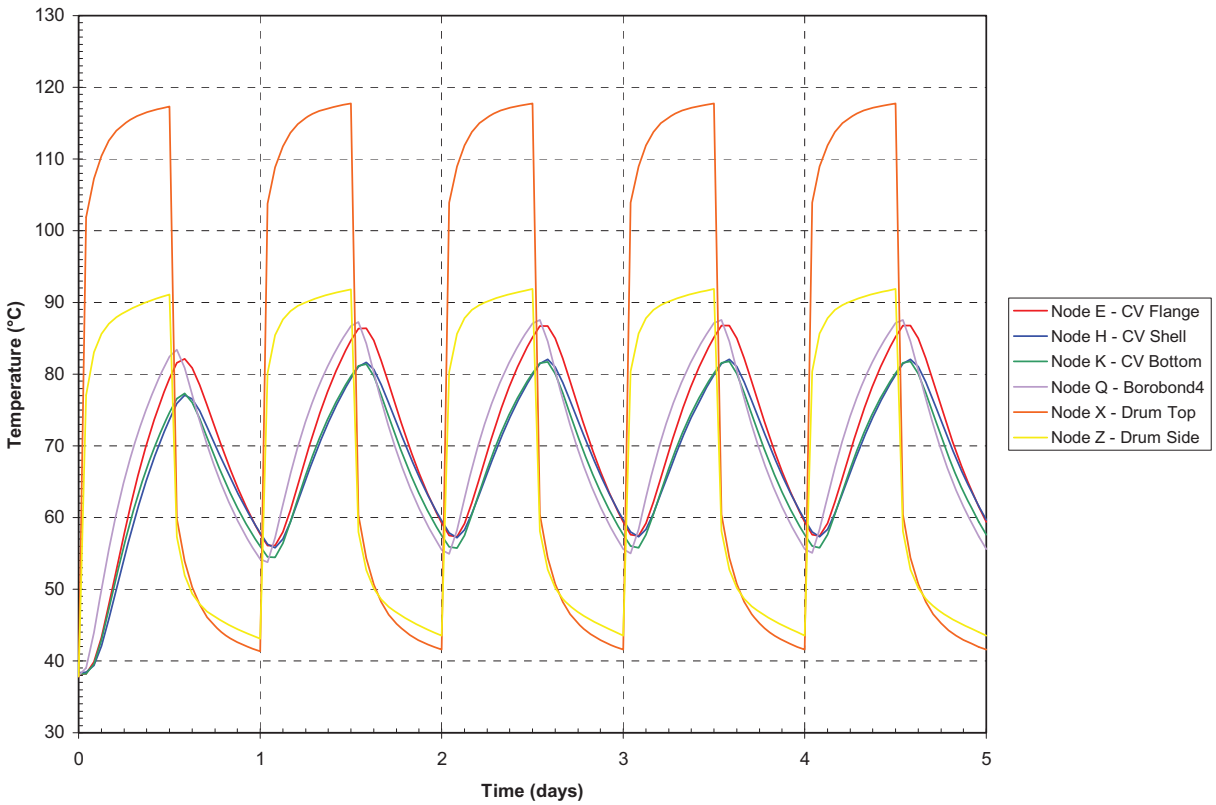

Figure 4. Transient temperatures of the ES-3100 shipping container for NCT (0.4 W content heat load) Kaolite density of 30 lbm/ft^3 (see Figure 2 for node locations).

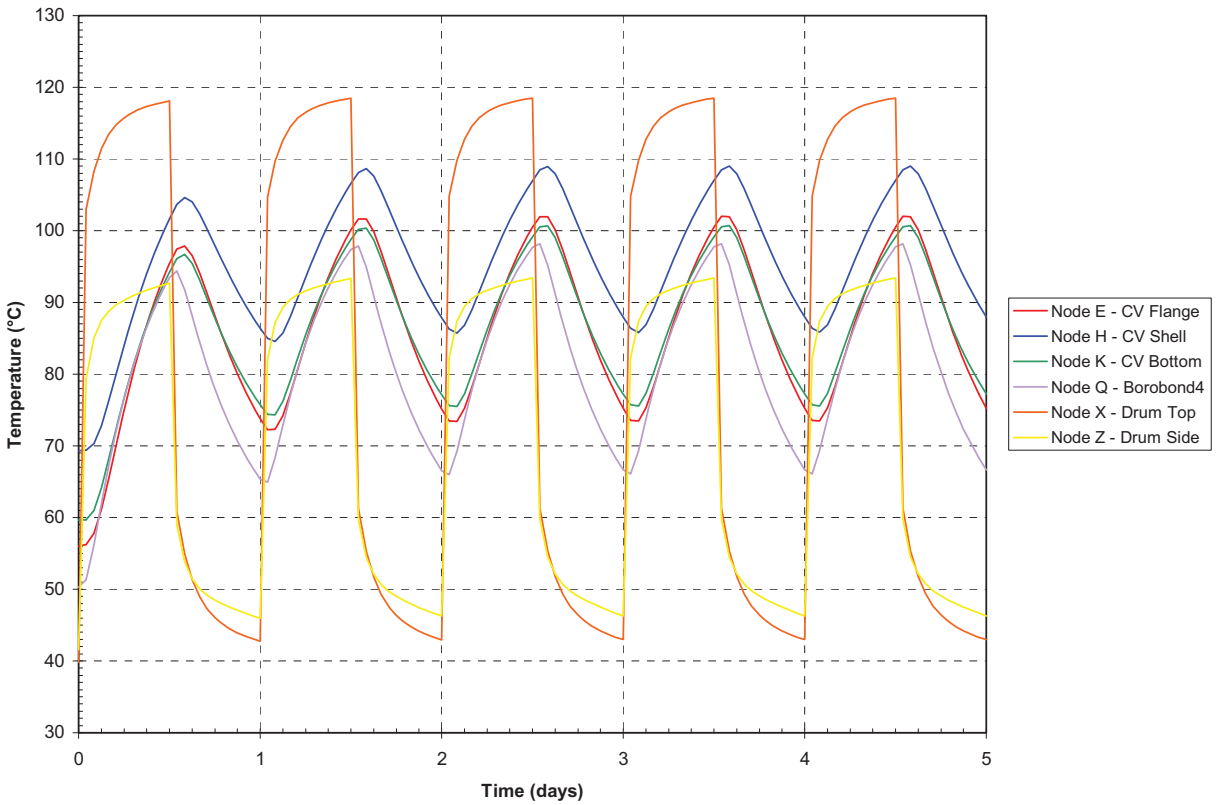

Figure 5. Transient temperatures of the ES-3100 shipping container for NCT (20 W content heat load) Kaolite density of 30 lbm/ft^3 (see Figure 2 for node locations).

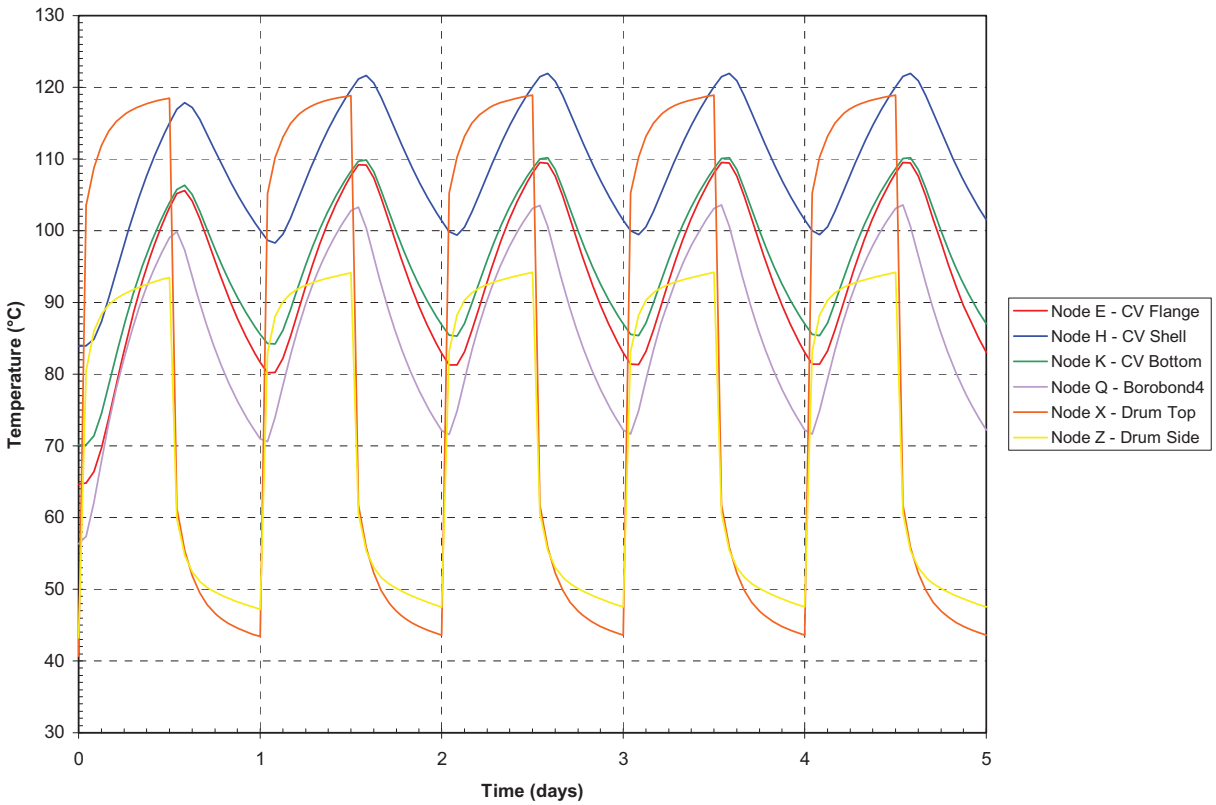

Figure 6. Transient temperatures of the ES-3100 shipping container for NCT (30 W content heat load)Kaolite density of 30 lbm/ft^3 (see Figure 2 for node locations).

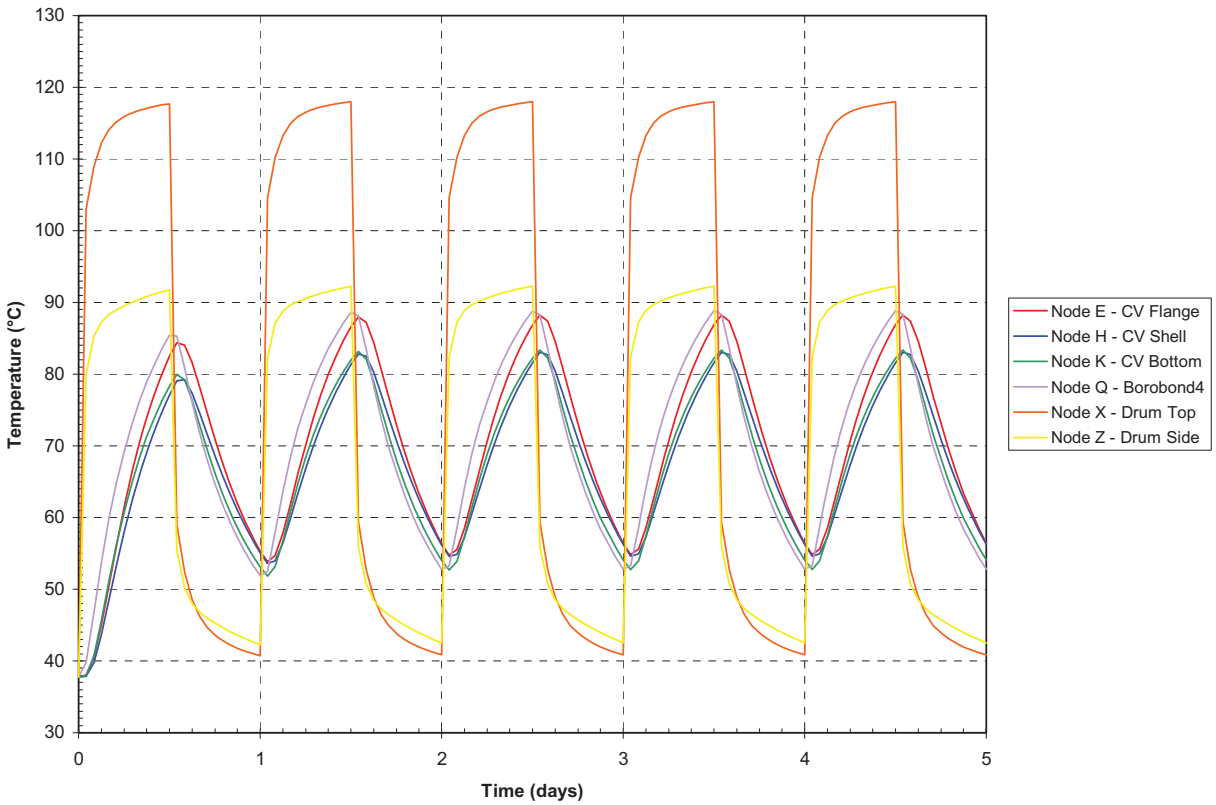

Figure 7. Transient temperatures of the ES-3100 shipping container for NCT (no content heat load) Kaolite density of 19.4 lbm/ft^3 (see Figure 2 for node locations).

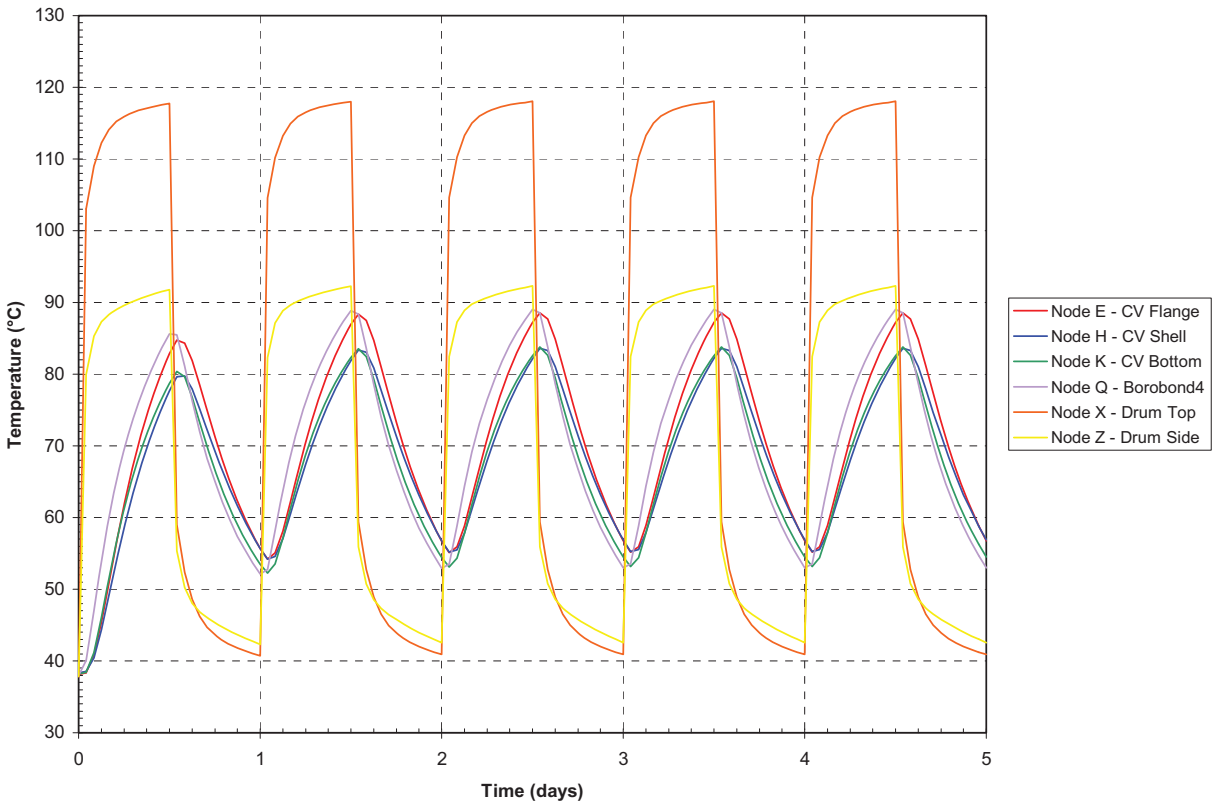

Figure 8. Transient temperatures of the ES-3100 shipping container for NCT (0.4 W content heat load) Kaolite density of 19.4 lbm/ft^3 (see Figure 2 for node locations).

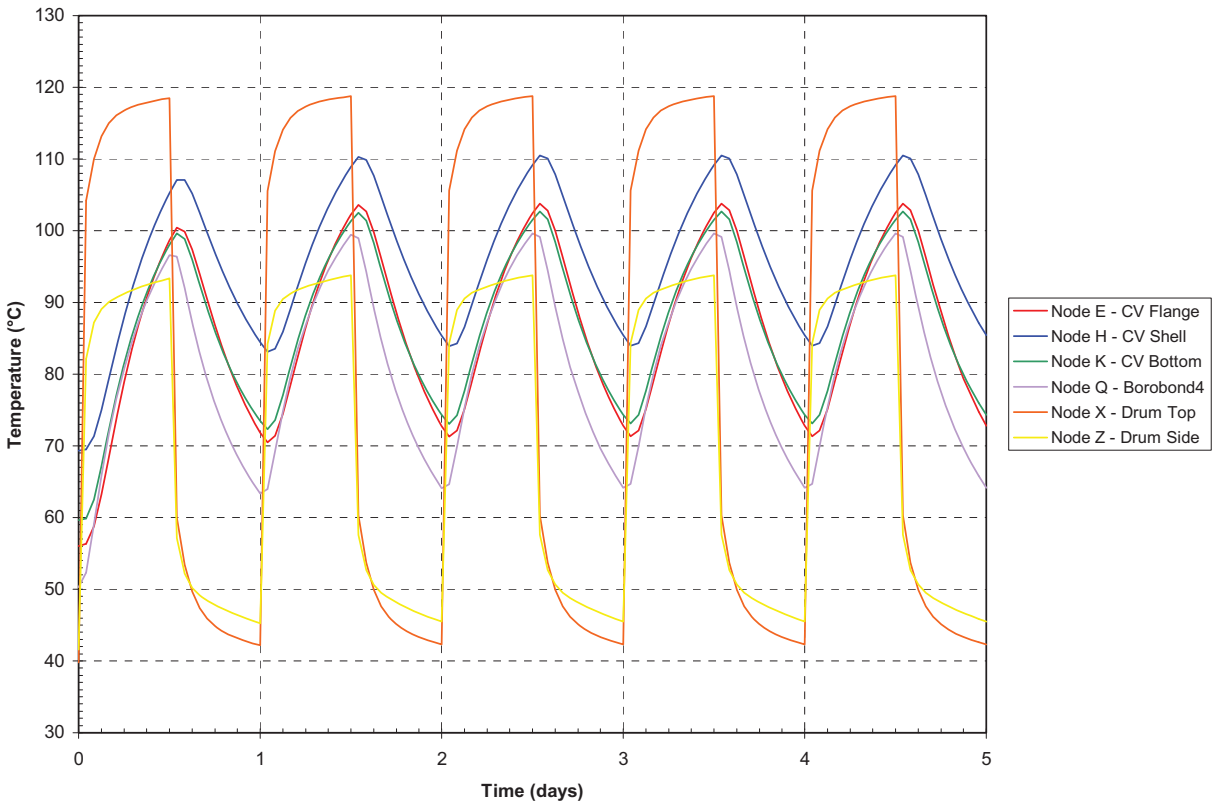

Figure 9. Transient temperatures of the ES-3100 shipping container for NCT (20 W content heat load) Kaolite density of 19.4 lbm/ft^3 (see Figure 2 for node locations).

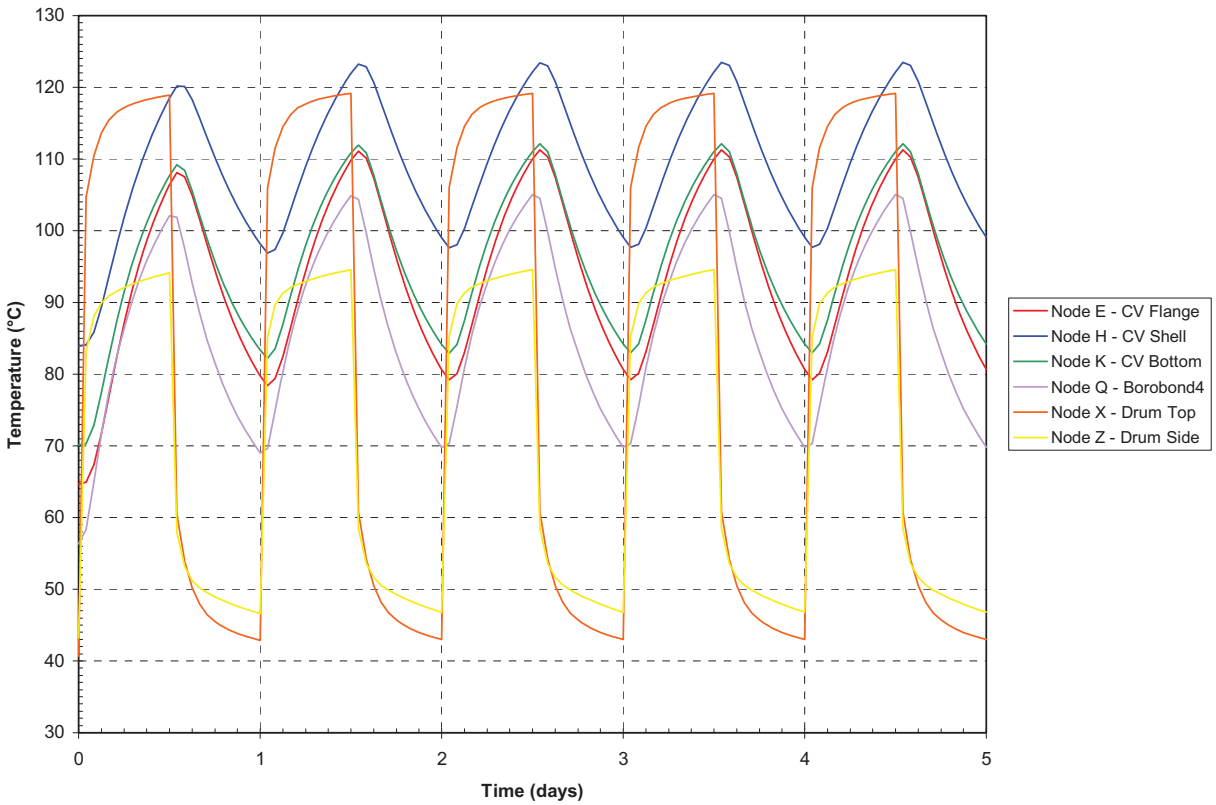

Figure 10. Transient temperatures of the ES-3100 shipping container for NCT (30 W content heat load) Kaolite density of 19.4 lbm/ft^3 (see Figure 2 for node locations).

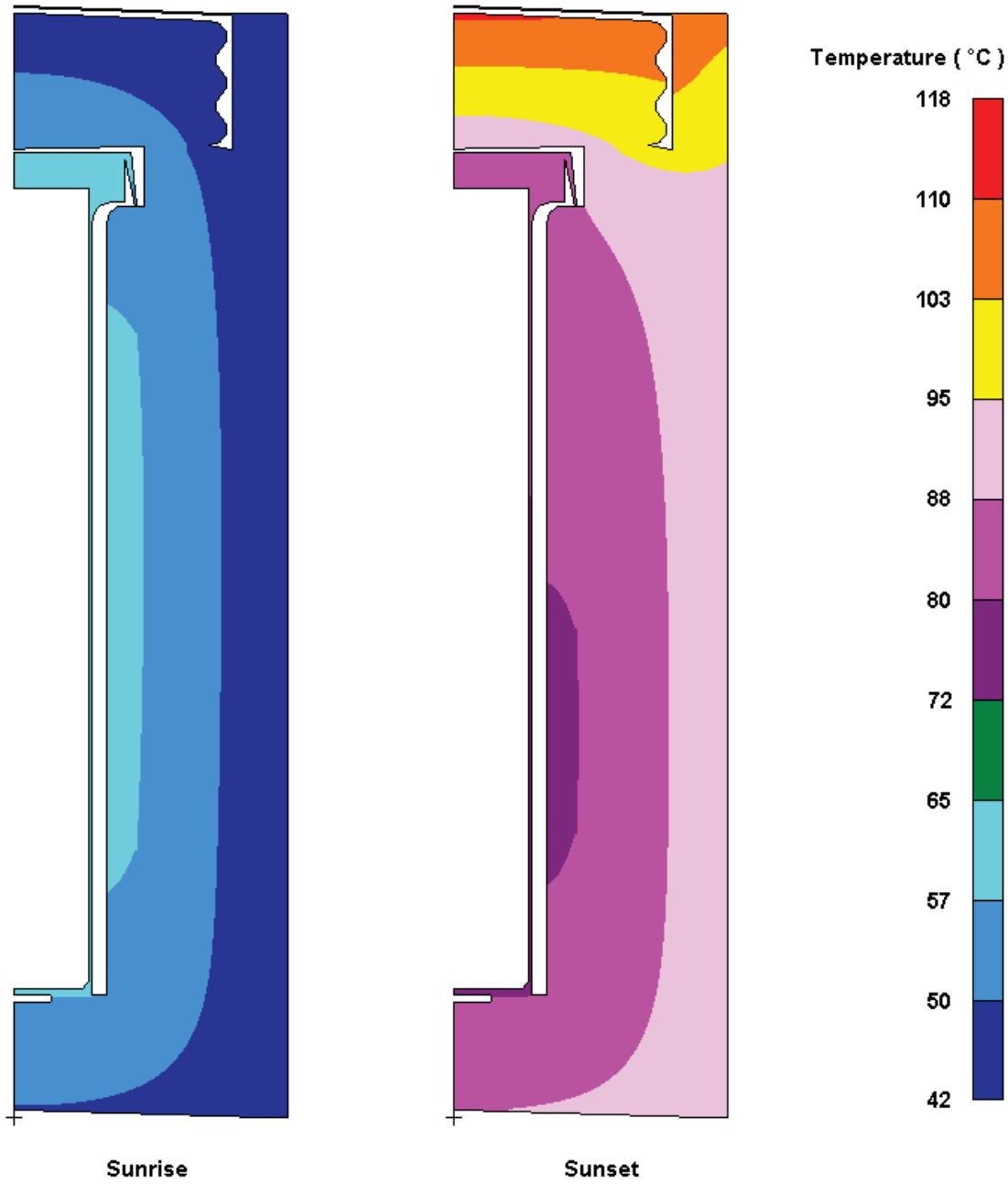

Figure 11. Temperature distribution in the ES-3100 shipping container for NCT (no content heat load)—Kaolite density of 30 lbm/ft^3—day 5 of transient analysis (elements representing air not shown for clarity).

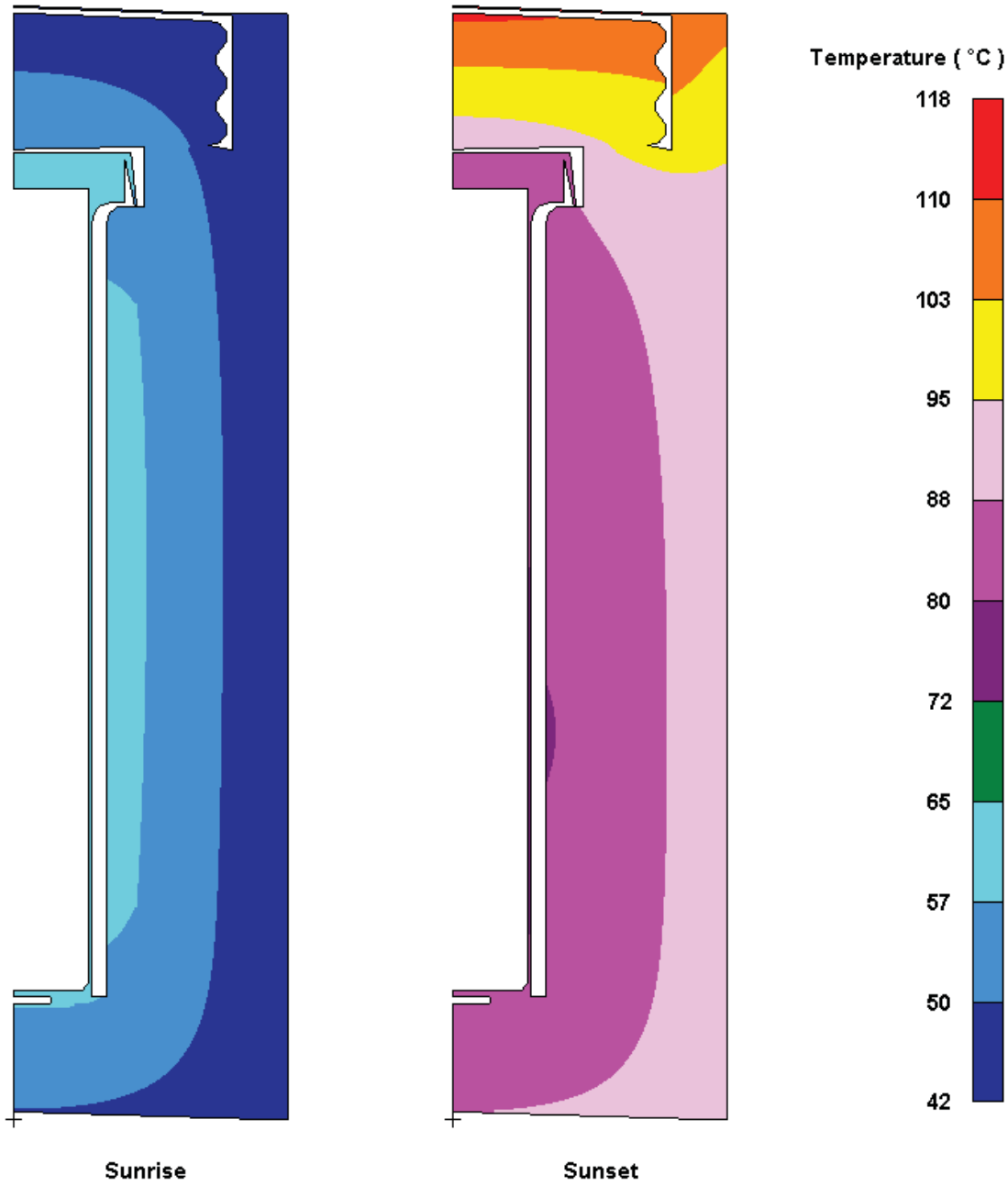

Figure 12. Temperature distribution in the ES-3100 shipping container for NCT (0.4 W content heat load)—Kaolite density of 30 lbm/ft^3—day 5 of transient analysis (elements representing air not shown for clarity).

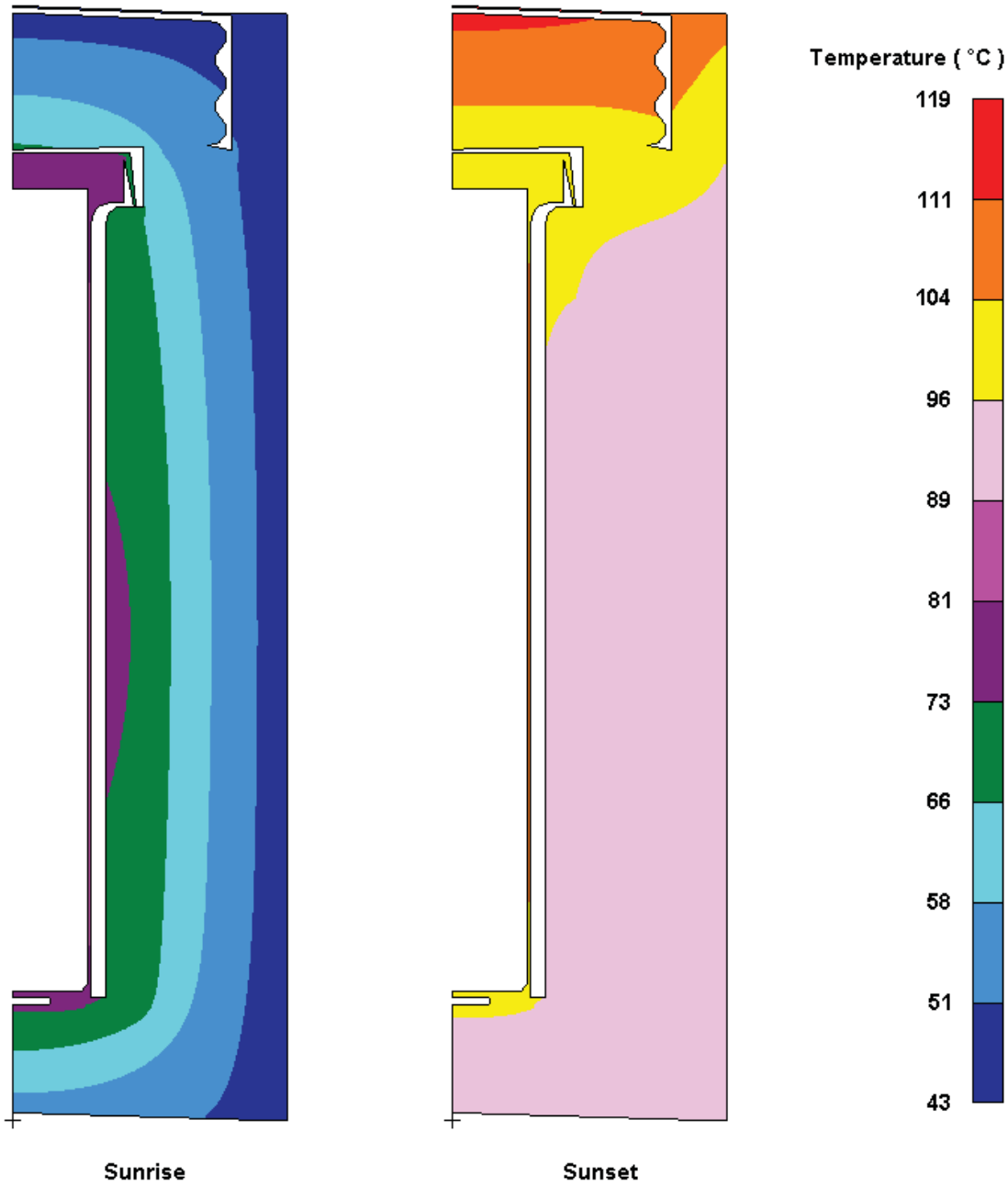

Figure 13. Temperature distribution in the ES-3100 shipping container for NCT (20 W content heat load)—Kaolite density of 30 lbm/ft^3—day 5 of transient analysis (elements representing air not shown for clarity).

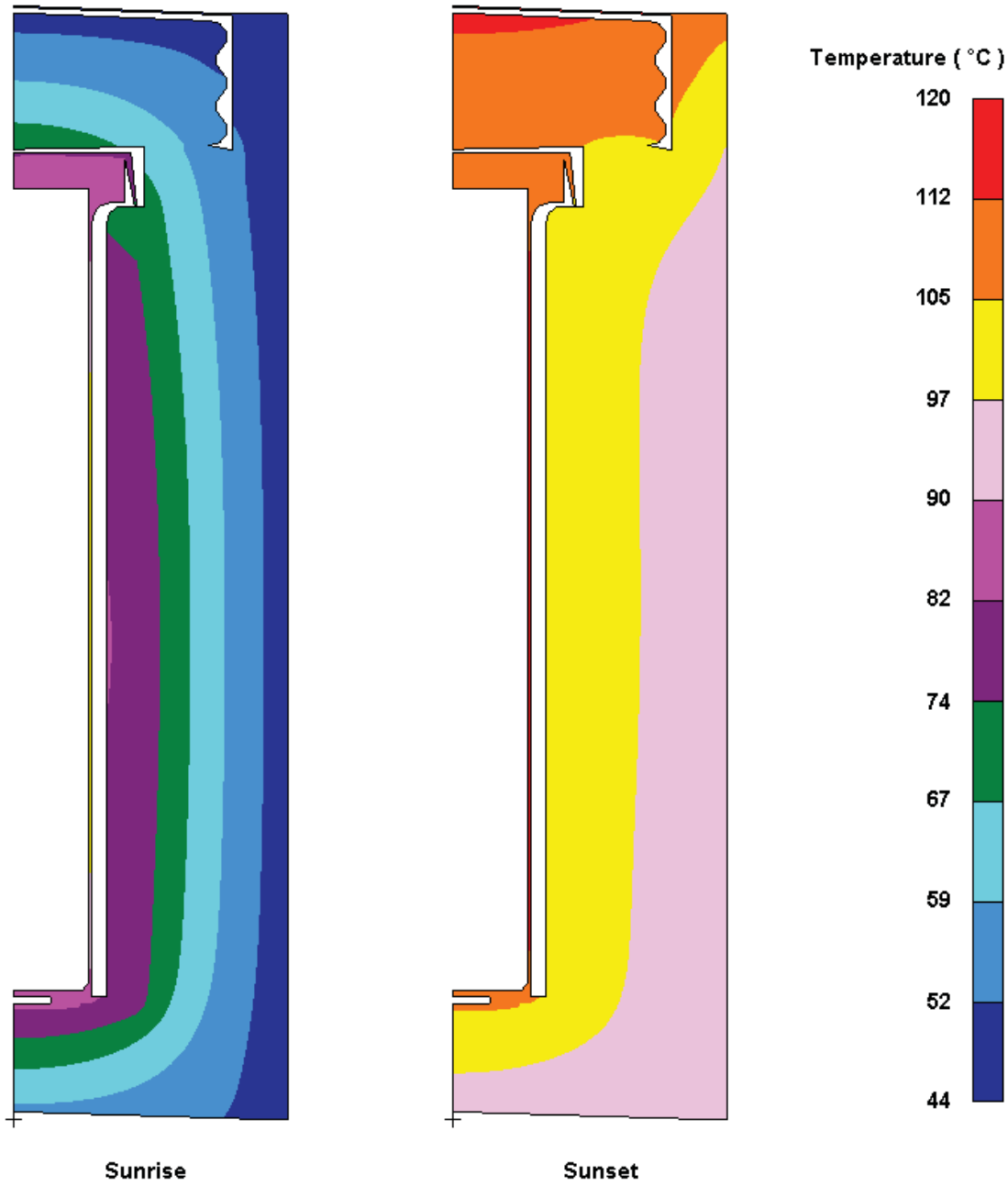

Figure 14. Temperature distribution in the ES-3100 shipping container for NCT (30 W content heat load)—Kaolite density of 30 lbm/ft^3—day 5 of transient analysis (elements representing air not shown for clarity).

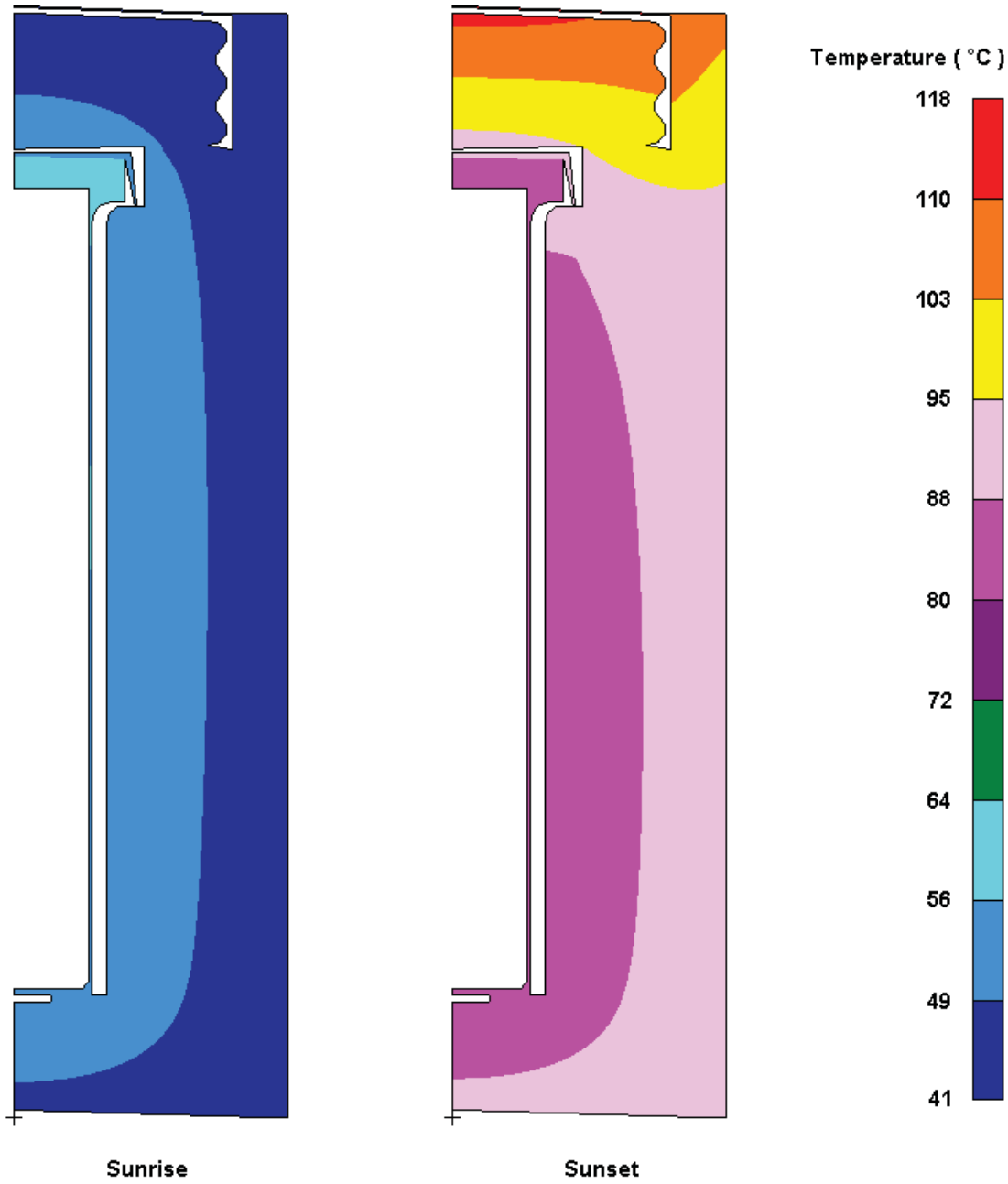

Figure 15. Temperature distribution in the ES-3100 shipping container for NCT (no content heat load)—Kaolite density of 19.4 lbm/ft^3—day 5 of transient analysis (elements representing air not shown for clarity).

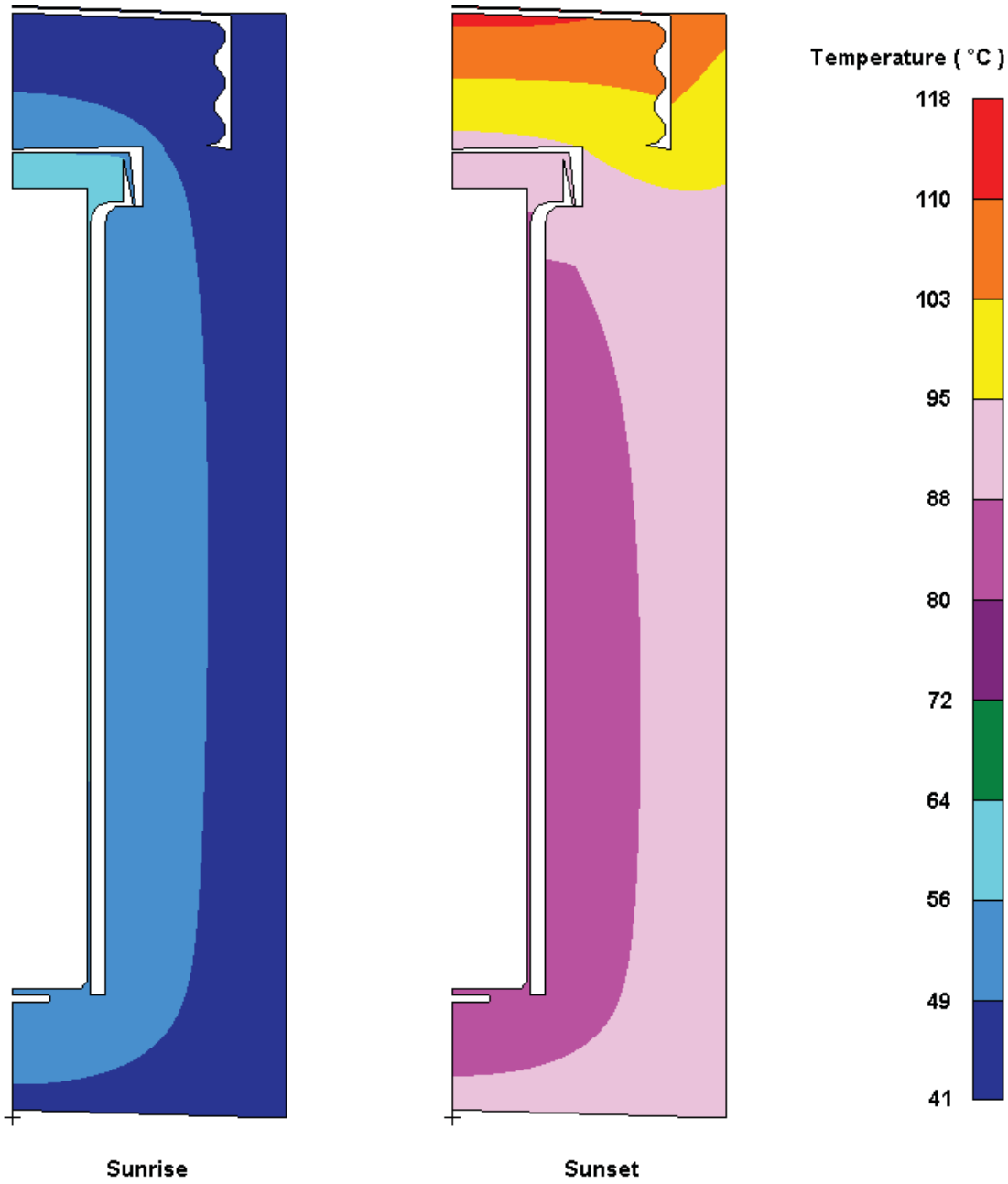

Figure 16. Temperature distribution in the ES-3100 shipping container for NCT (0.4 W content heat load)—Kaolite density of 19.4 lbm/ft^3—day 5 of transient analysis (elements representing air not shown for clarity).

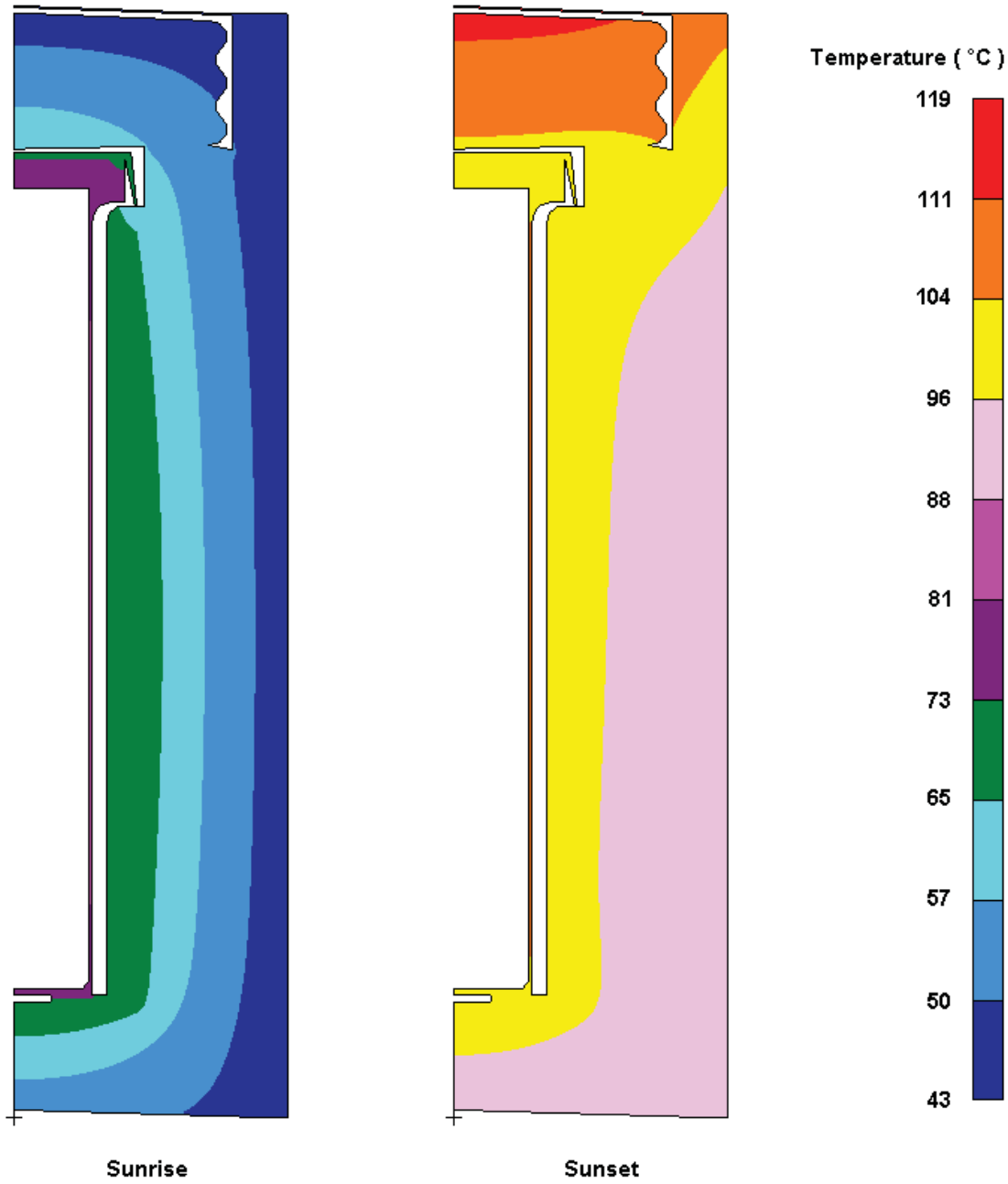

Figure 17. Temperature distribution in the ES-3100 shipping container for NCT (20 W content heat load)—Kaolite density of 19.4 lbm/ft^3—day 5 of transient analysis (elements representing air not shown for clarity).

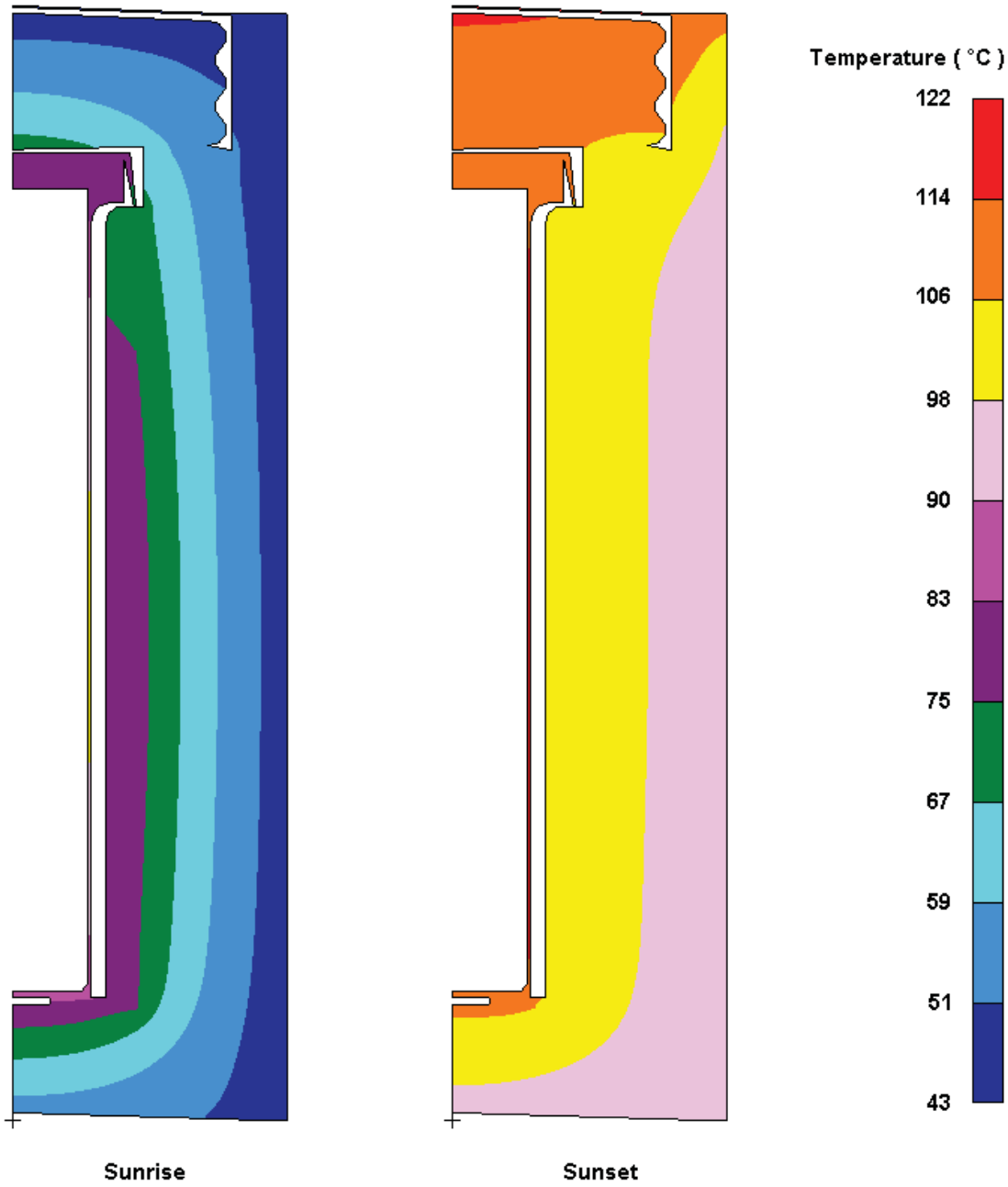

Figure 18. Temperature distribution in the ES-3100 shipping container for NCT (30 W content heat load)—Kaolite density of 19.4 lbm/ft^3—day 5 of transient analysis (elements representing air not shown for clarity).

Hypothetical Accident Conditions Analyses Results

Transient thermal analyses are performed on the finite element model of the ES-3100 shipping container (undamaged configuration) to simulate HAC as prescribed by 10 CFR 71.73(c)(4).[1] A 30-minute fire of 800°C (1472°F) is simulated by applying natural convection and radiant exchange boundary conditions to all external surfaces of the drum (assuming the drum is in a horizontal orientation) with content heat loads of 0, 0.4, 20, and 30 W and Kaolite densities of 30 (maximum density) and 19.4 lbm/ft^3 (minimum density). No heat flux boundary conditions simulating insolation are applied to the model during the 30-minute fire. The initial temperature distribution within the package having content heat loads of 0.4, 20, and 30 W is obtained from their respective steady-state analyses. The initial temperature distribution within the package having no content heat load (0 W) is assumed to be at a uniform temperature equal to the ambient temperature of 37.8°C (100°F).

Following the 30-minute fire transient analyses, 48-hour cool-down transient thermal analyses are performed using the temperature distribution at the end of the fire as the initial temperature distribution. During post-fire cool-down, natural convection and radiant exchange boundary conditions are applied to all external surfaces of the drum (assuming the drum is in a horizontal orientation). Additionally, cases are analyzed in which insolation is included during the post-fire cool-down. For the cases in which insolation is applied to the model during cool-down, insolation is applied during the first 12-hour period following the 30-minute fire, then alternated (off, then on) as was done for NCT.

The maximum temperatures calculated for the ES-3100 shipping container for HAC are summarized in Table 7 for the analyses using a Kaolite density of 30 lbm/ft^3 and Table 8 for the analyses using a Kaolite density of 19.4 lbm/ft^3. Temperature-history plots of several locations within the model are also depicted graphically in Figure 19 through Figure 22 for content heat loads of 0, 0.4, 20, and 30 W and a Kaolite density of 19.4 lbm/ft^3 (the graphs for the cases having a Kaolite density of 30 lbm/ft^3 are not shown because of their similarity to the presented graphs).

Table 7. ES-3100 shipping container HAC maximum temperatures—Kaolite density of 30 lbm/ft^3.

Content heat load (W)	Insolation during cool-down	Maximum temperature, °C (°F)						
		Node A[a] CV lid	Node E[a] CV flange at O-ring	Node H[a] CV shell (mid-elevation)	Node K[a] CV bottom (center)	Node Q[a] Borobond4 (top)	Node S[a] Borobond4 (mid-elevation)	Node T[a] Borobond4 (bottom)
0	No[b]	109.61 (229.29)	109.34 (228.81)	92.21 (197.98)	99.71 (211.47)	118.48 (245.26)	90.42 (194.76)	102.07 (215.73)
	Yes	116.91 (242.43)	116.74 (242.12)	104.22 (219.59)	106.13 (223.04)	122.46 (252.43)	103.28 (217.90)	107.63 (225.73)
0.4	No	109.93 (229.87)	109.66 (229.38)	92.78 (199.00)	100.11 (212.19)	118.69 (245.64)	90.73 (195.31)	102.38 (216.29)
	Yes	117.22 (243.00)	117.05 (242.68)	104.77 (220.58)	106.52 (223.74)	122.67 (252.81)	103.58 (218.45)	107.93 (226.28)
20	No	126.14 (259.05)	125.85 (258.53)	120.27 (248.48)	119.75 (247.56)	130.06 (266.11)	106.49 (223.67)	117.92 (244.25)
	Yes	133.07 (271.52)	132.85 (271.17)	131.38 (268.48)	125.90 (258.91)	134.05 (273.28)	118.96 (246.13)	123.31 (253.95)
30	No	134.00 (273.20)	133.69 (272.56)	133.41 (272.14)	129.43 (264.97)	135.69 (276.23)	114.38 (237.89)	125.62 (258.11)
	Yes	140.79 (285.42)	140.58 (285.05)	144.22 (291.59)	135.47 (275.85)	139.68 (283.42)	126.76 (260.17)	130.95 (267.71)

Notes: (a) See Figure 2 for node locations.
(b) Baseline case for ΔT comparisons.

Table 8. ES-3100 shipping container HAC maximum temperatures—Kaolite density of 19.4 lbm/ft^3.

Content heat load (W)	Insolation during cool-down	Maximum temperature, °C (°F)						
		Node A[a] CV lid	Node E[a] CV flange at O-ring	Node H[a] CV shell (mid-elevation)	Node K[a] CV bottom (center)	Node Q[a] Borobond4 (top)	Node S[a] Borobond4 (mid-elevation)	Node T[a] Borobond4 (bottom)
0	No[b]	114.95 (238.92)	114.69 (238.43)	95.48 (203.86)	105.98 (222.77)	129.89 (265.79)	93.95 (201.11)	109.65 (229.36)
	Yes	121.44 (250.60)	121.27 (250.28)	106.43 (223.58)	111.02 (231.83)	132.73 (270.92)	105.10 (221.19)	113.62 (236.51)
0.4	No	115.27 (239.49)	115.00 (239.00)	96.04 (204.87)	106.37 (223.47)	130.09 (266.17)	94.25 (201.65)	109.95 (229.91)
	Yes	121.75 (251.16)	121.58 (250.85)	106.97 (224.57)	111.41 (232.53)	132.94 (271.30)	105.41 (221.73)	113.92 (237.06)
20	No	131.51 (268.71)	131.22 (268.19)	123.43 (254.17)	126.00 (258.80)	141.29 (286.32)	109.98 (229.96)	125.44 (257.80)
	Yes	137.69 (279.84)	137.49 (279.48)	133.54 (272.37)	130.83 (267.49)	144.13 (291.44)	120.84 (249.51)	129.33 (264.79)
30	No	139.39 (282.90)	139.08 (282.25)	136.53 (277.75)	135.66 (276.19)	146.82 (296.28)	117.85 (244.14)	133.11 (271.60)
	Yes	145.45 (293.82)	145.24 (293.44)	146.35 (295.43)	140.42 (284.75)	149.67 (301.41)	128.65 (263.57)	136.97 (278.55)

Notes: (a) See Figure 2 for node locations.
(b) Baseline case for ΔT comparisons.

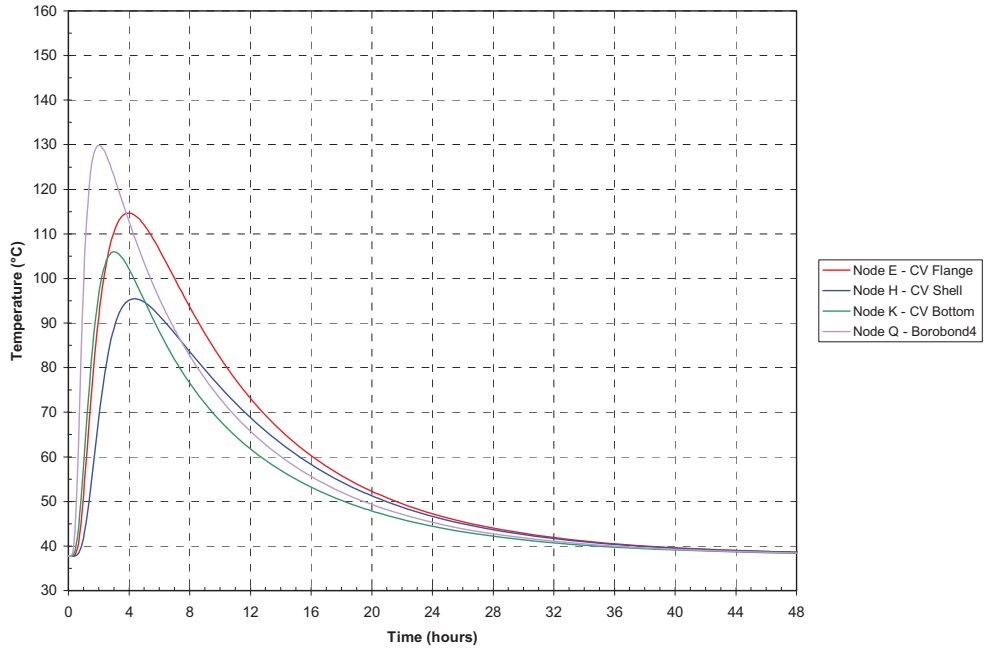

(a) No insolation during post-fire cool-down.

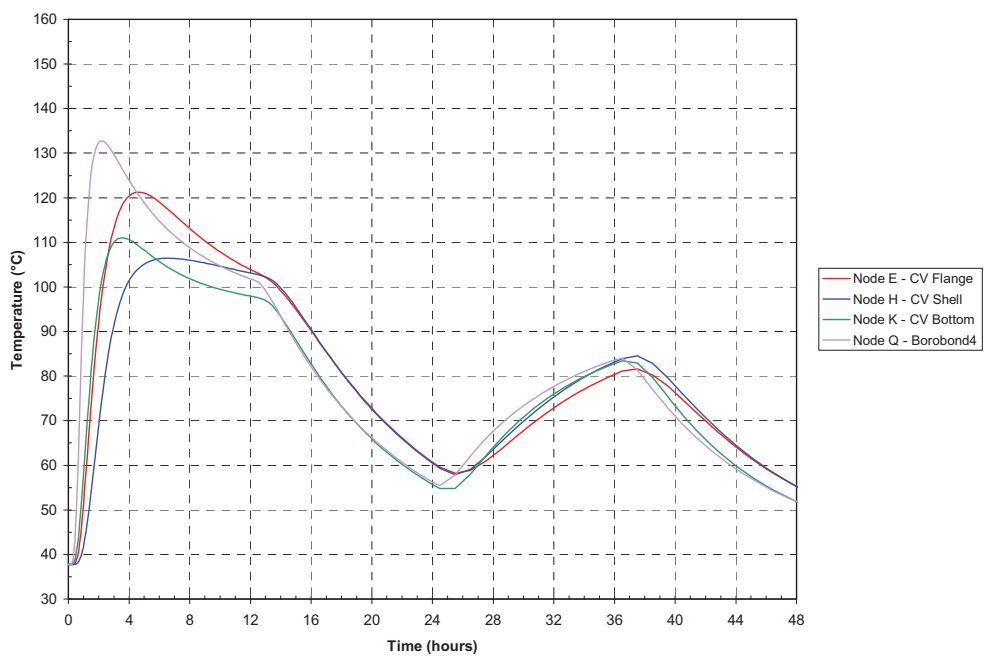

(b) Insolation during post-fire cool-down.

Figure 19. ES-3100 shipping container transient temperatures for HAC (no content heat load) Kaolite density of 19.4 lbm/ft^3 (see Figure 2 for node locations).

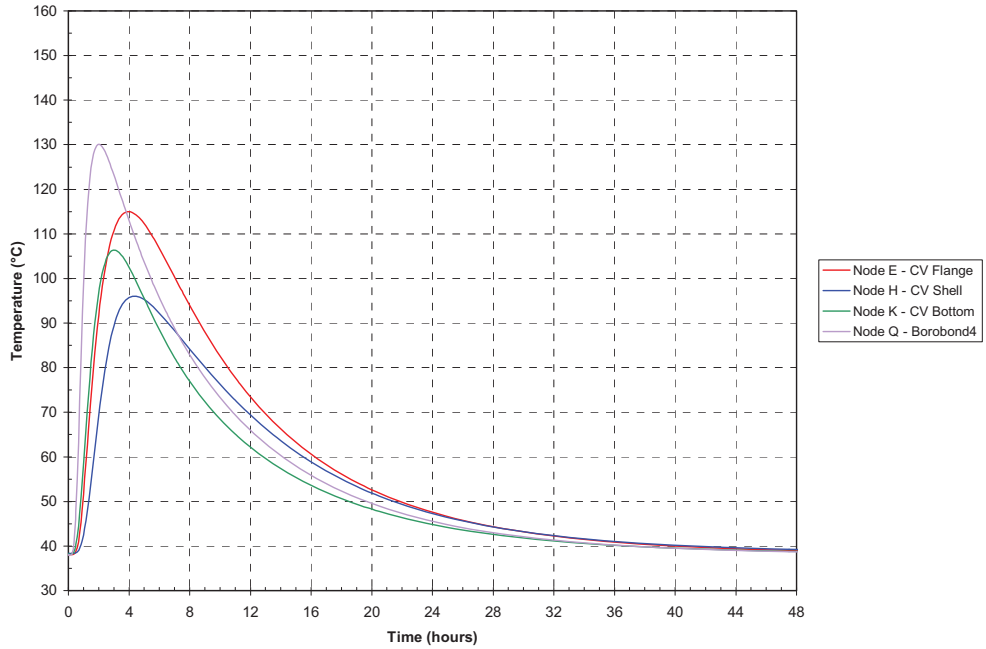

(a) No insolation during post-fire cool-down.

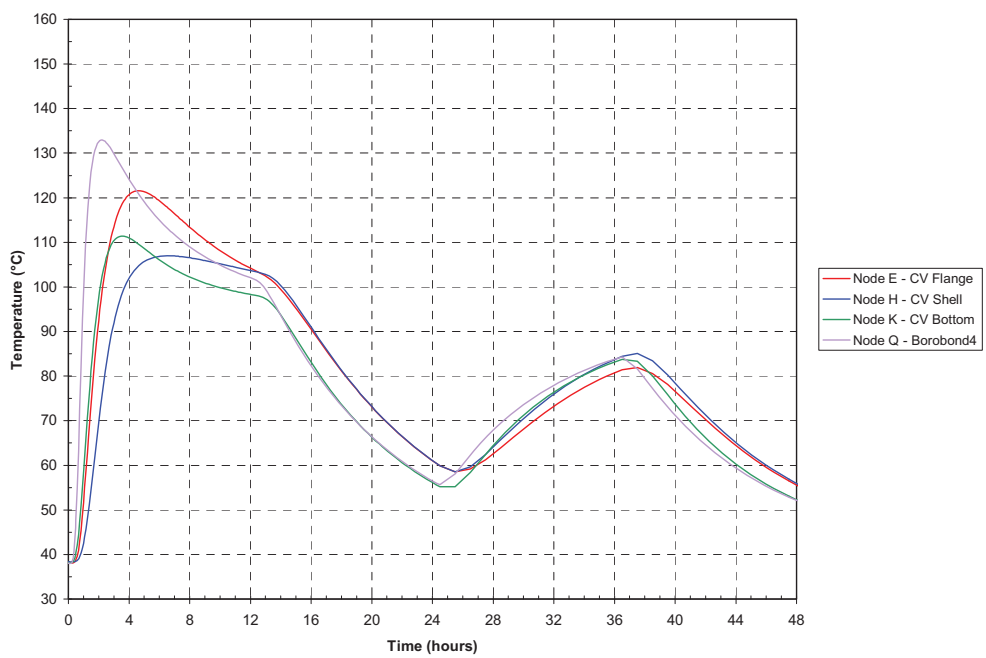

(b) Insolation during post-fire cool-down.

Figure 20. ES-3100 shipping container transient temperatures for HAC (0.4 W content heat load) Kaolite density of 19.4 lbm/ft^3 (see Figure 2 for node locations).

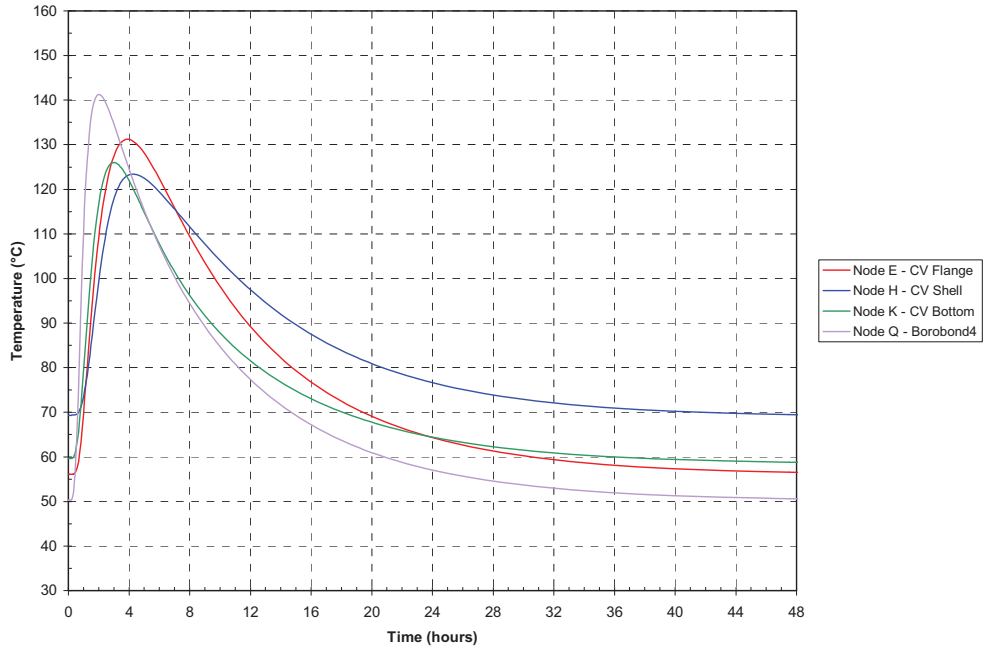

(a) No insolation during post-fire cool-down.

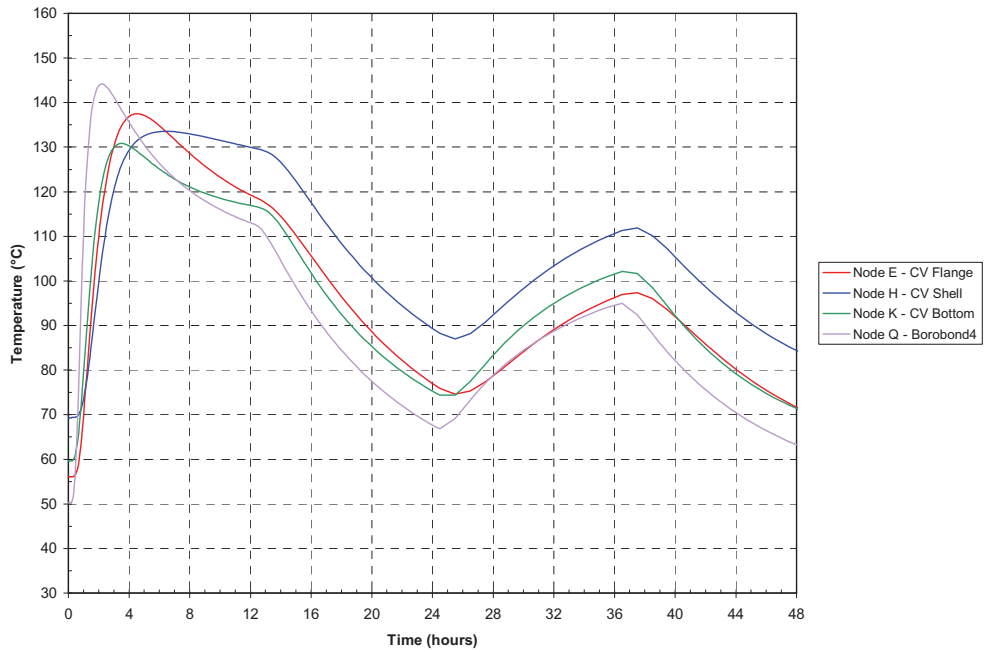

(b) Insolation during post-fire cool-down.

Figure 21. ES-3100 shipping container transient temperatures for HAC (20 W content heat load) Kaolite density of 19.4 lbm/ft^3 (see Figure 2 for node locations).

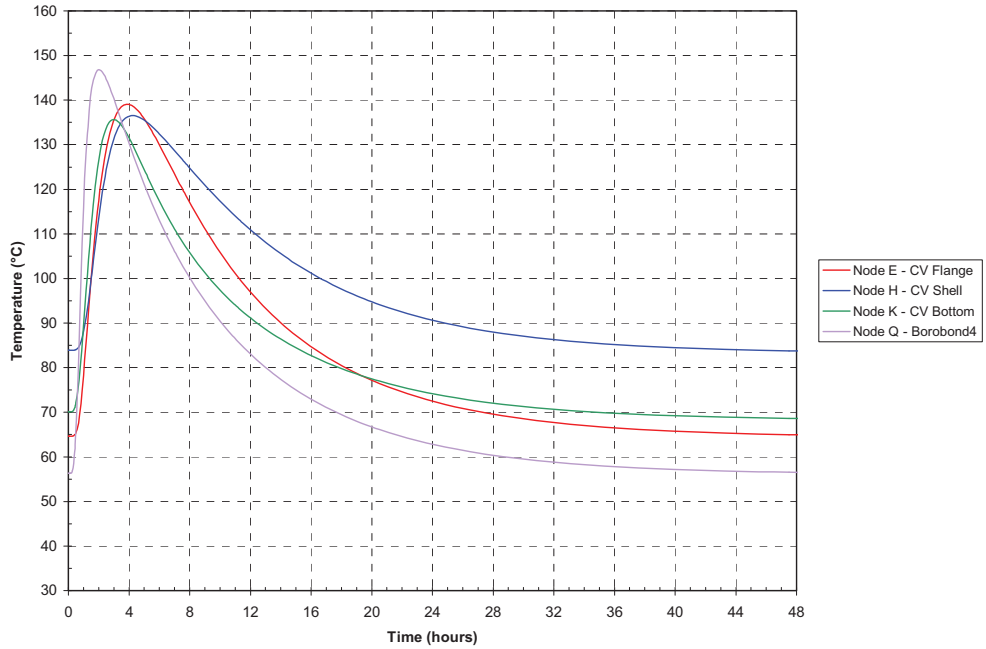

(a) No insolation during post-fire cool-down.

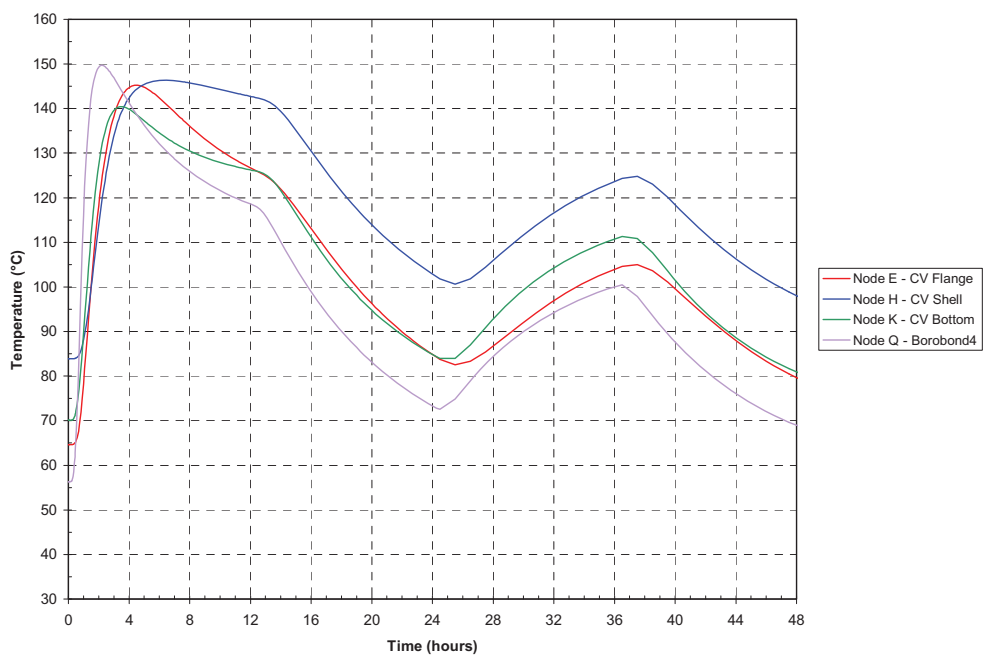

(b) Insolation during post-fire cool-down.

Figure 22. ES-3100 shipping container transient temperatures for HAC (30 W content heat load) Kaolite density of 19.4 lbm/ft^3 (see Figure 2 for node locations).

APPENDIX 3.6.1 REFERENCES

1. *Packaging and Transportation of Radioactive Materials*, U.S. Nuclear Regulatory Commission, Code of Federal Regulations, Title 10 – Energy, Part 71, 2003.

2. MSC.Patran 2004 Version 12.0.044, MacNeal Schwendler Corporation, 2004.

3. R. Siegel and J. R. Howell, *Thermal Radiation Heat Transfer*, Second Edition, Hemisphere Publishing Corporation, 1981.

4. F. P. Incropera and D. P. DeWitt, *Fundamentals of Heat and Mass Transfer*, Second Edition, John Wiley & Sons, New York, 1985.

5. *MSC.Patran 2003, Thermal User's Guide Volume 1, Thermal/Hydraulic Analysis*, MSC.Software Corporation, Santa Ana, CA, 2003.

6. J. C. Anderson and M. R. Feldman, *Thermal Modeling of Packages for Normal Conditions of Transport with Insolation*, Proceedings of the ASME Heat Transfer Division, HTD-Vol. 317-2, 1995, International Mechanical Engineering Congress and Exposition, November 1995.

7. P/VIEWFACTOR, Version 12.0.044, MacNeal Schwendler Corporation, 2004.

8. MSC.Patran Thermal, Version 12.0.044, MacNeal Schwendler Corporation, 2004.

THIS PAGE INTENTIONALLY LEFT BLANK.

Appendix 3.6.2

THERMAL EVALUATION OF THE ES-3100 SHIPPING CONTAINER FOR NCT AND HAC (FINAL DESIGN WITH CATALOG 277-4 NEUTRON ABSORBER)

THIS PAGE INTENTIONALLY LEFT BLANK.

Appendix 3.6.2

THERMAL EVALUATION OF THE ES-3100 SHIPPING CONTAINER FOR NCT AND HAC (FINAL DESIGN WITH CATALOG 277-4 NEUTRON ABSORBER)

INTRODUCTION

Thermal analyses of the ES-3100 shipping container are performed to determine the temperature distribution within the packaging during Normal Conditions of Transport (NCT) as specified in 10 CFR 71.71(c)(1).[1] Transient thermal analyses are performed by treating the problem as a cyclic transient with the incident heat flux due to solar radiation applied and not applied in alternating 12-hour periods.

Additionally, thermal analyses of the ES-3100 shipping container are performed to determine the thermal response of the packaging to Hypothetical Accident Conditions (HAC) as specified in 10 CFR 71.73(c)(4).[1] Since physical testing of the ES-3100 shipping container was conducted with no internal heat source or insolation during cool-down,[2] temperature increases due to internal heat loads of 0.4, 20, and 30 W as well as temperature increases due to the application of insolation during cool-down following the HAC fire are calculated. Although earlier revisions of 10 CFR 71 specifically state that insolation does not need to be evaluated before, during, or after HAC, the current version of 10 CFR 71 and associated guidance are unclear regarding the need for consideration following HAC testing. Since the Nuclear Regulatory Commission (NRC) has taken the position that insolation must be considered and evaluated following fire testing, analyses are conducted to determine the effect of insolation following the HAC fire on the ES-3100 shipping container. The predicted temperature increases may be used to adjust physical test data for those loads not included in the physical tests.

FINITE ELEMENT MODEL DESCRIPTION

A two-dimensional axisymmetric finite element model of the ES-3100 shipping container is constructed using MSC.Patran[3] and imported as an orphaned mesh into ABAQUS/CAE[4] for application of boundary conditions, interactions, and loads. The model is constructed of DCAX4 (four-node linear axisymmetric heat transfer quadrilateral) and DCAX3 (3-node linear axisymmetric heat transfer triangular) elements for evaluation for NCT and HAC. The actual contents of the ES-3100 shipping container are not specifically modeled—instead, the content source heat load (if desired) is modeled by applying a uniform heat flux to the inner surfaces of the containment vessel. This is a conservative approach in that package temperatures will not be reduced in a transient analysis by the heat capacity of the contents. A schematic of the finite element model is presented in Figure 1 with details of the upper and lower portions of the model shown in Figure 2 and Figure 3, respectively. The model consists of five materials: stainless steel (drum, liners, and containment vessel), Kaolite, neutron absorber, silicone rubber, and air in the gaps between the drum liner and containment vessel and between the drum liner and top plug. Degree-of-freedom “ties” are made at the interfaces of the different material regions in order to allow the heat to flow through the model. Thermal properties of the materials used in the analysis are presented in Table 1.

Heat is transferred to the model from the contents (i.e., decay heat of the contents) via heat flux boundary conditions applied to the inner surface of the elements representing the containment vessel. Additionally, solar heat fluxes are applied to the model during NCT and HAC post-fire cool-down via heat flux boundary conditions. The heat applied to the model via the boundary conditions is transferred through the model via conduction and thermal radiation. Heat is rejected from the external surfaces of the model via natural convection and thermal radiation boundary conditions.

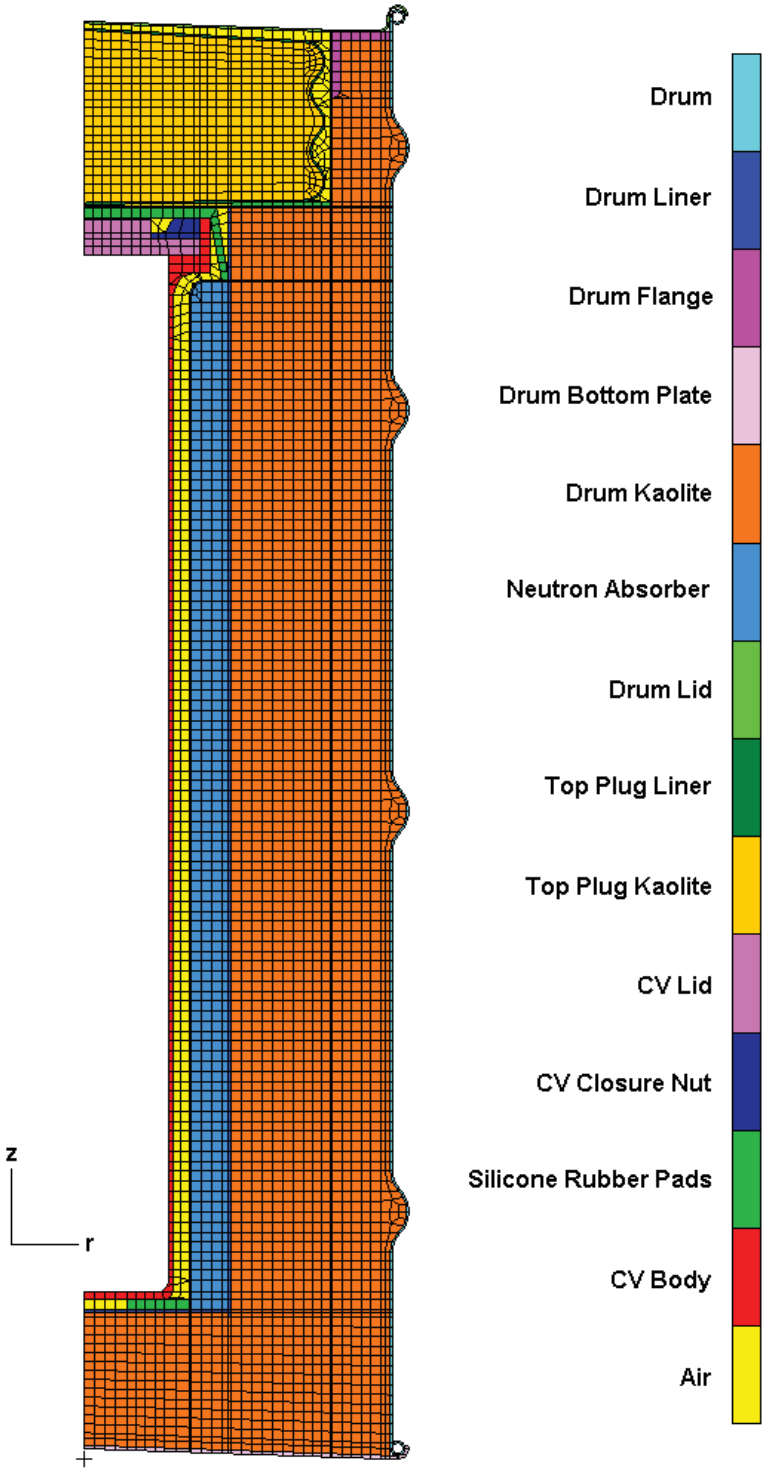

Figure 1. MSC.Patran axisymmetric finite element model of the ES-3100 shipping container.

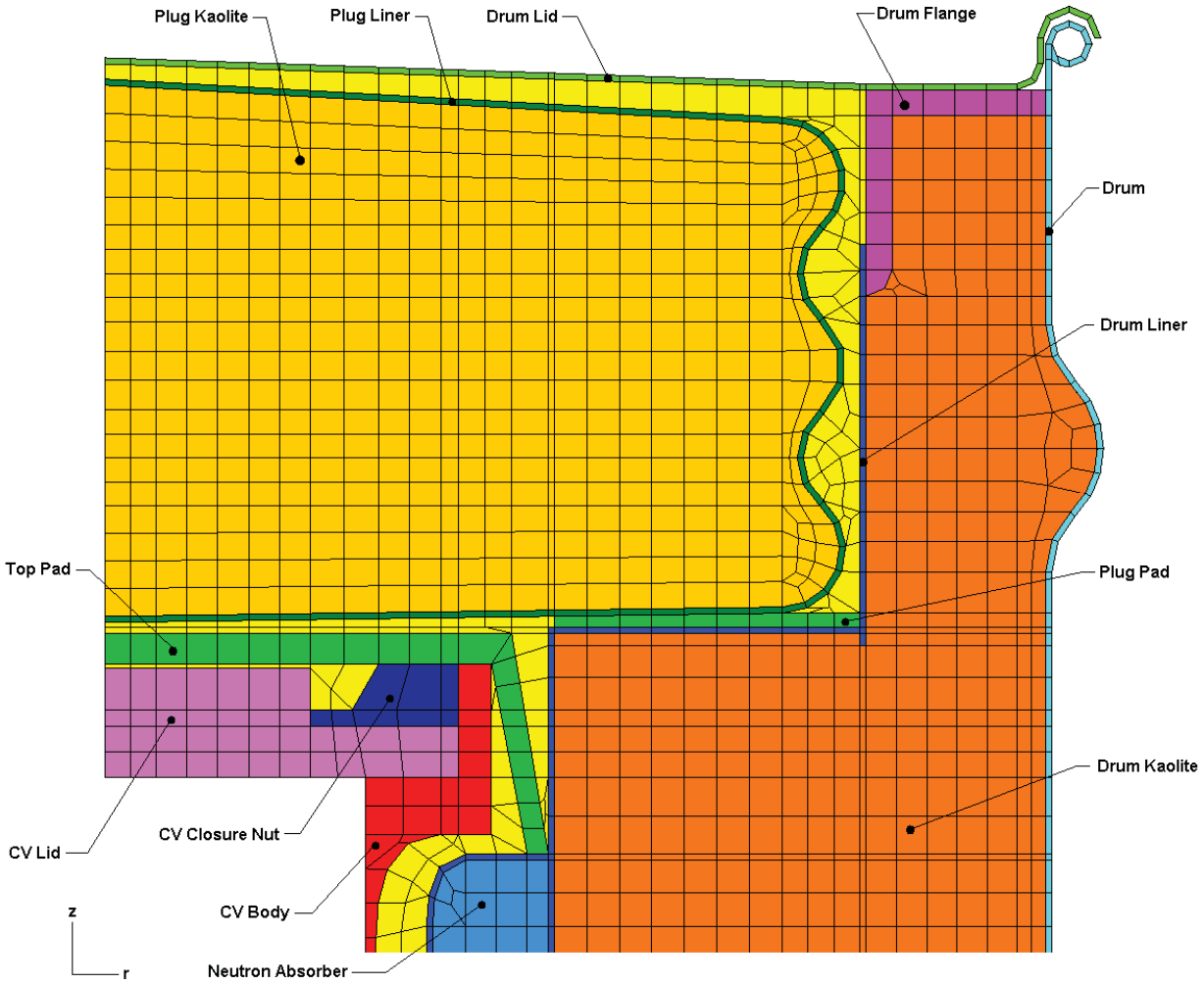

Figure 2. MSC.Patran axisymmetric finite element model of the ES-3100 shipping container (upper portion detail).

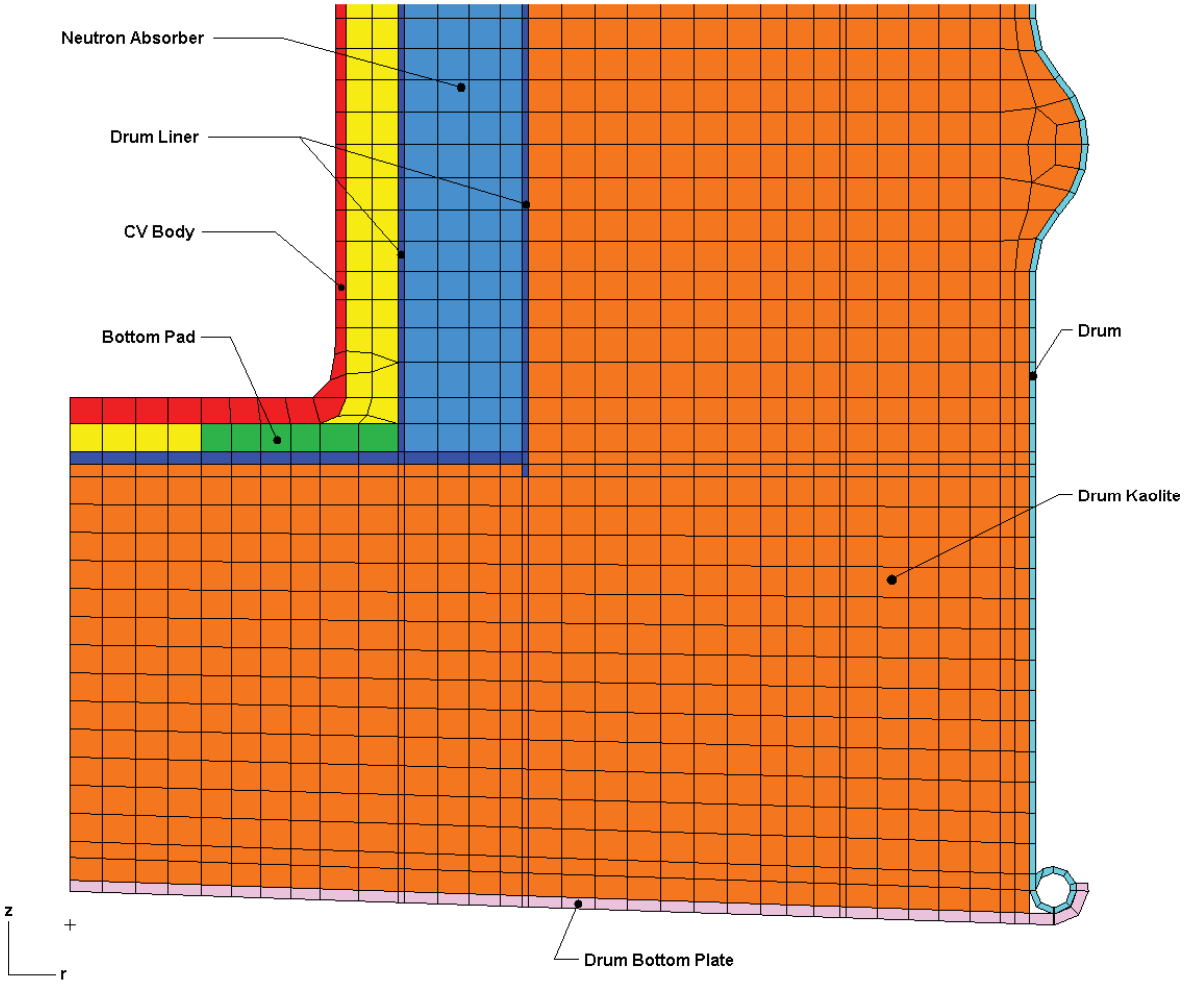

Figure 3. MSC.Patran axisymmetric finite element model of the ES-3100 shipping container (lower portion detail).

Table 1. Thermal properties of the materials used in the thermal analyses.

Material	Temperature (°F)	Thermal Conductivity (Btu/h-in.-°F)	Density (lbm/in.³)	Specific heat (Btu/lbm-°F)	Emissivity
Stainless steel	-279.67	0.443[a]	0.285[a]	0.065[a]	0.22[a]
	-99.67	0.607	–	0.096	–
	260.33	0.799	–	0.123	–
	620.33	0.953	–	0.133	–
	980.33	1.088	–	0.139	–
	1340.33	1.223	–	0.146	–
	1700.33	1.348	–	0.153	–
	2240.33	1.526	–	0.163	–
Kaolite 1600	68	0.0093[b]	0.011[c]	0.2[d]	–
	212	0.0091	–	–	–
	392	0.0081	–	–	–
	572	0.0072	–	–	–
	1112	0.0082	–	–	–
Neutron absorber (Catalog No. 277-4)	-31	0.0457[e]	0.0579[f]	0.125[e]	–
	73.4	0.0485	–	0.186	–
	140	0.0400	–	0.239	–
	212	0.0295	–	0.242	–
	302	0.0305	–	0.291	–
Silicone rubber	–	0.0161[g]	0.047[g]	0.300[g]	1.0[h]
Air	-9.67	1.074×10^{-3}[a]	4.064×10^{-5}[a],[i]	0.240[a]	–
	80.33	1.266×10^{-3}	–	0.241	–
	170.33	1.445×10^{-3}	–	0.241	–
	260.33	1.628×10^{-3}	–	0.242	–
	350.33	1.796×10^{-3}	–	0.244	–
	440.33	1.960×10^{-3}	–	0.246	–
	530.33	2.114×10^{-3}	–	0.248	–
	620.33	2.258×10^{-3}	–	0.251	–
	710.33	2.393×10^{-3}	–	0.254	–
	800.33	2.523×10^{-3}	–	0.257	–
	890.33	2.644×10^{-3}	–	0.260	–
	980.33	2.759×10^{-3}	–	0.263	–
	1070.33	2.870×10^{-3}	–	0.265	–
	1160.33	2.985×10^{-3}	–	0.268	–
	1250.33	3.096×10^{-3}	–	0.270	–
	1340.33	3.212×10^{-3}	–	0.273	–
	1520.33	3.443×10^{-3}	–	0.277	–

Notes:
(a) F. P. Incropera and D. P. DeWitt, *Fundamentals of Heat and Mass Transfer*, 2nd edition, John Wiley & Sons, New York, 1985.
(b) Hsin Wang, *Thermal Conductivity Measurements of Kaolite*, ORNL/TM-2003/49.
(c) Based on a baked density of 19.4 lbm/ft^3 (0.011 lbm/in^3). Specification JS-YMN3-801580-A003 requires a baked density of 22.4 ± 3 lbm/ft^3. Using a lower value for the Kaolite density results in higher temperatures on the containment vessel because the heat capacity of the Kaolite is minimized—allowing more heat to flow to the containment vessel; therefore, the thermal analyses are performed using a low-end density of 19.4 lbm/ft^3. The HAC analyses also consider a high-end density of 30 lbm/ft^3.
(d) FAX communication from J. W. Breuer of Thermal Ceramics, Engineering Department, August 11, 1995.
(e) W. D. Porter and H. Wang, *Thermophyical Properties of Heat Resistant Shielding Material*, ORNL/TM-2004/290, ORNL, Dec. 2004. Specific heat values are presented in MJ/m^3-K in ORNL/TM-2004/290—converted to mass-based units using a density of 105 lbm/ft^3.
(f) Based on a cured density of density of 100 lbm/ft^3 (0.0579 lbm/in^3). B. F. Smith and G. A. Byington, *Mechanical Properties of 277-4*, Y/DW-1987, January 19, 2005presents a range of measured densities between approximately 100 and 110 lbm/ft^3 for Catalog No. 277-4. Therefore, in order to minimize the heat capacity of the material and allow more heat to be transferred to the containment vessel, the lower-bound value is used. The HAC analyses also consider a high-end density of 110 lbm/ft^3.
(g) THERM 1.2, thermal properties database by R. A. Bailey.
(h) Conservatively modeled as 1.0.
(i) Constant density value evaluated at 100°F.

MODELED HEAT TRANSFER MECHANISMS

The heat transfer mechanisms included in the thermal model such, as thermal radiation, natural convection, and insolation (solar heat flux) are described in detail in the following sections.

Heat Transfer Between Package Exterior and Ambient

The heat transfer between the exterior of the package and the ambient (or fire) is modeled as a combination of radiant heat transfer and natural convection. The heat transfer due to radiant exchange with the environment is calculated as:[5]

$$q''_{rad} = \sigma F_e \left(T_s^{\,4} - T_a^{\,4}\right), \tag{1}$$

where σ = Stefan-Boltzmann constant,
F_e = overall exchange factor,
T_s = container outer surface temperature (absolute), and
T_a = ambient or fire temperature (absolute).

The overall interchange factor is calculated as:[5]

$$F_e = \left[\frac{1}{\dfrac{1}{\varepsilon_p} + \dfrac{A_p}{A_s}\left(\dfrac{1}{\varepsilon_s} - 1\right)}\right], \tag{2}$$

where ε_p = emissivity of package surface,
A_p = surface area of the package,
A_s = surface area of the surroundings, and
ε_s = emissivity of surroundings.

For NCT and the cool-down period following the HAC fire, the area of the surroundings is assumed to be much larger than the surface area of the package; therefore, Eq. 2 reduces to:

$$F_e \approx \varepsilon_p \,. \tag{3}$$

An emissivity value of 0.22,[6] which is typical of clean stainless steel, is assumed for the outer surfaces of the drum during NCT and during the cool-down period following the HAC fire. In reality, the outer surfaces of the drum will have a much higher emissivity following the HAC fire; therefore, this assumption is conservative.

During the HAC fire, the area of the surroundings is assumed to be approximately equal to the surface area of the drum; therefore, Eq. 2 reduces to:

$$F_e = \left[\frac{1}{\dfrac{1}{\varepsilon_p} + \dfrac{1}{\varepsilon_s} - 1}\right]. \tag{4}$$

During the HAC 30-minute fire, an emissivity of 0.8 is assumed for the drum, and an emissivity of 0.9 is assumed for the fire per the guidance of 10 CFR 71.74(c)(4).[1] This results in an overall exchange factor of 0.7347 during the HAC fire using Eq. 4.

The natural convection heat transfer from the package surface to the ambient air is calculated as:

$$q''_{convection} = h\left(T_s - T_a\right). \tag{5}$$

where h = natural convection heat transfer coefficient,
T_s = container outer surface temperature, and
T_a = ambient or fire temperature.

During the NCT transient thermal analyses and the steady-state thermal analyses (used to obtain the starting temperature distribution in the package for NCT and HAC when a content heat load is present), the shipping container is assumed to be in an upright (vertical) orientation. The top of the drum is modeled as a heated horizontal flat plate facing up using the following correlation:[6]

$$h = \left(\frac{k}{L}\right) C_1 \, Ra^{C_2}, \tag{6}$$

where k = thermal conductivity of air,
L = characteristic length (= D/4 per Ref. 6),
D = diameter of the package,
Ra = Rayleigh number,
C_1 = constant (see Table 2), and
C_2 = constant (see Table 2).

The Rayleigh number in Eq. 6 is defined as:

$$Ra = \frac{g \beta \Delta T L^3}{\nu \alpha}, \tag{7}$$

where g = acceleration of gravity,
β = coefficient of thermal expansion,
ΔT = temperature difference,
ν = kinematic viscosity [μ/ρ],
μ = absolute viscosity,
α = thermal diffusivity [$k/(\rho C_p)$],
ρ = density of air, and
C_p = specific heat of air.

The properties of air used in the natural convection calculations are presented in Table 3.

Table 2. Coefficients for natural convection correlations.

Coefficient	Rayleigh Number Range	Value
C_1	$10^4 < Ra < 10^7$ $10^7 < Ra < 10^{11}$	0.54 0.15
C_2	$10^4 < Ra < 10^7$ $10^7 < Ra < 10^{11}$	0.25 1/3
C_3	$Ra < 10^9$ $Ra > 10^9$	0.680 0.825
C_4	$Ra < 10^9$ $Ra > 10^9$	0.670 0.387
C_5	$Ra < 10^9$ $Ra > 10^9$	0.25 1/6
C_6	$Ra < 10^9$ $Ra > 10^9$	4/9 8/27
C_7	$Ra < 10^9$ $Ra > 10^9$	1 2

Source: F. P. Incropera and D. P. DeWitt, *Fundamentals of Heat and Mass Transfer*, 2nd ed., John Wiley & Sons, New York, 1985.

Table 3. Properties of air used in natural convection calculations.

Temperature (°F)	Thermal Conductivity (Btu/h-in.-°F)	Density (lbm/in.^{3})	Specific Heat (Btu/lbm-°F)	Kinematic Viscosity (in.^{2}/h)	Thermal Diffusivity (in.^{2}/h)	Prandtl Number
-9.67	1.074×10^{-3}	5.039×10^{-5}	0.240	6.384×10^{1}	8.872×10^{1}	0.720
80.33	1.266×10^{-3}	4.196×10^{-5}	0.241	8.867×10^{1}	1.255×10^{2}	0.707
170.33	1.445×10^{-3}	3.595×10^{-5}	0.241	1.167×10^{2}	1.668×10^{2}	0.700
260.33	1.628×10^{-3}	3.147×10^{-5}	0.242	1.474×10^{2}	2.137×10^{2}	0.690
350.33	1.796×10^{-3}	2.796×10^{-5}	0.244	1.807×10^{2}	2.634×10^{2}	0.686
440.33	1.960×10^{-3}	2.516×10^{-5}	0.246	2.164×10^{2}	3.164×10^{2}	0.684
530.33	2.114×10^{-3}	2.286×10^{-5}	0.248	2.543×10^{2}	3.722×10^{2}	0.683
620.33	2.258×10^{-3}	2.097×10^{-5}	0.251	2.940×10^{2}	4.291×10^{2}	0.685
710.33	2.393×10^{-3}	1.935×10^{-5}	0.254	3.360×10^{2}	4.871×10^{2}	0.690
800.33	2.523×10^{-3}	1.797×10^{-5}	0.257	3.800×10^{2}	5.468×10^{2}	0.695
890.33	2.644×10^{-3}	1.677×10^{-5}	0.260	4.261×10^{2}	6.082×10^{2}	0.702
980.33	2.759×10^{-3}	1.573×10^{-5}	0.263	4.739×10^{2}	6.696×10^{2}	0.709
1070.33	2.870×10^{-3}	1.480×10^{-5}	0.265	5.234×10^{2}	7.310×10^{2}	0.716
1160.33	2.985×10^{-3}	1.397×10^{-5}	0.268	5.742×10^{2}	7.979×10^{2}	0.720
1250.33	3.096×10^{-3}	1.324×10^{-5}	0.270	6.261×10^{2}	8.649×10^{2}	0.723
1340.33	3.212×10^{-3}	1.258×10^{-5}	0.273	6.802×10^{2}	9.374×10^{2}	0.726
1520.33	3.443×10^{-3}	1.144×10^{-5}	0.277	7.912×10^{2}	1.088×10^{3}	0.728

Source: F. P. Incropera and D. P. DeWitt, *Fundamentals of Heat and Mass Transfer*, 2nd ed., John Wiley & Sons, New York, 1985.

During the NCT transient thermal analyses and the steady-state thermal analyses, the sides of the drum are modeled as a vertical flat plate using the following correlation:[6]

$$h = \left(\frac{k}{L}\right)\left[C_3 + \frac{C_4\,Ra^{C_5}}{\left(1+\left[\frac{0.492}{Pr}\right]^{9/16}\right)^{C_6}}\right]^{C_7}, \tag{8}$$

where L = characteristic length = the drum height,
C_3 = constant (see Table 2),
C_4 = constant (see Table 2),
C_5 = constant (see Table 2),
C_6 = constant (see Table 2),
C_7 = constant (see Table 2), and
Pr = Prandtl number.

The bottom of the drum is conservatively modeled as adiabatic during the NCT transient analyses and the steady-state analyses.

During the HAC 30-minute fire and the post-fire cool-down, the shipping container is assumed to be in a horizontal orientation (as it is during furnace testing). As such, the top and bottom of the drum are modeled as vertical flat plates using Eq. 8 having a characteristic length, L, equivalent to the drum diameter, and the sides of the drum are modeled as a horizontal cylinder using the following correlation ($10^{-5} < Ra < 10^{12}$):[6]

$$h = \left(\frac{k}{D}\right)\left[0.60 + \frac{0.387\,Ra^{1/6}}{\left(1+\left[\frac{0.559}{Pr}\right]^{9/16}\right)^{8/27}}\right]^{2}, \tag{9}$$

where D = diameter of the package,

The calculated natural convection film coefficients used in the thermal analyses of the ES-3100 are presented graphically in Figure 4 and Figure 5 for NCT and HAC, respectively.

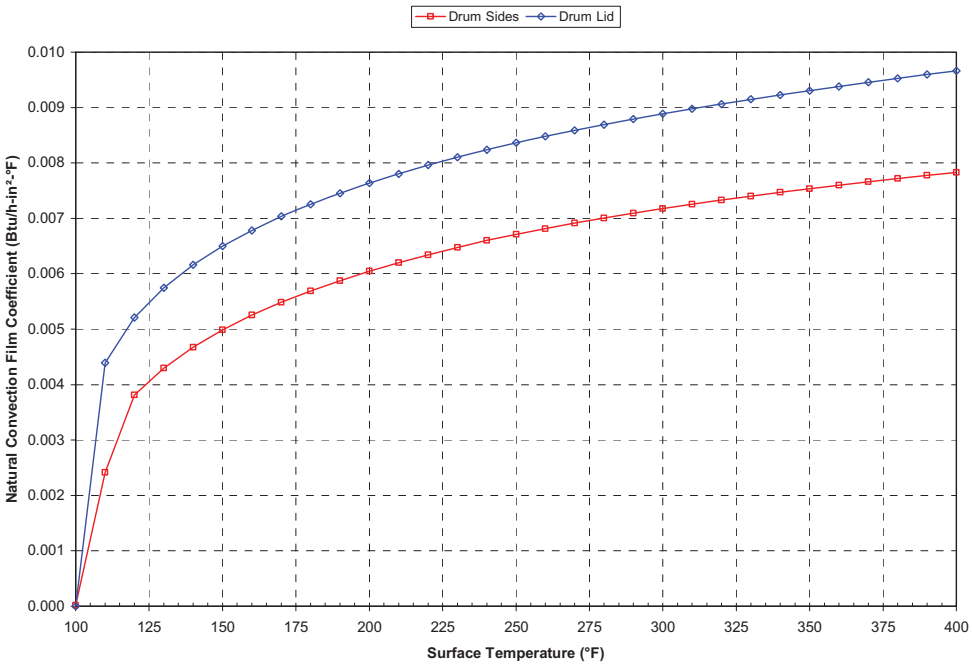

Figure 4. Natural convection film coefficients applied to the drum surfaces during NCT and steady-state conditions.

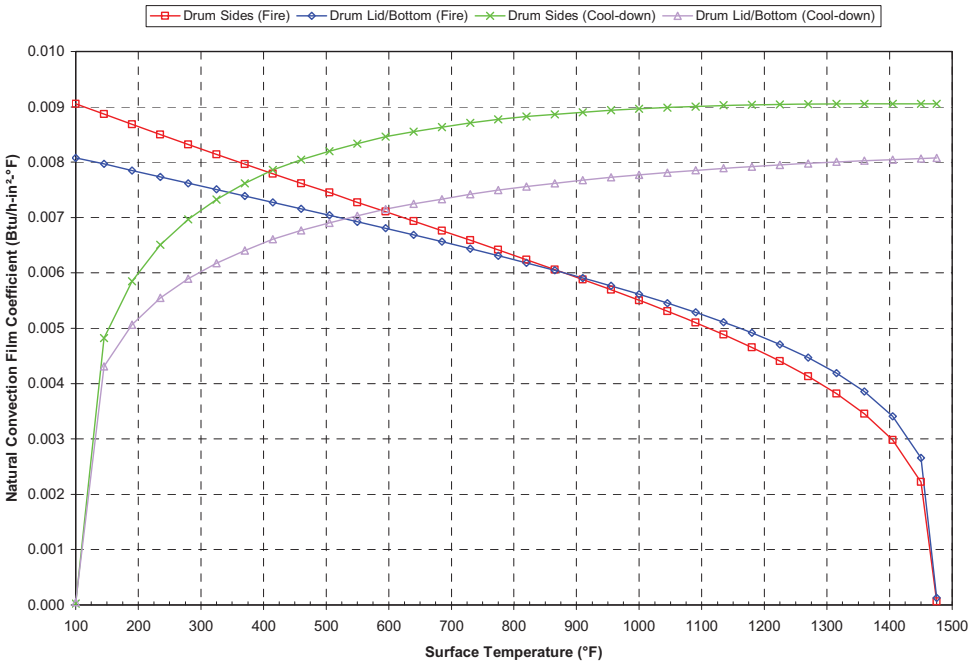

Figure 5. Natural convection film coefficients applied to the drum surfaces during HAC.

Insolation

The following insolation (incident solar radiation) data is required for NCT per 10 CFR 71.71(c)(1):[1]

Form and location of surface	Total insolation for a 12-hour period (cal/cm²)
Flat surfaces transported horizontally Base Other surfaces	 None 800
Flat surfaces not transported horizontally	200
Curved surfaces	400

The total insolation values specified in the previous table are for a 12-hour period. For analytical purposes, these values are "time-averaged" over the entire 12-hour period (i.e., divided by 12). Therefore, the incident solar heat fluxes ($q''_{solar,i}$) used in the analyses for NCT and cool-down following the HAC fire are as follows:

During NCT, the drum is in an upright (vertical) orientation; therefore, the following heat fluxes are applied to the external surfaces of the drum to represent insolation:

Top $$q''_{solar,i} = 1.7074\ \text{Btu/h-in.}^2, \tag{10}$$

Sides $$q''_{solar,i} = 0.8537\ \text{Btu/h-in.}^2, \tag{11}$$

Bottom $$q''_{solar,i} = 0. \tag{12}$$

During the cool-down period following the HAC 30-minute fire, the drum is assumed to be in a horizontal orientation; therefore, the following heat fluxes are applied to the external surfaces of the drum to represent insolation:

Top $$q''_{solar,i} = 0.4269\ \text{Btu/h-in.}^2, \tag{13}$$

Sides $$q''_{solar,i} = 0.8537\ \text{Btu/h-in.}^2, \tag{14}$$

Bottom $$q''_{solar,i} = 0.4269\ \text{Btu/h-in.}^2. \tag{15}$$

The insolation is applied as a square-wave function (i.e., alternating on and off in 12-hour periods) in the thermal analysis. The heat flux values presented in Eqs. 10–15 represent the insolation absorbed by the package surface since a drum absorptivity of 1.0 was conservatively assumed. An analytical study has been performed on a similar shipping package that investigated three methods of applying the insolation.[7] The three methods consisted of 1) performing a steady-state analysis assuming the insolation is applied continuously by distributing the heat flux evenly throughout a 24-hour period, 2) performing a transient analysis assuming the insolation is represented by a step function (i.e., applied and then not applied in 12-hour cycles, and 3) performing a transient analysis where the incident insolation is represented by a sinusoidal function that varies throughout the day. The results of the study indicate that the method used in applying the insolation has a significant effect on the temperatures of the outermost portions of the package. However, since the total insolation over any 24-hour period is the same for all cases, internal package temperatures are relatively unaffected by the way in which the insolation is applied. Since the containment vessel O-ring temperatures are of primary concern in this evaluation, the step function method for applying the insolation is suitable.

Heat Transfer Across Gaps in the Package

Heat transfer across all gaps in the package is modeled by a combination of radiant exchange and conduction. Natural convection heat transfer is not included across the gaps in the model. Scoping studies performed for a similar shipping package indicate that the heat transfer due to natural convection in relatively small gaps is approximately a factor of 6 times less than the heat transfer due to radiant exchange.[7] These calculations assumed a temperature difference of 9°F across the gap. Based on these previous calculations, the effect of neglecting the natural convection in the gap regions is minimal. The emissivity values used in the analysis for all internal radiating surfaces in the model are presented in Table 1.

Radiant exchange across gaps is modeled using the cavity radiation feature of ABAQUS/Standard.[8] For each cavity (or enclosure), radiation surfaces are defined as shown in Figure 6 and Figure 7.

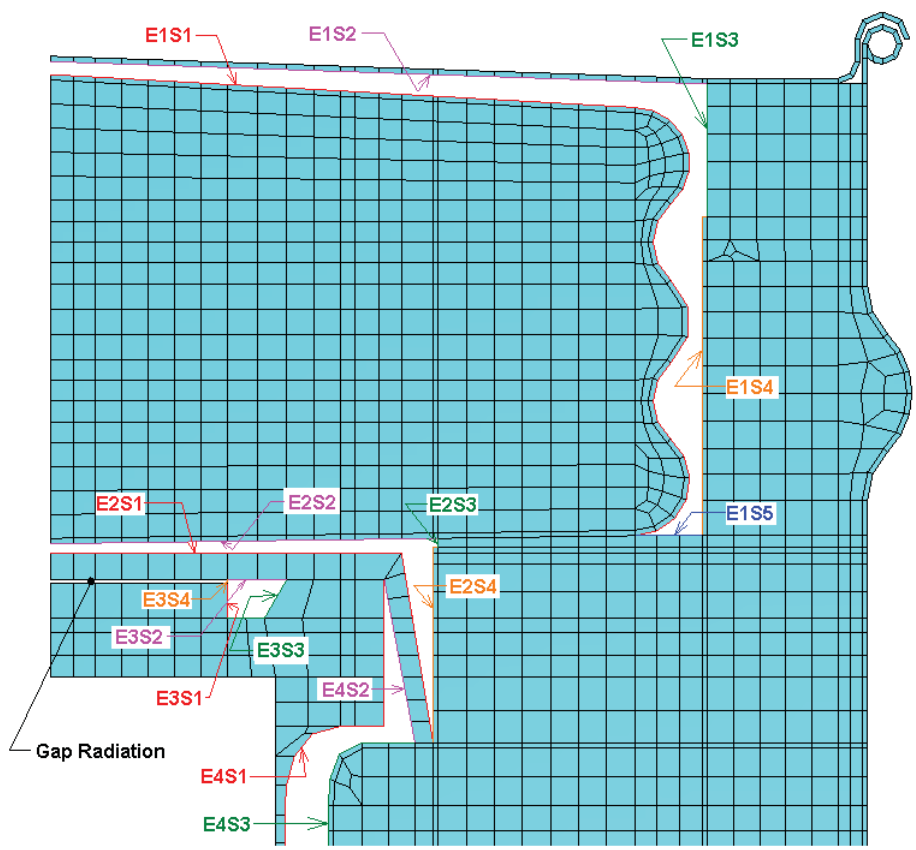

Figure 6. Radiation cavity surface definitions (top portion of the model).

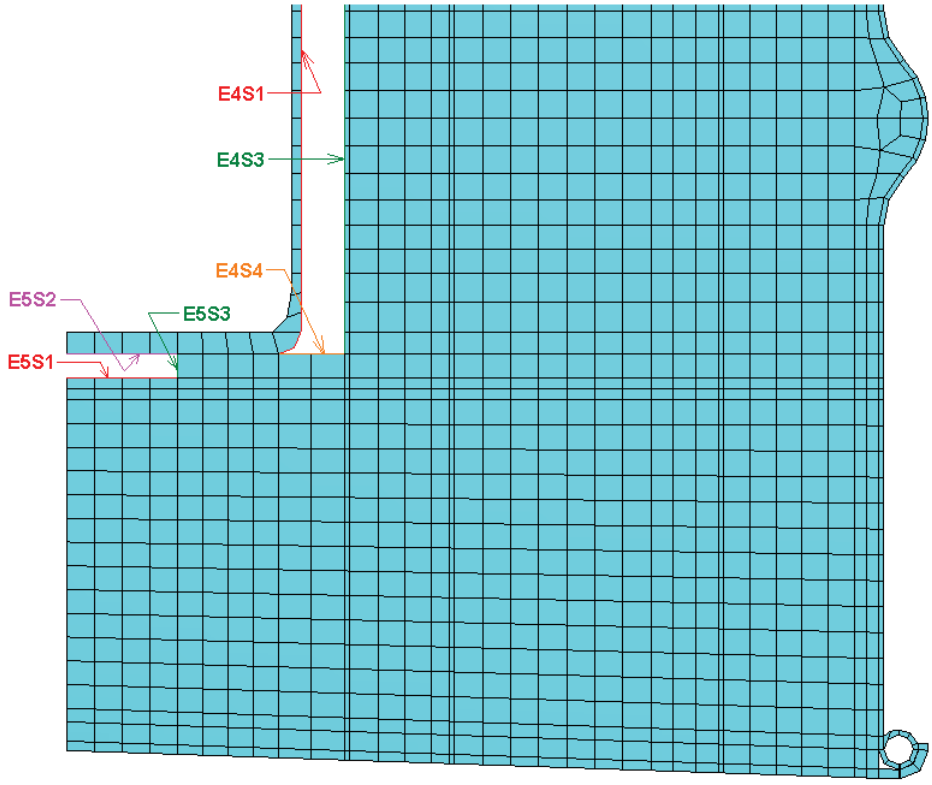

Figure 7. Radiation cavity surface definitions (bottom portion of the model).

As shown in Figure 6 and Figure 7, the various gaps in the model are divided into five separate cavities (designated 'E1' through 'E5' in the figures) with between three and five surfaces (designated 'S1' through 'S5' in the figures) in each cavity for radiation calculations. Because the gap between the CV lid and top pad is small in relation to its characteristic length, radiation exchange is modeled using the gap radiation feature in ABAQUS/Standard with a view factor of 1.0 assigned. As a result, a shell element (type DSAX1) is defined in the model with the radiation surface E3S4 (see Figure 6) superimposed to close off cavity 3. The DSAX1 element is assigned the properties of air, and surface E3S4 is assigned a small emissivity value of 0.01 since it is an imaginary surface used to close the cavity.

Content Heat Load

In order to simulate the decay heat generated by the ES-3100 shipping container contents, a uniform heat flux is applied to the element edges representing the inner surface of the containment vessel in the model. Content heat loads of 0, 0.4, 20, and 30 W are investigated in this report. The uniform heat flux (q''_{source}) for a given content heat load is calculated using the following equation:

$$q''_{source} = \frac{Q \times 3.4123}{2\left(\frac{\pi D_i^2}{4}\right) + \pi(D_i)(H)}, \tag{16}$$

where, Q = content heat load (W),
D_i = inside diameter of the containment vessel (5.06 in.),
H = height of the containment vessel cavity (31.00 in.).

Using Eq. 16, a content heat load of 0.4 W results in a uniform heat flux of 2.5608×10^{-3} Btu/h-in.^{2}, a content heat load of 20 W results in a uniform heat flux of 0.12804 Btu/h-in.^{2}, and a content heat load of 30 W results in a uniform heat flux of 0.19206 Btu/h-in.^{2}.

DISCUSSION OF ANALYTICAL RESULTS

All thermal analyses discussed in this report were performed using ABAQUS/Standard[8] on an Intel Pentium 4–based Microsoft Windows 2000 computer. Temperatures are monitored at selected locations in the model as shown in Figure 8 through Figure 11.

Steady-state Conditions Analyses Results

Steady-state thermal analyses are performed on the finite element model of the ES-3100 shipping container for three cases having content heat loads of 0.4, 20, and 30 W. The temperature distribution results from these analyses are used as the starting temperature distributions within the model when performing the transient thermal analyses for NCT and the HAC 30-minute fire. The boundary conditions for these steady-state analyses include a combination of thermal radiation exchange and natural convection applied to the top and sides of the drum using an ambient temperature of 100°F. The bottom of the drum is modeled as an adiabatic surface (i.e., no heat transfer). Additionally, the content heat load is simulated by applying a uniform heat flux to the surfaces of the elements representing the inner surface of the containment vessel. The calculated steady-state temperature distribution within the model of the ES-3100 shipping container for content heat loads of 0.4, 20, and 30 W is presented in Table 4.

As presented in Table 4, the maximum accessible surface temperature of the package when exposed to an ambient temperature of 100°F in the shade is 100.43°F (38.02°C), 114.39°F (45.77°C), and 120.08°F (48.93°C) for content heat loads of 0.4, 20, and 30 W, respectively.

Normal Conditions of Transport Analyses Results

Transient thermal analyses are performed on the finite element model of the ES-3100 shipping container to simulate NCT with content heat loads of 0, 0.4, 20, and 30 W. The insolation required for NCT per 10 CFR 71.71(c)(1)[1] is applied to the top and sides of the drum in alternating 12-hour periods (i.e., 12 hours on and 12 hours off) with the drum bottom remaining adiabatic during the transient thermal analysis. An ambient temperature of 100°F as stipulated in 10 CFR 71 is used in the NCT analysis. The initial temperature distribution within the package for the NCT transients was determined from steady-state analyses (with radiation and natural convection boundary conditions applied to the top and sides of the drum) for each internal heat load. For the case with no internal heat source (0 W), the initial temperature distribution within the package was assumed to be at a uniform 100°F. As with the steady-state analyses discussed previously, applying a uniform heat flux to the internal surfaces of the elements representing the containment vessel simulates the content heat load.

The transient thermal analyses simulate a five-day period of cyclic solar loading with 12 hours of insolation being applied at the beginning of each day (i.e., sunrise) followed by 12 hours in which there is no insolation to end the day (i.e., sunset). This five-day period allows for “quasi steady-state” conditions

to be reached. While the temperature of a particular node within the model changes with respect to time in the transient analyses, the maximum temperature that node reaches from day-to-day does not change once a "quasi steady-state" condition is reached. In particular, the maximum temperature of the key location on the containment vessel (i.e., at the O-ring) on day 5 is within 0.004°F of the maximum temperature of the same location on day 4.

The maximum temperatures of several locations within the model are summarized in Table 5 for content heat loads of 0, 0.4, 20, and 30 W. The maximum temperatures reported in Table 5 represent "quasi steady-state" conditions. Temperature-history plots of several locations within the model are also depicted graphically in Figure 12 through Figure 15 for various content heat loads. Additionally, temperature contours of the model at sunrise (0 hours), sunset (12 hours), and 68 to 70 minutes after sunset for a typical day (after the package temperatures reach "quasi steady-state") of the transient are presented in Figure 16 through Figure 19 for various content heat loads. The temperature contours at 68 to 70 minutes after sunset are presented because the temperature of the CV flange (i.e., O-ring location) peaks at this time. The elements representing the air between the drum liner and containment vessel and between the drum liner and top plug liner are not shown in the temperature contours presented in these figures so that the containment vessel temperature contours can be more easily viewed.

The maximum temperature in the model occurs at the top center of the drum lid in most instances. The drum lid maximum temperature is 243.86°F (117.70°C), 243.89°F (117.72°C), 245.32°F (118.51°C), and 246.03°F (118.91°C) for content heat loads of 0, 0.4, 20, and 30 W, respectively, and occurs at sunset in each case (see Table 5). For the case with a content heat load of 30 W, the maximum temperature in the model occurs in the sidewall of the CV approximately 80 minutes after sunset and is 252.87°F (122.71°C). The maximum temperature at the containment vessel O-ring is 189.28°F (87.38°C), 189.90°F (87.72°C), 217.07°F (102.82°C), and 230.51°F (110.28°C) for content heat loads of 0, 0.4, 20, and 30 W, respectively, and occurs at approximately 68 to 70 minutes after sunset in each case (see Table 5).

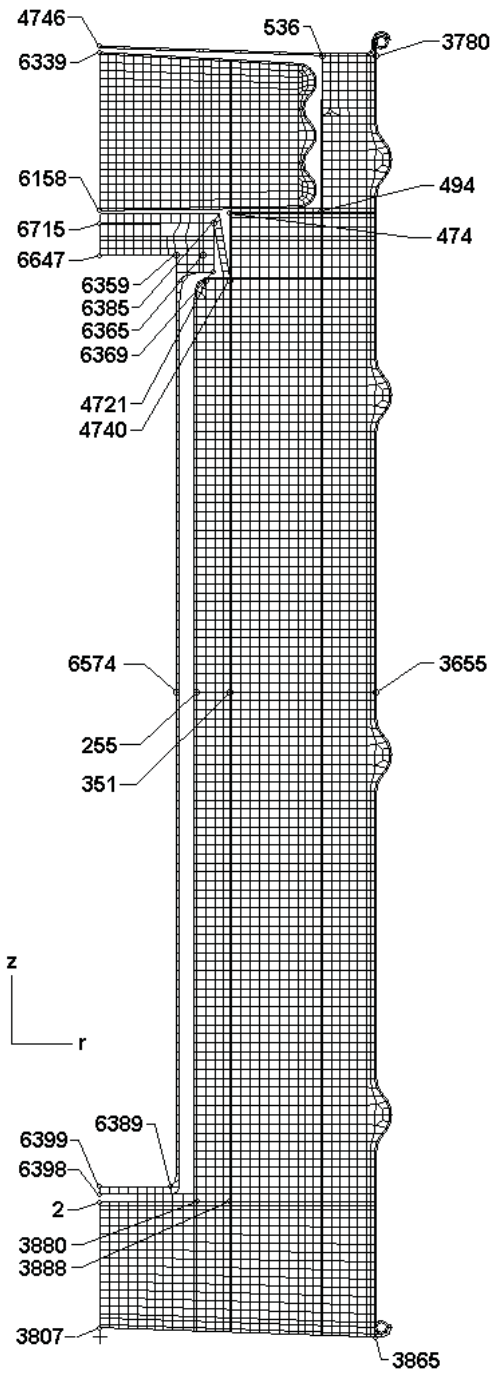

Node	r (in.)	z (in.)
2	0.000	4.505
255	3.180	21.528
351	4.300	21.528
474	4.300	37.535
494	7.325	37.535
536	7.385	42.755
3655	9.185	21.528
3780	9.185	42.755
3807	0.000	0.320
3865	9.185	0.008
3880	3.178	4.505
3888	4.300	4.505
4721	3.500	35.275
4740	4.300	35.275
4746	0.000	43.065
6158	0.000	37.579
6339	0.000	42.859
6359	2.530	36.075
6365	3.425	36.075
6369	3.750	35.525
6385	3.750	37.175
6389	2.310	5.025
6398	0.000	4.775
6399	0.000	5.025
6574	2.530	21.528
6647	0.000	36.075
6715	0.000	37.135

Figure 8. ABAQUS axisymmetric finite element model of the ES-3100 shipping container—nodal locations of interest defined in Table 3.4a (elements representing air not shown for clarity).

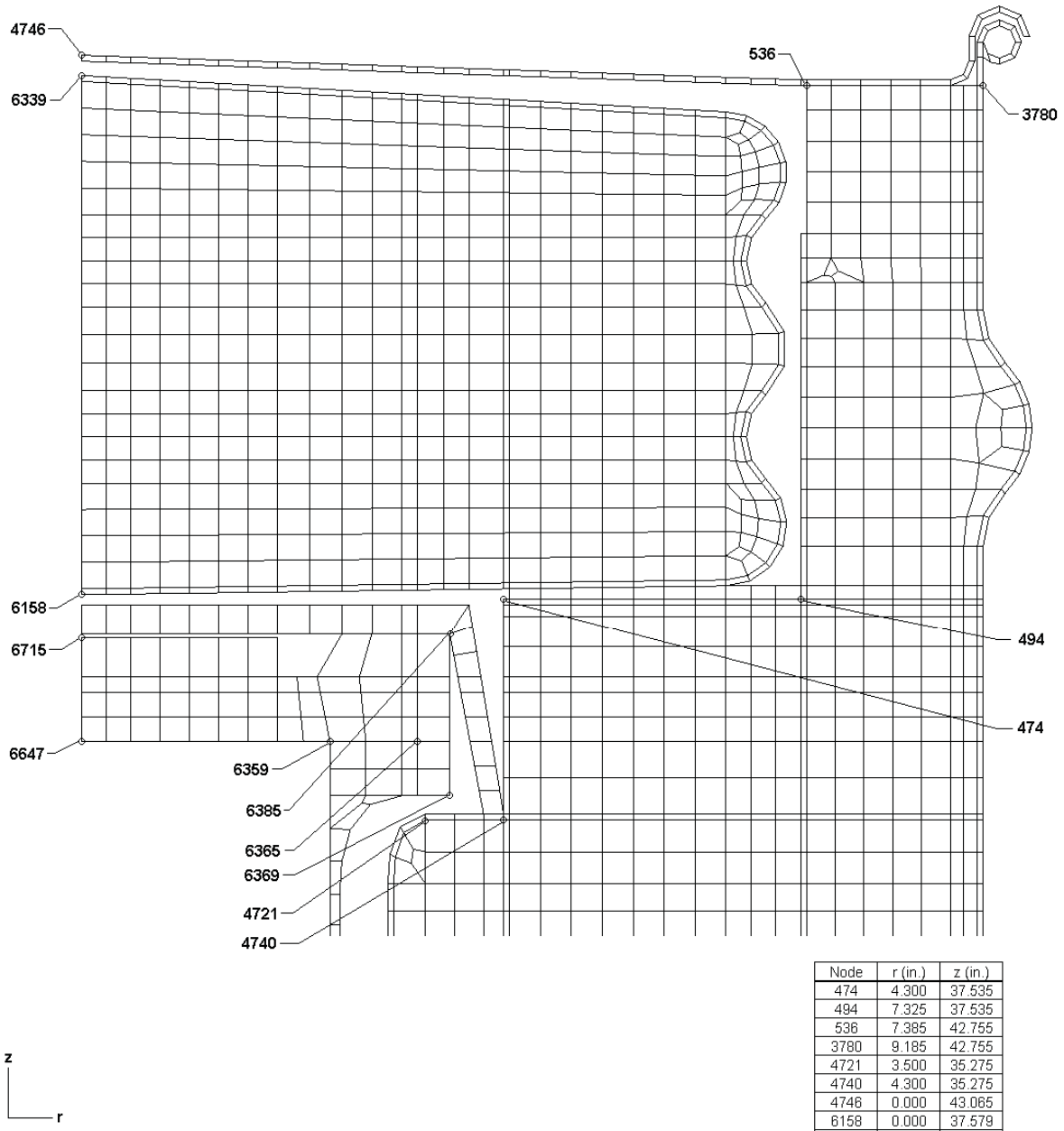

Node	r (in.)	z (in.)
474	4.300	37.535
494	7.325	37.535
536	7.385	42.755
3780	9.185	42.755
4721	3.500	35.275
4740	4.300	35.275
4746	0.000	43.065
6158	0.000	37.579
6339	0.000	42.859
6359	2.530	36.075
6365	3.425	36.075
6369	3.750	35.525
6385	3.750	37.175
6647	0.000	36.075
6715	0.000	37.135

Figure 9. ABAQUS axisymmetric finite element model of the ES-3100 shipping container—nodal locations of interest (elements representing air not shown for clarity), upper portion detail.

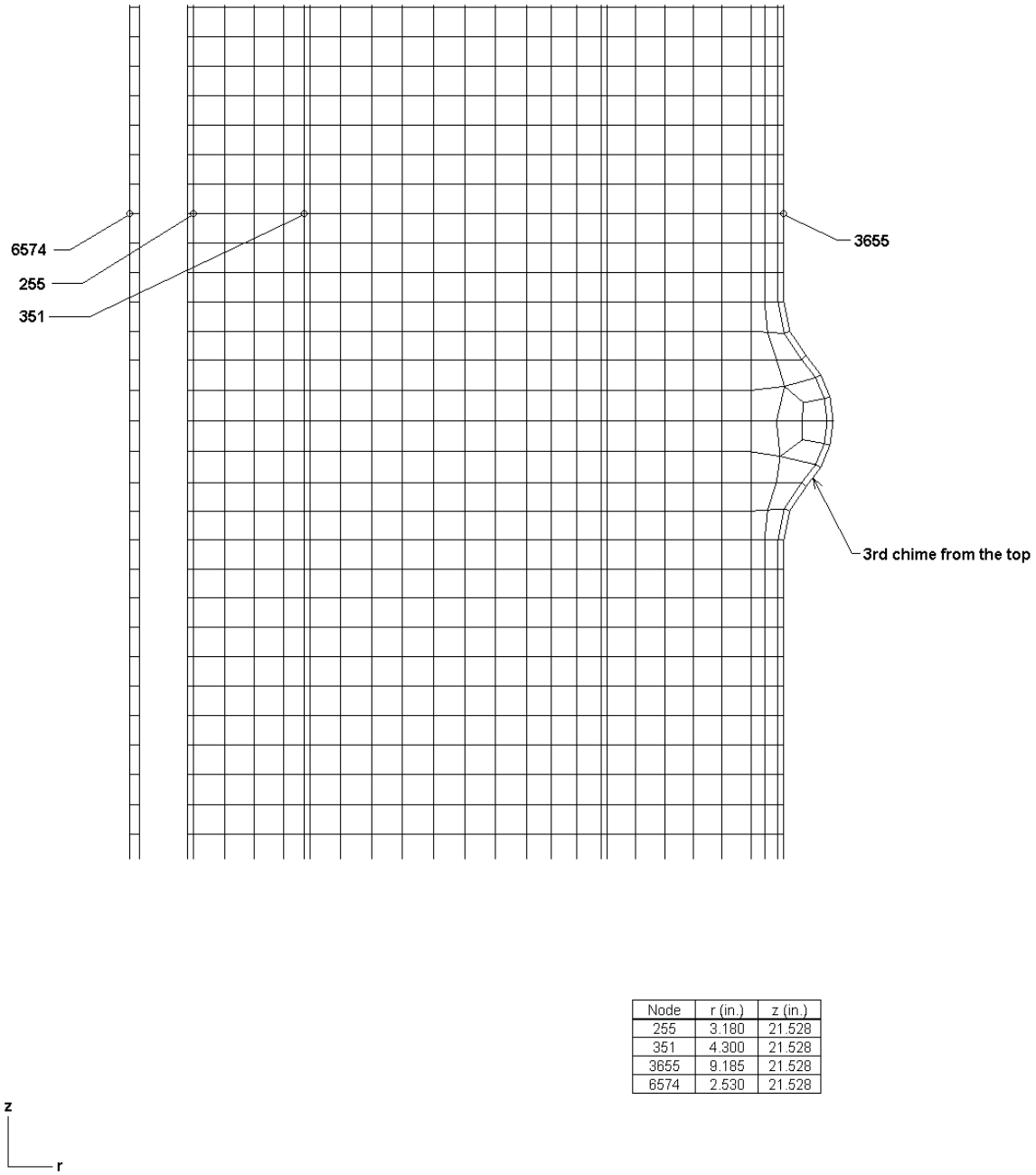

Node	r (in.)	z (in.)
255	3.180	21.528
351	4.300	21.528
3655	9.185	21.528
6574	2.530	21.528

Figure 10. ABAQUS axisymmetric finite element model of the ES-3100 shipping container—nodal locations of interest (elements representing air not shown for clarity), middle portion detail.

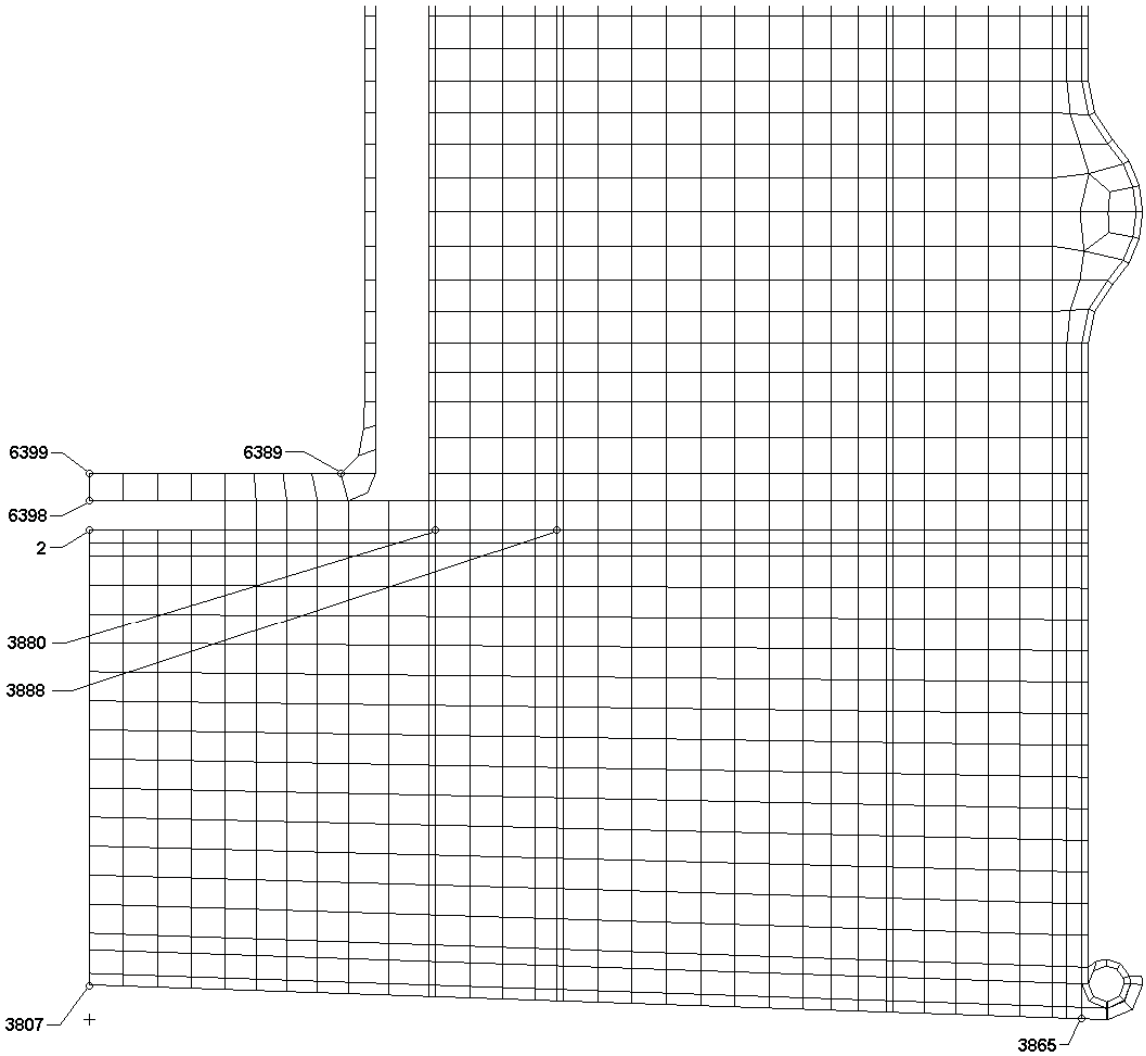

Node	r (in.)	z (in.)
2	0.000	4.505
3807	0.000	0.320
3865	9.185	0.008
3880	3.178	4.505
3888	4.300	4.505
6389	2.310	5.025
6398	0.000	4.775
6399	0.000	5.025

Figure 11. ABAQUS axisymmetric finite element model of the ES-3100 shipping container—nodal locations of interest (elements representing air not shown for clarity), lower portion detail.

Table 4. ES-3100 shipping container steady-state temperatures (100°F ambient temperature, no insolation).

Node map [a]	Node coordinates (in.)			Maximum steady-state temperature (°F)		
	No.	r	z	0.4 W	20 W	30 W
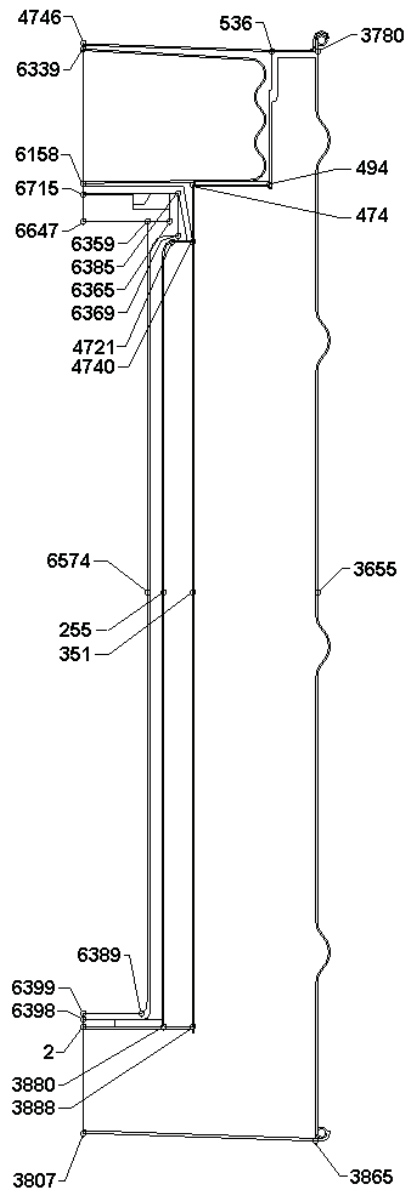	2	0.000	4.505	100.83	134.54	150.15
	255	3.180	21.528	100.75	131.57	146.21
	351	4.300	21.528	100.71	129.45	142.87
	474	4.300	37.535	100.46	117.90	125.67
	494	7.325	37.535	100.32	110.87	115.19
	536	7.385	42.755	100.21	105.50	107.19
	3655 [b]	9.185	21.528	100.28	107.58	109.92
	3780 [b]	9.185	42.755	100.21	105.29	106.89
	3807 [b]	0.000	0.320	100.43	114.39	120.08
	3865 [b]	9.185	0.008	100.32	108.97	111.97
	3880	3.178	4.505	100.74	130.48	144.23
	3888	4.300	4.505	100.71	128.60	141.42
	4721	3.500	35.275	100.59	124.08	134.90
	4740	4.300	35.275	100.57	122.92	133.15
	4746 [b]	0.000	43.065	100.20	104.99	106.43
	6158	0.000	37.579	100.57	123.14	133.42
	6339	0.000	42.859	100.25	107.42	110.04
	6359 [c]	2.530	36.075	100.80	133.51	148.56
	6365 [c]	3.425	36.075	100.79	133.33	148.28
	6369	3.750	35.525	100.79	133.27	148.20
	6385	3.750	37.175	100.78	132.85	147.58
	6389	2.310	5.025	100.97	141.27	160.06
	6398	0.000	4.775	100.96	140.91	159.55
	6399	0.000	5.025	100.96	140.94	159.60
	6574	2.530	21.528	101.33	157.70	183.56
	6647	0.000	36.075	100.80	133.56	148.63
	6715	0.000	37.135	100.79	133.40	148.40

Notes: (a) See Table 3.4a and Figs. 8–11 for details of node locations.
(b) These are nodes at the accessible surfaces of the package (i.e., the drum, drum lid, and drum bottom plate).
(c) Approximate location of the CV O-ring.

Table 5. ES-3100 shipping container maximum "quasi steady-state" temperatures during NCT with various content heat loads.

Node map [a]	Node coordinates (in.)			Maximum "quasi steady-state" temperature (°F)			
	No.	r	z	0 W	0.4 W	20 W	30 W
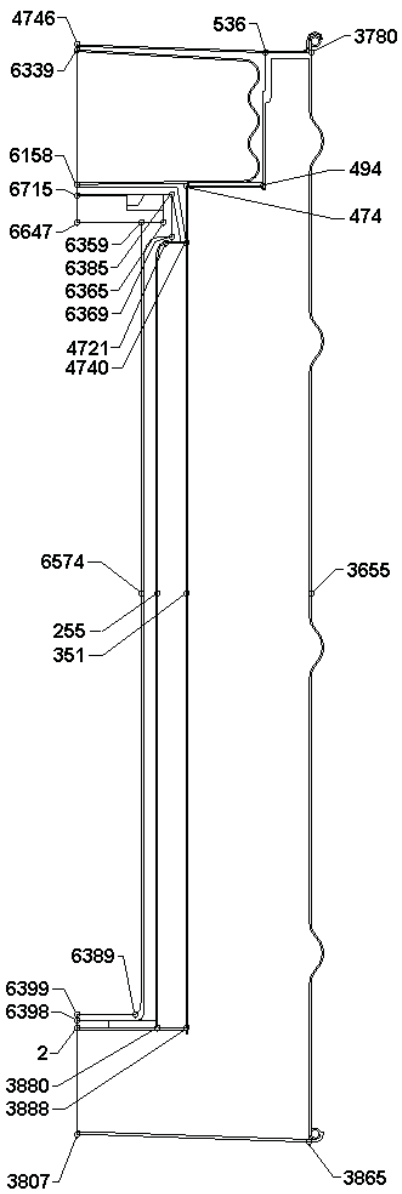	2	0.000	4.505	180.59	181.23	210.15	224.69
	255	3.180	21.528	179.33	179.93	207.32	221.43
	351	4.300	21.528	179.59	180.14	204.73	217.27
	474	4.300	37.535	198.88	199.20	212.72	219.58
	494	7.325	37.535	207.40	207.56	214.40	217.87
	536	7.385	42.755	226.44	226.49	228.31	229.24
	3655	9.185	21.528	198.09	198.15	200.81	202.16
	3780	9.185	42.755	223.47	223.51	225.13	225.95
	3807	0.000	0.320	190.48	190.70	199.84	204.43
	3865	9.185	0.008	195.87	195.97	199.91	201.90
	3880	3.178	4.505	180.72	181.28	206.65	219.52
	3888	4.300	4.505	181.03	181.55	205.08	217.01
	4721	3.500	35.275	189.45	189.90	209.53	219.47
	4740	4.300	35.275	190.56	190.98	209.37	218.68
	4746	0.000	43.065	243.86	243.89	245.32	246.03
	6158	0.000	37.579	198.42	198.84	217.12	226.32
	6339	0.000	42.859	233.98	234.06	237.32	238.95
	6359 [b]	2.530	36.075	189.28	189.90	217.07	230.51
	6365 [b]	3.425	36.075	189.27	189.88	216.88	230.23
	6369	3.750	35.525	189.23	189.85	216.79	230.12
	6385	3.750	37.175	189.39	190.00	216.57	229.72
	6389	2.310	5.025	179.94	180.70	215.75	233.27
	6398	0.000	4.775	179.99	180.76	215.52	232.92
	6399	0.000	5.025	179.99	180.76	215.55	232.96
	6574	2.530	21.528	179.27	180.35	229.19	252.87
	6647	0.000	36.075	189.40	190.02	217.24	230.72
	6715	0.000	37.135	189.44	190.06	217.14	230.54

Notes: (a) See Table 3.4a and Figs. 8–11 for details of node locations.
(b) Approximate location of the CV O-ring.

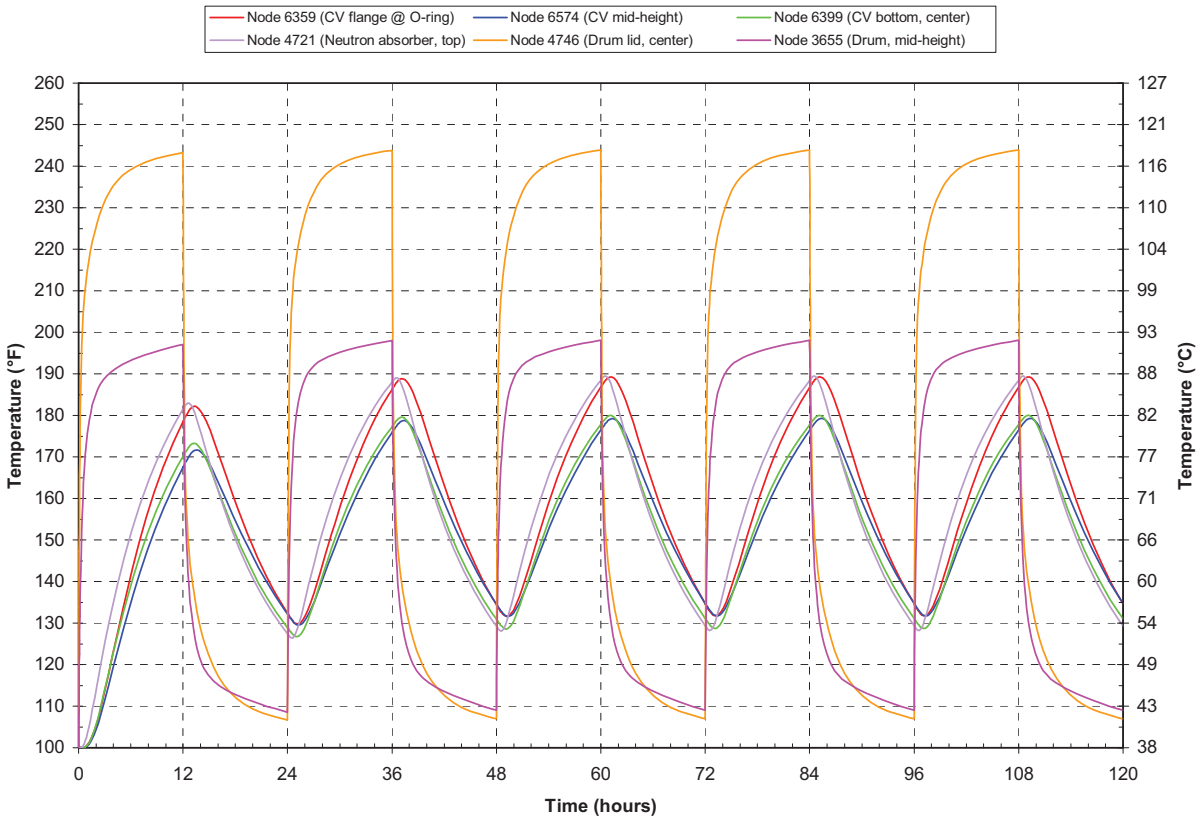

Figure 12. Transient temperatures of the ES-3100 shipping container for NCT (no content heat load) see Figure 8 through Figure 11 for node locations.

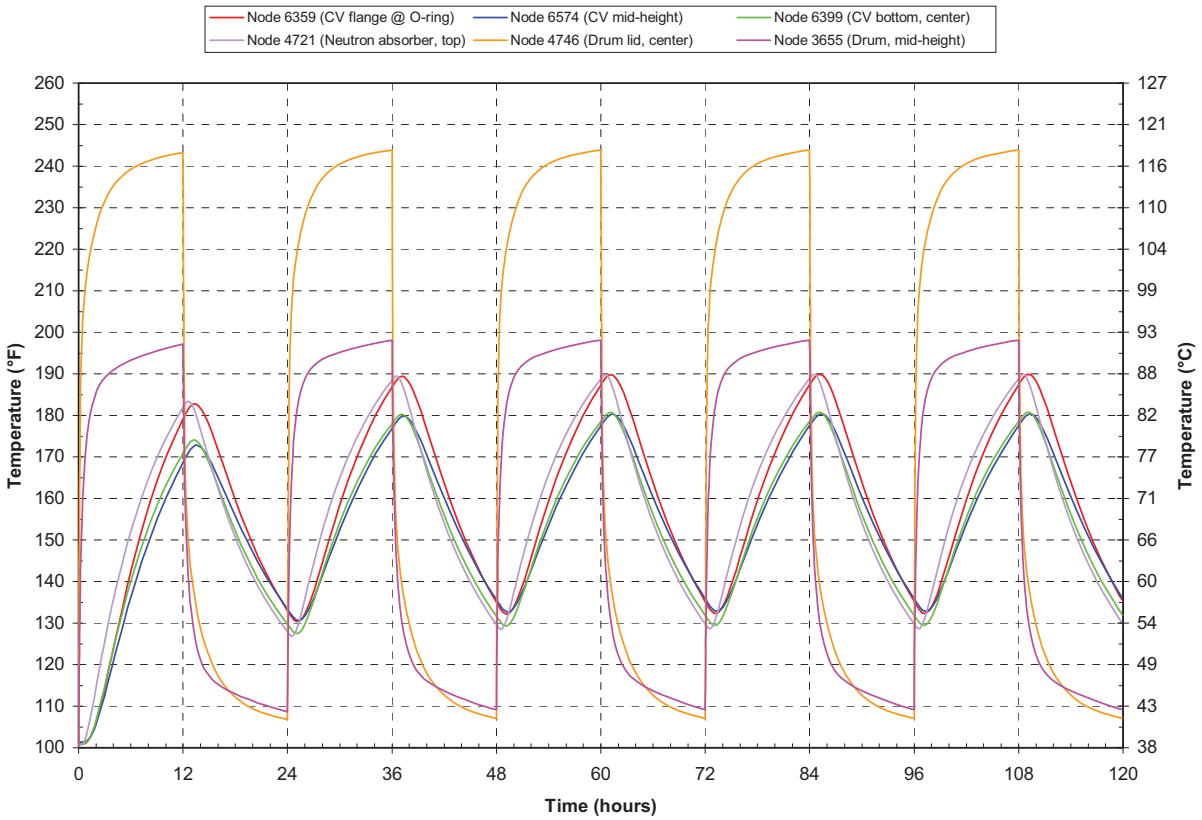

Figure 13. Transient temperatures of the ES-3100 shipping container for NCT (0.4 W content heat load) see Figure 8 through Figure 11 for node locations.

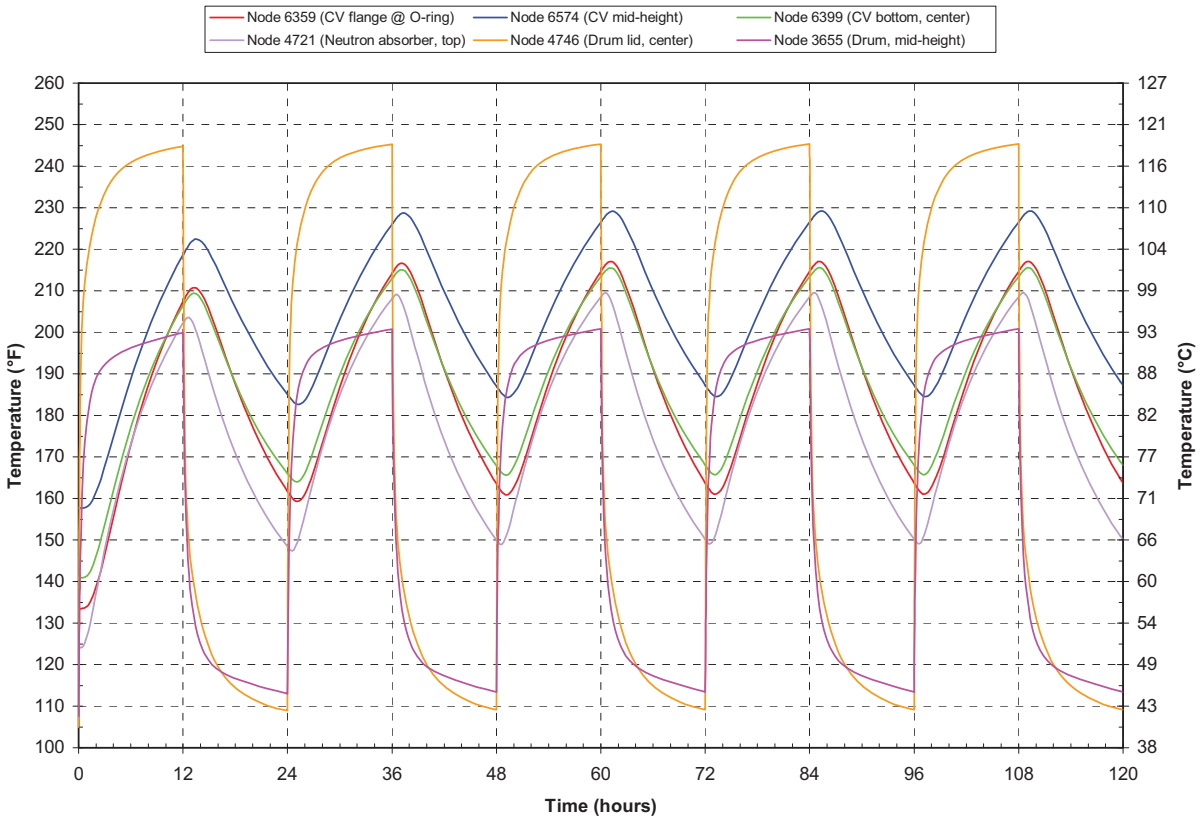

Figure 14. Transient temperatures of the ES-3100 shipping container for NCT (20 W content heat load) see Figure 8 through Figure 11 for node locations.

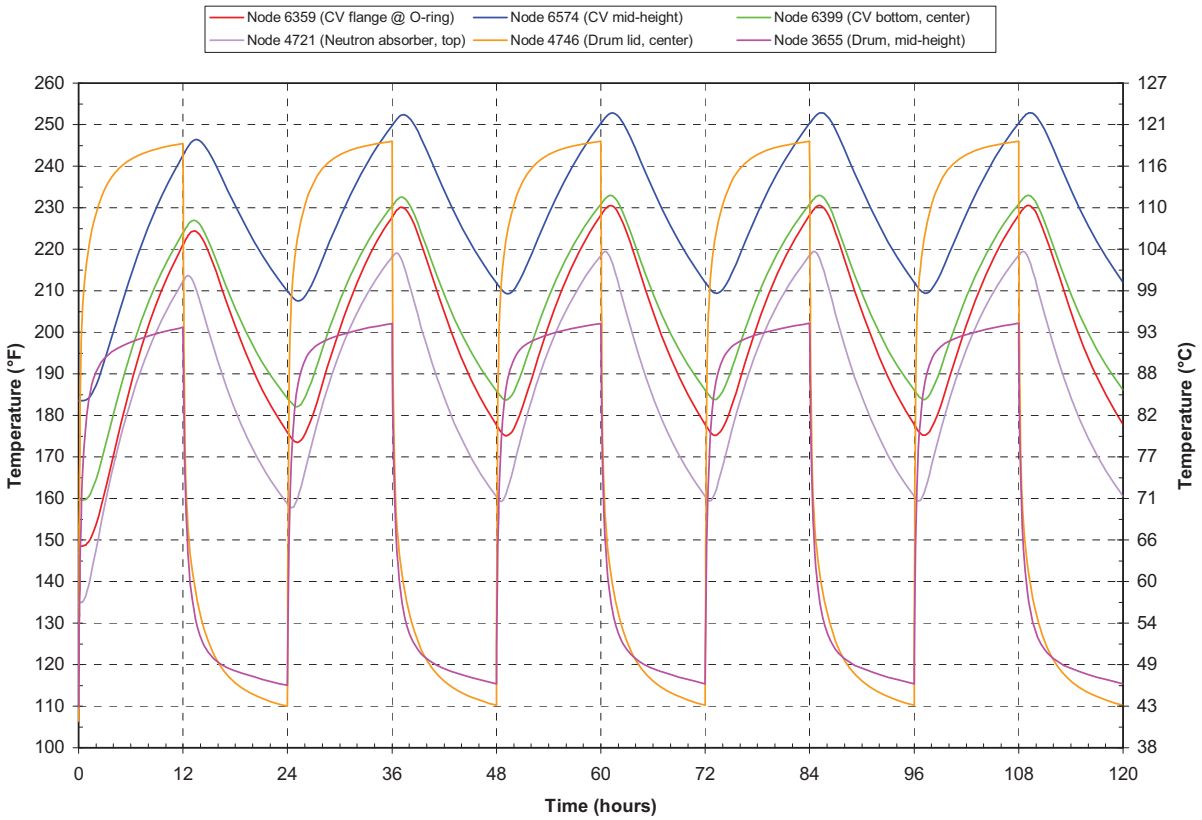

Figure 15. Transient temperatures of the ES-3100 shipping container for NCT (30 W content heat load) see Figure 8 through Figure 11 for node locations.

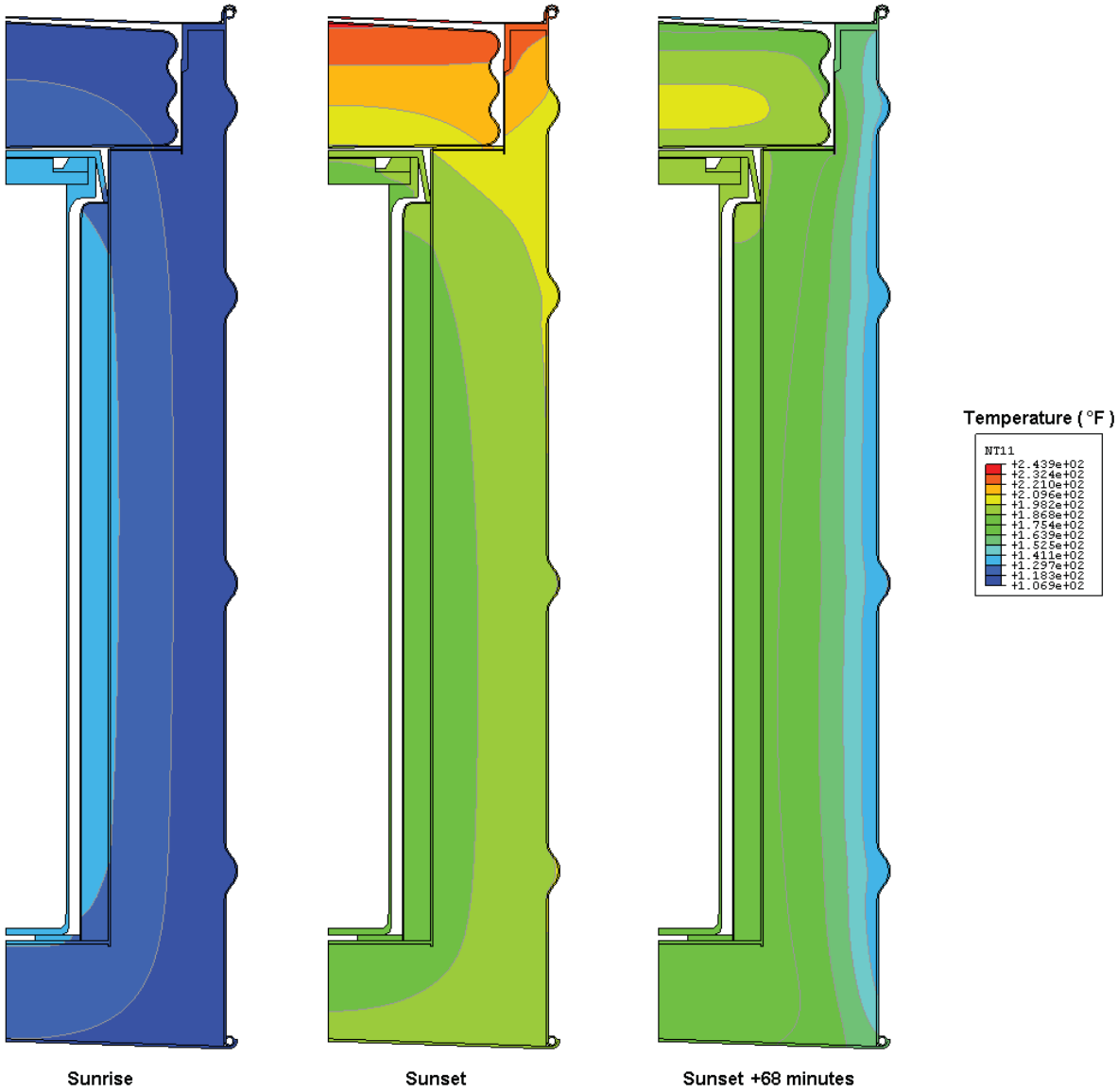

Figure 16. Temperature distribution in the ES-3100 shipping container for NCT (no content heat load) typical day of transient analysis (elements representing air not shown for clarity).

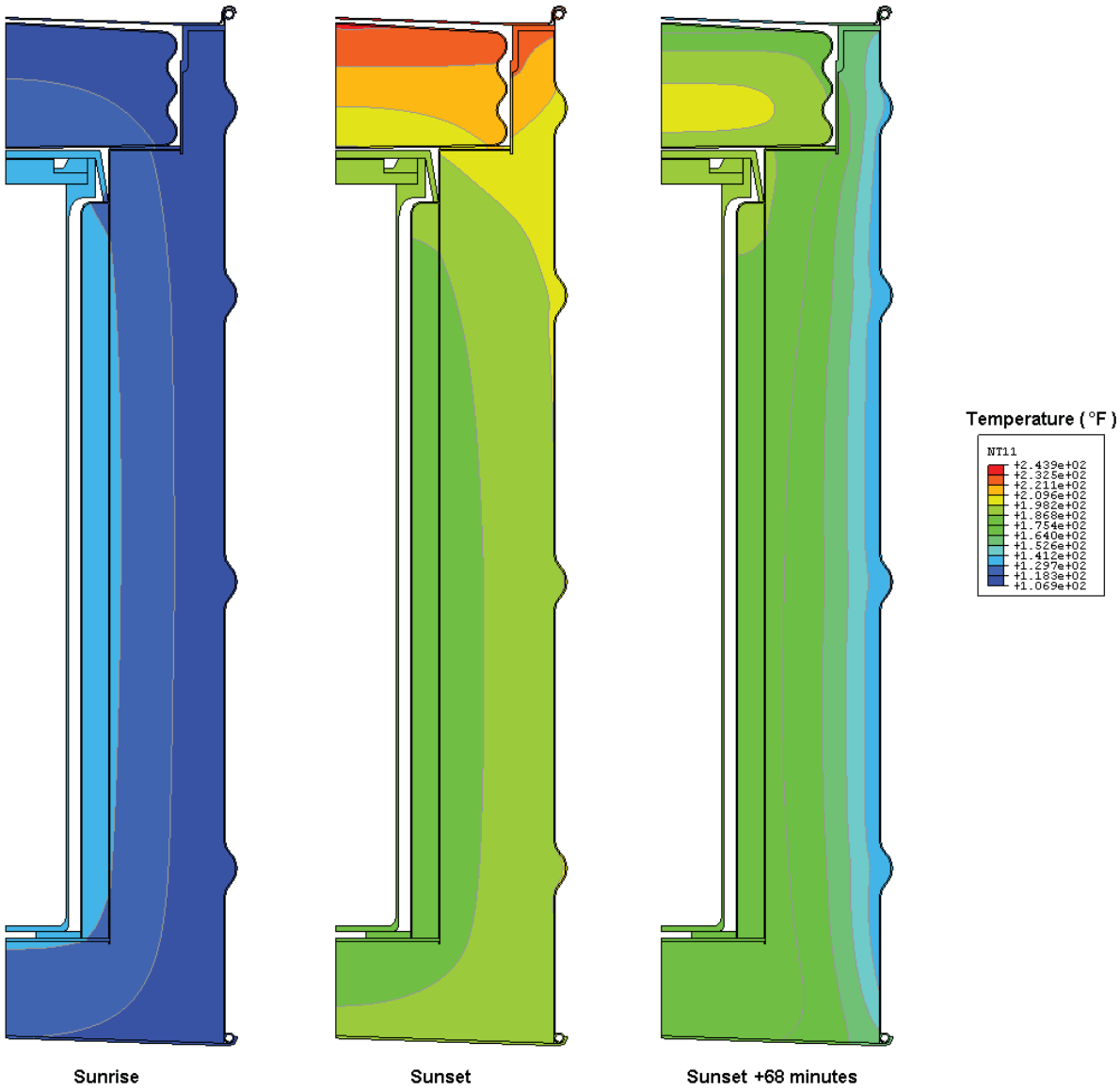

Figure 17. Temperature distribution in the ES-3100 shipping container for NCT (0.4 W content heat load) typical day of transient analysis (elements representing air not shown for clarity).

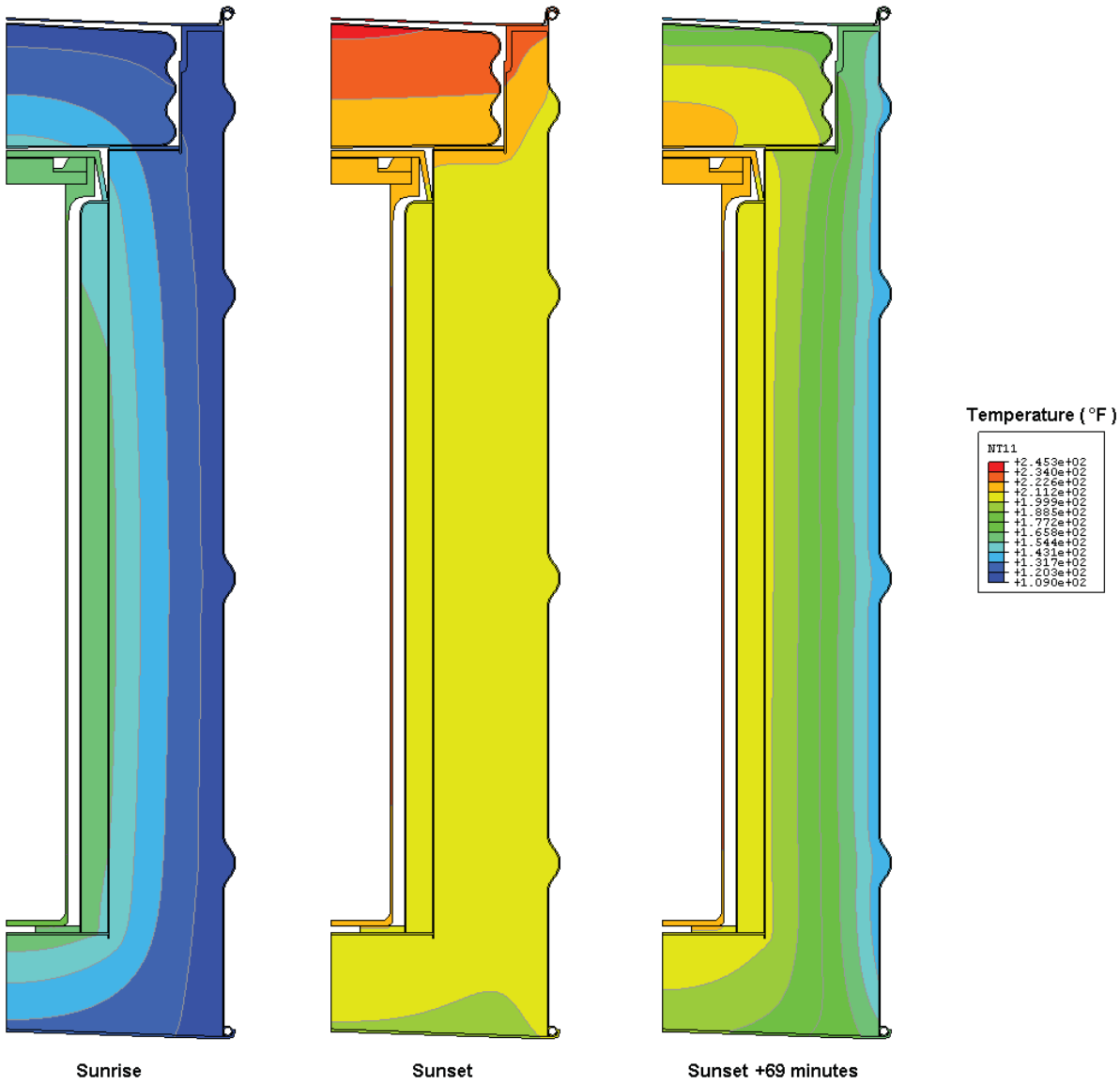

Figure 18. Temperature distribution in the ES-3100 shipping container for NCT (20 W content heat load) typical day of transient analysis (elements representing air not shown for clarity).

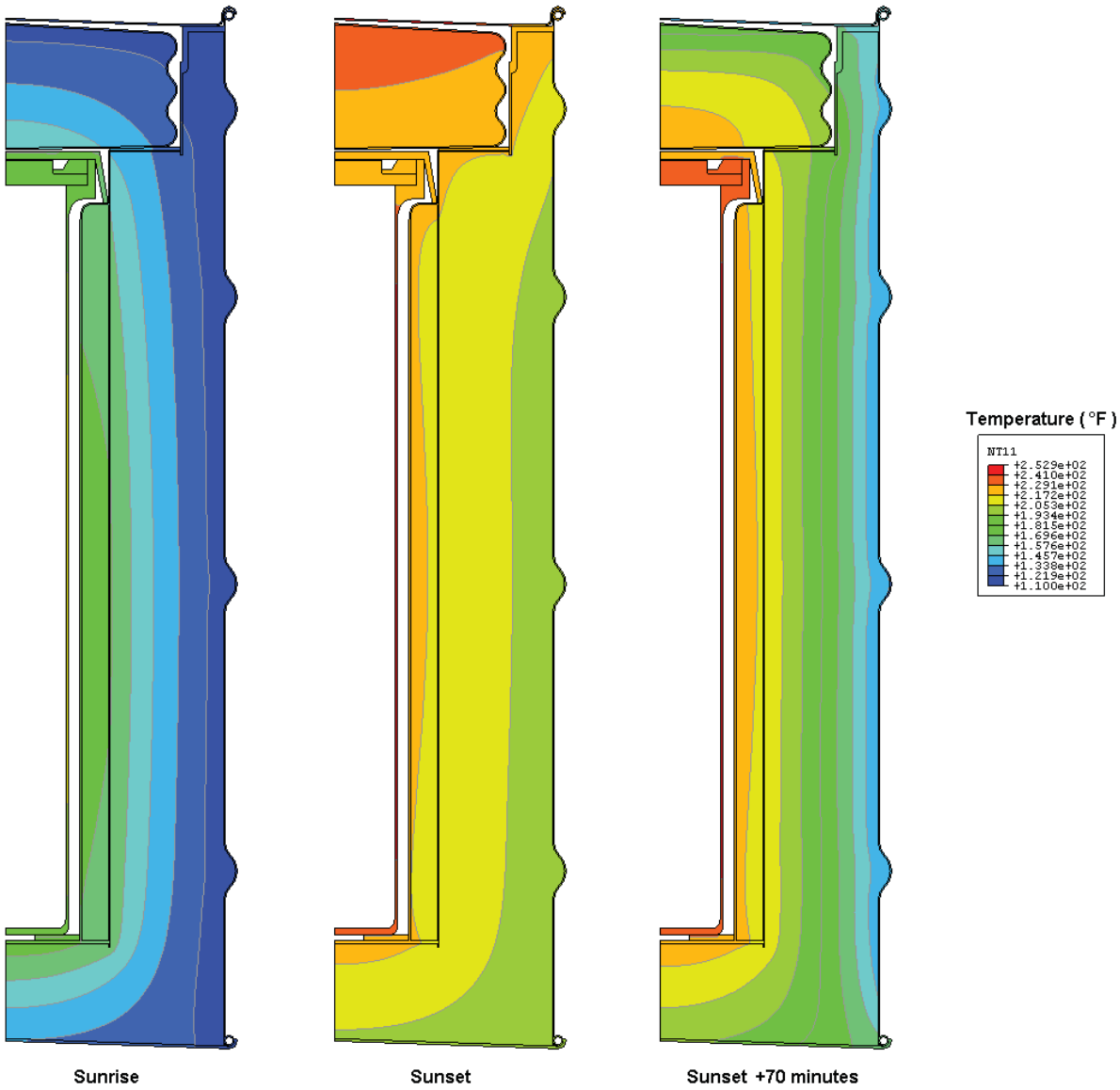

Figure 19. Temperature distribution in the ES-3100 shipping container for NCT (30 W content heat load) typical day of transient analysis (elements representing air not shown for clarity).

Hypothetical Accident Conditions Analyses Results

Transient thermal analyses are performed on the finite element model of the ES-3100 shipping container (undamaged configuration) to simulate HAC as prescribed by 10 CFR 71.73(c)(4).[1] A 30-minute fire of 1475°F (800°C) is simulated by applying natural convection and radiant exchange boundary conditions to all external surfaces of the drum (assuming the drum is in a horizontal orientation) with content heat loads of 0, 0.4, 20, and 30 W. There are no heat flux boundary conditions simulating insolation applied to the model before and during the 30-minute fire. The initial temperature distribution within the package having content heat loads of 0.4, 20, and 30 W is obtained from their respective steady-state analyses. The initial temperature distribution within the package having no content heat load (0 W) is assumed to be at a uniform temperature equal to the ambient temperature of 100°F (37.8°C). As with the steady-state analyses discussed previously, applying a uniform heat flux to the internal surfaces of the elements representing the containment vessel simulates the content heat load.

Following the 30-minute fire transient analyses, 48-hour cool-down transient thermal analyses are performed using the temperature distribution at the end of the fire as the initial temperature distribution. During post-fire cool-down, natural convection and radiant exchange boundary conditions are applied to all external surfaces of the drum (assuming the drum is in a horizontal orientation). Additionally, cases are analyzed in which insolation is included during the post-fire cool-down. For the cases in which insolation is applied to the model during cool-down, insolation is applied during the first 12-hour period following the 30-minute fire, then alternated (off, then on) as was done for NCT.

Based on previous analyses of a similar package[9] (see Appendix 3.6.1), it was noted that using the low-end density of Kaolite results in higher containment vessel temperatures than using the high-end density of Kaolite. For this reason, the NCT and HAC thermal analyses were run using a density of 19.4 lbm/ft^3 (see Table 1). Similarly, the low-end density of the neutron absorber (100 lbm/ft^3) was also used in these analyses. However, while using these low-end densities will result in higher temperatures to the containment vessel, using the high-end densities for these two materials will result in higher temperature differences from the baseline HAC case. Thus, runs are also made for heat loads of 0, 0.4, 20, and 30 W using a Kaolite density of 30 lbm/ft^3 and a neutron absorber density of 110 lbm/ft^3.

The maximum temperatures calculated for the ES-3100 shipping container for HAC are summarized in Table 6 for the analyses using a Kaolite density of 19.4 lbm/ft^3 and a neutron absorber density of 100 lbm/ft^3. The maximum temperatures calculated for the ES-3100 shipping container for HAC are summarized in Table 7 for the analyses using a Kaolite density of 30 lbm/ft^3 and a neutron absorber density of 110 lbm/ft^3. The thermal analyses that use the low-end density values for Kaolite and the neutron absorber achieve the higher package temperatures (see Table 6). Temperature-history plots of several locations within the model are also depicted graphically in Figure 20 through Figure 23 for content heat loads of 0, 0.4, 20, and 30 W for the analyses using a Kaolite density of 19.4 lbm/ft^3 and a neutron absorber density of 100 lbm/ft^3.

The HAC thermal analyses presented in this report are performed using a finite element model that represents an undamaged ES-3100 shipping container. While the cumulative damage from NCT and HAC drop tests, crush tests, and puncture tests, must be considered when evaluating the performance of the package to HAC, the temperature differences (i.e., adjustments) calculated from the data presented in Table 6 and Table 7 are of value when combined with the physical test data when making this assessment.

Table 6. ES-3100 shipping container HAC maximum temperatures (Kaolite density of 19.4 lbm/ft^3 and neutron absorber density of 100 lbm/ft^3).

Node map [a]	Node coordinates (in.)			HAC maximum temperature (°F)							
				0 W		0.4 W		20 W		30 W	
	No.	r	z	Insolation during cool-down?		Insolation during cool-down?		Insolation during cool-down?		Insolation during cool-down?	
				No [b]	Yes	No	Yes	No	Yes	No	Yes
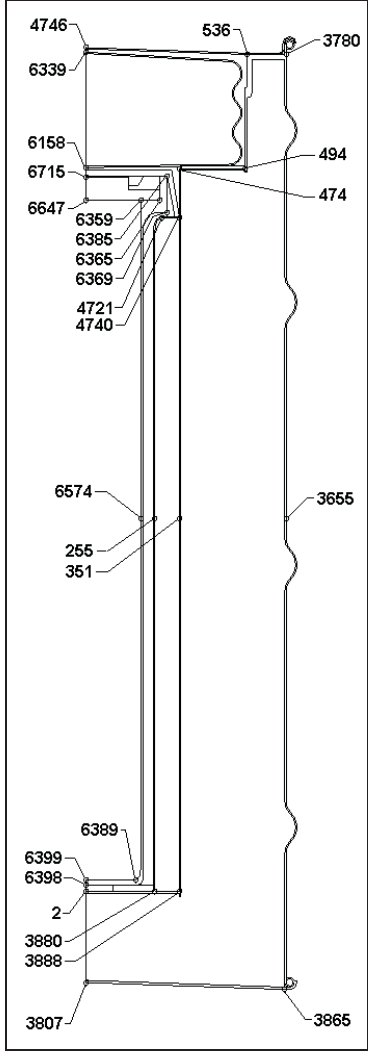	2	0.000	4.505	225.5	232.1	226.2	232.8	255.5	261.7	269.5	275.7
	255	3.180	21.528	194.5	212.5	195.2	213.2	223.8	241.3	237.8	255.3
	351	4.300	21.528	195.8	211.9	196.4	212.5	222.3	237.8	234.8	250.3
	474	4.300	37.535	392.9	395.0	393.2	395.4	407.6	409.7	414.2	416.3
	494	7.325	37.535	671.2	672.0	671.4	672.3	679.1	680.0	682.5	683.3
	536	7.385	42.755	1380.4	1380.4	1380.4	1380.4	1380.9	1380.9	1381.1	1381.1
	3655	9.185	21.528	1457.8	1457.8	1457.8	1457.8	1458.0	1458.0	1458.1	1458.1
	3780	9.185	42.755	1427.8	1427.8	1427.9	1427.9	1428.1	1428.1	1428.2	1428.2
	3807	0.000	0.320	1454.5	1454.5	1454.5	1454.5	1454.9	1454.9	1455.0	1455.0
	3865	9.185	0.008	1470.1	1470.1	1470.1	1470.1	1470.1	1470.1	1470.2	1470.2
	3880	3.178	4.505	230.6	236.4	231.2	237.0	257.1	262.5	269.4	274.8
	3888	4.300	4.505	236.9	241.7	237.5	242.3	261.5	266.1	272.9	277.5
	4721	3.500	35.275	245.7	252.8	246.2	253.3	266.8	273.8	276.6	283.6
	4740	4.300	35.275	258.4	263.5	258.8	264.0	278.1	283.1	287.1	292.1
	4746	0.000	43.065	1448.0	1448.0	1448.0	1448.0	1448.2	1448.2	1448.3	1448.3
	6158	0.000	37.579	308.7	311.6	309.1	312.0	328.3	331.2	337.3	340.2
	6339	0.000	42.859	1335.1	1335.1	1335.2	1335.2	1336.4	1336.4	1336.9	1336.9
	6359 [c]	2.530	36.075	236.7	247.6	237.3	248.3	266.2	276.6	279.8	289.9
	6365 [c]	3.425	36.075	236.6	247.6	237.3	248.3	266.0	276.4	279.5	289.7
	6369	3.750	35.525	236.5	247.6	237.2	248.2	265.8	276.2	279.3	289.5
	6385	3.750	37.175	237.3	248.2	237.9	248.8	266.1	276.4	279.4	289.5
	6389	2.310	5.025	219.0	227.4	219.9	228.2	255.3	263.1	272.2	279.9
	6398	0.000	4.775	219.7	227.9	220.5	228.7	255.6	263.3	272.5	280.0
	6399	0.000	5.025	219.7	227.9	220.5	228.7	255.6	263.3	272.5	280.0
	6574	2.530	21.528	196.1	214.9	197.3	216.0	246.7	263.8	269.9	286.5
	6647	0.000	36.075	237.2	248.0	237.9	248.6	266.8	277.0	280.4	290.4
	6715	0.000	37.135	237.4	248.1	238.0	248.8	266.8	277.0	280.4	290.4

Notes: (a) See Table 3.4a and Figs. 8–11 for details of node locations.
(b) Baseline case for ΔT comparisons.
(c) Approximate location of the CV O-ring.

Table 7. ES-3100 shipping container HAC maximum temperatures (Kaolite density of 30 lbm/ft^3 and neutron absorber density of 110 lbm/ft^3).

Node map [a]	Node coordinates (in.)			HAC maximum temperature (°F)							
				0 W		0.4 W		20 W		30 W	
	No.	r	z	Insolation during cool-down?		Insolation during cool-down?		Insolation during cool-down?		Insolation during cool-down?	
				No [b]	Yes	No	Yes	No	Yes	No	Yes
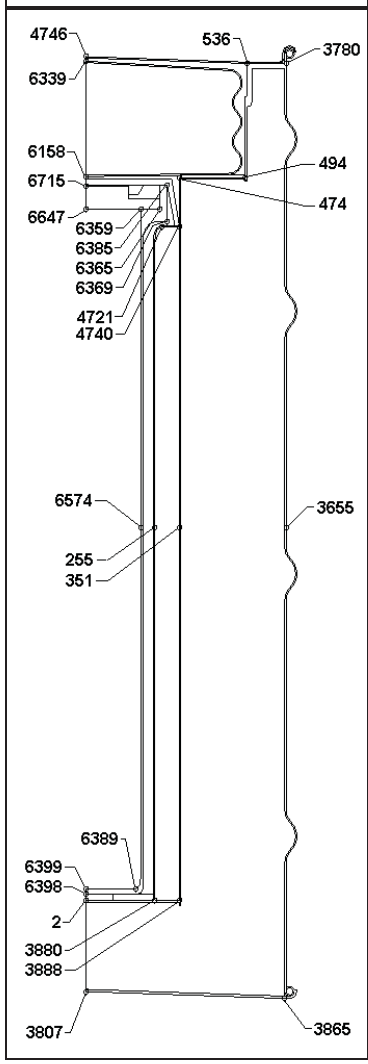	2	0.000	4.505	209.9	218.9	210.6	219.6	240.4	248.8	254.6	262.8
	255	3.180	21.528	185.5	207.7	186.1	208.4	215.1	236.6	229.3	250.6
	351	4.300	21.528	185.6	207.4	186.2	208.0	212.3	233.3	225.0	245.9
	474	4.300	37.535	342.9	345.5	343.3	345.9	358.1	360.7	365.0	367.5
	494	7.325	37.535	596.3	597.4	596.5	597.6	604.7	605.8	608.3	609.4
	536	7.385	42.755	1366.8	1366.8	1366.8	1366.8	1367.4	1367.4	1367.6	1367.6
	3655	9.185	21.528	1452.8	1452.8	1452.8	1452.8	1453.0	1453.0	1453.1	1453.1
	3780	9.185	42.755	1420.8	1420.8	1420.8	1420.8	1421.0	1421.0	1421.2	1421.2
	3807	0.000	0.320	1449.4	1449.4	1449.4	1449.4	1449.8	1449.8	1449.9	1449.9
	3865	9.185	0.008	1467.3	1467.3	1467.3	1467.3	1467.4	1467.4	1467.4	1467.4
	3880	3.178	4.505	213.1	221.4	213.7	222.0	240.0	247.9	252.5	260.3
	3888	4.300	4.505	217.0	224.4	217.6	225.0	242.1	249.1	253.8	260.7
	4721	3.500	35.275	228.0	237.5	228.5	238.0	249.7	259.0	259.7	269.0
	4740	4.300	35.275	236.5	243.8	236.9	244.3	256.7	263.9	266.0	273.2
	4746	0.000	43.065	1441.8	1441.8	1441.8	1441.8	1442.0	1442.0	1442.1	1442.1
	6158	0.000	37.579	277.3	281.8	277.8	282.3	297.5	302.0	306.7	311.2
	6339	0.000	42.859	1299.5	1299.5	1299.6	1299.6	1301.1	1301.1	1301.7	1301.7
	6359 [c]	2.530	36.075	225.1	237.3	225.8	237.9	254.7	266.1	268.3	279.6
	6365 [c]	3.425	36.075	225.0	237.3	225.7	237.9	254.5	266.0	268.1	279.3
	6369	3.750	35.525	224.9	237.2	225.6	237.8	254.3	265.8	267.9	279.2
	6385	3.750	37.175	225.5	237.6	226.2	238.3	254.6	266.1	268.0	279.2
	6389	2.310	5.025	205.3	215.9	206.2	216.8	242.0	251.9	259.2	268.9
	6398	0.000	4.775	205.8	216.3	206.7	217.1	242.2	252.0	259.2	268.8
	6399	0.000	5.025	205.8	216.3	206.7	217.1	242.2	252.0	259.3	268.8
	6574	2.530	21.528	187.8	209.1	189.0	210.2	238.9	258.4	262.4	281.3
	6647	0.000	36.075	225.6	237.7	226.3	238.3	255.2	266.5	268.9	280.0
	6715	0.000	37.135	225.8	237.8	226.4	238.4	255.2	266.5	268.9	280.0

Notes: (a) See Table 3.4a and Figs. 8–11 for details of node locations.
(b) Baseline case for ΔT comparisons.
(c) Approximate location of the CV O-ring.

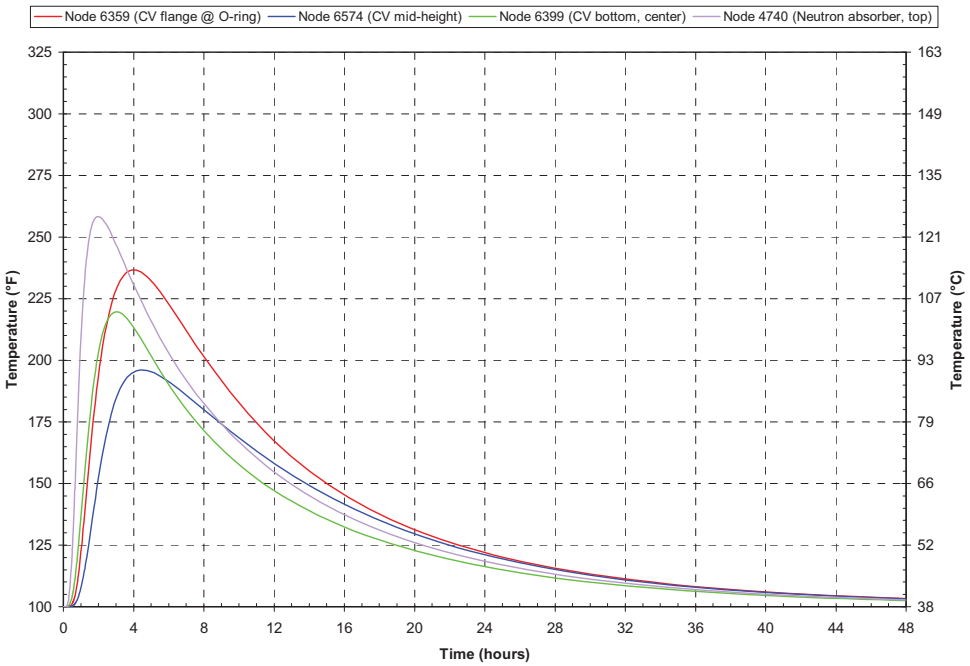

(a) No insolation during post-fire cool-down.

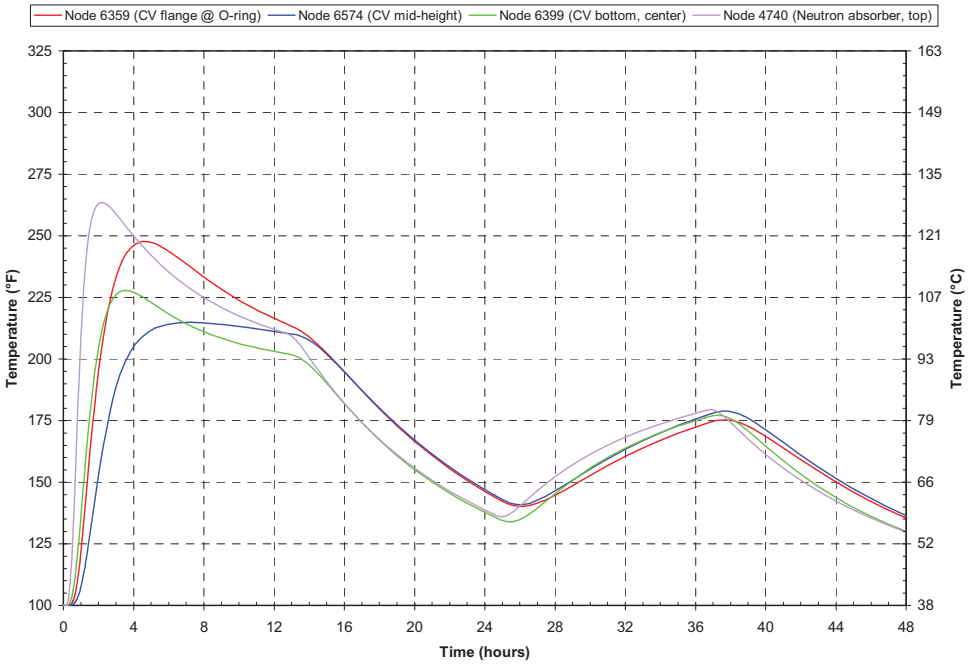

(b) Insolation during post-fire cool-down.

Figure 20. ES-3100 shipping container transient temperatures for HAC—no content heat load and lower bound Kaolite and neutron absorber densities (see Figure 8 through Figure 11 for node locations).

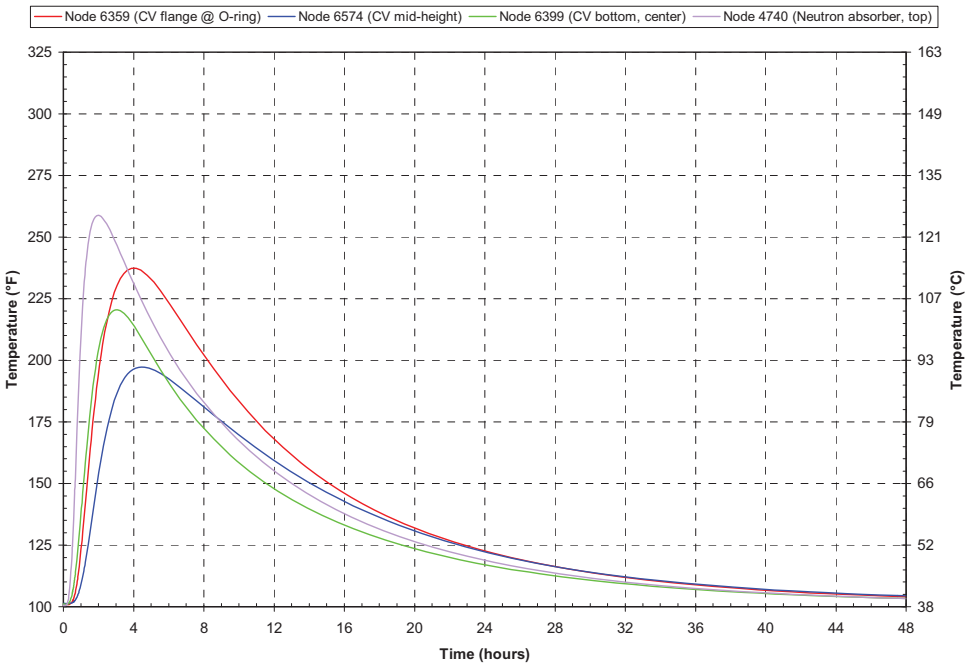

(a) No insolation during post-fire cool-down.

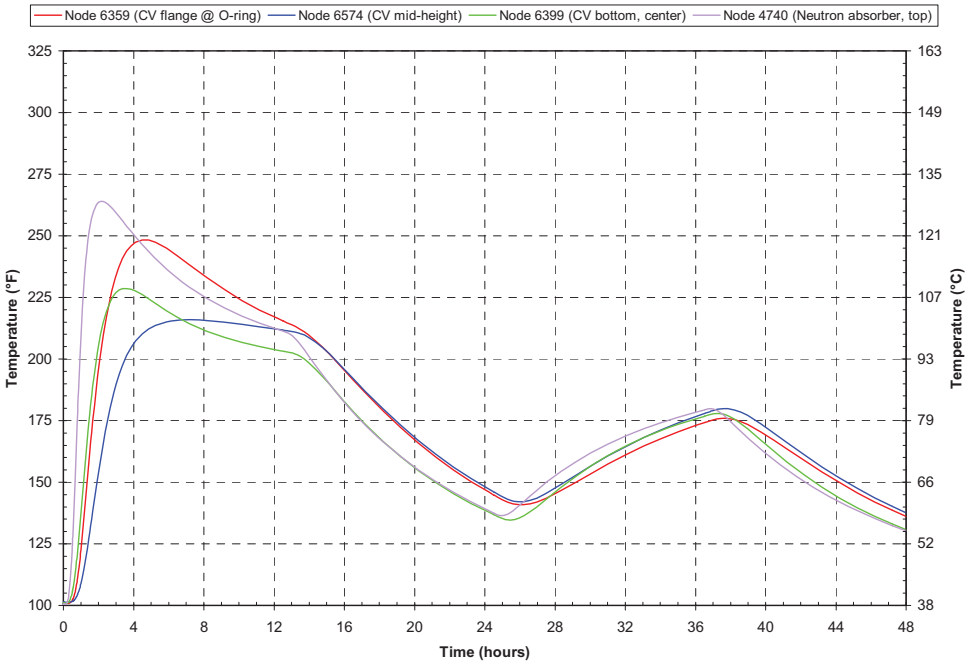

(b) Insolation during post-fire cool-down.

Figure 21. ES-3100 shipping container transient temperatures for HAC, 0.4 W content heat load and lower bound Kaolite and neutron absorber densities (see Figure 8 for through Figure 11 for node locations).

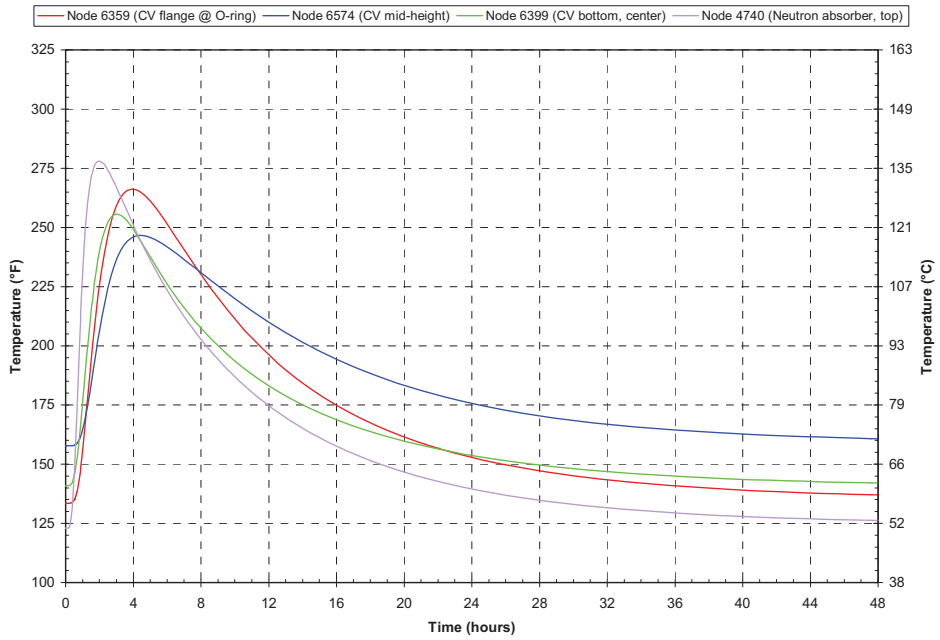

(a) No insolation during post-fire cool-down.

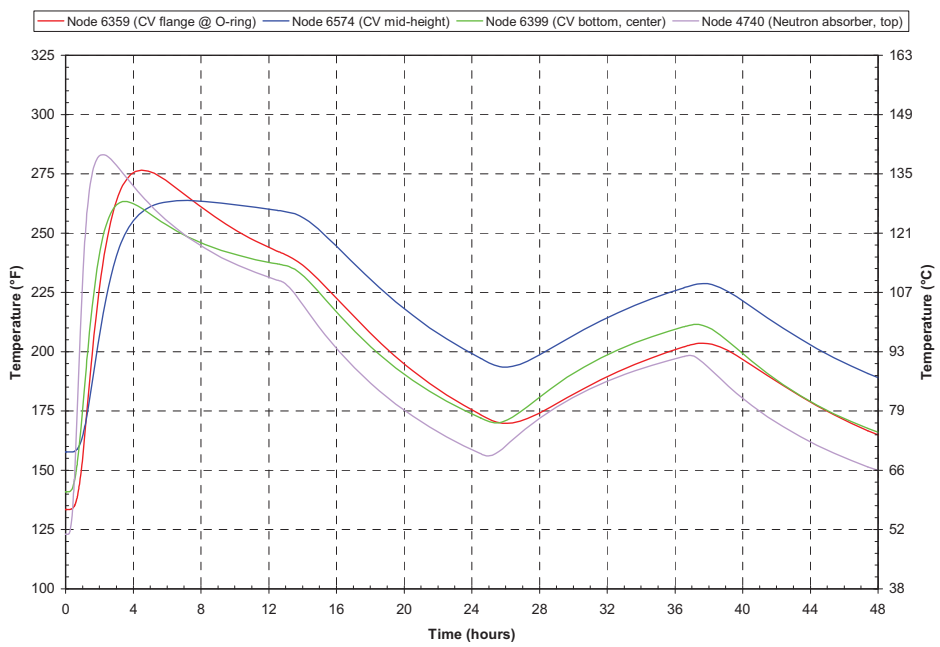

(b) Insolation during post-fire cool-down.

Figure 22. ES-3100 shipping container transient temperatures for HAC, 20 W content heat load and lower bound Kaolite and neutron absorber densities (see Figure 8 through Figure 11 for node locations).

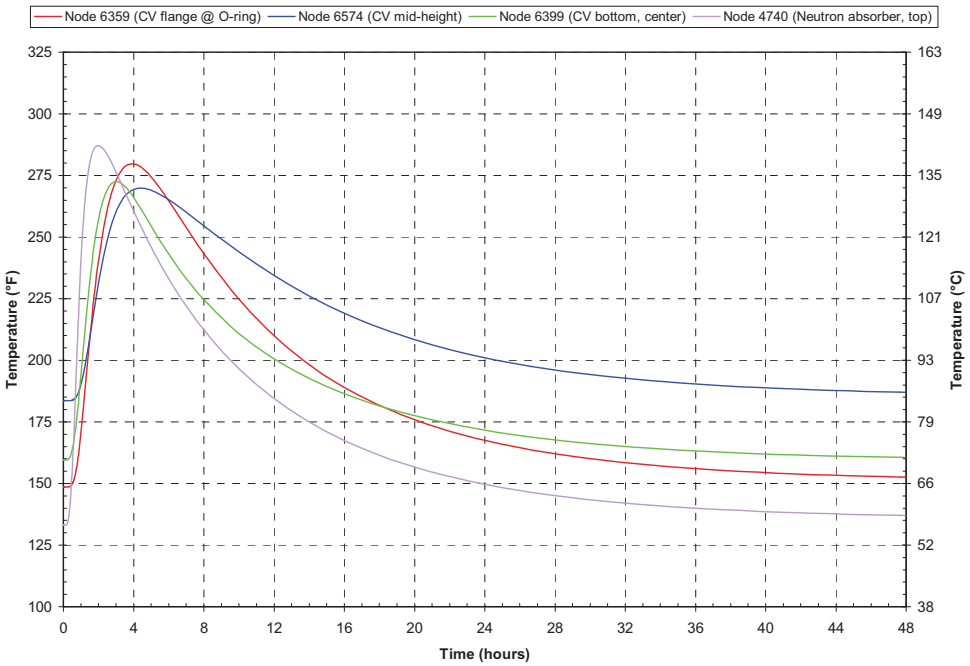

(a) No insolation during post-fire cool-down.

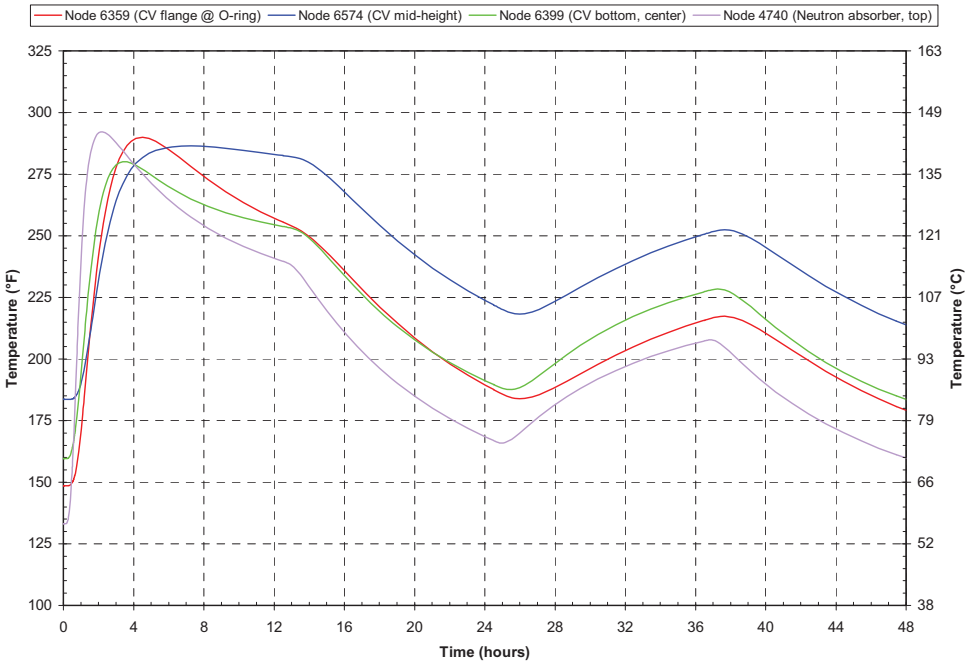

(b) Insolation during post-fire cool-down.

Figure 23. ES-3100 shipping container transient temperatures for HAC, 30 W content heat load and lower bound Kaolite and neutron absorber densities (see Figure 8 through Figure 11 for node locations)

APPENDIX 3.6.2 REFERENCES

1. *Packaging and Transportation of Radioactive Materials*, U.S. Nuclear Regulatory Commission, Code of Federal Regulations, Title 10 – Energy, Part 71, January 1, 2004.

2. L. S. Dickerson, M. R. Feldman, and R. D. Michaelhaugh, *Test Report of the ES-3100 Package*, Volumes 1–3, ORNL/NTRC-013, Rev. 0, Nuclear Science and Technology Division, Oak Ridge National Laboratory, Oak Ridge, Tennessee, September 10, 2004.

3. MSC. Patran 2004, Version 12.0.044, MacNeal Schwendler Corporation, 2004.

4. ABAQUS/CAE, Version 6.4-1, Build ID: 2003_09_29-11.18.28 46457, Abaqus, Inc., 2003.

5. R. Siegel and J. R. Howell, *Thermal Radiation Heat Transfer*, Second Edition, Hemisphere Publishing Corporation, 1981.

6. F. P. Incropera and D. P. DeWitt, *Fundamentals of Heat and Mass Transfer*, Second Edition, John Wiley & Sons, New York, 1985.

7. J. C. Anderson and M. R. Feldman, *Thermal Modeling of Packages for Normal Conditions of Transport with Insolation*, Proceedings of the ASME Heat Transfer Division, HTD-Vol. 317-2, 1995, International Mechanical Engineering Congress and Exposition, November 1995.

8. ABAQUS/Standard, Version 6.4-1, 2003_09_29-11.18.28 46457, Abaqus, Inc. , 2003.

9. P. A. Bales, *Thermal Analyses of the ES-3100 Shipping Container for NCT and HAC*, DAC-PKG-801699-A001, Rev. 1, BWXT Y-12, December 30, 2004.

THIS PAGE INTENTIONALLY LEFT BLANK.

Appendix 3.6.3

THERMAL STRESS EVALUATION OF THE ES-3100 SHIPPING CONTAINER DRUM BODY ASSEMBLY FOR NCT (FINAL DESIGN WITH CATALOG 277-4 NEUTRON ABSORBER)

THIS PAGE INTENTIONALLY LEFT BLANK.

Appendix 3.6.3

THERMAL STRESS EVALUATION OF THE ES-3100 SHIPPING CONTAINER DRUM BODY ASSEMBLY FOR NCT (FINAL DESIGN WITH CATALOG 277-4 NEUTRON ABSORBER)

INTRODUCTION

Static stress analyses of the ES-3100 shipping container are performed to determine the maximum thermal stresses within the packaging when exposed to Normal Conditions of Transport (NCT) as specified in 10 CFR 71.71(c)(1).[1] Transient thermal analyses were previously performed[2] (see Appendix 3.6.2) on the ES-3100 shipping container to determine its response to NCT. The thermal analyses treat the problem as a cyclic transient with the incident heat flux due to solar radiation applied and not applied in alternating 12-hour periods. The calculated temperature distributions within the drum body assembly for NCT at various times are then mapped onto the structural model, and static analyses are performed for each time step in the thermal analyses.

FINITE ELEMENT MODEL DESCRIPTION

A two-dimensional axisymmetric finite element model of the ES-3100 shipping container is constructed using MSC.Patran[3] and imported as an orphaned mesh into ABAQUS/CAE[4] for application of boundary conditions, interactions, and loads. The model is constructed of CAX4I (four-node bilinear axisymmetric quadrilateral, incompatible mode) elements for stress evaluation. These elements are chosen because they can accurately capture bending stresses with only one element through the thickness of a structure. A schematic of the finite element model is presented in Figure 1 with details of the upper and lower portions of the model shown in Figure 2 and Figure 3, respectively. The model consists of three materials: stainless steel (drum, drum bottom plate, and drum liner weldment), Kaolite, and neutron absorber. Details of the model are discussed in the following sections.

Surface-to-surface contact interactions are modeled between contacting surfaces in the static stress model. These interactions are shown graphically in Figure 2 and Figure 3. For all interactions, the tangential behavior is modeled as "frictionless" while the normal behavior is modeled as "hard contact." For the interactions modeled between the bottom of the neutron absorber and the drum liner and between the drum Kaolite bottom and the drum bottom plate, the contacting surfaces are not allowed to separate after contact is made.

The radial degree-of-freedom (U_r) of each node along the centerline of the model is fixed to simulate symmetry. Additionally, the axial degree-of-freedom (U_z) of one node on the drum bottom plate is fixed.

The temperatures calculated for NCT in Appendix 3.6.2 are stored in the 'NCT.fil' file for each of the content head loads analyzed. The temperature distribution for each time of interest is mapped onto the static stress model using the '`*Temperature`' keyword. The specific times of interest from the transient thermal analyses are at each increment in the final day/night cycle (after "quasi steady-state" is reached).

The mechanical properties of the materials used in the static stress analyses are presented in Table 1. The modulus of elasticity of Kaolite presented in Table 1 is calculated from the first two points of the compressive stress-strain assuming a Poisson's ratio of 0.01.[5]

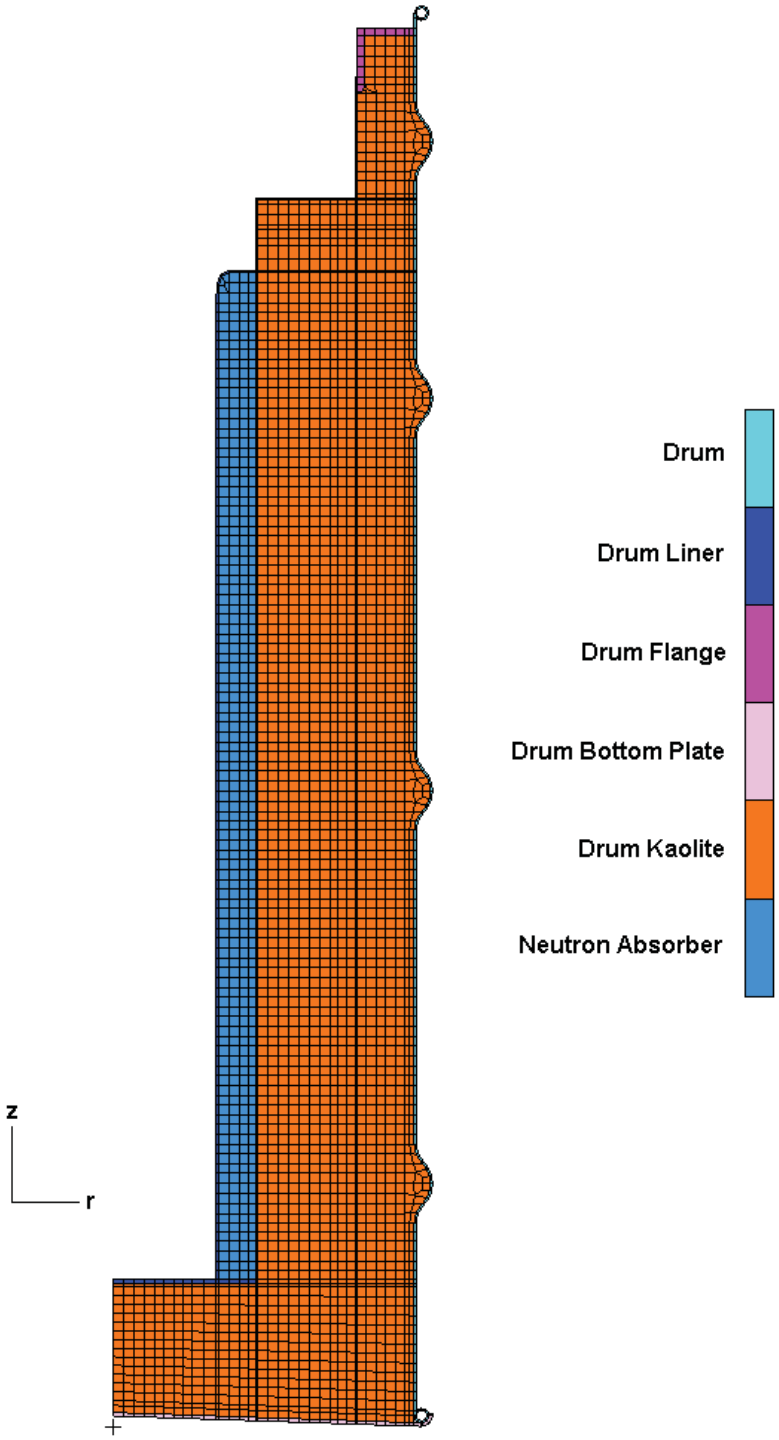

Figure 1. MSC.Patran axisymmetric finite element model of the ES-3100 shipping container drum body assembly.

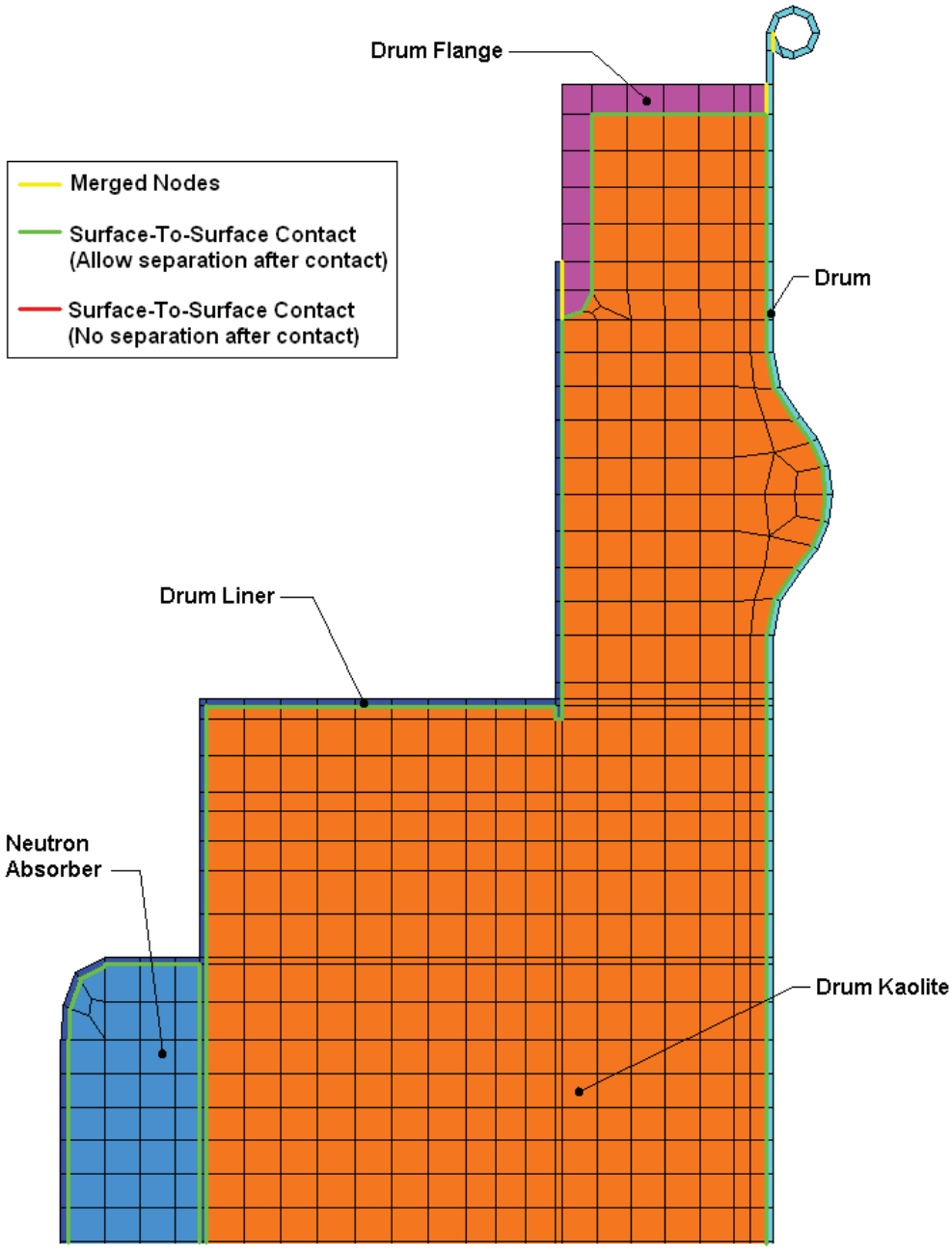

Figure 2. MSC.Patran axisymmetric finite element model of the ES-3100 shipping container drum body assembly (upper portion detail).

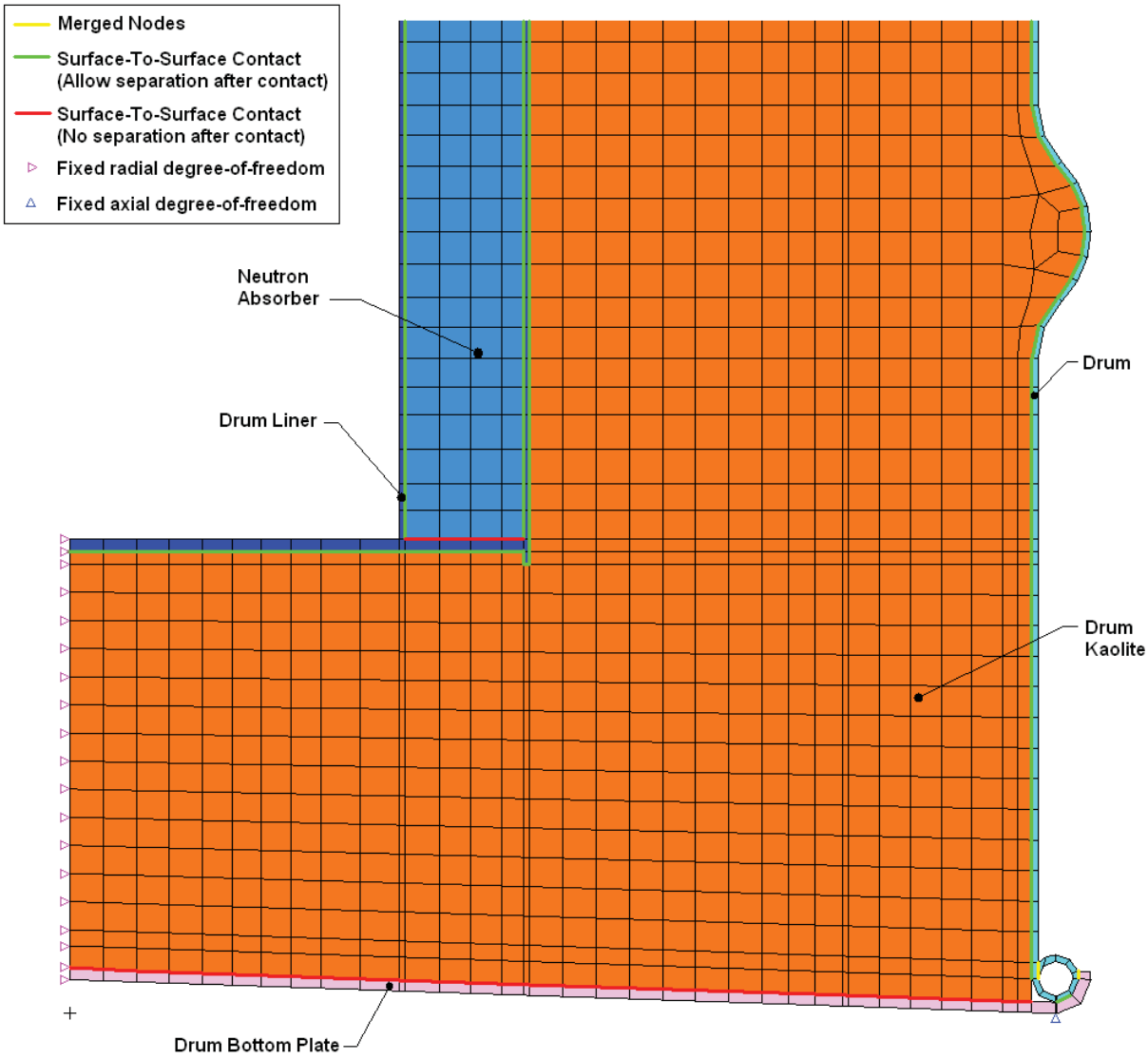

Figure 3. MSC.Patran axisymmetric finite element model of the ES-3100 shipping container drum body assembly (lower portion detail).

Table 1. Mechanical properties of the materials used in the static stress analyses.

Material	Temperature (°F)	Modulus of elasticity (psi)	Poisson's ratio	Density (lbm/in^3)	Coefficient of thermal expansion (in./in./°F)
Stainless Steel	-40	28.6×10^6 [(a)]	0.29 [(b)]	0.285 [(c)]	8.2×10^{-6} [(e)]
	100	28.14×10^6	–	–	8.6×10^{-6}
	200	27.6×10^6	–	–	8.9×10^{-6}
	300	27.0×10^6	–	–	9.2×10^{-6}
Kaolite	–	29,210 [(d)]	0.01 [(d)]	0.013 [(f)]	5.04×10^{-6} [(g)]
Neutron Absorber	-40	1.991×10^6 [(h)]	0.33 [(h)]	0.0608 [(h)]	7.056×10^{-6} [(i)]
	-4	–	–	–	7.222×10^{-6}
	32	–	–	–	7.222×10^{-6}
	70	0.984×10^6	0.28	–	–
	100	0.403×10^6	0.25	–	–
	104	–	–	–	7.000×10^{-6}
	140	–	–	–	6.444×10^{-6}
	176	–	–	–	5.778×10^{-6}
	212	–	–	–	5.389×10^{-6}
	248	–	–	–	5.056×10^{-6}
	284	–	–	–	4.889×10^{-6}
	302	–	–	–	4.833×10^{-6}

Notes:
(a) ASME Boiler and Pressure Vessel Code, Sect. II, Part D, Subpart 2, Tables TE-1, B column, and TM-1.
(b) R. A. Bailey, *Strain – A Material Database*, Lawrence Livermore National Laboratory, 1989.
(c) F. P. Incropera and D. P. DeWitt, *Fundamentals of Heat and Mass Transfer*, 2nd edition, John Wiley & Sons, New York, 1985.
(d) K. D. Handy, *Impact Analysis of ES3100 Design Concepts Using Borobond*, DAC-EA-801699-A001, BWXT Y-12, Oct. 2004. The Poisson's ratio of Kaolite is assumed to be a small value of 0.1.
(e) *Metallic Materials and Elements for Aerospace Vehicle Structures*, MIL-HDBK-5E, May 1986.
(f) Specification JS-YMN3-801580-A003 requires a baked density of 22.4 ± 3 lbm/ft^3.
(g) E-mail communication, Ken Moody (Thermal Ceramics, Inc.) to Paul Bales (BWXT Y-12), 12/9/04.
(h) B. F. Smith and G. A. Byington, Mechanical Properties of 277-4, Y/DW-1987, January 19, 2005.
(i) W. D. Porter and H. Wang, *Thermophysical Properties of Heat Resistant Shielding Material*, ORNL/TM-2004/290, ORNL, Dec. 2004. Coefficient of thermal expansion at each temperature taken as the maximum of values for Runs #2, #3, and #5.

DISCUSSION OF ANALYTICAL RESULTS

All static stress analyses discussed in this report were performed using ABAQUS/Standard[6] on an Intel Pentium 4–based Microsoft Windows 2000 computer. These analyses are sequential-coupled thermal/structural analyses.

As previously stated, the nodal temperature results for the final day/night cycle of the transient thermal analyses of the ES-3100 shipping container were stored in results files (NCT.fil) for each content heat load analyzed. Because automatic time-stepping was used in the transient thermal analyses, the number of increments stored in each 'NCT.fil' file differs for each content heat load analyzed. The static stress analyses of the ES-3100 are performed for each time increment analyzed in the thermal analyses for the final day/night cycle during NCT by copying the 'NCT.fil' and 'NCT.prt' files from the thermal analysis of interest to the directory where the stress analysis is being performed and entering the '`*Temperature`' keyword with the proper syntax for the time of interest. For example, for a content heat load of 0.4 W, the thermal stresses for time = 14.127 hours after sunrise (2.127 hours after sunset) on the final day/night

cycle (i.e., step = 11, increment = 29) are analyzed by entering the following keyword syntax via the keyword editor in ABAQUS/CAE:

```
*Temperature, file=NCT, bstep=11, binc=29, estep=11, einc=29
```

A separate static analysis is performed for each time step in the final day/night cycle of each thermal analysis for each content heat load.

The results of the static stress analyses for content heat loads of 0.4, 20, and 30 W are presented in Figure 4 through Figure 6. The stresses presented in these figures are the maximum nodal Mises stresses of each component at each point in time—as such, they don't necessarily occur at the same node location during the duration of the time period analyzed. The x-axes (i.e., time) are scaled in these figures such that the onset of sunrise on the final day/night cycle from the thermal analyses begins at time = 0 hours. Additionally, the stress (Mises) contours of the components of the finite element model are shown at various times in Figure 7 through Figure 11 for the case with a content heat load of 0.4 W. The time chosen for each stress contour plot coincides with the time that particular component reaches its maximum stress during the day/night cycle. The stress contours for the other heat loads investigated are similar to the 0.4 W case.

In addition to the static stress analyses performed for NCT, a static stress analysis is performed for exposure of the package to a -40°F ambient temperature (i.e., cold condition). A transient thermal analysis (24 hours in duration) is performed on the ES-3100 thermal model described in Appendix 3.6.2 to obtain the temperature distribution within the drum body assembly for exposure to cold conditions (see Appendix C for details). The package is assumed to be at an initial uniform temperature of 77°F, and no content heat load is applied. The natural convection coefficients (applied to the top and sides of the drum) are calculated for a -40°F ambient as described in Appendix 3.6.2 and are shown in Figure 12. A schematic of the thermal model showing several node locations for which the temperatures are tracked is presented in Figure 13. The transient temperatures calculated for cold conditions are presented in Figure 14 for several node locations. The maximum thermal stresses are presented in Figure 15 for this cold condition. Additionally, stress contours of the drum liner weldment, drum, and drum bottom plate are presented in Figure 16 through Figure 18 for the cold conditions at various times.

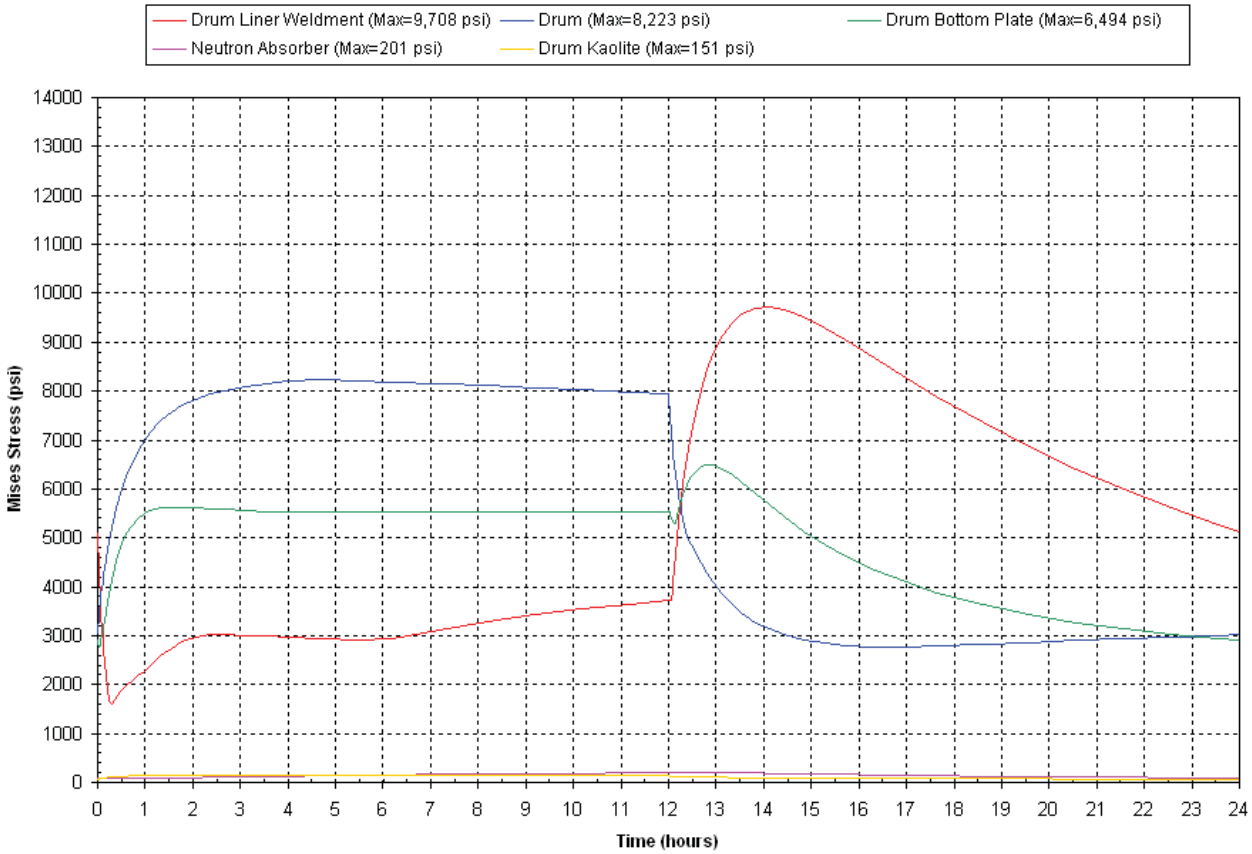

Figure 4. Thermal stresses (Mises) in the ES-3100 shipping container drum body assembly during a typical NCT day/night cycle—0.4 W content heat load.

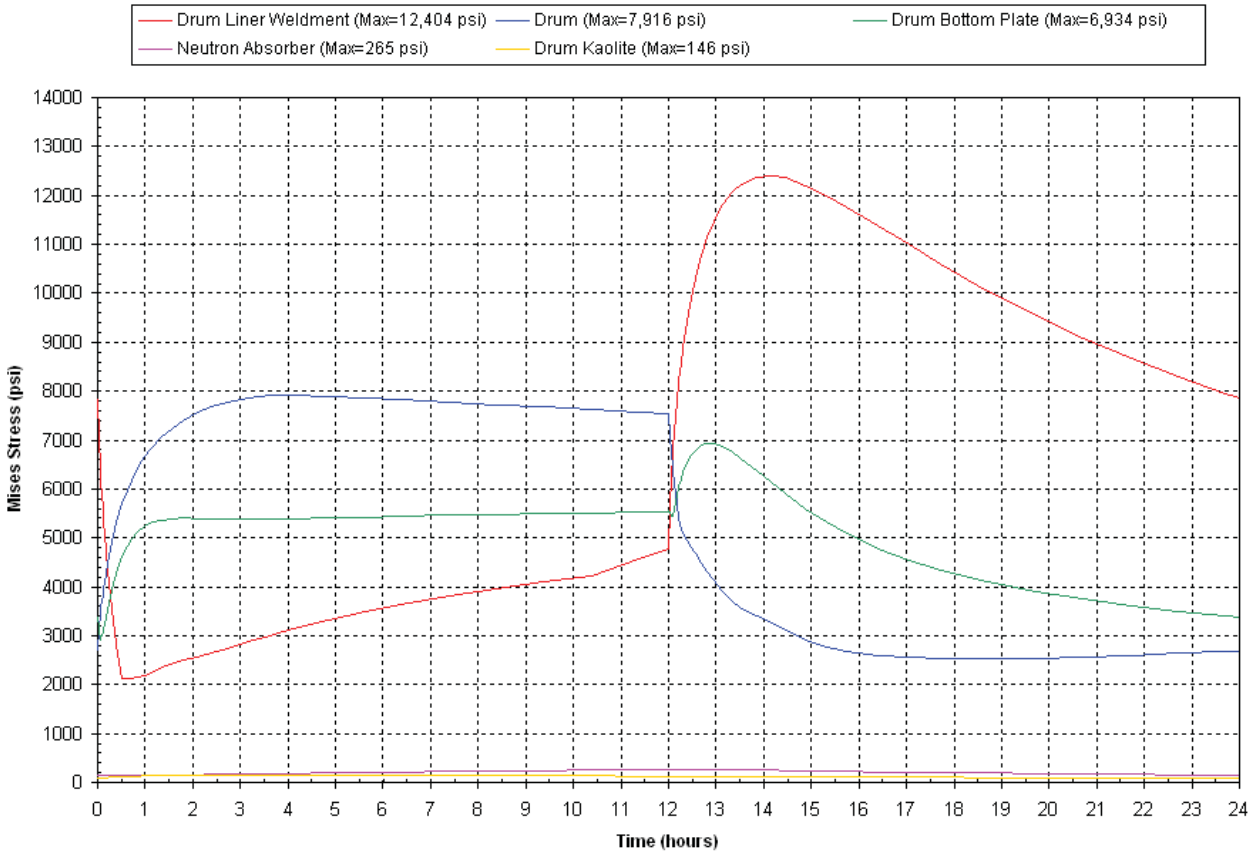

Figure 5. Thermal stresses (Mises) in the ES-3100 shipping container drum body assembly during a typical NCT day/night cycle—20 W content heat load.

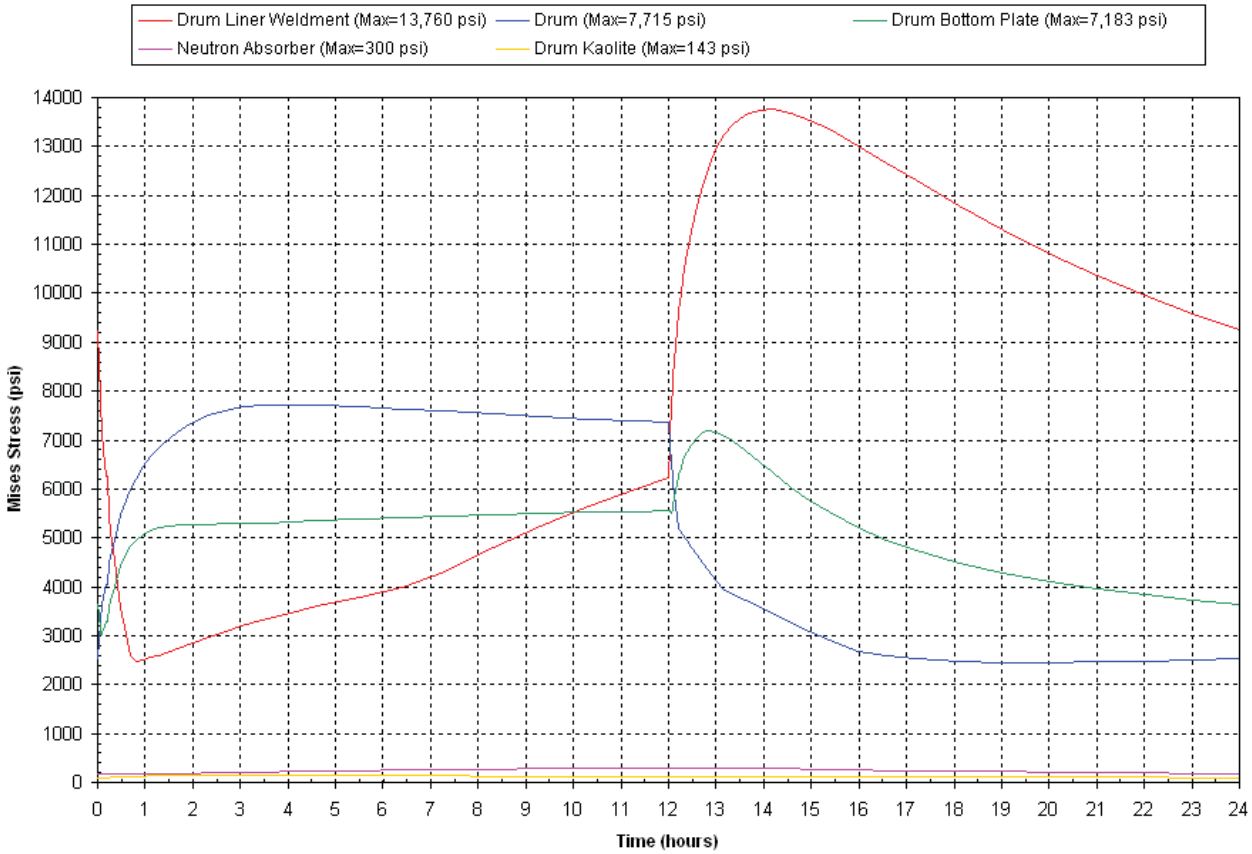

Figure 6. Thermal stresses (Mises) in the ES-3100 shipping container drum body assembly during a typical NCT day/night cycle—30 W content heat load.

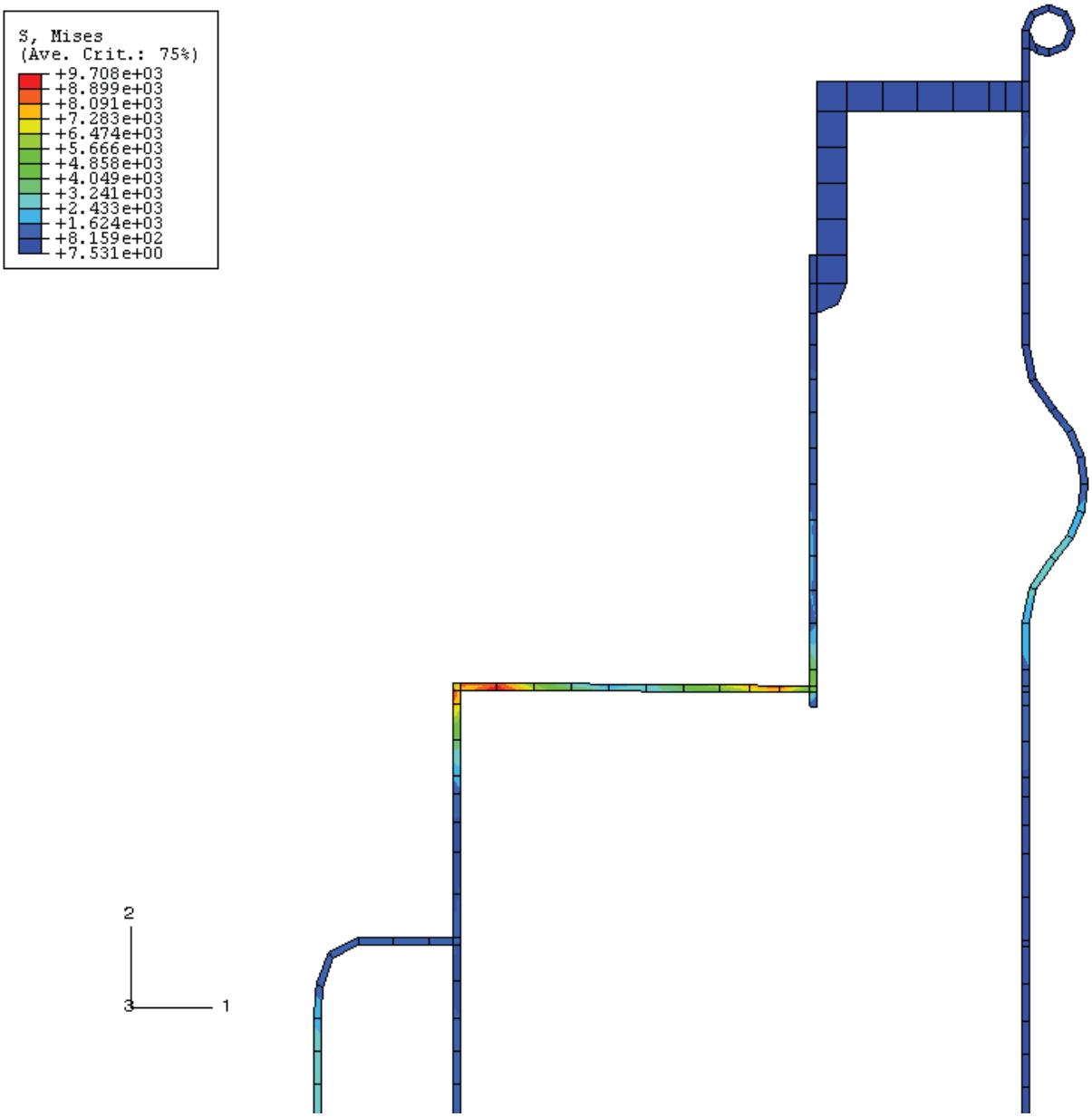

Figure 7. Drum/drum liner weldment Mises stresses (psi) during NCT at t = 14.127 hours (+2.127 hours after sunset)—0.4 W content heat load.

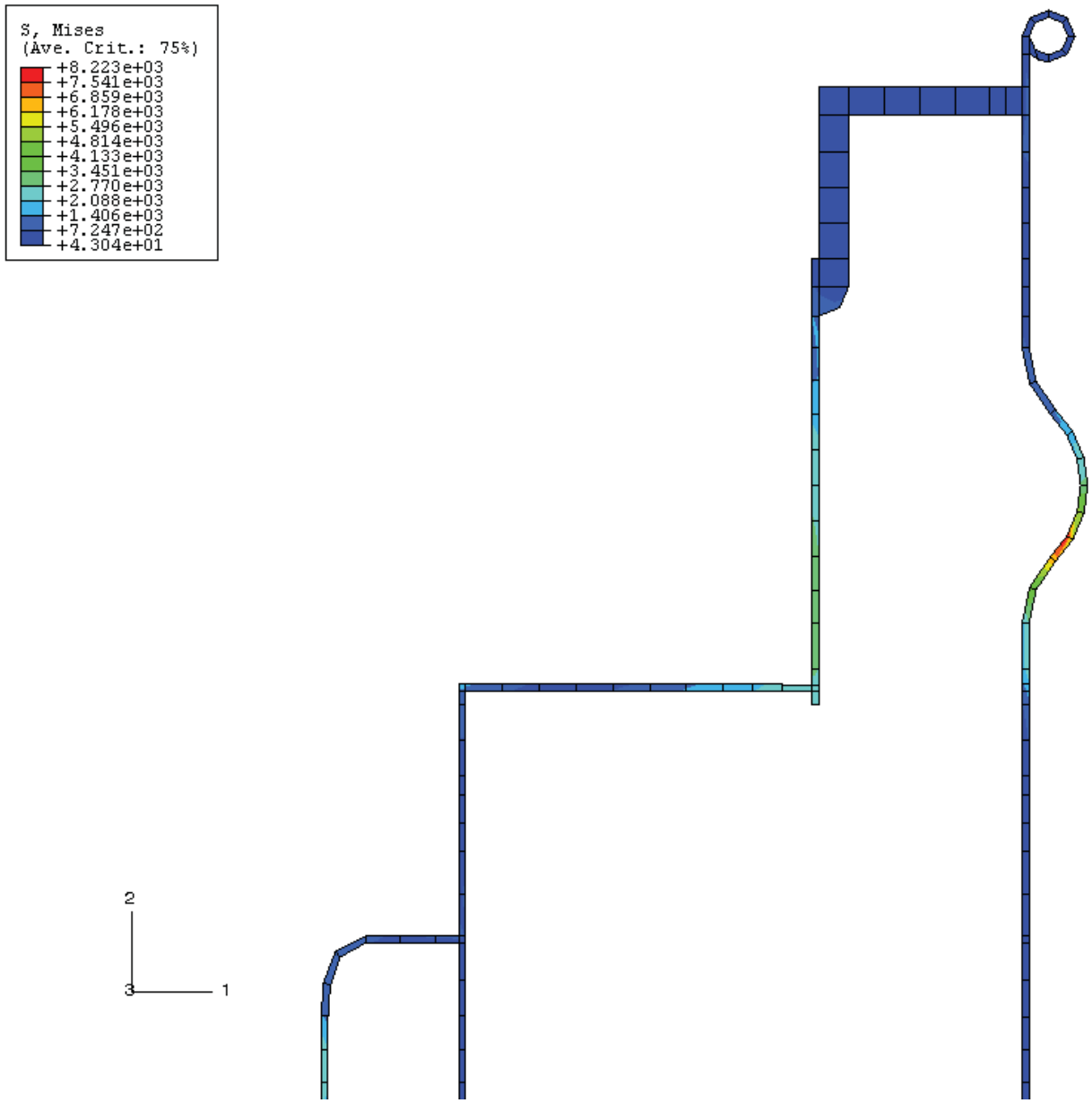

Figure 8. Drum/drum liner weldment Mises stresses (psi) during NCT at t = 4.724 hours (+4.724 hours after sunrise)—0.4 W content heat load.

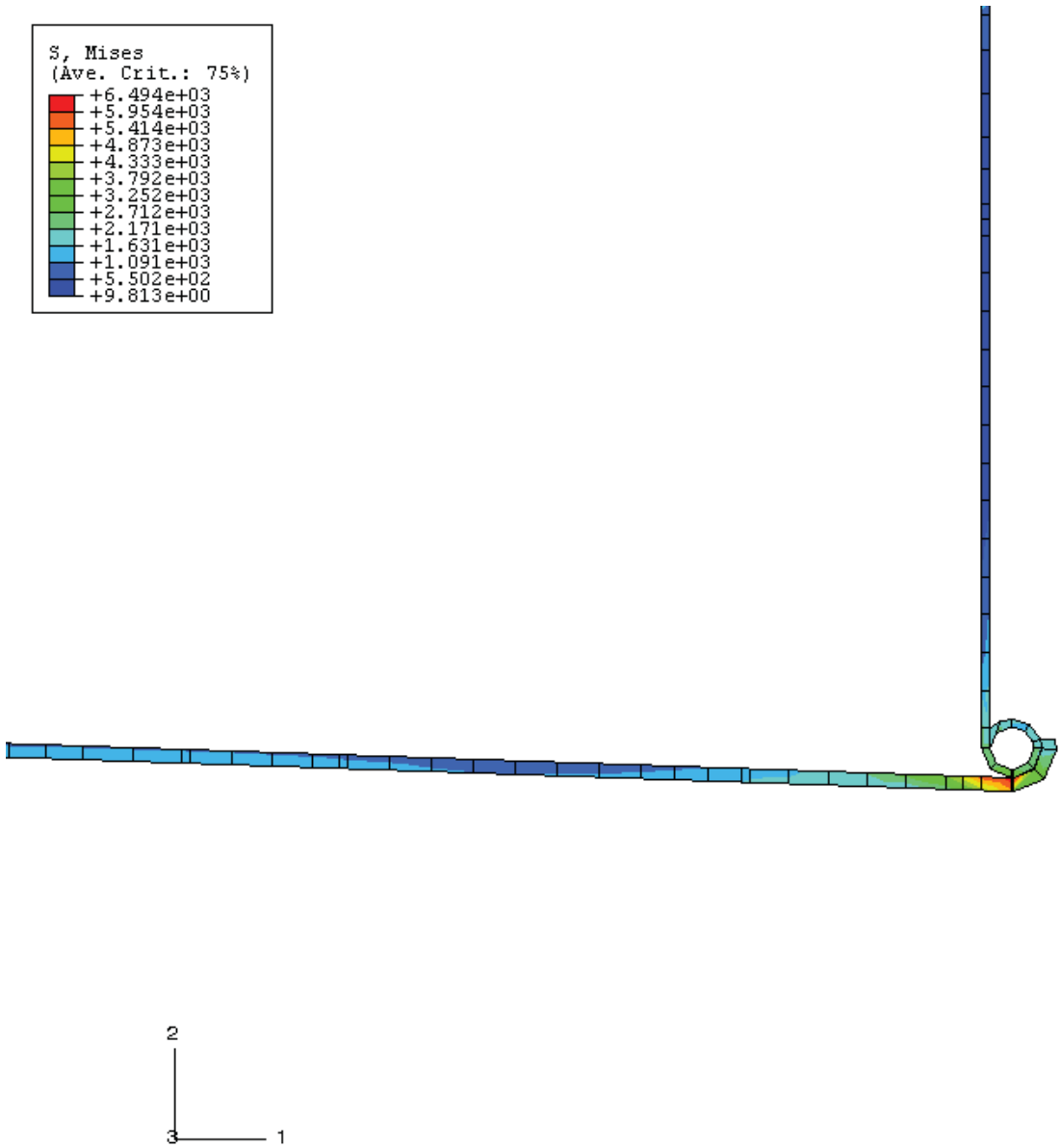

Figure 9. Drum/drum bottom plate Mises stresses (psi) during NCT at t = 12.814 hours (+0.814 hours after sunset)—0.4 W content heat load.

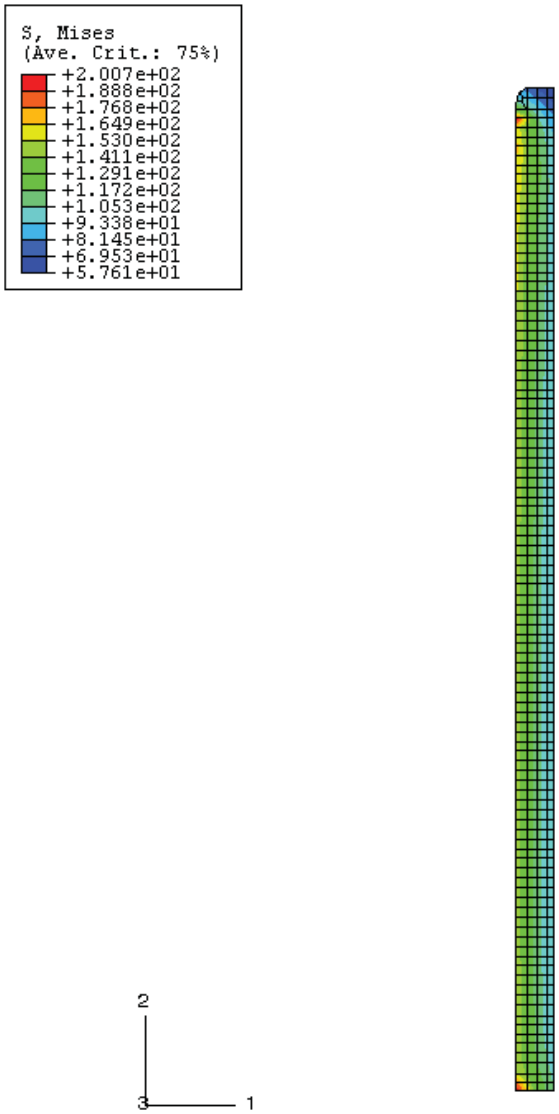

Figure 10. Neutron absorber Mises stresses (psi) during NCT at t = 12.867 hours (+0.867 hours after sunset)—0.4 W content heat load.

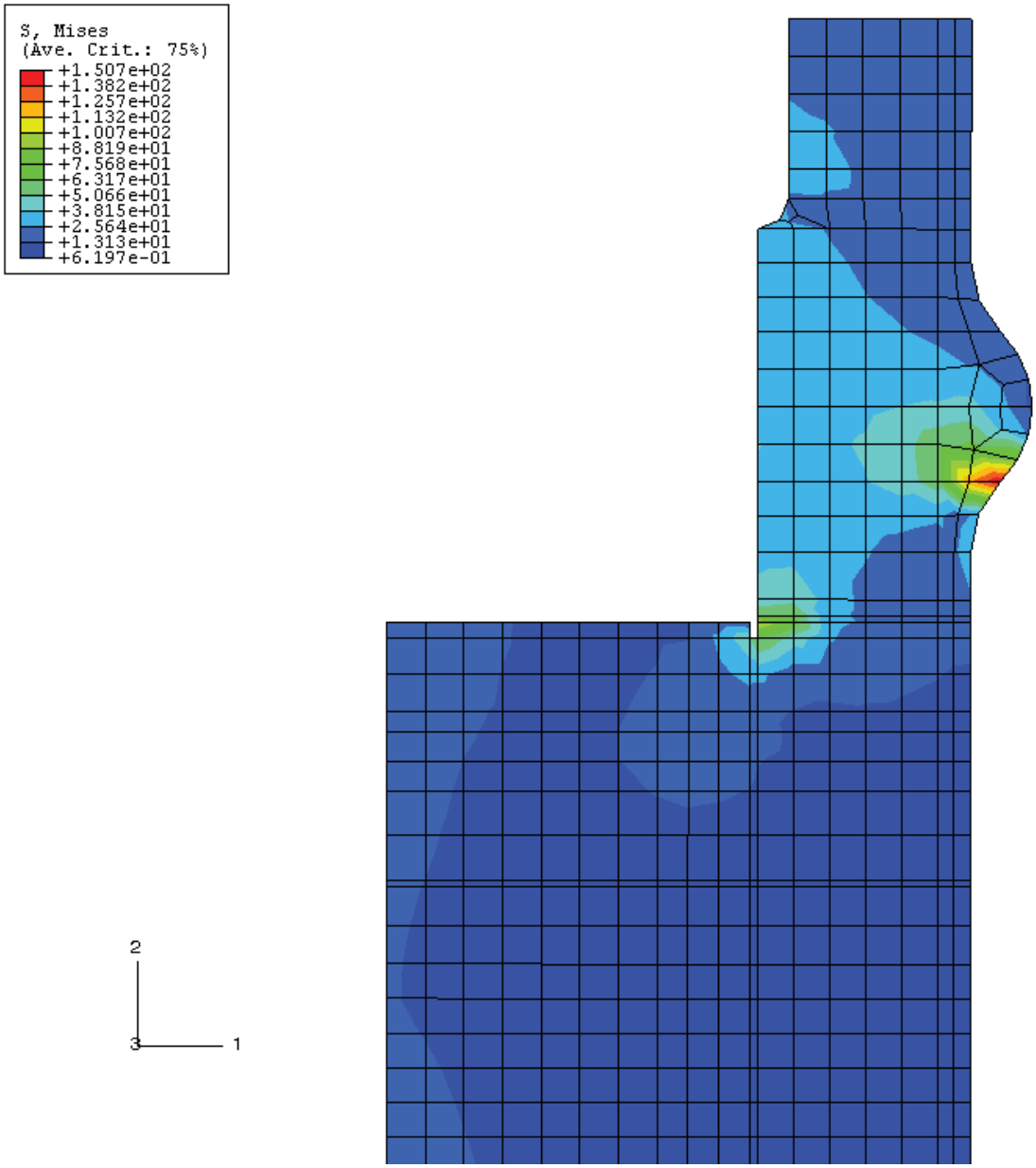

Figure 11. Drum Kaolite Mises stresses (psi) during NCT at t = 3.992 hours (+3.992 hours after sunrise)—0.4 W content heat load.

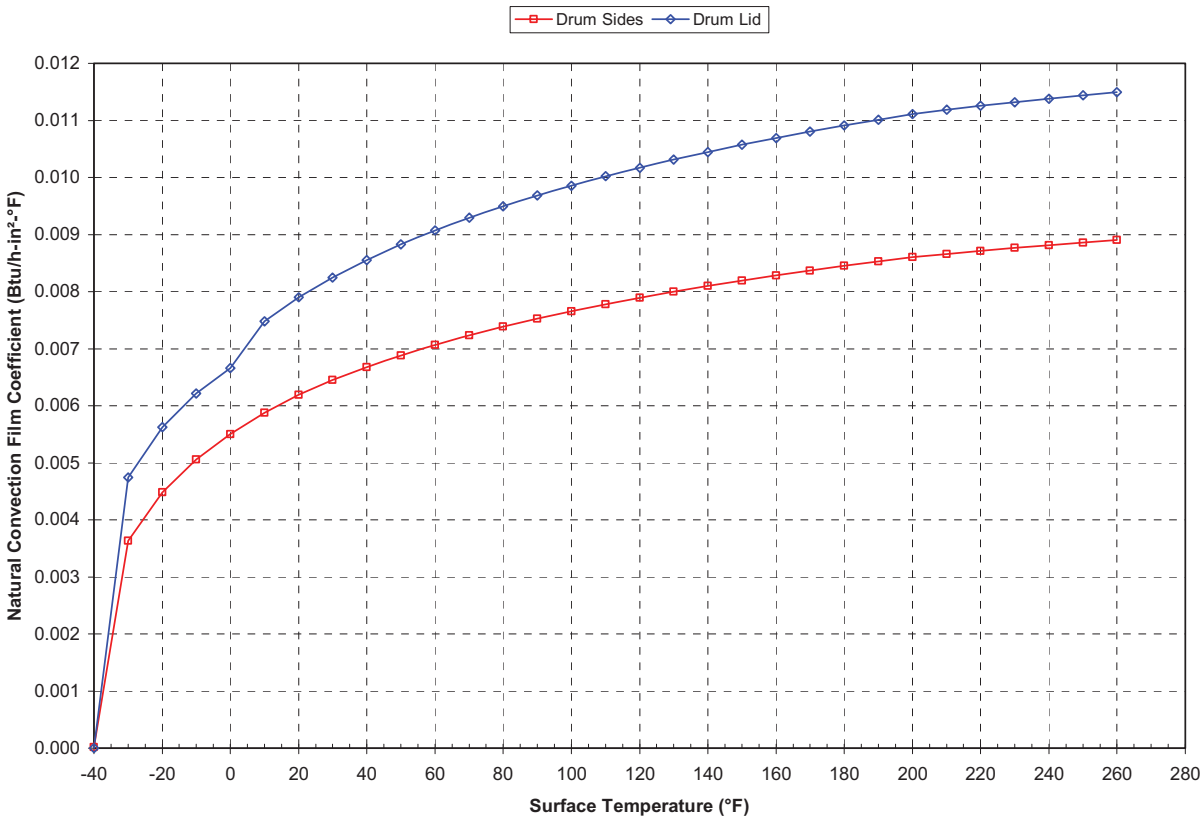

Figure 12. Natural convection film coefficients applied to the drum surfaces during cold conditions.

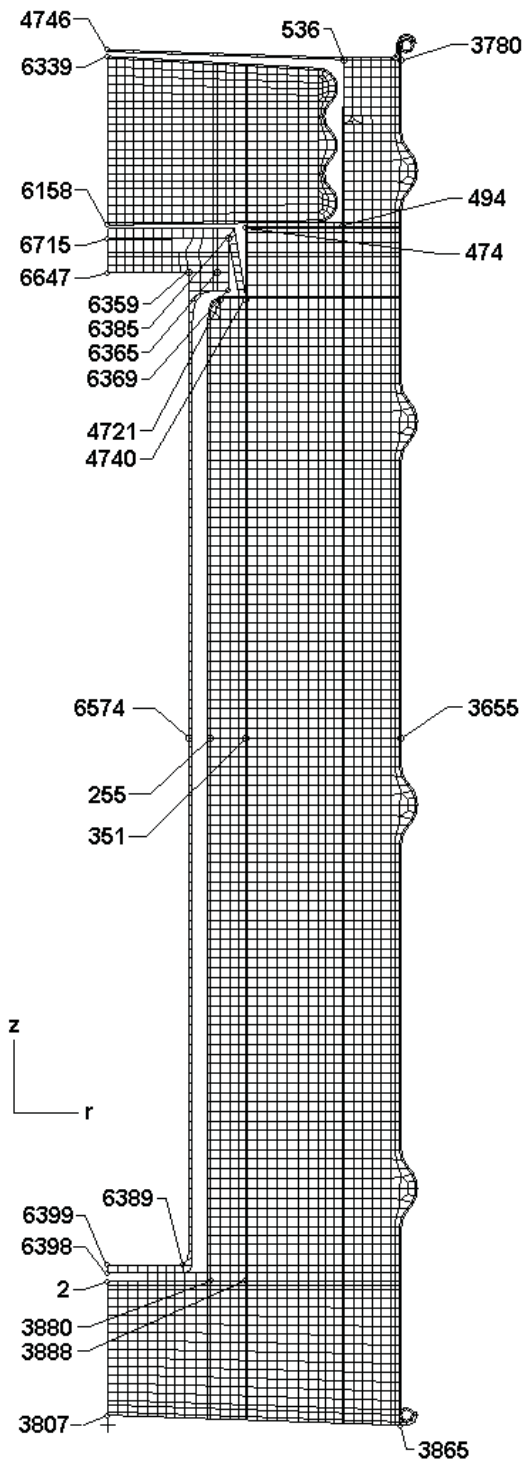

Node	r (in.)	z (in.)
2	0.000	4.505
255	3.180	21.528
351	4.300	21.528
474	4.300	37.535
494	7.325	37.535
536	7.385	42.755
3655	9.185	21.528
3780	9.185	42.755
3807	0.000	0.320
3865	9.185	0.008
3880	3.178	4.505
3888	4.300	4.505
4721	3.500	35.275
4740	4.300	35.275
4746	0.000	43.065
6158	0.000	37.579
6339	0.000	42.859
6359	2.530	36.075
6365	3.425	36.075
6369	3.750	35.525
6385	3.750	37.175
6389	2.310	5.025
6398	0.000	4.775
6399	0.000	5.025
6574	2.530	21.528
6647	0.000	36.075
6715	0.000	37.135

Figure 13. ABAQUS axisymmetric finite element thermal model of the ES-3100 shipping container—nodal locations of interest defined in Table 3.4a (elements representing air not shown for clarity).

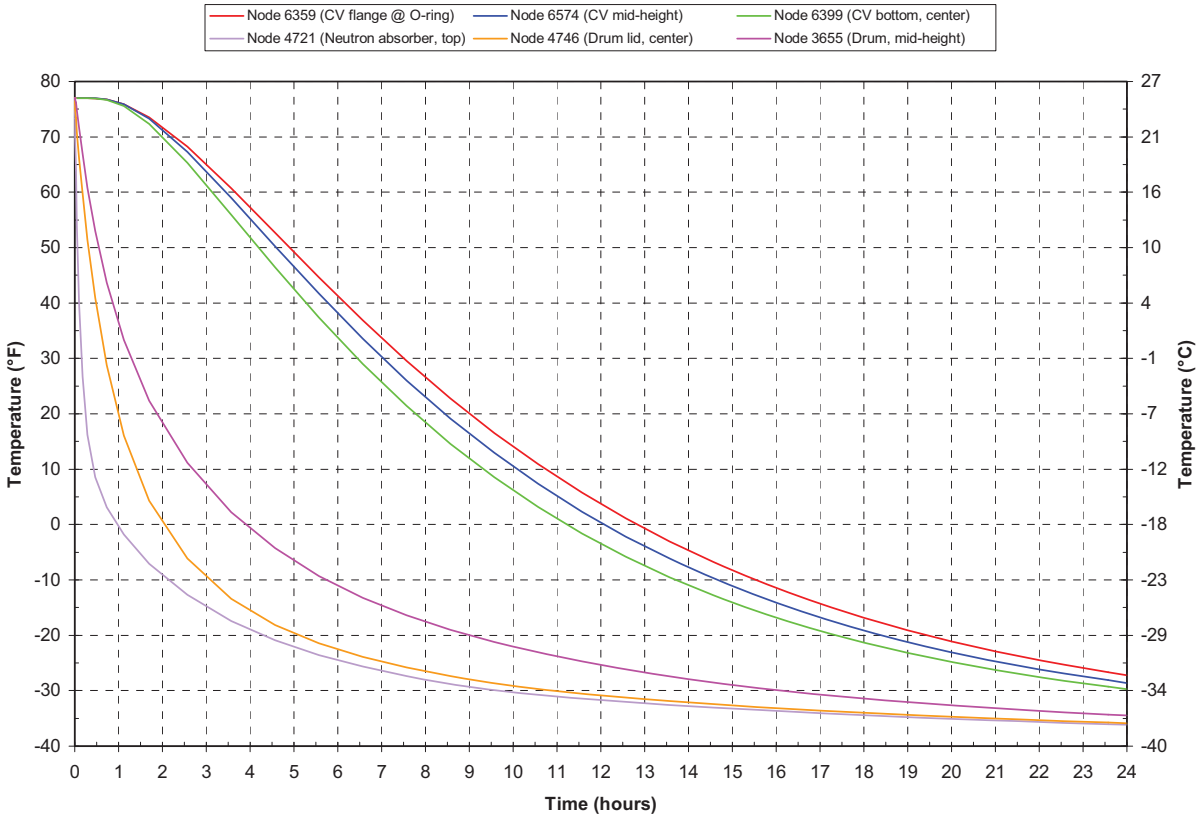

Figure 14. Transient temperatures of the ES-3100 shipping container for cold conditions (no content heat load) see Figure 13 for node locations.

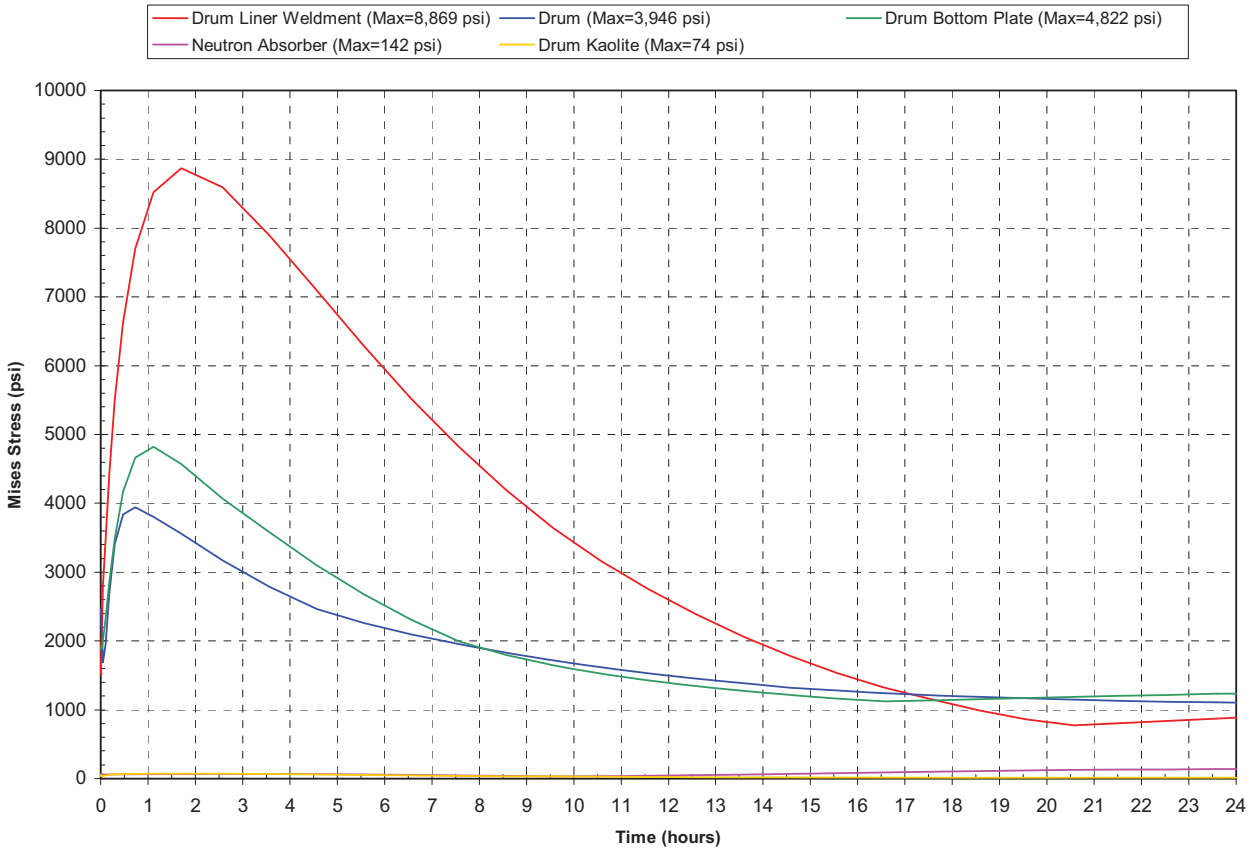

Figure 15. Thermal stresses (Mises) in the ES-3100 shipping container drum body assembly during cold conditions (-40°F ambient temperature)—no content heat load.

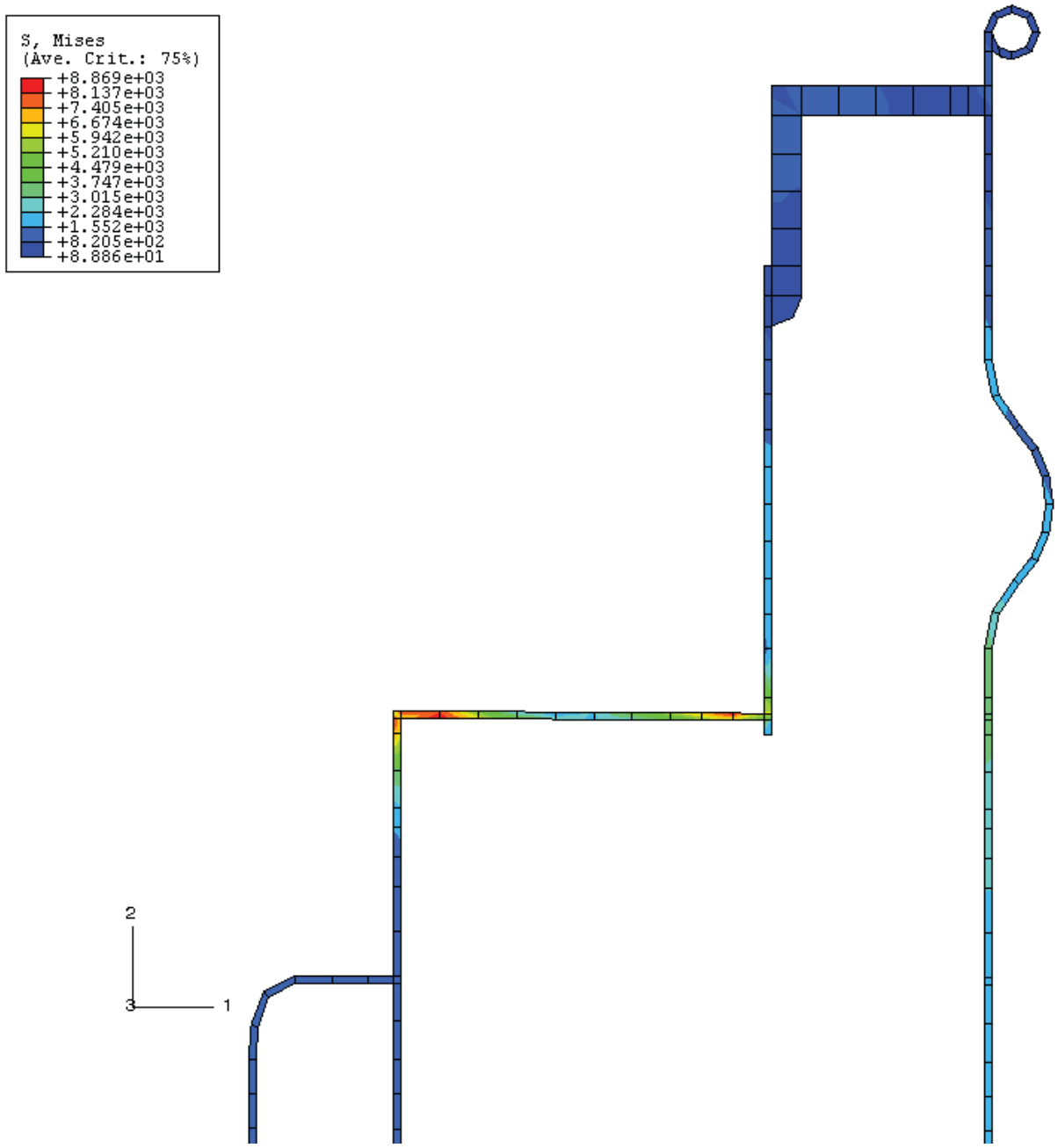

Figure 16. Drum/drum liner weldment Mises stresses (psi) during cold conditions at t = 1.698 hours—no content heat load.

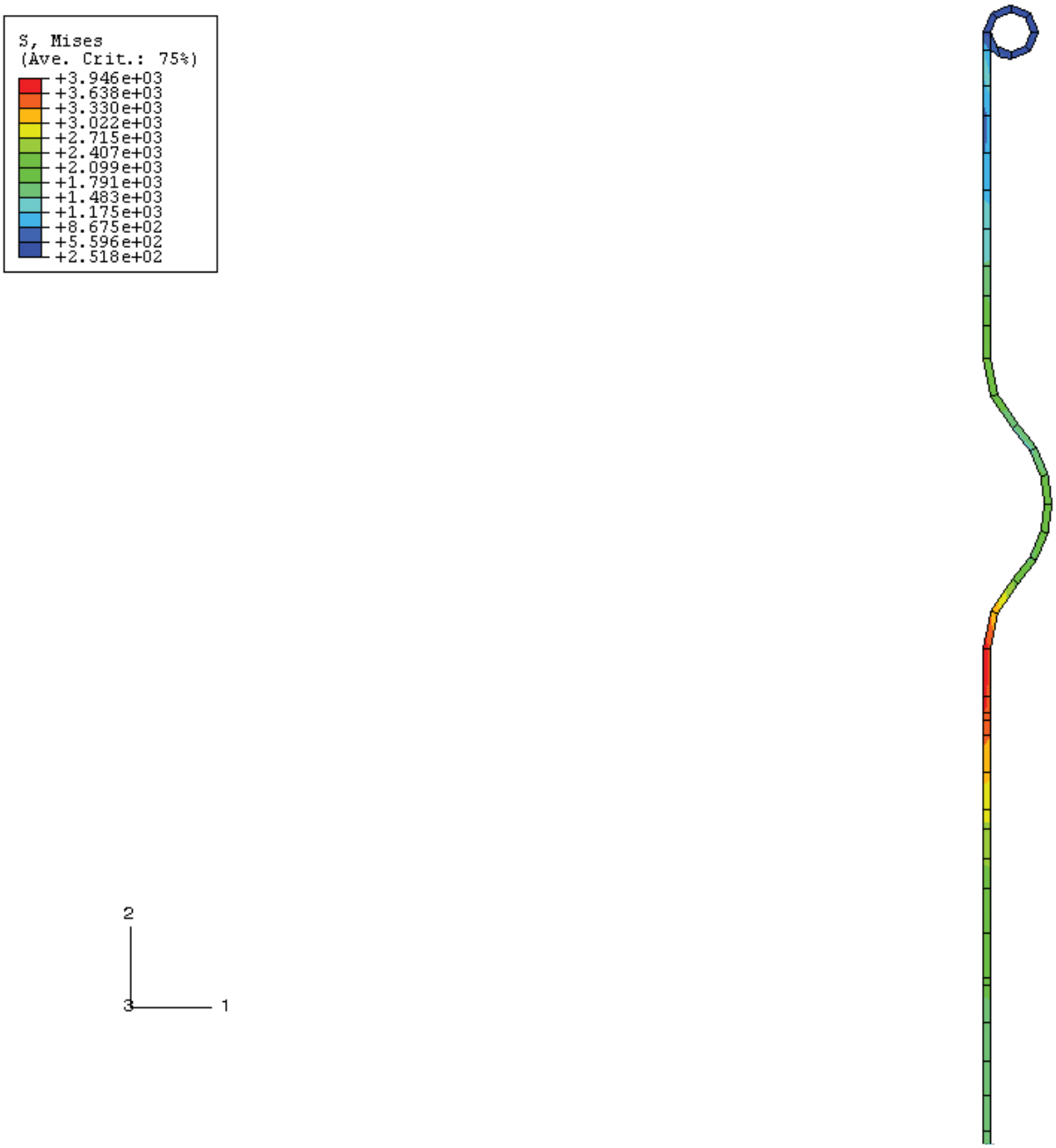

Figure 17. Drum Mises stresses (psi) during cold conditions at t = 0.726 hours — no content heat load.

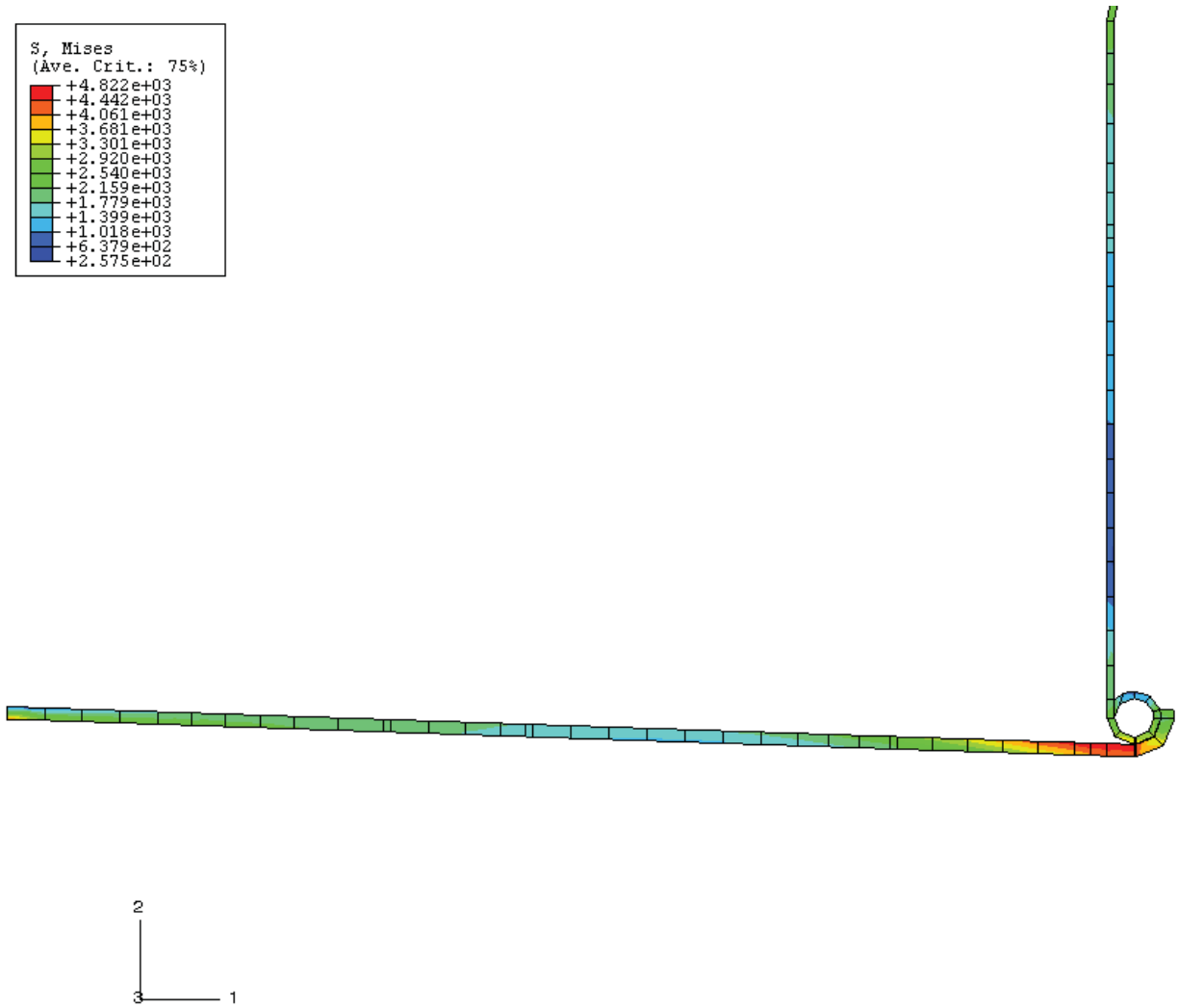

Figure 18. Drum bottom plate Mises stresses (psi) during cold conditions at t = 1.115 hours—no content heat load.

APPENDIX 3.6.3 REFERENCES

1. *Packaging and Transportation of Radioactive Materials*, U.S. Nuclear Regulatory Commission, Code of Federal Regulations, Title 10 – Energy, Part 71, January 1, 2004.

2. P. A. Bales, *Thermal Analyses of the ES-3100 Shipping Container for NCT and HAC (Final Design with 277-4 Neutron Absorber)*, DAC-PKG-801699-A002, Rev. 0, BWXT Y-12, January 31, 2005.

3. MSC. Patran 2004, Version 12.0.044, MacNeal Schwendler Corporation, 2004.

4. ABAQUS/CAE, Version 6.4-1, Build ID: 2003_09_29-11.18.28 46457, Abaqus, Inc., 2003.

5. K. D. Handy, *Impact Analysis of ES3100 Design Concepts Using Borobond*, DAC-EA-801699-A001, BWXT Y-12, Oct. 2004.

6. ABAQUS/Standard, Version 6.4-1, 2003_09-11.18.28 46457, Abaqus, Inc.

Appendix 3.6.4

CONTAINMENT VESSEL PRESSURE DUE TO NORMAL CONDITIONS OF TRANSPORT FOR THE PROPOSED CONTENTS

Prepared by: M. L. Goins
B&W Y-12
December 2007

Reviewed by: Paul Bales
B&W Y-12
January 2008

Revised by: Mark Stansberry
B&W Y-12
February 2009

Reviewed by: Drew Winder
B&W Y-12
February 2009

Revised by: Monty Goins
B&W Y-12
November 2010

Reviewed by: Drew Winder
B&W Y-12
December 2010

THIS PAGE INTENTIONALLY LEFT BLANK.

Appendix 3.6.4

CONTAINMENT VESSEL PRESSURE DUE TO NORMAL CONDITIONS OF TRANSPORT FOR THE PROPOSED CONTENTS

The following calculations determine the pressure of the containment vessel when subjected to the tests and conditions of Normal Condition of Transport per 10 CFR 71.71 for the most restrictive convenience can arrangements shipped in the ES-3100. The following packaging arrangements are evaluated for shipment:

1. one shipment will contain six cans with external dimensions of 4.25-in. diameter by 4.875-in. high;

2. one shipment will contain five cans with external dimensions of 4.25-in. diameter by 4.875-in. high and three can spacers, top can will be empty;

3. one shipment will contain three cans with external dimension of 4.25-in. diameter by 8.75-in. high and two can spacers;

4. one shipment will contain three cans with external dimension of 4.25-in. diameter by 10-in. high; and

5. one shipment will contain six cans with external dimension of 3.00-in. diameter by 4.75-in. high;

6. one shipment will contain three polyethylene bottles with external dimensions of 4.94-in. diameter by 8.7-in. high; and

7. one shipment will contain three Teflon FEP bottles with external dimensions of 4.69-in. diameter by 9.4-in. high.

To determine this pressure, the following assumptions have been made:

1. The HEU contents are loaded into convenience cans which are placed inside the ES-3100 containment vessel at standard temperature (T_{amb}) and pressure (P_t) [25°C (77°F) and 101.35 kPa (14.7 psia)] with air at a maximum relative humidity of 100%.

2. The convenience cans are assumed to not be sealed.

3. Polyethylene bagging of contents and/or convenience cans is limited to 500 g per containment vessel shipping arrangement.

4. If metal convenience cans are used, the total amount of polyethylene bagging and lifting slings is limited to 500 g per containment vessel shipping arrangement.

5. The mass of offgassing material (polyethylene bagging or bottles, Teflon bottles, silicone pads, lifting slings) is assumed to be 1490 g for the offgassing evaluation of containment vessel arrangement #7 and 500 g for containment vessel arrangement #6.

The offgassing material limits identified in assumptions 4 and 5 have been established based on the needs of shippers. All configurations are limited to 500 g of polyethylene in the form of bags, slings, and/or bottles. When the requirement to ship material in Teflon bottles arose, the upper limit of 1490 g of offgassing material was established. This limit is a combination of three Teflon bottles (330 g per bottle) and the original 500 g allowance for polyethylene material. These offgassing material limits have been used in calculations pertaining to containment vessel pressure, radioactive material leakage criteria, and criticality control. Therefore, portion of the safety basis of this shipping package has been based on these material limits.

Applying Dalton's law concerning a mixture of gases, the properties of each component are considered as though each component exists separately at the volume and temperature of the mixture. Therefore, the molar quantities of each constituent inside the containment vessel (i.e., dry air, water vapor, polyethylene bagging, and silicone rubber) must be calculated individually.

To calculate these molar properties, the void volume of the containment vessel must be determined. The volume inside an empty ES-3100 containment vessel was determined from Algor finite element software to be 637.18 in.^{3} (10,441.51 cm^3).

I. Molar quantity determination for dry air and water vapor

According to *Fundamentals of Classical Thermodynamics*,

> "Relative humidity (Φ) is defined as the ratio of the mole fraction in the mixture to the mole fraction of vapor in a saturated mixture at the same temperature and total pressure."

Since the vapor is considered an ideal gas, the definition reduces to the ratio of the partial pressure of the vapor (P_v) as it exists in the mixture to the saturation pressure of the vapor (P_g) at the same temperature.

Therefore,

$$\Phi = P_v / P_g .$$

From the above equation and interpolating the values given in Table A.1.1 of *Fundamentals of Classical Thermodynamics*, the partial pressure of the water vapor at saturation is:

$$P_v = 1.0\ (0.464)\ \text{psia},$$
$$P_v = 0.464\ \text{psia}.$$

The partial pressure of the dry air (P_a) in the volume:

$$P_a = P_t - P_v$$
$$= 14.7 - 0.464$$
$$= 14.236\ \text{psia}.$$

From the ideal gas law, the number of water vapor moles and dry air moles in the void volume (V_V) for each containment vessel arrangement (CVA) is calculated as follows:

$$n_v = \frac{P_v \cdot V_v}{R_u \cdot T_{amb} \cdot 12}, \quad n_a = \frac{P_a \cdot V_v}{R_u \cdot T_{amb} \cdot 12}$$

To determine the number of moles, the void volume of the air mixture must be determined. The void volume (V_V) in the containment vessel for each CVA is calculated as follows:

$$V_V = V_{ECV} - V_{SP} - V_{PB} - V_{SCC} - V_{CS} - V_{CH},$$

where

V_{ECV} = volume inside an empty containment vessel,
V_{SP} = silicone pad volume,
V_{PB} = polyethylene bagging or lifting sling volume,
V_{SCC} = structural volume of the convenience cans or bottles,
V_{CS} = external volume of the can spacers,
V_{CH} = external volume of the convenience can handles.

A summary for each CVA is shown in Table 1.

The bounding case based on the volumes listed in Table 1 is CVA 2 at 526.21 in.^{3}. To determine the minimum volume for this configuration, the mass limit of 15.13 kg of oxides is used in conjunction with the lowest density oxide of 7.3 kg/L (UO_3). The resulting volume is 15.13 kg / 7.3 kg/L × 1 ft^3 / 28.32 L × 1728 in.^{3} / ft^3 = 126.464 in.^{3}. Therefore, the bounding volume for CVA 2 is 526.21 in.^{3} – 126.464 in.^{3} = 399.746 in.^{3}.

Only CVA 7 can accommodate the uranyl nitrate crystals held in the Teflon bottles. CVA 7 is limited to 9.12 kg of the uranyl nitrate hexahydrate crystals and 11.9 kg of uranyl nitrate trihydrate crystals (see Appendix 3.6.7). For the bounding pressure calculation, the smallest resulting free volume in CVA 7 is then 578.72 – 11.9 kg / 2.81 kg/L × 1 ft^3 / 28.32 L × 1728 in.^{3} / ft^3 = 578.72 in.^{3} – 258.4 in.^{3} = 320.32 in.^{3}.

Using the above molar equations and bounding volumes, the number of moles for water vapor and dry air in the vessel for CVAs 2 and 7 are summarized in Table 2.

Table 1. Containment vessel void volume for each CVA

CVA		V_{ECV} (in.^{3})	V_{SP} [a] (in.^{3})	V_{PB} (in.^{3})	V_{SCC} (in.^{3})	V_{CS} (in.^{3})	V_{CH} (in.^{3})	V_V (in.^{3})
1	Six 4.875-in.-high cans Seven silicone pads Six can handles	637.18	9.35	30.51	7.84	0.00	1.02	588.46
2	Five 4.875-high cans Nine silicone pads Three Cat 277-4 spacers Eight can handles	637.18	12.03	30.51	6.47	60.60	1.36	526.21
3	Three 8.75-in.- high cans Two Cat 277-4 spacers Six silicone pads Five can handles	637.18	8.02	30.51	5.14	40.40	0.85	552.26
4	Three 10-in.-high cans Four silicone pads Three can handles	637.18	5.35	30.51	5.56	0.00	0.51	595.26
5	Six 4.75 in.-high nickel cans	637.18	0.00	30.51	12.64	0.00	1.02	593.01
6	Three 4.94 in. OD polyethylene bottles	637.18	0.00	9.46	21.05	0.00	0.00	606.67
7	Three 4.69 in. OD Teflon FEP bottles	637.18	0.00	30.51	27.95	0.00	0.00	578.72

[a] This assumes that the internal convenience cans, polyethylene or Teflon FEP bottles, and Cat 277-4 spacer cans are not sealed.

Table 2. Water vapor and dry air molar summary for each CVA

CVA	P_a (psia)	P_v (psia)	V_V (in.^{3})	R_u (ft-lb/lb-mole·R)	T_{amb} (R)	n_v (lb-mole)	n_a (lb-mole)
2	14.236	0.464	399.75	1545.32	537	1.0868E-05	5.7148E-04
7	14.236	0.464	320.32	1545.32	537	1.4926E-05	4.5793E-04

II. Molar quantity determination due to offgassing for each containment vessel arrangement

The maximum temperature calculated for the containment vessel is 87.81°C (190.06°F). This temperature is assumed to be constant throughout the containment vessel and contents. Therefore, the polyethylene bags, polyethylene bottles, Teflon FEP bottles, and silicone rubber can pads are assumed to be at this temperature.

Using the above calculated results and the specific gas generation of polyethylene bags and silicone rubber pad measurements at temperatures up to 170°C (338°F) conducted by the Y-12 Development Division, the amount of gas (V_{bo} and V_{po}) generated due to offgassing of the polyethylene bags and bottles, and silicone rubber can pads at any temperature is estimated by first determining the offgassing volume per unit mass at temperature and multiplying that by the total mass of the bags and can supports inside the containment vessel. Based on testing at a temperature of 93.33°C (200°F), no recordable offgassing occurred in the polyethylene bags and bottles, or silicone rubber pad material

as documented in Y/DZ-2585, Rev. 2 (Appendix 2.10.4). The value for Teflon FEP material offgassing volume per unit mass (V_{tf}) was obtained from Fig. 10 in Appendix 2.10.9. A value of ~0.12 to 0.13 cm^3/g@STP was recorded over a temperature range of 200 to 400°F. This value was conservatively doubled to 0.25 cm^3/g@STP. These values are used to determine the offgassing volumes as shown below:

$V_{po} = W_p \times 0.0 / 16.387\ (in.^3)$ (offgassing volume of silicone rubber pads)

$V_{bo} = W_b \times 0.0 / 16.387\ (in.^3)$ (offgassing volume of polyethylene bags and bottles or lifting sling)

$V_{tf} = W_{tf} \times 0.25 / 16.387\ (in.^3)$ (offgassing volume of Teflon bottles)

From the ideal gas law, the number of gas moles in the volume at standard temperature and pressure is as follows:

$$n_{io} = \frac{P_v \cdot V_i}{R_u \cdot T_{amb} \cdot 12}$$

A summary of the results obtained using the above equations for the bounding containment vessel arrangement is presented in Tables 3, 4, and 5.

Table 3. Molar quantity of gas generated due to the silicone rubber pad offgassing

CVA	W_p (g)	V_{po} (in.^{3})	P_V (psia)	R_u (ft-lb/lb-mole·R)	T_{amb} (R)	n_{po} (lb-mole)
2	240.09	0.00	14.7	1545.32	537	0.0000E+00
7	0.00	0.00	14.7	1545.32	537	0.0000E+00

Table 4. Molar quantity of gas generated due to the polyethylene bag, sling and bottle offgassing

CVA	W_b (g)	V_{bo} (in.^{3})	P_V (psia)	R_u (ft-lb/lb-mole·R)	T_{amb} (R)	n_{bo} (lb-mole)
2	500.00	0.00	14.7	1545.32	537	0.0000E+00
7	500.00	0.00	14.7	1545.32	537	0.0000E+00

Table 5. Molar quantity of gas generated due to the Teflon bottle offgassing

CVA	W_{tf} (g)	V_{tf} (in.^{3})	P_V (psia)	R_u (ft-lb/lb-mole·R)	T_{amb} (R)	n_{tf} (lb-mole)
7	990.00	15.10	14.7	1545.32	537	2.2296E-05

III. Gas generation due to radiolysis of water

Buildup of hydrogen gas (H_2) and oxygen gas (O_2) in the ES-3100 containment vessel due to radiolysis is incorporated into the pressure calculation by assuming that 5 mol % of the free volume is H_2. Since each mole of H_2 generated is accompanied by 0.5 mole of O_2, the concentration of H_2 will reach 5 mol % when volume of H_2 is 0.05405 times the initial void volume (see Sect. 3.6.7.8 of Appendix 3.6.7). Therefore, the volume of H_2 and O_2 in the void volume (V_v) is determined by the following expressions:

$$V_h = 0.05405 \times V_v \quad \text{and} \quad V_o = 0.5 \times V_h .$$

Using the ideal gas law, the number of gas moles of H_2 and O_2 in the volume at standard temperature and pressure is:

$$n_{r\text{-}H2} = \frac{P_v \cdot V_h}{R_u \cdot T_{amb} \cdot 12} \qquad n_{r\text{-}O2} = \frac{P_v \cdot V_o}{R_u \cdot T_{amb} \cdot 12}$$

where

$n_{r\text{-}H2}$ = individual molar quantity for H_2,
$n_{r\text{-}O2}$ = individual molar quantity for O_2,
V_h = volume of H_2 assumed generated by radiolysis,
V_o = volume of O_2 assumed generated by radiolysis.

A summary of the results for H_2 and O_2 generation due to radiolysis using the above equation is presented in Table 6.

Table 6. Molar quantity of oxygen and hydrogen gas generation due to radiolysis

CVA	V_v (in.^{3})	V_h (in.^{3})	V_o (in.^{3})	P_v (psia)	R_u (ft-lb/lb-mole · R)	T_{amb} (R)	$n_{r\text{-}H2}$ (lb-mole)	$n_{r\text{-}O2}$ (lb-mole)
1	399.75	21.61	10.80	14.7	1545.32	537.0	3.1895E-05	1.5948E-05
7	320.32	17.31	8.66	14.7	1545.32	537.0	2.5558E-05	1.2779E-05

IV. Molar quantity of gas generated due to the efflorescence of the uranyl nitrate crystals (UNX)

The uranyl nitrate crystals (UNX) in any hydrated state will decompose and lose water molecules at the temperature shown in Table 3.16 [87.81°C (190.06°F)]. The partial pressure of water vapor in this mixture is conservatively estimated to be the saturated vapor pressure (P_{sv}) of water at 87.81°C (190.06°F) or 9.344 psia. Using the ideal gas law, the molar quantity of water vapor (n_{wv}) in this volume at the maximum containment vessel temperature and the saturated vapor pressure is:

$$n_{wv} = \frac{P_{sv} \cdot V_v}{R_u \cdot T_{cv} \cdot 12}$$

$$n_{wv} = (9.344)\,(320.32) / (1545.32 \times 12 \times 650.06)$$
$$n_{wv} = 2.4829 \times 10^{-4} \text{ lb-moles}$$

where

n_{wv}	=	molar quantity for water vapor;
V_v	=	void volume of containment vessel;
T_{cv}	=	maximum temperature of containment vessel; and
P_{sv}	=	interpolated saturated vapor pressure of water at temperature from *Fundamentals of Classical Thermodynamics*, 2d ed, Table A.1.1, p. 650. (Van Wylen 1973)

V. Total pressure due to offgassing and NCT temperatures inside the containment vessel

The total pressure of the mixture at 87.81°C (190.06°F), P_T, for the bounding containment vessel arrangement is the pressure calculated using the sum of the previously calculated molar quantities of the gases in the containment vessel. Table 7 summarizes the molar constituents and total pressure of each bounding containment vessel arrangement. The following equation is used to calculate the final containment vessel pressure:

$$P_{87.81°C} = (\sum n_i \cdot R \cdot T \cdot 12) / V_{GMV} ,$$

where

n_i	=	individual molar quantity for each gas,
T	=	average gas temperature = 87.81°C (190.06°F),
V_{GMV}	=	V_v = gas mixture volume.

At −40°C (−40°F), the partial pressure of the water vapor is conservatively assumed to be zero. Therefore, the final pressure of the mixture at −40°C (−40°F) is calculated according to the ideal gas law based solely on the partial pressure of the air.

$$\frac{P_1 V_1}{T_1} = \frac{P_2 V_2}{T_2},$$

where

P_1	=	14.236 psi,	
T_1	=	77°F	= 536.67 R,
T_2	=	−40°F	= 419.67 R,
V_1	=	V_2.	

Rearranging and solving for P_2,

$$P_2 = P_1 (T_2/T_1),$$
$$P_2 = (14.236)(419.67/536.67) = 11.13 \text{ psia}.$$

Table 7. Total pressure inside the containment vessel at 87.81°C (190.06°F) [a]

CVA	n_a [b] (lb-mole)	n_v [b] (lb-mole)	n_{po} [b] (lb-mole)	n_{bo} [b] (lb-mole)	n_{tf} [b] (lb-mole)	n_{H2} [b] (lb-mole)	n_{O2} [b] (lb-mole)	n_T [b] (lb-mole)	P_T (psia)
2	5.7148E-04	1.8626E-05	0.0000E+00	0.0000E+00	0.0000E+00	3.1895E-05	1.5948E-05	6.3795E-04	19.238
7	4.5793E-04	2.4829E-04	0.0000E+00	0.0000E+00	2.2296E-05	2.5558E-05	1.2779E-05	7.6685E-04	28.859

[a] This assumes that the internal convenience cans, polyethylene or Teflon FEP bottles, and Cat 277-4 spacer cans are not sealed.

[b] n_a –molar quantity of dry air in the gas mixture;
n_v –molar quantity of water vapor in the gas mixture due primarily to efflorescence;
n_{po} –molar quantity of gas due to offgassing of the silicone rubber pads;
n_{bo} –molar quantity of gas due to offgassing of the polyethylene bags, bottles, and lifting sling;
n_{tf} –molar quantity of gas due to offgassing of the Teflon bottles;
n_{H2} –molar quantity of hydrogen gas due to radiolysis of water;
n_{O2} –molar quantity of oxygen gas due to radiolysis of water; and
n_T –total molar quantity in the gas mixture.

Appendix 3.6.5

CONTAINMENT VESSEL PRESSURE DUE TO HYPOTHETICAL ACCIDENT CONDITIONS FOR THE PROPOSED CONTENTS

Prepared by:	M. L. Goins B&W Y-12 December 2007
Reviewed by:	Paul Bales B&W Y-12 January 2008
Revised by:	Mark Stansberry B&W Y-12 February 2009
Reviewed by:	Drew Winder B&W Y-12 February 2009
Revised by:	Monty Goins B&W Y-12 November 2010
Reviewed by:	Drew Winder B&W Y-12 December 2010

THIS PAGE INTENTIONALLY LEFT BLANK.

Appendix 3.6.5

CONTAINMENT VESSEL PRESSURE DUE TO HYPOTHETICAL ACCIDENT CONDITIONS FOR THE PROPOSED CONTENTS

The following calculations determine the pressure of the containment vessel when subjected to the tests and conditions of Hypothetical Accident Conditions per 10 CFR 71.73 for the most restrictive convenience can arrangements shipped in the ES-3100 package. The following packaging arrangements are evaluated for shipment:

1. one shipment will contain six cans with external dimensions of 4.25-in. diam by 4.875-in. high;

2. one shipment will contain five cans with external dimensions of 4.25-in. diam by 4.875-in. high and three can spacers, the top can is empty;

3. one shipment will contain three cans with external dimensions of 4.25-in. diam by 8.75-in. high and 2 can spacers;

4. one shipment will contain three cans with external dimensions of 4.25-in. diam by 10-in. high;

5. one shipment will contain six nickel cans with external dimensions of 3.00-in. diam by 4.75-in. high;

6. one shipment will contain three polyethylene bottles with external dimensions of 4.94-in. diam by 8.7-in. high; and

7 one shipment will contain three Teflon FEP bottles with external dimensions of 4.69-in. diam by 9.4-in. high.

To determine this pressure, the following assumptions have been made:

1. The highly enriched uranium (HEU) contents are loaded into convenience cans and placed inside the ES-3100 containment vessel at standard temperature [25°C (77°F)] and at the maximum normal operating pressure (see Table 5 of Appendix 3.6.4) with air at a maximum relative humidity of 100%.

2. The convenience cans are assumed to not be sealed.

3. Polyethylene bagging of contents and/or convenience containers is limited to 500 g per containment vessel shipping arrangement.

4. If metal convenience cans are used, the total amount of polyethylene bagging and lifting slings is limited to 500 g per containment vessel shipping arrangement.

5. The mass of offgassing material (polyethylene bagging or bottles, Teflon bottles, silicone pads, lifting slings) is assumed to be 1490 g for the offgassing evaluation of containment vessel arrangement #7 and 500 g for containment vessel arrangement #6.

The offgassing material limits identified in assumptions 4 and 5 have been established based on the needs of shippers. All configurations are limited to 500 g of polyethylene in the form of bags, slings, and/or bottles. When the requirements to ship material in Teflon bottles arose, the upper limit of 1490 g of offgassing material was established. This limit is a combination of three Teflon bottles (990 g) and the original 500 g allowance for polyethylene material. These offgassing material limits have been used in calculations pertaining to containment vessel pressure, radioactive material leakage criteria, and criticality control. Therefore, portion of the safety basis of this shipping package has been based on these material limits.

Applying Dalton's law concerning a mixture of gases, the properties of each component are considered as though each component exists separately at the volume and temperature of the mixture. Therefore, the molar quantities of each constituent inside the containment vessel (i.e., dry air, water vapor, polyethylene bagging and bottles, silicone rubber pads, and teflon bottles) must be calculated individually.

To calculate these molar properties, the void volume of the containment vessel must be determined. The volume inside an empty ES-3100 containment vessel was determined from Algor finite element software to be 637.18 in.^{3} (10,441.51 cm^3).

I. Molar quantity determination based on MNOP

Table 1. Total pressure inside the containment vessel at 87.81°C (190.06°F) [a]

CVA	n_a [b] (lb-mole)	n_v [b] (lb-mole)	n_{po} [b] (lb-mole)	n_{bo} [b] (lb-mole)	n_{tf} [b] (lb-mole)	n_{H2} [b] (lb-mole)	n_{O2} [b] (lb-mole)	n_T [b] (lb-mole)	P_T (psia)
2	5.7148E-04	1.8626E-05	0.0000E+00	0.0000E+00	0.0000E+00	3.1895E-05	1.5948E-05	6.3795E-04	19.238
7	4.5793E-04	2.4829E-04	0.0000E+00	0.0000E+00	2.2296E-05	2.5558E-05	1.2779E-05	7.6685E-04	28.859

[a] This assumes that the internal convenience cans, polyethylene or Teflon FEP bottles, and Cat 277-4 spacer cans are not sealed.

[b] n_a –molar quantity of dry air in the gas mixture;
n_v –molar quantity of water vapor in the gas mixture due primarily to efflorescence;
n_{po} –molar quantity of gas due to offgassing of the silicone rubber pads;
n_{bo} –molar quantity of gas due to offgassing of the polyethylene bags, bottles, and lifting sling;
n_{tf} –molar quantity of gas due to offgassing of the Teflon bottles;
n_{H2} –molar quantity of hydrogen gas due to radiolysis of water;
n_{O2} –molar quantity of oxygen gas due to radiolysis of water; and
n_T –total molar quantity in the gas mixture.

To use the maximum normal operating pressure at standard temperature, the number of lb-mole of gas needs to be increased using the following equation:

$$n_{MNOP} = \frac{P_T \cdot V_v}{R_u \cdot T_{amb} \cdot 12}$$

Using the above molar equations, the total number of moles is summarized in Table 2.

Table 2. Molar summary at MNOP and 25°C (77°F)

CVA	P_T (psia)	V_V (in.^{3})	R_u (ft-lb/lb-mole·R)	T_{amb} (R)	n_{MNOP} (lb-mole)
2	19.238	399.75	1545.32	537	7.7228E-04
7	28.859	320.32	1545.32	537	9.2831E-04

II. Molar quantity determination due to offgassing for each containment vessel arrangement

To determine the maximum pressure inside the containment vessel as a result of thermal testing, the average adjusted gas temperature must be calculated based on the results shown in Sect. 3.5.3. The approach used is to divide the containment vessel volume into three distinct equal regions and then average the three together. The first volume is represented by the gas adjacent to the containment vessel lid and flange region and the top most convenience can. Based on the temperature recorded near the O-rings [116.11°C (241°F)] and the temperature recorded on the external surface of the convenience can [98.89°C (210°F)], the average temperature of the gas in this region is 107.50°C (225.50°F). Using the temperature adjustment of 25.11°C (45.20°F) for this region, the adjusted average temperature in the first region is 132.61°C (270.70°F). The second volume is represented by the gas adjacent to the second convenience can from the top. Based on the temperature recorded on the containment vessel wall and convenience can [92.78°C (199°F)], the average temperature of gas in this region is 92.78°C (199°F). Using the temperature adjustment of 27.89°C (50.20°F) for this region, the adjusted average temperature in the second region is 120.67°C (249.20°F). The third and final volume is represented by the gas adjacent to the bottom convenience can. Again, based on the convenience can temperature [87.78°C (190°F)] and the containment vessel end cap temperature [98.89°C (210°F), the average temperature of gas in this region is 93.33°C (200°F). Using the temperature adjustment of 24.94°C (44.90°F) for this region, the adjusted average temperature in the third region is 118.28°C (244.90°F). Averaging these three temperatures, an average adjusted gas temperature of 123.85°C (254.93°F) is determined for the containment vessel.

Using the above calculated results and the specific gas generation of polyethylene bags and silicone rubber pads measurements at temperatures up to 170°C (338°F) conducted by the Y-12 Development Division (Appendix 2.10.4), the amount of gas generated due to offgassing of the silicone rubber can pads, the polyethylene bags and bottles, and the Teflon FEP bottles at 123.85°C (254.93°F), (V_{po}, V_{bo}, and V_{tf}) is estimated by first determining the offgassing volume per unit mass at temperature and multiplying that by the total mass of the bags, bottles, slings, and silicone rubber can supports inside the containment vessel. Based on testing at an approximate temperature of 141.11°C (286.00°F), values of ~7.0 and ~0.8 cm3/g @STP for the polyethylene bagging and bottles, and silicone rubber pads, respectively, were taken from the curves for the offgassing volume per unit mass as documented in Y/DZ-2585, Rev. 2 (Appendix 2.10.4). The value for Teflon FEP material offgassing volume per unit mass (V_{tf}) was obtained from Fig. 10 in Appendix 2.10.9. A value of ~0.12 to 0.13 cm^3/g@STP

was recorded over a temperature range of 200 to 400°F. This value was conservatively doubled to 0.25 cm^3/g@STP. These values are used to determine the offgassing volume as shown below:

$V_{po} = W_p \times 0.8 / 16.387$ (in.^{3}) (offgassing volume of silicone rubber pads)

$V_{bo} = W_b \times 7.0 / 16.387$ (in.^{3}) (offgassing volume of polyethylene bags, bottles, and lifting sling)

$V_{tf} = W_{tf} \times 0.25 / 16.387$ (in.^{3}) (offgassing bottles of Teflon FEP bottles)

From the ideal gas law, the number of gas moles in the volume is as follows:

$$n_i = \frac{P_v \cdot V_i}{R_u \cdot T_{amb} \cdot 12}$$

A summary of the results obtained using the above equations for each containment vessel arrangement is presented in Tables 3, 4, and 5.

Table 3. Molar quantity of gas generated due to the silicone rubber pad offgassing

CVA	W_p (g)	V_{po} (in.^{3})	P_V (psia)	R_u (ft-lb/lb-mole·R)	T_{amb} (R)	n_{po} (lb-mole)
2	240.09	11.72	14.7	1545.32	537	1.7302E-05
7	0.00	0.00	14.7	1545.32	537	0.0000E+00

Table 4. Molar quantity of gas generated due to polyethylene bag, sling, and bottle offgassing

CVA	W_b (g)	V_{bo} (in.^{3})	P_V (psia)	R_u (ft-lb/lb-mole·R)	T_{amb} (R)	n_{bo} (lb-mole)
2	500.00	213.58	14.7	1545.32	537	3.1529E-04
7	500.00	213.58	14.7	1545.32	537	3.1529E-04

Table 5. Molar quantity of gas generated due to the Teflon FEP bottle offgassing

CVA	W_{tf} (g)	V_{tf} (in.^{3})	P_V (psia)	R_u (ft-lb/lb-mole·R)	T_{amb} (R)	n_{tf} (lb-mole)
7	990.00	15.10	14.7	1545.32	537	2.2296E-05

III. Gas generation due to radiolysis of water

Buildup of hydrogen gas (H_2) and oxygen gas (O_2) in the ES-3100 containment vessel due to radiolysis is incorporated into the pressure calculation by assuming that 5 mol % of the free volume is H_2. Since each mole of H_2 generated is accompanied by 0.5 mole of O_2, the concentration of H_2 will reach 5 mol % when volume of H_2 is 0.05405 times the initial void volume (see Sect. 3.6.7.8 of Appendix 3.6.7). Therefore, the volume of H_2 and O_2 in the void volume (V_v) is determined by the following expressions:

$$V_h = 0.05405 \times V_v \quad \text{and} \quad V_o = 0.5 \times V_h .$$

Using the ideal gas law, the number of gas moles of H_2 and O_2 in the volume at standard temperature and pressure is:

$$n_{r\text{-}H2} = \frac{P_v \cdot V_h}{R_u \cdot T_{amb} \cdot 12} \qquad n_{r\text{-}O2} = \frac{P_v \cdot V_o}{R_u \cdot T_{amb} \cdot 12}$$

where

$n_{r\text{-}H2}$ = individual molar quantity for H_2;
$n_{r\text{-}O2}$ = individual molar quantity for O_2;
V_h = volume of H_2 assumed generated by radiolysis;
V_o = volume of O_2 assumed generated by radiolysis.

A summary of the results for H_2 and O_2 generation due to radiolysis using the above equation is presented in Table 6.

Table 6. Molar quantity of oxygen and hydrogen gas generation due to radiolysis

CVA	V_v (in.^{3})	V_h (in.^{3})	V_o (in.^{3})	P_v (psia)	R_u (ft-lb/lb-mole · R)	T_{amb} (R)	$n_{r\text{-}H2}$ (lb-mole)	$n_{r\text{-}O2}$ (lb-mole)
1	399.75	21.61	10.80	14.7	1545.32	537.0	3.1895E-05	1.5948E-05
7	320.32	17.31	8.66	14.7	1545.32	537.0	2.5558E-05	1.2779E-05

IV. Molar quantity of gas generated due to the efflorescence nature of the uranyl nitrate crystals (UNX)

The uranyl nitrate crystals (UNX) in any hydrated state will decompose and lose water molecules at the average gas temperature shown in Sect. 3.4.3 [123.85°C (254.93°F)]. The partial pressure of water vapor in this mixture is conservatively estimated to be the saturated vapor pressure (P_{sv}) of water at 254.93°F or 32.460 psia. Using the ideal gas law, the molar quantity of water vapor (n_{wv}) in this volume at the maximum containment vessel temperature and the saturated vapor pressure is:

$$\begin{aligned} n_{wv} &= (P_{sv} \cdot V_v) / (R_u \cdot T_{cv} \cdot 12) \\ &= (32.460)\,(320.32) / (1545.32 \times 12 \times 714.93) \\ &= 7.8428 \times 10^{-4} \text{ lb-moles} \end{aligned}$$

where

n_v = individual molar quantity for water vapor;
V_v = void volume of containment vessel;
T_{cv} = average gas temperature inside the containment vessel; and
P_{sv} = interpolated saturated vapor pressure of water at temperature from *Fundamentals of Classical Thermodynamics*, 2d ed, Table A.1.1, p. 650. (Van Wylen 1973)

V. Total pressure due to offgassing and HAC temperatures inside the containment vessel

The total pressure of the mixture at 123.85°C (254.93°F), P_T, for each containment vessel arrangement is the pressure calculated using the sum of the previously calculated molar quantities of the gases in the containment vessel. Table 7 summarizes the molar constituents and total pressure of each containment vessel arrangement. The following equation is used to calculate the final containment vessel pressure:

$$P_{123.85°C} = (\sum n_i \cdot R \cdot T \cdot 12) / V_{GMV} ,$$

where

n_i = individual molar quantity for each gas,
T = average gas temperature = 123.85°C (254.93°F),
V_{GMV} = V_v = gas mixture volume.

Table 7. Total pressure inside the containment vessel at 123.85°C (254.93°F) [a]

CVA	n_{MNOP} [b] (lb-mole)	n_{po} [b] (lb-mole)	n_{bo} [b] (lb-mole)	n_{tf} [b] (lb-mole)	n_{r-H2} [b] (lb-mole)	n_{r-O2} [b] (lb-mole)	n_{wv} [b] (lb-mole)	n_T [b] (lb-mole)	P_T (psia)
2	7.7228E-04	1.7302E-05	3.1529E-04	0.0000E+00	3.1895E-05	1.5948E-05	0.0000E+00	1.1527E-03	38.236
7	9.2831E-04	0.0000E+00	3.1529E-04	2.2296E-05	2.5558E-05	1.2779E-05	7.8428E-04	2.0885E-03	86.441

[a] This assumes that the internal convenience cans, polyethylene or Teflon FEP bottles, and Cat 277-4 spacer cans are not sealed.

[b] n_{MNOP} –molar quantity of the gas mixture at maximum normal operating pressure at standard temperature [25°C (77°F)];
n_{po} –molar quantity of gas due to offgassing of the silicone rubber pads;
n_{bo} –molar quantity of gas due to offgassing of the polyethylene bags, bottles, and lifting sling;
n_{tf} –molar quantity of gas due to offgassing of the Teflon bottles;
n_{r-H2} –molar quantity of hydrogen gas due to radiolysis of water;
n_{r-O2} –molar quantity of oxygen gas due to radiolysis of water;
n_{WV} –molar quantity of water vapor due to efflorescence of UNX crystals; and
n_T –total molar quantity in the gas mixture.

Appendix 3.6.6

SILICONE RUBBER THERMAL PROPERTIES FROM THERM 1.2 DATABASE

The thermal properties for silicone rubber used in the thermal analyses of the ES-3100 shipping container were obtained from the THERM 1.2 Thermal Properties Database by R. A. Bailey. Since THERM 1.2 is not a publicly available program, screen captures from THERM 1.2 of the data for silicone rubber are presented in Figures 1 and 2 in English and SI units, respectively.

```
                 silicone rubber, medium k (see ref 5)
         ------------------------------------------------------------
         Density                                .04696548   lb/in**3
         Specific Heat                          .3          Btu/lb°F
         Conductivity                           .01612725   Btu/hr in°F
         Maximum Material Temp             545.0            °F

         silicone rubber, medium k (see ref 5)
         ------------------------------------------------------------
References:
    fleming p           private collection of plastics data           1968
                        materials engr  matl selector issue           1967
                        metals handbook  8th ed                       1961
    moyer j             private collection of thermal data            1968

Material properties quality
    Density                 -  Good data, or no way of estimating quality.
    Specific Heat           -  Poor or conflicting data.  Used best or average.
    Conductivity            -  Poor or conflicting data.  Used best or average.
    Transition Temperature  -  Good data, or no way of estimating quality.
    Latent Heat             -  No data.  Made no estimate.
    Specific Heat Tables    -  No data.  Made no estimate.
    Conductivity Tables     -  No data.  Made no estimate.
```

Figure 1. Silicone rubber thermal properties from Therm 1.2 (English units).

```
         silicone rubber, medium k (see ref 5)
         ------------------------------------------------------------
         Density                          1300.0          kg/m**3
         Specific Heat                    1255.2          J/kg°K
         Conductivity                         .33472      J/sec m°K
         Maximum Material Temp             558.15         °K

         silicone rubber, medium k (see ref 5)
         ------------------------------------------------------------
References:
    fleming p           private collection of plastics data           1968
                        materials engr  matl selector issue           1967
                        metals handbook  8th ed                       1961
    moyer j             private collection of thermal data            1968

Material properties quality
    Density                 -  Good data, or no way of estimating quality.
    Specific Heat           -  Poor or conflicting data.  Used best or average.
    Conductivity            -  Poor or conflicting data.  Used best or average.
    Transition Temperature  -  Good data, or no way of estimating quality.
    Latent Heat             -  No data.  Made no estimate.
    Specific Heat Tables    -  No data.  Made no estimate.
    Conductivity Tables     -  No data.  Made no estimate.
```

Figure 2. Silicone rubber thermal properties from Therm 1.2 (SI units).

Appendix 3.6.7

ESTIMATES OF HYDROGEN BUILDUP IN THE ES-3100 PACKAGE CONTAINING HIGHLY ENRICHED URANIUM

3.6.7.1 Summary

Table 3.6.7.1 below indicates that the ES-3100 package with a containment vessel arrangement (CVA) 2 (see Appendix 3.6.4) can accommodate a 15.13-kg load of uranium oxide with 3 wt % water if the time allowed to generate 5 mol % of hydrogen is assumed to be 1.20 years (14.4 months). For the same time period, with CVA 7, the ES-3100 can accommodate 4.75 kg of uranyl nitrate hexahydrate crystals (X=6, 21.6 wt % water) or 6.70 kg of uranyl nitrate trihydrate crystals (X=3, 12.1 wt % water). If the time allowed is assumed to be 0.5015 years (6.02 months), the ES-3100 can accommodate 9.12 kg of UN6 and 11.90 kg of UN3 crystals. For additional margin of safety (20%), the ES-3100 loading conditions will specify a hydrogen build-up time limit of 5 months and 12 months for these two UNX cases, instead of 6.02 and 14.4 months as analyzed, respectively.

Calculations of permeation and diffusion from closed convenience containers (bottles and cans) indicate that the steady-state concentration of hydrogen can be as high as 0.2 mol % when all conservative assumptions are used. These results do not take into account the leakage of hydrogen that will be experienced through the closed lid of these containers, which would result in a steady-state concentration lower than 0.2 mol %.

The calculated 0.2 mol % hydrogen initial steady-state concentration is accounted for in the mass loading allowables given in Table 3.6.7.1. As indicated, the time to reach 5 mol % hydrogen in the ES-3100 containment vessel (including the initial condition of 0.2 mol %) is 20% greater than the time allowed for shipping these materials (Sect. 1.2.3.8, condition 10). With this safety factor in place, and with other conservative assumptions, it will not be necessary to vent containers before loading into the ES-3100. The time limit for the shipment (5 or 12 months, as appropriate) begins when the containment vessel is sealed.

3.6.7.2 Introduction

There is a concern about the possible buildup of hydrogen gas (H_2) in the ES-3100 package, and it is necessary to show that the H_2 concentration in the package will not exceed 5 mol % in one year (established as a limit for the purposes of this analysis). The allowable materials include uranium oxide (UO_3, U_3O_8, and UO_2) and uranyl nitrate crystals [UNX or $UO_2(NO_3)_2 \bullet XH_2O$]. The water in UNX ranges from X=0 to X=6 (0 to 21.6 wt %) {molecular weights of uranyl nitrate [$UO_2(NO_3)_2$] and H_2O are 391 and 18, respectively, and $6 \times 18 / [391 + 6 \times 18] = 0.216$}. The water associated with oxides ranges from 0 to 3 wt % (Sect. 1.2.3). There is no liquid water (sorbed or interstitial) associated with other authorized contents. The air in the void spaces of the package contains water vapor (humidity). H_2 can be generated from water by radiolysis and/or chemical reaction. Radiolysis applies to any chemical form of HEU, but only the metal can have a chemical reaction with water. Radiolysis can also generate H_2 from other materials containing hydrogen (e.g., polyethylene bags). However, radiolysis of water is the major source of H_2 for uranium oxides and uranyl nitrate crystals.

Table 3.6.7.1. Summary of allowable weights

Weight (kg)	Water		Time to reach 5 mol % hydrogen	
	X	wt %	Years	Months
Oxides (U_3O_8, UO_2, UO_3) [CVA 2] [a]				
15.13		3.0	1.20	14.4
$UO_2(NO_3)_2 \times XH_2O$ [CVA 7] [b]				
4.75	6	21.6	1.20	14.4
6.70	3	12.1	1.20	14.4
9.12	6	21.6	0.5015	6.02
11.90	3	12.1	0.5015	6.02

[a] CVA 2 consists of five cans of which one is empty (see Sect. 3.1.4.1).
[b] CVA 7 consists of three Teflon bottles (see Sect. 3.1.4.1).

3.6.7.3 Hydrogen Generation by Chemical Reaction with Water

HEU metal can combine with the oxygen in water to release H_2. The only source of water for HEU metal is the humidity of the air initially in the void spaces of the package. The air is assumed to be at 25°C, 1 atm (101.3 kPa) and 100% relative humidity. The vapor pressure of water at 25°C is 3.1690 kPa (CRC Handbook, p. 6-8), so the initial concentration of water vapor is 3.1690 / 101.3 = 0.031 mole fraction. Since 1 mole of water vapor produces 1 mole of H_2 and the oxygen is bound up as solid uranium oxide, this reaction does not change the total gas pressure. Therefore, if all the water vapor reacts with the metal, the maximum concentration of H_2 is also 0.031 mole fraction, which is below the 5 mol % limit.

3.6.7.4 Radiation Energy Calculations

The radiation energy that drives radiolysis can be estimated from the decay rate and maximum decay energy of each radionuclide that makes up the HEU. The bounding information to calculate these terms and the results are given in Table 3.6.7.2.

The decay rate per gram of the nth radionuclide is

D_{Rn} = $[\ln(2) / T_{Hn}] \times A_N / MW_n$;
D_{Rn} = the decay rate of the nth radionuclide, atoms/y;
T_{Hn} = half life of the nth radionuclide, y;
A_N = Avogadro's number, 6.022×10^{23} molecules/mol; and
MW_n = the molecular (atomic) weight of the nth radionuclide, g/mol.

All the radionuclides in Table 3.6.7.2 are primarily α emitters, and the total rate of radiation dose is given as

$$D_E = \sum_{n=1}^{N} [wt\%_n \times D_{Rn} \times \alpha_{Mn}] / 100$$

Table 3.6.7.2. Radiation energy calculations

Nuclide	wt % [a]	MW [b] (g/mol)	T_H [b] (y)	α [b] (MeV)	D_R [c] [atms/(g y)]	Nuclide contr [c] [MeV/(g y)]
^{232}U	4.00E-06	232.0371	6.89E+01	5.414	2.61E+19	5.65E+12
^{233}U	6.00E-01	233.0396	1.59E+05	4.909	1.13E+16	3.32E+14
^{234}U	2.00E+00	234.0409	2.45E+05	4.856	7.28E+15	7.07E+14
^{235}U	5.49E+01	235.0439	7.04E+08	4.679	2.52E+12	6.48E+12
^{236}U	4.00E+01	236.0456	2.34E+07	4.569	7.56E+13	1.38E+14
^{238}U	0.00E+00	238.0508	4.46E+09	4.185	3.93E+11	0.00E+00
Transuranic	4.00E-03			5.476 [d]	4.73E+17	1.04E+14
^{237}Np	2.50E+00	237.0482	2.14E+06	4.957	8.23E+14	1.02E+14
Total	1.00E+02					1.39E+15

[a] wt % from Appendix 4.6.1 (Table 1). Maximum transuranic is 40 μg/gU and 0.60 MBq/gU activity.
[b] MW is molecular weight; T_H is half life; and α is the maximum energy emitted. (*CRC Handbook of Chemistry and Physics*, D. R. Lide, ed., 79th ed., CRC Press, Boca Raton, Fla., 1998, pp. 11-140 and 11-141)
[c] D_R is decay rate, and Nuclide contr is the contribution of each nuclide to the total rate of decay energy.
[d] Transuranic α assumed to be equal to ^{246}Cm.

where

D_E = the total rate of decay energy, Mev/(g y);
$wt\%_n$ = the weight percent of the nth radionuclide;
α_{Mn} = the α energy emitted in the decay of the nth radionuclide, MeV; and
N = the total number of radionuclides.

The above calculation of D_E for HEU is 1.39×10^{15} MeV/(g y).

3.6.7.5 Hydrogen Generation by Radiolysis from Polyethylene

Almost all the radiation energy from HEU is due to alpha particles with energies of 4–5 MeV (Table 3.6.7.2). These particles are not very penetrating and will only deposit their energy into materials that are in intimate contact with the uranium atoms (i.e., the water of hydration in uranyl nitrate crystals and the water associated with the oxides). The polyethylene is in the form of bottles and bags that surround the uranium and the only alpha particles that reach the polyethylene come from the outer range of alpha particle penetration within the HEU.

Equation 2 on page 6 in *Evaluation of Radiolysis-Induced Hydrogen Generation in DOT 6M Drums from INTEC* (WSRC-TR-2007-00200) gives the following expression for calculating the range of alpha particle penetration in the HEU (metal, oxide, or crystals).

$$R = 2.3 \times 10^{-6} \times (1.24 \times \alpha_{MA} - 2.62) \times (MW_A)^{1/2} / \rho$$

where

R	=	the range of alpha particle penetration in the HEU, m;
α_{MA}	=	the average α energy emitted by the HEU, ~4.9 MeV (Table 3.6.7.2);
MW_A	=	the average molecular weight of the HEU, ~235.5 g/mol (Table 3.6.7.2); and
ρ	=	the density of the HEU, g/cm^3.

The range increases with decreasing ρ, and the smallest value for ρ is about 1.5 g/cm^3 {the smallest approximate bulk density of HEU oxide from *Cost-Effectiveness of Utilizing Surplus Depleted Uranium (DU)*, [WM-4009]}. The resulting range is 8.1×10^{-5} m.

The radius of a polyethylene bottle is 0.0627 m [4.94-in. diam (Fig. 1.4), configuration designated as CVA 6]. If the HEU oxide fills the bottle, the alpha particles generated in the outer range come from the HEU between 0.0627 and ($0.0627 - 8.1 \times 10^{-5}$ m). For an infinite cylinder, the fraction of the total radiation within this range is $[(0.0627)^2 - (0.0627 - 8.1 \times 10^{-5})^2] / (0.0627)^2 = 0.00259$. Half of this radiation would be directed toward the center of the cylinder, and much of the outward-directed portion would be absorbed passing through the HEU. Consequently, the radiation absorbed by the polyethylene would be much less than 1% of that absorbed by the water, and the H_2 generated in the polyethylene would be correspondingly less than that generated in the water.

3.6.7.6 Hydrogen Generation by Radiolysis from Water

Assuming an infinite amount of water is available, the radiolytic hydrogen generation rate is given by the following expression (based on NUREG/CR-6673, p. 31, Eq. 4.7):

$$d(n_{H2}) / dt = (D_H / 100) \times [G(H_2) / A_N]$$

where

n_{H2}	=	the amount of hydrogen generated, mol;
t	=	time, y;
D_H	=	the decay energy absorbed by the water, eV/y; and
$G(H_2)$	=	a radiolytic hydrogen generation factor for alpha radiation in water, molecules H_2/100 eV absorbed by water.

3.6.7.7 Radiolytic Hydrogen Generation Factors for Alpha Radiation in Water

A bounding value for $G(H_2)$ with alpha radiation is 1.6 molecules H_2/100 eV absorbed by water. (NUREG/CR-6673, p. 12, Table 3.1) However, recent (2003) experimental data from Oak Ridge National Laboratory suggest lower $G(H_2)$ values [*Alpha Radiolysis of Sorbed Water on Uranium Oxides and Uranium Oxyfluorides* (ORNL/TM-2003/172) and *Water Sorption and Radiolysis Studies for Neptunium Oxides* (ORNL/TM-2003/194), included in this appendix]. Table 3.6.7.3 lists the $G(H_2)$ values derived from these experiments. The largest of the ORNL values (1.02) is used for the hydrogen generation calculations.

Table 3.6.7.3. $G(H_2)$ values derived from alpha radiolysis experiments

Sample description					Molecules/100 eV		
	$e^-(H_2O)$	$e^-(rem)$	f_{H2O}	Gf	G'(gas) [a]	$G'(H_2)$	$G(H_2)$
Icenhour and Toth, ORNL/TM-2003/172, 2003							
Fig. 3.3. Samp A-2-2, UO_3, 10% H_2O, 350°C	0.0556	0.3689	0.1000	0.1309	0.1507	0.1005	0.77
Fig. 3.5. Samp A-4-1 U_3O_8, 2% H_2O, 650°C	0.0111	0.4000	0.0200	0.0270	0.0113	0.0075	0.28
Icenhour et. al., ORNL/TM-2003/194, 2004							
Fig. 4.12. Samp Al 3, NpO_2, 8% H_2O, 650°C	0.0444	0.3728	0.0800	0.1065	0.1100	0.0733	0.69
Fig. 4.11. Samp Al 2, NpO_2, 1% H_2O, 650°C	0.0056	0.4012	0.0100	0.0137	0.0210	0.0140	1.02
Fig. 4.13. Samp Al 4, NpO_2, 1% H_2O, 800°C	0.0056	0.4012	0.0100	0.0137	0.0060	0.0040	0.29
Fig. 4.14. Samp Al 5, NpO_2, 0.5% H_2O, 650°C	0.0028	0.4032	0.0050	0.0068	0.0043	0.0029	0.42

[a] G'(gas) for ORNL/TM-2003/172 is based on a measured slope in Fig. 3.3 or 3.5. For ORNL/TM-2003/194, the values are listed on Figs. 4.11–4.14.

The G'(gas) value is the initial slope of the gas yield (mmol/g material) versus the decay energy (MGy) converted to units of molecules of gas per 100 eV. G'(gas) for ORNL/TM-2003/172 is based on a measured slope in Fig. 3.3 or 3.5 while the values for ORNL/TM-2003/194 are listed on Figs. 4.11–4.14. Figure 3.6.7.1 is from ORNL/TM-2003/172 (p. 9, Fig. 3.5) with lines added to outline the initial slope and facilitate reading values. From Fig. 3.6.7.1, the gas yield difference along the slope is 0.023 – (–0.0005) = 0.0235 millimol/g or $0.0235 \times A_N / 1000 = 1.42 \times 10^{19}$ molecules/g. The decay energy difference along the slope is 20.0 MGy or $20.0 \times 6.24 \times 10^{21} = 1.25 \times 10^{23}$ eV (6.24×10^{21} eV/g = 1 MGy). Therefore, G'(gas) is $1.42 \times 10^{19} / (1.25 \times 10^{23}) \times 100 = 0.0113$ molecules gas/100 eV. It is assumed the gas is due to the decomposition of H_2O and has a molar composition of 2/3 H_2 and 1/3 O_2. The derived $G'(H_2)$ is 2/3 of the G'(gas) value or 0.00756 molecules H_2/100 eV decay energy.

The radiation calculated in Table 3.6.7.2 is the decay energy rather than the energy absorbed by the water associated with the material. The energy absorbed by the associated water, D_H, is approximately equal to the decay energy, D_E, multiplied by the fraction of electrons associated with the water or

$$Gf = e^-(H_2O) / e^-(mat)$$

where

Gf = the fraction of electrons associated with the water;

$e^-(H_2O)$ = the number of electrons associated with the water, electrons/molecule;

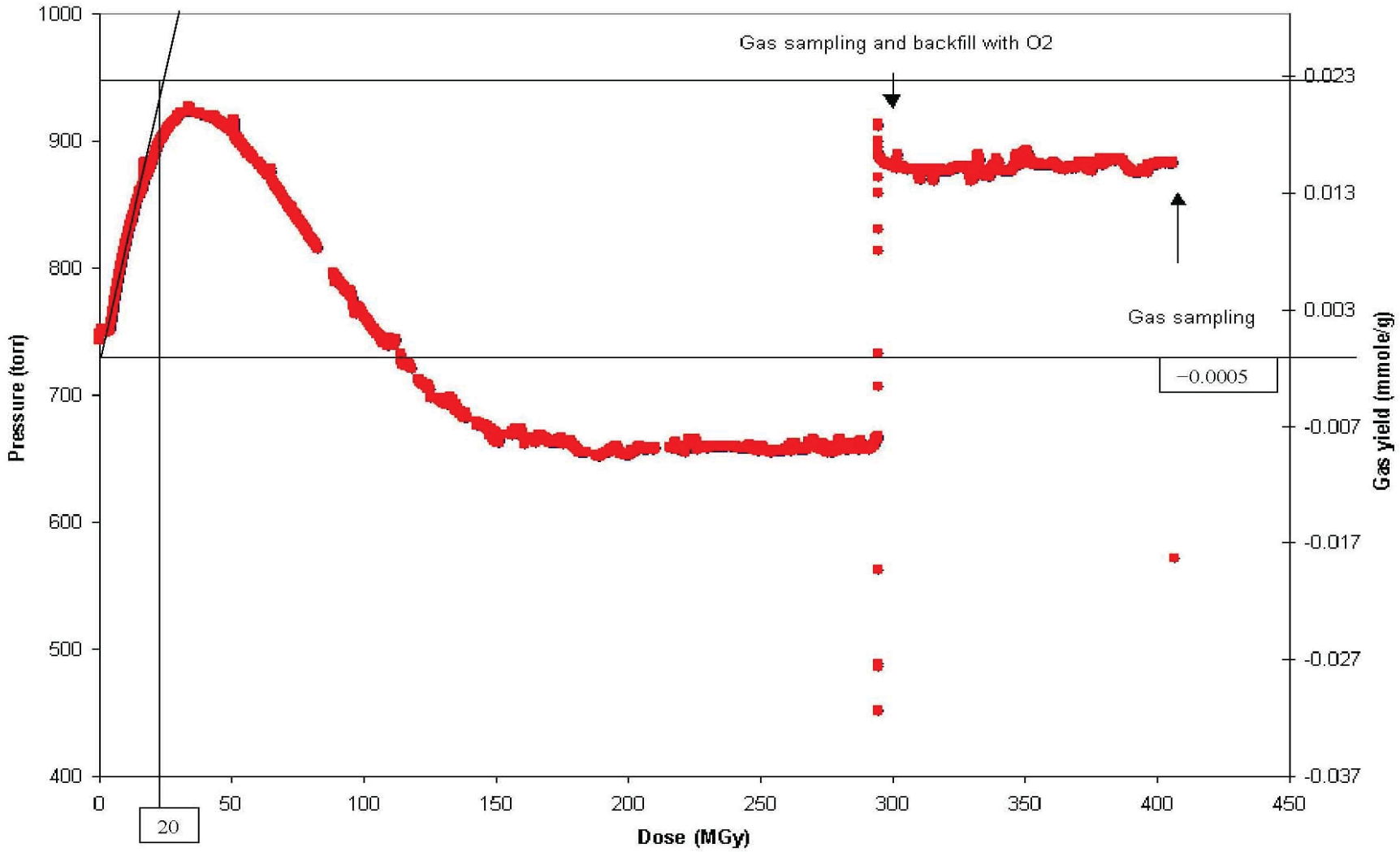

Fig. 3.6.7.1. Pressure and gas yield as a function of dose. Based on Fig. 3.5 in *Alpha Radiolysis of Sorbed Water on Uranium Oxides and Uranium Oxyfluorides* (ORNL/TM-2003/172), Sample A-4-1 (5.64 g U_3O_8 with 2 wt % H_2O, spiked with 0.0249 g ^{244}Cm).

$$e^-(mat) = \sum_{i=1}^{I} e^-(mat_i) =$$ the total number of electrons associated with the molecular species; electrons/molecule ;

$e^-(mat_i)$ = the contribution of the ith molecular species to $e^-(mat)$; and
I = the total number of molecular species. The energy absorbed by the water is
D_H = $Gf \times D_E$ and
$G'(H_2)$ = $Gf \times G(H_2) \rightarrow G(H_2) = G'(H_2) / Gf$.

Two methods to calculate Gf are reported in *Calculation of Hydrogen Generation Rates for Storage of Post-KIS Oxide in 9975 Shipping Containers* (Calculation No. N-CLC-K-00219, p. 9 and 10). In the more rigorous of the two methods, Gf is estimated from the material stoichiometry and molecular weights. Using this more rigorous method, $e^-(mat_i)$ is calculated as

$$e^-(mat_i) = f_i \times \sum_{i=1}^{J} [n_{i,j} \times Z_{i,j}] / MW_i$$

where

f_i = the weight fraction of the ith molecular species;
MW_i = the molecular weight of the ith species;
$n_{i,j}$ = the number of moles of the jth element in the ith species;
J = the total number of elements in the ith species; and
$Z_{i,j}$ = the atomic number of the jth element in the ith species.

According to the preceding equation, the expression for the number of electrons associated with the water is

$$e^-(H_2O) = f_{H2O} \times 10 / (16 + 2) = f_{H2O} \times 0.5556.$$

A mixture of water and U_3O_8 (assuming all the uranium is ^{235}U) is

$$e^-(mat) = f_{H2O} \times 0.5556 + f_{U3O8} \times (3 \times 92 + 8 \times 8) / (3 \times 235 + 8 \times 16)$$
$$= f_{H2O} \times 0.5556 + f_{U3O8} \times 0.4082$$

where

f_{H2O} = the weight fraction of water and
f_{U3O8} = the weight fraction of $U_3O_8 = 1 - f_{H2O}$ if no other material is present.

A $G'(H_2)$ value of 0.00756 molecules H_2/100 eV decay energy is derived from the experiment by Icenhour and Toth with a U_3O_8 sample (5.64 g) containing 2% water and spiked with 0.0249 g ^{244}Cm (ORNL/TM-2003/172, p. 7, Table 3.1). The mass of ^{244}Cm can be neglected, so the calculation of $G(H_2)$ for this sample is $e^-(H_2O) = 0.02 \times 0.5556 = 0.0111$; $e^-(mat) = 0.0111 + 0.98 \times 0.4082 = 0.4111$; $Gf = 0.0111 / 0.4111 = 0.0270$; and $G(H_2) = 0.00756 / 0.0270 = 0.280$ molecules H_2/100 eV absorbed by the water. Since the largest of the ORNL values (1.02) is used for the hydrogen generation calculations, the $G'(H_2)$ value for any other water content is the corresponding value of $Gf \times 1.02$.

To calculate Gf for $UO_2(NO_3)_2 \bullet XH_2O$, the two components are $UO_2(NO_3)_2$ and H_2O, where f_{H2O} is

$$f_{H2O} = X \times (2 + 16) / [235 + 2 \times 16 + 2 \times (14 + 3 \times 16) + X \times (2 + 16)]$$
$$= 1 / [1 + 391 / (X \times 18)]$$

$$e^-(mat) = f_{H2O} \times 0.5556 + f_{UN2O8} \times (92 + 8 \times 8 + 2 \times 7) / (391)$$
$$= f_{H2O} \times 0.5556 + f_{UN2O8} \times 0.4348$$

f_{UN2O8} = the weight fraction of $UO_2(NO_3)_2 = 1 - f_{H2O}$.

3.6.7.8 Time to Reach 5 mol %

The time at which the H_2 concentration in the void spaces of the package reaches 5 mol % depends on the H_2 generation rate and the volume of the void spaces. The void spaces are assumed to be initially filled with air at 25°C and 1 atm (101.3 kPa). The initial amount of air is given by

$$n_I = 101.3 \times V_{VT} / [8.3145 \times (25 + 273.15)]$$

where

n_I = the initial amount of air, mol;
V_{VT} = the total volume of the void spaces, L; and
8.3145 = the gas constant, J/(mol × K).

Since each mole of H_2 generated is accompanied by 0.5 mole of O_2, the concentration of H_2 will reach 5 mol % when

$$(n_{H2} + y \times n_I) / [1.5 \times (n_{H2} + y \times n_I) + n_I] = 0.05 \text{ or}$$
$$n_{H2} = (0.05405 - y) \times n_I$$

where

y is the initial mole fraction of hydrogen or 0.002.

The value of V_{VT} depends on the configuration and sizes of the convenience containers in the package and the amount of material in the containers. The configuration designated as CVA 7 is used for crystals and oxides may be placed in CVAs 1 through 6. The empty void volume (before the material is placed in the containers) is 9.4835 L (578.72 in.^{3}) for CVA 7 (Appendix 3.6.4, Table 1). The smallest (most conservative) empty void volume of CVAs 1 through 6 is 8.6230 L (526.21 in.^{3}) for CVA 2 (Appendix 3.6.4, Table 1).

If all the interstitial space is included, the total void volume is given by

$$V_{VT} = V_{BT} - Wt / \rho$$

where

V_{BT} = empty void volume, 8.6230 and 9.4835 L for CVA 2 and CVA 7, respectively;
Wt = the total weight of the material in the containers, kg; and
ρ = the theoretical density of the material in the containers, (10.97 kg/L for UO_2, 8.38 kg/L for U_3O_8, 7.3 kg/L for UO_3, and 2.81 kg/L for UNH). (CRC Handbook, p. 4-94)

Since UO_3 has the smallest theoretical density of the oxides, it will produce the smallest (most conservative) total volume of the void spaces.

As shown in Table 3.6.7.2, the bounding value of the decay energy is 1.39×10^{15} MeV/(g y). The fraction of uranium in UO_3 is $(1 - f_{H2O}) \times 235 / (235 + 3 \times 16) = 0.8055$ gU/g material for $f_{H2O} = 0.03$ (3% water). The corresponding fraction for crystals is $235 / [235 + 2 \times 16 + 2 \times (14 + 3 \times 16) + X \times (2 + 16)] = 0.4709$ gU/g material for X = 6 $[UO_2(NO_3)_2 \bullet 6H_2O]$. The decay energies are 1.12×10^{15} MeV/y g material for UO_3 with 3% H_2O and 6.57×10^{14} MeV/y g material for $UO_2(NO_3)_2 \bullet 6H_2O$.

The hydrogen generation rates for oxides (UO_2, U_3O_8, and UO_3) and uranyl nitrate crystals ($UO_2(NO_3)_2 \bullet XH_2O$) are calculated with the expression presented earlier in this appendix. The amounts of hydrogen for 5 mol % are divided by the corresponding generation rate to give the time to reach 5 mol %.

Table 3.6.7.4 gives the total weight of the material in the containers (Wt) that will generate enough hydrogen to reach 5 mol % in 1.20 or 0.5015 years as a function of the water content. The time limits for shipping the material are set at 1 year and 5 months and the additional 0.20 year allows a margin of safety in both cases. The water content considered is 3% for oxides and X values of 6 and 3 (21.64 and 12.13%) for crystals. As indicated in the table, the weight for UO_3 is the smallest for the oxides (15.13 kg).

The above calculations did not include the water from the humidity in the air. As indicated in Sect. 3.6.7.3, the mole fraction of water in the humid air is 0.031. Table 3.6.7.4 indicates the largest initial air in empty void volume is on the order of 0.32 moles so the water from the humidity in the air is on the order of $0.32 \times 0.031 = 0.01$ moles. The water content in the oxides is less than the crystals and is on the order of 3% so this water is on the order of $15{,}130 \times 0.03 / 18 = 25$ moles. Therefore, the radiolytic H_2 due to water from the humidity in the air is negligible.

3.6.7.9 Initial H_2 concentration

The results in Table 3.6.7.4 were calculated with the assumption that the initial H_2 concentrations were zero. It was suggested that a container stored for a long period of time would need to be vented before being placed in the ES-3100 in order to remove any H_2 that accumulated in the container during the storage period. An estimate of the accumulated H_2 is calculated in this section.

The H_2 generated in a container can leak out through tiny spaces in imperfect lids and by permeation or diffusion through the walls of the container. The largest leaks are through the tiny spaces but they are difficult to characterize. Consequently, this calculation conservatively considers only permeation and diffusion. Because permeation is usually a faster mechanism than diffusion and is more likely with plastics, the permeation model was used for the Teflon bottles. Since metals are not very permeable, the diffusion model was used for the cans.

The rate of gas loss through permeation is given by

$$d(n_P) / dt = P_m \times P \times A/\tau \times \rho_G$$

Table 3.6.7.4. Combinations of weight and water content that will generate 5 mol % hydrogen in 1.20 or 0.5015 years

Density (kg/L)	Weight (kg)	Total void volume (L)	Gas amounts (mol)		Water		Material uranium content (gU/g mat)	Annual radiation rate [MeV/(g mat y)]	Gf	G'(H_2) (molecules H_2/100 eV)	n_{H2} rate (mol/y)
			Initial air	H_2 for 5 mol %	X	(wt %)					
U Oxides (UO_2) [CVA 2]											
10.97	15.51	7.2095	0.29468	0.01593		3.0	0.8537	1.19E+15	0.0407	0.0416	1.27E-02
U Oxides (U_3O_8) [CVA 2]											
8.38	15.33	6.7939	0.27769	0.01501		3.0	0.8209	1.15E+15	0.0404	0.0412	1.20E-02
U Oxides (UO_3) [CVA 2]											
7.3	15.13	6.5511	0.26777	0.01447		3.0	0.8055	1.12E+15	0.0402	0.0410	1.16E-02
$UO_2(NO_3)_2 \cdot XH_2O$ [CVA 7]											
2.81	4.75	7.7946	0.31852	0.01722	6	21.64	0.4709	6.57E+14	0.2609	0.2661	1.38E-02
2.81	6.70	7.0981	0.29006	0.01568	3	12.13	0.5281	7.37E+14	0.1500	0.1530	1.25E-02
2.81	9.12	6.2389	0.25495	0.01378	6	21.64	0.4709	6.57E+14	0.2609	0.2661	2.65E-02
2.81	11.90	5.2494	0.21451	0.01160	3	12.13	0.5281	7.37E+14	0.1500	0.1530	2.23E-02

where

n_P is the amount of gas lost through permeation, mol;
P_m is the permeability, $cm^2/(Pa\ y)$;
P is the pressure increase over the initial value, Pa;
A is the cylindrical area of the Teflon bottle (4.69-in. diam × 9.4-in. tall, see Sect. 1), 893.5 cm^2 ;
τ is the thickness of the bottle (0.05-in. nominal thickness), 0.1270 cm; and
ρ_G is the gas density, 4.087×10^{-5} mol/cm^3 for an ideal gas at 25°C and 1 atm.

At steady state, the permeation rate is balanced by the gas generation rate.

$$1.5 \times d(n_{H2}) / dt = P_m \times P \times A/\tau \times \rho \quad \rightarrow \quad P = [1.5 \times d(n_{H2}) / dt] / [P_m \times A/\tau \times \rho_G]$$

where

$d(n_{H2}) / dt$ is the H_2 generation rate in the bottle due to radiolysis, mol/y and
1.5 is a factor to account for the oxygen released with the hydrogen.

The steady-state mole fraction is

$$f_{H2} = (2/3) \times P / P_0$$

where

f_{H2} = is the mole fraction of H_2 ;
2/3 is a factor to account for the fact that 1/3 of the pressure increase is due to oxygen; and
P_0 is the initial pressure in the bottle, 101325 Pa (1 atm).

The largest H_2 generation rate is 0.0265 mol/y (Table 3.6.7.4) for 3 Teflon bottles (see Sect. 3.1.4.1). The value for one bottle is 0.0265 / 3 = 0.00882 mol/y. Permeability values for Teflon bottles can be found at the Nalgene Labware Web site. In units of (cc • mm)/(m^2 • day • Bar), these permeability values are 4960 for N_2, 11,625 for O_2, and 34,100 for CO_2. The value for H_2 would be expected to be larger than these values; however, the smallest value (4960 for N_2) was conservatively assumed for H_2. When converted to consistent units, the permeability used for H_2 is 0.000181 $cm^2/(Pa \bullet y)$. With these values, the steady-state pressure rise is 254.1 Pa, and the H_2 mole fraction is 0.00167 or less than 0.2%.

The rate of H_2 loss through diffusion is given by

$$d(n_D) / dt = D \times C \times A/\tau$$

where

n_D is the amount of H_2 lost through diffusion, mol;
D is the diffusivity, cm^2/y; and
C is the H_2 concentration increase over the initial value, mol/cm^3.

At steady state, the diffusion rate is balanced by the H_2 generation rate.

$$d(n_{H2}) / dt = D \times C \times A/\tau \quad \rightarrow \quad C = [d(n_{H2}) / dt] / [D \times A/\tau]$$

The steady-state mole fraction is

$$f_{H2} = (V_C \times C) / n_I \ ; \quad n_I = V_C \times \rho_G \ \rightarrow \ f_{H2} = C / \rho_G$$

where

V_C is the volume of the can (4.25-in. diam × 4.88-in. tall; see Sect. 1), 1134.5 cm^3.

The largest H_2 generation rate (0.0265 mol/y, Table 3.6.7.4) is also conservatively applied to four cans (see Sect. 3.1.4.1), and the value for one can is 0.0265 / 4 = 0.00662 mol/y. The cylindrical area of the can is 420.4 cm^2, and the thickness is 0.0762 cm (0.03-in. nominal thickness for a nickel can). Presentation view graphs about hydrogen diffusion through metal pipelines indicate a wide range of diffusivity values at room temperatures and suggest that a value of about 5×10^{-7} cm^2/s is probably a low number for plain steel without welds or rough surfaces. (Sudersanam 2005) Using these values, the H_2 mole fraction is 0.00186, also less than 0.2%.

Both permeation and diffusion lead to H_2 concentrations less than 0.2 mole percent, which are negligible compared to the 5% limit. Also, these are conservative calculations in that they do not consider leaks through can and bottle closure lids, which are expected to be much larger. The small concentration (0.2 mol %) was used as an initial condition in the hydrogen generation calculations that gave rise to mass loadings and the time limits to complete shipment of this material. Therefore, it will not be necessary to vent the containers before loading them into an ES-3100 containment vessel.

Calculation Cover Sheet

Project N/A	Calculation No. N-CLC-K-00219	Project No. N/A
Title Calculation of Hydrogen Generation Rates for Storage of Post-KIS Oxide in 9975 Shipping Containers	Functional Classification General Services	Sheet 1 of 44
	Discipline Nuclear	
Calc Level ☒ Type 1 ☐ Type 2	Type 1 Calc Status ☐ Preliminary ☒ Confirmed	
Computer Program No. ☒ N/A	Version/Release No.	
Purpose and Objective NMM/Facilities Engineering has requested a calculation of hydrogen generation and accumulation rates inside the PCV of a 9975 shipping container for storage of impure plutonium oxide generated by the KIS process. Plans call for a hydrogen getter to be installed to absorb radiolytically generated hydrogen gas. Currently, the getter material has been qualified only for a period of six months. Sandia National Laboratory has an ongoing program to extent the qualification period. The request is for a calculation of the time required to reach the lower flammability limit, assuming that the getter suddenly fails at the end its qualification period.	DC/RO UNCLASSIFIED DOES NOT CONTAIN UCNI DC & Reviewing Official: James E. Laurinat (James E. Laurinat)	Date 6-5-07

Summary of Conclusion

Times to reach the LFL have been calculated for 38 MIS materials for which there was measurable radiolytic hydrogen generation. At the nominal moisture level for the MIS tests (approximately 0.5 weight % H_2O), the calculated time to LFL ranges from 12 days for Material ARF-102-85-295 calcined at 750 °C to 2400 days for several MIS's with the minimum reported hydrogen generation rate of 1 nmol/W/s. For moisture levels above 0.5 weight %, conservative bounds for times to LFL are calculated using extrapolated G values based on a weighted average of G values for bound and free water. Times to LFL based on these extrapolated G values drop off rapidly, reaching about 1.3 days for any hypothetical MIS item with 6 weight % H_2O. The bounding calculations predict that the hydrogen concentration inside the PCV will reach the LFL in a matter of days if the moisture level significantly exceeds 0.5 weight %. It should be stressed that it is unlikely that oxide materials with low G values will absorb high moisture contents from humid atmospheres. Materials that are likely to absorb significant moisture (namely, those that contain chloride salts) exhibited high G values during the MIS tests. The time required for the material with the highest gas generation rate, ARF-92-85-295 calcined at 750 °C, to reach the safety analysis pressure limit of 365 psig is 10.2 years at 0.5 wt % H_2O and 1.0 year at 6 wt % H_2O. Both times exceed anticipated storage times subsequent to a postulated getter material failure.

Revisions

Rev No.	Revision Description
0	Original issue
1	Added calculations for all MIS's. Changed basis from measured total gas generation rate to measured H_2 gas generation rate. Changed to more conservative extrapolation method for higher H_2O levels. Analyzed effect of gas mixing in getter can.
2	Changed maximum total radiolytic power from 2.5 to 5.0 watts to comply with revised interim safe storage criterion (ISSC). Listed limiting power in all table and graph captions.

Sign Off

Rev No.	Originator (Print) Sign/Date	Verification/Checking Method	Verifier/Checker (Print) Sign/Date	Manager (Print) Sign//Date
0				
1				
2	James E. Laurinat James E. Laurinat / 6-5-07	Document review.	Neal M. Askew Neal M. Askew / 6/5/07	Curtis W. Gardner Curtis W. Gardner 6/7/07

Additional Reviewer (Print) Todd D. Woodsmall	Signature Todd D. Woodsmall James E. Laurinat by telecon	Date 6-7-07
Design Authority (Print) N/A	Signature	Date
Release to Outside Agency (Print) N/A	Signature	Date

Security Classification of the Calculation
Unclassified

Table of Contents

Section	Page
1.0 Introduction	3
2.0 Description of Primary Containment Vessel and Other Enclosures	3
3.0 Input and Assumptions	3
4.0 Calculation of Hydrogen Gas Generation and Accumulation	6
5.0 Calculation Method	20
6.0 Open Items	20
7.0 Discussion of Results	20
8.0 Conclusion	21
9.0 References	25
Figures	26
Appendix A: Correspondence with Kirk Veirs Concerning H_2 Gas Generation Rates for MIS Samples	36
Appendix B: Analysis of Veirs and Co-workers Gas Generation Data for $CaCl_2$ and $MgCl_2$ Doped PuO_2 and Extrapolation of G values to Higher Moisture Levels	39

1.0 Introduction

NMM/Facilities Engineering has requested a calculation of hydrogen generation and accumulation rates inside the primary containment vessel (PCV) of a 9975 shipping container for storage of impure plutonium oxide generated by the K-Area Interim Surveillance (KIS) process. Plans call for a hydrogen getter to be installed to absorb hydrogen gas radiolytically generated by the impure plutonium oxide stored inside the PCV.[1,2] Currently, the getter material has been qualified only for a period of six months. Sandia National Laboratory has an ongoing program to extend the qualification period.[3] The NMM/FE request is for a calculation of the time required to reach the lower flammability limit, assuming that the getter suddenly fails at the end its qualification period. The time to reach the operating pressure limit of 365 psig set by the safety analysis for the 9975 shipping container[1] also is calculated for the worst case configuration.

This calculation note is a revision of a previous calculation note.[4] The previous calculation note reported hydrogen generation and accumulation rates for five typical oxide compositions, which are categorized by Material Identification and Surveillance (MIS) numbers. This revision includes all MIS categories for which measurable hydrogen generation rates have been reported. NMM Facilities Engineering has also requested an evaluation of the gas mixing inside the hydrogen getter material. In the original analysis of hydrogen concentration transients inside the PCV, the porous getter material was conservatively treated as an impermeable solid. A less conservative but more realistic model of mixing inside the getter is presented in this revised calculation note.

2.0 Description of Primary Containment Vessel and Other Enclosures

The impure oxide generated by the KIS process will be stored in 9975 shipping containers. Within the 9975 shipping container, the impure oxide will be confined within several nested vessels or structures, including a slip lid can (SLC), a heat-sealed plastic bag, a screw-lid convenience can (CC), a primary containment vessel (PCV), and a secondary containment vessel (SCV). The SLC, the plastic bag, and the CC each have a nuclear grade filter vent, while the PCV and the SCV are completely sealed. Therefore, the PCV can be considered to be the outermost vessel for hydrogen gas accumulation. Hydrogen gas will be generated by radiolysis of water absorbed on the impure oxide within the SLC. To minimize the oxygen concentrations within the PCV during storage, the gas space between the CC and the PCV will be inerted by purging with carbon dioxide (CO_2) gas until at least 75% of the air in this gas space is replaced with carbon dioxide.[1]

3.0 Input and Assumptions

Input items for the calculation of the radiolytically generated hydrogen concentrations in the SLC, the CC, and the PCV include the confinement vessel and bag dimensions, the volume occupied by the oxide and hydrogen getter materials, the rate of generation of

radiolytic energy in watts, the G value for the rate of hydrogen generation per unit decay energy, and the mass transfer coefficients for the leakage of gas through the can and bag filters.

The rate of radiolytic alpha energy given off by the stored oxide is limited to no more than 5 watts per PCV.[1] This bounding energy rate of 5 watts is used in this analysis in lieu of specifying the oxide weight and isotopic composition.

Can volumes are based on dimensions given in drawings.[5,6,7] The SLC has an outer diameter of 3.5 in. and a height of 6.0 in.[5] The wall thickness of the side wall and bottom is 0.062 in., and the lid wall thickness is 0.031 in.[5] The CC has a base that is smaller than the top portion of the can. The outer diameter of the base is 3.896 in., and the outer diameter of the top portion is 4.395 in.[6] The base is 0.75 in. high, and the top portion is 5.835 in. high; there is a transition between the two areas that is 0.54 in. high.[6] The side wall thickness is 0.042 in., and the bottom wall thickness is 0.06 in.[6] The CC lid has a top that is 0.312 in. high and a bottom threaded portion that is 0.275 in. high.[6] The outer diameter of the lid is flush with the outer can diameter. The PCV has an interior void volume of 313 in.^{3} when empty.[7]

A Nucfil® 019 filter is installed in the lid of both the SLC and the CC to provide ventilation. The manufacturer's literature states that the 019 filter has a height of 0.72 in. and an overall dimension equal to a diameter of 1.50 in. The 019 filter will transmit flow at a minimum rate of 200 mL/min for a 1.0 in. water column pressure differential. The hydrogen diffusivity for the 019 filter is 2.5×10^{-5} mol/s/mole fraction concentration difference at atmospheric pressure.

The SLC is placed within a heat-sealed bag with a single Nucfil® 036 filter before being inserted into the CC. The heat-sealed bag has a diameter which is approximately 0.375 in. larger than that of the SLC and is approximately 15 in. long before it is used to enclose the SLC. The wall thickness of the bag material is 0.004 in. According to the manufacturer's literature, the 036 filter has a diameter of 2.0 in. and a height of 0.2 in. The rated flow rate through the 036 filter is no less than 300 mL/min for a 1.0 in. water column pressure differential. The hydrogen diffusivity for the 036 filter is 9.0×10^{-5} mol/s/mole fraction concentration difference at atmospheric pressure.

Finally, a hydrogen getter and a microporous sieve are installed inside the PCV. The getter and microporous sieve are enclosed in separate Tyvek® bags and then double bagged within a third Tyvek® bag. The outer Tyvek® bag is encased within a perforated metal cylinder, as shown by Figure 1. The metal cylinder is 4.1 in. in diameter by 7 in. high. There are 375 g of getter material and 220 g of molecular sieve material within each metal cylinder. The getter material is Vacuum Energy HITOP® Hydrogen Getter based on Sandia National Laboratory's TS6D formulation, with an estimated bulk density of 0.65 g/cm^3 and a pycnometric density of 1.1 g/cm^3. The molecular sieve material is

---

® Nucfil is a registered trademark of Nuclear Filter Technology, Inc., of Golden, Colorado.
® Tyvek is a registered trademark of E. I. duPont de Nemours and Co., Inc., of Wilmington, Delaware.
® HITOP is a registered trademark of Vacuum Energy, Inc., of Cleveland, Ohio.

Type 3A, with an estimated bulk density of 0.67 g/cm^3 and a pycnometric density of 3.2 g/cm^3.

The Tyvek® bags are permeable to gases and vapors, so the gas spaces within the getter and molecular sieve bags can be considered part of the total open gas space within the PCV. Each bag is a Uline® S-5900 self-seal Tyvek® envelope, with dimensions before filling of 10.5 in. by 7.5 in. and an estimated weight of 0.018 lbm, or about 2.2 oz/yd^2. For Tyvek® bag material of this weight, the moisture vapor transmission rate (MVTR) has been measured to be 1615 g/m^2/day, using the Lyssy method, which typically records the water vapor transmission for a relative humidity differential of 90% at 100 °F.[8]

To reduce the oxygen concentration, the PCV gas space is purged with CO_2 during the packaging process. As indicated by the 9975 packaging procedure,[9] the minimum purge is 10 scfh for 15 min., followed by 3 scfh for 3 min.

Table 1 summarizes the gas space volumes within the SLC, the CC, the PCV, and the getter can. It is uncertain how the gas space between the SLC and the CC is partitioned, so this is treated as a single volume in the calculations. The flow resistances and diffusivities of the bag filter and the CC lid filter are combined using a reciprocal sum formula. The getter can and its contents are sufficiently permeable that the gas space within this can and the PCV can be combined, as is argued in Section 4.

G values for the rate of hydrogen generation are estimated using measurements provided by Veirs and co-workers from Los Alamos National Laboratory.[10] The hydrogen generation rate measurements were performed using "Small Scale Reactors" (SSR's) that are 1/500th the volume of a 3013 container. Results from the hydrogen generation rate measurements are listed by both SSR test number and by MIS designation (see Appendix A). The results are reported as G values that are given in units of nmole/s/W of alpha energy delivered to the absorbed water in the material. The reported G values are converted from a basis of the mass of absorbed water to a total mass basis so that they can be applied directly to the total rate of radiolytic energy generation in watts. This conversion is described in Section 4.

® Uline is a registered trademark of Uline Shipping Supply Specialists of Waukegan, Illinois.

Table 1. Volumes and Gas Spaces inside Confinement Vessels and Bag Enclosures

Description	Volume ($in.^3$)	Volume (cm^3)
Slip Lid Can Interior	52.3	857
Screw-Lid Convenience Can Interior	100.0	1639
Primary Containment Vessel Interior	313.0	5129
Hydrogen Getter and Microporous Sieve Can Interior	111.3	1824
Slip Lid Can Gas Space	30.9	507
Screw-Lid Convenience Can/Bag Gas Space	39.9	653
Hydrogen Getter and Microporous Sieve Can Gas Space	77.1	1264
Primary Containment Vessel Gas Space (Including Hydrogen Getter and Microporous Sieve Can Gas Space)	165.0	2703

4.0 Calculation of Hydrogen Gas Generation and Accumulation

The accumulation of hydrogen gas within the gas spaces enclosed by the SLC, the CC/sealed bag, and the PCV is calculated using transient mass transfer equations. The mass transfer equation for the SLC takes the form:

$$\frac{dm_{1,H_2}}{dt} = \frac{(10000)(24)(3600)WG'_{H_2}}{\left(1.602 \times 10^{-13}\right)N_A} - k_{019,H_2}\left(y_{1,H_2} - y_{2,H_2}\right) \qquad (1)$$

where

m_{1,H_2} = the number of moles of hydrogen gas in the SLC

t = the elapsed storage time in days

G'_{H_2} = the effective G value for hydrogen generation in molecules/100 eV

N_A = Avogadro's number (6.022×10^{23} molecules/mole)

k_{019,H_2} = the hydrogen diffusivity of the 019 filter in moles/day/mole fraction hydrogen gas

y_{1,H_2} = the volume fraction hydrogen in the gas in the SLC

y_{2,H_2} = the volume fraction hydrogen in the gas in the space between the SLC and the CC

W = rate of radiolytic energy generation in watts.

The term $\frac{(10000)(24)(3600)WG'_{H_2}}{N_A}$ represents the radiolytic hydrogen generation rate, and the term $k_{019,H_2}\left(y_{1,H_2} - y_{2,H_2}\right)$ represents the rate of transfer of hydrogen from the SLC to the CC.

Similar mass transfer equations are used to calculate the hydrogen accumulation in the gas spaces between the SLC and the CC and between the CC and the PCV. The equation for hydrogen accumulation in the space between the SLC and the CC is

$$\frac{dm_{2,H_2}}{dt} = k_{019,H_2}\left(y_{1,H_2} - y_{2,H_2}\right) - k_{019/036,H_2}\left(y_{2,H_2} - y_{3,H_2}\right) \qquad (2)$$

where

m_{2,H_2} = the number of moles of hydrogen gas in the space between the SLC and the CC

$k_{019/036,H_2}$ = the combined hydrogen diffusivity through the 036 bag filter and the 019 filter in the CC lid in moles/day/mole fraction hydrogen gas

y_{3,H_2} = the volume fraction hydrogen in the gas in the space between the CC and the PCV.

The combined diffusivity is given by the reciprocal sum of the two individual diffusivities for the bag and can lid filters:

$$k_{019/036,H_2} = \frac{k_{019,H_2} k_{036,H_2}}{k_{019,H_2} + k_{036,H_2}} \qquad (3)$$

where

k_{036,H_2} = the hydrogen diffusivity for the 036 bag filter.

The mass transfer equation for the gas space between the CC and the PCV is

$$\frac{dm_{3,H_2}}{dt} = k_{019/036,H_2}\left(y_{2,H_2} - y_{3,H_2}\right) \qquad (4)$$

where

m_{3,H_2} = the number of moles of hydrogen gas in the space between the CC and the PCV.

The hydrogen volume fractions are calculated by dividing the number of moles of hydrogen generated by the total number of moles. Thus,

$$y_{1,H_2} = \frac{m_{1,H_2}}{m_{1,i} + m_{1,H_2}} \tag{5}$$

$$y_{2,H_2} = \frac{m_{2,H_2}}{m_{2,i} + m_{2,H_2}} \tag{6}$$

and

$$y_{3,H_2} = \frac{m_{3,H_2}}{m_{3,i} + m_{3,H_2}} \tag{7}$$

where

$m_{1,i}$ = the initial number of moles of gas in the SLC

$m_{2.i}$ = the initial number of moles of gas in the space between the SLC and the CC

$m_{3,i}$ = the initial number of moles of gas in the space between the CC and the PCV

The initial number of moles of gas in the spaces inside the SLC, the CC, and the PCV are calculated using the ideal gas law, which, for these volumes takes the forms

$$m_{1,i} = \frac{PV_{SLC}}{R_g T} \tag{8}$$

$$m_{2,i} = \frac{PV_{CC}}{R_g T} \tag{9}$$

and

$$m_{3,i} = \frac{PV_{PCV}}{R_g T} \tag{10}$$

where

P = the pressure in atm
V_{SLC} = the gas space volume inside the SLC in cm^3
V_{CC} = the gas space volume between the CC and the SLC in cm^3
V_{PCV} = the gas space volume between the PCV and the CC in cm^3
R_g = gas law constant, cm^3 atm/gmol/K
T = temperature, K

The G value is estimated from radiolytic gas generation measurements performed by Veirs and co-workers at Los Alamos National Laboratory.[10] Veirs and co-workers expressed G values in terms of the alpha energy deposited in the water present in the material. The previous revision of this calculation note used total gas generation rates based on measured pressure increases.[4] In this revision, actual hydrogen gas generation rates are used (see Appendix A).

The alpha energy deposited in the absorbed moisture is approximately equal to the total radiolytic energy multiplied by the fraction of electrons associated with the water, $\frac{e^-(H_2O)}{e^-(mat)}$, where $e^-(H_2O)$ is the number of electrons associated with the water and $e^-(mat)$ is the number of electrons in all of the material, calculated by summing the contributions for all materials mat_i:

$$e^-(mat) = \sum_i e^-(mat_i) \tag{11}$$

Veirs recommends two methods to convert the G value based on the energy deposited in the water, defined here as G_{H_2}, to an effective G value applied to the entire radiolytic heat generation rate, defined here as G'_{H_2}. In the more rigorous of the two methods, the G value reported by Veirs and co-workers is multiplied by the fraction of the total number of electrons in the material that are associated with water, where this fraction is estimated from the material stoichiometry and molecular weights. According to this first method,

$$G'_{H_2} = G_{H_2} \frac{e^-(H_2O)}{e^-(mat)} \tag{12}$$

Veirs and co-workers used the following weighted average to calculate the number of electrons associated with each molecular species in the mixed oxide. For the ith material, the weight average is given by

$$e^{-}(mat_i) = mf_i \frac{\sum_j n_{i,j} Z_{i,j}}{MW_i} \tag{13}$$

where

m =the total mass of the material

f_i =the weight fraction of the ith molecular species

MW_i = the molecular weight of the ith species

$n_{i,j}$ = the number of moles of the jth element in the ith species

$Z_{i,j}$ = the atomic weight of the jth element in the ith species.

For general salt species, the fraction $\frac{\sum_j n_{i,j} Z_{i,j}}{MW_i}$ is estimated to be $\frac{1}{2}$.

According to the preceding equation, the expression for the number of electrons associated with the water is

$$e^{-}(H_2O) = mf_{H_2O} \frac{10}{18} \tag{14}$$

Assuming that the mixed oxide is comprised of a mixture of absorbed water, PuO_2, U_3O_8, and primarily chloride salts, the expression for the number of electrons associated with the entire material takes the form

$$e^{-}(mat) = m\left(f_{H_2O} \frac{10}{18} + f_{PuO_2} \frac{110}{271} + f_{U_3O_8} \frac{340}{833} + f_{salt} \frac{1}{2} \right) \tag{15}$$

The second method recommended by Veirs is simply to multiply the reported G value by the weight fraction of absorbed water and a bounding correction factor to account for the different weight fractions of hydrogen in water and oxides or salts. Veirs recommends a correction factor of 1.37 (see Appendix A). With this correction factor, the conversion formula becomes

$$G'_{H_2} = 1.37 f_{H_2O} G_{H_2} \tag{16}$$

This simplified bounding calculation is required because composition data were not provided for all MIS material types. Using hydrogen generation rate data for which MIS material compositions were provided, Figures 2 and 3 plot bounding equivalent G values for hydrogen generation from equation 16 against equivalent G values calculated using the more rigorous method given by equations 11 through 15. As these comparisons show, equation 16 both bounds and closely approximates the results of the more rigorous calculation method over the entire range of measured hydrogen gas generation rates. Since the bounding estimate from equation 16 does give an accurate estimate of the more

rigorous calculation, equation 16 is used to convert the G values reported by Veirs to equivalent G values for all MIS material types.

Effective G values calculated either by equations 11 through 15 or by equation 16 are linearly proportional to the moisture content for any given material. Extrapolation of effective G values to moisture levels higher than those for the Veirs measurements requires that the intrinsic G value G_{H_2} remain constant or that the effective G value G'_{H_2} vary linearly with moisture content as the moisture level increases. Recent gas generation experiments performed by Veirs and co-workers using PuO_2 doped with either magnesium chloride ($MgCl_2$) or calcium chloride ($CaCl_2$) salts show that the intrinsic G value G_{H_2} reaches a constant value at approximately 2 weight % H_2O and remains constant up to at least 6 weight % H_2O.[11] As might be expected, the value for G_{H_2} at high moisture levels approaches the value for hydrogen generation from free water, which is approximately 1.6 molec/100 eV.[12]

In keeping with these observations, G values for the MIS items are extrapolated to higher moisture levels by taking a weighted average of the measured G value at a moisture level of 0.5 weight % and the G value for free water for any moisture in excess of 0.5 weight %. The 0.5 weight % moisture is the nominal moisture level for the Veirs gas generation tests for the MIS items.[10] The use of a weighted average implies that the moisture is either tightly bound to the oxide so that it radiolyzes only to a slight degree or is present as much more loosely bound water of hydration of deliquescence. Appendix B provides details of the analysis of the Veirs data at elevated moisture levels[11] and the extrapolation of the MIS data[12] to elevated moisture levels.

Table 2 lists values for G'_{H_2} calculated from the hydrogen generation rates reported by Veirs (see Appendix A and equation 16). G values are listed for 38 of the 39 MIS designations; no rate is given for MIS Number ARF-102-85-114-1, for which no hydrogen generation was detected.

The hydrogen gas generation rate in mol/day is given by $\frac{G'_{H_2} W(10000)(24)(3600)}{(1.602e-13)N_A}$,

where

W = the radiolytic heat generation rate in watts.

Equations similar to equations 1 through 4 can be used to calculate the mixing of carbon dioxide gas within the PCV in the period following the carbon dioxide purge of the gas space between the PCV and the CC. The only changes are the elimination of the gas generation term in equation 1 and the substitution of a carbon dioxide diffusivity for the hydrogen diffusivity. The modified equations for carbon dioxide transfer in the gas space inside the SLC, the gas space between the SCL and the CC, and the gas space between the CC and the PCV, respectively, take the forms

$$\frac{dm_{1,CO_2}}{dt} = k_{019,CO_2}\left(y_{2,CO_2} - y_{1,CO_2}\right) \tag{17}$$

$$\frac{dm_{2,CO_2}}{dt} = k_{019,CO_2}\left(y_{1,CO_2} - y_{2,CO_2}\right) - k_{019/036,H_2}\left(y_{2,CO_2} - y_{3,CO_2}\right) \tag{18}$$

and

$$\frac{dm_{3,CO_2}}{dt} = k_{019/036,CO_2}\left(y_{2,CO_2} - y_{3,CO_2}\right) \tag{19}$$

where

m_{1,CO_2} = the number of moles of carbon dioxide gas in the SLC

k_{019,CO_2} = the carbon dioxide diffusivity of the 019 filter in moles/day/mole fraction carbon dioxide gas

y_{1,CO_2} = the volume fraction carbon dioxide in the gas in the SLC

m_{2,CO_2} = the number of moles of carbon dioxide gas in the space between the SLC and the CC

y_{2,CO_2} = the volume fraction carbon dioxide in the gas in the space between the SLC and the CC

m_{3,CO_2} = the number of moles of carbon dioxide gas in the space between the SLC and the CC

y_{3,CO_2} = the volume fraction carbon dioxide in the gas in the space between the CC and the PCV

$k_{019/036,CO_2}$ = the combined carbon dioxide diffusivity through the 036 bag filter and the 019 filter in the CC lid.

The combined diffusivity is given by the reciprocal sum of the two individual diffusivities for the bag and can lid filters:

$$k_{019/036,CO_2} = \frac{k_{019,CO_2} k_{036,CO_2}}{k_{019,CO_2} + k_{036,CO_2}} \tag{20}$$

The effective diffusivity of carbon dioxide through the filter vents is estimated by comparing binary diffusion coefficients for the diffusion of hydrogen and carbon dioxide gases into air. The binary diffusion coefficient for gases diffusing into air is given by the Fuller, Schettler, and Giddings correlation, which is[13]

Table 2. G Values for Measured H_2 Gas Generation Rates for LANL Mixed Oxides Typical of KIS Generated Oxides

SSR Number	MIS Number	G_{H_2}, 0.5 wt% H_2O, molec/100 eV
SSR122	7161856	2.64E-04
SSR123	TS707001	2.64E-04
SSR124	5501579	1.32E-04
SSR125	MT-1490	9.25E-04
SSR126	669194	4.69E-03
SSR127	CLLANL025	4.82E-03
SSR128	7242201	1.26E-03
SSR129A	5501407	1.26E-03
SSR130	C06032A	1.05E-02
SSR131	ARF-102-85-223	3.97E-03
SSR132	BLO-39-11-14-004	6.61E-05
SSR133	PSU-84-06-05	6.61E-05
SSR134	R441	1.06E-03
SSR135	SCP711-56	1.98E-04
SSR136	1000089	1.39E-03
SSR137	11589	5.35E-03
SSR138	53038	5.68E-03
SSR139	520610020	1.28E-02
SSR140	7242165	6.61E-05
SSR141	7242141 (fur ball)	3.30E-04
SSR142	PBO-47-09-012-023	1.32E-04
SSR143	ARF-102-85-355	6.61E-05
SSR144	ARF-102-85-365	4.63E-03
SSR145	64-85-12-1858	6.61E-05
SSR146	R438	5.29E-04
SSR147	CAN92	1.32E-04
SSR148	C0024A	2.64E-04
SSR149A	C00695	5.09E-03
SSR150	TS707013	7.27E-04
SSR151	7032282	2.38E-03
SSR152	41-85-08-1379B	1.32E-04
SSR153	63-88-06-121	1.65E-03
SSR154	ARF-102-85-114-1	0.00E+00
SSR155	ARF-102-85-295	1.31E-02
SSR155HT	ARF-102-85-295	5.22E-03
SSR156	PuF4-1	2.64E-04
SSR160	PMAXBS	4.96E-03
SSR161	PEOF1	6.61E-05
SSR162	MISSTD	4.63E-04

$$D_{AB} = \frac{0.001T^{1.75}\left(\frac{M_A + M_B}{M_A M_B}\right)^{0.5}}{P_a\left(\sum V_A^{1/3} + \sum V_B^{1/3}\right)^2} \tag{21}$$

where

T =the temperature in degrees K
M_A and M_B = the molecular weights of air and diffusing gas in g/mol
P_a = the pressure in atmospheres
$\sum V_A$ and $\sum V_B$ = molecular volumes, tabulated by Fuller, Schettler and Giddings.[12]

Comparative estimations of the diffusivities for hydrogen and carbon dioxide show that the ratio of the carbon dioxide and hydrogen diffusivities is bounded by the square root of the ratio of the molecular weights of hydrogen and carbon dioxide. The diffusivity also is inversely proportional to the square root of the gas molecular weight for slip flow and molecular (Knudsen) diffusion, as evidenced by the form of the slip flow correction factor.[14] Thus, conservative, lower bounds to the carbon diffusivities are given by

$$k_{019,CO_2} = \left(\frac{M_{H_2}}{M_{CO_2}}\right)^{0.5} k_{019,H_2} \tag{22}$$

and

$$k_{019/036,CO_2} = \left(\frac{M_{H_2}}{M_{CO_2}}\right)^{0.5} k_{019/036,H_2} \tag{23}$$

where

M_{H_2} and M_{CO_2} are the molecular weights of hydrogen and carbon dioxide, which are 2 and 44 g/mol, respectively.

The mixing of carbon dioxide following a purge which displaces 75% of the air in the gas space between the PCV and the CC with carbon dioxide is illustrated by Figure 4. Figure 4 shows that the concentration inside an empty SLC initially filled by air becomes equal to the mixed concentration inside the entire gas space within the PCV within about 18 hours. The diffusivity for hydrogen is predicted to be about 4.7 times greater than the diffusivity for carbon dioxide, so hydrogen gas should mix even faster than carbon dioxide gas. Because of this rapid mixing, the entire gas space within the PCV can be treated as a single mixed volume for flammability calculations to simplify the calculation of the approach to the LFL.

A question that needs to be resolved before the preceding model is applied is whether to treat the gas space inside the getter can as a well-mixed volume or as an effectively solid material that is impermeable to gas. It may be recalled that the getter and microporous sieve materials are enclosed within separate Tyvek® bags, double bagged within a third Tyvek® bag, and then encased within a perforated getter can. To treat the gas spaces within the getter can as being well-mixed, it is sufficient to demonstrate that the volume-average CO_2 concentration within getter can and the remaining gas space between the PCV and the CC reaches the purge criterion of 75 vol % CO_2 at the conclusion of the 18-min CO_2 purge. The reasoning is that the gas spaces inside and outside the getter can become well-mixed over the longer time spans of interest for subsequent hydrogen generation.

The CO_2 concentrations inside the inner Tyvek® bags at the end of the purge can be estimated by combining mass transfer equations for the gas spaces outside the inner bags with the solution of a radial diffusion equation for the gas space inside the inner bags. IN the mass transfer analysis, each Tyvek® bag is assumed to expand until it fills the getter can. The volume occupied by each inner bag is assumed to be proportional to the bulk volumes of the getter and microporous sieve materials. The surface area for diffusion of CO_2 is estimated by doubling the area of the rectangular bag shape prior to filling. Diffusion of CO_2 into the interior of the bags from the top and bottom ends is conservatively ignored. The volume between the outer Tyvek bag and the two inner bags is arbitrarily set at 25 cm^3.

If it is assumed that the gas spaces outside the bags and between the outer and inner bags remain well-mixed during the purge, then the CO_2 volume fractions inside and outside the bags can be calculated from the following mass transfer equations:

$$V_{PCV'} \frac{dy_{CO_2,PCV}}{dt} = Q_{purge}\left(1 - y_{CO_2,PCV}\right) - A_{Ty} k_{Ty}\left(y_{CO_2,PCV} - y_{CO_2,ob}\right) \quad (24)$$

$$V_{ob} \frac{dy_{CO_2,ob}}{dt} = A_{Ty} k_{Ty}\left(y_{CO_2,PCV} - y_{CO_2,ob}\right) \quad (25)$$

$$V_{gb} \frac{d\bar{y}_{CO_2,gb}}{dt} = A_{Ty} k_{Ty}\left(y_{CO_2,ob} - y_{CO_2,gb,s}\right) \quad (26)$$

and

$$V_{msb} \frac{d\bar{y}_{CO_2,msb}}{dt} = A_{Ty} k_{Ty}\left(y_{CO_2,ob} - y_{CO_2,msb,s}\right) \quad (27)$$

where

V_{PCV}' = the volume of the gas space inside the PCV but outside the getter can and the CC

$y_{CO_2,PCV}$ = the CO_2 volume fraction in the gas space outside the getter can

t = the elapsed time since the start of the purge

Q_{purge} = the purge flow rate

A_{Ty} = the surface area of the Tyvek® bag material

k_{Ty} = the diffusive permeability of the Tyvek®

V_{ob} = the volume of the gas space between the outer bag and the getter material and microporous sieve material bags

$y_{CO_2,ob}$ = the CO_2 volume fraction inside the outer bag

$y_{CO_2,gb,s}$ = the CO_2 volume fraction at the inside surface of the getter material bag

$y_{CO_2,msb,s}$ = the CO_2 volume fraction at the inside surface of the microporous sieve material bag

V_{gb} = the volume of the gas space inside the getter material bag

$\bar{y}_{CO_2,gb}$ = the average CO_2 volume fraction inside the getter material bag

V_{msb} = the volume of the gas space inside the microporous sieve material bag

$\bar{y}_{CO_2,msb}$ = the average CO_2 volume fraction inside the microporous sieve material bag

Equations 24 through 27 can be solved for the CO_2 concentration transients inside the PCV and the getter and microporous sieve material bags if the gas inside the bags is assumed to be well-mixed, so that

$$\bar{y}_{CO_2,gb} = y_{CO_2,gb,s} \tag{28}$$

and

$$\bar{y}_{CO_2,msb} = y_{CO_2,msb,s} \tag{29}$$

The solution to the mass transfer equations for well-mixed gases inside the Tyvek bags is obtained by numerical integration of equations 24 through 27. Figure 5 depicts the concentration transients from this integration. As Figure 5 shows, the calculated air concentration drops to 51 vol % in the getter bag and to 40 vol % in the microporous sieve bag at the end of the 18-min purge. In other words, the CO_2 concentration rises to 49 vol % in the getter bag and to 60 vol % in the microporous sieve bag.

The applicable solutions for radial diffusion within the Tyvek® bags are based on an assumption that the surface concentrations in the inner bags increase approximately linearly with time, so that

$$y_{CO_2,gb,s} = k_g t \tag{30}$$

and

$$y_{CO_2,msb,s} = k_{ms} t \tag{31}$$

where

k_g = the rate of increase in the volume fraction of CO_2 for diffusion across the Tyvek® getter bag surface

k_{ms} = the rate of increase in the volume fraction of CO_2 for diffusion across the Tyvek® microporous sieve bag surface

The solutions for radial diffusion inside the bags, with surface conditions given by equations 30 and 31, are:[15]

$$\bar{y}_{CO_2,gb} = k_g t - \frac{k_g r_{gc}^2}{8D_{eff}} + \frac{4k_g r_{gc}^2}{D_{eff}} \sum_{n=1}^{\infty} \frac{\exp\left(-\frac{\gamma_n^2 D_{eff} t}{r_{gc}^2}\right)}{\gamma_n^2} \tag{32}$$

and

$$\bar{y}_{CO_2,msb} = k_{ms} t - \frac{k_{ms} r_{gc}^2}{8D_{eff}} + \frac{4k_{ms} r_{gc}^2}{D_{eff}} \sum_{n=1}^{\infty} \frac{\exp\left(-\frac{\gamma_n^2 D_{eff} t}{r_{gc}^2}\right)}{\gamma_n^2} \tag{33}$$

where

r_{gc} = the getter can radius

$D_{eff,g}$ = the effective diffusivity for CO_2 in the gas space

γ_n = the nth root of Bessel's function of zero order

Equations 32 and 33 can be combined with equations 30 and 31 to give

$$\bar{y}_{CO_2,gb} = y_{CO_2,gb,s}\left(1 - \frac{r_{gc}^2}{8D_{eff}t} + \frac{4r_{gc}^2}{D_{eff}t}\sum_{n=1}^{\infty}\frac{\exp\left(-\frac{\gamma_n^2 D_{eff}t}{r_{gc}^2}\right)}{\gamma_n^2}\right) \tag{34}$$

$$\bar{y}_{CO_2,msb} = y_{CO_2,msb,s}\left(1 - \frac{r_{gc}^2}{8D_{eff}t} + \frac{4r_{gc}^2}{D_{eff}t}\sum_{n=1}^{\infty}\frac{\exp\left(-\frac{\gamma_n^2 D_{eff}t}{r_{gc}^2}\right)}{\gamma_n^2}\right) \tag{35}$$

The effective diffusivity for CO_2 in the gas spaces of the bags is calculated by dividing the binary molecular diffusion coefficient for CO_2 in air by a tortuosity conservatively set at a value of 2.5. The diffusivity does not need to be multiplied by the void fraction because the mass transfer analysis is applied only to the gas space within the inner bags. The expression for the effective diffusivity, D_{eff}, is

$$D_{eff} = \frac{D}{\tau} \tag{36}$$

where

D = molecular diffusion coefficient for CO_2 in air, calculated from equation 21
τ = tortuosity

The Bessel function terms on the right-hand sides of equations 34 and 35 do not contribute significantly to the overall solution. This is demonstrated by evaluating the first Bessel function term, whose root is given by[16]

$$\gamma_1 = 2.4048 \tag{37}$$

In the calculation of the relative volumes occupied by the getter and microporous sieve material bags, calculations of the bulk volume of each material and hence the void fraction are required. The void fraction is computed from a comparison of the pycnometric (or theoretical) density and the bulk density, using

$$\varepsilon = 1 - \frac{\rho_b}{\rho_{th}} \tag{38}$$

where

ρ_b = the bulk density

ρ_{th} = pycnometric or theoretical density

From equations 34 and 35, the average CO_2 concentrations in the getter and microporous sieve material bags are 6% lower than the concentrations at the bag surfaces at the conclusion of the purge. This translates to about 38 vol % CO_2 in the getter material bag and 48 vol % CO_2 in the microporous sieve material bag. From the solution to equations 24 through 27, the CO_2 concentrations in the outer Tyvek® bag is approximately 63 vol %, and the CO_2 concentration insde the PCV but outside the getter can is 99 vol %. The volume average CO_2 concentration at the end of the purge is 78.5 vol %, which slightly exceeds the minimum storage criterion of 75 vol % CO_2.[1] It may be concluded that the entire gas space within the PCV, including the gas space within the getter can, may be considered to be well-mixed for any time span for which there is significant hydrogen generation.

The preceding analysis is conservative in that it does not credit mixing through the top and bottom surfaces of the bags or any mixing subsequent to the purge. Additionally, the calculation of the concentration transients at the bag surfaces is inherently conservative because it treats the mixed concentrations in the transient terms in equations 25 and 26 as surface concentrations, and thus underestimates the rates of increase of the surface concentrations.

In a simplified approach in which the gas space within the PCV is treated as a single mixed volume, the mixed volume hydrogen gas concentration in vol %, y_{H_2}, is calculated from the equation

$$y_{H_2} = \frac{\dfrac{G'_{H_2} W (10000)(24)(3600)}{(1.602e-13) N_A \rho_M} t}{\dfrac{G'_{H_2} W (10000)(24)(3600)}{(1.602e-13) N_A \rho_M} t + V_t} \tag{39}$$

where

ρ_M = the gas density in mol/cm^3

V_t = the total gas space volume inside the PCV.

The gas density is evaluated using the ideal gas law:

$$\rho_M = \frac{P}{R_g T} \tag{40}$$

where

P = the initial pressure in atm
T = the absolute temperature in K
R_g = the gas law constant, 82.057 cm^3-atm/K.

The total gas space volume is the sum of the gas space volume between the CC and the PCV, V_{PCV}, the gas space volume between the CC and the SLC, V_{CC}, and the gas space volume inside the SLC, V_{SLC}, multiplied by the fraction of the SLC that is not occupied by the oxide. The inert gas volume is minimized and the LFL is reached the soonest if it is assumed that the oxide occupies the entire volume of the SLC. Consequently, the total volume is calculated without taking any credit for the volume inside the SLC, so that

$$V_t = V_{CC} + V_{PCV} \tag{41}$$

To calculate the time required to reach the LFL, the mixed gas space hydrogen concentration is set equal to the hydrogen concentration at the LFL. Thus,

$$y_{H_2} = y_{LFL} \tag{42}$$

A graphical correlation presented by Coward and Jones,[17] reproduced in Figure 6, gives the hydrogen LFL as a function of the percentage by volume of carbon dioxide in the original PCV atmosphere (prior to any hydrogen generation). For a 75% carbon dioxide purge of the gas space between the CC and the PCV, the carbon dioxide gas occupies 55% of the total mixed volume between the PCV and the SLC. At this dilution, y_{LFL}, from Figure 6, is approximately 5 vol %, or 0.05.

Equations 39 and 42 may be solved for the time to reach LFL to obtain

$$t = \frac{(1.602e-13)N_A \rho_M}{G'_{H_2} W(10000)(24)(3600)} \frac{y_{LFL} V_t}{(1 - y_{LFL})} \tag{43}$$

5.0 Calculation Method

All calculations were performed using Microsoft Excel spreadsheets.

6.0 Open Items

There are no open items associated with this calculation note.

7.0 Discussion of Results

Times to reach the LFL were calculated for the 38 MIS materials for which there was measurable hydrogen generation. Calculated hydrogen concentrations inside the PCV increased approximately linearly with time until the time the LFL was reached, as

indicated by Figure 7. Times to reach the LFL were calculated for arbitrary moisture levels ranging from 0.1 to 6 weight % H_2O, the maximum moisture content for which hydrogen generation rates have been measured. Results of these calculations are shown by Figures 8, 9, and 10. Tables 3 and 4 list the times to reach the LFL for each of the 38 MIS materials at varying moisture levels. At the nominal moisture level for the MIS tests (approximately 0.5 weight % H_2O), the time to reach the LFL varied from 12 days for Material ARF-92-85-295 calcined at 750 °C to 2400 days for several MIS's with the minimum reported hydrogen generation rate of 1 nmol/W/s. For moisture levels above 0.5 weight %, times to LFL are calculated using extrapolated G values based on a weighted average of G values for bound and free water. Times to LFL based on these extrapolated G values drop off rapidly, reaching about 1.3 days for any hypothetical MIS item with 6 weight % moisture. It should be stressed that it is unlikely that oxide materials with low G values will absorb high moisture contents from humid atmospheres. Materials that are likely to absorb significant moisture (namely, those that contain chloride salts) exhibited high G values during the MIS tests.

The time required for the material with the highest gas generation rate, ARF-92-85-295 calcined at 750 °C, to reach the safety analysis pressure limit of 365 psig is 10.2 years at 0.5 wt % H_2O and 1.0 year at 6 wt % H_2O. Both times exceed anticipated storage times subsequent to a postulated getter material failure.

Reported times to reach the LFL are computed under the assumption that the LFL is 5 vol % hydrogen. If the LFL were assumed to be 4 vol % hydrogen, as it would be in an air atmosphere, the times to LFL would be 0.8 times the reported values.

8.0 Conclusion

Times to reach the LFL have been calculated for 38 MIS materials for which there was measurable radiolytic hydrogen generation. At the nominal moisture level for the MIS tests (approximately 0.5 weight % H_2O), the calculated time to LFL ranges from 12 days for Material ARF-102-85-295 calcined at 750 °C to 2400 days for several MIS's with the minimum reported hydrogen generation rate of 1 nmol/W/s. For moisture levels above 0.5 weight %, conservative bounds for times to LFL are calculated using extrapolated G values based on a weighted average of G values for bound and free water. Times to LFL based on these extrapolated G values drop off rapidly, reaching about 1.3 days for any hypothetical MIS item with 6 weight % moisture. The bounding calculations predict that the hydrogen concentration inside the PCV will reach the LFL in a matter of days if the moisture level significantly exceeds 0.5 weight %. It should be stressed that it is unlikely that oxide materials with low G values will absorb high moisture contents from humid atmospheres. Materials that are likely to absorb significant moisture (namely, those that contain chloride salts) exhibited high G values during the MIS tests.

The time required for the material with the highest gas generation rate, ARF-92-85-295 calcined at 750 °C, to reach the safety analysis pressure limit of 365 psig is 10.2 years at 0.5 wt % H_2O and 1.0 year at 6 wt % H_2O. Both times exceed anticipated storage times subsequent to a postulated getter material failure.

The calculations are based on G values measured by Veirs and co-workers at Los Alamos National Laboratory, a LFL of 5 vol % for the hydrogen gas, and an approximation that the gas volume inside the PCV is well-mixed.

Reported times to reach the LFL are computed under the assumption that the LFL is 5 vol % hydrogen. If the LFL were assumed to be 4 vol % hydrogen, as it would be in an air atmosphere, the times to LFL would be 0.8 times the reported values.

Table 3. Times in Days to Reach the Hydrogen LFL at Moisture Levels between 0.1 and 0.9 wt %, for a Total Radiolytic Power of 5 watts

SSR No.	MIS No.	wt % H2O:	0.1	0.2	0.3	0.4	0.5	0.6	0.7	0.8	0.9
SSR122	7161856		3050	1525	1017	763	610	66	35	24	18
SSR123	TS707001		3050	1525	1017	763	610	66	35	24	18
SSR124	5501579		6100	3050	2033	1525	1220	69	36	24	18
SSR125	MT-1490		871	436	290	218	174	52	30	21	17
SSR126	669194		172	86	57	43	34	23	18	14	12
SSR127	CLLANL025		167	84	56	42	33	23	18	14	12
SSR128	7242201		642	321	214	161	128	47	29	21	16
SSR129A	5501407		642	321	214	161	128	47	29	21	16
SSR130	C06032A		77	38	26	19	15	13	11	9	8
SSR131	ARF-102-85-223		203	102	68	51	41	26	19	15	13
SSR132	BLO-39-11-14-004		12201	6100	4067	3050	2440	71	36	24	18
SSR133	PSU-84-06-05		12201	6100	4067	3050	2440	71	36	24	18
SSR134	R441		763	381	254	191	153	50	30	21	16
SSR135	SCP711-56		4067	2033	1356	1017	813	67	35	24	18
SSR136	1000089		581	290	194	145	116	45	28	20	16
SSR137	11589		151	75	50	38	30	21	17	14	11
SSR138	53038		142	71	47	35	28	20	16	13	11
SSR139	520610020		63	31	21	16	13	11	9	8	7
SSR140	7242165		12201	6100	4067	3050	2440	71	36	24	18
SSR141	7242141 (fur ball)		2440	1220	813	610	488	64	34	23	18
SSR142	PBO-47-09-012-023		6100	3050	2033	1525	1220	69	36	24	18
SSR143	ARF-102-85-355		12201	6100	4067	3050	2440	71	36	24	18
SSR144	ARF-102-85-365		174	87	58	44	35	24	18	14	12
SSR145	64-85-12-1858		12201	6100	4067	3050	2440	71	36	24	18
SSR146	R438		1525	763	508	381	305	59	33	23	17
SSR147	CAN92		6100	3050	2033	1525	1220	69	36	24	18
SSR148	C0024A		3050	1525	1017	763	610	66	35	24	18
SSR149A	C00695		158	79	53	40	32	22	17	14	12
SSR150	TS707013		1109	555	370	277	222	55	32	22	17
SSR151	7032282		339	169	113	85	68	35	24	18	14
SSR152	41-85-08-1379B		6100	3050	2033	1525	1220	69	36	24	18
SSR153	63-88-06-121		488	244	163	122	98	42	27	20	15
SSR155	ARF-102-85-295		62	31	21	15	12	11	9	8	7
SSR155HT	ARF-102-85-295		154	77	51	39	31	22	17	14	12
SSR156	PuF4-1		3050	1525	1017	763	610	66	35	24	18
SSR160	PMAXBS		163	81	54	41	33	23	17	14	12
SSR161	PEOF1		12201	6100	4067	3050	2440	71	36	24	18
SSR162	MISSTD		1743	871	581	436	349	61	33	23	17

Table 4. Times in Days to Reach the Hydrogen LFL at Moisture Levels between 2.0 and 6 wt %, for a Total Radiolytic Power of 5 watts

SSR No.	MIS No.	wt % H2O:	1	1.5	2	2.5	3	4	5	6
SSR122	7161856		14.4	7.3	4.9	3.7	2.9	2.1	1.6	1.3
SSR123	TS707001		14.4	7.3	4.9	3.7	2.9	2.1	1.6	1.3
SSR124	5501579		14.5	7.3	4.9	3.7	2.9	2.1	1.6	1.3
SSR125	MT-1490		13.6	7.1	4.8	3.6	2.9	2.1	1.6	1.3
SSR126	669194		10.3	6.1	4.3	3.3	2.7	2.0	1.6	1.3
SSR127	CLLANL025		10.2	6.0	4.3	3.3	2.7	2.0	1.6	1.3
SSR128	7242201		13.2	7.0	4.7	3.6	2.9	2.1	1.6	1.3
SSR129A	5501407		13.2	7.0	4.7	3.6	2.9	2.1	1.6	1.3
SSR130	C06032A		7.5	5.0	3.7	3.0	2.5	1.8	1.5	1.2
SSR131	ARF-102-85-223		10.8	6.2	4.4	3.4	2.7	2.0	1.6	1.3
SSR132	BLO-39-11-14-004		14.6	7.3	4.9	3.7	2.9	2.1	1.6	1.3
SSR133	PSU-84-06-05		14.6	7.3	4.9	3.7	2.9	2.1	1.6	1.3
SSR134	R441		13.4	7.0	4.8	3.6	2.9	2.1	1.6	1.3
SSR135	SCP711-56		14.5	7.3	4.9	3.7	2.9	2.1	1.6	1.3
SSR136	1000089		13.1	6.9	4.7	3.6	2.9	2.1	1.6	1.3
SSR137	11589		9.9	5.9	4.2	3.3	2.7	2.0	1.6	1.3
SSR138	53038		9.7	5.8	4.2	3.3	2.7	2.0	1.5	1.3
SSR139	520610020		6.8	4.6	3.5	2.8	2.4	1.8	1.4	1.2
SSR140	7242165		14.6	7.3	4.9	3.7	2.9	2.1	1.6	1.3
SSR141	7242141 (fur ball)		14.3	7.2	4.9	3.7	2.9	2.1	1.6	1.3
SSR142	PBO-47-09-012-023		14.5	7.3	4.9	3.7	2.9	2.1	1.6	1.3
SSR143	ARF-102-85-355		14.6	7.3	4.9	3.7	2.9	2.1	1.6	1.3
SSR144	ARF-102-85-365		10.3	6.1	4.3	3.3	2.7	2.0	1.6	1.3
SSR145	64-85-12-1858		14.6	7.3	4.9	3.7	2.9	2.1	1.6	1.3
SSR146	R438		14.0	7.2	4.8	3.6	2.9	2.1	1.6	1.3
SSR147	CAN92		14.5	7.3	4.9	3.7	2.9	2.1	1.6	1.3
SSR148	C0024A		14.4	7.3	4.9	3.7	2.9	2.1	1.6	1.3
SSR149A	C00695		10.0	6.0	4.2	3.3	2.7	2.0	1.6	1.3
SSR150	TS707013		13.8	7.1	4.8	3.6	2.9	2.1	1.6	1.3
SSR151	7032282		12.1	6.6	4.6	3.5	2.8	2.0	1.6	1.3
SSR152	41-85-08-1379B		14.5	7.3	4.9	3.7	2.9	2.1	1.6	1.3
SSR153	63-88-06-121		12.8	6.8	4.7	3.5	2.9	2.1	1.6	1.3
SSR155	ARF-102-85-295		6.7	4.6	3.5	2.8	2.4	1.8	1.4	1.2
SSR155HT	ARF-102-85-295		10.0	5.9	4.2	3.3	2.7	2.0	1.6	1.3
SSR156	PuF4-1		14.4	7.3	4.9	3.7	2.9	2.1	1.6	1.3
SSR160	PMAXBS		10.1	6.0	4.3	3.3	2.7	2.0	1.6	1.3
SSR161	PEOF1		14.6	7.3	4.9	3.7	2.9	2.1	1.6	1.3
SSR162	MISSTD		14.1	7.2	4.8	3.6	2.9	2.1	1.6	1.3

9.0 References

1. T. D. Woodsmall, "Implementation of the Interim Safe Storage Criteria in the 910-B Storage Vault," N-ESR-K-00004, Rev. 9, May 22, 2007 (or latest revision).
2. T. D. Woodsmall, "Packaging Reconfiguration for Repackaged Materials K Area Interim Surveillance Project (U)," M-TRT-K-00004, Rev. 1, February 6, 2006.
3. A. Nissen, G. Buffleben, and T. Shepodd, "Performance Testing of Aged Hydrogen Getters Against Criteria for Interim Safe Storage of Plutonium Bearing Materials," Sandia National Laboratory Report SAND2007-0095, January, 2007.
4. J. E. Laurinat, "Calculation of Hydrogen Generation Rates for Storage of Post-KIS Oxide in 9975 Shipping Containers," N-CLC-K-00219, Rev. 0, November 16, 2006.
5. Drawing SK-MWS081106-001, Rev. B, "Slip Lid Can Dimensional Requirements," October 5, 2006.
6. Drawing R-R2-F-0018, Rev. 5, "9975 Shipping Package: Primary and Secondary Containment Vessel Subassemblies (U)," June 30, 2004.
7. Drawing R-R1-F-0098, Rev. 2, "FB-Line Convenience Can Assembly and Details," February 23, 2004.
8. ASTM E 398-03, "Standard Test Method for Water Vapor Transmission Rate of Sheet Materials Using Dynamic Relative Humidity Measurement," ASTM International, West Conshohocken, Pennsylvania, May 10, 2003.
9. Procedure SOP-CSS-216-K, Draft K, "Venting a 9975 Container."
10. E. Kelly, L. Peppers, D. K. Veirs, and J. Berg, "3013 Container Statistical and Judgmental Samples Selected for Non Destructive Evaluation (NDE) in FY 2005," Los Alamos National Laboratory Report LA-UR-05-2193, March, 2005.
11. E. L. Garcia, M. A. Martinez, D. K. Veirs, J. M. Berg, and L. A. Worl, "Small-Scale Studies: Oxygen Generation and Corrosion," Los Alamos National Laboratory Document LA-UR-07-1371, January, 2007.
12. J. W. T. Spinks and R. J. Woods, An Introduction to Radiation Chemistry, 3rd ed., John Wiley and Sons, New York (1990).
13. D. W. Green, ed., Perry's Chemical Engineers' Handbook, 6th ed., p. 3-285.
14. D. W. Green, ed., Perry's Chemical Engineers' Handbook, 6th ed., pp. 5-32 to 5-33.
15. J. Crank, The Mathematics of Diffusion, Oxford University Press, London (1956), p. 70.
16. D. R. Lide, ed., CRC Handbook of Chemistry and Physics, 75th ed., CRC Press, Boca Raton, Florida (1994), pp. A-97 to A-98.
17. H. F. Coward and G. W. Jones, "Limits of Flammability of Gases and Vapors," Bureau of Mines Bulletin 503, U. S. Bureau of Mines, 1952.

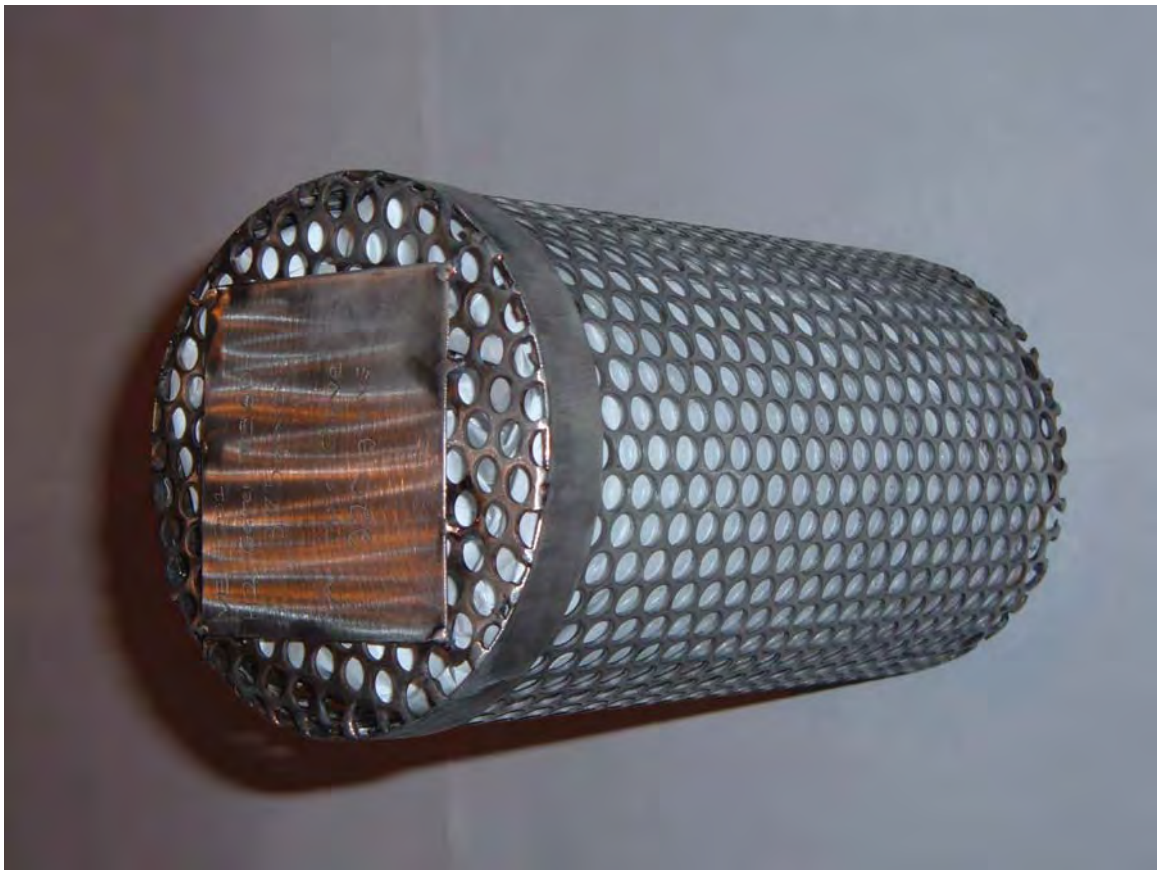

Figure 1. Getter Can with Getter and Microporous Sieve Bags

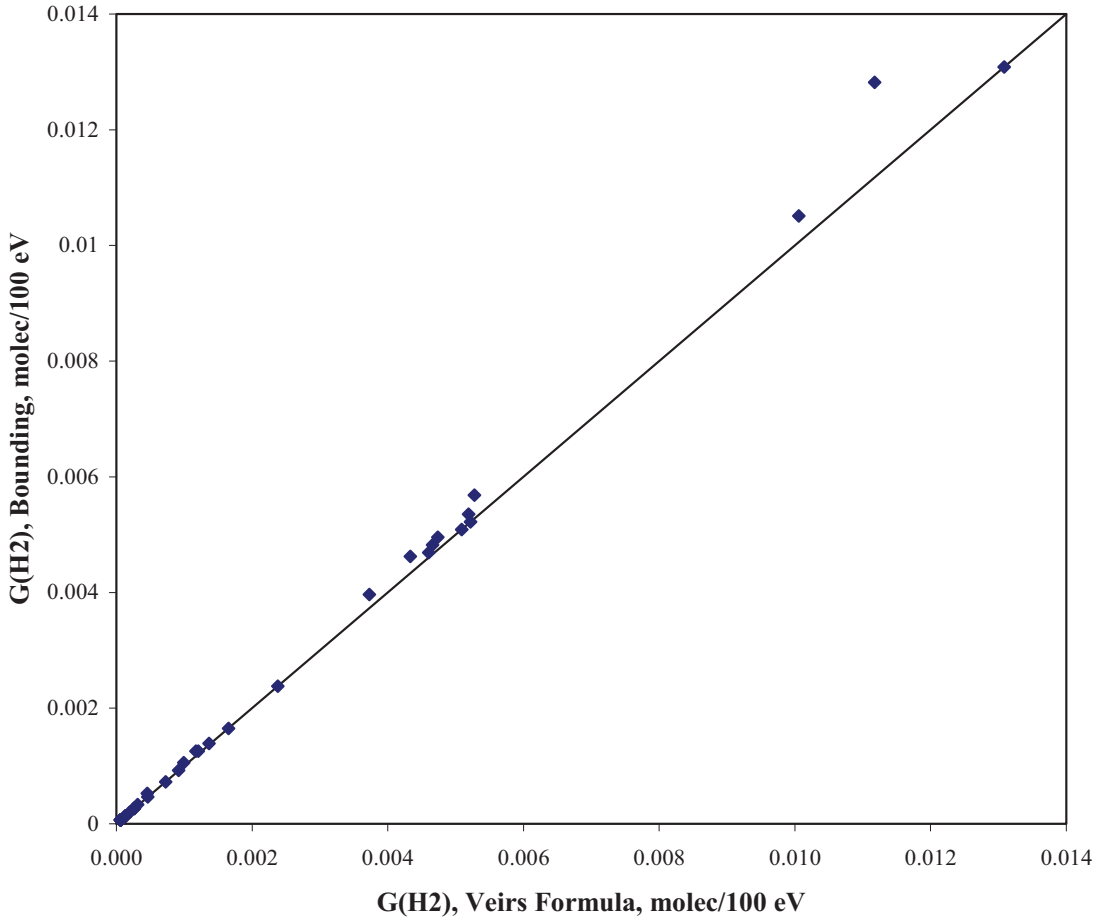

Figure 2. Comparison of Bounding G Value for Hydrogen Gas Generation from MIS Samples (from equation 16) with G Value from Veirs Conversion Formula (from equations 11 through 15), Using a Linear Scale

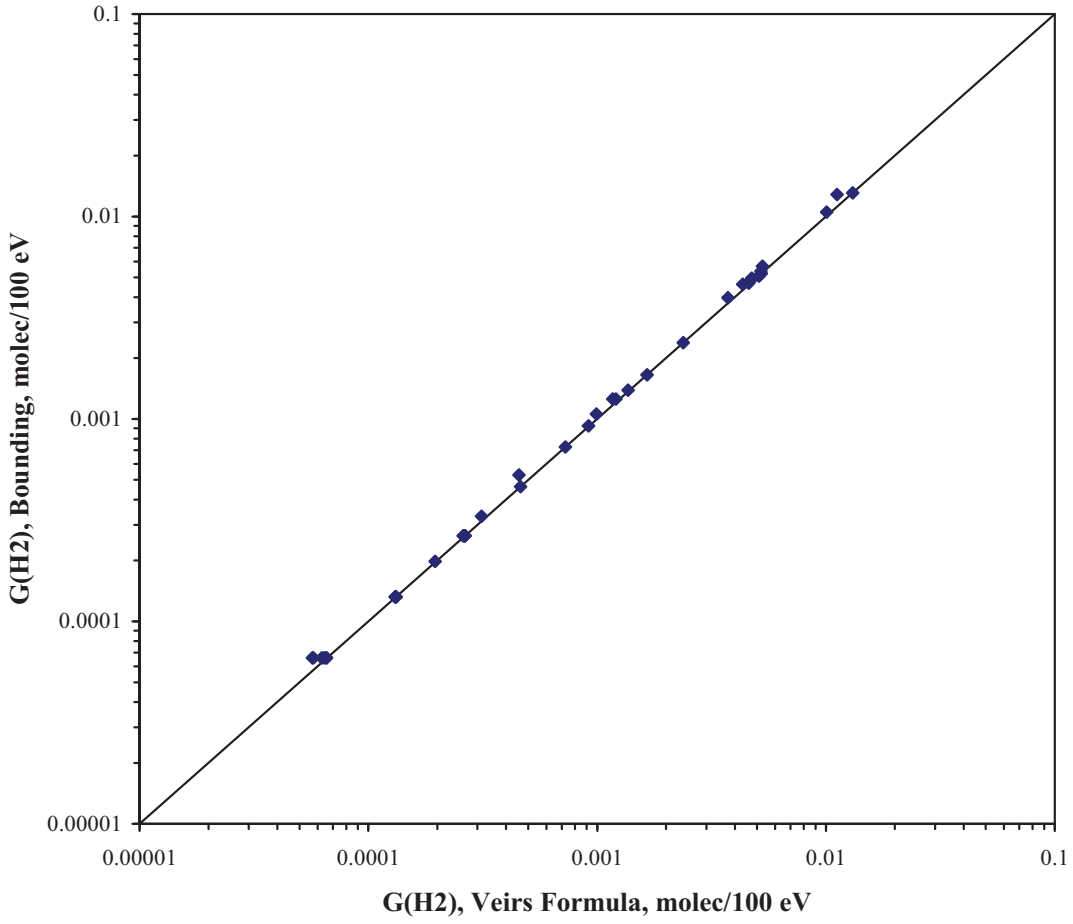

Figure 3. Comparison of Bounding G Value for Hydrogen Gas Generation from MIS Samples (from equation 16) with G Value from Veirs Conversion Formula (from equations 11 through 15), Using a Logarithmic Scale

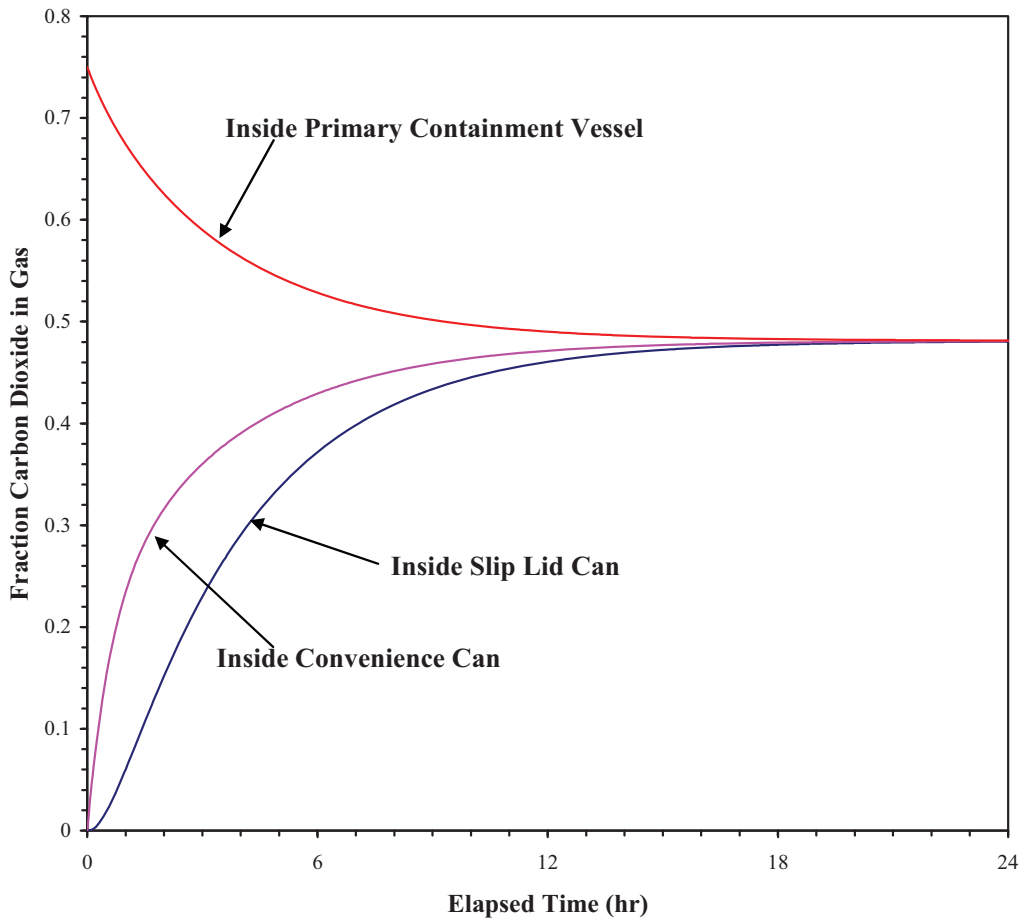

Figure 4. Variation of Carbon Dioxide Concentration during Initial Mixing after Purge, for Empty Slip Lid Can

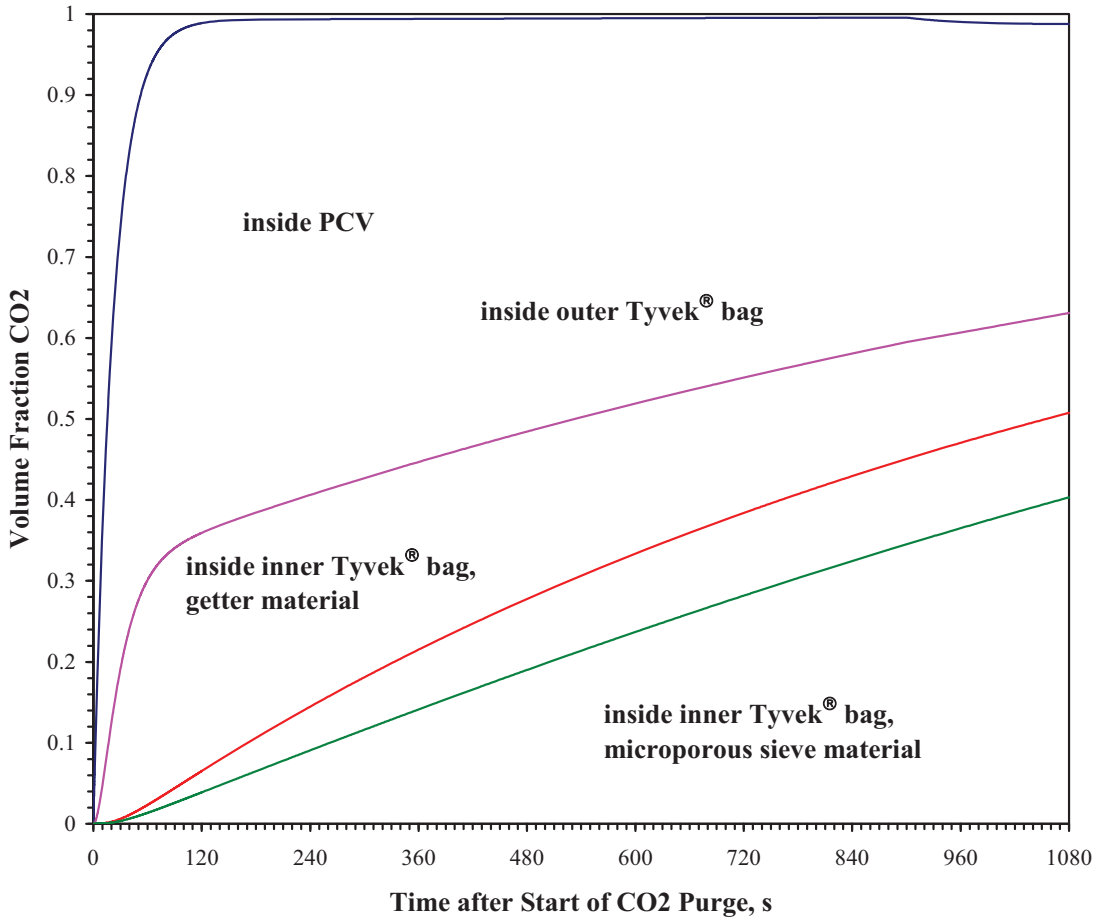

Figure 5. Variation of Carbon Dioxide Concentrations inside PCV, Getter Material Bag, and Microporous Sieve Material Bag during Purge

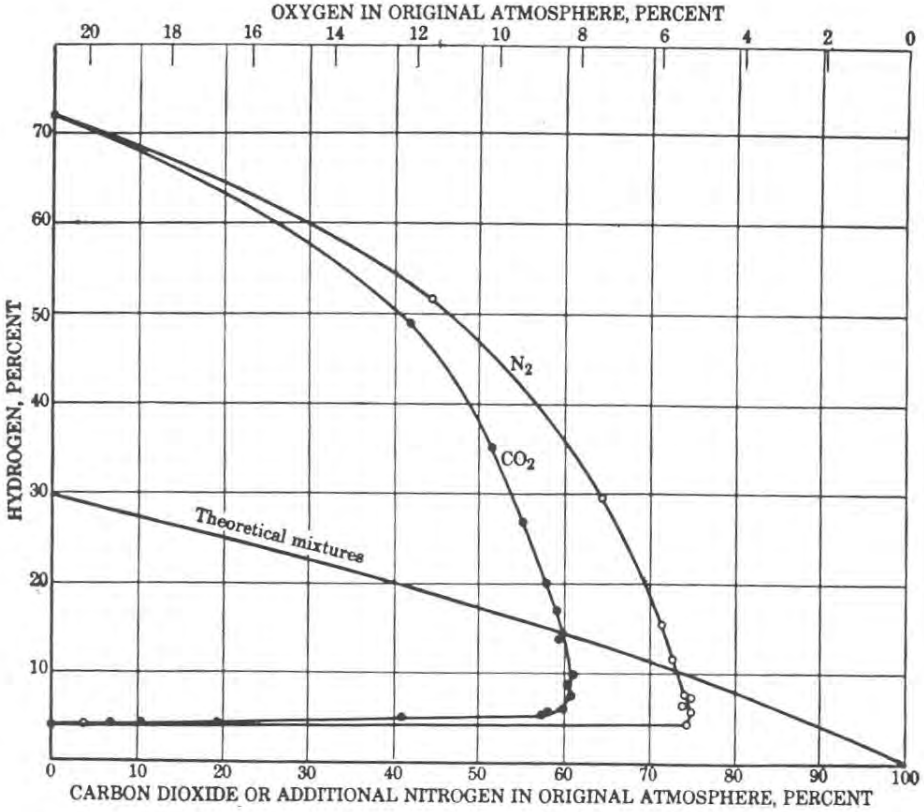

Figure 6. Variation of the Hydrogen Lower Flammability Limit with Carbon Dioxide Volume Fraction

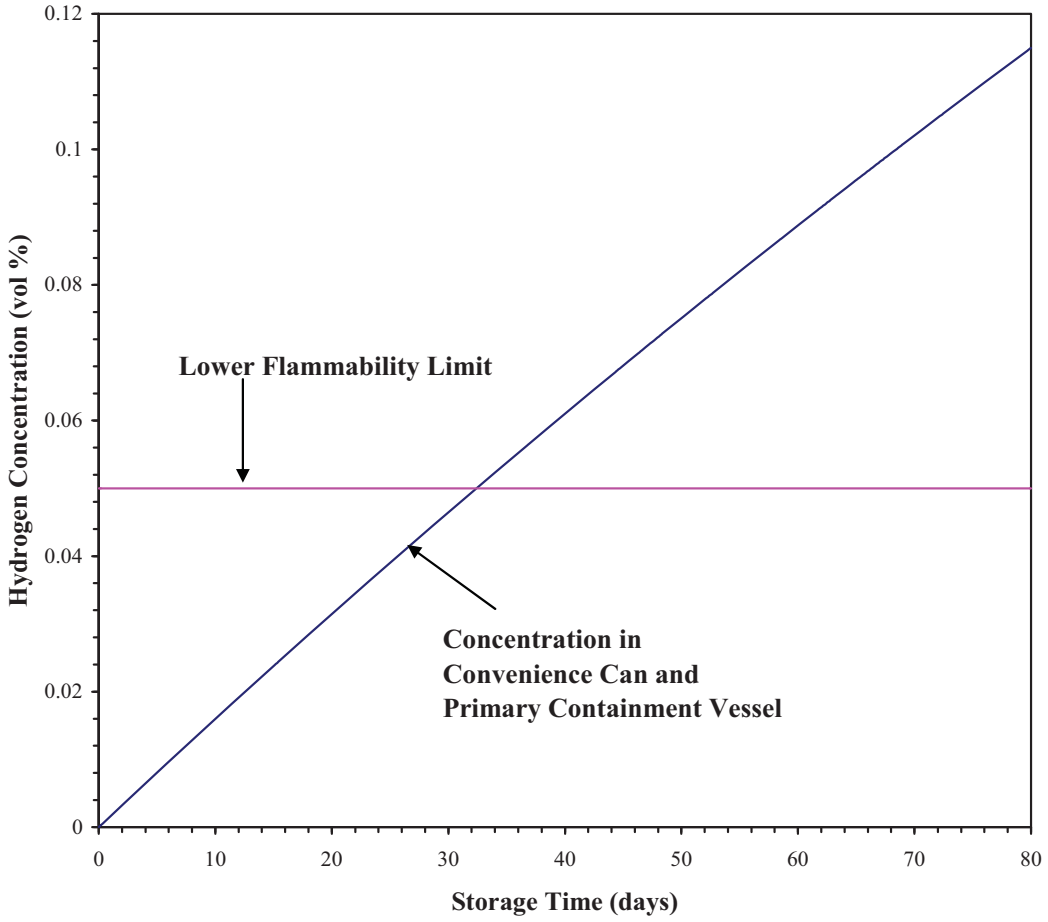

Figure 7. Approach to Lower Flammability Limit for MIS Material with Hypothetical G Value of 0.005 molec/100 eV, at a Total Radiolytic Power of 5 watts

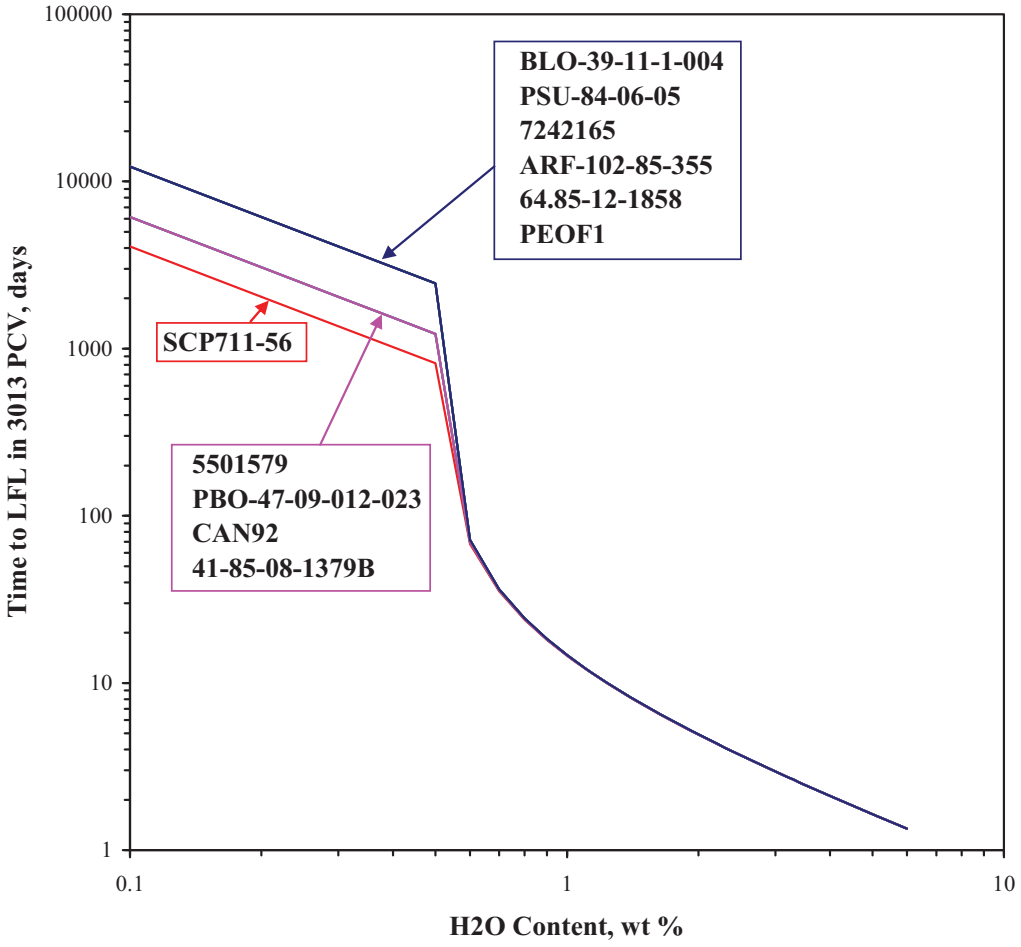

Figure 8. Variation of Time To Reach the LFL with Moisture Level, for MIS Materials with G Values Less Than 0.0002 molec/100 eV, at a Total Radiolytic Power of 5 watts

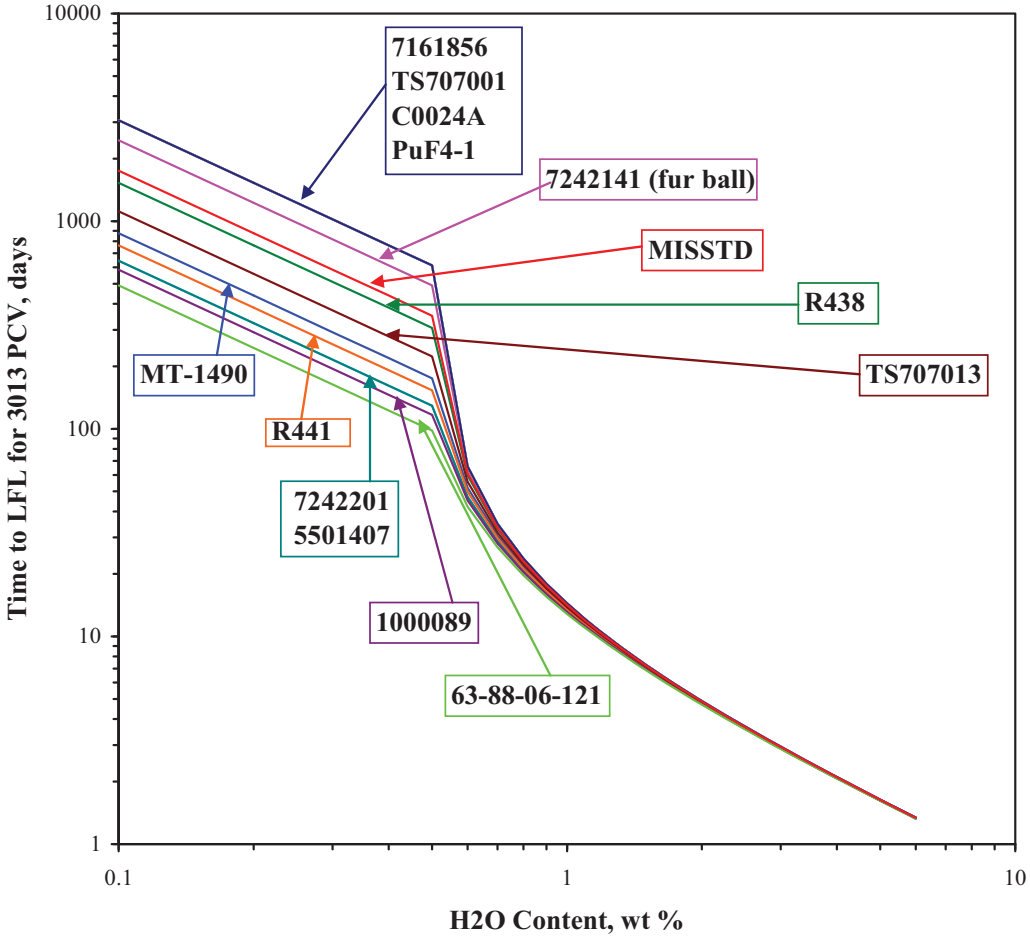

Figure 9. Variation of Time To Reach the LFL with Moisture Level, for MIS Materials with G Values between 0.0002 and 0.002 molec/100 eV, at a Total Radiolytic Power of 5 watts

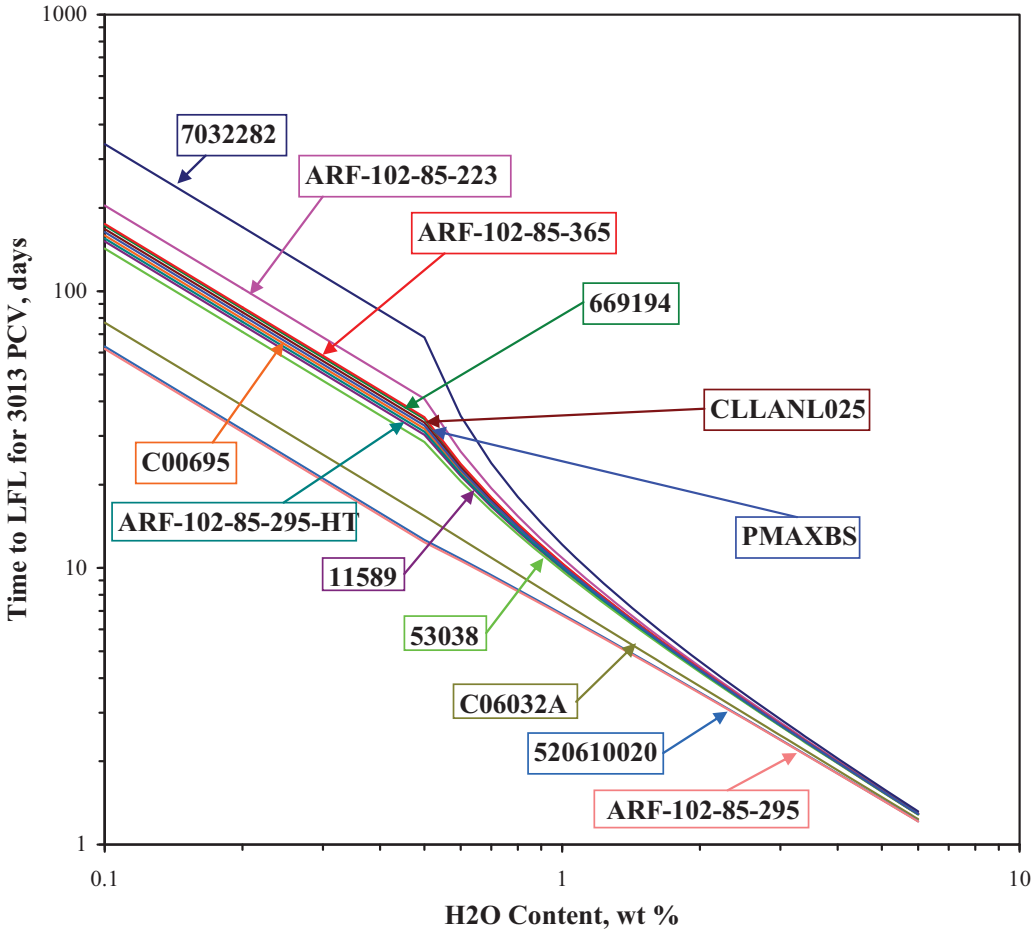

Figure 10. Variation of Time To Reach the LFL with Moisture Level, for MIS Materials with G Values Greater Than 0.002 molec/100 eV, at a Total Radiolytic Power of 5 watts

Appendix A: Correspondence with Kirk Veirs Concerning H_2 Gas Generation Rates for MIS Samples

Kirk Veirs <veirs@lanl.gov>
03/08/2007 06:53 PM
To
james.laurinat@srnl.doe.gov
cc
james.mcclard@srs.gov, todd.woodsmall@srs.gov
bcc

Subject
Re: Fw: additional data for other MIS numbers

James - attached please find a file that includes how to use the numbers to calculate the amount of hydrogen generated from represented materials. I had made a mistake - thinking on the fly leads to mistakes - in that the bounding factor adjusting the water wt% is 1.37 not 1.25. It's explained in the attached. Please don't hesitate to call me if things are not clear.

02/20/2007 11:45 AM
To
james.laurinat@srnl.doe.gov
cc
james.mcclard@srs.gov
Subject
Re: Fw: additional data for other MIS numbers

James – The following Table (Table A-1, author's note) contains the H_2 gas generation rates for all of the MIS samples. The Table includes our sample number, the MIS Sample ID that you are already familiar with, the initial H_2 gas generation rate based on gas composition analysis when the sample was first put into surveillance and the day at which the second gas composition analysis was taken, the day at which the second gas composition was determined for calculation of the initial H_2 gas generation rate, and finally, the rate calculated from the gas composition sample taken closest to one year and the initial gas composition. The difference between these numbers and the original numbers had are (1) the original numbers were based on overall pressure change and these numbers are based on the H_2 contribution to the overall pressure change, and (2) the original numbers was an average of the pressure rise the first week and the pressure rise at 10 months. In all MIS samples the observation is that the rate of rise of the H_2 gas composition is continually slowing down, so that the initial rates will always be larger than rates calculated from gas compositions at one year. Even smaller rates would be calculated for longer times. The rate is calculated as the number of moles produced per second per Watt of energy deposited into the water. The number of Watts deposited into the water is again calculated from the Wattage of the material and the number of

electrons due to the water ratioed to the number of electrons due to all of the material (actinides and salts). The H_2 gas generation rates for some of the samples are quite different from the rates calculated from the pressure rise. For instance the pressure rise in SSR135 is due mainly to CO_2; there is very little H_2.

(Note: The maximum of the initial rate and the one-year average rate is used to calculate the time to reach the LFL. Values reported by Veirs are converted to standard units of molec/100 eV by multiplying by the factor (6.022×10^{23} molec/mol) * (1×10^{-9} mol/nmol)(100)/(1.602×10^{-19} W s/eV).

In a subsequent telephone conversation, Kirk Veirs stated that gas generations tests SSR129 (MIS 5501407) and SSR149 (MIS C00695) had problems and were rerun as SSR129A and SSR149A. Consequently, the results for SSR129A and SSR149A are used for MIS 5501407 and C00695. He also stated that gas generation tests SSR155 and SSR155HT were for the same designation material calcined at different temperatures, 750 °C for SSR155 and 950 °C for SSR155HT. Times to LFL are calculated and reported using H_2 generation rates for both tests. No information was provided regarding gas generation tests SSR137 and SSR137A. Times to LFL are calculated and reported for H_2 generation rates from SSR137, since that test had higher gas generation rates than SSR137A.)

Table A-1. Hydrogen Generation Rates for MIS Materials

SSR No.	MIS ID	Initial rates		Rate average, 1-year
		H_2 generation rate (nmol sec^{-1} W^{-1})	Days valid	H_2 generation rate (nmol sec^{-1} W^{-1})
SSR122	7161856	4	29	1
SSR123	TS707001	4	57	0
SSR124	5501579	2	56	0
SSR125	MT-1490	14	35	3
SSR126	669194	71	63	21
SSR127	CLLANL025	73	63	39
SSR128	7242201	19	34	3
SSR129A	5501407	19	171	5
SSR130	C06032A	159	35	84
SSR131	ARF-102-85-223	60	99	33
SSR132	BLO-39-11-14-004	1	104	0
SSR133	PSU-84-06-05	0	28	1
SSR134	R441	16	30	7
SSR135	SCP711-56	0	27	3
SSR136	1000089	21	76	6
SSR137	11589	81	76	40
SSR138	53038	86	0.15	28
SSR139	520610020	194	7	90
SSR140	7242165	1	76	0
SSR141	7242141 (fur ball)	5	74	3
SSR142	PBO-47-09-012-023	2	63	0
SSR143	ARF-102-85-355	1	63	0
SSR144	ARF-102-85-365	70	61	43
SSR145	64-85-12-1858	0	19	1
SSR146	R438	5	19	8
SSR147	CAN92	2	229	2
SSR148	C00024A	4	229	4
SSR149A	C00695	77	1	25
SSR150	TS707013	11	216	7
SSR151	7032282	36	1	0
SSR152	41-85-08-1379B	2	216	1
SSR153	63-88-06-121	25	110	23
SSR155	ARF-102-85-295	198	175	164
SSR155HT	ARF-102-85-295	79	203	59
SSR156	PuF4-1	4	203	2
SSR160	PMAXBS	75	231	53
SSR161	PEOF1	1	232	1
SSR162	MISSTD	7	21	1

Appendix B: Analysis of Veirs and Co-Workers Gas Generation Data for $CaCl_2$ and $MgCl_2$ Doped PuO_2 and Extrapolation of G values to Higher Moisture Levels

Veirs and co-workers measured rates of pressure increase and gas generation for PuO_2 doped with nominally 5 weight % $CaCl_2$ or $MgCl_2$.[11] The PuO_2 and the chloride salts were mixed as powders and then calcined to either 800 °C (for $MgCl_2$) or 850 °C (for $CaCl_2$). Finally, measured amounts of water varying from 0.6 to 6 weight % were added to samples of the material in a humidification chamber, and the samples were placed in test vessels for gas generation tests. During the tests, corrosion of the test vessel interior was observed at moisture levels corresponding to 3.14 water of hydration for $CaCl_2$ and 4.51 waters of hydration for $MgCl_2$. In the absence of corrosion, most of the gas that was generated was hydrogen. If corrosion was present, then the radiolysis gases consisted of an approximately stoichiometric mixture of 2/3 hydrogen and 1/3 oxygen.

Rates of pressure increase and individual component gas generation were reported as a function of the number of waters of hydration added to the salt. Because the pressure measurements are somewhat more consistent and reliable than the direct measurements of gas generation rates, the analysis of the hydrogen gas generation rate and the G value is based on measured pressure increases. The intrinsic G value G_{H_2} (based on the water content) is calculated using the following set of equations:

$$G_{H_2} = \frac{e^{-}(mat)}{e^{-}(H_2O)} G'_{H_2} \qquad \text{(B-1)}$$

$$G'_{H_2} = \frac{1000 \times 1.602 \times 10^{-17}}{101325 \times 86400} \frac{V_g N_A \rho_M}{P_s\left(1 - \frac{m_{salt}}{m_{PuO_2}}\right)} \frac{dP}{dt} \qquad \text{(B-2)}$$

$$V_g = V_{tot} - \frac{m_{PuO_2}}{\rho_{PuO_2}} - \frac{m_{salt}}{\rho_{salt}} - \frac{m_{H_2O}}{\rho_{H_2O}} \qquad \text{(B-4)}$$

where

P_s = specific power for alpha radiolysis (2.05 W/g)

m_{salt} = mass of salt (either $CaCl_2$ or $MgCl_2$) in sample, g

m_{PuO_2} = mass of PuO_2 in sample, g

$\frac{dP}{dt}$ = reported rate of pressure increase, kPa/day

V_g = volume of gas space inside test vessel, cm^3

V_{tot} = total interior volume of test vessel, cm^3

m_{H_2O} = mass of water added to sample, g

ρ_{PuO_2} = theoretical density of PuO_2, g/cm^3

ρ_{salt} = theoretical density of salt, g/cm^3

ρ_{H_2O} = density of liquid water, g/cm^3

The number of waters of hydration is converted to a weight % moisture by

$$f_{H_2O} = \frac{\frac{18n_{H_2O}}{M_{salt}} f_{salt}}{1 + \frac{18n_{H_2O}}{M_{salt}} f_{salt}} \qquad \text{(B-5)}$$

where

n_{H_2O} = number of waters of hydration

M_{salt} = molecular weight of the salt, g/mol

All terms not defined in this appendix are defined in Section 4.

Tables B-1 and B-2 l report rates of pressure increase and intrinsic G values for the $CaCl_2$ and $MgCl_2$ doped PuO_2. Figure B-1 compares these G values with intrinsic G values for the MIS items, which are listed in Table B-3. As Figure B-1 shows, the intrinsic G values for the $CaCl_2$ and $MgCl_2$ doped materials approach constant values approximately equal to 2.1 and 1.2 molec/100 eV, respectively, above a moisture content of about 2 weight %. (In other words, the effective G values based on the entire mass, G'_{H_2}, increase linearly with the moisture level above 2 weight % moisture.) The intrinsic G values for the MIS items range from about 0.01 molec/100 eV up to the asymptotic maxima for the $CaCl_2$ and $MgCl_2$ doped materials.

It is noteworthy that intrinsic G values for the $CaCl_2$ and $MgCl_2$ doped materials, as well as the maximum G values reported for the MIS items, are of the same magnitude as the accepted G value for free water, which Spinks and Woods report to be

1.6 molec/100 eV.[12] The relatively close agreement between the maximum G values measured by Veirs and co-workers and the G value for water suggests that G values for MIS items at elevated moisture levels can be approximated by taking a weighted average of the reported G values for the MIS tests and the G value for free water. If the moisture level for the MIS tests is set at its average value of 0.5 weight % (0.005 as a weight fraction), then a simple weighted average formula takes the form

$$G_{H_2,pred} = \frac{0.005G_{H_2,MIS} + \left(f_{H_2O} - 0.005\right)G_{H_2,H_2O}}{f_{H_2O}} \qquad \text{(B-6)}$$

where

$G_{H_2,pred}$ = predicted intrinsic G value at the elevated moisture level, molec/100 eV

$G_{H_2,MIS}$ = measured intrinsic G value for the MIS item, molec/100 eV

G_{H_2,H_2O} = G value for free water, 1.6 molec/100 eV

Use of equation B-6 implies that the water absorbed by an MIS item is present as either a chemically bound constituent with a low propensity to be radiolyzed or as a water of hydration or deliquescence that radiolyzes about as readily as free water. The use of this weighted average also assumes that the MIS items are capable of absorbing the stated amount of moisture from humid atmospheres.

Table B-1. Pressure Increases for $CaCl_2$-Doped PuO_2 as a Function of Water Content

Waters of Hydration	Pressure Increase (kPa/day)	Water Content (weight %)	G_{H_2} (molec/100 eV)
0.77	0.57	0.62	0.69
1.30	1.79	1.04	1.27
1.99	2.93	1.58	1.35
2.53	6.43	2.00	2.32
3.14	10.00	2.47	2.41[a]
3.74	13.79	2.93	2.21[b]
4.39	17.14	3.42	2.33[b]
5.06	18.64	3.92	2.19[b]
5.67	21.00	4.38	2.18[b]
6.20	22.00	4.77	2.08[b]
6.83	23.64	5.23	2.02[b]
7.44	21.86	5.67	1.70[b]

Table B-2. Pressure Increases for $MgCl_2$-Doped PuO_2 as a Function of Water Content

Waters of Hydration	Pressure Increase (kPa/day)	Water Content (weight %)	G_{H_2} (molec/100 eV)
0.77	0.57	0.61	0.66
1.30	0.86	1.02	0.59
1.99	2.21	1.55	0.99
2.67	3.57	2.07	1.18
3.19	4.14	2.46	1.14
3.84	5.71	2.95	1.30
4.51	6.86	3.45	1.32
5.10	10.79	3.88	1.22[b]
5.59	12.57	4.24	1.29[b]
6.31	11.79	4.76	1.06[b]
6.93	13.86	5.20	1.13[b]
7.57	15.43	5.66	1.15[b]

Notes:
[a] G' value is calculated using 5/6 of the pressure increase, under the assumption that this data point is at the transition between generation of pure hydrogen and the generation of a stoichiometric mixture of 2/3 hydrogen and 1/3 oxygen (for corrosion conditions).
[b] G' value is calculated using 2/3 of the pressure increase, under the assumption that the gas generation is a stoichiometric mixture 2/3 hydrogen and 1/3 oxygen (for corrosion conditions).

Table B-3. Hydrogen Generation Rates for MIS Materials

SSR No.	MIS ID	Water Content (weight %)	G_{H_2} (molec/100 eV)
SSR122	7161856	0.54	0.039
SSR123	TS707001	0.36	0.039
SSR124	5501579	0.42	0.019
SSR125	MT-1490	0.51	0.135
SSR126	669194	0.45	0.685
SSR127	CLLANL025	0.47	0.704
SSR128	7242201	0.52	0.183
SSR129A	5501407	0.68	0.183
SSR130	C06032A	0.57	1.534
SSR131	ARF-102-85-223	0.58	0.579
SSR132	BLO-39-11-14-004	0.45	0.010
SSR133	PSU-84-06-05	0.45	0.010
SSR134	R441	0.42	0.154
SSR135	SCP711-56	0.19	0.029
SSR136	1000089	0.42	0.203
SSR137	11589	0.53	0.781
SSR138	53038	0.50	0.830
SSR139	5.21E+08	0.51	1.872
SSR140	7242165	0.48	0.010
SSR141	7242141 (fur ball)	0.45	0.048
SSR142	PBO-47-09-012-023	0.47	0.019
SSR143	ARF-102-85-355	0.46	0.010
SSR144	ARF-102-85-365	0.46	0.675
SSR145	64-85-12-1858	0.45	0.010
SSR146	R438	0.43	0.077
SSR147	CAN92	0.5[c]	0.019
SSR148	C0024A	0.5[c]	0.039
SSR149A	C00695	0.5[c]	0.743
SSR150	TS707013	0.5[c]	0.106
SSR151	7032282	0.5[c]	0.347
SSR152	41-85-08-1379B	0.5[c]	0.019
SSR153	63-88-06-121	0.5[c]	0.241
SSR154	ARF-102-85-114-1	0.5[c]	
SSR155	ARF-102-85-295	0.5[c]	1.910
SSR155HT	ARF-102-85-295	0.5[c]	0.762
SSR156	PuF4-1	0.5[c]	0.039
SSR160	PMAXBS	0.19	0.724
SSR161	PEOF1	0.08	0.010
SSR162	MISSTD	0.5[c]	0.068

Note:
[c] Water content is not reported. A nominal water content of 0.5 weight % is assumed.

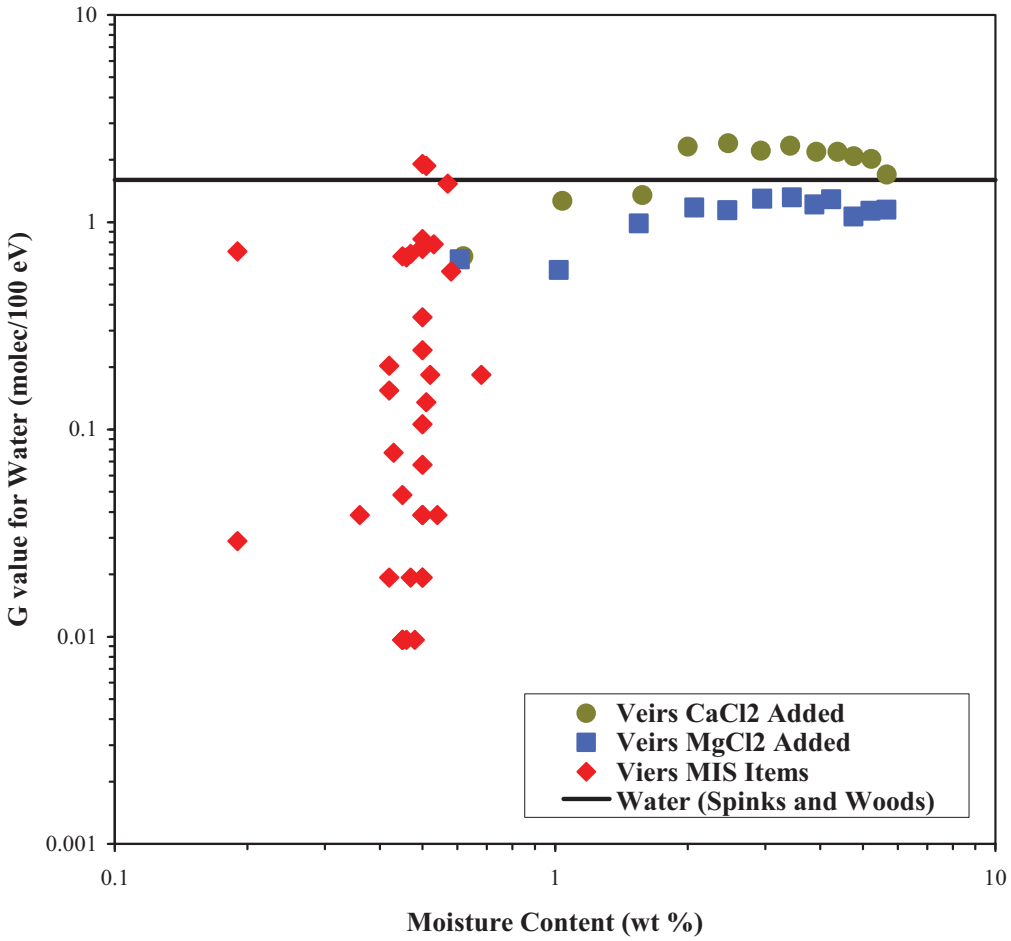

Figure B-1. Comparison of G Values Measured by Veirs and Co-Workers for $CaCl_2$ and $MgCl_2$ Doped PuO_2 and MIS Items with G Value for Water

COST-EFFECTIVENESS OF UTILIZING SURPLUS DEPLETED URANIUM (DU)

M. J. Haire, A. G. Croff
Oak Ridge National Laboratory*
Oak Ridge, Tennessee 37831-6166

ABSTRACT

About a billion pounds of surplus depleted uranium (DU) has been produced as a by-product of the uranium enrichment process for defense programs and civilian nuclear reactors at the gaseous diffusion plants at Oak Ridge, Tennessee; Paducah, Kentucky; and Portsmouth, Ohio. A project is under way to convert this DU hexafluoride (DUF_6) into a more stable oxide form that is predominately DU_3O_8. Baseline plans are to dispose of the conversion plant product in radioactive waste disposal facilities in Nevada or Utah. Finding a beneficial use for this material, rather than disposing of it, could save the U.S. government hundreds of millions, if not billions, of dollars.

This work reports estimated order-of-magnitude costs for DU_3O_8 packaging; transportation from Paducah, Kentucky; and disposal at the Nevada Test Site (NTS). Disposal charges were assumed to be $9/ft^3, based on discussions with NTS staff. The results cover a range of values, because the number of containers that results depends on the bulk density of the material that is produced and can range from 1.5 to 4.0 MT/m^3. The limiting criterion is 40,000 lb/truck load shipment, per U.S. Department of Transportation rules. The weight of a single container is assumed to be 0.53 MT, the amount contained in a 55-gal drum. The cost avoidance to the U.S. Department of Energy is estimated as follows:

Table I

Packaging		$93B170M
Transportation		$88B160M
Disposal		$60B100M
	Total	$241B430M

Some beneficial commercial uses of DU and their potential markets are described. The revenues from sales of casks constructed of DUO_2 composite materials are estimated to be as much as $0.5B/year.

INTRODUCTION

Naturally occurring uranium contains 0.71 wt % ^{235}U. In order for uranium to be useful in most nuclear applications, the concentration of the fissile isotope ^{235}U must be increased by a process called enrichment. The enrichment of uranium creates a by-product, depleted uranium (DU), in which the concentration of ^{235}U is <0.71 wt %. The U.S. government has ~500,000 MT of DU stored at U.S. Department of Energy (DOE) sites [1]. DU is the largest mass of nuclear material in the DOE inventory. This material, mostly in the form of DU hexafluoride (DUF_6), resulted from gaseous diffusion plant operations at Oak Ridge, Tennessee; Portsmouth, Ohio; and Paducah, Kentucky. The inventory of DUF_6, which is stored in large cylinders aboveground, is increasing at a rate of ~20,000 MT/year.

On August 29, 2002, DOE awarded a contract to Uranium Disposition Services, LLC, to convert the DUF_6 to a stable form and to dispose of any portion that might not be reused. The contract includes conversion facility design and construction; operation of two facilities located at enrichment plant sites in Portsmouth, Ohio, and Paducah, Kentucky; transportation of any portion of the product not destined for reuse; and disposal of that portion. The contract also includes near-term surveillance and maintenance of the DUF_6 cylinder inventory and shipment of the DUF_6 cylinders from Oak Ridge, Tennessee, to Portsmouth, Ohio, as well as incentives for reuse of the DU. Construction of the facilities will begin by July 31, 2004.

DOE is subject to a number of driving forces that encourage or require reuse of DUF_6 and research and development (R&D) toward this end. In the legal and regulatory arena, Public Law 102-486 [2] requires DOE to prepare a study that identifies DU tailings available for conversion to commercial use. Public Law 105-204 [3] requires that DOE undertake a good-faith effort to consider recycle (i.e., beneficial use) for DU. A Record of Decision was published in August 1999 [4]. In response to this legislation, DOE prepared a document, *Depleted Uranium Materials Use Roadmap* [5], which is a guide to R&D activities. The roadmap builds on the analysis performed and documented in the final *Programmatic Environmental Impact Statement for Alternative Strategies for the Long-Term Management and Use of Depleted Uranium Hexafluoride* [6]. An agreement [7] between DOE and the State of Ohio requires a continuing good-faith effort to find beneficial uses for DUF_6 and the production of annual reports that document progress in this area.

At least as important as the legal/regulatory driving forces is the desire to reduce the cost to the government for disposition of the DUF_6. Although DU has been used historically in applications ranging from munitions to counterweights to radiation shielding, the sum total of these applications would consume only a small fraction of the inventory. As a consequence, DOE is supporting a DU Uses R&D Program to create new uses for DU that might avoid some or all of the costs of DU disposition. The basis for this program is the previously mentioned *Roadmap* [5].

This paper summarizes the current status of the potential for DU uses to reduce the cost of DUF_6 disposition and the areas that are being investigated toward this end. However, none of the potential uses are sufficiently well developed to permit a rigorous economic analysis of the cost-effectiveness of DU reuse. Thus, the economic analysis in this paper will focus on framing the economic basis for reuse, the costs or cost ranges that are presently known, and discussion of uncertainties and possibilities.

BENEFIT TO DOE OF REUSE OF DU

The benefit to DOE of reuse of DU is cost savings. Such savings could be realized in two ways: (1) avoiding some or all of the potential cost to disposition the DU oxide product from the conversion plant by disposal and (2) receiving revenues from the sale of DU.

Avoiding DU Disposition Costs

Initial baseline disposition cost. The baseline approach for disposition of any unused DU oxide (primarily U_3O_8) conversion product is to package it in suitable containers and transport it from the conversion plants to the Nevada Test Site (NTS) or to Envirocare of Utah for near-surface disposal. The cost of disposing of the entire 500,000 MT inventory of DU as oxide at NTS was estimated [8] before the conversion contracts were awarded; the results are summarized in Table II.

Table II Estimated Cost for Disposition of DU Oxide Inventory at the NTS

Disposition Cost Component	Estimated Range of Cost, $M
Packaging	93B170
Transportation	88B160
Disposal	60B100
Total	241B430

The results cover a range of values because the number of containers required depends on the bulk density of the DU oxide product, which can range from 1.5 to 4.0 kg/L, depending on the conversion and packaging techniques used.

Optimized baseline disposition cost. Initial systems studies by the conversion contractor identified the opportunity to reduce the baseline disposition cost of the DU oxide product shown above by shipping the product to Envirocare=s disposal facility in Utah. This significantly reduces the disposition cost in three ways. First, rail shipment can be used at Envirocare whereas more costly truck shipment is the only means to access NTS. Second, the weight of a single package is limited to 430 kg at NTS whereas Envirocare can accept much larger packages (up to the size of an entire railcar). Third, container costs are reduced by the use of emptied DUF_6 cylinders to package the DU oxide product. Updated cost estimates have not yet been released but are believed to have a value in the $150B$200M range.

To the extent that beneficial uses are found for DU, the cost of disposition can be avoided by having the user take custody of the DU at the loading dock of the conversion plant. The DU product that is likely to be useful to potential users is uranium dioxide, which will require limited additional processing in the conversion plant to uniformly reduce the uranium to the +4 valence state. However, this step constitutes existing technology in nuclear fuel fabrication plants and is not expected to increase costs significantly.

Upper-bound baseline disposition cost. An important assumption in achieving the disposition cost described in the preceding section is that near-surface disposal of the DU oxide product is acceptable. This determination will be made as part of the National Environmental Policy Act (NEPA) process involving issuance of site-specific draft environmental impacts statements; soliciting comments thereon; and reconciling the comments, leading to a record of decision. The validity of this assumption is supported by the fact that various forms of DU from multiple DOE facilities have been disposed of at the Envirocare facility over a period of years. However, the validity of this assumption could be called into question for two reasons. First, the amount of DU involved in converting DOE=s entire inventory is much larger (at least 10 times greater) than that of all the DU previously disposed of. Second, the U.S. Nuclear Regulatory Commission is on record [9] as questioning the acceptability of near-surface disposal of DU at an enrichment plant that was proposed to be built in Louisiana. However, the applicability of this position to arid sites in the western United States is unknown.

If more confining disposal of the DU product were required, the baseline disposition cost could increase substantially. Estimates for more elaborate measures such as use of a consolidating matrix such as grout, use of engineered subsurface structures similar to concrete bunkers, or the requirements for disposal in deep mines or subsurface excavations have been estimated and range up to about $1500M [10].

Potential Revenues from Sale of DU

None of the potential uses of DU are yet sufficiently mature to assess their worth to the users with sufficient accuracy to allow potential revenues to be evaluated. Such worth could result from two sources. First, DU-based products could substitute for more expensive components. One example of this is substituting a DU-based geochemical barrier for repository waste package components presently composed of expensive degradation-resistant alloys such as titanium and Alloy C-22 (a high-nickel alloy). If the DU-based barrier can be substituted for the metal barriers without compromising protectiveness or causing other unacceptable impacts, then the metal barriers, which are estimated to cost $5B [11] might be eliminated while simultaneously using the entire DU inventory. Thus, in this application, the DU could be worth up to $10/kg DU ($5 × 10^9/$5 × 10^8 kg DU), although the fabrication cost of the DU-based barrier must be subtracted to establish the unit breakeven worth of DU. Using natural uranium in this application would not be economic, because, even in the presently depressed market, it sells for $20B$40/kg U. It is noteworthy that at $5/kg DU (net costs, allowing for fabrication), the revenues (cost avoidance by the repository program) from this application would be sufficient to pay the life-cycle cost of the entire DUF_6 conversion project.

A second potential economic advantage of DU is based on capitalizing on properties of uranium such as its high density and complex electronic structure to yield products having improved or even unique capabilities. One example of this is the use of DU-based materials of construction such as DUCRETEJ or a DU-steel cermet for spent fuel storage and transportation casks. The high density of these materials could result in reduced costs in two ways. Fewer shipments would be required (because each cask has a higher payload), and fewer casks would be required (because a separate transfer cask would not be needed to move spent fuel from water pools into dry storage at nuclear reactor sites) [9]. In addition to potential economic benefits, the use of such materials may offer nonquantifiable benefits such as increased resistance to accidental or deliberate breaching forces and reduced occupational dose from spent fuel transfer operations. Another example is the potential for DU dioxide to be used in semiconductor applications, such as in the manufacture of computer chips. The refractory nature of DU dioxide would yield a chip capable of withstanding high temperatures and also the high radiation fields typical of space applications. The magnitude of these benefits has not yet been estimated.

BENEFICIAL USES OF DU

A number of beneficial uses of the DUO_2 conversion plant product have been identified. Such uses can be divided into two groups: (1) those that consume the entire surplus DU inventory and (2) those that consume only a fraction of the inventory. High-volume uses [e.g., as new shielding materials for spent nuclear fuel (SNF) casks and as additional chemical barriers at geological SNF disposal sites] capitalize on the density and chemical identity of DUO_2. These uses are all in radiologically regulated applications.

High-value beneficial uses of DU capitalize on unique electronic properties of uranium. Examples of such uses would be in semiconductors, electrodes in batteries, and fuel cells, as well as in electrolysis of water to produce hydrogen, and in catalysts. These uses would be predominantly in radiologically unregulated areas. The benefits would be the potential for products having unique capabilities and significant revenues, if the appropriate application could be found.

High-Volume Uses

Repository Uses. The preponderance of SNF destined for disposal under current U.S. policies is Zircaloy-clad, low-enriched uranium dioxide fuels from light-water reactors. The resistance of the SNF disposal cask depends upon interaction of hot groundwater and humid air with the SNF and engineered barrier system over time. The SNF could be contained in a package composed of DUO_2-based engineered barriers. If this is

done, the chemical interaction of water and air with the DUO_2-based barriers should create conditions that delay water and air penetration to the spent fuel and reduce radionuclide release rates thereafter. Two approaches are envisioned: (1) filling the void spaces in the container with DUO_2 in a sand-like form and/or (2) building the SNF basket and/or package walls with a material made from DUO_2 cermet. The fill concept consists of inserting DUO_2 particles into a repository disposal package, completely filling the gap between fuel rods and between fuel assemblies. Such use is thought to have the potential to reduce (1) the rate at which groundwater might reach the fuel, (2) the dissolution rate and solubility of the fuel matrix, and (3) the diameter and weight of the overall package needed to achieve a specific dose rate. The DUO_2-steel cermet concept consists of DUO_2 particulates embedded in a continuous steel phase. Typical cermets use sandwich construction with clean uncontaminated steel layers on both sides of the cermet. It is envisioned that DUO_2-steel cermets could replace some steel components of a waste package shell and basket. The presence of DU should also reduce the likelihood of a criticality event over geologic time by lowering the average ^{235}U content. DUO_2 metal barriers could conceivably replace some of the $5B of engineered barriers at the geologic repository.

Research is being conducted to elucidate the nature and rate at which DUO_2, steel, groundwater, and air interact as a basis for determining whether DU-based engineered barriers can be substituted for other, more expensive barriers. If this appears promising, additional studies will be initiated to examine the impacts of DU-based engineered barriers on waste package and repository performance.

Shielding Applications. A large potential market for DU is in radiation shielding applications. Although DU metal has been used in such applications, its relatively high cost can be justified only when the need for high-density shielding offsets this cost. However, DU oxides (primarily DUO_2) could be used as a component of the primary shielding material in containers designed to store and, in some cases, dispose of SNF or high-level radioactive wastes. The high density of uranium compounds makes them excellent components as shields from photon radiation.

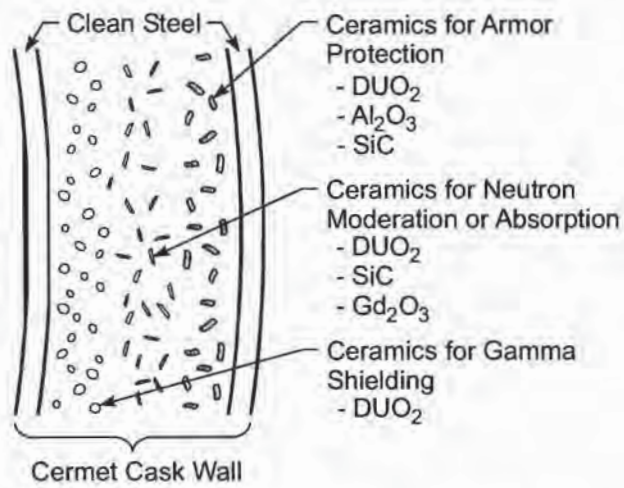

Fig. 1.

Two new uranium composite materials are envisioned for SNF storage and transport casks. One attractive new DU shielding material involves making a Aheavy@ concrete (e.g., DUCRETEJ), using a high-density DU compound as one of the components. If a DU compound is used to make the concrete, the same shielding performance could be achieved with up to one-half the thickness required of normal concrete, depending on the form of the DU [2]. To provide predictable structural strength, in this approach, the uranium compound is substituted for the coarse aggregate in conventional concrete and is enclosed between annular stainless steel shells that make up the body of the container.

The second new shielding material is DUO_2-steel cermet. Cask shells would be constructed of a cermet of DUO_2 particulates embedded in the steel, which in turn, would be contained between clean layers of steel (see figure). Because of the higher oxygen content associated with DUO_2, which moderates neutrons, cermets also have better shielding capabilities than steel. The cermet could also include a neutron absorber, such as gadolinium, for efficient absorption of neutrons.

There are ~131,000 pressurized-water reactor and 175,000 boiling-water reactor fuel assemblies that will be produced by U.S. nuclear power plants under the terms of their current licenses. Approximately 10,000 casks will be required for the storage and transport of commercial spent fuel to the repository [12]. It is estimated that 50–60 MT of DU will be required per cask to produce the "new generation" of DU casks to be used for spent fuel storage, transport, and disposal. The containment of DU composites within 10,000 casks that can be used in the United States alone will require the use of the total DOE DU inventory. The cost of material purchase and fabrication for conventional casks is in excess of $6B. The cost to procure materials for the fabrication of spent fuel and high-level-waste (HLW) containers within the engineered barrier at the geologic repository is estimated to be in excess of $14B. If DU composite materials can provide advances in radioactive material shielding and structural performance of casks, the estimated U.S. container cost of ~$14B can be significantly reduced using more uniform DU cask designs. The revenue from sales of DU casks is estimated to be as much as $0.5B/year.

Ongoing R&D is focused on confirming the long-term stability of candidate heavy concretes and on developing low-cost manufacturing techniques for large cermet shapes.

HIGH-VALUE USES

The DUF_6 Materials Use Roadmap [5] identifies the need for a science program to conceive and develop new potential uses for the DU conversion product. This need has led to the identification of a number of ideas that appear to be promising but where fundamental questions remain concerning the scientific feasibility. If only one or two of these potential uses were to prove feasible, a high-value market for DU could result, with attendant cost savings. Research is being conducted to ascertain the scientific feasibility of some of these high-value uses.

Uranium catalysts

U.S. industries and DOE must manage a variety of off-gas wastes consisting of complex volatile organic compounds. Ongoing research concentrates on a new class of nanoporous uranium oxide sol-gel catalysts doped with uranium oxides for destruction of a range of volatile organic contaminants, including alkanes, aromatics, and chlorinated organic compounds. Proof-of-principle experiments have been conducted, and optimal formulations are being sought. If performance meets expectations, uranium-based catalysts might replace high-cost platinum-based catalysts. The U.S. catalyst market is estimated to be ~$9B in 2003. Thus, a small niche in this market could be lucrative.

Uranium-based semiconductors

Uranium oxides have electrical and electronic properties that are equivalent, or superior, to those of conventional Si, Ge, and GaAs semiconductor materials. Thus, it appears that a new, higher-performance class of semiconductors is possible: uranium oxide–based semiconductors. Uranium oxides have characteristics that could give them significantly better performance than conventional semiconductor materials: operation at substantially higher temperatures and greater radiation and electromagnetic force resistance, qualities that could make them more suited for use in hazardous environments. A number of urania semiconductor devices are possible, including solar cells, thermophotovoltaic cells, and thermoelectric cells, as well as diodes and transistors. The semiconduction properties of solid-crystal DUO_2 with various dopants have been measured. A uranium-based diode and transistor have been constructed and tested. Replacing current silicon chips with DUO_2 chips would consume ~30,000 MTU/year. Assuming $20/kg U, this translates to more than $0.5B/year in revenues.

Urania fuel cells

Current solid oxide fuel cell (SOFC) technology is limited by relatively poor ion conductivity, erosion of electrodes and electrolyte due to surface interactions, and differences in thermal expansion of different materials at the electrode/electrolyte interface. Stabilized uranium oxides promise solutions to these problems. It is believed that stabilized uranium oxide films will be superior electrodes for SOFCs because of their higher mixed (electronic/ionic) conductivity, better stability, and improved structural compatibility with solid electrolytes. This work will lead to substantially improved components for SOFCs. The dollar value of a more efficient fuel cell is not estimated. The U.S. fuel cell market is estimated to be ~$12.6B in the year 2012.

Photoelectric hydrogen production

Photoelectric cells (PECs) are devices that provide a direct method for converting optical energy into either chemical or electrical form. In the case of conversion of optical energy into a chemical form, light strikes the PEC anode, resulting in the photoassisted dissociation of water into hydrogen and oxygen, thereby providing hydrogen fuel that can be stored and utilized at a later time. A number of semiconducting materials have been suggested for use as PEC anodes for the dissociation of water. However, electrode stability has proven to be a crucial problem in the realization of a workable PEC device. The most promising oxides that have been identified include pure UO_2 and uranium-doped potassium tantalite. The dollar value of a more cost-effective method of producing hydrogen has not been estimated. The hydrogen economy is currently about $2.5B/year and growing at a rate of 10%/year.

INTERNATIONAL COLLABORATIONS

The DU Uses R&D program engages in collaborative international activities to better understand the international situation concerning the disposition of DUF_6, provide credibility to U.S. efforts to beneficially use DU, and obtain the benefits of lower-cost or cost-shared research results. Currently, extensive collaborations are being conducted with the Russian Academy of Science and with Minatom.

CONCLUSIONS

The cost-effectiveness of using the DU oxide conversion product from facilities to convert DUF_6 to a more stable form depends on the magnitude of the avoided DU oxide disposition cost and potential revenues from the sale of DU-based products. The packaging, transportation, and disposal costs are expected to range from $150M to $200M but could be much higher if more elaborate waste forms or disposal technology were to be required. It is not yet possible to accurately estimate the revenues resulting from potential DU uses, which could consume a substantial portion of the DOE inventory. However, success concerning the better-developed potential applications related to spent fuel storage, spent fuel and waste transportation, and the repository could reduce or avoid costs measured in billions of dollars. Revenue from sale of casks made of DU composites could be as much as ~$0.5B/year. Other potential uses of DU still in the fundamental research stage might add substantially to this total if they are proven. The U.S. government has an ongoing program to investigate such uses and to develop the most promising of these technologies to the point that they are available for deployment.

REFERENCES

1 "Technology Assessment Report for the Long-Term Management of Depleted Uranium Hexafluoride," UCRL-ID-120372, Lawrence Livermore National Laboratory (June 1995).

2 Public Law 102-486, Energy Policy Act of 1992, Sect. 1016, 106 Stat 2949 (October 24, 1992).
3 Public Law 105-204, U.S. Congress (July 21, 1998).

4 "Record of Decision for the Long-Term Management and Use of Depleted Uranium Hexafluoride," *Fed. Regist.*, 64 (153), 43358 (August 10, 1999).

5 M. J. HAIRE and A. G. CROFF (eds.), "U.S. Department of Energy DUF_6 Materials Use Roadmap," ORNL-6968, Oak Ridge National Laboratory (August 2001).

6 U.S. DEPARTMENT OF ENERGY, "Final Programmatic Impact Statement for Alternative Strategies for Long-Term Management and Use of Depleted Uranium Hexafluoride," DOE/EIS-0269 (April 1999).

7 "Director=s Final Findings and Orders," Director, Ohio Environmental Protection Agency (February 24, 1998).

8 A. G. CROFF, J. R. HIGHTOWER, D. W. LEE, G. E. MICHAELS, N. L. RANEK, and J. R. TRABALKA, "Assessment of Preferred Depleted Uranium Disposal Forms," ORNL/TM-2000/161, Oak Ridge National Laboratory (June 2000).

9 U.S. NRC letter, docket number 70-3070, from John W. N. Hickey to W. Howard Arnold, President Louisiana Energy Services (September 22, 1992).

10 "Summary of the Cost Analysis Report for the Long-Term Management of Depleted Uranium Hexafluoride," UCRL-ID-127650, Lawrence Livermore National Laboratory (September 1997).

11 Personal communication, Paul Harrington, Yucca Mountain Project (October 7, 2003).

12 Personal communication, Archer Haskins, Holtec International (October 20, 2003).

FOOTNOTES

* Oak Ridge National Laboratory, managed by UT-Battelle, LLC, for the U.S. Department of Energy under contract DE-AC05-00OR22725.

The submitted manuscript has been authored by a contractor of the U.S. Government under contract DE-AC05-00OR22725. Accordingly, the U.S. Government retains a nonexclusive, royalty-free license to publish or reproduce the published form of this contribution, or allow others to do so, for U.S. Government purposes.

ORNL/TM-2003/172

Alpha Radiolysis of Sorbed Water on Uranium Oxides and Uranium Oxyfluorides

September 2003

Prepared by
A. S. Icenhour
L. M. Toth

DOCUMENT AVAILABILITY

Reports produced after January 1, 1996, are generally available free via the U.S. Department of Energy (DOE) Information Bridge:

Web site: http://www.osti.gov/bridge

Reports produced before January 1, 1996, may be purchased by members of the public from the following source:

National Technical Information Service
5285 Port Royal Road
Springfield, VA 22161
Telephone: 703-605-6000 (1-800-553-6847)
TDD: 703-487-4639
Fax: 703-605-6900
E-mail: info@ntis.fedworld.gov
Web site: http://www.ntis.gov/support/ordernowabout.htm

Reports are available to DOE employees, DOE contractors, Energy Technology Data Exchange (ETDE) representatives, and International Nuclear Information System (INIS) representatives from the following source:

Office of Scientific and Technical Information
P.O. Box 62
Oak Ridge, TN 37831
Telephone: 865-576-8401
Fax: 865-576-5728
E-mail: reports@adonis.osti.gov
Web site: http://www.osti.gov/contact.html

This report was prepared as an account of work sponsored by an agency of the United States Government. Neither the United States government nor any agency thereof, nor any of their employees, makes any warranty, express or implied, or assumes any legal liability or responsibility for the accuracy, completeness, or usefulness of any information, apparatus, product, or process disclosed, or represents that its use would not infringe privately owned rights. Reference herein to any specific commercial product, process, or service by trade name, trademark, manufacturer, or otherwise, does not necessarily constitute or imply its endorsement, recommendation, or favoring by the United States Government or any agency thereof. The views and opinions of authors expressed herein do not necessarily state or reflect those of the United States Government or any agency thereof.

ORNL/TM-2003/172

ALPHA RADIOLYSIS OF SORBED WATER ON URANIUM OXIDES AND URANIUM OXYFLUORIDES

A. S. Icenhour
L. M. Toth

Date Published: September 2003

Prepared by
OAK RIDGE NATIONAL LABORATORY
P.O. Box 2008
Oak Ridge, Tennessee 37831-6283
managed by
UT-Battelle, LLC
for the
U.S. DEPARTMENT OF ENERGY
under contract DE-AC05-00OR22725

THIS PAGE INTENTIONALLY LEFT BLANK.

CONTENTS

Page

LIST OF FIGURES v
LIST OF TABLES vii
ABSTRACT ix
1. INTRODUCTION 1
2. EXPERIMENTAL 2
  2.1 SAMPLE PREPARATION 2
  2.2 SAMPLE CONTAINERS 3
  2.3 DATA ACQUISITION 5
  2.4 SAMPLE ANALYSES 5
3. RESULTS 6
  3.1 PRESSURE MEASUREMENT 6
  3.2 GAS ANALYSIS 12
  3.3 X-RAY DIFFRACTION RESULTS FOR U_3O_8 AND UO_3 18
4. DISCUSSION 20
  4.1 UO_3 20
  4.2 U_3O_8 21
  4.3 UO_2F_2 22
  4.4 X-RAY DIFFRACTION 22
  4.5 SUMMARY 24
5. CONCLUSIONS 26
ACKNOWLEDGMENTS 26
REFERENCES 27

THIS PAGE INTENTIONALLY LEFT BLANK.

LIST OF FIGURES

Figure		Page
2.1	Comparison of alpha dose as a function of time for a U_3O_8 sample that consists of ^{238}U spiked with about 4400 ppm ^{244}Cm and one that consists of ^{233}U containing about 160 ppm ^{232}U.	2
2.2	Sample container and pressure transducer configuration used in the alpha radiolysis experiments.	4
2.3	Photograph of data acquisition system and glove box used for the experiments.	5
3.1	Pressure and gas yield as a function of dose for sample A-1 (UO_3 spiked with ^{244}Cm).	7
3.2	Pressure and gas yield as a function of dose for sample A-2-1 (UO_3 + 10 wt % H_2O, spiked with ^{244}Cm).	8
3.3	Pressure and gas yield as a function of dose for sample A-2-2 (UO_3 + 10 wt % H_2O, spiked with ^{244}Cm and followed by additional rinsing with NH_4OH to remove nitrates)	8
3.4	Pressure and gas yield as a function of dose for sample A-3 (U_3O_8 spiked with ^{244}Cm).	9
3.5	Pressure and gas yield as a function of dose for sample A-4-1 (U_3O_8 with 2 wt % H_2O, spiked with ^{244}Cm).	9
3.6	Pressure and gas yield as a function of dose for sample A-5 (UO_2F_2 wetted with ^{244}Cm solution and then dried)..	10
3.7	Pressure and gas yield as a function of dose for sample A-6 ($UO_2F_2 \bullet 1.7H_2O$ wetted with ^{244}Cm solution and then dried).	10
3.8	Calibration and rinse data for additional rinsing during preparation of A-2-2.	11

THIS PAGE INTENTIONALLY LEFT BLANK.

LIST OF TABLES

Table		Page
2.1	Example of radionuclide composition and dose contribution data for material used to spike uranium samples	3
2.2	Void volume of sample containers	4
3.1	Summary of irradiation experiments performed	7
3.2	Results of mass spectrometric analysis (volume percentage) of gas composition from UO_3 samples	12
3.3	Results of mass spectrometric analysis (volume percentage) of gas composition from U_3O_8 samples	13
3.4	Results of mass spectrometric analysis (volume percentage) of gas composition from UO_2F_2 samples	14
3.5	Comparison of gas composition (relative to argon) for a standard air composition and for irradiated UO_3 samples	16
3.6	Comparison of gas composition (relative to argon) for a standard air composition and for selected irradiated U_3O_8 samples	16
3.7	Comparison of gas composition (relative to argon) for a standard air composition and for selected irradiated UO_2F_2 samples	16
3.8	Estimated change in gas composition for selected experiments as a result of radiolysis	17
3.9	Estimate of hydrogen production as a percentage of moisture on sample	18
3.10	Estimated mole percentage of uranium oxidized by oxygen consumption	19
3.11	X-ray diffraction data for uranium oxides	19

THIS PAGE INTENTIONALLY LEFT BLANK.

ABSTRACT

The radiolysis of sorbed water and other impurities contained in actinide oxides has been the focus of a number of studies related to the establishment of criteria for the safe storage and transport of these materials. Gamma radiolysis studies have previously been performed on uranium oxides and oxyfluorides (UO_3, U_3O_8, and UO_2F_2) to evaluate the long-term storage characteristics of ^{233}U. This report describes a similar study for alpha radiolysis.

Uranium oxides and oxyfluorides (with ^{238}U as the surrogate for ^{233}U) were subjected to relatively high alpha radiation doses (235 to 634 MGy) by doping with ^{244}Cm. The typical irradiation time for these samples was about 1.5 years, which would be equivalent to more than 50 years irradiation by a ^{233}U sample. Both dry and wet (up to 10 wt % water) samples were examined in an effort to identify the gas pressure and composition changes that occurred as a result of radiolysis.

This study shows that several competing reactions occur during radiolysis, with the net effect that only very low pressures of hydrogen, nitrogen, and carbon dioxide are generated from the water, nitrate, and carbon impurities, respectively, associated with the oxides. In the absence of nitrate impurities, no pressures greater than 1000 torr are generated. Usually, however, the oxygen in the air atmosphere over the oxides is consumed with the corresponding oxidation of the uranium oxide. In the presence of up to 10 wt % water, the oxides first show a small pressure rise followed by a net decrease due to the oxygen consumption and the attainment of a steady-state pressure where the rate of generation of gaseous components is balanced by their recombination and/or consumption in the oxide phase.

These results clearly demonstrate that alpha radiolysis of either wet or dry ^{233}U oxides will not produce deleterious pressures or gaseous components that could compromise the long-term storage of these materials.

THIS PAGE INTENTIONALLY LEFT BLANK.

1. INTRODUCTION

The radiolysis of sorbed water and other impurities contained in actinide oxides has been the focus of a number of studies that centered on the establishment of criteria for the safe storage and transport of the oxides. These criteria are designed to prevent the production of large pressures or hazardous products (e.g., hydrogen and fluorine) that could be deleterious to storage containers and that might result in the release of radioactivity. Storage standards have been developed for both plutonium and uranium to address these concerns.[1,2] In support of the development of these standards, a number of radiolysis studies have been performed to evaluate the yields of radiolytic products (e.g., Refs. 3–8).

Uranium-233, which is stored primarily at Oak Ridge National Laboratory (ORNL), contains a contaminant isotope, ^{232}U, which has a daughter isotope, ^{208}Tl, that emits a 2.6-MeV gamma ray. Hence, these materials have a relatively high alpha activity as well as a large gamma radiation field, both of which complicate their handling. Experimental studies have been conducted on the gamma radiolysis of sorbed water on uranium oxides and on fluoride impurities in these oxides (primarily on uranium oxyfluorides).[3–5] These experiments have demonstrated that, with respect to gamma radiation, these materials can be safely stored. To complete the understanding of radiolysis in a ^{233}U oxide system, a similar set of experiments have been pursued to explore the effects of alpha radiolysis. In all of these experiments, ^{238}U was used as a surrogate for the $^{233}U/^{232}U$, with radiation supplied from a separate source. A surrogate alpha emitter, ^{244}Cm, was used in place of the $^{233}U/^{232}U$. The use of the surrogate alpha source offers the advantages of (1) a higher specific alpha activity, which provides for an accelerated experiment, and (2) the elimination of the use of $^{233}U/^{232}U$, which results in a significant personnel dose avoidance and more easily handled materials. This report documents the results of the alpha radiolysis experiments that have been performed on uranium oxides and oxyfluorides.

2. EXPERIMENTAL

2.1 SAMPLE PREPARATION

The surrogate uranium oxides were prepared by doping natural uranyl nitrate hexahydrate [$UO_2(NO_3)_2 \bullet 6H_2O$] with the desired amount of curium nitrate (~25 mg ^{244}Cm as a 0.04 *M* solution in 4 *N* HNO_3), coprecipitating the uranium and curium, and then calcining the precipitate. The procedure used was developed by first coprecipitating cerium and uranium. The chemical concentrations, rinsing steps, and calcination temperatures were thereby established.

Use of ^{244}Cm provided a dose rate about 37 times that which would be achieved if the sample was ^{233}U (with 160 ppm ^{232}U), as shown in Fig. 2.1. An example of the radionuclide composition for the ^{244}Cm solution and dose contribution data is presented in Table 2.1. Note that the ^{244}Cm solution contains a number of radioisotopes, and that while only 50 wt % of the material is ^{244}Cm, more than 99% of the dose is attributed to the ^{244}Cm.

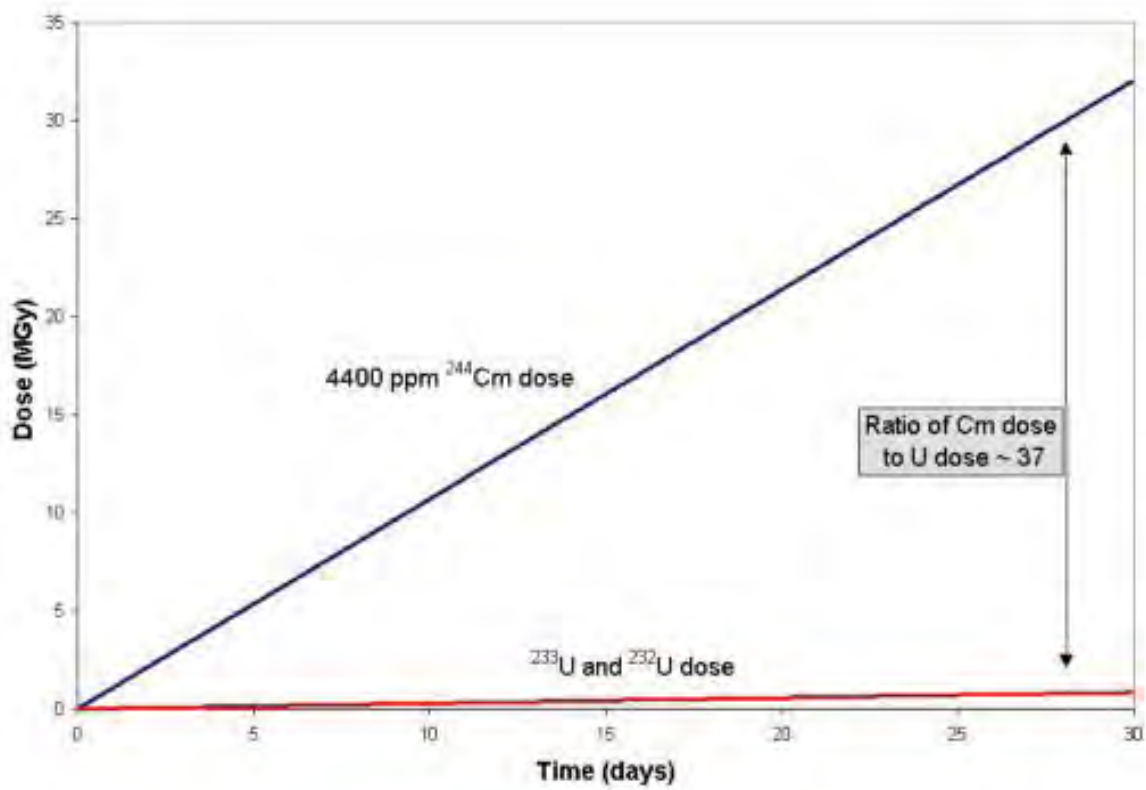

Fig 2.1. Comparison of alpha dose as a function of time for a U_3O_8 sample that consists of ^{238}U spiked with about 4400 ppm ^{244}Cm and one that consists of ^{233}U containing about 160 ppm ^{232}U.

Table 2.1. Example of radionuclide composition and dose contribution data for material used to spike uranium samples

Radionuclide	Half-life (years)	Specific activity (Ci/g)	Average alpha energy (MeV)	Composition (wt %)	Contribution to dose (%)
^{244}Cm	18.11	80.9	5.7965	50.34	99.74
^{245}Cm	8500	0.1717	5.363	1.36	0.01
^{246}Cm	4730	0.3072	5.376	7.31	0.05
^{247}Cm	1.56×10^7	9.20×10^5	4.9475	0.12	<<0.01
^{248}Cm	3.40×10^5	0.00424	4.6524	0.07	<<0.01
^{240}Pu	6563	0.22696	5.1549	40.04	0.20
^{241}Pu	14.4	103	0.000118	<<0.01	<<0.01
^{242}Pu	3.76×10^5	0.003926	4.89	<<0.01	<<0.01
^{243}Am	7380	0.1993	5.2656	0.76	<<0.01

The uranium and curium solutions were mixed and were then coprecipitated as a hydroxide in quartz tubes using concentrated ammonium hydroxide (NH_4OH). The precipitate was centrifuged and rinsed with NH_4OH. The precipitate was subsequently heated overnight to the appropriate temperature to obtain the desired oxide (about 350ºC for UO_3 and about 650ºC for U_3O_8). Uranyl fluoride samples could not be prepared by this method, because the UO_2F_2 could not be formed as a precipitate. Instead, UO_2F_2 was wetted with a curium nitrate solution and then dried overnight at 350ºC. This temperature was selected to be sufficiently high to decompose the nitrate but low enough to prevent disproportionation of the UO_2F_2. The samples were loaded into instrumented containers. Just prior to closure of the sample containers, the desired amount of water was added to each sample using a calibrated pipette.

2.2 SAMPLE CONTAINERS

The samples were placed in stainless steel containers, which were connected by a small-diameter stainless steel tube to a pressure transducer and to a valve (Fig. 2.2). These containers were constructed from a ½-in. Cajon VCR socket-weld gland that had a short piece of ½-in. tubing welded to it. The tubing was closed at one end with an 1/8-in.-thick disk. The overall length of the container was about 3.5 in. The container was closed with a VCR cap that was drilled through and had 1/16-in. tubing connected to it. The tubing led to a tee that was connected to a pressure transducer and a Nupro valve,

which was used for leak testing and withdrawal of gas samples. Filter gaskets (0.5-µm sintered frit) were used in the VCR face-sealed connections to prevent movement of particles and the spread of contamination. The void volume of the containers was measured by expanding helium from a known volume, and the measured volumes are shown in Table 2.2. Samples were prepared and loaded into the containers in a glove box at the ORNL Radiochemical Engineering Development Center.

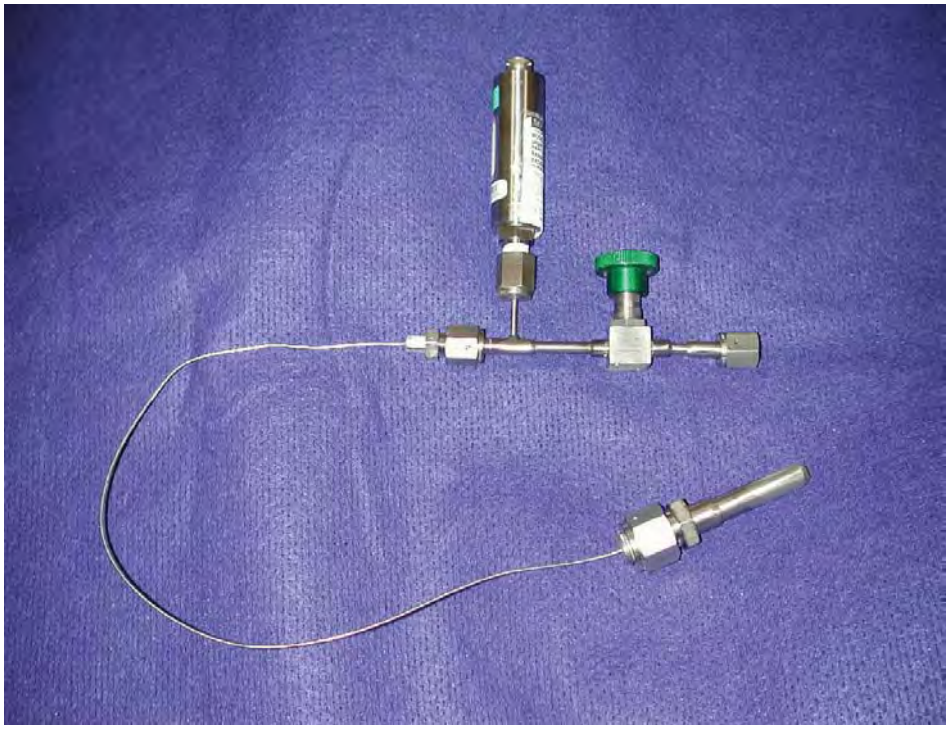

Fig. 2.2. Sample container and pressure transducer configuration used in the alpha radiolysis experiments.

Table 2.2 Void volume of sample containers

Container	Volume (cm^3)
A-1	12.6
A-2-1, A-2-2	12.9
A-3	12.7
A-4-1	12.4
A-5	12.7
A-6	12.3

2.3 DATA ACQUISITION

A computerized data acquisition system was used to record the pressure in the sample containers throughout the irradiations (Fig. 2.3). Validyne® hardware and software were used, providing up to eight data channels per card. Sensotec® pressure transducers (Model FPA) were used to measure the pressure. An Omega® Type K thermocouple was placed in contact with the exterior of one of the sample containers to obtain a representative temperature for each of the containers.

2.4 SAMPLE ANALYSES

During the irradiations, gas samples were periodically withdrawn and analyzed by mass spectrometry. Some samples were analyzed by X-ray diffraction (XRD) by loading capillaries with a small amount of ground sample and running XRD on a Debye-Scherrer camera using MoKα radiation. This very classic method for XRD analysis greatly minimized the amount of sample required and satisfied ALARA (as low as reasonably achievable) requirements for radiation exposure. During the preparation of one of the UO_3 samples, nitrate analyses were performed using a nitrate-specific electrode because it was suspected that radiolysis of residual nitrates contributed to an observed pressure increase.

Fig. 2.3. Photograph of data acquisition system and glove box used for the experiments.

3. RESULTS

The effects of alpha particle irradiation on the various wet and dry uranium oxide/oxyfluoride samples were studied by monitoring the pressure changes of the gas atmosphere in contact with them throughout the irradiation period followed by gas composition analyses of samples taken both on occasion during the experiment and at the end of the irradiation. Finally, XRD measurements were made on some of the oxides before and after irradiation to determine if any changes in the crystalline phases had occurred as a result of the alpha radiation exposure to the atmospheres in which they were in contact.

3.1 PRESSURE MEASUREMENT

Table 3.1 provides a summary of the irradiation experiments performed. Most of these samples were irradiated for more than 1.5 years with these relatively intense internal sources. The pressure data from each of the experiments are shown in Figs. 3.1–3.7 as gas yield (millimoles of gas per gram of sample) versus calculated dose. The gas yield was calculated using the ideal gas law. The dose to the sample was calculated based on the amount of ^{244}Cm present in the sample, assuming that all of the decay energy from the ^{244}Cm was deposited in the sample (i.e., in the uranium oxide or oxyfluoride plus the added H_2O).

Even after very long periods of alpha radiolysis, the pressures were generally observed to reach a limit ("plateau" or "steady-state" value) that is much lower than the net pressure expected from the radiolytic conversion of all the moisture to hydrogen and oxygen. These plateaus are usually preceded by some fluctuations that depend on the presence of water on the sample. Typical for the samples containing moisture is the appearance of a pressure rise that peaks and then proceeds downward to a steady-state value—one that is either slightly larger or smaller that the starting pressure of the system.

For dry UO_3 (Fig. 3.1), a slight decrease in pressure is followed by a steady growth to steady-state value of approximately 1000 torr. However, for a wetted UO_3 sample (Figs. 3.2 and 3.3), an initial rise is followed by a decrease in pressure to a steady-state value. Dry U_3O_8 and UO_2F_2 samples show only a progressive decrease to the limiting steady-state value, while the respective wetted samples show some increase in pressure, which is then followed by a decrease to a subatmospheric pressure.

Table 3.1. Summary of irradiation experiments performed

Experiment	Material	Mass (g)[a]	^{244}Cm added (mg)	Total dose (MGy)
A-1	UO_3	6.21	24.9	595
A-2-1	UO_3 + 10 wt % H_2O	5.90	25.0	329
A-2-2	UO_3 + 10 wt % H_2O[b]	5.86	24.9	235
A-3	U_3O_8	5.60	24.9	415
A-4-1	U_3O_8 + 2 wt % H_2O	5.64	24.9	406
A-5	UO_2F_2	4.93	25.0	634
A-6	UO_2F_2•1.7 H_2O (9 wt % H_2O)	4.86	25.0	595

[a]Mass of anhydrous material.

[b]Same method as that used for preparation of sample A-2-1, except that additional rinses were performed to reduce residual nitrates.

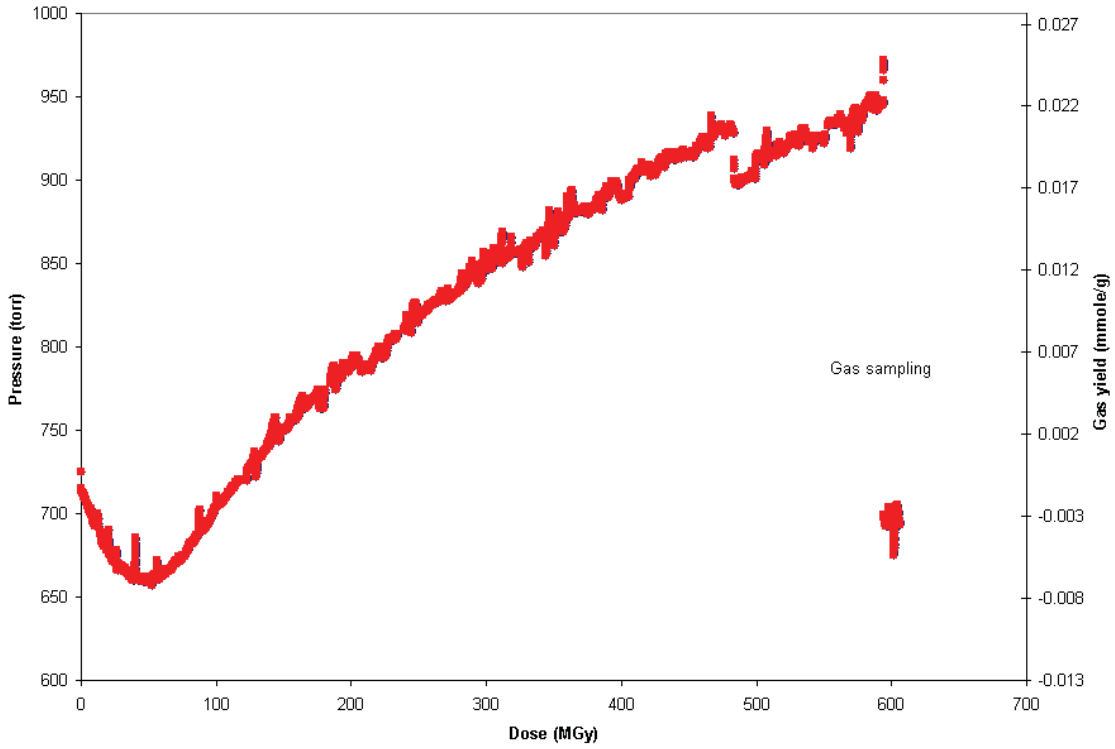

Fig. 3.1. Pressure and gas yield as a function of dose for sample A-1 (UO_3 spiked with ^{244}Cm).

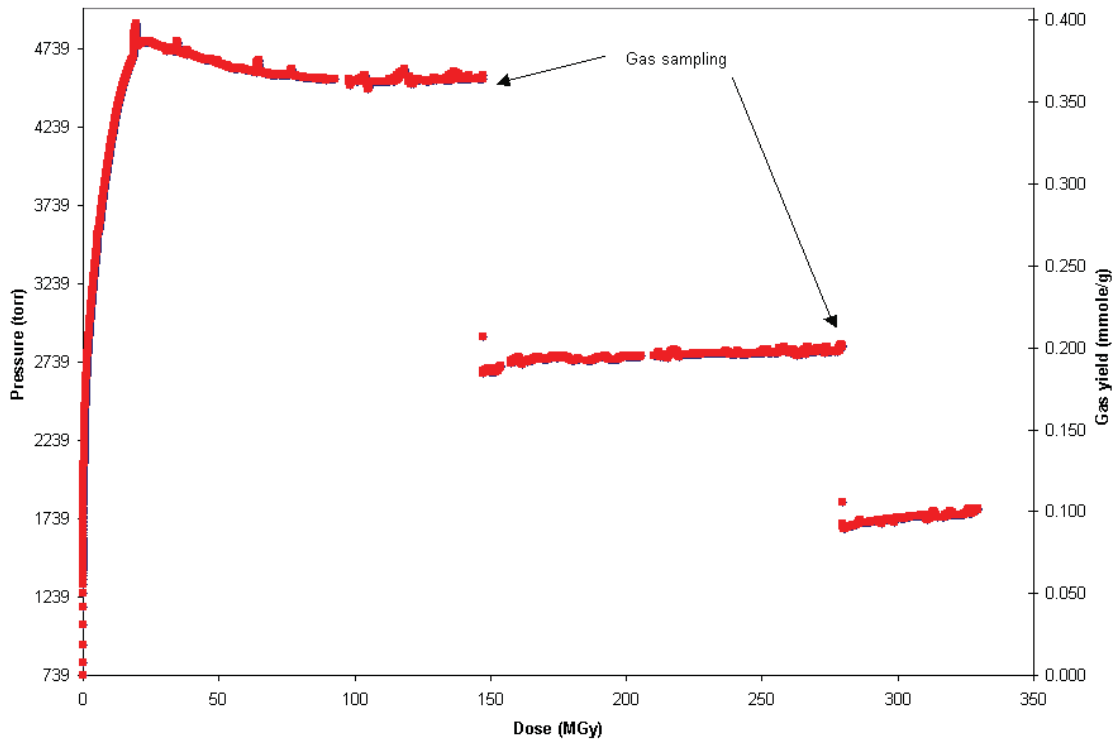

Fig. 3.2. Pressure and gas yield as a function of dose for sample A-2-1 (UO_3 + 10 wt % H_2O, spiked with ^{244}Cm).

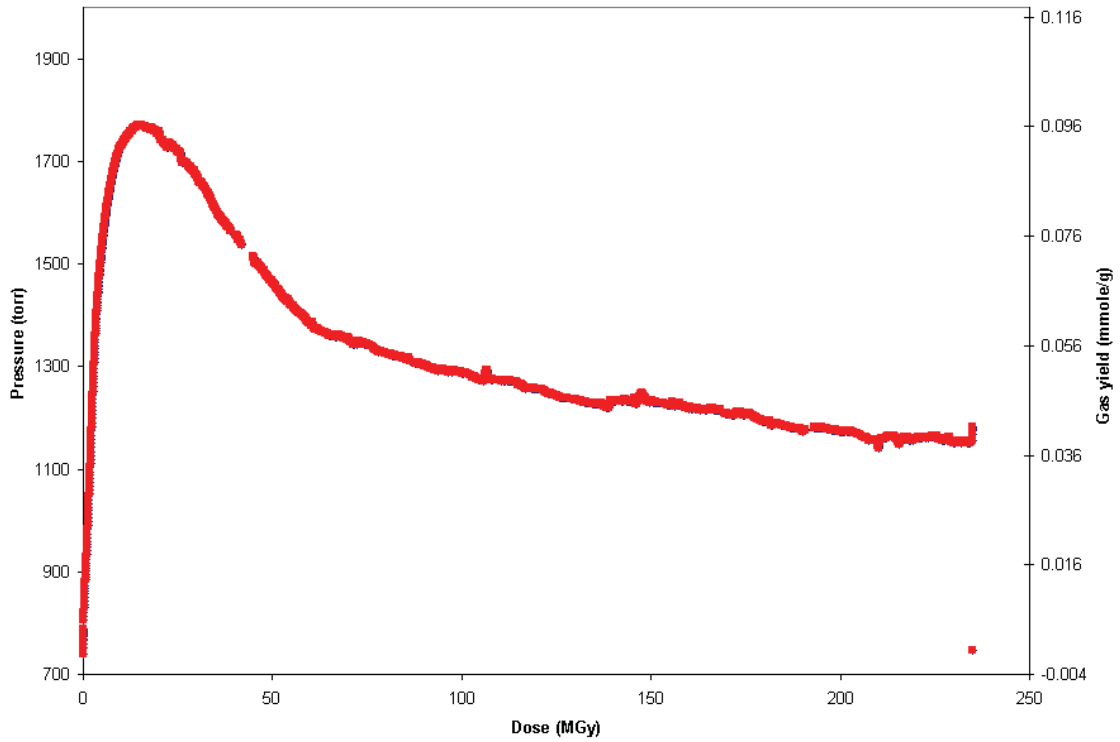

Fig. 3.3. Pressure and gas yield as a function of dose for sample A-2-2 (UO_3 + 10 wt % H_2O, spiked with ^{244}Cm and followed by additional rinsing with NH_4OH to remove nitrates).

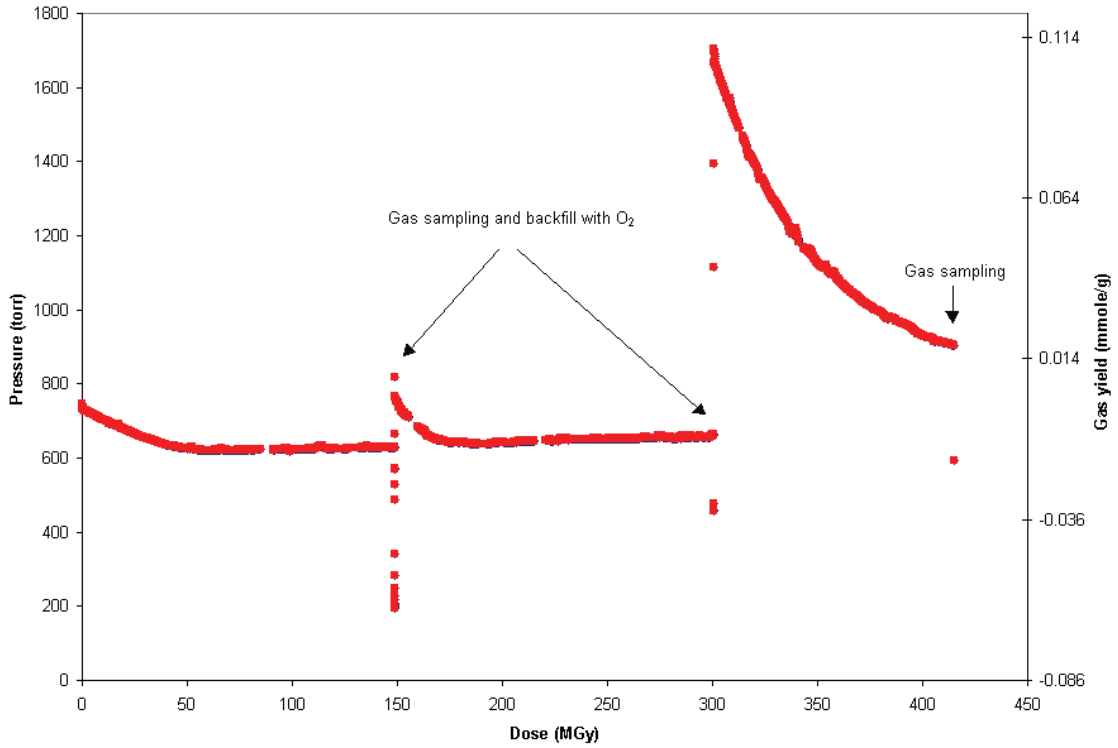

Fig. 3.4. Pressure and gas yield as a function of dose for sample A-3 (U_3O_8 spiked with ^{244}Cm).

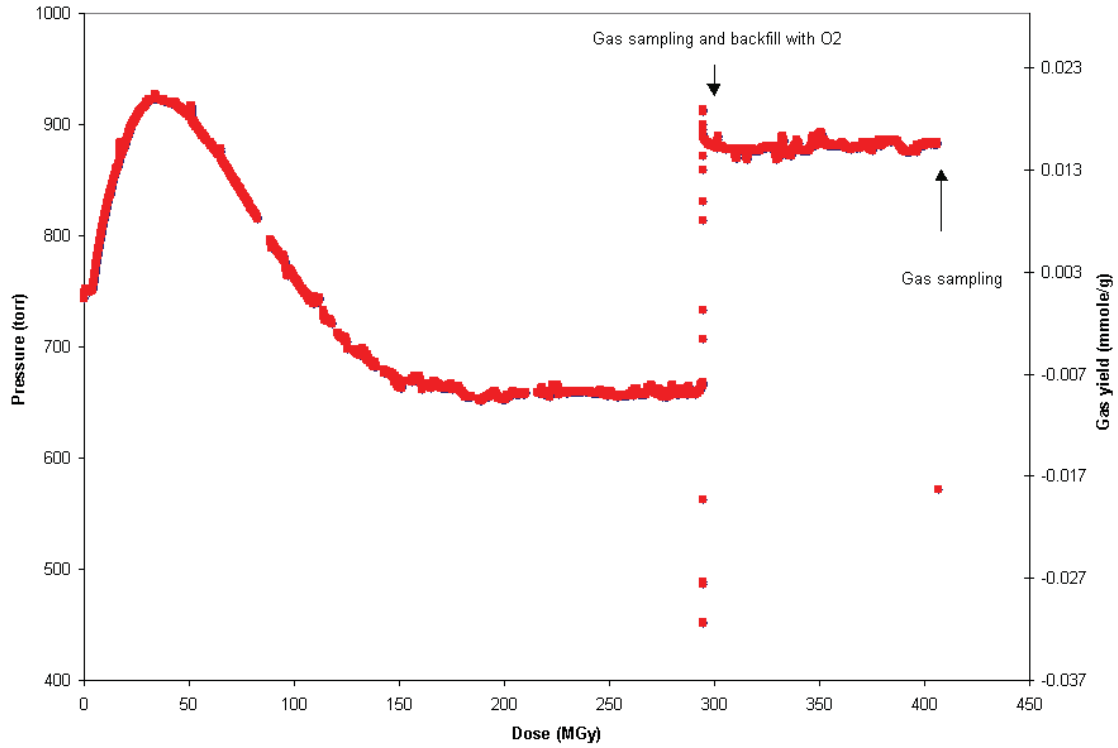

Fig. 3.5. Pressure and gas yield as a function of dose for sample A-4-1 (U_3O_8 with 2 wt % H_2O, spiked with ^{244}Cm).

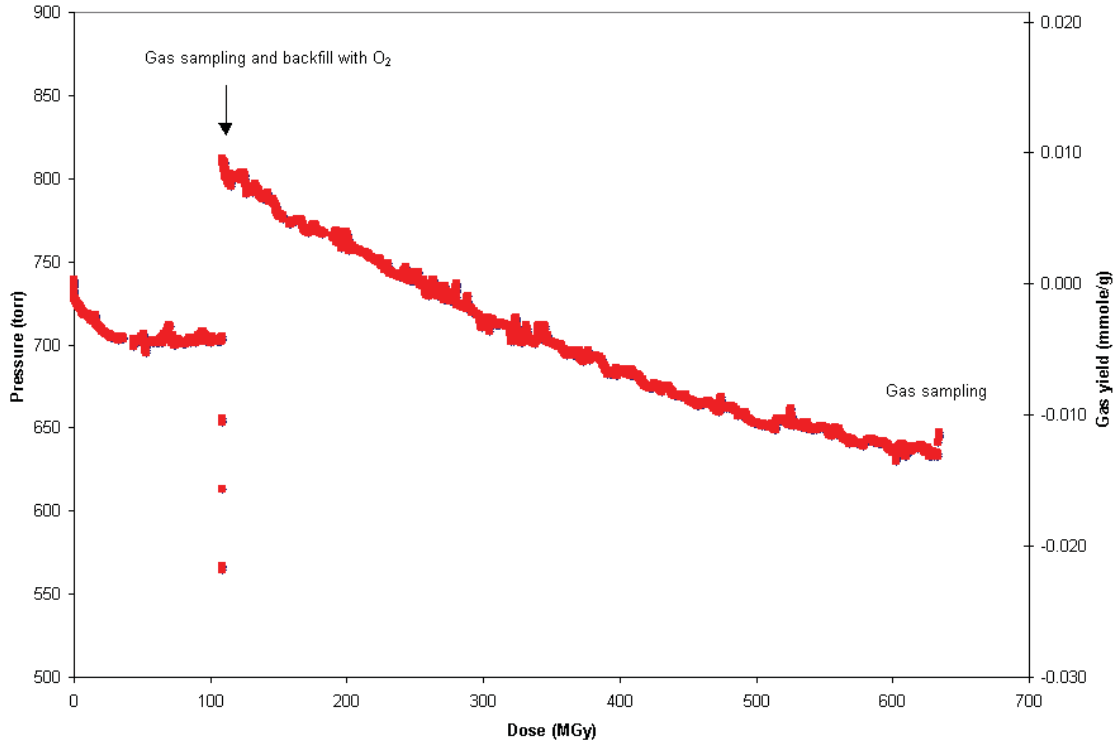

Fig. 3.6. Pressure and gas yield as a function of dose for sample A-5 (UO_2F_2 wetted with ^{244}Cm solution and then dried).

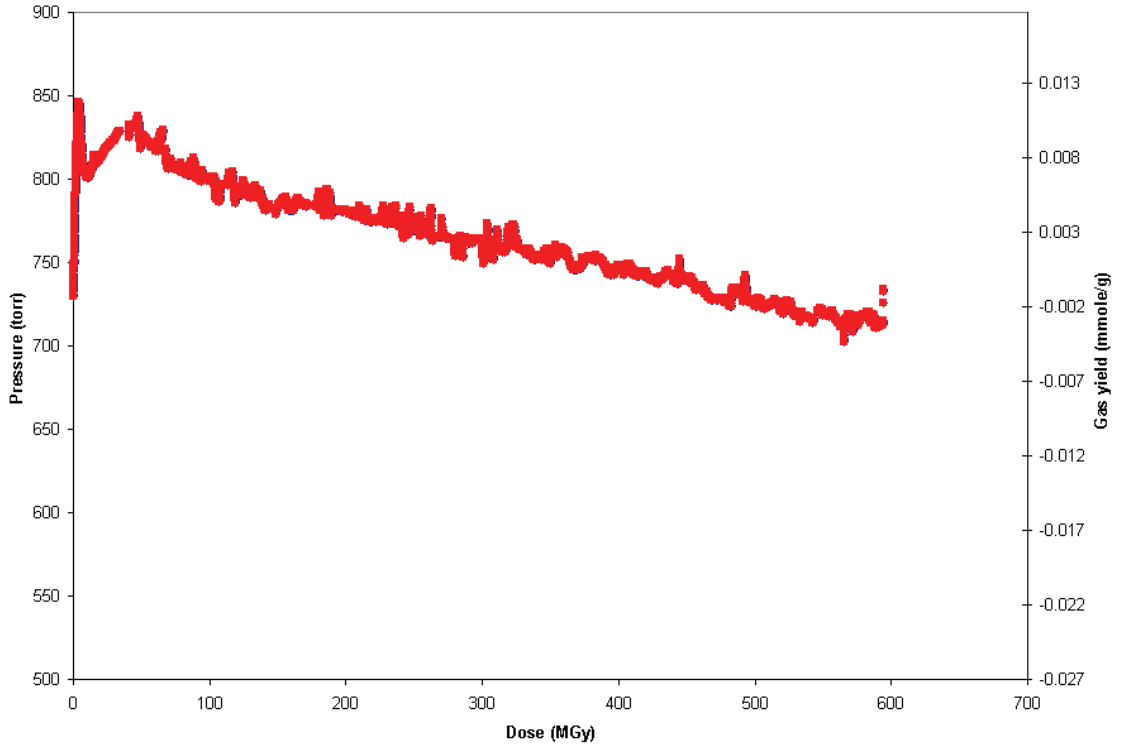

Fig. 3.7. Pressure and gas yield as a function of dose for sample A-6 (UO_2F_2•$1.7H_2O$ wetted with ^{244}Cm solution and then dried).

The only truly anomalous trend was seen with the first wetted UO_3 sample, which rapidly reached a relatively high (ultimate) steady-state pressure (Sample A-2-1, Fig. 3.2). Because the gas sample had an unusually high nitrogen content (see next section), it was suspected that the nitrate ion from the reagent material had not been sufficiently washed from the sample and that this residue was radiolyzing in addition to the uranium oxides and moisture.

Therefore, a repeat of this sample preparation and irradiation was deemed necessary but with more thorough washing of the sample after precipitation and separation from the mother liquor. The water from each rinse was monitored with a nitrate-specific ion electrode and compared with a calibration chart for nitrate ion in equivalent ionic strength solutions.* These results are given in Fig. 3.8, which shows that the nitrate concentration in the mother liquor was ~4.2 *M* and, after 5 rinses, was reduced to ~0.07 *M* in the final rinse. (Note that in the preparation of sample A-2-1, only one rinse was performed. Based on Fig. 3.8, this process would result in a rinse-solution nitrate concentration of ~1.5 *M*, or approximately 20 times that achieved for sample A-2-2.) This material was then dried and run with 10% added water to give a significantly lower steady-state pressure and an overall profile that better matched the other oxides. [Compare sample A-2-2 (Fig. 3.3) with, for example, sample A-4-1 (Fig. 3.5).]

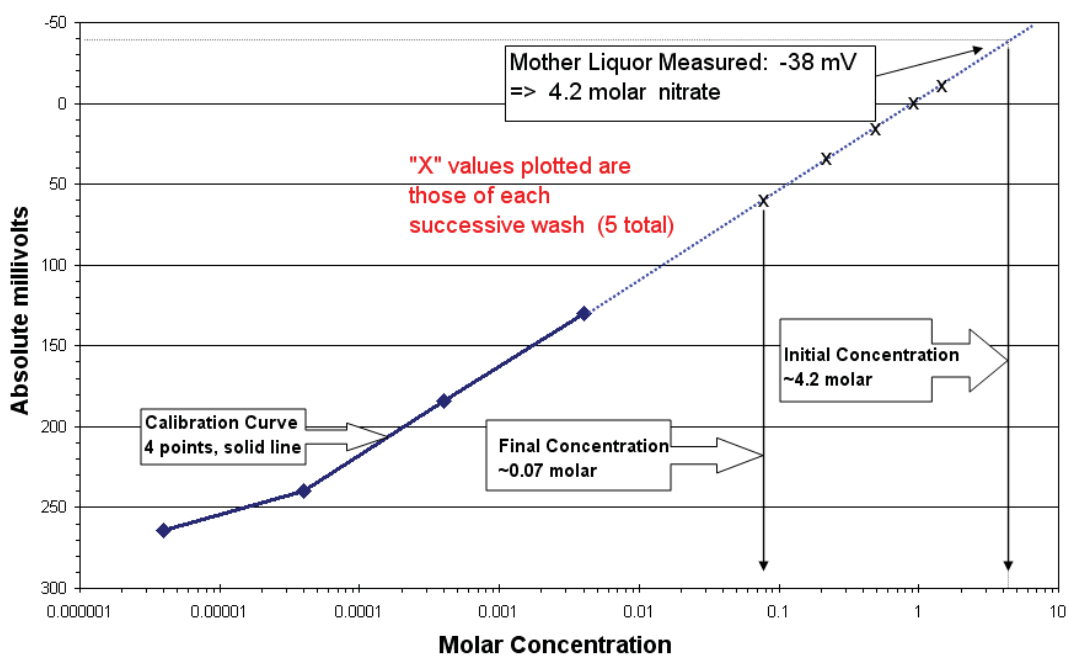

Fig. 3.8. Calibration and rinse data for additional rinsing during preparation of A-2-2.

*The measurement of nitrate ion in the wash solution was easier and less expensive than the more obvious direct destructive analysis of the solid sample.

The presence of nitrate ion impurity could not be a problem for the U_3O_8 and UO_2F_2 samples because these were prepared at temperatures above that at which nitrate decomposes. Furthermore, the gas analyses described in the following section confirm that nitrate ion was not a problem in these other two uranium compounds.

3.2 GAS ANALYSIS

Mass spectrometric gas analyses on periodic samples are presented in Tables 3.2–3.4 along with pressure and temperature data at the time of the sampling. The values labeled as "initial" are those at the beginning of the experiment or, in the case of multiple gas samples, the value just after sampling. The "final" values are taken just prior to withdrawal of the gas sample. Hence, these pressure values give a measure of the change during the period prior to sampling.

Table 3.2. Results of mass spectrometric analysis (volume percentage) of gas composition from UO_3 samples

	A-1 (UO_3 dry)	A-2-1 (UO_3 with 10 wt % H_2O)		A-2-2 (UO_3 with 10 wt % H_2O)
		First gas sample	Second gas sample	
Initial atmosphere	Air	Air	Modified air[a]	Air
Initial pressure[b] (torr)	725	739	2671	740
Initial temperature[c] (ºC)	27	29	25	29
Final pressure[c] (torr)	972	4572	2843	1183
Final temperature[c] (ºC)	29	25	27	29
CO_2	0.01	0.03	0.01	0.02
CO	<0.01			<0.01
Ar	0.3	0.08	0.09	0.2
O_2	0.92	1.32	0.6	1.01
N_2	82.8	89.2	89.09	96.68
NO_x[d]	0.37	0.2	0.05	0.32
H_2	0.002	0.24	0.37	0.72
He	15.59	8.84	9.7	1.05

[a] Composition remaining after first sample of A-2-1.
[b] Value at beginning of experiment or just after previous gas sampling operation.
[c] Value just prior to withdrawal of gas sample.
[d] Likely in the form N_2O.

Table 3.3. Results of mass spectrometric analysis (volume percentage) of gas composition from U_3O_8 samples

	A-3 (U_3O_8 dry)			A-4-1 (U_3O_8 with 2 wt % H_2O)	
	First gas sample	Second gas sample after backfill with O_2	Third gas sample after backfill with O_2	First gas sample	Second gas sample after backfill with O_2
Initial atmosphere	Air	Air/additional O_2[a]	Air/additional O_2[b]	Air	Air/additional O_2[c]
Initial pressure[d] (torr)	744	766	1701	743	912
Initial temperature[d] (ºC)	27	24	27	27	27
Final pressure[e] (torr)	629	663	906	668	883
Final temperature[e] (ºC)	24	27	24	27	25
CO_2	0.06	<.01	0.2	0.02	0.02
Ar	0.8	0.4	0.43	0.7	0.29
O_2	17.29	0.7	2.23	10.06	0.88
N_2	70.1	41.24	28.06	60.17	26.17
NO_x[f]		0.23	0.11	0.03	0.024
H_2	0.001	0.01	0.003	0.44	0.97
H_2O			0.4		0.2
He	11.66	57.4	68.56	28.08	71.44

[a] Composition remaining after first sample of A-3 plus backfilled with O_2.
[b] Composition remaining after second sample of A-3 plus backfilled with O_2.
[c] Composition remaining after first sample of A-4-1 plus backfilled with O_2.
[d] Value at beginning of experiment or just after previous gas sampling operation.
[e] Value just prior to withdrawal of gas sample.
[f] Likely in the form N_2O.

Table 3.4. Results of mass spectrometric analysis (volume percentage) of gas composition from UO_2F_2 samples

	A-5 (UO_2F_2 dry)		A-6 ($UO_2F_2 \bullet 1.7H_2O$)
	First gas sample	Second gas sample after O_2 addition	
Initial atmosphere	Air	Air/additional O_2[a]	Air
Initial pressure[b] (torr)	739	811	737
Initial temperature[b] (ºC)	27	24	27
Final pressure[c] (torr)	705	646	732
Final temperature[c] (ºC)	24	29	29
CO_2	0.1	1.2	1.86
CO		0.32	0.03
Ar	0.74	0.72	0.49
O_2	16.91	5.79	6.17
N_2	64.3	79.68	50.36
NO_x[d]		0.22	1.16
H_2	<0.001	0.007	8.15
He	18.05	12.06	31.78

[a] Composition remaining after first sample of A-5 plus backfilled with O_2.
[b] Value at beginning of experiment or just after previous gas sampling operation.
[c] Value just prior to withdrawal of gas sample.
[d] Likely in the form N_2O.

Results from the mass spectrometric analysis of the UO_3 samples are shown in Table 3.2. One gas sample was withdrawn at the end of experiment A-1. By contrast, because of the relatively large pressure rise seen for A-2-1, gas samples were taken at two different times from this container (see Fig. 3.2). A gas sample was withdrawn at the end of experiment A-2-2. The introduced helium seen here in the analysis is an artifact of the sampling method.

For the U_3O_8 experiments, a pressure decrease was evident and multiple gas samples were also withdrawn. Results of the mass spectrometric analysis of these samples are presented in Table 3.3. After the first gas sample of experiment A-3, the container was evacuated to about 200 torr and was then backfilled with oxygen to a total pressure of 766 torr. After withdrawal of the second gas sample from experiment A-3, the container pressure was about 458 torr (no further evacuation performed). This container was then backfilled with oxygen to a total pressure of 1701 torr. A similar operation was performed for experiment A-4-1. The pressure in A-4-1 was reduced to 450 torr as a result of withdrawal of the first gas sample. The container was then backfilled with oxygen to a total pressure of 912 torr. Because of the manifold configuration, some helium remained in the system and, as a result, the backfill gas was a mixture of helium and oxygen.

The mass spectrometric results for gas samples for the UO_2F_2 experiments are shown in Table 3.4. Two samples were withdrawn from A-5. After the first sample, the container was evacuated to about 200 torr and backfilled with a helium/oxygen mixture to a total pressure of 811 torr. A gas sample was withdrawn from A-6 at the end of the experiment.

The most significant general observation is that the hydrogen content of these gas samples is extremely low. It exceeds 1% of the total gas sample composition only in sample A-6. However, more careful evaluation of the mass spectrometric data is necessary in order to see the subtle trends that occur during the course of the radiolysis—as described in the following paragraph.

Some insight into the radiolytic effects on the samples can be gained by normalizing the measured gas composition with an inert component of the air, namely argon, that acts as an internal standard. This comparison for the UO_3 samples is shown in Table 3.5. Comparisons for selected U_3O_8 and UO_2F_2 samples are presented in Tables 3.6 and 3.7, respectively. Selected comparisons were made for these samples because, after initial gas withdrawal, the containers were evacuated and backfilled with oxygen. Table 3.8 presents the estimated change in gas composition (i.e., moles of oxygen and hydrogen formed or consumed) for selected experiments.* The standard air composition[9] was the assumed starting composition for each experiment.

---

*Because of the residual helium in the gas manifold, the exact composition of the gas resulting from the oxygen backfilling operation was not known. Consequently, estimates of changes in gas composition could not be made for containers that were backfilled with oxygen.

Table 3.5. Comparison of gas composition (relative to argon) for a standard air composition and for irradiated UO_3 samples

Ratio	Standard air composition[a]	A-1	A-2-1		A-2-2
			First gas sample	Second gas sample	
O_2:Ar	22.47	3.07	16.5	6.6	5.1
CO_2:Ar	0.03	0.03	0.38	0.11	0.1
N_2:Ar	83.98	276	1115	990	483
H_2:Ar	0.00005	0.007	3	4	4

[a] From *CRC Handbook of Chemistry and Physics*, 73rd ed., D. R. Lide, ed., CRC Press, Boca Raton, Florida, 1992.

Table 3.6. Comparison of gas composition (relative to argon) for a standard air composition and for selected irradiated U_3O_8 samples

Ratio	Standard air composition[a]	A-3 First gas sample	A-4-1 First gas sample
O_2:Ar	22.47	21.6	14.4
CO_2:Ar	0.03	0.08	0.03
N_2:Ar	83.98	87.6	85.9
H_2:Ar	0.00005	0.001	0.6

[a] From *CRC Handbook of Chemistry and Physics*, 73rd ed., D. R. Lide, ed., CRC Press, Boca Raton, Florida, 1992.

Table 3.7. Comparison of gas composition (relative to argon) for a standard air composition and for selected irradiated UO_2F_2 samples

Ratio	Standard air composition[a]	A-5 First gas sample	A-6
O_2:Ar	22.47	22.9	12.6
CO_2:Ar	0.03	0.14	3.8
N_2:Ar	83.98	86.9	103
H_2:Ar	0.00005	0	17

[a] From *CRC Handbook of Chemistry and Physics*, 73rd ed., D. R. Lide, ed., CRC Press, Boca Raton, Florida, 1992.

Table 3.8. Estimated change in gas composition for selected experiments as a result of radiolysis

Gas sample	ΔO_2 (mol)	ΔH_2 (mol)
A-1	-8.83×10^{-5}	1.45×10^{-8}
A-2-1 First gas sample	-5.34×10^{-5}	7.35×10^{-6}
A-2-1 Second gas sample	-1.22×10^{-5}	2.87×10^{-6}
A-2-2	-8.49×10^{-5}	5.13×10^{-6}
A-3 First gas sample	-2.01×10^{-5}	4.07×10^{-9}
A-4-1 First gas sample	-3.81×10^{-5}	2.57×10^{-6}
A-5 First gas sample	-5.06×10^{-6}	0
A-6	-5.26×10^{-5}	5.15×10^{-5}

For the UO_3 samples, the very high nitrogen content is evident by noting their nitrogen:argon ratios for all the samples, especially for sample A-2-1. It is also evident that the carbon dioxide is elevated, along with a slight amount of hydrogen. However, oxygen is depleted from all of these samples. Somewhat similarly, for U_3O_8, carbon dioxide is increased (sample A-3) and oxygen is decreased—but both to a lesser degree than in the UO_3 samples. Hydrogen is likewise only slightly increased, while there is little change in the nitrogen content (as compared to the UO_3 samples). For the UO_2F_2 samples, the only significant observations are increased carbon dioxide for both samples and some hydrogen generation and oxygen depletion for the wet sample, (A-6). Sample A-6 may also indicate a small amount of nitrogen production. The fact that neither HF nor fluorine was found is significant because these corrosive species were a concern for the long-term storage of uranium oxides that contain fluoride impurities.[3,5]

Finally, the hydrogen production for each of the wetted samples is shown in Table 3.9 by estimating the hydrogen production as a mole percentage of the available water. This table shows that only a very small amount of the water was radiolyzed to form hydrogen.

Table 3.9. Estimate of hydrogen production as a percentage of moisture on sample

Experiment	Initial H_2O content (mol)	Estimated H_2 production (mol)	Available H_2O radiolyzed (mol %)
A-2-1 (after second gas sample)	0.033	1.02×10^{-5}	0.03
A-2-2	0.033	5.13×10^{-6}	0.02
A-4-1 (after first gas sample)	0.0063	2.57×10^{-6}	0.04
A-6	0.027	5.15×10^{-5}	0.19

3.3 X-RAY DIFFRACTION RESULTS FOR U_3O_8 AND UO_3

XRD measurements were obtained for the uranium oxides before and after the alpha radiolysis experiments to determine if any measurable change in the crystalline form had occurred as a result of the radiolysis. The XRD patterns of the pure materials agreed with those reported in the literature[10–12] for the U_3O_8 and anhydrous UO_3 used in these experiments.

Realizing that 5% or more of a new crystalline phase would typically have to be present in order to be seen by XRD, an estimate of the possible extent of conversion to a new phase was made by noting the consumption of oxygen as measured in the gas analyses. Results of these estimates are presented in Table 3.10. Note that these estimates do not consider the oxidation of uranium directly by the radiolysis products of water. In some cases the estimated oxidation amounted to as much as 6%, thus giving some confidence that a new crystalline phase could, in principle, be detected under these conditions. However, limitations in length of irradiation time and the unavailability of more XRD measurements prevented a complete investigation from being made. Nevertheless, some interesting and supportive observations have resulted from these measurements.

After irradiation, the wetted samples showed a few new lines, notably at Mo ($\lambda = 0.70930$ Å) 2θ values of 5.48 and 17.57 for U_3O_8 and 6.62, 10.72, and 15.77 for UO_3 as shown in Table 3.11. The dry U_3O_8 showed weak lines at 2θ values of 8.03 and 8.73, while the dry UO_3 sample gave no XRD pattern at all.

Table 3.10. Estimated mole percentage of uranium oxidized by oxygen consumption

Experiment	Mol % U oxidized[a]
A-1	0.7
A-2-1	0.6
A-2-2	0.8
A-3	6
A-4-1	0.5

[a] Does not consider possible oxidation by-products from the radiolysis of water.

Table 3.11. X-ray diffraction data for uranium oxides[a]

U_3O_8		UO_3	
Unirradiated	A-4-1 after irradiation	Unirradiated	A-2-2 after irradiation
	5.48 m		6.62 s
6.57 w		8.03 s	7.97 s
9.87 s	9.82 s	9.33 w	9.42 w
11.87 m	12.02 s		10.72 w
12.57 w	12.72 w	11.58 vs	11.82 vs
15.57 s	15.52 s	12.48 vw	12.67 m
	16.67 vvw	14.33 m	14.12 m
	17.57 m		15.77 m
19.77 w	19.77 w	16.18 m	16.32 m
20.22 w	20.22 vw	19.08 w	18.87 w
21.15 w	20.82 w		19.72 w
23.12 s	23.17 s	20.68 m	20.57 m
24.07 vw	23.97 w	22.03 vw	22.82 w
	24.92 vw	23.53 w	23.72 w
25.87 vvw	25.97 w		
	26.92 vvw		
28.72 w	28.87 w		
	29.77 w		
	30.52 w		
31.17 vw	31.37 vw		
32.17 w	32.22 w		

[a] The 2θ values given are for MoKα radiation; the wavelength is 0.70930 Å. Intensities are denoted by the following: s = strong; m = medium; w = weak. The addition of the prefix "v" indicates "very."

4. DISCUSSION

In order to assess the effects of long-term self-irradiation by radioactive materials such as $^{232}U/^{233}U$ on a time scale that is reasonable in the laboratory, it is necessary to irradiate surrogate samples to equivalent doses but at a necessarily higher dose rate. Considering the higher dose rate supplied by the ^{244}Cm, the doses achieved correspond to more than 50 years of irradiation with a $^{233}U/^{232}U$ source, thus achieving the desired result of equivalent long-term irradiation exposure.

4.1 UO_3

Examination of Figs. 3.1–3.3 shows a net pressure increase for each of the samples. This increase is consistent with the presence of trace nitrate ion in the samples that is radiolyzed in addition to the uranium oxide and/or water that might be on the sample. In the case of the anhydrous UO_3 sample (A-1, Fig. 3.1), the pressure was seen to initially decrease and then slowly increase. The gas sample taken from A-1 (see Tables 3.2 and 3.5) revealed that nitrogen was produced and oxygen was consumed. Furthermore, it is apparent that some trace water, either as hydrate or adsorbed moisture, is radiolyzed along with the nitrate impurity, as confirmed by the presence of trace hydrogen in the gas sample. However, any oxygen produced is also consumed. It appears then that the initial pressure increase is a result of nitrogen generation, while the overall pressure decrease results from oxygen consumption.

A much more dramatic pressure rise was seen for sample A-2-1, which consisted of UO_3 with 10 wt % H_2O added (Fig. 3.2). For this sample, the pressure quickly rose to about 4750 torr and then slowly decreased as it appears a steady state was approached. After taking two gas samples of A-2-1, which resulted in a net decrease of the system pressure, the pressure appeared to rise very slowly towards a new plateau.

The gas analysis for the samples withdrawn from A-2-1 (Tables 3.2 and 3.5) clearly shows that nitrogen was produced and oxygen consumed. Only a small amount (<1 vol %) of hydrogen was produced. Hence, again it is seen that the initial rise in pressure results from nitrogen production, while the decrease from the peak is probably due to oxygen consumption. Ultimately, this combination of mechanisms approaches a steady-state value.

The results of more thorough rinsing of the sample to remove nitrate ion produced a situation in which much less nitrogen was generated, although such production was not completely eliminated. Consequently, a much lower overall steady-state pressure was achieved after irradiation of this material. The curve profile for this sample, A-2-2 (Fig. 3.3), is more typical of all the wet uranium oxide samples

(UO_3, U_3O_8, and UO_2F_2), where there is an initial rise in pressure followed by a steady decrease to a lower limiting value.

These results are interpreted as the combination of multiple mechanisms taking place in the system. First, water and nitrate are radiolyzed by energy transfer through the uranium/curium oxide lattice to form some oxygen, hydrogen, and nitrogen. The oxygen comes from both nitrate and water radiolysis. These gaseous components would eventually reach a steady state without a peaking and subsequent decrease of the pressure were it not for the advent of yet another mechanism—a process in which one of the components was consumed, namely oxygen. However, this reaction now occurs at a slower rate. This additional chemical mechanism will be described in greater detail following the discussion of the other uranium oxides.

4.2 U_3O_8

Figures 3.4 and 3.5 exhibit an overall pressure decrease with increasing dose. For the dry U_3O_8 sample (A-3, Fig. 3.4), the pressure decreases immediately upon initiation of the experiment and reaches a steady-state value. After the first gas sample, container A-3 was backfilled with a mixture of air and helium. The pressure again decreased to a steady-state value. After a second gas sample was withdrawn, container A-3 was once again pressurized—this time to a much higher pressure—with oxygen (and some residual helium). The pressure in A-3 again decreased and was approaching a steady state when a final gas sample was withdrawn and the experiment terminated. The first gas sample for A-3 (Tables 3.3, 3.6, and 3.8) shows slight evidence of oxygen consumption. However, the second and third gas samples from A-3 (Table 3.3) provide clear evidence of oxygen consumption.

The U_3O_8 sample that was loaded with 2 wt % water (A-4-1, Fig. 3.5) exhibited an initial pressure increase to a peak of about 920 torr and then a decrease to a steady-state pressure. A gas sample was withdrawn and the tube was repressurized with an oxygen/helium mixture. The pressure then decreased again to a steady-state value. A final gas sample was withdrawn at the conclusion of the experiment. The gas analysis (Tables 3.3, 3.6, and 3.8) shows that oxygen was depleted while some hydrogen was produced. The estimated hydrogen production at steady state (Table 3.8) cannot account for the entire pressure rise observed. However, it is likely that the rise is the result of the initial radiolysis of water—producing hydrogen and oxygen. Then back reactions (i.e., recombination of hydrogen and oxygen, and the other, slower oxygen consumption mechanism) result in the overall pressure decrease.

The second gas sample for experiment A-4-1 showed that almost all of the oxygen was consumed. Based on the small pressure change after the first gas sample, it is evident that the backfill gas was primarily helium with little oxygen.

Once again an initial increase in pressure occurs for a wet sample followed by a net pressure decrease and consumption of oxygen. For the corresponding dry sample, there is simply the consumption of oxygen with associated pressure decrease.

4.3 UO_2F_2

Figure 3.6 shows the pressure response for the alpha radiolysis of anhydrous UO_2F_2 (A-5). The pressure decreased to a steady state, at which point a gas sample was taken. The tube was evacuated to about 200 torr and was then backfilled with an oxygen/helium mixture. The pressure then slowly decreased and appears to approach a steady state again. A final gas sample was taken at the termination of experiment A-5. The analysis of the first gas sample from A-5 (Tables 3.4, 3.7, and 3.8) shows that a small amount of oxygen was consumed. The second gas sample (Table 3.4) showed consumption of the added oxygen. Neither HF nor fluorine was reported. Note that production of these corrosive species was a concern for the long-term storage of uranium oxides containing fluoride impurities.[3,5] The fact that none were found further demonstrates that these concerns were unwarranted.

The pressure response for the alpha radiolysis of $UO_2F_2 \bullet 1.7H_2O$ (A-6) presented in Figure 3.7 again exhibits an initial pressure increase followed by an overall pressure decrease similar to that for the other wet oxides. The gas analysis of the sample taken at the end of the experiment (Tables 3.4, 3.7, and 3.8) shows that oxygen was consumed while CO_2 and hydrogen were produced. Neither fluorine nor HF was seen in the gas analyses. The results for the alpha irradiation of UO_2F_2 are in sharp contrast to those seen for gamma irradiation,[3,5] where oxygen was found to be released from the UO_2F_2 matrix. Therefore, the type of radiation (alpha vs gamma) appears to play a significant role in the net radiolytic effect. Additionally, as shown in Ref. 3, the source of some of the hydrogen for moist UO_2F_2 was corrosion of the sample container. In a similar fashion, corrosion may also play some role in the production of hydrogen in the alpha radiolysis experiments.

4.4 X-RAY DIFFRACTION

The appearance of CO_2 in each of the samples might appear anomalous were it not for the realization that carbon is almost always present in sample preparations and yet goes undetected. When there is a source of oxygen and some means to oxidize the carbon (through elevated temperature or radiolysis), the carbon will combine with the oxygen and appear as CO_2. However, the amount of CO_2 is insufficient to account for all of the loss of oxygen seen in these experiments. Therefore, another mechanism for oxygen consumption must be present.

One such mechanism is through the oxidation of the uranium compound itself. Even in the radiation environment, this process would occur at a much slower rate since it is a gas–solid reaction and requires the diffusion of oxygen within the crystalline lattice. In order to establish such a mechanism, the XRD analyses were performed in a effort to identify a higher oxidation state of the uranium itself or an oxidized form of the uranium oxide compound.

Some additional lines were identified as a result of the XRD analysis. These, however, were insufficient to clearly establish oxidation in the current cases. Nevertheless, by comparison of these results with similar observations in the literature, it is apparent that the U_3O_8 form is oxidized to UO_3 while the UO_3 hydrate form is converted to a uranium peroxide. The production of uranium peroxide is most likely to occur in the wet samples where the hydroxyl radical is produced.

The line at 2θ of 5.48 for the irradiated U_3O_8 sample is typical of that for numerous uranyl oxide hydrates, namely the mono- and dihydrates.[12–14] Except for the line at 17.57, an insufficient number of additional lines exist to clearly identify this new crystalline phase by XRD. However, the data do indicate that the effect of radiation was to generate a new crystalline phase with the major XRD line that is consistent with a uranium oxide of higher oxidation state.

In a similar vein, the appearance of new lines after irradiation of wetted UO_3 indicates that it, too, has undergone some phase change as a result of alpha irradiation. In view of the consumption of oxygen (seen from the pressure decrease and gas analyses), we would suggest that some oxidation of the UO_3 has also occurred. Higher oxidation states than VI for uranium are not known, but peroxide forms of uranyl such as studtite and metastudtite have been reported in the literature.[15–17] These particular crystalline materials would have the formulae of $UO_3 \bullet H_2O_2 \bullet xH_2O$ (where x is either 2 or 4, corresponding to metastudtite and studtite, respectively) and are sometimes written as $UO_4 \bullet xH_2O$. The most intense lines in the XRD patterns for these studtites would be at 2θ values (MoKα radiation) of 7.94. Unfortunately, this line would appear on top of the strong line for anhydrous UO_3 at 8.03, thus precluding any firm evidence for the appearance of the peroxide form. However, by comparison with the U_3O_8 material, it would be consistent to interpret these results as suggesting that the UO_3 has undergone similar oxidation to form a crystalline peroxide species of U(VI).

Such oxidation has already been reported in the literature for much higher alpha irradiation fluxes from a cyclotron.[18] In this study, a UO_2 target in contact with leachant water was irradiated with alpha particles with fluxes up to 3.3×10^{11} α cm^{-2} s^{-1} . Post-irradiation examination of the UO_2 surface that had been in contact with the leachant water revealed the presence of extra lines attributed to metastudtite (i.e., hydrated uranium peroxide). In our case, the alpha flux at the surface of the particles of surface area = ~1 m^2/g is 7.5×10^6 α cm^{-2} s^{-1}. However, the exposure time in our experiments was of the order of 1 year compared with the 1-h exposure in the previous cyclotron experiment. The overall dose in our experiments is then up to 10 times less than that of the previous work.

While our results were consistent with those obtained in the previous work, it is not surprising that XRD lines of sufficient intensity were not obtained for definitive conclusions. Nevertheless, the formation of a uranium peroxide in the alpha irradiation of wet UO_3 is a plausible explanation for the results obtained. Furthermore, other authors have recently suggested that peroxide, formed by radiolysis, is incorporated into the uranium oxide matrix to form either studtite or metastudtite.[19]

Insufficient data were available to suggest an identity of the phase producing extra lines found as a result of the dry U_3O_8 radiolysis experiment. The conversion of the dry UO_3 to amorphous material suggests a phenomenon like that seen for other crystalline oxides[20] exposed to the effects of alpha irradiation. Such a metamict form is yet another possible result of irradiation and probably dependent on the absence of water in the sample.

4.5 SUMMARY

The overall mechanism observed in all of these oxide radiolysis experiments is one of several competing reactions. First, nitrate (if present) and water are radiolyzed to some extent at relatively rapid rates. These initial reactions account for the pressure spike in the wet and/or nitrate-containing samples. The water radiolysis, however, reaches a point at which back reactions of the radiolytic products, hydrogen and oxygen, reform the water by well-established radiolytic back-reaction mechanisms.[21,22] Occurring at a much slower rate is the consumption of oxygen through the uranium oxide oxidation process, producing the oxidized forms identified by other researchers and indicated here.

The alpha radiolysis of uranium oxides can be described in general for wet oxides as a modest pressure rise due to the water radiolysis followed by a net pressure decrease due to the oxidation of the uranium oxide form. If the oxide is dry, no initial pressure rise occurs. Only a steady decrease of the pressure (assuming oxygen is present) is noted as the uranium oxide is further oxidized.

The net result of this overall mechanism is that the pressure over these uranium oxides reaches a steady-state value, where the consumption of the radiolysis products is matched by their production. Except for the case in which there is a high level of residual nitrates, this steady-state pressure is unusually low—and, in many cases, less than the initial pressure of the system.* Furthermore, the concentration of hydrogen is negligible due to its recombination. Consequently, with the occurrence of numerous back reactions, there is no opportunity for the accumulation of hydrogen, or the overall pressure of the system, to build to intolerable limits.

---

* It is evident that efforts to remove nitrates by thermal decomposition are important. The production of U_3O_8 at reasonably high temperatures (400–600ºC) will eliminate nitrates.

An interesting comparison can be drawn by considering the maximum hydrogen pressure that could be achieved by radiolyzing all of the available water and the actual measured hydrogen pressure. The former, of course, is the conservative approach taken in storage standards. For example, total decomposition of all available water for sample A-2-1 would result in a hydrogen pressure of about 53,000 torr (~1000 psi). The total measured pressure for A-2-1 at steady state was about 4600 torr—a pressure increase due to nitrogen production (Table 3.2). Significantly, the hydrogen contribution to this pressure was only a small fraction (~0.24%) of the total pressure. Similar comparisons can be made for the U_3O_8 (A-4-1) and $UO_2F_2 \bullet 1.7H_2O$ (A-6), where total decomposition of the water would result in hydrogen pressures of about 10,000 torr (200 psi) and 45,000 torr (870 psi), respectively. Therefore, it is obvious from the experimental results that high pressures are not reached. In fact, both of these experiments exhibited a net pressure decrease, indicating that back reactions clearly play a strong role in limiting (or eliminating) the pressure increase from radiolysis.

5. CONCLUSIONS

The alpha radiolysis of uranium oxides has shown that several competing reactions are caused by the radioactive environment. These combine to produce pressure changes in closed containers holding these oxides that depend on the constituents in the atmosphere over the oxides and the presence of water or other impurities on the sample. However, none of these reactions produce excessively high pressures as predicted by the pedestrian assumption that any water associated with the samples will be converted entirely to hydrogen and oxygen. Instead, a steady-state pressure is reached at which back reactions quickly limit the accumulation of reaction products in the gas phase. Hydrogen is especially low as a result of radiolysis. Some oxidation of these oxides is possible if oxygen and/or hydroxyl radicals are present. Nevertheless, this oxidation process tends to function as yet another limiting "back reaction" to prevent the occurrence of excessive pressures in the system.

These results, combined with those from the earlier gamma radiolysis experiments, form the basis for resolving technical issues regarding the safe, long-term storage of these oxides and show that extraordinary measures are not required to remove all traces of moisture from the oxide.

ACKNOWLEDGMENTS

We are grateful to Dr. R. G. Haire of ORNL for the performance of the XRD analysis and his helpful advice. We also acknowledge the highly skilled assistance of C. E. Porter, R. D. Vandergrift, and L. K. Felker in the preparation and conduct of the experiments.

REFERENCES

1. *Criteria for Preparing and Packaging Plutonium Metals and Oxides for Long-term Storage*, DOE-STD-3013, U.S. Department of Energy, Washington, D.C.

2. *Criteria for Packaging and Storing Uranium-233-Bearing Materials*, DOE-STD-3028-2000, U.S. Department of Energy, Washington, D.C.

3. A. S. Icenhour, L. M. Toth, G. D. Del Cul, and L. F. Miller, "Gamma Radiolysis Studies of Uranyl Fluoride," *Radiochim. Acta* **90** (2), 109–22 (2002).

4. A. S. Icenhour, L. M. Toth, and H. Luo, *Water Sorption and Radiolysis Studies for Uranium Oxides*, ORNL/TM-2001/59, Oak Ridge National Laboratory, Oak Ridge, Tennessee, February 2002.

5. A. S. Icenhour and L. M. Toth, *A Gamma Radiolysis Study of $UO_2F_2 \cdot 0.4H_2O$ Using Spent Nuclear Fuel Elements from the High Flux Isotope Reactor*, ORNL/TM-2001/138, Oak Ridge National Laboratory, Oak Ridge, Tennessee, January 2002.

6. R. R. Livingston, *Gas Generation Test Support for Transportation and Storage of Plutonium Residue Materials*, WSRC-TR-99-00223, Westinghouse Savannah River Company, Savannah River Site, Aiken, South Carolina, August 1999.

7. R. R. Livingston and J. M. Duffey, *Effects of Plutonium Dioxide Moisture Content and Calcination Temperature on the Headspace Gas Composition of Sealed Containers*, WSRC-TR-2001-00420, Westinghouse Savannah River Company, Savannah River Site, Aiken, South Carolina, September 2001.

8. G. Bailey et al., *Gas Generation from Actinide Oxide Materials*, LA-13781-MS, Los Alamos National Laboratory, Los Alamos, New Mexico, December 2000.

9. *CRC Handbook of Chemistry and Physics*, 73rd ed., D. R. Lide, ed., CRC Press, Boca Raton, Florida, 1992.

10. S. Siegel, "The Crystal Structure of Trigonal U_3O_8,"*Acta Crystallogr.* **8**, 617–19 (1955).

11. K. Aykan and A. W. Sleight, "Characterization of Mixed Uranium Antimony Oxides $USbO_5$ and USb_3O_{10}," *J. Am. Ceram. Soc.* **53**, 427–31 (1970).

12. J. K. Dawson, E. Wait, K. Alcock, and D. R. Chilton, "Some Aspects of the System Uranium Trioxide–Water," *J. Chem. Soc.* **Part III**, 3531–40 (1956)

13. C. A. Wamser, J. Belle, E. Bernsohn, and B. Williamson, "The Constitution of the Uranates of Sodium," *J. Am. Chem. Soc.* **74**, 1020–22 (1952).

14. H. Dunn, *X-Ray Diffraction Data for Some Uranium Compounds*, ORNL-2092, Oak Ridge National Laboratory, Oak Ridge, Tennessee, August 1956

15. K. Walenta, "On Studtite and its Composition," *Am. Mineral.*, **59**, 166–71 (1974).

16. M. Deliens and P. Piret, "Metastudtite, $UO_4 \bullet 2H_2O$, a New Mineral from Shinkolobwe, Shaba, Zaire," *Am. Mineral.*, **68**, 456–58 (1983).

17. P. C. Debets, "X-ray Diffraction Data on Hydrated Uranium Peroxide," *J. Inorg. Nucl. Chem.*, **25**, 727–30 (1963).

18. G. Sattonnay et al., "Alpha-radiolysis Effects on UO_2 Alteration in Water," *J. Nucl. Mater.* **288**, 11–19 (2001).

19. P. C. Burns and K. Hughes, "Studtite $[(UO_2)(O_2)(H_2O)_2](H_2O)_2$: The First Structure of a Peroxide Mineral," *Am. Mineral*, **88**, 1165–68 (2003).

20. Hj. Matzke, "Radiation Damage in Crystalline Insulators, Oxides, and Ceramic Nuclear Fuels," *Radiat. Eff.* **64**, 3–33 (1982).

21. C. J. Hochanadel, "Effects of Cobalt Gamma-Radiation on Water and Aqueous Solutions," *J. Phys. Chem.* **56**(5), 587–94 (1952).

22. A. O. Allen, C. J. Hochanadel, J. A. Ghormley, and T. W. Davis, "Decomposition of Water and Aqueous Solutions Under Mixed Fast Neutron and Gamma Radiation," *J. Phys. Chem.* **56**(5), 575–86 (1952).

INTERNAL DISTRIBUTION

1. J. M. Begovich
2. P. J. Bereolos
3. W. D. Bond
4. T. B. Conley
5. G. D. Del Cul
6. D. Foster
7. J. N. Herndon
8. D. J. Hill
9–19. A. S. Icenhour
20. A. M. Krichinsky
21. S. C. Marschman
22. P. E. Osborne
23. F. J. Peretz
24. J. E. Rushton
25. D. W. Simmons
26–30. L. M. Toth
31. L. D. Trowbridge
32. R. M. Wham
33. D. F. Williams
34. ORNL OTIC–RC
35. NSTD DMC

EXTERNAL DISTRIBUTION

36. N. M. Askew, U.S. Department of Energy, Savannah River Site Operations Office, WSRC, Bldg. 773-A, Road 1A, Aiken, SC 29801
37. L. F. Blankner, U.S. Department of Energy, Oak Ridge Operations Office, Oak Ridge National Laboratory, UT-Battelle, Bethel Valley Road, Oak Ridge, TN 37831-6269
38. H. E. Clark, U.S. Department of Energy, Oak Ridge Operations Office, Oak Ridge National Laboratory, UT-Battelle, Bethel Valley Road, Oak Ridge, TN 37831-6269
39. C. H. Delegard, Pacific Northwest National Laboratory, 902 Battelle Blvd., P.O. Box 999, Richland, WA 99352
40. J. M. Duffey, U.S. Department of Energy, Savannah River Site Operations Office, WSRC, Bldg. 773-A, Road 1A, Aiken, SC 29801
41. P. G. Eller, U.S. Department of Energy, Los Alamos National Laboratory, P.O. Box 1663, Los Alamos, NM 87545
42. H. C. Johnson, U.S. Department of Energy, Headquarters, EM-21, Forrestal Bldg., 1000 Independence Ave. S.W., Washington, D.C. 20585
43. R. R. Livingston, U.S. Department of Energy, Savannah River Site Operations Office, WSRC, Bldg. 773-A, Road 1A, Aiken, SC 29801
44. R. E. Mason, U.S. Department of Energy, Los Alamos National Laboratory, P.O. Box 1663, Los Alamos, NM, 87545
45. L. Morales, U.S. Department of Energy, Los Alamos National Laboratory, P.O. Box 1663, Los Alamos, NM, 87545
46. M. T. Paffett, U.S. Department of Energy, Los Alamos National Laboratory, P.O. Box 1663, Los Alamos, NM, 87545
47. G. D. Roberson, U.S. Department of Energy, Albuquerque Operations Office, Bldg. 382-2, AL, Pennsylvania and H Street, Kirkland Air Force Base, Albuquerque, NM 87116
48. L. A. Worl, U.S. Department of Energy, Los Alamos National Laboratory, P.O. Box 1663, Los Alamos, NM 87545

THIS PAGE INTENTIONALLY LEFT BLANK.

WSRC-TR-2007-00200

Keywords: Radiolysis,
Hydrogen

Evaluation of Radiolysis-Induced Hydrogen Generation in DOT 6M Drums from INTEC

Savannah River National Laboratory
Materials Science and Technology

Publication Date: June 2007

Washington Savannah River Company
Savannah River Site
Aiken, SC 29808

This document was prepared in connection with work done under Contract No. DE-AC09-96SR18500 with the U. S. Department of Energy

DISCLAIMER

This report was prepared as an account of work sponsored by an agency of the United States Government. Neither the United States Government nor any agency thereof, nor any of their employees, makes any warranty, express or implied, or assumes any legal liability or responsibility for the accuracy, completeness, or usefulness of any information, apparatus, product, or process disclosed, or represents that its use would not infringe privately owned rights. Reference herein to any specific commercial product, process, or service by trade name, trademark, manufacturer, or otherwise does not necessarily constitute or imply its endorsement, recommendation, or favoring by the United States Government or any agency thereof. The views and opinions of authors expressed herein do not necessarily state or reflect those of the United States Government or any agency thereof.

DOCUMENT: **WSRC-TR-2007-00200**

TITLE: **Evaluation of Radiolysis-Induced Hydrogen Generation in DOT 6M Drums from INTEC**

APPROVALS

_____ **Date:** _____
D. W. Vinson, Author
SRNL-Materials Science and Technology

_____ **Date:** _____
N. E. Bibler, Technical Review
SRNL-Process Science and Engineering Section

_____ **Date:** _____
N. M. Askew, Technical Review
SRNL-Actinide Sciences Programs

_____ **Date:** _____
R. L. Sindelar, Manager
SRNL-Materials Science and Technology

_____ **Date:** _____
N. C. Iyer, Director
SRNL-Materials Science and Technology

_____ **Date:** _____
J. Bodkin, Customer
SFP-SFP Operations Engineering

_____ **Date:** _____
T. J. Spieker, Manager
SFP-SFP Operations Engineering

_____ **Date:** _____
R. W. Watkins
HMD-HB-Line Ph II Engineering

Table of Contents

Table of Contents ..... *iv*

List of Tables ..... *v*

List of Figures ..... *v*

1.0 Executive Summary *1*

2.0 Introduction *1*

3.0 Materials Description *1*

4.0 Calculational Approach and Methodology *5*

4.1 List of Assumptions **6**

4.2 Determination of the Absorbed Alpha Energy **8**

4.2.1 Total Alpha Energy Production 8

4.2.2 Parametric Evaluation of Fraction of Total Alpha Energy Absorbed by Bottle in Drums #3031 & #3598 9

4.2.3 Final Estimation of Hydrogen Generation in Drums #3031 & #3598 11

4.2.4 Hydrogen Production in DOT 6M drum #20102 13

5.0 Conclusions *13*

6.0 Reference *14*

List of Tables

Table 1 *Summary of the Uranium-Fissium Debris Contained in Three DOT 6M 30-gallon Drums* 5
Table 2 *Summary Table of Calculations for Power Density Determination*- 8
Table 3 *Summary Table of Calculations for Maximum Total Energy Generation due to Alpha Decay of Isotopes in HCL-1 and HCL-2 and 114/133 SAL* 9
Table 4 *Summary Table of Hydrogen Generation, Pressure Increase, and Concentration Results* 13
Table 5 *Summary Table of Results* 14

List of Figures

Figure 1 *Photograph of the recovered metallic pieces recovered from ICPP HCL.* 2
Figure 2 *Schematic representation of the packaging configuration for DOT 6M 30-gallon drums #3031 (Left) and #3598 (Right).* 3
Figure 3 *Schematic representation of the packaging configuration for DOT 6M 30-gallon drum #20102.* 4
Figure 4 *Photograph of the crimp-sealed tin can (114/133 SAL) that is stored in a 2R container within the DOT 6M 30-gallon drum #20102.* 5
Figure 5 *Schematic of the model used to determine fraction of alpha energy deposited in HDPE bottles in drum #3031, can HCL-1 and #3598, can HCL-2.* 10
Figure 6 *Hydrogen production rate as a function of modeled source density for drum #3031, can HCL-1.* 11
Figure 7 *Hydrogen production rate as a function of modeled source density for drum #3598, can HCL-2.* 12

1.0 EXECUTIVE SUMMARY

Three DOT 6M 30-gallon drums are scheduled to be shipped from the Idaho Nuclear Technology Engineering Center (INTEC) at the Idaho National Laboratory (INL) to L-Area at the Savannah River Site (SRS). These three drums contain radioactive materials that resulted from the material recovery effort following a small explosion that had occurred in the Idaho Chemical Processing Plant (ICPP) hot chemistry laboratory (HCL). In support of the shipment and subsequent storage of the three DOT 6M drums, an evaluation of the potential for molecular hydrogen production in the drums has been completed and documented herein. The potential sources of hydrogen evaluated in the current report include radiolytic decomposition of polymeric materials in the DOT 6M drums #3031 and #3598 and the radiolytic decomposition of water in drum #20102. No other potential sources have been identified based upon reported drum contents and packaging configuration.[1-2]

A parametric approach was used to evaluate the maximum quantity of molecular hydrogen that can be expected to evolve in two DOT 6M 30-gallon drums in support of receipt and subsequent interim storage prior to canyon processing. These drums are two of three drums scheduled for shipment from INTEC to SRS as part of the decommissioning effort of the INTEC facility. The three DOT 6M drums will be received at L-Area in SRS and stored for up to 13-years prior to final disposition at HB-Line in 2020. Results of the current analysis do not include parametric analysis of drum #20102 containing 114/133 SAL (salvage) which contains UO_3 powder. This drum has not been identified as containing polymeric materials and a conservative calculation indicates that the maximum gross molecular hydrogen production due to the radiolysis of adsorbed moisture would yield a production rate of 5.1-cm^3/yr, driven primarily by the large surface are to volume ratio of the oxide powder. The remaining two drums, #3031 and #3598 contain polymer bags and/or bottles that will be subject to radiolytically induced hydrogen gas generation due to decomposition of the polymers. Conservative values for hydrogen gas generation rates and rates of pressure increase within the drums have been determined based upon a number of inputs and assumptions. The results are that hydrogen will be produced at a rate of 1.93-cm^3/yr and 1.50-cm^3/yr, respectively for drums #3031 and #3598. Projected molecular hydrogen concentrations at 2020 have been calculated to remain below the lower flammability limit of 4% molecular hydrogen by volume in air.

2.0 INTRODUCTION

Three DOT 6M 30-gallon drums are planned to be shipped from the Idaho Nuclear Technology Engineering Center (INTEC) at the Idaho National Laboratory (INL) to L-Area at the Savannah River Site (SRS). These three drums contain radioactive materials that resulted from the material recovery effort following a small explosion that had occurred in the Idaho Chemical Processing Plant (ICPP) hot chemistry laboratory (HCL). The three DOT 6M drums would be received at L-Area in SRS and stored for up to 13-years prior to final disposition at HB-Line by 2020. In support of the shipment and subsequent storage of the three DOT 6M drums, an evaluation of the potential for molecular hydrogen production in the drums due to the radiolytic decomposition of the polymer bottles in drums #3031 and #3598 and due to radiolytic decomposition of water reported in drum #202102 has been completed and documented herein.

3.0 MATERIALS DESCRIPTION

Three DOT 6M 30-gallon drums are planned to be shipped from the Idaho Nuclear Technology Engineering Center to the Savannah River Site. The debris in each drum has been carefully characterized by personnel at the ICPP HCL.[3] Two of the three DOT 6M 30-gallon drums from INTEC, #3031 and #3598, contain a variety of materials that are characterized as quarter circles, pins, pellets, foils, wires, chips, turnings, and small filings/specks. The two largest pieces that are roughly shaped as quarter circles with a 5-cm radius and that are two centimeters thick are contained in drum #3598. They are

characterized as 4.5 wt % uranium fissium alloy which are contaminated with ^{239}Pu (200-400 ppm).[2] These two pieces are located in areas 7 and 14 of Figure 1. Figure 2 provides a graphical depiction of loading of the two 30 gallon DOT 6M drums. In drum #3598, the two quarter circles are each within a low-density polyethylene bag and the two bags within a 500-ml high-density polyethylene (HDPE) bottle. The HDPE bottle is closed with a screw cap and placed within a crimp-sealed tin can, HCL-2, that is placed inside the sealed 2R container within the DOT 6M 30-gallon drum. The can contains 1,190 grams of total uranium of which 617 grams are ^{235}U.

Drum #3031 contains the remaining metallic pieces shown in the photograph of Figure 1. These pieces are counted as 45 pins, 19 pellets, 7 foils, 4 wires, 3 chips, 131 turnings, and 1083 small filings/specks. These pieces are contained within a 500-ml HDPE bottle that is contained in a crimp-sealed tin can, HCL-1 that is sealed in the 2R container within the DOT 6M 30-gallon drum (see Figure 2). All of the pellets and chips and a majority of pins, foils, and small filing/specks are described as uranium fissium alloy low in zirconium. The uranium fissium alloy is 3.5 or 4.5 wt % fissium. The remaining material in this can consists of a small number of pins, foils, and small filing/specks that consist of a uranium alloy high in zirconium. Also stored in the can as foils, wires, turning, wire, and small filings/specks is a small quantity (gram amounts) of metal: Inconel, stainless steel (304), thorium, and nickel alloy. The material is contaminated with ^{239}Pu (200-400 ppm). The can, HCL-1, contains 290 grams of total uranium of which 255 grams are ^{235}U.

The third DOT 6M 30-gallon drum is labeled #20102 and contains material described as soil samples. The soil sample material is characterized as UO_3 granular powder, a high-grade uranium oxide product obtained from reprocessing fuel and scrap material at INTEC.[1] The material is comprised of 29 grams of total uranium, of which 26 grams are ^{235}U. In addition, this drum is reported to contain 0.45-g of water due to the hygroscopic nature of the uranium-oxide. This material is contained within the crimp sealed tin can 114/133 SAL shown in Figure 4 that is within the 2R inside the DOT 6M 30-gallon drum as depicted in Figure 3.

Figure 1 Photograph of the recovered metallic pieces recovered from ICPP HCL.

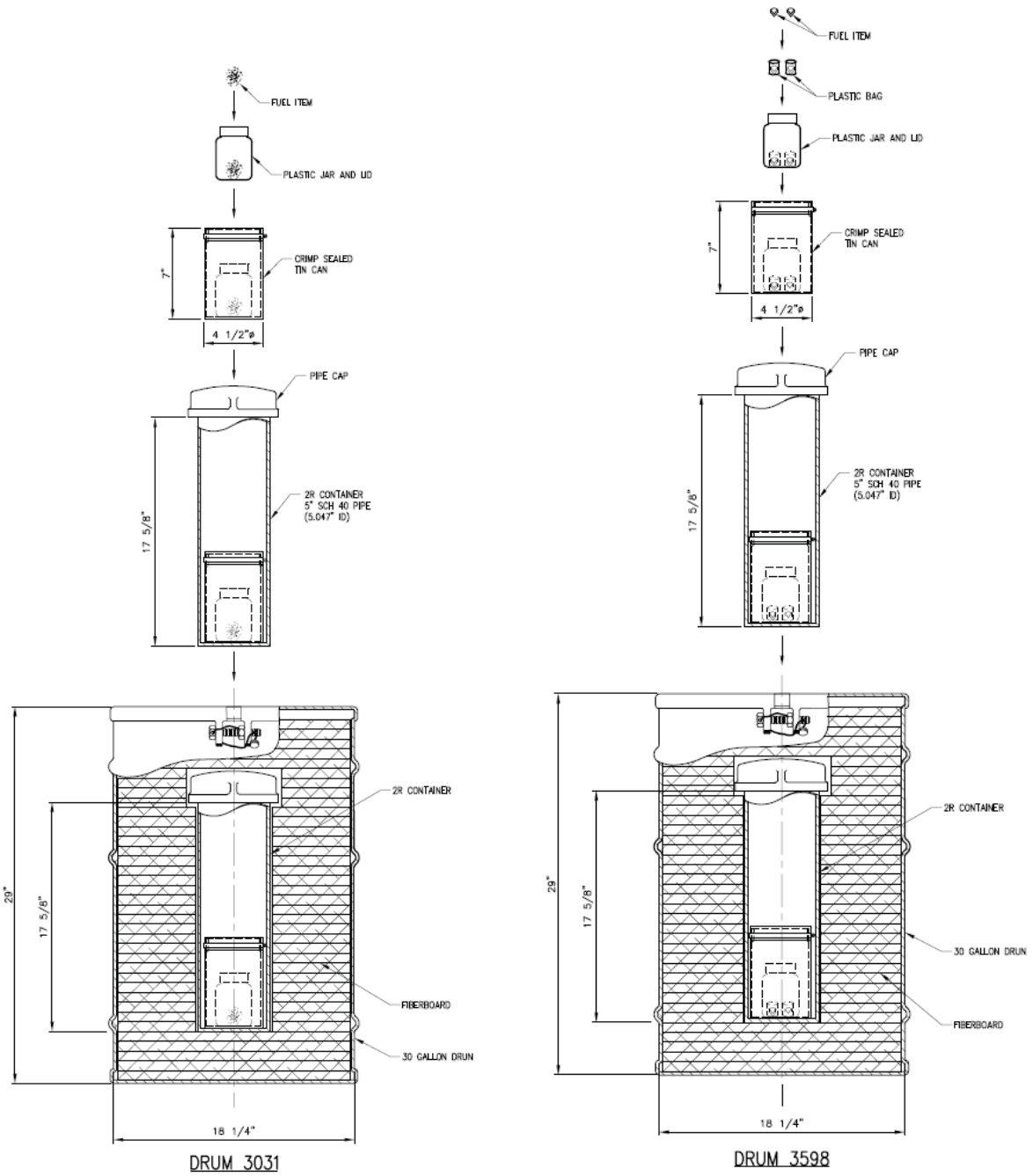

Figure 2 Schematic representation of the packaging configuration for DOT 6M 30-gallon drums #3031 (Left) and #3598 (Right).

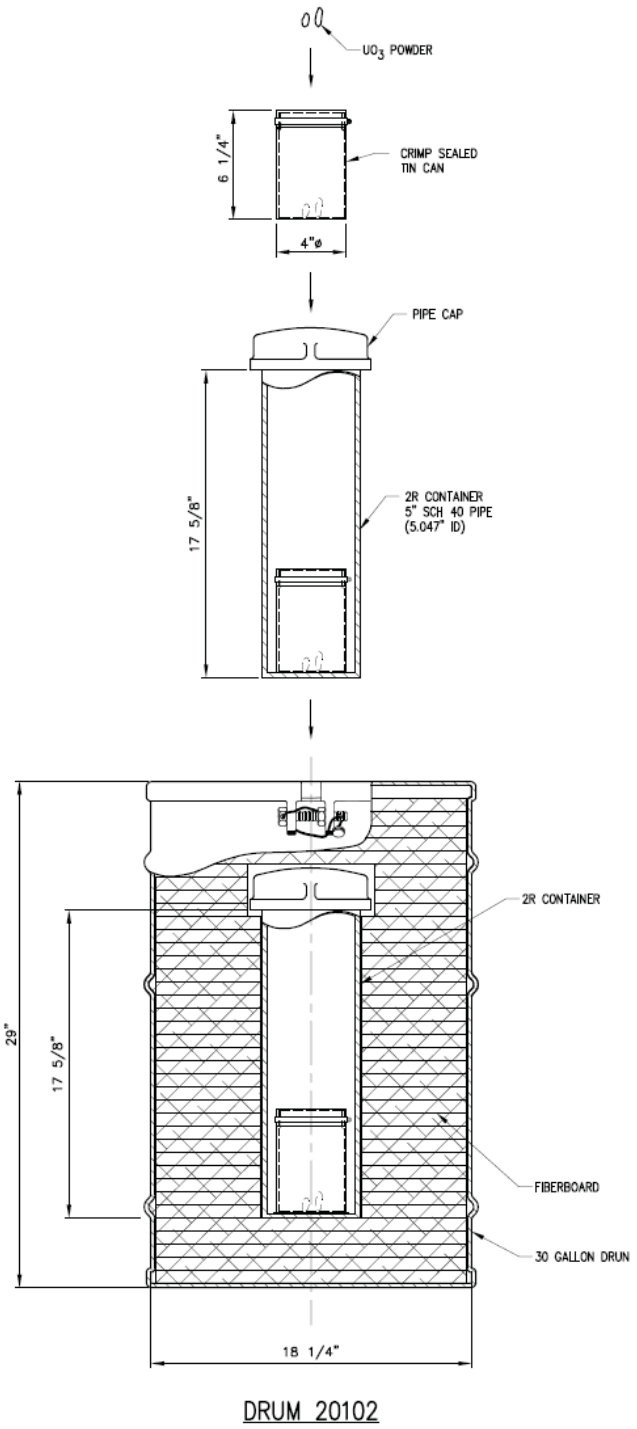

Figure 3 Schematic representation of the packaging configuration for DOT 6M 30-gallon drum #20102.

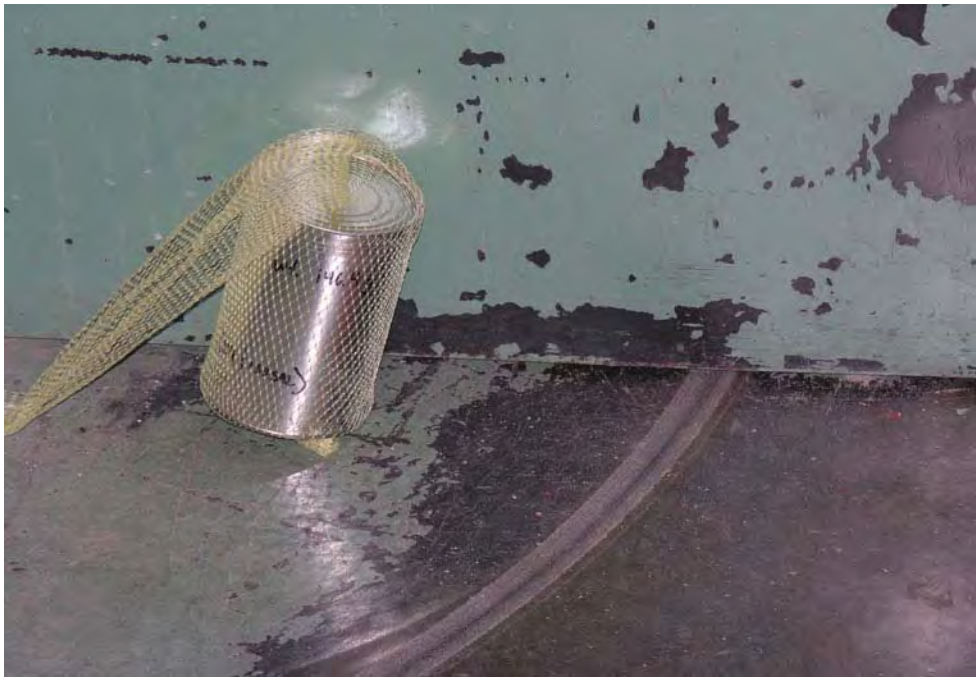

Figure 4 Photograph of the crimp-sealed tin can (114/133 SAL) that is stored in a 2R container within the DOT 6M 30-gallon drum #20102.

Table 1 Summary of the Uranium-Fissium Debris Contained in Three DOT 6M 30-gallon Drums

Can/Drum	Description	Form	Total U (g)	Total Pu (g)
HCL-1 #3031	Uranium-Fissium (3.5-4.5%)	45 pins, 19 pellets, 7 foils, 4 wires, 3 chips, 131 turnings, 1083 filings/specks	290	0.12
HCL-2 #3598	Uranium-Fissium (3.5-4.5%)	2 large quarter round chunks	1,190	0.48
114/133 SAL #20102	High-Grade UO_3 Powder	UO_3 Granular Powder	29	0

4.0 CALCULATIONAL APPROACH AND METHODOLOGY

The potential sources of hydrogen evaluated in the current report include radiolytic decomposition of polymeric materials in the DOT 6M drums #3031 and #3598 and the radiolytic decomposition of water in drum #20102. No other potential sources have been identified based upon reported drum contents and packaging configuration.[1-2]

Ionizing radiation causes radiolytic decomposition of polymers. The decomposition of polymers lead to the production of molecular hydrogen. The general approach used to develop an estimate of the potential for molecular hydrogen generation due to alpha radiolysis of polymers follows the approached used by Croft Associates for the SAFKEG package[4]. The rate of production of H_2 from decomposition of polymeric material in units of cm^3/sec (V_g) can be generally expressed as:

$$V_g = \left(D \times G \times k \times v / A_n \right) \qquad \text{(Eq. 1)}$$

where:
- D = alpha energy absorbed in the polymer (Watts),
- G = hydrogen gas generation constant (Molecules/MeV)
- k = conversion factor (6.24e12 Mev/J),
- v = volume of 1 mole of gas at STP (2.24e4 cm^3), and
- A_n = Avogadro's number (6.022e23 molecules).

For the current work, the alpha energy absorbed in the polymer, D, and the value of the hydrogen gas generation constant, G, are the two unknowns in Eq. 1. For the determination of D, it is necessary to determine the range of alpha particles in the various materials. The energy and material dependant range of an alpha particle in cm (R) is determined by the equation:[5-6]

$$R = 2.3 \times 10^{-4} \left(\frac{\sqrt{M}}{\rho} \right) \left(1.24 E_\alpha - 2.62 \right) \qquad \text{(Eq. 2)}$$

where:
- M = molecular weight of the medium (AMU),
- ρ = density of the medium (g/cm^3), and
- E_α = average alpha energy(MeV).

For the current work, the molecular weight and density of the medium and the average alpha energy are the three unknowns in Eq. 2. Having determined the volume of molecular hydrogen produced using Eq. 1, it is then possible to determine the pressure rise within the package as a function of time ($P_r(t)$) by the equation:[4]

$$P_r(t) = \left(P_a \times V_g \times t / V_c \right) \qquad \text{(Eq. 3)}$$

where:
- P_a = ambient pressure (1.0 bar abs),
- t = time (secs), and
- V_c = free volume of container (cm^3).

For the current work, the time, t, and free volume of the container, V_c are the two unknowns in Eq. 3. The next section of the report addresses the assumptions, methodology, and calculations used to develop a conservative estimate of the expected molecular hydrogen production due to the contents of the drums as described in the previous section.

4.1 List of Assumptions

1. The value of the hydrogen gas generation constant (G-value) is assumed equal 3.5 molecules/100 eV or 3.5×10^4 molecules/MeV. This value of G is taken from Reference 7 as the highest reported production rate for all polymers due to radiolytic decomposition by

incident alpha radiation. This assumption is conservative because no credit is taken for the dose dependent nature of radiation damage in the polymer. Increasing the dose absorbed by a polymer will decrease the effective G-value for hydrogen production due to the depletion of the matrix in the vicinity of the alpha-emitting radioactive source particle. Dose dependent G values are reported as less than 1/5th the value assumed in the current analysis.[8]

2. The value used for the molecular weight of the material in the HDPE bottles is 242-g/mole. This number is consistent with that of plutonium. This number bounds the actual effective molecular weight of the contents of the drums, since the contents include fissium elements whose weights are generally less than 100. This assumption is conservative as alpha range increases as the square-root of the molecular weight (see Eq. 2).
3. The bottle is modeled as a right-circular cylinder with a 4-cm radius and a height of 14.2-cm. This assumption is conservative as the surface area of the modeled ~700-ml bottle is greater than that of the expected 500-ml bottle actually used.
4. It is assumed that the materials in drums #3031 and #3598 are essentially dry. Unlike the materials in drum #20102, this material is not hygroscopic in nature and water content in these drums would be mostly limited to humidity in the facility. Radiolysis of bulk water in these two drums will not provide significant molecular hydrogen production relative to the production estimated for the production due to polymeric radiolytic decomposition. The short range of the alpha particles, the conservatism introduced by Assumption 1, and the G-value of 1.7×10^4 molecules/MeV[9] for H_2 generation from alpha radiolysis of water support this assumption.
5. The average alpha energy used in Eq. 2 is assumed equal to 5.25-MeV. This value bounds the alpha particles from all isotopes identified as being in the drums per the Appendix A and supporting documentation.
6. It is assumed that the free volume of the 2R containers and the crimp-sealed tin cans in the DOT 6M 30-gallon drums is equal to 90% of their physical volume. This assumption is conservative as the contents of the tin cans are expected to occupy less than 7% of the tin can and less than 3% of the 2R containers.[3] Increasing the free volume of the containers will further decrease the estimated pressure increase with time by Eq. 3.
7. It is assumed that only 50% of the alpha particles that are produced within range of the polymer surface contribute to the energy absorbed by the polymer. This assumption accounts for the fact that an isotropic source would generate 50% of its particles in a direction that takes the particle away from the polymer surface.
8. It is assumed that the methodology employed in the current parametric evaluation of the HDPE bottles whereby the source material is assumed to completely cover the inner surface of bottle with a homogeneous layer of variable density and related alpha particle range dictated by the layer thickness and the total source material available is sound and bounding.
9. It is assumed that the bags are not present in HCL-2. This is conservative because the surface area of source material in contact with the polymer bottle is significantly increased by ignoring the plastic bags based upon the current model.
10. It is assumed that there is no polymeric material in DOT 6M 30-gallon drum #20102. There is no indication of the presence of any polymeric bags or bottles as evidenced by the loading schematic shown in Figure 3.
11. It is assumed that the bottle is not an effective barrier to hydrogen migration for the pressure rise calculations. This is reasonable due to the high permeability of molecular hydrogen through polyethylene.[10] The crimp-sealed tin can is also ignored for pressure rise calculations for the 2R.
12. The start time for hydrogen accumulation calculations for drums #3031 and 3598 is assumed equal to 1992. This is a conservative assumption based upon the date at which the HCL crimp-sealed tin cans were loaded.[3]

13. The start time for the hydrogen accumulation calculations for drum #20102 is assumed equal to 2006.[11]
14. The 0.45-g of water reported for drum #20102[1] is assumed homogeneously mixed with alpha-producing uranium within the drum. That is to say that no credit is taken for the shielding effects of the UO_3 particles themselves in the current calculation. In addition, no credit is taken for recombination or reverse reactions by which molecular hydrogen is consumed to regenerate water molecules. This is a conservative assumption.

4.2 Determination of the Absorbed Alpha Energy

4.2.1 Total Alpha Energy Production

The total production of alpha particles generated in each of the crimp-sealed tin containers is completely dependent upon contents of the tin can. References 3-1 provide a list of the radioactive isotopes and quantities contained in each of the three DOT 6M 30-gallon drums. Tables 2 & 3 provide the alpha decay energy and isotopic content by weight for the three drums. Table 2 shows the calculation to determine the power density for each of the isotopes included in the 6M's. The power density is calculated as the product of the average alpha energy per alpha particle as obtained from the ENDF-VI decay library and the activity density of isotope as obtained from 10CFR71.[12] The total alpha energy generation due to radioactive decay can then be calculated and results are shown in Table 3, where the energy generation by isotope is the product of the power density and the total grams as obtained from the Appendix A documents.[1-2]

Table 2 Summary Table of Calculations for Power Density Determination[12-13]

Isotope	E_α (MeV)	E_α J/α	Activity Density (Ci/g)	Activity Density (Bq/g)	Power Density (Watts/g)
^{234}U	4.8419	7.76×10^{-13}	6.20×10^{-3}	2.29×10^{8}	1.78×10^{-4}
^{235}U	4.4709	7.16×10^{-13}	2.20×10^{-6}	8.14×10^{4}	5.83×10^{-8}
^{236}U	4.5563	7.30×10^{-13}	6.50×10^{-5}	2.41×10^{6}	1.76×10^{-6}
^{238}U	4.2610	6.83×10^{-13}	3.40×10^{-7}	1.26×10^{4}	8.59×10^{-9}
^{239}Pu	5.2375	8.39×10^{-13}	6.20×10^{-2}	2.29×10^{9}	1.92×10^{-3}
^{240}Pu	5.2429	8.40×10^{-13}	2.30×10^{-1}	8.51×10^{9}	7.15×10^{-3}

Table 3 Summary Table of Calculations for Maximum Total Energy Generation due to Alpha Decay of Isotopes in HCL-1 and HCL-2 and 114/133 SAL

Isotope	Composition by Can/Drum†			Power Density (Watts/g)	Energy Generation by Can/Drum		
	HCL-1 #3031 (grams)	HCL-2 #3598 (grams)	114/133 SAL #20102 (grams)		HCL-1 #3031 (Watts)	HCL-2 #3598 (Watts)	114/133 SAL #20102 (Watts)
^{234}U	2.17	6.25	0.22	1.78×10^{-4}	3.86E-04	1.11E-03	3.91E-05
^{235}U	255.00	617.00	26.00	5.83×10^{-8}	1.49E-05	3.60E-05	1.52E-06
^{236}U	0.93	1.09	0.1	1.76×10^{-6}	1.63E-06	1.91E-06	1.76E-07
^{238}U	31.90	565.66	2.68	8.59×10^{-9}	2.74E-07	4.86E-06	2.30E-08
Total U	290.00	1190.00	29.00		4.03E-04	1.15E-03	4.09E-05
^{239}Pu	0.11	0.46	—	1.92×10^{-3}	2.12E-04	8.85E-04	—
^{240}Pu	0.01	0.02	—	7.15×10^{-3}	7.15E-05	1.43E-04	—
Total Pu	0.12	0.48	—		2.83E-04	1.03E-03	—
Aggregate Total Energy Generation					**6.86E-04**	**2.18E-03**	**4.09E-05**

† Taken from Reference 3.

From Tables 2 & 3, it is determined that the total alpha energy production in HCL-1 and HCL-2 is 6.86×10^{-4}-Watts and 2.18×10^{-3}-Watts, respectively. The alpha energy generation rate for drum #20102 is used to determine the maximum molecular hydrogen generation rates in this drum due to the radiolytic decomposition of the water contents of this drum as prescribed in Section 4.2.4. This drum is not considered in the parametric calculations used to determine the maximum molecular hydrogen generation rate due to the radiolytic decomposition of the polymers in the two remaining drums. The approach to the determination of the fraction of alpha energy that contributes to the radiolytic decomposition of polymeric material in the two remaining drums, #3031 and #3598 is described in Section 4.2.2.

4.2.2 Parametric Evaluation of Fraction of Total Alpha Energy Absorbed by Bottle in Drums #3031 & #3598

A parametric approach was used in the evaluation to determine the maximum fraction of the total alpha particle energy that may be absorbed by the HDPE bottle. Figure 5 provides a schematic of the approach whereby the source material is assumed to occupy a homogeneous volume that is in contact with the inner surface of the HDPE bottle. The variables are the radius and height of the void region in the model (see Figure 5). As the radius and height vary as an increasing fraction of the bottle dimensions, the density of the source region is calculated as:

$$\rho_{source} = \frac{290.12 \; or \; 1190.48}{V_{bottle} - V_{void}} \qquad \text{(Eq. 4)}$$

where 290.12 or 1190.48 are used to represent the total source mass in grams in for drum #3031, can HCL-1 and drum #3598, can HCL-2, respectively, V_{bottle} is the total bottle volume of 714-cm^3. For the purpose of this calculation the value of V_{void} can vary from ~0-cm^3 to ~714-cm^3. As the void region increases in volume, the source region volume decreases and the density of the layer on the bottle increases as described in Eq. 4. The values of source region density calculated from Eq. 4 are used in Eq. 2 to determine the alpha range in the homogeneous source material region. The width of the contributing source region is equal to the alpha particle range. The calculated alpha particle range is then used to describe the contributing and noncontributing components of the source regions. The contributing mixture in Figure 5 is the homogeneous source region volume that is within the alpha range of the inner surface of the modeled cylindrical bottle. The total source region volume is the difference between the

bottle volume and the void region volume. The ratio of the contributing mixture volume divided by the total source region volume provides a conservative estimate of the fraction of alpha particle energy that is created within the range of an alpha particle of the surface of the HDPE bottle. This fraction is then applied to the total alpha particle energy in the last row of Table 3 to determine the energy generated by alpha decay in the contributing mixture volume. This total energy is then divided by a factor of 2 to account for the isotropic nature of the source material to result in the total energy that is absorbed in the polymer to generate molecular hydrogen (that is D in Eq. 1).

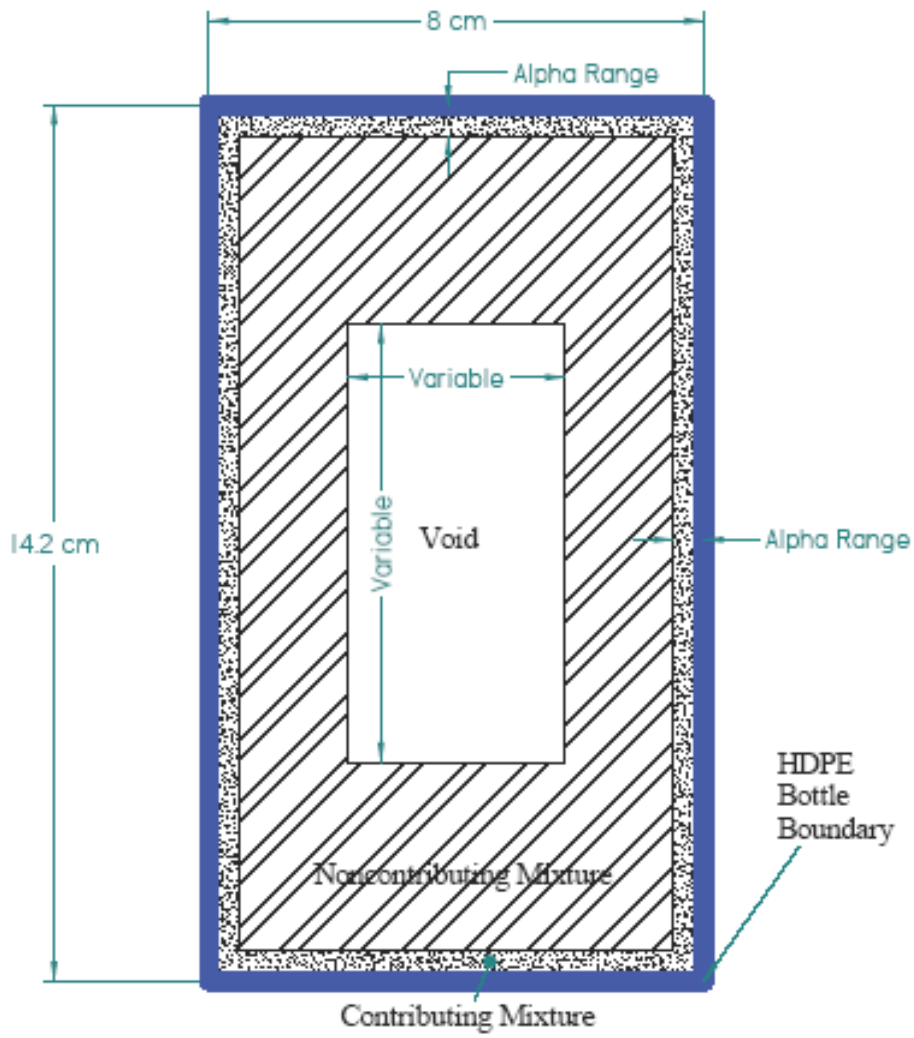

Figure 5 Schematic of the model used to determine fraction of alpha energy deposited in HDPE bottles in drum #3031, can HCL-1 and #3598, can HCL-2.

4.2.3 Final Estimation of Hydrogen Generation in Drums #3031 & #3598

The parametric approach as described in the previous section results in the consideration of hypothetical scenarios by which the modeled densities range from 0.4-g/cm^3 to more than 5000-g/cm^3. While these values are unrealistic, irregular material sizes and shapes and uncertainty in material composition and effective packing efficiency have instigated the current parametric methodology that evaluates all theoretically possible values of material and effective packing density. Although such densities are considered in order to bound analytically all possible material densities, it is expected that the actual material density would not achieve a density larger than that of uranium metal or about 18.9-g/cm^3. The plots of Figures 6 & 7show that the hydrogen production rates for drum #3031, can HCL-1 and drum #3598, can HCL-2 change only slightly as material density is increased above 18.9-g/cm^3. From this figure it is apparent that the maximum production rates are achieved as the material density is increased. This indicates that the shielding effect gained by the increased density of the source material, and decreased alpha particle range, as it is moved closer to the inner surface of the HDPE bottle effectively negates closer proximity of the alpha emitting material to the inner surface of the HDPE bottle.

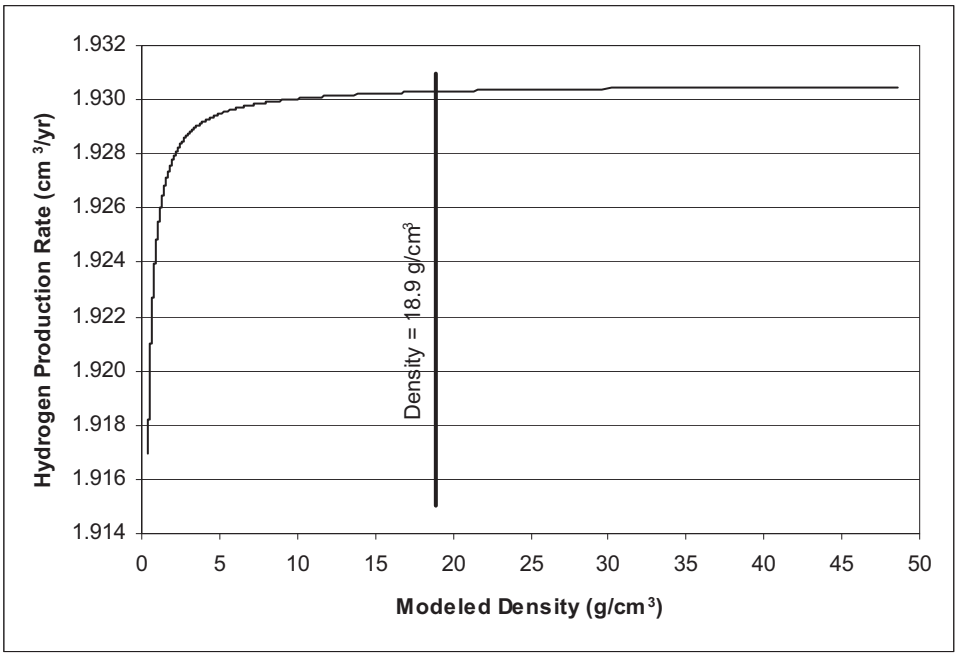

Figure 6 Hydrogen production rate as a function of modeled source density for drum #3031, can HCL-1.

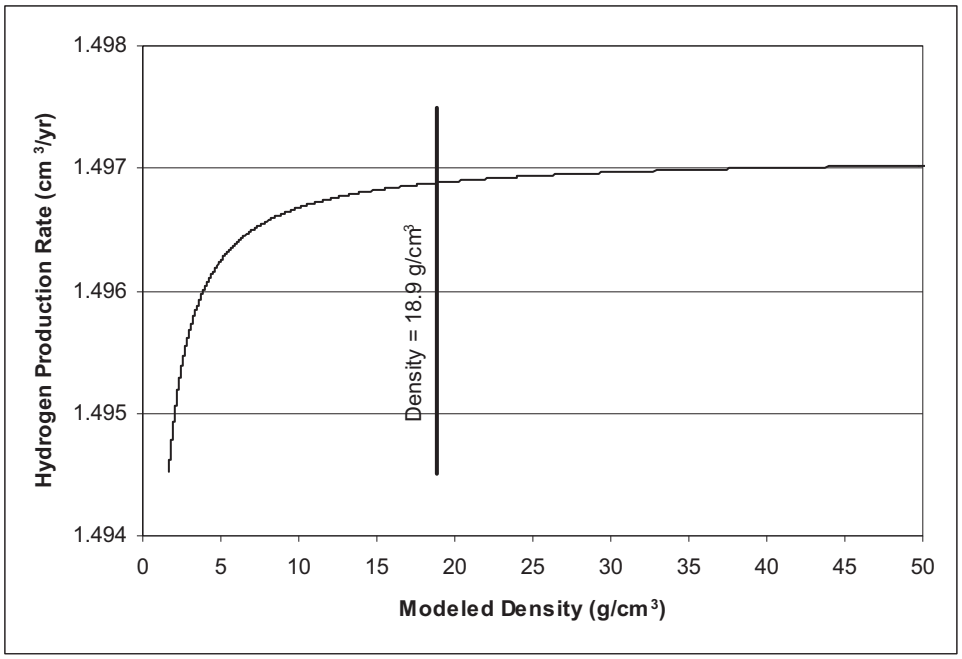

Figure 7 Hydrogen production rate as a function of modeled source density for drum #3598, can HCL-2.

The following calculation provides an illustration of the use of the current methodology in the determination of hydrogen production rate in the DOT 6M 30-gallon drums assuming a density of 18.9-g/cm^3. Based upon assumptions 2 and 5 in Section 4.1 and Eq. 2, the range of a 5.25 MeV alpha particle in source material contained within the HDPE bottle would be calculated as 7.36-µm. The assumed density of 18.9-g/cm^3 requires that the total mixture volume (that is the sum of the contributing and noncontributing volumes in Figure 5) equal 15.35-cm^3 and 62.99-cm^3, for drum #3031, can HCL-1 and drum #3598, can HCL-2, respectively. These values are determined as the material mass provided in Tables 1 & 3 divided by 18.9-g/cm^3. The contributing volume illustrated in Figure 5 is determined with the aid of assumption 3 for HDPE dimensions and the calculated alpha particle range of 7.36-µm. Based upon the dimensions provided in assumption 3, that is a 4-cm radius and a height of 14.2-cm, the total volume of the bottle is 713.76-cm^3. The material of density 18.9-g/cm^3 would occupy a space that is outside the cylinder whose radius is (4 - 0.000736)-cm and whose height is (14.2 – 2(0.000736))-cm. The volume of this bounding cylinder is determined to be 713.43-cm^3. The difference of the two volumes is the contributing volume of Figure 5 and is calculated to be 0.33-cm^3. A simple ratio of ½ of the contributing volume to the total mixture volume determines the fraction of generated alpha particles that are assumed to deposit their energy in the HDPE. By this method, the value of D in Eq. 1 is calculated to be equal to 7.53×10^{-6}-watts and 5.84×10^{-6}-watts, respectively for HCL-1 and HCL-2. Eq. 1 then yields 6.12×10^{-8}-cm^3/sec or 1.93-cm^3/yr for HCL-1 and 4.74×10^{-8}-cm^3/sec or 1.50-cm^3/yr for HCL-2.

Based upon the calculated hydrogen production rates at an assumed source material density of 18.9-g/cm^3, it is calculated that the molecular hydrogen production within HCL-1 will have generated 54-cm^3 of hydrogen in the 28-year period starting in 1992. This is equivalent to approximately 0.033-bar within the crimp sealed tin can and approximately 0.010-bar in the 2R within drum #3031. In the same time period, the production of molecular hydrogen in HCL-2 will have generated 42-cm^3 of hydrogen. This is equivalent to approximately 0.026-bar within the crimp sealed tin can and approximately 0.008-bar in the 2R within drum #3598. Table 4 provides a summary table of these calculations and results.

4.2.4 Hydrogen Production in DOT 6M drum #20102

The UO_3 material in DOT 6M 30-gallon drum #20102 is reported to contain adsorbed water in the amount of 0.45-g. This water is conservatively assumed homogeneously mixed with alpha-producing uranium within the drum. That is to say that no credit is taken for the shielding effects of the UO_3 particles themselves in the current calculation. Based upon this assumption, the total energy deposition rate of 4.09×10^{-5}-Watts is absorbed by the water within the drum. Applying this rate as D in Eq. 1 yields a volumetric hydrogen production rate of 1.61×10^{-7}-cm^3/sec or 5.09-cm^3/yr for drum #20102. This production rate would result in a total hydrogen concentration of 4.0% by volume in the crimp-sealed can at 2019 and a hydrogen concentration of 1.4% by volume in the 2R at 2020. The molecular hydrogen concentration within the crimp-sealed can remains below the lower flammability limit for hydrogen in air until 2019.

Table 4 Summary Table of Hydrogen Generation, Pressure Increase, and Concentration Results

	HCL-1 #3031	HCL-2 #3598	114/133 SAL #20102
H_2 Production Rate (cm^3/yr)	1.93	1.50	5.09
Pressure Increase in Can (bar/yr)	1.18E-03	9.12E-04	3.10E-03
Pressure Increase in 2R (bar/yr)	3.71E-04	2.88E-04	9.79E-04
H_2 Concentration in Can (% vol)	3.3†	2.6†	4.0‡
H_2 Concentration in 2R (% vol)	1.0†	0.8†	1.4†

† Concentration estimated at 2020.
‡ Concentration estimated at 2019.

5.0 CONCLUSIONS

Three DOT 6m 30-gallon drums will be received in L-Area at SRS and stored for up to 13-years prior to final disposition at HB-Line by 2019/2020. These drums are scheduled for shipment from INTEC to SRS as part of the decommissioning effort of the INTEC facility. Bounding values for hydrogen gas generation rates, rates of pressure increase within the drums, and projected molecular hydrogen concentrations at 2019/2020 have been determined for all three drums based upon the assumptions listed in Section 4.1. Two of these drums, #3031 and #3598 contain polymeric bags and/or bottles that will be subject to radiolysis induced hydrogen gas generation. The maximum quantity of molecular hydrogen that can be expected to evolve in two DOT 6M 30-gallon drums in support of receipt and subsequent interim storage prior to canyon processing has been estimated based on the alpha radiolysis of polymers. An upper bound estimate for alpha energy available for radiolysis of the polymeric materials was determined from the volume fraction occupied by material in the bottle packed within an alpha range of the inner surface of the HDPE bottles. A conservative estimation of the hydrogen generation in DOT 6M drum #20102, can 114/133 SAL that contains UO_3 powder due to the radiolytic decomposition of water has also been completed. The results are summarized in Table 5.

Table 5 Summary Table of Results

	HCL-1 #3031	HCL-2 #3598	114/133 SAL #20102
H_2 Production Rate (cm^3/yr)	1.93	1.50	5.09
Pressure Increase in Can (bar/yr)	1.18E-03	9.12E-04	3.10E-03
Pressure Increase in 2R (bar/yr)	3.71E-04	2.88E-04	9.79E-04
H_2 Concentration in Can (% vol)	3.3†	2.6†	4.0‡
H_2 Concentration in 2R (% vol)	1.0†	0.8†	1.4†

† Concentration estimated at 2020.
‡ Concentration estimated at 2019.

6.0 REFERENCE

1 ***"Appendix A: Idaho Cleanup Project, Nuclear Materials Completion,"*** Carol Nichols, DOESRAAD-06-075.1, Draft Document (December 21, 2006).

2 ***"Appendix A: Idaho Cleanup Project, Nuclear Materials Completion,"*** Carol Nichols, DOESRAAD-06-075, Draft Document (December 21, 2006).

3 DOE/ID-10368, ***"Uranium/Nitric Acid Processing Explosion at Idaho Chemical Processing Plant: Following-up Investigation Report"*** (September 1992).

4 R.A. Vaughn, **Calculation Sheet**, CS 2001/22, Issue C, Project No Y01/02/06 (December 17, 2002).

5 G.F. Knoll, **Radiation Detection and Measurement,** Second Edition, John-Wiley and Sons (1989).

6 H. Cember, **Introduction to Health Physics,** Second Edition, McGraw-Hill (1983).

7 J.R. Green, ***"Progress Report for the Enhancement of Radcalc: Isotope Database, Gamma Absorption Fractions, and G(H_2) Values,"*** WHC-SD-TP-RPT-014 (September 28, 1994).

8 U.S. Department of Energy (DOE), ***"CH-TRU Payload Appendices,"*** Rev. 1, U.S. Department of Energy, Carlsbad Field Office, Carlsbad, New Mexico (May 2005).

9 D.W. Vinson, N.E. Bibler, R.W. Deible, and R.L. Sindelar, ***"Evaluation of Hydrogen Generation from Radiolysis from Breached Spent Fuel,"*** American Nuclear Society Annual Meeting (September 19, 2002).

10 S. Pauly, ***"Permeability and Diffusion Data,"*** in **Polymer Handbook,** Fourth Edition, John Wiley & Sons, Inc. (1999).

11 C.F. Jones, ***"Soil Samples,"*** email communication to C. Nichols (Thu Jun 07 12:52:59 2007).

12 Code of Federal Regulations, 10CFR71.

13 ***"Evaluated Nuclear Structure Data File"*** − A Computer File of Evaluated Experimental Nuclear Data Maintained by the National Nuclear Data Center, Brookhaven National Laboratory ENDF/B-VI.

THIS PAGE INTENTIONALLY LEFT BLANK.

ORNL/TM-2003/194

Water Sorption and Radiolysis Studies for Neptunium Oxides

January 2004

Prepared by
A. S. Icenhour
R. M. Wham
R. R. Brunson
L. M. Toth

DOCUMENT AVAILABILITY

Reports produced after January 1, 1996, are generally available free via the U.S. Department of Energy (DOE) Information Bridge:

Web site: http://www.osti.gov/bridge

Reports produced before January 1, 1996, may be purchased by members of the public from the following source:

National Technical Information Service
5285 Port Royal Road
Springfield, VA 22161
Telephone: 703-605-6000 (1-800-553-6847)
TDD: 703-487-4639
Fax: 703-605-6900
E-mail: info@ntis.fedworld.gov
Web site: http://www.ntis.gov/support/ordernowabout.htm

Reports are available to DOE employees, DOE contractors, Energy Technology Data Exchange (ETDE) representatives, and International Nuclear Information System (INIS) representatives from the following source:

Office of Scientific and Technical Information
P.O. Box 62
Oak Ridge, TN 37831
Telephone: 865-576-8401
Fax: 865-576-5728
E-mail: reports@adonis.osti.gov
Web site: http://www.osti.gov/contact.html

This report was prepared as an account of work sponsored by an agency of the United States Government. Neither the United States government nor any agency thereof, nor any of their employees, makes any warranty, express or implied, or assumes any legal liability or responsibility for the accuracy, completeness, or usefulness of any information, apparatus, product, or process disclosed, or represents that its use would not infringe privately owned rights. Reference herein to any specific commercial product, process, or service by trade name, trademark, manufacturer, or otherwise, does not necessarily constitute or imply its endorsement, recommendation, or favoring by the United States Government or any agency thereof. The views and opinions of authors expressed herein do not necessarily state or reflect those of the United States Government or any agency thereof.

ORNL/TM-2003/194

WATER SORPTION AND RADIOLYSIS STUDIES FOR NEPTUNIUM OXIDES

A. S. Icenhour
R. M. Wham
R. R. Brunson
L. M. Toth

Date Published: January 2004

Prepared by
OAK RIDGE NATIONAL LABORATORY
P.O. Box 2008
Oak Ridge, Tennessee 37831-6285
managed by
UT-Battelle, LLC
for the
U.S. DEPARTMENT OF ENERGY
under contract DE-AC05-00OR22725

CONTENTS

Page

LIST OF FIGURES v
LIST OF TABLES vii
ACRONYMS, ABBREVIATIONS, AND DEFINITIONS ix
ABSTRACT xi
1. INTRODUCTION 1
2. BACKGROUND 2
3. EXPERIMENTAL 4
3.1 SAMPLE PREPARATION 4
3.2 WATER SORPTION STUDIES 4
3.3 RADIOLYSIS EXPERIMENTS 6
3.3.1 Gamma Irradiation Experiments 6
3.3.2 Alpha Radiolysis Experiments 11
3.4 SAMPLING AND ANALYSES 13
4. RESULTS AND DISCUSSION 14
4.1 WATER SORPTION EXPERIMENTS 14
4.2 GAMMA RADIOLYSIS EXPERIMENTS 14
4.2.1 Pressure Measurements 16
4.2.2 Gas Analyses 22
4.3 ALPHA RADIOLYSIS EXPERIMENTS 27
4.3.1 Pressure Measurements 28
4.3.2 Gas Analyses 31
4.4 OVERVIEW OF RADIOLYTIC MECHANISM 34
5. CONCLUSIONS 36
REFERENCES 37

LIST OF FIGURES

Figure		Page
2.1	Schematic depiction of neptunium processing and packaging.	3
3.1	ORNL ^{60}Co irradiator	7
3.2	Sample container and pressure transducer used in the ^{60}Co irradiations.	7
3.3	Irradiation chamber of ORNL ^{60}Co irradiator with sample containers installed.	8
3.4	Data acquisition computer in operation at the ORNL ^{60}Co source.	10
3.5	SNF elements in the HFIR SNF pool.	10
3.6	Schematic of the experimental configuration for gamma irradiation experiments with a HFIR SNF element.	10
3.7	Multiple-irradiation container used in HFIR SNF irradiations.	11
3.8	Comparison of doses to NpO_2 samples using 500 ppm ^{238}Pu and 7000 ppm ^{244}Cm.	12
3.9	Sample container and pressure transducer used in the alpha radiolysis experiments..	13
4.1	Moisture uptake data for NpO_2 prepared at 650ºC.	15
4.2	Pressure and gas yield as a function of dose for sample ^{60}Co Np Tube 1 [^{60}Co-irradiated NpO_2 (650ºC)].	17
4.3	Pressure and gas yield as a function of dose for sample ^{60}Co Np Tube 2 [^{60}Co-irradiated NpO_2 (650ºC) + 8 wt % H_2O].	17
4.4	Pressure and gas yield as a function of dose for sample ^{60}Co Np Tube 3 [^{60}Co-irradiated NpO_2 (650ºC) + 1 wt % H_2O].	18
4.5	Pressure and gas yield as a function of dose for sample ^{60}Co Np Tube 4 [^{60}Co-irradiated NpO_2 (800ºC) + 1 wt % H_2O].	19

LIST OF FIGURES (continued)

4.6 Pressure and gas yield as a function of dose for sample HFIR Np Tube 1 [HFIR SNF-irradiated NpO_2 (650ºC)]. 19

4.7 Pressure and gas yield as a function of dose for sample HFIR Np Tube 2 [HFIR SNF-irradiated NpO_2 (650ºC) + 1 wt % H_2O]. 20

4.8 Pressure and gas yield as a function of dose for sample HFIR Np Tube 3 [HFIR SNF-irradiated NpO_2 (650ºC) + 8 wt % H_2O]. 20

4.9 Pressure and gas yield as a function of dose for sample HFIR Np Tube 4 [HFIR SNF-irradiated NpO_2 (800ºC) + 1 wt % H_2O]. 21

4.10 Pressure and gas yield as a function of dose for sample Alpha Np Tube 1 [^{244}Cm alpha-irradiated NpO_2 (650ºC)]. 29

4.11 Pressure and gas yield as a function of dose for sample Alpha Np Tube 2 [^{244}Cm alpha-irradiated NpO_2 (650ºC) + 1 wt % H_2O]. 29

4.12 Pressure and gas yield as a function of dose for sample Alpha Np Tube 3 [^{244}Cm alpha-irradiated NpO_2 (650ºC) + 8 wt % H_2O]. 30

4.13 Pressure and gas yield as a function of dose for sample Alpha Np Tube 4 [^{244}Cm alpha-irradiated NpO_2 (800ºC) + 1 wt % H_2O]. 30

4.14 Pressure and gas yield as a function of dose for sample Alpha Np Tube 5 [^{244}Cm alpha-irradiated NpO_2 (650ºC) + 0.5 wt % H_2O]. 31

LIST OF TABLES

Table		Page
3.1	Neptunium isotopic data	5
3.2	Metal ion impurity in NpO_2 samples	5
3.3	Constant humidity control using sulfuric acid solutions	6
3.4	Volume of sample containers used in irradiation experiments	8
3.5	Example of radionuclide composition and dose contribution data for a NpO_2 sample spiked with ^{244}Cm	12
4.1	Summary of gamma irradiation experiments performed	16
4.2	Results of mass spectrometric analysis of gas composition from ^{60}Co-irradiated NpO_2 samples	23
4.3	Results of mass spectrometric analysis of gas composition from HFIR SNF-irradiated NpO_2 samples	24
4.4	Estimated change in gas composition for selected experiments as a result of radiolysis	25
4.5	Estimated H_2 production as a percentage of initial amount of water available for radiolysis	26
4.6	Summary of alpha irradiation experiments performed	27
4.7	Results of mass spectrometric analysis of gas composition from alpha-irradiated NpO_2 samples	32

ACRONYMS, ABBREVIATIONS, AND DEFINITIONS

ATR	Advanced Test Reactor
DOE	U.S. Department of Energy
G-value	the number of molecules of gas either produced or destroyed per 100 eV of energy deposited in the sample
HEPA	high-efficiency particulate air (filter)
HFIR	High Flux Isotope Reactor
INEEL	Idaho National Engineering and Environmental Laboratory
LANL	Los Alamos National Laboratory
MGy	megagray, 1 MGy = 10^6 J/kg (1 Gy = 100 rad)
ORNL	Oak Ridge National Laboratory
PCV	primary containment vessel
REDC	Radiochemical Engineering Development Center
SNF	spent nuclear fuel
SRS	Savannah River Site

ABSTRACT

Plans are to convert the ^{237}Np that is currently stored as a nitrate solution at the Savannah River Site to NpO_2 and then ship it to the Y-12 National Security Complex in Oak Ridge for interim storage. This material will serve as feedstock for the ^{238}Pu production program, and some will be periodically shipped to the Oak Ridge National Laboratory (ORNL) for fabrication into targets. The safe storage of this material requires an understanding of the radiolysis of moisture that is sorbed on the oxides, which, in turn, provides a basis for storage criteria (namely, moisture content). A two-component experimental program has been undertaken at ORNL to evaluate the radiolytic effects on NpO_2: (1) moisture uptake experiments and (2) radiolysis experiments using both gamma and alpha radiation.

These experiments have produced two key results. First, the water uptake experiments demonstrated that the 0.5 wt % moisture limit that has been typically established for similar materials (e.g., uranium and plutonium oxides) cannot be obtained in a practical environment. In fact, the uptake in a typical environment can be expected to be at least an order of magnitude lower than the limit.

The second key result is the establishment of steady-state pressure plateaus as a result of the radiolysis of sorbed moisture. These plateaus are the result of back reactions that limit the overall pressure increase and H_2 production. These results clearly demonstrate that 0.5 wt % H_2O on NpO_2 is safe for long-term storage—if such a moisture content could even be practically reached.

1. INTRODUCTION

The Department of Energy (DOE) Office of Space and Defense Power, NE-50, is reestablishing domestic production of ^{238}Pu using existing DOE facilities. The feed material for the production is ^{237}Np, which is currently stored at the Savannah River Site (SRS). This material will be stabilized as an oxide, packaged, and then transported to the Y-12 National Security Complex for interim storage. Y-12 will then transfer material as needed to Oak Ridge National Laboratory (ORNL). Target fabrication will occur at the Radiochemical Engineering Development Center (REDC) Building 7930. The High Flux Isotope Reactor (HFIR) at ORNL and the Advanced Test Reactor (ATR) at the Idaho National Engineering and Environmental Laboratory (INEEL) will be used to irradiate ^{237}Np-containing targets to produce ^{238}Pu. The irradiated targets will undergo chemical processing at the REDC to (1) recover ^{238}Pu for shipment to Los Alamos National Laboratory (LANL) and (2) recover ^{237}Np for recycle.

Safety issues concerning transportation and long-term storage of neptunium are of a particular concern to the program. The material and its packaging must comply with shipping standards as well as provide for safe storage.

One aspect relative to the safe transport and storage of NpO_2 is radiolysis of sorbed water. Current safety analyses assume that all of the water absorbed on the surface of the NpO_2 can be radiolyzed to gaseous hydrogen and oxygen, thus generating significant gas pressures within the storage containers. Also, the potential for detonation of the hydrogen has been identified as a safety issue for transportation. However, experimental work by Icenhour et al.[1–4] using uranium oxides and uranium oxyfluorides has demonstrated that radiolysis does not convert all of the water to H_2 and O_2 because of competing back reactions that result in a pressure plateau, demonstrating that a steady state has been reached. In some cases, the vessel actually goes to vacuum conditions as a result of the dominance of back reactions.

The use of high-dose-rate gamma and/or alpha irradiation capable of radiolyzing significant quantities of the proposed materials in a short period of time is the only practical way to achieve the necessary doses and thus assess potential long-term storage problems. A set of experiments was performed to irradiate NpO_2 samples that have sorbed moisture. This report provides a description of the experiments and the results.

2. BACKGROUND

The neptunium to be used as feed material currently exists in a nitrate solution in the SRS H-Canyon. The neptunium solution, which contains about 500 ppm ^{238}Pu,[5] will undergo chemical processing in a glove-box line (HB-Line Phase II) to remove impurities and convert it to an oxide as depicted in Fig. 2.1.

The neptunium solution first undergoes a feed adjustment to 6–8 *M* HNO_3. The adjusted solution is then fed into anion-exchange columns, where the neptunium nitrate complex absorbs, allowing most metal impurities to pass through the column. Next, a decontamination wash is performed to remove residual impurities. Finally, a weak nitric acid solution is passed through the column to elute the neptunium.

Once the anion-exchange process has been completed, the resulting neptunium solution is combined with oxalic acid, which forms an insoluble neptunium oxalic precipitant. This product is filtered, and the neptunium oxalate is then calcined at ~600ºC to convert the oxalate to oxide.

The oxide will be packaged in a can–bag–can configuration for shipment (Fig. 2.1). The inner can, which contains up to 6 kg neptunium, is a screw-top, food-pack convenience can. Because no gasket or sealing compounds are used on the closure, this inner can will not be gastight. The inner can is contained in a heat-sealed polyethylene bag, which has an installed HEPA (high-efficiency particulate air) filter. The can–bag will then be placed inside an outer can, which has a HEPA filter in its lid.* Finally, the can–bag–can will be placed inside a 9975 primary containment vessel (PCV).[6] SRS currently plans to evacuate the PCV and backfill with argon. Because of the installed HEPA filters and the screw-top lid on the inner can, the entire contents of the PCV will be evacuated and backfilled. This operation is expected to reduce the O_2 concentration inside the PCV to less than 5 vol %.

Concerns related to the long-term storage of the NpO_2 are the potential for container pressurization and/or the formation of H_2 as a result of radiolytic decomposition of moisture that is sorbed on the oxide. To address these concerns, NpO_2 radiolysis experiments have been conducted at ORNL using both gamma and alpha radiation sources. Samples of NpO_2 were prepared by the method expected to be used at SRS (i.e., oxalate precipitation and calcination). Moisture was added to the samples to simulate water uptake.

The equipment and experimental facilities described in this report have been used in similar studies concerning gamma irradiation of uranium oxides and fluoride salts with various amounts of sorbed water.[1–4]

---

*Because of ergonomic considerations, two bagged inner cans may be used instead of just one.

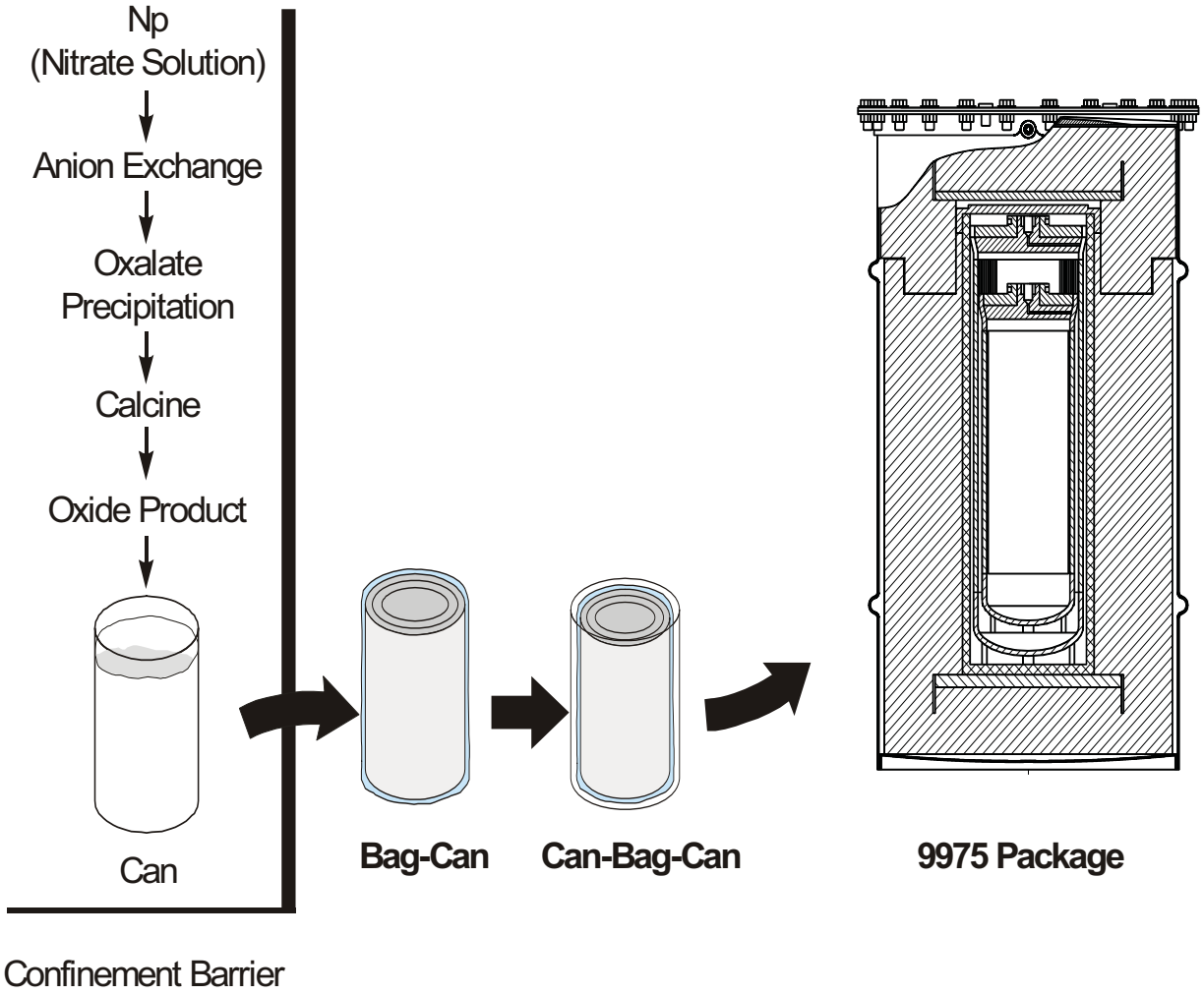

Fig. 2.1. Schematic depiction of neptunium processing and packaging.

3. EXPERIMENTAL

The experimental program was divided into three distinct activities: sample preparation, water sorption studies, and radiolysis experiments.

3.1 SAMPLE PREPARATION

Twelve samples of NpO_2 were prepared and then irradiated to evaluate radiolytic decomposition of water. The samples first underwent chemical processing at REDC Building 7930 to prepare the NpO_2 in a form similar to that expected from SRS.[7] The water content and the surface area of the samples were varied for the experiments.

In order to prepare NpO_2 for these experiments, a batch of 80–100 g of NpO_2 was dissolved in nitric acid. Some of the feed material was neptunium oxide originally obtained from LANL. The majority of the material had been processed using hydroxide precipitation, oxalate precipitation, and ion-exchange processing at the REDC. Because the neptunium product batches from the hydroxide precipitation and oxalate precipitation processes were calcined at 1400ºC, they were extremely difficult to dissolve. Therefore, these various sources of neptunium were dissolved in 8 *M* HNO_3 acid with 0.02 *M* NaF added to the solution, followed by heating over a period of about 24 h to promote the dissolution. After dissolution, the neptunium was adjusted to the 4+ valence state by addition of hydrazine followed by ascorbic acid. A slight excess of oxalic acid was then added to precipitate the neptunium as neptunium oxalate. The resulting material was filtered, dried, and fired to 650ºC to convert the oxalate to oxide.[*] Some material was fired at 800ºC to change the surface area. Tables 3.1 and 3.2 provide isotopic and chemical impurity results, respectively, from the analysis of NpO_2 prepared by the method described.

3.2 WATER SORPTION STUDIES

Neptunium oxide with varying amounts of sorbed water was needed for these experiments. The amount of water sorbed as a function of time was determined by placing these materials in a controlled-humidity environment. Humidities of 60 and 97.5% were used. The humidity was controlled by

[*]Note that at the time of this work, the exact calcination temperature had not yet been established. It is now expected that the SRS material will be fired at temperatures between 600 and 650ºC, depending on the capability of the furnace used. This temperature range will have no effect on the results or conclusions described in this report.

Table 3.1. Neptunium isotopic data

	Isotopic abundance (wt %)
^{237}Np	99.97361
$^{239/240}Pu$	0.02558
^{238}Pu	0.0008

Table 3.2. Metal ion impurity in NpO_2 samples

Element	Concentration (μg/g)
Al	$1.38 \times 10^4 \pm 1.38 \times 10^3$
B	$9.19 \times 10^3 \pm 9.19 \times 10^2$
Ba	$6.03 \times 10^3 \pm 6.03 \times 10^2$
Be	$4.25 \times 10^1 \pm 4.25$
Ca	$1.94 \times 10^4 \pm 1.91 \times 10^3$
Cu	$6.79 \times 10^2 \pm 8.49 \times 10^1$
Fe	$6.52 \times 10^3 \pm 1.36 \times 10^3$
K	$8.43 \times 10^3 \pm 2.08 \times 10^3$
Mg	$1.41 \times 10^4 \pm 1.31 \times 10^3$
Mn	$2.34 \times 10^2 \pm 4.25 \times 10^1$
Na	$5.44 \times 10^4 \pm 5.44 \times 10^3$
Sb	$3.27 \times 10^3 \pm 7.22 \times 10^2$
Sr	$3.40 \times 10^2 \pm 3.40 \times 10^1$

placing the NpO_2 sample in a small open glass container, which, in turn, was placed in a glass desiccator. The desiccant had been removed and was replaced with a small open container of dilute sulfuric acid to yield the desired humidity. The NpO_2 samples were periodically removed from the chamber and weighed to determine the uptake of water. Table 3.3 provides relative humidity data for a number of sulfuric acid solutions. (The vapor referred to is pure water.)

Table 3.3. Constant humidity control using sulfuric acid solutions[a]

Density of aqueous H_2SO_4 solution	Relative humidity (%)	Water vapor pressure at 20ºC (mm Hg)
1.00	100.0	17.4
1.05	97.5	17.0
1.10	93.9	16.3
1.15	88.8	15.4
1.20	80.5	14.0
1.25	70.4	12.2
1.30	58.3	10.1
1.35	47.2	8.3
1.40	37.1	6.5
1.50	18.8	3.3
1.60	8.5	1.5
1.70	3.2	0.6

[a]From *Handbook of Chemistry and Physics*, 41st ed., Chemical Rubber Publishing Co., Cleveland, 1959, p. 2500.

3.3 RADIOLYSIS EXPERIMENTS

Radiolysis experiments were performed using both gamma and alpha radiation. The equipment used for these experiments is described in Sects. 3.3.1 and 3.3.2.

3.3.1 Gamma Irradiation Experiments

Two different sources of gamma radiation were used: (1) the ORNL ^{60}Co irradiator and (2) the HFIR spent nuclear fuel (SNF) elements. In preparation of the samples, a calibrated pipette was used to add the desired amount of water.

3.3.1.1 ^{60}Co irradiation experiments

A J. L. Shepherd model 109-68 (serial no. 654) ^{60}Co gamma irradiator (shown in Fig. 3.1), providing a dose rate of about 10^5 rad/h, was used for the experiments. The sample container itself is shown in Fig. 3.2, while Fig. 3.3 shows the samples installed in the irradiator prior to being lowered into the device. A detailed description of the irradiator and the methods used to calculate the dose to the samples (for both the ^{60}Co source and HFIR SNF elements) is provided in Ref. 8.

The samples to be irradiated were placed in stainless steel containers, each of which had a small-diameter stainless steel tube connected at one end for pressure sensing and a capped opening at the other end for loading samples. The container was connected by small-diameter tubing to a stainless steel Nupro® valve and an MKS Baratron® pressure transducer (Type 127A). The material to be irradiated was loaded through a stainless steel VCR gland on one end of the container.

Preparation of sample containers for their insertion into the ^{60}Co irradiator consisted of leak checks, volume measurements, and loading of the samples into the containers. As part of their fabrication, the containers were leak checked with air to a pressure of about 6.8 atm (100 psia).

Just before their use, the containers were leak checked again, using both pressure (typically ~3 atm) and vacuum. The volume of the irradiation rig (i.e., the sample container, tubing, valve, and pressure transducer) was measured by expanding helium from a known volume into the rig, observing the pressure change, and applying the ideal gas law. The volume of each of the tubes used in the experiments is presented in Table 3.4.

Fig. 3.1. ORNL ^{60}Co irradiator.

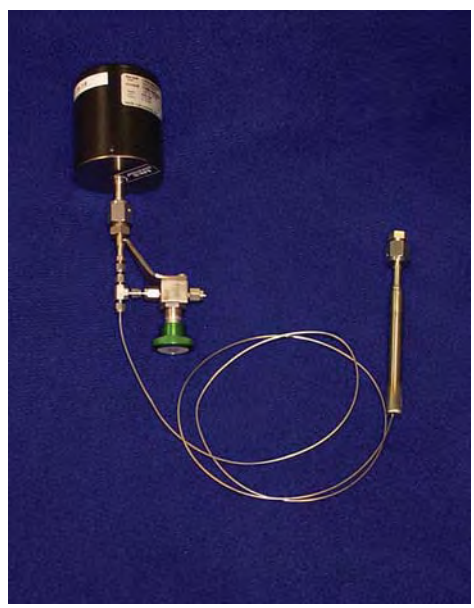

Fig. 3.2. Sample container and pressure transducer used in the ^{60}Co irradiations.

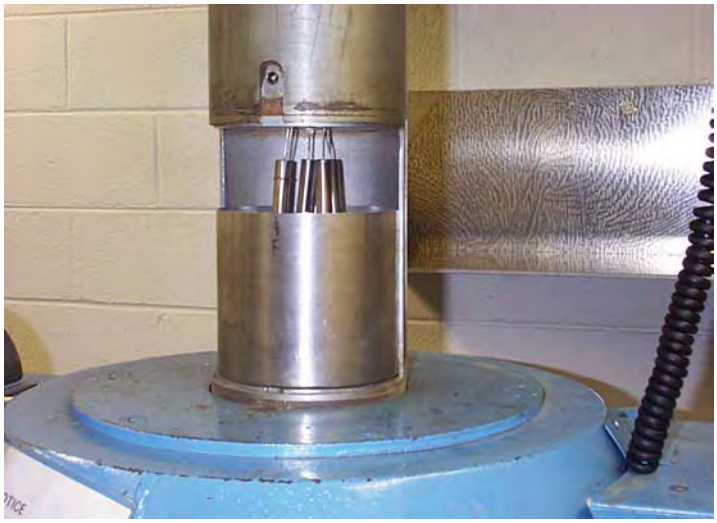

Fig. 3.3. Irradiation chamber of ORNL ^{60}Co irradiator with sample containers installed.

Table 3.4. Volume of sample containers used in irradiation experiments

Container	Volume (cm^3)
^{60}Co Np Tube 1	16.7
^{60}Co Np Tube 2	16.6
^{60}Co Np Tube 3	16.4
^{60}Co Np Tube 4	16.1
HFIR Np Tube 1	34.6
HFIR Np Tube 2	49.7
HFIR Np Tube 3	50.8
HFIR Np Tube 4	35.4
Alpha Np Tube 1	13.1
Alpha Np Tube 2	13.3
Alpha Np Tube 3	13.5
Alpha Np Tube 4	13.7
Alpha Np Tube 5	13.1

A computerized data acquisition system was used to collect data during each irradiation. Validyne® hardware and software were used, providing up to eight data channels per card. The data acquisition system is shown in Fig. 3.4. Typical parameters recorded during an irradiation included container pressure, temperature of selected containers, and ambient pressure and temperature.

3.3.1.2 HFIR SNF irradiation experiments

To obtain higher dose rates, the HFIR SNF gamma irradiation facility (shown in Fig. 3.5) was also used. Figure 3.6 depicts the experimental configuration for these irradiations. Samples can be irradiated in the HFIR SNF pool by inserting them into SNF elements. The SNF elements are cylindrical with a hollow center. In its storage position in the SNF pool, a cadmium sleeve inside the hollow region of the element absorbs neutrons. Hence, the hollow region of the fuel element primarily provides a gamma field for irradiation. The neutron flux in this region is about 100 neutrons • cm^{-2} • s^{-1}. The contribution of neutrons to the radiation damage is negligible when compared with the very large gamma field. Exposure rates vary from about 10^7 to 10^8 R/h, depending on the time since the discharge of the SNF from the reactor.

A multiple-irradiation container was used for the irradiation of four samples at once (Fig. 3.7). Small sample containers consisting of 1.27-cm-diam stainless steel tubing were placed inside an outer container, which was fabricated from 8.9-cm-diam, 44-cm-long stainless steel pipe. The outer container was closed at one end and had a Conflat flange on the other end. The flange contained five penetrations. Four were used to connect the smaller inner containers to 0.318-cm-diam stainless steel tubing, while the fifth connected the void volume of the outer container to 0.318-cm-diam stainless steel tubing. In each case, this tubing was about 6.1 m long and was connected to a pressure transducer and to a valve.

The volume of each of the sample containers, which included sampling lines and pressure transducers, is presented in Table 3.4. Before the experiment was transported to the HFIR for insertion in an SNF element, the samples were loaded in air and the outer container was pressurized to 1.7 atm (10 psig), as required by HFIR operations personnel.

Sensotec® (model FPA, 0–50 psia) pressure transducers were used for the four inner sample containers. A Kobold® (model KPK, 30 in. Hg to 100 psig) compound pressure transducer was used to monitor the pressure in the large outer vessel. A computerized data acquisition system was used to record the pressure throughout the experiments.

Fig. 3.4. Data acquisition computer in operation at the ORNL ^{60}Co source.

Fig. 3.5. SNF elements in the HFIR SNF pool.

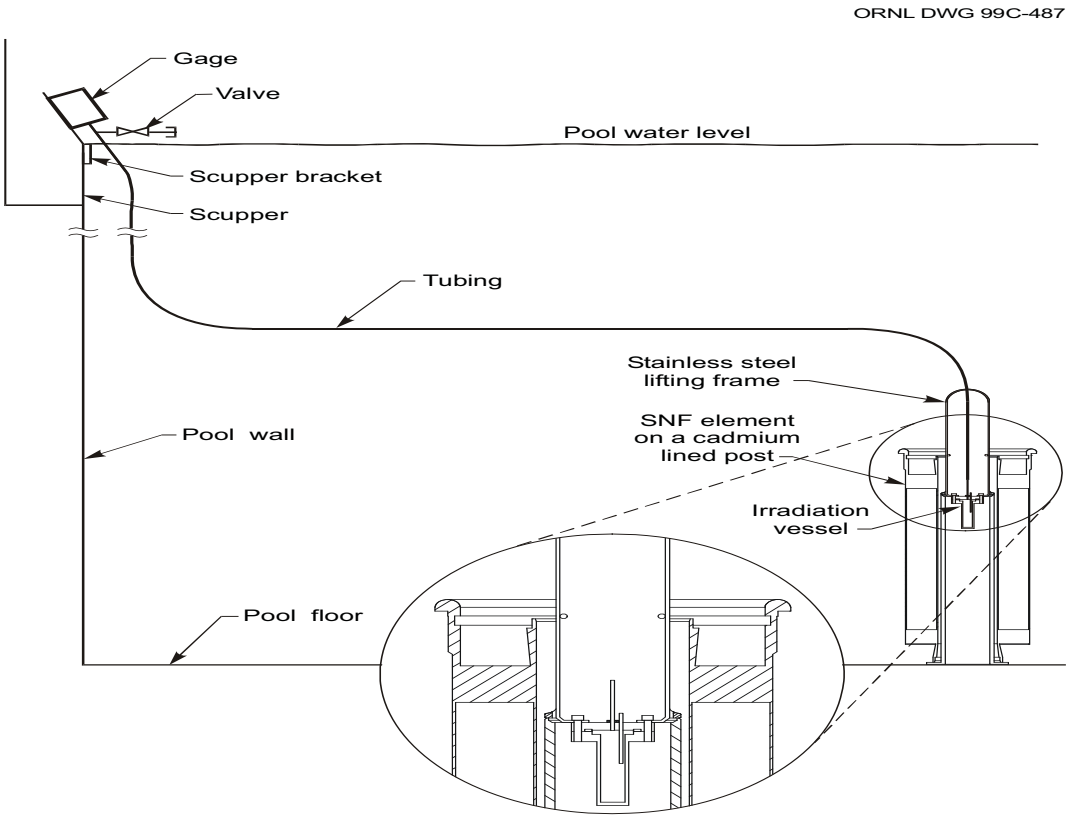

Fig. 3.6. Schematic of the experimental configuration for gamma irradiation experiments with a HFIR SNF element.

Fig. 3.7. Multiple-irradiation container used in HFIR SNF irradiations.

3.3.2 Alpha Radiolysis Experiments

To perform the alpha radiolysis experiments, neptunium samples were spiked with ^{244}Cm to mimic the dose from ^{238}Pu, but in a shorter time period reasonable for the present experimental study. Note that the neptunium in storage at SRS contains about 500 ppm ^{238}Pu. Samples of NpO_2 containing about 7000 ppm ^{244}Cm realized a dose rate about 70 times that for the SRS material, as illustrated in Figure 3.8. An example of the radionuclide composition and dose contribution data for the curium used is presented in Table 3.5. This table demonstrates that while 40 wt % of the material used to spike the samples was ^{240}Pu, more than 99% of the dose was delivered by the parent isotope, ^{244}Cm.

A portion of the dissolved neptunium was set aside for alpha radiolysis experiments. The neptunium was adjusted to the 4+ valence state and diluted to 1–2 *M* HNO_3. A small aliquot of ^{244}Cm was then mixed with the neptunium solution, and oxalic acid was added to form both neptunium and curium oxalate. The oxalate product was filtered, dried, and calcined at 650ºC. The resulting oxide was then divided into four samples, one of which was further heated to 800ºC.

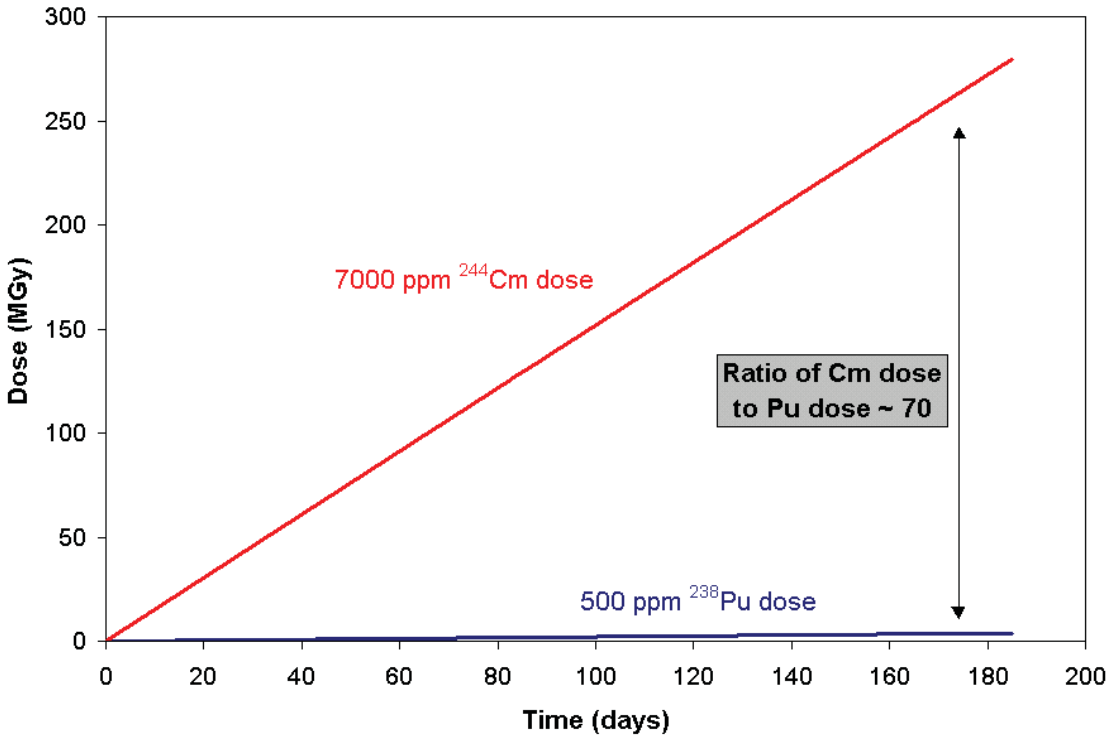

Fig. 3.8. Comparison of doses to NpO_2 samples using 500 ppm ^{238}Pu and 7000 ppm ^{244}Cm.

Table 3.5. Example of radionuclide composition and dose contribution data for a NpO_2 sample spiked with ^{244}Cm

Radionuclide	Half-life (years)	Specific activity (Ci/g)	Average alpha energy (MeV)	Composition (wt %)	Contribution to dose (%)
^{244}Cm	18.11	80.9	5.7965	50.34	99.74
^{245}Cm	8500	0.1717	5.363	1.36	0.01
^{246}Cm	4730	0.3072	5.376	7.31	0.05
^{247}Cm	1.56×10^{7}	9.20×10^{-5}	4.9475	0.12	2.34×10^{-7}
^{248}Cm	3.40×10^{5}	0.00424	4.6524	0.07	5.72×10^{-6}
^{240}Pu	6563	0.22696	5.1549	40.04	0.20
^{241}Pu	14.4	103	0.000118	2.01×10^{-6}	1.03×10^{-10}
^{242}Pu	3.76×10^{5}	0.003926	4.89	1.93×10^{-5}	1.57×10^{-9}
^{243}Am	7380	0.1993	5.2656	0.76	3.37×10^{-3}

The samples were placed in stainless steel containers, and the desired amount of water was then added. The containers were connected by a small-diameter stainless steel tube to a Sensotec pressure transducer and to a valve (Fig. 3.9). Filter gaskets (0.5-µm sintered frit) were used in the VCR face-sealed connections to prevent movement of particles and the spread of contamination. An Omega® Type K thermocouple was attached to the outside of each sample container. The void volume of the containers was measured by expanding helium from a known volume. (The measured volumes are shown in Table 3.4.) Samples were prepared and loaded into the containers in a glove box.

3.4 SAMPLING AND ANALYSES

At the completion of the irradiations, gas samples were withdrawn and analyzed by mass spectrometry.

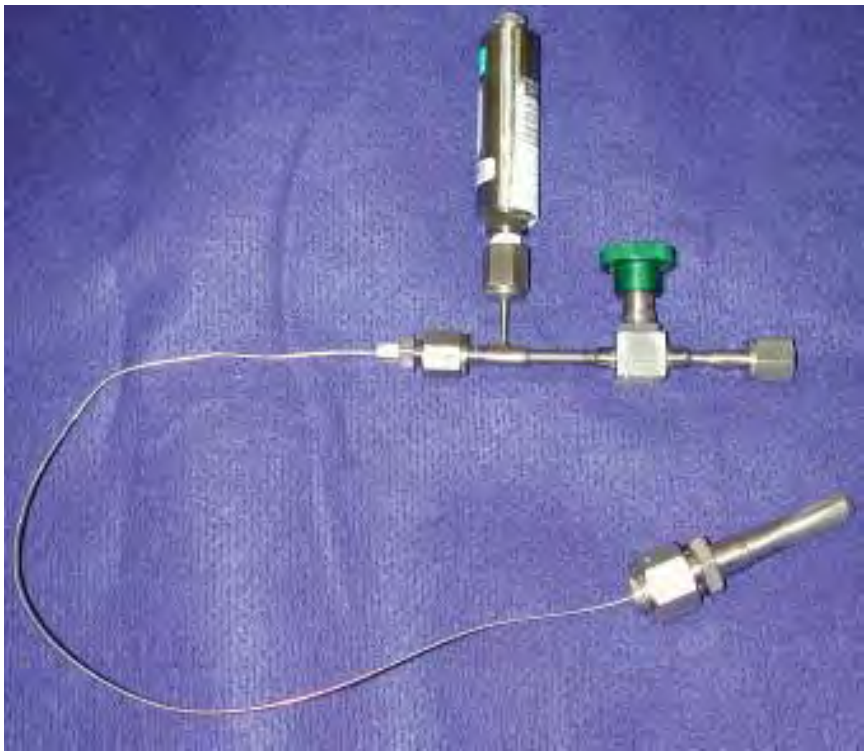

Fig. 3.9. Sample container and pressure transducer used in the alpha radiolysis experiments.

4. RESULTS AND DISCUSSION

4.1 WATER SORPTION EXPERIMENTS

The results for the water sorption on the samples prepared at 650ºC are shown in Fig. 4.1, where the weight gain (i.e., amount of water sorption) of the NpO_2 sample is depicted as a function of time for two different relative humidities. The sample exposed to the 97.5% humidity exhibited an increase in moisture uptake to a limiting value of about 1 wt %. Interestingly, at about 30 days, the lid to the chamber containing the sample was left off, thereby lowering the relative humidity over the sample to that of the glove box. The amount of moisture on the sample rapidly decreased, and, when the lid was replaced, the amount of moisture returned to the previous limit. For the sample exposed to the 60% humidity, a much lower moisture uptake limit was reached—about 0.02 wt %. A similar behavior was seen for the samples prepared at 800ºC (not shown in this report). For these samples, the maximum moisture uptake was 0.8 wt % in the 97.5% humidity, while the maximum was about 0.02 wt % in the 60% humidity.

The water sorption experiments showed that in practical humidities, NpO_2 sorbs very little water. Even in the case of extreme humidity (i.e., 97.5%), the sample prepared at 650ºC sorbed quantities of water only up to ~1 wt % (Fig. 4.1). Furthermore, this water was held very loosely on the surface—as demonstrated by the overnight occurrence described in the paragraph above. However, in the more normal operational case of 60% relative humidity, the maximum water uptake was about 0.02 wt %.

Taking these results in a broader perspective, it is worth noting that the plutonium and ^{233}U storage standards[9,10] have been set with the maximum acceptable moisture content at 0.5 wt %. With such precedents, we expect an identical limit will be established for the NpO_2 that is to be prepared at SRS. In light of the current moisture uptake data for the NpO_2 prepared at 650ºC, and based on similar results obtained at 75% relative humidity by the Savannah River Technology Center,[11] the storage standard limit of 0.5 wt % could never be reached in normal operating or storage conditions where humidity levels are controlled at 60–75%.

4.2 GAMMA RADIOLYSIS EXPERIMENTS

Irradiation experiments were conducted for a number of NpO_2 samples using either the ORNL ^{60}Co source or HFIR SNF elements. Table 4.1 provides a summary of the irradiation experiments performed. The results obtained from these radiolysis experiments are presented in Sects. 4.2.1 and 4.2.2.

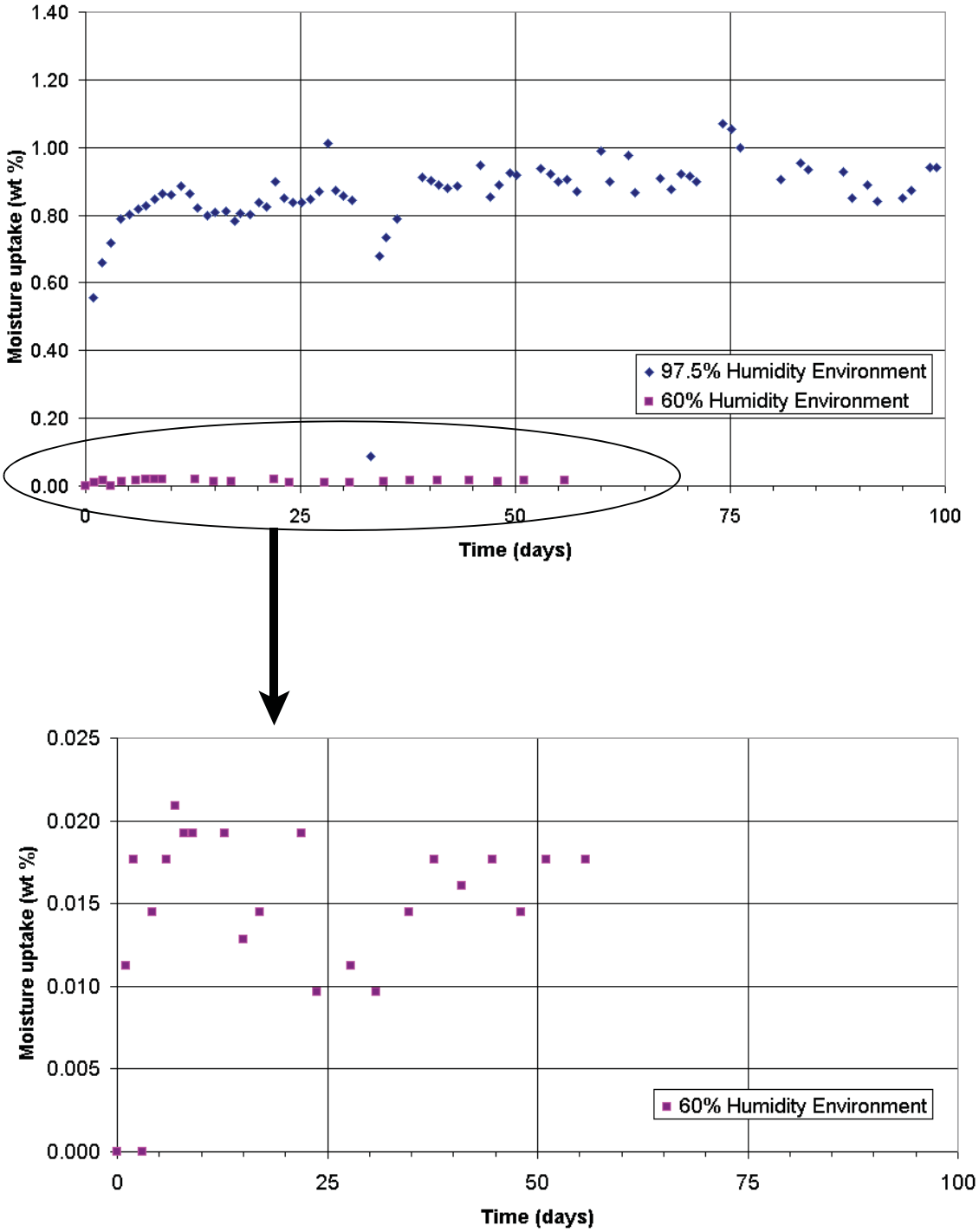

Fig. 4.1. Moisture uptake data for NpO_2 prepared at 650ºC.

Table 4.1. Summary of gamma irradiation experiments performed

Experiment	Material[a]	Mass (g)	Total dose (MGy)
^{60}Co Np Tube 1	NpO_2 (650ºC)	3.9593	4.2
^{60}Co Np Tube 2	NpO_2 (650ºC) + 8 wt % H_2O	4.3152	4.1
^{60}Co Np Tube 3	NpO_2 (650ºC) + 1 wt % H_2O	3.9832	4.2
^{60}Co Np Tube 4	NpO_2 (800ºC) + 1 wt % H_2O	3.9886	4.2
HFIR Np Tube 1	NpO_2 (650ºC)	3.9530	613
HFIR Np Tube 2	NpO_2 (650ºC) + 1 wt % H_2O	3.9908	612
HFIR Np Tube 3	NpO_2 (650ºC) + 8 wt % H_2O	4.2806	595
HFIR Np Tube 4	NpO_2 (800ºC) + 1 wt % H_2O	4.0227	611

[a] Value in parenthesis denotes preparation temperature.

4.2.1 Pressure Measurements

Pressure within the sample containers was monitored throughout the irradiations, and the pressure data from each of the gamma radiolysis experiments are shown in Figs. 4.2–4.9. The pressure and gas yield (millimoles of gas per gram of sample) are plotted as a function of dose in each of the figures. The gas yield was calculated using the ideal gas law.

Container temperatures in the ^{60}Co irradiator were measured to be about 28ºC. For the HFIR multiple-vessel irradiations, the temperature was estimated to average about 55ºC, based on earlier experiments.[3] For this earlier work, the temperature typically ranged from 50 to 60ºC, with several short transients upon insertion of the experiment into a fresh element. The difference in temperature between the ^{60}Co and HFIR irradiations did not appear to have a measurable effect on the irradiation results, other than accounting for the slight pressure differences due to gas expansion.

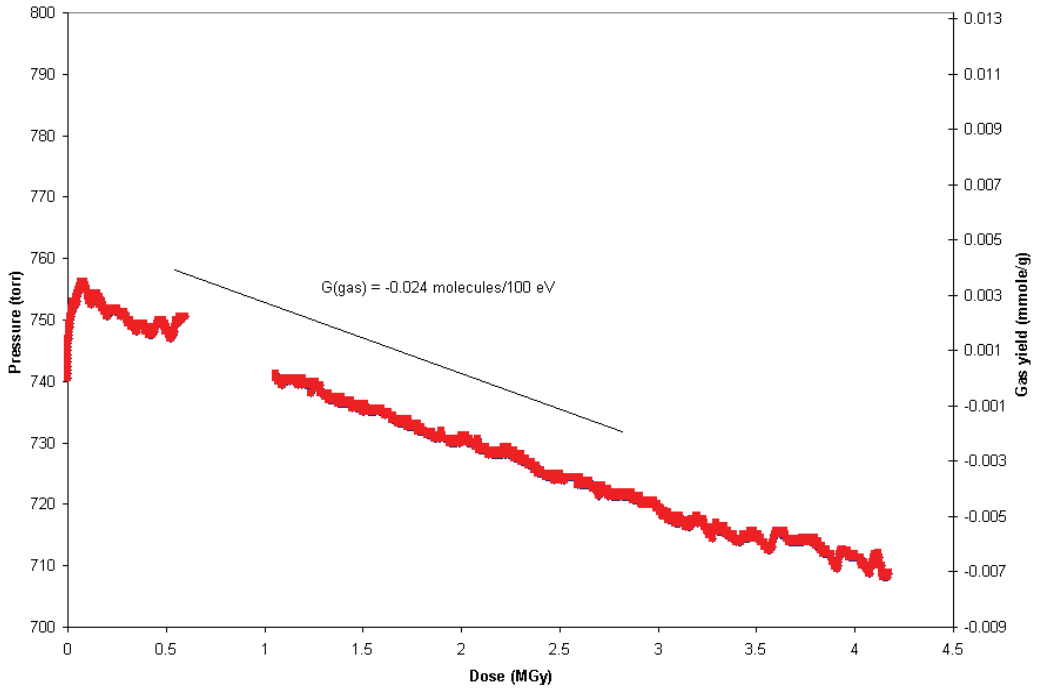

Fig. 4.2. Pressure and gas yield as a function of dose for sample ^{60}Co Np Tube 1 [^{60}Co-irradiated NpO_2 (650ºC)].

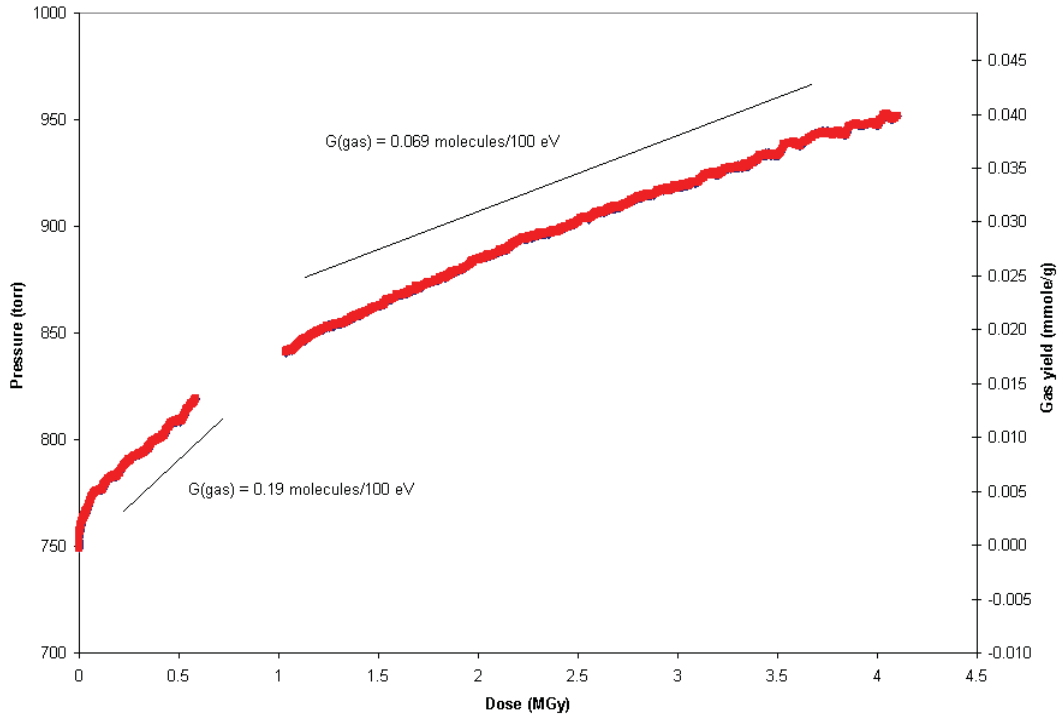

Fig. 4.3. Pressure and gas yield as a function of dose for sample ^{60}Co Np Tube 2 [^{60}Co-irradiated NpO_2 (650ºC) + 8 wt % H_2O].

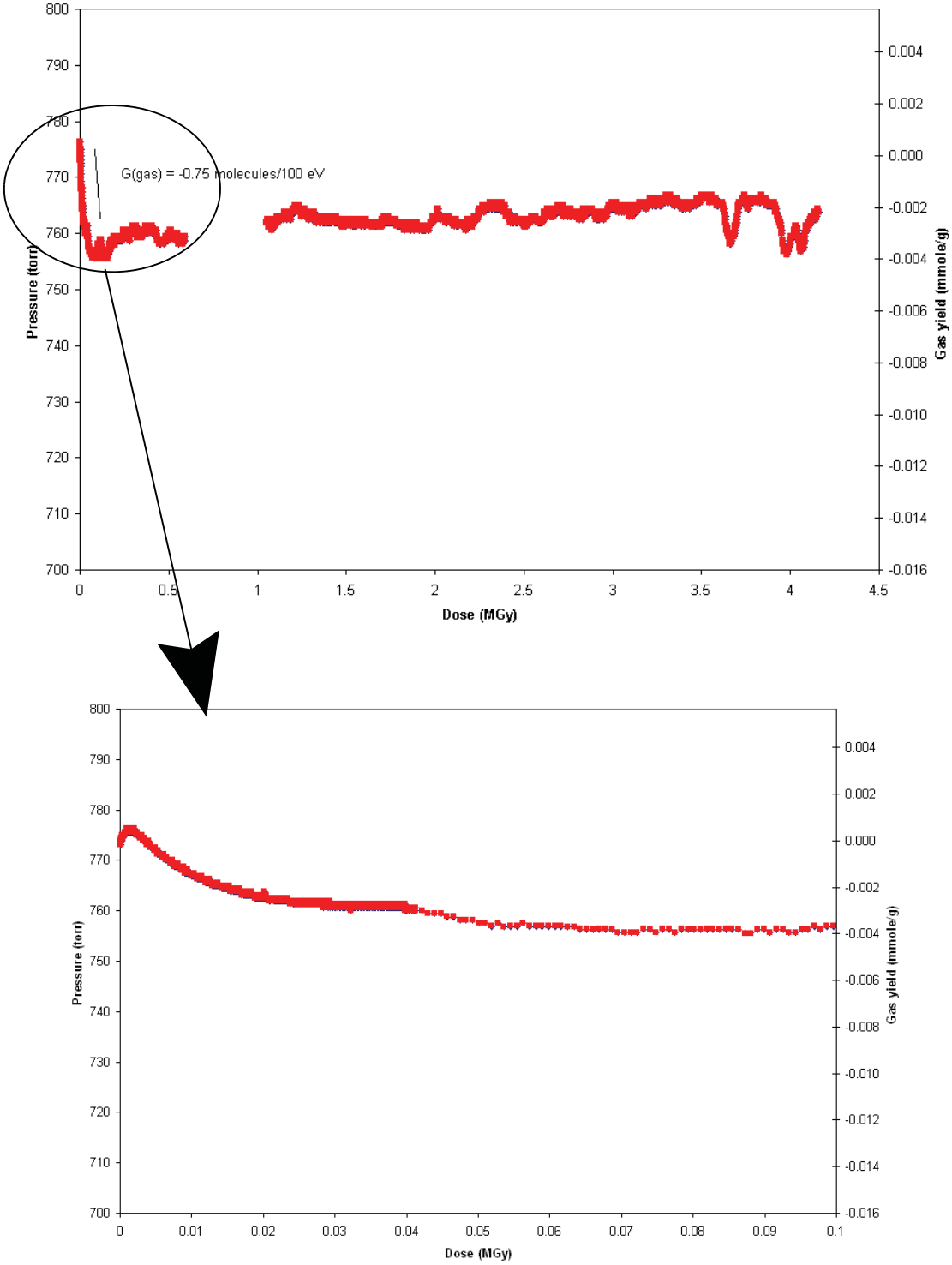

Fig. 4.4. Pressure and gas yield as a function of dose for sample ^{60}Co Np Tube 3 [^{60}Co-irradiated NpO_2 (650ºC) + 1 wt % H_2O].

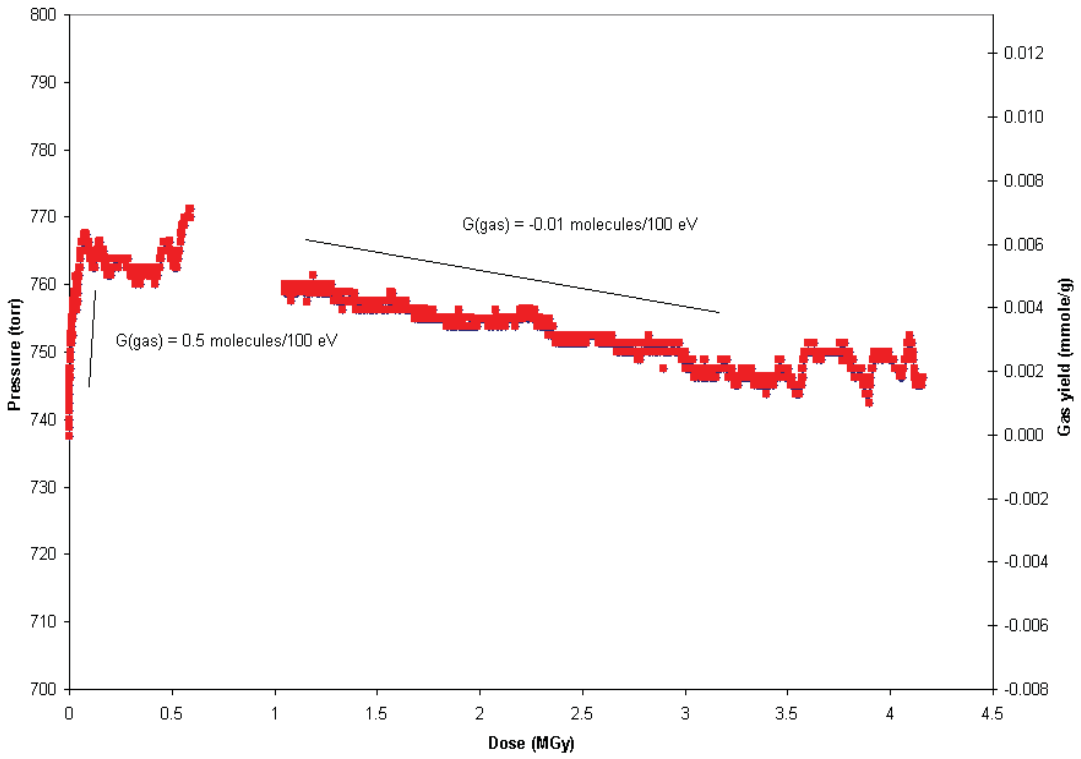

Fig. 4.5. Pressure and gas yield as a function of dose for sample ^{60}Co Np Tube 4 [^{60}Co-irradiated NpO_2 (800ºC) + 1 wt % H_2O].

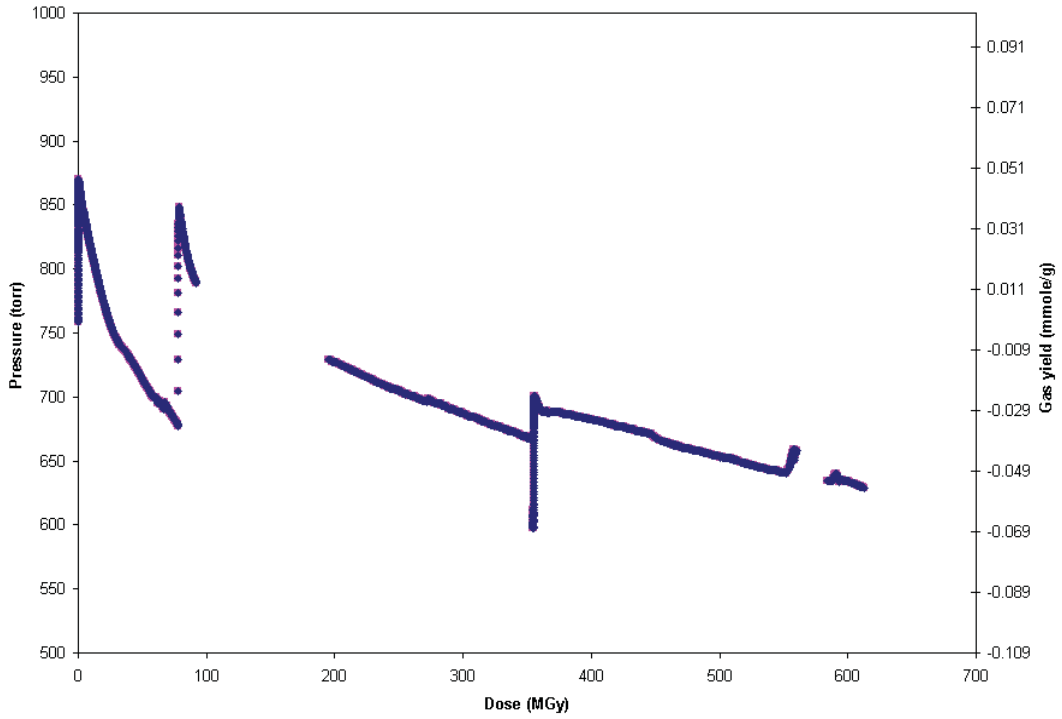

Fig. 4.6. Pressure and gas yield as a function of dose for sample HFIR Np Tube 1 [HFIR SNF-irradiated NpO_2 (650ºC)].

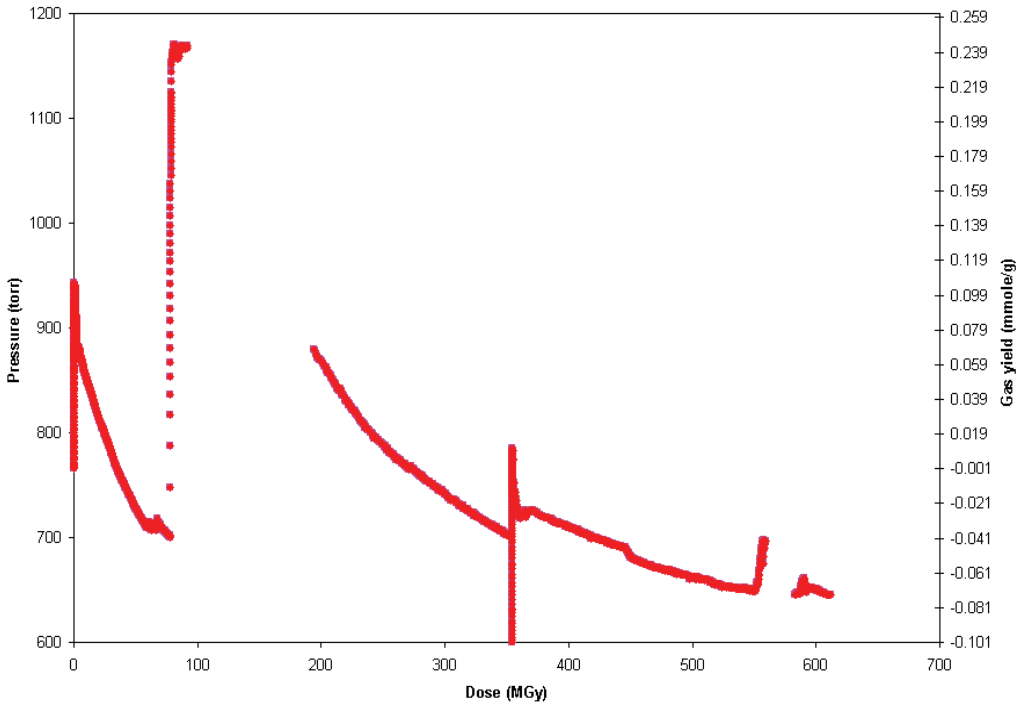

Fig. 4.7. Pressure and gas yield as a function of dose for sample HFIR Np Tube 2 [HFIR SNF-irradiated NpO_2 (650°C) + 1 wt % H_2O].

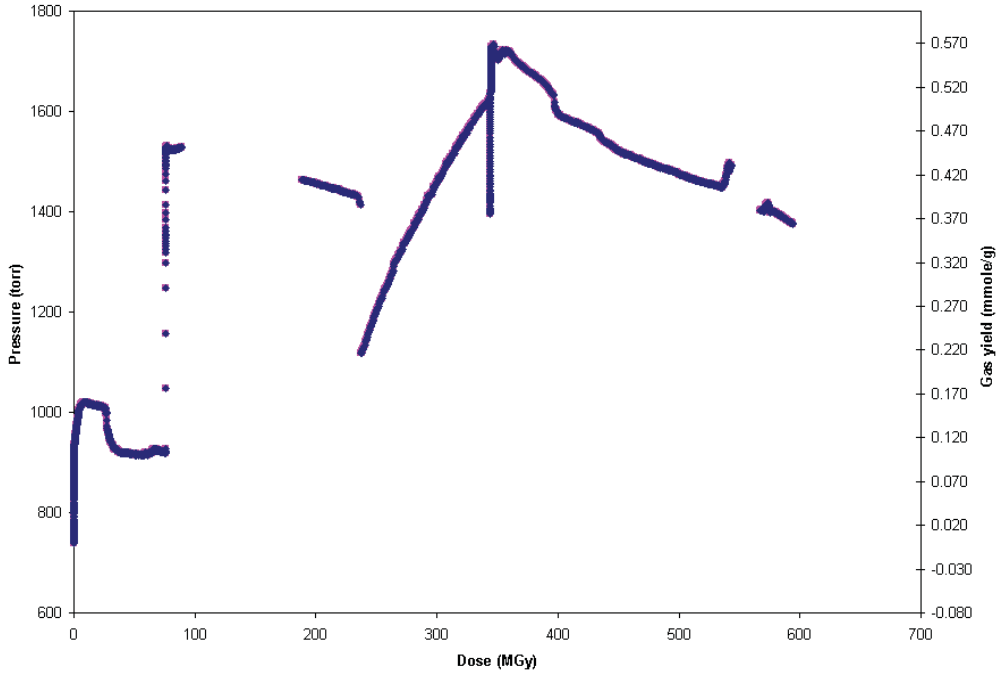

Fig. 4.8. Pressure and gas yield as a function of dose for sample HFIR Np Tube 3 [HFIR SNF-irradiated NpO_2 (650°C) + 8 wt % H_2O].

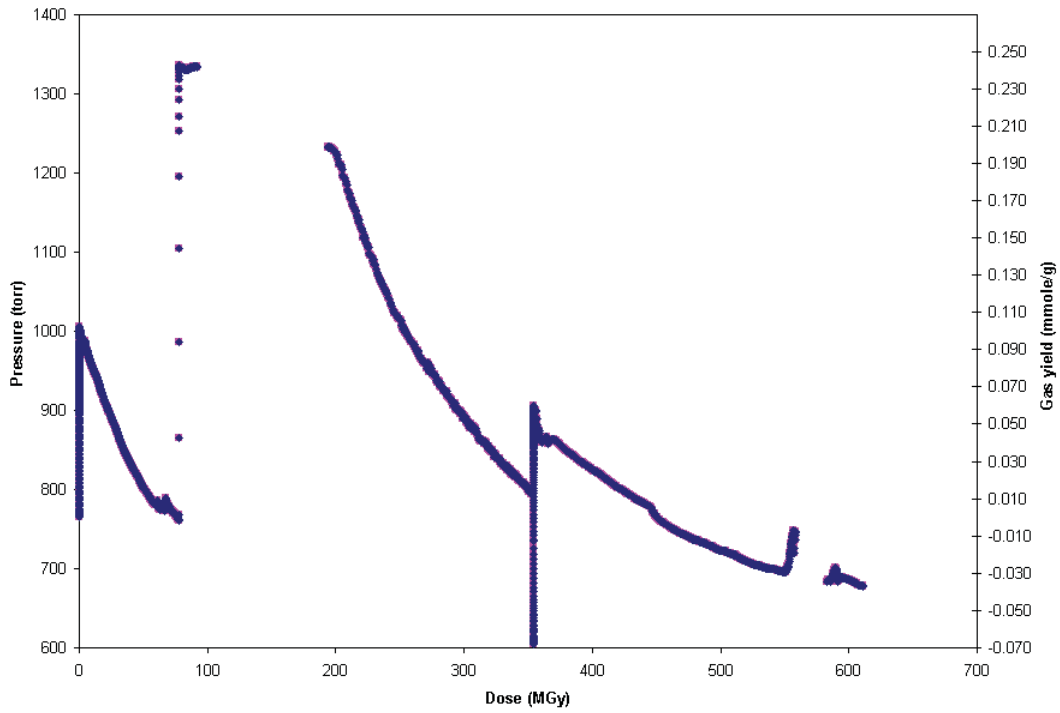

Fig. 4.9. Pressure and gas yield as a function of dose for sample HFIR Np Tube 4 [HFIR SNF-irradiated NpO_2 (800ºC) + 1 wt % H_2O].

The gap in the data for the ^{60}Co irradiations between about 0.5 and 1 MGy for Figs. 4.2–4.5 occurs because the data acquisition system was not working properly during that period. The slope of the gas yield vs dose curve gives (with unit conversion) the G-values that are indicated on the figures for the ^{60}Co experiments.

For the ^{60}Co experiments, the sample that was dry (Fig. 4.2) showed a small pressure increase, followed by a steady pressure decrease. Most of the increase can be attributed to the slight heating of the sample upon insertion into the irradiator. For the sample that contained 8 wt % moisture (Fig. 4.3), a steady pressure increase was seen. However, the rate of increase appears to slow with higher doses—as evidenced by the two G-values on the plot. This change in slope (G-value) is typical of an approach to a steady-state kinetic condition. The two ^{60}Co-irradiated samples that contained 1 wt % moisture showed a slightly different behavior. The sample prepared at 650ºC (Fig. 4.4) showed a small initial pressure increase (from about 773 to 778 torr, see insert), followed by a rather rapid pressure decrease to essentially a steady-state value of about 760 torr. The sample prepared at 800ºC (Fig. 4.5) had an initial pressure increase, which, similar to that presented in Fig. 4.4, could represent the combined effect of heating the sample (with a concomitant increase in vapor pressure of the moisture on the sample) and radiolysis of the moisture on the sample. Afterwards, the pressure was seen to steadily decrease.

For each of the HFIR SNF experiments (Figs. 4.6–4.9), a number of pressure transients are seen (i.e., at about 0, 90, and 350 MGy). These transients correspond to the insertion of the experiment into a fresh SNF element (i.e., one that was more recently discharged from the reactor and therefore of much greater gamma intensity).* The transient seen at about 550 MGy reflects an adjustment in the SNF pool temperature. The gap in the data shown in Figs. 4.6–4.9 between about 100 and 200 MGy occurred because the data acquisition system was not working properly during that period.

Each of the HFIR SNF-irradiated samples generally exhibited a similar behavior. Upon insertion into a fuel element, a pressure increase was observed, followed by a pressure decrease. In fact, if one disregards the transients, the overall trend is a pressure decrease. The increases during the transients are larger for the moisture-loaded samples (Figs. 4.7–4.9) than for the dry sample (Fig. 4.6). Again, the combined effects of heating and radiolysis are occurring during these transients.

In Fig. 4.8, which represents a HFIR sample that is heavily loaded with water, an additional transient is seen between about 220 and 350 MGy. The pressure is observed to quickly drop and then rise steadily. Otherwise, the behavior is very similar to that for the other samples. No explanation has been found for this transient, nor did time permit further exploration of this observation.

4.2.2 Gas Analyses

Results from the gas samples withdrawn from the containers at the completion of the irradiations are presented in Tables 4.2 and 4.3 for the ^{60}Co and the HFIR SNF experiments, respectively. Pressure and temperature data are also included in the tables. The values labeled as "initial" are those at the beginning of the experiment. The "final" values were taken just prior to withdrawal of the gas sample. As indicated in the tables, both the ^{60}Co and HFIR SNF experiments were loaded in air. However, there was a small amount of residual helium in each of the containers after leak testing.

To provide better insight into the change in the gas composition as a result of irradiation, the changes in the number of moles of O_2, CO_2, and H_2 were calculated by assuming that the starting sample atmosphere was the standard air composition (less any residual helium in the sample tubes).[12] The results of these calculations are shown in Table 4.4 . To put the measured H_2 yields in perspective, Table 4.5 provides the H_2 yields as a mole percentage of the initial amount of water available for radiolysis. Additionally, for the samples that had a net oxygen production, the O_2-plus-CO_2 yields as a mole percentage of the initial amount of water available for radiolysis are presented in Table 4.5.

The gas analysis for the ^{60}Co-irradiated samples containing ≤ 1 wt % H_2O showed, in general, O_2 consumption and a small amount of H_2 production (<1 vol %). A small amount of NO_x was also detected

* The insertion into a fresher element increases both the sample temperature and the radiolysis of any moisture that is present.

for each of the samples, which is a typical occurrence in the radiolysis of moist air.[13–15] Because this phenomenon is of no significance in the interpretation of the overall radiolysis experiments, it is not discussed further. The ^{60}Co-irradiated sample containing 8 wt % H_2O—which was clearly much greater than any amount of moisture possible by physi- or chemisorption—exhibited both H_2 and O_2 production. In fact, Table 4.4 shows that this production was nearly stoichiometric. For the 1 wt % moisture-laden samples, the O_2 consumption is nearly balanced by CO_2 production. For the dry NpO_2, the CO_2 production is about one-tenth the O_2 consumption. For each of the ^{60}Co-irradiated samples that contained water, a very small percentage of the available water was found as H_2 gas after irradiation (Table 4.5).

Table 4.2. Results of mass spectrometric analysis of gas composition from ^{60}Co-irradiated NpO_2 samples

	^{60}Co Np Tube 1 [NpO_2 (650°C)]	**^{60}Co Np Tube 2 [NpO_2 (650°C) + 8 wt % H_2O]**	**^{60}Co Np Tube 3 [NpO_2 (650°C) + 1 wt % H_2O]**	**^{60}Co Np Tube 4 [NpO_2 (800°C) + 1 wt % H_2O]**
Initial atmosphere	Air	Air	Air	Air
Initial pressure[a] (torr)	741	749	773	738
Initial temperature[a] (°C)	22	22	22	22
Final pressure[b] (torr)	709	952	764	746
Final temperature[b] (°C)	25	25	25	25
	Gas composition (vol %)			
CO_2	0.89	1.1	2.05	4.9
Ar	1.04	0.8	0.98	1.01
O_2	15.07	21.08	18.22	13.38
N_2	80.13	62.4	74.52	77.32
H_2	0.01	12.01	0.94	0.24
He	2.25	2.07	2.9	1.7
H_2O	0.48	0.35	0.1	0.09
NO_x	0.1	0.03	0.13	1.22

[a] Value at beginning of the experiment.
[b] Value just prior to withdrawal of gas sample.

Table 4.3. Results of mass spectrometric analysis of gas composition from HFIR SNF-irradiated NpO_2 samples

	HFIR Np Tube 1 [NpO_2 (650ºC)]	HFIR Np Tube 2 [NpO_2 (650ºC) + 1 wt % H_2O]	HFIR Np Tube 3 [NpO_2 (650ºC) + 8 wt % H_2O]	HFIR Np Tube 4 [NpO_2 (800ºC) + 1 wt % H_2O]
Initial atmosphere	Air	Air	Air	Air
Initial pressure[a] (torr)	759	766	739	766
Initial temperature[a,b] (ºC)	40	40	40	40
Final pressure[c] (torr)	629	645	1376	678
Final temperature[c,d] (ºC)	55	55	55	55
	Gas composition (vol %)			
CO_2	2.32	0.04	0.005	1.68
Ar	1.23	1.27	0.59	1.22
O_2	3.21	0.06	16.84	0.04
N_2	90.09	96.13	45.96	96.6
H_2	0.05	0.006	35.46	0.026
He	2.05	1.9	0.9	0.13
CO	0.1	<0.01	<0.01	<0.01
NO_x	0.9	0.54	0.16	0.15

[a] Value at beginning of the experiment.
[b] Typical SNF pool temperature.
[c] Value just prior to withdrawal of gas sample.
[d] Average temperature of container inside element (based on previous experiments).

Table 4.4. Estimated change in gas composition for selected experiments as a result of radiolysis

Experiment	Material[a]	Δ O_2 (mol)	Δ CO_2 (mol)	Δ H_2 (mol)
^{60}Co Np Tube 1	NpO_2 (650ºC)	-4.1×10^{-5}	5.3×10^{-6}	6.2×10^{-8}
^{60}Co Np Tube 2	NpO_2 (650ºC) + 8 wt % H_2O	3.9×10^{-5}	8.7×10^{-6}	9.8×10^{-5}
^{60}Co Np Tube 3	NpO_2 (650ºC) + 1 wt % H_2O	-1.7×10^{-5}	1.3×10^{-5}	6.2×10^{-6}
^{60}Co Np Tube 4	NpO_2 (800ºC) + 1 wt % H_2O	-4.5×10^{-5}	3.7×10^{-5}	1.5×10^{-6}
HFIR Np Tube 1	NpO_2 (650ºC)	-2.4×10^{-4}	2.4×10^{-5}	5.3×10^{-7}
HFIR Np Tube 2	NpO_2 (650ºC) + 1 wt % H_2O	-4.0×10^{-4}	2.4×10^{-8}	9.3×10^{-8}
HFIR Np Tube 3	NpO_2 (650ºC) + 8 wt % H_2O	1.8×10^{-4}	-4.2×10^{-7}	1.2×10^{-3}
HFIR Np Tube 4	NpO_2 (800º) + 1 wt % H_2O	-2.9×10^{-4}	1.9×10^{-5}	3.0×10^{-7}
Alpha Np Tube 1	NpO_2 (650ºC)	-5.4×10^{-5}	6.5×10^{-6}	8.7×10^{-7}
Alpha Np Tube 2	NpO_2 (650ºC) + 1 wt % H_2O	5.2×10^{-5}	-9.6×10^{-8}	1.1×10^{-4}
Alpha Np Tube 3 (first gas sample)	NpO_2 (650ºC) + 8 wt % H_2O	8.7×10^{-4}	1.2×10^{-6}	1.7×10^{-3}
Alpha Np Tube 4	NpO_2 (800ºC) + 1 wt % H_2O	7.5×10^{-6}	4.1×10^{-7}	8.1×10^{-5}
Alpha Np Tube 5	NpO_2 (650ºC) + 0.5 wt % H_2O	*b*	*b*	6.9×10^{-6}

[a] Value in parenthesis denotes preparation temperature.

[b] Excess O_2 was initially present in transducer region of sample; therefore, change in O_2 and CO_2 cannot be estimated.

Table 4.5. Estimated H_2 production as a percentage of initial amount of water available for radiolysis

Experiment	Material[a]	Ratio of H_2 production to water available for radiolysis (mol %)	Ratio of $O_2 + CO_2$ production to water available for radiolysis (mol %)
^{60}Co Np Tube 2	NpO_2 (650ºC) + 8 wt % H_2O	0.55	0.27
^{60}Co Np Tube 3	NpO_2 (650ºC) + 1 wt % H_2O	0.28	*b*
^{60}Co Np Tube 4	NpO_2 (800ºC) + 1 wt % H_2O	0.068	*b*
HFIR Np Tube 2	NpO_2 (650ºC) + 1 wt % H_2O	0.0042	*b*
HFIR Np Tube 3	NpO_2 (650ºC) + 8 wt % H_2O	6.7	0.99
HFIR Np Tube 4	NpO_2 (800ºC) + 1 wt % H_2O	0.014	*b*
Alpha Np Tube 2	NpO_2 (650ºC) + 1 wt % H_2O	6.8	3.2
Alpha Np Tube 3 (after first gas sample)	NpO_2 (650ºC) + 8 wt % H_2O	13	6.6
Alpha Np Tube 4	NpO_2 (800ºC) + 1 wt % H_2O	4.7	0.46
Alpha Np Tube 5	NpO_2 (650ºC) + 0.5 wt % H_2O	0.8	*c*

[a] Value in parenthesis denotes preparation temperature.
[b] For this sample, there was a net consumption of O_2.
[c] Not available, because the initial O_2 composition over the sample was not well known.

The NpO_2 samples containing ≤1 wt % H_2O that were irradiated in HFIR SNF elements (Figs. 4.6, 4.7, and 4.9) exhibited an overall pressure decrease. The gas analyses for these samples showed that the O_2 was almost completely consumed while only a trace of H_2 was produced. The CO_2 production was ≤10% of the O_2 consumption for HFIR Np Tube 1 and HFIR Np Tube 4. Only a trace of CO_2 was produced for HFIR Np Tube 2. By contrast, the sample containing 8% water (Fig. 4.8) had a net pressure increase. In this experiment, the pressure appeared to peak and then slowly decrease. The gas analysis for the 8% sample showed that a rather large amount of H_2 (~35 vol %, Table 4.3) was produced. It also appears from this table alone that a stoichiometric amount of O_2 was produced; however, closer examination of the net change in each component (Table 4.4) shows that the net O_2 production was 15% of the hydrogen production. Only in the case of HFIR Np Tube 3 was the H_2 production a significant fraction of the available H_2O (Table 4.5).

4.3 ALPHA RADIOLYSIS EXPERIMENTS

Table 4.6 provides a summary of the alpha irradiation experiments that were performed. Irradiation times ranged from 110 to 295 days. Considering the higher dose rate of the ^{244}Cm as compared with the ^{238}Pu (see Fig. 3.8), this would correspond to equivalent irradiation times ranging from 21 to 57 years for the SRS neptunium.

Table 4.6. Summary of alpha irradiation experiments performed

Experiment	Material[a]	Mass (g)	^{244}Cm added (mg)	Total dose (MGy)[b]
Alpha Np Tube 1	NpO_2 (650ºC)	2.95	18.72	280
Alpha Np Tube 2	NpO_2 (650ºC) + 1 wt % H_2O	2.96996	18.66	439
Alpha Np Tube 3	NpO_2 (650ºC) + 8 wt % H_2O	3.175	18.66	410
Alpha Np Tube 4	NpO_2 (800ºC) + 1 wt % H_2O	3.130	19.68	439
Alpha Np Tube 5	NpO_2 (650ºC) + 0.5 wt % H_2O	2.96475	18.72	166

[a]Value in parenthesis denotes preparation temperature.
[b]Dose calculated by depositing all of the alpha decay energy in the sample (i.e., NpO_2 + H_2O).

4.3.1 Pressure Measurements

Pressure within the sample containers was monitored throughout the irradiations, and the pressure data from each of the experiments are shown in Figs. 4.10–4.14. G-values, which were calculated from the slope of the curves, are also presented in these figures.

The dry NpO_2 sample (Fig. 4.10) exhibited a steady pressure decrease. As seen in Fig. 4.10, a gas sample was withdrawn from Alpha Np Tube 1 after a dose of about 140 MGy. The tube was then backfilled with O_2 to a total pressure of about 1350 torr. The pressure again decreased, although at what appears to be at a higher rate than previously seen. Additionally, with increasing dose, the pressure appears to approach a steady state. After about 280-MGy total dose, this tube (which contained dry NpO_2) was opened and 0.5 wt % moisture was added. This sample then became experiment Alpha Np Tube 5 (Fig. 4.14).

Both of the samples that contained 1 wt % moisture (Figs. 4.11 and 4.13) exhibited similar behavior. The pressure steadily increased and approached what appeared to be a plateau. A gas sample was withdrawn from Alpha Np Tube 2 (Fig. 4.11) after a dose of about 140 MGy. The tube was then vented to the glove box and isolated. The experiment continued, whereupon the pressure increased slightly, followed by an overall decrease. Hence, the plateau that was seen just before gas sampling was probably a peak—one that would have been followed by a pressure decrease had a gas sample not been withdrawn.

Similar to Alpha Np Tube 2, a gas sample was withdrawn from Alpha Np Tube 4 after a dose of about 140 MGy (Fig. 4.13). This tube was then vented to the glove box and resealed, and the experiment continued. Again, the pressure increased slightly, followed by a decrease.

For Alpha Np Tube 3 (Fig. 4.12), gas samples were withdrawn after about 80- and 130-MGy total dose. The tube was vented to the glove box (no gas sample taken) after a dose of almost 250 MGy. It was then resealed, and the experiment was continued. However, a final gas sample was not withdrawn. Throughout the irradiation of Alpha Np Tube 3, a steady pressure increase was noted. After each sample withdrawal or pressure reduction, the rate of pressure increase slowed, as shown by comparing the G-values for each segment. These decreasing G-values again indicate the approach to a steady state.

The sample that contained the 0.5 wt % moisture (Fig. 4.14) showed a steady pressure increase to a plateau. This sample had originally been the dry NpO_2 (Alpha Np Tube 1), which had been exposed to excess oxygen. As seen in Fig. 4.14, a gas sample was withdrawn from Alpha Np Tube 5 after a total dose of about 130 MGy.

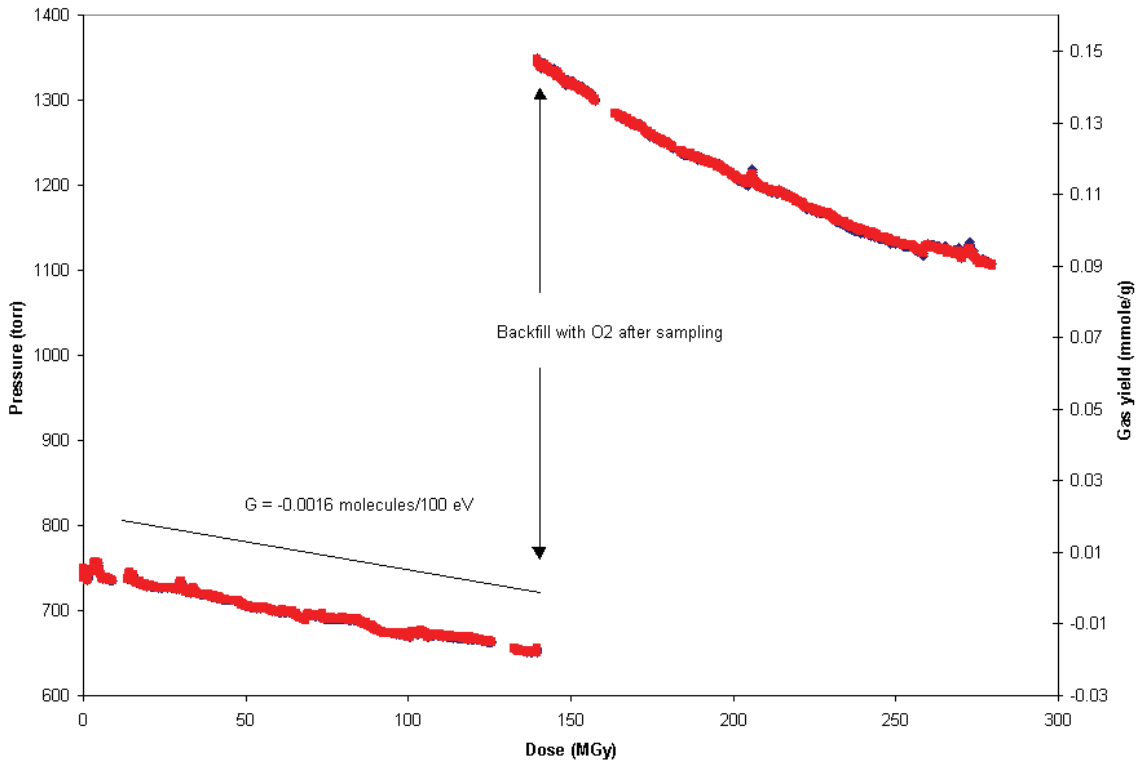

Fig. 4.10. Pressure and gas yield as a function of dose for sample Alpha Np Tube 1 [^{244}Cm alpha-irradiated NpO_2 (650ºC)].

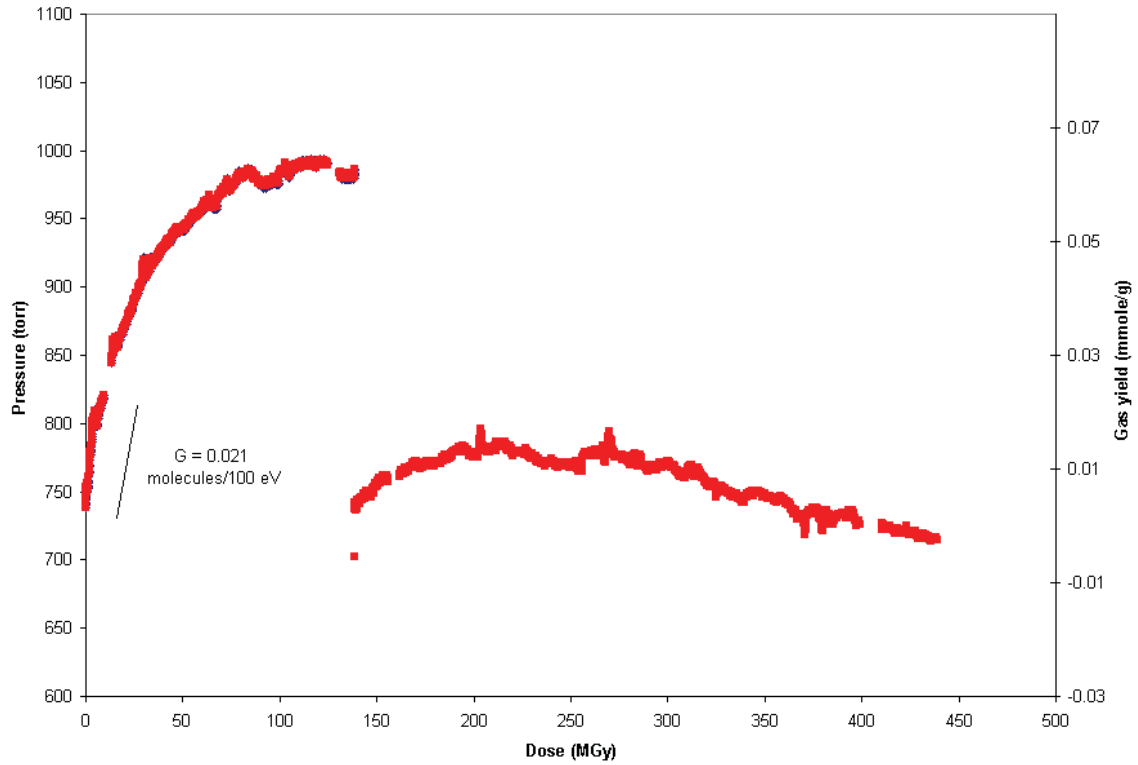

Fig. 4.11. Pressure and gas yield as a function of dose for sample Alpha Np Tube 2 [^{244}Cm alpha-irradiated NpO_2 (650º) + 1 wt % H_2O].

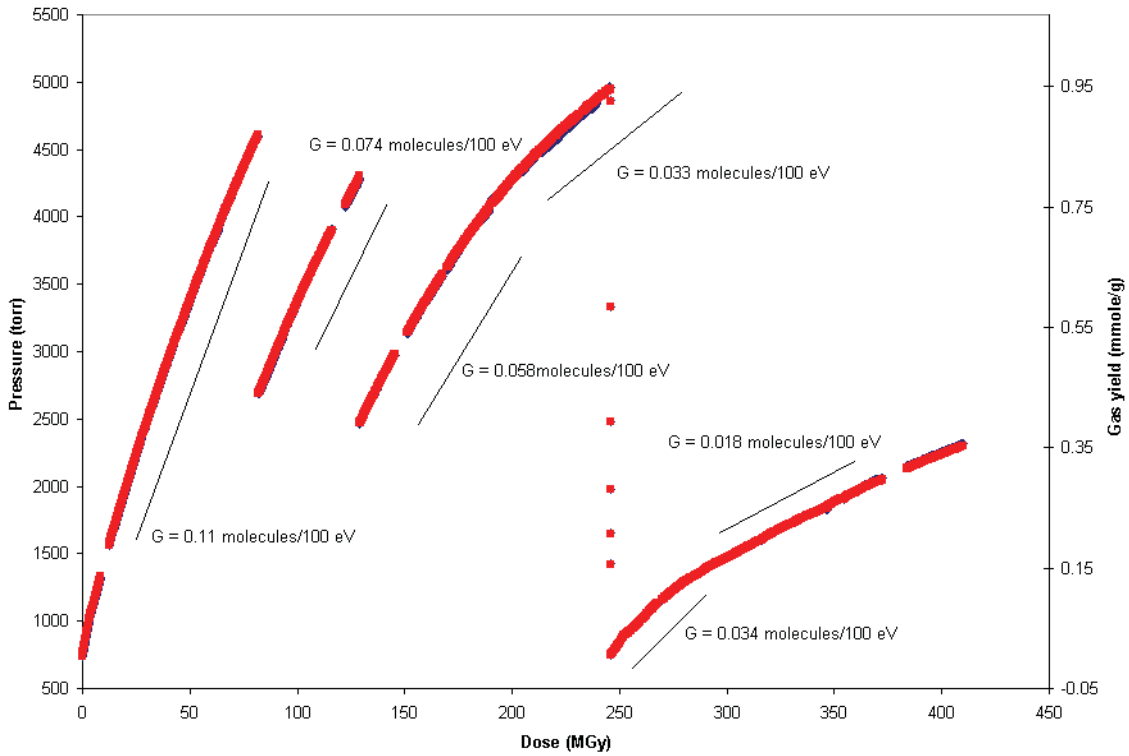

Fig. 4.12. Pressure and gas yield as a function of dose for sample Alpha Np Tube 3 [^{244}Cm alpha-irradiated NpO_2 (650ºC) + 8 wt % H_2O].

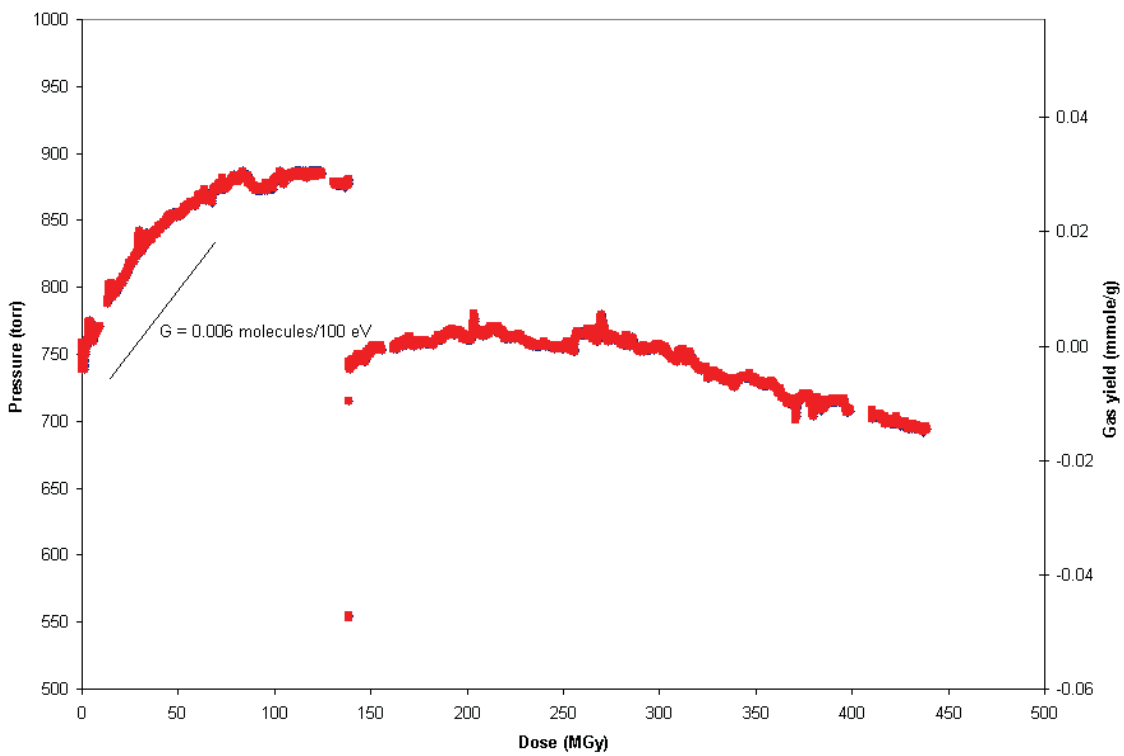

Fig. 4.13. Pressure and gas yield as a function of dose for sample Alpha Np Tube 4 [^{244}Cm alpha-irradiated NpO_2 (800ºC) + 1 wt % H_2O].

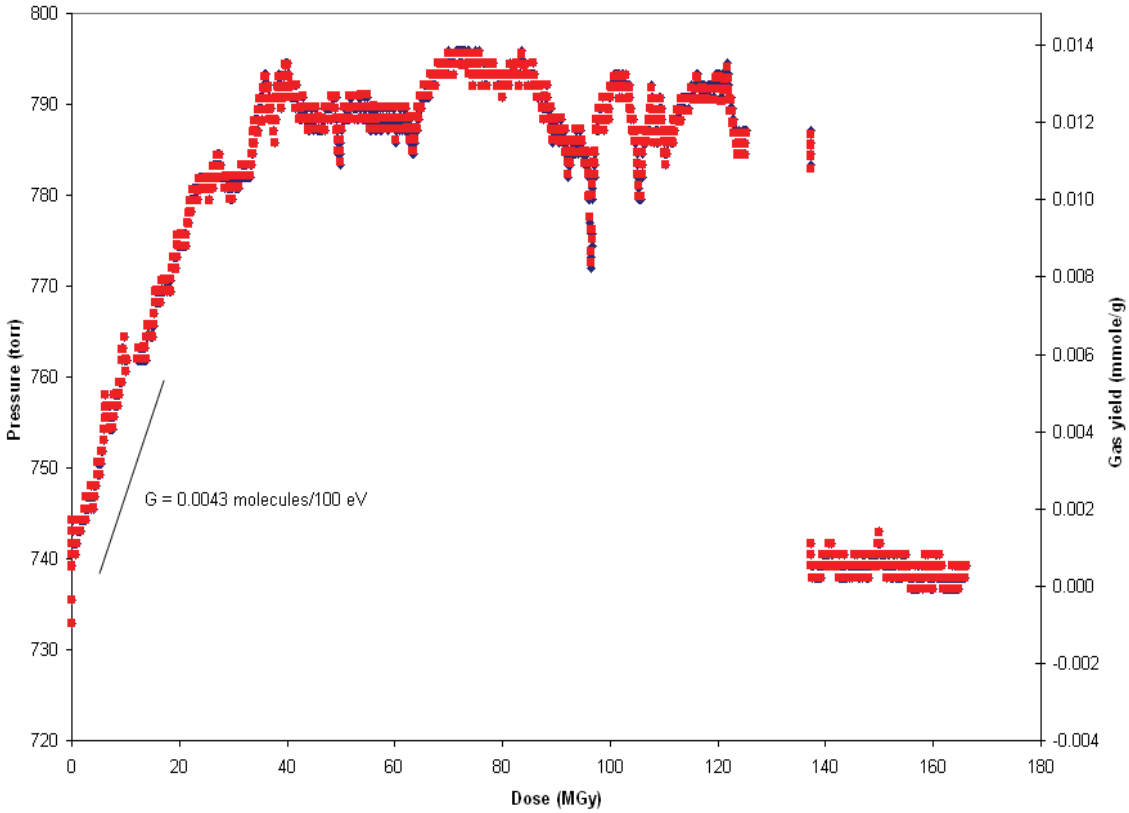

Fig. 4.14. Pressure and gas yield as a function of dose for sample Alpha Np Tube 5 [^{244}Cm alpha-irradiated NpO_2 (650°C) + 0.5 wt % H_2O].

4.3.2 Gas Analyses

Gas samples were periodically withdrawn from the containers during the experiments. Analytical results for these samples are presented in Table 4.7, which also includes pressure and temperature data. As in the gamma irradiation experiments, the values labeled as "initial" are those at the beginning of the experiment or, in the case of multiple gas samples, the value just after sampling. The "final" values are taken just prior to withdrawal of the gas sample.

The calculated changes in the moles of O_2, CO_2, and H_2 (assuming that the starting sample atmosphere was the standard air composition,[12] less any residual helium in the sample tubes) are shown in Table 4.4. (No such calculation was made for Alpha Np Tube 5. While air was present immediately over this sample, the sample initially had additional O_2 and helium that were present in the pressure-transducer region.) Table 4.5 provides (1) H_2 yields and (2) O_2-plus-CO_2 yields (for the samples that had a net oxygen production) as a mole percentage of the initial amount of water available for radiolysis.

Table 4.7. Results of mass spectrometric analysis of gas composition from alpha-irradiated NpO_2 samples

	Alpha Np Tube 1 NpO_2 (650ºC)	Alpha Np Tube 2 NpO_2 (650ºC) + 1 wt % H_2O	Alpha Np Tube 3 NpO_2 (650ºC) + 8 wt % H_2O		Alpha Np Tube 4 NpO_2 (800ºC) + 1 wt % H_2O	Alpha Np Tube 5 NpO_2 (650ºC) + 0.5 wt % H_2O
			First gas sample	Second gas sample		
Initial atmosphere	Air	Air	Air	First gas sample composition (no helium)	Air	Air/excess O_2[a]
Initial pressure[b] (torr)	739	738	740	2683	740	735
Initial temperature[b] (ºC)	19.5	17.2	18.3	18.9	19.5	19.8
Final pressure[c] (torr)	656	986	4601	4292	881	786
Final temperature[c] (ºC)	19.6	19.6	18.9	18.5	19.1	23.0
	Gas composition (vol %)					
CO_2	0.9	0.1	0.04	0.025	0.07	0.02
Ar	0.65	0.54	0.2	0.1	0.61	0.47
O_2	7.4	17.27	28.9	30.16	14.26	42.63
N_2	52.0	44.4	17.52	7.95	50.79	54.11
H_2	0.12	11.72	50.26	58.57	9.54	1.27
He[d]	38.03	25.55	2.85	2.97	23.92	1.09
H_2O	0.2	0.1		0.2	0.2	
NO_x	0.6	0.39	0.05	0.02	0.6	0.4
CH_4	0.004	0.003	<0.01	<0.01	0.005	<0.01
CO	<0.01	<0.01	<0.01	<0.01	<0.01	0.006

[a] Tube 5 was made by taking the Tube 1 experiment and adding 0.5 wt % water. Prior to this addition, Tube 1 had been backfilled with O_2. Because the pressure transducer and sampling line were not flushed with air prior to the water addition, the initial atmosphere in the pressure-transducer region likely had an excess of O_2. The atmosphere directly over the sample was air.

[b] Value at beginning of experiment or just after previous gas-sampling operation.

[c] Value just prior to withdrawal of gas sample.

[d] Helium was an artifact of the sampling method.

The dry NpO_2 sample that was irradiated with the alpha from ^{244}Cm (Fig. 4.10) showed a pressure decrease to vacuum (i.e., a pressure less than atmospheric). The gas sample from this experiment confirmed that O_2 was consumed. After the gas sample was withdrawn, this container was backfilled with O_2 and the sample pressure continued to decrease, likely from further O_2 consumption. (A final gas sample was not withdrawn.)

Both of the alpha-irradiated NpO_2 samples that had 1 wt % sorbed moisture exhibited a pressure increase to an apparent steady-state plateau at ~100–130 MGy (Figs. 4.11 and 4.13). The sample prepared at 650ºC increased about 250 torr, while that prepared at 800ºC increased about 140 torr. The steady-state plateau represents a situation in which back reactions (i.e., H_2 and O_2 recombination) balance forward reactions (i.e., H_2 and O_2 production). The gas analysis results for these two experiments revealed that both H_2 and O_2 were produced. For Alpha Np Tube 2, a stoichiometric mixture of H_2 and O_2 was present at the plateau. However, for Alpha Np Tube 4, the O_2 production was only about 10% of the H_2 production (Table 4.4). A small amount of NO_x was also detected. After sampling, both tubes were vented with the glove-box atmosphere and then closed. Both experiments showed a small pressure increase followed by a decrease, probably indicating the consumption of some excess O_2 in the system, as was seen before in other experiments. However, a final gas sample was not taken.

The alpha-irradiated NpO_2 sample that contained 8 wt % H_2O exhibited a steady increase in pressure (Fig. 4.12). The initial gas analysis of a sample taken after 80-MGy total dose showed that both H_2 and O_2 were produced in stoichiometric proportions. A second gas sample after about 130 MGy showed further H_2 and O_2 production. As indicated in Fig. 4.12, the pressure increased at a decreasing rate; however, for this experiment, a pressure plateau had not been reached by the time the experiment was terminated.

The alpha-irradiated NpO_2 sample containing 0.5 wt % H_2O (equivalent to the limit established for the SRS material) showed a small pressure increase to a steady-state plateau (Fig. 4.14). The gas analysis showed that H_2 was produced. A conclusion about the production or depletion of O_2 cannot be made for this sample because of excess O_2 in the pressure-transducer region.* However, any O_2 production should be bounded by the results from the 1 wt % experiments.

---

*Alpha Np Tube 5 was prepared by opening Alpha Np Tube 1 and adding 0.5 wt % H_2O. However, the atmosphere in the experimental rig was not purged. Although glove-box air was directly over the NpO_2 sample, it is likely that a slug of O_2-rich air (from the previous operations on Alpha Np Tube 1) resided in the transducer region of the experimental rig.

4.4 OVERVIEW OF RADIOLYTIC MECHANISM

All of these experiments demonstrate some common trends. First, water radiolysis alone is a rapid process relative to other chemical processes that are occurring simultaneously. Second, when the water content is $\leq 1\%$, the overall pressure in the system *generally* decreases (or peaks after small pressure increases and then decreases). Third, oxygen is both produced and consumed as a result of radiolytic reactions and, in the long-term, consumption will be the dominant effect.* This consumption is especially evident when oxygen is added during the course of the experiment (see Fig. 4.10). Fourth, limiting pressures (steady-state plateaus) are either reached or approached. Fifth, minor products such as CO_2 and NO_x are produced. All of these phenomena are consistent with previously reported fundamental reactions and are discussed separately below.

Water radiolysis was extensively studied more than a half century ago,[16,17] when it was shown not only that the water is dissociated into *primary radical products* (ultimately forming H_2, O_2 and H_2O_2), but also that these primary radical products cause back reactions limiting the overall amount of *ultimate products*. Thus, a steady-state condition is quickly reached in which no further accumulation of ultimate products occurs—one in which the rate of dissociation of water is balanced by its rate of formation. Consequently, extreme gas product pressures from the radiolysis of water are not ordinarily possible.

Accompanying these water radiolysis reactions is another reaction in which the oxygen over solid actinide oxides in such a radiolytically activated system can oxidize the actinide solid (at least partially) to a higher oxidation state. Evidence for this is clearly seen in the oxidation of uranium oxides to higher oxidation states.[4,18,19] While a direct measurement of the oxidation state of the NpO_2 was not made (e.g., via X-ray diffraction), the disappearance of oxygen in the presence of NpO_2 is interpreted as being the result of the formation of higher neptunium oxidation states (e.g., Np_2O_5)—a reaction mechanism analogous to that observed for the uranium oxides.[4] This reaction largely accounts for the net pressure decrease in the system through the consumption of oxygen.

By using the NpO_2 sample from Alpha Np Tube 1 for the Alpha Np Tube 5 experiment, the competing reactions of (1) O_2 generation and consumption by H_2O radiolytic chemistry were separated from (2) the NpO_2 oxidation reaction. In this case, the NpO_2 was "presaturated" with oxygen prior to the addition of water in the Tube 5 test; and when the water was added, only the water radiolysis chemistry was evident (i.e., water radiolysis and back reactions to reach a steady state). The experiment in Tube 5 then showed a gradual rise to a steady-state pressure. Had this NpO_2 sample not been presaturated with

---

*Note that both of the alpha-irradiated samples that contained 1% H_2O appeared to reach a plateau. However, after withdrawal of a gas sample, the net effect was a pressure decrease. This result indicates that in the long term, a slower-acting mechanism (i.e., one that is slower than the forward-reaction production of O_2) will result in net O_2 consumption.

oxygen, we would predict a profile more like that of Fig. 4.11—one in which after the water radiolysis and back reactions would initially dominate, but then the slower oxygen consumption reaction by the NpO_2 would commence and begin to reduce the total pressure of the system.

Additionally, it appears that the radiochemical kinetics of such reactions (radiolysis of water and oxidation of the NpO_2) may be influenced by the type of radiation. In the case of the highly penetrating gamma radiation, the radiolysis reaction response occurs rapidly, followed by a decrease resulting from the radiolytically influenced oxidation of the NpO_2. The overall character of the gamma radiolysis experiments is then one that is dominated by oxidation of NpO_2. For the alpha radiolysis experiments, it appears that radiolysis of water dominates for a longer period of time as compared with that observed in the gamma experiments.

Also associated with the above reactions are a number of *impurity* reactions in which the primary products of water radiolysis combine with the N_2 accompanying the O_2 in the air atmosphere over the sample or with the carbon that is ubiquitous in many oxide preparations. Thus, trace amounts of NO_x and CO_2 are common impurity by-products of such oxide/water radiolysis reactions.

We can therefore explain the overall chemistry taking place during these radiolysis reactions as being a combination of the above phenomena and not just one of these isolated fundamental processes. Initially, a pressure increase often occurs in the encapsulated system, representing both a slight temperature effect and, more importantly, radiolysis of sorbed water to form some hydrogen and oxygen. This water radiolysis would reach a steady-state pressure were it not for the reaction of oxygen with the actinide oxide to form a higher oxidation state of the actinide and thus decrease the oxygen content of the atmosphere over the system. Evidence for this is seen in the "dry" oxide radiolysis experiments, in which there is no pressure increase (because there is no water to be radiolyzed)—only oxygen consumption. When there is an excessive amount of moisture (e.g., 8%, a case in which water would have to actually condense and puddle on the oxide), the water radiolysis reaction is dominant. Nevertheless, even here, *all* of the water on the sample is not radiolyzed, because of the accompanying back reactions of the primary water radiolytic products (i.e., the radicals) with the water products (H_2, O_2, etc.).

5. CONCLUSIONS

Two key results were demonstrated in these experiments. First, the water uptake experiments clearly indicated that the 0.5 wt % moisture limit that has been typically established for similar materials (e.g., uranium and plutonium oxides)[9,10] cannot be obtained in a practical environment. In fact, the uptake in a typical environment can be expected to be at least an order of magnitude less than this limit.

The second key result is the establishment of steady-state plateaus. These plateaus illustrate the presence of back reactions that limit the overall pressure increase and H_2 production. For example, in the case of the NpO_2 alpha radiolysis experiments containing 1 wt % H_2O, total decomposition of all the H_2O into H_2 and O_2 would result in a pressure increase of about 3450 torr. However, for these experiments, the actual pressure increase was only 140–250 torr. Similarly, for the alpha-irradiated 0.5 wt % H_2O sample, total decomposition would result in a pressure increase of about 1750 torr, while a rise of only 50 torr was observed. These results clearly demonstrate that 0.5 wt % H_2O on NpO_2 is safe for long-term storage—if such a moisture content could ever be practically reached. Additionally, there is evidence that another mechanism plays a role in O_2 consumption; namely, radiolytically-influenced oxidation of the NpO_2. This mechanism further limits pressurization in the long term.

In setting the storage standards for the actinide oxides, it has customarily been assumed[9,10] that radiolysis of sorbed moisture would produce stoichiometric amounts of H_2 and O_2 and would continue until all of the water had been radiolyzed to these products. However, these results support the observations of other laboratories that *many other radiolytic reactions* are concurrently active in such radiolytic processes and thus limit the overall accumulation of these products.

REFERENCES

1. A. S. Icenhour, L. M. Toth, G. D. Del Cul, and L. F. Miller, "Gamma Radiolysis Studies of Uranyl Fluoride," *Radiochim. Acta* **90**, 109–122 (2002).

2. A. S. Icenhour and L. M. Toth, *Gamma Radiolysis Study of $UO_2F_2 \cdot 0.4\ H_2O$ Using Spent Nuclear Fuel Elements from the High Flux Isotope Reactor*, ORNL/TM-2001/138, UT-Battelle, LLC, Oak Ridge National Laboratory, Oak Ridge, Tennessee, January 2002.

3. A. S. Icenhour, L. M. Toth, and H. Luo, *Water Sorption and Gamma Radiolysis Studies for Uranium Oxides*, ORNL/TM-2001/59, UT-Battelle, LLC, Oak Ridge National Laboratory, Oak Ridge, Tennessee, February 2002.

4. A. S. Icenhour and L. M. Toth, *Alpha Radiolysis of Sorbed Water on Uranium Oxides and Uranium Oxyfluorides*, ORNL/TM-2003/172, UT-Battelle, LLC, Oak Ridge National Laboratory, Oak Ridge, Tennessee, September 2003.

5. "Np Oxide Material Specification Agreement between the Savannah River Site and the Oak Ridge National Laboratory for the transfer of Neptunium Oxide," NMM-PRG-2002-011.7, Rev. 0, December 2002.

6. "Np Oxide Packaging Agreement between the Savannah River Site and the Oak Ridge National Laboratory for the Transfer of Neptunium Oxide," CBU-HCP-2003-00033, Rev. 0, March 2003.

7. J. A. Porter, "Production Technology of Neptunium-237 and Plutonium-238," pp. 289–293 in *Proceedings of the Symposium on Production Technology of Neptunium-237 and Plutonium-238, 146th Meeting of the American Chemical Society, January 1964*, Vol. 3, Issue 4, American Chemical Society, Washington, D.C., 1964.

8. A. S. Icenhour, *Radiolytic Effects on Fluoride Impurities in a U_3O_8 Matrix*, ORNL/TM-2000/157, UT-Battelle, LLC, Oak Ridge National Laboratory, Oak Ridge, Tennessee, May 2000.

9. *Criteria for Packaging and Storing Uranium-233-Bearing Materials*, DOE-STD-3028-2000, U.S. Department of Energy, Washington, D.C.

10. *Criteria for Preparing and Packaging Plutonium Metals and Oxides for Long-term Storage*, DOE-STD-3013, U.S. Department of Energy, Washington, D.C.

11. J. M. Duffey and R. R. Livingston, *Characterization of Neptunium Oxide Generated Using the HB-Line Phase II Flowsheet*, WSRC-TR-2003-00388, Rev. 0, Westinghouse Savannah River Company, Savannah River Site, Aiken, S.C., August 2003.

12. *CRC Handbook of Chemistry and Physics*, 73rd ed., D. R. Lide, ed., CRC Press, Boca Raton, Florida, 1992.

13. W. Primak and L. H. Fuchs, "Nitrogen Fixation in a Nuclear Reactor," *Nucleonics* **13**(2), 38–41 (1955).

14. P. Harteck and S. Dondes, "Producing Chemicals with Reactor Radiations," *Nucleonics* **14**(7), 22–25 (1956).

15. A. R. Jones, "Radiation-Induced Reactions in the N_2-O_2-H_2O System," *Radiat. Res.* **10**, 655–663 (1959).

16. C. J. Hochanadel, "Effects of Cobalt Gamma-Radiation on Water and Aqueous Solutions," *J. Phys. Chem.* **56**(5), 587–94 (1952).

17. A. O. Allen, C. J. Hochanadel, J. A. Ghormley, and T. W. Davis, "Decomposition of Water and Aqueous Solutions Under Mixed Fast Neutron and Gamma Radiation," *J. Phys. Chem.* **56**(5), 575–86 (1952).

18. G. Sattonnay et al., "Alpha-Radiolysis Effects on UO_2 Alteration in Water," *J. Nucl. Mater.* **288**, 11–19 (2001).

19. P. C. Burns and K. Hughes, "Studtite $[(UO_2)(O_2)(H_2O)_2](H_2O)_2$: The First Structure of a Peroxide Mineral," *Am. Mineral.*, **88**, 1165–68 (2003).

INTERNAL DISTRIBUTION

1. C. W. Alexander
2. J. M. Begovich
3. W. D. Bond
4–5. R. R. Brunson
6. R. M. Canon
7. T. B. Conley
8. G. D. Del Cul
9. R. H. Elwood, Jr.
10. L. K. Felker
11. L. L. Gilpin
12. S. Goluoglu
13. M. A. Green
14. J. N. Herndon
15. D. J. Hill
16. C. M. Hopper
17–21. A. S. Icenhour
22. A. M. Krichinsky
23. B. E. Lewis
24. S. C. Marschman
25. D. E. Mueller
26. P. E. Osborne
27. C. V. Parks
28. D. A. Reed
29. J. E. Rushton
30. C. M. Simmons
31. D. W. Simmons
32. R. G. Taylor
33–34. L. M. Toth
35. L. D. Trowbridge
36. R. M. Westfall
37–41. R. M. Wham
42. D. F. Williams
43. NSTD DMC
44. OTIC–RC, OSTI, CRL

EXTERNAL DISTRIBUTION

45. N. M. Askew, U.S. Department of Energy, Savannah River Site Operations Office, WSRC, Bldg. 773-A, Road 1A, Aiken, SC 29801
46. L. W. Boyd, DOE-ORO, U.S. Department of Energy, P.O. Box 2008 MS-6269, Oak Ridge, TN 37831
47. W. R. Brock, BWXT–Y-12, LLC, P.O. Box 2009, Oak Ridge, TN 37831
48. W. P. Carroll, DOE-HQ, NE-40/Germantown Building, U.S. Department of Energy, 1000 Independence Ave. S.W., Washington, DC 20585-1290
49. S. O. Cox, BWXT–Y-12, LLC, P.O. Box 2009, Oak Ridge, TN 37831
50. C. H. Delegard, Pacific Northwest National Laboratory, 902 Battelle Blvd., P.O. Box 999, Richland, WA 99352
51. J. M. Duffey, U.S. Department of Energy, Savannah River Site Operations Office, WSRC, Bldg. 773-A, Road 1A, Aiken, SC 29801
52. P. G. Eller, U.S. Department of Energy, Los Alamos National Laboratory, P.O. Box 1663, Los Alamos, NM 87545
53. H. C. Johnson, U.S. Department of Energy, Headquarters, EM-21, Forrestal Bldg., 1000 Independence Ave. S.W., Washington, D.C. 20585
54. R. A. Just, BWXT–Y-12, LLC, P.O. Box 2009, Oak Ridge, TN 37831
55. H. J. Keener, BWXT–Y-12, LLC, P.O. Box 2009, Oak Ridge, TN 37831
56. E. Kendall, NNSA, U.S. Department of Energy, P.O. Box 2001 MS-8193, Oak Ridge, TN 37831
57. R. R. Livingston, U.S. Department of Energy, Savannah River Site Operations Office, WSRC, Bldg. 773-A, Road 1A, Aiken, SC 29801
58. R. E. Mason, U.S. Department of Energy, Los Alamos National Laboratory, P.O. Box 1663, Los Alamos, NM, 87545

59. R. C. McBroom, DOE-ORO, U.S. Department of Energy, P.O. Box 2008 MS-6269, Oak Ridge, TN 37831
60. S. R. Martin, Jr., DOE-ORO, U.S. Department of Energy, P.O. Box 2008 MS-6269, Oak Ridge, TN 37831
61. T. R. Miller, BWXT–Y-12, LLC, P.O. Box 2009, Oak Ridge, TN 37831
62. L. Morales, U.S. Department of Energy, Los Alamos National Laboratory, P.O. Box 1663, Los Alamos, NM, 87545
63. M. T. Paffett, U.S. Department of Energy, Los Alamos National Laboratory, P.O. Box 1663, Los Alamos, NM, 87545
64. M. J. Plaster, BWXT–Y-12, LLC, P.O. Box 2009, Oak Ridge, TN 37831
65. K. H. Reynolds, DOE-ORO, U.S. Department of Energy, P.O. Box 2008 MS-6269, Oak Ridge, TN 37831
66. G. D. Roberson, U.S. Department of Energy, Albuquerque Operations Office, Bldg. 382-2, AL, Pennsylvania and H Street, Kirkland Air Force Base, Albuquerque, NM 87116
67. L. A. Worl, U.S. Department of Energy, Los Alamos National Laboratory, P.O. Box 1663, Los Alamos, NM 87545

SECTION 3 REFERENCES

10 CFR 71, *Packaging and Transportation of Radioactive Material,* Jan. 1, 2007.

ABAQUS/Standard, Version 6.4-1, 2003-09-29-11.18.28 46457, Abaqus, Inc., 2003.

ASME Boiler and Pressure Vessel Code, An American National Standard, Materials, Sect. II, *Materials,* Part D, American Society of Mechanical Engineers, New York, 2001 ed. with 2002 and 2003 addenda.

ASME Boiler and Pressure Vessel Code, An American National Standard, Rules for Construction of Nuclear Power Facility Components, Sect. III, Div. 1, Subsection NB, American Society of Mechanical Engineers, New York, 2001 ed. with 2002 and 2003 addenda.

ASME Boiler and Pressure Vessel Code, An American National Standard, Welding and Brazing Qualifications, Sect. IX, American Society of Mechanical Engineers, New York, 2001 ed. with 2002 and 2003 addenda.

ASTM D-2000, *Standard Classification System for Rubber Products in Automotive Applications*, American Society for Testing and Materials, Philadelphia, current revision.

ASTM E-2230-02, *Standard Practice for Thermal Qualification of Type B Packages for Radioactive Materials,* ASTM International, West Conshohocken, Pa., 2002.

Bailey, R. A., *Strain—A Material Database*, Lawrence Livermore Natl. Lab., Nov. 18, 1987.

Bailey, R. A., *THERM 1.2, A Thermal Properties DataBase for the IBM PC*, Lawrence Livermore Natl. Lab., Nov. 18, 1987.

Byington, G. A., *Vibration Test Report of the ES-2M Shipping Package*, GAB1296-2, Lockheed Martin Energy Systems, Inc., Oak Ridge Y-12 Plant, Sept. 3, 1997.

CRC Handbook of Chemistry and Physics, D. R. Lide, ed., 79th ed., CRC Press, Boca Raton, Fla. 1998.

Incropera, F. P., and D. P. DeWitt, *Fundamentals of Heat and Mass Transfer*, 2nd ed., John Wiley & Sons, New York, 1985.

MIL-HDBK-5H, *Metallic Materials and Elements for Aerospace Vehicle Structures*, Dec. 1 1998.

MSC.Patran, Version 12.0.044, MacNeal Schwendler Corp., 2004.

Nalgene Labware, http://www.nalgenelabware.com/products/productList.asp?search=1&catalog_no=2101.

NUREG/CR-6673, *Hydrogen Generation in TRU Waste Transportation Packages*, Lawrence Livermore Natl. Lab., May 2000.

OO-PP-986, rev. D, *Procurement Specification for 70A Durometer Preformed Packing (O-rings)*, Lockheed Martin Energy Systems, Inc., Oak Ridge Y-12 Plant, Jan. 26, 1999.

Parker O-ring Handbook, Catalog ORD 5700A/US, Parker Hannifin Corp., O-ring Div., Lexington, Ky., 2001.

SG 140.1, *Combination Test Analysis/Method Used to Demonstrate Compliance to DOE Type B Packaging Thermal Test Requirements (30 Minute Fire Test)*, U.S. DOE, Albuquerque Field Office, Nuclear Explosive Safety Division, Feb. 10, 1992.

Sudarsanam, S. B., et al., UT-Battelle, Presentation to Hydrogen Pipeline R&D, Project Review Meeting, *Hydrogen permeability and Integrity of hydrogen transfer pipelines*, January 2005, http://www1.eere.energy.gov/hydrogenandfuelcells/pdfs/03_babu_transfer.pdf.

Van Wylen, G. J., and R. E. Sonntag, *Fundamentals of Classical Thermodynamics*, 2d ed., John Wiley & Sons, Inc., New York, 1973.

4. CONTAINMENT

Design analysis, full-scale testing, and similarity of the ES-3100 prototypes have been used to demonstrate that the ES-3100 package with highly enriched uranium (HEU) is in compliance with the applicable containment requirements of Title 10 Code of Federal Regulations, Part 71 (10 CFR 71). The containment requirements of 10 CFR 71.51 are shown in Table 4.1. A bounding load case has been established for the ES-3100 package, and it assumes that the maximum HEU content is 35.2 kg (Sect. 1.2.3.6) with a decay heat load of 0.4 W (Sect. 1.2.3.7). This decay heat load and the volumes established for the convenience cans, spacers, silicone rubber pads, and the containment vessel void volume are discussed in Sect. 3.1.2 and Appendix 3.6.4. Sections 2 and 3 of this safety analysis report (SAR) also examine the effects of the lightest weight HEU content [2.77 kg (6.11 lb)]. The evaluations in Sects. 2, 3, and 4 have demonstrated that the ES-3100 shipping package with HEU content weight ranging from 2.77 kg (6.11 lb) to 35.2 kg (77.60 lb) meets the containment requirements specified in 10 CFR 71 for all conditions of transport. A summary of the containment boundary design and fabrication acceptance basis is given in Table 4.2. No credit is taken for the various convenience cans' ability to protect the HEU contents from being released.

Table 4.1. Containment requirements of transport for Type B packages [a]

Condition	Allowable release rate
Normal Conditions of Transport (NCT)	$R_N = 10^{-6}$ A_2 per hour = 2.78×10^{-10} A_2 per second
Hypothetical Accident Conditions (HAC)	$R_A = A_2$ in 1 week = 1.65×10^{-6} A_2 per second
	For ^{85}Kr, a value of 10 A_2 in 1 week is used

[a] From ANSI N14.5-1997, Sects. 5.4.1 and 5.4.2, and 10 CFR 71.51(a)(1) and (a)(2)

Table 4.2. Summary of the containment vessel design and fabrication acceptance basis

Nominal empty weight	15.10 kg (33.29 lb)
Air fill medium temperature at loading	25°C (77°F)
Air fill medium pressure at loading	101.35 kPa (14.70 psia)
Hydrostatic pressure test	1034 ± 34 kPa (150 ± 5) gauge
Helium acceptance leakage rate [a]	$L_T \leq 2.0 \times 10^{-7}$ cm^3/s
Air acceptance leakage rate [a]	$L_T \leq 1 \times 10^{-7}$ ref-cm^3/s
Air preshipment leakage rate	$L_T \leq 1 \times 10^{-4}$ atm-cm^3/s

[a] Acceptance leakage testing includes fabrication, periodic (within 12 months of use), and maintenance testing. According to Sect. 2.1 of ANSI N14.5-1997, *leaktight* is defined as an air leakage rate of 1×10^{-7} ref-cm^3/s; under the same conditions, this air leakage rate is ~ equal to a helium leakage rate of 2×10^{-7} cm^3/s.

The analysis documented in Appendix 4.6.1 was conducted to establish the upper limit for the total activity and the maximum number of A_2s proposed for transport in the ES-3100 package. The maximum activity [3.2427×10^{-1} TBq (8.764 Ci)] of the contents occurs 10 years after initial fabrication. When the maximum activity-to-A_2 value (293.99) is reached at ~70 years from material fabrication, the corresponding activity is 3.2328×10^{-1} TBq (8.737 Ci). These values have been determined using a maximum of 35.2 kg of HEU with isotopic weight percents as shown in Table 4.3. By applying the

maximum weight percents of isotopes ^{233}U, ^{234}U, ^{236}U and by incorporating the traces of ^{232}U and the transuranic isotopes, the maximum activity, minimum A_2 value, and the minimum leakage requirements were determined for the proposed contents and are summarized in Tables 4.4, 4.5, and 4.6. The mass and isotopic concentrations used for the proposed content do not take into consideration limits based on shielding and subcriticality.

The initial composition of the content contains several isotopes of uranium (Sect. 1.2.3). As a result of radioactive decay, the ingrowth of uranium daughter products occurs, and these concentrations of daughter products will vary with time. The uranium isotopes and daughter products are considered a mixture of radionuclides, and the method for determining the mixture's A_2 value in Section IV, Appendix A, 10 CFR 71 is applied. The A_2 value for the most conservative set of contents defined in Sect. 1.2.3 has been calculated in Appendix 4.6.1. Since the HEU can be in the form of oxides (UO_2, UO_3, and U_3O_8), uranyl nitrate crystals (UNX), or metal and alloy, the calculation of the mixture's A_2 used the various uranium isotopic A_2 values for fast, medium, and slow lung absorption criteria shown in Table A-1 of Appendix A of 10 CFR 71.

The mass and material compositions analyzed in this section of the SAR are not limited by the combustible gas requirements stated in NUREG-1609, Sect. 4.5.2.3. NUREG-1609, Sect. 4.5.2.3, requires the applicant to demonstrate that any combustible gases generated in the package during a period of one year do not exceed 5% (by volume) of the free gas volume in any confined region of the package. No credit should be taken for getters, catalysts, or other recombination devices. The analysis conducted in Appendix 3.6.7 evaluates the different packaging arrangements for the generation of hydrogen gas due to the radiolysis of water vapor, free water, interstitial water, polyurethane bags, and polyurethane or Teflon bottles. By limiting the mass and the material distribution as shown in Appendix 3.6.7, the combustible gas concentration limit stated in NUREG-1609 is not exceeded. These limits are further shown in Tables 1.3 and 1.3a. Getters, catalysts, or other recombination devices are not employed in any of the containment vessel packaging arrangements. The analysis conducted in Appendix 3.6.4 predicts the maximum normal operating pressure inside the containment vessel for the various packaging arrangements and masses discussed previously. This appendix also includes the hydrogen gas generation predicted by Appendix 3.6.7.

4.1 DESCRIPTION OF THE CONTAINMENT BOUNDARY

As shown in Table 4.4, the number of A_2s proposed for shipping exceeds 30 but is less than 3000. In accordance with NUREG 1609, the containment vessel is a Category II vessel. Since this vessel may be used for future contents that exceed 3000 A_2, the containment vessel category has been elevated to a Category I vessel. Therefore, the containment vessel is designed (using nominal dimensions for each component), fabricated, and inspected in accordance with the American Society of Mechanical Engineers (ASME) *Boiler and Pressure Vessel Code*, Sect. III, Division I, Subsection NB and Section IX.

4.1.1 Containment Boundary

The containment boundary consists of the vessel's body, lid assembly, and inner O-ring (Sect. 1, Fig. 1.3). Only the inner O-ring is considered part of the boundary. The outer O-ring is provided to allow a post-assembly verification leak check. Two methods of fabrication may be used to fabricate the containment vessel body as shown on Drawing M2E801580A012 (Appendix 1.4.8). The first method uses a standard 5-in., schedule 40 stainless-steel pipe per ASME SA-312 Type TP304L, a machined flat-head bottom forging per ASME SA-182 Type F304L, and a machined top flange forging per ASME SA-182 Type F304L. The nominal outside diameter of the 5-in. schedule 40 pipe is machined to match the nominal wall thickness of 0.254 cm (0.100 in.). Each of these pieces is joined with

full-penetration circumferential weld as shown on sheet 2 of Drawing M2E801580A012 (Appendix 1.4.8). The weld filler material conforms to Sect. II, Part C, of the *ASME Boiler and Pressure Vessel Code*. All full-penetration welds are dye penetrant and radiographically inspected in accordance with Sect. III, Div. I, Sect. NB-5000, of the *ASME Boiler and Pressure Vessel Code*. The top flange is machined to match the schedule 40 stainless-steel 5-in. pipe, to provide two concentric half-dove-tailed O-ring grooves in the flat face, to provide locations for two 18-8 stainless-steel dowel pins, and to provide the threaded portion for closure using the lid assembly. The second method of fabrication uses forging, flow forming, or metal spinning to create the complete body (flat bottom, cylindrical body, and flange) from a single forged billet or bar with final material properties in accordance with ASME SA-182 Type F304L. Final machining of the top flange area is identical to that of the welded forging method. The lid assembly, which completes the containment boundary structure, consists of a sealing lid, closure nut, and external retaining ring (Drawing M2E801580A014, Appendix 1.4.8). The containment vessel sealing lid (Drawing M2E801580A015, Appendix 1.4.8) is machined from Type 304 stainless-steel bar with final material properties in accordance with ASME SA-479. The containment vessel closure nut is machined from a Nitronic 60 stainless-steel bar with material properties in accordance with ASME SA-479. These two components are held together using a WSM-400-S02 external retaining ring made from Type 302 stainless steel. The sealing lid is further machined to accept a ⅜-in.-16 swivel hoist ring bolt, to provide a leak-check port between the elastomeric O-rings, and notched along the perimeter to engage two dowel pins. The lid assembly, with the O-rings in place on the body, are joined together by torquing the closure nut and sealing lid assembly to 162.7 ± 6.78 N·m (120 ± 5 ft-lb). The sealing lid portion of the assembly is restrained from rotating during this torquing operation by the two dowel pins installed in the body flange. This torquing of the closure nut represents the positive fastening device used to satisfy the requirements of 10 CFR 71.43(c). The effectiveness of this closure system has been demonstrated by the NCT and HAC tests, which show that the complete containment system, including welds and O-ring seals, meet the leaktight criterion as defined in ANSI N14.5-1997 after the conclusion of the test series documented in *Test Report of the ES-3100 Package* (Appendix 2.10.7).

10 CFR 71.73(c) requires that the package containment vessel be immersed in 15 m (50 ft) of water, which is equivalent to an external pressure differential of 150 kPa (21.7 psi). The design analyses (Appendix 2.10.1) show that this vessel is conservatively rated for the 150-kPa (21.7-psi) external pressure differential requirement, as well as for an internal pressure differential of 699.82 kPa (101.5 psig). A summary of the containment boundary design and acceptance basis is given in Table 4.2.

The ES-3100 package has no connections, fittings, valves, tapped holes, or other devices that penetrate the containment boundary; therefore, the package does not allow continuous venting during transport. The leak test port on the containment vessel lid accesses the annulus between the two O-rings. Since the outer O-ring is not considered to be part of the containment boundary, this leak test port does not penetrate the containment boundary. Therefore, the requirements of 10 CFR 71.43(e) are not applicable.

The containment vessel O-rings (Drawing M2E801580A013, Appendix 1.4.8) are manufactured from an ethylene-propylene elastomer in accordance with specifications for 70A Durometer preformed packing developed at Y-12. These O-rings are rated for continuous service as a static face seal in the temperature range of −40 to 150°C (−40 to 302°F) [*Parker O-ring Handbook*, Fig. 2-24]. Tests conducted by Los Alamos National Laboratory (LANL) on a similar compound, ethylene-propylene rubber (EPDM), used as a static face seal, are documented in *SAFKEG 2863B Tests for Verification of O-ring Performance* (TR 96/12/20). The material compound for the LANL tests was certified to ASTM D-2000 as M3BA610A14B13F17. The ES-3100 package O-rings are also certified to ASTM D-2000 as M3BA712A14B13F17. The class of material in the LANL test is identical except that the durometer and tensile strengths are somewhat less than those of the ES-3100 package. Each material was tested in accordance with ASTM D-2137 for brittleness at −40°C (−40°F) without failure.

The leak test fixture, as reported in TR 96/12/20, provided a maximum compression of 25.7% in a static face seal configuration. The compression range provided by the flange and lid design of the ES-3100 package is 14.8 to 20.8% or 0.051 to 0.076 cm (0.020 to 0.030 in.) compression due to the half-dovetail design. Furthermore, *Parker O-ring Handbook* states that the minimum squeeze for all seals, regardless of cross-section, should be about 0.018 cm (0.007 in.). Since the minimum compression is 0.051 cm (0.020 in.) and the flange and lid with the closure nut have nearly identical coefficient of thermal expansion, the sealing performance at −40°C (−40°F) should not be degraded. Therefore, the performance of the ES-3100 O-rings should be representative of those documented in TR 96/12/20. These tests demonstrated that the O-rings were leaktight over the temperature range of −40 to 205°C (−40 to 401°F), which is greater than the operating temperature range of −40 to 141.22°C (−40 to 286.2°F) of the ES-3100 containment vessel (Table 3.17). In addition to component testing, an ES-3100 full-scale test unit (Test Unit-2) was chilled to ≤−40°C and later subjected to an NCT drop test and the entire HAC test battery. The containment vessel was leak tested and achieved "leaktight" status. Therefore, the continuous service temperature rating of the ethylene-propylene elastomer has been verified by testing.

4.1.2 Special Requirements for Plutonium

The highly enriched uranium contents have only trace amount of the transuranic isotopes. Therefore, this section is not applicable to the ES-3100 shipping container.

4.2 GENERAL CONSIDERATIONS

4.2.1 Type A Fissile Packages

The A_2 value of the proposed contents exceed the limits established for Type A packages.

4.2.2 Type B Packages

Requirements

(1) A Type B package, in addition to satisfying the requirements of 10 CFR 71.41–71.47, must be designed, constructed, and prepared for shipment so that under the tests specified in:

(a) Section 71.71 ("Normal conditions of transport"): There would be no loss or dispersal of radioactive contents as demonstrated to a sensitivity of 10^{-6} A_2/h, no significant increase in external surface radiation levels, and no substantial reduction in the effectiveness of the packaging; and

(b) Section 71.73 ("Hypothetical accident conditions"): There would be no escape of ^{85}Kr exceeding 10 A_2 in one week, no escape of other radioactive material exceeding a total amount A_2 in one week, and no external radiation dose rate exceeding 10 mSv/h (1 rem/h) at 1 m (40 in.) from the external surface of the package.

(2) Where mixtures of different radionuclides are present, the provisions of Appendix A, paragraph IV of this part shall apply, except that for ^{85}Kr, an effective A_2 value equal to 10 A_2 may be used.

(3) Compliance with the permitted activity release limits of paragraph (a) of this section may not depend on filters or on a mechanical cooling system.

Analysis. The A_2 value calculated for the ES-3100 shipping package has been determined in accordance with Appendix A of 10 CFR 71, documented in Appendix 4.6.1, and uses the proposed isotopic distribution shown in Table 4.3. Table 4.4 summarizes the results from Appendix 4.6.1 for the proposed contents from 0 to 70 years after original production.

Table 4.3. Isotopic mass and weight percent for the HEU contents [a]

Nuclide	Weight percent	Mass (g)
U-232	0.000004	0.001408
U-233	0.600000	211.200000
U-234	2.000000	704.000000
U-235	54.895996	19323.390592
U-236	40.000000	14080.000000
U-238	0.000000	0.000000
Transuranic	0.004000	1.408000
Np-237	2.500000	880.000000
Total	100.000000	35200.000000

[a] Weight percent values of individual isotopes are those that generate the largest activity within the allowable ranges presented in Sect. 1.2.3.

Table 4.4. Activity, A_2 value, and number of A_2 proposed for transport

Year	Fast absorption			Medium absorption			Slow absorption		
	Activity (TBq)	A_2 (TBq)	Act / A_2	Activity (TBq)	A_2 (TBq)	Act / A_2	Activity (TBq)	A_2 (TBq)	Act / A_2
0	3.185E-01	1.280E-03	2.489E+02	3.185E-01	1.226E-03	2.599E+02	3.185E-01	1.089E-03	2.926E+02
5	3.238E-01	1.295E-03	2.500E+02	3.238E-01	1.240E-03	2.610E+02	3.238E-01	1.103E-03	2.937E+02
10	3.243E-01	1.296E-03	2.502E+02	3.243E-01	1.241E-03	2.612E+02	3.243E-01	1.104E-03	2.938E+02
20	3.241E-01	1.295E-03	2.503E+02	3.241E-01	1.240E-03	2.613E+02	3.241E-01	1.103E-03	2.938E+02
30	3.239E-01	1.293E-03	2.504E+02	3.239E-01	1.239E-03	2.614E+02	3.239E-01	1.102E-03	2.938E+02
40	3.237E-01	1.292E-03	2.505E+02	3.237E-01	1.238E-03	2.615E+02	3.237E-01	1.101E-03	2.938E+02
50	3.235E-01	1.291E-03	2.506E+02	3.235E-01	1.237E-03	2.616E+02	3.235E-01	1.101E-03	2.939E+02
60	3.234E-01	1.290E-03	2.507E+02	3.234E-01	1.236E-03	2.617E+02	3.234E-01	1.100E-03	2.939E+02
70	3.233E-01	1.289E-03	2.508E+02	3.233E-01	1.235E-03	2.618E+02	3.233E-01	1.100E-03	2.940E+02

4.3 CONTAINMENT UNDER NORMAL CONDITIONS OF TRANSPORT (TYPE B PACKAGES)

Title 10 CFR 71.51(a)(1) specifies that there shall be no loss or dispersal of radioactive contents as demonstrated to a sensitivity of 10^{-6} A_2 per hour, no significant increase in external radiation levels, and no substantial reduction in the effectiveness of the packaging. The initial composition of the HEU contains several isotopes of uranium and transuranic contributors (Table 4.3). As a result of radioactive decay, uranium, transuranics, and daughter product isotopes are present in the HEU contents at varying concentrations depending on the length of decay time. The HEU, with its isotopes and daughter isotopes and contributions from unknown transuranic isotopes, qualifies as a mixture for A_2 determination (Appendix A of 10 CFR 71). The A_2 value and the maximum content activity-to-A_2 value ratio for this mixture have been calculated for several different decay times (Table 4.4). As calculated in Appendix 4.6.1, the A_2 value [1.0997×10^{-3} TBq (2.9720×10^{-2} Ci)] and the maximum content activity-to-A_2 ratio (293.99) used to qualify this package occurs at about 70 years of decay. As previously stated, these values have been determined using a bounding case maximum of 35.2 kg of HEU with isotopic weight percent values as shown in Table 4.3. The specified composition is a very conservative upper bound achieved by using the maximum weight percent values for the higher specific activity isotopes (^{232}U, ^{233}U, ^{234}U, and ^{236}U), including contributions from other transuranics and ^{237}Np.

The maximum activity, minimum A_2, and minimum leakage requirements were determined for this worst case scenario and are presented in Tables 4.4 and 4.5. These masses and isotopic concentrations were used for the proposed contents without regard to limits established based on shielding and subcriticality considerations. The actual mass limits affirmed for this shipping package are established in Sect. 1 (Table1.3). The analyses conducted in Appendix 4.6.2 assumes that the total mass of uranium for each component is available for release as an aerosol (worst case). From experimental tests, the maximum aerosol density containing uranium particulate was reported in *Leakage of Radioactive Powders from Containers* (Curren and Bond 1980) to be 9.0×10^{-6} g/cm^3. This aerosol density is used to calculate the total activity concentration in ANSI N14.5-1997, Section B.15, examples 13, 27, and 29.

The containment criteria for the ES-3100 package will be leaktight (defined in paragraph 2.1 of ANSI N14.5-1997 as having a leakage rate $\leq 1 \times 10^{-7}$ ref-cm^3/s) during the prototype tests. This leaktight criterion satisfies the design verification requirement stipulated in paragraph 7.2.4 of ANSI N14.5-1997. The requirements of ANSI N14.5-1997 are used for all stages of containment verification for the ES-3100 (i.e., design, fabrication, maintenance, periodic and preshipment).

The design, fabrication, maintenance and periodic leakage rate limit is 1×10^{-7} ref-cm^3/s air. The pass criterion for the preshipment leakage rate test, which demonstrates correct assembly of the containment vessels, is 1×10^{-4} ref-cm^3/s, which exceeds the requirements given in ANSI N14.5, paragraph 7.6.4. In accordance with the definition of sensitivity of a leakage test procedure provided in Sections 2 and 7.6.4 of ANSI N14.5-1997, the minimum acceptable leakage rate that the procedure needs to be capable of detecting is 1×10^{-3} ref-cm^3/s. The requirements for the ES-3100 exceed the regulatory criterion by specifying a leakage rate of $\leq 1 \times 10^{-4}$ ref-cm^3/s, and equipment used in accordance with Section 7.6.4 of ANSI N14.5-1997 would not detect this leakage. The preshipment, fabrication, maintenance and periodic leakage rate tests are required to be conducted on each containment vessel in accordance with ANSI N14.5 and are specified in Chapters 7 and 8. These leakage rates are not dependent on filters or mechanical cooling.

Table 4.5. Regulatory leakage criteria for NCT [a]

Verification activity	Fast absorption		Medium absorption		Slow absorption	
	L_{RN-air} (ref-cm^3/s)	L_{RN-He} (cm^3/s)	L_{RN-air} (ref-cm^3/s)	L_{RN-He} (cm^3/s)	L_{RN-air} (ref-cm^3/s)	L_{RN-He} (cm^3/s)
Design	2.6892E-03	2.9222E-03	2.5775E-03	2.8048E-03	2.2976E-03	2.5098E-03

[a] The procedure used to calculate the above criteria is shown in Appendix 4.6.2. This data has been extracted from Table 1 in Appendix 4.6.2.

Table 4.6. Containment vessel verification tests criteria for NCT

Test Type	Test Values	Leakage test procedure
Design and compliance leakage testing		
Design verification of O-ring seal (air)	$L_T \leq 1.0 \times 10^{-4}$ ref-cm^3/s	See Appendix 2.10.7
Design verification of containment vessel boundary (helium)	$L_T \leq 2.0 \times 10^{-7}$ cm^3/s	See Appendix 2.10.7
Verification leakage testing		
Fabrication, periodic, and maintenance (helium)	$L_T \leq 2.0 \times 10^{-7}$ cm^3/s	Y51-01-B2-R-140, Rev. A.1 (Appendix 8.3.1)
	$L_T \leq 1.0 \times 10^{-4}$ ref-cm^3/s	Y51-01-B2-R-074, Rev. A.1 (Appendix 7.5.1)

The complete design verification testing of the ES-3100 package for NCT was conducted on test unit TU-4. Since the containment vessel was assembled at ambient conditions, the pressure was nominally 101.35 kPa (14.70 psia) at 25°C (77°F). In accordance with 10 CFR 71.71(b), the initial pressure inside each containment vessel should be the maximum normal operating pressure (MNOP). As calculated in Appendix 3.6.4, the bounding case MNOP is 198.98 kPa (28.859 psia). The stresses at the maximum normal operating pressure [97.62 kPa (14.159 psig)] are insignificant compared to the allowable stresses (Table 2.21). O-ring grooves are designed and fabricated in accordance with guidance from the *Parker O-ring Handbook*. In accordance with Fig. 3-2 of the *Parker O-ring Handbook*, the durometer of the O-ring, and the tolerance gap from the production drawings, the O-ring should be able to withstand ~800 psig before anti-extrusion devices are required. Therefore, conducting a compliance test with the MNOP in the containment vessel will have little, if any, effect on the results.

Following the design verification testing of paragraphs 10 CFR 71.71(c)(5) through 71.71(c)(10) excluding 71.71(c)(8), Test Unit-4 was subjected to the sequential testing of paragraphs 10 CFR 71.73(c)(1) through (c)(4). Upon removal of the containment vessel from the drum assembly, the cavity between the O-rings was leak checked. This unit recorded a leak rate between the O-rings of 2.4773×10^{-5} ref-cm^3/s.

Following the O-ring leak test, the entire containment boundary of TU-4 was helium leak tested to a value $\leq 2 \times 10^{-7}$ cm^3/s, thereby verifying a leak-tight boundary. The leak-test procedure followed to verify this criteria is documented in the ES-3100 test plan (Appendix 2.10.7). The maximum recorded

helium leakage rate for this containment vessel was 2.0×10^{-7} cm^3/s after 20 min of testing. Visual inspection following the testing indicated that neither the vessel body, the O-rings, the seal areas, nor the vessel lid assembly were damaged during the tests. Pictures taken of the containment vessel top following testing showed that the closure nut had rotated a maximum of 0.15 cm (0.060 in.) from its original radial position obtained during assembly. Based on the pitch of the closure nut, this rotation translates into only 0.0013 cm (0.0005 in.) decompression of the O-rings. This compares to the original nominal compression of 0.064 cm (0.025 in.). Therefore, O-ring compression was maintained during compliance testing. Based on these results, the ES-3100 package meets and exceeds the containment criteria specified in 10 CFR 71.51 for NCT when used to ship the contents described in the introductory section of this chapter.

Following fabrication, the containment vessel undergoes hydrostatic pressure testing to 1034 kPa (150 psi) gauge. The hydrostatic test is conducted before the final leakage test. Following the hydrostatic pressure test, and prior to conducting the leakage test, the containment vessel and O-ring cavity must be thoroughly dried. Each vessel is then leak tested with either air or helium to $\leq 1 \times 10^{-7}$ ref-cm^3/s or 2×10^{-7} cm^3/s, respectively. This test ensures the containment vessel's integrity (walls, welds, inner O-ring seal) as delivered for use in accordance with paragraph 6.3.2 of ANSI N14.5-1997.

Following placement of the HEU content inside the containment vessel and joining the body and lid assembly, the volume between the containment vessel's O-ring seals is evacuated and checked to leak $\leq 1 \times 10^{-4}$ ref-cm^3/s. This leak-test procedure is a pressure rise air leak test prescribed in Section 7.1.2. This ensures that each containment vessel has been properly assembled in accordance with paragraph 7.6.4 of ANSI N14.5-1997.

The design verification tests were conducted following compliance tests in accordance with 10 CFR 71.71 and 71.73. The effectiveness of this closure system has been demonstrated by the NCT and HAC tests, which show that the complete containment system, including welds and O-ring seals, meet the leaktight criterion as defined in ANSI N14.5-1997 after the conclusion of the test series documented in *Test Report of the ES-3100 Package* (Appendix 2.10.7).

4.4 CONTAINMENT UNDER HYPOTHETICAL ACCIDENT CONDITIONS (TYPE B PACKAGES)

Requirements. A Type B package, in addition to satisfying the requirements of paragraphs 10 CFR 71.41 through 71.47, must be designed, constructed, and prepared for shipment so that under the tests specified in Sect. 71.73 ("Hypothetical Accident Conditions"), there would be no escape of ^{85}Kr exceeding 10 A_2 in one week, no escape of other radioactive material exceeding a total amount A_2 in one week, and no external radiation dose rate exceeding 10 mSv/h (1 rem/h) at 1 m (40 in.) from the external surface of the package.

Analysis. Calculations have been conducted in Appendix 4.6.2 to determine the regulatory leakage criteria to satisfy the above requirements. The results are shown in Table 4.7. These analyses assume that the total mass of uranium for each component is available for release as an aerosol (worst case). From experimental tests, the maximum aerosol density containing uranium particulate was reported by Curren and Bond to be 9.0×10^{-6} g/cm^3. This aerosol density is used to calculate the total activity concentration in ANSI N14.5-1997, Section B.15 examples 13, 27, and 29. Design leakage rate verification testing of the containment boundary (Table 4.8) was conducted on Test Units-1 through -6 and documented in test report (Appendix 2.10.7). Since each containment vessel was assembled at ambient conditions, the pressure was nominally 101.35 kPa (14.70 psi) at 25°C (77°F). In accordance

with 10 CFR 71.73(b), for these tests, the initial pressure inside each containment vessel should be the maximum normal operating pressure. As shown in Table 2.21, the stresses at the maximum normal operating pressure are insignificant compared to the allowable stresses. Therefore, conducting compliance testing with nominal pressure in the containment vessel would have little, if any, effect on the results. During the structural and thermal tests conducted on the ES-3100 for HAC, the drum experienced plastic deformation, and the insulation and impact limiter material experienced some deterioration, as anticipated (Sect. 2.7). The containment vessels did not exhibit any signs of damage and passed post-test leak tests and the subsequent 10 CFR 71.73(c)(5)–specified 0.9-m (3-ft) water immersion tests except for Test Unit-6. Test Unit-6 was subjected to the test specified by paragraph 10 CFR 71.73(c)(6). After completion of this test, the containment vessel was removed and the lid was drilled and tapped for a helium leak-check port. The entire containment boundary was then helium leak checked and passed the leaktight criteria. Also, no visible water was seen inside the inner O-ring groove of Test Unit-6 and no water was observed inside any of the other test units.

Table 4.7. Regulatory leakage criteria for HAC [a]

Verification activity	Fast absorption		Medium absorption		Slow absorption	
	$L_{RA\text{ - air}}$ (ref-cm^3/s)	$L_{RA\text{ - He}}$ (cm^3/s)	$L_{RA\text{ - air}}$ (ref-cm^3/s)	$L_{RA\text{ - He}}$ (cm^3/s)	$L_{RA\text{ - air}}$ (ref-cm^3/s)	$L_{RA\text{ - He}}$ (cm^3/s)
Design	5.6523	5.4158	5.4161	5.1909	4.8245	4.6273

[a] The procedure used to calculate the above criteria is shown in Appendix 4.6.2.

Table 4.8. Containment vessel design verification tests for HAC

Test Type	Test Values	Leakage test procedure
Design and compliance leakage testing		
Design verification of O-ring seal (air)	$L_T \leq 1.0 \times 10^{-4}$ ref-cm^3/s	See Appendix 2.10.7
Design verification of containment vessel boundary (helium)	$L_T \leq 2.0 \times 10^{-7}$ cm^3/s	See Appendix 2.10.7

To verify the entire containment boundary to the leaktight criteria, the containment vessels of Test Units-1 through -5 were helium leak tested using the procedure shown in the test report (Appendix 2.10.7). These test units had previously been subjected to the drop test stipulated in 10 CFR 71.71 (c)(6) and the sequential tests stipulated in 10 CFR 71.73 except for Test Unit-4, which had been first subjected to the testing in accordance with 10 CFR 71.71. The maximum recorded helium leak rate for any of these containment vessels was 2.0×10^{-7} cm^3/s after 20 min of testing on Test Unit-4 as documented in Section 5.2 of the test report (Appendix 2.10.7). Test Units-2 and -5 displayed some unusual pulsing action during leak testing. The peak amplitude changed after adding helium in a manner expected for diffusion through the O-rings rather than a rise immediately following the addition of helium that would indicate a leak to the outside of the containment vessel. This is further discussed and graphically presented in Sect. 5.2.2 of the ES-3100 test report (Appendix 2.10.7). These measured leakage rates verify that the containment vessels are leaktight in accordance with ANSI N14.5-1997. Therefore, the containment boundary of the ES-3100 package was maintained during the HAC testing.

The 35.2 kg of HEU content is unirradiated; therefore, only very small quantities of fission gas products will be produced from spontaneous fission and subcritical neutron induced fission. Fission gas products are produced in such small quantities that they have no measurable effect on the releasable content source term or containment vessel pressurization. Fission gas products will not be considered further in this SAR.

4.5 LEAKAGE RATE TESTS FOR TYPE B PACKAGES

The maximum allowable release of radioactive material allowed by 10 CFR 71.51(a)(2) under HAC is A_2 in one week. Title 10 CFR 71.51(a)(2) also specifies that there be no escape of ^{85}Kr exceeding 10 A_2 in one week. ANSI N14.5-1997 specifies the leakage test methods and leakage rates that are accepted in Nuclear Regulatory Commission (NRC) Regulatory Guide 7.4 as demonstrating that a package meets the 10 CFR 71.51(a)(2) requirements for containment. The containment criteria for the ES-3100 package will be leaktight, defined in ANSI N14.5 paragraph 2.1 as having a leakage rate $\leq 1 \times 10^{-7}$ ref-cm^3/s, during the prototype tests. This leaktight criterion satisfies the design verification requirement stipulated in paragraph 7.2.4 of ANSI N14.5-1997. The requirements of ANSI N14.5-1997 are used for all stages of containment verification for the ES-3100 (i.e., design, fabrication, maintenance, periodic and preshipment). The design, fabrication, maintenance and periodic leakage rate limit is 1×10^{-7} ref-cm^3/s air (or 2.0×10^{-7} cm^3/s helium). The pass criterion for the preshipment leakage rate test, which demonstrates correct assembly of the containment vessels, is 1×10^{-4} ref-cm^3/s, which exceeds the requirements given in ANSI N14.5-1997, paragraph 7.6.4. In accordance with the definition of sensitivity of a leakage test procedure provided in Sections 2 and 7.6.4 of ANSI N14.5-1997, the minimum acceptable leakage rate that the procedure needs to be capable of detecting is 1×10^{-3} ref-cm^3/s. The requirements for the ES-3100 exceed the regulatory criterion by specifying a leakage rate of $\leq 1 \times 10^{-4}$ ref-cm^3/s, and equipment used in accordance with Section 7.6.4 of ANSI N14.5-1997 would not detect this leakage. The preshipment, fabrication, maintenance, and periodic leakage rate tests are required to be conducted on each containment vessel in accordance with ANSI N14.5-1997 and are specified in Chapters 7 and 8. These leakage rates are not dependent on filters or mechanical cooling.

The requirements of ANSI N14.5-1997 are used for all stages of containment verification for the ES-3100; the design (HAC test) leakage rate limit is 1×10^{-7} ref-cm^3/s (which is defined as leaktight in ANSI N14.5-1997). The packaging has been shown to maintain containment before and after prototype testing by leakage tests performed for containment verification to the requirements of ANSI N14.5-1997. Test Unit-4's containment vessel was subjected to both the NCT and HAC tests. Test Units-1 through -5 were subjected to the free drop stipulated in 10 CFR 71.71(c)(7) and to the sequential HAC test stipulated in 10 CFR 71.73. Following these tests, each containment vessel was helium leak tested in accordance with the test plan. Again, the test results verified that the containment vessels were leaktight. Thus, there could be no release of radioactive materials from the containment vessels. These leakage rates are not dependent on filters or mechanical cooling. These measured leakage rates verify that the containment vessels are leaktight in accordance with ANSI N14.5-1997.

Therefore, the ES-3100 package meets the containment criteria as specified in 10 CFR 71.73 for HAC when shipping the proposed 35.2 kg of HEU in the containment vessel.

4.6 APPENDICES

Appendix	Description
4.6.1	DETERMINATION OF A_2 FOR THE ES-3100 PACKAGE WITH HEU CONTENTS
4.6.2	CALCULATION OF THE ES-3100 CONTAINMENT VESSEL'S REGULATORY REFERENCE AIR LEAKAGE RATES

THIS PAGE INTENTIONALLY LEFT BLANK.

Appendix 4.6.1

DETERMINATION OF A_2 FOR THE ES-3100 PACKAGE WITH HEU CONTENTS

Prepared by: Monty L. Goins
BWXT Y-12
November 2006

Reviewed by: G. A Byington
BWXT Y-12
November 2006

THIS PAGE INTENTIONALLY LEFT BLANK.

Appendix 4.6.1

DETERMINATION OF A_2 FOR THE ES-3100 PACKAGE WITH HEU CONTENTS

Introduction

The containment criteria for radioactive, fissile material packages are given in 10 CFR 71.51(a)(1) for Normal Conditions of Transport (NCT) ($\leq 10^{-6}$ A_2/h) and in 71.51(a)(2) for Hypothetical Accident Conditions (HAC) ($\leq A_2$ in a week). The A_2 value for this mixture of radioisotopes must be determined to establish the content containment criteria and to determine the maximum release quantity that is allowed by the regulations. These values for a mixture of isotopes are determined by the methodology given in 10 CFR 71, Appendix A, "Determination of A_1 and A_2," Sect. IV. The results of these analyses are used to demonstrate compliance of the ES-3100 package with the containment requirements of 10 CFR 71.

Scope

The A_2 value of the highly enriched uranium (HEU) content to be shipped is evaluated based on the mass and weight percents of HEU shown in Table 1 and defined in Sect. 1.2.3. The weight percents shown in Table 1 are the ones that generate the largest activity within the known weight percent ranges. Incorporating the new 10 CFR 71 A_2 values for the uranium isotopes, three different categories have been established based on the absorption rate of the uranium isotopes. The fast lung absorption, medium lung absorption and slow lung absorption categories are addressed in subsequent sections. By applying the maximum weight percents of isotopes ^{232}U, ^{233}U, ^{234}U, ^{236}U and by incorporating the traces of ^{237}Np and the transuranic isotopes, the maximum activity, minimum A_2 value, and the minimum leakage requirements were determined for each category of absorption for the HEU oxides, compounds, and metal pieces. The mass and isotopic concentrations used for the proposed content do not take into consideration limits based on shielding and subcriticality.

Table 1. Isotopic mass and weight percent for the HEU contents [a]

Nuclide	Weight percent	Mass (g)
U-232	0.000004	0.001408
U-233	0.600000	211.200000
U-234	2.000000	704.000000
U-235	54.895996	19323.390592
U-236	40.000000	14080.000000
U-238	0.000000	0.000000
Transuranic	0.004000	1.408000
Np-237	2.500000	880.000000
Total	100.000000	35200.000000

[a] Weight percents values of individual isotopes are those that generate the largest activity within the allowable ranges presented in Sect. 1.2.3.

According to 10 CFR 71, Appendix A, parent and daughter nuclides are considered to be a mixture of different nuclides than those of the parent nuclide. The radioactive decay of uranium (refer to the decay chains presented by Dr. David C. Kocher, *Radioactive Decay Data Tables* [Kocher 1981]) creates isotopes that will accumulate enough activity to exceed their respective criteria for limited quantities (*Shippers—General Requirements for Shipments and Packagings* [49 CFR 173.423], Table A-7, "Activity Limits for Limited Quantities, Instruments, and Articles") and for Type A quantities of radionuclides (10 CFR 71, Table A-1, "A_1 and A_2 Values for Radionuclides"). Furthermore, the A_2 value for the mixture will change over time as a result of radioactive decay. The analysis below shows that the A_2 value for this mixture reaches a minimum at initial fabrication, increases to the 10th year, and declines through the 70th year.

Analysis

Mass Tables. The mass and weight fractions for HEU isotopes used in the containment calculations are presented in Table 1. For conservatism, a small quantity of ^{232}U is assumed in this material at fabrication.

ORIGEN-S Results. The source terms of the isotopes in the mixtures were evaluated using the ORIGEN-S computer program (Parks 1984). The mass values for the parent and daughter products are presented in Table 2 for the time interval of 0–70 years. Contributions from the transuranics and ^{237}Np are held constant at each time interval during the 70-year evaluation.

The A_2 value of each mixture was calculated using the procedure shown in Tables 3, 4, and 5 for the above time intervals. The 70th year of decay represents the smallest value of A_2 and the maximum activity-to-A_2 value ratio (the smallest maximum allowable leakage rate within the time interval examined). A summary of the content activity and the A_2 value of the various configurations for the above time interval is given in Table 6.

From Section 1.2.3, the activity and mass concentrations for the transuranics are 6×10^5 Bq/gU and 40 µg/gU, respectively. Using a maximum uranium mass of 35.2 kg, the mass of transuranics is calculated to be 1.408 g and the activity is calculated to be 2.112×10^{-2} TBq. Dividing this activity by the mass results in a specific activity of 1.5×10^{-2} TBq/g. In accordance with 10 CFR 71, Appendix A, Table A-3 for "contents with no relevant data," an A_2 value of 9.0×10^{-5} TBq is obtained.

Section 1.2.3 gives a maximum concentration for Np-237 of 0.025 g/gU. Using a maximum uranium mass of 35.2 kg, the mass of Np-237 is calculated to be 880 g. This value is used in Tables 3, 4, and 5 of Appendix 4.6.1 for the Np-237 contents.

Results

The containment criteria analysis indicates that the HEU contents must be shipped in a Type B material package since their activities are greater than the A_2 value. The smallest A_2 value of 1.0997×10^{-3} TBq (2.9720×10^{-2} Ci) in conjunction with the maximum activity-to-A_2 value ratio of 293.99 occurs after about 70 years of decay for the assumed maximum 35.2 kg of HEU.

Table 2. Mass values of parent and daughter products for 35.2 kg of HEU

Isotope	0 years	5 years	10 years	20 years	30 years	40 years	50 years	60 years	70 years
Pb-210	0.0000E+00	1.4150E-10	1.0912E-09	8.1664E-09	2.5555E-08	5.6672E-08	1.0349E-07	1.6896E-07	2.5274E-07
Pb-212	0.0000E+00	1.8163E-08	2.0275E-08	1.8867E-08	1.7037E-08	1.5488E-08	1.3996E-08	1.2672E-08	1.1475E-08
Bi-210	0.0000E+00	8.7296E-14	6.7302E-13	5.0054E-12	1.5770E-11	3.4918E-11	6.3923E-11	1.0419E-10	1.5558E-10
Bi-212	0.0000E+00	1.7178E-09	1.9149E-09	1.7882E-09	1.6192E-09	1.4643E-09	1.3277E-09	1.2024E-09	1.0884E-09
Po-210	0.0000E+00	2.4077E-12	1.8586E-11	1.3798E-10	4.3507E-10	9.6448E-10	1.7670E-09	2.8653E-09	4.2944E-09
Rn-222	0.0000E+00	1.4150E-12	5.6602E-12	2.2598E-11	5.0829E-11	9.0112E-11	1.4080E-10	2.0205E-10	2.7526E-10
Ra-223	0.0000E+00	6.5313E-12	2.4734E-11	9.0047E-11	1.8454E-10	2.9951E-10	4.3091E-10	5.7390E-10	7.2463E-10
Ra-224	0.0000E+00	1.5770E-07	1.7600E-07	1.6474E-07	1.4925E-07	1.3489E-07	1.2207E-07	1.1053E-07	1.0011E-07
Ra-225	0.0000E+00	2.1120E-08	4.5619E-08	9.1238E-08	1.3686E-07	1.8227E-07	2.2810E-07	2.7245E-07	3.1891E-07
Ra-226	0.0000E+00	2.2035E-07	8.8000E-07	3.5200E-06	7.8848E-06	1.4010E-05	2.1894E-05	3.1469E-05	4.2803E-05
Ra-228	0.0000E+00	2.0557E-13	6.8992E-13	2.0557E-12	3.6186E-12	5.2378E-12	6.8710E-12	8.5184E-12	1.0166E-11
Ac-225	0.0000E+00	1.6896E-08	3.0835E-08	6.1670E-08	9.2506E-08	1.2313E-07	1.5396E-07	1.8459E-07	2.1542E-07
Ac-227	0.0000E+00	4.6183E-09	1.7565E-08	6.3574E-08	1.3043E-07	2.1256E-07	3.0531E-07	4.0579E-07	5.1207E-07
Ac-228	0.0000E+00	2.5062E-17	8.4198E-17	2.5062E-16	4.4070E-16	6.3923E-16	8.3917E-16	1.0391E-15	1.2404E-15
Th-227	0.0000E+00	1.0724E-11	4.0772E-11	1.4782E-10	3.0338E-10	4.9275E-10	7.0917E-10	9.4298E-10	1.1923E-09
Th-228	0.0000E+00	3.0694E-05	3.4214E-05	3.1962E-05	2.9005E-05	2.6189E-05	2.3795E-05	2.1542E-05	1.9430E-05
Th-229	0.0000E+00	6.3360E-03	9.0394E-03	1.8058E-02	2.7034E-02	3.6115E-02	4.4986E-02	5.4067E-02	6.3149E-02
Th-230	0.0000E+00	9.7856E-03	1.9501E-02	3.9072E-02	5.8573E-02	7.8144E-02	9.7856E-02	1.1686E-01	1.3658E-01
Th-231	0.0000E+00	7.8646E-08	7.8646E-08	7.8646E-08	7.8646E-08	7.8646E-08	7.8646E-08	7.8646E-08	7.8646E-08
Th-232	0.0000E+00	2.0416E-03	4.0973E-03	8.1946E-03	1.2292E-02	1.6333E-02	2.0416E-02	2.4640E-02	2.8723E-02
Th-234	0.0000E+00	0.0000E+00	0.0000E+00	0.0000E+00	0.0000E+00	0.0000E+00	0.0000E+00	0.0000E+00	0.0000E+00
Pa-231	0.0000E+00	9.3525E-05	1.8724E-04	3.7487E-04	5.6231E-04	7.4782E-04	9.3525E-04	1.1227E-03	1.3082E-03
Pa-233	0.0000E+00	0.0000E+00	0.0000E+00	0.0000E+00	0.0000E+00	0.0000E+00	0.0000E+00	0.0000E+00	0.0000E+00
U-232	1.4080E-03	1.3376E-03	1.2742E-03	1.1546E-03	1.0447E-03	9.4618E-04	8.5747E-04	7.7581E-04	7.0259E-04
U-233	2.1120E+02	2.1119E+02	2.1119E+02	2.1118E+02	2.1117E+02	2.1116E+02	2.1116E+02	2.1115E+02	2.1114E+02
U-234	7.0400E+02	7.0399E+02	7.0398E+02	7.0396E+02	7.0394E+02	7.0392E+02	7.0390E+02	7.0388E+02	7.0386E+02
U-235	1.9323E+04	1.9323E+04	1.9323E+04	1.9323E+04	1.9323E+04	1.9323E+04	1.9323E+04	1.9323E+04	1.9323E+04
U-236	1.4080E+04	1.4080E+04	1.4080E+04	1.4080E+04	1.4080E+04	1.4080E+04	1.4080E+04	1.4080E+04	1.4080E+04
U-238	0.0000E+00	0.0000E+00	0.0000E+00	0.0000E+00	0.0000E+00	0.0000E+00	0.0000E+00	0.0000E+00	0.0000E+00
Trans.	1.4080E+00	1.4080E+00	1.4080E+00	1.4080E+00	1.4080E+00	1.4080E+00	1.4080E+00	1.4080E+00	1.4080E+00
Np-237	8.8000E+02	8.8000E+02	8.8000E+02	8.8000E+02	8.8000E+02	8.8000E+02	8.8000E+02	8.8000E+02	8.8000E+02
Total	**3.5200E+04**	**3.5200E+04**	**3.5200E+04**	**3.5200E+04**	**3.5200E+04**	**3.5200E+04**	**3.5200E+04**	**3.5200E+04**	**3.5200E+04**

Table 3. A_2 value calculation for 35.2 kg HEU for fast absorption uranium at 70 years

Isotope	Mass at 70 years (g)	Specific activity (TBq/g)	Activity (TBq)	A_2 (TBq)	f(i) (TBq/TBq)	f(i) / A_2 (1/TBq)
Pb-210	2.5274E-07	2.8000E+00	7.0767E-07	5.0000E-02	2.1890E-06	4.3781E-05
Pb-212	1.1475E-08	5.1000E+04	5.8523E-04	2.0000E-01	1.8103E-03	9.0514E-03
Bi-210	1.5558E-10	4.6000E+03	7.1567E-07	6.0000E-01	2.2138E-06	3.6896E-06
Bi-212	1.0884E-09	5.4000E+05	5.8774E-04	6.0000E-01	1.8180E-03	3.0301E-03
Po-210	4.2944E-09	1.7000E+02	7.3005E-07	2.0000E-02	2.2583E-06	1.1291E-04
Rn-222	2.7526E-10	5.7000E+03	1.5690E-06	4.0000E-03	4.8533E-06	1.2133E-03
Ra-223	7.2463E-10	1.9000E+03	1.3768E-06	7.0000E-03	4.2588E-06	6.0841E-04
Ra-224	1.0011E-07	5.9000E+03	5.9065E-04	2.0000E-02	1.8271E-03	9.1353E-02
Ra-225	3.1891E-07	1.5000E+03	4.7837E-04	4.0000E-03	1.4797E-03	3.6993E-01
Ra-226	4.2803E-05	3.7000E-02	1.5837E-06	3.0000E-03	4.8989E-06	1.6330E-03
Ra-228	1.0166E-11	1.0000E+01	1.0166E-10	2.0000E-02	3.1446E-10	1.5723E-08
Ac-225	2.1542E-07	2.1000E+03	4.5238E-04	6.0000E-03	1.3994E-03	2.3323E-01
Ac-227	5.1207E-07	2.7000E+00	1.3826E-06	9.0000E-05	4.2768E-06	4.7519E-02
Ac-228	1.2404E-15	8.4000E+04	1.0419E-10	5.0000E-01	3.2230E-10	6.4460E-10
Th-227	1.1923E-09	1.1000E+03	1.3115E-06	5.0000E-03	4.0569E-06	8.1139E-04
Th-228	1.9430E-05	3.0000E+01	5.8290E-04	1.0000E-03	1.8031E-03	1.8031E+00
Th-229	6.3149E-02	7.9000E-03	4.9888E-04	5.0000E-04	1.5432E-03	3.0863E+00
Th-230	1.3658E-01	7.6000E-04	1.0380E-04	1.0000E-03	3.2109E-04	3.2109E-01
Th-231	7.8646E-08	2.0000E+04	1.5729E-03	2.0000E-02	4.8655E-03	2.4328E-01
Th-232	2.8723E-02	4.0000E-09	1.1489E-10	1.0000E+75	3.5539E-10	3.5539E-85
Pa-231	1.3082E-03	1.7000E-03	2.2239E-06	4.0000E-04	6.8793E-06	1.7198E-02
U-232	7.0259E-04	8.3000E-01	5.8315E-04	1.0000E-02	1.8039E-03	1.8039E-01
U-233	2.1114E+02	3.6000E-04	7.6010E-02	9.0000E-02	2.3512E-01	2.6125E+00
U-234	7.0386E+02	2.3000E-04	1.6189E-01	9.0000E-02	5.0077E-01	5.5641E+00
U-235	1.9323E+04	8.0000E-08	1.5458E-03	1.0000E+75	4.7817E-03	4.7817E-78
U-236	1.4080E+04	2.4000E-06	3.3792E-02	1.0000E+75	1.0453E-01	1.0453E-76
Transuranic	1.4080E+00	1.5000E-02	2.1120E-02	9.0000E-05	6.5330E-02	7.2588E+02
Np-237	8.8000E+02	2.6000E-05	2.2880E-02	2.0000E-03	7.0775E-02	3.5387E+01
Total Mass =	3.5200E+04	∑ Act. =	3.2328E-01		∑ f(i) / A_2 =	7.7585E+02

$$A_2\,(\text{mixture}) = \frac{1}{\sum f(i) / A_2} = \frac{1}{7.7586 \times 10^{2}\ (1/\text{TBq})} = 1.2889 \times 10^{-3}\ \text{TBq}$$

Table 4. A_2 value calculation for 35.2 kg HEU for medium absorption uranium at 70 years

Isotope	Mass at 70 years (g)	Specific activity (TBq/g)	Activity (TBq)	A_2 (TBq)	f(i) (TBq/TBq)	f(i) / A_2 (1/TBq)
Pb-210	2.5274E-07	2.8000E+00	7.0767E-07	5.0000E-02	2.1890E-06	4.3781E-05
Pb-212	1.1475E-08	5.1000E+04	5.8523E-04	2.0000E-01	1.8103E-03	9.0514E-03
Bi-210	1.5558E-10	4.6000E+03	7.1567E-07	6.0000E-01	2.2138E-06	3.6896E-06
Bi-212	1.0884E-09	5.4000E+05	5.8774E-04	6.0000E-01	1.8180E-03	3.0301E-03
Po-210	4.2944E-09	1.7000E+02	7.3005E-07	2.0000E-02	2.2583E-06	1.1291E-04
Rn-222	2.7526E-10	5.7000E+03	1.5690E-06	4.0000E-03	4.8533E-06	1.2133E-03
Ra-223	7.2463E-10	1.9000E+03	1.3768E-06	7.0000E-03	4.2588E-06	6.0841E-04
Ra-224	1.0011E-07	5.9000E+03	5.9065E-04	2.0000E-02	1.8271E-03	9.1353E-02
Ra-225	3.1891E-07	1.5000E+03	4.7837E-04	4.0000E-03	1.4797E-03	3.6993E-01
Ra-226	4.2803E-05	3.7000E-02	1.5837E-06	3.0000E-03	4.8989E-06	1.6330E-03
Ra-228	1.0166E-11	1.0000E+01	1.0166E-10	2.0000E-02	3.1446E-10	1.5723E-08
Ac-225	2.1542E-07	2.1000E+03	4.5238E-04	6.0000E-03	1.3994E-03	2.3323E-01
Ac-227	5.1207E-07	2.7000E+00	1.3826E-06	9.0000E-05	4.2768E-06	4.7519E-02
Ac-228	1.2404E-15	8.4000E+04	1.0419E-10	5.0000E-01	3.2230E-10	6.4460E-10
Th-227	1.1923E-09	1.1000E+03	1.3115E-06	5.0000E-03	4.0569E-06	8.1139E-04
Th-228	1.9430E-05	3.0000E+01	5.8290E-04	1.0000E-03	1.8031E-03	1.8031E+00
Th-229	6.3149E-02	7.9000E-03	4.9888E-04	5.0000E-04	1.5432E-03	3.0863E+00
Th-230	1.3658E-01	7.6000E-04	1.0380E-04	1.0000E-03	3.2109E-04	3.2109E-01
Th-231	7.8646E-08	2.0000E+04	1.5729E-03	2.0000E-02	4.8655E-03	2.4328E-01
Th-232	2.8723E-02	4.0000E-09	1.1489E-10	1.0000E+75	3.5539E-10	3.5539E-85
Pa-231	1.3082E-03	1.7000E-03	2.2239E-06	4.0000E-04	6.8793E-06	1.7198E-02
U-232	7.0259E-04	8.3000E-01	5.8315E-04	7.0000E-03	1.8039E-03	2.5769E-01
U-233	2.1114E+02	3.6000E-04	7.6010E-02	2.0000E-02	2.3512E-01	1.1756E+01
U-234	7.0386E+02	2.3000E-04	1.6189E-01	2.0000E-02	5.0077E-01	2.5038E+01
U-235	1.9323E+04	8.0000E-08	1.5458E-03	1.0000E+75	4.7817E-03	4.7817E-78
U-236	1.4080E+04	2.4000E-06	3.3792E-02	2.0000E-02	1.0453E-01	5.2264E+00
Transuranic	1.4080E+00	1.5000E-02	2.1120E-02	9.0000E-05	6.5330E-02	7.2589E+02
Np-237	8.8000E+02	2.6000E-05	2.2880E-02	2.0000E-03	7.0775E-02	3.5387E+01
Total Mass =	3.5200E+04	$\sum$ Act. =	3.2328E-01		$\sum$ f(i) / A_2 =	8.0978E+02

$$A_2\,(\text{mixture}) = \frac{1}{\sum f(i) / A_2} = \frac{1}{8.0978 \times 10^2\ (1/\text{TBq})} = 1.2349 \times 10^{-3}\ \text{TBq}$$

Table 5. A_2 value calculation for 35.2 kg HEU for slow absorption uranium at 70 years

Isotope	Mass at 70 years (g)	Specific activity (TBq/g)	Activity (TBq)	A_2 (TBq)	f(i) (TBq/TBq)	f(i) / A_2 (1/TBq)
Pb-210	2.5274E-07	2.8000E+00	7.0767E-07	5.0000E-02	2.1890E-06	4.3781E-05
Pb-212	1.1475E-08	5.1000E+04	5.8523E-04	2.0000E-01	1.8103E-03	9.0514E-03
Bi-210	1.5558E-10	4.6000E+03	7.1567E-07	6.0000E-01	2.2138E-06	3.6896E-06
Bi-212	1.0884E-09	5.4000E+05	5.8774E-04	6.0000E-01	1.8180E-03	3.0301E-03
Po-210	4.2944E-09	1.7000E+02	7.3005E-07	2.0000E-02	2.2583E-06	1.1291E-04
Rn-222	2.7526E-10	5.7000E+03	1.5690E-06	4.0000E-03	4.8533E-06	1.2133E-03
Ra-223	7.2463E-10	1.9000E+03	1.3768E-06	7.0000E-03	4.2588E-06	6.0841E-04
Ra-224	1.0011E-07	5.9000E+03	5.9065E-04	2.0000E-02	1.8271E-03	9.1353E-02
Ra-225	3.1891E-07	1.5000E+03	4.7837E-04	4.0000E-03	1.4797E-03	3.6993E-01
Ra-226	4.2803E-05	3.7000E-02	1.5837E-06	3.0000E-03	4.8989E-06	1.6330E-03
Ra-228	1.0166E-11	1.0000E+01	1.0166E-10	2.0000E-02	3.1446E-10	1.5723E-08
Ac-225	2.1542E-07	2.1000E+03	4.5238E-04	6.0000E-03	1.3994E-03	2.3323E-01
Ac-227	5.1207E-07	2.7000E+00	1.3826E-06	9.0000E-05	4.2768E-06	4.7519E-02
Ac-228	1.2404E-15	8.4000E+04	1.0419E-10	5.0000E-01	3.2230E-10	6.4460E-10
Th-227	1.1923E-09	1.1000E+03	1.3115E-06	5.0000E-03	4.0569E-06	8.1139E-04
Th-228	1.9430E-05	3.0000E+01	5.8290E-04	1.0000E-03	1.8031E-03	1.8031E+00
Th-229	6.3149E-02	7.9000E-03	4.9888E-04	5.0000E-04	1.5432E-03	3.0863E+00
Th-230	1.3658E-01	7.6000E-04	1.0380E-04	1.0000E-03	3.2109E-04	3.2109E-01
Th-231	7.8646E-08	2.0000E+04	1.5729E-03	2.0000E-02	4.8655E-03	2.4328E-01
Th-232	2.8723E-02	4.0000E-09	1.1489E-10	1.0000E+75	3.5539E-10	3.5539E-85
Pa-231	1.3082E-03	1.7000E-03	2.2239E-06	4.0000E-04	6.8793E-06	1.7198E-02
U-232	7.0259E-04	8.3000E-01	5.8315E-04	1.0000E-03	1.8039E-03	1.8039E+00
U-233	2.1114E+02	3.6000E-04	7.6010E-02	6.0000E-03	2.3512E-01	3.9187E+01
U-234	7.0386E+02	2.3000E-04	1.6189E-01	6.0000E-03	5.0077E-01	8.3461E+01
U-235	1.9323E+04	8.0000E-08	1.5458E-03	1.0000E+75	4.7817E-03	4.7817E-78
U-236	1.4080E+04	2.4000E-06	3.3792E-02	6.0000E-03	1.0453E-01	1.7421E+01
Transuranic	1.4080E+00	1.5000E-02	2.1120E-02	9.0000E-05	6.5330E-02	7.2589E+02
Np-237	8.8000E+02	2.6000E-05	2.2880E-02	2.0000E-03	7.0775E-02	3.5387E+01
Total Mass =	3.5200E+04	$\sum$ Act. =	3.2328E-01		$\sum$ f(i) / A_2 =	9.0938E+02

$$A_2\,(\text{mixture}) = \frac{1}{\sum f(i) / A_2} = \frac{1}{9.0937 \times 10^2\ (1/\text{TBq})} = 1.0997 \times 10^{-3}\ \text{TBq}$$

Table 6. Activity, A_2 value, and activity-to-A_2 ratio for the enriched uranium contents

Year	Activity (TBq)	A_2-Mixture (TBq)			Activity/A_2		
		Fast	Medium	Slow	Fast	Medium	Slow
0	3.1846E-01	1.2796E-03	1.2255E-03	1.0885E-03	248.87	259.86	292.57
5	3.2380E-01	1.2950E-03	1.2405E-03	1.1026E-03	250.04	261.03	293.68
10	3.2427E-01	1.2960E-03	1.2415E-03	1.1037E-03	250.21	261.20	293.81
20	3.2410E-01	1.2948E-03	1.2404E-03	1.1031E-03	250.31	261.29	293.82
30	3.2386E-01	1.2934E-03	1.2391E-03	1.1022E-03	250.40	261.38	293.82
40	3.2366E-01	1.2921E-03	1.2379E-03	1.1015E-03	250.49	261.47	293.84
50	3.2350E-01	1.2909E-03	1.2368E-03	1.1008E-03	250.59	261.56	293.87
60	3.2338E-01	1.2899E-03	1.2358E-03	1.1002E-03	250.71	261.68	293.93
70	3.2328E-01[a]	1.2889E-03	1.2349E-03	1.0997E-03[a]	250.82	261.79	293.99[a]

[a] The A_2, total activity, and activity-to-A_2 ratio values used in Appendix 4.6.2.

THIS PAGE INTENTIONALLY LEFT BLANK.

Appendix 4.6.2

CALCULATION OF THE ES-3100 CONTAINMENT VESSEL'S REGULATORY REFERENCE AIR LEAKAGE RATES

Prepared by: Monty L. Goins
BWXT Y-12
November 2006

Reviewed by: G. A. Byington
BWXT Y-12
November 2006

Revised by: Monty L. Goins
B & W Y-12
November 2010

Reviewed by: Drew Winder
B & W Y-12
December 2010

THIS PAGE INTENTIONALLY LEFT BLANK.

Appendix 4.6.2

CALCULATION OF THE ES-3100 CONTAINMENT VESSEL'S REGULATORY REFERENCE AIR LEAKAGE RATES

Introduction

The ES-3100 leak-testing requirements of the containment boundary are based on the smallest maximum allowable leakage rate generated from the maximum uranium content defined in Table 4.3. Section 5 of ANSI N14.5-1997 defines the maximum allowable leakage rate based on the maximum allowable release rate. These leakage rates, L_N and L_A, are the maximum allowable O-ring seal leakage rates for Normal Conditions of Transport (NCT) and Hypothetical Accident Conditions (HAC). The worst-case maximum allowable leakage rates are used to calculate an equivalent leakage hole diameter following ANSI N14.5-1997, Appendix B, for each condition of transport. This leakage hole diameter is used to calculate a reference air and a helium leakage rate for leak testing. A bounding mass for the highly enriched uranium (HEU) content of 35.2 kg is used in this calculation to certify the ES-3100 package for shipment. The maximum allowable leakage rates are calculated using this maximum content mass in a much more dispersive form (oxide powder) at the highest calculated pressures and temperatures. This appendix shows the procedure used to calculate the leak criteria for the uranium constituents in the "slow lung absorption" group. Table 1 shows the results of using this procedure for fast, medium, and slow absorption uranium constituents as a function of decay time.

HEU Content

Calculate R_N and R_A: Table 4.1

The maximum allowable release rate is based on using A_2.

$A_2 = 1.0997 \times 10^{-3}$ TBq, (2.9720×10^{-2} Ci). Table 6 (Appendix 4.6.1)

The containment requirements for NCT and HAC are:

$R_N = A_2 \times 10^{-6}$ TBq/h $= A_2 \times 2.78 \times 10^{-10}$ TBq/s, ANSI N14.5-1997 (Eq. 1)
$= 1.0997 \times 10^{-3} \times 2.78 \times 10^{-10}$ TBq/s,
$= 3.0570 \times 10^{-13}$ TBq/s, (8.2623×10^{-12} Ci/s).

$R_A = A_2$ (TBq/week),
$= A_2 \times 1.65 \times 10^{-6}$ (TBq/s), ANSI N14.5-1997 (Eq. 2)
$= 1.0997 \times 10^{-3} \times 1.65 \times 10^{-6}$ TBq/s,
$= 1.8144 \times 10^{-9}$ TBq/s, (4.9038×10^{-8} Ci/s). or limited to 10 A_2/week of ^{85}Kr

Following ANSI N14.5-1997, the medium aerosol activity must be calculated to determine the leakage rates.

m = total nuclide mass in the package available for release (g),
TotA = total activity in the package available for release (TBq),
TSA = total specific activity in the package available for release (TBq/g).

For HEU content:

$$\begin{aligned} TSA &= TotA / m, \\ &= 3.2328 \times 10^{-1}\ (TBq) / 35{,}200\ (g), && \text{Table 6 (Appendix 4.6.1)} \\ &= 9.1842 \times 10^{-6}\ TBq/g. \end{aligned}$$

$$\rho_P = 9 \times 10^{-6}\ g/cm^3. \qquad \text{The maximum density of powder aerosols in the fill gas}$$

For any packaging arrangement:

$$\begin{aligned} C_N &= \text{activity per unit volume of medium that could escape from the containment system } (TBq/cm^3). \\ &= TSA \times \rho_P, \\ &= 9.1842 \times 10^{-6}\ (TBq/g) \times 9 \times 10^{-6}\ (g/cm^3), \\ &= 8.2658 \times 10^{-11}\ TBq/cm^3. \end{aligned}$$

Using Curren's maximum aerosol density, $C_A = C_N$:

$$\begin{aligned} C_A &= \text{activity per unit volume of exiting gas } (TBq/cm^3), && \text{HAC} \\ &= 8.2658 \times 10^{-11}\ TBq/cm^3. \end{aligned}$$

Section 6.1 of ANSI N14.5-1997 calculates L_N with (Eq. 3) and L_A with (Eq. 4). L_N and L_A are the maximum allowable leakage rates for the containment vessel fill gas aerosol during NCT and HAC, respectively.

$$\begin{aligned} L_N &= \text{maximum allowable leakage rate for the medium for NCT } (TBq/cm^3), \\ &= R_N / C_N, && \text{ANSI N14.5-1997 (Eq. 3)} \\ &= 3.0570 \times 10^{-13}\ (TBq/s) / 8.2658 \times 10^{-11}\ (TBq/cm^3), \\ &= 3.6984 \times 10^{-3}\ cm^3/s. \end{aligned}$$

$$\begin{aligned} L_A &= \text{maximum allowable leakage rate for the medium for HAC } (TBq/cm^3), \\ &= R_A / C_A, \\ &= 1.8144 \times 10^{-9}\ (TBq/s) / 8.2658 \times 10^{-11}\ (TBq/cm^3), \\ &= 2.1951 \times 10^{1}\ cm^3/s. \end{aligned}$$

L_N and L_A correspond to the upstream volumetric leakage rate (L_u) at the upstream pressure (P_u) in the ANSI N14.5-1997 formulas for use later in this appendix. The reference air leakage rates $L_{R,N}$ and $L_{R,A}$ for NCT and HAC, based on the L_N and L_A, are then calculated using maximum temperatures and pressure combinations from Table 3.16 and Table 5 in Appendix 3.6.5.

Determination of the Leakage Test Procedure Requirements for the HEU Content

This calculation will examine the most conservative effects of a fully loaded containment vessel with an HEU mass of 35.2 kg. The smallest allowable leakage values are shown in Tables 4.5 and 4.7. The A_2 value and the maximum content activity-to-A_2 value ratio for this mixture were calculated for several different decay times (Table 6, Appendix 4.6.1). As calculated in Appendix 4.6.1, the A_2 value and the maximum content activity-to-A_2 ratio used to qualify this package occur at about 70 years of decay and are 1.0997×10^{-3} TBq (2.9720×10^{-2} Ci) and 293.99, respectively. These values are used to determine the leakage test procedural requirements when packaging any convenience cans/contents arrangements in the ES-3100 package. The convenience cans are sealed inside the containment vessel in

an environmentally controlled area. The ES-3100 package has been analyzed thermally in Sect. 3; it was evaluated at a maximum NCT gas temperature of 87.81°C (190.06°F) [100°F with solar insolation] and a maximum adjusted HAC gas temperature of 123.85°C (254.93°F).

The following analysis determines the maximum allowable O-ring seal air reference leakage rate for both NCT and HAC. The ANSI N14.5-1997 recommended method using a straight circular tube to model the leakage path is applied. Using this "standard" leakage hole model permits the calculation of equivalent reference leakage rates from which leak-test requirements can be established. Viscosity data for air and helium used in the following analyses were obtained from curve fitting routines at specific temperatures based on viscosity data for air (Handbook of Chemistry and Physics, 55th ed.) and helium (NBS Technical Note 631).

L_N and L_A correspond to the upstream volumetric leakage rate (L_u) at the upstream pressure (P_u).

$$L_N = 3.6984 \times 10^{-3}\ \text{cm}^3/\text{s},$$
$$L_A = 2.1951 \times 10^{1}\ \text{cm}^3/\text{s}.$$

Find the maximum pressure and temperature in the containment vessel:

Converting the temperature to degrees Kelvin:

$$T = 273.15 + T(°C),$$
$$= 273.15 + 5 / 9\ (°F - 32)\ (K).$$

$$T_N = 273.15 + 5 / 9\ (190.06°F - 32)\ (K), \qquad \text{(Sect. 3.4.1, for T = 190.06°F)}$$
$$= 360.961\ K. \qquad \text{NCT}$$

$$T_A = 273.15 + 5 / 9\ (254.93°F - 32)\ (K), \qquad \text{(Sect. 3.5.3, for T = 254.93°F)}$$
$$= 397.000\ K. \qquad \text{HAC}$$

Converting the pressures from psia to atmospheres:

$$P_N = P\ (psia) / 14.696\ (psia/atm), \qquad \text{where P is the pressure in Sect. 3.4.2}$$
$$= 28.859\ (psia) / 14.696\ (psia/atm), \qquad \text{NCT}$$
$$= 1.9637\ atm.$$

$$P_A = P\ (psia) / 14.696\ (psia/atm), \qquad \text{where P is the pressure in Sect. 3.5.3}$$
$$= 86.441\ (psia) / 14.696\ (psia/atm), \qquad \text{HAC}$$
$$= 5.8819\ atm.$$

NCT Leakage Hole Diameter for the HEU Content

The following calculations determine the leakage hole diameter that generates the maximum allowable leakage rate during NCT. To keep these calculations conservative, the maximum values for temperature and pressure were used as steady-state conditions for NCT.

Input data for NCT with air fill gas:

L_N	=	3.6984×10^{-3} cm^3/s,	Maximum upstream leakage
P_u	=	1.9637 atm,	Upstream pressure = 28.859 psia
P_d	=	0.2382 atm,	Downstream pressure = 3.5 psia, per 10 CFR 71.71(3)
a	=	0.3531 cm,	Leak path length, 0.139-in. O-ring section diameter
T	=	360.96 K,	Fill gas temperature = 190.06°F
μ	=	0.02141 cP,	Viscosity at temperature
M	=	29 g/g-mole.	Molecular weight of fill gas

The average pressure is:

$$P_a = (P_u + P_d) / 2,$$
$$= (1.9637 + 0.2382) / 2,$$
$$= 1.1009 \text{ atm.}$$

Average pressure during NCT

According to ANSI N14.5-1997, the flow leakage hole diameter is unknown. Therefore, the mass-like leakage flow rate must be calculated to calculate the average leakage flow rate.

Q is the mass-like leakage for flow using the upstream leakage, L_u, and pressure, P_u:

$$Q = P_u L_u, \quad \text{(Eq. B1)}$$
$$L_u = L_N. \quad \text{NCT leakage}$$

$$Q = (1.9637)(\text{atm})\,(3.6984 \times 10^{-3})(\text{cm}^3/\text{s}),$$
$$= 7.2628 \times 10^{-3} \text{ atm-cm}^3/\text{s}. \quad \text{NCT mass-like leakage rate}$$

$$Q = P_a L_a, \quad \text{(Eq. B1)}$$

$$L_a = Q / P_a = 7.2628 \times 10^{-3} \text{ (atm-cm}^3\text{/s) / (1.1009)(atm)},$$
$$= 6.5968 \times 10^{-3} \text{ cm}^3\text{/s}. \quad \text{NCT average leakage rate}$$

Solve equations B2–B4 from ANSI N14.5-1997:

$$L_a = (F_c + F_m)\,(P_u - P_d) \text{ cm}^3\text{/s}, \quad \text{(Eq. B2)}$$
$$= (F_c + F_m)\,(1.9637 - 0.2382),$$
$$= (1.7256)\,(F_c + F_m) \text{ cm}^3\text{/s}.$$

$$F_c = (2.49 \times 10^6)\, D^4 / (a\,\mu) \text{ (cm}^3\text{/atm-s)}, \quad \text{(Eq. B3)}$$
$$= (2.49 \times 10^6)\, D^4 / [(0.3531)\,(0.02141)],$$
$$= (3.2943 \times 10^8)\, D^4 \text{ cm}^3\text{/atm-s}.$$

$$F_m = (3.81 \times 10^3)\, D^3\, (T / M)^{.5} / (a\, P_a) \text{ (cm}^3\text{/atm-s)}, \quad \text{(Eq. B4)}$$
$$= (3.81 \times 10^3)\, D^3\, (360.96 / 29)^{.5} / [(0.3531)\,(1.1009)],$$
$$= (3.4581 \times 10^4)\, D^3 \text{ cm}^3\text{/atm-s}.$$

From the mass-like leakage calculation:

$$L_a = 6.5968 \times 10^{-3} \text{ cm}^3\text{/s}. \quad \text{NCT average leakage rate}$$

Find the leakage hole diameter that sets:

$$L_2 = L_a.$$

Using the equations:

$$L_2 = (1.7256)\,(F_c + F_m)\ \text{cm}^3/\text{s},$$
$$F_c = (3.2943 \times 10^8)\,D^4\ \text{cm}^3/\text{atm-s},$$
$$F_m = (3.4581 \times 10^4)\,D^3\ \text{cm}^3/\text{atm-s}.$$

To get a better guess on a new D use:

$$D = D_2\,(L_a / L_2)^{0.252}.$$

Now a guess must be made for D_2 to solve Eq. B2 for NCT:

D_2 = 0.001 cm, and solve for $L_a = 6.5968 \times 10^{-3}$ cm³/s. NCT average leakage rate

Diameter	F_c	F_m	L_2	L_a / L_2
1.0000E-03	3.2943E-04	3.4581E-05	6.2815E-04	1.0502E+01
1.9725E-03	4.9870E-03	2.6539E-04	9.0635E-03	7.2784E-01
1.8208E-03	3.6205E-03	2.0873E-04	6.6078E-03	9.9834E-01
1.8200E-03	3.6145E-03	2.0847E-04	6.5969E-03	9.9999E-01
1.8200E-03	3.6144E-03	2.0847E-04	6.5968E-03	1.0000E+00

The NCT leakage hole diameter for the HEU oxide content:

$D = 1.8200 \times 10^{-3}$ cm. NCT diameter

NCT Reference Air Leakage Rate for HEU Content

The leakage hole diameter found for the maximum allowable leakage rate for NCT will be used to determine the reference air leakage rate. O-ring seal leakage testing must ensure that no leakage is greater than the leakage generated by the hole diameter $D = 1.8200 \times 10^{-3}$ cm. Therefore, the NCT reference leakage flow rate ($L_{R,N}$) must be calculated to determine the allowable test leakage rate.

Input data for NCT reference air leakage rate:

D	=	1.8200×10^{-3} cm,	From NCT
a	=	0.3531 cm,	Leak path length, 0.139-in. O-ring section diameter
P_u	=	1.0 atm,	Upstream pressure
P_d	=	0.01 atm,	Downstream pressure
T	=	298 K,	Fill gas temperature, 77°F
M	=	29 g/g-mole,	Molecular weight of air
μ	=	0.0185 cP,	Viscosity of air at reference temperature

Calculate P_a:

$$P_a = (P_u + P_d) / 2,$$
$$= (1.0 + 0.01) /2,$$
$$= 0.505 \text{ atm.}$$ NCT average pressure

$$F_c = (2.49 \times 10^6)\, D^4 / (a\, \mu)\ (\text{cm}^3/\text{atm-s}),$$ (Eq. B3)
$$= (2.49 \times 10^6)\, (1.8200 \times 10^{-3})^4 / [(0.3531)\, (0.0185)],$$
$$= (3.8122 \times 10^8)\, (1.8200 \times 10^{-3})^4,$$
$$= 4.1827 \times 10^{-3}\ \text{cm}^3/\text{atm-s}.$$

$$F_m = (3.81 \times 10^3)\, D^3\, (T / M)^{.5} / (a\, P_a)\ (\text{cm}^3/\text{atm-s}),$$ (Eq. B4)
$$= (3.81 \times 10^3)\, (1.8200 \times 10^{-3})^3\, (298 / 29)^{.5} / [(0.3531)\, (0.505)],$$
$$= (6.8501 \times 10^4)\, (1.8200 \times 10^{-3})^3,$$
$$= 4.1296 \times 10^{-4}\ \text{cm}^3/\text{atm-s}.$$

$$L_u = (F_c + F_m)\, (P_u - P_d)\, (P_a / P_u)\ (\text{cm}^3/\text{s}),$$ (Eq. B5)
$$= (4.1827 \times 10^{-3} + 4.1296 \times 10^{-4})(\text{cm}^3/\text{atm-s})\ (1.0 - 0.01)(\text{atm})\ (0.505 / 1.0),$$
$$= (4.5957 \times 10^{-3})(\text{cm}^3/\text{atm-s})\ (0.49995)(\text{atm}),$$
$$= 2.2976 \times 10^{-3}\ \text{cm}^3/\text{s}.$$

The reference air leakage rate as defined in ANSI N14.5-1997, Sect. B.3, is the upstream leakage in air.

$$L_{RN,Air} = 2.2976 \times 10^{-3}\ \text{ref-cm}^3/\text{s}.$$ For HEU oxide content

The same equations can be used to calculate an allowable leakage rate using helium for leak testing.

$$M = 4\ \text{g/g-mole},$$ Molecular weight of helium
$$\mu = 0.0198\ \text{cP}.$$ Viscosity of helium at temperature

$$F_c = (2.49 \times 10^6)\, D^4 / (a\, \mu)\ (\text{cm}^3/\text{atm-s}),$$ (Eq. B3)
$$= (2.49 \times 10^6)\, (1.8200 \times 10^{-3})^4 / [(0.3531)\, (0.0198)],$$
$$= (3.5619 \times 10^8)\, (1.8200 \times 10^{-3})^4,$$
$$= 3.9081 \times 10^{-3}\ \text{cm}^3/\text{atm-s}.$$

$$F_m = (3.81 \times 10^3)\, D^3\, (T / M)^{.5} / (a\, P_a)\ (\text{cm}^3/\text{atm-s}),$$ (Eq. B4)
$$= (3.81 \times 10^3)\, (1.8200 \times 10^{-3})^3\, (298 / 4)^{.5} / [(0.3531)\, (0.505)],$$
$$= (1.8444 \times 10^5)\, (1.8200 \times 10^{-3})^3,$$
$$= 1.1119 \times 10^{-3}\ \text{cm}^3/\text{atm-s}.$$

$$L_u = (F_c + F_m)\, (P_u - P_d)\, (P_a / P_u)\ (\text{cm}^3/\text{s}),$$ (Eq. B5)
$$= (3.9081 \times 10^{-3} + 1.1119 \times 10^{-3})(\text{cm}^3/\text{atm-s})\ (1.0 - 0.01)(\text{atm})\ (0.505 / 1.0),$$
$$= (5.0200 \times 10^{-3})(\text{cm}^3/\text{atm-s})\ (0.49995)(\text{atm}),$$
$$= 2.5098 \times 10^{-3}\ \text{cm}^3/\text{s}.$$

The allowable leakage rate using helium for leak testing is:

$$L_{RN,\,He} = 2.5098 \times 10^{-3}\ \text{cm}^3/\text{s}.$$ NCT helium test value

HAC Leakage Hole Diameter for HEU Content

The calculation of a maximum allowable leakage rate hole diameter is based on the temperature and pressure of the fill gas aerosol for HAC, assuming the content is in an oxide powder form. Keeping this calculation conservative, the maximum values for temperature and pressure were used as steady-state conditions for a week. The maximum values were generated during the 30-min burn test for HAC.

Input data for HAC:

L_A	=	21.951 cm^3/s,	Maximum exit leakage
P_u	=	5.8819 atm,	Upstream pressure = 86.441 psia
P_d	=	1.0 atm,	Downstream pressure
T	=	397.000 K,	Fill gas temperature = 254.93 °F
μ	=	0.02297 cP,	Viscosity of air at temperature
M	=	29 g/g-mole,	Molecular weight of air
a	=	0.3531 cm.	Leak path length, 0.139-in. O-ring section diameter

$$P_a = (P_u + P_d) / 2$$
$$= (5.8819 + 1.0) / 2, \quad \text{HAC average pressure}$$
$$= 3.4410 \text{ atm.}$$

Q is the mass-like leakage for flow using the upstream leakage, L_u, and pressure, P_u:

$$Q = P_u L_u, \quad \text{(Eq. B1)}$$
$$L_u = L_A. \quad \text{HAC leakage}$$

$$Q = (5.8819)(\text{atm})\ (21.951)(\text{cm}^3/\text{s}),$$
$$= 129.116 \text{ atm-cm}^3/\text{s}. \quad \text{HAC mass-like leakage rate}$$

$$Q = P_a L_a, \quad \text{(Eq. B1)}$$

$$L_a = Q / P_a$$
$$= 129.116 \ (\text{atm-cm}^3/\text{s}) / (3.4410)(\text{atm}),$$
$$= 37.523 \text{ cm}^3/\text{s}. \quad \text{HAC average leakage rate}$$

Solve equations B2–B4 from ANSI N14.5-1997:

$$L_a = (F_c + F_m)\ (P_u - P_d)\ (\text{cm}^3/\text{s}), \quad \text{(Eq. B2)}$$
$$= (F_c + F_m)\ (5.8819 - 1.0),$$
$$= 4.8819\ (F_c + F_m) \text{ cm}^3/\text{s}.$$

$$F_c = (2.49 \times 10^6)\ D^4 / (\ a\ \mu\ )\ (\text{cm}^3/\text{atm-s}), \quad \text{(Eq. B3)}$$
$$= (2.49 \times 10^6)\ D^4 / [(0.3531)\ (0.02297)],$$
$$= (3.0706 \times 10^8)\ D^4 \text{ cm}^3/\text{atm-s}.$$

$$F_m = (3.81 \times 10^3)\ D^3\ (T / M)^{.5} / (a\ P_a)\ (\text{cm}^3/\text{atm-s}), \quad \text{(Eq. B4)}$$
$$= (3.81 \times 10^3)\ D^3\ (397.00 / 29)^{.5} / [(0.3531)\ (3.4410)],$$
$$= (1.1604 \times 10^4)\ D^3 \text{ cm}^3/\text{atm-s}.$$

From the mass-like leakage calculation:

L_a = 37.523 cm^3/s. HAC average leakage rate

Find the leakage hole diameter that sets:

$L_2 = L_a$.

Using the equations:

$$L_2 = 4.8819\ (F_c + F_m)\ cm^3/s,$$
$$F_c = (3.0706 \times 10^8)\ D^4\ cm^3/atm\text{-}s,$$
$$F_m = (1.1604 \times 10^4)\ D^3\ cm^3/atm\text{-}s.$$

To get a better guess on a new D use:

$$D = D_2\ (L_a / L_2)^{0.252}.$$

Now a guess must be made for D_2 to solve Eq. B2 for HAC:

D_2 = 0.01 (cm), and solve for L_a = 37.523 (cm^3/s). HAC average leakage rate

Diameter	F_c	F_m	L_2	L_a / L_2
1.0000E-02	3.0706E+00	1.1604E-02	1.5047E+01	2.4937E+00
1.2589E-02	7.7134E+00	2.3154E-02	3.7769E+01	9.9349E-01
1.2569E-02	7.6627E+00	2.3040E-02	3.7521E+01	1.0000E+00
1.2569E-02	7.6631E+00	2.3041E-02	3.7523E+01	1.0000E+00

The HAC leakage hole diameter for the HEU oxide content is:

D = 1.2569×10^{-2} cm. HAC diameter

HAC Reference Air Leakage Rate for HEU Content

The leakage hole diameter found for the maximum allowable leakage rate for HAC will be used to determine the reference air leakage rate. O-ring seal leakage testing must assure that no leakage is greater than the leakage generated by the hole diameter D = 1.2569×10^{-2} cm. Therefore, the HAC reference air leakage rate ($L_{R,\ A}$) must be calculated to determine the acceptable test leakage rate for post-HAC leakage testing.

Input data for HAC reference air leakage rate:

D = 1.2569×10^{-2} cm, From the HAC of transport
a = 0.3531 cm, Leak path length, 0.139-in. O-ring section diameter
P_u = 1.0 atm, Upstream pressure
P_d = 0.01 atm, Downstream pressure

$T = 298\ K,$ Fill gas temperature, 77°F
$M = 29\ g/g\text{-}mole,$ Molecular weight of air
$\mu = 0.0185\ cP.$ Viscosity at temperature

Calculate P_a:

$$P_a = (P_u + P_d) / 2$$
$$= 0.505\ atm.$$ HAC average pressure

$$F_c = (2.49 \times 10^6)\ D^4 / (a\ \mu)\ (cm^3/atm\text{-}s), \quad \text{(Eq. B3)}$$
$$= (2.49 \times 10^6)\ (1.2569 \times 10^{-2})^4 / [(0.3531)\ (0.0185)],$$
$$= (3.8122 \times 10^8)\ (1.2569 \times 10^{-2})^4,$$
$$= 9.5139\ cm^3/atm\text{-}s.$$

$$F_m = (3.81 \times 10^3)\ D^3\ (T / M)^{.5} / (a\ P_a)\ (cm^3/atm\text{-}s), \quad \text{(Eq. B4)}$$
$$= (3.81 \times 10^3)\ (1.2569 \times 10^{-2})^3\ (298 / 29)^{.5} / [(0.3531)\ (0.505)],$$
$$= (6.8501 \times 10^4)\ (1.2569 \times 10^{-2})^3,$$
$$= 1.3601 \times 10^{-1}\ cm^3/atm\text{-}s.$$

$$L_u = (F_c + F_m)\ (P_u - P_d)\ (P_a / P_u)\ (cm^3/s), \quad \text{(Eq. B5)}$$
$$= (9.5139 + 1.3601 \times 10^{-1})(cm^3/atm\text{-}s)\ (1.0 - 0.01)(atm)\ (0.505 / 1.0),$$
$$= (9.6499)(cm^3/atm\text{-}s)\ (0.49995)(atm),$$
$$= 4.8245\ cm^3/s.$$

The HAC reference air leakage rate as defined in ANSI N14.5-1997, Sect. B.3, is the upstream leakage in air.

$L_{RA,Air} = 4.8245\ ref\text{-}cm^3/s.$ for HEU oxide content

The same equations can be used to calculate an allowable leakage rate using helium for leak testing.

$M = 4\ g/g\text{-}mole,$ Molecular weight of helium
$\mu = 0.0198\ cP.$ Viscosity of helium at temperature

$$F_c = (2.49 \times 10^6)\ D^4 / (a\ \mu)\ (cm^3/atm\text{-}s), \quad \text{(Eq. B3)}$$
$$= (2.49 \times 10^6)\ (1.2569 \times 10^{-2})^4 / [(0.3531)\ (0.0198)],$$
$$= (3.5619 \times 10^8)\ (1.2569 \times 10^{-2})^4,$$
$$= 8.8892\ cm^3/atm\text{-}s.$$

$$F_m = (3.81 \times 10^3)\ D^3\ (T / M)^{0.5} / (a\ P_a)\ (cm^3/atm\text{-}s), \quad \text{(Eq. B4)}$$
$$= (3.81 \times 10^3)\ (1.2569 \times 10^{-2})^3\ (298 / 4)^{.5} / [(0.3531)\ (0.505)],$$
$$= (1.8444 \times 10^5)\ (1.2569 \times 10^{-2})^3,$$
$$= 3.6622 \times 10^{-1}\ cm^3/atm\text{-}s.$$

$$L_u = (F_c + F_m)\ (P_u - P_d)\ (P_a / P_u)\ (cm^3/s), \quad \text{(Eq. B5)}$$
$$= (8.8892 + 3.6622 \times 10^{-1})(cm^3/atm\text{-}s)\ (1.0 - 0.01)(atm)\ (0.505 / 1.0),$$
$$= (9.2554)(cm^3/atm\text{-}s)\ (0.49995)(atm),$$
$$= 4.6273\ cm^3/s.$$

The allowable leakage rate using helium for leak testing for HAC is:

$L_{RA,\ He} = 4.6273\ cm^3/s.$ HAC helium test value

Table 1. Regulatory leakage criteria for 35.2 kg of HEU

Years from fabrication		NCT		HAC	
		L_{RN-air} (ref-cm^3/s)	L_{RN-He} (cm^3/s)	L_{RA-air} (ref-cm^3/s)	L_{RA-He} (cm^3/s)
Fast absorption	0	2.7102E-03	2.9443E-03	5.6965E+00	5.4580E+00
	5	2.6976E-03	2.9311E-03	5.6700E+00	5.4327E+00
	10	2.6958E-03	2.9291E-03	5.6661E+00	5.4290E+00
	20	2.6947E-03	2.9279E-03	5.6637E+00	5.4268E+00
	30	2.6938E-03	2.9270E-03	5.6618E+00	5.4249E+00
	40	2.6928E-03	2.9260E-03	5.6597E+00	5.4230E+00
	50	2.6917E-03	2.9248E-03	5.6574E+00	5.4207E+00
	60	2.6905E-03	2.9236E-03	5.6549E+00	5.4184E+00
	70	2.6892E-03	2.9222E-03	5.6523E+00	5.4158E+00
Medium absorption	0	2.5965E-03	2.8247E-03	5.4562E+00	5.2291E+00
	5	2.5850E-03	2.8126E-03	5.4319E+00	5.2060E+00
	10	2.5833E-03	2.8109E-03	5.4284E+00	5.2026E+00
	20	2.5824E-03	2.8098E-03	5.4263E+00	5.2006E+00
	30	2.5816E-03	2.8090E-03	5.4246E+00	5.1990E+00
	40	2.5807E-03	2.8081E-03	5.4228E+00	5.1973E+00
	50	2.5797E-03	2.8071E-03	5.4207E+00	5.1953E+00
	60	2.5787E-03	2.8060E-03	5.4185E+00	5.1932E+00
	70	2.5775E-03	2.8048E-03	5.4161E+00	5.1909E+00
Slow absorption	0	2.3087E-03	2.5214E-03	4.8478E+00	4.6495E+00
	5	2.3000E-03	2.5123E-03	4.8295E+00	4.6320E+00
	10	2.2990E-03	2.5112E-03	4.8274E+00	4.6301E+00
	20	2.2989E-03	2.5111E-03	4.8272E+00	4.6299E+00
	30	2.2989E-03	2.5111E-03	4.8272E+00	4.6298E+00
	40	2.2988E-03	2.5110E-03	4.8269E+00	4.6296E+00
	50	2.2985E-03	2.5107E-03	4.8263E+00	4.6290E+00
	60	2.2981E-03	2.5103E-03	4.8255E+00	4.6282E+00
	70	2.2976E-03	2.5098E-03	4.8245E+00	4.6273E+00

SECTION 4 REFERENCES

10 CFR 71, *Packaging and Transportation of Radioactive Material,* Jan. 1, 2007.

49 CFR 173, *Shippers—General Requirements for Shipments and Packagings,* Oct. 1, 2007.

ANSI N14.5-1997, *Radioactive Materials—Leakage Tests on Packages for Shipment*, American Natl. Standards Institute, Feb. 5, 1998.

ASME Boiler and Pressure Vessel Code, An American National Standard, Sect. II, *Materials*, Part C, Specifications for Welding, Rods, Electrodes, and Filler Metals, American Society of Mechanical Engineers, New York, 2001 ed. with 2002 and 2003 addenda.

ASME Boiler and Pressure Vessel Code, An American National Standard, Rules for Construction of Nuclear Facility Components, Sect. III, Div. 1, Subsection NB, American Society of Mechanical Engineers, New York, 2001 ed. with 2002 and 2003 addenda.

ASME Boiler and Pressure Vessel Code, An American National Standard, Welding and Brazing Qualifications, Sect. IX, American Society of Mechanical Engineers, New York, 2001 ed. with 2002 and 2003 addenda.

Curren, W. D. and R. D. Bond, *Leakage of Radioactive Powders from Containers*, Proceedings of the Sixth International Symposium on Packaging and Transportation of Radioactive Material: PATRAM '80, West Berlin, F.R.G., November 10–14, 1980, pp. 463–471.

Kocher, D. C., *Radioactive Decay Data Tables, A Handbook of Decay Data for Application to Radiation Dosimetry and Radiological Assessments*, DOE/TIC-11026, U.S. DOE, Office of Scientific and Technical Information, 1981.

NUREG-1609, *Standard Review Plan for Transportation Packages for Radioactive Material*, U.S. NRC, Mar. 31, 1999.

Parker O-ring Handbook, Catalog ORD 5700/US, Parker Hannifin Corp., Lexington, Ky., 2001.

R.D. McCarty Cryogenics Division, National Bureau of Standards Technical Note 631 , Thermophysical Properties of Helium-43 from 2 to 1500 K with Pressures to 100 Atmospheres, pg 49, Nov. 1972.

Regulatory Guide 7.4, *Leakage Tests on Packages for Shipment of Radioactive Materials*, U.S. NRC, June 1975.

Robert C. Weast, Ph. D., Handbook of Chemistry and Physics, 55th ed., pg. F-13, 1974.

SCALE 4.1—System Module to Calculate Fuel Depletion, Actinide Transmutation Fission Product Buildup and Decay, and Associated Radiation Source Terms, Vol. 2, Sect. F, NUREG/CR-2000, C. V. Parks, ed., Radiation Shielding Information Center, Oak Ridge Natl. Lab., Dec. 1984.

TR 96/12/20, Issue A, *SAFKEG 2863B Tests for Verification of O-ring Performance*, Los Alamos Natl. Lab., Albuquerque, N.M., December 1996.

THIS PAGE INTENTIONALLY LEFT BLANK.

5. SHIELDING EVALUATION

This section describes the shielding evaluation performed for the shipment of up to 36 kg of highly enriched uranium (HEU) in the ES-3100 shipping package. The objective of this evaluation is to demonstrate, for both Normal Conditions of Transport (NCT) and Hypothetical Accident Conditions (HAC), compliance of this package with the performance requirements specified in Title 10 Code of Federal Regulations (CFR) 71 and 49 CFR 173.

5.1 DESCRIPTION OF SHIELDING DESIGN

5.1.1 Design Features

The ES-3100 package for NCT consists of stainless-steel convenience cans loaded with HEU material, spacer assemblies to support and position the convenience cans, the ES-3100 containment vessel, and an insulation-filled drum as shown in Appendix 1.4.1. None of the package materials are specifically designed for shielding gamma rays (photons), the primary contributor to external package dose rates. For HAC, it is assumed that the containment vessel and content remain intact, but all exterior packaging materials are removed. The geometry of the shielding analysis model is a conservative, cylindrical representation of the package. Two sets of contents have been investigated for the shielding analysis. These are 36 kg of HEU metal and 24 kg of HEU oxide powder. The analyses of these models have been performed such that the results and conclusions cover other proposed contents, in an equivalent or conservative manner. For the source calculation, the uranium is enriched at 92% ^{235}U and is assumed to contain 0.6% ^{233}U, 2.5% ^{237}Np, 40 ppb (parts per billion) ^{232}U, and 40 ppm (parts per million) plutonium.

5.1.2 Summary Table of Maximum Radiation Levels

The results of these shielding model evaluations, summarized in Tables 5.1 and 5.2, are the calculated dose rates at the locations indicated. The uncertainty associated with the results is one standard deviation of the mean (expressed as a percentage of the mean) of the Monte Carlo calculated results. As shown from the dose rates in the tables and the discussion in Sect. 5.3, the shielding evaluation demonstrates that the package meets all dose-rate limits for both NCT and HAC for all proposed contents.

5.2 SOURCE SPECIFICATION

The source for the calculated dose rates is from the decay and fission of the radioactive isotope contents. The isotopic content used in the shielding calculations is shown in Table 5.3. This composition was chosen to represent all proposed package contents. The primary contribution to the dose rates in Tables 5.1 and 5.2 is from decay of the ^{232}U isotope (this applies to any mix of the other uranium isotopes in Table 5.3). The photon and neutron source spectra are given in Tables 5.4 and 5.5. In Table 5.4, the group 6 photons are from the decay chain of ^{232}U. Group 18 photons were omitted from the source for the dose rate calculation due to negligible contribution from photons at these energies. Oxygen was not included in the uranium oxide source calculation, but the neutron source includes (α, n) neutrons from the UO_2 default option in the ORIGEN-S code (NUREG/CR-0200, rev. 6). The uranium metal source is assumed to be the same as that for the oxides, per unit HEU mass. Spontaneous fission neutrons are included in Table 5.5 spectrum. Induced fission neutrons and secondary photons are included in the dose rate calculations. Details of the source specifications and use in the dose rate calculations are given in the Sect. 5 appendices.

Table 5.1. Calculated external dose rates for the ES-3100 package with 36 kg of HEU metal contents (mrem/h) [a]

	Drum surface			One meter from surface [b]		
	Side	Top	Bottom	Side	Top	Bottom
			NCT			
Photon	92.264 ± 0.5%	38.746 ± 4.2%	77.410 ± 3.8%	6.441 ± 0.2%	1.419 ± 1.0%	1.450 ± 0.9%
Neutron [c]	1.767 ± 3.4%	0.144 ± 3.3%	3.690 ± 3.1%	0.062 ± 3.0%	0.028 ± 3.3%	0.084 ± 3.2%
Total	94.031 ± 0.5%	38.890 ± 4.2%	81.100 ± 3.8%	6.503 ± 0.2% [d]	1.447 ± 1.0%	1.534 ± 0.9%
Limit [e]	200	200	200	10	10	10
			HAC			
Photon	NA [f]	NA	NA	11.183 ± 0.2%	1.644 ± 0.9%	1.895 ± 0.9%
Neutron [c]	NA	NA	NA	0.029 ± 3.0%	0.007 ± 3.3%	0.018 ± 3.3%
Total	NA	NA	NA	11.212 ± 0.2%	1.651 ± 0.9%	1.913 ± 0.9%
Limit [g]	NA	NA	NA	1000	1000	1000

[a] MORSE-CGA Monte Carlo code results (ORNL-6174).
[b] Drum for NCT and containment vessel for HAC.
[c] Includes secondary photon dose rate (<1% of neutron dose rates).
[d] The radiation shielding transport index is 6.6.
[e] 10 CFR 71.47 and 49 CFR 173.441.
[f] Not applicable.
[g] 10 CFR 71.51.

Table 5.2. Calculated external dose rates for the ES-3100 package with 24 kg of HEU oxide contents (mrem/h) [a]

	Drum surface			One meter from surface [b]		
	Side	Top	Bottom	Side	Top	Bottom
			NCT			
Photon	82.201 ± 0.4%	14.315 ± 2.1%	62.208 ± 1.4%	4.975 ± 0.3%	1.249 ± 0.6%	1.519 ± 0.6%
Neutron [c]	1.035 ± 1.2%	0.084 ± 2.7%	2.181 ± 3.0%	0.038 ± 1.3%	0.016 ± 1.6%	0.047 ± 1.6%
Total	83.236 ± 0.4%	14.399 ± 2.1%	64.389 ± 1.4%	5.013 ± 0.3% [d]	1.265 ± 0.6%	1.566 ± 0.6%
Limit [e]	200	200	200	10	10	10
			HAC			
Photon	NA [f]	NA	NA	8.363 ± 0.4%	1.471 ± 1.2%	1.686 ± 1.2%
Neutron [c]	NA	NA	NA	0.027 ± 0.7%	0.010 ± 0.8%	0.018 ± 0.8%
Total	NA	NA	NA	8.390 ± 0.4%	1.481 ± 1.2%	1.704 ± 1.2%
Limit [g]	NA	NA	NA	1000	1000	1000

[a] MORSE-CGA Monte Carlo code results (ORNL-6174).
[b] Drum for NCT and containment vessel for HAC.
[c] Includes secondary photon dose rate (<1% of neutron dose rates).
[d] The radiation shielding transport index is 5.1.
[e] 10 CFR 71.47 and 49 CFR 173.441.
[f] Not applicable.
[g] 10 CFR 71.51.

5.3 DOSE RATE ANALYSIS MODELS

The photon and neutron sources from the radioactive content as described in the previous section, and listed in Tables 5.4 and 5.5, are input into the MORSE Monte Carlo radiation code to calculate the ES-3100 external package dose rates given in Tables 5.1 and 5.2. The packaging component drawings are shown in Appendix 1.4.1. A cylindrical model of this packaging and proposed HEU material content is shown in Fig. 5.1 and Table 5.6. The dose rate detector locations relative to the package model exterior are listed in Table 5.7. The materials and densities used in the calculational model are given in Table 5.8. These models are described in more detail in the input data and other information given in the Sect. 5 appendices. Kaolite is an insulation material, and Cat 277-4 is a criticality control material. Additional information on these two materials can be found in Sects. 1, 2, and 6.

Two proposed package contents have been analyzed: (1) 36 kg of HEU metal and (2) 24 kg of HEU oxide. The analyses of these models have been performed in a manner that covers other proposed contents, not analyzed, in an equivalent or conservative manner. Due to the simple source and packaging geometry, there are no radiation streaming paths from the source toward the package exterior. Each of the two models is analyzed for both photon and neutron sources, and for both NCT and HAC.

In addition to the analyses for the dose rates shown in Tables 5.1 and 5.2, many preliminary and auxiliary calculations were made for each model to ensure that all proposed content loadings in the ES-3100 vessel were covered. These extra analyses are necessary since only a content mass limit is specified for each shipment, and various geometric configurations must be investigated to determine if the maximum external package dose rates have been found. In some cases it is not possible, or practical, to find an exact maximum dose rate geometric configuration due to the statistical uncertainty of the calculation method, variations in model radius vs. height, variable densities, etc. The dose rate values shown in Tables 5.1 and 5.2 are all at or near possible maximum values for the package specifications given in Sect. 1. All package models investigated, including the preliminary and auxiliary models, are conservative.

Table 5.3. Radioisotope specification for all ES-3100 package analysis source calculations with HEU content and other nuclides per HEU unit weight

Isotope	wt %
^{232}U	0.000004
^{233}U	0.600000
^{234}U	2.000000
^{235}U	92.000000
^{236}U	1.000000
^{238}U	4.399996
^{237}Np	2.500000
Pu [a]	0.004000

[a] Nominal weapons-grade at 40 ppm plutonium by weight—see Appendix 5.5.1.

Table 5.4. Photon source for one gram of HEU for all contents [a]

Group number	Energy range (MeV)	Source (photons/s)
1	10.00–8.00	4.409×10^{-6}
2	8.00–6.50	2.552×10^{-5}
3	6.50–5.00	1.654×10^{-4}
4	5.00–4.00	5.106×10^{-4}
5	4.00–3.00	2.182×10^{-3}
6	3.00–2.50	$1.011 \times 10^{+4}$
7	2.50–2.00	1.011×10^{-1}
8	2.00–1.66	$9.761 \times 10^{+1}$
9	1.66–1.33	$1.101 \times 10^{+3}$
10	1.33–1.00	$3.426 \times 10^{+2}$
11	1.00–0.80	$1.595 \times 10^{+3}$
12	0.80–0.60	$4.620 \times 10^{+3}$
13	0.60–0.40	$2.347 \times 10^{+4}$
14	0.40–0.30	$1.977 \times 10^{+5}$
15	0.30–0.20	$4.550 \times 10^{+4}$
16	0.20–0.10	$1.150 \times 10^{+5}$
17	0.10–0.05	$3.534 \times 10^{+5}$
18 [b]	0.05–0.01	-
Total		$7.530 \times 10^{+5}$

[a] ORIGEN-S code results at 10½ years decay.
[b] Omitted in the dose rate calculations.

Table 5.5. Neutron source for one gram of HEU for all contents [a]

Group number	Energy range (MeV)	Source in uranium metal and oxide (neutrons/s)
1	$2.00 \times 10^{+1} – 6.43 \times 10^{+0}$	6.614×10^{-5}
2	$6.43 \times 10^{+0} – 3.00 \times 10^{+0}$	2.250×10^{-2}
3	$3.00 \times 10^{+0} – 1.85 \times 10^{+0}$	6.246×10^{-2}
4	$1.85 \times 10^{+0} – 1.40 \times 10^{+0}$	1.702×10^{-2}
5	$1.40 \times 10^{+0} – 9.00 \times 10^{-1}$	9.946×10^{-3}
6	$9.00 \times 10^{-1} – 4.00 \times 10^{-1}$	3.397×10^{-3}
7	$4.00 \times 10^{-1} – 1.00 \times 10^{-1}$	5.582×10^{-4}
8 [b]	$1.00 \times 10^{-1} – 1.70 \times 10^{-2}$	0
Total		1.160×10^{-1}

[a] ORIGEN-S results at 15 years decay.
[b] Source is zero for Groups 9–27.

Table 5.6. Geometric data for the shielding analysis models of the ES-3100 shipping package as shown in Fig. 5.1 for NCT. Each item is modeled as a cylinder or cylindrical shell. The content volume not identified (HEU metal photon shell model interior) is modeled as void. All materials interior to the containment vessel except the HEU material content are omitted. Each of the four content models is placed in the packaging to create four separate calculational models. All dimensions are in centimeters. For HAC, all material external to the containment vessel is omitted.

	Material	Outer radius	Base reference height [a]	Height [b] (h)	Side wall thickness	Top thickness	Bottom thickness
Content							
HEU metal shell photon model	HEU	6.35	11.195	76.2	0.6639	-	-
HEU metal neutron model	HEU	6.35	11.195	15.1003	-	-	-
Oxide photon model	UO_2	6.35	11.195	63.5	-	-	-
Oxide neutron model	UO_2	6.35	11.195	17.2864	-	-	-
Packaging (identical for all models)							
Inner vessel gap	void	6.4008	11.195	76.2	0.0508	-	-
ES-3100 containment vessel [c]	SS304 [e]	6.6548	10.56	77.47	0.254	0.635	0.635
Outer vessel gap	void	7.9248	10.56	77.47	1.27	-	-
Inner Cat 277-4 liner	SS304	8.0748	10.56	77.47	0.15	-	-
Criticality control material	Cat 277-4	10.9196	10.56	77.47	2.8448	-	-
Outer Cat 277-4 liner	SS304	11.0696	10.26	77.92	0.15	0.15	0.3
Upper insulation	Kaolite [d]	23.0275	88.18	19.385	-	-	-
Base and radial insulation	Kaolite	23.0275	0.26	87.92	11.9579	-	10
Drum	SS304	23.1775	0	107.715	0.15	0.15	0.26

[a] Measured from the lower drum base.
[b] Vessel interior content (and gap) height varies with density to preserve content mass.
[c] Upper flange and lid detail omitted.
[d] Modeled as void.
[e] 304 stainless steel.

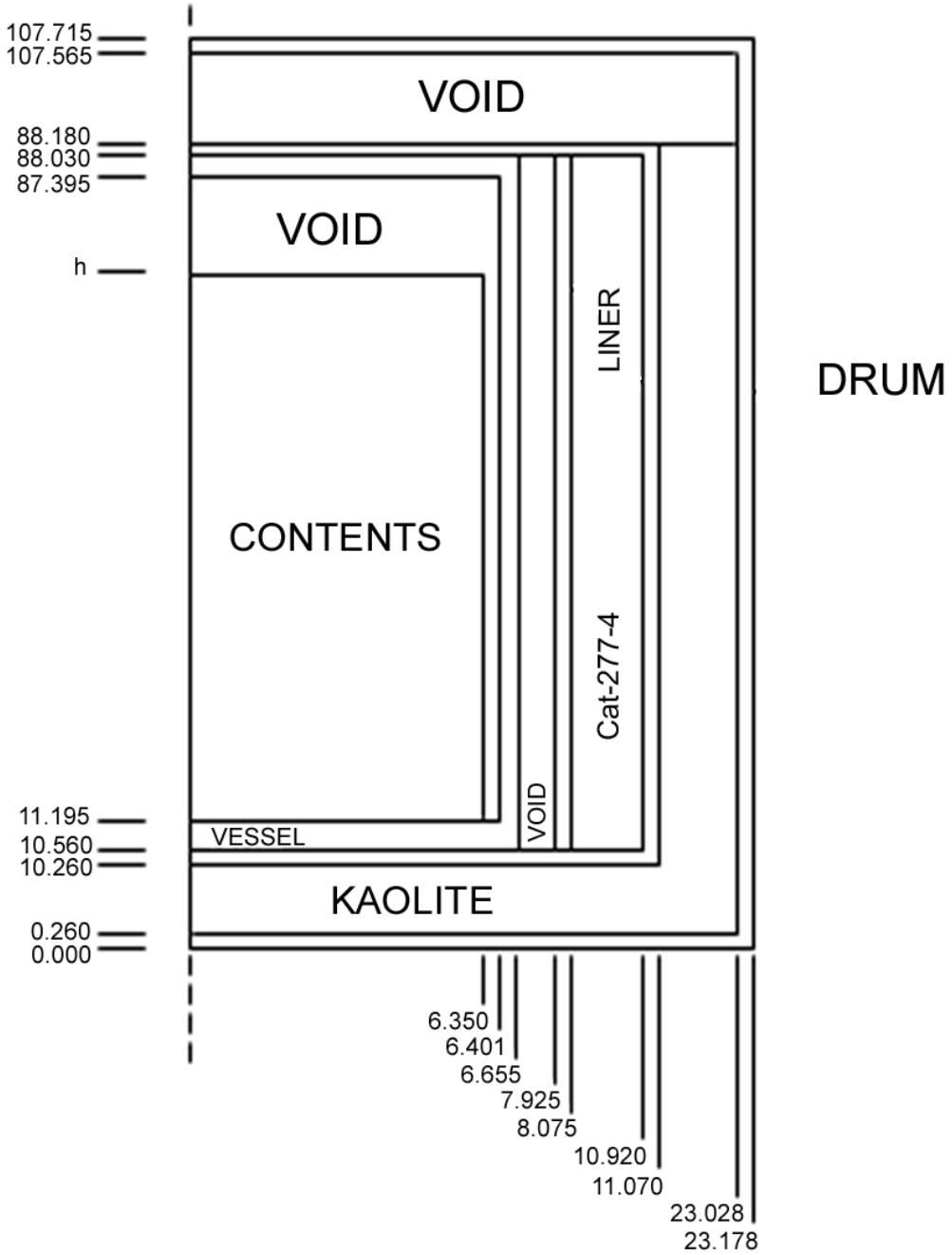

Fig. 5.1. Cylindrical calculational model of the ES-3100 shipping package for NCT. See Tables 5.6–5.8 for data on the contents, materials, and detector locations (not to scale; all dimensions are in centimeters). For HAC, all material external to the containment vessel is omitted.

Table 5.7. Detector locations relative to the drum for NCT and to the containment vessel for HAC

	Radius (cm)	H [a] (cm)
NCT detectors		
Side surface [b]	24.1775	49.2950
Top surface	0.0000	108.7150
Bottom surface	0.0000	–1.0000
Side 1 meter [b]	123.1775	49.2950
Top 1 meter	0.0000	207.7150
Bottom 1 meter	0.0000	–100.0000
HAC detectors		
Side 1 meter [b]	106.6548	49.2950
Top 1 meter	0.0000	188.0300
Bottom 1 meter	0.0000	–89.4400

[a] Height above drum base.
[b] Surface side location is at the axial mid-point of the content; values shown are for the first content in Table 5.6.

5.3.1 Packaging Model Conservative Features

Several conservative features applying to all content models are included in the packaging model. All material dimensions, thicknesses, and densities for the packaging are modeled at or less than specified or nominal values. All non-cylindrical detail has been omitted from the shielding models (see packaging drawings in Appendix 1.4.1). All minor items, such as the silicone rubber pads supporting the ES-3100 containment vessel, have been omitted. It was determined from preliminary analysis that the maximum axial external dose rates would occur relative to the package lower surface. All contents were modeled to contact the containment vessel lower surface, and the upper containment vessel geometry, containment vessel lid, and upper packaging, insulation, lids, covers, etc., were conservatively simplified and/or modeled as void (see Fig. 5.1).

All models of the vessel interior contain HEU material content only. All convenience cans, spacers, content wrappings, covers, supports, etc., are omitted. All contents are modeled as cylinders or cylindrical shells with the base resting on the lower vessel surface, with a maximum specified radius of 6.35 cm (the maximum allowable convenience can diameter is 5 in.), and with a height, inner radius (if any), and density adjusted for each specific model to preserve the content mass. In this conservative manner, it is possible to cover all specified combinations of can loadings and can and spacer placements with a minimum number of calculations. The geometric configuration of some of the cases investigated represents a situation where the maximum possible mass loading for a convenience can would be exceeded if the cans had been included in the model. However, the calculated dose rates from the models used will always exceed those from a model where the geometry is expanded so the can mass loadings are not exceeded and the internal vessel hardware is included. All the general, conservative items relative to the ES-3100 package shielding model are applied to each individual content model.

Table 5.8. Shielding model material specifications for the ES-3100 package with HEU content. Only the two principal uranium isotopes are used in the dose rate calculations. The uranium oxide density varies with the geometric model volume to preserve the 24-kg mass.

Material	Density (g/cm^3)	Constitute	Weight percent	Atomic density (atoms/barn-cm)
Uranium metal	18.82	^{235}U	95.00	4.582×10^{-2}
		^{238}U	5.00	2.381×10^{-3}
UO_2	10.960 [a]	O	11.98	4.941×10^{-2}
		^{235}U	83.62	2.349×10^{-2}
		^{238}U	4.40	1.221×10^{-3}
Stainless steel	7.92	Cr	19.00	1.743×10^{-2}
		Ni	9.50	7.721×10^{-3}
		Fe	69.50	5.936×10^{-2}
		Mn	2.00	1.736×10^{-3}
Cat 277-4	1.682	H	4.62	4.642×10^{-2}
		^{10}B	0.79	8.002×10^{-4}
		^{11}B	3.44	3.168×10^{-3}
		C	1.51	1.274×10^{-3}
		O	60.00	3.798×10^{-2}
		Mg	0.38	1.584×10^{-4}
		Al	21.16	7.944×10^{-3}
		Si	1.32	4.760×10^{-4}
		S	0.15	4.739×10^{-5}
		Na	0.13	5.728×10^{-5}
		Ca	6.18	1.562×10^{-3}
		Fe	0.32	5.804×10^{-5}
Kaolite	0.321	O	40.43	4.888×10^{-3}
		Na	1.45	1.219×10^{-4}
		Mg	7.86	6.251×10^{-4}
		Al	5.58	3.998×10^{-4}
		Si	16.12	1.110×10^{-3}
		Ca	23.40	1.129×10^{-3}
		Fe	5.16	1.786×10^{-4}

[a] Theoretical density— a density of 2.984 g/cm^3 is used in the Table 5.6 geometric model for photons.

5.3.2 Photon model for 36-kg HEU metal content

The HEU metal content in the ES-3100 may be many small, irregularly shaped pieces, each placed at some arbitrary orientation inside the convenience cans. Several conservative, regular geometry models have been devised to cover these and other proposed loadings. Some of these models violate, in a conservative manner, the volume capacity of a convenience can. The cans and spacers are omitted from the models.

The photon model for the dose rates shown in Table 5.1 is that given for the first content item in Table 5.6 (the HEU metal shell). Here, the content is a cylindrical shell the same height as the containment vessel model (76.2 cm). The inner radius of the shell, 5.6861 cm, was used to preserve the 36 kg HEU metal at 18.82 g/cm^3 for an outer radius of 6.35 cm. This case corresponds to a three-can loading configuration with a maximum of 12 kg in each 25.4-cm (10-in.) tall can.

Several 36-kg HEU metal cylindrical shell photon dose rate models were evaluated at lesser heights than the containment vessel inside height (in each case the shell wall thickness was adjusted to preserve the mass). The 1-m side photon dose rate in Table 5.1 is the calculated value for the entire analysis that gave the largest overall fraction of the regulatory limit, 65% of the 10-mrem/h limit. There was some increase in the side surface (not 1-m) photon dose at lesser shell heights. At ~50 cm content height, the maximum side surface dose rate for the shell model was calculated to be 98 mrem/h, 49% of the regulatory limit. This geometry would approximate a 12-kg loading in each of the 8.75-in. cans. The maximum calculated axial surface dose rate of 101 mrem/h was at the bottom drum surface for a shell height of 25 cm and inner radius of 4.0 cm, a gross conservative violation of an actual can loading.

The cylindrical shell representation of the HEU metal content is a convenient, conservative model for multiple possible loading configurations inside the vessel. Some other, more complicated, geometric radial models were also analyzed. The radial geometric cross-sections of these models are shown schematically in Fig. 5.2:

a. The cylindrical shell as described above.

b. A vertical flat plate across the center of the vessel. The maximum calculated photon package surface dose rate for a plate of dimensions 1.9766 cm × 12.7 cm × 76.2 cm was 63 mrem/h.

c. A cylindrical hemi-shell. The maximum calculated package surface photon dose rate was 69 mrem/h for an outer radius of 6.35 cm, an inner radius of 4.0436 cm, and a height of 50.8 cm.

d. A single solid rod placed against the side wall of the vessel. The maximum calculated package surface dose rate for a rod of radius 3.0966 cm and a height of 63.5 cm was 48 mrem/h.

e. A cylindrical segment (the shape a liquid would assume in a horizontal vessel). The maximum calculated package surface dose rate was calculated to be 71 mrem/h for a radius of 6.35 cm, an inner flat surface 11.495 cm across, and a height of 63.5 cm.

The variations in dose rates described here are due to the variations in source-detector point geometry and the self-absorption of photons in the source material. It may be possible to devise other geometric configurations that could produce slightly higher dose rates. However, it can be said with some certainty that the calculated photon dose rates for 36-kg HEU metal content defined in Table 5.3 should never exceed 110 mrem/h on the package surface, 7.6 mrem/h at one meter, and 16 mrem/h for HAC.

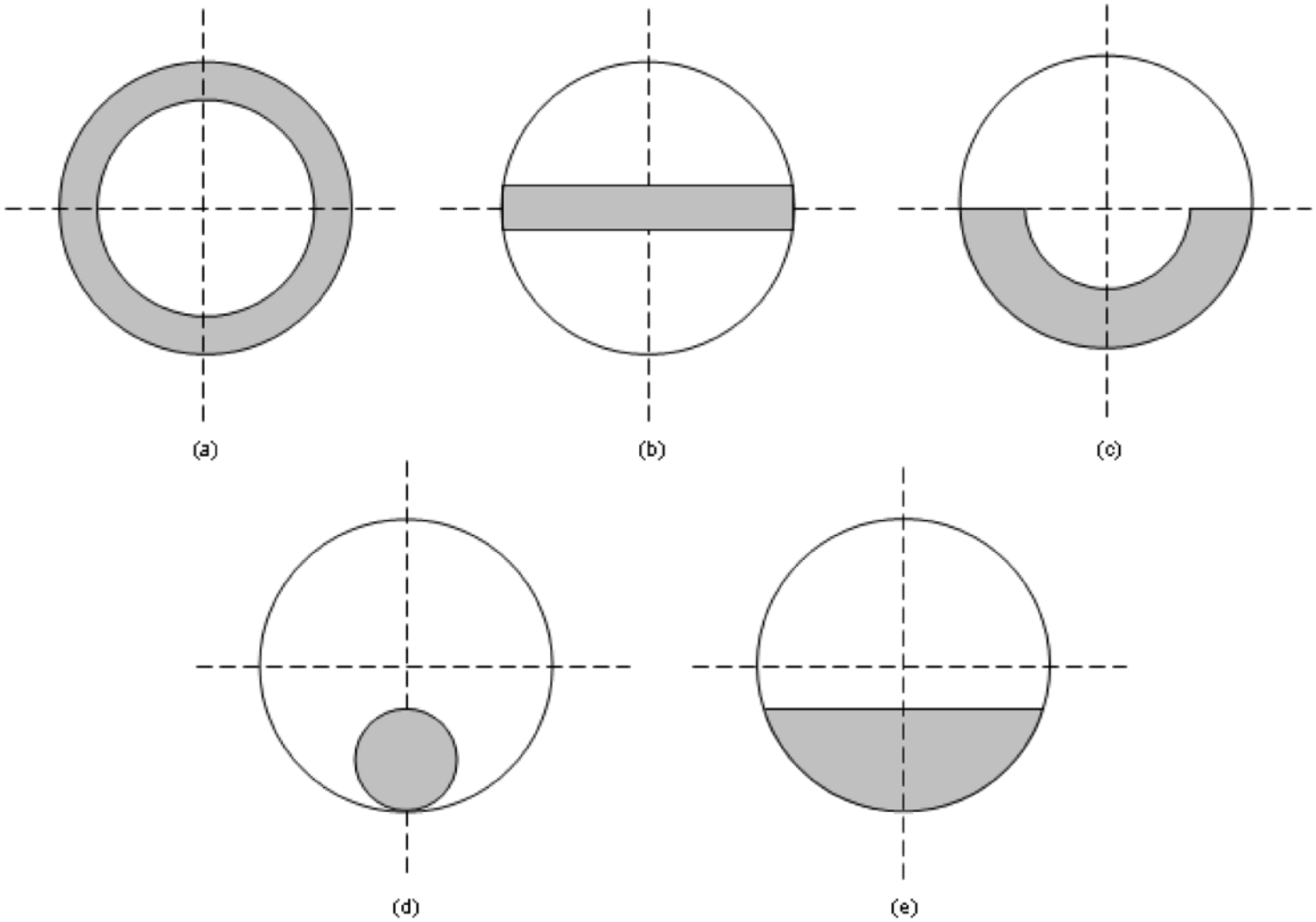

Fig. 5.2. ES-3100 HEU metal content radial (top view) geometric models. The 36-kg mass is conserved for each case. Detector locations were adjusted both vertically and radially from those given in Table 5.7 in the search for maximum external package dose rates for each case.

5.3.3 Neutron model for 36-kg HEU metal content

In the model for the neutron dose rates for the 36-kg HEU contents, it was assumed that all the uranium was a solid cylinder at the bottom of the vessel. The neutron results in Table 5.1 are from this configuration. This is a gross, conservative violation of a convenience can capacity, and no further investigation was made due to the low neutron dose rates obtained from this conservative model relative to the photon results.

5.3.4 Photon model for 24-kg HEU oxide content

A package photon dose rate calculation model was created to apply to 24 kg HEU oxide for all three common uranium oxides—UO_2, UO_3, and U_3O_8. The theoretical densities for these oxides are 10.96 g/cm^3, 7.29 g/cm^3, and 8.30 g/cm^3, respectively. In the package loading models, the convenience can locations are completely filled with oxide powder, and the actual densities, always less than theoretical values, will be the oxide mass divided by the model can volume.

The dose rate model excludes the convenience cans and spacers and it is represented by a solid cylinder of oxide resting on the vessel interior base. The cylinder radius is 6.35 cm, and the height is variable. The density is adjusted for each calculation to preserve the 24-kg oxide mass. The HEU mass is 21.126 kg for UO_2, the largest uranium mass of the three oxides for 24 kg of HEU oxide. In the dose rate calculations, the partial density of oxygen was set to zero, so that the analysis conservatively applies to all three oxides without regard to variations in the oxygen density. The photon dose rates in Table 5.2 are for a cylinder height of 63.5 cm. The 1-m dose rates are slightly higher for 76.2 cm height, and the surface values are slightly higher for a 50.8 cm height. The bottom dose rates approach the side values in Table 5.2 when the cylinder is compressed to the UO_2 theoretical density at the vessel bottom. From the various analyses, it can be stated that no calculated HEU oxide photon dose rates should exceed 90 mrem/h on the package surface, 6 mrem/h at one meter, and 12 mrem/h for HAC.

5.3.5 Neutron model for 24-kg HEU oxide content

The neutron model for the calculated values shown in Table 5.2 was for a solid cylinder of UO_2 at the containment vessel bottom. The density was 10.96 g/cm^3 and the height was 17.286 cm.

5.4 SHIELDING EVALUATION

Several computer programs were used in the shielding evaluation. These included the ORIGEN-S computer code, the CSASN analysis module, the ICE-S computer code, and the MORSE-CGA computer code. ORIGEN-S, CSASN, and ICE-S are parts of the SCALE code. MORSE-CGA is a stand-alone code. Brief descriptions of the programs are presented below.

1. ORIGEN-S is a general depletion and decay code. Given an initial isotopic distribution, materials are decayed to provide time-dependent, energy-grouped photon and neutron sources.

2. CSASN is a sequence of codes for performing resonance processing of neutron cross sections using the SCALE modules BONAMI-S and NITAWL-S.

3. ICE-S is a SCALE module used to format a cross-section library for MORSE-CGA.

4. MORSE-CGA is a general-purpose Monte Carlo code that treats multidimensional neutron, photon, and coupled problems in either a forward or an adjoint mode. Sources and detectors may be defined through user-supplied subroutines. Model definition is facilitated by combinatorial array geometry. Dose rates are calculated by the SAMBO analysis module.

Dose rates were calculated at the detector locations in Table 5.7 by converting the calculated photon and neutron fluxes using the American National Standards Institute (ANSI) conversion factors (ANSI/ANS-6.1.1). These factors for the energy groups used in the shielding evaluation are shown in Tables 5.9 and 5.10.

The results of these shielding model evaluations, summarized in Tables 5.1 and 5.2, are the calculated dose rates at the locations indicated. As shown from the dose rates in the tables and the discussion in Sect. 5.3, the shielding evaluation demonstrates that the package meets all dose-rate limits for both NCT and HAC. The shielding analyses were done in a conservative manner applicable to all proposed ES-3100 package contents listed in Sect. 1.2.3.

Table 5.9. ANSI standard photon flux-to-dose-rate conversion factors

Group number	Energy (MeV)	Factor (mrem/h)/(photons/s/cm^2)
1	10.00–8.00	8.771×10^{-3}
2	8.00–6.50	7.478×10^{-3}
3	6.50–5.00	6.374×10^{-3}
4	5.00–4.00	5.413×10^{-3}
5	4.00–3.00	4.622×10^{-3}
6	3.00–2.50	3.959×10^{-3}
7	2.50–2.00	3.468×10^{-3}
8	2.00–1.66	3.019×10^{-3}
9	1.66–1.33	2.627×10^{-3}
10	1.33–1.00	2.205×10^{-3}
11	1.00–0.80	1.832×10^{-3}
12	0.80–0.60	1.522×10^{-3}
13	0.60–0.40	1.172×10^{-3}
14	0.40–0.30	8.759×10^{-4}
15	0.30–0.20	6.306×10^{-4}
16	0.20–0.10	3.833×10^{-4}
17	0.10–0.05	2.669×10^{-4}
18	0.05–0.01	9.347×10^{-4}

Table 5.10. ANSI standard neutron flux-to-dose-rate conversion factors

Group number	Energy (MeV)	Factor (mrem/h)/(neutrons/s/cm^2)
1	$2.00 \times 10^{+1} – 6.43 \times 10^{+0}$	1.4916×10^{-1}
2	$6.43 \times 10^{+0} – 3.00 \times 10^{+0}$	1.4464×10^{-1}
3	$3.00 \times 10^{+0} – 1.85 \times 10^{+0}$	1.2701×10^{-1}
4	$1.85 \times 10^{+0} – 1.40 \times 10^{+0}$	1.2811×10^{-1}
5	$1.40 \times 10^{+0} – 9.00 \times 10^{-1}$	1.2977×10^{-1}
6	$9.00 \times 10^{-1} – 4.00 \times 10^{-1}$	1.0281×10^{-1}
7	$4.00 \times 10^{-1} – 1.00 \times 10^{-1}$	5.1183×10^{-2}
8	$1.00 \times 10^{-1} – 1.70 \times 10^{-2}$	1.2319×10^{-2}
9	$1.70 \times 10^{-2} – 3.00 \times 10^{-3}$	3.8365×10^{-3}
10	$3.00 \times 10^{-3} – 5.50 \times 10^{-4}$	3.7247×10^{-3}
11	$5.50 \times 10^{-4} – 1.00 \times 10^{-4}$	4.0150×10^{-3}
12	$1.00 \times 10^{-4} – 3.00 \times 10^{-5}$	4.2926×10^{-3}
13	$3.00 \times 10^{-5} – 1.00 \times 10^{-5}$	4.4744×10^{-3}
14	$1.00 \times 10^{-5} – 3.05 \times 10^{-6}$	4.5676×10^{-3}
15	$3.05 \times 10^{-6} – 1.77 \times 10^{-6}$	4.5581×10^{-3}
16	$1.77 \times 10^{-6} – 1.30 \times 10^{-6}$	4.5185×10^{-3}
17	$1.30 \times 10^{-6} – 1.13 \times 10^{-6}$	4.4879×10^{-3}
18	$1.13 \times 10^{-6} – 1.00 \times 10^{-6}$	4.4665×10^{-3}
19	$1.00 \times 10^{-6} – 8.00 \times 10^{-7}$	4.4345×10^{-3}
20	$8.00 \times 10^{-7} – 4.00 \times 10^{-7}$	4.3271×10^{-3}
21	$4.00 \times 10^{-7} – 3.25 \times 10^{-7}$	4.1975×10^{-3}
22	$3.25 \times 10^{-7} – 2.25 \times 10^{-7}$	4.0976×10^{-3}
23	$2.25 \times 10^{-7} – 1.00 \times 10^{-7}$	3.8390×10^{-3}
24	$1.00 \times 10^{-7} – 5.00 \times 10^{-8}$	3.6748×10^{-3}
25	$5.00 \times 10^{-8} – 3.00 \times 10^{-8}$	3.6748×10^{-3}
26	$3.00 \times 10^{-8} – 1.00 \times 10^{-8}$	3.6748×10^{-3}
27	$1.00 \times 10^{-8} – 1.00 \times 10^{-11}$	3.6748×10^{-3}

THIS PAGE INTENTIONALLY LEFT BLANK.

5.5 APPENDICES

Appendix	Descriptions
5.5.1	ORIGEN INPUT DATA FROM TABLE 5.3
5.5.2	CSASN AND ICE INPUT FROM TABLE 5.8
5.5.3	MORSE ROUTINES AND INPUT DATA

THIS PAGE INTENTIONALLY LEFT BLANK.

Appendix 5.5.1

ORIGEN INPUT DATA FROM TABLE 5.3

This file is for generation of the photon spectra in Table 5.4 and the metal and oxide neutron data in Table 5.5. The concentration for each isotope is given based on 1 g of HEU.

```
#origen
0$$ 6 13 a8 26 e
1$$ 1 t
master photon
3$$ 21 0 1 -88 6 a16 2 a33 18
4** a4 1-70 t
35$$ 0 t
56$$ 0 10 a13 13 5 3 a17 2 e
57** 0 e t
es3100 uranium metal and oxides
one gram HEU
60** 8 9 10 10.5 11 12 15 20 40 50
65$$ a7 1 a25 1 a28 1 a31 1 a49 1 e
73$$ 922320 922340 922350 922360 922380
     922330 942380 942390 932370
     942400 942410 942420 952410
74** 0.4000-07 .020000 0.92000 .010000 0.04399996
     6.00-03 8.00-09 3.7032-05 0.025
     2.60-06 2.24-07 1.60-08 1.20-07
75$$ 2 2 2 2 2 2 2 2 2 2 2 2 2
81$$ 2 0 26 1 e
82$$ 2 2 2 2 2 2 2 2 0 0
83** 10+6 8+6 6.5+6 5+6 4+6 3+6 2.5+6 2+6 1.66+6 1.33+6 1+6 .8+6
     .6+6 .4+6 .3+6 .2+6 .1+6 .05+6 .01+6 t
               8
               9
              10
              10.5
              11
              12
              15
              20
56$$ f0 t
end
```

Appendix 5.5.2

CSASN AND ICE INPUT FROM TABLE 5.8

This file is the input data for the generation and preparation (format) of the cross-section data used in the MORSE code. The data generated from this input file can be used for all MORSE media input cases. Oxygen is omitted from the oxide models, and HEU is assumed to be all U-235 in the neutron models in the MORSE data. The atomic densities for all dose rate calculations in Appendix 5.5.3 cases are given, or indicated, in Table 5.8.

```
=csasn
es3100: morse-cg cross section library
27n-18couple
multiregion
  arbmu02      10.9600  3  0  0  0   8016  11.9800
                                     92235  83.6200
                                     92238   4.4000   1 1.0000 293.0 end
  arbmsst       7.9200  4  0  0  0  26304  69.5000
                                     24304  19.0000
                                     28304   9.5000
                                     25055   2.0000   2 1.0000 293.0 end
  arbmcat       1.6820 12  0  0  0   1001   4.6200
                                      5010   0.7900
                                      5011   3.4400
                                      6012   1.5100
                                      8016  60.0000
                                     12000   0.3800
                                     13027  21.1600
                                     14000   1.3200
                                     16000   0.1500
                                     11023   0.1300
                                     20000   6.1800
                                     26304   0.3200  3 1.0000 293.0 end
  arbmkoa       0.3210  7  0  0  0   8016  40.4300
                                     11023   1.4500
                                     12000   7.8600
                                     13027   5.8600
                                     14000  16.1200
                                     20000  23.4000
                                     26304   5.1600   4 1.0000 293.0 end
end comp
spherical end
  1  1.0     noextermod
end zone
end
=ice
es31 ice : morse cross section library
-1$$ a3 2200 e
1$$ 26 26 0 10 0 0 1 1t
2$$ 1 2 3 4 5 6 7 8 9 10 11 12 13 14 15 16 17 18 19 20 21 22 23 24
       25 26
3$$ 1008016 1092235 1092238
    2024304 2025055 2026304 2028304
    3001001 3005010 3005011 3006012 3008016 3012000 3013027
    3014000 3016000 3011023 3020000 3026304
    4008016 4011023 4012000 4013027 4014000 4020000 4026304
4** 26r1.0
5$$ 26r10
7$$ 3 16 60 0 0 0 e 2t
9$$ 258I1 260
10$$ 1 1452 27 3t
end
```

Appendix 5.5.3

MORSE ROUTINES AND INPUT DATA

Included here are the routines and input files used for the dose rate calculations for the results in Tables 5.1 and 5.2. For each case, there are two routines, INSCOR and SOURCE, followed by the NCT and the HAC input. The normalization is given in INSCOR, which is the appropriate Total value in Tables 5.4 or 5.5 times the content mass. The spatial and energy distributions for the photon and neutron sources from Tables 5.4 and 5.5 are in the data statements in the SOURCE routine. Induced fission and secondary photons are included in the MORSE calculation. It is assumed that the energy group distribution of induced fissions is the same as for the spectra in Table 5.5. The photon source is biased, and weight corrected, so that half of all primary photons are selected in group 6 from Table 5.4.

For each case, the input data for NCT and HAC follow the two routines. For the HAC cases, all material external to the containment vessel is set to void and the detectors (now three) are set one meter from the external vessel surface. The 24-kg oxide neutron case, similar to the 36-kg metal neutron case, is not shown.

```
      subroutine inscor
       common /pdet/   nd,     nne,    ne,     nt,     na,     nresp,
      1                nex,    nexnd,  nend,   ndnr,   ntnr,   ntne,
      2                nane,   ntndnr, ntnend, nanend, locrsp, locxd,
      3                locib,  locco,  loct,   locud,  locsd,  locqe,
      4                locqt,  locqte, locqae, lmax,   efirst, egtop
       common bc(1)
       do 100 i = 1,nd
         bc(locxd + 5*nd + i) = 2.711e+10
100    continue
       return
       end
       subroutine source( ig,u,v,w,x,y,z,
      1                   wate,med,ag,isour,itstr,ngpqt3,ddf,
      2                   isbias,nmtg )
       dimension spect(1,18)
       data xst,yst,zst /0.000,0.0,11.195/
       data cyl_ht/76.200/
c40ppb u232
       data (spect(1,k),k=1,18) /
      1  4.409e-6,2.552e-5,1.654e-4,5.106e-4, 2.182e-3,7.429e+5,
      2  1.011e-1,9.761e+1,1.101e+3,
      3  3.426e+2,1.595e+3, 4.620e+03,
      4  2.347e+04,1.977e+5,4.550e+4,1.150e+5,3.534e+5,0.000e-00/
       data icall / 1 /
       if (icall) 10,10,5
5      icall = 0
       r02 = 5.6861**2
       r12 = 6.3500**2
        i=1
        sum=0.0
         do 92 j = 1,nmtg
92         sum = sum + spect(i,j)
         spect(i,1) = spect(i,1) / sum
         do 93 j = 2,nmtg
93         spect(i,j) = spect(i,j-1) + spect(i,j) / sum
10     continue
       r1 = fltrnf( 0 )
       call azirn( sinang,cosang )
       rad = sqrt( r1 * r12 + ( 1.0 - r1 ) * r02 )
       x = rad * sinang + xst
       y = rad * cosang + yst
       z = zst + fltrnf( 0 ) * cyl_ht
       i=1
       rn = fltrnf( 0 )
       do 94 j = 1,nmtg
         if ( rn .le. spect(i,j) ) goto 95
94     continue
       j = nmtg
95     ig = j
c40ppb u232
       if(ig.ne.6)wate=wate*1.97315
       if(ig.eq.6)wate=wate*0.026853
       return
       end
```

```
es3100 package nct 36kg u metal 40 ppb u232
 $$ 500 850 500    1    0   17   18   18    0    0  99.    4    0
 $$  0    0    0    0  **  1.0 1.0000e-5 1.0000e+4       1.0 2.2000e+5
 **    0.0       0.0       0.0       0.0       0.0       0.0       0.0
 **
 10.000e+6 8.0000e+6 6.5000e+6 5.0000e+6 4.0000e+6 3.0000e+6 2.5000e+6
 2.0000e+6 1.6600e+6 1.3300e+6 1.0000e+6 0.8000e+6 0.6000e+6 0.4000e+6
 0.3000e+6 0.2000e+6 0.1000e+6 0.0500e+6
 b1a303a31a34
 $$   1    1    0    0    0    1   18
 $$   1    1   10    1    1    1 **   0.1    .001       .010  5.000e-01
 $$  11    1   14    1    1    1 **   1.0    .010       .100  5.000e-01
 $$  15    1   18    1    1    1 **   10.    .100       1.00  5.000e-01
 $$  -1    9r0
    0    0    0    0
    0    0                heu in es-3100 36kg cylinder model
    0    0    1    0
  rcc    1    0.000   0.0   11.1950   0.00   0.0  76.2000   5.6861
  rcc    2    0.000   0.0   11.1950   0.00   0.0  76.2000   6.3500
  rcc    3    0.000   0.0   11.1950   0.00   0.0  76.2000   6.4008
  rcc    4    0.000   0.0   10.5600   0.00   0.0  77.4700   6.6548
  rcc    5    0.000   0.0   10.5600   0.00   0.0  77.4700   7.9248
  rcc    6    0.000   0.0   10.5600   0.00   0.0  77.4700   8.0748
  rcc    7    0.000   0.0   10.5600   0.00   0.0  77.4700  10.9196
  rcc    8    0.000   0.0   10.2600   0.00   0.0  77.9200  11.0696
  rcc    9    0.000   0.0    0.2600   0.00   0.0  87.9200  23.0275
  rcc   10    0.000   0.0    0.2600   0.00   0.0 107.3050  23.0275
  rcc   11    0.000   0.0    0.0000   0.00   0.0 107.7150  23.1775
  sph   12      0.0      0.0     0.0       1000.
  sph   13      0.0      0.0     0.0       2000.
  end
  vid           1
  con           2     -1
  vid           3     -2
  sst           4     -3
  vid           5     -4
  sst           6     -5
  bor           7     -6
  sst           8     -7
  kao           9     -8
  vid          10     -9
  sst          11    -10
  vid          12    -11
  vix          13    -12
  end
    1    1    1    1    1    1    1    1    1    1    1    1    1
  13z
 1000    1 1000    2 1000    2    3    2    4 1000    2 1000    0
    0
27N18P LIBRARY (P5)
 $$ 0    0   18   18   45   60   16    4   26  26    6    3    1    3
    0    0    0    0    0    0    0   20    0    0    0
    1    2    3    4    5    6   11   12   13   14   15   16   21   22
   23   24   25   26   31   32   33   34   35   36   41   42   43   44
   45   46   51   52   53   54   55   56   61   62   63   64   65   66
   71   72   73   74   75   76   81   82   83   84   85   86   91   92
   93   94   95   96  101  102  103  104  105  106  111  112  113  114
  115  116  121  122  123  124  125  126  131  132  133  134  135  136
  141  142  143  144  145  146  151  152  153  154  155  156  161  162
  163  164  165  166  171  172  173  174  175  176  181  182  183  184
  185  186  191  192  193  194  195  196  201  202  203  204  205  206
  211  212  213  214  215  216  221  222  223  224  225  226  231  232
  233  234  235  236  241  242  243  244  245  246  251  252  253  254
```

```
  255  256
 $$ 1   12 ** 1.0000e-9
 $$ 1    2 ** 4.5820e-2
 $$ 1   -3 ** 2.3810e-3
 $$ 2    5 ** 1.7360e-3
 $$ 2    6 ** 5.9360e-2
 $$ 2    7 ** 7.7210e-3
 $$ 2   -4 ** 1.7430e-2
 $$ 3    8 ** 4.6420e-2
 $$ 3    9 ** 8.0020e-4
 $$ 3   10 ** 3.1680e-3
 $$ 3   11 ** 1.2740e-3
 $$ 3   12 ** 3.7980e-2
 $$ 3   13 ** 1.5840e-4
 $$ 3   14 ** 7.9440e-3
 $$ 3   15 ** 4.7600e-4
 $$ 3   16 ** 4.7390e-5
 $$ 3   17 ** 5.7280e-5
 $$ 3   18 ** 1.5620e-3
 $$ 3  -19 ** 5.8040e-5
 $$ 4   20 ** 4.8880e-3
 $$ 4   21 ** 1.2190e-4
 $$ 4   22 ** 6.2510e-4
 $$ 4   23 ** 3.9980e-4
 $$ 4   24 ** 1.1100e-3
 $$ 4   25 ** 1.1290e-3
 $$ 4  -26 ** 1.7860e-4
SAMBO ANALYSIS INPUT DATA
 $$   6    0    0    0    0    1    1    2
 **
   24.1775 0.0 49.295
   0.0 0.0  -1.00
   0.0 0.0  108.715
   123.1775 0.0 49.295
   0.0 0.0 -100.00
   0.0 0.0  207.7150
UNCOLLIDED AND TOTAL PHOTON DOSE RATES
ANSI STANDARD GAMMA DOSE RATES
 **
 8.7716e-3 7.4785e-3 6.3748e-3 5.4136e-3 4.6221e-3 3.9596e-3 3.4686e-3
 3.0192e-3 2.6276e-3 2.2051e-3 1.8326e-3 1.5228e-3 1.1725e-3 8.7594e-4
 6.3061e-4 3.8338e-4 2.6693e-4 9.3472e-4
```

```
es3100 package hac 36kg u metal 40 ppb u232
 $$ 500 850 500    1    0   17   18   18    0    0  99.    4    0
 $$  0    0    0    0  **  1.0 1.0000e-5 1.0000e+4       1.0 2.2000e+5
 **    0.0       0.0       0.0       0.0       0.0       0.0       0.0
 **
 10.000e+6 8.0000e+6 6.5000e+6 5.0000e+6 4.0000e+6 3.0000e+6 2.5000e+6
 2.0000e+6 1.6600e+6 1.3300e+6 1.0000e+6 0.8000e+6 0.6000e+6 0.4000e+6
 0.3000e+6 0.2000e+6 0.1000e+6 0.0500e+6
 b1a303a31a34
 $$   1    1    0    0    0    1   18
 $$   1    1   10    1    1    1 **   0.1    .001       .010  5.000e-01
 $$  11    1   14    1    1    1 **   1.0    .010       .100  5.000e-01
 $$  15    1   18    1    1    1 **   10.    .100       1.00  5.000e-01
 $$  -1    9r0
    0    0    0    0
    0    0                heu in es-3100 36kg cylinder model
    0    0    1    0
  rcc    1    0.000   0.0   11.1950   0.00   0.0  76.2000   5.6861
  rcc    2    0.000   0.0   11.1950   0.00   0.0  76.2000   6.3500
  rcc    3    0.000   0.0   11.1950   0.00   0.0  76.2000   6.4008
  rcc    4    0.000   0.0   10.5600   0.00   0.0  77.4700   6.6548
  rcc    5    0.000   0.0   10.5600   0.00   0.0  77.4700   7.9248
  rcc    6    0.000   0.0   10.5600   0.00   0.0  77.4700   8.0748
  rcc    7    0.000   0.0   10.5600   0.00   0.0  77.4700  10.9196
  rcc    8    0.000   0.0   10.2600   0.00   0.0  77.9200  11.0696
  rcc    9    0.000   0.0    0.2600   0.00   0.0  87.9200  23.0275
  rcc   10    0.000   0.0    0.2600   0.00   0.0 107.3050  23.0275
  rcc   11    0.000   0.0    0.0000   0.00   0.0 107.7150  23.1775
  sph   12      0.0      0.0     0.0       1000.
  sph   13      0.0      0.0     0.0       2000.
  end
  vid           1
  con           2     -1
  vid           3     -2
  sst           4     -3
  vid           5     -4
  sst           6     -5
  bor           7     -6
  sst           8     -7
  kao           9     -8
  vid          10     -9
  sst          11    -10
  vid          12    -11
  vix          13    -12
  end
    1    1    1    1    1    1    1    1    1    1    1    1    1
  13z
 1000   1 1000   2 1000 1000 1000 1000 1000 1000 1000 1000    0
    0
27N18P LIBRARY (P5)
 $$ 0    0   18   18   45   60   16    4   26  26    6    3    1    3
    0    0    0    0    0    0    0   20    0    0    0
    1    2    3    4    5    6   11   12   13   14   15   16   21   22
   23   24   25   26   31   32   33   34   35   36   41   42   43   44
   45   46   51   52   53   54   55   56   61   62   63   64   65   66
   71   72   73   74   75   76   81   82   83   84   85   86   91   92
   93   94   95   96  101  102  103  104  105  106  111  112  113  114
  115  116  121  122  123  124  125  126  131  132  133  134  135  136
  141  142  143  144  145  146  151  152  153  154  155  156  161  162
  163  164  165  166  171  172  173  174  175  176  181  182  183  184
  185  186  191  192  193  194  195  196  201  202  203  204  205  206
  211  212  213  214  215  216  221  222  223  224  225  226  231  232
  233  234  235  236  241  242  243  244  245  246  251  252  253  254
```

```
  255  256
 $$ 1   12 ** 1.0000e-9
 $$ 1    2 ** 4.5820e-2
 $$ 1   -3 ** 2.3810e-3
 $$ 2    5 ** 1.7360e-3
 $$ 2    6 ** 5.9360e-2
 $$ 2    7 ** 7.7210e-3
 $$ 2   -4 ** 1.7430e-2
 $$ 3    8 ** 4.6420e-2
 $$ 3    9 ** 8.0020e-4
 $$ 3   10 ** 3.1680e-3
 $$ 3   11 ** 1.2740e-3
 $$ 3   12 ** 3.7980e-2
 $$ 3   13 ** 1.5840e-4
 $$ 3   14 ** 7.9440e-3
 $$ 3   15 ** 4.7600e-4
 $$ 3   16 ** 4.7390e-5
 $$ 3   17 ** 5.7280e-5
 $$ 3   18 ** 1.5620e-3
 $$ 3  -19 ** 5.8040e-5
 $$ 4   20 ** 4.8880e-3
 $$ 4   21 ** 1.2190e-4
 $$ 4   22 ** 6.2510e-4
 $$ 4   23 ** 3.9980e-4
 $$ 4   24 ** 1.1100e-3
 $$ 4   25 ** 1.1290e-3
 $$ 4  -26 ** 1.7860e-4
SAMBO ANALYSIS INPUT DATA
 $$   3    0    0    0    0    1    1    2
 **
   106.6548 0.0 49.295
   0.0 0.0 -89.440
   0.0 0.0 188.03
UNCOLLIDED AND TOTAL PHOTON DOSE RATES
ANSI STANDARD GAMMA DOSE RATES
 **
 8.7716e-3 7.4785e-3 6.3748e-3 5.4136e-3 4.6221e-3 3.9596e-3 3.4686e-3
 3.0192e-3 2.6276e-3 2.2051e-3 1.8326e-3 1.5228e-3 1.1725e-3 8.7594e-4
 6.3061e-4 3.8338e-4 2.6693e-4 9.3472e-4
```

```
      subroutine inscor
      common /pdet/   nd,     nne,    ne,     nt,     na,     nresp,
     1                nex,    nexnd,  nend,   ndnr,   ntnr,   ntne,
     2                nane,   ntndnr, ntnend, nanend, locrsp, locxd,
     3                locib,  locco,  loct,   locud,  locsd,  locqe,
     4                locqt,  locqte, locqae, lmax,   efirst, egtop
      common bc(1)
      do 100 i = 1,nd
        bc(locxd + 5*nd + i) = 4.1800e+03
100   continue
      return
      end
      subroutine source( ig,u,v,w,x,y,z,
     1                   wate,med,ag,isour,itstr,ngpqt3,ddf,
     2                   isbias,nmtg )
     dimension spect(1,8)
      data xst,yst,zst /0.000,0.0, 11.1950/
      data cyl_ht/15.1003/
      data (spect(1,k),k=1,8) /
     1 6.614e-5,2.250e-2,6.246e-2,1.702e-2,9.946e-3,3.397e-3,
     2 5.582e-4,0.000e+0/
      data icall / 1 /
      if (icall) 10,10,5
5     icall = 0
      r11 = 6.3500
       i=1
       sum=0.0
        do 92 j = 1,8
92        sum = sum + spect(i,j)
        spect(i,1) = spect(i,1) / sum
        do 93 j = 2,8
93        spect(i,j) = spect(i,j-1) + spect(i,j) / sum
10    continue
      r1 = fltrnf( 0 )
      call azirn( sinang,cosang )
      rad = sqrt( r1)* r11
      x = rad * sinang + xst
      y = rad * cosang + yst
      z = zst + fltrnf( 0 ) * cyl_ht
      i=1
      rn = fltrnf( 0 )
      do 94 j = 1,8
        if ( rn .le. spect(i,j) ) goto 95
94    continue
      j = 8
95    ig = j
      return
      end
```

```
es3100 package nct 36kg u metal neutrons
 $$ 200  850  200   1   27   18   27   45    0    0  60.    4    0
 $$   0    0    0    0  **   1.0 1.0000e-5 1.0000e+4       1.0 2.2000e+5
 $$    0.0       0.0       0.0       0.0       0.0       0.0       0.0
 **
 2.0000e+7 6.4300e+6 3.0000e+6 1.8500e+6 1.4000e+6 9.0000e+5 4.0000e+5
 1.0000e+5 1.7000e+4 3.0000e+3 5.5000e+2 1.0000e+2 3.0000e+1 1.0000e+1
 3.0500e+0 1.7700e+0 1.3000e+0 1.1300e+0 1.0000e+0 8.0000e-1 4.0000e-1
 3.2500e-1 2.2500e-1 9.9999e-2 5.0000e-2 3.0000e-2 1.0000e-2 1.0000e+7
 8.0000e+6 6.5000e+6 5.0000e+6 4.0000e+6 3.0000e+6 2.5000e+6 2.0000e+6
 1.6600e+6 1.3300e+6 1.0000e+6 0.8000e+6 0.6000e+6 0.4000e+6 0.3000e+6
 0.2000e+6 0.1000e+6 0.0500e+6
 b3a343b203a1
 $$   1    1    0    0    0    1   45
 $$   1    1    9    1    1    1 **   50.    .050       .500  5.000e-01
 $$  10    1   27    1    1    1 **   50.    1.00       10.0  5.000e-01
 $$  28    1   45    1    1    1 **   20.    .500       2.00  5.000e-01
 $$  -1    9r0
 $$ 0    1    0    0
 ** 1.0
 **
 6.6140e-5 2.250e-2 6.246e-2 1.702e-2 9.946e-3 3.397e-3 5.582e-4
 0.0000e-0 19z
 **   27z
 **   27z
 **   27z
 ** 27r.01
    0    0            heu in es-3100 36kg cylinder model
    0    0    1    0
  rcc    1    0.000   0.0   11.1950   0.00   0.0  15.1003   0.0001
  rcc    2    0.000   0.0   11.1950   0.00   0.0  15.1003   6.3500
  rcc    3    0.000   0.0   11.1950   0.00   0.0  76.2000   6.4008
  rcc    4    0.000   0.0   10.5600   0.00   0.0  77.4700   6.6548
  rcc    5    0.000   0.0   10.5600   0.00   0.0  77.4700   7.9248
  rcc    6    0.000   0.0   10.5600   0.00   0.0  77.4700   8.0748
  rcc    7    0.000   0.0   10.5600   0.00   0.0  77.4700  10.9196
  rcc    8    0.000   0.0   10.2600   0.00   0.0  77.9200  11.0696
  rcc    9    0.000   0.0    0.2600   0.00   0.0  87.9200  23.0275
  rcc   10    0.000   0.0    0.2600   0.00   0.0 107.3050  23.0275
  rcc   11    0.000   0.0    0.0000   0.00   0.0 107.7150  23.1775
  sph   12      0.0      0.0     0.0       1000.
  sph   13      0.0      0.0     0.0       2000.
  end
  vid           1
  con           2     -1
  vid           3     -2
  sst           4     -3
  vid           5     -4
  sst           6     -5
  bor           7     -6
  sst           8     -7
  kao           9     -8
  vid          10     -9
  sst          11    -10
  vid          12    -11
  vix          13    -12
  end
    1    1    1    1    1    1    1    1    1    1    1    1    1
  13z
 1000    1 1000    2 1000    2    3    2    4 1000    2 1000    0
    0
27N18P LIBRARY (P5)
 $$ 27   27   18   18   45   60   16   4    26   26    6    3    1    3
```

```
    0    0    0    0    0    0    0   20    0    0    0
    1    2    3    4    5    6   11   12   13   14   15   16   21   22
   23   24   25   26   31   32   33   34   35   36   41   42   43   44
   45   46   51   52   53   54   55   56   61   62   63   64   65   66
   71   72   73   74   75   76   81   82   83   84   85   86   91   92
   93   94   95   96  101  102  103  104  105  106  111  112  113  114
  115  116  121  122  123  124  125  126  131  132  133  134  135  136
  141  142  143  144  145  146  151  152  153  154  155  156  161  162
  163  164  165  166  171  172  173  174  175  176  181  182  183  184
  185  186  191  192  193  194  195  196  201  202  203  204  205  206
  211  212  213  214  215  216  221  222  223  224  225  226  231  232
  233  234  235  236  241  242  243  244  245  246  251  252  253  254
  255  256
 $$ 1   12 ** 1.0000e-9
 $$ 1    2 ** 4.8240e-2
 $$ 1   -3 ** 1.2210e-9
 $$ 2    5 ** 1.7360e-3
 $$ 2    6 ** 5.9360e-2
 $$ 2    7 ** 7.7210e-3
 $$ 2   -4 ** 1.7430e-2
 $$ 3    8 ** 4.6420e-2
 $$ 3    9 ** 8.0020e-4
 $$ 3   10 ** 3.1680e-3
 $$ 3   11 ** 1.2740e-3
 $$ 3   12 ** 3.7980e-2
 $$ 3   13 ** 1.5840e-4
 $$ 3   14 ** 7.9440e-3
 $$ 3   15 ** 4.7600e-4
 $$ 3   16 ** 4.7390e-5
 $$ 3   17 ** 5.7280e-5
 $$ 3   18 ** 1.5620e-3
 $$ 3  -19 ** 5.8040e-5
 $$ 4   20 ** 4.8880e-3
 $$ 4   21 ** 1.2190e-4
 $$ 4   22 ** 6.2510e-4
 $$ 4   23 ** 3.9980e-4
 $$ 4   24 ** 1.1100e-3
 $$ 4   25 ** 1.1290e-3
 $$ 4  -26 ** 1.7860e-4
SAMBO ANALYSIS INPUT DATA
 $$   6    0    0    0    0    3    1    2
 **
   24.1775 0.0  18.745
   0.0 0.0 -1.000
   0.0 0.0  108.715
   123.1775 0.0  18.745
   0.0 0.0 -100.00
   0.0 0.0  207.7150
uncollided and total photon dose rates
ansi standard neutron dose rates :
 **
 1.4916e-1 1.4464e-1 1.2701e-1 1.2811e-1 1.2977e-1 1.0281e-1 5.1183e-2
 1.2319e-2 3.8365e-3 3.7247e-3 4.0150e-3 4.2926e-3 4.4744e-3 4.5676e-3
 4.5581e-3 4.5185e-3 4.4879e-3 4.4665e-3 4.4345e-3 4.3271e-3 4.1975e-3
 4.0976e-3 3.8390e-3 3.6748e-3 3.6748e-3 3.6748e-3 3.6748e-3
 18r0.0
ansi standard photon dose rates :
 **
 27r0.0
 8.7716e-3 7.4785e-3 6.3748e-3 5.4136e-3 4.6221e-3 3.9596e-3 3.4686e-3
 3.0192e-3 2.6276e-3 2.2051e-3 1.8326e-3 1.5228e-3 1.1725e-3 8.7594e-4
 6.3061e-4 3.8338e-4 2.6693e-4 9.3472e-4
ansi standard total dose rates :
```

```
 **
 1.4916e-1 1.4464e-1 1.2701e-1 1.2811e-1 1.2977e-1 1.0281e-1 5.1183e-2
 1.2319e-2 3.8365e-3 3.7247e-3 4.0150e-3 4.2926e-3 4.4744e-3 4.5676e-3
 4.5581e-3 4.5185e-3 4.4879e-3 4.4665e-3 4.4345e-3 4.3271e-3 4.1975e-3
 4.0976e-3 3.8390e-3 3.6748e-3 3.6748e-3 3.6748e-3 3.6748e-3
 8.7716e-3 7.4785e-3 6.3748e-3 5.4136e-3 4.6221e-3 3.9596e-3 3.4686e-3
 3.0192e-3 2.6276e-3 2.2051e-3 1.8326e-3 1.5228e-3 1.1725e-3 8.7594e-4
 6.3061e-4 3.8338e-4 2.6693e-4 9.3472e-4



es3100 package hac 36kg u metal neutrons
 $$ 200  850  200   1   27   18   27   45    0    0  60.    4    0
 $$   0    0    0    0  **   1.0 1.0000e-5 1.0000e+4       1.0 2.2000e+5
 $$    0.0       0.0       0.0       0.0       0.0       0.0       0.0
 **
 2.0000e+7 6.4300e+6 3.0000e+6 1.8500e+6 1.4000e+6 9.0000e+5 4.0000e+5
 1.0000e+5 1.7000e+4 3.0000e+3 5.5000e+2 1.0000e+2 3.0000e+1 1.0000e+1
 3.0500e+0 1.7700e+0 1.3000e+0 1.1300e+0 1.0000e+0 8.0000e-1 4.0000e-1
 3.2500e-1 2.2500e-1 9.9999e-2 5.0000e-2 3.0000e-2 1.0000e-2 1.0000e+7
 8.0000e+6 6.5000e+6 5.0000e+6 4.0000e+6 3.0000e+6 2.5000e+6 2.0000e+6
 1.6600e+6 1.3300e+6 1.0000e+6 0.8000e+6 0.6000e+6 0.4000e+6 0.3000e+6
 0.2000e+6 0.1000e+6 0.0500e+6
 b3a343b203a1
 $$   1    1    0    0    0    1   45
 $$   1    1    9    1    1    1 **   50.    .050       .500  5.000e-01
 $$  10    1   27    1    1    1 **   50.    1.00       10.0  5.000e-01
 $$  28    1   45    1    1    1 **   20.    .500       2.00  5.000e-01
 $$  -1    9r0
 $$ 0    1    0    0
 ** 1.0
 **
 6.6140e-5 2.107e-2 5.841e-2 1.593e-2 9.334e-3 3.219e-3 5.304e-4
 0.0000e-0 19z
 **   27z
 **   27z
 **   27z
 ** 27r.01
    0    0            heu in es-3100 36kg cylinder model
    0    0    1    0
  rcc    1    0.000   0.0   11.1950   0.00   0.0  15.1003   0.0001
  rcc    2    0.000   0.0   11.1950   0.00   0.0  15.1003   6.3500
  rcc    3    0.000   0.0   11.1950   0.00   0.0  76.2000   6.4008
  rcc    4    0.000   0.0   10.5600   0.00   0.0  77.4700   6.6548
  rcc    5    0.000   0.0   10.5600   0.00   0.0  77.4700   7.9248
  rcc    6    0.000   0.0   10.5600   0.00   0.0  77.4700   8.0748
  rcc    7    0.000   0.0   10.5600   0.00   0.0  77.4700  10.9196
  rcc    8    0.000   0.0   10.2600   0.00   0.0  77.9200  11.0696
  rcc    9    0.000   0.0    0.2600   0.00   0.0  87.9200  23.0275
  rcc   10    0.000   0.0    0.2600   0.00   0.0 107.3050  23.0275
  rcc   11    0.000   0.0    0.0000   0.00   0.0 107.7150  23.1775
  sph   12      0.0      0.0     0.0       1000.
  sph   13      0.0      0.0     0.0       2000.
  end
  vid           1
  con           2     -1
  vid           3     -2
  sst           4     -3
  vid           5     -4
  sst           6     -5
  bor           7     -6
  sst           8     -7
  kao           9     -8
```

```
  vid          10     -9
  sst          11    -10
  vid          12    -11
  vix          13    -12
  end
    1    1    1    1    1    1    1    1    1    1    1    1    1
  13z
 1000    1 1000    2 1000 1000 1000 1000 1000 1000 1000 1000     0
    0
27N18P LIBRARY (P5)
 $$ 27   27   18   18   45   60   16   4    26   26    6    3    1    3
    0    0    0    0    0    0    0   20    0    0    0
    1    2    3    4    5    6   11   12   13   14   15   16   21   22
   23   24   25   26   31   32   33   34   35   36   41   42   43   44
   45   46   51   52   53   54   55   56   61   62   63   64   65   66
   71   72   73   74   75   76   81   82   83   84   85   86   91   92
   93   94   95   96  101  102  103  104  105  106  111  112  113  114
  115  116  121  122  123  124  125  126  131  132  133  134  135  136
  141  142  143  144  145  146  151  152  153  154  155  156  161  162
  163  164  165  166  171  172  173  174  175  176  181  182  183  184
  185  186  191  192  193  194  195  196  201  202  203  204  205  206
  211  212  213  214  215  216  221  222  223  224  225  226  231  232
  233  234  235  236  241  242  243  244  245  246  251  252  253  254
  255  256
 $$ 1   12 ** 1.0000e-9
 $$ 1    2 ** 4.8240e-2
 $$ 1   -3 ** 1.2210e-9
 $$ 2    5 ** 1.7360e-3
 $$ 2    6 ** 5.9360e-2
 $$ 2    7 ** 7.7210e-3
 $$ 2   -4 ** 1.7430e-2
 $$ 3    8 ** 4.6420e-2
 $$ 3    9 ** 8.0020e-4
 $$ 3   10 ** 3.1680e-3
 $$ 3   11 ** 1.2740e-3
 $$ 3   12 ** 3.7980e-2
 $$ 3   13 ** 1.5840e-4
 $$ 3   14 ** 7.9440e-3
 $$ 3   15 ** 4.7600e-4
 $$ 3   16 ** 4.7390e-5
 $$ 3   17 ** 5.7280e-5
 $$ 3   18 ** 1.5620e-3
 $$ 3  -19 ** 5.8040e-5
 $$ 4   20 ** 4.8880e-3
 $$ 4   21 ** 1.2190e-4
 $$ 4   22 ** 6.2510e-4
 $$ 4   23 ** 3.9980e-4
 $$ 4   24 ** 1.1100e-3
 $$ 4   25 ** 1.1290e-3
 $$ 4  -26 ** 1.7860e-4
SAMBO ANALYSIS INPUT DATA
 $$   3   0    0    0    0    3    1    2
 **
   106.6548 0.0  18.745
   0.0 0.0 -89.44
   0.0 0.0 188.03
uncollided and total photon dose rates
ansi standard neutron dose rates :
 **
 1.4916e-1 1.4464e-1 1.2701e-1 1.2811e-1 1.2977e-1 1.0281e-1 5.1183e-2
 1.2319e-2 3.8365e-3 3.7247e-3 4.0150e-3 4.2926e-3 4.4744e-3 4.5676e-3
 4.5581e-3 4.5185e-3 4.4879e-3 4.4665e-3 4.4345e-3 4.3271e-3 4.1975e-3
 4.0976e-3 3.8390e-3 3.6748e-3 3.6748e-3 3.6748e-3 3.6748e-3
```

```
 18r0.0
ansi standard photon dose rates :
 **
 27r0.0
 8.7716e-3 7.4785e-3 6.3748e-3 5.4136e-3 4.6221e-3 3.9596e-3 3.4686e-3
 3.0192e-3 2.6276e-3 2.2051e-3 1.8326e-3 1.5228e-3 1.1725e-3 8.7594e-4
 6.3061e-4 3.8338e-4 2.6693e-4 9.3472e-4
ansi standard total dose rates :
 **
 1.4916e-1 1.4464e-1 1.2701e-1 1.2811e-1 1.2977e-1 1.0281e-1 5.1183e-2
 1.2319e-2 3.8365e-3 3.7247e-3 4.0150e-3 4.2926e-3 4.4744e-3 4.5676e-3
 4.5581e-3 4.5185e-3 4.4879e-3 4.4665e-3 4.4345e-3 4.3271e-3 4.1975e-3
 4.0976e-3 3.8390e-3 3.6748e-3 3.6748e-3 3.6748e-3 3.6748e-3
 8.7716e-3 7.4785e-3 6.3748e-3 5.4136e-3 4.6221e-3 3.9596e-3 3.4686e-3
 3.0192e-3 2.6276e-3 2.2051e-3 1.8326e-3 1.5228e-3 1.1725e-3 8.7594e-4
 6.3061e-4 3.8338e-4 2.6693e-4 9.3472e-4
```

```
      subroutine inscor
       common /pdet/   nd,     nne,    ne,     nt,     na,     nresp,
      1                nex,    nexnd,  nend,   ndnr,   ntnr,   ntne,
      2                nane,   ntndnr, ntnend, nanend, locrsp, locxd,
      3                locib,  locco,  loct,   locud,  locsd,  locqe,
      4                locqt,  locqte, locqae, lmax,   efirst, egtop
       common bc(1)
       do 100 i = 1,nd
         bc(locxd + 5*nd + i) = 2.7110e+10*24./36.*0.88024
100    continue
       return
       end
       subroutine source( ig,u,v,w,x,y,z,
      1                   wate,med,ag,isour,itstr,ngpqt3,ddf,
      2                   isbias,nmtg )
       dimension spect(1,18)
       data xst,yst,zst /0.000,0.0,11.195/
        data cyl_ht/63.500/
c40ppb u232
       data (spect(1,k),k=1,18) /
      1  4.409e-6,2.552e-5,1.654e-4,5.106e-4, 2.182e-3,7.429e+5,
      2  1.011e-1,9.761e+1,1.101e+3,
      3  3.426e+2,1.595e+3, 4.620e+03,
      4  2.347e+04,1.977e+5,4.550e+4,1.150e+5,3.534e+5,0.000e-00/
       data icall / 1 /
       if (icall) 10,10,5
5      icall = 0
c      r02 = 5.6861**2
       r02 = 0.0001**2
       r12 = 6.3500**2
        i=1
        sum=0.0
         do 92 j = 1,nmtg
92         sum = sum + spect(i,j)
         spect(i,1) = spect(i,1) / sum
         do 93 j = 2,nmtg
93         spect(i,j) = spect(i,j-1) + spect(i,j) / sum
10     continue
       r1 = fltrnf( 0 )
       call azirn( sinang,cosang )
       rad = sqrt( r1 * r12 + ( 1.0 - r1 ) * r02 )
       x = rad * sinang + xst
       y = rad * cosang + yst
       z = zst + fltrnf( 0 ) * cyl_ht
       i=1
       rn = fltrnf( 0 )
       do 94 j = 1,nmtg
         if ( rn .le. spect(i,j) ) goto 95
94     continue
       j = nmtg
95     ig = j
c40ppb u232
       if(ig.ne.6)wate=wate*1.97315
       if(ig.eq.6)wate=wate*0.026853
       return
       end
```

```
 es3100 package photon nct 24kg u oxide 40 ppb u232
 $$ 500 850 500    1    0   17   18   18    0    0  99.    4    0
 $$  0    0    0    0  **  1.0 1.0000e-5 1.0000e+4       1.0 2.2000e+5
 **    0.0       0.0       0.0       0.0       0.0       0.0       0.0
 **
 10.000e+6 8.0000e+6 6.5000e+6 5.0000e+6 4.0000e+6 3.0000e+6 2.5000e+6
 2.0000e+6 1.6600e+6 1.3300e+6 1.0000e+6 0.8000e+6 0.6000e+6 0.4000e+6
 0.3000e+6 0.2000e+6 0.1000e+6 0.0500e+6
 b1a303a31a34
 $$   1    1    0    0    0    1   18
 $$   1    1   10    1    1    1 **   0.1    .001       .010  5.000e-01
 $$  11    1   14    1    1    1 **   1.0    .010       .100  5.000e-01
 $$  15    1   18    1    1    1 **   10.    .100       1.00  5.000e-01
 $$  -1    9r0
    0    0    0    0
    0    0                oxide in es-3100 24kg cylinder model
    0    0    1    0
  rcc    1    0.000   0.0   11.1950   0.00   0.0  63.5000   0.0001
  rcc    2    0.000   0.0   11.1950   0.00   0.0  63.5000   6.3500
  rcc    3    0.000   0.0   11.1950   0.00   0.0  76.2000   6.4008
  rcc    4    0.000   0.0   10.5600   0.00   0.0  77.4700   6.6548
  rcc    5    0.000   0.0   10.5600   0.00   0.0  77.4700   7.9248
  rcc    6    0.000   0.0   10.5600   0.00   0.0  77.4700   8.0748
  rcc    7    0.000   0.0   10.5600   0.00   0.0  77.4700  10.9196
  rcc    8    0.000   0.0   10.2600   0.00   0.0  77.9200  11.0696
  rcc    9    0.000   0.0    0.2600   0.00   0.0  87.9200  23.0275
  rcc   10    0.000   0.0    0.2600   0.00   0.0 107.3050  23.0275
  rcc   11    0.000   0.0    0.0000   0.00   0.0 107.7150  23.1775
  sph   12      0.0      0.0     0.0       1000.
  sph   13      0.0      0.0     0.0       2000.
  end
  vid           1
  con           2     -1
  vid           3     -2
  sst           4     -3
  vid           5     -4
  sst           6     -5
  bor           7     -6
  sst           8     -7
  kao           9     -8
  vid          10     -9
  sst          11    -10
  vid          12    -11
  vix          13    -12
  end
    1    1    1    1    1    1    1    1    1    1    1    1    1
  13z
 1000    1 1000    2 1000    2    3    2    4 1000    2 1000    0
    0
27N18P LIBRARY (P5)
 $$ 0    0   18   18   45   60   16    4   26  26    6    3    1    3
    0    0    0    0    0    0    0   20    0    0    0
    1    2    3    4    5    6   11   12   13   14   15   16   21   22
   23   24   25   26   31   32   33   34   35   36   41   42   43   44
   45   46   51   52   53   54   55   56   61   62   63   64   65   66
   71   72   73   74   75   76   81   82   83   84   85   86   91   92
   93   94   95   96  101  102  103  104  105  106  111  112  113  114
  115  116  121  122  123  124  125  126  131  132  133  134  135  136
  141  142  143  144  145  146  151  152  153  154  155  156  161  162
  163  164  165  166  171  172  173  174  175  176  181  182  183  184
  185  186  191  192  193  194  195  196  201  202  203  204  205  206
  211  212  213  214  215  216  221  222  223  224  225  226  231  232
  233  234  235  236  241  242  243  244  245  246  251  252  253  254
```

```
  255  256
 $$ 1   12 ** 1.0000e-9
 $$ 1    2 ** 6.3940e-3
 $$ 1   -3 ** 3.3220e-4
 $$ 2    5 ** 1.7360e-3
 $$ 2    6 ** 5.9360e-2
 $$ 2    7 ** 7.7210e-3
 $$ 2   -4 ** 1.7430e-2
 $$ 3    8 ** 4.6420e-2
 $$ 3    9 ** 8.0020e-4
 $$ 3   10 ** 3.1680e-3
 $$ 3   11 ** 1.2740e-3
 $$ 3   12 ** 3.7980e-2
 $$ 3   13 ** 1.5840e-4
 $$ 3   14 ** 7.9440e-3
 $$ 3   15 ** 4.7600e-4
 $$ 3   16 ** 4.7390e-5
 $$ 3   17 ** 5.7280e-5
 $$ 3   18 ** 1.5620e-3
 $$ 3  -19 ** 5.8040e-5
 $$ 4   20 ** 4.8880e-3
 $$ 4   21 ** 1.2190e-4
 $$ 4   22 ** 6.2510e-4
 $$ 4   23 ** 3.9980e-4
 $$ 4   24 ** 1.1100e-3
 $$ 4   25 ** 1.1290e-3
 $$ 4  -26 ** 1.7860e-4
SAMBO ANALYSIS INPUT DATA
 $$   6    0    0    0    0    1    1    2
 **
   24.1775 0.0 42.945
   0.0 0.0  -1.00
   0.0 0.0  108.715
   123.1775 0.0 42.945
   0.0 0.0 -100.00
   0.0 0.0  207.715
UNCOLLIDED AND TOTAL PHOTON DOSE RATES
ANSI STANDARD GAMMA DOSE RATES
 **
 8.7716e-3 7.4785e-3 6.3748e-3 5.4136e-3 4.6221e-3 3.9596e-3 3.4686e-3
 3.0192e-3 2.6276e-3 2.2051e-3 1.8326e-3 1.5228e-3 1.1725e-3 8.7594e-4
 6.3061e-4 3.8338e-4 2.6693e-4 9.3472e-4
```

```
es3100 package photon hac 24kg u oxide 40 ppb u232
 $$ 500 850 500    1    0   17   18   18    0    0  99.    4    0
 $$  0    0    0    0  **  1.0 1.0000e-5 1.0000e+4       1.0 2.2000e+5
 **    0.0       0.0       0.0       0.0       0.0       0.0       0.0
 **
 10.000e+6 8.0000e+6 6.5000e+6 5.0000e+6 4.0000e+6 3.0000e+6 2.5000e+6
 2.0000e+6 1.6600e+6 1.3300e+6 1.0000e+6 0.8000e+6 0.6000e+6 0.4000e+6
 0.3000e+6 0.2000e+6 0.1000e+6 0.0500e+6
 b1a303a31a34
 $$   1    1    0    0    0    1   18
 $$   1    1   10    1    1    1 **   0.1    .001       .010  5.000e-01
 $$  11    1   14    1    1    1 **   1.0    .010       .100  5.000e-01
 $$  15    1   18    1    1    1 **   10.    .100       1.00  5.000e-01
 $$  -1    9r0
    0    0    0    0
    0    0                oxide in es-3100 24kg cylinder model
    0    0    1    0
  rcc    1    0.000   0.0   11.1950   0.00   0.0  63.5000   0.0001
  rcc    2    0.000   0.0   11.1950   0.00   0.0  63.5000   6.3500
  rcc    3    0.000   0.0   11.1950   0.00   0.0  76.2000   6.4008
  rcc    4    0.000   0.0   10.5600   0.00   0.0  77.4700   6.6548
  rcc    5    0.000   0.0   10.5600   0.00   0.0  77.4700   7.9248
  rcc    6    0.000   0.0   10.5600   0.00   0.0  77.4700   8.0748
  rcc    7    0.000   0.0   10.5600   0.00   0.0  77.4700  10.9196
  rcc    8    0.000   0.0   10.2600   0.00   0.0  77.9200  11.0696
  rcc    9    0.000   0.0    0.2600   0.00   0.0  87.9200  23.0275
  rcc   10    0.000   0.0    0.2600   0.00   0.0 107.3050  23.0275
  rcc   11    0.000   0.0    0.0000   0.00   0.0 107.7150  23.1775
  sph   12      0.0      0.0     0.0       1000.
  sph   13      0.0      0.0     0.0       2000.
  end
  vid           1
  con           2     -1
  vid           3     -2
  sst           4     -3
  vid           5     -4
  sst           6     -5
  bor           7     -6
  sst           8     -7
  kao           9     -8
  vid          10     -9
  sst          11    -10
  vid          12    -11
  vix          13    -12
  end
    1    1    1    1    1    1    1    1    1    1    1    1    1
  13z
 1000    1 1000    2 1000 1000 1000 1000 1000 1000 1000 1000    0
    0
27N18P LIBRARY (P5)
 $$ 0    0   18   18   45   60   16    4   26  26    6    3    1    3
    0    0    0    0    0    0    0   20    0    0    0
    1    2    3    4    5    6   11   12   13   14   15   16   21   22
   23   24   25   26   31   32   33   34   35   36   41   42   43   44
   45   46   51   52   53   54   55   56   61   62   63   64   65   66
   71   72   73   74   75   76   81   82   83   84   85   86   91   92
   93   94   95   96  101  102  103  104  105  106  111  112  113  114
  115  116  121  122  123  124  125  126  131  132  133  134  135  136
  141  142  143  144  145  146  151  152  153  154  155  156  161  162
  163  164  165  166  171  172  173  174  175  176  181  182  183  184
  185  186  191  192  193  194  195  196  201  202  203  204  205  206
  211  212  213  214  215  216  221  222  223  224  225  226  231  232
  233  234  235  236  241  242  243  244  245  246  251  252  253  254
```

```
  255  256
 $$ 1   12 ** 1.0000e-9
 $$ 1    2 ** 6.3940e-3
 $$ 1   -3 ** 3.3220e-4
 $$ 2    5 ** 1.7360e-3
 $$ 2    6 ** 5.9360e-2
 $$ 2    7 ** 7.7210e-3
 $$ 2   -4 ** 1.7430e-2
 $$ 3    8 ** 4.6420e-2
 $$ 3    9 ** 8.0020e-4
 $$ 3   10 ** 3.1680e-3
 $$ 3   11 ** 1.2740e-3
 $$ 3   12 ** 3.7980e-2
 $$ 3   13 ** 1.5840e-4
 $$ 3   14 ** 7.9440e-3
 $$ 3   15 ** 4.7600e-4
 $$ 3   16 ** 4.7390e-5
 $$ 3   17 ** 5.7280e-5
 $$ 3   18 ** 1.5620e-3
 $$ 3  -19 ** 5.8040e-5
 $$ 4   20 ** 4.8880e-3
 $$ 4   21 ** 1.2190e-4
 $$ 4   22 ** 6.2510e-4
 $$ 4   23 ** 3.9980e-4
 $$ 4   24 ** 1.1100e-3
 $$ 4   25 ** 1.1290e-3
 $$ 4  -26 ** 1.7860e-4
SAMBO ANALYSIS INPUT DATA
 $$   3    0    0    0    0    1    1    2
 **
  106.6548 0.0 42.945
   0.0 0.0 -89.440
   0.0 0.0 188.03
UNCOLLIDED AND TOTAL PHOTON DOSE RATES
ANSI STANDARD GAMMA DOSE RATES
 **
 8.7716e-3 7.4785e-3 6.3748e-3 5.4136e-3 4.6221e-3 3.9596e-3 3.4686e-3
 3.0192e-3 2.6276e-3 2.2051e-3 1.8326e-3 1.5228e-3 1.1725e-3 8.7594e-4
 6.3061e-4 3.8338e-4 2.6693e-4 9.3472e-4
```

THIS PAGE INTENTIONALLY LEFT BLANK.

SECTION 5 REFERENCES

10 CFR 71, *Packaging and Transportation of Radioactive Material*, Jan. 1, 2007.

49 CFR 173, *Shippers—General Requirements for Shipments and Packagings*, Oct. 1, 2007.

ANSI/ANS-6.1.1, *Neutron and Gamma Ray Flux-to-Dose-Rate Factors,* American Natl. Standards Institute, American Nuclear Society, La Grange, Ill., 1977.

MORSE-CGA, *Monte Carlo Radiation Transport Code with Array Geometry Capability,* ORNL-6174, M. B. Emmett, Oak Ridge Natl. Lab., April 1985.

SCALE: A Modular Code System for Performing Standardized Computer Analyses for Licensing Evaluation, C. V. Parks, ed., NUREG/CR-0200, rev. 6, ORNL/NUREG/CSD-2/R6, May 2000.

THIS PAGE INTENTIONALLY LEFT BLANK.

6. CRITICALITY EVALUATION

This section describes the criticality safety evaluation of the Y-12 National Security Complex (Y-12) Model ES-3100 package with highly enriched uranium (HEU) metal or alloys of aluminum, molybednum, or zirconium (specific information for alloys are addressed in Sects. 6.2.1, 6.2.4, 6.3.2, 6.4, 6.4.1, and 6.6.1.), or HEU oxide, or highly enriched uranyl nitrate crystals (UNX). HEU metal may be solid shapes (cylinders, bars, buttons, slugs, unirradiated TRIGA fuel) or broken metal pieces of unspecified geometric shapes. Physical testing of Type-B fissile material packages for surface transportation conducted in accordance with the physical testing requirements of 10 CFR 71 is limited to the ES-3100 packaging and non-fissile dummy contents. Consequently, analytic methods are used to demonstrate compliance of the ES-3100 package with the applicable performance requirements in 10 CFR 71. The specific requirements investigated for compliance in this evaluation are contained in 10 CFR 71.55, "General Requirements of all Fissile Material Packages," and 10 CFR 71.59, "Standards for Arrays of Fissile Material Packages." Physical testing of Type-B fissile material packages transported by air is not conducted for the ES-3100. Analytic methods are also used to demonstrate compliance of the ES-3100 package with the requirements of 10 CFR 71.55(f). This is accomplished by demonstrating compliance of the package with the more stringent requirements of the International Atomic Energy Agency (IAEA) for situations where the conditions of the fissile material package following the tests cannot be demonstrated. (TS-G-1.1, Sect. 680.2)

6.1 DESCRIPTION OF THE CRITICALITY DESIGN

6.1.1 Design Features

The principal design feature of interest in the criticality evaluation of the Model ES-3100 package is the containment/outer drum system (Drawing No. M2E801580A031, Appendix 1.4.8). The ES-3100 package uses a single containment system (Drawing No. M2E801580A011, Appendix 1.4.8) to contain the HEU contents. The containment is a high-integrity, watertight, post-load leak-testable, stainless-steel vessel (Fig. 1.2). The outer drum system (Drawing M2E801580A001, Appendix 1.4.8) is a recessed, double-compartment body with a removable top for insertion and removal of the containment vessel. The body weldment liner outer cavity and the top plug weldment contain Kaolite 1600™ (Kaolite), a thermal insulation material that protects the containment vessel from thermal absorption, shock and impact. The body weldment liner inner cavity contains a neutron poison, "277-4," which serves as a strong neutron absorber. Other sections of this report (Sects. 2, 3, and 4) demonstrate the integrity of the ES-3100 package [i.e., that this single containment vessel remains intact and watertight under the Normal Conditions of Transport (NCT) and Hypothetical Accident Conditions (HAC)].

Typical shipping configurations inside the ES-3100 containment vessel are illustrated in Fig. 1.4. The 277-4 canned spacers will only be used for contents shipped in metal convenience cans. Three 4.25-in.-diam × 10.0-in.-tall or six 4.25-in.-diam × 4.88-in.-tall convenience cans separated by can pads may be placed inside the 31-in.-tall cavity of the ES-3100 containment vessel (Drawing M2E801580A035, Appendix 1.4.8). Other can arrangements fit inside the containment vessel, such as three 4.25-in.-diam × 8.75-in.-tall or five 4.25-in.-diam × 4.88-in.-tall convenience cans. Both of these can arrangements include can pads and 277-4 canned spacers with overall dimensions of 4.25-in. diam × 1.82-in. height (Drawing M2E801580A026 or M2E801580A043, Appendix 1.4.8). Nickel alloy cans are ~3-in. diam × 4.75-in.-tall. Up to three Teflon bottles (4.69-in. diam × 9.4-in. tall) or three polyethylene bottles (4.94-in. diam × 8.7-in. tall) will fit inside the containment vessel; however, 277-4 canned spacers are not used with these configurations.

A modified convenience can may be used to package the TRIGA contents that do not fit inside these containers. A 17.5 in.-tall convenience can is constructed from two 4.25-in.-diam × 8.75-in.-tall cans brazed together.

Credit is not taken in this criticality analysis for fissile material spacing provided by the presence of the convenience cans or bottles inside the containment vessel. These containers are not manufactured to the *ASME Boiler and Pressure Vessel Code*, Sect. III, Subsection NG, or better.

6.1.2 Summary of the Criticality Evaluation

Testing conducted in accordance with the physical testing requirements of 10 CFR 71 demonstrated that water leakage into the containment is not a credible event under the NCT and HAC. However, credit for the high-integrity, watertight containment is not taken in this criticality evaluation, as agreed upon during discussions held at public meetings at the U.S. Nuclear Regulatory Commission. (Docket 71-9315)

10 CFR 71.55(b) requires the evaluation of water leakage into the containment vessel or leakage of liquid contents out of the containment vessel and of other conditions that produce maximum reactivity in the single package. For solid uranium contents, water leakage conditions are simulated by flooding all regions outside and inside of the containment vessel, including the sealed convenience cans. For liquid uranium contents, water leakage conditions are simulated by flooding all regions outside the containment vessel except the containment vessel well. Uranyl nitrate (UN) solution resides inside both the containment vessel well and the containment vessel, including the Teflon bottles. For this evaluation, a flooded containment vessel under full water reflection is also analyzed. Under such leakage conditions, the calculated neutron multiplication factor ($k_{eff} + 2\sigma$) for the ES-3100 package with HEU contents is lower than the upper subcritical limit (USL) for a subcritical system. Water inleakage into the containment vessel or liquid content leakage out of the containment vessel will not produce a criticality in the containment vessel of a disassembled package or an assembled single package. Therefore, the Model ES-3100 shipping package complies with all of the requirements of 10 CFR 71.55(b, d).

Credit for the high-integrity, watertight containment is not taken either in the single package analysis [10 CFR 71.55(d, e)] or in the array analysis [10 CFR 71.59(a)(1)] of undamaged packages. In the evaluation of undamaged packages under 10 CFR 71.59(a)(1) and the evaluation of damaged packages under 10 CFR 71.59(a)(2), the containment vessel is flooded with water, providing moderation to such an extent as to cause maximum reactivity of the content consistent with the chemical and physical form of the material present. Solid HEU, <u>not solution HEU</u>, is being shipped in the ES-3100. Consequently, in the evaluation of damaged packages under 10 CFR 71.59(a)(2), the leakage out of the containment vessel of content moderated to such an extent as to cause maximum reactivity consistent with the physical and chemical form of material is not considered credible HAC, based on results for tests specified in 10 CFR 71.73. Because credit for the high-integrity, watertight containment is not fully taken in this criticality evaluation, the fissile material mass loading limits are very conservative.

The NCT tests under 10 CFR 71.71 and the HAC tests under 10 CFR 71.73 demonstrate that containment is not breached. Nevertheless, containment vessel flooding is assumed in the criticality calculations performed for the derivation of fissile material loading limits. The 7.1–10.1 kg quantities of evaluation water in both the NCT and HAC criticality calculations are not actually present in the containment vessel. Simulation of this condition in the criticality calculations produces fissile material content that is more reactive than actual.

The 7.1–10.1 kg quantity of evaluation water does not necessarily bound reasonable amounts of hydrogenous packing material present inside the containment vessel when the fissile material is in particulate form (primarily HEU oxides and UNH crystals) or must be evaluated as particulate matter (broken metal). Packing materials include can pads, polyethylene bags, vinyl tape, and polyethylene or Teflon bottles, if used. An administrative criticality control is used to restrict the amount of hydrogenous packing material normally present inside the containment vessel (Item 7 in Sect. 6.2.4.)

Under NCT and HAC, three parameters that affect criticality and may vary during transport of the Model ES-3100 package are the number of packages transported, the amount of water present in the package, and the volatile (organic) constituents of the package. The number of packages transported is a parameter limited by the criticality safety index (CSI) established by this criticality evaluation. Both the amount of water present inside the package and the volatile constituents of the package are parameters for the following reasons. First, the inherent water content of the Kaolite in NCT and water absorption/retention by the Kaolite in HAC are unknowns. Second, volatile constituents can be driven off at the high temperatures of HAC. These parameters determine a variety of competing effects that govern the fission process, including, but not limited to, mass, moderation, absorption, and reflection. To ensure that all effects are adequately included in this criticality evaluation, the range of these parameters is evaluated. The moisture fraction inside the containment vessel (MOCFR) and the moisture fraction of the package external to the containment vessel (MOIFR) are varied from the dry to the flooded condition.

It is possible for accidents to be significantly more severe in the air transport mode than in the surface transport mode. Thus, the performance requirements for packages designed to be transported by air are more stringent. These requirements address separate aspects of the accident assessment and apply only to the criticality evaluation of an individual package under isolation. (TS-G-1.1) For a fissile material package designed to be transported by air, 10 CFR 71.55(f) requires that the criticality evaluation demonstrate that the package be subcritical assuming reflection by 20 cm (7.9 in.) of water but no water inleakage when subjected to the sequential application of the HAC free drop and crush tests of 10 CFR 71.73(c)(1 and 2) and the modified puncture and thermal tests of 10 CFR 71.55(f)(1)(iii and iv).

The ES-3100 package was not subjected to physical testing of Type-B fissile material packages transported by air. Instead, analytic methods are used to demonstrate compliance of the ES-3100 package with the requirements of 10 CFR 71.55(f). This is accomplished by demonstrating compliance of the package with the more stringent requirements imposed by the IAEA for situations where the conditions of the fissile material package following the tests cannot be demonstrated. (TS-G-1.1, Sect. 680.2) Section 680.2 of TS-G-1.1 states that worst-case assumptions regarding the geometric arrangement of the package and contents should be made in the criticality evaluation taking into account all moderating and structural components of the packaging. The assumptions should be in conformity with the potential worst-case effects of the mechanical and thermal tests, and all package orientations should be considered for the analysis. Subcriticality must be demonstrated after due consideration of such aspects as the efficiency of the moderator, loss of neutron absorbers, rearrangement of packaging components and contents, geometry changes, and temperature effects. Given that the requirements of 10 CFR 71.55(f) mirror the IAEA requirements of TS-R-1, Sect. 680, for Type B(U) fissile material packages, this approach is considered an acceptable one.

The following criticality safety evaluation shows that the Model ES-3100 package with designated content satisfies the requirements of 10 CFR 71.55 and 71.59 for surface transport, and of 10 CFR 71.55(f) for air transport. Designated contents are solid HEU metal shapes (cylinders, bars, buttons, billets, slugs, and unirradiated TRIGA fuel); HEU broken metal contents of unspecified geometric shapes; HEU products or skull oxides; or UNX crystals. HEU skull oxides are distinguished from product oxides (UO_2, U_3O_8, or UO_3) as being a residue of graphite and oxidized uranium (U_3O_8)

recovered in the casting process. The criticality evaluation of these contents is addressed in the main subsections of this chapter. The loading capability of the Model ES-3100 package for HEU product oxide has been extended by the assignment of a CSI value of 0.4 to the package. The criticality evaluation supporting this increased capability is addressed in Appendix 6.9.9.

Tables 6.1a–6.1e pertain to surface-only modes of transportation. The column headings across the tables identify content and 277-4 canned spacer configurations. The tables are organized into groups of rows, which identify the defining calculations for addressing the performance requirements of 10 CFR 71.55(b), 71.55(d), 71.55(e), or 71.59 (see "Conditions" column). The defining calculations are also discussed in Sects. 6.4, 6.5, or 6.6, as appropriate. The KENO V.a input listings for the calculations are provided in Appendix 6.9.7. The rows within the groups cite the specific requirements stated in the CFR paragraphs and provide details regarding how these conditions are addressed or treated in the defining calculations for each content and 277-4 canned spacer configuration listed in a table column. Tables 6.1a and 6.1b summarize the results of the evaluation for solid HEU metal shapes, Table 6.1c for HEU broken metal, Table 6.1d for HEU product and skull oxide, and Table 6.1e for UNX crystals and unirradiated TRIGA fuel elements.

The evaluation limits for solid HEU metal shapes listed in the column headings of Table 6.1a are expressed in terms of the diameter for a cylinder and the length-width of the geometric cross section for a square bar. These values are established by the size of the convenience can opening through which these contents are inserted. Potential fissile (^{235}U) mass loading limits for these contents are given in the information blocks where a description of the content appears for the fissile material "in the most reactive credible configuration."

The fissile (^{235}U) or uranium masses listed in the column headings of Tables 6.1b–6.1e indicate evaluation limits for the associated content configurations. In the case of slugs (Table 6.1b), the ^{235}U evaluation limits represent the fissile content contained in the slugs with maximum tolerances applied. In the case of broken metal (Table 6.1c), the ^{235}U evaluation limits represent the maximum amount of ^{235}U adequately subcritical in a flooded, reflected containment vessel as conservatively applied over the indicated range of enrichment. For HEU enrichments $\leq$60%, the 35.32-kg package limit on the amount of HEU to be shipped in an ES-3100 becomes the evaluation limit. For HEU oxide (Table 6.1d) and UNX crystals (Table 6.1e), the ^{235}U evaluation limits correspond to the 24-kg package limit on the amount of HEU oxide or UNX crystals to be shipped. For HEU skull oxide (Table 6.1d), the ^{235}U evaluation limit represents a maximum derived from the evaluation of an inventory at Y-12. For unirradiated TRIGA reactor fuel elements (Table 6.1e), the ^{235}U evaluation limit represents a maximum for the fuel manufacturer's product line.

The NCT and HAC array analyses [10 CFR 71.59(1), (2)] may reveal reductions in the potential loading limits for content and 277-4 canned spacer configurations initially identified in the single package calculations [10 CFR 71.55(b), (d), and (e)] of Tables 6.1a–6.1e. This occurs in order to achieve fissile material loadings which are at or below the subcritical safety limit. These reduced loading limits are identified as "**load-limited to**" values in the "CSI" rows.

Table 6.2a summarizes the fissile loading limits derived from Tables 6.1a–6.1e for surface-only transport mode. The fissile loading limits pertaining to the air-transport mode summarized in Table 6.2b are derived from the air-transport analysis addressed in Sect. 6.7. The loading limit for packages under mixed-mode transportation is taken as the most restrictive limit for either mode (surface or air transport).

Table 6.1a. Summary of criticality evaluation for solid HEU metal cylinders and bars

Conditions	cylinders (d ≤ 3.24 in.) no can spacers	cylinders (d ≤ 3.24 in.) with can spacers	square bars (l,w ≤ 2.29 in.) no can spacers	cylinders (3.24 < d ≤ 4.25 in.) no can spacers	cylinders (3.24 < d ≤ 4.25 in.) with can spacers
General requirements for each fissile package (§71.55)					
"A package used for shipment of fissile material must be so designed and constructed and its contents so limited that it would be subcritical if water were to leak into the containment system, . . . so that under the following conditions, maximum reactivity of the fissile material would be attained:" (Paragraph "b")	$k_{eff} + 2\sigma \leq 0.9228$ cvcrcyt11_21_1	$k_{eff} + 2\sigma \leq 0.8866$ cvcrcyt11_36_2	$k_{eff} + 2\sigma \leq 0.8787$ cvcrsqt11_36_1	$k_{eff} + 2\sigma \leq 0.9215$ cvcrcyct11_17_1	$k_{eff} + 2\sigma \leq 0.9202$ cvcrcyct11_32_2
(1) the most reactive credible configuration consistent with the chemical and physical form of the material,	3 stacked cylinders (d = 3.24 in.) 1 cylinder per convenience can, no can spacers, 21,000g ^{235}U	3 stacked cylinders (d = 3.24 in.) 1 cylinder per convenience can, with can spacers, 36,000g ^{235}U	3 stacked bars (l,w = 2.29 in.) 1 bar per convenience can, no can spacers, 36,000g ^{235}U	3 stacked cylinders (d = 4.25 in.) 1 cylinder per convenience can, no can spacers, 17,000g ^{235}U	3 stacked cylinders (d = 4.25 in.) 1 cylinder per convenience can, with can spacers, 32,000g ^{235}U
(2) moderation by water to the most reactive credible extent,	flooding of the containment vessel	same	same	same	same
(3) close full reflection of the containment system by water on all sides, or such greater reflection of the containment system as may be provided by the surrounding material of the packaging.	30.48 cm H_2O surrounding the containment vessel	same	same	same	same

Table 6.1a. Summary of criticality evaluation for solid HEU metal cylinders and bars

Conditions	cylinders (d ≤ 3.24 in.) no can spacers	cylinders (d ≤ 3.24 in.) with can spacers	square bars (l,w ≤ 2.29 in.) no can spacers	cylinders (3.24 < d ≤ 4.25 in.) no can spacers	cylinders (3.24 < d ≤ 4.25 in.) with can spacers
"A package used for shipment of fissile material must be so designed and constructed and its contents so limited under the tests specified in §71.71 (Normal Conditions of Transport) . . ." (Paragraph "d")					
(1) the contents would be subcritical,	$k_{eff} + 2\sigma \leq 0.9035$ ncsrcyt11_21_1_15	$k_{eff} + 2\sigma \leq 0.8731$ ncsrcyt11_36_2_15	$k_{eff} + 2\sigma \leq 0.8652$ ncsrsqt11_36_1_15	$k_{eff} + 2\sigma \leq 0.8941$ ncsrcyct11_17_1_15	$k_{eff} + 2\sigma \leq 0.8946$ ncsrcyct11_32_2_15
(2) the geometric form of the package contents would not be substantially altered,	3 stacked cylinders (d = 3.24 in.) 1 cylinder per convenience can, no can spacers, 21,000g ^{235}U	3 stacked cylinders (d = 3.24 in.) 1 cylinder per convenience can, with can spacers, 36,000g ^{235}U	3 stacked bars (l,w = 2.29 in.) 1 bar per convenience can, no can spacers, 36,000g ^{235}U	3 stacked cylinders (d = 4.25 in.) 1 cylinder per convenience can, no can spacers, 17,000g ^{235}U	3 stacked cylinders (d = 4.25 in.) 1 cylinder per convenience can, with can spacers, 32,000g ^{235}U
(3) there would be no leakage of water into the containment system unless, in the evaluation of undamaged packages under §71.59(a)(1), it has been assumed that moderation is present to such an extent as to cause maximum reactivity consistent with the chemical and physical form of the material,	moderation is present to such an extent as to cause maximum reactivity	same	same	same	same
(4) there will be no substantial reduction in the effectiveness of the packaging	30.48 cm H_2O surrounding the drum (d=18.37 in., h=43.5 in.)	same	same	same	same

Table 6.1a. Summary of criticality evaluation for solid HEU metal cylinders and bars

Conditions	cylinders ($d \leq 3.24$ in.) no can spacers	cylinders ($d \leq 3.24$ in.) with can spacers	square bars ($l,w \leq 2.29$ in.) no can spacers	cylinders ($3.24 < d \leq 4.25$ in.) no can spacers	cylinders ($3.24 < d \leq 4.25$ in.) with can spacers
"A package used for shipment of fissile material must be so designed and constructed and its contents so limited that under the tests specified in §71.73 (Hypothetical Accident Conditions) the package would be subcritical. For this determination, it must be assumed that:" (Paragraph "e")	$k_{eff} + 2\sigma \leq 0.9044$ hcsrcyt12_21_1_15	$k_{eff} + 2\sigma \leq 0.8734$ hcsrcyt12_36_2_15	$k_{eff} + 2\sigma \leq 0.8642$ hcsrsqt12_36_1_15	$k_{eff} + 2\sigma \leq 0.8979$ hcsrcyct12_17_1_15	$k_{eff} + 2\sigma \leq 0.8977$ hcsrcyct12_32_2_15
(1) the fissile material is in the most reactive credible configuration consistent with the chemical and physical form of the contents,	3 stacked cylinders (d = 3.24 in.) 1 cylinder per convenience can, no can spacers, 21,000g ^{235}U	3 stacked cylinders (d = 3.24 in.) 1 cylinder per convenience can, with can spacers, 36,000g ^{235}U	3 stacked bars (l,w = 2.29 in.) 1 bar per convenience can, no can spacers, 36,000g ^{235}U	3 stacked cylinders (d = 4.25 in.) 1 cylinder per convenience can, no can spacers, 17,000g ^{235}U	3 stacked cylinders (d = 4.25 in.) 1 cylinder per convenience can, with can spacers, 32,000g ^{235}U
(2) water moderation occurs to the most reactive credible extent consistent with the chemical and physical form of content,	flooding of the package	same	same	same	same
(3) there is full reflection by water on all sides, as close as is consistent with the damage condition of the package.	30.48 cm H_2O surrounding the reduced diameter drum (d=17.20 in., h=43.5 in.)	same	same	same	same

Table 6.1a. Summary of criticality evaluation for solid HEU metal cylinders and bars

Conditions	cylinders (d ≤ 3.24 in.) no can spacers	cylinders (d ≤ 3.24 in.) with can spacers	square bars (l,w ≤ 2.29 in.) no can spacers	cylinders (3.24 < d ≤ 4.25 in.) no can spacers	cylinders (3.24 < d ≤ 4.25 in.) with can spacers
Standards for arrays of fissile material packages (§71.59)					
" . . . the designer of a fissile material package shall derive a number "N" based on all the following conditions being satisfied, assuming packages are stacked together in any arrangement and with close reflection on all sides of the stack by water:" (Paragraph "a")					
Transport index based on nuclear criticality control, CSI = 0.0	**load-limited to 18,000g ^{235}U no can spacers**	**load-limited to 30,000g ^{235}U can spacers**	**load-limited to 30,000g ^{235}U no can spacers**	**load-limited to 15,000g ^{235}U no can spacers**	**load-limited to 25,000g ^{235}U can spacers**
(1) five times "N" undamaged packages with nothing between the packages would be subcritical,	$k_{eff} + 2\sigma \leq 0.9237$ nciacyt11_18_1_3	$k_{eff} + 2\sigma \leq 0.9195$ nciacyt11_30_2_3	$k_{eff} + 2\sigma \leq 0.9219$ nciasqt11_30_1_3	$k_{eff} + 2\sigma \leq 0.8992$ nciacyct11_15_1_3	$k_{eff} + 2\sigma \leq 0.9147$ nciacyct11_25_2_3
(2) two times "N" damaged packages, if each package were subject to the tests specified in §71.73 (Hypothetical Accident Conditions) would be subcritical with optimum interspersed hydrogenous moderation,	$k_{eff} + 2\sigma \leq 0.9230$ hciacyt12_18_1_3	$k_{eff} + 2\sigma \leq 0.9220$ hciacyt12_30_2_3	$k_{eff} + 2\sigma \leq 0.9221$ hciasqt12_30_1_3	$k_{eff} + 2\sigma \leq 0.8986$ hciacyct12_15_1_3	$k_{eff} + 2\sigma \leq 0.9156$ hciacyct12_25_2_3
(3) the value of "N" not <0.5.	N(1,2) = ∞	same	same	same	same
Transport index based on nuclear criticality control, CSI = 0.0			**load-limited to 36,000g ^{235}U can spacers**		
(1) five times "N" undamaged packages			$k_{eff} + 2\sigma \leq 0.8961$ nciasqt11_36_2_3		
(2) two times "N" damaged packages, ...			$k_{eff} + 2\sigma \leq 0.8946$ hciasqt12_36_2_3		
(3) the value of "N"			N(1,2) = ∞		

Table 6.1b. Summary of criticality evaluation for solid HEU metal slugs

Conditions	slugs, no can spacers enr. ≤ 100% ≤ 18,277 g ^{235}U	slugs with can spacers 80% < enr. ≤ 100% < 36,555 g ^{235}U	slugs with can spacers enr. ≤ 80% < 36,555 g ^{235}U
General requirements for each fissile package (§71.55)			
"A package used for shipment of fissile material must be so designed and constructed and its contents so limited that it would be subcritical if water were to leak into the containment system, . . . so that under the following conditions, maximum reactivity of the fissile material would be attained:" (Paragraph "b")	$k_{eff} + 2\sigma \leq 0.9098$ cvcr5st11_1_1	$k_{eff} + 2\sigma \leq 0.9029$ cvcr5st11_2_2	
(1) the most reactive credible configuration consistent with the chemical and physical form of the material,	cluster of 5 slugs (d = 1.5625 in., h = 2.0625 in.) per convenience can, no can spacers, 18,277 g ^{235}U	cluster of 10 slugs stacked 2 high per convenience can, can spacers, 36,555 g ^{235}U	
(2) moderation by water to the most reactive credible extent,	flooding of the containment vessel	same	
(3) close full reflection of the containment system by water on all sides, or such greater reflection of the containment system as may be provided by the surrounding material of the packaging.	30.48 cm H_2O surrounding the containment vessel	same	

Table 6.1b. Summary of criticality evaluation for solid HEU metal slugs

Conditions	slugs, no can spacers enr. ≤ 100% ≤ 18,277 g ^{235}U	slugs with can spacers 80% < enr. ≤ 100% < 36,555 g ^{235}U	slugs with can spacers enr. ≤ 80% < 36,555 g ^{235}U
"A package used for shipment of fissile material must be so designed and constructed and its contents so limited under the tests specified in §71.71 (Normal Conditions of Transport) . . ." (Paragraph "d")			
(1) the contents would be subcritical,	$k_{eff} + 2\sigma \leq 0.8834$ ncsr5st11_1_1_15	$k_{eff} + 2\sigma \leq 0.8781$ ncsr5st11_2_2_15	
(2) the geometric form of the package contents would not be substantially altered,	cluster of 5 slugs (d = 1.5625 in., h = 2.0625 in.) per convenience can, no can spacers, 18,277 g ^{235}U	cluster of 10 slugs stacked 2 high per convenience can, can spacers, 36,555 g ^{235}U	
(3) there would be no leakage of water into the containment system unless, in the evaluation of undamaged packages under §71.59(a)(1), it has been assumed that moderation is present to such an extent as to cause maximum reactivity consistent with the chemical and physical form of the material,	moderation is present to such an extent as to cause maximum reactivity	same	
(4) there will be no substantial reduction in the effectiveness of the packaging	30.48 cm H_2O surrounding the drum (d=18.37 in., h=43.5 in.)	same	

Table 6.1b. Summary of criticality evaluation for solid HEU metal slugs

Conditions	slugs, no can spacers enr. ≤ 100% ≤ 18,277 g ^{235}U	slugs with can spacers 80% < enr. ≤ 100% < 36,555 g ^{235}U	slugs with can spacers enr. ≤ 80% < 36,555 g ^{235}U
"A package used for shipment of fissile material must be so designed and constructed and its contents so limited that under the tests specified in §71.73 (Hypothetical Accident Conditions) the package would be subcritical. For this determination, it must be assumed that:" (Paragraph "e")	$k_{eff} + 2\sigma \leq 0.8860$ hcsr5st12_1_1_15	$k_{eff} + 2\sigma \leq 0.8772$ hcsr5st12_2_2_15	
(1) the fissile material is in the most reactive credible configuration consistent with the chemical and physical form of the contents,	cluster of 5 slugs (d = 1.5625 in., h = 2.0625 in.) per convenience can, no can spacers, 18,277 g ^{235}U	cluster of 10 slugs stacked 2 high per convenience can, can spacers, 36,555 g ^{235}U	
(2) water moderation occurs to the most reactive credible extent consistent with the chemical and physical form of content,	flooding of the package	same	
(3) there is full reflection by water on all sides, as close as is consistent with the damage condition of the package.	30.48 cm H_2O surrounding the reduced diameter drum (d=17.20 in., h=43.5 in.)	same	

Table 6.1b. Summary of criticality evaluation for solid HEU metal slugs

Conditions	slugs, no can spacers enr. ≤ 100% ≤ 18,277 g ^{235}U	slugs with can spacers 80% < enr. ≤ 100% < 36,555 g ^{235}U	slugs with can spacers enr. ≤ 80% < 36,555 g ^{235}U
Standards for arrays of fissile material packages (§71.59)			
" . . . the designer of a fissile material package shall derive a number "N" based on all the following conditions being satisfied, assuming packages are stacked together in any arrangement and with close reflection on all sides of the stack by water: " (Paragraph "a")			
Transport index based on nuclear criticality control, CSI = 0.0	**load-limited to enr. ≤ 95%, 17,374 g ^{235}U no can spacers**	**load-limited to 80% < enr. ≤ 95% 24,324 g ^{235}U can spacers**	**load-limited to enr. ≤ 80%, 29,318 g ^{235}U can spacers**
(1) five times "N" undamaged packages with nothing between the packages would be subcritical,	$k_{eff} + 2\sigma \leq 0.9077$ ncia5st11_1_1_7_3	$k_{eff} + 2\sigma \leq 0.8936$ ncia70st11_2_7_3	$k_{eff} + 2\sigma \leq 0.9085$ ncia5est11_2_2_5_3
(2) two times "N" damaged packages, if each package were subject to the tests specified in §71.73 (Hypothetical Accident Conditions) would be subcritical with optimum interspersed hydrogenous moderation,	$k_{eff} + 2\sigma \leq 0.9029$ hcia5est12_1_1_7_3	$k_{eff} + 2\sigma \leq 0.8946$ hcia70st12_2_7_3	$k_{eff} + 2\sigma \leq 0.9100$ hcia5est12_2_2_5_3
(3) the value of "N" not <0.5.	N(1,2) = ∞	same	same

Table 6.1b. Summary of criticality evaluation for solid HEU metal slugs

Conditions	slugs, no can spacers enr. ≤ 100% ≤ 18,277 g ^{235}U	slugs with can spacers 80% < enr. ≤ 100% < 36,555 g ^{235}U	slugs with can spacers enr. ≤ 80% < 36,555 g ^{235}U
Transport index based on nuclear criticality control, CSI = 0.4	**load-limited to enr. ≤ 95%, 17,374 g ^{235}U no can spacers**	**load-limited to 80% < enr. ≤ 95% 34,749 g ^{235}U can spacers**	**load-limited to enr. ≤ 80%, 29,318 g ^{235}U can spacers**
(1) five times "N" undamaged packages	bounded by CSI=0	$k_{eff} + 2\sigma \leq 0.9200$ ncf15est11_2_2_7_3	$k_{eff} + 2\sigma \leq 0.8643$ ncf15est11_2_2_5_3
(2) two times "N" damaged packages, ...	bounded by CSI=0	$k_{eff} + 2\sigma \leq 0.9056$ hcf25est12_2_2_7_3	$k_{eff} + 2\sigma \leq 0.8556$ hcf25est12_2_2_5_3
(3) the value of "N"	N(1,2) = 202/162	same	same

Table 6.1c. Summary of criticality evaluation for solid HEU metal of unspecified geometric shapes characterized as broken metal

Conditions	95% < enr. ≤ 100% ≤ 25,894g ^{235}U	90% < enr. ≤95% ≤ 27,252g ^{235}U	80% < enr. ≤90% ≤ 28,334g ^{235}U	70% < enr. ≤80% ≤ 28,184g ^{235}U	60% < enr. ≤70% ≤ 24,693g ^{235}U	enr. ≤60% ≤ 35,320g Uranium
General requirements for each fissile package (§71.55)						
"A package used for shipment of fissile material must be so designed and constructed and its contents so limited that it would be subcritical if water were to leak into the containment system, . . . so that under the following conditions, maximum reactivity of the fissile material would be attained:" (Paragraph "b")	$k_{eff} + 2\sigma \leq 0.9181$ cvr3lha_26_1_8_15	$k_{eff} + 2\sigma \leq 0.9206$ cvr3lha_29_1_7_15	$k_{eff} + 2\sigma \leq 0.9224$ cvr3lha_32_1_6_15	$k_{eff} + 2\sigma \leq 0.8927$ cvr3lha_36_1_5_15	$k_{eff} + 2\sigma \leq 0.8620$ cvr3lha_36_1_4_15	$k_{eff} + 2\sigma \leq 0.8289$ cvr3lha_36_1_3_15
(1) the most reactive credible configuration consistent with the chemical and physical form of the material,	A mixture of HEU metal and water is homogenized over the internal volume of an assumed content lattice, one per can location. The square footprint of the content lattice is circumscribed by the inner wall of the containment vessel. The amount of water in the flooded containment vessel is calculated on the basis that the convenience can steel is replaced with water. Can pads and spacers not used. See Appendix 6.9.3, Sect. 6.9.3.1, for justification of the content model.					
(2) moderation by water to the most reactive credible extent,	flooding of the containment vessel					
(3) close full reflection of the containment system by water on all sides, or such greater reflection of the containment system as may be provided by the surrounding material of the packaging.	30.48 cm H_2O surrounding the containment vessel					

Table 6.1c. Summary of criticality evaluation for solid HEU metal of unspecified geometric shapes characterized as broken metal

Conditions	95% < enr. ≤ 100% ≤ 25,894g ^{235}U	90% < enr. ≤95% ≤ 27,252g ^{235}U	80% < enr. ≤90% ≤ 28,334g ^{235}U	70% < enr. ≤80% ≤ 28,184g ^{235}U	60% < enr. ≤70% ≤ 24,693g ^{235}U	enr. ≤60% ≤ 35,320g Uranium
"A package used for shipment of fissile material must be so designed and constructed and its contents so limited under the tests specified in §71.71 (Normal Conditions of Transport) . . ." (Paragraph "d")						
(1) the contents would be subcritical,	$k_{eff} + 2\sigma \leq 0.8908$ (ncsrbmt11_36_1_15)					
(2) the geometric form of the package contents would not be substantially altered,	A mixture of HEU metal and water is homogenized over the internal volume of the containment vessel. The amount of water in the flooded containment vessel is calculated on the basis that the convenience can steel is replaced with water. Can pads and spacers not used.					
(3) there would be no leakage of water into the containment system unless, in the evaluation of undamaged packages under §71.59(a)(1), it has been assumed that moderation is present to such an extent as to cause maximum reactivity consistent with the chemical and physical form of the material,	moderation is present to such an extent as to cause maximum reactivity					
(4) there will be no substantial reduction in the effectiveness of the packaging	30.48 cm H_2O surrounding the drum (d = 18.37 in., h = 43.5 in.)					

Table 6.1c. Summary of criticality evaluation for solid HEU metal of unspecified geometric shapes characterized as broken metal

Conditions	95% < enr. ≤ 100% ≤ 25,894g ^{235}U	90% < enr. ≤95% ≤ 27,252g ^{235}U	80% < enr. ≤90% ≤ 28,334g ^{235}U	70% < enr. ≤80% ≤ 28,184g ^{235}U	60% < enr. ≤70% ≤ 24,693g ^{235}U	enr. ≤60% ≤ 35,320g Uranium
"A package used for shipment of fissile material must be so designed and constructed and its contents so limited that under the tests specified in §71.73 (Hypothetical Accident Conditions) the package would be subcritical. For this determination, it must be assumed that:" (Paragraph "e")	$k_{eff} + 2\sigma \leq 0.8912$ (hcsrbmt12_36_1_15)					
(1) the fissile material is in the most reactive credible configuration consistent with the chemical and physical form of the contents,	A mixture of HEU metal and water is homogenized over the internal volume of the containment vessel. The amount of water in the flooded containment vessel is calculated on the basis that the convenience can steel is replaced with water. Can pads and spacers not used.					
(2) water moderation occurs to the most reactive credible extent consistent with the chemical and physical form of content,	flooding of the package					
(3) there is full reflection by water on all sides, as close as is consistent with the damage condition of the package.	30.48 cm H_2O surrounding the reduced diameter drum (d = 17.20 in., h = 43.5 in.)					

Table 6.1c. Summary of criticality evaluation for solid HEU metal of unspecified geometric shapes characterized as broken metal

Conditions	95% < enr. ≤ 100% ≤ 25,894g ^{235}U	90% < enr. ≤95% ≤ 27,252g ^{235}U	80% < enr. ≤90% ≤ 28,334g ^{235}U	70% < enr. ≤80% ≤ 28,184g ^{235}U	60% < enr. ≤70% ≤ 24,693g ^{235}U	enr. ≤60% ≤ 35,320g Uranium
Standards for arrays of fissile material packages (§71.59)						
" . . . the designer of a fissile material package shall derive a number "N" based on all the following conditions being satisfied, assuming packages are stacked together in any arrangement and with close reflection on all sides of the stack by water: " (Paragraph "a")						
Transport index based on nuclear criticality control, CSI = 0.0	**can spacers are required**	**can spacers are required**	**can spacers are required**	**load-limited to 2,967g ^{235}U no can spacers**	**load-limited to 3,249g ^{235}U no can spacers**	**load-limited to 5,577g Uranium no can spacers**
(1) five times "N" undamaged packages with nothing between the packages would be subcritical,	Not applicable	Not applicable	Not applicable	$k_{eff} + 2\sigma \leq 0.9213$ nciabmt11_4_1_5_3	$k_{eff} + 2\sigma \leq 0.9207$ nciabmt11_5_1_4_3	$k_{eff} + 2\sigma \leq 0.9152$ nciabmt11_6_1_3_3
(2) two times "N" damaged packages, if each package were subject to the tests specified in §71.73 (Hypothetical Accident Conditions) would be subcritical with optimum interspersed hydrogenous moderation,	Not applicable	Not applicable	Not applicable	$k_{eff} + 2\sigma \leq 0.9248$ hciabmt12_4_1_5_3	$k_{eff} + 2\sigma \leq 0.9235$ hciabmt12_5_1_4_3	$k_{eff} + 2\sigma \leq 0.9127$ hciabmt12_6_1_3_3
(3) the value of "N" cannot be <0.5.	Not applicable	Not applicable	Not applicable	N(1,2) = ∞	same	same

Table 6.1c. Summary of criticality evaluation for solid HEU metal of unspecified geometric shapes characterized as broken metal

Conditions	95% < enr. ≤ 100% ≤ 25,894g ^{235}U	90% < enr. ≤95% ≤ 27,252g ^{235}U	80% < enr. ≤90% ≤ 28,334g ^{235}U	70% < enr. ≤80% ≤ 28,184g ^{235}U	60% < enr. ≤70% ≤ 24,693g ^{235}U	enr. ≤60% ≤ 35,320g Uranium
Transport index based on nuclear criticality control, CSI = 0.0	**load-limited to 2,774g ^{235}U can spacers**	**load-limited to 3,516g ^{235}U can spacers**	**load-limited to 3,333g ^{235}U can spacers**	**load-limited to 4,450g ^{235}U can spacers**	**load-limited to 5,198g ^{235}U can spacers**	**load-limited to 11,154g Uranium can spacers**
(1) five times "N" undamaged packages ...	$k_{eff} + 2\sigma \leq 0.9041$ nciabmt11_3_2_8_3	$k_{eff} + 2\sigma \leq 0.9199$ nciabmt11_4_2_7_3	$k_{eff} + 2\sigma \leq 0.9084$ nciabmt11_4_2_6_3	$k_{eff} + 2\sigma \leq 0.9224$ nciabmt11_6_2_5_3	$k_{eff} + 2\sigma \leq 0.9218$ nciabmt11_8_2_4_3	$k_{eff} + 2\sigma \leq 0.9181$ nciabmt11_12_2_3_3
(2) two times "N" damaged packages, ...	$k_{eff} + 2\sigma \leq 0.9050$ hciabmt12_3_2_8_3	$k_{eff} + 2\sigma \leq 0.9237$ hciabmt12_4_2_7_3	$k_{eff} + 2\sigma \leq 0.9091$ hciabmt12_4_2_6_3	$k_{eff} + 2\sigma \leq 0.9230$ hciabmt12_6_2_5_3	$k_{eff} + 2\sigma \leq 0.9209$ hciabmt12_8_2_4_3	$k_{eff} + 2\sigma \leq 0.9205$ hciabmt12_12_2_3_3
(3) the value of "N" ...	N(1,2) = ∞	same	same	same	same	same
Transport index based on nuclear criticality control, CSI = 0.4	**can spacers are required**	**can spacers are required**	**can spacers are required**	**load-limited to 5,192g ^{235}U no can spacers**	**load-limited to 5,848g ^{235}U no can spacers**	**load-limited to 14,872g Uranium no can spacers**
(1) five times "N" undamaged packages	Not applicable	Not applicable	Not applicable	$k_{eff} + 2\sigma \leq 0.9235$ ncf1bmt11_7_1_5_3	$k_{eff} + 2\sigma \leq 0.9216$ ncf1bmt11_9_1_4_3	$k_{eff} + 2\sigma \leq 0.9225$ ncf1bmt11_15_1_3_3
(2) two times "N" damaged packages, ...	Not applicable	Not applicable	Not applicable	$k_{eff} + 2\sigma \leq 0.9064$ hcf2bmt12_8_1_5_3	$k_{eff} + 2\sigma \leq 0.9118$ hcf2bmt12_12_1_4_3	$k_{eff} + 2\sigma \leq 0.9072$ hcf2bmt12_18_1_3_3
(3) the value of "N" ...	Not applicable	Not applicable	Not applicable	N(1,2) = 202/162	same	same
Transport index based on nuclear criticality control, CSI = 0.4	**load-limited to 5,549g ^{235}U can spacers**	**load-limited to 6,154g ^{235}U can spacers**	**load-limited to 7,500g ^{235}U can spacers**	**load-limited to 8,900g ^{235}U can spacers**	**load-limited to 12,996g ^{235}U can spacers**	**load-limited to 28,813g Uranium can spacers**
(1) five times "N" undamaged packages	$k_{eff} + 2\sigma \leq 0.9241$ ncf1bmt11_6_2_8_3	$k_{eff} + 2\sigma \leq 0.9220$ ncf1bmt11_7_2_7_3	$k_{eff} + 2\sigma \leq 0.9203$ ncf1bmt11_9_2_6_3	$k_{eff} + 2\sigma \leq 0.9187$ ncf1bmt11_12_2_5_3	$k_{eff} + 2\sigma \leq 0.9245$ ncf1bmt11_19_2_4_3	$k_{eff} + 2\sigma \leq 0.9235$ ncf1bmt11_29_2_3_3
(2) two times "N" damaged packages, ...	$k_{eff} + 2\sigma \leq 0.9244$ hcf2bmt12_8_2_8_3	$k_{eff} + 2\sigma \leq 0.9232$ hcf2bmt12_11_2_7_3	$k_{eff} + 2\sigma \leq 0.9192$ hcf2bmt12_12_2_6_3	$k_{eff} + 2\sigma \leq 0.8964$ hcf2bmt12_12_2_5_3	$k_{eff} + 2\sigma \leq 0.9005$ hcf2bmt12_19_2_4_3	$k_{eff} + 2\sigma \leq 0.9112$ hcf2bmt12_36_2_3_3
(3) the value of "N"	N(1,2) = 202/162	same	same	same	same	same

Table 6.1c. Summary of criticality evaluation for solid HEU metal of unspecified geometric shapes characterized as broken metal

Conditions	95% < enr. ≤ 100% ≤ 25,894g ^{235}U	90% < enr. ≤95% ≤ 27,252g ^{235}U	80% < enr. ≤90% ≤ 28,334g ^{235}U	70% < enr. ≤80% ≤ 28,184g ^{235}U	60% < enr. ≤70% ≤ 24,693g ^{235}U	enr. ≤60% ≤ 35,320g Uranium
Transport index based on nuclear criticality control, CSI = 0.8	**can spacers are required**	**can spacers are required**	**can spacers are required**	**load-limited to 8,900g ^{235}U no can spacers**	**load-limited to 13,646g ^{235}U no can spacers**	**load-limited to 28,814g Uranium no can spacers**
(1) five times "N" undamaged packages	Not applicable	Not applicable	Not applicable	$k_{eff} + 2\sigma \leq 0.9216$ ncf2bmt11_12_1_5_3	$k_{eff} + 2\sigma \leq 0.9234$ ncf2bmt11_20_1_4_3	$k_{eff} + 2\sigma \leq 0.9205$ ncf2bmt11_29_1_3_3
(2) two times "N" damaged packages, ...	Not applicable	Not applicable	Not applicable	$k_{eff} + 2\sigma \leq 0.9012$ hcf3bmt12_12_1_5_3	$k_{eff} + 2\sigma \leq 0.9065$ hcf3bmt12_20_1_4_3	$k_{eff} + 2\sigma \leq 0.9022$ hcf3bmt12_29_1_3_3
(3) the value of "N"	Not applicable	Not applicable	Not applicable	same	same	same
Transport index based on nuclear criticality control, CSI = 0.8	**load-limited to 9,248g ^{235}U can spacers**	**load-limited to 10,549g ^{235}U can spacers**	**load-limited to 12,500g ^{235}U can spacers**	**load-limited to 16,317g ^{235}U can spacers**	**load-limited to 20,793g ^{235}U can spacers**	**35,320g Uranium can spacers**
(1) five times "N" undamaged packages	$k_{eff} + 2\sigma \leq 0.9233$ ncf2bmt11_10_2_8_3	$k_{eff} + 2\sigma \leq 0.9221$ ncf2bmt11_12_2_7_3	$k_{eff} + 2\sigma \leq 0.9220$ ncf2bmt11_14_2_6_3	$k_{eff} + 2\sigma \leq 0.9193$ ncf2bmt11_21_2_5_3	$k_{eff} + 2\sigma \leq 0.9233$ ncf2bmt11_30_2_4_3	$k_{eff} + 2\sigma \leq 0.9064$ ncf2bmt11_36_2_3_3
(2) two times "N" damaged packages, ...	$k_{eff} + 2\sigma \leq 0.9090$ hcf3bmt12_10_2_8_3	$k_{eff} + 2\sigma \leq 0.9005$ hcf3bmt12_12_2_7_3	$k_{eff} + 2\sigma \leq 0.9042$ hcf3bmt12_14_2_6_3	$k_{eff} + 2\sigma \leq 0.9022$ hcf3bmt12_21_2_5_3	$k_{eff} + 2\sigma \leq 0.9019$ hcf3bmt12_30_2_4_3	$k_{eff} + 2\sigma \leq 0.8850$ hcf3bmt12_36_2_3_3
(3) the value of "N"	N(1,2) = 64/73	same	same	same	same	same
Transport index based on nuclear criticality control, CSI = 2.0 *	**can spacers are required**	**can spacers are required**	**can spacers are required**	**load-limited to 17,059g ^{235}U no can spacers**	**load-limited to 21,444g ^{235}U no can spacers**	**35,320g Uranium no can spacers**
(1) five times "N" undamaged packages	Not applicable	Not applicable	Not applicable	$k_{eff} + 2\sigma \leq 0.9223$ ncf3bmt11_22_1_5_3	$k_{eff} + 2\sigma \leq 0.9216$ ncf3bmt11_31_1_4_3	$k_{eff} + 2\sigma \leq 0.9045$ ncf3bmt11_36_1_3_3
(2) two times "N" damaged packages, ...	Not applicable	Not applicable	Not applicable	$k_{eff} + 2\sigma \leq 0.8852$ hcf4bmt12_22_1_5_3	$k_{eff} + 2\sigma \leq 0.8858$ hcf4bmt12_31_1_4_3	$k_{eff} + 2\sigma \leq 0.8705$ hcf4bmt12_36_1_3_3
(3) the value of "N"	Not applicable	Not applicable	Not applicable	N(1,2) = 29/25	same	same

Table 6.1c. Summary of criticality evaluation for solid HEU metal of unspecified geometric shapes characterized as broken metal

Conditions	95% < enr. ≤ 100% ≤ 25,894g ^{235}U	90% < enr. ≤95% ≤ 27,252g ^{235}U	80% < enr. ≤90% ≤ 28,334g ^{235}U	70% < enr. ≤80% ≤ 28,184g ^{235}U	60% < enr. ≤70% ≤ 24,693g ^{235}U	enr. ≤60% ≤ 35,320g Uranium
Transport index based on nuclear criticality control, CSI = 2.0 *	**load-limited to 13,872g ^{235}U can spacers**	**load-limited to 18,461g ^{235}U can spacers**	**load-limited to 20,000g ^{235}U can spacers**	**load-limited to 25,218g ^{235}U can spacers**	**24,692g ^{235}U can spacers**	**35,320g Uranium can spacers**
(1) five times "N" undamaged packages	$k_{eff} + 2\sigma \leq 0.9204$ ncf3bmt11_14_2_8_3	$k_{eff} + 2\sigma \leq 0.9239$ ncf3bmt11_20_2_7_3	$k_{eff} + 2\sigma \leq 0.9213$ ncf3bmt11_23_2_6_3	$k_{eff} + 2\sigma \leq 0.9216$ ncf3bmt11_32_2_5_3	$k_{eff} + 2\sigma \leq 0.9035$ ncf3bmt11_36_2_4_3	$k_{eff} + 2\sigma \leq 0.8745$ ncf3bmt11_36_2_3_3
(2) two times "N" damaged packages, ...	$k_{eff} + 2\sigma \leq 0.8877$ hcf4bmt12_14_2_8_3	$k_{eff} + 2\sigma \leq 0.8914$ hcf4bmt12_20_2_7_3	$k_{eff} + 2\sigma \leq 0.8851$ hcf4bmt12_23_2_6_3	$k_{eff} + 2\sigma \leq 0.8884$ hcf4bmt12_32_2_5_3	$k_{eff} + 2\sigma \leq 0.8684$ hcf4bmt12_36_2_4_3	$k_{eff} + 2\sigma \leq 0.8412$ hcf4bmt12_36_2_3_3
(3) the value of "N"	N(1,2) = 29/25	same	same	same	same	same
Transport index based on nuclear criticality control, CSI = 3.2 **	**can spacers are required**	**can spacers are required**	**can spacers are required**	**load-limited to 27,443g ^{235}U no can spacers**	**24,692g ^{235}U no can spacers**	**35,320g Uranium no can spacers**
(1) five times "N" undamaged packages	Not applicable	Not applicable	Not applicable	$k_{eff} + 2\sigma \leq 0.9226$ ncf5bmt11_35_1_5_3	$k_{eff} + 2\sigma \leq 0.9030$ ncf5bmt11_36_1_4_3	$k_{eff} + 2\sigma \leq 0.8743$ ncf5bmt11_36_1_3_3
(2) two times "N" damaged packages, ...	Not applicable	Not applicable	Not applicable	$k_{eff} + 2\sigma \leq 0.9052$ hcf5bmt12_35_1_5_3	$k_{eff} + 2\sigma \leq 0.8819$ hcf5bmt12_36_1_4_3	$k_{eff} + 2\sigma \leq 0.8542$ hcf5bmt12_36_1_3_3
(3) the value of "N"	Not applicable	Not applicable	Not applicable	N(1,2) = 16/24	same	same
Transport index based on nuclear criticality control, CSI = 3.2 **	**load-limited to 24,969g ^{235}U can spacers**	**load-limited to 26,373g ^{235}U can spacers**	**28,334g ^{235}U can spacers**	**28,184g ^{235}U can spacers**	**24,692g ^{235}U can spacers**	**35,320g Uranium can spacers**
(1) five times "N" undamaged packages	$k_{eff} + 2\sigma \leq 0.9249$ ncf5bmt11_25_2_8_3	$k_{eff} + 2\sigma \leq 0.9196$ ncf5bmt11_28_2_7_3	$k_{eff} + 2\sigma \leq 0.9246$ ncf5bmt11_35_2_6_3	$k_{eff} + 2\sigma \leq 0.8974$ ncf5bmt11_36_2_5_3	$k_{eff} + 2\sigma \leq 0.8736$ ncf5bmt11_36_2_4_3	$k_{eff} + 2\sigma \leq 0.8445$ ncf5bmt11_36_2_3_3
(2) two times "N" damaged packages, ...	$k_{eff} + 2\sigma \leq 0.9089$ hcf5bmt12_25_2_8_3	$k_{eff} + 2\sigma \leq 0.8981$ hcf5bmt12_28_2_7_3	$k_{eff} + 2\sigma \leq 0.9032$ hcf5bmt12_35_2_6_3	$k_{eff} + 2\sigma \leq 0.8804$ hcf5bmt12_36_2_5_3	$k_{eff} + 2\sigma \leq 0.8532$ hcf5bmt12_36_2_4_3	$k_{eff} + 2\sigma \leq 0.8265$ hcf5bmt12_36_2_3_3
(3) the value of "N"	N(1,2) = 16/24	same	same	same	same	same

* Neutron multiplication factors and "N" are shown for an NCT array size of 7×7×3 and an HAC array size of 5×5×2; both arrays are nearly cubic arrangements. An HAC array size is not available for CSI=1.8; therefore, CSI for NCT at 1.8 is rounded up to 2.0 as shown.

** Neutron multiplication factors and "N" are shown for an NCT array size of 27×3 and an HAC array size of 16×3; where packages in the planar dimension are in explicit triangular-pitch arrangement and stacked three high in the vertical direction. An NCT array size of 81 packages gives a CSI value of 3.12 (50/16), while an HAC array size of 48 packages gives a CSI value of 2.08 (50/24). The specified CSI value of 3.2 is the larger of the two numbers rounded up to the nearest tenth decimal place as shown.

Table 6.1d. Summary of criticality evaluation for HEU product and skull oxide

Conditions	HEU product oxide ≤ 21,125g ^{235}U	HEU skull oxide ≤ 15,673g ^{235}U and ≤ 921g C
General requirements for each fissile package (§71.55)		
"A package used for shipment of fissile material must be so designed and constructed and its contents so limited that it would be subcritical if water were to leak into the containment system, . . . so that under the following conditions, maximum reactivity of the fissile material would be attained:" (Paragraph "b")	$k_{eff} + 2\sigma \leq 0.9143$ (cvcrpdoxt11_1_3_24_15)	$k_{eff} + 2\sigma \leq 0.8497$ (cvcrsk3cc_9_15_17)
(1) the most reactive credible configuration consistent with the chemical and physical form of the material,	HEU oxide at the bulk density is assumed dispersed in the containment vessel, where the oxide fills the containment vessel to a height determined by the oxide mass. The oxide is saturated with water. Water fills the void region above the oxide content, but this amount of water is reduced by an amount equivalent to the volume occupied by can spacers. The can pads, spacer can, and convenience can steel are replaced by water. See Sect. 6.9.3.1 for justification of the content model.	same
(2) moderation by water to the most reactive credible extent,	flooding of the containment vessel	same
(3) close full reflection of the containment system by water on all sides, or such greater reflection of the containment system as may be provided by the surrounding material of the packaging.	30.48 cm H_2O surrounding the containment vessel	same

Table 6.1d. Summary of criticality evaluation for HEU product and skull oxide

Conditions	HEU product oxide ≤ 21,125g ^{235}U	HEU skull oxide ≤ 15,673g ^{235}U and ≤ 921g C
"A package used for shipment of fissile material must be so designed and constructed and its contents so limited under the tests specified in §71.71 (Normal Conditions of Transport) . . ." (Paragraph "d")		
(1) the contents would be subcritical,	$k_{eff} + 2\sigma \leq 0.8166$ (ncsrpdoxt11_1_3_24)	$k_{eff} + 2\sigma \leq 0.7410$ (ncsrsk_9_15)
(2) the geometric form of the package contents would not be substantially altered,	HEU oxide at the bulk density is assumed dispersed in the containment vessel, where the oxide fills the containment vessel to a height determined by the oxide mass. The oxide is saturated with water. Water fills the void region above the oxide content, but this amount of water is reduced by an amount equivalent to the volume occupied by can spacers. The can pads, spacer can, and convenience can steel are replaced by water.	same
(3) there would be no leakage of water into the containment system unless, in the evaluation of undamaged packages under §71.59(a)(1), it has been assumed that moderation is present to such an extent as to cause maximum reactivity consistent with the chemical and physical form of the material,	moderation is present to such an extent as to cause maximum reactivity	same
(4) there will be no substantial reduction in the effectiveness of the packaging	30.48 cm H_2O surrounding the drum (d = 18.37 in., h = 43.5 in.)	same

Table 6.1d. Summary of criticality evaluation for HEU product and skull oxide

Conditions	HEU product oxide ≤ 21,125g ^{235}U	HEU skull oxide ≤ 15,673g ^{235}U and ≤ 921g C
"A package used for shipment of fissile material must be so designed and constructed and its contents so limited that under the tests specified in §71.73 (Hypothetical Accident Conditions) the package would be subcritical. For this determination, it must be assumed that:" (Paragraph "e")	$k_{eff} + 2\sigma \leq 0.8187$ (hcsrpdoxt12_1_3_24)	$k_{eff} + 2\sigma \leq 0.7410$ (hcsrsk_9_15)
(1) the fissile material is in the most reactive credible configuration consistent with the chemical and physical form of the contents,	HEU oxide at the bulk density is assumed dispersed in the containment vessel, where the oxide fills the containment vessel to a height determined by the oxide mass. The oxide is saturated with water. Water fills the void region above the oxide content, but this amount of water is reduced by an amount equivalent to the volume occupied by can spacers. The can pads, spacer can, and convenience can steel are replaced by water.	same
(2) water moderation occurs to the most reactive credible extent consistent with the chemical and physical form of content,	flooding of the package	same
(3) there is full reflection by water on all sides, as close as is consistent with the damage condition of the package.	30.48 cm H_2O surrounding the reduced diameter drum, (d = 17.20 in., h = 43.5 in.)	same

Table 6.1d. Summary of criticality evaluation for HEU product and skull oxide

Conditions	HEU product oxide ≤ 21,125g ^{235}U	HEU skull oxide ≤ 15,673g ^{235}U and ≤ 921g C
Standards for arrays of fissile material packages (§71.59)		
" . . . the designer of a fissile material package shall derive a number "N" based on all the following conditions being satisfied, assuming packages are stacked together in any arrangement and with close reflection on all sides of the stack by water: " (Paragraph "a")		
Transport index based on nuclear criticality control, CSI = 0.0	**load-limited to 9,682g ^{235}U no can spacers**	**load-limited to 15,673g ^{235}U no can spacers**
(1) five times "N" undamaged packages with nothing between the packages would be subcritical,	$k_{eff} + 2\sigma \leq 0.9201$ nciapdoxt11_1_1_11_3	$k_{eff} + 2\sigma \leq 0.7562$ nciask_9_15
(2) two times "N" damaged packages, if each package were subject to the tests specified in §71.73 (Hypothetical Accident Conditions) would be subcritical with optimum interspersed hydrogenous moderation,	$k_{eff} + 2\sigma \leq 0.9247$ hciapdoxt12_1_1_11_3	$k_{eff} + 2\sigma \leq 0.7599$ hciask_9_15
(3) the value of "N" cannot be <0.5.	$N(1,2) = \infty$	same

Table 6.1e. Summary of criticality evaluation for UNX crystals and unirradiated TRIGA reactor fuel elements

Conditions	UNX crystals ≤ 11,303g ^{235}U	unirradiated TRIGA fuel elements ≤ 921g ^{235}U
General requirements for each fissile package (§71.55)		
"A package used for shipment of fissile material must be so designed and constructed and its contents so limited that it would be subcritical if water were to leak into the containment system, . . . so that under the following conditions, maximum reactivity of the fissile material would be attained:" (Paragraph "b")	$k_{eff} + 2\sigma \leq 0.8630$ (cvcrpunhct11_10_15)	$k_{eff} + 2\sigma \leq 0.5274$ (cvcrtriga_1_15)
(1) the most reactive credible configuration consistent with the chemical and physical form of the material,	UNX crystals are homogenized with water over the internal volume of the containment vessel consistent with the high solubility properties of UNX. Can spacers are not used. Hydrogenous packing material represented by 500 g.	Three 5-in tall sectioned pieces of $UZrH_x$ from a cylindrical TRIGA fuel element per convenience can. Sectioned pieces arranged in triangular pitch. No can spacers. Convenience can steel replaced by water.
(2) moderation by water to the most reactive credible extent,	flooding of the containment vessel	same
(3) close full reflection of the containment system by water on all sides, or such greater reflection of the containment system as may be provided by the surrounding material of the packaging.	30.48 cm H_2O surrounding the containment vessel	same

Table 6.1e. Summary of criticality evaluation for UNX crystals and unirradiated TRIGA reactor fuel elements

Conditions	UNX crystals ≤ 11,303g ^{235}U	unirradiated TRIGA fuel elements ≤ 921g ^{235}U
"A package used for shipment of fissile material must be so designed and constructed and its contents so limited under the tests specified in §71.71 (Normal Conditions of Transport) . . ." (Paragraph "d")		
(1) the contents would be subcritical,	$k_{eff} + 2\sigma \leq 0.7526$ (ncsrpunhct11_8_15)	$k_{eff} + 2\sigma \leq 0.4950$ (ncsrtriga_1_15_15)
(2) the geometric form of the package contents would not be substantially altered,	UNX crystals are homogenized with water over the internal volume of the containment vessel consistent with the high solubility properties of UNX. Can spacers are not used. Hydrogenous packing material represented by 500 g.	Three 5-in tall sectioned pieces of $UZrH_x$ from a cylindrical TRIGA fuel element per convenience can. Sectioned pieces arranged in triangular pitch. No can spacers. Convenience can steel replaced by water.
(3) there would be no leakage of water into the containment system unless, in the evaluation of undamaged packages under §71.59(a)(1), it has been assumed that moderation is present to such an extent as to cause maximum reactivity consistent with the chemical and physical form of the material,	moderation is present to such an extent as to cause maximum reactivity	same
(4) there will be no substantial reduction in the effectiveness of the packaging	30.48 cm H_2O surrounding the drum (d = 18.37 in., h = 43.5 in.)	same

Table 6.1e. Summary of criticality evaluation for UNX crystals and unirradiated TRIGA reactor fuel elements

Conditions	UNX crystals ≤ 11,303g ^{235}U	unirradiated TRIGA fuel elements ≤ 921g ^{235}U
"A package used for shipment of fissile material must be so designed and constructed and its contents so limited that under the tests specified in §71.73 (Hypothetical Accident Conditions) the package would be subcritical. For this determination, it must be assumed that:" (Paragraph "e")	$k_{eff} + 2\sigma \leq 0.8144$ (icsrpunhct12_15_15)	$k_{eff} + 2\sigma \leq 0.4945$ (hcsrtriga_1_15_15)
(1) the fissile material is in the most reactive credible configuration consistent with the chemical and physical form of the contents,	UNX crystals are homogenized with water over the internal volume of the containment vessel consistent with the high solubility properties of UNX. Can spacers are not used. Hydrogenous packing material represented by 500 g.	Three 5-in tall sectioned pieces of $UZrH_x$ from a cylindrical TRIGA fuel element per convenience can. Sectioned pieces arranged in triangular pitch. No can spacers. Convenience can steel replaced by water.
(2) water moderation occurs to the most reactive credible extent consistent with the chemical and physical form of content,	flooding of the package	same
(3) there is full reflection by water on all sides, as close as is consistent with the damage condition of the package.	30.48 cm H_2O surrounding the reduced diameter drum, (d = 17.20 in., h = 43.5 in.)	same

Table 6.1e. Summary of criticality evaluation for UNX crystals and unirradiated TRIGA reactor fuel elements

Conditions	UNX crystals ≤ 11,303g ^{235}U	unirradiated TRIGA fuel elements ≤ 921g ^{235}U
Standards for arrays of fissile material packages (§71.59)		
" . . . the designer of a fissile material package shall derive a number "N" based on all the following conditions being satisfied, assuming packages are stacked together in any arrangement and with close reflection on all sides of the stack by water: " (Paragraph "a")		
Transport index based on nuclear criticality control, CSI = 0.0	**load-limited to 3297g ^{235}U no can spacers**	**no can spacers**
(1) five times "N" undamaged packages with nothing between the packages would be subcritical,	$k_{eff} + 2\sigma \leq 0.9199$ nciapunhct11_7_3	$k_{eff} + 2\sigma \leq 0.5254$ nciatriga_1_15_3
(2) two times "N" damaged packages, if each package were subject to the tests specified in §71.73 (Hypothetical Accident Conditions) would be subcritical with optimum interspersed hydrogenous moderation,	$k_{eff} + 2\sigma \leq 0.9180$ hciapunhct12_7_3	$k_{eff} + 2\sigma \leq 0.5261$ hciatriga_1_15_3
(3) the value of "N" cannot be <0.5.	$N(1,2) = \infty$	same
Transport index based on nuclear criticality control, CSI = 0.0	**can spacers**	**can spacers**
(1) five times "N" undamaged packages	**not applicable**	$k_{eff} + 2\sigma \leq 0.4421$ nciatriga_2_15_3
(2) two times "N" damaged packages, ...	**not applicable**	$k_{eff} + 2\sigma \leq 0.4427$ hciatriga_2_15_3
(3) the value of "N"	**not applicable**	$N(1,2) = \infty$

Table 6.1e. Summary of criticality evaluation for UNX crystals and unirradiated TRIGA reactor fuel elements

Conditions	UNX crystals ≤ 11,303g ^{235}U	unirradiated TRIGA fuel elements ≤ 921g ^{235}U
Transport index based on nuclear criticality control, CSI = 0.4	**load-limited to 11,303g ^{235}U no can spacers**	**no can spacers**
(1) five times "N" undamaged packages	$k_{eff} + 2\sigma \leq 0.8730$ ncf1punhct11_24_3	bounded by CSI=0
(2) two times "N" damaged packages, ...	$k_{eff} + 2\sigma \leq 0.8423$ hcf2punhct12_24_3	bounded by CSI=0
(3) the value of "N"	N(1,2) = 202/162	same
Transport index based on nuclear criticality control, CSI = 0.4	**can spacers**	**can spacers**
(1) five times "N" undamaged packages	**not applicable**	bounded by CSI=0
(2) two times "N" damaged packages, ...	**not applicable**	bounded by CSI=0
(3) the value of "N"	**not applicable**	N(1,2) = 202/162

Table 6.2a. HEU fissile material mass loading limits (case name) for surface-only modes of transportation

Solid HEU metal of specified geometric shapes						
Transport index based on nuclear criticality control	**cylinders (d ≤ 3.24 in.)**	**cylinders (3.24 in. < d ≤ 4.25 in.)**	**bars**	**slugs [a] enr. ≤ 95%**	**slugs [b] 80% < enr. ≤ 95%**	**slugs [b] enr. ≤ 80%**
No can spacers						
CSI = 0.0	18,000 g ^{235}U (nciacyt11_18_1_3)	15,000 g ^{235}U (nciacyct11_15_1_3)	30,000 g ^{235}U (hciasqt12_30_1_3)	17,374 g ^{235}U (ncia5st11_1_1_7_3)	-	-
With can spacers						
CSI = 0.0	30,000 g ^{235}U (nciacyt11_30_2_3)	25,000 g ^{235}U (nciacyct11_25_2_3)	36,000 g ^{235}U (nciasqt11_36_2_3)	-	24,324 g ^{235}U (hcia70st12_2_7_3)	29,318 g ^{235}U (hcia5est12_2_2_5_3)
CSI = 0.4	-	-	-	-	34,749 g ^{235}U [b] (ncf15est11_2_2_7_3)	29,318 g ^{235}U (ncf15est11_2_2_5_3)
Solid HEU metal of unspecified geometric shapes characterized as broken metal [d]						
Transport index based on nuclear criticality control	**95% < enr. ≤ 100%**	**90% < enr. ≤95%**	**80% < enr. ≤90%**	**70% < enr. ≤80%**	**60% < enr. ≤70%**	**enr. ≤60%**
No can spacers						
CSI = 0.0	can spacers required	can spacers required	can spacers required	2,967 g ^{235}U (hciabmt12_4_1_5_3)	3,249 g ^{235}U (hciabmt12_5_1_4_3)	5,576 g Uranium (nciabmt11_6_1_3_3)
CSI = 0.4	can spacers required	can spacers required	can spacers required	5,192 g ^{235}U (ncf1bmt11_7_1_5_3)	5,848 g ^{235}U (ncf1bmt11_9_1_4_3)	14,872 g Uranium (ncf1bmt11_15_1_3_3)
CSI = 0.8	can spacers required	can spacers required	can spacers required	8,900 g ^{235}U (ncf2bmt11_12_1_5_3)	13,646 g ^{235}U (ncf2bmt11_20_1_4_3)	28,814 g Uranium (ncf2bmt11_29_1_3_3)
CSI = 2.0	can spacers required	can spacers required	can spacers required	17,059 g ^{235}U (ncf3bmt11_22_1_5_3)	21,444 g ^{235}U (ncf3bmt11_31_1_4_3)	35,320 g Uranium (ncf3bmt11_36_1_3_3)
CSI = 3.2	can spacers required	can spacers required	can spacers required	27,692 g ^{235}U (ncf5bmt11_35_1_5_3)	24,692 g ^{235}U (ncf5bmt11_36_1_4_3)	35,320 g Uranium (ncf5bmt11_36_1_3_3)
With can spacers						
CSI = 0.0	2,774 g ^{235}U (hciabmt12_3_2_8_3)	3,516 g ^{235}U (hciabmt12_4_2_7_3)	3,333 g ^{235}U (hciabmt12_4_2_6_3)	4,450 g ^{235}U (hciabmt12_6_2_5_3)	5,198 g ^{235}U (nciabmt11_8_2_4_3)	11,154 g Uranium (hciabmt12_12_2_3_3)
CSI = 0.4	5,549 g ^{235}U (ncf1bmt11_6_2_8_3)	6,154 g ^{235}U (ncf1bmt11_7_2_7_3)	7,500 g ^{235}U (ncf1bmt11_9_2_6_3)	8,900 g ^{235}U (ncf1bmt11_12_2_5_3)	12,996 g ^{235}U (ncf1bmt11_19_2_4_3)	28,813 g Uranium (ncf1bmt11_29_2_3_3)
CSI = 0.8	9,248 g ^{235}U (ncf2bmt11_10_2_8_3)	10,549 g ^{235}U (ncf2bmt11_12_2_7_3)	12,500 g ^{235}U (ncf2bmt11_14_2_6_3)	16,317 g ^{235}U (ncf2bmt11_21_2_5_3)	20,793 g ^{235}U (ncf2bmt11_30_2_4_3)	35,320 g Uranium (ncf2bmt11_36_2_3_3)
CSI = 2.0	13,872 g ^{235}U (ncf3bmt11_14_2_8_3)	18,461 g ^{235}U (ncf3bmt11_20_2_7_3)	20,000 g ^{235}U (ncf3bmt11_23_2_6_3)	25,218 g ^{235}U (ncf3bmt11_32_2_5_3)	24,692 g ^{235}U (ncf3bmt11_36_2_4_3)	35,320 g Uranium (ncf3bmt11_36_2_3_3)
CSI = 3.2	24,969 g ^{235}U (ncf5bmt11_25_2_8_3)	26,373 g ^{235}U (ncf5bmt11_28_2_7_3)	28,334 g ^{235}U (ncf5bmt11_35_2_6_3)	28,184 g ^{235}U (ncf5bmt11_36_2_5_3)	24,692 g ^{235}U (ncf5bmt11_36_2_4_3)	35,320 g Uranium (ncf5bmt11_36_2_3_3)

Table 6.2a. HEU fissile material mass loading limits (case name) for surface-only modes of transportation

HEU oxide and UNX crystals					
Transport index based on nuclear criticality control	**HEU product oxide, no can spacers**	**HEU skull oxide, no can spacers**	**UNX crystals, no can spacers**	**unirradiated TRIGA fuel elements, no can spacers [c]**	
				20% enrichment	70% enrichment
CSI = 0.0	9,682 g ^{235}U (hciapdoxt12_1_1_11_3)	15,673 g ^{235}U and 921 g C (nciask_9_15)	3,297 g ^{235}U (nciapunhct11_7_3)	921 g ^{235}U (nciatriga_1_15_3)	408 g ^{235}U (nciatriga70_1_15_3)
CSI = 0.4	12,323 g ^{235}U [e] (5hcf2pdoxt12_1_1_11_3)	-	11,303 g ^{235}U (ncf1punhct11_24_3)	-	-

[a] When can spacers **are not** used, the mass limit = 17,374 g ^{235}U.
[b] When can spacers are used, a greater fissile mass limit is permissible based on enrichment. For CSI=0 and enrichments above 80 wt%, the fissile mass must be reduced below the volumetric limit. For CSI=0.4, fissile mass is volumetrically limited by the size of the slugs. Note that within a fixed volume, the HEU mass increases slightly with decreasing enrichment.
[c] For ground transport, TRIGA reactor fuel element content will be limited to three fuel sections ("meats") per loaded convenience can and up to three loaded cans per package. The TRIGA fuel content may also be configured as clad fuel rods, each rod derived from a single TRIGA fuel element. A ~15 inch long rod consists of the three fuel pellets and an exterior sheath of clad, where protruding clad at each end has been crimped in. Clad fuel rods will be packed into convenience cans, with a maximum of three fuel rods per loaded convenience can and one loaded can per containment vessel.
[d] Uranium/aluminum, uranium/molybdenum, and uranium/zirconium alloys may be loaded to the broken metal mass limits by assuming the mass of the alloy is all uranium.
[e] See Appendix 6.9.9.

Table 6.2b. HEU fissile material mass loading limits for air transport mode of transportation

Solid HEU metal of specified geometric shapes					
One per convenience can	**cylinders (d = 3.24 in.)**	**cylinders (3.24 < d ≤ 4.25 in.)**	**bars**	**slugs**	
	500g ^{235}U	500g ^{235}U	500g ^{235}U	500g ^{235}U	
Solid HEU metal of unspecified geometric shapes characterized as broken metal					
	enr. ≤ 20%			**20% < enr. ≤ 100%**	
	700g ^{235}U			500g ^{235}U	
HEU oxide, UNX crystals, unirradiated TRIGA fuel elements					
	HEU product oxide	**HEU skull oxide**	**UNX crystals**	**unirradiated TRIGA [a]**	
				20% enrichment	**70% enrichment**
	not allowed	**not allowed**	**not allowed**	716g ^{235}U	408g ^{235}U

[a] For air transport, TRIGA reactor fuel element content will be limited to fuel sections or clad fuel rods as described for surface-only modes of transportation in footnote "c" of Table 6.2a and the fissile mass limit specified herein, whichever is more limiting.

The oxide and compounds are packaged for air transport under limits specified in Table 6.2b for unirradiated TRIGA fuel elements. Per package limits for these items are a maximum of 716 g ^{235}U at enrichments not exceeding 20 wt% and a maximum of 408 g ^{235}U for content enrichments greater than 20 wt%.

The criticality evaluation demonstrates that the ES-3100 packaging with the HEU content satisfies the requirements for single packages and for arrays of fissile material packages when the packages are load-limited as specified in Tables 6.2a and 6.2b (reproduced in Table 1.3) under the conditions identified in Sect. 6.2.4.

6.1.3 Criticality Safety Index

A CSI is assigned to the Model ES-3100 package on the basis of an adequate margin of subcriticality for the single package and arrays of packages for both NCT and HAC. Values for the CSI given in Tables 6.2a and 6.2b (Table 1.3) are based on the uranium and the ^{235}U mass of the content and on the presence of 277-4 canned spacers as defined in Sect. 6.2.2.

The CSI is determined from bounding calculations using KENO V.a models of the containment vessel, the single package, and arrays of packages. (SCALE, Vol. 2, Sect. F11) It is a dimensionless number used to limit the number of packages in a conveyance for nuclear criticality safety control. The CSI is the larger of the CSI values for NCT and for HAC. For NCT, the CSI is equal to 50 divided by the allowable number of packages "N" that can be shipped, where the allowable number of packages is one-fifth of the maximum array size that is calculated to be subcritical. For HAC, the CSI is equal to 50 divided by the allowable number of packages "N" that can be shipped, where the allowable number of packages is one-half of the maximum array size that is calculated to be subcritical. The CSI is a calculated number rounded up to the nearest first decimal.

The array sizes examined in this evaluation are infinite, 13×13×6, 9×9×4, 7×7×3, 5×5×2, explicit triangular pitch (ETP) 27×3 for NCT, ETP 16×3 for HAC, and the degenerate single unit. For NCT, the "N" and corresponding CSI values for arrays determined to be adequately subcritical are as follows: N = ∞, CSI = 0; N = 202, CSI = 0.3; N = 64, CSI = 0.8; N = 29, CSI = 1.8; N = 10, CSI = 5.0; and N = 16, CSI = 3.2. For HAC, the "N" and corresponding CSI values for arrays determined to be adequately subcritical are as follows: N = ∞, CSI = 0; N = 507, CSI = 0.1; N =162, CSI = 0.4; N = 73, CSI = 0.7; N = 25, CSI = 2.0; and N = 24, CSI = 2.1. Absent an exact correspondence of CSI values for the NCT and HAC, the following arrays results were selected for rounded CSI values as indicated in Tables 6.1a–6.1d:

- infinite arrays evaluated for both NCT and HAC [designated as "(1,2)"], where N(1,2) = ∞ for a CSI = 0;
- 13×13×6 evaluated for NCT and 9×9×4 evaluated for HAC where N(1,2) = (202,162) for a CSI = 0.4;
- 9×9×4 evaluated for NCT and 7×7×3 evaluated for HAC where N(1,2) = (64,73) for a CSI = 0.8;
- 7×7×3 evaluated for NCT and 5×5×2 evaluated for HAC where N(1,2) = (29,25) for a CSI = 2.0; and
- 27×3 evaluated for NCT and 16×3 evaluated for HAC where N(1,2) = (16,24) for a CSI = 3.2.

6.2 PACKAGE CONTENTS

The **package content** is defined as the HEU fissile material, bottles, convenience cans, canned spacers, can pads, and the associated packing materials (plastic bags, pads, tape, etc.) inside the ES-3100 containment vessel.

6.2.1 Fissile Material Contents

The per-package HEU mass loadings considered in the criticality evaluation range from 1000 to 36,000 g for uranium metal and from 1000 to 24,000 g for uranium oxide and UNX crystals. The HEU mass may include nonradioactive contaminants and trace elements or materials in the HEU.

The bounding types of HEU content evaluated in this criticality analysis are 4.25-in.- and 3.24-in.-diam cylinders; 2.29-in.-square bars; 1.5-in.-diam × 2-in.-tall slugs; cubes ranging from 0.25 to 1 in. on a side; broken metal pieces of unspecified geometric shapes; skull oxide; uranium oxide; UNX crystals; and unirradiated TRIGA reactor fuel elements.

The term "broken metal pieces" is used to describe an HEU content without restrictions on shape or size other than a minimum size limit (spontaneous ignition), a maximum mass limit (criticality control), a minimum enrichment (the lower limit for HEU at 19 wt % ^{235}U in uranium), and the capacity limits of the convenience cans. The content geometry envelope encompasses regular, uniform shapes and sizes as well as irregular shapes and sizes.

The density of HEU metal ranges from 18.811 to 19.003 g/cm^3 for HEU metal, corresponding to enrichments ranging from 100 to 19 wt % ^{235}U. Theoretical (crystalline) densities for HEU oxide are 10.96 g/cm^3, 8.30 g/cm^3, and 7.29 g/cm^3 for UO_2, U_3O_8, and UO_3, respectively. However, bulk densities of product oxide are typically on the order of 2.0 to 6.54 g/cm^3. With increased moderation of fissile mass possible at these lower densities, only "less-than-theoretical" mass loadings would actually be achieved. Skull oxides are a mixture of U_3O_8 and graphite, having densities on the order of 2.44 g/cm^3 for poured material and 2.78 g/cm^3 for tamped (packed) material. Combined water saturation and crystallization of the HEU oxide is not expected in the HAC because UO_2 and UO_3 are non-hygroscopic and U_3O_8 is only mildly hygroscopic. The density of UNX crystals varies depending on the degree of hydration. The most reactive form of $UO_2(NO_3)\bullet xH_2O$ is with 6 molecules of hydration, having a density of 2.79 g/cm^3. UNX crystals are highly soluble in nitric acid and mildly soluble in water. Dissolution of UNX crystals in water is assumed in this criticality evaluation. The content geometry envelope encompasses both regular, uniform clumps and densities, and irregular clumps and densities.

The approximate 40 stock items of TRIGA fuel are cataloged as one of the four basic types: a standard element, an instrumented element, a fuel follower control rod, or a cluster assembly. The active region of TRIGA element consists of three 5-in long sections "fuel meats" of uranium zirconium hydride ($UZrH_x$). The "x" in $UZrH_x$ equals 1.6 in all cases except for two stock items where x = equals 1.0 and the fissile content is < 40 g ^{235}U. The clad thickness is ~0.02 inches for a TRIGA fuel element with stainless steel cladding and ~0.03 inches for an element with aluminum cladding.

Solid form TRIGA fuel is either 20 or 70 wt % enriched in ^{235}U and has specific dimensional characteristics for its designed function. For the 20 wt % enriched TRIGA elements, the active fuel diameters are 1.44 in., 1.41 in., 1.40 in., 1.37 in., 1.34 in., or 1.31 in. The uranium weight fractions are 45 wt %, 30 wt %, 20 wt %, 12 wt %, and 8.5 wt %. The TRIGA element with a maximum fissile content of 307 g ^{235}U in 1,560 g U is 45 wt% U in $UZrH_x$ and has a computed density of ~8.6 g/cm^3 (Appendix 6.9.3.1). For the 70 wt % enriched TRIGA fuel, the active fuel diameter is 1.44 inches in the standard element and instrumented element, and 1.31 inches in the fuel follower control rod. Both the

standard element and instrumented elements contain ~136 g ^{235}U in 194 g U while the fuel follower control rod contains ~113 g ^{235}U in 162 g U. The 70 wt % enriched TRIGA fuel is 8.5 wt% U in $UZrH_x$ and has a computed density of ~5.7 g/cm^3 (Appendix 6.9.3.1).

In preparation for shipment in the ES-3100, the unirradiated TRIGA fuel elements may be disassembled and the fuel sections removed from the thin-wall cladding. The TRIGA fuel may also be configured as clad fuel rods. Each clad fuel rod will be derived from a single TRIGA fuel element by removal of the stainless steel or aluminum clad beyond the plenum adjacent to the axial ends of the active fuel section. Each ~15 inch long rod consists of the 3 fuel pellets and an exterior sheath of clad, where the protruding clad at each end has been crimped in.

The 0.02 in thick sheath of stainless steel clad adds ~179 g to the mass of the active fuel for the standard element or instrumented element with 1.48 in. overall diameter, and ~163 g to active fuel mass for the fuel follower control rod with 1.35 in. overall diameter. Allowance for ½ in. of residual stainless steel crimped on each end of the clad fuel rod adds ~11 to 12 g stainless steel to these amounts. Likewise, the 0.03 in thick sheath of aluminum clad adds ~90 g to the mass of the active fuel for the 1.47 in. diameter standard element or instrumented element. Allowance for ½ in. of residual aluminum crimped on each end of the clad fuel rod adds ~6 g aluminum.

Skull oxides, uranium alloys of aluminum, molybdenum, or zirconium and unirradiated TRIGA reactor fuel elements are evaluated where composition data is for material in the as-manufactured condition. A maximum enrichment of 100 wt % is used for HEU metal, oxide and UNX crystals in the criticality calculations strictly for the purpose of maximizing reactivity, even though HEU enrichment ranges from 19 to 97.7 wt % ^{235}U. Although mass loading limits for oxide and crystals are based on 100% enrichment, the actual enrichment is expected to be less than the stated maximum, with the remainder of the uranium being primarily ^{238}U. The HEU mass may also include nonradioactive contaminants and trace elements or materials in the HEU.

No intact weapon part or component will be shipped in this package. Weapon parts or components that have been reduced to "broken metal pieces" or processed into HEU oxide and meet the additional content requirements identified in Sect. 6.2.4 may be shipped in this package.

6.2.2 Convenience Cans, Teflon and Polyethylene Bottles, and 277-4 Canned Spacers

HEU fissile material to be shipped in the ES-3100 package will be placed in stainless steel, tin-plated carbon steel, or nickel alloy convenience cans or polyethylene or Teflon bottles. Can lids may be welded, press fit, slip lid, or crimp seal types; bottle lids are screw cap type. Convenience cans and bottles are used to hold the HEU for shipment in the ES-3100 package and to assure that the inside of the containment vessel does not become contaminated with HEU under NCT. The HEU metal or oxide content may be wrapped or bagged in polyethylene, and the convenience cans may also be wrapped in polyethylene to further reduce the possibility of radioactive contamination of the packaging. Nylon straps may be used for handling the nickel alloy cans. Masses of the convenience cans and packing materials are in addition to the fissile material mass.

Three 4.25-in.-diam × 10.0-in.-tall or six 4.25-in.-diam × 4.88-in.-tall convenience cans, separated by can pads, may be placed inside the 31-in.-tall cavity of the ES-3100 containment vessel (Fig. 1.4). The convenience cans may have press-fit or crimp-seal lids. The size of solid content placed inside a convenience can is physically limited by both the can opening and the usable height of the convenience can. Other can arrangements fit inside the containment vessel, such as three 4.25-in.-diam × 8.75-in.-tall convenience cans or five 4.25-in.-diam × 4.88-in.-tall convenience cans. Both of these can arrangements include can pads and 277-4 canned spacers. Nickel alloy cans to

be used exclusively for HEU oxide content are ~3-in. diam × 4.75-in. tall. Three Teflon bottles (4.69-in. diam × 9.4-in. tall) or three polyethylene bottles (4.94-in. diam × 8.76-in. tall) fit inside the containment vessel; however, 277-4 canned spacers are not used with these configurations.

A modified convenience can may be used to package the TRIGA components that do not fit inside these containers. A 17.5 in.-tall convenience can is constructed from two 4.25-in.-diam × 8.75-in.-tall cans brazed together.

The can pad and 277-4 canned spacer have overall dimensions of 4.25-in. diam × 1.82-in. height (Drawing M2E801580A026 or M2E801580A043, Appendix 1.4.8). A carbon steel or stainless-steel spacer can with a lid has a usable cavity with dimensions of 4.13-in. diam × 1.37-in. height, which nominally allows for ~510 g of neutron poison material.

6.2.3 Packing Materials

Polyethylene bags may be used for contamination control to hold the HEU material that is packed into a convenience can. Realistically, the number of polyethylene bags used to bag content and wrap a convenience can would be six bags at most. Given that each bag weighs ~28 g, this results in a maximum of ~510 g of polyethylene per ES-3100 package. Possible additional sources of hydrogenous material inside the containment vessel include can pads and vinyl tape.

Polyethylene bottles (~85 g) may be used to pack HEU oxide; however, polyethylene bags are not used for packing HEU oxide. While polyethylene bags may be used to bag the 85 g polyethylene bottles, the amount of hydrogenous packing material inside the containment vessel is limited to an equivalent 500 g polyethylene. Non-metallic containers such as polyethylene or Teflon (~303 g) may be used to pack UNH crystals. Likewise, polyethylene bags are not used for packing the UNH crystals and the amount of hydrogenous packing material inside the containment vessel is limited to an equivalent 500 g polyethylene.

Normally, the H/X ratio inside the containment vessel is specified as an administrative control used to restrict both the amount of hydrogenous packing material normally used inside the containment vessel and other sources of moisture present in the fissile content. The total amount of hydrogen inside the containment vessel is used in the determination of package H/X ratio (i.e., the ratio of the number of hydrogen atoms "H" to the number of fissile atoms "X," where the hydrogen atoms are those of the content, including absorbed moisture and of the packing material both inside and outside of the convenience cans). However, containment vessel flooding is assumed in calculations performed for the derivation of fissile material loading limits. This simulated condition produces fissile material content that is more reactive than actual.

The 7.1–10.1 kg quantity of evaluation water required in both the NCT and HAC criticality calculations bounds reasonable amounts of hydrogenous packing material present inside the ES-3100 containment vessel for solid HEU metal content (cylinders, bars, buttons, slugs, unirradiated TRIGA fuel, and research-related fuel components fissile material). The hydrogenous packing material encompasses the solid fissile material but is not interspersed within it.

However, the 7.1–10.1 kg quantity of evaluation water does not necessarily bound reasonable amounts of hydrogenous packing material present inside the containment vessel when the fissile material is in particulate form (primarily HEU oxides and UNH crystals) or must be evaluated in particulate form (broken metal). An administrative criticality control is used to restrict the amount of hydrogenous packing material normally present inside the containment vessel (see Item 7 in Sect. 6.2.4).

6.2.4 Package Content Loading Restrictions

Loading restrictions based upon the results of the criticality safety calculations presented in Sects. 6.4 and 6.5 are as follows:

(1) HEU fissile material to be shipped in the ES-3100 package shall be placed in stainless steel, tin-plated carbon steel or nickel-plated carbon steel convenience cans or polyethylene or Teflon bottles. The can lids may be welded, press fit, slip lid, or crimp seal types; bottle lids are screw cap type.

(2) The content shall not exceed the "per package" fissile material mass loading limits specified in Tables 6.2a and 6.2b, and 277-4 canned spacers shall be used as indicated for criticality control.

(3) Where 277-4 canned spacers are required, not greater than one-third of the permissible package content for that category indicated in Tables 6.2a or 6.2b shall be loaded in any vacancy between or adjacent to canned spacers inside the containment vessel. The content mass loading may be further restricted based on structural, mechanical, and practical considerations (see Sects. 1 and 2).

(4) As shown in Fig. 1.4, the ES-3100 package may carry up to six loaded convenience cans. In situations where the plan for loading the containment vessel calls for the use of empty convenience cans to fill the containment vessel, the heavier cans shall be loaded into the bottom of the upright shipping container, and the empty cans shall be placed above them.

(5) The presence of uranium isotopes is limited on a weight-percent basis as follows: $^{232}U \leq 40$ ppb U, $^{234}U \leq 2.0$ wt % U, $^{235}U \leq 100.0$ wt % U, and $^{236}U \leq 40.0$ wt % U.

(6) With the exception of slug content and unirradiated TRIGA reactor fuel element content, solid HEU metal or alloy content of specified geometric shapes shall be one item per loaded convenience can. HEU bulk metal or alloy content not covered by the specified geometric shapes (cylinder, square bar, billet, slug, or unirradiated TRIGA fuel element contents) will be in the HEU broken metal category, and so limited.

(7) The package content is defined as the HEU fissile material, bottles, the convenience cans, the can spacers, and the associated packing materials (plastic bags, pads, tape, etc.) inside the ES-3100 containment vessel. The amount of hydrogenous packing material inside the containment vessel shall not exceed an equivalent mass of 500 g polyethylene. The only hydrogenous packing materials that can be used in the containment vessel when shipping HEU broken metal content are those that have a hydrogen density less than or equal to water.

(8) The mass of unidentified constituents of an HEU fissile material to be loaded into the ES-3100 will be counted against the fissile mass loading limit. The HEU fissile material will not contain unevaluated moderating materials.

(9) The CSI is determined on the basis of the uranium enrichment and total ^{235}U mass in the package and the fissile material shape or form.

6.3 GENERAL CONSIDERATIONS

The ES-3100 packaging configuration is shown on Drawing M2E801580A031 (Appendix 1.4.8). KENO V.a modeling of this configuration with the maximum allowable contents (Sect. 6.2) for a variety of array sizes and array conditions yields bounding calculations that determine the package's CSI (Tables 6.1a–6.1e). Can spacers are used as indicated in Table 6.2a and 6.2b for the purpose of reducing neutronic interaction between the contents of the package, aiding in maintaining the $k_{eff} + 2\sigma$ below the USL for the ES-3100 package. Key input listings are provided in Appendix 6.9.7.

The HEU content of a package is in one of the following forms: metal of a specified geometric shape, metal of an unspecified shape characterized as broken metal, uranium or skull oxide, UNX crystals, or unirradiated TRIGA reactor fuel elements. The bounding types of HEU content evaluated in this criticality analysis are: 4.25-in.- and 3.24-in.-diam cylinders; 2.29-in.-square bars; 1.5-in.-diam × 2-in.-tall slugs; cubes ranging from 0.25 to 1 in. on a side; broken metal pieces of unspecified geometric shapes; product and skull oxide; UNH crystals; and unirradiated TRIGA reactor fuel elements. Uranyl nitrate hexahydrate (UNH) has a chemical formula of $UO_2(NO_3)_2 + 6\ H_2O$. This most reactive form is used as the bounding composition for UNX crystals in the criticality evaluation. TRIGA fuel elements are 1.44-in.-diam × 15-in.-tall cylinders of $UZrH_x$ containing <310 g ^{235}U. Fuel elements are sectioned into three equal length pieces. Calculations demonstrate that these contents are bounded by 3.24-in.-diam HEU metal cylinders. Evaluation of the 3.93-in.-diam × 9.5-in.-tall U-Al cylinders is covered under the evaluation of the 4.25-in.-diam HEU metal cylinders. The evaluation of the U-Mo content is covered under the assessment of HEU contents at 95 wt % enrichment.

HEU metal shapes are distributed in an optimum arrangement in the flooded containment vessel. For the single package and the array calculations, the HEU broken metal is modeled as a homogeneous mixture of uranium metal and water filling the interior of a flooded containment vessel. This representation bounds the heterogeneous configuration of metal pieces interspersed with hydrogenous packing material inside of wrapped convenience cans. (Appendix 6.9.3., Sect. 6.9.3.1) Water soluble UNH crystalline content is modeled as a homogeneous mixture of UN and water filling the interior of the containment vessel.

No credit is taken for the fissile material spacing, neutron absorption, or free volume reduction provided by the presence of can pads, spacer can steel, and convenience cans inside the containment vessel. Water is substituted for polyethylene bagging which may be in use as packing material for both the content placed inside the convenience can and the cans themselves. Pads of steel turnings rolled up into a disk-like shape may also be present in the ES-3100 package, in use as cushioning and for reducing the free volume inside the convenience cans. This steel packing material acts as a neutron absorber and is excluded from the calculation model.

Criticality calculations are performed for the containment vessel under full water reflection whereby the water content inside the containment vessel is varied from dry to fully flooded conditions. These calculations demonstrate that the fully flooded condition is most reactive. The containment vessel is flooded in the single-unit calculation model and the infinite and finite array calculation models for both the NCT and HAC evaluations.

The KENO V.a models discussed in the following sections are the single-unit calculation model (Sect. 6.3.1.1), the infinite and finite array calculation models (Sect. 6.3.1.2), the HAC calculation models (Sect. 6.3.1.3), and the air transport models (Sect. 6.3.1.4). The single-unit calculation model is evaluated with a vacuum boundary condition and with full water reflection. The finite array calculation model is evaluated in arrays consisting of packages stacked in 13×13×6, 9×9×4, 7×7×3, 5×5×2, ETP 27×3 and ETP 16×3 arrangements with full water reflection at the array boundary. The ETP arrangements are used specifically for defining smaller array configurations with a high CSI value.

The geometry of the ES-3100 package is depicted in Drawing No. M2E801580A001 (Appendix 1.4.8). Calculation models of this geometry for evaluating NCT and HAC must be constructed for the single-unit, infinite array and finite arrays within the constraints and capabilities of KENO V.a. As shown in the drawing, the ES-3100 geometry is complex. Given KENO V.a's constraints and capabilities, two methods may be used to evaluate these complex geometries: simplify the geometries with conservative approximations or construct accurate geometries from simple components. Both methods yield valid results; however, the latter method is chosen for this analysis in order to maximize accuracy and to eliminate unnecessary conservatism.

6.3.1 Model Configuration

A detailed ES-3100 geometry model is accurately constructed using many simple geometric shapes. The selection of these components is governed by two of KENO V.a's geometry constraints: geometry regions must be composed of uniform and homogeneous materials and exterior regions must completely enclose interior regions. It is apparent from Drawing No. M2E801580A001 (Appendix 1.4.8) that these constraints could not be simultaneously applied to the entire ES-3100 package. However, these constraints could be applied to vertical segments of the package. Segments (i.e., simple components) are defined by starting at the bottom of the package and defining geometry regions radially outward until the drum surface is reached. A vertical segment is extended upward to the point where the KENO V.a constraints are violated. This vertical position is the termination point of a segment (i.e., the interface with the adjacent segment above it). The vertical segments are constructed accordingly, ignoring the minor variations in the ES-3100 geometry (i.e., radii of curvature, beveled edges, nuts and bolts). The KENO V.a geometry model for the ES-3100 is then assembled from the vertical segments. The resulting calculation model geometry includes the HEU content, 277-4 canned spacers, the containment vessel, the stainless-steel liner, the inner-liner cavity filled with 277-4, the outer-liner cavity filled with Kaolite, the Kaolite top plug and steel shell, the silicon rubber spacers, and the stainless-steel drum.

6.3.1.1 Single-unit packaging calculation model

The single-unit packaging calculation model is comprised of the geometry model, material compositions, and boundary conditions. Figures 6.1–6.5 depict section views of the geometry model used to evaluate a single ES-3100 package. Excluding minor variations in the ES-3100 geometry (i.e., radii of curvature, beveled edges, nuts and bolts), the single-unit packaging calculation model is an accurate representation of the ES-3100 geometry.

Figure 6.1 depicts a vertical section view of an ES-3100 package with the content of three loaded convenience cans and 277-4 can spacers inside the containment vessel. The fissile material contents shown are HEU cylinders, but convenience cans are not modeled. As illustrated in Fig. 6.1, credit is not taken for fissile material spacing provided by convenience cans inside the containment vessel. Appendix 6.9.1 provides wire-frame schematic and isometric diagrams depicting other fissile material contents considered in this criticality calculation.

Figures 6.2–6.5 depict vertical section views at various elevations in the package. The dimensions and the material specifications of any element of the ES-3100 single-unit packaging model may be obtained directly from the KENO V.a input listings in Appendix 6.9.7. The vertical segments (KENO V.a geometry unit numbers) are denoted in parenthesis to the right of the dimensions. The dimensions are given in units of centimeters. Material specification data for the single-unit packaging calculation model are provided in Sect. 6.3.2.

The single-unit calculation model is evaluated as both a bare system (i.e., with a vacuum boundary condition) and as a reflected system with 30.48 cm (1 ft) of water surrounding the package for effectively infinite water reflection.

10 CFR 71.55(b) requires evaluation of water leakage into the containment system disregarding any performance capability demonstrated by physical testing per 10 CFR 71.71 and 71.73. In conjunction, 10 CFR 71.55(b)(3) also requires evaluation of the efficiency of the packaging as an external reflector to the containment vessel. The test case is defined as a flooded package. All regions within the water-reflected, single-unit packaging calculation model are flooded with water. The reference case is defined as a water-reflected flooded containment vessel. This calculation model is a modification of the water-reflected, single-unit packaging calculation model where all regions of the packaging external to the containment vessel are replaced with full density water.

6.3.1.2 Infinite and finite array packaging calculation models

Array packaging calculation models like the single-unit packaging calculation model are comprised of geometry, material compositions, and boundary conditions. Figures 6.6–6.10 depict section views of the geometry model used to evaluate an array of ES-3100 packages. The array geometry model incorporates a 7.0% reduction in the inside diameter of the ES-3100 drum. This reduction of the drum's inside diameter produces an array density equivalent to drums in a tightly packed, triangular pitch configuration. (O'Dell and Schlesser 1991) Since all array calculations in this evaluation use a square pitch package configuration, using the 7.0% reduction in diameter of uniform-shaped packages avoids the use of a nonconservative lattice arrangement in the array analysis.

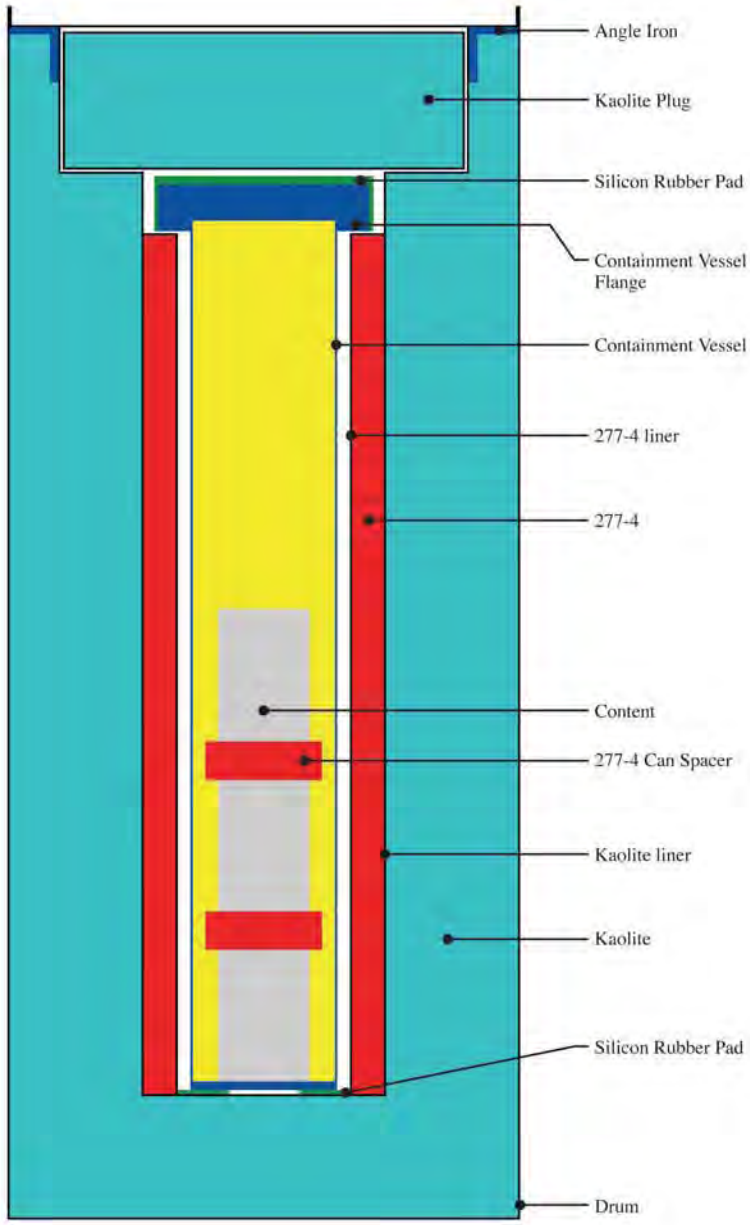

YGG 06-0182

Fig. 6.1. R/Z section view of ES-3100 single-unit packaging model.

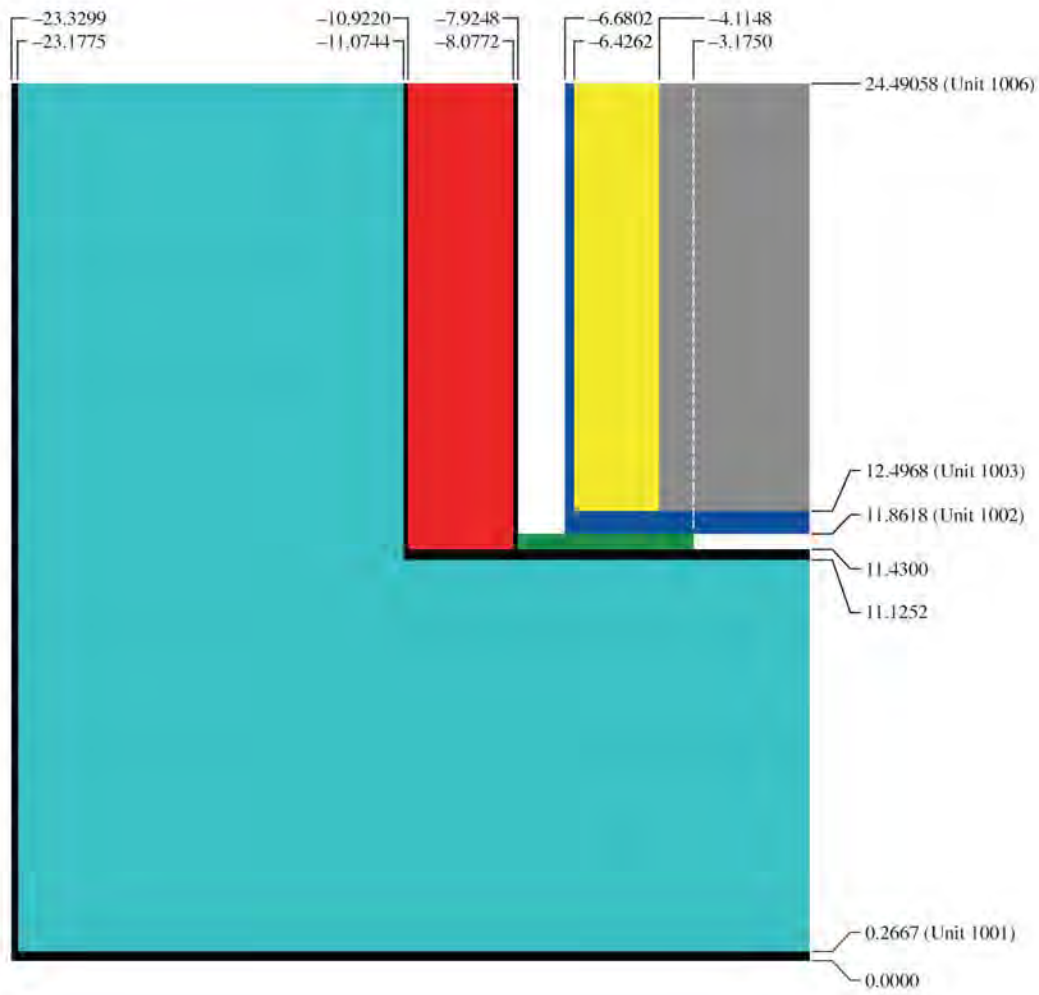

Fig. 6.2. R/Z section view at bottom of ES-3100 single-unit packaging showing KENO V.a geometry units 1001–1003, and 1006 (partial). Dimensions are in centimeters.

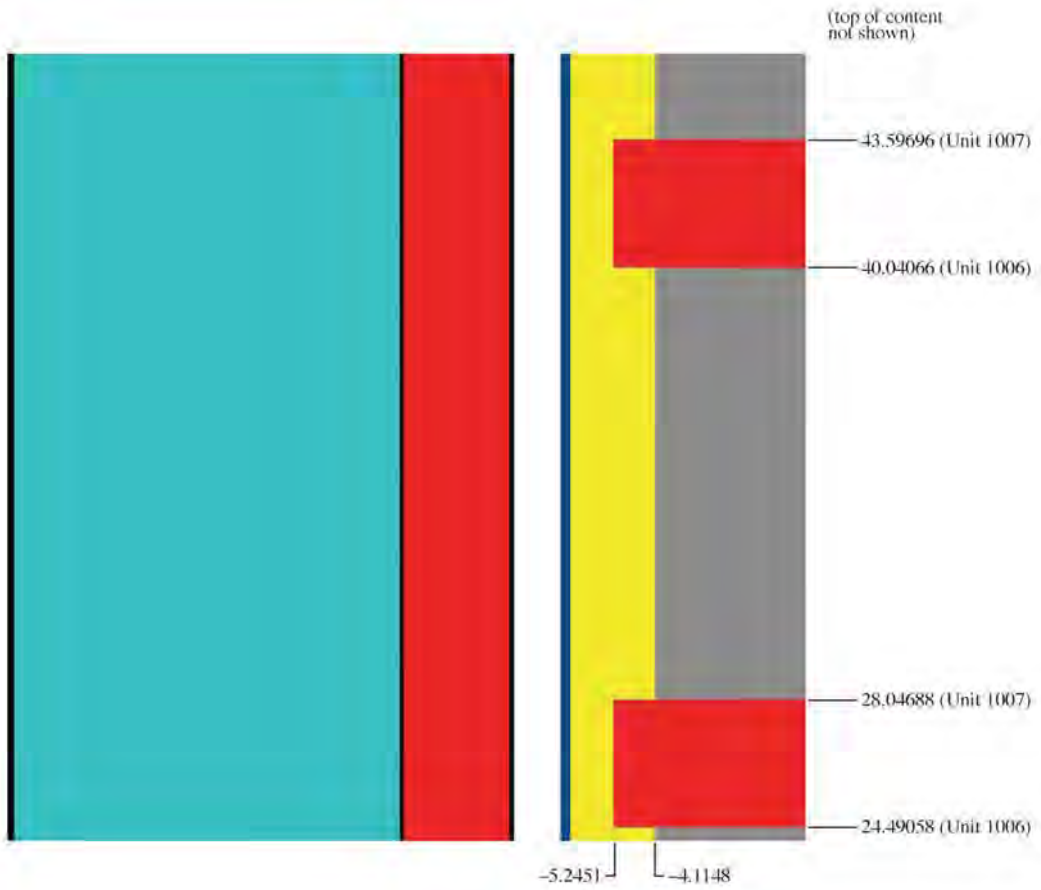

Fig. 6.3. R/Z section view at center of the ES-3100 single-unit packaging showing KENO V.a geometry units 1006 (partial), 1007, and 1008 (partial). Dimensions are in centimeters.

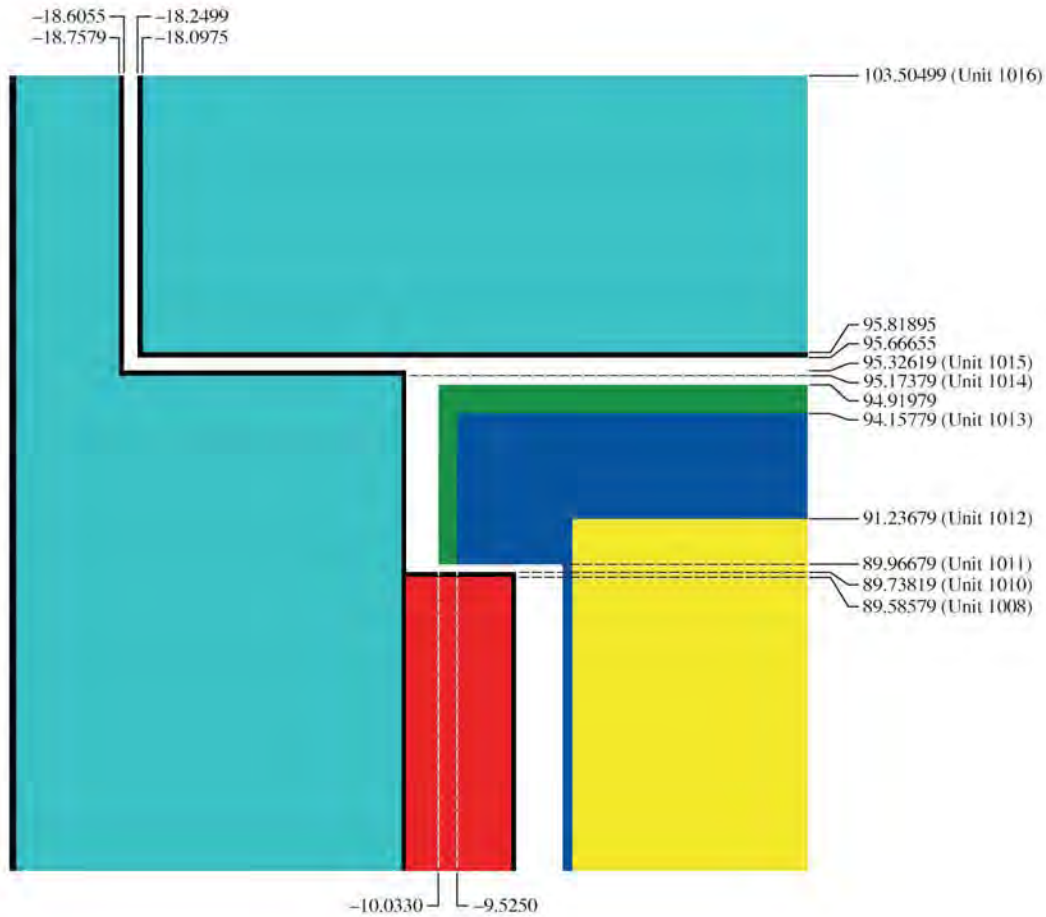

Fig. 6.4. R/Z section view of near top of the ES-3100 single-unit packaging showing KENO V.a geometry units 1008 (partial) and 1010–1016. Dimensions are in centimeters.

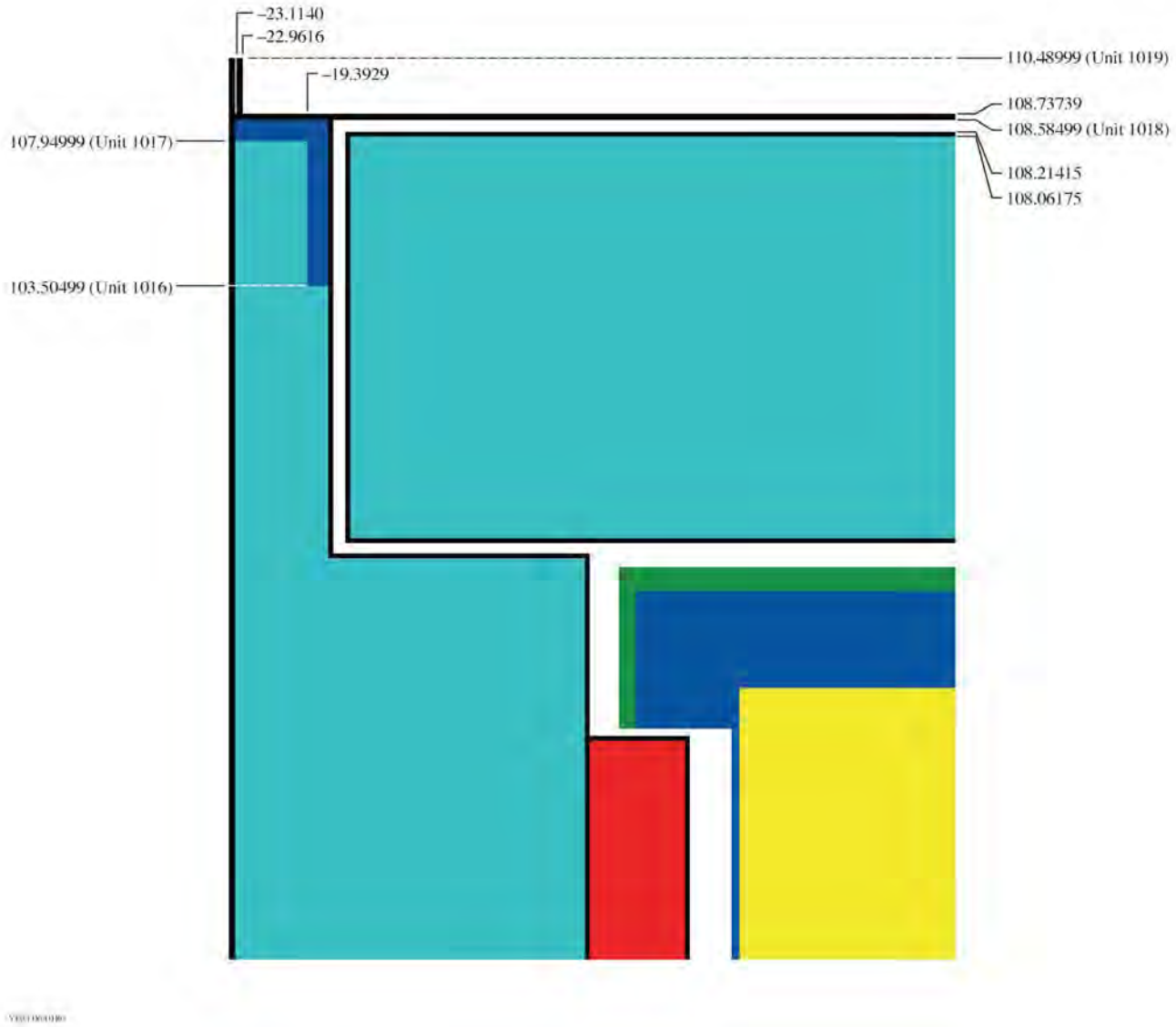

Fig. 6.5. R/Z section view at the top of the ES-3100 single-unit packaging showing KENO V.a geometry units 1016–1019. Dimensions are in centimeters.

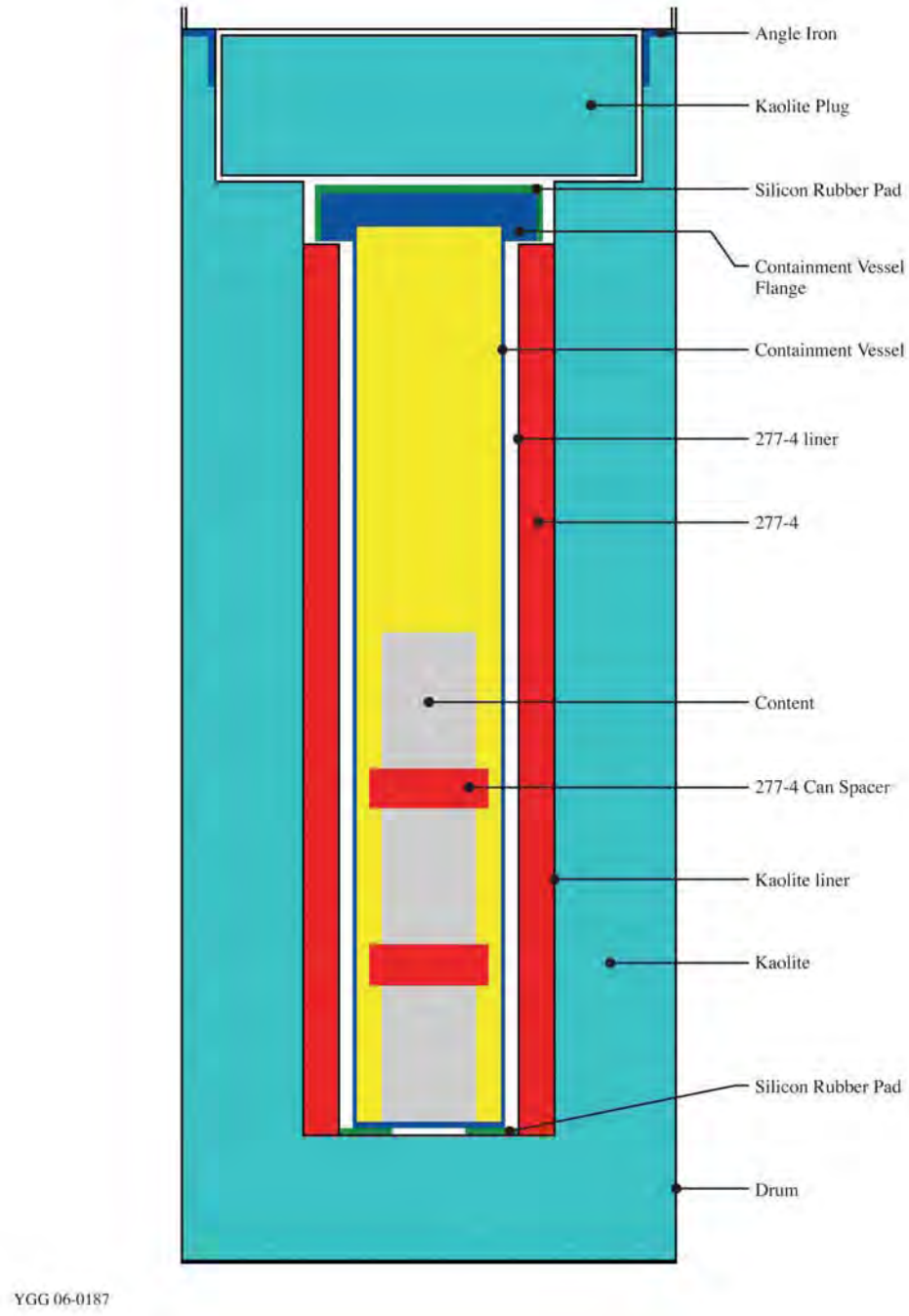

Fig. 6.6. R/Z section view of ES-3100 array packaging model with a 7% reduction in the drum's inner diameter.

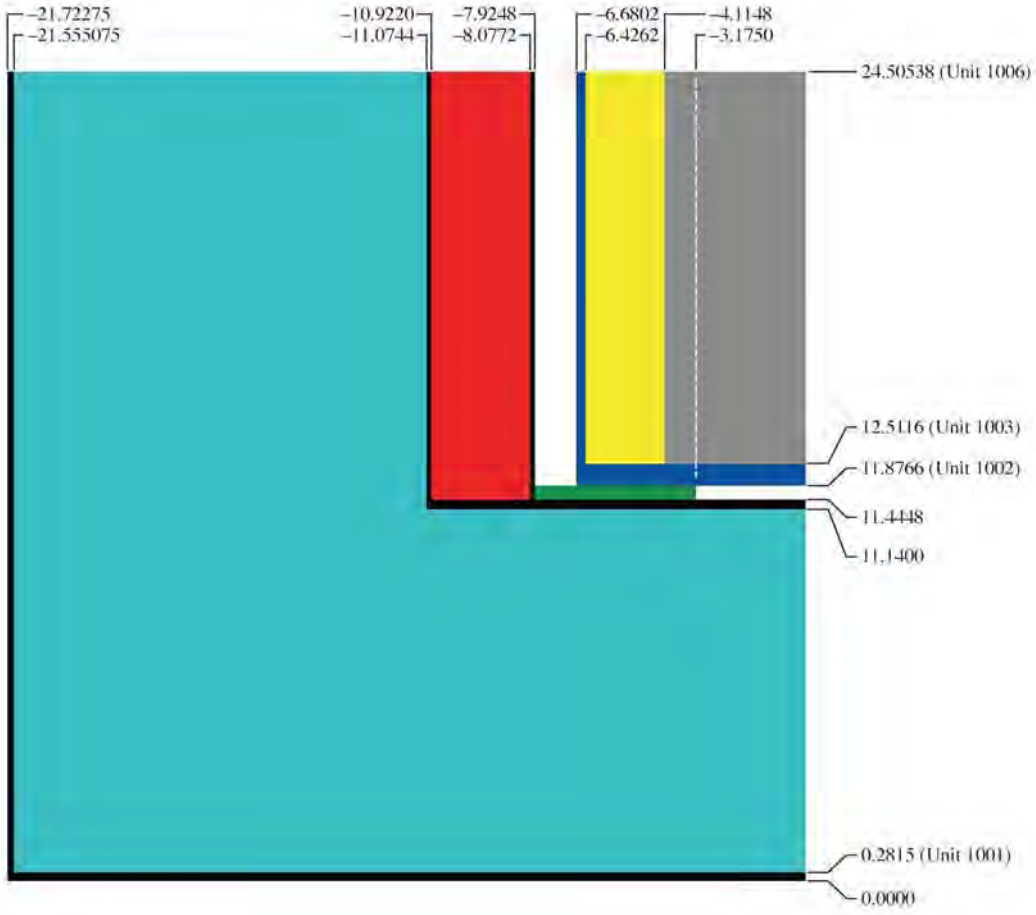

Fig. 6.7. R/Z section view at the bottom of the ES-3100 array packaging showing KENO V.a geometry units 1001–1003, and 1006 (partial). Dimensions are in centimeters.

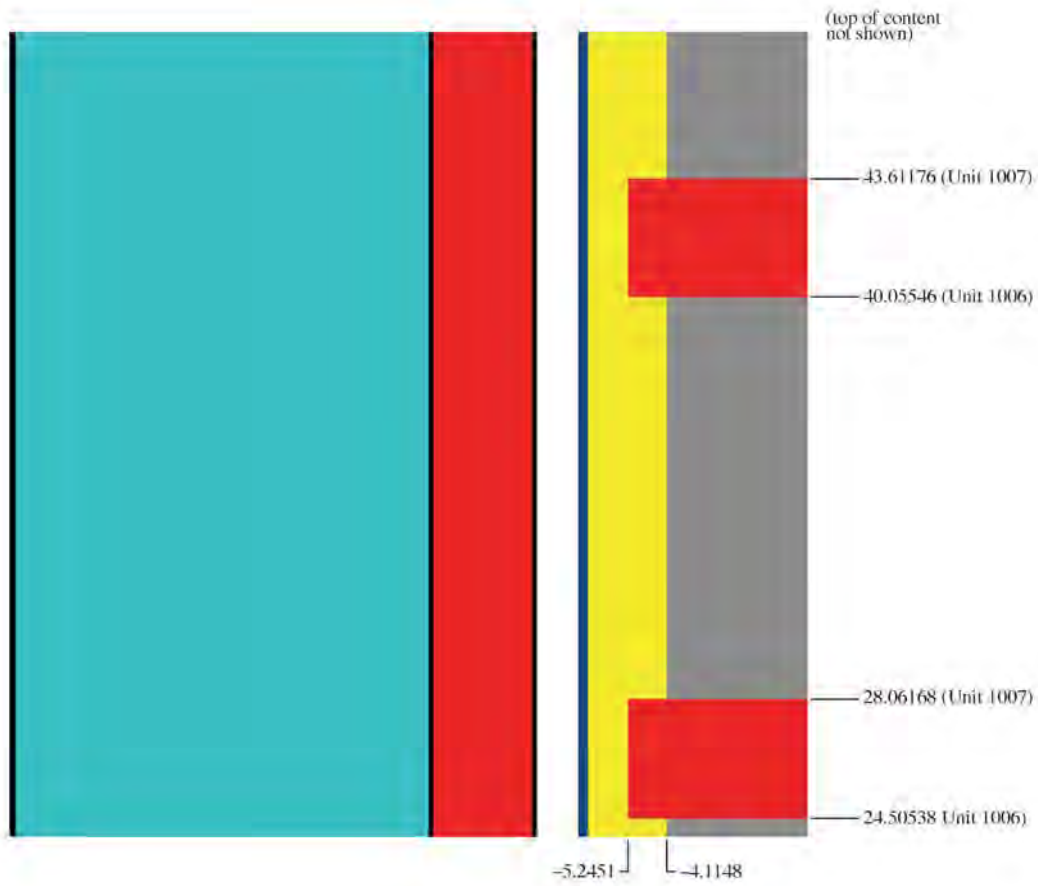

Fig. 6.8. R/Z section view at the center of the ES-3100 array packaging showing KENO V.a geometry units 1006 (partial), 1007, and 1008 (partial). Dimensions are in centimeters.

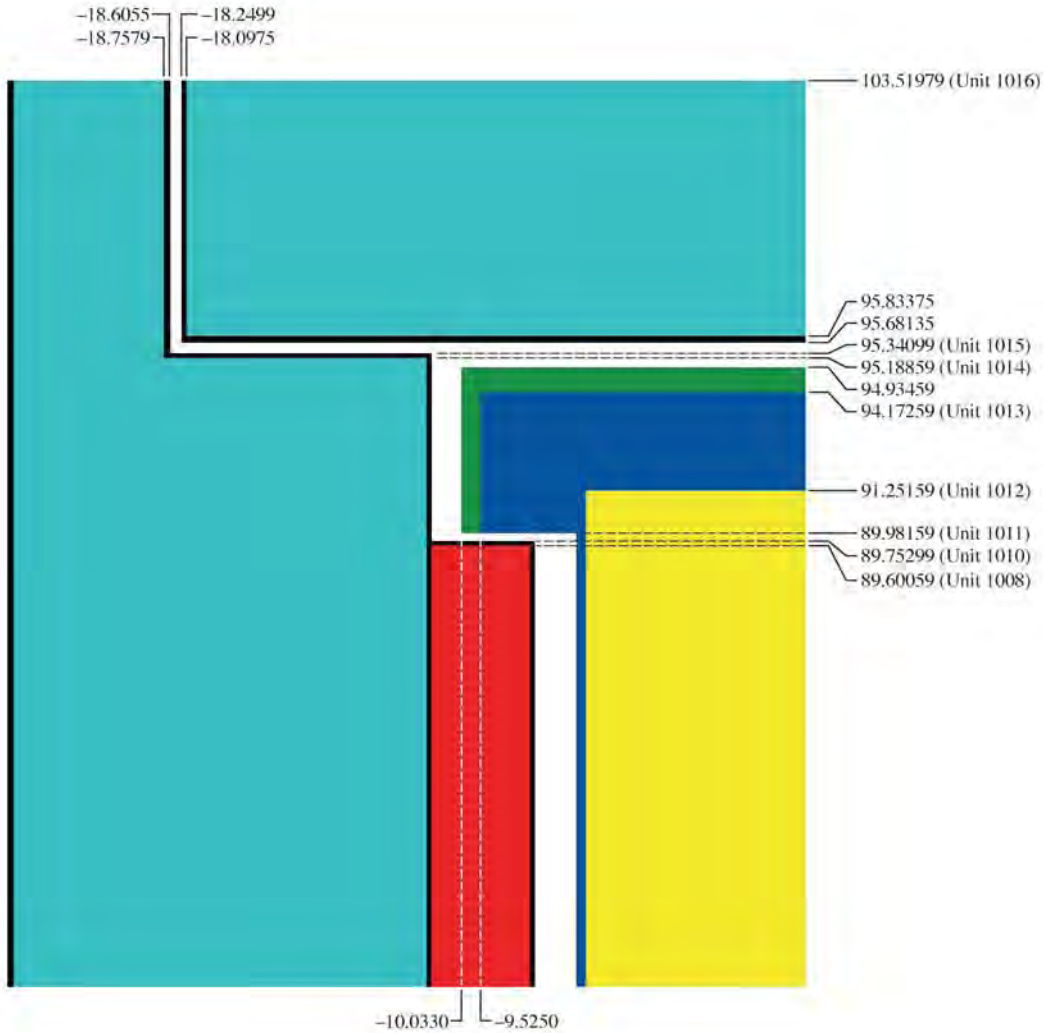

Fig. 6.9. R/Z section view of near top of the ES-3100 array packaging showing KENO V.a geometry units 1008 (partial) and 1010–1016. Dimensions are in centimeters.

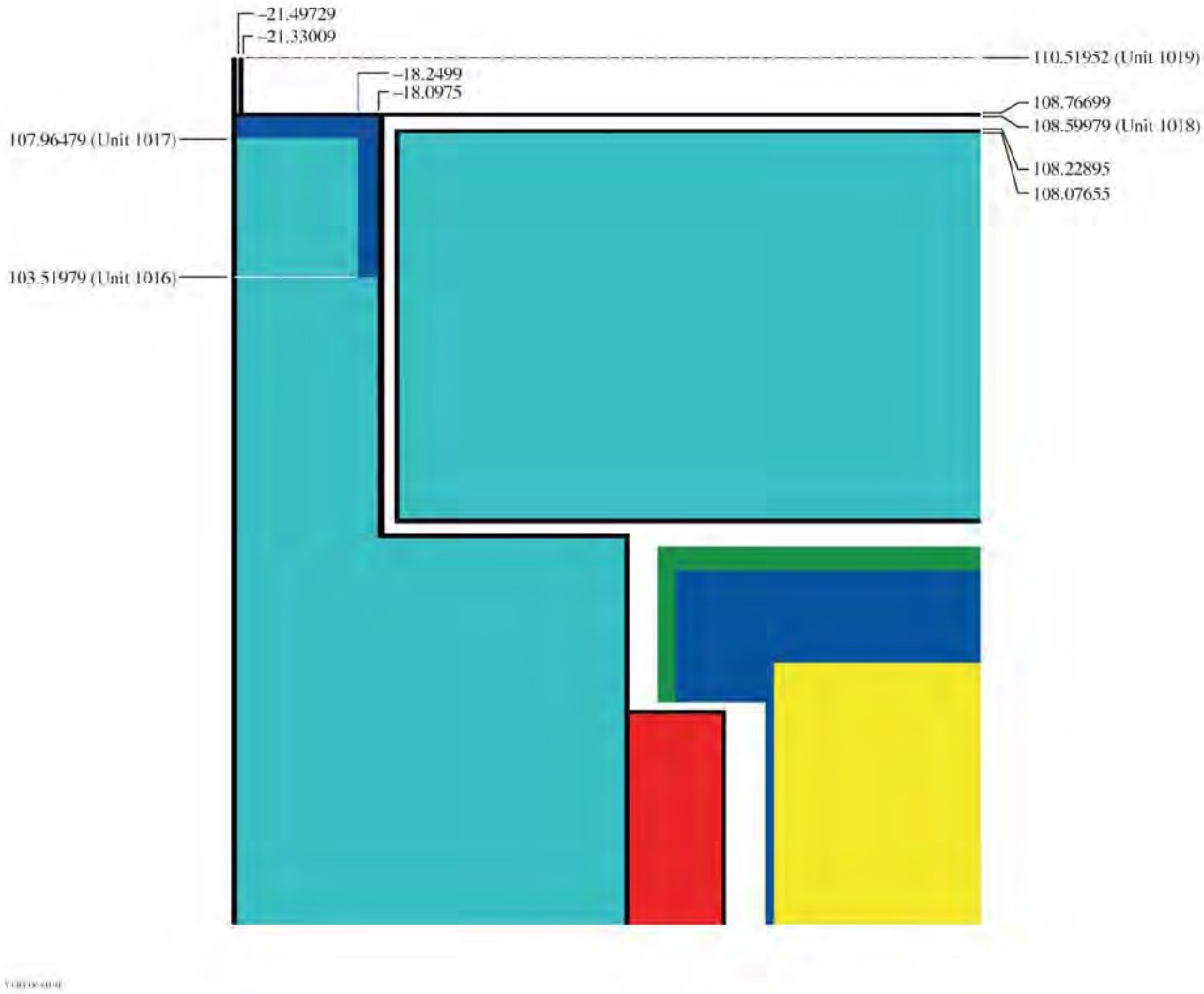

Fig. 6.10. R/Z section view at the top of the ES-3100 array packaging showing KENO V.a geometry units 1016–1019. Dimensions are in centimeters.

As seen in Drawings M2E801580A002 and M2E801580A003 (Appendix 1.4.8), a 7.0% reduction of the inside diameter of the ES-3100 drum affects the masses of the drum, the modified 2 × 2 × ¼ in. angle (angle iron), and the Kaolite refractory material. Also, a 7.0% reduction in diameter affects the mass of interstitial water between the ES-3100 packages of a tightly packed array. To maintain the correct mass of these materials in the array packaging calculation model, the drum's outside diameter, the density of the steel in the angle iron, the density of Kaolite, and the density of interstitial water are modified. Excluding modifications required to simulate a triangular pitch and minor variations in the ES-3100 geometry (i.e., radii of curvature, beveled edges, nuts and bolts), the array geometry model is an accurate model of the ES-3100 geometry.

In the array geometry model, the drum outside diameter is 43.444550 cm (17.104154 in.) (21.722275-cm radius used as the input value), and the drum inside diameter is 43.11015 cm (16.972500 in.) (21.555075-cm radius). This inside diameter corresponds to 93% of the inside diameter of the ES-3100 drum, and the drum outer diameter is modified to maintain drum mass. The angle iron outside diameter is identical to the drum inside diameter. To maintain mass, the angle iron steel, the liner outer-cavity Kaolite, and interstitial water densities are modified by factors of 1.25705, 1.22252, and 1.16235, respectively. Excluding the modifications to drum and angle iron dimensions, the dimensions of any element of the ES-3100 array geometry model may be obtained directly from Appendix 6.9.7. Material specification data from the array calculation models are provided in Sect. 6.3.2.

O'Dell and Schlesser equate modeling triangular arrays with square pitch arrays, provided that the outer dimension of the array is reduced by a factor of 0.9306 and that the mass of materials is maintained. The actual reduction factors (ratio of the reduced radii to the single unit radii) for the Kaolite of the body weldment and for the angle iron is slightly <0.9306. Given that the array packages are closer than required by O'Dell and Schlesser, the array models are conservative with respect to their reduced radii.

The finite array calculation model is evaluated with arrays of packages stacked in 13×13×6, 9×9×4, 7×7×3, and 5×5×2 arrangements where the arrays are surrounded with 30 cm (~1 ft) of water as a boundary condition representative of full water reflection. These arrays are nearly cubic in shape for optimum reactivity of the array, thus eliminating the need for placing limitations on array configurations in terms of stack height, width, and depth.

The KENO V.a users manual (SCALE, Vol. 2, Sect. F11) describes the input statements for an ETP model of cylinders in a close-pack array. This technique is adapted for modeling the ES-3100 in small compact array configurations. The ETP geometry model is much more complicated than the reduced-diameter approximation model described previously, but it yields smaller package configurations with correspondingly higher CSI values than the 7×7×3 and 5×5×2 package arrangements. Use of the ETP geometry specification allows for constructing compact package arrangements of 27×3 (27 packages in the horizontal plane stacked 3 packages high) and 16×3 packages.

6.3.1.3 Calculation models for damaged packages

Sections 2, 3, and 4 of this report address the overall integrity of the Model ES-3100 package in tests for NCT and HAC. (ORNL/NTRC-013) From a dimensional viewpoint, the only physical changes of interest for criticality safety occurred as a result of the 9-m (30-ft) drop test, the crush test, and the 1-m (40-in.) puncture test. There was significant crushing of the drum rim at the point of impact from the 9-m (30-ft) drop test and an indentation on the drum side from the 1-m (40-in.) puncture test. Even though significant crushing of the drum mid-section and bottom occurs, the effective center-to-center spacing of the contents actually increases under HAC. Selective rearrangement of alternating packages would be required to achieve a more compact array; however, this event is not credible.

The deformation of the outer diameters of the drum as predicted by finite element analysis is presented in Table 6.3. These diameters measured along the 90–270° and 0–180° axes are specified at five node points located along the vertical axis of an upright package. These node points are designated in a downward direction from the top of the drum as "UR," "MUR," "MR," "MLR," and "LR." Equivalent circular diameters for representing the deformed drum in the calculation models for the HAC study (Appendix 6.9.2) are based on the assumption that the drum cross section at each deformation point is ellipsoidal.

The package water content in the void spaces external to the containment vessel and the interstitial spaces between drums is varied in the calculation model while maintaining the Kaolite in the dry condition. At a low moisture content where neutronic interaction between packages of an array is greatest, there is no statistically significant difference in the calculated neutron multiplication factor for package models based on the "MR," "MLR," and "LR" node points. At high moisture content where a statistically significant difference in the calculated neutron multiplication factor occurs, the packages of an array are nearly isolated. The slight increase in k_{eff} at the smaller diameters is not numerically significant. A calculation model based on the "MLR" node point is used to represent HAC.

As concluded in Sect. 6.9.2.3, the criticality analysis of an array of HAC packages based on the "MLR" package model (diameter = 17.20 in.) in rectangular pitch bounds the analysis of damaged packages (diameter = 17.26 in.) in close-pack array configurations. Considering both the irregular shape of the deformed drums and the fact that overall (maximum) dimensions rather than a mean or minimum dimension for a damaged package would establish array spacing—this assumption is a reasonable one, and the model is conservative.

The neutron poison, Kaolite refractory material, and stainless-steel components of the ES-3100 package were not significantly damaged during thermal testing. The principal material change of consequence that occurred during the thermal test was the loss of volatile material (Sect. 2.7.4). No loss of volatile material other than steam from the Kaolite was experienced during prototype testing of the Model ES-3100 package.

Physical damage is significant in terms of criticality safety when the amount of volatile hydrogenous material available for interstitial moderation is reduced. Conversely, the package could be saturated with water during water immersion conditions. Both possibilities affect only the amount of interstitial moderation. The representation of the changes to material composition from temperature extremes and water intrusion is addressed in Sect. 6.3.2.

In the case of broken metal content, the ETP geometry specification using the "MLR" package model (diameter = 17.20 in.) produces a 16×3 package configuration having a correspondingly higher CSI value than a 5×5×2 package arrangement. This allows for a greater fissile payload.

6.3.1.4 Calculation models for catastrophically-damaged packages (air-transport)

It is possible for accidents to be substantially more severe in the air transport mode than in the surface transport mode. Thus, the performance requirements for packages designed to be transported by air are more stringent. Regulatory Guide 7.9 states that the criticality evaluation should evaluate a single package under the expanded accident conditions specific in 10 CFR 71.55(f).

Table 6.3. Deformation of 18.37-in.-diam ES-3100 drum projected by finite element analysis Case "3100 RUN1HL Lower Bound Kaolite May 2004"

Deformation point	FEA node	Diameter at 90° (in.)	Diameter at 180° (in.)	Equivalent circular diameter (in.)
UR	098194	20.02	15.60	17.67
MUR	100238	20.74	15.07	17.68
MR	101589	20.74	14.18	17.15
MLR	103012	22.00	13.44	17.20
LR	105786	20.92	12.92	16.44

For a fissile material package designed to be transported by air, 10 CFR 71.55(f) requires the criticality evaluation demonstrate that the package be subcritical, assuming no water inleakage and reflection by 20 cm (7.9 in.) of water, when subjected to the sequential application of the HAC free drop and crush tests of 10 CFR 71.73(c)(1 and 2) and the modified puncture and thermal tests of 10 CFR 71.55(f)(1)(iii and iv).

Physical testing of Type-B fissile material packages transported by air was not conducted for the ES-3100. In lieu of testing, criticality calculations are performed using calculation models that conform to the basic requirements of 10 CFR 71.55(f) regarding both the reflection of the package by 20 cm of water and the absence of water inleakage. In addition, the air-transport calculation models incorporate features exhibiting the worst-case assumptions made regarding the geometric arrangement of the packaging and package contents. No credit is taken for the geometric form of the package content. Spherical geometry is used to represent the ultimate configuration of the ES-3100 package which undergoes catastrophic destruction.

The criticality analysis for air transport does not credit the ES-3100 for maintaining the geometry configuration of the packaged content. Fissile material is configured spherical in shape for optimization of neutron multiplication. Also, the criticality analysis does not credit the ES-3100 packaging for structural integrity of the containment and the confinement. The reactivity "enhancing" materials of the packaging and of the accident environment may be interspersed with the fissile material content. However, selective removal of the neutron absorbing material of the package (i.e., Kaolite and stainless steel) accompanied by retention of the moderating constituents of the neutron absorbing material (i.e., bound water in the Kaolite) is not a credible condition. Moreover, a calculation model where the fissile material is homogenized with moderating material, is only an appropriate representation when the fissile material content being shipped consists of numerous solid pieces uranium ("broken metal"), oxide, or crystals. Homogenization of fissile material with moderating material is not performed with exclusive preference given to specific constituents of the moderating material.

A set of six calculation models are constructed in order to determine the worst case or most reactive configuration with consideration given to the efficiency of moderators, loss of neutron absorbers, rearrangement of packaging components and contents, geometry changes, and temperature effects. The fissile material component is dry in each case.

Model 1 (Fig. 6.11) represents the fissile material content configured into a spherical core with a 20.0-cm thick water reflector. All ES-3100 packaging material (Kaolite, stainless steel, 277-4 neutron poison, etc.) is excluded from Model 1. The fissile material content considered in the calculation model consists of a specific material form: solid HEU metal (7 – 10 kg ^{235}U); TRIGA fuel (10 kg $UZrH_x$ having 921 g ^{235}U); or broken HEU metal (≤ 7 kg ^{235}U). The presence of hydrogenous packing material inside the containment vessel is also addressed in this calculation model. 513 g of polyethylene is used to represent a maximum amount of hydrogenous packing material in the ES-3100. For 7 kg ^{235}U HEU homogenized with 513 g of polyethylene, the radius of the core is 6.0547 cm. The parametric variation of both the ^{235}U mass and the enrichment in Model 1 is used to establish a reference point for the evaluation neutron reflection and absorption effects on k_{eff} provided by the stainless steel and Kaolite packaging material, addressed separately in Models 2 and 3.

Model 2 (Fig. 6.12) represents a spherical core of Model 1 blanketed by a variable-thickness shell of stainless steel, and a 20.0 cm thick water reflector external to the shell. The shell at maximum thickness corresponds to the 66,133 g stainless steel of the containment vessel and the liner and drum assembly. For 7 kg ^{235}U HEU metal, the radius of the core is 6.0547 cm while the outer radius of the stainless steel shell is 13.0264 cm.

Model 3 (Fig. 6.13) is configured the same as Model 2 with the exception that the variable-thickness shell is composed of the Kaolite instead of stainless steel. At maximum shell thickness, the 128,034 g of Kaolite corresponds to the mass of water-saturated Kaolite inside the drum body weldment and the drum top plug. The 76,819 g of saturation water corresponds to the amount of water in the Kaolite cast-slurry prior to baking. For 7 kg ^{235}U HEU metal, the radius of the core is 6.0547 cm while the outer radius of the Kaolite shell is 31.0814 cm. The parametric variation of shell thickness in Models 2 and 3 is performed for the purpose of evaluating the effect on k_{eff} of neutron reflection and absorption provided by each packaging material.

Models 1–3 are applicable for establishing loading limits for air transport packages having a single piece or several pieces of solid HEU metal where the integrity of the content can be established based on package tests or dynamic impact simulations per Type-C test criteria. Otherwise, the criticality evaluation of additional accident models is required for those situations where: (1) data is not available or is inadequate for discounting fragmentation of the fissile content in the air transport accident, or (2) the fissile material is in a physical form (crystals, oxide, or multiple pieces of solids) having the potential to blend with the other material of the package in the air transport accident.

Fig. 6.11. Model 1.
7 kg ^{235}U (red) reflected by 20 cm of water (blue).

Fig. 6.12. Model 2.
7 kg ^{235}U (red) blanketed by a stainless-steel shell (gray), reflected by 20 cm of water (blue).

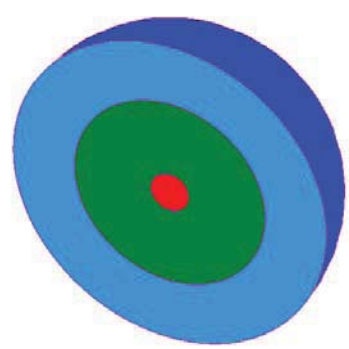

Fig. 6.13. Model 3.
7 kg ^{235}U (red) blanketed by a Kaolite shell (green), reflected by 20 cm of water (blue).

Model 4 (Fig. 6.14) depicts a spherical core of broken metal homogenized with water-saturated Kaolite and hydrogenous packing materials inside the containment vessel represented by 513 g of polyethylene. A 20-cm thick water reflector blankets the spherical core. All other ES-3100 packaging material (stainless steel, 277-4 neutron poison, etc.) is excluded from Model 4. For 25 kg of HEU (5 kg of ^{235}U), the radius of the homogenized core ranges from 31.4499 cm with dry Kaolite to 39.1608 cm with water saturated Kaolite. Model 4 also applies to TRIGA fuel content.

Model 5 (Fig. 6.15) is an extension of Model 3 applied to the case of TRIGA fuel and broken metal contents. Excess water from saturated Kaolite is homogenized with the fissile material in the core. For 25 kg of HEU where 5 kg of ^{235}U is homogenized with 513 g of polyethylene and 7,461 g of excess water from water saturated Kaolite, the radius of the spherical core is 13.0681 cm. The exterior Kaolite shell containing 69,357.9 g of water and the 51,214.9 g of vermiculite-cement constituents, has an outer radius of 31.7599 cm. At the extreme condition where the entire 74,614.0 g of excess water excess from the water saturated Kaolite is homogenized with the core, the radius of the spherical core is 26.3485 cm. The exterior shell of dry Kaolite, containing 2204.7 g of bound water and 51,214.9 g of vermiculite cement constituents, has an outer radius of 36.3668 cm. Although an unlimited amount of moderator could be imparted from the environment, optimum moderation is addressed simply by considering the full range of potential moisture from the Kaolite interspersed with pieces of fissile material.

Model 6 (Fig. 6.16) is configured similarly to Model 4 with the exception that only a partial amount of broken metal resides in the homogenized core. The remainder of the fissile material is modeled as a shell external to the spherical core and internal to the 20.0 cm thick water reflector. The amount of fissile material in the homogenized core is varied in 500 g increments from the full amount of Model 5 minus 500 g to a minimum amount of 500 g HEU. In the case of 25 kg of broken metal where 4.5 kg of ^{235}U is homogenized with 513 g of polyethylene and water-saturated Kaolite, the radius of the core is 39.1539 cm while the outer radius of the exterior 0.5 kg shell of ^{235}U is 39.1609 cm. In the case where 0.5 kg of ^{235}U is homogenized with 513 g of polyethylene and water-saturated Kaolite, the radius of core is 39.0992 cm while the outer radius of the exterior 4.5 kg shell of ^{235}U is 39.1609 cm. Model 6 addresses potential redistribution of fissile material consisting of multiple pieces, specifically the broken metal content. The parametric variation of shell thickness in Model 6 is performed for the purpose of evaluating the effect on k_{eff} of moderation efficiency of the core and enhanced neutron multiplication of the shell.

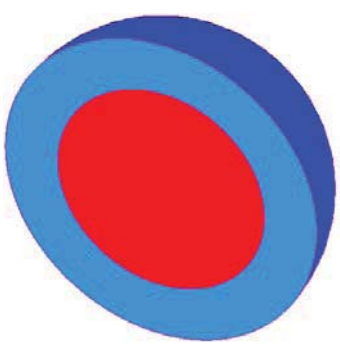

Fig. 6.14. Model 4. Homogenized sphere of 5 kg ^{235}U, polyethylene, and water saturated Kaolite (red), reflected by 20 cm of water (blue).

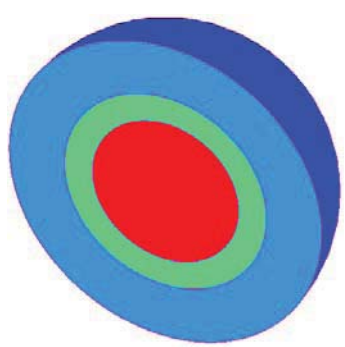

Fig. 6.15. Model 5. Homogenized sphere of 5 kg ^{235}U and excess moisture from Kaolite (red), blanketed by Kaolite shell (lt. green), reflected by 20 cm of water (blue).

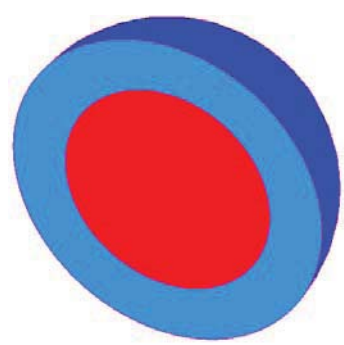

Fig. 6.16. Model 6. Homogenized sphere of 4.5 kg ^{235}U, polyethylene, and water saturated Kaolite (red); blanketed by shell of 0.5 kg ^{235}U (not visible), reflected by 20 cm of water (blue).

Models 1–6 are applicable to air transport of the ES-3100 package given that the physical integrity of the fissile content following the air transport accident can not be established, or that the physical form of fissile material content may be multiple solid pieces or oxide.

6.3.2 Material Properties

Criticality calculation models include the definition of material compositions in the geometry model for both NCT and HAC. The materials which affect nuclear criticality safety and may be present in the ES-3100 package during these conditions are fissile material content (HEU metal, aluminum, molybdenum, and zirconium alloys of uranium, HEU product or skull oxide, UNX crystals, or $UZrH_x$), stainless steel, 277-4 neutron poison, Kaolite, silicon rubber, Teflon or polyethylene, and various amounts of water. Other materials are present in the package (e.g., tin-coated steel convenience cans, nylon bagging, rubber O-rings, and trace impurities). However, these other materials are not present in amounts that will significantly affect the reactivity of the package. Detailed discussion of the package content and packaging materials is contained in Appendix 6.9.3. Specific topics are summarized in this section as required to support the discussion of the criticality calculations presented in Sects. 6.4–6.6.

277-4 neutron poison is designed to maximize the hydrogen content necessary for thermalizing fast neutrons for capture in the boron constituent. 277-4 is a formulation of Thermo Electron Corporation's Cat 277-0, a boron carbide additive, and water. This mixture is cast and dried. "Loss On Drying" (LOD) tests are used to measure the amount of water in the as manufactured 277-4 casting. The as-manufactured neutron poison material at 100 lb/ft^3 and 31.8% LOD has a hydrogen concentration of 3.56 wt % and a natural boron concentration of 4.359 wt %. (DAC-PKG-801624-A001, Table 5)

The testing of 277-4 reveals that the material will dehydrate at elevated temperatures. Test specimens were dried at 250°F for 168 hours to reach the NCT state, and weight measurements were taken. These specimens where subsequently heated to 320°F for 4 hours to reach the HAC state, and weight measurements were again taken. The compositions of 277-4 at NCT and HAC states were derived by adjustment of the formulation specification for measured losses taking into account the statistical variations in the data. Conservation of mass for non-volatiles was observed in the derivation of material specifications based upon testing. Given that hydrogen presence is key to the effectiveness of the neutron poison, conservative material specifications were derived for minimum hydrogen content and minimum material density.

The NCT material specification for 277-4 at minimum density (95.39 lb/ft^3) and minimum hydrogen (25.15% LOD) is given in Table 11 of DAC-PKG-801624-A001. The average density of 277-4 in the ES-3100 package used for NCT calculations in KENO V.a is 1.52797 g/cm^3; the boron constituent is 7.31015e-2 g/cm^3; the residual base is 1.07070 g/cm^3; and the water component is 3.84169e-01 g/cm^3 (Appendix 6.9.3, Table 6.9.3.3-2). The HAC material specification at minimum density (95.32 lb/ft^3) and minimum hydrogen (25.09% LOD) is given in Table 12 of DAC-PKG-801624-A001. The average density of 277-4 used for HAC calculations in KENO V.a is 1.52680 g/cm^3; the boron constituent is 7.31015e-2 g/cm^3; the residual base is 1.07071 g/cm^3; and the water component is 3.82995e-1 g/cm^3 (Appendix 6.9.3, Table 6.9.3.3-3).

A set of 20 canned spacer assemblies as-manufactured has an average weight of 591.55 g. On average, the weight of an empty can with a lid is 86.05 g, and the 277-4 is 505.5 g. On the basis of volumetric measurements, the neutron poison is ~10.075 oz or 297.95 cm^3. The resultant 277-4 density is 1.6966 g/cm^3. The corresponding minimum mass is 473.84 g (given that the 277-4 material inside the spacer can is ≥4.07-in. diam and 1.31-in. thickness). Based on model dimensions of 4.13-in. diam × 1.37-in. height and use of composition data from Table 11 of DAC-PKG-801624-A001

(as-manufactured material at minimum density and hydrogen), the mass of neutron poison in the calculation model of the canned spacer is conservatively modeled as 457.15 g.

The density of 277-4 in the liner inner cavity is further reduced by a factor of 0.966893 because the actual volume of neutron poison is 12,831.4 cm^3 in the package, but 13,270.8 cm^3 is used in the calculation model. Also, guidance in Sect. 6.5.3.2 of NUREG-1609 requires that 75% of elemental boron be used in the material specification. Consequently, the minimum weight of 277-4 in the liner inner cavity of the calculation models is 19.37 kg (42.71 lb) for NCT and 19.36 kg (42.67 lb) for HAC, determined from the input density and the volume of the 277-4 region calculated by KENO V.a.

Kaolite is a lightweight, low thermal conductivity, refractory material that is used in the ES-3100 package between the drum and the inner liner. Kaolite is formed by mixing a dry constituent powder with water, pouring the mixture into a casting form, and curing and baking the cast. For NCT, the average density of Kaolite in the Model ES-3100 package is 0.34438 g/cm^3, and the residual water is 0.01493 g/cm^3 (Appendix 6.9.3, Sect. 6.9.3.4). The nominal weights of Kaolite in the liner outer cavity and in the top plug as determined from the input density and the region volumes calculated by KENO V.a are 49.04 kg (108.1 lb) and 4.37 kg (9.63 lb), respectively.

Kaolite is a nonvolatile refractory material, not significantly damaged by thermal excursions associated with HAC. It is assumed that upon immersion, a cured and dried casting will absorb a quantity of water equal to that required during preparation. This assumption is valid because the casting is fully saturated with water prior to curing and baking, and the casting does not change volume significantly during baking. The maximum water content of Kaolite refractory material is the water content of manufacture (1.5 g water per gram dry Kaolite) equivalent to a density of 0.51655 g/cm^3. For the single package, water saturation in the Kaolite region maximizes the effect of self-reflection in the surrounding package. This condition is assumed in the NCT single package calculations. For an array of packages, neutronic interaction between packages is maximized when the minimum amount of water is present in the Kaolite, which occurs in the as-manufactured condition. A volume fraction of 1.0 in the material specification corresponds to the water-saturated condition, while a volume fraction of 0.0289 corresponds to the dry condition.

The fissile material content packed into the containment vessel is ordinarily dry. Given that a flooded containment vessel is assumed for both NCT and HAC, the concurrent condition where the water-saturated Kaolite is baked dry beyond the as-manufactured condition while the containment vessel remains flooded is considered not credible. Therefore, the as-manufactured condition is assumed for the Kaolite water content in the HAC array analysis.

All other material compositions for HAC are identical to the material compositions for NCT. For the HAC calculation model, the densities for the Kaolite in the body weldment liner inner cavity, the stainless steel of the angle iron, and the drum steel are adjusted to correspond with changes in dimensions. However, the atomic densities do not change in the HAC calculation model because mass is conserved.

The material composition used in the calculation model for the containment vessel, the drum liner, and the drum is Type 304 stainless steel at a density of 7.94 g/cm^3. The density and composition of the 304 stainless steel for the drum is taken from the Standard Composition Library of the Standardized Computer Analysis for Licensing Evaluation (SCALE) code system. The nominal weights of these components, as determined by input density and volume calculated by KENO V.a, are 14.9 kg (32.85 lb) for the containment vessel, 15.67 kg (34.55 lb) for the drum liner, and 25.44 kg (56.1 lb) for the drum.

The amount of hydrogenous packaging material used for packing the content in the containment vessel is an unknown variable. Polyethylene with a density of 0.92 g/cm^3 and a molecular formula of CH_2 has the greatest hydrogen density of potential packing materials. Although polyethylene bags are generally used in packing for contamination control, the exact mass of the polyethylene bags used is unknown. Multiple bags may be used to package the contents and to enclose the convenience cans, or bags may be omitted altogether. Realistically, the number of polyethylene bags used to bag the contents and wrap a convenience can would be six bags at most. Given that each bag weighs ~28 g, this results in a maximum of ~510 g of polyethylene per ES-3100 package. Possibly additional sources of hydrogenous material inside the containment vessel include can pads, vinyl tape, and polyethylene (~85 g) or Teflon (~303 g) bottles.

For the criticality calculations, the sources of hydrogen contained in packing materials are not distinguished from other sources of hydrogen inherent in the fissile material content. Therefore, packing material mass is defined as all sources of hydrogenous packing materials inside the containment vessel plus the actual moisture in the content as constituent (the bonded hydrogen in UNX crystals or impurities in the oxide.) Given content moisture is not to exceed 6 wt %, the amount of hydrogenous material inside the containment vessel is not expected to exceed 2,400 g.

Containment vessel flooding is assumed in calculations performed for the derivation of fissile material loading limits. Even though both the NCT tests under 10 CFR 71.71 and the HAC tests under 10 CFR 71.73 demonstrate that containment is not breached, this simulated condition produces package configurations in the criticality calculations that are more reactive than the actual package configurations. The 7.1–10.1 kg quantities of evaluation water required in both the NCT and HAC criticality calculations bound reasonable amounts of hydrogenous material and inherent moisture of fissile material (primarily HEU oxides) present inside the containment vessel (2,400 g).

HAC alter only the amount of volatile hydrogenous material contained in the package external to the containment vessel (Sect. 2.7.3). High temperatures may reduce the hydrogenous material content of the Kaolite. Conversely, water intrusion may increase the hydrogenous material content in the package. Thus, the package's range of possible volatile hydrogenous material content varies from none, caused by high temperatures, to the maximum possible value caused by water intrusion.

Table 6.4 lists the material, density, atomic or isotopic constituent, and atomic or isotopic weight percent as basic data for materials used in the single-unit packaging and array calculation models in this criticality safety evaluation for NCT and HAC, respectively. Appendix 6.9.3 provides the rationale, justification, or both for using the basic data for computing atomic densities listed in Table 6.4.

6.3.3 Computer Codes and Cross-Section Libraries

The Criticality Safety Analysis Sequences within the SCALE modular code system provide automated, problem-dependent, cross-section processing followed by calculation of the neutron multiplication factor (k_{eff}) for the system being modeled. (NUREG/CR-200, rev. 6) Initiated by "=csas25" appearing on the first line in the user input, the CSAS module runs the CSAS25 control sequence. The cross-section processing functional modules BONAMI (NUREG/CR-200, rev. 6) and NITAWL-II (NUREG/CR-200, rev. 6) are activated, providing resonance-corrected cross sections to the multigroup Monte Carlo functional module, KENO V.a (NUREG/CR-200, rev. 6). Using the processed cross sections, KENO V.a calculates the k_{eff} of three-dimensional system models. The geometric modeling capabilities available in KENO V.a, coupled with the automated cross-section processing, allow complex, three-dimensional systems to be easily analyzed.

Table 6.4. Material compositions used in the ES-3100 calculation models

Material	Mix. No.	Theoretical density input parameter (g/cm^3)[a]	Volume fraction	Constituent	Atomic weight	Weight fraction	Atomic density (atoms/b-cm)
Fissile material contents							
Uranium (solid metal)	1	18.81109	1.0	^{235}U	235.0441	1.00	4.81970E-02
				^{238}U	238.0510	0.00	0.0000E+00
Uranium (solid metal)	1	18.82298	1.0	^{235}U	235.0441	0.95	4.58156E-02
				^{238}U	238.0510	0.05	2.38089E-03
Uranium (solid metal)	1	18.83488	1.0	^{235}U	235.0441	0.90	4.34317E-02
				^{238}U	238.0510	0.10	4.76479E-03
Uranium (solid metal)	1	18.85873	1.0	^{235}U	235.0441	0.80	3.86548E-02
				^{238}U	238.0510	0.20	9.54164E-03
Uranium (solid metal)	1	18.88264	1.0	^{235}U	235.0441	0.70	3.38659E-02
				^{238}U	238.0510	0.30	1.43306E-02
Uranium (solid metal)	1	18.90661	1.0	^{235}U	235.0441	0.60	2.90647E-02
				^{238}U	238.0510	0.40	1.91317E-02
Uranium (solid metal)	1	18.95474	1.0	^{235}U	235.0441	0.40	1.94258E-02
				^{238}U	238.0510	0.60	2.87707E-02
Uranium (solid metal)	1	19.00554	1.0	^{235}U	235.0441	0.19	9.25199E-03
				^{238}U	238.0510	0.81	3.89445E-02
Uranium oxide (UO_2)	1	6.94256	1.0	H	1.0077	0.6490	2.69208E-02
				O	15.9904	16.4340	4.29699E-02
				^{235}U	235.0441	82.9170	1.47490E-02
Uranium oxide (U_3O_8)	1	6.75167	1.0	H	1.0077	0.3510	1.41552E-02
				O	15.9904	17.6620	4.49101E-02
				^{235}U	235.0441	81.9870	1.41826E-02
Uranium oxide (UO_3)	1	6.64270	1.0	H	1.0077	0.1730	6.86795E-03
				O	15.9904	18.0650	4.51925E-02
				^{235}U	235.0441	81.7620	1.39155E-02
Skull oxide	1	3.34850	1.0	H	1.0077	1.9000	3.80225E-02
(UO_3+graphite)				C	12.0001	11.9173	2.00261E-02
				O	15.9904	25.9923	3.27786E-02
				^{235}U	235.0441	56.0976	4.81282E-03
				^{238}U	238.0510	4.0929	3.46713E-04
UNH crystals	1	2.50804	1.0	H	1.0077	2.9770	4.46274E-02
(24000.0 g)				N	14.0033	5.2570	5.66985E-03
[$UO_2(NO_3)_2$+$6H_2O$]				O	15.9904	47.6480	4.50055E-02
				^{235}U	235.0441	44.1180	2.83495E-03
UNH crystals	1	1.56439	1.0	H	1.0077	6.2525	5.84562E-02
(9000.0 g)				N	14.0033	3.1604	2.12620E-03
[$UO_2(NO_3)_2$+$6H_2O$]				O	15.9904	64.0630	3.77431E-02
				^{235}U	235.0441	26.5240	1.06311E-03

Table 6.4. Material compositions used in the ES-3100 calculation models

Material	Mix. No.	Theoretical density input parameter (g/cm^3)[a]	Volume fraction	Constituent	Atomic weight	Weight fraction	Atomic density (atoms/b-cm)
UNH crystals	1	1.50149	1.0	H	1.0077	6.6172	5.93782E-02
(8000.0 g)				N	14.0033	2.9270	1.89000E-03
$[UO_2(NO_3)_2+6H_2O]$				O	15.9904	65.8907	3.72591E-02
				^{235}U	235.0441	24.5651	9.45006E-04
UNH crystals	1	1.06111	1.0	H	1.0077	10.3811	6.58313E-02
(1000.1 g)				N	14.0033	0.5178	2.36275E-04
$[UO_2(NO_3)_2+6H_2O]$				O	15.9904	84.7556	3.38697E-02
				^{235}U	235.0441	4.3455	9.45006E-04
~20% enriched UZrH	1	8.65974	1.0	H	1.0078	0.9554	4.94386E-02
(3466.7 g)				Zr	91.2196	54.0447	3.08972E-02
				^{235}U	235.0441	8.8558	1.96487E-03
				^{238}U	238.0510	36.1441	7.91816E-03
~70% enriched UZrH	1	5.70132	1.0	H	1.0078	1.5894	5.41480E-02
(2282.4 g)				Zr	91.2196	89.9107	3.38410E-02
				^{235}U	235.0441	5.9588	8.67175E-04
				^{238}U	238.0510	2.5413	3.69825E-04
Single-unit calculation models (NCT)							
277-4	2	1.50970	1.0	H	1.0077	2.84745	2.56909E-02
canned spacer				^{10}B	10.0130	0.65907	5.98418E-04
Table 11 data: [b]				^{11}B	11.0096	2.97264	2.45475E-03
as-manufactured,				C	12.0001	1.36094	1.03107E-03
minimum density and				N	14.0033	0.01000	6.49252E-06
hydrogen				O	15.9904	53.39650	3.03592E-02
				Na	22.9895	0.08326	3.29274E-05
				Mg	24.3048	0.23957	8.96150E-05
				Al	26.9818	27.69370	9.33137E-03
				Si	28.0853	1.74979	5.66427E-04
				S	32.0634	0.21865	6.19983E-05
				Ca	40.0803	8.39267	1.90373E-03
				Fe	55.8447	0.37575	6.11714E-05
Water-flooded CV	3	0.9982	1.0	H	1.0077	11.1909	6.67536E-02
				O	15.9904	88.8091	3.33856E-02
SS304	8	7.9400	1.0	C	12.0001	0.0800	3.18772E-04
containment				Si	28.0853	1.0000	1.70252E-03
vessel body				P	30.9741	0.0450	6.94680E-05
16.60 lb				Cr	51.9957	19.0000	1.74726E-02
but 15.74 lb used				Mn	54.9379	2.0000	1.74071E-03
				Fe	55.8447	68.3750	5.85446E-02
				Ni	58.6872	9.5000	7.74020E-03

Table 6.4. Material compositions used in the ES-3100 calculation models

Material	Mix. No.	Theoretical density input parameter (g/cm^3)[a]	Volume fraction	Constituent	Atomic weight	Weight fraction	Atomic density (atoms/b-cm)
SS304	9	7.9400	0.97267	C	12.0001	0.0800	3.10060E-04
containment vessel				Si	28.0853	1.0000	1.65599E-03
lower flange				P	30.9741	0.0450	6.75695E-05
used 3.36 lb				Cr	51.9957	19.0000	1.69951E-02
				Mn	54.9379	2.0000	1.69314E-03
				Fe	55.8447	68.3750	5.69445E-02
				Ni	58.6872	9.5000	7.52866E-03
SS304	10	7.9400	0.94348	C	12.0001	0.0800	3.00755E-04
containment vessel				Si	28.0853	1.0000	1.60629E-03
upper flange				P	30.9741	0.0450	6.55417E-05
used 13.75 lb				Cr	51.9957	19.0000	1.64850E-02
				Mn	54.9379	2.0000	1.64233E-03
				Fe	55.8447	68.3750	5.52356E-02
				Ni	58.6872	9.5000	7.30272E-03
277-4	11	1.45971	1.0	H	1.0077	2.84746	2.48404E-02
filling CV				^{10}B	10.0130	0.65907	5.78606E-04
inner-liner cavity				^{11}B	11.0096	2.97265	2.37348E-03
Table 11 data: [b]				C	12.0001	1.36094	9.96935E-04
as-manufactured,				N	14.0033	0.01000	6.27756E-06
minimum density and				O	15.9904	53.39660	2.93541E-02
hydrogen				Na	22.9895	0.08326	3.18372E-05
				Mg	24.3048	0.23957	8.66479E-05
				Al	26.9818	27.69360	9.02241E-03
				Si	28.0853	1.74979	5.47673E-04
				S	32.0634	0.21865	5.99456E-05
				Ca	40.0803	8.39266	1.84069E-03
				Fe	55.8447	0.37575	5.91461E-05
Kaolite	12	(body weldment)					
Al_2O_3		0.34864	0.096	Al	26.9818	52.9390	3.95461E-04
				O	15.9904	47.0610	—
SiO_2		0.34864	0.367	Si	28.0853	46.7570	1.28281E-03
				O	15.9904	53.2430	—
Fe_2O_3		0.34864	0.067	Fe	55.8447	69.9540	1.76211E-04
				O	15.9904	30.0460	—
TiO_2		0.34864	0.012	Ti	47.8793	59.9530	3.15486E-05
				O	15.9904	40.0470	—
CaO		0.34864	0.307	Ca	40.0803	71.4810	1.14955E-03
				O	15.9904	28.5180	—
MgO		0.34864	0.131	Mg	24.3048	60.3170	6.82560E-04
				O	15.9904	39.6830	—
Na_2O		0.34864	0.020	Na	22.9895	74.1960	1.35522E-04

Table 6.4. Material compositions used in the ES-3100 calculation models

Material	Mix. No.	Theoretical density input parameter (g/cm^3)[a]	Volume fraction	Constituent	Atomic weight	Weight fraction	Atomic density (atoms/b-cm)
				O	15.9904	25.8040	—
Total O		—	—	—	15.9904	—	5.39065E-03
Water	12	0.52294	1.0	H	1.0077	11.1909	3.49711E-02
				O	15.9904	88.8091	1.74856E-02
Kaolite	13	(top plug)					
Al_2O_3		0.33241	0.096	Al	26.9818	52.9390	3.77052E-04
				O	15.9904	47.0610	—
SiO_2		0.33241	0.367	Si	28.0853	46.7570	1.22309E-03
				O	15.9904	53.2430	—
Fe_2O_3		0.33241	0.067	Fe	55.8447	69.9540	1.68008E-04
				O	15.9904	30.0460	—
TiO_2		0.33241	0.012	Ti	47.8793	59.9530	3.00799E-05
				O	15.9904	40.0470	—
CaO		0.33241	0.307	Ca	40.0803	71.4810	1.09604E-03
				O	15.9904	28.5180	—
MgO		0.33241	0.131	Mg	24.3048	60.3170	6.50785E-04
				O	15.9904	39.6830	—
Na_2O		0.33241	0.020	Na	22.9895	74.1960	1.29213E-04
				O	15.9904	25.8040	—
Total O		—	—	—	15.9904	—	5.13975E-03
Water	13	0.49860	1.0	H	1.0077	11.1909	3.33433E-02
				O	15.9904	88.8091	1.66717E-02
Silicon rubber pads	14	1.21791	1.0	H	1.0077	8.1562	5.93660E-02
				C	12.0001	32.3774	1.97887E-02
				O	15.9904	21.5782	9.89729E-03
				Si	28.0853	37.8882	9.89432E-03
Water—CV well	15	0.9982	variable	H	1.0077	11.1909	variable
				O	15.9904	88.8091	variable
SS304 liner	16	7.94	1.0	C	12.0001	0.0800	3.18772E-04
				Si	28.0853	1.0000	1.70252E-03
				P	30.9741	0.0450	6.94680E-05
				Cr	51.9957	19.0000	1.74726E-02
				Mn	54.9379	2.0000	1.74071E-03
				Fe	55.8447	68.3750	5.85446E-02
				Ni	58.6872	9.5000	7.74020E-03
SS304 plug cover used 9.907 lb	17	7.94	1.06388	C	12.0001	0.0800	3.39135E-04
				Si	28.0853	1.0000	1.81128E-03
				P	30.9741	0.0450	7.39056E-05
				Cr	51.9957	19.0000	1.85887E-02
				Mn	54.9379	2.0000	1.85191E-03
				Fe	55.8447	68.3750	6.22844E-02

Table 6.4. Material compositions used in the ES-3100 calculation models

Material	Mix. No.	Theoretical density input parameter (g/cm^3)[a]	Volume fraction	Constituent	Atomic weight	Weight fraction	Atomic density (atoms/b-cm)
				Ni	58.6872	9.5000	8.23464E-03
SS304 angle iron	18	7.94	1.0	C	12.0001	0.0800	3.18772E-04
				Si	28.0853	1.0000	1.70252E-03
				P	30.9741	0.0450	6.94680E-05
				Cr	51.9957	19.0000	1.74726E-02
				Mn	54.9379	2.0000	1.74071E-03
				Fe	55.8447	68.3750	5.85446E-02
				Ni	58.6872	9.5000	7.74020E-03
SS304 steel drum	19	7.94	1.0	C	12.0001	0.0800	3.18772E-04
				Si	28.0853	1.0000	1.70252E-03
				P	30.9741	0.0450	6.94680E-05
				Cr	51.9957	19.0000	1.74726E-02
				Mn	54.9379	2.0000	1.74071E-03
				Fe	55.8447	68.3750	5.85446E-02
				Ni	58.6872	9.5000	7.74020E-03
Water—interstitial	20	0.9982	variable	H	1.0077	11.1909	variable
				O	15.9904	88.8091	variable
Water—reflector	21	0.9982	1.0	H	1.0077	11.1909	6.67536E-02
				O	15.9904	88.8091	3.33856E-02
Array calculation models (NCT)							
Kaolite	12	(body weldment)					
Al_2O_3		0.42622	0.096	Al	26.9818	52.9390	4.83460E-04
				O	15.9904	47.0610	—
SiO_2		0.42622	0.367	Si	28.0853	46.7570	1.56821E-03
				O	15.9904	53.2430	—
Fe_2O_3		0.42622	0.067	Fe	55.8447	69.9540	2.15422E-04
				O	15.9904	30.0460	—
TiO_2		0.42622	0.012	Ti	47.8793	59.9530	3.85688E-05
				O	15.9904	40.0470	—
CaO		0.42622	0.307	Ca	40.0803	71.4810	1.40535E-03
				O	15.9904	28.5180	—
MgO		0.42622	0.131	Mg	24.3048	60.3170	8.34444E-04
				O	15.9904	39.6830	—
Na_2O		0.42622	0.020	Na	22.9895	74.1960	1.65678E-04
				O	15.9904	25.8040	—
Total O		—	—	—	15.9904	—	6.58477E-03
Water	12	0.63931	0.287	H	1.0077	11.1909	1.22702E-03
				O	15.9904	88.8091	6.13510E-04

Table 6.4. Material compositions used in the ES-3100 calculation models

Material	Mix. No.	Theoretical density input parameter (g/cm^3)[a]	Volume fraction	Constituent	Atomic weight	Weight fraction	Atomic density (atoms/b-cm)
Kaolite	13	(top plug)					
Al_2O_3		0.33241	0.096	Al	26.9818	52.9390	3.77052E-04
				O	15.9904	47.0610	—
SiO_2		0.33241	0.367	Si	28.0853	46.7570	1.22309E-03
				O	15.9904	53.2430	—
Fe_2O_3		0.33241	0.067	Fe	55.8447	69.9540	1.68008E-04
				O	15.9904	30.0460	—
TiO_2		0.33241	0.012	Ti	47.8793	59.9530	3.00799E-05
				O	15.9904	40.0470	—
CaO		0.33241	0.307	Ca	40.0803	71.4810	1.09604E-03
				O	15.9904	28.5180	—
MgO		0.33241	0.131	Mg	24.3048	60.3170	6.50785E-04
				O	15.9904	39.6830	—
Na_2O		0.33241	0.020	Na	22.9895	74.1960	1.29213E-04
				O	15.9904	25.8040	—
Total O		—	—	—	15.9904	—	5.13548E-03
Water	13	0.49860	0.0287	H	1.0077	11.1909	9.56954E-04
				O	15.9904	88.8091	4.78477E-04
SS304 angle iron	18	7.94	1.25705	C	12.0001	0.0800	4.00712E-04
				Si	28.0853	1.0000	2.14015E-03
				P	30.9741	0.0450	8.73248E-05
				Cr	51.9957	19.0000	2.19639E-02
				Mn	54.9379	2.0000	2.18816E-03
				Fe	55.8447	68.3750	7.35934E-02
				Ni	58.6872	9.5000	9.72982E-03
SS304 steel drum	19	7.94	0.99981	C	12.0001	0.0800	3.18711E-04
				Si	28.0853	1.0000	1.70220E-03
				P	30.9741	0.0450	6.94548E-05
				Cr	51.9957	19.0000	1.74693E-02
				Mn	54.9379	2.0000	1.74038E-03
				Fe	55.8447	68.3750	5.85334E-02
				Ni	58.6872	9.5000	7.73873E-03
Water—reflector	21	1.16235	1.0	H	1.0077	11.1909	7.75911E-06
				O	15.9904	88.8091	3.88058E-06

Table 6.4. Material compositions used in the ES-3100 calculation models

Material	Mix. No.	Theoretical density input parameter (g/cm^3)[a]	Volume fraction	Constituent	Atomic weight	Weight fraction	Atomic density (atoms/b-cm)
Single-unit calculation models (HAC) same as NCT except as follows:							
277-4	2	1.50853	1.0	H	1.0077	2.84094	2.56124E-02
canned spacer				^{10}B	10.0130	0.65958	5.98418E-04
Table 12 data: [b]				^{11}B	11.0096	2.97494	2.45475E-03
as-manufactured,				C	12.0001	1.36193	1.03103E-03
minimum density and				N	14.0033	0.01001	6.49258E-06
hydrogen				O	15.9904	53.36920	3.03202E-02
				Na	22.9895	0.08333	3.29277E-05
				Mg	24.3048	0.23976	8.96158E-05
				Al	26.9818	27.71520	9.33140E-03
				Si	28.0853	1.75109	5.66409E-04
				S	32.0634	0.21882	6.19989E-05
				Ca	40.0803	8.39916	1.90373E-03
				Fe	55.8447	0.37604	6.11720E-05
277-4	11	1.45858	1.0	H	1.0077	2.84097	2.47645E-02
filling CV				^{10}B	10.0130	0.65959	5.78606E-04
inner-liner cavity				^{11}B	11.0096	2.97496	2.37348E-03
Table 12 data: [b]				C	12.0001	1.36193	9.96883E-04
as-manufactured,				N	14.0033	0.01001	6.27756E-06
minimum density and				O	15.9904	53.36930	2.93162E-02
hydrogen				Na	22.9895	0.08333	3.18372E-05
				Mg	24.3048	0.23976	8.66479E-05
				Al	26.9818	27.71510	9.02236E-03
				Si	28.0853	1.75109	5.47651E-04
				S	32.0634	0.21882	5.99456E-05
				Ca	40.0803	8.39913	1.84068E-03
				Fe	55.8447	0.37604	5.91461E-05
Kaolite	12	(body weldment)					
Al_2O_3		0.41898	0.096	Al	26.9818	52.9390	4.75248E-04
				O	15.9904	47.0610	—
SiO_2		0.41898	0.367	Si	28.0853	46.7570	1.54162E-03
				O	15.9904	53.2430	—
Fe_2O_3		0.41898	0.067	Fe	55.8447	69.9540	2.11763E-04
				O	15.9904	30.0460	—
TiO_2		0.41898	0.012	Ti	47.8793	59.9530	3.79136E-05
				O	15.9904	40.0470	—
CaO		0.41898	0.307	Ca	40.0803	71.4810	1.38148E-03
				O	15.9904	28.5180	—
MgO		0.41898	0.131	Mg	24.3048	60.3170	8.20270E-04
				O	15.9904	39.6830	—

Table 6.4. Material compositions used in the ES-3100 calculation models

Material	Mix. No.	Theoretical density input parameter (g/cm^3)[a]	Volume fraction	Constituent	Atomic weight	Weight fraction	Atomic density (atoms/b-cm)
Na_2O		0.41898	0.020	Na	22.9895	74.1960	1.62864E-04
				O	15.9904	25.8040	—
Total O		—	—	—	15.9904	—	6.47830E-03
Water	12	0.62843	1.0	H	1.0077	11.1909	4.20256E-02
				O	15.9904	88.8091	2.10128E-02
SS304 angle iron	18	7.94	1.23239	C	12.0001	0.0800	3.92851E-04
				Si	28.0853	1.0000	2.09817E-03
				P	30.9741	0.0450	8.56117E-05
				Cr	51.9957	19.0000	2.15330E-02
				Mn	54.9379	2.0000	2.14524E-03
				Fe	55.8447	68.3750	7.21497E-02
				Ni	58.6872	9.5000	9.53894E-03
SS304 steel drum	19	7.94	1.08401	C	12.0001	0.0800	3.45552E-04
				Si	28.0853	1.0000	1.84555E-03
				P	30.9741	0.0450	7.53040E-05
				Cr	51.9957	19.0000	1.89405E-02
				Mn	54.9379	2.0000	1.88695E-03
				Fe	55.8447	68.3750	6.34629E-02
				Ni	58.6872	9.5000	8.39045E-03
Array calculation models (HAC) same as NCT except as follows:							
Kaolite	12	(body weldment)					
Al_2O_3		0.42622	0.096	Al	26.9818	52.9390	4.83460E-04
				O	15.9904	47.0610	—
SiO_2		0.42622	0.367	Si	28.0853	46.7570	1.56821E-03
				O	15.9904	53.2430	—
Fe_2O_3		0.42622	0.067	Fe	55.8447	69.9540	2.15422E-04
				O	15.9904	30.0460	—
TiO_2		0.42622	0.012	Ti	47.8793	59.9530	3.85688E-05
				O	15.9904	40.0470	—
CaO		0.42622	0.307	Ca	40.0803	71.4810	1.40535E-03
				O	15.9904	28.5180	—
MgO		0.42622	0.131	Mg	24.3048	60.3170	8.34444E-04
				O	15.9904	39.6830	—
Na_2O		0.42622	0.020	Na	22.9895	74.1960	1.65678E-04
				O	15.9904	25.8040	—
Total O		—	—	—	15.9904	—	6.58477E-03
Water	12	0.63931	0.287	H	1.0077	11.1909	1.22702E-03
				O	15.9904	88.8091	6.13510E-04

Table 6.4. Material compositions used in the ES-3100 calculation models

Material	Mix. No.	Theoretical density input parameter (g/cm^3)[a]	Volume fraction	Constituent	Atomic weight	Weight fraction	Atomic density (atoms/b-cm)
Kaolite	13	(top plug)					
Al_2O_3		0.33241	0.096	Al	26.9818	52.9390	3.77052E-04
				O	15.9904	47.0610	—
SiO_2		0.33241	0.367	Si	28.0853	46.7570	1.22309E-03
				O	15.9904	53.2430	—
Fe_2O_3		0.33241	0.067	Fe	55.8447	69.9540	1.68008E-04
				O	15.9904	30.0460	—
TiO_2		0.33241	0.012	Ti	47.8793	59.9530	3.00799E-05
				O	15.9904	40.0470	—
CaO		0.33241	0.307	Ca	40.0803	71.4810	1.09604E-03
				O	15.9904	28.5180	—
MgO		0.33241	0.131	Mg	24.3048	60.3170	6.50785E-04
				O	15.9904	39.6830	—
Na_2O		0.33241	0.020	Na	22.9895	74.1960	1.29213E-04
				O	15.9904	25.8040	—
Total O		—	—	—	15.9904	—	5.13548E-03
Water	13	0.49860	0.0287	H	1.0077	11.1909	9.56954E-04
				O	15.9904	88.8091	4.78477E-04
SS304 angle iron	18	7.94	1.25705	C	12.0001	0.0800	4.00712E-04
				Si	28.0853	1.0000	2.14015E-03
				P	30.9741	0.0450	8.73248E-05
				Cr	51.9957	19.0000	2.19639E-02
				Mn	54.9379	2.0000	2.18816E-03
				Fe	55.8447	68.3750	7.35934E-02
				Ni	58.6872	9.5000	9.72982E-03
SS304 steel drum	19	7.94	0.99981	C	12.0001	0.0800	3.18711E-04
				Si	28.0853	1.0000	1.70220E-03
				P	30.9741	0.0450	6.94548E-05
				Cr	51.9957	19.0000	1.74693E-02
				Mn	54.9379	2.0000	1.74038E-03
				Fe	55.8447	68.3750	5.85334E-02
				Ni	58.6872	9.5000	7.73873E-03
Water—reflector	21	1.16235	1.0	H	1.0077	11.1909	7.75911E-06
				O	15.9904	88.8091	3.88058E-06

[a] The theoretical density input parameter is specified for each material such that the required (or desired) mass of material is represented in the KENO V.a calculation model. The mass of material is computed by KENO V.a as the product of the theoretical density input parameter times the volume fraction times the volume of the geometry region in which the material resides in the calculation model.

[b] DAC-PKG-801624-A001.

The CSAS25 control sequence and the 238-group ENDF/B-V cross-section library in SCALE are used for all calculations. The control sequence, functional modules, and cross-section library are summarized in the following paragraphs.

The CSAS25 control sequence reads user-specified input data, which include the required cross-section library, specifications for mixtures, information for resonance processing of nuclides (size, geometry, and temperature), and a detailed geometry model for KENO V.a. Physical and neutronic information not specified but required by the functional modules (such as theoretical density, molecular weights, and average resonance region background cross sections) is supplied by the Standard Composition Library or calculated by the Materials Information Processor. The Standard Composition Library (NUREG/CR-200, rev. 6) consists of a standard composition directory and table, an isotopic distribution directory and table, and a nuclide information table. The Materials Information Processor (NUREG/CR-200, rev. 6) checks the input data pertaining to cross-section preparation and prepares binary input files for the applicable functional modules BONAMI and NITAWL-II.

The standardized automated procedures process SCALE cross sections using the Bondarenko method (via BONAMI) and the Nordheim integral method (via NITAWL-II) to provide a resonance-corrected cross-section library based on the physical characteristics of the problem being analyzed.

BONAMI performs resonance shielding through the application of the Bondarenko shielding factor method. BONAMI reads the master format library and applies the Bondarenko correction to all nuclides that have Bondarenko data. BONAMI produces a Bondarenko-corrected master format library which is read by NITAWL-II.

NITAWL-II applies the Nordheim Integral Treatment to perform neutron cross-section processing in the resonance energy range for nuclides that have ENDF/B resonance parameter data. This technique involves the numerical integration of ENDF/B resonance parameters using a calculated flux distribution, which is based on the calculated collision density across each resonance and subsequent weighing of the reaction cross section to the desired broad group structure. In the CSAS sequence, NITAWL-II assembles the group-to-group transfer arrays from the elastic and inelastic scattering components and performs other tasks to produce a problem-dependent, working cross-section library which can be used by KENO.

KENO V.a, a multigroup Monte Carlo computer code, is used to determine k_{eff} for multidimensional systems. The basic geometrical bodies allowed in KENO V.a for defining models are cuboids, spheres, cylinders, hemispheres, and hemicylinders. KENO V.a has the following major characteristics:

- enhanced geometry package that allows arrays to be defined and positioned throughout the model;
- P_n scattering treatment;
- extended use of differential albedo reflection;
- printer plots for checking the input model;
- energy-dependent data supergrouping;
- restart capability; and
- origin specifications for cuboids, spheres, cylinders, hemicylinders, and hemispheres.

The 238-group ENDF/B-V master cross-section library in SCALE is activated in the CSAS25 control sequence by specifying 238GROUPNDF5 (238GR) as the cross-section library name. The 238-GROUP ENDF/B-V [neutron cross-section] library is a general-purpose criticality analysis library and the most complete library available in SCALE 4.4a. The library contains data for all nuclides (more than 300) available in ENDF/B-V processed by the AMPX-77 systems. It also contains data for ENDF/B-VI evaluations of ^{14}N, ^{15}N, ^{16}O, ^{154}Eu, and ^{155}Eu. The library has 148 fast groups and 90 thermal groups (below 3 eV). Most resonance nuclides in the 238 group have resonance data (to be processed by NITAWL-II in the resolved resonance range) and Bondarenko factors (to be processed by BONAMI) for the unresolved range. The 238-group library contains resolved resonance data for s-wave, p-wave, and d-wave resonances **R** = 0, **R** = 1, and **R** = 2, respectively. These data can have a significant effect on results for under-moderated, intermediate-energy problems. Resonance structures in several light-to-intermediate mass "nonresonance" ENDF nuclides (i.e., ^{7}Li, ^{19}F, ^{27}Al, ^{28}Si) are accounted for using Bondarenko shielding factors. These structures can also be important in intermediate energy problems.

All nuclides in the 238-group library use the same weighting spectrum, consisting of:

- Maxwellian spectrum (peak at 300 K) from 10^{-5} to 0.125 eV,
- a 1/E spectrum from 0.125 eV to 67.4 keV,
- a fission spectrum (effective temperature at 1.273 MeV) from 67.4 keV to 10 MeV, and
- a 1/E spectrum from 10 to 20 MeV.

The k_{eff} values for each KENO V.a case are based on 500,000 neutron histories produced by running for 215 generations with 2,500 neutrons per generation and truncating the first 15 generations of data. The convergence of the KENO V.a calculation is related to trends in the average calculated k_{eff}. In general, the KENO V.a output table of k_{eff} by Generation Skipped is reviewed for trends. If no trends are observed, the calculation is accepted, and the reported value of k_{eff} is the one with the most neutron histories. Usually there is no statistically significant difference between this result and the one with the smallest standard deviation.

No manual cross-section adjustment is performed for the criticality safety evaluation. The cross-section processing is performed automatically in the CSAS25 code sequence making use of the available cross-section treatment options as appropriate.

The CSAS control module, the associated functional modules, cross sections, and databases used in this evaluation reside in the verified configuration control area designated **/vcc/scale4.4a** on a Hewlett Packard Series 9000 J Class workstation at the Y-12 Safety Analysis Engineering organization in Oak Ridge, Tennessee. The detailed input and computer output for the criticality safety evaluation of the ES-3100 shipping container with HEU reside in a configuration control area **/archive/ylf717_Rv2** on the workstation. Input listings of the key cases indicated in Tables 6.1a–6.1e are provided in Appendix 6.9.7.

6.3.4 Demonstration of Maximum Reactivity

10 CFR 71.55(b) requires the evaluation of water leakage into the containment vessel, leakage of liquid contents out of the containment vessel, and other conditions which produce maximum reactivity in the single package. For solid uranium contents, water leakage conditions are simulated by flooding all regions outside and inside of the containment vessel, including the sealed convenience cans. For liquid uranium contents, water leakage conditions are simulated by flooding all regions outside the containment vessel except the containment vessel well. Uranyl nitrate solution resides inside both the containment vessel, including the sealed convenience cans, and the well external to the containment vessel. According

to the 10 CFR 71.55(b) requirement, a flooded containment vessel under full water reflection is also evaluated.

Credit for the high-integrity, watertight containment is not taken either in the single package analysis [10 CFR 71.55 (d, e)] or in the array analysis [10 CFR 71.59 (a)(1)] of undamaged packages. In the evaluation of undamaged packages under 10 CFR 71.59 (a)(1) and the evaluation of damaged packages under 10 CFR 71.59 (a)(2), the containment vessel is flooded with water, providing moderation to such an extent as to cause maximum reactivity of the content consistent with the chemical and physical form of the material present. Solid HEU, not solution HEU, is being shipped in the ES-3100. Consequently, in the evaluation of damaged packages under 10 CFR 71.59 (a)(2), the leakage out of the containment vessel of content moderated to such an extent as to cause maximum reactivity consistent with the physical and chemical form of the material is not considered credible HAC, based on results for tests specified in 10 CFR 71.73.

Contents are generally dry, and only small quantities of hydrogenous packing materials are used. However, credit for the high-integrity, watertight containment is not taken in this criticality evaluation. (Meeting, Docket 71-9315) Fissile material loading is restricted such that if a containment vessel were flooded, it would be adequately subcritical under full water reflection. But instead of loading limits being established in accordance with conditions of confinement and containment as demonstrated under the NCT and HAC tests, these single-unit fissile material loading limits are severely reduced on the basis of the array calculations where all of the containment vessels of the packages in an array are assumed to be flooded but each packaging is dry. This has the effect of maximizing both the neutron source and neutronic interaction between packages. Because credit for the high-integrity, watertight containment is not fully taken in this criticality evaluation, the fissile material mass loading limits developed as a result are very conservative.

Section 6.3.1 provides dimensional data for content and package models, and Sect. 6.3.2 provides material composition data used in the calculation models. Appendix 6.9.3 provides justification for the composition data used in the evaluation. These sections and this appendix describe how the packaging dimensions and materials are optimized to produce a conservative model by reducing neutron absorbing materials and maximizing the reactivity of the fissile material content through the inclusion of water in the containment vessel.

As described in Sect. 6.3.1.1, a geometry region is defined by dimensions and the type of material contained therein. The amount of material within a region is quantified in terms of the density, material volume fraction, and the volume of the region (Sect. 6.3.2). The term “water fraction” means the fraction of the maximum specific gravity of water possible for any geometry region in the ES-3100 package. Therefore, the water content is the fraction of the maximum specific gravity of water possible in a material in the ES-3100 package when flooded.

The maximum value for the void regions (spaces external to the containment vessel) is 1.0 for both single-unit and array geometries. For the geometry regions containing Kaolite, the maximum values are 0.51655 for the single unit and 0.63931 for the array. For the geometry regions containing 277-4, the maximum value is 0.6942 for both the single-unit and array geometries. The same single-unit values are used in the array calculation models because the 277-4–bearing regions do not require adjustment for the close-pack approximation (Sect. 6.3.1.2).

In general, boundary condition specifications are not required in KENO V.a, so that calculation models analyzed using KENO V.a require no special boundary conditions. However, in this evaluation, the infinite array cases use a single package with a reduced radius modeled with spectral reflection on all faces of a surrounding cuboid. The energies and angular dependence of the neutrons are treated such that an infinite system with no neutron leakage is simulated.

For simplicity, the NCT and HAC sets of calculations were performed for selected ES-3100 array sizes by varying the water content of the ES-3100 package external to the containment vessel from zero to its maximum value. This technique bounds all NCT and HAC; however, only the relevant calculation results are used in determination of the CSI for criticality purposes.

Although four decimal places are shown for k_{eff} values in result tables, the actual accuracy of the code, for a particular calculation, may be on the order of ± 0.02–0.03 based on the spread in results for benchmark calculations (Y/DD-896/R1 and Y/DD-972R1, Appendix 6.9.8). Also, the standard deviation of the mean for a particular calculation is on the order of 0.001 for benchmark cases and somewhat higher for the package calculations. Therefore, numerical values are considered physically meaningful or significant to the third decimal place. The primary reason for reporting four (or five) decimal places for a calculation result is to confirm that the result reported actually originated from a given output file. A value of 0.925 is the USL used for this safety analysis report (Sect. 6.8.3).

6.4 SINGLE PACKAGE EVALUATION

The HEU content of a package is in one of the following forms: metal of a specified geometric shape; metal of an unspecified shape characterized as broken metal; uranium oxide; or UNH crystals. The bounding types of HEU content evaluated in this criticality analysis are 3.24-in. and 4.25-in.-diam cylinders; 2.29-in.-square bars; 1.5-in.-diam × 2-in.-tall slugs; cubes ranging from 0.25 to 1 in. on a side; broken metal pieces of unspecified geometric shapes; product oxide; skull oxide; UNH crystals; and unirradiated TRIGA reactor fuel elements.

Dimensions for bounding calculation models of a TRIGA fuel section are 1.44 inches in diameter × 5 in. tall. The 20% enrichment fuel contains more fissile mass than the 70% enrichment fuel on account of a higher uranium weight fraction and associated material density. A 20 wt % enriched TRIGA fuel element with 45 wt % U contains ≤307 g ^{235}U; whereas, a 70 wt % enriched TRIGA fuel with 8.5 wt % U contains ≤136 g ^{235}U. The physical parameters which characterize the TRIGA fuel are enrichment, uranium weight fraction, and the fuel diameter. (Appendix 6.9.3.1). These parameters are addressed in this section demonstrating that the calculation models are bounding in the criticality evaluation.

Alloys of uranium may include aluminum, molybdenum, or zirconium. Uranium-aluminum (U-Al) alloy is typically 70 to 95 wt % aluminum. Uranium-molybdenum (U-Mo) alloys are typically 1.5 to 12 wt % molybdenum. U-Mo alloys may be plated with, clad with, or contain traces of aluminum, gold, stainless steel, nickel, and/or chromium. The enrichment of U-Al, U-Mo, and U-Zr alloys range from 92.65 to 93.21 wt % ^{235}U.

Where scattering media (aluminum, molybdenum, or zirconium) is counted as multiplying media (^{235}U), the alloy is conservatively assessed. Consider a canned content of U-Al which contains 940 g of uranium, 600 g of ^{235}U, and 4070 g of aluminum. In determining compliance with a loading limit, the loading of this content would be on the basis that the material contains 4670 g ^{235}U rather than 600 g ^{235}U.

6.4.1 Solid HEU Metal of Specified Geometric Shapes

For bare and reflected single packages with HEU metal content, the neutron multiplication factor increases as a function of the ^{235}U mass and the moisture fraction of the package external to the containment vessel (MOIFR). For example, consider the ES-3100 package loaded with three convenience cans for a total of 36,000 g ^{235}U. Each press-fit lid type can contains a single 3.24-in.-diam, 12,000 g cylinder of ^{235}U. The $k_{eff} + 2\sigma$ values in the bare package increase from 0.911 to 0.955 with increasing moisture fraction of the package external to the containment vessel (MOIFR), Cases **ncsbcyt11_36_1_1** through **ncsbcyt11_36_1_15** (Appendix 6.9.6, Table 6.9.6-2). The $k_{eff} + 2\sigma$ values increase from 0.918 to 0.955 with increasing MOIFR in the water-reflected package, Cases **ncsrcyt11_36_1_1** through **ncsrcyt11_36_1_15** (Appendix 6.9.6, Table 6.9.6-2). The addition of water to the package reduces the neutron leakage fraction (NLF), thereby increasing k_{eff}. Water reflection external to a flooded package is inconsequential to package reactivity as a comparison of results for Cases **ncsbcyt11_36_1_15** and **ncsrcyt11_36_1_15** indicates.

In this series of calculations using the ES-3100 package model with NCT geometry (Cases **ncsrcyt11_36_1_1** through **ncsrcyt11_36_1_15)**, the MOIFR is varied uniformly over the package model with the exception of the neutron poison of the body weldment liner inner cavity and the flooded containment vessel. The single-unit case with a MOIFR = 1.0 pertains specifically to the flooded drum under conditions specified in 10 CFR 71.55(b). This pseudo-HAC condition is more reactive than either the true NCT where both the containment vessel and Kaolite are dry [10 CFR 71.55(d)] or this evaluation for NCT where the containment vessel is flooded and the Kaolite is dry (in the as-manufactured condition, MOIFR ~ 0.0289). At MOIFR = 1.0, external water reflection of the package is inconsequential to package reactivity. Moisture in the Kaolite and in the recesses of the package acts as a close reflector that decreases neutron leakage away from the package.

The single-unit case with a MOIFR = 1e-20 pertains specifically to a package under pseudo-HAC where both the Kaolite and the recesses of the package do not contain **any** water or bound hydrogen. This configuration is less reactive than the cases for Kaolite in the as-manufactured condition or water-saturated Kaolite because water in the Kaolite will provide some neutron moderation and reflection of neutrons back into the content.

Single package reactivity changes slightly between the bare and reflected conditions, while NLF changes considerably over the range of water fractions. This behavior illustrates the dependence of package reactivity on internal conditions of the package. Bare packages with low MOIFR values manifest low reactivity ($k_{eff} = 0.911$) and high neutron leakage (NLF = 0.47). These parameters indicate that fast neutrons scattered in the packaging do not slow down significantly but escape the package. Consequently, neutron interaction between these packages when they are configured into an array is high. Bare packages with MOIFR values >1e-2 manifest increasing k_{eff} values (from 0.911 to 0.955) and reduced NLF values (from 0.47 to 0.18). The increase in k_{eff} occurs due to water present in the regions of the package external to the content which reflects neutrons back into the HEU content that would otherwise escape the package.

A series of calculations are performed using the calculation model of a water-reflected containment vessel loaded with 3.24-in.–diam cylinders. The three cylinders are aligned as depicted in Fig. 6.9.1-1 (Appendix 6.9.1) but in very close proximity due to the omission of can spacers. A parametric variation of water density from zero to 1.0 sp gr inside the containment vessel is performed for establishing moderation by water to the most credible extent. The calculated $k_{eff} + 2\sigma$ values for Cases **cvcrcyt11_36_1_1** through **cvcrcyt11_36_1_15** (Appendix 6.9.6, Table 6.9.6-1) increase monotonically from 0.907 to 0.974 with increasing moisture fraction inside the containment vessel (MOCFR). Maximum reactivity of the fissile material occurs in the flooded containment vessel.

10 CFR 71.55(b)(3) requires evaluation of the efficiency of the packaging as an external reflector to the containment vessel. Comparison of the calculated $k_{eff} + 2\sigma$ value for Case **cvcrcyt11_36_1_15** to the value for Case **ncsrcyt11_36_1_15** reveals that the flooded containment vessel under full water reflection is a more reactive configuration than the containment vessel inside a flooded ES-3100 packaging. The ES-3100 package is not as efficient a reflector as full water reflection provided to the flooded containment vessel. For this reason, calculation results for the flooded containment vessel rather than a flooded package are reported in Tables 6.1a (and Tables 6.1b–6.1e) for the evaluation of 10 CFR 71.55(b) requirements.

Examination of the results for Cases **cvcrcyt11_36_1** through **cvcrcyt11_18_1** indicates that an adequately subcritical loading is achieved when the mass loading is limited to 21,000 g ^{235}U (Case **cvcrcyt11_21_1**). Case **cvcrcyt11_36_2** reveals that the 277-4 canned spacers are adequate for mass loading >18,000 g ^{235}U but ≤36,000 g ^{235}U. These potential fissile (^{235}U) mass loading limits derived through the evaluation of 10 CFR 71.55(b) are listed in Table 6.1a in the information block where a description of the content appears for fissile material "the most reactive credible configuration consistent with the chemical and physical form of the content,". The final mass loading limit is derived at the conclusion of the array analysis for these content configurations.

The NCT tests under 10 CFR 71.71 and the HAC tests under 10 CFR 71.73 demonstrate that containment is not breached. Nevertheless, containment vessel flooding is assumed in the criticality calculations performed for the derivation of fissile material loading limits. The 7.1–10.1 kg quantities of evaluation water in both the NCT and HAC criticality calculations are not actually present in the containment vessel. Simulation of this condition in the criticality calculations produces fissile material content that is more reactive than actual. The evaluation water required in both the NCT and HAC criticality calculations bounds reasonable amounts of hydrogenous material present inside the containment vessel for solid HEU shapes.

Consider Case **cvcrcyt11_21_1** as the reference case where the calculated $k_{eff} + 2\sigma = 0.923$ (Table 6.9.6-1). The fissile material content is 21,000 g HEU metal at 100% enrichment and a density of 18.81109 g/cm^3. Three HEU cylinders (3.24 in. in diameter and 2.75425-in. tall) are stacked end-to-end starting at 0.0005 cm above the bottom of the containment vessel. The stack height is 20.98987 cm where each cylinder is separated by a 0.0001-cm–thick 277-4 canned spacer and 0.0012 cm of moderating material. Effectively, this configuration does not have 277-4 canned spacers, and no polyethylene is used in this calculation model. The water-filled cavity above the content is 57.74963 cm in height. As the input listing for Case **cvcrcyt11_21_1** (Appendix 6.9.7) indicates, ~9083 g of **evaluation** water fills the flooded containment vessel and the calculated H/X ratio is ~11.29. The calculated H/X ratio for the HEU content wrapped in 500 g polyethylene (hydrogenous packing material) inside a dry containment vessel is ~0.80.

Case **cvcrpcyt11_21_1** is the same as reference Case **cvcrcyt11_21_1,** except that 500 g polyethylene wraps three HEU cylinders with a uniform thickness of 0.54956 cm. The three wrapped HEU cylinders are stacked end-to-end starting at 0.0005 cm above the bottom of the containment vessel. Each wrapped cylinder is separated by a 0.0001-cm–thick 277-4 canned spacer and 0.0012 cm of moderating material resulting in a stack height of 24.28733 cm. The water-filled cavity above the content is 57.74963 cm in height. At a density of 0.9200 g/cm^3, 500 g polyethylene adds 543.47826 cm^3 to the volume of the content and reduces the free volume of the containment vessel by an equal amount. As indicated in the case title card, 8540.1 g of **evaluation** water fills the flooded containment vessel. The 500 g polyethylene increases the overall H/X ratio inside the flooded containment vessel to 11.41. The calculated $k_{eff} + 2\sigma$ is 0.908 for this configuration (Table 6.9.6-1). While polyethylene having a greater hydrogen density than water is a slightly better moderating material than water, the presence of polyethylene in the calculation model provides separation between the fissile

material resulting in a slight reduction in the calculated $k_{eff} + 2\sigma$ value. Case **cvdcrpcyt11_21_1** is the same as Case **cvcrpcyt11_21_1**, except that the containment vessel is dry. The calculated $k_{eff} + 2\sigma$ is 0.847 for Case **cvdcrpcyt11_21_1** (Table 6.9.6-1). The calculated $k_{eff} + 2\sigma$ value of 0.923 for reference Case **cvcrcyt11_21_1** without polyethylene is greater than the values for Cases **cvcrpcyt11_21_1** and **cvdcrpcyt11_21_1** with polyethylene. In the case of solid HEU shapes, the 7.1–10.1 kg quantities of evaluation water required in both the NCT and HAC criticality calculations bound reasonable amounts of hydrogenous material present inside the containment vessel.

Because convenience cans are not credited for providing configuration control in the containment vessel, it is possible for the fissile material to be spaced farther apart than shown in Fig. 6.9.1-1. A series of cases was run to evaluate the axial spacing of content inside the containment vessel. As shown in Table 6.9.6-3b, the separation distances between adjacent cylinders range from 0.0 to 8.75 in. (12.225 cm). Zero separation occurs when the base surfaces of adjacent cylinders are flush with the 277-4 canned spacer between them. Figure 6.9.1-1b depicts a section view of the containment vessel with 3.24-in.-diam cylinders at 4.826 and 0.254 cm separation. The calculated $k_{eff}+2\sigma$ values for Cases **ncsrcyat11_1_2_15** through **ncsrcyat11_12_2_15** (Table 6.9.6-3c) decrease with increasing separation distance. Loading configurations where solid HEU of specified geometric shape is axially positioned in contact with the can spacers are the most reactive ones.

Case **hcsrcyt12_36_1_15** (Appendix 6.9.6, Table 6.9.6-3) represents the HAC model of the damaged ES-3100 package, where the outer dimensions of the package are reduced accordingly and the entire package is flooded with the exception of the neutron poison of the body weldment liner inner cavity. The containment vessel well is flooded with water, and the Kaolite contains maximum water content. This single-unit case with a MOIFR = 1.0 pertains specifically to the flooded drum under conditions specified in 10 CFR 71.55(e). The $k_{eff} + 2\sigma = 0.955$ for this HAC. The changes in both the outer dimensions of the package and the compositions of the Kaolite and 277-4 due to HAC result in an ~0.002 change in the neutron multiplication factor.

Repeated for 4.25-in.-diam cylinders (Appendix 6.9.6, Tables 6.9.6-6 and 6.9.6-7); 2.29-in.-square bars (Tables 6.9.6-4 and 6.9.6-5); and 1.5-in.-diam × 2-in.-tall slugs (Tables 6.9.6-8 and 6.9.6-9), this type of analysis for the 3.24-in.-diam cylinders demonstrates that single packages with restricted fissile material (^{235}U) loading remain subcritical over the entire range of water content or MOIFR. HEU bulk metal or alloy content not covered by the specified geometric shapes (cylinder, square bar, or slug contents) will be in the HEU broken metal category, and so limited.

Each TRIGA fuel element for shipment in the ES-3100 is to be disassembled. The active fuel consisting of three 5-in.-tall cylinders of $UZrH_{1.6}$ is to be packed into a metal-type convenience can. (Section 6.2.1) The use of three loaded convenience cans in the ES-3100 is assumed in the criticality calculation models for ground transport. However, credit is only taken for vertical spacing provided by canned spacers when present. For configurations where canned spacers are not used, the TRIGA content is assumed stacked end-to-end. The three cylinders of the active fuel are modeled in triangular-pitch configuration within the radial boundary of the convenience can(s). The pitch used in the criticality calculation models for the NCT and HAC ground transport is 4.9809 cm (1.96 in.).

As shown in Table 6.9.6-19b, a set of parametric cases were run where the triangular pitch for the fuel content is varied from 1.44 in. (fuel sections touching) to 2.413 in. (fuel sections at maximum separation and touching the inner boundary of the convenience can). As shown in Fig. 6.16a, the calculated $k_{eff} + 2\sigma$ values increase slightly from 0.48 to an asymptotic value of ~ 0.53 at a pitch of 2.121 in. or a foci of 3.1106 cm (Table 6.9.6-19b). The foci of 2.8757 cm. for the TRIGA fuel sections used in the criticality calculation models, corresponds to a 1.96 in. pitch. The calculated $k_{eff} + 2\sigma$ value is 0.527 for Case **cvcrtriga_1_15** (Table 6.9.6-19a) indicating that the configuration is in the range of optimum moderation. Moreover, the calculated $k_{eff} + 2\sigma$ value is substantially below the USL. (The foci is the distance perpendicular from the CV's vertical axis to the center of each fuel section. The value is obtained from the computer input listing on the comment line for geometry Unit 1006 which reads: " -2.875700 minus-y location lower cylinder. ")

Parametric cases were also run as a function of the moisture fraction ("mocfr") in the CV. As shown in Fig. 6.16b, the $k_{eff} + 2\sigma$ values decrease with decreasing water content in the CV; and content spacing has less of an effect on k_{eff} at lower at the lower fractions.

The first of the three physical parameters which characterize the TRIGA fuel is enrichment. Table 6.9.6-19a presents results for 20 % enriched and 70 % enriched TRIGA fuel where the diameter of the active fuel is 1.44 in. The calculated $k_{eff} + 2\sigma$ values for TRIGA fuel content at the lower enrichment is greater than for the fuel with the higher enrichment due to the greater quantity of fissile isotope present. The 20% enriched TRIGA fuel is considered the bounding content.

The second physical parameter which characterizes the TRIGA fuel is the uranium weight fraction. For a TRIGA fuel enriched to 20 wt % ^{235}U in U, the uranium weight fractions for the $UZrH_{1.6}$ fuel are: 45 wt %; 30 wt %; 20 wt %; 12 wt %; and 8.5 wt % U. A set of parametric cases were run where the uranium weight fraction is varied from the minimum value of 8.5 wt % to the maximum value of 45 wt %. Additionally, moderation in the containment vessel is varied from the dry to the flooded condition. As shown in Fig. 6.16c, the $k_{eff} + 2\sigma$ values decrease with both decreasing uranium weight fraction and decreasing water content in the CV. Details are provided in Table 6.9.6-19c.

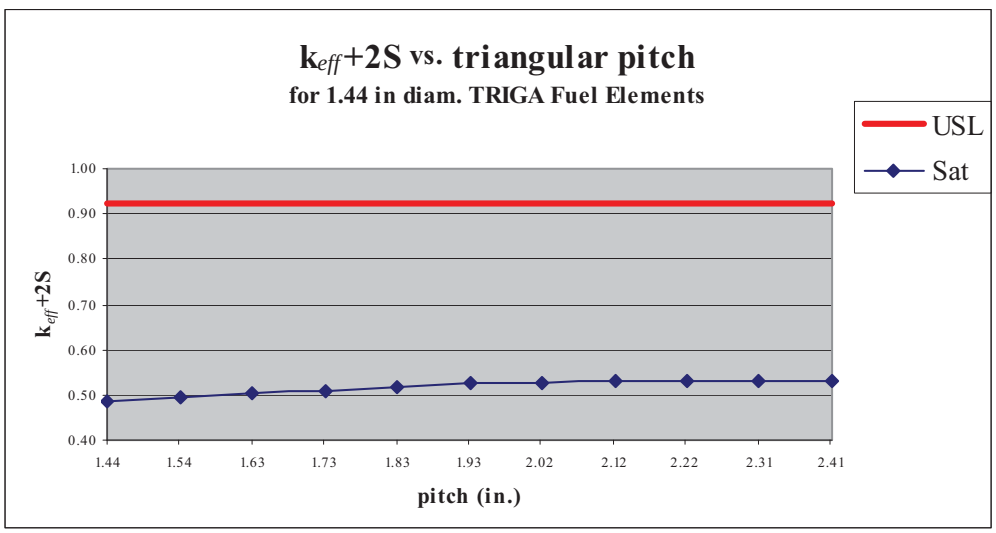

Fig. 6.16a. $k_{eff} + 2\sigma$ versus pitch for triangular arrangement of content in CV.

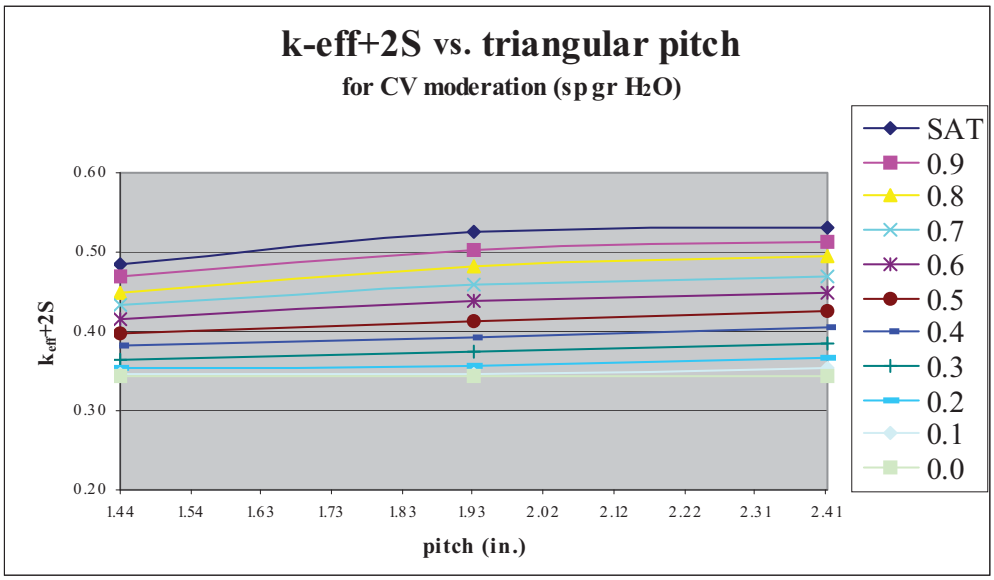

Fig. 6.16b. k_{eff} + 2σ versus triangular pitch over range of CV moderation.

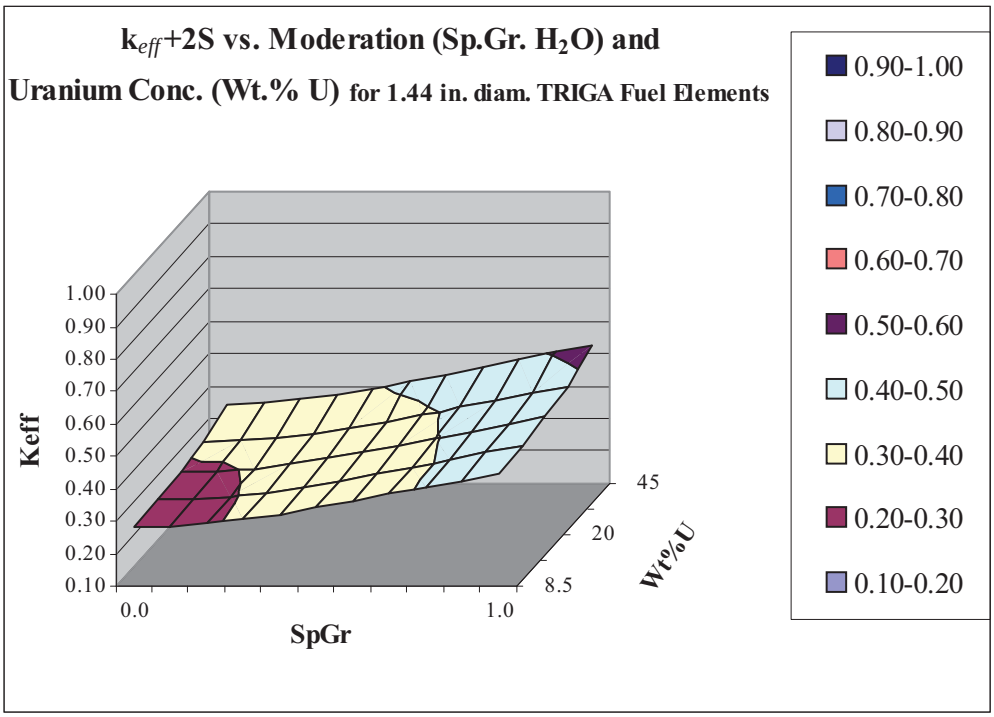

Fig. 6.16c. k_{eff} + 2σ as a function of uranium weight fraction and moderation.

Third physical parameter which characterizes the TRIGA fuel is active fuel diameter. The active fuel diameters are: 1.44 in.; 1.41 in.; 1.40 in.; 1.37 in.; 1.34in.; and 1.31 in. The smaller the diameter, the less the amount of ^{235}U is present resulting in lower k_{eff} + 2σ values, as demonstrated later in this section.

Cases **cvcrtriga_1_1** through **cvcrtriga_1_15** (Appendix 6.9.6, Table 6.9.6-19a) represent the TRIGA fuel content in a flooded containment vessel, reflected by 30.48 cm of water. The flooded containment vessel under full water reflection is a more reactive configuration than the containment vessel inside of flooded ES-3100 packaging, Case **ncsrtriga_1_15_15** (Appendix 6.9.6, Table 6.9.6-20a). Further examination of the results in Table 6.9.6-20a indicates the content loading is adequately subcritical loading and that 277-4 canned spacers are not required for criticality control. Comparison of results for the NCT Case **ncsrtriga_1_15_15** and the HAC **hcsrtriga_1_15_15**, both with $k_{eff} + 2\sigma = 0.495$, reveal that changes to the packaging external to the containment vessel due to the HAC do not result in an appreciable change in the neutron multiplication factor for the single package.

Cases **ncsrtriga70_1_1_1** through **ncsrtriga70_1_15_15** (Appendix 6.9.6, Table 6.9.6-20b) represent the 70 % enriched TRIGA fuel content in a flooded ES-3100 package, reflected by 30.48 cm of water. Comparison of results for these cases with results for the 20 % enriched TRIGA fuel (Cases **ncsrtriga_1_1_1** through **ncsrtriga_1_15_15**) confirm that the 20 % enriched TRIGA fuel is the bounding content.

Cases **ncsrT70_131_1_1_15** through **ncsrT70_131_1_15_15** (Appendix 6.9.6, Table 6.9.6-20c) represent the 1.31 in. diameter TRIGA fuel content in a flooded ES-3100 package, reflected by 30.48 cm of water. Comparison of results for these cases with results for the larger 1.44 in. diameter TRIGA fuel content (Cases **ncsrtriga70_1_1_1** through ncsrtriga70_1_15_15) confirm that the 1.44 in. diameter TRIGA fuel is the bounding content.

10 CFR 71.55(d)(2) requires the geometric form of a package's content not be substantially altered under the NCT. Also, 10 CFR 7155(e)(1) requires that the package be adequately subcritical under HAC with the package contents in the most reactive credible configuration. However, conclusions about damage to the fuel content can not be extrapolated from test data because a mock (test weight) content rather than actual TRIGA content is evaluated in the NCT and HAC tests of 10 CFR 71.71 and 10 CFR 71.73. Consequently, one way for addressing these requirements is to model the content in an extremely damaged condition and make a determination of subcriticality through a series of criticality calculations. Cases **ncsrt55d2_ 1_1_1**5 through **ncsrt55d2_1_15_15** (Appendix 6.9.6, Table 6.9.6-20d) represent TRIGA fuel content homogenized with variable density water over the free volume of the containment vessel, where the ES-3100 packaging is flooded and reflected by 30.48 cm of water. The variable density water ranges from the dry containment condition to the fully flooded condition. Credit for physical integrity of the content is not taken in this set of cases which model the substantially altered content. The calculation results in Table 6.9.6-20d indicate extremely damaged content (Case **ncsrt55d2_1_15_15** with $k_{eff} + 2\sigma = 0.611$) is more reactive than the unaltered configuration (Case **ncsrtriga_1_15_15** with $k_{eff} + 2\sigma = 0.403$). Nevertheless, both cases are adequately below the USL of 0.925 and the requirement of 10 CFR 71.55(d)(2) is satisfied. Given that changes external to the containment vessel due to the HAC do not result in an appreciable change in the neutron multiplication for the single package, similar results are expected for the cases demonstrating compliance with 10 CFR 7155(e)(1).

The shipping configuration for disassembled TRIGA fuel addressed in this subsection is not the only permissible shipping configuration for TRIGA fuel in the ES-3100. TRIGA fuel may also be configured as clad fuel rods (Appendix 6.9.3.1). Each 15 in. long rod is derived from a single TRIGA fuel element. The clad fuel rod consists of the 3 fuel pellets and the exterior sheath of stainless steel or aluminum clad. Clad fuel rods are packed into stainless steel or tin-plated carbon steel convenience cans with a maximum of three fuel rods per loaded convenience can. This shipping configuration requires that only one convenience can is loaded with clad fuel rods.

Except for a 0.02 in. thick sheath of stainless steel clad added to the exterior surface of the $UZrH_{1.6}$, a calculation model for the clad fuel rod configuration is essentially the same as the NCT shipping configuration model for disassembled TRIGA fuel. A 0.02 in thickness of stainless steel is insignificant for an external reflection. As illustrated in Fig. 6.21 (Sect. 6.7.2), stainless steel up to several cm in thickness acts as a neutron absorber. Several inches in thickness are required for neutron multiplication to increase from neutron reflection by the stainless steel. The NCT shipping configuration model for disassembled TRIGA fuel is bounding. The same applies for TRIGA fuel with aluminum clad.

A clad fuel rod with 1.44 in. diameter fuel pellets contains 2,282.4 g $UZrH_x$ (Appendix 6.9.3.1) and ~179 to 191 g of stainless steel. Stainless steel tends to act as a neutron absorber; moreover, its presence as clad in the TRIGA fuel content replaces water moderator otherwise present in the geometry configuration of TRIGA fuel meats. When stainless steel is homogenized with the $UZrH_{1.6}$ as in the calculation model for package content in the extremely damaged condition [10 CFR 71.55(d)(2) and 10 CFR 7155(e)(1)], the stainless steel acts more effectively as a neutron absorber. However, the amount of stainless steel added and water displaced is not expected to have a statistically significant affect on neutron multiplication. Thus, the HAC shipping configuration model for disassembled TRIGA fuel (bare fuel meats) is bounding.

A clad fuel rod with 1.41 in. diameter fuel pellets contains ~2,188 g $UZrH_x$ and ~90 to 96 g of aluminum. While aluminum tends to act as a neutron scatter, its presence in the TRIGA fuel content replaces water moderator otherwise present in the geometry configuration of TRIGA fuel meats. The amount of aluminum added and water displaced is not sufficient to have a statistically significant affect on neutron multiplication. Thus, the HAC shipping configuration model for disassembled TRIGA fuel is also bounding for aluminum clad TRIGA fuel content.

The TRIGA content is to be transported by air; consequently, additional discussion is included in Sect. 6.7.

The 1.5-in.–diam × 2-in.–tall slugs may be packed up to ten items per press-fit lid type convenience can and up to twelve items per crimp-lid type convenience can. With nominal dimensions, each slug weighs ~1,090 g. With +1/16 in. tolerance on both the diameter and height, each slug in the calculation model weighs ~1218 g. As described in Appendix 6.9.1, different arrangements of slugs in the convenience cans are possible. A configuration of slugs in a flooded reflected containment vessel must be shown to be adequately subcritical and so limited either by the use of 277-4 canned spacers, by limitation of fissile mass, or by both.

Several slug arrangements depicted in Fig. 6.9.1-4b are evaluated for demonstrating that the most conservative arrangement of slugs is being analyzed. The blue marker shown in Fig. 6.9.1-4c depicts the 4.13-in. diam of the canned spacer. Content within a configuration radius of 2.125 in. (5.4 cm) are within the boundary of the convenience can wall. The convenience cans are not modeled and contents are allowed to project beyond the convenience can wall boundary. The slugs are modeled only as 100 wt % ^{235}U for this portion of the criticality evaluation. Cases **cvcr5st11_1_1**, **cvcr5est11_1_1**, **cvcr50st11_1**, **cvcr5e0st11_1**, **cvcr5u0st11_1**, and **cvcr5l0st11_1** depict very different spacing arrangements with five slugs per convenience can, three cans per package. The statistical difference in the calculated "$k_{eff} + 2\sigma$" values is insignificant. Cases **cvcr6e0st11_1** and **cvcr6st11_1_1** depict arrangements with six slugs per convenience can, and Case **cvcr70st11_1** depicts seven slugs per convenience can. (Considerable deformation of the 4.25-in.–diam convenience can wall is required to achieve all but the simple pentagonal-ring arrangement of slugs.) Calculation results reveal the primary dependence of the "$k_{eff} + 2\sigma$" value is on the fissile mass loading and the secondary dependence is on the arrangement and spacing of slugs. The calculation results presented in Table 6.9.6-8 (Appendix 6.9.6) for a flooded containment vessel indicate that only five slugs per convenience

can (18,277 g ^{235}U per package) may be loaded without the use of 277-4 canned spacers (Cases **cvcr5st11_1_1** and **cvcr5est11_1_1**). Further evaluation of the single package and array configurations are required. Also, results highlighted in red indicate that 277-4 canned spacers are required for the slug content.

The sensitivity of k_{eff} to the space between slugs arranged in a pentagonal ring is evident in the calculation results for Cases **cvcr5st11_1_2** and **cvcr5est11_1_2,** which model content for three convenience cans, each location with two pentagonal rings (10 slugs) per can. These two configurations represent degrees of separation between adjacent neighbors in the pentagonal rings of 0.0 cm and 1.0 cm, respectively. The most reactive configuration occurs when the slugs are spaced 1.0 cm apart from direct contact with adjacent neighbors in the pentagonal rings. Because positioning devices are not used in the convenience cans to control spacing and prevent an optimal arrangement of contents from occurring, both calculation models for slug arrangement are the basis for additional calculations where 277-4 canned spacers may not be required.

Cases **cvcr5st11_2_1**, **cvcr5est11_2_1**, **cvcr50st11_2**, **cvcr5e0st11_2**, **cvcr5u0st11_2**, and **cvcr5l0st11_2** represent the different spacing arrangements with five slugs per convenience can, three cans per package, and cans separated by canned spacers. Likewise, Cases **cvcr6e0st11_2** and **cvcr6st11_2_1** represent arrangements with six slugs per convenience can, three can per package, and cans separated by can spacers. Case **cvcr70st11_2** represents seven slugs per convenience can. While the differences in the calculated "$k_{eff} + 2\sigma$" values for equal numbers of slugs per can are $\leq$ 0.006, the "$k_{eff} + 2\sigma$" values are significantly below the USL. Again, the calculation results presented in Table 6.9.6-8 (Appendix 6.9.6) for these cases reveal the primary dependence of the "$k_{eff} + 2\sigma$" value is on fissile mass loading, and the secondary dependence is on the arrangement and spacing of slugs.

Case **cvcr6e0st11_2** models three sets of slugs, six slugs in a pentagonal ring with one slug in the center, and each set of slugs separated by a 277-4 canned spacer. Cases **cv0r6e0st11_2** and **cvwr6e0st11_2** are variations of the reference case where the 1.4-in. spacer is replaced with void in the first case and is replaced with water in the second case. Comparison of the "$k_{eff} + 2\sigma$" values between Cases **cvcr6e0st11_2** and **cv0r6e0st11_2** reveals that the spacers reduce k_{eff} by ~ 0.03. Comparison of the "$k_{eff} + 2\sigma$" values for Cases **cvcr6e0st11_2** and **cvwr6e0st11_2** reveals that axial spacing of the content provided by the content cans inside the containment vessel serves to reduce k_{eff}.

The calculation results presented in Table 6.9.1-8 for a flooded containment vessel indicate that up to ten slugs per convenience can (36,555 g ^{235}U per package) *might* be loaded when 277-4 canned spacers are used. Conceivable arrangements are considered in Cases **cvcr5st11_2_2**, **cvcr5est11_2_2**, **cvcr6e4st11_2**, and **cvcr73st11_2**, (Table 6.9.6-8). Suitability is contingent on the results of single package and array calculations.

Cases **ncsr5est11_2_1_1** through **ncsr5est11_2_1_15** (Appendix 6.9.6, Table 6.9.6-9) model a reflected package with one pentagonal ring of slugs per content location with 277-4 canned spacers between content locations and HEU content at 100 wt % ^{235}U. The $k_{eff} + 2\sigma$ values range from a low value of 0.688 to 0.736. These results show that the most reactive configuration is the flooded condition with MOIFR=1.0.

As shown by the cylindrical content calculation models, the ES-3100 package is not as an efficient reflector as full water reflection provided to the flooded containment vessel. This is also true for content loadings of one pentagonal ring of slugs per content location without 277-4 canned spacers between locations and HEU content at 100 wt % ^{235}U. For Cases **cvcr5est11_1_1** and **ncsr5est11_1_1_15**, the $k_{eff} + 2\sigma$ values are 0.910 and 0.871, respectively. Likewise, the $k_{eff} + 2\sigma$ values

are 0.901 and 0.867 for content loadings of two pentagonal rings of slugs per content location with 277-4 canned spacers between locations, Cases **cvcr5est11_2_2** and **ncsr5est11_2_2_15**, respectively.

For the flooded containment vessel under full water reflection and loaded with the slugs in a pentagonal arrangement and 277-4 canned spacers between content locations, the $k_{eff} + 2\sigma$ value is 0.903, Case **cvcr5st11_2_2.** [10 CFR 71.55(b)] This value is below the USL value of 0.925. For packages with the required 1.4-in. spacers, the calculated $k_{eff} + 2\sigma$ value is 0.878 for the water-reflected package, Case **ncsr5st11_2_2_15**. [10 CFR 71.55(d)] Case **hcsr5st11_02_2_15** represents the HAC model of the damaged ES-3100 package, where the outer dimensions of the package are reduced accordingly and the entire package is flooded except the neutron poison of the body weldment liner inner cavity. This single-unit case with a MOIFR = 1.0 pertains specifically to the flooded drum under conditions specified in 10 CFR 71.55(e). The $k_{eff} + 2\sigma$ value is 0.872 for this HAC. The changes in both the outer dimensions of the package and the compositions of the Kaolite and 277-4 due to HAC result in an ~0.001 change in the neutron multiplication factor.

6.4.2 HEU Solid Metal of Unspecified Geometric Shapes or HEU Broken Metal

Like packages with HEU metal, the neutron multiplication factor for reflected single packages with HEU broken metal increases as a function of the ^{235}U mass and the MOIFR. For example, consider the ES-3100 package loaded with three convenience cans for a total of 35,142 g ^{235}U. The $k_{eff} + 2\sigma$ values range from 0.814 to 0.891 with increasing MOIFR in the water-reflected package [Cases **ncsrbmt11_36_1_1** through **ncsrbmt11_36_1_15** (Appendix 6.9.6, Table 6.9.6-11)]. The addition of water to the package reduces the NLF, thereby increasing k_{eff}.

For the containment vessel loaded with the broken metal content but without 277-4 canned spacers between content locations, the $k_{eff} + 2\sigma$ values increase from 0.751 to 0.949 as the water content in the containment vessel increases [Cases **cvr3lha_36_1_8_1** through **cvr3lha_36_1_8_15** (Appendix 6.9.6, Table 6.9.6-10, and Appendix 6.9.3, Fig. 6.9.3.1-5)]. Cases **cvr3lha_36_1_8_15** through **cvr3lha_36_1_1_15** model the flooded containment vessel with 35 kg of broken HEU metal where the enrichment ranges from 100 to 19 wt % ^{235}U. The result for Case **cvr3lha_36_1_6_15** indicates that for an enrichment of 90 wt % ^{235}U, the mass loading cannot exceed 31,482 g in the absence of canned spacers. However, the application of this limit to higher enrichment material is non-conservative, as illustrated by the result for Case **cvr3lha_26_1_8_15**. (The results for cases highlighted in yellow indicate potential limits.) As the enrichment increases, the mass loading limit decreases (from 28,334 g to 25,894 g in this example) due to less ^{238}U for neutron absorption.

For the flooded containment vessel under full water reflection and loaded with the broken metal content and 277-4 canned spacers between content locations, the $k_{eff} + 2\sigma = 0.876$, Case **cvr3lha_36_2_8_15** [10 CFR 71.55(b)]. For packages loaded with the broken metal content and 277-4 canned spacers between content locations, the calculated $k_{eff} + 2\sigma$ value is 0.872, Case **ncsrbmt11_36_2_15** [10 CFR 71.55(d)]. Case **hcsrbmt12_36_2_15** (Appendix 6.9.6, Table 6.9.6-11) represents the HAC model of the damaged ES-3100 package, where the outer dimensions of the package are reduced accordingly and the entire package is flooded except the neutron poison of the body weldment liner inner cavity. This single-unit case with a MOIFR = 1.0 pertains specifically to the flooded drum under conditions specified in 10 CFR 71.55(e). The $k_{eff} + 2\sigma = 0.874$ for this HAC condition. The changes in both the outer dimensions of the package and the compositions of the Kaolite and 277-4 due to HAC result in an ~0.002 change in the neutron multiplication factor.

6.4.3 HEU Oxide

HEU product oxide content is non-hygroscopic or mildly hygroscopic. While bulk densities of product oxides are typically on the order of 6.54 g/cm^3, the bulk density of HEU oxides considered for shipment in the ES-3100 ranges from 2.0 to 6.54 g/cm^3. HEU skull oxide is a less dense form of U_3O_8 intermixed with graphite. Of interest are those compositions with carbon/fissile uranium (C/^{235}U) ratios up to 2.3×10^5 µg C/g^{235}U. The quantity of fissile uranium is extremely low where even higher C/^{235}U ratios are present.

HEU product oxide content may be packed in polyethylene bottles or metal convenience cans; HEU skull oxide content is packed in metal convenience cans. Polyethylene bottles and hydrogenous packing material are represented by 500 g polyethylene. While both the size and shape of the polyethylene bottles prevents the use of 277-4 canned spacers with product oxide loadings, the 10-in. height of the metal convenience cans eliminates the use of 277-4 canned spacers for product or skull oxide content packaged in these size cans. However, the convenience cans are not modeled in this criticality evaluation and this analysis is performed from the standpoint that metal-type convenience cans may be used for both oxide types.

HEU oxide content is not considered a "rigid" content like solid or broken HEU metal. For the calculation models of HEU oxides, the polyethylene is homogenized with the saturated bulk oxide. At a density of 0.9200 g/cm^3, polyethylene adds 543.47826 cm^3 to the volume of the saturated bulk oxide and reduces the free volume of the containment vessel by an equal amount. The evaluation water in the void region of the containment vessel fills the volume of the containment vessel that not occupied by oxide content. (The void region of the containment vessel is defined as the containment vessel volume minus the oxide content volume.) Because of the differences in densities and compositions, product oxides are addressed separately from skull oxides.

Like packages with HEU metal or broken metal, the neutron multiplication factor for reflected single packages with HEU oxide increases as a function of increasing MOIFR and decreases with decreasing ^{235}U mass. For example, consider the ES-3100 package loaded with oxide at 6.54 g/cm^3 in three convenience cans for a total of 24,000 g UO_2 (21,125 g ^{235}U). The $k_{eff} + 2\sigma$ values range from 0.724 to 0.804 with increasing MOIFR in the reflected package [Cases **ncsrpoxt11_1_24_1** through **ncsrpoxt11_1_24_15** (Table 6.9.6-13)]. The addition of water to the package reduces the NLF, thereby increasing k_{eff}. The flooded, reflected package is the most reactive single package configuration; consequently, MOIFR is treated as a constant rather than a variable in subsequent "**pdox**" cases.

Parametric calculations are performed for oxide content loadings in a flooded, reflected package by varying the oxide bulk density from 6.54 g/cm^3 to a lower value limited by the capacity of the convenience cans. The maximum content capacity of the ES-3100 is ~6,975 cm^3, where each of three 4.25-in.-diam × 10.0-in.-tall convenience cans has a capacity of ~2,375 cm^3. As shown in Table 6.9.6-13a, calculations for a loading of 24,000 g UO_2 are performed at bulk densities of 6.54 g/cm^3, 5.0 g/cm^3, and 4.0 g/cm^3, but not 3.0 g/cm^3 because the capacity of the convenience cans is exceeded for this mass loading. Note that Case **ncsrpoxt11_1_24_15** (Table 6.9.6-13) is identical to Case **ncsrpdoxt11_1_5_24** (Table 6.9.6-13a). Results for the parametric Cases **ncsrpdoxt11_1_*n*_24**, **ncsrpdoxt11_1_*n*_20**, and **ncsrpdoxt11_1_*n*_15** reveal the consistent increase in the $k_{eff} + 2\sigma$ values as the bulk density decreases. This increase in neutron multiplication is due to the increased moderation of the HEU oxide.

Cases **ncsrpdoxt11_1_*n*_14** for UO_2 (12,323 g ^{235}U), **ncsrpdoxt11_2_*n*_14** for U_3O_8 (11,850 g ^{235}U), and **ncsrpdoxt11_3_*n*_14** for UO_3 (11,627 g ^{235}U) evaluate the ES-3100 package loaded with 14 kg oxide over the range of bulk density "*n*". The $k_{eff} + 2\sigma$ values reveal a consistent increase over the range of density. Results for Cases **ncsrpdoxt11_2_1_14** and **ncsrpdoxt11_3_1_14** indicate that both the U_3O_8 content ($k_{eff} + 2\sigma = 0.778$) and the UO_3 content ($k_{eff} + 2\sigma = 0.760$) are bounded by the UO_2 content ($k_{eff} + 2\sigma = 0.814$). Even though the capacity of the convenience cans is exceeded by 25 g, these cases are retained for the purpose of illustrating this point.

Results for a reflected containment vessel loaded with HEU oxide reveal the same trends in the $k_{eff} + 2\sigma$ values as do results for the reflected package; however, the $k_{eff} + 2\sigma$ values are ~0.1 greater in the containment vessel cases. For the flooded containment vessel loaded with UO_2, the $k_{eff} + 2\sigma$ values increase from 0.838 to 0.911 with decreasing bulk density [Cases **cvcrpdoxt11_1_5_14_15** through **cvcrpdoxt11_1_1_14_15** (Table 6.9.6-12 and Fig. 6.9.1-6)]. For the dry containment vessel, the $k_{eff} + 2\sigma$ values increase from 0.824 to 0.912 [Cases **cvcrpdoxt11_1_5_14_1** through **cvcrpdoxt11_1_1_14_1** (Table 6.9.6-12 and Fig. 6.9.1-6)]. Comparison of results for high density UO_2 oxide saturated with 862 g water reveals a small increase in $k_{eff} + 2\sigma$ from 0.824 to 0.838 due to flooding of the containment vessel. Comparison of results for low density UO_2 oxide saturated with 5,712 g water reveals an insignificant increase in $k_{eff} + 2\sigma$ due to flooding of the containment vessel, [Cases **cvcrpdoxt11_1_5_14_15** and **cvcrpdoxt11_1_5_14_1** (Table 6.9.6-12 and Fig. 6.9.1-6)].

Cases **cvcrpdoxt11_1_11_14_15** through **cvcrpdoxt11_1_1_14_15** demonstrate that the $k_{eff} + 2\sigma$ values decrease for decreased mass loadings of HEU oxide at constant bulk density.

For the flooded containment vessel under full water reflection containment, the $k_{eff} + 2\sigma$ value is 0.914, Case **cvcrpdoxt11_1_3_24_15**. [10 CFR 71.55(b)] The $k_{eff} + 2\sigma$ value is 0.817 for water-reflected package, Case **ncsrpdoxt11_1_3_24**. [10 CFR 71.55(d)] Case **hcsrpdoxt12_1_3_24** (Table 6.9.6-13a) represents the HAC model of the damaged ES-3100 package, where the outer dimensions of the package are reduced accordingly and the entire package is flooded except the neutron poison of the body weldment liner inner cavity. This single-unit case pertains specifically to the flooded drum under conditions specified in 10 CFR 71.55(e). The $k_{eff} + 2\sigma$ value is 0.819 for this HAC condition. The changes in both the outer dimensions of the package and the compositions of the Kaolite and 277-4 due to HAC result in an ~0.002 change in the neutron multiplication factor.

Cases **cvcrsk3cc_1_15_17** through **cvcrsk3cc_10_15_17** (Appendix 6.9.6, Table 6.9.6-17) evaluate the 10 skull oxide compositions identified Table 6.9.3.1-3b, where the containment vessel is loaded with 3 convenience cans. The fissile enrichment is ~70 wt % ^{235}U for contents "**sk3cc_1**" through "**sk3cc_5**" and ~38 wt % ^{235}U for contents "**sk3cc_6**" through "**sk3cc_8**." The observed maximums of 7.1 kg skull oxide and ~93.2 wt % ^{235}U enrichment present in 292 convenience cans are the basis for the hypothetical contents "**sk3cc_9**" and "**sk3cc_10**," where unidentified material is treated as ^{235}U and the carbon content is either maximized or minimized. Content "**sk3cc_10**" differs from "**sk3cc_9**" in that 921 g of graphite in the skull oxide is replaced with 921 g ^{235}U in the form of U_3O_8. Content "**sk3cc_10**" is more representative of high enrichment skull oxides where < 85 g of graphite is present. For each of the 10 content models, 513 g of the skull oxide content is modeled as polyethylene, representing the potential use of hydrogenous packing material. The U_3O_8 content ranges from 8 to 21 kg, while the ^{235}U content ranges from 3.7 to 16.4 kg. The graphite content ranges from 0 to 921 g C, and the C/^{235}U ratio ranges from 0 to 223,432 µg C/g ^{235}U. For Cases **cvcrsk3cc_1_15_17** through **cvcrsk3cc_10_15_17** at both saturation moisture and full graphite content, the $k_{eff} + 2\sigma$ values range from 0.759 to 0.855 in the flooded, water-reflected containment vessel. Cases **cvcrsk3cc_9_15_17** and **cvcrsk3cc_10_15_17** reveal that $k_{eff} + 2\sigma$ increases slightly when the 921 g of carbon in the skull oxide is replaced with 726 g ^{235}U in the form of U_3O_8.

Cases **cvcrsk3cc_4_1_1** through **cvcrsk3cc_4_*m*_*g*** evaluate the effects of moisture and skull oxide graphite content on reactivity. The case designator "***m***" ranges from 1 to 15, signifying the variation in moisture; "***g***" ranges from 1 to 17, signifying the variation in graphite. Examination of results indicates that moisture content has a predominate effect on the neutron multiplication factor, while variation in graphite content has a minor effect. The peak $k_{eff} + 2\sigma$ value occurs at saturated moisture and full graphite content.

Cases **ncsrsk_1_15** through **ncsrsk_10_15** (Appendix 6.9.6, Table 6.9.6-18a) model the 10 skull oxide compositions in a flooded containment vessel in a water reflected package. The $k_{eff} + 2\sigma$ values range from 0.641 to 0.745. Likewise, Cases **hcsrsk_1_15** through **hcsrsk_10_15** (Appendix 6.9.6, Table 6.9.6-18b) evaluate infinite arrays damage packages. The $k_{eff} + 2\sigma$ values ranging from 0.658 to 0.767 are not statistically significantly different from the NCT case results.

Cases **ncsrsk_9_1** through **ncsrsk_9_15** evaluate the bounding skull oxide content containing ~19.9 kg U_3O_8 and 921 g graphite, where the saturation moisture is varied from 0 to 3801 g water. Likewise, Cases **ncsrsk_10_1** through **ncsrsk_10_15** evaluate the skull oxide content containing ~20.8 kg U_3O_8 where the 921 g of graphite in the skull oxide is replaced with 726 g ^{235}U in the form of U_3O_8. The $k_{eff} + 2\sigma$ values range from 0.403 to 0.741 in the former set of cases and range from 0.404 to 0.746 in the latter set of cases. The $k_{eff} + 2\sigma$ values are well below the USL value of 0.925, indicating that canned spacers are not required for criticality control. Moreover, these results indicate that moisture content has a predominate effect on the neutron multiplication factor, while the graphite content has an insignificant effect.

6.4.4 UNH Crystals

UNH crystal content is to be packed in Teflon bottles, which may be placed in polyethylene bags. The Teflon bottles are not credited for containing the UNH crystal content. The 277-4 canned spacers are not used in this packing configuration. Teflon is polytetrafluoroethylene (or Polyethylene Tetrafluoride) having a monomer formula of C_2F_4 with a melting point of ~280°C (536°F). Teflon will not melt at the much lower containment vessel inner wall temperatures associated with NCT and HAC. The use of Teflon and polyethylene packing material is conservatively represented by 500 g of polyethylene in the calculation model. UNH crystal content is not considered a "rigid" content like solid or broken HEU metal. Like HEU oxide content, the UNH crystal content is homogenized with the polyethylene.

Unlike the other HEU contents, UNH crystals are soluble in water. The most reactive content condition occurs at an optimum solution concentration derived from the UNH crystal loading and the volume of water flooding the containment vessel. Both flooding of the containment vessel and a reduced loading of UNH crystals going into solution is required to achieve the most reactive configuration.

Consider a flooded containment vessel with the UNH crystals in solution and no polyethylene. For Cases **cvcrunhct11_24_1** through **cvcrunhct11_1_1** (Table 6.9.6-14), the $k_{eff} + 2\sigma$ values range from 0.823 to 0.609 and optimum concentration occurs at ~9,000 g UNH (Case **cvcrunhct11_9_1**, $k_{eff} + 2\sigma = 0.857$). Consider a flooded containment vessel with a solution of UNH crystals homogenized with 500 g polyethylene. For Cases **cvcrpunhct11_24_15** through **cvcrpunhct11_1_15** (Table 6.9.6-14), the $k_{eff} + 2\sigma$ values range from 0.827 to 0.613 and optimum concentration occurs at ~10,000 g UNH (Case **cvcrpunhct11_10_15**, $k_{eff} + 2\sigma = 0.863$). The replacement of water with 500 g of polyethylene in the latter set of cases results in changes to the neutron multiplication factor on the order of ~0.004 to 0.006. The concentration for a 24,000 g loading in both set of cases is 1,106 g ^{235}U per liter of flooded containment vessel. In the calculation of the uranium concentration, the solution volume is not reduced by the volume of polyethylene because polyethylene is homogenized with UNH in the solution.

For Cases **cvcrpunhct11_24_1** through **cvcrpunhct11_1_1** (Table 6.9.6-14), the homogenized UNH crystals and polyethylene are dispersed over a dry containment vessel. The $k_{eff} + 2\sigma$ values range from 0.769 to 0.251 as the mass loading decreases. Comparison with results for corresponding Cases **cvcrpunhct11_24_15** through **cvcrpunhct11_1_15** for a flooded containment vessel reveals that the most reactive content condition occurs for UNH in the solution state.

For Cases **cvcrbpunhct11_24_15** through **cvcrbpunhct11_1_15** (Table 6.9.6-14), homogenized UNH crystals and polyethylene are settled on the bottom of the containment vessel and the residual volume above it is flooded. The $k_{eff} + 2\sigma$ values range from 0.817 to 0.553 as the mass loading decreases. For Cases **cvcrbpunhct11_24_1** through **cvcrbpunhct11_1_1**, the residual volume above the content is dry. Likewise, the $k_{eff} + 2\sigma$ values range from 0.815 to 0.478 as the mass loading decreases.

Comparison of results for corresponding Cases **cvdrpunhct11_*n*_1** and **cvcrbpunhct11_*n*_15** reveal greater changes in the k_{eff} values occurring at the lower mass loadings when dispersed content is settled to the bottom of the containment vessel. Nevertheless, interspersed moderation has a dominant effect on k_{eff} occurring when settled content goes into solution (Case **cvcrbpunhct11_10_15** vs Case **cvcrpunhct11_10_15**).

Similar to packages loaded with HEU metal, broken metal, or oxide, the neutron multiplication factor for a reflected single package with UNH crystals increases as a function of MOIFR. Consider the ES-3100 package loaded with bottles for a total of 24,000 g UNH crystals (11,303 g ^{235}U). For Cases **ncsrunhct11_24_1_1** through **ncsrunhct11_24_1_15** (Table 6.9.6-15), the $k_{eff} + 2\sigma$ values range from 0.605 to 0.702 with increasing MOIFR in the water-reflected package. For Cases **ncsrpunhct11_24_1** and **ncsrpunhct11_24_15** (Table 6.9.6-15), the $k_{eff} + 2\sigma$ values range from 0.609 to 0.708 with increasing MOIFR in the water-reflected package. These cases confirm that the replacement of water with 500 g of polyethylene results in changes to the neutron multiplication factor on the order of ~0.004 to 0.006.

For a flooded containment vessel with UNH crystals in solution, the $k_{eff} + 2\sigma$ values range from 0.702 to 0.646 [Cases **ncsrunhct11_24_1_15** through **ncsrunhct11_2_1_15** (Table 6.9.6-15)]. Similarly, for a flooded containment vessel with a solution of UNH crystals homogenized with 500 g of polyethylene, the $k_{eff} + 2\sigma$ values range from 0.708 to 0.545 [Cases **ncsrpunhct11_24_15** through **ncsrpunhct11_1_15** (Table 6.9.6-15)]. At optimal concentration (~8,000 g UNH), the calculated $k_{eff} + 2\sigma$ value is 0.863 for Case **cvcrpunhct11_10_15** and $k_{eff} + 2\sigma = 0.753$ for Case **ncsrpunhct11_8_15**. The water-reflected containment vessel is more reactive than the water-reflected package; therefore, the result for Case **cvcrpunhct11_10_15** is reported. [10 CFR 71.55(b)] The result for Case **ncsrpunhct11_8_15** having the maximum $k_{eff} + 2\sigma$ value is reported for the NCT water-reflected package. [10 CFR 71.55(d)]

Unlike solid HEU metal and oxide content, which are confined to the containment vessel and only water leakage into the containment vessel need be considered, the evaluation of UNH crystal content for compliance with 10 CFR 71.55(b) also requires that the leakage of liquid HEU contents out of the containment be addressed. This is because UNH crystals are soluble in water and would dissolve in the water flooding the containment vessel and the containment vessel well. For a content loading of 24,000 g UNH, the uranium concentration inside the containment vessel drops from 1,106 g ^{235}U/L to 710 g ^{235}U/L. Optimum solution concentrations occurs for fissile mass loadings of ~15,000 g UNH. In the calculation of the uranium concentration, the solution volume is not reduced by the volume of polyethylene because polyethylene is homogenized with UNH in the solution.

Cases **hcsrpunhct12_8_15** (Table 6.9.6-15) and **icsrpunhct12_15_15** (Table 6.9.6-16) represent the HAC model of the damaged ES-3100 package where the outer dimensions of the package are reduced accordingly. For Case **hcsrpunhct12_8_15**, the dilution of the UNH crystals is confined to the containment vessel, and maximum reactivity occurs at ~8000 g UNH homogenized with 500 g polyethylene. For Case **icsrpunhct12_15_15**, UNH crystals are dissolved in the water flooding the containment vessel and the containment vessel well. The fissile material is uniformly distributed over the volume of the containment vessel and the well, but the polyethylene is confined to the containment vessel. Maximum reactivity occurs at ~15,000 g UNH. These single-unit cases with a MOIFR = 1.0 pertain specifically to the flooded drum under conditions specified in 10 CFR 71.55(e), where the $k_{eff} + 2\sigma$ values are 0.752 and 0.814 for this HAC condition. The result for Case **icsrpunhct12_15_15** having the maximum $k_{eff} + 2\sigma$ value is reported for the HAC water-reflected package. [10 CFR 71.55(e)]

6.5 EVALUATION OF PACKAGE ARRAYS UNDER NORMAL CONDITIONS OF TRANSPORT

For the NCT array evaluation of ES-3100 packages, the package content is confined within the containment vessel, consistent with the result of the tests specified in §71.71 (Normal Conditions of Transport). The array sizes examined in this evaluation are infinite, 13×13×6, 9×9×4, 7×7×3, 5×5×2, ETP 27×3, and the degenerate single unit. The "N" and corresponding CSI values for arrays determined to be adequately subcritical are as follows: N = ∞, CSI = 0; N = 202, CSI = 0.3; N = 64, CSI = 0.8; N = 29, CSI = 1.7; and N = 16, CSI = 3.2. All arrays, except the infinite array, are reflected with 30 cm (1 ft) of water. These arrays are nearly cubic in shape for optimum array reactivity, thus eliminating the need for placing criticality controls on package arrangements in terms of stack height, width, and depth of an array. The array configurations and the range of water contents (Table 6.4) evaluated bound all possible packaging arrangements and moderation conditions for NCT.

6.5.1 Solid HEU Metal of Specified Geometric Shapes

For infinite and finite arrays of packages with HEU metal, the neutron multiplication factor increases as a function of the ^{235}U mass and decreases as a function of MOIFR. For example, consider the ES-3100 package loaded with three convenience cans for a total of 36,000 g ^{235}U where each can contains a 3.24-in.-diam cylinder. For package content without 277-4 canned spacers, the $k_{eff} + 2\sigma$ values range from 1.027 to 0.963 with increasing MOIFR in the package [Cases **nciacyt11_36_1_1** through **nciacyt11_36_1_15** (Appendix 6.9.6, Table 6.9.6-3)]. For package content with 277-4 canned spacers, the $k_{eff} + 2\sigma$ values range from 0.957 to 0.880 with increasing MOIFR in the package [Cases **nciacyt11_36_2_1** through **nciacyt11_36_2_15** (Appendix 6.9.6, Table 6.9.6-3)].

The effect of increasing the water content of the array is straightforward. As interspersed water is added to the packages of an array, two reactivity effects occur in series. The first effect is the tendency for reactivity to remain constant due to controlled neutron interaction between the packages of the array. For an infinite array where neutrons cannot escape from the system, neutrons are scattered about the array. In the MOIFR range of 1e-20 to 1e-02, both the interspersed moderator inside the packages of the dry array and the interstitial moderator between the package drums of the array are not sufficient for neutron thermalization and absorption to occur in the adjacent packaging materials. However, hydrogen in the 277-4 provides moderation, and neutrons are absorbed in the interspersed boron of this neutron poison. This results in a subcritical system with near constant neutron multiplication factors over the range of MOIFR. The second effect is the tendency for reactivity to decrease due to internal moderation in packages of the array. The introduction of water above ~0.01 MOIFR shows the effect of isolating the individual array units from each other. The neutron multiplication factor approaches k_{eff} for the single, water-reflected unit at a full-content water fraction (MOIFR = 1.0).

The array case with a water fraction of MOIFR = 1e-04 pertains specifically to packages under NCT where the Kaolite and recesses of the package external to the containment vessel do not contain any residual moisture. This NCT case is more reactive than all other NCT cases where more moisture is present in the Kaolite and recesses of the package. Interspersed water between the containment vessels in the array will reduce neutronic interaction between the flooded contents because neutrons are absorbed in the hydrogen of the water. As more water is added, the packages of the array become isolated, and array reactivity ($k_{eff} + 2\sigma = 0.880$, Case **nciacyt11_36_2_1**5) approaches the reactivity of the single unit ($k_{eff} + 2\sigma = 0.873$, Case **ncsrcyt11_36_2_1**5).

Repeated for 4.25-in.-diam cylinders (Appendix 6.9.6, Table 6.9.6-7); 2.29-in. -square bars (Table 6.9.6-5); and 1.5-in.-diam × 2-in.-tall slugs (Table 6.9.6-9), this type of analysis for the 3.24-in.-diam cylinders demonstrates that arrays of packages with restricted fissile material (^{235}U) loading remain subcritical over the entire range of water content or MOIFR. HEU bulk metal or alloy content not covered by the specified geometric shapes (cylinder, square bar, or slug contents) will be in the HEU broken metal category, and so limited.

Cases **nciatriga_1_1_3** through **nciatriga_1_15_3** (Appendix 6.9.6, Table 6.9.6-20a) represent infinite arrays of packages containing the bounding TRIGA fuel content (20 % enrichment with 45 wt % U containing 307 g ^{235}U), without 277-4 canned spacers. The MOIFR is set at 1.0e-04 such that neutronic interaction between packages is maximized. For these cases, the $k_{eff} + 2\sigma$ values increase from 0.218 to 0.525 as MOIFR increases. The $k_{eff} + 2\sigma = 0.525$ for Case **nciatriga_1_15_3** is substantially below the USL value of 0.925, indicating that canned spacers are not required for criticality control.

As stated in Sect. 6.4.1, 10 CFR 71.55(d)(2) requires the geometric form of a package's content not be substantially altered under the NCT. Similarly, 10 CFR 71.55(e)(1) requires that the package be adequately subcritical under HAC with the package contents in the most reactive credible configuration. Even though visible signs of damage to the metal convenience can have not been observed resulting from the regulatory tests, conclusions about damage to the TRIGA fuel content are not extrapolated from test data. The regulatory requirements are addressed by modeling the TRIGA fuel content in an extremely damaged condition. A series of criticality calculations is performed for making a determination of subcriticality. Cases **nciat55d2_1_1_3** through **ncia55d2_1_15_3** (Appendix 6.9.6, Table 6.9.6-20d) represent TRIGA fuel content homogenized with variable density water over the free volume of the containment vessel. The packaging is flooded in each ES-3100 package of the infinite array. The variable density water ranges from the dry containment condition to the fully flooded condition. Credit for physical integrity of the content is not taken in this set of cases which model the substantially altered content. The calculation results in Table 6.9.6-20d indicate extremely damaged content (Case **nciat55d2_1_15_3** with $k_{eff} + 2\sigma = 0.716$) is more reactive than the unaltered configuration (Case **nciatriga_1_15_3** with $k_{eff} + 2\sigma = 0.442$). Nevertheless, both cases are adequately below the USL of 0.925 and the requirement of 10 CFR 71.55(d)(2) is satisfied. Given that changes external to the containment vessel due to the HAC do not result in an appreciable change in neutron multiplication for an array of packages, similar results are expected for the cases demonstrating compliance with 10 CFR 71.55(e)(1).

For TRIGA fuel content as clad fuel rods, the amount of clad added (stainless steel as a neutron absorber or aluminum as a neutron scatter) and corresponding amount of water moderator displaced by the clad is not expected to have a statistically significant affect on the calculated k_{eff}. Thus, the NCT shipping configuration model for disassembled TRIGA fuel (bare fuel meats) bounds shipping configuration model for TRIGA fuel configured as clad fuel rods (Appendix 6.9.3.1).

The array results for three slug configurations presented in Table 6.9.6-9 (Appendix 6.9.6) are for five or ten slugs touching or spaced apart in a pentagonal ring (Cases **ncia5st11** and **ncia5est11**) and for seven slugs formed by a hexagonal ring of slugs with one slug in the center of the ring **(ncia70st11**). These cases are used to establish the mass loading limitations, which in turn limit the number of slugs in the package to less than the number required to assemble a critical configuration.

Cases **ncia5est11_1_1_8_3** through **ncia5est11_1_1_1_3** (Appendix 6.9.6, Table 6.9.6-9) represent infinite arrays of packages containing 18,277 g U without 277-4 canned spacers. For these cases, the $k_{eff} + 2\sigma$ values increase from 0.550 to 0.924 as the enrichment is increased from 19.0 wt % to 100.0 wt % ^{235}U. The $k_{eff} + 2\sigma$ value is 0.924 for Case **ncia5est11_1_1_8_3**, which is below the USL of 0.925. Likewise, the $k_{eff} + 2\sigma$ values for Cases **ncia5st11_1_1_8_3** through **ncia5st11_1_1_1_3** increase from 0.521 to 0.929 as the enrichment is increased. However, the $k_{eff} + 2\sigma$ value is 0.929 for Case **ncia5st11_1_1_8_3**, which is slightly above the USL of 0.925. For simplification of the criticality evaluation, the maximum enrichment is limited to 95% and the corresponding fissile mass limit is 17,374 g ^{235}U. For Cases **ncia5st11_1_1_7_3** and **ncia5est11_1_1_7_3**, the $k_{eff} + 2\sigma$ values are below the USL. Moreover, the values are not statistically different.

Cases **ncia70st11_2_8_3** through **ncia70st11_2_1_3** (Appendix 6.9.6, Table 6.9.6-9) represent infinite arrays of packages containing 25,588 g U with 277-4 canned spacers. For these cases, the $k_{eff} + 2\sigma$ values increase from 0.473 to 0.915 as the enrichment is increased from 19.0 wt % to 100.0 wt % ^{235}U. The $k_{eff} + 2\sigma$ value of 0.894 for Case **ncia70st11_2_7_3** at the 95% enrichment limit is adequately below the USL of 0.925.

Cases **ncia5est11_2_2_8_3** through **ncia5est11_2_2_1_3** (Appendix 6.9.6, Table 6.9.6-9) represent infinite arrays of packages containing 36,555 g ^{235}U with 277-4 canned spacers. For these cases, the $k_{eff} + 2\sigma$ values increase from 0.583 to 0.983 as the enrichment is increased from 19.0 wt % to 100.0 wt % ^{235}U. At 80 wt % ^{235}U, the $k_{eff} + 2\sigma$ value (0.908) for Case **ncia5est11_2_2_5_3** with spaced-apart slugs is just below the USL. Similarly, Case **ncia5st11_2_2_5_3** with touching slugs has a calculated $k_{eff} + 2\sigma$ value of 0.902. Therefore, a restriction on mass and enrichment for slug content is that for ≤80 wt % ^{235}U, the mass of ^{235}U in the package must not exceed 29,318 g as a prerequisite for the shipment of the package slug content and with 277-4 canned spacers under a CSI = 0.0.

Cases **ncf15est11_2_2_8_3** through **ncf15est11_2_2_1_3** (Appendix 6.9.6, Table 6.9.6-9) represent a 13 × 13 × 6 array of packages containing 36,555 g ^{235}U with 277-4 canned spacers for which the corresponding rounded CSI = 0.4. For these cases, the $k_{eff} + 2\sigma$ values increase from 0.548 to 0.938 as the enrichment is increased from 19.0 wt % to 100.0 wt % ^{235}U. Case **ncf15est11_2_2_7_3** at 95 wt % ^{235}U with $k_{eff} + 2\sigma = 0.920$ is below the USL of 0.925 to permit increasing the limit on enrichment for mass loadings of ≤34.7 kg uranium metal.

The CSI determinations provided in this section are contingent upon satisfactory results under the HAC evaluation (Sect. 6.6.1).

6.5.2 HEU Solid Metal of Unspecified Geometric Shapes or HEU Broken Metal

Like packages with HEU metal, the neutron multiplication factor for arrays of packages with HEU broken metal decreases as a function of MOIFR and increases as a function of the ^{235}U mass. For example, consider the ES-3100 package loaded with three convenience cans for a total of 35,142 g ^{235}U and no canned spacers between content locations. The $k_{eff} + 2\sigma$ values range from 1.138 to 0.913 with increasing MOIFR [Cases **nciabmt11_36_1_8_1** through **nciabmt11_36_1_8_15** (Appendix 6.9.6, Table 6.9.6-11)]. The introduction of water above ~0.01 MOIFR shows the effect of isolating the

individual array units from each other. Array reactivity ($k_{eff} + 2\sigma = 0.913$) approaches the reactivity of the water-saturated, water-reflected single package Case **ncsrbmt11_36_1_15** ($k_{eff} + 2\sigma = 0.891$).

In the series of calculations using the ES-3100 package model with NCT geometry (Cases **nciabmt11_1_*n*_*m*_3** through **nciabmt11_*36*_*n*_*m*_3**), the enrichment of the content is varied from 19 wt % to 100 wt % ^{235}U. These array cases with a water fraction of MOIFR = 1e-04 pertain specifically to NCT packages where both the neutron poison of the body weldment liner inner cavity and the Kaolite are dry (in the as-manufactured condition) and both the recesses of the package external to the containment vessel and the interstitial space between the drums of the array do not contain any residual moisture. As stated before, this NCT case is more reactive than all other NCT cases where more moisture is present in the Kaolite and recesses of the package. Increased interspersed water between the containment vessels in the array will reduce neutronic interaction between the flooded contents to a point where the packages of the array become isolated.

Ranges of enrichment are specified in Table 6.1b (10 CFR 71.59) for identifying fissile mass loading limits for HEU broken metal. Consider specifically enrichments >95 wt % ^{235}U. The containment vessel calculations (Case **cvr3lha_36_1_8_15** versus Case **cvr3lha_36_2_8_15**) indicate that 277-4 canned spacers are required in this enrichment range, where the maximum evaluated fissile mass loading of 35,142 g ^{235}U is possible. However, the fissile mass loading must be limited to 2,774 g ^{235}U (Case **nciabmt11_3_2_8_3**) in order for the $k_{eff} + 2\sigma$ value (= 0.904) to be below the USL of 0.925. This fissile mass limit is conservative when applied to enrichments only slightly greater than 95 wt % ^{235}U. A reduction in the enrichment within the range of 80 to 95 wt % ^{235}U (Cases **nciabmt11_4_2_7_3** and **nciabmt11_4_2_6_3**) does not result in a sufficient reduction in the $k_{eff} + 2\sigma$ from neutron absorption in ^{238}U to allow for increased mass loadings. Therefore, the uranium mass limit remains at ~2774 g, while the fissile mass loading limit decreases with the reduction in enrichment as illustrated in Table 6.1b. As stated previously, these fissile mass loading limits for a CSI = 0 are contingent upon the infinite array of damaged packages also being adequately subcritical for HAC (Sect. 6.6.2).

This evaluation technique for determination of mass loading limits for enrichment intervals is repeated over the range of HEU enrichments identified in Table 6.1b. At HEU enrichment <60 wt % ^{235}U, the evaluated package mass loading limit of 35 kg uranium is achieved, so further delineation of fissile mass loading limits is not required.

The loading limits for HEU solid metal of unspecified geometric shapes or for HEU broken metal are summarized in Table 6.2a based on array calculations performed using the uniform dispersal approximation "**cha**" model (Fig. 6.9.1-5d). The calculation results on which the determination of the loading limits is based are summarized in Table 6.1c.

As discussed in Appendix 6.9.1, the "**cha**" model is a first-order approximation model. The 500 g polyethylene representing the use of hydrogenous packing material is replaced with water in the flooded containment vessel. Broken metal and water is homogenized as a uranium "solution" and uniformly dispersed over the entire volume of the containment vessel. The vertical location of the 277-4 canned spacers inside the containment vessel is based on a fixed HEU packing fraction of ~0.59. The use of this large packing fraction results in minimum separation between canned spacers, which minimizes the size of the lower and middle content locations and maximizes the size of the upper content location. Reactivity of the containment vessel is driven by the oversized upper content location having a proportionately greater amount of fissile material. Conversely, the use of a small packing fraction (~0.2) in the "**cha**" model would result in greater separation between the canned spacers, which increases the size of the lower and middle content locations while reducing the size of the upper content location. Reactivity of the containment vessel would decrease as the proportions of fissile material in the content

regions equalize. Calculations based on a packing fraction of ~0.59 bound similar cases based on lower packing fractions.

The "**cha**" model is characteristic of the situation where the dimensions of the broken metal pieces are sufficiently small to allow pieces of HEU to pass between the void spaces formed between the inner wall of the containment vessel and the exterior wall of the canned spacers.

As shown in Fig. 6.9.3.1-3, HEU broken metal content typically consists of irregular pieces, sufficiently large (0.5 in. to several inches on a side), that will not pass between the 277-4 canned spacer locations. The packing fraction calculation model "**fl**" and the dispersed content calculation model "**fd**" better represent broken metal content which does not pass between the canned spacer locations. Inside the containment vessel, the content locations between canned spacers are established based on a variable packing fraction for HEU broken metal ranging from 0.2 to 0.6. The 500 g polyethylene is included in the flooded containment vessel. HEU broken metal, polyethylene and water are homogenized as a uranium "solution" residing within the content locations (Figs. 6.9.1-5e and 6.9.1-5f) rather than distributed uniformly over the containment vessel (Fig. 6.9.1-5d). The "**fl**" model defines the upper content location based on packing fraction while the "**fd**" model defines the upper content location as the entire region above the upper canned spacer.

NCT cases for the "**fl**" and "**fd**" calculation models are documented in Table 6.9.6-11b. The reference case results based on the uniform dispersal approximation "**cha**" model are highlighted. The corresponding cases for the packaging fraction ("**fl**") and for the dispersed content ("**fd**") calculation models are given in the rows below the reference case. Consider Case **nciabmt11_4_1_5_3** where the quantity of HEU content in the model is calculated based on a discrete number of 1-in. cubes. The HEU in corresponding Cases **nciapbmflt11_1_*n*_4_5** and **nciapbmfdt11_1_*n*_4_5** is not limited to fractional kilogram quantities based on whole cubes as in Case **nciabmt11_4_1_5_3**. Instead, the intended whole kilogram quantities of HEU are evaluated as a function of the packing fraction ("***n***") in the "... flt11_1_***n***_ ..." and "... fdt11_1_***n***_ ..." cases.

An increase of ~0.08 in the $k_{eff} + 2\sigma$ values is observed as the packing fraction is reduced and more water is homogenized with the fissile material, (i.e., Cases **nciapbmtfl11_1_6_4_5** through **nciapbmtfl11_1_2_4_5**, Table 6.9.6-11b). As the packing fraction is reduced and the volume of the content location increases accordingly, neutron multiplication increases due to increased moderation of the fissile material. A considerable increase of ~0.22 in the $k_{eff} + 2\sigma$ values is observed when fissile material in the upper can location is homogenized with water in the upper content location and dispersed over that region, (i.e., Case **nciapbmtfl11_1_6_4_5** vs Case **nciapbmtfd11_1_6_4_5**, Table 6.9.6-11b). Nevertheless, the $k_{eff} + 2\sigma$ values for the packaging fraction "**fl**" and dispersed content calculation "**fd**" models are lower than values for the corresponding uniform dispersal approximation "**cha**" model. The "**cha**" model evaluated without polyethylene bounds results for the more realistic "**fl**" and "**fd**" models evaluated with 500 g polyethylene and the HEU content of the package confined to the specific content locations.

Powder, particulate, or small pieces of HEU potentially present in broken metal are capable of passing between content locations. The quantity of this material, potentially present, represents a small fraction of the total HEU broken metal content. However, the placement of a limit on content size for criticality control is not adopted as a package content loading restriction (Sect. 6.2.4) Instead, the loading limits established based on the "**cha**" model are retained, recognizing that the use of polyethylene is not addressed in "**cha**" model. Therefore, the only hydrogenous packing materials that can be used in the containment vessel when broken metal content is present are those that have a hydrogen density less than or equal to water (Sect. 6.2.4, Item 7).

6.5.3 HEU Oxide

Like packages with HEU metal or broken metal, the neutron multiplication factor for an NCT array of packages with HEU product oxide decreases as a function of decreasing ^{235}U mass [parametric Cases **nciapdoxt11_1_*n*_24_3**, **nciapdoxt11_1_*n*_20_3**, **nciapdoxt11_1_*n*_15_3**, **nciapdoxt11_1_*n*_12_3**, **nciapdoxt11_1_*n*_11_3**, and **nciapdoxt11_1_1_10_3** through **nciapdoxt11_1_1_6_3** (Table 6.9.6-13b)]. For these NCT cases, the MOIFR is set at 1.0E-04 such that neutronic interaction between packages of an array is maximized. Results for the parametric cases reveal the same consistent increase in the $k_{eff} + 2\sigma$ values with decreasing bulk density as observed in the single package calculation results (Sect. 6.4.3). Results for Cases **nciapdoxt11_1_*n*_11_3** and **nciapdoxt11_1_1_10_3** through **nciapdoxt11_1_1_6_3** demonstrate that over the range of HEU oxide bulk densities from 6.54 to 2.0 g/cm^3, the $k_{eff} + 2\sigma$ values are below the USL of 0.925.

Cases **nciask_1_15** through **nciask_10_15** (Appendix 6.9.6, Table 6.9.6-18) evaluate infinite arrays of packages having the 10 skull oxide compositions described in Sect. 6.4.3. The MOIFR is set at 1.0e-04 such that neutronic interaction between packages is maximized. The $k_{eff} + 2\sigma$ values, ranging from 0.656 to 0.764, are substantially below the below the USL value of 0.925, indicating that canned spacers are not required for criticality control.

The CSI is 0.0 for an infinite array of packages having product oxide content with a bulk density ≥2.0 g/cm^3 and with a maximum of 9,682 g ^{235}U or having skull oxide content with a maximum of 16,399 g ^{235}U and 921 g graphite. The suitability of this determination is contingent upon satisfactory results under the HAC evaluation (Sect. 6.6.3.)

6.5.4 UNH Crystals

Unlike the HEU metal, broken metal, or oxide content, UNH crystals are soluble in water (Sect. 6.4.4). The most reactive content condition occurs at an optimum solution concentration derived from the UNH crystal loading and the volume of water flooding the containment vessel. Both flooding of the containment vessel and a reduced loading of UNH crystals going into solution is required to achieve the most reactive configuration.

Similar to packages with HEU metal, broken metal, or oxide, the neutron multiplication factor for an array of packages with UNH crystals decreases as a function of increasing MOIFR. Cases **nciaunhct11_8_24_1_1** through **nciaunhct11_8_24_1_15** for content without polyethylene and Cases **nciapunhct11_24_1** and **nciapunhct11_24_15** for content with 500 g polyethylene (Table 6.9.6-15) reveal the effect of isolating the individual array units from each other with the introduction of water above ~0.01 MOIFR. Array reactivity ($k_{eff} + 2\sigma = 0.721$ without polyethylene and 0.729 with polyethylene) approaches the reactivity of the water-saturated, water-reflected single-unit package ($k_{eff} + 2\sigma = 0.702$ without polyethylene and 0.708 with polyethylene).

In a series of NCT calculations (Cases **nciapunhct11_*nn*_3**), the $k_{eff} + 2\sigma$ values are above the USL of 0.925 for mass loadings between 8,000 and 24,000 g UNH crystals. Credit is not taken for water tightness that is demonstrated by the NCT (and HAC) tests. Therefore, mass loading is limited to 7,000 g UNH crystals. The CSI is 0.0 [10 CFR 71.59(a)(1) and 10 CFR 71.59(b)] for ES-3100 packages having a maximum of 3,297 g ^{235}U. The suitability of this determination depends upon satisfactory results under the HAC evaluation of Sect. 6.6.4. [10 CFR 71.59(a)(2) and 10 CFR 71.59(b)]

The $k_{eff} + 2\sigma$ values are expected to range from subcritical to critical for array configurations where UNH crystals are dissolved in the water flooding the containment vessel and the containment vessel well. This requires intrusion of water into the containment vessel, dissolving of UNH crystals in the influent, and leakage of solution out of the containment vessels in each package of an array (catastrophic failure of all packages in an infinite array). Given that loss of containment is deemed not credible by merit of the 10 CFR 71.71 and 10 CFR 71.73 tests performed on the ES-3100, this accident condition is not credible.

For Cases **ncf1punhct12_*nn*_3**, the $k_{eff} + 2\sigma$ values are below the USL of 0.925. Given that the results for NCT and HAC (Sect. 6.6.4) are adequately subcritical, packages may be shipped under a CSI = 0.4 for packages with a maximum of 24,000 g UNH crystals. [10 CFR 71.59(a)(1) and 10 CFR 71.59(b)]. Likewise, the suitability of this determination depends upon satisfactory results under the HAC evaluation of Sect. 6.6.4.

6.6 EVALUATION OF PACKAGE ARRAYS UNDER HYPOTHETICAL ACCIDENT CONDITIONS

Except for UNH crystals, the package content is confined within the containment vessel for the HAC array evaluation of ES-3100 packages, consistent with the result of the tests specified in 10 CFR 71.73 (Hypothetical Accident Conditions). The array sizes examined in this evaluation are infinite, 13×13×6, 9×9×4, 7×7×3, 5×5×2, ETP 16×3, and the degenerate single unit. The "N" and corresponding CSI values for arrays determined to be adequately subcritical are as follows: N = ∞, CSI = 0; N =162, CSI = 0.4; N = 73, CSI = 0.7; N = 25, CSI = 2.0; and N = 24, CSI = 2.1. All arrays, except the infinite array, are reflected with 30 cm (1 ft) of water. These array are nearly cubic in shape for optimum reactivity of the array, thus eliminating the need for placing criticality controls on package arrangements in terms of stack height, width, and depth of an array. The array configurations and the range of water contents (Table 6.4) evaluated bound all possible packaging arrangements and moderation conditions for HAC.

For the single damaged package, and for infinite and finite arrays of damaged packages with HEU metal, HEU oxide, or UNH crystal content, the neutron multiplication factor changes as a function of the ^{235}U mass, MOIFR, or applicable solution concentration in the same manner as in an array of undamaged packages.

6.6.1 Solid HEU Metal of Specified Geometric Shapes

For infinite and finite arrays of damaged packages with HEU metal, the neutron multiplication factor increases as a function of the ^{235}U mass and decreases as a function of MOIFR. For example, consider the ES-3100 package loaded with three convenience cans that contain a 3.24-in.-diam cylinder with 12,000 g ^{235}U for a total of 36,000 g ^{235}U. For package content without 277-4 canned spacers, the $k_{eff} + 2\sigma$ values range from 1.027 to 0.967 with increasing MOIFR in the damaged packages [Cases **hciacyct12_36_1_1** through **hciacyt12_36_1_15** (Appendix 6.9.6, Table 6.9.6-3)]. For package content with 277-4 canned spacers, the $k_{eff} + 2\sigma$ values range from 0.956 to 0.884 with increasing MOIFR in the damaged package [Cases **hciacyt12_36_2_1** through **hciacyt12_36_2_15** (Appendix 6.9.6, Table 6.9.6-3)].

The introduction of water above ~0.01 MOIFR shows the effect of isolating the individual array units from each other. The neutron multiplication factor approaches k_{eff} for the single, water-reflected unit at a full content-water fraction (MOIFR = 1.0). Comparison of these results with the corresponding NCT cases (Sect. 6.5.1.) indicates no significant differences. This result is as expected given that the neutron multiplication in an infinite array is independent of pitch between fissile contents but is dependent on changes in mass and moderation in the array. The changes in both the outer dimensions and the compositions of the Kaolite and 277-4 of the ES-3100 package due to HAC result in changes to the neutron multiplication factor on the order of ~0.001 to 0.002.

Repeated for 4.25-in.-diam cylinders (Appendix 6.9.6, Table 6.9.6-7); 2.29-in.-square bars (Table 6.9.6-5); and 1.5-in.-diam × 2-in.-tall slugs (Table 6.9.6-9), this type of analysis for the 3.24-in.-diam cylinders demonstrates that arrays of damaged packages with restricted fissile material (^{235}U) loading remain subcritical over the entire range of water content or MOIFR. HEU bulk metal or alloy content not covered by the specified geometric shapes (cylinder, square bar, or slug contents) will be in the HEU broken metal category, and so limited.

Cases **hciatriga_1_1_3** through **hciatriga_1_15_3** (Appendix 6.9.6, Table 6.9.6-20) represent infinite arrays of damaged packages containing the bounding TRIGA fuel content (20 % enrichment with 45 wt % U containing 307 g ^{235}U), without 277-4 canned spacers. For these cases, the $k_{eff} + 2\sigma$ values increase from 0.218 to 0.526 as MOIFR increases. The $k_{eff} + 2\sigma = 0.526$ for Case **hciatriga_1_15_3** is substantially below the USL of 0.925, indicating that canned spacers are not required for criticality control. Given that the results for NCT (Sect. 6.5.2) and HAC are adequately subcritical, packages with TRIGA fuel content ≤921 g ^{235}U may be shipped under a CSI = 0.

As stated in Sect. 6.5.1, calculation results presented in Table 6.9.6-20d for an infinite array of ES-3100 packages (NCT packaging with extremely damaged TRIGA fuel content) is substantially below the USL of 0.925. Similar results are expected for an infinite array of ES-3100 packages (HAC packaging with extremely damaged TRIGA fuel content) given that changes external to the containment vessel due to the HAC do not result in an appreciable change in the neutron multiplication for the an array of packages. Therefore, the 10 CFR 71.55(e)(1) requirement that the package be adequately subcritical under HAC with the package contents in the most reactive credible configuration is satisfied.

The array results for three slug configurations presented in Table 6.9.6-9 (Appendix 6.9.6) are for five or ten slugs touching or spaced apart in a pentagonal ring (Cases **hcia5st12** and **hcia5est12**) and for seven slugs formed by a hexagonal ring of slugs with one slug in the center of the ring **(hcia70st12**). These cases are used to establish the mass loading limitations for damaged packages, which in turn limit the number of slugs in the package to less than the number required to assemble a critical configuration.

Cases **hcia5est12_1_1_8_3** through **hcia5est12_1_1_1_3** and Cases **hcia5st12_1_1_8_3** through **hcia5st12_1_1_1_3** (Appendix 6.9.6, Table 6.9.6-9) represent infinite arrays of damaged packages containing 18,277 g U without 277-4 canned spacers. Infinite array Cases **hcia70st11_2_8_3** through **hcia70st11_2_1_3** represent damaged packages containing 25,588 g U with 277-4 canned spacers while Cases **hcia5est12_2_2_8_3** through **hcia5est12_2_2_1_3** represent damaged packages containing 36,558 g U also with 277-4 canned spacers. Cases **hcf25est12_2_2_8_3** through **hcf25est12_2_2_1_3** represent a 9 × 9 × 4 array of damaged packages containing 36,558 g U with 277-4 canned spacers. The $k_{eff} + 2\sigma$ values for these cases representing arrays of damaged packages are slightly less than values for the corresponding cases representing undamaged packages. (The changes in both the outer dimensions of the package and the compositions of the Kaolite and 277-4 due to HAC result in an ~0.001 change in the neutron multiplication factor.) Therefore, the prospective CSI values determined in the NCT evaluation (Sect. 6.5.1) for arrays of undamaged packages with slug content are controlling.

6.6.2 HEU Solid Metal of Unspecified Geometric Shapes or HEU Broken Metal

Consider the ES-3100 package loaded with three convenience cans for a total of 35,142 g ^{235}U with no canned spacers between content locations. The $k_{eff} + 2\sigma$ values range from 1.14 to 0.939 with increasing MOIFR, Cases **hciabmt12_36_1_8_1** through **hciabmt12_36_1_8_15** (Appendix 6.9.6, Table 6.9.6-11). The introduction of water above ~0.01 MOIFR shows the effect of isolating the individual array units from each other. Array reactivity ($k_{eff} + 2\sigma = 0.939$) approaches the reactivity of the water-saturated, water-reflected single package ($k_{eff} + 2\sigma = 0.891$, Case **hcsrbmt12_36_1_15**, Table 6.9.6-11).

Cases **hciabmt12_1_*nn_mm*_3** through **hciabmt12_36_*nn_mm*_3** model the ES-3100 with the reduced-diameter HAC package model where the enrichment of the content is varied from 60 wt % to 100 wt % ^{235}U. These array cases with MOIFR = 1e-04 pertain specifically to HAC packages where the neutron poison of the body weldment liner inner cavity is at 90% moisture content, but the Kaolite is dry (in the as-manufactured condition), and neither recess of the package external to the containment vessel and the interstitial space between the drums of the array contains any residual moisture. As stated before, this HAC case is more reactive than all other HAC cases where more moisture is present in the Kaolite and recesses of the package. Increasing the interspersed water between the containment vessels in the array will reduce neutronic interaction between the flooded contents to a point where the packages of the array become isolated.

Ranges of enrichment are specified in Table 6.1b (10 CFR 71.59) for identifying fissile mass loading limits for HEU broken metal. Consider specifically enrichments >95 wt % ^{235}U. The containment vessel calculations (Case **cvr3lha_36_1_8_15** versus Case **cvr3lha_36_2_8_15**, Appendix 6.9.6, Table 6.9.6-10) indicate that 277-4 canned spacers are required in this enrichment range, where the maximum evaluated mass loading of 35,142 g ^{235}U is possible. However, the fissile mass loading must be limited to 2774 g ^{235}U (Case **hciabmt12_3_2_8_3**) in order for the $k_{eff} + 2\sigma$ value (= 0.905) to be below the USL of 0.925. This fissile mass limit is conservative when applied to enrichments only slightly greater than 95 wt % ^{235}U. Given that the results for NCT (Sect. 6.5.2) and HAC are adequately subcritical, packages ≤2774 g ^{235}U and enrichment >95 wt % ^{235}U may be shipped under a CSI = 0.

This evaluation technique for determination of mass loading limits for enrichment intervals is repeated over the range of HEU enrichments. At HEU enrichment <60 wt % ^{235}U, the package mass loading limit is achieved, so no further delineation is required.

The loading limits for HEU solid metal of unspecified geometric shapes or for HEU broken metal are summarized in Table 6.2a based on array calculations performed using the uniform dispersal approximation "**cha**" model (Fig. 6.9.1-5d). The calculation results on which the determination of the loading limits is based are summarized in Table 6.1c.

As discussed in Sect. 6.5.2, criticality calculations with the "**cha**" model for a packing fraction of ~0.59 bound similar cases at the lower packing fractions. The "**cha**" model is characteristic of the situation where the dimensions of the broken metal pieces are sufficiently small to allow for HEU to pass between void space formed between the inner wall of the containment vessel and the exterior wall of each canned spacer.

As shown in Fig. 6.9.3.1-3, HEU broken metal content typically consists of irregular pieces, sufficiently large (0.5 in. to several inches on a side), that will not pass between the 277-4 canned spacer locations. The packing fraction calculation model "**fl**" and the dispersed content calculation model "**fd**" better represent broken metal content which does not pass between the canned spacer locations.

HAC cases are documented in Table 6.9.6-11c. The reference case results based on the uniform dispersal approximation "**cha**" model are highlighted. The corresponding cases for the packaging fraction ("**fl**") and for the dispersed content ("**fd**") calculation models are given in the rows below the reference case.

An increase of ~0.08 in the $k_{eff} + 2\sigma$ values is observed as the packing fraction is reduced and more water is homogenized with the fissile material (i.e., Cases **hciapbmtfl11_1_6_4_5** through **hciapbmtfl11_1_2_4_5**, Table 6.9.6-11c). As the packing fraction is reduced and the volume of the content location is increased, moderation of the fissile material increases. A considerable increase of ~0.22 in the $k_{eff} + 2\sigma$ values is observed when fissile material in the upper can location is homogenized with water in the upper content location and dispersed over that region (i.e., Case **hciapbmtfl11_1_6_4_5** vs Case **hciapbmtfd11_1_6_4_5**, Table 6.9.6-11c). Nevertheless, the $k_{eff} + 2\sigma$ values for the packaging fraction "**fl**" and dispersed content calculation "**fd**" models are lower than values for the corresponding uniform dispersal approximation "**cha**" model. The "**cha**" model evaluated without polyethylene bounds results for the more realistic "**fl**" and "**fd**" models evaluated with 500 g polyethylene and the HEU content of the package confined to the specific content locations.

Powder, particulate, or small pieces of HEU potentially present in broken metal are capable of passing between content locations. The quantity of this material, potentially present, represents a small fraction of the total HEU broken metal content. However, the placement of a limit on content size for criticality control is not adopted as a package content loading restriction (Sect. 6.2.4). Instead, the loading limits established based on the "**cha**" model are retained, recognizing that the use of polyethylene is not addressed in "**cha**" model. Therefore, the only hydrogenous packing materials that can be used in the containment vessel when broken metal content is present are those that have a hydrogen density less than or equal to water (Sect. 6.2.4, Item 7).

6.6.3 HEU Oxide

Like packages with HEU metal or broken metal, the neutron multiplication factor for an array of HAC packages with HEU product oxide decreases as a function of decreasing ^{235}U mass [parametric Cases **hciapdoxt11_1_*n*_24_3**, **hciapdoxt11_1_*n*_20_3**, **hciapdoxt11_1_*n*_15_3**, **hciapdoxt11_1_*n*_12_3**, **hciapdoxt11_1_*n*_11_3**, and **hciapdoxt11_1_1_10_3** through **hciapdoxt11_1_1_6_3** (Table 6.9.6-13b)]. For these HAC cases, the MOIFR is set at 1.0E-04 such that neutronic interaction between packages of an array is maximized. Results for the parametric cases reveal the same consistent increase in the $k_{eff} + 2\sigma$ values with decreasing bulk density as observed in the single package calculation results (Sect. 6.4.3). Results for Cases **hciapdoxt11_1_*n*_11_3** and **hciapdoxt11_1_1_10_3** through **hciapdoxt11_1_1_6_3** demonstrate that over the range of HEU oxide bulk densities from 6.54 to 2.0 g/cm^3, the $k_{eff} + 2\sigma$ values are below the USL of 0.925. Given that the results for NCT (Sect. 6.5.3) and HAC are adequately subcritical, packages may be shipped under a CSI = 0.0 for an infinite array of packages having product oxide with a maximum of 9,682 g ^{235}U.

Cases **hciask_1_15** through **hciask_10_15** (Appendix 6.9.6, Table 6.9.6-18b) evaluate infinite arrays of damaged packages having the 10 skull oxide compositions described in Sect. 6.4.3. The differences between the HAC case results and the NCT case results are not statistically significant. The $k_{eff} + 2\sigma$ values, ranging from 0.658 to 0.767, are substantially below the USL value of 0.925. Given that the results for NCT (Sect. 6.5.3) and HAC are adequately subcritical, packages may be shipped under a CSI = 0.0 for an infinite array of packages having skull oxide content with a maximum of 16,399 g ^{235}U and 921 g graphite.

6.6.4 UNH Crystals

Unlike the HEU metal, broken metal, or oxide content, UNH crystals are soluble in water (Sect. 6.4.4). The most reactive content condition occurs at an optimum solution concentration derived from the UNH crystal loading and the volume of water flooding the containment vessel. Both flooding of the containment vessel and a reduced loading of UNH crystals going into solution is required to achieve the most reactive configuration.

Similar to packages with HEU metal, broken metal, or oxide, the neutron multiplication factor for an array of damaged packages with UNH crystals decreases as a function of increasing MOIFR. Cases **hciaunhct12_8_24_1_1** through **hciaunhct12_8_24_1_15** for content without polyethylene and Cases **hciapunhct12_24_1** and **hciapunhct12_24_15** for content with 500 g polyethylene (Table 6.9.6-15) reveal the effect of isolating the individual array units from each other with the introduction of water above ~0.01 MOIFR. Array reactivity ($k_{eff} + 2\sigma = 0.729$ without polyethylene and 0.733 with polyethylene) approaches the reactivity of the water-saturated, water-reflected unit single package ($k_{eff} + 2\sigma = 0.704$ without polyethylene and 0.711 with polyethylene).

In a series of HAC calculations (Cases **hciapunhct11_*nn*_3**), the calculated $k_{eff} + 2\sigma$ values are below the USL of 0.925 for loading with <8,000 g UNH crystals. Given that the results for NCT (Sect. 6.5.4) and HAC are adequately subcritical, the CSI is 0.0 [10 CFR 71.59(a)(2) and 10 CFR 71.59(b)] for packages having a maximum of 3,297 g ^{235}U.

The $k_{eff} + 2\sigma$ values are expected to range from subcritical to critical for array configurations where UNH crystals are dissolved in the water flooding the containment vessel and the containment vessel well. This requires intrusion of water into the containment vessel, dissolving of UNH crystals in the influent, and leakage of solution out of the containment vessels in each package of an array. The leakage out of the containment vessel of content moderated "to such an extent as to cause maximum reactivity consistent with the physical and chemical form of material" is not considered credible HAC based on results for tests specified in 10 CFR 71.73.

In a series of HAC calculations (Cases **hcf2punhct12_*nn*_3**), the calculated $k_{eff} + 2\sigma$ values are below the USL of 0.925. Given that the results for NCT (Sect. 6.5.4) and HAC are adequately subcritical, packages may be shipped under a CSI = 0.4 for packages with a maximum of 24,000 g UNH crystals.

6.7 FISSILE MATERIAL PACKAGES FOR AIR TRANSPORT

A series of calculations are performed for determining the most reactive configuration of the content and surrounding packaging material in an ES-3100 package that undergoes catastrophic destruction. Fissile content mass loadings that remain under the USL for these catastrophic events are identified. Subcriticality is demonstrated after due consideration of such aspects as the efficiency of moderator, loss of neutron absorbers, rearrangement of packaging components and contents, geometry changes and temperature effects. The seven calculation models used in this evaluation are described in Sect 6.3.1.4. Key model dimensions and parameters are tabulated in Tables 6.9.6-21 through 6.9.6-23, Appendix 6.9.6.

6.7.1 Results for Solid HEU, One Piece per Convenience Can

Cases **atdmr_10_8** through **atdmr_7_1** (Table 6.9.6-21, Appendix 6.9.6) pertain to Model 1 (Fig. 6.11, Section 6.3.1.4). HEU solid or broken metal of three convenience cans is homogenized with 513 g of polyethylene, representing the potential use of hydrogenous packing materials in the ES-3100. The fissile core is configured into a spherical shape with an exterior 20 cm water reflector. As shown in Fig. 6.17 and Table 6.9.6-21, the $k_{eff} + 2\sigma$ values decrease as a function of both enrichment and ^{235}U mass. The $k_{eff} + 2\sigma$ values are substantially below the USL of 0.925. The $k_{eff} + 2\sigma$ value for 7 kg of HEU at 100 % enrichment is 0.792.

Cases **atdmsr_7_8_11** through **atdmsr_7_1_1** (Table 6.9.6-21, Appendix 6.9.6) pertain to Model 2 (Fig. 6.12, Section 6.3.1.4). The fissile core of Model 1 is blanketed with a variable thickness stainless steel shell and an exterior 20 cm water reflector. As shown in Fig. 6.18 and Table 6.9.6-21, the maximum $k_{eff} + 2\sigma$ values occur at zero stainless steel thickness. The $k_{eff} + 2\sigma$ value for 7 kg of HEU at 100% enrichment and zero stainless steel thickness is 0.793. The $k_{eff} + 2\sigma$ values decrease to minimum values for steel thicknesses of 0.99 cm at 100 % enrichment and thicknesses of 1.47 cm at 19 % enrichment while the NLF decreases from ~ 0.07 to 0.06. The NLF continues to decrease to a value of 0.03 as stainless steel is added up to the 66,133 g amount of the containment vessel and the liner and drum assembly. At maximum stainless steel thickness, the $k_{eff} + 2\sigma$ values increase to within 0.02 of the values for zero stainless steel thickness. The stainless steel of the ES-3100 packaging is not as effective a reflector as the 20 cm water surrounding the core. The overall effect of adding the stainless steel of the ES-3100 packaging to the configuration is the reduction in the neutron multiplication factor for the system. The $k_{eff} + 2\sigma$ values are substantially below the USL of 0.925.

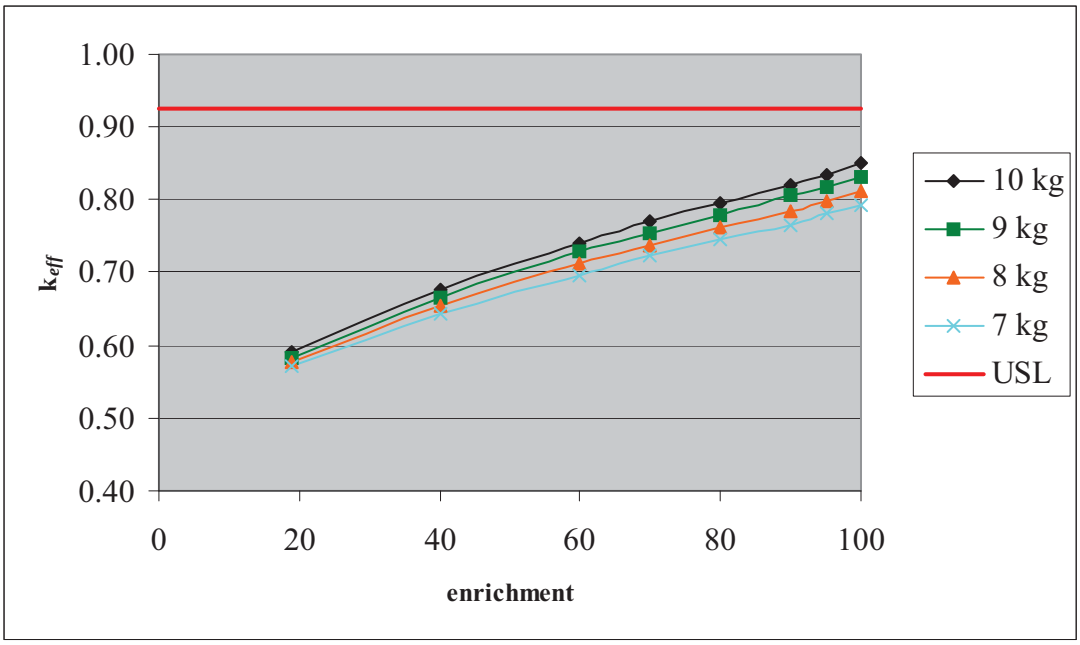

Fig. 6.17. K_{eff} vs. enrichment (wt % ^{235}U) for HEU ranging from 7 to 10 kg.

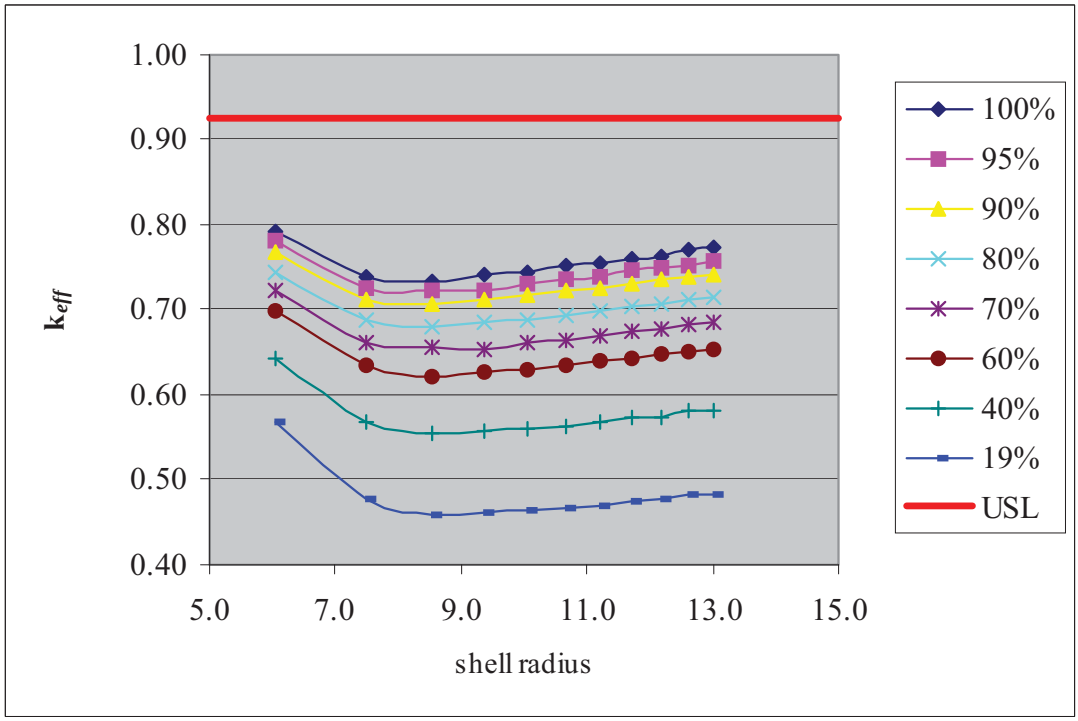

Fig. 6.18. K_{eff} vs. stainless steel shell radius (cm) for 7 kg HEU with enrichments ranging from 19 to 100 wt % ^{235}U.

Cases **atdmkr_7_8_11** through **atdmkr_7_1_1** (Table 6.9.6-21, Appendix 6.9.6) pertain to Model 3 (Fig. 6.13, Section 6.3.1.4). The fissile core of Model 1 is blanketed with a variable thickness Kaolite shell and an exterior 20 cm water reflector. As shown in Fig. 6.19 and Table 6.9.6-21, the maximum $k_{eff} + 2\sigma$ values occur at a Kaolite shell thickness of zero. For 7 kg of HEU at 100 % enrichment, the $k_{eff} + 2\sigma$ value is 0.793. $K_{eff} + 2\sigma$ values decrease to asymptotic values at shell radii of ~14.74 cm (Kaolite thicknesses of ~ 8.66 cm) while the NLF decreases from ~ 0.07 to 0.03. The NLF continues to decrease to a value of 0.006 as water-saturated Kaolite is added up to the 128,034 g pre-bake amount inside the body weldment outer liner and the drum top plug. The asymptotic values for $k_{eff} + 2\sigma$ are ~ 0.043 below maximum $k_{eff} + 2\sigma$ values which occur at zero Kaolite thickness.

Cases **atdmdkr_7_8_11** through **atdmdkr_7_8_1** (Table 6.9.6-21, Appendix 6.9.6) pertain to Model 3 (Fig. 6.13, Section 6.3.1.4), where dry Kaolite is being evaluated consistent with test results of 10 CFR 71.55(d). Only 7 kg of HEU at 100 % enrichment is evaluated in these cases. As shown in Fig. 6.20 and Table 6.9.6-21, the $k_{eff} + 2\sigma$ value decreases to a minimum value at a shell radius of 31.08 cm (dry Kaolite thickness of 25.03 cm). The NLF decreases gradually from ~ 0.07 to 0.05 as NCT Kaolite is added up to the amount contained inside the body weldment outer liner and the drum top plug. Neutron leakage from a configuration with the NCT Kaolite of the ES-3100 packaging is much greater than leakage from one with water-saturated Kaolite. Over the range of moisture content, the Kaolite of the ES-3100 packaging is not as effective a reflector as the 20 cm water surrounding the core. The overall effect of adding Kaolite to the system is the reduction in neutron multiplication in the system. The $k_{eff} + 2\sigma$ values are substantially below the USL of 0.925.

A uranium alloy is conservatively assessed when scattering media (aluminum, molybdenum, or zirconium) is treated as multiplying media (^{235}U) in the calculation models. Thus, limits established for HEU metal apply to the alloy.

6.7.2 Results for TRIGA Fuel Elements, Three Pieces per Convenience Can

Case **atdzr** pertains to Model 1 (Fig. 6.11, Section 6.3.1.4), in which 10.4 kg of $UZrH_x$ (921 g ^{235}U) of three TRIGA fuel elements is homogenized with 513 g polyethylene. The fissile core is configured into a spherical shape with an exterior 20 cm water reflector. The $k_{eff} + 2\sigma$ value of 0.679 (Table 6.9.6-22, Appendix 6.9.6) is substantially below the USL of 0.925.

Cases **atdzsr_11** through **atdzsr_1** pertain to Model 2 (Fig. 6.12, Section 6.3.1.4). The fissile core of Model 1 is blanketed with a variable thickness stainless steel shell with an exterior 20 cm water reflector. As shown in Fig. 6.21 and Table 6.9.6-22 (Appendix 6.9.6), the $k_{eff} + 2\sigma$ value decreases to minimum value for a stainless steel thickness of 1.87 cm while the NLF decreases from ~ 0.06 to 0.05. The NLF decreases to 0.03 as stainless steel is added up to the 66,133 g amount of the containment vessel and the liner and drum assembly. At maximum stainless steel thickness, the $k_{eff} + 2\sigma$ values increase to within 0.058 of the values for zero stainless steel thickness. The overall effect of adding stainless steel to the system is the reduction in neutron multiplication in the system. The $k_{eff} + 2\sigma$ values are substantially below the USL of 0.925.

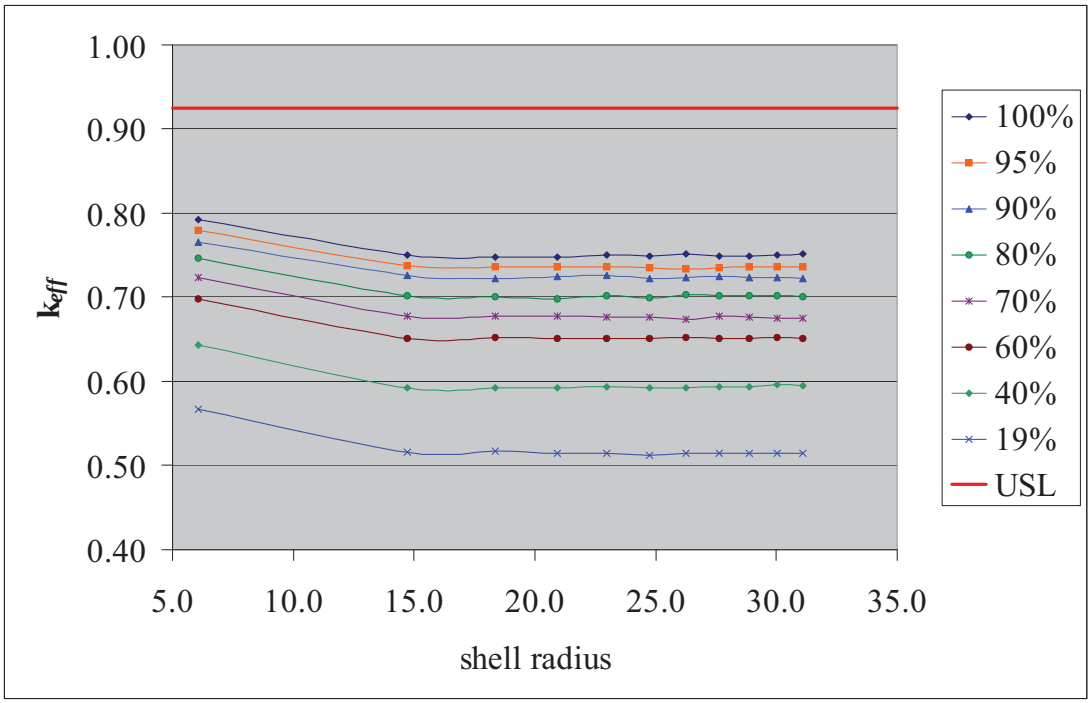

Fig. 6.19. K_{eff} vs. Kaolite shell radius (cm) for 7 kg HEU with enrichments ranging from 19 to 100 wt % ^{235}U.

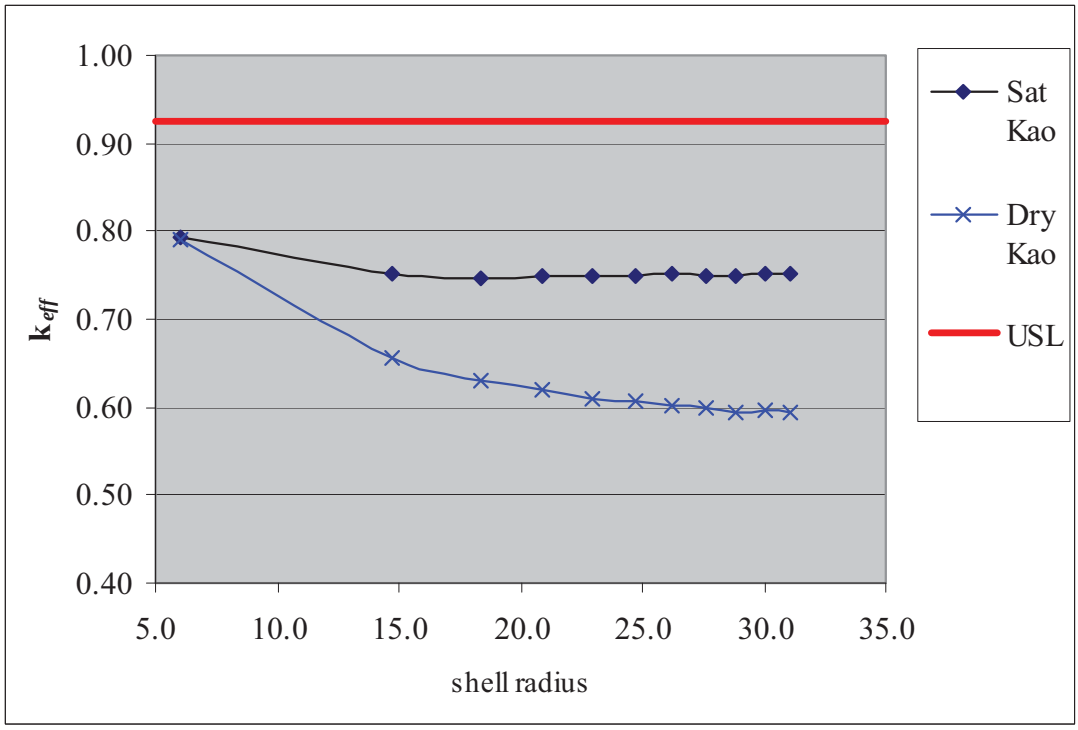

Fig. 6.20. K_{eff} vs. shell radius (cm) for dry and water-saturated Kaolite for 7 kg HEU at 100% enrichment.

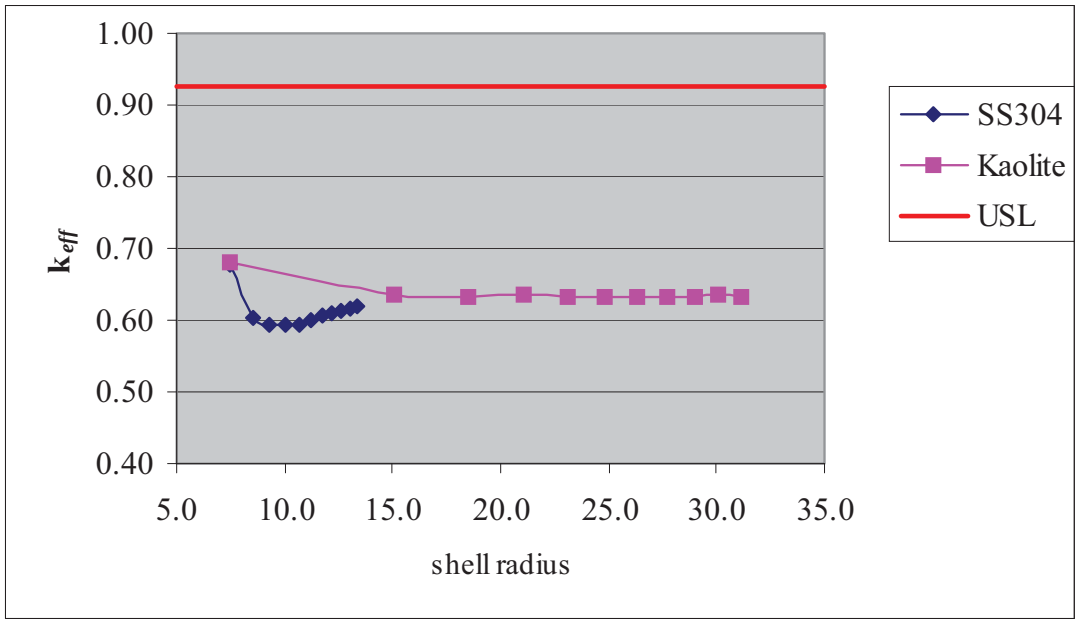

Fig. 6.21. K_{eff} vs shell radius (cm) for 10.4 kg core of $UZrH_x$ with stainless steel or Kaolite shell.

Cases **atdzkr_11** through **atdzkr_1** pertain to Model 3 (Fig. 6.13, Section 6.3.1.4). The fissile core of Model 1 is blanketed with a variable thickness Kaolite shell with an exterior 20 cm water reflector. As shown in Fig. 6.21 and Table 6.9.6-22 (Appendix 6.9.6), the $k_{eff} + 2\sigma$ values decrease to an asymptotic value at a shell radius of 18.54 cm (Kaolite thickness of 11.08 cm.) The NLF decreases from ~ 0.06 to 0.02. The NLF continues to decrease to a value of 0.006 as water-saturated Kaolite is added up to the 128,034 g pre-bake amount contained inside the body weldment outer liner and the drum top plug. The asymptotic value for $k_{eff} + 2\sigma$ is ~ 0.048 below the maximum $k_{eff} + 2\sigma$ value at zero Kaolite thickness. The overall effect of adding water-saturated Kaolite to the system is the reduction in neutron multiplication in the system. The $k_{eff} + 2\sigma$ values are substantially below the USL of 0.925.

Cases **athzpkr_11** through **athzpkr_1** pertain to Model 4 (Fig. 6.14, Section 6.3.1.4). The homogenized core of Model 4 consists of $UZrH_x$, 500 g of polyethylene, and Kaolite. For this set of parametric cases, the Kaolite water content ranges from the water-saturated (maximum radius) to the dry condition (minimum radius) [Table 6.9.6-22, Appendix 6.9.6]. As shown in Fig. 6.22 and Table 6.9.6-22, the $k_{eff} + 2\sigma$ value remains constant at ~0.468 until the moisture content drops to 60% at a core radius of 37.17 cm. The $k_{eff} + 2\sigma$ value decreases to a minimum value of 0.306 at the dry Kaolite condition. The homogenization of the Kaolite shell and the fissile material core from Model 3 produces two competing effects in Model 4:

- addition of Kaolite expands the fissile material core, reducing neutron multiplication (evident in the comparison of results for Cases **athzphr_11** and **atdzkr_11**), and
- the addition of the water in the Kaolite increases neutron multiplication.

Consequently, the scenario of water penetration of fissile material core requires evaluation.

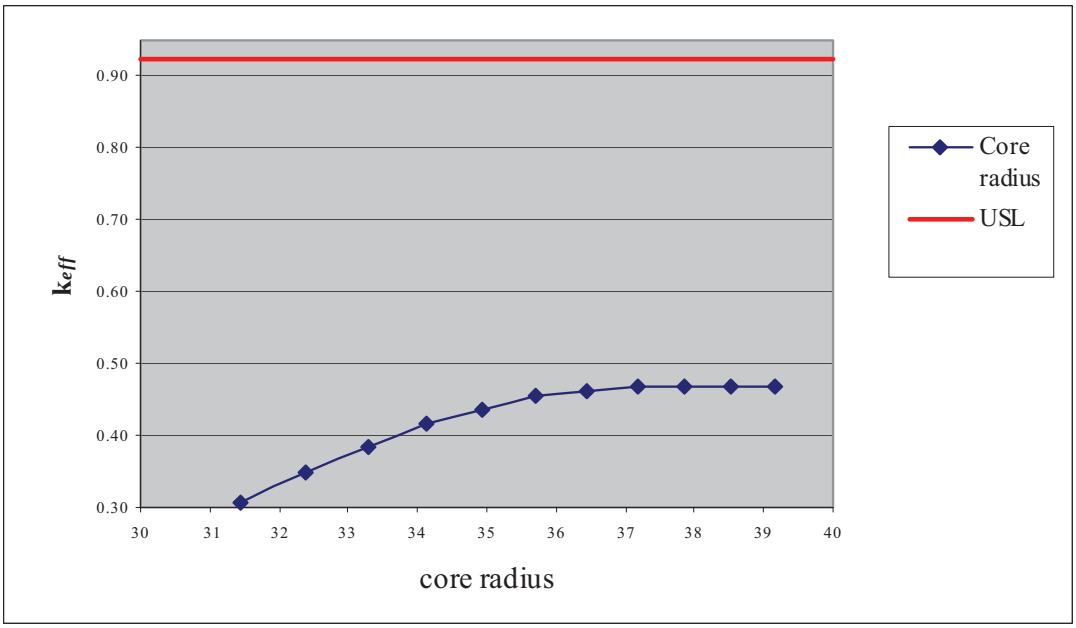

Fig. 6.22. K_{eff} vs. core radius (cm) for homogenized core of $UZrH_x$, 500 g polyethylene, and Kaolite where the Kaolite water content ranges from the dry to the water-saturated condition.

Cases **athzpwskr_9_11** through **athzpwskr_9_1** pertain to Model 5 (Fig. 6.15, Section 6.3.1.4). Model 5 is a variation of Model 3, which represents a fissile material core blanketed with water-saturated Kaolite and reflected by 20 cm of water. In Model 5, excess water from the Kaolite shell is assumed to penetrate the core. As shown in Fig. 6.23 and Table 6.9.6-22a (Appendix 6.9.6), the $k_{eff} + 2\sigma$ value increases to a maximum of 0.962 with the addition of 14,922 g of excess water into the fissile material core. As more water is added to the core, the core becomes overmoderated and the $k_{eff} + 2\sigma$ value decreases below the subcritical limit.

In the absence of Part 71.55(f) Test data or dynamic impact simulations per Type-C test criteria, the assumption of water penetration of the fissile material core is valid under the severe air transport evaluation criteria. Models 5 is applicable to air transport of the ES-3100 package given that the geometric form of the TRIGA fuel content following the air transport accident can not be established.

Additional case results are presented in Table 6.9.6-22a (Cases **athzpwskr_8_11** through **athzpwskr_6_1**) where the number of fuel segments is reduced from 9 items in a package to 6 items where the content remains subcritical over the entire range of moderation. As shown in Fig. 6.23 and Table 6.9.6-22a (Appendix 6.9.6), the $k_{eff} + 2\sigma$ value increases to a maximum of 0.911with the addition of 14,922 g of excess water into the fissile material core for a package loading of 716 g ^{235}U. As more water is added to the core, the core becomes overmoderated and the $k_{eff} + 2\sigma$ value decreases to 0.601.

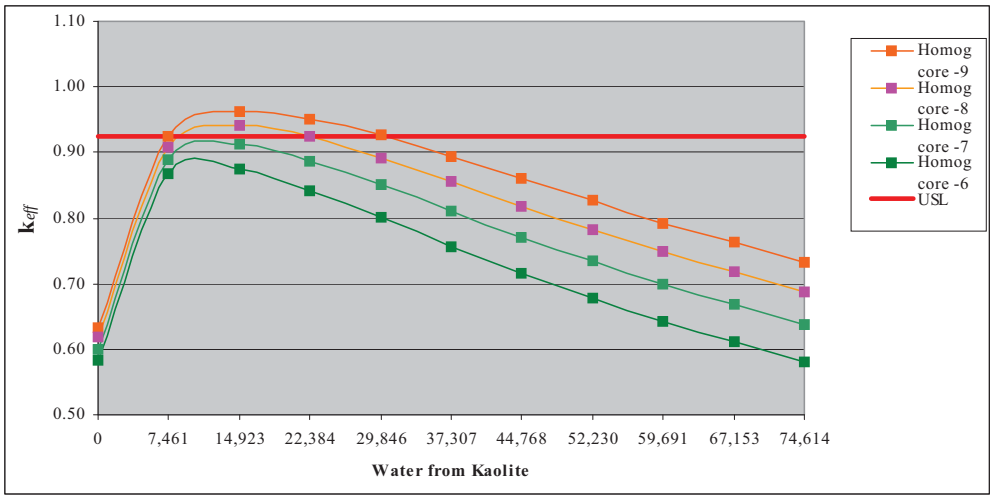

Fig. 6.23. k_{eff} vs. excess water from Kaolite for fissile core blanketed with a variable thickness Kaolite shell.

Model 6 (Fig. 6.16, Section 6.3.1.4) pertains to the case where fissile material from the homogenized core of Model 4 forms a shell external to the core. Given that the total amount of fissile material is limited to 716 g ^{235}U, the quantity is not sufficient to form a critical configuration. As shown in Section 6.7.3, this is apparent even if kilogram quantities of additional fissile material were located in the shell adjacent to the core.

6.7.3 Results for HEU Broken Metal, More Than One Piece per Convenience Can

The results for Models 1–3 are presented in Sect. 6.7.1. Cases **athmpkr_12_8_11** through **athmpkr_8_8_1** (Table 6.9.6-23, Appendix 6.9.6) pertain to Model 4 (Fig. 6.14, Section 6.3.1.4) for broken metal loadings in the range of 4–7 kg ^{235}U for uranium at 100% enrichment and Kaolite water content from dry to water saturation values. Cases **athmpkr_12_1_11** through **athmpkr_10_1_1** pertain to loadings in the range of 5–7 kg ^{235}U for uranium at 20% enrichment and Kaolite water content from dry to water saturation values. The $k_{eff} + 2\sigma$ values are adequately below the USL of 0.925 for mass loadings up to 4,000 g ^{235}U at 100% enrichment and up to 6,000 g ^{235}U at 20% enrichment.

Cases **athmpwskr_12_8_11** through **athmpwskr_2_8_1** (Table 6.9.6-23, Appendix 6.9.6) pertain to Model 5 (Fig. 6.15, Section 6.3.1.4) for mass loadings in the range of 1–7 kg ^{235}U for uranium at 100% enrichment and for core water content over the range of excess water from the Kaolite shell. As shown in Fig. 6.24 and Table 6.9.6-23 (Appendix 6.9.6), the $k_{eff} + 2\sigma$ values are significantly above the USL.

Cases **athmpwskr_12_1_11** through **athmpwskr_2_1_1** and Cases **athm2pwskr_5_1_11** through **athm2pwskr_2_1_1** pertain to mass loadings in the range of 7–0.6 kg ^{235}U for uranium at 20% enrichment and core water content over the range of excess water from the Kaolite shell. As shown in Fig. 6.25 and Table 6.9.6-23 (Appendix 6.9.6), the $k_{eff} + 2\sigma$ values are adequately below the USL of 0.925 for mass loadings up to 700 g ^{235}U at 20% enrichment. This signifies the fissile mass loading limit for HEU broken metal content to be shipped by air transport. Therefore, the evaluation of Model 6 is focused on this limit.

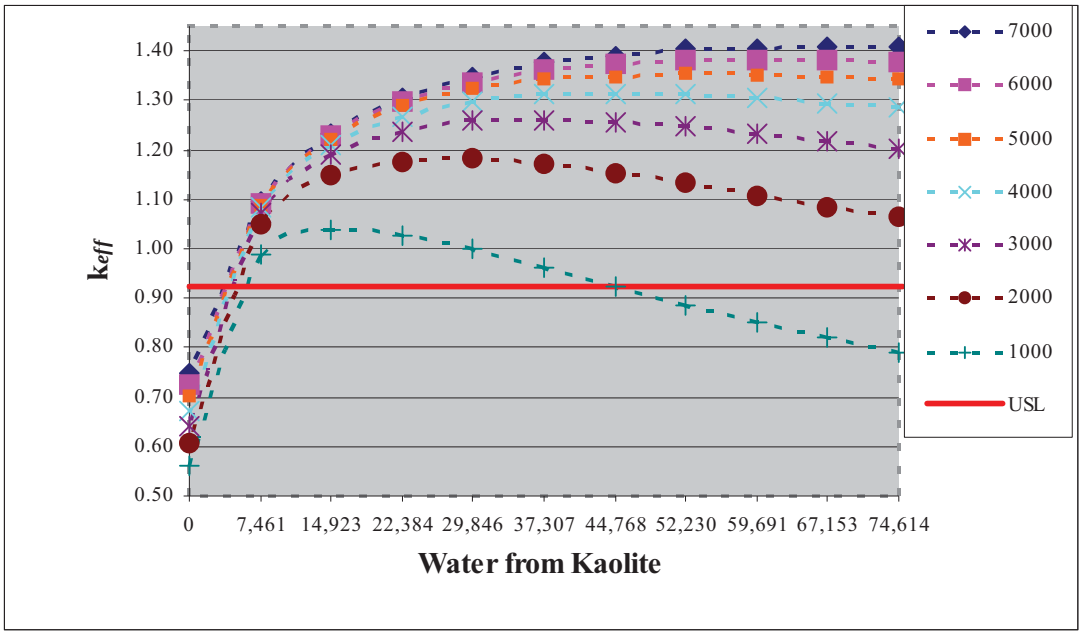

Fig. 6.24. K_{eff} vs. excess water from Kaolite for core of 1–7 kg enriched HEU broken metal at 100% enrichment, core blanketed with a variable thickness Kaolite shell.

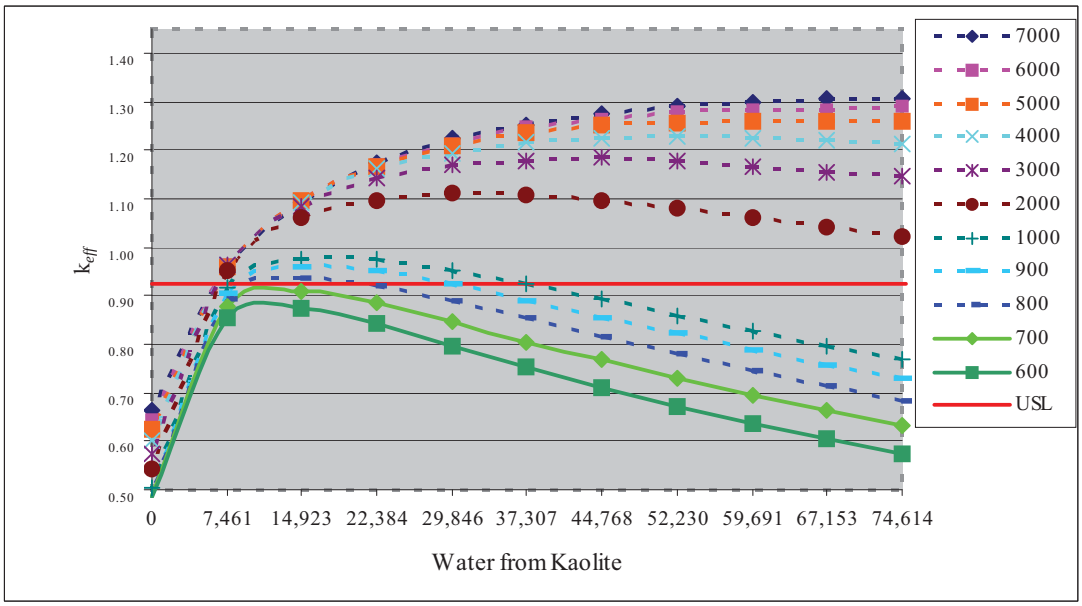

Fig. 6.25. K_{eff} vs. excess water from Kaolite for core 20% enriched HEU broken metal (0.6–7 kg ^{235}U), core blanketed with a variable thickness Kaolite shell.

Cases **athmpkmr_6_1_1_11** through **athmpwskr_1_6_1_1** (Table 6.9.6-23, Appendix 6.9.6) pertain to Model 6 (Fig. 6.16, Section 6.3.1.4), where fissile material from the homogenized core of Model 4 forms a shell external to the core. Cases **athmpkmr_6_1_1_11** through **athmpkmr_6_1_1_1** represent 3 kg ^{235}U in the core and 0.5 kg ^{235}U in the shell (17.5 kg total HEU at 20% enrichment) with the water content of the Kaolite ranging from the water-saturated to the dry condition. In the subsequent series of cases, the $k_{eff} + 2\sigma$ values decrease as HEU is moved from the core to the shell in 2.5 kg increments. Although the total HEU of 17.5 kg greatly exceeds the 3.5 kg limit identified in the evaluation of Model 5, all $k_{eff} + 2\sigma$ values are adequately below the USL of 0.925.

As stated previously, uranium alloy is conservatively assessed when the aluminum, molybdenum, or zirconium constituents are modeled as ^{235}U. Thus, limits established for HEU metal apply to the uranium alloys of aluminum, molybednum, or zirconium.

6.7.4 Conclusions

Given that the results for catastrophic damage are adequately subcritical, ES-3100 packages may be shipped via air transport with:

- Solid or broken HEU metal or U-Al alloy with up to 700 g ^{235}U,
- 3 fuel sections ("meats") of $UZrH_x$ per loaded convenience can and up to 3 loaded cans per package where the ^{235}U does not exceed 716 g at 20% enrichment or 408 g ^{235}U at 70%,
- ~15 inch long clad fuel rods, each rod derived from a single TRIGA fuel element, and where per package ^{235}U does not exceed 716 g at 20% enrichment or 408 g ^{235}U at 70%, or

6.8 BENCHMARK EXPERIMENTS

6.8.1 Applicability of Benchmark Experiments

The criticality validation is specific to uranium, plutonium, and uranium-233 systems encompassing a substantial subset of the database used to prepare the Organization for Economic Cooperation and Development (OECD) Handbook, Volumes I–VI. The benchmark specifications are intended for use by criticality safety engineers to validate the application of criticality calculation techniques such as SCALE 4.4a. Example calculations presented in the handbook do not constitute a validation of the codes or cross-section data sets by themselves, but the Handbook information can be and has been used to validate SCALE 4.4a by competent nuclear criticality safety persons.

The data from the benchmark experiments involving uranium represent a sufficiently wide range of enrichments and physical and chemical forms to cover many existing or presently planned activities for Y-12. These include enriched uranium with ^{235}U only and natural and depleted uranium, as well as highly enriched uranium, intermediate enriched uranium, and low enriched uranium. Data analyzed from critical experiments in this validation include systems having fast, intermediate, and thermal neutron energy spectra, and they include materials in various physical and chemical forms such as uranium metals, solutions, and oxide compounds. With the benchmark experiments that are directly applicable to uranium systems, there is a high level of confidence that the calculated results presented in this evaluation are sufficiently accurate to establish the safety of the package under both NCT and HAC. This conclusion is based on the validation of the code and cross-section library described in Sect. 6.3.3.

6.8.2 Details of Benchmark Calculations

The validation of CSAS25 control module of SCALE 4.4a with the 238-group ENDF/B-V cross-section library is documented in Y/DD-896/R1 and Y/DD-972R1 (Appendix 6.9.8). Y/DD-896/R1 addresses the establishment of bias, bias trends, and uncertainty associated with the use of SCALE 4.4a for performance of criticality calculations. This evaluation is directed at uranium systems consisting of fissile and fissionable material in metallic, solution, and other physical forms, as well as plutonium and ^{233}U systems, as described in the OECD Handbook. [NEA/NSC/DOC(95)03] The focus is on comparison of k_{eff} with the associated experimental results for establishment of bias, bias trends, and uncertainty as a final step. Compiled data for 1217 critical experiments are used as the basis for the calculation models. The calculated results from SCALE 4.4a using the 238-group ENDF/B-V cross-section library have been compared with reported results for the benchmark experiments. Comparison of results demonstrates that SCALE 4.4a run on the SAE HP J-5600 unclassified workstation (CMODB) produces the same results within the statistical uncertainty of the Monte Carlo calculations as reported by the OECD for the experiments.

Y/DD-972R1 (Appendix 6.9.8) addresses determining USL and for incorporating uncertainty and margin into this USL. Y/DD-972R1 establishes subcritical limits determined through an evaluation of statistical parameters of calculation results for critical experiments. The correlating parameters (i.e., mass, enrichment, geometry, absorption, moderation, reflection) and values for applying additional margin to the subcritical limits are application dependent. The determination of correlating parameters and additional margin is an integral part of the process analysis for a particular application. For the critical experiment results, no correlation between calculation results and neutron energy causing fission was found. As such, this document does not specify “final” USL values as has been done in the past.

6.8.3 Bias Determination

The USL is based on the non-parametric statistics-based lower tolerance limit (LTL) for greater than 0.99/99% where there is a probability of greater than 0.99 that 99% of the population is greater than a specified result, reduced by additional margin. From Table 1 of Y/DD-972R1 (Appendix 6.9.8), the LTL combining bias and bias uncertainty is 0.975 for uranium systems, including HEU metal. Tables 4.2, 4.3, and 4.4 of Y/DD-896/R1 (Appendix 6.9.8) list the maximum (positive) and minimum (negative) biases for HEU (metal, compound, solution), IEU (metal, compound) and LEU (compound, solution) systems. Since the positive bias is conservatively treated as a “zero” bias in the validation analysis, the negative bias is applied to determine the USL for the systems. The minimum bias for the HEU, IEU, and LEU systems is given as −0.14356, −0.0055 and −0.0247, respectively.

The minimum result for the HEU systems is from one of four k-infinite models, which are somewhat different than the actual benchmark experiments. As discussed in Sect 5.3 of Y/DD-896/R1, four outlier results are for benchmark experiments that were modeled infinite in extent. The models required additional interpretation and adjustment from the actual finite experiment configuration to create an infinite benchmark model. After eliminating the outlier models from the bias determination, the minimum bias determined from data in Y/DD-896/R1, Table 4.2, is −0.0203 for HEU systems.

The global minimum bias for these uranium systems [−0.0247 (conservatively rounded to −0.025)] is applied to all uranium enrichments. Ordinarily, the USL would be 0.955 where an additional margin of subcriticality of 0.02 is subtracted from the LTL of 0.975. However, NUREG/CR-5661 provides guidance that the USL should be established with a minimum margin of subcriticality of 0.05. Thus, the USL is equal to 0.95 plus the minimum bias (−0.025), giving a value of 0.925.

6.9 APPENDICES

Appendix	Description
6.9.1	FISSILE CONTENT AND PACKAGING MODELS
6.9.2	HAC PACKAGE MODEL
6.9.3	PACKAGE MATERIAL COMPOSITIONS
6.9.4	QUALIFICATION OF A NEUTRON ABSORBER MATERIAL FOR THE ES-3100
6.9.5	MISCELLANEOUS INFORMATION AND DATA
6.9.6	ABRIDGED SUMMARY TABLES OF CRITICALITY CALCULATION RESULTS
6.9.7	INPUT LISTINGS OF ES-3100 CALCULATION MODELS FOR SELECT CASES
6.9.8	Y/DD-896/R1, *CRITICAL EXPERIMENT BENCHMARK CALCULATIONS WITH CSAS25 FROM SCALE4.4a FOR CRITICALITY SAFETY ANALYSES ON THE HP J-5600 UNCLASSIFIED WORKSTATION (CMODB)* AND Y/DD-972R1, *DETERMINATION OF THE UPPER SUBCRITICAL LIMIT FOR CRITICALITY CALCULATIONS FOR CRITICALITY SAFETY ANALYSES*
6.9.9	CRITICALITY EVALUATION FOR INCREASING THE FISSILE LOADING LIMIT FOR HEU OXIDE IN THE ES-3100
6.9.10	Y/DD-1220, *CRITICAL EXPERIMENT BENCHMARK CALCULATIONS WITH CSAS25 FROM SCALE5 FOR CRITICALITY SAFETY ANALYSES ON THE HP zx6000 UNCLASSIFIED WORKSTATION (CMODD)* AND Y/DD-1221, *DETERMINATION OF THE UPPER SUBCRITICAL LIMIT FOR CRITICALITY CALCULATIONS FOR CRITICALITY SAFETY ANALYSES*

THIS PAGE INTENTIONALLY LEFT BLANK.

Appendix 6.9.1

FISSILE CONTENT AND PACKAGING MODELS

THIS PAGE INTENTIONALLY LEFT BLANK.

Appendix 6.9.1

FISSILE CONTENT AND PACKAGING MODELS

Calculation model for solid HEU metal, 3.24-in.-diam cylinders. Figure 6.9.1-1 depicts the wire-mesh view of the 3.24-in.-diam highly enriched uranium (HEU) cylindrical content configuration inside the containment vessel. The interstitial water has been removed for illustration purposes. As can be seen from Fig. 6.9.1-1, the cylindrical content model contains one cylinder per convenience can and 1.4-in.-thick 277-4 canned spacers between the can locations. Cylinders are at the maximum diameter that will fit through the opening of a press-fit lid type convenience can. The cylindrical content shown is at the maximum mass loading; the height of the cylinders may change depending upon the mass loading. Figure 6.9.1-1b depicts a section view of the containment vessel with 3.24-in.-diam cylinders at 4.826 and 0.254 cm separation.

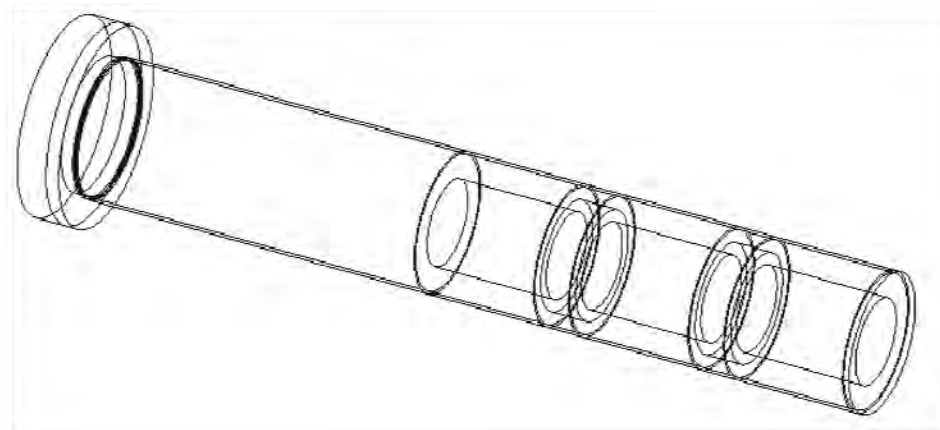

Fig. 6.9.1-1. Containment vessel containing 3.24-in.-diam cylinders and 1.4-in.-thick 277-4 canned spacers.

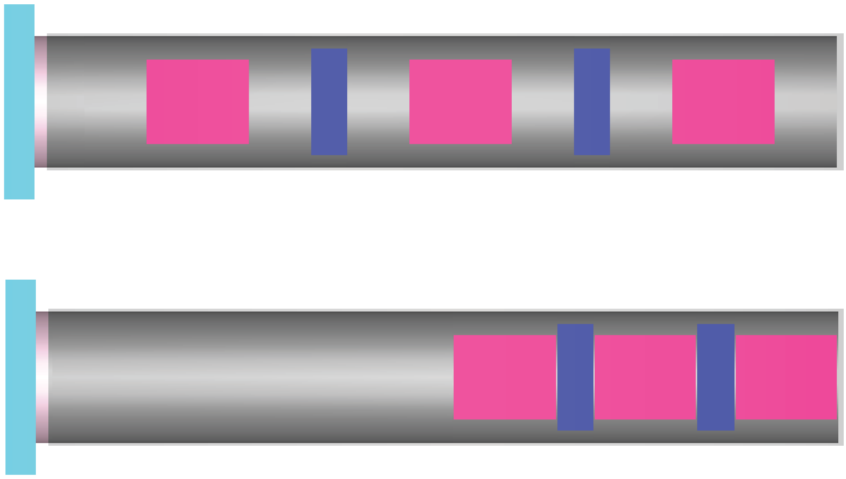

Fig. 6.9.1-1b. Section view of the containment vessel depicting 4.826 and 0.254 cm separation distances for 3.24-in.-diam cylinders (pink) with 1.4-in.-thick canned spacers (blue).

Calculation model for solid HEU metal, 4.25-in.-diam cylinders. Figure 6.9.1-2 depicts the wire-mesh view of the 4.25-in.-diam HEU cylindrical content configuration inside the containment vessel. The interstitial water has been removed for illustration purposes. As can be seen from Fig. 6.9.1-2, the cylindrical content model contains one cylinder per convenience can and 1.4-in.-thick 277-4 canned spacers between the can locations. Cylinders are at the maximum diameter that will fit through the opening of a crimp-seal lid type convenience can. The cylindrical content shown is at the maximum mass loading; the height of the cylinders may change depending upon the mass loading.

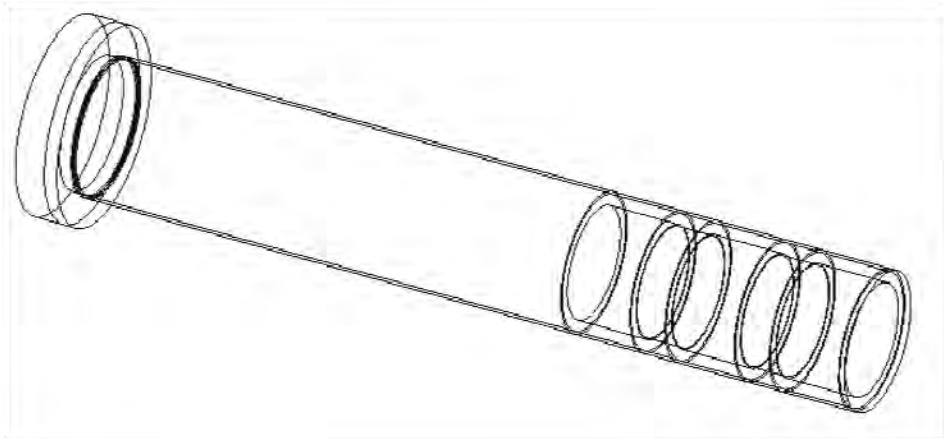

Fig. 6.9.1-2. Containment vessel containing 4.25-in.-diam cylinders and 1.4-in.-thick 277-4 canned spacers.

Calculation model for solid HEU metal, bars. Figure 6.9.1-3 depicts the wire-mesh view of the 2.29-in.-square HEU bar content configuration inside the containment vessel. The interstitial water inside the containment vessel has been removed for illustration purposes. The square bar content model contains one bar per convenience can and 1.4-in.-thick 277-4 canned spacers between the can locations. The 2.29-in.-square bar is the largest size that will fit through the 3.24-in.-diam opening of a press-fit lid type convenience can. Similar to the cylindrical model, the height of the square bar is dependent upon the HEU mass.

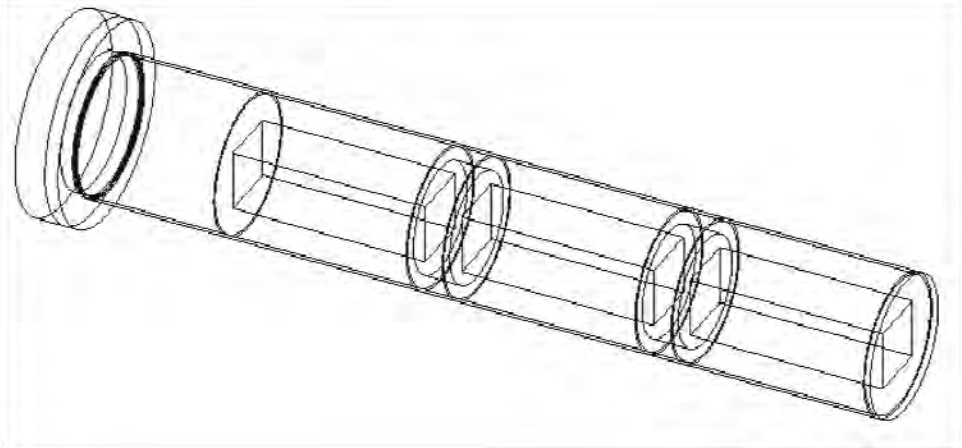

Fig. 6.9.1-3. Containment vessel containing 2.29-in.-square bars and 1.4-in.-thick 277-4 canned spacers.

Calculation model for solid HEU metal, slugs. Figure 6.9.1-4 depicts the wire-mesh view of a pentagonal ring configuration of the 1.5-in.-diam × 2.0-in.-tall slugs inside the containment vessel. The axial centerline of each slug is located 1.27598 in. from the origin of the pentagon such that a tight fitting configuration of slugs is modeled (i.e., there are no gaps between adjacent slugs). The slug content model contains two rings of the 1.5-in.-diam × 2.0-in.-tall slugs per convenience can and the 277-4 canned spacers between the convenience cans locations. The interstitial water inside the containment vessel has been removed for illustration purposes. Figure 6.9.1-4b depicts typical slug configurations that were evaluated.

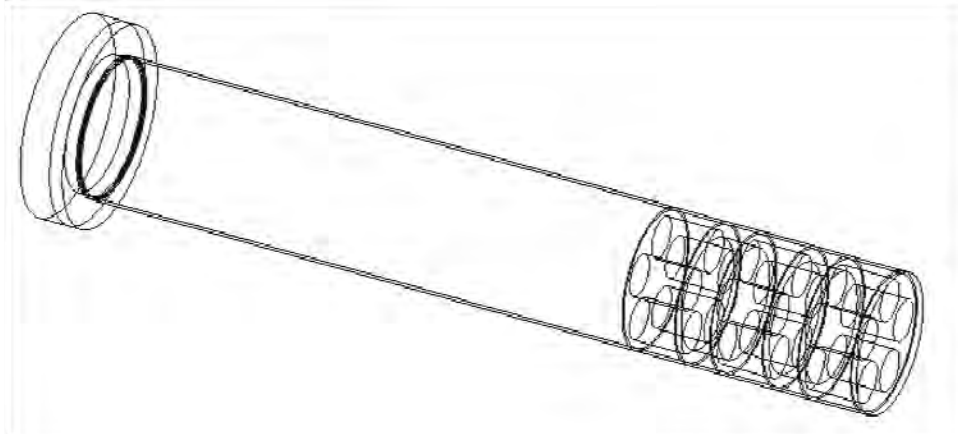

Fig. 6.9.1-4. Containment vessel containing the 1.5-in.-diam × 2.0-in.-tall slugs in a pentagonal ring configuration with 0.0-cm spacing between slugs and 1.4-in.-thick 277-4 canned spacers.

A 1.5-in.–diam × 2.0-in.–tall slug was modeled with a maximum tolerance of 1/16 in. applied to both the radius and height. The resulting dimensions are 1.984375 cm in radius and 5.23875 cm in height; the calculated volume of a single slug is 64.80746 cm^3. For 100% enriched uranium (density = 18.81109 g/cm^3), the calculated mass of 15 slugs is 18,286.5 g. Subsequently, the radius of each slug was reduced by 0.0005 cm thus eliminating a geometry intersection error in KENO V.a which occurs when the hole option is used to place slugs into an encompassing piece of the geometry unit. In the case of a pentagonal ring with spaced-apart slugs (Case **cvcr5est11_1_1**, Fig. 6.9.1-4b), the calculated volume reported for 15 slugs in KENO V.a is 971.622 cm^3 and the corresponding mass is 18277.3 g or 1,218.5 g per slug. This reduction in mass of 0.6333 g per slug is insignificant when considering the mass of a slug is nominally 1,089 g.

The maximum tolerance slug was also used in other slug geometry configurations, such as, “cvcr5s”, “cvcr6e0s”, “cvcr6s”, “cvcr70s”, “cvcr6e4s”, and “cvcr73s” orientations shown in Fig. 6.9.1-4b. For the pentagonal geometry configuration with slugs stacked two high in a ring (Case **cvcr5est11_1_2** or **cvcr5st11_1_2**), the model volume and mass of the slugs are twice the values of the single ring (Case **cvcr5est11_1_1** or **cvcr5st11_1_1**). For a pentagonal geometry configuration with a central slug (“cvcr6e0s”) and the hexagonal geometry configuration (“cvcr6"), the calculated volume reported in KENO V.a is 1,165.95 cm^3 and the corresponding mass is 21,932.7 g. For a hexagonal geometry configuration with a central slug (“cvcr70s”), the calculated volume reported in KENO V.a is 1,360.27 cm^3 and the corresponding mass is 25,588.2 g. For the compact ten-slug-per-can configurations (“cvcr5est”, “cvcr5est”, “cvcr6e4s”, and “cvcr73s”), the calculated volume reported in KENO V.a is 1,943.24 cm^3, and the corresponding mass is 36,554.6 g.

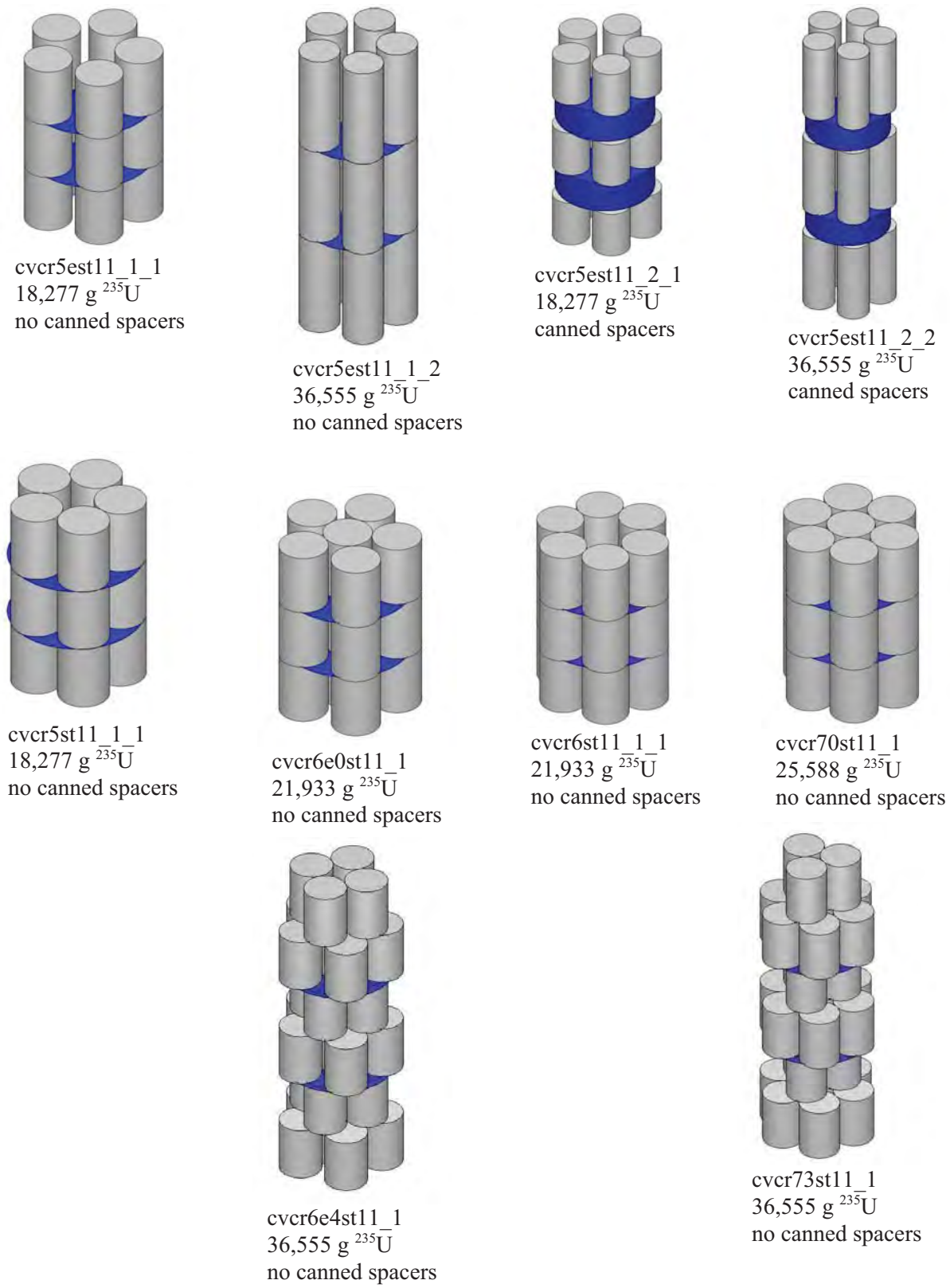

Fig. 6.9.1-4b. Isometric views for typical slug configurations. Blue marker depicted for configurations without 1.4-in.-thick 277-4 canned spacers.

Several slug arrangements were evaluated for demonstrating that the most conservative arrangement of slugs has been analyzed. Figure 6.9.1-4c depicts radial section views of the containment vessel showing the slugs (pink) in relation to the footprint (blue) for a 4.25-in.–diam (5.3975-cm) convenience can. Cases **cvcr5st11_1_1**, **cvcr5est11_1_1**, **cvcr5e0st11_1** , **cvcr5u0st11_1**, and **cvcr5l0st11_1** depict different arrangements with five slugs per convenience can, three cans per package. Cases **cvcr6e0st11_1_1** and **cvcr6st11_1_1** depict arrangements with six slugs per convenience can, and Case **cvcr70st11_1** depicts seven slugs per convenience can. (Considerable deformation of a 4.25-in.–diam convenience can wall is required to achieve all but the simple pentagonal-ring arrangement of slugs.) The 277-4 canned spacers are not present in these calculation models.

Calculation models for solid HEU metal of unspecified geometric shapes characterized as broken metal. The intended use of the "broken metal" category is for shipment of solid HEU metal of unspecified geometric shape characterized as broken metal, packed in 4.25-in.-diam convenience cans where the packing fraction would not exceed 0.59. The packing fraction is a parameter which characterizes the volume that broken metal occupies. A typical broken metal content is depicted in Fig. 6.9.3.1-3 where the packing fraction for content in a convenience can ranges from 0.2 to ~0.6.

In the criticality evaluation of broken metal, convenience cans are not credited for containing the content nor for maintaining spacing between the 277-4 canned spacers. Consequently, the shape and size of the broken metal pieces establishes the separation between canned spacers which in turn determines the size of the HEU content locations inside the containment vessel. Given the irregular shape of broken metal, the packing fraction is the parameter which quantifies the volume of space that the broken metal occupies. The use of a large packing fraction (~0.6) results in minimum separation between canned spacers which minimizes the size of the lower and middle content locations and maximizes the size of the upper content location. Reactivity of the containment vessel is driven by the oversized upper content location. Conversely, the use of a small packing fraction (~0.2) February 16, 2009results in greater separation between the canned spacers which increases the size of the lower and middle content locations while reducing the size of the upper content location. Reactivity of the containment vessel decreases accordingly.

The "**sqa**", "**lha**", and "**cha**" calculation models are devised for evaluating broken metal in the idealized forms described in the following paragraphs. The heights of the lower can locations and separation between the first and second 277-4 canned spacers inside the containment vessel are conservatively established on the basis that broken metal is confined within a rectangular lattice formed by the unit cells of fissile material having a packing fraction of ~0.59.

In the "sqa" model for HEU broken metal, a uniform-size metal cube is contained inside a unit cell of content. The unit cells are configured into arrays with one array for each can location inside the containment vessel. HEU metal cubes ranging in size from 1.0 to 0.25 in. are correspondingly arranged into 3 × 3, 6 × 6, or 12 × 12 configurations with ***N*** layers stacked vertically. A rectangular lattice of unit cells is defined by a square prism circumscribed by the wall of the containment vessel with an inner diameter of 5.06 in. (12.8524 cm). The width and depth of the square base is 3.57796 in. (9.08802 cm). The height of the lattice is determined by both the size of a cube and the number of layers of cubes required for a given HEU mass loading.

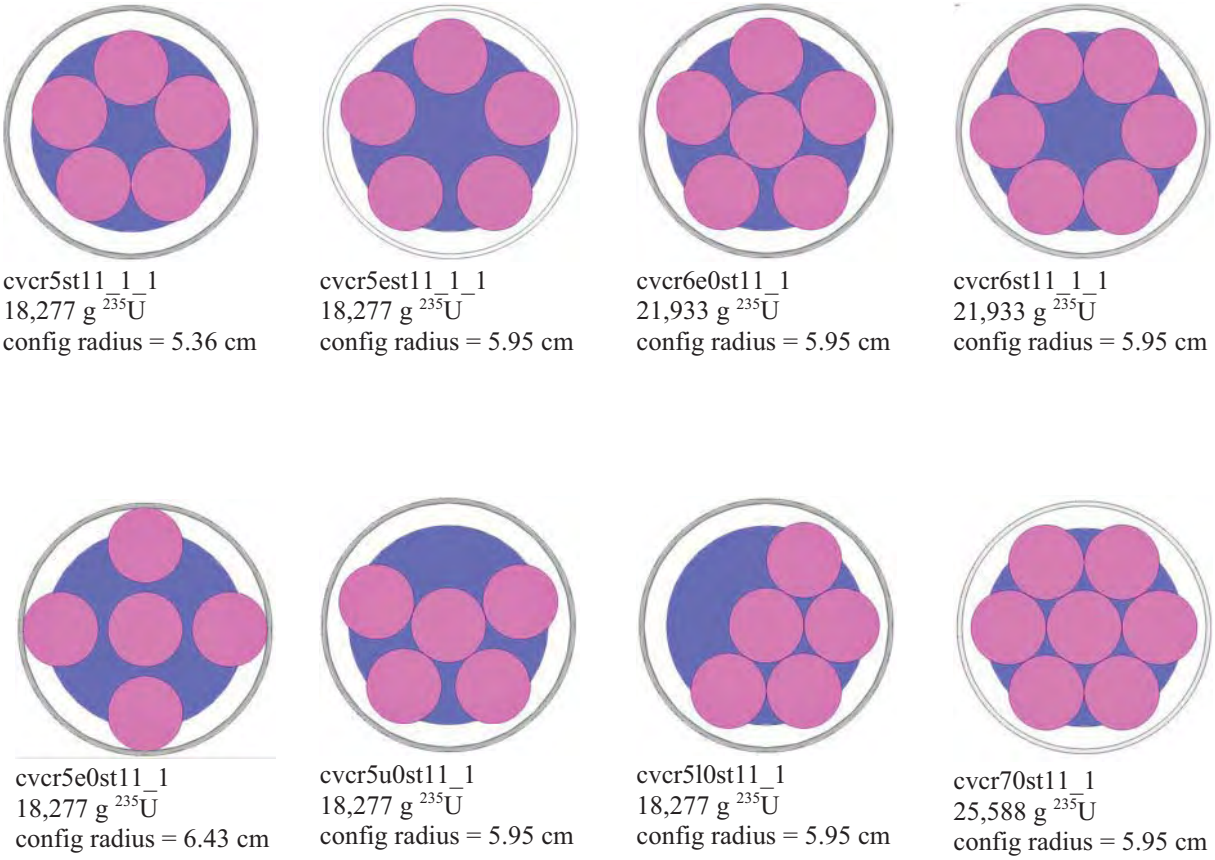

Fig. 6.9.1-4c. Plan view of slug configurations in the confines of the containment vessel. Blue marker depicts 4.25-in.–diam wall of the convenience can.

Figure 6.9.1-5 depicts a wire mesh view of the containment vessel and lid with three 12 × 12 × 18 arrays of HEU content separated by 277-4 canned spacers. Figure 6.9.1-5b depicts an isometric view of this same content with the **evaluation** water surrounding the HEU removed for illustration. The corner unit cells touch the inside wall of the containment vessel. The HEU cubes are centered within the individual unit cells and uniform spacing between cubes is modeled. The 277-4 canned spacers are modeled as cylindrical disks with dimensions of 4.13-in. diam × 1.37-in. height.

Uranium mass is reduced in the calculation model by removing one or more cubes from the array and filling these vacancies with water. The location of the 277-4 canned spacers between the arrays of cubes decreases as complete layers of cubes are removed from each array. The volume of the containment vessel above the top layer of the top array of cubes is filled with full-density water.

In the "lha" model of HEU broken metal, the metal cubes of the "sqa" model are homogeneously mixed with **evaluation** water within the square prism of the "sqa" model. Figure 6.9.1-5c depicts an isometric view of the "lha" model. The boundaries of each square prism shown in the figure are defined by the 12 × 12 × 18 array of unit cells of the explicit "sqa" model. Each prism contains the same mass of HEU and **evaluation** water that the respective explicit cube model contains. The volume outside the prisms and the canned spacers is filled with full density water.

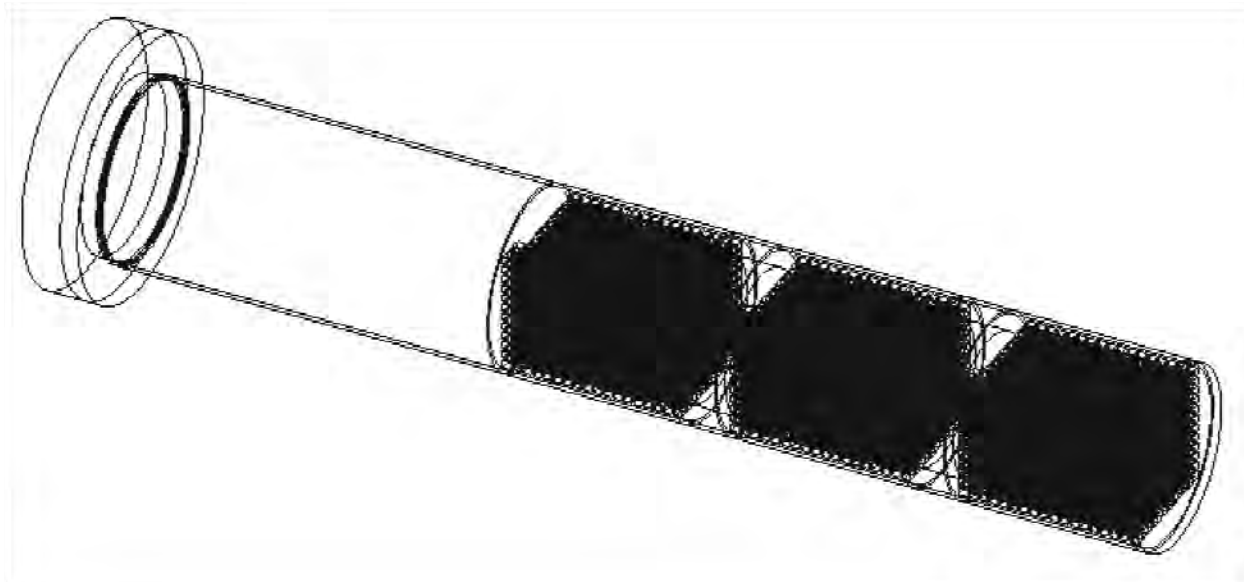

Fig. 6.9.1-5. Wire mesh view of the "sqa" model with three 12 × 12 × 18 lattices of HEU broken metal as 1-in. cubes separated by 1.4-in. 277-4 canned spacers.

In the "cha" model of HEU broken metal, the metal cubes of the "sqa" model are homogeneously mixed with the **evaluation** water within the free volume of the containment vessel. Figure 6.9.1-5d depicts an isometric view of the "cha" model. The 277-4 canned spacers are positioned for similarity with the "sqa" and "lha" models using the height of the prism, defined in this case by the 12 × 12 × 18 array of unit cells of the explicit "sqa" model. The mass of HEU and **evaluation** water of the explicit "sqa" model is preserved.

Once the locations of the canned spacers in the containment vessel are established based on the height of the square prism, the HEU broken metal and evaluation water inside the containment vessel are homogenized over the internal volume of the 12.8524-cm-diam containment vessel not being occupied by the canned spacers. The homogenization of fissile material with moderator to represent discrete solid HEU metal of unspecified geometric shape characterized as broken metal is unquestionably bounding only when the overall volume (and shape) containing HEU and interstitial moderator between the pieces of HEU is preserved in the approximation model.

In the "cha" model, the uniform dispersal of the homogenized HEU and evaluation water over the residual internal volume of the containment vessel has the effect of relocating ^{235}U from the two lower can locations into the upper can location. When the 277-4 canned spacers are present, the neutronic coupling of can locations is weak and the reactivity of the packaged content is determined by the reactivity of the largest can location. This model may not be conservative when canned spacers are absent because nothing would prevent settling of content inside the containment vessel into a single mass given that the convenience cans are not credited for containing the content nor for maintaining spacing between the contents of each can.

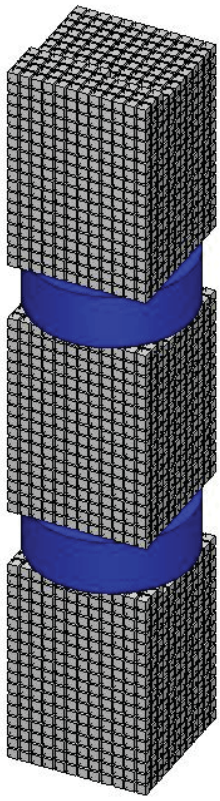

Fig. 6.9.1-5b. Detailed isometric view of the explicit "sqa" model for HEU broken metal. Three 12 × 12 × 18 lattices of 1-in. cubes separated by 1.4-in. 277-4 spacers are shown.

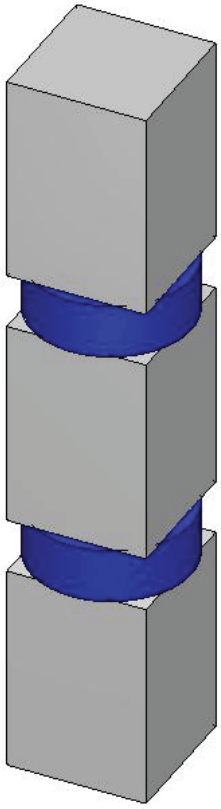

Fig. 6.9.1-5c. Isometric view of the homogeneous "lha" model with HEU homogeneously mixed with evaluation water within the rectangular lattices formed by the units cells.

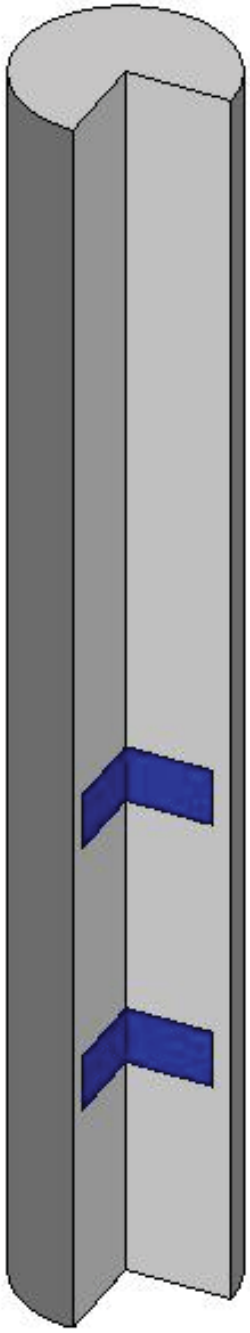

Fig. 6.9.1-5d. Isometric view of the homogeneous "cha" model with HEU homogeneously mixed with evaluation water within the interior of the containment vessel.

As stated in Sect. 6.9.3.1, the "cha" model is used to represent broken metal in single packages and the array of packages under NCT and HAC. For addressing the issue that the uniform dispersal approximation model ("cha") may not be conservative, especially when the 277-4 canned spacers are absent, the settling of content may be evaluated by establishing the material geometry and composition based on a maximum packing fraction. The packing fraction calculation model is described for this purpose.

In the packing fraction model, the material within a variable height can location is evaluated over the range of packing fractions from loosely packed material (PF ~0.2) to densely packed material (PF ~0.6). The height of can locations is determined based on the packing fraction instead of the fictitious cube stacking algorithm which was used in the "cha" uniform dispersal approximation model. The height of can locations used in the packing fraction calculation model is given by the following formula:

$$hgt = [(HEU_{vol} / PF) + Poly_{vol}] / CV_{area}$$

(500 grams of polyethylene is included in the calculation model to represent the potential use of packing material.)

Fig. 6.9.1-5e depicts a section view of the containment vessel for the packing fraction calculation model. The height of the lower, middle, and upper can locations are equal. Only in the upper location does the can location coincide with the content location. The "**fl**" is used in the case name to designate calculations are based on the packing fraction model.

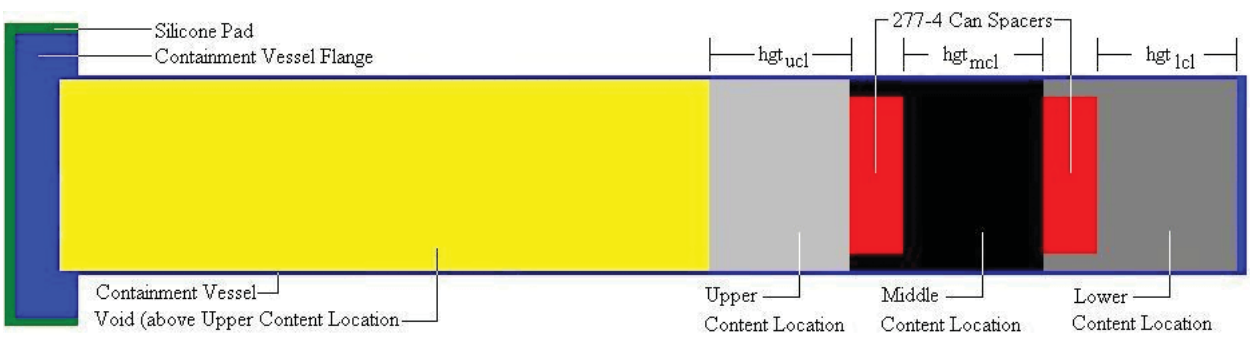

Fig. 6.9.1-5e. Section view of the containment vessel for the packaging fraction calculation model depicting the content locations for broken metal. The height (hgt) of the upper, middle, and lower can locations are determined by the HEU packing fraction.

The volume fractions for material constituents in the middle and lower content locations are calculated as follows:

$$VF_{HEU} = HEU_{vol} / (hgt \times CV_{area} + Spacer_{void})$$

where HEU_{vol} is the volume of HEU at theoretical density and $Spacer_{void}$ is the volume of the void region between the CV wall an the can spacer assumed filled with evaluation water.

$$VF_{H2O} = [(HEU_{vol} / PF) - HEU_{vol} + Spacer_{void}] / (hgt \times CV_{area} + Spacer_{void})$$

$$VF_{Poly} = Poly_{vol} / (hgt \times CV_{area} + Spacer_{void})$$

The volume fractions for material constituents in the upper content location are calculated as follows:

$$VF_{HEU} = HEU_{vol} / (hgt \times CV_{area})$$

$$VF_{H2O} = [(HEU_{vol} / PF) - HEU_{vol}] / (hgt \times CV_{area})$$

$$VF_{Poly} = Poly_{vol} / (hgt \times CV_{area})$$

The void region above the upper content location (Vol_{above}) is filled with full density water.

In addressing the issue that the uniform dispersal approximation "cha" model may not be conservative because homogenization of HEU is performed over a much larger volume and shape than the HEU content conceivably occupies, the effect of dispersing content within a can location may be evaluated using a variation of the packing fraction calculation model. The dispersed content calculation model is described for this purpose.

In the dispersed content calculation model, the HEU, the polyethylene, and the evaluation water of the upper content location is homogenized over the entire volume of this location. Figure 6.9.1-5f depicts a section view of the containment vessel for the dispersed content calculation model. The height of the lower and middle content locations are equal while the height of the upper content location extends to the top of the containment vessel cavity. The "**fd**" designation in the case name is used to identify the dispersed content calculation model.

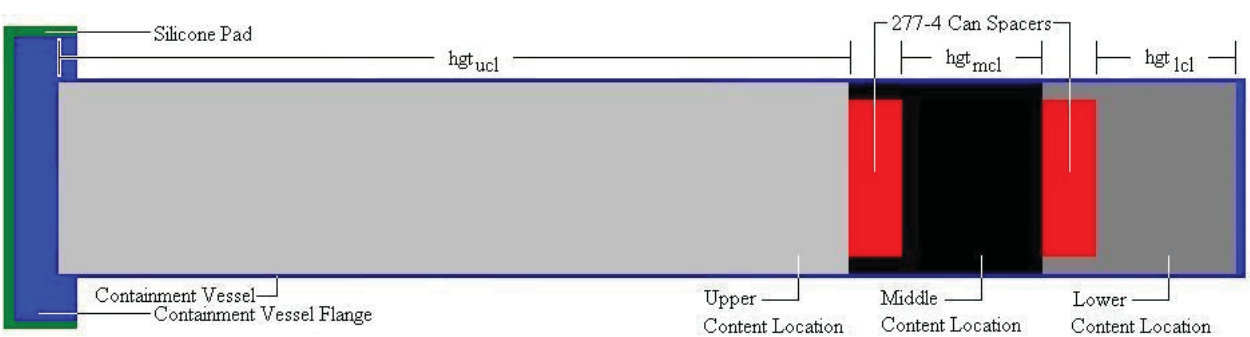

Fig. 6.9.1-5f. Section view of the containment vessel in the dispersed content calculation model depicting the content locations for broken metal. The height (hgt) of the middle and lower content locations are determined by the HEU packing fraction. The height of the upper content location extends to the top of the containment vessel cavity.

The volume fractions for material constituents in the middle and lower content locations are specified the same as in the "**fl**" model. However, the volume fractions for material constituents dispersed into the upper content location are calculated as follows:

$$VF_{HEU} = HEU_{vol} / (hgt \times CV_{area} + Vol_{above})$$

where Vol_{above} is the void region above the upper can location into which the content is dispersed.

$$VF_{H2O} = [(HEU_{vol} / PF) - HEU_{vol} + Vol_{above}] / (hgt \times CV_{area} + Vol_{above})$$

$$VF_{H2O} = Poly_{vol} / (hgt \times CV_{area} + Vol_{above})$$

For example, consider reference Case **hciabmt12_4_1_5_3** (Table 6.9.6-11) which defines the loading limit for broken metal in the 70% < enr. ≤ 80% range where canned spacers are not used in the containment vessel. In revised Case **hciapbmflt12_1_6_4_5**, HEU broken metal with a packing fraction of 0.6, the 500 g of polyethylene and evaluation water in each can location is homogenized over the content location. Case **hciapbmflt12_1_2_4_5** is the same as Case **hciapbmflt12_1_6_4_5**, except the packing fraction is 0.2. In Case **hciapbmfdt12_1_6_4_5**, HEU broken metal with a packing fraction of 0.6, the 500 g of polyethylene and evaluation water in each content location is homogenized over the content location. Case **hciapbmfdt12_1_2_4_5** is the same as Case **hciapbmfdt12_1_6_4_5,** except the packing fraction is 0.2. Table 6.9.1.0 provides details for the packing fraction and dispersed content calculation models.

Table 6.9.1.0. Details for the packing fraction "fl" and dispersed content "fd" calculation models

Location	Height (cm)	Material	Density × VF × region volume	HEU (g)	Water (g)	Polyethylene (g)
*Case **hciapbmflt12_1_6_4_5**, packing fraction = 0.6*						
Lower	2.30470	HEU	(18.85873)(0.23645)(299.031)	1333.4		
		Water	(0.9982)(1.5773e-01)(299.031)		47.1	
		Poly	(0.9200)(6.0582e-01)(299.031)			166.7
Spacer	0.00030	Water	(0.9982)(8.64286E-03)		0.0	
Middle	2.30470	HEU	(18.85873)(0.23645)(299.031)	1333.4		
		Water	(0.9982)(1.5773e-01)(299.031)		47.1	
		Poly	(0.9200)(6.0582e-01)(299.031)			166.7
Spacer	0.00030	Water	(0.9982)(8.64286E-03)		0.0	
Top	2.30470	HEU	(18.85873)(0.23647)(299.001)	1333.4		
		Water	(0.9982)(1.5765e-01)(299.001)		47.1	
		Poly	(0.9200)(6.0588e-01)(299.001)			166.7
Above	71.82530	Water	(0.9982)(1.0)(9318.28)		9301.5	
Total	78.74000			4000.2	9442.8	500.0
*Case **hciapbmflt12_1_2_4_5**, packing fraction = 0.2*						
Lower	4.12133	HEU	(18.85873)(0.13223)(534.713)	1333.4		
		Water	(0.9982)(5.2897e-01)(534.713)		282.3	
		Poly	(0.9200)(3.3880e-01)(534.713)			166.7
Spacer	0.00030	Water	(0.9982)(8.64286E-03)		0.0	
Middle	4.12133	HEU	(18.85873)(0.13223)(534.713)	1333.4		
		Water	(0.9982)(5.2897e-01)(534.713)		282.3	
		Poly	(0.9200)(3.3880e-01)(534.713)			166.7
Spacer	0.00030	Water	(0.9982)(8.64286E-03)		0.0	
Top	4.12133	HEU	(18.85873)(0.13224)(534.682)	1333.4		
		Water	(0.9982)(5.2895e-01)(534.682)		282.3	
		Poly	(0.9200)(3.3882e-01)(534.682)			166.7

Table 6.9.1.0. Details for the packing fraction "fl" and dispersed content "fd" calculation models

Location	Height (cm)	Material	Density × VF × region volume	HEU (g)	Water (g)	Polyethylene (g)
Above	66.37541	Water	(0.9982)(1.0)(8.61124E+03)		8595.7	
Total	78.74000			4000.2	9442.7	500.0
*Case **hciapbmfdt12_1_6_4_5**, packing fraction = 0.6*						
Lower	2.30470	HEU	(18.85873)(0.23645)(299.031)	1333.4		
		Water	(0.9982)(1.5773e-01)(299.031)		47.1	
		Poly	(0.9200)(6.0582e-01)(299.031)			166.7
Spacer	0.00030	Water	(0.9982)(8.64286E-03)		0.0	
Middle	2.30470	HEU	(18.85873)(0.23645)(299.031)	1333.4		
		Water	(0.9982)(1.5773e-01)(299.031)		47.1	
		Poly	(0.9200)(6.0582e-01)(299.031)			166.7
Spacer	0.00030	Water	(0.9982)(8.64286E-03)		0.0	
Top	74.13000	HEU	(18.85873)(0.00735)(9617.28)	1333.4		
		Water	(0.9982)(9.7381e-01)(9617.28)		9348.5	
		Poly	(0.9200)(1.8837e-02)(9617.28)			166.7
Total	78.74000			4000.2	9442.7	500.0
*Case **hciapbmfdt12_1_2_4_5**, packing fraction = 0.2*						
Lower	4.12133	HEU	(18.85873)(0.13223)(534.713)	1333.4		
		Water	(0.9982)(5.2897e-01)(534.713)		282.3	
		Poly	(0.9200)(3.3880e-01)(534.713)			166.7
Spacer	0.00030	Water	(0.9982)(8.64286E-03)		0.0	
Middle	4.12133	HEU	(18.85873)(0.13223)(534.713)	1333.4		
		Water	(0.9982)(5.2897e-01)(534.713)		282.3	
		Poly	(0.9200)(3.3880e-01)(534.713)			166.7
Spacer	0.00030	Water	(0.9982)(8.64286E-03)		0.0	
Top	4.12133	HEU	(18.8587)(0.00773)(9145.92)	1333.3		
		Water	(0.9982)(9.7246e-01)(9145.92)		8878.0	
		Poly	(0.9200)(1.9808e-02)(9145.92)			166.7
Total	12.36459			4000.1	9442.7	500.0

Calculation model for solid HEU of unspecified geometric shape, HEU oxides. Figure 6.9.1-6 depicts the wire-mesh view of the HEU oxide content inside the containment vessel. The interstitial water inside the containment vessel has been removed for illustration purposes. The HEU oxide mixture at bulk density is located at the bottom of the containment vessel and fills the space to the wall of the containment vessel. The height of the HEU oxide mixture is dependant upon the mass loading.

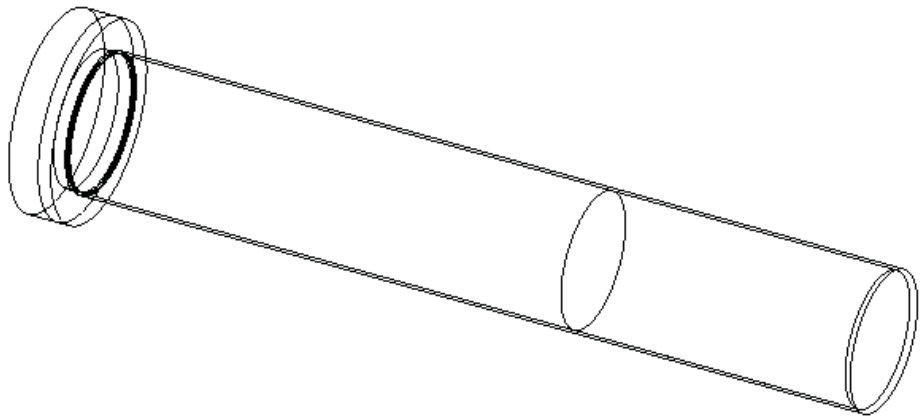

Fig. 6.9.1-6. Wire-mesh view of the containment vessel containing the HEU oxide mixture.

HEU product oxide is assumed to be saturated with water in the criticality calculation models. Maximum saturation in the oxide material occurs in a volume defined as the difference between the specific volume of bulk oxide and the minimum specific volume of the product oxide. Product oxide has a bulk density of 6.54 g/cm^3 or a specific volume of 0.152905 cm^3/g (Sect. 6.9.3.1). UO_2 has a theoretical density of 10.96 g/cm^3 or a minimum specific volume of 0.091241 cm^3/g. Therefore, the maximum volume per gram of UO_2 available for saturation by water is 0.061664 cm^3/g. Additionally, an assumed maximum of 500 g of polyethylene is homogenized with the water-saturated product oxide. The homogenized oxide containing polyethylene (density = 0.92 g/cm^3) occupies an additional 543.47826 cm^3.

The height of polyethylene homogenized with water-saturated product oxide inside the containment vessel is calculated by dividing the volume of the homogenized oxide by the internal area of the base of the containment vessel. The area of the base is 129.73536 cm^2 for the containment vessel with an inner diameter of 5.06 in. (12.8524 cm). The height of the void space above the homogenized oxide is calculated by subtracting the homogenized oxide height from the 78.84-cm (31.0-in.) inside height of the containment vessel.

As an example, consider Case **cvcrpoxt11_1_21_15** where 21,000 g of UO_2 (18,484.3 g ^{235}U) is saturated with 1,292.62 g water (Table 6.9.6-12). The calculated H/X ratio for the water saturated product oxide is 1.83. The water-saturated product oxide homogenized with 500 g of polyethylene rises to a height of ~28.93955 cm inside the containment vessel. The 6,460.87 cm^3 of void space is flooded with 6449.2 g of evaluation water, such that the calculated H/X ratio inside the containment vessel is 11.84. The 500 g of polyethylene adds 0.90 to the calculated H/X ratio of water-saturated product oxide. The calculated H/X ratio for the water-saturated product oxide homogenized with 500 g of polyethylene in a dry containment vessel is 1.83 + 0.90 = 2.73 (Case **cvcrpoxt11_1_21_1**). In all cases, the H/X ratio is a computed value rather than an evaluation parameter.

The same modeling technique is applied to product oxides of U_3O_8 and UO_3. U_3O_8 has a theoretical density of 8.30 g/cm^3 or a minimum specific volume of 0.120482 cm^3/g. UO_3 has a theoretical density of 7.29 g/cm^3 or a minimum specific volume of 0.137174 cm^3/g. The maximum volumes per gram of U_3O_8 and UO_3 available for saturation by water are 0.032423 cm^3/g and 0.015731 cm^3/g, respectively.

The eight skull oxide content compositions described in Table 6.9.3.1-3b for evaluating skull oxide are derived from 292 samples of canned skull oxide. Two additional compositions are listed in the table for addressing skull oxides with an enrichment of 93.2 wt %. The skull oxide content is assumed to be U_3O_8 plus polyethylene, graphite, and unidentified material. A maximum of 513 g of polyethylene is assumed to be present in the skull oxide content. The volume of skull oxide content in the containment vessel (**vsoc**) is calculated as the grams of skull oxide content (**gsoc**) divided by the bulk density of the skull oxide content (**densoc**). The height of skull oxide content inside the containment vessel is calculated by dividing the volume of skull oxide content (**vsoc**) by the internal area of the base of the containment vessel (129.73536 cm^3).

Calculation model for solid HEU of unspecified geometric shape, UNH crystals. Figure 6.9.1-7 depicts the wire-mesh view of the UNH crystal content inside the containment vessel. A solution of UNH crystals dissolved in water fills the entire volume of the containment vessel.

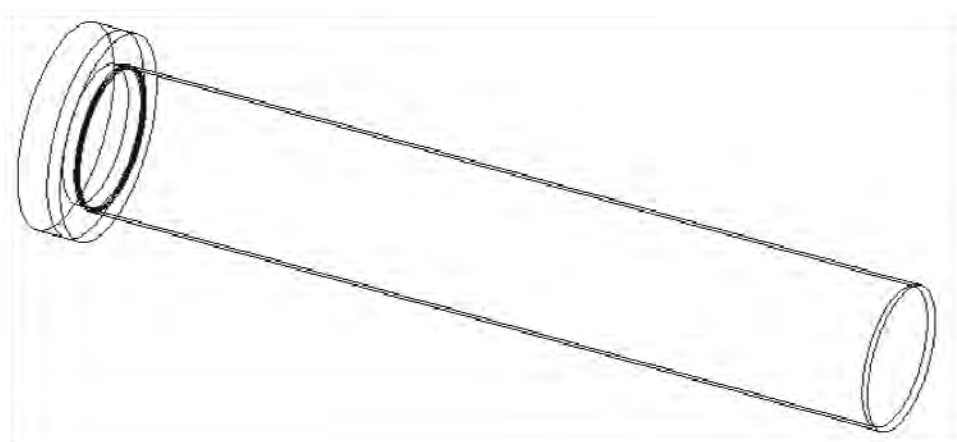

Fig. 6.9.1-7. Wire-mesh view of the containment vessel containing the UNH crystal mixture.

Table 6.9.1.1 provides details of the calculation models used to establish the mass loading limits identified in Table 6.2a for surface-only modes of transportation. The table provides exact dimensions of the fissile material used in the analyses; the mass of fissile material, enrichment, and density of the fissile material used in the analysis; moderating properties of materials inside the containment vessel (water, hydrogenous packing material, represented by polyethylene, etc.), moderator density and h/x ratios; and arrangement of the fissile material including amount of spacing (if any) between the fissile material and/or 277-4 canned spacers. In the creation of a generalized geometry model for treatment of 277-4 canned spacers, the use of a non-zero thickness spacer was required by KENO V.a. An insignificant thickness of 0.0001 cm was used for representing this imaginary region.

Table 6.9.1.1. Details of calculation models used to establish mass loading limits for surface-only modes of transportation identified in Table 6.2a

Case	Dimensions (cm)	Enrichment (wt. % ^{235}U)	Density (g/cm^3)
Cylinders (d ≤ 3.24 in.)			
nciacyt11_18_1_3	r = 4.1148 cm h = 5.99639 cm	100	18.81109
The moderator is full density water (0.9982 g/cm^3) surrounding three stacked cylindrical contents. The contents have an overall stack height of 17.99171 cm (7.08335 in.). No polyethylene was used in this model. Each cylindrical content is separated by a 0.0001 cm 277-4 canned spacer and 0.0012 cm of moderating material. The bottom cylinder has a 0.0005 cm gap between it and the bottom of the containment vessel. The contents sit in the exact center on the bottom of the CV. Therefore, the cylinder content has 2.3114 cm of moderating material around each side and 60.74779 cm of moderating material above. The modeled material masses are: 18 kg ^{235}U, 9.2418 kg H_2O, resulting in an h/x ratio of ~13.40.			
nciacyt11_30_2_3	r = 4.11480 cm h = 9.99399 cm	100	18.81109
The moderator is full density water (0.9982 g/cm^3) surrounding three stacked cylindrical contents separated by 277-4 canned spacers between each cylindrical content. The contents (uranium and spacers) have an overall stack height of 37.09657 cm (14.60495 in.). No polyethylene was used in this model. Each cylindrical content is separated by a 3.5561 cm spacer and 0.0012 cm of moderating material. The bottom cylinder has a 0.0005 cm gap between it and the bottom of the containment vessel. The contents sit in the exact center on the bottom of the CV. Therefore, the cylinder content has 2.3114 cm of moderating material around each side and 41.64293 cm of moderating material above. The modeled material masses are: 30 kg ^{235}U, 7.9915 kg H_2O, resulting in an h/x ratio of ~6.95.			
Cylinders (3.24 in. < d ≤ 4.25 in.)			
nciacyct11_15_1_3	r = 5.39750 cm h = 2.90416 cm	100	18.81109
The moderator is full density water (0.9982 g/cm^3) surrounding three stacked cylindrical contents separated by 277-4 canned spacers. The contents have an overall stack height of 8.71508 cm (3.43133 in.). No polyethylene was used in this model. Each cylindrical content is separated by a 0.0001 cm spacer and 0.0012 cm of moderating material. The bottom cylinder has a 0.0005 cm gap between it and the bottom of the containment vessel. The contents sit in the exact center on the bottom of the CV. Therefore, the cylinder content has 1.0287 cm of moderating material around each side and 70.02442 cm of moderating material above. The modeled material masses are: 15 kg ^{235}U, 9.4010 kg H_2O, resulting in an h/x ratio of ~16.36.			
nciacyct11_25_2_3	r = 5.39750 cm h = 4.84031 cm	100	18.81109
The moderator is full density water (0.9982 g/cm^3) surrounding three stacked cylindrical contents separated by 277-4 canned spacers. The contents have an overall stack height of 21.63433 cm (8.517453 in.). No polyethylene was used in this model. Each cylindrical content is separated by a 3.5561 cm spacer and 0.0012 cm of moderating material. The bottom cylinder has a 0.0005 cm gap between it and the bottom of the containment vessel. The contents sit in the exact center on the bottom of the CV. Therefore, the cylinder content has 1.0287 cm of moderating material around each side and 57.10417 cm of moderating material above. The modeled material masses are: 25 kg ^{235}U, 8.2568 kg H_2O, resulting in an h/x ratio of ~8.62.			

Table 6.9.1.1. Details of calculation models used to establish mass loading limits for surface-only modes of transportation identified in Table 6.2a

Case	Dimensions (cm)	Enrichment (wt. % ^{235}U)	Density (g/cm^3)
Bars			
hciasqt12_30_1_3	x = 5.81920 cm y = 5.81920 cm z = 15.69855 cm	100	18.81109
The moderator is full density water (0.9982 g/cm^3) surrounding three stacked square or cuboid contents separated by 277-4 canned spacers. The contents have an overall stack height of 47.09825 cm (18.54262 in.). No polyethylene was used in this model. Each cuboid content is separated by a 0.0001 cm spacer and 0.0012 cm of moderating material. The bottom cuboid has a 0.0005 cm gap between it and the bottom of the containment vessel. The contents sit in the exact center on the bottom of the CV. Therefore, the cuboid content is surrounded by moderating material ranging from 3.6166 to 2.4144 cm (center to outer edge) and 31.64125 cm of moderating material above. The modeled material masses are: 30 kg ^{235}U, 8.6050 kg H_2O, resulting in an h/x ratio of ~7.49.			
nciasqt11_36_2_3	x = 5.81920 cm y = 5.81920 cm z = 18.83826 cm	100	18.81109
The moderator is full density water (0.9982 g/cm^3) surrounding three stacked square or cuboid contents separated by 277-4 canned spacers. The contents have an overall stack height of 63.62938 cm (25.05094 in.). No polyethylene was used in this model. Each cuboid content is separated by a 3.5561 cm spacer and 0.0012 cm of moderating material. The bottom cuboid has a 0.0005 cm gap between it and the bottom of the containment vessel. Therefore, the cuboid content is surrounded by moderating material ranging from 3.6166 to 2.4144 cm (center to outer edge) and 15.11012 cm of moderating material above. The modeled material masses are: 36 kg ^{235}U, 7.6731 kg H_2O, resulting in an h/x ratio of ~5.56.			
Slugs (enr. ≤ 95%–no can spacers)			
ncia5st11_1_1_7_3	r = 1.983875 cm h = 5.23875 cm	95	18.82298
The moderator is full density water (0.9982 g/cm^3) surrounding three stacked pentagonal rings of slug content separated by 277-4 canned spacers. (Slugs are inserted into the cylindrical geometry segment of the containment vessel using the hole option.) The contents have an overall stack height of 15.71885 cm (6.18852 in.). No polyethylene is used in this model. Each ring is separated by a 0.0001 cm spacer and 0.0012 cm of moderating material. The bottom ring of slugs has a 0.0005 cm gap between it and the bottom of the containment vessel. Above the stack of slugs is 63.02065 cm of moderating material. The modeled material masses are: 18.288 kg U (17.374 kg ^{235}U), 9.2269 kg H_2O, resulting in an h/x ratio of ~13.86. The loading arrangement of slugs is depicted in Fig. 6.9.1-4b for the Case **cvcr5st11_1_1**.			
Slugs (80% < enr. ≤ 95%–with can spacers)			
hcia70st12_2_7_3	r = 1.983875 cm h = 5.23875 cm	95	18.82298
The moderator is full density water (0.9982 g/cm^3) surrounding three stacked rings of slugs, each ring with a central slug surrounded by slugs in a hexagonal pattern. (Slugs are inserted into the cylindrical geometry segment of the containment vessel using the hole option.) Each ring is separated by a 277-4 canned spacer. The contents (uranium and spacers) have an overall stack height of 22.83085 cm (8.98852 in.). No polyethylene was used in this model. Each ring is separated by a 3.5561 cm spacer and 0.0012 cm of moderating material. The bottom ring has a 0.0005 cm gap between it and the bottom of the containment vessel. The stack of slugs has 55.90865 cm of moderating material above. The modeled material masses are: 25.604 kg U (24.324 kg ^{235}U), 8.2253 kg H_2O, resulting in an h/x ratio of ~8.83. The loading arrangement of slugs is similar to that depicted in Fig. 6.9.1-4b for the Case **cvcr70st11_1** except that the canned spacers are present.			

Table 6.9.1.1. Details of calculation models used to establish mass loading limits for surface-only modes of transportation identified in Table 6.2a

Case	Dimensions (cm)	Enrichment (wt. % ^{235}U)	Density (g/cm^3)
ncf15est11_2_2_7_3	r = 1.983875 cm h = 5.23875 cm	95	18.82298
The moderator is full density water (0.9982 g/cm^3) surrounding three rings of double stacked slugs, each ring separated by a 277-4 canned spacer. (Slugs are inserted into the cylindrical geometry segment of the containment vessel using the hole option.) The contents (uranium and spacers) have an overall stack height of 22.83085 cm (8.98852 in.). No polyethylene was used in this model. Each ring is separated by a 3.5561 cm spacer and 0.0012 cm of moderating material. The bottom ring has a 0.0005 cm gap between it and the bottom of the containment vessel. The stack of slugs has 55.90865 cm of moderating material above. The modeled material masses are: 36.578 kg U (34.749 kg ^{235}U), 7.6434 kg H_2O, resulting in an h/x ratio of ~5.74. The loading arrangement of slugs is depicted in Fig. 6.9.1-4b for the Case **cvcr5est11_2_2**.			
Slugs (enr. ≤ 80%–with can spacers)			
hcia5est12_2_2_5_3	r = 1.983875 cm h = 5.23875 cm	80	18.85873
The moderator is full density water (0.9982 g/cm^3) surrounding three rings of double stacked slugs, each ring separated by a 277-4 canned spacer. (Slugs are inserted into the cylindrical geometry segment of the containment vessel using the hole option.) The contents (uranium and spacers) have an overall stack height of 22.83085 cm (8.98852 in.). No polyethylene was used in this model. Each ring is separated by a 3.5561 cm spacer and 0.0012 cm of moderating material. The bottom ring has a 0.0005 cm gap between it and the bottom of the containment vessel. The stack of slugs has 55.90865 cm of moderating material above. The modeled material masses are: 36.647 kg U (29.318 kg ^{235}U), 7.6434 kg H_2O, resulting in an h/x ratio of ~6.80. The loading arrangement of slugs is depicted in Fig. 6.9.1-4b for the Case **cvcr5est11_2_2**.			
ncf15est11_2_2_5_3	r = 1.983875 cm h = 5.23875 cm	80	18.85873
The moderator is full density water (0.9982 g/cm^3) surrounding three rings of double stacked slugs, each ring separated by a 277-4 canned spacer. (Slugs are inserted into the cylindrical geometry segment of the containment vessel using the hole option.) The contents (uranium and spacers) have an overall stack height of 22.83085 cm (8.98852 in.). No polyethylene was used in this model. Each ring is separated by a 3.5561 cm spacer and 0.0012 cm of moderating material. The bottom ring has a 0.0005 cm gap between it and the bottom of the containment vessel. The stack of slugs has 55.90865 cm of moderating material above. The modeled material masses are: 36.647 kg U (29.318 kg ^{235}U), 7.6434 kg H_2O, resulting in an h/x ratio of ~6.80. The loading arrangement of slugs is depicted in Fig. 6.9.1-4b for the Case **cvcr5est11_2_2**.			
Broken Metal for CSI=0.0			
hciabmt12_4_1_5_3	r = 6.52620 cm h = 78.74000 cm	80	18.85873
The uranium "broken metal" content is homogenized with a moderator of water with a specific gravity of 1.0×10^{-4} over the interior volume of the containment vessel. No 277-4 canned spacers are used in this calculation. No polyethylene was used in this calculation. Since the contents are homogenized over the internal volume of the containment vessel, there is no moderating material between the content and the containment vessel walls. The modeled material masses are: 3.7085 kg U (2.9668 kg ^{235}U), 10.0007 kg H_2O, resulting in an h/x ratio of ~87.98.			

Table 6.9.1.1. Details of calculation models used to establish mass loading limits for surface-only modes of transportation identified in Table 6.2a

Case	Dimensions (cm)	Enrichment (wt. % ^{235}U)	Density (g/cm^3)
hciabmt12_5_1_4_3	r = 6.52620 cm h = 78.74000 cm	70	18.88264
The uranium "broken metal" content is homogenized with a moderator of water with a specific gravity of 1.0×10^{-4} over the interior volume of the containment vessel. No 277-4 canned spacers are used in this calculation. No polyethylene was used in this calculation. Since the contents are homogenized over the internal volume of the containment vessel, there is no moderating material between the content and the containment vessel walls. The modeled material masses are: 4.6415 kg U (3.2490 kg ^{235}U), 9.9516 kg H_2O, resulting in an h/x ratio of ~79.95.			
nciabmt11_6_1_3_3	r = 6.52620 cm h = 78.74000 cm	60	18.90661
The uranium "broken metal" content is homogenized with a moderator of water with a specific gravity of 1.0×10^{-4} over the interior volume of the containment vessel. No 277-4 canned spacers are used in this calculation. No polyethylene was used in this calculation. Since the contents are homogenized over the internal volume of the containment vessel, there is no moderating material between the content and the containment vessel walls. The modeled material masses are: 5.5768 kg U (3.3461 kg ^{235}U), 9.9025 kg H_2O, resulting in an h/x ratio of ~77.24.			
hciabmt12_3_2_8_3	r = 6.52620 cm h = 78.74000 cm	100	18.81109
The uranium "broken metal" content is homogenized with a moderator of water with a specific gravity of 1.0×10^{-4} over the interior volume of the containment vessel. The 277-4 canned spacers with a thickness of 3.5561 cm (1.4000 in.) are used and are modeled at 3.02984 cm and 9.61638 cm above the bottom of the containment vessel. No polyethylene was used in this calculation. Since the contents are homogenized over the internal volume of the containment vessel, there is no moderating material between the content and the containment vessel walls or the spacers. The modeled material masses are: 2.7743 kg ^{235}U, 9.4362 kg H_2O, resulting in an h/x ratio of ~88.78.			
hciabmt12_4_2_7_3	r = 6.52620 cm h = 78.74000 cm	95	18.82298
The uranium "broken metal" content is homogenized with a moderator of water with a specific gravity of 1.0×10^{-4} over the interior volume of the containment vessel. The 277-4 canned spacers with a thickness of 3.5561 cm (1.4000 in.) are used and are modeled at 3.02984 cm and 9.61638 cm above the bottom of the containment vessel. No polyethylene was used in this calculation. Since the contents are homogenized over the internal volume of the containment vessel, there is no moderating material between the content and the containment vessel walls or the spacers. The modeled material masses are: 3.7014 kg U (3.5164 kg ^{235}U), 9.3871 kg H_2O, resulting in an h/x ratio of ~69.68.			
hciabmt12_4_2_6_3	r = 6.52620 cm h = 78.74000 cm	90	18.83488
The uranium "broken metal" content is homogenized with a moderator of water with a specific gravity of 1.0×10^{-4} over the interior volume of the containment vessel. The 277-4 canned spacers with a thickness of 3.5561 cm (1.4000 in.) are used and are modeled at 3.02984 cm and 9.61638 cm above the bottom of the containment vessel. No polyethylene was used in this calculation. Since the contents are homogenized over the internal volume of the containment vessel, there is no moderating material between the content and the containment vessel walls or the spacers. The modeled material masses are: 3.7038 kg U (3.3334 kg ^{235}U), 9.3871 kg H_2O, resulting in an h/x ratio of ~73.50.			

Table 6.9.1.1. Details of calculation models used to establish mass loading limits for surface-only modes of transportation identified in Table 6.2a

Case	Dimensions (cm)	Enrichment (wt. % ^{235}U)	Density (g/cm^3)
hciabmt12_6_2_5_3	r = 6.52620 cm h = 78.74000 cm	80	18.85873
The uranium "broken metal" content is homogenized with a moderator of water with a specific gravity of 1.0×10^{-4} over the interior volume of the containment vessel. The 277-4 canned spacers with a thickness of 3.5561 cm (1.4000 in.) are used and are modeled at 3.02984 cm and 9.61638 cm above the bottom of the containment vessel. No polyethylene was used in this calculation. Since the contents are homogenized over the internal volume of the containment vessel, there is no moderating material between the content and the containment vessel walls or the spacers. The modeled material masses are: 5.5627 kg U (4.4502 kg ^{235}U), 9.2890 kg H_2O, resulting in an h/x ratio of ~54.48.			
nciabmt11_8_2_4_3	r = 6.52620 cm h = 78.74000 cm	70	18.88264
The uranium "broken metal" content is homogenized with a moderator of water with a specific gravity of 1.0×10^{-4} over the interior volume of the containment vessel. The 277-4 canned spacers with a thickness of 3.5561 cm (1.4000 in.) are used and are modeled at 3.02984 cm and 9.61638 cm above the bottom of the containment vessel. No polyethylene was used in this calculation. Since the contents are homogenized over the internal volume of the containment vessel, there is no moderating material between the content and the containment vessel walls or the spacers. The modeled material masses are: 7.4263 kg U (5.1984 kg ^{235}U), 9.1908 kg H_2O, resulting in an h/x ratio of ~46.15.			
hciabmt12_12_2_3_3	r = 6.52620 cm h = 78.74000 cm	60	18.90661
The uranium "broken metal" content is homogenized with a moderator of water with a specific gravity of 1.0×10^{-4} over the interior volume of the containment vessel. The 277-4 canned spacers with a thickness of 3.5561 cm (1.4000 in.) are used and are modeled at 3.02984 cm and 9.61638 cm above the bottom of the containment vessel. No polyethylene was used in this calculation. Since the contents are homogenized over the internal volume of the containment vessel, there is no moderating material between the content and the containment vessel walls or the spacers. The modeled material masses are: 11.1537 kg U (6.6922 kg ^{235}U), 8.9945 kg H_2O, resulting in an h/x ratio of ~35.08.			
Broken Metal for CSI=0.4			
ncf1bmt11_7_1_5_3	r = 6.52620 cm h = 78.74000 cm	80	18.85873
The uranium "broken metal" content is homogenized with a moderator of water with a specific gravity of 1.0×10^{-4} over the interior volume of the containment vessel. No 277-4 canned spacers are used in this calculation. No polyethylene was used in this calculation. Since the contents are homogenized over the internal volume of the containment vessel, there is no moderating material between the content and the containment vessel walls. The modeled material masses are: 6.4898 kg U (5.1919 kg ^{235}U), 9.8535 kg H_2O, resulting in an h/x ratio of ~49.54.			
ncf1bmt11_9_1_4_3	r = 6.52620 cm h = 78.74000 cm	70	18.88264
The uranium "broken metal" content is homogenized with a moderator of water with a specific gravity of 1.0×10^{-4} over the interior volume of the containment vessel. No 277-4 canned spacers are used in this calculation. No polyethylene was used in this calculation. Since the contents are homogenized over the internal volume of the containment vessel, there is no moderating material between the content and the containment vessel walls. The modeled material masses are: 8.3546 kg U (5.8482 kg ^{235}U), 9.7553 kg H_2O, resulting in an h/x ratio of ~43.54.			

Table 6.9.1.1. Details of calculation models used to establish mass loading limits for surface-only modes of transportation identified in Table 6.2a

Case	Dimensions (cm)	Enrichment (wt. % ^{235}U)	Density (g/cm^3)
ncf1bmt11_15_1_3_3	r = 6.52620 cm h = 78.74000 cm	60	18.90661
The uranium "broken metal" content is homogenized with a moderator of water with a specific gravity of 1.0×10^{-4} over the interior volume of the containment vessel. No 277-4 canned spacers are used in this calculation. No polyethylene was used in this calculation. Since the contents are homogenized over the internal volume of the containment vessel, there is no moderating material between the content and the containment vessel walls. The modeled material masses are: 14.8715 kg U (8.9229 kg ^{235}U), 9.4118 kg H_2O, resulting in an h/x ratio of ~27.53.			
ncf1bmt11_6_2_8_3	r = 6.52620 cm h = 78.74000 cm	100	18.81109
The uranium "broken metal" content is homogenized with a moderator of water with a specific gravity of 1.0×10^{-4} over the interior volume of the containment vessel. The 277-4 canned spacers with a thickness of 3.5561 cm (1.4000 in.) are used and are modeled at 3.02984 cm and 9.61638 cm above the bottom of the containment vessel. No polyethylene was used in this calculation. Since the contents are homogenized over the internal volume of the containment vessel, there is no moderating material between the content and the containment vessel walls or the spacers. The modeled material masses are: 5.5487 kg ^{235}U, 9.2890 kg H_2O, resulting in an h/x ratio of ~43.70.			
ncf1bmt11_7_2_7_3	r = 6.52620 cm h = 78.74000 cm	95	18.82298
The uranium "broken metal" content is homogenized with a moderator of water with a specific gravity of 1.0×10^{-4} over the interior volume of the containment vessel. The 277-4 canned spacers with a thickness of 3.5561 cm (1.4000 in.) are used and are modeled at 3.02984 cm and 9.61638 cm above the bottom of the containment vessel. No polyethylene was used in this calculation. Since the contents are homogenized over the internal volume of the containment vessel, there is no moderating material between the content and the containment vessel walls or the spacers. The modeled material masses are: 6.4775 kg U (6.1536 kg ^{235}U), 9.2399 kg H_2O, resulting in an h/x ratio of ~39.19.			
ncf1bmt11_9_2_6_3	r = 6.52620 cm h = 78.74000 cm	90	18.83488
The uranium "broken metal" content is homogenized with a moderator of water with a specific gravity of 1.0×10^{-4} over the interior volume of the containment vessel. The 277-4 canned spacers with a thickness of 3.5561 cm (1.4000 in.) are used and are modeled at 3.02984 cm and 9.61638 cm above the bottom of the containment vessel. No polyethylene was used in this calculation. Since the contents are homogenized over the internal volume of the containment vessel, there is no moderating material between the content and the containment vessel walls or the spacers. The modeled material masses are: 8.3335 kg U (7.5002 kg ^{235}U), 9.1417 kg H_2O, resulting in an h/x ratio of ~31.81.			
ncf1bmt11_12_2_5_3	r = 6.52620 cm h = 78.74000 cm	80	18.85873
The uranium "broken metal" content is homogenized with a moderator of water with a specific gravity of 1.0×10^{-4} over the interior volume of the containment vessel. The 277-4 canned spacers with a thickness of 3.5561 cm (1.4000 in.) are used and are modeled at 3.02984 cm and 9.61638 cm above the bottom of the containment vessel. No polyethylene was used in this calculation. Since the contents are homogenized over the internal volume of the containment vessel, there is no moderating material between the content and the containment vessel walls or the spacers. The modeled material masses are: 11.1254 kg U (8.9003 kg ^{235}U), 8.9945 kg H_2O, resulting in an h/x ratio of ~26.38.			

Table 6.9.1.1. Details of calculation models used to establish mass loading limits for surface-only modes of transportation identified in Table 6.2a

Case	Dimensions (cm)	Enrichment (wt. % ^{235}U)	Density (g/cm^3)
ncf1bmt11_19_2_4_3	r = 6.52620 cm h = 78.74000 cm	70	18.88264
The uranium "broken metal" content is homogenized with a moderator of water with a specific gravity of 1.0×10^{-4} over the interior volume of the containment vessel. The 277-4 canned spacers with a thickness of 3.5561 cm (1.4000 in.) are used and are modeled at 3.02984 cm and 9.61638 cm above the bottom of the containment vessel. No polyethylene was used in this calculation. Since the contents are homogenized over the internal volume of the containment vessel, there is no moderating material between the content and the containment vessel walls or the spacers. The modeled material masses are: 18.5659 kg U (12.9961 kg ^{235}U), 8.6019 kg H_2O, resulting in an h/x ratio of ~17.28.			
ncf1bmt11_29_2_3_3	r = 6.52620 cm h = 78.74000 cm	60	18.90661
The uranium "broken metal" content is homogenized with a moderator of water with a specific gravity of 1.0×10^{-4} over the interior volume of the containment vessel. The 277-4 canned spacers with a thickness of 3.5561 cm (1.4000 in.) are used and are modeled at 3.02984 cm and 9.61638 cm above the bottom of the containment vessel. No polyethylene was used in this calculation. Since the contents are homogenized over the internal volume of the containment vessel, there is no moderating material between the content and the containment vessel walls or the spacers. The modeled material masses are: 28.8136 kg U (17.2882 kg ^{235}U), 8.0621 kg H_2O, resulting in an h/x ratio of ~12.17.			
Broken metal for CSI=0.8			
ncf2bmt11_12_1_5_3	r = 6.52620 cm h = 78.74000 cm	80	18.85873
The uranium "broken metal" content is homogenized with a moderator of water with a specific gravity of 1.0×10^{-4} over the interior volume of the containment vessel. No 277-4 canned spacers are used in this calculation. No polyethylene was used in this calculation. Since the contents are homogenized over the internal volume of the containment vessel, there is no moderating material between the content and the containment vessel walls. The modeled material masses are: 11.1254 kg U (8.9003 kg ^{235}U), 9.6081 kg H_2O, resulting in an h/x ratio of ~28.18.			
ncf2bmt11_20_1_4_3	r = 6.52620 cm h = 78.74000 cm	70	18.88264
The uranium "broken metal" content is homogenized with a moderator of water with a specific gravity of 1.0×10^{-4} over the interior volume of the containment vessel. No 277-4 canned spacers are used in this calculation. No polyethylene was used in this calculation. Since the contents are homogenized over the internal volume of the containment vessel, there is no moderating material between the content and the containment vessel walls. The modeled material masses are: 19.4942 kg U (13.6459 kg ^{235}U), 9.1664 kg H_2O, resulting in an h/x ratio of ~17.53.			
ncf2bmt11_29_1_3_3	r = 6.52620 cm h = 78.74000 cm	60	18.90661
The uranium "broken metal" content is homogenized with a moderator of water with a specific gravity of 1.0×10^{-4} over the interior volume of the containment vessel. No 277-4 canned spacers are used in this calculation. No polyethylene was used in this calculation. Since the contents are homogenized over the internal volume of the containment vessel, there is no moderating material between the content and the containment vessel walls. The modeled material masses are: 28.8136 kg U (17.2882 kg ^{235}U), 8.6757 kg H_2O, resulting in an h/x ratio of ~13.10.			

Table 6.9.1.1. Details of calculation models used to establish mass loading limits for surface-only modes of transportation identified in Table 6.2a

Case	Dimensions (cm)	Enrichment (wt. % ^{235}U)	Density (g/cm^3)
ncf2bmt11_10_2_8_3	r = 6.52620 cm h = 78.74000 cm	100	18.81109
The uranium "broken metal" content is homogenized with a moderator of water with a specific gravity of 1.0×10^{-4} over the interior volume of the containment vessel. The 277-4 canned spacers with a thickness of 3.5561 cm (1.4000 in.) are used and are modeled at 3.02984 cm and 9.61638 cm above the bottom of the containment vessel. No polyethylene was used in this calculation. Since the contents are homogenized over the internal volume of the containment vessel, there is no moderating material between the content and the containment vessel walls or the spacers. The modeled material masses are: 9.2478 kg ^{235}U, 9.0927 kg H_2O, resulting in an h/x ratio of ~25.66.			
ncf2bmt11_12_2_7_3	r = 6.52620 cm h = 78.74000 cm	95	18.82298
The uranium "broken metal" content is homogenized with a moderator of water with a specific gravity of 1.0×10^{-4} over the interior volume of the containment vessel. The 277-4 canned spacers with a thickness of 3.5561 cm (1.4000 in.) are used and are modeled at 3.02984 cm and 9.61638 cm above the bottom of the containment vessel. No polyethylene was used in this calculation. Since the contents are homogenized over the internal volume of the containment vessel, there is no moderating material between the content and the containment vessel walls or the spacers. The modeled material masses are: 11.1043 kg U (10.5491 kg ^{235}U), 8.9945 kg H_2O, resulting in an h/x ratio of ~22.25.			
ncf2bmt11_14_2_6_3	r = 6.52620 cm h = 78.74000 cm	90	18.83488
The uranium "broken metal" content is homogenized with a moderator of water with a specific gravity of 1.0×10^{-4} over the interior volume of the containment vessel. The 277-4 canned spacers with a thickness of 3.5561 cm (1.4000 in.) are used and are modeled at 3.02984 cm and 9.61638 cm above the bottom of the containment vessel. No polyethylene was used in this calculation. Since the contents are homogenized over the internal volume of the containment vessel, there is no moderating material between the content and the containment vessel walls or the spacers. The modeled material masses are: 13.8892 kg U (12.5003 kg ^{235}U), 8.8473 kg H_2O, resulting in an h/x ratio of ~31.81.			
ncf2bmt11_21_2_5_3	r = 6.52620 cm h = 78.74000 cm	80	18.85873
The uranium "broken metal" content is homogenized with a moderator of water with a specific gravity of 1.0×10^{-4} over the interior volume of the containment vessel. The 277-4 canned spacers with a thickness of 3.5561 cm (1.4000 in.) are used and are modeled at 3.02984 cm and 9.61638 cm above the bottom of the containment vessel. No polyethylene was used in this calculation. Since the contents are homogenized over the internal volume of the containment vessel, there is no moderating material between the content and the containment vessel walls or the spacers. The modeled material masses are: 20.3966 kg U (16.3173 kg ^{235}U), 8.5038 kg H_2O, resulting in an h/x ratio of ~13.60.			
ncf2bmt11_30_2_4_3	r = 6.52620 cm h = 78.74000 cm	70	18.88264
The uranium "broken metal" content is homogenized with a moderator of water with a specific gravity of 1.0×10^{-4} over the interior volume of the containment vessel. The 277-4 canned spacers with a thickness of 3.5561 cm (1.4000 in.) are used and are modeled at 3.02984 cm and 9.61638 cm above the bottom of the containment vessel. No polyethylene was used in this calculation. Since the contents are homogenized over the internal volume of the containment vessel, there is no moderating material between the content and the containment vessel walls or the spacers. The modeled material masses are: 29.7054 kg U (20.7938 kg ^{235}U), 8.0131 kg H_2O, resulting in an h/x ratio of ~10.06.			

Table 6.9.1.1. Details of calculation models used to establish mass loading limits for surface-only modes of transportation identified in Table 6.2a

Case	Dimensions (cm)	Enrichment (wt. % ^{235}U)	Density (g/cm^3)
ncf2bmt11_36_2_3_3	r = 6.52620 cm h = 78.74000 cm	60	18.90661
The uranium "broken metal" content is homogenized with a moderator of water with a specific gravity of 1.0×10^{-4} over the interior volume of the containment vessel. The 277-4 canned spacers with a thickness of 3.5561 cm (1.4000 in.) are used and are modeled at 3.02984 cm and 9.61638 cm above the bottom of the containment vessel. No polyethylene was used in this calculation. Since the contents are homogenized over the internal volume of the containment vessel, there is no moderating material between the content and the containment vessel walls or the spacers. The modeled material masses are: 35.3199 kg U (21.1920 kg ^{235}U), 7.7186 kg H_2O, resulting in an h/x ratio of ~9.51.			
Broken metal for CSI=2.0			
ncf3bmt11_22_1_5_3	r = 6.52620 cm h = 78.74000 cm	80	18.85873
The uranium "broken metal" content is homogenized with a moderator of water with a specific gravity of 1.0×10^{-4} over the interior volume of the containment vessel. No 277-4 canned spacers are used in this calculation. No polyethylene was used in this calculation. Since the contents are homogenized over the internal volume of the containment vessel, there is no moderating material between the content and the containment vessel walls. The modeled material masses are: 21.3237 kg U (17.0590 kg ^{235}U), 9.0683 kg H_2O, resulting in an h/x ratio of ~13.87.			
ncf3bmt11_31_1_4_3	r = 6.52620 cm h = 78.74000 cm	70	18.88264
The uranium "broken metal" content is homogenized with a moderator of water with a specific gravity of 1.0×10^{-4} over the interior volume of the containment vessel. No 277-4 canned spacers are used in this calculation. No polyethylene was used in this calculation. Since the contents are homogenized over the internal volume of the containment vessel, there is no moderating material between the content and the containment vessel walls. The modeled material masses are: 30.6337 kg U (21.4436 kg ^{235}U), 8.5776 kg H_2O, resulting in an h/x ratio of ~10.44.			
ncf3bmt11_36_1_3_3	r = 6.52620 cm h = 78.74000 cm	60	18.90661
The uranium "broken metal" content is homogenized with a moderator of water with a specific gravity of 1.0×10^{-4} over the interior volume of the containment vessel. No 277-4 canned spacers are used in this calculation. No polyethylene was used in this calculation. Since the contents are homogenized over the internal volume of the containment vessel, there is no moderating material between the content and the containment vessel walls or the spacers. The modeled material masses are: 35.3199 kg U (21.1920 kg ^{235}U), 8.3322 kg H_2O, resulting in an h/x ratio of ~10.26.			
ncf3bmt11_14_2_8_3	r = 6.52620 cm h = 78.74000 cm	100	18.81109
The uranium "broken metal" content is homogenized with a moderator of water with a specific gravity of 1.0×10^{-4} over the interior volume of the containment vessel. The 277-4 canned spacers with a thickness of 3.5561 cm (1.4000 in.) are used and are modeled at 3.02984 cm and 9.61638 cm above the bottom of the containment vessel. No polyethylene was used in this calculation. Since the contents are homogenized over the internal volume of the containment vessel, there is no moderating material between the content and the containment vessel walls or the spacers. The modeled material masses are: 13.8716 kg ^{235}U, 8.8473 kg H_2O, resulting in an h/x ratio of ~16.65.			

Table 6.9.1.1. Details of calculation models used to establish mass loading limits for surface-only modes of transportation identified in Table 6.2a

Case	Dimensions (cm)	Enrichment (wt. % ^{235}U)	Density (g/cm^3)
ncf3bmt11_20_2_7_3	r = 6.52620 cm h = 78.74000 cm	95	18.82298
The uranium "broken metal" content is homogenized with a moderator of water with a specific gravity of 1.0×10^{-4} over the interior volume of the containment vessel. The 277-4 canned spacers with a thickness of 3.5561 cm (1.4000 in.) are used and are modeled at 3.02984 cm and 9.61638 cm above the bottom of the containment vessel. No polyethylene was used in this calculation. Since the contents are homogenized over the internal volume of the containment vessel, there is no moderating material between the content and the containment vessel walls or the spacers. The modeled material masses are: 19.4326 kg U (18.4609 kg ^{235}U), 8.5529 kg H_2O, resulting in an h/x ratio of ~12.09.			
ncf3bmt11_23_2_6_3	r = 6.52620 cm h = 78.74000 cm	90	18.83488
The uranium "broken metal" content is homogenized with a moderator of water with a specific gravity of 1.0×10^{-4} over the interior volume of the containment vessel. The 277-4 canned spacers with a thickness of 3.5561 cm (1.4000 in.) are used and are modeled at 3.02984 cm and 9.61638 cm above the bottom of the containment vessel. No polyethylene was used in this calculation. Since the contents are homogenized over the internal volume of the containment vessel, there is no moderating material between the content and the containment vessel walls or the spacers. The modeled material masses are: 22.2227 kg U (20.0004 kg ^{235}U), 8.4057 kg H_2O, resulting in an h/x ratio of ~10.97.			
ncf3bmt11_32_2_5_3	r = 6.52620 cm h = 78.74000 cm	80	18.85873
The uranium "broken metal" content is homogenized with a moderator of water with a specific gravity of 1.0×10^{-4} over the interior volume of the containment vessel. The 277-4 canned spacers with a thickness of 3.5561 cm (1.4000 in.) are used and are modeled at 3.02984 cm and 9.61638 cm above the bottom of the containment vessel. No polyethylene was used in this calculation. Since the contents are homogenized over the internal volume of the containment vessel, there is no moderating material between the content and the containment vessel walls or the spacers. The modeled material masses are: 31.5220 kg U (25.2176 kg ^{235}U), 7.9149 kg H_2O, resulting in an h/x ratio of ~8.19.			
ncf3bmt11_36_2_4_3	r = 6.52620 cm h = 78.74000 cm	70	18.88264
The uranium "broken metal" content is homogenized with a moderator of water with a specific gravity of 1.0×10^{-4} over the interior volume of the containment vessel. The 277-4 canned spacers with a thickness of 3.5561 cm (1.4000 in.) are used and are modeled at 3.02984 cm and 9.61638 cm above the bottom of the containment vessel. No polyethylene was used in this calculation. Since the contents are homogenized over the internal volume of the containment vessel, there is no moderating material between the content and the containment vessel walls or the spacers. The modeled material masses are: 35.2751 kg U (24.6926 kg ^{235}U), 7.7186 kg H_2O, resulting in an h/x ratio of ~8.16.			
ncf3bmt11_36_2_3_3	r = 6.52620 cm h = 78.74000 cm	60	18.90661
The uranium "broken metal" content is homogenized with a moderator of water with a specific gravity of 1.0×10^{-4} over the interior volume of the containment vessel. The 277-4 canned spacers with a thickness of 3.5561 cm (1.4000 in.) are used and are modeled at 3.02984 cm and 9.61638 cm above the bottom of the containment vessel. No polyethylene was used in this calculation. Since the contents are homogenized over the internal volume of the containment vessel, there is no moderating material between the content and the containment vessel walls or the spacers. The modeled material masses are: 35.3199 kg U (21.1920 kg ^{235}U), 7.7186 kg H_2O, resulting in an h/x ratio of ~9.51.			

Table 6.9.1.1. Details of calculation models used to establish mass loading limits for surface-only modes of transportation identified in Table 6.2a

Case	Dimensions (cm)	Enrichment (wt. % ^{235}U)	Density (g/cm^3)
Broken metal for CSI=3.2			
ncf5bmt11_35_1_5_3	r = 6.52620 cm h = 78.74000 cm	80	18.85873
The uranium "broken metal" content is homogenized with a moderator of water with a specific gravity of 1.0×10^{-4} over the interior volume of the containment vessel. No 277-4 canned spacers are used in this calculation. No polyethylene was used in this calculation. Since the contents are homogenized over the internal volume of the containment vessel, there is no moderating material between the content and the containment vessel walls. The modeled material masses are: 34.3034 kg U (27.4427 kg ^{235}U), 8.3813 kg H_2O, resulting in an h/x ratio of ~7.97.			
ncf5bmt11_36_1_4_3	r = 6.52620 cm h = 78.74000 cm	70	18.88264
The uranium "broken metal" content is homogenized with a moderator of water with a specific gravity of 1.0×10^{-4} over the interior volume of the containment vessel. No 277-4 canned spacers are used in this calculation. No polyethylene was used in this calculation. Since the contents are homogenized over the internal volume of the containment vessel, there is no moderating material between the content and the containment vessel walls. The modeled material masses are: 35.2751 kg U (24.9626 kg ^{235}U), 8.3322 kg H_2O, resulting in an h/x ratio of ~8.81.			
ncf5bmt11_36_1_3_3	r = 6.52620 cm h = 78.74000 cm	60	18.90661
The uranium "broken metal" content is homogenized with a moderator of water with a specific gravity of 1.0×10^{-4} over the interior volume of the containment vessel. No 277-4 canned spacers are used in this calculation. No polyethylene was used in this calculation. Since the contents are homogenized over the internal volume of the containment vessel, there is no moderating material between the content and the containment vessel walls. The modeled material masses are: 35.3199 kg U (21.1920 kg ^{235}U), 8.3322 kg H_2O, resulting in an h/x ratio of ~10.26.			
ncf5bmt11_25_2_8_3	r = 6.52620 cm h = 78.74000 cm	100	18.81109
The uranium "broken metal" content is homogenized with a moderator of water with a specific gravity of 1.0×10^{-4} over the interior volume of the containment vessel. The 277-4 canned spacers with a thickness of 3.5561 cm (1.4000 in.) are used and are modeled at 3.02984 cm and 9.61638 cm above the bottom of the containment vessel. No polyethylene was used in this calculation. Since the contents are homogenized over the internal volume of the containment vessel, there is no moderating material between the content and the containment vessel walls or the spacers. The modeled material masses are: 24.9689 kg ^{235}U, 8.2584 kg H_2O, resulting in an h/x ratio of ~8.63.			
ncf5bmt11_28_2_7_3	r = 6.52620 cm h = 78.74000 cm	95	18.82298
The uranium "broken metal" content is homogenized with a moderator of water with a specific gravity of 1.0×10^{-4} over the interior volume of the containment vessel. The 277-4 canned spacers with a thickness of 3.5561 cm (1.4000 in.) are used and are modeled at 3.02984 cm and 9.61638 cm above the bottom of the containment vessel. No polyethylene was used in this calculation. Since the contents are homogenized over the internal volume of the containment vessel, there is no moderating material between the content and the containment vessel walls or the spacers. The modeled material masses are: 27.7608 kg U (26.3728 kg ^{235}U), 8.1112 kg H_2O, resulting in an h/x ratio of ~8.03.			

Table 6.9.1.1. Details of calculation models used to establish mass loading limits for surface-only modes of transportation identified in Table 6.2a

Case	Dimensions (cm)	Enrichment (wt. % ^{235}U)	Density (g/cm^3)
ncf5bmt11_35_2_6_3	r = 6.52620 cm h = 78.74000 cm	90	18.83488
The uranium "broken metal" content is homogenized with a moderator of water with a specific gravity of 1.0×10^{-4} over the interior volume of the containment vessel. The 277-4 canned spacers with a thickness of 3.5561 cm (1.4000 in.) are used and are modeled at 3.02984 cm and 9.61638 cm above the bottom of the containment vessel. No polyethylene was used in this calculation. Since the contents are homogenized over the internal volume of the containment vessel, there is no moderating material between the content and the containment vessel walls or the spacers. The modeled material masses are: 34.2600 kg U (30.8340 kg ^{235}U), 7.7677 kg H_2O, resulting in an h/x ratio of ~6.58.			
ncf5bmt11_36_2_5_3	r = 6.52620 cm h = 78.74000 cm	80	18.85873
The uranium "broken metal" content is homogenized with a moderator of water with a specific gravity of 1.0×10^{-4} over the interior volume of the containment vessel. The 277-4 canned spacers with a thickness of 3.5561 cm (1.4000 in.) are used and are modeled at 3.02984 cm and 9.61638 cm above the bottom of the containment vessel. No polyethylene was used in this calculation. Since the contents are homogenized over the internal volume of the containment vessel, there is no moderating material between the content and the containment vessel walls or the spacers. The modeled material masses are: 35.2305 kg U (28.1844 kg ^{235}U), 7.7186 kg H_2O, resulting in an h/x ratio of ~7.15.			
ncf5bmt11_36_2_4_3	r = 6.52620 cm h = 78.74000 cm	70	18.88264
The uranium "broken metal" content is homogenized with a moderator of water with a specific gravity of 1.0×10^{-4} over the interior volume of the containment vessel. The 277-4 canned spacers with a thickness of 3.5561 cm (1.4000 in.) are used and are modeled at 3.02984 cm and 9.61638 cm above the bottom of the containment vessel. No polyethylene was used in this calculation. Since the contents are homogenized over the internal volume of the containment vessel, there is no moderating material between the content and the containment vessel walls or the spacers. The modeled material masses are: 35.2751 kg U (24.6926 kg ^{235}U), 7.7186 kg H_2O, resulting in an h/x ratio of ~8.16.			
ncf5bmt11_36_2_3_3	r = 6.52620 cm h = 78.74000 cm	60	18.90661
The uranium "broken metal" content is homogenized with a moderator of water with a specific gravity of 1.0×10^{-4} over the interior volume of the containment vessel. The 277-4 canned spacers with a thickness of 3.5561 cm (1.4000 in.) are used and are modeled at 3.02984 cm and 9.61638 cm above the bottom of the containment vessel. No polyethylene was used in this calculation. Since the contents are homogenized over the internal volume of the containment vessel, there is no moderating material between the content and the containment vessel walls or the spacers. The modeled material masses are: 35.3199 kg U (21.1920 kg ^{235}U), 7.7186 kg H_2O, resulting in an h/x ratio of ~9.51.			

Table 6.9.1.1. Details of calculation models used to establish mass loading limits for surface-only modes of transportation identified in Table 6.2a

Case	Dimensions (cm)	Enrichment (wt. % ^{235}U)	Density (g/cm^3)
Product oxide			
nciaoxt11_1_24_1_3	r = 6.42620 cm h = 28.18623 cm	100	6.54000
The HEU product oxide is dispersed within the containment vessel to a height determined by the mass of the product oxide. The product oxide is saturated with a moderator of full density water (0.9982 g/cm^3). No polyethylene is used in this analysis. Since the product oxide content is assumed to be dispersed within the containment vessel, there are no gaps between the content and the containment vessel wall or bottom. There are 50.55377 cm of moderator above the product oxide content. No 277-4 canned spacers are used in this analysis. The modeled material masses are: 24.00 kg UO_2, 21.1249 kg ^{235}U, 6.5339 kg H_2O, resulting in an h/x ratio of ~9.90.			
Skull oxide			
nciask_9_15	r = 6.42620 cm h = 28.18623 cm	100	6.54000
The skull oxide is dispersed within the containment vessel to a height determined by the mass of the skull oxide. The skull oxide is saturated with a moderator of full density water (0.9982 g/cm^3). No polyethylene is used in this analysis. Since the skull oxide content is assumed to be dispersed within the containment vessel, there are no gaps between the content and the containment vessel wall or bottom. There are 50.55377 cm of moderator above the skull oxide content. No 277-4 canned spacers are used in this analysis. The modeled material masses are: 21.3000 kg skull oxide, 19.8653 kg U_3O_8, 15.6728 kg ^{235}U, 3.8014 kg H_2O, resulting in an h/x ratio of ~7.43.			
UNX crystals			
nciaunhct11_8_8_1_3	r = 6.42620 cm h = 78.74000 cm	100	2.79329
The UNX crystals are homogenized with a moderator of full density water (0.9982 g/cm^3) dispersed over the entire inner volume of the containment vessel. There is no gap between the homogenized UNX crystals and the containment vessel bottom or sides. Since the content is homogenized over the inner volume of the containment vessel, no moderating material is above the content. No 277-4 canned spacers were used in this model. The modeled material masses are 7.0 kg UNX crystals; 3.2968 kg ^{235}U, and 7.6954 kg H_2O, resulting in an h/x ratio of ~72.92.			
nciaunhct11_8_24_1_3	r = 6.42620 cm h = 78.74000 cm	100	2.79329
The UNX crystals are homogenized with a moderator of full density water (0.9982 g/cm3) dispersed over the entire inner volume of the containment vessel. There is no gap between the homogenized UNX crystals and the containment vessel bottom or sides. Since the content is homogenized over the inner volume of the containment vessel, no moderating material is above the content. No 277-4 canned spacers were used in this model. The modeled material masses are 24.0 kg UNX crystals, 11.3031 kg ^{235}U, and 1.6204 kg H2O, resulting in an h/x ratio of ~15.74.			

Table 6.9.1.1. Details of calculation models used to establish mass loading limits for surface-only modes of transportation identified in Table 6.2a

Case	Dimensions (cm)	Enrichment (wt. % ^{235}U)	Density (g/cm^3)
TRIGA fuel			
nciatriga_1_15_3	r = 1.8288 cm h = 12.7000 cm	20	8.65974
The moderator is full density water (0.9982 g/cm^3) surrounding three stacked "bundles" of three Triga fuel elements separated by 277-4 canned spacers. The content has an overall height of 38.10310 cm (15.00122 in.). No polyethylene was used in this model. Each content is separated by a 0.0001 cm spacer and 0.0012 cm of moderating material. The bottom content has a 0.0005 cm gap between it and the bottom of the containment vessel. The contents sit in the exact center on the bottom of the CV. The modeled material masses are 10.4 kg $UZrH_x$, 0.9210 kg ^{235}U, and 8.9982 kg H_2O, resulting in an h/x ratio of ~255.01.			
nciatriga70_1_15_3	r = 1.8288 cm h = 12.7000 cm	70	5.70132
The moderator is full density water (0.9982 g/cm^3) surrounding three stacked "bundles" of three Triga fuel elements separated by 277-4 canned spacers. The content has an overall height of 38.10310 cm (15.00122 in.). No polyethylene was used in this model. Each content is separated by a 0.0001 cm spacer and 0.0012 cm of moderating material. The bottom content has a 0.0005 cm gap between it and the bottom of the containment vessel. The contents sit in the exact center on the bottom of the CV. The modeled material masses are 6.8471 kg $UZrH_x$, 0.4080 kg ^{235}U, and 8.9982 kg H_2O, resulting in an h/x ratio of ~575.64.			

Appendix 6.9.2

HAC PACKAGE MODEL

THIS PAGE INTENTIONALLY LEFT BLANK.

Appendix 6.9.2

HAC PACKAGE MODEL

6.9.2.1 PREDICTION OF HAC DAMAGE IN THE ES-3100 PACKAGE

Finite element analysis of an ES-3100 package under Hypothetical Accident Conditions (HAC) is used to predict the deformed outer diameters of the drum at node points along the vertical axis of an upright package. Selected node points are designated in a downward direction from the top of the drum as "UR," "MUR," "MR," "MLR," and "LR." Table 6.9.2.1-1 lists diameters at the five node points measured along the 90–270° and 0–180° axes. These dimensions represent major and minor axes at each deformation point on the assumption that the drum cross section is ellipsoidal. A corresponding equivalent circular diameter is also listed for each node point in Table 6.9.2.1-1.

A set of KENO V.a calculation models based on reduced package diameters at the "MR," "MLR," and "LR" deformation points are derived from the Normal Conditions of Transport (NCT) geometry model. These geometry models are evaluated for the purpose of establishing a bounding geometry model for representing the ES-3100 package under HAC. The primary changes made to the KENO V.a geometry input statements in the NCT model are reductions in the drum's radii. The change to the drum's inner radius also affects the outer radius of both the angle iron and the Kaolite located inside the containment vessel outer liner. The volume fractions for these materials are adjusted in the KENO V.a calculation models so that material masses of the affected package components are conserved. Table 6.9.2.1-2 provides data for transforming the KENO V.a calculation model from an NCT model into an HAC model.

6.9.2.2 CRITICALITY CALCULATIONS

Sets of criticality calculations are performed for the "MR," "MLR," and "LR" models at five different package water contents over the range of HAC. The five package water contents of the void spaces external to the containment vessel and the interstitial space between drums are as follows: 1e-20 spg water, 1e-04 spg water, 0.1 spg water, 0.3 spg water, and 1.0 spg water. The water content in the Kaolite corresponds to the dry condition (VF= 0.0287) where neutronic interaction between the packages of an array is maximized.

An infinite array of packages is evaluated in order to eliminate any biases arising from spectral leakage effects in the reflector of the finite array. The k_{eff} values for each KENO V.a case are based on 500,000 neutron histories produced by running for 215 generations with 2,500 neutrons per generation and truncating the first 15 generations of data. Each package modeled has 36 kg of 100% enriched uranium in the form of broken metal content.

Each case is rerun using a different starting random number in order to produce sets of computed k_{eff} values that are statistically independent. The random starting number, the mean value (k_{eff}), and the corresponding standard error (s_i) computed for ten individual runs are shown in Tables 6.9.2.2-1, -2, and -3. The same statistical method (described in DAC-FS-900000-A014) used in the evaluation of Kaolite models (Appendix 6.9.3, Sect. 6.9.3.4) is also used here for determining whether or not differences in neutronic performance between the package models are statistically significant.

Table 6.9.2.1-1. Deformation of the ES-3100 drum at five node points, projected by finite element analysis "Case 3100 RUN1HL Lower Bound Kaolite May 2004"

Deformation point	FEA node	Diameter at 90° (in.)	Diameter at 180° (in.)	Equivalent circular diameter	
				(in.)	(cm)
UR	098194	20.02	15.60	17.6724	44.8878
MUR	100238	20.74	15.07	17.6791	44.9050
MR	101589	20.74	14.18	17.1492	43.5588
MLR	103012	22.00	13.44	17.1954	43.6762
LR	105786	20.92	12.92	16.4404	41.7586

Table 6.9.2.1-2. Parameter changes for converting an NCT package model into an HAC package model

Parameter	Reference NCT package model	HAC model at MR node point of package	HAC model at MLR node point of package	HAC model at LR node point of package
Package Model Dimension				
OR_{Drum} (cm)	23.32990	21.77942	21.83809	20.87929
IR_{Drum} (cm)	23.17750	21.62702	21.68569	20.72689
$th_{Drum\ wall}$ (cm)	0.15240	0.15240	0.15240	0.15240
OR_{Lid} (cm)	23.11400	21.56352	21.62219	20.66339
IR_{Lid} (cm)	22.96160	21.41112	21.46979	20.51099
$th_{Kaolite}$ (cm)	12.10310	10.55262	10.61129	9.65249
Kaolite of the Body Weldment Inner Liner				
Mass (g)	117563.0	97080.4	97829.7	85839.8
Volume (cm^3)	134888.0	111387.0	112246.0	98489.5
Volume fraction multiplier [a]	–	1.21099	1.20171	1.36956
VF for water component of Kaolite	0.52294	0.63327 [b]	0.62843 [b]	0.71620 [b]
VF for dry mix component of Kaolite	0.34864	0.42220 [b]	0.41897 [b]	0.47749 [b]
Angle Iron				
Mass (g)	5621.76	4521.40	4561.66	3917.54
Volume (cm^3)	708.030	569.446	574.516	493.393
VF	1.0	1.24337	1.23239	1.43502
Drum Steel				
Mass (g)	25446.3	23397.6	23474.2	22231.2
Volume (cm^3)	3204.82	2946.80	2956.50	2799.90
VF	1.0	1.08756	1.08401	1.14462

[a] Volume fraction multiplier is an NCT density multiplier for conserving mass in components having modified volumes in the HAC calculation models.

[b] Volume Fraction (VF) for Kaolite components calculated by multiplying the VF used in the NCT model by volume fraction multiplier for the HAC model.

Table 6.9.2.2-1. Neutron multiplication factors with standard deviations for the ES-3100 package models at the "MR" and "MLR" node points

moifr	Random Number	"A" cases	k_{eff}	s	"B" cases	k_{eff}	s
1.0e-20	109E77866CF6	mrandnum_01_01	1.04965	0.00119	lrrandnum_01_01	1.05093	0.00133
1.0e-20	16AA4A58735C	mrandnum_01_02	1.05132	0.00131	lrrandnum_01_02	1.05009	0.00118
1.0e-20	1814171B652A	mrandnum_01_03	1.05368	0.00123	lrrandnum_01_03	1.05057	0.00118
1.0e-20	1A423B9472C7	mrandnum_01_04	1.05165	0.00145	lrrandnum_01_04	1.05066	0.00120
1.0e-20	20E876D82248	mrandnum_01_05	1.05344	0.00106	lrrandnum_01_05	1.04882	0.00129
1.0e-20	3F6E65CA7440	mrandnum_01_06	1.05188	0.00157	lrrandnum_01_06	1.05316	0.00127
1.0e-20	479D21DB7509	mrandnum_01_07	1.05149	0.00148	lrrandnum_01_07	1.05229	0.00134
1.0e-20	55D4371D3A23	mrandnum_01_08	1.05083	0.00113	lrrandnum_01_08	1.05186	0.00131
1.0e-20	6E1A14672B8F	mrandnum_01_09	1.04910	0.00106	lrrandnum_01_09	1.05236	0.00113
1.0e-20	77A0308C0E44	mrandnum_01_10	1.05254	0.00106	lrrandnum_01_10	1.05098	0.00120
1.0e-04	109E77866CF6	mrandnum_03_01	1.04994	0.00132	lrrandnum_03_01	1.05122	0.00123
1.0e-04	16AA4A58735C	mrandnum_03_02	1.05023	0.00118	lrrandnum_03_02	1.05324	0.00121
1.0e-04	1814171B652A	mrandnum_03_03	1.05090	0.00139	lrrandnum_03_03	1.05143	0.00123
1.0e-04	1A423B9472C7	mrandnum_03_04	1.05072	0.00115	lrrandnum_03_04	1.05048	0.00121
1.0e-04	20E876D82248	mrandnum_03_05	1.05052	0.00119	lrrandnum_03_05	1.05095	0.00137
1.0e-04	3F6E65CA7440	mrandnum_03_06	1.05383	0.00131	lrrandnum_03_06	1.05029	0.00119
1.0e-04	479D21DB7509	mrandnum_03_07	1.05205	0.00153	lrrandnum_03_07	1.05124	0.00108
1.0e-04	55D4371D3A23	mrandnum_03_08	1.05343	0.00106	lrrandnum_03_08	1.05080	0.00116
1.0e-04	6E1A14672B8F	mrandnum_03_09	1.04831	0.00132	lrrandnum_03_09	1.05074	0.00122
1.0e-04	77A0308C0E44	mrandnum_03_10	1.05353	0.00111	lrrandnum_03_10	1.05094	0.00111
0.10	109E77866CF6	mrandnum_06_01	0.97948	0.00120	lrrandnum_06_01	0.98315	0.00118
0.10	16AA4A58735C	mrandnum_06_02	0.98104	0.00125	lrrandnum_06_02	0.98605	0.00124
0.10	1814171B652A	mrandnum_06_03	0.98056	0.00134	lrrandnum_06_03	0.98690	0.00120
0.10	1A423B9472C7	mrandnum_06_04	0.97895	0.00114	lrrandnum_06_04	0.98347	0.00126
0.10	20E876D82248	mrandnum_06_05	0.98058	0.00113	lrrandnum_06_05	0.98770	0.00124
0.10	3F6E65CA7440	mrandnum_06_06	0.97966	0.00119	lrrandnum_06_06	0.98734	0.00140
0.10	479D21DB7509	mrandnum_06_07	0.97953	0.00145	lrrandnum_06_07	0.98417	0.00133
0.10	55D4371D3A23	mrandnum_06_08	0.97993	0.00130	lrrandnum_06_08	0.98712	0.00136
0.10	6E1A14672B8F	mrandnum_06_09	0.97972	0.00138	lrrandnum_06_09	0.98533	0.00142
0.10	77A0308C0E44	mrandnum_06_10	0.98157	0.00134	lrrandnum_06_10	0.98412	0.00116
0.30	109E77866CF6	mrandnum_08_01	0.93412	0.00118	lrrandnum_08_01	0.93910	0.00146
0.30	16AA4A58735C	mrandnum_08_02	0.93227	0.00138	lrrandnum_08_02	0.93757	0.00117
0.30	1814171B652A	mrandnum_08_03	0.93390	0.00131	lrrandnum_08_03	0.93940	0.00146
0.30	1A423B9472C7	mrandnum_08_04	0.93252	0.00144	lrrandnum_08_04	0.93676	0.00130
0.30	20E876D82248	mrandnum_08_05	0.93334	0.00132	lrrandnum_08_05	0.93851	0.00111
0.30	3F6E65CA7440	mrandnum_08_06	0.93168	0.00132	lrrandnum_08_06	0.93914	0.00149
0.30	479D21DB7509	mrandnum_08_07	0.93514	0.00123	lrrandnum_08_07	0.94011	0.00131
0.30	55D4371D3A23	mrandnum_08_08	0.93564	0.00132	lrrandnum_08_08	0.93900	0.00139
0.30	6E1A14672B8F	mrandnum_08_09	0.93597	0.00136	lrrandnum_08_09	0.93781	0.00117
0.30	77A0308C0E44	mrandnum_08_10	0.93525	0.00128	lrrandnum_08_10	0.93965	0.00118

Table 6.9.2.2-1. Neutron multiplication factors with standard deviations for the ES-3100 package models at the "MR" and "MLR" node points

moifr	Random Number	"A" cases	k_{eff}	s	"B" cases	k_{eff}	s
1.00	109E77866CF6	mrandnum_15_01	0.93103	0.00139	lrrandnum_15_01	0.93344	0.00126
1.00	16AA4A58735C	mrandnum_15_02	0.93082	0.00131	lrrandnum_15_02	0.93281	0.00121
1.00	1814171B652A	mrandnum_15_03	0.92890	0.00148	lrrandnum_15_03	0.93468	0.00132
1.00	1A423B9472C7	mrandnum_15_04	0.93062	0.00145	lrrandnum_15_04	0.93592	0.00126
1.00	20E876D82248	mrandnum_15_05	0.93055	0.00125	lrrandnum_15_05	0.93251	0.00143
1.00	3F6E65CA7440	mrandnum_15_06	0.92950	0.00117	lrrandnum_15_06	0.93374	0.00121
1.00	479D21DB7509	mrandnum_15_07	0.92952	0.00116	lrrandnum_15_07	0.93572	0.00138
1.00	55D4371D3A23	mrandnum_15_08	0.92805	0.00154	lrrandnum_15_08	0.93498	0.00145
1.00	6E1A14672B8F	mrandnum_15_09	0.93117	0.00140	lrrandnum_15_09	0.93224	0.00114
1.00	77A0308C0E44	mrandnum_15_10	0.93218	0.00120	lrrandnum_15_10	0.93158	0.00131

Table 6.9.2.2-2.Neutron multiplication factors with standard deviations for the ES-3100 package models at the "MLR" and "LR" node points

moifr	Random Number	"A" cases	k_{eff}	s	"B" cases	k_{eff}	s
1.0e-20	109E77866CF6	mlrrandnum_01_01	1.05024	0.00139	lrrandnum_01_01	1.05093	0.00133
1.0e-20	16AA4A58735C	mlrrandnum_01_02	1.05051	0.00135	lrrandnum_01_02	1.05009	0.00118
1.0e-20	1814171B652A	mlrrandnum_01_03	1.05121	0.00128	lrrandnum_01_03	1.05057	0.00118
1.0e-20	1A423B9472C7	mlrrandnum_01_04	1.04954	0.00120	lrrandnum_01_04	1.05066	0.00120
1.0e-20	20E876D82248	mlrrandnum_01_05	1.05249	0.00110	lrrandnum_01_05	1.04882	0.00129
1.0e-20	3F6E65CA7440	mlrrandnum_01_06	1.04924	0.00132	lrrandnum_01_06	1.05316	0.00127
1.0e-20	479D21DB7509	mlrrandnum_01_07	1.05105	0.00111	lrrandnum_01_07	1.05229	0.00134
1.0e-20	55D4371D3A23	mlrrandnum_01_08	1.05039	0.00129	lrrandnum_01_08	1.05186	0.00131
1.0e-20	6E1A14672B8F	mlrrandnum_01_09	1.05161	0.00125	lrrandnum_01_09	1.05236	0.00113
1.0e-20	77A0308C0E44	mlrrandnum_01_10	1.05041	0.00129	lrrandnum_01_10	1.05098	0.00120
1.0e-04	109E77866CF6	mlrrandnum_03_01	1.05108	0.00151	lrrandnum_03_01	1.05122	0.00123
1.0e-04	16AA4A58735C	mlrrandnum_03_02	1.05245	0.00116	lrrandnum_03_02	1.05324	0.00121
1.0e-04	1814171B652A	mlrrandnum_03_03	1.05169	0.00138	lrrandnum_03_03	1.05143	0.00123
1.0e-04	1A423B9472C7	mlrrandnum_03_04	1.05303	0.00102	lrrandnum_03_04	1.05048	0.00121
1.0e-04	20E876D82248	mlrrandnum_03_05	1.05191	0.00115	lrrandnum_03_05	1.05095	0.00137
1.0e-04	3F6E65CA7440	mlrrandnum_03_06	1.05017	0.00110	lrrandnum_03_06	1.05029	0.00119
1.0e-04	479D21DB7509	mlrrandnum_03_07	1.05232	0.00128	lrrandnum_03_07	1.05124	0.00108
1.0e-04	55D4371D3A23	mlrrandnum_03_08	1.05100	0.00144	lrrandnum_03_08	1.05080	0.00116
1.0e-04	6E1A14672B8F	mlrrandnum_03_09	1.05046	0.00145	lrrandnum_03_09	1.05074	0.00122
1.0e-04	77A0308C0E44	mlrrandnum_03_10	1.05130	0.00134	lrrandnum_03_10	1.05094	0.00111

Table 6.9.2.2-2.Neutron multiplication factors with standard deviations for the ES-3100 package models at the "MLR" and "LR" node points

moifr	Random Number	"A" cases	k_{eff}	s	"B" cases	k_{eff}	s
0.1	109E77866CF6	mlrrandnum_06_01	0.98071	0.00129	lrrandnum_06_01	0.98315	0.00118
0.1	16AA4A58735C	mlrrandnum_06_02	0.98006	0.00110	lrrandnum_06_02	0.98605	0.00124
0.1	1814171B652A	mlrrandnum_06_03	0.98043	0.00116	lrrandnum_06_03	0.98690	0.00120
0.1	1A423B9472C7	mlrrandnum_06_04	0.98253	0.00109	lrrandnum_06_04	0.98347	0.00126
0.1	20E876D82248	mlrrandnum_06_05	0.98256	0.00135	lrrandnum_06_05	0.98770	0.00124
0.1	3F6E65CA7440	mlrrandnum_06_06	0.98093	0.00127	lrrandnum_06_06	0.98734	0.00140
0.1	479D21DB7509	mlrrandnum_06_07	0.97959	0.00127	lrrandnum_06_07	0.98417	0.00133
0.1	55D4371D3A23	mlrrandnum_06_08	0.98033	0.00111	lrrandnum_06_08	0.98712	0.00136
0.1	6E1A14672B8F	mlrrandnum_06_09	0.97940	0.00117	lrrandnum_06_09	0.98533	0.00142
0.1	77A0308C0E44	mlrrandnum_06_10	0.98318	0.00134	lrrandnum_06_10	0.98412	0.00116
0.3	109E77866CF6	mlrrandnum_08_01	0.93254	0.00147	lrrandnum_08_01	0.93910	0.00146
0.3	16AA4A58735C	mlrrandnum_08_02	0.93186	0.00142	lrrandnum_08_02	0.93757	0.00117
0.3	1814171B652A	mlrrandnum_08_03	0.93200	0.00135	lrrandnum_08_03	0.93940	0.00146
0.3	1A423B9472C7	mlrrandnum_08_04	0.93197	0.00150	lrrandnum_08_04	0.93676	0.00130
0.3	20E876D82248	mlrrandnum_08_05	0.93601	0.00124	lrrandnum_08_05	0.93851	0.00111
0.3	3F6E65CA7440	mlrrandnum_08_06	0.93249	0.00118	lrrandnum_08_06	0.93914	0.00149
0.3	479D21DB7509	mlrrandnum_08_07	0.93299	0.00128	lrrandnum_08_07	0.94011	0.00131
0.3	55D4371D3A23	mlrrandnum_08_08	0.93500	0.00133	lrrandnum_08_08	0.93900	0.00139
0.3	6E1A14672B8F	mlrrandnum_08_09	0.93201	0.00122	lrrandnum_08_09	0.93781	0.00117
0.3	77A0308C0E44	mlrrandnum_08_10	0.93238	0.00153	lrrandnum_08_10	0.93965	0.00118
1.0	109E77866CF6	mlrrandnum_15_01	0.93180	0.00126	lrrandnum_15_01	0.93344	0.00126
1.0	16AA4A58735C	mlrrandnum_15_02	0.93020	0.00159	lrrandnum_15_02	0.93281	0.00121
1.0	1814171B652A	mlrrandnum_15_03	0.92956	0.00117	lrrandnum_15_03	0.93468	0.00132
1.0	1A423B9472C7	mlrrandnum_15_04	0.92837	0.00165	lrrandnum_15_04	0.93592	0.00126
1.0	20E876D82248	mlrrandnum_15_05	0.93220	0.00120	lrrandnum_15_05	0.93251	0.00143
1.0	3F6E65CA7440	mlrrandnum_15_06	0.93177	0.00141	lrrandnum_15_06	0.93374	0.00121
1.0	479D21DB7509	mlrrandnum_15_07	0.93217	0.00144	lrrandnum_15_07	0.93572	0.00138
1.0	55D4371D3A23	mlrrandnum_15_08	0.92921	0.00125	lrrandnum_15_08	0.93498	0.00145
1.0	6E1A14672B8F	mlrrandnum_15_09	0.92980	0.00177	lrrandnum_15_09	0.93224	0.00114
1.0	77A0308C0E44	mlrrandnum_15_10	0.93070	0.00126	lrrandnum_15_10	0.93158	0.00131

Table 6.9.2.2-3.Neutron multiplication factors with standard deviations for the ES-3100 package models at the "MR" and "LR" node points

moifr	Random Number	"A" cases	k_{eff}	s	"B" cases	k_{eff}	s
1.0e-20	109E77866CF6	mrandnum_01_01	1.04965	0.00119	lrrandnum_01_01	1.05093	0.00133
1.0e-20	16AA4A58735C	mrandnum_01_02	1.05132	0.00131	lrrandnum_01_02	1.05009	0.00118
1.0e-20	1814171B652A	mrandnum_01_03	1.05368	0.00123	lrrandnum_01_03	1.05057	0.00118
1.0e-20	1A423B9472C7	mrandnum_01_04	1.05165	0.00145	lrrandnum_01_04	1.05066	0.00120
1.0e-20	20E876D82248	mrandnum_01_05	1.05344	0.00106	lrrandnum_01_05	1.04882	0.00129
1.0e-20	3F6E65CA7440	mrandnum_01_06	1.05188	0.00157	lrrandnum_01_06	1.05316	0.00127
1.0e-20	479D21DB7509	mrandnum_01_07	1.05149	0.00148	lrrandnum_01_07	1.05229	0.00134
1.0e-20	55D4371D3A23	mrandnum_01_08	1.05083	0.00113	lrrandnum_01_08	1.05186	0.00131
1.0e-20	6E1A14672B8F	mrandnum_01_09	1.04910	0.00106	lrrandnum_01_09	1.05236	0.00113
1.0e-20	77A0308C0E44	mrandnum_01_10	1.05254	0.00106	lrrandnum_01_10	1.05098	0.00120
1.0e-04	109E77866CF6	mrandnum_03_01	1.04994	0.00132	lrrandnum_03_01	1.05122	0.00123
1.0e-04	16AA4A58735C	mrandnum_03_02	1.05023	0.00118	lrrandnum_03_02	1.05324	0.00121
1.0e-04	1814171B652A	mrandnum_03_03	1.05090	0.00139	lrrandnum_03_03	1.05143	0.00123
1.0e-04	1A423B9472C7	mrandnum_03_04	1.05072	0.00115	lrrandnum_03_04	1.05048	0.00121
1.0e-04	20E876D82248	mrandnum_03_05	1.05052	0.00119	lrrandnum_03_05	1.05095	0.00137
1.0e-04	3F6E65CA7440	mrandnum_03_06	1.05383	0.00131	lrrandnum_03_06	1.05029	0.00119
1.0e-04	479D21DB7509	mrandnum_03_07	1.05205	0.00153	lrrandnum_03_07	1.05124	0.00108
1.0e-04	55D4371D3A23	mrandnum_03_08	1.05343	0.00106	lrrandnum_03_08	1.05080	0.00116
1.0e-04	6E1A14672B8F	mrandnum_03_09	1.04831	0.00132	lrrandnum_03_09	1.05074	0.00122
1.0e-04	77A0308C0E44	mrandnum_03_10	1.05353	0.00111	lrrandnum_03_10	1.05094	0.00111
0.10	109E77866CF6	mrandnum_06_01	0.97948	0.00120	lrrandnum_06_01	0.98315	0.00118
0.10	16AA4A58735C	mrandnum_06_02	0.98104	0.00125	lrrandnum_06_02	0.98605	0.00124
0.10	1814171B652A	mrandnum_06_03	0.98056	0.00134	lrrandnum_06_03	0.98690	0.00120
0.10	1A423B9472C7	mrandnum_06_04	0.97895	0.00114	lrrandnum_06_04	0.98347	0.00126
0.10	20E876D82248	mrandnum_06_05	0.98058	0.00113	lrrandnum_06_05	0.98770	0.00124
0.10	3F6E65CA7440	mrandnum_06_06	0.97966	0.00119	lrrandnum_06_06	0.98734	0.00140
0.10	479D21DB7509	mrandnum_06_07	0.97953	0.00145	lrrandnum_06_07	0.98417	0.00133
0.10	55D4371D3A23	mrandnum_06_08	0.97993	0.00130	lrrandnum_06_08	0.98712	0.00136
0.10	6E1A14672B8F	mrandnum_06_09	0.97972	0.00138	lrrandnum_06_09	0.98533	0.00142
0.10	77A0308C0E44	mrandnum_06_10	0.98157	0.00134	lrrandnum_06_10	0.98412	0.00116
0.30	109E77866CF6	mrandnum_08_01	0.93412	0.00118	lrrandnum_08_01	0.93910	0.00146
0.30	16AA4A58735C	mrandnum_08_02	0.93227	0.00138	lrrandnum_08_02	0.93757	0.00117
0.30	1814171B652A	mrandnum_08_03	0.93390	0.00131	lrrandnum_08_03	0.93940	0.00146
0.30	1A423B9472C7	mrandnum_08_04	0.93252	0.00144	lrrandnum_08_04	0.93676	0.00130
0.30	20E876D82248	mrandnum_08_05	0.93334	0.00132	lrrandnum_08_05	0.93851	0.00111
0.30	3F6E65CA7440	mrandnum_08_06	0.93168	0.00132	lrrandnum_08_06	0.93914	0.00149
0.30	479D21DB7509	mrandnum_08_07	0.93514	0.00123	lrrandnum_08_07	0.94011	0.00131
0.30	55D4371D3A23	mrandnum_08_08	0.93564	0.00132	lrrandnum_08_08	0.93900	0.00139
0.30	6E1A14672B8F	mrandnum_08_09	0.93597	0.00136	lrrandnum_08_09	0.93781	0.00117
0.30	77A0308C0E44	mrandnum_08_10	0.93525	0.00128	lrrandnum_08_10	0.93965	0.00118

Table 6.9.2.2-3.Neutron multiplication factors with standard deviations for the ES-3100 package models at the "MR" and "LR" node points

moifr	Random Number	"A" cases	k_{eff}	s	"B" cases	k_{eff}	s
1.00	109E77866CF6	mrandnum_15_01	0.93103	0.00139	lrrandnum_15_01	0.93344	0.00126
1.00	16AA4A58735C	mrandnum_15_02	0.93082	0.00131	lrrandnum_15_02	0.93281	0.00121
1.00	1814171B652A	mrandnum_15_03	0.92890	0.00148	lrrandnum_15_03	0.93468	0.00132
1.00	1A423B9472C7	mrandnum_15_04	0.93062	0.00145	lrrandnum_15_04	0.93592	0.00126
1.00	20E876D82248	mrandnum_15_05	0.93055	0.00125	lrrandnum_15_05	0.93251	0.00143
1.00	3F6E65CA7440	mrandnum_15_06	0.92950	0.00117	lrrandnum_15_06	0.93374	0.00121
1.00	479D21DB7509	mrandnum_15_07	0.92952	0.00116	lrrandnum_15_07	0.93572	0.00138
1.00	55D4371D3A23	mrandnum_15_08	0.92805	0.00154	lrrandnum_15_08	0.93498	0.00145
1.00	6E1A14672B8F	mrandnum_15_09	0.93117	0.00140	lrrandnum_15_09	0.93224	0.00114
1.00	77A0308C0E44	mrandnum_15_10	0.93218	0.00120	lrrandnum_15_10	0.93158	0.00131

6.9.2.3 STATISTICAL EVALUATION

An evaluation of KENO V.a calculation results is made to determine if there is a statistically significant difference between the mean k_{eff} for the "MR" and "MLR" models, for the "MLR" and "LR" models, and for the "MR" and "LR" models. Cases are classified into five groups based on the amount of water assumed to be present in the shipping package. The symbol "I" is used to specify the case. The mean difference and standard deviation for each of the five sets of pair-wise differences are defined as follows:

(a) $d_i = (k_{effBi} - k_{effAi})/n$ and
(b) $s_{di} = \sqrt{[\, [\, n\Sigma d_i^{\,2} - (\,\Sigma d_i\,)^2 \,] / n(n-1) \,]}$ (conservatively defined for the t-test appropriate for small sample sizes),

where A_i and B_i denote the model types, and n denotes the sample size of ten. It is reasonable to assume that the paired differences have been randomly selected from a normally distributed population of paired differences with mean (μ_d) and standard deviation (σ_d), then the sampling distribution of

$$(d - \mu_d) / (s_d/\sqrt{n})$$

is a *t* distribution having n-1 degrees of freedom.

The evaluation of the mean differences (d_i) for the 10 sets of cases is accomplished through hypothesis testing, a statistical tool used to provide evidence that a difference exists or does not exist. The t_i values are given in Table 6.9.2.3-1. A value of 3.25 is obtained from the standard table for critical values for the t distribution from which the decision to accept or reject the null hypothesis H_0 is made with a Type I error probability (α) of 0.01.

For $|t| < 3.25$, the H_o hypothesis is not rejected. Acceptance of the null hypothesis is the result of insufficient evidence to reject it. Thus, it can be concluded that the mean estimates of the difference in k_{eff} between the "MR" and "MLR" calculation models, between the "MLR" and "LR" calculation models, and between the "MR" and "LR" calculation models are not statistically significant for the dry condition where neutronic interaction between packages is significant. Also, the mean estimate of the difference in k_{eff} between the "MR" and "MLR" calculation models is not statistically significant for wet or flooded conditions where the packages of the array become isolated.

Table 6.9.2.3-1. T-test values for establishing the statistical significance of the differences in calculated k_{eff} values for the ES-3100 package models at the "MR," "MLR," and "LR" node points

moifr	"MR" cases (k_{eff})	"MLR" cases (k_{eff})	d_i	S_{di}	t[a]
1.0E-20	1.05154	1.05075	0.00089	1.58991e-03	1.77
1.0E-04	1.05146	1.05165	-0.00019	2.17840e-03	-0.28
0.1	0.98008	0.98091	-0.00087	1.33870e-03	-2.06
0.3	0.93404	0.93300	0.00106	1.88912e-03	1.77
1.0	0.93030	0.93067	-0.00034	1.68664e-03	-0.65
moifr	**"MLR" cases (k_{eff})**	**"LR" cases (k_{eff})**	**d_i**	**S_{di}**	**t**
1.0E-20	1.05075	1.05116	-0.00050	1.92087e-03	-0.83
1.0E-04	1.05165	1.05113	0.00041	9.36819e-04	1.38
0.1	0.98091	0.98546	-0.00456	2.28535e-03	-6.31
0.3	0.93300	0.93863	-0.00578	1.59574e-03	-11.45
1.0	0.93067	0.93369	-0.00318	2.30797e-03	-4.36
moifr	**"MR" cases (k_{eff})**	**"LR" cases (k_{eff})**	**d_i**	**S_{di}**	**t**
1.0E-20	1.05154	1.05116	0.00039	2.35840e-03	0.52
1.0E-04	1.05146	1.05113	0.00021	2.19813e-03	0.31
0.10	0.98008	0.98546	-0.00543	1.66324e-03	-10.33
0.30	0.93404	0.93863	-0.00472	1.46294e-03	-10.21
1.00	0.93030	0.93369	-0.00353	2.50750e-03	-4.45

[a] critical value = 3.25 for 10 cases.

For $|t| > 3.25$, the H_o hypothesis is rejected. Therefore, it can be concluded that the mean estimate of the difference in k_{eff} between the "MLR" and "LR" calculation models, and between the "MR" and "LR" calculation models, is statistically significant for wet or flooded conditions where the packages of the array become isolated. The negative t-values indicate that the calculated k_{eff} value for the "LR" model is slightly higher than for the "MR" and "MLR" models. This result is consistent with an expected increase in k_{eff} due to "tighter or closer" water reflector surrounding the package content.

Although flattening of the side of the package represents a reduction in the diameter of the drum, the points at which minimum flattening occurs provide an indication of the reduction of lattice spacing between packages of an array under HAC. The composite of the minimum deformation points at perpendicular axes (90–270° and 0–180°) represents the modified lattice spacing in an array of ES-3100 packages. As illustrated in Table 6.9.2.3-2, the equivalent diameter of the package for "composite" lattice spacing is not significantly different from the 18.37-in. diameter of the pre-test package. Even though significant crushing of the drum midsection and bottom occurs, the effective center-to-center spacing of the contents actually increases under HAC. Selective rearrangement of alternating packages would be required to achieve a more compact array; however, this event is not credible.

As described in Sect. 6.3.1.2, a close-pack (triangular-pitch) array of packages would be represented by a reduced package in a rectangular-pitch configuration. For HAC, the 17.26-in. reduced diameter for the "composite close-pack" package is slightly larger than the 17.20-in. diameter of the "MLR" calculation model used in the HAC calculations of Sect. 6.6. Therefore, packages evaluated with the "MLR" calculation model of packages in a rectangular-pitch configuration are deemed adequate for the HAC criticality evaluation. Considering both the irregular shape of the deformed drums and that array spacing is determined by overall (maximum) dimensions rather than by mean or minimum dimensions of a damaged package, the use of the "MLR" model for representing the ES-3100 package under HAC is conservative and bounding.

Table 6.9.2.3-2. Deformation of the ES-3100 drum projected by finite element analysis "Case 3100 RUN1HL Lower Bound Kaolite May 2004"

	FEA node	Diameter at 90° (in.)	Diameter at 180° (in.)	Equivalent circular diameter (in.)
Composite	103012/098194	22.00	15.60	18.56
Pre-test drum	-	18.37	18.37	
Pre-test, close-pack	-	17.08	17.08	
Composite, close-pack	103012/098194	-	-	17.26

THIS PAGE INTENTIONALLY LEFT BLANK.

Appendix 6.9.3

PACKAGE MATERIAL COMPOSITIONS

THIS PAGE INTENTIONALLY LEFT BLANK.

Appendix 6.9.3

PACKAGE MATERIAL COMPOSITIONS

Table 6.4 (Sect. 6.3.2) provides basic information for deriving the compositions for the ES-3100 package (Figs. 6.1 and 6.2). The atomic densities presented in Table 6.4 can be verified using additional information provided in Appendix 6.9.5. The following sections provide the rationale, the justification, or both for the material compositions used in the criticality calculations.

6.9.3.1 HEU AND UNIRRADIATED TRIGA CONTENTS

HEU considered for shipment in the ES-3100 is categorized into the following material forms: highly enriched uranium (HEU) solid or broken metal; HEU oxide; uranyl nitrate hexahydrate (UNH) crystals. In the interest of adding conservatism, uranium is modeled as ^{235}U and ^{238}U, while the ^{234}U and ^{236}U isotopes are excluded. Any positive change in neutron multiplication represented by the presence of the ^{234}U is covered by the higher than actual ^{235}U content. (Rothe et al. 1978) The theoretical density of 100 wt % ^{235}U HEU is 18.8111 g/cm^3. This value is determined by adjusting the density of natural uranium included in the SCALE Standard Composition Library with 100 wt % weight factors. The theoretical density of HEU oxide types are 10.96 g/cm^3 for UO_2, 8.30 g/cm^3 for U_3O_8, and 7.29 g/cm^3 for UO_3. The theoretical density of UNH crystals is 2.79 g/cm^3. Table 6.9.3.1-1 provides details of the calculated weight percentages input to KENO V.a calculated on the basis of the stoichiometric formula of $UO_2(NO_3)_2+6H_2O$ and crystalline density. The maximum enrichment considered in the analysis is 100 wt % ^{235}U, although actual material enrichments are lower. The unirradiated solid form TRIGA fuel is uranium zirconium hydride ($UZrH_x$) where "x" is ≤2, having a density of 8.65 g/cm^3.

Table 6.9.3.1-1. Calculation of constituent weight-percentage values for uranyl nitrate hexahydrate crystals used in KENO V.a calculation models

Avogadro No. (N_o)	6.0221370E+23					
UNH						
$UO_2(NO_3)_2+6H_2O$	Atoms/Molecule	At. wt [a]	Mole. wt.	wt %	calc. Ni	NiAi
Hydrogen	12	1.0078	12.0936	2.4233	4.0401e+22	4.0716e+22
Nitrogen	2	14.0031	28.0062	5.6117	6.7333e+21	9.4286e+22
Oxygen	14	15.9949	223.9286	44.8690	4.7132e+22	7.5388e+23
U-235		235.0441		100.0000		
U-238		238.0510		0.0000		
Uranium	1	235.0441	235.0441	47.0962	3.3666e+21	7.9130e+23
			499.0725	100.0002		
summations				100.0002	9.7633e+22	1.6802e+24
At. Wt. material						
assumed density	2.7900					
den.=($\sum N_iA_i$)/No						2.7900

[a] *Source*: *Nuclides and Isotopes*, 14th ed., General Electric Company, 1989.

HEU broken metal. The critical mass of fissile material is dependent on factors such as the form and shape of the material, bulk density if the material is broken into pieces, and the enrichment. Broken metal can be compared to the minimum critical mass of submerged metal lattices of regular-shaped fissile material. Using experimental data, the approximation of a heterogeneous mixture of fissile material and moderator to a homogenous mixture is justified as follows.

Figure 6.9.3.1-1 depicts the experimentally determined minimum critical mass of U (~ 94) lattices immersed in water as a function of the volume-to-surface area ratio of the fissile element. (TID-7028). The critical mass is shown to increase from 850 g to 21 kg over the range of volume-to-surface ratios from 0 to 0.18 in. The critical mass is nearly constant in the range of volume-to-surface ratios from 0.18 to 0.8 in. For pieces greater than 1-in. cubes, the minimum critical mass will not be less than 21 kg. For smaller pieces, the minimum critical mass is a nearly linear function of the volume-to-surface-area ratio of the fissile element.

Figure 6.9.3.1-2 depicts the experimentally determined minimum critical mass of U (~ 94) metal water and solution systems as a function of the concentration of ^{235}U. The figure with added data reveals that: (1) a minimum critical mass exists for each metal lattice system plotted, and (2) as the bulk density of uranium or the uranium concentration increases, the curves for the critical mass of metal lattice systems converge with the curve for highly enriched solution experiments or the curve for calculated homogenous metal water mixtures. Conversely stated, the critical mass is greater for a heterogenous system than for a homogenous system, and this difference increases as the H/X ratio increases. Therefore, the practice of approximating a heterogeneous mixture of fissile material and moderator as a homogenous mixture is justifiable and also conservative at the higher H/X ratios.

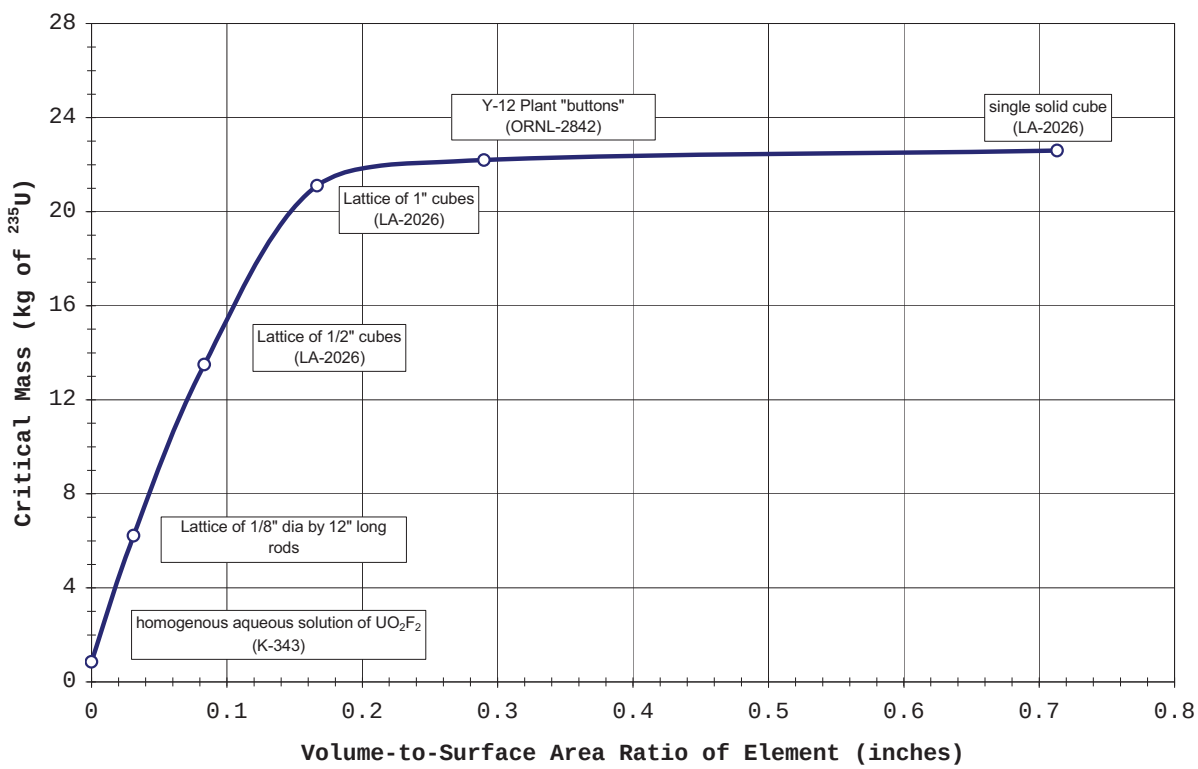

Fig. 6.9.3.1-1. Experimentally determined minimum critical mass U(~94) metal lattices immersed in water as a function of volume-to-surface area ratio of fissile material. *Source*: H. C. Paxton et al., *Critical Dimensions of Systems Containing 235U,* TID-7028, Los Alamos Scientific Lab. and Oak Ridge Natl. Lab., June 1964, Fig. 19. Y-12 data have been added.

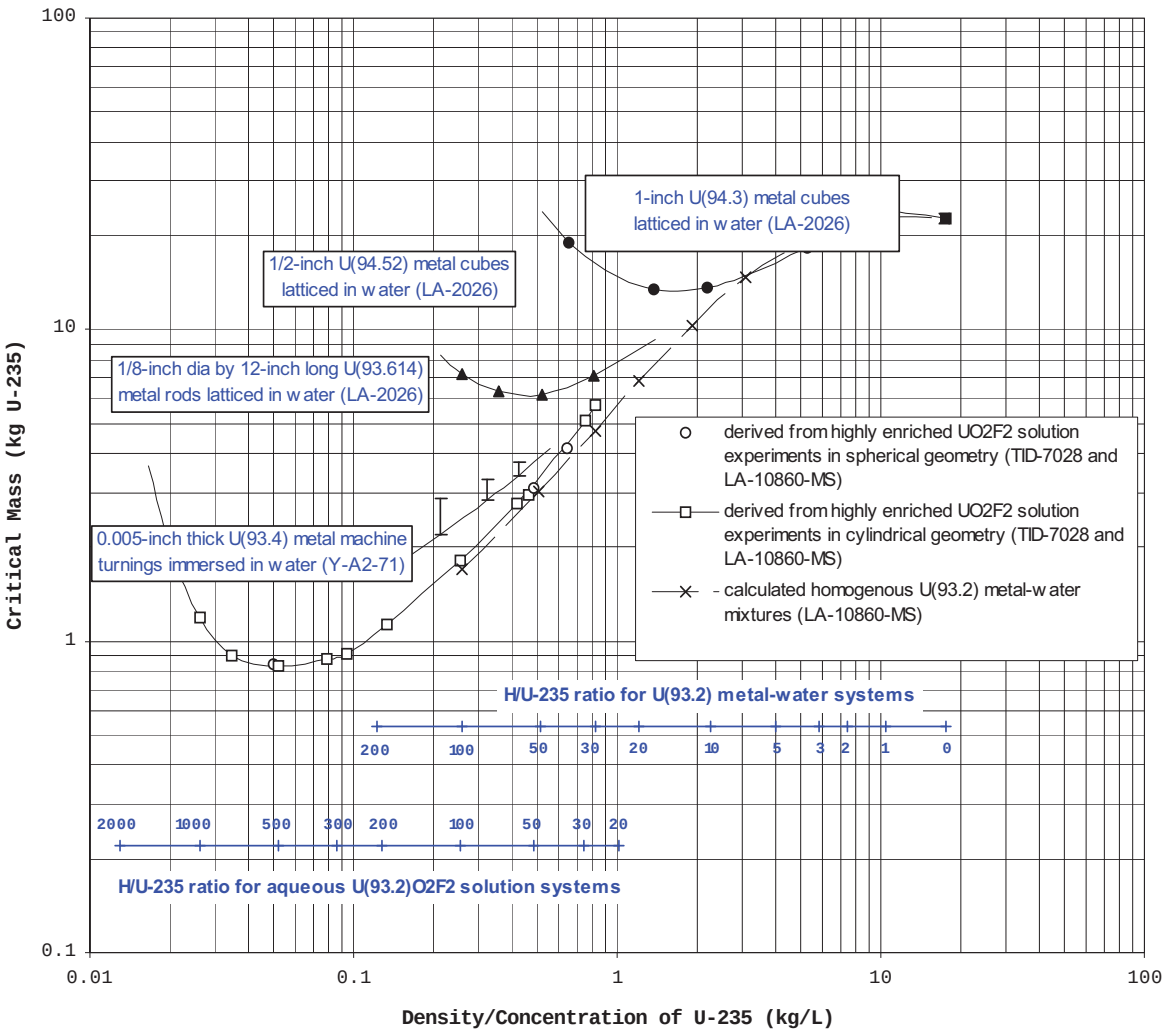

Fig. 6.9.3.1-2. Experimentally determined minimum critical mass of U(~94) metal water and solution systems as a function of the concentration of ^{235}U. *Sources*: A. W. Krass, *Survey of Experimental Data Concerning the Critical Mass of Highly Enriched Uranium–Water Systems*, CCG-365, Lockheed Martin Energy systems, Inc., Oak Ridge Y-12 Plant, July 13, 2000, Fig. 1. Y-12 data added.

Approximating broken metal as a homogenous mixture of uranium and water requires a defined space within which masses of the components are conserved. This space is generally characterized by a lattice constructed of unit cells and defined by the dimensions of the fissile material being approximated.

The broken HEU metal consists of large, irregular pieces ranging from 0.5 in. to several inches on a side as shown in Fig. 6.9.3.1-3. A lattice of cubes is chosen to represent broken metal inside the ES-3100 containment vessel. Due to the constraints of KENO V.a, an idealized configuration is defined by a square lattice circumscribed by the inner wall of the containment vessel. Water fills the truncated cylindrical regions between the inner wall of the containment vessel and the vertical faces of the lattice. Two additional models are developed to evaluate conservatism at various stages of model approximations for broken metal.

Fig. 6.9.3.1-3. Pan of HEU broken metal.

Together, these models include an explicit arrangement of HEU metal cubes forming a compact rectangular lattice inside the containment vessel, HEU metal homogeneously mixed with water within the rectangular lattice formed by the unit cells, and HEU metal homogeneously mixed with water within the volume of the containment vessel.

Parameters varied in each of these three models include (1) the cube size in the explicit model from 1.0 in. to 0.25 in. on a side, (2) water moderation inside the containment vessel from dry to the fully flooded condition, (3) enrichment from 100.0 wt % ^{235}U to 20.0 wt % ^{235}U, (4) thickness of the 277-4 canned spacers located between each convenience can, and (5) the mass of the uranium metal at each content location. One-quarter inch, 0.5-in., and 1.0-in. cubes are selected to evaluate "approach-to-homogeneity" of broken metal in this idealized form. The corresponding array configurations for 0.25-in., 0.5-in., and 1.0-in. cubes are 12 × 12 × N, 6 × 6 × N, and 3 × 3 × N. The N-th layer of unit cells for a given mass loading may not all contain HEU metal; the empty cells are filled with water. Nevertheless, a slight variation still arises in the total mass of HEU metal between these array configurations given whole cubes are contained in the calculation models.

The results for the calculation models representing the various configurations of broken uranium metal are shown in the Table 6.9.3.1-2. As the explicitly modeled cubes become smaller in size, the calculated k_{eff} values for the explicit "sqa" models approach values for the "lha" models where HEU metal cubes are homogenized with water within the rectangular lattice formed by the unit cells of the array. A representative or converged k_{eff} value is 0.87 for increasing by smaller cubes based on calculation results for the "lha" models. The "lha" results indicate a slight difference between the k_{eff} values for the three array sizes; these differences are attributed to the difference in the HEU for the arrays of whole cubes.

Table 6.9.3.1-2. Summary for evaluation of HEU broken metal models (95 wt % ^{235}U) in a flooded containment vessel, 1.4-in. canned spacers and full water reflection of containment vessel

Array type	U (g)	^{235}U (g)	H_2O (g)	h/x	k_{eff}	σ	$k_{eff} + 2\sigma$
discrete array of cubes ("sqa" cases)							
3 × 3 × *n*	35,164	33,406	7,719	6.03	0.8352	0.0012	0.84
6 × 6 × *n*	35,973	34,175	7,676	5.86	0.8559	0.0011	0.86
12 × 12 × *n*	35,988	34,188	7,765	5.86	0.8603	0.0012	0.86
cubes homogenized within footprint of lattice ("lha" cases)							
3 × 3 × *n*	35,164	33,406	7,719	6.03	0.8586	0.0011	0.86
6 × 6 × *n*	35,988	34,188	7,675	5.86	0.8650	0.0012	0.87
12 × 12 × *n*	35,988	34,188	7,675	5.86	0.8677	0.0010	0.87
cubes homogenized within containment vessel ("cha" cases)							
3 × 3 × *n*	35,164	33,406	7,719	6.03	0.9427	0.0013	0.95
6 × 6 × *n*	35,973	34,175	7,676	5.86	0.9495	0.0015	0.95
12 × 12 × *n*	35,988	34,188	7,675	5.86	0.9517	0.0016	0.95

Calculation results for the "cha" models, where arrays of cubes are fully homogenized with the water for the flooded containment vessel, indicate the highest k_{eff} values. The neutron multiplication factor jumps from 0.87 to 0.95. This model is deemed to be overly conservative when applied to broken metal for the following reasons.

- HEU metal does not dissolve in water.
- HEU metal is not in an oxide or powder form that will absorb moisture or readily mix and become homogenized with the water inside the flooded containment vessel.
- Because HEU metal is much denser than water, it will not float and become distributed throughout a flooded containment vessel; instead it will gravitate toward the bottom of the containment vessel.

The calculation results for the homogeneous mixture model of HEU metal and water within a rectangular lattice bound results for the explicit model. Also, the homogenization over the entire volume of the containment vessel is deemed overly conservative. For these reasons, the "lha" model is chosen to represent HEU broken metal inside the flooded containment vessel under full water reflection. For conservatism, the "cha" model is chosen to represent broken metal in single packages and the array of packages under NCT and HAC. Details regarding the "sqa", "lha", and "cha" calculation models are presented in Appendix 6.9.1.

<u>HEU Oxide.</u> Theoretical (crystalline) densities for HEU oxide are 10.96 g/cm^3, 8.30 g/cm^3, and 7.29 g/cm^3 for UO_2, U_3O_8, and UO_3, respectively. While bulk densities of product oxides with enrichments ranging from 19 to 100 wt % ^{235}U are typically on the order of 6.54 g/cm^3, the bulk density of HEU oxides considered for shipment in the ES-3100 ranges from 2.0 to 6.54 g/cm^3. Therefore, only less-than-theoretical mass loadings would actually be achieved. Skull oxides are a mixture of graphite and U_3O_8 with densities on the order of 2.44 g/cm^3 for poured material and 2.78 g/cm^3 for tapped material. The combined water saturation and crystallization of the HEU oxide are not expected in the HAC, given that UO_2 and UO_3 are non-hygroscopic while U_3O_8 is only mildly hygroscopic. Table 6.9.3.1-3 provides summary data for 292 samples of canned skull oxide.

Table 6.9.3.1-3. Summary data for 292 samples of skull oxide

Statistic	wt % U	wt % ^{235}U	µg C/g U	µg C /g ^{235}U	Net Wt (g)	U Wt (g)	^{235}U Wt (g)
Maximum	84.52	93.19	171,000	252,861	**7,072**	5,938	4,165
Minimum	12.93	20.28	13	17	442	312	221
Median	81.66	37.62	5,590	13,910	4,448	3,541	1,414
Mean	79.64	45.02	16,968	41,333	4,419	3,532	1,563
Std Dev	6.87	16.40	24,304	59,027	745	698	606

Values of wt % U, wt % ^{235}U, µg C/g U, etc. for a given statistic (maximum, minimum, medium, or mean) do not occur simultaneously in a specific sample. Inspection of sample data reveals the following characteristics:

(1) the fissile material content is ≤221 g ^{235}U in samples with concentrations up to 252,861 µg C/g^{235}U,
(2) the enrichment is 93.2 wt % ^{235}U for samples with concentrations in the range of 12,600 to 18,600 µg C/gU,
(3) the enrichment ranges from 60 to 70.2 wt % ^{235}U for samples with concentrations in the range of 3,231 to 87,720 µg C/gU, and
(4) the enrichment ranges from 37 to 38 wt % ^{235}U for samples with concentrations in the range of 400 to 233,366 µg C/gU.

Eight skull oxide compositions representative of 292 samples of canned skull oxide were selected for establishing the bounding content calculation models. The skull oxide content is assumed to be U_3O_8 plus graphite, polyethylene, and unidentified material. Two additional compositions were derived for addressing skull oxides with an enrichment of 93.2 wt % ^{235}U where unidentified material is treated as ^{235}U and the carbon content is either maximized or minimized. Treatment of the unidentified material as fissile material in the criticality analysis assures that its presence in skull oxide does not increase reactivity beyond what is considered in the bounding analysis.

The composition of the skull oxide content is given in terms of the following parameters: the grams skull oxide content in a content can (**gramskul**), the content bulk density (**densoc**), the wt % uranium in skull oxide content (**wtpuskul**), the wt % ^{235}U in uranium (**wtpu25u**), and the grams of graphite in the content can (**gramg**). Values for the content specification parameters are provided in Table 6.9.3.1-3b.

Table 6.9.3.1-3b. Content specification parameters for skull oxide content

Content	gramskul (g)	densoc (g/cm^3)	wtpuskul (wt %)	wtpu25u (wt %)	gramg (g)
sk_01	3863	1.899	58.92	69.78	139
sk_02	4978	2.447	66.15	69.42	168
sk_03	4607	1.981	72.77	69.88	124
sk_04	5082	2.186	82.77	70.07	20
sk_05	7072	3.042	83.97	69.91	9
sk_06	5037	2.476	72.53	37.61	307
sk_07	4385	2.156	75.15	37.55	203
sk_08	4550	2.237	72.57	37.73	87
sk_09	7100	3.054	78.95	93.20	307
sk_10	7100	3.054	82.61	93.20	1.0E-05

The information in Table 6.9.3.1-3c is derived from the content specification parameters of Table 6.9.3.1-3b on the assumption that 513 g of polyethylene is present in the skull oxide content in three content locations inside the containment vessel.

The amount of skull oxide content (Column 2, Table 6.9.3.1-3c) is **gsoc** = 3.0 × **gramskul**.

The amount of uranium in the skull oxide content (Column 6, Table 6.9.3.1-3c) is
gusoc = **gsoc** × **wtpuskul** / 100.0.

The amount of ^{235}U (Column 7, Table 6.9.3.1-3c) is **gr235** = **gusoc** × **wtpu25u** / 100.0.

The amount of graphite in the skull oxide content (Column 8, Table 6.9.3.1-3c) is **ggsoc** = 3.0 × **gramg**.

The micrograms graphite per gram uranium in skull oxide content (Column 9, Table 6.9.3.1-3c) is
mggraphgu = **ggsoc** × 1.0e6 / **gusoc**.

The amount of U_3O_8 in the skull oxide content (**guox**) [Column 3, Table 6.9.3.1-3c] is
guox = **gusoc** / **wtpuuox**,

where **gusoc** (Column 6, Table 6.9.3.1-3c),
wtpuuox is the weight percent uranium in uranium oxide, and
wtpuuox = **mwu** / (**mwu** + **mwo**),

where **mwu** = (3){(235.0441 × wtpu25u) + [238.0510 × (100 − wtpu25u)]} /100.0 and
mwo = (8)(15.9949).

The amount of unidentified material in skull oxide content (**gramunid**) [Column 12, Table 6.9.3.1-3c] is
gramunid = (**gsoc** − **guox** − **ggsoc** − **grampoly**)

Skull oxide content is assumed to be saturated with water. The amount of saturation moisture (**gmsatm**) [Column 4, Table 6.9.3.1-3c] is **gmsatm** = 0.9982 × **volsatm**,

where **volsatm** is the volume of saturation moisture in the skull oxide content and
volsatm = **vsox** − **volminsox**

The volume of skull oxide (**vsox**) in the containment vessel is
vsox = (**gsoc** / **densoc**) − (**grampoly** / **denpoly**),

where **gsoc** (Column 2, Table 6.9.3.1-3c),
densoc is the bulk density of skull oxide content,
grampoly is the 513 g of polyethylene, and
denpoly is the density of polyethylene, 0.92 g/cm^3.

The minimum volume of skull oxide (**volminsox**) in the containment vessel is
volminsox = (**gsoc** − **grampoly** − **gramunid**) / **dnsoxtheo**,

where **gsoc** (column 2, Table 6.9.3.1-3c),
grampoly (513 g),
gramunid (column 12, Table 6.9.3.1-3c), and
dnsoxtheo is the theoretical density of skull oxide.

Table 6.9.3.1-3c. Canned skull oxide (SO) content for ES-3100 calculation models, assuming 513 g polyethylene present and can spacers absent.

Content	SO (g)	UOx (g)	Sat. H_2O (g)	SO h/x	U (g)	^{235}U (g)	C (g)	µg C/ g ^{235}U	CV H_2O (g)	CV h/x	Unident (g)
sk_01	11,589	8,063	4,468	28.09	6,828	4,765	417	87,518	4,105	50.58	2,596[a]
sk_02	14,934	11,665	4,015	17.79	9,879	6,858	504	73,492	4,105	33.41	2,252[a]
sk_03	13,821	11,876	4,893	20.62	10,058	7,028	372	52,930	3,233	32.62	1,060[a]
sk_04	15,246	14,900	4,599	15.52	12,619	8,842	60	6,786	3,235	25.07	-227[b]
sk_05	21,216	21,036	3,869	9.49	17,815	12,455	27	2,168	3,235	16.27	-360[b]
sk_06	15,111	12,933	3,765	28.02	10,960	4,122	921	223,432	4,105	54.01	744[a]
sk_07	13,155	11,666	3,989	32.68	9,886	3,712	609	164,054	4,106	61.55	367[a]
sk_08	13,650	11,689	4,068	33.01	9,906	3,737	261	69,834	4,106	61.69	1,187[a]
sk_09	21,300	19,865	3,801	7.43	16,816	15,673	921	58,764	3,235	12.82	1
sk_10	21,300	20,786	3,905	7.27	17,596	16,399	0	0	3,235	12.41	1

[a] Positive value specifies grams of miscellaneous neutron absorber elements in content, modeled as water.
[b] Negative value specifies grams of excess polyethylene included in the content model.

The theoretical density of skull oxide (**dnsoxtheo**) is
dnsoxtheo = (**ggsoc** + **guox**) / [(**ggsoc** / **dnctheo**) + (**guox** / **dnuoxtheo**)],

where **ggsoc** (Column 8, Table 6.9.3.1-3c),
guox (Column 3, Table 6.9.3.1-3c),
dnuoxtheo is the theoretical density of U_3O_8, 8.3 g/cm^3, and
dnctheo is the theoretical density of graphite, 4.2 g/cm^3.

The hydrogen to fissile uranium ratio of canned skull (Column 5, Table 6.9.3.1-3c) is
sochtox = {[(**gmsatm** × **wtphwat**) + (**grampoly** × **wtphpoly**)] × **atwu25**} / (**gr235** × **atwth** × 100.0),

where **gmsatm** (column 4, Table 6.9.3.1-3c),
wtphwat is the weight percent hydrogen in water, 11.1913%,
grampoly (513 g),
wtphpoly is the weight percent hydrogen in polyethylene, 14.3811%,
atwu25 is the atomic weight of ^{235}U, 235.0441,
gr235 (column 7, Table 6.9.3.1-3c), and
atwth is the atomic weight of hydrogen, 1.0078.

The amount of water in the voided region of the CV (column 10, Table 6.9.3.1-3c) is
gwatcv = 0.9982 × **volvcv**,

where **volvcv** is the void volume of the CV and
volvcv = (**cvarea** × **cvih**) − (**gsoc** / **densoc**),

where **cvarea** is the internal area (129.73536 cm^2) of the CV,
cvih is the internal height (78.74 cm),
gsoc (column 2, Table 6.9.3.1-3c), and
densoc (Table 6.9.3.1-3b).

The hydrogen to fissile uranium ratio inside the containment vessel (Column 11, Table 6.9.3.1-3c) is
htox = ⟨{[(**gmsatm** + **gwatcv**) × **wtphwat**] + [**grampoly** × **wtphpoly**]}
× **atwu25**⟩ / (**gr235** × **atwth** × 100.0),

where **gmsatm** (column 4, Table 6.9.3.1-3c),
gwatcv is the amount of water in the voided region of CV,
wtphwat is the weight percent hydrogen in water, 11.1913%,
grampoly (513 g),
wtphpoly is the weight percent hydrogen in polyethylene, 14.3811%,
atwu25 is the atomic weight of ^{235}U, 235.0441,
gr235 (Column 7, Table 6.9.3.1-3c), and
atwth is the atomic weight of hydrogen, 1.0078.

Unirradiated TRIGA reactor fuel. TRIGA fuel is uranium zirconium hydride ($UZrH_x$), an alloy of uranium metal homogeneously dispersed as fine particles in a zirconium hydride matrix. The fuel is stable because uranium hydride does not form to any considerable extent. Moreover, uranium hydride has never been detected in the photomicrographic evaluations of TRIGA fuel.

The General Atomics catalog of stock items lists approximately 40 TRIGA fuel elements classified into four basic types: standard element, instrumented element, fuel-follower control rod, or cluster assembly. The TRIGA element active fuel region consists of three 5-in long sections "fuel meats" of $UZrH_x$. The H/Z atom ratio "x" in $UZrH_x$ equals 1.6 in all cases except for two stock items. For these cases, x = equals 1.0 and the fissile content is < 40 g ^{235}U. The unirradiated solid form TRIGA fuel is identified as either 20 % enriched or 70 % enriched, and has dimensions and material properties specific to its design function. Table 1.4 provides a summary description.

The fuel diameter for the 20 % enriched TRIGA elements is either 1.44 in., 1.41 in., 1.40 in., 1.37 in., 1.34 in., or 1.31 in. The uranium composition of the fuel is 45 wt %, 30 wt %, 20 wt %, 12 wt %, and 8.5 wt %. As illustrated in Table 6.9.3.1.4-a, the TRIGA element with a maximum fissile content of 307 g ^{235}U in 1,560 g U, 45 wt% U in $UZrH_x$, and a H/Zr atom ratio of 1.6 has a computed fuel density of ~8.66 g/cm^3. The calculated number density (N_i) for each element or isotope is also given. The TRIGA fuel element with a fuel diameter of 1.44 inches contains 3,466.7 g $UZrH_x$. Further evaluation of the manufacturers data reveals that fuel density is proportional to the uranium weight fraction. Calculated density values are: 8.6597 g/cm^3 for 45 wt% U in $UZrH_x$, 6.8995 g/cm^3 for 30 wt% U in $UZrH_x$, 6.2825 g/cm^3 for 20 wt% U in $UZrH_x$, 5.9328 g/cm^3 for 12 wt% U in $UZrH_x$, and 5.7895 g/cm^3 for 8.5 wt% U in $UZrH_x$.

The active fuel diameter for 70 % enriched TRIGA fuel is 1.44 inches in both the standard element and instrumented element, and 1.31 inches in the fuel follower control rod. The uranium composition of the fuel is 8.5 wt %. The standard element and instrumented elements contain ~136 g ^{235}U in 194 g U while the fuel follower control rod contains ~113 g ^{235}U in 162 g U. As the calculation in Table 6.9.3.1.4-b illustrates, the 70 wt % enriched TRIGA fuel has a computed density of ~5.70 g/cm^3. The TRIGA fuel element with a fuel diameter of 1.44 inches contains 2,282.4 g $UZrH_x$ while the element with a fuel diameter of 1.31 inches contains 1,888.9 g $UZrH_x$.

The clad thickness is ~0.02 inches for a TRIGA fuel element with stainless steel cladding and ~0.03 inches for an element with aluminum cladding. In preparation for shipment in the ES-3100, a TRIGA fuel element is disassembled, the fuel meats are removed from the thin cladding and packed into convenience cans.

Table 6.9.3.1-4a. Calculation of constituent weight-percentage values for 20 wt % enriched uranium-zirconium hydride content in KENO V.a calculation models

Avogadro No. (N_o) = 6.0221370e+23

U(ZrH_x) atom	wt %	x	mass (g)	at. wt.		calc. N_i	N_iA_i
Hydrogen	0.9554	1.6		1.00780	1.6125	4.9439E+22	4.9824E+22
Zirconium	54.0447	1		91.21960	91.2196	3.0897E+22	2.8184E+24
u-235	19.6795		307.0	235.04410			
u-238	80.3205			238.05099			
uranium	45.0000		1560.0	237.45318	75.9535	9.8830E+21	2.3468E+24
	100.0001				168.7856		
summations	100.0001					9.0219E+22	5.2150E+24
At. wt molecule							
Volume (cm^3)	400.3200						
Mass (g)	3466.66667						
density (g/cm^3)	8.65974						
den.=(∑NiAi)/No							8.6597

Table 6.9.3.1-4b. Calculation of constituent weight-percentage values for 70 wt % enriched uranium-zirconium hydride content in KENO V.a calculation models

Avogadro No. (N_o) = 6.0221370e+23

U(ZrH_x) atom	wt %	x	mass (g)	at. wt		calc. N_i	N_iA_i
Hydrogen	1.5894	1.6		1.00780	1.6125	5.4148e+22	5.4571e+22
Zirconium	89.9107	1		91.21960	91.2196	3.3841e+22	3.0870e+24
u-235	70.1031		136.0	235.04410			
u-238	29.8969			238.05099			
uranium	8.5000		194.0	235.93508	8.6237	1.2370e+21	2.9184e+23
	100.0001				101.4558		
summations	100.0001					8.9227e+22	3.4334e+24
At. wt molecule							
Volume (cm^3)	400.3200						
Mass (g)	2282.35294						
density (g/cm^3)	5.70132						
den.=(∑NiAi)/No							5.7013

The TRIGA fuel may also be configured as clad fuel rods. Each clad fuel rod will be derived from a single TRIGA fuel element by removal of the stainless steel or aluminum clad extending beyond the plenum adjacent to the axial ends of the active fuel section. Each ~15 inch long rod consists of the 3 fuel pellets and an exterior sheath of stainless steel or aluminum clad, where the protruding clad at each end has been crimped in. The fuel rods will be packed into stainless steel or tin-plated carbon steel convenience cans, with a maximum of three fuel rods per loaded convenience can. This shipping configuration requires a minimum of two convenience cans; where only one convenience can is loaded with clad fuel rods. The loaded can is 17.5 inches tall while the empty one is 8.75 inches tall. Although can spacers are not required for criticality control, can spacers or stainless steel pads may be used to take up free volume over the 31 in. internal height of the containment vessel. The maximum quantity of fissile material per package is 408 g ^{235}U.

The clad fuel rod with 1.44 inch diameter fuel pellets contains 2,282.4 g $UZrH_x$ while rod with the 1.31 inch diameter fuel pellets contains 1,888.9 g $UZrH_x$. The 0.02 in thick sheath of stainless steel clad adds ~179 g to the mass of the active fuel for the 1.48 in. diameter standard element or instrumented element, and ~163 g to active fuel mass for the 1.35 in. diameter fuel follower control rod. Allowance for 1/2 in. of residual stainless steel crimped on each end of the clad fuel rod adds ~11 - 12 g stainless steel to these amounts. Likewise, the 0.03 in thick sheath of aluminum clad adds ~90 g to the mass of the active fuel for the 1.47 in. diameter standard element or instrumented element. Allowance for 1/2 in. of residual aluminum crimped on each end of the clad fuel rod adds ~6 g aluminum.

6.9.3.2 TYPE 304 STAINLESS STEEL

The metallic components of the ES-3100 package are composed of type 304 stainless steel. These include the containment vessel, the convenience cans, the drum liner, and the drum. Type 304 stainless steel with a density of 7.9400 g/cm^3 is included as a material in the SCALE Standard Composition Library.

6.9.3.3 277-4 NEUTRON ABSORBER

Catalog No. 277 dry mix is a proprietary mixture of Thermo Electron Corporation for producing a heat-resistant shielding material which combines the most effective shielding components into a single homogeneous composite. The shielding composite material is designed to maximize the hydrogen content necessary for thermalizing fast neutrons for capture in the boron constituent. Widely used in nuclear power plant applications, the heat-resistant shielding material is capable of retaining a significant portion of its shielding properties up to 230°C (450°F). The recommended operating limit is 350°F, which is well above HAC temperatures expected inside the body weldment liner inner cavity and canned spacers.

The 277-4 neutron absorber material used in the ES-3100 is a formulation of Cat 277-0 dry mix, a boron carbide additive, and water. 277-4 is produced through a quality-controlled batch process of dry blending, wet mixing, vibration casting, and timed cure. (Equipment Specification JS-YMN3-801580-A005, Appendix 1.4.5*)* "Loss On Drying" (LOD) tests are used to measure the amount of water in the as-manufactured 277-4 casting. The as-manufactured 277-4 at 100 lb/ft^3 and 31.8 % LOD has a hydrogen concentration of 3.56 wt % and a natural boron concentration of 4.359 wt %. (DAC-PKG-801624-A001, Table 5)

The ability of 277-4 to perform its function depends upon the masses of hydrogen and ^{10}B locked inside the high alumina borated cement cast into the body weldment liner inner cavity and the spacer

cans. A calculated amount of boron carbide is added to Cat 277-0 dry mix for producing as-manufactured 277-4 material with a volumetric isotopic concentration >7.621 × 10^{20} at/cm^3 of ^{10}B. The additive is boron carbide (B_4C) with small amount of a frit-like compound and trace amounts of unaccounted elements (0.17 wt %). Boron carbide has a theoretical density from 2.45 to 2.52 g/cm^3. The boron carbide grit partical sizes used are also small after passing through mesh sizes of 200 and 40 (63 to 355 μm). 277-4 contains a large amount of hydrated alumina, also known as aluminum trihydrate [$Al(OH)_3$]. It is a nonabrasive powder with a specific gravity of 2.42. Given that both materials are of like density and similar partial size, separation and in homogeneity of 277-4 material is not expected during the controlled vibration casting process.

Table 6.9.3.3-1 provides detailed elemental composition data derived for as-manufactured neutron absorber material at 100 lb/ft^3 and 31.8% LOD. This material description allows for clear specification of reduced boron and water contents required in the evaluation of NCT and HAC. As shown in Table 6.9.3.3-1, both the water and boron components are extracted from the material specification for the neutron absorber, and the constituent weight percents are recalculated accordingly (green box). 277-4 is specified in KENO V.a as three arbitrary materials: **arbmnpmx** with a density of 1.02276 g/cm^3, **arbmnph2o** with a density of 0.509253 g/cm^3, and **arbmboron** with a density of 6.98257e-02 g/cm^3. Model densities for 277-4 inside the body weldment liner inner cavity are reduced by a factor of 0.966893 to account for a material gap at the top of the liner. This material description allows for clear specification of reduced boron and water contents required in the evaluation of NCT and HAC.

The testing of 277-4 reveals that the material will dehydrate at elevated temperatures. Test specimens were dried at 250°F for 168 hours to reach the NCT state, and weight measurements were taken. These specimens where subsequently heated to 320°F for 4 hours to reach the HAC state, and weight measurements were again taken. The compositions of 277 at NCT and HAC states were derived by adjustment of the formulation specification for measured losses taking into account the statistical variations in the data. Conservation of mass for nonvolatile materials was observed in the derivation of material specifications based upon testing. Given that hydrogen must be present for the neutron absorber to be effective, conservative material specifications were derived for minimum hydrogen content and minimum material density.

Tables 6.9.3.3-2 and 6.9.3.3-3 respectively provide NCT and HAC composition data for as-manufactured 277-4 material at minimum density and hydrogen content. Respectively, Tables 6.9.3.3-4 and 6.9.3.3-5 provide NCT and HAC composition data or as-manufactured neutron absorber material at minimum density and boron content. Because the amount of ^{10}B present in the neutron absorber material is near saturation, a change in the hydrogen concentration has a major effect on the neutron multiplication factor, while a change in the amount of boron has a minor effect.

The neutron absorbing material used in the ES-3100 Shipping Package will perform as analyzed. The analysis of 277-4 with criticality calculations is adequate in lieu of neutron transmission testing for the demonstration of acceptable performance by experimental means. Criticality calculations show boron content is adequate and k_{eff} is not dependent on absolute (microscopic) homogeneity. Geometry characteristics of the ES-3100 system preclude the need for uniformity in boron areal density as a prerequisite for criticality safety control. The neutron absorbing material will be fabricated under strict quality control and accepted for use under an NQA-1 compliant quality assurance (QA) program. A QA-approved mixing process provides a method for creating an exact mix for the neutron absorber during ES-3100 fabrication. An important part of this QA-approved process is a 277-4 material verification and acceptance testing program. The following discussion elaborates on these key points:

Table 6.9.3.3-1. Calculation of constituent weight-percentage values used in KENO V.a calculation models for as-manufactured 277-4 at minimum acceptable density and boron content [a]

			arbmboron	arbmnpmx	arbmnph2o			arbmboron	arbmnpmx	arbmnph2o
31.8% LOD	**At. wt**	**lb/ft^3**	**lb/ft^3**	**lb/ft^3**	**lb/ft^3**		**NID**	**Wt %**	**Wt %**	**Wt %**
H	1.0078	3.5579			3.5579	**H**	1001			11.1913%
B10	10.0129	0.7911	0.7911			**B10**	5010	18.1482%		
B11	11.0093	3.5680	3.5680			**B11**	5011	81.8518%		
C	12.0000	1.2251		1.2251		**C**	6012		1.9187%	
N	14.0031	0.0090		0.0090		**N**	7014		0.0141%	
O	15.9949	55.9620		27.7281	28.2339	**O**	8016		43.4275%	88.8087%
Na	22.9895	0.0750		0.0750		**Na**	11023		0.1175%	
Mg	24.3051	0.2156		0.2156		**Mg**	12000		0.3377%	
Al	26.9818	24.9306		24.9306		**Al**	13027		39.0461%	
Si	28.0853	1.5752		1.5752		**Si**	14000		2.4671%	
S	32.0636	0.1969		0.1969		**S**	16000		0.3084%	
Ca	40.0803	7.5553		7.5553		**Ca**	20000		11.8331%	
Fe	55.8447	0.3383		0.3383		**Fe**	24000		0.5298%	
Totals		100.0000	4.3591	63.8491	31.7918			100.00%	100.00%	100.00%
H_2O	18.0105									
density (g/cm^3)		1.601838e+00	6.982572e-02	1.022759e+00	5.092532e-01	spacer density (g/cm^3)	1.601838e+00	6.98257e-02	1.02276e+00	5.09253e-01
						liner density (g/cm^3)	1.548806e+00	6.75140e-02	9.88899e-01	4.92393e-01
						liner den. multiplier	0.966893			

a *Source*: G. A. Byington, *Mixing Weights and Elemental Composition of 277-4 Neutron Poison Used in the ES-3100*, DAC-PKG-801624-A001, BWXT Y-12, Y-12 National Security Complex, Jan. 25, 2006, Table 5.

Table 6.9.3.3-2. Calculation of constituent weight-percentage values used in KENO V.a calculation models for NCT as-manufactured 277-4 at minimum density and hydrogen content [a]

			arbmboron	arbmnpmx	arbmnph2o			arbmboron	arbmnpmx	arbmnph2o
	At. wt	lb/ft^3	lb/ft^3	lb/ft^3	lb/ft^3		NID	Wt %	Wt %	Wt %
H	1.0078	2.6840			2.6840	**H**	1001			11.1913%
B10	10.0129	0.8282	0.8282			**B10**	5010	18.1479%		
B11	11.0093	3.7354	3.7354			**B11**	5011	81.8520%		
C	12.0000	1.2826		1.2826		**C**	6012		1.9189%	
N	14.0031	0.0094		0.0094		**N**	7014		0.0141%	
O	15.9949	50.3252		29.0262		**O**	8016		43.4251%	
O	15.9949				21.2990	**O**	8016			88.8087%
Na	22.9895	0.0785		0.0785		**Na**	11023		0.1174%	
Mg	24.3051	0.2258		0.2258		**Mg**	12000		0.3378%	
Al	26.9818	26.1004		26.1004		**Al**	13027		39.0479%	
Si	28.0853	1.6491		1.6491		**Si**	14000		2.4672%	
S	32.0636	0.2061		0.2061		**S**	16000		0.3083%	
Ca	40.0803	7.9098		7.9098		**Ca**	20000		11.8336%	
Fe	55.8447	0.3541		0.3541		**Fe**	24000		0.5298%	
Totals		95.3886	4.5636	66.8420	23.9830			100.00%	100.00%	100.00%
H_2O	18.0105									
density (g/cm^3)		1.527971e+00	7.310148e-02	1.070700e+00	3.841692e-01	spacer density (g/cm^3)	1.527971e+00	7.31015e-02	1.07070e+00	3.84169e-01
						liner density (g/cm^3)	1.477385e+00	7.06813e-02	1.03525e+00	3.71451e-01
						liner den. multiplier	0.966893			

a *Source*: G. A. Byington, *Mixing Weights and Elemental Composition of 277-4 Neutron Poison Used in the ES-3100*, DAC-PKG-801624-A001, BWXT Y-12, Y-12 National Security Complex, Jan. 25, 2006, Table 11.

Table 6.9.3.3-3. Calculation of constituent weight-percentage values used in KENO V.a calculation models for HAC as-manufactured 277-4 at minimum density and hydrogen content [a]

			arbmboron	arbmnpmx	arbmnph2o			arbmboron	arbmnpmx	arbmnph2o
	At. wt	lb/ft^3	lb/ft^3	lb/ft^3	lb/ft^3		NID	Wt %	Wt %	Wt %
H	1.0078	2.6758			2.6758	**H**	1001			11.1913%
B10	10.0129	0.8282	0.8282			**N10**	5010	18.1479%		
B11	11.0093	3.7354	3.7354			**N11**	5011	81.8520%		
C	12.0000	1.2826		1.2826		**V**	6012		1.9188%	
N	14.0031	0.0094		0.0094		**N**	7014		0.0141%	
O	15.9949	50.2605		29.0265		**O**	8016		43.4254%	
O	15.9949				21.2340	**O**	8016			88.8087%
Na	22.9895	0.0785		0.0785		**Na**	11023		0.1174%	
Mg	24.3051	0.2258		0.2258		**,g**	12000		0.3378%	
Al	26.9818	26.1004		26.1004		**Al**	13027		39.0477%	
Si	28.0853	1.6491		1.6491		**Si**	14000		2.4671%	
S	32.0636	0.2061		0.2061		**S**	16000		0.3083%	
Ca	40.0803	7.9098		7.9098		**Ca**	20000		11.8335%	
Fe	55.8447	0.3541		0.3541		**Fe**	24000		0.5298%	
Totals		95.3157	4.5636	66.8423	23.9098			100.00%	100.00%	100.00%
H_2O	18.0105									
density (g/cm^3)		1.52680e+00	7.31015e-02	1.07071e+00	3.82995e-01	spacer density (g/cm^3)	1.52680e+00	7.31015e-02	1.07071e+00	3.82995e-01
						liner density (g/cm^3)	1.47626e+00	7.06813e-02	1.03526e+00	3.70316e-01
						liner den. multiplier	0.966893			

a *Source*: G. A. Byington, *Mixing Weights and Elemental Composition of 277-4 Neutron Poison Used in the ES-3100*, DAC-PKG-801624-A001, BWXT Y-12, Y-12 National Security Complex, Jan. 25, 2006, Table 12.

Table 6.9.3.3-4. Calculation of constituent weight-percentage values used in KENO V.a calculation models for NCT as-manufactured 277-4 at minimum density and boron content [a]

			arbmboron	arbmnpmx	arbmnph2o			arbmboron	arbmnpmx	arbmnph2o
	At. wt	lb/ft^3	lb/ft^3	lb/ft^3	lb/ft^3		NID	Wt %	Wt %	Wt %
H	1.0078	2.9617			2.9617	**H**	1001			11.1913%
B10	10.0129	0.7911	0.7911			**B10**	5010	18.1482%		
B11	11.0093	3.5680	3.5680			**B11**	5011	81.8517%		
C	12.0000	1.2251		1.2251		**C**	6012		1.9188%	
N	14.0031	0.0090		0.0090		**N**	7014		0.0141%	
O	15.9949	51.2291		27.7264		**O**	8016		43.4260%	
O	15.9949				23.5027	**O**	8016			88.8087%
Na	22.9895	0.0750		0.0750		**Na**	11023		0.1175%	
Mg	24.3051	0.2156		0.2156		**Mg**	12000		0.3377%	
Al	26.9818	24.9306		24.9306		**Al**	13027		39.0472%	
Si	28.0853	1.5752		1.5752		**Si**	14000		2.4671%	
S	32.0636	0.1969		0.1969		**S**	16000		0.3084%	
Ca	40.0803	7.5553		7.5553		**Ca**	20000		11.8334%	
Fe	55.8447	0.3383		0.3383		**Fe**	24000		0.5299%	
Totals		94.6709	4.3591	63.8474	26.4644			100.00%	100.00%	100.00%
H_2O	18.0105									
density (g/cm^3)		1.516474e+00	6.982572e-02	1.022731e+00	4.239172e-01	spacer density (g/cm^3)	1.516474e+00	6.98257e-02	1.02273e+00	4.23917e-01
						liner density (g/cm^3)	1.466269e+00	6.75140e-02	9.88872e-01	4.09883e-01
						liner den. multiplier	0.966893			

a *Source*: G. A. Byington, *Mixing Weights and Elemental Composition of 277-4 Neutron Poison Used in the ES-3100*, DAC-PKG-801624-A001, BWXT Y-12, Y-12 National Security Complex, Jan. 25, 2006, Table 13.

Table 6.9.3.3-5. Calculation of constituent weight-percentage values used in KENO V.a calculation models for HAC as-manufactured 277-4 at minimum density and boron content [a]

			arbmboron	arbmnpmx	arbmnph2o			arbmboron	arbmnpmx	arbmnph2o
	At. wt	lb/ft^3	lb/ft^3	lb/ft^3	lb/ft^3		NID	Wt %	Wt %	Wt %
H	1.0078	2.9524			2.9524	**H**	1001			11.1913%
B10	10.0129	0.7911	0.7911			**B10**	5010	18.1482%		
B11	11.0093	3.5680	3.5680			**B11**	5011	81.8517%		
C	12.0000	1.2251		1.2251		**C**	6012		1.9188%	
N	14.0031	0.0090		0.0090		**N**	7014		0.0141%	
O	15.9949	51.1551		27.7262		**O**	8016		43.4258%	
O	15.9949				23.4289	**O**	8016			88.8087%
Na	22.9895	0.0750		0.0750		**Na**	11023		0.1175%	
Mg	24.3051	0.2156		0.2156		**Mg**	12000		0.3377%	
Al	26.9818	24.9306		24.9306		**Al**	13027		39.0473%	
Si	28.0853	1.5752		1.5752		**Si**	14000		2.4671%	
S	32.0636	0.1969		0.1969		**S**	16000		0.3084%	
Ca	40.0803	7.5553		7.5553		**Ca**	20000		11.8334%	
Fe	55.8447	0.3383		0.3383		**Fe**	24000		0.5299%	
Totals		94.5876	4.3591	63.8472	26.3813			100.00%	100.00%	100.00%
H_2O	18.0105									
density (g/cm^3)		1.515140e+00	6.982572e-02	1.022728e+00	4.225861e-01	spacer density (g/cm^3)	1.515140e+00	6.98257e-02	1.02273e+00	4.22586e-01
						liner density (g/cm^3)	1.464979e+00	6.75140e-02	9.88869e-01	4.08596e-01
						liner den. multiplier	0.966893			

a *Source*: G. A. Byington, *Mixing Weights and Elemental Composition of 277-4 Neutron Poison Used in the ES-3100*, DAC-PKG-801624-A001, BWXT Y-12, Y-12 National Security Complex, Jan. 25, 2006, Table 14.

The analysis of 277-4 with criticality calculations is adequate in lieu of neutron transmission testing for the demonstration of acceptable performance. Early on in the licensing process, Borobond 4 was selected as the neutron absorber material for use in the ES-3100 package. The decision to use Borobond 4 in the ES-3100 was made because of favorable experience with its use in the Highly Enriched Uranium (HEU) Rackable Can Storage Box (RCSB), an element of the new state-of-the art HEU storage facility at the Y-12 National Security Complex (Y-12). From an economic standpoint, however, Borobond 4 proved not to be a viable option for the small quantities needed for the ES-3100 project. 277-4 neutron absorber material, which has very similar nuclear material properties to Borobond 4, was then selected as an alternative.

Both the RCSB and the ES-3100 are fast systems in the normal condition when the HEU fissile material is essentially unmoderated. A key factor for an effective neutron absorber is that hydrogen should be present for moderation, and it should be interspersed with boron-10 (^{10}B), thus promoting neutron capture. The potential for neutron streaming through an absorber is significant when a hydrogenous moderator is absent, as in the case of an aluminum boron-carbide matrix (a Boral alloy).

Borobond 4 is a ceramicrete material with slightly greater than 4 wt % boron carbide (B_4C). The boron carbide powder is micro encapsulated by the crystalline matrix of the ceramic; therefore, leaching out the boron is not feasible. In Borobond 4, 100 wt % of the B_4C has a particle size <500 µm; 90 wt % of the other constituents range from <164 µm to <36 µm. Given the differences in particle size, the potential for separation in the mixing process is real.

Some of the questions regarding the use of 277-4 as a neutron poison in the ES-3100 were previously addressed regarding the use of Borobond 4 in the RCSB. Radiography was performed on Borobond 4 samples ranging in thickness from 1.0 to 1.5 in. Inspections revealed little or no visual differences, indicating uniformity of the Borobond 4. For 277-4 where the B_4C grit is on the order of 200 µm, the potential for separation is reduced.

Measurements from neutron transmission tests on Borobond 4 for determination of areal density indicated greater boron content than was physically present. This is due to the presence of elements besides the aluminum and boron (principally hydrogen, oxygen and other low and intermediate-Z elements). From these measurements, credit for 90 wt % boron in a criticality calculation was established as an adequate adjustment. Given the similarity of 277-4 to Borobond 4 (a ceramic-cement composite shielding material, with a similar elemental composition, more uniform particle size, and the same boron content), the 75% credit for boron content applied in the ES-3100 criticality calculations is an adequate enough correction for the efficiency of the material.

Criticality calculations show boron content is adequate and k_{eff} is not dependent on absolute (microscopic) homogeneity. The boron concentration calculations presented here model an infinite array of ES-3100 packages with the boron concentration of Cat 277-4 uniformly varied inside the body weldment inner liner. While the Cat 277-4 described herein is an earlier formulation of the neutron absorber material, the behavior characteristics being demonstrated for Cat 277-4 apply to the revised formulation, 277-4.

Credit for only 75% of the boron is taken in the specification of Cat 277-4. Each package in the array contains 2.774 kg of ^{235}U in broken metal form uniformly distributed inside the containment vessel. The presence of just the hydrogenous cement matrix in the inner liner reduces k_{eff} to 1.132 from a value of 1.35 without the cement matrix. As an initial 1 wt % natural boron is added to the high alumina cement system (Table 6.9.3.3-6), the calculated k_{eff} based on 75% of the boron present drops significantly. Cat 277-4 with 4.2284 wt % natural boron in the minimum cast density of 100 lb/ft^3 (1.60 g/cc) has an acceptable mixture concentration, generating a k_{eff} of 0.88. The saturation value for boron content is reached at ~8 wt %. This near doubling of the boron content results in ~4% decrease in k_{eff} to an asymptotic value of ~0.85.

The density of Cat 277-4 is the sum of constituent densities: the boron density, the base-material density, and the water density. In the calculation model, the density of water in Cat 277-4 is 0.48210 g/cm^3 (not shown in Table 6.9.3.3-6). Canned spacers are omitted from the calculation model. Credit for only 75% of the boron is taken in each parametric calculation. The volume of the 277-4 in the body weldment inner liner cavity is 1.32708×10^4 cm^3.

Table 6.9.3.3-6. Effect of boron concentration on array neutron multiplication

100%B (wt %)	Boron density (g/cm^3)	Base material density (g/cm^3)	NP277-4 mass (g)	Case name	$k_{eff} \pm 2\sigma$ (@75% B)
0.01	0.00016	1.11775	21232.6	nbiabm_kvsb_1	1.13199 +/- 0.00138
0.1	0.0016	1.11631	2.12279E+04	nbiabm_kvsb_2	1.07944 +/- 0.00145
1	0.016	1.10191	2.11801E+04	nbiabm_kvsb_3	0.95564 +/- 0.00129
2	0.032	1.08591	2.11270E+04	nbiabm_kvsb_4	0.91708 +/- 0.00135
3	0.048	1.06991	2.10739E+04	nbiabm_kvsb_5	0.89396 +/- 0.00117
4.2284	0.068614	1.04930	2.10056E+04	nbiabm_kvsb_6	0.87985 +/- 0.00145
6	9.6000E-02	1.02191.	2.09147E+04	nbiabm_kvsb_7	0.86029 +/- 0.00151
8	1.2800E-01	0.98991	2.08085E+04	nbiabm_kvsb_8	0.84769 +/- 0.00150
10	0.16	0.95791	2.07024E+04	nbiabm_kvsb_9	0.84086 +/- 0.00142

NUREG 1609 recommended that only 75% of the minimum boron density be credited in criticality evaluation in order to address the issue of non-homogeneity of ^{10}B in the neutron absorber material. The boron non-homogenity calculations presented here model an infinite array of ES-3100 packages with the boron concentration of Cat 277-4 varying along the vertical height of the body weldment inner liner. However, the total amount of boron in each package is fixed. Each package in the array contains 2.774 kg of ^{235}U in broken metal form uniformly distributed inside the containment vessel. Two sets of calculations are evaluated with this model to address the effects of boron distribution in the ES-3100 inner liner.

In one set of cases, the inner cavity is divided vertically into three equal-volume regions. The density in one region is increased to 95% of the minimum boron density, while the boron density in the

other two regions is decreased to 65%, thus preserving the amount of neutron absorber material in the package. In the other set of cases, the inner cavity is divided vertically into four equal volume regions, but two regions are combined. This creates two quarter-sized regions and one half-size region. The density in the half-size region is increased to 95% of the minimum boron density, while the density in the quarter-sized regions is decreased to 55%, thus preserving the amount of neutron absorber in the package. In both sets of calculations, the high-density region was shifted upward in the package to examine the effect of boron distribution.

As shown in Figures 6.9.3.3-2 and 6.9.3.3-3, the effect of non-homogeneity of boron in the ES-3100 liner on k_{eff} is not statistically significant. The "65% - 95% - 65%" nonhomogeneous boron distribution represents a relative standard deviation of 23.1% in boron concentration. Given the controls on method of manufacture and installation of the neutron absorber material, these calculated conditions bound the expected physical distribution of boron with a large degree of conservatism.

Geometry characteristics of the ES-3100 system preclude the need for uniformity in boron areal density as a prerequisite for criticality safety control. The ISG-15 provides crucial guidance for controlling areal density in a geometry configuration where one-dimensional effects are significant, such as a distributed source separated by thin Boral sheets (aluminum and boron carbide) which range in thickness from 0.075 to 0.4 in. In this example, Boral aluminum sheets are placed between fissile fuel rods just a few inches away and only become efficient when the low-enriched fissile material is placed in a sea of hydrogenous moderator. The cylindrical thickness of the ES-3100 cast neutron absorber material (Cat 277-4) is 1.12 in., which is about three times thicker than the largest Boral sheet. Its purpose in the ES-3100 is to provide criticality safety control for arrays of packages.

In the ES-3100, the proposed fissile mass loads are separated by at least one drum diameter (19.36 in.). Drawing M2E801580A031 in Appendix 1.4.8 shows the cross-section view of the many different layers of materials that are between the fissile mass loads in adjacent packages in an array. The direct neutron transport path between dispersed fissile material (assuming a neutron passes through the following thickness of materials at a normal angle to the closest neighboring package) is:

- fissile material,
- 0.100 in. 304 stainless-steel containment vessel wall,
- air gap,
- 0.06 in. 304 stainless-steel inner liner wall,
- 1.12 in. of 277-4 neutron absorber material,
- 0.06 in. 304 stainless-steel outer liner wall,
- 4.77 in. of Kaolite,
- 0.06 in. 304 stainless-steel outer drum wall, and
- air gap,

followed by the reverse:

- 0.06 in. stainless-steel outer drum wall,
- 4.77 in. of Kaolite,
- 0.06 in. 304 stainless-steel outer liner wall,
- 1.12 in. of 277-4 neutron absorber material,
- 0.06 in. 304 stainless-steel inner liner wall,
- air gap,
- 0.100 in. 304 stainless-steel containment vessel wall, and
- back into a fissile material.

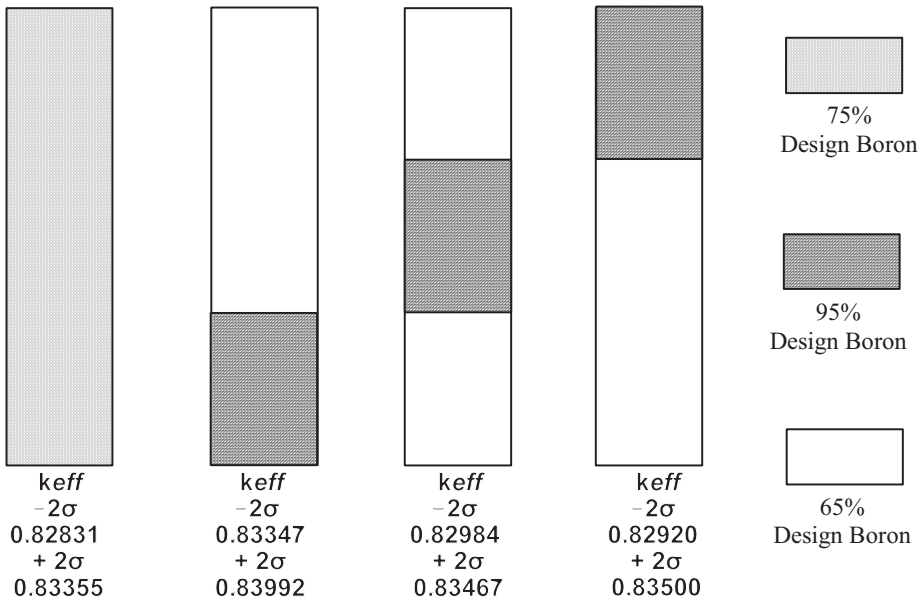

Fig. 6.9.3.3-2. Three equal-region models for evaluation of non-homogeneity in the boron distribution.

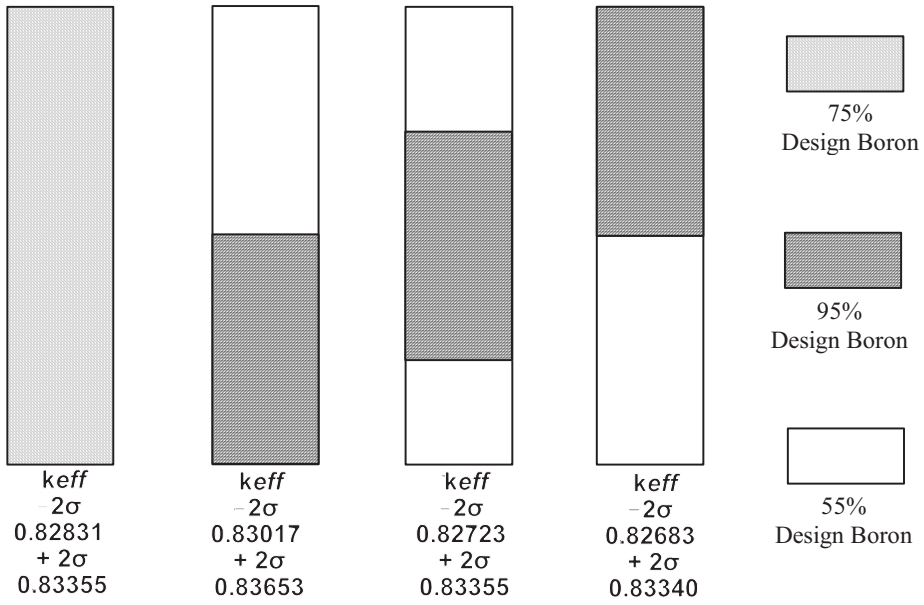

Fig. 6.9.3.3-3. Non-uniform region model for evaluation of non-homogeneity in the boron distribution.

At the shortest distance between fissile materials, neutrons travel through the 1.12 in. (2.8448 cm) of 277-4 neutron absorber material and 0.28 in. (0.7112 cm) of 304 stainless steel at least twice, with the high probability of several neutron scattering collisions along the way. Thus, the mean free path in the package is much smaller than the separation between the fissile material of adjacent packages.

In contrast to a Boral sheet application, the neutron absorber component of the ES-3100 package physically represents a significant fraction of the total container volume and is large in comparison to the potential fissile material volume. Furthermore, the neutron absorber component consists of boron dispersed throughout a hydraulic cement matrix with a high neutron scattering potential. The net result is that sensitivity to angular and spatial variations in the areal density of ^{10}B in the neutron absorber volume is eliminated.

The neutron absorbing material will be fabricated under strict quality control and accepted for use under an NQA-1 compliant QA program. The original equipment specification for the production of 277-4 neutron absorber material used a proprietary mixture from the Thermo Electron Corporation that combined high alumina cement and a boron grit (Cat 277-4). The manufacturing process for the neutron absorber was revised in order to obtain details necessary for material characterization and to achieve process control for ensuring consistency of absorber material among lots.

A two-part system of dry-blend components is now employed rather than relying on a single base material (a premixed powder of high alumina cement and boron grit). Thermo Electron Corporation's proprietary high-alumina cement without boron grit (Cat 277-0) is mixed on-site with boron carbide by the ES-3100 manufacturer under strict quality controls. A single batch is mixed on a per package basis. The boron carbide used in this process is strictly controlled. Boron carbide is specified per ASTM C 750-03, "Nuclear-Grade Boron Carbide Powder," in the Type 1 category. The grit size is controlled to $\leq$100 µm or a grit size of 120 per ANSI B74-12, with 100% passing a 120USS mesh.

The new formulation designated "277-4" is produced through a quality-controlled batch process of dry blending, wet mixing, vibration casting, and timed cure. (Equipment Specification JS-YMN3-801580-A005, Appendix 1.4.5) The plan is to control the purity, boron carbide particle size, chemistry, measurements, weights, mixing, recording, casting, and testing using one batch per each shipping package (and its two companion spacer cans). A design analysis calculation shows all of the calculations used in mixing and determines (from the minimum acceptable chemical purities) the volumetric densities in g/cm^3 and an areal density in g/cm^3 of ^{10}B. (DAC-PKG-801624-A001) These values will prove the acceptability of the mixing specifications.

An important part of this approach is a QA-approved 277-4 material verification and acceptance testing program. The applicant plans on performing 100% acceptance testing on the criticality safety significant properties of density, ^{10}B interaction (neutron absorption), and hydrogen content. The acceptance density shall be the as cast density in the drum to 105−5+10 lb/ft^3 and shall be determined as shown in Appendix 1.4.5. To test the other properties, two companion sample cans shall be cast from each batch used to cast a shipping container (the manufacturer will cast a fresh batch for each shipping container). The companion sample cans shall also have their density verified. The ^{10}B interaction will be tested in the manner described in Appendix A of the 277-4 specification (Appendix 1.4.5). Initially, a new set of 277-4–certified cans will be cast using the newly proposed casting specification with the QA plan described previously. Then, on a companion sample can for each batch pour, a Prompt Gamma-ray Neutron Activation Analysis (PGNAA) test will be used to neutronically test the ^{10}B for absorption. To pass the PGNAA test, the sample can results must be within the results obtained for the 277-4 certified standards, in units of Average Net Count rate (ANC/second) ±4 standard deviations. The second companion sample can will be used to test for hydrogen content using an LOD test as described in

Appendix 1.4.5. Upon successful completion of the density, PGNAA, and LOD testing, the ES-3100 neutron absorber material will be accepted for use.

6.9.3.4 KAOLITE 1600

Kaolite 1600, manufactured by Thermal Ceramics of Augusta, Georgia [telephone number (404) 796-4200], is a super-lightweight, low thermal conductivity, castable material designed for backup insulation up to 1600°F. The material is obtained as a dry powder with the chemical composition given in Table 6.9.3.4-1. The powder is mixed with water in a water-to-powder ratio of 14.5 qt per 20-lb bag. The mixture is poured into the drum body weldment or top plug, vibrated to eliminate voids, and then dried and fired to form the finished product. (Rowland, 2001) The density of the fired material is ~25 lb/ft^3. It is assumed that the wet mixture contains the maximum water possible. This value (14.5 qt per 20 lb) is therefore used to determine the maximum water content of the fired product,

$$\rho_{max} = \frac{14.5\ \text{qt}}{20\ \text{lb dry}} \times \frac{25\ \text{lb}}{\text{ft}^3} \times \frac{0.946\ \ell}{1\ \text{qt}} \times \frac{998.2\ \text{g}}{\ell} \times \frac{35.32\ \text{ft}^3}{10^6\ \text{cm}^3} = \frac{0.6045\ \text{g}}{\text{cm}^3}$$

Table 6.9.3.4-1. Kaolite 1600 chemical composition, percent fired basis

Component	Weight percent	Component	Weight percent
Al_2O_3	9.6	CaO	30.7
SiO_2	36.7	MgO	13.1
Fe_2O_3	6.7	Na_2O	2.0
TiO_2	1.2		

Tables 6.9.3.4-2 and 6.9.3.4-3 provide detailed information regarding the weight measurements taken during the casting of Kaolite 1600 for the production of a series of drum body weldment and top plug parts for a similar package (the BWXT Y-12 Model ES-2100). The mean values for the amount of Kaolite and water present after baking are 107.08 lb of Kaolite and 4.8 lb of water in the drum body weldment, and 16.99 lb of Kaolite and 0.58 lb of water in the top plug. An ES-2100 package contains, on the average, 124.07 lb (56,276.91 g) of Kaolite and 5.38 lb (2,440.32 g) of water. Given that the average volume is 5.72 ft^3, the average density of Kaolite is 22.63 lb/ft^3 (0.3625 g/cm^3).

The volume of the Kaolite region in the KENO models is 1.63417 × 5 cm^3. For NCT, the density of Kaolite is 0.34438 g/cm^3, and the density of water is 0.01493 g/cm^3. The data in Tables 6.9.3.4-2 and 6.9.3.4-3 indicate that the Kaolite may have as little as 1.90 lb (861.82 g) of water after baking (Part Serial Number 97) such that the corresponding density of water is 0.00527 g/cm^3. For the water-flooded HAC, the amount of water is assumed not to exceed the amount present before baking. The package would contain on the average 186.10 lb (84,413.1 g) of water such that the corresponding density is 0.51655 g/cm^3. The full range of NCT and HAC conditions would be covered by a variation of water in the Kaolite from 0 g/cm^3 to 0.51655 g/cm^3 in a calculation model.

Table 6.9.3.4-2. Fabrication data, before and after baking the drum body weldment parts of the ES-2100 shipping package

								before baking			after baking		
Part Serial Number	clean & empty (lb)	filled with water (lb)	before baking (lb)	after baking (lb)	density after baking (lb/ft^3)	water conditions (lb)	volume (ft^3)	Kaolite and water (lb)	Kaolite (lb)	water (lb)	Kaolite and water (lb)	Kaolite (lb)	water (lb)
97	87.5	393.5	356.5	197.0	22.29	306.00	4.91	269.00	107.60	161.40	109.50	107.60	1.90
98	87.5	393.5	356.5	198.5	22.60	306.00	4.91	269.00	107.60	161.40	111.00	107.60	3.40
54	87.5	395.0	356.5	199.0	22.59	307.50	4.94	269.00	107.60	161.40	111.50	107.60	3.90
87	87.5	394.0	353.5	196.5	22.16	306.50	4.92	266.00	106.40	159.60	109.00	106.40	2.60
2	88.0	394.0	360.0	202.5	23.31	306.00	4.91	272.00	108.80	163.20	114.50	108.80	5.70
4	88.0	395.5	360.0	203.0	23.30	307.50	4.94	272.00	108.80	163.20	115.00	108.80	6.20
42	88.0	394.5	356.5	199.5	22.66	306.50	4.92	268.50	107.40	161.10	111.50	107.40	4.10
43	88.0	396.0	357.5	198.0	22.25	308.00	4.94	269.50	107.80	161.70	110.00	107.80	2.20
94	87.0	393.5	361.5	205.0	23.98	306.50	4.92	274.50	109.80	164.70	118.00	109.80	8.20
35	88.0	394.5	363.5	208.0	24.39	306.50	4.92	275.50	110.20	165.30	120.00	110.20	9.80
3	87.0	393.0	364.0	206.0	24.23	306.00	4.91	277.00	110.80	166.20	119.00	110.80	8.20
44	88.0	394.0	356.5	204.5	23.72	306.00	4.91	268.50	107.40	161.10	116.50	107.40	9.10
32	88.0	396.0	355.0	198.5	22.35	308.00	4.94	267.00	106.80	160.20	110.50	106.80	3.70
33	87.5	394.0	351.0	197.5	22.36	306.50	4.92	263.50	105.40	158.10	110.00	105.40	4.60
58	87.5	394.5	351.5	196.5	22.12	307.00	4.93	264.00	105.60	158.40	109.00	105.60	3.40
4	87.5	394.0	343.0	192.5	21.34	306.50	4.92	255.50	102.20	153.30	105.00	102.20	2.80
22	87.5	394.5	352.0	196.0	22.02	307.00	4.93	264.50	105.80	158.70	108.50	105.80	2.70
27	88.0	395.5	352.5	196.5	21.98	307.50	4.94	264.50	105.80	158.70	108.50	105.80	2.70
28	87.5	394.5	350.5	199.0	22.63	307.00	4.93	263.00	105.20	157.80	111.50	105.20	6.30
30	87.5	395.0	352.0	200.0	22.79	307.50	4.94	264.50	105.80	158.70	112.50	105.80	6.70
27	88.0	395.5	352.5	196.5	21.98	307.50	4.94	264.50	105.80	158.70	108.50	105.80	2.70
mean	87.67	394.50	355.36	199.55	22.72	306.83	4.93	267.69	107.08	160.61	111.88	107.08	4.80
std. dev.					0.8132						100%	95.71%	4.29%
computed on means					22.72	306.83	4.93	267.69	107.08	160.61	111.88	107.08	4.80

Table 6.9.3.4-3. Fabrication data, before and after baking the top plug parts of the ES-2100 shipping package

								before baking			after baking		
Part Serial Number	clean & empty (lb)	filled with water (lb)	before baking (lb)	after baking (lb)	density after baking (lb/ft^3)	water conditions (lb)	volume (ft^3)	Kaolite and water (lb)	Kaolite (lb)	water (lb)	Kaolite and water (lb)	Kaolite (lb)	water (lb)
97	10.5	60.0	53.5	28.5	22.65	49.50	0.79	43.00	17.20	25.80	18.00	17.20	0.80
83	10.5	59.0	50.5	27.0	50.50	27.00	50.50	27.00	16.00	24.00	16.00	24.00	16.00
86	10.5	60.0	50.5	27.5	21.40	49.50	0.79	40.00	16.00	24.00	17.00	16.00	1.00
87	10.5	59.0	53.0	28.5	23.12	48.50	0.78	42.50	17.00	25.50	18.00	17.00	1.00
28	11.0	59.0	53.0	28.5	22.71	48.00	0.77	42.00	16.80	25.20	17.50	16.80	0.70
23	10.5	59.5	52.5	28.0	22.25	49.00	0.79	42.00	16.80	25.20	17.50	16.80	0.70
24	10.5	59.0	53.5	28.5	23.12	48.50	0.78	43.00	17.20	25.80	18.00	17.20	0.80
25	10.5	58.5	54.0	29.0	24.01	48.00	0.77	43.50	17.40	26.10	18.50	17.40	1.10
26	10.5	59.0	54.0	29.0	23.76	48.50	0.78	43.50	17.40	26.10	18.50	17.40	1.10
27	10.5	60.0	54.5	29.0	23.28	49.50	0.79	44.00	17.60	26.40	18.50	17.60	0.90
0	10.5	60.0	52.0	27.0	20.77	49.50	0.79	41.50	16.60	24.90	16.50	16.60	-0.10[a]
20	10.5	60.0	53.5	28.0	22.03	49.50	0.79	43.00	17.20	25.80	17.50	17.20	0.30
22	10.5	60.0	54.0	28.5	22.65	49.50	0.79	43.50	17.40	26.10	18.00	17.40	0.60
21	10.5	61.0	53.0	28.0	21.59	50.50	0.81	42.50	17.00	25.50	17.50	17.00	0.50
19	10.5	60.0	53.0	27.5	21.40	49.50	0.79	42.50	17.00	25.50	17.00	17.00	0.00
11	10.5	60.0	52.5	28.0	22.03	49.50	0.79	42.00	16.80	25.20	17.50	16.80	0.70
14	10.5	60.0	52.5	27.5	21.40	49.50	0.79	42.00	16.80	25.20	17.00	16.80	0.20
15	10.5	60.5	54.0	28.0	21.80	50.00	0.80	43.50	17.40	26.10	17.50	17.40	0.10
16	10.5	59.0	52.0	27.5	21.84	48.50	0.78	41.50	16.60	24.90	17.00	16.60	0.40
17	10.5	60.5	54.5	28.5	22.43	50.00	0.80	44.00	17.60	26.40	18.00	17.60	0.40
mean	10.52	59.70	53.00	28.10	23.74	48.10	3.28	42.48	16.99	25.48	17.58	16.99	0.58
std. dev.					6.3565						100%	96.67%	3.33%
computed on means					22.27	49.18	0.79	42.48	16.99	25.48	17.58	16.99	0.58

[a] No explanation is given for the negative amount of water in Part 0. Also, the smaller percentage of water present in the top plug compared with to the drum body weldment is attributed to the larger surface-to-volume ratio, which results in better drying of the parts.

The Kaolite components of ES-3100 shipping package had not been manufactured at the time this criticality safety evaluation was performed. Given the lack of production data for ES-3100 Kaolite, a material specification (mass and density) was derived from data for ES-2100 production units. This specification, denoted "as-manufactured" (AM) Kaolite, was used for the ES-3100 criticality calculations. This ES-2100 shipping package is similar in design to the ES-3100 currently being evaluated.

The Kaolite production process was re-evaluated and improved following the production of ES-3100 units. (Y/DW-1890) Test samples were produced. These were classified into three groups: high density, medium density, and low density. The predominate number of samples fell into the medium density category (22.04 lb/ft^3), representing the expected, improved Kaolite production process. (Y/DW-1890, Appendix 2.10.4, Table 5) A material specification for use in criticality calculations was derived from the medium density "test sample" (TS) Kaolite data. However, the TS data are based on small sample volumes, whereas the AM data represents the entire package. Taking into consideration both the potential for scaling error and the uncertainty of how representative the test samples are of the manufactured ES-2100 units, the criticality safety packaging analysts chose to utilize the material specification derived from AM data rather than TS data in the criticality calculations for the ES-3100 safety analysis report.

A set of criticality calculations was performed for each of the packaging material specifications (i.e., the TS and the AM Kaolite) using three package water contents to represent the range of NCT and HAC. Y-12 statisticians were asked to determine whether or not the observed differences in neutronic performance are statistically significant for a package modeled with the TS specification versus one modeled with the AM specification. The purpose of this discussion is to summarize this comparison (DAC-FS-900000-A014) and draw conclusions.

Criticality Calculations. Each case is rerun using a different starting random number in order to produce computed k_{eff} values that are statistically independent. Table 6.9.3.4-4 presents the random starting number, the mean value (k_{eff}) and corresponding standard error (s_i) computed for 10 individual runs of each case.

Three sets of criticality calculations were run for both the AM Kaolite and TS Kaolite. One set of calculaitons is for dry Kaolite (i.e., low water content, IS = 1e-04 sp gr water); another set is for normal moisture Kaolite (i.e., NCT water content); and the third set is for flooded Kaolite (i.e., high water content, IS = 1.0 sp gr water). These conditions span the range of NCT and HAC addressed in the criticality evaluation. An infinite array of packages was evaluated in order to eliminate any biases arising from spectral leakage effects in the reflector of the finite array. Each package was modeled having 36 kg of 100% enriched uranium in the form of 3.24-in. diameter cylinder content. The k_{eff} values for each KENO V.a case are based on 500,000 neutron histories produced by running for 215 generations with 2,500 neutrons per generation and truncating the first 15 generations of data.

Statistical evaluation. A review of KENO V.a calculation results was made to determine if a statistically significant difference exists between the mean k_{eff} for the TS Kaolite specification and the AM Kaolite material specifications used in the criticality evaluation of the ES-3100 shipping package. Case results were classified into three groups (i.e., low water content, medium water content, or high water content) depending on the amount of water present in the ES-3100 shipping package. The symbol "I" is used to specify the group. The mean difference and standard deviation for each of the three (3) sets of pair-wise differences was defined as follows:

(a) $d_i = (k_{effBi} - k_{effAi})/n$ and
(b) $s_{di} = \sqrt{[\, [\, n\Sigma d_i^{\,2} - (\,\Sigma d_i\,)^2 \,] / n(n-1) \,]}$ (conservatively defined for the t-test appropriate for small sample sizes)

Table 6.9.3.4-4. Data for the statistical evaluation of "as-manufactured"and "test sample" Kaolite

As-Manufactured Kaolite				Test Sample Kaolite			
Case name	**Random number**	**k_{eff}**	**s_i**	**Case name**	**Random number**	**k_{eff}**	**s_i**
Group 1 – Low water content							
esrandnum_01_01_in	109E77866CF	1.00274	0.00138	mdrandnum_01_01_in	109E77866CF	1.00170	0.00125
esrandnum_01_02_in	16AA4A58735	1.00224	0.00120	mdrandnum_01_02_in	16AA4A58735	1.00416	0.00116
esrandnum_01_03_in	1814171B652	1.00121	0.00107	mdrandnum_01_03_in	1814171B652	1.00208	0.00125
esrandnum_01_04_in	1A423B9472C	1.00367	0.00118	mdrandnum_01_04_in	1A423B9472C	1.00271	0.00131
esrandnum_01_05_in	20E876D8224	1.00290	0.00133	mdrandnum_01_05_in	20E876D8224	1.00406	0.00125
esrandnum_01_06_in	3F6E65CA744	1.00266	0.00137	mdrandnum_01_06_in	3F6E65CA744	1.00418	0.00124
esrandnum_01_07_in	479D21DB750	1.00393	0.00108	mdrandnum_01_07_in	479D21DB750	1.00193	0.00133
esrandnum_01_08_in	55D4371D3A2	1.00313	0.00113	mdrandnum_01_08_in	55D4371D3A2	1.00196	0.00105
esrandnum_01_09_in	6E1A14672B8	1.00343	0.00119	mdrandnum_01_09_in	6E1A14672B8	1.00503	0.00118
esrandnum_01_10_in	77A0308C0E4	1.00229	0.00113	mdrandnum_01_10_in	77A0308C0E4	1.00358	0.00108
Group 2 – NCT medium density							
esrandnum_06_01_in	109E77866CF	0.99025	0.00119	mdrandnum_06_01_in	109E77866CF	0.98323	0.00118
esrandnum_06_02_in	16AA4A58735	0.98863	0.00128	mdrandnum_06_02_in	16AA4A58735	0.98630	0.00108
esrandnum_06_03_in	1814171B652	0.98811	0.00120	mdrandnum_06_03_in	1814171B652	0.98328	0.00125
esrandnum_06_04_in	1A423B9472C	0.98933	0.00114	mdrandnum_06_04_in	1A423B9472C	0.98487	0.00112
esrandnum_06_05_in	20E876D8224	0.98869	0.00103	mdrandnum_06_05_in	20E876D8224	0.98559	0.00109
esrandnum_06_06_in	3F6E65CA744	0.98854	0.00117	mdrandnum_06_06_in	3F6E65CA744	0.98412	0.00106
esrandnum_06_07_in	479D21DB750	0.98900	0.00119	mdrandnum_06_07_in	479D21DB750	0.98395	0.00118
esrandnum_06_08_in	55D4371D3A2	0.98844	0.00113	mdrandnum_06_08_in	55D4371D3A2	0.98546	0.00114
esrandnum_06_09_in	6E1A14672B8	0.99007	0.00126	mdrandnum_06_09_in	6E1A14672B8	0.98424	0.00121
esrandnum_06_10_in	77A0308C0E4	0.99028	0.00122	mdrandnum_06_10_in	77A0308C0E4	0.98465	0.00118
Group 3 – High water content							
esrandnum_09_01_in	109E77866CF	0.92872	0.00118	mdrandnum_09_01_in	109E77866CF	0.92800	0.00123
esrandnum_09_02_in	16AA4A58735	0.92800	0.00110	mdrandnum_09_02_in	16AA4A58735	0.92817	0.00107
esrandnum_09_03_in	1814171B652	0.92844	0.00118	mdrandnum_09_03_in	1814171B652	0.92770	0.00115
esrandnum_09_04_in	1A423B9472C	0.92780	0.00123	mdrandnum_09_04_in	1A423B9472C	0.92763	0.00126
esrandnum_09_05_in	20E876D8224	0.92783	0.00134	mdrandnum_09_05_in	20E876D8224	0.92584	0.00105
esrandnum_09_06_in	3F6E65CA744	0.92809	0.00128	mdrandnum_09_06_in	3F6E65CA744	0.92853	0.00112
esrandnum_09_07_in	479D21DB750	0.92725	0.00111	mdrandnum_09_07_in	479D21DB750	0.92682	0.00111
esrandnum_09_08_in	55D4371D3A2	0.92622	0.00126	mdrandnum_09_08_in	55D4371D3A2	0.92706	0.00116
esrandnum_09_09_in	6E1A14672B8	0.92925	0.00132	mdrandnum_09_09_in	6E1A14672B8	0.92733	0.00110
esrandnum_09_10_in	77A0308C0E4	0.92757	0.00114	mdrandnum_09_10_in	77A0308C0E4	0.92886	0.00132

where A_i denotes the TS by group classification, B_i the AM by group classification, and n the sample size of ten (10). It is reasonable to assume that the paired differences have been randomly selected from a normally distributed population of paired differences with mean μ_d and standard deviation σ_d. Therefore, the sampling distribution of

$$(d - \mu_d) / (s_d/\sqrt{n})$$

is a *t*-distribution having n-1 degrees of freedom.

The evaluation of the mean differences (d_i) for the 10 set of cases is accomplished through hypothesis testing, a statistical tool used to provide evidence that a difference exists or does not exist. The t_i values are 0.70, 10.0 and 0.95 for dry Kaolite, for NCT Kaolite, and for flooded Kaolite, respectively. A value of 3.25 is obtained from the standard table for critical values for the t distribution, from which the decision to accept or reject the null hypothesis H_0 is made with a Type I error probability (α) of 0.01. For $t < 3.25$, the H_o hypothesis is not rejected. Acceptance of the null hypothesis is the result of insufficient evidence to reject it. Thus, it can be concluded that the mean estimate of the difference of the AM Kaolite is not significantly different from the mean of the TS Kaolite for both dry and flooded Kaolite. For $t > 3.25$, the H_o hypothesis is rejected. Therefore, it can be concluded that the mean estimate of the difference of the AM Kaolite is significantly different from the mean of the TS Kaolite for the normal moisture Kaolite. The mean k_{eff} for AM Kaolite is significantly greater than the mean k_{eff} of the TS Kaolite; therefore, the use of the AM specification in the ES-3100 criticality calculations is conservative and bounding. Details of the statistical evaluation are documented in Reference DAC-FS-900000-A014.

6.9.3.5 WATER

Water is used in various regions of the models to simulate HAC as an interstitial moderator and as a reflector. When used at full density, the density of water is 0.9982 g/cm^3. (SCALE, Vol. 3, Sect. M8)

6.9.3.6 CALCULATION OF EQUIVALENT WATER MASS FOR POLYETHYLENE

In the calculation models for evaluation of NCT, water may be substituted for the polyethylene composition of bags present in the package. Based on hydrogen density, 1285.14 g of water are equivalent to 1000 g of polyethylene for nuclear criticality safety calculations. The equivalent water mass is calculated as follows:
Hydrogen in 1 kg of polyethylene [$(CH_2)_2$, molecular weight = 28.0312; density = 0.92]:

$$1 \text{ kg polyethylene} = \frac{1000 \text{ g}}{0.92 \text{ g/cm}^3} = 1087.0197 \text{ cm}^3$$

$$\text{H number density} = \frac{(0.92)(4)(6.02252\times10^{23})}{(28.0312)(10^{24})} = 7.906502\times10^{-2} \text{at/bn-cm}$$

$$\text{H in 1 kg} = (1087.0197\text{cm}^3)(7.906502\times10^{-2}) = 85.945234 \text{ at-cm}^2\text{/bn}$$

Grams of water [H_2O, molecular weight = 18.0110; density = 0.9982] with hydrogen content equivalent to 1 kg of polyethylene:

$$\text{equivalent g of } H_2O = \frac{(85.945234)(18.0110)(10^{24})}{(2)(6.02252\times10^{23})} = 1285.1427 \text{ g}$$

THIS PAGE INTENTIOANLLY LEFT BLANK.

Appendix 6.9.4

QUALIFICATION OF A NEUTRON ABSORBER MATERIAL FOR THE ES-3100

THIS PAGE INTENTIONALLY LEFT BLANK.

Appendix 6.9.4

QUALIFICATION OF A NEUTRON ABSORBER MATERIAL FOR THE ES-3100

6.9.4.1 INTRODUCTION

277-4 is a formulation of Thermo Electron Corporation's Cat. 277-0, a boron carbide additive and water. 277-4 is a neutron radiation shielding product and is one of several materials in its class that have been evaluated as a candidate neutron absorber system for a variety of nuclear criticality safety applications by the Y-12 National Security Complex (Y-12). This class of materials is characterized as a dispersion of $^{nat}B_4C$ particulate* throughout a hardened hydraulic cement or binder, resulting in a high-hydrogen, borated material system. It offers many advantages for typical Y-12 applications over other classes of materials such as borated aluminum because a neutron moderator and neutron absorber are both integral to the solid material system itself. The separate addition of another neutron moderating material such as water or polyethylene is not required in order for it to function effectively.

Computational methods of analysis in simple geometry permit direct comparison of neutron absorber system performance for nuclear criticality safety applications. The measure of comparison is the neutron interaction potential between two parallel 0.745-cm-thick slabs of infinite extent of ^{235}U metal at a density of 18.81 g/cm^3. The slabs are separated by a variable thickness of material and reflected by a 60-cm thickness of the same material (Fig. 6.9.4.1-1). Each material is modeled as an idealized homogenous mixture of elements based on nominal density and constituent proportions (Table 6.9.4.1-1). The result is expressed in terms of calculated k_{eff} † as influenced by the thickness of the candidate material between the two parallel slabs (see Fig. 6.9.4.1-2).

The least effective neutron absorber material systems are those with low hydrogen content and low neutron absorption cross section (e.g., ordinary concrete). The performance of concrete that contains $^{nat}B_4C$ particulate (e.g., borated concrete) is improved, but it is still hindered by its low hydrogen content. This is a function of the proportion and type of cement in the typical concrete mixture (i.e., a low proportion of lime- and silica-based Portland cement). Ordinary water is also included for comparison because of its high hydrogen content, but its performance is also limited by a low total mass density and low neutron absorption cross section.

As expected, materials with high hydrogen content and high boron content (e.g., 277-4, borated ceramics, and borated polymers) are predicted to be the most effective neutron absorber systems. Although the mechanical and thermal properties of such systems can vary significantly, their nuclear properties are dictated almost exclusively by the relative proportion and content of ^{10}B and H and the total mass density of the material system. These things being equal, the nuclear performance of any material in this class (i.e., 277-4, borated ceramics, and borated polymers) is representative of the others.

---

*277-4 is an improved variant of the Cat 277 product ca. 2000 which was originally formulated as a dispersion of ^{nat}Borosilicate glass granules rather than the current practice of using $^{nat}B_4C$ particulate.

†SCALE 4.4a, CSAS25 code sequence for KENO V.a with the 238-group ENDF B-IV neutron cross-section library on the Y-12 SAE Hewlett-Packard J5600 workstation (CMODB).

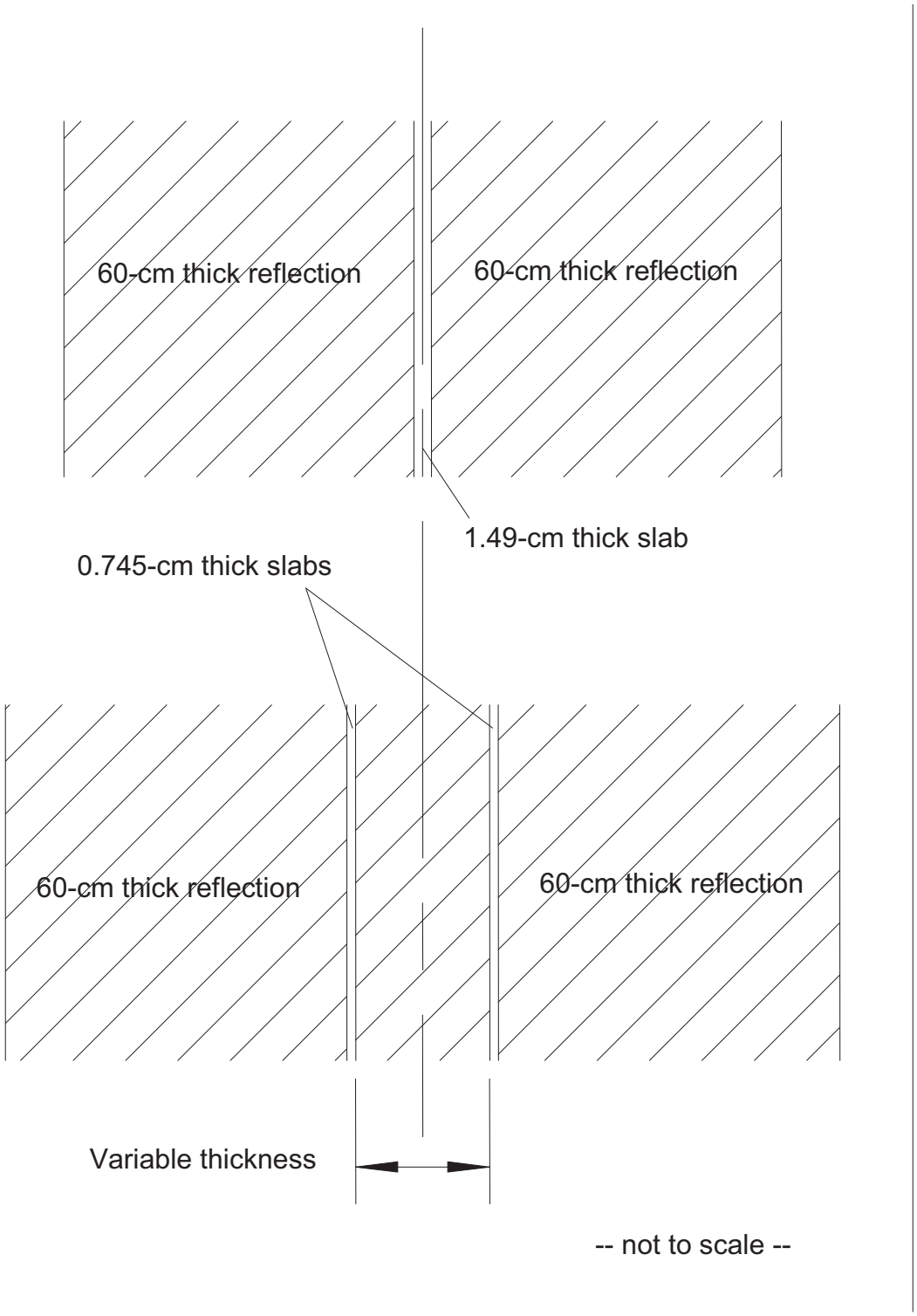

Fig. 6.9.4.1-1. Physical model of parallel ^{235}U metal slabs of infinite extent reflected and separated by various candidate neutron absorber materials.

Table 6.9.4.1-1. Nominal elemental and isotopic compositions of idealized material models for comparison of various neutron absorbers (atoms/barn·cm)

	Ordinary Concrete A 2.147 g/cm^3	Ordinary Concrete B 2.299 g/cm^3	Water 0.9982 g/cm^3	Borated Concrete 2.563 g/cm^3	Cat 277[a] 1.68 g/cm^3	Borated Ceramic 1.91 g/cm^3	Borated Polymer 1.717 g/cm^3	^{235}U Metal 18.81 g/cm^3
H	4.2581e-03	8.5010e-03	6.6751e-02	4.2900e-03	3.3800e-02	2.7200e-02	5.7600e-02	
B-10				1.7600e-04	2.8400e-04	2.6500e-03	9.4600e-04	
B-11				6.8100e-04	1.1800e-03	1.1000e-02	3.9200e-03	
C	1.1348e-02	2.0217e-02		9.0000e-04		4.2600e-03	2.3500e-02	
N							1.3800e-03	
O	4.0370e-02	3.5511e-02	3.3376e-02	4.2400e-02	3.7100e-02	3.2900e-02	2.5900e-02	
Na	7.9356e-05	1.6299e-05		6.7100e-05	2.6000e-04	7.9200e-05		
Mg	5.0111e-03	1.8602e-03		2.3000e-04	2.0800e-04	2.3300e-03		
Al	3.7660e-04	5.5580e-04		2.2900e-03	8.9700e-03	1.7400e-03	7.7000e-03	
Si	1.9382e-03	1.7000e-03		1.1800e-02	7.6700e-04	3.2300e-03		
P						2.1200e-03		
S	1.0013e-04			9.6300e-05	6.0000e-05	7.7800e-05		
Cl	1.9074e-05							
K	3.1231e-04	4.0300e-05		3.1600e-04		2.3100e-03		
Ca	7.3008e-03	1.1101e-02		3.1200e-03	2.2300e-03	2.4600e-04		
Ti	4.0183e-05					7.0800e-05		
Mn	1.2050e-05			1.4000e-04				
Fe	1.2954e-04	1.9301e-04		4.6200e-03	4.8900e-05	5.2000e-04		
U-235								4.8200e-02

[a] The ^{10}B content of this material model for Cat 277 is based on its ca. 2000 formulation using crushed borosilicate glass rather than the current practice of using $^{nat}B_4C$ particulate. This particular formulation is roughly equivalent to ~2% $^{nat}B_4C$ particulate (i.e., equivalent ^{10}B content, by weight). For otherwise identical H and B-10 content, this difference is unimportant relative to its nuclear performance as an idealized homogeneous mixture of elements. However, the current use of more than 5% $^{nat}B_4C$ particulate (by weight) is preferred due to reasons relating to the method of preparation, chemical reaction, and placement of 277-4 and uniformity of ^{10}B distribution in the cured product. As with all the materials in this class, the amount of H and ^{10}B in the finished product is determined by the relative proportions of its major constituents, which are tailored to the requirements of the specific application.

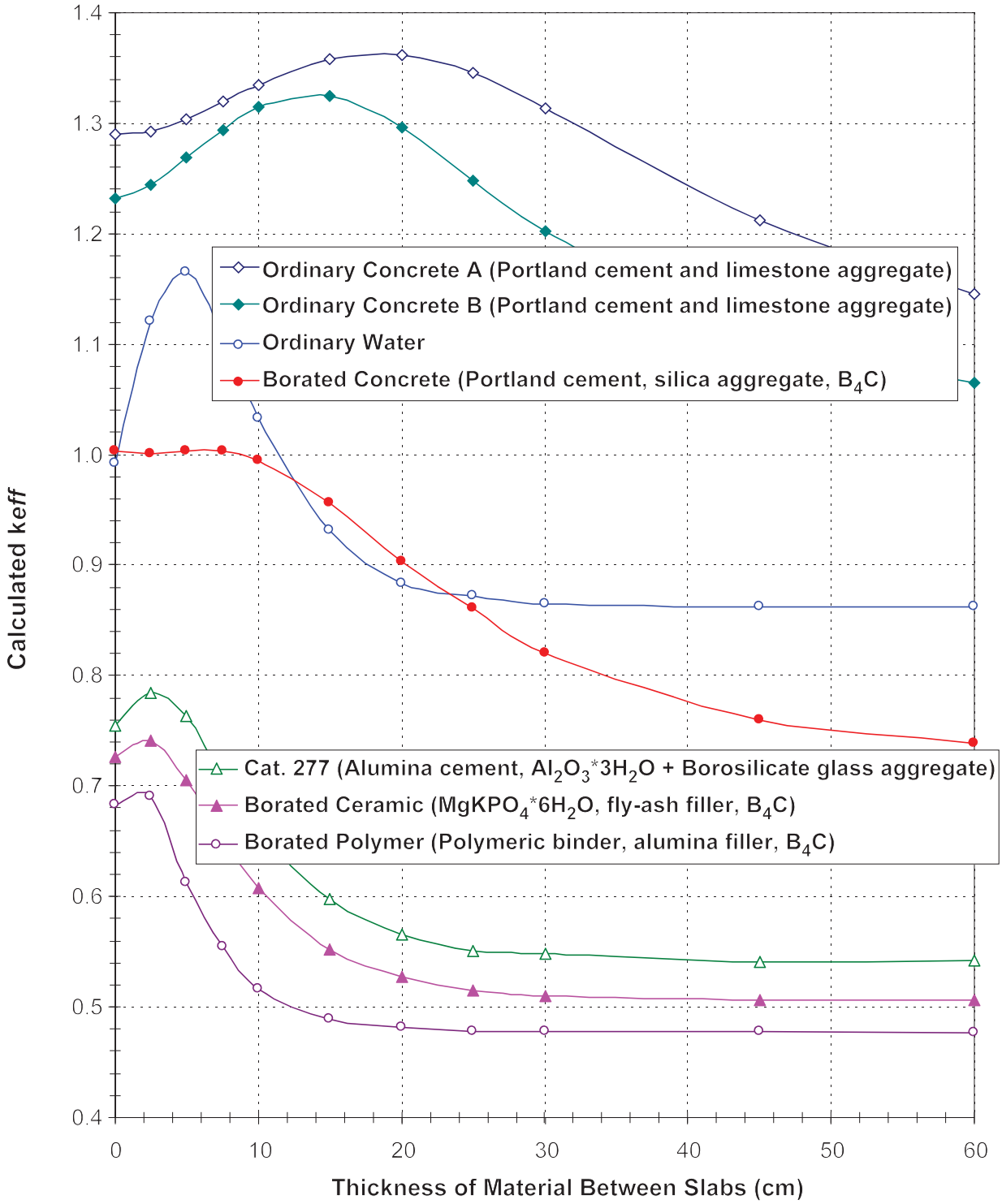

Fig. 6.9.4.1-2. The effect of various materials on neutron interaction between parallel slabs of ^{235}U metal of infinite extent.

6.9.4.2 PERFORMANCE TESTING

To investigate the performance of this class of neutron absorbing materials further, Y-12 has studied neutron radiography and neutron transmission measurements on several samples of a borated ceramic. Like 277-4, the borated ceramic is also a dispersion of $^{nat}B_4C$ particulate throughout a hardened hydraulic crystalline solid material matrix for which the binder phase is $MgKPO_4 \cdot 6H_2O$ rather than the hydrates of CaO and Al_2O_3. In fact, the more finely divided $^{nat}B_4C$ particulate specified for 277-4 is a slight advantage over the modestly coarser particulate in the borated ceramic. As shown below in Table 6.9.4.2-1, the relative proportion and content of H and ^{10}B and their total mass density are very similar. The small differences between the nuclear properties of their associated low- and intermediate-Z elements (i.e., oxides of Mg, Al, P, K, and Ca) are negligible. Thus, performance and the most significant factors affecting performance are nearly identical for both materials, so the results of neutron radiography and neutron transmission for the borated ceramic samples are judged applicable to 277-4 specimens of similar dimension.

Table 6.9.4.2-1. Comparison of nominal values for 277-4 and borated ceramic samples subjected to neutron radiography and neutron transmission testing.

Attribute	Cat 277 Original Formulation ca. 2000	277-4 ES-3100 Formulation as Cured	Borated Ceramic Samples for Testing
Principal Binder Phase(s)	Hydrates of CaO and Al_2O_3	Hydrates of CaO and Al_2O_3	$MgKPO_4 \cdot 6H_2O$
Neutron Absorber Particle Size	^{nat}Borosilicate glass granules 90 wt % <2360 µm 65 wt % <1180 µm 40 wt % <600 µm 15 wt % <102 µm 0 wt % <150 µm	$^{nat}B_4C$ particulate 100 wt % <102 µm	$^{nat}B_4C$ particulate 100 wt % <559 µm 90 wt % <356 µm 40 wt % <254 µm 3 wt % <122 µm 0 wt % <63 µm
Filler Material(s)	$Al_2O_3 \cdot 3H_2O$	$Al_2O_3 \cdot 3H_2O$	Class F Coal Fly-ash
Total Mass Density	1.68 g/cm^3	1.60 g/cm^3	1.91 g/cm^3
Total H_2O content	0.51 g/cm^3	0.51 g/cm^3	0.49 g/cm^3
Total ^{10}B content	0.005 g/cm^3	0.013 g/cm^3	0.012 g/cm^3

Samples were prepared from sectioned pieces of a single specimen from a vertically oriented mold measuring 10 × 10 × ~30 cm tall, as illustrated in Fig. 6.9.4.2-1 (nominally 4 × 4 × 12 in. tall). One specimen was prepared by the normal method of mixing and preparation for the borated ceramic material. Sectioning the first specimen resulted in two thick samples designated “1 of 2” and “2 of 2” which each measured 10-cm wide by ~30-cm long by ~2.4-cm thick (nominally 1-in. thick). A second specimen was prepared by abnormal methods intended to produce non-homogeneity (i.e., poorly mixed using retardants followed by excessive and extended vibration of the mold after installation). Sectioning this specimen resulted in two thin samples designated “062d1bc” and “062d1bd” which each measured 10-cm wide by ~30-cm long by ~1.2-cm thick (nominally 0.5-in. thick). The samples were delivered to the Breazeale Nuclear Reactor Building at Pennsylvania State University for inspection. Upon completion of inspection for all four samples as received, a thick sample “1 of 2” and a thin sample “062d1bc” were dehydrated by heating to 140°C to eliminate interference by hydrogen, and all four samples were tested again.

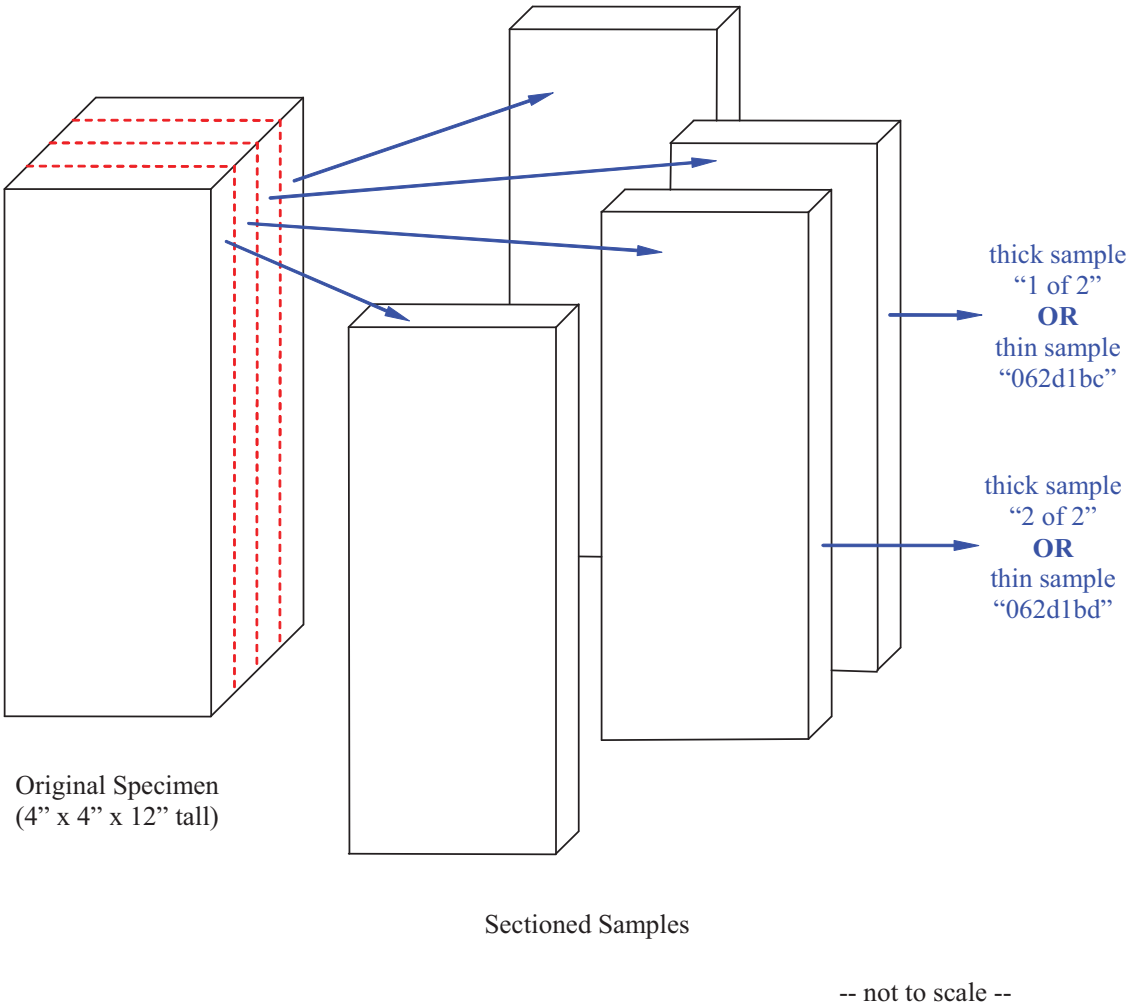

Fig. 6.9.4.2-1. Illustration of sectioning plan for borated ceramic samples for neutron radiography and neutron transmission measurements.

All four samples were qualitatively inspected for visual defects and subjected to neutron radiographic inspection. The inspections were intended to identify any variations in image luminance, which would indicate a variation in homogeneity and density. Neutron transmission measurements were calibrated to results for thin ZrB_2 reference coupons sandwiched with thick aluminum metal. The ^{10}B areal densities of the thin reference coupons ranged from 5.32 mg/cm^2 to 57.04 mg/cm^2 over a total ZrB_2 + Al reference thickness of 24.21–24.98 mm. By comparison, the thick samples contain an idealized ^{10}B areal density of 28.8 mg/cm^2 (i.e., 0.012 g/cm^3 over a 2.4-cm thickness), and the thin samples contain an idealized ^{10}B areal density of 14.4 mg/cm^2 (i.e., 0.012 g/cm^3 over a 1.2-cm thickness).

Radiographic examination of both thick samples "1 of 2" and "2 of 2" indicated uniformity of composition and density (see Fig. 6.9.4.2-2). Even after dehydration of thick sample "1 of 2," radioscopic examination indicated uniformity of composition and density. Initial neutron transmission results for both thick samples "1 of 2" and "2 of 2" indicated that neutron transmission was very low. In fact, the interference due to the hydrogen content implies an equivalent ^{10}B areal density measurement of ~67 ± 4 mg/cm^2. This is more than twice the actual physical value of 28.8 mg/cm^2. Only after thick sample of "1 of 2" is dehydrated and tested again do the results of neutron transmission measurements more accurately reflect the actual physical ^{10}B content. In fact, the average measured value of 27.419 mg/cm^2 at eleven points along the long axis of the dehydrated sample "1 of 2" is more than 95% of the actual physical value of 28.8 mg/cm^2 and varies no more than a few percent from one end to the other (see Tables 6.9.4.2-2 and 6.9.4.2-3).

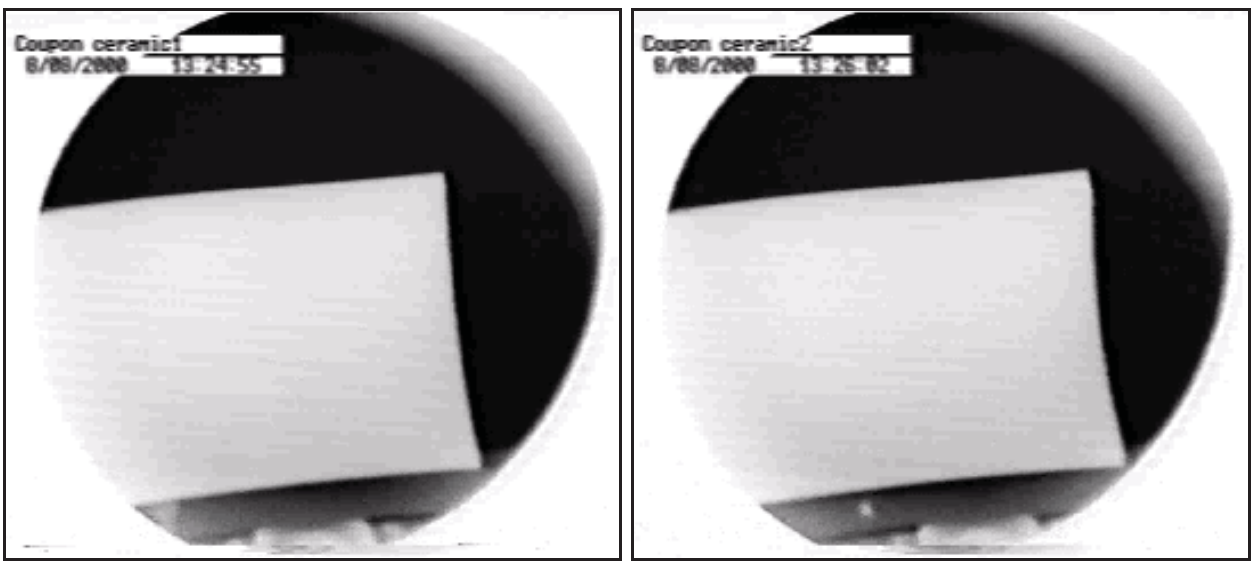

Fig. 6.9.4.2-2. Radiographic images of thick samples "1 of 2" (left) and "2 of 2" (right) indicating uniformity of composition and density.

Table 6.9.4.2-2. Results of neutron transmission measurements of thick samples

	Equivalent ^{10}B Areal Density (mg/cm^2)		
	End	**Center**	**End**
sample "1 of 2"	66.419	68.673	71.003
sample "2 of 2"	65.0	68.25	69.708
sample "1 of 2" (dehydrated)	27.586	27.191	28.555
sample "2 of 2" (re-test)	63.687	65.966	65.572

Table 6.9.4.2-3. Neutron transmission measurements of thick sample "1 of 2" after dehydration

Point of Measurement (uniform intervals from one end to the other)	Equivalent ^{10}B Areal Density (mg/cm^2)	Deviation from Average (%)
1	27.586	+0.6 %
2	26.909	-1.9 %
3	27.039	-1.4 %
4	27.358	-0.2 %
5	27.286	-0.5 %
6	27.191	-0.8 %
7	27.375	-0.2 %
8	27.179	-0.8 %
9	27.236	-0.7 %
10	27.897	-0.9 %
11	28.555	+4.1 %
Average	**27.419**	

Radiographic examination of both thin samples “062d1bc” and “062d1bd” indicates areas of nonuniformity and spots of lower neutron attenuation, along with greater dissimilarity between the samples themselves (see Fig. 6.9.4.2-3). Many of these areas and spots remained evident by radiographic examination even after dehydration of thin sample “062d1bc” and are attributed to physical voids revealed during visual inspection. Again, initial neutron transmission measurements implied a greater-than-actual equivalent ^{10}B areal density due to the interference of hydrogen (i.e., measured values averaged ~23.3 mg $^{10}B/cm^2$ rather than the actual value of 14.4 mg $^{10}B/cm^2$).

Measurements repeated after dehydration of sample “062d1bc” more correctly estimate the equivalent ^{10}B areal density to be ~11.1 mg/cm^2, which is ~77% of the actual physical ^{10}B content. Again, the relative values vary only a few percent from one end of the sample to the other (see Table 6.9.4.2-4). However, the measured values of a dehydrated sample in this case are known to be biased low. First, the total thicknesses of the ZrB_2 + Al reference coupons for calibration were ~24.21 to 24.98-mm compared to the 1.2-cm thickness of “062d1bc.” Second, the total mass density of the sample is ~1.4 to 1.5 g/cm^3 after dehydration compared to an Al mass density of ~2.7 g/cm^3 for the ZrB_2 + Al reference coupons. This indicates that even the performance of the thin samples (i.e., 1.2-cm thickness) exhibiting non-uniformity of composition and density is only marginally reduced from that of the idealized, homogenous material model with respect to neutron absorber efficiency.

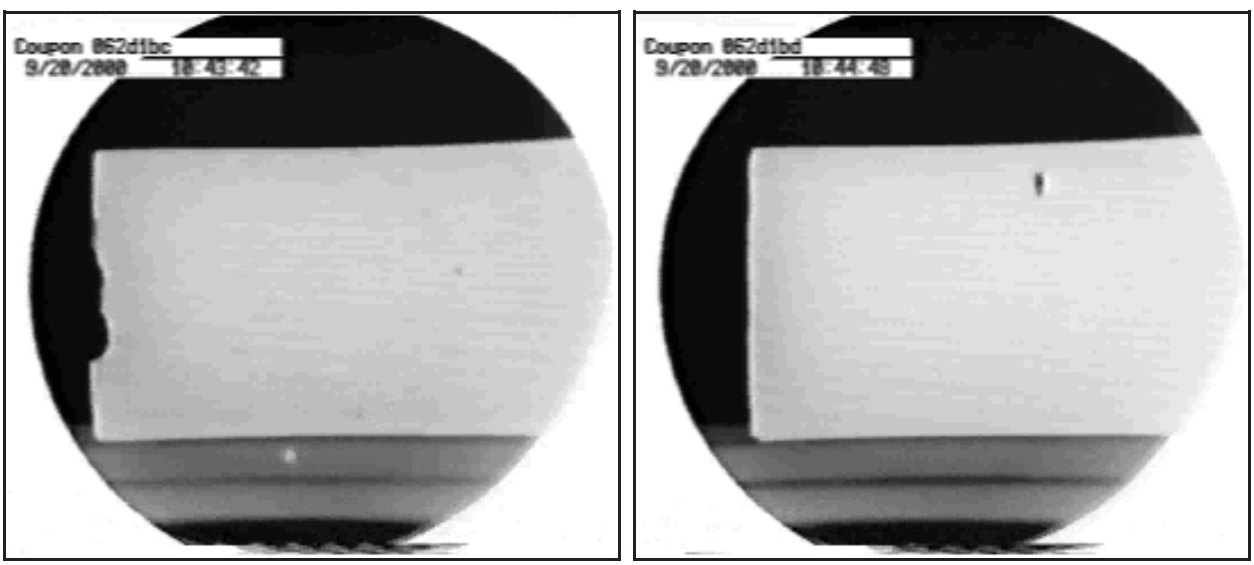

Fig. 6.9.4.2-3. Radiographic images of thin samples “062d1bc” (left) and “062d1bd” (right) indicating non-uniformity of composition and density and dissimilarity of samples.

Table 6.9.4.2-4. Neutron transmission results for dehydrated thin sample "062d1bc" and re-test of thin sample "062d1bd"

Position of Measurement (see Fig. 6.9.4.2-4)	Minimum Equivalent ^{10}B Areal Density (mg/cm^2)			
	Dehydrated Thin Sample "062d1bc"		Re-Test of Thin Sample "062d1bd"	
	Line A	Line B	Line A	Line B
1	12.227	11.781	25.909	25.154
2	11.776	11.462	24.390	25.344
3	11.388	11.252	24.257	24.645
4	10.554	10.462	25.341	24.885
5	10.432	10.528	24.646	25.483
6	10.754	11.728	25.450	25.712
7	10.396	11.534	25.761	23.063
8	11.166	10.221	24.522	25.257
9	10.875	10.459	23.113	23.882
10	11.051	10.676	25.270	23.724
11	11.258	11.214	24.922	25.355
Combined Average	11.1		24.8	

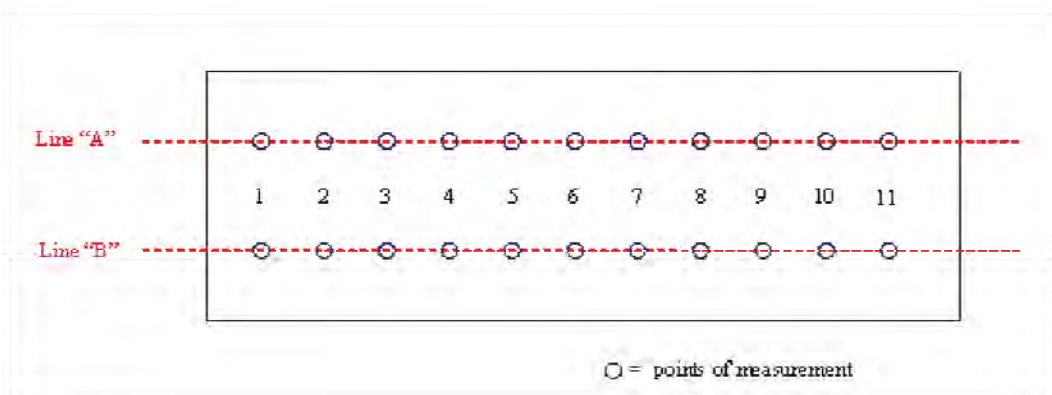

Fig. 6.9.4-6. Illustration of measurement plan for neutron transmission measurements of thin samples "062d1bc" and "062d1bd."

6.9.4.2.3 CONCLUSIONS

Provided that 277-4 is prepared in a controlled manner to ensure the proper specification and proportioning of batch constituents, thorough mixing of the wet slurry, and correct placement and installation to prevent large physical voids, a credible technical justification exists to credit no less than 75% f the $^{nat}B_4C$ particulate and its other constituents, by weight, as an idealized homogenous mixture for nuclear criticality safety analysis of the ES-3100. There is no evidence of non-homogeneity, neutron self-shielding effects, or neutron streaming effects in borated hydraulic cement or ceramic material systems for thicknesses of 2.4-cm or more. The qualification of 277-4 for use in the design and construction of the ES-3100 described herein is based on sound nuclear engineering principles and direct application of performance test results for such material systems.

Appendix 6.9.5

MISCELLANEOUS INFORMATION AND DATA

THIS PAGE INTENTIONALLY LEFT BLANK.

Appendix 6.9.5

MISCELLANEOUS INFORMATION AND DATA

Table 6.9.5.1 provides the atomic weights of the elements and isotopes of the materials used in this criticality safety evaluation. Atomic weights and isotopic weight percents of the naturally occurring materials are those taken from the Materials Information Processor in the SCALE Standard Composition Library.

Table 6.9.5.2 provides the molecular weights and weight percents of the corresponding elements and isotopes of the various compounds. The weight percents shown in this table are the input to KENO V.a. (NUREG/CR-0200, rev. 6)

Table 6.9.5.3 provides equations for determining atomic densities. These equations were derived based on the assumption that all constituents in the mixture are volume additive. Although these equations with their corresponding subscripts are for mixtures of elements, isotopes, or both, all except Equation (2) can be applied to compounds if the user substitutes certain subscript notations and meaning changes. For example, in Equations (1a) and (1b), the atomic weight becomes the molecular weight and the subscript "m" for mixture changes to the subscript "c" for compound. Likewise, in Equations (3a) and (3b), the atomic weight becomes the molecular weight, and the atom fraction (n_i) becomes the stoichiometric proportion of the elements making up the molecule. In Equations (3)–(5), the atom fraction (n_i) becomes the stoichiometric proportion (the element number subscript in the molecular formula), whose sum does not equal unity. Equation (2) is applicable only to the theoretical density of mixtures; it does not apply to the density of compounds.

Table 6.9.5.1. Atomic weights

Element or isotope	Atomic weight
H	1.0078
C	12.0000
O	15.9954
N	14.0033
Na	22.9895
Mg	24.3051
Al	26.9818
Si	28.0853
Ca	40.0803
Ti	47.8789
Cr	51.9957
Mn	54.9380
Fe	55.8447
Ni	58.6868
Zr	91.2196
^{235}U	235.0442
^{238}U	238.0510

Table 6.9.5.2. Molecular weights

Compound	Molecular or atomic weight	Weight percent in compound	Stoichiometric composition
Kaolite 1600™			
Alumina	-	9.6	Al_2O_3
Al	26.9818	52.92507	
O	15.9954	47.07493	
Silica	-	36.7	SiO_2
Si	28.0853	46.74349	
O	15.9954	53.25651	
Ferric Oxide	-	6.7	Fe_2O_3
Fe	55.8447	69.94330	
O	15.9954	30.05670	
Titanium Oxide	-	1.2	TiO_2
Ti	47.8789	59.95084	
O	15.9954	40.04916	
Calcium Oxide	-	30.7	CaO
Ca	40.0803	71.47009	
O	15.9954	28.52991	
Magnesium Oxide	-	13.1	MgO
Mg	24.3051	60.30359	
O	15.9954	39.69641	
Alkalies	-	2.0	Na_2O
Na	22.9895	74.18575	
O	15.9954	25.81425	

Table 6.9.5.3. Useful equations

N_m	=	$\rho_m N_o / A_m$.	(1a)
N_i	=	$w_i \rho_m N_o / A_i$.	(1b)
ρ_m	=	$1/\Sigma w_i/\rho_i$.	(2)
A_m	=	$1/\Sigma w_i/A_i$.	(3a)
	=	$\Sigma n_i A_i$	(3b)
w_i	=	m_i/m_m .	(4a)
	=	$n_i A_i / \Sigma n_i A_i$.	(4b)
n_i	=	N_i/N_m .	(5a)
	=	$(w_i/A_i)/\Sigma(w_i/A_i)$.	(5b)

where

N_o	=	0.602252×10^{24} (atoms/mole) Avogadro's number,
N	=	atom density (atoms/cm^3), $N_m = \Sigma N_i$,
ρ	=	density (g/cm^3) ,
A	=	atomic mass (g-mole) ,
w	=	weight fraction, $\Sigma w_i = 1$,
n	=	atom fraction, $\Sigma n_i = 1$,
subscript "m"	=	of the mixture ,
subscript "i"	=	i^{th} component of the mixture ,
(atoms/cm^3)(1/10^{24})	=	atoms/barn-cm.

Appendix 6.9.6

ABRIDGED SUMMARY TABLES OF CRITICALITY CALCULATION RESULTS

THIS PAGE INTENTIONALLY LEFT BLANK.

Appendix 6.9.6

ABRIDGED SUMMARY TABLES OF CRITICALITY CALCULATION RESULTS

This appendix contains the summary tables for calculation results identified in Sects. 6.4, 6.5, 6.6, and 6.7 of this document. The CV calculation model is a modification of the water-reflected, single-unit package calculation model where the packaging regions external to the containment vessel are replaced with full density water. The index is as follows:

CYLINDER CONTENT

Table 6.9.6-1 Results for the 3.24-in.-diam cylinder HEU content in CV calculation model.

Table 6.9.6-2 Results for the 3.24-in.-diam cylinder HEU content in bare and water reflected package calculation models.

Table 6.9.6-3 Results for the 3.24-in.-diam cylinder HEU content in package calculation models.

Table 6.9.6-3b Results for spacing of 3.24 in.-diameter cylinder HEU metal content in CV calculation model.

Table 6.9.6-3c Results for spacing of 3.24 in.-diameter cylinder HEU metal content in packaging calculation model.

SQUARE BAR CONTENT

Table 6.9.6-4 Results for the 2.29-in square bar HEU content in CV calculation model.

Table 6.9.6-5 Results for the 2.29-in square bar HEU content in packaging calculation model.

CYLINDER CONTENT

Table 6.9.6-6 Results for the 4.25-in.-diam cylinder HEU content in CV calculation model.

Table 6.9.6-7 Results for the 4.25-in.-diam cylinder HEU content in packaging calculation models.

SLUGS CONTENT

Table 6.9.6-8 Results for 1.5-in.-diam × 2.0-in.-tall slug HEU metal content in CV calculation model.

Table 6.9.6-9 Results for the 1.5-in.-diam × 2.0-in.-tall slug HEU metal content in packaging calculation model.

BROKEN METAL CONTENT

Table 6.9.6-10 Results for HEU broken metal content in CV calculation model.

Table 6.9.6-11 Results for HEU broken metal content in packaging calculation model.

Table 6.9.6-11b Comparison of NCT results for HEU broken metal content in ES-3100 NCT packaging calculation models

Table 6.9.6-11c Comparison of HAC results for HEU broken metal content in ES-3100 HAC packaging calculation models

HEU PRODUCT OXIDE CONTENT

Table 6.9.6-12 Results for HEU oxide content in CV calculation model.

Table 6.9.6-13 Results for HEU product oxide content at 6.54 g/cm^3 in single-unit packaging calculation model.

Table 6.9.6-13a Results for HEU oxide content in single-unit packaging calculation model.

Table 6.9.6-13b Results for HEU oxide content in array packaging calculation model.

UNX CRYSTAL CONTENT

Table 6.9.6-14 Results for UNX crystal content in CV calculation model.

Table 6.9.6-15 Results for UNX crystal content in packaging calculation model.

Table 6.9.6-16 Results for leakage of UNX crystal content out of containment vessel.

HEU SKULL OXIDE CONTENT

Table 6.9.6-17 Results for skull oxide (SO) content in CV calculation model.

Table 6.9.6-18a NCT results for SO content in packaging calculation model.

Table 6.9.6-18b HAC results for SO content in packaging calculation model.

UNIRRADIATED TRIGA REACTOR FUEL ELEMENT CONTENT

Table 6.9.6-19a Results for $UZrH_x$ content in CV calculation model.

Table 6.9.6-19b Results for $UZrH_x$ content spacing in CV calculation model.

Table 6.9.6-19c Results for $UZrH_x$ content uranium weight fraction in CV calculation model.

Table 6.9.6-20a Results for $UZrH_x$ content at 19.7 wt % ^{235}U in packaging calculation model.

Table 6.9.6-20b Results for $UZrH_x$ content at 70.1 wt % ^{235}U in packaging calculation model.

Table 6.9.6-20c Results for 1.31 in. Smaller diameter $UZrH_x$ at 70.1 wt % ^{235}U content in packaging calculation model.

Table 6.9.6-20d Results for 1.31 in. smaller diameter $UZrH_x$ at 19.7 wt % ^{235}U content in packaging calculation model.

AIR TRANSPORT CONTENT

Table 6.9.6-21 Results for solid HEU metal content for air transportation.

Table 6.9.6-22a Results for TRIGA ($UZrH_x$) fuel element content at 19.7 wt % ^{235}U for air transportation.

Table 6.9.6-22b Results for TRIGA ($UZrH_x$) fuel element content at 70.1 wt % ^{235}U for air transportation.

Table 6.9.6-23 Results for HEU broken metal content for air transport.

THIS PAGE INTENTIONALLY LEFT BLANK.

Table 6.9.6-1. Results for 3.24 in.-diameter cylinder HEU metal content in CV calculation model

case name	np (in.)	U (g)	^{235}U (g)	H_2O (g)	h/x	mocfr	k_{eff}	σ	$k_{eff}+2σ$				
flooded containment vessel, reflected													
no can spacers (np thickness = 0.0 in.)													
cvcrcyt11_36_1_1	0.0	36000	36000	0	0.00	1.0e-20	0.90460	0.00107	0.90673				
cvcrcyt11_36_1_6	0.0	36000	36000	829	0.60	1.0e-01	0.90726	0.00124	0.90973				
cvcrcyt11_36_1_7	0.0	36000	36000	1657	1.20	2.0e-01	0.91182	0.00120	0.91422				
cvcrcyt11_36_1_8	0.0	36000	36000	2486	1.80	3.0e-01	0.91690	0.00139	0.91967				
cvcrcyt11_36_1_9	0.0	36000	36000	3315	2.40	4.0e-01	0.92263	0.00119	0.92500				
cvcrcyt11_36_1_10	0.0	36000	36000	4143	3.00	5.0e-01	0.92840	0.00115	0.93071				
cvcrcyt11_36_1_11	0.0	36000	36000	4972	3.60	6.0e-01	0.93827	0.00112	0.94050				
cvcrcyt11_36_1_12	0.0	36000	36000	5801	4.21	7.0e-01	0.94633	0.00127	0.94886				
cvcrcyt11_36_1_13	0.0	36000	36000	6629	4.81	8.0e-01	0.95397	0.00120	0.95636				
cvcrcyt11_36_1_14	0.0	36000	36000	7458	5.41	9.0e-01	0.96276	0.00137	0.96551				
cvcrcyt11_36_1_15	0.0	36000	36000	8287	6.01	1.0e+00	0.97121	0.00125	0.97371				
cvcrcyt11_36_1	0.0	36000	36000	8287	6.01	1.0e+00	0.97121	0.00125	0.97371				
cvcrcyt11_35_1	0.0	35000	35000	8340	6.22	1.0e+00	0.96937	0.00120	0.97177				
cvcrcyt11_34_1	0.0	34000	34000	8393	6.44	1.0e+00	0.96886	0.00120	0.97126				
cvcrcyt11_33_1	0.0	33000	33000	8446	6.68	1.0e+00	0.96531	0.00111	0.96754				
cvcrcyt11_32_1	0.0	32000	32000	8499	6.93	1.0e+00	0.96360	0.00120	0.96600				
cvcrcyt11_31_1	0.0	31000	31000	8552	7.20	1.0e+00	0.95960	0.00122	0.96205				
cvcrcyt11_30_1	0.0	30000	30000	8605	7.49	1.0e+00	0.95842	0.00128	0.96097				
cvcrcyt11_29_1	0.0	29000	29000	8658	7.79	1.0e+00	0.95488	0.00115	0.95717				
cvcrcyt11_28_1	0.0	28000	28000	8711	8.12	1.0e+00	0.95409	0.00118	0.95645				
cvcrcyt11_27_1	0.0	27000	27000	8764	8.47	1.0e+00	0.94797	0.00113	0.95023				
cvcrcyt11_26_1	0.0	26000	26000	8817	8.85	1.0e+00	0.94376	0.00124	0.94623				

Table 6.9.6-1. Results for 3.24 in.-diameter cylinder HEU metal content in CV calculation model

case name	np (in.)	U (g)	^{235}U (g)	H_2O (g)	h/x	mocfr	k_{eff}	σ	$k_{eff}+2σ$				
cvcrcyt11_25_1	0.0	25000	25000	8870	9.26	1.0e+00	0.94075	0.00141	0.94357				
cvcrcyt11_24_1	0.0	24000	24000	8923	9.70	1.0e+00	0.93510	0.00133	0.93776				
cvcrcyt11_23_1	0.0	23000	23000	8977	10.19	1.0e+00	0.93038	0.00130	0.93298				
cvcrcyt11_22_1	0.0	22000	22000	9030	10.71	1.0e+00	0.92658	0.00106	0.92870				
cvcrcyt11_21_1	0.0	21000	21000	9083	11.29	1.0e+00	0.92046	0.00118	0.92282				
cvcrcyt11_20_1	0.0	20000	20000	9136	11.92	1.0e+00	0.91168	0.00125	0.91418				
cvcrcyt11_19_1	0.0	19000	19000	9189	12.62	1.0e+00	0.90618	0.00128	0.90874				
cvcrcyt11_18_1	0.0	18000	18000	9242	13.40	1.0e+00	0.89978	0.00124	0.90226				
with can spacers (np thickness=1.4 in.)													
cvcrcyt11_36_2_1	1.4	36000	36000	0	0.00	1.0e-20	0.83041	0.00103	0.83248				
cvcrcyt11_36_2_6	1.4	36000	36000	767	0.56	1.0e-01	0.82885	0.00106	0.83096				
cvcrcyt11_36_2_7	1.4	36000	36000	1535	1.11	2.0e-01	0.83022	0.00104	0.83230				
cvcrcyt11_36_2_8	1.4	36000	36000	2302	1.67	3.0e-01	0.83492	0.00104	0.83699				
cvcrcyt11_36_2_9	1.4	36000	36000	3069	2.23	4.0e-01	0.84066	0.00123	0.84311				
cvcrcyt11_36_2_10	1.4	36000	36000	3837	2.78	5.0e-01	0.84789	0.00102	0.84993				
cvcrcyt11_36_2_11	1.4	36000	36000	4604	3.34	6.0e-01	0.85423	0.00101	0.85624				
cvcrcyt11_36_2_12	1.4	36000	36000	5371	3.89	7.0e-01	0.86190	0.00106	0.86403				
cvcrcyt11_36_2_13	1.4	36000	36000	6139	4.45	8.0e-01	0.86687	0.00118	0.86923				
cvcrcyt11_36_2_14	1.4	36000	36000	6906	5.01	9.0e-01	0.87589	0.00113	0.87816				
cvcrcyt11_36_2_15	1.4	36000	36000	7673	5.56	1.0e+00	0.88436	0.00111	0.88657				
cvcrcyt11_36_2	1.4	36000	36000	7673	5.56	1.0e+00	0.88436	0.00111	0.88657				
cvcrcyt11_35_2	1.4	35000	35000	7726	5.76	1.0e+00	0.88274	0.00108	0.88491				
cvcrcyt11_34_2	1.4	34000	34000	7779	5.97	1.0e+00	0.87740	0.00119	0.87977				
cvcrcyt11_33_2	1.4	33000	33000	7832	6.19	1.0e+00	0.87234	0.00112	0.87459				

Table 6.9.6-1. Results for 3.24 in.-diameter cylinder HEU metal content in CV calculation model

case name	np (in.)	U (g)	^{235}U (g)	H_2O (g)	h/x	mocfr	k_{eff}	σ	$k_{eff}+2σ$				
cvcrcyt11_32_2	1.4	32000	32000	7885	6.43	1.0e+00	0.86817	0.00108	0.87033				
cvcrcyt11_31_2	1.4	31000	31000	7938	6.68	1.0e+00	0.86047	0.00124	0.86295				
cvcrcyt11_30_2	1.4	30000	30000	7992	6.95	1.0e+00	0.85525	0.00117	0.85760				
flooded containment vessel, reflected, no can spacers (np thickness = 0.0 in.)													
no polyethylene													
cvcrcyt11_21_1	0.0	21000	21000	9083	11.29	1.0e+00	0.92046	0.00118	0.92282				
500 g polyethylene													
cvcrpcyt11_21_1	0.0	21000	21000	8540	11.41	1.0e+00	0.90599	0.00107	0.90814				
dry containment vessel, reflected, no can spacers (np thickness = 0.0 in.)													
500 g polyethylene													
cvdcrpcyt11_21_1	0.0	21000	21000	0.0	0.80	1.0e+00	0.84505	0.00105	0.84716				

Table 6.9.6-2. Results for 3.24 in.-diameter cylinder HEU metal content in bare and water reflected packaging calculation models

case name	U (g)	^{235}U (g)	H_2O (g)	h/x	moifr	nlf	k_{eff}	σ	$k_{eff}+2σ$	case name	nlf	k_{eff}	σ	$k_{eff}+2σ$
content in flooded CV, single package bare										**content in flooded CV, single package reflected**				
no can spacers (np thickness = 0.0 in.)										**no can spacers (np thickness = 0.0 in.)**				
ncsbcyt11_36_1_1	36000	36000	8287	6.01	1.0e-20	0.4744	0.90856	0.00115	0.91087	ncsrcyt11_36_1_1	0.0021	0.91542	0.00120	0.91782
ncsbcyt11_36_1_2	36000	36000	8287	6.01	1.0e-05	0.4749	0.90825	0.00100	0.91026	ncsrcyt11_36_1_2	0.0021	0.91477	0.00123	0.91724
ncsbcyt11_36_1_3	36000	36000	8287	6.01	1.0e-04	0.4747	0.90817	0.00121	0.91059	ncsrcyt11_36_1_3	0.0022	0.91550	0.00111	0.91772
ncsbcyt11_36_1_4	36000	36000	8287	6.01	1.0e-03	0.4744	0.90926	0.00134	0.91194	ncsrcyt11_36_1_4	0.0022	0.91636	0.00117	0.91869
ncsbcyt11_36_1_5	36000	36000	8287	6.01	1.0e-02	0.4730	0.90883	0.00108	0.91100	ncsrcyt11_36_1_5	0.0022	0.91537	0.00109	0.91755
ncsbcyt11_36_1_6	36000	36000	8287	6.01	1.0e-01	0.4510	0.91550	0.00112	0.91774	ncsrcyt11_36_1_6	0.0019	0.92121	0.00133	0.92386
ncsbcyt11_36_1_8	36000	36000	8287	6.01	3.0e-01	0.3899	0.92546	0.00134	0.92814	ncsrcyt11_36_1_8	0.0016	0.92807	0.00112	0.93032

Table 6.9.6-2. Results for 3.24 in.-diameter cylinder HEU metal content in bare and water reflected packaging calculation models

case name	U (g)	^{235}U (g)	H_2O (g)	h/x	moifr	nlf	k_{eff}	σ	$k_{eff}+2σ$	case name	nlf	k_{eff}	σ	$k_{eff}+2σ$
ncsbcyt11_36_1_15	36000	36000	8287	6.01	1.0e+00	0.1823	0.95215	0.00119	0.95454	ncsrcyt11_36_1_15	0.0007	0.95213	0.00129	0.95472
ncsbcyt11_36_1_15	36000	36000	8287	6.01	1.0e+00	0.1823	0.95215	0.00119	0.95454	ncsrcyt11_36_1_15	0.0007	0.95213	0.00129	0.95472
ncsbcyt11_35_1_15	35000	35000	8340	6.22	1.0e+00	0.1838	0.94834	0.00122	0.95077	ncsrcyt11_35_1_15	0.0008	0.94870	0.00107	0.95083
ncsbcyt11_34_1_15	34000	34000	8393	6.44	1.0e+00	0.1842	0.94748	0.00113	0.94975	ncsrcyt11_34_1_15	0.0008	0.94742	0.00124	0.94990
ncsbcyt11_33_1_15	33000	33000	8446	6.68	1.0e+00	0.1853	0.94613	0.00118	0.94850	ncsrcyt11_33_1_15	0.0008	0.94478	0.00119	0.94716
ncsbcyt11_32_1_15	32000	32000	8499	6.93	1.0e+00	0.1863	0.94237	0.00106	0.94448	ncsrcyt11_32_1_15	0.0007	0.94247	0.00111	0.94468
ncsbcyt11_31_1_15	31000	31000	8552	7.20	1.0e+00	0.1867	0.94052	0.00106	0.94264	ncsrcyt11_31_1_15	0.0008	0.94091	0.00107	0.94306
ncsbcyt11_30_1_15	30000	30000	8605	7.49	1.0e+00	0.1882	0.93819	0.00110	0.94039	ncsrcyt11_30_1_15	0.0007	0.94139	0.00137	0.94412
ncsbcyt11_29_1_15	29000	29000	8658	7.79	1.0e+00	0.1894	0.93483	0.00104	0.93692	ncsrcyt11_29_1_15	0.0007	0.93406	0.00108	0.93622
ncsbcyt11_28_1_15	28000	28000	8711	8.12	1.0e+00	0.1894	0.93339	0.00102	0.93543	ncsrcyt11_28_1_15	0.0008	0.93012	0.00124	0.93261
ncsbcyt11_27_1_15	27000	27000	8764	8.47	1.0e+00	0.1911	0.92636	0.00112	0.92860	ncsrcyt11_27_1_15	0.0008	0.92820	0.00122	0.93064
ncsbcyt11_26_1_15	26000	26000	8817	8.85	1.0e+00	0.1919	0.92366	0.00115	0.92597	ncsrcyt11_26_1_15	0.0008	0.92396	0.00141	0.92679
ncsbcyt11_25_1_15	25000	25000	8870	9.26	1.0e+00	0.1928	0.92122	0.00122	0.92366	ncsrcyt11_25_1_15	0.0008	0.91761	0.00102	0.91966
ncsbcyt11_24_1_15	24000	24000	8923	9.70	1.0e+00	0.1948	0.91432	0.00108	0.91648	ncsrcyt11_24_1_15	0.0008	0.91466	0.00107	0.91680
ncsbcyt11_23_1_15	23000	23000	8977	10.19	1.0e+00	0.1965	0.91055	0.00130	0.91314	ncsrcyt11_23_1_15	0.0008	0.91172	0.00116	0.91403
ncsbcyt11_22_1_15	22000	22000	9030	10.71	1.0e+00	0.1969	0.90695	0.00121	0.90936	ncsrcyt11_22_1_15	0.0008	0.90680	0.00153	0.90986
ncsbcyt11_21_1_15	21000	21000	9083	11.29	1.0e+00	0.1984	0.90241	0.00124	0.90490	ncsrcyt11_21_1_15	0.0009	0.90125	0.00113	0.90352
ncsbcyt11_20_1_15	20000	20000	9136	11.92	1.0e+00	0.2007	0.89477	0.00125	0.89726	ncsrcyt11_20_1_15	0.0009	0.89481	0.00109	0.89698
ncsbcyt11_19_1_15	19000	19000	9189	12.62	1.0e+00	0.2026	0.88819	0.00113	0.89044	ncsrcyt11_19_1_15	0.0008	0.88857	0.00136	0.89129
ncsbcyt11_18_1_15	18000	18000	9242	13.40	1.0e+00	0.2037	0.88255	0.00126	0.88507	ncsrcyt11_18_1_15	0.0008	0.88157	0.00127	0.88410
with can spacers (np thickness = 1.4 in.)										**with can spacers (np thickness = 1.4 in.)**				
ncsbcyt11_36_2_1	36000	36000	7673	5.56	1.0e-20	0.4882	0.83390	0.00106	0.83603	ncsrcyt11_36_2_1	0.0022	0.83904	0.00110	0.84125
ncsbcyt11_36_2_2	36000	36000	7673	5.56	1.0e-05	0.4879	0.83481	0.00142	0.83764	ncsrcyt11_36_2_2	0.0021	0.84122	0.00110	0.84342
ncsbcyt11_36_2_3	36000	36000	7673	5.56	1.0e-04	0.4883	0.83383	0.00100	0.83583	ncsrcyt11_36_2_3	0.0022	0.84013	0.00106	0.84225

Table 6.9.6-2. Results for 3.24 in.-diameter cylinder HEU metal content in bare and water reflected packaging calculation models

case name	U (g)	^{235}U (g)	H_2O (g)	h/x	moifr	nlf	k_{eff}	σ	$k_{eff}+2σ$	case name	nlf	k_{eff}	σ	$k_{eff}+2σ$
ncsbcyt11_36_2_4	36000	36000	7673	5.56	1.0e-03	0.4880	0.83530	0.00126	0.83783	ncsrcyt11_36_2_4	0.0022	0.84001	0.00112	0.84224
ncsbcyt11_36_2_5	36000	36000	7673	5.56	1.0e-02	0.4861	0.83461	0.00120	0.83702	ncsrcyt11_36_2_5	0.0021	0.84128	0.00115	0.84359
ncsbcyt11_36_2_6	36000	36000	7673	5.56	1.0e-01	0.4642	0.83979	0.00110	0.84199	ncsrcyt11_36_2_6	0.0020	0.84524	0.00116	0.84755
ncsbcyt11_36_2_8	36000	36000	7673	5.56	3.0e-01	0.4000	0.84736	0.00123	0.84982	ncsrcyt11_36_2_8	0.0016	0.84947	0.00103	0.85153
ncsbcyt11_36_2_15	36000	36000	7673	5.56	1.0e+00	0.1881	0.87048	0.00109	0.87266	ncsrcyt11_36_2_15	0.0008	0.87062	0.00122	0.87305
ncsbcyt11_36_2_15	36000	36000	7673	5.56	1.0e+00	0.1881	0.87048	0.00109	0.87266	ncsrcyt11_36_2_15	0.0008	0.87062	0.00122	0.87305
ncsbcyt11_35_2_15	35000	35000	7726	5.76	1.0e+00	0.1879	0.86609	0.00114	0.86836	ncsrcyt11_35_2_15	0.0007	0.86649	0.00118	0.86886
ncsbcyt11_34_2_15	34000	34000	7779	5.97	1.0e+00	0.1885	0.86151	0.00103	0.86358	ncsrcyt11_34_2_15	0.0008	0.86038	0.00129	0.86296
ncsbcyt11_33_2_15	33000	33000	7832	6.19	1.0e+00	0.1901	0.85729	0.00099	0.85927	ncsrcyt11_33_2_15	0.0007	0.85903	0.00106	0.86115
ncsbcyt11_32_2_15	32000	32000	7885	6.43	1.0e+00	0.1908	0.85350	0.00116	0.85582	ncsrcyt11_32_2_15	0.0007	0.85357	0.00108	0.85573
ncsbcyt11_31_2_15	31000	31000	7938	6.68	1.0e+00	0.1922	0.84914	0.00108	0.85129	ncsrcyt11_31_2_15	0.0008	0.84895	0.00123	0.85142
ncsbcyt11_30_2_15	30000	30000	7992	6.95	1.0e+00	0.1913	0.84250	0.00100	0.84450	ncsrcyt11_30_2_15	0.0008	0.84343	0.00114	0.84572

Table 6.9.6-3. Results for 3.24 in.-diameter cylinder HEU metal content in packaging calculation model

case name	np (in)	U (g)	^{235}U (g)	H_2O (g)	h/x	moifr	k_{eff}	σ	$k_{eff}+2σ$	case name	k_{eff}	σ	$k_{eff}+2σ$
content in flooded containment vessel, single package reflected													
NCT										HAC			
no can spacers (np thickness = 0.0 in.)													
ncsrcyt11_36_1_1	0.0	36000	36000	8287	6.01	1.0e-20	0.91542	0.00120	0.91782	hcsrcyt12_36_1_1	0.91636	0.00117	0.91869
ncsrcyt11_36_1_2	0.0	36000	36000	8287	6.01	1.0e-05	0.91477	0.00123	0.91724	hcsrcyt12_36_1_2	0.91593	0.00138	0.91869
ncsrcyt11_36_1_3	0.0	36000	36000	8287	6.01	1.0e-04	0.91550	0.00111	0.91772	hcsrcyt12_36_1_3	0.91660	0.00134	0.91929
ncsrcyt11_36_1_4	0.0	36000	36000	8287	6.01	1.0e-03	0.91636	0.00117	0.91869	hcsrcyt12_36_1_4	0.91565	0.00122	0.91810

Table 6.9.6-3. Results for 3.24 in.-diameter cylinder HEU metal content in packaging calculation model

case name	np (in)	U (g)	^{235}U (g)	H_2O (g)	h/x	moifr	k_{eff}	σ	$k_{eff}+2σ$	case name	k_{eff}	σ	$k_{eff}+2σ$
ncsrcyt11_36_1_5	0.0	36000	36000	8287	6.01	1.0e-02	0.91537	0.00109	0.91755	hcsrcyt12_36_1_5	0.91489	0.00120	0.91729
ncsrcyt11_36_1_6	0.0	36000	36000	8287	6.01	1.0e-01	0.92121	0.00133	0.92386	hcsrcyt12_36_1_6	0.92198	0.00104	0.92407
ncsrcyt11_36_1_8	0.0	36000	36000	8287	6.01	3.0e-01	0.92807	0.00112	0.93032	hcsrcyt12_36_1_8	0.92950	0.00125	0.93201
ncsrcyt11_36_1_15	0.0	36000	36000	8287	6.01	1.0e+00	0.95213	0.00129	0.95472	hcsrcyt12_36_1_15	0.95112	0.00120	0.95353
ncsrcyt11_36_1_15	0.0	36000	36000	8287	6.01	1.0e+00	0.95213	0.00129	0.95472	hcsrcyt12_36_1_15	0.95112	0.00120	0.95353
ncsrcyt11_35_1_15	0.0	35000	35000	8340	6.22	1.0e+00	0.94870	0.00107	0.95083	hcsrcyt12_35_1_15	0.94915	0.00120	0.95155
ncsrcyt11_34_1_15	0.0	34000	34000	8393	6.44	1.0e+00	0.94742	0.00124	0.94990	hcsrcyt12_34_1_15	0.94863	0.00113	0.95088
ncsrcyt11_33_1_15	0.0	33000	33000	8446	6.68	1.0e+00	0.94478	0.00119	0.94716	hcsrcyt12_33_1_15	0.94610	0.00123	0.94856
ncsrcyt11_32_1_15	0.0	32000	32000	8499	6.93	1.0e+00	0.94247	0.00111	0.94468	hcsrcyt12_32_1_15	0.94528	0.00141	0.94810
ncsrcyt11_31_1_15	0.0	31000	31000	8552	7.20	1.0e+00	0.94091	0.00107	0.94306	hcsrcyt12_31_1_15	0.94090	0.00107	0.94304
ncsrcyt11_30_1_15	0.0	30000	30000	8605	7.49	1.0e+00	0.94139	0.00137	0.94412	hcsrcyt12_30_1_15	0.94035	0.00120	0.94275
ncsrcyt11_29_1_15	0.0	29000	29000	8658	7.79	1.0e+00	0.93406	0.00108	0.93622	hcsrcyt12_29_1_15	0.93540	0.00112	0.93765
ncsrcyt11_28_1_15	0.0	28000	28000	8711	8.12	1.0e+00	0.93012	0.00124	0.93261	hcsrcyt12_28_1_15	0.93239	0.00118	0.93475
ncsrcyt11_27_1_15	0.0	27000	27000	8764	8.47	1.0e+00	0.92820	0.00122	0.93064	hcsrcyt12_27_1_15	0.93043	0.00144	0.93331
ncsrcyt11_26_1_15	0.0	26000	26000	8817	8.85	1.0e+00	0.92396	0.00141	0.92679	hcsrcyt12_26_1_15	0.92632	0.00119	0.92870
ncsrcyt11_25_1_15	0.0	25000	25000	8870	9.26	1.0e+00	0.91761	0.00102	0.91966	hcsrcyt12_25_1_15	0.92218	0.00109	0.92436
ncsrcyt11_24_1_15	0.0	24000	24000	8923	9.70	1.0e+00	0.91466	0.00107	0.91680	hcsrcyt12_24_1_15	0.91688	0.00117	0.91922
ncsrcyt11_23_1_15	0.0	23000	23000	8977	10.19	1.0e+00	0.91172	0.00116	0.91403	hcsrcyt12_23_1_15	0.91134	0.00119	0.91371
ncsrcyt11_22_1_15	0.0	22000	22000	9030	10.71	1.0e+00	0.90680	0.00153	0.90986	hcsrcyt12_22_1_15	0.90850	0.00113	0.91077
ncsrcyt11_21_1_15	0.0	21000	21000	9083	11.29	1.0e+00	0.90125	0.00113	0.90352	hcsrcyt12_21_1_15	0.90188	0.00124	0.90437
ncsrcyt11_20_1_15	0.0	20000	20000	9136	11.92	1.0e+00	0.89481	0.00109	0.89698	hcsrcyt12_20_1_15	0.89612	0.00115	0.89842
ncsrcyt11_19_1_15	0.0	19000	19000	9189	12.62	1.0e+00	0.88857	0.00136	0.89129	hcsrcyt12_19_1_15	0.89080	0.00122	0.89323
ncsrcyt11_18_1_15	0.0	18000	18000	9242	13.40	1.0e+00	0.88157	0.00127	0.88410	hcsrcyt12_18_1_15	0.88276	0.00128	0.88532

Table 6.9.6-3. Results for 3.24 in.-diameter cylinder HEU metal content in packaging calculation model

case name	np (in)	U (g)	^{235}U (g)	H_2O (g)	h/x	moifr	k_{eff}	σ	$k_{eff}+2σ$	case name	k_{eff}	σ	$k_{eff}+2σ$
with can spacers (np thickness = 1.4 in.)													
ncsrcyt11_36_2_1	1.4	36000	36000	7673	5.56	1.0e-20	0.83904	0.00110	0.84125	hcsrcyt12_36_2_1	0.84250	0.00103	0.84456
ncsrcyt11_36_2_2	1.4	36000	36000	7673	5.56	1.0e-05	0.84122	0.00110	0.84342	hcsrcyt12_36_2_2	0.84146	0.00118	0.84382
ncsrcyt11_36_2_3	1.4	36000	36000	7673	5.56	1.0e-04	0.84013	0.00106	0.84225	hcsrcyt12_36_2_3	0.84182	0.00105	0.84392
ncsrcyt11_36_2_4	1.4	36000	36000	7673	5.56	1.0e-03	0.84001	0.00112	0.84224	hcsrcyt12_36_2_4	0.83975	0.00103	0.84181
ncsrcyt11_36_2_5	1.4	36000	36000	7673	5.56	1.0e-02	0.84128	0.00115	0.84359	hcsrcyt12_36_2_5	0.84070	0.00129	0.84328
ncsrcyt11_36_2_6	1.4	36000	36000	7673	5.56	1.0e-01	0.84524	0.00116	0.84755	hcsrcyt12_36_2_6	0.84484	0.00127	0.84738
ncsrcyt11_36_2_8	1.4	36000	36000	7673	5.56	3.0e-01	0.84947	0.00103	0.85153	hcsrcyt12_36_2_8	0.85159	0.00102	0.85364
ncsrcyt11_36_2_15	1.4	36000	36000	7673	5.56	1.0e+00	0.87062	0.00122	0.87305	hcsrcyt12_36_2_15	0.87110	0.00117	0.87344
ncsrcyt11_36_2_15	1.4	36000	36000	7673	5.56	1.0e+00	0.87062	0.00122	0.87305	hcsrcyt12_36_2_15	0.87110	0.00117	0.87344
ncsrcyt11_35_2_15	1.4	35000	35000	7726	5.76	1.0e+00	0.86649	0.00118	0.86886	hcsrcyt12_35_2_15	0.86666	0.00110	0.86886
ncsrcyt11_34_2_15	1.4	34000	34000	7779	5.97	1.0e+00	0.86038	0.00129	0.86296	hcsrcyt12_34_2_15	0.86109	0.00117	0.86343
ncsrcyt11_33_2_15	1.4	33000	33000	7832	6.19	1.0e+00	0.85903	0.00106	0.86115	hcsrcyt12_33_2_15	0.86022	0.00123	0.86267
ncsrcyt11_32_2_15	1.4	32000	32000	7885	6.43	1.0e+00	0.85357	0.00108	0.85573	hcsrcyt12_32_2_15	0.85544	0.00096	0.85736
ncsrcyt11_31_2_15	1.4	31000	31000	7938	6.68	1.0e+00	0.84895	0.00123	0.85142	hcsrcyt12_31_2_15	0.84745	0.00105	0.84956
ncsrcyt11_30_2_15	1.4	30000	30000	7992	6.95	1.0e+00	0.84343	0.00114	0.84572	hcsrcyt12_30_2_15	0.84390	0.00112	0.84615
content in flooded containment vessel, array packaging model for CSI=0.0													
NCT										**HAC**			
no can spacers (np thickness = 0.0 in.)													
nciacyt11_36_1_1	0.0	36000	36000	8287	6.01	1.0e-20	1.02410	0.00125	1.02660	hciacyt12_36_1_1	1.02427	0.00120	1.02667
nciacyt11_36_1_2	0.0	36000	36000	8287	6.01	1.0e-05	1.02380	0.00124	1.02628	hciacyt12_36_1_2	1.02384	0.00130	1.02644
nciacyt11_36_1_3	0.0	36000	36000	8287	6.01	1.0e-04	1.02208	0.00111	1.02430	hciacyt12_36_1_3	1.02390	0.00135	1.02660
nciacyt11_36_1_4	0.0	36000	36000	8287	6.01	1.0e-03	1.02276	0.00134	1.02545	hciacyt12_36_1_4	1.02441	0.00122	1.02684
nciacyt11_36_1_5	0.0	36000	36000	8287	6.01	1.0e-02	1.01749	0.00124	1.01997	hciacyt12_36_1_5	1.01867	0.00114	1.02094

Table 6.9.6-3. Results for 3.24 in.-diameter cylinder HEU metal content in packaging calculation model

case name	np (in)	U (g)	^{235}U (g)	H_2O (g)	h/x	moifr	k_{eff}	σ	$k_{eff}+2σ$	case name	k_{eff}	σ	$k_{eff}+2σ$
nciacyt11_36_1_6	0.0	36000	36000	8287	6.01	1.0e-01	0.98560	0.00118	0.98797	hciacyt12_36_1_6	0.98825	0.00112	0.99048
nciacyt11_36_1_8	0.0	36000	36000	8287	6.01	3.0e-01	0.96228	0.00116	0.96461	hciacyt12_36_1_8	0.96519	0.00122	0.96763
nciacyt11_36_1_15	0.0	36000	36000	8287	6.01	1.0e+00	0.96088	0.00119	0.96326	hciacyt12_36_1_15	0.96417	0.00119	0.96655
nciacyt11_36_1_3	0.0	36000	36000	8287	6.01	1.0e-04	1.02208	0.00111	1.02430	hciacyt12_36_1_3	1.02390	0.00135	1.02660
nciacyt11_35_1_3	0.0	35000	35000	8340	6.22	1.0e-04	1.01930	0.00118	1.02166	hciacyt12_35_1_3	1.01912	0.00127	1.02165
nciacyt11_34_1_3	0.0	34000	34000	8393	6.44	1.0e-04	1.01654	0.00130	1.01914	hciacyt12_34_1_3	1.01860	0.00104	1.02068
nciacyt11_33_1_3	0.0	33000	33000	8446	6.68	1.0e-04	1.01121	0.00116	1.01353	hciacyt12_33_1_3	1.01077	0.00142	1.01361
nciacyt11_32_1_3	0.0	32000	32000	8499	6.93	1.0e-04	1.00876	0.00134	1.01144	hciacyt12_32_1_3	1.00943	0.00114	1.01171
nciacyt11_31_1_3	0.0	31000	31000	8552	7.20	1.0e-04	1.00544	0.00116	1.00777	hciacyt12_31_1_3	1.00148	0.00102	1.00353
nciacyt11_30_1_3	0.0	30000	30000	8605	7.49	1.0e-04	0.99921	0.00131	1.00182	hciacyt12_30_1_3	0.99963	0.00138	1.00238
nciacyt11_29_1_3	0.0	29000	29000	8658	7.79	1.0e-04	0.99494	0.00121	0.99736	hciacyt12_29_1_3	0.99453	0.00117	0.99687
nciacyt11_28_1_3	0.0	28000	28000	8711	8.12	1.0e-04	0.98905	0.00124	0.99152	hciacyt12_28_1_3	0.99159	0.00123	0.99405
nciacyt11_27_1_3	0.0	27000	27000	8764	8.47	1.0e-04	0.98520	0.00115	0.98750	hciacyt12_27_1_3	0.98720	0.00122	0.98963
nciacyt11_26_1_3	0.0	26000	26000	8817	8.85	1.0e-04	0.97887	0.00117	0.98120	hciacyt12_26_1_3	0.97870	0.00130	0.98129
nciacyt11_25_1_3	0.0	25000	25000	8870	9.26	1.0e-04	0.97441	0.00118	0.97676	hciacyt12_25_1_3	0.97501	0.00106	0.97713
nciacyt11_24_1_3	0.0	24000	24000	8923	9.70	1.0e-04	0.96997	0.00115	0.97228	hciacyt12_24_1_3	0.96945	0.00122	0.97188
nciacyt11_23_1_3	0.0	23000	23000	8977	10.19	1.0e-04	0.96203	0.00122	0.96447	hciacyt12_23_1_3	0.96228	0.00121	0.96469
nciacyt11_22_1_3	0.0	22000	22000	9030	10.71	1.0e-04	0.95256	0.00110	0.95475	hciacyt12_22_1_3	0.95313	0.00138	0.95589
nciacyt11_21_1_3	0.0	21000	21000	9083	11.29	1.0e-04	0.94755	0.00114	0.94982	hciacyt12_21_1_3	0.94735	0.00121	0.94976
nciacyt11_20_1_3	0.0	20000	20000	9136	11.92	1.0e-04	0.93967	0.00124	0.94215	hciacyt12_20_1_3	0.94131	0.00113	0.94357
nciacyt11_19_1_3	0.0	19000	19000	9189	12.62	1.0e-04	0.93107	0.00113	0.93334	hciacyt12_19_1_3	0.92967	0.00120	0.93207
nciacyt11_18_1_3	0.0	18000	18000	9242	13.40	1.0e-04	0.92165	0.00100	0.92366	hciacyt12_18_1_3	0.92083	0.00110	0.92302
nciacyt11_15_1_3	0.0	15000	15000	9401	16.36	1.0e-04	0.88925	0.00111	0.89146	hciacyt12_15_1_3	0.88802	0.00116	0.89034
nciacyt11_12_1_3	0.0	12000	12000	9560	20.79	1.0e-04	0.84430	0.00103	0.84636	hciacyt12_12_1_3	0.84558	0.00110	0.84777

Table 6.9.6-3. Results for 3.24 in.-diameter cylinder HEU metal content in packaging calculation model

case name	np (in)	U (g)	^{235}U (g)	H_2O (g)	h/x	moifr	k_{eff}	σ	$k_{eff}+2σ$	case name	k_{eff}	σ	$k_{eff}+2σ$
nciacyt11_9_1_3	0.0	9000	9000	9719	28.19	1.0e-04	0.78552	0.00116	0.78784	hciacyt12_9_1_3	0.78464	0.00132	0.78728
nciacyt11_6_1_3	0.0	6000	6000	9879	42.97	1.0e-04	0.69176	0.00119	0.69414	hciacyt12_6_1_3	0.69169	0.00122	0.69413
nciacyt11_3_1_3	0.0	3000	3000	10038	87.33	1.0e-04	0.53217	0.00084	0.53385	hciacyt12_3_1_3	0.53298	0.00091	0.53481
with can spacers (np thickness = 1.4 in.)													
nciacyt11_36_2_1	1.4	36000	36000	7673	5.56	1.0e-20	0.95474	0.00109	0.95693	hciacyt12_36_2_1	0.95429	0.00106	0.95641
nciacyt11_36_2_2	1.4	36000	36000	7673	5.56	1.0e-05	0.95402	0.00119	0.95640	hciacyt12_36_2_2	0.95522	0.00105	0.95732
nciacyt11_36_2_3	1.4	36000	36000	7673	5.56	1.0e-04	0.95362	0.00105	0.95571	hciacyt12_36_2_3	0.95319	0.00139	0.95596
nciacyt11_36_2_4	1.4	36000	36000	7673	5.56	1.0e-03	0.95222	0.00128	0.95478	hciacyt12_36_2_4	0.95333	0.00116	0.95564
nciacyt11_36_2_5	1.4	36000	36000	7673	5.56	1.0e-02	0.94649	0.00110	0.94869	hciacyt12_36_2_5	0.94837	0.00124	0.95084
nciacyt11_36_2_6	1.4	36000	36000	7673	5.56	1.0e-01	0.91268	0.00128	0.91524	hciacyt12_36_2_6	0.91591	0.00121	0.91834
nciacyt11_36_2_8	1.4	36000	36000	7673	5.56	3.0e-01	0.88453	0.00140	0.88733	hciacyt12_36_2_8	0.89062	0.00119	0.89300
nciacyt11_36_2_15	1.4	36000	36000	7673	5.56	1.0e+00	0.87822	0.00106	0.88034	hciacyt12_36_2_15	0.88152	0.00135	0.88423
nciacyt11_36_2_3	1.4	36000	36000	7673	5.56	1.0e-04	0.95362	0.00105	0.95571	hciacyt12_36_2_3	0.95319	0.00139	0.95596
nciacyt11_35_2_3	1.4	35000	35000	7726	5.76	1.0e-04	0.94906	0.00125	0.95156	hciacyt12_35_2_3	0.94788	0.00129	0.95046
nciacyt11_34_2_3	1.4	34000	34000	7779	5.97	1.0e-04	0.94393	0.00136	0.94664	hciacyt12_34_2_3	0.94428	0.00130	0.94687
nciacyt11_33_2_3	1.4	33000	33000	7832	6.19	1.0e-04	0.93703	0.00114	0.93930	hciacyt12_33_2_3	0.93708	0.00122	0.93952
nciacyt11_32_2_3	1.4	32000	32000	7885	6.43	1.0e-04	0.92940	0.00125	0.93191	hciacyt12_32_2_3	0.93065	0.00109	0.93283
nciacyt11_31_2_3	1.4	31000	31000	7938	6.68	1.0e-04	0.92483	0.00119	0.92721	hciacyt12_31_2_3	0.92625	0.00125	0.92874
nciacyt11_30_2_3	1.4	30000	30000	7992	6.95	1.0e-04	0.91737	0.00106	0.91949	hciacyt12_30_2_3	0.91983	0.00107	0.92198
nciacyt11_29_2_3	1.4	29000	29000	8045	7.24	1.0e-04	0.91253	0.00116	0.91484	hciacyt12_29_2_3	0.91204	0.00107	0.91419
nciacyt11_28_2_3	1.4	28000	28000	8098	7.55	1.0e-04	0.90504	0.00117	0.90737	hciacyt12_28_2_3	0.90515	0.00100	0.90716
nciacyt11_27_2_3	1.4	27000	27000	8151	7.88	1.0e-04	0.89967	0.00121	0.90208	hciacyt12_27_2_3	0.89749	0.00097	0.89942
nciacyt11_26_2_3	1.4	26000	26000	8204	8.24	1.0e-04	0.89129	0.00107	0.89343	hciacyt12_26_2_3	0.88997	0.00124	0.89246
nciacyt11_25_2_3	1.4	25000	25000	8257	8.62	1.0e-04	0.88183	0.00104	0.88391	hciacyt12_25_2_3	0.88253	0.00129	0.88511

Table 6.9.6-3. Results for 3.24 in.-diameter cylinder HEU metal content in packaging calculation model

case name	np (in)	U (g)	^{235}U (g)	H_2O (g)	h/x	moifr	k_{eff}	σ	$k_{eff}+2σ$	case name	k_{eff}	σ	$k_{eff}+2σ$
nciacyt11_24_2_3	1.4	24000	24000	8310	9.04	1.0e-04	0.87406	0.00117	0.87640	hciacyt12_24_2_3	0.87448	0.00117	0.87681
nciacyt11_23_2_3	1.4	23000	23000	8363	9.49	1.0e-04	0.86345	0.00109	0.86564	hciacyt12_23_2_3	0.86388	0.00119	0.86626
nciacyt11_22_2_3	1.4	22000	22000	8416	9.98	1.0e-04	0.85413	0.00107	0.85627	hciacyt12_22_2_3	0.85333	0.00109	0.85551
nciacyt11_21_2_3	1.4	21000	21000	8469	10.53	1.0e-04	0.84424	0.00109	0.84642	hciacyt12_21_2_3	0.84414	0.00111	0.84636
nciacyt11_20_2_3	1.4	20000	20000	8522	11.12	1.0e-04	0.83545	0.00106	0.83756	hciacyt12_20_2_3	0.83388	0.00099	0.83585
nciacyt11_19_2_3	1.4	19000	19000	8575	11.78	1.0e-04	0.82051	0.00130	0.82311	hciacyt12_19_2_3	0.82263	0.00109	0.82480
nciacyt11_18_2_3	1.4	18000	18000	8628	12.51	1.0e-04	0.81105	0.00122	0.81350	hciacyt12_18_2_3	0.81076	0.00113	0.81301
nciacyt11_15_2_3	1.4	15000	15000	8787	15.29	1.0e-04	0.76734	0.00107	0.76948	hciacyt12_15_2_3	0.76757	0.00102	0.76960
nciacyt11_12_2_3	1.4	12000	12000	8947	19.46	1.0e-04	0.71377	0.00097	0.71571	hciacyt12_12_2_3	0.71466	0.00102	0.71669
nciacyt11_9_2_3	1.4	9000	9000	9106	26.41	1.0e-04	0.64515	0.00110	0.64734	hciacyt12_9_2_3	0.64486	0.00103	0.64692
nciacyt11_6_2_3	1.4	6000	6000	9265	40.30	1.0e-04	0.54772	0.00094	0.54960	hciacyt12_6_2_3	0.54697	0.00098	0.54893
nciacyt11_3_2_3	1.4	3000	3000	9424	81.99	1.0e-04	0.39773	0.00080	0.39933	hciacyt12_3_2_3	0.39723	0.00087	0.39896

Table 6.9.6-3b. Results for spacing of 3.24 in.-diameter cylinder HEU metal content in CV calculation model

case name	np (in.)	^{235}U (g)	H_2O (g)	h/x	separation (cm)	moifr	k_{eff}	σ	$k_{eff}+2σ$				
content in flooded containment vessel, reflected													
NCT													
separation is the distance between the 3.24 in.-diameter cylinders (an additional 1.4 in. is provided by the can spacer)													
cvcrcyat11_1_2	1.4	30000	7992	6.95	0.000	1.0e+00	0.85525	0.00117	0.85760				
cvcrcyat11_2_2	1.4	30000	7992	6.95	0.254	1.0e+00	0.85568	0.00100	0.85768				
cvcrcyat11_3_2	1.4	30000	7992	6.95	0.762	1.0e+00	0.85058	0.00110	0.85278				
cvcrcyat11_4_2	1.4	30000	7992	6.95	1.270	1.0e+00	0.84834	0.00124	0.85082				
cvcrcyat11_5_2	1.4	30000	7992	6.95	1.778	1.0e+00	0.84241	0.00123	0.84488				

Table 6.9.6-3b. Results for spacing of 3.24 in.-diameter cylinder HEU metal content in CV calculation model

case name	np (in.)	^{235}U (g)	H_2O (g)	h/x	separation (cm)	moifr	k_{eff}	σ	$k_{eff}+2\sigma$				
cvcrcyat11_6_2	1.4	30000	7992	6.95	2.286	1.0e+00	0.83866	0.00099	0.84063				
cvcrcyat11_7_2	1.4	30000	7992	6.95	2.794	1.0e+00	0.83549	0.00117	0.83782				
cvcrcyat11_8_2	1.4	30000	7992	6.95	3.302	1.0e+00	0.83213	0.00126	0.83465				
cvcrcyat11_9_2	1.4	30000	7992	6.95	3.810	1.0e+00	0.82984	0.00125	0.83233				
cvcrcyat11_10_2	1.4	30000	7992	6.95	4.318	1.0e+00	0.82777	0.00105	0.82986				
cvcrcyat11_11_2	1.4	30000	7992	6.95	4.826	1.0e+00	0.82499	0.00116	0.82731				
cvcrcyat11_12_2	1.4	30000	7992	6.95	12.230	1.0e+00	0.80870	0.00121	0.81113				

Table 6.9.6-3c. Results for spacing of 3.24 in.-diameter cylinder HEU metal content in packaging calculation model

case name	np (in.)	^{235}U (g)	H_2O (g)	h/x	separation (cm)	moifr	k_{eff}	σ	$k_{eff}+2\sigma$				
content in flooded containment vessel, single package reflected													
NCT													
separation is the distance between the 3.24 in.-diameter cylinders (an additional 1.4 in. is provided by the canned spacer)													
ncsrcyat11_1_2_15	1.4	30000	7992	6.95	0.000	1.0e+00	0.84343	0.00114	0.84572				
ncsrcyat11_2_2_15	1.4	30000	7992	6.95	0.254	1.0e+00	0.84249	0.00111	0.84472				
ncsrcyat11_3_2_15	1.4	30000	7992	6.95	0.762	1.0e+00	0.83638	0.00103	0.83845				
ncsrcyat11_4_2_15	1.4	30000	7992	6.95	1.270	1.0e+00	0.83416	0.00110	0.83636				
ncsrcyat11_5_2_15	1.4	30000	7992	6.95	1.778	1.0e+00	0.82786	0.00128	0.83043				
ncsrcyat11_6_2_15	1.4	30000	7992	6.95	2.286	1.0e+00	0.82516	0.00113	0.82743				
ncsrcyat11_7_2_15	1.4	30000	7992	6.95	2.794	1.0e+00	0.82161	0.00116	0.82393				
ncsrcyat11_8_2_15	1.4	30000	7992	6.95	3.302	1.0e+00	0.82004	0.00114	0.82232				
ncsrcyat11_9_2_15	1.4	30000	7992	6.95	3.810	1.0e+00	0.81641	0.00101	0.81843				
ncsrcyat11_10_2_15	1.4	30000	7992	6.95	4.318	1.0e+00	0.81362	0.00109	0.81581				

Table 6.9.6-3c. Results for spacing of 3.24 in.-diameter cylinder HEU metal content in packaging calculation model

case name	np (in.)	^{235}U (g)	H_2O (g)	h/x	separation (cm)	moifr	k_{eff}	σ	$k_{eff}+2σ$				
ncsrcyat11_11_2_15	1.4	30000	7992	6.95	4.826	1.0e+00	0.81218	0.00104	0.81426				
ncsrcyat11_12_2_15	1.4	30000	7992	6.95	12.230	1.0e+00	0.79592	0.00100	0.79793				

Table 6.9.6-4. Results for 2.29 in.-square bar HEU metal content in CV calculation model

case name	np (in)	U (g)	^{235}U (g)	H_2O (g)	h/x	mocfr	k_{eff}	σ	$k_{eff}+2σ$				
flooded containment vessel, reflected													
no can spacers (np thickness = 0.0 in.)													
cvcrsqt11_36_1	0.0	36000	36000	8287	6.01	1.0e+00	0.87614	0.00128	0.87869				
cvcrsqt11_35_1	0.0	35000	35000	8340	6.22	1.0e+00	0.87560	0.00111	0.87781				
cvcrsqt11_34_1	0.0	34000	34000	8393	6.44	1.0e+00	0.87541	0.00126	0.87794				
cvcrsqt11_33_1	0.0	33000	33000	8446	6.68	1.0e+00	0.87396	0.00108	0.87612				
cvcrsqt11_32_1	0.0	32000	32000	8499	6.93	1.0e+00	0.87319	0.00119	0.87556				
cvcrsqt11_31_1	0.0	31000	31000	8552	7.20	1.0e+00	0.86993	0.00116	0.87225				
cvcrsqt11_30_1	0.0	30000	30000	8605	7.49	1.0e+00	0.87046	0.00120	0.87286				
cvcrsqt11_29_1	0.0	29000	29000	8658	7.79	1.0e+00	0.86852	0.00107	0.87067				
cvcrsqt11_28_1	0.0	28000	28000	8711	8.12	1.0e+00	0.86740	0.00113	0.86966				
cvcrsqt11_27_1	0.0	27000	27000	8764	8.47	1.0e+00	0.86366	0.00116	0.86597				
cvcrsqt11_26_1	0.0	26000	26000	8817	8.85	1.0e+00	0.86498	0.00138	0.86773				
cvcrsqt11_25_1	0.0	25000	25000	8870	9.26	1.0e+00	0.86077	0.00121	0.86319				
cvcrsqt11_24_1	0.0	24000	24000	8923	9.70	1.0e+00	0.85955	0.00138	0.86231				
cvcrsqt11_23_1	0.0	23000	23000	8977	10.19	1.0e+00	0.85604	0.00106	0.85816				
cvcrsqt11_22_1	0.0	22000	22000	9030	10.71	1.0e+00	0.85211	0.00103	0.85417				
cvcrsqt11_21_1	0.0	21000	21000	9083	11.29	1.0e+00	0.84970	0.00118	0.85206				

Table 6.9.6-4. Results for 2.29 in.-square bar HEU metal content in CV calculation model

case name	np (in)	U (g)	^{235}U (g)	H_2O (g)	h/x	mocfr	k_{eff}	σ	$k_{eff}+2σ$				
cvcrsqt11_20_1	0.0	20000	20000	9136	11.92	1.0e+00	0.84694	0.00119	0.84931				
cvcrsqt11_19_1	0.0	19000	19000	9189	12.62	1.0e+00	0.84285	0.00109	0.84503				
cvcrsqt11_18_1	0.0	18000	18000	9242	13.40	1.0e+00	0.83888	0.00115	0.84117				
with can spacers (np thickness=1.4 in.)													
cvcrsqt11_36_2	1.4	36000	36000	7673	5.56	1.0e+00	0.82217	0.00098	0.82414				
cvcrsqt11_35_2	1.4	35000	35000	7726	5.76	1.0e+00	0.81622	0.00130	0.81881				
cvcrsqt11_34_2	1.4	34000	34000	7779	5.97	1.0e+00	0.81548	0.00103	0.81755				
cvcrsqt11_33_2	1.4	33000	33000	7832	6.19	1.0e+00	0.81272	0.00118	0.81508				
cvcrsqt11_32_2	1.4	32000	32000	7885	6.43	1.0e+00	0.80782	0.00120	0.81022				
cvcrsqt11_31_2	1.4	31000	31000	7938	6.68	1.0e+00	0.80495	0.00109	0.80712				
cvcrsqt11_30_2	1.4	30000	30000	7992	6.95	1.0e+00	0.80163	0.00117	0.80397				

Table 6.9.6-5. Results for 2.29 in.-square bar HEU metal content in packaging calculation model

case name	np (in)	U (g)	^{235}U (g)	H_2O (g)	h/x	moifr	k_{eff}	σ	$k_{eff}+2σ$	case name	k_{eff}	σ	$k_{eff}+2σ$
content in flooded containment vessel, single package reflected													
NCT										**HAC**			
no can spacers (np thickness = 0.0 in.)													
ncsrsqt11_36_1_1	0.0	36000	36000	8287	6.01	1.0e-20	0.82940	0.00124	0.83189	hcsrsqt12_36_1_1	0.83133	0.00125	0.83384
ncsrsqt11_36_1_2	0.0	36000	36000	8287	6.01	1.0e-05	0.83107	0.00107	0.83320	hcsrsqt12_36_1_2	0.83168	0.00121	0.83409
ncsrsqt11_36_1_3	0.0	36000	36000	8287	6.01	1.0e-04	0.83051	0.00120	0.83292	hcsrsqt12_36_1_3	0.83088	0.00103	0.83293
ncsrsqt11_36_1_4	0.0	36000	36000	8287	6.01	1.0e-03	0.82981	0.00116	0.83213	hcsrsqt12_36_1_4	0.83030	0.00122	0.83273
ncsrsqt11_36_1_5	0.0	36000	36000	8287	6.01	1.0e-02	0.82859	0.00123	0.83105	hcsrsqt12_36_1_5	0.83244	0.00126	0.83496
ncsrsqt11_36_1_6	0.0	36000	36000	8287	6.01	1.0e-01	0.83608	0.00123	0.83853	hcsrsqt12_36_1_6	0.83502	0.00119	0.83739

Table 6.9.6-5. Results for 2.29 in.-square bar HEU metal content in packaging calculation model

case name	np (in)	U (g)	^{235}U (g)	H_2O (g)	h/x	moifr	k_{eff}	σ	$k_{eff}+2σ$	case name	k_{eff}	σ	$k_{eff}+2σ$
ncsrsqt11_36_1_8	0.0	36000	36000	8287	6.01	3.0e-01	0.84146	0.00118	0.84382	hcsrsqt12_36_1_8	0.84236	0.00115	0.84465
ncsrsqt11_36_1_15	0.0	36000	36000	8287	6.01	1.0e+00	0.86253	0.00131	0.86516	hcsrsqt12_36_1_15	0.86198	0.00112	0.86422
ncsrsqt11_36_1_15	0.0	36000	36000	8287	6.01	1.0e+00	0.86253	0.00131	0.86516	hcsrsqt12_36_1_15	0.86198	0.00112	0.86422
ncsrsqt11_35_1_15	0.0	35000	35000	8340	6.22	1.0e+00	0.86041	0.00112	0.86265	hcsrsqt12_35_1_15	0.86067	0.00121	0.86309
ncsrsqt11_34_1_15	0.0	34000	34000	8393	6.44	1.0e+00	0.85820	0.00129	0.86078	hcsrsqt12_34_1_15	0.85896	0.00102	0.86101
ncsrsqt11_33_1_15	0.0	33000	33000	8446	6.68	1.0e+00	0.85708	0.00106	0.85920	hcsrsqt12_33_1_15	0.86064	0.00110	0.86285
ncsrsqt11_32_1_15	0.0	32000	32000	8499	6.93	1.0e+00	0.85769	0.00107	0.85983	hcsrsqt12_32_1_15	0.85800	0.00110	0.86020
ncsrsqt11_31_1_15	0.0	31000	31000	8552	7.20	1.0e+00	0.85495	0.00127	0.85749	hcsrsqt12_31_1_15	0.85333	0.00123	0.85580
ncsrsqt11_30_1_15	0.0	30000	30000	8605	7.49	1.0e+00	0.85270	0.00120	0.85510	hcsrsqt12_30_1_15	0.85520	0.00132	0.85784
ncsrsqt11_29_1_15	0.0	29000	29000	8658	7.79	1.0e+00	0.85067	0.00119	0.85305	hcsrsqt12_29_1_15	0.85348	0.00114	0.85575
ncsrsqt11_28_1_15	0.0	28000	28000	8711	8.12	1.0e+00	0.85223	0.00111	0.85446	hcsrsqt12_28_1_15	0.85043	0.00101	0.85246
ncsrsqt11_27_1_15	0.0	27000	27000	8764	8.47	1.0e+00	0.84973	0.00121	0.85214	hcsrsqt12_27_1_15	0.85029	0.00111	0.85250
ncsrsqt11_26_1_15	0.0	26000	26000	8817	8.85	1.0e+00	0.84838	0.00127	0.85091	hcsrsqt12_26_1_15	0.84829	0.00115	0.85058
ncsrsqt11_25_1_15	0.0	25000	25000	8870	9.26	1.0e+00	0.84598	0.00113	0.84824	hcsrsqt12_25_1_15	0.84583	0.00105	0.84792
ncsrsqt11_24_1_15	0.0	24000	24000	8923	9.70	1.0e+00	0.84390	0.00111	0.84611	hcsrsqt12_24_1_15	0.84296	0.00112	0.84521
ncsrsqt11_23_1_15	0.0	23000	23000	8977	10.19	1.0e+00	0.84101	0.00108	0.84317	hcsrsqt12_23_1_15	0.84241	0.00129	0.84499
ncsrsqt11_22_1_15	0.0	22000	22000	9030	10.71	1.0e+00	0.83888	0.00112	0.84111	hcsrsqt12_22_1_15	0.83951	0.00107	0.84164
ncsrsqt11_21_1_15	0.0	21000	21000	9083	11.29	1.0e+00	0.83473	0.00112	0.83696	hcsrsqt12_21_1_15	0.83577	0.00128	0.83832
ncsrsqt11_20_1_15	0.0	20000	20000	9136	11.92	1.0e+00	0.83029	0.00110	0.83250	hcsrsqt12_20_1_15	0.83094	0.00103	0.83300
ncsrsqt11_19_1_15	0.0	19000	19000	9189	12.62	1.0e+00	0.82676	0.00107	0.82889	hcsrsqt12_19_1_15	0.82652	0.00113	0.82879
ncsrsqt11_18_1_15	0.0	18000	18000	9242	13.40	1.0e+00	0.82247	0.00121	0.82489	hcsrsqt12_18_1_15	0.82440	0.00112	0.82664
with can spacers (np thickness = 1.4 in.)													
ncsrsqt11_36_2_1	1.4	36000	36000	7673	5.56	1.0e-20	0.78167	0.00104	0.78375	hcsrsqt12_36_2_1	0.78308	0.00128	0.78563
ncsrsqt11_36_2_2	1.4	36000	36000	7673	5.56	1.0e-05	0.78210	0.00112	0.78434	hcsrsqt12_36_2_2	0.78549	0.00112	0.78772

Table 6.9.6-5. Results for 2.29 in.-square bar HEU metal content in packaging calculation model

case name	np (in)	U (g)	^{235}U (g)	H_2O (g)	h/x	moifr	k_{eff}	σ	$k_{eff}+2σ$	case name	k_{eff}	σ	$k_{eff}+2σ$
ncsrsqt11_36_2_3	1.4	36000	36000	7673	5.56	1.0e-04	0.78209	0.00104	0.78417	hcsrsqt12_36_2_3	0.78508	0.00119	0.78746
ncsrsqt11_36_2_4	1.4	36000	36000	7673	5.56	1.0e-03	0.78414	0.00111	0.78636	hcsrsqt12_36_2_4	0.78484	0.00121	0.78727
ncsrsqt11_36_2_5	1.4	36000	36000	7673	5.56	1.0e-02	0.78141	0.00137	0.78415	hcsrsqt12_36_2_5	0.78362	0.00114	0.78591
ncsrsqt11_36_2_6	1.4	36000	36000	7673	5.56	1.0e-01	0.78591	0.00113	0.78818	hcsrsqt12_36_2_6	0.78757	0.00108	0.78972
ncsrsqt11_36_2_8	1.4	36000	36000	7673	5.56	3.0e-01	0.79206	0.00130	0.79466	hcsrsqt12_36_2_8	0.79070	0.00128	0.79327
ncsrsqt11_36_2_15	1.4	36000	36000	7673	5.56	1.0e+00	0.80894	0.00103	0.81101	hcsrsqt12_36_2_15	0.80856	0.00110	0.81077
ncsrsqt11_36_2_15	1.4	36000	36000	7673	5.56	1.0e+00	0.80894	0.00103	0.81101	hcsrsqt12_36_2_15	0.80856	0.00110	0.81077
ncsrsqt11_35_2_15	1.4	35000	35000	7726	5.76	1.0e+00	0.80583	0.00113	0.80808	hcsrsqt12_35_2_15	0.80522	0.00112	0.80747
ncsrsqt11_34_2_15	1.4	34000	34000	7779	5.97	1.0e+00	0.80341	0.00125	0.80591	hcsrsqt12_34_2_15	0.80255	0.00107	0.80469
ncsrsqt11_33_2_15	1.4	33000	33000	7832	6.19	1.0e+00	0.80213	0.00108	0.80429	hcsrsqt12_33_2_15	0.79972	0.00096	0.80164
ncsrsqt11_32_2_15	1.4	32000	32000	7885	6.43	1.0e+00	0.79784	0.00124	0.80032	hcsrsqt12_32_2_15	0.79750	0.00118	0.79985
ncsrsqt11_31_2_15	1.4	31000	31000	7938	6.68	1.0e+00	0.79226	0.00107	0.79440	hcsrsqt12_31_2_15	0.79447	0.00099	0.79646
ncsrsqt11_30_2_15	1.4	30000	30000	7992	6.95	1.0e+00	0.79192	0.00110	0.79412	hcsrsqt12_30_2_15	0.79053	0.00108	0.79268
content in flooded containment vessel, array packaging model for CSI=0.0													
NCT										**HAC**			
no can spacers (np thickness = 0.0 in.)													
nciasqt11_36_1_3	0.0	36000	36000	8287	6.01	1.0e-04	0.93786	0.00112	0.94011	hciasqt12_36_1_3	0.93760	0.00119	0.93998
nciasqt11_35_1_3	0.0	35000	35000	8340	6.22	1.0e-04	0.93414	0.00107	0.93629	hciasqt12_35_1_3	0.93524	0.00130	0.93785

Table 6.9.6-5. Results for 2.29 in.-square bar HEU metal content in packaging calculation model

case name	np (in)	U (g)	^{235}U (g)	H_2O (g)	h/x	moifr	k_{eff}	σ	$k_{eff}+2σ$	case name	k_{eff}	σ	$k_{eff}+2σ$
nciasqt11_34_1_3	0.0	34000	34000	8393	6.44	1.0e-04	0.93004	0.00116	0.93235	hciasqt12_34_1_3	0.92962	0.00116	0.93195
nciasqt11_33_1_3	0.0	33000	33000	8446	6.68	1.0e-04	0.92897	0.00121	0.93139	hciasqt12_33_1_3	0.92744	0.00120	0.92984
nciasqt11_32_1_3	0.0	32000	32000	8499	6.93	1.0e-04	0.92703	0.00119	0.92942	hciasqt12_32_1_3	0.92854	0.00110	0.93073
nciasqt11_31_1_3	0.0	31000	31000	8552	7.20	1.0e-04	0.92403	0.00109	0.92621	hciasqt12_31_1_3	0.92290	0.00105	0.92499
nciasqt11_30_1_3	0.0	30000	30000	8605	7.49	1.0e-04	0.91959	0.00114	0.92188	hciasqt12_30_1_3	0.91960	0.00125	0.92211
nciasqt11_29_1_3	0.0	29000	29000	8658	7.79	1.0e-04	0.91544	0.00122	0.91787	hciasqt12_29_1_3	0.91645	0.00138	0.91922
nciasqt11_28_1_3	0.0	28000	28000	8711	8.12	1.0e-04	0.91153	0.00123	0.91399	hciasqt12_28_1_3	0.91477	0.00122	0.91722
nciasqt11_27_1_3	0.0	27000	27000	8764	8.47	1.0e-04	0.90851	0.00099	0.91050	hciasqt12_27_1_3	0.91066	0.00119	0.91305
nciasqt11_26_1_3	0.0	26000	26000	8817	8.85	1.0e-04	0.90835	0.00125	0.91084	hciasqt12_26_1_3	0.90452	0.00124	0.90699
nciasqt11_25_1_3	0.0	25000	25000	8870	9.26	1.0e-04	0.90272	0.00115	0.90501	hciasqt12_25_1_3	0.90142	0.00116	0.90374
nciasqt11_24_1_3	0.0	24000	24000	8923	9.70	1.0e-04	0.89930	0.00123	0.90177	hciasqt12_24_1_3	0.89640	0.00120	0.89881
nciasqt11_23_1_3	0.0	23000	23000	8977	10.19	1.0e-04	0.89380	0.00120	0.89619	hciasqt12_23_1_3	0.89613	0.00135	0.89882
nciasqt11_22_1_3	0.0	22000	22000	9030	10.71	1.0e-04	0.88934	0.00105	0.89144	hciasqt12_22_1_3	0.88839	0.00106	0.89051
nciasqt11_21_1_3	0.0	21000	21000	9083	11.29	1.0e-04	0.88358	0.00109	0.88576	hciasqt12_21_1_3	0.88413	0.00118	0.88649
nciasqt11_20_1_3	0.0	20000	20000	9136	11.92	1.0e-04	0.87812	0.00123	0.88058	hciasqt12_20_1_3	0.87811	0.00124	0.88058
nciasqt11_19_1_3	0.0	19000	19000	9189	12.62	1.0e-04	0.87206	0.00108	0.87423	hciasqt12_19_1_3	0.87171	0.00118	0.87408
nciasqt11_18_1_3	0.0	18000	18000	9242	13.40	1.0e-04	0.86772	0.00140	0.87052	hciasqt12_18_1_3	0.86555	0.00119	0.86794
nciasqt11_15_1_3	0.0	15000	15000	9401	16.36	1.0e-04	0.84518	0.00119	0.84756	hciasqt12_15_1_3	0.84416	0.00102	0.84620
nciasqt11_12_1_3	0.0	12000	12000	9560	20.79	1.0e-04	0.81425	0.00113	0.81651	hciasqt12_12_1_3	0.81332	0.00101	0.81534
nciasqt11_9_1_3	0.0	9000	9000	9719	28.19	1.0e-04	0.76947	0.00115	0.77178	hciasqt12_9_1_3	0.77066	0.00107	0.77280
nciasqt11_6_1_3	0.0	6000	6000	9879	42.97	1.0e-04	0.69668	0.00099	0.69866	hciasqt12_6_1_3	0.69648	0.00101	0.69850
nciasqt11_3_1_3	0.0	3000	3000	10038	87.33	1.0e-04	0.55857	0.00089	0.56036	hciasqt12_3_1_3	0.55806	0.00092	0.55989
with can spacers (np thickness = 1.4 in.)													
nciasqt11_36_2_3	1.4	36000	36000	7673	5.56	1.0e-04	0.89382	0.00114	0.89610	hciasqt12_36_2_3	0.89230	0.00114	0.89458
nciasqt11_35_2_3	1.4	35000	35000	7726	5.76	1.0e-04	0.88604	0.00105	0.88813	hciasqt12_35_2_3	0.88890	0.00130	0.89150

Table 6.9.6-5. Results for 2.29 in.-square bar HEU metal content in packaging calculation model

case name	np (in)	U (g)	^{235}U (g)	H_2O (g)	h/x	moifr	k_{eff}	σ	$k_{eff}+2σ$	case name	k_{eff}	σ	$k_{eff}+2σ$
nciasqt11_34_2_3	1.4	34000	34000	7779	5.97	1.0e-04	0.88480	0.00105	0.88690	hciasqt12_34_2_3	0.88544	0.00139	0.88822
nciasqt11_33_2_3	1.4	33000	33000	7832	6.19	1.0e-04	0.87854	0.00118	0.88090	hciasqt12_33_2_3	0.87897	0.00106	0.88110
nciasqt11_32_2_3	1.4	32000	32000	7885	6.43	1.0e-04	0.87561	0.00104	0.87768	hciasqt12_32_2_3	0.87638	0.00121	0.87880
nciasqt11_31_2_3	1.4	31000	31000	7938	6.68	1.0e-04	0.86867	0.00123	0.87114	hciasqt12_31_2_3	0.87222	0.00105	0.87432
nciasqt11_30_2_3	1.4	30000	30000	7992	6.95	1.0e-04	0.86347	0.00122	0.86590	hciasqt12_30_2_3	0.86614	0.00121	0.86855
nciasqt11_29_2_3	1.4	29000	29000	8045	7.24	1.0e-04	0.85781	0.00109	0.86000	hciasqt12_29_2_3	0.85842	0.00113	0.86068
nciasqt11_28_2_3	1.4	28000	28000	8098	7.55	1.0e-04	0.85401	0.00119	0.85640	hciasqt12_28_2_3	0.85399	0.00116	0.85630
nciasqt11_27_2_3	1.4	27000	27000	8151	7.88	1.0e-04	0.84755	0.00127	0.85009	hciasqt12_27_2_3	0.84935	0.00125	0.85184
nciasqt11_26_2_3	1.4	26000	26000	8204	8.24	1.0e-04	0.84285	0.00119	0.84522	hciasqt12_26_2_3	0.84287	0.00106	0.84500
nciasqt11_25_2_3	1.4	25000	25000	8257	8.62	1.0e-04	0.83719	0.00124	0.83967	hciasqt12_25_2_3	0.83683	0.00113	0.83910
nciasqt11_24_2_3	1.4	24000	24000	8310	9.04	1.0e-04	0.82927	0.00102	0.83132	hciasqt12_24_2_3	0.83192	0.00111	0.83414
nciasqt11_23_2_3	1.4	23000	23000	8363	9.49	1.0e-04	0.82375	0.00132	0.82638	hciasqt12_23_2_3	0.82315	0.00124	0.82562
nciasqt11_22_2_3	1.4	22000	22000	8416	9.98	1.0e-04	0.81735	0.00107	0.81950	hciasqt12_22_2_3	0.81490	0.00105	0.81700
nciasqt11_21_2_3	1.4	21000	21000	8469	10.53	1.0e-04	0.80580	0.00118	0.80817	hciasqt12_21_2_3	0.81021	0.00121	0.81263
nciasqt11_20_2_3	1.4	20000	20000	8522	11.12	1.0e-04	0.79977	0.00110	0.80197	hciasqt12_20_2_3	0.80091	0.00116	0.80324
nciasqt11_19_2_3	1.4	19000	19000	8575	11.78	1.0e-04	0.79125	0.00109	0.79343	hciasqt12_19_2_3	0.79175	0.00113	0.79400
nciasqt11_18_2_3	1.4	18000	18000	8628	12.51	1.0e-04	0.78165	0.00110	0.78386	hciasqt12_18_2_3	0.78285	0.00110	0.78505
nciasqt11_15_2_3	1.4	15000	15000	8787	15.29	1.0e-04	0.74822	0.00105	0.75032	hciasqt12_15_2_3	0.74548	0.00107	0.74762
nciasqt11_12_2_3	1.4	12000	12000	8947	19.46	1.0e-04	0.70519	0.00106	0.70732	hciasqt12_12_2_3	0.70419	0.00105	0.70628
nciasqt11_9_2_3	1.4	9000	9000	9106	26.41	1.0e-04	0.64473	0.00106	0.64685	hciasqt12_9_2_3	0.64451	0.00101	0.64653
nciasqt11_6_2_3	1.4	6000	6000	9265	40.30	1.0e-04	0.55778	0.00097	0.55972	hciasqt12_6_2_3	0.55888	0.00098	0.56084
nciasqt11_3_2_3	1.4	3000	3000	9424	81.99	1.0e-04	0.41347	0.00085	0.41517	hciasqt12_3_2_3	0.41398	0.00074	0.41545

Table 6.9.6-6. Results for 4.25 in.-diameter cylinder HEU metal content in CV calculation model

case name	np (in)	U (g)	^{235}U (g)	H_2O (g)	h/x	mocfr	k_{eff}	σ	$k_{eff}+2σ$				
flooded containment vessel, reflected													
no can spacers (np thickness = 0.0 in.)													
cvcrcyct11_36_1	0.0	36000	36000	8287	6.01	1.0e+00	1.06320	0.00115	1.06549				
cvcrcyct11_35_1	0.0	35000	35000	8340	6.22	1.0e+00	1.06114	0.00121	1.06356				
cvcrcyct11_34_1	0.0	34000	34000	8393	6.44	1.0e+00	1.05675	0.00122	1.05919				
cvcrcyct11_33_1	0.0	33000	33000	8446	6.68	1.0e+00	1.04990	0.00112	1.05214				
cvcrcyct11_32_1	0.0	32000	32000	8499	6.93	1.0e+00	1.04469	0.00123	1.04714				
cvcrcyct11_31_1	0.0	31000	31000	8552	7.20	1.0e+00	1.04101	0.00104	1.04310				
cvcrcyct11_30_1	0.0	30000	30000	8605	7.49	1.0e+00	1.03487	0.00117	1.03722				
cvcrcyct11_29_1	0.0	29000	29000	8658	7.79	1.0e+00	1.02817	0.00115	1.03046				
cvcrcyct11_28_1	0.0	28000	28000	8711	8.12	1.0e+00	1.02183	0.00125	1.02433				
cvcrcyct11_27_1	0.0	27000	27000	8764	8.47	1.0e+00	1.01524	0.00109	1.01742				
cvcrcyct11_26_1	0.0	26000	26000	8817	8.85	1.0e+00	1.00971	0.00116	1.01203				
cvcrcyct11_25_1	0.0	25000	25000	8870	9.26	1.0e+00	1.00149	0.00136	1.00420				
cvcrcyct11_24_1	0.0	24000	24000	8923	9.70	1.0e+00	0.99327	0.00137	0.99600				
cvcrcyct11_23_1	0.0	23000	23000	8977	10.19	1.0e+00	0.98432	0.00124	0.98680				
cvcrcyct11_22_1	0.0	22000	22000	9030	10.71	1.0e+00	0.97759	0.00112	0.97984				
cvcrcyct11_21_1	0.0	21000	21000	9083	11.29	1.0e+00	0.96672	0.00116	0.96904				
cvcrcyct11_20_1	0.0	20000	20000	9136	11.92	1.0e+00	0.95743	0.00128	0.95999				
cvcrcyct11_19_1	0.0	19000	19000	9189	12.62	1.0e+00	0.94629	0.00118	0.94866				
cvcrcyct11_18_1	0.0	18000	18000	9242	13.40	1.0e+00	0.93349	0.00114	0.93576				
cvcrcyct11_17_1	0.0	17000	17000	9295	14.27	1.0e+00	0.91942	0.00105	0.92152				
cvcrcyct11_16_1	0.0	16000	16000	9348	15.25	1.0e+00	0.90458	0.00120	0.90699				
cvcrcyct11_15_1	0.0	15000	15000	9401	16.36	1.0e+00	0.88788	0.00107	0.89002				

Table 6.9.6-6. Results for 4.25 in.-diameter cylinder HEU metal content in CV calculation model

case name	np (in)	U (g)	^{235}U (g)	H_2O (g)	h/x	mocfr	k_{eff}	σ	$k_{eff}+2σ$				
with can spacers (np thickness=1.4 in.)													
cvcrcyct11_36_2	1.4	36000	36000	7673	5.56	1.0e+00	0.94321	0.00111	0.94543				
cvcrcyct11_35_2	1.4	35000	35000	7726	5.76	1.0e+00	0.93828	0.00114	0.94056				
cvcrcyct11_34_2	1.4	34000	34000	7779	5.97	1.0e+00	0.93114	0.00129	0.93372				
cvcrcyct11_33_2	1.4	33000	33000	7832	6.19	1.0e+00	0.92558	0.00124	0.92805				
cvcrcyct11_32_2	1.4	32000	32000	7885	6.43	1.0e+00	0.91799	0.00111	0.92021				
cvcrcyct11_31_2	1.4	31000	31000	7938	6.68	1.0e+00	0.91146	0.00114	0.91375				
cvcrcyct11_30_2	1.4	30000	30000	7992	6.95	1.0e+00	0.90499	0.00117	0.90734				

Table 6.9.6-7. Results for 4.25 in.-diameter cylinder HEU metal content in packaging calculation model

case name	np (in)	U (g)	^{235}U (g)	H_2O (g)	h/x	moifr	k_{eff}	σ	$k_{eff}+2σ$	case name	k_{eff}	σ	$k_{eff}+2σ$
content in flooded containment vessel, single package reflected													
NCT										HAC			
no can spacers (np thickness = 0.0 in.)													
ncsrcyct11_36_1_1	0.0	36000	36000	8286.7	6.01	1.0e-20	0.98628	0.00107	0.98841	hcsrcyct12_36_1_1	0.98723	0.00126	0.98975
ncsrcyct11_36_1_2	0.0	36000	36000	8286.7	6.01	1.0e-05	0.98712	0.00138	0.98988	hcsrcyct12_36_1_2	0.98582	0.00120	0.98823
ncsrcyct11_36_1_3	0.0	36000	36000	8287	6.01	1.0e-04	0.98624	0.00119	0.98861	hcsrcyct12_36_1_3	0.98691	0.00113	0.98917
ncsrcyct11_36_1_4	0.0	36000	36000	8287	6.01	1.0e-03	0.98433	0.00102	0.98637	hcsrcyct12_36_1_4	0.98537	0.00111	0.98759
ncsrcyct11_36_1_5	0.0	36000	36000	8287	6.01	1.0e-02	0.98646	0.00103	0.98852	hcsrcyct12_36_1_5	0.98809	0.00110	0.99028
ncsrcyct11_36_1_6	0.0	36000	36000	8287	6.01	1.0e-01	0.99092	0.00127	0.99346	hcsrcyct12_36_1_6	0.99096	0.00099	0.99295
ncsrcyct11_36_1_8	0.0	36000	36000	8287	6.01	3.0e-01	1.00000	0.00123	1.00246	hcsrcyct12_36_1_8	1.00334	0.00119	1.00572
ncsrcyct11_36_1_15	0.0	36000	36000	8287	6.01	1.0e+00	1.03142	0.00144	1.03430	hcsrcyct12_36_1_15	1.03141	0.00116	1.03374
ncsrcyct11_36_1_15	0.0	36000	36000	8287	6.01	1.0e+00	1.03142	0.00144	1.03430	hcsrcyct12_36_1_15	1.03141	0.00116	1.03374

Table 6.9.6-7. Results for 4.25 in.-diameter cylinder HEU metal content in packaging calculation model

case name	np (in)	U (g)	^{235}U (g)	H_2O (g)	h/x	moifr	k_{eff}	σ	$k_{eff}+2σ$	case name	k_{eff}	σ	$k_{eff}+2σ$
ncsrcyct11_35_1_15	0.0	35000	35000	8340	6.22	1.0e+00	1.02816	0.00115	1.03045	hcsrcyct12_35_1_15	1.03309	0.00126	1.03561
ncsrcyct11_34_1_15	0.0	34000	34000	8393	6.44	1.0e+00	1.02658	0.00113	1.02884	hcsrcyct12_34_1_15	1.02529	0.00124	1.02776
ncsrcyct11_33_1_15	0.0	33000	33000	8446	6.68	1.0e+00	1.01975	0.00114	1.02203	hcsrcyct12_33_1_15	1.02060	0.00124	1.02308
ncsrcyct11_32_1_15	0.0	32000	32000	8499	6.93	1.0e+00	1.01647	0.00104	1.01854	hcsrcyct12_32_1_15	1.01688	0.00114	1.01916
ncsrcyct11_31_1_15	0.0	31000	31000	8552	7.20	1.0e+00	1.00952	0.00114	1.01179	hcsrcyct12_31_1_15	1.01218	0.00144	1.01505
ncsrcyct11_30_1_15	0.0	30000	30000	8605	7.49	1.0e+00	1.00434	0.00123	1.00679	hcsrcyct12_30_1_15	1.00757	0.00117	1.00992
ncsrcyct11_29_1_15	0.0	29000	29000	8658	7.79	1.0e+00	1.00074	0.00106	1.00287	hcsrcyct12_29_1_15	1.00071	0.00139	1.00348
ncsrcyct11_28_1_15	0.0	28000	28000	8711	8.12	1.0e+00	0.99381	0.00135	0.99652	hcsrcyct12_28_1_15	0.99442	0.00129	0.99700
ncsrcyct11_27_1_15	0.0	27000	27000	8764	8.47	1.0e+00	0.98595	0.00094	0.98782	hcsrcyct12_27_1_15	0.99057	0.00119	0.99296
ncsrcyct11_26_1_15	0.0	26000	26000	8817	8.85	1.0e+00	0.97783	0.00117	0.98017	hcsrcyct12_26_1_15	0.98010	0.00135	0.98281
ncsrcyct11_25_1_15	0.0	25000	25000	8870	9.26	1.0e+00	0.97189	0.00126	0.97440	hcsrcyct12_25_1_15	0.97263	0.00118	0.97499
ncsrcyct11_24_1_15	0.0	24000	24000	8923	9.70	1.0e+00	0.96439	0.00121	0.96681	hcsrcyct12_24_1_15	0.96656	0.00113	0.96881
ncsrcyct11_23_1_15	0.0	23000	23000	8977	10.19	1.0e+00	0.95375	0.00130	0.95635	hcsrcyct12_23_1_15	0.95783	0.00118	0.96018
ncsrcyct11_22_1_15	0.0	22000	22000	9030	10.71	1.0e+00	0.94744	0.00132	0.95008	hcsrcyct12_22_1_15	0.94901	0.00143	0.95187
ncsrcyct11_21_1_15	0.0	21000	21000	9083	11.29	1.0e+00	0.93842	0.00127	0.94095	hcsrcyct12_21_1_15	0.93880	0.00126	0.94132
ncsrcyct11_20_1_15	0.0	20000	20000	9136	11.92	1.0e+00	0.92684	0.00118	0.92920	hcsrcyct12_20_1_15	0.92929	0.00124	0.93176
ncsrcyct11_19_1_15	0.0	19000	19000	9189	12.62	1.0e+00	0.91527	0.00109	0.91745	hcsrcyct12_19_1_15	0.91879	0.00101	0.92081
ncsrcyct11_18_1_15	0.0	18000	18000	9242	13.40	1.0e+00	0.90374	0.00111	0.90597	hcsrcyct12_18_1_15	0.90716	0.00105	0.90927
ncsrcyct11_17_1_15	0.0	17000	17000	9295	14.27	1.0e+00	0.89147	0.00133	0.89412	hcsrcyct12_17_1_15	0.89585	0.00104	0.89794
ncsrcyct11_16_1_15	0.0	16000	16000	9348	15.25	1.0e+00	0.87788	0.00101	0.87990	hcsrcyct12_16_1_15	0.87933	0.00118	0.88168
ncsrcyct11_15_1_15	0.0	15000	15000	9401	16.36	1.0e+00	0.86209	0.00110	0.86429	hcsrcyct12_15_1_15	0.86488	0.00110	0.86708
with can spacers (np thickness = 1.4 in.)													
ncsrcyct11_36_2_1	1.4	36000	36000	7673	5.56	1.0e-20	0.87502	0.00112	0.87725	hcsrcyct12_36_2_1	0.87543	0.00107	0.87757
ncsrcyct11_36_2_2	1.4	36000	36000	7673	5.56	1.0e-05	0.87474	0.00108	0.87691	hcsrcyct12_36_2_2	0.87795	0.00117	0.88029
ncsrcyct11_36_2_3	1.4	36000	36000	7673	5.56	1.0e-04	0.87595	0.00126	0.87846	hcsrcyct12_36_2_3	0.87675	0.00112	0.87899

Table 6.9.6-7. Results for 4.25 in.-diameter cylinder HEU metal content in packaging calculation model

case name	np (in)	U (g)	^{235}U (g)	H_2O (g)	h/x	moifr	k_{eff}	σ	$k_{eff}+2σ$	case name	k_{eff}	σ	$k_{eff}+2σ$
ncsrcyct11_36_2_4	1.4	36000	36000	7673	5.56	1.0e-03	0.87655	0.00100	0.87856	hcsrcyct12_36_2_4	0.87798	0.00106	0.88011
ncsrcyct11_36_2_5	1.4	36000	36000	7673	5.56	1.0e-02	0.87634	0.00104	0.87843	hcsrcyct12_36_2_5	0.87876	0.00109	0.88094
ncsrcyct11_36_2_6	1.4	36000	36000	7673	5.56	1.0e-01	0.87971	0.00102	0.88174	hcsrcyct12_36_2_6	0.88317	0.00111	0.88539
ncsrcyct11_36_2_8	1.4	36000	36000	7673	5.56	3.0e-01	0.88865	0.00115	0.89094	hcsrcyct12_36_2_8	0.89169	0.00103	0.89375
ncsrcyct11_36_2_15	1.4	36000	36000	7673	5.56	1.0e+00	0.91608	0.00120	0.91847	hcsrcyct12_36_2_15	0.91815	0.00118	0.92050
ncsrcyct11_36_2_15	1.4	36000	36000	7673	5.56	1.0e+00	0.91608	0.00120	0.91847	hcsrcyct12_36_2_15	0.91815	0.00118	0.92050
ncsrcyct11_35_2_15	1.4	35000	35000	7726	5.76	1.0e+00	0.91190	0.00116	0.91422	hcsrcyct12_35_2_15	0.91300	0.00117	0.91534
ncsrcyct11_34_2_15	1.4	34000	34000	7779	5.97	1.0e+00	0.90497	0.00112	0.90721	hcsrcyct12_34_2_15	0.90616	0.00116	0.90848
ncsrcyct11_33_2_15	1.4	33000	33000	7832	6.19	1.0e+00	0.90032	0.00120	0.90272	hcsrcyct12_33_2_15	0.90269	0.00118	0.90506
ncsrcyct11_32_2_15	1.4	32000	32000	7885	6.43	1.0e+00	0.89251	0.00102	0.89455	hcsrcyct12_32_2_15	0.89526	0.00120	0.89766
ncsrcyct11_31_2_15	1.4	31000	31000	7938	6.68	1.0e+00	0.88531	0.00136	0.88803	hcsrcyct12_31_2_15	0.88765	0.00108	0.88981
ncsrcyct11_30_2_15	1.4	30000	30000	7992	6.95	1.0e+00	0.88012	0.00120	0.88252	hcsrcyct12_30_2_15	0.88005	0.00120	0.88246
content in flooded containment vessel, array packaging model for CSI=0.0													
NCT										**HAC**			
no can spacers (np thickness = 0.0 in.)													
nciacyct11_36_1_3	0.0	36000	36000	8287	6.01	1.0e-04	1.10334	0.00135	1.10604	hciacyct12_36_1_3	1.10722	0.00119	1.10961
nciacyct11_35_1_3	0.0	35000	35000	8340	6.22	1.0e-04	1.10128	0.00116	1.10360	hciacyct12_35_1_3	1.10067	0.00114	1.10295
nciacyct11_34_1_3	0.0	34000	34000	8393	6.44	1.0e-04	1.09399	0.00125	1.09648	hciacyct12_34_1_3	1.09477	0.00124	1.09726
nciacyct11_33_1_3	0.0	33000	33000	8446	6.68	1.0e-04	1.08794	0.00127	1.09048	hciacyct12_33_1_3	1.08942	0.00134	1.09210
nciacyct11_32_1_3	0.0	32000	32000	8499	6.93	1.0e-04	1.08183	0.00131	1.08444	hciacyct12_32_1_3	1.08089	0.00128	1.08346
nciacyct11_31_1_3	0.0	31000	31000	8552	7.20	1.0e-04	1.07391	0.00114	1.07619	hciacyct12_31_1_3	1.07627	0.00101	1.07829
nciacyct11_30_1_3	0.0	30000	30000	8605	7.49	1.0e-04	1.06840	0.00131	1.07102	hciacyct12_30_1_3	1.06781	0.00107	1.06994
nciacyct11_29_1_3	0.0	29000	29000	8658	7.79	1.0e-04	1.06070	0.00108	1.06286	hciacyct12_29_1_3	1.05946	0.00121	1.06188
nciacyct11_28_1_3	0.0	28000	28000	8711	8.12	1.0e-04	1.05398	0.00116	1.05630	hciacyct12_28_1_3	1.05253	0.00102	1.05457

Table 6.9.6-7. Results for 4.25 in.-diameter cylinder HEU metal content in packaging calculation model

case name	np (in)	U (g)	^{235}U (g)	H_2O (g)	h/x	moifr	k_{eff}	σ	$k_{eff}+2σ$	case name	k_{eff}	σ	$k_{eff}+2σ$
nciacyct11_27_1_3	0.0	27000	27000	8764	8.47	1.0e-04	1.04385	0.00142	1.04670	hciacyct12_27_1_3	1.04481	0.00121	1.04723
nciacyct11_26_1_3	0.0	26000	26000	8817	8.85	1.0e-04	1.03489	0.00124	1.03736	hciacyct12_26_1_3	1.03688	0.00118	1.03923
nciacyct11_25_1_3	0.0	25000	25000	8870	9.26	1.0e-04	1.02495	0.00128	1.02751	hciacyct12_25_1_3	1.02706	0.00120	1.02946
nciacyct11_24_1_3	0.0	24000	24000	8923	9.70	1.0e-04	1.01610	0.00120	1.01850	hciacyct12_24_1_3	1.01634	0.00118	1.01870
nciacyct11_23_1_3	0.0	23000	23000	8977	10.19	1.0e-04	1.00723	0.00108	1.00938	hciacyct12_23_1_3	1.00427	0.00110	1.00648
nciacyct11_22_1_3	0.0	22000	22000	9030	10.71	1.0e-04	0.99573	0.00122	0.99817	hciacyct12_22_1_3	0.99481	0.00112	0.99705
nciacyct11_21_1_3	0.0	21000	21000	9083	11.29	1.0e-04	0.98149	0.00122	0.98393	hciacyct12_21_1_3	0.98514	0.00127	0.98768
nciacyct11_20_1_3	0.0	20000	20000	9136	11.92	1.0e-04	0.97377	0.00104	0.97585	hciacyct12_20_1_3	0.97210	0.00120	0.97450
nciacyct11_19_1_3	0.0	19000	19000	9189	12.62	1.0e-04	0.95985	0.00127	0.96240	hciacyct12_19_1_3	0.95807	0.00143	0.96092
nciacyct11_18_1_3	0.0	18000	18000	9242	13.40	1.0e-04	0.94375	0.00137	0.94649	hciacyct12_18_1_3	0.94639	0.00124	0.94887
nciacyct11_15_1_3	0.0	15000	15000	9401	16.36	1.0e-04	0.89699	0.00109	0.89917	hciacyct12_15_1_3	0.89646	0.00108	0.89862
nciacyct11_12_1_3	0.0	12000	12000	9560	20.79	1.0e-04	0.83537	0.00118	0.83772	hciacyct12_12_1_3	0.83858	0.00118	0.84093
nciacyct11_9_1_3	0.0	9000	9000	9719	28.19	1.0e-04	0.76061	0.00121	0.76303	hciacyct12_9_1_3	0.75657	0.00112	0.75882
nciacyct11_6_1_3	0.0	6000	6000	9879	42.97	1.0e-04	0.64959	0.00106	0.65172	hciacyct12_6_1_3	0.64940	0.00109	0.65157
nciacyct11_3_1_3	0.0	3000	3000	10038	87.33	1.0e-04	0.48405	0.00103	0.48611	hciacyct12_3_1_3	0.48552	0.00096	0.48745
with can spacers (np thickness = 1.4 in.)													
nciacyct11_36_2_3	1.4	36000	36000	7673	5.56	1.0e-04	1.01018	0.00139	1.01297	hciacyct12_36_2_3	1.01024	0.00120	1.01263
nciacyct11_35_2_3	1.4	35000	35000	7726	5.76	1.0e-04	1.00029	0.00110	1.00249	hciacyct12_35_2_3	1.00083	0.00105	1.00293
nciacyct11_34_2_3	1.4	34000	34000	7779	5.97	1.0e-04	0.99523	0.00100	0.99723	hciacyct12_34_2_3	0.99499	0.00116	0.99731
nciacyct11_33_2_3	1.4	33000	33000	7832	6.19	1.0e-04	0.98713	0.00110	0.98932	hciacyct12_33_2_3	0.98922	0.00108	0.99139
nciacyct11_32_2_3	1.4	32000	32000	7885	6.43	1.0e-04	0.97809	0.00109	0.98028	hciacyct12_32_2_3	0.98046	0.00098	0.98242
nciacyct11_31_2_3	1.4	31000	31000	7938	6.68	1.0e-04	0.96968	0.00130	0.97227	hciacyct12_31_2_3	0.96951	0.00147	0.97246
nciacyct11_30_2_3	1.4	30000	30000	7992	6.95	1.0e-04	0.96031	0.00132	0.96295	hciacyct12_30_2_3	0.96156	0.00107	0.96370
nciacyct11_29_2_3	1.4	29000	29000	8045	7.24	1.0e-04	0.95128	0.00117	0.95362	hciacyct12_29_2_3	0.95414	0.00120	0.95654
nciacyct11_28_2_3	1.4	28000	28000	8098	7.55	1.0e-04	0.94378	0.00138	0.94654	hciacyct12_28_2_3	0.94376	0.00138	0.94652

Table 6.9.6-7. Results for 4.25 in.-diameter cylinder HEU metal content in packaging calculation model

case name	np (in)	U (g)	^{235}U (g)	H_2O (g)	h/x	moifr	k_{eff}	σ	$k_{eff}+2σ$	case name	k_{eff}	σ	$k_{eff}+2σ$
nciacyct11_27_2_3	1.4	27000	27000	8151	7.88	1.0e-04	0.93234	0.00111	0.93456	hciacyct12_27_2_3	0.93273	0.00132	0.93536
nciacyct11_26_2_3	1.4	26000	26000	8204	8.24	1.0e-04	0.92078	0.00104	0.92287	hciacyct12_26_2_3	0.92390	0.00128	0.92646
nciacyct11_25_2_3	1.4	25000	25000	8257	8.62	1.0e-04	0.91264	0.00100	0.91465	hciacyct12_25_2_3	0.91352	0.00105	0.91562
nciacyct11_24_2_3	1.4	24000	24000	8310	9.04	1.0e-04	0.89955	0.00124	0.90203	hciacyct12_24_2_3	0.90170	0.00109	0.90388
nciacyct11_23_2_3	1.4	23000	23000	8363	9.49	1.0e-04	0.89118	0.00128	0.89374	hciacyct12_23_2_3	0.89159	0.00128	0.89414
nciacyct11_22_2_3	1.4	22000	22000	8416	9.98	1.0e-04	0.87715	0.00098	0.87910	hciacyct12_22_2_3	0.87791	0.00103	0.87997
nciacyct11_21_2_3	1.4	21000	21000	8469	10.53	1.0e-04	0.86679	0.00109	0.86898	hciacyct12_21_2_3	0.86482	0.00106	0.86693
nciacyct11_20_2_3	1.4	20000	20000	8522	11.12	1.0e-04	0.85029	0.00131	0.85292	hciacyct12_20_2_3	0.85207	0.00119	0.85445
nciacyct11_19_2_3	1.4	19000	19000	8575	11.78	1.0e-04	0.83585	0.00110	0.83805	hciacyct12_19_2_3	0.83631	0.00101	0.83833
nciacyct11_18_2_3	1.4	18000	18000	8628	12.51	1.0e-04	0.82112	0.00105	0.82323	hciacyct12_18_2_3	0.82020	0.00108	0.82236
nciacyct11_15_2_3	1.4	15000	15000	8787	15.29	1.0e-04	0.77012	0.00102	0.77216	hciacyct12_15_2_3	0.77067	0.00099	0.77265
nciacyct11_12_2_3	1.4	12000	12000	8947	19.46	1.0e-04	0.70996	0.00113	0.71222	hciacyct12_12_2_3	0.70716	0.00100	0.70915
nciacyct11_9_2_3	1.4	9000	9000	9106	26.41	1.0e-04	0.38338	0.00093	0.38524	hciacyct12_9_2_3	0.62982	0.00097	0.63175
nciacyct11_6_2_3	1.4	6000	6000	9265	40.30	1.0e-04	0.63066	0.00100	0.63267	hciacyct12_6_2_3	0.52901	0.00100	0.53101
nciacyct11_3_2_3	1.4	3000	3000	9424	81.99	1.0e-04	0.52971	0.00101	0.53173	hciacyct12_3_2_3	0.38124	0.00075	0.38274

Table 6.9.6-8. Results for 1.5in.-diameter x 2.0 in.-tall slug HEU metal content in CV calculation model

case name	np (in)	U (g)	^{235}U (g)	H_2O (g)	h/x	mocfr	k_{eff}	σ	$k_{eff}+2σ$	content description
flooded containment vessel, reflected										
no can spacers (np thickness = 0.0 in.)										
cvcr5st11_1_1	0.0	18277	18277	9227	13.18	1.0e+00	0.90734	0.00123	0.90980	5 slugs in a pentagonal ring
cvcr5est11_1_1	0.0	18277	18277	9227	13.18	1.0e+00	0.90718	0.00119	0.90955	5 slugs in a pentagonal ring, extended spacing
cvcr50st11_1	0.0	18277	18277	9227	13.18	1.0e+00	0.90671	0.00120	0.90911	5 slugs in cruciform pattern

Table 6.9.6-8. Results for 1.5in.-diameter x 2.0 in.-tall slug HEU metal content in CV calculation model

case name	np (in)	U (g)	^{235}U (g)	H_2O (g)	h/x	mocfr	k_{eff}	σ	$k_{eff}+2σ$	content description
cvcr5e0st11_1	0.0	18277	18277	9227	13.18	1.0e+00	0.90690	0.00124	0.90938	5 slugs in cruciform pattern, extended spacing
cvcr5u0st11_1	0.0	18277	18277	9227	13.18	1.0e+00	0.90690	0.00122	0.90935	5 slugs in four pointed star pattern
cvcr5l0st11_1	0.0	18277	18277	9227	13.18	1.0e+00	0.90660	0.00113	0.90885	5 slugs, filled hex. Ring with 2 slugs missing
cvcr6st11_1_1	0.0	21933	21933	9033	10.75	1.0e+00	0.95173	0.00118	0.95409	6 slugs in a hexagonal ring
cvcr6e0st11_1	0.0	21933	21933	9033	10.75	1.0e+00	0.95531	0.00106	0.95742	6 slugs in pentagonal ring with center slug
cvcr70st11_1	0.0	25588	25588	8839	9.02	1.0e+00	0.99827	0.00135	1.00097	7 slugs in hexagonal ring with center slug
cvcr5st11_1_2	0.0	36555	36555	8257	5.90	1.0e+00	0.99909	0.00125	1.00158	10 slugs in stacked pentagonal rings
cvcr5est11_1_2	0.0	36555	36555	8257	5.90	1.0e+00	1.00409	0.00136	1.00681	10 slugs in stacked pent. rings, extended spacing
cvcr6e4st11_1	0.0	36555	36555	8257	5.90	1.0e+00	1.00361	0.00134	1.00630	10 slugs, lower 6 slugs in hex ring, upper 4 in square
cvcr73st11_1	0.0	36555	36555	8257	5.90	1.0e+00	1.00523	0.00127	1.00776	10 slugs, lower 7 slugs in hex ring, upper 3 in triangle
cvcr6st11_1_2	0.0	43865	43865	7869	4.68	1.0e+00	1.05336	0.00130	1.05597	12 slugs in stacked hexagonal rings
with can spacers (np thickness=1.4 in.)										
cvcr5st11_2_1	1.4	18277	18277	8613	12.30	1.0e+00	0.76864	0.00113	0.77089	5 slugs in a pentagonal ring
cvcr5est11_2_1	1.4	18277	18277	8613	12.30	1.0e+00	0.76420	0.00102	0.76624	5 slugs in a pentagonal ring, extended spacing
cvcr50st11_2	1.4	18277	18277	8613	12.30	1.0e+00	0.76929	0.00117	0.77163	5 slugs in cruciform pattern
cvcr5e0st11_2	1.4	18277	18277	8613	12.30	1.0e+00	0.76532	0.00127	0.76785	5 slugs in cruciform pattern, extended spacing
cvcr5u0st11_2	1.4	18277	18277	8613	12.30	1.0e+00	0.76953	0.00108	0.77168	5 slugs in four pointed star pattern
cvcr5l0st11_2	1.4	18277	18277	8613	12.30	1.0e+00	0.77162	0.00102	0.77366	5 slugs, filled hex. Ring with 2 slugs missing
cvcr6st11_2_1	1.4	21933	21933	8419	10.02	1.0e+00	0.81300	0.00148	0.81596	6 slugs in a hexagonal ring
cvcr6e0st11_2	1.4	21933	21933	8419	10.02	1.0e+00	0.81943	0.00116	0.82176	6 slugs in pentagonal ring with center slug
cvcr70st11_2	1.4	25588	25588	8225	8.39	1.0e+00	0.86296	0.00104	0.86503	7 slugs in hexagonal ring with center slug
cvcr5st11_2_2	1.4	36555	36555	7643	5.46	1.0e+00	0.90058	0.00115	0.90287	10 slugs in stacked pentagonal rings
cvcr5est11_2_2	1.4	36555	36555	7643	5.46	1.0e+00	0.89862	0.00121	0.90104	10 slugs in stacked pent. rings, extended spacing
cvcr6e4st11_2	1.4	36555	36555	7643	5.46	1.0e+00	0.89991	0.00109	0.90209	10 slugs, lower 6 slugs in hex ring, upper 4 in square

Table 6.9.6-8. Results for 1.5in.-diameter x 2.0 in.-tall slug HEU metal content in CV calculation model

case name	np (in)	U (g)	^{235}U (g)	H_2O (g)	h/x	mocfr	k_{eff}	σ	$k_{eff}+2σ$	content description
cvcr73st11_2	1.4	36555	36555	7643	5.46	1.0e+00	0.89922	0.00109	0.90139	10 slugs, lower 7 slugs in hex ring, upper 3 in triangle
cvcr6st11_2_2	1.4	43865	43865	7256	4.32	1.0e+00	0.94962	0.00126	0.95213	12 slugs in stacked hexagonal rings
evaluation of model approximations in no can spacer configurations (np thickness=0.0002 in.)										
cvcr6e0st11_1	0.0	21933	21933	9033	10.75	1.0e+00	0.95531	0.00106	0.95742	6 slugs in pentagonal ring with center slug
cv0r6e0s_1	0.0	21933	21933	9033	10.75	1.0e+00	0.95418	0.00135	0.95689	0.0002 cm thick spacers voided in above model
cvwr6e0s_1	0.0	21933	21933	9033	10.75	1.0e+00	0.95384	0.00117	0.95618	0.0002 cm thick spacers replaced with water in above
cvcr70st11_1	0.0	25588	25588	8839	9.02	1.0e+00	0.99827	0.00135	1.00097	7 slugs, hex ring with slug in center
cv0r70s_1	0.0	25588	25588	8839	9.02	1.0e+00	0.99814	0.00118	1.00051	0.0002 cm thick spacers voided in above model
cvwr70s_1	0.0	25588	25588	8839	9.02	1.0e+00	0.99847	0.00120	1.00088	0.0002 cm thick spacers flooded in above model
evaluation of model approximations in configurations with can spacers (np thickness=1.4 in.)										
cvcr6e0st11_2	1.4	21933	21933	8419	10.02	1.0e+00	0.81943	0.00116	0.82176	6 slugs in pentagonal ring with center slug
cv0r6e0s_2	1.4	21933	21933	8419	10.02	1.0e+00	0.84682	0.00118	0.84918	1.4 in thick spacers voided in above model
cvcr6e0st11_1	0.0	21933	21933	9033	10.75	1.0e+00	0.95531	0.00106	0.95742	6 slugs in pentagonal ring with center slug
cvwr6e0s_2	1.4	21933	21933	9033	10.75	1.0e+00	0.89988	0.00138	0.90263	1.4 in thick spacers replace with water
cvcr70st11_2	1.4	25588	25588	8225	8.39	1.0e+00	0.86296	0.00104	0.86503	7 slugs, hex ring with slug in center
cv0r70s_2	1.4	25588	25588	8225	8.39	1.0e+00	0.88250	0.00110	0.88470	1.4 in thick spacers voided in above model
cvcr70st11_1	0.0	25588	25588	8839	9.02	1.0e+00	0.99827	0.00135	1.00097	7 slugs, hex ring with slug in center
cvwr70s_2	1.4	25588	25588	8839	9.02	1.0e+00	0.93953	0.00111	0.94175	1.4 in thick spacers replace with water

Table 6.9.6-9. Results for 1.5in.-diameter x 2.0 in.-tall slug HEU metal content in packaging calculation model

case name	enr	U (g)	^{235}U (g)	H_2O (g)	h/x	moifr	k_{eff}	σ	$k_{eff}+2σ$	case name	k_{eff}	σ	$k_{eff}+2σ$
content in flooded containment vessel, single package reflected													
NCT										HAC			
no can spacers (np thickness = 0.0 in.)													
ncsr5est11_1_1_15	100	18277	18277	9227	13.18	1.0e+00	0.86857	0.00128	0.87113	hcsr5est12_1_1_15	0.87319	0.00116	0.87551
ncsr5st11_1_1_15	100	18277	18277	9227	13.18	1.0e+00	0.88102	0.00119	0.88339	hcsr5st12_1_1_15	0.88322	0.00142	0.88606
ncsr6st11_1_1_15	100	21933	21933	9033	10.75	1.0e+00	0.91461	0.00110	0.91680				
ncsr5est11_1_2_15	100	36555	36555	8257	5.90	1.0e+00	0.96511	0.00123	0.96756	hcsr5est12_1_2_15	0.96512	0.00128	0.96768
ncsr5st11_1_2_15	100	36555	36555	8257	5.90	1.0e+00	0.96727	0.00116	0.96960	hcsr5st12_1_2_15	0.97082	0.00124	0.97330
ncsr6e4st11_1_1	100	36555	36555	8257	5.90	1.0e-20	0.92156	0.00105	0.92367				
ncsr6e4st11_1_2	100	36555	36555	8257	5.90	1.0e-05	0.92051	0.00114	0.92279				
ncsr6e4st11_1_3	100	36555	36555	8257	5.90	1.0e-04	0.92239	0.00107	0.92453				
ncsr6e4st11_1_4	100	36555	36555	8257	5.90	1.0e-03	0.91834	0.00126	0.92086				
ncsr6e4st11_1_5	100	36555	36555	8257	5.90	1.0e-02	0.92233	0.00111	0.92455				
ncsr6e4st11_1_6	100	36555	36555	8257	5.90	1.0e-01	0.92584	0.00123	0.92830				
ncsr6e4st11_1_8	100	36555	36555	8257	5.90	3.0e-01	0.93741	0.00125	0.93990				
ncsr6e4st11_1_15	100	36555	36555	8257	5.90	1.0e+00	0.97010	0.00114	0.97238				
ncsr73st11_1_1	100	36555	36555	8257	5.90	1.0e-20	0.92144	0.00127	0.92399				
ncsr73st11_1_2	100	36555	36555	8257	5.90	1.0e-05	0.92591	0.00108	0.92808				
ncsr73st11_1_3	100	36555	36555	8257	5.90	1.0e-04	0.92106	0.00121	0.92348				
ncsr73st11_1_4	100	36555	36555	8257	5.90	1.0e-03	0.92326	0.00122	0.92570				
ncsr73st11_1_5	100	36555	36555	8257	5.90	1.0e-02	0.92213	0.00113	0.92439				
ncsr73st11_1_6	100	36555	36555	8257	5.90	1.0e-01	0.92784	0.00111	0.93007				

Table 6.9.6-9. Results for 1.5in.-diameter x 2.0 in.-tall slug HEU metal content in packaging calculation model

case name	enr	U (g)	^{235}U (g)	H_2O (g)	h/x	moifr	k_{eff}	σ	$k_{eff}+2σ$	case name	k_{eff}	σ	$k_{eff}+2σ$
ncsr73st11_1_8	100	36555	36555	8257	5.90	3.0e-01	0.93898	0.00115	0.94128				
ncsr73st11_1_15	100	36555	36555	8257	5.90	1.0e+00	0.96854	0.00128	0.97110				
ncsr6st11_1_2_15	100	43865	43865	7869	4.68	1.0e+00	1.01197	0.00132	1.01461				
with can spacers (np thickness = 1.4 in.)													
ncsr5est11_2_1_1	100	18277	18277	8613	12.30	1.0e-20	0.68597	0.00122	0.68841	hcsr5est12_2_1_1	0.68926	0.00101	0.69128
ncsr5est11_2_1_2	100	18277	18277	8613	12.30	1.0e-05	0.68486	0.00101	0.68688	hcsr5est12_2_1_2	0.68645	0.00110	0.68866
ncsr5est11_2_1_3	100	18277	18277	8613	12.30	1.0e-04	0.68766	0.00128	0.69022	hcsr5est12_2_1_3	0.68796	0.00105	0.69007
ncsr5est11_2_1_4	100	18277	18277	8613	12.30	1.0e-03	0.68729	0.00120	0.68969	hcsr5est12_2_1_4	0.68815	0.00098	0.69010
ncsr5est11_2_1_5	100	18277	18277	8613	12.30	1.0e-02	0.68465	0.00128	0.68720	hcsr5est12_2_1_5	0.69008	0.00097	0.69201
ncsr5est11_2_1_6	100	18277	18277	8613	12.30	1.0e-01	0.68906	0.00105	0.69117	hcsr5est12_2_1_6	0.69613	0.00117	0.69847
ncsr5est11_2_1_8	100	18277	18277	8613	12.30	3.0e-01	0.70289	0.00101	0.70491	hcsr5est12_2_1_8	0.70357	0.00107	0.70571
ncsr5est11_2_1_15	100	18277	18277	8613	12.30	1.0e+00	0.73412	0.00109	0.73629	hcsr5est12_2_1_15	0.73557	0.00101	0.73759
ncsr5st11_2_1_1	100	18277	18277	8613	12.30	1.0e-20	0.70896	0.00096	0.71087				
ncsr5st11_2_1_2	100	18277	18277	8613	12.30	1.0e-05	0.70901	0.00095	0.71092				
ncsr5st11_2_1_3	100	18277	18277	8613	12.30	1.0e-04	0.71109	0.00096	0.71300				
ncsr5st11_2_1_4	100	18277	18277	8613	12.30	1.0e-03	0.70980	0.00102	0.71184				
ncsr5st11_2_1_5	100	18277	18277	8613	12.30	1.0e-02	0.71089	0.00103	0.71294				
ncsr5st11_2_1_6	100	18277	18277	8613	12.30	1.0e-01	0.71505	0.00112	0.71729				
ncsr5st11_2_1_8	100	18277	18277	8613	12.30	3.0e-01	0.72364	0.00121	0.72605				
ncsr5st11_2_1_15	100	18277	18277	8613	12.30	1.0e+00	0.74773	0.00114	0.75001	hcsr5st12_2_1_15	0.74885	0.00101	0.75087
ncsr6st11_2_1_1	100	21933	21933	8419	10.02	1.0e-20	0.73305	0.00104	0.73514				
ncsr6st11_2_1_2	100	21933	21933	8419	10.02	1.0e-05	0.73284	0.00105	0.73494				

Table 6.9.6-9. Results for 1.5in.-diameter x 2.0 in.-tall slug HEU metal content in packaging calculation model

case name	enr	U (g)	^{235}U (g)	H_2O (g)	h/x	moifr	k_{eff}	σ	$k_{eff}+2σ$	case name	k_{eff}	σ	$k_{eff}+2σ$
ncsr6st11_2_1_3	100	21933	21933	8419	10.02	1.0e-04	0.73419	0.00111	0.73641				
ncsr6st11_2_1_4	100	21933	21933	8419	10.02	1.0e-03	0.73339	0.00106	0.73551				
ncsr6st11_2_1_5	100	21933	21933	8419	10.02	1.0e-02	0.73282	0.00101	0.73484				
ncsr6st11_2_1_6	100	21933	21933	8419	10.02	1.0e-01	0.73962	0.00104	0.74170				
ncsr6st11_2_1_8	100	21933	21933	8419	10.02	3.0e-01	0.74981	0.00112	0.75206				
ncsr6st11_2_1_15	100	21933	21933	8419	10.02	1.0e+00	0.78295	0.00118	0.78531				
ncsr5est11_2_2_1	100	36555	36555	7643	5.46	1.0e-20	0.81441	0.00102	0.81646	hcsr5est12_2_2_1	0.81949	0.00126	0.82202
ncsr5est11_2_2_2	100	36555	36555	7643	5.46	1.0e-05	0.81751	0.00107	0.81966	hcsr5est12_2_2_2	0.81765	0.00108	0.81981
ncsr5est11_2_2_3	100	36555	36555	7643	5.46	1.0e-04	0.81443	0.00110	0.81664	hcsr5est12_2_2_3	0.81691	0.00115	0.81922
ncsr5est11_2_2_4	100	36555	36555	7643	5.46	1.0e-03	0.81628	0.00124	0.81876	hcsr5est12_2_2_4	0.81854	0.00123	0.82100
ncsr5est11_2_2_5	100	36555	36555	7643	5.46	1.0e-02	0.81513	0.00118	0.81749	hcsr5est12_2_2_5	0.81898	0.00104	0.82106
ncsr5est11_2_2_6	100	36555	36555	7643	5.46	1.0e-01	0.82099	0.00114	0.82326	hcsr5est12_2_2_6	0.82414	0.00111	0.82636
ncsr5est11_2_2_8	100	36555	36555	7643	5.46	3.0e-01	0.83205	0.00109	0.83424	hcsr5est12_2_2_8	0.83469	0.00107	0.83683
ncsr5est11_2_2_15	100	36555	36555	7643	5.46	1.0e+00	0.86471	0.00124	0.86719	hcsr5est12_2_2_15	0.86591	0.00115	0.86822
ncsr5st11_2_2_1	100	36555	36555	7643	5.46	1.0e-20	0.83654	0.00109	0.83872				
ncsr5st11_2_2_2	100	36555	36555	7643	5.46	1.0e-05	0.83389	0.00104	0.83597				
ncsr5st11_2_2_3	100	36555	36555	7643	5.46	1.0e-04	0.83615	0.00113	0.83841				
ncsr5st11_2_2_4	100	36555	36555	7643	5.46	1.0e-03	0.83524	0.00141	0.83806				
ncsr5st11_2_2_5	100	36555	36555	7643	5.46	1.0e-02	0.83580	0.00109	0.83797				
ncsr5st11_2_2_6	100	36555	36555	7643	5.46	1.0e-01	0.84206	0.00110	0.84426				
ncsr5st11_2_2_8	100	36555	36555	7643	5.46	3.0e-01	0.85011	0.00135	0.85281				
ncsr5st11_2_2_15	100	36555	36555	7643	5.46	1.0e+00	0.87549	0.00131	0.87810	hcsr5st12_2_2_15	0.87483	0.00116	0.87715

Table 6.9.6-9. Results for 1.5in.-diameter x 2.0 in.-tall slug HEU metal content in packaging calculation model

case name	enr	U (g)	^{235}U (g)	H_2O (g)	h/x	moifr	k_{eff}	σ	$k_{eff}+2σ$	case name	k_{eff}	σ	$k_{eff}+2σ$
ncsr6e4st11_2_1	100	36555	36555	7643	5.46	1.0e-20	0.83636	0.00110	0.83857				
ncsr6e4st11_2_2	100	36555	36555	7643	5.46	1.0e-05	0.83532	0.00112	0.83757				
ncsr6e4st11_2_3	100	36555	36555	7643	5.46	1.0e-04	0.83689	0.00118	0.83924				
ncsr6e4st11_2_4	100	36555	36555	7643	5.46	1.0e-03	0.83744	0.00114	0.83972				
ncsr6e4st11_2_5	100	36555	36555	7643	5.46	1.0e-02	0.83615	0.00122	0.83858				
ncsr6e4st11_2_6	100	36555	36555	7643	5.46	1.0e-01	0.84173	0.00127	0.84426				
ncsr6e4st11_2_8	100	36555	36555	7643	5.46	3.0e-01	0.84987	0.00113	0.85213				
ncsr6e4st11_2_15	100	36555	36555	7643	5.46	1.0e+00	0.87722	0.00131	0.87984				
ncsr73st11_2_1	100	36555	36555	7643	5.46	1.0e-20	0.83665	0.00111	0.83887				
ncsr73st11_2_2	100	36555	36555	7643	5.46	1.0e-05	0.83570	0.00116	0.83801				
ncsr73st11_2_3	100	36555	36555	7643	5.46	1.0e-04	0.83716	0.00115	0.83946				
ncsr73st11_2_4	100	36555	36555	7643	5.46	1.0e-03	0.83728	0.00117	0.83961				
ncsr73st11_2_5	100	36555	36555	7643	5.46	1.0e-02	0.83790	0.00116	0.84023				
ncsr73st11_2_6	100	36555	36555	7643	5.46	1.0e-01	0.84068	0.00120	0.84309				
ncsr73st11_2_8	100	36555	36555	7643	5.46	3.0e-01	0.84928	0.00106	0.85139				
ncsr73st11_2_15	100	36555	36555	7643	5.46	1.0e+00	0.87257	0.00099	0.87455				
ncsr6st11_2_2_1	100	43865	43865	7256	4.32	1.0e-20	0.86427	0.00104	0.86636				
ncsr6st11_2_2_2	100	43865	43865	7256	4.32	1.0e-05	0.86386	0.00108	0.86601				
ncsr6st11_2_2_3	100	43865	43865	7256	4.32	1.0e-04	0.86637	0.00117	0.86870				
ncsr6st11_2_2_4	100	43865	43865	7256	4.32	1.0e-03	0.86498	0.00125	0.86747				
ncsr6st11_2_2_5	100	43865	43865	7256	4.32	1.0e-02	0.86541	0.00116	0.86773				
ncsr6st11_2_2_6	100	43865	43865	7256	4.32	1.0e-01	0.87070	0.00111	0.87292				

Table 6.9.6-9. Results for 1.5in.-diameter x 2.0 in.-tall slug HEU metal content in packaging calculation model

case name	enr	U (g)	^{235}U (g)	H_2O (g)	h/x	moifr	k_{eff}	σ	$k_{eff}+2σ$	case name	k_{eff}	σ	$k_{eff}+2σ$
ncsr6st11_2_2_8	100	43865	43865	7256	4.32	3.0e-01	0.88148	0.00122	0.88392				
ncsr6st11_2_2_15	100	43865	43865	7256	4.32	1.0e+00	0.91478	0.00118	0.91713				
content in flooded containment vessel, array packaging model for CSI=0.0													
NCT										**HAC**			
no can spacers (np thickness = 0.0 in.)													
ncia5est11_1_1_8_3	100	18277	18277	9227	13.18	1.0e-04	0.92163	0.00126	0.92414	hcia5est12_1_1_8_3	0.91941	0.00126	0.92194
ncia5est11_1_1_7_3	95	18289	17374	9227	13.86	1.0e-04	0.90412	0.00109	0.90630	hcia5est12_1_1_7_3	0.90066	0.00110	0.90285
ncia5est11_1_1_5_3	90	18324	14659	9227	16.43	1.0e-04	0.85207	0.00110	0.85427	hcia5est12_1_1_6_3	0.88401	0.00108	0.88616
ncia5est11_1_1_4_3	80	18347	12843	9227	18.75	1.0e-04	0.81402	0.00108	0.81617	hcia5est12_1_1_5_3	0.84983	0.00117	0.85217
ncia5est11_1_1_6_3	70	18300	16470	9227	14.62	1.0e-04	0.88510	0.00118	0.88746	hcia5est12_1_1_4_3	0.81368	0.00111	0.81590
ncia5est11_1_1_3_3	60	18370	11022	9227	21.85	1.0e-04	0.77131	0.00109	0.77349	hcia5est12_1_1_3_3	0.77296	0.00113	0.77523
ncia5est11_1_1_2_3	40	18417	7367	9227	32.69	1.0e-04	0.67736	0.00103	0.67943	hcia5est12_1_1_2_3	0.67968	0.00108	0.68184
ncia5est11_1_1_1_3	19	18466	3509	9227	68.64	1.0e-04	0.54780	0.00092	0.54964	hcia5est12_1_1_1_3	0.54586	0.00117	0.54819
ncia5st11_1_1_8_3	100	18277	18277	9227	13.18	1.0e-04	0.92611	0.00127	0.92865	hcia5st12_1_1_8_3	0.92609	0.00110	0.92829
ncia5st11_1_1_7_3	95	18289	17374	9227	13.86	1.0e-04	0.90538	0.00116	0.90769	hcia5st12_1_1_7_3	0.90683	0.00113	0.90909
ncia5st11_1_1_5_3	90	18324	14659	9227	16.43	1.0e-04	0.88586	0.00112	0.88811	hcia5st12_1_1_6_3	0.88827	0.00110	0.89046
ncia5st11_1_1_4_3	80	18347	12843	9227	18.75	1.0e-04	0.84871	0.00124	0.85119	hcia5st12_1_1_5_3	0.85050	0.00113	0.85276
ncia5st11_1_1_6_3	70	18300	16470	9227	14.62	1.0e-04	0.80834	0.00102	0.81037	hcia5st12_1_1_4_3	0.80870	0.00112	0.81094
ncia5st11_1_1_3_3	60	18370	11022	9227	21.85	1.0e-04	0.76467	0.00098	0.76663	hcia5st12_1_1_3_3	0.76245	0.00105	0.76454
ncia5st11_1_1_2_3	40	18417	7367	9227	32.69	1.0e-04	0.66040	0.00106	0.66252	hcia5st12_1_1_2_3	0.65955	0.00097	0.66149
ncia5st11_1_1_1_3	19	18466	3509	9227	68.64	1.0e-04	0.51929	0.00090	0.52109	hcia5st12_1_1_1_3	0.51805	0.00084	0.51973
with can spacers (np thickness = 1.4 in.)													
ncia5est11_2_1_8_3	100	18277	18277	8613	12.30	1.0e-04	0.80353	0.00113	0.80580	hcia5est12_2_1_8_3	0.80594	0.00121	0.80835
ncia5est11_2_1_7_3	95	18289	17374	8613	12.94	1.0e-04	0.78741	0.00118	0.78977	hcia5est12_2_1_7_3	0.78684	0.00107	0.78898

Table 6.9.6-9. Results for 1.5in.-diameter x 2.0 in.-tall slug HEU metal content in packaging calculation model

case name	enr	U (g)	^{235}U (g)	H_2O (g)	h/x	moifr	k_{eff}	σ	$k_{eff}+2σ$	case name	k_{eff}	σ	$k_{eff}+2σ$
ncia5est11_2_1_6_3	90	18300	16470	8613	13.65	1.0e-04	0.77061	0.00112	0.77285	hcia5est12_2_1_6_3	0.77268	0.00114	0.77496
ncia5est11_2_1_5_3	80	18324	14659	8613	15.34	1.0e-04	0.73732	0.00118	0.73969	hcia5est12_2_1_5_3	0.73645	0.00094	0.73834
ncia5est11_2_1_4_3	70	18347	12843	8613	17.51	1.0e-04	0.70261	0.00108	0.70477	hcia5est12_2_1_4_3	0.70418	0.00107	0.70631
ncia5est11_2_1_3_3	60	18370	11022	8613	20.40	1.0e-04	0.66332	0.00094	0.66520	hcia5est12_2_1_3_3	0.66396	0.00114	0.66624
ncia5est11_2_1_2_3	40	18417	7367	8613	30.52	1.0e-04	0.57466	0.00097	0.57660	hcia5est12_2_1_2_3	0.57526	0.00080	0.57687
ncia5est11_2_1_1_3	19	18466	3509	8613	64.08	1.0e-04	0.45117	0.00082	0.45280	hcia5est12_2_1_1_3	0.45114	0.00084	0.45281
ncia70st11_2_8_3	100	25588	25588	8225	8.39	1.0e-04	0.91300	0.00104	0.91507	hcia70st12_2_8_3	0.91329	0.00111	0.91551
ncia70st11_2_7_3	95	25604	24324	8225	8.83	1.0e-04	0.89143	0.00108	0.89360	hcia70st12_2_7_3	0.89210	0.00124	0.89457
ncia70st11_2_6_3	90	25621	23059	8225	9.31	1.0e-04	0.87368	0.00108	0.87585	hcia70st12_2_6_3	0.87198	0.00113	0.87425
ncia70st11_2_5_3	80	25653	20522	8225	10.46	1.0e-04	0.83357	0.00110	0.83577	hcia70st12_2_5_3	0.83150	0.00106	0.83362
ncia70st11_2_4_3	70	25686	17980	8225	11.94	1.0e-04	0.78606	0.00105	0.78816	hcia70st12_2_4_3	0.78783	0.00099	0.78981
ncia70st11_2_3_3	60	25718	15431	8225	13.91	1.0e-04	0.73820	0.00099	0.74017	hcia70st12_2_3_3	0.73745	0.00100	0.73944
ncia70st11_2_2_3	40	25784	10313	8225	20.82	1.0e-04	0.62591	0.00090	0.62771	hcia70st12_2_2_3	0.62664	0.00107	0.62878
ncia70st11_2_1_3	19	25853	4912	8225	43.71	1.0e-04	0.47179	0.00077	0.47333	hcia70st12_2_1_3	0.47178	0.00086	0.47349
ncia5est11_2_2_8_3	100	36555	36555	7643	5.46	1.0e-04	0.98202	0.00112	0.98425	hcia5est12_2_2_8_3	0.98033	0.00111	0.98254
ncia5est11_2_2_7_3	95	36578	34749	7643	5.74	1.0e-04	0.96108	0.00119	0.96346	hcia5est12_2_2_7_3	0.96166	0.00113	0.96392
ncia5est11_2_2_6_3	90	36601	32941	7643	6.06	1.0e-04	0.94424	0.00134	0.94692	hcia5est12_2_2_6_3	0.94560	0.00118	0.94796
ncia5est11_2_2_5_3	80	36647	29318	7643	6.80	1.0e-04	0.90628	0.00109	0.90846	hcia5est12_2_2_5_3	0.90763	0.00117	0.90997
ncia5est11_2_2_4_3	70	36694	25686	7643	7.77	1.0e-04	0.86606	0.00104	0.86814	hcia5est12_2_2_4_3	0.86855	0.00104	0.87064
ncia5est11_2_2_3_3	60	36740	22044	7643	9.05	1.0e-04	0.82451	0.00098	0.82647	hcia5est12_2_2_3_3	0.82536	0.00115	0.82767
ncia5est11_2_2_2_3	40	36834	14734	7643	13.54	1.0e-04	0.72349	0.00093	0.72535	hcia5est12_2_2_2_3	0.72285	0.00114	0.72513
ncia5est11_2_2_1_3	19	36932	7017	7643	28.43	1.0e-04	0.58171	0.00100	0.58370	hcia5est12_2_2_1_3	0.58235	0.00096	0.58427

Table 6.9.6-9. Results for 1.5in.-diameter x 2.0 in.-tall slug HEU metal content in packaging calculation model

case name	enr	U (g)	^{235}U (g)	H_2O (g)	h/x	moifr	k_{eff}	σ	$k_{eff}+2σ$	case name	k_{eff}	σ	$k_{eff}+2σ$
ncia5st11_2_2_8_3	100	36555	36555	7643	5.46	1.0e-04	0.97720	0.00133	0.97986	hcia5st12_2_2_8_3	0.97562	0.00123	0.97807
ncia5st11_2_2_7_3	95	36578	34749	7643	5.74	1.0e-04	0.95854	0.00105	0.96064	hcia5st12_2_2_7_3	0.95594	0.00097	0.95789
ncia5st11_2_2_6_3	90	36601	32941	7643	6.06	1.0e-04	0.93619	0.00132	0.93883	hcia5st12_2_2_6_3	0.93579	0.00110	0.93800
ncia5st11_2_2_5_3	80	36647	29318	7643	6.80	1.0e-04	0.90011	0.00117	0.90244	hcia5st12_2_2_5_3	0.89786	0.00154	0.90095
ncia5st11_2_2_4_3	70	36694	25686	7643	7.77	1.0e-04	0.85499	0.00102	0.85703	hcia5st12_2_2_4_3	0.85363	0.00119	0.85601
ncia5st11_2_2_3_3	60	36740	22044	7643	9.05	1.0e-04	0.80868	0.00116	0.81101	hcia5st12_2_2_3_3	0.80882	0.00105	0.81091
ncia5st11_2_2_2_3	40	36834	14734	7643	13.54	1.0e-04	0.70077	0.00098	0.70274	hcia5st12_2_2_2_3	0.70205	0.00105	0.70415
ncia5st11_2_2_1_3	19	36932	7017	7643	28.43	1.0e-04	0.55139	0.00095	0.55330	hcia5st12_2_2_1_3	0.55187	0.00101	0.55389
content in flooded containment vessel, array packaging model for CSI=0.4													
NCT										**HAC**			
no can spacers (np thickness = 0.0 in.)													
ncf15est11_1_1_8_3	100	18277	18277	9227	13.18	1.0e-04	0.87707	0.00119	0.87944	hcf25est12_1_1_8_3	0.86992	0.00106	0.87204
ncf15est11_1_1_7_3	95	18289	17374	9227	13.86	1.0e-04	0.86115	0.00120	0.86354	hcf25est12_1_1_7_3	0.85401	0.00126	0.85652
ncf15est11_1_1_6_3	90	18300	16470	9227	14.62	1.0e-04	0.84672	0.00112	0.84896	hcf25est12_1_1_6_3	0.83451	0.00102	0.83656
ncf15est11_1_1_5_3	80	18324	14659	9227	16.43	1.0e-04	0.81108	0.00109	0.81327	hcf25est12_1_1_5_3	0.80144	0.00107	0.80358
ncf15est11_1_1_4_3	70	18347	12843	9227	18.75	1.0e-04	0.77287	0.00112	0.77510	hcf25est12_1_1_4_3	0.76516	0.00111	0.76739
ncf15est11_1_1_3_3	60	18370	11022	9227	21.85	1.0e-04	0.73211	0.00114	0.73440	hcf25est12_1_1_3_3	0.72484	0.00118	0.72719
ncf15est11_1_1_2_3	40	18417	7367	9227	32.69	1.0e-04	0.64270	0.00105	0.64480	hcf25est12_1_1_2_3	0.63366	0.00107	0.63580
ncf15est11_1_1_1_3	19	18466	3509	9227	68.64	1.0e-04	0.51398	0.00088	0.51573	hcf25est12_1_1_1_3	0.51052	0.00094	0.51241
with can spacers (np thickness = 1.4 in.)													
ncf15est11_2_1_8_3	100	18277	18277	8613	12.30	1.0e-04	0.76015	0.00112	0.76239	hcf25est12_2_1_8_3	0.75353	0.00102	0.75558
ncf15est11_2_1_7_3	95	18289	17374	8613	12.94	1.0e-04	0.74428	0.00129	0.74686	hcf25est12_2_1_7_3	0.73938	0.00109	0.74156
ncf15est11_2_1_6_3	90	18300	16470	8613	13.65	1.0e-04	0.72783	0.00107	0.72998	hcf25est12_2_1_6_3	0.72401	0.00105	0.72611
ncf15est11_2_1_5_3	80	18324	14659	8613	15.34	1.0e-04	0.69813	0.00098	0.70009	hcf25est12_2_1_5_3	0.69017	0.00089	0.69195
ncf15est11_2_1_4_3	70	18347	12843	8613	17.51	1.0e-04	0.66593	0.00098	0.66789	hcf25est12_2_1_4_3	0.65691	0.00113	0.65916

Table 6.9.6-9. Results for 1.5in.-diameter x 2.0 in.-tall slug HEU metal content in packaging calculation model

case name	enr	U (g)	^{235}U (g)	H_2O (g)	h/x	moifr	k_{eff}	σ	$k_{eff}+2σ$	case name	k_{eff}	σ	$k_{eff}+2σ$
ncf15est11_2_1_3_3	60	18370	11022	8613	20.40	1.0e-04	0.62541	0.00096	0.62733	hcf25est12_2_1_3_3	0.61903	0.00111	0.62125
ncf15est11_2_1_2_3	40	18417	7367	8613	30.52	1.0e-04	0.54139	0.00091	0.54320	hcf25est12_2_1_2_3	0.53450	0.00087	0.53625
ncf15est11_2_1_1_3	19	18466	3509	8613	64.08	1.0e-04	0.42329	0.00080	0.42489	hcf25est12_2_1_1_3	0.41671	0.00077	0.41825
ncf15est11_2_2_8_3	100	36555	36555	7643	5.46	1.0e-04	0.93621	0.00109	0.93839	hcf25est12_2_2_8_3	0.92186	0.00104	0.92394
ncf15est11_2_2_7_3	95	36578	34749	7643	5.74	1.0e-04	0.91732	0.00132	0.91995	hcf25est12_2_2_7_3	0.90286	0.00137	0.90560
ncf15est11_2_2_6_3	90	36601	32941	7643	6.06	1.0e-04	0.89754	0.00118	0.89990	hcf25est12_2_2_6_3	0.88774	0.00119	0.89013
ncf15est11_2_2_5_3	80	36647	29318	7643	6.80	1.0e-04	0.86210	0.00109	0.86428	hcf25est12_2_2_5_3	0.85335	0.00111	0.85557
ncf15est11_2_2_4_3	70	36694	25686	7643	7.77	1.0e-04	0.82389	0.00121	0.82631	hcf25est12_2_2_4_3	0.81165	0.00110	0.81386
ncf15est11_2_2_3_3	60	36740	22044	7643	9.05	1.0e-04	0.78278	0.00120	0.78519	hcf25est12_2_2_3_3	0.77147	0.00114	0.77375
ncf15est11_2_2_2_3	40	36834	14734	7643	13.54	1.0e-04	0.68461	0.00116	0.68692	hcf25est12_2_2_2_3	0.67454	0.00112	0.67679
ncf15est11_2_2_1_3	19	36932	7017	7643	28.43	1.0e-04	0.54624	0.00099	0.54823	hcf25est12_2_2_1_3	0.53779	0.00105	0.53989

Table 6.9.6-10. Results for HEU broken metal content in CV calculation model

case name	np (in)	enr. (wt%)	U (g)	^{235}U (g)	H_2O (g)	h/x	mocfr	k_{eff}	σ	$k_{eff}+2σ$				
broken metal as 1-in. cubes, flooded containment vessel, reflected														
no can spacers (np thickness = 0.0 in.)														
cvr3sqa_36_1_8_15	0.0	100	35142	35142	8332	6.19	1.0e+00	0.93455	0.00107	0.93668				
cvr3sqa_36_1_7_15	0.0	95	35164	33406	8332	6.51	1.0e+00	0.91663	0.00128	0.91920				
cvr3sqa_36_1_6_15	0.0	90	35186	31667	8332	6.87	1.0e+00	0.90133	0.00123	0.90379				
cvr3sqa_36_1_5_15	0.0	80	35230	28184	8332	7.72	1.0e+00	0.87330	0.00119	0.87567				
cvr3sqa_36_1_4_15	0.0	70	35275	24693	8332	8.81	1.0e+00	0.84424	0.00113	0.84650				
cvr3sqa_36_1_3_15	0.0	60	35320	21192	8332	10.26	1.0e+00	0.81162	0.00124	0.81410				

Table 6.9.6-10. Results for HEU broken metal content in CV calculation model

case name	np (in)	enr. (wt%)	U (g)	^{235}U (g)	H_2O (g)	h/x	mocfr	k_{eff}	σ	$k_{eff}+2σ$				
cvr3sqa_36_1_2_15	0.0	40	35410	14164	8332	15.35	1.0e+00	0.73700	0.00098	0.73896				
cvr3sqa_36_1_1_15	0.0	19	35505	6746	8332	32.24	1.0e+00	0.63755	0.00119	0.63992				
cvr3sqa_36_1_8_1	0.0	100	35142	35142	0	0.00	1.0e-20	0.78442	0.00112	0.78667				
cvr3sqa_36_1_8_6	0.0	100	35142	35142	833	0.62	1.0e-01	0.79134	0.00116	0.79366				
cvr3sqa_36_1_8_7	0.0	100	35142	35142	1666	1.24	2.0e-01	0.80350	0.00113	0.80577				
cvr3sqa_36_1_8_8	0.0	100	35142	35142	2500	1.86	3.0e-01	0.81548	0.00107	0.81761				
cvr3sqa_36_1_8_9	0.0	100	35142	35142	3333	2.48	4.0e-01	0.83048	0.00122	0.83293				
cvr3sqa_36_1_8_10	0.0	100	35142	35142	4166	3.09	5.0e-01	0.84727	0.00122	0.84971				
cvr3sqa_36_1_8_11	0.0	100	35142	35142	4999	3.71	6.0e-01	0.86174	0.00123	0.86420				
cvr3sqa_36_1_8_12	0.0	100	35142	35142	5832	4.33	7.0e-01	0.87977	0.00118	0.88213				
cvr3sqa_36_1_8_13	0.0	100	35142	35142	6666	4.95	8.0e-01	0.89818	0.00110	0.90037				
cvr3sqa_36_1_8_14	0.0	100	35142	35142	7499	5.57	9.0e-01	0.91611	0.00118	0.91846				
cvr3sqa_36_1_8_15	0.0	100	35142	35142	8332	6.19	1.0e+00	0.93455	0.00107	0.93668				
with can spacers (np thickness = 1.4 in.)														
cvr3sqa_36_2_8_15	1.4	100	35142	35142	7719	5.73	1.0e+00	0.85151	0.00123	0.85397				
cvr3sqa_36_2_7_15	1.4	95	35164	33406	7719	6.03	1.0e+00	0.83521	0.00123	0.83766				
cvr3sqa_36_2_6_15	1.4	90	35186	31667	7719	6.36	1.0e+00	0.82166	0.00125	0.82415				
cvr3sqa_36_2_5_15	1.4	80	35230	28184	7719	7.15	1.0e+00	0.78928	0.00112	0.79152				
cvr3sqa_36_2_4_15	1.4	70	35275	24693	7719	8.16	1.0e+00	0.75994	0.00113	0.76220				
cvr3sqa_36_2_3_15	1.4	60	35320	21192	7719	9.51	1.0e+00	0.72673	0.00112	0.72898				
cvr3sqa_36_2_2_15	1.4	40	35410	14164	7719	14.22	1.0e+00	0.65008	0.00102	0.65213				
cvr3sqa_36_2_1_15	1.4	19	35505	6746	7719	29.86	1.0e+00	0.54677	0.00102	0.54881				

Table 6.9.6-10. Results for HEU broken metal content in CV calculation model

case name	np (in)	enr. (wt%)	U (g)	^{235}U (g)	H_2O (g)	h/x	mocfr	k_{eff}	σ	$k_{eff}+2σ$				
broken metal as lattice homogenized 1-in. cubes, flooded containment vessel, reflected														
no can spacers (np thickness = 0.0 in.)														
cvr3lha_36_1_8_1	0.0	100	35142	35142	0	0.00	1.0e-20	0.74814	0.00123	0.75060				
cvr3lha_36_1_8_6	0.0	100	35142	35142	833	0.62	1.0e-01	0.76415	0.00125	0.76665				
cvr3lha_36_1_8_7	0.0	100	35142	35142	1666	1.24	2.0e-01	0.77899	0.00102	0.78103				
cvr3lha_36_1_8_8	0.0	100	35142	35142	2500	1.86	3.0e-01	0.79660	0.00143	0.79946				
cvr3lha_36_1_8_9	0.0	100	35142	35142	3333	2.48	4.0e-01	0.81635	0.00113	0.81861				
cvr3lha_36_1_8_10	0.0	100	35142	35142	4166	3.09	5.0e-01	0.83767	0.00109	0.83986				
cvr3lha_36_1_8_11	0.0	100	35142	35142	4999	3.71	6.0e-01	0.85716	0.00116	0.85949				
cvr3lha_36_1_8_12	0.0	100	35142	35142	5832	4.33	7.0e-01	0.88187	0.00114	0.88415				
cvr3lha_36_1_8_13	0.0	100	35142	35142	6666	4.95	8.0e-01	0.90182	0.00109	0.90399				
cvr3lha_36_1_8_14	0.0	100	35142	35142	7499	5.57	9.0e-01	0.92553	0.00148	0.92849				
cvr3lha_36_1_8_15	0.0	100	35142	35142	8332	6.19	1.0e+00	0.94654	0.00126	0.94906				
cvr3lha_36_1_8_15	0.0	100	35142	35142	8332	6.19	1.0e+00	0.94654	0.00126	0.94906				
cvr3lha_36_1_7_15	0.0	95	35164	33406	8332	6.51	1.0e+00	0.93172	0.00115	0.93403				
cvr3lha_36_1_6_15	0.0	90	35186	31667	8332	6.87	1.0e+00	0.91744	0.00126	0.91995				
cvr3lha_36_1_5_15	0.0	80	35230	28184	8332	7.72	1.0e+00	0.89049	0.00113	0.89274				
cvr3lha_36_1_4_15	0.0	70	35275	24693	8332	8.81	1.0e+00	0.85930	0.00133	0.86196				
cvr3lha_36_1_3_15	0.0	60	35320	21192	8332	10.26	1.0e+00	0.82623	0.00131	0.82886				
cvr3lha_36_1_2_15	0.0	40	35410	14164	8332	15.35	1.0e+00	0.75317	0.00110	0.75536				
cvr3lha_36_1_1_15	0.0	19	35505	6746	8332	32.24	1.0e+00	0.65522	0.00102	0.65726				
cvr3lha_36_1_8_15	0.0	100	35142	35142	8332	6.19	1.0e+00	0.94654	0.00126	0.94906				
cvr3lha_35_1_8_15	0.0	100	34217	34217	8381	6.39	1.0e+00	0.94183	0.00106	0.94396				

Table 6.9.6-10. Results for HEU broken metal content in CV calculation model

case name	np (in)	enr. (wt%)	U (g)	^{235}U (g)	H_2O (g)	h/x	mocfr	k_{eff}	σ	$k_{eff}+2σ$
cvr3lha_34_1_8_15	0.0	100	33292	33292	8430	6.61	1.0e+00	0.93673	0.00125	0.93922
cvr3lha_33_1_8_15	0.0	100	32367	32367	8479	6.84	1.0e+00	0.95706	0.00123	0.95952
cvr3lha_32_1_8_15	0.0	100	31442	31442	8528	7.08	1.0e+00	0.94986	0.00142	0.95271
cvr3lha_31_1_8_15	0.0	100	30518	30518	8578	7.34	1.0e+00	0.94716	0.00118	0.94953
cvr3lha_30_1_8_15	0.0	100	29593	29593	8627	7.61	1.0e+00	0.93908	0.00127	0.94162
cvr3lha_29_1_8_15	0.0	100	28668	28668	8676	7.90	1.0e+00	0.93306	0.00126	0.93557
cvr3lha_28_1_8_15	0.0	100	27743	27743	8725	8.21	1.0e+00	0.93059	0.00137	0.93333
cvr3lha_27_1_8_15	0.0	100	26818	26818	8774	8.54	1.0e+00	0.92502	0.00139	0.92780
cvr3lha_26_1_8_15	0.0	100	25894	25894	8823	8.89	1.0e+00	0.91519	0.00145	0.91810
cvr3lha_25_1_8_15	0.0	100	24969	24969	8872	9.27	1.0e+00	0.91200	0.00125	0.91451
cvr3lha_24_1_8_15	0.0	100	23119	23119	8970	10.13	1.0e+00	0.92028	0.00106	0.92241
cvr3lha_23_1_8_15	0.0	100	22195	22195	9019	10.61	1.0e+00	0.91201	0.00115	0.91430
cvr3lha_22_1_8_15	0.0	100	21270	21270	9068	11.13	1.0e+00	0.90500	0.00138	0.90777
cvr3lha_21_1_8_15	0.0	100	20345	20345	9117	11.70	1.0e+00	0.89763	0.00133	0.90030
cvr3lha_31_1_7_15	0.0	95	30537	29010	8578	7.72	1.0e+00	0.92875	0.00129	0.93134
cvr3lha_30_1_7_15	0.0	95	29612	28131	8627	8.00	1.0e+00	0.92618	0.00111	0.92840
cvr3lha_29_1_7_15	0.0	95	28686	27252	8676	8.31	1.0e+00	0.91841	0.00107	0.92055
cvr3lha_28_1_7_15	0.0	95	27761	26373	8725	8.63	1.0e+00	0.91075	0.00124	0.91322
cvr3lha_27_1_7_15	0.0	95	26835	25494	8774	8.98	1.0e+00	0.90920	0.00117	0.91153
cvr3lha_33_1_6_15	0.0	90	32408	29167	8479	7.59	1.0e+00	0.92553	0.00126	0.92804
cvr3lha_32_1_6_15	0.0	90	31482	28334	8528	7.86	1.0e+00	0.92000	0.00119	0.92238
cvr3lha_31_1_6_15	0.0	90	30556	27501	8578	8.14	1.0e+00	0.91758	0.00132	0.92021

Table 6.9.6-10. Results for HEU broken metal content in CV calculation model

case name	np (in)	enr. (wt%)	U (g)	^{235}U (g)	H_2O (g)	h/x	mocfr	k_{eff}	σ	$k_{eff}+2σ$
cvr3lha_36_1_5_15	0.0	80	35230	28184	8332	7.72	1.0e+00	0.89049	0.00113	0.89274
cvr3lha_35_1_5_15	0.0	80	34303	27443	8381	7.97	1.0e+00	0.88496	0.00111	0.88719
cvr3lha_34_1_5_15	0.0	80	33376	26701	8430	8.24	1.0e+00	0.88044	0.00106	0.88256
cvr3lha_33_1_5_15	0.0	80	32449	25959	8479	8.53	1.0e+00	0.89355	0.00112	0.89579
cvr3lha_32_1_5_15	0.0	80	31522	25218	8528	8.83	1.0e+00	0.88961	0.00146	0.89253
cvr3lha_31_1_5_15	0.0	80	30595	24476	8578	9.15	1.0e+00	0.88752	0.00141	0.89034
cvr3lha_36_1_4_15	0.0	70	35275	24693	8332	8.81	1.0e+00	0.85930	0.00133	0.86196
cvr3lha_35_1_4_15	0.0	70	34347	24043	8381	9.10	1.0e+00	0.85473	0.00113	0.85698
cvr3lha_34_1_4_15	0.0	70	33419	23393	8430	9.41	1.0e+00	0.85237	0.00129	0.85496
cvr3lha_33_1_4_15	0.0	70	32490	22743	8479	9.73	1.0e+00	0.86299	0.00121	0.86542
cvr3lha_32_1_4_15	0.0	70	31562	22093	8528	10.08	1.0e+00	0.85876	0.00132	0.86140
cvr3lha_31_1_4_15	0.0	70	30634	21444	8578	10.44	1.0e+00	0.85471	0.00125	0.85720
cvr3lha_36_1_3_15	0.0	60	35320	21192	8332	10.26	1.0e+00	0.82623	0.00131	0.82886
cvr3lha_36_1_2_15	0.0	40	35410	14164	8332	15.35	1.0e+00	0.75317	0.00110	0.75536
cvr3lha_36_1_1_15	0.0	19	35505	6746	8332	32.24	1.0e+00	0.65522	0.00102	0.65726
cvr3lha_36_2_8_15	1.4	100	35142	35142	7719	5.73	1.0e+00	0.87286	0.00134	0.87554
cvr3lha_36_2_7_15	1.4	95	35164	33406	7719	6.03	1.0e+00	0.85858	0.00109	0.86077
cvr3lha_36_2_6_15	1.4	90	35186	31667	7719	6.36	1.0e+00	0.84459	0.00107	0.84672
cvr3lha_36_2_5_15	1.4	80	35230	28184	7719	7.15	1.0e+00	0.81698	0.00127	0.81952
cvr3lha_36_2_4_15	1.4	70	35275	24693	7719	8.16	1.0e+00	0.78484	0.00122	0.78727

Table 6.9.6-10. Results for HEU broken metal content in CV calculation model

case name	np (in)	enr. (wt%)	U (g)	^{235}U (g)	H_2O (g)	h/x	mocfr	k_{eff}	σ	$k_{eff}+2σ$
cvr3lha_36_2_3_15	1.4	60	35320	21192	7719	9.51	1.0e+00	0.75584	0.00105	0.75795
cvr3lha_36_2_2_15	1.4	40	35410	14164	7719	14.22	1.0e+00	0.68360	0.00131	0.68623
cvr3lha_36_2_1_15	1.4	19	35505	6746	7719	29.86	1.0e+00	0.58144	0.00104	0.58352
broken metal as 1-in. cubes fully homogenized with water for flooded containment vessel, reflected										
no can spacers (np thickness = 0.0 in.)										
cvr3cha_36_1_8_1	0.0	100	35142	35142	0	0.00	1.0e+00	0.61068	0.00099	0.61266
cvr3cha_36_1_8_6	0.0	100	35142	35142	833	0.62	1.0e+00	0.64671	0.00117	0.64905
cvr3cha_36_1_8_7	0.0	100	35142	35142	1666	1.24	1.0e+00	0.68117	0.00106	0.68329
cvr3cha_36_1_8_8	0.0	100	35142	35142	2500	1.86	1.0e+00	0.71931	0.00121	0.72174
cvr3cha_36_1_8_9	0.0	100	35142	35142	3333	2.48	1.0e+00	0.75910	0.00125	0.76160
cvr3cha_36_1_8_10	0.0	100	35142	35142	4166	3.09	1.0e+00	0.79344	0.00123	0.79589
cvr3cha_36_1_8_11	0.0	100	35142	35142	4999	3.71	1.0e+00	0.83513	0.00132	0.83777
cvr3cha_36_1_8_12	0.0	100	35142	35142	5832	4.33	1.0e+00	0.87270	0.00117	0.87504
cvr3cha_36_1_8_13	0.0	100	35142	35142	6666	4.95	1.0e+00	0.90988	0.00115	0.91219
cvr3cha_36_1_8_14	0.0	100	35142	35142	7499	5.57	1.0e+00	0.94696	0.00136	0.94968
cvr3cha_36_1_8_15	0.0	100	35142	35142	8332	6.19	1.0e+00	0.98062	0.00128	0.98318
cvr3cha_36_1_8_15	0.0	100	35142	35142	8332	6.19	1.0e+00	0.98062	0.00128	0.98318
cvr3cha_36_1_7_15	0.0	95	35164	33406	8332	6.51	1.0e+00	0.96729	0.00134	0.96997
cvr3cha_36_1_6_15	0.0	90	35186	31667	8332	6.87	1.0e+00	0.95443	0.00144	0.95731
cvr3cha_36_1_5_15	0.0	80	35230	28184	8332	7.72	1.0e+00	0.93639	0.00114	0.93867
cvr3cha_36_1_4_15	0.0	70	35275	24693	8332	8.81	1.0e+00	0.91729	0.00125	0.91978
cvr3cha_36_1_3_15	0.0	60	35320	21192	8332	10.26	1.0e+00	0.89768	0.00137	0.90042

Table 6.9.6-10. Results for HEU broken metal content in CV calculation model

case name	np (in)	enr. (wt%)	U (g)	^{235}U (g)	H_2O (g)	h/x	mocfr	k_{eff}	σ	$k_{eff}+2σ$				
cvr3cha_36_1_2_15	0.0	40	35410	14164	8332	15.35	1.0e+00	0.85347	0.00132	0.85612				
cvr3cha_36_1_1_15	0.0	19	35505	6746	8332	32.24	1.0e+00	0.78799	0.00132	0.79064				
with can spacers (np thickness = 1.4 in.)														
cvr3cha_36_2_8_15	1.4	100	35142	35142	7719	5.73	1.0e+00	0.96066	0.00128	0.96321				
cvr3cha_36_2_7_15	1.4	95	35164	33406	7719	6.03	1.0e+00	0.94267	0.00127	0.94521				
cvr3cha_36_2_6_15	1.4	90	35186	31667	7719	6.36	1.0e+00	0.93250	0.00117	0.93484				
cvr3cha_36_2_5_15	1.4	80	35230	28184	7719	7.15	1.0e+00	0.91364	0.00126	0.91615				
cvr3cha_36_2_4_15	1.4	70	35275	24693	7719	8.16	1.0e+00	0.89707	0.00125	0.89957				
cvr3cha_36_2_3_15	1.4	60	35320	21192	7719	9.51	1.0e+00	0.87509	0.00121	0.87751				
cvr3cha_36_2_2_15	1.4	40	35410	14164	7719	14.22	1.0e+00	0.82672	0.00135	0.82943				
cvr3cha_36_2_1_15	1.4	19	35505	6746	7719	29.86	1.0e+00	0.76024	0.00148	0.76320				

Table 6.9.6-11. Results for HEU broken metal content in packaging calculation model

case name	np (in)	enr. (wt%)	U (g)	^{235}U (g)	H_2O (g)	h/x	moifr	k_{eff}	σ	$k_{eff}+2σ$	case name	k_{eff}	σ	$k_{eff}+2σ$
content in flooded containment vessel, single package reflected														
NCT											**HAC**			
no can spacers (np thickness = 0.0 in.)														
ncsrbmt11_36_1_1	0.0	100	35142	35142	8332	6.19	1.0e-20	0.81144	0.00127	0.81397	hcsrbmt12_36_1_1	0.81597	0.00140	0.81877
ncsrbmt11_36_1_2	0.0	100	35142	35142	8332	6.19	1.0e-05	0.81278	0.00143	0.81563	hcsrbmt12_36_1_2	0.81496	0.00123	0.81741
ncsrbmt11_36_1_3	0.0	100	35142	35142	8332	6.19	1.0e-04	0.81066	0.00124	0.81314	hcsrbmt12_36_1_3	0.81490	0.00149	0.81787
ncsrbmt11_36_1_4	0.0	100	35142	35142	8332	6.19	1.0e-03	0.81064	0.00142	0.81347	hcsrbmt12_36_1_4	0.81512	0.00157	0.81826
ncsrbmt11_36_1_5	0.0	100	35142	35142	8332	6.19	1.0e-02	0.81069	0.00138	0.81346	hcsrbmt12_36_1_5	0.81594	0.00126	0.81846
ncsrbmt11_36_1_6	0.0	100	35142	35142	8332	6.19	1.0e-01	0.81880	0.00126	0.82132	hcsrbmt12_36_1_6	0.82255	0.00126	0.82507

Table 6.9.6-11. Results for HEU broken metal content in packaging calculation model

case name	np (in)	enr. (wt%)	U (g)	^{235}U (g)	H_2O (g)	h/x	moifr	k_{eff}	σ	$k_{eff}+2σ$	case name	k_{eff}	σ	$k_{eff}+2σ$
ncsrbmt11_36_1_8	0.0	100	35142	35142	8332	6.19	3.0e-01	0.83502	0.00115	0.83732	hcsrbmt12_36_1_8	0.83846	0.00125	0.84095
ncsrbmt11_36_1_15	0.0	100	35142	35142	8332	6.19	1.0e+00	0.88830	0.00122	0.89075	hcsrbmt12_36_1_15	0.88841	0.00140	0.89122
ncsrbmt11_36_1_15	0.0	100	35142	35142	8332	6.19	1.0e+00	0.88830	0.00122	0.89075				
ncsrbmt11_35_1_15	0.0	100	34217	34217	8381	6.39	1.0e+00	0.88662	0.00129	0.88921				
ncsrbmt11_34_1_15	0.0	100	33292	33292	8430	6.61	1.0e+00	0.88622	0.00119	0.88860				
ncsrbmt11_33_1_15	0.0	100	32367	32367	8479	6.84	1.0e+00	0.88175	0.00127	0.88429				
ncsrbmt11_32_1_15	0.0	100	31442	31442	8529	7.08	1.0e+00	0.88109	0.00124	0.88357				
ncsrbmt11_31_1_15	0.0	100	30518	30518	8578	7.34	1.0e+00	0.87995	0.00126	0.88247				
ncsrbmt11_30_1_15	0.0	100	29593	29593	8627	7.61	1.0e+00	0.87410	0.00144	0.87697				
ncsrbmt11_29_1_15	0.0	100	28668	28668	8676	7.90	1.0e+00	0.87385	0.00118	0.87621				
ncsrbmt11_28_1_15	0.0	100	27743	27743	8725	8.21	1.0e+00	0.87237	0.00119	0.87474				
ncsrbmt11_27_1_15	0.0	100	26819	26819	8774	8.54	1.0e+00	0.86800	0.00126	0.87053				
ncsrbmt11_26_1_15	0.0	100	25894	25894	8823	8.89	1.0e+00	0.86869	0.00123	0.87115				
ncsrbmt11_25_1_15	0.0	100	24969	24969	8872	9.27	1.0e+00	0.86558	0.00152	0.86862				
ncsrbmt11_24_1_15	0.0	100	23119	23119	8970	10.13	1.0e+00	0.85827	0.00123	0.86074				
ncsrbmt11_23_1_15	0.0	100	22195	22195	9019	10.61	1.0e+00	0.85657	0.00134	0.85924				
ncsrbmt11_22_1_15	0.0	100	21270	21270	9068	11.13	1.0e+00	0.85373	0.00156	0.85686				
ncsrbmt11_21_1_15	0.0	100	20345	20345	9117	11.70	1.0e+00	0.85521	0.00126	0.85774				
ncsrbmt11_20_1_15	0.0	100	19420	19420	9166	12.32	1.0e+00	0.84989	0.00157	0.85303				
ncsrbmt11_19_1_15	0.0	100	18496	18496	9216	13.00	1.0e+00	0.85069	0.00155	0.85378				
ncsrbmt11_18_1_15	0.0	100	17571	17571	9265	13.76	1.0e+00	0.84676	0.00182	0.85039				
ncsrbmt11_17_1_15	0.0	100	16646	16646	9314	14.60	1.0e+00	0.84566	0.00147	0.84859				
ncsrbmt11_16_1_15	0.0	100	15721	15721	9363	15.54	1.0e+00	0.84458	0.00125	0.84708				
ncsrbmt11_15_1_15	0.0	100	14796	14796	9412	16.60	1.0e+00	0.83932	0.00148	0.84229				

Table 6.9.6-11. Results for HEU broken metal content in packaging calculation model

case name	np (in)	enr. (wt%)	U (g)	^{235}U (g)	H_2O (g)	h/x	moifr	k_{eff}	σ	$k_{eff}+2σ$	case name	k_{eff}	σ	$k_{eff}+2σ$
ncsrbmt11_14_1_15	0.0	100	13872	13872	9461	17.80	1.0e+00	0.83752	0.00133	0.84019				
ncsrbmt11_13_1_15	0.0	100	12947	12947	9510	19.17	1.0e+00	0.83532	0.00151	0.83834				
ncsrbmt11_12_1_15	0.0	100	11097	11097	9608	22.60	1.0e+00	0.82792	0.00133	0.83057				
ncsrbmt11_11_1_15	0.0	100	10173	10173	9657	24.78	1.0e+00	0.82643	0.00127	0.82898				
ncsrbmt11_10_1_15	0.0	100	9248	9248	9706	27.39	1.0e+00	0.82649	0.00160	0.82968				
ncsrbmt11_9_1_15	0.0	100	8323	8323	9755	30.59	1.0e+00	0.81840	0.00140	0.82119				
ncsrbmt11_8_1_15	0.0	100	7398	7398	9804	34.59	1.0e+00	0.81808	0.00170	0.82148				
ncsrbmt11_7_1_15	0.0	100	6473	6473	9854	39.73	1.0e+00	0.81130	0.00152	0.81434				
ncsrbmt11_6_1_15	0.0	100	5549	5549	9903	46.58	1.0e+00	0.80480	0.00140	0.80761				
ncsrbmt11_5_1_15	0.0	100	4624	4624	9952	56.17	1.0e+00	0.79723	0.00124	0.79971				
ncsrbmt11_4_1_15	0.0	100	3699	3699	10001	70.56	1.0e+00	0.78533	0.00133	0.78799				
ncsrbmt11_3_1_15	0.0	100	2774	2774	10050	94.55	1.0e+00	0.76796	0.00152	0.77099				
ncsrbmt11_2_1_15	0.0	100	1850	1850	10099	142.51	1.0e+00	0.73495	0.00142	0.73778				
ncsrbmt11_1_1_15	0.0	100	925	925	10148	286.41	1.0e+00	0.65230	0.00132	0.65494				
with can spacers (np thickness = 1.4 in.)														
ncsrbmt11_36_2_1	1.4	100	35142	35142	7719	5.73	1.0e-20	0.79252	0.00122	0.79496	hcsrbmt12_36_2_1	0.79368	0.00134	0.79636
ncsrbmt11_36_2_2	1.4	100	35142	35142	7719	5.73	1.0e-05	0.79014	0.00147	0.79309	hcsrbmt12_36_2_2	0.79487	0.00120	0.79727
ncsrbmt11_36_2_3	1.4	100	35142	35142	7719	5.73	1.0e-04	0.79182	0.00134	0.79450	hcsrbmt12_36_2_3	0.79667	0.00135	0.79938
ncsrbmt11_36_2_4	1.4	100	35142	35142	7719	5.73	1.0e-03	0.79144	0.00116	0.79376	hcsrbmt12_36_2_4	0.79705	0.00133	0.79971
ncsrbmt11_36_2_5	1.4	100	35142	35142	7719	5.73	1.0e-02	0.78918	0.00111	0.79141	hcsrbmt12_36_2_5	0.79627	0.00135	0.79898
ncsrbmt11_36_2_6	1.4	100	35142	35142	7719	5.73	1.0e-01	0.80114	0.00117	0.80348	hcsrbmt12_36_2_6	0.80431	0.00130	0.80691
ncsrbmt11_36_2_8	1.4	100	35142	35142	7719	5.73	3.0e-01	0.81416	0.00141	0.81698	hcsrbmt12_36_2_8	0.82035	0.00119	0.82273
ncsrbmt11_36_2_15	1.4	100	35142	35142	7719	5.73	1.0e+00	0.86924	0.00119	0.87162	hcsrbmt12_36_2_15	0.87124	0.00142	0.87408

Table 6.9.6-11. Results for HEU broken metal content in packaging calculation model

case name	np (in)	enr. (wt%)	U (g)	^{235}U (g)	H_2O (g)	h/x	moifr	k_{eff}	σ	$k_{eff}+2σ$	case name	k_{eff}	σ	$k_{eff}+2σ$
ncsrbmt11_36_2_15	1.4	100	35142	35142	7719	5.73	1.0e+00	0.86924	0.00119	0.87162				
ncsrbmt11_35_2_15	1.4	100	34217	34217	7768	5.93	1.0e+00	0.86697	0.00130	0.86957				
ncsrbmt11_34_2_15	1.4	100	33292	33292	7817	6.13	1.0e+00	0.86435	0.00138	0.86712				
ncsrbmt11_33_2_15	1.4	100	32367	32367	7866	6.34	1.0e+00	0.86988	0.00130	0.87249				
ncsrbmt11_32_2_15	1.4	100	31442	31442	7915	6.57	1.0e+00	0.86598	0.00145	0.86889				
ncsrbmt11_31_2_15	1.4	100	30518	30518	7964	6.81	1.0e+00	0.86432	0.00153	0.86739				
ncsrbmt11_30_2_15	1.4	100	29593	29593	8013	7.07	1.0e+00	0.85951	0.00163	0.86277				
ncsrbmt11_29_2_15	1.4	100	28668	28668	8062	7.34	1.0e+00	0.85938	0.00134	0.86206				
ncsrbmt11_28_2_15	1.4	100	27743	27743	8111	7.63	1.0e+00	0.85890	0.00133	0.86157				
ncsrbmt11_27_2_15	1.4	100	26819	26819	8160	7.94	1.0e+00	0.85736	0.00143	0.86023				
ncsrbmt11_26_2_15	1.4	100	25894	25894	8209	8.28	1.0e+00	0.85189	0.00129	0.85447				
ncsrbmt11_25_2_15	1.4	100	24969	24969	8258	8.63	1.0e+00	0.84986	0.00148	0.85281				
ncsrbmt11_24_2_15	1.4	100	23119	23119	8357	9.43	1.0e+00	0.85225	0.00131	0.85488				
ncsrbmt11_23_2_15	1.4	100	22195	22195	8406	9.89	1.0e+00	0.84824	0.00142	0.85108				
ncsrbmt11_22_2_15	1.4	100	21270	21270	8455	10.38	1.0e+00	0.84600	0.00135	0.84869				
ncsrbmt11_21_2_15	1.4	100	20345	20345	8504	10.91	1.0e+00	0.84406	0.00150	0.84706				
ncsrbmt11_20_2_15	1.4	100	19420	19420	8553	11.50	1.0e+00	0.83992	0.00126	0.84244				
ncsrbmt11_19_2_15	1.4	100	18496	18496	8602	12.14	1.0e+00	0.83869	0.00134	0.84138				
ncsrbmt11_18_2_15	1.4	100	17571	17571	8651	12.85	1.0e+00	0.83488	0.00152	0.83793				
ncsrbmt11_17_2_15	1.4	100	16646	16646	8700	13.64	1.0e+00	0.83409	0.00130	0.83669				
ncsrbmt11_16_2_15	1.4	100	15721	15721	8749	14.53	1.0e+00	0.83520	0.00135	0.83789				
ncsrbmt11_15_2_15	1.4	100	14796	14796	8798	15.52	1.0e+00	0.83427	0.00129	0.83686				
ncsrbmt11_14_2_15	1.4	100	13872	13872	8847	16.65	1.0e+00	0.83162	0.00157	0.83476				
ncsrbmt11_13_2_15	1.4	100	12947	12947	8896	17.94	1.0e+00	0.82907	0.00147	0.83201				
ncsrbmt11_12_2_15	1.4	100	11097	11097	8995	21.16	1.0e+00	0.82195	0.00149	0.82493				

Table 6.9.6-11. Results for HEU broken metal content in packaging calculation model

case name	np (in)	enr. (wt%)	U (g)	^{235}U (g)	H_2O (g)	h/x	moifr	k_{eff}	σ	$k_{eff}+2σ$	case name	k_{eff}	σ	$k_{eff}+2σ$
ncsrbmt11_11_2_15	1.4	100	10173	10173	9044	23.20	1.0e+00	0.81845	0.00120	0.82084				
ncsrbmt11_10_2_15	1.4	100	9248	9248	9093	25.66	1.0e+00	0.81508	0.00142	0.81792				
ncsrbmt11_9_2_15	1.4	100	8323	8323	9142	28.67	1.0e+00	0.81075	0.00138	0.81351				
ncsrbmt11_8_2_15	1.4	100	7398	7398	9191	32.43	1.0e+00	0.81425	0.00169	0.81764				
ncsrbmt11_7_2_15	1.4	100	6473	6473	9240	37.26	1.0e+00	0.80774	0.00155	0.81084				
ncsrbmt11_6_2_15	1.4	100	5549	5549	9289	43.70	1.0e+00	0.80060	0.00138	0.80336				
ncsrbmt11_5_2_15	1.4	100	4624	4624	9338	52.71	1.0e+00	0.79537	0.00167	0.79870				
ncsrbmt11_4_2_15	1.4	100	3699	3699	9387	66.24	1.0e+00	0.78379	0.00136	0.78651				
ncsrbmt11_3_2_15	1.4	100	2774	2774	9436	88.78	1.0e+00	0.76586	0.00130	0.76846				
ncsrbmt11_2_2_15	1.4	100	1850	1850	9485	133.86	1.0e+00	0.73246	0.00135	0.73516				
ncsrbmt11_1_2_15	1.4	100	925	925	9534	269.10	1.0e+00	0.65664	0.00150	0.65963				
content in flooded containment vessel, array packaging model for CSI=0.0														
NCT											**HAC**			
no can spacers (np thickness = 0.0 in.)														
nciabmt11_36_1_8_1	0.0	100	35142	35142	8332	6.19	1.0e-20	1.13613	0.00121	1.13855	hciabmt12_36_1_8_1	1.13721	0.00124	1.13969
nciabmt11_36_1_8_2	0.0	100	35142	35142	8332	6.19	1.0e-05	1.13830	0.00153	1.14135	hciabmt12_36_1_8_2	1.13634	0.00114	1.13862
nciabmt11_36_1_8_3	0.0	100	35142	35142	8332	6.19	1.0e-04	1.13709	0.00121	1.13952	hciabmt12_36_1_8_3	1.13700	0.00127	1.13954
nciabmt11_36_1_8_4	0.0	100	35142	35142	8332	6.19	1.0e-03	1.13450	0.00115	1.13679	hciabmt12_36_1_8_4	1.13567	0.00121	1.13809
nciabmt11_36_1_8_5	0.0	100	35142	35142	8332	6.19	1.0e-02	1.11154	0.00120	1.11394	hciabmt12_36_1_8_5	1.12232	0.00129	1.12490
nciabmt11_36_1_8_6	0.0	100	35142	35142	8332	6.19	1.0e-01	0.98653	0.00121	0.98894	hciabmt12_36_1_8_6	1.03049	0.00115	1.03278
nciabmt11_36_1_8_8	0.0	100	35142	35142	8332	6.19	3.0e-01	0.91622	0.00135	0.91892	hciabmt12_36_1_8_8	0.95566	0.00126	0.95818
nciabmt11_36_1_8_15	0.0	100	35142	35142	8332	6.19	1.0e+00	0.91008	0.00124	0.91255	hciabmt12_36_1_8_15	0.93645	0.00120	0.93884
nciabmt11_7_1_5_3	0.0	80	6490	5192	9854	49.54	1.0e-04	0.96163	0.00130	0.96423	hciabmt12_7_1_5_3	0.96193	0.00149	0.96490
nciabmt11_6_1_5_3	0.0	80	5563	4450	9903	58.08	1.0e-04	0.95210	0.00130	0.95471	hciabmt12_6_1_5_3	0.95164	0.00139	0.95442

Table 6.9.6-11. Results for HEU broken metal content in packaging calculation model

case name	np (in)	enr. (wt%)	U (g)	^{235}U (g)	H_2O (g)	h/x	moifr	k_{eff}	σ	$k_{eff}+2σ$	case name	k_{eff}	σ	$k_{eff}+2σ$
nciabmt11_5_1_5_3	0.0	80	4636	3709	9952	70.04	1.0e-04	0.93892	0.00161	0.94215	hciabmt12_5_1_5_3	0.93880	0.00141	0.94162
nciabmt11_4_1_5_3	0.0	80	3709	2967	10001	87.98	1.0e-04	0.91835	0.00149	0.92133	hciabmt12_4_1_5_3	0.92156	0.00160	0.92476
nciabmt11_3_1_5_3	0.0	80	2781	2225	10050	117.89	1.0e-04	0.89262	0.00129	0.89520	hciabmt12_3_1_5_3	0.89109	0.00160	0.89430
nciabmt11_9_1_4_3	0.0	70	8355	5848	9755	43.54	1.0e-04	0.95952	0.00130	0.96213	hciabmt12_9_1_4_3	0.95495	0.00150	0.95795
nciabmt11_8_1_4_3	0.0	70	7426	5198	9804	49.23	1.0e-04	0.94887	0.00152	0.95191	hciabmt12_8_1_4_3	0.95267	0.00156	0.95578
nciabmt11_7_1_4_3	0.0	70	6498	4549	9854	56.54	1.0e-04	0.94082	0.00132	0.94346	hciabmt12_7_1_4_3	0.94409	0.00125	0.94659
nciabmt11_6_1_4_3	0.0	70	5570	3899	9903	66.29	1.0e-04	0.92987	0.00119	0.93225	hciabmt12_6_1_4_3	0.93280	0.00123	0.93526
nciabmt11_5_1_4_3	0.0	70	4642	3249	9952	79.95	1.0e-04	0.91799	0.00136	0.92070	hciabmt12_5_1_4_3	0.92053	0.00147	0.92347
nciabmt11_10_1_3_3	0.0	60	9295	5577	9706	45.43	1.0e-04	0.94106	0.00152	0.94409	hciabmt12_10_1_3_3	0.94167	0.00126	0.94419
nciabmt11_9_1_3_3	0.0	60	8365	5019	9755	50.73	1.0e-04	0.93671	0.00123	0.93918	hciabmt12_9_1_3_3	0.93973	0.00135	0.94242
nciabmt11_8_1_3_3	0.0	60	7436	4462	9804	57.36	1.0e-04	0.92907	0.00129	0.93166	hciabmt12_8_1_3_3	0.93016	0.00128	0.93273
nciabmt11_7_1_3_3	0.0	60	6506	3904	9854	65.88	1.0e-04	0.92171	0.00118	0.92407	hciabmt12_7_1_3_3	0.92300	0.00130	0.92560
nciabmt11_6_1_3_3	0.0	60	5577	3346	9903	77.24	1.0e-04	0.91221	0.00147	0.91515	hciabmt12_6_1_3_3	0.91017	0.00128	0.91274
with can spacers (np thickness = 1.4 in.)														
nciabmt11_36_2_8_1	1.4	100	35142	35142	7719	5.73	1.0e-20	1.11012	0.00118	1.11249	hciabmt12_36_2_8_1	1.11021	0.00115	1.11250
nciabmt11_36_2_8_2	1.4	100	35142	35142	7719	5.73	1.0e-05	1.10934	0.00103	1.11141	hciabmt12_36_2_8_2	1.10929	0.00137	1.11202
nciabmt11_36_2_8_3	1.4	100	35142	35142	7719	5.73	1.0e-04	1.10991	0.00131	1.11252	hciabmt12_36_2_8_3	1.10922	0.00112	1.11145
nciabmt11_36_2_8_4	1.4	100	35142	35142	7719	5.73	1.0e-03	1.10774	0.00123	1.11020	hciabmt12_36_2_8_4	1.10732	0.00115	1.10963
nciabmt11_36_2_8_5	1.4	100	35142	35142	7719	5.73	1.0e-02	1.08309	0.00140	1.08589	hciabmt12_36_2_8_5	1.09559	0.00114	1.09786
nciabmt11_36_2_8_6	1.4	100	35142	35142	7719	5.73	1.0e-01	0.95955	0.00128	0.96212	hciabmt12_36_2_8_6	1.00216	0.00124	1.00463
nciabmt11_36_2_8_8	1.4	100	35142	35142	7719	5.73	3.0e-01	0.88829	0.00112	0.89053	hciabmt12_36_2_8_8	0.92859	0.00158	0.93175
nciabmt11_36_2_8_15	1.4	100	35142	35142	7719	5.73	1.0e+00	0.88638	0.00158	0.88953	hciabmt12_36_2_8_15	0.91405	0.00147	0.91698

Table 6.9.6-11. Results for HEU broken metal content in packaging calculation model

case name	np (in)	enr. (wt%)	U (g)	^{235}U (g)	H_2O (g)	h/x	moifr	k_{eff}	σ	$k_{eff}+2σ$	case name	k_{eff}	σ	$k_{eff}+2σ$
nciabmt11_5_2_8_3	1.4	100	4624	4624	9338	52.71	1.0e-04	0.94785	0.00147	0.95079	hciabmt12_5_2_8_3	0.95226	0.00143	0.95511
nciabmt11_4_2_8_3	1.4	100	3699	3699	9387	66.24	1.0e-04	0.92504	0.00170	0.92845	hciabmt12_4_2_8_3	0.93069	0.00142	0.93352
nciabmt11_3_2_8_3	1.4	100	2774	2774	9436	88.78	1.0e-04	0.90131	0.00139	0.90409	hciabmt12_3_2_8_3	0.90243	0.00127	0.90497
nciabmt11_2_2_8_3	1.4	100	1850	1850	9485	133.86	1.0e-04	0.85414	0.00141	0.85696	hciabmt12_2_2_8_3	0.85600	0.00123	0.85846
nciabmt11_1_2_8_3	1.4	100	925	925	9534	269.10	1.0e-04	0.74985	0.00124	0.75232	hciabmt12_1_2_8_3	0.75078	0.00135	0.75347
nciabmt11_6_2_7_3	1.4	95	5552	5275	9289	45.97	1.0e-04	0.95078	0.00124	0.95327	hciabmt12_6_2_7_3	0.95399	0.00153	0.95704
nciabmt11_5_2_7_3	1.4	95	4627	4396	9338	55.45	1.0e-04	0.93742	0.00130	0.94002	hciabmt12_5_2_7_3	0.93696	0.00142	0.93981
nciabmt11_4_2_7_3	1.4	95	3701	3516	9387	69.68	1.0e-04	0.91690	0.00149	0.91987	hciabmt12_4_2_7_3	0.92094	0.00140	0.92374
nciabmt11_3_2_7_3	1.4	95	2776	2637	9436	93.39	1.0e-04	0.89089	0.00127	0.89343	hciabmt12_3_2_7_3	0.89250	0.00144	0.89537
nciabmt11_2_2_7_3	1.4	95	1851	1758	9485	140.81	1.0e-04	0.84225	0.00143	0.84510	hciabmt12_2_2_7_3	0.84604	0.00135	0.84875
nciabmt11_6_2_6_3	1.4	90	5556	5000	9289	48.49	1.0e-04	0.93703	0.00127	0.93956	hciabmt12_6_2_6_3	0.93967	0.00130	0.94227
nciabmt11_5_2_6_3	1.4	90	4630	4167	9338	58.49	1.0e-04	0.92640	0.00142	0.92925	hciabmt12_5_2_6_3	0.92390	0.00155	0.92700
nciabmt11_4_2_6_3	1.4	90	3704	3333	9387	73.50	1.0e-04	0.90541	0.00147	0.90835	hciabmt12_4_2_6_3	0.90643	0.00133	0.90909
nciabmt11_3_2_6_3	1.4	90	2778	2500	9436	98.52	1.0e-04	0.87970	0.00157	0.88283	hciabmt12_3_2_6_3	0.87916	0.00154	0.88224
nciabmt11_2_2_6_3	1.4	90	1852	1667	9485	148.54	1.0e-04	0.83371	0.00129	0.83628	hciabmt12_2_2_6_3	0.83414	0.00130	0.83674
nciabmt11_8_2_5_3	1.4	80	7417	5934	9191	40.43	1.0e-04	0.94131	0.00162	0.94455	hciabmt12_8_2_5_3	0.93963	0.00149	0.94261
nciabmt11_7_2_5_3	1.4	80	6490	5192	9240	46.45	1.0e-04	0.92939	0.00127	0.93193	hciabmt12_7_2_5_3	0.93070	0.00160	0.93391
nciabmt11_6_2_5_3	1.4	80	5563	4450	9289	54.48	1.0e-04	0.91981	0.00127	0.92235	hciabmt12_6_2_5_3	0.91987	0.00157	0.92301
nciabmt11_5_2_5_3	1.4	80	4636	3709	9338	65.72	1.0e-04	0.90533	0.00127	0.90787	hciabmt12_5_2_5_3	0.90772	0.00136	0.91044
nciabmt11_4_2_5_3	1.4	80	3709	2967	9387	82.59	1.0e-04	0.88537	0.00136	0.88808	hciabmt12_4_2_5_3	0.88792	0.00150	0.89092

Table 6.9.6-11. Results for HEU broken metal content in packaging calculation model

case name	np (in)	enr. (wt%)	U (g)	^{235}U (g)	H_2O (g)	h/x	moifr	k_{eff}	σ	$k_{eff}+2σ$	case name	k_{eff}	σ	$k_{eff}+2σ$
nciabmt11_11_2_4_3	1.4	70	10211	7148	9044	33.02	1.0e-04	0.93094	0.00141	0.93376	hciabmt12_11_2_4_3	0.93119	0.00138	0.93395
nciabmt11_10_2_4_3	1.4	70	9283	6498	9093	36.52	1.0e-04	0.92534	0.00139	0.92813	hciabmt12_10_2_4_3	0.92795	0.00129	0.93052
nciabmt11_9_2_4_3	1.4	70	8355	5848	9142	40.80	1.0e-04	0.91866	0.00122	0.92110	hciabmt12_9_2_4_3	0.92290	0.00125	0.92540
nciabmt11_8_2_4_3	1.4	70	7426	5198	9191	46.15	1.0e-04	0.91902	0.00137	0.92175	hciabmt12_8_2_4_3	0.91835	0.00126	0.92086
nciabmt11_7_2_4_3	1.4	70	6498	4549	9240	53.02	1.0e-04	0.90863	0.00152	0.91166	hciabmt12_7_2_4_3	0.91042	0.00137	0.91316
nciabmt11_15_2_3_3	1.4	60	14872	8923	8798	25.74	1.0e-04	0.93047	0.00133	0.93313	hciabmt12_15_2_3_3	0.93032	0.00114	0.93259
nciabmt11_14_2_3_3	1.4	60	13942	8365	8847	27.61	1.0e-04	0.92560	0.00138	0.92837	hciabmt12_14_2_3_3	0.92828	0.00143	0.93115
nciabmt11_13_2_3_3	1.4	60	12083	7250	8946	32.21	1.0e-04	0.91963	0.00126	0.92214	hciabmt12_13_2_3_3	0.92389	0.00124	0.92638
nciabmt11_12_2_3_3	1.4	60	11154	6692	8995	35.08	1.0e-04	0.91502	0.00155	0.91812	hciabmt12_12_2_3_3	0.91776	0.00138	0.92053
nciabmt11_11_2_3_3	1.4	60	10224	6135	9044	38.48	1.0e-04	0.90892	0.00140	0.91172	hciabmt12_11_2_3_3	0.91237	0.00133	0.91503
content in flooded containment vessel, array packaging model for CSI=0.4														
NCT											**HAC**			
no can spacers (np thickness = 0.0 in.)														
											hcf2bmt12_11_1_5_3	0.91900	0.00131	0.92163
											hcf2bmt12_10_1_5_3	0.91775	0.00161	0.92097
											hcf2bmt12_9_1_5_3	0.91229	0.00127	0.91483
ncf1bmt11_8_1_5_3	0.0	80	7417	5934	9804	43.13	1.0e-04	0.92824	0.00156	0.93135	hcf2bmt12_8_1_5_3	0.90367	0.00138	0.90643
ncf1bmt11_7_1_5_3	0.0	80	6490	5192	9854	49.54	1.0e-04	0.92088	0.00131	0.92349				
ncf1bmt11_6_1_5_3	0.0	80	5563	4450	9903	58.08	1.0e-04	0.91164	0.00153	0.91470				
ncf1bmt11_5_1_5_3	0.0	80	4636	3709	9952	70.04	1.0e-04	0.90130	0.00135	0.90400				
ncf1bmt11_4_1_5_3	0.0	80	3709	2967	10001	87.98	1.0e-04	0.88094	0.00128	0.88350				
											hcf2bmt12_15_1_4_3	0.91711	0.00152	0.92016
											hcf2bmt12_14_1_4_3	0.91432	0.00164	0.91760

Table 6.9.6-11. Results for HEU broken metal content in packaging calculation model

case name	np (in)	enr. (wt%)	U (g)	^{235}U (g)	H_2O (g)	h/x	moifr	k_{eff}	σ	$k_{eff}+2σ$	case name	k_{eff}	σ	$k_{eff}+2σ$
ncf1bmt11_13_1_4_3	0.0	70	12996	9097	9510	27.28	1.0e-04	0.93558	0.00138	0.93834	hcf2bmt12_13_1_4_3	0.91429	0.00141	0.91711
ncf1bmt11_12_1_4_3	0.0	70	11140	7798	9608	32.16	1.0e-04	0.92957	0.00130	0.93217	hcf2bmt12_12_1_4_3	0.90853	0.00161	0.91175
ncf1bmt11_11_1_4_3	0.0	70	10211	7148	9657	35.26	1.0e-04	0.92397	0.00139	0.92675				
ncf1bmt11_10_1_4_3	0.0	70	9283	6498	9706	38.99	1.0e-04	0.92240	0.00135	0.92510				
ncf1bmt11_9_1_4_3	0.0	70	8355	5848	9755	43.54	1.0e-04	0.91886	0.00139	0.92163				
											hcf2bmt12_21_1_3_3	0.91091	0.00139	0.91369
											hcf2bmt12_20_1_3_3	0.90915	0.00144	0.91203
ncf1bmt11_19_1_3_3	0.0	60	18589	11154	9216	21.57	1.0e-04	0.92771	0.00137	0.93044	hcf2bmt12_19_1_3_3	0.90638	0.00160	0.90958
ncf1bmt11_18_1_3_3	0.0	60	17660	10596	9265	22.82	1.0e-04	0.92867	0.00148	0.93164	hcf2bmt12_18_1_3_3	0.90466	0.00124	0.90715
ncf1bmt11_17_1_3_3	0.0	60	16731	10038	9314	24.22	1.0e-04	0.92948	0.00113	0.93173				
ncf1bmt11_16_1_3_3	0.0	60	15801	9481	9363	25.78	1.0e-04	0.92252	0.00158	0.92569				
ncf1bmt11_15_1_3_3	0.0	60	14872	8923	9412	27.53	1.0e-04	0.91999	0.00123	0.92246				
ncf1bmt11_14_1_3_3	0.0	60	13942	8365	9461	29.52	1.0e-04	0.91961	0.00144	0.92248				
with can spacers (np thickness = 1.4 in.)														
											hcf2bmt12_10_2_8_3	0.93154	0.00152	0.93458
ncf1bmt11_9_2_8_3	1.4	100	8323	8323	9142	28.67	1.0e-04	0.94429	0.00138	0.94704	hcf2bmt12_9_2_8_3	0.92329	0.00147	0.92622
ncf1bmt11_8_2_8_3	1.4	100	7398	7398	9191	32.43	1.0e-04	0.94337	0.00169	0.94674	hcf2bmt12_8_2_8_3	0.92153	0.00144	0.92442
ncf1bmt11_7_2_8_3	1.4	100	6473	6473	9240	37.26	1.0e-04	0.93117	0.00172	0.93460				
ncf1bmt11_6_2_8_3	1.4	100	5549	5549	9289	43.70	1.0e-04	0.92119	0.00147	0.92412				
											hcf2bmt12_13_2_7_3	0.93389	0.00167	0.93722
											hcf2bmt12_12_2_7_3	0.92649	0.00146	0.92941
ncf1bmt11_11_2_7_3	1.4	95	10179	9670	9044	24.41	1.0e-04	0.94326	0.00139	0.94604	hcf2bmt12_11_2_7_3	0.92061	0.00130	0.92320
ncf1bmt11_10_2_7_3	1.4	95	9254	8791	9093	27.00	1.0e-04	0.93829	0.00154	0.94138	hcf2bmt12_10_2_7_3	0.91423	0.00145	0.91712

Table 6.9.6-11. Results for HEU broken metal content in packaging calculation model

case name	np (in)	enr. (wt%)	U (g)	^{235}U (g)	H_2O (g)	h/x	moifr	k_{eff}	σ	$k_{eff}+2σ$	case name	k_{eff}	σ	$k_{eff}+2σ$
ncf1bmt11_9_2_7_3	1.4	95	8328	7912	9142	30.16	1.0e-04	0.93239	0.00181	0.93600	hcf2bmt12_9_2_7_3	0.90883	0.00137	0.91156
ncf1bmt11_8_2_7_3	1.4	95	7403	7033	9191	34.11	1.0e-04	0.92812	0.00144	0.93100				
ncf1bmt11_7_2_7_3	1.4	95	6478	6154	9240	39.19	1.0e-04	0.91938	0.00130	0.92199				
											hcf2bmt12_15_2_6_3	0.93106	0.00129	0.93364
											hcf2bmt12_14_2_6_3	0.92492	0.00129	0.92749
ncf1bmt11_13_2_6_3	1.4	90	12963	11667	8896	19.90	1.0e-04	0.94806	0.00123	0.95052	hcf2bmt12_13_2_6_3	0.92272	0.00138	0.92548
ncf1bmt11_12_2_6_3	1.4	90	11111	10000	8995	23.48	1.0e-04	0.93464	0.00123	0.93710	hcf2bmt12_12_2_6_3	0.91625	0.00149	0.91924
ncf1bmt11_11_2_6_3	1.4	90	10185	9167	9044	25.75	1.0e-04	0.93068	0.00148	0.93363	hcf2bmt12_11_2_6_3	0.91097	0.00136	0.91370
ncf1bmt11_10_2_6_3	1.4	90	9260	8334	9093	28.48	1.0e-04	0.92732	0.00150	0.93032				
ncf1bmt11_9_2_6_3	1.4	90	8334	7500	9142	31.81	1.0e-04	0.91744	0.00145	0.92034				
ncf1bmt11_8_2_6_3	1.4	90	7408	6667	9191	35.98	1.0e-04	0.91952	0.00133	0.92218				
ncf1bmt11_17_2_5_3	1.4	80	16688	13351	8700	17.01	1.0e-04	0.93531	0.00128	0.93787	hcf2bmt12_17_2_5_3	0.91255	0.00114	0.91482
ncf1bmt11_16_2_5_3	1.4	80	15761	12609	8749	18.11	1.0e-04	0.93511	0.00160	0.93832	hcf2bmt12_16_2_5_3	0.91363	0.00123	0.91608
ncf1bmt11_15_2_5_3	1.4	80	14834	11867	8798	19.35	1.0e-04	0.93431	0.00141	0.93713	hcf2bmt12_15_2_5_3	0.91038	0.00115	0.91268
ncf1bmt11_14_2_5_3	1.4	80	13907	11125	8847	20.76	1.0e-04	0.92939	0.00133	0.93205	hcf2bmt12_14_2_5_3	0.90762	0.00139	0.91041
ncf1bmt11_13_2_5_3	1.4	80	12980	10384	8896	22.36	1.0e-04	0.92453	0.00131	0.92715	hcf2bmt12_13_2_5_3	0.90539	0.00137	0.90812
ncf1bmt11_12_2_5_3	1.4	80	11125	8900	8995	26.38	1.0e-04	0.91584	0.00142	0.91868	hcf2bmt12_12_2_5_3	0.89295	0.00174	0.89642
ncf1bmt11_24_2_4_3	1.4	70	23207	16245	8357	13.43	1.0e-04	0.93515	0.00143	0.93801	hcf2bmt12_24_2_4_3	0.91356	0.00125	0.91606
ncf1bmt11_23_2_4_3	1.4	70	22279	15595	8406	14.07	1.0e-04	0.93264	0.00113	0.93490	hcf2bmt12_23_2_4_3	0.91116	0.00113	0.91342
ncf1bmt11_22_2_4_3	1.4	70	21351	14946	8455	14.77	1.0e-04	0.93058	0.00128	0.93314	hcf2bmt12_22_2_4_3	0.90737	0.00145	0.91027
ncf1bmt11_21_2_4_3	1.4	70	20422	14296	8504	15.53	1.0e-04	0.92635	0.00112	0.92859	hcf2bmt12_21_2_4_3	0.90516	0.00140	0.90796
ncf1bmt11_20_2_4_3	1.4	70	19494	13646	8553	16.36	1.0e-04	0.92535	0.00141	0.92818	hcf2bmt12_20_2_4_3	0.90283	0.00136	0.90555

Table 6.9.6-11. Results for HEU broken metal content in packaging calculation model

case name	np (in)	enr. (wt%)	U (g)	^{235}U (g)	H_2O (g)	h/x	moifr	k_{eff}	σ	$k_{eff}+2σ$	case name	k_{eff}	σ	$k_{eff}+2σ$
ncf1bmt11_19_2_4_3	1.4	70	18566	12996	8602	17.28	1.0e-04	0.92097	0.00177	0.92450	hcf2bmt12_19_2_4_3	0.89757	0.00144	0.90046
ncf1bmt11_18_2_4_3	1.4	70	17638	12346	8651	18.29	1.0e-04	0.91681	0.00140	0.91961	hcf2bmt12_18_2_4_3	0.89367	0.00144	0.89656
ncf1bmt11_36_2_3_3	1.4	60	35320	21192	7719	9.51	1.0e-04	0.93212	0.00121	0.93455	hcf2bmt12_36_2_3_3	0.90846	0.00137	0.91121
ncf1bmt11_35_2_3_3	1.4	60	34391	20634	7768	9.83	1.0e-04	0.93168	0.00129	0.93426	hcf2bmt12_35_2_3_3	0.90742	0.00118	0.90977
ncf1bmt11_34_2_3_3	1.4	60	33461	20077	7817	10.16	1.0e-04	0.93079	0.00145	0.93368	hcf2bmt12_34_2_3_3	0.90657	0.00134	0.90925
ncf1bmt11_33_2_3_3	1.4	60	32532	19519	7866	10.52	1.0e-04	0.92781	0.00131	0.93042	hcf2bmt12_33_2_3_3	0.90603	0.00117	0.90837
ncf1bmt11_32_2_3_3	1.4	60	31602	18961	7915	10.90	1.0e-04	0.92550	0.00131	0.92811	hcf2bmt12_32_2_3_3	0.90015	0.00127	0.90270
ncf1bmt11_31_2_3_3	1.4	60	30673	18404	7964	11.29	1.0e-04	0.92597	0.00128	0.92853	hcf2bmt12_31_2_3_3	0.90333	0.00122	0.90577
ncf1bmt11_30_2_3_3	1.4	60	29743	17846	8013	11.72	1.0e-04	0.92361	0.00120	0.92601	hcf2bmt12_30_2_3_3	0.89683	0.00144	0.89971
ncf1bmt11_29_2_3_3	1.4	60	28814	17288	8062	12.17	1.0e-04	0.92063	0.00143	0.92350				
content in flooded containment vessel, array packaging model for CSI=0.8														
NCT											**HAC**			
no can spacers (np thickness = 0.0 in.)														
ncf2bmt11_17_1_5_3	0.0	80	16688	13351	9314	18.21	1.0e-04	0.93655	0.00144	0.93942	hcf3bmt12_17_1_5_3	0.92003	0.00129	0.92262
ncf2bmt11_16_1_5_3	0.0	80	15761	12609	9363	19.38	1.0e-04	0.93242	0.00143	0.93529	hcf3bmt12_16_1_5_3	0.91399	0.00148	0.91694
ncf2bmt11_15_1_5_3	0.0	80	14834	11867	9412	20.70	1.0e-04	0.92982	0.00135	0.93251	hcf3bmt12_15_1_5_3	0.91169	0.00139	0.91448
ncf2bmt11_14_1_5_3	0.0	80	13907	11125	9461	22.20	1.0e-04	0.92699	0.00137	0.92972	hcf3bmt12_14_1_5_3	0.90943	0.00135	0.91213
ncf2bmt11_13_1_5_3	0.0	80	12980	10384	9510	23.90	1.0e-04	0.92634	0.00138	0.92909	hcf3bmt12_13_1_5_3	0.90348	0.00133	0.90615
ncf2bmt11_12_1_5_3	0.0	80	11125	8900	9608	28.18	1.0e-04	0.91826	0.00166	0.92158	hcf3bmt12_12_1_5_3	0.89805	0.00155	0.90115
ncf2bmt11_21_1_4_3	0.0	70	20422	14296	9117	16.65	1.0e-04	0.92723	0.00123	0.92968				
ncf2bmt11_20_1_4_3	0.0	70	19494	13646	9166	17.53	1.0e-04	0.92094	0.00124	0.92342	hcf3bmt12_20_1_4_3	0.90398	0.00124	0.90646
ncf2bmt11_19_1_4_3	0.0	70	18566	12996	9216	18.51	1.0e-04	0.92341	0.00144	0.92629	hcf3bmt12_19_1_4_3	0.90150	0.00151	0.90452
ncf2bmt11_18_1_4_3	0.0	70	17638	12346	9265	19.59	1.0e-04	0.91814	0.00135	0.92085	hcf3bmt12_18_1_4_3	0.89955	0.00134	0.90222

Table 6.9.6-11. Results for HEU broken metal content in packaging calculation model

case name	np (in)	enr. (wt%)	U (g)	^{235}U (g)	H_2O (g)	h/x	moifr	k_{eff}	σ	$k_{eff}+2σ$	case name	k_{eff}	σ	$k_{eff}+2σ$
ncf2bmt11_17_1_4_3	0.0	70	16709	11697	9314	20.78	1.0e-04	0.91793	0.00133	0.92058	hcf3bmt12_17_1_4_3	0.89730	0.00133	0.89996
ncf2bmt11_16_1_4_3	0.0	70	15781	11047	9363	22.12	1.0e-04	0.91629	0.00133	0.91895	hcf3bmt12_16_1_4_3	0.89458	0.00122	0.89702
ncf2bmt11_15_1_4_3	0.0	70	14853	10397	9412	23.63	1.0e-04	0.91068	0.00125	0.91317	hcf3bmt12_15_1_4_3	0.89088	0.00130	0.89347
ncf2bmt11_36_1_3_3	0.0	60	35320	21192	8332	10.26	1.0e-04	0.93348	0.00105	0.93558	hcf3bmt12_36_1_3_3	0.91223	0.00113	0.91450
ncf2bmt11_35_1_3_3	0.0	60	34391	20634	8381	10.60	1.0e-04	0.93036	0.00127	0.93290	hcf3bmt12_35_1_3_3	0.91033	0.00128	0.91288
ncf2bmt11_34_1_3_3	0.0	60	33461	20077	8430	10.96	1.0e-04	0.92584	0.00127	0.92837	hcf3bmt12_34_1_3_3	0.90950	0.00126	0.91202
ncf2bmt11_33_1_3_3	0.0	60	32532	19519	8479	11.34	1.0e-04	0.92680	0.00142	0.92965	hcf3bmt12_33_1_3_3	0.90720	0.00143	0.91007
ncf2bmt11_32_1_3_3	0.0	60	31602	18961	8529	11.74	1.0e-04	0.92588	0.00144	0.92877	hcf3bmt12_32_1_3_3	0.90425	0.00126	0.90678
ncf2bmt11_31_1_3_3	0.0	60	30673	18404	8578	12.17	1.0e-04	0.92420	0.00123	0.92665	hcf3bmt12_31_1_3_3	0.90271	0.00118	0.90506
ncf2bmt11_30_1_3_3	0.0	60	29743	17846	8627	12.62	1.0e-04	0.92236	0.00165	0.92566	hcf3bmt12_30_1_3_3	0.90323	0.00138	0.90599
ncf2bmt11_29_1_3_3	0.0	60	28814	17288	8676	13.10	1.0e-04	0.91822	0.00113	0.92047	hcf3bmt12_29_1_3_3	0.89982	0.00121	0.90224
with can spacers (np thickness = 1.4 in.)														
ncf2bmt11_12_2_8_3	1.4	100	11097	11097	8995	21.16	1.0e-04	0.93137	0.00124	0.93385	hcf3bmt12_12_2_8_3	0.91417	0.00139	0.91696
ncf2bmt11_11_2_8_3	1.4	100	10173	10173	9044	23.20	1.0e-04	0.92641	0.00144	0.92928	hcf3bmt12_11_2_8_3	0.91315	0.00164	0.91642
ncf2bmt11_10_2_8_3	1.4	100	9248	9248	9093	25.66	1.0e-04	0.92058	0.00138	0.92334	hcf3bmt12_10_2_8_3	0.90570	0.00166	0.90902
ncf2bmt11_9_2_8_3	1.4	100	8323	8323	9142	28.67	1.0e-04	0.91671	0.00138	0.91947	hcf3bmt12_9_2_8_3	0.89648	0.00131	0.89911
ncf2bmt11_8_2_8_3	1.4	100	7398	7398	9191	32.43	1.0e-04	0.91365	0.00171	0.91706	hcf3bmt12_8_2_8_3	0.89682	0.00139	0.89960
ncf2bmt11_7_2_8_3	1.4	100	6473	6473	9240	37.26	1.0e-04	0.90684	0.00166	0.91016	hcf3bmt12_7_2_8_3	0.88907	0.00143	0.89192
ncf2bmt11_6_2_8_3	1.4	100	5549	5549	9289	43.70	1.0e-04	0.89705	0.00145	0.89995	hcf3bmt12_6_2_8_3	0.87797	0.00166	0.88130
ncf2bmt11_14_2_7_3	1.4	95	13880	13186	8847	17.51	1.0e-04	0.93174	0.00131	0.93437	hcf3bmt12_14_2_7_3	0.91453	0.00162	0.91777
ncf2bmt11_13_2_7_3	1.4	95	12955	12307	8896	18.87	1.0e-04	0.92685	0.00140	0.92965	hcf3bmt12_13_2_7_3	0.91006	0.00135	0.91276
ncf2bmt11_12_2_7_3	1.4	95	11104	10549	8995	22.25	1.0e-04	0.91939	0.00136	0.92210	hcf3bmt12_12_2_7_3	0.89784	0.00132	0.90048
ncf2bmt11_11_2_7_3	1.4	95	10179	9670	9044	24.41	1.0e-04	0.91215	0.00134	0.91483	hcf3bmt12_11_2_7_3	0.89423	0.00146	0.89715

Table 6.9.6-11. Results for HEU broken metal content in packaging calculation model

case name	np (in)	enr. (wt%)	U (g)	^{235}U (g)	H_2O (g)	h/x	moifr	k_{eff}	σ	$k_{eff}+2σ$	case name	k_{eff}	σ	$k_{eff}+2σ$
ncf2bmt11_10_2_7_3	1.4	95	9254	8791	9093	27.00	1.0e-04	0.90898	0.00126	0.91151	hcf3bmt12_10_2_7_3	0.89121	0.00159	0.89438
ncf2bmt11_9_2_7_3	1.4	95	8328	7912	9142	30.16	1.0e-04	0.90123	0.00147	0.90416	hcf3bmt12_9_2_7_3	0.88311	0.00145	0.88602
ncf2bmt11_16_2_6_3	1.4	90	15741	14167	8749	16.12	1.0e-04	0.92855	0.00124	0.93103	hcf3bmt12_16_2_6_3	0.91007	0.00134	0.91276
ncf2bmt11_15_2_6_3	1.4	90	14815	13334	8798	17.22	1.0e-04	0.92599	0.00107	0.92813	hcf3bmt12_15_2_6_3	0.90421	0.00136	0.90693
ncf2bmt11_14_2_6_3	1.4	90	13889	12500	8847	18.47	1.0e-04	0.91938	0.00131	0.92200	hcf3bmt12_14_2_6_3	0.90163	0.00129	0.90422
ncf2bmt11_13_2_6_3	1.4	90	12963	11667	8896	19.90	1.0e-04	0.91387	0.00110	0.91607	hcf3bmt12_13_2_6_3	0.89824	0.00123	0.90069
ncf2bmt11_12_2_6_3	1.4	90	11111	10000	8995	23.48	1.0e-04	0.90989	0.00135	0.91258	hcf3bmt12_12_2_6_3	0.88832	0.00136	0.89105
ncf2bmt11_11_2_6_3	1.4	90	10185	9167	9044	25.75	1.0e-04	0.90334	0.00152	0.90637	hcf3bmt12_11_2_6_3	0.88574	0.00168	0.88911
ncf2bmt11_10_2_6_3	1.4	90	9260	8334	9093	28.48	1.0e-04	0.89868	0.00172	0.90212	hcf3bmt12_10_2_6_3	0.87986	0.00134	0.88254
ncf2bmt11_9_2_6_3	1.4	90	8334	7500	9142	31.81	1.0e-04	0.89190	0.00154	0.89499	hcf3bmt12_9_2_6_3	0.87453	0.00140	0.87733
											hcf3bmt12_24_2_5_3	0.90790	0.00134	0.91058
											hcf3bmt12_23_2_5_3	0.90282	0.00121	0.90523
ncf2bmt11_22_2_5_3	1.4	80	21324	17059	8455	12.94	1.0e-04	0.92358	0.00131	0.92619	hcf3bmt12_22_2_5_3	0.90006	0.00139	0.90284
ncf2bmt11_21_2_5_3	1.4	80	20397	16317	8504	13.60	1.0e-04	0.91640	0.00145	0.91930	hcf3bmt12_21_2_5_3	0.89948	0.00134	0.90216
ncf2bmt11_20_2_5_3	1.4	80	19470	15576	8553	14.33	1.0e-04	0.91428	0.00133	0.91694	hcf3bmt12_20_2_5_3	0.89698	0.00122	0.89941
ncf2bmt11_19_2_5_3	1.4	80	18542	14834	8602	15.14	1.0e-04	0.91020	0.00130	0.91281	hcf3bmt12_19_2_5_3	0.89282	0.00129	0.89541
ncf2bmt11_18_2_5_3	1.4	80	17615	14092	8651	16.02	1.0e-04	0.90784	0.00135	0.91054	hcf3bmt12_18_2_5_3	0.88897	0.00125	0.89148
ncf2bmt11_17_2_5_3	1.4	80	16688	13351	8700	17.01	1.0e-04	0.90364	0.00123	0.90610	hcf3bmt12_17_2_5_3	0.88452	0.00123	0.88697
ncf2bmt11_16_2_5_3	1.4	80	15761	12609	8749	18.11	1.0e-04	0.90402	0.00132	0.90666	hcf3bmt12_16_2_5_3	0.88688	0.00121	0.88929
ncf2bmt11_15_2_5_3	1.4	80	14834	11867	8798	19.35	1.0e-04	0.90496	0.00145	0.90786	hcf3bmt12_15_2_5_3	0.88496	0.00135	0.88765
ncf2bmt11_33_2_4_3	1.4	70	32490	22743	7866	9.03	1.0e-04	0.92631	0.00120	0.92871	hcf3bmt12_33_2_4_3	0.90516	0.00118	0.90752
ncf2bmt11_32_2_4_3	1.4	70	31562	22093	7915	9.35	1.0e-04	0.92304	0.00128	0.92560	hcf3bmt12_32_2_4_3	0.90236	0.00135	0.90507

Table 6.9.6-11. Results for HEU broken metal content in packaging calculation model

case name	np (in)	enr. (wt%)	U (g)	^{235}U (g)	H_2O (g)	h/x	moifr	k_{eff}	σ	$k_{eff}+2σ$	case name	k_{eff}	σ	$k_{eff}+2σ$
ncf2bmt11_31_2_4_3	1.4	70	30634	21444	7964	9.69	1.0e-04	0.92250	0.00132	0.92514	hcf3bmt12_31_2_4_3	0.90127	0.00111	0.90349
ncf2bmt11_30_2_4_3	1.4	70	29705	20794	8013	10.06	1.0e-04	0.92048	0.00138	0.92325	hcf3bmt12_30_2_4_3	0.89944	0.00124	0.90192
ncf2bmt11_29_2_4_3	1.4	70	28777	20144	8062	10.45	1.0e-04	0.91607	0.00135	0.91878	hcf3bmt12_29_2_4_3	0.89544	0.00139	0.89823
ncf2bmt11_28_2_4_3	1.4	70	27849	19494	8111	10.86	1.0e-04	0.91338	0.00129	0.91596	hcf3bmt12_28_2_4_3	0.89451	0.00127	0.89706
ncf2bmt11_27_2_4_3	1.4	70	26921	18844	8160	11.30	1.0e-04	0.91255	0.00127	0.91510	hcf3bmt12_27_2_4_3	0.88990	0.00135	0.89261
ncf2bmt11_36_2_3_3	1.4	60	35320	21192	7719	9.51	1.0e-04	0.90382	0.00130	0.90642	hcf3bmt12_36_2_3_3	0.88262	0.00120	0.88503
ncf2bmt11_35_2_3_3	1.4	60	34391	20634	7768	9.83	1.0e-04	0.90020	0.00136	0.90291	hcf3bmt12_35_2_3_3	0.87857	0.00132	0.88120
ncf2bmt11_34_2_3_3	1.4	60	33461	20077	7817	10.16	1.0e-04	0.89689	0.00121	0.89932	hcf3bmt12_34_2_3_3	0.87717	0.00111	0.87939
ncf2bmt11_33_2_3_3	1.4	60	32532	19519	7866	10.52	1.0e-04	0.89834	0.00117	0.90069	hcf3bmt12_33_2_3_3	0.87502	0.00127	0.87757
ncf2bmt11_32_2_3_3	1.4	60	31602	18961	7915	10.90	1.0e-04	0.89483	0.00136	0.89755	hcf3bmt12_32_2_3_3	0.87552	0.00129	0.87809
ncf2bmt11_31_2_3_3	1.4	60	30673	18404	7964	11.29	1.0e-04	0.89450	0.00137	0.89723	hcf3bmt12_31_2_3_3	0.87475	0.00139	0.87752
ncf2bmt11_30_2_3_3	1.4	60	29743	17846	8013	11.72	1.0e-04	0.89227	0.00133	0.89493	hcf3bmt12_30_2_3_3	0.87454	0.00121	0.87695
content in flooded containment vessel, array packaging model for CSI=2.0														
NCT											**HAC**			
no can spacers (np thickness = 0.0 in.)														
ncf3bmt11_24_1_5_3	0.0	80	23178	18542	8970	12.63	1.0e-04	0.92510	0.00131	0.92772	hcf4bmt12_24_1_5_3	0.88778	0.00138	0.89054
ncf3bmt11_23_1_5_3	0.0	80	22251	17801	9019	13.22	1.0e-04	0.92307	0.00144	0.92595	hcf4bmt12_23_1_5_3	0.88545	0.00131	0.88806
ncf3bmt11_22_1_5_3	0.0	80	21324	17059	9068	13.87	1.0e-04	0.91977	0.00125	0.92228	hcf4bmt12_22_1_5_3	0.88238	0.00140	0.88519
ncf3bmt11_21_1_5_3	0.0	80	20397	16317	9117	14.58	1.0e-04	0.91607	0.00134	0.91876	hcf4bmt12_21_1_5_3	0.87917	0.00128	0.88173
ncf3bmt11_20_1_5_3	0.0	80	19470	15576	9166	15.36	1.0e-04	0.91812	0.00123	0.92059	hcf4bmt12_20_1_5_3	0.87731	0.00132	0.87995
ncf3bmt11_36_1_4_3	0.0	70	35275	24693	8332	8.81	1.0e-04	0.93179	0.00144	0.93467	hcf4bmt12_36_1_4_3	0.89390	0.00117	0.89625
ncf3bmt11_35_1_4_3	0.0	70	34347	24043	8381	9.10	1.0e-04	0.92998	0.00125	0.93248	hcf4bmt12_35_1_4_3	0.89164	0.00140	0.89444
ncf3bmt11_34_1_4_3	0.0	70	33419	23393	8430	9.41	1.0e-04	0.92792	0.00128	0.93049	hcf4bmt12_34_1_4_3	0.88829	0.00123	0.89075

Table 6.9.6-11. Results for HEU broken metal content in packaging calculation model

case name	np (in)	enr. (wt%)	U (g)	^{235}U (g)	H_2O (g)	h/x	moifr	k_{eff}	σ	$k_{eff}+2σ$	case name	k_{eff}	σ	$k_{eff}+2σ$
ncf3bmt11_33_1_4_3	0.0	70	32490	22743	8479	9.73	1.0e-04	0.92421	0.00134	0.92690	hcf4bmt12_33_1_4_3	0.88600	0.00117	0.88834
ncf3bmt11_32_1_4_3	0.0	70	31562	22093	8529	10.08	1.0e-04	0.92329	0.00131	0.92591	hcf4bmt12_32_1_4_3	0.88581	0.00140	0.88861
ncf3bmt11_31_1_4_3	0.0	70	30634	21444	8578	10.44	1.0e-04	0.91896	0.00132	0.92160	hcf4bmt12_31_1_4_3	0.88314	0.00132	0.88577
ncf3bmt11_36_1_3_3	0.0	60	35320	21192	8332	10.26	1.0e-04	0.90201	0.00123	0.90447	hcf4bmt12_36_1_3_3	0.86792	0.00130	0.87053
ncf3bmt11_35_1_3_3	0.0	60	34391	20634	8381	10.60	1.0e-04	0.90103	0.00130	0.90363	hcf4bmt12_35_1_3_3	0.86477	0.00150	0.86777
ncf3bmt11_34_1_3_3	0.0	60	33461	20077	8430	10.96	1.0e-04	0.89984	0.00147	0.90278	hcf4bmt12_34_1_3_3	0.86396	0.00137	0.86670
ncf3bmt11_33_1_3_3	0.0	60	32532	19519	8479	11.34	1.0e-04	0.89745	0.00130	0.90004	hcf4bmt12_33_1_3_3	0.86136	0.00134	0.86404
ncf3bmt11_32_1_3_3	0.0	60	31602	18961	8529	11.74	1.0e-04	0.89310	0.00137	0.89585	hcf4bmt12_32_1_3_3	0.86115	0.00124	0.86362
ncf3bmt11_31_1_3_3	0.0	60	30673	18404	8578	12.17	1.0e-04	0.89440	0.00135	0.89711	hcf4bmt12_31_1_3_3	0.85909	0.00151	0.86212
with can spacers (np thickness = 1.4 in.)														
ncf3bmt11_19_2_8_3	1.4	100	18496	18496	8602	12.14	1.0e-04	0.93577	0.00135	0.93847	hcf4bmt12_19_2_8_3	0.89811	0.00149	0.90110
ncf3bmt11_18_2_8_3	1.4	100	17571	17571	8651	12.85	1.0e-04	0.93186	0.00154	0.93494	hcf4bmt12_18_2_8_3	0.89794	0.00151	0.90096
ncf3bmt11_17_2_8_3	1.4	100	16646	16646	8700	13.64	1.0e-04	0.92731	0.00135	0.93002	hcf4bmt12_17_2_8_3	0.89377	0.00134	0.89644
ncf3bmt11_16_2_8_3	1.4	100	15721	15721	8749	14.53	1.0e-04	0.92992	0.00126	0.93244	hcf4bmt12_16_2_8_3	0.89138	0.00121	0.89379
ncf3bmt11_15_2_8_3	1.4	100	14796	14796	8798	15.52	1.0e-04	0.92597	0.00134	0.92865	hcf4bmt12_15_2_8_3	0.89085	0.00130	0.89345
ncf3bmt11_14_2_8_3	1.4	100	13872	13872	8847	16.65	1.0e-04	0.91788	0.00124	0.92037	hcf4bmt12_14_2_8_3	0.88486	0.00143	0.88772
ncf3bmt11_13_2_8_3	1.4	100	12947	12947	8896	17.94	1.0e-04	0.91410	0.00116	0.91642	hcf4bmt12_13_2_8_3	0.88161	0.00147	0.88454
ncf3bmt11_12_2_8_3	1.4	100	11097	11097	8995	21.16	1.0e-04	0.90586	0.00164	0.90915	hcf4bmt12_12_2_8_3	0.87451	0.00129	0.87708
ncf3bmt11_11_2_8_3	1.4	100	10173	10173	9044	23.20	1.0e-04	0.90034	0.00144	0.90322	hcf4bmt12_11_2_8_3	0.86789	0.00129	0.87047
ncf3bmt11_24_2_7_3	1.4	95	23134	21977	8357	9.92	1.0e-04	0.93439	0.00143	0.93724	hcf4bmt12_24_2_7_3	0.89896	0.00122	0.90141
ncf3bmt11_23_2_7_3	1.4	95	22209	21098	8406	10.40	1.0e-04	0.93453	0.00131	0.93716	hcf4bmt12_23_2_7_3	0.89761	0.00131	0.90024
ncf3bmt11_22_2_7_3	1.4	95	21283	20219	8455	10.91	1.0e-04	0.92992	0.00130	0.93252	hcf4bmt12_22_2_7_3	0.89290	0.00142	0.89574
ncf3bmt11_21_2_7_3	1.4	95	20358	19340	8504	11.48	1.0e-04	0.92588	0.00136	0.92860	hcf4bmt12_21_2_7_3	0.89171	0.00135	0.89441

Table 6.9.6-11. Results for HEU broken metal content in packaging calculation model

case name	np (in)	enr. (wt%)	U (g)	^{235}U (g)	H_2O (g)	h/x	moifr	k_{eff}	σ	$k_{eff}+2σ$	case name	k_{eff}	σ	$k_{eff}+2σ$
ncf3bmt11_20_2_7_3	1.4	95	19433	18461	8553	12.09	1.0e-04	0.92140	0.00126	0.92392	hcf4bmt12_20_2_7_3	0.88860	0.00138	0.89135
ncf3bmt11_19_2_7_3	1.4	95	18507	17582	8602	12.77	1.0e-04	0.91794	0.00128	0.92049	hcf4bmt12_19_2_7_3	0.88544	0.00131	0.88806
ncf3bmt11_18_2_7_3	1.4	95	17582	16703	8651	13.52	1.0e-04	0.91432	0.00143	0.91717	hcf4bmt12_18_2_7_3	0.87916	0.00119	0.88154
ncf3bmt11_28_2_6_3	1.4	90	27778	25001	8111	8.47	1.0e-04	0.93537	0.00113	0.93763	hcf4bmt12_28_2_6_3	0.89885	0.00127	0.90138
ncf3bmt11_27_2_6_3	1.4	90	26852	24167	8160	8.81	1.0e-04	0.93322	0.00129	0.93581	hcf4bmt12_27_2_6_3	0.89628	0.00137	0.89902
ncf3bmt11_26_2_6_3	1.4	90	25927	23334	8209	9.18	1.0e-04	0.92880	0.00119	0.93117	hcf4bmt12_26_2_6_3	0.89189	0.00127	0.89443
ncf3bmt11_25_2_6_3	1.4	90	24075	21667	8308	10.01	1.0e-04	0.92446	0.00149	0.92745	hcf4bmt12_25_2_6_3	0.88877	0.00144	0.89165
ncf3bmt11_24_2_6_3	1.4	90	23149	20834	8357	10.47	1.0e-04	0.92270	0.00138	0.92547	hcf4bmt12_24_2_6_3	0.88731	0.00129	0.88990
ncf3bmt11_23_2_6_3	1.4	90	22223	20000	8406	10.97	1.0e-04	0.91857	0.00138	0.92133	hcf4bmt12_23_2_6_3	0.88245	0.00133	0.88512
ncf3bmt11_22_2_6_3	1.4	90	21297	19167	8455	11.51	1.0e-04	0.91639	0.00145	0.91929	hcf4bmt12_22_2_6_3	0.87838	0.00119	0.88076
ncf3bmt11_34_2_5_3	1.4	80	33376	26701	7817	7.64	1.0e-04	0.92540	0.00127	0.92795	hcf4bmt12_34_2_5_3	0.88608	0.00131	0.88869
ncf3bmt11_33_2_5_3	1.4	80	32449	25959	7866	7.91	1.0e-04	0.92436	0.00140	0.92716	hcf4bmt12_33_2_5_3	0.88749	0.00156	0.89061
ncf3bmt11_32_2_5_3	1.4	80	31522	25218	7915	8.19	1.0e-04	0.91919	0.00120	0.92159	hcf4bmt12_32_2_5_3	0.88581	0.00130	0.88841
ncf3bmt11_31_2_5_3	1.4	80	30595	24476	7964	8.49	1.0e-04	0.91747	0.00126	0.92000	hcf4bmt12_31_2_5_3	0.88299	0.00141	0.88582
ncf3bmt11_36_2_4_3	1.4	70	35275	24693	7719	8.16	1.0e-04	0.90114	0.00120	0.90353	hcf4bmt12_36_2_4_3	0.86624	0.00106	0.86835
ncf3bmt11_35_2_4_3	1.4	70	34347	24043	7768	8.43	1.0e-04	0.89908	0.00131	0.90169	hcf4bmt12_35_2_4_3	0.86262	0.00143	0.86549
ncf3bmt11_34_2_4_3	1.4	70	33419	23393	7817	8.72	1.0e-04	0.89841	0.00115	0.90070	hcf4bmt12_34_2_4_3	0.86008	0.00129	0.86265
ncf3bmt11_36_2_3_3	1.4	60	35320	21192	7719	9.51	1.0e-04	0.87206	0.00120	0.87446	hcf4bmt12_36_2_3_3	0.83873	0.00122	0.84116
ncf3bmt11_35_2_3_3	1.4	60	34391	20634	7768	9.83	1.0e-04	0.86988	0.00123	0.87235	hcf4bmt12_35_2_3_3	0.83470	0.00130	0.83731
ncf3bmt11_34_2_3_3	1.4	60	33461	20077	7817	10.16	1.0e-04	0.86818	0.00130	0.87078	hcf4bmt12_34_2_3_3	0.83204	0.00117	0.83439

Table 6.9.6-11. Results for HEU broken metal content in packaging calculation model

case name	np (in)	enr. (wt%)	U (g)	^{235}U (g)	H_2O (g)	h/x	moifr	k_{eff}	σ	$k_{eff}+2σ$	case name	k_{eff}	σ	$k_{eff}+2σ$
content in flooded containment vessel, array packaging model for CSI=3.1														
NCT											**HAC**			
no can spacers (np thickness = 0.0 in.)														
nctf5bmt11_36_1_5_3	0.0	80	35231	28184	8332	7.72	1.0e-04	0.92519	0.00130	0.92779	hctf5bmt12_36_1_5_3	0.90361	0.00119	0.90600
nctf5bmt11_35_1_5_3	0.0	80	34303	27443	8381	7.97	1.0e-04	0.91980	0.00138	0.92255	hctf5bmt12_35_1_5_3	0.90246	0.00137	0.90520
nctf5bmt11_34_1_5_3	0.0	80	33376	26701	8430	8.24	1.0e-04	0.92113	0.00138	0.92389	hctf5bmt12_34_1_5_3	0.89974	0.00136	0.90246
nctf5bmt11_33_1_5_3	0.0	80	32449	25959	8479	8.53	1.0e-04	0.91846	0.00117	0.92079	hctf5bmt12_33_1_5_3	0.89587	0.00129	0.89845
nctf5bmt11_32_1_5_3	0.0	80	31522	25218	8529	8.83	1.0e-04	0.91556	0.00119	0.91795	hctf5bmt12_32_1_5_3	0.89459	0.00148	0.89755
nctf5bmt11_36_1_4_3	0.0	70	35275	24693	8332	8.81	1.0e-04	0.90020	0.00139	0.90299	hctf5bmt12_36_1_4_3	0.87905	0.00142	0.88188
nctf5bmt11_35_1_4_3	0.0	70	34347	24043	8381	9.10	1.0e-04	0.89748	0.00118	0.89984	hctf5bmt12_35_1_4_3	0.87388	0.00126	0.87639
nctf5bmt11_34_1_4_3	0.0	70	33419	23393	8430	9.41	1.0e-04	0.89206	0.00115	0.89437	hctf5bmt12_34_1_4_3	0.87550	0.00150	0.87851
nctf5bmt11_36_1_3_3	0.0	60	35320	21192	8332	10.26	1.0e-04	0.87170	0.00131	0.87433	hctf5bmt12_36_1_3_3	0.85181	0.00121	0.85423
nctf5bmt11_35_1_3_3	0.0	60	34391	20634	8381	10.60	1.0e-04	0.87122	0.00146	0.87414	hctf5bmt12_35_1_3_3	0.85100	0.00135	0.85369
with can spacers (np thickness = 1.4 in.)														
nctf5bmt11_26_2_8_3	1.4	100	25894	25894	8209	8.28	1.0e-04	0.92880	0.00114	0.93108	hctf5bmt12_26_2_8_3	0.90779	0.00115	0.91009
nctf5bmt11_25_2_8_3	1.4	100	24969	24969	8258	8.63	1.0e-04	0.92250	0.00118	0.92485	hctf5bmt12_25_2_8_3	0.90619	0.00136	0.90890
nctf5bmt11_24_2_8_3	1.4	100	23119	23119	8357	9.43	1.0e-04	0.92133	0.00137	0.92406	hctf5bmt12_24_2_8_3	0.90163	0.00125	0.90413
nctf5bmt11_23_2_8_3	1.4	100	22195	22195	8406	9.89	1.0e-04	0.92154	0.00124	0.92401	hctf5bmt12_23_2_8_3	0.90028	0.00150	0.90329
nctf5bmt11_22_2_8_3	1.4	100	21270	21270	8455	10.38	1.0e-04	0.91455	0.00141	0.91737	hctf5bmt12_22_2_8_3	0.89693	0.00148	0.89990
nctf5bmt11_21_2_8_3	1.4	100	20345	20345	8504	10.91	1.0e-04	0.91027	0.00140	0.91306	hctf5bmt12_21_2_8_3	0.89420	0.00140	0.89700
nctf5bmt11_30_2_7_3	1.4	95	29612	28131	8013	7.43	1.0e-04	0.92409	0.00126	0.92660	hctf5bmt12_30_2_7_3	0.90413	0.00129	0.90670
nctf5bmt11_29_2_7_3	1.4	95	28686	27252	8062	7.72	1.0e-04	0.92175	0.00160	0.92495	hctf5bmt12_29_2_7_3	0.90149	0.00125	0.90400

Table 6.9.6-11. Results for HEU broken metal content in packaging calculation model

case name	np (in)	enr. (wt%)	U (g)	^{235}U (g)	H_2O (g)	h/x	moifr	k_{eff}	σ	$k_{eff}+2σ$	case name	k_{eff}	σ	$k_{eff}+2σ$
nctf5bmt11_28_2_7_3	1.4	95	27761	26373	8111	8.03	1.0e-04	0.91662	0.00149	0.91960	hctf5bmt12_28_2_7_3	0.89554	0.00127	0.89809
nctf5bmt11_27_2_7_3	1.4	95	26835	25494	8160	8.35	1.0e-04	0.91290	0.00112	0.91515	hctf5bmt12_27_2_7_3	0.89349	0.00120	0.89588
nctf5bmt11_26_2_7_3	1.4	95	25910	24615	8209	8.71	1.0e-04	0.90934	0.00124	0.91182	hctf5bmt12_26_2_7_3	0.88954	0.00116	0.89187
nctf5bmt11_25_2_7_3	1.4	95	24985	23736	8258	9.08	1.0e-04	0.90900	0.00116	0.91131	hctf5bmt12_25_2_7_3	0.88811	0.00120	0.89051
nctf5bmt11_24_2_7_3	1.4	95	23134	21977	8357	9.92	1.0e-04	0.90460	0.00146	0.90752	hctf5bmt12_24_2_7_3	0.88850	0.00132	0.89113
nctf5bmt11_35_2_6_3	1.4	90	34260	30834	7768	6.58	1.0e-04	0.92200	0.00132	0.92464	hctf5bmt12_35_2_6_3	0.90072	0.00123	0.90318
nctf5bmt11_34_2_6_3	1.4	90	33334	30001	7817	6.80	1.0e-04	0.91799	0.00130	0.92059	hctf5bmt12_34_2_6_3	0.89921	0.00112	0.90145
nctf5bmt11_33_2_6_3	1.4	90	32408	29167	7866	7.04	1.0e-04	0.91789	0.00136	0.92061	hctf5bmt12_33_2_6_3	0.89931	0.00137	0.90206
nctf5bmt11_32_2_6_3	1.4	90	31482	28334	7915	7.29	1.0e-04	0.91514	0.00113	0.91740	hctf5bmt12_32_2_6_3	0.89395	0.00118	0.89631
nctf5bmt11_36_2_5_3	1.4	80	35231	28184	7719	7.15	1.0e-04	0.89457	0.00141	0.89739	hctf5bmt12_36_2_5_3	0.87726	0.00158	0.88041
nctf5bmt11_35_2_5_3	1.4	80	34303	27443	7768	7.39	1.0e-04	0.89528	0.00129	0.89787	hctf5bmt12_35_2_5_3	0.87420	0.00120	0.87660
nctf5bmt11_34_2_5_3	1.4	80	33376	26701	7817	7.64	1.0e-04	0.89346	0.00115	0.89576	hctf5bmt12_34_2_5_3	0.87530	0.00122	0.87775
nctf5bmt11_36_2_4_3	1.4	70	35275	24693	7719	8.16	1.0e-04	0.87119	0.00121	0.87361	hctf5bmt12_36_2_4_3	0.85030	0.00147	0.85323
nctf5bmt11_35_2_4_3	1.4	70	34347	24043	7768	8.43	1.0e-04	0.86740	0.00110	0.86959	hctf5bmt12_35_2_4_3	0.84958	0.00107	0.85173
nctf5bmt11_36_2_3_3	1.4	60	35320	21192	7719	9.51	1.0e-04	0.84212	0.00121	0.84454	hctf5bmt12_36_2_3_3	0.82413	0.00117	0.82647
nctf5bmt11_35_2_3_3	1.4	60	34391	20634	7768	9.83	1.0e-04	0.83953	0.00135	0.84223	hctf5bmt12_35_2_3_3	0.82142	0.00125	0.82393

Table 6.9.6-11b. Comparison of NCT results for HEU broken metal content in ES-3100 NCT packaging calculation models.
Reference results for content homogenized over volume of containment vessel are highlighted. Results shown below the reference results are for modified cases where the HEU packaging fraction varies from 0.2 to 0.6 and the content is homogenized with 500 g polyethylene.

nciabmt11	np (in.)	enr. (wt %)	U (g)	^{235}U (g)	H_2O (g)	h/x	moifr	k_{eff}	σ	$k_{eff}+2σ$				
nciapbmflt11	np (in.)	PF	U (g)	^{235}U (g)	H_2O (g)	h/x	moifr	k_{eff}	σ	$k_{eff}+2σ$	nciapbmfdt11	k_{eff}	σ	$k_{eff}+2σ$
content in flooded containment vessel, array packaging model for CSI=0.0														
no can spacers (np thickness = 0.0 in.)														
_4_1_5_3	0.0	80.0	3709	2967	10001	87.98	1.0e-04	0.91835	0.00149	0.92133				
_1_2_4_5	0.0	0.2	4000	3200	9443	82.26	1.0e-04	0.68903	0.00121	0.69146	_1_2_4_5	0.85247	0.00116	0.85479
_1_3_4_5	0.0	0.3	4000	3200	9443	82.26	1.0e-04	0.65516	0.00136	0.65788	_1_3_4_5	0.84236	0.00121	0.84477
_1_4_4_5	0.0	0.4	4000	3200	9443	82.26	1.0e-04	0.63720	0.00123	0.63965	_1_4_4_5	0.83993	0.00137	0.84267
_1_5_4_5	0.0	0.5	4000	3200	9443	82.26	1.0e-04	0.62195	0.00105	0.62405	_1_5_4_5	0.83701	0.00126	0.83953
_1_6_4_5	0.0	0.6	4000	3200	9443	82.26	1.0e-04	0.61282	0.00101	0.61484	_1_6_4_5	0.83523	0.00118	0.83758
_5_1_4_3	0.0	70.0	4642	3249	9952	79.95	1.0e-04	0.91799	0.00136	0.92070				
_1_2_5_4	0.0	0.2	5000	3500	9390	74.82	1.0e-04	0.70497	0.00140	0.70778	_1_2_5_4	0.85830	0.00155	0.86140
_1_3_5_4	0.0	0.3	5000	3500	9390	74.82	1.0e-04	0.66703	0.00120	0.66942	_1_3_5_4	0.85296	0.00124	0.85545
_1_4_5_4	0.0	0.4	5000	3500	9390	74.82	1.0e-04	0.64665	0.00120	0.64904	_1_4_5_4	0.84681	0.00155	0.84991
_1_5_5_4	0.0	0.5	5000	3500	9390	74.82	1.0e-04	0.63242	0.00127	0.63496	_1_5_5_4	0.84544	0.00142	0.84827
_1_6_5_4	0.0	0.6	5000	3500	9390	74.82	1.0e-04	0.62104	0.00129	0.62362	_1_6_5_4	0.84411	0.00122	0.84656
_6_1_3_3	0.0	60.0	5577	3346	9903	77.24	1.0e-04	0.91221	0.00147	0.91515				
_1_2_6_3	0.0	0.2	6000	3600	9338	72.36	1.0e-04	0.71137	0.00124	0.71386	_1_2_6_3	0.85681	0.00117	0.85916
_1_3_6_3	0.0	0.3	6000	3600	9338	72.36	1.0e-04	0.67406	0.00124	0.67654	_1_3_6_3	0.85226	0.00126	0.85478
_1_4_6_3	0.0	0.4	6000	3600	9338	72.36	1.0e-04	0.65407	0.00115	0.65637	_1_4_6_3	0.84813	0.00119	0.85052
_1_5_6_3	0.0	0.5	6000	3600	9338	72.36	1.0e-04	0.63393	0.00117	0.63626	_1_5_6_3	0.84385	0.00128	0.84642
_1_6_6_3	0.0	0.6	6000	3600	9338	72.36	1.0e-04	0.62196	0.00126	0.62449	_1_6_6_3	0.84286	0.00127	0.84541

Table 6.9.6-11b. Comparison of NCT results for HEU broken metal content in ES-3100 NCT packaging calculation models.
Reference results for content homogenized over volume of containment vessel are highlighted. Results shown below the reference results are for modified cases where the HEU packaging fraction varies from 0.2 to 0.6 and the content is homogenized with 500 g polyethylene.

nciabmt11	np (in.)	enr. (wt %)	U (g)	^{235}U (g)	H_2O (g)	h/x	moifr	k_{eff}	σ	$k_{eff}+2σ$				
nciapbmflt11	np (in.)	PF	U (g)	^{235}U (g)	H_2O (g)	h/x	moifr	k_{eff}	σ	$k_{eff}+2σ$	nciapbmfdt11	k_{eff}	σ	$k_{eff}+2σ$
with can spacers (np thickness = 1.4 in.)														
_3_2_8_3	1.4	100.0	2774	2774	9436	88.78	1.0e-04	0.90131	0.00139	0.90409				
_2_2_3_8	1.4	0.2	3000	3000	8882	82.86	1.0e-04	0.57463	0.00111	0.57684	_2_2_3_8	0.81623	0.00130	0.81883
_2_3_3_8	1.4	0.3	3000	3000	8882	82.86	1.0e-04	0.54703	0.00098	0.54900	_2_3_3_8	0.81643	0.00134	0.81912
_2_4_3_8	1.4	0.4	3000	3000	8882	82.86	1.0e-04	0.53274	0.00097	0.53467	_2_4_3_8	0.81357	0.00122	0.81600
_2_5_3_8	1.4	0.5	3000	3000	8882	82.86	1.0e-04	0.52613	0.00105	0.52822	_2_5_3_8	0.81038	0.00125	0.81288
_2_6_3_8	1.4	0.6	3000	3000	8882	82.86	1.0e-04	0.51882	0.00092	0.52065	_2_6_3_8	0.81249	0.00116	0.81482
_4_2_7_3	1.4	95.0	3701	3516	9387	69.68	1.0e-04	0.91690	0.00149	0.91987				
_2_2_4_7	1.4	0.2	4000	3800	8829	65.05	1.0e-04	0.61562	0.00115	0.61792	_2_2_4_7	0.85451	0.00154	0.85759
_2_3_4_7	1.4	0.3	4000	3800	8829	65.05	1.0e-04	0.58602	0.00121	0.58843	_2_3_4_7	0.84752	0.00128	0.85009
_2_4_4_7	1.4	0.4	4000	3800	8829	65.05	1.0e-04	0.56904	0.00124	0.57153	_2_4_4_7	0.84935	0.00118	0.85170
_2_5_4_7	1.4	0.5	4000	3800	8829	65.05	1.0e-04	0.55712	0.00096	0.55904	_2_5_4_7	0.84837	0.00138	0.85113
_2_6_4_7	1.4	0.6	4000	3800	8829	65.05	1.0e-04	0.55125	0.00100	0.55326	_2_6_4_7	0.84715	0.00114	0.84943
_4_2_6_3	1.4	90.0	3704	3333	9387	73.50	1.0e-04	0.90541	0.00147	0.90835				
_2_2_4_6	1.4	0.2	4000	3600	8829	68.67	1.0e-04	0.60511	0.00103	0.60717	_2_2_4_6	0.84248	0.00138	0.84524
_2_3_4_6	1.4	0.3	4000	3600	8829	68.67	1.0e-04	0.57445	0.00092	0.57628	_2_3_4_6	0.83740	0.00119	0.83978
_2_4_4_6	1.4	0.4	4000	3600	8829	68.67	1.0e-04	0.55835	0.00103	0.56041	_2_4_4_6	0.83957	0.00113	0.84184
_2_5_4_6	1.4	0.5	4000	3600	8829	68.67	1.0e-04	0.54727	0.00106	0.54939	_2_5_4_6	0.83601	0.00137	0.83875
_2_6_4_6	1.4	0.6	4000	3600	8829	68.67	1.0e-04	0.53974	0.00107	0.54189	_2_6_4_6	0.83732	0.00140	0.84011

Table 6.9.6-11b. Comparison of NCT results for HEU broken metal content in ES-3100 NCT packaging calculation models.
Reference results for content homogenized over volume of containment vessel are highlighted. Results shown below the reference results are for modified cases where the HEU packaging fraction varies from 0.2 to 0.6 and the content is homogenized with 500 g polyethylene.

nciabmt11	np (in.)	enr. (wt %)	U (g)	^{235}U (g)	H_2O (g)	h/x	moifr	k_{eff}	σ	$k_{eff}+2σ$				
nciapbmflt11	np (in.)	PF	U (g)	^{235}U (g)	H_2O (g)	h/x	moifr	k_{eff}	σ	$k_{eff}+2σ$	nciapbmfdt11	k_{eff}	σ	$k_{eff}+2σ$
_6_2_5_3	1.4	80.0	5563	4450	9289	54.48	1.0e-04	0.91981	0.00127	0.92235				
_2_2_6_5	1.4	0.2	6000	4800	8723	50.93	1.0e-04	0.66266	0.00117	0.66500	_2_2_6_5	0.87671	0.00141	0.87952
_2_3_6_5	1.4	0.3	6000	4800	8723	50.93	1.0e-04	0.62900	0.00108	0.63116	_2_3_6_5	0.87268	0.00141	0.87551
_2_4_6_5	1.4	0.4	6000	4800	8723	50.93	1.0e-04	0.60636	0.00106	0.60848	_2_4_6_5	0.87070	0.00137	0.87344
_2_5_6_5	1.4	0.5	6000	4800	8723	50.93	1.0e-04	0.59549	0.00110	0.59769	_2_5_6_5	0.87064	0.00126	0.87316
_2_6_6_5	1.4	0.6	6000	4800	8723	50.93	1.0e-04	0.58580	0.00104	0.58789	_2_6_6_5	0.86937	0.00136	0.87209
_8_2_4_3	1.4	70.0	7426	5198	9191	46.15	1.0e-04	0.91902	0.00137	0.92175				
_2_2_8_4	1.4	0.2	8000	5600	8618	43.16	1.0e-04	0.69894	0.00117	0.70128	_2_2_8_4	0.88757	0.00154	0.89065
_2_3_8_4	1.4	0.3	8000	5600	8618	43.16	1.0e-04	0.65861	0.00101	0.66064	_2_3_8_4	0.88142	0.00149	0.88440
_2_4_8_4	1.4	0.4	8000	5600	8618	43.16	1.0e-04	0.63538	0.00119	0.63775	_2_4_8_4	0.88292	0.00164	0.88621
_2_5_8_4	1.4	0.5	8000	5600	8618	43.16	1.0e-04	0.62021	0.00120	0.62260	_2_5_8_4	0.88202	0.00141	0.88484
_2_6_8_4	1.4	0.6	8000	5600	8618	43.16	1.0e-04	0.61023	0.00116	0.61255	_2_6_8_4	0.88175	0.00132	0.88439
_12_2_3_3	1.4	60.0	11154	6692	8995	35.08	1.0e-04	0.91502	0.00155	0.91812				
_2_2_12_3	1.4	0.2	12000	7200	8407	32.81	1.0e-04	0.75340	0.00124	0.75588	_2_2_12_3	0.90142	0.00133	0.90409
_2_3_12_3	1.4	0.3	12000	7200	8407	32.81	1.0e-04	0.71017	0.00101	0.71220	_2_3_12_3	0.90203	0.00119	0.90441
_2_4_12_3	1.4	0.4	12000	7200	8407	32.81	1.0e-04	0.68355	0.00103	0.68561	_2_4_12_3	0.89718	0.00145	0.90009
_2_5_12_3	1.4	0.5	12000	7200	8407	32.81	1.0e-04	0.66830	0.00090	0.67011	_2_5_12_3	0.90008	0.00114	0.90237
_2_6_12_3	1.4	0.6	12000	7200	8407	32.81	1.0e-04	0.65711	0.00100	0.65912	_2_6_12_3	0.89900	0.00120	0.90140

Table 6.9.6-11c. Comparison of HAC results for HEU broken metal content in ES-3100 HAC packaging calculation models.
Reference results for content homogenized over volume of containment vessel are highlighted. Results are for modified cases where the HEU packaging fraction varies from 0.2 to 0.6 and the content is homogenized with 500 g polyethylene.

hciabmt12	np (in.)	enr. (wt %)	U (g)	^{235}U (g)	H_2O (g)	h/x	moifr	k_{eff}	σ	$k_{eff}+2σ$				
hciapbmflt12	np (in.)	PF	U (g)	^{235}U (g)	H_2O (g)	h/x	moifr	k_{eff}	σ	$k_{eff}+2σ$	hciapbmfdt12	k_{eff}	σ	$k_{eff}+2σ$
content in flooded containment vessel, array packaging model for CSI=0.0														
no can spacers (np thickness = 0.0 in.)														
_4_1_5_3	0.0	80.0	3709	2967	10001	87.98	1.0e-04	0.92156	0.00160	0.92476				
_1_2_4_5	0.0	0.2	4000	3200	9443	82.26	1.0e-04	0.69676	0.00134	0.69944	_1_2_4_5	0.85244	0.00119	0.85481
_1_3_4_5	0.0	0.3	4000	3200	9443	82.26	1.0e-04	0.66231	0.00119	0.66469	_1_3_4_5	0.84158	0.00146	0.84451
_1_4_4_5	0.0	0.4	4000	3200	9443	82.26	1.0e-04	0.64127	0.00133	0.64392	_1_4_4_5	0.84036	0.00120	0.84276
_1_5_4_5	0.0	0.5	4000	3200	9443	82.26	1.0e-04	0.62704	0.00115	0.62934	_1_5_4_5	0.83647	0.00127	0.83901
_1_6_4_5	0.0	0.6	4000	3200	9443	82.26	1.0e-04	0.61943	0.00110	0.62164	_1_6_4_5	0.83721	0.00128	0.83977
_5_1_4_3	0.0	70.0	4642	3249	9952	79.95	1.0e-04	0.92053	0.00147	0.92347				
_1_2_5_4	0.0	0.2	5000	3500	9390	74.82	1.0e-04	0.71271	0.00111	0.71494	_1_2_5_4	0.86056	0.00125	0.86305
_1_3_5_4	0.0	0.3	5000	3500	9390	74.82	1.0e-04	0.67372	0.00145	0.67662	_1_3_5_4	0.85614	0.00119	0.85851
_1_4_5_4	0.0	0.4	5000	3500	9390	74.82	1.0e-04	0.65481	0.00129	0.65738	_1_4_5_4	0.84829	0.00144	0.85117
_1_5_5_4	0.0	0.5	5000	3500	9390	74.82	1.0e-04	0.63822	0.00113	0.64047	_1_5_5_4	0.84683	0.00118	0.84919
_1_6_5_4	0.0	0.6	5000	3500	9390	74.82	1.0e-04	0.62688	0.00106	0.62899	_1_6_5_4	0.84497	0.00128	0.84754
_6_1_3_3	0.0	60.0	5577	3346	9903	77.24	1.0e-04	0.91017	0.00128	0.91274				
_1_2_6_3	0.0	0.2	6000	3600	9338	72.36	1.0e-04	0.71739	0.00119	0.71977	_1_2_6_3	0.85989	0.00142	0.86273
_1_3_6_3	0.0	0.3	6000	3600	9338	72.36	1.0e-04	0.68131	0.00126	0.68383	_1_3_6_3	0.85119	0.00113	0.85345
_1_4_6_3	0.0	0.4	6000	3600	9338	72.36	1.0e-04	0.65662	0.00118	0.65898	_1_4_6_3	0.84466	0.00126	0.84718
_1_5_6_3	0.0	0.5	6000	3600	9338	72.36	1.0e-04	0.63993	0.00109	0.64211	_1_5_6_3	0.84460	0.00144	0.84749
_1_6_6_3	0.0	0.6	6000	3600	9338	72.36	1.0e-04	0.62949	0.00119	0.63187	_1_6_6_3	0.84243	0.00125	0.84493

Table 6.9.6-11c. Comparison of HAC results for HEU broken metal content in ES-3100 HAC packaging calculation models.
Reference results for content homogenized over volume of containment vessel are highlighted. Results are for modified cases where the HEU packaging fraction varies from 0.2 to 0.6 and the content is homogenized with 500 g polyethylene.

hciabmt12	np (in.)	enr. (wt %)	U (g)	^{235}U (g)	H_2O (g)	h/x	moifr	k_{eff}	σ	$k_{eff}+2σ$				
hciapbmflt12	np (in.)	PF	U (g)	^{235}U (g)	H_2O (g)	h/x	moifr	k_{eff}	σ	$k_{eff}+2σ$	hciapbmfdt12	k_{eff}	σ	$k_{eff}+2σ$
with can spacers (np thickness = 1.4 in.)														
_3_2_8_3	1.4	100.0	2774	2774	9436	88.78	1.0e-04	0.90243	0.00127	0.90497				
_2_2_3_8	1.4	0.2	3000	3000	8882	82.86	1.0e-04	0.57951	0.00103	0.58157	_2_2_3_8	0.81782	0.00115	0.82012
_2_3_3_8	1.4	0.3	3000	3000	8882	82.86	1.0e-04	0.55359	0.00094	0.55547	_2_3_3_8	0.81514	0.00148	0.81810
_2_4_3_8	1.4	0.4	3000	3000	8882	82.86	1.0e-04	0.53870	0.00102	0.54075	_2_4_3_8	0.81423	0.00122	0.81666
_2_5_3_8	1.4	0.5	3000	3000	8882	82.86	1.0e-04	0.52950	0.00097	0.53143	_2_5_3_8	0.81351	0.00131	0.81613
_2_6_3_8	1.4	0.6	3000	3000	8882	82.86	1.0e-04	0.52360	0.00120	0.52599	_2_6_3_8	0.81065	0.00127	0.81320
_4_2_7_3	1.4	95.0	3701	3516	9387	69.68	1.0e-04	0.92094	0.00140	0.92374				
_2_2_4_7	1.4	0.2	4000	3800	8829	65.05	1.0e-04	0.62129	0.00113	0.62355	_2_2_4_7	0.85574	0.00150	0.85874
_2_3_4_7	1.4	0.3	4000	3800	8829	65.05	1.0e-04	0.59045	0.00106	0.59256	_2_3_4_7	0.85080	0.00142	0.85364
_2_4_4_7	1.4	0.4	4000	3800	8829	65.05	1.0e-04	0.57686	0.00095	0.57875	_2_4_4_7	0.84954	0.00126	0.85205
_2_5_4_7	1.4	0.5	4000	3800	8829	65.05	1.0e-04	0.56383	0.00096	0.56576	_2_5_4_7	0.84837	0.00159	0.85155
_2_6_4_7	1.4	0.6	4000	3800	8829	65.05	1.0e-04	0.55861	0.00120	0.56100	_2_6_4_7	0.85112	0.00127	0.85366
_4_2_6_3	1.4	90.0	3704	3333	9387	73.50	1.0e-04	0.90643	0.00133	0.90909				
_2_2_4_6	1.4	0.2	4000	3600	8829	68.67	1.0e-04	0.61197	0.00116	0.61429	_2_2_4_6	0.84318	0.00154	0.84626
_2_3_4_6	1.4	0.3	4000	3600	8829	68.67	1.0e-04	0.58023	0.00112	0.58248	_2_3_4_6	0.83944	0.00123	0.84190
_2_4_4_6	1.4	0.4	4000	3600	8829	68.67	1.0e-04	0.56418	0.00111	0.56641	_2_4_4_6	0.83754	0.00123	0.84000
_2_5_4_6	1.4	0.5	4000	3600	8829	68.67	1.0e-04	0.55222	0.00100	0.55423	_2_5_4_6	0.83876	0.00144	0.84163
_2_6_4_6	1.4	0.6	4000	3600	8829	68.67	1.0e-04	0.54866	0.00099	0.55063	_2_6_4_6	0.83719	0.00119	0.83958

Table 6.9.6-11c. Comparison of HAC results for HEU broken metal content in ES-3100 HAC packaging calculation models.
Reference results for content homogenized over volume of containment vessel are highlighted. Results are for modified cases where the HEU packaging fraction varies from 0.2 to 0.6 and the content is homogenized with 500 g polyethylene.

hciabmt12	np (in.)	enr. (wt %)	U (g)	^{235}U (g)	H_2O (g)	h/x	moifr	k_{eff}	σ	$k_{eff}+2σ$				
hciapbmflt12	np (in.)	PF	U (g)	^{235}U (g)	H_2O (g)	h/x	moifr	k_{eff}	σ	$k_{eff}+2σ$	hciapbmfdt12	k_{eff}	σ	$k_{eff}+2σ$
_6_2_5_3	1.4	80.0	5563	4450	9289	54.48	1.0e-04	0.91987	0.00157	0.92301				
_2_2_6_5	1.4	0.2	6000	4800	8723	50.93	1.0e-04	0.67004	0.00099	0.67203	_2_2_6_5	0.87714	0.00150	0.88015
_2_3_6_5	1.4	0.3	6000	4800	8723	50.93	1.0e-04	0.63588	0.00098	0.63783	_2_3_6_5	0.87335	0.00149	0.87633
_2_4_6_5	1.4	0.4	6000	4800	8723	50.93	1.0e-04	0.61580	0.00114	0.61809	_2_4_6_5	0.87067	0.00120	0.87306
_2_5_6_5	1.4	0.5	6000	4800	8723	50.93	1.0e-04	0.60063	0.00111	0.60284	_2_5_6_5	0.87386	0.00137	0.87660
_2_6_6_5	1.4	0.6	6000	4800	8723	50.93	1.0e-04	0.59340	0.00097	0.59534	_2_6_6_5	0.87070	0.00141	0.87353
_8_2_4_3	1.4	70.0	7426	5198	9191	46.15	1.0e-04	0.91835	0.00126	0.92086				
_2_2_8_4	1.4	0.2	8000	5600	8618	43.16	1.0e-04	0.70405	0.00125	0.70655	_2_2_8_4	0.88804	0.00136	0.89077
_2_3_8_4	1.4	0.3	8000	5600	8618	43.16	1.0e-04	0.66628	0.00114	0.66856	_2_3_8_4	0.88503	0.00118	0.88740
_2_4_8_4	1.4	0.4	8000	5600	8618	43.16	1.0e-04	0.64431	0.00125	0.64681	_2_4_8_4	0.88186	0.00141	0.88467
_2_5_8_4	1.4	0.5	8000	5600	8618	43.16	1.0e-04	0.62989	0.00106	0.63201	_2_5_8_4	0.88416	0.00142	0.88701
_2_6_8_4	1.4	0.6	8000	5600	8618	43.16	1.0e-04	0.61934	0.00096	0.62126	_2_6_8_4	0.88358	0.00130	0.88618
_12_2_3_3	1.4	60.0	11154	6692	8995	35.08	1.0e-04	0.91776	0.00138	0.92053				
_2_2_12_3	1.4	0.2	12000	7200	8407	32.81	1.0e-04	0.75872	0.00115	0.76102	_2_2_12_3	0.90576	0.00134	0.90845
_2_3_12_3	1.4	0.3	12000	7200	8407	32.81	1.0e-04	0.71743	0.00106	0.71954	_2_3_12_3	0.90165	0.00138	0.90440
_2_4_12_3	1.4	0.4	12000	7200	8407	32.81	1.0e-04	0.69072	0.00115	0.69301	_2_4_12_3	0.90012	0.00124	0.90260
_2_5_12_3	1.4	0.5	12000	7200	8407	32.81	1.0e-04	0.67462	0.00099	0.67660	_2_5_12_3	0.89870	0.00124	0.90118
_2_6_12_3	1.4	0.6	12000	7200	8407	32.81	1.0e-04	0.66490	0.00106	0.66702	_2_6_12_3	0.90032	0.00117	0.90267

Table 6.9.6-12. Results for HEU oxide content in CV calculation model

case name (cvcrpdoxt11)	Ox (g)	^{235}U (g)	Ox density (g/cm^3)	Ox volume (cm^3)	Sat. H_2O (g)	CV H_2O (g)	h/x	mocfr	k_{eff}	σ	k_{eff}+2σ
UO_2 content, 500 g polyethylene, flooded containment vessel, reflected											
_1_3_24_15	24000	21125	4.00	6000	3803	3665	10.02	1.0e+00	0.91157	0.00138	0.91434
_1_4_24_15	24000	21125	5.00	4800	2606	4863	10.02	1.0e+00	0.90264	0.00139	0.90541
_1_5_24_15	24000	21125	6.54	5000	1477	5991	10.02	1.0e+00	0.89152	0.00115	0.89382
_1_2_20_15	20000	17604	3.00	6667	4833	3000	12.57	1.0e+00	0.90943	0.00117	0.91177
_1_3_20_15	20000	17604	4.00	5000	3170	4663	12.57	1.0e+00	0.89797	0.00129	0.90055
_1_4_20_15	20000	17604	5.00	4000	2171	5662	12.57	1.0e+00	0.89035	0.00121	0.89278
_1_5_20_15	20000	17604	6.54	3058	1231	6602	12.57	1.0e+00	0.87565	0.00112	0.87789
_1_2_15_15	15000	13203	3.00	5000	3625	4664	17.66	1.0e+00	0.89891	0.00138	0.90166
_1_3_15_15	15000	13203	4.00	3750	2377	5911	17.66	1.0e+00	0.87963	0.00116	0.88195
_1_4_15_15	15000	13203	5.00	3000	1629	6660	17.66	1.0e+00	0.86309	0.00134	0.86578
_1_5_15_15	15000	13203	6.54	2294	923	7365	17.66	1.0e+00	0.84270	0.00121	0.84513
14,000 g UO_2 content, 500 g polyethylene, flooded containment vessel, reflected											
_1_1_14_15	14000	12323	2.00	7000	5712	2667	19.11	1.0e+00	0.90801	0.00154	0.91110
_1_2_14_15	14000	12323	3.00	4667	3383	4996	19.11	1.0e+00	0.89261	0.00124	0.89510
_1_3_14_15	14000	12323	4.00	3500	2219	6161	19.11	1.0e+00	0.87604	0.00119	0.87842
_1_4_14_15	14000	12323	5.00	2800	1520	6860	19.11	1.0e+00	0.85585	0.00139	0.85863
_1_5_14_15	14000	12323	6.54	2141	862	7518	19.11	1.0e+00	0.83530	0.00112	0.83755
14,000 g U_3O_8 content, 500 g polyethylene, flooded containment vessel, reflected											
_2_1_14_15	14000	11850	2.00	7000	5304	2667	18.97	1.0e+00	0.88331	0.00144	0.88620
_2_2_14_15	14000	11850	3.00	4667	2975	4996	18.97	1.0e+00	0.85075	0.00129	0.85333
_2_3_14_15	14000	11850	4.00	3500	1810	6161	18.97	1.0e+00	0.82386	0.00123	0.82632
_2_4_14_15	14000	11850	5.00	2800	1111	6860	18.97	1.0e+00	0.79922	0.00143	0.80209
_2_5_14_15	14000	11850	6.54	2141	453	7518	18.97	1.0e+00	0.76510	0.00114	0.76738

Table 6.9.6-12. Results for HEU oxide content in CV calculation model

case name (cvcrpdoxt11)	Ox (g)	^{235}U (g)	Ox density (g/cm^3)	Ox volume (cm^3)	Sat. H_2O (g)	CV H_2O (g)	h/x	mocfr	k_{eff}	σ	$k_{eff}+2σ$
14,000 g UO_3 content, 500 g polyethylene, flooded containment vessel, reflected											
_3_1_14_15	14000	11627	2.00	7000	5071	2667	18.81	1.0e+00	0.86835	0.00122	0.87079
_3_2_14_15	14000	11627	3.00	4667	2741	4996	18.81	1.0e+00	0.83069	0.00119	0.83307
_3_3_14_15	14000	11627	4.00	3500	1577	6161	18.81	1.0e+00	0.79457	0.00132	0.79720
_3_4_14_15	14000	11627	5.00	2800	878	6860	18.81	1.0e+00	0.76399	0.00140	0.76679
_3_5_14_15	14000	11627	6.54	2141	220	7518	18.81	1.0e+00	0.72235	0.00127	0.72490
14,000 g UO_2 content, 500 g polyethylene, dry containment vessel, reflected											
_1_1_14_1	14000	12323	2.00	7000	5712	0	13.46	1.0e-20	0.90869	0.00156	0.91180
_1_2_14_1	14000	12323	3.00	4667	3383	0	8.53	1.0e-20	0.88628	0.00144	0.88916
_1_3_14_1	14000	12323	4.00	3500	2219	0	6.06	1.0e-20	0.86750	0.00131	0.87012
_1_4_14_1	14000	12323	5.00	2800	1520	0	4.58	1.0e-20	0.84555	0.00151	0.84857
_1_5_14_1	14000	12323	6.54	2141	862	0	3.19	1.0e-20	0.82157	0.00109	0.82375
UO_2 content, 2.0 g/cm^3 oxide density , 500 g polyethylene, flooded containment vessel, reflected											
_1_1_14_15	14000	12323	2.00	7000	5712	2667	19.11	1.0e+00	0.90801	0.00154	0.91110
_1_1_13_15	13000	11443	2.00	6500	5304	3166	20.79	1.0e+00	0.91011	0.00123	0.91258
_1_1_12_15	12000	10562	2.00	6000	4896	3665	22.74	1.0e+00	0.90176	0.00141	0.90457
_1_1_11_15	11000	9682	2.00	5500	4488	4164	25.06	1.0e+00	0.89737	0.00154	0.90044
_1_1_10_15	10000	8802	2.00	5000	4080	4663	27.83	1.0e+00	0.89620	0.00130	0.89880
_1_1_9_15	9000	7922	2.00	4500	3672	5163	31.23	1.0e+00	0.88551	0.00161	0.88872
_1_1_8_15	8000	7042	2.00	4000	3264	5662	35.47	1.0e+00	0.87598	0.00157	0.87912
_1_1_7_15	7000	6162	2.00	3500	2856	6161	40.92	1.0e+00	0.86765	0.00148	0.87061
_1_1_6_15	6000	5281	2.00	3000	2448	6660	48.19	1.0e+00	0.85412	0.00120	0.85652
_1_1_5_15	5000	4401	2.00	2500	2040	7159	58.37	1.0e+00	0.83022	0.00138	0.83298
_1_1_4_15	4000	3521	2.00	2000	1632	7658	73.63	1.0e+00	0.80856	0.00156	0.81168

Table 6.9.6-12. Results for HEU oxide content in CV calculation model

case name (cvcrpdoxt11)	Ox (g)	^{235}U (g)	Ox density (g/cm^3)	Ox volume (cm^3)	Sat. H_2O (g)	CV H_2O (g)	h/x	mocfr	k_{eff}	σ	k_{eff}+2σ
_1_1_3_15	3000	2641	2.00	1500	1224	8157	99.08	1.0e+00	0.77245	0.00147	0.77539
_1_1_2_15	2000	1761	2.00	1000	816	8656	149.96	1.0e+00	0.72062	0.00132	0.72326
_1_1_1_15	1000	880	2.00	500	408	9155	302.58	1.0e+00	0.63401	0.00126	0.63653

Table 6.9.6-13. Results for HEU product oxide content at 6.54 g/cm^3 in single-unit packaging calculation model

case name	Ox (g)	^{235}U (g)	Sat. H_2O (g)	CV H_2O (g)	h/x	moifr	k_{eff}	σ	k_{eff}+2σ	case name	k_{eff}	σ	k_{eff}+2σ
UO_2 content and 500 g polyethylene in flooded containment vessel, single package reflected													
NCT										HAC			
ncsrpoxt11_1_24_1	24000	21125	1477	5991	10.02	1.0e-20	0.72148	0.00120	0.72388				
ncsrpoxt11_1_24_2	24000	21125	1477	5991	10.02	1.0e-05	0.71942	0.00107	0.72156				
ncsrpoxt11_1_24_3	24000	21125	1477	5991	10.02	0.0e+00	0.71790	0.00122	0.72035				
ncsrpoxt11_1_24_4	24000	21125	1477	5991	10.02	1.0e-03	0.72072	0.00154	0.72380				
ncsrpoxt11_1_24_5	24000	21125	1477	5991	10.02	1.0e-02	0.71999	0.00123	0.72244				
ncsrpoxt11_1_24_6	24000	21125	1477	5991	10.02	1.0e-01	0.72828	0.00103	0.73035				
ncsrpoxt11_1_24_8	24000	21125	1477	5991	10.02	3.0e-01	0.74362	0.00123	0.74607				
ncsrpoxt11_1_24_15	24000	21125	1477	5991	10.02	1.0e+00	0.80222	0.00108	0.80438				

Table 6.9.6-13a. Results for HEU oxide content in single-unit packaging calculation model

case name (ncsrpdoxt11)	Ox (g)	^{235}U (g)	Ox den. (g/cm^3)	Ox vol. (cm^3)	Sat. H_2O (g)	CV H_2O (g)	h/x	k_{eff}	σ	k_{eff}+2σ	case name (hcsrpdoxt12)	k_{eff}	σ	k_{eff}+2σ
UO_2 content and 500 g polyethylene in flooded containment vessel, flooded package														
NCT											**HAC**			
_1_3_24	24000	21125	4.00	6000	3803	3665	10.02	0.81371	0.00144	0.81659	_1_3_24	0.81599	0.00133	0.81865
_1_4_24	24000	21125	5.00	4800	2606	4863	10.02	0.80666	0.00111	0.80887	_1_4_24	0.81112	0.00119	0.81350
_1_5_24	24000	21125	6.54	3670	1477	5991	10.02	0.80222	0.00108	0.80438	_1_5_24	0.80624	0.00114	0.80852
_1_2_20	20000	17604	3.00	6667	4833	3000	12.57	0.81352	0.00155	0.81662	_1_2_20	0.81200	0.00136	0.81472
_1_3_20	20000	17604	4.00	5000	3170	4663	12.57	0.80451	0.00124	0.80698	_1_3_20	0.80524	0.00118	0.80760
_1_4_20	20000	17604	5.00	4000	2171	5662	12.57	0.79655	0.00129	0.79914	_1_4_20	0.79813	0.00137	0.80087
_1_5_20	20000	17604	6.54	3058	1231	6602	12.57	0.78510	0.00133	0.78775	_1_5_20	0.78801	0.00121	0.79043
_1_2_15	15000	13203	3.00	5000	3625	4664	17.66	0.79666	0.00133	0.79933	_1_2_15	0.79891	0.00149	0.80189
_1_3_15	15000	13203	4.00	3750	2377	5911	17.66	0.78374	0.00123	0.78619	_1_3_15	0.78801	0.00130	0.79061
_1_4_15	15000	13203	5.00	3000	1629	6660	17.66	0.77585	0.00104	0.77794	_1_4_15	0.77767	0.00131	0.78028
_1_5_15	15000	13203	6.54	2294	923	7365	17.66	0.75988	0.00120	0.76228	_1_5_15	0.76047	0.00122	0.76291
UO_2, content and 500 g polyethylene in flooded containment vessel, flooded package														
NCT											**HAC**			
_1_1_14	14000	12323	2.00	7000	5712	2667	19.11	0.81144	0.00130	0.81403	_1_1_14	0.80983	0.00147	0.81276
_1_2_14	14000	12323	3.00	4667	3383	4996	19.11	0.79632	0.00134	0.79900	_1_2_14	0.79412	0.00155	0.79722
_1_3_14	14000	12323	4.00	3500	2219	6161	19.11	0.78024	0.00138	0.78300	_1_3_14	0.78251	0.00141	0.78533
_1_4_14	14000	12323	5.00	2800	1520	6860	19.11	0.76867	0.00119	0.77106	_1_4_14	0.77186	0.00130	0.77446
_1_5_14	14000	12323	6.54	2141	862	7518	19.11	0.75106	0.00143	0.75393	_1_5_14	0.75712	0.00132	0.75975
UO_3 content and 500 g polyethylene in flooded containment vessel, flooded package														
_2_1_14	14000	11850	2.00	7000	5304	2667	18.97	0.77449	0.00162	0.77772	_2_1_14	0.77571	0.00138	0.77847
_2_2_14	14000	11850	3.00	4667	2975	4996	18.97	0.75132	0.00141	0.75415	_2_2_14	0.74985	0.00135	0.75256
_2_3_14	14000	11850	4.00	3500	1810	6161	18.97	0.72213	0.00119	0.72452	_2_3_14	0.72485	0.00112	0.72708

Table 6.9.6-13a. Results for HEU oxide content in single-unit packaging calculation model

case name (ncsrpdoxt11)	Ox (g)	^{235}U (g)	Ox den. (g/cm^3)	Ox vol. (cm^3)	Sat. H_2O (g)	CV H_2O (g)	h/x	k_{eff}	σ	k_{eff}+2σ	case name (hcsrpdoxt12)	k_{eff}	σ	k_{eff}+2σ
_2_4_14	14000	11850	5.00	2800	1111	6860	18.97	0.70025	0.00132	0.70289	_2_4_14	0.70229	0.00135	0.70498
_2_5_14	14000	11850	6.54	2141	453	7518	18.97	0.66897	0.00140	0.67177	_2_5_14	0.67431	0.00107	0.67645
U_3O_8 content and 500 g polyethylene in flooded containment vessel, flooded package														
_3_1_14	14000	11627	2.00	7000	5071	2667	18.81	0.75704	0.00138	0.75980	_3_1_14	0.75676	0.00139	0.75954
_3_2_14	14000	11627	3.00	4667	2741	4996	18.81	0.72097	0.00124	0.72345	_3_2_14	0.72300	0.00121	0.72542
_3_3_14	14000	11627	4.00	3500	1577	6161	18.81	0.69035	0.00114	0.69263	_3_3_14	0.69274	0.00112	0.69498
_3_4_14	14000	11627	5.00	2800	878	6860	18.81	0.66080	0.00123	0.66326	_3_4_14	0.66443	0.00115	0.66674
_3_5_14	14000	11627	6.54	2141	220	7518	18.81	0.62168	0.00129	0.62427	_3_5_14	0.62544	0.00118	0.62780

Table 6.9.6-13b. Results for HEU oxide content in array packaging calculation model

case name (nciapdoxt11)	Ox (g)	^{235}U (g)	Ox den. (g/cm^3)	Ox vol. (cm^3)	Sat. H_2O (g)	CV H_2O (g)	h/x	k_{eff}	σ	k_{eff}+2σ	case name (hciapdoxt12)	k_{eff}	σ	k_{eff}+2σ
UO_2 content and 500 g polyethylene in flooded containment vessel, array packaging model for CSI=0.0														
NCT											HAC			
_1_3_24_3	24000	21125	4.00	6000	3803	3665	10.02	0.96758	0.00121	0.97000	_1_3_24_3	0.96822	0.00124	0.97070
_1_4_24_3	24000	21125	5.00	4800	2606	4863	10.02	0.94340	0.00119	0.94578	_1_4_24_3	0.94131	0.00115	0.94360
_1_5_24_3	24000	21125	6.54	3670	1477	5991	10.02	0.91495	0.00134	0.91764	_1_5_24_3	0.91666	0.00106	0.91878
_1_2_20_3	20000	17604	3.00	6667	4833	3000	12.57	0.97118	0.00122	0.97363	_1_2_20_3	0.97255	0.00139	0.97532
_1_3_20_3	20000	17604	4.00	5000	3170	4663	12.57	0.93543	0.00122	0.93786	_1_3_20_3	0.93616	0.00141	0.93897
_1_4_20_3	20000	17604	5.00	4000	2171	5662	12.57	0.91167	0.00117	0.91401	_1_4_20_3	0.91202	0.00126	0.91453
_1_5_20_3	20000	17604	6.54	3058	1231	6602	12.57	0.88413	0.00124	0.88661	_1_5_20_3	0.88426	0.00137	0.88700
_1_2_15_3	15000	13203	3.00	5000	3625	4664	17.66	0.92181	0.00128	0.92438	_1_2_15_3	0.92129	0.00139	0.92407
_1_3_15_3	15000	13203	4.00	3750	2377	5911	17.66	0.88533	0.00117	0.88767	_1_3_15_3	0.88414	0.00125	0.88663

Table 6.9.6-13b. Results for HEU oxide content in array packaging calculation model

case name (nciapdoxt11)	Ox (g)	^{235}U (g)	Ox den. (g/cm^3)	Ox vol. (cm^3)	Sat. H_2O (g)	CV H_2O (g)	h/x	k_{eff}	σ	k_{eff}+2σ	case name (hciapdoxt12)	k_{eff}	σ	k_{eff}+2σ
_1_4_15_3	15000	13203	5.00	3000	1628	6660	17.66	0.86168	0.00116	0.86400	_1_4_15_3	0.86039	0.00117	0.86273
_1_5_15_3	15000	13203	6.54	2294	923	7365	17.66	0.83434	0.00122	0.83678	_1_5_15_3	0.83140	0.00111	0.83363
_1_1_12_3	12000	10562	2.00	6000	4896	3665	22.74	0.93409	0.00140	0.93688	_1_1_12_3	0.93732	0.00137	0.94006
_1_2_12_3	12000	10562	3.00	4000	2900	5662	22.74	0.88391	0.00131	0.88652	_1_2_12_3	0.88387	0.00121	0.88630
_1_3_12_3	12000	10562	4.00	3000	1902	6660	22.74	0.85157	0.00111	0.85379	_1_3_12_3	0.84658	0.00133	0.84925
_1_4_12_3	12000	10562	5.00	2400	1303	7259	22.74	0.82574	0.00128	0.82831	_1_4_12_3	0.82349	0.00119	0.82587
_1_5_12_3	12000	10562	6.54	1835	739	7823	22.74	0.79328	0.00110	0.79548	_1_5_12_3	0.79233	0.00121	0.79475
_1_1_11_3	11000	9682	2.00	5500	4488	4164	25.06	0.91822	0.00129	0.92079	_1_1_11_3	0.92203	0.00134	0.92471
_1_2_11_3	11000	9682	3.00	3667	2658	5994	25.06	0.86689	0.00129	0.86946	_1_2_11_3	0.87093	0.00135	0.87364
_1_3_11_3	11000	9682	4.00	2750	1743	6909	25.06	0.83492	0.00133	0.83757	_1_3_11_3	0.83515	0.00124	0.83763
_1_4_11_3	11000	9682	5.00	2200	1194	7458	25.06	0.80930	0.00149	0.81227	_1_4_11_3	0.80948	0.00129	0.81205
_1_5_11_3	11000	9682	6.54	1682	677	7976	25.06	0.77906	0.00100	0.78106	_1_5_11_3	0.77935	0.00118	0.78171
_1_1_10_3	10000	8802	2.00	5000	4080	4663	27.83	0.90471	0.00131	0.90733	_1_1_10_3	0.90600	0.00128	0.90856
_1_1_9_3	9000	7922	2.00	4500	3672	5163	31.23	0.88936	0.00137	0.89210	_1_1_9_3	0.88714	0.00123	0.88960
_1_1_8_3	8000	7042	2.00	4000	3264	5662	35.47	0.86854	0.00144	0.87141	_1_1_8_3	0.86980	0.00145	0.87270
_1_1_7_3	7000	6162	2.00	3500	2856	6161	40.92	0.84876	0.00125	0.85126	_1_1_7_3	0.84926	0.00133	0.85192
_1_1_6_3	6000	5281	2.00	3000	2448	6660	48.19	0.82546	0.00127	0.82800	_1_1_6_3	0.82275	0.00135	0.82544
UO_2, UO_3, or U_3O_8 content and 500 g polyethylene in flooded containment vessel, array packaging model for CSI=0.0														
_1_1_7_3	7000	6162	2.00	3500	2856	6161	40.92	0.84876	0.00125	0.85126	_1_1_7_3	0.84926	0.00133	0.85192
_2_1_7_3	7000	5925	2.00	3500	2652	6161	41.65	0.81721	0.00130	0.81980	_2_1_7_3	0.81943	0.00125	0.82194
_3_1_7_3	7000	5813	2.00	3500	2535	6161	41.93	0.80044	0.00129	0.80302	_3_1_7_3	0.80086	0.00134	0.80355

Table 6.9.6-14. Results for UNX crystal content in CV calculation model

case name	unh (g)	^{235}U (g)	unh H_2O (g)	CV H_2O (g)	h/x	gU/l	mocfr	k_{eff}	σ	k_{eff}+2σ				
UNH crystal content, 0 g polyethylene, flooded containment vessel, reflected														
cvcrunhct11_24_1	24000	11303	5197	1620	15.74	1106	1.0e+00	0.82007	0.00128	0.82262				
cvcrunhct11_23_1	23000	10832	4980	1978	16.77	1060	1.0e+00	0.82120	0.00129	0.82378				
cvcrunhct11_22_1	22000	10361	4764	2335	17.88	1014	1.0e+00	0.82675	0.00122	0.82919				
cvcrunhct11_21_1	21000	9890	4547	2693	19.11	968	1.0e+00	0.82938	0.00118	0.83174				
cvcrunhct11_20_1	20000	9419	4331	3050	20.45	922	1.0e+00	0.83221	0.00129	0.83480				
cvcrunhct11_19_1	19000	8948	4114	3407	21.94	876	1.0e+00	0.83423	0.00152	0.83728				
cvcrunhct11_18_1	18000	8477	3898	3765	23.59	830	1.0e+00	0.83622	0.00128	0.83878				
cvcrunhct11_17_1	17000	8006	3681	4122	25.44	784	1.0e+00	0.84032	0.00167	0.84365				
cvcrunhct11_16_1	16000	7536	3464	4479	27.51	738	1.0e+00	0.84509	0.00151	0.84811				
cvcrunhct11_15_1	15000	7064	3248	4837	29.87	692	1.0e+00	0.84402	0.00133	0.84667				
cvcrunhct11_14_1	14000	6594	3031	5194	32.56	645	1.0e+00	0.84915	0.00130	0.85175				
cvcrunhct11_13_1	13000	6123	2815	5551	35.67	599	1.0e+00	0.84986	0.00127	0.85241				
cvcrunhct11_12_1	12000	5652	2598	5909	39.29	553	1.0e+00	0.85138	0.00159	0.85456				
cvcrunhct11_11_1	11000	5181	2382	6266	43.57	507	1.0e+00	0.85137	0.00136	0.85408				
cvcrunhct11_10_1	10000	4710	2165	6623	48.71	461	1.0e+00	0.85062	0.00149	0.85359				
cvcrunhct11_9_1	9000	4239	1949	6981	54.99	415	1.0e+00	0.85423	0.00147	0.85718				
cvcrunhct11_8_1	8000	3768	1732	7338	62.83	369	1.0e+00	0.84783	0.00152	0.85088				
cvcrunhct11_7_1	7000	3297	1516	7695	72.92	323	1.0e+00	0.84713	0.00166	0.85044				
cvcrunhct11_6_1	6000	2826	1299	8053	86.38	277	1.0e+00	0.83915	0.00151	0.84218				
cvcrunhct11_5_1	5000	2355	1083	8410	105.2	231	1.0e+00	0.82865	0.00177	0.83220				
cvcrunhct11_4_1	4000	1884	866	8768	133.5	184	1.0e+00	0.81158	0.00162	0.81483				
cvcrunhct11_3_1	3000	1413	650	9125	180.6	138	1.0e+00	0.78282	0.00120	0.78522				

Table 6.9.6-14. Results for UNX crystal content in CV calculation model

case name	unh (g)	^{235}U (g)	unh H_2O (g)	CV H_2O (g)	h/x	gU/l	mocfr	k_{eff}	σ	$k_{eff}+2σ$				
cvcrunhct11_2_1	2000	942	433	9482	274.7	92	1.0e+00	0.73150	0.00114	0.73377				
cvcrunhct11_1_1	1000	471	217	9840	557.2	46	1.0e+00	0.60716	0.00106	0.60927				
UNH crystal content, 500 g polyethylene, flooded containment vessel, reflected														
cvcrpunhct11_24_15	24000	11303	5197	1078	15.97	1106	1.0e+00	0.82422	0.00129	0.82681				
cvcrpunhct11_23_15	23000	10832	4980	1435	17.01	1060	1.0e+00	0.82842	0.00146	0.83134				
cvcrpunhct11_22_15	22000	10361	4764	1793	18.13	1014	1.0e+00	0.83462	0.00156	0.83773				
cvcrpunhct11_21_15	21000	9890	4547	2150	19.37	968	1.0e+00	0.83608	0.00149	0.83906				
cvcrpunhct11_20_15	20000	9419	4331	2507	20.73	922	1.0e+00	0.84111	0.00143	0.84397				
cvcrpunhct11_19_15	19000	8948	4114	2865	22.23	876	1.0e+00	0.84084	0.00135	0.84355				
cvcrpunhct11_18_15	18000	8477	3898	3222	23.90	830	1.0e+00	0.84379	0.00138	0.84654				
cvcrpunhct11_17_15	17000	8006	3681	3579	25.76	784	1.0e+00	0.84513	0.00147	0.84807				
cvcrpunhct11_16_15	16000	7536	3464	3937	27.86	738	1.0e+00	0.84809	0.00132	0.85072				
cvcrpunhct11_15_15	15000	7064	3248	4294	30.24	692	1.0e+00	0.85178	0.00146	0.85470				
cvcrpunhct11_14_15	14000	6594	3031	4652	32.96	645	1.0e+00	0.85473	0.00134	0.85741				
cvcrpunhct11_13_15	13000	6123	2815	5009	36.09	599	1.0e+00	0.85544	0.00134	0.85812				
cvcrpunhct11_12_15	12000	5652	2598	5366	39.75	553	1.0e+00	0.85658	0.00142	0.85941				
cvcrpunhct11_11_15	11000	5181	2382	5724	44.07	507	1.0e+00	0.85830	0.00152	0.86133				
cvcrpunhct11_10_15	10000	4710	2165	6081	49.26	461	1.0e+00	0.85943	0.00176	0.86296				
cvcrpunhct11_9_15	9000	4239	1949	6438	55.60	415	1.0e+00	0.85882	0.00139	0.86161				
cvcrpunhct11_8_15	8000	3768	1732	6796	63.53	369	1.0e+00	0.85472	0.00116	0.85705				
cvcrpunhct11_7_15	7000	3297	1516	7153	73.72	323	1.0e+00	0.84975	0.00143	0.85261				
cvcrpunhct11_6_15	6000	2826	1299	7510	87.31	277	1.0e+00	0.84484	0.00132	0.84748				
cvcrpunhct11_5_15	5000	2355	1083	7868	106.33	231	1.0e+00	0.83459	0.00167	0.83793				
cvcrpunhct11_4_15	4000	1884	866	8225	134.85	184	1.0e+00	0.82093	0.00142	0.82378				

Table 6.9.6-14. Results for UNX crystal content in CV calculation model

case name	unh (g)	^{235}U (g)	unh H_2O (g)	CV H_2O (g)	h/x	gU/l	mocfr	k_{eff}	σ	$k_{eff}+2σ$
cvcrpunhct11_3_15	3000	1413	650	8582	182.42	138	1.0e+00	0.78968	0.00130	0.79228
cvcrpunhct11_2_15	2000	942	433	8940	277.51	92	1.0e+00	0.73500	0.00145	0.73791
cvcrpunhct11_1_15	1000	471	217	9297	562.74	46	1.0e+00	0.61053	0.00118	0.61289
UNH crystal content, 500 g polyethylene, dry containment vessel, reflected										
cvcrpunhct11_24_1	24000	11303	5197	0	13.48	1106.5	1.0e-20	0.76603	0.00145	0.76893
cvcrpunhct11_23_1	23000	10832	4980	0	13.55	1060.4	1.0e-20	0.75118	0.00132	0.75382
cvcrpunhct11_22_1	22000	10361	4764	0	13.62	1014.3	1.0e-20	0.73265	0.00133	0.73531
cvcrpunhct11_21_1	21000	9890	4547	0	13.70	968.2	1.0e-20	0.71276	0.00125	0.71527
cvcrpunhct11_20_1	20000	9419	4331	0	13.78	922.1	1.0e-20	0.69662	0.00146	0.69955
cvcrpunhct11_19_1	19000	8948	4114	0	13.87	876.0	1.0e-20	0.67992	0.00144	0.68279
cvcrpunhct11_18_1	18000	8477	3898	0	13.98	829.9	1.0e-20	0.66144	0.00115	0.66374
cvcrpunhct11_17_1	17000	8006	3681	0	14.09	783.8	1.0e-20	0.64482	0.00128	0.64738
cvcrpunhct11_16_1	16000	7536	3464	0	14.23	737.7	1.0e-20	0.62404	0.00110	0.62624
cvcrpunhct11_15_1	15000	7064	3248	0	14.37	691.5	1.0e-20	0.60835	0.00125	0.61085
cvcrpunhct11_14_1	14000	6594	3031	0	14.54	645.5	1.0e-20	0.58778	0.00113	0.59003
cvcrpunhct11_13_1	13000	6123	2815	0	14.74	599.4	1.0e-20	0.56892	0.00115	0.57123
cvcrpunhct11_12_1	12000	5652	2598	0	14.97	553.2	1.0e-20	0.55059	0.00129	0.55317
cvcrpunhct11_11_1	11000	5181	2382	0	15.24	507.1	1.0e-20	0.53268	0.00108	0.53485
cvcrpunhct11_10_1	10000	4710	2165	0	15.56	461.0	1.0e-20	0.51381	0.00135	0.51650
cvcrpunhct11_9_1	9000	4239	1949	0	15.96	414.9	1.0e-20	0.49374	0.00111	0.49596
cvcrpunhct11_8_1	8000	3768	1732	0	16.45	368.8	1.0e-20	0.47312	0.00106	0.47524
cvcrpunhct11_7_1	7000	3297	1516	0	17.09	322.7	1.0e-20	0.45221	0.00108	0.45437
cvcrpunhct11_6_1	6000	2826	1299	0	17.93	276.6	1.0e-20	0.43063	0.00114	0.43290
cvcrpunhct11_5_1	5000	2355	1083	0	19.12	230.5	1.0e-20	0.40936	0.00103	0.41141

Table 6.9.6-14. Results for UNX crystal content in CV calculation model

case name	unh (g)	^{235}U (g)	unh H_2O (g)	CV H_2O (g)	h/x	gU/l	mocfr	k_{eff}	σ	$k_{eff}+2σ$				
cvcrpunhct11_4_1	4000	1884	866	0	20.90	184.4	1.0e-20	0.38394	0.00105	0.38603				
cvcrpunhct11_3_1	3000	1413	650	0	23.87	138.3	1.0e-20	0.35655	0.00096	0.35846				
cvcrpunhct11_2_1	2000	942	433	0	29.80	92.2	1.0e-20	0.31381	0.00093	0.31566				
cvcrpunhct11_1_1	1000	471	217	0	47.60	46.1	1.0e-20	0.24974	0.00079	0.25132				
500 g polyethylene and undissolved UNH crystals, flooded containment vessel, reflected														
cvcrbpunhct11_24_15	24000	11303	5197	1078	15.97	NA	1.0e+00	0.81439	0.00135	0.81710				
cvcrbpunhct11_23_15	23000	10832	4980	1435	17.01	NA	1.0e+00	0.81243	0.00128	0.81498				
cvcrbpunhct11_22_15	22000	10361	4764	1793	18.13	NA	1.0e+00	0.81092	0.00139	0.81369				
cvcrbpunhct11_21_15	21000	9890	4547	2150	19.37	NA	1.0e+00	0.80901	0.00135	0.81172				
cvcrbpunhct11_20_15	20000	9419	4331	2507	20.73	NA	1.0e+00	0.80864	0.00168	0.81200				
cvcrbpunhct11_19_15	19000	8948	4114	2865	22.23	NA	1.0e+00	0.80344	0.00145	0.80635				
cvcrbpunhct11_18_15	18000	8477	3898	3222	23.90	NA	1.0e+00	0.80646	0.00132	0.80911				
cvcrbpunhct11_17_15	17000	8006	3681	3579	25.76	NA	1.0e+00	0.80294	0.00134	0.80563				
cvcrbpunhct11_16_15	16000	7536	3465	3937	27.86	NA	1.0e+00	0.79909	0.00115	0.80139				
cvcrbpunhct11_15_15	15000	7064	3248	4294	30.24	NA	1.0e+00	0.79593	0.00133	0.79858				
cvcrbpunhct11_14_15	14000	6594	3031	4652	32.96	NA	1.0e+00	0.79487	0.00109	0.79705				
cvcrbpunhct11_13_15	13000	6123	2815	5009	36.09	NA	1.0e+00	0.78728	0.00118	0.78964				
cvcrbpunhct11_12_15	12000	5652	2598	5366	39.75	NA	1.0e+00	0.78337	0.00127	0.78592				
cvcrbpunhct11_11_15	11000	5181	2382	5724	44.07	NA	1.0e+00	0.77773	0.00122	0.78017				
cvcrbpunhct11_10_15	10000	4710	2165	6081	49.26	NA	1.0e+00	0.77009	0.00154	0.77317				
cvcrbpunhct11_9_15	9000	4239	1949	6438	55.60	NA	1.0e+00	0.76494	0.00133	0.76760				
cvcrbpunhct11_8_15	8000	3768	1732	6796	63.53	NA	1.0e+00	0.75339	0.00148	0.75635				
cvcrbpunhct11_7_15	7000	3297	1516	7153	73.72	NA	1.0e+00	0.74139	0.00149	0.74437				
cvcrbpunhct11_6_15	6000	2826	1299	7510	87.31	NA	1.0e+00	0.72740	0.00134	0.73009				

Table 6.9.6-14. Results for UNX crystal content in CV calculation model

case name	unh (g)	^{235}U (g)	unh H_2O (g)	CV H_2O (g)	h/x	gU/l	mocfr	k_{eff}	σ	$k_{eff}+2σ$
cvcrbpunhct11_5_15	5000	2355	1083	7868	6.33	NA	1.0e+00	0.70988	0.00128	0.71244
cvcrbpunhct11_4_15	4000	1884	866	8225	34.85	NA	1.0e+00	0.68707	0.00137	0.68981
cvcrbpunhct11_3_15	3000	1413	650	8582	82.42	NA	1.0e+00	0.65613	0.00136	0.65885
cvcrbpunhct11_2_15	2000	942	433	8940	77.51	NA	1.0e+00	0.61167	0.00117	0.61402
cvcrbpunhct11_1_15	1000	471	217	9297	62.74	NA	1.0e+00	0.55043	0.00140	0.55324
500 g polyethylene and undissolved UNH crystals, dry containment vessel, reflected										
cvcrbpunhct11_24_1	24000	11303	5197	0	13.48	NA	1.0e-20	0.81264	0.00142	0.81548
cvcrbpunhct11_23_1	23000	10832	4980	0	13.55	NA	1.0e-20	0.81127	0.00129	0.81384
cvcrbpunhct11_22_1	22000	10361	4764	0	13.62	NA	1.0e-20	0.80828	0.00121	0.81069
cvcrbpunhct11_21_1	21000	9890	4547	0	13.70	NA	1.0e-20	0.80873	0.00122	0.81117
cvcrbpunhct11_20_1	20000	9419	4331	0	13.78	NA	1.0e-20	0.80508	0.00132	0.80773
cvcrbpunhct11_19_1	19000	8948	4114	0	13.87	NA	1.0e-20	0.80364	0.00150	0.80664
cvcrbpunhct11_18_1	18000	8477	3898	0	13.98	NA	1.0e-20	0.80002	0.00170	0.80343
cvcrbpunhct11_17_1	17000	8006	3681	0	14.09	NA	1.0e-20	0.79969	0.00165	0.80298
cvcrbpunhct11_16_1	16000	7536	3465	0	14.23	NA	1.0e-20	0.79458	0.00144	0.79746
cvcrbpunhct11_15_1	15000	7064	3248	0	14.37	NA	1.0e-20	0.79130	0.00141	0.79411
cvcrbpunhct11_14_1	14000	6594	3031	0	14.54	NA	1.0e-20	0.78794	0.00127	0.79048
cvcrbpunhct11_13_1	13000	6123	2815	0	14.74	NA	1.0e-20	0.78506	0.00137	0.78781
cvcrbpunhct11_12_1	12000	5652	2598	0	14.97	NA	1.0e-20	0.78061	0.00121	0.78303
cvcrbpunhct11_11_1	11000	5181	2382	0	15.24	NA	1.0e-20	0.77102	0.00125	0.77352
cvcrbpunhct11_10_1	10000	4710	2165	0	15.56	NA	1.0e-20	0.76415	0.00129	0.76673
cvcrbpunhct11_9_1	9000	4239	1949	0	15.96	NA	1.0e-20	0.75589	0.00141	0.75872
cvcrbpunhct11_8_1	8000	3768	1732	0	16.45	NA	1.0e-20	0.74147	0.00151	0.74449
cvcrbpunhct11_7_1	7000	3297	1516	0	17.09	NA	1.0e-20	0.72828	0.00125	0.73077

Table 6.9.6-14. Results for UNX crystal content in CV calculation model

case name	unh (g)	^{235}U (g)	unh H_2O (g)	CV H_2O (g)	h/x	gU/l	mocfr	k_{eff}	σ	$k_{eff}+2σ$				
cvcrbpunhct11_6_1	6000	2826	1299	0	17.93	NA	1.0e-20	0.71077	0.00122	0.71321				
cvcrbpunhct11_5_1	5000	2355	1083	0	19.12	NA	1.0e-20	0.68823	0.00137	0.69096				
cvcrbpunhct11_4_1	4000	1884	866	0	20.90	NA	1.0e-20	0.66016	0.00146	0.66309				
cvcrbpunhct11_3_1	3000	1413	650	0	23.87	NA	1.0e-20	0.61922	0.00144	0.62211				
cvcrbpunhct11_2_1	2000	942	433	0	29.80	NA	1.0e-20	0.56205	0.00129	0.56462				
cvcrbpunhct11_1_1	1000	471	217	0	47.60	NA	1.0e-20	0.47544	0.00110	0.47765				

Table 6.9.6-15. Results for UNX crystal content in packaging calculation model

case name	unh (g)	^{235}U (g)	unh H_2O (g)	CV H_2O (g)	h/x	gU/l	moifr	k_{eff}	σ	$k_{eff}+2σ$	case name	k_{eff}	σ	$k_{eff}+2σ$
UNH crystal content, 0 g polyethylene in flooded containment vessel, single package reflected														
NCT											**HAC**			
ncsrunhct11_24_1_1	24000	11303	5197	1620	15.74	1106	1.0e-20	0.60250	0.00130	0.60510	hcsrunhct12_24_1_1	0.60528	0.00129	0.60786
ncsrunhct11_24_1_2	24000	11303	5197	1620	15.74	1106	1.0e-05	0.59895	0.00119	0.60134	hcsrunhct12_24_1_2	0.60289	0.00142	0.60574
ncsrunhct11_24_1_3	24000	11303	5197	1620	15.74	1106	1.0e-04	0.59947	0.00124	0.60194	hcsrunhct12_24_1_3	0.60552	0.00130	0.60812
ncsrunhct11_24_1_4	24000	11303	5197	1620	15.74	1106	1.0e-03	0.60331	0.00132	0.60595	hcsrunhct12_24_1_4	0.60265	0.00112	0.60489
ncsrunhct11_24_1_5	24000	11303	5197	1620	15.74	1106	1.0e-02	0.60398	0.00118	0.60635	hcsrunhct12_24_1_5	0.60426	0.00152	0.60731
ncsrunhct11_24_1_6	24000	11303	5197	1620	15.74	1106	1.0e-01	0.61004	0.00142	0.61287	hcsrunhct12_24_1_6	0.61378	0.00127	0.61632
ncsrunhct11_24_1_8	24000	11303	5197	1620	15.74	1106	3.0e-01	0.63238	0.00143	0.63524	hcsrunhct12_24_1_8	0.63556	0.00128	0.63813
ncsrunhct11_24_1_15	24000	11303	5197	1620	15.74	1106	1.0e+00	0.69882	0.00142	0.70166	hcsrunhct12_24_1_15	0.70190	0.00129	0.70448
ncsrunhct11_24_1_15	24000	11303	5197	1620	15.74	1106	1.0e+00	0.69882	0.00142	0.70166	hcsrunhct12_24_1_15	0.70190	0.00129	0.70448
ncsrunhct11_23_1_15	23000	10832	4980	1978	16.77	1060	1.0e+00	0.70360	0.00134	0.70628	hcsrunhct12_23_1_15	0.70555	0.00129	0.70813

Table 6.9.6-15. Results for UNX crystal content in packaging calculation model

case name	unh (g)	^{235}U (g)	unh H_2O (g)	CV H_2O (g)	h/x	gU/l	moifr	k_{eff}	σ	$k_{eff}+2σ$	case name	k_{eff}	σ	$k_{eff}+2σ$
ncsrunhct11_22_1_15	22000	10361	4764	2335	17.88	1014	1.0e+00	0.70899	0.00132	0.71163	hcsrunhct12_22_1_15	0.70899	0.00136	0.71171
ncsrunhct11_21_1_15	21000	9890	4547	2693	19.11	968	1.0e+00	0.71172	0.00133	0.71438	hcsrunhct12_21_1_15	0.71348	0.00158	0.71664
ncsrunhct11_20_1_15	20000	9419	4331	3050	20.45	922	1.0e+00	0.71256	0.00123	0.71501	hcsrunhct12_20_1_15	0.71623	0.00117	0.71858
ncsrunhct11_19_1_15	19000	8948	4114	3407	21.94	876	1.0e+00	0.71780	0.00132	0.72045	hcsrunhct12_19_1_15	0.71798	0.00132	0.72063
ncsrunhct11_18_1_15	18000	8477	3898	3765	23.59	830	1.0e+00	0.72130	0.00139	0.72407	hcsrunhct12_18_1_15	0.72545	0.00149	0.72843
ncsrunhct11_17_1_15	17000	8006	3681	4122	25.44	784	1.0e+00	0.72340	0.00161	0.72663	hcsrunhct12_17_1_15	0.72589	0.00134	0.72856
ncsrunhct11_16_1_15	16000	7536	3464	4479	27.51	738	1.0e+00	0.72816	0.00141	0.73098	hcsrunhct12_16_1_15	0.73042	0.00147	0.73336
ncsrunhct11_15_1_15	15000	7064	3248	4837	29.87	692	1.0e+00	0.73150	0.00149	0.73449	hcsrunhct12_15_1_15	0.73525	0.00151	0.73827
ncsrunhct11_14_1_15	14000	6594	3031	5194	32.56	645	1.0e+00	0.73255	0.00135	0.73524	hcsrunhct12_14_1_15	0.73405	0.00150	0.73704
ncsrunhct11_13_1_15	13000	6123	2815	5551	35.67	599	1.0e+00	0.73488	0.00128	0.73745	hcsrunhct12_13_1_15	0.73722	0.00159	0.74040
ncsrunhct11_12_1_15	12000	5652	2598	5909	39.29	553	1.0e+00	0.73982	0.00146	0.74274	hcsrunhct12_12_1_15	0.74114	0.00126	0.74366
ncsrunhct11_11_1_15	11000	5181	2382	6266	43.57	507	1.0e+00	0.74059	0.00156	0.74370	hcsrunhct12_11_1_15	0.74104	0.00187	0.74477
ncsrunhct11_10_1_15	10000	4710	2165	6623	48.71	461	1.0e+00	0.74238	0.00148	0.74533	hcsrunhct12_10_1_15	0.74247	0.00134	0.74514
ncsrunhct11_9_1_15	9000	4239	1949	6981	54.99	415	1.0e+00	0.74214	0.00135	0.74484	hcsrunhct12_9_1_15	0.74537	0.00150	0.74836
ncsrunhct11_8_1_15	8000	3768	1732	7338	62.83	369	1.0e+00	0.74436	0.00146	0.74728	hcsrunhct12_8_1_15	0.74169	0.00176	0.74521
ncsrunhct11_7_1_15	7000	3297	1516	7695	72.92	323	1.0e+00	0.73972	0.00146	0.74265	hcsrunhct12_7_1_15	0.74201	0.00129	0.74459
ncsrunhct11_6_1_15	6000	2826	1299	8053	86.38	277	1.0e+00	0.73458	0.00147	0.73752	hcsrunhct12_6_1_15	0.73491	0.00155	0.73802
ncsrunhct11_5_1_15	5000	2355	1083	8410	105.22	231	1.0e+00	0.72880	0.00143	0.73166	hcsrunhct12_5_1_15	0.72804	0.00151	0.73107
ncsrunhct11_4_1_15	4000	1884	866	8768	133.47	184	1.0e+00	0.71269	0.00158	0.71585	hcsrunhct12_4_1_15	0.71463	0.00147	0.71758
ncsrunhct11_3_1_15	3000	1413	650	9125	180.57	138	1.0e+00	0.68768	0.00137	0.69042	hcsrunhct12_3_1_15	0.69065	0.00121	0.69306
ncsrunhct11_2_1_15	2000	942	433	9482	274.74	92	1.0e+00	0.64383	0.00118	0.64619	hcsrunhct12_2_1_15	0.64813	0.00131	0.65076
UNH crystal content, 500 g polyethylene in flooded containment vessel, single package reflected														
ncsrpunhct11_24_1	24000	11303	5197	1078	15.97	1106	1e-20	0.60653	0.00140	0.60932	hcsrpunhct12_24_1	0.60988	0.00142	0.61273
ncsrpunhct11_24_15	24000	11303	5197	1078	15.97	1106	1e+00	0.70571	0.00135	0.70841	hcsrpunhct12_24_15	0.70886	0.00133	0.71152

Table 6.9.6-15. Results for UNX crystal content in packaging calculation model

case name	unh (g)	^{235}U (g)	unh H_2O (g)	CV H_2O (g)	h/x	gU/l	moifr	k_{eff}	σ	$k_{eff}+2σ$	case name	k_{eff}	σ	$k_{eff}+2σ$
ncsrpunhct11_24_15	24000	11303	5197	1078	15.97	1106	1e+00	0.70571	0.00135	0.70841	hcsrpunhct12_24_15	0.70886	0.00133	0.71152
ncsrpunhct11_23_15	23000	10832	4980	1435	17.01	1060	1e+00	0.71244	0.00130	0.71504	hcsrpunhct12_23_15	0.71209	0.00121	0.71452
ncsrpunhct11_22_15	22000	10361	4764	1793	18.13	1014	1e+00	0.71524	0.00158	0.71841	hcsrpunhct12_22_15	0.71753	0.00126	0.72006
ncsrpunhct11_21_15	21000	9890	4547	2150	19.37	968	1e+00	0.71747	0.00154	0.72055	hcsrpunhct12_21_15	0.71997	0.00137	0.72270
ncsrpunhct11_20_15	20000	9419	4331	2507	20.73	922	1e+00	0.72176	0.00151	0.72479	hcsrpunhct12_20_15	0.72403	0.00130	0.72663
ncsrpunhct11_19_15	19000	8948	4114	2865	22.23	876	1e+00	0.72616	0.00138	0.72891	hcsrpunhct12_19_15	0.72647	0.00141	0.72929
ncsrpunhct11_18_15	18000	8477	3898	3222	23.90	830	1e+00	0.72901	0.00163	0.73227	hcsrpunhct12_18_15	0.73343	0.00131	0.73606
ncsrpunhct11_17_15	17000	8006	3681	3579	25.76	784	1e+00	0.73255	0.00127	0.73508	hcsrpunhct12_17_15	0.73387	0.00128	0.73643
ncsrpunhct11_16_15	16000	7536	3465	3937	27.86	738	1e+00	0.73515	0.00152	0.73818	hcsrpunhct12_16_15	0.73768	0.00152	0.74073
ncsrpunhct11_15_15	15000	7064	3248	4294	30.24	692	1e+00	0.74097	0.00126	0.74349	hcsrpunhct12_15_15	0.74006	0.00132	0.74270
ncsrpunhct11_14_15	14000	6594	3031	4652	32.96	645	1e+00	0.74169	0.00135	0.74438	hcsrpunhct12_14_15	0.74240	0.00141	0.74522
ncsrpunhct11_13_15	13000	6123	2815	5009	36.09	599	1e+00	0.74466	0.00139	0.74744	hcsrpunhct12_13_15	0.74534	0.00141	0.74815
ncsrpunhct11_12_15	12000	5652	2598	5366	39.75	553	1e+00	0.74381	0.00142	0.74666	hcsrpunhct12_12_15	0.74529	0.00132	0.74794
ncsrpunhct11_11_15	11000	5181	2382	5724	44.07	507	1e+00	0.74858	0.00146	0.75151	hcsrpunhct12_11_15	0.74980	0.00139	0.75259
ncsrpunhct11_10_15	10000	4710	2165	6081	49.26	461	1e+00	0.74595	0.00140	0.74875	hcsrpunhct12_10_15	0.74967	0.00141	0.75249
ncsrpunhct11_9_15	9000	4239	1949	6438	55.60	415	1e+00	0.74868	0.00167	0.75202	hcsrpunhct12_9_15	0.75260	0.00164	0.75587
ncsrpunhct11_8_15	8000	3768	1732	6796	63.53	369	1e+00	0.74978	0.00139	0.75255	hcsrpunhct12_8_15	0.74914	0.00120	0.75155
ncsrpunhct11_7_15	7000	3297	1516	7153	73.72	323	1e+00	0.74628	0.00147	0.74922	hcsrpunhct12_7_15	0.74708	0.00155	0.75018
ncsrpunhct11_6_15	6000	2826	1299	7510	87.31	277	1e+00	0.74259	0.00122	0.74503	hcsrpunhct12_6_15	0.74481	0.00150	0.74781
ncsrpunhct11_5_15	5000	2355	1083	7868	106.33	231	1e+00	0.73226	0.00133	0.73492	hcsrpunhct12_5_15	0.73303	0.00153	0.73609
ncsrpunhct11_4_15	4000	1884	866	8225	134.85	184	1e+00	0.72045	0.00145	0.72334	hcsrpunhct12_4_15	0.71942	0.00168	0.72279
ncsrpunhct11_3_15	3000	1413	650	8582	182.42	138	1e+00	0.69669	0.00167	0.70003	hcsrpunhct12_3_15	0.69613	0.00139	0.69891

Table 6.9.6-15. Results for UNX crystal content in packaging calculation model

case name	unh (g)	^{235}U (g)	unh H_2O (g)	CV H_2O (g)	h/x	gU/l	moifr	k_{eff}	σ	$k_{eff}+2σ$	case name	k_{eff}	σ	$k_{eff}+2σ$
ncsrpunhct11_2_15	2000	942	433	8940	277.51	92	1e+00	0.65100	0.00112	0.65324	hcsrpunhct12_2_15	0.65137	0.00149	0.65436
ncsrpunhct11_1_15	1000	471	217	9297	562.74	46	1e+00	0.54270	0.00116	0.54501	hcsrpunhct12_1_15	0.54296	0.00099	0.54494
UNH crystal content, 0 g polyethylene in flooded containment vessel, array packaging calculation model for CSI=0.0														
NCT											**HAC**			
nciaunhct11_8_24_1_1	24000	11303	5197	1620	15.74	1106	1.0e-20	0.91485	0.00136	0.91756	hciaunhct12_8_24_1_1	0.91665	0.00134	0.91933
nciaunhct11_8_24_1_2	24000	11303	5197	1620	15.74	1106	1.0e-05	0.91420	0.00120	0.91659	hciaunhct12_8_24_1_2	0.91708	0.00131	0.91969
nciaunhct11_8_24_1_3	24000	11303	5197	1620	15.74	1106	1.0e-04	0.91426	0.00123	0.91672	hciaunhct12_8_24_1_3	0.91632	0.00112	0.91856
nciaunhct11_8_24_1_4	24000	11303	5197	1620	15.74	1106	1.0e-03	0.91095	0.00119	0.91333	hciaunhct12_8_24_1_4	0.91159	0.00120	0.91399
nciaunhct11_8_24_1_5	24000	11303	5197	1620	15.74	1106	1.0e-02	0.88904	0.00117	0.89138	hciaunhct12_8_24_1_5	0.89357	0.00127	0.89610
nciaunhct11_8_24_1_6	24000	11303	5197	1620	15.74	1106	1.0e-01	0.77132	0.00109	0.77350	hciaunhct12_8_24_1_6	0.78417	0.00129	0.78676
nciaunhct11_8_24_1_8	24000	11303	5197	1620	15.74	1106	3.0e-01	0.71012	0.00130	0.71272	hciaunhct12_8_24_1_8	0.71917	0.00135	0.72188
nciaunhct11_8_24_1_15	24000	11303	5197	1620	15.74	1106	1.0e+00	0.71873	0.00134	0.72140	hciaunhct12_8_24_1_15	0.72598	0.00147	0.72892
nciaunhct11_8_24_1_3	24000	11303	5197	1620	15.74	1106	1.0e-04	0.91426	0.00123	0.91672	hciaunhct12_8_24_1_3	0.91632	0.00112	0.91856
nciaunhct11_8_12_1_3	12000	5652	2598	5909	39.29	553	1.0e-04	0.93016	0.00130	0.93277	hciaunhct12_8_12_1_3	0.92942	0.00157	0.93256
nciaunhct11_8_11_1_3	11000	5181	2382	6266	43.57	507	1.0e-04	0.92825	0.00132	0.93090	hciaunhct12_8_11_1_3	0.92834	0.00152	0.93138
nciaunhct11_8_10_1_3	10000	4710	2165	6623	48.71	461	1.0e-04	0.92490	0.00152	0.92794	hciaunhct12_8_10_1_3	0.92555	0.00137	0.92828
nciaunhct11_8_9_1_3	9000	4239	1949	6981	54.99	415	1.0e-04	0.92044	0.00124	0.92293	hciaunhct12_8_9_1_3	0.92360	0.00136	0.92631
nciaunhct11_8_8_1_3	8000	3768	1732	7338	62.83	369	1.0e-04	0.91662	0.00121	0.91905	hciaunhct12_8_8_1_3	0.91875	0.00144	0.92163
nciaunhct11_8_7_1_3	7000	3297	1516	7695	72.92	323	1.0e-04	0.91132	0.00140	0.91411	hciaunhct12_8_7_1_3	0.90978	0.00135	0.91247
nciaunhct11_8_6_1_3	6000	2826	1299	8053	86.38	277	1.0e-04	0.90036	0.00128	0.90293	hciaunhct12_8_6_1_3	0.89938	0.00150	0.90238
nciaunhct11_8_5_1_3	5000	2355	1083	8410	105.22	231	1.0e-04	0.88578	0.00141	0.88860	hciaunhct12_8_5_1_3	0.88489	0.00149	0.88788
nciaunhct11_8_4_1_3	4000	1884	866	8768	133.47	184	1.0e-04	0.86530	0.00119	0.86769	hciaunhct12_8_4_1_3	0.86326	0.00139	0.86604
nciaunhct11_8_3_1_3	3000	1413	650	9125	180.57	138	1.0e-04	0.82655	0.00120	0.82895	hciaunhct12_8_3_1_3	0.83005	0.00118	0.83242

Table 6.9.6-15. Results for UNX crystal content in packaging calculation model

case name	unh (g)	^{235}U (g)	unh H_2O (g)	CV H_2O (g)	h/x	gU/l	moifr	k_{eff}	σ	$k_{eff}+2σ$	case name	k_{eff}	σ	$k_{eff}+2σ$
nciaunhct11_8_2_1_3	2000	942	433	9482	274.74	92	1.0e-04	0.76783	0.00123	0.77029	hciaunhct12_8_2_1_3	0.76545	0.00129	0.76804
nciaunhct11_8_1_1_3	1000	471	217	9840	557.20	46	1.0e-04	0.62610	0.00112	0.62834	hciaunhct12_8_1_1_3	0.62341	0.00104	0.62549
UNH crystal content, 500 g polyethylene in flooded containment vessel, array packaging calculation model for CSI=0.0														
nciapunhct11_24_1	24000	11303	5197	1078	15.97	1106	1e-20	0.92205	0.00118	0.92442	hciapunhct12_24_1	0.92136	0.00123	0.92383
nciapunhct11_24_15	24000	11303	5197	1078	15.97	1106	1e+00	0.72649	0.00128	0.72905	hciapunhct12_24_15	0.73087	0.00128	0.73343
nciapunhct11_24_3	24000	11303	5197	1078	15.97	1106	1e-04	0.92258	0.00141	0.92539	hciapunhct12_24_3	0.92172	0.00124	0.92419
nciapunhct11_16_3	16000	7536	3465	3937	27.86	738	1e-04	0.93498	0.00131	0.93759	hciapunhct12_16_3	0.93544	0.00130	0.93804
nciapunhct11_15_3	15000	7064	3248	4294	30.24	692	1e-04	0.93400	0.00139	0.93678	hciapunhct12_15_3	0.93500	0.00136	0.93771
nciapunhct11_14_3	14000	6594	3031	4652	32.96	645	1e-04	0.93374	0.00153	0.93680	hciapunhct12_14_3	0.93539	0.00135	0.93810
nciapunhct11_8_3	8000	3768	1732	6796	63.53	369	1e-04	0.92190	0.00144	0.92478	hciapunhct12_8_3	0.92270	0.00159	0.92589
nciapunhct11_7_3	7000	3297	1516	7153	73.72	323	1e-04	0.91677	0.00157	0.91991	hciapunhct12_7_3	0.91538	0.00132	0.91803
nciapunhct11_1_3	1000	471	217	9297	562.74	46	1e-04	0.62819	0.00115	0.63049	hciapunhct12_1_3	0.62885	0.00109	0.63103
UNH crystal content, 0 g polyethylene in flooded containment vessel, array packaging calculation model for CSI=0.4														
NCT											**HAC**			
ncf1unhct11_8_24_1_3	24000	11303	5197	1620	15.74	1106	1.0e-04	0.86774	0.00127	0.87027	hcf2unhct12_8_24_1_3	0.82915	0.00145	0.83205
ncf1unhct11_8_12_1_3	12000	5652	2598	5909	39.29	553	1.0e-04	0.88287	0.00133	0.88554	hcf2unhct12_8_12_1_3	0.85267	0.00165	0.85597
ncf1unhct11_8_11_1_3	11000	5181	2382	6266	43.57	507	1.0e-04	0.88535	0.00133	0.88802	hcf2unhct12_8_11_1_3	0.85565	0.00134	0.85833
ncf1unhct11_8_10_1_3	10000	4710	2165	6623	48.71	461	1.0e-04	0.88182	0.00140	0.88461	hcf2unhct12_8_10_1_3	0.85153	0.00132	0.85416
ncf1unhct11_8_1_1_3	1000	471	217	9840	557.20	46	1.0e-04	0.60011	0.00143	0.60297	hcf2unhct12_8_1_1_3	0.58199	0.00107	0.58414
UNH crystal content, 500 g polyethylene in flooded containment vessel, array packaging calculation model for CSI=0.4														
ncf1punhct11_24_3	24000	11303	5197	1078	15.97	1106	1e-04	0.87035	0.00135	0.87304	hcf2punhct12_24_3	0.83958	0.00135	0.84227
ncf1punhct11_15_3	15000	7064	3248	4294	30.24	692	1e-04	0.89208	0.00154	0.89516	hcf2punhct12_15_3	0.86102	0.00149	0.86400

Table 6.9.6-15. Results for UNX crystal content in packaging calculation model

case name	unh (g)	^{235}U (g)	unh H_2O (g)	CV H_2O (g)	h/x	gU/l	moifr	k_{eff}	σ	$k_{eff}+2σ$	case name	k_{eff}	σ	$k_{eff}+2σ$
ncf1punhct11_14_3	14000	6594	3031	4652	32.96	645	1e-04	0.89354	0.00152	0.89658	hcf2punhct12_14_3	0.85954	0.00131	0.86216
ncf1punhct11_1_3	1000	471	217	9297	562.74	46	1e-04	0.60481	0.00118	0.60718	hcf2punhct12_1_3	0.58731	0.00119	0.58968

Table 6.9.6-16. Results for leakage of UNX crystal content out of containment vessel

case name	U (g)	^{235}U (g)	unh H_2O (g)	CV H_2O (g)	h/x	CV gU/l	moifr	k_{eff}	σ	$k_{eff}+2σ$				
UNH crystal content, 0 g polyethylene in flooded containment vessel, out leakage, single package reflected														
HAC														
icsrunhct12_24_1_1	24000	11303	5197	4875	30.14	687	1.0e-20	0.78331	0.00139	0.78609				
icsrunhct12_24_1_2	24000	11303	5197	4875	30.14	687	1.0e-05	0.78291	0.00159	0.78610				
icsrunhct12_24_1_3	24000	11303	5197	4875	30.14	687	1.0e-04	0.78197	0.00153	0.78503				
icsrunhct12_24_1_4	24000	11303	5197	4875	30.14	687	1.0e-03	0.78003	0.00145	0.78294				
icsrunhct12_24_1_5	24000	11303	5197	4875	30.14	687	1.0e-02	0.78443	0.00140	0.78723				
icsrunhct12_24_1_6	24000	11303	5197	4875	30.14	687	1.0e-01	0.78426	0.00151	0.78729				
icsrunhct12_24_1_8	24000	11303	5197	4875	30.14	687	3.0e-01	0.78841	0.00153	0.79146				
icsrunhct12_24_1_15	24000	11303	5197	4875	30.14	687	1.0e+00	0.79193	0.00164	0.79521				
icsrunhct12_24_1_15	24000	11303	5197	4875	30.14	687	1.0e+00	0.79193	0.00164	0.79521				
icsrunhct12_23_1_15	23000	10832	4980	5097	31.79	658	1.0e+00	0.79465	0.00130	0.79724				
icsrunhct12_22_1_15	22000	10361	4764	5318	33.59	629	1.0e+00	0.79665	0.00145	0.79956				
icsrunhct12_21_1_15	21000	9890	4547	5540	35.56	601	1.0e+00	0.79533	0.00156	0.79845				
icsrunhct12_20_1_15	20000	9419	4331	5762	37.73	572	1.0e+00	0.79937	0.00179	0.80295				
icsrunhct12_19_1_15	19000	8948	4114	5984	40.13	544	1.0e+00	0.80059	0.00135	0.80329				

Table 6.9.6-16. Results for leakage of UNX crystal content out of containment vessel

case name	U (g)	^{235}U (g)	unh H_2O (g)	CV H_2O (g)	h/x	CV gU/l	moifr	k_{eff}	σ	k_{eff}+2σ				
icsrunhct12_18_1_15	18000	8477	3898	6205	42.79	515	1.0e+00	0.79930	0.00144	0.80219				
icsrunhct12_17_1_15	17000	8006	3681	6427	45.77	486	1.0e+00	0.80320	0.00153	0.80626				
icsrunhct12_16_1_15	16000	7536	3464	6649	49.11	458	1.0e+00	0.80113	0.00142	0.80396				
icsrunhct12_15_1_15	15000	7064	3248	6871	52.91	429	1.0e+00	0.80445	0.00148	0.80740				
icsrunhct12_14_1_15	14000	6594	3031	7092	57.24	401	1.0e+00	0.79995	0.00124	0.80243				
icsrunhct12_13_1_15	13000	6123	2815	7314	62.25	372	1.0e+00	0.80425	0.00139	0.80703				
icsrunhct12_12_1_15	12000	5652	2598	7536	68.09	343	1.0e+00	0.79843	0.00129	0.80100				
icsrunhct12_11_1_15	11000	5181	2382	7758	74.98	315	1.0e+00	0.80002	0.00147	0.80297				
icsrunhct12_10_1_15	10000	4710	2165	7979	83.26	286	1.0e+00	0.79540	0.00162	0.79864				
icsrunhct12_9_1_15	9000	4239	1949	8201	93.38	257	1.0e+00	0.79147	0.00156	0.79459				
icsrunhct12_8_1_15	8000	3768	1732	8423	106.03	229	1.0e+00	0.78224	0.00165	0.78553				
icsrunhct12_7_1_15	7000	3297	1516	8645	122.29	200	1.0e+00	0.77559	0.00131	0.77821				
icsrunhct12_6_1_15	6000	2826	1299	8866	143.98	172	1.0e+00	0.76261	0.00136	0.76532				
icsrunhct12_5_1_15	5000	2355	1083	9088	174.33	143	1.0e+00	0.74504	0.00138	0.74781				
icsrunhct12_4_1_15	4000	1884	866	9310	219.86	114	1.0e+00	0.72070	0.00131	0.72333				
icsrunhct12_3_1_15	3000	1413	650	9532	295.76	86	1.0e+00	0.68185	0.00131	0.68447				
icsrunhct12_2_1_15	2000	942	433	9753	447.52	57	1.0e+00	0.61401	0.00117	0.61635				
icsrunhct12_1_1_15	1000	471	217	9975	902.71	29	1.0e+00	0.47625	0.00103	0.47831				
UNH crystal content, 500 g polyethylene in flooded containment vessel, out leakage, single package reflected														
icsrpunhct12_24_1	24000	11303	5197	4444	30.37	710	1e-20	0.79145	0.00146	0.79436				
icsrpunhct12_24_15	24000	11303	5197	4444	30.37	710	1e+00	0.80433	0.00145	0.80723				
icsrpunhct12_24_15	24000	11303	5197	4444	30.37	710	1e+00	0.80433	0.00145	0.80723				
icsrpunhct12_23_15	23000	10832	4980	4661	32.03	680	1e+00	0.80343	0.00127	0.80597				
icsrpunhct12_22_15	22000	10361	4764	4878	33.84	651	1e+00	0.80375	0.00125	0.80625				

Table 6.9.6-16. Results for leakage of UNX crystal content out of containment vessel

case name	U (g)	^{235}U (g)	unh H_2O (g)	CV H_2O (g)	h/x	CV gU/l	moifr	k_{eff}	σ	$k_{eff}+2\sigma$
icsrpunhct12_21_15	21000	9890	4547	5095	35.83	621	1e+00	0.80639	0.00161	0.80961
icsrpunhct12_20_15	20000	9419	4331	5312	38.01	592	1e+00	0.80696	0.00144	0.80984
icsrpunhct12_19_15	19000	8948	4114	5529	40.42	562	1e+00	0.80928	0.00157	0.81242
icsrpunhct12_18_15	18000	8477	3898	5746	43.10	533	1e+00	0.80687	0.00138	0.80963
icsrpunhct12_17_15	17000	8006	3681	5963	46.09	503	1e+00	0.80989	0.00164	0.81317
icsrpunhct12_16_15	16000	7536	3464	6180	49.46	473	1e+00	0.80777	0.00162	0.81101
icsrpunhct12_15_15	15000	7064	3248	6398	53.28	444	1e+00	0.81131	0.00154	0.81439
icsrpunhct12_14_15	14000	6594	3031	6615	57.64	414	1e+00	0.80815	0.00162	0.81139
icsrpunhct12_13_15	13000	6123	2815	6832	62.67	385	1e+00	0.80680	0.00133	0.80947
icsrpunhct12_12_15	12000	5652	2598	7049	68.55	355	1e+00	0.80665	0.00151	0.80967
icsrpunhct12_11_15	11000	5181	2382	7266	75.49	325	1e+00	0.80422	0.00157	0.80736
icsrpunhct12_10_15	10000	4710	2165	7483	83.82	296	1e+00	0.80093	0.00148	0.80388
icsrpunhct12_9_15	9000	4239	1949	7700	94.00	266	1e+00	0.79650	0.00144	0.79937
icsrpunhct12_8_15	8000	3768	1732	7918	106.72	237	1e+00	0.79302	0.00182	0.79667
icsrpunhct12_7_15	7000	3297	1516	8135	123.08	207	1e+00	0.78234	0.00156	0.78546
icsrpunhct12_6_15	6000	2826	1299	8352	144.90	178	1e+00	0.76957	0.00175	0.77308
icsrpunhct12_5_15	5000	2355	1083	8569	175.44	148	1e+00	0.75295	0.00147	0.75588
icsrpunhct12_4_15	4000	1884	866	8786	221.24	118	1e+00	0.72610	0.00127	0.72864
icsrpunhct12_3_15	3000	1413	650	9003	297.61	89	1e+00	0.68788	0.00134	0.69055
icsrpunhct12_2_15	2000	942	433	9220	450.29	59	1e+00	0.61943	0.00119	0.62182
icsrpunhct12_1_15	1000	471	217	9437	908.25	30	1e+00	0.47924	0.00105	0.48134

Table 6.9.6-17. Results for skull oxide (SO) content in CV calculation model

case name	SO (g)	UO_3 (g)	Sat. H_2O (g)	SO h/x	U (g)	^{235}U (g)	C (g)	mg C/ g ^{235}U	CV H_2O (g)	CV h/x	Unident. (g)	k_{eff}	σ	$k_{eff}+2σ$
flooded containment vessel, reflected														
513 g polyethylene, no can spacers														
cvcrsk3cc_1_15_17	11589	8063	4468	28.09	6828	4765	417	87518	4105	50.58	2596	0.82806	0.00135	0.83075
cvcrsk3cc_2_15_17	14934	11665	4015	17.79	9879	6858	504	73492	4105	33.41	2252	0.81716	0.00136	0.81989
cvcrsk3cc_3_15_17	13821	11876	4893	20.62	10058	7028	372	52930	3233	32.62	1060	0.82909	0.00144	0.83197
cvcrsk3cc_4_15_17	15246	14900	4599	15.52	12619	8842	60	6786	3235	25.07	-227	0.82622	0.00154	0.82930
cvcrsk3cc_5_15_17	21216	21036	3869	9.49	17815	12455	27	2168	3235	16.27	-360	0.81061	0.00116	0.81293
cvcrsk3cc_6_15_17	15111	12933	3765	28.02	10960	4122	921	223432	4105	54.01	744	0.75711	0.00110	0.75932
cvcrsk3cc_7_15_17	13155	11666	3989	32.68	9886	3712	609	164054	4106	61.55	367	0.76196	0.00136	0.76469
cvcrsk3cc_8_15_17	13650	11689	4068	33.01	9906	3737	261	69834	4106	61.69	1187	0.76713	0.00137	0.76988
cvcrsk3cc_9_15_17	21300	19865	3801	7.43	16816	15673	921	58764	3235	12.82	1	0.84737	0.00114	0.84965
cvcrsk3cc_10_15_17	21300	20786	3905	7.27	17596	16399	0	0	3235	12.41	1	0.85155	0.00148	0.85451
cvcrsk3cc_4_1_1	15246	14900	0	1.95	12619	8842	0.00	0	0	1.95	-227	0.49030	0.00095	0.49220
cvcrsk3cc_4_1_2	15246	14900	0	1.95	12619	8842	3.75	424	0	1.95	-227	0.49148	0.00090	0.49328
cvcrsk3cc_4_1_3	15246	14900	0	1.95	12619	8842	7.50	848	0	1.95	-227	0.49081	0.00095	0.49270
cvcrsk3cc_4_1_4	15246	14900	0	1.95	12619	8842	11.25	1272	0	1.95	-227	0.49337	0.00123	0.49584
cvcrsk3cc_4_1_5	15246	14900	0	1.95	12619	8842	15.00	1696	0	1.95	-227	0.49100	0.00105	0.49309
cvcrsk3cc_4_1_6	15246	14900	0	1.95	12619	8842	18.75	2120	0	1.95	-227	0.49125	0.00112	0.49348
cvcrsk3cc_4_1_7	15246	14900	0	1.95	12619	8842	22.50	2545	0	1.95	-227	0.49155	0.00104	0.49363
cvcrsk3cc_4_1_8	15246	14900	0	1.95	12619	8842	26.25	2969	0	1.95	-227	0.49300	0.00105	0.49510
cvcrsk3cc_4_1_9	15246	14900	0	1.95	12619	8842	30.00	3393	0	1.95	-227	0.49295	0.00117	0.49530
cvcrsk3cc_4_1_10	15246	14900	0	1.95	12619	8842	33.75	3817	0	1.95	-227	0.49206	0.00092	0.49391
cvcrsk3cc_4_1_11	15246	14900	0	1.95	12619	8842	37.50	4241	0	1.95	-227	0.49004	0.00115	0.49233

Table 6.9.6-17. Results for skull oxide (SO) content in CV calculation model

case name	SO (g)	UO_3 (g)	Sat. H_2O (g)	SO h/x	U (g)	^{235}U (g)	C (g)	mg C/ g ^{235}U	CV H_2O (g)	CV h/x	Unident. (g)	k_{eff}	σ	$k_{eff}+2σ$
cvcrsk3cc_4_1_12	15246	14900	0	1.95	12619	8842	41.25	4665	0	1.95	-227	0.49325	0.00116	0.49558
cvcrsk3cc_4_1_13	15246	14900	0	1.95	12619	8842	45.00	5089	0	1.95	-227	0.49242	0.00093	0.49429
cvcrsk3cc_4_1_14	15246	14900	0	1.95	12619	8842	48.75	5513	0	1.95	-227	0.49328	0.00119	0.49566
cvcrsk3cc_4_1_15	15246	14900	0	1.95	12619	8842	52.50	5937	0	1.95	-227	0.49139	0.00117	0.49373
cvcrsk3cc_4_1_16	15246	14900	0	1.95	12619	8842	56.25	6362	0	1.95	-227	0.49068	0.00105	0.49278
cvcrsk3cc_4_1_17	15246	14900	0	1.95	12619	8842	60.00	6786	0	1.95	-227	0.49303	0.00100	0.49502
cvcrsk3cc_4_6_1	15246	14900	460	3.3	12619	8842	0.00	0	323.51	4.26	-227	0.52088	0.00109	0.52306
cvcrsk3cc_4_6_2	15246	14900	460	3.3	12619	8842	3.75	424	323.51	4.26	-227	0.52247	0.00114	0.52474
cvcrsk3cc_4_6_3	15246	14900	460	3.3	12619	8842	7.50	848	323.51	4.26	-227	0.52250	0.00116	0.52482
cvcrsk3cc_4_6_4	15246	14900	460	3.3	12619	8842	11.25	1272	323.51	4.26	-227	0.52325	0.00103	0.52531
cvcrsk3cc_4_6_5	15246	14900	460	3.3	12619	8842	15.00	1696	323.51	4.26	-227	0.52252	0.00116	0.52485
cvcrsk3cc_4_6_6	15246	14900	460	3.3	12619	8842	18.75	2120	323.51	4.26	-227	0.52123	0.00113	0.52348
cvcrsk3cc_4_6_7	15246	14900	460	3.3	12619	8842	22.50	2545	323.51	4.26	-227	0.52156	0.00098	0.52353
cvcrsk3cc_4_6_8	15246	14900	460	3.3	12619	8842	26.25	2969	323.51	4.26	-227	0.52048	0.00106	0.52260
cvcrsk3cc_4_6_9	15246	14900	460	3.3	12619	8842	30.00	3393	323.51	4.26	-227	0.52115	0.00100	0.52315
cvcrsk3cc_4_6_10	15246	14900	460	3.3	12619	8842	33.75	3817	323.51	4.26	-227	0.52271	0.00114	0.52500
cvcrsk3cc_4_6_11	15246	14900	460	3.3	12619	8842	37.50	4241	323.51	4.26	-227	0.52221	0.00127	0.52474
cvcrsk3cc_4_6_12	15246	14900	460	3.3	12619	8842	41.25	4665	323.51	4.26	-227	0.52079	0.00104	0.52287
cvcrsk3cc_4_6_13	15246	14900	460	3.3	12619	8842	45.00	5089	323.51	4.26	-227	0.52323	0.00110	0.52543
cvcrsk3cc_4_6_14	15246	14900	460	3.3	12619	8842	48.75	5513	323.51	4.26	-227	0.52202	0.00129	0.52459
cvcrsk3cc_4_6_15	15246	14900	460	3.3	12619	8842	52.50	5937	323.51	4.26	-227	0.52288	0.00094	0.52476
cvcrsk3cc_4_6_16	15246	14900	460	3.3	12619	8842	56.25	6362	323.51	4.26	-227	0.52179	0.00106	0.52391
cvcrsk3cc_4_6_17	15246	14900	460	3.3	12619	8842	60.00	6786	323.51	4.26	-227	0.52265	0.00108	0.52481

Table 6.9.6-17. Results for skull oxide (SO) content in CV calculation model

case name	SO (g)	UO_3 (g)	Sat. H_2O (g)	SO h/x	U (g)	^{235}U (g)	C (g)	mg C/ g ^{235}U	CV H_2O (g)	CV h/x	Unident. (g)	k_{eff}	σ	$k_{eff}+2σ$
cvcrsk3cc_4_7_1	15246	14900	920	4.66	12619	8842	0.00	0	647.03	6.57	-227	0.55466	0.00117	0.55699
cvcrsk3cc_4_7_2	15246	14900	920	4.66	12619	8842	3.75	424	647.03	6.57	-227	0.55192	0.00105	0.55402
cvcrsk3cc_4_7_3	15246	14900	920	4.66	12619	8842	7.50	848	647.03	6.57	-227	0.55432	0.00118	0.55668
cvcrsk3cc_4_7_4	15246	14900	920	4.66	12619	8842	11.25	1272	647.03	6.57	-227	0.55387	0.00107	0.55600
cvcrsk3cc_4_7_5	15246	14900	920	4.66	12619	8842	15.00	1696	647.03	6.57	-227	0.55390	0.00102	0.55595
cvcrsk3cc_4_7_6	15246	14900	920	4.66	12619	8842	18.75	2120	647.03	6.57	-227	0.55272	0.00112	0.55496
cvcrsk3cc_4_7_7	15246	14900	920	4.66	12619	8842	22.50	2545	647.03	6.57	-227	0.55292	0.00118	0.55529
cvcrsk3cc_4_7_8	15246	14900	920	4.66	12619	8842	26.25	2969	647.03	6.57	-227	0.55262	0.00111	0.55484
cvcrsk3cc_4_7_9	15246	14900	920	4.66	12619	8842	30.00	3393	647.03	6.57	-227	0.55242	0.00108	0.55457
cvcrsk3cc_4_7_10	15246	14900	920	4.66	12619	8842	33.75	3817	647.03	6.57	-227	0.55457	0.00137	0.55732
cvcrsk3cc_4_7_11	15246	14900	920	4.66	12619	8842	37.50	4241	647.03	6.57	-227	0.55376	0.00117	0.55610
cvcrsk3cc_4_7_12	15246	14900	920	4.66	12619	8842	41.25	4665	647.03	6.57	-227	0.55283	0.00131	0.55545
cvcrsk3cc_4_7_13	15246	14900	920	4.66	12619	8842	45.00	5089	647.03	6.57	-227	0.55393	0.00118	0.55630
cvcrsk3cc_4_7_14	15246	14900	920	4.66	12619	8842	48.75	5513	647.03	6.57	-227	0.55181	0.00107	0.55395
cvcrsk3cc_4_7_15	15246	14900	920	4.66	12619	8842	52.50	5937	647.03	6.57	-227	0.55425	0.00107	0.55640
cvcrsk3cc_4_7_16	15246	14900	920	4.66	12619	8842	56.25	6362	647.03	6.57	-227	0.55377	0.00105	0.55587
cvcrsk3cc_4_7_17	15246	14900	920	4.66	12619	8842	60.00	6786	647.03	6.57	-227	0.55425	0.00101	0.55628
cvcrsk3cc_4_8_1	15246	14900	1380	6.02	12619	8842	0.00	0	970.54	8.88	-227	0.58801	0.00133	0.59068
cvcrsk3cc_4_8_2	15246	14900	1380	6.02	12619	8842	3.75	424	970.54	8.88	-227	0.58867	0.00114	0.59095
cvcrsk3cc_4_8_3	15246	14900	1380	6.02	12619	8842	7.50	848	970.54	8.88	-227	0.58712	0.00112	0.58936
cvcrsk3cc_4_8_4	15246	14900	1380	6.02	12619	8842	11.25	1272	970.54	8.88	-227	0.58657	0.00115	0.58887
cvcrsk3cc_4_8_5	15246	14900	1380	6.02	12619	8842	15.00	1696	970.54	8.88	-227	0.58720	0.00105	0.58930

Table 6.9.6-17. Results for skull oxide (SO) content in CV calculation model

case name	SO (g)	UO_3 (g)	Sat. H_2O (g)	SO h/x	U (g)	^{235}U (g)	C (g)	mg C/ g ^{235}U	CV H_2O (g)	CV h/x	Unident. (g)	k_{eff}	σ	$k_{eff}+2σ$
cvcrsk3cc_4_8_6	15246	14900	1380	6.02	12619	8842	18.75	2120	970.54	8.88	-227	0.58418	0.00122	0.58663
cvcrsk3cc_4_8_7	15246	14900	1380	6.02	12619	8842	22.50	2545	970.54	8.88	-227	0.58706	0.00118	0.58943
cvcrsk3cc_4_8_8	15246	14900	1380	6.02	12619	8842	26.25	2969	970.54	8.88	-227	0.58528	0.00110	0.58748
cvcrsk3cc_4_8_9	15246	14900	1380	6.02	12619	8842	30.00	3393	970.54	8.88	-227	0.58452	0.00119	0.58689
cvcrsk3cc_4_8_10	15246	14900	1380	6.02	12619	8842	33.75	3817	970.54	8.88	-227	0.58645	0.00113	0.58870
cvcrsk3cc_4_8_11	15246	14900	1380	6.02	12619	8842	37.50	4241	970.54	8.88	-227	0.58475	0.00109	0.58694
cvcrsk3cc_4_8_12	15246	14900	1380	6.02	12619	8842	41.25	4665	970.54	8.88	-227	0.58633	0.00110	0.58853
cvcrsk3cc_4_8_13	15246	14900	1380	6.02	12619	8842	45.00	5089	970.54	8.88	-227	0.58553	0.00107	0.58766
cvcrsk3cc_4_8_14	15246	14900	1380	6.02	12619	8842	48.75	5513	970.54	8.88	-227	0.58632	0.00118	0.58869
cvcrsk3cc_4_8_15	15246	14900	1380	6.02	12619	8842	52.50	5937	970.54	8.88	-227	0.58543	0.00106	0.58756
cvcrsk3cc_4_8_16	15246	14900	1380	6.02	12619	8842	56.25	6362	970.54	8.88	-227	0.58716	0.00123	0.58962
cvcrsk3cc_4_8_17	15246	14900	1380	6.02	12619	8842	60.00	6786	970.54	8.88	-227	0.58845	0.00113	0.59071
cvcrsk3cc_4_9_1	15246	14900	1840	7.38	12619	8842	0.00	0	1294.06	11.2	-227	0.62013	0.00104	0.62220
cvcrsk3cc_4_9_2	15246	14900	1840	7.38	12619	8842	3.75	424	1294.06	11.2	-227	0.61947	0.00123	0.62193
cvcrsk3cc_4_9_3	15246	14900	1840	7.38	12619	8842	7.50	848	1294.06	11.2	-227	0.62178	0.00112	0.62402
cvcrsk3cc_4_9_4	15246	14900	1840	7.38	12619	8842	11.25	1272	1294.06	11.2	-227	0.62009	0.00108	0.62225
cvcrsk3cc_4_9_5	15246	14900	1840	7.38	12619	8842	15.00	1696	1294.06	11.2	-227	0.61950	0.00114	0.62178
cvcrsk3cc_4_9_6	15246	14900	1840	7.38	12619	8842	18.75	2120	1294.06	11.2	-227	0.62035	0.00102	0.62240
cvcrsk3cc_4_9_7	15246	14900	1840	7.38	12619	8842	22.50	2545	1294.06	11.2	-227	0.61820	0.00111	0.62042
cvcrsk3cc_4_9_8	15246	14900	1840	7.38	12619	8842	26.25	2969	1294.06	11.2	-227	0.62037	0.00127	0.62290
cvcrsk3cc_4_9_9	15246	14900	1840	7.38	12619	8842	30.00	3393	1294.06	11.2	-227	0.62084	0.00111	0.62306
cvcrsk3cc_4_9_10	15246	14900	1840	7.38	12619	8842	33.75	3817	1294.06	11.2	-227	0.61977	0.00114	0.62205
cvcrsk3cc_4_9_11	15246	14900	1840	7.38	12619	8842	37.50	4241	1294.06	11.2	-227	0.61997	0.00123	0.62243

Table 6.9.6-17. Results for skull oxide (SO) content in CV calculation model

case name	SO (g)	UO_3 (g)	Sat. H_2O (g)	SO h/x	U (g)	^{235}U (g)	C (g)	mg C/ g ^{235}U	CV H_2O (g)	CV h/x	Unident. (g)	k_{eff}	σ	$k_{eff}+2σ$
cvcrsk3cc_4_9_12	15246	14900	1840	7.38	12619	8842	41.25	4665	1294.06	11.2	-227	0.62097	0.00112	0.62320
cvcrsk3cc_4_9_13	15246	14900	1840	7.38	12619	8842	45.00	5089	1294.06	11.2	-227	0.62013	0.00126	0.62266
cvcrsk3cc_4_9_14	15246	14900	1840	7.38	12619	8842	48.75	5513	1294.06	11.2	-227	0.62028	0.00109	0.62245
cvcrsk3cc_4_9_15	15246	14900	1840	7.38	12619	8842	52.50	5937	1294.06	11.2	-227	0.62003	0.00107	0.62216
cvcrsk3cc_4_9_16	15246	14900	1840	7.38	12619	8842	56.25	6362	1294.06	11.2	-227	0.62193	0.00107	0.62408
cvcrsk3cc_4_9_17	15246	14900	1840	7.38	12619	8842	60.00	6786	1294.06	11.2	-227	0.62122	0.00117	0.62356
cvcrsk3cc_4_10_1	15246	14900	2300	8.73	12619	8842	0.00	0	1617.57	13.51	-227	0.65504	0.00131	0.65766
cvcrsk3cc_4_10_2	15246	14900	2300	8.73	12619	8842	3.75	424	1617.57	13.51	-227	0.65421	0.00099	0.65618
cvcrsk3cc_4_10_3	15246	14900	2300	8.73	12619	8842	7.50	848	1617.57	13.51	-227	0.65445	0.00123	0.65692
cvcrsk3cc_4_10_4	15246	14900	2300	8.73	12619	8842	11.25	1272	1617.57	13.51	-227	0.65392	0.00127	0.65646
cvcrsk3cc_4_10_5	15246	14900	2300	8.73	12619	8842	15.00	1696	1617.57	13.51	-227	0.65599	0.00134	0.65868
cvcrsk3cc_4_10_6	15246	14900	2300	8.73	12619	8842	18.75	2120	1617.57	13.51	-227	0.65239	0.00107	0.65454
cvcrsk3cc_4_10_7	15246	14900	2300	8.73	12619	8842	22.50	2545	1617.57	13.51	-227	0.65356	0.00101	0.65558
cvcrsk3cc_4_10_8	15246	14900	2300	8.73	12619	8842	26.25	2969	1617.57	13.51	-227	0.65451	0.00134	0.65719
cvcrsk3cc_4_10_9	15246	14900	2300	8.73	12619	8842	30.00	3393	1617.57	13.51	-227	0.65576	0.00140	0.65855
cvcrsk3cc_4_10_10	15246	14900	2300	8.73	12619	8842	33.75	3817	1617.57	13.51	-227	0.65386	0.00121	0.65629
cvcrsk3cc_4_10_11	15246	14900	2300	8.73	12619	8842	37.50	4241	1617.57	13.51	-227	0.65645	0.00113	0.65871
cvcrsk3cc_4_10_12	15246	14900	2300	8.73	12619	8842	41.25	4665	1617.57	13.51	-227	0.65406	0.00130	0.65666
cvcrsk3cc_4_10_13	15246	14900	2300	8.73	12619	8842	45.00	5089	1617.57	13.51	-227	0.65406	0.00120	0.65646
cvcrsk3cc_4_10_14	15246	14900	2300	8.73	12619	8842	48.75	5513	1617.57	13.51	-227	0.65484	0.00126	0.65736
cvcrsk3cc_4_10_15	15246	14900	2300	8.73	12619	8842	52.50	5937	1617.57	13.51	-227	0.65420	0.00128	0.65675
cvcrsk3cc_4_10_16	15246	14900	2300	8.73	12619	8842	56.25	6362	1617.57	13.51	-227	0.65433	0.00123	0.65679
cvcrsk3cc_4_10_17	15246	14900	2300	8.73	12619	8842	60.00	6786	1617.57	13.51	-227	0.65399	0.00123	0.65646

Table 6.9.6-17. Results for skull oxide (SO) content in CV calculation model

case name	SO (g)	UO_3 (g)	Sat. H_2O (g)	SO h/x	U (g)	^{235}U (g)	C (g)	mg C/ g ^{235}U	CV H_2O (g)	CV h/x	Unident. (g)	k_{eff}	σ	$k_{eff}+2σ$
cvcrsk3cc_4_11_1	15246	14900	2760	10.09	12619	8842	0.00	0	1941.09	15.82	-227	0.68728	0.00114	0.68956
cvcrsk3cc_4_11_2	15246	14900	2760	10.09	12619	8842	3.75	424	1941.09	15.82	-227	0.68899	0.00121	0.69141
cvcrsk3cc_4_11_3	15246	14900	2760	10.09	12619	8842	7.50	848	1941.09	15.82	-227	0.68815	0.00113	0.69041
cvcrsk3cc_4_11_4	15246	14900	2760	10.09	12619	8842	11.25	1272	1941.09	15.82	-227	0.68967	0.00117	0.69200
cvcrsk3cc_4_11_5	15246	14900	2760	10.09	12619	8842	15.00	1696	1941.09	15.82	-227	0.68936	0.00133	0.69201
cvcrsk3cc_4_11_6	15246	14900	2760	10.09	12619	8842	18.75	2120	1941.09	15.82	-227	0.68713	0.00127	0.68966
cvcrsk3cc_4_11_7	15246	14900	2760	10.09	12619	8842	22.50	2545	1941.09	15.82	-227	0.68933	0.00141	0.69216
cvcrsk3cc_4_11_8	15246	14900	2760	10.09	12619	8842	26.25	2969	1941.09	15.82	-227	0.68808	0.00130	0.69068
cvcrsk3cc_4_11_9	15246	14900	2760	10.09	12619	8842	30.00	3393	1941.09	15.82	-227	0.69012	0.00114	0.69239
cvcrsk3cc_4_11_10	15246	14900	2760	10.09	12619	8842	33.75	3817	1941.09	15.82	-227	0.68913	0.00148	0.69208
cvcrsk3cc_4_11_11	15246	14900	2760	10.09	12619	8842	37.50	4241	1941.09	15.82	-227	0.68961	0.00139	0.69239
cvcrsk3cc_4_11_12	15246	14900	2760	10.09	12619	8842	41.25	4665	1941.09	15.82	-227	0.68779	0.00113	0.69005
cvcrsk3cc_4_11_13	15246	14900	2760	10.09	12619	8842	45.00	5089	1941.09	15.82	-227	0.69197	0.00114	0.69425
cvcrsk3cc_4_11_14	15246	14900	2760	10.09	12619	8842	48.75	5513	1941.09	15.82	-227	0.68861	0.00114	0.69090
cvcrsk3cc_4_11_15	15246	14900	2760	10.09	12619	8842	52.50	5937	1941.09	15.82	-227	0.68815	0.00127	0.69069
cvcrsk3cc_4_11_16	15246	14900	2760	10.09	12619	8842	56.25	6362	1941.09	15.82	-227	0.69041	0.00131	0.69303
cvcrsk3cc_4_11_17	15246	14900	2760	10.09	12619	8842	60.00	6786	1941.09	15.82	-227	0.68744	0.00129	0.69003
cvcrsk3cc_4_12_1	15246	14900	3220	11.45	12619	8842	0.00	0	2264.6	18.13	-227	0.72168	0.00119	0.72405
cvcrsk3cc_4_12_2	15246	14900	3220	11.45	12619	8842	3.75	424	2264.6	18.13	-227	0.72398	0.00131	0.72660
cvcrsk3cc_4_12_3	15246	14900	3220	11.45	12619	8842	7.50	848	2264.6	18.13	-227	0.72501	0.00142	0.72786
cvcrsk3cc_4_12_4	15246	14900	3220	11.45	12619	8842	11.25	1272	2264.6	18.13	-227	0.72327	0.00132	0.72592
cvcrsk3cc_4_12_5	15246	14900	3220	11.45	12619	8842	15.00	1696	2264.6	18.13	-227	0.72278	0.00124	0.72526

Table 6.9.6-17. Results for skull oxide (SO) content in CV calculation model

case name	SO (g)	UO_3 (g)	Sat. H_2O (g)	SO h/x	U (g)	^{235}U (g)	C (g)	mg C/ g ^{235}U	CV H_2O (g)	CV h/x	Unident. (g)	k_{eff}	σ	$k_{eff}+2σ$
cvcrsk3cc_4_12_6	15246	14900	3220	11.45	12619	8842	18.75	2120	2264.6	18.13	-227	0.72081	0.00142	0.72364
cvcrsk3cc_4_12_7	15246	14900	3220	11.45	12619	8842	22.50	2545	2264.6	18.13	-227	0.72286	0.00141	0.72568
cvcrsk3cc_4_12_8	15246	14900	3220	11.45	12619	8842	26.25	2969	2264.6	18.13	-227	0.72457	0.00118	0.72693
cvcrsk3cc_4_12_9	15246	14900	3220	11.45	12619	8842	30.00	3393	2264.6	18.13	-227	0.72295	0.00126	0.72547
cvcrsk3cc_4_12_10	15246	14900	3220	11.45	12619	8842	33.75	3817	2264.6	18.13	-227	0.71959	0.00131	0.72221
cvcrsk3cc_4_12_11	15246	14900	3220	11.45	12619	8842	37.50	4241	2264.6	18.13	-227	0.72351	0.00106	0.72563
cvcrsk3cc_4_12_12	15246	14900	3220	11.45	12619	8842	41.25	4665	2264.6	18.13	-227	0.72291	0.00139	0.72570
cvcrsk3cc_4_12_13	15246	14900	3220	11.45	12619	8842	45.00	5089	2264.6	18.13	-227	0.72324	0.00125	0.72574
cvcrsk3cc_4_12_14	15246	14900	3220	11.45	12619	8842	48.75	5513	2264.6	18.13	-227	0.72395	0.00143	0.72680
cvcrsk3cc_4_12_15	15246	14900	3220	11.45	12619	8842	52.50	5937	2264.6	18.13	-227	0.72591	0.00111	0.72814
cvcrsk3cc_4_12_16	15246	14900	3220	11.45	12619	8842	56.25	6362	2264.6	18.13	-227	0.72242	0.00146	0.72535
cvcrsk3cc_4_12_17	15246	14900	3220	11.45	12619	8842	60.00	6786	2264.6	18.13	-227	0.72398	0.00117	0.72631
cvcrsk3cc_4_13_1	15246	14900	3679	12.81	12619	8842	0.00	0	2588.12	20.45	-227	0.75630	0.00133	0.75896
cvcrsk3cc_4_13_2	15246	14900	3679	12.81	12619	8842	3.75	424	2588.12	20.45	-227	0.75574	0.00132	0.75838
cvcrsk3cc_4_13_3	15246	14900	3679	12.81	12619	8842	7.50	848	2588.12	20.45	-227	0.75761	0.00136	0.76032
cvcrsk3cc_4_13_4	15246	14900	3679	12.81	12619	8842	11.25	1272	2588.12	20.45	-227	0.75747	0.00147	0.76042
cvcrsk3cc_4_13_5	15246	14900	3679	12.81	12619	8842	15.00	1696	2588.12	20.45	-227	0.75674	0.00120	0.75914
cvcrsk3cc_4_13_6	15246	14900	3679	12.81	12619	8842	18.75	2120	2588.12	20.45	-227	0.75883	0.00137	0.76157
cvcrsk3cc_4_13_7	15246	14900	3679	12.81	12619	8842	22.50	2545	2588.12	20.45	-227	0.75912	0.00125	0.76162
cvcrsk3cc_4_13_8	15246	14900	3679	12.81	12619	8842	26.25	2969	2588.12	20.45	-227	0.75690	0.00131	0.75952
cvcrsk3cc_4_13_9	15246	14900	3679	12.81	12619	8842	30.00	3393	2588.12	20.45	-227	0.75692	0.00123	0.75938
cvcrsk3cc_4_13_10	15246	14900	3679	12.81	12619	8842	33.75	3817	2588.12	20.45	-227	0.75676	0.00123	0.75923
cvcrsk3cc_4_13_11	15246	14900	3679	12.81	12619	8842	37.50	4241	2588.12	20.45	-227	0.75541	0.00134	0.75808

Table 6.9.6-17. Results for skull oxide (SO) content in CV calculation model

case name	SO (g)	UO_3 (g)	Sat. H_2O (g)	SO h/x	U (g)	^{235}U (g)	C (g)	mg C/ g ^{235}U	CV H_2O (g)	CV h/x	Unident. (g)	k_{eff}	σ	$k_{eff}+2σ$
cvcrsk3cc_4_13_12	15246	14900	3679	12.81	12619	8842	41.25	4665	2588.12	20.45	-227	0.75894	0.00141	0.76176
cvcrsk3cc_4_13_13	15246	14900	3679	12.81	12619	8842	45.00	5089	2588.12	20.45	-227	0.75688	0.00137	0.75963
cvcrsk3cc_4_13_14	15246	14900	3679	12.81	12619	8842	48.75	5513	2588.12	20.45	-227	0.75618	0.00140	0.75898
cvcrsk3cc_4_13_15	15246	14900	3679	12.81	12619	8842	52.50	5937	2588.12	20.45	-227	0.75806	0.00143	0.76092
cvcrsk3cc_4_13_16	15246	14900	3679	12.81	12619	8842	56.25	6362	2588.12	20.45	-227	0.75838	0.00131	0.76100
cvcrsk3cc_4_13_17	15246	14900	3679	12.81	12619	8842	60.00	6786	2588.12	20.45	-227	0.75890	0.00130	0.76150
cvcrsk3cc_4_14_1	15246	14900	4139	14.16	12619	8842	0.00	0	2911.63	22.76	-227	0.78934	0.00142	0.79219
cvcrsk3cc_4_14_2	15246	14900	4139	14.16	12619	8842	3.75	424	2911.63	22.76	-227	0.79102	0.00153	0.79408
cvcrsk3cc_4_14_3	15246	14900	4139	14.16	12619	8842	7.50	848	2911.63	22.76	-227	0.78792	0.00140	0.79073
cvcrsk3cc_4_14_4	15246	14900	4139	14.16	12619	8842	11.25	1272	2911.63	22.76	-227	0.78817	0.00122	0.79061
cvcrsk3cc_4_14_5	15246	14900	4139	14.16	12619	8842	15.00	1696	2911.63	22.76	-227	0.79185	0.00133	0.79451
cvcrsk3cc_4_14_6	15246	14900	4139	14.16	12619	8842	18.75	2120	2911.63	22.76	-227	0.78935	0.00155	0.79244
cvcrsk3cc_4_14_7	15246	14900	4139	14.16	12619	8842	22.50	2545	2911.63	22.76	-227	0.79031	0.00139	0.79310
cvcrsk3cc_4_14_8	15246	14900	4139	14.16	12619	8842	26.25	2969	2911.63	22.76	-227	0.79032	0.00119	0.79269
cvcrsk3cc_4_14_9	15246	14900	4139	14.16	12619	8842	30.00	3393	2911.63	22.76	-227	0.79075	0.00125	0.79326
cvcrsk3cc_4_14_10	15246	14900	4139	14.16	12619	8842	33.75	3817	2911.63	22.76	-227	0.78950	0.00127	0.79203
cvcrsk3cc_4_14_11	15246	14900	4139	14.16	12619	8842	37.50	4241	2911.63	22.76	-227	0.79226	0.00132	0.79490
cvcrsk3cc_4_14_12	15246	14900	4139	14.16	12619	8842	41.25	4665	2911.63	22.76	-227	0.79141	0.00129	0.79400
cvcrsk3cc_4_14_13	15246	14900	4139	14.16	12619	8842	45.00	5089	2911.63	22.76	-227	0.79226	0.00131	0.79488
cvcrsk3cc_4_14_14	15246	14900	4139	14.16	12619	8842	48.75	5513	2911.63	22.76	-227	0.79139	0.00140	0.79418
cvcrsk3cc_4_14_15	15246	14900	4139	14.16	12619	8842	52.50	5937	2911.63	22.76	-227	0.79157	0.00136	0.79429
cvcrsk3cc_4_14_16	15246	14900	4139	14.16	12619	8842	56.25	6362	2911.63	22.76	-227	0.78883	0.00118	0.79119
cvcrsk3cc_4_14_17	15246	14900	4139	14.16	12619	8842	60.00	6786	2911.63	22.76	-227	0.79251	0.00163	0.79576

Table 6.9.6-17. Results for skull oxide (SO) content in CV calculation model

case name	SO (g)	UO_3 (g)	Sat. H_2O (g)	SO h/x	U (g)	^{235}U (g)	C (g)	mg C/ g ^{235}U	CV H_2O (g)	CV h/x	Unident. (g)	k_{eff}	σ	$k_{eff}+2σ$
cvcrsk3cc_4_15_1	15246	14900	4599	15.52	12619	8842	0.00	0	3235.15	25.07	-227	0.82370	0.00143	0.82655
cvcrsk3cc_4_15_2	15246	14900	4599	15.52	12619	8842	3.75	424	3235.15	25.07	-227	0.82249	0.00121	0.82491
cvcrsk3cc_4_15_3	15246	14900	4599	15.52	12619	8842	7.50	848	3235.15	25.07	-227	0.82289	0.00125	0.82539
cvcrsk3cc_4_15_4	15246	14900	4599	15.52	12619	8842	11.25	1272	3235.15	25.07	-227	0.82409	0.00117	0.82643
cvcrsk3cc_4_15_5	15246	14900	4599	15.52	12619	8842	15.00	1696	3235.15	25.07	-227	0.82541	0.00127	0.82794
cvcrsk3cc_4_15_6	15246	14900	4599	15.52	12619	8842	18.75	2120	3235.15	25.07	-227	0.82424	0.00123	0.82669
cvcrsk3cc_4_15_7	15246	14900	4599	15.52	12619	8842	22.50	2545	3235.15	25.07	-227	0.82476	0.00182	0.82841
cvcrsk3cc_4_15_8	15246	14900	4599	15.52	12619	8842	26.25	2969	3235.15	25.07	-227	0.82419	0.00142	0.82702
cvcrsk3cc_4_15_9	15246	14900	4599	15.52	12619	8842	30.00	3393	3235.15	25.07	-227	0.82530	0.00145	0.82820
cvcrsk3cc_4_15_10	15246	14900	4599	15.52	12619	8842	33.75	3817	3235.15	25.07	-227	0.82433	0.00155	0.82742
cvcrsk3cc_4_15_11	15246	14900	4599	15.52	12619	8842	37.50	4241	3235.15	25.07	-227	0.82379	0.00142	0.82663
cvcrsk3cc_4_15_12	15246	14900	4599	15.52	12619	8842	41.25	4665	3235.15	25.07	-227	0.82450	0.00146	0.82742
cvcrsk3cc_4_15_13	15246	14900	4599	15.52	12619	8842	45.00	5089	3235.15	25.07	-227	0.82666	0.00109	0.82883
cvcrsk3cc_4_15_14	15246	14900	4599	15.52	12619	8842	48.75	5513	3235.15	25.07	-227	0.82521	0.00125	0.82772
cvcrsk3cc_4_15_15	15246	14900	4599	15.52	12619	8842	52.50	5937	3235.15	25.07	-227	0.82544	0.00120	0.82784
cvcrsk3cc_4_15_16	15246	14900	4599	15.52	12619	8842	56.25	6362	3235.15	25.07	-227	0.82578	0.00133	0.82844
cvcrsk3cc_4_15_17	15246	14900	4599	15.52	12619	8842	60.00	6786	3235.15	25.07	-227	0.82622	0.00154	0.82930
cvcrsk3cc_6_1_17	15111	12933	0	4.17	10960	4122	921	223432	0	4.17	744	0.44158	0.00098	0.44355
cvcrsk3cc_6_6_17	15111	12933	377	6.56	10960	4122	921	223432	410	9.16	744	0.46812	0.00103	0.47018
cvcrsk3cc_6_7_17	15111	12933	753	8.94	10960	4122	921	223432	821	14.14	744	0.49580	0.00108	0.49797
cvcrsk3cc_6_8_17	15111	12933	1130	11.33	10960	4122	921	223432	1231	19.12	744	0.52824	0.00111	0.53046
cvcrsk3cc_6_9_17	15111	12933	1506	13.71	10960	4122	921	223432	1642	24.11	744	0.55880	0.00129	0.56139

Table 6.9.6-17. Results for skull oxide (SO) content in CV calculation model

case name	SO (g)	UO_3 (g)	Sat. H_2O (g)	SO h/x	U (g)	^{235}U (g)	C (g)	mg C/ g ^{235}U	CV H_2O (g)	CV h/x	Unident. (g)	k_{eff}	σ	$k_{eff}+2σ$
cvcrsk3cc_6_10_17	15111	12933	1883	16.09	10960	4122	921	223432	2052	29.09	744	0.58946	0.00103	0.59153
cvcrsk3cc_6_11_17	15111	12933	2259	18.48	10960	4122	921	223432	2463	34.07	744	0.62334	0.00130	0.62593
cvcrsk3cc_6_12_17	15111	12933	2636	20.86	10960	4122	921	223432	2873	39.06	744	0.65813	0.00115	0.66044
cvcrsk3cc_6_13_17	15111	12933	3012	23.25	10960	4122	921	223432	3284	44.04	744	0.69032	0.00104	0.69240
cvcrsk3cc_6_14_17	15111	12933	3389	25.63	10960	4122	921	223432	3694	49.02	744	0.72104	0.00142	0.72388
cvcrsk3cc_6_15_17	15111	12933	3765	28.02	10960	4122	921	223432	4105	54.01	744	0.75711	0.00110	0.75932

Table 6.9.6-18a. NCT results for skull oxide (SO) content in packaging calculation model

case name	SO (g)	U_3O_8 (g)	Sat. H_2O (g)	SO h/x	U (g)	^{235}U (g)	C (g)	mg C/ g ^{235}U	CV H_2O (g)	CV h/x	Unident. (g)	k_{eff}	σ	$k_{eff}+2σ$
content in flooded CV, NCT single package, reflected														
513 g polyethylene, no can spacers														
ncsrsk_1_15	11589	8063	4468	28.09	6828	4765	417	87518	4105	50.58	2596	0.71933	0.00154	0.72241
ncsrsk_2_15	14934	11665	4015	17.79	9879	6858	504	73492	4105	33.41	2252	0.70319	0.00144	0.70606
ncsrsk_3_15	13821	11876	4893	20.62	10058	7028	372	52930	3233	32.62	1060	0.71916	0.00128	0.72172
ncsrsk_4_15	15246	14900	4599	15.52	12619	8842	60	6786	3235	25.07	-227	0.71123	0.00145	0.71413
ncsrsk_5_15	21216	21036	3869	9.49	17815	12455	27	2168	3235	16.27	-360	0.69577	0.00139	0.69855
ncsrsk_6_15	15111	12933	3765	28.02	10960	4122	921	223432	4105	54.01	744	0.63803	0.00171	0.64146
ncsrsk_7_15	13155	11666	3989	32.68	9886	3712	609	164054	4106	61.55	367	0.65018	0.00127	0.65271
ncsrsk_8_15	13650	11689	4068	33.01	9906	3737	261	69834	4106	61.69	1187	0.65349	0.00128	0.65604
ncsrsk_9_15	21300	19865	3801	7.43	16816	15673	921	58764	3235	12.82	1	0.73837	0.00130	0.74096
ncsrsk_10_15	21300	20786	3905	7.27	17596	16399	0	0	3235	12.41	1	0.74201	0.00149	0.74499

Table 6.9.6-18a. NCT results for skull oxide (SO) content in packaging calculation model

case name	SO (g)	U_3O_8 (g)	Sat. H_2O (g)	SO h/x	U (g)	^{235}U (g)	C (g)	mg C/ g ^{235}U	CV H_2O (g)	CV h/x	Unident. (g)	k_{eff}	σ	k_{eff}+2σ
ncsrsk_9_1	21300	19865	0	1.10	16816	15673	921	58764	0	1.10	1	0.40142	0.00078	0.40297
ncsrsk_9_6	21300	19865	380	1.73	16816	15673	921	58764	324	2.27	1	0.43142	0.00096	0.43334
ncsrsk_9_7	21300	19865	760	2.36	16816	15673	921	58764	647	3.44	1	0.46578	0.00099	0.46776
ncsrsk_9_8	21300	19865	1140	3.00	16816	15673	921	58764	971	4.61	1	0.49839	0.00107	0.50053
ncsrsk_9_9	21300	19865	1521	3.63	16816	15673	921	58764	1294	5.79	1	0.53148	0.00124	0.53397
ncsrsk_9_10	21300	19865	1901	4.26	16816	15673	921	58764	1618	6.96	1	0.56633	0.00122	0.56877
ncsrsk_9_11	21300	19865	2281	4.90	16816	15673	921	58764	1941	8.13	1	0.60204	0.00118	0.60441
ncsrsk_9_12	21300	19865	2661	5.53	16816	15673	921	58764	2265	9.30	1	0.63600	0.00119	0.63839
ncsrsk_9_13	21300	19865	3041	6.16	16816	15673	921	58764	2588	10.47	1	0.67128	0.00130	0.67389
ncsrsk_9_14	21300	19865	3421	6.80	16816	15673	921	58764	2912	11.64	1	0.70363	0.00130	0.70623
ncsrsk_9_15	21300	19865	3801	7.43	16816	15673	921	58764	3235	12.82	1	0.73837	0.00130	0.74096
ncsrsk_10_1	21300	20786	0	1.05	17596	16399	0	0	0	1.05	1	0.40278	0.00079	0.40436
ncsrsk_10_6	21300	20786	391	1.67	17596	16399	0	0	324	2.19	1	0.43497	0.00093	0.43683
ncsrsk_10_7	21300	20786	781	2.29	17596	16399	0	0	647	3.32	1	0.46764	0.00104	0.46971
ncsrsk_10_8	21300	20786	1172	2.91	17596	16399	0	0	971	4.46	1	0.50067	0.00103	0.50274
ncsrsk_10_9	21300	20786	1562	3.54	17596	16399	0	0	1294	5.60	1	0.53570	0.00129	0.53828
ncsrsk_10_10	21300	20786	1953	4.16	17596	16399	0	0	1618	6.73	1	0.57116	0.00119	0.57355
ncsrsk_10_11	21300	20786	2343	4.78	17596	16399	0	0	1941	7.87	1	0.60642	0.00131	0.60904
ncsrsk_10_12	21300	20786	2734	5.40	17596	16399	0	0	2265	9.00	1	0.63938	0.00118	0.64175
ncsrsk_10_13	21300	20786	3124	6.02	17596	16399	0	0	2588	10.14	1	0.67610	0.00123	0.67856
ncsrsk_10_14	21300	20786	3515	6.64	17596	16399	0	0	2912	11.28	1	0.70857	0.00115	0.71087
ncsrsk_10_15	21300	20786	3905	7.27	17596	16399	0	0	3235	12.41	1	0.74201	0.00149	0.74499

Table 6.9.6-18a. NCT results for skull oxide (SO) content in packaging calculation model

case name	SO (g)	U_3O_8 (g)	Sat. H_2O (g)	SO h/x	U (g)	^{235}U (g)	C (g)	mg C/ g ^{235}U	CV H_2O (g)	CV h/x	Unident. (g)	k_{eff}	σ	$k_{eff}+2σ$
content in flooded containment vessel, NCT array packaging calculation model for CSI=0.0														
513 g polyethylene, no can spacers														
nciask_1_15	11589	8063	4468	28.09	6828	4765	417	87518	4105	50.58	2596	0.73555	0.00130	0.73814
nciask_2_15	14934	11665	4015	17.79	9879	6858	504	73492	4105	33.41	2252	0.72258	0.00122	0.72503
nciask_3_15	13821	11876	4893	20.62	10058	7028	372	52930	3233	32.62	1060	0.73483	0.00120	0.73724
nciask_4_15	15246	14900	4599	15.52	12619	8842	60	6786	3235	25.07	-227	0.72783	0.00122	0.73027
nciask_5_15	21216	21036	3869	9.49	17815	12455	27	2168	3235	16.27	-360	0.71163	0.00123	0.71409
nciask_6_15	15111	12933	3765	28.02	10960	4122	921	223432	4105	54.01	744	0.65333	0.00109	0.65551
nciask_7_15	13155	11666	3989	32.68	9886	3712	609	164054	4106	61.55	367	0.66124	0.00107	0.66339
nciask_8_15	13650	11689	4068	33.01	9906	3737	261	69834	4106	61.69	1187	0.66664	0.00124	0.66912
nciask_9_15	21300	19865	3801	7.43	16816	15673	921	58764	3235	12.82	1	0.75365	0.00127	0.75620
nciask_10_15	21300	20786	3905	7.27	17596	16399	0	0	3235	12.41	1	0.76141	0.00140	0.76422
nciask_6_1	15111	12933	0	4.17	10960	4122	921	223432	0	4.17	744	0.26223	0.00069	0.26361
nciask_6_6	15111	12933	377	6.56	10960	4122	921	223432	410	9.16	744	0.29333	0.00078	0.29489
nciask_6_7	15111	12933	753	8.94	10960	4122	921	223432	821	14.14	744	0.32968	0.00084	0.33136
nciask_6_8	15111	12933	1130	11.33	10960	4122	921	223432	1231	19.12	744	0.36777	0.00088	0.36953
nciask_6_9	15111	12933	1506	13.71	10960	4122	921	223432	1642	24.11	744	0.40621	0.00127	0.40874
nciask_6_10	15111	12933	1883	16.09	10960	4122	921	223432	2052	29.09	744	0.44807	0.00116	0.45039
nciask_6_11	15111	12933	2259	18.48	10960	4122	921	223432	2463	34.07	744	0.49212	0.00111	0.49435
nciask_6_12	15111	12933	2636	20.86	10960	4122	921	223432	2873	39.06	744	0.53233	0.00122	0.53477
nciask_6_13	15111	12933	3012	23.25	10960	4122	921	223432	3284	44.04	744	0.57192	0.00123	0.57439
nciask_6_14	15111	12933	3389	25.63	10960	4122	921	223432	3694	49.02	744	0.61188	0.00136	0.61460
nciask_6_15	15111	12933	3765	28.02	10960	4122	921	223432	4105	54.01	744	0.65333	0.00109	0.65551

Table 6.9.6-18a. NCT results for skull oxide (SO) content in packaging calculation model

case name	SO (g)	U_3O_8 (g)	Sat. H_2O (g)	SO h/x	U (g)	^{235}U (g)	C (g)	mg C/ g ^{235}U	CV H_2O (g)	CV h/x	Unident. (g)	k_{eff}	σ	$k_{eff}+2σ$
nciask_9_1	21300	19865	0	1.1	16816	15673	921	58764	0	1.10	1	0.41949	0.00093	0.42134
nciask_9_6	21300	19865	380	1.73	16816	15673	921	58764	324	2.27	1	0.45272	0.00092	0.45456
nciask_9_7	21300	19865	760	2.36	16816	15673	921	58764	647	3.44	1	0.48472	0.00116	0.48704
nciask_9_8	21300	19865	1140	3	16816	15673	921	58764	971	4.61	1	0.51805	0.00111	0.52027
nciask_9_9	21300	19865	1521	3.63	16816	15673	921	58764	1294	5.79	1	0.55105	0.00116	0.55336
nciask_9_10	21300	19865	1901	4.26	16816	15673	921	58764	1618	6.96	1	0.58571	0.00105	0.58780
nciask_9_11	21300	19865	2281	4.9	16816	15673	921	58764	1941	8.13	1	0.62158	0.00114	0.62386
nciask_9_12	21300	19865	2661	5.53	16816	15673	921	58764	2265	9.30	1	0.65700	0.00141	0.65983
nciask_9_13	21300	19865	3041	6.16	16816	15673	921	58764	2588	10.47	1	0.68964	0.00125	0.69214
nciask_9_14	21300	19865	3421	6.8	16816	15673	921	58764	2912	11.64	1	0.72169	0.00141	0.72451
nciask_9_15	21300	19865	3801	7.43	16816	15673	921	58764	3235	12.82	1	0.75365	0.00127	0.75620
nciask_10_1	21300	20786	0	1.05	17596	16399	0	0	0	1.05	1	0.42530	0.00082	0.42693
nciask_10_6	21300	20786	391	1.67	17596	16399	0	0	324	2.19	1	0.45517	0.00080	0.45677
nciask_10_7	21300	20786	781	2.29	17596	16399	0	0	647	3.32	1	0.48754	0.00099	0.48952
nciask_10_8	21300	20786	1172	2.91	17596	16399	0	0	971	4.46	1	0.52247	0.00101	0.52448
nciask_10_9	21300	20786	1562	3.54	17596	16399	0	0	1294	5.60	1	0.55799	0.00107	0.56013
nciask_10_10	21300	20786	1953	4.16	17596	16399	0	0	1618	6.73	1	0.59209	0.00104	0.59416
nciask_10_11	21300	20786	2343	4.78	17596	16399	0	0	1941	7.87	1	0.62721	0.00107	0.62935
nciask_10_12	21300	20786	2734	5.4	17596	16399	0	0	2265	9.00	1	0.65769	0.00115	0.65999
nciask_10_13	21300	20786	3124	6.02	17596	16399	0	0	2588	10.14	1	0.69394	0.00131	0.69655
nciask_10_14	21300	20786	3515	6.64	17596	16399	0	0	2912	11.28	1	0.72808	0.00150	0.73109
nciask_10_15	21300	20786	3905	7.27	17596	16399	0	0	3235	12.41	1	0.76141	0.00140	0.76422

Table 6.9.6-18b. HAC results for skull oxide (SO) content in packaging calculation model

case name	SO (g)	U_3O_8 (g)	Sat. H_2O (g)	SO h/x	U (g)	^{235}U (g)	C (g)	mg C/ g ^{235}U	CV H_2O (g)	CV h/x	Unident. (g)	k_{eff}	σ	$k_{eff}+2σ$
content in flooded CV, HAC single package, reflected														
513 g polyethylene, no can spacers														
hcsrsk_1_15	11589	8063	4468	28.09	6828	4765	417	87518	4105	50.58	2596	0.72049	0.00145	0.72339
hcsrsk_2_15	14934	11665	4015	17.79	9879	6858	504	73492	4105	33.41	2252	0.70717	0.00140	0.70997
hcsrsk_3_15	13821	11876	4893	20.62	10058	7028	372	52930	3233	32.62	1060	0.72081	0.00136	0.72353
hcsrsk_4_15	15246	14900	4599	15.52	12619	8842	60	6786	3235	25.07	-227	0.71449	0.00128	0.71706
hcsrsk_5_15	21216	21036	3869	9.49	17815	12455	27	2168	3235	16.27	-360	0.69845	0.00134	0.70113
hcsrsk_6_15	15111	12933	3765	28.02	10960	4122	921	223432	4105	54.01	744	0.63787	0.00140	0.64066
hcsrsk_7_15	13155	11666	3989	32.68	9886	3712	609	164054	4106	61.55	367	0.64910	0.00150	0.65210
hcsrsk_8_15	13650	11689	4068	33.01	9906	3737	261	69834	4106	61.69	1187	0.65332	0.00140	0.65613
hcsrsk_9_15	21300	19865	3801	7.43	16816	15673	921	58764	3235	12.82	1	0.73855	0.00121	0.74096
hcsrsk_10_15	21300	20786	3905	7.27	17596	16399	0	0	3235	12.41	1	0.74359	0.00118	0.74595
hcsrsk_9_1	21300	19865	0	1.10	16816	15673	921	58764	0	1.10	1	0.40344	0.00080	0.40505
hcsrsk_9_6	21300	19865	380	1.73	16816	15673	921	58764	324	2.27	1	0.43432	0.00091	0.43614
hcsrsk_9_7	21300	19865	760	2.36	16816	15673	921	58764	647	3.44	1	0.46617	0.00090	0.46796
hcsrsk_9_8	21300	19865	1140	3.00	16816	15673	921	58764	971	4.61	1	0.49951	0.00104	0.50160
hcsrsk_9_9	21300	19865	1521	3.63	16816	15673	921	58764	1294	5.79	1	0.53428	0.00114	0.53656
hcsrsk_9_10	21300	19865	1901	4.26	16816	15673	921	58764	1618	6.96	1	0.57081	0.00102	0.57286
hcsrsk_9_11	21300	19865	2281	4.90	16816	15673	921	58764	1941	8.13	1	0.60569	0.00111	0.60792
hcsrsk_9_12	21300	19865	2661	5.53	16816	15673	921	58764	2265	9.30	1	0.63704	0.00125	0.63955
hcsrsk_9_13	21300	19865	3041	6.16	16816	15673	921	58764	2588	10.47	1	0.67153	0.00139	0.67431

Table 6.9.6-18b. HAC results for skull oxide (SO) content in packaging calculation model

case name	SO (g)	U_3O_8 (g)	Sat. H_2O (g)	SO h/x	U (g)	^{235}U (g)	C (g)	mg C/ g ^{235}U	CV H_2O (g)	CV h/x	Unident. (g)	k_{eff}	σ	$k_{eff}+2σ$
hcsrsk_9_14	21300	19865	3421	6.80	16816	15673	921	58764	2912	11.64	1	0.70545	0.00113	0.70770
hcsrsk_9_15	21300	19865	3801	7.43	16816	15673	921	58764	3235	12.82	1	0.73855	0.00121	0.74096
hcsrsk_10_1	21300	20786	0	1.05	17596	16399	0	0	0	1.05	1	0.40569	0.00088	0.40745
hcsrsk_10_6	21300	20786	391	1.67	17596	16399	0	0	324	2.19	1	0.43659	0.00086	0.43832
hcsrsk_10_7	21300	20786	781	2.29	17596	16399	0	0	647	3.32	1	0.47008	0.00095	0.47198
hcsrsk_10_8	21300	20786	1172	2.91	17596	16399	0	0	971	4.46	1	0.50524	0.00097	0.50717
hcsrsk_10_9	21300	20786	1562	3.54	17596	16399	0	0	1294	5.60	1	0.53928	0.00102	0.54133
hcsrsk_10_10	21300	20786	1953	4.16	17596	16399	0	0	1618	6.73	1	0.57494	0.00115	0.57724
hcsrsk_10_11	21300	20786	2343	4.78	17596	16399	0	0	1941	7.87	1	0.60702	0.00111	0.60924
hcsrsk_10_12	21300	20786	2734	5.40	17596	16399	0	0	2265	9.00	1	0.64205	0.00132	0.64469
hcsrsk_10_13	21300	20786	3124	6.02	17596	16399	0	0	2588	10.14	1	0.67634	0.00138	0.67911
hcsrsk_10_14	21300	20786	3515	6.64	17596	16399	0	0	2912	11.28	1	0.71259	0.00144	0.71547
hcsrsk_10_15	21300	20786	3905	7.27	17596	16399	0	0	3235	12.41	1	0.74359	0.00118	0.74595
content in flooded containment vessel, HAC array packaging calculation model for CSI=0.0														
513 g polyethylene, no can spacers														
hciask_1_15	11589	8063	4468	28.09	6828	4765	417	87518	4105	50.58	2596	0.73896	0.00132	0.74159
hciask_2_15	14934	11665	4015	17.79	9879	6858	504	73492	4105	33.41	2252	0.72435	0.00127	0.72689
hciask_3_15	13821	11876	4893	20.62	10058	7028	372	52930	3233	32.62	1060	0.73900	0.00130	0.74160
hciask_4_15	15246	14900	4599	15.52	12619	8842	60	6786	3235	25.07	-227	0.73199	0.00123	0.73445
hciask_5_15	21216	21036	3869	9.49	17815	12455	27	2168	3235	16.27	-360	0.71601	0.00117	0.71835
hciask_6_15	15111	12933	3765	28.02	10960	4122	921	223432	4105	54.01	744	0.65587	0.00125	0.65837
hciask_7_15	13155	11666	3989	32.68	9886	3712	609	164054	4106	61.55	367	0.66608	0.00159	0.66925
hciask_8_15	13650	11689	4068	33.01	9906	3737	261	69834	4106	61.69	1187	0.66948	0.00153	0.67255

Table 6.9.6-18b. HAC results for skull oxide (SO) content in packaging calculation model

case name	SO (g)	U_3O_8 (g)	Sat. H_2O (g)	SO h/x	U (g)	^{235}U (g)	C (g)	mg C/ g ^{235}U	CV H_2O (g)	CV h/x	Unident. (g)	k_{eff}	σ	$k_{eff}+2σ$
hciask_9_15	21300	19865	3801	7.43	16816	15673	921	58764	3235	12.82	1	0.75757	0.00116	0.75989
hciask_10_15	21300	20786	3905	7.27	17596	16399	0	0	3235	12.41	1	0.76462	0.00131	0.76725
hciask_6_1	15111	12933	0	4.17	10960	4122	921	223432	0	4.17	744	0.26620	0.00075	0.26769
hciask_6_6	15111	12933	377	6.56	10960	4122	921	223432	411	9.16	744	0.29787	0.00085	0.29957
hciask_6_7	15111	12933	753	8.94	10960	4122	921	223432	821	14.14	744	0.33370	0.00085	0.33539
hciask_6_8	15111	12933	1130	11.33	10960	4122	921	223432	1231	19.12	744	0.37226	0.00098	0.37422
hciask_6_9	15111	12933	1506	13.71	10960	4122	921	223432	1642	24.11	744	0.41300	0.00083	0.41465
hciask_6_10	15111	12933	1883	16.09	10960	4122	921	223432	2052	29.09	744	0.45192	0.00106	0.45403
hciask_6_11	15111	12933	2259	18.48	10960	4122	921	223432	2463	34.07	744	0.49341	0.00113	0.49566
hciask_6_12	15111	12933	2636	20.86	10960	4122	921	223432	2873	39.06	744	0.53469	0.00111	0.53691
hciask_6_13	15111	12933	3012	23.25	10960	4122	921	223432	3284	44.04	744	0.57324	0.00123	0.57571
hciask_6_14	15111	12933	3389	25.63	10960	4122	921	223432	3694	49.02	744	0.61596	0.00125	0.61847
hciask_6_15	15111	12933	3765	28.02	10960	4122	921	223432	4105	54.01	744	0.65587	0.00125	0.65837
hciask_9_1	21300	19865	0	1.10	16816	15673	921	58764	0	1.10	1	0.42753	0.00091	0.42935
hciask_9_6	21300	19865	380	1.73	16816	15673	921	58764	324	2.27	1	0.45603	0.00103	0.45808
hciask_9_7	21300	19865	760	2.36	16816	15673	921	58764	647	3.44	1	0.48912	0.00101	0.49114
hciask_9_8	21300	19865	1140	3.00	16816	15673	921	58764	971	4.61	1	0.52104	0.00109	0.52322
hciask_9_9	21300	19865	1521	3.63	16816	15673	921	58764	1294	5.79	1	0.55643	0.00104	0.55851
hciask_9_10	21300	19865	1901	4.26	16816	15673	921	58764	1618	6.96	1	0.59193	0.00105	0.59403
hciask_9_11	21300	19865	2281	4.90	16816	15673	921	58764	1941	8.13	1	0.62726	0.00109	0.62945
hciask_9_12	21300	19865	2661	5.53	16816	15673	921	58764	2265	9.30	1	0.65952	0.00106	0.66163
hciask_9_13	21300	19865	3041	6.16	16816	15673	921	58764	2588	10.47	1	0.69094	0.00127	0.69348

Table 6.9.6-18b. HAC results for skull oxide (SO) content in packaging calculation model

case name	SO (g)	U_3O_8 (g)	Sat. H_2O (g)	SO h/x	U (g)	^{235}U (g)	C (g)	mg C/ g ^{235}U	CV H_2O (g)	CV h/x	Unident. (g)	k_{eff}	σ	$k_{eff}+2σ$
hciask_9_14	21300	19865	3421	6.80	16816	15673	921	58764	2912	11.64	1	0.72863	0.00116	0.73095
hciask_9_15	21300	19865	3801	7.43	16816	15673	921	58764	3235	12.82	1	0.75757	0.00116	0.75989
hciask_10_1	21300	20786	0	1.05	17596	16399	0	0	0	1.05	1	0.43087	0.00111	0.43308
hciask_10_6	21300	20786	391	1.67	17596	16399	0	0	324	2.19	1	0.46066	0.00092	0.46250
hciask_10_7	21300	20786	781	2.29	17596	16399	0	0	647	3.32	1	0.49381	0.00097	0.49574
hciask_10_8	21300	20786	1172	2.91	17596	16399	0	0	971	4.46	1	0.52679	0.00113	0.52906
hciask_10_9	21300	20786	1562	3.54	17596	16399	0	0	1294	5.60	1	0.56200	0.00121	0.56442
hciask_10_10	21300	20786	1953	4.16	17596	16399	0	0	1618	6.73	1	0.59673	0.00118	0.59908
hciask_10_11	21300	20786	2343	4.78	17596	16399	0	0	1941	7.87	1	0.63042	0.00109	0.63260
hciask_10_12	21300	20786	2734	5.40	17596	16399	0	0	2265	9.00	1	0.66502	0.00116	0.66735
hciask_10_13	21300	20786	3124	6.02	17596	16399	0	0	2588	10.14	1	0.69780	0.00108	0.69997
hciask_10_14	21300	20786	3515	6.64	17596	16399	0	0	2912	11.28	1	0.73223	0.00123	0.73470
hciask_10_15	21300	20786	3905	7.27	17596	16399	0	0	3235	12.41	1	0.76462	0.00131	0.76725
nciask_10_14	21300	20786	3515	6.64	17596	16399	0	0	2912	11.28	1	0.72808	0.00150	0.73109
nciask_10_15	21300	20786	3905	7.27	17596	16399	0	0	3235	12.41	1	0.76141	0.00140	0.76422

Table 6.9.6-19a. Results for $UZrH_x$ content in CV calculation model

case name	np	$UZrH_x$ (g)	^{235}U (g)	H_2O (g)	h/x	mocfr	k_{eff}	σ	$k_{eff}+2σ$				
TRIGA ($UZrH_x$) fuel content at 19.7 wt % ^{235}U, 500 g CH_2, containment vessel, reflected													
no can spacers (np thickness = 0.0 in.)													
cvcrtriga_1_1	0.0	10,400	921	0	0.00	1.0e-20	0.34219	0.00107	0.34432				
cvcrtriga_1_6	0.0	10,400	921	900	25.50	1.0e-01	0.34704	0.00101	0.34905				
cvcrtriga_1_7	0.0	10,400	921	1,800	51.00	2.0e-01	0.35869	0.00094	0.36057				
cvcrtriga_1_8	0.0	10,400	921	2,700	76.50	3.0e-01	0.37291	0.00103	0.37496				
cvcrtriga_1_9	0.0	10,400	921	3,599	102.00	4.0e-01	0.38978	0.00115	0.39209				
cvcrtriga_1_10	0.0	10,400	921	4,499	127.50	5.0e-01	0.41521	0.00099	0.41719				
cvcrtriga_1_11	0.0	10,400	921	5,399	153.00	6.0e-01	0.43399	0.00108	0.43616				
cvcrtriga_1_12	0.0	10,400	921	6,299	178.50	7.0e-01	0.45681	0.00116	0.45914				
cvcrtriga_1_13	0.0	10,400	921	7,199	204.00	8.0e-01	0.48121	0.00136	0.48393				
cvcrtriga_1_14	0.0	10,400	921	8,098	229.51	9.0e-01	0.50284	0.00114	0.50511				
cvcrtriga_1_15	0.0	10,400	921	8,998	255.01	1.0e+00	0.52494	0.00120	0.52735				
can spacers (np thickness = 1.4 in.)													
cvcrtriga_2_15	1.4	10,400	921	8,385	237.62	1.0e+00	0.42157	0.00099	0.42354				
TRIGA ($UZrH_x$) fuel content at 70.1 wt % ^{235}U, 500 g CH_2, containment vessel, reflected													
no can spacers (np thickness = 0.0 in.)													
cvcrtriga_70_1_1	0.0	6,847	408	0	0.00	1.0e+00	0.29196	0.00097	0.29391				
cvcrtriga_70_1_6	0.0	6,847	408	900	57.56	1.0e+00	0.30096	0.00102	0.30300				
cvcrtriga_70_1_7	0.0	6,847	408	1,800	115.13	1.0e+00	0.31496	0.00089	0.31674				
cvcrtriga_70_1_8	0.0	6,847	408	2,700	172.69	1.0e+00	0.33376	0.00106	0.33588				
cvcrtriga_70_1_9	0.0	6,847	408	3,599	230.26	1.0e+00	0.35363	0.00100	0.35564				

Table 6.9.6-19a. Results for $UZrH_x$ content in CV calculation model

case name	np	$UZrH_x$ (g)	^{235}U (g)	H_2O (g)	h/x	mocfr	k_{eff}	σ	$k_{eff}+2σ$				
cvcrtriga_70_1_10	0.0	6,847	408	4,499	287.82	1.0e+00	0.37761	0.00098	0.37956				
cvcrtriga_70_1_11	0.0	6,847	408	5,399	345.38	1.0e+00	0.40017	0.00120	0.40257				
cvcrtriga_70_1_12	0.0	6,847	408	6,299	402.95	1.0e+00	0.42263	0.00109	0.42481				
cvcrtriga_70_1_13	0.0	6,847	408	7,199	460.51	1.0e+00	0.44607	0.00120	0.44848				
cvcrtriga_70_1_14	0.0	6,847	408	8,098	518.07	1.0e+00	0.46618	0.00104	0.46827				
cvcrtriga_70_1_15	0.0	6,847	408	8,998	575.64	1.0e+00	0.48847	0.00130	0.49107				
can spacers (np thickness = 1.4 in.)													
cvcrtriga_70_2_15	1.4	6,847	408	8,385	536.39	1.0e+00	0.38372	0.00112	0.38596				

Table 6.9.6-19b. Results for $UZrH_x$ content spacing in CV calculation model

case name	$UZrH_x$ (g)	^{235}U (g)	H_2O (g)	h/x	pitch (cm)	pitch (in	k_{eff}	σ	$k_{eff}+2σ$
TRIGA ($UZrH_x$) fuel content at 19.7 wt % ^{235}U, triangular pitch spacing from touching sections to sections touching convenience can									
500 g CH_2 in cc, no can spacers (np thickness = 0.0 in.), containment vessel, reflected									
mocfr=1.0									
cvT20ptch_1_15_1	10,400	921	8,998	255.01	2.11201	1.440	0.48176	0.00106	0.48387
cvT20ptch_1_15_2	10,400	921	8,998	255.01	2.25466	1.537	0.49373	0.00119	0.49612
cvT20ptch_1_15_3	10,400	921	8,998	255.01	2.39731	1.635	0.50012	0.00131	0.50274
cvT20ptch_1_15_4	10,400	921	8,998	255.01	2.53996	1.732	0.50823	0.00110	0.51044
cvT20ptch_1_15_5	10,400	921	8,998	255.01	2.68261	1.829	0.51676	0.00126	0.51928
cvT20ptch_1_15_6	10,400	921	8,998	255.01	2.82526	1.927	0.52300	0.00115	0.52530
cvT20ptch_1_15_7	10,400	921	8,998	255.01	2.96791	2.024	0.52511	0.00127	0.52766
cvT20ptch_1_15_8	10,400	921	8,998	255.01	3.11056	2.121	0.52789	0.00116	0.53022

Table 6.9.6-19b. Results for $UZrH_x$ content spacing in CV calculation model

case name	$UZrH_x$ (g)	^{235}U (g)	H_2O (g)	h/x	pitch (cm)	pitch (in	k_{eff}	σ	k_{eff}+2σ
cvT20ptch_1_15_9	10,400	921	8,998	255.01	3.25321	2.218	0.52959	0.00109	0.53177
cvT20ptch_1_15_10	10,400	921	8,998	255.01	3.39586	2.316	0.52841	0.00115	0.53072
cvT20ptch_1_15_11	10,400	921	8,998	255.01	3.53851	2.413	0.52767	0.00109	0.52985
mocfr=0.9									
cvT20ptch_1_14_1	10,400	921	8,098	229.51	2.11201	1.440	0.46727	0.00112	0.46951
cvT20ptch_1_14_6	10,400	921	8,098	229.51	2.82526	1.927	0.50042	0.00110	0.50263
cvT20ptch_1_14_11	10,400	921	8,098	229.51	3.53851	2.413	0.51015	0.00114	0.51244
mocfr=0.8									
cvT20ptch_1_13_1	10,400	921	7,199	204.00	2.11201	1.440	0.44680	0.00107	0.44894
cvT20ptch_1_13_6	10,400	921	7,199	204.00	2.82526	1.927	0.47920	0.00102	0.48124
cvT20ptch_1_13_11	10,400	921	7,199	204.00	3.53851	2.413	0.49183	0.00115	0.49413
mocfr=0.7									
cvT20ptch_1_12_1	10,400	921	6,299	178.50	2.11201	1.440	0.43179	0.00117	0.43413
cvT20ptch_1_12_6	10,400	921	6,299	178.50	2.82526	1.927	0.45630	0.00123	0.45875
cvT20ptch_1_12_11	10,400	921	6,299	178.50	3.53851	2.413	0.46790	0.00112	0.47014
mocfr=0.6									
cvT20ptch_1_11_1	10,400	921	5,399	153.00	2.11201	1.440	0.41313	0.00109	0.41531
cvT20ptch_1_11_6	10,400	921	5,399	153.00	2.82526	1.927	0.43561	0.00115	0.43792
cvT20ptch_1_11_11	10,400	921	5,399	153.00	3.53851	2.413	0.44764	0.00100	0.44964
mocfr=0.5									
cvT20ptch_1_10_1	10,400	921	4,499	127.50	2.11201	1.440	0.39451	0.00106	0.39664
cvT20ptch_1_10_6	10,400	921	4,499	127.50	2.82526	1.927	0.41120	0.00128	0.41376
cvT20ptch_1_10_11	10,400	921	4,499	127.50	3.53851	2.413	0.42438	0.00120	0.42678

Table 6.9.6-19b. Results for $UZrH_x$ content spacing in CV calculation model

case name	$UZrH_x$ (g)	^{235}U (g)	H_2O (g)	h/x	pitch (cm)	pitch (in	k_{eff}	σ	k_{eff}+2σ
mocfr=0.4									
cvT20ptch_1_9_1	10,400	921	3,599	102.00	2.11201	1.440	0.38008	0.00097	0.38203
cvT20ptch_1_9_6	10,400	921	3,599	102.00	2.82526	1.927	0.39106	0.00098	0.39303
cvT20ptch_1_9_11	10,400	921	3,599	102.00	3.53851	2.413	0.40267	0.00126	0.40519
mocfr=0.3									
cvT20ptch_1_8_1	10,400	921	2,700	76.50	2.11201	1.440	0.36348	0.00091	0.36531
cvT20ptch_1_8_6	10,400	921	2,700	76.50	2.82526	1.927	0.37106	0.00102	0.37309
cvT20ptch_1_8_11	10,400	921	2,700	76.50	3.53851	2.413	0.38210	0.00098	0.38406
mocfr=0.2									
cvT20ptch_1_7_1	10,400	921	1,800	51.00	2.11201	1.440	0.35255	0.00094	0.35443
cvT20ptch_1_7_6	10,400	921	1,800	51.00	2.82526	1.927	0.35542	0.00089	0.35721
cvT20ptch_1_7_11	10,400	921	1,800	51.00	3.53851	2.413	0.36444	0.00091	0.36627
mocfr=0.1									
cvT20ptch_1_6_1	10,400	921	900	25.50	2.11201	1.440	0.34383	0.00115	0.34612
cvT20ptch_1_6_6	10,400	921	900	25.50	2.82526	1.927	0.34516	0.00093	0.34703
cvT20ptch_1_6_11	10,400	921	900	25.50	3.53851	2.413	0.35189	0.00102	0.35394
mocfr=1.0e-20									
cvT20ptch_1_1_1	10,400	921	0	0.00	2.11201	1.440	0.34314	0.00084	0.34482
cvT20ptch_1_1_6	10,400	921	0	0.00	2.82526	1.927	0.34273	0.00089	0.34452
cvT20ptch_1_1_11	10,400	921	0	0.00	3.53851	2.413	0.34291	0.00087	0.34466

Table 6.9.6-19c. Results for $UZrH_x$ content uranium weight fraction in CV calculation model

case name	$UZrH_x$ (g)	^{235}U (g)	H_2O (g)	h/x	mocfr	k_{eff}	σ	$k_{eff}+2σ$
TRIGA ($UZrH_x$) fuel content at 19.7 wt % ^{235}U, variation of uranium weight fraction in content								
500 g CH_2 in cc, no can spacers (np thickness = 0.0 in.), containment vessel, reflected								
45 Wt.% U								
cvTE20U45_1_15	10,400	921	8,998	255.01	1.0e+00	0.52494	0.00120	0.52735
cvTE20U45_1_14	10,400	921	8,098	229.51	9.0e-01	0.50284	0.00114	0.50511
cvTE20U45_1_13	10,400	921	7,199	204.00	8.0e-01	0.48121	0.00136	0.48393
cvTE20U45_1_12	10,400	921	6,299	178.50	7.0e-01	0.45681	0.00116	0.45914
cvTE20U45_1_11	10,400	921	5,399	153.00	6.0e-01	0.43399	0.00108	0.43616
cvTE20U45_1_10	10,400	921	4,499	127.50	5.0e-01	0.41521	0.00099	0.41719
cvTE20U45_1_9	10,400	921	3,599	102.00	4.0e-01	0.38978	0.00115	0.39209
cvTE20U45_1_8	10,400	921	2,700	76.50	3.0e-01	0.37291	0.00103	0.37496
cvTE20U45_1_7	10,400	921	1,800	51.00	2.0e-01	0.35869	0.00094	0.36057
cvTE20U45_1_6	10,400	921	900	25.50	1.0e-01	0.34704	0.00101	0.34905
cvTE20U45_1_1	10,400	921	0	0.00	1.0e-20	0.34219	0.00107	0.34432
30 Wt.% U								
cvTE20U30_1_15	8,250	489	8,998	480.29	1.0e+00	0.47671	0.00135	0.47942
cvTE20U30_1_14	8,250	489	8,098	432.26	9.0e-01	0.45562	0.00105	0.45772
cvTE20U30_1_13	8,250	489	7,199	384.23	8.0e-01	0.43218	0.00113	0.43445
cvTE20U30_1_12	8,250	489	6,299	336.20	7.0e-01	0.41165	0.00096	0.41356
cvTE20U30_1_11	8,250	489	5,399	288.17	6.0e-01	0.38706	0.00099	0.38903
cvTE20U30_1_10	8,250	489	4,499	240.14	5.0e-01	0.36759	0.00092	0.36944
cvTE20U30_1_9	8,250	489	3,599	192.11	4.0e-01	0.34766	0.00094	0.34954
cvTE20U30_1_8	8,250	489	2,700	144.09	3.0e-01	0.33073	0.00086	0.33245
cvTE20U30_1_7	8,250	489	1,800	96.06	2.0e-01	0.31555	0.00082	0.31720

Table 6.9.6-19c. Results for $UZrH_x$ content uranium weight fraction in CV calculation model

case name	$UZrH_x$ (g)	^{235}U (g)	H_2O (g)	h/x	mocfr	k_{eff}	σ	$k_{eff}+2σ$
cvTE20U30_1_6	8,250	489	900	48.03	1.0e-01	0.31018	0.00092	0.31202
cvTE20U30_1_01	8,250	489	0	0.00	1.0e-20	0.30488	0.00083	0.30654
20 Wt.% U								
cvTE20U20_1_15	7,545	297	8,998	790.78	1.0e+00	0.46046	0.00121	0.46289
cvTE20U20_1_14	7,545	297	8,098	711.70	9.0e-01	0.43928	0.00114	0.44156
cvTE20U20_1_13	7,545	297	7,199	632.62	8.0e-01	0.41486	0.00108	0.41702
cvTE20U20_1_12	7,545	297	6,299	553.54	7.0e-01	0.39584	0.00113	0.39809
cvTE20U20_1_11	7,545	297	5,399	474.47	6.0e-01	0.37399	0.00106	0.37612
cvTE20U20_1_10	7,545	297	4,499	395.39	5.0e-01	0.35345	0.00100	0.35545
cvTE20U20_1_9	7,545	297	3,599	316.31	4.0e-01	0.33290	0.00098	0.33486
cvTE20U20_1_8	7,545	297	2,700	237.23	3.0e-01	0.31513	0.00103	0.31719
cvTE20U20_1_7	7,545	297	1,800	158.16	2.0e-01	0.30148	0.00101	0.30350
cvTE20U20_1_6	7,545	297	900	79.08	1.0e-01	0.29354	0.00089	0.29532
cvTE20U20_1_1	7,545	297	0	0.00	1.0e-20	0.29227	0.00083	0.29392
12 Wt.% U								
cvTE20U12_1_15	7,125	168	8,998	1397.90	1.0e+00	0.44948	0.00108	0.45163
cvTE20U12_1_14	7,125	168	8,098	1258.10	9.0e-01	0.43067	0.00106	0.43280
cvTE20U12_1_13	7,125	168	7,199	1118.30	8.0e-01	0.40699	0.00098	0.40894
cvTE20U12_1_12	7,125	168	6,299	978.59	7.0e-01	0.38549	0.00098	0.38744
cvTE20U12_1_11	7,125	168	5,399	838.79	6.0e-01	0.36416	0.00089	0.36595
cvTE20U12_1_10	7,125	168	4,499	698.99	5.0e-01	0.34375	0.00106	0.34586
cvTE20U12_1_9	7,125	168	3,599	559.19	4.0e-01	0.32505	0.00108	0.32721
cvTE20U12_1_8	7,125	168	2,700	419.40	3.0e-01	0.30767	0.00087	0.30940
cvTE20U12_1_7	7,125	168	1,800	279.60	2.0e-01	0.29545	0.00076	0.29698

Table 6.9.6-19c. Results for $UZrH_x$ content uranium weight fraction in CV calculation model

case name	$UZrH_x$ (g)	^{235}U (g)	H_2O (g)	h/x	mocfr	k_{eff}	σ	$k_{eff}+2σ$
cvTE20U12_1_6	7,125	168	900	139.80	1.0e-01	0.28602	0.00086	0.28774
cvTE20U12_1_1	7,125	168	0	0.00	1.0e-20	0.28442	0.00079	0.28601
8.5 Wt.% U								
cvTE20U8p5_1_15	6,953	117	8,998	2007.30	1.0e+00	0.44412	0.00115	0.44643
cvTE20U8p5_1_14	6,953	117	8,098	1806.60	9.0e-01	0.42328	0.00110	0.42549
cvTE20U8p5_1_13	6,953	117	7,199	1605.80	8.0e-01	0.40452	0.00100	0.40652
cvTE20U8p5_1_12	6,953	117	6,299	1405.10	7.0e-01	0.38253	0.00122	0.38496
cvTE20U8p5_1_11	6,953	117	5,399	1204.40	6.0e-01	0.35988	0.00111	0.36209
cvTE20U8p5_1_10	6,953	117	4,499	1003.60	5.0e-01	0.33974	0.00099	0.34173
cvTE20U8p5_1_9	6,953	117	3,599	802.94	4.0e-01	0.31938	0.00090	0.32118
cvTE20U8p5_1_8	6,953	117	2,700	602.20	3.0e-01	0.30560	0.00084	0.30729
cvTE20U8p5_1_7	6,953	117	1,800	401.47	2.0e-01	0.29237	0.00085	0.29407
cvTE20U8p5_1_6	6,953	117	900	200.73	1.0e-01	0.28287	0.00104	0.28495
cvTE20U8p5_1_1	6,953	117	0	0.00	1.0e-20	0.28060	0.00080	0.28219
500 g CH_2 in cc, can spacers (np thickness = 1.4 in.), containment vessel, reflected								
cvTE20U45_02_15	10,400	921	8,385	237.62	1.0e+00	0.42157	0.00099	0.42354
cvTE20U30_02_15	8,250	489	8,385	447.54	1.0e+00	0.37862	0.00092	0.38046
cvTE20U20_02_15	7,545	297	8,385	736.86	1.0e+00	0.36052	0.00089	0.36229
cvTE20U12_02_15	7,125	168	8,385	1302.60	1.0e+00	0.35193	0.00100	0.35392
cvTE20U8p5_02_15	6,953	117	8,385	1870.40	1.0e+00	0.34847	0.00108	0.35064

Table 6.9.6-20a. Results for $UZrH_x$ content at 19.7 wt % ^{235}U in packaging calculation model

case name	np (in)	$UZrH_x$ (g)	^{235}U (g)	H_2O (g)	h/x	mocfr/ moifr	k_{eff}	σ	$k_{eff}+2σ$	case name	k_{eff}	σ	$k_{eff}+2σ$
content in flooded containment vessel, single package reflected													
NCT										HAC			
no can spacers (np thickness = 0.0 in.)													
mocfr													
ncsrtriga_1_1_15	0.0	10,400	921	0	0.00	1.0e-20	0.19699	0.00072	0.19844	hcsrtriga_1_1_15	0.19912	0.00071	0.20055
ncsrtriga_1_6_15	0.0	10,400	921	900	25.50	1.0e-01	0.22100	0.00077	0.22253	hcsrtriga_1_6_15	0.22405	0.00077	0.22559
ncsrtriga_1_7_15	0.0	10,400	921	1,800	51.00	2.0e-02	0.25006	0.00081	0.25167	hcsrtriga_1_7_15	0.25119	0.00075	0.25268
ncsrtriga_1_8_15	0.0	10,400	921	2,700	76.50	3.0e-01	0.27901	0.00083	0.28067	hcsrtriga_1_8_15	0.28071	0.00086	0.28243
ncsrtriga_1_9_15	0.0	10,400	921	3,599	102.00	4.0e-01	0.31206	0.00097	0.31399	hcsrtriga_1_9_15	0.31333	0.00093	0.31520
ncsrtriga_1_10_15	0.0	10,400	921	4,499	127.50	5.0e-01	0.34408	0.00096	0.34601	hcsrtriga_1_10_15	0.34576	0.00103	0.34781
ncsrtriga_1_11_15	0.0	10,400	921	5,399	153.00	6.0e-01	0.37488	0.00093	0.37674	hcsrtriga_1_11_15	0.37800	0.00111	0.38023
ncsrtriga_1_12_15	0.0	10,400	921	6,299	178.50	7.0e-01	0.40792	0.00107	0.41006	hcsrtriga_1_12_15	0.40683	0.00105	0.40893
ncsrtriga_1_13_15	0.0	10,400	921	7,199	204.00	8.0e-01	0.43782	0.00116	0.44013	hcsrtriga_1_13_15	0.43867	0.00123	0.44113
ncsrtriga_1_14_15	0.0	10,400	921	8,098	229.51	9.0e-01	0.46460	0.00106	0.46672	hcsrtriga_1_14_15	0.46627	0.00120	0.46867
ncsrtriga_1_15_15	0.0	10,400	921	8,998	255.01	1.0e+00	0.49295	0.00104	0.49503	hcsrtriga_1_15_15	0.49247	0.00103	0.49454
moifr													
ncsrtriga_1_15_1	0.0	10,400	921	8,998	255.01	1.0e-20	0.44499	0.00100	0.44700	hcsrtriga_1_15_1	0.44706	0.00104	0.44914
ncsrtriga_1_15_2	0.0	10,400	921	8,998	255.01	1.0e-05	0.44282	0.00109	0.44500	hcsrtriga_1_15_2	0.44626	0.00100	0.44825
ncsrtriga_1_15_3	0.0	10,400	921	8,998	255.01	1.0e-04	0.44454	0.00120	0.44693	hcsrtriga_1_15_3	0.44469	0.00125	0.44719
ncsrtriga_1_15_4	0.0	10,400	921	8,998	255.01	1.0e-03	0.44553	0.00111	0.44774	hcsrtriga_1_15_4	0.44692	0.00113	0.44918
ncsrtriga_1_15_5	0.0	10,400	921	8,998	255.01	1.0e-02	0.44389	0.00121	0.44631	hcsrtriga_1_15_5	0.44565	0.00104	0.44773
ncsrtriga_1_15_6	0.0	10,400	921	8,998	255.01	1.0e-01	0.44801	0.00104	0.45008	hcsrtriga_1_15_6	0.45115	0.00120	0.45356
ncsrtriga_1_15_8	0.0	10,400	921	8,998	255.01	3.0e-01	0.45921	0.00143	0.46207	hcsrtriga_1_15_8	0.46090	0.00112	0.46314
ncsrtriga_1_15_15	0.0	10,400	921	8,998	255.01	1.0e+00	0.49295	0.00104	0.49503	hcsrtriga_1_15_15	0.49247	0.00103	0.49454

Table 6.9.6-20a. Results for $UZrH_x$ content at 19.7 wt % ^{235}U in packaging calculation model

case name	np (in)	$UZrH_x$ (g)	^{235}U (g)	H_2O (g)	h/x	mocfr/ moifr	k_{eff}	σ	$k_{eff}+2σ$	case name	k_{eff}	σ	$k_{eff}+2σ$
with can spacers (np thickness = 1.4 in.)													
mocfr													
ncsrtriga_2_1_15	1.4	10,400	921	0	0.00	1.0e-20	0.16519	0.00060	0.16640	hcsrtriga_2_1_15	0.16449	0.00062	0.16573
ncsrtriga_2_6_15	1.4	10,400	921	839	23.76	1.0e-01	0.18078	0.00063	0.18204	hcsrtriga_2_6_15	0.18163	0.00061	0.18284
ncsrtriga_2_7_15	1.4	10,400	921	1,677	47.52	2.0e-01	0.20001	0.00066	0.20133	hcsrtriga_2_7_15	0.20112	0.00072	0.20256
ncsrtriga_2_8_15	1.4	10,400	921	2,515	71.29	3.0e-01	0.22235	0.00085	0.22405	hcsrtriga_2_8_15	0.22446	0.00079	0.22603
ncsrtriga_2_9_15	1.4	10,400	921	3,354	95.05	4.0e-01	0.24785	0.00076	0.24936	hcsrtriga_2_9_15	0.24932	0.00079	0.25090
ncsrtriga_2_10_15	1.4	10,400	921	4,192	118.81	5.0e-01	0.27336	0.00091	0.27517	hcsrtriga_2_10_15	0.27427	0.00084	0.27595
ncsrtriga_2_11_15	1.4	10,400	921	5,031	142.57	6.0e-01	0.29864	0.00105	0.30075	hcsrtriga_2_11_15	0.30007	0.00090	0.30188
ncsrtriga_2_12_15	1.4	10,400	921	5,869	166.33	7.0e-01	0.32492	0.00094	0.32680	hcsrtriga_2_12_15	0.32594	0.00113	0.32820
ncsrtriga_2_13_15	1.4	10,400	921	6,708	190.09	8.0e-01	0.35137	0.00101	0.35339	hcsrtriga_2_13_15	0.35174	0.00101	0.35375
ncsrtriga_2_14_15	1.4	10,400	921	7,546	213.86	9.0e-01	0.37602	0.00105	0.37812	hcsrtriga_2_14_15	0.37666	0.00093	0.37852
ncsrtriga_2_15_15	1.4	10,400	921	8,385	237.62	1.0e+00	0.40040	0.00106	0.40252	hcsrtriga_2_15_15	0.40020	0.00112	0.40244
moifr													
ncsrtriga_2_15_1	1.4	10,400	921	8,385	237.62	1.0e-20	0.36082	0.00102	0.36286	hcsrtriga_2_15_1	0.36370	0.00103	0.36576
ncsrtriga_2_15_2	1.4	10,400	921	8,385	237.62	1.0e-05	0.36163	0.00105	0.36373	hcsrtriga_2_15_2	0.36457	0.00097	0.36651
ncsrtriga_2_15_3	1.4	10,400	921	8,385	237.62	1.0e-04	0.36349	0.00115	0.36579	hcsrtriga_2_15_3	0.36369	0.00107	0.36584
ncsrtriga_2_15_4	1.4	10,400	921	8,385	237.62	1.0e-03	0.36368	0.00093	0.36554	hcsrtriga_2_15_4	0.36290	0.00107	0.36503
ncsrtriga_2_15_5	1.4	10,400	921	8,385	237.62	1.0e-02	0.36298	0.00111	0.36520	hcsrtriga_2_15_5	0.36275	0.00112	0.36498
ncsrtriga_2_15_6	1.4	10,400	921	8,385	237.62	1.0e-01	0.36587	0.00090	0.36766	hcsrtriga_2_15_6	0.37015	0.00095	0.37205
ncsrtriga_2_15_8	1.4	10,400	921	8,385	237.62	3.0e-01	0.37454	0.00104	0.37662	hcsrtriga_2_15_8	0.37482	0.00099	0.37680
ncsrtriga_2_15_15	1.4	10,400	921	8,385	237.62	1.0e+00	0.40040	0.00106	0.40252	hcsrtriga_2_15_15	0.40020	0.00112	0.40244

Table 6.9.6-20a. Results for $UZrH_x$ content at 19.7 wt % ^{235}U in packaging calculation model

case name	np (in)	$UZrH_x$ (g)	^{235}U (g)	H_2O (g)	h/x	mocfr/ moifr	k_{eff}	σ	$k_{eff}+2σ$	case name	k_{eff}	σ	$k_{eff}+2σ$
content in flooded containment vessel, array packaging model for CSI=0.0													
NCT										HAC			
no can spacers (np thickness = 0.0 in.)													
moifr													
nciatriga_1_1_3	0.0	10,400	921	0	0.00	1.0e-04	0.21653	0.00055	0.21763	hciatriga_1_1_3	0.21640	0.00062	0.21763
nciatriga_1_6_3	0.0	10,400	921	900	25.50	1.0e-04	0.24325	0.00064	0.24453	hciatriga_1_6_3	0.24355	0.00069	0.24493
nciatriga_1_7_3	0.0	10,400	921	1,800	51.00	1.0e-04	0.27402	0.00079	0.27561	hciatriga_1_7_3	0.27398	0.00073	0.27544
nciatriga_1_8_3	0.0	10,400	921	2,700	76.50	1.0e-04	0.30790	0.00105	0.30999	hciatriga_1_8_3	0.30795	0.00081	0.30958
nciatriga_1_9_3	0.0	10,400	921	3,599	102.00	1.0e-04	0.34171	0.00109	0.34390	hciatriga_1_9_3	0.34285	0.00108	0.34500
nciatriga_1_10_3	0.0	10,400	921	4,499	127.50	1.0e-04	0.37614	0.00108	0.37830	hciatriga_1_10_3	0.37487	0.00101	0.37689
nciatriga_1_11_3	0.0	10,400	921	5,399	153.00	1.0e-04	0.40944	0.00101	0.41146	hciatriga_1_11_3	0.40922	0.00099	0.41120
nciatriga_1_12_3	0.0	10,400	921	6,299	178.50	1.0e-04	0.44034	0.00116	0.44267	hciatriga_1_12_3	0.44217	0.00104	0.44426
nciatriga_1_13_3	0.0	10,400	921	7,199	204.00	1.0e-04	0.46949	0.00102	0.47153	hciatriga_1_13_3	0.46841	0.00104	0.47049
nciatriga_1_14_3	0.0	10,400	921	8,098	229.51	1.0e-04	0.49678	0.00102	0.49881	hciatriga_1_14_3	0.49952	0.00113	0.50179
nciatriga_1_15_3	0.0	10,400	921	8,998	255.01	1.0e-04	0.52325	0.00109	0.52543	hciatriga_1_15_3	0.52373	0.00117	0.52606
with can spacers (np thickness = 1.4 in.)													
nciatriga_2_1_3	1.4	10,400	921	0	0.00	1.0e-04	0.19663	0.00056	0.19775	hciatriga_2_1_3	0.19533	0.00058	0.19648
nciatriga_2_6_3	1.4	10,400	921	839	23.76	1.0e-04	0.21458	0.00063	0.21583	hciatriga_2_6_3	0.21404	0.00062	0.21528
nciatriga_2_7_3	1.4	10,400	921	1,677	47.52	1.0e-04	0.23878	0.00069	0.24017	hciatriga_2_7_3	0.23939	0.00065	0.24068
nciatriga_2_8_3	1.4	10,400	921	2,515	71.29	1.0e-04	0.26268	0.00095	0.26458	hciatriga_2_8_3	0.26265	0.00073	0.26410
nciatriga_2_9_3	1.4	10,400	921	3,354	95.05	1.0e-04	0.28930	0.00075	0.29081	hciatriga_2_9_3	0.29016	0.00077	0.29169
nciatriga_2_10_3	1.4	10,400	921	4,192	118.81	1.0e-04	0.31695	0.00092	0.31879	hciatriga_2_10_3	0.31775	0.00088	0.31951
nciatriga_2_11_3	1.4	10,400	921	5,031	142.57	1.0e-04	0.34183	0.00090	0.34364	hciatriga_2_11_3	0.34164	0.00096	0.34355
nciatriga_2_12_3	1.4	10,400	921	5,869	166.33	1.0e-04	0.36766	0.00092	0.36949	hciatriga_2_12_3	0.36733	0.00102	0.36937

Table 6.9.6-20a. Results for $UZrH_x$ content at 19.7 wt % ^{235}U in packaging calculation model

case name	np (in)	$UZrH_x$ (g)	^{235}U (g)	H_2O (g)	h/x	mocfr/ moifr	k_{eff}	σ	$k_{eff}+2σ$	case name	k_{eff}	σ	$k_{eff}+2σ$
nciatriga_2_13_3	1.4	10,400	921	6,708	190.09	1.0e-04	0.39176	0.00122	0.39420	hciatriga_2_13_3	0.39342	0.00103	0.39547
nciatriga_2_14_3	1.4	10,400	921	7,546	213.86	1.0e-04	0.41783	0.00101	0.41986	hciatriga_2_14_3	0.41760	0.00108	0.41976
nciatriga_2_15_3	1.4	10,400	921	8,385	237.62	1.0e-04	0.43993	0.00109	0.44211	hciatriga_2_15_3	0.44034	0.00119	0.44271

Table 6.9.6-20b. Results for $UZrH_x$ content at 70.1 wt % ^{235}U in packaging calculation model

case name	np (in)	$UZrH_x$ (g)	^{235}U (g)	H_2O (g)	h/x	mocfr/ moifr	k_{eff}	σ	$k_{eff}+2σ$	case name	k_{eff}	σ	$k_{eff}+2σ$
content in flooded containment vessel, single package reflected													
NCT										HAC			
no can spacers (np thickness = 0.0 in.)													
moifr													
ncsrtriga70_1_1_15	0.0	6,847	408	0	0.00	1.0e+00	0.15814	0.00073	0.15960	hcsrtriga70_1_1_15	0.15823	0.00062	0.15947
ncsrtriga70_1_6_15	0.0	6,847	408	900	57.56	1.0e+00	0.18268	0.00068	0.18403	hcsrtriga70_1_6_15	0.18526	0.00075	0.18676
ncsrtriga70_1_7_15	0.0	6,847	408	1,800	115.13	1.0e+00	0.21248	0.00074	0.21396	hcsrtriga70_1_7_15	0.21376	0.00082	0.21540
ncsrtriga70_1_8_15	0.0	6,847	408	2,700	172.69	1.0e+00	0.24596	0.00086	0.24769	hcsrtriga70_1_8_15	0.24666	0.00081	0.24829
ncsrtriga70_1_9_15	0.0	6,847	408	3,599	230.26	1.0e+00	0.27756	0.00103	0.27963	hcsrtriga70_1_9_15	0.27837	0.00085	0.28007
ncsrtriga70_1_10_15	0.0	6,847	408	4,499	287.82	1.0e+00	0.30903	0.00102	0.31107	hcsrtriga70_1_10_15	0.31172	0.00101	0.31374
ncsrtriga70_1_11_15	0.0	6,847	408	5,399	345.38	1.0e+00	0.34331	0.00121	0.34573	hcsrtriga70_1_11_15	0.34406	0.00110	0.34626
ncsrtriga70_1_12_15	0.0	6,847	408	6,299	402.95	1.0e+00	0.37320	0.00129	0.37578	hcsrtriga70_1_12_15	0.37419	0.00109	0.37637
ncsrtriga70_1_13_15	0.0	6,847	408	7,199	460.51	1.0e+00	0.40369	0.00106	0.40581	hcsrtriga70_1_13_15	0.40592	0.00110	0.40811
ncsrtriga70_1_14_15	0.0	6,847	408	8,098	518.07	1.0e+00	0.43096	0.00129	0.43353	hcsrtriga70_1_14_15	0.42993	0.00109	0.43212
ncsrtriga70_1_15_15	0.0	6,847	408	8,998	575.64	1.0e+00	0.45846	0.00117	0.46080	hcsrtriga70_1_15_15	0.45656	0.00108	0.45872

Table 6.9.6-20b. Results for $UZrH_x$ content at 70.1 wt % ^{235}U in packaging calculation model

case name	np (in)	$UZrH_x$ (g)	^{235}U (g)	H_2O (g)	h/x	mocfr/ moifr	k_{eff}	σ	$k_{eff}+2σ$	case name	k_{eff}	σ	$k_{eff}+2σ$
moifr													
ncsrtriga70_1_15_1	0.0	6,847	408	8,998	575.64	1.0e-20	0.40894	0.00119	0.41131	hcsrtriga70_1_15_1_	0.41076	0.00122	0.41320
ncsrtriga70_1_15_2	0.0	6,847	408	8,998	575.64	1.0e-05	0.40806	0.00115	0.41036	hcsrtriga70_1_15_2	0.41073	0.00130	0.41332
ncsrtriga70_1_15_3	0.0	6,847	408	8,998	575.64	1.0e-04	0.40992	0.00118	0.41228	hcsrtriga70_1_15_3	0.41080	0.00120	0.41319
ncsrtriga70_1_15_4	0.0	6,847	408	8,998	575.64	1.0e-03	0.41084	0.00110	0.41304	hcsrtriga70_1_15_4	0.41181	0.00115	0.41412
ncsrtriga70_1_15_5	0.0	6,847	408	8,998	575.64	1.0e-02	0.41069	0.00116	0.41300	hcsrtriga70_1_15_5	0.41159	0.00124	0.41407
ncsrtriga70_1_15_6	0.0	6,847	408	8,998	575.64	1.0e-01	0.41431	0.00107	0.41644	hcsrtriga70_1_15_6	0.41621	0.00123	0.41868
ncsrtriga70_1_15_8	0.0	6,847	408	8,998	575.64	3.0e-01	0.42523	0.00129	0.42780	hcsrtriga70_1_15_8	0.42893	0.00120	0.43133
ncsrtriga70_1_15_15	0.0	6,847	408	8,998	575.64	1.0e+00	0.45846	0.00117	0.46080	hcsrtriga70_1_15_15	0.45656	0.00108	0.45872
with can spacers (np thickness = 1.4 in.)													
moifr													
ncsrtriga70_2_1_15	1.4	6,847	408	0	0.00	1.0e+00	0.12174	0.00059	0.12291	hcsrtriga70_2_1_15	0.12413	0.00057	0.12528
ncsrtriga70_2_6_15	1.4	6,847	408	839	53.64	1.0e+00	0.14017	0.00063	0.14143	hcsrtriga70_2_6_15	0.14097	0.00061	0.14220
ncsrtriga70_2_7_15	1.4	6,847	408	1,677	107.28	1.0e+00	0.16109	0.00066	0.16241	hcsrtriga70_2_7_15	0.16260	0.00068	0.16396
ncsrtriga70_2_8_15	1.4	6,847	408	2,515	160.92	1.0e+00	0.18174	0.00080	0.18335	hcsrtriga70_2_8_15	0.18552	0.00067	0.18686
ncsrtriga70_2_9_15	1.4	6,847	408	3,354	214.55	1.0e+00	0.20707	0.00076	0.20859	hcsrtriga70_2_9_15	0.20911	0.00077	0.21064
ncsrtriga70_2_10_15	1.4	6,847	408	4,192	268.19	1.0e+00	0.23324	0.00089	0.23503	hcsrtriga70_2_10_15	0.23447	0.00074	0.23595
ncsrtriga70_2_11_15	1.4	6,847	408	5,031	321.83	1.0e+00	0.26093	0.00080	0.26254	hcsrtriga70_2_11_15	0.26039	0.00085	0.26209
ncsrtriga70_2_12_15	1.4	6,847	408	5,869	375.47	1.0e+00	0.28710	0.00084	0.28878	hcsrtriga70_2_12_15	0.28784	0.00093	0.28970
ncsrtriga70_2_13_15	1.4	6,847	408	6,708	429.11	1.0e+00	0.30929	0.00098	0.31124	hcsrtriga70_2_13_15	0.31105	0.00093	0.31291
ncsrtriga70_2_14_15	1.4	6,847	408	7,546	482.75	1.0e+00	0.33473	0.00114	0.33702	hcsrtriga70_2_14_15	0.33634	0.00094	0.33822
ncsrtriga70_2_15_15	1.4	6,847	408	8,385	536.39	1.0e+00	0.35776	0.00116	0.36008	hcsrtriga70_2_15_15	0.35922	0.00110	0.36142
moifr													
ncsrtriga70_2_15_1	1.4	6,847	408	8,385	536.39	1.0e-20	0.32321	0.00094	0.32508	hcsrtriga70_2_15_1	0.32561	0.00106	0.32774
ncsrtriga70_2_15_2	1.4	6,847	408	8,385	536.39	1.0e-05	0.32283	0.00092	0.32467	hcsrtriga70_2_15_2	0.32441	0.00099	0.32639

Table 6.9.6-20b. Results for $UZrH_x$ content at 70.1 wt % ^{235}U in packaging calculation model

case name	np (in)	$UZrH_x$ (g)	^{235}U (g)	H_2O (g)	h/x	mocfr/ moifr	k_{eff}	σ	$k_{eff}+2σ$	case name	k_{eff}	σ	$k_{eff}+2σ$
ncsrtriga70_2_15_3	1.4	6,847	408	8,385	536.39	1.0e-04	0.32432	0.00088	0.32608	hcsrtriga70_2_15_3	0.32423	0.00102	0.32628
ncsrtriga70_2_15_4	1.4	6,847	408	8,385	536.39	1.0e-03	0.32279	0.00104	0.32488	hcsrtriga70_2_15_4	0.32600	0.00111	0.32822
ncsrtriga70_2_15_5	1.4	6,847	408	8,385	536.39	1.0e-02	0.32448	0.00105	0.32658	hcsrtriga70_2_15_5	0.32622	0.00093	0.32808
ncsrtriga70_2_15_6	1.4	6,847	408	8,385	536.39	1.0e-01	0.32871	0.00097	0.33065	hcsrtriga70_2_15_6	0.32929	0.00110	0.33150
ncsrtriga70_2_15_8	1.4	6,847	408	8,385	536.39	3.0e-01	0.33627	0.00091	0.33809	hcsrtriga70_2_15_8	0.33709	0.00106	0.33920
ncsrtriga70_2_15_15	1.4	6,847	408	8,385	536.39	1.0e+00	0.35776	0.00116	0.36008	hcsrtriga70_2_15_15	0.35922	0.00110	0.36142
content in flooded containment vessel, array packaging model for CSI=0.0													
NCT										**HAC**			
no can spacers (np thickness = 0.0 in.)													
moifr													
nciatriga70_1_1_3	0.0	6,847	408	0	0.00	1.0e-04	0.16525	0.00063	0.16651	hciatriga70_1_1_3	0.16514	0.00067	0.16648
nciatriga70_1_6_3	0.0	6,847	408	900	57.56	1.0e-04	0.19360	0.00070	0.19500	hciatriga70_1_6_3	0.19280	0.00066	0.19411
nciatriga70_1_7_3	0.0	6,847	408	1,800	115.13	1.0e-04	0.22946	0.00076	0.23099	hciatriga70_1_7_3	0.23027	0.00076	0.23179
nciatriga70_1_8_3	0.0	6,847	408	2,700	172.69	1.0e-04	0.26461	0.00087	0.26635	hciatriga70_1_8_3	0.26463	0.00074	0.26612
nciatriga70_1_9_3	0.0	6,847	408	3,599	230.26	1.0e-04	0.30186	0.00095	0.30375	hciatriga70_1_9_3	0.30020	0.00084	0.30187
nciatriga70_1_10_3	0.0	6,847	408	4,499	287.82	1.0e-04	0.33608	0.00095	0.33798	hciatriga70_1_10_3	0.33776	0.00089	0.33954
nciatriga70_1_11_3	0.0	6,847	408	5,399	345.38	1.0e-04	0.37069	0.00105	0.37279	hciatriga70_1_11_3	0.37191	0.00104	0.37400
nciatriga70_1_12_3	0.0	6,847	408	6,299	402.95	1.0e-04	0.40431	0.00110	0.40651	hciatriga70_1_12_3	0.40368	0.00099	0.40567
nciatriga70_1_13_3	0.0	6,847	408	7,199	460.51	1.0e-04	0.43185	0.00143	0.43472	hciatriga70_1_13_3	0.43386	0.00141	0.43668
nciatriga70_1_14_3	0.0	6,847	408	8,098	518.07	1.0e-04	0.46029	0.00122	0.46272	hciatriga70_1_14_3	0.46036	0.00120	0.46277
nciatriga70_1_15_3	0.0	6,847	408	8,998	575.64	1.0e-04	0.48628	0.00123	0.48875	hciatriga70_1_15_3	0.48653	0.00107	0.48868
with can spacers (np thickness = 1.4 in.)													
nciatriga70_2_1_3	1.4	6,847	408	0	0.00	1.0e-04	0.14342	0.00054	0.14450	hciatriga70_2_1_3	0.14299	0.00055	0.14410
nciatriga70_2_6_3	1.4	6,847	408	839	53.64	1.0e-04	0.16333	0.00057	0.16446	hciatriga70_2_6_3	0.16444	0.00071	0.16586
nciatriga70_2_7_3	1.4	6,847	408	1,677	107.28	1.0e-04	0.18886	0.00069	0.19024	hciatriga70_2_7_3	0.18870	0.00075	0.19020

Table 6.9.6-20b. Results for $UZrH_x$ content at 70.1 wt % ^{235}U in packaging calculation model

case name	np (in)	$UZrH_x$ (g)	^{235}U (g)	H_2O (g)	h/x	mocfr/ moifr	k_{eff}	σ	$k_{eff}+2σ$	case name	k_{eff}	σ	$k_{eff}+2σ$
nciatriga70_2_8_3	1.4	6,847	408	2,515	160.92	1.0e-04	0.21548	0.00077	0.21703	hciatriga70_2_8_3	0.21709	0.00079	0.21867
nciatriga70_2_9_3	1.4	6,847	408	3,354	214.55	1.0e-04	0.24403	0.00092	0.24587	hciatriga70_2_9_3	0.24443	0.00082	0.24606
nciatriga70_2_10_3	1.4	6,847	408	4,192	268.19	1.0e-04	0.27230	0.00090	0.27410	hciatriga70_2_10_3	0.27167	0.00077	0.27321
nciatriga70_2_11_3	1.4	6,847	408	5,031	321.83	1.0e-04	0.29818	0.00092	0.30003	hciatriga70_2_11_3	0.29902	0.00096	0.30093
nciatriga70_2_12_3	1.4	6,847	408	5,869	375.47	1.0e-04	0.32583	0.00081	0.32745	hciatriga70_2_12_3	0.32607	0.00087	0.32781
nciatriga70_2_13_3	1.4	6,847	408	6,708	429.11	1.0e-04	0.35008	0.00102	0.35212	hciatriga70_2_13_3	0.34964	0.00088	0.35140
nciatriga70_2_14_3	1.4	6,847	408	7,546	482.75	1.0e-04	0.37201	0.00116	0.37434	hciatriga70_2_14_3	0.37167	0.00099	0.37364
nciatriga70_2_15_3	1.4	6,847	408	8,385	536.39	1.0e-04	0.39529	0.00120	0.39769	hciatriga70_2_15_3	0.39403	0.00109	0.39622

Table 6.9.6-20c. Results for 1.31 in. smaller diameter $UZrH_x$ content at 70.1 wt % ^{235}U in packaging calculation model

case name	np (in)	$UZrH_x$ (g)	^{235}U (g)	H_2O (g)	h/x	mocfr/ moifr	k_{eff}	σ	$k_{eff}+2σ$	case name	k_{eff}	σ	$k_{eff}+2σ$
1.31 in. diameter content in flooded containment vessel, single package reflected													
NCT													
no can spacers (np thickness = 0.0 in.)													
mocfr													
ncsrT70_131_1_1_15	0.0	5,667	338	0	0.00	1.0e+00	0.12864	0.00055	0.12974				
ncsrT70_131_1_6_15	0.0	5,667	338	920	71.15	1.0e+00	0.15144	0.00066	0.15276				
ncsrT70_131_1_7_15	0.0	5,667	338	1,841	142.31	1.0e+00	0.18245	0.00065	0.18375				
ncsrT70_131_1_8_15	0.0	5,667	338	2,762	213.46	1.0e+00	0.21360	0.00085	0.21530				
ncsrT70_131_1_9_15	0.0	5,667	338	3,682	284.61	1.0e+00	0.24688	0.00096	0.24880				
ncsrT70_131_1_10_15	0.0	5,667	338	4,602	355.77	1.0e+00	0.28138	0.00101	0.28340				
ncsrT70_131_1_11_15	0.0	5,667	338	5,523	426.92	1.0e+00	0.31377	0.00098	0.31574				

Table 6.9.6-20c. Results for 1.31 in. smaller diameter $UZrH_x$ content at 70.1 wt % ^{235}U in packaging calculation model

case name	np (in)	$UZrH_x$ (g)	^{235}U (g)	H_2O (g)	h/x	mocfr/ moifr	k_{eff}	σ	$k_{eff}+2σ$	case name	k_{eff}	σ	$k_{eff}+2σ$
ncsrT70_131_1_12_15	0.0	5,667	338	6,443	498.07	1.0e+00	0.34582	0.00107	0.34797				
ncsrT70_131_1_13_15	0.0	5,667	338	7,364	569.23	1.0e+00	0.37661	0.00103	0.37867				
ncsrT70_131_1_14_15	0.0	5,667	338	8,284	640.38	1.0e+00	0.40376	0.00110	0.40597				
ncsrT70_131_1_15_15	0.0	5,667	338	9,205	711.53	1.0e+00	0.43000	0.00103	0.43206				
moifr													
ncsrT70_131_1_15_1	0.0	5,667	338	9,205	711.53	1.0e-20	0.38521	0.00136	0.38793				
ncsrT70_131_1_15_2	0.0	5,667	338	9,205	711.53	1.0e-05	0.38339	0.00098	0.38536				
ncsrT70_131_1_15_3	0.0	5,667	338	9,205	711.53	1.0e-04	0.38633	0.00100	0.38834				
ncsrT70_131_1_15_4	0.0	5,667	338	9,205	711.53	1.0e-03	0.38417	0.00096	0.38610				
ncsrT70_131_1_15_5	0.0	5,667	338	9,205	711.53	1.0e-02	0.38613	0.00108	0.38829				
ncsrT70_131_1_15_6	0.0	5,667	338	9,205	711.53	1.0e-01	0.39026	0.00098	0.39222				
ncsrT70_131_1_15_8	0.0	5,667	338	9,205	711.53	3.0e-01	0.40187	0.00122	0.40430				
ncsrT70_131_1_15_15	0.0	5,667	338	9,205	711.53	1.0e+00	0.43000	0.00103	0.43206				
1.31 in. diameter content content in flooded containment vessel, array packaging model for CSI=0.0													
NCT													
no can spacers (np thickness = 0.0 in.)													
moifr													
nciaT70_131_1_1_3	0.0	5,667	338	0	0.00	1.0e-04	0.12954	0.00047	0.13048				
nciaT70_131_1_6_3	0.0	5,667	338	920	71.15	1.0e-04	0.15804	0.00057	0.15918				
nciaT70_131_1_7_3	0.0	5,667	338	1,841	142.31	1.0e-04	0.19290	0.00064	0.19417				
nciaT70_131_1_8_3	0.0	5,667	338	2,762	213.46	1.0e-04	0.22844	0.00085	0.23015				
nciaT70_131_1_9_3	0.0	5,667	338	3,682	284.61	1.0e-04	0.26752	0.00081	0.26914				

Table 6.9.6-20c. Results for 1.31 in. smaller diameter $UZrH_x$ content at 70.1 wt % ^{235}U in packaging calculation model

case name	np (in)	$UZrH_x$ (g)	^{235}U (g)	H_2O (g)	h/x	mocfr/ moifr	k_{eff}	σ	$k_{eff}+2σ$	case name	k_{eff}	σ	$k_{eff}+2σ$
nciaT70_131_1_10_3	0.0	5,667	338	4,602	355.77	1.0e-04	0.30500	0.00096	0.30692				
nciaT70_131_1_11_3	0.0	5,667	338	5,523	426.92	1.0e-04	0.33850	0.00107	0.34064				
nciaT70_131_1_12_3	0.0	5,667	338	6,443	498.07	1.0e-04	0.37139	0.00102	0.37342				
nciaT70_131_1_13_3	0.0	5,667	338	7,364	569.23	1.0e-04	0.40245	0.00098	0.40441				
nciaT70_131_1_14_3	0.0	5,667	338	8,284	640.38	1.0e-04	0.43010	0.00115	0.43241				
nciaT70_131_1_15_3	0.0	5,667	338	9,205	711.53	1.0e-04	0.45804	0.00122	0.46047				

Table 6.9.6-20d. Results for $UZrH_x$ content at 19.7 wt % ^{235}U in packaging calculation model

case name	np (in)	$UZrH_x$ (g)	^{235}U (g)	H_2O (g)	h/x	mocfr/ moifr	k_{eff}	σ	$k_{eff}+2σ$	case name	k_{eff}	σ	$k_{eff}+2σ$
homogenized content in flooded containment vessel, single package reflected [10 CFR 71.55(d)(2)]													
NCT													
no can spacers (np thickness = 0.0 in.)													
mocfr													
ncsrt55d2_1_1_15	0.0	10,400	921	0	0.00	1.0e+00	0.11370	0.00054	0.11477				
ncsrt55d2_1_6_15	0.0	10,400	921	900	25.50	1.0e+00	0.15074	0.00061	0.15196				
ncsrt55d2_1_7_15	0.0	10,400	921	1,800	51.00	1.0e+00	0.19298	0.00070	0.19439				
ncsrt55d2_1_8_15	0.0	10,400	921	2,700	76.50	1.0e+00	0.24182	0.00082	0.24346				
ncsrt55d2_1_9_15	0.0	10,400	921	3,599	102.00	1.0e+00	0.29424	0.00084	0.29591				
ncsrt55d2_1_10_15	0.0	10,400	921	4,499	127.50	1.0e+00	0.34858	0.00100	0.35059				
ncsrt55d2_1_11_15	0.0	10,400	921	5,399	153.00	1.0e+00	0.40341	0.00119	0.40579				
ncsrt55d2_1_12_15	0.0	10,400	921	6,299	178.50	1.0e+00	0.45802	0.00109	0.46020				

Table 6.9.6-20d. Results for $UZrH_x$ content at 19.7 wt % ^{235}U in packaging calculation model

case name	np (in)	$UZrH_x$ (g)	^{235}U (g)	H_2O (g)	h/x	mocfr/ moifr	k_{eff}	σ	$k_{eff}+2σ$	case name	k_{eff}	σ	$k_{eff}+2σ$
ncsrt55d2_1_13_15	0.0	10,400	921	7,199	204.00	1.0e+00	0.51163	0.00121	0.51404				
ncsrt55d2_1_14_15	0.0	10,400	921	8,098	229.51	1.0e+00	0.56264	0.00129	0.56521				
ncsrt55d2_1_15_15	0.0	10,400	921	8,998	255.01	1.0e+00	0.60824	0.00136	0.61095				
moifr													
ncsrt55d2_1_15_15	0.0	10,400	921	8,998	255.01	1.0e+00	0.60824	0.00136	0.61095				
ncsrt55d2_1_15_8	0.0	10,400	921	8,998	255.01	3.0e-01	0.55284	0.00122	0.55528				
ncsrt55d2_1_15_6	0.0	10,400	921	8,998	255.01	1.0e-01	0.53397	0.00114	0.53626				
ncsrt55d2_1_15_5	0.0	10,400	921	8,998	255.01	1.0e-02	0.52373	0.00115	0.52604				
ncsrt55d2_1_15_4	0.0	10,400	921	8,998	255.01	1.0e-03	0.52361	0.00124	0.52609				
ncsrt55d2_1_15_3	0.0	10,400	921	8,998	255.01	1.0e-04	0.52050	0.00116	0.52283				
ncsrt55d2_1_15_2	0.0	10,400	921	8,998	255.01	1.0e-05	0.52366	0.00123	0.52611				
ncsrt55d2_1_15_1	0.0	10,400	921	8,998	255.01	1.0e-20	0.52390	0.00120	0.52631				
with can spacers (np thickness = 1.4 in.)													
mocfr													
ncsrt55d2_2_1_15	1.4	10,400	921	0	0.00	1.0e+00	0.10877	0.00048	0.10972				
ncsrt55d2_2_6_15	1.4	10,400	921	839	23.76	1.0e+00	0.14519	0.00062	0.14643				
ncsrt55d2_2_7_15	1.4	10,400	921	1,677	47.52	1.0e+00	0.18564	0.00082	0.18729				
ncsrt55d2_2_8_15	1.4	10,400	921	2,515	71.29	1.0e+00	0.23269	0.00095	0.23459				
ncsrt55d2_2_9_15	1.4	10,400	921	3,354	95.05	1.0e+00	0.28305	0.00082	0.28469				
ncsrt55d2_2_10_15	1.4	10,400	921	4,192	118.81	1.0e+00	0.33734	0.00105	0.33944				
ncsrt55d2_2_11_15	1.4	10,400	921	5,031	142.57	1.0e+00	0.39111	0.00128	0.39367				
ncsrt55d2_2_12_15	1.4	10,400	921	5,869	166.33	1.0e+00	0.44324	0.00114	0.44553				

Table 6.9.6-20d. Results for $UZrH_x$ content at 19.7 wt % ^{235}U in packaging calculation model

case name	np (in)	$UZrH_x$ (g)	^{235}U (g)	H_2O (g)	h/x	mocfr/ moifr	k_{eff}	σ	$k_{eff}+2σ$	case name	k_{eff}	σ	$k_{eff}+2σ$
ncsrt55d2_2_13_15	1.4	10,400	921	6,708	190.09	1.0e+00	0.49696	0.00128	0.49951				
ncsrt55d2_2_14_15	1.4	10,400	921	7,546	213.86	1.0e+00	0.54756	0.00093	0.54942				
ncsrt55d2_2_15_15	1.4	10,400	921	8,385	237.62	1.0e+00	0.59538	0.00144	0.59825				
moifr													
ncsrt55d2_2_15_15	1.4	10,400	921	8,385	237.62	1.0e+00	0.59538	0.00144	0.59825				
ncsrt55d2_2_15_8	1.4	10,400	921	8,385	237.62	3.0e-01	0.53671	0.00112	0.53895				
ncsrt55d2_2_15_6	1.4	10,400	921	8,385	237.62	1.0e-01	0.52002	0.00107	0.52217				
ncsrt55d2_2_15_5	1.4	10,400	921	8,385	237.62	1.0e-02	0.50958	0.00123	0.51204				
ncsrt55d2_2_15_4	1.4	10,400	921	8,385	237.62	1.0e-03	0.50803	0.00111	0.51024				
ncsrt55d2_2_15_3	1.4	10,400	921	8,385	237.62	1.0e-04	0.50785	0.00116	0.51018				
ncsrt55d2_2_15_2	1.4	10,400	921	8,385	237.62	1.0e-05	0.50851	0.00117	0.51086				
ncsrt55d2_2_15_1	1.4	10,400	921	8,385	237.62	1.0e-20	0.50763	0.00113	0.50989				
homogenized content in flooded containment vessel, array packaging model for CSI=0.0 [10 CFR 71.55(d)(2)]													
NCT													
no can spacers (np thickness = 0.0 in.)													
moifr													
nciat55d2_1_1_3	0.0	10400	921	0	0.00	1.0e-04	0.13090	0.00039	0.13168				
nciat55d2_1_6_3	0.0	10400	921	900	25.50	1.0e-04	0.18600	0.00056	0.18713				
nciat55d2_1_7_3	0.0	10400	921	1,800	51.00	1.0e-04	0.24841	0.00078	0.24997				
nciat55d2_1_8_3	0.0	10400	921	2,700	76.50	1.0e-04	0.31679	0.00074	0.31826				
nciat55d2_1_9_3	0.0	10400	921	3,599	102.00	1.0e-04	0.38338	0.00097	0.38531				
nciat55d2_1_10_3	0.0	10400	921	4,499	127.50	1.0e-04	0.44808	0.00093	0.44993				
nciat55d2_1_11_3	0.0	10400	921	5,399	153.00	1.0e-04	0.51062	0.00096	0.51254				

Table 6.9.6-20d. Results for $UZrH_x$ content at 19.7 wt % ^{235}U in packaging calculation model

case name	np (in)	$UZrH_x$ (g)	^{235}U (g)	H_2O (g)	h/x	mocfr/ moifr	k_{eff}	σ	k_{eff}+2σ	case name	k_{eff}	σ	k_{eff}+2σ
nciat55d2_1_12_3	0.0	10400	921	6,299	178.50	1.0e-04	0.56869	0.00104	0.57076				
nciat55d2_1_13_3	0.0	10400	921	7,198	204.00	1.0e-04	0.62259	0.00112	0.62484				
nciat55d2_1_14_3	0.0	10400	921	8,098	229.51	1.0e-04	0.67077	0.00100	0.67276				
nciat55d2_1_15_3	0.0	10400	921	8,998	255.01	1.0e-04	0.71379	0.00131	0.71641				
with can spacers (np thickness = 1.4 in.)													
nciat55d2_02_1_3	1.4	10400	921	0	0.00	1.0e-04	0.12620	0.00039	0.12697				
nciat55d2_02_6_3	1.4	10400	921	838	23.76	1.0e-04	0.17224	0.00043	0.17310				
nciat55d2_02_7_3	1.4	10400	921	1,677	47.52	1.0e-04	0.22779	0.00057	0.22894				
nciat55d2_02_8_3	1.4	10400	921	2,515	71.29	1.0e-04	0.28723	0.00081	0.28884				
nciat55d2_02_9_3	1.4	10400	921	3,354	95.05	1.0e-04	0.34934	0.00079	0.35091				
nciat55d2_02_10_3	1.4	10400	921	4,192	118.81	1.0e-04	0.40899	0.00097	0.41094				
nciat55d2_02_11_3	1.4	10400	921	5,031	142.57	1.0e-04	0.46775	0.00101	0.46977				
nciat55d2_02_12_3	1.4	10400	921	5,869	166.33	1.0e-04	0.52454	0.00105	0.52664				
nciat55d2_02_13_3	1.4	10400	921	6,708	190.09	1.0e-04	0.57561	0.00105	0.57771				
nciat55d2_02_14_3	1.4	10400	921	7,546	213.86	1.0e-04	0.62437	0.00100	0.62637				
nciat55d2_02_15_3	1.4	10400	921	8,385	237.62	1.0e-04	0.66968	0.00118	0.67203				

Table 6.9.6-21. Results for solid HEU metal content for air transportation

case name	^{235}U (g)	CH_2 (g)	H_2O (g)	Kaolite (g)	htox	Rc (cm)	H_2O (g)	Kao (g)	Shell (g)	Rs (cm)	nlf	k_{eff}	σ	k_{eff} + 2σ
compromised package, HEU in spherical configuration, 20.0 cm water reflector														
10,000g HEU														
atdmr_10_8	10,000	513	na	na	1.72	6.3828	na	na	na	na	0.0699	0.84749	0.00166	0.85080
atdmr_10_7	9,500	513	na	na	1.81	6.3821	na	na	na	na	0.0700	0.83119	0.00116	0.83352

Table 6.9.6-21. Results for solid HEU metal content for air transportation

case name	^{235}U (g)	CH_2 (g)	H_2O (g)	Kaolite (g)	htox	Rc (cm)	H_2O (g)	Kao (g)	Shell (g)	Rs (cm)	nlf	k_{eff}	σ	$k_{eff} + 2\sigma$
atdmr_10_6	9,000	513	na	na	1.91	6.3814	na	na	na	na	0.0704	0.81788	0.00124	0.82037
atdmr_10_5	8,000	513	na	na	2.15	6.3801	na	na	na	na	0.0703	0.79457	0.00108	0.79673
atdmr_10_4	7,000	513	na	na	2.46	6.3788	na	na	na	na	0.0708	0.76800	0.00105	0.77010
atdmr_10_3	6,000	513	na	na	2.87	6.3775	na	na	na	na	0.0708	0.73829	0.00119	0.74067
atdmr_10_2	4,000	513	na	na	4.30	6.3749	na	na	na	na	0.0707	0.67494	0.00115	0.67723
atdmr_10_1	1,900	513	na	na	9.06	6.3721	na	na	na	na	0.0714	0.58800	0.00115	0.59030
9,000g HEU														
atdmr_9_8	9,000	513	na	na	1.91	6.2772	na	na	na	na	0.0709	0.82760	0.00126	0.83012
atdmr_9_7	8,550	513	na	na	2.01	6.2766	na	na	na	na	0.0706	0.81397	0.00109	0.81615
atdmr_9_6	8,100	513	na	na	2.12	6.2760	na	na	na	na	0.0709	0.80283	0.00125	0.80533
atdmr_9_5	7,200	513	na	na	2.39	6.2747	na	na	na	na	0.0713	0.77712	0.00131	0.77973
atdmr_9_4	6,300	513	na	na	2.73	6.2735	na	na	na	na	0.0713	0.75186	0.00109	0.75403
atdmr_9_3	5,400	513	na	na	3.19	6.2723	na	na	na	na	0.0717	0.72734	0.00146	0.73025
atdmr_9_2	3,600	513	na	na	4.78	6.2698	na	na	na	na	0.0716	0.66431	0.00106	0.66642
atdmr_9_1	1,710	513	na	na	10.06	6.2673	na	na	na	na	0.0722	0.58032	0.00113	0.58259
8,000g HEU														
atdmr_8_7	7,600	513	na	na	2.26	6.1674	na	na	na	na	0.0715	0.79619	0.00117	0.79853
atdmr_8_6	7,200	513	na	na	2.39	6.1668	na	na	na	na	0.0727	0.78301	0.00116	0.78533
atdmr_8_5	6,400	513	na	na	2.69	6.1657	na	na	na	na	0.0719	0.75965	0.00114	0.76193
atdmr_8_4	5,600	513	na	na	3.07	6.1646	na	na	na	na	0.0716	0.73554	0.00108	0.73771
atdmr_8_3	4,800	513	na	na	3.58	6.1634	na	na	na	na	0.0726	0.70989	0.00097	0.71182
atdmr_8_2	3,200	513	na	na	5.38	6.1612	na	na	na	na	0.0728	0.65175	0.00102	0.65379
atdmr_8_1	1,520	513	na	na	11.32	6.1588	na	na	na	na	0.0733	0.57379	0.00106	0.57592

Table 6.9.6-21. Results for solid HEU metal content for air transportation

case name	^{235}U (g)	CH_2 (g)	H_2O (g)	Kaolite (g)	htox	Rc (cm)	H_2O (g)	Kao (g)	Shell (g)	Rs (cm)	nlf	k_{eff}	σ	$k_{eff} + 2σ$
7,000g HEU														
atdmr_7_8	7,000	513	na	na	2.46	6.0547	na	na	na	na	0.0727	0.78948	0.00115	0.79178
atdmr_7_7	6,650	513	na	na	2.59	6.0541	na	na	na	na	0.0729	0.77766	0.00132	0.78030
atdmr_7_6	6,300	513	na	na	2.73	6.0536	na	na	na	na	0.0730	0.76315	0.00123	0.76560
atdmr_7_5	5,600	513	na	na	3.07	6.0526	na	na	na	na	0.0732	0.74249	0.00125	0.74499
atdmr_7_4	4,900	513	na	na	3.51	6.0516	na	na	na	na	0.0727	0.72132	0.00116	0.72365
atdmr_7_3	4,200	513	na	na	4.10	6.0506	na	na	na	na	0.0741	0.69486	0.00105	0.69696
atdmr_7_2	2,800	513	na	na	6.15	6.0485	na	na	na	na	0.0735	0.64123	0.00116	0.64355
atdmr_7_1	1,330	513	na	na	12.94	6.0464	na	na	na	na	0.0737	0.56794	0.00130	0.57053
compromised package, HEU in spherical configuration, Kaolite shell, 20.0 cm water reflector														
7,000g HEU 100% enrichment														
atdmsr_7_8_11	7,000	513	na	na	2.46	6.0547	na	na	66,133.1	13.0264	0.0300	0.76978	0.00129	0.77236
atdmsr_7_8_10	7,000	513	na	na	2.46	6.0547	na	na	59,519.8	12.6235	0.0314	0.76732	0.00118	0.76967
atdmsr_7_8_9	7,000	513	na	na	2.46	6.0547	na	na	52,906.5	12.1930	0.0330	0.76002	0.00125	0.76252
atdmsr_7_8_8	7,000	513	na	na	2.46	6.0547	na	na	46,293.2	11.7298	0.0345	0.75671	0.00121	0.75913
atdmsr_7_8_7	7,000	513	na	na	2.46	6.0547	na	na	39,679.9	11.2268	0.0374	0.75221	0.00109	0.75438
atdmsr_7_8_6	7,000	513	na	na	2.46	6.0547	na	na	33,066.6	10.6742	0.0395	0.75004	0.00120	0.75245
atdmsr_7_8_5	7,000	513	na	na	2.46	6.0547	na	na	26,453.3	10.0575	0.0423	0.74240	0.00101	0.74442
atdmsr_7_8_4	7,000	513	na	na	2.46	6.0547	na	na	19,839.9	9.3542	0.0466	0.73769	0.00151	0.74072
atdmsr_7_8_3	7,000	513	na	na	2.46	6.0547	na	na	13,226.6	8.5255	0.0516	0.73211	0.00120	0.73452
atdmsr_7_8_2	7,000	513	na	na	2.46	6.0547	na	na	6,613.3	7.4937	0.0589	0.73646	0.00124	0.73894
atdmsr_7_8_1	7,000	513	na	na	2.46	6.0547	na	na	0.0	6.0548	0.0728	0.79093	0.00117	0.79327
7,000g HEU 95% enrichment														
atdmsr_7_7_11	6,650	513	na	na	2.59	6.0541	na	na	66,133.1	13.0263	0.0295	0.75467	0.00115	0.75698
atdmsr_7_7_10	6,650	513	na	na	2.59	6.0541	na	na	59,519.8	12.6234	0.0312	0.75071	0.00123	0.75317

Table 6.9.6-21. Results for solid HEU metal content for air transportation

case name	^{235}U (g)	CH_2 (g)	H_2O (g)	Kaolite (g)	htox	Rc (cm)	H_2O (g)	Kao (g)	Shell (g)	Rs (cm)	nlf	k_{eff}	σ	$k_{eff} + 2\sigma$
atdmsr_7_7_9	6,650	513	na	na	2.59	6.0541	na	na	52,906.5	12.1929	0.0328	0.74594	0.00128	0.74850
atdmsr_7_7_8	6,650	513	na	na	2.59	6.0541	na	na	46,293.2	11.7297	0.0348	0.74333	0.00108	0.74549
atdmsr_7_7_7	6,650	513	na	na	2.59	6.0541	na	na	39,679.9	11.2267	0.0368	0.73698	0.00117	0.73932
atdmsr_7_7_6	6,650	513	na	na	2.59	6.0541	na	na	33,066.6	10.6740	0.0397	0.73239	0.00125	0.73489
atdmsr_7_7_5	6,650	513	na	na	2.59	6.0541	na	na	26,453.3	10.0573	0.0428	0.72809	0.00142	0.73093
atdmsr_7_7_4	6,650	513	na	na	2.59	6.0541	na	na	19,839.9	9.3540	0.0461	0.72160	0.00110	0.72381
atdmsr_7_7_3	6,650	513	na	na	2.59	6.0541	na	na	13,226.6	8.5252	0.0514	0.71946	0.00121	0.72189
atdmsr_7_7_2	6,650	513	na	na	2.59	6.0541	na	na	6,613.3	7.4934	0.0596	0.72377	0.00105	0.72587
atdmsr_7_7_1	6,650	513	na	na	2.59	6.0541	na	na	0.0	6.0542	0.0727	0.77941	0.00138	0.78218
7,000g HEU 90% enrichment														
atdmsr_7_6_11	6,300	513	na	na	2.73	6.0536	na	na	66,133.1	13.0262	0.0298	0.74002	0.00123	0.74248
atdmsr_7_6_10	6,300	513	na	na	2.73	6.0536	na	na	59,519.8	12.6233	0.0309	0.73640	0.00130	0.73899
atdmsr_7_6_9	6,300	513	na	na	2.73	6.0536	na	na	52,906.5	12.1928	0.0326	0.73341	0.00130	0.73601
atdmsr_7_6_8	6,300	513	na	na	2.73	6.0536	na	na	46,293.2	11.7296	0.0350	0.72745	0.00117	0.72978
atdmsr_7_6_7	6,300	513	na	na	2.73	6.0536	na	na	39,679.9	11.2265	0.0371	0.72397	0.00125	0.72647
atdmsr_7_6_6	6,300	513	na	na	2.73	6.0536	na	na	33,066.6	10.6739	0.0396	0.71997	0.00111	0.72219
atdmsr_7_6_5	6,300	513	na	na	2.73	6.0536	na	na	26,453.3	10.0572	0.0422	0.71532	0.00112	0.71755
atdmsr_7_6_4	6,300	513	na	na	2.73	6.0536	na	na	19,839.9	9.3538	0.0466	0.70916	0.00125	0.71166
atdmsr_7_6_3	6,300	513	na	na	2.73	6.0536	na	na	13,226.6	8.5250	0.0518	0.70456	0.00108	0.70672
atdmsr_7_6_2	6,300	513	na	na	2.73	6.0536	na	na	6,613.3	7.4931	0.0590	0.71101	0.00110	0.71322
atdmsr_7_6_1	6,300	513	na	na	2.73	6.0536	na	na	0.0	6.0537	0.0735	0.76667	0.00126	0.76920
7,000g HEU 80% enrichment														
atdmsr_7_5_11	5,600	513	na	na	3.07	6.0526	na	na	66,133.1	13.0260	0.0297	0.71137	0.00112	0.71362
atdmsr_7_5_10	5,600	513	na	na	3.07	6.0526	na	na	59,519.8	12.6230	0.0314	0.70938	0.00141	0.71220
atdmsr_7_5_9	5,600	513	na	na	3.07	6.0526	na	na	52,906.5	12.1925	0.0329	0.70515	0.00096	0.70706

Table 6.9.6-21. Results for solid HEU metal content for air transportation

case name	^{235}U (g)	CH_2 (g)	H_2O (g)	Kaolite (g)	htox	Rc (cm)	H_2O (g)	Kao (g)	Shell (g)	Rs (cm)	nlf	k_{eff}	σ	$k_{eff} + 2\sigma$
atdmsr_7_5_8	5,600	513	na	na	3.07	6.0526	na	na	46,293.2	11.7293	0.0346	0.70045	0.00120	0.70285
atdmsr_7_5_7	5,600	513	na	na	3.07	6.0526	na	na	39,679.9	11.2262	0.0366	0.69582	0.00122	0.69826
atdmsr_7_5_6	5,600	513	na	na	3.07	6.0526	na	na	33,066.6	10.6736	0.0396	0.69115	0.00124	0.69363
atdmsr_7_5_5	5,600	513	na	na	3.07	6.0526	na	na	26,453.3	10.0568	0.0428	0.68561	0.00118	0.68797
atdmsr_7_5_4	5,600	513	na	na	3.07	6.0526	na	na	19,839.9	9.3534	0.0463	0.68277	0.00124	0.68525
atdmsr_7_5_3	5,600	513	na	na	3.07	6.0526	na	na	13,226.6	8.5244	0.0515	0.67737	0.00102	0.67940
atdmsr_7_5_2	5,600	513	na	na	3.07	6.0526	na	na	6,613.3	7.4924	0.0593	0.68540	0.00103	0.68746
atdmsr_7_5_1	5,600	513	na	na	3.07	6.0526	na	na	0.0	6.0527	0.0729	0.74261	0.00120	0.74501
7,000g HEU70% enrichment														
atdmsr_7_4_11	4,900	513	na	na	3.51	6.0516	na	na	66,133.1	13.0258	0.0300	0.68306	0.00121	0.68547
atdmsr_7_4_10	4,900	513	na	na	3.51	6.0516	na	na	59,519.8	12.6228	0.0312	0.67927	0.00127	0.68181
atdmsr_7_4_9	4,900	513	na	na	3.51	6.0516	na	na	52,906.5	12.1923	0.0328	0.67583	0.00137	0.67857
atdmsr_7_4_8	4,900	513	na	na	3.51	6.0516	na	na	46,293.2	11.7290	0.0349	0.67138	0.00121	0.67380
atdmsr_7_4_7	4,900	513	na	na	3.51	6.0516	na	na	39,679.9	11.2259	0.0369	0.66709	0.00108	0.66925
atdmsr_7_4_6	4,900	513	na	na	3.51	6.0516	na	na	33,066.6	10.6732	0.0399	0.66244	0.00101	0.66446
atdmsr_7_4_5	4,900	513	na	na	3.51	6.0516	na	na	26,453.3	10.0564	0.0431	0.65826	0.00111	0.66048
atdmsr_7_4_4	4,900	513	na	na	3.51	6.0516	na	na	19,839.9	9.3530	0.0465	0.65222	0.00119	0.65460
atdmsr_7_4_3	4,900	513	na	na	3.51	6.0516	na	na	13,226.6	8.5239	0.0518	0.65245	0.00126	0.65497
atdmsr_7_4_2	4,900	513	na	na	3.51	6.0516	na	na	6,613.3	7.4917	0.0599	0.65772	0.00118	0.66008
atdmsr_7_4_1	4,900	513	na	na	3.51	6.0516	na	na	0.0	6.0517	0.0733	0.72043	0.00123	0.72290
7,000g HEU 60% enrichment														
atdmsr_7_3_11	4,200	513	na	na	4.10	6.0506	na	na	66,133.1	13.0256	0.0299	0.65025	0.00135	0.65295
atdmsr_7_3_10	4,200	513	na	na	4.10	6.0506	na	na	59,519.8	12.6226	0.0314	0.64822	0.00112	0.65045
atdmsr_7_3_9	4,200	513	na	na	4.10	6.0506	na	na	52,906.5	12.1920	0.0330	0.64480	0.00112	0.64705
atdmsr_7_3_8	4,200	513	na	na	4.10	6.0506	na	na	46,293.2	11.7288	0.0351	0.63950	0.00103	0.64156

Table 6.9.6-21. Results for solid HEU metal content for air transportation

case name	^{235}U (g)	CH_2 (g)	H_2O (g)	Kaolite (g)	htox	Rc (cm)	H_2O (g)	Kao (g)	Shell (g)	Rs (cm)	nlf	k_{eff}	σ	$k_{eff} + 2\sigma$
atdmsr_7_3_7	4,200	513	na	na	4.10	6.0506	na	na	39,679.9	11.2257	0.0371	0.63712	0.00119	0.63950
atdmsr_7_3_6	4,200	513	na	na	4.10	6.0506	na	na	33,066.6	10.6729	0.0397	0.63245	0.00093	0.63431
atdmsr_7_3_5	4,200	513	na	na	4.10	6.0506	na	na	26,453.3	10.0561	0.0428	0.62613	0.00113	0.62838
atdmsr_7_3_4	4,200	513	na	na	4.10	6.0506	na	na	19,839.9	9.3525	0.0468	0.62494	0.00105	0.62705
atdmsr_7_3_3	4,200	513	na	na	4.10	6.0506	na	na	13,226.6	8.5234	0.0517	0.61900	0.00116	0.62132
atdmsr_7_3_2	4,200	513	na	na	4.10	6.0506	na	na	6,613.3	7.4911	0.0595	0.63166	0.00116	0.63399
atdmsr_7_3_1	4,200	513	na	na	4.10	6.0506	na	na	0.0	6.0507	0.0734	0.69589	0.00112	0.69813
7,000g HEU 40% enrichment														
atdmsr_7_2_11	2,800	513	na	na	6.15	6.0485	na	na	66,133.1	13.0251	0.0303	0.57913	0.00106	0.58126
atdmsr_7_2_10	2,800	513	na	na	6.15	6.0485	na	na	59,519.8	12.6221	0.0311	0.57855	0.00114	0.58083
atdmsr_7_2_9	2,800	513	na	na	6.15	6.0485	na	na	52,906.5	12.1915	0.0332	0.57213	0.00121	0.57455
atdmsr_7_2_8	2,800	513	na	na	6.15	6.0485	na	na	46,293.2	11.7282	0.0350	0.56971	0.00124	0.57219
atdmsr_7_2_7	2,800	513	na	na	6.15	6.0485	na	na	39,679.9	11.2251	0.0372	0.56672	0.00109	0.56890
atdmsr_7_2_6	2,800	513	na	na	6.15	6.0485	na	na	33,066.6	10.6722	0.0391	0.56156	0.00107	0.56371
atdmsr_7_2_5	2,800	513	na	na	6.15	6.0485	na	na	26,453.3	10.0553	0.0424	0.55753	0.00109	0.55972
atdmsr_7_2_4	2,800	513	na	na	6.15	6.0485	na	na	19,839.9	9.3517	0.0467	0.55519	0.00116	0.55752
atdmsr_7_2_3	2,800	513	na	na	6.15	6.0485	na	na	13,226.6	8.5224	0.0521	0.55309	0.00103	0.55515
atdmsr_7_2_2	2,800	513	na	na	6.15	6.0485	na	na	6,613.3	7.4897	0.0592	0.56497	0.00103	0.56704
atdmsr_7_2_1	2,800	513	na	na	6.15	6.0485	na	na	0.0	6.0486	0.0738	0.64051	0.00108	0.64267
7,000g HEU 20% enrichment														
atdmsr_7_1_11	1,330	513	na	na	12.94	6.0464	na	na	66,133.1	13.0247	0.0300	0.47937	0.00107	0.48151
atdmsr_7_1_10	1,330	513	na	na	12.94	6.0464	na	na	59,519.8	12.6216	0.0315	0.47895	0.00120	0.48136
atdmsr_7_1_9	1,330	513	na	na	12.94	6.0464	na	na	52,906.5	12.1910	0.0330	0.47468	0.00117	0.47702
atdmsr_7_1_8	1,330	513	na	na	12.94	6.0464	na	na	46,293.2	11.7276	0.0349	0.47179	0.00102	0.47383
atdmsr_7_1_7	1,330	513	na	na	12.94	6.0464	na	na	39,679.9	11.2244	0.0372	0.46614	0.00113	0.46841

Table 6.9.6-21. Results for solid HEU metal content for air transportation

case name	^{235}U (g)	CH_2 (g)	H_2O (g)	Kaolite (g)	htox	Rc (cm)	H_2O (g)	Kao (g)	Shell (g)	Rs (cm)	nlf	k_{eff}	σ	$k_{eff} + 2σ$
atdmsr_7_1_6	1,330	513	na	na	12.94	6.0464	na	na	33,066.6	10.6715	0.0393	0.46445	0.00093	0.46632
atdmsr_7_1_5	1,330	513	na	na	12.94	6.0464	na	na	26,453.3	10.0545	0.0430	0.46287	0.00096	0.46480
atdmsr_7_1_4	1,330	513	na	na	12.94	6.0464	na	na	19,839.9	9.3508	0.0469	0.45842	0.00094	0.46031
atdmsr_7_1_3	1,330	513	na	na	12.94	6.0464	na	na	13,226.6	8.5213	0.0525	0.45781	0.00095	0.45971
atdmsr_7_1_2	1,330	513	na	na	12.94	6.0464	na	na	6,613.3	7.4883	0.0602	0.47487	0.00114	0.47715
atdmsr_7_1_1	1,330	513	na	na	12.94	6.0464	na	na	0.0	6.0465	0.0733	0.56625	0.00104	0.56833
compromised package, HEU in spherical configuration, none-to-water saturated Kaolite shell, 20.0 cm water reflector														
7,000g HEU 100% enrichment														
atdmkr_7_8_11	7,000	513	na	na	2.46	6.0547	76,819.4	51,214.9	128,034.0	31.0814	0.0057	0.74873	0.00152	0.75178
atdmkr_7_8_10	7,000	513	na	na	2.46	6.0547	69,137.2	46,093.4	115,230.6	30.0170	0.0065	0.74821	0.00123	0.75067
atdmkr_7_8_9	7,000	513	na	na	2.46	6.0547	61,455.3	40,971.9	102,427.2	28.8712	0.0074	0.74665	0.00112	0.74889
atdmkr_7_8_8	7,000	513	na	na	2.46	6.0547	53,773.4	35,850.4	89,623.8	27.6264	0.0083	0.74610	0.00123	0.74856
atdmkr_7_8_7	7,000	513	na	na	2.46	6.0547	46,091.5	30,728.9	76,820.4	26.2581	0.0094	0.74918	0.00119	0.75155
atdmkr_7_8_6	7,000	513	na	na	2.46	6.0547	38,409.6	25,607.5	64,017.0	24.7300	0.0110	0.74664	0.00118	0.74901
atdmkr_7_8_5	7,000	513	na	na	2.46	6.0547	30,727.6	20,486.0	51,213.6	22.9853	0.0128	0.74760	0.00134	0.75027
atdmkr_7_8_4	7,000	513	na	na	2.46	6.0547	23,045.7	15,364.5	38,410.2	20.9259	0.0161	0.74585	0.00118	0.74821
atdmkr_7_8_3	7,000	513	na	na	2.46	6.0547	15,363.8	10,243.0	25,606.8	18.3540	0.0206	0.74498	0.00117	0.74733
atdmkr_7_8_2	7,000	513	na	na	2.46	6.0547	7,681.9	5,121.5	12,803.4	14.7399	0.0296	0.74816	0.00123	0.75063
atdmkr_7_8_1	7,000	513	na	na	2.46	6.0547	0.0	0.0	0.0	6.0548	0.0730	0.78994	0.00131	0.79257
7,000g HEU 95% enrichment														
atdmkr_7_7_11	6,650	513	na	na	2.59	6.0541	76,819.4	51,214.9	128,034.0	31.0814	0.0058	0.73331	0.00141	0.73613
atdmkr_7_7_10	6,650	513	na	na	2.59	6.0541	69,137.2	46,093.4	115,230.6	30.0170	0.0064	0.73430	0.00130	0.73690
atdmkr_7_7_9	6,650	513	na	na	2.59	6.0541	61,455.3	40,971.9	102,427.2	28.8712	0.0073	0.73397	0.00103	0.73603
atdmkr_7_7_8	6,650	513	na	na	2.59	6.0541	53,773.4	35,850.4	89,623.8	27.6264	0.0081	0.73295	0.00123	0.73541
atdmkr_7_7_7	6,650	513	na	na	2.59	6.0541	46,091.5	30,728.9	76,820.4	26.2581	0.0094	0.73168	0.00112	0.73392

Table 6.9.6-21. Results for solid HEU metal content for air transportation

case name	^{235}U (g)	CH_2 (g)	H_2O (g)	Kaolite (g)	htox	Rc (cm)	H_2O (g)	Kao (g)	Shell (g)	Rs (cm)	nlf	k_{eff}	σ	$k_{eff} + 2\sigma$
atdmkr_7_7_6	6,650	513	na	na	2.59	6.0541	38,409.6	25,607.5	64,017.0	24.7300	0.0110	0.73221	0.00132	0.73484
atdmkr_7_7_5	6,650	513	na	na	2.59	6.0541	30,727.6	20,486.0	51,213.6	22.9853	0.0130	0.73422	0.00121	0.73664
atdmkr_7_7_4	6,650	513	na	na	2.59	6.0541	23,045.7	15,364.5	38,410.2	20.9259	0.0159	0.73389	0.00107	0.73604
atdmkr_7_7_3	6,650	513	na	na	2.59	6.0541	15,363.8	10,243.0	25,606.8	18.3539	0.0208	0.73441	0.00117	0.73675
atdmkr_7_7_2	6,650	513	na	na	2.59	6.0541	7,681.9	5,121.5	12,803.4	14.7398	0.0298	0.73565	0.00118	0.73801
atdmkr_7_7_1	6,650	513	na	na	2.59	6.0541	0.0	0.0	0.0	6.0542	0.0729	0.77722	0.00126	0.77975
7,000g HEU 90% enrichment														
atdmkr_7_6_11	6,300	513	na	na	2.73	6.0536	76,819.4	51,214.9	128,034.0	31.0814	0.0059	0.72011	0.00123	0.72257
atdmkr_7_6_10	6,300	513	na	na	2.73	6.0536	69,137.2	46,093.4	115,230.6	30.0169	0.0066	0.72046	0.00133	0.72312
atdmkr_7_6_9	6,300	513	na	na	2.73	6.0536	61,455.3	40,971.9	102,427.2	28.8711	0.0074	0.72075	0.00115	0.72306
atdmkr_7_6_8	6,300	513	na	na	2.73	6.0536	53,773.4	35,850.4	89,623.8	27.6264	0.0081	0.72144	0.00139	0.72422
atdmkr_7_6_7	6,300	513	na	na	2.73	6.0536	46,091.5	30,728.9	76,820.4	26.2580	0.0095	0.72118	0.00124	0.72366
atdmkr_7_6_6	6,300	513	na	na	2.73	6.0536	38,409.6	25,607.5	64,017.0	24.7299	0.0109	0.71958	0.00123	0.72204
atdmkr_7_6_5	6,300	513	na	na	2.73	6.0536	30,727.6	20,486.0	51,213.6	22.9853	0.0130	0.72335	0.00122	0.72580
atdmkr_7_6_4	6,300	513	na	na	2.73	6.0536	23,045.7	15,364.5	38,410.2	20.9258	0.0159	0.72261	0.00128	0.72517
atdmkr_7_6_3	6,300	513	na	na	2.73	6.0536	15,363.8	10,243.0	25,606.8	18.3539	0.0211	0.71961	0.00116	0.72192
atdmkr_7_6_2	6,300	513	na	na	2.73	6.0536	7,681.9	5,121.5	12,803.4	14.7397	0.0300	0.72437	0.00112	0.72661
atdmkr_7_6_1	6,300	513	na	na	2.73	6.0536	0.0	0.0	0.0	6.0537	0.0727	0.76352	0.00123	0.76598
7,000g HEU 80% enrichment														
atdmkr_7_5_11	5,600	513	na	na	3.07	6.0526	76,819.4	51,214.9	128,034.0	31.0813	0.0060	0.69823	0.00124	0.70071
atdmkr_7_5_10	5,600	513	na	na	3.07	6.0526	69,137.2	46,093.4	115,230.6	30.0169	0.0065	0.69888	0.00124	0.70137
atdmkr_7_5_9	5,600	513	na	na	3.07	6.0526	61,455.3	40,971.9	102,427.2	28.8711	0.0073	0.69842	0.00148	0.70138
atdmkr_7_5_8	5,600	513	na	na	3.07	6.0526	53,773.4	35,850.4	89,623.8	27.6263	0.0081	0.70030	0.00109	0.70248
atdmkr_7_5_7	5,600	513	na	na	3.07	6.0526	46,091.5	30,728.9	76,820.4	26.2580	0.0092	0.70044	0.00126	0.70297
atdmkr_7_5_6	5,600	513	na	na	3.07	6.0526	38,409.6	25,607.5	64,017.0	24.7299	0.0108	0.69703	0.00110	0.69924

Table 6.9.6-21. Results for solid HEU metal content for air transportation

case name	^{235}U (g)	CH_2 (g)	H_2O (g)	Kaolite (g)	htox	Rc (cm)	H_2O (g)	Kao (g)	Shell (g)	Rs (cm)	nlf	k_{eff}	σ	$k_{eff} + 2\sigma$
atdmkr_7_5_5	5,600	513	na	na	3.07	6.0526	30,727.6	20,486.0	51,213.6	22.9852	0.0127	0.69957	0.00122	0.70202
atdmkr_7_5_4	5,600	513	na	na	3.07	6.0526	23,045.7	15,364.5	38,410.2	20.9257	0.0159	0.69622	0.00108	0.69838
atdmkr_7_5_3	5,600	513	na	na	3.07	6.0526	15,363.8	10,243.0	25,606.8	18.3538	0.0203	0.69848	0.00117	0.70081
atdmkr_7_5_2	5,600	513	na	na	3.07	6.0526	7,681.9	5,121.5	12,803.4	14.7395	0.0297	0.69932	0.00130	0.70193
atdmkr_7_5_1	5,600	513	na	na	3.07	6.0526	0.0	0.0	0.0	6.0527	0.0732	0.74467	0.00118	0.74704
7,000g HEU 70% enrichment														
atdmkr_7_4_11	4,900	513	na	na	3.51	6.0516	76,819.4	51,214.9	128,034.0	31.0813	0.0060	0.67338	0.00112	0.67561
atdmkr_7_4_10	4,900	513	na	na	3.51	6.0516	69,137.2	46,093.4	115,230.6	30.0169	0.0066	0.67336	0.00119	0.67574
atdmkr_7_4_9	4,900	513	na	na	3.51	6.0516	61,455.3	40,971.9	102,427.2	28.8711	0.0073	0.67359	0.00118	0.67595
atdmkr_7_4_8	4,900	513	na	na	3.51	6.0516	53,773.4	35,850.4	89,623.8	27.6263	0.0082	0.67522	0.00122	0.67767
atdmkr_7_4_7	4,900	513	na	na	3.51	6.0516	46,091.5	30,728.9	76,820.4	26.2579	0.0095	0.67169	0.00110	0.67389
atdmkr_7_4_6	4,900	513	na	na	3.51	6.0516	38,409.6	25,607.5	64,017.0	24.7298	0.0110	0.67452	0.00113	0.67679
atdmkr_7_4_5	4,900	513	na	na	3.51	6.0516	30,727.6	20,486.0	51,213.6	22.9851	0.0129	0.67401	0.00133	0.67667
atdmkr_7_4_4	4,900	513	na	na	3.51	6.0516	23,045.7	15,364.5	38,410.2	20.9256	0.0159	0.67488	0.00118	0.67725
atdmkr_7_4_3	4,900	513	na	na	3.51	6.0516	15,363.8	10,243.0	25,606.8	18.3536	0.0207	0.67501	0.00120	0.67742
atdmkr_7_4_2	4,900	513	na	na	3.51	6.0516	7,681.9	5,121.5	12,803.4	14.7393	0.0299	0.67480	0.00129	0.67737
atdmkr_7_4_1	4,900	513	na	na	3.51	6.0516	0.0	0.0	0.0	6.0517	0.0725	0.72119	0.00137	0.72393
7,000g HEU 60% enrichment														
atdmkr_7_3_11	4,200	513	na	na	4.10	6.0506	76,819.4	51,214.9	128,034.0	31.0813	0.0058	0.64845	0.00127	0.65099
atdmkr_7_3_10	4,200	513	na	na	4.10	6.0506	69,137.2	46,093.4	115,230.6	30.0168	0.0064	0.64981	0.00121	0.65224
atdmkr_7_3_9	4,200	513	na	na	4.10	6.0506	61,455.3	40,971.9	102,427.2	28.8710	0.0073	0.64800	0.00123	0.65045
atdmkr_7_3_8	4,200	513	na	na	4.10	6.0506	53,773.4	35,850.4	89,623.8	27.6262	0.0084	0.64931	0.00113	0.65157
atdmkr_7_3_7	4,200	513	na	na	4.10	6.0506	46,091.5	30,728.9	76,820.4	26.2579	0.0094	0.65002	0.00105	0.65213
atdmkr_7_3_6	4,200	513	na	na	4.10	6.0506	38,409.6	25,607.5	64,017.0	24.7297	0.0109	0.64947	0.00105	0.65157
atdmkr_7_3_5	4,200	513	na	na	4.10	6.0506	30,727.6	20,486.0	51,213.6	22.9851	0.0131	0.64780	0.00128	0.65036

Table 6.9.6-21. Results for solid HEU metal content for air transportation

case name	^{235}U (g)	CH_2 (g)	H_2O (g)	Kaolite (g)	htox	Rc (cm)	H_2O (g)	Kao (g)	Shell (g)	Rs (cm)	nlf	k_{eff}	σ	$k_{eff} + 2σ$
atdmkr_7_3_4	4,200	513	na	na	4.10	6.0506	23,045.7	15,364.5	38,410.2	20.9256	0.0161	0.64888	0.00112	0.65112
atdmkr_7_3_3	4,200	513	na	na	4.10	6.0506	15,363.8	10,243.0	25,606.8	18.3535	0.0207	0.65026	0.00104	0.65233
atdmkr_7_3_2	4,200	513	na	na	4.10	6.0506	7,681.9	5,121.5	12,803.4	14.7392	0.0298	0.64866	0.00107	0.65081
atdmkr_7_3_1	4,200	513	na	na	4.10	6.0506	0.0	0.0	0.0	6.0507	0.0733	0.69563	0.00132	0.69828
7,000g HEU 40% enrichment														
atdmkr_7_2_11	2,800	513	na	na	6.15	6.0485	76,819.4	51,214.9	128,034.0	31.0812	0.0059	0.59232	0.00100	0.59432
atdmkr_7_2_10	2,800	513	na	na	6.15	6.0485	69,137.2	46,093.4	115,230.6	30.0167	0.0064	0.59431	0.00098	0.59626
atdmkr_7_2_9	2,800	513	na	na	6.15	6.0485	61,455.3	40,971.9	102,427.2	28.8709	0.0072	0.59123	0.00117	0.59357
atdmkr_7_2_8	2,800	513	na	na	6.15	6.0485	53,773.4	35,850.4	89,623.8	27.6261	0.0082	0.59177	0.00110	0.59398
atdmkr_7_2_7	2,800	513	na	na	6.15	6.0485	46,091.5	30,728.9	76,820.4	26.2578	0.0096	0.59056	0.00120	0.59296
atdmkr_7_2_6	2,800	513	na	na	6.15	6.0485	38,409.6	25,607.5	64,017.0	24.7296	0.0110	0.59052	0.00121	0.59294
atdmkr_7_2_5	2,800	513	na	na	6.15	6.0485	30,727.6	20,486.0	51,213.6	22.9849	0.0133	0.59140	0.00116	0.59372
atdmkr_7_2_4	2,800	513	na	na	6.15	6.0485	23,045.7	15,364.5	38,410.2	20.9254	0.0160	0.58984	0.00115	0.59215
atdmkr_7_2_3	2,800	513	na	na	6.15	6.0485	15,363.8	10,243.0	25,606.8	18.3533	0.0207	0.59072	0.00102	0.59275
atdmkr_7_2_2	2,800	513	na	na	6.15	6.0485	7,681.9	5,121.5	12,803.4	14.7388	0.0304	0.59025	0.00114	0.59254
atdmkr_7_2_1	2,800	513	na	na	6.15	6.0485	0.0	0.0	0.0	6.0486	0.0732	0.64138	0.00114	0.64366
7,000g HEU 20% enrichment														
atdmkr_7_1_11	1,330	513	na	na	12.94	6.0464	76,819.4	51,214.9	128,034.0	31.0811	0.0058	0.51279	0.00108	0.51495
atdmkr_7_1_10	1,330	513	na	na	12.94	6.0464	69,137.2	46,093.4	115,230.6	30.0167	0.0066	0.51316	0.00104	0.51523
atdmkr_7_1_9	1,330	513	na	na	12.94	6.0464	61,455.3	40,971.9	102,427.2	28.8708	0.0074	0.51271	0.00095	0.51460
atdmkr_7_1_8	1,330	513	na	na	12.94	6.0464	53,773.4	35,850.4	89,623.8	27.6260	0.0080	0.51226	0.00101	0.51429
atdmkr_7_1_7	1,330	513	na	na	12.94	6.0464	46,091.5	30,728.9	76,820.4	26.2576	0.0094	0.51273	0.00107	0.51487
atdmkr_7_1_6	1,330	513	na	na	12.94	6.0464	38,409.6	25,607.5	64,017.0	24.7295	0.0108	0.51071	0.00095	0.51262
atdmkr_7_1_5	1,330	513	na	na	12.94	6.0464	30,727.6	20,486.0	51,213.6	22.9848	0.0132	0.51334	0.00090	0.51514
atdmkr_7_1_4	1,330	513	na	na	12.94	6.0464	23,045.7	15,364.5	38,410.2	20.9252	0.0160	0.51289	0.00114	0.51517

Table 6.9.6-21. Results for solid HEU metal content for air transportation

case name	^{235}U (g)	CH_2 (g)	H_2O (g)	Kaolite (g)	htox	Rc (cm)	H_2O (g)	Kao (g)	Shell (g)	Rs (cm)	nlf	k_{eff}	σ	k_{eff} + 2σ
atdmkr_7_1_3	1,330	513	na	na	12.94	6.0464	15,363.8	10,243.0	25,606.8	18.3531	0.0209	0.51438	0.00127	0.51692
atdmkr_7_1_2	1,330	513	na	na	12.94	6.0464	7,681.9	5,121.5	12,803.4	14.7385	0.0304	0.51402	0.00103	0.51608
atdmkr_7_1_1	1,330	513	na	na	12.94	6.0464	0.0	0.0	0.0	6.0465	0.0739	0.56475	0.00101	0.56677
compromised package, HEU in spherical configuration, none-to-dry Kaolite shell, 20.0 cm water reflector														
7,000g HEU 100% enrichment														
atdmdkr_7_8_11	7,000	513	na	na	2.46	6.0547	2,204.7	51,214.9	53,419.1	31.0814	0.0487	0.59229	0.00094	0.59417
atdmdkr_7_8_10	7,000	513	na	na	2.46	6.0547	1,984.2	46,093.4	48,077.2	30.0170	0.0500	0.59518	0.00088	0.59695
atdmdkr_7_8_9	7,000	513	na	na	2.46	6.0547	1,763.8	40,971.9	42,735.3	28.8712	0.0506	0.59249	0.00102	0.59453
atdmdkr_7_8_8	7,000	513	na	na	2.46	6.0547	1,543.3	35,850.4	37,393.3	27.6264	0.0516	0.59743	0.00105	0.59953
atdmdkr_7_8_7	7,000	513	na	na	2.46	6.0547	1,322.8	30,728.9	32,051.4	26.2581	0.0529	0.59965	0.00135	0.60235
atdmdkr_7_8_6	7,000	513	na	na	2.46	6.0547	1,102.4	25,607.4	26,709.5	24.7300	0.0541	0.60453	0.00113	0.60679
atdmdkr_7_8_5	7,000	513	na	na	2.46	6.0547	881.9	20,486.0	21,367.6	22.9853	0.0557	0.60794	0.00108	0.61010
atdmdkr_7_8_4	7,000	513	na	na	2.46	6.0547	661.4	15,364.5	16,025.7	20.9259	0.0574	0.61664	0.00108	0.61879
atdmdkr_7_8_3	7,000	513	na	na	2.46	6.0547	440.9	10,243.0	10,683.8	18.3540	0.0603	0.62837	0.00115	0.63068
atdmdkr_7_8_2	7,000	513	na	na	2.46	6.0547	220.5	5,121.5	5,341.9	14.7399	0.0653	0.65279	0.00107	0.65492
atdmdkr_7_8_1	7,000	513	na	na	2.46	6.0547	0.0	0.0	0.0	6.0548	0.0727	0.78877	0.00123	0.79123

Table 6.9.6-22a. Results for TRIGA ($UZrH_x$) fuel element content at 19.7 wt % ^{235}U for air transportation

case name	^{235}U (g)	CH_2 (g)	H_2O (g)	Kaolite (g)	htox	Rc (cm)	H_2O (g)	Kaolite (g)	Shell (g)	Rs (cm)	nlf	k_{eff}	σ	k_{eff} + 2σ
compromised package, 10,400 g $UZrH_x$ in spherical configuration, 20.0 cm water reflector														
atdzr	921	500	na	na	43.37	7.4677	na	na	na	na	0.0617	0.67633	0.00116	0.67906
compromised package, 10,400 g $UZrH_x$ in spherical configuration, steel shell, 20.0 cm water reflector														
atdzsr_11	921	500	na	na	43.37	7.4677	na	na	66,133.0	13.3978	0.0271	0.61692	0.00121	0.61933
atdzsr_10	921	500	na	na	43.37	7.4677	na	na	59,520.0	13.0179	0.0285	0.61377	0.00109	0.61595

Table 6.9.6-22a. Results for TRIGA ($UZrH_x$) fuel element content at 19.7 wt % ^{235}U for air transportation

case name	^{235}U (g)	CH_2 (g)	H_2O (g)	Kaolite (g)	htox	Rc (cm)	H_2O (g)	Kaolite (g)	Shell (g)	Rs (cm)	nlf	k_{eff}	σ	k_{eff} + 2σ
atdzsr_9	921	500	na	na	43.37	7.4677	na	na	52,907.0	12.6144	0.0301	0.60931	0.00156	0.61243
atdzsr_8	921	500	na	na	43.37	7.4677	na	na	46,293.0	12.1833	0.0315	0.60602	0.00132	0.60867
atdzsr_7	921	500	na	na	43.37	7.4677	na	na	39,680.0	11.7193	0.0332	0.60256	0.00138	0.60533
atdzsr_6	921	500	na	na	43.37	7.4677	na	na	33,067.0	11.2153	0.0356	0.59752	0.00129	0.60010
atdzsr_5	921	500	na	na	43.37	7.4677	na	na	26,453.0	10.6615	0.0379	0.59162	0.00109	0.59381
atdzsr_4	921	500	na	na	43.37	7.4677	na	na	19,840.0	10.0432	0.0407	0.59012	0.00116	0.59243
atdzsr_3	921	500	na	na	43.37	7.4677	na	na	13,227.0	9.3377	0.0458	0.58978	0.00116	0.59210
atdzsr_2	921	500	na	na	43.37	7.4677	na	na	6,613.0	8.5055	0.0515	0.60131	0.00135	0.60401
atdzsr_1	921	500	na	na	43.37	7.4677	na	na	0.0	7.4677	0.0614	0.67521	0.00128	0.67777
compromised package, 10,400 g $UZrH_x$ in spherical configuration, Kaolite shell, 20.0 cm water reflector														
atdzkr_11	921	500	na	na	43.37	7.4677	76,819.4	51,214.9	128,034.0	31.1484	0.0057	0.62901	0.00121	0.63143
atdzkr_10	921	500	na	na	43.37	7.4677	69,137.4	46,093.4	115,230.8	30.0888	0.0062	0.63269	0.00123	0.63515
atdzkr_9	921	500	na	na	43.37	7.4677	61,455.5	40,971.9	102,427.4	28.9488	0.0070	0.62940	0.00134	0.63207
atdzkr_8	921	500	na	na	43.37	7.4677	53,773.5	35,850.4	89,624.0	27.7111	0.0078	0.63130	0.00124	0.63379
atdzkr_7	921	500	na	na	43.37	7.4677	46,091.6	30,728.9	76,820.5	26.3518	0.0086	0.62935	0.00117	0.63168
atdzkr_6	921	500	na	na	43.37	7.4677	38,409.7	25,607.4	64,017.1	24.8355	0.0106	0.63103	0.00126	0.63355
atdzkr_5	921	500	na	na	43.37	7.4677	30,727.7	20,486.0	51,213.7	23.1074	0.0124	0.63018	0.00125	0.63267
atdzkr_4	921	500	na	na	43.37	7.4677	23,045.8	15,364.5	38,410.3	21.0729	0.0150	0.63155	0.00144	0.63442
atdzkr_3	921	500	na	na	43.37	7.4677	15,363.9	10,243.0	25,606.8	18.5444	0.0196	0.63021	0.00146	0.63312
atdzkr_2	921	500	na	na	43.37	7.4677	7,681.9	5,121.5	12,803.4	15.0324	0.0277	0.63366	0.00133	0.63631
atdzkr_1	921	500	na	na	43.37	7.4677	0.0	0.0	0.0	7.4678	0.0607	0.67680	0.00134	0.67948
compromised package, homogenous core of $UZrH_x$, polyethylene, and Kaolite in spherical configuration, 20.0 cm water reflector														
athzpkr_11	921	500	76,819.0	51,214.9	2,220.00	39.1541	na	na	na	na	0.0289	0.46690	0.00060	0.46810
athzpkr_10	921	500	69,357.0	51,214.9	2,008.00	38.5142	na	na	na	na	0.0308	0.46634	0.00070	0.46774
athzpkr_9	921	500	61,896.0	51,214.9	1,797.00	37.8524	na	na	na	na	0.0325	0.46794	0.00072	0.46938

Table 6.9.6-22a. Results for TRIGA ($UZrH_x$) fuel element content at 19.7 wt % ^{235}U for air transportation

case name	^{235}U (g)	CH_2 (g)	H_2O (g)	Kaolite (g)	htox	Rc (cm)	H_2O (g)	Kaolite (g)	Shell (g)	Rs (cm)	nlf	k_{eff}	σ	k_{eff} + 2σ
athzpkr_8	921	500	54,435.0	51,214.9	1,586.00	37.1666	na	na	na	na	0.0345	0.46711	0.00071	0.46854
athzpkr_7	921	500	46,973.0	51,214.9	1,374.00	36.4545	na	na	na	na	0.0372	0.45900	0.00080	0.46060
athzpkr_6	921	500	39,512.0	51,214.9	1,163.00	35.7134	na	na	na	na	0.0397	0.45205	0.00087	0.45379
athzpkr_5	921	500	32,050.0	51,214.9	951.60	34.9402	na	na	na	na	0.0430	0.43464	0.00080	0.43623
athzpkr_4	921	500	24,589.0	51,214.9	740.20	34.1312	na	na	na	na	0.0465	0.41318	0.00082	0.41482
athzpkr_3	921	500	17,127.0	51,214.9	528.70	33.2819	na	na	na	na	0.0519	0.38374	0.00080	0.38535
athzpkr_2	921	500	9,666.2	51,214.9	317.30	32.3869	na	na	na	na	0.0585	0.34609	0.00090	0.34789
athzpkr_1	921	500	2,204.7	51,214.9	105.80	31.4395	na	na	na	na	0.0672	0.30481	0.00079	0.30639
compromised package, homogenous core ($UZrH_x$, polyethylene, and water from Kaolite shell), 20.0 cm water reflector														
9 fuel segments (10,400 g $UZrH_x$)														
athzpwskr_9_11	921	500	74,614.0	na	2157.00	26.3337	2,204.7	51,214.9	53,419.6	36.3591	0.0137	0.73042	0.00074	0.73191
athzpwskr_9_10	921	500	67,153.0	na	1946.00	25.4464	9,666.2	51,214.9	60,881.0	35.9034	0.0129	0.76078	0.00082	0.76243
athzpwskr_9_9	921	500	59,691.0	na	1735.00	24.4924	17,127.6	51,214.9	68,342.5	35.4359	0.0126	0.79105	0.00088	0.79281
athzpwskr_9_8	921	500	52,230.0	na	1523.00	23.4577	24,589.1	51,214.9	75,803.9	34.9557	0.0117	0.82427	0.00113	0.82653
athzpwskr_9_7	921	500	44,768.0	na	1312.00	22.3227	32,050.6	51,214.9	83,265.4	34.4620	0.0110	0.85846	0.00090	0.86026
athzpwskr_9_6	921	500	37,307.0	na	1100.00	21.0588	39,512.0	51,214.9	90,726.9	33.9536	0.0107	0.89274	0.00105	0.89485
athzpwskr_9_5	921	500	29,845.0	na	889.10	19.6216	46,973.5	51,214.9	98,188.3	33.4296	0.0097	0.92524	0.00117	0.92758
athzpwskr_9_4	921	500	22,384.0	na	677.70	17.9360	54,435.0	51,214.9	105,649.0	32.8886	0.0091	0.94825	0.00123	0.95071
athzpwskr_9_3	921	500	14,922.0	na	466.20	15.8548	61,896.4	51,214.9	113,111.0	32.3292	0.0080	0.95910	0.00127	0.96164
athzpwskr_9_2	921	500	7,461.5	na	254.80	13.0078	69,357.9	51,214.9	120,572.0	31.7498	0.0069	0.92258	0.00137	0.92531
athzpwskr_9_1	921	500	0.0	na	43.37	7.4677	76,819.4	51,214.9	128,034.0	31.1484	0.0056	0.63068	0.00143	0.63354
8 fuel segments (9,244 g $UZrH_x$)														
athzpwskr_8_11	819	500	74,614.0		2424.00	26.3184	2,204.7	51,214.9	53,419.6	36.3510	0.0137	0.68550	0.00068	0.68685
athzpwskr_8_10	819	500	67,153.0		2186.00	25.4300	9,666.2	51,214.9	60,881.0	35.8952	0.0132	0.71544	0.00084	0.71712
athzpwskr_8_9	819	500	59,691.0		1948.00	24.4747	17,127.6	51,214.9	68,342.5	35.4274	0.0127	0.74694	0.00091	0.74875

Table 6.9.6-22a. Results for TRIGA ($UZrH_x$) fuel element content at 19.7 wt % ^{235}U for air transportation

case name	^{235}U (g)	CH_2 (g)	H_2O (g)	Kaolite (g)	htox	Rc (cm)	H_2O (g)	Kaolite (g)	Shell (g)	Rs (cm)	nlf	k_{eff}	σ	k_{eff} + 2σ
athzpwskr_8_8	819	500	52,230.0		1710.00	23.4384	24,589.1	51,214.9	75,803.9	34.9470	0.0118	0.78124	0.00105	0.78334
athzpwskr_8_7	819	500	44,768.0		1472.00	22.3014	32,050.6	51,214.9	83,265.4	34.4530	0.0112	0.81614	0.00081	0.81776
athzpwskr_8_6	819	500	37,307.0		1235.00	21.0348	39,512.0	51,214.9	90,726.9	33.9444	0.0102	0.85317	0.00091	0.85499
athzpwskr_8_5	819	500	29,845.0		997.20	19.5940	46,973.5	51,214.9	98,188.3	33.4201	0.0095	0.88863	0.00106	0.89075
athzpwskr_8_4	819	500	22,384.0		759.30	17.9029	54,435.0	51,214.9	105,649.0	32.8788	0.0089	0.92262	0.00120	0.92503
athzpwskr_8_3	819	500	14,922.0		521.40	15.8124	61,896.4	51,214.9	113,111.0	32.3191	0.0080	0.93749	0.00145	0.94039
athzpwskr_8_2	819	500	7,461.5		283.50	12.9447	69,357.9	51,214.9	120,572.0	31.7393	0.0071	0.90663	0.00114	0.90892
athzpwskr_8_1	819	500	0.0		45.65	7.2723	76,819.4	51,214.9	128,034.0	31.1374	0.0054	0.61678	0.00122	0.61922
7 fuel segments (8,089g $UZrH_x$)														
athzpwskr_7_11	716	500	74,614.0		2767.00	26.3031	2,204.7	51,214.9	53,419.6	36.3430	0.0139	0.63543	0.00076	0.63695
athzpwskr_7_10	716	500	67,153.0		2495.00	25.4135	9,666.2	51,214.9	60,881.0	35.8869	0.0131	0.66621	0.00060	0.66742
athzpwskr_7_9	716	500	59,691.0		2223.00	24.4570	17,127.6	51,214.9	68,342.5	35.4190	0.0125	0.69724	0.00074	0.69872
athzpwskr_7_8	716	500	52,230.0		1951.00	23.4191	24,589.1	51,214.9	75,803.9	34.9383	0.0118	0.73306	0.00095	0.73496
athzpwskr_7_7	716	500	44,768.0		1679.00	22.2800	32,050.6	51,214.9	83,265.4	34.4441	0.0111	0.76887	0.00095	0.77077
athzpwskr_7_6	716	500	37,307.0		1407.00	21.0108	39,512.0	51,214.9	90,726.9	33.9352	0.0106	0.80872	0.00103	0.81078
athzpwskr_7_5	716	500	29,845.0		1136.00	19.5663	46,973.5	51,214.9	98,188.3	33.4106	0.0096	0.84859	0.00119	0.85097
athzpwskr_7_4	716	500	22,384.0		864.10	17.8697	54,435.0	51,214.9	105,649.0	32.8690	0.0089	0.88532	0.00101	0.88735
athzpwskr_7_3	716	500	14,922.0		592.30	15.7698	61,896.4	51,214.9	113,111.0	32.3089	0.0081	0.90821	0.00168	0.91157
athzpwskr_7_2	716	500	7,461.5		320.40	12.8811	69,357.9	51,214.9	120,572.0	31.7287	0.0071	0.88554	0.00160	0.88875
athzpwskr_7_1	716	500	0.0		48.57	7.0657	76,819.4	51,214.9	128,034.0	31.1265	0.0057	0.59808	0.00127	0.60062
6 fuel segments (6,933 g $UZrH_x$)														
athzpwskr_6_11	614	500	74,614.0		3224.00	26.2877	2,204.7	51,214.9	53,419.6	36.3349	0.0138	0.58035	0.00069	0.58174
athzpwskr_6_10	614	500	67,153.0		2907.00	25.3971	9,666.2	51,214.9	60,881.0	35.8787	0.0134	0.60885	0.00077	0.61039
athzpwskr_6_9	614	500	59,691.0		2589.00	24.4392	17,127.6	51,214.9	68,342.5	35.4105	0.0124	0.64015	0.00062	0.64140
athzpwskr_6_8	614	500	52,230.0		2272.00	23.3997	24,589.1	51,214.9	75,803.9	34.9296	0.0120	0.67689	0.00071	0.67830

Table 6.9.6-22a. Results for TRIGA ($UZrH_x$) fuel element content at 19.7 wt % ^{235}U for air transportation

case name	^{235}U (g)	CH_2 (g)	H_2O (g)	Kaolite (g)	htox	Rc (cm)	H_2O (g)	Kaolite (g)	Shell (g)	Rs (cm)	nlf	k_{eff}	σ	k_{eff} + 2σ
athzpwskr_6_7	614	500	44,768.0		1955.00	22.2586	32,050.6	51,214.9	83,265.4	34.4351	0.0108	0.71368	0.00081	0.71530
athzpwskr_6_6	614	500	37,307.0		1638.00	20.9867	39,512.0	51,214.9	90,726.9	33.9260	0.0103	0.75489	0.00118	0.75725
athzpwskr_6_5	614	500	29,845.0		1321.00	19.5385	46,973.5	51,214.9	98,188.3	33.4011	0.0096	0.79977	0.00091	0.80159
athzpwskr_6_4	614	500	22,384.0		1004.00	17.8364	54,435.0	51,214.9	105,649.0	32.8592	0.0089	0.83986	0.00099	0.84184
athzpwskr_6_3	614	500	14,922.0		686.80	15.7270	61,896.4	51,214.9	113,111.0	32.2987	0.0079	0.87249	0.00118	0.87484
athzpwskr_6_2	614	500	7,461.5		369.60	12.8167	69,357.9	51,214.9	120,572.0	31.7182	0.0070	0.86601	0.00123	0.86846
athzpwskr_6_1	614	500	0.0		52.47	6.8462	76,819.4	51,214.9	128,034.0	31.1155	0.0054	0.58104	0.00119	0.58341

Table 6.9.6-22b. Results for TRIGA ($UZrH_x$) fuel element content at 70.1 wt % ^{235}U for air transportation

case name	^{235}U (g)	CH_2 (g)	H_2O (g)	Kaolite (g)	htox	Rc (cm)	H_2O (g)	Kaolite (g)	Shell (g)	Rs (cm)	nlf	k_{eff}	σ	k_{eff} + 2σ
compromised package, 6847g $UZrH_x$ in spherical configuration, 20.0 cm water reflector														
atdzr_70	408	500	na	na	103.30	7.4677	na	na	na	na	0.0624	0.67908	0.00139	0.68187
compromised package, 6,847 g $UZrH_x$ in spherical configuration, steel shell, 20.0 cm water reflector														
atdzsr_70_11	408	500	na	na	103.30	7.4677	na	na	66,133.1	13.3978	0.0280	0.62618	0.00125	0.62868
atdzsr_70_10	408	500	na	na	103.30	7.4677	na	na	59,519.8	13.0179	0.0296	0.62153	0.00132	0.62417
atdzsr_70_9	408	500	na	na	103.30	7.4677	na	na	52,906.5	12.6144	0.0306	0.61874	0.00131	0.62135
atdzsr_70_8	408	500	na	na	103.30	7.4677	na	na	46,293.2	12.1833	0.0323	0.61302	0.00159	0.61619
atdzsr_70_7	408	500	na	na	103.30	7.4677	na	na	39,679.9	11.7193	0.0343	0.60579	0.00123	0.60825
atdzsr_70_6	408	500	na	na	103.30	7.4677	na	na	33,066.6	11.2153	0.0368	0.60315	0.00128	0.60571
atdzsr_70_5	408	500	na	na	103.30	7.4677	na	na	26,453.3	10.6615	0.0392	0.59802	0.00120	0.60043
atdzsr_70_4	408	500	na	na	103.30	7.4677	na	na	19,839.9	10.0432	0.0427	0.58654	0.00123	0.58900
atdzsr_70_3	408	500	na	na	103.30	7.4677	na	na	13,226.6	9.3377	0.0470	0.58790	0.00125	0.59040
atdzsr_70_2	408	500	na	na	103.30	7.4677	na	na	6,613.3	8.5055	0.0529	0.59739	0.00132	0.60003
atdzsr_70_1	408	500	na	na	103.30	7.4677	na	na	0.0	7.4677	0.0627	0.67646	0.00125	0.67896

Table 6.9.6-22b. Results for TRIGA ($UZrH_x$) fuel element content at 70.1 wt % ^{235}U for air transportation

case name	^{235}U (g)	CH_2 (g)	H_2O (g)	Kaolite (g)	htox	Rc (cm)	H_2O (g)	Kaolite (g)	Shell (g)	Rs (cm)	nlf	k_{eff}	σ	k_{eff} + 2σ
compromised package, 6,847 g $UZrH_x$ in spherical configuration, Kaolite shell, 20.0 cm water reflector														
atdzkr_70_11	408	500	na	na	103.30	7.4677	76,819.1	51,214.9	128,034.0	31.1484	0.0059	0.62875	0.00163	0.63201
atdzkr_70_10	408	500	na	na	103.30	7.4677	69,137.2	46,093.4	115,230.6	30.0888	0.0065	0.63092	0.00145	0.63382
atdzkr_70_9	408	500	na	na	103.30	7.4677	61,455.3	40,971.9	102,427.2	28.9488	0.0071	0.62976	0.00120	0.63217
atdzkr_70_8	408	500	na	na	103.30	7.4677	53,773.4	35,850.4	89,623.8	27.7111	0.0081	0.62727	0.00127	0.62981
atdzkr_70_7	408	500	na	na	103.30	7.4677	46,091.5	30,728.9	76,820.4	26.3518	0.0091	0.63196	0.00132	0.63460
atdzkr_70_6	408	500	na	na	103.30	7.4677	38,409.6	25,607.4	64,017.0	24.8355	0.0105	0.63124	0.00126	0.63376
atdzkr_70_5	408	500	na	na	103.30	7.4677	30,727.6	20,486.0	51,213.6	23.1074	0.0128	0.62913	0.00120	0.63153
atdzkr_70_4	408	500	na	na	103.30	7.4677	23,045.7	15,364.5	38,410.2	21.0729	0.0155	0.62943	0.00124	0.63192
atdzkr_70_3	408	500	na	na	103.30	7.4677	15,363.8	10,243.0	25,606.8	18.5444	0.0198	0.62910	0.00118	0.63146
atdzkr_70_2	408	500	na	na	103.30	7.4677	7,681.9	5,121.5	12,803.4	15.0324	0.0288	0.62962	0.00139	0.63240
atdzkr_70_1	408	500	na	na	103.30	7.4677	0.0	0.0	0.0	7.4677	0.0629	0.67511	0.00143	0.67798
compromised package, homogenous core of 6,847 g $UZrH_x$, polyethylene, and Kaolite in spherical configuration, 20.0 cm water reflector														
athzpkr_70_11	408	500	76,819.0	51,214.9	5017.00	39.1541	na	na	na	na	0.0290	0.26748	0.00033	0.26814
athzpkr_70_10	408	500	69,357.0	51,214.9	4540.00	38.5142	na	na	na	na	0.0307	0.27025	0.00042	0.27108
athzpkr_70_9	408	500	61,896.0	51,214.9	4063.00	37.8524	na	na	na	na	0.0325	0.27525	0.00044	0.27612
athzpkr_70_8	408	500	54,435.0	51,214.9	3585.00	37.1666	na	na	na	na	0.0347	0.27839	0.00046	0.27931
athzpkr_70_7	408	500	46,973.0	51,214.9	3108.00	36.4545	na	na	na	na	0.0369	0.27822	0.00049	0.27920
athzpkr_70_6	408	500	39,512.0	51,214.9	2631.00	35.7134	na	na	na	na	0.0398	0.27705	0.00056	0.27818
athzpkr_70_5	408	500	32,050.0	51,214.9	2153.00	34.9402	na	na	na	na	0.0427	0.27191	0.00049	0.27289
athzpkr_70_4	408	500	24,589.0	51,214.9	1676.00	34.1312	na	na	na	na	0.0473	0.26332	0.00052	0.26437
athzpkr_70_3	408	500	17,127.0	51,214.9	1199.00	33.2819	na	na	na	na	0.0519	0.25025	0.00056	0.25138
athzpkr_70_2	408	500	9,666.2	51,214.9	721.60	32.3869	na	na	na	na	0.0591	0.22951	0.00053	0.23057
athzpkr_70_1	408	500	2,204.7	51,214.9	244.30	31.4395	na	na	na	na	0.0679	0.20646	0.00055	0.20755

Table 6.9.6-22b. Results for TRIGA ($UZrH_x$) fuel element content at 70.1 wt % ^{235}U for air transportation

case name	^{235}U (g)	CH_2 (g)	H_2O (g)	Kaolite (g)	htox	Rc (cm)	H_2O (g)	Kaolite (g)	Shell (g)	Rs (cm)	nlf	k_{eff}	σ	k_{eff} + 2σ
compromised package, homogenous core (6,847 g $UZrH_x$, polyethylene, and water from Kaolite shell), 20.0 cm water reflector														
athzpwskr_70_11	408	500	74,614.0	na	4876.00	26.3337	2,204.7	51,214.9	53,419.6	36.3591	0.0134	0.44499	0.00044	0.44586
athzpwskr_70_10	408	500	67,153.0	na	4399.00	25.4464	9,666.2	51,214.9	60,881.0	35.9034	0.0130	0.47137	0.00054	0.47245
athzpwskr_70_9	408	500	59,691.0	na	3921.00	24.4924	17,127.6	51,214.9	68,342.5	35.4359	0.0123	0.50131	0.00054	0.50240
athzpwskr_70_8	408	500	52,230.0	na	3444.00	23.4577	24,589.1	51,214.9	75,803.9	34.9557	0.0118	0.53602	0.00064	0.53731
athzpwskr_70_7	408	500	44,768.0	na	2967.00	22.3227	32,050.6	51,214.9	83,265.4	34.4620	0.0111	0.57515	0.00057	0.57630
athzpwskr_70_6	408	500	37,307.0	na	2489.00	21.0588	39,512.0	51,214.9	90,726.9	33.9536	0.0104	0.62110	0.00071	0.62252
athzpwskr_70_5	408	500	29,845.0	na	2012.00	19.6216	46,973.5	51,214.9	98,188.3	33.4296	0.0096	0.67041	0.00078	0.67197
athzpwskr_70_4	408	500	22,384.0	na	1535.00	17.9360	54,435.0	51,214.9	105,649.0	32.8886	0.0087	0.72604	0.00103	0.72811
athzpwskr_70_3	408	500	14,922.0	na	1057.00	15.8548	61,896.4	51,214.9	113,111.0	32.3292	0.0078	0.78713	0.00124	0.78961
athzpwskr_70_2	408	500	7,461.5	na	580.60	13.0078	69,357.9	51,214.9	120,572.0	31.7498	0.0069	0.82138	0.00139	0.82415
athzpwskr_70_1	408	500	0.0	na	103.30	7.4677	76,819.4	51,214.9	128,034.0	31.1484	0.0057	0.62877	0.00145	0.63168

Table 6.9.6-23. Results for HEU broken metal content for air transportation

case name	^{235}U (g)	CH_2 (g)	H_2O (g)	Kaolite (g)	htox	Rc (cm)	H_2O (g)	Kao (g)	Shell (g)	Rs (cm)	nlf	k_{eff}	σ	k_{eff} + 2σ
compromised package, HEU in spherical configuration, 20.0 cm water reflector (See Table 6.9.6-21)														
compromised package, HEU in spherical configuration, Kaolite shell, 20.0 cm water reflector (See Table 6.9.6-21)														
compromised package, HEU in spherical configuration, Kaolite shell, 20.0 cm water reflector (See Table 6.9.6-21)														
compromised package, homogenous core of HEU broken metal, polyethylene, and Kaolite in spherical configuration, 20.0 cm water reflector														
7,000g HEU 100% enrichment														
athmpkr_12_8_11	7,000	513	76,819.0	51,214.9	288.80	39.11173	na	na	na	na	0.0303	1.02117	0.00126	1.02369
athmpkr_12_8_10	7,000	513	69,357.0	51,214.9	261.00	38.47048	na	na	na	na	0.0316	1.00126	0.00127	1.00381
athmpkr_12_8_9	7,000	513	61,896.0	51,214.9	233.20	37.80710	na	na	na	na	0.0329	0.97483	0.00132	0.97746
athmpkr_12_8_8	7,000	513	54,435.0	51,214.9	205.40	37.11959	na	na	na	na	0.0351	0.94449	0.00130	0.94709

Table 6.9.6-23. Results for HEU broken metal content for air transportation

case name	^{235}U (g)	CH_2 (g)	H_2O (g)	Kaolite (g)	htox	Rc (cm)	H_2O (g)	Kao (g)	Shell (g)	Rs (cm)	nlf	k_{eff}	σ	$k_{eff} + 2σ$
athmpkr_12_8_7	7,000	513	46,973.0	51,214.9	177.60	36.40562	na	na	na	na	0.0373	0.90773	0.00123	0.91019
athmpkr_12_8_6	7,000	513	39,512.0	51,214.9	149.70	35.66249	na	na	na	na	0.0405	0.86356	0.00129	0.86614
athmpkr_12_8_5	7,000	513	32,050.0	51,214.9	121.90	34.88702	na	na	na	na	0.0438	0.80722	0.00131	0.80984
athmpkr_12_8_4	7,000	513	24,589.0	51,214.9	94.14	34.07546	na	na	na	na	0.0473	0.74163	0.00124	0.74411
athmpkr_12_8_3	7,000	513	17,127.0	51,214.9	66.32	33.22329	na	na	na	na	0.0522	0.66883	0.00119	0.67121
athmpkr_12_8_2	7,000	513	9,666.2	51,214.9	38.50	32.32500	na	na	na	na	0.0579	0.58476	0.00116	0.58707
athmpkr_12_8_1	7,000	513	2,204.7	51,214.9	10.68	31.37380	na	na	na	na	0.0660	0.49910	0.00115	0.50141
6,000g HEU 100% enrichment														
athmpkr_11_8_11	6,000	513	76,819.0	51,214.9	337.00	39.10897	na	na	na	na	0.0296	0.99414	0.00136	0.99686
athmpkr_11_8_10	6,000	513	69,357.0	51,214.9	304.50	38.46762	na	na	na	na	0.0317	0.97423	0.00134	0.97691
athmpkr_11_8_9	6,000	513	61,896.0	51,214.9	272.10	37.80414	na	na	na	na	0.0333	0.94998	0.00135	0.95269
athmpkr_11_8_8	6,000	513	54,435.0	51,214.9	239.60	37.11651	na	na	na	na	0.0351	0.92270	0.00139	0.92549
athmpkr_11_8_7	6,000	513	46,973.0	51,214.9	207.20	36.40242	na	na	na	na	0.0378	0.88445	0.00148	0.88741
athmpkr_11_8_6	6,000	513	39,512.0	51,214.9	174.70	35.65916	na	na	na	na	0.0408	0.84157	0.00122	0.84401
athmpkr_11_8_5	6,000	513	32,050.0	51,214.9	142.20	34.88355	na	na	na	na	0.0435	0.79067	0.00131	0.79329
athmpkr_11_8_4	6,000	513	24,589.0	51,214.9	109.80	34.07182	na	na	na	na	0.0472	0.72721	0.00132	0.72984
athmpkr_11_8_3	6,000	513	17,127.0	51,214.9	77.38	33.21946	na	na	na	na	0.0521	0.65397	0.00117	0.65630
athmpkr_11_8_2	6,000	513	9,666.2	51,214.9	44.92	32.32095	na	na	na	na	0.0576	0.57446	0.00112	0.57670
athmpkr_11_8_1	6,000	513	2,204.7	51,214.9	12.46	31.36950	na	na	na	na	0.0668	0.48779	0.00112	0.49002
5,000g HEU 100% enrichment														
athmpkr_10_8_11	5,000	513	76,819.0	51,214.9	404.40	39.10620	na	na	na	na	0.0294	0.95646	0.00121	0.95888
athmpkr_10_8_10	5,000	513	69,357.0	51,214.9	365.50	38.46476	na	na	na	na	0.0314	0.94048	0.00114	0.94276
athmpkr_10_8_9	5,000	513	61,896.0	51,214.9	326.50	37.80118	na	na	na	na	0.0330	0.91763	0.00150	0.92063
athmpkr_10_8_8	5,000	513	54,435.0	51,214.9	287.60	37.11344	na	na	na	na	0.0354	0.89037	0.00129	0.89296
athmpkr_10_8_7	5,000	513	46,973.0	51,214.9	248.60	36.39923	na	na	na	na	0.0373	0.85732	0.00122	0.85977

Table 6.9.6-23. Results for HEU broken metal content for air transportation

case name	^{235}U (g)	CH_2 (g)	H_2O (g)	Kaolite (g)	htox	Rc (cm)	H_2O (g)	Kao (g)	Shell (g)	Rs (cm)	nlf	k_{eff}	σ	$k_{eff} + 2σ$
athmpkr_10_8_6	5,000	513	39,512.0	51,214.9	209.70	35.65583	na	na	na	na	0.0401	0.81566	0.00126	0.81819
athmpkr_10_8_5	5,000	513	32,050.0	51,214.9	170.70	34.88007	na	na	na	na	0.0434	0.76481	0.00134	0.76750
athmpkr_10_8_4	5,000	513	24,589.0	51,214.9	131.80	34.06818	na	na	na	na	0.0473	0.70780	0.00130	0.71040
athmpkr_10_8_3	5,000	513	17,127.0	51,214.9	92.85	33.21562	na	na	na	na	0.0522	0.63560	0.00122	0.63804
athmpkr_10_8_2	5,000	513	9,666.2	51,214.9	53.90	32.31690	na	na	na	na	0.0586	0.55806	0.00122	0.56051
athmpkr_10_8_1	5,000	513	2,204.7	51,214.9	14.95	31.36520	na	na	na	na	0.0670	0.47312	0.00116	0.47544
4,500g HEU 100% enrichment														
athmpkr_9_8_11	4,500	513	76,819.0	51,214.9	449.30	39.10482	na	na	na	na	0.0298	0.93346	0.00133	0.93612
athmpkr_9_8_10	4,500	513	69,357.0	51,214.9	406.10	38.46333	na	na	na	na	0.0313	0.91551	0.00143	0.91836
athmpkr_9_8_9	4,500	513	61,896.0	51,214.9	362.80	37.79970	na	na	na	na	0.0335	0.89522	0.00152	0.89826
athmpkr_9_8_8	4,500	513	54,435.0	51,214.9	319.50	37.11191	na	na	na	na	0.0353	0.87213	0.00126	0.87465
athmpkr_9_8_7	4,500	513	46,973.0	51,214.9	276.20	36.39763	na	na	na	na	0.0377	0.84048	0.00133	0.84313
athmpkr_9_8_6	4,500	513	39,512.0	51,214.9	233.00	35.65417	na	na	na	na	0.0404	0.80226	0.00125	0.80476
athmpkr_9_8_5	4,500	513	32,050.0	51,214.9	189.70	34.87833	na	na	na	na	0.0437	0.75194	0.00122	0.75439
athmpkr_9_8_4	4,500	513	24,589.0	51,214.9	146.40	34.06635	na	na	na	na	0.0476	0.69314	0.00112	0.69538
athmpkr_9_8_3	4,500	513	17,127.0	51,214.9	103.10	33.21370	na	na	na	na	0.0524	0.62629	0.00119	0.62867
athmpkr_9_8_2	4,500	513	9,666.2	51,214.9	59.89	32.31488	na	na	na	na	0.0584	0.54872	0.00115	0.55101
athmpkr_9_8_1	4,500	513	2,204.7	51,214.9	16.61	31.36305	na	na	na	na	0.0669	0.46796	0.00115	0.47026
4,000g HEU 100% enrichment														
athmpkr_8_8_11	4,000	513	76,819.0	51,214.9	505.50	39.10344	na	na	na	na	0.0298	0.90432	0.00121	0.90674
athmpkr_8_8_10	4,000	513	69,357.0	51,214.9	456.80	38.46190	na	na	na	na	0.0319	0.88942	0.00129	0.89199
athmpkr_8_8_9	4,000	513	61,896.0	51,214.9	408.10	37.79822	na	na	na	na	0.0334	0.87153	0.00115	0.87382
athmpkr_8_8_8	4,000	513	54,435.0	51,214.9	359.50	37.11037	na	na	na	na	0.0350	0.84664	0.00127	0.84918
athmpkr_8_8_7	4,000	513	46,973.0	51,214.9	310.80	36.39604	na	na	na	na	0.0370	0.82052	0.00118	0.82288
athmpkr_8_8_6	4,000	513	39,512.0	51,214.9	262.10	35.65250	na	na	na	na	0.0405	0.77971	0.00116	0.78203

Table 6.9.6-23. Results for HEU broken metal content for air transportation

case name	^{235}U (g)	CH_2 (g)	H_2O (g)	Kaolite (g)	htox	Rc (cm)	H_2O (g)	Kao (g)	Shell (g)	Rs (cm)	nlf	k_{eff}	σ	$k_{eff} + 2σ$
athmpkr_8_8_5	4,000	513	32,050.0	51,214.9	213.40	34.87659	na	na	na	na	0.0435	0.73454	0.00143	0.73739
athmpkr_8_8_4	4,000	513	24,589.0	51,214.9	164.70	34.06453	na	na	na	na	0.0481	0.67953	0.00135	0.68224
athmpkr_8_8_3	4,000	513	17,127.0	51,214.9	116.00	33.21179	na	na	na	na	0.0526	0.61370	0.00125	0.61620
athmpkr_8_8_2	4,000	513	9,666.2	51,214.9	67.38	32.31285	na	na	na	na	0.0589	0.53800	0.00112	0.54024
athmpkr_8_8_1	4,000	513	2,204.7	51,214.9	18.69	31.36090	na	na	na	na	0.0672	0.45619	0.00091	0.45801
35,000g HEU 20% enrichment														
athmpkr_12_1_11	7,000	513	76,819.0	51,214.9	57.78	39.18804	na	na	na	na	0.0301	0.96192	0.00133	0.96459
athmpkr_12_1_10	7,000	513	69,357.0	51,214.9	52.21	38.54934	na	na	na	na	0.0314	0.94161	0.00143	0.94448
athmpkr_12_1_9	7,000	513	61,896.0	51,214.9	46.65	37.88874	na	na	na	na	0.0329	0.91690	0.00128	0.91946
athmpkr_12_1_8	7,000	513	54,435.0	51,214.9	41.09	37.20427	na	na	na	na	0.0348	0.88747	0.00124	0.88995
athmpkr_12_1_7	7,000	513	46,973.0	51,214.9	35.52	36.49364	na	na	na	na	0.0374	0.85152	0.00140	0.85433
athmpkr_12_1_6	7,000	513	39,512.0	51,214.9	29.96	35.75421	na	na	na	na	0.0399	0.80727	0.00130	0.80988
athmpkr_12_1_5	7,000	513	32,050.0	51,214.9	24.39	34.98285	na	na	na	na	0.0428	0.75729	0.00132	0.75994
athmpkr_12_1_4	7,000	513	24,589.0	51,214.9	18.83	34.17589	na	na	na	na	0.0463	0.70008	0.00133	0.70274
athmpkr_12_1_3	7,000	513	17,127.0	51,214.9	13.26	33.32891	na	na	na	na	0.0504	0.63481	0.00122	0.63725
athmpkr_12_1_2	7,000	513	9,666.2	51,214.9	7.70	32.43654	na	na	na	na	0.0564	0.56213	0.00123	0.56458
athmpkr_12_1_1	7,000	513	2,204.7	51,214.9	2.14	31.49217	na	na	na	na	0.0641	0.48853	0.00108	0.49068
30,000g HEU 20% enrichment														
athmpkr_11_1_11	6,000	513	76,819.0	51,214.9	67.41	39.17440	na	na	na	na	0.0295	0.93897	0.00126	0.94150
athmpkr_11_1_10	6,000	513	69,357.0	51,214.9	60.92	38.53524	na	na	na	na	0.0308	0.91990	0.00112	0.92213
athmpkr_11_1_9	6,000	513	61,896.0	51,214.9	54.43	37.87415	na	na	na	na	0.0328	0.89565	0.00141	0.89848
athmpkr_11_1_8	6,000	513	54,435.0	51,214.9	47.93	37.18914	na	na	na	na	0.0350	0.86704	0.00129	0.86961
athmpkr_11_1_7	6,000	513	46,973.0	51,214.9	41.44	36.47792	na	na	na	na	0.0373	0.83339	0.00110	0.83560
athmpkr_11_1_6	6,000	513	39,512.0	51,214.9	34.95	35.73782	na	na	na	na	0.0395	0.79255	0.00152	0.79560
athmpkr_11_1_5	6,000	513	32,050.0	51,214.9	28.46	34.96573	na	na	na	na	0.0426	0.74225	0.00124	0.74473

Table 6.9.6-23. Results for HEU broken metal content for air transportation

case name	^{235}U (g)	CH_2 (g)	H_2O (g)	Kaolite (g)	htox	Rc (cm)	H_2O (g)	Kao (g)	Shell (g)	Rs (cm)	nlf	k_{eff}	σ	$k_{eff} + 2σ$
athmpkr_11_1_4	6,000	513	24,589.0	51,214.9	21.97	34.15796	na	na	na	na	0.0467	0.68601	0.00131	0.68863
athmpkr_11_1_3	6,000	513	17,127.0	51,214.9	15.48	33.31005	na	na	na	na	0.0513	0.62146	0.00116	0.62378
athmpkr_11_1_2	6,000	513	9,666.2	51,214.9	8.98	32.41663	na	na	na	na	0.0569	0.55015	0.00105	0.55225
athmpkr_11_1_1	6,000	513	2,204.7	51,214.9	2.49	31.47105	na	na	na	na	0.0648	0.47666	0.00112	0.47889
25,000g HEU 20% enrichment														
athmpkr_10_1_11	5,000	513	76,819.0	51,214.9	80.89	39.16075	na	na	na	na	0.0298	0.90855	0.00127	0.91109
athmpkr_10_1_10	5,000	513	69,357.0	51,214.9	73.10	38.52114	na	na	na	na	0.0313	0.88989	0.00113	0.89214
athmpkr_10_1_9	5,000	513	61,896.0	51,214.9	65.31	37.85955	na	na	na	na	0.0333	0.86764	0.00140	0.87044
athmpkr_10_1_8	5,000	513	54,435.0	51,214.9	57.52	37.17399	na	na	na	na	0.0349	0.84114	0.00150	0.84413
athmpkr_10_1_7	5,000	513	46,973.0	51,214.9	49.73	36.46217	na	na	na	na	0.0375	0.81229	0.00117	0.81463
athmpkr_10_1_6	5,000	513	39,512.0	51,214.9	41.94	35.72142	na	na	na	na	0.0399	0.77026	0.00129	0.77285
athmpkr_10_1_5	5,000	513	32,050.0	51,214.9	34.15	34.94860	na	na	na	na	0.0428	0.72521	0.00110	0.72741
athmpkr_10_1_4	5,000	513	24,589.0	51,214.9	26.36	34.14000	na	na	na	na	0.0464	0.66966	0.00118	0.67201
athmpkr_10_1_3	5,000	513	17,127.0	51,214.9	18.57	33.29117	na	na	na	na	0.0513	0.60484	0.00106	0.60696
athmpkr_10_1_2	5,000	513	9,666.2	51,214.9	10.78	32.39669	na	na	na	na	0.0569	0.53554	0.00110	0.53774
athmpkr_10_1_1	5,000	513	2,204.7	51,214.9	2.99	31.44989	na	na	na	na	0.0657	0.46235	0.00101	0.46436
compromised package, homogenous core (HEU broken metal, polyethylene, and water from Kaolite shell), 20.0 cm water reflector														
7,000g HEU 100% enrichment														
athmpwskr_12_8_11	7,000	513	74,614.0	na	280.60	26.23990	2,204.7	51,214.9	53,419.6	36.3100	0.0147	1.40566	0.00163	1.40891
athmpwskr_12_8_10	7,000	513	67,153.0	na	252.80	25.34586	9,666.2	51,214.9	60,881.0	35.8530	0.0143	1.40534	0.00159	1.40851
athmpwskr_12_8_9	7,000	513	59,691.0	na	225.00	24.38387	17,127.6	51,214.9	68,342.5	35.3842	0.0132	1.40155	0.00136	1.40427
athmpwskr_12_8_8	7,000	513	52,230.0	na	197.20	23.33933	24,589.1	51,214.9	75,803.9	34.9026	0.0127	1.39948	0.00148	1.40243
athmpwskr_12_8_7	7,000	513	44,768.0	na	169.30	22.19184	32,050.6	51,214.9	83,265.4	34.4073	0.0120	1.38745	0.00140	1.39024
athmpwskr_12_8_6	7,000	513	37,307.0	na	141.50	20.91156	39,512.0	51,214.9	90,726.9	33.8973	0.0112	1.37472	0.00171	1.37815
athmpwskr_12_8_5	7,000	513	29,845.0	na	113.70	19.45176	46,973.5	51,214.9	98,188.3	33.3715	0.0101	1.34516	0.00143	1.34802

Table 6.9.6-23. Results for HEU broken metal content for air transportation

case name	^{235}U (g)	CH_2 (g)	H_2O (g)	Kaolite (g)	htox	Rc (cm)	H_2O (g)	Kao (g)	Shell (g)	Rs (cm)	nlf	k_{eff}	σ	$k_{eff} + 2σ$
athmpwskr_12_8_4	7,000	513	22,384.0	na	85.92	17.73212	54,435.0	51,214.9	105,649.0	32.8286	0.0092	1.30120	0.00174	1.30468
athmpwskr_12_8_3	7,000	513	14,922.0	na	58.10	15.59253	61,896.4	51,214.9	113,111.0	32.2671	0.0082	1.23073	0.00150	1.23372
athmpwskr_12_8_2	7,000	513	7,461.5	na	30.28	12.61277	69,357.9	51,214.9	120,572.0	31.6853	0.0074	1.09181	0.00180	1.09541
athmpwskr_12_8_1	7,000	513	0.0	na	2.46	6.05465	76,819.4	51,214.9	128,034.0	31.0814	0.0059	0.74568	0.00119	0.74806
6,000g HEU 100% enrichment														
athmpwskr_11_8_11	6,000	513	74,614.0	na	327.40	26.23375	2,204.7	51,214.9	53,419.6	36.3067	0.0146	1.37327	0.00128	1.37583
athmpwskr_11_8_10	6,000	513	67,153.0	na	294.90	25.33928	9,666.2	51,214.9	60,881.0	35.8498	0.0141	1.37801	0.00135	1.38071
athmpwskr_11_8_9	6,000	513	59,691.0	na	262.50	24.37676	17,127.6	51,214.9	68,342.5	35.3808	0.0133	1.37898	0.00144	1.38186
athmpwskr_11_8_8	6,000	513	52,230.0	na	230.00	23.33156	24,589.1	51,214.9	75,803.9	34.8991	0.0127	1.37963	0.00145	1.38253
athmpwskr_11_8_7	6,000	513	44,768.0	na	197.60	22.18325	32,050.6	51,214.9	83,265.4	34.4037	0.0115	1.37069	0.00134	1.37337
athmpwskr_11_8_6	6,000	513	37,307.0	na	165.10	20.90188	39,512.0	51,214.9	90,726.9	33.8936	0.0113	1.35827	0.00151	1.36128
athmpwskr_11_8_5	6,000	513	29,845.0	na	132.70	19.44057	46,973.5	51,214.9	98,188.3	33.3677	0.0102	1.33346	0.00169	1.33684
athmpwskr_11_8_4	6,000	513	22,384.0	na	100.20	17.71865	54,435.0	51,214.9	105,649.0	32.8247	0.0092	1.29338	0.00156	1.29649
athmpwskr_11_8_3	6,000	513	14,922.0	na	67.78	15.57511	61,896.4	51,214.9	113,111.0	32.2630	0.0083	1.22486	0.00149	1.22783
athmpwskr_11_8_2	6,000	513	7,461.5	na	35.33	12.58612	69,357.9	51,214.9	120,572.0	31.6811	0.0072	1.08845	0.00153	1.09150
athmpwskr_11_8_1	6,000	513	0.0	na	2.87	5.93698	76,819.4	51,214.9	128,034.0	31.0770	0.0059	0.72381	0.00141	0.72662
5,000g HEU 100% enrichment														
athmpwskr_10_8_11	5,000	513	74,614.0	na	392.90	26.22760	2,204.7	51,214.9	53,419.6	36.3035	0.0146	1.33984	0.00131	1.34246
athmpwskr_10_8_10	5,000	513	67,153.0	na	353.90	25.33269	9,666.2	51,214.9	60,881.0	35.8465	0.0138	1.34369	0.00132	1.34633
athmpwskr_10_8_9	5,000	513	59,691.0	na	315.00	24.36964	17,127.6	51,214.9	68,342.5	35.3774	0.0132	1.34600	0.00155	1.34910
athmpwskr_10_8_8	5,000	513	52,230.0	na	276.00	23.32378	24,589.1	51,214.9	75,803.9	34.8956	0.0123	1.35066	0.00167	1.35399
athmpwskr_10_8_7	5,000	513	44,768.0	na	237.10	22.17465	32,050.6	51,214.9	83,265.4	34.4001	0.0118	1.34411	0.00181	1.34774
athmpwskr_10_8_6	5,000	513	37,307.0	na	198.10	20.89219	39,512.0	51,214.9	90,726.9	33.8899	0.0109	1.33905	0.00153	1.34211
athmpwskr_10_8_5	5,000	513	29,845.0	na	159.20	19.42937	46,973.5	51,214.9	98,188.3	33.3639	0.0102	1.32129	0.00137	1.32402
athmpwskr_10_8_4	5,000	513	22,384.0	na	120.20	17.70517	54,435.0	51,214.9	105,649.0	32.8207	0.0093	1.28519	0.00134	1.28787

Table 6.9.6-23. Results for HEU broken metal content for air transportation

case name	^{235}U (g)	CH_2 (g)	H_2O (g)	Kaolite (g)	htox	Rc (cm)	H_2O (g)	Kao (g)	Shell (g)	Rs (cm)	nlf	k_{eff}	σ	$k_{eff} + 2σ$
athmpwskr_10_8_3	5,000	513	14,922.0	na	81.34	15.55766	61,896.4	51,214.9	113,111.0	32.2590	0.0084	1.21735	0.00195	1.22124
athmpwskr_10_8_2	5,000	513	7,461.5	na	42.39	12.55935	69,357.9	51,214.9	120,572.0	31.6769	0.0074	1.08329	0.00161	1.08651
athmpwskr_10_8_1	5,000	513	0.0	na	3.44	5.81446	76,819.4	51,214.9	128,034.0	31.0727	0.0059	0.69818	0.00115	0.70048
4,000g HEU 100% enrichment														
athmpwskr_8_8_11	4,000	513	74,614.0	na	491.10	26.22145	2,204.7	51,214.9	53,419.6	36.3003	0.0144	1.28173	0.00151	1.28476
athmpwskr_8_8_10	4,000	513	67,153.0	na	442.40	25.32609	9,666.2	51,214.9	60,881.0	35.8432	0.0139	1.29257	0.00121	1.29500
athmpwskr_8_8_9	4,000	513	59,691.0	na	393.80	24.36251	17,127.6	51,214.9	68,342.5	35.3741	0.0133	1.30185	0.00134	1.30454
athmpwskr_8_8_8	4,000	513	52,230.0	na	345.10	23.31600	24,589.1	51,214.9	75,803.9	34.8922	0.0126	1.30836	0.00146	1.31127
athmpwskr_8_8_7	4,000	513	44,768.0	na	296.40	22.16604	32,050.6	51,214.9	83,265.4	34.3966	0.0117	1.31084	0.00173	1.31430
athmpwskr_8_8_6	4,000	513	37,307.0	na	247.70	20.88250	39,512.0	51,214.9	90,726.9	33.8863	0.0110	1.30781	0.00164	1.31109
athmpwskr_8_8_5	4,000	513	29,845.0	na	199.00	19.41816	46,973.5	51,214.9	98,188.3	33.3601	0.0100	1.29559	0.00152	1.29863
athmpwskr_8_8_4	4,000	513	22,384.0	na	150.30	17.69166	54,435.0	51,214.9	105,649.0	32.8168	0.0093	1.26284	0.00131	1.26545
athmpwskr_8_8_3	4,000	513	14,922.0	na	101.60	15.54016	61,896.4	51,214.9	113,111.0	32.2549	0.0083	1.20481	0.00156	1.20793
athmpwskr_8_8_2	4,000	513	7,461.5	na	52.99	12.53248	69,357.9	51,214.9	120,572.0	31.6727	0.0075	1.08009	0.00169	1.08346
athmpwskr_8_8_1	4,000	513	0.0	na	4.30	5.68653	76,819.4	51,214.9	128,034.0	31.0683	0.0059	0.66987	0.00120	0.67228
3,000g HEU 100% enrichment														
athmpwskr_6_8_11	3,000	513	74,614.0	na	654.90	26.21530	2,204.7	51,214.9	53,419.6	36.2971	0.0143	1.19922	0.00120	1.20161
athmpwskr_6_8_10	3,000	513	67,153.0	na	589.90	25.31949	9,666.2	51,214.9	60,881.0	35.8399	0.0137	1.21615	0.00114	1.21844
athmpwskr_6_8_9	3,000	513	59,691.0	na	525.00	24.35538	17,127.6	51,214.9	68,342.5	35.3707	0.0133	1.23018	0.00144	1.23305
athmpwskr_6_8_8	3,000	513	52,230.0	na	460.10	23.30822	24,589.1	51,214.9	75,803.9	34.8887	0.0122	1.24414	0.00166	1.24745
athmpwskr_6_8_7	3,000	513	44,768.0	na	395.20	22.15743	32,050.6	51,214.9	83,265.4	34.3930	0.0114	1.25133	0.00159	1.25450
athmpwskr_6_8_6	3,000	513	37,307.0	na	330.30	20.87279	39,512.0	51,214.9	90,726.9	33.8826	0.0108	1.25789	0.00155	1.26100
athmpwskr_6_8_5	3,000	513	29,845.0	na	265.40	19.40693	46,973.5	51,214.9	98,188.3	33.3563	0.0101	1.25398	0.00171	1.25740
athmpwskr_6_8_4	3,000	513	22,384.0	na	200.40	17.67814	54,435.0	51,214.9	105,649.0	32.8129	0.0091	1.23478	0.00161	1.23799
athmpwskr_6_8_3	3,000	513	14,922.0	na	135.50	15.52262	61,896.4	51,214.9	113,111.0	32.2508	0.0085	1.18809	0.00160	1.19128

Table 6.9.6-23. Results for HEU broken metal content for air transportation

case name	^{235}U (g)	CH_2 (g)	H_2O (g)	Kaolite (g)	htox	Rc (cm)	H_2O (g)	Kao (g)	Shell (g)	Rs (cm)	nlf	k_{eff}	σ	$k_{eff} + 2σ$
athmpwskr_6_8_2	3,000	513	7,461.5	na	70.65	12.50549	69,357.9	51,214.9	120,572.0	31.6685	0.0073	1.06995	0.00163	1.07321
athmpwskr_6_8_1	3,000	513	0.0	na	5.74	5.55258	76,819.4	51,214.9	128,034.0	31.0639	0.0060	0.63966	0.00095	0.64155
2,000g HEU 100% enrichment														
athmpwskr_4_8_11	2,000	513	74,614.0	na	982.30	26.20914	2,204.7	51,214.9	53,419.6	36.2939	0.0140	1.06299	0.00106	1.06511
athmpwskr_4_8_10	2,000	513	67,153.0	na	884.90	25.31289	9,666.2	51,214.9	60,881.0	35.8366	0.0137	1.08184	0.00119	1.08421
athmpwskr_4_8_9	2,000	513	59,691.0	na	787.60	24.34825	17,127.6	51,214.9	68,342.5	35.3673	0.0130	1.10555	0.00127	1.10808
athmpwskr_4_8_8	2,000	513	52,230.0	na	690.20	23.30043	24,589.1	51,214.9	75,803.9	34.8852	0.0122	1.13134	0.00127	1.13387
athmpwskr_4_8_7	2,000	513	44,768.0	na	592.80	22.14881	32,050.6	51,214.9	83,265.4	34.3894	0.0116	1.15079	0.00124	1.15327
athmpwskr_4_8_6	2,000	513	37,307.0	na	495.40	20.86308	39,512.0	51,214.9	90,726.9	33.8789	0.0111	1.16711	0.00141	1.16993
athmpwskr_4_8_5	2,000	513	29,845.0	na	398.10	19.39569	46,973.5	51,214.9	98,188.3	33.3525	0.0098	1.17872	0.00167	1.18207
athmpwskr_4_8_4	2,000	513	22,384.0	na	300.70	17.66459	54,435.0	51,214.9	105,649.0	32.8089	0.0090	1.17375	0.00144	1.17664
athmpwskr_4_8_3	2,000	513	14,922.0	na	203.30	15.50504	61,896.4	51,214.9	113,111.0	32.2468	0.0083	1.14657	0.00155	1.14967
athmpwskr_4_8_2	2,000	513	7,461.5	na	105.90	12.47838	69,357.9	51,214.9	120,572.0	31.6643	0.0074	1.04637	0.00136	1.04909
athmpwskr_4_8_1	2,000	513	0.0	na	8.60	5.41183	76,819.4	51,214.9	128,034.0	31.0595	0.0061	0.60330	0.00119	0.60569
1,000g HEU 100% enrichment														
athmpwskr_2_8_11	1,000	513	74,614.0	na	1964.0	26.20298	2,204.7	51,214.9	53,419.6	36.2907	0.0141	0.78675	0.00095	0.78864
athmpwskr_2_8_10	1,000	513	67,153.0	na	1769.0	25.30629	9,666.2	51,214.9	60,881.0	35.8333	0.0133	0.81910	0.00090	0.82091
athmpwskr_2_8_9	1,000	513	59,691.0	na	1575.0	24.34111	17,127.6	51,214.9	68,342.5	35.3639	0.0128	0.84934	0.00112	0.85158
athmpwskr_2_8_8	1,000	513	52,230.0	na	1380.0	23.29264	24,589.1	51,214.9	75,803.9	34.8817	0.0122	0.88411	0.00113	0.88637
athmpwskr_2_8_7	1,000	513	44,768.0	na	1185.0	22.14018	32,050.6	51,214.9	83,265.4	34.3858	0.0114	0.92300	0.00099	0.92498
athmpwskr_2_8_6	1,000	513	37,307.0	na	990.90	20.85335	39,512.0	51,214.9	90,726.9	33.8752	0.0105	0.95883	0.00112	0.96106
athmpwskr_2_8_5	1,000	513	29,845.0	na	796.20	19.38444	46,973.5	51,214.9	98,188.3	33.3487	0.0099	0.99564	0.00140	0.99844
athmpwskr_2_8_4	1,000	513	22,384.0	na	601.40	17.65102	54,435.0	51,214.9	105,649.0	32.8050	0.0093	1.02565	0.00138	1.02840
athmpwskr_2_8_3	1,000	513	14,922.0	na	406.70	15.48743	61,896.4	51,214.9	113,111.0	32.2427	0.0080	1.03421	0.00144	1.03710

Table 6.9.6-23. Results for HEU broken metal content for air transportation

case name	^{235}U (g)	CH_2 (g)	H_2O (g)	Kaolite (g)	htox	Rc (cm)	H_2O (g)	Kao (g)	Shell (g)	Rs (cm)	nlf	k_{eff}	σ	$k_{eff} + 2σ$
athmpwskr_2_8_2	1,000	513	7,461.5	na	211.90	12.45115	69,357.9	51,214.9	120,572.0	31.6600	0.0071	0.98526	0.00145	0.98817
athmpwskr_2_8_1	1,000	513	0.0	na	17.21	5.26336	76,819.4	51,214.9	128,034.0	31.0551	0.0060	0.55815	0.00111	0.56036
35,000g HEU 20% enrichment														
athmpwskr_12_1_11	7,000	513	74,614.0	na	56.13	26.40867	2,204.7	51,214.9	53,419.6	36.3984	0.0146	1.30444	0.00132	1.30708
athmpwskr_12_1_10	7,000	513	67,153.0	na	50.57	25.52662	9,666.2	51,214.9	60,881.0	35.9438	0.0136	1.30153	0.00156	1.30465
athmpwskr_12_1_9	7,000	513	59,691.0	na	45.01	24.57901	17,127.6	51,214.9	68,342.5	35.4774	0.0131	1.29397	0.00141	1.29679
athmpwskr_12_1_8	7,000	513	52,230.0	na	39.44	23.55208	24,589.1	51,214.9	75,803.9	34.9983	0.0122	1.28559	0.00158	1.28875
athmpwskr_12_1_7	7,000	513	44,768.0	na	33.88	22.42682	32,050.6	51,214.9	83,265.4	34.5058	0.0115	1.27331	0.00148	1.27627
athmpwskr_12_1_6	7,000	513	37,307.0	na	28.31	21.17566	39,512.0	51,214.9	90,726.9	33.9988	0.0110	1.24850	0.00147	1.25144
athmpwskr_12_1_5	7,000	513	29,845.0	na	22.75	19.75607	46,973.5	51,214.9	98,188.3	33.4762	0.0100	1.21970	0.00148	1.22267
athmpwskr_12_1_4	7,000	513	22,384.0	na	17.18	18.09653	54,435.0	51,214.9	105,649.0	32.9367	0.0091	1.17002	0.00139	1.17279
athmpwskr_12_1_3	7,000	513	14,922.0	na	11.62	16.05945	61,896.4	51,214.9	113,111.0	32.3790	0.0081	1.09036	0.00129	1.09294
athmpwskr_12_1_2	7,000	513	7,461.5	na	6.06	13.30882	69,357.9	51,214.9	120,572.0	31.8014	0.0072	0.95817	0.00131	0.96080
athmpwskr_12_1_1	7,000	513	0.0	na	0.49	8.30498	76,819.4	51,214.9	128,034.0	31.2020	0.0058	0.65983	0.00100	0.66184
30,000g HEU 20% enrichment														
athmpwskr_11_1_11	6,000	513	74,614.0	na	65.49	26.37861	2,204.7	51,214.9	53,419.6	36.3826	0.0145	1.28729	0.00151	1.29031
athmpwskr_11_1_10	6,000	513	67,153.0	na	59.00	25.49445	9,666.2	51,214.9	60,881.0	35.9276	0.0141	1.28153	0.00149	1.28451
athmpwskr_11_1_9	6,000	513	59,691.0	na	52.51	24.54430	17,127.6	51,214.9	68,342.5	35.4607	0.0128	1.27980	0.00155	1.28290
athmpwskr_11_1_8	6,000	513	52,230.0	na	46.02	23.51428	24,589.1	51,214.9	75,803.9	34.9812	0.0123	1.27508	0.00136	1.27780
athmpwskr_11_1_7	6,000	513	44,768.0	na	39.52	22.38512	32,050.6	51,214.9	83,265.4	34.4882	0.0118	1.26109	0.00154	1.26418
athmpwskr_11_1_6	6,000	513	37,307.0	na	33.03	21.12886	39,512.0	51,214.9	90,726.9	33.9807	0.0109	1.24331	0.00126	1.24582
athmpwskr_11_1_5	6,000	513	29,845.0	na	26.54	19.70228	46,973.5	51,214.9	98,188.3	33.4575	0.0102	1.20965	0.00156	1.21277
athmpwskr_11_1_4	6,000	513	22,384.0	na	20.05	18.03237	54,435.0	51,214.9	105,649.0	32.9174	0.0090	1.16727	0.00150	1.17026
athmpwskr_11_1_3	6,000	513	14,922.0	na	13.56	15.97785	61,896.4	51,214.9	113,111.0	32.3590	0.0082	1.09306	0.00155	1.09615

Table 6.9.6-23. Results for HEU broken metal content for air transportation

case name	^{235}U (g)	CH_2 (g)	H_2O (g)	Kaolite (g)	htox	Rc (cm)	H_2O (g)	Kao (g)	Shell (g)	Rs (cm)	nlf	k_{eff}	σ	$k_{eff} + 2σ$
athmpwskr_11_1_2	6,000	513	7,461.5	na	7.07	13.18955	69,357.9	51,214.9	120,572.0	31.7807	0.0072	0.95881	0.00135	0.96150
athmpwskr_11_1_1	6,000	513	0.0	na	0.57	7.98959	76,819.4	51,214.9	128,034.0	31.1805	0.0058	0.64202	0.00097	0.64395
25,000g HEU 20% enrichment														
athmpwskr_10_1_11	5,000	513	74,614.0	na	78.59	26.34849	2,204.7	51,214.9	53,419.6	36.3668	0.0147	1.25666	0.00148	1.25962
athmpwskr_10_1_10	5,000	513	67,153.0	na	70.80	25.46220	9,666.2	51,214.9	60,881.0	35.9114	0.0137	1.25683	0.00146	1.25975
athmpwskr_10_1_9	5,000	513	59,691.0	na	63.01	24.50950	17,127.6	51,214.9	68,342.5	35.4441	0.0129	1.25832	0.00126	1.26084
athmpwskr_10_1_8	5,000	513	52,230.0	na	55.22	23.47635	24,589.1	51,214.9	75,803.9	34.9641	0.0124	1.25363	0.00147	1.25658
athmpwskr_10_1_7	5,000	513	44,768.0	na	47.43	22.34325	32,050.6	51,214.9	83,265.4	34.4706	0.0113	1.24695	0.00140	1.24974
athmpwskr_10_1_6	5,000	513	37,307.0	na	39.64	21.08185	39,512.0	51,214.9	90,726.9	33.9625	0.0106	1.23226	0.00154	1.23533
athmpwskr_10_1_5	5,000	513	29,845.0	na	31.85	19.64819	46,973.5	51,214.9	98,188.3	33.4388	0.0100	1.20506	0.00163	1.20832
athmpwskr_10_1_4	5,000	513	22,384.0	na	24.06	17.96775	54,435.0	51,214.9	105,649.0	32.8981	0.0093	1.16366	0.00132	1.16630
athmpwskr_10_1_3	5,000	513	14,922.0	na	16.27	15.89541	61,896.4	51,214.9	113,111.0	32.3390	0.0082	1.09217	0.00162	1.09540
athmpwskr_10_1_2	5,000	513	7,461.5	na	8.48	13.06807	69,357.9	51,214.9	120,572.0	31.7599	0.0070	0.95867	0.00128	0.96122
athmpwskr_10_1_1	5,000	513	0.0	na	0.69	7.64711	76,819.4	51,214.9	128,034.0	31.1589	0.0061	0.62222	0.00118	0.62457
20,000g HEU 20% enrichment														
athmpwskr_8_1_11	4,000	513	74,614.0	na	98.24	26.31829	2,204.7	51,214.9	53,419.6	36.3510	0.0145	1.21178	0.00126	1.21429
athmpwskr_8_1_10	4,000	513	67,153.0	na	88.50	25.42986	9,666.2	51,214.9	60,881.0	35.8951	0.0138	1.21697	0.00145	1.21987
athmpwskr_8_1_9	4,000	513	59,691.0	na	78.76	24.47459	17,127.6	51,214.9	68,342.5	35.4274	0.0129	1.22166	0.00110	1.22386
athmpwskr_8_1_8	4,000	513	52,230.0	na	69.02	23.43829	24,589.1	51,214.9	75,803.9	34.9470	0.0122	1.22547	0.00134	1.22815
athmpwskr_8_1_7	4,000	513	44,768.0	na	59.29	22.30123	32,050.6	51,214.9	83,265.4	34.4530	0.0118	1.22053	0.00127	1.22307
athmpwskr_8_1_6	4,000	513	37,307.0	na	49.55	21.03464	39,512.0	51,214.9	90,726.9	33.9444	0.0107	1.21326	0.00137	1.21600
athmpwskr_8_1_5	4,000	513	29,845.0	na	39.81	19.59380	46,973.5	51,214.9	98,188.3	33.4200	0.0102	1.19193	0.00131	1.19455
athmpwskr_8_1_4	4,000	513	22,384.0	na	30.07	17.90266	54,435.0	51,214.9	105,649.0	32.8787	0.0090	1.15762	0.00164	1.16090
athmpwskr_8_1_3	4,000	513	14,922.0	na	20.34	15.81211	61,896.4	51,214.9	113,111.0	32.3190	0.0082	1.08959	0.00153	1.09264

Table 6.9.6-23. Results for HEU broken metal content for air transportation

case name	^{235}U (g)	CH_2 (g)	H_2O (g)	Kaolite (g)	htox	Rc (cm)	H_2O (g)	Kao (g)	Shell (g)	Rs (cm)	nlf	k_{eff}	σ	$k_{eff} + 2σ$
athmpwskr_8_1_2	4,000	513	7,461.5	na	10.60	12.94430	69,357.9	51,214.9	120,572.0	31.7392	0.0074	0.96034	0.00139	0.96313
athmpwskr_8_1_1	4,000	513	0.0	na	0.86	7.27085	76,819.4	51,214.9	128,034.0	31.1374	0.0058	0.59785	0.00112	0.60008
15,000g HEU 20% enrichment														
athmpwskr_6_1_11	3,000	513	74,614.0	na	130.90	26.28803	2,204.7	51,214.9	53,419.6	36.3351	0.0142	1.14239	0.00134	1.14507
athmpwskr_6_1_10	3,000	513	67,153.0	na	118.00	25.39744	9,666.2	51,214.9	60,881.0	35.8789	0.0137	1.15284	0.00120	1.15523
athmpwskr_6_1_9	3,000	513	59,691.0	na	105.00	24.43959	17,127.6	51,214.9	68,342.5	35.4107	0.0131	1.16521	0.00121	1.16764
athmpwskr_6_1_8	3,000	513	52,230.0	na	92.03	23.40012	24,589.1	51,214.9	75,803.9	34.9298	0.0120	1.17283	0.00145	1.17574
athmpwskr_6_1_7	3,000	513	44,768.0	na	79.05	22.25905	32,050.6	51,214.9	83,265.4	34.4353	0.0113	1.18127	0.00164	1.18456
athmpwskr_6_1_6	3,000	513	37,307.0	na	66.06	20.98721	39,512.0	51,214.9	90,726.9	33.9262	0.0109	1.17504	0.00155	1.17814
athmpwskr_6_1_5	3,000	513	29,845.0	na	53.08	19.53911	46,973.5	51,214.9	98,188.3	33.4013	0.0100	1.16750	0.00146	1.17042
athmpwskr_6_1_4	3,000	513	22,384.0	na	40.10	17.83709	54,435.0	51,214.9	105,649.0	32.8594	0.0091	1.13986	0.00148	1.14283
athmpwskr_6_1_3	3,000	513	14,922.0	na	27.11	15.72792	61,896.4	51,214.9	113,111.0	32.2989	0.0082	1.08027	0.00151	1.08330
athmpwskr_6_1_2	3,000	513	7,461.5	na	14.13	12.81811	69,357.9	51,214.9	120,572.0	31.7184	0.0071	0.95952	0.00150	0.96252
athmpwskr_6_1_1	3,000	513	0.0	na	1.15	6.85101	76,819.4	51,214.9	128,034.0	31.1157	0.0058	0.57184	0.00092	0.57368
6,000g HEU 20% enrichment														
athmpwskr_4_1_11	2,000	513	74,614.0	na	196.40	26.25769	2,204.7	51,214.9	53,419.6	36.3193	0.0142	1.01841	0.00110	1.02061
athmpwskr_4_1_10	2,000	513	67,153.0	na	177.00	25.36494	9,666.2	51,214.9	60,881.0	35.8626	0.0138	1.04003	0.00121	1.04246
athmpwskr_4_1_9	2,000	513	59,691.0	na	157.50	24.40448	17,127.6	51,214.9	68,342.5	35.3940	0.0129	1.05800	0.00096	1.05992
athmpwskr_4_1_8	2,000	513	52,230.0	na	138.00	23.36182	24,589.1	51,214.9	75,803.9	34.9126	0.0121	1.07916	0.00129	1.08174
athmpwskr_4_1_7	2,000	513	44,768.0	na	118.50	22.21671	32,050.6	51,214.9	83,265.4	34.4176	0.0116	1.09162	0.00115	1.09393
athmpwskr_4_1_6	2,000	513	37,307.0	na	99.10	20.93956	39,512.0	51,214.9	90,726.9	33.9080	0.0107	1.10489	0.00122	1.10732
athmpwskr_4_1_5	2,000	513	29,845.0	na	79.62	19.48411	46,973.5	51,214.9	98,188.3	33.3825	0.0101	1.10960	0.00160	1.11281
athmpwskr_4_1_4	2,000	513	22,384.0	na	60.15	17.77103	54,435.0	51,214.9	105,649.0	32.8400	0.0091	1.09428	0.00143	1.09713
athmpwskr_4_1_3	2,000	513	14,922.0	na	40.67	15.64281	61,896.4	51,214.9	113,111.0	32.2789	0.0081	1.05881	0.00155	1.06191

Table 6.9.6-23. Results for HEU broken metal content for air transportation

case name	^{235}U (g)	CH_2 (g)	H_2O (g)	Kaolite (g)	htox	Rc (cm)	H_2O (g)	Kao (g)	Shell (g)	Rs (cm)	nlf	k_{eff}	σ	$k_{eff} + 2σ$
athmpwskr_4_1_2	2,000	513	7,461.5	na	21.20	12.68939	69,357.9	51,214.9	120,572.0	31.6976	0.0072	0.95084	0.00134	0.95353
athmpwskr_4_1_1	2,000	513	0.0	na	1.72	6.37224	76,819.4	51,214.9	128,034.0	31.0941	0.0059	0.54033	0.00105	0.54242
5,000g HEU 20% enrichment														
athmpwskr_2_1_11	1,000	513	74,614.0	na	392.90	26.22729	2,204.7	51,214.9	53,419.6	36.3034	0.0139	0.76722	0.00089	0.76900
athmpwskr_2_1_10	1,000	513	67,153.0	na	353.90	25.33235	9,666.2	51,214.9	60,881.0	35.8463	0.0132	0.79602	0.00086	0.79774
athmpwskr_2_1_9	1,000	513	59,691.0	na	315.00	24.36928	17,127.6	51,214.9	68,342.5	35.3773	0.0127	0.82462	0.00105	0.82673
athmpwskr_2_1_8	1,000	513	52,230.0	na	276.00	23.32339	24,589.1	51,214.9	75,803.9	34.8954	0.0120	0.85817	0.00098	0.86014
athmpwskr_2_1_7	1,000	513	44,768.0	na	237.10	22.17421	32,050.6	51,214.9	83,265.4	34.4000	0.0112	0.88947	0.00112	0.89172
athmpwskr_2_1_6	1,000	513	37,307.0	na	198.10	20.89170	39,512.0	51,214.9	90,726.9	33.8898	0.0104	0.92204	0.00129	0.92462
athmpwskr_2_1_5	1,000	513	29,845.0	na	159.20	19.42880	46,973.5	51,214.9	98,188.3	33.3637	0.0098	0.95114	0.00115	0.95345
athmpwskr_2_1_4	1,000	513	22,384.0	na	120.20	17.70449	54,435.0	51,214.9	105,649.0	32.8205	0.0092	0.97244	0.00110	0.97465
athmpwskr_2_1_3	1,000	513	14,922.0	na	81.34	15.55677	61,896.4	51,214.9	113,111.0	32.2588	0.0083	0.97325	0.00168	0.97660
athmpwskr_2_1_2	1,000	513	7,461.5	na	42.39	12.55800	69,357.9	51,214.9	120,572.0	31.6767	0.0073	0.91381	0.00132	0.91644
athmpwskr_2_1_1	1,000	513	0.0	na	3.44	5.80813	76,819.4	51,214.9	128,034.0	31.0724	0.0059	0.50206	0.00118	0.50441
4,500g HEU 20% enrichment														
athm2pwskr_5_1_11	900	513	74,614.0	na	436.60	26.2243	2,204.7	51,214.9	53,419.6	36.3018	0.0138	0.72669	0.00082	0.72832
athm2pwskr_5_1_10	900	513	67,153.0	na	393.30	25.3291	9,666.2	51,214.9	60,881.0	35.8447	0.0131	0.75662	0.00084	0.75830
athm2pwskr_5_1_9	900	513	59,691.0	na	350.00	24.3658	17,127.6	51,214.9	68,342.5	35.3756	0.0127	0.78606	0.00091	0.78788
athm2pwskr_5_1_8	900	513	52,230.0	na	306.70	23.3195	24,589.1	51,214.9	75,803.9	34.8937	0.0120	0.82194	0.00094	0.82382
athm2pwskr_5_1_7	900	513	44,768.0	na	263.40	22.1700	32,050.6	51,214.9	83,265.4	34.3982	0.0112	0.85385	0.00090	0.85565
athm2pwskr_5_1_6	900	513	37,307.0	na	220.20	20.8869	39,512.0	51,214.9	90,726.9	33.8879	0.0109	0.88893	0.00106	0.89105
athm2pwskr_5_1_5	900	513	29,845.0	na	176.90	19.4233	46,973.5	51,214.9	98,188.3	33.3618	0.0098	0.92125	0.00114	0.92352
athm2pwskr_5_1_4	900	513	22,384.0	na	133.60	17.6978	54,435.0	51,214.9	105,649.0	32.8186	0.0088	0.94828	0.00112	0.95052
athm2pwskr_5_1_3	900	513	14,922.0	na	90.38	15.5481	61,896.4	51,214.9	113,111.0	32.2567	0.0081	0.95553	0.00128	0.95810

Table 6.9.6-23. Results for HEU broken metal content for air transportation

case name	^{235}U (g)	CH_2 (g)	H_2O (g)	Kaolite (g)	htox	Rc (cm)	H_2O (g)	Kao (g)	Shell (g)	Rs (cm)	nlf	k_{eff}	σ	$k_{eff} + 2σ$
athm2pwskr_5_1_2	900	513	7,461.5	na	47.10	12.5447	69,357.9	51,214.9	120,572.0	31.6746	0.0072	0.90112	0.00143	0.90398
athm2pwskr_5_1_1	900	513	0.0	na	3.82	5.7454	76,819.4	51,214.9	128,034.0	31.0703	0.0060	0.49483	0.00115	0.49712
4,000g HEU 20% enrichment														
athm2pwskr_4_1_11	800	513	74,614.0	na	491.10	26.2212	2,204.7	51,214.9	53,419.6	36.3002	0.0139	0.68165	0.00072	0.68308
athm2pwskr_4_1_10	800	513	67,153.0	na	442.40	25.3258	9,666.2	51,214.9	60,881.0	35.8430	0.0131	0.71140	0.00080	0.71299
athm2pwskr_4_1_9	800	513	59,691.0	na	393.80	24.3622	17,127.6	51,214.9	68,342.5	35.3739	0.0124	0.74377	0.00085	0.74547
athm2pwskr_4_1_8	800	513	52,230.0	na	345.10	23.3157	24,589.1	51,214.9	75,803.9	34.8920	0.0120	0.77769	0.00081	0.77931
athm2pwskr_4_1_7	800	513	44,768.0	na	296.40	22.1657	32,050.6	51,214.9	83,265.4	34.3964	0.0116	0.81374	0.00077	0.81528
athm2pwskr_4_1_6	800	513	37,307.0	na	247.70	20.8821	39,512.0	51,214.9	90,726.9	33.8861	0.0106	0.85125	0.00097	0.85319
athm2pwskr_4_1_5	800	513	29,845.0	na	199.00	19.4177	46,973.5	51,214.9	98,188.3	33.3599	0.0098	0.88803	0.00130	0.89063
athm2pwskr_4_1_4	800	513	22,384.0	na	150.30	17.6911	54,435.0	51,214.9	105,649.0	32.8166	0.0089	0.91753	0.00124	0.92001
athm2pwskr_4_1_3	800	513	14,922.0	na	101.60	15.5395	61,896.4	51,214.9	113,111.0	32.2547	0.0081	0.93454	0.00150	0.93755
athm2pwskr_4_1_2	800	513	7,461.5	na	52.99	12.5314	69,357.9	51,214.9	120,572.0	31.6725	0.0071	0.89101	0.00130	0.89362
athm2pwskr_4_1_1	800	513	0.0	na	4.30	5.6812	76,819.4	51,214.9	128,034.0	31.0681	0.0059	0.49028	0.00108	0.49244
3,500g HEU 20% enrichment														
athm2pwskr_3_1_11	700	513	74,614.0	na	561.30	26.2182	2,204.7	51,214.9	53,419.6	36.2986	0.0139	0.63180	0.00067	0.63314
athm2pwskr_3_1_10	700	513	67,153.0	na	505.70	25.3226	9,666.2	51,214.9	60,881.0	35.8414	0.0131	0.66242	0.00078	0.66397
athm2pwskr_3_1_9	700	513	59,691.0	na	450.00	24.3587	17,127.6	51,214.9	68,342.5	35.3722	0.0126	0.69361	0.00081	0.69524
athm2pwskr_3_1_8	700	513	52,230.0	na	394.40	23.3118	24,589.1	51,214.9	75,803.9	34.8903	0.0120	0.72803	0.00083	0.72969
athm2pwskr_3_1_7	700	513	44,768.0	na	338.70	22.1614	32,050.6	51,214.9	83,265.4	34.3946	0.0112	0.76553	0.00089	0.76731
athm2pwskr_3_1_6	700	513	37,307.0	na	283.10	20.8773	39,512.0	51,214.9	90,726.9	33.8843	0.0104	0.80365	0.00089	0.80542
athm2pwskr_3_1_5	700	513	29,845.0	na	227.40	19.4122	46,973.5	51,214.9	98,188.3	33.3581	0.0100	0.84452	0.00099	0.84649
athm2pwskr_3_1_4	700	513	22,384.0	na	171.80	17.6844	54,435.0	51,214.9	105,649.0	32.8147	0.0091	0.88253	0.00104	0.88461
athm2pwskr_3_1_3	700	513	14,922.0	na	116.20	15.5308	61,896.4	51,214.9	113,111.0	32.2527	0.0081	0.90492	0.00126	0.90744

Table 6.9.6-23. Results for HEU broken metal content for air transportation

case name	^{235}U (g)	CH_2 (g)	H_2O (g)	Kaolite (g)	htox	Rc (cm)	H_2O (g)	Kao (g)	Shell (g)	Rs (cm)	nlf	k_{eff}	σ	$k_{eff} + 2σ$
athm2pwskr_3_1_2	700	513	7,461.5	na	60.56	12.5180	69,357.9	51,214.9	120,572.0	31.6704	0.0073	0.87397	0.00159	0.87716
athm2pwskr_3_1_1	700	513	0.0	na	4.92	5.6156	76,819.4	51,214.9	128,034.0	31.0659	0.0059	0.48609	0.00103	0.48815
3,000g HEU 20% enrichment														
athm2pwskr_2_1_11	600	513	74,614.0	na	654.90	26.2151	2,204.7	51,214.9	53,419.6	36.2970	0.0140	0.57444	0.00056	0.57557
athm2pwskr_2_1_10	600	513	67,153.0	na	589.90	25.3193	9,666.2	51,214.9	60,881.0	35.8398	0.0132	0.60498	0.00063	0.60623
athm2pwskr_2_1_9	600	513	59,691.0	na	525.00	24.3552	17,127.6	51,214.9	68,342.5	35.3706	0.0128	0.63499	0.00090	0.63678
athm2pwskr_2_1_8	600	513	52,230.0	na	460.10	23.3080	24,589.1	51,214.9	75,803.9	34.8886	0.0121	0.66999	0.00083	0.67164
athm2pwskr_2_1_7	600	513	44,768.0	na	395.20	22.1572	32,050.6	51,214.9	83,265.4	34.3929	0.0114	0.70932	0.00087	0.71106
athm2pwskr_2_1_6	600	513	37,307.0	na	330.30	20.8725	39,512.0	51,214.9	90,726.9	33.8825	0.0108	0.75066	0.00084	0.75234
athm2pwskr_2_1_5	600	513	29,845.0	na	265.40	19.4066	46,973.5	51,214.9	98,188.3	33.3562	0.0099	0.79472	0.00098	0.79669
athm2pwskr_2_1_4	600	513	22,384.0	na	200.40	17.6777	54,435.0	51,214.9	105,649.0	32.8128	0.0088	0.83915	0.00127	0.84169
athm2pwskr_2_1_3	600	513	14,922.0	na	135.50	15.5221	61,896.4	51,214.9	113,111.0	32.2507	0.0081	0.86959	0.00135	0.87228
athm2pwskr_2_1_2	600	513	7,461.5	na	70.65	12.5047	69,357.9	51,214.9	120,572.0	31.6684	0.0073	0.85284	0.00128	0.85540
athm2pwskr_2_1_1	600	513	0.0	na	5.74	5.5484	76,819.4	51,214.9	128,034.0	31.0638	0.0060	0.48105	0.00114	0.48333
compromised package, homogenous core (HEU broken metal, polyethylene, and Kaolite), HEU shell, 20.0 cm water reflector														
17,500 g HEU														
athmpkmr_6_1_1_11	3,000	513	76,819.4	51,214.9	134.82	39.13343	na	na	500.0	39.1404	0.0305	0.82671	0.00116	0.82904
athmpkmr_6_1_1_10	3,000	513	69,357.9	51,214.9	121.83	38.49290	na	na	500.0	38.5001	0.0316	0.81988	0.00107	0.82201
athmpkmr_6_1_1_9	3,000	513	61,896.4	51,214.9	108.85	37.83031	na	na	500.0	37.8377	0.0331	0.80737	0.00168	0.81074
athmpkmr_6_1_1_8	3,000	513	54,435.0	51,214.9	95.87	37.14367	na	na	500.0	37.1514	0.0350	0.78879	0.00127	0.79133
athmpkmr_6_1_1_7	3,000	513	46,973.5	51,214.9	82.88	36.43065	na	na	500.0	36.4386	0.0381	0.76393	0.00123	0.76638
athmpkmr_6_1_1_6	3,000	513	39,512.0	51,214.9	69.90	35.68857	na	na	500.0	35.6969	0.0399	0.73508	0.00126	0.73759
athmpkmr_6_1_1_5	3,000	513	32,050.6	51,214.9	56.92	34.91428	na	na	500.0	34.9230	0.0435	0.69610	0.00112	0.69835
athmpkmr_6_1_1_4	3,000	513	24,589.1	51,214.9	43.93	34.10403	na	na	500.0	34.1131	0.0465	0.64833	0.00105	0.65043
athmpkmr_6_1_1_3	3,000	513	17,127.6	51,214.9	30.95	33.25334	na	na	500.0	33.2629	0.0515	0.58834	0.00116	0.59066

Table 6.9.6-23. Results for HEU broken metal content for air transportation

case name	^{235}U (g)	CH_2 (g)	H_2O (g)	Kaolite (g)	htox	Rc (cm)	H_2O (g)	Kao (g)	Shell (g)	Rs (cm)	nlf	k_{eff}	σ	$k_{eff} + 2σ$
athmpkmr_6_1_1_2	3,000	513	9,666.2	51,214.9	17.97	32.35674	na	na	500.0	32.3668	0.0567	0.51967	0.00102	0.52172
athmpkmr_6_1_1_1	3,000	513	2,204.7	51,214.9	4.98	31.40750	na	na	500.0	31.4182	0.0648	0.44668	0.00102	0.44873
17,500 g HEU														
athmpkmr_5_2_1_11	2,500	513	76,819.4	51,214.9	161.78	39.12659	na	na	1,000.0	39.1404	0.0308	0.81054	0.00107	0.81268
athmpkmr_5_2_1_10	2,500	513	69,357.9	51,214.9	146.20	38.48583	na	na	1,000.0	38.5001	0.0321	0.80744	0.00111	0.80966
athmpkmr_5_2_1_9	2,500	513	61,896.4	51,214.9	130.62	37.82300	na	na	1,000.0	37.8377	0.0337	0.79514	0.00117	0.79749
athmpkmr_5_2_1_8	2,500	513	54,435.0	51,214.9	115.04	37.13608	na	na	1,000.0	37.1514	0.0354	0.78193	0.00117	0.78426
athmpkmr_5_2_1_7	2,500	513	46,973.5	51,214.9	99.46	36.42276	na	na	1,000.0	36.4386	0.0380	0.76122	0.00146	0.76414
athmpkmr_5_2_1_6	2,500	513	39,512.0	51,214.9	83.88	35.68035	na	na	1,000.0	35.6969	0.0402	0.73648	0.00125	0.73898
athmpkmr_5_2_1_5	2,500	513	32,050.6	51,214.9	68.30	34.90569	na	na	1,000.0	34.9230	0.0432	0.69977	0.00121	0.70218
athmpkmr_5_2_1_4	2,500	513	24,589.1	51,214.9	52.72	34.09503	na	na	1,000.0	34.1131	0.0465	0.65426	0.00101	0.65627
athmpkmr_5_2_1_3	2,500	513	17,127.6	51,214.9	37.14	33.24387	na	na	1,000.0	33.2629	0.0508	0.59580	0.00122	0.59824
athmpkmr_5_2_1_2	2,500	513	9,666.2	51,214.9	21.56	32.34674	na	na	1,000.0	32.3668	0.0557	0.52943	0.00102	0.53147
athmpkmr_5_2_1_1	2,500	513	2,204.7	51,214.9	5.98	31.39688	na	na	1,000.0	31.4182	0.0640	0.45232	0.00099	0.45429
17,500 g HEU														
athmpkmr_4_3_1_11	2,000	513	76,819.4	51,214.9	202.23	39.11975	na	na	1,500.0	39.1404	0.0315	0.78278	0.00117	0.78512
athmpkmr_4_3_1_10	2,000	513	69,357.9	51,214.9	182.75	38.47876	na	na	1,500.0	38.5001	0.0322	0.78073	0.00097	0.78267
athmpkmr_4_3_1_9	2,000	513	61,896.4	51,214.9	163.28	37.81568	na	na	1,500.0	37.8377	0.0341	0.77618	0.00112	0.77842
athmpkmr_4_3_1_8	2,000	513	54,435.0	51,214.9	143.80	37.12848	na	na	1,500.0	37.1514	0.0359	0.76473	0.00117	0.76706
athmpkmr_4_3_1_7	2,000	513	46,973.5	51,214.9	124.33	36.41487	na	na	1,500.0	36.4386	0.0381	0.74931	0.00113	0.75157
athmpkmr_4_3_1_6	2,000	513	39,512.0	51,214.9	104.85	35.67213	na	na	1,500.0	35.6969	0.0401	0.72799	0.00111	0.73021
athmpkmr_4_3_1_5	2,000	513	32,050.6	51,214.9	85.38	34.89710	na	na	1,500.0	34.9230	0.0432	0.69825	0.00112	0.70049
athmpkmr_4_3_1_4	2,000	513	24,589.1	51,214.9	65.90	34.08602	na	na	1,500.0	34.1131	0.0461	0.65621	0.00111	0.65843
athmpkmr_4_3_1_3	2,000	513	17,127.6	51,214.9	46.43	33.23440	na	na	1,500.0	33.2629	0.0506	0.60270	0.00125	0.60519

Table 6.9.6-23. Results for HEU broken metal content for air transportation

case name	^{235}U (g)	CH_2 (g)	H_2O (g)	Kaolite (g)	htox	Rc (cm)	H_2O (g)	Kao (g)	Shell (g)	Rs (cm)	nlf	k_{eff}	σ	$k_{eff} + 2σ$
athmpkmr_4_3_1_2	2,000	513	9,666.2	51,214.9	26.95	32.33673	na	na	1,500.0	32.3668	0.0552	0.53659	0.00100	0.53859
athmpkmr_4_3_1_1	2,000	513	2,204.7	51,214.9	7.48	31.38626	na	na	1,500.0	31.4182	0.0626	0.46023	0.00105	0.46233
17,500 g HEU														
athmpkmr_3_4_1_11	1,500	513	76,819.4	51,214.9	269.63	39.11291	na	na	2,000.0	39.1404	0.0323	0.74454	0.00111	0.74677
athmpkmr_3_4_1_10	1,500	513	69,357.9	51,214.9	243.67	38.47169	na	na	2,000.0	38.5001	0.0332	0.74408	0.00106	0.74619
athmpkmr_3_4_1_9	1,500	513	61,896.4	51,214.9	217.70	37.80835	na	na	2,000.0	37.8377	0.0348	0.74205	0.00101	0.74407
athmpkmr_3_4_1_8	1,500	513	54,435.0	51,214.9	191.73	37.12089	na	na	2,000.0	37.1514	0.0366	0.73801	0.00109	0.74020
athmpkmr_3_4_1_7	1,500	513	46,973.5	51,214.9	165.77	36.40697	na	na	2,000.0	36.4386	0.0381	0.72624	0.00099	0.72823
athmpkmr_3_4_1_6	1,500	513	39,512.0	51,214.9	139.80	35.66390	na	na	2,000.0	35.6969	0.0400	0.71184	0.00109	0.71402
athmpkmr_3_4_1_5	1,500	513	32,050.6	51,214.9	113.83	34.88850	na	na	2,000.0	34.9230	0.0422	0.68601	0.00108	0.68817
athmpkmr_3_4_1_4	1,500	513	24,589.1	51,214.9	87.87	34.07701	na	na	2,000.0	34.1131	0.0460	0.65133	0.00126	0.65385
athmpkmr_3_4_1_3	1,500	513	17,127.6	51,214.9	61.90	33.22491	na	na	2,000.0	33.2629	0.0500	0.60077	0.00107	0.60290
athmpkmr_3_4_1_2	1,500	513	9,666.2	51,214.9	35.93	32.32672	na	na	2,000.0	32.3668	0.0547	0.54059	0.00105	0.54270
athmpkmr_3_4_1_1	1,500	513	2,204.7	51,214.9	9.97	31.37562	na	na	2,000.0	31.4182	0.0615	0.46420	0.00093	0.46605
17,500 g HEU														
athmpkmr_2_5_1_11	1,000	513	76,819.4	51,214.9	404.45	39.10606	na	na	2,500.0	39.1404	0.0330	0.68332	0.00087	0.68506
athmpkmr_2_5_1_10	1,000	513	69,357.9	51,214.9	365.50	38.46461	na	na	2,500.0	38.5001	0.0338	0.68976	0.00107	0.69191
athmpkmr_2_5_1_9	1,000	513	61,896.4	51,214.9	326.55	37.80103	na	na	2,500.0	37.8377	0.0350	0.69285	0.00095	0.69475
athmpkmr_2_5_1_8	1,000	513	54,435.0	51,214.9	287.60	37.11329	na	na	2,500.0	37.1514	0.0365	0.69207	0.00120	0.69447
athmpkmr_2_5_1_7	1,000	513	46,973.5	51,214.9	248.65	36.39907	na	na	2,500.0	36.4386	0.0383	0.69082	0.00098	0.69278
athmpkmr_2_5_1_6	1,000	513	39,512.0	51,214.9	209.70	35.65566	na	na	2,500.0	35.6969	0.0399	0.68238	0.00101	0.68440
athmpkmr_2_5_1_5	1,000	513	32,050.6	51,214.9	170.75	34.87989	na	na	2,500.0	34.9230	0.0429	0.66578	0.00110	0.66798
athmpkmr_2_5_1_4	1,000	513	24,589.1	51,214.9	131.80	34.06799	na	na	2,500.0	34.1131	0.0457	0.63892	0.00106	0.64104
athmpkmr_2_5_1_3	1,000	513	17,127.6	51,214.9	92.85	33.21543	na	na	2,500.0	33.2629	0.0491	0.59774	0.00102	0.59979

Table 6.9.6-23. Results for HEU broken metal content for air transportation

case name	^{235}U (g)	CH_2 (g)	H_2O (g)	Kaolite (g)	htox	Rc (cm)	H_2O (g)	Kao (g)	Shell (g)	Rs (cm)	nlf	k_{eff}	σ	k_{eff} + 2σ
athmpkmr_2_5_1_2	1,000	513	9,666.2	51,214.9	53.90	32.31670	na	na	2,500.0	32.3668	0.0535	0.54129	0.00121	0.54371
athmpkmr_2_5_1_1	1,000	513	2,204.7	51,214.9	14.95	31.36499	na	na	2,500.0	31.4182	0.0599	0.46802	0.00098	0.46999
17,500 g HEU														
athmpkmr_1_6_1_11	500	513	76,819.4	51,214.9	808.90	39.09921	na	na	3,000.0	39.1404	0.0342	0.59914	0.00103	0.60120
athmpkmr_1_6_1_10	500	513	69,357.9	51,214.9	731.00	38.45754	na	na	3,000.0	38.5001	0.0350	0.60911	0.00091	0.61092
athmpkmr_1_6_1_9	500	513	61,896.4	51,214.9	653.10	37.79370	na	na	3,000.0	37.8377	0.0362	0.61744	0.00087	0.61919
athmpkmr_1_6_1_8	500	513	54,435.0	51,214.9	575.20	37.10569	na	na	3,000.0	37.1514	0.0375	0.62582	0.00099	0.62780
athmpkmr_1_6_1_7	500	513	46,973.5	51,214.9	497.30	36.39117	na	na	3,000.0	36.4386	0.0389	0.63123	0.00105	0.63332
athmpkmr_1_6_1_6	500	513	39,512.0	51,214.9	419.40	35.64743	na	na	3,000.0	35.6969	0.0407	0.63132	0.00115	0.63362
athmpkmr_1_6_1_5	500	513	32,050.6	51,214.9	341.50	34.87129	na	na	3,000.0	34.9230	0.0427	0.62606	0.00126	0.62858
athmpkmr_1_6_1_4	500	513	24,589.1	51,214.9	263.60	34.05897	na	na	3,000.0	34.1131	0.0450	0.61361	0.00122	0.61605
athmpkmr_1_6_1_3	500	513	17,127.6	51,214.9	185.70	33.20594	na	na	3,000.0	33.2629	0.0485	0.58503	0.00102	0.58706
athmpkmr_1_6_1_2	500	513	9,666.2	51,214.9	107.80	32.30667	na	na	3,000.0	32.3668	0.0527	0.53799	0.00104	0.54007
athmpkmr_1_6_1_1	500	513	2,204.7	51,214.9	29.90	31.35434	na	na	3,000.0	31.4182	0.0577	0.47057	0.00099	0.47255

THIS PAGE INTENTIONALLY LEFT BLANK.

Appendix 6.9.7

INPUT LISTINGS OF ES-3100 CALCULATION MODELS FOR SELECT CASES

This appendix contains selected input listing for calculations identified Tables 6.1a-e and Sects. 6.4, 6.5, and 6.6 of this document, and Sect. 6.7 on air transport. These listings are a few taken from Y/LF-718.

THIS PAGE INTENTIONALLY LEFT BLANK.

ES-3100 Input file - Results table crosswalk

Case	Description	Input File	Results Table
cvcrcyt11_21_1	3 cyl, 0.0 in np, 21000 gU (21000 g ^{235}U, 9082.6 g H_2O, h/x=11.29)	6-359	6-204
cvcrcyt11_36_2	3 cyl, 1.4 in np, 36000 gU (36000 g ^{235}U, 7673.1 g H_2O, h/x=5.56)	6-360	6-204
cvcrsqt11_36_1	3 bar, 0.0 in np, 36000 gU (36000 g ^{235}U, 8286.7 g H_2O, h/x=6.01)	6-362	6-214
cvcrcyct11_17_1	3 cyl, 0.0 in np, 17000 gU (17000 g ^{235}U, 9294.9 g H_2O, h/x=14.27)	6-364	6-220
cvcrcyct11_32_2	3 cyl, 1.4 in np, 32000 gU (32000 g ^{235}U, 7885.3 g H_2O, h/x= 6.43)	6-366	6-221
cvcr5est11_1_1	0.0 in np, 18286.5 gU (18286.5 g ^{235}U, 9226.6 g H_2O, h/x=13.75)	6-368	6-225
cvcr6e4st11_1	1.4 in np, 36573.0 gU (36573.0 g ^{235}U, 7642.7 g H_2O, h/x= 5.45)	6-372	6-226
cvcr70st11_2	0.0 in np, 25601.1 gU (25601.1 g ^{235}U, 8838.5 g H_2O, h/x= 9.01)	6-376	6-226
cvr3sqa_26_1_8_15	0.0 in np, 25893.7 gU (25893.7 g ^{235}U, 8822.9 g H_2O, h/x= 8.89)	6-380	N/A[a]
cvr3lha_26_1_8_15	0.0 in np, 25893.7 gU (25893.7 g ^{235}U, 8822.9 g H_2O, h/x= 8.89)	6-382	6-238
cvr3cha_26_1_8_15	0.0 in np, 25893.7 gU (25893.7 g ^{235}U, 8822.9 g H_2O, h/x= 8.89)	6-384	N/A[a]
cvcrpdoxt11_1_5_24_15	0.0 in. np, disp. 24,000 g UO_2 (21,124.9 g ^{235}U, 1,477.3 g Sat.H_2O), 4 g H_2O CV, h/x= 10.02)	6-387	6-265
cvcrsk3cc_9_15_17	0.0 in np, 21300g SOC (19865.3g UOx, 15672.8 g ^{235}U, 921.0 g C, h/x=12.82)	6-390	6-284
cvcrunhct11_9_1	0.0 in np, disp. 9000 gUNHc (4238.7 g ^{235}U, 6980.8 g H_2O, h/x=54.99)	6-392	6-271
cvcrtriga_1_15	0.0 in np, 10400.0 gUZrHx (921.0 g ^{235}U, 8998.2 g H_2O, h/x=255.01)	6-393	6-301
ncsrcyt11_21_1_15	3 cyl, 0.0 in np, 21000 gU (21000 g ^{235}U, 9082.6 g H_2O, h/x=11.29)	6-395	6-206
nciacyct11_25_2_3	3 cyl, 1.4 in np, 25000 gU (25000 g ^{235}U, 8256.8 g H_2O, h/x= 8.62)	6-400	6-225
hciacyct12_25_2_3	3 cyl, 1.4 in np, 25000 gU (25000 g ^{235}U, 8256.8 g H_2O, h/x= 8.62)	6-404	6-225
ncia70st11_2_8_3	1.4 in np, 25601.1 gU (25601.1 g ^{235}U, 8224.9 g H_2O, h/x= 8.39)	6-408	6-233

ES-3100 Input file - Results table crosswalk

Case	Description	Input File	Results Table
ncia5est11_2_2_5_3	1.4 in np, 36647 gU (29318 g ^{235}U, 7642.7 g H_2O, h/x= 6.80)	6-414	6-233
nciabmt11_4_1_5_3	0.0 in np, 3708.5 gU (2966.8 g ^{235}U, 10000.7 g H_2O, h/x=87.98)	6-419	6-246
hctf5bmt12_25_2_8_3	1.4 in np, 24968.9 gU (24968.9 g ^{235}U, 8258.4 g H_2O, h/x= 8.63)	6-424	6-257
nciaoxt11_1_24_1_3	0.0 in np, disp. 24000 gUO_2 (21124.9 g ^{235}U, 6533.9 g H_2O, h/x= 9.90)	6-439	N/A
nciask_9_15	0.0 in np, 21300g SOC (19865.3g UOx, 15672.8 g ^{235}U, 921.0 g C, h/x=12.82)	6-443	6-295
ncsrunhct11_9_1_15	0.0 in np, disp. 9000 gUNHc (4238.7 g ^{235}U, 6980.8 g H_2O, h/x=54.99)	6-447	6-277
icsrunhct12_15_1_15	0.0 in. np, disp. 15,000.0 g UNHc (7064.4 g ^{235}U, 6870.7 g H_2O, h/x=52.91)	6-451	6-282
ncsrtriga_1_15_15	0.0 in np, 10400.0 gUZrHx (921.0 g ^{235}U, 8998.2 g H_2O, h/x=255.01)	6-455	6-308
nciatriga_1_15_3	0.0 in np, 10400.0 gUZrHx (921.0 g ^{235}U, 8998.2 g H_2O, h/x=255.01)	6-460	6-310
atdmr_7_8	7000 gU, 7000 g^{235}U, 513.0 gCH_2, h/x=2.46, Rc=6.05465cm	6-464	6-321
atdmsr_7_8_11	7000 gU, 7000 g^{235}U, 513.0 gCH_2, h/x=2.46, Rc=6.05465cm, 661331. gSS, Rs=13.0264cm	6-465	6-321
atdmkr_7_8_11	7000 gU, 7000 g^{235}U, 513.0 gCH_2, h/x=2.46, Rc=6.05465cm, 128034.0gKao,Rk=31.0814cm	6-466	6-325
atdzr	10400.0 gUZrHx (921.0 g ^{235}U, 500.0 gCH_2, h/x=43.37), Rc=7.46774cm	6-467	6-329
athzpkr_11	10400.0 gUZrHx (921.g ^{235}U, 500.0 gCH_2, 76819 gH_2O, h/x=2220), Rc=39.15407cm	6-468	6-330
athzpwskr_9_11	10400 gUZrHx, 921.0 g^{235}U, 500.0 gCH_2, 74614 gH_2O, h/x=2157, Rc=26.33372cm, Rs=36.35905cm	6-469	6-331
athmpkr_8_8_11	4000 gUZrHx, 4000 g^{235}U, 513. gCH_2, 76819 gH_2O, h/x=505.5, Rc=39.10344cm	6-470	6-337
athmpwskr_2_8_11	1000gUZrHx, 1000. g ^{235}U, 513. gCH_2, 74614 gH_2O, h/x=1964, Rc=26.20298cm, Rs=36.29068cm	6-471	6-342
athm2pwskr_3_1_3	3500 gUZrHx, 700. g^{235}U, 513. gCH_2, 14922 gH_2O, h/x=116.2, Rc=15.53077cm, Rs=32.25271cm	6-473	6-347
athmpkmr_2_5_1_11	17.5kgU,(1000. g^{235}U, 513. gCH_2, 76819 gH_2O, h/x=404.45, Rc=39.10606cm, Rs=39.14036cm	6-475	6-350

ES-3100 Input file - Results table crosswalk

Case	Description	Input File	Results Table
cvcrtriga_1_1	0.0 in np, 10400.0 gUZrHx (921.0 g ^{235}U, 0.0 gH_2O hx= 0.00)	6-476	6-301
cvcrtriga_1_15	0.0 in np, 10400.0 gUZrHx (921.0 g ^{235}U, 8998.2 gH_2O hx= 0.00)	6-479	6-301
cvcrtriga_2_15	1.4 in np, 10400.0 gUZrHx (921.0 g ^{235}U, 8384.6 g H_2O, h/x=237.62)	6-483	6-301
cvcrtriga_70_1_1	0.0 in np, 6847.1 gUZrHx (408.0 g ^{235}U, 0.0 g H_2O, h/x=0.0)	6-486	6-301
cvcrtriga_70_1_15	0.0 in np, 6847.1 gUZrHx (408.0 g ^{235}U, 8998.2 g H_2O, h/x=575.64)	6-489	6-302
cvcrtriga_70_2_15	1.4 in np, 6847.1 gUZrHx (408.0 g ^{235}U, 8384.6 g H_2O, h/x=536.39)	6-492	6-302
ncsrtriga_1_15_15	0.0 in np, 10400.0 gUZrHx (921.0 g ^{235}U, 8998.2 g H_2O, h/x=255.01)	6-496	6-308
ncsrtriga70_1_15_15	0.0 in np, 6847.1 gUZrHx (408.0 g ^{235}U, 8998.2 g H_2O, h/x=575.64)	6-500	6-311
ncsrt55d2_1_15_15	0.0 in np, 10400.0 gUZrHx (921.0 g ^{235}U, 8998.2 g H_2O, h/x=255.01)	6-505	6-317
hcsrtriga_1_15_15	0.0 in np, 10400.0 gUZrHx (921.0 g ^{235}U, 8998.2 g H_2O, h/x=255.01)	6-509	6-308
hcsrtriga70_1_15_15	0.0 in np, 6847.1 gUZrHx (408.0 g ^{235}U, 8998.2 g H_2O, h/x=575.64)	6-513	6-311
nciatriga_1_15_3	0.0 in np, 10400.0 gUZrHx (921.0 g ^{235}U, 8998.2 g H_2O, h/x=255.01)	6-518	6-310
nciatriga70_1_15_3	0.0 in np, 6847.1 gUZrHx (408.0 g ^{235}U, 8998.2 g H_2O, h/x=575.64)	6-522	6-313
hciatriga_1_15_3	0.0 in np, 10400.0 gUZrHx (921.0 g ^{235}U, 8998.2 g H_2O, h/x=255.01)	6-527	6-310
hciatriga70_1_15_3	0.0 in np, 6847.1 gUZrHx (408.0 g ^{235}U, 8998.2 g H_2O, h/x=575.64)	6-531	6-313
ncsrT70_131_1_15_15	0.0in np, 5666.6 gUZrHx(337.7 g^{235}U, 9204.9 gH_2O hx=711.53), fr=1.0e+00	6-536	6-315
nciaT70_131_1_15_3	0.0in np, 5666.6 gUZrHx(337.7 g^{235}U, 9204.9 gH_2O hx=711.53), fr=1.0e-04	6-540	6-316
cvcrcyat11_2_2	3 cyl, 1.4 in. np, 30,000 g U (30,000 g ^{235}U, 7,991.5 g H_2O, hx=6.95), sep=4.826	6-545	6-212
cvcrcyat11_11_2	3 cyl, 1.4 in. np, 30,000 g U (30,000 g ^{235}U, 7,991.5 g H_2O, hx=6.95), sep=4.826	6-548	6-213

ES-3100 Input file - Results table crosswalk

Case	Description	Input File	Results Table
cvcrpunhct11_10_15	10,000.2 g UNHc (4,709.7 g ^{235}U, 2,165.3 g H_2O) 6,080 g H_2O CV, hx=49.26	6-551	6-272
cvcrbpunhct11_24_15	24,000.2 g UNHc (11,303.1 g ^{235}U, 5,196.7 g H_2O) 1,077.9 g H_2O CV, hx=15.97	6-555	6-274
nciapbmflt11_1_6_4_5	0.0 in. np, 4,000.2 g U (3,200.2 g ^{235}U), 9,442.7 g H_2O CV, hx=82.26 fr=0.0001	6-557	6-259
nciapbmfdt11_1_6_4_5	0.0 in. np, 4,000.2 g U (3,200.2 g ^{235}U), 9,442.7 g H_2O CV, hx=82.26	6-562	6-259
ncsrpunhct11_15_15	8,000.1 g UNHc (3,767.7 g ^{235}U, 1,732.2 g H_2O) 6,795.6 g H_2O CV hx= 63.53	6-568	6-278
icsrpunhct12_15_15	15,000.0 g UNHc (7,064.4 g ^{235}U, 3,247.9 g H_2O) 6,397.6 g H_2O CV, hx=53.28	6-572	6-283

[a] Input files included in appendix for comparison with bounding model but not recorded in results tables.

```
=csas25    parm=size=3000000
cvcrcyt11 3cyl,0.0in thk np,21000.0gU(21000.0g235, 9082.6gH2O hx= 11.29),fr=1.0e+00
238groupndf5 infhommedium
'HEU volume =1116.36286, SPACER volume    0.00000'
'HEU wrapped dry content can hx=0.80, CV void volume 9098.99908'
uranium  1 den=18.81109 1.0 293      92235  100.00
                                     92238   0.000               end
'np277-4: spacer (NCT_MD&H)'
'NCT min.den.(95.3886 lb/ft3) and hydrogen'
'np277-4 min.den.= 1.527971 = (95.3886 lb/ft3)(453.59 g/lb)/(28316.84 cm3/ft3)'
'use 75% of boron in calculations per NUREG-1609 Section 6.5.3.2'
arbmboron 7.31015e-2  2 0 0 0    5010   18.1479
                                 5011   81.8520    2  0.7500  293  end
arbmnpmx  1.07070e+0 10 0 0 0    6012    1.9189
                                 7014    0.0141
                                 8016   43.4251
                                11023    0.1174
                                12000    0.3378
                                13027   39.0479
                                14000    2.4672
                                16000    0.3083
                                20000   11.8336
                                26000    0.5298    2  1.0000  293  end
arbmnph2o 3.84169e-1  2 0 0 0    1001   11.1913
                                 8016   88.8087    2  1.0000  293  end
'flooded containmment vessel and content cans -- 10 CFR 71.55(d)(3)'
arbmwicv   0.9982   2 0 0 0    1001   11.1913
                               8016   88.8087    3  1.0     293  end
'steel: containment vessel body 16.60 lb but use 15.74 lb'
ss304                                            8  1.0     293  end
'steel: cv flange lower use 3.36 lb'
ss304                                            9  0.97267 293  end
'steel: cv flange upper use 13.75 lb'
ss304                                           10  0.94348 293  end
'reflective water'
arbmh20r   0.9982   2 0 0 0    1001   11.1913
                               8016   88.8087   21  1.0     293  end
end comp
cvcrcyt11 3cyl,0.0in thk np,21000.0gU(21000.0g235, 9082.6gH2O,hx= 11.29),fr=1.0e+00
read parameters nub=yes npg=2500 gen=215 nsk=15 tme=100 end parameters
read boun       all=vac                         end boun
read geometry
unit 1001
'drum bottom flat cover [Elev= 0.105 in. at top of unit]'
'cylinder  19 1   24.587200    0.26670   0.0     com='extended radius not used'
 cuboid    21 1 4p24.587200    0.26670   0.0     com='drum chine outer radius'
unit 1002
'above drum bottom flat cover and below containment vessel [Elev= 4.670 in.]'
 cuboid    21 1 4p24.587200   11.59510   0.0     com='drum chine outer radius'
unit 1003
'cv bottom [Elev= 4.920 in.]'
 cylinder  8  1    6.680200    0.63500   0.0     com='cv bottom'
 cuboid    21 1 4p24.587200    0.63500   0.0     com='drum chine outer radius'
unit 1006
'content (collapsed) [Elev= 7.675 in.]'
 cylinder  1  1    4.114800     6.99579   0.0     com='cylindrical content'
 cylinder  3  1    6.426200    6.99629  -0.0005  com='cv well cavity'
 cylinder  8  1    6.680200    6.99629  -0.0005  com='cv below 1st step'
 cuboid    21 1 4p24.587200    6.99629  -0.0005  com='drum chine outer radius'
unit 1007
'np277_4 spacer [Elev= 7.675 in.]'
 cylinder  2  1    5.24510     0.00010   0.0     com='np spacer'
 cylinder  3  1    6.426200    0.00020  -0.0001  com='cv well cavity'
 cylinder  8  1    6.680200    0.00020  -0.0001  com='cv below 1st step'
 cuboid    21 1 4p24.587200    0.00020  -0.0001  com='drum chine outer radius'
unit 1008
'top of content stack to bottom of 1st step [Elev=35.270 in.]'
'20.99097             stack height (content spacers)       CALCULATED
 cylinder  3  1    6.426200   56.09803   0.0     com='cv well cavity'
 cylinder  8  1    6.680200   56.09803   0.0     com='cv below 1st step'
 cuboid    21 1 4p24.587200   56.09803   0.0     com='drum chine outer radius'
```

```
unit 1010
'cv at 1st step in liner [Elev=35.330 in.]'
 cylinder  3  1    6.426200    0.15240   0.0     com='cv well cavity'
 cylinder  8  1    6.680200    0.15240   0.0     com='cv at 1st step'
 cuboid    21 1 4p24.587200    0.15240   0.0     com='drum chine outer radius'
unit 1011
'vertical gap between 1st step in liner and cv flange [Elev=35.420 in.]'
 cylinder  3  1    6.426200    0.22860   0.0     com='cv well cavity'
 cylinder  8  1    6.680200    0.22860   0.0     com='cv at gap btwn step-flng'
 cuboid    21 1 4p24.587200    0.22860   0.0     com='drum chine outer radius'
unit 1012
'cv flange to top of cv well [Elev=35.920 in.]'
 cylinder  3  1    6.426200    1.27000   0.0     com='cavity'
 cylinder  9  1    9.525000    1.27000   0.0     com='flange to top of well'
 cuboid    21 1 4p24.587200    1.27000   0.0     com='drum chine outer radius'
unit 1013
'cv flange above cv well [Elev=37.070 in.]'
 cylinder  10 1    9.525000    2.92100   0.0     com='flange above cv well'
 cuboid    21 1 4p24.587200    2.92100   0.0     com='drum chine outer radius'
unit 1014
'plugpad2 below liner 2nd step [Elev=37.470 in.]'
 cuboid    21 1 4p24.587200    1.01600   0.0     com='drum chine outer radius'
unit 1015
'2nd step in liner [Elev=37.530 in.]'
 cuboid    21 1 4p24.587200    0.15240   0.0     com='drum chine outer radius'
unit 1016
'abv 2nd step in liner to bottom of angle iron [Elev=40.750 in.]'
 cuboid    21 1 4p24.587200    8.17880   0.0     com='drum chine outer radius'
unit 1017
'bottom of angle iron to bend in angle iron [Elev=42.500 in.]'
 cuboid    21 1 4p24.587200    4.44500   0.0     com='drum chine outer radius'
unit 1018
'bend in angle iron to top of angle iron [Elev=42.750 in.]'
 cuboid    21 1 4p24.587200    0.63500   0.0     com='drum chine outer radius'
unit 1019
'drum lid and lip [Elev=43.500 in.]'
 cuboid    21 1 4p24.587200    1.90500   0.0     com='drum chine outer radius'
global
unit 1020
'es3100 drum [Elev=43.500 in.]'
array 3         2r-24.587200     0.0
'cuboid     0  1 4p24.587200    110.4905  0.0    com='bare package'
 cuboid    21  1 4p55.067200   140.9700 -30.48   com='reflected package'
'cuboid    20  1 4p22.889718    110.5048  0.0    com='interstital array space'
'global
'unit 1021
'array 4   3r0.0
'reflector  21 2  6r3.0  10
end geometry
read array
ara=3 nux=1 nuy=1 nuz=19 fill
1001 1002 1003 1006 1007 1006 1007 1006 1008 1010
1011 1012 1013 1014 1015 1016 1017 1018 1019        end fill
'ara=4 nux=13 nuy=13 nuz=06 fill f1020               end fill
end array
'read bias id=500 2  11  end bias
read start nst=0
end start
end data
end


=csas25    parm=size=3000000
cvcrcyt11 3cyl,1.4in thk np,36000.0gU(36000.0g235, 7673.1gH2O hx=  5.56),fr=1.0e+00
238groupndf5 infhommedium
'HEU volume =1913.76490, SPACER volume  614.68012'
'HEU wrapped dry content can hx=0.47, CV void volume 7686.91692'
uranium  1 den=18.81109 1.0 293      92235  100.00
                                     92238   0.000               end
'np277-4: spacer (NCT_MD&H)'
'NCT min.den.(95.3886 lb/ft3) and hydrogen'
```

```
'np277-4 min.den.= 1.527971 = (95.3886 lb/ft3)(453.59 g/lb)/(28316.84 cm3/ft3)'
'use 75% of boron in calculations per NUREG-1609 Section 6.5.3.2'
arbmboron 7.31015e-2  2 0 0 0    5010   18.1479
                                 5011   81.8520    2  0.7500  293  end
arbmnpmx  1.07070e+0 10 0 0 0    6012    1.9189
                                 7014    0.0141
                                 8016   43.4251
                                11023    0.1174
                                12000    0.3378
                                13027   39.0479
                                14000    2.4672
                                16000    0.3083
                                20000   11.8336
                                26000    0.5298    2  1.0000  293  end
arbmnph2o 3.84169e-1  2 0 0 0    1001   11.1913
                                 8016   88.8087    2  1.0000  293  end
'flooded containmment vessel and content cans -- 10 CFR 71.55(d)(3)'
arbmwicv   0.9982   2 0 0 0    1001   11.1913
                               8016   88.8087    3  1.0     293  end
'steel: containment vessel body 16.60 lb but use 15.74 lb'
ss304                                            8  1.0     293  end
'steel: cv flange lower use 3.36 lb'
ss304                                            9  0.97267 293  end
'steel: cv flange upper use 13.75 lb'
ss304                                           10  0.94348 293  end
'reflective water'
arbmh20r   0.9982   2 0 0 0    1001   11.1913
                               8016   88.8087   21  1.0     293  end
end comp
cvcrcyt11 3cyl,1.4in thk np,36000.0gU(36000.0g235, 7673.1gH2O,hx=  5.56),fr=1.0e+00
read parameters nub=yes npg=2500 gen=215 nsk=15 tme=100 end parameters
read boun       all=vac                         end boun
read geometry
unit 1001
'drum bottom flat cover [Elev= 0.105 in. at top of unit]'
'cylinder  19 1   24.587200    0.26670   0.0     com='extended radius not used'
 cuboid    21 1 4p24.587200    0.26670   0.0     com='drum chine outer radius'
unit 1002
'above drum bottom flat cover and below containment vessel [Elev= 4.670 in.]'
 cuboid    21 1 4p24.587200   11.59510   0.0     com='drum chine outer radius'
unit 1003
'cv bottom [Elev= 4.920 in.]'
 cylinder  8  1    6.680200    0.63500   0.0     com='cv bottom'
 cuboid    21 1 4p24.587200    0.63500   0.0     com='drum chine outer radius'
unit 1006
'content (collapsed) [Elev= 9.642 in.]'
 cylinder  1  1    4.114800    11.99278   0.0     com='cylindrical content'
 cylinder  3  1    6.426200   11.99328  -0.0005  com='cv well cavity'
 cylinder  8  1    6.680200   11.99328  -0.0005  com='cv below 1st step'
 cuboid    21 1 4p24.587200   11.99328  -0.0005  com='drum chine outer radius'
unit 1007
'np277_4 spacer [Elev=11.042 in.]'
 cylinder  2  1    5.24510     3.55610   0.0     com='np spacer'
 cylinder  3  1    6.426200    3.55620  -0.0001  com='cv well cavity'
 cylinder  8  1    6.680200    3.55620  -0.0001  com='cv below 1st step'
 cuboid    21 1 4p24.587200    3.55620  -0.0001  com='drum chine outer radius'
unit 1008
'top of content stack to bottom of 1st step [Elev=35.270 in.]'
'43.09395             stack height (content spacers)       CALCULATED
 cylinder  3  1    6.426200   33.99505   0.0     com='cv well cavity'
 cylinder  8  1    6.680200   33.99505   0.0     com='cv below 1st step'
 cuboid    21 1 4p24.587200   33.99505   0.0     com='drum chine outer radius'
unit 1010
'cv at 1st step in liner [Elev=35.330 in.]'
 cylinder  3  1    6.426200    0.15240   0.0     com='cv well cavity'
 cylinder  8  1    6.680200    0.15240   0.0     com='cv at 1st step'
 cuboid    21 1 4p24.587200    0.15240   0.0     com='drum chine outer radius'
unit 1011
'vertical gap between 1st step in liner and cv flange [Elev=35.420 in.]'
 cylinder  3  1    6.426200    0.22860   0.0     com='cv well cavity'
 cylinder  8  1    6.680200    0.22860   0.0     com='cv at gap btwn step-flng'
```

```
 cuboid    21 1 4p24.587200    0.22860   0.0     com='drum chine outer radius'
unit 1012
'cv flange to top of cv well [Elev=35.920 in.]'
 cylinder  3  1    6.426200    1.27000   0.0     com='cavity'
 cylinder  9  1    9.525000    1.27000   0.0     com='flange to top of well'
 cuboid    21 1 4p24.587200    1.27000   0.0     com='drum chine outer radius'
unit 1013
'cv flange above cv well [Elev=37.070 in.]'
 cylinder  10 1    9.525000    2.92100   0.0     com='flange above cv well'
 cuboid    21 1 4p24.587200    2.92100   0.0     com='drum chine outer radius'
unit 1014
'plugpad2 below liner 2nd step [Elev=37.470 in.]'
 cuboid    21 1 4p24.587200    1.01600   0.0     com='drum chine outer radius'
unit 1015
'2nd step in liner [Elev=37.530 in.]'
 cuboid    21 1 4p24.587200    0.15240   0.0     com='drum chine outer radius'
unit 1016
'abv 2nd step in liner to bottom of angle iron [Elev=40.750 in.]'
 cuboid    21 1 4p24.587200    8.17880   0.0     com='drum chine outer radius'
unit 1017
'bottom of angle iron to bend in angle iron [Elev=42.500 in.]'
 cuboid    21 1 4p24.587200    4.44500   0.0     com='drum chine outer radius'
unit 1018
'bend in angle iron to top of angle iron [Elev=42.750 in.]'
 cuboid    21 1 4p24.587200    0.63500   0.0     com='drum chine outer radius'
unit 1019
'drum lid and lip [Elev=43.500 in.]'
 cuboid    21 1 4p24.587200    1.90500   0.0     com='drum chine outer radius'
global
unit 1020
'es3100 drum [Elev=43.500 in.]'
array 3         2r-24.587200     0.0
'cuboid     0  1 4p24.587200    110.4905  0.0    com='bare package'
 cuboid    21  1 4p55.067200   140.9700 -30.48   com='reflected package'
'cuboid    20  1 4p22.889718    110.5048  0.0    com='interstital array space'
'global
'unit 1021
'array 4   3r0.0
'reflector  21 2  6r3.0  10
end geometry
read array
ara=3 nux=1 nuy=1 nuz=19 fill
1001 1002 1003 1006 1007 1006 1007 1006 1008 1010
1011 1012 1013 1014 1015 1016 1017 1018 1019        end fill
'ara=4 nux=13 nuy=13 nuz=06 fill f1020               end fill
end array
'read bias id=500 2  11  end bias
read start nst=0
end start
end data
end


=csas25    parm=size=3000000
cvcrsqt11 3bar,0.0in thk np,36000.0gU(36000.0g235, 8286.7gH2O hx=  6.01),fr=1.0e+00
238groupndf5 infhommedium
'HEU volume =1913.76490, SPACER volume    0.00000'
'HEU wrapped dry content can hx=0.47, CV void volume 8301.59704'
uranium  1 den=18.81109 1.0 293      92235  100.00
                                     92238   0.000               end
'np277-4: spacer (NCT_MD&H)'
'NCT min.den.(95.3886 lb/ft3) and hydrogen'
'np277-4 min.den.= 1.527971 = (95.3886 lb/ft3)(453.59 g/lb)/(28316.84 cm3/ft3)'
'use 75% of boron in calculations per NUREG-1609 Section 6.5.3.2'
arbmboron 7.31015e-2  2 0 0 0    5010   18.1479
                                 5011   81.8520    2  0.7500  293  end
arbmnpmx  1.07070e+0 10 0 0 0    6012    1.9189
                                 7014    0.0141
                                 8016   43.4251
                                11023    0.1174
                                12000    0.3378
```

```
                                13027   39.0479
                                14000    2.4672
                                16000    0.3083
                                20000   11.8336
                                26000    0.5298    2  1.0000  293  end
arbmnph2o 3.84169e-1  2 0 0 0    1001   11.1913
                                 8016   88.8087    2  1.0000  293  end
'flooded containmment vessel and content cans -- 10 CFR 71.55(d)(3)'
arbmwicv   0.9982   2 0 0 0    1001   11.1913
                               8016   88.8087    3  1.0     293  end
'steel: containment vessel body 16.60 lb but use 15.74 lb'
ss304                                          8  1.0     293  end
'steel: cv flange lower use 3.36 lb'
ss304                                          9  0.97267 293  end
'steel: cv flange upper use 13.75 lb'
ss304                                         10  0.94348 293  end
'reflective water'
arbmh20r   0.9982   2 0 0 0    1001   11.1913
                               8016   88.8087   21  1.0     293  end
end comp
cvcrsqt11 3bar,0.0in thk np,36000.0gU(36000.0g235, 8286.7gH2O,hx=  6.01),fr=1.0e+00
read parameters nub=yes npg=2500 gen=215 nsk=15 tme=100 end parameters
read boun       all=vac                        end boun
read geometry
unit 1001
'drum bottom flat cover [Elev= 0.105 in. at top of unit]'
'cylinder  19 1   24.587200    0.26670   0.0     com='extended radius not used'
 cuboid    21 1 4p24.587200    0.26670   0.0     com='drum chine outer radius'
unit 1002
'above drum bottom flat cover and below containment vessel [Elev= 4.670 in.]'
 cuboid    21 1 4p24.587200   11.59510   0.0     com='drum chine outer radius'
unit 1003
'cv bottom [Elev= 4.920 in.]'
 cylinder  8  1    6.680200    0.63500   0.0     com='cv bottom'
 cuboid    21 1 4p24.587200    0.63500   0.0     com='drum chine outer radius'
unit 1006
'content (collapsed) [Elev=12.337 in.]'
 cuboid    1  1  4p2.909600    18.83826   0.0     com='block content'
 cylinder  3  1    6.426200   18.83876  -0.0005  com='cv well cavity'
 cylinder  8  1    6.680200   18.83876  -0.0005  com='cv below 1st step'
 cuboid    21 1 4p24.587200   18.83876  -0.0005  com='drum chine outer radius'
unit 1007
'np277_4 spacer [Elev=12.337 in.]'
 cylinder  2  1    5.24510     0.00010   0.0     com='np spacer'
 cylinder  3  1    6.426200    0.00020  -0.0001  com='cv well cavity'
 cylinder  8  1    6.680200    0.00020  -0.0001  com='cv below 1st step'
 cuboid    21 1 4p24.587200    0.00020  -0.0001  com='drum chine outer radius'
unit 1008
'top of content stack to bottom of 1st step [Elev=35.270 in.]'
'56.51838             stack height (content spacers)       CALCULATED
 cylinder  3  1    6.426200   20.57062   0.0     com='cv well cavity'
 cylinder  8  1    6.680200   20.57062   0.0     com='cv below 1st step'
 cuboid    21 1 4p24.587200   20.57062   0.0     com='drum chine outer radius'
unit 1010
'cv at 1st step in liner [Elev=35.330 in.]'
 cylinder  3  1    6.426200    0.15240   0.0     com='cv well cavity'
 cylinder  8  1    6.680200    0.15240   0.0     com='cv at 1st step'
 cuboid    21 1 4p24.587200    0.15240   0.0     com='drum chine outer radius'
unit 1011
'vertical gap between 1st step in liner and cv flange [Elev=35.420 in.]'
 cylinder  3  1    6.426200    0.22860   0.0     com='cv well cavity'
 cylinder  8  1    6.680200    0.22860   0.0     com='cv at gap btwn step-flng'
 cuboid    21 1 4p24.587200    0.22860   0.0     com='drum chine outer radius'
unit 1012
'cv flange to top of cv well [Elev=35.920 in.]'
 cylinder  3  1    6.426200    1.27000   0.0     com='cavity'
 cylinder  9  1    9.525000    1.27000   0.0     com='flange to top of well'
 cuboid    21 1 4p24.587200    1.27000   0.0     com='drum chine outer radius'
unit 1013
'cv flange above cv well [Elev=37.070 in.]'
 cylinder  10 1    9.525000    2.92100   0.0     com='flange above cv well'
```

```
 cuboid    21 1 4p24.587200    2.92100   0.0     com='drum chine outer radius'
unit 1014
'plugpad2 below liner 2nd step [Elev=37.470 in.]'
 cuboid    21 1 4p24.587200    1.01600   0.0     com='drum chine outer radius'
unit 1015
'2nd step in liner [Elev=37.530 in.]'
 cuboid    21 1 4p24.587200    0.15240   0.0     com='drum chine outer radius'
unit 1016
'abv 2nd step in liner to bottom of angle iron [Elev=40.750 in.]'
 cuboid    21 1 4p24.587200    8.17880   0.0     com='drum chine outer radius'
unit 1017
'bottom of angle iron to bend in angle iron [Elev=42.500 in.]'
 cuboid    21 1 4p24.587200    4.44500   0.0     com='drum chine outer radius'
unit 1018
'bend in angle iron to top of angle iron [Elev=42.750 in.]'
 cuboid    21 1 4p24.587200    0.63500   0.0     com='drum chine outer radius'
unit 1019
'drum lid and lip [Elev=43.500 in.]'
 cuboid    21 1 4p24.587200    1.90500   0.0     com='drum chine outer radius'
global
unit 1020
'es3100 drum [Elev=43.500 in.]'
array 3         2r-24.587200     0.0
'cuboid     0  1 4p24.587200    110.4905  0.0    com='bare package'
 cuboid    21  1 4p55.067200   140.9700 -30.48   com='reflected package'
'cuboid    20  1 4p22.889718    110.5048  0.0    com='interstital array space'
'global
'unit 1021
'array 4   3r0.0
'reflector  21 2  6r3.0  10
end geometry
read array
ara=3 nux=1 nuy=1 nuz=19 fill
1001 1002 1003 1006 1007 1006 1007 1006 1008 1010
1011 1012 1013 1014 1015 1016 1017 1018 1019        end fill
'ara=4 nux=13 nuy=13 nuz=06 fill f1020               end fill
end array
'read bias id=500 2  11  end bias
read start nst=0
end start
end data
end


=csas25    parm=size=3000000
cvcrcyct11 3cyl,0.0in thk np,17000.1gU(17000.1g235, 9294.9gH2O hx= 14.27),fr=1.0e+00
238groupndf5 infhommedium
'HEU volume = 903.72763, SPACER volume    0.00000'
'HEU wrapped dry content can hx=0.99, CV void volume 9311.63431'
uranium  1 den=18.81109 1.0 293      92235  100.00
                                     92238   0.000               end
'np277-4: spacer (NCT_MD&H)'
'NCT min.den.(95.3886 lb/ft3) and hydrogen'
'np277-4 min.den.= 1.527971 = (95.3886 lb/ft3)(453.59 g/lb)/(28316.84 cm3/ft3)'
'use 75% of boron in calculations per NUREG-1609 Section 6.5.3.2'
arbmboron 7.31015e-2  2 0 0 0    5010   18.1479
                                 5011   81.8520    2  0.7500  293  end
arbmnpmx  1.07070e+0 10 0 0 0    6012    1.9189
                                 7014    0.0141
                                 8016   43.4251
                                11023    0.1174
                                12000    0.3378
                                13027   39.0479
                                14000    2.4672
                                16000    0.3083
                                20000   11.8336
                                26000    0.5298    2  1.0000  293  end
arbmnph2o 3.84169e-1  2 0 0 0    1001   11.1913
                                 8016   88.8087    2  1.0000  293  end
'flooded containmment vessel and content cans -- 10 CFR 71.55(d)(3)'
arbmwicv   0.9982   2 0 0 0    1001   11.1913
```

```
                              8016   88.8087    3  1.0     293  end
'steel: containment vessel body 16.60 lb but use 15.74 lb'
ss304                                            8  1.0     293  end
'steel: cv flange lower use 3.36 lb'
ss304                                            9  0.97267 293  end
'steel: cv flange upper use 13.75 lb'
ss304                                           10  0.94348 293  end
'reflective water'
arbmh20r   0.9982   2 0 0 0    1001   11.1913
                              8016   88.8087   21  1.0     293  end
end comp
cvcrcyct11 3cyl,0.0in thk np,17000.1gU(17000.1g235, 9294.9gH2O,hx= 14.27),fr=1.0e+00
read parameters nub=yes npg=2500 gen=215 nsk=15 tme=100 end parameters
read boun       all=vac                          end boun
read geometry
unit 1001
'drum bottom flat cover [Elev= 0.105 in. at top of unit]'
'cylinder  19 1   24.587200    0.26670   0.0     com='extended radius not used'
 cuboid    21 1 4p24.587200    0.26670   0.0     com='drum chine outer radius'
unit 1002
'above drum bottom flat cover and below containment vessel [Elev= 4.670 in.]'
 cuboid    21 1 4p24.587200   11.59510   0.0     com='drum chine outer radius'
unit 1003
'cv bottom [Elev= 4.920 in.]'
 cylinder  8  1    6.680200    0.63500   0.0     com='cv bottom'
 cuboid    21 1 4p24.587200    0.63500   0.0     com='drum chine outer radius'
unit 1006
'content (collapsed) [Elev= 6.216 in.]'
 cylinder  1  1    5.397500     3.29140   0.0     com='cylindrical content'
 cylinder  3  1    6.426200    3.29190  -0.0005  com='cv well cavity'
 cylinder  8  1    6.680200    3.29190  -0.0005  com='cv below 1st step'
 cuboid    21 1 4p24.587200    3.29190  -0.0005  com='drum chine outer radius'
unit 1007
'np277_4 spacer [Elev= 6.216 in.]'
 cylinder  2  1    5.24510     0.00010   0.0     com='np spacer'
 cylinder  3  1    6.426200    0.00020  -0.0001  com='cv well cavity'
 cylinder  8  1    6.680200    0.00020  -0.0001  com='cv below 1st step'
 cuboid    21 1 4p24.587200    0.00020  -0.0001  com='drum chine outer radius'
unit 1008
'top of content stack to bottom of 1st step [Elev=35.270 in.]'
' 9.87781             stack height (content spacers)       CALCULATED
 cylinder  3  1    6.426200   67.21119   0.0     com='cv well cavity'
 cylinder  8  1    6.680200   67.21119   0.0     com='cv below 1st step'
 cuboid    21 1 4p24.587200   67.21119   0.0     com='drum chine outer radius'
unit 1010
'cv at 1st step in liner [Elev=35.330 in.]'
 cylinder  3  1    6.426200    0.15240   0.0     com='cv well cavity'
 cylinder  8  1    6.680200    0.15240   0.0     com='cv at 1st step'
 cuboid    21 1 4p24.587200    0.15240   0.0     com='drum chine outer radius'
unit 1011
'vertical gap between 1st step in liner and cv flange [Elev=35.420 in.]'
 cylinder  3  1    6.426200    0.22860   0.0     com='cv well cavity'
 cylinder  8  1    6.680200    0.22860   0.0     com='cv at gap btwn step-flng'
 cuboid    21 1 4p24.587200    0.22860   0.0     com='drum chine outer radius'
unit 1012
'cv flange to top of cv well [Elev=35.920 in.]'
 cylinder  3  1    6.426200    1.27000   0.0     com='cavity'
 cylinder  9  1    9.525000    1.27000   0.0     com='flange to top of well'
 cuboid    21 1 4p24.587200    1.27000   0.0     com='drum chine outer radius'
unit 1013
'cv flange above cv well [Elev=37.070 in.]'
 cylinder  10 1    9.525000    2.92100   0.0     com='flange above cv well'
 cuboid    21 1 4p24.587200    2.92100   0.0     com='drum chine outer radius'
unit 1014
'plugpad2 below liner 2nd step [Elev=37.470 in.]'
 cuboid    21 1 4p24.587200    1.01600   0.0     com='drum chine outer radius'
unit 1015
'2nd step in liner [Elev=37.530 in.]'
 cuboid    21 1 4p24.587200    0.15240   0.0     com='drum chine outer radius'
unit 1016
'abv 2nd step in liner to bottom of angle iron [Elev=40.750 in.]'
```

```
 cuboid    21 1 4p24.587200    8.17880   0.0     com='drum chine outer radius'
unit 1017
'bottom of angle iron to bend in angle iron [Elev=42.500 in.]'
 cuboid    21 1 4p24.587200    4.44500   0.0     com='drum chine outer radius'
unit 1018
'bend in angle iron to top of angle iron [Elev=42.750 in.]'
 cuboid    21 1 4p24.587200    0.63500   0.0     com='drum chine outer radius'
unit 1019
'drum lid and lip [Elev=43.500 in.]'
 cuboid    21 1 4p24.587200    1.90500   0.0     com='drum chine outer radius'
global
unit 1020
'es3100 drum [Elev=43.500 in.]'
array 3         2r-24.587200     0.0
'cuboid     0  1 4p24.587200    110.4905  0.0    com='bare package'
 cuboid    21  1 4p55.067200   140.9700 -30.48   com='reflected package'
'cuboid    20  1 4p22.889718    110.5048  0.0    com='interstital array space'
'global
'unit 1021
'array 4   3r0.0
'reflector  21 2  6r3.0  10
end geometry
read array
ara=3 nux=1 nuy=1 nuz=19 fill
1001 1002 1003 1006 1007 1006 1007 1006 1008 1010
1011 1012 1013 1014 1015 1016 1017 1018 1019        end fill
'ara=4 nux=13 nuy=13 nuz=06 fill f1020               end fill
end array
'read bias id=500 2  11  end bias
read start nst=0
end start
end data
end


=csas25    parm=size=3000000
cvcrcyct11 3cyl,1.4in thk np,32000.1gU(32000.1g235, 7885.3gH2O hx=  6.43),fr=1.0e+00
238groupndf5 infhommedium
'HEU volume =1701.12968, SPACER volume  614.68012'
'HEU wrapped dry content can hx=0.52, CV void volume 7899.55215'
uranium  1 den=18.81109 1.0 293      92235  100.00
                                     92238   0.000               end
'np277-4: spacer (NCT_MD&H)'
'NCT min.den.(95.3886 lb/ft3) and hydrogen'
'np277-4 min.den.= 1.527971 = (95.3886 lb/ft3)(453.59 g/lb)/(28316.84 cm3/ft3)'
'use 75% of boron in calculations per NUREG-1609 Section 6.5.3.2'
arbmboron 7.31015e-2  2 0 0 0    5010   18.1479
                                 5011   81.8520    2  0.7500  293  end
arbmnpmx  1.07070e+0 10 0 0 0    6012    1.9189
                                 7014    0.0141
                                 8016   43.4251
                                11023    0.1174
                                12000    0.3378
                                13027   39.0479
                                14000    2.4672
                                16000    0.3083
                                20000   11.8336
                                26000    0.5298    2  1.0000  293  end
arbmnph2o 3.84169e-1  2 0 0 0    1001   11.1913
                                 8016   88.8087    2  1.0000  293  end
'flooded containmment vessel and content cans -- 10 CFR 71.55(d)(3)'
arbmwicv   0.9982   2 0 0 0    1001   11.1913
                               8016   88.8087    3  1.0     293  end
'steel: containment vessel body 16.60 lb but use 15.74 lb'
ss304                                            8  1.0     293  end
'steel: cv flange lower use 3.36 lb'
ss304                                            9  0.97267 293  end
'steel: cv flange upper use 13.75 lb'
ss304                                           10  0.94348 293  end
'reflective water'
arbmh20r   0.9982   2 0 0 0    1001   11.1913
```

```
                                8016   88.8087   21  1.0     293  end
end comp
cvcrcyct11 3cyl,1.4in thk np,32000.1gU(32000.1g235, 7885.3gH2O,hx=  6.43),fr=1.0e+00
read parameters nub=yes npg=2500 gen=215 nsk=15 tme=100 end parameters
read boun       all=vac                         end boun
read geometry
unit 1001
'drum bottom flat cover [Elev= 0.105 in. at top of unit]'
'cylinder  19 1   24.587200    0.26670   0.0     com='extended radius not used'
 cuboid    21 1 4p24.587200    0.26670   0.0     com='drum chine outer radius'
unit 1002
'above drum bottom flat cover and below containment vessel [Elev= 4.670 in.]'
 cuboid    21 1 4p24.587200   11.59510   0.0     com='drum chine outer radius'
unit 1003
'cv bottom [Elev= 4.920 in.]'
 cylinder  8  1    6.680200    0.63500   0.0     com='cv bottom'
 cuboid    21 1 4p24.587200    0.63500   0.0     com='drum chine outer radius'
unit 1006
'content (collapsed) [Elev= 7.360 in.]'
 cylinder  1  1    5.397500     6.19557   0.0     com='cylindrical content'
 cylinder  3  1    6.426200    6.19607  -0.0005  com='cv well cavity'
 cylinder  8  1    6.680200    6.19607  -0.0005  com='cv below 1st step'
 cuboid    21 1 4p24.587200    6.19607  -0.0005  com='drum chine outer radius'
unit 1007
'np277_4 spacer [Elev= 8.760 in.]'
 cylinder  2  1    5.24510     3.55610   0.0     com='np spacer'
 cylinder  3  1    6.426200    3.55620  -0.0001  com='cv well cavity'
 cylinder  8  1    6.680200    3.55620  -0.0001  com='cv below 1st step'
 cuboid    21 1 4p24.587200    3.55620  -0.0001  com='drum chine outer radius'
unit 1008
'top of content stack to bottom of 1st step [Elev=35.270 in.]'
'25.70230             stack height (content spacers)       CALCULATED
 cylinder  3  1    6.426200   51.38670   0.0     com='cv well cavity'
 cylinder  8  1    6.680200   51.38670   0.0     com='cv below 1st step'
 cuboid    21 1 4p24.587200   51.38670   0.0     com='drum chine outer radius'
unit 1010
'cv at 1st step in liner [Elev=35.330 in.]'
 cylinder  3  1    6.426200    0.15240   0.0     com='cv well cavity'
 cylinder  8  1    6.680200    0.15240   0.0     com='cv at 1st step'
 cuboid    21 1 4p24.587200    0.15240   0.0     com='drum chine outer radius'
unit 1011
'vertical gap between 1st step in liner and cv flange [Elev=35.420 in.]'
 cylinder  3  1    6.426200    0.22860   0.0     com='cv well cavity'
 cylinder  8  1    6.680200    0.22860   0.0     com='cv at gap btwn step-flng'
 cuboid    21 1 4p24.587200    0.22860   0.0     com='drum chine outer radius'
unit 1012
'cv flange to top of cv well [Elev=35.920 in.]'
 cylinder  3  1    6.426200    1.27000   0.0     com='cavity'
 cylinder  9  1    9.525000    1.27000   0.0     com='flange to top of well'
 cuboid    21 1 4p24.587200    1.27000   0.0     com='drum chine outer radius'
unit 1013
'cv flange above cv well [Elev=37.070 in.]'
 cylinder  10 1    9.525000    2.92100   0.0     com='flange above cv well'
 cuboid    21 1 4p24.587200    2.92100   0.0     com='drum chine outer radius'
unit 1014
'plugpad2 below liner 2nd step [Elev=37.470 in.]'
 cuboid    21 1 4p24.587200    1.01600   0.0     com='drum chine outer radius'
unit 1015
'2nd step in liner [Elev=37.530 in.]'
 cuboid    21 1 4p24.587200    0.15240   0.0     com='drum chine outer radius'
unit 1016
'abv 2nd step in liner to bottom of angle iron [Elev=40.750 in.]'
 cuboid    21 1 4p24.587200    8.17880   0.0     com='drum chine outer radius'
unit 1017
'bottom of angle iron to bend in angle iron [Elev=42.500 in.]'
 cuboid    21 1 4p24.587200    4.44500   0.0     com='drum chine outer radius'
unit 1018
'bend in angle iron to top of angle iron [Elev=42.750 in.]'
 cuboid    21 1 4p24.587200    0.63500   0.0     com='drum chine outer radius'
unit 1019
'drum lid and lip [Elev=43.500 in.]'
```

```
 cuboid    21 1 4p24.587200    1.90500   0.0     com='drum chine outer radius'
global
unit 1020
'es3100 drum [Elev=43.500 in.]'
array 3         2r-24.587200     0.0
'cuboid     0  1 4p24.587200    110.4905  0.0    com='bare package'
 cuboid    21  1 4p55.067200   140.9700 -30.48   com='reflected package'
'cuboid    20  1 4p22.889718    110.5048  0.0    com='interstital array space'
'global
'unit 1021
'array 4   3r0.0
'reflector  21 2  6r3.0  10
end geometry
read array
ara=3 nux=1 nuy=1 nuz=19 fill
1001 1002 1003 1006 1007 1006 1007 1006 1008 1010
1011 1012 1013 1014 1015 1016 1017 1018 1019        end fill
'ara=4 nux=13 nuy=13 nuz=06 fill f1020               end fill
end array
'read bias id=500 2  11  end bias
read start nst=0
end start
end data
end


=csas25    parm=size=3000000
cvcr5est11,0.0in np,18277.3gU(18277.3g235, 9226.9gH2O hx= 13.18),fr=1.0e+00
238groupndf5 infhommedium
'HEU volume = 971.62217, SPACER volume    0.01729'
'HEU wrapped dry content can hx=0.92, CV void volume 9243.50194'
uranium  1 den=18.81109 1.0 293      92235  100.00
                                     92238   0.000               end
'np277-4: spacer (NCT_MD&H)'
'NCT min.den.(95.3886 lb/ft3) and hydrogen'
'np277-4 min.den.= 1.527971 = (95.3886 lb/ft3)(453.59 g/lb)/(28316.84 cm3/ft3)'
'use 75% of boron in calculations per NUREG-1609 Section 6.5.3.2'
arbmboron 7.31015e-2  2 0 0 0    5010   18.1479
                                 5011   81.8520    2  0.7500  293  end
arbmnpmx  1.07070e+0 10 0 0 0    6012    1.9189
                                 7014    0.0141
                                 8016   43.4251
                                11023    0.1174
                                12000    0.3378
                                13027   39.0479
                                14000    2.4672
                                16000    0.3083
                                20000   11.8336
                                26000    0.5298    2  1.0000  293  end
arbmnph2o 3.84169e-1  2 0 0 0    1001   11.1913
                                 8016   88.8087    2  1.0000  293  end
'flooded containmment vessel and content cans -- 10 CFR 71.55(d)(3)'
arbmwicv   0.9982   2 0 0 0    1001   11.1913
                               8016   88.8087    3  1.0     293  end
'steel: containment vessel body 16.60 lb but use 15.74 lb'
ss304                                            8  1.0     293  end
'steel: cv flange lower use 3.36 lb'
ss304                                            9  0.97267 293  end
'steel: cv flange upper use 13.75 lb'
ss304                                           10  0.94348 293  end
'np277-4: confinement -- neutron poison inner liner (NCT_MD&H)'
'actual vol.= 1.31846e4 cm3 = (8.0457422e2 in3)(16.387064)'
'den.multiplier = 1.31846e4 cm3 (actual vol.) / 1.32708e4 cm3 (model vol.)'
'np277-4 min.den.= 1.527971 = (95.3886 lb/ft3)(453.59 g/lb)/(28316.84 cm3/ft3)'
'density = 1.518047 = (den.mult)(np277-4 min.den.) = 0.9935052*1.527971'
'use 75% of boron in calculations per NUREG-1609 Section 6.5.3.2'
arbmboron 7.26267e-2  2 0 0 0    5010   18.1479
                                 5011   81.8520   11  0.7500  293  end
arbmnpmx  1.06375e+0 10 0 0 0    6012    1.9189
                                 7014    0.0141
                                 8016   43.4251
```

```
                                11023    0.1174
                                12000    0.3378
                                13027   39.0479
                                14000    2.4672
                                16000    0.3083
                                20000   11.8336
                                26000    0.5298   11  1.0000  293  end
arbmnph2o 3.81674e-1  2 0 0 0    1001   11.1913
                                 8016   88.8087   11  1.0000  293  end
'kaolite 1600 body'
'sing.unit.density= (den.mult)(min.den.)'
' for arbmh20k = 1.012373*0.51655,  for rest = 1.012373*0.34438'
'den.mult= 1.36557e5 cm3 (actual vol.) / 1.34888e5 cm3 (model vol.)'
'actual vol.= 1.36557e5 cm3 = (28316.84 cm3/ft3)(108.33188 lb)/(22.464 lb/ft3)'
arbmh2ok   0.52294  2 0 0 0    1001   11.1913
                                8016   88.8087   12  1       293  end
arbmal2o3  0.34864  2 0 0 0   13027   52.9390
                                8016   47.0610   12  0.096   293  end
arbmsio2   0.34864  2 0 0 0   14000   46.7570
                                8016   53.2430   12  0.367   293  end
arbmfe2o3  0.34864  2 0 0 0   26000   69.9540
                                8016   30.0460   12  0.067   293  end
arbmtio2   0.34864  2 0 0 0   22000   59.9535
                                8016   40.0465   12  0.012   293  end
arbmcao    0.34864  2 0 0 0   20000   71.4815
                                8016   28.5185   12  0.307   293  end
arbmmgo    0.34864  2 0 0 0   12000   60.3169
                                8016   39.6831   12  0.131   293  end
arbmna2o   0.34864  2 0 0 0   11023   74.1961
                                8016   25.8039   12  0.020   293  end
'kaolite 1600 top plug'
'sing.unit.density= (den.mult)(min.den.)'
' for arbmh20k = 0.965246*0.51655,  for rest = 0.965246*0.34438'
'den.mult= 1.21592e4 cm3 (actual vol.) / 1.25970e4 cm3 (model vol.)'
'actual vol.= 1.21592e4 cm3 = (28316.84 cm3/ft3)(9.646 lb)/(22.464 lb/ft3)'
arbmh2ok   0.49860  2 0 0 0    1001   11.1913
                                8016   88.8087   13  1       293  end
arbmal2o3  0.33241  2 0 0 0   13027   52.9390
                                8016   47.0610   13  0.096   293  end
arbmsio2   0.33241  2 0 0 0   14000   46.7570
                                8016   53.2430   13  0.367   293  end
arbmfe2o3  0.33241  2 0 0 0   26000   69.9540
                                8016   30.0460   13  0.067   293  end
arbmtio2   0.33241  2 0 0 0   22000   59.9535
                                8016   40.0465   13  0.012   293  end
arbmcao    0.33241  2 0 0 0   20000   71.4815
                                8016   28.5185   13  0.307   293  end
arbmmgo    0.33241  2 0 0 0   12000   60.3169
                                8016   39.6831   13  0.131   293  end
arbmna2o   0.33241  2 0 0 0   11023   74.1961
                                8016   25.8039   13  0.020   293  end
'silicone rubber pads'
arbmsiru   1.21791  4 0 0 0    6012   32.3767
                                1001    8.1573
                                8016   21.5782
                               14000   37.8878   14  1.0     293  end
'void space external to containment vessel'
arbmwecv   0.9982   2 0 0 0    1001   11.1913
                                8016   88.8087   15  1       293  end
'steel: liner'
ss304                                           16  1.0     293  end
'steel: plug cover (pc) use 9.907 lb'
ss304                                           17  1.06388 293  end
'steel: angle iron (ai) for single units'
ss304                                           18  1.0     293  end
'steel: angle iron (ai) for arrays'
'array density is multiplied by a volume fraction 7.08030/5.63249'
'ss304                                           18  1.25705 293  end
'steel: drum steel for single units'
ss304                                           19  1.0     293  end
'steel: drum steel for arrays'
```

```
'array density is multiplied by a volume fraction 3.20482/3.20544'
'ss304                                          19  0.99981 293  end
'void space external to drum'
'array density is multiplied by a volume ratio 8.11698/6.98323'
'arbmwed    1.16026  2 0 0 0    1001   11.1913
'                               8016   88.8087   20  1       293  end
'reflective water'
arbmh20r   0.9982   2 0 0 0    1001   11.1913
                                8016   88.8087   21  1.0     293  end
end comp
cvcr5est11,0.0in np,18277.3gU(18277.3g235, 9226.9gH2O,hx= 13.18),fr=1.0e+00
read parameters nub=yes npg=2500 gen=215 nsk=15 tme=100 end parameters
read boun       all=vac                         end boun
read geometry
unit 1001
'drum bottom flat cover [Elev= 0.105 in. at top of unit]'
'cylinder  19 1   24.587200    0.26670   0.0     com='extended radius not used'
 cuboid    21 1 4p24.587200    0.26670   0.0     com='drum chine outer radius'
unit 1002
'above drum bottom flat cover and below containment vessel [Elev= 4.670 in.]'
 cuboid    21 1 4p24.587200   11.59510   0.0     com='drum chine outer radius'
unit 1003
'cv bottom [Elev= 4.920 in.]'
 cylinder  8  1    6.680200    0.63500   0.0     com='cv bottom'
 cuboid    21 1 4p24.587200    0.63500   0.0     com='drum chine outer radius'
unit 1004
'1st content can (collapsed) [Elev= 6.983 in.]'
'Reference CRC 29 Ed. pg 105'
'side of pentagon denoted spent'
'radius of inscribed circle in pentagon denoted icrpent'
'radius of circumscribed circle outside pentagon denoted ccrpent'
'ccrpent equals 0.85065 times spent'
'icrpent equals 0.68819 times spent'
'side of pentagon equals diameter of a cylinder fit into cc'
'radius of cc equals ccrpent plus radius of cylinder fit into cc'
'radius of ccrpent equal diamater of slug'
' 3.96875 radius of circumscribed circle'
' 2.33277 half of side of pentagon'
' 3.21078 radius of inscribed circle'
' 3.77452 x axis location of 2nd cyl in cc'
' 1.22642 y axis location of 2nd cyl in cc'
 cylinder  3  1    6.426200    5.23925  -0.0005  com='cv well cavity'
 hole  1020    0.0       3.96875 0.0        com='cy1 (0,ccrpent)'
 hole  1020    3.77452   1.22642 0.0        com='cy2 (xtwo,ytwo)'
 hole  1020    2.33277  -3.21078 0.0        com='cy3 (hspent,-icrpent)'
 hole  1020   -2.33277  -3.21078 0.0        com='cy4 (-hspent,-icrpent)'
 hole  1020   -3.77452   1.22642 0.0        com='cy5 (-xtwo,ytwo)'
 cylinder  8  1    6.680200    5.23925  -0.0005  com='cv below 1st step'
 cuboid    21 1 4p24.587200    5.23925  -0.0005  com='drum chine outer radius'
unit 1005
'np277_4 spacer [Elev= 6.983 in.]'
 cylinder  2  1    5.24510     0.00010   0.0     com='np spacer'
 cylinder  3  1    6.426200    0.00020  -0.0001  com='cv well cavity'
 cylinder  8  1    6.680200    0.00020  -0.0001  com='cv below 1st step'
 cuboid    21 1 4p24.587200    0.00020  -0.0001  com='drum chine outer radius'
unit 1006
'2nd content can (collapsed) [Elev= 9.046 in.]'
 cylinder  3  1    6.426200    5.23925  -0.0005  com='cv well cavity'
 hole  1021    0.0       3.96875 0.0        com='cy1 (0,ccrpent)'
 hole  1021    3.77452   1.22642 0.0        com='cy2 (xtwo,ytwo)'
 hole  1021    2.33277  -3.21078 0.0        com='cy3 (hspent,-icrpent)'
 hole  1021   -2.33277  -3.21078 0.0        com='cy4 (-hspent,-icrpent)'
 hole  1021   -3.77452   1.22642 0.0        com='cy5 (-xtwo,ytwo)'
 cylinder  8  1    6.680200    5.23925  -0.0005  com='cv below 1st step'
 cuboid    21 1 4p24.587200    5.23925  -0.0005  com='drum chine outer radius'
unit 1007
'np277_4 spacer [Elev= 9.046 in.]'
 cylinder  2  1    5.24510     0.00010   0.0     com='np spacer'
 cylinder  3  1    6.426200    0.00020  -0.0001  com='cv well cavity'
 cylinder  8  1    6.680200    0.00020  -0.0001  com='cv below 1st step'
 cuboid    21 1 4p24.587200    0.00020  -0.0001  com='drum chine outer radius'
```

```
unit 1008
'3rd content can (collapsed) [Elev= 9.046 in.]'
 cylinder  3  1    6.426200    5.23925  -0.0005  com='cv well cavity'
 hole  1022    0.0       3.96875 0.0        com='cy1 (0,ccrpent)'
 hole  1022    3.77452   1.22642 0.0        com='cy2 (xtwo,ytwo)'
 hole  1022    2.33277  -3.21078 0.0        com='cy3 (hspent,-icrpent)'
 hole  1022   -2.33277  -3.21078 0.0        com='cy4 (-hspent,-icrpent)'
 hole  1022   -3.77452   1.22642 0.0        com='cy5 (-xtwo,ytwo)'
 cylinder  8  1    6.680200    5.23925  -0.0005  com='cv below 1st step'
 cuboid    21 1 4p24.587200    5.23925  -0.0005  com='drum chine outer radius'
unit 1009
'top of content stack to bottom of 1st step [Elev=35.270 in.]'
'15.72155             stack height (content spacers)       CALCULATED
 cylinder  3  1    6.426200   61.36745   0.0     com='cv well cavity'
 cylinder  8  1    6.680200   61.36745   0.0     com='cv below 1st step'
 cuboid    21 1 4p24.587200   61.36745   0.0     com='drum chine outer radius'
unit 1010
'cv at 1st step in liner [Elev=35.330 in.]'
 cylinder  3  1    6.426200    0.15240   0.0     com='cv well cavity'
 cylinder  8  1    6.680200    0.15240   0.0     com='cv at 1st step'
 cuboid    21 1 4p24.587200    0.15240   0.0     com='drum chine outer radius'
unit 1011
'vertical gap between 1st step in liner and cv flange [Elev=35.420 in.]'
 cylinder  3  1    6.426200    0.22860   0.0     com='cv well cavity'
 cylinder  8  1    6.680200    0.22860   0.0     com='cv at gap btwn step-flng'
 cuboid    21 1 4p24.587200    0.22860   0.0     com='drum chine outer radius'
unit 1012
'cv flange to top of cv well [Elev=35.920 in.]'
 cylinder  3  1    6.426200    1.27000   0.0     com='cavity'
 cylinder  9  1    9.525000    1.27000   0.0     com='flange to top of well'
 cuboid    21 1 4p24.587200    1.27000   0.0     com='drum chine outer radius'
unit 1013
'cv flange above cv well [Elev=37.070 in.]'
 cylinder  10 1    9.525000    2.92100   0.0     com='flange above cv well'
 cuboid    21 1 4p24.587200    2.92100   0.0     com='drum chine outer radius'
unit 1014
'plugpad2 below liner 2nd step [Elev=37.470 in.]'
 cuboid    21 1 4p24.587200    1.01600   0.0     com='drum chine outer radius'
unit 1015
'2nd step in liner [Elev=37.530 in.]'
 cuboid    21 1 4p24.587200    0.15240   0.0     com='drum chine outer radius'
unit 1016
'abv 2nd step in liner to bottom of angle iron [Elev=40.750 in.]'
 cuboid    21 1 4p24.587200    8.17880   0.0     com='drum chine outer radius'
unit 1017
'bottom of angle iron to bend in angle iron [Elev=42.500 in.]'
 cuboid    21 1 4p24.587200    4.44500   0.0     com='drum chine outer radius'
unit 1018
'bend in angle iron to top of angle iron [Elev=42.750 in.]'
 cuboid    21 1 4p24.587200    0.63500   0.0     com='drum chine outer radius'
unit 1019
'drum lid and lip [Elev=43.500 in.]'
 cuboid    21 1 4p24.587200    1.90500   0.0     com='drum chine outer radius'
unit 1020
'HEU cylinder content, 3.96875cm diameter by  5.23875cm height'
'  64.77481cm3 single slug volume'
 cylinder  1  1    1.983875  5.23875   0.0       com='cyl'
unit 1021
'HEU cylinder content, 3.96875cm diameter by  5.23875cm height'
'  64.77481cm3 single slug volume'
 cylinder  1  1    1.983875  5.23875   0.0       com='cyl'
unit 1022
'HEU cylinder content, 3.96875cm diameter by  5.23875cm height'
'  64.77481cm3 single slug volume'
 cylinder  1  1    1.983875  5.23875   0.0       com='cyl'
global
unit 1023
'es3100 drum [Elev=43.500 in.]'
array 3         2r-24.587200     0.0
'cuboid     0  1 4p24.587200    110.4905  0.0    com='bare package'
 cuboid    21  1 4p55.067200   140.9700 -30.48   com='reflected package'
```

```
'cuboid    20  1 4p22.889718    110.5048  0.0    com='interstital array space'
'global
'unit 1025
'array 4   3r0.0
'reflector  21 2  6r3.0  10
end geometry
read array
ara=3 nux=1 nuy=1 nuz=19 fill
1001 1002 1003 1004 1005 1006 1007 1008 1009 1010
1011 1012 1013 1014 1015 1016 1017 1018 1019        end fill
'ara=4 nux=13 nuy=13 nuz=06 fill f1023               end fill
end array
'read bias id=500 2  11  end bias
read start nst=0
end start
end data
end


=csas25    parm=size=3000000
cvcr6e4st11,0.0in np,36554.5gU(36554.5g235, 8257.0gH2O hx=  5.90),fr=1.0e+00
238groupndf5 infhommedium
'HEU volume =1943.24434, SPACER volume    0.01729'
'HEU wrapped dry content can hx=0.46, CV void volume 8271.87977'
uranium  1 den=18.81109 1.0 293      92235  100.00
                                     92238   0.000               end
'np277-4: spacer (NCT_MD&H)'
'NCT min.den.(95.3886 lb/ft3) and hydrogen'
'np277-4 min.den.= 1.527971 = (95.3886 lb/ft3)(453.59 g/lb)/(28316.84 cm3/ft3)'
'use 75% of boron in calculations per NUREG-1609 Section 6.5.3.2'
arbmboron 7.31015e-2  2 0 0 0    5010   18.1479
                                 5011   81.8520    2  0.7500  293  end
arbmnpmx  1.07070e+0 10 0 0 0    6012    1.9189
                                 7014    0.0141
                                 8016   43.4251
                                11023    0.1174
                                12000    0.3378
                                13027   39.0479
                                14000    2.4672
                                16000    0.3083
                                20000   11.8336
                                26000    0.5298    2  1.0000  293  end
arbmnph2o 3.84169e-1  2 0 0 0    1001   11.1913
                                 8016   88.8087    2  1.0000  293  end
'flooded containmment vessel and content cans -- 10 CFR 71.55(d)(3)'
arbmwicv   0.9982   2 0 0 0    1001   11.1913
                               8016   88.8087    3  1.0     293  end
'steel: containment vessel body 16.60 lb but use 15.74 lb'
ss304                                            8  1.0     293  end
'steel: cv flange lower use 3.36 lb'
ss304                                            9  0.97267 293  end
'steel: cv flange upper use 13.75 lb'
ss304                                           10  0.94348 293  end
'np277-4: confinement -- neutron poison inner liner (NCT_MD&H)'
'actual vol.= 1.31846e4 cm3 = (8.0457422e2 in3)(16.387064)'
'den.multiplier = 1.31846e4 cm3 (actual vol.) / 1.32708e4 cm3 (model vol.)'
'np277-4 min.den.= 1.527971 = (95.3886 lb/ft3)(453.59 g/lb)/(28316.84 cm3/ft3)'
'density = 1.518047 = (den.mult)(np277-4 min.den.) = 0.9935052*1.527971'
'use 75% of boron in calculations per NUREG-1609 Section 6.5.3.2'
arbmboron 7.26267e-2  2 0 0 0    5010   18.1479
                                 5011   81.8520   11  0.7500  293  end
arbmnpmx  1.06375e+0 10 0 0 0    6012    1.9189
                                 7014    0.0141
                                 8016   43.4251
                                11023    0.1174
                                12000    0.3378
                                13027   39.0479
                                14000    2.4672
                                16000    0.3083
                                20000   11.8336
                                26000    0.5298   11  1.0000  293  end
```

```
arbmnph2o 3.81674e-1  2 0 0 0    1001   11.1913
                                 8016   88.8087   11  1.0000  293  end
'kaolite 1600 body'
'sing.unit.density= (den.mult)(min.den.)'
' for arbmh20k = 1.012373*0.51655,  for rest = 1.012373*0.34438'
'den.mult= 1.36557e5 cm3 (actual vol.) / 1.34888e5 cm3 (model vol.)'
'actual vol.= 1.36557e5 cm3 = (28316.84 cm3/ft3)(108.33188 lb)/(22.464 lb/ft3)'
arbmh2ok   0.52294  2 0 0 0    1001   11.1913
                                8016   88.8087   12  1       293  end
arbmal2o3  0.34864  2 0 0 0   13027   52.9390
                                8016   47.0610   12  0.096   293  end
arbmsio2   0.34864  2 0 0 0   14000   46.7570
                                8016   53.2430   12  0.367   293  end
arbmfe2o3  0.34864  2 0 0 0   26000   69.9540
                                8016   30.0460   12  0.067   293  end
arbmtio2   0.34864  2 0 0 0   22000   59.9535
                                8016   40.0465   12  0.012   293  end
arbmcao    0.34864  2 0 0 0   20000   71.4815
                                8016   28.5185   12  0.307   293  end
arbmmgo    0.34864  2 0 0 0   12000   60.3169
                                8016   39.6831   12  0.131   293  end
arbmna2o   0.34864  2 0 0 0   11023   74.1961
                                8016   25.8039   12  0.020   293  end
'kaolite 1600 top plug'
'sing.unit.density= (den.mult)(min.den.)'
' for arbmh20k = 0.965246*0.51655,  for rest = 0.965246*0.34438'
'den.mult= 1.21592e4 cm3 (actual vol.) / 1.25970e4 cm3 (model vol.)'
'actual vol.= 1.21592e4 cm3 = (28316.84 cm3/ft3)(9.646 lb)/(22.464 lb/ft3)'
arbmh2ok   0.49860  2 0 0 0    1001   11.1913
                                8016   88.8087   13  1       293  end
arbmal2o3  0.33241  2 0 0 0   13027   52.9390
                                8016   47.0610   13  0.096   293  end
arbmsio2   0.33241  2 0 0 0   14000   46.7570
                                8016   53.2430   13  0.367   293  end
arbmfe2o3  0.33241  2 0 0 0   26000   69.9540
                                8016   30.0460   13  0.067   293  end
arbmtio2   0.33241  2 0 0 0   22000   59.9535
                                8016   40.0465   13  0.012   293  end
arbmcao    0.33241  2 0 0 0   20000   71.4815
                                8016   28.5185   13  0.307   293  end
arbmmgo    0.33241  2 0 0 0   12000   60.3169
                                8016   39.6831   13  0.131   293  end
arbmna2o   0.33241  2 0 0 0   11023   74.1961
                                8016   25.8039   13  0.020   293  end
'silicone rubber pads'
arbmsiru   1.21791  4 0 0 0    6012   32.3767
                                1001    8.1573
                                8016   21.5782
                               14000   37.8878   14  1.0     293  end
'void space external to containment vessel'
arbmwecv   0.9982   2 0 0 0    1001   11.1913
                                8016   88.8087   15  1       293  end
'steel: liner'
ss304                                           16  1.0     293  end
'steel: plug cover (pc) use 9.907 lb'
ss304                                           17  1.06388 293  end
'steel: angle iron (ai) for single units'
ss304                                           18  1.0     293  end
'steel: angle iron (ai) for arrays'
'array density is multiplied by a volume fraction 7.08030/5.63249'
'ss304                                           18  1.25705 293  end
'steel: drum steel for single units'
ss304                                           19  1.0     293  end
'steel: drum steel for arrays'
'array density is multiplied by a volume fraction 3.20482/3.20544'
'ss304                                           19  0.99981 293  end
'void space external to drum'
'array density is multiplied by a volume ratio 8.11698/6.98323'
'arbmwed    1.16026  2 0 0 0    1001   11.1913
'                               8016   88.8087   20  1       293  end
'reflective water'
```

```
arbmh20r   0.9982   2 0 0 0    1001   11.1913
                               8016   88.8087   21  1.0     293  end
end comp
cvcr6e4st11,0.0in np,36554.5gU(36554.5g235, 8257.0gH2O,hx=  5.90),fr=1.0e+00
read parameters nub=yes npg=2500 gen=215 nsk=15 tme=100 end parameters
read boun       all=vac                         end boun
read geometry
unit 1001
'drum bottom flat cover [Elev= 0.105 in. at top of unit]'
'cylinder  19 1   24.587200    0.26670   0.0     com='extended radius not used'
 cuboid    21 1 4p24.587200    0.26670   0.0     com='drum chine outer radius'
unit 1002
'above drum bottom flat cover and below containment vessel [Elev= 4.670 in.]'
 cuboid    21 1 4p24.587200   11.59510   0.0     com='drum chine outer radius'
unit 1003
'cv bottom [Elev= 4.920 in.]'
 cylinder  8  1    6.680200    0.63500   0.0     com='cv bottom'
 cuboid    21 1 4p24.587200    0.63500   0.0     com='drum chine outer radius'
unit 1004
'1st content can (collapsed) [Elev= 9.045 in.]'
'Reference CRC 29 Ed. pg 105'
'side of pentagon denoted spent'
'radius of inscribed circle in pentagon denoted icrpent'
'radius of circumscribed circle outside pentagon denoted ccrpent'
'ccrpent equals 0.85065 times spent'
'icrpent equals 0.68819 times spent'
'side of pentagon equals diameter of a cylinder fit into cc'
'radius of cc equals ccrpent plus radius of cylinder fit into cc'
'radius of ccrpent equal diamater of slug'
' 3.96925 radius of circumscribed circle'
' 2.33307 half of side of pentagon'
' 3.21119 radius of inscribed circle'
' 3.77499 x axis location of 2nd cyl in cc'
' 1.22658 y axis location of 2nd cyl in cc'
 cylinder  3  1    6.426200   10.47800  -0.0005  com='cv well cavity'
 hole  1020    0.0       3.96925 0.0        com='cy1 (0,ccrpent)'
 hole  1020    3.77499   1.22658 0.0        com='cy2 (xtwo,ytwo)'
 hole  1020    2.33307  -3.21119 0.0        com='cy3 (hspent,-icrpent)'
 hole  1020   -2.33307  -3.21119 0.0        com='cy4 (-hspent,-icrpent)'
 hole  1020   -3.77499   1.22658 0.0        com='cy5 (-xtwo,ytwo)'
 hole  1020    0.0       0.0    0.0        com='cy6 (0,0)'
 hole  1020    2.80704   0.0 5.23875      com='cy7'
 hole  1020   -2.80704   0.0 5.23875      com='cy8'
 hole  1020    0.0     2.80704 5.23875      com='cy9'
 hole  1020    0.0    -2.80704 5.23875      com='cy10'
 cylinder  8  1    6.680200   10.47800  -0.0005  com='cv below 1st step'
 cuboid    21 1 4p24.587200   10.47800  -0.0005  com='drum chine outer radius'
unit 1005
'np277_4 spacer [Elev= 9.046 in.]'
 cylinder  2  1    5.24510     0.00010   0.0     com='np spacer'
 cylinder  3  1    6.426200    0.00020  -0.0001  com='cv well cavity'
 cylinder  8  1    6.680200    0.00020  -0.0001  com='cv below 1st step'
 cuboid    21 1 4p24.587200    0.00020  -0.0001  com='drum chine outer radius'
unit 1006
'2nd content can (collapsed) [Elev=13.171 in.]'
 cylinder  3  1    6.426200   10.47800  -0.0005  com='cv well cavity'
 hole  1021    0.0       3.96925 0.0        com='cy1 (0,ccrpent)'
 hole  1021    3.77499   1.22658 0.0        com='cy2 (xtwo,ytwo)'
 hole  1021    2.33307  -3.21119 0.0        com='cy3 (hspent,-icrpent)'
 hole  1021   -2.33307  -3.21119 0.0        com='cy4 (-hspent,-icrpent)'
 hole  1021   -3.77499   1.22658 0.0        com='cy5 (-xtwo,ytwo)'
 hole  1021    0.0       0.0    0.0        com='cy6 (0,0)'
 hole  1021    2.80704   0.0 5.23875      com='cy7'
 hole  1021   -2.80704   0.0 5.23875      com='cy8'
 hole  1021    0.0     2.80704 5.23875      com='cy9'
 hole  1021    0.0    -2.80704 5.23875      com='cy10'
 cylinder  8  1    6.680200   10.47800  -0.0005  com='cv below 1st step'
 cuboid    21 1 4p24.587200   10.47800  -0.0005  com='drum chine outer radius'
unit 1007
'np277_4 spacer [Elev=13.171 in.]'
 cylinder  2  1    5.24510     0.00010   0.0     com='np spacer'
```

```
 cylinder  3  1    6.426200    0.00020  -0.0001  com='cv well cavity'
 cylinder  8  1    6.680200    0.00020  -0.0001  com='cv below 1st step'
 cuboid    21 1 4p24.587200    0.00020  -0.0001  com='drum chine outer radius'
unit 1008
'3rd content can (collapsed) [Elev=13.171 in.]'
 cylinder  3  1    6.426200   10.47800  -0.0005  com='cv well cavity'
 hole  1022    0.0       3.96925 0.0        com='cy1 (0,ccrpent)'
 hole  1022    3.77499   1.22658 0.0        com='cy2 (xtwo,ytwo)'
 hole  1022    2.33307  -3.21119 0.0        com='cy3 (hspent,-icrpent)'
 hole  1022   -2.33307  -3.21119 0.0        com='cy4 (-hspent,-icrpent)'
 hole  1022   -3.77499   1.22658 0.0        com='cy5 (-xtwo,ytwo)'
 hole  1022    0.0       0.0    0.0        com='cy6 (0,0)'
 hole  1022    2.80704   0.0 5.23875      com='cy7'
 hole  1022   -2.80704   0.0 5.23875      com='cy8'
 hole  1022    0.0     2.80704 5.23875      com='cy9'
 hole  1022    0.0    -2.80704 5.23875      com='cy10'
 cylinder  8  1    6.680200   10.47800  -0.0005  com='cv below 1st step'
 cuboid    21 1 4p24.587200   10.47800  -0.0005  com='drum chine outer radius'
unit 1009
'top of content stack to bottom of 1st step [Elev=35.270 in.]'
'31.43780             stack height (content spacers)       CALCULATED
 cylinder  3  1    6.426200   45.65120   0.0     com='cv well cavity'
 cylinder  8  1    6.680200   45.65120   0.0     com='cv below 1st step'
 cuboid    21 1 4p24.587200   45.65120   0.0     com='drum chine outer radius'
unit 1010
'cv at 1st step in liner [Elev=35.330 in.]'
 cylinder  3  1    6.426200    0.15240   0.0     com='cv well cavity'
 cylinder  8  1    6.680200    0.15240   0.0     com='cv at 1st step'
 cuboid    21 1 4p24.587200    0.15240   0.0     com='drum chine outer radius'
unit 1011
'vertical gap between 1st step in liner and cv flange [Elev=35.420 in.]'
 cylinder  3  1    6.426200    0.22860   0.0     com='cv well cavity'
 cylinder  8  1    6.680200    0.22860   0.0     com='cv at gap btwn step-flng'
 cuboid    21 1 4p24.587200    0.22860   0.0     com='drum chine outer radius'
unit 1012
'cv flange to top of cv well [Elev=35.920 in.]'
 cylinder  3  1    6.426200    1.27000   0.0     com='cavity'
 cylinder  9  1    9.525000    1.27000   0.0     com='flange to top of well'
 cuboid    21 1 4p24.587200    1.27000   0.0     com='drum chine outer radius'
unit 1013
'cv flange above cv well [Elev=37.070 in.]'
 cylinder  10 1    9.525000    2.92100   0.0     com='flange above cv well'
 cuboid    21 1 4p24.587200    2.92100   0.0     com='drum chine outer radius'
unit 1014
'plugpad2 below liner 2nd step [Elev=37.470 in.]'
 cuboid    21 1 4p24.587200    1.01600   0.0     com='drum chine outer radius'
unit 1015
'2nd step in liner [Elev=37.530 in.]'
 cuboid    21 1 4p24.587200    0.15240   0.0     com='drum chine outer radius'
unit 1016
'abv 2nd step in liner to bottom of angle iron [Elev=40.750 in.]'
 cuboid    21 1 4p24.587200    8.17880   0.0     com='drum chine outer radius'
unit 1017
'bottom of angle iron to bend in angle iron [Elev=42.500 in.]'
 cuboid    21 1 4p24.587200    4.44500   0.0     com='drum chine outer radius'
unit 1018
'bend in angle iron to top of angle iron [Elev=42.750 in.]'
 cuboid    21 1 4p24.587200    0.63500   0.0     com='drum chine outer radius'
unit 1019
'drum lid and lip [Elev=43.500 in.]'
 cuboid    21 1 4p24.587200    1.90500   0.0     com='drum chine outer radius'
unit 1020
'HEU cylinder content, 3.96875cm diameter by  5.23875cm height'
'  64.77481cm3 single slug volume'
 cylinder  1  1    1.983875  5.23875   0.0       com='cyl'
unit 1021
'HEU cylinder content, 3.96875cm diameter by  5.23875cm height'
'  64.77481cm3 single slug volume'
 cylinder  1  1    1.983875  5.23875   0.0       com='cyl'
unit 1022
'HEU cylinder content, 3.96875cm diameter by  5.23875cm height'
```

```
'  64.77481cm3 single slug volume'
 cylinder  1  1    1.983875  5.23875   0.0       com='cyl'
global
unit 1023
'es3100 drum [Elev=43.500 in.]'
array 3         2r-24.587200     0.0
'cuboid     0  1 4p24.587200    110.4905  0.0    com='bare package'
 cuboid    21  1 4p55.067200   140.9700 -30.48   com='reflected package'
'cuboid    20  1 4p22.889718    110.5048  0.0    com='interstital array space'
'global
'unit 1025
'array 4   3r0.0
'reflector  21 2  6r3.0  10
end geometry
read array
ara=3 nux=1 nuy=1 nuz=19 fill
1001 1002 1003 1004 1005 1006 1007 1008 1009 1010
1011 1012 1013 1014 1015 1016 1017 1018 1019        end fill
'ara=4 nux=13 nuy=13 nuz=06 fill f1023               end fill
end array
'read bias id=500 2  11  end bias
read start nst=0
end start
end data
end


=csas25    parm=size=3000000
cvcr70st11,1.4in np,25588.2gU(25588.2g235, 8225.3gH2O hx=  8.39),fr=1.0e+00
238groupndf5 infhommedium
'HEU volume =1360.27104, SPACER volume  614.69740'
'HEU wrapped dry content can hx=0.66, CV void volume 8240.17295'
uranium  1 den=18.81109 1.0 293      92235  100.00
                                     92238   0.000               end
'np277-4: spacer (NCT_MD&H)'
'NCT min.den.(95.3886 lb/ft3) and hydrogen'
'np277-4 min.den.= 1.527971 = (95.3886 lb/ft3)(453.59 g/lb)/(28316.84 cm3/ft3)'
'use 75% of boron in calculations per NUREG-1609 Section 6.5.3.2'
arbmboron 7.31015e-2  2 0 0 0    5010   18.1479
                                 5011   81.8520    2  0.7500  293  end
arbmnpmx  1.07070e+0 10 0 0 0    6012    1.9189
                                 7014    0.0141
                                 8016   43.4251
                                11023    0.1174
                                12000    0.3378
                                13027   39.0479
                                14000    2.4672
                                16000    0.3083
                                20000   11.8336
                                26000    0.5298    2  1.0000  293  end
arbmnph2o 3.84169e-1  2 0 0 0    1001   11.1913
                                 8016   88.8087    2  1.0000  293  end
'flooded containmment vessel and content cans -- 10 CFR 71.55(d)(3)'
arbmwicv   0.9982   2 0 0 0    1001   11.1913
                               8016   88.8087    3  1.0     293  end
'steel: containment vessel body 16.60 lb but use 15.74 lb'
ss304                                            8  1.0     293  end
'steel: cv flange lower use 3.36 lb'
ss304                                            9  0.97267 293  end
'steel: cv flange upper use 13.75 lb'
ss304                                           10  0.94348 293  end
'np277-4: confinement -- neutron poison inner liner (NCT_MD&H)'
'actual vol.= 1.31846e4 cm3 = (8.0457422e2 in3)(16.387064)'
'den.multiplier = 1.31846e4 cm3 (actual vol.) / 1.32708e4 cm3 (model vol.)'
'np277-4 min.den.= 1.527971 = (95.3886 lb/ft3)(453.59 g/lb)/(28316.84 cm3/ft3)'
'density = 1.518047 = (den.mult)(np277-4 min.den.) = 0.9935052*1.527971'
'use 75% of boron in calculations per NUREG-1609 Section 6.5.3.2'
arbmboron 7.26267e-2  2 0 0 0    5010   18.1479
                                 5011   81.8520   11  0.7500  293  end
arbmnpmx  1.06375e+0 10 0 0 0    6012    1.9189
                                 7014    0.0141
```

```
                                 8016   43.4251
                                11023    0.1174
                                12000    0.3378
                                13027   39.0479
                                14000    2.4672
                                16000    0.3083
                                20000   11.8336
                                26000    0.5298   11  1.0000  293  end
arbmnph2o 3.81674e-1  2 0 0 0    1001   11.1913
                                 8016   88.8087   11  1.0000  293  end
'kaolite 1600 body'
'sing.unit.density= (den.mult)(min.den.)'
' for arbmh20k = 1.012373*0.51655,  for rest = 1.012373*0.34438'
'den.mult= 1.36557e5 cm3 (actual vol.) / 1.34888e5 cm3 (model vol.)'
'actual vol.= 1.36557e5 cm3 = (28316.84 cm3/ft3)(108.33188 lb)/(22.464 lb/ft3)'
arbmh2ok   0.52294  2 0 0 0    1001   11.1913
                                8016   88.8087   12  1       293  end
arbmal2o3  0.34864  2 0 0 0   13027   52.9390
                                8016   47.0610   12  0.096   293  end
arbmsio2   0.34864  2 0 0 0   14000   46.7570
                                8016   53.2430   12  0.367   293  end
arbmfe2o3  0.34864  2 0 0 0   26000   69.9540
                                8016   30.0460   12  0.067   293  end
arbmtio2   0.34864  2 0 0 0   22000   59.9535
                                8016   40.0465   12  0.012   293  end
arbmcao    0.34864  2 0 0 0   20000   71.4815
                                8016   28.5185   12  0.307   293  end
arbmmgo    0.34864  2 0 0 0   12000   60.3169
                                8016   39.6831   12  0.131   293  end
arbmna2o   0.34864  2 0 0 0   11023   74.1961
                                8016   25.8039   12  0.020   293  end
'kaolite 1600 top plug'
'sing.unit.density= (den.mult)(min.den.)'
' for arbmh20k = 0.965246*0.51655,  for rest = 0.965246*0.34438'
'den.mult= 1.21592e4 cm3 (actual vol.) / 1.25970e4 cm3 (model vol.)'
'actual vol.= 1.21592e4 cm3 = (28316.84 cm3/ft3)(9.646 lb)/(22.464 lb/ft3)'
arbmh2ok   0.49860  2 0 0 0    1001   11.1913
                                8016   88.8087   13  1       293  end
arbmal2o3  0.33241  2 0 0 0   13027   52.9390
                                8016   47.0610   13  0.096   293  end
arbmsio2   0.33241  2 0 0 0   14000   46.7570
                                8016   53.2430   13  0.367   293  end
arbmfe2o3  0.33241  2 0 0 0   26000   69.9540
                                8016   30.0460   13  0.067   293  end
arbmtio2   0.33241  2 0 0 0   22000   59.9535
                                8016   40.0465   13  0.012   293  end
arbmcao    0.33241  2 0 0 0   20000   71.4815
                                8016   28.5185   13  0.307   293  end
arbmmgo    0.33241  2 0 0 0   12000   60.3169
                                8016   39.6831   13  0.131   293  end
arbmna2o   0.33241  2 0 0 0   11023   74.1961
                                8016   25.8039   13  0.020   293  end
'silicone rubber pads'
arbmsiru   1.21791  4 0 0 0    6012   32.3767
                                1001    8.1573
                                8016   21.5782
                               14000   37.8878   14  1.0     293  end
'void space external to containment vessel'
arbmwecv   0.9982   2 0 0 0    1001   11.1913
                                8016   88.8087   15  1       293  end
'steel: liner'
ss304                                           16  1.0     293  end
'steel: plug cover (pc) use 9.907 lb'
ss304                                           17  1.06388 293  end
'steel: angle iron (ai) for single units'
ss304                                           18  1.0     293  end
'steel: angle iron (ai) for arrays'
'array density is multiplied by a volume fraction 7.08030/5.63249'
'ss304                                           18  1.25705 293  end
'steel: drum steel for single units'
ss304                                           19  1.0     293  end
```

```
'steel: drum steel for arrays'
'array density is multiplied by a volume fraction 3.20482/3.20544'
'ss304                                          19  0.99981 293  end
'void space external to drum'
'array density is multiplied by a volume ratio 8.11698/6.98323'
'arbmwed    1.16026  2 0 0 0    1001   11.1913
'                               8016   88.8087   20  1       293  end
'reflective water'
arbmh20r   0.9982   2 0 0 0    1001   11.1913
                                8016   88.8087   21  1.0     293  end
end comp
cvcr70st11,1.4in np,25588.2gU(25588.2g235, 8225.3gH2O,hx=  8.39),fr=1.0e+00
read parameters nub=yes npg=2500 gen=215 nsk=15 tme=100 end parameters
read boun       all=vac                         end boun
read geometry
unit 1001
'drum bottom flat cover [Elev= 0.105 in. at top of unit]'
'cylinder  19 1   24.587200    0.26670   0.0     com='extended radius not used'
 cuboid    21 1 4p24.587200    0.26670   0.0     com='drum chine outer radius'
unit 1002
'above drum bottom flat cover and below containment vessel [Elev= 4.670 in.]'
 cuboid    21 1 4p24.587200   11.59510   0.0     com='drum chine outer radius'
unit 1003
'cv bottom [Elev= 4.920 in.]'
 cylinder  8  1    6.680200    0.63500   0.0     com='cv bottom'
 cuboid    21 1 4p24.587200    0.63500   0.0     com='drum chine outer radius'
unit 1004
'1st content can (collapsed) [Elev= 6.983 in.]'
'3.437212   plus-y location cylinders'
'-3.437212  minus-y location cylinders'
'1.984375   plus-x location cylinders'
'-1.984375  minus-x location cylinders'
 cylinder  3  1    6.426200    5.23925  -0.0005  com='cv well cavity'
 hole  1020   -3.968750   0.0       0.0     com='cy1 (2cymx,0)'
 hole  1020   -1.984375   3.437212  0.0     com='cy2 (cymx,cypy)'
 hole  1020    1.984375   3.437212  0.0     com='cy3 (cypx,cypy)'
 hole  1020    3.968750   0.0       0.0     com='cy4 (2cypx,0)'
 hole  1020    1.984375  -3.437212  0.0     com='cy5 (cypx,cymx)'
 hole  1020   -1.984375  -3.437212  0.0     com='cy6 (cymx,cymy)'
 hole  1020    0.0        0.0       0.0     com='cy7 (0,0)'
 cylinder  8  1    6.680200    5.23925  -0.0005  com='cv below 1st step'
 cuboid    21 1 4p24.587200    5.23925  -0.0005  com='drum chine outer radius'
unit 1005
'np277_4 spacer [Elev= 8.383 in.]'
 cylinder  2  1    5.24510     3.55610   0.0     com='np spacer'
 cylinder  3  1    6.426200    3.55620  -0.0001  com='cv well cavity'
 cylinder  8  1    6.680200    3.55620  -0.0001  com='cv below 1st step'
 cuboid    21 1 4p24.587200    3.55620  -0.0001  com='drum chine outer radius'
unit 1006
'2nd content can (collapsed) [Elev=10.446 in.]'
 cylinder  3  1    6.426200    5.23925  -0.0005  com='cv well cavity'
 hole  1021   -3.968750   0.0       0.0     com='cy1 (2cymx,0)'
 hole  1021   -1.984375   3.437212  0.0     com='cy2 (cymx,cypy)'
 hole  1021    1.984375   3.437212  0.0     com='cy3 (cypx,cypy)'
 hole  1021    3.968750   0.0       0.0     com='cy4 (2cypx,0)'
 hole  1021    1.984375  -3.437212  0.0     com='cy5 (cypx,cymx)'
 hole  1021   -1.984375  -3.437212  0.0     com='cy6 (cymx,cymy)'
 hole  1021    0.0        0.0       0.0     com='cy7 (0,0)'
 cylinder  8  1    6.680200    5.23925  -0.0005  com='cv below 1st step'
 cuboid    21 1 4p24.587200    5.23925  -0.0005  com='drum chine outer radius'
unit 1007
'np277_4 spacer [Elev=11.846 in.]'
 cylinder  2  1    5.24510     3.55610   0.0     com='np spacer'
 cylinder  3  1    6.426200    3.55620  -0.0001  com='cv well cavity'
 cylinder  8  1    6.680200    3.55620  -0.0001  com='cv below 1st step'
 cuboid    21 1 4p24.587200    3.55620  -0.0001  com='drum chine outer radius'
unit 1008
'3rd content can (collapsed) [Elev=10.446 in.]'
 cylinder  3  1    6.426200    5.23925  -0.0005  com='cv well cavity'
 hole  1022   -3.968750   0.0       0.0     com='cy1 (2cymx,0)'
 hole  1022   -1.984375   3.437212  0.0     com='cy2 (cymx,cypy)'
```

```
 hole  1022    1.984375   3.437212  0.0     com='cy3 (cypx,cypy)'
 hole  1022    3.968750   0.0       0.0     com='cy4 (2cypx,0)'
 hole  1022    1.984375  -3.437212  0.0     com='cy5 (cypx,cymx)'
 hole  1022   -1.984375  -3.437212  0.0     com='cy6 (cymx,cymy)'
 hole  1022    0.0        0.0       0.0     com='cy7 (0,0)'
 cylinder  8  1    6.680200    5.23925  -0.0005  com='cv below 1st step'
 cuboid    21 1 4p24.587200    5.23925  -0.0005  com='drum chine outer radius'
unit 1009
'top of content stack to bottom of 1st step [Elev=35.270 in.]'
'22.83355             stack height (content spacers)       CALCULATED
 cylinder  3  1    6.426200   54.25545   0.0     com='cv well cavity'
 cylinder  8  1    6.680200   54.25545   0.0     com='cv below 1st step'
 cuboid    21 1 4p24.587200   54.25545   0.0     com='drum chine outer radius'
unit 1010
'cv at 1st step in liner [Elev=35.330 in.]'
 cylinder  3  1    6.426200    0.15240   0.0     com='cv well cavity'
 cylinder  8  1    6.680200    0.15240   0.0     com='cv at 1st step'
 cuboid    21 1 4p24.587200    0.15240   0.0     com='drum chine outer radius'
unit 1011
'vertical gap between 1st step in liner and cv flange [Elev=35.420 in.]'
 cylinder  3  1    6.426200    0.22860   0.0     com='cv well cavity'
 cylinder  8  1    6.680200    0.22860   0.0     com='cv at gap btwn step-flng'
 cuboid    21 1 4p24.587200    0.22860   0.0     com='drum chine outer radius'
unit 1012
'cv flange to top of cv well [Elev=35.920 in.]'
 cylinder  3  1    6.426200    1.27000   0.0     com='cavity'
 cylinder  9  1    9.525000    1.27000   0.0     com='flange to top of well'
 cuboid    21 1 4p24.587200    1.27000   0.0     com='drum chine outer radius'
unit 1013
'cv flange above cv well [Elev=37.070 in.]'
 cylinder  10 1    9.525000    2.92100   0.0     com='flange above cv well'
 cuboid    21 1 4p24.587200    2.92100   0.0     com='drum chine outer radius'
unit 1014
'plugpad2 below liner 2nd step [Elev=37.470 in.]'
 cuboid    21 1 4p24.587200    1.01600   0.0     com='drum chine outer radius'
unit 1015
'2nd step in liner [Elev=37.530 in.]'
 cuboid    21 1 4p24.587200    0.15240   0.0     com='drum chine outer radius'
unit 1016
'abv 2nd step in liner to bottom of angle iron [Elev=40.750 in.]'
 cuboid    21 1 4p24.587200    8.17880   0.0     com='drum chine outer radius'
unit 1017
'bottom of angle iron to bend in angle iron [Elev=42.500 in.]'
 cuboid    21 1 4p24.587200    4.44500   0.0     com='drum chine outer radius'
unit 1018
'bend in angle iron to top of angle iron [Elev=42.750 in.]'
 cuboid    21 1 4p24.587200    0.63500   0.0     com='drum chine outer radius'
unit 1019
'drum lid and lip [Elev=43.500 in.]'
 cuboid    21 1 4p24.587200    1.90500   0.0     com='drum chine outer radius'
unit 1020
'HEU cylinder content, 3.96875cm diameter by  5.23875cm height'
'  64.77481cm3 single slug volume'
 cylinder  1  1    1.983875  5.23875   0.0       com='cyl'
unit 1021
'HEU cylinder content, 3.96875cm diameter by  5.23875cm height'
'  64.77481cm3 single slug volume'
 cylinder  1  1    1.983875  5.23875   0.0       com='cyl'
unit 1022
'HEU cylinder content, 3.96875cm diameter by  5.23875cm height'
'  64.77481cm3 single slug volume'
 cylinder  1  1    1.983875  5.23875   0.0       com='cyl'
global
unit 1023
'es3100 drum [Elev=43.500 in.]'
array 3         2r-24.587200     0.0
'cuboid     0  1 4p24.587200    110.4905  0.0    com='bare package'
 cuboid    21  1 4p55.067200   140.9700 -30.48   com='reflected package'
'cuboid    20  1 4p22.889718    110.5048  0.0    com='interstital array space'
'global
'unit 1025
```

```
'array 4   3r0.0
'reflector  21 2  6r3.0  10
end geometry
read array
ara=3 nux=1 nuy=1 nuz=19 fill
1001 1002 1003 1004 1005 1006 1007 1008 1009 1010
1011 1012 1013 1014 1015 1016 1017 1018 1019        end fill
'ara=4 nux=13 nuy=13 nuz=06 fill f1023               end fill
end array
'read bias id=500 2  11  end bias
read start nst=0
end start
end data
end


=csas25    parm=size=3000000
cvr 3x3sqa,0.0in thk np,25893.7gU(25893.7g235, 8822.9gH2O hx=  8.89),fr=1.0e+00
238groupndf5 infhommedium
'HEU volume =1376.51338, SPACER volume    0.00000'
'HEU wrapped dry content can hx=0.65, CV void volume 8838.84856'
uranium  1 den=18.81109 1.0 293      92235  100.00
                                     92238   0.000               end
'np277-4: spacer (NCT_MD&H)'
'NCT min.den.(95.3886 lb/ft3) and hydrogen'
'np277-4 min.den.= 1.527971 = (95.3886 lb/ft3)(453.59 g/lb)/(28316.84 cm3/ft3)'
'use 75% of boron in calculations per NUREG-1609 Section 6.5.3.2'
arbmboron 7.31015e-2  2 0 0 0    5010   18.1479
                                 5011   81.8520    2  0.7500  293  end
arbmnpmx  1.07072e+0 10 0 0 0    6012    1.9188
                                 7014    0.0141
                                 8016   43.4264
                                11023    0.1174
                                12000    0.3378
                                13027   39.0470
                                14000    2.4671
                                16000    0.3083
                                20000   11.8333
                                26000    0.5297    2  1.0000  293  end
arbmnph2o 3.84144e-1  2 0 0 0    1001   11.1913
                                 8016   88.8087    2  1.0000  293  end
'void space internal to containmment vessel -- including content cans'
arbmwicv   0.9982   2 0 0 0    1001   11.1913
                               8016   88.8087    3  1       293  end
'steel: containment vessel body 16.60 lb but use 15.74 lb'
ss304                                            8  1.0     293  end
'steel: cv flange lower use 3.36 lb'
ss304                                            9  0.97267 293  end
'steel: cv flange upper use 13.75 lb'
ss304                                           10  0.94348 293  end
'reflective water'
arbmh20r   0.9982   2 0 0 0    1001   11.1913
                               8016   88.8087   21  1.0     293  end
end comp
cvr 3x3sqa,0.0in thk np,25893.7gU(25893.7g235, 8822.9gH2O,hx=  8.89),fr=1.0e+00
read parameters nub=yes npg=2500 gen=215 nsk=15 tme=100 end parameters
read boun       all=vac                         end boun
read geometry
unit 1001
'drum bottom flat cover [Elev= 0.105 in. at top of unit]'
 cuboid    21 1 4p24.587200    0.26670   0.0     com='drum chine outer radius'
unit 1002
'above drum bottom flat cover and below containment vessel [Elev= 4.670 in.]'
 cuboid    21 1 4p24.587200   11.59510   0.0     com='drum chine outer radius'
unit 1003
'cv bottom [Elev= 4.920 in.]'
 cylinder  8  1    6.680200    0.63500   0.0     com='cv bottom'
 cuboid    21 1 4p24.587200    0.63500   0.0     com='drum chine outer radius'
unit 1004
'cubical content, stacked per cc'
'    9.08802     3.57796 lattice width-depth'
```

```
'    2.54000     1.00000 cube dimension'
'    1.27000     0.50000 cube half-dimension'
'   16.38706     1.00000 volume of HEU cube in unit cell'
'  308.25850             HEU mass one cube'
'   28                   number of HEU cubes per can'
' 8631.23808             HEU mass of cubes in cc'
'    3           3       number of cubes in -x direction'
'    3           3       number of cubes in -y direction'
'    9           9       number of HEU cubes in a layer'
'    4    VARIABLE       number of HEU layers in z-axis'
'    1    VARIABLE       number of HEU cubes in top layer modulus(Z%N)'
'    8    VARIABLE       number of HEU voids in top layer'
'    ara=1 nux=3 nuy=3 nuz=4   fill 28r1004  8r1005      end fill'
'    0.48924     0.19261 gap dimension                       CALCULATED
'    3.02924     1.19261 unit cell dimension                 CALCULATED
'    1.51462     0.59631 unit cell half-dimension            CALCULATED
'   27.79719     1.69629 volume of unit cell                 CALCULATED
'   11.41013     0.69629 volume of water gap in unit cell    CALCULATED
 cuboid    1  1  6p1.26990                       com='content cube'
 cuboid    3  1  6p1.51452                       com='unit cell'
unit 1005
'cubical void, filler for layers'
 cuboid    3  1  6p1.51452                       com='unit cell'
unit 1006
'content (collapsed) [Elev= 9.691 in.]'
' 4.54386     1.78892 half width-depth lattice            CALCULATED'
'12.11696             height lattice                      CALCULATED'
 array 1         2r-4.54386      0.0
 cuboid    3  1  4p4.54386     12.1169   0.0     com='content-array'
 cylinder  3  1    6.426200   12.11746  -0.0005  com='cv well cavity'
 cylinder  8  1    6.680200   12.11746  -0.0005  com='cv below 1st step'
 cuboid    21 1 4p24.587200   12.11746  -0.0005  com='drum chine outer radius'
unit 1007
'np277_4 spacer [Elev= 9.691 in.]'
 cylinder  2  1    5.24510     0.00010   0.0     com='np spacer'
 cylinder  3  1    6.426200    0.00020  -0.0001  com='cv well cavity'
 cylinder  8  1    6.680200    0.00020  -0.0001  com='cv below 1st step'
 cuboid    21 1 4p24.587200    0.00020  -0.0001  com='drum chine outer radius'
unit 1008
'top of content stack to bottom of 1st step [Elev=35.270 in.]'
'36.35448             stack height (content spacers)       CALCULATED
 cylinder  3  1    6.426200   40.73452   0.0     com='cv well cavity'
 cylinder  8  1    6.680200   40.73452   0.0     com='cv below 1st step'
 cuboid    21 1 4p24.587200   40.73452   0.0     com='drum chine outer radius'
unit 1010
'cv at 1st step in liner [Elev=35.330 in.]'
 cylinder  3  1    6.426200    0.15240   0.0     com='cv well cavity'
 cylinder  8  1    6.680200    0.15240   0.0     com='cv at 1st step'
 cuboid    21 1 4p24.587200    0.15240   0.0     com='drum chine outer radius'
unit 1011
'vertical gap between 1st step in liner and cv flange [Elev=35.420 in.]'
 cylinder  3  1    6.426200    0.22860   0.0     com='cv well cavity'
 cylinder  8  1    6.680200    0.22860   0.0     com='cv at gap btwn step-flng'
 cuboid    21 1 4p24.587200    0.22860   0.0     com='drum chine outer radius'
unit 1012
'cv flange to top of cv well [Elev=35.920 in.]'
 cylinder  3  1    6.426200    1.27000   0.0     com='cavity'
 cylinder  9  1    9.525000    1.27000   0.0     com='flange to top of well'
 cuboid    21 1 4p24.587200    1.27000   0.0     com='drum chine outer radius'
unit 1013
'cv flange above cv well [Elev=37.070 in.]'
 cylinder  10 1    9.525000    2.92100   0.0     com='flange above cv well'
 cuboid    21 1 4p24.587200    2.92100   0.0     com='drum chine outer radius'
unit 1014
'plugpad2 below liner 2nd step [Elev=37.470 in.]'
 cuboid    21 1 4p24.587200    1.01600   0.0     com='drum chine outer radius'
unit 1015
'2nd step in liner [Elev=37.530 in.]'
 cuboid    21 1 4p24.587200    0.15240   0.0     com='drum chine outer radius'
unit 1016
'abv 2nd step in liner to bottom of angle iron [Elev=40.750 in.]'
```

```
 cuboid    21 1 4p24.587200    8.17880   0.0     com='drum chine outer radius'
unit 1017
'bottom of angle iron to bend in angle iron [Elev=42.500 in.]'
 cuboid    21 1 4p24.587200    4.44500   0.0     com='drum chine outer radius'
unit 1018
'bend in angle iron to top of angle iron [Elev=42.750 in.]'
 cuboid    21 1 4p24.587200    0.63500   0.0     com='drum chine outer radius'
unit 1019
'drum lid and lip [Elev=43.500 in.]'
 cuboid    21 1 4p24.587200    1.90500   0.0     com='drum chine outer radius'
global
unit 1020
'es3100 drum [Elev=43.500 in.]'
 array 3   2r-24.587200     0.0
'cuboid     0  1 4p24.587200    110.4905  0.0    com='bare package'
 cuboid    21  1 4p55.067200   140.9700 -30.48   com='reflected package'
'cuboid    20  1 4p22.889718    110.5048  0.0    com='interstital array space'
'global
'unit 1021
'array 4   3r0.0
'reflector  21 2  6r3.0  10
end geometry
read array
ara=1 nux=3 nuy=3 nuz=4   fill 28r1004  8r1005      end fill
ara=3 nux=1 nuy=1 nuz=19 fill
1001 1002 1003 1006 1007 1006 1007 1006 1008 1010
1011 1012 1013 1014 1015 1016 1017 1018 1019        end fill
'ara=4 nux=13 nuy=13 nuz=06 fill f1020               end fill
end array
'read bias id=500 2  11  end bias
read start nst=0
end start
end data
end


=csas25    parm=size=3000000
cvr 3x3lha,0.0in thk np,25893.7gU(25893.7g235, 8822.9gH2O hx=  8.89),fr=1.0e+00
238groupndf5 infhommedium
'HEU volume =1376.51338, SPACER volume    0.00000'
'HEU wrapped dry content can hx=0.65, CV void volume 8838.84856'
uranium  1 den=18.81109 0.45852 293      92235  100.00
                                     92238   0.000               end
arbmh20i   0.54051  2 0 0 0    1001   11.1913
                               8016   88.8087    1  1       293  end
'np277-4: spacer (NCT_MD&H)'
'NCT min.den.(95.3886 lb/ft3) and hydrogen'
'np277-4 min.den.= 1.527971 = (95.3886 lb/ft3)(453.59 g/lb)/(28316.84 cm3/ft3)'
'use 75% of boron in calculations per NUREG-1609 Section 6.5.3.2'
arbmboron 7.31015e-2  2 0 0 0    5010   18.1479
                                 5011   81.8520    2  0.7500  293  end
arbmnpmx  1.07072e+0 10 0 0 0    6012    1.9188
                                 7014    0.0141
                                 8016   43.4264
                                11023    0.1174
                                12000    0.3378
                                13027   39.0470
                                14000    2.4671
                                16000    0.3083
                                20000   11.8333
                                26000    0.5297    2  1.0000  293  end
arbmnph2o 3.84144e-1  2 0 0 0    1001   11.1913
                                 8016   88.8087    2  1.0000  293  end
'void space internal to containmment vessel -- including content cans'
arbmwicv   0.9982   2 0 0 0    1001   11.1913
                               8016   88.8087    3  1       293  end
'steel: containment vessel body 16.60 lb but use 15.74 lb'
ss304                                             8  1.0     293  end
'steel: cv flange lower use 3.36 lb'
ss304                                             9  0.97267 293  end
'steel: cv flange upper use 13.75 lb'
```

```
ss304                                          10  0.94348 293  end
'reflective water'
arbmh20r   0.9982   2 0 0 0    1001   11.1913
                               8016   88.8087   21  1.0     293  end
end comp
cvr 3x3lha,0.0in thk np,25893.7gU(25893.7g235, 8822.9gH2O,hx=  8.89),fr=1.0e+00
read parameters nub=yes npg=2500 gen=215 nsk=15 tme=100 end parameters
read boun       all=vac                        end boun
read geometry
unit 1001
'drum bottom flat cover [Elev= 0.105 in. at top of unit]'
 cuboid    21 1 4p24.587200    0.26670   0.0     com='drum chine outer radius'
unit 1002
'above drum bottom flat cover and below containment vessel [Elev= 4.670 in.]'
 cuboid    21 1 4p24.587200   11.59510   0.0     com='drum chine outer radius'
unit 1003
'cv bottom [Elev= 4.920 in.]'
 cylinder  8  1    6.680200    0.63500   0.0     com='cv bottom'
 cuboid    21 1 4p24.587200    0.63500   0.0     com='drum chine outer radius'
unit 1004
'cubical content, stacked per cc'
'    9.08802     3.57796 lattice width-depth'
'    2.54000     1.00000 cube dimension'
'    1.27000     0.50000 cube half-dimension'
'   16.38706     1.00000 volume of HEU cube in unit cell'
'  308.25850             HEU mass one cube'
'   28                   number of HEU cubes per can'
' 8631.23808             HEU mass of cubes in cc'
'    3           3       number of cubes in -x direction'
'    3           3       number of cubes in -y direction'
'    9           9       number of HEU cubes in a layer'
'    4    VARIABLE       number of HEU layers in z-axis'
'    1    VARIABLE       number of HEU cubes in top layer modulus(Z%N)'
'    8    VARIABLE       number of HEU voids in top layer'
'    ara=1 nux=3 nuy=3 nuz=4   fill 28r1004  8r1005      end fill'
'    0.48924     0.19261 gap dimension                       CALCULATED
'    3.02924     1.19261 unit cell dimension                 CALCULATED
'    1.51462     0.59631 unit cell half-dimension            CALCULATED
'   27.79719     1.69629 volume of unit cell                 CALCULATED
'   11.41013     0.69629 volume of water gap in unit cell    CALCULATED
' 1000.69893             lattice volume in cc                CALCULATED
'  541.86113             moderator volume in lattice in cc   CALCULATED
'  458.83779             HEU volume in lattice in cc         CALCULATED
'    0.45852             volume fraction of HEU in lattice'  CALCULATED
'    0.54051             bulk dens of water in lattice in cc CALCULATED
 cuboid    1  1  6p1.51452                      com='unit cell'
unit 1005
'cubical void, filler for layers'
 cuboid    1  1  6p1.51452                      com='unit cell'
unit 1006
'content (collapsed) [Elev= 9.691 in.]'
' 4.54386     1.78892 half width-depth lattice            CALCULATED'
'12.11696             height lattice                      CALCULATED'
'array 1         2r-4.54386      0.0'
 cuboid    1  1  4p4.54386     12.1169   0.0     com='homog. content-array'
 cylinder  3  1    6.426200   12.11746  -0.0005  com='cv well cavity'
 cylinder  8  1    6.680200   12.11746  -0.0005  com='cv below 1st step'
 cuboid    21 1 4p24.587200   12.11746  -0.0005  com='drum chine outer radius'
unit 1007
'np277_4 spacer [Elev= 9.691 in.]'
 cylinder  2  1    5.24510     0.00010   0.0     com='np spacer'
 cylinder  3  1    6.426200    0.00020  -0.0001  com='cv well cavity'
 cylinder  8  1    6.680200    0.00020  -0.0001  com='cv below 1st step'
 cuboid    21 1 4p24.587200    0.00020  -0.0001  com='drum chine outer radius'
unit 1008
'top of content stack to bottom of 1st step [Elev=35.270 in.]'
'36.35448             stack height (content spacers)       CALCULATED
 cylinder  3  1    6.426200   40.73452   0.0     com='cv well cavity'
 cylinder  8  1    6.680200   40.73452   0.0     com='cv below 1st step'
 cuboid    21 1 4p24.587200   40.73452   0.0     com='drum chine outer radius'
unit 1010
```

```
'cv at 1st step in liner [Elev=35.330 in.]'
 cylinder  3  1    6.426200    0.15240   0.0     com='cv well cavity'
 cylinder  8  1    6.680200    0.15240   0.0     com='cv at 1st step'
 cuboid    21 1 4p24.587200    0.15240   0.0     com='drum chine outer radius'
unit 1011
'vertical gap between 1st step in liner and cv flange [Elev=35.420 in.]'
 cylinder  3  1    6.426200    0.22860   0.0     com='cv well cavity'
 cylinder  8  1    6.680200    0.22860   0.0     com='cv at gap btwn step-flng'
 cuboid    21 1 4p24.587200    0.22860   0.0     com='drum chine outer radius'
unit 1012
'cv flange to top of cv well [Elev=35.920 in.]'
 cylinder  3  1    6.426200    1.27000   0.0     com='cavity'
 cylinder  9  1    9.525000    1.27000   0.0     com='flange to top of well'
 cuboid    21 1 4p24.587200    1.27000   0.0     com='drum chine outer radius'
unit 1013
'cv flange above cv well [Elev=37.070 in.]'
 cylinder  10 1    9.525000    2.92100   0.0     com='flange above cv well'
 cuboid    21 1 4p24.587200    2.92100   0.0     com='drum chine outer radius'
unit 1014
'plugpad2 below liner 2nd step [Elev=37.470 in.]'
 cuboid    21 1 4p24.587200    1.01600   0.0     com='drum chine outer radius'
unit 1015
'2nd step in liner [Elev=37.530 in.]'
 cuboid    21 1 4p24.587200    0.15240   0.0     com='drum chine outer radius'
unit 1016
'abv 2nd step in liner to bottom of angle iron [Elev=40.750 in.]'
 cuboid    21 1 4p24.587200    8.17880   0.0     com='drum chine outer radius'
unit 1017
'bottom of angle iron to bend in angle iron [Elev=42.500 in.]'
 cuboid    21 1 4p24.587200    4.44500   0.0     com='drum chine outer radius'
unit 1018
'bend in angle iron to top of angle iron [Elev=42.750 in.]'
 cuboid    21 1 4p24.587200    0.63500   0.0     com='drum chine outer radius'
unit 1019
'drum lid and lip [Elev=43.500 in.]'
 cuboid    21 1 4p24.587200    1.90500   0.0     com='drum chine outer radius'
global
unit 1020
'es3100 drum [Elev=43.500 in.]'
 array 3   2r-24.587200     0.0
'cuboid     0  1 4p24.587200    110.4905  0.0    com='bare package'
 cuboid    21  1 4p55.067200   140.9700 -30.48   com='reflected package'
'cuboid    20  1 4p22.889718    110.5048  0.0    com='interstital array space'
'global
'unit 1021
'array 4   3r0.0
'reflector  21 2  6r3.0  10
end geometry
read array
ara=1 nux=3 nuy=3 nuz=4   fill 28r1004  8r1005      end fill
ara=3 nux=1 nuy=1 nuz=19 fill
1001 1002 1003 1006 1007 1006 1007 1006 1008 1010
1011 1012 1013 1014 1015 1016 1017 1018 1019        end fill
'ara=4 nux=13 nuy=13 nuz=06 fill f1020               end fill
end array
'read bias id=500 2  11  end bias
read start nst=0
end start
end data
end


=csas25    parm=size=3000000
cvr 3x3cha,0.0in thk np,25893.7gU(25893.7g235, 8822.9gH2O hx=  8.89),fr=1.0e+00
238groupndf5 infhommedium
'HEU volume =1376.51338, SPACER volume    0.00000'
'HEU wrapped dry content can hx=0.65, CV void volume 8838.84856'
uranium  1 den=18.81109 0.13475 293      92235  100.00
                                   92238   0.000               end
arbmh20i   0.86369  2 0 0 0    1001   11.1913
                               8016   88.8087    1  1       293  end
```

```
'np277-4: spacer (NCT_MD&H)'
'NCT min.den.(95.3886 lb/ft3) and hydrogen'
'np277-4 min.den.= 1.527971 = (95.3886 lb/ft3)(453.59 g/lb)/(28316.84 cm3/ft3)'
'use 75% of boron in calculations per NUREG-1609 Section 6.5.3.2'
arbmboron 7.31015e-2  2 0 0 0    5010   18.1479
                                 5011   81.8520    2  0.7500  293  end
arbmnpmx  1.07072e+0 10 0 0 0    6012    1.9188
                                 7014    0.0141
                                 8016   43.4264
                                11023    0.1174
                                12000    0.3378
                                13027   39.0470
                                14000    2.4671
                                16000    0.3083
                                20000   11.8333
                                26000    0.5297    2  1.0000  293  end
arbmnph2o 3.84144e-1  2 0 0 0    1001   11.1913
                                 8016   88.8087    2  1.0000  293  end
'void space internal to containmment vessel -- including content cans'
arbmwicv   0.9982   2 0 0 0    1001   11.1913
                               8016   88.8087    3  1       293  end
'steel: containment vessel body 16.60 lb but use 15.74 lb'
ss304                                            8  1.0     293  end
'steel: cv flange lower use 3.36 lb'
ss304                                            9  0.97267 293  end
'steel: cv flange upper use 13.75 lb'
ss304                                           10  0.94348 293  end
'reflective water'
arbmh20r   0.9982   2 0 0 0    1001   11.1913
                               8016   88.8087   21  1.0     293  end
end comp
cvr 3x3cha,0.0in thk np,25893.7gU(25893.7g235, 8822.9gH2O,hx=  8.89),fr=1.0e+00
read parameters nub=yes npg=2500 gen=215 nsk=15 tme=100 end parameters
read boun       all=vac                         end boun
read geometry
unit 1001
'drum bottom flat cover [Elev= 0.105 in. at top of unit]'
 cuboid    21 1 4p24.587200    0.26670   0.0     com='drum chine outer radius'
unit 1002
'above drum bottom flat cover and below containment vessel [Elev= 4.670 in.]'
 cuboid    21 1 4p24.587200   11.59510   0.0     com='drum chine outer radius'
unit 1003
'cv bottom [Elev= 4.920 in.]'
 cylinder  8  1    6.680200    0.63500   0.0     com='cv bottom'
 cuboid    21 1 4p24.587200    0.63500   0.0     com='drum chine outer radius'
unit 1004
'cubical content, stacked per cc'
'    9.08802     3.57796 lattice width-depth'
'    2.54000     1.00000 cube dimension'
'    1.27000     0.50000 cube half-dimension'
'   16.38706     1.00000 volume of HEU cube in unit cell'
'  308.25850             HEU mass one cube'
'   28                   number of HEU cubes per can'
' 8631.23808             HEU mass of cubes in cc'
'    3           3       number of cubes in -x direction'
'    3           3       number of cubes in -y direction'
'    9           9       number of HEU cubes in a layer'
'    4    VARIABLE       number of HEU layers in z-axis'
'    1    VARIABLE       number of HEU cubes in top layer modulus(Z%N)'
'    8    VARIABLE       number of HEU voids in top layer'
'    ara=1 nux=3 nuy=3 nuz=4   fill 28r1004  8r1005      end fill'
'    0.48924     0.19261 gap dimension                       CALCULATED
'    3.02924     1.19261 unit cell dimension                 CALCULATED
'    1.51462     0.59631 unit cell half-dimension            CALCULATED
'   27.79719     1.69629 volume of unit cell                 CALCULATED
'   11.41013     0.69629 volume of water gap in unit cell    CALCULATED
' 1000.69893             lattice volume in cc                CALCULATED
'  541.86113             moderator volume in lattice in cc   CALCULATED
'  458.83779             HEU volume in lattice in cc         CALCULATED
'    0.13475             volume fraction of HEU in CV        CALCULATED
'    0.86369             bulk dens of water in CV            CALCULATED
```

```
 cuboid    1  1  6p1.51452                       com='unit cell'
unit 1005
'cubical void, filler for layers'
 cuboid    1  1  6p1.51452                       com='unit cell'
unit 1006
'content (collapsed) [Elev= 9.691 in.]'
' 4.54386     1.78892 half width-depth lattice            CALCULATED'
'12.11696             height lattice                      CALCULATED'
'array 1         2r-4.54386      0.0'
 cuboid    1  1  4p4.54386     12.1169   0.0     com='homog. content-array'
 cylinder  1  1    6.426200   12.11746  -0.0005  com='cv well cavity'
 cylinder  8  1    6.680200   12.11746  -0.0005  com='cv below 1st step'
 cuboid    21 1 4p24.587200   12.11746  -0.0005  com='drum chine outer radius'
unit 1007
'np277_4 spacer [Elev= 9.691 in.]'
 cylinder  2  1    5.24510     0.00010   0.0     com='np spacer'
 cylinder  1  1    6.426200    0.00020  -0.0001  com='cv well cavity'
 cylinder  8  1    6.680200    0.00020  -0.0001  com='cv below 1st step'
 cuboid    21 1 4p24.587200    0.00020  -0.0001  com='drum chine outer radius'
unit 1008
'top of content stack to bottom of 1st step [Elev=35.270 in.]'
'36.35448             stack height (content spacers)       CALCULATED
 cylinder  1  1    6.426200   40.73452   0.0     com='cv well cavity'
 cylinder  8  1    6.680200   40.73452   0.0     com='cv below 1st step'
 cuboid    21 1 4p24.587200   40.73452   0.0     com='drum chine outer radius'
unit 1010
'cv at 1st step in liner [Elev=35.330 in.]'
 cylinder  1  1    6.426200    0.15240   0.0     com='cv well cavity'
 cylinder  8  1    6.680200    0.15240   0.0     com='cv at 1st step'
 cuboid    21 1 4p24.587200    0.15240   0.0     com='drum chine outer radius'
unit 1011
'vertical gap between 1st step in liner and cv flange [Elev=35.420 in.]'
 cylinder  1  1    6.426200    0.22860   0.0     com='cv well cavity'
 cylinder  8  1    6.680200    0.22860   0.0     com='cv at gap btwn step-flng'
 cuboid    21 1 4p24.587200    0.22860   0.0     com='drum chine outer radius'
unit 1012
'cv flange to top of cv well [Elev=35.920 in.]'
 cylinder  1  1    6.426200    1.27000   0.0     com='cavity'
 cylinder  9  1    9.525000    1.27000   0.0     com='flange to top of well'
 cuboid    21 1 4p24.587200    1.27000   0.0     com='drum chine outer radius'
unit 1013
'cv flange above cv well [Elev=37.070 in.]'
 cylinder  10 1    9.525000    2.92100   0.0     com='flange above cv well'
 cuboid    21 1 4p24.587200    2.92100   0.0     com='drum chine outer radius'
unit 1014
'plugpad2 below liner 2nd step [Elev=37.470 in.]'
 cuboid    21 1 4p24.587200    1.01600   0.0     com='drum chine outer radius'
unit 1015
'2nd step in liner [Elev=37.530 in.]'
 cuboid    21 1 4p24.587200    0.15240   0.0     com='drum chine outer radius'
unit 1016
'abv 2nd step in liner to bottom of angle iron [Elev=40.750 in.]'
 cuboid    21 1 4p24.587200    8.17880   0.0     com='drum chine outer radius'
unit 1017
'bottom of angle iron to bend in angle iron [Elev=42.500 in.]'
 cuboid    21 1 4p24.587200    4.44500   0.0     com='drum chine outer radius'
unit 1018
'bend in angle iron to top of angle iron [Elev=42.750 in.]'
 cuboid    21 1 4p24.587200    0.63500   0.0     com='drum chine outer radius'
unit 1019
'drum lid and lip [Elev=43.500 in.]'
 cuboid    21 1 4p24.587200    1.90500   0.0     com='drum chine outer radius'
global
unit 1020
'es3100 drum [Elev=43.500 in.]'
 array 3   2r-24.587200     0.0
'cuboid     0  1 4p24.587200    110.4905  0.0    com='bare package'
 cuboid    21  1 4p55.067200   140.9700 -30.48   com='reflected package'
'cuboid    20  1 4p22.889718    110.5048  0.0    com='interstital array space'
'global
'unit 1021
```

```
'array 4   3r0.0
'reflector  21 2  6r3.0  10
end geometry
read array
ara=1 nux=3 nuy=3 nuz=4   fill 28r1004  8r1005      end fill
ara=3 nux=1 nuy=1 nuz=19 fill
1001 1002 1003 1006 1007 1006 1007 1006 1008 1010
1011 1012 1013 1014 1015 1016 1017 1018 1019        end fill
'ara=4 nux=13 nuy=13 nuz=06 fill f1020               end fill
end array
'read bias id=500 2  11  end bias
read start nst=0
end start
end data
end
```

*(This case name is actually **cvcrpdoxt11_1_5_24_15**.)*

```
=csas25    parm=size=3000000
cvcrpoxt11,24000.0gUO2 (21124.9g235)1477.3gSH2O 5991.4gH2Ocv hx= 10.02 fr=1
238groupndf5 infhommedium
'HEU volume =3669.72477 HEU oxide, bulk density of oxide in cans=  6.54000 g/cm3'
'oxide= 24000.0 g, sat.h2o in HEU oxide=1477.3 g, oxide h/x= 1.83'
'poly (packed or wrapped) dry content h/x=0.79, CV void volume 6002.15891'
arbmuox    5.69638   2 0 0 0  92235   88.0203
                               8016   11.9797    1  1.0000  293  end
arbmastm  3.5063e-01  2 0 0 0  1001   11.1913
                               8016   88.8087    1  1.0000  293  end
arbmpoly  1.1867e-01  2 0 0 0  1001   14.3798
                               6012   85.6202    1  1.0000  293  end
'np277-4: spacer (NCT_MD&H)'
'NCT min.den.(95.3886 lb/ft3) and hydrogen'
'np277-4 min.den.= 1.527971 = (95.3886 lb/ft3)(453.59 g/lb)/(28316.84 cm3/ft3)'
'use 75% of boron in calculations per NUREG-1609 Section 6.5.3.2'
arbmboron 7.31015e-2  2 0 0 0    5010   18.1479
                                 5011   81.8520    2  0.7500  293  end
arbmnpmx  1.07070e+0 10 0 0 0    6012    1.9189
                                 7014    0.0141
                                 8016   43.4251
                                11023    0.1174
                                12000    0.3378
                                13027   39.0479
                                14000    2.4672
                                16000    0.3083
                                20000   11.8336
                                26000    0.5298    2  1.0000  293  end
arbmnph2o 3.84169e-1  2 0 0 0    1001   11.1913
                                 8016   88.8087    2  1.0000  293  end
'flooded containmment vessel and content cans -- 10 CFR 71.55(d)(3)'
arbmwicv  9.9820e-01  2 0 0 0   1001   11.1913
                               8016   88.8087    3  1       293  end
'steel: containment vessel body 16.60 lb but use 15.74 lb'
ss304                                            8  1.0     293  end
'steel: cv flange lower use 3.36 lb'
ss304                                            9  0.97267 293  end
'steel: cv flange upper use 13.75 lb'
ss304                                           10  0.94348 293  end
'np277-4: confinement -- neutron poison inner liner (NCT_MD&H)'
'actual vol.= 1.31846e4 cm3 = (8.0457422e2 in3)(16.387064)'
'den.multiplier = 1.31846e4 cm3 (actual vol.) / 1.32708e4 cm3 (model vol.)'
'np277-4 min.den.= 1.527971 = (95.3886 lb/ft3)(453.59 g/lb)/(28316.84 cm3/ft3)'
'density = 1.518047 = (den.mult)(np277-4 min.den.) = 0.9935052*1.527971'
'use 75% of boron in calculations per NUREG-1609 Section 6.5.3.2'
arbmboron 7.26267e-2  2 0 0 0    5010   18.1479
                                 5011   81.8520   11  0.7500  293  end
arbmnpmx  1.06375e+0 10 0 0 0    6012    1.9189
                                 7014    0.0141
                                 8016   43.4251
                                11023    0.1174
                                12000    0.3378
                                13027   39.0479
                                14000    2.4672
```

```
                                16000    0.3083
                                20000   11.8336
                                26000    0.5298   11  1.0000  293  end
arbmnph2o 3.81674e-1  2 0 0 0    1001   11.1913
                                 8016   88.8087   11  1.0000  293  end
'kaolite 1600 body'
'sing.unit.density= (den.mult)(min.den.)'
' for arbmh20k = 1.012373*0.51655,  for rest = 1.012373*0.34438'
'den.mult= 1.36557e5 cm3 (actual vol.) / 1.34888e5 cm3 (model vol.)'
'actual vol.= 1.36557e5 cm3 = (28316.84 cm3/ft3)(108.33188 lb)/(22.464 lb/ft3)'
arbmh2ok   0.52294  2 0 0 0    1001   11.1913
                                8016   88.8087   12  1       293  end
arbmal2o3  0.34864  2 0 0 0   13027   52.9390
                                8016   47.0610   12  0.096   293  end
arbmsio2   0.34864  2 0 0 0   14000   46.7570
                                8016   53.2430   12  0.367   293  end
arbmfe2o3  0.34864  2 0 0 0   26000   69.9540
                                8016   30.0460   12  0.067   293  end
arbmtio2   0.34864  2 0 0 0   22000   59.9535
                                8016   40.0465   12  0.012   293  end
arbmcao    0.34864  2 0 0 0   20000   71.4815
                                8016   28.5185   12  0.307   293  end
arbmmgo    0.34864  2 0 0 0   12000   60.3169
                                8016   39.6831   12  0.131   293  end
arbmna2o   0.34864  2 0 0 0   11023   74.1961
                                8016   25.8039   12  0.020   293  end
'kaolite 1600 top plug'
'sing.unit.density= (den.mult)(min.den.)'
' for arbmh20k = 0.965246*0.51655,  for rest = 0.965246*0.34438'
'den.mult= 1.21592e4 cm3 (actual vol.) / 1.25970e4 cm3 (model vol.)'
'actual vol.= 1.21592e4 cm3 = (28316.84 cm3/ft3)(9.646 lb)/(22.464 lb/ft3)'
arbmh2ok   0.49860  2 0 0 0    1001   11.1913
                                8016   88.8087   13  1       293  end
arbmal2o3  0.33241  2 0 0 0   13027   52.9390
                                8016   47.0610   13  0.096   293  end
arbmsio2   0.33241  2 0 0 0   14000   46.7570
                                8016   53.2430   13  0.367   293  end
arbmfe2o3  0.33241  2 0 0 0   26000   69.9540
                                8016   30.0460   13  0.067   293  end
arbmtio2   0.33241  2 0 0 0   22000   59.9535
                                8016   40.0465   13  0.012   293  end
arbmcao    0.33241  2 0 0 0   20000   71.4815
                                8016   28.5185   13  0.307   293  end
arbmmgo    0.33241  2 0 0 0   12000   60.3169
                                8016   39.6831   13  0.131   293  end
arbmna2o   0.33241  2 0 0 0   11023   74.1961
                                8016   25.8039   13  0.020   293  end
'silicone rubber pads'
arbmsiru   1.21791  4 0 0 0    6012   32.3767
                                1001    8.1573
                                8016   21.5782
                               14000   37.8878   14  1.0     293  end
'void space external to containment vessel'
arbmwecv   0.9982   2 0 0 0    1001   11.1913
                                8016   88.8087   15  1       293  end
'steel: liner'
ss304                                           16  1.0     293  end
'steel: plug cover (pc) use 9.907 lb'
ss304                                           17  1.06388 293  end
steel: angle iron (ai) for single units'
ss304                                           18  1.0     293  end
'steel: angle iron (ai) for arrays'
'array density is multiplied by a volume fraction 7.08030/5.63249'
'ss304                                           18  1.25705 293  end
'steel: drum steel for single units'
ss304                                           19  1.0     293  end
'steel: drum steel for arrays'
'array density is multiplied by a volume fraction 3.20482/3.20544'
'ss304                                           19  0.99981 293  end
'void space external to drum'
'array density is multiplied by a volume ratio 8.11698/6.98323'
```

```
'arbmwed    1.16026  2 0 0 0    1001   11.1913
'                               8016   88.8087   20  1       293  end
'reflective water'
arbmh20r   0.9982   2 0 0 0    1001   11.1913
                               8016   88.8087   21  1.0     293  end
end comp
cvcrpoxt11,24000.0gUO2 (21124.9g235)1477.3gSH2O 5991.4gH2Ocv,hx= 10.02 fr=1
read parameters nub=yes npg=2500 gen=215 nsk=15 tme=100 end parameters
read boun       all=vac                         end boun
read geometry
unit 1001
'drum bottom flat cover [Elev= 0.105 in. at top of unit]'
'cylinder  19 1   24.587200    0.26670   0.0     com='extended radius not used'
 cuboid    21 1 4p24.587200    0.26670   0.0     com='drum chine outer radius'
unit 1002
'above drum bottom flat cover and below containment vessel [Elev= 4.670 in.]'
 cuboid    21 1 4p24.587200   11.59510   0.0     com='drum chine outer radius'
unit 1003
'cv bottom to bottom of 1st step [Elev=35.270 in.]'
 cylinder  3  1    6.426200   77.72400  33.11036 com='cavity abv HEU'
 cylinder  1  1    6.426200   77.72400   0.63500 com='HEU content'
 cylinder  8  1    6.680200   77.72400   0.0     com='cv bottom'
 cuboid    21 1 4p24.587200   77.72400   0.0     com='drum chine outer radius'
unit 1010
'cv at 1st step in liner [Elev=35.330 in.]'
 cylinder  3  1    6.426200    0.15240   0.00000 com='cavity abv HEU'
 cylinder  1  1    6.426200    0.15240   0.0     com='HEU content'
 cylinder  8  1    6.680200    0.15240   0.0     com='cv at 1st step'
 cuboid    21 1 4p24.587200    0.15240   0.0     com='drum chine outer radius'
unit 1011
'vertical gap between 1st step in liner and cv flange [Elev=35.420 in.]'
 cylinder  3  1    6.426200    0.22860   0.00000 com='cavity abv HEU'
 cylinder  1  1    6.426200    0.22860   0.0     com='HEU content'
 cylinder  8  1    6.680200    0.22860   0.0     com='cv at gap btwn step-flng'
 cuboid    21 1 4p24.587200    0.22860   0.0     com='drum chine outer radius'
unit 1012
'cv flange to top of cv well [Elev=35.920 in.]'
 cylinder  3  1    6.426200    1.27000   0.00000 com='cavity abv HEU'
 cylinder  1  1    6.426200    1.27000   0.0     com='HEU content'
 cylinder  9  1    9.525000    1.27000   0.0     com='flange to top of well'
 cuboid    21 1 4p24.587200    1.27000   0.0     com='drum chine outer radius'
unit 1013
'cv flange above cv well [Elev=37.070 in.]'
 cylinder  10 1    9.525000    2.92100   0.0     com='flange above cv well'
 cuboid    21 1 4p24.587200    2.92100   0.0     com='drum chine outer radius'
unit 1014
'plugpad2 below liner 2nd step [Elev=37.470 in.]'
 cuboid    21 1 4p24.587200    1.01600   0.0     com='drum chine outer radius'
unit 1015
'2nd step in liner [Elev=37.530 in.]'
 cuboid    21 1 4p24.587200    0.15240   0.0     com='drum chine outer radius'
unit 1016
'abv 2nd step in liner to bottom of angle iron [Elev=40.750 in.]'
 cuboid    21 1 4p24.587200    8.17880   0.0     com='drum chine outer radius'
unit 1017
'bottom of angle iron to bend in angle iron [Elev=42.500 in.]'
 cuboid    21 1 4p24.587200    4.44500   0.0     com='drum chine outer radius'
unit 1018
'bend in angle iron to top of angle iron [Elev=42.750 in.]'
 cuboid    21 1 4p24.587200    0.63500   0.0     com='drum chine outer radius'
unit 1019
'drum lid and lip [Elev=43.500 in.]'
 cuboid    21 1 4p24.587200    1.90500   0.0     com='drum chine outer radius'
global
unit 1020
'es3100 drum [Elev=43.500 in.]'
array 3         2r-24.587200     0.0
'cuboid     0  1 4p24.587200    110.4905  0.0    com='bare package'
 cuboid    21  1 4p55.067200   140.9700 -30.48   com='reflected package'
'cuboid    20  1 4p22.889718    110.5048  0.0    com='interstital array space'
'global
```

```
'unit 1021
'array 4   3r0.0
'reflector  21 2  6r3.0  10
end geometry
read array
ara=3 nux=1 nuy=1 nuz=13 fill
1001 1002 1003 1010
1011 1012 1013 1014 1015 1016 1017 1018 1019        end fill
'ara=4 nux=13 nuy=13 nuz=06 fill f1020               end fill
end array
'read bias id=500 2  11  end bias
read start nst=0
end start
end data
end


csas25    parm=size=3000000
cvcrsk3cc,0.0,21300.0g soc(19865.3uox,15672.8u235,  921.0c),hx= 12.82,fr=1.0e+00
238groupndf5 infhommedium
'  cm3: Skull oxide content 6974.5, SPACER    0.0, CV void 3240.9; CV htox=12.82'
'g/cm3: Skull oxide content  3.05400'
'U3O8   (19865.33gUOX,16816.3gU,15672.8g235U, 3801.4g.sat.H2O, HX=  7.43)'
'Carbon (  921.00gC,   58764.1mgC/g235U)'
'Poly   (  513.00gCH2)'
'Other  (    0.67gUnident (assumed H2O)'
''
'Increm (  921.0gC,15672.8g235U,   58764.1mgC/g235U)'
'GREP1:21300.00 19865.33 3.8014e+03    7.43 16816.35 15672.84   921.00  58764.1
'GREP2: 3235.07   513.00      12.82    0.67  1.0e+00
''
arbmuox    2.84830    3 0 0 0  92235   78.8954
                               92238    5.7563
                                8016   15.3483    1  1.0000  293  end
arbmc     1.3205e-01  1 0 0 0   6012  100.0000    1  1.0000  293  end
arbmastm  5.4505e-01  2 0 0 0   1001   11.1913
                                8016   88.8087    1  1.0000  293  end
arbmpoly   0.07355    2 0 0 0   1001   14.3798
                                6012   85.6202    1  1.0000  293  end
'np277-4: spacer (NCT_MD&H)'
'NCT min.den.(95.3886 lb/ft3) and hydrogen'
'np277-4 min.den.= 1.527971 = (95.3886 lb/ft3)(453.59 g/lb)/(28316.84 cm3/ft3)'
'use 75% of boron in calculations per NUREG-1609 Section 6.5.3.2'
arbmboron 7.31015e-2  2 0 0 0    5010   18.1479
                                 5011   81.8520    2  0.7500  293  end
arbmnpmx  1.07070e+0 10 0 0 0    6012    1.9189
                                 7014    0.0141
                                 8016   43.4251
                                11023    0.1174
                                12000    0.3378
                                13027   39.0479
                                14000    2.4672
                                16000    0.3083
                                20000   11.8336
                                26000    0.5298    2  1.0000  293  end
arbmnph2o 3.84169e-1  2 0 0 0    1001   11.1913
                                 8016   88.8087    2  1.0000  293  end
'flooded containmment vessel and content cans -- 10 CFR 71.55(d)(3)'
arbmwicv  9.9820e-01  2 0 0 0   1001   11.1913
                               8016   88.8087    3  1.0     293  end
'steel: containment vessel body 16.60 lb but use 15.74 lb'
ss304                                            8  1.0     293  end
'steel: cv flange lower use 3.36 lb'
ss304                                            9  0.97267 293  end
'steel: cv flange upper use 13.75 lb'
ss304                                           10  0.94348 293  end
'reflective water'
arbmh20r   0.9982   2 0 0 0    1001   11.1913
                               8016   88.8087   21  1.0     293  end
end comp
cvcrsk3cc,0.0,21300.0g soc(19865.3uox,15672.8u235,  921.0c),hx= 12.82 fr=1.0e+00
```

```
read parameters nub=yes npg=2500 gen=215 nsk=15 tme=100 end parameters
read boun       all=vac                         end boun
read geometry
unit 1001
'drum bottom flat cover [Elev= 0.105 in. at top of unit]'
 cuboid    21 1 4p24.587200    0.26670   0.0     com='drum chine outer radius'
unit 1002
'above drum bottom flat cover and below containment vessel [Elev= 4.670 in.]'
 cuboid    21 1 4p24.587200   11.59510   0.0     com='drum chine outer radius'
unit 1003
'cv bottom to bottom of 1st step [Elev=35.270 in.]'
 cylinder  3  1    6.426200   77.72400  54.39413 com='cavity abv HEU'
 cylinder  1  1    6.426200   77.72400   0.63500 com='HEU content'
 cylinder  8  1    6.680200   77.72400   0.0     com='cv bottom'
 cuboid    21 1 4p24.587200   77.72400   0.0     com='drum chine outer radius'
unit 1010
'cv at 1st step in liner [Elev=35.330 in.]'
 cylinder  3  1    6.426200    0.15240   0.00000 com='cavity abv HEU'
 cylinder  1  1    6.426200    0.15240   0.0     com='HEU content'
 cylinder  8  1    6.680200    0.15240   0.0     com='cv at 1st step'
 cuboid    21 1 4p24.587200    0.15240   0.0     com='drum chine outer radius'
unit 1011
'vertical gap between 1st step in liner and cv flange [Elev=35.420 in.]'
 cylinder  3  1    6.426200    0.22860   0.00000 com='cavity abv HEU'
 cylinder  1  1    6.426200    0.22860   0.0     com='HEU content'
 cylinder  8  1    6.680200    0.22860   0.0     com='cv at gap btwn step-flng'
 cuboid    21 1 4p24.587200    0.22860   0.0     com='drum chine outer radius'
unit 1012
'cv flange to top of cv well [Elev=35.920 in.]'
 cylinder  3  1    6.426200    1.27000   0.00000 com='cavity abv HEU'
 cylinder  1  1    6.426200    1.27000   0.0     com='HEU content'
 cylinder  9  1    9.525000    1.27000   0.0     com='flange to top of well'
 cuboid    21 1 4p24.587200    1.27000   0.0     com='drum chine outer radius'
unit 1013
'cv flange above cv well [Elev=37.070 in.]'
 cylinder  10 1    9.525000    2.92100   0.0     com='flange above cv well'
 cuboid    21 1 4p24.587200    2.92100   0.0     com='drum chine outer radius'
unit 1014
'plugpad2 below liner 2nd step [Elev=37.470 in.]'
 cuboid    21 1 4p24.587200    1.01600   0.0     com='drum chine outer radius'
unit 1015
'2nd step in liner [Elev=37.530 in.]'
 cuboid    21 1 4p24.587200    0.15240   0.0     com='drum chine outer radius'
unit 1016
'abv 2nd step in liner to bottom of angle iron [Elev=40.750 in.]'
 cuboid    21 1 4p24.587200    8.17880   0.0     com='drum chine outer radius'
unit 1017
'bottom of angle iron to bend in angle iron [Elev=42.500 in.]'
 cuboid    21 1 4p24.587200    4.44500   0.0     com='drum chine outer radius'
unit 1018
'bend in angle iron to top of angle iron [Elev=42.750 in.]'
 cuboid    21 1 4p24.587200    0.63500   0.0     com='drum chine outer radius'
unit 1019
'drum lid and lip [Elev=43.500 in.]'
 cuboid    21 1 4p24.587200    1.90500   0.0     com='drum chine outer radius'
global
unit 1020
'es3100 drum [Elev=43.500 in.]'
array 3         2r-24.587200     0.0
'cuboid     0  1 4p24.587200    110.4905  0.0    com='bare package'
 cuboid    21  1 4p55.067200   140.9700 -30.48   com='reflected package'
'cuboid    20  1 4p22.889718    110.5048  0.0    com='interstital array space'
'global
'unit 1021
'array 4   3r0.0
'reflector  21 2  6r3.0  10
end geometry
read array
ara=3 nux=1 nuy=1 nuz=13 fill
1001 1002 1003 1010
1011 1012 1013 1014 1015 1016 1017 1018 1019        end fill
```

```
'ara=4 nux=13 nuy=13 nuz=06 fill f1020               end fill
end array
'read bias id=500 2  11  end bias
read start nst=0
end start
end data
end


=csas25    parm=size=3000000
cvcrunhct11 0.0innp,disp. 9000.0gUNHc( 4238.7g235, 6980.8gH2O hx= 54.99),fr=1.0e+00
238groupndf5 infhommedium
'U(enr)O2(NO3)2+6H2O [2.81 g/cc for U(nat)], gU/L= 414.9296'
'UNH crystals in cans  2.79329 g/cm3. wrapped dry content can hx=3.96'
arbmunh    2.79329  5 0 0 0   92235   47.0962
                              92238    0.0000
                               1001    2.4232
                               7014    5.6116
                               8016   44.8690    1  0.31541 293  end
arbmh2oc  6.8336e-01  2 0 0 0  1001   11.1913
                               8016   88.8087    1  1.0000  293  end
'np277-4: spacer (NCT_MD&H)'
'NCT min.den.(95.3886 lb/ft3) and hydrogen'
'np277-4 min.den.= 1.527971 = (95.3886 lb/ft3)(453.59 g/lb)/(28316.84 cm3/ft3)'
'use 75% of boron in calculations per NUREG-1609 Section 6.5.3.2'
arbmboron 7.31015e-2  2 0 0 0    5010   18.1479
                                 5011   81.8520    2  0.7500  293  end
arbmnpmx  1.07070e+0 10 0 0 0    6012    1.9189
                                 7014    0.0141
                                 8016   43.4251
                                11023    0.1174
                                12000    0.3378
                                13027   39.0479
                                14000    2.4672
                                16000    0.3083
                                20000   11.8336
                                26000    0.5298    2  1.0000  293  end
arbmnph2o 3.84169e-1  2 0 0 0    1001   11.1913
                                 8016   88.8087    2  1.0000  293  end
'flooded containmment vessel and content cans -- 10 CFR 71.55(d)(3)'
arbmwicv  6.8336e-01  2 0 0 0   1001   11.1913
                                8016   88.8087     3  1.0     293  end
'steel: containment vessel body 16.60 lb but use 15.74 lb'
ss304                                            8  1.0     293  end
'steel: cv flange lower use 3.36 lb'
ss304                                            9  0.97267 293  end
'steel: cv flange upper use 13.75 lb'
ss304                                           10  0.94348 293  end
'reflective water'
arbmh20r   0.9982   2 0 0 0    1001   11.1913
                               8016   88.8087   21  1.0     293  end
end comp
cvcrunhct11 0.0innp,disp. 9000.0gUNHc( 4238.7g235, 6980.8gH2O,hx= 54.99),fr=1.0e+00
read parameters nub=yes npg=2500 gen=215 nsk=15 tme=100 end parameters
read boun       all=vac                         end boun
read geometry
unit 1001
'drum bottom flat cover [Elev= 0.105 in. at top of unit]'
'cylinder  19 1   24.587200    0.26670   0.0     com='extended radius not used'
 cuboid    21 1 4p24.587200    0.26670   0.0     com='drum chine outer radius'
unit 1002
'above drum bottom flat cover and below containment vessel [Elev= 4.670 in.]'
 cuboid    21 1 4p24.587200   11.59510   0.0     com='drum chine outer radius'
unit 1003
'cv bottom to bottom of 1st step [Elev=35.270 in.]'
 cylinder  1  1    6.426200   77.72400   0.63500 com='HEU content'
 cylinder  8  1    6.680200   77.72400   0.0     com='cv bottom'
 cuboid    21 1 4p24.587200   77.72400   0.0     com='drum chine outer radius'
unit 1010
'cv at 1st step in liner [Elev=35.330 in.]'
 cylinder  1  1    6.426200    0.15240   0.0     com='HEU content'
```

```
 cylinder  8  1    6.680200    0.15240   0.0     com='cv at 1st step'
 cuboid    21 1 4p24.587200    0.15240   0.0     com='drum chine outer radius'
unit 1011
'vertical gap between 1st step in liner and cv flange [Elev=35.420 in.]'
 cylinder  1  1    6.426200    0.22860   0.0     com='HEU content'
 cylinder  8  1    6.680200    0.22860   0.0     com='cv at gap btwn step-flng'
 cuboid    21 1 4p24.587200    0.22860   0.0     com='drum chine outer radius'
unit 1012
'cv flange to top of cv well [Elev=35.920 in.]'
 cylinder  1  1    6.426200    1.27000   0.0     com='HEU content'
 cylinder  9  1    9.525000    1.27000   0.0     com='flange to top of well'
 cuboid    21 1 4p24.587200    1.27000   0.0     com='drum chine outer radius'
unit 1013
'cv flange above cv well [Elev=37.070 in.]'
 cylinder  10 1    9.525000    2.92100   0.0     com='flange above cv well'
 cuboid    21 1 4p24.587200    2.92100   0.0     com='drum chine outer radius'
unit 1014
'plugpad2 below liner 2nd step [Elev=37.470 in.]'
 cuboid    21 1 4p24.587200    1.01600   0.0     com='drum chine outer radius'
unit 1015
'2nd step in liner [Elev=37.530 in.]'
 cuboid    21 1 4p24.587200    0.15240   0.0     com='drum chine outer radius'
unit 1016
'abv 2nd step in liner to bottom of angle iron [Elev=40.750 in.]'
 cuboid    21 1 4p24.587200    8.17880   0.0     com='drum chine outer radius'
unit 1017
'bottom of angle iron to bend in angle iron [Elev=42.500 in.]'
 cuboid    21 1 4p24.587200    4.44500   0.0     com='drum chine outer radius'
unit 1018
'bend in angle iron to top of angle iron [Elev=42.750 in.]'
 cuboid    21 1 4p24.587200    0.63500   0.0     com='drum chine outer radius'
unit 1019
'drum lid and lip [Elev=43.500 in.]'
 cuboid    21 1 4p24.587200    1.90500   0.0     com='drum chine outer radius'
global
unit 1020
'es3100 drum [Elev=43.500 in.]'
array 3         2r-24.587200     0.0
'cuboid     0  1 4p24.587200    110.4905  0.0    com='bare package'
 cuboid    21  1 4p55.067200   140.9700 -30.48   com='reflected package'
'cuboid    20  1 4p22.889718    110.5048  0.0    com='interstital array space'
'global
'unit 1021
'array 4   3r0.0
'reflector  21 2  6r3.0  10
end geometry
read array
ara=3 nux=1 nuy=1 nuz=13 fill
1001 1002 1003 1010
1011 1012 1013 1014 1015 1016 1017 1018 1019        end fill
'ara=4 nux=13 nuy=13 nuz=06 fill f1020               end fill
end array
'read bias id=500 2  11  end bias
read start nst=0
end start
end data
end


=csas25    parm=size=3000000
cvcrtriga 0.0in thk np,10400.0gUZrHx(  921.0g235, 8998.2gH2O hx=255.01),fr=1.0e+00
238groupndf5 infhommedium
'TRIGA volume =1200.95996, SPACER volume    0.00000'
'TRIGA wrapped dry content can hx=18.2, CV void volume 9014.40198'
arbmtriga  8.65974  4 0 0 0    1001    0.9554
                              40000   54.0446
                              92235    8.8558
                              92238   36.1442    1  1.0     293  end
'np277-4: spacer (NCT_MD&H)'
'NCT min.den.(95.3886 lb/ft3) and hydrogen'
'np277-4 min.den.= 1.527971 = (95.3886 lb/ft3)(453.59 g/lb)/(28316.84 cm3/ft3)'
```

```
'use 75% of boron in calculations per NUREG-1609 Section 6.5.3.2'
arbmboron 7.31015e-2  2 0 0 0    5010   18.1479
                                 5011   81.8520    2  0.7500  293  end
arbmnpmx  1.07070e+0 10 0 0 0    6012    1.9189
                                 7014    0.0141
                                 8016   43.4251
                                11023    0.1174
                                12000    0.3378
                                13027   39.0479
                                14000    2.4672
                                16000    0.3083
                                20000   11.8336
                                26000    0.5298    2  1.0000  293  end
arbmnph2o 3.84169e-1  2 0 0 0    1001   11.1913
                                 8016   88.8087    2  1.0000  293  end
'flooded containmment vessel and content cans -- 10 CFR 71.55(d)(3)'
arbmwicv   0.9982   2 0 0 0    1001   11.1913
                               8016   88.8087    3  1       293  end
'steel: containment vessel body 16.60 lb but use 15.74 lb'
ss304                                            8  1.0     293  end
'steel: cv flange lower use 3.36 lb'
ss304                                            9  0.97267 293  end
'steel: cv flange upper use 13.75 lb'
ss304                                           10  0.94348 293  end
'reflective water'
arbmh20r   0.9982   2 0 0 0    1001   11.1913
                               8016   88.8087   21  1.0     293  end
end comp
cvcrtriga 0.0in thk np,10400.0gUZrHx(  921.0g235, 8998.2gH2O,hx=255.01),fr=1.0e+00
read parameters nub=yes npg=2500 gen=215 nsk=15 tme=100 end parameters
read boun       all=vac                         end boun
read geometry
unit 1001
'drum bottom flat cover [Elev= 0.105 in. at top of unit]'
 cuboid    21 1 4p24.587200    0.26670   0.0     com='drum chine outer radius'
unit 1002
'above drum bottom flat cover and below containment vessel [Elev= 4.670 in.]'
 cuboid    21 1 4p24.587200   11.59510   0.0     com='drum chine outer radius'
unit 1003
'cv bottom [Elev= 4.920 in.]'
 cylinder  8  1    6.680200    0.63500   0.0     com='cv bottom'
 cuboid    21 1 4p24.587200    0.63500   0.0     com='drum chine outer radius'
unit 1004
'UZrHx fuel element'
 cylinder  1  1    1.828800   12.70000   0.0     com='cylindrical content'
unit 1006
'content (collapsed) [Elev= 9.920 in.]'
'1.437900   plus-y location upper cylinders'
'-2.875700  minus-y location lower cylinder'
'2.490443   plus-x location upper cylinder'
'-2.490443  minus-x location upper cylinder'
 cylinder  3  1    6.426200   12.70050  -0.0005  com='cv well cavity'
 hole  1004   -2.490443  1.437900  0.0     com='cyl1'
 hole  1004    2.490443  1.437900  0.0     com='cyl2'
 hole  1004    0.0      -2.875700  0.0     com='cyl3'
 cylinder  8  1    6.680200   12.70050  -0.0005  com='cv below 1st step'
 cuboid    21 1 4p24.587200   12.70050  -0.0005  com='drum chine outer radius'
unit 1007
'np277_4 spacer [Elev= 9.921 in.]'
 cylinder  2  1    5.24510     0.00010   0.0     com='np spacer'
 cylinder  3  1    6.426200    0.00020  -0.0001  com='cv well cavity'
 cylinder  8  1    6.680200    0.00020  -0.0001  com='cv below 1st step'
 cuboid    21 1 4p24.587200    0.00020  -0.0001  com='drum chine outer radius'
unit 1008
'top of content stack to bottom of 1st step [Elev=35.270 in.]'
'38.10360             stack height (content spacers)       CALCULATED
 cylinder  3  1    6.426200   38.98540   0.0     com='cv well cavity'
 cylinder  8  1    6.680200   38.98540   0.0     com='cv below 1st step'
 cuboid    21 1 4p24.587200   38.98540   0.0     com='drum chine outer radius'
unit 1010
'cv at 1st step in liner [Elev=35.330 in.]'
```

```
 cylinder  3  1    6.426200    0.15240   0.0     com='cv well cavity'
 cylinder  8  1    6.680200    0.15240   0.0     com='cv at 1st step'
 cuboid    21 1 4p24.587200    0.15240   0.0     com='drum chine outer radius'
unit 1011
'vertical gap between 1st step in liner and cv flange [Elev=35.420 in.]'
 cylinder  3  1    6.426200    0.22860   0.0     com='cv well cavity'
 cylinder  8  1    6.680200    0.22860   0.0     com='cv at gap btwn step-flng'
 cuboid    21 1 4p24.587200    0.22860   0.0     com='drum chine outer radius'
unit 1012
'cv flange to top of cv well [Elev=35.920 in.]'
 cylinder  3  1    6.426200    1.27000   0.0     com='cavity'
 cylinder  9  1    9.525000    1.27000   0.0     com='flange to top of well'
 cuboid    21 1 4p24.587200    1.27000   0.0     com='drum chine outer radius'
unit 1013
'cv flange above cv well [Elev=37.070 in.]'
 cylinder  10 1    9.525000    2.92100   0.0     com='flange above cv well'
 cuboid    21 1 4p24.587200    2.92100   0.0     com='drum chine outer radius'
unit 1014
'plugpad2 below liner 2nd step [Elev=37.470 in.]'
 cuboid    21 1 4p24.587200    1.01600   0.0     com='drum chine outer radius'
unit 1015
'2nd step in liner [Elev=37.530 in.]'
 cuboid    21 1 4p24.587200    0.15240   0.0     com='drum chine outer radius'
unit 1016
'abv 2nd step in liner to bottom of angle iron [Elev=40.750 in.]'
 cuboid    21 1 4p24.587200    8.17880   0.0     com='drum chine outer radius'
unit 1017
'bottom of angle iron to bend in angle iron [Elev=42.500 in.]'
 cuboid    21 1 4p24.587200    4.44500   0.0     com='drum chine outer radius'
unit 1018
'bend in angle iron to top of angle iron [Elev=42.750 in.]'
 cuboid    21 1 4p24.587200    0.63500   0.0     com='drum chine outer radius'
unit 1019
'drum lid and lip [Elev=43.500 in.]'
 cuboid    21 1 4p24.587200    1.90500   0.0     com='drum chine outer radius'
global
unit 1020
'es3100 drum [Elev=43.500 in.]'
array 3         2r-24.587200     0.0
'cuboid     0  1 4p24.587200    110.4905  0.0    com='bare package'
 cuboid    21  1 4p55.067200   140.9700 -30.48   com='reflected package'
'cuboid    20  1 4p22.889718    110.5048  0.0    com='interstital array space'
'global
'unit 1021
'array 4   3r0.0
'reflector  21 2  6r3.0  10
end geometry
read array
ara=3 nux=1 nuy=1 nuz=19 fill
1001 1002 1003 1006 1007 1006 1007 1006 1008 1010
1011 1012 1013 1014 1015 1016 1017 1018 1019        end fill
'ara=4 nux=13 nuy=13 nuz=06 fill f1020               end fill
end array
'read bias id=500 2  11  end bias
read start nst=0
end start
end data
end


=csas25    parm=size=3000000
ncsrcyt11 3cyl,0.0in thk np,21000.0gU(21000.0g235, 9082.6gH2O hx= 11.29),fr=1.0e+00
238groupndf5 infhommedium
'HEU volume =1116.36286, SPACER volume    0.00000'
'HEU wrapped dry content can hx=0.80, CV void volume 9098.99908'
uranium  1 den=18.81109 1.0 293      92235  100.00
                                     92238   0.000               end
'np277-4: spacer (NCT_MD&H)'
'NCT min.den.(95.3886 lb/ft3) and hydrogen'
'np277-4 min.den.= 1.527971 = (95.3886 lb/ft3)(453.59 g/lb)/(28316.84 cm3/ft3)'
'use 75% of boron in calculations per NUREG-1609 Section 6.5.3.2'
```

```
arbmboron 7.31015e-2  2 0 0 0    5010   18.1479
                                 5011   81.8520    2  0.7500  293  end
arbmnpmx  1.07070e+0 10 0 0 0    6012    1.9189
                                 7014    0.0141
                                 8016   43.4251
                                11023    0.1174
                                12000    0.3378
                                13027   39.0479
                                14000    2.4672
                                16000    0.3083
                                20000   11.8336
                                26000    0.5298    2  1.0000  293  end
arbmnph2o 3.84169e-1  2 0 0 0    1001   11.1913
                                 8016   88.8087    2  1.0000  293  end
'flooded containmment vessel and content cans -- 10 CFR 71.55(d)(3)'
arbmwicv   0.9982   2 0 0 0    1001   11.1913
                               8016   88.8087    3  1.0     293  end
'steel: containment vessel body 16.60 lb but use 15.74 lb'
ss304                                            8  1.0     293  end
'steel: cv flange lower use 3.36 lb'
ss304                                            9  0.97267 293  end
'steel: cv flange upper use 13.75 lb'
ss304                                           10  0.94348 293  end
'np277-4: confinement -- neutron poison inner liner (NCT_MD&H)'
'actual vol.= 1.28314e4 cm3 = (7.83023e2 in3)(16.387064)'
'den.multiplier = 1.28314e4 cm3 (actual vol.) / 1.32708e4 cm3 (model vol.)'
'np277-4 min.den.= 1.527971 = (95.3886 lb/ft3)(453.59 g/lb)/(28316.84 cm3/ft3)'
'density = 1.477385 = (den.mult)(np277-4 min.den.) = 0.9668933*1.527971'
'use 75% of boron in calculations per NUREG-1609 Section 6.5.3.2'
arbmboron 7.06813e-2  2 0 0 0    5010   18.1479
                                 5011   81.8520   11  0.7500  293  end
arbmnpmx  1.03525e+0 10 0 0 0    6012    1.9189
                                 7014    0.0141
                                 8016   43.4251
                                11023    0.1174
                                12000    0.3378
                                13027   39.0479
                                14000    2.4672
                                16000    0.3083
                                20000   11.8336
                                26000    0.5298   11  1.0000  293  end
arbmnph2o 3.71451e-1  2 0 0 0    1001   11.1913
                                 8016   88.8087   11  1.0000  293  end
'kaolite 1600 body'
'sing.unit.density= (den.mult)(min.den.)'
' for arbmh20k = 1.012373*0.51655,  for rest = 1.012373*0.34438'
'den.mult= 1.36557e5 cm3 (actual vol.) / 1.34888e5 cm3 (model vol.)'
'actual vol.= 1.36557e5 cm3 = (28316.84 cm3/ft3)(108.33188 lb)/(22.464 lb/ft3)'
arbmh2ok   0.52294  2 0 0 0    1001   11.1913
                               8016   88.8087   12  1       293  end
arbmal2o3  0.34864  2 0 0 0   13027   52.9390
                               8016   47.0610   12  0.096   293  end
arbmsio2   0.34864  2 0 0 0   14000   46.7570
                               8016   53.2430   12  0.367   293  end
arbmfe2o3  0.34864  2 0 0 0   26000   69.9540
                               8016   30.0460   12  0.067   293  end
arbmtio2   0.34864  2 0 0 0   22000   59.9535
                               8016   40.0465   12  0.012   293  end
arbmcao    0.34864  2 0 0 0   20000   71.4815
                               8016   28.5185   12  0.307   293  end
arbmmgo    0.34864  2 0 0 0   12000   60.3169
                               8016   39.6831   12  0.131   293  end
arbmna2o   0.34864  2 0 0 0   11023   74.1961
                               8016   25.8039   12  0.020   293  end
'kaolite 1600 top plug'
'sing.unit.density= (den.mult)(min.den.)'
' for arbmh20k = 0.965246*0.51655,  for rest = 0.965246*0.34438'
'den.mult= 1.21592e4 cm3 (actual vol.) / 1.25970e4 cm3 (model vol.)'
'actual vol.= 1.21592e4 cm3 = (28316.84 cm3/ft3)(9.646 lb)/(22.464 lb/ft3)'
arbmh2ok   0.49860  2 0 0 0    1001   11.1913
                               8016   88.8087   13  1       293  end
```

```
arbmal2o3  0.33241  2 0 0 0   13027   52.9390
                               8016   47.0610   13  0.096   293  end
arbmsio2   0.33241  2 0 0 0   14000   46.7570
                               8016   53.2430   13  0.367   293  end
arbmfe2o3  0.33241  2 0 0 0   26000   69.9540
                               8016   30.0460   13  0.067   293  end
arbmtio2   0.33241  2 0 0 0   22000   59.9535
                               8016   40.0465   13  0.012   293  end
arbmcao    0.33241  2 0 0 0   20000   71.4815
                               8016   28.5185   13  0.307   293  end
arbmmgo    0.33241  2 0 0 0   12000   60.3169
                               8016   39.6831   13  0.131   293  end
arbmna2o   0.33241  2 0 0 0   11023   74.1961
                               8016   25.8039   13  0.020   293  end
'silicone rubber pads'
arbmsiru   1.21791  4 0 0 0    6012   32.3767
                               1001    8.1573
                               8016   21.5782
                              14000   37.8878   14  1.0     293  end
'void space external to containment vessel'
arbmwecv   0.9982   2 0 0 0    1001   11.1913
                               8016   88.8087   15  1       293  end
'steel: liner'
ss304                                            16  1.0     293  end
'steel: plug cover (pc) use 9.907 lb'
ss304                                            17  1.06388 293  end
'steel: angle iron (ai) for single units'
ss304                                            18  1.0     293  end
'steel: angle iron (ai) for arrays'
'array density is multiplied by a volume fraction 7.08030/5.63249'
'ss304                                            18  1.25705 293  end
'steel: drum steel for single units'
ss304                                            19  1.0     293  end
'steel: drum steel for arrays'
'array density is multiplied by a volume fraction 3.20482/3.20544'
'ss304                                            19  0.99981 293  end
'void space external to drum'
'array density is multiplied by a volume ratio 8.11698/6.98323'
'arbmwed    1.16026  2 0 0 0    1001   11.1913
'                               8016   88.8087   20  1       293  end
'reflective water'
arbmh20r   0.9982   2 0 0 0    1001   11.1913
                               8016   88.8087   21  1.0     293  end
end comp
ncsrcyt11 3cyl,0.0in thk np,21000.0gU(21000.0g235, 9082.6gH2O,hx= 11.29),fr=1.0e+00
read parameters nub=yes npg=2500 gen=215 nsk=15 tme=100 end parameters
read boun       all=vac                          end boun
read geometry
unit 1001
'drum bottom flat cover [Elev= 0.105 in. at top of unit]'
'cylinder  19 1   24.587200    0.26670   0.0     com='extended radius not used'
 cylinder  19 1   23.329900    0.26670   0.0     com='drum bottom flat cover'
 cuboid    21 1 4p24.587200    0.26670   0.0     com='drum chine outer radius'
unit 1002
'above drum bottom flat cover and below containment vessel [Elev= 4.670 in.]'
 cylinder  15 1    3.175000   11.59510  11.16330 com='void in pad-1'
 cylinder  14 1    7.924800   11.59510  11.16330 com='pad-1'
 cylinder  16 1    8.077200   11.59510  11.16330 com='np277_4 liner'
 cylinder  11 1   10.922000   11.59510  11.16330 com='np277_4'
 cylinder  16 1   11.074400   11.59510  10.85850 com='kaolite liner bottom'
 cylinder  12 1   23.177500   11.59510   0.0     com='kaolite'
 cylinder  19 1   23.329900   11.59510   0.0     com='drum'
 cuboid    21 1 4p24.587200   11.59510   0.0     com='drum chine outer radius'
unit 1003
'cv bottom [Elev= 4.920 in.]'
 cylinder  8  1    6.680200    0.63500   0.0     com='cv bottom'
 cylinder  15 1    7.924800    0.63500   0.0     com='void btw cv-np liner'
 cylinder  16 1    8.077200    0.63500   0.0     com='np277_4 liner'
 cylinder  11 1   10.922000    0.63500   0.0     com='np277_4'
 cylinder  16 1   11.074400    0.63500   0.0     com='kaolite liner'
 cylinder  12 1   23.177500    0.63500   0.0     com='kaolite'
```

```
 cylinder  19 1   23.329900    0.63500   0.0     com='drum'
 cuboid    21 1 4p24.587200    0.63500   0.0     com='drum chine outer radius'
unit 1006
'content (collapsed) [Elev= 7.675 in.]'
 cylinder  1  1    4.114800     6.99579   0.0     com='cylindrical content'
 cylinder  3  1    6.426200    6.99629  -0.0005  com='cv well cavity'
 cylinder  8  1    6.680200    6.99629  -0.0005  com='cv below 1st step'
 cylinder  15 1    7.924800    6.99629  -0.0005  com='void btw cv-np liner'
 cylinder  16 1    8.077200    6.99629  -0.0005  com='np277_4 liner'
 cylinder  11 1   10.922000    6.99629  -0.0005  com='np277_4'
 cylinder  16 1   11.074400    6.99629  -0.0005  com='kaolite liner'
 cylinder  12 1   23.177500    6.99629  -0.0005  com='kaolite'
 cylinder  19 1   23.329900    6.99629  -0.0005  com='drum'
 cuboid    21 1 4p24.587200    6.99629  -0.0005  com='drum chine outer radius'
unit 1007
'np277_4 spacer [Elev= 7.675 in.]'
 cylinder  2  1    5.24510     0.00010   0.0     com='np spacer'
 cylinder  3  1    6.426200    0.00020  -0.0001  com='cv well cavity'
 cylinder  8  1    6.680200    0.00020  -0.0001  com='cv below 1st step'
 cylinder  15 1    7.924800    0.00020  -0.0001  com='void btw cv-np liner'
 cylinder  16 1    8.077200    0.00020  -0.0001  com='np277_4 liner'
 cylinder  11 1   10.922000    0.00020  -0.0001  com='np277_4'
 cylinder  16 1   11.074400    0.00020  -0.0001  com='kaolite liner'
 cylinder  12 1   23.177500    0.00020  -0.0001  com='kaolite'
 cylinder  19 1   23.329900    0.00020  -0.0001  com='drum'
 cuboid    21 1 4p24.587200    0.00020  -0.0001  com='drum chine outer radius'
unit 1008
'top of content stack to bottom of 1st step [Elev=35.270 in.]'
'20.99097             stack height (content spacers)       CALCULATED
 cylinder  3  1    6.426200   56.09803   0.0     com='cv well cavity'
 cylinder  8  1    6.680200   56.09803   0.0     com='cv below 1st step'
 cylinder  15 1    7.924800   56.09803   0.0     com='void btw cv-np liner'
 cylinder  16 1    8.077200   56.09803   0.0     com='np277_4 liner'
 cylinder  11 1   10.922000   56.09803   0.0     com='np277_4'
 cylinder  16 1   11.074400   56.09803   0.0     com='kaolite liner'
 cylinder  12 1   23.177500   56.09803   0.0     com='kaolite'
 cylinder  19 1   23.329900   56.09803   0.0     com='drum'
 cuboid    21 1 4p24.587200   56.09803   0.0     com='drum chine outer radius'
unit 1010
'cv at 1st step in liner [Elev=35.330 in.]'
 cylinder  3  1    6.426200    0.15240   0.0     com='cv well cavity'
 cylinder  8  1    6.680200    0.15240   0.0     com='cv at 1st step'
 cylinder  15 1    7.924800    0.15240   0.0     com='void btw cv and liner'
 cylinder  16 1   11.074400    0.15240   0.0     com='liner 1st step'
 cylinder  12 1   23.177500    0.15240   0.0     com='kaolite'
 cylinder  19 1   23.329900    0.15240   0.0     com='drum'
 cuboid    21 1 4p24.587200    0.15240   0.0     com='drum chine outer radius'
unit 1011
'vertical gap between 1st step in liner and cv flange [Elev=35.420 in.]'
 cylinder  3  1    6.426200    0.22860   0.0     com='cv well cavity'
 cylinder  8  1    6.680200    0.22860   0.0     com='cv at gap btwn step-flng'
 cylinder  15 1   10.922000    0.22860   0.0     com='void btw cv and liner'
 cylinder  16 1   11.074400    0.22860   0.0     com='liner wall'
 cylinder  12 1   23.177500    0.22860   0.0     com='kaolite'
 cylinder  19 1   23.329900    0.22860   0.0     com='drum'
 cuboid    21 1 4p24.587200    0.22860   0.0     com='drum chine outer radius'
unit 1012
'cv flange to top of cv well [Elev=35.920 in.]'
 cylinder  3  1    6.426200    1.27000   0.0     com='cavity'
 cylinder  9  1    9.525000    1.27000   0.0     com='flange to top of well'
 cylinder  15 1    9.525000    1.27000   0.0     com='void btw cv and pad-2'
 cylinder  14 1   10.033000    1.27000   0.0     com='pad-2'
 cylinder  15 1   10.922000    1.27000   0.0     com='void btw cv and liner'
 cylinder  16 1   11.074400    1.27000   0.0     com='liner wall'
 cylinder  12 1   23.177500    1.27000   0.0     com='kaolite'
 cylinder  19 1   23.329900    1.27000   0.0     com='drum'
 cuboid    21 1 4p24.587200    1.27000   0.0     com='drum chine outer radius'
unit 1013
'cv flange above cv well [Elev=37.070 in.]'
 cylinder  10 1    9.525000    2.92100   0.0     com='flange above cv well'
 cylinder  15 1    9.525000    2.92100   0.0     com='void btw cv and pad-2'
```

```
 cylinder  14 1   10.033000    2.92100   0.0     com='pad-2'
 cylinder  15 1   10.922000    2.92100   0.0     com='void btw pad2 and liner'
 cylinder  16 1   11.074400    2.92100   0.0     com='liner wall'
 cylinder  12 1   23.177500    2.92100   0.0     com='kaolite'
 cylinder  19 1   23.329900    2.92100   0.0     com='drum'
 cuboid    21 1 4p24.587200    2.92100   0.0     com='drum chine outer radius'
unit 1014
'plugpad2 below liner 2nd step [Elev=37.470 in.]'
 cylinder  14 1   10.033000    0.76200   0.0     com='pad-2'
 cylinder  15 1   10.922000    1.01600   0.0     com='void btw pad2 and liner'
 cylinder  16 1   11.074400    1.01600   0.0     com='liner wall'
 cylinder  12 1   23.177500    1.01600   0.0     com='kaolite'
 cylinder  19 1   23.329900    1.01600   0.0     com='drum'
 cuboid    21 1 4p24.587200    1.01600   0.0     com='drum chine outer radius'
unit 1015
'2nd step in liner [Elev=37.530 in.]'
 cylinder  15 1   10.922000    0.15240   0.0     com='void abv pad2'
 cylinder  16 1   18.757900    0.15240   0.0     com='liner 2nd step'
 cylinder  12 1   23.177500    0.15240   0.0     com='kaolite'
 cylinder  19 1   23.329900    0.15240   0.0     com='drum'
 cuboid    21 1 4p24.587200    0.15240   0.0     com='drum chine outer radius'
unit 1016
'abv 2nd step in liner to bottom of angle iron [Elev=40.750 in.]'
 cylinder  13 1   18.097500    8.17880   0.49276 com='plug kaolite'
 cylinder  17 1   18.249900    8.17880   0.34036 com='sides of plug case'
 cylinder  15 1   18.605500    8.17880   0.0     com='void: plug to liner'
 cylinder  16 1   18.757900    8.17880   0.0     com='liner wall'
 cylinder  12 1   23.177500    8.17880   0.0     com='kaolite'
 cylinder  19 1   23.329900    8.17880   0.0     com='drum'
 cuboid    21 1 4p24.587200    8.17880   0.0     com='drum chine outer radius'
unit 1017
'bottom of angle iron to bend in angle iron [Elev=42.500 in.]'
 cylinder  13 1   18.097500    4.44500   0.0     com='plug kaolite'
 cylinder  17 1   18.249900    4.44500   0.0     com='sides of plug case'
 cylinder  15 1   18.605500    4.44500   0.0     com='void: plug to liner'
 cylinder  16 1   18.757900    4.44500   0.0     com='liner wall'
 cylinder  18 1   19.392900    4.44500   0.0     com='lower angle iron'
 cylinder  12 1   23.177500    4.44500   0.0     com='kaolite'
 cylinder  19 1   23.329900    4.44500   0.0     com='drum'
 cuboid    21 1 4p24.587200    4.44500   0.0     com='drum chine outer radius'
unit 1018
'bend in angle iron to top of angle iron [Elev=42.750 in.]'
 cylinder  13 1   18.097500    0.11176   0.0     com='plug kaolite'
 cylinder  17 1   18.249900    0.26416   0.0     com='sides of plug case'
 cylinder  15 1   18.605500    0.63500   0.0     com='void: plug to liner'
 cylinder  16 1   18.757900    0.63500   0.0     com='liner wall'
 cylinder  18 1   23.177500    0.63500   0.0     com='bend section of ai'
 cylinder  19 1   23.329900    0.63500   0.0     com='drum'
 cuboid    21 1 4p24.587200    0.63500   0.0     com='drum chine outer radius'
unit 1019
'drum lid and lip [Elev=43.500 in.]'
 cylinder  21 1   22.961600    1.90500   0.15240 com='void above lid'
 cylinder  19 1   23.114000    1.90500   0.0     com='drum lid'
 cylinder  21 1   23.177500    1.90500   0.0     com='void btw lid - drum wall'
 cylinder  19 1   23.329900    1.90500   0.0     com='drum'
 cuboid    21 1 4p24.587200    1.90500   0.0     com='drum chine outer radius'
global
unit 1020
'es3100 drum [Elev=43.500 in.]'
array 3         2r-24.587200     0.0
'cuboid     0  1 4p24.587200    110.4905  0.0    com='bare package'
 cuboid    21  1 4p55.067200   140.9700 -30.48   com='reflected package'
'cuboid    20  1 4p22.889718    110.5048  0.0    com='interstital array space'
'global
'unit 1021
'array 4   3r0.0
'reflector  21 2  6r3.0  10
end geometry
read array
ara=3 nux=1 nuy=1 nuz=19 fill
1001 1002 1003 1006 1007 1006 1007 1006 1008 1010
```

```
1011 1012 1013 1014 1015 1016 1017 1018 1019        end fill
'ara=4 nux=13 nuy=13 nuz=06 fill f1020               end fill
end array
'read bias id=500 2  11  end bias
read start nst=0
end start
end data
end


=csas25    parm=size=3000000
nciacyct11 3cyl,1.4in thk np,25000.2gU(25000.2g235, 8256.8gH2O hx=  8.62),fr=1.0e-04
238groupndf5 infhommedium
'HEU volume =1329.01404, SPACER volume  614.68012'
'HEU wrapped dry content can hx=0.67, CV void volume 8271.66778'
uranium  1 den=18.81109 1.0 293      92235  100.00
                                     92238   0.000               end
'np277-4: spacer (NCT_MD&H)'
'NCT min.den.(95.3886 lb/ft3) and hydrogen'
'np277-4 min.den.= 1.527971 = (95.3886 lb/ft3)(453.59 g/lb)/(28316.84 cm3/ft3)'
'use 75% of boron in calculations per NUREG-1609 Section 6.5.3.2'
arbmboron 7.31015e-2  2 0 0 0    5010   18.1479
                                 5011   81.8520    2  0.7500  293  end
arbmnpmx  1.07070e+0 10 0 0 0    6012    1.9189
                                 7014    0.0141
                                 8016   43.4251
                                11023    0.1174
                                12000    0.3378
                                13027   39.0479
                                14000    2.4672
                                16000    0.3083
                                20000   11.8336
                                26000    0.5298    2  1.0000  293  end
arbmnph2o 3.84169e-1  2 0 0 0    1001   11.1913
                                 8016   88.8087    2  1.0000  293  end
'flooded containmment vessel and content cans -- 10 CFR 71.55(d)(3)'
arbmwicv   0.9982   2 0 0 0    1001   11.1913
                               8016   88.8087    3  1.0     293  end
'steel: containment vessel body 16.60 lb but use 15.74 lb'
ss304                                            8  1.0     293  end
'steel: cv flange lower use 3.36 lb'
ss304                                            9  0.97267 293  end
'steel: cv flange upper use 13.75 lb'
ss304                                           10  0.94348 293  end
'np277-4: confinement -- neutron poison inner liner (NCT_MD&H)'
'actual vol.= 1.28314e4 cm3 = (7.83023e2 in3)(16.387064)'
'den.multiplier = 1.28314e4 cm3 (actual vol.) / 1.32708e4 cm3 (model vol.)'
'np277-4 min.den.= 1.527971 = (95.3886 lb/ft3)(453.59 g/lb)/(28316.84 cm3/ft3)'
'density = 1.477385 = (den.mult)(np277-4 min.den.) = 0.9668933*1.527971'
'use 75% of boron in calculations per NUREG-1609 Section 6.5.3.2'
arbmboron 7.06813e-2  2 0 0 0    5010   18.1479
                                 5011   81.8520   11  0.7500  293  end
arbmnpmx  1.03525e+0 10 0 0 0    6012    1.9189
                                 7014    0.0141
                                 8016   43.4251
                                11023    0.1174
                                12000    0.3378
                                13027   39.0479
                                14000    2.4672
                                16000    0.3083
                                20000   11.8336
                                26000    0.5298   11  1.0000  293  end
arbmnph2o 3.71451e-1  2 0 0 0    1001   11.1913
                                 8016   88.8087   11  1.0000  293  end
'kaolite 1600 body'
'sing.unit.density= (den.mult)(min.den.)'
' for arbmh20k = 1.012373*0.51655,  for rest = 1.012373*0.34438'
'den.mult= 1.36557e5 cm3 (actual vol.) / 1.34888e5 cm3 (model vol.)'
'actual vol.= 1.36557e5 cm3 = (28316.84 cm3/ft3)(108.33188 lb)/(22.464 lb/ft3)'
'nct array densities are s.u.dens. multiplied by volume ratio 1.34888/1.10336'
arbmh2ok   0.63931  2 0 0 0    1001   11.1913
```

```
                                8016   88.8087   12  0.0287  293  end
arbmal2o3  0.42622  2 0 0 0   13027   52.9390
                                8016   47.0610   12  0.096   293  end
arbmsio2   0.42622  2 0 0 0   14000   46.7570
                                8016   53.2430   12  0.367   293  end
arbmfe2o3  0.42622  2 0 0 0   26000   69.9540
                                8016   30.0460   12  0.067   293  end
arbmtio2   0.42622  2 0 0 0   22000   59.9535
                                8016   40.0465   12  0.012   293  end
arbmcao    0.42622  2 0 0 0   20000   71.4815
                                8016   28.5185   12  0.307   293  end
arbmmgo    0.42622  2 0 0 0   12000   60.3169
                                8016   39.6831   12  0.131   293  end
arbmna2o   0.42622  2 0 0 0   11023   74.1961
                                8016   25.8039   12  0.020   293  end
'kaolite 1600 top plug'
'sing.unit.density= (den.mult)(min.den.)'
' for arbmh20k = 0.965246*0.51655,  for rest = 0.965246*0.34438'
'den.mult= 1.21592e4 cm3 (actual vol.) / 1.25970e4 cm3 (model vol.)'
'actual vol.= 1.21592e4 cm3 = (28316.84 cm3/ft3)(9.646 lb)/(22.464 lb/ft3)'
arbmh2ok   0.49860  2 0 0 0    1001   11.1913
                                8016   88.8087   13  0.0287  293  end
arbmal2o3  0.33241  2 0 0 0   13027   52.9390
                                8016   47.0610   13  0.096   293  end
arbmsio2   0.33241  2 0 0 0   14000   46.7570
                                8016   53.2430   13  0.367   293  end
arbmfe2o3  0.33241  2 0 0 0   26000   69.9540
                                8016   30.0460   13  0.067   293  end
arbmtio2   0.33241  2 0 0 0   22000   59.9535
                                8016   40.0465   13  0.012   293  end
arbmcao    0.33241  2 0 0 0   20000   71.4815
                                8016   28.5185   13  0.307   293  end
arbmmgo    0.33241  2 0 0 0   12000   60.3169
                                8016   39.6831   13  0.131   293  end
arbmna2o   0.33241  2 0 0 0   11023   74.1961
                                8016   25.8039   13  0.020   293  end
'silicone rubber pads'
arbmsiru   1.21791  4 0 0 0    6012   32.3767
                                1001    8.1573
                                8016   21.5782
                               14000   37.8878   14  1.0     293  end
'void space external to containment vessel'
arbmwecv   0.9982   2 0 0 0    1001   11.1913
                                8016   88.8087   15  0.0001  293  end
'steel: liner'
ss304                                             16  1.0     293  end
'steel: plug cover (pc) use 9.907 lb'
ss304                                             17  1.06388 293  end
'steel: angle iron (ai) for single units'
'ss304                                             18  1.0     293  end
'steel: angle iron (ai) for arrays'
'array density is multiplied by a volume fraction 7.08030/5.63249'
ss304                                             18  1.25705 293  end
'steel: drum steel for single units'
'ss304                                             19  1.0     293  end
'steel: drum steel for arrays'
'array density is multiplied by a volume fraction 3.20482/3.20544'
ss304                                             19  0.99981 293  end
'void space external to drum'
'array density is multiplied by a volume ratio 8.11698/6.98323'
arbmwed    1.16026  2 0 0 0    1001   11.1913
                                8016   88.8087   20  0.0001  293  end
'reflective water'
'arbmh20r   0.9982   2 0 0 0    1001   11.1913
'                               8016   88.8087   21  1.0     293  end
end comp
nciacyct11 3cyl,1.4in thk np,25000.2gU(25000.2g235, 8256.8gH2O,hx=  8.62),fr=1.0e-04
read parameters nub=yes npg=2500 gen=215 nsk=15 tme=100 end parameters
read boun       all=specular                      end boun
read geometry
unit 1001
```

```
'drum bottom flat cover [Elev= 0.111 in. at top of unit]'
'cylinder  19 1   22.866096    0.28150   0.0     com='extended radius not used'
 cylinder  19 1   21.722275    0.28150   0.0     com='drum bottom flat cover'
 cuboid    20 1 4p22.866096    0.28150   0.0     com='drum chine outer radius'
unit 1002
'above drum bottom flat cover and below containment vessel [Elev= 4.676 in.]'
 cylinder  15 1    3.175000   11.59510  11.16330 com='void in pad-1'
 cylinder  14 1    7.924800   11.59510  11.16330 com='pad-1'
 cylinder  16 1    8.077200   11.59510  11.16330 com='np277_4 liner'
 cylinder  11 1   10.922000   11.59510  11.16330 com='np277_4'
 cylinder  16 1   11.074400   11.59510  10.85850 com='kaolite liner bottom'
 cylinder  12 1   21.555075   11.59510   0.0     com='kaolite'
 cylinder  19 1   21.722275   11.59510   0.0     com='drum'
 cuboid    20 1 4p22.866096   11.59510   0.0     com='drum chine outer radius'
unit 1003
'cv bottom [Elev= 4.926 in.]'
 cylinder  8  1    6.680200    0.63500   0.0     com='cv bottom'
 cylinder  15 1    7.924800    0.63500   0.0     com='void btw cv-np liner'
 cylinder  16 1    8.077200    0.63500   0.0     com='np277_4 liner'
 cylinder  11 1   10.922000    0.63500   0.0     com='np277_4'
 cylinder  16 1   11.074400    0.63500   0.0     com='kaolite liner'
 cylinder  12 1   21.555075    0.63500   0.0     com='kaolite'
 cylinder  19 1   21.722275    0.63500   0.0     com='drum'
 cuboid    20 1 4p22.866096    0.63500   0.0     com='drum chine outer radius'
unit 1006
'content (collapsed) [Elev= 6.832 in.]'
 cylinder  1  1    5.397500     4.84031   0.0     com='cylindrical content'
 cylinder  3  1    6.426200    4.84081  -0.0005  com='cv well cavity'
 cylinder  8  1    6.680200    4.84081  -0.0005  com='cv below 1st step'
 cylinder  15 1    7.924800    4.84081  -0.0005  com='void btw cv-np liner'
 cylinder  16 1    8.077200    4.84081  -0.0005  com='np277_4 liner'
 cylinder  11 1   10.922000    4.84081  -0.0005  com='np277_4'
 cylinder  16 1   11.074400    4.84081  -0.0005  com='kaolite liner'
 cylinder  12 1   21.555075    4.84081  -0.0005  com='kaolite'
 cylinder  19 1   21.722275    4.84081  -0.0005  com='drum'
 cuboid    20 1 4p22.866096    4.84081  -0.0005  com='drum chine outer radius'
unit 1007
'np277_4 spacer [Elev= 8.232 in.]'
 cylinder  2  1    5.24510     3.55610   0.0     com='np spacer'
 cylinder  3  1    6.426200    3.55620  -0.0001  com='cv well cavity'
 cylinder  8  1    6.680200    3.55620  -0.0001  com='cv below 1st step'
 cylinder  15 1    7.924800    3.55620  -0.0001  com='void btw cv-np liner'
 cylinder  16 1    8.077200    3.55620  -0.0001  com='np277_4 liner'
 cylinder  11 1   10.922000    3.55620  -0.0001  com='np277_4'
 cylinder  16 1   11.074400    3.55620  -0.0001  com='kaolite liner'
 cylinder  12 1   21.555075    3.55620  -0.0001  com='kaolite'
 cylinder  19 1   21.722275    3.55620  -0.0001  com='drum'
 cuboid    20 1 4p22.866096    3.55620  -0.0001  com='drum chine outer radius'
unit 1008
'top of content stack to bottom of 1st step [Elev=35.276 in.]'
'21.63653             stack height (content spacers)       CALCULATED
 cylinder  3  1    6.426200   55.45247   0.0     com='cv well cavity'
 cylinder  8  1    6.680200   55.45247   0.0     com='cv below 1st step'
 cylinder  15 1    7.924800   55.45247   0.0     com='void btw cv-np liner'
 cylinder  16 1    8.077200   55.45247   0.0     com='np277_4 liner'
 cylinder  11 1   10.922000   55.45247   0.0     com='np277_4'
 cylinder  16 1   11.074400   55.45247   0.0     com='kaolite liner'
 cylinder  12 1   21.555075   55.45247   0.0     com='kaolite'
 cylinder  19 1   21.722275   55.45247   0.0     com='drum'
 cuboid    20 1 4p22.866096   55.45247   0.0     com='drum chine outer radius'
unit 1010
'cv at 1st step in liner [Elev=35.336 in.]'
 cylinder  3  1    6.426200    0.15240   0.0     com='cv well cavity'
 cylinder  8  1    6.680200    0.15240   0.0     com='cv at 1st step'
 cylinder  15 1    7.924800    0.15240   0.0     com='void btw cv and liner'
 cylinder  16 1   11.074400    0.15240   0.0     com='liner 1st step'
 cylinder  12 1   21.555075    0.15240   0.0     com='kaolite'
 cylinder  19 1   21.722275    0.15240   0.0     com='drum'
 cuboid    20 1 4p22.866096    0.15240   0.0     com='drum chine outer radius'
unit 1011
'vertical gap between 1st step in liner and cv flange [Elev=35.426 in.]'
```

```
 cylinder  3  1    6.426200    0.22860   0.0     com='cv well cavity'
 cylinder  8  1    6.680200    0.22860   0.0     com='cv at gap btwn step-flng'
 cylinder  15 1   10.922000    0.22860   0.0     com='void btw cv and liner'
 cylinder  16 1   11.074400    0.22860   0.0     com='liner wall'
 cylinder  12 1   21.555075    0.22860   0.0     com='kaolite'
 cylinder  19 1   21.722275    0.22860   0.0     com='drum'
 cuboid    20 1 4p22.866096    0.22860   0.0     com='drum chine outer radius'
unit 1012
'cv flange to top of cv well [Elev=35.926 in.]'
 cylinder  3  1    6.426200    1.27000   0.0     com='cavity'
 cylinder  9  1    9.525000    1.27000   0.0     com='flange to top of well'
 cylinder  15 1    9.525000    1.27000   0.0     com='void btw cv and pad-2'
 cylinder  14 1   10.033000    1.27000   0.0     com='pad-2'
 cylinder  15 1   10.922000    1.27000   0.0     com='void btw cv and liner'
 cylinder  16 1   11.074400    1.27000   0.0     com='liner wall'
 cylinder  12 1   21.555075    1.27000   0.0     com='kaolite'
 cylinder  19 1   21.722275    1.27000   0.0     com='drum'
 cuboid    20 1 4p22.866096    1.27000   0.0     com='drum chine outer radius'
unit 1013
'cv flange above cv well [Elev=37.076 in.]'
 cylinder  10 1    9.525000    2.92100   0.0     com='flange above cv well'
 cylinder  15 1    9.525000    2.92100   0.0     com='void btw cv and pad-2'
 cylinder  14 1   10.033000    2.92100   0.0     com='pad-2'
 cylinder  15 1   10.922000    2.92100   0.0     com='void btw pad2 and liner'
 cylinder  16 1   11.074400    2.92100   0.0     com='liner wall'
 cylinder  12 1   21.555075    2.92100   0.0     com='kaolite'
 cylinder  19 1   21.722275    2.92100   0.0     com='drum'
 cuboid    20 1 4p22.866096    2.92100   0.0     com='drum chine outer radius'
unit 1014
'plugpad2 below liner 2nd step [Elev=37.476 in.]'
 cylinder  14 1   10.033000    0.76200   0.0     com='pad-2'
 cylinder  15 1   10.922000    1.01600   0.0     com='void btw pad2 and liner'
 cylinder  16 1   11.074400    1.01600   0.0     com='liner wall'
 cylinder  12 1   21.555075    1.01600   0.0     com='kaolite'
 cylinder  19 1   21.722275    1.01600   0.0     com='drum'
 cuboid    20 1 4p22.866096    1.01600   0.0     com='drum chine outer radius'
unit 1015
'2nd step in liner [Elev=37.536 in.]'
 cylinder  15 1   10.922000    0.15240   0.0     com='void abv pad2'
 cylinder  16 1   18.757900    0.15240   0.0     com='liner 2nd step'
 cylinder  12 1   21.555075    0.15240   0.0     com='kaolite'
 cylinder  19 1   21.722275    0.15240   0.0     com='drum'
 cuboid    20 1 4p22.866096    0.15240   0.0     com='drum chine outer radius'
unit 1016
'abv 2nd step in liner to bottom of angle iron [Elev=40.756 in.]'
 cylinder  13 1   18.097500    8.17880   0.49276 com='plug kaolite'
 cylinder  17 1   18.249900    8.17880   0.34036 com='sides of plug case'
 cylinder  15 1   18.605500    8.17880   0.0     com='void: plug to liner'
 cylinder  16 1   18.757900    8.17880   0.0     com='liner wall'
 cylinder  12 1   21.555075    8.17880   0.0     com='kaolite'
 cylinder  19 1   21.722275    8.17880   0.0     com='drum'
 cuboid    20 1 4p22.866096    8.17880   0.0     com='drum chine outer radius'
unit 1017
'bottom of angle iron to bend in angle iron [Elev=42.506 in.]'
 cylinder  13 1   18.097500    4.44500   0.0     com='plug kaolite'
 cylinder  17 1   18.249900    4.44500   0.0     com='sides of plug case'
 cylinder  15 1   18.605500    4.44500   0.0     com='void: plug to liner'
 cylinder  16 1   18.757900    4.44500   0.0     com='liner wall'
 cylinder  18 1   19.392900    4.44500   0.0     com='lower angle iron'
 cylinder  12 1   21.555075    4.44500   0.0     com='kaolite'
 cylinder  19 1   21.722275    4.44500   0.0     com='drum'
 cuboid    20 1 4p22.866096    4.44500   0.0     com='drum chine outer radius'
unit 1018
'bend in angle iron to top of angle iron [Elev=42.756 in.]'
 cylinder  13 1   18.097500    0.11176   0.0     com='plug kaolite'
 cylinder  17 1   18.249900    0.26416   0.0     com='sides of plug case'
 cylinder  15 1   18.605500    0.63500   0.0     com='void: plug to liner'
 cylinder  16 1   18.757900    0.63500   0.0     com='liner wall'
 cylinder  18 1   21.555075    0.63500   0.0     com='bend section of ai'
 cylinder  19 1   21.722275    0.63500   0.0     com='drum'
 cuboid    20 1 4p22.866096    0.63500   0.0     com='drum chine outer radius'
```

```
unit 1019
'drum lid and lip [Elev=43.512 in.]'
 cylinder  20 1   21.330090    1.91973   0.16720 com='void above lid'
 cylinder  19 1   21.497290    1.91973   0.0     com='drum lid'
 cylinder  20 1   21.555075    1.91973   0.0     com='void btw lid - drum wall'
 cylinder  19 1   21.722275    1.91973   0.0     com='drum'
 cuboid    20 1 4p22.866096    1.91973   0.0     com='drum chine outer radius'
global
unit 1020
'es3100 drum [Elev=43.512 in.]'
array 3         2r-22.866096     0.0
'cuboid     0  1 4p24.587200    110.4900  0.0    com='bare package'
'cuboid    21  1 4p55.067200   140.9700 -30.48   com='reflected package'
 cuboid    20  1 4p22.866096    110.5197  0.0    com='interstital array space'
'global
'unit 1021
'array 4   3r0.0
'reflector  21 2  6r3.0  10
end geometry
read array
ara=3 nux=1 nuy=1 nuz=19 fill
1001 1002 1003 1006 1007 1006 1007 1006 1008 1010
1011 1012 1013 1014 1015 1016 1017 1018 1019        end fill
'ara=4 nux=13 nuy=13 nuz=06 fill f1020               end fill
end array
'read bias id=500 2  11  end bias
read start nst=0
end start
end data
end


=csas25    parm=size=3000000
hciacyct12 3cyl,1.4in thk np,25000.2gU(25000.2g235, 8256.8gH2O hx=  8.62),fr=1.0e-04
238groupndf5 infhommedium
'HEU wrapped dry content can hx=0.67, CV void volume 8271.66778'
uranium  1 den=18.81109 1.0 293      92235  100.00
                                     92238   0.000               end
'np277-4: spacer (HAC_MD&H)'
'HAC min.den.(95.3157 lb/ft3) and hydrogen'
'np277-4 min.den.= 1.526803 = (95.3157 lb/ft3)(453.59 g/lb)/(28316.84 cm3/ft3)'
'use 75% of boron in calculations per NUREG-1609 Section 6.5.3.2'
arbmboron 7.31015e-2  2 0 0 0    5010   18.1479
                                 5011   81.8520    2  0.7500  293  end
arbmnpmx  1.07071e+0 10 0 0 0    6012    1.9188
                                 7014    0.0141
                                 8016   43.4254
                                11023    0.1174
                                12000    0.3378
                                13027   39.0477
                                14000    2.4671
                                16000    0.3083
                                20000   11.8335
                                26000    0.5298    2  1.0000  293  end
arbmnph2o 3.82995e-1  2 0 0 0    1001   11.1913
                                 8016   88.8087    2  1.0000  293  end
'flooded containmment vessel and content cans -- 10 CFR 71.55(d)(3)'
arbmwicv   0.9982   2 0 0 0    1001   11.1913
                               8016   88.8087    3  1.0     293  end
'steel: containment vessel body 16.60 lb but use 15.74 lb'
ss304                                            8  1.0     293  end
'steel: cv flange lower use 3.36 lb'
ss304                                            9  0.97267 293  end
'steel: cv flange upper use 13.75 lb'
ss304                                           10  0.94348 293  end
'np277-4: confinement -- neutron poison inner liner (HAC_MD&H)'
'actual vol.= 1.28314e4 cm3 = (7.83023e2 in3)(16.387064)'
'den.multiplier = 1.28314e4 cm3 (actual vol.) / 1.32708e4 cm3 (model vol.)'
'np277-4 min.den.= 1.526803 = (95.3157 lb/ft3)(453.59 g/lb)/(28316.84 cm3/ft3)'
'density = 1.476265 = (den.mult)(np277-4 min.den.) = 0.9668933*1.526803'
'use 75% of boron in calculations per NUREG-1609 Section 6.5.3.2'
```

```
arbmboron 7.06813e-2  2 0 0 0    5010   18.1479
                                 5011   81.8520   11  0.7500  293  end
arbmnpmx  1.03525e+0 10 0 0 0    6012    1.9188
                                 7014    0.0141
                                 8016   43.4254
                                11023    0.1174
                                12000    0.3378
                                13027   39.0477
                                14000    2.4671
                                16000    0.3083
                                20000   11.8335
                                26000    0.5298   11  1.0000  293  end
arbmnph2o 3.70316e-1  2 0 0 0    1001   11.1913
                                 8016   88.8087   11  1.0000  293  end
'kaolite 1600 body'
'nct.sing.unit.density= (den.mult)(min.den.)'
' for arbmh20k 0.52294 = 1.012373*0.51655, for rest 0.34864 = 1.012373*0.34438'
'den.mult= 1.36557e5 cm3 (actual vol.) / 1.34888e5 cm3 (model vol.)'
'actual vol.= 1.36557e5 cm3 = (28316.84 cm3/ft3)(108.33188 lb)/(22.464 lb/ft3)'
'hac.s.u.dens= (hac.mult)(nct.s.u.dens)'
'hac.mult = 1.34888e5 cm3 (nct vol.)/ 1.12246e5 cm3 (model vol.)'
' for arbmh2ok 0.62843 = 1.20172*0.52294,   for rest = 1.20172*0.34864'
'hac array densities are hac s.u.dens.'
arbmh2ok   0.62843  2 0 0 0    1001   11.1913
                                8016   88.8087   12  0.0287  293  end
arbmal2o3  0.41898  2 0 0 0   13027   52.9390
                                8016   47.0610   12  0.096   293  end
arbmsio2   0.41898  2 0 0 0   14000   46.7570
                                8016   53.2430   12  0.367   293  end
arbmfe2o3  0.41898  2 0 0 0   26000   69.9540
                                8016   30.0460   12  0.067   293  end
arbmtio2   0.41898  2 0 0 0   22000   59.9535
                                8016   40.0465   12  0.012   293  end
arbmcao    0.41898  2 0 0 0   20000   71.4815
                                8016   28.5185   12  0.307   293  end
arbmmgo    0.41898  2 0 0 0   12000   60.3169
                                8016   39.6831   12  0.131   293  end
arbmna2o   0.41898  2 0 0 0   11023   74.1961
                                8016   25.8039   12  0.020   293  end
'kaolite 1600 top plug'
'sing.unit.density= (den.mult)(min.den.)'
' for arbmh20k = 0.965246*0.51655,  for rest = 0.965246*0.34438'
'den.mult= 1.21592e4 cm3 (actual vol.) / 1.25970e4 cm3 (model vol.)'
'actual vol.= 1.21592e4 cm3 = (28316.84 cm3/ft3)(9.646 lb)/(22.464 lb/ft3)'
arbmh2ok   0.49860  2 0 0 0    1001   11.1913
                                8016   88.8087   13  0.0287  293  end
arbmal2o3  0.33241  2 0 0 0   13027   52.9390
                                8016   47.0610   13  0.096   293  end
arbmsio2   0.33241  2 0 0 0   14000   46.7570
                                8016   53.2430   13  0.367   293  end
arbmfe2o3  0.33241  2 0 0 0   26000   69.9540
                                8016   30.0460   13  0.067   293  end
arbmtio2   0.33241  2 0 0 0   22000   59.9535
                                8016   40.0465   13  0.012   293  end
arbmcao    0.33241  2 0 0 0   20000   71.4815
                                8016   28.5185   13  0.307   293  end
arbmmgo    0.33241  2 0 0 0   12000   60.3169
                                8016   39.6831   13  0.131   293  end
arbmna2o   0.33241  2 0 0 0   11023   74.1961
                                8016   25.8039   13  0.020   293  end
'silicone rubber pads'
arbmsiru   1.21791  4 0 0 0    6012   32.3767
                                1001    8.1573
                                8016   21.5782
                               14000   37.8878   14  1.0     293  end
'void space external to containment vessel'
arbmwecv   0.9982   2 0 0 0    1001   11.1913
                                8016   88.8087   15  0.0001  293  end
'steel: liner'
ss304                                           16  1.0     293  end
'steel: plug cover (pc) use 9.907 lb'
```

```
ss304                                          17  1.06388 293  end
'steel: angle iron (ai) for HAC'
'nct density is multiplied by volume fraction 7.08030/5.74516'
ss304                                          18  1.23239 293  end
'steel: drum steel for HAC'
'nct density is multiplied by volume fraction 3.20482/2.95645'
ss304                                          19  1.08401 293  end
'void space external to drum'
'array density is assumed not reduced by hac'
arbmwed    0.9982   2 0 0 0    1001   11.1913
                                8016   88.8087   20  0.0001  293  end
'reflective water'
'arbmh20r   0.9982   2 0 0 0    1001   11.1913
'                                8016   88.8087   21  1.0     293  end
end comp
hciacyct12 3cyl,1.4in thk np,25000.2gU(25000.2g235, 8256.8gH2O,hx=  8.62),fr=1.0e-04
read parameters nub=yes npg=2500 gen=215 nsk=15 tme=100 end parameters
read boun       all=specular                   end boun
read geometry
unit 1001
'drum bottom flat cover [Elev= 0.105 in. at top of unit]'
'cylinder  19 1   21.838092    0.26670   0.0     com='extended radius not used'
 cylinder  19 1   21.838092    0.26670   0.0     com='drum bottom flat cover'
 cuboid    20 1 4p21.838092    0.26670   0.0     com='drum(chine)outer radius'
unit 1002
'above drum bottom flat cover and below containment vessel [Elev= 4.670 in.]'
 cylinder  15 1    3.175000   11.59510  11.16330 com='void in pad-1'
 cylinder  14 1    7.924800   11.59510  11.16330 com='pad-1'
 cylinder  16 1    8.077200   11.59510  11.16330 com='np277_4 liner'
 cylinder  11 1   10.922000   11.59510  11.16330 com='np277_4'
 cylinder  16 1   11.074400   11.59510  10.85850 com='kaolite liner bottom'
 cylinder  12 1   21.685692   11.59510   0.0     com='kaolite'
 cylinder  19 1   21.838092   11.59510   0.0     com='drum'
 cuboid    20 1 4p21.838092   11.59510   0.0     com='drum(chine)outer radius'
unit 1003
'cv bottom [Elev= 4.920 in.]'
 cylinder  8  1    6.680200    0.63500   0.0     com='cv bottom'
 cylinder  15 1    7.924800    0.63500   0.0     com='void btw cv-np liner'
 cylinder  16 1    8.077200    0.63500   0.0     com='np277_4 liner'
 cylinder  11 1   10.922000    0.63500   0.0     com='np277_4'
 cylinder  16 1   11.074400    0.63500   0.0     com='kaolite liner'
 cylinder  12 1   21.685692    0.63500   0.0     com='kaolite'
 cylinder  19 1   21.838092    0.63500   0.0     com='drum'
 cuboid    20 1 4p21.838092    0.63500   0.0     com='drum(chine)outer radius'
unit 1006
'content (collapsed) [Elev= 6.826 in.]'
 cylinder  1  1    5.397500     4.84031   0.0     com='cylindrical content'
 cylinder  3  1    6.426200    4.84081  -0.0005  com='cv well cavity'
 cylinder  8  1    6.680200    4.84081  -0.0005  com='cv below 1st step'
 cylinder  15 1    7.924800    4.84081  -0.0005  com='void btw cv-np liner'
 cylinder  16 1    8.077200    4.84081  -0.0005  com='np277_4 liner'
 cylinder  11 1   10.922000    4.84081  -0.0005  com='np277_4'
 cylinder  16 1   11.074400    4.84081  -0.0005  com='kaolite liner'
 cylinder  12 1   21.685692    4.84081  -0.0005  com='kaolite'
 cylinder  19 1   21.838092    4.84081  -0.0005  com='drum'
 cuboid    20 1 4p21.838092    4.84081  -0.0005  com='drum(chine)outer radius'
unit 1007
'np277_4 spacer [Elev= 8.226 in.]'
 cylinder  2  1    5.24510     3.55610   0.0     com='np spacer'
 cylinder  3  1    6.426200    3.55620  -0.0001  com='cv well cavity'
 cylinder  8  1    6.680200    3.55620  -0.0001  com='cv below 1st step'
 cylinder  15 1    7.924800    3.55620  -0.0001  com='void btw cv-np liner'
 cylinder  16 1    8.077200    3.55620  -0.0001  com='np277_4 liner'
 cylinder  11 1   10.922000    3.55620  -0.0001  com='np277_4'
 cylinder  16 1   11.074400    3.55620  -0.0001  com='kaolite liner'
 cylinder  12 1   21.685692    3.55620  -0.0001  com='kaolite'
 cylinder  19 1   21.838092    3.55620  -0.0001  com='drum'
 cuboid    20 1 4p21.838092    3.55620  -0.0001  com='drum(chine)outer radius'
unit 1008
'top of content stack to bottom of 1st step [Elev=35.270 in.]'
'21.63653             stack height (content spacers)       CALCULATED
```

```
 cylinder  3  1    6.426200   55.45247   0.0     com='cv well cavity'
 cylinder  8  1    6.680200   55.45247   0.0     com='cv below 1st step'
 cylinder  15 1    7.924800   55.45247   0.0     com='void btw cv-np liner'
 cylinder  16 1    8.077200   55.45247   0.0     com='np277_4 liner'
 cylinder  11 1   10.922000   55.45247   0.0     com='np277_4'
 cylinder  16 1   11.074400   55.45247   0.0     com='kaolite liner'
 cylinder  12 1   21.685692   55.45247   0.0     com='kaolite'
 cylinder  19 1   21.838092   55.45247   0.0     com='drum'
 cuboid    20 1 4p21.838092   55.45247   0.0     com='drum(chine)outer radius'
unit 1010
'cv at 1st step in liner [Elev=35.330 in.]'
 cylinder  3  1    6.426200    0.15240   0.0     com='cv well cavity'
 cylinder  8  1    6.680200    0.15240   0.0     com='cv at 1st step'
 cylinder  15 1    7.924800    0.15240   0.0     com='void btw cv and liner'
 cylinder  16 1   11.074400    0.15240   0.0     com='liner 1st step'
 cylinder  12 1   21.685692    0.15240   0.0     com='kaolite'
 cylinder  19 1   21.838092    0.15240   0.0     com='drum'
 cuboid    20 1 4p21.838092    0.15240   0.0     com='drum(chine)outer radius'
unit 1011
'vertical gap between 1st step in liner and cv flange [Elev=35.420 in.]'
 cylinder  3  1    6.426200    0.22860   0.0     com='cv well cavity'
 cylinder  8  1    6.680200    0.22860   0.0     com='cv at gap btwn step-flng'
 cylinder  15 1   10.922000    0.22860   0.0     com='void btw cv and liner'
 cylinder  16 1   11.074400    0.22860   0.0     com='liner wall'
 cylinder  12 1   21.685692    0.22860   0.0     com='kaolite'
 cylinder  19 1   21.838092    0.22860   0.0     com='drum'
 cuboid    20 1 4p21.838092    0.22860   0.0     com='drum(chine)outer radius'
unit 1012
'cv flange to top of cv well [Elev=35.920 in.]'
 cylinder  3  1    6.426200    1.27000   0.0     com='cavity'
 cylinder  9  1    9.525000    1.27000   0.0     com='flange to top of well'
 cylinder  15 1    9.525000    1.27000   0.0     com='void btw cv and pad-2'
 cylinder  14 1   10.033000    1.27000   0.0     com='pad-2'
 cylinder  15 1   10.922000    1.27000   0.0     com='void btw cv and liner'
 cylinder  16 1   11.074400    1.27000   0.0     com='liner wall'
 cylinder  12 1   21.685692    1.27000   0.0     com='kaolite'
 cylinder  19 1   21.838092    1.27000   0.0     com='drum'
 cuboid    20 1 4p21.838092    1.27000   0.0     com='drum(chine)outer radius'
unit 1013
'cv flange above cv well [Elev=37.070 in.]'
 cylinder  10 1    9.525000    2.92100   0.0     com='flange above cv well'
 cylinder  15 1    9.525000    2.92100   0.0     com='void btw cv and pad-2'
 cylinder  14 1   10.033000    2.92100   0.0     com='pad-2'
 cylinder  15 1   10.922000    2.92100   0.0     com='void btw pad2 and liner'
 cylinder  16 1   11.074400    2.92100   0.0     com='liner wall'
 cylinder  12 1   21.685692    2.92100   0.0     com='kaolite'
 cylinder  19 1   21.838092    2.92100   0.0     com='drum'
 cuboid    20 1 4p21.838092    2.92100   0.0     com='drum(chine)outer radius'
unit 1014
'plugpad2 below liner 2nd step [Elev=37.470 in.]'
 cylinder  14 1   10.033000    0.76200   0.0     com='pad-2'
 cylinder  15 1   10.922000    1.01600   0.0     com='void btw pad2 and liner'
 cylinder  16 1   11.074400    1.01600   0.0     com='liner wall'
 cylinder  12 1   21.685692    1.01600   0.0     com='kaolite'
 cylinder  19 1   21.838092    1.01600   0.0     com='drum'
 cuboid    20 1 4p21.838092    1.01600   0.0     com='drum(chine)outer radius'
unit 1015
'2nd step in liner [Elev=37.530 in.]'
 cylinder  15 1   10.922000    0.15240   0.0     com='void abv pad2'
 cylinder  16 1   18.757900    0.15240   0.0     com='liner 2nd step'
 cylinder  12 1   21.685692    0.15240   0.0     com='kaolite'
 cylinder  19 1   21.838092    0.15240   0.0     com='drum'
 cuboid    20 1 4p21.838092    0.15240   0.0     com='drum(chine)outer radius'
unit 1016
'abv 2nd step in liner to bottom of angle iron [Elev=40.750 in.]'
 cylinder  13 1   18.097500    8.17880   0.49276 com='plug kaolite'
 cylinder  17 1   18.249900    8.17880   0.34036 com='sides of plug case'
 cylinder  15 1   18.605500    8.17880   0.0     com='void: plug to liner'
 cylinder  16 1   18.757900    8.17880   0.0     com='liner wall'
 cylinder  12 1   21.685692    8.17880   0.0     com='kaolite'
 cylinder  19 1   21.838092    8.17880   0.0     com='drum'
```

```
 cuboid    20 1 4p21.838092    8.17880   0.0     com='drum(chine)outer radius'
unit 1017
'bottom of angle iron to bend in angle iron [Elev=42.500 in.]'
 cylinder  13 1   18.097500    4.44500   0.0     com='plug kaolite'
 cylinder  17 1   18.249900    4.44500   0.0     com='sides of plug case'
 cylinder  15 1   18.605500    4.44500   0.0     com='void: plug to liner'
 cylinder  16 1   18.757900    4.44500   0.0     com='liner wall'
 cylinder  18 1   19.392900    4.44500   0.0     com='lower angle iron'
 cylinder  12 1   21.685692    4.44500   0.0     com='kaolite'
 cylinder  19 1   21.838092    4.44500   0.0     com='drum'
 cuboid    20 1 4p21.838092    4.44500   0.0     com='drum(chine)outer radius'
unit 1018
'bend in angle iron to top of angle iron [Elev=42.750 in.]'
 cylinder  13 1   18.097500    0.11176   0.0     com='plug kaolite'
 cylinder  17 1   18.249900    0.26416   0.0     com='sides of plug case'
 cylinder  15 1   18.605500    0.63500   0.0     com='void: plug to liner'
 cylinder  16 1   18.757900    0.63500   0.0     com='liner wall'
 cylinder  18 1   21.685692    0.63500   0.0     com='bend section of ai'
 cylinder  19 1   21.838092    0.63500   0.0     com='drum'
 cuboid    20 1 4p21.838092    0.63500   0.0     com='drum(chine)outer radius'
unit 1019
'drum lid and lip [Elev=43.500 in.]'
 cylinder  20 1   21.469792    1.90500   0.15240 com='void above lid'
 cylinder  19 1   21.622192    1.90500   0.0     com='drum lid'
 cylinder  20 1   21.685692    1.90500   0.0     com='void btw lid - drum wall'
 cylinder  19 1   21.838092    1.90500   0.0     com='drum'
 cuboid    20 1 4p21.838092    1.90500   0.0     com='drum(chine)outer radius'
global
unit 1020
'es3100 drum [Elev=43.500 in.]'
array 3         2r-21.838092     0.0
'cuboid     0  1 4p21.838092    110.4905  0.0    com='bare package'
'cuboid    21  1 4p52.318092   140.9700 -30.48   com='reflected package'
 cuboid    20  1 4p22.889718    110.5048  0.0    com='interstital array space'
'global
'unit 1021
'array 4   3r0.0
'reflector  21 2  6r3.0  10
end geometry
read array
ara=3 nux=1 nuy=1 nuz=19 fill
1001 1002 1003 1006 1007 1006 1007 1006 1008 1010
1011 1012 1013 1014 1015 1016 1017 1018 1019        end fill
'ara=4 nux=13 nuy=13 nuz=06 fill f1020               end fill
end array
'read bias id=500 2  11  end bias
read start nst=0
end start
end data
end


=csas25    parm=size=3000000
ncia70st11,1.4in np,25588.2gU(25588.2g235, 8225.3gH2O hx=  8.39),fr=1.0e-04
238groupndf5 infhommedium
'HEU volume =1360.27104, SPACER volume  614.69740'
'HEU wrapped dry content can hx=0.66, CV void volume 8240.17295'
uranium  1 den=18.81109 1.0 293      92235  100.00
                                     92238   0.000               end
'np277-4: spacer (NCT_MD&H)'
'NCT min.den.(95.3886 lb/ft3) and hydrogen'
'np277-4 min.den.= 1.527971 = (95.3886 lb/ft3)(453.59 g/lb)/(28316.84 cm3/ft3)'
'use 75% of boron in calculations per NUREG-1609 Section 6.5.3.2'
arbmboron 7.31015e-2  2 0 0 0    5010   18.1479
                                 5011   81.8520    2  0.7500  293  end
arbmnpmx  1.07070e+0 10 0 0 0    6012    1.9189
                                 7014    0.0141
                                 8016   43.4251
                                11023    0.1174
                                12000    0.3378
                                13027   39.0479
```

```
                                14000    2.4672
                                16000    0.3083
                                20000   11.8336
                                26000    0.5298    2  1.0000  293  end
arbmnph2o 3.84169e-1  2 0 0 0    1001   11.1913
                                 8016   88.8087    2  1.0000  293  end
'flooded containmment vessel and content cans -- 10 CFR 71.55(d)(3)'
arbmwicv   0.9982   2 0 0 0    1001   11.1913
                               8016   88.8087    3  1.0     293  end
'steel: containment vessel body 16.60 lb but use 15.74 lb'
ss304                                            8  1.0     293  end
'steel: cv flange lower use 3.36 lb'
ss304                                            9  0.97267 293  end
'steel: cv flange upper use 13.75 lb'
ss304                                           10  0.94348 293  end
'np277-4: confinement -- neutron poison inner liner (NCT_MD&H)'
'actual vol.= 1.28314e4 cm3 = (7.83023e2 in3)(16.387064)'
'den.multiplier = 1.28314e4 cm3 (actual vol.) / 1.32708e4 cm3 (model vol.)'
'np277-4 min.den.= 1.527971 = (95.3886 lb/ft3)(453.59 g/lb)/(28316.84 cm3/ft3)'
'density = 1.477385 = (den.mult)(np277-4 min.den.) = 0.9668933*1.527971'
'use 75% of boron in calculations per NUREG-1609 Section 6.5.3.2'
arbmboron 7.06813e-2  2 0 0 0    5010   18.1479
                                 5011   81.8520   11  0.7500  293  end
arbmnpmx  1.03525e+0 10 0 0 0    6012    1.9189
                                 7014    0.0141
                                 8016   43.4251
                                11023    0.1174
                                12000    0.3378
                                13027   39.0479
                                14000    2.4672
                                16000    0.3083
                                20000   11.8336
                                26000    0.5298   11  1.0000  293  end
arbmnph2o 3.71451e-1  2 0 0 0    1001   11.1913
                                 8016   88.8087   11  1.0000  293  end
'kaolite 1600 body'
'sing.unit.density= (den.mult)(min.den.)'
' for arbmh20k = 1.012373*0.51655,  for rest = 1.012373*0.34438'
'den.mult= 1.36557e5 cm3 (actual vol.) / 1.34888e5 cm3 (model vol.)'
'actual vol.= 1.36557e5 cm3 = (28316.84 cm3/ft3)(108.33188 lb)/(22.464 lb/ft3)'
arbmh2ok   0.63931  2 0 0 0    1001   11.1913
                               8016   88.8087   12  0.0287  293  end
arbmal2o3  0.42622  2 0 0 0   13027   52.9390
                               8016   47.0610   12  0.096   293  end
arbmsio2   0.42622  2 0 0 0   14000   46.7570
                               8016   53.2430   12  0.367   293  end
arbmfe2o3  0.42622  2 0 0 0   26000   69.9540
                               8016   30.0460   12  0.067   293  end
arbmtio2   0.42622  2 0 0 0   22000   59.9535
                               8016   40.0465   12  0.012   293  end
arbmcao    0.42622  2 0 0 0   20000   71.4815
                               8016   28.5185   12  0.307   293  end
arbmmgo    0.42622  2 0 0 0   12000   60.3169
                               8016   39.6831   12  0.131   293  end
arbmna2o   0.42622  2 0 0 0   11023   74.1961
                               8016   25.8039   12  0.020   293  end
'kaolite 1600 top plug'
'sing.unit.density= (den.mult)(min.den.)'
' for arbmh20k = 0.965246*0.51655,  for rest = 0.965246*0.34438'
'den.mult= 1.21592e4 cm3 (actual vol.) / 1.25970e4 cm3 (model vol.)'
'actual vol.= 1.21592e4 cm3 = (28316.84 cm3/ft3)(9.646 lb)/(22.464 lb/ft3)'
arbmh2ok   0.49860  2 0 0 0    1001   11.1913
                               8016   88.8087   13  0.0287  293  end
arbmal2o3  0.33241  2 0 0 0   13027   52.9390
                               8016   47.0610   13  0.096   293  end
arbmsio2   0.33241  2 0 0 0   14000   46.7570
                               8016   53.2430   13  0.367   293  end
arbmfe2o3  0.33241  2 0 0 0   26000   69.9540
                               8016   30.0460   13  0.067   293  end
arbmtio2   0.33241  2 0 0 0   22000   59.9535
                               8016   40.0465   13  0.012   293  end
```

```
arbmcao    0.33241  2 0 0 0   20000   71.4815
                               8016   28.5185   13  0.307   293  end
arbmmgo    0.33241  2 0 0 0   12000   60.3169
                               8016   39.6831   13  0.131   293  end
arbmna2o   0.33241  2 0 0 0   11023   74.1961
                               8016   25.8039   13  0.020   293  end
'silicone rubber pads'
arbmsiru   1.21791  4 0 0 0    6012   32.3767
                               1001    8.1573
                               8016   21.5782
                              14000   37.8878   14  1.0     293  end
'void space external to containment vessel'
arbmwecv   0.9982   2 0 0 0    1001   11.1913
                               8016   88.8087   15  0.0001  293  end
'steel: liner'
ss304                                            16  1.0     293  end
'steel: plug cover (pc) use 9.907 lb'
ss304                                            17  1.06388 293  end
'steel: angle iron (ai) for single units'
'ss304                                            18  1.0     293  end
'steel: angle iron (ai) for arrays'
'array density is multiplied by a volume fraction 7.08030/5.63249'
ss304                                            18  1.25705 293  end
'steel: drum steel for single units'
'ss304                                            19  1.0     293  end
'steel: drum steel for arrays'
'array density is multiplied by a volume fraction 3.20482/3.20544'
ss304                                            19  0.99981 293  end
'void space external to drum'
'array density is multiplied by a volume ratio 8.11698/6.98323'
arbmwed    1.16026  2 0 0 0    1001   11.1913
                               8016   88.8087   20  0.0001  293  end
'reflective water'
'arbmh20r   0.9982   2 0 0 0    1001   11.1913
'                               8016   88.8087   21  1.0     293  end
end comp
ncia70st11,1.4in np,25588.2gU(25588.2g235, 8225.3gH2O,hx=  8.39),fr=1.0e-04
read parameters nub=yes npg=2500 gen=215 nsk=15 tme=100 end parameters
read boun       all=specular                     end boun
read geometry
unit 1001
'drum bottom flat cover [Elev= 0.111 in. at top of unit]'
'cylinder  19 1   22.866096    0.28150   0.0     com='extended radius not used'
 cylinder  19 1   21.722275    0.28150   0.0     com='drum bottom flat cover'
 cuboid    20 1 4p22.866096    0.28150   0.0     com='drum chine outer radius'
unit 1002
'above drum bottom flat cover and below containment vessel [Elev= 4.676 in.]'
 cylinder  15 1    3.175000   11.59510  11.16330 com='void in pad-1'
 cylinder  14 1    7.924800   11.59510  11.16330 com='pad-1'
 cylinder  16 1    8.077200   11.59510  11.16330 com='np277_4 liner'
 cylinder  11 1   10.922000   11.59510  11.16330 com='np277_4'
 cylinder  16 1   11.074400   11.59510  10.85850 com='kaolite liner bottom'
 cylinder  12 1   21.555075   11.59510   0.0     com='kaolite'
 cylinder  19 1   21.722275   11.59510   0.0     com='drum'
 cuboid    20 1 4p22.866096   11.59510   0.0     com='drum chine outer radius'
unit 1003
'cv bottom [Elev= 4.926 in.]'
 cylinder  8  1    6.680200    0.63500   0.0     com='cv bottom'
 cylinder  15 1    7.924800    0.63500   0.0     com='void btw cv-np liner'
 cylinder  16 1    8.077200    0.63500   0.0     com='np277_4 liner'
 cylinder  11 1   10.922000    0.63500   0.0     com='np277_4'
 cylinder  16 1   11.074400    0.63500   0.0     com='kaolite liner'
 cylinder  12 1   21.555075    0.63500   0.0     com='kaolite'
 cylinder  19 1   21.722275    0.63500   0.0     com='drum'
 cuboid    20 1 4p22.866096    0.63500   0.0     com='drum chine outer radius'
unit 1004
'1st content can (collapsed) [Elev= 6.989 in.]'
'3.437212   plus-y location cylinders'
'-3.437212  minus-y location cylinders'
'1.984375   plus-x location cylinders'
'-1.984375  minus-x location cylinders'
```

```
 cylinder  3  1    6.426200    5.23925  -0.0005  com='cv well cavity'
 hole  1020   -3.968750   0.0       0.0     com='cy1 (2cymx,0)'
 hole  1020   -1.984375   3.437212  0.0     com='cy2 (cymx,cypy)'
 hole  1020    1.984375   3.437212  0.0     com='cy3 (cypx,cypy)'
 hole  1020    3.968750   0.0       0.0     com='cy4 (2cypx,0)'
 hole  1020    1.984375  -3.437212  0.0     com='cy5 (cypx,cymx)'
 hole  1020   -1.984375  -3.437212  0.0     com='cy6 (cymx,cymy)'
 hole  1020    0.0        0.0       0.0     com='cy7 (0,0)'
 cylinder  8  1    6.680200    5.23925  -0.0005  com='cv below 1st step'
 cylinder  15 1    7.924800    5.23925  -0.0005  com='void btw cv-np liner'
 cylinder  16 1    8.077200    5.23925  -0.0005  com='np277_4 liner'
 cylinder  11 1   10.922000    5.23925  -0.0005  com='np277_4'
 cylinder  16 1   11.074400    5.23925  -0.0005  com='kaolite liner'
 cylinder  12 1   21.555075    5.23925  -0.0005  com='kaolite'
 cylinder  19 1   21.722275    5.23925  -0.0005  com='drum'
 cuboid    20 1 4p22.866096    5.23925  -0.0005  com='drum chine outer radius'
unit 1005
'np277_4 spacer [Elev= 8.389 in.]'
 cylinder  2  1    5.24510     3.55610   0.0     com='np spacer'
 cylinder  3  1    6.426200    3.55620  -0.0001  com='cv well cavity'
 cylinder  8  1    6.680200    3.55620  -0.0001  com='cv below 1st step'
 cylinder  15 1    7.924800    3.55620  -0.0001  com='void btw cv-np liner'
 cylinder  16 1    8.077200    3.55620  -0.0001  com='np277_4 liner'
 cylinder  11 1   10.922000    3.55620  -0.0001  com='np277_4'
 cylinder  16 1   11.074400    3.55620  -0.0001  com='kaolite liner'
 cylinder  12 1   21.555075    3.55620  -0.0001  com='kaolite'
 cylinder  19 1   21.722275    3.55620  -0.0001  com='drum'
 cuboid    20 1 4p22.866096    3.55620  -0.0001  com='drum chine outer radius'
unit 1006
'2nd content can (collapsed) [Elev=10.452 in.]'
 cylinder  3  1    6.426200    5.23925  -0.0005  com='cv well cavity'
 hole  1021   -3.968750   0.0       0.0     com='cy1 (2cymx,0)'
 hole  1021   -1.984375   3.437212  0.0     com='cy2 (cymx,cypy)'
 hole  1021    1.984375   3.437212  0.0     com='cy3 (cypx,cypy)'
 hole  1021    3.968750   0.0       0.0     com='cy4 (2cypx,0)'
 hole  1021    1.984375  -3.437212  0.0     com='cy5 (cypx,cymx)'
 hole  1021   -1.984375  -3.437212  0.0     com='cy6 (cymx,cymy)'
 hole  1021    0.0        0.0       0.0     com='cy7 (0,0)'
 cylinder  8  1    6.680200    5.23925  -0.0005  com='cv below 1st step'
 cylinder  15 1    7.924800    5.23925  -0.0005  com='void btw cv-np liner'
 cylinder  16 1    8.077200    5.23925  -0.0005  com='np277_4 liner'
 cylinder  11 1   10.922000    5.23925  -0.0005  com='np277_4'
 cylinder  16 1   11.074400    5.23925  -0.0005  com='kaolite liner'
 cylinder  12 1   21.555075    5.23925  -0.0005  com='kaolite'
 cylinder  19 1   21.722275    5.23925  -0.0005  com='drum'
 cuboid    20 1 4p22.866096    5.23925  -0.0005  com='drum chine outer radius'
unit 1007
'np277_4 spacer [Elev=11.852 in.]'
 cylinder  2  1    5.24510     3.55610   0.0     com='np spacer'
 cylinder  3  1    6.426200    3.55620  -0.0001  com='cv well cavity'
 cylinder  8  1    6.680200    3.55620  -0.0001  com='cv below 1st step'
 cylinder  15 1    7.924800    3.55620  -0.0001  com='void btw cv-np liner'
 cylinder  16 1    8.077200    3.55620  -0.0001  com='np277_4 liner'
 cylinder  11 1   10.922000    3.55620  -0.0001  com='np277_4'
 cylinder  16 1   11.074400    3.55620  -0.0001  com='kaolite liner'
 cylinder  12 1   21.555075    3.55620  -0.0001  com='kaolite'
 cylinder  19 1   21.722275    3.55620  -0.0001  com='drum'
 cuboid    20 1 4p22.866096    3.55620  -0.0001  com='drum chine outer radius'
unit 1008
'3rd content can (collapsed) [Elev=10.452 in.]'
 cylinder  3  1    6.426200    5.23925  -0.0005  com='cv well cavity'
 hole  1022   -3.968750   0.0       0.0     com='cy1 (2cymx,0)'
 hole  1022   -1.984375   3.437212  0.0     com='cy2 (cymx,cypy)'
 hole  1022    1.984375   3.437212  0.0     com='cy3 (cypx,cypy)'
 hole  1022    3.968750   0.0       0.0     com='cy4 (2cypx,0)'
 hole  1022    1.984375  -3.437212  0.0     com='cy5 (cypx,cymx)'
 hole  1022   -1.984375  -3.437212  0.0     com='cy6 (cymx,cymy)'
 hole  1022    0.0        0.0       0.0     com='cy7 (0,0)'
 cylinder  8  1    6.680200    5.23925  -0.0005  com='cv below 1st step'
 cylinder  15 1    7.924800    5.23925  -0.0005  com='void btw cv-np liner'
 cylinder  16 1    8.077200    5.23925  -0.0005  com='np277_4 liner'
```

```
 cylinder  11 1   10.922000    5.23925  -0.0005  com='np277_4'
 cylinder  16 1   11.074400    5.23925  -0.0005  com='kaolite liner'
 cylinder  12 1   21.555075    5.23925  -0.0005  com='kaolite'
 cylinder  19 1   21.722275    5.23925  -0.0005  com='drum'
 cuboid    20 1 4p22.866096    5.23925  -0.0005  com='drum chine outer radius'
unit 1009
'top of content stack to bottom of 1st step [Elev=35.276 in.]'
'22.83355             stack height (content spacers)       CALCULATED
 cylinder  3  1    6.426200   54.25545   0.0     com='cv well cavity'
 cylinder  8  1    6.680200   54.25545   0.0     com='cv below 1st step'
 cylinder  15 1    7.924800   54.25545   0.0     com='void btw cv-np liner'
 cylinder  16 1    8.077200   54.25545   0.0     com='np277_4 liner'
 cylinder  11 1   10.922000   54.25545   0.0     com='np277_4'
 cylinder  16 1   11.074400   54.25545   0.0     com='kaolite liner'
 cylinder  12 1   21.555075   54.25545   0.0     com='kaolite'
 cylinder  19 1   21.722275   54.25545   0.0     com='drum'
 cuboid    20 1 4p22.866096   54.25545   0.0     com='drum chine outer radius'
unit 1010
'cv at 1st step in liner [Elev=35.336 in.]'
 cylinder  3  1    6.426200    0.15240   0.0     com='cv well cavity'
 cylinder  8  1    6.680200    0.15240   0.0     com='cv at 1st step'
 cylinder  15 1    7.924800    0.15240   0.0     com='void btw cv and liner'
 cylinder  16 1   11.074400    0.15240   0.0     com='liner 1st step'
 cylinder  12 1   21.555075    0.15240   0.0     com='kaolite'
 cylinder  19 1   21.722275    0.15240   0.0     com='drum'
 cuboid    20 1 4p22.866096    0.15240   0.0     com='drum chine outer radius'
unit 1011
'vertical gap between 1st step in liner and cv flange [Elev=35.426 in.]'
 cylinder  3  1    6.426200    0.22860   0.0     com='cv well cavity'
 cylinder  8  1    6.680200    0.22860   0.0     com='cv at gap btwn step-flng'
 cylinder  15 1   10.922000    0.22860   0.0     com='void btw cv and liner'
 cylinder  16 1   11.074400    0.22860   0.0     com='liner wall'
 cylinder  12 1   21.555075    0.22860   0.0     com='kaolite'
 cylinder  19 1   21.722275    0.22860   0.0     com='drum'
 cuboid    20 1 4p22.866096    0.22860   0.0     com='drum chine outer radius'
unit 1012
'cv flange to top of cv well [Elev=35.926 in.]'
 cylinder  3  1    6.426200    1.27000   0.0     com='cavity'
 cylinder  9  1    9.525000    1.27000   0.0     com='flange to top of well'
 cylinder  15 1    9.525000    1.27000   0.0     com='void btw cv and pad-2'
 cylinder  14 1   10.033000    1.27000   0.0     com='pad-2'
 cylinder  15 1   10.922000    1.27000   0.0     com='void btw cv and liner'
 cylinder  16 1   11.074400    1.27000   0.0     com='liner wall'
 cylinder  12 1   21.555075    1.27000   0.0     com='kaolite'
 cylinder  19 1   21.722275    1.27000   0.0     com='drum'
 cuboid    20 1 4p22.866096    1.27000   0.0     com='drum chine outer radius'
unit 1013
'cv flange above cv well [Elev=37.076 in.]'
 cylinder  10 1    9.525000    2.92100   0.0     com='flange above cv well'
 cylinder  15 1    9.525000    2.92100   0.0     com='void btw cv and pad-2'
 cylinder  14 1   10.033000    2.92100   0.0     com='pad-2'
 cylinder  15 1   10.922000    2.92100   0.0     com='void btw pad2 and liner'
 cylinder  16 1   11.074400    2.92100   0.0     com='liner wall'
 cylinder  12 1   21.555075    2.92100   0.0     com='kaolite'
 cylinder  19 1   21.722275    2.92100   0.0     com='drum'
 cuboid    20 1 4p22.866096    2.92100   0.0     com='drum chine outer radius'
unit 1014
'plugpad2 below liner 2nd step [Elev=37.476 in.]'
 cylinder  14 1   10.033000    0.76200   0.0     com='pad-2'
 cylinder  15 1   10.922000    1.01600   0.0     com='void btw pad2 and liner'
 cylinder  16 1   11.074400    1.01600   0.0     com='liner wall'
 cylinder  12 1   21.555075    1.01600   0.0     com='kaolite'
 cylinder  19 1   21.722275    1.01600   0.0     com='drum'
 cuboid    20 1 4p22.866096    1.01600   0.0     com='drum chine outer radius'
unit 1015
'2nd step in liner [Elev=37.536 in.]'
 cylinder  15 1   10.922000    0.15240   0.0     com='void abv pad2'
 cylinder  16 1   18.757900    0.15240   0.0     com='liner 2nd step'
 cylinder  12 1   21.555075    0.15240   0.0     com='kaolite'
 cylinder  19 1   21.722275    0.15240   0.0     com='drum'
 cuboid    20 1 4p22.866096    0.15240   0.0     com='drum chine outer radius'
```

```
unit 1016
'abv 2nd step in liner to bottom of angle iron [Elev=40.756 in.]'
 cylinder  13 1   18.097500    8.17880   0.49276 com='plug kaolite'
 cylinder  17 1   18.249900    8.17880   0.34036 com='sides of plug case'
 cylinder  15 1   18.605500    8.17880   0.0     com='void: plug to liner'
 cylinder  16 1   18.757900    8.17880   0.0     com='liner wall'
 cylinder  12 1   21.555075    8.17880   0.0     com='kaolite'
 cylinder  19 1   21.722275    8.17880   0.0     com='drum'
 cuboid    20 1 4p22.866096    8.17880   0.0     com='drum chine outer radius'
unit 1017
'bottom of angle iron to bend in angle iron [Elev=42.506 in.]'
 cylinder  13 1   18.097500    4.44500   0.0     com='plug kaolite'
 cylinder  17 1   18.249900    4.44500   0.0     com='sides of plug case'
 cylinder  15 1   18.605500    4.44500   0.0     com='void: plug to liner'
 cylinder  16 1   18.757900    4.44500   0.0     com='liner wall'
 cylinder  18 1   19.392900    4.44500   0.0     com='lower angle iron'
 cylinder  12 1   21.555075    4.44500   0.0     com='kaolite'
 cylinder  19 1   21.722275    4.44500   0.0     com='drum'
 cuboid    20 1 4p22.866096    4.44500   0.0     com='drum chine outer radius'
unit 1018
'bend in angle iron to top of angle iron [Elev=42.756 in.]'
 cylinder  13 1   18.097500    0.11176   0.0     com='plug kaolite'
 cylinder  17 1   18.249900    0.26416   0.0     com='sides of plug case'
 cylinder  15 1   18.605500    0.63500   0.0     com='void: plug to liner'
 cylinder  16 1   18.757900    0.63500   0.0     com='liner wall'
 cylinder  18 1   21.555075    0.63500   0.0     com='bend section of ai'
 cylinder  19 1   21.722275    0.63500   0.0     com='drum'
 cuboid    20 1 4p22.866096    0.63500   0.0     com='drum chine outer radius'
unit 1019
'drum lid and lip [Elev=43.512 in.]'
 cylinder  20 1   21.330090    1.91973   0.16720 com='void above lid'
 cylinder  19 1   21.497290    1.91973   0.0     com='drum lid'
 cylinder  20 1   21.555075    1.91973   0.0     com='void btw lid - drum wall'
 cylinder  19 1   21.722275    1.91973   0.0     com='drum'
 cuboid    20 1 4p22.866096    1.91973   0.0     com='drum chine outer radius'
unit 1020
'HEU cylinder content, 3.96875cm diameter by  5.23875cm height'
'  64.77481cm3 single slug volume'
 cylinder  1  1    1.983875  5.23875   0.0       com='cyl'
unit 1021
'HEU cylinder content, 3.96875cm diameter by  5.23875cm height'
'  64.77481cm3 single slug volume'
 cylinder  1  1    1.983875  5.23875   0.0       com='cyl'
unit 1022
'HEU cylinder content, 3.96875cm diameter by  5.23875cm height'
'  64.77481cm3 single slug volume'
 cylinder  1  1    1.983875  5.23875   0.0       com='cyl'
global
unit 1023
'es3100 drum [Elev=43.512 in.]'
array 3         2r-22.866096     0.0
'cuboid     0  1 4p24.587200    110.4900  0.0    com='bare package'
'cuboid    21  1 4p55.067200   140.9700 -30.48   com='reflected package'
 cuboid    20  1 4p22.866096    110.5197  0.0    com='interstital array space'
'global
'unit 1025
'array 4   3r0.0
'reflector  21 2  6r3.0  10
end geometry
read array
ara=3 nux=1 nuy=1 nuz=19 fill
1001 1002 1003 1004 1005 1006 1007 1008 1009 1010
1011 1012 1013 1014 1015 1016 1017 1018 1019        end fill
'ara=4 nux=13 nuy=13 nuz=06 fill f1023               end fill
end array
'read bias id=500 2  11  end bias
read start nst=0
end start
end data
end
```

*(This case name is actually **ncia5est11_2_2_5_3**.)*

```
=csas25    parm=size=3000000
ncia5est11,0.0in np,73294.2gU(58635.4g235, 6317.2gH2O hx=  2.81),fr=1.0e-04
238groupndf5 infhommedium
'HEU volume =3886.48867, SPACER volume    0.01729'
'HEU wrapped dry content can hx=0.57, CV void volume 6328.63543'
uranium  1 den=18.85873 1.0 293      92235  80.000
                                     92238  20.000               end
'np277-4: spacer (NCT_MD&H)'
'NCT min.den.(95.3886 lb/ft3) and hydrogen'
'np277-4 min.den.= 1.527971 = (95.3886 lb/ft3)(453.59 g/lb)/(28316.84 cm3/ft3)'
'use 75% of boron in calculations per NUREG-1609 Section 6.5.3.2'
arbmboron 7.31015e-2  2 0 0 0    5010   18.1479
                                 5011   81.8520    2  0.7500  293  end
arbmnpmx  1.07070e+0 10 0 0 0    6012    1.9189
                                 7014    0.0141
                                 8016   43.4251
                                11023    0.1174
                                12000    0.3378
                                13027   39.0479
                                14000    2.4672
                                16000    0.3083
                                20000   11.8336
                                26000    0.5298    2  1.0000  293  end
arbmnph2o 3.84169e-1  2 0 0 0    1001   11.1913
                                 8016   88.8087    2  1.0000  293  end
'flooded containmment vessel and content cans -- 10 CFR 71.55(d)(3)'
arbmwicv   0.9982   2 0 0 0    1001   11.1913
                               8016   88.8087    3  1.0     293  end
'steel: containment vessel body 16.60 lb but use 15.74 lb'
ss304                                            8  1.0     293  end
'steel: cv flange lower use 3.36 lb'
ss304                                            9  0.97267 293  end
'steel: cv flange upper use 13.75 lb'
ss304                                           10  0.94348 293  end
'np277-4: confinement -- neutron poison inner liner (NCT_MD&H)'
'actual vol.= 1.28314e4 cm3 = (7.83023e2 in3)(16.387064)'
'den.multiplier = 1.28314e4 cm3 (actual vol.) / 1.32708e4 cm3 (model vol.)'
'np277-4 min.den.= 1.527971 = (95.3886 lb/ft3)(453.59 g/lb)/(28316.84 cm3/ft3)'
'density = 1.477385 = (den.mult)(np277-4 min.den.) = 0.9668933*1.527971'
'use 75% of boron in calculations per NUREG-1609 Section 6.5.3.2'
arbmboron 7.06813e-2  2 0 0 0    5010   18.1479
                                 5011   81.8520   11  0.7500  293  end
arbmnpmx  1.03525e+0 10 0 0 0    6012    1.9189
                                 7014    0.0141
                                 8016   43.4251
                                11023    0.1174
                                12000    0.3378
                                13027   39.0479
                                14000    2.4672
                                16000    0.3083
                                20000   11.8336
                                26000    0.5298   11  1.0000  293  end
arbmnph2o 3.71451e-1  2 0 0 0    1001   11.1913
                                 8016   88.8087   11  1.0000  293  end
'kaolite 1600 body'
'sing.unit.density= (den.mult)(min.den.)'
' for arbmh20k = 1.012373*0.51655,  for rest = 1.012373*0.34438'
'den.mult= 1.36557e5 cm3 (actual vol.) / 1.34888e5 cm3 (model vol.)'
'actual vol.= 1.36557e5 cm3 = (28316.84 cm3/ft3)(108.33188 lb)/(22.464 lb/ft3)'
arbmh2ok   0.63931  2 0 0 0    1001   11.1913
                               8016   88.8087   12  0.0287  293  end
arbmal2o3  0.42622  2 0 0 0   13027   52.9390
                               8016   47.0610   12  0.096   293  end
arbmsio2   0.42622  2 0 0 0   14000   46.7570
                               8016   53.2430   12  0.367   293  end
arbmfe2o3  0.42622  2 0 0 0   26000   69.9540
                               8016   30.0460   12  0.067   293  end
arbmtio2   0.42622  2 0 0 0   22000   59.9535
                               8016   40.0465   12  0.012   293  end
arbmcao    0.42622  2 0 0 0   20000   71.4815
```

```
                                8016   28.5185   12  0.307   293  end
arbmmgo    0.42622  2 0 0 0   12000   60.3169
                                8016   39.6831   12  0.131   293  end
arbmna2o   0.42622  2 0 0 0   11023   74.1961
                                8016   25.8039   12  0.020   293  end
'kaolite 1600 top plug'
'sing.unit.density= (den.mult)(min.den.)'
' for arbmh20k = 0.965246*0.51655,  for rest = 0.965246*0.34438'
'den.mult= 1.21592e4 cm3 (actual vol.) / 1.25970e4 cm3 (model vol.)'
'actual vol.= 1.21592e4 cm3 = (28316.84 cm3/ft3)(9.646 lb)/(22.464 lb/ft3)'
arbmh2ok   0.49860  2 0 0 0    1001   11.1913
                                8016   88.8087   13  0.0287  293  end
arbmal2o3  0.33241  2 0 0 0   13027   52.9390
                                8016   47.0610   13  0.096   293  end
arbmsio2   0.33241  2 0 0 0   14000   46.7570
                                8016   53.2430   13  0.367   293  end
arbmfe2o3  0.33241  2 0 0 0   26000   69.9540
                                8016   30.0460   13  0.067   293  end
arbmtio2   0.33241  2 0 0 0   22000   59.9535
                                8016   40.0465   13  0.012   293  end
arbmcao    0.33241  2 0 0 0   20000   71.4815
                                8016   28.5185   13  0.307   293  end
arbmmgo    0.33241  2 0 0 0   12000   60.3169
                                8016   39.6831   13  0.131   293  end
arbmna2o   0.33241  2 0 0 0   11023   74.1961
                                8016   25.8039   13  0.020   293  end
'silicone rubber pads'
arbmsiru   1.21791  4 0 0 0    6012   32.3767
                                1001    8.1573
                                8016   21.5782
                               14000   37.8878   14  1.0     293  end
'void space external to containment vessel'
arbmwecv   0.9982   2 0 0 0    1001   11.1913
                                8016   88.8087   15  0.0001  293  end
'steel: liner'
ss304                                           16  1.0     293  end
'steel: plug cover (pc) use 9.907 lb'
ss304                                           17  1.06388 293  end
'steel: angle iron (ai) for single units'
'ss304                                           18  1.0     293  end
'steel: angle iron (ai) for arrays'
'array density is multiplied by a volume fraction 7.08030/5.63249'
ss304                                           18  1.25705 293  end
'steel: drum steel for single units'
'ss304                                           19  1.0     293  end
'steel: drum steel for arrays'
'array density is multiplied by a volume fraction 3.20482/3.20544'
ss304                                           19  0.99981 293  end
'void space external to drum'
'array density is multiplied by a volume ratio 8.11698/6.98323'
arbmwed    1.16026  2 0 0 0    1001   11.1913
                                8016   88.8087   20  0.0001  293  end
'reflective water'
'arbmh20r   0.9982   2 0 0 0    1001   11.1913
'                                8016   88.8087   21  1.0     293  end
end comp
ncia5est11,0.0in np,73294.2gU(58635.4g235, 6317.2gH2O,hx=  2.81),fr=1.0e-04
read parameters nub=yes npg=2500 gen=215 nsk=15 tme=100 end parameters
read boun       all=specular                    end boun
read geometry
unit 1001
'drum bottom flat cover [Elev= 0.111 in. at top of unit]'
'cylinder  19 1   22.866096    0.28150   0.0     com='extended radius not used'
 cylinder  19 1   21.722275    0.28150   0.0     com='drum bottom flat cover'
 cuboid    20 1 4p22.866096    0.28150   0.0     com='drum chine outer radius'
unit 1002
'above drum bottom flat cover and below containment vessel [Elev= 4.676 in.]'
 cylinder  15 1    3.175000   11.59510  11.16330 com='void in pad-1'
 cylinder  14 1    7.924800   11.59510  11.16330 com='pad-1'
 cylinder  16 1    8.077200   11.59510  11.16330 com='np277_4 liner'
 cylinder  11 1   10.922000   11.59510  11.16330 com='np277_4'
```

```
 cylinder  16 1   11.074400   11.59510  10.85850 com='kaolite liner bottom'
 cylinder  12 1   21.555075   11.59510   0.0     com='kaolite'
 cylinder  19 1   21.722275   11.59510   0.0     com='drum'
 cuboid    20 1 4p22.866096   11.59510   0.0     com='drum chine outer radius'
unit 1003
'cv bottom [Elev= 4.926 in.]'
 cylinder  8  1    6.680200    0.63500   0.0     com='cv bottom'
 cylinder  15 1    7.924800    0.63500   0.0     com='void btw cv-np liner'
 cylinder  16 1    8.077200    0.63500   0.0     com='np277_4 liner'
 cylinder  11 1   10.922000    0.63500   0.0     com='np277_4'
 cylinder  16 1   11.074400    0.63500   0.0     com='kaolite liner'
 cylinder  12 1   21.555075    0.63500   0.0     com='kaolite'
 cylinder  19 1   21.722275    0.63500   0.0     com='drum'
 cuboid    20 1 4p22.866096    0.63500   0.0     com='drum chine outer radius'
unit 1004
'1st content can (collapsed) [Elev= 9.051 in.]'
'Reference CRC 29 Ed. pg 105'
'side of pentagon denoted spent'
'radius of inscribed circle in pentagon denoted icrpent'
'radius of circumscribed circle outside pentagon denoted ccrpent'
'ccrpent equals 0.85065 times spent'
'icrpent equals 0.68819 times spent'
'side of pentagon equals diameter of a cylinder fit into cc'
'radius of cc equals ccrpent plus radius of cylinder fit into cc'
'radius of ccrpent equal diamater of slug'
' 3.96875 radius of circumscribed circle'
' 2.33277 half of side of pentagon'
' 3.21078 radius of inscribed circle'
' 3.77452 x axis location of 2nd cyl in cc'
' 1.22642 y axis location of 2nd cyl in cc'
 cylinder  3  1    6.426200   10.47800  -0.0005  com='cv well cavity'
 hole  1020    0.0       3.96875 0.0        com='cy1 (0,ccrpent)'
 hole  1020    3.77452   1.22642 0.0        com='cy2 (xtwo,ytwo)'
 hole  1020    2.33277  -3.21078 0.0        com='cy3 (hspent,-icrpent)'
 hole  1020   -2.33277  -3.21078 0.0        com='cy4 (-hspent,-icrpent)'
 hole  1020   -3.77452   1.22642 0.0        com='cy5 (-xtwo,ytwo)'
 cylinder  8  1    6.680200   10.47800  -0.0005  com='cv below 1st step'
 cylinder  15 1    7.924800   10.47800  -0.0005  com='void btw cv-np liner'
 cylinder  16 1    8.077200   10.47800  -0.0005  com='np277_4 liner'
 cylinder  11 1   10.922000   10.47800  -0.0005  com='np277_4'
 cylinder  16 1   11.074400   10.47800  -0.0005  com='kaolite liner'
 cylinder  12 1   21.555075   10.47800  -0.0005  com='kaolite'
 cylinder  19 1   21.722275   10.47800  -0.0005  com='drum'
 cuboid    20 1 4p22.866096   10.47800  -0.0005  com='drum chine outer radius'
unit 1005
'np277_4 spacer [Elev= 9.051 in.]'
 cylinder  2  1    5.24510     0.00010   0.0     com='np spacer'
 cylinder  3  1    6.426200    0.00020  -0.0001  com='cv well cavity'
 cylinder  8  1    6.680200    0.00020  -0.0001  com='cv below 1st step'
 cylinder  15 1    7.924800    0.00020  -0.0001  com='void btw cv-np liner'
 cylinder  16 1    8.077200    0.00020  -0.0001  com='np277_4 liner'
 cylinder  11 1   10.922000    0.00020  -0.0001  com='np277_4'
 cylinder  16 1   11.074400    0.00020  -0.0001  com='kaolite liner'
 cylinder  12 1   21.555075    0.00020  -0.0001  com='kaolite'
 cylinder  19 1   21.722275    0.00020  -0.0001  com='drum'
 cuboid    20 1 4p22.866096    0.00020  -0.0001  com='drum chine outer radius'
unit 1006
'2nd content can (collapsed) [Elev=13.177 in.]'
 cylinder  3  1    6.426200   10.47800  -0.0005  com='cv well cavity'
 hole  1021    0.0       3.96875 0.0        com='cy1 (0,ccrpent)'
 hole  1021    3.77452   1.22642 0.0        com='cy2 (xtwo,ytwo)'
 hole  1021    2.33277  -3.21078 0.0        com='cy3 (hspent,-icrpent)'
 hole  1021   -2.33277  -3.21078 0.0        com='cy4 (-hspent,-icrpent)'
 hole  1021   -3.77452   1.22642 0.0        com='cy5 (-xtwo,ytwo)'
 cylinder  8  1    6.680200   10.47800  -0.0005  com='cv below 1st step'
 cylinder  15 1    7.924800   10.47800  -0.0005  com='void btw cv-np liner'
 cylinder  16 1    8.077200   10.47800  -0.0005  com='np277_4 liner'
 cylinder  11 1   10.922000   10.47800  -0.0005  com='np277_4'
 cylinder  16 1   11.074400   10.47800  -0.0005  com='kaolite liner'
 cylinder  12 1   21.555075   10.47800  -0.0005  com='kaolite'
 cylinder  19 1   21.722275   10.47800  -0.0005  com='drum'
```

```
 cuboid    20 1 4p22.866096   10.47800  -0.0005  com='drum chine outer radius'
unit 1007
'np277_4 spacer [Elev=13.177 in.]'
 cylinder  2  1    5.24510     0.00010   0.0     com='np spacer'
 cylinder  3  1    6.426200    0.00020  -0.0001  com='cv well cavity'
 cylinder  8  1    6.680200    0.00020  -0.0001  com='cv below 1st step'
 cylinder  15 1    7.924800    0.00020  -0.0001  com='void btw cv-np liner'
 cylinder  16 1    8.077200    0.00020  -0.0001  com='np277_4 liner'
 cylinder  11 1   10.922000    0.00020  -0.0001  com='np277_4'
 cylinder  16 1   11.074400    0.00020  -0.0001  com='kaolite liner'
 cylinder  12 1   21.555075    0.00020  -0.0001  com='kaolite'
 cylinder  19 1   21.722275    0.00020  -0.0001  com='drum'
 cuboid    20 1 4p22.866096    0.00020  -0.0001  com='drum chine outer radius'
unit 1008
'3rd content can (collapsed) [Elev=13.177 in.]'
 cylinder  3  1    6.426200   10.47800  -0.0005  com='cv well cavity'
 hole  1022    0.0       3.96875 0.0        com='cy1 (0,ccrpent)'
 hole  1022    3.77452   1.22642 0.0        com='cy2 (xtwo,ytwo)'
 hole  1022    2.33277  -3.21078 0.0        com='cy3 (hspent,-icrpent)'
 hole  1022   -2.33277  -3.21078 0.0        com='cy4 (-hspent,-icrpent)'
 hole  1022   -3.77452   1.22642 0.0        com='cy5 (-xtwo,ytwo)'
 cylinder  8  1    6.680200   10.47800  -0.0005  com='cv below 1st step'
 cylinder  15 1    7.924800   10.47800  -0.0005  com='void btw cv-np liner'
 cylinder  16 1    8.077200   10.47800  -0.0005  com='np277_4 liner'
 cylinder  11 1   10.922000   10.47800  -0.0005  com='np277_4'
 cylinder  16 1   11.074400   10.47800  -0.0005  com='kaolite liner'
 cylinder  12 1   21.555075   10.47800  -0.0005  com='kaolite'
 cylinder  19 1   21.722275   10.47800  -0.0005  com='drum'
 cuboid    20 1 4p22.866096   10.47800  -0.0005  com='drum chine outer radius'
unit 1009
'top of content stack to bottom of 1st step [Elev=35.276 in.]'
'31.43780             stack height (content spacers)       CALCULATED
 cylinder  3  1    6.426200   45.65120   0.0     com='cv well cavity'
 cylinder  8  1    6.680200   45.65120   0.0     com='cv below 1st step'
 cylinder  15 1    7.924800   45.65120   0.0     com='void btw cv-np liner'
 cylinder  16 1    8.077200   45.65120   0.0     com='np277_4 liner'
 cylinder  11 1   10.922000   45.65120   0.0     com='np277_4'
 cylinder  16 1   11.074400   45.65120   0.0     com='kaolite liner'
 cylinder  12 1   21.555075   45.65120   0.0     com='kaolite'
 cylinder  19 1   21.722275   45.65120   0.0     com='drum'
 cuboid    20 1 4p22.866096   45.65120   0.0     com='drum chine outer radius'
unit 1010
'cv at 1st step in liner [Elev=35.336 in.]'
 cylinder  3  1    6.426200    0.15240   0.0     com='cv well cavity'
 cylinder  8  1    6.680200    0.15240   0.0     com='cv at 1st step'
 cylinder  15 1    7.924800    0.15240   0.0     com='void btw cv and liner'
 cylinder  16 1   11.074400    0.15240   0.0     com='liner 1st step'
 cylinder  12 1   21.555075    0.15240   0.0     com='kaolite'
 cylinder  19 1   21.722275    0.15240   0.0     com='drum'
 cuboid    20 1 4p22.866096    0.15240   0.0     com='drum chine outer radius'
unit 1011
'vertical gap between 1st step in liner and cv flange [Elev=35.426 in.]'
 cylinder  3  1    6.426200    0.22860   0.0     com='cv well cavity'
 cylinder  8  1    6.680200    0.22860   0.0     com='cv at gap btwn step-flng'
 cylinder  15 1   10.922000    0.22860   0.0     com='void btw cv and liner'
 cylinder  16 1   11.074400    0.22860   0.0     com='liner wall'
 cylinder  12 1   21.555075    0.22860   0.0     com='kaolite'
 cylinder  19 1   21.722275    0.22860   0.0     com='drum'
 cuboid    20 1 4p22.866096    0.22860   0.0     com='drum chine outer radius'
unit 1012
'cv flange to top of cv well [Elev=35.926 in.]'
 cylinder  3  1    6.426200    1.27000   0.0     com='cavity'
 cylinder  9  1    9.525000    1.27000   0.0     com='flange to top of well'
 cylinder  15 1    9.525000    1.27000   0.0     com='void btw cv and pad-2'
 cylinder  14 1   10.033000    1.27000   0.0     com='pad-2'
 cylinder  15 1   10.922000    1.27000   0.0     com='void btw cv and liner'
 cylinder  16 1   11.074400    1.27000   0.0     com='liner wall'
 cylinder  12 1   21.555075    1.27000   0.0     com='kaolite'
 cylinder  19 1   21.722275    1.27000   0.0     com='drum'
 cuboid    20 1 4p22.866096    1.27000   0.0     com='drum chine outer radius'
unit 1013
```

```
'cv flange above cv well [Elev=37.076 in.]'
 cylinder  10 1    9.525000    2.92100   0.0     com='flange above cv well'
 cylinder  15 1    9.525000    2.92100   0.0     com='void btw cv and pad-2'
 cylinder  14 1   10.033000    2.92100   0.0     com='pad-2'
 cylinder  15 1   10.922000    2.92100   0.0     com='void btw pad2 and liner'
 cylinder  16 1   11.074400    2.92100   0.0     com='liner wall'
 cylinder  12 1   21.555075    2.92100   0.0     com='kaolite'
 cylinder  19 1   21.722275    2.92100   0.0     com='drum'
 cuboid    20 1 4p22.866096    2.92100   0.0     com='drum chine outer radius'
unit 1014
'plugpad2 below liner 2nd step [Elev=37.476 in.]'
 cylinder  14 1   10.033000    0.76200   0.0     com='pad-2'
 cylinder  15 1   10.922000    1.01600   0.0     com='void btw pad2 and liner'
 cylinder  16 1   11.074400    1.01600   0.0     com='liner wall'
 cylinder  12 1   21.555075    1.01600   0.0     com='kaolite'
 cylinder  19 1   21.722275    1.01600   0.0     com='drum'
 cuboid    20 1 4p22.866096    1.01600   0.0     com='drum chine outer radius'
unit 1015
'2nd step in liner [Elev=37.536 in.]'
 cylinder  15 1   10.922000    0.15240   0.0     com='void abv pad2'
 cylinder  16 1   18.757900    0.15240   0.0     com='liner 2nd step'
 cylinder  12 1   21.555075    0.15240   0.0     com='kaolite'
 cylinder  19 1   21.722275    0.15240   0.0     com='drum'
 cuboid    20 1 4p22.866096    0.15240   0.0     com='drum chine outer radius'
unit 1016
'abv 2nd step in liner to bottom of angle iron [Elev=40.756 in.]'
 cylinder  13 1   18.097500    8.17880   0.49276 com='plug kaolite'
 cylinder  17 1   18.249900    8.17880   0.34036 com='sides of plug case'
 cylinder  15 1   18.605500    8.17880   0.0     com='void: plug to liner'
 cylinder  16 1   18.757900    8.17880   0.0     com='liner wall'
 cylinder  12 1   21.555075    8.17880   0.0     com='kaolite'
 cylinder  19 1   21.722275    8.17880   0.0     com='drum'
 cuboid    20 1 4p22.866096    8.17880   0.0     com='drum chine outer radius'
unit 1017
'bottom of angle iron to bend in angle iron [Elev=42.506 in.]'
 cylinder  13 1   18.097500    4.44500   0.0     com='plug kaolite'
 cylinder  17 1   18.249900    4.44500   0.0     com='sides of plug case'
 cylinder  15 1   18.605500    4.44500   0.0     com='void: plug to liner'
 cylinder  16 1   18.757900    4.44500   0.0     com='liner wall'
 cylinder  18 1   19.392900    4.44500   0.0     com='lower angle iron'
 cylinder  12 1   21.555075    4.44500   0.0     com='kaolite'
 cylinder  19 1   21.722275    4.44500   0.0     com='drum'
 cuboid    20 1 4p22.866096    4.44500   0.0     com='drum chine outer radius'
unit 1018
'bend in angle iron to top of angle iron [Elev=42.756 in.]'
 cylinder  13 1   18.097500    0.11176   0.0     com='plug kaolite'
 cylinder  17 1   18.249900    0.26416   0.0     com='sides of plug case'
 cylinder  15 1   18.605500    0.63500   0.0     com='void: plug to liner'
 cylinder  16 1   18.757900    0.63500   0.0     com='liner wall'
 cylinder  18 1   21.555075    0.63500   0.0     com='bend section of ai'
 cylinder  19 1   21.722275    0.63500   0.0     com='drum'
 cuboid    20 1 4p22.866096    0.63500   0.0     com='drum chine outer radius'
unit 1019
'drum lid and lip [Elev=43.512 in.]'
 cylinder  20 1   21.330090    1.91973   0.16720 com='void above lid'
 cylinder  19 1   21.497290    1.91973   0.0     com='drum lid'
 cylinder  20 1   21.555075    1.91973   0.0     com='void btw lid - drum wall'
 cylinder  19 1   21.722275    1.91973   0.0     com='drum'
 cuboid    20 1 4p22.866096    1.91973   0.0     com='drum chine outer radius'
unit 1020
'HEU cylinder content, 3.96875cm diameter by 10.47750cm height'
' 129.54962cm3 single slug volume'
 cylinder  1  1    1.983875  10.4775   0.0       com='cyl'
unit 1021
'HEU cylinder content, 3.96875cm diameter by 10.47750cm height'
' 129.54962cm3 single slug volume'
 cylinder  1  1    1.983875  10.4775   0.0       com='cyl'
unit 1022
'HEU cylinder content, 3.96875cm diameter by 10.47750cm height'
' 129.54962cm3 single slug volume'
 cylinder  1  1    1.983875  10.4775   0.0       com='cyl'
```

```
global
unit 1023
'es3100 drum [Elev=43.512 in.]'
array 3         2r-22.866096     0.0
'cuboid     0  1 4p24.587200    110.4900  0.0    com='bare package'
'cuboid    21  1 4p55.067200   140.9700 -30.48   com='reflected package'
 cuboid    20  1 4p22.866096    110.5197  0.0    com='interstital array space'
'global
'unit 1025
'array 4   3r0.0
'reflector  21 2  6r3.0  10
end geometry
read array
ara=3 nux=1 nuy=1 nuz=19 fill
1001 1002 1003 1004 1005 1006 1007 1008 1009 1010
1011 1012 1013 1014 1015 1016 1017 1018 1019        end fill
'ara=4 nux=13 nuy=13 nuz=06 fill f1023               end fill
end array
'read bias id=500 2  11  end bias
read start nst=0
end start
end data
end


=csas25    parm=size=3000000
nciabmt11,0.0in thk np, 3708.5gU( 2966.8g235,10000.7gH2O hx= 87.98),fr=1.0e-04
238groupndf5 infhommedium
'HEU volume = 196.64477, SPACER volume    0.00000'
'HEU wrapped dry content can hx=5.65, CV void volume 10018.7171'
uranium  1 den=18.85873 0.01925 293      92235  80.000
                                     92238  20.000               end
arbmh20i   0.97898  2 0 0 0    1001   11.1913
                               8016   88.8087    1  1.0000  293  end
'np277-4: spacer (NCT_MD&H)'
'NCT min.den.(95.3886 lb/ft3) and hydrogen'
'np277-4 min.den.= 1.527971 = (95.3886 lb/ft3)(453.59 g/lb)/(28316.84 cm3/ft3)'
'use 75% of boron in calculations per NUREG-1609 Section 6.5.3.2'
arbmboron 7.31015e-2  2 0 0 0    5010   18.1479
                                 5011   81.8520    2  0.7500  293  end
arbmnpmx  1.07070e+0 10 0 0 0    6012    1.9189
                                 7014    0.0141
                                 8016   43.4251
                                11023    0.1174
                                12000    0.3378
                                13027   39.0479
                                14000    2.4672
                                16000    0.3083
                                20000   11.8336
                                26000    0.5298    2  1.0000  293  end
arbmnph2o 3.84169e-1  2 0 0 0    1001   11.1913
                                 8016   88.8087    2  1.0000  293  end
'flooded containmment vessel and content cans -- 10 CFR 71.55(d)(3)'
arbmwicv   0.9982   2 0 0 0    1001   11.1913
                               8016   88.8087    3  1.0     293  end
'steel: containment vessel body 16.60 lb but use 15.74 lb'
ss304                                            8  1.0     293  end
'steel: cv flange lower use 3.36 lb'
ss304                                            9  0.97267 293  end
'steel: cv flange upper use 13.75 lb'
ss304                                           10  0.94348 293  end
'np277-4: confinement -- neutron poison inner liner (NCT_MD&H)'
'actual vol.= 1.28314e4 cm3 = (7.83023e2 in3)(16.387064)'
'den.multiplier = 1.28314e4 cm3 (actual vol.) / 1.32708e4 cm3 (model vol.)'
'np277-4 min.den.= 1.527971 = (95.3886 lb/ft3)(453.59 g/lb)/(28316.84 cm3/ft3)'
'density = 1.477385 = (den.mult)(np277-4 min.den.) = 0.9668933*1.527971'
'use 75% of boron in calculations per NUREG-1609 Section 6.5.3.2'
arbmboron 7.06813e-2  2 0 0 0    5010   18.1479
                                 5011   81.8520   11  0.7500  293  end
arbmnpmx  1.03525e+0 10 0 0 0    6012    1.9189
                                 7014    0.0141
```

```
                                 8016   43.4251
                                11023    0.1174
                                12000    0.3378
                                13027   39.0479
                                14000    2.4672
                                16000    0.3083
                                20000   11.8336
                                26000    0.5298   11  1.0000  293  end
arbmnph2o 3.71451e-1  2 0 0 0    1001   11.1913
                                 8016   88.8087   11  1.0000  293  end
'kaolite 1600 body'
'sing.unit.density= (den.mult)(min.den.)'
' for arbmh20k = 1.012373*0.51655,  for rest = 1.012373*0.34438'
'den.mult= 1.36557e5 cm3 (actual vol.) / 1.34888e5 cm3 (model vol.)'
'actual vol.= 1.36557e5 cm3 = (28316.84 cm3/ft3)(108.33188 lb)/(22.464 lb/ft3)'
'nct array densities are s.u.dens. multiplied by volume ratio 1.34888/1.10336'
arbmh2ok   0.63931  2 0 0 0    1001   11.1913
                               8016   88.8087   12  0.0287  293  end
arbmal2o3  0.42622  2 0 0 0   13027   52.9390
                               8016   47.0610   12  0.096   293  end
arbmsio2   0.42622  2 0 0 0   14000   46.7570
                               8016   53.2430   12  0.367   293  end
arbmfe2o3  0.42622  2 0 0 0   26000   69.9540
                               8016   30.0460   12  0.067   293  end
arbmtio2   0.42622  2 0 0 0   22000   59.9535
                               8016   40.0465   12  0.012   293  end
arbmcao    0.42622  2 0 0 0   20000   71.4815
                               8016   28.5185   12  0.307   293  end
arbmmgo    0.42622  2 0 0 0   12000   60.3169
                               8016   39.6831   12  0.131   293  end
arbmna2o   0.42622  2 0 0 0   11023   74.1961
                               8016   25.8039   12  0.020   293  end
'kaolite 1600 top plug'
'sing.unit.density= (den.mult)(min.den.)'
' for arbmh20k = 0.965246*0.51655,  for rest = 0.965246*0.34438'
'den.mult= 1.21592e4 cm3 (actual vol.) / 1.25970e4 cm3 (model vol.)'
'actual vol.= 1.21592e4 cm3 = (28316.84 cm3/ft3)(9.646 lb)/(22.464 lb/ft3)'
arbmh2ok   0.49860  2 0 0 0    1001   11.1913
                               8016   88.8087   13  0.0287  293  end
arbmal2o3  0.33241  2 0 0 0   13027   52.9390
                               8016   47.0610   13  0.096   293  end
arbmsio2   0.33241  2 0 0 0   14000   46.7570
                               8016   53.2430   13  0.367   293  end
arbmfe2o3  0.33241  2 0 0 0   26000   69.9540
                               8016   30.0460   13  0.067   293  end
arbmtio2   0.33241  2 0 0 0   22000   59.9535
                               8016   40.0465   13  0.012   293  end
arbmcao    0.33241  2 0 0 0   20000   71.4815
                               8016   28.5185   13  0.307   293  end
arbmmgo    0.33241  2 0 0 0   12000   60.3169
                               8016   39.6831   13  0.131   293  end
arbmna2o   0.33241  2 0 0 0   11023   74.1961
                               8016   25.8039   13  0.020   293  end
'silicone rubber pads'
arbmsiru   1.21791  4 0 0 0    6012   32.3767
                               1001    8.1573
                               8016   21.5782
                              14000   37.8878   14  1.0     293  end
'void space external to containment vessel'
arbmwecv   0.9982   2 0 0 0    1001   11.1913
                               8016   88.8087   15  0.0001  293  end
'steel: liner'
ss304                                            16  1.0     293  end
'steel: plug cover (pc) use 9.907 lb'
ss304                                            17  1.06388 293  end
'steel: angle iron (ai) for single units'
'ss304                                            18  1.0     293  end
'steel: angle iron (ai) for arrays'
'array density is multiplied by a volume fraction 7.08030/5.63249'
ss304                                            18  1.25705 293  end
'steel: drum steel for single units'
```

```
'ss304                                          19  1.0     293  end
'steel: drum steel for arrays'
'array density is multiplied by a volume fraction 3.20482/3.20544'
ss304                                          19  0.99981 293  end
'void space external to drum'
'array density is multiplied by a volume ratio 8.11698/6.98323'
arbmwed    1.16026  2 0 0 0    1001   11.1913
                                8016   88.8087   20  0.0001  293  end
'reflective water'
'arbmh20r   0.9982   2 0 0 0    1001   11.1913
'                               8016   88.8087   21  1.0     293  end
end comp
nciabmt11,0.0in thk np, 3708.5gU( 2966.8g235,10000.7gH2O,hx= 87.98),fr=1.0e-04
read parameters nub=yes npg=2500 gen=215 nsk=15 tme=100 end parameters
read boun       all=specular                   end boun
read geometry
unit 1001
'drum bottom flat cover [Elev= 0.111 in. at top of unit]'
'cylinder  19 1   22.866096    0.28150   0.0     com='extended radius not used'
 cylinder  19 1   21.722275    0.28150   0.0     com='drum bottom flat cover'
 cuboid    20 1 4p22.866096    0.28150   0.0     com='drum chine outer radius'
unit 1002
'above drum bottom flat cover and below containment vessel [Elev= 4.676 in.]'
 cylinder  15 1    3.175000   11.59510  11.16330 com='void in pad-1'
 cylinder  14 1    7.924800   11.59510  11.16330 com='pad-1'
 cylinder  16 1    8.077200   11.59510  11.16330 com='np277_4 liner'
 cylinder  11 1   10.922000   11.59510  11.16330 com='np277_4'
 cylinder  16 1   11.074400   11.59510  10.85850 com='kaolite liner bottom'
 cylinder  12 1   21.555075   11.59510   0.0     com='kaolite'
 cylinder  19 1   21.722275   11.59510   0.0     com='drum'
 cuboid    20 1 4p22.866096   11.59510   0.0     com='drum chine outer radius'
unit 1003
'cv bottom [Elev= 4.926 in.]'
 cylinder  8  1    6.680200    0.63500   0.0     com='cv bottom'
 cylinder  15 1    7.924800    0.63500   0.0     com='void btw cv-np liner'
 cylinder  16 1    8.077200    0.63500   0.0     com='np277_4 liner'
 cylinder  11 1   10.922000    0.63500   0.0     com='np277_4'
 cylinder  16 1   11.074400    0.63500   0.0     com='kaolite liner'
 cylinder  12 1   21.555075    0.63500   0.0     com='kaolite'
 cylinder  19 1   21.722275    0.63500   0.0     com='drum'
 cuboid    20 1 4p22.866096    0.63500   0.0     com='drum chine outer radius'
unit 1004
'cubical content, stacked per cc'
'    9.08802     3.57796 lattice width-depth'
'    2.54000     1.00000 cube dimension'
'    1.27000     0.50000 cube half-dimension'
'   16.38706     1.00000 volume of HEU cube in unit cell'
'  309.03922             HEU mass one cube'
'   4                    number of HEU cubes per can'
' 1236.15687             HEU mass of cubes in cc'
'    3           3       number of cubes in -x direction'
'    3           3       number of cubes in -y direction'
'    9           9       number of HEU cubes in a layer'
'    1    VARIABLE       number of HEU layers in z-axis'
'    4    VARIABLE       number of HEU cubes in top layer modulus(Z%N)'
'    5    VARIABLE       number of HEU voids in top layer'
'    ara=1 nux=3 nuy=3 nuz=1   fill  4r1004  5r1005      end fill'
'    0.48924     0.19261 gap dimension                       CALCULATED
'    3.02924     1.19261 unit cell dimension                 CALCULATED
'    1.51462     0.59631 unit cell half-dimension            CALCULATED
'   27.79719     1.69629 volume of unit cell                 CALCULATED
'   11.41013     0.69629 volume of water gap in unit cell    CALCULATED
'  250.17473             lattice volume in cc                CALCULATED
'  184.62648             moderator volume in lattice in cc   CALCULATED
'   65.54826             HEU volume in lattice in cc         CALCULATED
'    0.01925             volume fraction of HEU in CV        CALCULATED
'    0.97898             bulk dens of water in CV            CALCULATED
 cuboid    1  1  6p1.51452                       com='unit cell'
unit 1005
'cubical void, filler for layers'
 cuboid    1  1  6p1.51452                       com='unit cell'
```

```
unit 1006
'content (collapsed) [Elev= 6.119 in.]'
' 4.54386     1.78892 half width-depth lattice             CALCULATED'
' 3.02924             height lattice                       CALCULATED'
'array 1         2r-4.54386      0.0'
 cuboid    1  1  4p4.54386     3.02924   0.0     com='homog. content-array'
 cylinder  1  1    6.426200    3.02974  -0.0005  com='cv well cavity'
 cylinder  8  1    6.680200    3.02974  -0.0005  com='cv below 1st step'
 cylinder  15 1    7.924800    3.02974  -0.0005  com='void btw cv-np liner'
 cylinder  16 1    8.077200    3.02974  -0.0005  com='np277_4 liner'
 cylinder  11 1   10.922000    3.02974  -0.0005  com='np277_4'
 cylinder  16 1   11.074400    3.02974  -0.0005  com='kaolite liner'
 cylinder  12 1   21.555075    3.02974  -0.0005  com='kaolite'
 cylinder  19 1   21.722275    3.02974  -0.0005  com='drum'
 cuboid    20 1 4p22.866096    3.02974  -0.0005  com='drum chine outer radius'
unit 1007
'np277_4 spacer [Elev= 6.119 in.]'
 cylinder  2  1    5.24510     0.00010   0.0     com='np spacer'
 cylinder  1  1    6.426200    0.00020  -0.0001  com='cv well cavity'
 cylinder  8  1    6.680200    0.00020  -0.0001  com='cv below 1st step'
 cylinder  15 1    7.924800    0.00020  -0.0001  com='void btw cv-np liner'
 cylinder  16 1    8.077200    0.00020  -0.0001  com='np277_4 liner'
 cylinder  11 1   10.922000    0.00020  -0.0001  com='np277_4'
 cylinder  16 1   11.074400    0.00020  -0.0001  com='kaolite liner'
 cylinder  12 1   21.555075    0.00020  -0.0001  com='kaolite'
 cylinder  19 1   21.722275    0.00020  -0.0001  com='drum'
 cuboid    20 1 4p22.866096    0.00020  -0.0001  com='drum chine outer radius'
unit 1008
'top of content stack to bottom of 1st step [Elev=35.276 in.]'
' 9.09132             stack height (content spacers)       CALCULATED
 cylinder  1  1    6.426200   67.99768   0.0     com='cv well cavity'
 cylinder  8  1    6.680200   67.99768   0.0     com='cv below 1st step'
 cylinder  15 1    7.924800   67.99768   0.0     com='void btw cv-np liner'
 cylinder  16 1    8.077200   67.99768   0.0     com='np277_4 liner'
 cylinder  11 1   10.922000   67.99768   0.0     com='np277_4'
 cylinder  16 1   11.074400   67.99768   0.0     com='kaolite liner'
 cylinder  12 1   21.555075   67.99768   0.0     com='kaolite'
 cylinder  19 1   21.722275   67.99768   0.0     com='drum'
 cuboid    20 1 4p22.866096   67.99768   0.0     com='drum chine outer radius'
unit 1010
'cv at 1st step in liner [Elev=35.336 in.]'
 cylinder  1  1    6.426200    0.15240   0.0     com='cv well cavity'
 cylinder  8  1    6.680200    0.15240   0.0     com='cv at 1st step'
 cylinder  15 1    7.924800    0.15240   0.0     com='void btw cv and liner'
 cylinder  16 1   11.074400    0.15240   0.0     com='liner 1st step'
 cylinder  12 1   21.555075    0.15240   0.0     com='kaolite'
 cylinder  19 1   21.722275    0.15240   0.0     com='drum'
 cuboid    20 1 4p22.866096    0.15240   0.0     com='drum chine outer radius'
unit 1011
'vertical gap between 1st step in liner and cv flange [Elev=35.426 in.]'
 cylinder  1  1    6.426200    0.22860   0.0     com='cv well cavity'
 cylinder  8  1    6.680200    0.22860   0.0     com='cv at gap btwn step-flng'
 cylinder  15 1   10.922000    0.22860   0.0     com='void btw cv and liner'
 cylinder  16 1   11.074400    0.22860   0.0     com='liner wall'
 cylinder  12 1   21.555075    0.22860   0.0     com='kaolite'
 cylinder  19 1   21.722275    0.22860   0.0     com='drum'
 cuboid    20 1 4p22.866096    0.22860   0.0     com='drum chine outer radius'
unit 1012
'cv flange to top of cv well [Elev=35.926 in.]'
 cylinder  1  1    6.426200    1.27000   0.0     com='cavity'
 cylinder  9  1    9.525000    1.27000   0.0     com='flange to top of well'
 cylinder  15 1    9.525000    1.27000   0.0     com='void btw cv and pad-2'
 cylinder  14 1   10.033000    1.27000   0.0     com='pad-2'
 cylinder  15 1   10.922000    1.27000   0.0     com='void btw cv and liner'
 cylinder  16 1   11.074400    1.27000   0.0     com='liner wall'
 cylinder  12 1   21.555075    1.27000   0.0     com='kaolite'
 cylinder  19 1   21.722275    1.27000   0.0     com='drum'
 cuboid    20 1 4p22.866096    1.27000   0.0     com='drum chine outer radius'
unit 1013
'cv flange above cv well [Elev=37.076 in.]'
 cylinder  10 1    9.525000    2.92100   0.0     com='flange above cv well'
```

```
 cylinder  15 1    9.525000    2.92100   0.0     com='void btw cv and pad-2'
 cylinder  14 1   10.033000    2.92100   0.0     com='pad-2'
 cylinder  15 1   10.922000    2.92100   0.0     com='void btw pad2 and liner'
 cylinder  16 1   11.074400    2.92100   0.0     com='liner wall'
 cylinder  12 1   21.555075    2.92100   0.0     com='kaolite'
 cylinder  19 1   21.722275    2.92100   0.0     com='drum'
 cuboid    20 1 4p22.866096    2.92100   0.0     com='drum chine outer radius'
unit 1014
'plugpad2 below liner 2nd step [Elev=37.476 in.]'
 cylinder  14 1   10.033000    0.76200   0.0     com='pad-2'
 cylinder  15 1   10.922000    1.01600   0.0     com='void btw pad2 and liner'
 cylinder  16 1   11.074400    1.01600   0.0     com='liner wall'
 cylinder  12 1   21.555075    1.01600   0.0     com='kaolite'
 cylinder  19 1   21.722275    1.01600   0.0     com='drum'
 cuboid    20 1 4p22.866096    1.01600   0.0     com='drum chine outer radius'
unit 1015
'2nd step in liner [Elev=37.536 in.]'
 cylinder  15 1   10.922000    0.15240   0.0     com='void abv pad2'
 cylinder  16 1   18.757900    0.15240   0.0     com='liner 2nd step'
 cylinder  12 1   21.555075    0.15240   0.0     com='kaolite'
 cylinder  19 1   21.722275    0.15240   0.0     com='drum'
 cuboid    20 1 4p22.866096    0.15240   0.0     com='drum chine outer radius'
unit 1016
'abv 2nd step in liner to bottom of angle iron [Elev=40.756 in.]'
 cylinder  13 1   18.097500    8.17880   0.49276 com='plug kaolite'
 cylinder  17 1   18.249900    8.17880   0.34036 com='sides of plug case'
 cylinder  15 1   18.605500    8.17880   0.0     com='void: plug to liner'
 cylinder  16 1   18.757900    8.17880   0.0     com='liner wall'
 cylinder  12 1   21.555075    8.17880   0.0     com='kaolite'
 cylinder  19 1   21.722275    8.17880   0.0     com='drum'
 cuboid    20 1 4p22.866096    8.17880   0.0     com='drum chine outer radius'
unit 1017
'bottom of angle iron to bend in angle iron [Elev=42.506 in.]'
 cylinder  13 1   18.097500    4.44500   0.0     com='plug kaolite'
 cylinder  17 1   18.249900    4.44500   0.0     com='sides of plug case'
 cylinder  15 1   18.605500    4.44500   0.0     com='void: plug to liner'
 cylinder  16 1   18.757900    4.44500   0.0     com='liner wall'
 cylinder  18 1   19.392900    4.44500   0.0     com='lower angle iron'
 cylinder  12 1   21.555075    4.44500   0.0     com='kaolite'
 cylinder  19 1   21.722275    4.44500   0.0     com='drum'
 cuboid    20 1 4p22.866096    4.44500   0.0     com='drum chine outer radius'
unit 1018
'bend in angle iron to top of angle iron [Elev=42.756 in.]'
 cylinder  13 1   18.097500    0.11176   0.0     com='plug kaolite'
 cylinder  17 1   18.249900    0.26416   0.0     com='sides of plug case'
 cylinder  15 1   18.605500    0.63500   0.0     com='void: plug to liner'
 cylinder  16 1   18.757900    0.63500   0.0     com='liner wall'
 cylinder  18 1   21.555075    0.63500   0.0     com='bend section of ai'
 cylinder  19 1   21.722275    0.63500   0.0     com='drum'
 cuboid    20 1 4p22.866096    0.63500   0.0     com='drum chine outer radius'
unit 1019
'drum lid and lip [Elev=43.512 in.]'
 cylinder  20 1   21.330090    1.91973   0.16720 com='void above lid'
 cylinder  19 1   21.497290    1.91973   0.0     com='drum lid'
 cylinder  20 1   21.555075    1.91973   0.0     com='void btw lid - drum wall'
 cylinder  19 1   21.722275    1.91973   0.0     com='drum'
 cuboid    20 1 4p22.866096    1.91973   0.0     com='drum chine outer radius'
global
unit 1020
'es3100 drum [Elev=43.512 in.]'
array 3         2r-22.866096     0.0
'cuboid     0  1 4p24.587200    110.4900  0.0    com='bare package'
'cuboid    21  1 4p55.067200   140.9700 -30.48   com='reflected package'
 cuboid    20  1 4p22.866096    110.5197  0.0    com='interstital array space'
'global
'unit 1021
'array 4   3r0.0
'reflector  21 2  6r3.0  10
end geometry
read array
ara=1 nux=3 nuy=3 nuz=1   fill  4r1004  5r1005      end fill
```

```
ara=3 nux=1 nuy=1 nuz=19 fill
1001 1002 1003 1006 1007 1006 1007 1006 1008 1010
1011 1012 1013 1014 1015 1016 1017 1018 1019        end fill
'ara=4 nux=13 nuy=13 nuz=06 fill f1020               end fill
end array
'read bias id=500 2  11  end bias
read start nst=0
end start
end data
end


=csas25    parm=size=4000000
hctf5bmt12,1.4in thk np,24968.9gU(24968.9g235, 8258.4gH2O hx=  8.63),fr=1.0e-04
238groupndf5 infhommedium
'HEU wrapped dry content can hx=0.67, CV void volume 8273.32964'
uranium  1 den=18.81109 0.13826 293      92235  100.00
                                     92238   0.000               end
arbmh20i   0.86019  2 0 0 0    1001   11.1913
                               8016   88.8087    1  1.0000  293  end
'np277-4: spacer (HAC_MD&H)'
'HAC min.den.(95.3157 lb/ft3) and hydrogen'
'np277-4 min.den.= 1.526803 = (95.3157 lb/ft3)(453.59 g/lb)/(28316.84 cm3/ft3)'
'use 75% of boron in calculations per NUREG-1609 Section 6.5.3.2'
arbmboron 7.31015e-2  2 0 0 0    5010   18.1479
                                 5011   81.8520    2  0.7500  293  end
arbmnpmx  1.07071e+0 10 0 0 0    6012    1.9188
                                 7014    0.0141
                                 8016   43.4254
                                11023    0.1174
                                12000    0.3378
                                13027   39.0477
                                14000    2.4671
                                16000    0.3083
                                20000   11.8335
                                26000    0.5298    2  1.0000  293  end
arbmnph2o 3.82995e-1  2 0 0 0    1001   11.1913
                                 8016   88.8087    2  1.0000  293  end
'flooded containmment vessel and content cans -- 10 CFR 71.55(d)(3)'
arbmwicv   0.9982   2 0 0 0    1001   11.1913
                               8016   88.8087    3  1.0     293  end
'steel: containment vessel body 16.60 lb but use 15.74 lb'
ss304                                            8  1.0     293  end
'steel: cv flange lower use 3.36 lb'
ss304                                            9  0.97267 293  end
'steel: cv flange upper use 13.75 lb'
ss304                                           10  0.94348 293  end
'np277-4: confinement -- neutron poison inner liner (HAC_MD&H)'
'actual vol.= 1.28314e4 cm3 = (7.83023e2 in3)(16.387064)'
'den.multiplier = 1.28314e4 cm3 (actual vol.) / 1.32708e4 cm3 (model vol.)'
'np277-4 min.den.= 1.526803 = (95.3157 lb/ft3)(453.59 g/lb)/(28316.84 cm3/ft3)'
'density = 1.476265 = (den.mult)(np277-4 min.den.) = 0.9668933*1.526803'
'use 75% of boron in calculations per NUREG-1609 Section 6.5.3.2'
arbmboron 7.06813e-2  2 0 0 0    5010   18.1479
                                 5011   81.8520   11  0.7500  293  end
arbmnpmx  1.03525e+0 10 0 0 0    6012    1.9188
                                 7014    0.0141
                                 8016   43.4254
                                11023    0.1174
                                12000    0.3378
                                13027   39.0477
                                14000    2.4671
                                16000    0.3083
                                20000   11.8335
                                26000    0.5298   11  1.0000  293  end
arbmnph2o 3.70316e-1  2 0 0 0    1001   11.1913
                                 8016   88.8087   11  1.0000  293  end
'kaolite 1600 body'
'nct.sing.unit.density= (den.mult)(min.den.)'
' for arbmh20k 0.52294 = 1.012373*0.51655, for rest 0.34864 = 1.012373*0.34438'
'den.mult= 1.36557e5 cm3 (actual vol.) / 1.34888e5 cm3 (model vol.)'
```

```
'actual vol.= 1.36557e5 cm3 = (28316.84 cm3/ft3)(108.33188 lb)/(22.464 lb/ft3)'
'hac.s.u.dens= (hac.mult)(nct.s.u.dens)'
'hac.mult = 1.34888e5 cm3 (nct vol.)/ 1.12246e5 cm3 (model vol.)'
' for arbmh2ok 0.62843 = 1.20172*0.52294,   for rest = 1.20172*0.34864'
'hac array densities are hac s.u.dens.'
arbmh2ok   0.62843  2 0 0 0    1001   11.1913
                                8016   88.8087   12  0.0287  293  end
arbmal2o3  0.41898  2 0 0 0   13027   52.9390
                                8016   47.0610   12  0.096   293  end
arbmsio2   0.41898  2 0 0 0   14000   46.7570
                                8016   53.2430   12  0.367   293  end
arbmfe2o3  0.41898  2 0 0 0   26000   69.9540
                                8016   30.0460   12  0.067   293  end
arbmtio2   0.41898  2 0 0 0   22000   59.9535
                                8016   40.0465   12  0.012   293  end
arbmcao    0.41898  2 0 0 0   20000   71.4815
                                8016   28.5185   12  0.307   293  end
arbmmgo    0.41898  2 0 0 0   12000   60.3169
                                8016   39.6831   12  0.131   293  end
arbmna2o   0.41898  2 0 0 0   11023   74.1961
                                8016   25.8039   12  0.020   293  end
'kaolite 1600 top plug'
'sing.unit.density= (den.mult)(min.den.)'
' for arbmh20k = 0.965246*0.51655,  for rest = 0.965246*0.34438'
'den.mult= 1.21592e4 cm3 (actual vol.) / 1.25970e4 cm3 (model vol.)'
'actual vol.= 1.21592e4 cm3 = (28316.84 cm3/ft3)(9.646 lb)/(22.464 lb/ft3)'
arbmh2ok   0.49860  2 0 0 0    1001   11.1913
                                8016   88.8087   13  0.0287  293  end
arbmal2o3  0.33241  2 0 0 0   13027   52.9390
                                8016   47.0610   13  0.096   293  end
arbmsio2   0.33241  2 0 0 0   14000   46.7570
                                8016   53.2430   13  0.367   293  end
arbmfe2o3  0.33241  2 0 0 0   26000   69.9540
                                8016   30.0460   13  0.067   293  end
arbmtio2   0.33241  2 0 0 0   22000   59.9535
                                8016   40.0465   13  0.012   293  end
arbmcao    0.33241  2 0 0 0   20000   71.4815
                                8016   28.5185   13  0.307   293  end
arbmmgo    0.33241  2 0 0 0   12000   60.3169
                                8016   39.6831   13  0.131   293  end
arbmna2o   0.33241  2 0 0 0   11023   74.1961
                                8016   25.8039   13  0.020   293  end
'silicone rubber pads'
arbmsiru   1.21791  4 0 0 0    6012   32.3767
                                1001    8.1573
                                8016   21.5782
                               14000   37.8878   14  1.0     293  end
'void space external to containment vessel'
arbmwecv   0.9982   2 0 0 0    1001   11.1913
                                8016   88.8087   15  0.0001  293  end
'steel: liner'
ss304                                           16  1.0     293  end
'steel: plug cover (pc) use 9.907 lb'
ss304                                           17  1.06388 293  end
'steel: angle iron (ai) for HAC'
'nct density is multiplied by volume fraction 7.08030/5.74516 for HAC'
ss304                                           18  1.23239 293  end
'steel: drum steel for HAC'
'nct density is multiplied by volume fraction 3.20482/2.95645 for HAC'
ss304                                           19  1.08401 293  end
'void space external to drum'
arbmwed    0.9982   2 0 0 0    1001   11.1913
                                8016   88.8087   20  0.0001  293  end
'reflective water'
arbmh20r   0.9982   2 0 0 0    1001   11.1913
                                8016   88.8087   21  1.0     293  end
end comp
more data dab=400 end
hctf5bmt12,1.4in thk np,24968.9gU(24968.9g235, 8258.4gH2O,hx=  8.63),fr=1.0e-04
read parameters nub=yes npg=2500 gen=215 nsk=15 tme=100 nb8=400 end parameters
read boun       all=specular                    end boun
```

```
read geometry
unit 1001
'drum bottom flat cover [Elev= 0.105 in. at top of unit]'
'zhemicyl-y  19 1   21.838092    0.26620   0.00050 com='extend radius not used'
 zhemicyl-y  19 1   21.838092    0.26620   0.00050 com='drum bottom flat cover'
unit 1002
'above drum bottom flat cover and below containment vessel [Elev= 4.670 in.]'
 zhemicyl-y  15 1    3.175000   11.59460  11.16330 com='void in pad-1'
 zhemicyl-y  14 1    7.924800   11.59460  11.16330 com='pad-1'
 zhemicyl-y  16 1    8.077200   11.59460  11.16330 com='np277_4 liner'
 zhemicyl-y  11 1   10.922000   11.59460  11.16330 com='np277_4'
 zhemicyl-y  16 1   11.074400   11.59460  10.85850 com='kaolite liner bottom'
 zhemicyl-y  12 1   21.685692   11.59460   0.00050 com='kaolite'
 zhemicyl-y  19 1   21.838092   11.59460   0.00050 com='drum'
unit 1003
'cv bottom [Elev= 4.920 in.]'
 zhemicyl-y  8  1    6.680200    0.63450   0.00050 com='cv bottom'
 zhemicyl-y  15 1    7.924800    0.63450   0.00050 com='void btw cv-np liner'
 zhemicyl-y  16 1    8.077200    0.63450   0.00050 com='np277_4 liner'
 zhemicyl-y  11 1   10.922000    0.63450   0.00050 com='np277_4'
 zhemicyl-y  16 1   11.074400    0.63450   0.00050 com='kaolite liner'
 zhemicyl-y  12 1   21.685692    0.63450   0.00050 com='kaolite'
 zhemicyl-y  19 1   21.838092    0.63450   0.00050 com='drum'
unit 1004
'cubical content, stacked per cc'
'    9.08802     3.57796 lattice width-depth'
'    2.54000     1.00000 cube dimension'
'    1.27000     0.50000 cube half-dimension'
'   16.38706     1.00000 volume of HEU cube in unit cell'
'  308.25850             HEU mass one cube'
'   27                   number of HEU cubes per can'
' 8322.97957             HEU mass of cubes in cc'
'    3           3       number of cubes in -x direction'
'    3           3       number of cubes in -y direction'
'    9           9       number of HEU cubes in a layer'
'    4    VARIABLE       number of HEU layers in z-axis'
'    0    VARIABLE       number of HEU cubes in top layer modulus(Z%N)'
'    9    VARIABLE       number of HEU voids in top layer'
'    ara=1 nux=3 nuy=3 nuz=4   fill 27r1004  9r1005      end fill'
'    0.48924     0.19261 gap dimension                       CALCULATED
'    3.02924     1.19261 unit cell dimension                 CALCULATED
'    1.51462     0.59631 unit cell half-dimension            CALCULATED
'   27.79719     1.69629 volume of unit cell                 CALCULATED
'   11.41013     0.69629 volume of water gap in unit cell    CALCULATED
' 1000.69893             lattice volume in cc                CALCULATED
'  558.24820             moderator volume in lattice in cc   CALCULATED
'  442.45073             HEU volume in lattice in cc         CALCULATED
'    0.13826             volume fraction of HEU in CV        CALCULATED
'    0.86019             bulk dens of water in CV            CALCULATED
 cuboid    1  1  6p1.51452                      com='unit cell'
unit 1005
'cubical void, filler for layers'
 cuboid    1  1  6p1.51452                      com='unit cell'
unit 1006
'content (collapsed) [Elev= 9.691 in.]'
' 4.54386     1.78892 half width-depth lattice            CALCULATED'
'12.11696             height lattice                      CALCULATED'
'array 1         2r-4.54386      0.0'
 cuboid  1  1  2p4.54386 0.0 -4.54386 12.1169 0.0005 com='homog. content-array'
 zhemicyl-y  1  1    6.426200   12.11696   0.00050 com='cv well cavity'
 zhemicyl-y  8  1    6.680200   12.11696   0.00050 com='cv below 1st step'
 zhemicyl-y  15 1    7.924800   12.11696   0.00050 com='void btw cv-np liner'
 zhemicyl-y  16 1    8.077200   12.11696   0.00050 com='np277_4 liner'
 zhemicyl-y  11 1   10.922000   12.11696   0.00050 com='np277_4'
 zhemicyl-y  16 1   11.074400   12.11696   0.00050 com='kaolite liner'
 zhemicyl-y  12 1   21.685692   12.11696   0.00050 com='kaolite'
 zhemicyl-y  19 1   21.838092   12.11696   0.00050 com='drum'
unit 1007
'np277_4 spacer [Elev=11.091 in.]'
 zhemicyl-y  2  1    5.24510     3.55660   0.00050 com='np spacer'
 zhemicyl-y  1  1    6.426200    3.55660   0.00050 com='cv well cavity'
```

```
 zhemicyl-y  8  1    6.680200    3.55660   0.00050 com='cv below 1st step'
 zhemicyl-y  15 1    7.924800    3.55660   0.00050 com='void btw cv-np liner'
 zhemicyl-y  16 1    8.077200    3.55660   0.00050 com='np277_4 liner'
 zhemicyl-y  11 1   10.922000    3.55660   0.00050 com='np277_4'
 zhemicyl-y  16 1   11.074400    3.55660   0.00050 com='kaolite liner'
 zhemicyl-y  12 1   21.685692    3.55660   0.00050 com='kaolite'
 zhemicyl-y  19 1   21.838092    3.55660   0.00050 com='drum'
unit 1008
'top of content stack to bottom of 1st step [Elev=35.270 in.]'
'43.46828             stack height (content spacers)       CALCULATED
 zhemicyl-y  1  1    6.426200   33.62022   0.00050 com='cv well cavity'
 zhemicyl-y  8  1    6.680200   33.62022   0.00050 com='cv below 1st step'
 zhemicyl-y  15 1    7.924800   33.62022   0.00050 com='void btw cv-np liner'
 zhemicyl-y  16 1    8.077200   33.62022   0.00050 com='np277_4 liner'
 zhemicyl-y  11 1   10.922000   33.62022   0.00050 com='np277_4'
 zhemicyl-y  16 1   11.074400   33.62022   0.00050 com='kaolite liner'
 zhemicyl-y  12 1   21.685692   33.62022   0.00050 com='kaolite'
 zhemicyl-y  19 1   21.838092   33.62022   0.00050 com='drum'
unit 1010
'cv at 1st step in liner [Elev=35.330 in.]'
 zhemicyl-y  1  1    6.426200    0.15190   0.00050 com='cv well cavity'
 zhemicyl-y  8  1    6.680200    0.15190   0.00050 com='cv at 1st step'
 zhemicyl-y  15 1    7.924800    0.15190   0.00050 com='void btw cv and liner'
 zhemicyl-y  16 1   11.074400    0.15190   0.00050 com='liner 1st step'
 zhemicyl-y  12 1   21.685692    0.15190   0.00050 com='kaolite'
 zhemicyl-y  19 1   21.838092    0.15190   0.00050 com='drum'
unit 1011
'vertical gap between 1st step in liner and cv flange [Elev=35.420 in.]'
 zhemicyl-y  1  1    6.426200    0.22810   0.00050 com='cv well cavity'
 zhemicyl-y  8  1    6.680200    0.22810   0.00050 com='cv gap btw step-flng'
 zhemicyl-y  15 1   10.922000    0.22810   0.00050 com='void btw cv and liner'
 zhemicyl-y  16 1   11.074400    0.22810   0.00050 com='liner wall'
 zhemicyl-y  12 1   21.685692    0.22810   0.00050 com='kaolite'
 zhemicyl-y  19 1   21.838092    0.22810   0.00050 com='drum'
unit 1012
'cv flange to top of cv well [Elev=35.920 in.]'
 zhemicyl-y  1  1    6.426200    1.26950   0.00050 com='cavity'
 zhemicyl-y  9  1    9.525000    1.26950   0.00050 com='flange to top of well'
 zhemicyl-y  15 1    9.525000    1.26950   0.00050 com='void btw cv and pad-2'
 zhemicyl-y  14 1   10.033000    1.26950   0.00050 com='pad-2'
 zhemicyl-y  15 1   10.922000    1.26950   0.00050 com='void btw cv and liner'
 zhemicyl-y  16 1   11.074400    1.26950   0.00050 com='liner wall'
 zhemicyl-y  12 1   21.685692    1.26950   0.00050 com='kaolite'
 zhemicyl-y  19 1   21.838092    1.26950   0.00050 com='drum'
unit 1013
'cv flange above cv well [Elev=37.070 in.]'
 zhemicyl-y  10 1    9.525000    2.92050   0.00050 com='flange above cv well'
 zhemicyl-y  15 1    9.525000    2.92050   0.00050 com='void btw cv and pad-2'
 zhemicyl-y  14 1   10.033000    2.92050   0.00050 com='pad-2'
 zhemicyl-y  15 1   10.922000    2.92050   0.00050 com='void btw pad2-liner'
 zhemicyl-y  16 1   11.074400    2.92050   0.00050 com='liner wall'
 zhemicyl-y  12 1   21.685692    2.92050   0.00050 com='kaolite'
 zhemicyl-y  19 1   21.838092    2.92050   0.00050 com='drum'
unit 1014
'plugpad2 below liner 2nd step [Elev=37.470 in.]'
 zhemicyl-y  14 1   10.033000    0.76150   0.00050 com='pad-2'
 zhemicyl-y  15 1   10.922000    1.01550   0.00050 com='void btw pad2-liner'
 zhemicyl-y  16 1   11.074400    1.01550   0.00050 com='liner wall'
 zhemicyl-y  12 1   21.685692    1.01550   0.00050 com='kaolite'
 zhemicyl-y  19 1   21.838092    1.01550   0.00050 com='drum'
unit 1015
'2nd step in liner [Elev=37.530 in.]'
 zhemicyl-y  15 1   10.922000    0.15190   0.00050 com='void abv pad2'
 zhemicyl-y  16 1   18.757900    0.15190   0.00050 com='liner 2nd step'
 zhemicyl-y  12 1   21.685692    0.15190   0.00050 com='kaolite'
 zhemicyl-y  19 1   21.838092    0.15190   0.00050 com='drum'
unit 1016
'abv 2nd step in liner to bottom of angle iron [Elev=40.750 in.]'
 zhemicyl-y  13 1   18.097500    8.17830   0.49276 com='plug kaolite'
 zhemicyl-y  17 1   18.249900    8.17830   0.34036 com='sides of plug case'
 zhemicyl-y  15 1   18.605500    8.17830   0.00050 com='void: plug to liner'
```

```
 zhemicyl-y  16 1   18.757900    8.17830   0.00050 com='liner wall'
 zhemicyl-y  12 1   21.685692    8.17830   0.00050 com='kaolite'
 zhemicyl-y  19 1   21.838092    8.17830   0.00050 com='drum'
unit 1017
'bottom of angle iron to bend in angle iron [Elev=42.500 in.]'
 zhemicyl-y  13 1   18.097500    4.44450   0.00050 com='plug kaolite'
 zhemicyl-y  17 1   18.249900    4.44450   0.00050 com='sides of plug case'
 zhemicyl-y  15 1   18.605500    4.44450   0.00050 com='void: plug to liner'
 zhemicyl-y  16 1   18.757900    4.44450   0.00050 com='liner wall'
 zhemicyl-y  18 1   19.392900    4.44450   0.00050 com='lower angle iron'
 zhemicyl-y  12 1   21.685692    4.44450   0.00050 com='kaolite'
 zhemicyl-y  19 1   21.838092    4.44450   0.00050 com='drum'
unit 1018
'bend in angle iron to top of angle iron [Elev=42.750 in.]'
 zhemicyl-y  13 1   18.097500    0.11126   0.00050 com='plug kaolite'
 zhemicyl-y  17 1   18.249900    0.26366   0.00050 com='sides of plug case'
 zhemicyl-y  15 1   18.605500    0.63450   0.00050 com='void: plug to liner'
 zhemicyl-y  16 1   18.757900    0.63450   0.00050 com='liner wall'
 zhemicyl-y  18 1   21.685692    0.63450   0.00050 com='bend section of ai'
 zhemicyl-y  19 1   21.838092    0.63450   0.00050 com='drum'
unit 1019
'drum lid and lip [Elev=43.500 in.]'
 zhemicyl-y  20 1   21.469792    1.90450   0.15240 com='void above lid'
 zhemicyl-y  19 1   21.622192    1.90450   0.00050 com='drum lid'
 zhemicyl-y  20 1   21.685692    1.90450   0.00050 com='void btw lid-drumwall'
 zhemicyl-y  19 1   21.838092    1.90450   0.00050 com='drum'
unit 2001
'drum bottom flat cover [Elev= 0.105 in. at top of unit]'
'zhemicyl+y  19 1   21.838092    0.26620   0.00050 com='extended radius not used'
 zhemicyl+y  19 1   21.838092    0.26620   0.00050 com='drum bottom flat cover'
unit 2002
'above drum bottom flat cover and below containment vessel [Elev= 4.670 in.]'
 zhemicyl+y  15 1    3.175000   11.59460  11.16330 com='void in pad-1'
 zhemicyl+y  14 1    7.924800   11.59460  11.16330 com='pad-1'
 zhemicyl+y  16 1    8.077200   11.59460  11.16330 com='np277_4 liner'
 zhemicyl+y  11 1   10.922000   11.59460  11.16330 com='np277_4'
 zhemicyl+y  16 1   11.074400   11.59460  10.85850 com='kaolite liner bottom'
 zhemicyl+y  12 1   21.685692   11.59460   0.00050 com='kaolite'
 zhemicyl+y  19 1   21.838092   11.59460   0.00050 com='drum'
unit 2003
'cv bottom [Elev= 4.920 in.]'
 zhemicyl+y  8  1    6.680200    0.63450   0.00050 com='cv bottom'
 zhemicyl+y  15 1    7.924800    0.63450   0.00050 com='void btw cv-np liner'
 zhemicyl+y  16 1    8.077200    0.63450   0.00050 com='np277_4 liner'
 zhemicyl+y  11 1   10.922000    0.63450   0.00050 com='np277_4'
 zhemicyl+y  16 1   11.074400    0.63450   0.00050 com='kaolite liner'
 zhemicyl+y  12 1   21.685692    0.63450   0.00050 com='kaolite'
 zhemicyl+y  19 1   21.838092    0.63450   0.00050 com='drum'
unit 2006
'content (collapsed) [Elev= 9.691 in.]'
 zhemicyl+y  1  1    6.426200   12.11696   0.00050 com='cv well cavity'
 zhemicyl+y  8  1    6.680200   12.11696   0.00050 com='cv below 1st step'
 zhemicyl+y  15 1    7.924800   12.11696   0.00050 com='void btw cv-np liner'
 zhemicyl+y  16 1    8.077200   12.11696   0.00050 com='np277_4 liner'
 zhemicyl+y  11 1   10.922000   12.11696   0.00050 com='np277_4'
 zhemicyl+y  16 1   11.074400   12.11696   0.00050 com='kaolite liner'
 zhemicyl+y  12 1   21.685692   12.11696   0.00050 com='kaolite'
 zhemicyl+y  19 1   21.838092   12.11696   0.00050 com='drum'
unit 2007
'np277_4 spacer [Elev=11.091 in.]'
 zhemicyl+y  2  1    5.24510     3.55660   0.00050 com='np spacer'
 zhemicyl+y  1  1    6.426200    3.55660   0.00050 com='cv well cavity'
 zhemicyl+y  8  1    6.680200    3.55660   0.00050 com='cv below 1st step'
 zhemicyl+y  15 1    7.924800    3.55660   0.00050 com='void btw cv-np liner'
 zhemicyl+y  16 1    8.077200    3.55660   0.00050 com='np277_4 liner'
 zhemicyl+y  11 1   10.922000    3.55660   0.00050 com='np277_4'
 zhemicyl+y  16 1   11.074400    3.55660   0.00050 com='kaolite liner'
 zhemicyl+y  12 1   21.685692    3.55660   0.00050 com='kaolite'
 zhemicyl+y  19 1   21.838092    3.55660   0.00050 com='drum'
unit 2008
'top of content stack to bottom of 1st step [Elev=35.270 in.]'
```

```
 zhemicyl+y  1  1    6.426200   33.62022   0.00050 com='cv well cavity'
 zhemicyl+y  8  1    6.680200   33.62022   0.00050 com='cv below 1st step'
 zhemicyl+y  15 1    7.924800   33.62022   0.00050 com='void btw cv-np liner'
 zhemicyl+y  16 1    8.077200   33.62022   0.00050 com='np277_4 liner'
 zhemicyl+y  11 1   10.922000   33.62022   0.00050 com='np277_4'
 zhemicyl+y  16 1   11.074400   33.62022   0.00050 com='kaolite liner'
 zhemicyl+y  12 1   21.685692   33.62022   0.00050 com='kaolite'
 zhemicyl+y  19 1   21.838092   33.62022   0.00050 com='drum'
unit 2010
'cv at 1st step in liner [Elev=35.330 in.]'
 zhemicyl+y  1  1    6.426200    0.15190   0.00050 com='cv well cavity'
 zhemicyl+y  8  1    6.680200    0.15190   0.00050 com='cv at 1st step'
 zhemicyl+y  15 1    7.924800    0.15190   0.00050 com='void btw cv and liner'
 zhemicyl+y  16 1   11.074400    0.15190   0.00050 com='liner 1st step'
 zhemicyl+y  12 1   21.685692    0.15190   0.00050 com='kaolite'
 zhemicyl+y  19 1   21.838092    0.15190   0.00050 com='drum'
unit 2011
'vertical gap between 1st step in liner and cv flange [Elev=35.420 in.]'
 zhemicyl+y  1  1    6.426200    0.22810   0.00050 com='cv well cavity'
 zhemicyl+y  8  1    6.680200    0.22810   0.00050 com='cv gap btw step-flng'
 zhemicyl+y  15 1   10.922000    0.22810   0.00050 com='void btw cv and liner'
 zhemicyl+y  16 1   11.074400    0.22810   0.00050 com='liner wall'
 zhemicyl+y  12 1   21.685692    0.22810   0.00050 com='kaolite'
 zhemicyl+y  19 1   21.838092    0.22810   0.00050 com='drum'
unit 2012
'cv flange to top of cv well [Elev=35.920 in.]'
 zhemicyl+y  1  1    6.426200    1.26950   0.00050 com='cavity'
 zhemicyl+y  9  1    9.525000    1.26950   0.00050 com='flange to top of well'
 zhemicyl+y  15 1    9.525000    1.26950   0.00050 com='void btw cv and pad-2'
 zhemicyl+y  14 1   10.033000    1.26950   0.00050 com='pad-2'
 zhemicyl+y  15 1   10.922000    1.26950   0.00050 com='void btw cv and liner'
 zhemicyl+y  16 1   11.074400    1.26950   0.00050 com='liner wall'
 zhemicyl+y  12 1   21.685692    1.26950   0.00050 com='kaolite'
 zhemicyl+y  19 1   21.838092    1.26950   0.00050 com='drum'
unit 2013
'cv flange above cv well [Elev=37.070 in.]'
 zhemicyl+y  10 1    9.525000    2.92050   0.00050 com='flange above cv well'
 zhemicyl+y  15 1    9.525000    2.92050   0.00050 com='void btw cv and pad-2'
 zhemicyl+y  14 1   10.033000    2.92050   0.00050 com='pad-2'
 zhemicyl+y  15 1   10.922000    2.92050   0.00050 com='void btw pad2-liner'
 zhemicyl+y  16 1   11.074400    2.92050   0.00050 com='liner wall'
 zhemicyl+y  12 1   21.685692    2.92050   0.00050 com='kaolite'
 zhemicyl+y  19 1   21.838092    2.92050   0.00050 com='drum'
unit 2014
'plugpad2 below liner 2nd step [Elev=37.470 in.]'
 zhemicyl+y  14 1   10.033000    0.76150   0.00050 com='pad-2'
 zhemicyl+y  15 1   10.922000    1.01550   0.00050 com='void btw pad2-liner'
 zhemicyl+y  16 1   11.074400    1.01550   0.00050 com='liner wall'
 zhemicyl+y  12 1   21.685692    1.01550   0.00050 com='kaolite'
 zhemicyl+y  19 1   21.838092    1.01550   0.00050 com='drum'
unit 2015
'2nd step in liner [Elev=37.530 in.]'
 zhemicyl+y  15 1   10.922000    0.15190   0.00050 com='void abv pad2'
 zhemicyl+y  16 1   18.757900    0.15190   0.00050 com='liner 2nd step'
 zhemicyl+y  12 1   21.685692    0.15190   0.00050 com='kaolite'
 zhemicyl+y  19 1   21.838092    0.15190   0.00050 com='drum'
unit 2016
'abv 2nd step in liner to bottom of angle iron [Elev=40.750 in.]'
 zhemicyl+y  13 1   18.097500    8.17830   0.49276 com='plug kaolite'
 zhemicyl+y  17 1   18.249900    8.17830   0.34036 com='sides of plug case'
 zhemicyl+y  15 1   18.605500    8.17830   0.00050 com='void: plug to liner'
 zhemicyl+y  16 1   18.757900    8.17830   0.00050 com='liner wall'
 zhemicyl+y  12 1   21.685692    8.17830   0.00050 com='kaolite'
 zhemicyl+y  19 1   21.838092    8.17830   0.00050 com='drum'
unit 2017
'bottom of angle iron to bend in angle iron [Elev=42.500 in.]'
 zhemicyl+y  13 1   18.097500    4.44450   0.00050 com='plug kaolite'
 zhemicyl+y  17 1   18.249900    4.44450   0.00050 com='sides of plug case'
 zhemicyl+y  15 1   18.605500    4.44450   0.00050 com='void: plug to liner'
 zhemicyl+y  16 1   18.757900    4.44450   0.00050 com='liner wall'
 zhemicyl+y  18 1   19.392900    4.44450   0.00050 com='lower angle iron'
```

```
 zhemicyl+y  12 1   21.685692    4.44450   0.00050 com='kaolite'
 zhemicyl+y  19 1   21.838092    4.44450   0.00050 com='drum'
unit 2018
'bend in angle iron to top of angle iron [Elev=42.750 in.]'
 zhemicyl+y  13 1   18.097500    0.11126   0.00050 com='plug kaolite'
 zhemicyl+y  17 1   18.249900    0.26366   0.00050 com='sides of plug case'
 zhemicyl+y  15 1   18.605500    0.63450   0.00050 com='void: plug to liner'
 zhemicyl+y  16 1   18.757900    0.63450   0.00050 com='liner wall'
 zhemicyl+y  18 1   21.685692    0.63450   0.00050 com='bend section of ai'
 zhemicyl+y  19 1   21.838092    0.63450   0.00050 com='drum'
unit 2019
'drum lid and lip [Elev=43.500 in.]'
 zhemicyl+y  20 1   21.469792    1.90450   0.15240 com='void above lid'
 zhemicyl+y  19 1   21.622192    1.90450   0.00050 com='drum lid'
 zhemicyl+y  20 1   21.685692    1.90450   0.00050 com='void btw lid-drumwall'
 zhemicyl+y  19 1   21.838092    1.90450   0.00050 com='drum'
unit 3001
'drum bottom flat cover [Elev= 0.105 in. at top of unit]'
'zhemicyl-x  19 1   21.838092    0.26620   0.00050 com='extended radius not used'
 zhemicyl-x  19 1   21.838092    0.26620   0.00050 com='drum bottom flat cover'
unit 3002
'above drum bottom flat cover and below containment vessel [Elev= 4.670 in.]'
 zhemicyl-x  15 1    3.175000   11.59460  11.16330 com='void in pad-1'
 zhemicyl-x  14 1    7.924800   11.59460  11.16330 com='pad-1'
 zhemicyl-x  16 1    8.077200   11.59460  11.16330 com='np277_4 liner'
 zhemicyl-x  11 1   10.922000   11.59460  11.16330 com='np277_4'
 zhemicyl-x  16 1   11.074400   11.59460  10.85850 com='kaolite liner bottom'
 zhemicyl-x  12 1   21.685692   11.59460   0.00050 com='kaolite'
 zhemicyl-x  19 1   21.838092   11.59460   0.00050 com='drum'
unit 3003
'cv bottom [Elev= 4.920 in.]'
 zhemicyl-x  8  1    6.680200    0.63450   0.00050 com='cv bottom'
 zhemicyl-x  15 1    7.924800    0.63450   0.00050 com='void btw cv-np liner'
 zhemicyl-x  16 1    8.077200    0.63450   0.00050 com='np277_4 liner'
 zhemicyl-x  11 1   10.922000    0.63450   0.00050 com='np277_4'
 zhemicyl-x  16 1   11.074400    0.63450   0.00050 com='kaolite liner'
 zhemicyl-x  12 1   21.685692    0.63450   0.00050 com='kaolite'
 zhemicyl-x  19 1   21.838092    0.63450   0.00050 com='drum'
unit 3006
'content (collapsed) [Elev= 9.691 in.]'
 zhemicyl-x  1  1    6.426200   12.11696   0.00050 com='cv well cavity'
 zhemicyl-x  8  1    6.680200   12.11696   0.00050 com='cv below 1st step'
 zhemicyl-x  15 1    7.924800   12.11696   0.00050 com='void btw cv-np liner'
 zhemicyl-x  16 1    8.077200   12.11696   0.00050 com='np277_4 liner'
 zhemicyl-x  11 1   10.922000   12.11696   0.00050 com='np277_4'
 zhemicyl-x  16 1   11.074400   12.11696   0.00050 com='kaolite liner'
 zhemicyl-x  12 1   21.685692   12.11696   0.00050 com='kaolite'
 zhemicyl-x  19 1   21.838092   12.11696   0.00050 com='drum'
unit 3007
'np277_4 spacer [Elev=11.091 in.]'
 zhemicyl-x  2  1    5.24510     3.55660   0.00050 com='np spacer'
 zhemicyl-x  1  1    6.426200    3.55660   0.00050 com='cv well cavity'
 zhemicyl-x  8  1    6.680200    3.55660   0.00050 com='cv below 1st step'
 zhemicyl-x  15 1    7.924800    3.55660   0.00050 com='void btw cv-np liner'
 zhemicyl-x  16 1    8.077200    3.55660   0.00050 com='np277_4 liner'
 zhemicyl-x  11 1   10.922000    3.55660   0.00050 com='np277_4'
 zhemicyl-x  16 1   11.074400    3.55660   0.00050 com='kaolite liner'
 zhemicyl-x  12 1   21.685692    3.55660   0.00050 com='kaolite'
 zhemicyl-x  19 1   21.838092    3.55660   0.00050 com='drum'
unit 3008
'top of content stack to bottom of 1st step [Elev=35.270 in.]'
 zhemicyl-x  1  1    6.426200   33.62022   0.00050 com='cv well cavity'
 zhemicyl-x  8  1    6.680200   33.62022   0.00050 com='cv below 1st step'
 zhemicyl-x  15 1    7.924800   33.62022   0.00050 com='void btw cv-np liner'
 zhemicyl-x  16 1    8.077200   33.62022   0.00050 com='np277_4 liner'
 zhemicyl-x  11 1   10.922000   33.62022   0.00050 com='np277_4'
 zhemicyl-x  16 1   11.074400   33.62022   0.00050 com='kaolite liner'
 zhemicyl-x  12 1   21.685692   33.62022   0.00050 com='kaolite'
 zhemicyl-x  19 1   21.838092   33.62022   0.00050 com='drum'
unit 3010
'cv at 1st step in liner [Elev=35.330 in.]'
```

```
 zhemicyl-x  1  1    6.426200    0.15190   0.00050 com='cv well cavity'
 zhemicyl-x  8  1    6.680200    0.15190   0.00050 com='cv at 1st step'
 zhemicyl-x  15 1    7.924800    0.15190   0.00050 com='void btw cv and liner'
 zhemicyl-x  16 1   11.074400    0.15190   0.00050 com='liner 1st step'
 zhemicyl-x  12 1   21.685692    0.15190   0.00050 com='kaolite'
 zhemicyl-x  19 1   21.838092    0.15190   0.00050 com='drum'
unit 3011
'vertical gap between 1st step in liner and cv flange [Elev=35.420 in.]'
 zhemicyl-x  1  1    6.426200    0.22810   0.00050 com='cv well cavity'
 zhemicyl-x  8  1    6.680200    0.22810   0.00050 com='cv gap btw step-flng'
 zhemicyl-x  15 1   10.922000    0.22810   0.00050 com='void btw cv and liner'
 zhemicyl-x  16 1   11.074400    0.22810   0.00050 com='liner wall'
 zhemicyl-x  12 1   21.685692    0.22810   0.00050 com='kaolite'
 zhemicyl-x  19 1   21.838092    0.22810   0.00050 com='drum'
unit 3012
'cv flange to top of cv well [Elev=35.920 in.]'
 zhemicyl-x  1  1    6.426200    1.26950   0.00050 com='cavity'
 zhemicyl-x  9  1    9.525000    1.26950   0.00050 com='flange to top of well'
 zhemicyl-x  15 1    9.525000    1.26950   0.00050 com='void btw cv and pad-2'
 zhemicyl-x  14 1   10.033000    1.26950   0.00050 com='pad-2'
 zhemicyl-x  15 1   10.922000    1.26950   0.00050 com='void btw cv and liner'
 zhemicyl-x  16 1   11.074400    1.26950   0.00050 com='liner wall'
 zhemicyl-x  12 1   21.685692    1.26950   0.00050 com='kaolite'
 zhemicyl-x  19 1   21.838092    1.26950   0.00050 com='drum'
unit 3013
'cv flange above cv well [Elev=37.070 in.]'
 zhemicyl-x  10 1    9.525000    2.92050   0.00050 com='flange above cv well'
 zhemicyl-x  15 1    9.525000    2.92050   0.00050 com='void btw cv and pad-2'
 zhemicyl-x  14 1   10.033000    2.92050   0.00050 com='pad-2'
 zhemicyl-x  15 1   10.922000    2.92050   0.00050 com='void btw pad2-liner'
 zhemicyl-x  16 1   11.074400    2.92050   0.00050 com='liner wall'
 zhemicyl-x  12 1   21.685692    2.92050   0.00050 com='kaolite'
 zhemicyl-x  19 1   21.838092    2.92050   0.00050 com='drum'
unit 3014
'plugpad2 below liner 2nd step [Elev=37.470 in.]'
 zhemicyl-x  14 1   10.033000    0.76150   0.00050 com='pad-2'
 zhemicyl-x  15 1   10.922000    1.01550   0.00050 com='void btw pad2-liner'
 zhemicyl-x  16 1   11.074400    1.01550   0.00050 com='liner wall'
 zhemicyl-x  12 1   21.685692    1.01550   0.00050 com='kaolite'
 zhemicyl-x  19 1   21.838092    1.01550   0.00050 com='drum'
unit 3015
'2nd step in liner [Elev=37.530 in.]'
 zhemicyl-x  15 1   10.922000    0.15190   0.00050 com='void abv pad2'
 zhemicyl-x  16 1   18.757900    0.15190   0.00050 com='liner 2nd step'
 zhemicyl-x  12 1   21.685692    0.15190   0.00050 com='kaolite'
 zhemicyl-x  19 1   21.838092    0.15190   0.00050 com='drum'
unit 3016
'abv 2nd step in liner to bottom of angle iron [Elev=40.750 in.]'
 zhemicyl-x  13 1   18.097500    8.17830   0.49276 com='plug kaolite'
 zhemicyl-x  17 1   18.249900    8.17830   0.34036 com='sides of plug case'
 zhemicyl-x  15 1   18.605500    8.17830   0.00050 com='void: plug to liner'
 zhemicyl-x  16 1   18.757900    8.17830   0.00050 com='liner wall'
 zhemicyl-x  12 1   21.685692    8.17830   0.00050 com='kaolite'
 zhemicyl-x  19 1   21.838092    8.17830   0.00050 com='drum'
unit 3017
'bottom of angle iron to bend in angle iron [Elev=42.500 in.]'
 zhemicyl-x  13 1   18.097500    4.44450   0.00050 com='plug kaolite'
 zhemicyl-x  17 1   18.249900    4.44450   0.00050 com='sides of plug case'
 zhemicyl-x  15 1   18.605500    4.44450   0.00050 com='void: plug to liner'
 zhemicyl-x  16 1   18.757900    4.44450   0.00050 com='liner wall'
 zhemicyl-x  18 1   19.392900    4.44450   0.00050 com='lower angle iron'
 zhemicyl-x  12 1   21.685692    4.44450   0.00050 com='kaolite'
 zhemicyl-x  19 1   21.838092    4.44450   0.00050 com='drum'
unit 3018
'bend in angle iron to top of angle iron [Elev=42.750 in.]'
 zhemicyl-x  13 1   18.097500    0.11126   0.00050 com='plug kaolite'
 zhemicyl-x  17 1   18.249900    0.26366   0.00050 com='sides of plug case'
 zhemicyl-x  15 1   18.605500    0.63450   0.00050 com='void: plug to liner'
 zhemicyl-x  16 1   18.757900    0.63450   0.00050 com='liner wall'
 zhemicyl-x  18 1   21.685692    0.63450   0.00050 com='bend section of ai'
 zhemicyl-x  19 1   21.838092    0.63450   0.00050 com='drum'
```

```
unit 3019
'drum lid and lip [Elev=43.500 in.]'
 zhemicyl-x  20 1   21.469792    1.90450   0.15240 com='void above lid'
 zhemicyl-x  19 1   21.622192    1.90450   0.00050 com='drum lid'
 zhemicyl-x  20 1   21.685692    1.90450   0.00050 com='void btw lid-drumwall'
 zhemicyl-x  19 1   21.838092    1.90450   0.00050 com='drum'
unit 4001
'drum bottom flat cover [Elev= 0.105 in. at top of unit]'
'zhemicyl+x  19 1   21.838092    0.26620   0.00050 com='extended radius not used'
 zhemicyl+x  19 1   21.838092    0.26620   0.00050 com='drum bottom flat cover'
unit 4002
'above drum bottom flat cover and below containment vessel [Elev= 4.670 in.]'
 zhemicyl+x  15 1    3.175000   11.59460  11.16330 com='void in pad-1'
 zhemicyl+x  14 1    7.924800   11.59460  11.16330 com='pad-1'
 zhemicyl+x  16 1    8.077200   11.59460  11.16330 com='np277_4 liner'
 zhemicyl+x  11 1   10.922000   11.59460  11.16330 com='np277_4'
 zhemicyl+x  16 1   11.074400   11.59460  10.85850 com='kaolite liner bottom'
 zhemicyl+x  12 1   21.685692   11.59460   0.00050 com='kaolite'
 zhemicyl+x  19 1   21.838092   11.59460   0.00050 com='drum'
unit 4003
'cv bottom [Elev= 4.920 in.]'
 zhemicyl+x  8  1    6.680200    0.63450   0.00050 com='cv bottom'
 zhemicyl+x  15 1    7.924800    0.63450   0.00050 com='void btw cv-np liner'
 zhemicyl+x  16 1    8.077200    0.63450   0.00050 com='np277_4 liner'
 zhemicyl+x  11 1   10.922000    0.63450   0.00050 com='np277_4'
 zhemicyl+x  16 1   11.074400    0.63450   0.00050 com='kaolite liner'
 zhemicyl+x  12 1   21.685692    0.63450   0.00050 com='kaolite'
 zhemicyl+x  19 1   21.838092    0.63450   0.00050 com='drum'
unit 4006
'content (collapsed) [Elev= 9.691 in.]'
 zhemicyl+x  1  1    6.426200   12.11696   0.00050 com='cv well cavity'
 zhemicyl+x  8  1    6.680200   12.11696   0.00050 com='cv below 1st step'
 zhemicyl+x  15 1    7.924800   12.11696   0.00050 com='void btw cv-np liner'
 zhemicyl+x  16 1    8.077200   12.11696   0.00050 com='np277_4 liner'
 zhemicyl+x  11 1   10.922000   12.11696   0.00050 com='np277_4'
 zhemicyl+x  16 1   11.074400   12.11696   0.00050 com='kaolite liner'
 zhemicyl+x  12 1   21.685692   12.11696   0.00050 com='kaolite'
 zhemicyl+x  19 1   21.838092   12.11696   0.00050 com='drum'
unit 4007
'np277_4 spacer [Elev=11.091 in.]'
 zhemicyl+x  2  1    5.24510     3.55660   0.00050 com='np spacer'
 zhemicyl+x  1  1    6.426200    3.55660   0.00050 com='cv well cavity'
 zhemicyl+x  8  1    6.680200    3.55660   0.00050 com='cv below 1st step'
 zhemicyl+x  15 1    7.924800    3.55660   0.00050 com='void btw cv-np liner'
 zhemicyl+x  16 1    8.077200    3.55660   0.00050 com='np277_4 liner'
 zhemicyl+x  11 1   10.922000    3.55660   0.00050 com='np277_4'
 zhemicyl+x  16 1   11.074400    3.55660   0.00050 com='kaolite liner'
 zhemicyl+x  12 1   21.685692    3.55660   0.00050 com='kaolite'
 zhemicyl+x  19 1   21.838092    3.55660   0.00050 com='drum'
unit 4008
'top of content stack to bottom of 1st step [Elev=35.270 in.]'
 zhemicyl+x  1  1    6.426200   33.62022   0.00050 com='cv well cavity'
 zhemicyl+x  8  1    6.680200   33.62022   0.00050 com='cv below 1st step'
 zhemicyl+x  15 1    7.924800   33.62022   0.00050 com='void btw cv-np liner'
 zhemicyl+x  16 1    8.077200   33.62022   0.00050 com='np277_4 liner'
 zhemicyl+x  11 1   10.922000   33.62022   0.00050 com='np277_4'
 zhemicyl+x  16 1   11.074400   33.62022   0.00050 com='kaolite liner'
 zhemicyl+x  12 1   21.685692   33.62022   0.00050 com='kaolite'
 zhemicyl+x  19 1   21.838092   33.62022   0.00050 com='drum'
unit 4010
'cv at 1st step in liner [Elev=35.330 in.]'
 zhemicyl+x  1  1    6.426200    0.15190   0.00050 com='cv well cavity'
 zhemicyl+x  8  1    6.680200    0.15190   0.00050 com='cv at 1st step'
 zhemicyl+x  15 1    7.924800    0.15190   0.00050 com='void btw cv and liner'
 zhemicyl+x  16 1   11.074400    0.15190   0.00050 com='liner 1st step'
 zhemicyl+x  12 1   21.685692    0.15190   0.00050 com='kaolite'
 zhemicyl+x  19 1   21.838092    0.15190   0.00050 com='drum'
unit 4011
'vertical gap between 1st step in liner and cv flange [Elev=35.420 in.]'
 zhemicyl+x  1  1    6.426200    0.22810   0.00050 com='cv well cavity'
 zhemicyl+x  8  1    6.680200    0.22810   0.00050 com='cv gap btw step-flng'
```

```
 zhemicyl+x  15 1   10.922000    0.22810   0.00050 com='void btw cv and liner'
 zhemicyl+x  16 1   11.074400    0.22810   0.00050 com='liner wall'
 zhemicyl+x  12 1   21.685692    0.22810   0.00050 com='kaolite'
 zhemicyl+x  19 1   21.838092    0.22810   0.00050 com='drum'
unit 4012
'cv flange to top of cv well [Elev=35.920 in.]'
 zhemicyl+x  1  1    6.426200    1.26950   0.00050 com='cavity'
 zhemicyl+x  9  1    9.525000    1.26950   0.00050 com='flange to top of well'
 zhemicyl+x  15 1    9.525000    1.26950   0.00050 com='void btw cv and pad-2'
 zhemicyl+x  14 1   10.033000    1.26950   0.00050 com='pad-2'
 zhemicyl+x  15 1   10.922000    1.26950   0.00050 com='void btw cv and liner'
 zhemicyl+x  16 1   11.074400    1.26950   0.00050 com='liner wall'
 zhemicyl+x  12 1   21.685692    1.26950   0.00050 com='kaolite'
 zhemicyl+x  19 1   21.838092    1.26950   0.00050 com='drum'
unit 4013
'cv flange above cv well [Elev=37.070 in.]'
 zhemicyl+x  10 1    9.525000    2.92050   0.00050 com='flange above cv well'
 zhemicyl+x  15 1    9.525000    2.92050   0.00050 com='void btw cv and pad-2'
 zhemicyl+x  14 1   10.033000    2.92050   0.00050 com='pad-2'
 zhemicyl+x  15 1   10.922000    2.92050   0.00050 com='void btw pad2-liner'
 zhemicyl+x  16 1   11.074400    2.92050   0.00050 com='liner wall'
 zhemicyl+x  12 1   21.685692    2.92050   0.00050 com='kaolite'
 zhemicyl+x  19 1   21.838092    2.92050   0.00050 com='drum'
unit 4014
'plugpad2 below liner 2nd step [Elev=37.470 in.]'
 zhemicyl+x  14 1   10.033000    0.76150   0.00050 com='pad-2'
 zhemicyl+x  15 1   10.922000    1.01550   0.00050 com='void btw pad2-liner'
 zhemicyl+x  16 1   11.074400    1.01550   0.00050 com='liner wall'
 zhemicyl+x  12 1   21.685692    1.01550   0.00050 com='kaolite'
 zhemicyl+x  19 1   21.838092    1.01550   0.00050 com='drum'
unit 4015
'2nd step in liner [Elev=37.530 in.]'
 zhemicyl+x  15 1   10.922000    0.15190   0.00050 com='void abv pad2'
 zhemicyl+x  16 1   18.757900    0.15190   0.00050 com='liner 2nd step'
 zhemicyl+x  12 1   21.685692    0.15190   0.00050 com='kaolite'
 zhemicyl+x  19 1   21.838092    0.15190   0.00050 com='drum'
unit 4016
'abv 2nd step in liner to bottom of angle iron [Elev=40.750 in.]'
 zhemicyl+x  13 1   18.097500    8.17830   0.49276 com='plug kaolite'
 zhemicyl+x  17 1   18.249900    8.17830   0.34036 com='sides of plug case'
 zhemicyl+x  15 1   18.605500    8.17830   0.00050 com='void: plug to liner'
 zhemicyl+x  16 1   18.757900    8.17830   0.00050 com='liner wall'
 zhemicyl+x  12 1   21.685692    8.17830   0.00050 com='kaolite'
 zhemicyl+x  19 1   21.838092    8.17830   0.00050 com='drum'
unit 4017
'bottom of angle iron to bend in angle iron [Elev=42.500 in.]'
 zhemicyl+x  13 1   18.097500    4.44450   0.00050 com='plug kaolite'
 zhemicyl+x  17 1   18.249900    4.44450   0.00050 com='sides of plug case'
 zhemicyl+x  15 1   18.605500    4.44450   0.00050 com='void: plug to liner'
 zhemicyl+x  16 1   18.757900    4.44450   0.00050 com='liner wall'
 zhemicyl+x  18 1   19.392900    4.44450   0.00050 com='lower angle iron'
 zhemicyl+x  12 1   21.685692    4.44450   0.00050 com='kaolite'
 zhemicyl+x  19 1   21.838092    4.44450   0.00050 com='drum'
unit 4018
'bend in angle iron to top of angle iron [Elev=42.750 in.]'
 zhemicyl+x  13 1   18.097500    0.11126   0.00050 com='plug kaolite'
 zhemicyl+x  17 1   18.249900    0.26366   0.00050 com='sides of plug case'
 zhemicyl+x  15 1   18.605500    0.63450   0.00050 com='void: plug to liner'
 zhemicyl+x  16 1   18.757900    0.63450   0.00050 com='liner wall'
 zhemicyl+x  18 1   21.685692    0.63450   0.00050 com='bend section of ai'
 zhemicyl+x  19 1   21.838092    0.63450   0.00050 com='drum'
unit 4019
'drum lid and lip [Elev=43.500 in.]'
 zhemicyl+x  20 1   21.469792    1.90450   0.15240 com='void above lid'
 zhemicyl+x  19 1   21.622192    1.90450   0.00050 com='drum lid'
 zhemicyl+x  20 1   21.685692    1.90450   0.00050 com='void btw lid-drumwall'
 zhemicyl+x  19 1   21.838092    1.90450   0.00050 com='drum'
unit 5001
'drum bottom flat cover [Elev= 0.105 in. at top of unit]'
 cuboid    20 1 2p21.839092  2p37.826417   0.26670   0.0
 hole 1001 0.0   37.826417   0.0
```

```
 hole 2001 0.0  -37.826417   0.0
 hole 3001  21.839092   0.0   0.0
 hole 4001 -21.839092   0.0   0.0
unit 5002
'above drum bottom flat cover and below containment vessel [Elev= 4.670 in.]'
 cuboid    20 1 2p21.839092  2p37.826417  11.59510   0.0
 hole 1002 0.0   37.826417   0.0
 hole 2002 0.0  -37.826417   0.0
 hole 3002  21.839092   0.0   0.0
 hole 4002 -21.839092   0.0   0.0
unit 5003
'cv bottom [Elev= 4.920 in.]'
 cuboid    20 1 2p21.839092  2p37.826417   0.63500   0.0
 hole 1003 0.0   37.826417   0.0
 hole 2003 0.0  -37.826417   0.0
 hole 3003  21.839092   0.0   0.0
 hole 4003 -21.839092   0.0   0.0
unit 5006
'content (collapsed) [Elev= 9.691 in.]'
 cuboid    20 1 2p21.839092  2p37.826417  12.11746   0.0
 hole 1006 0.0   37.826417   0.0
 hole 2006 0.0  -37.826417   0.0
 hole 3006  21.839092   0.0   0.0
 hole 4006 -21.839092   0.0   0.0
unit 5007
'np277_4 spacer [Elev=11.091 in.]'
 cuboid    20 1 2p21.839092  2p37.826417   3.55710   0.0
 hole 1007 0.0   37.826417   0.0
 hole 2007 0.0  -37.826417   0.0
 hole 3007  21.839092   0.0   0.0
 hole 4007 -21.839092   0.0   0.0
unit 5008
'top of content stack to bottom of 1st step [Elev=35.270 in.]'
 cuboid    20 1 2p21.839092  2p37.826417  33.62072   0.0
 hole 1008 0.0   37.826417   0.0
 hole 2008 0.0  -37.826417   0.0
 hole 3008  21.839092   0.0   0.0
 hole 4008 -21.839092   0.0   0.0
unit 5010
'cv at 1st step in liner [Elev=35.330 in.]'
 cuboid    20 1 2p21.839092  2p37.826417   0.15240   0.0
 hole 1010 0.0   37.826417   0.0
 hole 2010 0.0  -37.826417   0.0
 hole 3010  21.839092   0.0   0.0
 hole 4010 -21.839092   0.0   0.0
unit 5011
'vertical gap between 1st step in liner and cv flange [Elev=35.420 in.]'
 cuboid    20 1 2p21.839092  2p37.826417   0.22860   0.0
 hole 1011 0.0   37.826417   0.0
 hole 2011 0.0  -37.826417   0.0
 hole 3011  21.839092   0.0   0.0
 hole 4011 -21.839092   0.0   0.0
unit 5012
'cv flange to top of cv well [Elev=35.920 in.]'
 cuboid    20 1 2p21.839092  2p37.826417   1.27000   0.0
 hole 1012 0.0   37.826417   0.0
 hole 2012 0.0  -37.826417   0.0
 hole 3012  21.839092   0.0   0.0
 hole 4012 -21.839092   0.0   0.0
unit 5013
'cv flange above cv well [Elev=37.070 in.]'
 cuboid    20 1 2p21.839092  2p37.826417   2.92100   0.0
 hole 1013 0.0   37.826417   0.0
 hole 2013 0.0  -37.826417   0.0
 hole 3013  21.839092   0.0   0.0
 hole 4013 -21.839092   0.0   0.0
unit 5014
'plugpad2 below liner 2nd step [Elev=37.470 in.]'
 cuboid    20 1 2p21.839092  2p37.826417   1.01600   0.0
 hole 1014 0.0   37.826417   0.0
 hole 2014 0.0  -37.826417   0.0
```

```
 hole 3014  21.839092   0.0   0.0
 hole 4014 -21.839092   0.0   0.0
unit 5015
'2nd step in liner [Elev=37.530 in.]'
 cuboid    20 1 2p21.839092  2p37.826417   0.15240   0.0
 hole 1015 0.0   37.826417   0.0
 hole 2015 0.0  -37.826417   0.0
 hole 3015  21.839092   0.0   0.0
 hole 4015 -21.839092   0.0   0.0
unit 5016
'abv 2nd step in liner to bottom of angle iron [Elev=40.750 in.]'
 cuboid    20 1 2p21.839092  2p37.826417   8.17880   0.0
 hole 1016 0.0   37.826417   0.0
 hole 2016 0.0  -37.826417   0.0
 hole 3016  21.839092   0.0   0.0
 hole 4016 -21.839092   0.0   0.0
unit 5017
'bottom of angle iron to bend in angle iron [Elev=42.500 in.]'
 cuboid    20 1 2p21.839092  2p37.826417   4.44500   0.0
 hole 1017 0.0   37.826417   0.0
 hole 2017 0.0  -37.826417   0.0
 hole 3017  21.839092   0.0   0.0
 hole 4017 -21.839092   0.0   0.0
unit 5018
'bend in angle iron to top of angle iron [Elev=42.750 in.]'
 cuboid    20 1 2p21.839092  2p37.826417   0.63500   0.0
 hole 1018 0.0   37.826417   0.0
 hole 2018 0.0  -37.826417   0.0
 hole 3018  21.839092   0.0   0.0
 hole 4018 -21.839092   0.0   0.0
unit 5019
'drum lid and lip [Elev=43.500 in.]'
 cuboid    20 1 2p21.839092  2p37.826417   1.90500   0.0
 hole 1019 0.0   37.826417   0.0
 hole 2019 0.0  -37.826417   0.0
 hole 3019  21.839092   0.0   0.0
 hole 4019 -21.839092   0.0   0.0
unit 5020
'es3100 drum [Elev=43.500 in.]'
array 3         -21.839092   -37.826417    0.0
 cuboid    20  1 2p21.839592 2p37.826917 110.4905 0.0 com='interst. array space'
unit 6001
'drum bottom flat cover'
 cuboid    20  1 2p21.839092 0.0 -21.839092  0.26670 0.0
 hole 1001 0.0   0.0   0.0
unit 6002
'above drum bottom flat cover and below containment vessel'
 cuboid    20  1 2p21.839092 0.0 -21.839092 11.59510 0.0
 hole 1002 0.0   0.0   0.0
unit 6003
'cv bottom'
 cuboid    20  1 2p21.839092 0.0 -21.839092  0.63500 0.0
 hole 1003 0.0   0.0   0.0
unit 6006
'drum stand'
'content (collapsed)'
 cuboid    20  1 2p21.839092 0.0 -21.839092 12.11746 0.0
 hole 1006 0.0   0.0   0.0
unit 6007
'np277_4 spacer'
 cuboid    20  1 2p21.839092 0.0 -21.839092  3.55710 0.0
 hole 1007 0.0   0.0   0.0
unit 6008
'top of content stack to bottom of 1st step'
 cuboid    20  1 2p21.839092 0.0 -21.839092 33.62072 0.0
 hole 1008 0.0   0.0   0.0
unit 6010
'cv at 1st step in liner'
 cuboid    20  1 2p21.839092 0.0 -21.839092  0.15240 0.0
 hole 1010 0.0   0.0   0.0
unit 6011
```

```
'vertical gap between 1st step in liner and cv flange'
 cuboid    20  1 2p21.839092 0.0 -21.839092  0.22860 0.0
 hole 1011 0.0   0.0   0.0
unit 6012
'cv flange to top of cv well'
 cuboid    20  1 2p21.839092 0.0 -21.839092  1.27000 0.0
 hole 1012 0.0   0.0   0.0
unit 6013
'cv flange above cv well'
 cuboid    20  1 2p21.839092 0.0 -21.839092  2.92100 0.0
 hole 1013 0.0   0.0   0.0
unit 6014
'plugpad2 below liner 2nd step'
 cuboid    20  1 2p21.839092 0.0 -21.839092  1.01600 0.0
 hole 1014 0.0   0.0   0.0
unit 6015
'2nd step in liner'
 cuboid    20  1 2p21.839092 0.0 -21.839092  0.15240 0.0
 hole 1015 0.0   0.0   0.0
unit 6016
'abv 2nd step in liner to bottom of angle iron'
 cuboid    20  1 2p21.839092 0.0 -21.839092  8.17880 0.0
 hole 1016 0.0   0.0   0.0
unit 6017
'bottom of angle iron to bend in angle iron'
 cuboid    20  1 2p21.839092 0.0 -21.839092  4.44500 0.0
 hole 1017 0.0   0.0   0.0
unit 6018
'bend in angle iron to top of angle iron'
 cuboid    20  1 2p21.839092 0.0 -21.839092  0.63500 0.0
 hole 1018 0.0   0.0   0.0
unit 6019
'drum lid and lip'
 cuboid    20  1 2p21.839092 0.0 -21.839092  1.90500 0.0
 hole 1019 0.0   0.0   0.0
unit 6020
'es3100 drum'
array 4         2r-21.839092     0.0
 cuboid    20  1 2p21.839592 0.0005 -21.839592 110.4905 0.0
unit 7001
 cuboid    20  1 2p21.839092 21.839092 0.0  0.26670 0.0
 hole 2001 0.0   0.0   0.0
unit 7002
 cuboid    20  1 2p21.839092 21.839092 0.0 11.59510 0.0
 hole 2002 0.0   0.0   0.0
unit 7003
 cuboid    20  1 2p21.839092 21.839092 0.0  0.63500 0.0
 hole 2003 0.0   0.0   0.0
unit 7006
 cuboid    20  1 2p21.839092 21.839092 0.0 12.11746 0.0
 hole 2006 0.0   0.0   0.0
unit 7007
 cuboid    20  1 2p21.839092 21.839092 0.0  3.55710 0.0
 hole 2007 0.0   0.0   0.0
unit 7008
 cuboid    20  1 2p21.839092 21.839092 0.0 33.62072 0.0
 hole 2008 0.0   0.0   0.0
unit 7010
 cuboid    20  1 2p21.839092 21.839092 0.0  0.15240 0.0
 hole 2010 0.0   0.0   0.0
unit 7011
 cuboid    20  1 2p21.839092 21.839092 0.0  0.22860 0.0
 hole 2011 0.0   0.0   0.0
unit 7012
 cuboid    20  1 2p21.839092 21.839092 0.0  1.27000 0.0
 hole 2012 0.0   0.0   0.0
unit 7013
 cuboid    20  1 2p21.839092 21.839092 0.0  2.92100 0.0
 hole 2013 0.0   0.0   0.0
unit 7014
 cuboid    20  1 2p21.839092 21.839092 0.0  1.01600 0.0
```

```
 hole 2014 0.0   0.0   0.0
unit 7015
 cuboid    20  1 2p21.839092 21.839092 0.0  0.15240 0.0
 hole 2015 0.0   0.0   0.0
unit 7016
 cuboid    20  1 2p21.839092 21.839092 0.0  8.17880 0.0
 hole 2016 0.0   0.0   0.0
unit 7017
 cuboid    20  1 2p21.839092 21.839092 0.0  4.44500 0.0
 hole 2017 0.0   0.0   0.0
unit 7018
 cuboid    20  1 2p21.839092 21.839092 0.0  0.63500 0.0
 hole 2018 0.0   0.0   0.0
unit 7019
 cuboid    20  1 2p21.839092 21.839092 0.0  1.90500 0.0
 hole 2019 0.0   0.0   0.0
unit 7020
'es3100 drum'
array 5         -21.839092     0.0     0.0
 cuboid    20  1 2p21.839592 21.839592 -0.0005 110.4905 0.0
unit 8001
 cuboid    20  1 0.0 -21.839092 2p37.826417  0.26670 0.0
 hole 3001 0.0   0.0   0.0
unit 8002
 cuboid    20  1 0.0 -21.839092 2p37.826417 11.59510 0.0
 hole 3002 0.0   0.0   0.0
unit 8003
 cuboid    20  1 0.0 -21.839092 2p37.826417  0.63500 0.0
 hole 3003 0.0   0.0   0.0
unit 8006
 cuboid    20  1 0.0 -21.839092 2p37.826417 12.11746 0.0
 hole 3006 0.0   0.0   0.0
unit 8007
 cuboid    20  1 0.0 -21.839092 2p37.826417  3.55710 0.0
 hole 3007 0.0   0.0   0.0
unit 8008
 cuboid    20  1 0.0 -21.839092 2p37.826417 33.62072 0.0
 hole 3008 0.0   0.0   0.0
unit 8010
 cuboid    20  1 0.0 -21.839092 2p37.826417  0.15240 0.0
 hole 3010 0.0   0.0   0.0
unit 8011
 cuboid    20  1 0.0 -21.839092 2p37.826417  0.22860 0.0
 hole 3011 0.0   0.0   0.0
unit 8012
 cuboid    20  1 0.0 -21.839092 2p37.826417  1.27000 0.0
 hole 3012 0.0   0.0   0.0
unit 8013
 cuboid    20  1 0.0 -21.839092 2p37.826417  2.92100 0.0
 hole 3013 0.0   0.0   0.0
unit 8014
 cuboid    20  1 0.0 -21.839092 2p37.826417  1.01600 0.0
 hole 3014 0.0   0.0   0.0
unit 8015
 cuboid    20  1 0.0 -21.839092 2p37.826417  0.15240 0.0
 hole 3015 0.0   0.0   0.0
unit 8016
 cuboid    20  1 0.0 -21.839092 2p37.826417  8.17880 0.0
 hole 3016 0.0   0.0   0.0
unit 8017
 cuboid    20  1 0.0 -21.839092 2p37.826417  4.44500 0.0
 hole 3017 0.0   0.0   0.0
unit 8018
 cuboid    20  1 0.0 -21.839092 2p37.826417  0.63500 0.0
 hole 3018 0.0   0.0   0.0
unit 8019
 cuboid    20  1 0.0 -21.839092 2p37.826417  1.90500 0.0
 hole 3019 0.0   0.0   0.0
unit 8020
'es3100 drum'
array 6         -21.839092    -37.826417    0.0
```

```
 cuboid    20  1 0.0005 -21.839592 2p37.826917 110.4905 0.0
unit 9001
 cuboid    20  1 21.839092 0.0 2p37.826417  0.26670 0.0
 hole 4001 0.0   0.0   0.0
unit 9002
 cuboid    20  1 21.839092 0.0 2p37.826417 11.59510 0.0
 hole 4002 0.0   0.0   0.0
unit 9003
 cuboid    20  1 21.839092 0.0 2p37.826417  0.63500 0.0
 hole 4003 0.0   0.0   0.0
unit 9006
 cuboid    20  1 21.839092 0.0 2p37.826417 12.11746 0.0
 hole 4006 0.0   0.0   0.0
unit 9007
 cuboid    20  1 21.839092 0.0 2p37.826417  3.55710 0.0
 hole 4007 0.0   0.0   0.0
unit 9008
 cuboid    20  1 21.839092 0.0 2p37.826417 33.62072 0.0
 hole 4008 0.0   0.0   0.0
unit 9010
 cuboid    20  1 21.839092 0.0 2p37.826417  0.15240 0.0
 hole 4010 0.0   0.0   0.0
unit 9011
 cuboid    20  1 21.839092 0.0 2p37.826417  0.22860 0.0
 hole 4011 0.0   0.0   0.0
unit 9012
 cuboid    20  1 21.839092 0.0 2p37.826417  1.27000 0.0
 hole 4012 0.0   0.0   0.0
unit 9013
 cuboid    20  1 21.839092 0.0 2p37.826417  2.92100 0.0
 hole 4013 0.0   0.0   0.0
unit 9014
 cuboid    20  1 21.839092 0.0 2p37.826417  1.01600 0.0
 hole 4014 0.0   0.0   0.0
unit 9015
 cuboid    20  1 21.839092 0.0 2p37.826417  0.15240 0.0
 hole 4015 0.0   0.0   0.0
unit 9016
 cuboid    20  1 21.839092 0.0 2p37.826417  8.17880 0.0
 hole 4016 0.0   0.0   0.0
unit 9017
 cuboid    20  1 21.839092 0.0 2p37.826417  4.44500 0.0
 hole 4017 0.0   0.0   0.0
unit 9018
 cuboid    20  1 21.839092 0.0 2p37.826417  0.63500 0.0
 hole 4018 0.0   0.0   0.0
unit 9019
 cuboid    20  1 21.839092 0.0 2p37.826417  1.90500 0.0
 hole 4019 0.0   0.0   0.0
unit 9020
'es3100 drum'
array 7         0.0    -37.826417    0.0
 cuboid    20  1 21.839592 -0.0005 2p37.826917 110.4905 0.0
unit 9021
 cuboid    20  1 21.839092 0.0 21.839092 0.0  0.26670 0.0
unit 9022
 cuboid    20  1 21.839092 0.0 21.839092 0.0 11.59510 0.0
unit 9023
 cuboid    20  1 21.839092 0.0 21.839092 0.0  0.63500 0.0
unit 9026
 cuboid    20  1 21.839092 0.0 21.839092 0.0 12.11746 0.0
unit 9027
 cuboid    20  1 21.839092 0.0 21.839092 0.0  3.55710 0.0
unit 9028
 cuboid    20  1 21.839092 0.0 21.839092 0.0 33.62072 0.0
unit 9030
 cuboid    20  1 21.839092 0.0 21.839092 0.0  0.15240 0.0
unit 9031
 cuboid    20  1 21.839092 0.0 21.839092 0.0  0.22860 0.0
unit 9032
 cuboid    20  1 21.839092 0.0 21.839092 0.0  1.27000 0.0
```

```
unit 9033
 cuboid    20  1 21.839092 0.0 21.839092 0.0  2.92100 0.0
unit 9034
 cuboid    20  1 21.839092 0.0 21.839092 0.0  1.01600 0.0
unit 9035
 cuboid    20  1 21.839092 0.0 21.839092 0.0  0.15240 0.0
unit 9036
 cuboid    20  1 21.839092 0.0 21.839092 0.0  8.17880 0.0
unit 9037
 cuboid    20  1 21.839092 0.0 21.839092 0.0  4.44500 0.0
unit 9038
 cuboid    20  1 21.839092 0.0 21.839092 0.0  0.63500 0.0
unit 9039
 cuboid    20  1 21.839092 0.0 21.839092 0.0  1.90500 0.0
unit 9040
'array end space'
array 8         0.0    0.0    0.0
 cuboid    20  1 21.839592 -0.0005 21.839592 -0.0005 110.4905 0.0
global
unit 9050
array 9    3r0.0
reflector  21 2  6r3.0  10
end geometry
read array
ara=1 nux=3 nuy=3 nuz=4   fill 27r1004  9r1005      end fill
ara=3 nux=1 nuy=1 nuz=19 fill
5001 5002 5003 5006 5007 5006 5007 5006 5008 5010
5011 5012 5013 5014 5015 5016 5017 5018 5019       end fill
ara=4 nux=1 nuy=1 nuz=19                               fill
6001 6002 6003 6006 6007 6006 6007 6006 6008 6010
6011 6012 6013 6014 6015 6016 6017 6018 6019       end fill
ara=5 nux=1 nuy=1 nuz=19                               fill
7001 7002 7003 7006 7007 7006 7007 7006 7008 7010
7011 7012 7013 7014 7015 7016 7017 7018 7019       end fill
ara=6 nux=1 nuy=1 nuz=19                               fill
8001 8002 8003 8006 8007 8006 8007 8006 8008 8010
8011 8012 8013 8014 8015 8016 8017 8018 8019       end fill
ara=7 nux=1 nuy=1 nuz=19                               fill
9001 9002 9003 9006 9007 9006 9007 9006 9008 9010
9011 9012 9013 9014 9015 9016 9017 9018 9019       end fill
ara=8 nux=1 nuy=1 nuz=19                               fill
9021 9022 9023 9026 9027 9026 9027 9026 9028 9030
9031 9032 9033 9034 9035 9036 9037 9038 9039       end fill
ara=9 nux=7 nuy=3 nuz=3                                fill
9040 5r6020 9040 8020 5r5020 9020 9040 5r7020 9040 2q21 end fill
end array
read bias id=500 2  11  end bias
read start nst=0
end start
end data
end


=csas25    parm=size=3000000
nciaoxt11,0.0in np,disp.24000.0gUO2 (21124.9g235, 6533.9gH2O hx=  9.90),fr=1.0e-04
238groupndf5 infhommedium
'HEU volume =3669.72477, SPACER volume    0.00000'
'HEU oxide, bulk density of oxide in cans=  6.54000 g/cm3'
'wrapped dry content can hx=0.79, CV void volume 6545.63717'
'oxide= 24000.0 g, sat. moisture in HEU oxide=1477.3 g, oxide htox= 1.83'
arbmuox    6.54000   2 0 0 0  92235   88.0203
                               8016   11.9797    1  1.0000  293  end
arbmastm  4.0256e-01  2 0 0 0   1001   11.1913
                               8016   88.8087    1  1.0000  293  end
'np277-4: spacer (NCT_MD&H)'
'NCT min.den.(95.3886 lb/ft3) and hydrogen'
'np277-4 min.den.= 1.527971 = (95.3886 lb/ft3)(453.59 g/lb)/(28316.84 cm3/ft3)'
'use 75% of boron in calculations per NUREG-1609 Section 6.5.3.2'
arbmboron 7.31015e-2  2 0 0 0    5010   18.1479
                                 5011   81.8520    2  0.7500  293  end
arbmnpmx  1.07070e+0 10 0 0 0    6012    1.9189
```

```
                                 7014    0.0141
                                 8016   43.4251
                                11023    0.1174
                                12000    0.3378
                                13027   39.0479
                                14000    2.4672
                                16000    0.3083
                                20000   11.8336
                                26000    0.5298    2  1.0000  293  end
arbmnph2o 3.84169e-1  2 0 0 0    1001   11.1913
                                 8016   88.8087    2  1.0000  293  end
'flooded containmment vessel and content cans -- 10 CFR 71.55(d)(3)'
arbmwicv  9.9820e-01  2 0 0 0   1001   11.1913
                               8016   88.8087    3  1.0     293  end
'steel: containment vessel body 16.60 lb but use 15.74 lb'
ss304                                            8  1.0     293  end
'steel: cv flange lower use 3.36 lb'
ss304                                            9  0.97267 293  end
'steel: cv flange upper use 13.75 lb'
ss304                                           10  0.94348 293  end
'np277-4: confinement -- neutron poison inner liner (NCT_MD&H)'
'actual vol.= 1.28314e4 cm3 = (7.83023e2 in3)(16.387064)'
'den.multiplier = 1.28314e4 cm3 (actual vol.) / 1.32708e4 cm3 (model vol.)'
'np277-4 min.den.= 1.527971 = (95.3886 lb/ft3)(453.59 g/lb)/(28316.84 cm3/ft3)'
'density = 1.477385 = (den.mult)(np277-4 min.den.) = 0.9668933*1.527971'
'use 75% of boron in calculations per NUREG-1609 Section 6.5.3.2'
arbmboron 7.06813e-2  2 0 0 0    5010   18.1479
                                 5011   81.8520   11  0.7500  293  end
arbmnpmx  1.03525e+0 10 0 0 0    6012    1.9189
                                 7014    0.0141
                                 8016   43.4251
                                11023    0.1174
                                12000    0.3378
                                13027   39.0479
                                14000    2.4672
                                16000    0.3083
                                20000   11.8336
                                26000    0.5298   11  1.0000  293  end
arbmnph2o 3.71451e-1  2 0 0 0    1001   11.1913
                                 8016   88.8087   11  1.0000  293  end
'kaolite 1600 body'
'sing.unit.density= (den.mult)(min.den.)'
' for arbmh20k = 1.012373*0.51655,  for rest = 1.012373*0.34438'
'den.mult= 1.36557e5 cm3 (actual vol.) / 1.34888e5 cm3 (model vol.)'
'actual vol.= 1.36557e5 cm3 = (28316.84 cm3/ft3)(108.33188 lb)/(22.464 lb/ft3)'
'nct array densities are s.u.dens. multiplied by volume ratio 1.34888/1.10336'
arbmh2ok   0.63931  2 0 0 0    1001   11.1913
                               8016   88.8087   12  0.0287  293  end
arbmal2o3  0.42622  2 0 0 0   13027   52.9390
                               8016   47.0610   12  0.096   293  end
arbmsio2   0.42622  2 0 0 0   14000   46.7570
                               8016   53.2430   12  0.367   293  end
arbmfe2o3  0.42622  2 0 0 0   26000   69.9540
                               8016   30.0460   12  0.067   293  end
arbmtio2   0.42622  2 0 0 0   22000   59.9535
                               8016   40.0465   12  0.012   293  end
arbmcao    0.42622  2 0 0 0   20000   71.4815
                               8016   28.5185   12  0.307   293  end
arbmmgo    0.42622  2 0 0 0   12000   60.3169
                               8016   39.6831   12  0.131   293  end
arbmna2o   0.42622  2 0 0 0   11023   74.1961
                               8016   25.8039   12  0.020   293  end
'kaolite 1600 top plug'
'sing.unit.density= (den.mult)(min.den.)'
' for arbmh20k = 0.965246*0.51655,  for rest = 0.965246*0.34438'
'den.mult= 1.21592e4 cm3 (actual vol.) / 1.25970e4 cm3 (model vol.)'
'actual vol.= 1.21592e4 cm3 = (28316.84 cm3/ft3)(9.646 lb)/(22.464 lb/ft3)'
arbmh2ok   0.49860  2 0 0 0    1001   11.1913
                               8016   88.8087   13  0.0287  293  end
arbmal2o3  0.33241  2 0 0 0   13027   52.9390
                               8016   47.0610   13  0.096   293  end
```

```
arbmsio2   0.33241  2 0 0 0   14000   46.7570
                               8016   53.2430   13  0.367   293  end
arbmfe2o3  0.33241  2 0 0 0   26000   69.9540
                               8016   30.0460   13  0.067   293  end
arbmtio2   0.33241  2 0 0 0   22000   59.9535
                               8016   40.0465   13  0.012   293  end
arbmcao    0.33241  2 0 0 0   20000   71.4815
                               8016   28.5185   13  0.307   293  end
arbmmgo    0.33241  2 0 0 0   12000   60.3169
                               8016   39.6831   13  0.131   293  end
arbmna2o   0.33241  2 0 0 0   11023   74.1961
                               8016   25.8039   13  0.020   293  end
'silicone rubber pads'
arbmsiru   1.21791  4 0 0 0    6012   32.3767
                               1001    8.1573
                               8016   21.5782
                              14000   37.8878   14  1.0     293  end
'void space external to containment vessel'
arbmwecv   0.9982   2 0 0 0    1001   11.1913
                               8016   88.8087   15  0.0001  293  end
'steel: liner'
ss304                                            16  1.0     293  end
'steel: plug cover (pc) use 9.907 lb'
ss304                                            17  1.06388 293  end
'steel: angle iron (ai) for single units'
'ss304                                            18  1.0     293  end
'steel: angle iron (ai) for arrays'
'array density is multiplied by a volume fraction 7.08030/5.63249'
ss304                                            18  1.25705 293  end
'steel: drum steel for single units'
'ss304                                            19  1.0     293  end
'steel: drum steel for arrays'
'array density is multiplied by a volume fraction 3.20482/3.20544'
ss304                                            19  0.99981 293  end
'void space external to drum'
'array density is multiplied by a volume ratio 8.11698/6.98323'
arbmwed    1.16026  2 0 0 0    1001   11.1913
                               8016   88.8087   20  0.0001  293  end
'reflective water'
'arbmh20r   0.9982   2 0 0 0    1001   11.1913
'                               8016   88.8087   21  1.0     293  end
end comp
nciaoxt11,0.0in np,disp.24000.0gUO2 (21124.9g235, 6533.9gH2O,hx=  9.90),fr=1.0e-04
read parameters nub=yes npg=2500 gen=215 nsk=15 tme=100 end parameters
read boun       all=specular                     end boun
read geometry
unit 1001
'drum bottom flat cover [Elev= 0.111 in. at top of unit]'
'cylinder  19 1   22.866096    0.28150   0.0     com='extended radius not used'
 cylinder  19 1   21.722275    0.28150   0.0     com='drum bottom flat cover'
 cuboid    20 1 4p22.866096    0.28150   0.0     com='drum chine outer radius'
unit 1002
'above drum bottom flat cover and below containment vessel [Elev= 4.676 in.]'
 cylinder  15 1    3.175000   11.59510  11.16330 com='void in pad-1'
 cylinder  14 1    7.924800   11.59510  11.16330 com='pad-1'
 cylinder  16 1    8.077200   11.59510  11.16330 com='np277_4 liner'
 cylinder  11 1   10.922000   11.59510  11.16330 com='np277_4'
 cylinder  16 1   11.074400   11.59510  10.85850 com='kaolite liner bottom'
 cylinder  12 1   21.555075   11.59510   0.0     com='kaolite'
 cylinder  19 1   21.722275   11.59510   0.0     com='drum'
 cuboid    20 1 4p22.866096   11.59510   0.0     com='drum chine outer radius'
unit 1003
'cv bottom to bottom of 1st step [Elev=35.276 in.]'
 cylinder  3  1    6.426200   77.72400  28.92123 com='cavity abv HEU'
 cylinder  1  1    6.426200   77.72400   0.63500 com='HEU content'
 cylinder  8  1    6.680200   77.72400   0.0     com='cv bottom'
 cylinder  15 1    7.924800   77.72400   0.0     com='void btw cv-np liner'
 cylinder  16 1    8.077200   77.72400   0.0     com='np277_4 liner'
 cylinder  11 1   10.922000   77.72400   0.0     com='np277_4'
 cylinder  16 1   11.074400   77.72400   0.0     com='kaolite liner'
 cylinder  12 1   21.555075   77.72400   0.0     com='kaolite'
```

```
 cylinder  19 1   21.722275   77.72400   0.0     com='drum'
 cuboid    20 1 4p22.866096   77.72400   0.0     com='drum chine outer radius'
unit 1010
'cv at 1st step in liner [Elev=35.336 in.]'
 cylinder  3  1    6.426200    0.15240   0.00000 com='cavity abv HEU'
 cylinder  1  1    6.426200    0.15240   0.0     com='HEU content'
 cylinder  8  1    6.680200    0.15240   0.0     com='cv at 1st step'
 cylinder  15 1    7.924800    0.15240   0.0     com='void btw cv and liner'
 cylinder  16 1   11.074400    0.15240   0.0     com='liner 1st step'
 cylinder  12 1   21.555075    0.15240   0.0     com='kaolite'
 cylinder  19 1   21.722275    0.15240   0.0     com='drum'
 cuboid    20 1 4p22.866096    0.15240   0.0     com='drum chine outer radius'
unit 1011
'vertical gap between 1st step in liner and cv flange [Elev=35.426 in.]'
 cylinder  3  1    6.426200    0.22860   0.00000 com='cavity abv HEU'
 cylinder  1  1    6.426200    0.22860   0.0     com='HEU content'
 cylinder  8  1    6.680200    0.22860   0.0     com='cv at gap btwn step-flng'
 cylinder  15 1   10.922000    0.22860   0.0     com='void btw cv and liner'
 cylinder  16 1   11.074400    0.22860   0.0     com='liner wall'
 cylinder  12 1   21.555075    0.22860   0.0     com='kaolite'
 cylinder  19 1   21.722275    0.22860   0.0     com='drum'
 cuboid    20 1 4p22.866096    0.22860   0.0     com='drum chine outer radius'
unit 1012
'cv flange to top of cv well [Elev=35.926 in.]'
 cylinder  3  1    6.426200    1.27000   0.00000 com='cavity abv HEU'
 cylinder  1  1    6.426200    1.27000   0.0     com='HEU content'
 cylinder  9  1    9.525000    1.27000   0.0     com='flange to top of well'
 cylinder  15 1    9.525000    1.27000   0.0     com='void btw cv and pad-2'
 cylinder  14 1   10.033000    1.27000   0.0     com='pad-2'
 cylinder  15 1   10.922000    1.27000   0.0     com='void btw cv and liner'
 cylinder  16 1   11.074400    1.27000   0.0     com='liner wall'
 cylinder  12 1   21.555075    1.27000   0.0     com='kaolite'
 cylinder  19 1   21.722275    1.27000   0.0     com='drum'
 cuboid    20 1 4p22.866096    1.27000   0.0     com='drum chine outer radius'
unit 1013
'cv flange above cv well [Elev=37.076 in.]'
 cylinder  10 1    9.525000    2.92100   0.0     com='flange above cv well'
 cylinder  15 1    9.525000    2.92100   0.0     com='void btw cv and pad-2'
 cylinder  14 1   10.033000    2.92100   0.0     com='pad-2'
 cylinder  15 1   10.922000    2.92100   0.0     com='void btw pad2 and liner'
 cylinder  16 1   11.074400    2.92100   0.0     com='liner wall'
 cylinder  12 1   21.555075    2.92100   0.0     com='kaolite'
 cylinder  19 1   21.722275    2.92100   0.0     com='drum'
 cuboid    20 1 4p22.866096    2.92100   0.0     com='drum chine outer radius'
unit 1014
'plugpad2 below liner 2nd step [Elev=37.476 in.]'
 cylinder  14 1   10.033000    0.76200   0.0     com='pad-2'
 cylinder  15 1   10.922000    1.01600   0.0     com='void btw pad2 and liner'
 cylinder  16 1   11.074400    1.01600   0.0     com='liner wall'
 cylinder  12 1   21.555075    1.01600   0.0     com='kaolite'
 cylinder  19 1   21.722275    1.01600   0.0     com='drum'
 cuboid    20 1 4p22.866096    1.01600   0.0     com='drum chine outer radius'
unit 1015
'2nd step in liner [Elev=37.536 in.]'
 cylinder  15 1   10.922000    0.15240   0.0     com='void abv pad2'
 cylinder  16 1   18.757900    0.15240   0.0     com='liner 2nd step'
 cylinder  12 1   21.555075    0.15240   0.0     com='kaolite'
 cylinder  19 1   21.722275    0.15240   0.0     com='drum'
 cuboid    20 1 4p22.866096    0.15240   0.0     com='drum chine outer radius'
unit 1016
'abv 2nd step in liner to bottom of angle iron [Elev=40.756 in.]'
 cylinder  13 1   18.097500    8.17880   0.49276 com='plug kaolite'
 cylinder  17 1   18.249900    8.17880   0.34036 com='sides of plug case'
 cylinder  15 1   18.605500    8.17880   0.0     com='void: plug to liner'
 cylinder  16 1   18.757900    8.17880   0.0     com='liner wall'
 cylinder  12 1   21.555075    8.17880   0.0     com='kaolite'
 cylinder  19 1   21.722275    8.17880   0.0     com='drum'
 cuboid    20 1 4p22.866096    8.17880   0.0     com='drum chine outer radius'
unit 1017
'bottom of angle iron to bend in angle iron [Elev=42.506 in.]'
 cylinder  13 1   18.097500    4.44500   0.0     com='plug kaolite'
```

```
 cylinder  17 1   18.249900    4.44500   0.0     com='sides of plug case'
 cylinder  15 1   18.605500    4.44500   0.0     com='void: plug to liner'
 cylinder  16 1   18.757900    4.44500   0.0     com='liner wall'
 cylinder  18 1   19.392900    4.44500   0.0     com='lower angle iron'
 cylinder  12 1   21.555075    4.44500   0.0     com='kaolite'
 cylinder  19 1   21.722275    4.44500   0.0     com='drum'
 cuboid    20 1 4p22.866096    4.44500   0.0     com='drum chine outer radius'
unit 1018
'bend in angle iron to top of angle iron [Elev=42.756 in.]'
 cylinder  13 1   18.097500    0.11176   0.0     com='plug kaolite'
 cylinder  17 1   18.249900    0.26416   0.0     com='sides of plug case'
 cylinder  15 1   18.605500    0.63500   0.0     com='void: plug to liner'
 cylinder  16 1   18.757900    0.63500   0.0     com='liner wall'
 cylinder  18 1   21.555075    0.63500   0.0     com='bend section of ai'
 cylinder  19 1   21.722275    0.63500   0.0     com='drum'
 cuboid    20 1 4p22.866096    0.63500   0.0     com='drum chine outer radius'
unit 1019
'drum lid and lip [Elev=43.512 in.]'
 cylinder  20 1   21.330090    1.91973   0.16720 com='void above lid'
 cylinder  19 1   21.497290    1.91973   0.0     com='drum lid'
 cylinder  20 1   21.555075    1.91973   0.0     com='void btw lid - drum wall'
 cylinder  19 1   21.722275    1.91973   0.0     com='drum'
 cuboid    20 1 4p22.866096    1.91973   0.0     com='drum chine outer radius'
global
unit 1020
'es3100 drum [Elev=43.512 in.]'
array 3         2r-22.866096     0.0
'cuboid     0  1 4p24.587200    1120.337  0.0    com='bare package'
'cuboid    21  1 4p55.067200   1150.817 -30.48   com='reflected package'
 cuboid    20  1 4p22.866096    110.5197  0.0    com='interstital array space'
'global
'unit 1021
'array 4   3r0.0
'reflector  21 2  6r3.0  10
end geometry
read array
ara=3 nux=1 nuy=1 nuz=13 fill
1001 1002 1003 1010
1011 1012 1013 1014 1015 1016 1017 1018 1019        end fill
'ara=4 nux=13 nuy=13 nuz=06 fill f1020               end fill
end array
'read bias id=500 2  11  end bias
read start nst=0
end start
end data
end


=csas25    parm=size=3000000
nciask,0.0 21300.0g soc(19865.3uox,15672.8u235,  921.0c),hx= 12.82,fr=1.0e+00
238groupndf5 infhommedium
'  cm3: Skull oxide content 6974.5, SPACER    0.0, CV void 3240.9; CV htox=12.82'
'g/cm3: Skull oxide content  3.05400'
'U3O8   (19865.33gUOX,16816.3gU,15672.8g235U, 3801.4g.sat.H2O, HX=  7.43)'
'Carbon (  921.00gC,   58764.1mgC/g235U)'
'Poly   (  513.00gCH2)'
'Other  (    0.67gUnident (assumed H2O)'
''
'Increm (  921.0gC,15672.8g235U,   58764.1mgC/g235U)'
'GREP1:21300.00 19865.33 3.8014e+03    7.43 16816.35 15672.84   921.00  58764.1
'GREP2: 3235.07   513.00      12.82    0.67  1.0e+00
''
arbmuox    2.84830    3 0 0 0  92235   78.8954
                                92238    5.7563
                                 8016   15.3483    1  1.0000  293  end
arbmc     1.3205e-01  1 0 0 0   6012  100.0000    1  1.0000  293  end
arbmastm  5.4505e-01  2 0 0 0   1001   11.1913
                                 8016   88.8087    1  1.0000  293  end
arbmpoly   0.07355    2 0 0 0   1001   14.3798
                                 6012   85.6202    1  1.0000  293  end
'np277-4: spacer (NCT_MD&H)'
```

```
'NCT min.den.(95.3886 lb/ft3) and hydrogen'
'np277-4 min.den.= 1.527971 = (95.3886 lb/ft3)(453.59 g/lb)/(28316.84 cm3/ft3)'
'use 75% of boron in calculations per NUREG-1609 Section 6.5.3.2'
arbmboron 7.31015e-2  2 0 0 0    5010   18.1479
                                 5011   81.8520    2  0.7500  293  end
arbmnpmx  1.07070e+0 10 0 0 0    6012    1.9189
                                 7014    0.0141
                                 8016   43.4251
                                11023    0.1174
                                12000    0.3378
                                13027   39.0479
                                14000    2.4672
                                16000    0.3083
                                20000   11.8336
                                26000    0.5298    2  1.0000  293  end
arbmnph2o 3.84169e-1  2 0 0 0    1001   11.1913
                                 8016   88.8087    2  1.0000  293  end
'flooded containmment vessel and content cans -- 10 CFR 71.55(d)(3)'
arbmwicv  9.9820e-01  2 0 0 0   1001   11.1913
                               8016   88.8087    3  1       293  end
'steel: containment vessel body 16.60 lb but use 15.74 lb'
ss304                                            8  1.0     293  end
'steel: cv flange lower use 3.36 lb'
ss304                                            9  0.97267 293  end
'steel: cv flange upper use 13.75 lb'
ss304                                           10  0.94348 293  end
'np277-4: confinement -- neutron poison inner liner (NCT_MD&H)'
'actual vol.= 1.28314e4 cm3 = (7.83023e2 in3)(16.387064)'
'den.multiplier = 1.28314e4 cm3 (actual vol.) / 1.32708e4 cm3 (model vol.)'
'np277-4 min.den.= 1.527971 = (95.3886 lb/ft3)(453.59 g/lb)/(28316.84 cm3/ft3)'
'density = 1.477385 = (den.mult)(np277-4 min.den.) = 0.9668933*1.527971'
'use 75% of boron in calculations per NUREG-1609 Section 6.5.3.2'
arbmboron 7.06813e-2  2 0 0 0    5010   18.1479
                                 5011   81.8520   11  0.7500  293  end
arbmnpmx  1.03525e+0 10 0 0 0    6012    1.9189
                                 7014    0.0141
                                 8016   43.4251
                                11023    0.1174
                                12000    0.3378
                                13027   39.0479
                                14000    2.4672
                                16000    0.3083
                                20000   11.8336
                                26000    0.5298   11  1.0000  293  end
arbmnph2o 3.71451e-1  2 0 0 0    1001   11.1913
                                 8016   88.8087   11  1.0000  293  end
'kaolite 1600 body'
'sing.unit.density= (den.mult)(min.den.)'
' for arbmh20k = 1.012373*0.51655,  for rest = 1.012373*0.34438'
'den.mult= 1.36557e5 cm3 (actual vol.) / 1.34888e5 cm3 (model vol.)'
'actual vol.= 1.36557e5 cm3 = (28316.84 cm3/ft3)(108.33188 lb)/(22.464 lb/ft3)'
'nct array densities are s.u.dens. multiplied by volume ratio 1.34888/1.10336'
arbmh2ok   0.63931  2 0 0 0    1001   11.1913
                               8016   88.8087   12  0.0287  293  end
arbmal2o3  0.42622  2 0 0 0   13027   52.9390
                               8016   47.0610   12  0.096   293  end
arbmsio2   0.42622  2 0 0 0   14000   46.7570
                               8016   53.2430   12  0.367   293  end
arbmfe2o3  0.42622  2 0 0 0   26000   69.9540
                               8016   30.0460   12  0.067   293  end
arbmtio2   0.42622  2 0 0 0   22000   59.9535
                               8016   40.0465   12  0.012   293  end
arbmcao    0.42622  2 0 0 0   20000   71.4815
                               8016   28.5185   12  0.307   293  end
arbmmgo    0.42622  2 0 0 0   12000   60.3169
                               8016   39.6831   12  0.131   293  end
arbmna2o   0.42622  2 0 0 0   11023   74.1961
                               8016   25.8039   12  0.020   293  end
'kaolite 1600 top plug'
'sing.unit.density= (den.mult)(min.den.)'
' for arbmh20k = 0.965246*0.51655,  for rest = 0.965246*0.34438'
```

```
'den.mult= 1.21592e4 cm3 (actual vol.) / 1.25970e4 cm3 (model vol.)'
'actual vol.= 1.21592e4 cm3 = (28316.84 cm3/ft3)(9.646 lb)/(22.464 lb/ft3)'
arbmh2ok   0.49860  2 0 0 0    1001   11.1913
                               8016   88.8087   13  0.0287  293  end
arbmal2o3  0.33241  2 0 0 0   13027   52.9390
                               8016   47.0610   13  0.096   293  end
arbmsio2   0.33241  2 0 0 0   14000   46.7570
                               8016   53.2430   13  0.367   293  end
arbmfe2o3  0.33241  2 0 0 0   26000   69.9540
                               8016   30.0460   13  0.067   293  end
arbmtio2   0.33241  2 0 0 0   22000   59.9535
                               8016   40.0465   13  0.012   293  end
arbmcao    0.33241  2 0 0 0   20000   71.4815
                               8016   28.5185   13  0.307   293  end
arbmmgo    0.33241  2 0 0 0   12000   60.3169
                               8016   39.6831   13  0.131   293  end
arbmna2o   0.33241  2 0 0 0   11023   74.1961
                               8016   25.8039   13  0.020   293  end
'silicone rubber pads'
arbmsiru   1.21791  4 0 0 0    6012   32.3767
                               1001    8.1573
                               8016   21.5782
                              14000   37.8878   14  1.0     293  end
'void space external to containment vessel'
arbmwecv   0.9982   2 0 0 0    1001   11.1913
                               8016   88.8087   15  1       293  end
'steel: liner'
ss304                                            16  1.0     293  end
'steel: plug cover (pc) use 9.907 lb'
ss304                                            17  1.06388 293  end
'steel: angle iron (ai) for single units'
'ss304                                            18  1.0     293  end
'steel: angle iron (ai) for arrays'
'array density is multiplied by a volume fraction 7.08030/5.63249'
ss304                                            18  1.25705 293  end
'steel: drum steel for single units'
'ss304                                            19  1.0     293  end
'steel: drum steel for arrays'
'array density is multiplied by a volume fraction 3.20482/3.20544'
ss304                                            19  0.99981 293  end
'void space external to drum'
'array density is multiplied by a volume ratio 8.11698/6.98323'
arbmwed    1.16026  2 0 0 0    1001   11.1913
                               8016   88.8087   20  1       293  end
'reflective water'
'arbmh20r   0.9982   2 0 0 0    1001   11.1913
'                               8016   88.8087   21  1.0     293  end
end comp
nciask,0.0,21300.0g soc(19865.3uox,15672.8u235,  921.0c),hx= 12.82 fr=1.0e+00
read parameters nub=yes npg=2500 gen=215 nsk=15 tme=100 end parameters
read boun       all=specular                     end boun
read geometry
unit 1001
'drum bottom flat cover [Elev= 0.111 in. at top of unit]'
'cylinder  19 1   22.866096    0.28150   0.0     com='extended radius not used'
 cylinder  19 1   21.722275    0.28150   0.0     com='drum bottom flat cover'
 cuboid    20 1 4p22.866096    0.28150   0.0     com='drum chine outer radius'
unit 1002
'above drum bottom flat cover and below containment vessel [Elev= 4.676 in.]'
 cylinder  15 1    3.175000   11.59510  11.16330 com='void in pad-1'
 cylinder  14 1    7.924800   11.59510  11.16330 com='pad-1'
 cylinder  16 1    8.077200   11.59510  11.16330 com='np277_4 liner'
 cylinder  11 1   10.922000   11.59510  11.16330 com='np277_4'
 cylinder  16 1   11.074400   11.59510  10.85850 com='kaolite liner bottom'
 cylinder  12 1   21.555075   11.59510   0.0     com='kaolite'
 cylinder  19 1   21.722275   11.59510   0.0     com='drum'
 cuboid    20 1 4p22.866096   11.59510   0.0     com='drum chine outer radius'
unit 1003
'cv bottom to bottom of 1st step [Elev=35.276 in.]'
 cylinder  3  1    6.426200   77.72400  54.39413 com='cavity abv HEU'
 cylinder  1  1    6.426200   77.72400   0.63500 com='HEU content'
```

```
 cylinder  8  1    6.680200   77.72400   0.0     com='cv bottom'
 cylinder  15 1    7.924800   77.72400   0.0     com='void btw cv-np liner'
 cylinder  16 1    8.077200   77.72400   0.0     com='np277_4 liner'
 cylinder  11 1   10.922000   77.72400   0.0     com='np277_4'
 cylinder  16 1   11.074400   77.72400   0.0     com='kaolite liner'
 cylinder  12 1   21.555075   77.72400   0.0     com='kaolite'
 cylinder  19 1   21.722275   77.72400   0.0     com='drum'
 cuboid    20 1 4p22.866096   77.72400   0.0     com='drum chine outer radius'
unit 1010
'cv at 1st step in liner [Elev=35.336 in.]'
 cylinder  3  1    6.426200    0.15240   0.00000 com='cavity abv HEU'
 cylinder  1  1    6.426200    0.15240   0.0     com='HEU content'
 cylinder  8  1    6.680200    0.15240   0.0     com='cv at 1st step'
 cylinder  15 1    7.924800    0.15240   0.0     com='void btw cv and liner'
 cylinder  16 1   11.074400    0.15240   0.0     com='liner 1st step'
 cylinder  12 1   21.555075    0.15240   0.0     com='kaolite'
 cylinder  19 1   21.722275    0.15240   0.0     com='drum'
 cuboid    20 1 4p22.866096    0.15240   0.0     com='drum chine outer radius'
unit 1011
'vertical gap between 1st step in liner and cv flange [Elev=35.426 in.]'
 cylinder  3  1    6.426200    0.22860   0.00000 com='cavity abv HEU'
 cylinder  1  1    6.426200    0.22860   0.0     com='HEU content'
 cylinder  8  1    6.680200    0.22860   0.0     com='cv at gap btwn step-flng'
 cylinder  15 1   10.922000    0.22860   0.0     com='void btw cv and liner'
 cylinder  16 1   11.074400    0.22860   0.0     com='liner wall'
 cylinder  12 1   21.555075    0.22860   0.0     com='kaolite'
 cylinder  19 1   21.722275    0.22860   0.0     com='drum'
 cuboid    20 1 4p22.866096    0.22860   0.0     com='drum chine outer radius'
unit 1012
'cv flange to top of cv well [Elev=35.926 in.]'
 cylinder  3  1    6.426200    1.27000   0.00000 com='cavity abv HEU'
 cylinder  1  1    6.426200    1.27000   0.0     com='HEU content'
 cylinder  9  1    9.525000    1.27000   0.0     com='flange to top of well'
 cylinder  15 1    9.525000    1.27000   0.0     com='void btw cv and pad-2'
 cylinder  14 1   10.033000    1.27000   0.0     com='pad-2'
 cylinder  15 1   10.922000    1.27000   0.0     com='void btw cv and liner'
 cylinder  16 1   11.074400    1.27000   0.0     com='liner wall'
 cylinder  12 1   21.555075    1.27000   0.0     com='kaolite'
 cylinder  19 1   21.722275    1.27000   0.0     com='drum'
 cuboid    20 1 4p22.866096    1.27000   0.0     com='drum chine outer radius'
unit 1013
'cv flange above cv well [Elev=37.076 in.]'
 cylinder  10 1    9.525000    2.92100   0.0     com='flange above cv well'
 cylinder  15 1    9.525000    2.92100   0.0     com='void btw cv and pad-2'
 cylinder  14 1   10.033000    2.92100   0.0     com='pad-2'
 cylinder  15 1   10.922000    2.92100   0.0     com='void btw pad2 and liner'
 cylinder  16 1   11.074400    2.92100   0.0     com='liner wall'
 cylinder  12 1   21.555075    2.92100   0.0     com='kaolite'
 cylinder  19 1   21.722275    2.92100   0.0     com='drum'
 cuboid    20 1 4p22.866096    2.92100   0.0     com='drum chine outer radius'
unit 1014
'plugpad2 below liner 2nd step [Elev=37.476 in.]'
 cylinder  14 1   10.033000    0.76200   0.0     com='pad-2'
 cylinder  15 1   10.922000    1.01600   0.0     com='void btw pad2 and liner'
 cylinder  16 1   11.074400    1.01600   0.0     com='liner wall'
 cylinder  12 1   21.555075    1.01600   0.0     com='kaolite'
 cylinder  19 1   21.722275    1.01600   0.0     com='drum'
 cuboid    20 1 4p22.866096    1.01600   0.0     com='drum chine outer radius'
unit 1015
'2nd step in liner [Elev=37.536 in.]'
 cylinder  15 1   10.922000    0.15240   0.0     com='void abv pad2'
 cylinder  16 1   18.757900    0.15240   0.0     com='liner 2nd step'
 cylinder  12 1   21.555075    0.15240   0.0     com='kaolite'
 cylinder  19 1   21.722275    0.15240   0.0     com='drum'
 cuboid    20 1 4p22.866096    0.15240   0.0     com='drum chine outer radius'
unit 1016
'abv 2nd step in liner to bottom of angle iron [Elev=40.756 in.]'
 cylinder  13 1   18.097500    8.17880   0.49276 com='plug kaolite'
 cylinder  17 1   18.249900    8.17880   0.34036 com='sides of plug case'
 cylinder  15 1   18.605500    8.17880   0.0     com='void: plug to liner'
 cylinder  16 1   18.757900    8.17880   0.0     com='liner wall'
```

```
 cylinder  12 1   21.555075    8.17880   0.0     com='kaolite'
 cylinder  19 1   21.722275    8.17880   0.0     com='drum'
 cuboid    20 1 4p22.866096    8.17880   0.0     com='drum chine outer radius'
unit 1017
'bottom of angle iron to bend in angle iron [Elev=42.506 in.]'
 cylinder  13 1   18.097500    4.44500   0.0     com='plug kaolite'
 cylinder  17 1   18.249900    4.44500   0.0     com='sides of plug case'
 cylinder  15 1   18.605500    4.44500   0.0     com='void: plug to liner'
 cylinder  16 1   18.757900    4.44500   0.0     com='liner wall'
 cylinder  18 1   19.392900    4.44500   0.0     com='lower angle iron'
 cylinder  12 1   21.555075    4.44500   0.0     com='kaolite'
 cylinder  19 1   21.722275    4.44500   0.0     com='drum'
 cuboid    20 1 4p22.866096    4.44500   0.0     com='drum chine outer radius'
unit 1018
'bend in angle iron to top of angle iron [Elev=42.756 in.]'
 cylinder  13 1   18.097500    0.11176   0.0     com='plug kaolite'
 cylinder  17 1   18.249900    0.26416   0.0     com='sides of plug case'
 cylinder  15 1   18.605500    0.63500   0.0     com='void: plug to liner'
 cylinder  16 1   18.757900    0.63500   0.0     com='liner wall'
 cylinder  18 1   21.555075    0.63500   0.0     com='bend section of ai'
 cylinder  19 1   21.722275    0.63500   0.0     com='drum'
 cuboid    20 1 4p22.866096    0.63500   0.0     com='drum chine outer radius'
unit 1019
'drum lid and lip [Elev=43.512 in.]'
 cylinder  20 1   21.330090    1.91973   0.16720 com='void above lid'
 cylinder  19 1   21.497290    1.91973   0.0     com='drum lid'
 cylinder  20 1   21.555075    1.91973   0.0     com='void btw lid - drum wall'
 cylinder  19 1   21.722275    1.91973   0.0     com='drum'
 cuboid    20 1 4p22.866096    1.91973   0.0     com='drum chine outer radius'
global
unit 1020
'es3100 drum [Elev=43.512 in.]'
array 3         2r-22.866096     0.0
'cuboid     0  1 4p24.587200    1120.337  0.0    com='bare package'
'cuboid    21  1 4p55.067200   1150.817 -30.48   com='reflected package'
 cuboid    20  1 4p22.866096    110.5197  0.0    com='interstital array space'
'global
'unit 1021
'array 4   3r0.0
'reflector  21 2  6r3.0  10
end geometry
read array
ara=3 nux=1 nuy=1 nuz=13 fill
1001 1002 1003 1010
1011 1012 1013 1014 1015 1016 1017 1018 1019        end fill
'ara=4 nux=13 nuy=13 nuz=06 fill f1020               end fill
end array
'read bias id=500 2  11  end bias
read start nst=0
end start
end data
end


=csas25    parm=size=3000000
ncsrunhct11 0.0innp,disp. 9000.0gUNHc( 4238.7g235, 6980.8gH2O hx= 54.99),fr=1.0e+00
238groupndf5 infhommedium
'U(enr)O2(NO3)2+6H2O [2.81 g/cc for U(nat)], gU/L= 414.9296'
'UNH crystals in cans  2.79329 g/cm3. wrapped dry content can hx=3.96'
arbmunh    2.79329  5 0 0 0   92235   47.0962
                              92238    0.0000
                               1001    2.4232
                               7014    5.6116
                               8016   44.8690    1  0.31541 293  end
arbmh2oc  6.8336e-01  2 0 0 0  1001   11.1913
                               8016   88.8087    1  1.0000  293  end
'np277-4: spacer (NCT_MD&H)'
'NCT min.den.(95.3886 lb/ft3) and hydrogen'
'np277-4 min.den.= 1.527971 = (95.3886 lb/ft3)(453.59 g/lb)/(28316.84 cm3/ft3)'
'use 75% of boron in calculations per NUREG-1609 Section 6.5.3.2'
arbmboron 7.31015e-2  2 0 0 0    5010   18.1479
```

```
                                 5011   81.8520    2  0.7500  293  end
arbmnpmx  1.07070e+0 10 0 0 0    6012    1.9189
                                 7014    0.0141
                                 8016   43.4251
                                11023    0.1174
                                12000    0.3378
                                13027   39.0479
                                14000    2.4672
                                16000    0.3083
                                20000   11.8336
                                26000    0.5298    2  1.0000  293  end
arbmnph2o 3.84169e-1  2 0 0 0    1001   11.1913
                                 8016   88.8087    2  1.0000  293  end
'flooded containmment vessel and content cans -- 10 CFR 71.55(d)(3)'
arbmwicv  6.8336e-01  2 0 0 0   1001   11.1913
                                8016   88.8087     3  1.0     293  end
'steel: containment vessel body 16.60 lb but use 15.74 lb'
ss304                                              8  1.0     293  end
'steel: cv flange lower use 3.36 lb'
ss304                                              9  0.97267 293  end
'steel: cv flange upper use 13.75 lb'
ss304                                             10  0.94348 293  end
'np277-4: confinement -- neutron poison inner liner (NCT_MD&H)'
'actual vol.= 1.28314e4 cm3 = (7.83023e2 in3)(16.387064)'
'den.multiplier = 1.28314e4 cm3 (actual vol.) / 1.32708e4 cm3 (model vol.)'
'np277-4 min.den.= 1.527971 = (95.3886 lb/ft3)(453.59 g/lb)/(28316.84 cm3/ft3)'
'density = 1.477385 = (den.mult)(np277-4 min.den.) = 0.9668933*1.527971'
'use 75% of boron in calculations per NUREG-1609 Section 6.5.3.2'
arbmboron 7.06813e-2  2 0 0 0    5010   18.1479
                                 5011   81.8520   11  0.7500  293  end
arbmnpmx  1.03525e+0 10 0 0 0    6012    1.9189
                                 7014    0.0141
                                 8016   43.4251
                                11023    0.1174
                                12000    0.3378
                                13027   39.0479
                                14000    2.4672
                                16000    0.3083
                                20000   11.8336
                                26000    0.5298   11  1.0000  293  end
arbmnph2o 3.71451e-1  2 0 0 0    1001   11.1913
                                 8016   88.8087   11  1.0000  293  end
'kaolite 1600 body'
'sing.unit.density= (den.mult)(min.den.)'
' for arbmh20k = 1.012373*0.51655,  for rest = 1.012373*0.34438'
'den.mult= 1.36557e5 cm3 (actual vol.) / 1.34888e5 cm3 (model vol.)'
'actual vol.= 1.36557e5 cm3 = (28316.84 cm3/ft3)(108.33188 lb)/(22.464 lb/ft3)'
arbmh2ok   0.52294  2 0 0 0    1001   11.1913
                               8016   88.8087   12  1       293  end
arbmal2o3  0.34864  2 0 0 0   13027   52.9390
                               8016   47.0610   12  0.096   293  end
arbmsio2   0.34864  2 0 0 0   14000   46.7570
                               8016   53.2430   12  0.367   293  end
arbmfe2o3  0.34864  2 0 0 0   26000   69.9540
                               8016   30.0460   12  0.067   293  end
arbmtio2   0.34864  2 0 0 0   22000   59.9535
                               8016   40.0465   12  0.012   293  end
arbmcao    0.34864  2 0 0 0   20000   71.4815
                               8016   28.5185   12  0.307   293  end
arbmmgo    0.34864  2 0 0 0   12000   60.3169
                               8016   39.6831   12  0.131   293  end
arbmna2o   0.34864  2 0 0 0   11023   74.1961
                               8016   25.8039   12  0.020   293  end
'kaolite 1600 top plug'
'sing.unit.density= (den.mult)(min.den.)'
' for arbmh20k = 0.965246*0.51655,  for rest = 0.965246*0.34438'
'den.mult= 1.21592e4 cm3 (actual vol.) / 1.25970e4 cm3 (model vol.)'
'actual vol.= 1.21592e4 cm3 = (28316.84 cm3/ft3)(9.646 lb)/(22.464 lb/ft3)'
arbmh2ok   0.49860  2 0 0 0    1001   11.1913
                               8016   88.8087   13  1       293  end
arbmal2o3  0.33241  2 0 0 0   13027   52.9390
```

```
                                8016   47.0610   13  0.096   293  end
arbmsio2   0.33241  2 0 0 0   14000   46.7570
                                8016   53.2430   13  0.367   293  end
arbmfe2o3  0.33241  2 0 0 0   26000   69.9540
                                8016   30.0460   13  0.067   293  end
arbmtio2   0.33241  2 0 0 0   22000   59.9535
                                8016   40.0465   13  0.012   293  end
arbmcao    0.33241  2 0 0 0   20000   71.4815
                                8016   28.5185   13  0.307   293  end
arbmmgo    0.33241  2 0 0 0   12000   60.3169
                                8016   39.6831   13  0.131   293  end
arbmna2o   0.33241  2 0 0 0   11023   74.1961
                                8016   25.8039   13  0.020   293  end
'silicone rubber pads'
arbmsiru   1.21791  4 0 0 0    6012   32.3767
                                1001    8.1573
                                8016   21.5782
                               14000   37.8878   14  1.0     293  end
'void space external to containment vessel'
arbmwecv   0.9982   2 0 0 0    1001   11.1913
                                8016   88.8087   15  1       293  end
'steel: liner'
ss304                                            16  1.0     293  end
'steel: plug cover (pc) use 9.907 lb'
ss304                                            17  1.06388 293  end
'steel: angle iron (ai) for single units'
ss304                                            18  1.0     293  end
'steel: angle iron (ai) for arrays'
'array density is multiplied by a volume fraction 7.08030/5.63249'
'ss304                                            18  1.25705 293  end
'steel: drum steel for single units'
ss304                                            19  1.0     293  end
'steel: drum steel for arrays'
'array density is multiplied by a volume fraction 3.20482/3.20544'
'ss304                                            19  0.99981 293  end
'void space external to drum'
'array density is multiplied by a volume ratio 8.11698/6.98323'
'arbmwed    1.16026  2 0 0 0    1001   11.1913
'                                8016   88.8087   20  1       293  end
'reflective water'
arbmh20r   0.9982   2 0 0 0    1001   11.1913
                                8016   88.8087   21  1.0     293  end
end comp
ncsrunhct11 0.0innp,disp. 9000.0gUNHc( 4238.7g235, 6980.8gH2O,hx= 54.99),fr=1.0e+00
read parameters nub=yes npg=2500 gen=215 nsk=15 tme=100 end parameters
read boun       all=vac                          end boun
read geometry
unit 1001
'drum bottom flat cover [Elev= 0.105 in. at top of unit]'
'cylinder  19 1   24.587200    0.26670   0.0     com='extended radius not used'
 cylinder  19 1   23.329900    0.26670   0.0     com='drum bottom flat cover'
 cuboid    21 1 4p24.587200    0.26670   0.0     com='drum chine outer radius'
unit 1002
'above drum bottom flat cover and below containment vessel [Elev= 4.670 in.]'
 cylinder  15 1    3.175000   11.59510  11.16330 com='void in pad-1'
 cylinder  14 1    7.924800   11.59510  11.16330 com='pad-1'
 cylinder  16 1    8.077200   11.59510  11.16330 com='np277_4 liner'
 cylinder  11 1   10.922000   11.59510  11.16330 com='np277_4'
 cylinder  16 1   11.074400   11.59510  10.85850 com='kaolite liner bottom'
 cylinder  12 1   23.177500   11.59510   0.0     com='kaolite'
 cylinder  19 1   23.329900   11.59510   0.0     com='drum'
 cuboid    21 1 4p24.587200   11.59510   0.0     com='drum chine outer radius'
unit 1003
'cv bottom to bottom of 1st step [Elev=35.270 in.]'
 cylinder  1  1    6.426200   77.72400   0.63500 com='HEU content'
 cylinder  8  1    6.680200   77.72400   0.0     com='cv bottom'
 cylinder  15 1    7.924800   77.72400   0.0     com='void btw cv-np liner'
 cylinder  16 1    8.077200   77.72400   0.0     com='np277_4 liner'
 cylinder  11 1   10.922000   77.72400   0.0     com='np277_4'
 cylinder  16 1   11.074400   77.72400   0.0     com='kaolite liner'
 cylinder  12 1   23.177500   77.72400   0.0     com='kaolite'
```

```
 cylinder  19 1   23.329900   77.72400   0.0     com='drum'
 cuboid    21 1 4p24.587200   77.72400   0.0     com='drum chine outer radius'
unit 1010
'cv at 1st step in liner [Elev=35.330 in.]'
 cylinder  1  1    6.426200    0.15240   0.0     com='HEU content'
 cylinder  8  1    6.680200    0.15240   0.0     com='cv at 1st step'
 cylinder  15 1    7.924800    0.15240   0.0     com='void btw cv and liner'
 cylinder  16 1   11.074400    0.15240   0.0     com='liner 1st step'
 cylinder  12 1   23.177500    0.15240   0.0     com='kaolite'
 cylinder  19 1   23.329900    0.15240   0.0     com='drum'
 cuboid    21 1 4p24.587200    0.15240   0.0     com='drum chine outer radius'
unit 1011
'vertical gap between 1st step in liner and cv flange [Elev=35.420 in.]'
 cylinder  1  1    6.426200    0.22860   0.0     com='HEU content'
 cylinder  8  1    6.680200    0.22860   0.0     com='cv at gap btwn step-flng'
 cylinder  15 1   10.922000    0.22860   0.0     com='void btw cv and liner'
 cylinder  16 1   11.074400    0.22860   0.0     com='liner wall'
 cylinder  12 1   23.177500    0.22860   0.0     com='kaolite'
 cylinder  19 1   23.329900    0.22860   0.0     com='drum'
 cuboid    21 1 4p24.587200    0.22860   0.0     com='drum chine outer radius'
unit 1012
'cv flange to top of cv well [Elev=35.920 in.]'
 cylinder  1  1    6.426200    1.27000   0.0     com='HEU content'
 cylinder  9  1    9.525000    1.27000   0.0     com='flange to top of well'
 cylinder  15 1    9.525000    1.27000   0.0     com='void btw cv and pad-2'
 cylinder  14 1   10.033000    1.27000   0.0     com='pad-2'
 cylinder  15 1   10.922000    1.27000   0.0     com='void btw cv and liner'
 cylinder  16 1   11.074400    1.27000   0.0     com='liner wall'
 cylinder  12 1   23.177500    1.27000   0.0     com='kaolite'
 cylinder  19 1   23.329900    1.27000   0.0     com='drum'
 cuboid    21 1 4p24.587200    1.27000   0.0     com='drum chine outer radius'
unit 1013
'cv flange above cv well [Elev=37.070 in.]'
 cylinder  10 1    9.525000    2.92100   0.0     com='flange above cv well'
 cylinder  15 1    9.525000    2.92100   0.0     com='void btw cv and pad-2'
 cylinder  14 1   10.033000    2.92100   0.0     com='pad-2'
 cylinder  15 1   10.922000    2.92100   0.0     com='void btw pad2 and liner'
 cylinder  16 1   11.074400    2.92100   0.0     com='liner wall'
 cylinder  12 1   23.177500    2.92100   0.0     com='kaolite'
 cylinder  19 1   23.329900    2.92100   0.0     com='drum'
 cuboid    21 1 4p24.587200    2.92100   0.0     com='drum chine outer radius'
unit 1014
'plugpad2 below liner 2nd step [Elev=37.470 in.]'
 cylinder  14 1   10.033000    0.76200   0.0     com='pad-2'
 cylinder  15 1   10.922000    1.01600   0.0     com='void btw pad2 and liner'
 cylinder  16 1   11.074400    1.01600   0.0     com='liner wall'
 cylinder  12 1   23.177500    1.01600   0.0     com='kaolite'
 cylinder  19 1   23.329900    1.01600   0.0     com='drum'
 cuboid    21 1 4p24.587200    1.01600   0.0     com='drum chine outer radius'
unit 1015
'2nd step in liner [Elev=37.530 in.]'
 cylinder  15 1   10.922000    0.15240   0.0     com='void abv pad2'
 cylinder  16 1   18.757900    0.15240   0.0     com='liner 2nd step'
 cylinder  12 1   23.177500    0.15240   0.0     com='kaolite'
 cylinder  19 1   23.329900    0.15240   0.0     com='drum'
 cuboid    21 1 4p24.587200    0.15240   0.0     com='drum chine outer radius'
unit 1016
'abv 2nd step in liner to bottom of angle iron [Elev=40.750 in.]'
 cylinder  13 1   18.097500    8.17880   0.49276 com='plug kaolite'
 cylinder  17 1   18.249900    8.17880   0.34036 com='sides of plug case'
 cylinder  15 1   18.605500    8.17880   0.0     com='void: plug to liner'
 cylinder  16 1   18.757900    8.17880   0.0     com='liner wall'
 cylinder  12 1   23.177500    8.17880   0.0     com='kaolite'
 cylinder  19 1   23.329900    8.17880   0.0     com='drum'
 cuboid    21 1 4p24.587200    8.17880   0.0     com='drum chine outer radius'
unit 1017
'bottom of angle iron to bend in angle iron [Elev=42.500 in.]'
 cylinder  13 1   18.097500    4.44500   0.0     com='plug kaolite'
 cylinder  17 1   18.249900    4.44500   0.0     com='sides of plug case'
 cylinder  15 1   18.605500    4.44500   0.0     com='void: plug to liner'
 cylinder  16 1   18.757900    4.44500   0.0     com='liner wall'
```

```
 cylinder  18 1   19.392900    4.44500   0.0     com='lower angle iron'
 cylinder  12 1   23.177500    4.44500   0.0     com='kaolite'
 cylinder  19 1   23.329900    4.44500   0.0     com='drum'
 cuboid    21 1 4p24.587200    4.44500   0.0     com='drum chine outer radius'
unit 1018
'bend in angle iron to top of angle iron [Elev=42.750 in.]'
 cylinder  13 1   18.097500    0.11176   0.0     com='plug kaolite'
 cylinder  17 1   18.249900    0.26416   0.0     com='sides of plug case'
 cylinder  15 1   18.605500    0.63500   0.0     com='void: plug to liner'
 cylinder  16 1   18.757900    0.63500   0.0     com='liner wall'
 cylinder  18 1   23.177500    0.63500   0.0     com='bend section of ai'
 cylinder  19 1   23.329900    0.63500   0.0     com='drum'
 cuboid    21 1 4p24.587200    0.63500   0.0     com='drum chine outer radius'
unit 1019
'drum lid and lip [Elev=43.500 in.]'
 cylinder  21 1   22.961600    1.90500   0.15240 com='void above lid'
 cylinder  19 1   23.114000    1.90500   0.0     com='drum lid'
 cylinder  21 1   23.177500    1.90500   0.0     com='void btw lid - drum wall'
 cylinder  19 1   23.329900    1.90500   0.0     com='drum'
 cuboid    21 1 4p24.587200    1.90500   0.0     com='drum chine outer radius'
global
unit 1020
'es3100 drum [Elev=43.500 in.]'
array 3         2r-24.587200     0.0
'cuboid     0  1 4p24.587200    110.4905  0.0    com='bare package'
 cuboid    21  1 4p55.067200   140.9700 -30.48   com='reflected package'
'cuboid    20  1 4p22.889718    110.5048  0.0    com='interstital array space'
'global
'unit 1021
'array 4   3r0.0
'reflector  21 2  6r3.0  10
end geometry
read array
ara=3 nux=1 nuy=1 nuz=13 fill
1001 1002 1003 1010
1011 1012 1013 1014 1015 1016 1017 1018 1019        end fill
'ara=4 nux=13 nuy=13 nuz=06 fill f1020               end fill
end array
'read bias id=500 2  11  end bias
read start nst=0
end start
end data
end


=csas25    parm=size=3000000
icsrunhct12 0.0innp,disp.15000.0gUNHc( 7064.4g235, 6870.7gH2O hx= 52.91),fr=1.0e+00
238groupndf5 infhommedium
'U(enr)O2(NO3)2+6H2O [2.81 g/cc for U(nat)], gU/L= 429.1329 dispersed'
'UNH crystals in cans  2.79329 g/cm3. wrapped dry content can hx=2.37'
'UNHc in cv   9308.07449 g.'
'water in cv  6870.67680 g.'
arbmunh    2.79329  5 0 0 0   92235   47.0962
                              92238    0.0000
                               1001    2.4232
                               7014    5.6116
                               8016   44.8690    1  0.32620 293  end
arbmh2oc   0.99820  2 0 0 0    1001   11.1913
                               8016   88.8087    1  0.67380 293  end
'np277-4: spacer (HAC_MD&H)'
'HAC min.den.(95.3157 lb/ft3) and hydrogen'
'np277-4 min.den.= 1.526803 = (95.3157 lb/ft3)(453.59 g/lb)/(28316.84 cm3/ft3)'
'use 75% of boron in calculations per NUREG-1609 Section 6.5.3.2'
arbmboron 7.31015e-2  2 0 0 0    5010   18.1479
                                 5011   81.8520    2  0.7500  293  end
arbmnpmx  1.07071e+0 10 0 0 0    6012    1.9188
                                 7014    0.0141
                                 8016   43.4254
                                11023    0.1174
                                12000    0.3378
                                13027   39.0477
```

```
                                14000    2.4671
                                16000    0.3083
                                20000   11.8335
                                26000    0.5298    2  1.0000  293  end
arbmnph2o 3.82995e-1  2 0 0 0    1001   11.1913
                                 8016   88.8087    2  1.0000  293  end
'flooded containmment vessel and content cans -- 10 CFR 71.55(d)(3)'
arbmwicv  9.9820e-01  2 0 0 0    1001   11.1913
                                 8016   88.8087    3  1.0     293  end
'steel: containment vessel body 16.60 lb but use 15.74 lb'
ss304                                            8  1.0     293  end
'steel: cv flange lower use 3.36 lb'
ss304                                            9  0.97267 293  end
'steel: cv flange upper use 13.75 lb'
ss304                                           10  0.94348 293  end
'np277-4: confinement -- neutron poison inner liner (HAC_MD&H)'
'actual vol.= 1.31846e4 cm3 = (8.0457422e2 in3)(16.387064)'
'den.multiplier = 1.31846e4 cm3 (actual vol.) / 1.32708e4 cm3 (model vol.)'
'np277-4 min.den.= 1.526803 = (95.3157 lb/ft3)(453.59 g/lb)/(28316.84 cm3/ft3)'
'density = 1.516887 = (den.mult)(np277-4 min.den.) = 0.9935052*1.526803'
'use 75% of boron in calculations per NUREG-1609 Section 6.5.3.2'
arbmboron 7.26267e-2  2 0 0 0    5010   18.1479
                                 5011   81.8520   11  0.7500  293  end
arbmnpmx  1.06375e+0 10 0 0 0    6012    1.9188
                                 7014    0.0141
                                 8016   43.4254
                                11023    0.1174
                                12000    0.3378
                                13027   39.0477
                                14000    2.4671
                                16000    0.3083
                                20000   11.8335
                                26000    0.5298   11  1.0000  293  end
arbmnph2o 3.80508e-1  2 0 0 0    1001   11.1913
                                 8016   88.8087   11  1.0000  293  end
'kaolite 1600 body'
'nct.sing.unit.density= (den.mult)(min.den.)'
' for arbmh20k 0.52294 = 1.012373*0.51655, for rest 0.34864 = 1.012373*0.34438'
'den.mult= 1.36557e5 cm3 (actual vol.) / 1.34888e5 cm3 (model vol.)'
'actual vol.= 1.36557e5 cm3 = (28316.84 cm3/ft3)(108.33188 lb)/(22.464 lb/ft3)'
'hac.s.u.dens= (hac.mult)(nct.s.u.dens)'
'hac.mult = 1.34888e5 cm3 (nct vol.)/ 1.12246e5 cm3 (model vol.)'
' for arbmh2ok 0.62843 = 1.20172*0.52294,   for rest = 1.20172*0.34864'
arbmh2ok   0.62843  2 0 0 0    1001   11.1913
                               8016   88.8087   12  1       293  end
arbmal2o3  0.41898  2 0 0 0   13027   52.9390
                               8016   47.0610   12  0.096   293  end
arbmsio2   0.41898  2 0 0 0   14000   46.7570
                               8016   53.2430   12  0.367   293  end
arbmfe2o3  0.41898  2 0 0 0   26000   69.9540
                               8016   30.0460   12  0.067   293  end
arbmtio2   0.41898  2 0 0 0   22000   59.9535
                               8016   40.0465   12  0.012   293  end
arbmcao    0.41898  2 0 0 0   20000   71.4815
                               8016   28.5185   12  0.307   293  end
arbmmgo    0.41898  2 0 0 0   12000   60.3169
                               8016   39.6831   12  0.131   293  end
arbmna2o   0.41898  2 0 0 0   11023   74.1961
                               8016   25.8039   12  0.020   293  end
'kaolite 1600 top plug'
'sing.unit.density= (den.mult)(min.den.)'
' for arbmh20k = 0.965246*0.51655,  for rest = 0.965246*0.34438'
'den.mult= 1.21592e4 cm3 (actual vol.) / 1.25970e4 cm3 (model vol.)'
'actual vol.= 1.21592e4 cm3 = (28316.84 cm3/ft3)(9.646 lb)/(22.464 lb/ft3)'
arbmh2ok   0.49860  2 0 0 0    1001   11.1913
                               8016   88.8087   13  1       293  end
arbmal2o3  0.33241  2 0 0 0   13027   52.9390
                               8016   47.0610   13  0.096   293  end
arbmsio2   0.33241  2 0 0 0   14000   46.7570
                               8016   53.2430   13  0.367   293  end
arbmfe2o3  0.33241  2 0 0 0   26000   69.9540
```

```
                                8016   30.0460   13  0.067   293  end
arbmtio2   0.33241  2 0 0 0   22000   59.9535
                                8016   40.0465   13  0.012   293  end
arbmcao    0.33241  2 0 0 0   20000   71.4815
                                8016   28.5185   13  0.307   293  end
arbmmgo    0.33241  2 0 0 0   12000   60.3169
                                8016   39.6831   13  0.131   293  end
arbmna2o   0.33241  2 0 0 0   11023   74.1961
                                8016   25.8039   13  0.020   293  end
'silicone rubber pads'
arbmsiru   1.21791  4 0 0 0    6012   32.3767
                                1001    8.1573
                                8016   21.5782
                               14000   37.8878   14  1.0     293  end
'void space external to containment vessel'
'UNHc in cv well   5691.92551 g.'
'water in cv well  4201.44688 g.'
arbmunh    2.79329  5 0 0 0   92235   47.0962
                               92238    0.0000
                                1001    2.4232
                                7014    5.6116
                                8016   44.8690   15  0.32620 293  end
arbmh2oc   0.99820  2 0 0 0    1001   11.1913
                                8016   88.8087   15  0.67380 293  end
'steel: liner'
ss304                                            16  1.0     293  end
'steel: plug cover (pc) use 9.907 lb'
ss304                                            17  1.06388 293  end
'steel: angle iron (ai) for HAC'
'nct density is multiplied by volume fraction 7.08030/5.74516'
ss304                                            18  1.23239 293  end
'steel: drum steel for HAC'
'nct density is multiplied by volume fraction 3.20482/2.95645'
ss304                                            19  1.08401 293  end
'void space external to drum'
'array density is assumed not reduced by hac'
'arbmwed    0.9982   2 0 0 0    1001   11.1913
'                               8016   88.8087   20  1       293  end
'reflective water'
arbmh20r   0.9982   2 0 0 0    1001   11.1913
                                8016   88.8087   21  1.0     293  end
end comp
icsrunhct12 0.0innp,disp.15000.0gUNHc( 7064.4g235, 6870.7gH2O,hx= 52.91),fr=1.0e+00
read parameters nub=yes npg=2500 gen=215 nsk=15 tme=100 end parameters
read boun       all=vac                          end boun
read geometry
unit 1001
'drum bottom flat cover [Elev= 0.105 in. at top of unit]'
'cylinder  19 1   21.838092    0.26670   0.0     com='extended radius not used'
 cylinder  19 1   21.838092    0.26670   0.0     com='drum bottom flat cover'
 cuboid    21 1 4p21.838092    0.26670   0.0     com='drum(chine)outer radius'
unit 1002
'above drum bottom flat cover and below containment vessel [Elev= 4.670 in.]'
'v1002=1.36748e+01  '
 cylinder  15 1    3.175000   11.59510  11.16330 com='void in pad-1'
 cylinder  14 1    7.924800   11.59510  11.16330 com='pad-1'
 cylinder  16 1    8.077200   11.59510  11.16330 com='np277_4 liner'
 cylinder  11 1   10.922000   11.59510  11.16330 com='np277_4'
 cylinder  16 1   11.074400   11.59510  10.85850 com='kaolite liner bottom'
 cylinder  12 1   21.685692   11.59510   0.0     com='kaolite'
 cylinder  19 1   21.838092   11.59510   0.0     com='drum'
 cuboid    21 1 4p21.838092   11.59510   0.0     com='drum(chine)outer radius'
unit 1003
'cv bottom to bottom of 1st step [Elev=35.270 in.]'
'v1003=4.43850e+03  '
 cylinder  1  1    6.426200   77.72400   0.63500 com='HEU content'
 cylinder  8  1    6.680200   77.72400   0.0     com='cv bottom'
 cylinder  15 1    7.924800   77.72400   0.0     com='void btw cv-np liner'
 cylinder  16 1    8.077200   77.72400   0.0     com='np277_4 liner'
 cylinder  11 1   10.922000   77.72400   0.0     com='np277_4'
 cylinder  16 1   11.074400   77.72400   0.0     com='kaolite liner'
```

```
 cylinder  12 1   21.685692   77.72400   0.0     com='kaolite'
 cylinder  19 1   21.838092   77.72400   0.0     com='drum'
 cuboid    21 1 4p21.838092   77.72400   0.0     com='drum(chine)outer radius'
unit 1010
'cv at 1st step in liner [Elev=35.330 in.]'
'v1010=8.70294e+00  '
 cylinder  1  1    6.426200    0.15240   0.0     com='HEU content'
 cylinder  8  1    6.680200    0.15240   0.0     com='cv at 1st step'
 cylinder  15 1    7.924800    0.15240   0.0     com='void btw cv and liner'
 cylinder  16 1   11.074400    0.15240   0.0     com='liner 1st step'
 cylinder  12 1   21.685692    0.15240   0.0     com='kaolite'
 cylinder  19 1   21.838092    0.15240   0.0     com='drum'
 cuboid    21 1 4p21.838092    0.15240   0.0     com='drum(chine)outer radius'
unit 1011
'vertical gap between 1st step in liner and cv flange [Elev=35.420 in.]'
'v1011=5.36220e+01  '
 cylinder  1  1    6.426200    0.22860   0.0     com='HEU content'
 cylinder  8  1    6.680200    0.22860   0.0     com='cv at gap btwn step-flng'
 cylinder  15 1   10.922000    0.22860   0.0     com='void btw cv and liner'
 cylinder  16 1   11.074400    0.22860   0.0     com='liner wall'
 cylinder  12 1   21.685692    0.22860   0.0     com='kaolite'
 cylinder  19 1   21.838092    0.22860   0.0     com='drum'
 cuboid    21 1 4p21.838092    0.22860   0.0     com='drum(chine)outer radius'
unit 1012
'cv flange to top of cv well [Elev=35.920 in.]'
'v1012=7.43264e+01  '
 cylinder  1  1    6.426200    1.27000   0.0     com='HEU content'
 cylinder  9  1    9.525000    1.27000   0.0     com='flange to top of well'
 cylinder  15 1    9.525000    1.27000   0.0     com='void btw cv and pad-2'
 cylinder  14 1   10.033000    1.27000   0.0     com='pad-2'
 cylinder  15 1   10.922000    1.27000   0.0     com='void btw cv and liner'
 cylinder  16 1   11.074400    1.27000   0.0     com='liner wall'
 cylinder  12 1   21.685692    1.27000   0.0     com='kaolite'
 cylinder  19 1   21.838092    1.27000   0.0     com='drum'
 cuboid    21 1 4p21.838092    1.27000   0.0     com='drum(chine)outer radius'
unit 1013
'cv flange above cv well [Elev=37.070 in.]'
'v1013=1.70951e+02  '
 cylinder  10 1    9.525000    2.92100   0.0     com='flange above cv well'
 cylinder  15 1    9.525000    2.92100   0.0     com='void btw cv and pad-2'
 cylinder  14 1   10.033000    2.92100   0.0     com='pad-2'
 cylinder  15 1   10.922000    2.92100   0.0     com='void btw pad2 and liner'
 cylinder  16 1   11.074400    2.92100   0.0     com='liner wall'
 cylinder  12 1   21.685692    2.92100   0.0     com='kaolite'
 cylinder  19 1   21.838092    2.92100   0.0     com='drum'
 cuboid    21 1 4p21.838092    2.92100   0.0     com='drum(chine)outer radius'
unit 1014
'plugpad2 below liner 2nd step [Elev=37.470 in.]'
'v1014=1.39785e+02  '
 cylinder  14 1   10.033000    0.76200   0.0     com='pad-2'
 cylinder  15 1   10.922000    1.01600   0.0     com='void btw pad2 and liner'
 cylinder  16 1   11.074400    1.01600   0.0     com='liner wall'
 cylinder  12 1   21.685692    1.01600   0.0     com='kaolite'
 cylinder  19 1   21.838092    1.01600   0.0     com='drum'
 cuboid    21 1 4p21.838092    1.01600   0.0     com='drum(chine)outer radius'
unit 1015
'2nd step in liner [Elev=37.530 in.]'
'v1015=5.71136e+01  '
 cylinder  15 1   10.922000    0.15240   0.0     com='void abv pad2'
 cylinder  16 1   18.757900    0.15240   0.0     com='liner 2nd step'
 cylinder  12 1   21.685692    0.15240   0.0     com='kaolite'
 cylinder  19 1   21.838092    0.15240   0.0     com='drum'
 cuboid    21 1 4p21.838092    0.15240   0.0     com='drum(chine)outer radius'
unit 1016
'abv 2nd step in liner to bottom of angle iron [Elev=40.750 in.]'
'v1016=6.92877e+02  '
 cylinder  13 1   18.097500    8.17880   0.49276 com='plug kaolite'
 cylinder  17 1   18.249900    8.17880   0.34036 com='sides of plug case'
 cylinder  15 1   18.605500    8.17880   0.0     com='void: plug to liner'
 cylinder  16 1   18.757900    8.17880   0.0     com='liner wall'
 cylinder  12 1   21.685692    8.17880   0.0     com='kaolite'
```

```
 cylinder  19 1   21.838092    8.17880   0.0     com='drum'
 cuboid    21 1 4p21.838092    8.17880   0.0     com='drum(chine)outer radius'
unit 1017
'bottom of angle iron to bend in angle iron [Elev=42.500 in.]'
'v1017=1.83014e+02  '
 cylinder  13 1   18.097500    4.44500   0.0     com='plug kaolite'
 cylinder  17 1   18.249900    4.44500   0.0     com='sides of plug case'
 cylinder  15 1   18.605500    4.44500   0.0     com='void: plug to liner'
 cylinder  16 1   18.757900    4.44500   0.0     com='liner wall'
 cylinder  18 1   19.392900    4.44500   0.0     com='lower angle iron'
 cylinder  12 1   21.685692    4.44500   0.0     com='kaolite'
 cylinder  19 1   21.838092    4.44500   0.0     com='drum'
 cuboid    21 1 4p21.838092    4.44500   0.0     com='drum(chine)outer radius'
unit 1018
'bend in angle iron to top of angle iron [Elev=42.750 in.]'
'v1018=4.14168e+02  '
'Volume cv well=6.24674e+03  '
 cylinder  13 1   18.097500    0.11176   0.0     com='plug kaolite'
 cylinder  17 1   18.249900    0.26416   0.0     com='sides of plug case'
 cylinder  15 1   18.605500    0.63500   0.0     com='void: plug to liner'
 cylinder  16 1   18.757900    0.63500   0.0     com='liner wall'
 cylinder  18 1   21.685692    0.63500   0.0     com='bend section of ai'
 cylinder  19 1   21.838092    0.63500   0.0     com='drum'
 cuboid    21 1 4p21.838092    0.63500   0.0     com='drum(chine)outer radius'
unit 1019
'drum lid and lip [Elev=43.500 in.]'
 cylinder  21 1   21.469792    1.90500   0.15240 com='void above lid'
 cylinder  19 1   21.622192    1.90500   0.0     com='drum lid'
 cylinder  21 1   21.685692    1.90500   0.0     com='void btw lid - drum wall'
 cylinder  19 1   21.838092    1.90500   0.0     com='drum'
 cuboid    21 1 4p21.838092    1.90500   0.0     com='drum(chine)outer radius'
global
unit 1020
'es3100 drum [Elev=43.500 in.]'
array 3         2r-21.838092     0.0
'cuboid     0  1 4p21.838092    110.4905  0.0    com='bare package'
 cuboid    21  1 4p52.318092   140.9700 -30.48   com='reflected package'
'cuboid    20  1 4p22.889718    110.5048  0.0    com='interstital array space'
'global
'unit 1021
'array 4   3r0.0
'reflector  21 2  6r3.0  10
end geometry
read array
ara=3 nux=1 nuy=1 nuz=13 fill
1001 1002 1003 1010
1011 1012 1013 1014 1015 1016 1017 1018 1019        end fill
'ara=4 nux=13 nuy=13 nuz=06 fill f1020               end fill
end array
'read bias id=500 2  11  end bias
read start nst=0
end start
end data
end


=csas25    parm=size=3000000
ncsrtriga 0.0in thk np,10400.0gUZrHx(  921.0g235, 8998.2gH2O hx=255.01),fr=1.0e+00
238groupndf5 infhommedium
'TRIGA volume =1200.95996, SPACER volume    0.00000'
'TRIGA wrapped dry content can hx=18.2, CV void volume 9014.40198'
arbmtriga  8.65974  4 0 0 0    1001    0.9554
                              40000   54.0446
                              92235    8.8558
                              92238   36.1442    1  1.0     293  end
'np277-4: spacer (NCT_MD&H)'
'NCT min.den.(95.3886 lb/ft3) and hydrogen'
'np277-4 min.den.= 1.527971 = (95.3886 lb/ft3)(453.59 g/lb)/(28316.84 cm3/ft3)'
'use 75% of boron in calculations per NUREG-1609 Section 6.5.3.2'
arbmboron 7.31015e-2  2 0 0 0    5010   18.1479
                                 5011   81.8520    2  0.7500  293  end
```

```
arbmnpmx  1.07070e+0 10 0 0 0    6012    1.9189
                                 7014    0.0141
                                 8016   43.4251
                                11023    0.1174
                                12000    0.3378
                                13027   39.0479
                                14000    2.4672
                                16000    0.3083
                                20000   11.8336
                                26000    0.5298    2  1.0000  293  end
arbmnph2o 3.84169e-1  2 0 0 0    1001   11.1913
                                 8016   88.8087    2  1.0000  293  end
'flooded containmment vessel and content cans -- 10 CFR 71.55(d)(3)'
arbmwicv   0.9982   2 0 0 0    1001   11.1913
                               8016   88.8087    3  1       293  end
'steel: containment vessel body 16.60 lb but use 15.74 lb'
ss304                                            8  1.0     293  end
'steel: cv flange lower use 3.36 lb'
ss304                                            9  0.97267 293  end
'steel: cv flange upper use 13.75 lb'
ss304                                           10  0.94348 293  end
'np277-4: confinement -- neutron poison inner liner (NCT_MD&H)'
'actual vol.= 1.28314e4 cm3 = (7.83023e2 in3)(16.387064)'
'den.multiplier = 1.28314e4 cm3 (actual vol.) / 1.32708e4 cm3 (model vol.)'
'np277-4 min.den.= 1.527971 = (95.3886 lb/ft3)(453.59 g/lb)/(28316.84 cm3/ft3)'
'density = 1.477385 = (den.mult)(np277-4 min.den.) = 0.9668933*1.527971'
'use 75% of boron in calculations per NUREG-1609 Section 6.5.3.2'
arbmboron 7.06813e-2  2 0 0 0    5010   18.1479
                                 5011   81.8520   11  0.7500  293  end
arbmnpmx  1.03525e+0 10 0 0 0    6012    1.9189
                                 7014    0.0141
                                 8016   43.4251
                                11023    0.1174
                                12000    0.3378
                                13027   39.0479
                                14000    2.4672
                                16000    0.3083
                                20000   11.8336
                                26000    0.5298   11  1.0000  293  end
arbmnph2o 3.71451e-1  2 0 0 0    1001   11.1913
                                 8016   88.8087   11  1.0000  293  end
'kaolite 1600 body'
'sing.unit.density= (den.mult)(min.den.)'
' for arbmh20k = 1.012373*0.51655,  for rest = 1.012373*0.34438'
'den.mult= 1.36557e5 cm3 (actual vol.) / 1.34888e5 cm3 (model vol.)'
'actual vol.= 1.36557e5 cm3 = (28316.84 cm3/ft3)(108.33188 lb)/(22.464 lb/ft3)'
arbmh2ok   0.52294  2 0 0 0    1001   11.1913
                               8016   88.8087   12  1       293  end
arbmal2o3  0.34864  2 0 0 0   13027   52.9390
                               8016   47.0610   12  0.096   293  end
arbmsio2   0.34864  2 0 0 0   14000   46.7570
                               8016   53.2430   12  0.367   293  end
arbmfe2o3  0.34864  2 0 0 0   26000   69.9540
                               8016   30.0460   12  0.067   293  end
arbmtio2   0.34864  2 0 0 0   22000   59.9535
                               8016   40.0465   12  0.012   293  end
arbmcao    0.34864  2 0 0 0   20000   71.4815
                               8016   28.5185   12  0.307   293  end
arbmmgo    0.34864  2 0 0 0   12000   60.3169
                               8016   39.6831   12  0.131   293  end
arbmna2o   0.34864  2 0 0 0   11023   74.1961
                               8016   25.8039   12  0.020   293  end
'kaolite 1600 top plug'
'sing.unit.density= (den.mult)(min.den.)'
' for arbmh20k = 0.965246*0.51655,  for rest = 0.965246*0.34438'
'den.mult= 1.21592e4 cm3 (actual vol.) / 1.25970e4 cm3 (model vol.)'
'actual vol.= 1.21592e4 cm3 = (28316.84 cm3/ft3)(9.646 lb)/(22.464 lb/ft3)'
arbmh2ok   0.49860  2 0 0 0    1001   11.1913
                               8016   88.8087   13  1       293  end
arbmal2o3  0.33241  2 0 0 0   13027   52.9390
                               8016   47.0610   13  0.096   293  end
```

```
arbmsio2   0.33241  2 0 0 0   14000   46.7570
                              8016   53.2430   13  0.367   293  end
arbmfe2o3  0.33241  2 0 0 0   26000   69.9540
                              8016   30.0460   13  0.067   293  end
arbmtio2   0.33241  2 0 0 0   22000   59.9535
                              8016   40.0465   13  0.012   293  end
arbmcao    0.33241  2 0 0 0   20000   71.4815
                              8016   28.5185   13  0.307   293  end
arbmmgo    0.33241  2 0 0 0   12000   60.3169
                              8016   39.6831   13  0.131   293  end
arbmna2o   0.33241  2 0 0 0   11023   74.1961
                              8016   25.8039   13  0.020   293  end
'silicone rubber pads'
arbmsiru   1.21791  4 0 0 0    6012   32.3767
                              1001    8.1573
                              8016   21.5782
                             14000   37.8878   14  1.0     293  end
'void space external to containment vessel'
arbmwecv   0.9982   2 0 0 0    1001   11.1913
                              8016   88.8087   15  1       293  end
'steel: liner'
ss304                                           16  1.0     293  end
'steel: plug cover (pc) use 9.907 lb'
ss304                                           17  1.06388 293  end
'steel: angle iron (ai) for single units'
ss304                                           18  1.0     293  end
'steel: angle iron (ai) for arrays'
'array density is multiplied by a volume fraction 7.08030/5.63249'
'ss304                                           18  1.25705 293  end
'steel: drum steel for single units'
ss304                                           19  1.0     293  end
'steel: drum steel for arrays'
'array density is multiplied by a volume fraction 3.20482/3.20544'
'ss304                                           19  0.99981 293  end
'void space external to drum'
'array density is multiplied by a volume ratio 8.11698/6.98323'
'arbmwed    1.16026  2 0 0 0    1001   11.1913
'                              8016   88.8087   20  1       293  end
'reflective water'
arbmh20r   0.9982   2 0 0 0    1001   11.1913
                              8016   88.8087   21  1.0     293  end
end comp
ncsrtriga 0.0in thk np,10400.0gUZrHx(  921.0g235, 8998.2gH2O,hx=255.01),fr=1.0e+00
read parameters nub=yes npg=2500 gen=215 nsk=15 tme=100 end parameters
read boun       all=vac                         end boun
read geometry
unit 1001
'drum bottom flat cover [Elev= 0.105 in. at top of unit]'
'cylinder  19 1   24.587200    0.26670   0.0     com='extended radius not used'
 cylinder  19 1   23.329900    0.26670   0.0     com='drum bottom flat cover'
 cuboid    21 1 4p24.587200    0.26670   0.0     com='drum chine outer radius'
unit 1002
'above drum bottom flat cover and below containment vessel [Elev= 4.670 in.]'
 cylinder  15 1    3.175000   11.59510  11.16330 com='void in pad-1'
 cylinder  14 1    7.924800   11.59510  11.16330 com='pad-1'
 cylinder  16 1    8.077200   11.59510  11.16330 com='np277_4 liner'
 cylinder  11 1   10.922000   11.59510  11.16330 com='np277_4'
 cylinder  16 1   11.074400   11.59510  10.85850 com='kaolite liner bottom'
 cylinder  12 1   23.177500   11.59510   0.0     com='kaolite'
 cylinder  19 1   23.329900   11.59510   0.0     com='drum'
 cuboid    21 1 4p24.587200   11.59510   0.0     com='drum chine outer radius'
unit 1003
'cv bottom [Elev= 4.920 in.]'
 cylinder  8  1    6.680200    0.63500   0.0     com='cv bottom'
 cylinder  15 1    7.924800    0.63500   0.0     com='void btw cv-np liner'
 cylinder  16 1    8.077200    0.63500   0.0     com='np277_4 liner'
 cylinder  11 1   10.922000    0.63500   0.0     com='np277_4'
 cylinder  16 1   11.074400    0.63500   0.0     com='kaolite liner'
 cylinder  12 1   23.177500    0.63500   0.0     com='kaolite'
 cylinder  19 1   23.329900    0.63500   0.0     com='drum'
 cuboid    21 1 4p24.587200    0.63500   0.0     com='drum chine outer radius'
```

```
unit 1004
'UZrHx fuel element'
 cylinder  1  1    1.828800   12.70000   0.0     com='cylindrical content'
unit 1006
'content (collapsed) [Elev= 9.920 in.]'
'1.437900   plus-y location upper cylinders'
'-2.875700  minus-y location lower cylinder'
'2.490443   plus-x location upper cylinder'
'-2.490443  minus-x location upper cylinder'
 cylinder  3  1    6.426200   12.70050  -0.0005  com='cv well cavity'
 hole  1004   -2.490443  1.437900  0.0     com='cyl1'
 hole  1004    2.490443  1.437900  0.0     com='cyl2'
 hole  1004    0.0      -2.875700  0.0     com='cyl3'
 cylinder  8  1    6.680200   12.70050  -0.0005  com='cv below 1st step'
 cylinder  15 1    7.924800   12.70050  -0.0005  com='void btw cv-np liner'
 cylinder  16 1    8.077200   12.70050  -0.0005  com='np277_4 liner'
 cylinder  11 1   10.922000   12.70050  -0.0005  com='np277_4'
 cylinder  16 1   11.074400   12.70050  -0.0005  com='kaolite liner'
 cylinder  12 1   23.177500   12.70050  -0.0005  com='kaolite'
 cylinder  19 1   23.329900   12.70050  -0.0005  com='drum'
 cuboid    21 1 4p24.587200   12.70050  -0.0005  com='drum chine outer radius'
unit 1007
'np277_4 spacer [Elev= 9.921 in.]'
 cylinder  2  1    5.24510     0.00010   0.0     com='np spacer'
 cylinder  3  1    6.426200    0.00020  -0.0001  com='cv well cavity'
 cylinder  8  1    6.680200    0.00020  -0.0001  com='cv below 1st step'
 cylinder  15 1    7.924800    0.00020  -0.0001  com='void btw cv-np liner'
 cylinder  16 1    8.077200    0.00020  -0.0001  com='np277_4 liner'
 cylinder  11 1   10.922000    0.00020  -0.0001  com='np277_4'
 cylinder  16 1   11.074400    0.00020  -0.0001  com='kaolite liner'
 cylinder  12 1   23.177500    0.00020  -0.0001  com='kaolite'
 cylinder  19 1   23.329900    0.00020  -0.0001  com='drum'
 cuboid    21 1 4p24.587200    0.00020  -0.0001  com='drum chine outer radius'
unit 1008
'top of content stack to bottom of 1st step [Elev=35.270 in.]'
'38.10360             stack height (content spacers)       CALCULATED
 cylinder  3  1    6.426200   38.98540   0.0     com='cv well cavity'
 cylinder  8  1    6.680200   38.98540   0.0     com='cv below 1st step'
 cylinder  15 1    7.924800   38.98540   0.0     com='void btw cv-np liner'
 cylinder  16 1    8.077200   38.98540   0.0     com='np277_4 liner'
 cylinder  11 1   10.922000   38.98540   0.0     com='np277_4'
 cylinder  16 1   11.074400   38.98540   0.0     com='kaolite liner'
 cylinder  12 1   23.177500   38.98540   0.0     com='kaolite'
 cylinder  19 1   23.329900   38.98540   0.0     com='drum'
 cuboid    21 1 4p24.587200   38.98540   0.0     com='drum chine outer radius'
unit 1010
'cv at 1st step in liner [Elev=35.330 in.]'
 cylinder  3  1    6.426200    0.15240   0.0     com='cv well cavity'
 cylinder  8  1    6.680200    0.15240   0.0     com='cv at 1st step'
 cylinder  15 1    7.924800    0.15240   0.0     com='void btw cv and liner'
 cylinder  16 1   11.074400    0.15240   0.0     com='liner 1st step'
 cylinder  12 1   23.177500    0.15240   0.0     com='kaolite'
 cylinder  19 1   23.329900    0.15240   0.0     com='drum'
 cuboid    21 1 4p24.587200    0.15240   0.0     com='drum chine outer radius'
unit 1011
'vertical gap between 1st step in liner and cv flange [Elev=35.420 in.]'
 cylinder  3  1    6.426200    0.22860   0.0     com='cv well cavity'
 cylinder  8  1    6.680200    0.22860   0.0     com='cv at gap btwn step-flng'
 cylinder  15 1   10.922000    0.22860   0.0     com='void btw cv and liner'
 cylinder  16 1   11.074400    0.22860   0.0     com='liner wall'
 cylinder  12 1   23.177500    0.22860   0.0     com='kaolite'
 cylinder  19 1   23.329900    0.22860   0.0     com='drum'
 cuboid    21 1 4p24.587200    0.22860   0.0     com='drum chine outer radius'
unit 1012
'cv flange to top of cv well [Elev=35.920 in.]'
 cylinder  3  1    6.426200    1.27000   0.0     com='cavity'
 cylinder  9  1    9.525000    1.27000   0.0     com='flange to top of well'
 cylinder  15 1    9.525000    1.27000   0.0     com='void btw cv and pad-2'
 cylinder  14 1   10.033000    1.27000   0.0     com='pad-2'
 cylinder  15 1   10.922000    1.27000   0.0     com='void btw cv and liner'
 cylinder  16 1   11.074400    1.27000   0.0     com='liner wall'
```

```
 cylinder  12 1   23.177500    1.27000   0.0     com='kaolite'
 cylinder  19 1   23.329900    1.27000   0.0     com='drum'
 cuboid    21 1 4p24.587200    1.27000   0.0     com='drum chine outer radius'
unit 1013
'cv flange above cv well [Elev=37.070 in.]'
 cylinder  10 1    9.525000    2.92100   0.0     com='flange above cv well'
 cylinder  15 1    9.525000    2.92100   0.0     com='void btw cv and pad-2'
 cylinder  14 1   10.033000    2.92100   0.0     com='pad-2'
 cylinder  15 1   10.922000    2.92100   0.0     com='void btw pad2 and liner'
 cylinder  16 1   11.074400    2.92100   0.0     com='liner wall'
 cylinder  12 1   23.177500    2.92100   0.0     com='kaolite'
 cylinder  19 1   23.329900    2.92100   0.0     com='drum'
 cuboid    21 1 4p24.587200    2.92100   0.0     com='drum chine outer radius'
unit 1014
'plugpad2 below liner 2nd step [Elev=37.470 in.]'
 cylinder  14 1   10.033000    0.76200   0.0     com='pad-2'
 cylinder  15 1   10.922000    1.01600   0.0     com='void btw pad2 and liner'
 cylinder  16 1   11.074400    1.01600   0.0     com='liner wall'
 cylinder  12 1   23.177500    1.01600   0.0     com='kaolite'
 cylinder  19 1   23.329900    1.01600   0.0     com='drum'
 cuboid    21 1 4p24.587200    1.01600   0.0     com='drum chine outer radius'
unit 1015
'2nd step in liner [Elev=37.530 in.]'
 cylinder  15 1   10.922000    0.15240   0.0     com='void abv pad2'
 cylinder  16 1   18.757900    0.15240   0.0     com='liner 2nd step'
 cylinder  12 1   23.177500    0.15240   0.0     com='kaolite'
 cylinder  19 1   23.329900    0.15240   0.0     com='drum'
 cuboid    21 1 4p24.587200    0.15240   0.0     com='drum chine outer radius'
unit 1016
'abv 2nd step in liner to bottom of angle iron [Elev=40.750 in.]'
 cylinder  13 1   18.097500    8.17880   0.49276 com='plug kaolite'
 cylinder  17 1   18.249900    8.17880   0.34036 com='sides of plug case'
 cylinder  15 1   18.605500    8.17880   0.0     com='void: plug to liner'
 cylinder  16 1   18.757900    8.17880   0.0     com='liner wall'
 cylinder  12 1   23.177500    8.17880   0.0     com='kaolite'
 cylinder  19 1   23.329900    8.17880   0.0     com='drum'
 cuboid    21 1 4p24.587200    8.17880   0.0     com='drum chine outer radius'
unit 1017
'bottom of angle iron to bend in angle iron [Elev=42.500 in.]'
 cylinder  13 1   18.097500    4.44500   0.0     com='plug kaolite'
 cylinder  17 1   18.249900    4.44500   0.0     com='sides of plug case'
 cylinder  15 1   18.605500    4.44500   0.0     com='void: plug to liner'
 cylinder  16 1   18.757900    4.44500   0.0     com='liner wall'
 cylinder  18 1   19.392900    4.44500   0.0     com='lower angle iron'
 cylinder  12 1   23.177500    4.44500   0.0     com='kaolite'
 cylinder  19 1   23.329900    4.44500   0.0     com='drum'
 cuboid    21 1 4p24.587200    4.44500   0.0     com='drum chine outer radius'
unit 1018
'bend in angle iron to top of angle iron [Elev=42.750 in.]'
 cylinder  13 1   18.097500    0.11176   0.0     com='plug kaolite'
 cylinder  17 1   18.249900    0.26416   0.0     com='sides of plug case'
 cylinder  15 1   18.605500    0.63500   0.0     com='void: plug to liner'
 cylinder  16 1   18.757900    0.63500   0.0     com='liner wall'
 cylinder  18 1   23.177500    0.63500   0.0     com='bend section of ai'
 cylinder  19 1   23.329900    0.63500   0.0     com='drum'
 cuboid    21 1 4p24.587200    0.63500   0.0     com='drum chine outer radius'
unit 1019
'drum lid and lip [Elev=43.500 in.]'
 cylinder  21 1   22.961600    1.90500   0.15240 com='void above lid'
 cylinder  19 1   23.114000    1.90500   0.0     com='drum lid'
 cylinder  21 1   23.177500    1.90500   0.0     com='void btw lid - drum wall'
 cylinder  19 1   23.329900    1.90500   0.0     com='drum'
 cuboid    21 1 4p24.587200    1.90500   0.0     com='drum chine outer radius'
global
unit 1020
'es3100 drum [Elev=43.500 in.]'
array 3         2r-24.587200     0.0
'cuboid     0  1 4p24.587200    110.4905  0.0    com='bare package'
 cuboid    21  1 4p55.067200   140.9700 -30.48   com='reflected package'
'cuboid    20  1 4p22.889718    110.5048  0.0    com='interstital array space'
'global
```

```
'unit 1021
'array 4   3r0.0
'reflector  21 2  6r3.0  10
end geometry
read array
ara=3 nux=1 nuy=1 nuz=19 fill
1001 1002 1003 1006 1007 1006 1007 1006 1008 1010
1011 1012 1013 1014 1015 1016 1017 1018 1019        end fill
'ara=4 nux=13 nuy=13 nuz=06 fill f1020               end fill
end array
'read bias id=500 2  11  end bias
read start nst=0
end start
end data
end


=csas25    parm=size=3000000
nciatriga 0.0in thk np,10400.0gUZrHx(  921.0g235, 8998.2gH2O hx=255.01),fr=1.0e-04
238groupndf5 infhommedium
'TRIGA volume =1200.95996, SPACER volume    0.00000'
'TRIGA wrapped dry content can hx=18.2, CV void volume 9014.40198'
arbmtriga  8.65974  4 0 0 0    1001    0.9554
                              40000   54.0446
                              92235    8.8558
                              92238   36.1442    1  1.0     293  end
'np277-4: spacer (NCT_MD&H)'
'NCT min.den.(95.3886 lb/ft3) and hydrogen'
'np277-4 min.den.= 1.527971 = (95.3886 lb/ft3)(453.59 g/lb)/(28316.84 cm3/ft3)'
'use 75% of boron in calculations per NUREG-1609 Section 6.5.3.2'
arbmboron 7.31015e-2  2 0 0 0    5010   18.1479
                                 5011   81.8520    2  0.7500  293  end
arbmnpmx  1.07070e+0 10 0 0 0    6012    1.9189
                                 7014    0.0141
                                 8016   43.4251
                                11023    0.1174
                                12000    0.3378
                                13027   39.0479
                                14000    2.4672
                                16000    0.3083
                                20000   11.8336
                                26000    0.5298    2  1.0000  293  end
arbmnph2o 3.84169e-1  2 0 0 0    1001   11.1913
                                 8016   88.8087    2  1.0000  293  end
'flooded containmment vessel and content cans -- 10 CFR 71.55(d)(3)'
arbmwicv   0.9982   2 0 0 0    1001   11.1913
                              8016   88.8087    3  1       293  end
'steel: containment vessel body 16.60 lb but use 15.74 lb'
ss304                                            8  1.0     293  end
'steel: cv flange lower use 3.36 lb'
ss304                                            9  0.97267 293  end
'steel: cv flange upper use 13.75 lb'
ss304                                           10  0.94348 293  end
'np277-4: confinement -- neutron poison inner liner (NCT_MD&H)'
'actual vol.= 1.28314e4 cm3 = (7.83023e2 in3)(16.387064)'
'den.multiplier = 1.28314e4 cm3 (actual vol.) / 1.32708e4 cm3 (model vol.)'
'np277-4 min.den.= 1.527971 = (95.3886 lb/ft3)(453.59 g/lb)/(28316.84 cm3/ft3)'
'density = 1.477385 = (den.mult)(np277-4 min.den.) = 0.9668933*1.527971'
'use 75% of boron in calculations per NUREG-1609 Section 6.5.3.2'
arbmboron 7.06813e-2  2 0 0 0    5010   18.1479
                                 5011   81.8520   11  0.7500  293  end
arbmnpmx  1.03525e+0 10 0 0 0    6012    1.9189
                                 7014    0.0141
                                 8016   43.4251
                                11023    0.1174
                                12000    0.3378
                                13027   39.0479
                                14000    2.4672
                                16000    0.3083
                                20000   11.8336
                                26000    0.5298   11  1.0000  293  end
```

```
arbmnph2o 3.71451e-1  2 0 0 0    1001   11.1913
                                 8016   88.8087   11  1.0000  293  end
'kaolite 1600 body'
'sing.unit.density= (den.mult)(min.den.)'
' for arbmh20k = 1.012373*0.51655,  for rest = 1.012373*0.34438'
'den.mult= 1.36557e5 cm3 (actual vol.) / 1.34888e5 cm3 (model vol.)'
'actual vol.= 1.36557e5 cm3 = (28316.84 cm3/ft3)(108.33188 lb)/(22.464 lb/ft3)'
'nct array densities are s.u.dens. multiplied by volume ratio 1.34888/1.10336'
arbmh2ok   0.63931  2 0 0 0    1001   11.1913
                               8016   88.8087   12  0.0287  293  end
arbmal2o3  0.42622  2 0 0 0   13027   52.9390
                               8016   47.0610   12  0.096   293  end
arbmsio2   0.42622  2 0 0 0   14000   46.7570
                               8016   53.2430   12  0.367   293  end
arbmfe2o3  0.42622  2 0 0 0   26000   69.9540
                               8016   30.0460   12  0.067   293  end
arbmtio2   0.42622  2 0 0 0   22000   59.9535
                               8016   40.0465   12  0.012   293  end
arbmcao    0.42622  2 0 0 0   20000   71.4815
                               8016   28.5185   12  0.307   293  end
arbmmgo    0.42622  2 0 0 0   12000   60.3169
                               8016   39.6831   12  0.131   293  end
arbmna2o   0.42622  2 0 0 0   11023   74.1961
                               8016   25.8039   12  0.020   293  end
'kaolite 1600 top plug'
'sing.unit.density= (den.mult)(min.den.)'
' for arbmh20k = 0.965246*0.51655,  for rest = 0.965246*0.34438'
'den.mult= 1.21592e4 cm3 (actual vol.) / 1.25970e4 cm3 (model vol.)'
'actual vol.= 1.21592e4 cm3 = (28316.84 cm3/ft3)(9.646 lb)/(22.464 lb/ft3)'
arbmh2ok   0.49860  2 0 0 0    1001   11.1913
                               8016   88.8087   13  0.0287  293  end
arbmal2o3  0.33241  2 0 0 0   13027   52.9390
                               8016   47.0610   13  0.096   293  end
arbmsio2   0.33241  2 0 0 0   14000   46.7570
                               8016   53.2430   13  0.367   293  end
arbmfe2o3  0.33241  2 0 0 0   26000   69.9540
                               8016   30.0460   13  0.067   293  end
arbmtio2   0.33241  2 0 0 0   22000   59.9535
                               8016   40.0465   13  0.012   293  end
arbmcao    0.33241  2 0 0 0   20000   71.4815
                               8016   28.5185   13  0.307   293  end
arbmmgo    0.33241  2 0 0 0   12000   60.3169
                               8016   39.6831   13  0.131   293  end
arbmna2o   0.33241  2 0 0 0   11023   74.1961
                               8016   25.8039   13  0.020   293  end
'silicone rubber pads'
arbmsiru   1.21791  4 0 0 0    6012   32.3767
                               1001    8.1573
                               8016   21.5782
                              14000   37.8878   14  1.0     293  end
'void space external to containment vessel'
arbmwecv   0.9982   2 0 0 0    1001   11.1913
                               8016   88.8087   15  0.0001  293  end
'steel: liner'
ss304                                            16  1.0     293  end
'steel: plug cover (pc) use 9.907 lb'
ss304                                            17  1.06388 293  end
'steel: angle iron (ai) for single units'
'ss304                                            18  1.0     293  end
'steel: angle iron (ai) for arrays'
'array density is multiplied by a volume fraction 7.08030/5.63249'
ss304                                            18  1.25705 293  end
'steel: drum steel for single units'
'ss304                                            19  1.0     293  end
'steel: drum steel for arrays'
'array density is multiplied by a volume fraction 3.20482/3.20544'
ss304                                            19  0.99981 293  end
'void space external to drum'
'array density is multiplied by a volume ratio 8.11698/6.98323'
arbmwed    1.16026  2 0 0 0    1001   11.1913
                               8016   88.8087   20  0.0001  293  end
```

```
'reflective water'
'arbmh20r   0.9982   2 0 0 0    1001   11.1913
'                               8016   88.8087   21  1.0     293  end
end comp
nciatriga 0.0in thk np,10400.0gUZrHx(  921.0g235, 8998.2gH2O,hx=255.01),fr=1.0e-04
read parameters nub=yes npg=2500 gen=215 nsk=15 tme=100 end parameters
read boun       all=specular                    end boun
read geometry
unit 1001
'drum bottom flat cover [Elev= 0.111 in. at top of unit]'
'cylinder  19 1   22.866096    0.28150   0.0     com='extended radius not used'
 cylinder  19 1   21.722275    0.28150   0.0     com='drum bottom flat cover'
 cuboid    20 1 4p22.866096    0.28150   0.0     com='drum chine outer radius'
unit 1002
'above drum bottom flat cover and below containment vessel [Elev= 4.676 in.]'
 cylinder  15 1    3.175000   11.59510  11.16330 com='void in pad-1'
 cylinder  14 1    7.924800   11.59510  11.16330 com='pad-1'
 cylinder  16 1    8.077200   11.59510  11.16330 com='np277_4 liner'
 cylinder  11 1   10.922000   11.59510  11.16330 com='np277_4'
 cylinder  16 1   11.074400   11.59510  10.85850 com='kaolite liner bottom'
 cylinder  12 1   21.555075   11.59510   0.0     com='kaolite'
 cylinder  19 1   21.722275   11.59510   0.0     com='drum'
 cuboid    20 1 4p22.866096   11.59510   0.0     com='drum chine outer radius'
unit 1003
'cv bottom [Elev= 4.926 in.]'
 cylinder  8  1    6.680200    0.63500   0.0     com='cv bottom'
 cylinder  15 1    7.924800    0.63500   0.0     com='void btw cv-np liner'
 cylinder  16 1    8.077200    0.63500   0.0     com='np277_4 liner'
 cylinder  11 1   10.922000    0.63500   0.0     com='np277_4'
 cylinder  16 1   11.074400    0.63500   0.0     com='kaolite liner'
 cylinder  12 1   21.555075    0.63500   0.0     com='kaolite'
 cylinder  19 1   21.722275    0.63500   0.0     com='drum'
 cuboid    20 1 4p22.866096    0.63500   0.0     com='drum chine outer radius'
unit 1004
'UZrHx fuel element'
 cylinder  1  1    1.828800   12.70000   0.0     com='cylindrical content'
unit 1006
'content (collapsed) [Elev= 9.926 in.]'
'1.437900   plus-y location upper cylinders'
'-2.875700  minus-y location lower cylinder'
'2.490443   plus-x location upper cylinder'
'-2.490443  minus-x location upper cylinder'
 cylinder  3  1    6.426200   12.70050  -0.0005  com='cv well cavity'
 hole  1004   -2.490443  1.437900  0.0     com='cyl1'
 hole  1004    2.490443  1.437900  0.0     com='cyl2'
 hole  1004    0.0      -2.875700  0.0     com='cyl3'
 cylinder  8  1    6.680200   12.70050  -0.0005  com='cv below 1st step'
 cylinder  15 1    7.924800   12.70050  -0.0005  com='void btw cv-np liner'
 cylinder  16 1    8.077200   12.70050  -0.0005  com='np277_4 liner'
 cylinder  11 1   10.922000   12.70050  -0.0005  com='np277_4'
 cylinder  16 1   11.074400   12.70050  -0.0005  com='kaolite liner'
 cylinder  12 1   21.555075   12.70050  -0.0005  com='kaolite'
 cylinder  19 1   21.722275   12.70050  -0.0005  com='drum'
 cuboid    20 1 4p22.866096   12.70050  -0.0005  com='drum chine outer radius'
unit 1007
'np277_4 spacer [Elev= 9.926 in.]'
 cylinder  2  1    5.24510     0.00010   0.0     com='np spacer'
 cylinder  3  1    6.426200    0.00020  -0.0001  com='cv well cavity'
 cylinder  8  1    6.680200    0.00020  -0.0001  com='cv below 1st step'
 cylinder  15 1    7.924800    0.00020  -0.0001  com='void btw cv-np liner'
 cylinder  16 1    8.077200    0.00020  -0.0001  com='np277_4 liner'
 cylinder  11 1   10.922000    0.00020  -0.0001  com='np277_4'
 cylinder  16 1   11.074400    0.00020  -0.0001  com='kaolite liner'
 cylinder  12 1   21.555075    0.00020  -0.0001  com='kaolite'
 cylinder  19 1   21.722275    0.00020  -0.0001  com='drum'
 cuboid    20 1 4p22.866096    0.00020  -0.0001  com='drum chine outer radius'
unit 1008
'top of content stack to bottom of 1st step [Elev=35.276 in.]'
'38.10360             stack height (content spacers)       CALCULATED
 cylinder  3  1    6.426200   38.98540   0.0     com='cv well cavity'
 cylinder  8  1    6.680200   38.98540   0.0     com='cv below 1st step'
```

```
 cylinder  15 1    7.924800   38.98540   0.0     com='void btw cv-np liner'
 cylinder  16 1    8.077200   38.98540   0.0     com='np277_4 liner'
 cylinder  11 1   10.922000   38.98540   0.0     com='np277_4'
 cylinder  16 1   11.074400   38.98540   0.0     com='kaolite liner'
 cylinder  12 1   21.555075   38.98540   0.0     com='kaolite'
 cylinder  19 1   21.722275   38.98540   0.0     com='drum'
 cuboid    20 1 4p22.866096   38.98540   0.0     com='drum chine outer radius'
unit 1010
'cv at 1st step in liner [Elev=35.336 in.]'
 cylinder  3  1    6.426200    0.15240   0.0     com='cv well cavity'
 cylinder  8  1    6.680200    0.15240   0.0     com='cv at 1st step'
 cylinder  15 1    7.924800    0.15240   0.0     com='void btw cv and liner'
 cylinder  16 1   11.074400    0.15240   0.0     com='liner 1st step'
 cylinder  12 1   21.555075    0.15240   0.0     com='kaolite'
 cylinder  19 1   21.722275    0.15240   0.0     com='drum'
 cuboid    20 1 4p22.866096    0.15240   0.0     com='drum chine outer radius'
unit 1011
'vertical gap between 1st step in liner and cv flange [Elev=35.426 in.]'
 cylinder  3  1    6.426200    0.22860   0.0     com='cv well cavity'
 cylinder  8  1    6.680200    0.22860   0.0     com='cv at gap btwn step-flng'
 cylinder  15 1   10.922000    0.22860   0.0     com='void btw cv and liner'
 cylinder  16 1   11.074400    0.22860   0.0     com='liner wall'
 cylinder  12 1   21.555075    0.22860   0.0     com='kaolite'
 cylinder  19 1   21.722275    0.22860   0.0     com='drum'
 cuboid    20 1 4p22.866096    0.22860   0.0     com='drum chine outer radius'
unit 1012
'cv flange to top of cv well [Elev=35.926 in.]'
 cylinder  3  1    6.426200    1.27000   0.0     com='cavity'
 cylinder  9  1    9.525000    1.27000   0.0     com='flange to top of well'
 cylinder  15 1    9.525000    1.27000   0.0     com='void btw cv and pad-2'
 cylinder  14 1   10.033000    1.27000   0.0     com='pad-2'
 cylinder  15 1   10.922000    1.27000   0.0     com='void btw cv and liner'
 cylinder  16 1   11.074400    1.27000   0.0     com='liner wall'
 cylinder  12 1   21.555075    1.27000   0.0     com='kaolite'
 cylinder  19 1   21.722275    1.27000   0.0     com='drum'
 cuboid    20 1 4p22.866096    1.27000   0.0     com='drum chine outer radius'
unit 1013
'cv flange above cv well [Elev=37.076 in.]'
 cylinder  10 1    9.525000    2.92100   0.0     com='flange above cv well'
 cylinder  15 1    9.525000    2.92100   0.0     com='void btw cv and pad-2'
 cylinder  14 1   10.033000    2.92100   0.0     com='pad-2'
 cylinder  15 1   10.922000    2.92100   0.0     com='void btw pad2 and liner'
 cylinder  16 1   11.074400    2.92100   0.0     com='liner wall'
 cylinder  12 1   21.555075    2.92100   0.0     com='kaolite'
 cylinder  19 1   21.722275    2.92100   0.0     com='drum'
 cuboid    20 1 4p22.866096    2.92100   0.0     com='drum chine outer radius'
unit 1014
'plugpad2 below liner 2nd step [Elev=37.476 in.]'
 cylinder  14 1   10.033000    0.76200   0.0     com='pad-2'
 cylinder  15 1   10.922000    1.01600   0.0     com='void btw pad2 and liner'
 cylinder  16 1   11.074400    1.01600   0.0     com='liner wall'
 cylinder  12 1   21.555075    1.01600   0.0     com='kaolite'
 cylinder  19 1   21.722275    1.01600   0.0     com='drum'
 cuboid    20 1 4p22.866096    1.01600   0.0     com='drum chine outer radius'
unit 1015
'2nd step in liner [Elev=37.536 in.]'
 cylinder  15 1   10.922000    0.15240   0.0     com='void abv pad2'
 cylinder  16 1   18.757900    0.15240   0.0     com='liner 2nd step'
 cylinder  12 1   21.555075    0.15240   0.0     com='kaolite'
 cylinder  19 1   21.722275    0.15240   0.0     com='drum'
 cuboid    20 1 4p22.866096    0.15240   0.0     com='drum chine outer radius'
unit 1016
'abv 2nd step in liner to bottom of angle iron [Elev=40.756 in.]'
 cylinder  13 1   18.097500    8.17880   0.49276 com='plug kaolite'
 cylinder  17 1   18.249900    8.17880   0.34036 com='sides of plug case'
 cylinder  15 1   18.605500    8.17880   0.0     com='void: plug to liner'
 cylinder  16 1   18.757900    8.17880   0.0     com='liner wall'
 cylinder  12 1   21.555075    8.17880   0.0     com='kaolite'
 cylinder  19 1   21.722275    8.17880   0.0     com='drum'
 cuboid    20 1 4p22.866096    8.17880   0.0     com='drum chine outer radius'
unit 1017
```

```
'bottom of angle iron to bend in angle iron [Elev=42.506 in.]'
 cylinder  13 1   18.097500    4.44500   0.0     com='plug kaolite'
 cylinder  17 1   18.249900    4.44500   0.0     com='sides of plug case'
 cylinder  15 1   18.605500    4.44500   0.0     com='void: plug to liner'
 cylinder  16 1   18.757900    4.44500   0.0     com='liner wall'
 cylinder  18 1   19.392900    4.44500   0.0     com='lower angle iron'
 cylinder  12 1   21.555075    4.44500   0.0     com='kaolite'
 cylinder  19 1   21.722275    4.44500   0.0     com='drum'
 cuboid    20 1 4p22.866096    4.44500   0.0     com='drum chine outer radius'
unit 1018
'bend in angle iron to top of angle iron [Elev=42.756 in.]'
 cylinder  13 1   18.097500    0.11176   0.0     com='plug kaolite'
 cylinder  17 1   18.249900    0.26416   0.0     com='sides of plug case'
 cylinder  15 1   18.605500    0.63500   0.0     com='void: plug to liner'
 cylinder  16 1   18.757900    0.63500   0.0     com='liner wall'
 cylinder  18 1   21.555075    0.63500   0.0     com='bend section of ai'
 cylinder  19 1   21.722275    0.63500   0.0     com='drum'
 cuboid    20 1 4p22.866096    0.63500   0.0     com='drum chine outer radius'
unit 1019
'drum lid and lip [Elev=43.512 in.]'
 cylinder  20 1   21.330090    1.91973   0.16720 com='void above lid'
 cylinder  19 1   21.497290    1.91973   0.0     com='drum lid'
 cylinder  20 1   21.555075    1.91973   0.0     com='void btw lid - drum wall'
 cylinder  19 1   21.722275    1.91973   0.0     com='drum'
 cuboid    20 1 4p22.866096    1.91973   0.0     com='drum chine outer radius'
global
unit 1020
'es3100 drum [Elev=43.512 in.]'
array 3         2r-22.866096     0.0
'cuboid     0  1 4p24.587200    110.4900  0.0    com='bare package'
'cuboid    21  1 4p55.067200   140.9700 -30.48   com='reflected package'
 cuboid    20  1 4p22.866096    110.5197  0.0    com='interstital array space'
'global
'unit 1021
'array 4   3r0.0
'reflector  21 2  6r3.0  10
end geometry
read array
ara=3 nux=1 nuy=1 nuz=19 fill
1001 1002 1003 1006 1007 1006 1007 1006 1008 1010
1011 1012 1013 1014 1015 1016 1017 1018 1019        end fill
'ara=4 nux=13 nuy=13 nuz=06 fill f1020               end fill
end array
'read bias id=500 2  11  end bias
read start nst=0
end start
end data
end


=csas25    parm=size=300000
atdmr,[ 7000.0U, 7000.0U235,513.0CH2]g htox= 2.46,Rc= 6.05465cm
238groupndf5 multiregion
'HEU volume = 372.12095'
'U= 7000.0g, poly=513.0g, content hx=2.46'
'core htox= 2.46'
uranium  1 den=18.81109 0.4002 293  92235  100.00
                                    92238   0.000                end
arbmpoly   0.92000   2 0 0 0   1001   14.3798
                               6012   85.6202    1  0.5998  293  end
'reflective water'
arbmh20r   0.9982   2 0 0 0    1001   11.1913
                               8016   88.8087    7  1.0000  293  end
end comp
spherical end
1   6.05465
7  26.05465
end zone
atdmr,[ 7000.0U, 7000.0U235,513.0CH2]g htox= 2.46 Rc= 6.05465cm
read parameters nub=yes npg=2500 gen=215 nsk=15 tme=100 end parameters
'Mass of fm in core region   = 7000.00000 g'
```

```
'Mass of poly in core region =  513.00000 g'
'Mass of core region         = 7513.00000 g'
'Vol of fm                   =  372.12095 cm3'
'Vol of poly                 =  557.60870 cm3'
'Volume of core region       =  929.72965 cm3'
'Calculate HTOX ratio for use of 513.0 grams can pads,vinyl tape, polyethylene in CV'
'hydrogen to fissile uranium ratio  =   2.4580'
read geometry
global
unit 1001
'fissile material dry core with 20.0 cm water reflection'
sphere  1  1   6.05465  com='HEU core'
sphere  7  1  26.05465  com='20.0 cm water reflector'
end geometry
end data
end


=csas25    parm=size=300000
atdmsr,[ 7000.0U, 7000.0U235,513.0CH2]g htox= 2.46,Rc= 6.05465cm, 66133.1gSS,Rs=13.0264cm
238groupndf5 multiregion
'HEU volume = 372.12095'
'U= 7000.0g, poly=513.0g, content hx=2.46'
'core htox= 2.46'
uranium  1 den=18.81109 0.4002 293  92235  100.00
                                    92238   0.000                end
arbmpoly   0.92000   2 0 0 0   1001   14.3798
                               6012   85.6202    1  0.5998  293  end
'steel: cv, drum liner, plug liner, angle iron, drum'
ss304                                            3  1.0     293  end
'reflective water'
arbmh20r   0.9982   2 0 0 0    1001   11.1913
                               8016   88.8087    7  1.0000  293  end
end comp
spherical end
1   6.05465
3  13.02645
7  33.02645
end zone
atdmsr,[ 7000.0U, 7000.0U235,513.0CH2]g htox= 2.46 Rc= 6.05465cm, 66133.1gSS,Rs=13.0264cm
read parameters nub=yes npg=2500 gen=215 nsk=15 tme=100 end parameters
'Mass of fm in core region   = 7000.00000 g'
'Mass of poly in core region =  513.00000 g'
'Mass of core region         = 7513.00000 g'
'Vol of fm                   =  372.12095 cm3'
'Vol of poly                 =  557.60870 cm3'
'Volume of core region       =  929.72965 cm3'
'Calculate HTOX ratio for use of 513.0 grams can pads,vinyl tape, polyethylene in CV'
'hydrogen to fissile uranium ratio  =   2.4580'
' '
'Mass of steel is derived from the mass of the steel in the CV,'
'steel liner, plug liner, angle iron and drum.  The mass of each'
'was taken directly from Case hciabmt12_36_1_8_1_in.output'
'Model volume taken as stainless steel mass divided by ss density'
'total mass of ss304=  66133.15000'
'total volume of ss304= 8329.1'
'maximum ss304 radius = 13.02635'
read geometry
global
unit 1001
'fissile material dry core, ss304 shell, 20.0 cm h2o reflector'
'increase ss304 shell by equal volume increments'
'8.32911e+02  cm3  volume of increment'
'9258.841 cm3               accumulative volume of core and ss304'
'13.02645 cm                accumulative radius of ss304 shell'
'6.61331e+04  g             accumulative mass of ss304 shell'
sphere  1  1   6.05465  com='HEU core'
sphere  3  1  13.02645  com='ss304 shell around HEU core'
sphere  7  1  33.02645  com='20cm h2o reflector around ss304 shell'
end geometry
end data
```

```
end


=csas25    parm=size=300000
atdmkr,[ 7000.0U, 7000.0U235,513.0CH2]g htox= 2.46,Rc= 6.05465cm,128034.0gKao,Rk=31.0814cm
238groupndf5 multiregion
'HEU volume = 372.12095'
'U= 7000.0g, poly=513.0g, content hx=2.46'
'core htox= 2.46'
uranium  1 den=18.81109 0.4002 293  92235  100.00
                                    92238   0.000                end
arbmpoly   0.92000   2 0 0 0   1001   14.3798
                               6012   85.6202    1  0.5998  293  end
'kaolite 1600 body'
'nct.sing.unit.density= (den.mult)(min.den.)'
' for arbmh20k 0.52294 = 1.012373*0.51655, for rest 0.34864 = 1.012373*0.34438'
'den.mult= 1.36557e5 cm3 (actual vol.) / 1.34888e5 cm3 (model vol.)'
'actual vol.= 1.36557e5 cm3 = (28316.84 cm3/ft3)(108.33188 lb)/(22.464 lb/ft3)'
'hac.s.u.dens= (hac.mult)(nct.s.u.dens)'
'hac.mult = 1.34888e5 cm3 (nct vol.)/ 1.12246e5 cm3 (model vol.)'
' for arbmh2ok 0.62843 = 1.20172*0.52294,   for rest = 1.20172*0.34864'
'hac array densities are hac s.u.dens.'
arbmh2ok   0.62843  2 0 0 0    1001   11.1913
                               8016   88.8087    4  0.0287  293  end
arbmal2o3  0.41898  2 0 0 0   13027   52.9390
                               8016   47.0610    4  0.096   293  end
arbmsio2   0.41898  2 0 0 0   14000   46.7570
                               8016   53.2430    4  0.367   293  end
arbmfe2o3  0.41898  2 0 0 0   26000   69.9540
                               8016   30.0460    4  0.067   293  end
arbmtio2   0.41898  2 0 0 0   22000   59.9535
                               8016   40.0465    4  0.012   293  end
arbmcao    0.41898  2 0 0 0   20000   71.4815
                               8016   28.5185    4  0.307   293  end
arbmmgo    0.41898  2 0 0 0   12000   60.3169
                               8016   39.6831    4  0.131   293  end
arbmna2o   0.41898  2 0 0 0   11023   74.1961
                               8016   25.8039    4  0.020   293  end
'kaolite 1600 top plug'
'sing.unit.density= (den.mult)(min.den.)'
' for arbmh20k = 0.965246*0.51655,  for rest = 0.965246*0.34438'
'den.mult= 1.21592e4 cm3 (actual vol.) / 1.25970e4 cm3 (model vol.)'
'actual vol.= 1.21592e4 cm3 = (28316.84 cm3/ft3)(9.646 lb)/(22.464 lb/ft3)'
arbmh2ok   0.49860  2 0 0 0    1001   11.1913
                               8016   88.8087    5  0.0287  293  end
arbmal2o3  0.33241  2 0 0 0   13027   52.9390
                               8016   47.0610    5  0.096   293  end
arbmsio2   0.33241  2 0 0 0   14000   46.7570
                               8016   53.2430    5  0.367   293  end
arbmfe2o3  0.33241  2 0 0 0   26000   69.9540
                               8016   30.0460    5  0.067   293  end
arbmtio2   0.33241  2 0 0 0   22000   59.9535
                               8016   40.0465    5  0.012   293  end
arbmcao    0.33241  2 0 0 0   20000   71.4815
                               8016   28.5185    5  0.307   293  end
arbmmgo    0.33241  2 0 0 0   12000   60.3169
                               8016   39.6831    5  0.131   293  end
arbmna2o   0.33241  2 0 0 0   11023   74.1961
                               8016   25.8039    5  0.020   293  end
'kaolite 1600 combined'
'sing.unit.density= (den.mult)(min.den.)'
' for arbmh20k = 1.191224*0.51655,  for rest = 1.191224*0.34438'
'den.mult= 1.48716e5 cm3 (actual vol.) / 1.24843e5 cm3 (model vol.)'
'actual body vol.= 1.36557e5 cm3 = (28316.84 cm3/ft3)(108.33188 lb)/(22.464 lb/ft3)'
'actual plug vol.= 1.21592e4 cm3 = (28316.84 cm3/ft3)(9.646 lb)/(22.464 lb/ft3)'
'total Kaolite volume=1.48716e5 cm3 =  1.36557e5 + 1.21592e4 cm3'
'model body vol.= 1.12246e5 cm3'
'model plug vol.= 1.25970e4 cm3'
'total model volume=1.24843e5 cm3 =  1.12246e5 + 1.25970e4 cm3'
arbmh2ok   0.61533  2 0 0 0    1001   11.1913
                               8016   88.8087    6  1.0e+00  293  end
```

```
arbmal2o3  0.41023  2 0 0 0   13027   52.9390
                               8016   47.0610    6  0.096   293  end
arbmsio2   0.41023  2 0 0 0   14000   46.7570
                               8016   53.2430    6  0.367   293  end
arbmfe2o3  0.41023  2 0 0 0   26000   69.9540
                               8016   30.0460    6  0.067   293  end
arbmtio2   0.41023  2 0 0 0   22000   59.9535
                               8016   40.0465    6  0.012   293  end
arbmcao    0.41023  2 0 0 0   20000   71.4815
                               8016   28.5185    6  0.307   293  end
arbmmgo    0.41023  2 0 0 0   12000   60.3169
                               8016   39.6831    6  0.131   293  end
arbmna2o   0.41023  2 0 0 0   11023   74.1961
                               8016   25.8039    6  0.020   293  end
'reflective water'
arbmh20r   0.9982   2 0 0 0    1001   11.1913
                               8016   88.8087    7  1.0000  293  end
end comp
spherical end
1   6.05465
6  31.08141
7  51.08141
end zone
atdmkr,[ 7000.0U, 7000.0U235,513.0CH2]g htox= 2.46 Rc= 6.05465cm,128034.0gKao,Rk=31.0814cm
read parameters nub=yes npg=2500 gen=215 nsk=15 tme=100 end parameters
'Mass of fm in core region   = 7000.00000 g'
'Mass of poly in core region =  513.00000 g'
'Mass of core region         = 7513.00000 g'
'Vol of fm                   =  372.12095 cm3'
'Vol of poly                 =  557.60870 cm3'
'Volume of core region       =  929.72965 cm3'
'Calculate HTOX ratio for use of 513.0 grams can pads,vinyl tape, polyethylene in CV'
'hydrogen to fissile uranium ratio  =   2.4580'
read geometry
global
unit 1001
'fissile material dry core with 20.0 cm water reflection'
'fissile material dry core, kaolite shell, 20.0 cm h2o reflector'
'maximum kaolite radius =  31.08131 cm'
'increase kaolite shell by equal volume increments'
'1.24843e+04  cm3 volume of increment'
'125772.7 cm3 accumulative volume of core and kaolite'
'31.08141 cm accumulative radius of kaolite shell'
'1.28034e+05  g accumulative mass of kaolite shell'
sphere  1  1   6.05465  com='HEU core'
sphere  6  1  31.08141  com='kaolite shell around HEU core'
sphere  7  1  51.08141  com='20cm h2o reflector around kaolite shell'
end geometry
end data
end


=csas25    parm=size=300000
atdzr,[10400.UZrHx, 921.0U235,500.0CH2]g htox=43.37,Rc= 7.46774cm
238groupndf5 multiregion
'UZrHx=10400.0g, poly=500.0g, content hx=18.2'
'core htox=43.37'
arbmtriga  8.65974  4 0 0 0    1001    0.9554
                              40000   54.0446
                              92235    8.8558
                              92238   36.1442    1  0.6885 293  end
arbmpoly   0.92000   2 0 0 0   1001   14.3798
                               6012   85.6202    1  0.3115  293  end
'reflective water'
arbmh20r   0.9982   2 0 0 0    1001   11.1913
                               8016   88.8087    7  1.0000  293  end
end comp
spherical end
1   7.46774
7  27.46774
end zone
```

```
atdzr,[10400.UZrHx, 921.0U235,500.0CH2]g htox=43.37 Rc= 7.46774cm
read parameters nub=yes npg=2500 gen=215 nsk=15 tme=100 end parameters
'Mass of fm in core region   = 10400.0010 g'
'Mass of poly in core region =  500.00000 g'
'Mass of core region         = 10900.0010 g'
'Vol of fm                   = 1200.95996 cm3'
'Vol of poly                 =  543.47826 cm3'
'Volume of core region       = 1744.43822 cm3'
'Calculate HTOX ratio for use of 500.0 grams can pads,vinyl tape, polyethylene in CV'
'hydrogen to fissile uranium ratio  =  43.3700'
read geometry
global
unit 1001
'fissile material dry core with 20.0 cm water reflection'
sphere  1  1   7.46774  com='HEU core'
sphere  7  1  27.46774  com='20.0 cm water reflector'
end geometry
end data
end


=csas25    parm=size=300000
athzpkr,[10400.UZrHx, 921.0U235,500.0CH2,76819.H2O]g htox=2220.,Rc=39.15407cm
238groupndf5 multiregion
'UZrHx=10400.0g, poly=500.0g, content hx=18.2'
'H2O in Kaolite= 76819.4g, homogenized htox=2220.'
arbmtriga  8.65974  4 0 0 0    1001    0.9554
                              40000   54.0446
                              92235    8.8558
                              92238   36.1442    1  0.0048 293  end
arbmpoly   0.92000   2 0 0 0    1001   14.3798
                                6012   85.6202    1  0.0022  293  end
arbmh2ok   0.61533   2 0 0 0    1001   11.1913
                                8016   88.8087    1  0.4965   293  end
arbmal2o3  0.20369   2 0 0 0   13027   52.9390
                                8016   47.0610    1  0.096   293  end
arbmsio2   0.20369   2 0 0 0   14000   46.7570
                                8016   53.2430    1  0.367   293  end
arbmfe2o3  0.20369   2 0 0 0   26000   69.9540
                                8016   30.0460    1  0.067   293  end
arbmtio2   0.20369   2 0 0 0   22000   59.9535
                                8016   40.0465    1  0.012   293  end
arbmcao    0.20369   2 0 0 0   20000   71.4815
                                8016   28.5185    1  0.307   293  end
arbmmgo    0.20369   2 0 0 0   12000   60.3169
                                8016   39.6831    1  0.131   293  end
arbmna2o   0.20369   2 0 0 0   11023   74.1961
                                8016   25.8039    1  0.020   293  end
'reflective water'
arbmh20r   0.9982   2 0 0 0    1001   11.1913
                                8016   88.8087    7  1.0000  293  end
end comp
spherical end
1  39.15407
7  59.15407
end zone
athzpkr,[10400.UZrHx, 921.0U235,500.0CH2,76819.H2O]g htox=2220. Rc=39.15407cm
read parameters nub=yes npg=2500 gen=215 nsk=15 tme=100 end parameters
'                             CHECK=> 76819.64 g'
'Minimum mass of water from Kaolite = 2204.715 g'
'                             CHECK=> 2204.724 g'
'Mass of kao from Kaolite = 51214.88 g'
'                             CHECK=> 51214.34 g'
' '
'Calculate the mass of water contained in the homogenized region'
'Mass of fm in homogenized region   = 10400.0010 g'
'Mass of poly in homogenized region =  500.00000 g'
'Mass of h2o in homogenized region  = 76819.3531 g'
'Mass of kao in homogenized region  = 51214.8849 g'
'Mass of homogenized region         = 138934.239 g'
'Vol of homogenized fm              = 1200.95996 cm3'
```

```
'Vol of poly                        =  543.47826 cm3'
'Vol of h2o                         = 124842.528 cm3'
'Vol of kao                         = 124844.318 cm3'
'Volume of homogenized region       = 251431.285 cm3'
'Calculate HTOX ratio for use of 500.0 grams can pads,vinyl tape, polyethylene in CV'
'hydrogen to fissile uranium ratio  = 2220.409'
read geometry
global
unit 1001
'fissile material homogenized with Kaolite, 20.0 cm refl'
sphere  1  1  39.15407  com='HEU core/water mixture'
sphere  7  1  59.15407  com='20.0 cm water reflector'
end geometry
end data
end


=csas25    parm=size=300000
athzpwskr,[10400.UZrHx, 921.0U235,500.0CH2,74614.H2O]g
htox=2157.,Rc=26.33372cm,53419.6,Rs=36.35905cm
238groupndf5 multiregion
'UZrHx=10400.0g, poly=500.0g, content hx=18.2'
'H2O in Kaolite= 74614.6g, homogenized htox=2157.'
arbmtriga  8.65974  4 0 0 0    1001    0.9554
                              40000   54.0446
                              92235    8.8558
                              92238   36.1442    1  1.5700e-02   293  end
arbmpoly   0.92000   2 0 0 0   1001   14.3798
                               6012   85.6202    1  7.1049e-03    293  end
arbmkh2o   0.9982    2 0 0 0   1001   11.1913
                               8016   88.8087    1  9.7719e-01    293  end
'kaolite 1600 shell'
arbmh2ok 1.7660e-02  2 0 0 0   1001   11.1913
                               8016   88.8087    2  1.000   293  end
arbmal2o3  0.41023   2 0 0 0   13027   52.9390
                               8016   47.0610    2  0.096   293  end
arbmsio2   0.41023   2 0 0 0   14000   46.7570
                               8016   53.2430    2  0.367   293  end
arbmfe2o3  0.41023   2 0 0 0   26000   69.9540
                               8016   30.0460    2  0.067   293  end
arbmtio2   0.41023   2 0 0 0   22000   59.9535
                               8016   40.0465    2  0.012   293  end
arbmcao    0.41023   2 0 0 0   20000   71.4815
                               8016   28.5185    2  0.307   293  end
arbmmgo    0.41023   2 0 0 0   12000   60.3169
                               8016   39.6831    2  0.131   293  end
arbmna2o   0.41023   2 0 0 0   11023   74.1961
                               8016   25.8039    2  0.020   293  end
'reflective water'
arbmh2or   0.9982   2 0 0 0    1001   11.1913
                               8016   88.8087    8  1.0000  293  end
end comp
spherical end
1  26.33372
2  36.35905
8  56.35905
end zone
athzpwskr,[10400.UZrHx, 921.0U235,500.0CH2,74614.H2O]g htox=2157.
Rc=26.33372cm,53419.6,Rs=36.35905cm
read parameters nub=yes npg=2500 gen=215 nsk=15 tme=100 end parameters
'                              CHECK=> 76819.64 g'
'Minimum mass of water from Kaolite = 2204.715 g'
'                              CHECK=> 2204.724 g'
'Mass of kao from Kaolite = 51214.88 g'
'                              CHECK=> 51214.34 g'
' '
'Calculate the mass of water contained in the homogenized region'
'Mass of fm in homogenized region   = 10400.0010 g'
'Mass of poly in homogenized region =  500.00000 g'
'Mass of h2o in homogenized region  = 74614.6376 g'
'Mass of homogenized region         = 85514.6387 g'
```

```
'Vol of homogenized fm              = 1200.95996 cm3'
'Vol of poly                        =  543.47826 cm3'
'Vol of h2o                         = 74749.1862 cm3'
'Volume of homogenized region       = 76493.6244 cm3'
'Calculate HTOX ratio for use of 500.0 grams can pads,vinyl tape, polyethylene in CV'
'hydrogen to fissile uranium ratio  = 2157.928'
' '
'Mass of h2o in shell region        = 2204.71543 g'
'Mass of kao in shell region        = 51214.8849 g'
'Mass of kaolite in shell           = 53419.6003 g'
'Volume of kaolite in shell region  = 124843.000 cm3'
read geometry
global
unit 1001
'fissile material homogenized with water of Kaolite, 20.0 cm refl'
'Radius of homogenized mix          =   26.33372 cm'
'Radius of kaolite shell                 =   36.35905 cm'
sphere  1  1  26.33372  com='HEU core/water mixture'
sphere  2  1  36.35905  com='radius of kaolite shell'
sphere  8  1  56.35905  com='20.0 cm water reflector'
end geometry
end data
end


=csas25    parm=size=300000
athmpkr,[ 4000.0U, 4000.0U235,513.0CH2,76819.H2O]g htox=505.5,Rc=39.10344cm
238groupndf5 multiregion
'wrapped dry content can hx=4.30''HEU= 4000.0g, H2O in Kaolite= 76819.4g, poly=513.0g htox=505.5'
uranium  1 den=18.81109 8.4901e-04   293   92235  100.00
                                           92238    0.000               end
arbmpoly   0.92000   2 0 0 0    1001   14.3798
                                6012   85.6202    1  2.2264e-03    293  end
arbmh2ok   0.61533   2 0 0 0    1001   11.1913
                                8016   88.8087    1  4.9846e-01    293  end
arbmal2o3  0.20449   2 0 0 0   13027   52.9390
                                8016   47.0610    1  0.096   293  end
arbmsio2   0.20449   2 0 0 0   14000   46.7570
                                8016   53.2430    1  0.367   293  end
arbmfe2o3  0.20449   2 0 0 0   26000   69.9540
                                8016   30.0460    1  0.067   293  end
arbmtio2   0.20449   2 0 0 0   22000   59.9535
                                8016   40.0465    1  0.012   293  end
arbmcao    0.20449   2 0 0 0   20000   71.4815
                                8016   28.5185    1  0.307   293  end
arbmmgo    0.20449   2 0 0 0   12000   60.3169
                                8016   39.6831    1  0.131   293  end
arbmna2o   0.20449   2 0 0 0   11023   74.1961
                                8016   25.8039    1  0.020   293  end
'reflective water'
arbmh20r   0.9982   2 0 0 0    1001   11.1913
                               8016   88.8087    7  1.0000  293  end
end comp
spherical end
1  39.10344
7  59.10344
end zone
athmpkr,[ 4000.0U, 4000.0U235,513.0CH2,76819.H2O]g htox=505.5 Rc=39.10344cm
read parameters nub=yes npg=2500 gen=215 nsk=15 tme=100 end parameters
'Maximum mass of water from Kaolite = 76819.35 g'
'                              CHECK=> 76819.64 g'
'Minimum mass of water from Kaolite = 2204.715 g'
'                              CHECK=> 2204.724 g'
'Mass of kao from Kaolite = 51214.88 g'
'                              CHECK=> 51214.34 g'
' '
'Calculate the mass of water contained in the homogenized region'
'Mass of homogenized fm             = 4000.00000 g'
'Mass of poly in homogenized region =  513.00000 g'
'Mass of h2o in homogenized region  = 76819.3531 g'
'Mass of kao in homogenized region  = 51214.8849 g'
```

```
'Mass of homogenized region         = 132547.238 g'
'Vol of homogenized fm              =  212.64054 cm3'
'Vol of h2o                         = 124842.528 cm3'
'Vol of kao                         = 124844.318 cm3'
'Volume of homogenized region       = 250457.096 cm3'
'Calculate HTOX ratio for use of 513.0 grams can pads,vinyl tape, polyethylene in CV'
'hydrogen to fissile uranium ratio  = 505.5652'
read geometry
global
unit 1001
'fissile material homogenized with Kaolite, 20.0 cm refl'
sphere  1  1  39.10344  com='HEU core/water mixture'
sphere  7  1  59.10344  com='20.0 cm water reflector'
end geometry
end data
end


csas25    parm=size=300000
athmpwskr,[ 1000.0U, 1000.0U235,513.0CH2,74614.H2O]g
htox=1964.,Rc=26.20298cm,53419.6,Rs=36.29068cm
238groupndf5 multiregion
'wrapped dry content can hx=17.2'
'HEU= 1000.0g, H2O in Kaolite= 74614.6g, poly=513.0g htox=1964.'
uranium  1 den=18.81109 7.0542e-04   293   92235  100.00
                                            92238    0.000               end
arbmpoly   0.92000   2 0 0 0   1001   14.3798
                               6012   85.6202    1  7.3993e-03    293  end
arbmkh2o   0.9982    2 0 0 0   1001   11.1913
                               8016   88.8087    1  9.9190e-01    293  end
'kaolite 1600 shell'
arbmh2ok 1.7660e-02  2 0 0 0   1001   11.1913
                               8016   88.8087    2  1.000   293  end
arbmal2o3  0.41023   2 0 0 0   13027   52.9390
                               8016   47.0610    2  0.096   293  end
arbmsio2   0.41023   2 0 0 0   14000   46.7570
                               8016   53.2430    2  0.367   293  end
arbmfe2o3  0.41023   2 0 0 0   26000   69.9540
                               8016   30.0460    2  0.067   293  end
arbmtio2   0.41023   2 0 0 0   22000   59.9535
                               8016   40.0465    2  0.012   293  end
arbmcao    0.41023   2 0 0 0   20000   71.4815
                               8016   28.5185    2  0.307   293  end
arbmmgo    0.41023   2 0 0 0   12000   60.3169
                               8016   39.6831    2  0.131   293  end
arbmna2o   0.41023   2 0 0 0   11023   74.1961
                               8016   25.8039    2  0.020   293  end
'flooded containment vessel and content cans -- 10 CFR 71.55(d)(3)'
arbmwicv   0.9982   2 0 0 0    1001   11.1913
                               8016   88.8087    3  1.0     293  end
'steel: cv body, lower flange, upper flange, drum liner'
ss304                                            4  1.0     293  end
'kaolite 1600 body'
'nct.sing.unit.density= (den.mult)(min.den.)'
' for arbmh20k 0.52294 = 1.012373*0.51655, for rest 0.34864 = 1.012373*0.34438'
'den.mult= 1.36557e5 cm3 (actual vol.) / 1.34888e5 cm3 (model vol.)'
'actual vol.= 1.36557e5 cm3 = (28316.84 cm3/ft3)(108.33188 lb)/(22.464 lb/ft3)'
'hac.s.u.dens= (hac.mult)(nct.s.u.dens)'
'hac.mult = 1.34888e5 cm3 (nct vol.)/ 1.12246e5 cm3 (model vol.)'
' for arbmh2ok 0.62843 = 1.20172*0.52294,   for rest = 1.20172*0.34864'
'hac array densities are hac s.u.dens.'
arbmh2ok   0.62843  2 0 0 0    1001   11.1913
                               8016   88.8087    5  0.0287  293  end
arbmal2o3  0.41898  2 0 0 0   13027   52.9390
                               8016   47.0610    5  0.096   293  end
arbmsio2   0.41898  2 0 0 0   14000   46.7570
                               8016   53.2430    5  0.367   293  end
arbmfe2o3  0.41898  2 0 0 0   26000   69.9540
                               8016   30.0460    5  0.067   293  end
arbmtio2   0.41898  2 0 0 0   22000   59.9535
                               8016   40.0465    5  0.012   293  end
```

```
arbmcao    0.41898  2 0 0 0   20000   71.4815
                               8016   28.5185    5  0.307   293  end
arbmmgo    0.41898  2 0 0 0   12000   60.3169
                               8016   39.6831    5  0.131   293  end
arbmna2o   0.41898  2 0 0 0   11023   74.1961
                               8016   25.8039    5  0.020   293  end
'kaolite 1600 top plug'
'sing.unit.density= (den.mult)(min.den.)'
' for arbmh20k = 0.965246*0.51655,  for rest = 0.965246*0.34438'
'den.mult= 1.21592e4 cm3 (actual vol.) / 1.25970e4 cm3 (model vol.)'
'actual vol.= 1.21592e4 cm3 = (28316.84 cm3/ft3)(9.646 lb)/(22.464 lb/ft3)'
arbmh2ok   0.49860  2 0 0 0    1001   11.1913
                               8016   88.8087    6  0.0287  293  end
arbmal2o3  0.33241  2 0 0 0   13027   52.9390
                               8016   47.0610    6  0.096   293  end
arbmsio2   0.33241  2 0 0 0   14000   46.7570
                               8016   53.2430    6  0.367   293  end
arbmfe2o3  0.33241  2 0 0 0   26000   69.9540
                               8016   30.0460    6  0.067   293  end
arbmtio2   0.33241  2 0 0 0   22000   59.9535
                               8016   40.0465    6  0.012   293  end
arbmcao    0.33241  2 0 0 0   20000   71.4815
                               8016   28.5185    6  0.307   293  end
arbmmgo    0.33241  2 0 0 0   12000   60.3169
                               8016   39.6831    6  0.131   293  end
arbmna2o   0.33241  2 0 0 0   11023   74.1961
                               8016   25.8039    6  0.020   293  end
'kaolite 1600 combined'
'sing.unit.density= (den.mult)(min.den.)'
' for arbmh20k = 1.191224*0.51655,  for rest = 1.191224*0.34438'
'den.mult= 1.48716e5 cm3 (actual vol.) / 1.24843e5 cm3 (model vol.)'
'actual body vol.= 1.36557e5 cm3 = (28316.84 cm3/ft3)(108.33188 lb)/(22.464 lb/ft3)'
'actual plug vol.= 1.21592e4 cm3 = (28316.84 cm3/ft3)(9.646 lb)/(22.464 lb/ft3)'
'total Kaolite volume=1.48716e5 cm3 =  1.36557e5 + 1.21592e4 cm3'
'model body vol.= 1.12246e5 cm3'
'model plug vol.= 1.25970e4 cm3'
'total model volume=1.24843e5 cm3 =  1.12246e5 + 1.25970e4 cm3'
arbmh2ok   0.61533  2 0 0 0    1001   11.1913
                               8016   88.8087    7  0.0287  293  end
arbmal2o3  0.41023  2 0 0 0   13027   52.9390
                               8016   47.0610    7  0.096   293  end
arbmsio2   0.41023  2 0 0 0   14000   46.7570
                               8016   53.2430    7  0.367   293  end
arbmfe2o3  0.41023  2 0 0 0   26000   69.9540
                               8016   30.0460    7  0.067   293  end
arbmtio2   0.41023  2 0 0 0   22000   59.9535
                               8016   40.0465    7  0.012   293  end
arbmcao    0.41023  2 0 0 0   20000   71.4815
                               8016   28.5185    7  0.307   293  end
arbmmgo    0.41023  2 0 0 0   12000   60.3169
                               8016   39.6831    7  0.131   293  end
arbmna2o   0.41023  2 0 0 0   11023   74.1961
                               8016   25.8039    7  0.020   293  end
'reflective water'
arbmh2or   0.9982   2 0 0 0    1001   11.1913
                               8016   88.8087    8  1.0000  293  end
end comp
spherical end
1  26.20298
2  36.29068
8  56.29068
end zone
athmpwkr,[ 1000.0U, 1000.0U235,513.0CH2,74614.H2O]g htox=1964.
Rc=26.20298cm,53419.6,Rs=36.29068cm
read parameters nub=yes npg=2500 gen=215 nsk=15 tme=100 end parameters
'Maximum mass of water from Kaolite = 76819.35 g'
'                            CHECK=> 76819.64 g'
'Minimum mass of water from Kaolite = 2204.715 g'
'                            CHECK=> 2204.724 g'
'Mass of kao from Kaolite = 51214.88 g'
'                            CHECK=> 51214.34 g'
```

```
' '
'Calculate the mass of water contained in the homogenized region'
'Mass of homogenized fm             = 1000.00000 g'
'Mass of poly in homogenized region =  513.00000 g'
'Mass of h2o in homogenized region  = 74614.6376 g'
'Mass of homogenized region         = 76127.6376 g'
'Vol of homogenized fm              =   53.16014 cm3'
'Vol of poly                        =  557.60870 cm3'
'Vol of h2o                         = 74749.1862 cm3'
'Volume of homogenized region       = 75359.9550 cm3'
'Calculate HTOX ratio for use of 513.0 grams can pads,vinyl tape, polyethylene in CV'
'hydrogen to fissile uranium ratio  = 1964.715'
' '
'Mass of h2o in shell region        = 2204.71543 g'
'Mass of kao in shell region        = 51214.8849 g'
'Mass of kaolite in shell           = 53419.6003 g'
'Volume of kaolite in shell region  = 124843.000 cm3'
read geometry
global
unit 1001
'Radius of homogenized mix          =   26.20298 cm'
'Radius of kaolite shell                 =   36.29068 cm'
sphere  1  1  26.20298  com='HEU core/water mixture'
sphere  2  1  36.29068  com='radius of kaolite shell'
sphere  8  1  56.29068  com='20.0 cm water reflector'
end geometry
end data
end


=csas25    parm=size=300000
athm2pwskr,[ 3500.0U,  700.0U235,513.0CH2,14922.H2O]g
htox=116.2,Rc=15.53077cm,113111.,Rs=32.25271cm
238groupndf5 multiregion
'wrapped dry content can hx=24.5'
'HEU= 3500.0g, H2O in Kaolite= 14922.9g, poly=513.0g htox=116.2'
uranium  1 den=19.00312 1.1737e-02   293   92235  20.000
                                            92238   80.000               end
arbmpoly   0.92000   2 0 0 0   1001   14.3798
                               6012   85.6202    1  3.5535e-02    293  end
arbmkh2o   0.9982    2 0 0 0   1001   11.1913
                               8016   88.8087    1  9.5273e-01    293  end
'kaolite 1600 shell'
arbmh2ok 4.9579e-01  2 0 0 0   1001   11.1913
                               8016   88.8087    2  1.000   293  end
arbmal2o3  0.41023   2 0 0 0   13027   52.9390
                               8016   47.0610    2  0.096   293  end
arbmsio2   0.41023   2 0 0 0   14000   46.7570
                               8016   53.2430    2  0.367   293  end
arbmfe2o3  0.41023   2 0 0 0   26000   69.9540
                               8016   30.0460    2  0.067   293  end
arbmtio2   0.41023   2 0 0 0   22000   59.9535
                               8016   40.0465    2  0.012   293  end
arbmcao    0.41023   2 0 0 0   20000   71.4815
                               8016   28.5185    2  0.307   293  end
arbmmgo    0.41023   2 0 0 0   12000   60.3169
                               8016   39.6831    2  0.131   293  end
arbmna2o   0.41023   2 0 0 0   11023   74.1961
                               8016   25.8039    2  0.020   293  end
'flooded containment vessel and content cans -- 10 CFR 71.55(d)(3)'
arbmwicv   0.9982   2 0 0 0    1001   11.1913
                               8016   88.8087    3  1.0     293  end
'steel: cv body, lower flange, upper flange, drum liner'
ss304                                             4  1.0     293  end
'kaolite 1600 body'
'nct.sing.unit.density= (den.mult)(min.den.)'
' for arbmh20k 0.52294 = 1.012373*0.51655, for rest 0.34864 = 1.012373*0.34438'
'den.mult= 1.36557e5 cm3 (actual vol.) / 1.34888e5 cm3 (model vol.)'
'actual vol.= 1.36557e5 cm3 = (28316.84 cm3/ft3)(108.33188 lb)/(22.464 lb/ft3)'
'hac.s.u.dens= (hac.mult)(nct.s.u.dens)'
'hac.mult = 1.34888e5 cm3 (nct vol.)/ 1.12246e5 cm3 (model vol.)'
```

```
' for arbmh2ok 0.62843 = 1.20172*0.52294,   for rest = 1.20172*0.34864'
'hac array densities are hac s.u.dens.'
arbmh2ok   0.62843  2 0 0 0    1001   11.1913
                                8016   88.8087    5  0.0287  293  end
arbmal2o3  0.41898  2 0 0 0   13027   52.9390
                                8016   47.0610    5  0.096   293  end
arbmsio2   0.41898  2 0 0 0   14000   46.7570
                                8016   53.2430    5  0.367   293  end
arbmfe2o3  0.41898  2 0 0 0   26000   69.9540
                                8016   30.0460    5  0.067   293  end
arbmtio2   0.41898  2 0 0 0   22000   59.9535
                                8016   40.0465    5  0.012   293  end
arbmcao    0.41898  2 0 0 0   20000   71.4815
                                8016   28.5185    5  0.307   293  end
arbmmgo    0.41898  2 0 0 0   12000   60.3169
                                8016   39.6831    5  0.131   293  end
arbmna2o   0.41898  2 0 0 0   11023   74.1961
                                8016   25.8039    5  0.020   293  end
'kaolite 1600 top plug'
'sing.unit.density= (den.mult)(min.den.)'
' for arbmh20k = 0.965246*0.51655,  for rest = 0.965246*0.34438'
'den.mult= 1.21592e4 cm3 (actual vol.) / 1.25970e4 cm3 (model vol.)'
'actual vol.= 1.21592e4 cm3 = (28316.84 cm3/ft3)(9.646 lb)/(22.464 lb/ft3)'
arbmh2ok   0.49860  2 0 0 0    1001   11.1913
                                8016   88.8087    6  0.0287  293  end
arbmal2o3  0.33241  2 0 0 0   13027   52.9390
                                8016   47.0610    6  0.096   293  end
arbmsio2   0.33241  2 0 0 0   14000   46.7570
                                8016   53.2430    6  0.367   293  end
arbmfe2o3  0.33241  2 0 0 0   26000   69.9540
                                8016   30.0460    6  0.067   293  end
arbmtio2   0.33241  2 0 0 0   22000   59.9535
                                8016   40.0465    6  0.012   293  end
arbmcao    0.33241  2 0 0 0   20000   71.4815
                                8016   28.5185    6  0.307   293  end
arbmmgo    0.33241  2 0 0 0   12000   60.3169
                                8016   39.6831    6  0.131   293  end
arbmna2o   0.33241  2 0 0 0   11023   74.1961
                                8016   25.8039    6  0.020   293  end
'kaolite 1600 combined'
'sing.unit.density= (den.mult)(min.den.)'
' for arbmh20k = 1.191224*0.51655,  for rest = 1.191224*0.34438'
'den.mult= 1.48716e5 cm3 (actual vol.) / 1.24843e5 cm3 (model vol.)'
'actual body vol.= 1.36557e5 cm3 = (28316.84 cm3/ft3)(108.33188 lb)/(22.464 lb/ft3)'
'actual plug vol.= 1.21592e4 cm3 = (28316.84 cm3/ft3)(9.646 lb)/(22.464 lb/ft3)'
'total Kaolite volume=1.48716e5 cm3 =  1.36557e5 + 1.21592e4 cm3'
'model body vol.= 1.12246e5 cm3'
'model plug vol.= 1.25970e4 cm3'
'total model volume=1.24843e5 cm3 =  1.12246e5 + 1.25970e4 cm3'
arbmh2ok   0.61533  2 0 0 0    1001   11.1913
                                8016   88.8087    7  0.0287  293  end
arbmal2o3  0.41023  2 0 0 0   13027   52.9390
                                8016   47.0610    7  0.096   293  end
arbmsio2   0.41023  2 0 0 0   14000   46.7570
                                8016   53.2430    7  0.367   293  end
arbmfe2o3  0.41023  2 0 0 0   26000   69.9540
                                8016   30.0460    7  0.067   293  end
arbmtio2   0.41023  2 0 0 0   22000   59.9535
                                8016   40.0465    7  0.012   293  end
arbmcao    0.41023  2 0 0 0   20000   71.4815
                                8016   28.5185    7  0.307   293  end
arbmmgo    0.41023  2 0 0 0   12000   60.3169
                                8016   39.6831    7  0.131   293  end
arbmna2o   0.41023  2 0 0 0   11023   74.1961
                                8016   25.8039    7  0.020   293  end
'reflective water'
arbmh2or   0.9982   2 0 0 0    1001   11.1913
                                8016   88.8087    8  1.0000  293  end
end comp
spherical end
1  15.53077
```

```
2  32.25271
8  52.25271
end zone
athmpwkr,[ 3500.0U,  700.0U235,513.0CH2,14922.H2O]g htox=116.2
Rc=15.53077cm,113111.,Rs=32.25271cm
read parameters nub=yes npg=2500 gen=215 nsk=15 tme=100 end parameters
'Maximum mass of water from Kaolite = 76819.35 g'
'                             CHECK=> 76819.64 g'
'Minimum mass of water from Kaolite = 2204.715 g'
'                             CHECK=> 2204.724 g'
'Mass of kao from Kaolite = 51214.88 g'
'                             CHECK=> 51214.34 g'
' '
'Calculate the mass of water contained in the homogenized region'
'Mass of homogenized fm            = 3500.00000 g'
'Mass of poly in homogenized region =  513.00000 g'
'Mass of h2o in homogenized region  = 14922.9275 g'
'Mass of homogenized region         = 18935.9275 g'
'Vol of homogenized fm              =  184.18032 cm3'
'Vol of poly                        =  557.60870 cm3'
'Vol of h2o                         = 14949.8372 cm3'
'Volume of homogenized region       = 15691.6262 cm3'
'Calculate HTOX ratio for use of 513.0 grams can pads,vinyl tape, polyethylene in CV'
'hydrogen to fissile uranium ratio  = 116.2023'
' '
'Mass of h2o in shell region        = 61896.4255 g'
'Mass of kao in shell region        = 51214.8849 g'
'Mass of kaolite in shell           = 113111.310 g'
'Volume of kaolite in shell region  = 124843.000 cm3'
read geometry
global
unit 1001
'Radius of homogenized mix          =   15.53077 cm'
'Radius of kaolite shell                 =   32.25271 cm'
sphere  1  1  15.53077  com='HEU core/water mixture'
sphere  2  1  32.25271  com='radius of kaolite shell'
sphere  8  1  52.25271  com='20.0 cm water reflector'
end geometry
end data
end


=csas25    parm=size=300000
athmpkmr,17.5kgU,[1000.0U235,513.0CH2,76819.4H2O]g
htox=404.45,Rc=39.10606cm,2500.0U235,Rs=39.14036cm
238groupndf5 multiregion
'dry CV hx=4.92 for 17.5 kilograms HEU metal wrapped content'
'Core  1000.0g235U,513.0g Poly, 76819.4gH2O in Kaolite.  htox=404.4'
uranium  1 den=19.00312 1.0503e-03   293   92235  20.000
                                            92238   80.00                end
arbmpoly   0.92000   2 0 0 0    1001   14.3798
                                6012   85.6202    1  2.2259e-03    293  end
arbmh2ok   0.61533   2 0 0 0    1001   11.1913
                                8016   88.8087    1  4.9836e-01    293  end
arbmal2o3  0.20444   2 0 0 0   13027   52.9390
                                8016   47.0610    1  0.096   293  end
arbmsio2   0.20444   2 0 0 0   14000   46.7570
                                8016   53.2430    1  0.367   293  end
arbmfe2o3  0.20444   2 0 0 0   26000   69.9540
                                8016   30.0460    1  0.067   293  end
arbmtio2   0.20444   2 0 0 0   22000   59.9535
                                8016   40.0465    1  0.012   293  end
arbmcao    0.20444   2 0 0 0   20000   71.4815
                                8016   28.5185    1  0.307   293  end
arbmmgo    0.20444   2 0 0 0   12000   60.3169
                                8016   39.6831    1  0.131   293  end
arbmna2o   0.20444   2 0 0 0   11023   74.1961
                                8016   25.8039    1  0.020   293  end
uranium  2 den=19.00312  1.0   293   92235  20.000
                                      92238   80.00               end
'reflective water'
```

```
arbmh2or   0.9982   2 0 0 0    1001   11.1913
                               8016   88.8087    8  1.0000  293  end
end comp
spherical end
1  39.10606
2  39.14036
8  59.14036
end zone
athmpkmr,17.5kgU,[1000.0U235,513.0CH2,76819.4H2O]g htox=404.45
Rc=39.10606cm,2500.0U235,Rs=39.14036cm
read parameters nub=yes npg=2500 gen=215 nsk=15 tme=100 end parameters
'Maximum mass of water from Kaolite = 76819.35 g'
'                             CHECK=> 76819.64 g'
'Minimum mass of water from Kaolite = 2204.715 g'
'                             CHECK=> 2204.724 g'
'Mass of kao from Kaolite = 51214.88 g'
'                             CHECK=> 51214.34 g'
' '
'Calculate the mass of water contained in the homogenized region'
'Mass of homogenized fissile U     = 5000.00000 g'
'Mass of poly in homogenized region=  513.00000 g'
'Mass of h2o in homogenized region = 76819.3531 g'
'Mass of kao in homogenized region = 51214.8849 g'
'Mass of homogenized core region   = 133547.238 g'
'Vol of homogenized fissile U      =  263.11475 cm3'
'Vol of poly                       =  557.60870 cm3'
'Vol of h2o                        = 124842.528 cm3'
'Vol of kao                        = 124844.318 cm3'
'Volume of homogenized core region = 250507.570 cm3'
'Calculate HTOX ratio for use of 513.0 grams can pads,vinyl tape, polyethylene in CV'
'Core hydrogen to fissile U ratio  = 404.4521'
' '
read geometry
global
unit 1001
'fissile material, homog, remaining fm as shell around mixture, 20.0 cm refl'
'Radius of homogenized core         =   39.10606 cm'
'Mass of fm shell                   = 12500.0000 g'
'Vol of fm shell                    =  657.78687 cm3'
'Radius of fm shell                 =   39.14036 cm'
sphere  1  1  39.10606  com='HEU core/water mixture'
sphere  2  1  39.14036  com='radius of fissile material shell'
sphere  8  1  59.14036  com='20.0 cm water reflector'
end geometry
end data
end


=csas25    parm=size=3000000
cvcrtriga 0.0in thk np,10400.0gUZrHx(  921.0g235,    0.0gH2O hx=  0.00),fr=1.0e+00
238groupndf5 infhommedium
'TRIGA volume =1200.95996, SPACER volume    0.00000'
'TRIGA wrapped dry content can hx=18.2, CV void volume 9014.40198'
arbmtriga  8.65974  4 0 0 0    1001    0.9554
                              40000   54.0446
                              92235    8.8558
                              92238   36.1442    1  1.0     293  end
'np277-4: spacer (NCT_MD&H)'
'NCT min.den.(95.3886 lb/ft3) and hydrogen'
'np277-4 min.den.= 1.527971 = (95.3886 lb/ft3)(453.59 g/lb)/(28316.84 cm3/ft3)'
'use 75% of boron in calculations per NUREG-1609 Section 6.5.3.2'
arbmboron 7.31015e-2  2 0 0 0    5010   18.1479
                                 5011   81.8520    2  0.7500  293  end
arbmnpmx  1.07070e+0 10 0 0 0    6012    1.9189
                                 7014    0.0141
                                 8016   43.4251
                                11023    0.1174
                                12000    0.3378
                                13027   39.0479
                                14000    2.4672
                                16000    0.3083
```

```
                                20000   11.8336
                                26000    0.5298    2  1.0000  293  end
arbmnph2o 3.84169e-1  2 0 0 0    1001   11.1913
                                 8016   88.8087    2  1.0000  293  end
'flooded containmment vessel and content cans -- 10 CFR 71.55(d)(3)'
arbmwicv   0.9982   2 0 0 0    1001   11.1913
                               8016   88.8087    3  1e-20   293  end
'steel: containment vessel body 16.60 lb but use 15.74 lb'
ss304                                            8  1.0     293  end
'steel: cv flange lower use 3.36 lb'
ss304                                            9  0.97267 293  end
'steel: cv flange upper use 13.75 lb'
ss304                                           10  0.94348 293  end
'np277-4: confinement -- neutron poison inner liner (NCT_MD&H)'
'actual vol.= 1.31846e4 cm3 = (8.0457422e2 in3)(16.387064)'
'den.multiplier = 1.31846e4 cm3 (actual vol.) / 1.32708e4 cm3 (model vol.)'
'np277-4 min.den.= 1.527971 = (95.3886 lb/ft3)(453.59 g/lb)/(28316.84 cm3/ft3)'
'density = 1.518047 = (den.mult)(np277-4 min.den.) = 0.9935052*1.527971'
'use 75% of boron in calculations per NUREG-1609 Section 6.5.3.2'
arbmboron 7.26267e-2  2 0 0 0    5010   18.1479
                                 5011   81.8520   11  0.7500  293  end
arbmnpmx  1.06375e+0 10 0 0 0    6012    1.9189
                                 7014    0.0141
                                 8016   43.4251
                                11023    0.1174
                                12000    0.3378
                                13027   39.0479
                                14000    2.4672
                                16000    0.3083
                                20000   11.8336
                                26000    0.5298   11  1.0000  293  end
arbmnph2o 3.81674e-1  2 0 0 0    1001   11.1913
                                 8016   88.8087   11  1.0000  293  end
'kaolite 1600 body'
'sing.unit.density= (den.mult)(min.den.)'
' for arbmh20k = 1.012373*0.51655,  for rest = 1.012373*0.34438'
'den.mult= 1.36557e5 cm3 (actual vol.) / 1.34888e5 cm3 (model vol.)'
'actual vol.= 1.36557e5 cm3 = (28316.84 cm3/ft3)(108.33188 lb)/(22.464 lb/ft3)'
arbmh2ok   0.52294  2 0 0 0    1001   11.1913
                               8016   88.8087   12  1       293  end
arbmal2o3  0.34864  2 0 0 0   13027   52.9390
                               8016   47.0610   12  0.096   293  end
arbmsio2   0.34864  2 0 0 0   14000   46.7570
                               8016   53.2430   12  0.367   293  end
arbmfe2o3  0.34864  2 0 0 0   26000   69.9540
                               8016   30.0460   12  0.067   293  end
arbmtio2   0.34864  2 0 0 0   22000   59.9535
                               8016   40.0465   12  0.012   293  end
arbmcao    0.34864  2 0 0 0   20000   71.4815
                               8016   28.5185   12  0.307   293  end
arbmmgo    0.34864  2 0 0 0   12000   60.3169
                               8016   39.6831   12  0.131   293  end
arbmna2o   0.34864  2 0 0 0   11023   74.1961
                               8016   25.8039   12  0.020   293  end
'kaolite 1600 top plug'
'sing.unit.density= (den.mult)(min.den.)'
' for arbmh20k = 0.965246*0.51655,  for rest = 0.965246*0.34438'
'den.mult= 1.21592e4 cm3 (actual vol.) / 1.25970e4 cm3 (model vol.)'
'actual vol.= 1.21592e4 cm3 = (28316.84 cm3/ft3)(9.646 lb)/(22.464 lb/ft3)'
arbmh2ok   0.49860  2 0 0 0    1001   11.1913
                               8016   88.8087   13  1       293  end
arbmal2o3  0.33241  2 0 0 0   13027   52.9390
                               8016   47.0610   13  0.096   293  end
arbmsio2   0.33241  2 0 0 0   14000   46.7570
                               8016   53.2430   13  0.367   293  end
arbmfe2o3  0.33241  2 0 0 0   26000   69.9540
                               8016   30.0460   13  0.067   293  end
arbmtio2   0.33241  2 0 0 0   22000   59.9535
                               8016   40.0465   13  0.012   293  end
arbmcao    0.33241  2 0 0 0   20000   71.4815
                               8016   28.5185   13  0.307   293  end
```

```
arbmmgo    0.33241  2 0 0 0   12000   60.3169
                               8016   39.6831   13  0.131   293  end
arbmna2o   0.33241  2 0 0 0   11023   74.1961
                               8016   25.8039   13  0.020   293  end
'silicone rubber pads'
arbmsiru   1.21791  4 0 0 0    6012   32.3767
                               1001    8.1573
                               8016   21.5782
                              14000   37.8878   14  1.0     293  end
'void space external to containment vessel'
arbmwecv   0.9982   2 0 0 0    1001   11.1913
                               8016   88.8087   15  1       293  end
'steel: liner'
ss304                                            16  1.0     293  end
'steel: plug cover (pc) use 9.907 lb'
ss304                                            17  1.06388 293  end
'steel: angle iron (ai) for single units'
ss304                                            18  1.0     293  end
'steel: angle iron (ai) for arrays'
'array density is multiplied by a volume fraction 7.08030/5.63249'
'ss304                                            18  1.25705 293  end
'steel: drum steel for single units'
ss304                                            19  1.0     293  end
'steel: drum steel for arrays'
'array density is multiplied by a volume fraction 3.20482/3.20544'
'ss304                                            19  0.99981 293  end
'void space external to drum'
'array density is multiplied by a volume ratio 8.11698/6.98323'
'arbmwed    1.16026  2 0 0 0    1001   11.1913
'                               8016   88.8087   20  1       293  end
'reflective water'
arbmh20r   0.9982   2 0 0 0    1001   11.1913
                               8016   88.8087   21  1.0     293  end
end comp
cvcrtriga 0.0in thk np,10400.0gUZrHx(  921.0g235,    0.0gH2O,hx=  0.00),fr=1.0e+00
read parameters nub=yes npg=2500 gen=215 nsk=15 tme=100 end parameters
read boun       all=vac                          end boun
read geometry
unit 1001
'drum bottom flat cover [Elev= 0.105 in. at top of unit]'
 cuboid    21 1 4p24.587200    0.26670   0.0     com='drum chine outer radius'
unit 1002
'above drum bottom flat cover and below containment vessel [Elev= 4.670 in.]'
 cuboid    21 1 4p24.587200   11.59510   0.0     com='drum chine outer radius'
unit 1003
'cv bottom [Elev= 4.920 in.]'
 cylinder  8  1    6.680200    0.63500   0.0     com='cv bottom'
 cuboid    21 1 4p24.587200    0.63500   0.0     com='drum chine outer radius'
unit 1004
'UZrHx fuel element'
 cylinder  1  1    1.828800   12.70000   0.0     com='cylindrical content'
unit 1006
'content (collapsed) [Elev= 9.920 in.]'
'1.437900   plus-y location upper cylinders'
'-2.875700  minus-y location lower cylinder'
'2.490443   plus-x location upper cylinder'
'-2.490443  minus-x location upper cylinder'
 cylinder  3  1    6.426200   12.70050  -0.0005  com='cv well cavity'
 hole  1004   -2.490443  1.437900  0.0     com='cyl1'
 hole  1004    2.490443  1.437900  0.0     com='cyl2'
 hole  1004    0.0      -2.875700  0.0     com='cyl3'
 cylinder  8  1    6.680200   12.70050  -0.0005  com='cv below 1st step'
 cuboid    21 1 4p24.587200   12.70050  -0.0005  com='drum chine outer radius'
unit 1007
'np277_4 spacer [Elev= 9.921 in.]'
 cylinder  2  1    5.24510     0.00010   0.0     com='np spacer'
 cylinder  3  1    6.426200    0.00020  -0.0001  com='cv well cavity'
 cylinder  8  1    6.680200    0.00020  -0.0001  com='cv below 1st step'
 cuboid    21 1 4p24.587200    0.00020  -0.0001  com='drum chine outer radius'
unit 1008
'top of content stack to bottom of 1st step [Elev=35.270 in.]'
```

```
'38.10360             stack height (content spacers)       CALCULATED
 cylinder  3  1    6.426200   38.98540   0.0     com='cv well cavity'
 cylinder  8  1    6.680200   38.98540   0.0     com='cv below 1st step'
 cuboid    21 1 4p24.587200   38.98540   0.0     com='drum chine outer radius'
unit 1010
'cv at 1st step in liner [Elev=35.330 in.]'
 cylinder  3  1    6.426200    0.15240   0.0     com='cv well cavity'
 cylinder  8  1    6.680200    0.15240   0.0     com='cv at 1st step'
 cuboid    21 1 4p24.587200    0.15240   0.0     com='drum chine outer radius'
unit 1011
'vertical gap between 1st step in liner and cv flange [Elev=35.420 in.]'
 cylinder  3  1    6.426200    0.22860   0.0     com='cv well cavity'
 cylinder  8  1    6.680200    0.22860   0.0     com='cv at gap btwn step-flng'
 cuboid    21 1 4p24.587200    0.22860   0.0     com='drum chine outer radius'
unit 1012
'cv flange to top of cv well [Elev=35.920 in.]'
 cylinder  3  1    6.426200    1.27000   0.0     com='cavity'
 cylinder  9  1    9.525000    1.27000   0.0     com='flange to top of well'
 cuboid    21 1 4p24.587200    1.27000   0.0     com='drum chine outer radius'
unit 1013
'cv flange above cv well [Elev=37.070 in.]'
 cylinder  10 1    9.525000    2.92100   0.0     com='flange above cv well'
 cuboid    21 1 4p24.587200    2.92100   0.0     com='drum chine outer radius'
unit 1014
'plugpad2 below liner 2nd step [Elev=37.470 in.]'
 cuboid    21 1 4p24.587200    1.01600   0.0     com='drum chine outer radius'
unit 1015
'2nd step in liner [Elev=37.530 in.]'
 cuboid    21 1 4p24.587200    0.15240   0.0     com='drum chine outer radius'
unit 1016
'abv 2nd step in liner to bottom of angle iron [Elev=40.750 in.]'
 cuboid    21 1 4p24.587200    8.17880   0.0     com='drum chine outer radius'
unit 1017
'bottom of angle iron to bend in angle iron [Elev=42.500 in.]'
 cuboid    21 1 4p24.587200    4.44500   0.0     com='drum chine outer radius'
unit 1018
'bend in angle iron to top of angle iron [Elev=42.750 in.]'
 cuboid    21 1 4p24.587200    0.63500   0.0     com='drum chine outer radius'
unit 1019
'drum lid and lip [Elev=43.500 in.]'
 cuboid    21 1 4p24.587200    1.90500   0.0     com='drum chine outer radius'
global
unit 1020
'es3100 drum [Elev=43.500 in.]'
array 3         2r-24.587200     0.0
'cuboid     0  1 4p24.587200    110.4905  0.0    com='bare package'
 cuboid    21  1 4p55.067200   140.9700 -30.48   com='reflected package'
'cuboid    20  1 4p22.889718    110.5048  0.0    com='interstital array space'
'global
'unit 1021
'array 4   3r0.0
'reflector  21 2  6r3.0  10
end geometry
read array
ara=3 nux=1 nuy=1 nuz=19 fill
1001 1002 1003 1006 1007 1006 1007 1006 1008 1010
1011 1012 1013 1014 1015 1016 1017 1018 1019        end fill
'ara=4 nux=13 nuy=13 nuz=06 fill f1020               end fill
end array
'read bias id=500 2  11  end bias
read start nst=0
end start
end data
end


=csas25    parm=size=3000000
cvcrtriga 0.0in thk np,10400.0gUZrHx(  921.0g235, 8998.2gH2O hx=255.01),fr=1.0e+00
238groupndf5 infhommedium
'TRIGA volume =1200.95996, SPACER volume    0.00000'
'TRIGA wrapped dry content can hx=18.2, CV void volume 9014.40198'
```

```
arbmtriga  8.65974  4 0 0 0    1001    0.9554
                              40000   54.0446
                              92235    8.8558
                              92238   36.1442    1  1.0     293  end
'np277-4: spacer (NCT_MD&H)'
'NCT min.den.(95.3886 lb/ft3) and hydrogen'
'np277-4 min.den.= 1.527971 = (95.3886 lb/ft3)(453.59 g/lb)/(28316.84 cm3/ft3)'
'use 75% of boron in calculations per NUREG-1609 Section 6.5.3.2'
arbmboron 7.31015e-2  2 0 0 0    5010   18.1479
                                 5011   81.8520    2  0.7500  293  end
arbmnpmx  1.07070e+0 10 0 0 0    6012    1.9189
                                 7014    0.0141
                                 8016   43.4251
                                11023    0.1174
                                12000    0.3378
                                13027   39.0479
                                14000    2.4672
                                16000    0.3083
                                20000   11.8336
                                26000    0.5298    2  1.0000  293  end
arbmnph2o 3.84169e-1  2 0 0 0    1001   11.1913
                                 8016   88.8087    2  1.0000  293  end
'flooded containmment vessel and content cans -- 10 CFR 71.55(d)(3)'
arbmwicv   0.9982   2 0 0 0    1001   11.1913
                              8016   88.8087    3  1       293  end
'steel: containment vessel body 16.60 lb but use 15.74 lb'
ss304                                           8  1.0     293  end
'steel: cv flange lower use 3.36 lb'
ss304                                           9  0.97267 293  end
'steel: cv flange upper use 13.75 lb'
ss304                                          10  0.94348 293  end
'np277-4: confinement -- neutron poison inner liner (NCT_MD&H)'
'actual vol.= 1.31846e4 cm3 = (8.0457422e2 in3)(16.387064)'
'den.multiplier = 1.31846e4 cm3 (actual vol.) / 1.32708e4 cm3 (model vol.)'
'np277-4 min.den.= 1.527971 = (95.3886 lb/ft3)(453.59 g/lb)/(28316.84 cm3/ft3)'
'density = 1.518047 = (den.mult)(np277-4 min.den.) = 0.9935052*1.527971'
'use 75% of boron in calculations per NUREG-1609 Section 6.5.3.2'
arbmboron 7.26267e-2  2 0 0 0    5010   18.1479
                                 5011   81.8520   11  0.7500  293  end
arbmnpmx  1.06375e+0 10 0 0 0    6012    1.9189
                                 7014    0.0141
                                 8016   43.4251
                                11023    0.1174
                                12000    0.3378
                                13027   39.0479
                                14000    2.4672
                                16000    0.3083
                                20000   11.8336
                                26000    0.5298   11  1.0000  293  end
arbmnph2o 3.81674e-1  2 0 0 0    1001   11.1913
                                 8016   88.8087   11  1.0000  293  end
'kaolite 1600 body'
'sing.unit.density= (den.mult)(min.den.)'
' for arbmh20k = 1.012373*0.51655,  for rest = 1.012373*0.34438'
'den.mult= 1.36557e5 cm3 (actual vol.) / 1.34888e5 cm3 (model vol.)'
'actual vol.= 1.36557e5 cm3 = (28316.84 cm3/ft3)(108.33188 lb)/(22.464 lb/ft3)'
arbmh2ok   0.52294  2 0 0 0    1001   11.1913
                               8016   88.8087   12  1       293  end
arbmal2o3  0.34864  2 0 0 0   13027   52.9390
                               8016   47.0610   12  0.096   293  end
arbmsio2   0.34864  2 0 0 0   14000   46.7570
                               8016   53.2430   12  0.367   293  end
arbmfe2o3  0.34864  2 0 0 0   26000   69.9540
                               8016   30.0460   12  0.067   293  end
arbmtio2   0.34864  2 0 0 0   22000   59.9535
                               8016   40.0465   12  0.012   293  end
arbmcao    0.34864  2 0 0 0   20000   71.4815
                               8016   28.5185   12  0.307   293  end
arbmmgo    0.34864  2 0 0 0   12000   60.3169
                               8016   39.6831   12  0.131   293  end
arbmna2o   0.34864  2 0 0 0   11023   74.1961
```

```
                              8016   25.8039   12  0.020   293  end
'kaolite 1600 top plug'
'sing.unit.density= (den.mult)(min.den.)'
' for arbmh20k = 0.965246*0.51655,  for rest = 0.965246*0.34438'
'den.mult= 1.21592e4 cm3 (actual vol.) / 1.25970e4 cm3 (model vol.)'
'actual vol.= 1.21592e4 cm3 = (28316.84 cm3/ft3)(9.646 lb)/(22.464 lb/ft3)'
arbmh2ok   0.49860  2 0 0 0    1001   11.1913
                              8016   88.8087   13  1       293  end
arbmal2o3  0.33241  2 0 0 0   13027   52.9390
                              8016   47.0610   13  0.096   293  end
arbmsio2   0.33241  2 0 0 0   14000   46.7570
                              8016   53.2430   13  0.367   293  end
arbmfe2o3  0.33241  2 0 0 0   26000   69.9540
                              8016   30.0460   13  0.067   293  end
arbmtio2   0.33241  2 0 0 0   22000   59.9535
                              8016   40.0465   13  0.012   293  end
arbmcao    0.33241  2 0 0 0   20000   71.4815
                              8016   28.5185   13  0.307   293  end
arbmmgo    0.33241  2 0 0 0   12000   60.3169
                              8016   39.6831   13  0.131   293  end
arbmna2o   0.33241  2 0 0 0   11023   74.1961
                              8016   25.8039   13  0.020   293  end
'silicone rubber pads'
arbmsiru   1.21791  4 0 0 0    6012   32.3767
                              1001    8.1573
                              8016   21.5782
                             14000   37.8878   14  1.0     293  end
'void space external to containment vessel'
arbmwecv   0.9982   2 0 0 0    1001   11.1913
                              8016   88.8087   15  1       293  end
'steel: liner'
ss304                                           16  1.0     293  end
'steel: plug cover (pc) use 9.907 lb'
ss304                                           17  1.06388 293  end
'steel: angle iron (ai) for single units'
ss304                                           18  1.0     293  end
'steel: angle iron (ai) for arrays'
'array density is multiplied by a volume fraction 7.08030/5.63249'
'ss304                                           18  1.25705 293  end
'steel: drum steel for single units'
ss304                                           19  1.0     293  end
'steel: drum steel for arrays'
'array density is multiplied by a volume fraction 3.20482/3.20544'
'ss304                                           19  0.99981 293  end
'void space external to drum'
'array density is multiplied by a volume ratio 8.11698/6.98323'
'arbmwed    1.16026  2 0 0 0    1001   11.1913
'                              8016   88.8087   20  1       293  end
'reflective water'
arbmh20r   0.9982   2 0 0 0    1001   11.1913
                              8016   88.8087   21  1.0     293  end
end comp
cvcrtriga 0.0in thk np,10400.0gUZrHx(  921.0g235, 8998.2gH2O,hx=255.01),fr=1.0e+00
read parameters nub=yes npg=2500 gen=215 nsk=15 tme=100 end parameters
read boun       all=vac                         end boun
read geometry
unit 1001
'drum bottom flat cover [Elev= 0.105 in. at top of unit]'
 cuboid    21 1 4p24.587200    0.26670   0.0     com='drum chine outer radius'
unit 1002
'above drum bottom flat cover and below containment vessel [Elev= 4.670 in.]'
 cuboid    21 1 4p24.587200   11.59510   0.0     com='drum chine outer radius'
unit 1003
'cv bottom [Elev= 4.920 in.]'
 cylinder  8  1    6.680200    0.63500   0.0     com='cv bottom'
 cuboid    21 1 4p24.587200    0.63500   0.0     com='drum chine outer radius'
unit 1004
'UZrHx fuel element'
 cylinder  1  1    1.828800   12.70000   0.0     com='cylindrical content'
unit 1006
'content (collapsed) [Elev= 9.920 in.]'
```

```
'1.437900   plus-y location upper cylinders'
'-2.875700  minus-y location lower cylinder'
'2.490443   plus-x location upper cylinder'
'-2.490443  minus-x location upper cylinder'
 cylinder  3  1    6.426200   12.70050  -0.0005  com='cv well cavity'
 hole  1004   -2.490443  1.437900  0.0     com='cyl1'
 hole  1004    2.490443  1.437900  0.0     com='cyl2'
 hole  1004    0.0      -2.875700  0.0     com='cyl3'
 cylinder  8  1    6.680200   12.70050  -0.0005  com='cv below 1st step'
 cuboid    21 1 4p24.587200   12.70050  -0.0005  com='drum chine outer radius'
unit 1007
'np277_4 spacer [Elev= 9.921 in.]'
 cylinder  2  1    5.24510     0.00010   0.0     com='np spacer'
 cylinder  3  1    6.426200    0.00020  -0.0001  com='cv well cavity'
 cylinder  8  1    6.680200    0.00020  -0.0001  com='cv below 1st step'
 cuboid    21 1 4p24.587200    0.00020  -0.0001  com='drum chine outer radius'
unit 1008
'top of content stack to bottom of 1st step [Elev=35.270 in.]'
'38.10360             stack height (content spacers)       CALCULATED
 cylinder  3  1    6.426200   38.98540   0.0     com='cv well cavity'
 cylinder  8  1    6.680200   38.98540   0.0     com='cv below 1st step'
 cuboid    21 1 4p24.587200   38.98540   0.0     com='drum chine outer radius'
unit 1010
'cv at 1st step in liner [Elev=35.330 in.]'
 cylinder  3  1    6.426200    0.15240   0.0     com='cv well cavity'
 cylinder  8  1    6.680200    0.15240   0.0     com='cv at 1st step'
 cuboid    21 1 4p24.587200    0.15240   0.0     com='drum chine outer radius'
unit 1011
'vertical gap between 1st step in liner and cv flange [Elev=35.420 in.]'
 cylinder  3  1    6.426200    0.22860   0.0     com='cv well cavity'
 cylinder  8  1    6.680200    0.22860   0.0     com='cv at gap btwn step-flng'
 cuboid    21 1 4p24.587200    0.22860   0.0     com='drum chine outer radius'
unit 1012
'cv flange to top of cv well [Elev=35.920 in.]'
 cylinder  3  1    6.426200    1.27000   0.0     com='cavity'
 cylinder  9  1    9.525000    1.27000   0.0     com='flange to top of well'
 cuboid    21 1 4p24.587200    1.27000   0.0     com='drum chine outer radius'
unit 1013
'cv flange above cv well [Elev=37.070 in.]'
 cylinder  10 1    9.525000    2.92100   0.0     com='flange above cv well'
 cuboid    21 1 4p24.587200    2.92100   0.0     com='drum chine outer radius'
unit 1014
'plugpad2 below liner 2nd step [Elev=37.470 in.]'
 cuboid    21 1 4p24.587200    1.01600   0.0     com='drum chine outer radius'
unit 1015
'2nd step in liner [Elev=37.530 in.]'
 cuboid    21 1 4p24.587200    0.15240   0.0     com='drum chine outer radius'
unit 1016
'abv 2nd step in liner to bottom of angle iron [Elev=40.750 in.]'
 cuboid    21 1 4p24.587200    8.17880   0.0     com='drum chine outer radius'
unit 1017
'bottom of angle iron to bend in angle iron [Elev=42.500 in.]'
 cuboid    21 1 4p24.587200    4.44500   0.0     com='drum chine outer radius'
unit 1018
'bend in angle iron to top of angle iron [Elev=42.750 in.]'
 cuboid    21 1 4p24.587200    0.63500   0.0     com='drum chine outer radius'
unit 1019
'drum lid and lip [Elev=43.500 in.]'
 cuboid    21 1 4p24.587200    1.90500   0.0     com='drum chine outer radius'
global
unit 1020
'es3100 drum [Elev=43.500 in.]'
array 3         2r-24.587200     0.0
'cuboid     0  1 4p24.587200    110.4905  0.0    com='bare package'
 cuboid    21  1 4p55.067200   140.9700 -30.48   com='reflected package'
'cuboid    20  1 4p22.889718    110.5048  0.0    com='interstital array space'
'global
'unit 1021
'array 4   3r0.0
'reflector  21 2  6r3.0  10
end geometry
```

```
read array
ara=3 nux=1 nuy=1 nuz=19 fill
1001 1002 1003 1006 1007 1006 1007 1006 1008 1010
1011 1012 1013 1014 1015 1016 1017 1018 1019        end fill
'ara=4 nux=13 nuy=13 nuz=06 fill f1020               end fill
end array
'read bias id=500 2  11  end bias
read start nst=0
end start
end data
end


=csas25    parm=size=3000000
cvcrtriga 1.4in thk np,10400.0gUZrHx(  921.0g235, 8384.6gH2O hx=237.62),fr=1.0e+00
238groupndf5 infhommedium
'TRIGA volume =1200.95996, SPACER volume  614.68012'
'TRIGA wrapped dry content can hx=18.2, CV void volume 8399.72186'
arbmtriga  8.65974  4 0 0 0    1001    0.9554
                              40000   54.0446
                              92235    8.8558
                              92238   36.1442    1  1.0     293  end
'np277-4: spacer (NCT_MD&H)'
'NCT min.den.(95.3886 lb/ft3) and hydrogen'
'np277-4 min.den.= 1.527971 = (95.3886 lb/ft3)(453.59 g/lb)/(28316.84 cm3/ft3)'
'use 75% of boron in calculations per NUREG-1609 Section 6.5.3.2'
arbmboron 7.31015e-2  2 0 0 0    5010   18.1479
                                 5011   81.8520    2  0.7500  293  end
arbmnpmx  1.07070e+0 10 0 0 0    6012    1.9189
                                 7014    0.0141
                                 8016   43.4251
                                11023    0.1174
                                12000    0.3378
                                13027   39.0479
                                14000    2.4672
                                16000    0.3083
                                20000   11.8336
                                26000    0.5298    2  1.0000  293  end
arbmnph2o 3.84169e-1  2 0 0 0    1001   11.1913
                                 8016   88.8087    2  1.0000  293  end
'flooded containmment vessel and content cans -- 10 CFR 71.55(d)(3)'
arbmwicv   0.9982   2 0 0 0    1001   11.1913
                              8016   88.8087    3  1       293  end
'steel: containment vessel body 16.60 lb but use 15.74 lb'
ss304                                            8  1.0     293  end
'steel: cv flange lower use 3.36 lb'
ss304                                            9  0.97267 293  end
'steel: cv flange upper use 13.75 lb'
ss304                                           10  0.94348 293  end
'np277-4: confinement -- neutron poison inner liner (NCT_MD&H)'
'actual vol.= 1.31846e4 cm3 = (8.0457422e2 in3)(16.387064)'
'den.multiplier = 1.31846e4 cm3 (actual vol.) / 1.32708e4 cm3 (model vol.)'
'np277-4 min.den.= 1.527971 = (95.3886 lb/ft3)(453.59 g/lb)/(28316.84 cm3/ft3)'
'density = 1.518047 = (den.mult)(np277-4 min.den.) = 0.9935052*1.527971'
'use 75% of boron in calculations per NUREG-1609 Section 6.5.3.2'
arbmboron 7.26267e-2  2 0 0 0    5010   18.1479
                                 5011   81.8520   11  0.7500  293  end
arbmnpmx  1.06375e+0 10 0 0 0    6012    1.9189
                                 7014    0.0141
                                 8016   43.4251
                                11023    0.1174
                                12000    0.3378
                                13027   39.0479
                                14000    2.4672
                                16000    0.3083
                                20000   11.8336
                                26000    0.5298   11  1.0000  293  end
arbmnph2o 3.81674e-1  2 0 0 0    1001   11.1913
                                 8016   88.8087   11  1.0000  293  end
'kaolite 1600 body'
'sing.unit.density= (den.mult)(min.den.)'
```

```
' for arbmh20k = 1.012373*0.51655,  for rest = 1.012373*0.34438'
'den.mult= 1.36557e5 cm3 (actual vol.) / 1.34888e5 cm3 (model vol.)'
'actual vol.= 1.36557e5 cm3 = (28316.84 cm3/ft3)(108.33188 lb)/(22.464 lb/ft3)'
arbmh2ok   0.52294  2 0 0 0    1001   11.1913
                               8016   88.8087   12  1       293  end
arbmal2o3  0.34864  2 0 0 0   13027   52.9390
                               8016   47.0610   12  0.096   293  end
arbmsio2   0.34864  2 0 0 0   14000   46.7570
                               8016   53.2430   12  0.367   293  end
arbmfe2o3  0.34864  2 0 0 0   26000   69.9540
                               8016   30.0460   12  0.067   293  end
arbmtio2   0.34864  2 0 0 0   22000   59.9535
                               8016   40.0465   12  0.012   293  end
arbmcao    0.34864  2 0 0 0   20000   71.4815
                               8016   28.5185   12  0.307   293  end
arbmmgo    0.34864  2 0 0 0   12000   60.3169
                               8016   39.6831   12  0.131   293  end
arbmna2o   0.34864  2 0 0 0   11023   74.1961
                               8016   25.8039   12  0.020   293  end
'kaolite 1600 top plug'
'sing.unit.density= (den.mult)(min.den.)'
' for arbmh20k = 0.965246*0.51655,  for rest = 0.965246*0.34438'
'den.mult= 1.21592e4 cm3 (actual vol.) / 1.25970e4 cm3 (model vol.)'
'actual vol.= 1.21592e4 cm3 = (28316.84 cm3/ft3)(9.646 lb)/(22.464 lb/ft3)'
arbmh2ok   0.49860  2 0 0 0    1001   11.1913
                               8016   88.8087   13  1       293  end
arbmal2o3  0.33241  2 0 0 0   13027   52.9390
                               8016   47.0610   13  0.096   293  end
arbmsio2   0.33241  2 0 0 0   14000   46.7570
                               8016   53.2430   13  0.367   293  end
arbmfe2o3  0.33241  2 0 0 0   26000   69.9540
                               8016   30.0460   13  0.067   293  end
arbmtio2   0.33241  2 0 0 0   22000   59.9535
                               8016   40.0465   13  0.012   293  end
arbmcao    0.33241  2 0 0 0   20000   71.4815
                               8016   28.5185   13  0.307   293  end
arbmmgo    0.33241  2 0 0 0   12000   60.3169
                               8016   39.6831   13  0.131   293  end
arbmna2o   0.33241  2 0 0 0   11023   74.1961
                               8016   25.8039   13  0.020   293  end
'silicone rubber pads'
arbmsiru   1.21791  4 0 0 0    6012   32.3767
                               1001    8.1573
                               8016   21.5782
                              14000   37.8878   14  1.0     293  end
'void space external to containment vessel'
arbmwecv   0.9982   2 0 0 0    1001   11.1913
                               8016   88.8087   15  1       293  end
'steel: liner'
ss304                                            16  1.0     293  end
'steel: plug cover (pc) use 9.907 lb'
ss304                                            17  1.06388 293  end
'steel: angle iron (ai) for single units'
ss304                                            18  1.0     293  end
'steel: angle iron (ai) for arrays'
'array density is multiplied by a volume fraction 7.08030/5.63249'
'ss304                                            18  1.25705 293  end
'steel: drum steel for single units'
ss304                                            19  1.0     293  end
'steel: drum steel for arrays'
'array density is multiplied by a volume fraction 3.20482/3.20544'
'ss304                                            19  0.99981 293  end
'void space external to drum'
'array density is multiplied by a volume ratio 8.11698/6.98323'
'arbmwed    1.16026  2 0 0 0    1001   11.1913
'                               8016   88.8087   20  1       293  end
'reflective water'
arbmh20r   0.9982   2 0 0 0    1001   11.1913
                               8016   88.8087   21  1.0     293  end
end comp
cvcrtriga 1.4in thk np,10400.0gUZrHx(  921.0g235, 8384.6gH2O,hx=237.62),fr=1.0e+00
```

```
read parameters nub=yes npg=2500 gen=215 nsk=15 tme=100 end parameters
read boun       all=vac                         end boun
read geometry
unit 1001
'drum bottom flat cover [Elev= 0.105 in. at top of unit]'
 cuboid    21 1 4p24.587200    0.26670   0.0     com='drum chine outer radius'
unit 1002
'above drum bottom flat cover and below containment vessel [Elev= 4.670 in.]'
 cuboid    21 1 4p24.587200   11.59510   0.0     com='drum chine outer radius'
unit 1003
'cv bottom [Elev= 4.920 in.]'
 cylinder  8  1    6.680200    0.63500   0.0     com='cv bottom'
 cuboid    21 1 4p24.587200    0.63500   0.0     com='drum chine outer radius'
unit 1004
'UZrHx fuel element'
 cylinder  1  1    1.828800   12.70000   0.0     com='cylindrical content'
unit 1006
'content (collapsed) [Elev= 9.920 in.]'
'1.437900   plus-y location upper cylinders'
'-2.875700  minus-y location lower cylinder'
'2.490443   plus-x location upper cylinder'
'-2.490443  minus-x location upper cylinder'
 cylinder  3  1    6.426200   12.70050  -0.0005  com='cv well cavity'
 hole  1004   -2.490443  1.437900  0.0     com='cyl1'
 hole  1004    2.490443  1.437900  0.0     com='cyl2'
 hole  1004    0.0      -2.875700  0.0     com='cyl3'
 cylinder  8  1    6.680200   12.70050  -0.0005  com='cv below 1st step'
 cuboid    21 1 4p24.587200   12.70050  -0.0005  com='drum chine outer radius'
unit 1007
'np277_4 spacer [Elev=11.321 in.]'
 cylinder  2  1    5.24510     3.55610   0.0     com='np spacer'
 cylinder  3  1    6.426200    3.55620  -0.0001  com='cv well cavity'
 cylinder  8  1    6.680200    3.55620  -0.0001  com='cv below 1st step'
 cuboid    21 1 4p24.587200    3.55620  -0.0001  com='drum chine outer radius'
unit 1008
'top of content stack to bottom of 1st step [Elev=35.270 in.]'
'45.21560             stack height (content spacers)       CALCULATED
 cylinder  3  1    6.426200   31.87340   0.0     com='cv well cavity'
 cylinder  8  1    6.680200   31.87340   0.0     com='cv below 1st step'
 cuboid    21 1 4p24.587200   31.87340   0.0     com='drum chine outer radius'
unit 1010
'cv at 1st step in liner [Elev=35.330 in.]'
 cylinder  3  1    6.426200    0.15240   0.0     com='cv well cavity'
 cylinder  8  1    6.680200    0.15240   0.0     com='cv at 1st step'
 cuboid    21 1 4p24.587200    0.15240   0.0     com='drum chine outer radius'
unit 1011
'vertical gap between 1st step in liner and cv flange [Elev=35.420 in.]'
 cylinder  3  1    6.426200    0.22860   0.0     com='cv well cavity'
 cylinder  8  1    6.680200    0.22860   0.0     com='cv at gap btwn step-flng'
 cuboid    21 1 4p24.587200    0.22860   0.0     com='drum chine outer radius'
unit 1012
'cv flange to top of cv well [Elev=35.920 in.]'
 cylinder  3  1    6.426200    1.27000   0.0     com='cavity'
 cylinder  9  1    9.525000    1.27000   0.0     com='flange to top of well'
 cuboid    21 1 4p24.587200    1.27000   0.0     com='drum chine outer radius'
unit 1013
'cv flange above cv well [Elev=37.070 in.]'
 cylinder  10 1    9.525000    2.92100   0.0     com='flange above cv well'
 cuboid    21 1 4p24.587200    2.92100   0.0     com='drum chine outer radius'
unit 1014
'plugpad2 below liner 2nd step [Elev=37.470 in.]'
 cuboid    21 1 4p24.587200    1.01600   0.0     com='drum chine outer radius'
unit 1015
'2nd step in liner [Elev=37.530 in.]'
 cuboid    21 1 4p24.587200    0.15240   0.0     com='drum chine outer radius'
unit 1016
'abv 2nd step in liner to bottom of angle iron [Elev=40.750 in.]'
 cuboid    21 1 4p24.587200    8.17880   0.0     com='drum chine outer radius'
unit 1017
'bottom of angle iron to bend in angle iron [Elev=42.500 in.]'
 cuboid    21 1 4p24.587200    4.44500   0.0     com='drum chine outer radius'
```

```
unit 1018
'bend in angle iron to top of angle iron [Elev=42.750 in.]'
 cuboid    21 1 4p24.587200    0.63500   0.0     com='drum chine outer radius'
unit 1019
'drum lid and lip [Elev=43.500 in.]'
 cuboid    21 1 4p24.587200    1.90500   0.0     com='drum chine outer radius'
global
unit 1020
'es3100 drum [Elev=43.500 in.]'
array 3         2r-24.587200     0.0
'cuboid     0  1 4p24.587200    110.4905  0.0    com='bare package'
 cuboid    21  1 4p55.067200   140.9700 -30.48   com='reflected package'
'cuboid    20  1 4p22.889718    110.5048  0.0    com='interstital array space'
'global
'unit 1021
'array 4   3r0.0
'reflector  21 2  6r3.0  10
end geometry
read array
ara=3 nux=1 nuy=1 nuz=19 fill
1001 1002 1003 1006 1007 1006 1007 1006 1008 1010
1011 1012 1013 1014 1015 1016 1017 1018 1019        end fill
'ara=4 nux=13 nuy=13 nuz=06 fill f1020               end fill
end array
'read bias id=500 2  11  end bias
read start nst=0
end start
end data
end


=csas25    parm=size=3000000
cvcrtriga_70 0.0in thk np, 6847.1gUZrHx(  408.0g235,    0.0gH2O hx=  0.00),fr=1.0e+00
238groupndf5 infhommedium
'TRIGA volume =1200.95996, SPACER volume    0.00000'
'TRIGA wrapped dry content can hx=41.1, CV void volume 9014.40198'
arbmtriga  5.70132  4 0 0 0    1001    1.5894
                              40000   89.9107
                              92235    5.9587
                              92238    2.5412    1  1.0     293  end
'np277-4: spacer (NCT_MD&H)'
'NCT min.den.(95.3886 lb/ft3) and hydrogen'
'np277-4 min.den.= 1.527971 = (95.3886 lb/ft3)(453.59 g/lb)/(28316.84 cm3/ft3)'
'use 75% of boron in calculations per NUREG-1609 Section 6.5.3.2'
arbmboron 7.31015e-2  2 0 0 0    5010   18.1479
                                 5011   81.8520    2  0.7500  293  end
arbmnpmx  1.07070e+0 10 0 0 0    6012    1.9189
                                 7014    0.0141
                                 8016   43.4251
                                11023    0.1174
                                12000    0.3378
                                13027   39.0479
                                14000    2.4672
                                16000    0.3083
                                20000   11.8336
                                26000    0.5298    2  1.0000  293  end
arbmnph2o 3.84169e-1  2 0 0 0    1001   11.1913
                                 8016   88.8087    2  1.0000  293  end
'flooded containmment vessel and content cans -- 10 CFR 71.55(d)(3)'
arbmwicv   0.9982   2 0 0 0    1001   11.1913
                               8016   88.8087    3  1e-20   293  end
'steel: containment vessel body 16.60 lb but use 15.74 lb'
ss304                                            8  1.0     293  end
'steel: cv flange lower use 3.36 lb'
ss304                                            9  0.97267 293  end
'steel: cv flange upper use 13.75 lb'
ss304                                           10  0.94348 293  end
'np277-4: confinement -- neutron poison inner liner (NCT_MD&H)'
'actual vol.= 1.31846e4 cm3 = (8.0457422e2 in3)(16.387064)'
'den.multiplier = 1.31846e4 cm3 (actual vol.) / 1.32708e4 cm3 (model vol.)'
'np277-4 min.den.= 1.527971 = (95.3886 lb/ft3)(453.59 g/lb)/(28316.84 cm3/ft3)'
```

```
'density = 1.518047 = (den.mult)(np277-4 min.den.) = 0.9935052*1.527971'
'use 75% of boron in calculations per NUREG-1609 Section 6.5.3.2'
arbmboron 7.26267e-2  2 0 0 0    5010   18.1479
                                 5011   81.8520   11  0.7500  293  end
arbmnpmx  1.06375e+0 10 0 0 0    6012    1.9189
                                 7014    0.0141
                                 8016   43.4251
                                11023    0.1174
                                12000    0.3378
                                13027   39.0479
                                14000    2.4672
                                16000    0.3083
                                20000   11.8336
                                26000    0.5298   11  1.0000  293  end
arbmnph2o 3.81674e-1  2 0 0 0    1001   11.1913
                                 8016   88.8087   11  1.0000  293  end
'kaolite 1600 body'
'sing.unit.density= (den.mult)(min.den.)'
' for arbmh20k = 1.012373*0.51655,  for rest = 1.012373*0.34438'
'den.mult= 1.36557e5 cm3 (actual vol.) / 1.34888e5 cm3 (model vol.)'
'actual vol.= 1.36557e5 cm3 = (28316.84 cm3/ft3)(108.33188 lb)/(22.464 lb/ft3)'
arbmh2ok   0.52294  2 0 0 0    1001   11.1913
                               8016   88.8087   12  1       293  end
arbmal2o3  0.34864  2 0 0 0   13027   52.9390
                               8016   47.0610   12  0.096   293  end
arbmsio2   0.34864  2 0 0 0   14000   46.7570
                               8016   53.2430   12  0.367   293  end
arbmfe2o3  0.34864  2 0 0 0   26000   69.9540
                               8016   30.0460   12  0.067   293  end
arbmtio2   0.34864  2 0 0 0   22000   59.9535
                               8016   40.0465   12  0.012   293  end
arbmcao    0.34864  2 0 0 0   20000   71.4815
                               8016   28.5185   12  0.307   293  end
arbmmgo    0.34864  2 0 0 0   12000   60.3169
                               8016   39.6831   12  0.131   293  end
arbmna2o   0.34864  2 0 0 0   11023   74.1961
                               8016   25.8039   12  0.020   293  end
'kaolite 1600 top plug'
'sing.unit.density= (den.mult)(min.den.)'
' for arbmh20k = 0.965246*0.51655,  for rest = 0.965246*0.34438'
'den.mult= 1.21592e4 cm3 (actual vol.) / 1.25970e4 cm3 (model vol.)'
'actual vol.= 1.21592e4 cm3 = (28316.84 cm3/ft3)(9.646 lb)/(22.464 lb/ft3)'
arbmh2ok   0.49860  2 0 0 0    1001   11.1913
                               8016   88.8087   13  1       293  end
arbmal2o3  0.33241  2 0 0 0   13027   52.9390
                               8016   47.0610   13  0.096   293  end
arbmsio2   0.33241  2 0 0 0   14000   46.7570
                               8016   53.2430   13  0.367   293  end
arbmfe2o3  0.33241  2 0 0 0   26000   69.9540
                               8016   30.0460   13  0.067   293  end
arbmtio2   0.33241  2 0 0 0   22000   59.9535
                               8016   40.0465   13  0.012   293  end
arbmcao    0.33241  2 0 0 0   20000   71.4815
                               8016   28.5185   13  0.307   293  end
arbmmgo    0.33241  2 0 0 0   12000   60.3169
                               8016   39.6831   13  0.131   293  end
arbmna2o   0.33241  2 0 0 0   11023   74.1961
                               8016   25.8039   13  0.020   293  end
'silicone rubber pads'
arbmsiru   1.21791  4 0 0 0    6012   32.3767
                               1001    8.1573
                               8016   21.5782
                              14000   37.8878   14  1.0     293  end
'void space external to containment vessel'
arbmwecv   0.9982   2 0 0 0    1001   11.1913
                               8016   88.8087   15  1       293  end
'steel: liner'
ss304                                            16  1.0     293  end
'steel: plug cover (pc) use 9.907 lb'
ss304                                            17  1.06388 293  end
'steel: angle iron (ai) for single units'
```

```
ss304                                          18  1.0     293  end
'steel: angle iron (ai) for arrays'
'array density is multiplied by a volume fraction 7.08030/5.63249'
'ss304                                          18  1.25705 293  end
'steel: drum steel for single units'
ss304                                          19  1.0     293  end
'steel: drum steel for arrays'
'array density is multiplied by a volume fraction 3.20482/3.20544'
'ss304                                          19  0.99981 293  end
'void space external to drum'
'array density is multiplied by a volume ratio 8.11698/6.98323'
'arbmwed    1.16026  2 0 0 0    1001   11.1913
'                               8016   88.8087   20  1       293  end
'reflective water'
arbmh20r   0.9982   2 0 0 0    1001   11.1913
                                8016   88.8087   21  1.0     293  end
end comp
cvcrtriga_70 0.0in thk np, 6847.1gUZrHx(  408.0g235,    0.0gH2O,hx=  0.00),fr=1.0e+00
read parameters nub=yes npg=2500 gen=215 nsk=15 tme=100 end parameters
read boun       all=vac                         end boun
read geometry
unit 1001
'drum bottom flat cover [Elev= 0.105 in. at top of unit]'
 cuboid    21 1 4p24.587200    0.26670   0.0     com='drum chine outer radius'
unit 1002
'above drum bottom flat cover and below containment vessel [Elev= 4.670 in.]'
 cuboid    21 1 4p24.587200   11.59510   0.0     com='drum chine outer radius'
unit 1003
'cv bottom [Elev= 4.920 in.]'
 cylinder  8  1    6.680200    0.63500   0.0     com='cv bottom'
 cuboid    21 1 4p24.587200    0.63500   0.0     com='drum chine outer radius'
unit 1004
'UZrHx fuel element'
 cylinder  1  1    1.828800   12.70000   0.0     com='cylindrical content'
unit 1006
'content (collapsed) [Elev= 9.920 in.]'
'1.437900   plus-y location upper cylinders'
'-2.875700  minus-y location lower cylinder'
'2.490443   plus-x location upper cylinder'
'-2.490443  minus-x location upper cylinder'
 cylinder  3  1    6.426200   12.70050  -0.0005  com='cv well cavity'
 hole  1004   -2.490443  1.437900  0.0     com='cyl1'
 hole  1004    2.490443  1.437900  0.0     com='cyl2'
 hole  1004    0.0      -2.875700  0.0     com='cyl3'
 cylinder  8  1    6.680200   12.70050  -0.0005  com='cv below 1st step'
 cuboid    21 1 4p24.587200   12.70050  -0.0005  com='drum chine outer radius'
unit 1007
'np277_4 spacer [Elev= 9.921 in.]'
 cylinder  2  1    5.24510     0.00010   0.0     com='np spacer'
 cylinder  3  1    6.426200    0.00020  -0.0001  com='cv well cavity'
 cylinder  8  1    6.680200    0.00020  -0.0001  com='cv below 1st step'
 cuboid    21 1 4p24.587200    0.00020  -0.0001  com='drum chine outer radius'
unit 1008
'top of content stack to bottom of 1st step [Elev=35.270 in.]'
'38.10360             stack height (content spacers)       CALCULATED
 cylinder  3  1    6.426200   38.98540   0.0     com='cv well cavity'
 cylinder  8  1    6.680200   38.98540   0.0     com='cv below 1st step'
 cuboid    21 1 4p24.587200   38.98540   0.0     com='drum chine outer radius'
unit 1010
'cv at 1st step in liner [Elev=35.330 in.]'
 cylinder  3  1    6.426200    0.15240   0.0     com='cv well cavity'
 cylinder  8  1    6.680200    0.15240   0.0     com='cv at 1st step'
 cuboid    21 1 4p24.587200    0.15240   0.0     com='drum chine outer radius'
unit 1011
'vertical gap between 1st step in liner and cv flange [Elev=35.420 in.]'
 cylinder  3  1    6.426200    0.22860   0.0     com='cv well cavity'
 cylinder  8  1    6.680200    0.22860   0.0     com='cv at gap btwn step-flng'
 cuboid    21 1 4p24.587200    0.22860   0.0     com='drum chine outer radius'
unit 1012
'cv flange to top of cv well [Elev=35.920 in.]'
 cylinder  3  1    6.426200    1.27000   0.0     com='cavity'
```

```
 cylinder  9  1    9.525000    1.27000   0.0     com='flange to top of well'
 cuboid    21 1 4p24.587200    1.27000   0.0     com='drum chine outer radius'
unit 1013
'cv flange above cv well [Elev=37.070 in.]'
 cylinder  10 1    9.525000    2.92100   0.0     com='flange above cv well'
 cuboid    21 1 4p24.587200    2.92100   0.0     com='drum chine outer radius'
unit 1014
'plugpad2 below liner 2nd step [Elev=37.470 in.]'
 cuboid    21 1 4p24.587200    1.01600   0.0     com='drum chine outer radius'
unit 1015
'2nd step in liner [Elev=37.530 in.]'
 cuboid    21 1 4p24.587200    0.15240   0.0     com='drum chine outer radius'
unit 1016
'abv 2nd step in liner to bottom of angle iron [Elev=40.750 in.]'
 cuboid    21 1 4p24.587200    8.17880   0.0     com='drum chine outer radius'
unit 1017
'bottom of angle iron to bend in angle iron [Elev=42.500 in.]'
 cuboid    21 1 4p24.587200    4.44500   0.0     com='drum chine outer radius'
unit 1018
'bend in angle iron to top of angle iron [Elev=42.750 in.]'
 cuboid    21 1 4p24.587200    0.63500   0.0     com='drum chine outer radius'
unit 1019
'drum lid and lip [Elev=43.500 in.]'
 cuboid    21 1 4p24.587200    1.90500   0.0     com='drum chine outer radius'
global
unit 1020
'es3100 drum [Elev=43.500 in.]'
array 3         2r-24.587200     0.0
'cuboid     0  1 4p24.587200    110.4905  0.0    com='bare package'
 cuboid    21  1 4p55.067200   140.9700 -30.48   com='reflected package'
'cuboid    20  1 4p22.889718    110.5048  0.0    com='interstital array space'
'global
'unit 1021
'array 4   3r0.0
'reflector  21 2  6r3.0  10
end geometry
read array
ara=3 nux=1 nuy=1 nuz=19 fill
1001 1002 1003 1006 1007 1006 1007 1006 1008 1010
1011 1012 1013 1014 1015 1016 1017 1018 1019        end fill
'ara=4 nux=13 nuy=13 nuz=06 fill f1020               end fill
end array
'read bias id=500 2  11  end bias
read start nst=0
end start
end data
end


=csas25    parm=size=3000000
cvcrtriga_70 0.0in thk np, 6847.1gUZrHx(  408.0g235, 8998.2gH2O hx=575.64),fr=1.0e+00
238groupndf5 infhommedium
'TRIGA volume =1200.95996, SPACER volume    0.00000'
'TRIGA wrapped dry content can hx=41.1, CV void volume 9014.40198'
arbmtriga  5.70132  4 0 0 0    1001    1.5894
                              40000   89.9107
                              92235    5.9587
                              92238    2.5412    1  1.0     293  end
'np277-4: spacer (NCT_MD&H)'
'NCT min.den.(95.3886 lb/ft3) and hydrogen'
'np277-4 min.den.= 1.527971 = (95.3886 lb/ft3)(453.59 g/lb)/(28316.84 cm3/ft3)'
'use 75% of boron in calculations per NUREG-1609 Section 6.5.3.2'
arbmboron 7.31015e-2  2 0 0 0    5010   18.1479
                                 5011   81.8520    2  0.7500  293  end
arbmnpmx  1.07070e+0 10 0 0 0    6012    1.9189
                                 7014    0.0141
                                 8016   43.4251
                                11023    0.1174
                                12000    0.3378
                                13027   39.0479
                                14000    2.4672
```

```
                                16000    0.3083
                                20000   11.8336
                                26000    0.5298    2  1.0000  293  end
arbmnph2o 3.84169e-1  2 0 0 0    1001   11.1913
                                 8016   88.8087    2  1.0000  293  end
'flooded containmment vessel and content cans -- 10 CFR 71.55(d)(3)'
arbmwicv   0.9982   2 0 0 0    1001   11.1913
                               8016   88.8087    3  1       293  end
'steel: containment vessel body 16.60 lb but use 15.74 lb'
ss304                                            8  1.0     293  end
'steel: cv flange lower use 3.36 lb'
ss304                                            9  0.97267 293  end
'steel: cv flange upper use 13.75 lb'
ss304                                           10  0.94348 293  end
'np277-4: confinement -- neutron poison inner liner (NCT_MD&H)'
'actual vol.= 1.31846e4 cm3 = (8.0457422e2 in3)(16.387064)'
'den.multiplier = 1.31846e4 cm3 (actual vol.) / 1.32708e4 cm3 (model vol.)'
'np277-4 min.den.= 1.527971 = (95.3886 lb/ft3)(453.59 g/lb)/(28316.84 cm3/ft3)'
'density = 1.518047 = (den.mult)(np277-4 min.den.) = 0.9935052*1.527971'
'use 75% of boron in calculations per NUREG-1609 Section 6.5.3.2'
arbmboron 7.26267e-2  2 0 0 0    5010   18.1479
                                 5011   81.8520   11  0.7500  293  end
arbmnpmx  1.06375e+0 10 0 0 0    6012    1.9189
                                 7014    0.0141
                                 8016   43.4251
                                11023    0.1174
                                12000    0.3378
                                13027   39.0479
                                14000    2.4672
                                16000    0.3083
                                20000   11.8336
                                26000    0.5298   11  1.0000  293  end
arbmnph2o 3.81674e-1  2 0 0 0    1001   11.1913
                                 8016   88.8087   11  1.0000  293  end
'kaolite 1600 body'
'sing.unit.density= (den.mult)(min.den.)'
' for arbmh20k = 1.012373*0.51655,  for rest = 1.012373*0.34438'
'den.mult= 1.36557e5 cm3 (actual vol.) / 1.34888e5 cm3 (model vol.)'
'actual vol.= 1.36557e5 cm3 = (28316.84 cm3/ft3)(108.33188 lb)/(22.464 lb/ft3)'
arbmh2ok   0.52294  2 0 0 0    1001   11.1913
                               8016   88.8087   12  1       293  end
arbmal2o3  0.34864  2 0 0 0   13027   52.9390
                               8016   47.0610   12  0.096   293  end
arbmsio2   0.34864  2 0 0 0   14000   46.7570
                               8016   53.2430   12  0.367   293  end
arbmfe2o3  0.34864  2 0 0 0   26000   69.9540
                               8016   30.0460   12  0.067   293  end
arbmtio2   0.34864  2 0 0 0   22000   59.9535
                               8016   40.0465   12  0.012   293  end
arbmcao    0.34864  2 0 0 0   20000   71.4815
                               8016   28.5185   12  0.307   293  end
arbmmgo    0.34864  2 0 0 0   12000   60.3169
                               8016   39.6831   12  0.131   293  end
arbmna2o   0.34864  2 0 0 0   11023   74.1961
                               8016   25.8039   12  0.020   293  end
'kaolite 1600 top plug'
'sing.unit.density= (den.mult)(min.den.)'
' for arbmh20k = 0.965246*0.51655,  for rest = 0.965246*0.34438'
'den.mult= 1.21592e4 cm3 (actual vol.) / 1.25970e4 cm3 (model vol.)'
'actual vol.= 1.21592e4 cm3 = (28316.84 cm3/ft3)(9.646 lb)/(22.464 lb/ft3)'
arbmh2ok   0.49860  2 0 0 0    1001   11.1913
                               8016   88.8087   13  1       293  end
arbmal2o3  0.33241  2 0 0 0   13027   52.9390
                               8016   47.0610   13  0.096   293  end
arbmsio2   0.33241  2 0 0 0   14000   46.7570
                               8016   53.2430   13  0.367   293  end
arbmfe2o3  0.33241  2 0 0 0   26000   69.9540
                               8016   30.0460   13  0.067   293  end
arbmtio2   0.33241  2 0 0 0   22000   59.9535
                               8016   40.0465   13  0.012   293  end
arbmcao    0.33241  2 0 0 0   20000   71.4815
```

```
                                8016   28.5185   13  0.307   293  end
arbmmgo    0.33241  2 0 0 0   12000   60.3169
                                8016   39.6831   13  0.131   293  end
arbmna2o   0.33241  2 0 0 0   11023   74.1961
                                8016   25.8039   13  0.020   293  end
'silicone rubber pads'
arbmsiru   1.21791  4 0 0 0    6012   32.3767
                                1001    8.1573
                                8016   21.5782
                               14000   37.8878   14  1.0     293  end
'void space external to containment vessel'
arbmwecv   0.9982   2 0 0 0    1001   11.1913
                                8016   88.8087   15  1       293  end
'steel: liner'
ss304                                            16  1.0     293  end
'steel: plug cover (pc) use 9.907 lb'
ss304                                            17  1.06388 293  end
'steel: angle iron (ai) for single units'
ss304                                            18  1.0     293  end
'steel: angle iron (ai) for arrays'
'array density is multiplied by a volume fraction 7.08030/5.63249'
'ss304                                            18  1.25705 293  end
'steel: drum steel for single units'
ss304                                            19  1.0     293  end
'steel: drum steel for arrays'
'array density is multiplied by a volume fraction 3.20482/3.20544'
'ss304                                            19  0.99981 293  end
'void space external to drum'
'array density is multiplied by a volume ratio 8.11698/6.98323'
'arbmwed    1.16026  2 0 0 0    1001   11.1913
'                                8016   88.8087   20  1       293  end
'reflective water'
arbmh20r   0.9982   2 0 0 0    1001   11.1913
                                8016   88.8087   21  1.0     293  end
end comp
cvcrtriga_70 0.0in thk np, 6847.1gUZrHx(  408.0g235, 8998.2gH2O,hx=575.64),fr=1.0e+00
read parameters nub=yes npg=2500 gen=215 nsk=15 tme=100 end parameters
read boun       all=vac                          end boun
read geometry
unit 1001
'drum bottom flat cover [Elev= 0.105 in. at top of unit]'
 cuboid    21 1 4p24.587200    0.26670   0.0     com='drum chine outer radius'
unit 1002
'above drum bottom flat cover and below containment vessel [Elev= 4.670 in.]'
 cuboid    21 1 4p24.587200   11.59510   0.0     com='drum chine outer radius'
unit 1003
'cv bottom [Elev= 4.920 in.]'
 cylinder  8  1    6.680200    0.63500   0.0     com='cv bottom'
 cuboid    21 1 4p24.587200    0.63500   0.0     com='drum chine outer radius'
unit 1004
'UZrHx fuel element'
 cylinder  1  1    1.828800   12.70000   0.0     com='cylindrical content'
unit 1006
'content (collapsed) [Elev= 9.920 in.]'
'1.437900   plus-y location upper cylinders'
'-2.875700  minus-y location lower cylinder'
'2.490443   plus-x location upper cylinder'
'-2.490443  minus-x location upper cylinder'
 cylinder  3  1    6.426200   12.70050  -0.0005  com='cv well cavity'
 hole  1004   -2.490443  1.437900  0.0     com='cyl1'
 hole  1004    2.490443  1.437900  0.0     com='cyl2'
 hole  1004    0.0      -2.875700  0.0     com='cyl3'
 cylinder  8  1    6.680200   12.70050  -0.0005  com='cv below 1st step'
 cuboid    21 1 4p24.587200   12.70050  -0.0005  com='drum chine outer radius'
unit 1007
'np277_4 spacer [Elev= 9.921 in.]'
 cylinder  2  1    5.24510     0.00010   0.0     com='np spacer'
 cylinder  3  1    6.426200    0.00020  -0.0001  com='cv well cavity'
 cylinder  8  1    6.680200    0.00020  -0.0001  com='cv below 1st step'
 cuboid    21 1 4p24.587200    0.00020  -0.0001  com='drum chine outer radius'
unit 1008
```

```
'top of content stack to bottom of 1st step [Elev=35.270 in.]'
'38.10360             stack height (content spacers)       CALCULATED
 cylinder  3  1    6.426200   38.98540   0.0     com='cv well cavity'
 cylinder  8  1    6.680200   38.98540   0.0     com='cv below 1st step'
 cuboid    21 1 4p24.587200   38.98540   0.0     com='drum chine outer radius'
unit 1010
'cv at 1st step in liner [Elev=35.330 in.]'
 cylinder  3  1    6.426200    0.15240   0.0     com='cv well cavity'
 cylinder  8  1    6.680200    0.15240   0.0     com='cv at 1st step'
 cuboid    21 1 4p24.587200    0.15240   0.0     com='drum chine outer radius'
unit 1011
'vertical gap between 1st step in liner and cv flange [Elev=35.420 in.]'
 cylinder  3  1    6.426200    0.22860   0.0     com='cv well cavity'
 cylinder  8  1    6.680200    0.22860   0.0     com='cv at gap btwn step-flng'
 cuboid    21 1 4p24.587200    0.22860   0.0     com='drum chine outer radius'
unit 1012
'cv flange to top of cv well [Elev=35.920 in.]'
 cylinder  3  1    6.426200    1.27000   0.0     com='cavity'
 cylinder  9  1    9.525000    1.27000   0.0     com='flange to top of well'
 cuboid    21 1 4p24.587200    1.27000   0.0     com='drum chine outer radius'
unit 1013
'cv flange above cv well [Elev=37.070 in.]'
 cylinder  10 1    9.525000    2.92100   0.0     com='flange above cv well'
 cuboid    21 1 4p24.587200    2.92100   0.0     com='drum chine outer radius'
unit 1014
'plugpad2 below liner 2nd step [Elev=37.470 in.]'
 cuboid    21 1 4p24.587200    1.01600   0.0     com='drum chine outer radius'
unit 1015
'2nd step in liner [Elev=37.530 in.]'
 cuboid    21 1 4p24.587200    0.15240   0.0     com='drum chine outer radius'
unit 1016
'abv 2nd step in liner to bottom of angle iron [Elev=40.750 in.]'
 cuboid    21 1 4p24.587200    8.17880   0.0     com='drum chine outer radius'
unit 1017
'bottom of angle iron to bend in angle iron [Elev=42.500 in.]'
 cuboid    21 1 4p24.587200    4.44500   0.0     com='drum chine outer radius'
unit 1018
'bend in angle iron to top of angle iron [Elev=42.750 in.]'
 cuboid    21 1 4p24.587200    0.63500   0.0     com='drum chine outer radius'
unit 1019
'drum lid and lip [Elev=43.500 in.]'
 cuboid    21 1 4p24.587200    1.90500   0.0     com='drum chine outer radius'
global
unit 1020
'es3100 drum [Elev=43.500 in.]'
array 3         2r-24.587200     0.0
'cuboid     0  1 4p24.587200    110.4905  0.0    com='bare package'
 cuboid    21  1 4p55.067200   140.9700 -30.48   com='reflected package'
'cuboid    20  1 4p22.889718    110.5048  0.0    com='interstital array space'
'global
'unit 1021
'array 4   3r0.0
'reflector  21 2  6r3.0  10
end geometry
read array
ara=3 nux=1 nuy=1 nuz=19 fill
1001 1002 1003 1006 1007 1006 1007 1006 1008 1010
1011 1012 1013 1014 1015 1016 1017 1018 1019        end fill
'ara=4 nux=13 nuy=13 nuz=06 fill f1020               end fill
end array
'read bias id=500 2  11  end bias
read start nst=0
end start
end data
end


=csas25    parm=size=3000000
cvcrtriga_70 1.4in thk np, 6847.1gUZrHx(  408.0g235, 8384.6gH2O hx=536.39),fr=1.0e+00
238groupndf5 infhommedium
'TRIGA volume =1200.95996, SPACER volume  614.68012'
```

```
'TRIGA wrapped dry content can hx=41.1, CV void volume 8399.72186'
arbmtriga  5.70132  4 0 0 0    1001    1.5894
                              40000   89.9107
                              92235    5.9587
                              92238    2.5412    1  1.0     293  end
'np277-4: spacer (NCT_MD&H)'
'NCT min.den.(95.3886 lb/ft3) and hydrogen'
'np277-4 min.den.= 1.527971 = (95.3886 lb/ft3)(453.59 g/lb)/(28316.84 cm3/ft3)'
'use 75% of boron in calculations per NUREG-1609 Section 6.5.3.2'
arbmboron 7.31015e-2  2 0 0 0    5010   18.1479
                                 5011   81.8520    2  0.7500  293  end
arbmnpmx  1.07070e+0 10 0 0 0    6012    1.9189
                                 7014    0.0141
                                 8016   43.4251
                                11023    0.1174
                                12000    0.3378
                                13027   39.0479
                                14000    2.4672
                                16000    0.3083
                                20000   11.8336
                                26000    0.5298    2  1.0000  293  end
arbmnph2o 3.84169e-1  2 0 0 0    1001   11.1913
                                 8016   88.8087    2  1.0000  293  end
'flooded containmment vessel and content cans -- 10 CFR 71.55(d)(3)'
arbmwicv   0.9982   2 0 0 0    1001   11.1913
                               8016   88.8087    3  1       293  end
'steel: containment vessel body 16.60 lb but use 15.74 lb'
ss304                                            8  1.0     293  end
'steel: cv flange lower use 3.36 lb'
ss304                                            9  0.97267 293  end
'steel: cv flange upper use 13.75 lb'
ss304                                           10  0.94348 293  end
'np277-4: confinement -- neutron poison inner liner (NCT_MD&H)'
'actual vol.= 1.31846e4 cm3 = (8.0457422e2 in3)(16.387064)'
'den.multiplier = 1.31846e4 cm3 (actual vol.) / 1.32708e4 cm3 (model vol.)'
'np277-4 min.den.= 1.527971 = (95.3886 lb/ft3)(453.59 g/lb)/(28316.84 cm3/ft3)'
'density = 1.518047 = (den.mult)(np277-4 min.den.) = 0.9935052*1.527971'
'use 75% of boron in calculations per NUREG-1609 Section 6.5.3.2'
arbmboron 7.26267e-2  2 0 0 0    5010   18.1479
                                 5011   81.8520   11  0.7500  293  end
arbmnpmx  1.06375e+0 10 0 0 0    6012    1.9189
                                 7014    0.0141
                                 8016   43.4251
                                11023    0.1174
                                12000    0.3378
                                13027   39.0479
                                14000    2.4672
                                16000    0.3083
                                20000   11.8336
                                26000    0.5298   11  1.0000  293  end
arbmnph2o 3.81674e-1  2 0 0 0    1001   11.1913
                                 8016   88.8087   11  1.0000  293  end
'kaolite 1600 body'
'sing.unit.density= (den.mult)(min.den.)'
' for arbmh20k = 1.012373*0.51655,  for rest = 1.012373*0.34438'
'den.mult= 1.36557e5 cm3 (actual vol.) / 1.34888e5 cm3 (model vol.)'
'actual vol.= 1.36557e5 cm3 = (28316.84 cm3/ft3)(108.33188 lb)/(22.464 lb/ft3)'
arbmh2ok   0.52294  2 0 0 0    1001   11.1913
                               8016   88.8087   12  1       293  end
arbmal2o3  0.34864  2 0 0 0   13027   52.9390
                               8016   47.0610   12  0.096   293  end
arbmsio2   0.34864  2 0 0 0   14000   46.7570
                               8016   53.2430   12  0.367   293  end
arbmfe2o3  0.34864  2 0 0 0   26000   69.9540
                               8016   30.0460   12  0.067   293  end
arbmtio2   0.34864  2 0 0 0   22000   59.9535
                               8016   40.0465   12  0.012   293  end
arbmcao    0.34864  2 0 0 0   20000   71.4815
                               8016   28.5185   12  0.307   293  end
arbmmgo    0.34864  2 0 0 0   12000   60.3169
                               8016   39.6831   12  0.131   293  end
```

```
arbmna2o   0.34864  2 0 0 0   11023   74.1961
                               8016   25.8039   12  0.020   293  end
'kaolite 1600 top plug'
'sing.unit.density= (den.mult)(min.den.)'
' for arbmh20k = 0.965246*0.51655,  for rest = 0.965246*0.34438'
'den.mult= 1.21592e4 cm3 (actual vol.) / 1.25970e4 cm3 (model vol.)'
'actual vol.= 1.21592e4 cm3 = (28316.84 cm3/ft3)(9.646 lb)/(22.464 lb/ft3)'
arbmh2ok   0.49860  2 0 0 0    1001   11.1913
                               8016   88.8087   13  1       293  end
arbmal2o3  0.33241  2 0 0 0   13027   52.9390
                               8016   47.0610   13  0.096   293  end
arbmsio2   0.33241  2 0 0 0   14000   46.7570
                               8016   53.2430   13  0.367   293  end
arbmfe2o3  0.33241  2 0 0 0   26000   69.9540
                               8016   30.0460   13  0.067   293  end
arbmtio2   0.33241  2 0 0 0   22000   59.9535
                               8016   40.0465   13  0.012   293  end
arbmcao    0.33241  2 0 0 0   20000   71.4815
                               8016   28.5185   13  0.307   293  end
arbmmgo    0.33241  2 0 0 0   12000   60.3169
                               8016   39.6831   13  0.131   293  end
arbmna2o   0.33241  2 0 0 0   11023   74.1961
                               8016   25.8039   13  0.020   293  end
'silicone rubber pads'
arbmsiru   1.21791  4 0 0 0    6012   32.3767
                               1001    8.1573
                               8016   21.5782
                              14000   37.8878   14  1.0     293  end
'void space external to containment vessel'
arbmwecv   0.9982   2 0 0 0    1001   11.1913
                               8016   88.8087   15  1       293  end
'steel: liner'
ss304                                            16  1.0     293  end
'steel: plug cover (pc) use 9.907 lb'
ss304                                            17  1.06388 293  end
'steel: angle iron (ai) for single units'
ss304                                            18  1.0     293  end
'steel: angle iron (ai) for arrays'
'array density is multiplied by a volume fraction 7.08030/5.63249'
'ss304                                            18  1.25705 293  end
'steel: drum steel for single units'
ss304                                            19  1.0     293  end
'steel: drum steel for arrays'
'array density is multiplied by a volume fraction 3.20482/3.20544'
'ss304                                            19  0.99981 293  end
'void space external to drum'
'array density is multiplied by a volume ratio 8.11698/6.98323'
'arbmwed    1.16026  2 0 0 0    1001   11.1913
'                               8016   88.8087   20  1       293  end
'reflective water'
arbmh20r   0.9982   2 0 0 0    1001   11.1913
                               8016   88.8087   21  1.0     293  end
end comp
cvcrtriga_70 1.4in thk np, 6847.1gUZrHx(  408.0g235, 8384.6gH2O,hx=536.39),fr=1.0e+00
read parameters nub=yes npg=2500 gen=215 nsk=15 tme=100 end parameters
read boun       all=vac                          end boun
read geometry
unit 1001
'drum bottom flat cover [Elev= 0.105 in. at top of unit]'
 cuboid    21 1 4p24.587200    0.26670   0.0     com='drum chine outer radius'
unit 1002
'above drum bottom flat cover and below containment vessel [Elev= 4.670 in.]'
 cuboid    21 1 4p24.587200   11.59510   0.0     com='drum chine outer radius'
unit 1003
'cv bottom [Elev= 4.920 in.]'
 cylinder  8  1    6.680200    0.63500   0.0     com='cv bottom'
 cuboid    21 1 4p24.587200    0.63500   0.0     com='drum chine outer radius'
unit 1004
'UZrHx fuel element'
 cylinder  1  1    1.828800   12.70000   0.0     com='cylindrical content'
unit 1006
```

```
'content (collapsed) [Elev= 9.920 in.]'
'1.437900   plus-y location upper cylinders'
'-2.875700  minus-y location lower cylinder'
'2.490443   plus-x location upper cylinder'
'-2.490443  minus-x location upper cylinder'
 cylinder  3  1    6.426200   12.70050  -0.0005  com='cv well cavity'
 hole  1004   -2.490443  1.437900  0.0     com='cyl1'
 hole  1004    2.490443  1.437900  0.0     com='cyl2'
 hole  1004    0.0      -2.875700  0.0     com='cyl3'
 cylinder  8  1    6.680200   12.70050  -0.0005  com='cv below 1st step'
 cuboid    21 1 4p24.587200   12.70050  -0.0005  com='drum chine outer radius'
unit 1007
'np277_4 spacer [Elev=11.321 in.]'
 cylinder  2  1    5.24510     3.55610   0.0     com='np spacer'
 cylinder  3  1    6.426200    3.55620  -0.0001  com='cv well cavity'
 cylinder  8  1    6.680200    3.55620  -0.0001  com='cv below 1st step'
 cuboid    21 1 4p24.587200    3.55620  -0.0001  com='drum chine outer radius'
unit 1008
'top of content stack to bottom of 1st step [Elev=35.270 in.]'
'45.21560             stack height (content spacers)       CALCULATED
 cylinder  3  1    6.426200   31.87340   0.0     com='cv well cavity'
 cylinder  8  1    6.680200   31.87340   0.0     com='cv below 1st step'
 cuboid    21 1 4p24.587200   31.87340   0.0     com='drum chine outer radius'
unit 1010
'cv at 1st step in liner [Elev=35.330 in.]'
 cylinder  3  1    6.426200    0.15240   0.0     com='cv well cavity'
 cylinder  8  1    6.680200    0.15240   0.0     com='cv at 1st step'
 cuboid    21 1 4p24.587200    0.15240   0.0     com='drum chine outer radius'
unit 1011
'vertical gap between 1st step in liner and cv flange [Elev=35.420 in.]'
 cylinder  3  1    6.426200    0.22860   0.0     com='cv well cavity'
 cylinder  8  1    6.680200    0.22860   0.0     com='cv at gap btwn step-flng'
 cuboid    21 1 4p24.587200    0.22860   0.0     com='drum chine outer radius'
unit 1012
'cv flange to top of cv well [Elev=35.920 in.]'
 cylinder  3  1    6.426200    1.27000   0.0     com='cavity'
 cylinder  9  1    9.525000    1.27000   0.0     com='flange to top of well'
 cuboid    21 1 4p24.587200    1.27000   0.0     com='drum chine outer radius'
unit 1013
'cv flange above cv well [Elev=37.070 in.]'
 cylinder  10 1    9.525000    2.92100   0.0     com='flange above cv well'
 cuboid    21 1 4p24.587200    2.92100   0.0     com='drum chine outer radius'
unit 1014
'plugpad2 below liner 2nd step [Elev=37.470 in.]'
 cuboid    21 1 4p24.587200    1.01600   0.0     com='drum chine outer radius'
unit 1015
'2nd step in liner [Elev=37.530 in.]'
 cuboid    21 1 4p24.587200    0.15240   0.0     com='drum chine outer radius'
unit 1016
'abv 2nd step in liner to bottom of angle iron [Elev=40.750 in.]'
 cuboid    21 1 4p24.587200    8.17880   0.0     com='drum chine outer radius'
unit 1017
'bottom of angle iron to bend in angle iron [Elev=42.500 in.]'
 cuboid    21 1 4p24.587200    4.44500   0.0     com='drum chine outer radius'
unit 1018
'bend in angle iron to top of angle iron [Elev=42.750 in.]'
 cuboid    21 1 4p24.587200    0.63500   0.0     com='drum chine outer radius'
unit 1019
'drum lid and lip [Elev=43.500 in.]'
 cuboid    21 1 4p24.587200    1.90500   0.0     com='drum chine outer radius'
global
unit 1020
'es3100 drum [Elev=43.500 in.]'
array 3         2r-24.587200     0.0
'cuboid     0  1 4p24.587200    110.4905  0.0    com='bare package'
 cuboid    21  1 4p55.067200   140.9700 -30.48   com='reflected package'
'cuboid    20  1 4p22.889718    110.5048  0.0    com='interstital array space'
'global
'unit 1021
'array 4   3r0.0
'reflector  21 2  6r3.0  10
```

```
end geometry
read array
ara=3 nux=1 nuy=1 nuz=19 fill
1001 1002 1003 1006 1007 1006 1007 1006 1008 1010
1011 1012 1013 1014 1015 1016 1017 1018 1019        end fill
'ara=4 nux=13 nuy=13 nuz=06 fill f1020               end fill
end array
'read bias id=500 2  11  end bias
read start nst=0
end start
end data
end


=csas25    parm=size=3000000
ncsrtriga 0.0in thk np,10400.0gUZrHx(  921.0g235, 8998.2gH2O hx=255.01),fr=1.0e+00
238groupndf5 infhommedium
'TRIGA volume =1200.95996, SPACER volume    0.00000'
'TRIGA wrapped dry content can hx=18.2, CV void volume 9014.40198'
arbmtriga  8.65974  4 0 0 0    1001    0.9554
                              40000   54.0446
                              92235    8.8558
                              92238   36.1442    1  1.0     293  end
'np277-4: spacer (NCT_MD&H)'
'NCT min.den.(95.3886 lb/ft3) and hydrogen'
'np277-4 min.den.= 1.527971 = (95.3886 lb/ft3)(453.59 g/lb)/(28316.84 cm3/ft3)'
'use 75% of boron in calculations per NUREG-1609 Section 6.5.3.2'
arbmboron 7.31015e-2  2 0 0 0    5010   18.1479
                                 5011   81.8520    2  0.7500  293  end
arbmnpmx  1.07070e+0 10 0 0 0    6012    1.9189
                                 7014    0.0141
                                 8016   43.4251
                                11023    0.1174
                                12000    0.3378
                                13027   39.0479
                                14000    2.4672
                                16000    0.3083
                                20000   11.8336
                                26000    0.5298    2  1.0000  293  end
arbmnph2o 3.84169e-1  2 0 0 0    1001   11.1913
                                 8016   88.8087    2  1.0000  293  end
'flooded containmment vessel and content cans -- 10 CFR 71.55(d)(3)'
arbmwicv   0.9982   2 0 0 0    1001   11.1913
                              8016   88.8087    3  1       293  end
'steel: containment vessel body 16.60 lb but use 15.74 lb'
ss304                                            8  1.0     293  end
'steel: cv flange lower use 3.36 lb'
ss304                                            9  0.97267 293  end
'steel: cv flange upper use 13.75 lb'
ss304                                           10  0.94348 293  end
'np277-4: confinement -- neutron poison inner liner (NCT_MD&H)'
'actual vol.= 1.28314e4 cm3 = (7.83023e2 in3)(16.387064)'
'den.multiplier = 1.28314e4 cm3 (actual vol.) / 1.32708e4 cm3 (model vol.)'
'np277-4 min.den.= 1.527971 = (95.3886 lb/ft3)(453.59 g/lb)/(28316.84 cm3/ft3)'
'density = 1.477385 = (den.mult)(np277-4 min.den.) = 0.9668933*1.527971'
'use 75% of boron in calculations per NUREG-1609 Section 6.5.3.2'
arbmboron 7.06813e-2  2 0 0 0    5010   18.1479
                                 5011   81.8520   11  0.7500  293  end
arbmnpmx  1.03525e+0 10 0 0 0    6012    1.9189
                                 7014    0.0141
                                 8016   43.4251
                                11023    0.1174
                                12000    0.3378
                                13027   39.0479
                                14000    2.4672
                                16000    0.3083
                                20000   11.8336
                                26000    0.5298   11  1.0000  293  end
arbmnph2o 3.71451e-1  2 0 0 0    1001   11.1913
                                 8016   88.8087   11  1.0000  293  end
'kaolite 1600 body'
```

```
'sing.unit.density= (den.mult)(min.den.)'
' for arbmh20k = 1.012373*0.51655,  for rest = 1.012373*0.34438'
'den.mult= 1.36557e5 cm3 (actual vol.) / 1.34888e5 cm3 (model vol.)'
'actual vol.= 1.36557e5 cm3 = (28316.84 cm3/ft3)(108.33188 lb)/(22.464 lb/ft3)'
arbmh2ok   0.52294  2 0 0 0    1001   11.1913
                               8016   88.8087   12  1       293  end
arbmal2o3  0.34864  2 0 0 0   13027   52.9390
                               8016   47.0610   12  0.096   293  end
arbmsio2   0.34864  2 0 0 0   14000   46.7570
                               8016   53.2430   12  0.367   293  end
arbmfe2o3  0.34864  2 0 0 0   26000   69.9540
                               8016   30.0460   12  0.067   293  end
arbmtio2   0.34864  2 0 0 0   22000   59.9535
                               8016   40.0465   12  0.012   293  end
arbmcao    0.34864  2 0 0 0   20000   71.4815
                               8016   28.5185   12  0.307   293  end
arbmmgo    0.34864  2 0 0 0   12000   60.3169
                               8016   39.6831   12  0.131   293  end
arbmna2o   0.34864  2 0 0 0   11023   74.1961
                               8016   25.8039   12  0.020   293  end
'kaolite 1600 top plug'
'sing.unit.density= (den.mult)(min.den.)'
' for arbmh20k = 0.965246*0.51655,  for rest = 0.965246*0.34438'
'den.mult= 1.21592e4 cm3 (actual vol.) / 1.25970e4 cm3 (model vol.)'
'actual vol.= 1.21592e4 cm3 = (28316.84 cm3/ft3)(9.646 lb)/(22.464 lb/ft3)'
arbmh2ok   0.49860  2 0 0 0    1001   11.1913
                               8016   88.8087   13  1       293  end
arbmal2o3  0.33241  2 0 0 0   13027   52.9390
                               8016   47.0610   13  0.096   293  end
arbmsio2   0.33241  2 0 0 0   14000   46.7570
                               8016   53.2430   13  0.367   293  end
arbmfe2o3  0.33241  2 0 0 0   26000   69.9540
                               8016   30.0460   13  0.067   293  end
arbmtio2   0.33241  2 0 0 0   22000   59.9535
                               8016   40.0465   13  0.012   293  end
arbmcao    0.33241  2 0 0 0   20000   71.4815
                               8016   28.5185   13  0.307   293  end
arbmmgo    0.33241  2 0 0 0   12000   60.3169
                               8016   39.6831   13  0.131   293  end
arbmna2o   0.33241  2 0 0 0   11023   74.1961
                               8016   25.8039   13  0.020   293  end
'silicone rubber pads'
arbmsiru   1.21791  4 0 0 0    6012   32.3767
                               1001    8.1573
                               8016   21.5782
                              14000   37.8878   14  1.0     293  end
'void space external to containment vessel'
arbmwecv   0.9982   2 0 0 0    1001   11.1913
                               8016   88.8087   15  1       293  end
'steel: liner'
ss304                                            16  1.0     293  end
'steel: plug cover (pc) use 9.907 lb'
ss304                                            17  1.06388 293  end
'steel: angle iron (ai) for single units'
ss304                                            18  1.0     293  end
'steel: angle iron (ai) for arrays'
'array density is multiplied by a volume fraction 7.08030/5.63249'
'ss304                                            18  1.25705 293  end
'steel: drum steel for single units'
ss304                                            19  1.0     293  end
'steel: drum steel for arrays'
'array density is multiplied by a volume fraction 3.20482/3.20544'
'ss304                                            19  0.99981 293  end
'void space external to drum'
'array density is multiplied by a volume ratio 8.11698/6.98323'
'arbmwed    1.16026  2 0 0 0    1001   11.1913
'                               8016   88.8087   20  1       293  end
'reflective water'
arbmh20r   0.9982   2 0 0 0    1001   11.1913
                               8016   88.8087   21  1.0     293  end
end comp
```

```
ncsrtriga 0.0in thk np,10400.0gUZrHx(  921.0g235, 8998.2gH2O,hx=255.01),fr=1.0e+00
read parameters nub=yes npg=2500 gen=215 nsk=15 tme=100 end parameters
read boun       all=vac                         end boun
read geometry
unit 1001
'drum bottom flat cover [Elev= 0.105 in. at top of unit]'
'cylinder  19 1   24.587200    0.26670   0.0     com='extended radius not used'
 cylinder  19 1   23.329900    0.26670   0.0     com='drum bottom flat cover'
 cuboid    21 1 4p24.587200    0.26670   0.0     com='drum chine outer radius'
unit 1002
'above drum bottom flat cover and below containment vessel [Elev= 4.670 in.]'
 cylinder  15 1    3.175000   11.59510  11.16330 com='void in pad-1'
 cylinder  14 1    7.924800   11.59510  11.16330 com='pad-1'
 cylinder  16 1    8.077200   11.59510  11.16330 com='np277_4 liner'
 cylinder  11 1   10.922000   11.59510  11.16330 com='np277_4'
 cylinder  16 1   11.074400   11.59510  10.85850 com='kaolite liner bottom'
 cylinder  12 1   23.177500   11.59510   0.0     com='kaolite'
 cylinder  19 1   23.329900   11.59510   0.0     com='drum'
 cuboid    21 1 4p24.587200   11.59510   0.0     com='drum chine outer radius'
unit 1003
'cv bottom [Elev= 4.920 in.]'
 cylinder  8  1    6.680200    0.63500   0.0     com='cv bottom'
 cylinder  15 1    7.924800    0.63500   0.0     com='void btw cv-np liner'
 cylinder  16 1    8.077200    0.63500   0.0     com='np277_4 liner'
 cylinder  11 1   10.922000    0.63500   0.0     com='np277_4'
 cylinder  16 1   11.074400    0.63500   0.0     com='kaolite liner'
 cylinder  12 1   23.177500    0.63500   0.0     com='kaolite'
 cylinder  19 1   23.329900    0.63500   0.0     com='drum'
 cuboid    21 1 4p24.587200    0.63500   0.0     com='drum chine outer radius'
unit 1004
'UZrHx fuel element'
 cylinder  1  1    1.828800   12.70000   0.0     com='cylindrical content'
unit 1006
'content (collapsed) [Elev= 9.920 in.]'
'1.437900   plus-y location upper cylinders'
'-2.875700  minus-y location lower cylinder'
'2.490443   plus-x location upper cylinder'
'-2.490443  minus-x location upper cylinder'
 cylinder  3  1    6.426200   12.70050  -0.0005  com='cv well cavity'
 hole  1004   -2.490443  1.437900  0.0     com='cyl1'
 hole  1004    2.490443  1.437900  0.0     com='cyl2'
 hole  1004    0.0      -2.875700  0.0     com='cyl3'
 cylinder  8  1    6.680200   12.70050  -0.0005  com='cv below 1st step'
 cylinder  15 1    7.924800   12.70050  -0.0005  com='void btw cv-np liner'
 cylinder  16 1    8.077200   12.70050  -0.0005  com='np277_4 liner'
 cylinder  11 1   10.922000   12.70050  -0.0005  com='np277_4'
 cylinder  16 1   11.074400   12.70050  -0.0005  com='kaolite liner'
 cylinder  12 1   23.177500   12.70050  -0.0005  com='kaolite'
 cylinder  19 1   23.329900   12.70050  -0.0005  com='drum'
 cuboid    21 1 4p24.587200   12.70050  -0.0005  com='drum chine outer radius'
unit 1007
'np277_4 spacer [Elev= 9.921 in.]'
 cylinder  2  1    5.24510     0.00010   0.0     com='np spacer'
 cylinder  3  1    6.426200    0.00020  -0.0001  com='cv well cavity'
 cylinder  8  1    6.680200    0.00020  -0.0001  com='cv below 1st step'
 cylinder  15 1    7.924800    0.00020  -0.0001  com='void btw cv-np liner'
 cylinder  16 1    8.077200    0.00020  -0.0001  com='np277_4 liner'
 cylinder  11 1   10.922000    0.00020  -0.0001  com='np277_4'
 cylinder  16 1   11.074400    0.00020  -0.0001  com='kaolite liner'
 cylinder  12 1   23.177500    0.00020  -0.0001  com='kaolite'
 cylinder  19 1   23.329900    0.00020  -0.0001  com='drum'
 cuboid    21 1 4p24.587200    0.00020  -0.0001  com='drum chine outer radius'
unit 1008
'top of content stack to bottom of 1st step [Elev=35.270 in.]'
'38.10360             stack height (content spacers)       CALCULATED
 cylinder  3  1    6.426200   38.98540   0.0     com='cv well cavity'
 cylinder  8  1    6.680200   38.98540   0.0     com='cv below 1st step'
 cylinder  15 1    7.924800   38.98540   0.0     com='void btw cv-np liner'
 cylinder  16 1    8.077200   38.98540   0.0     com='np277_4 liner'
 cylinder  11 1   10.922000   38.98540   0.0     com='np277_4'
 cylinder  16 1   11.074400   38.98540   0.0     com='kaolite liner'
```

```
 cylinder  12 1   23.177500   38.98540   0.0     com='kaolite'
 cylinder  19 1   23.329900   38.98540   0.0     com='drum'
 cuboid    21 1 4p24.587200   38.98540   0.0     com='drum chine outer radius'
unit 1010
'cv at 1st step in liner [Elev=35.330 in.]'
 cylinder  3  1    6.426200    0.15240   0.0     com='cv well cavity'
 cylinder  8  1    6.680200    0.15240   0.0     com='cv at 1st step'
 cylinder  15 1    7.924800    0.15240   0.0     com='void btw cv and liner'
 cylinder  16 1   11.074400    0.15240   0.0     com='liner 1st step'
 cylinder  12 1   23.177500    0.15240   0.0     com='kaolite'
 cylinder  19 1   23.329900    0.15240   0.0     com='drum'
 cuboid    21 1 4p24.587200    0.15240   0.0     com='drum chine outer radius'
unit 1011
'vertical gap between 1st step in liner and cv flange [Elev=35.420 in.]'
 cylinder  3  1    6.426200    0.22860   0.0     com='cv well cavity'
 cylinder  8  1    6.680200    0.22860   0.0     com='cv at gap btwn step-flng'
 cylinder  15 1   10.922000    0.22860   0.0     com='void btw cv and liner'
 cylinder  16 1   11.074400    0.22860   0.0     com='liner wall'
 cylinder  12 1   23.177500    0.22860   0.0     com='kaolite'
 cylinder  19 1   23.329900    0.22860   0.0     com='drum'
 cuboid    21 1 4p24.587200    0.22860   0.0     com='drum chine outer radius'
unit 1012
'cv flange to top of cv well [Elev=35.920 in.]'
 cylinder  3  1    6.426200    1.27000   0.0     com='cavity'
 cylinder  9  1    9.525000    1.27000   0.0     com='flange to top of well'
 cylinder  15 1    9.525000    1.27000   0.0     com='void btw cv and pad-2'
 cylinder  14 1   10.033000    1.27000   0.0     com='pad-2'
 cylinder  15 1   10.922000    1.27000   0.0     com='void btw cv and liner'
 cylinder  16 1   11.074400    1.27000   0.0     com='liner wall'
 cylinder  12 1   23.177500    1.27000   0.0     com='kaolite'
 cylinder  19 1   23.329900    1.27000   0.0     com='drum'
 cuboid    21 1 4p24.587200    1.27000   0.0     com='drum chine outer radius'
unit 1013
'cv flange above cv well [Elev=37.070 in.]'
 cylinder  10 1    9.525000    2.92100   0.0     com='flange above cv well'
 cylinder  15 1    9.525000    2.92100   0.0     com='void btw cv and pad-2'
 cylinder  14 1   10.033000    2.92100   0.0     com='pad-2'
 cylinder  15 1   10.922000    2.92100   0.0     com='void btw pad2 and liner'
 cylinder  16 1   11.074400    2.92100   0.0     com='liner wall'
 cylinder  12 1   23.177500    2.92100   0.0     com='kaolite'
 cylinder  19 1   23.329900    2.92100   0.0     com='drum'
 cuboid    21 1 4p24.587200    2.92100   0.0     com='drum chine outer radius'
unit 1014
'plugpad2 below liner 2nd step [Elev=37.470 in.]'
 cylinder  14 1   10.033000    0.76200   0.0     com='pad-2'
 cylinder  15 1   10.922000    1.01600   0.0     com='void btw pad2 and liner'
 cylinder  16 1   11.074400    1.01600   0.0     com='liner wall'
 cylinder  12 1   23.177500    1.01600   0.0     com='kaolite'
 cylinder  19 1   23.329900    1.01600   0.0     com='drum'
 cuboid    21 1 4p24.587200    1.01600   0.0     com='drum chine outer radius'
unit 1015
'2nd step in liner [Elev=37.530 in.]'
 cylinder  15 1   10.922000    0.15240   0.0     com='void abv pad2'
 cylinder  16 1   18.757900    0.15240   0.0     com='liner 2nd step'
 cylinder  12 1   23.177500    0.15240   0.0     com='kaolite'
 cylinder  19 1   23.329900    0.15240   0.0     com='drum'
 cuboid    21 1 4p24.587200    0.15240   0.0     com='drum chine outer radius'
unit 1016
'abv 2nd step in liner to bottom of angle iron [Elev=40.750 in.]'
 cylinder  13 1   18.097500    8.17880   0.49276 com='plug kaolite'
 cylinder  17 1   18.249900    8.17880   0.34036 com='sides of plug case'
 cylinder  15 1   18.605500    8.17880   0.0     com='void: plug to liner'
 cylinder  16 1   18.757900    8.17880   0.0     com='liner wall'
 cylinder  12 1   23.177500    8.17880   0.0     com='kaolite'
 cylinder  19 1   23.329900    8.17880   0.0     com='drum'
 cuboid    21 1 4p24.587200    8.17880   0.0     com='drum chine outer radius'
unit 1017
'bottom of angle iron to bend in angle iron [Elev=42.500 in.]'
 cylinder  13 1   18.097500    4.44500   0.0     com='plug kaolite'
 cylinder  17 1   18.249900    4.44500   0.0     com='sides of plug case'
 cylinder  15 1   18.605500    4.44500   0.0     com='void: plug to liner'
```

```
 cylinder  16 1   18.757900    4.44500   0.0     com='liner wall'
 cylinder  18 1   19.392900    4.44500   0.0     com='lower angle iron'
 cylinder  12 1   23.177500    4.44500   0.0     com='kaolite'
 cylinder  19 1   23.329900    4.44500   0.0     com='drum'
 cuboid    21 1 4p24.587200    4.44500   0.0     com='drum chine outer radius'
unit 1018
'bend in angle iron to top of angle iron [Elev=42.750 in.]'
 cylinder  13 1   18.097500    0.11176   0.0     com='plug kaolite'
 cylinder  17 1   18.249900    0.26416   0.0     com='sides of plug case'
 cylinder  15 1   18.605500    0.63500   0.0     com='void: plug to liner'
 cylinder  16 1   18.757900    0.63500   0.0     com='liner wall'
 cylinder  18 1   23.177500    0.63500   0.0     com='bend section of ai'
 cylinder  19 1   23.329900    0.63500   0.0     com='drum'
 cuboid    21 1 4p24.587200    0.63500   0.0     com='drum chine outer radius'
unit 1019
'drum lid and lip [Elev=43.500 in.]'
 cylinder  21 1   22.961600    1.90500   0.15240 com='void above lid'
 cylinder  19 1   23.114000    1.90500   0.0     com='drum lid'
 cylinder  21 1   23.177500    1.90500   0.0     com='void btw lid - drum wall'
 cylinder  19 1   23.329900    1.90500   0.0     com='drum'
 cuboid    21 1 4p24.587200    1.90500   0.0     com='drum chine outer radius'
global
unit 1020
'es3100 drum [Elev=43.500 in.]'
array 3         2r-24.587200     0.0
'cuboid     0  1 4p24.587200    110.4905  0.0    com='bare package'
 cuboid    21  1 4p55.067200   140.9700 -30.48   com='reflected package'
'cuboid    20  1 4p22.889718    110.5048  0.0    com='interstital array space'
'global
'unit 1021
'array 4   3r0.0
'reflector  21 2  6r3.0  10
end geometry
read array
ara=3 nux=1 nuy=1 nuz=19 fill
1001 1002 1003 1006 1007 1006 1007 1006 1008 1010
1011 1012 1013 1014 1015 1016 1017 1018 1019        end fill
'ara=4 nux=13 nuy=13 nuz=06 fill f1020               end fill
end array
'read bias id=500 2  11  end bias
read start nst=0
end start
end data
end


=csas25    parm=size=3000000
ncsrtriga_70 0.0in thk np, 6847.1gUZrHx(  408.0g235, 8998.2gH2O hx=575.64),fr=1.0e+00
238groupndf5 infhommedium
'TRIGA volume =1200.95996, SPACER volume    0.00000'
'TRIGA wrapped dry content can hx=41.1, CV void volume 9014.40198'
arbmtriga  5.70132  4 0 0 0    1001    1.5894
                              40000   89.9107
                              92235    5.9587
                              92238    2.5412    1  1.0     293  end
'np277-4: spacer (NCT_MD&H)'
'NCT min.den.(95.3886 lb/ft3) and hydrogen'
'np277-4 min.den.= 1.527971 = (95.3886 lb/ft3)(453.59 g/lb)/(28316.84 cm3/ft3)'
'use 75% of boron in calculations per NUREG-1609 Section 6.5.3.2'
arbmboron 7.31015e-2  2 0 0 0    5010   18.1479
                                 5011   81.8520    2  0.7500  293  end
arbmnpmx  1.07070e+0 10 0 0 0    6012    1.9189
                                 7014    0.0141
                                 8016   43.4251
                                11023    0.1174
                                12000    0.3378
                                13027   39.0479
                                14000    2.4672
                                16000    0.3083
                                20000   11.8336
                                26000    0.5298    2  1.0000  293  end
```

```
arbmnph2o 3.84169e-1  2 0 0 0    1001   11.1913
                                 8016   88.8087    2  1.0000  293  end
'flooded containmment vessel and content cans -- 10 CFR 71.55(d)(3)'
arbmwicv   0.9982   2 0 0 0    1001   11.1913
                                8016   88.8087    3  1       293  end
'steel: containment vessel body 16.60 lb but use 15.74 lb'
ss304                                            8  1.0     293  end
'steel: cv flange lower use 3.36 lb'
ss304                                            9  0.97267 293  end
'steel: cv flange upper use 13.75 lb'
ss304                                           10  0.94348 293  end
'np277-4: confinement -- neutron poison inner liner (NCT_MD&H)'
'actual vol.= 1.28314e4 cm3 = (7.83023e2 in3)(16.387064)'
'den.multiplier = 1.28314e4 cm3 (actual vol.) / 1.32708e4 cm3 (model vol.)'
'np277-4 min.den.= 1.527971 = (95.3886 lb/ft3)(453.59 g/lb)/(28316.84 cm3/ft3)'
'density = 1.477385 = (den.mult)(np277-4 min.den.) = 0.9668933*1.527971'
'use 75% of boron in calculations per NUREG-1609 Section 6.5.3.2'
arbmboron 7.06813e-2  2 0 0 0    5010   18.1479
                                 5011   81.8520   11  0.7500  293  end
arbmnpmx  1.03525e+0 10 0 0 0    6012    1.9189
                                 7014    0.0141
                                 8016   43.4251
                                11023    0.1174
                                12000    0.3378
                                13027   39.0479
                                14000    2.4672
                                16000    0.3083
                                20000   11.8336
                                26000    0.5298   11  1.0000  293  end
arbmnph2o 3.71451e-1  2 0 0 0    1001   11.1913
                                 8016   88.8087   11  1.0000  293  end
'kaolite 1600 body'
'sing.unit.density= (den.mult)(min.den.)'
' for arbmh20k = 1.012373*0.51655,  for rest = 1.012373*0.34438'
'den.mult= 1.36557e5 cm3 (actual vol.) / 1.34888e5 cm3 (model vol.)'
'actual vol.= 1.36557e5 cm3 = (28316.84 cm3/ft3)(108.33188 lb)/(22.464 lb/ft3)'
arbmh2ok   0.52294  2 0 0 0    1001   11.1913
                                8016   88.8087   12  1       293  end
arbmal2o3  0.34864  2 0 0 0   13027   52.9390
                                8016   47.0610   12  0.096   293  end
arbmsio2   0.34864  2 0 0 0   14000   46.7570
                                8016   53.2430   12  0.367   293  end
arbmfe2o3  0.34864  2 0 0 0   26000   69.9540
                                8016   30.0460   12  0.067   293  end
arbmtio2   0.34864  2 0 0 0   22000   59.9535
                                8016   40.0465   12  0.012   293  end
arbmcao    0.34864  2 0 0 0   20000   71.4815
                                8016   28.5185   12  0.307   293  end
arbmmgo    0.34864  2 0 0 0   12000   60.3169
                                8016   39.6831   12  0.131   293  end
arbmna2o   0.34864  2 0 0 0   11023   74.1961
                                8016   25.8039   12  0.020   293  end
'kaolite 1600 top plug'
'sing.unit.density= (den.mult)(min.den.)'
' for arbmh20k = 0.965246*0.51655,  for rest = 0.965246*0.34438'
'den.mult= 1.21592e4 cm3 (actual vol.) / 1.25970e4 cm3 (model vol.)'
'actual vol.= 1.21592e4 cm3 = (28316.84 cm3/ft3)(9.646 lb)/(22.464 lb/ft3)'
arbmh2ok   0.49860  2 0 0 0    1001   11.1913
                                8016   88.8087   13  1       293  end
arbmal2o3  0.33241  2 0 0 0   13027   52.9390
                                8016   47.0610   13  0.096   293  end
arbmsio2   0.33241  2 0 0 0   14000   46.7570
                                8016   53.2430   13  0.367   293  end
arbmfe2o3  0.33241  2 0 0 0   26000   69.9540
                                8016   30.0460   13  0.067   293  end
arbmtio2   0.33241  2 0 0 0   22000   59.9535
                                8016   40.0465   13  0.012   293  end
arbmcao    0.33241  2 0 0 0   20000   71.4815
                                8016   28.5185   13  0.307   293  end
arbmmgo    0.33241  2 0 0 0   12000   60.3169
                                8016   39.6831   13  0.131   293  end
```

```
arbmna2o   0.33241  2 0 0 0   11023   74.1961
                              8016   25.8039   13  0.020   293  end
'silicone rubber pads'
arbmsiru   1.21791  4 0 0 0    6012   32.3767
                              1001    8.1573
                              8016   21.5782
                             14000   37.8878   14  1.0     293  end
'void space external to containment vessel'
arbmwecv   0.9982   2 0 0 0    1001   11.1913
                              8016   88.8087   15  1       293  end
'steel: liner'
ss304                                           16  1.0     293  end
'steel: plug cover (pc) use 9.907 lb'
ss304                                           17  1.06388 293  end
'steel: angle iron (ai) for single units'
ss304                                           18  1.0     293  end
'steel: angle iron (ai) for arrays'
'array density is multiplied by a volume fraction 7.08030/5.63249'
'ss304                                           18  1.25705 293  end
'steel: drum steel for single units'
ss304                                           19  1.0     293  end
'steel: drum steel for arrays'
'array density is multiplied by a volume fraction 3.20482/3.20544'
'ss304                                           19  0.99981 293  end
'void space external to drum'
'array density is multiplied by a volume ratio 8.11698/6.98323'
'arbmwed    1.16026  2 0 0 0    1001   11.1913
'                              8016   88.8087   20  1       293  end
'reflective water'
arbmh20r   0.9982   2 0 0 0    1001   11.1913
                              8016   88.8087   21  1.0     293  end
end comp
ncsrtriga_70 0.0in thk np, 6847.1gUZrHx(  408.0g235, 8998.2gH2O,hx=575.64),fr=1.0e+00
read parameters nub=yes npg=2500 gen=215 nsk=15 tme=100 end parameters
read boun       all=vac                         end boun
read geometry
unit 1001
'drum bottom flat cover [Elev= 0.105 in. at top of unit]'
'cylinder  19 1   24.587200    0.26670   0.0     com='extended radius not used'
 cylinder  19 1   23.329900    0.26670   0.0     com='drum bottom flat cover'
 cuboid    21 1 4p24.587200    0.26670   0.0     com='drum chine outer radius'
unit 1002
'above drum bottom flat cover and below containment vessel [Elev= 4.670 in.]'
 cylinder  15 1    3.175000   11.59510  11.16330 com='void in pad-1'
 cylinder  14 1    7.924800   11.59510  11.16330 com='pad-1'
 cylinder  16 1    8.077200   11.59510  11.16330 com='np277_4 liner'
 cylinder  11 1   10.922000   11.59510  11.16330 com='np277_4'
 cylinder  16 1   11.074400   11.59510  10.85850 com='kaolite liner bottom'
 cylinder  12 1   23.177500   11.59510   0.0     com='kaolite'
 cylinder  19 1   23.329900   11.59510   0.0     com='drum'
 cuboid    21 1 4p24.587200   11.59510   0.0     com='drum chine outer radius'
unit 1003
'cv bottom [Elev= 4.920 in.]'
 cylinder  8  1    6.680200    0.63500   0.0     com='cv bottom'
 cylinder  15 1    7.924800    0.63500   0.0     com='void btw cv-np liner'
 cylinder  16 1    8.077200    0.63500   0.0     com='np277_4 liner'
 cylinder  11 1   10.922000    0.63500   0.0     com='np277_4'
 cylinder  16 1   11.074400    0.63500   0.0     com='kaolite liner'
 cylinder  12 1   23.177500    0.63500   0.0     com='kaolite'
 cylinder  19 1   23.329900    0.63500   0.0     com='drum'
 cuboid    21 1 4p24.587200    0.63500   0.0     com='drum chine outer radius'
unit 1004
'UZrHx fuel element'
 cylinder  1  1    1.828800   12.70000   0.0     com='cylindrical content'
unit 1006
'content (collapsed) [Elev= 9.920 in.]'
'1.437900   plus-y location upper cylinders'
'-2.875700  minus-y location lower cylinder'
'2.490443   plus-x location upper cylinder'
'-2.490443  minus-x location upper cylinder'
 cylinder  3  1    6.426200   12.70050  -0.0005  com='cv well cavity'
```

```
 hole  1004   -2.490443  1.437900  0.0     com='cyl1'
 hole  1004    2.490443  1.437900  0.0     com='cyl2'
 hole  1004    0.0      -2.875700  0.0     com='cyl3'
 cylinder  8  1    6.680200   12.70050  -0.0005  com='cv below 1st step'
 cylinder  15 1    7.924800   12.70050  -0.0005  com='void btw cv-np liner'
 cylinder  16 1    8.077200   12.70050  -0.0005  com='np277_4 liner'
 cylinder  11 1   10.922000   12.70050  -0.0005  com='np277_4'
 cylinder  16 1   11.074400   12.70050  -0.0005  com='kaolite liner'
 cylinder  12 1   23.177500   12.70050  -0.0005  com='kaolite'
 cylinder  19 1   23.329900   12.70050  -0.0005  com='drum'
 cuboid    21 1 4p24.587200   12.70050  -0.0005  com='drum chine outer radius'
unit 1007
'np277_4 spacer [Elev= 9.921 in.]'
 cylinder  2  1    5.24510     0.00010   0.0     com='np spacer'
 cylinder  3  1    6.426200    0.00020  -0.0001  com='cv well cavity'
 cylinder  8  1    6.680200    0.00020  -0.0001  com='cv below 1st step'
 cylinder  15 1    7.924800    0.00020  -0.0001  com='void btw cv-np liner'
 cylinder  16 1    8.077200    0.00020  -0.0001  com='np277_4 liner'
 cylinder  11 1   10.922000    0.00020  -0.0001  com='np277_4'
 cylinder  16 1   11.074400    0.00020  -0.0001  com='kaolite liner'
 cylinder  12 1   23.177500    0.00020  -0.0001  com='kaolite'
 cylinder  19 1   23.329900    0.00020  -0.0001  com='drum'
 cuboid    21 1 4p24.587200    0.00020  -0.0001  com='drum chine outer radius'
unit 1008
'top of content stack to bottom of 1st step [Elev=35.270 in.]'
'38.10360             stack height (content spacers)       CALCULATED
 cylinder  3  1    6.426200   38.98540   0.0     com='cv well cavity'
 cylinder  8  1    6.680200   38.98540   0.0     com='cv below 1st step'
 cylinder  15 1    7.924800   38.98540   0.0     com='void btw cv-np liner'
 cylinder  16 1    8.077200   38.98540   0.0     com='np277_4 liner'
 cylinder  11 1   10.922000   38.98540   0.0     com='np277_4'
 cylinder  16 1   11.074400   38.98540   0.0     com='kaolite liner'
 cylinder  12 1   23.177500   38.98540   0.0     com='kaolite'
 cylinder  19 1   23.329900   38.98540   0.0     com='drum'
 cuboid    21 1 4p24.587200   38.98540   0.0     com='drum chine outer radius'
unit 1010
'cv at 1st step in liner [Elev=35.330 in.]'
 cylinder  3  1    6.426200    0.15240   0.0     com='cv well cavity'
 cylinder  8  1    6.680200    0.15240   0.0     com='cv at 1st step'
 cylinder  15 1    7.924800    0.15240   0.0     com='void btw cv and liner'
 cylinder  16 1   11.074400    0.15240   0.0     com='liner 1st step'
 cylinder  12 1   23.177500    0.15240   0.0     com='kaolite'
 cylinder  19 1   23.329900    0.15240   0.0     com='drum'
 cuboid    21 1 4p24.587200    0.15240   0.0     com='drum chine outer radius'
unit 1011
'vertical gap between 1st step in liner and cv flange [Elev=35.420 in.]'
 cylinder  3  1    6.426200    0.22860   0.0     com='cv well cavity'
 cylinder  8  1    6.680200    0.22860   0.0     com='cv at gap btwn step-flng'
 cylinder  15 1   10.922000    0.22860   0.0     com='void btw cv and liner'
 cylinder  16 1   11.074400    0.22860   0.0     com='liner wall'
 cylinder  12 1   23.177500    0.22860   0.0     com='kaolite'
 cylinder  19 1   23.329900    0.22860   0.0     com='drum'
 cuboid    21 1 4p24.587200    0.22860   0.0     com='drum chine outer radius'
unit 1012
'cv flange to top of cv well [Elev=35.920 in.]'
 cylinder  3  1    6.426200    1.27000   0.0     com='cavity'
 cylinder  9  1    9.525000    1.27000   0.0     com='flange to top of well'
 cylinder  15 1    9.525000    1.27000   0.0     com='void btw cv and pad-2'
 cylinder  14 1   10.033000    1.27000   0.0     com='pad-2'
 cylinder  15 1   10.922000    1.27000   0.0     com='void btw cv and liner'
 cylinder  16 1   11.074400    1.27000   0.0     com='liner wall'
 cylinder  12 1   23.177500    1.27000   0.0     com='kaolite'
 cylinder  19 1   23.329900    1.27000   0.0     com='drum'
 cuboid    21 1 4p24.587200    1.27000   0.0     com='drum chine outer radius'
unit 1013
'cv flange above cv well [Elev=37.070 in.]'
 cylinder  10 1    9.525000    2.92100   0.0     com='flange above cv well'
 cylinder  15 1    9.525000    2.92100   0.0     com='void btw cv and pad-2'
 cylinder  14 1   10.033000    2.92100   0.0     com='pad-2'
 cylinder  15 1   10.922000    2.92100   0.0     com='void btw pad2 and liner'
 cylinder  16 1   11.074400    2.92100   0.0     com='liner wall'
```

```
 cylinder  12 1   23.177500    2.92100   0.0     com='kaolite'
 cylinder  19 1   23.329900    2.92100   0.0     com='drum'
 cuboid    21 1 4p24.587200    2.92100   0.0     com='drum chine outer radius'
unit 1014
'plugpad2 below liner 2nd step [Elev=37.470 in.]'
 cylinder  14 1   10.033000    0.76200   0.0     com='pad-2'
 cylinder  15 1   10.922000    1.01600   0.0     com='void btw pad2 and liner'
 cylinder  16 1   11.074400    1.01600   0.0     com='liner wall'
 cylinder  12 1   23.177500    1.01600   0.0     com='kaolite'
 cylinder  19 1   23.329900    1.01600   0.0     com='drum'
 cuboid    21 1 4p24.587200    1.01600   0.0     com='drum chine outer radius'
unit 1015
'2nd step in liner [Elev=37.530 in.]'
 cylinder  15 1   10.922000    0.15240   0.0     com='void abv pad2'
 cylinder  16 1   18.757900    0.15240   0.0     com='liner 2nd step'
 cylinder  12 1   23.177500    0.15240   0.0     com='kaolite'
 cylinder  19 1   23.329900    0.15240   0.0     com='drum'
 cuboid    21 1 4p24.587200    0.15240   0.0     com='drum chine outer radius'
unit 1016
'abv 2nd step in liner to bottom of angle iron [Elev=40.750 in.]'
 cylinder  13 1   18.097500    8.17880   0.49276 com='plug kaolite'
 cylinder  17 1   18.249900    8.17880   0.34036 com='sides of plug case'
 cylinder  15 1   18.605500    8.17880   0.0     com='void: plug to liner'
 cylinder  16 1   18.757900    8.17880   0.0     com='liner wall'
 cylinder  12 1   23.177500    8.17880   0.0     com='kaolite'
 cylinder  19 1   23.329900    8.17880   0.0     com='drum'
 cuboid    21 1 4p24.587200    8.17880   0.0     com='drum chine outer radius'
unit 1017
'bottom of angle iron to bend in angle iron [Elev=42.500 in.]'
 cylinder  13 1   18.097500    4.44500   0.0     com='plug kaolite'
 cylinder  17 1   18.249900    4.44500   0.0     com='sides of plug case'
 cylinder  15 1   18.605500    4.44500   0.0     com='void: plug to liner'
 cylinder  16 1   18.757900    4.44500   0.0     com='liner wall'
 cylinder  18 1   19.392900    4.44500   0.0     com='lower angle iron'
 cylinder  12 1   23.177500    4.44500   0.0     com='kaolite'
 cylinder  19 1   23.329900    4.44500   0.0     com='drum'
 cuboid    21 1 4p24.587200    4.44500   0.0     com='drum chine outer radius'
unit 1018
'bend in angle iron to top of angle iron [Elev=42.750 in.]'
 cylinder  13 1   18.097500    0.11176   0.0     com='plug kaolite'
 cylinder  17 1   18.249900    0.26416   0.0     com='sides of plug case'
 cylinder  15 1   18.605500    0.63500   0.0     com='void: plug to liner'
 cylinder  16 1   18.757900    0.63500   0.0     com='liner wall'
 cylinder  18 1   23.177500    0.63500   0.0     com='bend section of ai'
 cylinder  19 1   23.329900    0.63500   0.0     com='drum'
 cuboid    21 1 4p24.587200    0.63500   0.0     com='drum chine outer radius'
unit 1019
'drum lid and lip [Elev=43.500 in.]'
 cylinder  21 1   22.961600    1.90500   0.15240 com='void above lid'
 cylinder  19 1   23.114000    1.90500   0.0     com='drum lid'
 cylinder  21 1   23.177500    1.90500   0.0     com='void btw lid - drum wall'
 cylinder  19 1   23.329900    1.90500   0.0     com='drum'
 cuboid    21 1 4p24.587200    1.90500   0.0     com='drum chine outer radius'
global
unit 1020
'es3100 drum [Elev=43.500 in.]'
array 3         2r-24.587200     0.0
'cuboid     0  1 4p24.587200    110.4905  0.0    com='bare package'
 cuboid    21  1 4p55.067200   140.9700 -30.48   com='reflected package'
'cuboid    20  1 4p22.889718    110.5048  0.0    com='interstital array space'
'global
'unit 1021
'array 4   3r0.0
'reflector  21 2  6r3.0  10
end geometry
read array
ara=3 nux=1 nuy=1 nuz=19 fill
1001 1002 1003 1006 1007 1006 1007 1006 1008 1010
1011 1012 1013 1014 1015 1016 1017 1018 1019        end fill
'ara=4 nux=13 nuy=13 nuz=06 fill f1020               end fill
end array
```

```
'read bias id=500 2  11  end bias
read start nst=0
end start
end data
end


=csas25    parm=size=3000000
ncsrt55d2 0.0in thk np,10400.0gUZrHx(  921.0g235, 8998.2gH2O hx=255.01),fr=1.0e+00
238groupndf5 infhommedium
'TRIGA volume =1200.95996, SPACER volume    0.00000'
'TRIGA wrapped dry content can hx=18.2, CV void volume 9014.40198'
arbmtriga  8.65974  4 0 0 0    1001    0.9554
                              40000   54.0446
                              92235    8.8558
                              92238   36.1442    1   0.11756  293  end
arbmwicv 9.9820e-01  2 0 0 0   1001   11.1913
                               8016   88.8087    1   0.88244  293  end
'np277-4: spacer (NCT_MD&H)'
'NCT min.den.(95.3886 lb/ft3) and hydrogen'
'np277-4 min.den.= 1.527971 = (95.3886 lb/ft3)(453.59 g/lb)/(28316.84 cm3/ft3)'
'use 75% of boron in calculations per NUREG-1609 Section 6.5.3.2'
arbmboron 7.31015e-2  2 0 0 0    5010   18.1479
                                 5011   81.8520    2  0.7500  293  end
arbmnpmx  1.07070e+0 10 0 0 0    6012    1.9189
                                 7014    0.0141
                                 8016   43.4251
                                11023    0.1174
                                12000    0.3378
                                13027   39.0479
                                14000    2.4672
                                16000    0.3083
                                20000   11.8336
                                26000    0.5298    2  1.0000  293  end
arbmnph2o 3.84169e-1  2 0 0 0    1001   11.1913
                                 8016   88.8087    2  1.0000  293  end
'flooded containmment vessel and content cans -- 10 CFR 71.55(d)(3)'
arbmwicv   0.9982   2 0 0 0    1001   11.1913
                               8016   88.8087    3  1       293  end
'steel: containment vessel body 16.60 lb but use 15.74 lb'
ss304                                            8  1.0     293  end
'steel: cv flange lower use 3.36 lb'
ss304                                            9  0.97267 293  end
'steel: cv flange upper use 13.75 lb'
ss304                                           10  0.94348 293  end
'np277-4: confinement -- neutron poison inner liner (NCT_MD&H)'
'actual vol.= 1.28314e4 cm3 = (7.83023e2 in3)(16.387064)'
'den.multiplier = 1.28314e4 cm3 (actual vol.) / 1.32708e4 cm3 (model vol.)'
'np277-4 min.den.= 1.527971 = (95.3886 lb/ft3)(453.59 g/lb)/(28316.84 cm3/ft3)'
'density = 1.477385 = (den.mult)(np277-4 min.den.) = 0.9668933*1.527971'
'use 75% of boron in calculations per NUREG-1609 Section 6.5.3.2'
arbmboron 7.06813e-2  2 0 0 0    5010   18.1479
                                 5011   81.8520   11  0.7500  293  end
arbmnpmx  1.03525e+0 10 0 0 0    6012    1.9189
                                 7014    0.0141
                                 8016   43.4251
                                11023    0.1174
                                12000    0.3378
                                13027   39.0479
                                14000    2.4672
                                16000    0.3083
                                20000   11.8336
                                26000    0.5298   11  1.0000  293  end
arbmnph2o 3.71451e-1  2 0 0 0    1001   11.1913
                                 8016   88.8087   11  1.0000  293  end
'kaolite 1600 body'
'sing.unit.density= (den.mult)(min.den.)'
' for arbmh20k = 1.012373*0.51655,  for rest = 1.012373*0.34438'
'den.mult= 1.36557e5 cm3 (actual vol.) / 1.34888e5 cm3 (model vol.)'
'actual vol.= 1.36557e5 cm3 = (28316.84 cm3/ft3)(108.33188 lb)/(22.464 lb/ft3)'
arbmh2ok   0.52294  2 0 0 0    1001   11.1913
```

```
                                8016   88.8087   12  1       293  end
arbmal2o3  0.34864  2 0 0 0   13027   52.9390
                                8016   47.0610   12  0.096   293  end
arbmsio2   0.34864  2 0 0 0   14000   46.7570
                                8016   53.2430   12  0.367   293  end
arbmfe2o3  0.34864  2 0 0 0   26000   69.9540
                                8016   30.0460   12  0.067   293  end
arbmtio2   0.34864  2 0 0 0   22000   59.9535
                                8016   40.0465   12  0.012   293  end
arbmcao    0.34864  2 0 0 0   20000   71.4815
                                8016   28.5185   12  0.307   293  end
arbmmgo    0.34864  2 0 0 0   12000   60.3169
                                8016   39.6831   12  0.131   293  end
arbmna2o   0.34864  2 0 0 0   11023   74.1961
                                8016   25.8039   12  0.020   293  end
'kaolite 1600 top plug'
'sing.unit.density= (den.mult)(min.den.)'
' for arbmh20k = 0.965246*0.51655,  for rest = 0.965246*0.34438'
'den.mult= 1.21592e4 cm3 (actual vol.) / 1.25970e4 cm3 (model vol.)'
'actual vol.= 1.21592e4 cm3 = (28316.84 cm3/ft3)(9.646 lb)/(22.464 lb/ft3)'
arbmh2ok   0.49860  2 0 0 0    1001   11.1913
                                8016   88.8087   13  1       293  end
arbmal2o3  0.33241  2 0 0 0   13027   52.9390
                                8016   47.0610   13  0.096   293  end
arbmsio2   0.33241  2 0 0 0   14000   46.7570
                                8016   53.2430   13  0.367   293  end
arbmfe2o3  0.33241  2 0 0 0   26000   69.9540
                                8016   30.0460   13  0.067   293  end
arbmtio2   0.33241  2 0 0 0   22000   59.9535
                                8016   40.0465   13  0.012   293  end
arbmcao    0.33241  2 0 0 0   20000   71.4815
                                8016   28.5185   13  0.307   293  end
arbmmgo    0.33241  2 0 0 0   12000   60.3169
                                8016   39.6831   13  0.131   293  end
arbmna2o   0.33241  2 0 0 0   11023   74.1961
                                8016   25.8039   13  0.020   293  end
'silicone rubber pads'
arbmsiru   1.21791  4 0 0 0    6012   32.3767
                                1001    8.1573
                                8016   21.5782
                               14000   37.8878   14  1.0     293  end
'void space external to containment vessel'
arbmwecv   0.9982   2 0 0 0    1001   11.1913
                                8016   88.8087   15  1       293  end
'steel: liner'
ss304                                           16  1.0     293  end
'steel: plug cover (pc) use 9.907 lb'
ss304                                           17  1.06388 293  end
'steel: angle iron (ai) for single units'
ss304                                           18  1.0     293  end
'steel: angle iron (ai) for arrays'
'array density is multiplied by a volume fraction 7.08030/5.63249'
'ss304                                           18  1.25705 293  end
'steel: drum steel for single units'
ss304                                           19  1.0     293  end
'steel: drum steel for arrays'
'array density is multiplied by a volume fraction 3.20482/3.20544'
'ss304                                           19  0.99981 293  end
'void space external to drum'
'array density is multiplied by a volume ratio 8.11698/6.98323'
'arbmwed    1.16026  2 0 0 0    1001   11.1913
'                                8016   88.8087   20  1       293  end
'reflective water'
arbmh20r   0.9982   2 0 0 0    1001   11.1913
                                8016   88.8087   21  1.0     293  end
end comp
ncsrt55d2 0.0in thk np,10400.0gUZrHx(  921.0g235, 8998.2gH2O,hx=255.01),fr=1.0e+00
read parameters nub=yes npg=2500 gen=215 nsk=15 tme=100 end parameters
read boun       all=vac                         end boun
read geometry
unit 1001
```

```
'drum bottom flat cover [Elev= 0.105 in. at top of unit]'
'cylinder  19 1   24.587200    0.26670   0.0     com='extended radius not used'
 cylinder  19 1   23.329900    0.26670   0.0     com='drum bottom flat cover'
 cuboid    21 1 4p24.587200    0.26670   0.0     com='drum chine outer radius'
unit 1002
'above drum bottom flat cover and below containment vessel [Elev= 4.670 in.]'
 cylinder  15 1    3.175000   11.59510  11.16330 com='void in pad-1'
 cylinder  14 1    7.924800   11.59510  11.16330 com='pad-1'
 cylinder  16 1    8.077200   11.59510  11.16330 com='np277_4 liner'
 cylinder  11 1   10.922000   11.59510  11.16330 com='np277_4'
 cylinder  16 1   11.074400   11.59510  10.85850 com='kaolite liner bottom'
 cylinder  12 1   23.177500   11.59510   0.0     com='kaolite'
 cylinder  19 1   23.329900   11.59510   0.0     com='drum'
 cuboid    21 1 4p24.587200   11.59510   0.0     com='drum chine outer radius'
unit 1003
'cv bottom [Elev= 4.920 in.]'
 cylinder  8  1    6.680200    0.63500   0.0     com='cv bottom'
 cylinder  15 1    7.924800    0.63500   0.0     com='void btw cv-np liner'
 cylinder  16 1    8.077200    0.63500   0.0     com='np277_4 liner'
 cylinder  11 1   10.922000    0.63500   0.0     com='np277_4'
 cylinder  16 1   11.074400    0.63500   0.0     com='kaolite liner'
 cylinder  12 1   23.177500    0.63500   0.0     com='kaolite'
 cylinder  19 1   23.329900    0.63500   0.0     com='drum'
 cuboid    21 1 4p24.587200    0.63500   0.0     com='drum chine outer radius'
unit 1006
'content (collapsed) [Elev= 9.920 in.]'
 cylinder  1  1    6.426200   12.70050  -0.0005  com='cv well cavity'
 cylinder  8  1    6.680200   12.70050  -0.0005  com='cv below 1st step'
 cylinder  15 1    7.924800   12.70050  -0.0005  com='void btw cv-np liner'
 cylinder  16 1    8.077200   12.70050  -0.0005  com='np277_4 liner'
 cylinder  11 1   10.922000   12.70050  -0.0005  com='np277_4'
 cylinder  16 1   11.074400   12.70050  -0.0005  com='kaolite liner'
 cylinder  12 1   23.177500   12.70050  -0.0005  com='kaolite'
 cylinder  19 1   23.329900   12.70050  -0.0005  com='drum'
 cuboid    21 1 4p24.587200   12.70050  -0.0005  com='drum chine outer radius'
unit 1007
'np277_4 spacer [Elev= 9.921 in.]'
 cylinder  2  1    5.24510     0.00010   0.0     com='np spacer'
 cylinder  1  1    6.426200    0.00020  -0.0001  com='cv well cavity'
 cylinder  8  1    6.680200    0.00020  -0.0001  com='cv below 1st step'
 cylinder  15 1    7.924800    0.00020  -0.0001  com='void btw cv-np liner'
 cylinder  16 1    8.077200    0.00020  -0.0001  com='np277_4 liner'
 cylinder  11 1   10.922000    0.00020  -0.0001  com='np277_4'
 cylinder  16 1   11.074400    0.00020  -0.0001  com='kaolite liner'
 cylinder  12 1   23.177500    0.00020  -0.0001  com='kaolite'
 cylinder  19 1   23.329900    0.00020  -0.0001  com='drum'
 cuboid    21 1 4p24.587200    0.00020  -0.0001  com='drum chine outer radius'
unit 1008
'top of content stack to bottom of 1st step [Elev=35.270 in.]'
'38.10360             stack height (content spacers)       CALCULATED
 cylinder  1  1    6.426200   38.98540   0.0     com='cv well cavity'
 cylinder  8  1    6.680200   38.98540   0.0     com='cv below 1st step'
 cylinder  15 1    7.924800   38.98540   0.0     com='void btw cv-np liner'
 cylinder  16 1    8.077200   38.98540   0.0     com='np277_4 liner'
 cylinder  11 1   10.922000   38.98540   0.0     com='np277_4'
 cylinder  16 1   11.074400   38.98540   0.0     com='kaolite liner'
 cylinder  12 1   23.177500   38.98540   0.0     com='kaolite'
 cylinder  19 1   23.329900   38.98540   0.0     com='drum'
 cuboid    21 1 4p24.587200   38.98540   0.0     com='drum chine outer radius'
unit 1010
'cv at 1st step in liner [Elev=35.330 in.]'
 cylinder  1  1    6.426200    0.15240   0.0     com='cv well cavity'
 cylinder  8  1    6.680200    0.15240   0.0     com='cv at 1st step'
 cylinder  15 1    7.924800    0.15240   0.0     com='void btw cv and liner'
 cylinder  16 1   11.074400    0.15240   0.0     com='liner 1st step'
 cylinder  12 1   23.177500    0.15240   0.0     com='kaolite'
 cylinder  19 1   23.329900    0.15240   0.0     com='drum'
 cuboid    21 1 4p24.587200    0.15240   0.0     com='drum chine outer radius'
unit 1011
'vertical gap between 1st step in liner and cv flange [Elev=35.420 in.]'
 cylinder  1  1    6.426200    0.22860   0.0     com='cv well cavity'
```

```
 cylinder  8  1    6.680200    0.22860   0.0     com='cv at gap btwn step-flng'
 cylinder  15 1   10.922000    0.22860   0.0     com='void btw cv and liner'
 cylinder  16 1   11.074400    0.22860   0.0     com='liner wall'
 cylinder  12 1   23.177500    0.22860   0.0     com='kaolite'
 cylinder  19 1   23.329900    0.22860   0.0     com='drum'
 cuboid    21 1 4p24.587200    0.22860   0.0     com='drum chine outer radius'
unit 1012
'cv flange to top of cv well [Elev=35.920 in.]'
 cylinder  1  1    6.426200    1.27000   0.0     com='cavity'
 cylinder  9  1    9.525000    1.27000   0.0     com='flange to top of well'
 cylinder  15 1    9.525000    1.27000   0.0     com='void btw cv and pad-2'
 cylinder  14 1   10.033000    1.27000   0.0     com='pad-2'
 cylinder  15 1   10.922000    1.27000   0.0     com='void btw cv and liner'
 cylinder  16 1   11.074400    1.27000   0.0     com='liner wall'
 cylinder  12 1   23.177500    1.27000   0.0     com='kaolite'
 cylinder  19 1   23.329900    1.27000   0.0     com='drum'
 cuboid    21 1 4p24.587200    1.27000   0.0     com='drum chine outer radius'
unit 1013
'cv flange above cv well [Elev=37.070 in.]'
 cylinder  10 1    9.525000    2.92100   0.0     com='flange above cv well'
 cylinder  15 1    9.525000    2.92100   0.0     com='void btw cv and pad-2'
 cylinder  14 1   10.033000    2.92100   0.0     com='pad-2'
 cylinder  15 1   10.922000    2.92100   0.0     com='void btw pad2 and liner'
 cylinder  16 1   11.074400    2.92100   0.0     com='liner wall'
 cylinder  12 1   23.177500    2.92100   0.0     com='kaolite'
 cylinder  19 1   23.329900    2.92100   0.0     com='drum'
 cuboid    21 1 4p24.587200    2.92100   0.0     com='drum chine outer radius'
unit 1014
'plugpad2 below liner 2nd step [Elev=37.470 in.]'
 cylinder  14 1   10.033000    0.76200   0.0     com='pad-2'
 cylinder  15 1   10.922000    1.01600   0.0     com='void btw pad2 and liner'
 cylinder  16 1   11.074400    1.01600   0.0     com='liner wall'
 cylinder  12 1   23.177500    1.01600   0.0     com='kaolite'
 cylinder  19 1   23.329900    1.01600   0.0     com='drum'
 cuboid    21 1 4p24.587200    1.01600   0.0     com='drum chine outer radius'
unit 1015
'2nd step in liner [Elev=37.530 in.]'
 cylinder  15 1   10.922000    0.15240   0.0     com='void abv pad2'
 cylinder  16 1   18.757900    0.15240   0.0     com='liner 2nd step'
 cylinder  12 1   23.177500    0.15240   0.0     com='kaolite'
 cylinder  19 1   23.329900    0.15240   0.0     com='drum'
 cuboid    21 1 4p24.587200    0.15240   0.0     com='drum chine outer radius'
unit 1016
'abv 2nd step in liner to bottom of angle iron [Elev=40.750 in.]'
 cylinder  13 1   18.097500    8.17880   0.49276 com='plug kaolite'
 cylinder  17 1   18.249900    8.17880   0.34036 com='sides of plug case'
 cylinder  15 1   18.605500    8.17880   0.0     com='void: plug to liner'
 cylinder  16 1   18.757900    8.17880   0.0     com='liner wall'
 cylinder  12 1   23.177500    8.17880   0.0     com='kaolite'
 cylinder  19 1   23.329900    8.17880   0.0     com='drum'
 cuboid    21 1 4p24.587200    8.17880   0.0     com='drum chine outer radius'
unit 1017
'bottom of angle iron to bend in angle iron [Elev=42.500 in.]'
 cylinder  13 1   18.097500    4.44500   0.0     com='plug kaolite'
 cylinder  17 1   18.249900    4.44500   0.0     com='sides of plug case'
 cylinder  15 1   18.605500    4.44500   0.0     com='void: plug to liner'
 cylinder  16 1   18.757900    4.44500   0.0     com='liner wall'
 cylinder  18 1   19.392900    4.44500   0.0     com='lower angle iron'
 cylinder  12 1   23.177500    4.44500   0.0     com='kaolite'
 cylinder  19 1   23.329900    4.44500   0.0     com='drum'
 cuboid    21 1 4p24.587200    4.44500   0.0     com='drum chine outer radius'
unit 1018
'bend in angle iron to top of angle iron [Elev=42.750 in.]'
 cylinder  13 1   18.097500    0.11176   0.0     com='plug kaolite'
 cylinder  17 1   18.249900    0.26416   0.0     com='sides of plug case'
 cylinder  15 1   18.605500    0.63500   0.0     com='void: plug to liner'
 cylinder  16 1   18.757900    0.63500   0.0     com='liner wall'
 cylinder  18 1   23.177500    0.63500   0.0     com='bend section of ai'
 cylinder  19 1   23.329900    0.63500   0.0     com='drum'
 cuboid    21 1 4p24.587200    0.63500   0.0     com='drum chine outer radius'
unit 1019
```

```
'drum lid and lip [Elev=43.500 in.]'
 cylinder  21 1   22.961600    1.90500   0.15240 com='void above lid'
 cylinder  19 1   23.114000    1.90500   0.0     com='drum lid'
 cylinder  21 1   23.177500    1.90500   0.0     com='void btw lid - drum wall'
 cylinder  19 1   23.329900    1.90500   0.0     com='drum'
 cuboid    21 1 4p24.587200    1.90500   0.0     com='drum chine outer radius'
global
unit 1020
'es3100 drum [Elev=43.500 in.]'
array 3         2r-24.587200     0.0
'cuboid     0  1 4p24.587200    110.4905  0.0    com='bare package'
 cuboid    21  1 4p55.067200   140.9700 -30.48   com='reflected package'
'cuboid    20  1 4p22.889718    110.5048  0.0    com='interstital array space'
'global
'unit 1021
'array 4   3r0.0
'reflector  21 2  6r3.0  10
end geometry
read array
ara=3 nux=1 nuy=1 nuz=19 fill
1001 1002 1003 1006 1007 1006 1007 1006 1008 1010
1011 1012 1013 1014 1015 1016 1017 1018 1019        end fill
'ara=4 nux=13 nuy=13 nuz=06 fill f1020               end fill
end array
'read bias id=500 2  11  end bias
read start nst=0
end start
end data
end


=csas25    parm=size=3000000
hcsrtriga 0.0in thk np,10400.0gUZrHx(  921.0g235, 8998.2gH2O hx=255.01),fr=1.0e+00
238groupndf5 infhommedium
'TRIGA volume =1200.95996, SPACER volume    0.00000'
'TRIGA wrapped dry content can hx=18.2, CV void volume 9014.40198'
arbmtriga  8.65974  4 0 0 0    1001    0.9554
                              40000   54.0446
                              92235    8.8558
                              92238   36.1442    1  1.0     293  end
'flooded containmment vessel and content cans -- 10 CFR 71.55(d)(3)'
'np277-4: spacer (HAC_MD&H)'
'HAC min.den.(95.3157 lb/ft3) and hydrogen'
'np277-4 min.den.= 1.526803 = (95.3157 lb/ft3)(453.59 g/lb)/(28316.84 cm3/ft3)'
'use 75% of boron in calculations per NUREG-1609 Section 6.5.3.2'
arbmboron 7.31015e-2  2 0 0 0    5010   18.1479
                                 5011   81.8520    2  0.7500  293  end
arbmnpmx  1.07071e+0 10 0 0 0    6012    1.9188
                                 7014    0.0141
                                 8016   43.4254
                                11023    0.1174
                                12000    0.3378
                                13027   39.0477
                                14000    2.4671
                                16000    0.3083
                                20000   11.8335
                                26000    0.5298    2  1.0000  293  end
arbmnph2o 3.82995e-1  2 0 0 0    1001   11.1913
                                 8016   88.8087    2  1.0000  293  end
'flooded containmment vessel and content cans -- 10 CFR 71.55(d)(3)'
arbmwicv   0.9982   2 0 0 0    1001   11.1913
                               8016   88.8087    3  1       293  end
'steel: containment vessel body 16.60 lb but use 15.74 lb'
ss304                                            8  1.0     293  end
'steel: cv flange lower use 3.36 lb'
ss304                                            9  0.97267 293  end
'steel: cv flange upper use 13.75 lb'
ss304                                           10  0.94348 293  end
'np277-4: confinement -- neutron poison inner liner (HAC_MD&H)'
'actual vol.= 1.28314e4 cm3 = (7.83023e2 in3)(16.387064)'
'den.multiplier = 1.28314e4 cm3 (actual vol.) / 1.32708e4 cm3 (model vol.)'
```

```
'np277-4 min.den.= 1.526803 = (95.3157 lb/ft3)(453.59 g/lb)/(28316.84 cm3/ft3)'
'density = 1.476265 = (den.mult)(np277-4 min.den.) = 0.9668933*1.526803'
'use 75% of boron in calculations per NUREG-1609 Section 6.5.3.2'
arbmboron 7.06813e-2  2 0 0 0    5010   18.1479
                                 5011   81.8520   11  0.7500  293  end
arbmnpmx  1.03525e+0 10 0 0 0    6012    1.9188
                                 7014    0.0141
                                 8016   43.4254
                                11023    0.1174
                                12000    0.3378
                                13027   39.0477
                                14000    2.4671
                                16000    0.3083
                                20000   11.8335
                                26000    0.5298   11  1.0000  293  end
arbmnph2o 3.70316e-1  2 0 0 0    1001   11.1913
                                 8016   88.8087   11  1.0000  293  end
'kaolite 1600 body'
'nct.sing.unit.density= (den.mult)(min.den.)'
' for arbmh20k 0.52294 = 1.012373*0.51655, for rest 0.34864 = 1.012373*0.34438'
'den.mult= 1.36557e5 cm3 (actual vol.) / 1.34888e5 cm3 (model vol.)'
'actual vol.= 1.36557e5 cm3 = (28316.84 cm3/ft3)(108.33188 lb)/(22.464 lb/ft3)'
'hac.s.u.dens= (hac.mult)(nct.s.u.dens)'
'hac.mult = 1.34888e5 cm3 (nct vol.)/ 1.12246e5 cm3 (model vol.)'
' for arbmh2ok 0.62843 = 1.20172*0.52294,   for rest = 1.20172*0.34864'
arbmh2ok   0.62843  2 0 0 0    1001   11.1913
                               8016   88.8087   12  1       293  end
arbmal2o3  0.41898  2 0 0 0   13027   52.9390
                               8016   47.0610   12  0.096   293  end
arbmsio2   0.41898  2 0 0 0   14000   46.7570
                               8016   53.2430   12  0.367   293  end
arbmfe2o3  0.41898  2 0 0 0   26000   69.9540
                               8016   30.0460   12  0.067   293  end
arbmtio2   0.41898  2 0 0 0   22000   59.9535
                               8016   40.0465   12  0.012   293  end
arbmcao    0.41898  2 0 0 0   20000   71.4815
                               8016   28.5185   12  0.307   293  end
arbmmgo    0.41898  2 0 0 0   12000   60.3169
                               8016   39.6831   12  0.131   293  end
arbmna2o   0.41898  2 0 0 0   11023   74.1961
                               8016   25.8039   12  0.020   293  end
'kaolite 1600 top plug'
'sing.unit.density= (den.mult)(min.den.)'
' for arbmh20k = 0.965246*0.51655,  for rest = 0.965246*0.34438'
'den.mult= 1.21592e4 cm3 (actual vol.) / 1.25970e4 cm3 (model vol.)'
'actual vol.= 1.21592e4 cm3 = (28316.84 cm3/ft3)(9.646 lb)/(22.464 lb/ft3)'
arbmh2ok   0.49860  2 0 0 0    1001   11.1913
                               8016   88.8087   13  1       293  end
arbmal2o3  0.33241  2 0 0 0   13027   52.9390
                               8016   47.0610   13  0.096   293  end
arbmsio2   0.33241  2 0 0 0   14000   46.7570
                               8016   53.2430   13  0.367   293  end
arbmfe2o3  0.33241  2 0 0 0   26000   69.9540
                               8016   30.0460   13  0.067   293  end
arbmtio2   0.33241  2 0 0 0   22000   59.9535
                               8016   40.0465   13  0.012   293  end
arbmcao    0.33241  2 0 0 0   20000   71.4815
                               8016   28.5185   13  0.307   293  end
arbmmgo    0.33241  2 0 0 0   12000   60.3169
                               8016   39.6831   13  0.131   293  end
arbmna2o   0.33241  2 0 0 0   11023   74.1961
                               8016   25.8039   13  0.020   293  end
'silicone rubber pads'
arbmsiru   1.21791  4 0 0 0    6012   32.3767
                               1001    8.1573
                               8016   21.5782
                              14000   37.8878   14  1.0     293  end
'void space external to containment vessel'
arbmwecv   0.9982   2 0 0 0    1001   11.1913
                               8016   88.8087   15  1       293  end
'steel: liner'
```

```
ss304                                          16  1.0     293  end
'steel: plug cover (pc) use 9.907 lb'
ss304                                          17  1.06388 293  end
'steel: angle iron (ai) for HAC'
'nct density is multiplied by volume fraction 7.08030/5.74516'
ss304                                          18  1.23239 293  end
'steel: drum steel for HAC'
'nct density is multiplied by volume fraction 3.20482/2.95645'
ss304                                          19  1.08401 293  end
'void space external to drum'
'array density is assumed not reduced by hac'
'arbmwed    0.9982   2 0 0 0    1001   11.1913
'                               8016   88.8087   20  1       293  end
'reflective water'
arbmh20r   0.9982   2 0 0 0    1001   11.1913
                                8016   88.8087   21  1.0     293  end
end comp
hcsrtriga 0.0in thk np,10400.0gU(  921.0g235, 8998.2gH2O,hx=255.01),fr=1.0e+00
read parameters nub=yes npg=2500 gen=215 nsk=15 tme=100 end parameters
read boun       all=vac                        end boun
read geometry
unit 1001
'drum bottom flat cover [Elev= 0.105 in. at top of unit]'
'cylinder  19 1   21.838092    0.26670   0.0     com='extended radius not used'
 cylinder  19 1   21.838092    0.26670   0.0     com='drum bottom flat cover'
 cuboid    21 1 4p21.838092    0.26670   0.0     com='drum(chine)outer radius'
unit 1002
'above drum bottom flat cover and below containment vessel [Elev= 4.670 in.]'
 cylinder  15 1    3.175000   11.59510  11.16330 com='void in pad-1'
 cylinder  14 1    7.924800   11.59510  11.16330 com='pad-1'
 cylinder  16 1    8.077200   11.59510  11.16330 com='np277_4 liner'
 cylinder  11 1   10.922000   11.59510  11.16330 com='np277_4'
 cylinder  16 1   11.074400   11.59510  10.85850 com='kaolite liner bottom'
 cylinder  12 1   21.685692   11.59510   0.0     com='kaolite'
 cylinder  19 1   21.838092   11.59510   0.0     com='drum'
 cuboid    21 1 4p21.838092   11.59510   0.0     com='drum(chine)outer radius'
unit 1003
'cv bottom [Elev= 4.920 in.]'
 cylinder  8  1    6.680200    0.63500   0.0     com='cv bottom'
 cylinder  15 1    7.924800    0.63500   0.0     com='void btw cv-np liner'
 cylinder  16 1    8.077200    0.63500   0.0     com='np277_4 liner'
 cylinder  11 1   10.922000    0.63500   0.0     com='np277_4'
 cylinder  16 1   11.074400    0.63500   0.0     com='kaolite liner'
 cylinder  12 1   21.685692    0.63500   0.0     com='kaolite'
 cylinder  19 1   21.838092    0.63500   0.0     com='drum'
 cuboid    21 1 4p21.838092    0.63500   0.0     com='drum(chine)outer radius'
unit 1004
'UZrHx fuel element'
 cylinder  1  1    1.828800   12.70000   0.0     com='cylindrical content'
unit 1006
'content (collapsed) [Elev= 9.920 in.]'
'1.437900   plus-y location upper cylinders'
'-2.875700  minus-y location lower cylinder'
'2.490443   plus-x location upper cylinder'
'-2.490443  minus-x location upper cylinder'
 cylinder  3  1    6.426200   12.70050  -0.0005  com='cv well cavity'
 hole  1004   -2.490443  1.437900  0.0     com='cyl1'
 hole  1004    2.490443  1.437900  0.0     com='cyl2'
 hole  1004    0.0      -2.875700  0.0     com='cyl3'
 cylinder  8  1    6.680200   12.70050  -0.0005  com='cv below 1st step'
 cylinder  15 1    7.924800   12.70050  -0.0005  com='void btw cv-np liner'
 cylinder  16 1    8.077200   12.70050  -0.0005  com='np277_4 liner'
 cylinder  11 1   10.922000   12.70050  -0.0005  com='np277_4'
 cylinder  16 1   11.074400   12.70050  -0.0005  com='kaolite liner'
 cylinder  12 1   21.685692   12.70050  -0.0005  com='kaolite'
 cylinder  19 1   21.838092   12.70050  -0.0005  com='drum'
 cuboid    21 1 4p21.838092   12.70050  -0.0005  com='drum chine outer radius'
unit 1007
'np277_4 spacer [Elev= 9.921 in.]'
 cylinder  2  1    5.24510     0.00010   0.0     com='np spacer'
 cylinder  3  1    6.426200    0.00020  -0.0001  com='cv well cavity'
```

```
 cylinder  8  1    6.680200    0.00020  -0.0001  com='cv below 1st step'
 cylinder  15 1    7.924800    0.00020  -0.0001  com='void btw cv-np liner'
 cylinder  16 1    8.077200    0.00020  -0.0001  com='np277_4 liner'
 cylinder  11 1   10.922000    0.00020  -0.0001  com='np277_4'
 cylinder  16 1   11.074400    0.00020  -0.0001  com='kaolite liner'
 cylinder  12 1   21.685692    0.00020  -0.0001  com='kaolite'
 cylinder  19 1   21.838092    0.00020  -0.0001  com='drum'
 cuboid    21 1 4p21.838092    0.00020  -0.0001  com='drum(chine)outer radius'
unit 1008
'top of content stack to bottom of 1st step [Elev=35.270 in.]'
'38.10360             stack height (content spacers)       CALCULATED
 cylinder  3  1    6.426200   38.98540   0.0     com='cv well cavity'
 cylinder  8  1    6.680200   38.98540   0.0     com='cv below 1st step'
 cylinder  15 1    7.924800   38.98540   0.0     com='void btw cv-np liner'
 cylinder  16 1    8.077200   38.98540   0.0     com='np277_4 liner'
 cylinder  11 1   10.922000   38.98540   0.0     com='np277_4'
 cylinder  16 1   11.074400   38.98540   0.0     com='kaolite liner'
 cylinder  12 1   21.685692   38.98540   0.0     com='kaolite'
 cylinder  19 1   21.838092   38.98540   0.0     com='drum'
 cuboid    21 1 4p21.838092   38.98540   0.0     com='drum(chine)outer radius'
unit 1010
'cv at 1st step in liner [Elev=35.330 in.]'
 cylinder  3  1    6.426200    0.15240   0.0     com='cv well cavity'
 cylinder  8  1    6.680200    0.15240   0.0     com='cv at 1st step'
 cylinder  15 1    7.924800    0.15240   0.0     com='void btw cv and liner'
 cylinder  16 1   11.074400    0.15240   0.0     com='liner 1st step'
 cylinder  12 1   21.685692    0.15240   0.0     com='kaolite'
 cylinder  19 1   21.838092    0.15240   0.0     com='drum'
 cuboid    21 1 4p21.838092    0.15240   0.0     com='drum(chine)outer radius'
unit 1011
'vertical gap between 1st step in liner and cv flange [Elev=35.420 in.]'
 cylinder  3  1    6.426200    0.22860   0.0     com='cv well cavity'
 cylinder  8  1    6.680200    0.22860   0.0     com='cv at gap btwn step-flng'
 cylinder  15 1   10.922000    0.22860   0.0     com='void btw cv and liner'
 cylinder  16 1   11.074400    0.22860   0.0     com='liner wall'
 cylinder  12 1   21.685692    0.22860   0.0     com='kaolite'
 cylinder  19 1   21.838092    0.22860   0.0     com='drum'
 cuboid    21 1 4p21.838092    0.22860   0.0     com='drum(chine)outer radius'
unit 1012
'cv flange to top of cv well [Elev=35.920 in.]'
 cylinder  3  1    6.426200    1.27000   0.0     com='cavity'
 cylinder  9  1    9.525000    1.27000   0.0     com='flange to top of well'
 cylinder  15 1    9.525000    1.27000   0.0     com='void btw cv and pad-2'
 cylinder  14 1   10.033000    1.27000   0.0     com='pad-2'
 cylinder  15 1   10.922000    1.27000   0.0     com='void btw cv and liner'
 cylinder  16 1   11.074400    1.27000   0.0     com='liner wall'
 cylinder  12 1   21.685692    1.27000   0.0     com='kaolite'
 cylinder  19 1   21.838092    1.27000   0.0     com='drum'
 cuboid    21 1 4p21.838092    1.27000   0.0     com='drum(chine)outer radius'
unit 1013
'cv flange above cv well [Elev=37.070 in.]'
 cylinder  10 1    9.525000    2.92100   0.0     com='flange above cv well'
 cylinder  15 1    9.525000    2.92100   0.0     com='void btw cv and pad-2'
 cylinder  14 1   10.033000    2.92100   0.0     com='pad-2'
 cylinder  15 1   10.922000    2.92100   0.0     com='void btw pad2 and liner'
 cylinder  16 1   11.074400    2.92100   0.0     com='liner wall'
 cylinder  12 1   21.685692    2.92100   0.0     com='kaolite'
 cylinder  19 1   21.838092    2.92100   0.0     com='drum'
 cuboid    21 1 4p21.838092    2.92100   0.0     com='drum(chine)outer radius'
unit 1014
'plugpad2 below liner 2nd step [Elev=37.470 in.]'
 cylinder  14 1   10.033000    0.76200   0.0     com='pad-2'
 cylinder  15 1   10.922000    1.01600   0.0     com='void btw pad2 and liner'
 cylinder  16 1   11.074400    1.01600   0.0     com='liner wall'
 cylinder  12 1   21.685692    1.01600   0.0     com='kaolite'
 cylinder  19 1   21.838092    1.01600   0.0     com='drum'
 cuboid    21 1 4p21.838092    1.01600   0.0     com='drum(chine)outer radius'
unit 1015
'2nd step in liner [Elev=37.530 in.]'
 cylinder  15 1   10.922000    0.15240   0.0     com='void abv pad2'
 cylinder  16 1   18.757900    0.15240   0.0     com='liner 2nd step'
```

```
 cylinder  12 1   21.685692    0.15240   0.0     com='kaolite'
 cylinder  19 1   21.838092    0.15240   0.0     com='drum'
 cuboid    21 1 4p21.838092    0.15240   0.0     com='drum(chine)outer radius'
unit 1016
'abv 2nd step in liner to bottom of angle iron [Elev=40.750 in.]'
 cylinder  13 1   18.097500    8.17880   0.49276 com='plug kaolite'
 cylinder  17 1   18.249900    8.17880   0.34036 com='sides of plug case'
 cylinder  15 1   18.605500    8.17880   0.0     com='void: plug to liner'
 cylinder  16 1   18.757900    8.17880   0.0     com='liner wall'
 cylinder  12 1   21.685692    8.17880   0.0     com='kaolite'
 cylinder  19 1   21.838092    8.17880   0.0     com='drum'
 cuboid    21 1 4p21.838092    8.17880   0.0     com='drum(chine)outer radius'
unit 1017
'bottom of angle iron to bend in angle iron [Elev=42.500 in.]'
 cylinder  13 1   18.097500    4.44500   0.0     com='plug kaolite'
 cylinder  17 1   18.249900    4.44500   0.0     com='sides of plug case'
 cylinder  15 1   18.605500    4.44500   0.0     com='void: plug to liner'
 cylinder  16 1   18.757900    4.44500   0.0     com='liner wall'
 cylinder  18 1   19.392900    4.44500   0.0     com='lower angle iron'
 cylinder  12 1   21.685692    4.44500   0.0     com='kaolite'
 cylinder  19 1   21.838092    4.44500   0.0     com='drum'
 cuboid    21 1 4p21.838092    4.44500   0.0     com='drum(chine)outer radius'
unit 1018
'bend in angle iron to top of angle iron [Elev=42.750 in.]'
 cylinder  13 1   18.097500    0.11176   0.0     com='plug kaolite'
 cylinder  17 1   18.249900    0.26416   0.0     com='sides of plug case'
 cylinder  15 1   18.605500    0.63500   0.0     com='void: plug to liner'
 cylinder  16 1   18.757900    0.63500   0.0     com='liner wall'
 cylinder  18 1   21.685692    0.63500   0.0     com='bend section of ai'
 cylinder  19 1   21.838092    0.63500   0.0     com='drum'
 cuboid    21 1 4p21.838092    0.63500   0.0     com='drum(chine)outer radius'
unit 1019
'drum lid and lip [Elev=43.500 in.]'
 cylinder  21 1   21.469792    1.90500   0.15240 com='void above lid'
 cylinder  19 1   21.622192    1.90500   0.0     com='drum lid'
 cylinder  21 1   21.685692    1.90500   0.0     com='void btw lid - drum wall'
 cylinder  19 1   21.838092    1.90500   0.0     com='drum'
 cuboid    21 1 4p21.838092    1.90500   0.0     com='drum(chine)outer radius'
global
unit 1020
'es3100 drum [Elev=43.500 in.]'
array 3         2r-21.838092     0.0
'cuboid     0  1 4p21.838092    110.4905  0.0    com='bare package'
 cuboid    21  1 4p52.318092   140.9700 -30.48   com='reflected package'
'cuboid    20  1 4p22.889718    110.5048  0.0    com='interstital array space'
'global
'unit 1021
'array 4   3r0.0
'reflector  21 2  6r3.0  10
end geometry
read array
ara=3 nux=1 nuy=1 nuz=19 fill
1001 1002 1003 1006 1007 1006 1007 1006 1008 1010
1011 1012 1013 1014 1015 1016 1017 1018 1019        end fill
'ara=4 nux=13 nuy=13 nuz=06 fill f1020               end fill
end array
'read bias id=500 2  11  end bias
read start nst=0
end start
end data
end


=csas25    parm=size=3000000
hcsrtriag_70 0.0in thk np, 6847.1gUZrHx(  408.0g235, 8998.2gH2O hx=575.64),fr=1.0e+00
238groupndf5 infhommedium
'TRIGA volume =1200.95996, SPACER volume    0.00000'
'TRIGA wrapped dry content can hx=41.1, CV void volume 9014.40198'
arbmtriga  5.70132  4 0 0 0    1001    1.5894
                              40000   89.9107
                              92235    5.9587
```

```
                              92238    2.5412    1  1.0     293  end
'flooded containmment vessel and content cans -- 10 CFR 71.55(d)(3)'
'np277-4: spacer (HAC_MD&H)'
'HAC min.den.(95.3157 lb/ft3) and hydrogen'
'np277-4 min.den.= 1.526803 = (95.3157 lb/ft3)(453.59 g/lb)/(28316.84 cm3/ft3)'
'use 75% of boron in calculations per NUREG-1609 Section 6.5.3.2'
arbmboron 7.31015e-2  2 0 0 0    5010   18.1479
                                  5011   81.8520    2  0.7500  293  end
arbmnpmx  1.07071e+0 10 0 0 0    6012    1.9188
                                  7014    0.0141
                                  8016   43.4254
                                 11023    0.1174
                                 12000    0.3378
                                 13027   39.0477
                                 14000    2.4671
                                 16000    0.3083
                                 20000   11.8335
                                 26000    0.5298    2  1.0000  293  end
arbmnph2o 3.82995e-1  2 0 0 0    1001   11.1913
                                  8016   88.8087    2  1.0000  293  end
'flooded containmment vessel and content cans -- 10 CFR 71.55(d)(3)'
arbmwicv   0.9982   2 0 0 0    1001   11.1913
                               8016   88.8087    3  1       293  end
'steel: containment vessel body 16.60 lb but use 15.74 lb'
ss304                                            8  1.0     293  end
'steel: cv flange lower use 3.36 lb'
ss304                                            9  0.97267 293  end
'steel: cv flange upper use 13.75 lb'
ss304                                           10  0.94348 293  end
'np277-4: confinement -- neutron poison inner liner (HAC_MD&H)'
'actual vol.= 1.28314e4 cm3 = (7.83023e2 in3)(16.387064)'
'den.multiplier = 1.28314e4 cm3 (actual vol.) / 1.32708e4 cm3 (model vol.)'
'np277-4 min.den.= 1.526803 = (95.3157 lb/ft3)(453.59 g/lb)/(28316.84 cm3/ft3)'
'density = 1.476265 = (den.mult)(np277-4 min.den.) = 0.9668933*1.526803'
'use 75% of boron in calculations per NUREG-1609 Section 6.5.3.2'
arbmboron 7.06813e-2  2 0 0 0    5010   18.1479
                                  5011   81.8520   11  0.7500  293  end
arbmnpmx  1.03525e+0 10 0 0 0    6012    1.9188
                                  7014    0.0141
                                  8016   43.4254
                                 11023    0.1174
                                 12000    0.3378
                                 13027   39.0477
                                 14000    2.4671
                                 16000    0.3083
                                 20000   11.8335
                                 26000    0.5298   11  1.0000  293  end
arbmnph2o 3.70316e-1  2 0 0 0    1001   11.1913
                                  8016   88.8087   11  1.0000  293  end
'kaolite 1600 body'
'nct.sing.unit.density= (den.mult)(min.den.)'
' for arbmh20k 0.52294 = 1.012373*0.51655, for rest 0.34864 = 1.012373*0.34438'
'den.mult= 1.36557e5 cm3 (actual vol.) / 1.34888e5 cm3 (model vol.)'
'actual vol.= 1.36557e5 cm3 = (28316.84 cm3/ft3)(108.33188 lb)/(22.464 lb/ft3)'
'hac.s.u.dens= (hac.mult)(nct.s.u.dens)'
'hac.mult = 1.34888e5 cm3 (nct vol.)/ 1.12246e5 cm3 (model vol.)'
' for arbmh2ok 0.62843 = 1.20172*0.52294,   for rest = 1.20172*0.34864'
arbmh2ok   0.62843  2 0 0 0    1001   11.1913
                               8016   88.8087   12  1       293  end
arbmal2o3  0.41898  2 0 0 0   13027   52.9390
                               8016   47.0610   12  0.096   293  end
arbmsio2   0.41898  2 0 0 0   14000   46.7570
                               8016   53.2430   12  0.367   293  end
arbmfe2o3  0.41898  2 0 0 0   26000   69.9540
                               8016   30.0460   12  0.067   293  end
arbmtio2   0.41898  2 0 0 0   22000   59.9535
                               8016   40.0465   12  0.012   293  end
arbmcao    0.41898  2 0 0 0   20000   71.4815
                               8016   28.5185   12  0.307   293  end
arbmmgo    0.41898  2 0 0 0   12000   60.3169
                               8016   39.6831   12  0.131   293  end
```

```
arbmna2o   0.41898  2 0 0 0   11023   74.1961
                               8016   25.8039   12  0.020   293  end
'kaolite 1600 top plug'
'sing.unit.density= (den.mult)(min.den.)'
' for arbmh20k = 0.965246*0.51655,  for rest = 0.965246*0.34438'
'den.mult= 1.21592e4 cm3 (actual vol.) / 1.25970e4 cm3 (model vol.)'
'actual vol.= 1.21592e4 cm3 = (28316.84 cm3/ft3)(9.646 lb)/(22.464 lb/ft3)'
arbmh2ok   0.49860  2 0 0 0    1001   11.1913
                               8016   88.8087   13  1       293  end
arbmal2o3  0.33241  2 0 0 0   13027   52.9390
                               8016   47.0610   13  0.096   293  end
arbmsio2   0.33241  2 0 0 0   14000   46.7570
                               8016   53.2430   13  0.367   293  end
arbmfe2o3  0.33241  2 0 0 0   26000   69.9540
                               8016   30.0460   13  0.067   293  end
arbmtio2   0.33241  2 0 0 0   22000   59.9535
                               8016   40.0465   13  0.012   293  end
arbmcao    0.33241  2 0 0 0   20000   71.4815
                               8016   28.5185   13  0.307   293  end
arbmmgo    0.33241  2 0 0 0   12000   60.3169
                               8016   39.6831   13  0.131   293  end
arbmna2o   0.33241  2 0 0 0   11023   74.1961
                               8016   25.8039   13  0.020   293  end
'silicone rubber pads'
arbmsiru   1.21791  4 0 0 0    6012   32.3767
                               1001    8.1573
                               8016   21.5782
                              14000   37.8878   14  1.0     293  end
'void space external to containment vessel'
arbmwecv   0.9982   2 0 0 0    1001   11.1913
                               8016   88.8087   15  1       293  end
'steel: liner'
ss304                                            16  1.0     293  end
'steel: plug cover (pc) use 9.907 lb'
ss304                                            17  1.06388 293  end
'steel: angle iron (ai) for HAC'
'nct density is multiplied by volume fraction 7.08030/5.74516'
ss304                                            18  1.23239 293  end
'steel: drum steel for HAC'
'nct density is multiplied by volume fraction 3.20482/2.95645'
ss304                                            19  1.08401 293  end
'void space external to drum'
'array density is assumed not reduced by hac'
'arbmwed    0.9982   2 0 0 0    1001   11.1913
'                               8016   88.8087   20  1       293  end
'reflective water'
arbmh20r   0.9982   2 0 0 0    1001   11.1913
                               8016   88.8087   21  1.0     293  end
end comp
hcsrtriag_70 0.0in thk np, 6847.1gU(  408.0g235, 8998.2gH2O,hx=575.64),fr=1.0e+00
read parameters nub=yes npg=2500 gen=215 nsk=15 tme=100 end parameters
read boun       all=vac                          end boun
read geometry
unit 1001
'drum bottom flat cover [Elev= 0.105 in. at top of unit]'
'cylinder  19 1   21.838092    0.26670   0.0     com='extended radius not used'
 cylinder  19 1   21.838092    0.26670   0.0     com='drum bottom flat cover'
 cuboid    21 1 4p21.838092    0.26670   0.0     com='drum(chine)outer radius'
unit 1002
'above drum bottom flat cover and below containment vessel [Elev= 4.670 in.]'
 cylinder  15 1    3.175000   11.59510  11.16330 com='void in pad-1'
 cylinder  14 1    7.924800   11.59510  11.16330 com='pad-1'
 cylinder  16 1    8.077200   11.59510  11.16330 com='np277_4 liner'
 cylinder  11 1   10.922000   11.59510  11.16330 com='np277_4'
 cylinder  16 1   11.074400   11.59510  10.85850 com='kaolite liner bottom'
 cylinder  12 1   21.685692   11.59510   0.0     com='kaolite'
 cylinder  19 1   21.838092   11.59510   0.0     com='drum'
 cuboid    21 1 4p21.838092   11.59510   0.0     com='drum(chine)outer radius'
unit 1003
'cv bottom [Elev= 4.920 in.]'
 cylinder  8  1    6.680200    0.63500   0.0     com='cv bottom'
```

```
 cylinder  15 1    7.924800    0.63500   0.0     com='void btw cv-np liner'
 cylinder  16 1    8.077200    0.63500   0.0     com='np277_4 liner'
 cylinder  11 1   10.922000    0.63500   0.0     com='np277_4'
 cylinder  16 1   11.074400    0.63500   0.0     com='kaolite liner'
 cylinder  12 1   21.685692    0.63500   0.0     com='kaolite'
 cylinder  19 1   21.838092    0.63500   0.0     com='drum'
 cuboid    21 1 4p21.838092    0.63500   0.0     com='drum(chine)outer radius'
unit 1004
'UZrHx fuel element'
 cylinder  1  1    1.828800   12.70000   0.0     com='cylindrical content'
unit 1006
'content (collapsed) [Elev= 9.920 in.]'
'1.437900   plus-y location upper cylinders'
'-2.875700  minus-y location lower cylinder'
'2.490443   plus-x location upper cylinder'
'-2.490443  minus-x location upper cylinder'
 cylinder  3  1    6.426200   12.70050  -0.0005  com='cv well cavity'
 hole  1004   -2.490443  1.437900  0.0     com='cyl1'
 hole  1004    2.490443  1.437900  0.0     com='cyl2'
 hole  1004    0.0      -2.875700  0.0     com='cyl3'
 cylinder  8  1    6.680200   12.70050  -0.0005  com='cv below 1st step'
 cylinder  15 1    7.924800   12.70050  -0.0005  com='void btw cv-np liner'
 cylinder  16 1    8.077200   12.70050  -0.0005  com='np277_4 liner'
 cylinder  11 1   10.922000   12.70050  -0.0005  com='np277_4'
 cylinder  16 1   11.074400   12.70050  -0.0005  com='kaolite liner'
 cylinder  12 1   21.685692   12.70050  -0.0005  com='kaolite'
 cylinder  19 1   21.838092   12.70050  -0.0005  com='drum'
 cuboid    21 1 4p21.838092   12.70050  -0.0005  com='drum chine outer radius'
unit 1007
'np277_4 spacer [Elev= 9.921 in.]'
 cylinder  2  1    5.24510     0.00010   0.0     com='np spacer'
 cylinder  3  1    6.426200    0.00020  -0.0001  com='cv well cavity'
 cylinder  8  1    6.680200    0.00020  -0.0001  com='cv below 1st step'
 cylinder  15 1    7.924800    0.00020  -0.0001  com='void btw cv-np liner'
 cylinder  16 1    8.077200    0.00020  -0.0001  com='np277_4 liner'
 cylinder  11 1   10.922000    0.00020  -0.0001  com='np277_4'
 cylinder  16 1   11.074400    0.00020  -0.0001  com='kaolite liner'
 cylinder  12 1   21.685692    0.00020  -0.0001  com='kaolite'
 cylinder  19 1   21.838092    0.00020  -0.0001  com='drum'
 cuboid    21 1 4p21.838092    0.00020  -0.0001  com='drum(chine)outer radius'
unit 1008
'top of content stack to bottom of 1st step [Elev=35.270 in.]'
'38.10360             stack height (content spacers)       CALCULATED
 cylinder  3  1    6.426200   38.98540   0.0     com='cv well cavity'
 cylinder  8  1    6.680200   38.98540   0.0     com='cv below 1st step'
 cylinder  15 1    7.924800   38.98540   0.0     com='void btw cv-np liner'
 cylinder  16 1    8.077200   38.98540   0.0     com='np277_4 liner'
 cylinder  11 1   10.922000   38.98540   0.0     com='np277_4'
 cylinder  16 1   11.074400   38.98540   0.0     com='kaolite liner'
 cylinder  12 1   21.685692   38.98540   0.0     com='kaolite'
 cylinder  19 1   21.838092   38.98540   0.0     com='drum'
 cuboid    21 1 4p21.838092   38.98540   0.0     com='drum(chine)outer radius'
unit 1010
'cv at 1st step in liner [Elev=35.330 in.]'
 cylinder  3  1    6.426200    0.15240   0.0     com='cv well cavity'
 cylinder  8  1    6.680200    0.15240   0.0     com='cv at 1st step'
 cylinder  15 1    7.924800    0.15240   0.0     com='void btw cv and liner'
 cylinder  16 1   11.074400    0.15240   0.0     com='liner 1st step'
 cylinder  12 1   21.685692    0.15240   0.0     com='kaolite'
 cylinder  19 1   21.838092    0.15240   0.0     com='drum'
 cuboid    21 1 4p21.838092    0.15240   0.0     com='drum(chine)outer radius'
unit 1011
'vertical gap between 1st step in liner and cv flange [Elev=35.420 in.]'
 cylinder  3  1    6.426200    0.22860   0.0     com='cv well cavity'
 cylinder  8  1    6.680200    0.22860   0.0     com='cv at gap btwn step-flng'
 cylinder  15 1   10.922000    0.22860   0.0     com='void btw cv and liner'
 cylinder  16 1   11.074400    0.22860   0.0     com='liner wall'
 cylinder  12 1   21.685692    0.22860   0.0     com='kaolite'
 cylinder  19 1   21.838092    0.22860   0.0     com='drum'
 cuboid    21 1 4p21.838092    0.22860   0.0     com='drum(chine)outer radius'
unit 1012
```

```
'cv flange to top of cv well [Elev=35.920 in.]'
 cylinder  3  1    6.426200    1.27000   0.0     com='cavity'
 cylinder  9  1    9.525000    1.27000   0.0     com='flange to top of well'
 cylinder  15 1    9.525000    1.27000   0.0     com='void btw cv and pad-2'
 cylinder  14 1   10.033000    1.27000   0.0     com='pad-2'
 cylinder  15 1   10.922000    1.27000   0.0     com='void btw cv and liner'
 cylinder  16 1   11.074400    1.27000   0.0     com='liner wall'
 cylinder  12 1   21.685692    1.27000   0.0     com='kaolite'
 cylinder  19 1   21.838092    1.27000   0.0     com='drum'
 cuboid    21 1 4p21.838092    1.27000   0.0     com='drum(chine)outer radius'
unit 1013
'cv flange above cv well [Elev=37.070 in.]'
 cylinder  10 1    9.525000    2.92100   0.0     com='flange above cv well'
 cylinder  15 1    9.525000    2.92100   0.0     com='void btw cv and pad-2'
 cylinder  14 1   10.033000    2.92100   0.0     com='pad-2'
 cylinder  15 1   10.922000    2.92100   0.0     com='void btw pad2 and liner'
 cylinder  16 1   11.074400    2.92100   0.0     com='liner wall'
 cylinder  12 1   21.685692    2.92100   0.0     com='kaolite'
 cylinder  19 1   21.838092    2.92100   0.0     com='drum'
 cuboid    21 1 4p21.838092    2.92100   0.0     com='drum(chine)outer radius'
unit 1014
'plugpad2 below liner 2nd step [Elev=37.470 in.]'
 cylinder  14 1   10.033000    0.76200   0.0     com='pad-2'
 cylinder  15 1   10.922000    1.01600   0.0     com='void btw pad2 and liner'
 cylinder  16 1   11.074400    1.01600   0.0     com='liner wall'
 cylinder  12 1   21.685692    1.01600   0.0     com='kaolite'
 cylinder  19 1   21.838092    1.01600   0.0     com='drum'
 cuboid    21 1 4p21.838092    1.01600   0.0     com='drum(chine)outer radius'
unit 1015
'2nd step in liner [Elev=37.530 in.]'
 cylinder  15 1   10.922000    0.15240   0.0     com='void abv pad2'
 cylinder  16 1   18.757900    0.15240   0.0     com='liner 2nd step'
 cylinder  12 1   21.685692    0.15240   0.0     com='kaolite'
 cylinder  19 1   21.838092    0.15240   0.0     com='drum'
 cuboid    21 1 4p21.838092    0.15240   0.0     com='drum(chine)outer radius'
unit 1016
'abv 2nd step in liner to bottom of angle iron [Elev=40.750 in.]'
 cylinder  13 1   18.097500    8.17880   0.49276 com='plug kaolite'
 cylinder  17 1   18.249900    8.17880   0.34036 com='sides of plug case'
 cylinder  15 1   18.605500    8.17880   0.0     com='void: plug to liner'
 cylinder  16 1   18.757900    8.17880   0.0     com='liner wall'
 cylinder  12 1   21.685692    8.17880   0.0     com='kaolite'
 cylinder  19 1   21.838092    8.17880   0.0     com='drum'
 cuboid    21 1 4p21.838092    8.17880   0.0     com='drum(chine)outer radius'
unit 1017
'bottom of angle iron to bend in angle iron [Elev=42.500 in.]'
 cylinder  13 1   18.097500    4.44500   0.0     com='plug kaolite'
 cylinder  17 1   18.249900    4.44500   0.0     com='sides of plug case'
 cylinder  15 1   18.605500    4.44500   0.0     com='void: plug to liner'
 cylinder  16 1   18.757900    4.44500   0.0     com='liner wall'
 cylinder  18 1   19.392900    4.44500   0.0     com='lower angle iron'
 cylinder  12 1   21.685692    4.44500   0.0     com='kaolite'
 cylinder  19 1   21.838092    4.44500   0.0     com='drum'
 cuboid    21 1 4p21.838092    4.44500   0.0     com='drum(chine)outer radius'
unit 1018
'bend in angle iron to top of angle iron [Elev=42.750 in.]'
 cylinder  13 1   18.097500    0.11176   0.0     com='plug kaolite'
 cylinder  17 1   18.249900    0.26416   0.0     com='sides of plug case'
 cylinder  15 1   18.605500    0.63500   0.0     com='void: plug to liner'
 cylinder  16 1   18.757900    0.63500   0.0     com='liner wall'
 cylinder  18 1   21.685692    0.63500   0.0     com='bend section of ai'
 cylinder  19 1   21.838092    0.63500   0.0     com='drum'
 cuboid    21 1 4p21.838092    0.63500   0.0     com='drum(chine)outer radius'
unit 1019
'drum lid and lip [Elev=43.500 in.]'
 cylinder  21 1   21.469792    1.90500   0.15240 com='void above lid'
 cylinder  19 1   21.622192    1.90500   0.0     com='drum lid'
 cylinder  21 1   21.685692    1.90500   0.0     com='void btw lid - drum wall'
 cylinder  19 1   21.838092    1.90500   0.0     com='drum'
 cuboid    21 1 4p21.838092    1.90500   0.0     com='drum(chine)outer radius'
global
```

```
unit 1020
'es3100 drum [Elev=43.500 in.]'
array 3         2r-21.838092     0.0
'cuboid     0  1 4p21.838092    110.4905  0.0    com='bare package'
 cuboid    21  1 4p52.318092   140.9700 -30.48   com='reflected package'
'cuboid    20  1 4p22.889718    110.5048  0.0    com='interstital array space'
'global
'unit 1021
'array 4   3r0.0
'reflector  21 2  6r3.0  10
end geometry
read array
ara=3 nux=1 nuy=1 nuz=19 fill
1001 1002 1003 1006 1007 1006 1007 1006 1008 1010
1011 1012 1013 1014 1015 1016 1017 1018 1019        end fill
'ara=4 nux=13 nuy=13 nuz=06 fill f1020               end fill
end array
'read bias id=500 2  11  end bias
read start nst=0
end start
end data
end


=csas25    parm=size=3000000
nciatriga 0.0in thk np,10400.0gUZrHx(  921.0g235, 8998.2gH2O hx=255.01),fr=1.0e-04
238groupndf5 infhommedium
'TRIGA volume =1200.95996, SPACER volume    0.00000'
'TRIGA wrapped dry content can hx=18.2, CV void volume 9014.40198'
arbmtriga  8.65974  4 0 0 0    1001    0.9554
                              40000   54.0446
                              92235    8.8558
                              92238   36.1442    1  1.0     293  end
'np277-4: spacer (NCT_MD&H)'
'NCT min.den.(95.3886 lb/ft3) and hydrogen'
'np277-4 min.den.= 1.527971 = (95.3886 lb/ft3)(453.59 g/lb)/(28316.84 cm3/ft3)'
'use 75% of boron in calculations per NUREG-1609 Section 6.5.3.2'
arbmboron 7.31015e-2  2 0 0 0    5010   18.1479
                                 5011   81.8520    2  0.7500  293  end
arbmnpmx  1.07070e+0 10 0 0 0    6012    1.9189
                                 7014    0.0141
                                 8016   43.4251
                                11023    0.1174
                                12000    0.3378
                                13027   39.0479
                                14000    2.4672
                                16000    0.3083
                                20000   11.8336
                                26000    0.5298    2  1.0000  293  end
arbmnph2o 3.84169e-1  2 0 0 0    1001   11.1913
                                 8016   88.8087    2  1.0000  293  end
'flooded containmment vessel and content cans -- 10 CFR 71.55(d)(3)'
arbmwicv   0.9982   2 0 0 0    1001   11.1913
                               8016   88.8087    3  1       293  end
'steel: containment vessel body 16.60 lb but use 15.74 lb'
ss304                                            8  1.0     293  end
'steel: cv flange lower use 3.36 lb'
ss304                                            9  0.97267 293  end
'steel: cv flange upper use 13.75 lb'
ss304                                           10  0.94348 293  end
'np277-4: confinement -- neutron poison inner liner (NCT_MD&H)'
'actual vol.= 1.28314e4 cm3 = (7.83023e2 in3)(16.387064)'
'den.multiplier = 1.28314e4 cm3 (actual vol.) / 1.32708e4 cm3 (model vol.)'
'np277-4 min.den.= 1.527971 = (95.3886 lb/ft3)(453.59 g/lb)/(28316.84 cm3/ft3)'
'density = 1.477385 = (den.mult)(np277-4 min.den.) = 0.9668933*1.527971'
'use 75% of boron in calculations per NUREG-1609 Section 6.5.3.2'
arbmboron 7.06813e-2  2 0 0 0    5010   18.1479
                                 5011   81.8520   11  0.7500  293  end
arbmnpmx  1.03525e+0 10 0 0 0    6012    1.9189
                                 7014    0.0141
                                 8016   43.4251
```

```
                                11023    0.1174
                                12000    0.3378
                                13027   39.0479
                                14000    2.4672
                                16000    0.3083
                                20000   11.8336
                                26000    0.5298   11  1.0000  293  end
arbmnph2o 3.71451e-1  2 0 0 0    1001   11.1913
                                 8016   88.8087   11  1.0000  293  end
'kaolite 1600 body'
'sing.unit.density= (den.mult)(min.den.)'
' for arbmh20k = 1.012373*0.51655,  for rest = 1.012373*0.34438'
'den.mult= 1.36557e5 cm3 (actual vol.) / 1.34888e5 cm3 (model vol.)'
'actual vol.= 1.36557e5 cm3 = (28316.84 cm3/ft3)(108.33188 lb)/(22.464 lb/ft3)'
'nct array densities are s.u.dens. multiplied by volume ratio 1.34888/1.10336'
arbmh2ok   0.63931  2 0 0 0    1001   11.1913
                               8016   88.8087   12  0.0287  293  end
arbmal2o3  0.42622  2 0 0 0   13027   52.9390
                               8016   47.0610   12  0.096   293  end
arbmsio2   0.42622  2 0 0 0   14000   46.7570
                               8016   53.2430   12  0.367   293  end
arbmfe2o3  0.42622  2 0 0 0   26000   69.9540
                               8016   30.0460   12  0.067   293  end
arbmtio2   0.42622  2 0 0 0   22000   59.9535
                               8016   40.0465   12  0.012   293  end
arbmcao    0.42622  2 0 0 0   20000   71.4815
                               8016   28.5185   12  0.307   293  end
arbmmgo    0.42622  2 0 0 0   12000   60.3169
                               8016   39.6831   12  0.131   293  end
arbmna2o   0.42622  2 0 0 0   11023   74.1961
                               8016   25.8039   12  0.020   293  end
'kaolite 1600 top plug'
'sing.unit.density= (den.mult)(min.den.)'
' for arbmh20k = 0.965246*0.51655,  for rest = 0.965246*0.34438'
'den.mult= 1.21592e4 cm3 (actual vol.) / 1.25970e4 cm3 (model vol.)'
'actual vol.= 1.21592e4 cm3 = (28316.84 cm3/ft3)(9.646 lb)/(22.464 lb/ft3)'
arbmh2ok   0.49860  2 0 0 0    1001   11.1913
                               8016   88.8087   13  0.0287  293  end
arbmal2o3  0.33241  2 0 0 0   13027   52.9390
                               8016   47.0610   13  0.096   293  end
arbmsio2   0.33241  2 0 0 0   14000   46.7570
                               8016   53.2430   13  0.367   293  end
arbmfe2o3  0.33241  2 0 0 0   26000   69.9540
                               8016   30.0460   13  0.067   293  end
arbmtio2   0.33241  2 0 0 0   22000   59.9535
                               8016   40.0465   13  0.012   293  end
arbmcao    0.33241  2 0 0 0   20000   71.4815
                               8016   28.5185   13  0.307   293  end
arbmmgo    0.33241  2 0 0 0   12000   60.3169
                               8016   39.6831   13  0.131   293  end
arbmna2o   0.33241  2 0 0 0   11023   74.1961
                               8016   25.8039   13  0.020   293  end
'silicone rubber pads'
arbmsiru   1.21791  4 0 0 0    6012   32.3767
                               1001    8.1573
                               8016   21.5782
                              14000   37.8878   14  1.0     293  end
'void space external to containment vessel'
arbmwecv   0.9982   2 0 0 0    1001   11.1913
                               8016   88.8087   15  0.0001  293  end
'steel: liner'
ss304                                            16  1.0     293  end
'steel: plug cover (pc) use 9.907 lb'
ss304                                            17  1.06388 293  end
'steel: angle iron (ai) for single units'
'ss304                                            18  1.0     293  end
'steel: angle iron (ai) for arrays'
'array density is multiplied by a volume fraction 7.08030/5.63249'
ss304                                            18  1.25705 293  end
'steel: drum steel for single units'
'ss304                                            19  1.0     293  end
```

```
'steel: drum steel for arrays'
'array density is multiplied by a volume fraction 3.20482/3.20544'
ss304                                          19  0.99981 293  end
'void space external to drum'
'array density is multiplied by a volume ratio 8.11698/6.98323'
arbmwed    1.16026  2 0 0 0    1001   11.1913
                                8016   88.8087   20  0.0001  293  end
'reflective water'
'arbmh20r   0.9982   2 0 0 0    1001   11.1913
'                                8016   88.8087   21  1.0     293  end
end comp
nciatriga 0.0in thk np,10400.0gUZrHx(  921.0g235, 8998.2gH2O,hx=255.01),fr=1.0e-04
read parameters nub=yes npg=2500 gen=215 nsk=15 tme=100 end parameters
read boun       all=specular                   end boun
read geometry
unit 1001
'drum bottom flat cover [Elev= 0.111 in. at top of unit]'
'cylinder  19 1   22.866096    0.28150   0.0     com='extended radius not used'
 cylinder  19 1   21.722275    0.28150   0.0     com='drum bottom flat cover'
 cuboid    20 1 4p22.866096    0.28150   0.0     com='drum chine outer radius'
unit 1002
'above drum bottom flat cover and below containment vessel [Elev= 4.676 in.]'
 cylinder  15 1    3.175000   11.59510  11.16330 com='void in pad-1'
 cylinder  14 1    7.924800   11.59510  11.16330 com='pad-1'
 cylinder  16 1    8.077200   11.59510  11.16330 com='np277_4 liner'
 cylinder  11 1   10.922000   11.59510  11.16330 com='np277_4'
 cylinder  16 1   11.074400   11.59510  10.85850 com='kaolite liner bottom'
 cylinder  12 1   21.555075   11.59510   0.0     com='kaolite'
 cylinder  19 1   21.722275   11.59510   0.0     com='drum'
 cuboid    20 1 4p22.866096   11.59510   0.0     com='drum chine outer radius'
unit 1003
'cv bottom [Elev= 4.926 in.]'
 cylinder  8  1    6.680200    0.63500   0.0     com='cv bottom'
 cylinder  15 1    7.924800    0.63500   0.0     com='void btw cv-np liner'
 cylinder  16 1    8.077200    0.63500   0.0     com='np277_4 liner'
 cylinder  11 1   10.922000    0.63500   0.0     com='np277_4'
 cylinder  16 1   11.074400    0.63500   0.0     com='kaolite liner'
 cylinder  12 1   21.555075    0.63500   0.0     com='kaolite'
 cylinder  19 1   21.722275    0.63500   0.0     com='drum'
 cuboid    20 1 4p22.866096    0.63500   0.0     com='drum chine outer radius'
unit 1004
'UZrHx fuel element'
 cylinder  1  1    1.828800   12.70000   0.0     com='cylindrical content'
unit 1006
'content (collapsed) [Elev= 9.926 in.]'
'1.437900   plus-y location upper cylinders'
'-2.875700  minus-y location lower cylinder'
'2.490443   plus-x location upper cylinder'
'-2.490443  minus-x location upper cylinder'
 cylinder  3  1    6.426200   12.70050  -0.0005  com='cv well cavity'
 hole  1004   -2.490443  1.437900  0.0     com='cyl1'
 hole  1004    2.490443  1.437900  0.0     com='cyl2'
 hole  1004    0.0      -2.875700  0.0     com='cyl3'
 cylinder  8  1    6.680200   12.70050  -0.0005  com='cv below 1st step'
 cylinder  15 1    7.924800   12.70050  -0.0005  com='void btw cv-np liner'
 cylinder  16 1    8.077200   12.70050  -0.0005  com='np277_4 liner'
 cylinder  11 1   10.922000   12.70050  -0.0005  com='np277_4'
 cylinder  16 1   11.074400   12.70050  -0.0005  com='kaolite liner'
 cylinder  12 1   21.555075   12.70050  -0.0005  com='kaolite'
 cylinder  19 1   21.722275   12.70050  -0.0005  com='drum'
 cuboid    20 1 4p22.866096   12.70050  -0.0005  com='drum chine outer radius'
unit 1007
'np277_4 spacer [Elev= 9.926 in.]'
 cylinder  2  1    5.24510     0.00010   0.0     com='np spacer'
 cylinder  3  1    6.426200    0.00020  -0.0001  com='cv well cavity'
 cylinder  8  1    6.680200    0.00020  -0.0001  com='cv below 1st step'
 cylinder  15 1    7.924800    0.00020  -0.0001  com='void btw cv-np liner'
 cylinder  16 1    8.077200    0.00020  -0.0001  com='np277_4 liner'
 cylinder  11 1   10.922000    0.00020  -0.0001  com='np277_4'
 cylinder  16 1   11.074400    0.00020  -0.0001  com='kaolite liner'
 cylinder  12 1   21.555075    0.00020  -0.0001  com='kaolite'
```

```
 cylinder  19 1   21.722275    0.00020  -0.0001  com='drum'
 cuboid    20 1 4p22.866096    0.00020  -0.0001  com='drum chine outer radius'
unit 1008
'top of content stack to bottom of 1st step [Elev=35.276 in.]'
'38.10360             stack height (content spacers)       CALCULATED
 cylinder  3  1    6.426200   38.98540   0.0     com='cv well cavity'
 cylinder  8  1    6.680200   38.98540   0.0     com='cv below 1st step'
 cylinder  15 1    7.924800   38.98540   0.0     com='void btw cv-np liner'
 cylinder  16 1    8.077200   38.98540   0.0     com='np277_4 liner'
 cylinder  11 1   10.922000   38.98540   0.0     com='np277_4'
 cylinder  16 1   11.074400   38.98540   0.0     com='kaolite liner'
 cylinder  12 1   21.555075   38.98540   0.0     com='kaolite'
 cylinder  19 1   21.722275   38.98540   0.0     com='drum'
 cuboid    20 1 4p22.866096   38.98540   0.0     com='drum chine outer radius'
unit 1010
'cv at 1st step in liner [Elev=35.336 in.]'
 cylinder  3  1    6.426200    0.15240   0.0     com='cv well cavity'
 cylinder  8  1    6.680200    0.15240   0.0     com='cv at 1st step'
 cylinder  15 1    7.924800    0.15240   0.0     com='void btw cv and liner'
 cylinder  16 1   11.074400    0.15240   0.0     com='liner 1st step'
 cylinder  12 1   21.555075    0.15240   0.0     com='kaolite'
 cylinder  19 1   21.722275    0.15240   0.0     com='drum'
 cuboid    20 1 4p22.866096    0.15240   0.0     com='drum chine outer radius'
unit 1011
'vertical gap between 1st step in liner and cv flange [Elev=35.426 in.]'
 cylinder  3  1    6.426200    0.22860   0.0     com='cv well cavity'
 cylinder  8  1    6.680200    0.22860   0.0     com='cv at gap btwn step-flng'
 cylinder  15 1   10.922000    0.22860   0.0     com='void btw cv and liner'
 cylinder  16 1   11.074400    0.22860   0.0     com='liner wall'
 cylinder  12 1   21.555075    0.22860   0.0     com='kaolite'
 cylinder  19 1   21.722275    0.22860   0.0     com='drum'
 cuboid    20 1 4p22.866096    0.22860   0.0     com='drum chine outer radius'
unit 1012
'cv flange to top of cv well [Elev=35.926 in.]'
 cylinder  3  1    6.426200    1.27000   0.0     com='cavity'
 cylinder  9  1    9.525000    1.27000   0.0     com='flange to top of well'
 cylinder  15 1    9.525000    1.27000   0.0     com='void btw cv and pad-2'
 cylinder  14 1   10.033000    1.27000   0.0     com='pad-2'
 cylinder  15 1   10.922000    1.27000   0.0     com='void btw cv and liner'
 cylinder  16 1   11.074400    1.27000   0.0     com='liner wall'
 cylinder  12 1   21.555075    1.27000   0.0     com='kaolite'
 cylinder  19 1   21.722275    1.27000   0.0     com='drum'
 cuboid    20 1 4p22.866096    1.27000   0.0     com='drum chine outer radius'
unit 1013
'cv flange above cv well [Elev=37.076 in.]'
 cylinder  10 1    9.525000    2.92100   0.0     com='flange above cv well'
 cylinder  15 1    9.525000    2.92100   0.0     com='void btw cv and pad-2'
 cylinder  14 1   10.033000    2.92100   0.0     com='pad-2'
 cylinder  15 1   10.922000    2.92100   0.0     com='void btw pad2 and liner'
 cylinder  16 1   11.074400    2.92100   0.0     com='liner wall'
 cylinder  12 1   21.555075    2.92100   0.0     com='kaolite'
 cylinder  19 1   21.722275    2.92100   0.0     com='drum'
 cuboid    20 1 4p22.866096    2.92100   0.0     com='drum chine outer radius'
unit 1014
'plugpad2 below liner 2nd step [Elev=37.476 in.]'
 cylinder  14 1   10.033000    0.76200   0.0     com='pad-2'
 cylinder  15 1   10.922000    1.01600   0.0     com='void btw pad2 and liner'
 cylinder  16 1   11.074400    1.01600   0.0     com='liner wall'
 cylinder  12 1   21.555075    1.01600   0.0     com='kaolite'
 cylinder  19 1   21.722275    1.01600   0.0     com='drum'
 cuboid    20 1 4p22.866096    1.01600   0.0     com='drum chine outer radius'
unit 1015
'2nd step in liner [Elev=37.536 in.]'
 cylinder  15 1   10.922000    0.15240   0.0     com='void abv pad2'
 cylinder  16 1   18.757900    0.15240   0.0     com='liner 2nd step'
 cylinder  12 1   21.555075    0.15240   0.0     com='kaolite'
 cylinder  19 1   21.722275    0.15240   0.0     com='drum'
 cuboid    20 1 4p22.866096    0.15240   0.0     com='drum chine outer radius'
unit 1016
'abv 2nd step in liner to bottom of angle iron [Elev=40.756 in.]'
 cylinder  13 1   18.097500    8.17880   0.49276 com='plug kaolite'
```

```
 cylinder  17 1   18.249900    8.17880   0.34036 com='sides of plug case'
 cylinder  15 1   18.605500    8.17880   0.0     com='void: plug to liner'
 cylinder  16 1   18.757900    8.17880   0.0     com='liner wall'
 cylinder  12 1   21.555075    8.17880   0.0     com='kaolite'
 cylinder  19 1   21.722275    8.17880   0.0     com='drum'
 cuboid    20 1 4p22.866096    8.17880   0.0     com='drum chine outer radius'
unit 1017
'bottom of angle iron to bend in angle iron [Elev=42.506 in.]'
 cylinder  13 1   18.097500    4.44500   0.0     com='plug kaolite'
 cylinder  17 1   18.249900    4.44500   0.0     com='sides of plug case'
 cylinder  15 1   18.605500    4.44500   0.0     com='void: plug to liner'
 cylinder  16 1   18.757900    4.44500   0.0     com='liner wall'
 cylinder  18 1   19.392900    4.44500   0.0     com='lower angle iron'
 cylinder  12 1   21.555075    4.44500   0.0     com='kaolite'
 cylinder  19 1   21.722275    4.44500   0.0     com='drum'
 cuboid    20 1 4p22.866096    4.44500   0.0     com='drum chine outer radius'
unit 1018
'bend in angle iron to top of angle iron [Elev=42.756 in.]'
 cylinder  13 1   18.097500    0.11176   0.0     com='plug kaolite'
 cylinder  17 1   18.249900    0.26416   0.0     com='sides of plug case'
 cylinder  15 1   18.605500    0.63500   0.0     com='void: plug to liner'
 cylinder  16 1   18.757900    0.63500   0.0     com='liner wall'
 cylinder  18 1   21.555075    0.63500   0.0     com='bend section of ai'
 cylinder  19 1   21.722275    0.63500   0.0     com='drum'
 cuboid    20 1 4p22.866096    0.63500   0.0     com='drum chine outer radius'
unit 1019
'drum lid and lip [Elev=43.512 in.]'
 cylinder  20 1   21.330090    1.91973   0.16720 com='void above lid'
 cylinder  19 1   21.497290    1.91973   0.0     com='drum lid'
 cylinder  20 1   21.555075    1.91973   0.0     com='void btw lid - drum wall'
 cylinder  19 1   21.722275    1.91973   0.0     com='drum'
 cuboid    20 1 4p22.866096    1.91973   0.0     com='drum chine outer radius'
global
unit 1020
'es3100 drum [Elev=43.512 in.]'
array 3         2r-22.866096     0.0
'cuboid     0  1 4p24.587200    110.4900  0.0    com='bare package'
'cuboid    21  1 4p55.067200   140.9700 -30.48   com='reflected package'
 cuboid    20  1 4p22.866096    110.5197  0.0    com='interstital array space'
'global
'unit 1021
'array 4   3r0.0
'reflector  21 2  6r3.0  10
end geometry
read array
ara=3 nux=1 nuy=1 nuz=19 fill
1001 1002 1003 1006 1007 1006 1007 1006 1008 1010
1011 1012 1013 1014 1015 1016 1017 1018 1019        end fill
'ara=4 nux=13 nuy=13 nuz=06 fill f1020               end fill
end array
'read bias id=500 2  11  end bias
read start nst=0
end start
end data
end


=csas25    parm=size=3000000
nciatriga_70 0.0in thk np, 6847.1gUZrHx(  408.0g235, 8998.2gH2O hx=575.64),fr=1.0e-04
238groupndf5 infhommedium
'TRIGA volume =1200.95996, SPACER volume    0.00000'
'TRIGA wrapped dry content can hx=41.1, CV void volume 9014.40198'
arbmtriga  5.70132  4 0 0 0    1001    1.5894
                              40000   89.9107
                              92235    5.9587
                              92238    2.5412    1  1.0     293  end
'np277-4: spacer (NCT_MD&H)'
'NCT min.den.(95.3886 lb/ft3) and hydrogen'
'np277-4 min.den.= 1.527971 = (95.3886 lb/ft3)(453.59 g/lb)/(28316.84 cm3/ft3)'
'use 75% of boron in calculations per NUREG-1609 Section 6.5.3.2'
arbmboron 7.31015e-2  2 0 0 0    5010   18.1479
```

```
                                 5011   81.8520    2  0.7500  293  end
arbmnpmx  1.07070e+0 10 0 0 0    6012    1.9189
                                 7014    0.0141
                                 8016   43.4251
                                11023    0.1174
                                12000    0.3378
                                13027   39.0479
                                14000    2.4672
                                16000    0.3083
                                20000   11.8336
                                26000    0.5298    2  1.0000  293  end
arbmnph2o 3.84169e-1  2 0 0 0    1001   11.1913
                                 8016   88.8087    2  1.0000  293  end
'flooded containmment vessel and content cans -- 10 CFR 71.55(d)(3)'
arbmwicv   0.9982   2 0 0 0    1001   11.1913
                               8016   88.8087    3  1       293  end
'steel: containment vessel body 16.60 lb but use 15.74 lb'
ss304                                            8  1.0     293  end
'steel: cv flange lower use 3.36 lb'
ss304                                            9  0.97267 293  end
'steel: cv flange upper use 13.75 lb'
ss304                                           10  0.94348 293  end
'np277-4: confinement -- neutron poison inner liner (NCT_MD&H)'
'actual vol.= 1.28314e4 cm3 = (7.83023e2 in3)(16.387064)'
'den.multiplier = 1.28314e4 cm3 (actual vol.) / 1.32708e4 cm3 (model vol.)'
'np277-4 min.den.= 1.527971 = (95.3886 lb/ft3)(453.59 g/lb)/(28316.84 cm3/ft3)'
'density = 1.477385 = (den.mult)(np277-4 min.den.) = 0.9668933*1.527971'
'use 75% of boron in calculations per NUREG-1609 Section 6.5.3.2'
arbmboron 7.06813e-2  2 0 0 0    5010   18.1479
                                 5011   81.8520   11  0.7500  293  end
arbmnpmx  1.03525e+0 10 0 0 0    6012    1.9189
                                 7014    0.0141
                                 8016   43.4251
                                11023    0.1174
                                12000    0.3378
                                13027   39.0479
                                14000    2.4672
                                16000    0.3083
                                20000   11.8336
                                26000    0.5298   11  1.0000  293  end
arbmnph2o 3.71451e-1  2 0 0 0    1001   11.1913
                                 8016   88.8087   11  1.0000  293  end
'kaolite 1600 body'
'sing.unit.density= (den.mult)(min.den.)'
' for arbmh20k = 1.012373*0.51655,  for rest = 1.012373*0.34438'
'den.mult= 1.36557e5 cm3 (actual vol.) / 1.34888e5 cm3 (model vol.)'
'actual vol.= 1.36557e5 cm3 = (28316.84 cm3/ft3)(108.33188 lb)/(22.464 lb/ft3)'
'nct array densities are s.u.dens. multiplied by volume ratio 1.34888/1.10336'
arbmh2ok   0.63931  2 0 0 0    1001   11.1913
                               8016   88.8087   12  0.0287  293  end
arbmal2o3  0.42622  2 0 0 0   13027   52.9390
                               8016   47.0610   12  0.096   293  end
arbmsio2   0.42622  2 0 0 0   14000   46.7570
                               8016   53.2430   12  0.367   293  end
arbmfe2o3  0.42622  2 0 0 0   26000   69.9540
                               8016   30.0460   12  0.067   293  end
arbmtio2   0.42622  2 0 0 0   22000   59.9535
                               8016   40.0465   12  0.012   293  end
arbmcao    0.42622  2 0 0 0   20000   71.4815
                               8016   28.5185   12  0.307   293  end
arbmmgo    0.42622  2 0 0 0   12000   60.3169
                               8016   39.6831   12  0.131   293  end
arbmna2o   0.42622  2 0 0 0   11023   74.1961
                               8016   25.8039   12  0.020   293  end
'kaolite 1600 top plug'
'sing.unit.density= (den.mult)(min.den.)'
' for arbmh20k = 0.965246*0.51655,  for rest = 0.965246*0.34438'
'den.mult= 1.21592e4 cm3 (actual vol.) / 1.25970e4 cm3 (model vol.)'
'actual vol.= 1.21592e4 cm3 = (28316.84 cm3/ft3)(9.646 lb)/(22.464 lb/ft3)'
arbmh2ok   0.49860  2 0 0 0    1001   11.1913
                               8016   88.8087   13  0.0287  293  end
```

```
arbmal2o3  0.33241  2 0 0 0   13027   52.9390
                               8016   47.0610   13  0.096   293  end
arbmsio2   0.33241  2 0 0 0   14000   46.7570
                               8016   53.2430   13  0.367   293  end
arbmfe2o3  0.33241  2 0 0 0   26000   69.9540
                               8016   30.0460   13  0.067   293  end
arbmtio2   0.33241  2 0 0 0   22000   59.9535
                               8016   40.0465   13  0.012   293  end
arbmcao    0.33241  2 0 0 0   20000   71.4815
                               8016   28.5185   13  0.307   293  end
arbmmgo    0.33241  2 0 0 0   12000   60.3169
                               8016   39.6831   13  0.131   293  end
arbmna2o   0.33241  2 0 0 0   11023   74.1961
                               8016   25.8039   13  0.020   293  end
'silicone rubber pads'
arbmsiru   1.21791  4 0 0 0    6012   32.3767
                               1001    8.1573
                               8016   21.5782
                              14000   37.8878   14  1.0     293  end
'void space external to containment vessel'
arbmwecv   0.9982   2 0 0 0    1001   11.1913
                               8016   88.8087   15  0.0001  293  end
'steel: liner'
ss304                                            16  1.0     293  end
'steel: plug cover (pc) use 9.907 lb'
ss304                                            17  1.06388 293  end
'steel: angle iron (ai) for single units'
'ss304                                            18  1.0     293  end
'steel: angle iron (ai) for arrays'
'array density is multiplied by a volume fraction 7.08030/5.63249'
ss304                                            18  1.25705 293  end
'steel: drum steel for single units'
'ss304                                            19  1.0     293  end
'steel: drum steel for arrays'
'array density is multiplied by a volume fraction 3.20482/3.20544'
ss304                                            19  0.99981 293  end
'void space external to drum'
'array density is multiplied by a volume ratio 8.11698/6.98323'
arbmwed    1.16026  2 0 0 0    1001   11.1913
                               8016   88.8087   20  0.0001  293  end
'reflective water'
'arbmh20r   0.9982   2 0 0 0    1001   11.1913
'                               8016   88.8087   21  1.0     293  end
end comp
nciatriga_70 0.0in thk np, 6847.1gUZrHx(  408.0g235, 8998.2gH2O,hx=575.64),fr=1.0e-04
read parameters nub=yes npg=2500 gen=215 nsk=15 tme=100 end parameters
read boun       all=specular                     end boun
read geometry
unit 1001
'drum bottom flat cover [Elev= 0.111 in. at top of unit]'
'cylinder  19 1   22.866096    0.28150   0.0     com='extended radius not used'
 cylinder  19 1   21.722275    0.28150   0.0     com='drum bottom flat cover'
 cuboid    20 1 4p22.866096    0.28150   0.0     com='drum chine outer radius'
unit 1002
'above drum bottom flat cover and below containment vessel [Elev= 4.676 in.]'
 cylinder  15 1    3.175000   11.59510  11.16330 com='void in pad-1'
 cylinder  14 1    7.924800   11.59510  11.16330 com='pad-1'
 cylinder  16 1    8.077200   11.59510  11.16330 com='np277_4 liner'
 cylinder  11 1   10.922000   11.59510  11.16330 com='np277_4'
 cylinder  16 1   11.074400   11.59510  10.85850 com='kaolite liner bottom'
 cylinder  12 1   21.555075   11.59510   0.0     com='kaolite'
 cylinder  19 1   21.722275   11.59510   0.0     com='drum'
 cuboid    20 1 4p22.866096   11.59510   0.0     com='drum chine outer radius'
unit 1003
'cv bottom [Elev= 4.926 in.]'
 cylinder  8  1    6.680200    0.63500   0.0     com='cv bottom'
 cylinder  15 1    7.924800    0.63500   0.0     com='void btw cv-np liner'
 cylinder  16 1    8.077200    0.63500   0.0     com='np277_4 liner'
 cylinder  11 1   10.922000    0.63500   0.0     com='np277_4'
 cylinder  16 1   11.074400    0.63500   0.0     com='kaolite liner'
 cylinder  12 1   21.555075    0.63500   0.0     com='kaolite'
```

```
 cylinder  19 1   21.722275    0.63500   0.0     com='drum'
 cuboid    20 1 4p22.866096    0.63500   0.0     com='drum chine outer radius'
unit 1004
'UZrHx fuel element'
 cylinder  1  1    1.828800   12.70000   0.0     com='cylindrical content'
unit 1006
'content (collapsed) [Elev= 9.926 in.]'
'1.437900   plus-y location upper cylinders'
'-2.875700  minus-y location lower cylinder'
'2.490443   plus-x location upper cylinder'
'-2.490443  minus-x location upper cylinder'
 cylinder  3  1    6.426200   12.70050  -0.0005  com='cv well cavity'
 hole  1004   -2.490443  1.437900  0.0     com='cyl1'
 hole  1004    2.490443  1.437900  0.0     com='cyl2'
 hole  1004    0.0      -2.875700  0.0     com='cyl3'
 cylinder  8  1    6.680200   12.70050  -0.0005  com='cv below 1st step'
 cylinder  15 1    7.924800   12.70050  -0.0005  com='void btw cv-np liner'
 cylinder  16 1    8.077200   12.70050  -0.0005  com='np277_4 liner'
 cylinder  11 1   10.922000   12.70050  -0.0005  com='np277_4'
 cylinder  16 1   11.074400   12.70050  -0.0005  com='kaolite liner'
 cylinder  12 1   21.555075   12.70050  -0.0005  com='kaolite'
 cylinder  19 1   21.722275   12.70050  -0.0005  com='drum'
 cuboid    20 1 4p22.866096   12.70050  -0.0005  com='drum chine outer radius'
unit 1007
'np277_4 spacer [Elev= 9.926 in.]'
 cylinder  2  1    5.24510     0.00010   0.0     com='np spacer'
 cylinder  3  1    6.426200    0.00020  -0.0001  com='cv well cavity'
 cylinder  8  1    6.680200    0.00020  -0.0001  com='cv below 1st step'
 cylinder  15 1    7.924800    0.00020  -0.0001  com='void btw cv-np liner'
 cylinder  16 1    8.077200    0.00020  -0.0001  com='np277_4 liner'
 cylinder  11 1   10.922000    0.00020  -0.0001  com='np277_4'
 cylinder  16 1   11.074400    0.00020  -0.0001  com='kaolite liner'
 cylinder  12 1   21.555075    0.00020  -0.0001  com='kaolite'
 cylinder  19 1   21.722275    0.00020  -0.0001  com='drum'
 cuboid    20 1 4p22.866096    0.00020  -0.0001  com='drum chine outer radius'
unit 1008
'top of content stack to bottom of 1st step [Elev=35.276 in.]'
'38.10360             stack height (content spacers)       CALCULATED
 cylinder  3  1    6.426200   38.98540   0.0     com='cv well cavity'
 cylinder  8  1    6.680200   38.98540   0.0     com='cv below 1st step'
 cylinder  15 1    7.924800   38.98540   0.0     com='void btw cv-np liner'
 cylinder  16 1    8.077200   38.98540   0.0     com='np277_4 liner'
 cylinder  11 1   10.922000   38.98540   0.0     com='np277_4'
 cylinder  16 1   11.074400   38.98540   0.0     com='kaolite liner'
 cylinder  12 1   21.555075   38.98540   0.0     com='kaolite'
 cylinder  19 1   21.722275   38.98540   0.0     com='drum'
 cuboid    20 1 4p22.866096   38.98540   0.0     com='drum chine outer radius'
unit 1010
'cv at 1st step in liner [Elev=35.336 in.]'
 cylinder  3  1    6.426200    0.15240   0.0     com='cv well cavity'
 cylinder  8  1    6.680200    0.15240   0.0     com='cv at 1st step'
 cylinder  15 1    7.924800    0.15240   0.0     com='void btw cv and liner'
 cylinder  16 1   11.074400    0.15240   0.0     com='liner 1st step'
 cylinder  12 1   21.555075    0.15240   0.0     com='kaolite'
 cylinder  19 1   21.722275    0.15240   0.0     com='drum'
 cuboid    20 1 4p22.866096    0.15240   0.0     com='drum chine outer radius'
unit 1011
'vertical gap between 1st step in liner and cv flange [Elev=35.426 in.]'
 cylinder  3  1    6.426200    0.22860   0.0     com='cv well cavity'
 cylinder  8  1    6.680200    0.22860   0.0     com='cv at gap btwn step-flng'
 cylinder  15 1   10.922000    0.22860   0.0     com='void btw cv and liner'
 cylinder  16 1   11.074400    0.22860   0.0     com='liner wall'
 cylinder  12 1   21.555075    0.22860   0.0     com='kaolite'
 cylinder  19 1   21.722275    0.22860   0.0     com='drum'
 cuboid    20 1 4p22.866096    0.22860   0.0     com='drum chine outer radius'
unit 1012
'cv flange to top of cv well [Elev=35.926 in.]'
 cylinder  3  1    6.426200    1.27000   0.0     com='cavity'
 cylinder  9  1    9.525000    1.27000   0.0     com='flange to top of well'
 cylinder  15 1    9.525000    1.27000   0.0     com='void btw cv and pad-2'
 cylinder  14 1   10.033000    1.27000   0.0     com='pad-2'
```

```
 cylinder  15 1   10.922000    1.27000   0.0     com='void btw cv and liner'
 cylinder  16 1   11.074400    1.27000   0.0     com='liner wall'
 cylinder  12 1   21.555075    1.27000   0.0     com='kaolite'
 cylinder  19 1   21.722275    1.27000   0.0     com='drum'
 cuboid    20 1 4p22.866096    1.27000   0.0     com='drum chine outer radius'
unit 1013
'cv flange above cv well [Elev=37.076 in.]'
 cylinder  10 1    9.525000    2.92100   0.0     com='flange above cv well'
 cylinder  15 1    9.525000    2.92100   0.0     com='void btw cv and pad-2'
 cylinder  14 1   10.033000    2.92100   0.0     com='pad-2'
 cylinder  15 1   10.922000    2.92100   0.0     com='void btw pad2 and liner'
 cylinder  16 1   11.074400    2.92100   0.0     com='liner wall'
 cylinder  12 1   21.555075    2.92100   0.0     com='kaolite'
 cylinder  19 1   21.722275    2.92100   0.0     com='drum'
 cuboid    20 1 4p22.866096    2.92100   0.0     com='drum chine outer radius'
unit 1014
'plugpad2 below liner 2nd step [Elev=37.476 in.]'
 cylinder  14 1   10.033000    0.76200   0.0     com='pad-2'
 cylinder  15 1   10.922000    1.01600   0.0     com='void btw pad2 and liner'
 cylinder  16 1   11.074400    1.01600   0.0     com='liner wall'
 cylinder  12 1   21.555075    1.01600   0.0     com='kaolite'
 cylinder  19 1   21.722275    1.01600   0.0     com='drum'
 cuboid    20 1 4p22.866096    1.01600   0.0     com='drum chine outer radius'
unit 1015
'2nd step in liner [Elev=37.536 in.]'
 cylinder  15 1   10.922000    0.15240   0.0     com='void abv pad2'
 cylinder  16 1   18.757900    0.15240   0.0     com='liner 2nd step'
 cylinder  12 1   21.555075    0.15240   0.0     com='kaolite'
 cylinder  19 1   21.722275    0.15240   0.0     com='drum'
 cuboid    20 1 4p22.866096    0.15240   0.0     com='drum chine outer radius'
unit 1016
'abv 2nd step in liner to bottom of angle iron [Elev=40.756 in.]'
 cylinder  13 1   18.097500    8.17880   0.49276 com='plug kaolite'
 cylinder  17 1   18.249900    8.17880   0.34036 com='sides of plug case'
 cylinder  15 1   18.605500    8.17880   0.0     com='void: plug to liner'
 cylinder  16 1   18.757900    8.17880   0.0     com='liner wall'
 cylinder  12 1   21.555075    8.17880   0.0     com='kaolite'
 cylinder  19 1   21.722275    8.17880   0.0     com='drum'
 cuboid    20 1 4p22.866096    8.17880   0.0     com='drum chine outer radius'
unit 1017
'bottom of angle iron to bend in angle iron [Elev=42.506 in.]'
 cylinder  13 1   18.097500    4.44500   0.0     com='plug kaolite'
 cylinder  17 1   18.249900    4.44500   0.0     com='sides of plug case'
 cylinder  15 1   18.605500    4.44500   0.0     com='void: plug to liner'
 cylinder  16 1   18.757900    4.44500   0.0     com='liner wall'
 cylinder  18 1   19.392900    4.44500   0.0     com='lower angle iron'
 cylinder  12 1   21.555075    4.44500   0.0     com='kaolite'
 cylinder  19 1   21.722275    4.44500   0.0     com='drum'
 cuboid    20 1 4p22.866096    4.44500   0.0     com='drum chine outer radius'
unit 1018
'bend in angle iron to top of angle iron [Elev=42.756 in.]'
 cylinder  13 1   18.097500    0.11176   0.0     com='plug kaolite'
 cylinder  17 1   18.249900    0.26416   0.0     com='sides of plug case'
 cylinder  15 1   18.605500    0.63500   0.0     com='void: plug to liner'
 cylinder  16 1   18.757900    0.63500   0.0     com='liner wall'
 cylinder  18 1   21.555075    0.63500   0.0     com='bend section of ai'
 cylinder  19 1   21.722275    0.63500   0.0     com='drum'
 cuboid    20 1 4p22.866096    0.63500   0.0     com='drum chine outer radius'
unit 1019
'drum lid and lip [Elev=43.512 in.]'
 cylinder  20 1   21.330090    1.91973   0.16720 com='void above lid'
 cylinder  19 1   21.497290    1.91973   0.0     com='drum lid'
 cylinder  20 1   21.555075    1.91973   0.0     com='void btw lid - drum wall'
 cylinder  19 1   21.722275    1.91973   0.0     com='drum'
 cuboid    20 1 4p22.866096    1.91973   0.0     com='drum chine outer radius'
global
unit 1020
'es3100 drum [Elev=43.512 in.]'
array 3         2r-22.866096     0.0
'cuboid     0  1 4p24.587200    110.4900  0.0    com='bare package'
'cuboid    21  1 4p55.067200   140.9700 -30.48   com='reflected package'
```

```
 cuboid    20  1 4p22.866096    110.5197  0.0    com='interstital array space'
'global
'unit 1021
'array 4   3r0.0
'reflector  21 2  6r3.0  10
end geometry
read array
ara=3 nux=1 nuy=1 nuz=19 fill
1001 1002 1003 1006 1007 1006 1007 1006 1008 1010
1011 1012 1013 1014 1015 1016 1017 1018 1019        end fill
'ara=4 nux=13 nuy=13 nuz=06 fill f1020               end fill
end array
'read bias id=500 2  11  end bias
read start nst=0
end start
end data
end


=csas25    parm=size=3000000
hciatriga 0.0in thk np,10400.0gUZrHx(  921.0g235, 8998.2gH2O hx=255.01),fr=1.0e-04
238groupndf5 infhommedium
'TRIGA volume =1200.95996, SPACER volume    0.00000'
'TRIGA wrapped dry content can hx=18.2, CV void volume 9014.40198'
arbmtriga  8.65974  4 0 0 0    1001    0.9554
                              40000   54.0446
                              92235    8.8558
                              92238   36.1442    1  1.0     293  end
'np277-4: spacer (HAC_MD&H)'
'HAC min.den.(95.3157 lb/ft3) and hydrogen'
'np277-4 min.den.= 1.526803 = (95.3157 lb/ft3)(453.59 g/lb)/(28316.84 cm3/ft3)'
'use 75% of boron in calculations per NUREG-1609 Section 6.5.3.2'
arbmboron 7.31015e-2  2 0 0 0    5010   18.1479
                                 5011   81.8520    2  0.7500  293  end
arbmnpmx  1.07071e+0 10 0 0 0    6012    1.9188
                                 7014    0.0141
                                 8016   43.4254
                                11023    0.1174
                                12000    0.3378
                                13027   39.0477
                                14000    2.4671
                                16000    0.3083
                                20000   11.8335
                                26000    0.5298    2  1.0000  293  end
arbmnph2o 3.82995e-1  2 0 0 0    1001   11.1913
                                 8016   88.8087    2  1.0000  293  end
'flooded containmment vessel and content cans -- 10 CFR 71.55(d)(3)'
arbmwicv   0.9982   2 0 0 0    1001   11.1913
                               8016   88.8087    3  1       293  end
'steel: containment vessel body 16.60 lb but use 15.74 lb'
ss304                                            8  1.0     293  end
'steel: cv flange lower use 3.36 lb'
ss304                                            9  0.97267 293  end
'steel: cv flange upper use 13.75 lb'
ss304                                           10  0.94348 293  end
'np277-4: confinement -- neutron poison inner liner (HAC_MD&H)'
'actual vol.= 1.28314e4 cm3 = (7.83023e2 in3)(16.387064)'
'den.multiplier = 1.28314e4 cm3 (actual vol.) / 1.32708e4 cm3 (model vol.)'
'np277-4 min.den.= 1.526803 = (95.3157 lb/ft3)(453.59 g/lb)/(28316.84 cm3/ft3)'
'density = 1.476265 = (den.mult)(np277-4 min.den.) = 0.9668933*1.526803'
'use 75% of boron in calculations per NUREG-1609 Section 6.5.3.2'
arbmboron 7.06813e-2  2 0 0 0    5010   18.1479
                                 5011   81.8520   11  0.7500  293  end
arbmnpmx  1.03525e+0 10 0 0 0    6012    1.9188
                                 7014    0.0141
                                 8016   43.4254
                                11023    0.1174
                                12000    0.3378
                                13027   39.0477
                                14000    2.4671
                                16000    0.3083
```

```
                                20000   11.8335
                                26000    0.5298   11  1.0000  293  end
arbmnph2o 3.70316e-1  2 0 0 0    1001   11.1913
                                 8016   88.8087   11  1.0000  293  end
'kaolite 1600 body'
'nct.sing.unit.density= (den.mult)(min.den.)'
' for arbmh20k 0.52294 = 1.012373*0.51655, for rest 0.34864 = 1.012373*0.34438'
'den.mult= 1.36557e5 cm3 (actual vol.) / 1.34888e5 cm3 (model vol.)'
'actual vol.= 1.36557e5 cm3 = (28316.84 cm3/ft3)(108.33188 lb)/(22.464 lb/ft3)'
'hac.s.u.dens= (hac.mult)(nct.s.u.dens)'
'hac.mult = 1.34888e5 cm3 (nct vol.)/ 1.12246e5 cm3 (model vol.)'
' for arbmh2ok 0.62843 = 1.20172*0.52294,   for rest = 1.20172*0.34864'
'hac array densities are hac s.u.dens.'
arbmh2ok   0.62843  2 0 0 0    1001   11.1913
                                8016   88.8087   12  0.0287  293  end
arbmal2o3  0.41898  2 0 0 0   13027   52.9390
                                8016   47.0610   12  0.096   293  end
arbmsio2   0.41898  2 0 0 0   14000   46.7570
                                8016   53.2430   12  0.367   293  end
arbmfe2o3  0.41898  2 0 0 0   26000   69.9540
                                8016   30.0460   12  0.067   293  end
arbmtio2   0.41898  2 0 0 0   22000   59.9535
                                8016   40.0465   12  0.012   293  end
arbmcao    0.41898  2 0 0 0   20000   71.4815
                                8016   28.5185   12  0.307   293  end
arbmmgo    0.41898  2 0 0 0   12000   60.3169
                                8016   39.6831   12  0.131   293  end
arbmna2o   0.41898  2 0 0 0   11023   74.1961
                                8016   25.8039   12  0.020   293  end
'kaolite 1600 top plug'
'sing.unit.density= (den.mult)(min.den.)'
' for arbmh20k = 0.965246*0.51655,  for rest = 0.965246*0.34438'
'den.mult= 1.21592e4 cm3 (actual vol.) / 1.25970e4 cm3 (model vol.)'
'actual vol.= 1.21592e4 cm3 = (28316.84 cm3/ft3)(9.646 lb)/(22.464 lb/ft3)'
arbmh2ok   0.49860  2 0 0 0    1001   11.1913
                                8016   88.8087   13  0.0287  293  end
arbmal2o3  0.33241  2 0 0 0   13027   52.9390
                                8016   47.0610   13  0.096   293  end
arbmsio2   0.33241  2 0 0 0   14000   46.7570
                                8016   53.2430   13  0.367   293  end
arbmfe2o3  0.33241  2 0 0 0   26000   69.9540
                                8016   30.0460   13  0.067   293  end
arbmtio2   0.33241  2 0 0 0   22000   59.9535
                                8016   40.0465   13  0.012   293  end
arbmcao    0.33241  2 0 0 0   20000   71.4815
                                8016   28.5185   13  0.307   293  end
arbmmgo    0.33241  2 0 0 0   12000   60.3169
                                8016   39.6831   13  0.131   293  end
arbmna2o   0.33241  2 0 0 0   11023   74.1961
                                8016   25.8039   13  0.020   293  end
'silicone rubber pads'
arbmsiru   1.21791  4 0 0 0    6012   32.3767
                                1001    8.1573
                                8016   21.5782
                               14000   37.8878   14  1.0     293  end
'void space external to containment vessel'
arbmwecv   0.9982   2 0 0 0    1001   11.1913
                                8016   88.8087   15  0.0001  293  end
'steel: liner'
ss304                                           16  1.0     293  end
'steel: plug cover (pc) use 9.907 lb'
ss304                                           17  1.06388 293  end
'steel: angle iron (ai) for HAC'
'nct density is multiplied by volume fraction 7.08030/5.74516'
ss304                                           18  1.23239 293  end
'steel: drum steel for HAC'
'nct density is multiplied by volume fraction 3.20482/2.95645'
ss304                                           19  1.08401 293  end
'void space external to drum'
'array density is assumed not reduced by hac'
arbmwed    0.9982   2 0 0 0    1001   11.1913
```

```
                                8016   88.8087   20  0.0001  293  end
'reflective water'
'arbmh20r   0.9982   2 0 0 0    1001   11.1913
'                               8016   88.8087   21  1.0     293  end
end comp
hciatriga 0.0in thk np,10400.0gUZrHx(  921.0g235, 8998.2gH2O,hx=255.01),fr=1.0e-04
read parameters nub=yes npg=2500 gen=215 nsk=15 tme=100 end parameters
read boun       all=specular                    end boun
read geometry
unit 1001
'drum bottom flat cover [Elev= 0.105 in. at top of unit]'
'cylinder  19 1   21.838092    0.26670   0.0     com='extended radius not used'
 cylinder  19 1   21.838092    0.26670   0.0     com='drum bottom flat cover'
 cuboid    20 1 4p21.838092    0.26670   0.0     com='drum(chine)outer radius'
unit 1002
'above drum bottom flat cover and below containment vessel [Elev= 4.670 in.]'
 cylinder  15 1    3.175000   11.59510  11.16330 com='void in pad-1'
 cylinder  14 1    7.924800   11.59510  11.16330 com='pad-1'
 cylinder  16 1    8.077200   11.59510  11.16330 com='np277_4 liner'
 cylinder  11 1   10.922000   11.59510  11.16330 com='np277_4'
 cylinder  16 1   11.074400   11.59510  10.85850 com='kaolite liner bottom'
 cylinder  12 1   21.685692   11.59510   0.0     com='kaolite'
 cylinder  19 1   21.838092   11.59510   0.0     com='drum'
 cuboid    20 1 4p21.838092   11.59510   0.0     com='drum(chine)outer radius'
unit 1003
'cv bottom [Elev= 4.920 in.]'
 cylinder  8  1    6.680200    0.63500   0.0     com='cv bottom'
 cylinder  15 1    7.924800    0.63500   0.0     com='void btw cv-np liner'
 cylinder  16 1    8.077200    0.63500   0.0     com='np277_4 liner'
 cylinder  11 1   10.922000    0.63500   0.0     com='np277_4'
 cylinder  16 1   11.074400    0.63500   0.0     com='kaolite liner'
 cylinder  12 1   21.685692    0.63500   0.0     com='kaolite'
 cylinder  19 1   21.838092    0.63500   0.0     com='drum'
 cuboid    20 1 4p21.838092    0.63500   0.0     com='drum(chine)outer radius'
unit 1004
'UZrHx fuel element'
 cylinder  1  1    1.828800   12.70000   0.0     com='cylindrical content'
unit 1006
'content (collapsed) [Elev= 9.920 in.]'
'1.437900   plus-y location upper cylinders'
'-2.875700  minus-y location lower cylinder'
'2.490443   plus-x location upper cylinder'
'-2.490443  minus-x location upper cylinder'
 cylinder  3  1    6.426200   12.70050  -0.0005  com='cv well cavity'
 hole  1004   -2.490443  1.437900  0.0     com='cyl1'
 hole  1004    2.490443  1.437900  0.0     com='cyl2'
 hole  1004    0.0      -2.875700  0.0     com='cyl3'
 cylinder  8  1    6.680200   12.70050  -0.0005  com='cv below 1st step'
 cylinder  15 1    7.924800   12.70050  -0.0005  com='void btw cv-np liner'
 cylinder  16 1    8.077200   12.70050  -0.0005  com='np277_4 liner'
 cylinder  11 1   10.922000   12.70050  -0.0005  com='np277_4'
 cylinder  16 1   11.074400   12.70050  -0.0005  com='kaolite liner'
 cylinder  12 1   21.685692   12.70050  -0.0005  com='kaolite'
 cylinder  19 1   21.838092   12.70050  -0.0005  com='drum'
 cuboid    20 1 4p21.838092   12.70050  -0.0005  com='drum chine outer radius'
unit 1007
'np277_4 spacer [Elev= 9.921 in.]'
 cylinder  2  1    5.24510     0.00010   0.0     com='np spacer'
 cylinder  3  1    6.426200    0.00020  -0.0001  com='cv well cavity'
 cylinder  8  1    6.680200    0.00020  -0.0001  com='cv below 1st step'
 cylinder  15 1    7.924800    0.00020  -0.0001  com='void btw cv-np liner'
 cylinder  16 1    8.077200    0.00020  -0.0001  com='np277_4 liner'
 cylinder  11 1   10.922000    0.00020  -0.0001  com='np277_4'
 cylinder  16 1   11.074400    0.00020  -0.0001  com='kaolite liner'
 cylinder  12 1   21.685692    0.00020  -0.0001  com='kaolite'
 cylinder  19 1   21.838092    0.00020  -0.0001  com='drum'
 cuboid    20 1 4p21.838092    0.00020  -0.0001  com='drum(chine)outer radius'
unit 1008
'top of content stack to bottom of 1st step [Elev=35.270 in.]'
'38.10360             stack height (content spacers)       CALCULATED
 cylinder  3  1    6.426200   38.98540   0.0     com='cv well cavity'
```

```
 cylinder  8  1    6.680200   38.98540   0.0     com='cv below 1st step'
 cylinder  15 1    7.924800   38.98540   0.0     com='void btw cv-np liner'
 cylinder  16 1    8.077200   38.98540   0.0     com='np277_4 liner'
 cylinder  11 1   10.922000   38.98540   0.0     com='np277_4'
 cylinder  16 1   11.074400   38.98540   0.0     com='kaolite liner'
 cylinder  12 1   21.685692   38.98540   0.0     com='kaolite'
 cylinder  19 1   21.838092   38.98540   0.0     com='drum'
 cuboid    20 1 4p21.838092   38.98540   0.0     com='drum(chine)outer radius'
unit 1010
'cv at 1st step in liner [Elev=35.330 in.]'
 cylinder  3  1    6.426200    0.15240   0.0     com='cv well cavity'
 cylinder  8  1    6.680200    0.15240   0.0     com='cv at 1st step'
 cylinder  15 1    7.924800    0.15240   0.0     com='void btw cv and liner'
 cylinder  16 1   11.074400    0.15240   0.0     com='liner 1st step'
 cylinder  12 1   21.685692    0.15240   0.0     com='kaolite'
 cylinder  19 1   21.838092    0.15240   0.0     com='drum'
 cuboid    20 1 4p21.838092    0.15240   0.0     com='drum(chine)outer radius'
unit 1011
'vertical gap between 1st step in liner and cv flange [Elev=35.420 in.]'
 cylinder  3  1    6.426200    0.22860   0.0     com='cv well cavity'
 cylinder  8  1    6.680200    0.22860   0.0     com='cv at gap btwn step-flng'
 cylinder  15 1   10.922000    0.22860   0.0     com='void btw cv and liner'
 cylinder  16 1   11.074400    0.22860   0.0     com='liner wall'
 cylinder  12 1   21.685692    0.22860   0.0     com='kaolite'
 cylinder  19 1   21.838092    0.22860   0.0     com='drum'
 cuboid    20 1 4p21.838092    0.22860   0.0     com='drum(chine)outer radius'
unit 1012
'cv flange to top of cv well [Elev=35.920 in.]'
 cylinder  3  1    6.426200    1.27000   0.0     com='cavity'
 cylinder  9  1    9.525000    1.27000   0.0     com='flange to top of well'
 cylinder  15 1    9.525000    1.27000   0.0     com='void btw cv and pad-2'
 cylinder  14 1   10.033000    1.27000   0.0     com='pad-2'
 cylinder  15 1   10.922000    1.27000   0.0     com='void btw cv and liner'
 cylinder  16 1   11.074400    1.27000   0.0     com='liner wall'
 cylinder  12 1   21.685692    1.27000   0.0     com='kaolite'
 cylinder  19 1   21.838092    1.27000   0.0     com='drum'
 cuboid    20 1 4p21.838092    1.27000   0.0     com='drum(chine)outer radius'
unit 1013
'cv flange above cv well [Elev=37.070 in.]'
 cylinder  10 1    9.525000    2.92100   0.0     com='flange above cv well'
 cylinder  15 1    9.525000    2.92100   0.0     com='void btw cv and pad-2'
 cylinder  14 1   10.033000    2.92100   0.0     com='pad-2'
 cylinder  15 1   10.922000    2.92100   0.0     com='void btw pad2 and liner'
 cylinder  16 1   11.074400    2.92100   0.0     com='liner wall'
 cylinder  12 1   21.685692    2.92100   0.0     com='kaolite'
 cylinder  19 1   21.838092    2.92100   0.0     com='drum'
 cuboid    20 1 4p21.838092    2.92100   0.0     com='drum(chine)outer radius'
unit 1014
'plugpad2 below liner 2nd step [Elev=37.470 in.]'
 cylinder  14 1   10.033000    0.76200   0.0     com='pad-2'
 cylinder  15 1   10.922000    1.01600   0.0     com='void btw pad2 and liner'
 cylinder  16 1   11.074400    1.01600   0.0     com='liner wall'
 cylinder  12 1   21.685692    1.01600   0.0     com='kaolite'
 cylinder  19 1   21.838092    1.01600   0.0     com='drum'
 cuboid    20 1 4p21.838092    1.01600   0.0     com='drum(chine)outer radius'
unit 1015
'2nd step in liner [Elev=37.530 in.]'
 cylinder  15 1   10.922000    0.15240   0.0     com='void abv pad2'
 cylinder  16 1   18.757900    0.15240   0.0     com='liner 2nd step'
 cylinder  12 1   21.685692    0.15240   0.0     com='kaolite'
 cylinder  19 1   21.838092    0.15240   0.0     com='drum'
 cuboid    20 1 4p21.838092    0.15240   0.0     com='drum(chine)outer radius'
unit 1016
'abv 2nd step in liner to bottom of angle iron [Elev=40.750 in.]'
 cylinder  13 1   18.097500    8.17880   0.49276 com='plug kaolite'
 cylinder  17 1   18.249900    8.17880   0.34036 com='sides of plug case'
 cylinder  15 1   18.605500    8.17880   0.0     com='void: plug to liner'
 cylinder  16 1   18.757900    8.17880   0.0     com='liner wall'
 cylinder  12 1   21.685692    8.17880   0.0     com='kaolite'
 cylinder  19 1   21.838092    8.17880   0.0     com='drum'
 cuboid    20 1 4p21.838092    8.17880   0.0     com='drum(chine)outer radius'
```

```
unit 1017
'bottom of angle iron to bend in angle iron [Elev=42.500 in.]'
 cylinder  13 1   18.097500    4.44500   0.0     com='plug kaolite'
 cylinder  17 1   18.249900    4.44500   0.0     com='sides of plug case'
 cylinder  15 1   18.605500    4.44500   0.0     com='void: plug to liner'
 cylinder  16 1   18.757900    4.44500   0.0     com='liner wall'
 cylinder  18 1   19.392900    4.44500   0.0     com='lower angle iron'
 cylinder  12 1   21.685692    4.44500   0.0     com='kaolite'
 cylinder  19 1   21.838092    4.44500   0.0     com='drum'
 cuboid    20 1 4p21.838092    4.44500   0.0     com='drum(chine)outer radius'
unit 1018
'bend in angle iron to top of angle iron [Elev=42.750 in.]'
 cylinder  13 1   18.097500    0.11176   0.0     com='plug kaolite'
 cylinder  17 1   18.249900    0.26416   0.0     com='sides of plug case'
 cylinder  15 1   18.605500    0.63500   0.0     com='void: plug to liner'
 cylinder  16 1   18.757900    0.63500   0.0     com='liner wall'
 cylinder  18 1   21.685692    0.63500   0.0     com='bend section of ai'
 cylinder  19 1   21.838092    0.63500   0.0     com='drum'
 cuboid    20 1 4p21.838092    0.63500   0.0     com='drum(chine)outer radius'
unit 1019
'drum lid and lip [Elev=43.500 in.]'
 cylinder  20 1   21.469792    1.90500   0.15240 com='void above lid'
 cylinder  19 1   21.622192    1.90500   0.0     com='drum lid'
 cylinder  20 1   21.685692    1.90500   0.0     com='void btw lid - drum wall'
 cylinder  19 1   21.838092    1.90500   0.0     com='drum'
 cuboid    20 1 4p21.838092    1.90500   0.0     com='drum(chine)outer radius'
global
unit 1020
'es3100 drum [Elev=43.500 in.]'
array 3         2r-21.838092     0.0
'cuboid     0  1 4p21.838092    110.4905  0.0    com='bare package'
'cuboid    21  1 4p52.318092   140.9700 -30.48   com='reflected package'
 cuboid    20  1 4p22.889718    110.5048  0.0    com='interstital array space'
'global
'unit 1021
'array 4   3r0.0
'reflector  21 2  6r3.0  10
end geometry
read array
ara=3 nux=1 nuy=1 nuz=19 fill
1001 1002 1003 1006 1007 1006 1007 1006 1008 1010
1011 1012 1013 1014 1015 1016 1017 1018 1019        end fill
'ara=4 nux=13 nuy=13 nuz=06 fill f1020               end fill
end array
'read bias id=500 2  11  end bias
read start nst=0
end start
end data
end


=csas25    parm=size=3000000
hciatriga_70 0.0in thk np, 6847.1gUZrHx(  408.0g235, 8998.2gH2O hx=575.64),fr=1.0e-04
238groupndf5 infhommedium
'TRIGA volume =1200.95996, SPACER volume    0.00000'
'TRIGA wrapped dry content can hx=41.1, CV void volume 9014.40198'
arbmtriga  5.70132  4 0 0 0    1001    1.5894
                              40000   89.9107
                              92235    5.9587
                              92238    2.5412    1  1.0     293  end
'np277-4: spacer (HAC_MD&H)'
'HAC min.den.(95.3157 lb/ft3) and hydrogen'
'np277-4 min.den.= 1.526803 = (95.3157 lb/ft3)(453.59 g/lb)/(28316.84 cm3/ft3)'
'use 75% of boron in calculations per NUREG-1609 Section 6.5.3.2'
arbmboron 7.31015e-2  2 0 0 0    5010   18.1479
                                 5011   81.8520    2  0.7500  293  end
arbmnpmx  1.07071e+0 10 0 0 0    6012    1.9188
                                 7014    0.0141
                                 8016   43.4254
                                11023    0.1174
                                12000    0.3378
```

```
                                13027   39.0477
                                14000    2.4671
                                16000    0.3083
                                20000   11.8335
                                26000    0.5298    2  1.0000  293  end
arbmnph2o 3.82995e-1  2 0 0 0    1001   11.1913
                                 8016   88.8087    2  1.0000  293  end
'flooded containmment vessel and content cans -- 10 CFR 71.55(d)(3)'
arbmwicv   0.9982   2 0 0 0    1001   11.1913
                               8016   88.8087    3  1       293  end
'steel: containment vessel body 16.60 lb but use 15.74 lb'
ss304                                            8  1.0     293  end
'steel: cv flange lower use 3.36 lb'
ss304                                            9  0.97267 293  end
'steel: cv flange upper use 13.75 lb'
ss304                                           10  0.94348 293  end
'np277-4: confinement -- neutron poison inner liner (HAC_MD&H)'
'actual vol.= 1.28314e4 cm3 = (7.83023e2 in3)(16.387064)'
'den.multiplier = 1.28314e4 cm3 (actual vol.) / 1.32708e4 cm3 (model vol.)'
'np277-4 min.den.= 1.526803 = (95.3157 lb/ft3)(453.59 g/lb)/(28316.84 cm3/ft3)'
'density = 1.476265 = (den.mult)(np277-4 min.den.) = 0.9668933*1.526803'
'use 75% of boron in calculations per NUREG-1609 Section 6.5.3.2'
arbmboron 7.06813e-2  2 0 0 0    5010   18.1479
                                 5011   81.8520   11  0.7500  293  end
arbmnpmx  1.03525e+0 10 0 0 0    6012    1.9188
                                 7014    0.0141
                                 8016   43.4254
                                11023    0.1174
                                12000    0.3378
                                13027   39.0477
                                14000    2.4671
                                16000    0.3083
                                20000   11.8335
                                26000    0.5298   11  1.0000  293  end
arbmnph2o 3.70316e-1  2 0 0 0    1001   11.1913
                                 8016   88.8087   11  1.0000  293  end
'kaolite 1600 body'
'nct.sing.unit.density= (den.mult)(min.den.)'
' for arbmh20k 0.52294 = 1.012373*0.51655, for rest 0.34864 = 1.012373*0.34438'
'den.mult= 1.36557e5 cm3 (actual vol.) / 1.34888e5 cm3 (model vol.)'
'actual vol.= 1.36557e5 cm3 = (28316.84 cm3/ft3)(108.33188 lb)/(22.464 lb/ft3)'
'hac.s.u.dens= (hac.mult)(nct.s.u.dens)'
'hac.mult = 1.34888e5 cm3 (nct vol.)/ 1.12246e5 cm3 (model vol.)'
' for arbmh2ok 0.62843 = 1.20172*0.52294,   for rest = 1.20172*0.34864'
'hac array densities are hac s.u.dens.'
arbmh2ok   0.62843  2 0 0 0    1001   11.1913
                               8016   88.8087   12  0.0287  293  end
arbmal2o3  0.41898  2 0 0 0   13027   52.9390
                               8016   47.0610   12  0.096   293  end
arbmsio2   0.41898  2 0 0 0   14000   46.7570
                               8016   53.2430   12  0.367   293  end
arbmfe2o3  0.41898  2 0 0 0   26000   69.9540
                               8016   30.0460   12  0.067   293  end
arbmtio2   0.41898  2 0 0 0   22000   59.9535
                               8016   40.0465   12  0.012   293  end
arbmcao    0.41898  2 0 0 0   20000   71.4815
                               8016   28.5185   12  0.307   293  end
arbmmgo    0.41898  2 0 0 0   12000   60.3169
                               8016   39.6831   12  0.131   293  end
arbmna2o   0.41898  2 0 0 0   11023   74.1961
                               8016   25.8039   12  0.020   293  end
'kaolite 1600 top plug'
'sing.unit.density= (den.mult)(min.den.)'
' for arbmh20k = 0.965246*0.51655,  for rest = 0.965246*0.34438'
'den.mult= 1.21592e4 cm3 (actual vol.) / 1.25970e4 cm3 (model vol.)'
'actual vol.= 1.21592e4 cm3 = (28316.84 cm3/ft3)(9.646 lb)/(22.464 lb/ft3)'
arbmh2ok   0.49860  2 0 0 0    1001   11.1913
                               8016   88.8087   13  0.0287  293  end
arbmal2o3  0.33241  2 0 0 0   13027   52.9390
                               8016   47.0610   13  0.096   293  end
arbmsio2   0.33241  2 0 0 0   14000   46.7570
```

```
                                8016   53.2430   13  0.367   293  end
arbmfe2o3  0.33241  2 0 0 0   26000   69.9540
                                8016   30.0460   13  0.067   293  end
arbmtio2   0.33241  2 0 0 0   22000   59.9535
                                8016   40.0465   13  0.012   293  end
arbmcao    0.33241  2 0 0 0   20000   71.4815
                                8016   28.5185   13  0.307   293  end
arbmmgo    0.33241  2 0 0 0   12000   60.3169
                                8016   39.6831   13  0.131   293  end
arbmna2o   0.33241  2 0 0 0   11023   74.1961
                                8016   25.8039   13  0.020   293  end
'silicone rubber pads'
arbmsiru   1.21791  4 0 0 0    6012   32.3767
                                1001    8.1573
                                8016   21.5782
                               14000   37.8878   14  1.0     293  end
'void space external to containment vessel'
arbmwecv   0.9982   2 0 0 0    1001   11.1913
                                8016   88.8087   15  0.0001  293  end
'steel: liner'
ss304                                            16  1.0     293  end
'steel: plug cover (pc) use 9.907 lb'
ss304                                            17  1.06388 293  end
'steel: angle iron (ai) for HAC'
'nct density is multiplied by volume fraction 7.08030/5.74516'
ss304                                            18  1.23239 293  end
'steel: drum steel for HAC'
'nct density is multiplied by volume fraction 3.20482/2.95645'
ss304                                            19  1.08401 293  end
'void space external to drum'
'array density is assumed not reduced by hac'
arbmwed    0.9982   2 0 0 0    1001   11.1913
                                8016   88.8087   20  0.0001  293  end
'reflective water'
'arbmh20r   0.9982   2 0 0 0    1001   11.1913
'                               8016   88.8087   21  1.0     293  end
end comp
hciatriga_70 0.0in thk np, 6847.1gUZrHx(  408.0g235, 8998.2gH2O,hx=575.64),fr=1.0e-04
read parameters nub=yes npg=2500 gen=215 nsk=15 tme=100 end parameters
read boun       all=specular                     end boun
read geometry
unit 1001
'drum bottom flat cover [Elev= 0.105 in. at top of unit]'
'cylinder  19 1   21.838092    0.26670   0.0     com='extended radius not used'
 cylinder  19 1   21.838092    0.26670   0.0     com='drum bottom flat cover'
 cuboid    20 1 4p21.838092    0.26670   0.0     com='drum(chine)outer radius'
unit 1002
'above drum bottom flat cover and below containment vessel [Elev= 4.670 in.]'
 cylinder  15 1    3.175000   11.59510  11.16330 com='void in pad-1'
 cylinder  14 1    7.924800   11.59510  11.16330 com='pad-1'
 cylinder  16 1    8.077200   11.59510  11.16330 com='np277_4 liner'
 cylinder  11 1   10.922000   11.59510  11.16330 com='np277_4'
 cylinder  16 1   11.074400   11.59510  10.85850 com='kaolite liner bottom'
 cylinder  12 1   21.685692   11.59510   0.0     com='kaolite'
 cylinder  19 1   21.838092   11.59510   0.0     com='drum'
 cuboid    20 1 4p21.838092   11.59510   0.0     com='drum(chine)outer radius'
unit 1003
'cv bottom [Elev= 4.920 in.]'
 cylinder  8  1    6.680200    0.63500   0.0     com='cv bottom'
 cylinder  15 1    7.924800    0.63500   0.0     com='void btw cv-np liner'
 cylinder  16 1    8.077200    0.63500   0.0     com='np277_4 liner'
 cylinder  11 1   10.922000    0.63500   0.0     com='np277_4'
 cylinder  16 1   11.074400    0.63500   0.0     com='kaolite liner'
 cylinder  12 1   21.685692    0.63500   0.0     com='kaolite'
 cylinder  19 1   21.838092    0.63500   0.0     com='drum'
 cuboid    20 1 4p21.838092    0.63500   0.0     com='drum(chine)outer radius'
unit 1004
'UZrHx fuel element'
 cylinder  1  1    1.828800   12.70000   0.0     com='cylindrical content'
unit 1006
'content (collapsed) [Elev= 9.920 in.]'
```

```
'1.437900   plus-y location upper cylinders'
'-2.875700  minus-y location lower cylinder'
'2.490443   plus-x location upper cylinder'
'-2.490443  minus-x location upper cylinder'
 cylinder  3  1    6.426200   12.70050  -0.0005  com='cv well cavity'
 hole  1004   -2.490443  1.437900  0.0     com='cyl1'
 hole  1004    2.490443  1.437900  0.0     com='cyl2'
 hole  1004    0.0      -2.875700  0.0     com='cyl3'
 cylinder  8  1    6.680200   12.70050  -0.0005  com='cv below 1st step'
 cylinder  15 1    7.924800   12.70050  -0.0005  com='void btw cv-np liner'
 cylinder  16 1    8.077200   12.70050  -0.0005  com='np277_4 liner'
 cylinder  11 1   10.922000   12.70050  -0.0005  com='np277_4'
 cylinder  16 1   11.074400   12.70050  -0.0005  com='kaolite liner'
 cylinder  12 1   21.685692   12.70050  -0.0005  com='kaolite'
 cylinder  19 1   21.838092   12.70050  -0.0005  com='drum'
 cuboid    20 1 4p21.838092   12.70050  -0.0005  com='drum chine outer radius'
unit 1007
'np277_4 spacer [Elev= 9.921 in.]'
 cylinder  2  1    5.24510     0.00010   0.0     com='np spacer'
 cylinder  3  1    6.426200    0.00020  -0.0001  com='cv well cavity'
 cylinder  8  1    6.680200    0.00020  -0.0001  com='cv below 1st step'
 cylinder  15 1    7.924800    0.00020  -0.0001  com='void btw cv-np liner'
 cylinder  16 1    8.077200    0.00020  -0.0001  com='np277_4 liner'
 cylinder  11 1   10.922000    0.00020  -0.0001  com='np277_4'
 cylinder  16 1   11.074400    0.00020  -0.0001  com='kaolite liner'
 cylinder  12 1   21.685692    0.00020  -0.0001  com='kaolite'
 cylinder  19 1   21.838092    0.00020  -0.0001  com='drum'
 cuboid    20 1 4p21.838092    0.00020  -0.0001  com='drum(chine)outer radius'
unit 1008
'top of content stack to bottom of 1st step [Elev=35.270 in.]'
'38.10360             stack height (content spacers)       CALCULATED
 cylinder  3  1    6.426200   38.98540   0.0     com='cv well cavity'
 cylinder  8  1    6.680200   38.98540   0.0     com='cv below 1st step'
 cylinder  15 1    7.924800   38.98540   0.0     com='void btw cv-np liner'
 cylinder  16 1    8.077200   38.98540   0.0     com='np277_4 liner'
 cylinder  11 1   10.922000   38.98540   0.0     com='np277_4'
 cylinder  16 1   11.074400   38.98540   0.0     com='kaolite liner'
 cylinder  12 1   21.685692   38.98540   0.0     com='kaolite'
 cylinder  19 1   21.838092   38.98540   0.0     com='drum'
 cuboid    20 1 4p21.838092   38.98540   0.0     com='drum(chine)outer radius'
unit 1010
'cv at 1st step in liner [Elev=35.330 in.]'
 cylinder  3  1    6.426200    0.15240   0.0     com='cv well cavity'
 cylinder  8  1    6.680200    0.15240   0.0     com='cv at 1st step'
 cylinder  15 1    7.924800    0.15240   0.0     com='void btw cv and liner'
 cylinder  16 1   11.074400    0.15240   0.0     com='liner 1st step'
 cylinder  12 1   21.685692    0.15240   0.0     com='kaolite'
 cylinder  19 1   21.838092    0.15240   0.0     com='drum'
 cuboid    20 1 4p21.838092    0.15240   0.0     com='drum(chine)outer radius'
unit 1011
'vertical gap between 1st step in liner and cv flange [Elev=35.420 in.]'
 cylinder  3  1    6.426200    0.22860   0.0     com='cv well cavity'
 cylinder  8  1    6.680200    0.22860   0.0     com='cv at gap btwn step-flng'
 cylinder  15 1   10.922000    0.22860   0.0     com='void btw cv and liner'
 cylinder  16 1   11.074400    0.22860   0.0     com='liner wall'
 cylinder  12 1   21.685692    0.22860   0.0     com='kaolite'
 cylinder  19 1   21.838092    0.22860   0.0     com='drum'
 cuboid    20 1 4p21.838092    0.22860   0.0     com='drum(chine)outer radius'
unit 1012
'cv flange to top of cv well [Elev=35.920 in.]'
 cylinder  3  1    6.426200    1.27000   0.0     com='cavity'
 cylinder  9  1    9.525000    1.27000   0.0     com='flange to top of well'
 cylinder  15 1    9.525000    1.27000   0.0     com='void btw cv and pad-2'
 cylinder  14 1   10.033000    1.27000   0.0     com='pad-2'
 cylinder  15 1   10.922000    1.27000   0.0     com='void btw cv and liner'
 cylinder  16 1   11.074400    1.27000   0.0     com='liner wall'
 cylinder  12 1   21.685692    1.27000   0.0     com='kaolite'
 cylinder  19 1   21.838092    1.27000   0.0     com='drum'
 cuboid    20 1 4p21.838092    1.27000   0.0     com='drum(chine)outer radius'
unit 1013
'cv flange above cv well [Elev=37.070 in.]'
```

```
 cylinder  10 1    9.525000    2.92100   0.0     com='flange above cv well'
 cylinder  15 1    9.525000    2.92100   0.0     com='void btw cv and pad-2'
 cylinder  14 1   10.033000    2.92100   0.0     com='pad-2'
 cylinder  15 1   10.922000    2.92100   0.0     com='void btw pad2 and liner'
 cylinder  16 1   11.074400    2.92100   0.0     com='liner wall'
 cylinder  12 1   21.685692    2.92100   0.0     com='kaolite'
 cylinder  19 1   21.838092    2.92100   0.0     com='drum'
 cuboid    20 1 4p21.838092    2.92100   0.0     com='drum(chine)outer radius'
unit 1014
'plugpad2 below liner 2nd step [Elev=37.470 in.]'
 cylinder  14 1   10.033000    0.76200   0.0     com='pad-2'
 cylinder  15 1   10.922000    1.01600   0.0     com='void btw pad2 and liner'
 cylinder  16 1   11.074400    1.01600   0.0     com='liner wall'
 cylinder  12 1   21.685692    1.01600   0.0     com='kaolite'
 cylinder  19 1   21.838092    1.01600   0.0     com='drum'
 cuboid    20 1 4p21.838092    1.01600   0.0     com='drum(chine)outer radius'
unit 1015
'2nd step in liner [Elev=37.530 in.]'
 cylinder  15 1   10.922000    0.15240   0.0     com='void abv pad2'
 cylinder  16 1   18.757900    0.15240   0.0     com='liner 2nd step'
 cylinder  12 1   21.685692    0.15240   0.0     com='kaolite'
 cylinder  19 1   21.838092    0.15240   0.0     com='drum'
 cuboid    20 1 4p21.838092    0.15240   0.0     com='drum(chine)outer radius'
unit 1016
'abv 2nd step in liner to bottom of angle iron [Elev=40.750 in.]'
 cylinder  13 1   18.097500    8.17880   0.49276 com='plug kaolite'
 cylinder  17 1   18.249900    8.17880   0.34036 com='sides of plug case'
 cylinder  15 1   18.605500    8.17880   0.0     com='void: plug to liner'
 cylinder  16 1   18.757900    8.17880   0.0     com='liner wall'
 cylinder  12 1   21.685692    8.17880   0.0     com='kaolite'
 cylinder  19 1   21.838092    8.17880   0.0     com='drum'
 cuboid    20 1 4p21.838092    8.17880   0.0     com='drum(chine)outer radius'
unit 1017
'bottom of angle iron to bend in angle iron [Elev=42.500 in.]'
 cylinder  13 1   18.097500    4.44500   0.0     com='plug kaolite'
 cylinder  17 1   18.249900    4.44500   0.0     com='sides of plug case'
 cylinder  15 1   18.605500    4.44500   0.0     com='void: plug to liner'
 cylinder  16 1   18.757900    4.44500   0.0     com='liner wall'
 cylinder  18 1   19.392900    4.44500   0.0     com='lower angle iron'
 cylinder  12 1   21.685692    4.44500   0.0     com='kaolite'
 cylinder  19 1   21.838092    4.44500   0.0     com='drum'
 cuboid    20 1 4p21.838092    4.44500   0.0     com='drum(chine)outer radius'
unit 1018
'bend in angle iron to top of angle iron [Elev=42.750 in.]'
 cylinder  13 1   18.097500    0.11176   0.0     com='plug kaolite'
 cylinder  17 1   18.249900    0.26416   0.0     com='sides of plug case'
 cylinder  15 1   18.605500    0.63500   0.0     com='void: plug to liner'
 cylinder  16 1   18.757900    0.63500   0.0     com='liner wall'
 cylinder  18 1   21.685692    0.63500   0.0     com='bend section of ai'
 cylinder  19 1   21.838092    0.63500   0.0     com='drum'
 cuboid    20 1 4p21.838092    0.63500   0.0     com='drum(chine)outer radius'
unit 1019
'drum lid and lip [Elev=43.500 in.]'
 cylinder  20 1   21.469792    1.90500   0.15240 com='void above lid'
 cylinder  19 1   21.622192    1.90500   0.0     com='drum lid'
 cylinder  20 1   21.685692    1.90500   0.0     com='void btw lid - drum wall'
 cylinder  19 1   21.838092    1.90500   0.0     com='drum'
 cuboid    20 1 4p21.838092    1.90500   0.0     com='drum(chine)outer radius'
global
unit 1020
'es3100 drum [Elev=43.500 in.]'
array 3         2r-21.838092     0.0
'cuboid     0  1 4p21.838092    110.4905  0.0    com='bare package'
'cuboid    21  1 4p52.318092   140.9700 -30.48   com='reflected package'
 cuboid    20  1 4p22.889718    110.5048  0.0    com='interstital array space'
'global
'unit 1021
'array 4   3r0.0
'reflector  21 2  6r3.0  10
end geometry
read array
```

```
ara=3 nux=1 nuy=1 nuz=19 fill
1001 1002 1003 1006 1007 1006 1007 1006 1008 1010
1011 1012 1013 1014 1015 1016 1017 1018 1019        end fill
'ara=4 nux=13 nuy=13 nuz=06 fill f1020               end fill
end array
'read bias id=500 2  11  end bias
read start nst=0
end start
end data
end


=csas25    parm=size=3000000
ncsrT70131 0.0in thk np, 5666.6gUZrHx(  337.7g235, 9204.9gH2O hx=711.53),fr=1.0e+00
238groupndf5 infhommedium
'TRIGA volume = 993.90789, SPACER volume    0.00000'
'TRIGA wrapped dry content can hx=49.6, CV void volume 9221.45406'
arbmtriga  5.70132  4 0 0 0    1001    1.5894
                              40000   89.9107
                              92235    5.9587
                              92238    2.5412    1  1.0     293  end
'np277-4: spacer (NCT_MD&H)'
'NCT min.den.(95.3886 lb/ft3) and hydrogen'
'np277-4 min.den.= 1.527971 = (95.3886 lb/ft3)(453.59 g/lb)/(28316.84 cm3/ft3)'
'use 75% of boron in calculations per NUREG-1609 Section 6.5.3.2'
arbmboron 7.31015e-2  2 0 0 0    5010   18.1479
                                 5011   81.8520    2  0.7500  293  end
arbmnpmx  1.07070e+0 10 0 0 0    6012    1.9189
                                 7014    0.0141
                                 8016   43.4251
                                11023    0.1174
                                12000    0.3378
                                13027   39.0479
                                14000    2.4672
                                16000    0.3083
                                20000   11.8336
                                26000    0.5298    2  1.0000  293  end
arbmnph2o 3.84169e-1  2 0 0 0    1001   11.1913
                                 8016   88.8087    2  1.0000  293  end
'flooded containmment vessel and content cans -- 10 CFR 71.55(d)(3)'
arbmwicv   0.9982   2 0 0 0    1001   11.1913
                               8016   88.8087    3  1       293  end
'steel: containment vessel body 16.60 lb but use 15.74 lb'
ss304                                            8  1.0     293  end
'steel: cv flange lower use 3.36 lb'
ss304                                            9  0.97267 293  end
'steel: cv flange upper use 13.75 lb'
ss304                                           10  0.94348 293  end
'np277-4: confinement -- neutron poison inner liner (NCT_MD&H)'
'actual vol.= 1.28314e4 cm3 = (7.83023e2 in3)(16.387064)'
'den.multiplier = 1.28314e4 cm3 (actual vol.) / 1.32708e4 cm3 (model vol.)'
'np277-4 min.den.= 1.527971 = (95.3886 lb/ft3)(453.59 g/lb)/(28316.84 cm3/ft3)'
'density = 1.477385 = (den.mult)(np277-4 min.den.) = 0.9668933*1.527971'
'use 75% of boron in calculations per NUREG-1609 Section 6.5.3.2'
arbmboron 7.06813e-2  2 0 0 0    5010   18.1479
                                 5011   81.8520   11  0.7500  293  end
arbmnpmx  1.03525e+0 10 0 0 0    6012    1.9189
                                 7014    0.0141
                                 8016   43.4251
                                11023    0.1174
                                12000    0.3378
                                13027   39.0479
                                14000    2.4672
                                16000    0.3083
                                20000   11.8336
                                26000    0.5298   11  1.0000  293  end
arbmnph2o 3.71451e-1  2 0 0 0    1001   11.1913
                                 8016   88.8087   11  1.0000  293  end
'kaolite 1600 body'
'sing.unit.density= (den.mult)(min.den.)'
' for arbmh20k = 1.012373*0.51655,  for rest = 1.012373*0.34438'
```

```
'den.mult= 1.36557e5 cm3 (actual vol.) / 1.34888e5 cm3 (model vol.)'
'actual vol.= 1.36557e5 cm3 = (28316.84 cm3/ft3)(108.33188 lb)/(22.464 lb/ft3)'
arbmh2ok   0.52294  2 0 0 0    1001   11.1913
                               8016   88.8087   12  1       293  end
arbmal2o3  0.34864  2 0 0 0   13027   52.9390
                               8016   47.0610   12  0.096   293  end
arbmsio2   0.34864  2 0 0 0   14000   46.7570
                               8016   53.2430   12  0.367   293  end
arbmfe2o3  0.34864  2 0 0 0   26000   69.9540
                               8016   30.0460   12  0.067   293  end
arbmtio2   0.34864  2 0 0 0   22000   59.9535
                               8016   40.0465   12  0.012   293  end
arbmcao    0.34864  2 0 0 0   20000   71.4815
                               8016   28.5185   12  0.307   293  end
arbmmgo    0.34864  2 0 0 0   12000   60.3169
                               8016   39.6831   12  0.131   293  end
arbmna2o   0.34864  2 0 0 0   11023   74.1961
                               8016   25.8039   12  0.020   293  end
'kaolite 1600 top plug'
'sing.unit.density= (den.mult)(min.den.)'
' for arbmh20k = 0.965246*0.51655,  for rest = 0.965246*0.34438'
'den.mult= 1.21592e4 cm3 (actual vol.) / 1.25970e4 cm3 (model vol.)'
'actual vol.= 1.21592e4 cm3 = (28316.84 cm3/ft3)(9.646 lb)/(22.464 lb/ft3)'
arbmh2ok   0.49860  2 0 0 0    1001   11.1913
                               8016   88.8087   13  1       293  end
arbmal2o3  0.33241  2 0 0 0   13027   52.9390
                               8016   47.0610   13  0.096   293  end
arbmsio2   0.33241  2 0 0 0   14000   46.7570
                               8016   53.2430   13  0.367   293  end
arbmfe2o3  0.33241  2 0 0 0   26000   69.9540
                               8016   30.0460   13  0.067   293  end
arbmtio2   0.33241  2 0 0 0   22000   59.9535
                               8016   40.0465   13  0.012   293  end
arbmcao    0.33241  2 0 0 0   20000   71.4815
                               8016   28.5185   13  0.307   293  end
arbmmgo    0.33241  2 0 0 0   12000   60.3169
                               8016   39.6831   13  0.131   293  end
arbmna2o   0.33241  2 0 0 0   11023   74.1961
                               8016   25.8039   13  0.020   293  end
'silicone rubber pads'
arbmsiru   1.21791  4 0 0 0    6012   32.3767
                               1001    8.1573
                               8016   21.5782
                              14000   37.8878   14  1.0     293  end
'void space external to containment vessel'
arbmwecv   0.9982   2 0 0 0    1001   11.1913
                               8016   88.8087   15  1       293  end
'steel: liner'
ss304                                            16  1.0     293  end
'steel: plug cover (pc) use 9.907 lb'
ss304                                            17  1.06388 293  end
'steel: angle iron (ai) for single units'
ss304                                            18  1.0     293  end
'steel: angle iron (ai) for arrays'
'array density is multiplied by a volume fraction 7.08030/5.63249'
'ss304                                            18  1.25705 293  end
'steel: drum steel for single units'
ss304                                            19  1.0     293  end
'steel: drum steel for arrays'
'array density is multiplied by a volume fraction 3.20482/3.20544'
'ss304                                            19  0.99981 293  end
'void space external to drum'
'array density is multiplied by a volume ratio 8.11698/6.98323'
'arbmwed    1.16026  2 0 0 0    1001   11.1913
'                               8016   88.8087   20  1       293  end
'reflective water'
arbmh20r   0.9982   2 0 0 0    1001   11.1913
                               8016   88.8087   21  1.0     293  end
end comp
ncsrT70131 0.0in thk np, 5666.6gUZrHx(  337.7g235, 9204.9gH2O,hx=711.53),fr=1.0e+00
read parameters nub=yes npg=2500 gen=215 nsk=15 tme=100 end parameters
```

```
read boun       all=vac                         end boun
read geometry
unit 1001
'drum bottom flat cover [Elev= 0.105 in. at top of unit]'
'cylinder  19 1   24.587200    0.26670   0.0     com='extended radius not used'
 cylinder  19 1   23.329900    0.26670   0.0     com='drum bottom flat cover'
 cuboid    21 1 4p24.587200    0.26670   0.0     com='drum chine outer radius'
unit 1002
'above drum bottom flat cover and below containment vessel [Elev= 4.670 in.]'
 cylinder  15 1    3.175000   11.59510  11.16330 com='void in pad-1'
 cylinder  14 1    7.924800   11.59510  11.16330 com='pad-1'
 cylinder  16 1    8.077200   11.59510  11.16330 com='np277_4 liner'
 cylinder  11 1   10.922000   11.59510  11.16330 com='np277_4'
 cylinder  16 1   11.074400   11.59510  10.85850 com='kaolite liner bottom'
 cylinder  12 1   23.177500   11.59510   0.0     com='kaolite'
 cylinder  19 1   23.329900   11.59510   0.0     com='drum'
 cuboid    21 1 4p24.587200   11.59510   0.0     com='drum chine outer radius'
unit 1003
'cv bottom [Elev= 4.920 in.]'
 cylinder  8  1    6.680200    0.63500   0.0     com='cv bottom'
 cylinder  15 1    7.924800    0.63500   0.0     com='void btw cv-np liner'
 cylinder  16 1    8.077200    0.63500   0.0     com='np277_4 liner'
 cylinder  11 1   10.922000    0.63500   0.0     com='np277_4'
 cylinder  16 1   11.074400    0.63500   0.0     com='kaolite liner'
 cylinder  12 1   23.177500    0.63500   0.0     com='kaolite'
 cylinder  19 1   23.329900    0.63500   0.0     com='drum'
 cuboid    21 1 4p24.587200    0.63500   0.0     com='drum chine outer radius'
unit 1004
'UZrHx fuel element'
 cylinder  1  1    1.663700   12.70000   0.0     com='cylindrical content'
unit 1006
'content (collapsed) [Elev= 9.920 in.]'
'1.437900   plus-y location upper cylinders'
'-2.875700  minus-y location lower cylinder'
'2.490443   plus-x location upper cylinder'
'-2.490443  minus-x location upper cylinder'
 cylinder  3  1    6.426200   12.70050  -0.0005  com='cv well cavity'
 hole  1004   -2.490443  1.437900  0.0     com='cyl1'
 hole  1004    2.490443  1.437900  0.0     com='cyl2'
 hole  1004    0.0      -2.875700  0.0     com='cyl3'
 cylinder  8  1    6.680200   12.70050  -0.0005  com='cv below 1st step'
 cylinder  15 1    7.924800   12.70050  -0.0005  com='void btw cv-np liner'
 cylinder  16 1    8.077200   12.70050  -0.0005  com='np277_4 liner'
 cylinder  11 1   10.922000   12.70050  -0.0005  com='np277_4'
 cylinder  16 1   11.074400   12.70050  -0.0005  com='kaolite liner'
 cylinder  12 1   23.177500   12.70050  -0.0005  com='kaolite'
 cylinder  19 1   23.329900   12.70050  -0.0005  com='drum'
 cuboid    21 1 4p24.587200   12.70050  -0.0005  com='drum chine outer radius'
unit 1007
'np277_4 spacer [Elev= 9.921 in.]'
 cylinder  2  1    5.24510     0.00010   0.0     com='np spacer'
 cylinder  3  1    6.426200    0.00020  -0.0001  com='cv well cavity'
 cylinder  8  1    6.680200    0.00020  -0.0001  com='cv below 1st step'
 cylinder  15 1    7.924800    0.00020  -0.0001  com='void btw cv-np liner'
 cylinder  16 1    8.077200    0.00020  -0.0001  com='np277_4 liner'
 cylinder  11 1   10.922000    0.00020  -0.0001  com='np277_4'
 cylinder  16 1   11.074400    0.00020  -0.0001  com='kaolite liner'
 cylinder  12 1   23.177500    0.00020  -0.0001  com='kaolite'
 cylinder  19 1   23.329900    0.00020  -0.0001  com='drum'
 cuboid    21 1 4p24.587200    0.00020  -0.0001  com='drum chine outer radius'
unit 1008
'top of content stack to bottom of 1st step [Elev=35.270 in.]'
'38.10360             stack height (content spacers)       CALCULATED
 cylinder  3  1    6.426200   38.98540   0.0     com='cv well cavity'
 cylinder  8  1    6.680200   38.98540   0.0     com='cv below 1st step'
 cylinder  15 1    7.924800   38.98540   0.0     com='void btw cv-np liner'
 cylinder  16 1    8.077200   38.98540   0.0     com='np277_4 liner'
 cylinder  11 1   10.922000   38.98540   0.0     com='np277_4'
 cylinder  16 1   11.074400   38.98540   0.0     com='kaolite liner'
 cylinder  12 1   23.177500   38.98540   0.0     com='kaolite'
 cylinder  19 1   23.329900   38.98540   0.0     com='drum'
```

```
 cuboid    21 1 4p24.587200   38.98540   0.0     com='drum chine outer radius'
unit 1010
'cv at 1st step in liner [Elev=35.330 in.]'
 cylinder  3  1    6.426200    0.15240   0.0     com='cv well cavity'
 cylinder  8  1    6.680200    0.15240   0.0     com='cv at 1st step'
 cylinder  15 1    7.924800    0.15240   0.0     com='void btw cv and liner'
 cylinder  16 1   11.074400    0.15240   0.0     com='liner 1st step'
 cylinder  12 1   23.177500    0.15240   0.0     com='kaolite'
 cylinder  19 1   23.329900    0.15240   0.0     com='drum'
 cuboid    21 1 4p24.587200    0.15240   0.0     com='drum chine outer radius'
unit 1011
'vertical gap between 1st step in liner and cv flange [Elev=35.420 in.]'
 cylinder  3  1    6.426200    0.22860   0.0     com='cv well cavity'
 cylinder  8  1    6.680200    0.22860   0.0     com='cv at gap btwn step-flng'
 cylinder  15 1   10.922000    0.22860   0.0     com='void btw cv and liner'
 cylinder  16 1   11.074400    0.22860   0.0     com='liner wall'
 cylinder  12 1   23.177500    0.22860   0.0     com='kaolite'
 cylinder  19 1   23.329900    0.22860   0.0     com='drum'
 cuboid    21 1 4p24.587200    0.22860   0.0     com='drum chine outer radius'
unit 1012
'cv flange to top of cv well [Elev=35.920 in.]'
 cylinder  3  1    6.426200    1.27000   0.0     com='cavity'
 cylinder  9  1    9.525000    1.27000   0.0     com='flange to top of well'
 cylinder  15 1    9.525000    1.27000   0.0     com='void btw cv and pad-2'
 cylinder  14 1   10.033000    1.27000   0.0     com='pad-2'
 cylinder  15 1   10.922000    1.27000   0.0     com='void btw cv and liner'
 cylinder  16 1   11.074400    1.27000   0.0     com='liner wall'
 cylinder  12 1   23.177500    1.27000   0.0     com='kaolite'
 cylinder  19 1   23.329900    1.27000   0.0     com='drum'
 cuboid    21 1 4p24.587200    1.27000   0.0     com='drum chine outer radius'
unit 1013
'cv flange above cv well [Elev=37.070 in.]'
 cylinder  10 1    9.525000    2.92100   0.0     com='flange above cv well'
 cylinder  15 1    9.525000    2.92100   0.0     com='void btw cv and pad-2'
 cylinder  14 1   10.033000    2.92100   0.0     com='pad-2'
 cylinder  15 1   10.922000    2.92100   0.0     com='void btw pad2 and liner'
 cylinder  16 1   11.074400    2.92100   0.0     com='liner wall'
 cylinder  12 1   23.177500    2.92100   0.0     com='kaolite'
 cylinder  19 1   23.329900    2.92100   0.0     com='drum'
 cuboid    21 1 4p24.587200    2.92100   0.0     com='drum chine outer radius'
unit 1014
'plugpad2 below liner 2nd step [Elev=37.470 in.]'
 cylinder  14 1   10.033000    0.76200   0.0     com='pad-2'
 cylinder  15 1   10.922000    1.01600   0.0     com='void btw pad2 and liner'
 cylinder  16 1   11.074400    1.01600   0.0     com='liner wall'
 cylinder  12 1   23.177500    1.01600   0.0     com='kaolite'
 cylinder  19 1   23.329900    1.01600   0.0     com='drum'
 cuboid    21 1 4p24.587200    1.01600   0.0     com='drum chine outer radius'
unit 1015
'2nd step in liner [Elev=37.530 in.]'
 cylinder  15 1   10.922000    0.15240   0.0     com='void abv pad2'
 cylinder  16 1   18.757900    0.15240   0.0     com='liner 2nd step'
 cylinder  12 1   23.177500    0.15240   0.0     com='kaolite'
 cylinder  19 1   23.329900    0.15240   0.0     com='drum'
 cuboid    21 1 4p24.587200    0.15240   0.0     com='drum chine outer radius'
unit 1016
'abv 2nd step in liner to bottom of angle iron [Elev=40.750 in.]'
 cylinder  13 1   18.097500    8.17880   0.49276 com='plug kaolite'
 cylinder  17 1   18.249900    8.17880   0.34036 com='sides of plug case'
 cylinder  15 1   18.605500    8.17880   0.0     com='void: plug to liner'
 cylinder  16 1   18.757900    8.17880   0.0     com='liner wall'
 cylinder  12 1   23.177500    8.17880   0.0     com='kaolite'
 cylinder  19 1   23.329900    8.17880   0.0     com='drum'
 cuboid    21 1 4p24.587200    8.17880   0.0     com='drum chine outer radius'
unit 1017
'bottom of angle iron to bend in angle iron [Elev=42.500 in.]'
 cylinder  13 1   18.097500    4.44500   0.0     com='plug kaolite'
 cylinder  17 1   18.249900    4.44500   0.0     com='sides of plug case'
 cylinder  15 1   18.605500    4.44500   0.0     com='void: plug to liner'
 cylinder  16 1   18.757900    4.44500   0.0     com='liner wall'
 cylinder  18 1   19.392900    4.44500   0.0     com='lower angle iron'
```

```
 cylinder  12 1   23.177500    4.44500   0.0     com='kaolite'
 cylinder  19 1   23.329900    4.44500   0.0     com='drum'
 cuboid    21 1 4p24.587200    4.44500   0.0     com='drum chine outer radius'
unit 1018
'bend in angle iron to top of angle iron [Elev=42.750 in.]'
 cylinder  13 1   18.097500    0.11176   0.0     com='plug kaolite'
 cylinder  17 1   18.249900    0.26416   0.0     com='sides of plug case'
 cylinder  15 1   18.605500    0.63500   0.0     com='void: plug to liner'
 cylinder  16 1   18.757900    0.63500   0.0     com='liner wall'
 cylinder  18 1   23.177500    0.63500   0.0     com='bend section of ai'
 cylinder  19 1   23.329900    0.63500   0.0     com='drum'
 cuboid    21 1 4p24.587200    0.63500   0.0     com='drum chine outer radius'
unit 1019
'drum lid and lip [Elev=43.500 in.]'
 cylinder  21 1   22.961600    1.90500   0.15240 com='void above lid'
 cylinder  19 1   23.114000    1.90500   0.0     com='drum lid'
 cylinder  21 1   23.177500    1.90500   0.0     com='void btw lid - drum wall'
 cylinder  19 1   23.329900    1.90500   0.0     com='drum'
 cuboid    21 1 4p24.587200    1.90500   0.0     com='drum chine outer radius'
global
unit 1020
'es3100 drum [Elev=43.500 in.]'
array 3         2r-24.587200     0.0
'cuboid     0  1 4p24.587200    110.4905  0.0    com='bare package'
 cuboid    21  1 4p55.067200   140.9700 -30.48   com='reflected package'
'cuboid    20  1 4p22.889718    110.5048  0.0    com='interstital array space'
'global
'unit 1021
'array 4   3r0.0
'reflector  21 2  6r3.0  10
end geometry
read array
ara=3 nux=1 nuy=1 nuz=19 fill
1001 1002 1003 1006 1007 1006 1007 1006 1008 1010
1011 1012 1013 1014 1015 1016 1017 1018 1019        end fill
'ara=4 nux=13 nuy=13 nuz=06 fill f1020               end fill
end array
'read bias id=500 2  11  end bias
read start nst=0
end start
end data
end


=csas25    parm=size=3000000
nciaT70131 0.0in thk np, 5666.6gUZrHx(  337.7g235, 9204.9gH2O hx=711.53),fr=1.0e-04
238groupndf5 infhommedium
'TRIGA volume = 993.90789, SPACER volume    0.00000'
'TRIGA wrapped dry content can hx=49.6, CV void volume 9221.45406'
arbmtriga  5.70132  4 0 0 0    1001    1.5894
                              40000   89.9107
                              92235    5.9587
                              92238    2.5412    1  1.0     293  end
'np277-4: spacer (NCT_MD&H)'
'NCT min.den.(95.3886 lb/ft3) and hydrogen'
'np277-4 min.den.= 1.527971 = (95.3886 lb/ft3)(453.59 g/lb)/(28316.84 cm3/ft3)'
'use 75% of boron in calculations per NUREG-1609 Section 6.5.3.2'
arbmboron 7.31015e-2  2 0 0 0    5010   18.1479
                                 5011   81.8520    2  0.7500  293  end
arbmnpmx  1.07070e+0 10 0 0 0    6012    1.9189
                                 7014    0.0141
                                 8016   43.4251
                                11023    0.1174
                                12000    0.3378
                                13027   39.0479
                                14000    2.4672
                                16000    0.3083
                                20000   11.8336
                                26000    0.5298    2  1.0000  293  end
arbmnph2o 3.84169e-1  2 0 0 0    1001   11.1913
                                 8016   88.8087    2  1.0000  293  end
```

```
'flooded containmment vessel and content cans -- 10 CFR 71.55(d)(3)'
arbmwicv   0.9982   2 0 0 0    1001   11.1913
                               8016   88.8087    3  1       293  end
'steel: containment vessel body 16.60 lb but use 15.74 lb'
ss304                                            8  1.0     293  end
'steel: cv flange lower use 3.36 lb'
ss304                                            9  0.97267 293  end
'steel: cv flange upper use 13.75 lb'
ss304                                           10  0.94348 293  end
'np277-4: confinement -- neutron poison inner liner (NCT_MD&H)'
'actual vol.= 1.28314e4 cm3 = (7.83023e2 in3)(16.387064)'
'den.multiplier = 1.28314e4 cm3 (actual vol.) / 1.32708e4 cm3 (model vol.)'
'np277-4 min.den.= 1.527971 = (95.3886 lb/ft3)(453.59 g/lb)/(28316.84 cm3/ft3)'
'density = 1.477385 = (den.mult)(np277-4 min.den.) = 0.9668933*1.527971'
'use 75% of boron in calculations per NUREG-1609 Section 6.5.3.2'
arbmboron 7.06813e-2  2 0 0 0    5010   18.1479
                                 5011   81.8520   11  0.7500  293  end
arbmnpmx  1.03525e+0 10 0 0 0    6012    1.9189
                                 7014    0.0141
                                 8016   43.4251
                                11023    0.1174
                                12000    0.3378
                                13027   39.0479
                                14000    2.4672
                                16000    0.3083
                                20000   11.8336
                                26000    0.5298   11  1.0000  293  end
arbmnph2o 3.71451e-1  2 0 0 0    1001   11.1913
                                 8016   88.8087   11  1.0000  293  end
'kaolite 1600 body'
'sing.unit.density= (den.mult)(min.den.)'
' for arbmh20k = 1.012373*0.51655,  for rest = 1.012373*0.34438'
'den.mult= 1.36557e5 cm3 (actual vol.) / 1.34888e5 cm3 (model vol.)'
'actual vol.= 1.36557e5 cm3 = (28316.84 cm3/ft3)(108.33188 lb)/(22.464 lb/ft3)'
'nct array densities are s.u.dens. multiplied by volume ratio 1.34888/1.10336'
arbmh2ok   0.63931  2 0 0 0    1001   11.1913
                               8016   88.8087   12  0.0287  293  end
arbmal2o3  0.42622  2 0 0 0   13027   52.9390
                               8016   47.0610   12  0.096   293  end
arbmsio2   0.42622  2 0 0 0   14000   46.7570
                               8016   53.2430   12  0.367   293  end
arbmfe2o3  0.42622  2 0 0 0   26000   69.9540
                               8016   30.0460   12  0.067   293  end
arbmtio2   0.42622  2 0 0 0   22000   59.9535
                               8016   40.0465   12  0.012   293  end
arbmcao    0.42622  2 0 0 0   20000   71.4815
                               8016   28.5185   12  0.307   293  end
arbmmgo    0.42622  2 0 0 0   12000   60.3169
                               8016   39.6831   12  0.131   293  end
arbmna2o   0.42622  2 0 0 0   11023   74.1961
                               8016   25.8039   12  0.020   293  end
'kaolite 1600 top plug'
'sing.unit.density= (den.mult)(min.den.)'
' for arbmh20k = 0.965246*0.51655,  for rest = 0.965246*0.34438'
'den.mult= 1.21592e4 cm3 (actual vol.) / 1.25970e4 cm3 (model vol.)'
'actual vol.= 1.21592e4 cm3 = (28316.84 cm3/ft3)(9.646 lb)/(22.464 lb/ft3)'
arbmh2ok   0.49860  2 0 0 0    1001   11.1913
                               8016   88.8087   13  0.0287  293  end
arbmal2o3  0.33241  2 0 0 0   13027   52.9390
                               8016   47.0610   13  0.096   293  end
arbmsio2   0.33241  2 0 0 0   14000   46.7570
                               8016   53.2430   13  0.367   293  end
arbmfe2o3  0.33241  2 0 0 0   26000   69.9540
                               8016   30.0460   13  0.067   293  end
arbmtio2   0.33241  2 0 0 0   22000   59.9535
                               8016   40.0465   13  0.012   293  end
arbmcao    0.33241  2 0 0 0   20000   71.4815
                               8016   28.5185   13  0.307   293  end
arbmmgo    0.33241  2 0 0 0   12000   60.3169
                               8016   39.6831   13  0.131   293  end
arbmna2o   0.33241  2 0 0 0   11023   74.1961
```

```
                              8016   25.8039   13  0.020   293  end
'silicone rubber pads'
arbmsiru   1.21791  4 0 0 0    6012   32.3767
                              1001    8.1573
                              8016   21.5782
                             14000   37.8878   14  1.0     293  end
'void space external to containment vessel'
arbmwecv   0.9982   2 0 0 0    1001   11.1913
                              8016   88.8087   15  0.0001  293  end
'steel: liner'
ss304                                           16  1.0     293  end
'steel: plug cover (pc) use 9.907 lb'
ss304                                           17  1.06388 293  end
'steel: angle iron (ai) for single units'
'ss304                                           18  1.0     293  end
'steel: angle iron (ai) for arrays'
'array density is multiplied by a volume fraction 7.08030/5.63249'
ss304                                           18  1.25705 293  end
'steel: drum steel for single units'
'ss304                                           19  1.0     293  end
'steel: drum steel for arrays'
'array density is multiplied by a volume fraction 3.20482/3.20544'
ss304                                           19  0.99981 293  end
'void space external to drum'
'array density is multiplied by a volume ratio 8.11698/6.98323'
arbmwed    1.16026  2 0 0 0    1001   11.1913
                              8016   88.8087   20  0.0001  293  end
'reflective water'
'arbmh20r   0.9982   2 0 0 0    1001   11.1913
'                              8016   88.8087   21  1.0     293  end
end comp
nciaT70131 0.0in thk np, 5666.6gUZrHx(  337.7g235, 9204.9gH2O,hx=711.53),fr=1.0e-04
read parameters nub=yes npg=2500 gen=215 nsk=15 tme=100 end parameters
read boun       all=specular                    end boun
read geometry
unit 1001
'drum bottom flat cover [Elev= 0.111 in. at top of unit]'
'cylinder  19 1   22.866096    0.28150   0.0     com='extended radius not used'
 cylinder  19 1   21.722275    0.28150   0.0     com='drum bottom flat cover'
 cuboid    20 1 4p22.866096    0.28150   0.0     com='drum chine outer radius'
unit 1002
'above drum bottom flat cover and below containment vessel [Elev= 4.676 in.]'
 cylinder  15 1    3.175000   11.59510  11.16330 com='void in pad-1'
 cylinder  14 1    7.924800   11.59510  11.16330 com='pad-1'
 cylinder  16 1    8.077200   11.59510  11.16330 com='np277_4 liner'
 cylinder  11 1   10.922000   11.59510  11.16330 com='np277_4'
 cylinder  16 1   11.074400   11.59510  10.85850 com='kaolite liner bottom'
 cylinder  12 1   21.555075   11.59510   0.0     com='kaolite'
 cylinder  19 1   21.722275   11.59510   0.0     com='drum'
 cuboid    20 1 4p22.866096   11.59510   0.0     com='drum chine outer radius'
unit 1003
'cv bottom [Elev= 4.926 in.]'
 cylinder  8  1    6.680200    0.63500   0.0     com='cv bottom'
 cylinder  15 1    7.924800    0.63500   0.0     com='void btw cv-np liner'
 cylinder  16 1    8.077200    0.63500   0.0     com='np277_4 liner'
 cylinder  11 1   10.922000    0.63500   0.0     com='np277_4'
 cylinder  16 1   11.074400    0.63500   0.0     com='kaolite liner'
 cylinder  12 1   21.555075    0.63500   0.0     com='kaolite'
 cylinder  19 1   21.722275    0.63500   0.0     com='drum'
 cuboid    20 1 4p22.866096    0.63500   0.0     com='drum chine outer radius'
unit 1004
'UZrHx fuel element'
 cylinder  1  1    1.663700   12.70000   0.0     com='cylindrical content'
unit 1006
'content (collapsed) [Elev= 9.926 in.]'
'1.437900   plus-y location upper cylinders'
'-2.875700  minus-y location lower cylinder'
'2.490443   plus-x location upper cylinder'
'-2.490443  minus-x location upper cylinder'
 cylinder  3  1    6.426200   12.70050  -0.0005  com='cv well cavity'
 hole  1004   -2.490443  1.437900  0.0     com='cyl1'
```

```
 hole  1004    2.490443  1.437900  0.0     com='cyl2'
 hole  1004    0.0      -2.875700  0.0     com='cyl3'
 cylinder  8  1    6.680200   12.70050  -0.0005  com='cv below 1st step'
 cylinder  15 1    7.924800   12.70050  -0.0005  com='void btw cv-np liner'
 cylinder  16 1    8.077200   12.70050  -0.0005  com='np277_4 liner'
 cylinder  11 1   10.922000   12.70050  -0.0005  com='np277_4'
 cylinder  16 1   11.074400   12.70050  -0.0005  com='kaolite liner'
 cylinder  12 1   21.555075   12.70050  -0.0005  com='kaolite'
 cylinder  19 1   21.722275   12.70050  -0.0005  com='drum'
 cuboid    20 1 4p22.866096   12.70050  -0.0005  com='drum chine outer radius'
unit 1007
'np277_4 spacer [Elev= 9.926 in.]'
 cylinder  2  1    5.24510     0.00010   0.0     com='np spacer'
 cylinder  3  1    6.426200    0.00020  -0.0001  com='cv well cavity'
 cylinder  8  1    6.680200    0.00020  -0.0001  com='cv below 1st step'
 cylinder  15 1    7.924800    0.00020  -0.0001  com='void btw cv-np liner'
 cylinder  16 1    8.077200    0.00020  -0.0001  com='np277_4 liner'
 cylinder  11 1   10.922000    0.00020  -0.0001  com='np277_4'
 cylinder  16 1   11.074400    0.00020  -0.0001  com='kaolite liner'
 cylinder  12 1   21.555075    0.00020  -0.0001  com='kaolite'
 cylinder  19 1   21.722275    0.00020  -0.0001  com='drum'
 cuboid    20 1 4p22.866096    0.00020  -0.0001  com='drum chine outer radius'
unit 1008
'top of content stack to bottom of 1st step [Elev=35.276 in.]'
'38.10360             stack height (content spacers)       CALCULATED
 cylinder  3  1    6.426200   38.98540   0.0     com='cv well cavity'
 cylinder  8  1    6.680200   38.98540   0.0     com='cv below 1st step'
 cylinder  15 1    7.924800   38.98540   0.0     com='void btw cv-np liner'
 cylinder  16 1    8.077200   38.98540   0.0     com='np277_4 liner'
 cylinder  11 1   10.922000   38.98540   0.0     com='np277_4'
 cylinder  16 1   11.074400   38.98540   0.0     com='kaolite liner'
 cylinder  12 1   21.555075   38.98540   0.0     com='kaolite'
 cylinder  19 1   21.722275   38.98540   0.0     com='drum'
 cuboid    20 1 4p22.866096   38.98540   0.0     com='drum chine outer radius'
unit 1010
'cv at 1st step in liner [Elev=35.336 in.]'
 cylinder  3  1    6.426200    0.15240   0.0     com='cv well cavity'
 cylinder  8  1    6.680200    0.15240   0.0     com='cv at 1st step'
 cylinder  15 1    7.924800    0.15240   0.0     com='void btw cv and liner'
 cylinder  16 1   11.074400    0.15240   0.0     com='liner 1st step'
 cylinder  12 1   21.555075    0.15240   0.0     com='kaolite'
 cylinder  19 1   21.722275    0.15240   0.0     com='drum'
 cuboid    20 1 4p22.866096    0.15240   0.0     com='drum chine outer radius'
unit 1011
'vertical gap between 1st step in liner and cv flange [Elev=35.426 in.]'
 cylinder  3  1    6.426200    0.22860   0.0     com='cv well cavity'
 cylinder  8  1    6.680200    0.22860   0.0     com='cv at gap btwn step-flng'
 cylinder  15 1   10.922000    0.22860   0.0     com='void btw cv and liner'
 cylinder  16 1   11.074400    0.22860   0.0     com='liner wall'
 cylinder  12 1   21.555075    0.22860   0.0     com='kaolite'
 cylinder  19 1   21.722275    0.22860   0.0     com='drum'
 cuboid    20 1 4p22.866096    0.22860   0.0     com='drum chine outer radius'
unit 1012
'cv flange to top of cv well [Elev=35.926 in.]'
 cylinder  3  1    6.426200    1.27000   0.0     com='cavity'
 cylinder  9  1    9.525000    1.27000   0.0     com='flange to top of well'
 cylinder  15 1    9.525000    1.27000   0.0     com='void btw cv and pad-2'
 cylinder  14 1   10.033000    1.27000   0.0     com='pad-2'
 cylinder  15 1   10.922000    1.27000   0.0     com='void btw cv and liner'
 cylinder  16 1   11.074400    1.27000   0.0     com='liner wall'
 cylinder  12 1   21.555075    1.27000   0.0     com='kaolite'
 cylinder  19 1   21.722275    1.27000   0.0     com='drum'
 cuboid    20 1 4p22.866096    1.27000   0.0     com='drum chine outer radius'
unit 1013
'cv flange above cv well [Elev=37.076 in.]'
 cylinder  10 1    9.525000    2.92100   0.0     com='flange above cv well'
 cylinder  15 1    9.525000    2.92100   0.0     com='void btw cv and pad-2'
 cylinder  14 1   10.033000    2.92100   0.0     com='pad-2'
 cylinder  15 1   10.922000    2.92100   0.0     com='void btw pad2 and liner'
 cylinder  16 1   11.074400    2.92100   0.0     com='liner wall'
 cylinder  12 1   21.555075    2.92100   0.0     com='kaolite'
```

```
 cylinder  19 1   21.722275    2.92100   0.0     com='drum'
 cuboid    20 1 4p22.866096    2.92100   0.0     com='drum chine outer radius'
unit 1014
'plugpad2 below liner 2nd step [Elev=37.476 in.]'
 cylinder  14 1   10.033000    0.76200   0.0     com='pad-2'
 cylinder  15 1   10.922000    1.01600   0.0     com='void btw pad2 and liner'
 cylinder  16 1   11.074400    1.01600   0.0     com='liner wall'
 cylinder  12 1   21.555075    1.01600   0.0     com='kaolite'
 cylinder  19 1   21.722275    1.01600   0.0     com='drum'
 cuboid    20 1 4p22.866096    1.01600   0.0     com='drum chine outer radius'
unit 1015
'2nd step in liner [Elev=37.536 in.]'
 cylinder  15 1   10.922000    0.15240   0.0     com='void abv pad2'
 cylinder  16 1   18.757900    0.15240   0.0     com='liner 2nd step'
 cylinder  12 1   21.555075    0.15240   0.0     com='kaolite'
 cylinder  19 1   21.722275    0.15240   0.0     com='drum'
 cuboid    20 1 4p22.866096    0.15240   0.0     com='drum chine outer radius'
unit 1016
'abv 2nd step in liner to bottom of angle iron [Elev=40.756 in.]'
 cylinder  13 1   18.097500    8.17880   0.49276 com='plug kaolite'
 cylinder  17 1   18.249900    8.17880   0.34036 com='sides of plug case'
 cylinder  15 1   18.605500    8.17880   0.0     com='void: plug to liner'
 cylinder  16 1   18.757900    8.17880   0.0     com='liner wall'
 cylinder  12 1   21.555075    8.17880   0.0     com='kaolite'
 cylinder  19 1   21.722275    8.17880   0.0     com='drum'
 cuboid    20 1 4p22.866096    8.17880   0.0     com='drum chine outer radius'
unit 1017
'bottom of angle iron to bend in angle iron [Elev=42.506 in.]'
 cylinder  13 1   18.097500    4.44500   0.0     com='plug kaolite'
 cylinder  17 1   18.249900    4.44500   0.0     com='sides of plug case'
 cylinder  15 1   18.605500    4.44500   0.0     com='void: plug to liner'
 cylinder  16 1   18.757900    4.44500   0.0     com='liner wall'
 cylinder  18 1   19.392900    4.44500   0.0     com='lower angle iron'
 cylinder  12 1   21.555075    4.44500   0.0     com='kaolite'
 cylinder  19 1   21.722275    4.44500   0.0     com='drum'
 cuboid    20 1 4p22.866096    4.44500   0.0     com='drum chine outer radius'
unit 1018
'bend in angle iron to top of angle iron [Elev=42.756 in.]'
 cylinder  13 1   18.097500    0.11176   0.0     com='plug kaolite'
 cylinder  17 1   18.249900    0.26416   0.0     com='sides of plug case'
 cylinder  15 1   18.605500    0.63500   0.0     com='void: plug to liner'
 cylinder  16 1   18.757900    0.63500   0.0     com='liner wall'
 cylinder  18 1   21.555075    0.63500   0.0     com='bend section of ai'
 cylinder  19 1   21.722275    0.63500   0.0     com='drum'
 cuboid    20 1 4p22.866096    0.63500   0.0     com='drum chine outer radius'
unit 1019
'drum lid and lip [Elev=43.512 in.]'
 cylinder  20 1   21.330090    1.91973   0.16720 com='void above lid'
 cylinder  19 1   21.497290    1.91973   0.0     com='drum lid'
 cylinder  20 1   21.555075    1.91973   0.0     com='void btw lid - drum wall'
 cylinder  19 1   21.722275    1.91973   0.0     com='drum'
 cuboid    20 1 4p22.866096    1.91973   0.0     com='drum chine outer radius'
global
unit 1020
'es3100 drum [Elev=43.512 in.]'
array 3         2r-22.866096     0.0
'cuboid     0  1 4p24.587200    110.4900  0.0    com='bare package'
'cuboid    21  1 4p55.067200   140.9700 -30.48   com='reflected package'
 cuboid    20  1 4p22.866096    110.5197  0.0    com='interstital array space'
'global
'unit 1021
'array 4   3r0.0
'reflector  21 2  6r3.0  10
end geometry
read array
ara=3 nux=1 nuy=1 nuz=19 fill
1001 1002 1003 1006 1007 1006 1007 1006 1008 1010
1011 1012 1013 1014 1015 1016 1017 1018 1019        end fill
'ara=4 nux=13 nuy=13 nuz=06 fill f1020               end fill
end array
'read bias id=500 2  11  end bias
```

```
read start nst=0
end start
end data
end


=csas25    parm=size=3000000
cvcrcyat11 3cyl,1.4in thk np,(30000.0g235, 7991.5gH2O hx=  6.95),sep=0.254,fr=1.0e+00
238groupndf5 infhommedium
'HEU volume =1594.80409, SPACER volume  614.68012'
'HEU wrapped dry content can hx=0.56, CV void volume 8005.87774'
uranium  1 den=18.81109 1.0 293      92235  100.00
                                     92238   0.000               end
'np277-4: spacer (NCT_MD&H)'
'NCT min.den.(95.3886 lb/ft3) and hydrogen'
'np277-4 min.den.= 1.527971 = (95.3886 lb/ft3)(453.59 g/lb)/(28316.84 cm3/ft3)'
'use 75% of boron in calculations per NUREG-1609 Section 6.5.3.2'
arbmboron 7.31015e-2  2 0 0 0    5010   18.1479
                                 5011   81.8520    2  0.7500  293  end
arbmnpmx  1.07070e+0 10 0 0 0    6012    1.9189
                                 7014    0.0141
                                 8016   43.4251
                                11023    0.1174
                                12000    0.3378
                                13027   39.0479
                                14000    2.4672
                                16000    0.3083
                                20000   11.8336
                                26000    0.5298    2  1.0000  293  end
arbmnph2o 3.84169e-1  2 0 0 0    1001   11.1913
                                 8016   88.8087    2  1.0000  293  end
'flooded containmment vessel and content cans -- 10 CFR 71.55(d)(3)'
arbmwicv   0.9982   2 0 0 0    1001   11.1913
                               8016   88.8087    3  1       293  end
'steel: containment vessel body 16.60 lb but use 15.74 lb'
ss304                                            8  1.0     293  end
'steel: cv flange lower use 3.36 lb'
ss304                                            9  0.97267 293  end
'steel: cv flange upper use 13.75 lb'
ss304                                           10  0.94348 293  end
'np277-4: confinement -- neutron poison inner liner (NCT_MD&H)'
'actual vol.= 1.31846e4 cm3 = (8.0457422e2 in3)(16.387064)'
'den.multiplier = 1.31846e4 cm3 (actual vol.) / 1.32708e4 cm3 (model vol.)'
'np277-4 min.den.= 1.527971 = (95.3886 lb/ft3)(453.59 g/lb)/(28316.84 cm3/ft3)'
'density = 1.518047 = (den.mult)(np277-4 min.den.) = 0.9935052*1.527971'
'use 75% of boron in calculations per NUREG-1609 Section 6.5.3.2'
arbmboron 7.26267e-2  2 0 0 0    5010   18.1479
                                 5011   81.8520   11  0.7500  293  end
arbmnpmx  1.06375e+0 10 0 0 0    6012    1.9189
                                 7014    0.0141
                                 8016   43.4251
                                11023    0.1174
                                12000    0.3378
                                13027   39.0479
                                14000    2.4672
                                16000    0.3083
                                20000   11.8336
                                26000    0.5298   11  1.0000  293  end
arbmnph2o 3.81674e-1  2 0 0 0    1001   11.1913
                                 8016   88.8087   11  1.0000  293  end
'kaolite 1600 body'
'sing.unit.density= (den.mult)(min.den.)'
' for arbmh2ok = 1.012373*0.51655,  for rest = 1.012373*0.34438'
'den.mult= 1.36557e5 cm3 (actual vol.) / 1.34888e5 cm3 (model vol.)'
'actual vol.= 1.36557e5 cm3 = (28316.84 cm3/ft3)(108.33188 lb)/(22.464 lb/ft3)'
arbmh2ok   0.52294  2 0 0 0    1001   11.1913
                               8016   88.8087   12  1       293  end
arbmal2o3  0.34864  2 0 0 0   13027   52.9390
                               8016   47.0610   12  0.096   293  end
arbmsio2   0.34864  2 0 0 0   14000   46.7570
                               8016   53.2430   12  0.367   293  end
```

```
arbmfe2o3  0.34864  2 0 0 0   26000   69.9540
                               8016   30.0460   12  0.067   293  end
arbmtio2   0.34864  2 0 0 0   22000   59.9535
                               8016   40.0465   12  0.012   293  end
arbmcao    0.34864  2 0 0 0   20000   71.4815
                               8016   28.5185   12  0.307   293  end
arbmmgo    0.34864  2 0 0 0   12000   60.3169
                               8016   39.6831   12  0.131   293  end
arbmna2o   0.34864  2 0 0 0   11023   74.1961
                               8016   25.8039   12  0.020   293  end
'kaolite 1600 top plug'
'sing.unit.density= (den.mult)(min.den.)'
' for arbmh20k = 0.965246*0.51655,  for rest = 0.965246*0.34438'
'den.mult= 1.21592e4 cm3 (actual vol.) / 1.25970e4 cm3 (model vol.)'
'actual vol.= 1.21592e4 cm3 = (28316.84 cm3/ft3)(9.646 lb)/(22.464 lb/ft3)'
arbmh2ok   0.49860  2 0 0 0    1001   11.1913
                               8016   88.8087   13  1       293  end
arbmal2o3  0.33241  2 0 0 0   13027   52.9390
                               8016   47.0610   13  0.096   293  end
arbmsio2   0.33241  2 0 0 0   14000   46.7570
                               8016   53.2430   13  0.367   293  end
arbmfe2o3  0.33241  2 0 0 0   26000   69.9540
                               8016   30.0460   13  0.067   293  end
arbmtio2   0.33241  2 0 0 0   22000   59.9535
                               8016   40.0465   13  0.012   293  end
arbmcao    0.33241  2 0 0 0   20000   71.4815
                               8016   28.5185   13  0.307   293  end
arbmmgo    0.33241  2 0 0 0   12000   60.3169
                               8016   39.6831   13  0.131   293  end
arbmna2o   0.33241  2 0 0 0   11023   74.1961
                               8016   25.8039   13  0.020   293  end
'silicone rubber pads'
arbmsiru   1.21791  4 0 0 0    6012   32.3767
                               1001    8.1573
                               8016   21.5782
                              14000   37.8878   14  1.0     293  end
'void space external to containment vessel'
arbmwecv   0.9982   2 0 0 0    1001   11.1913
                               8016   88.8087   15  1       293  end
'steel: liner'
ss304                                            16  1.0     293  end
'steel: plug cover (pc) use 9.907 lb'
ss304                                            17  1.06388 293  end
'steel: angle iron (ai) for single units'
ss304                                            18  1.0     293  end
'steel: angle iron (ai) for arrays'
'array density is multiplied by a volume fraction 7.08030/5.63249'
'ss304                                            18  1.25705 293  end
'steel: drum steel for single units'
ss304                                            19  1.0     293  end
'steel: drum steel for arrays'
'array density is multiplied by a volume fraction 3.20482/3.20544'
'ss304                                            19  0.99981 293  end
'void space external to drum'
'array density is multiplied by a volume ratio 8.11698/6.98323'
'arbmwed    1.16026  2 0 0 0    1001   11.1913
'                               8016   88.8087   20  1       293  end
'reflective water'
arbmh20r   0.9982   2 0 0 0    1001   11.1913
                               8016   88.8087   21  1.0     293  end
end comp
cvcrcyat11 3cyl,1.4in thk np,(30000.0g235, 7991.5gH2O,hx=  6.95),sep=0.254,fr=1.0e+00
read parameters nub=yes npg=2500 gen=215 nsk=15 tme=100 end parameters
read boun       all=vac                          end boun
read geometry
unit 1001
'drum bottom flat cover [Elev= 0.105 in. at top of unit]'
'cylinder  19 1   24.587200    0.26670   0.0     com='extended radius not used'
 cuboid    21 1 4p24.587200    0.26670   0.0     com='drum chine outer radius'
unit 1002
'above drum bottom flat cover and below containment vessel [Elev= 4.670 in.]'
```

```
 cuboid    21 1 4p24.587200   11.59510   0.0     com='drum chine outer radius'
unit 1003
'cv bottom [Elev= 4.920 in.]'
 cylinder  8  1    6.680200    0.63500   0.0     com='cv bottom'
 cuboid    21 1 4p24.587200    0.63500   0.0     com='drum chine outer radius'
unit 1006
'content (centered) [Elev= 8.955 in.]'
 cylinder  1  1    4.114800   10.12099   0.12700    com='cylindrical content'
 cylinder  3  1    6.426200   10.24849  -0.0005  com='cv well cavity'
 cylinder  8  1    6.680200   10.24849  -0.0005  com='cv below 1st step'
 cuboid    21 1 4p24.587200   10.24849  -0.0005  com='drum chine outer radius'
unit 1007
'np277_4 spacer [Elev=10.355 in.]'
 cylinder  2  1    5.24510     3.55610   0.0     com='np spacer'
 cylinder  3  1    6.426200    3.55620  -0.0001  com='cv well cavity'
 cylinder  8  1    6.680200    3.55620  -0.0001  com='cv below 1st step'
 cuboid    21 1 4p24.587200    3.55620  -0.0001  com='drum chine outer radius'
unit 1008
'top of content stack to bottom of 1st step [Elev=35.270 in.]'
'37.85956             stack height (content spacers)       CALCULATED
 cylinder  3  1    6.426200   39.22944   0.0     com='cv well cavity'
 cylinder  8  1    6.680200   39.22944   0.0     com='cv below 1st step'
 cuboid    21 1 4p24.587200   39.22944   0.0     com='drum chine outer radius'
unit 1010
'cv at 1st step in liner [Elev=35.330 in.]'
 cylinder  3  1    6.426200    0.15240   0.0     com='cv well cavity'
 cylinder  8  1    6.680200    0.15240   0.0     com='cv at 1st step'
 cuboid    21 1 4p24.587200    0.15240   0.0     com='drum chine outer radius'
unit 1011
'vertical gap between 1st step in liner and cv flange [Elev=35.420 in.]'
 cylinder  3  1    6.426200    0.22860   0.0     com='cv well cavity'
 cylinder  8  1    6.680200    0.22860   0.0     com='cv at gap btwn step-flng'
 cuboid    21 1 4p24.587200    0.22860   0.0     com='drum chine outer radius'
unit 1012
'cv flange to top of cv well [Elev=35.920 in.]'
 cylinder  3  1    6.426200    1.27000   0.0     com='cavity'
 cylinder  9  1    9.525000    1.27000   0.0     com='flange to top of well'
 cuboid    21 1 4p24.587200    1.27000   0.0     com='drum chine outer radius'
unit 1013
'cv flange above cv well [Elev=37.070 in.]'
 cylinder  10 1    9.525000    2.92100   0.0     com='flange above cv well'
 cuboid    21 1 4p24.587200    2.92100   0.0     com='drum chine outer radius'
unit 1014
'plugpad2 below liner 2nd step [Elev=37.470 in.]'
 cuboid    21 1 4p24.587200    1.01600   0.0     com='drum chine outer radius'
unit 1015
'2nd step in liner [Elev=37.530 in.]'
 cuboid    21 1 4p24.587200    0.15240   0.0     com='drum chine outer radius'
unit 1016
'abv 2nd step in liner to bottom of angle iron [Elev=40.750 in.]'
 cuboid    21 1 4p24.587200    8.17880   0.0     com='drum chine outer radius'
unit 1017
'bottom of angle iron to bend in angle iron [Elev=42.500 in.]'
 cuboid    21 1 4p24.587200    4.44500   0.0     com='drum chine outer radius'
unit 1018
'bend in angle iron to top of angle iron [Elev=42.750 in.]'
 cuboid    21 1 4p24.587200    0.63500   0.0     com='drum chine outer radius'
unit 1019
'drum lid and lip [Elev=43.500 in.]'
 cuboid    21 1 4p24.587200    1.90500   0.0     com='drum chine outer radius'
global
unit 1020
'es3100 drum [Elev=43.500 in.]'
array 3         2r-24.587200     0.0
'cuboid     0  1 4p24.587200    110.4905  0.0    com='bare package'
 cuboid    21  1 4p55.067200   140.9700 -30.48   com='reflected package'
'cuboid    20  1 4p22.889718    110.5048  0.0    com='interstital array space'
'global
'unit 1021
'array 4   3r0.0
'reflector  21 2  6r3.0  10
```

```
end geometry
read array
ara=3 nux=1 nuy=1 nuz=19 fill
1001 1002 1003 1006 1007 1006 1007 1006 1008 1010
1011 1012 1013 1014 1015 1016 1017 1018 1019        end fill
'ara=4 nux=13 nuy=13 nuz=06 fill f1020               end fill
end array
'read bias id=500 2  11  end bias
read start nst=0
end start
end data
end


=csas25    parm=size=3000000
cvcrcyat11 3cyl,1.4in thk np,(30000.0g235, 7991.5gH2O hx=  6.95),sep=4.826,fr=1.0e+00
238groupndf5 infhommedium
'HEU volume =1594.80409, SPACER volume  614.68012'
'HEU wrapped dry content can hx=0.56, CV void volume 8005.87774'
uranium  1 den=18.81109 1.0 293      92235  100.00
                                     92238   0.000               end
'np277-4: spacer (NCT_MD&H)'
'NCT min.den.(95.3886 lb/ft3) and hydrogen'
'np277-4 min.den.= 1.527971 = (95.3886 lb/ft3)(453.59 g/lb)/(28316.84 cm3/ft3)'
'use 75% of boron in calculations per NUREG-1609 Section 6.5.3.2'
arbmboron 7.31015e-2  2 0 0 0    5010   18.1479
                                 5011   81.8520    2  0.7500  293  end
arbmnpmx  1.07070e+0 10 0 0 0    6012    1.9189
                                 7014    0.0141
                                 8016   43.4251
                                11023    0.1174
                                12000    0.3378
                                13027   39.0479
                                14000    2.4672
                                16000    0.3083
                                20000   11.8336
                                26000    0.5298    2  1.0000  293  end
arbmnph2o 3.84169e-1  2 0 0 0    1001   11.1913
                                 8016   88.8087    2  1.0000  293  end
'flooded containmment vessel and content cans -- 10 CFR 71.55(d)(3)'
arbmwicv   0.9982   2 0 0 0    1001   11.1913
                               8016   88.8087    3  1       293  end
'steel: containment vessel body 16.60 lb but use 15.74 lb'
ss304                                            8  1.0     293  end
'steel: cv flange lower use 3.36 lb'
ss304                                            9  0.97267 293  end
'steel: cv flange upper use 13.75 lb'
ss304                                           10  0.94348 293  end
'np277-4: confinement -- neutron poison inner liner (NCT_MD&H)'
'actual vol.= 1.31846e4 cm3 = (8.0457422e2 in3)(16.387064)'
'den.multiplier = 1.31846e4 cm3 (actual vol.) / 1.32708e4 cm3 (model vol.)'
'np277-4 min.den.= 1.527971 = (95.3886 lb/ft3)(453.59 g/lb)/(28316.84 cm3/ft3)'
'density = 1.518047 = (den.mult)(np277-4 min.den.) = 0.9935052*1.527971'
'use 75% of boron in calculations per NUREG-1609 Section 6.5.3.2'
arbmboron 7.26267e-2  2 0 0 0    5010   18.1479
                                 5011   81.8520   11  0.7500  293  end
arbmnpmx  1.06375e+0 10 0 0 0    6012    1.9189
                                 7014    0.0141
                                 8016   43.4251
                                11023    0.1174
                                12000    0.3378
                                13027   39.0479
                                14000    2.4672
                                16000    0.3083
                                20000   11.8336
                                26000    0.5298   11  1.0000  293  end
arbmnph2o 3.81674e-1  2 0 0 0    1001   11.1913
                                 8016   88.8087   11  1.0000  293  end
'kaolite 1600 body'
'sing.unit.density= (den.mult)(min.den.)'
' for arbmh20k = 1.012373*0.51655,  for rest = 1.012373*0.34438'
```

```
'den.mult= 1.36557e5 cm3 (actual vol.) / 1.34888e5 cm3 (model vol.)'
'actual vol.= 1.36557e5 cm3 = (28316.84 cm3/ft3)(108.33188 lb)/(22.464 lb/ft3)'
arbmh2ok   0.52294  2 0 0 0    1001   11.1913
                               8016   88.8087   12  1       293  end
arbmal2o3  0.34864  2 0 0 0   13027   52.9390
                               8016   47.0610   12  0.096   293  end
arbmsio2   0.34864  2 0 0 0   14000   46.7570
                               8016   53.2430   12  0.367   293  end
arbmfe2o3  0.34864  2 0 0 0   26000   69.9540
                               8016   30.0460   12  0.067   293  end
arbmtio2   0.34864  2 0 0 0   22000   59.9535
                               8016   40.0465   12  0.012   293  end
arbmcao    0.34864  2 0 0 0   20000   71.4815
                               8016   28.5185   12  0.307   293  end
arbmmgo    0.34864  2 0 0 0   12000   60.3169
                               8016   39.6831   12  0.131   293  end
arbmna2o   0.34864  2 0 0 0   11023   74.1961
                               8016   25.8039   12  0.020   293  end
'kaolite 1600 top plug'
'sing.unit.density= (den.mult)(min.den.)'
' for arbmh20k = 0.965246*0.51655,  for rest = 0.965246*0.34438'
'den.mult= 1.21592e4 cm3 (actual vol.) / 1.25970e4 cm3 (model vol.)'
'actual vol.= 1.21592e4 cm3 = (28316.84 cm3/ft3)(9.646 lb)/(22.464 lb/ft3)'
arbmh2ok   0.49860  2 0 0 0    1001   11.1913
                               8016   88.8087   13  1       293  end
arbmal2o3  0.33241  2 0 0 0   13027   52.9390
                               8016   47.0610   13  0.096   293  end
arbmsio2   0.33241  2 0 0 0   14000   46.7570
                               8016   53.2430   13  0.367   293  end
arbmfe2o3  0.33241  2 0 0 0   26000   69.9540
                               8016   30.0460   13  0.067   293  end
arbmtio2   0.33241  2 0 0 0   22000   59.9535
                               8016   40.0465   13  0.012   293  end
arbmcao    0.33241  2 0 0 0   20000   71.4815
                               8016   28.5185   13  0.307   293  end
arbmmgo    0.33241  2 0 0 0   12000   60.3169
                               8016   39.6831   13  0.131   293  end
arbmna2o   0.33241  2 0 0 0   11023   74.1961
                               8016   25.8039   13  0.020   293  end
'silicone rubber pads'
arbmsiru   1.21791  4 0 0 0    6012   32.3767
                               1001    8.1573
                               8016   21.5782
                              14000   37.8878   14  1.0     293  end
'void space external to containment vessel'
arbmwecv   0.9982   2 0 0 0    1001   11.1913
                               8016   88.8087   15  1       293  end
'steel: liner'
ss304                                            16  1.0     293  end
'steel: plug cover (pc) use 9.907 lb'
ss304                                            17  1.06388 293  end
'steel: angle iron (ai) for single units'
ss304                                            18  1.0     293  end
'steel: angle iron (ai) for arrays'
'array density is multiplied by a volume fraction 7.08030/5.63249'
'ss304                                            18  1.25705 293  end
'steel: drum steel for single units'
ss304                                            19  1.0     293  end
'steel: drum steel for arrays'
'array density is multiplied by a volume fraction 3.20482/3.20544'
'ss304                                            19  0.99981 293  end
'void space external to drum'
'array density is multiplied by a volume ratio 8.11698/6.98323'
'arbmwed    1.16026  2 0 0 0    1001   11.1913
'                               8016   88.8087   20  1       293  end
'reflective water'
arbmh20r   0.9982   2 0 0 0    1001   11.1913
                               8016   88.8087   21  1.0     293  end
end comp
cvcrcyat11 3cyl,1.4in thk np,(30000.0g235, 7991.5gH2O,hx=  6.95),sep=4.826,fr=1.0e+00
read parameters nub=yes npg=2500 gen=215 nsk=15 tme=100 end parameters
```

```
read boun       all=vac                         end boun
read geometry
unit 1001
'drum bottom flat cover [Elev= 0.105 in. at top of unit]'
'cylinder  19 1   24.587200    0.26670   0.0     com='extended radius not used'
 cuboid    21 1 4p24.587200    0.26670   0.0     com='drum chine outer radius'
unit 1002
'above drum bottom flat cover and below containment vessel [Elev= 4.670 in.]'
 cuboid    21 1 4p24.587200   11.59510   0.0     com='drum chine outer radius'
unit 1003
'cv bottom [Elev= 4.920 in.]'
 cylinder  8  1    6.680200    0.63500   0.0     com='cv bottom'
 cuboid    21 1 4p24.587200    0.63500   0.0     com='drum chine outer radius'
unit 1006
'content (centered) [Elev=10.755 in.]'
 cylinder  1  1    4.114800   12.40699   2.41300    com='cylindrical content'
 cylinder  3  1    6.426200   14.82049  -0.0005  com='cv well cavity'
 cylinder  8  1    6.680200   14.82049  -0.0005  com='cv below 1st step'
 cuboid    21 1 4p24.587200   14.82049  -0.0005  com='drum chine outer radius'
unit 1007
'np277_4 spacer [Elev=12.155 in.]'
 cylinder  2  1    5.24510     3.55610   0.0     com='np spacer'
 cylinder  3  1    6.426200    3.55620  -0.0001  com='cv well cavity'
 cylinder  8  1    6.680200    3.55620  -0.0001  com='cv below 1st step'
 cuboid    21 1 4p24.587200    3.55620  -0.0001  com='drum chine outer radius'
unit 1008
'top of content stack to bottom of 1st step [Elev=35.270 in.]'
'51.57556             stack height (content spacers)       CALCULATED
 cylinder  3  1    6.426200   25.51344   0.0     com='cv well cavity'
 cylinder  8  1    6.680200   25.51344   0.0     com='cv below 1st step'
 cuboid    21 1 4p24.587200   25.51344   0.0     com='drum chine outer radius'
unit 1010
'cv at 1st step in liner [Elev=35.330 in.]'
 cylinder  3  1    6.426200    0.15240   0.0     com='cv well cavity'
 cylinder  8  1    6.680200    0.15240   0.0     com='cv at 1st step'
 cuboid    21 1 4p24.587200    0.15240   0.0     com='drum chine outer radius'
unit 1011
'vertical gap between 1st step in liner and cv flange [Elev=35.420 in.]'
 cylinder  3  1    6.426200    0.22860   0.0     com='cv well cavity'
 cylinder  8  1    6.680200    0.22860   0.0     com='cv at gap btwn step-flng'
 cuboid    21 1 4p24.587200    0.22860   0.0     com='drum chine outer radius'
unit 1012
'cv flange to top of cv well [Elev=35.920 in.]'
 cylinder  3  1    6.426200    1.27000   0.0     com='cavity'
 cylinder  9  1    9.525000    1.27000   0.0     com='flange to top of well'
 cuboid    21 1 4p24.587200    1.27000   0.0     com='drum chine outer radius'
unit 1013
'cv flange above cv well [Elev=37.070 in.]'
 cylinder  10 1    9.525000    2.92100   0.0     com='flange above cv well'
 cuboid    21 1 4p24.587200    2.92100   0.0     com='drum chine outer radius'
unit 1014
'plugpad2 below liner 2nd step [Elev=37.470 in.]'
 cuboid    21 1 4p24.587200    1.01600   0.0     com='drum chine outer radius'
unit 1015
'2nd step in liner [Elev=37.530 in.]'
 cuboid    21 1 4p24.587200    0.15240   0.0     com='drum chine outer radius'
unit 1016
'abv 2nd step in liner to bottom of angle iron [Elev=40.750 in.]'
 cuboid    21 1 4p24.587200    8.17880   0.0     com='drum chine outer radius'
unit 1017
'bottom of angle iron to bend in angle iron [Elev=42.500 in.]'
 cuboid    21 1 4p24.587200    4.44500   0.0     com='drum chine outer radius'
unit 1018
'bend in angle iron to top of angle iron [Elev=42.750 in.]'
 cuboid    21 1 4p24.587200    0.63500   0.0     com='drum chine outer radius'
unit 1019
'drum lid and lip [Elev=43.500 in.]'
 cuboid    21 1 4p24.587200    1.90500   0.0     com='drum chine outer radius'
global
unit 1020
'es3100 drum [Elev=43.500 in.]'
```

```
array 3         2r-24.587200     0.0
'cuboid     0  1 4p24.587200    110.4905  0.0    com='bare package'
 cuboid    21  1 4p55.067200   140.9700 -30.48   com='reflected package'
'cuboid    20  1 4p22.889718    110.5048  0.0    com='interstital array space'
'global
'unit 1021
'array 4   3r0.0
'reflector  21 2  6r3.0  10
end geometry
read array
ara=3 nux=1 nuy=1 nuz=19 fill
1001 1002 1003 1006 1007 1006 1007 1006 1008 1010
1011 1012 1013 1014 1015 1016 1017 1018 1019        end fill
'ara=4 nux=13 nuy=13 nuz=06 fill f1020               end fill
end array
'read bias id=500 2  11  end bias
read start nst=0
end start
end data
end


=csas25    parm=size=3000000
cvcrpunhct11 10000.2gUNHc( 4709.7g235,2165.3gH2O) 6080.8gH2Ocv hx= 49.26 fr=1.0e+00
238groupndf5 infhommedium
'U(enr)O2(NO3)2+6H2O [2.81 g/cc for U(nat)]  2.79329 g/cm3, hx=12.0, gU/L= 461.0422'
'dry content (poly packed or wrapped) h/x=3.56, CV void volume 6091.80676 cm3'
arbmunh    2.79329  5 0 0 0   92235   47.0962
                              92238    0.0000
                               1001    2.4232
                               7014    5.6116
                               8016   44.8690    1  3.5046e-01   293  end
arbmh2oc   0.99820  2 0 0 0  1001   11.1913
                               8016   88.8087    1  5.9634e-01   293  end
arbmpoly   0.92000  2 0 0 0  1001   14.3798
                               6012   85.6202    1  5.3202e-02   293  end
'np277-4: spacer (NCT_MD&H)'
'NCT min.den.(95.3886 lb/ft3) and hydrogen'
'np277-4 min.den.= 1.527971 = (95.3886 lb/ft3)(453.59 g/lb)/(28316.84 cm3/ft3)'
'use 75% of boron in calculations per NUREG-1609 Section 6.5.3.2'
arbmboron 7.31015e-2  2 0 0 0    5010   18.1479
                                 5011   81.8520    2  0.7500  293  end
arbmnpmx  1.07070e+0 10 0 0 0    6012    1.9189
                                 7014    0.0141
                                 8016   43.4251
                                11023    0.1174
                                12000    0.3378
                                13027   39.0479
                                14000    2.4672
                                16000    0.3083
                                20000   11.8336
                                26000    0.5298    2  1.0000  293  end
arbmnph2o 3.84169e-1  2 0 0 0    1001   11.1913
                                 8016   88.8087    2  1.0000  293  end
'flooded containmment vessel and content cans -- 10 CFR 71.55(d)(3)'
arbmwicv  5.9526e-01  2 0 0 0   1001   11.1913
                                8016   88.8087     3  1.0     293  end
'steel: containment vessel body 16.60 lb but use 15.74 lb'
ss304                                            8  1.0     293  end
'steel: cv flange lower use 3.36 lb'
ss304                                            9  0.97267 293  end
'steel: cv flange upper use 13.75 lb'
ss304                                           10  0.94348 293  end
'np277-4: confinement -- neutron poison inner liner (NCT_MD&H)'
'actual vol.= 1.31846e4 cm3 = (8.0457422e2 in3)(16.387064)'
'den.multiplier = 1.31846e4 cm3 (actual vol.) / 1.32708e4 cm3 (model vol.)'
'np277-4 min.den.= 1.527971 = (95.3886 lb/ft3)(453.59 g/lb)/(28316.84 cm3/ft3)'
'density = 1.518047 = (den.mult)(np277-4 min.den.) = 0.9935052*1.527971'
'use 75% of boron in calculations per NUREG-1609 Section 6.5.3.2'
arbmboron 7.26267e-2  2 0 0 0    5010   18.1479
                                 5011   81.8520   11  0.7500  293  end
```

```
arbmnpmx  1.06375e+0 10 0 0 0    6012    1.9189
                                 7014    0.0141
                                 8016   43.4251
                                11023    0.1174
                                12000    0.3378
                                13027   39.0479
                                14000    2.4672
                                16000    0.3083
                                20000   11.8336
                                26000    0.5298   11  1.0000  293  end
arbmnph2o 3.81674e-1  2 0 0 0    1001   11.1913
                                 8016   88.8087   11  1.0000  293  end
'kaolite 1600 body'
'sing.unit.density= (den.mult)(min.den.)'
' for arbmh20k = 1.012373*0.51655,  for rest = 1.012373*0.34438'
'den.mult= 1.36557e5 cm3 (actual vol.) / 1.34888e5 cm3 (model vol.)'
'actual vol.= 1.36557e5 cm3 = (28316.84 cm3/ft3)(108.33188 lb)/(22.464 lb/ft3)'
arbmh2ok   0.52294  2 0 0 0    1001   11.1913
                               8016   88.8087   12  1       293  end
arbmal2o3  0.34864  2 0 0 0   13027   52.9390
                               8016   47.0610   12  0.096   293  end
arbmsio2   0.34864  2 0 0 0   14000   46.7570
                               8016   53.2430   12  0.367   293  end
arbmfe2o3  0.34864  2 0 0 0   26000   69.9540
                               8016   30.0460   12  0.067   293  end
arbmtio2   0.34864  2 0 0 0   22000   59.9535
                               8016   40.0465   12  0.012   293  end
arbmcao    0.34864  2 0 0 0   20000   71.4815
                               8016   28.5185   12  0.307   293  end
arbmmgo    0.34864  2 0 0 0   12000   60.3169
                               8016   39.6831   12  0.131   293  end
arbmna2o   0.34864  2 0 0 0   11023   74.1961
                               8016   25.8039   12  0.020   293  end
'kaolite 1600 top plug'
'sing.unit.density= (den.mult)(min.den.)'
' for arbmh20k = 0.965246*0.51655,  for rest = 0.965246*0.34438'
'den.mult= 1.21592e4 cm3 (actual vol.) / 1.25970e4 cm3 (model vol.)'
'actual vol.= 1.21592e4 cm3 = (28316.84 cm3/ft3)(9.646 lb)/(22.464 lb/ft3)'
arbmh2ok   0.49860  2 0 0 0    1001   11.1913
                               8016   88.8087   13  1       293  end
arbmal2o3  0.33241  2 0 0 0   13027   52.9390
                               8016   47.0610   13  0.096   293  end
arbmsio2   0.33241  2 0 0 0   14000   46.7570
                               8016   53.2430   13  0.367   293  end
arbmfe2o3  0.33241  2 0 0 0   26000   69.9540
                               8016   30.0460   13  0.067   293  end
arbmtio2   0.33241  2 0 0 0   22000   59.9535
                               8016   40.0465   13  0.012   293  end
arbmcao    0.33241  2 0 0 0   20000   71.4815
                               8016   28.5185   13  0.307   293  end
arbmmgo    0.33241  2 0 0 0   12000   60.3169
                               8016   39.6831   13  0.131   293  end
arbmna2o   0.33241  2 0 0 0   11023   74.1961
                               8016   25.8039   13  0.020   293  end
'silicone rubber pads'
arbmsiru   1.21791  4 0 0 0    6012   32.3767
                               1001    8.1573
                               8016   21.5782
                              14000   37.8878   14  1.0     293  end
'void space external to containment vessel'
arbmwecv   0.9982   2 0 0 0    1001   11.1913
                               8016   88.8087   15  1       293  end
'steel: liner'
ss304                                            16  1.0     293  end
'steel: plug cover (pc) use 9.907 lb'
ss304                                            17  1.06388 293  end
'steel: angle iron (ai) for single units'
ss304                                            18  1.0     293  end
'steel: angle iron (ai) for arrays'
'array density is multiplied by a volume fraction 7.08030/5.63249'
'ss304                                            18  1.25705 293  end
```

```
'steel: drum steel for single units'
ss304                                          19  1.0     293  end
'steel: drum steel for arrays'
'array density is multiplied by a volume fraction 3.20482/3.20544'
'ss304                                          19  0.99981 293  end
'void space external to drum'
'array density is multiplied by a volume ratio 8.11698/6.98323'
'arbmwed    1.16026  2 0 0 0    1001   11.1913
'                               8016   88.8087   20  1       293  end
'reflective water'
arbmh20r   0.9982   2 0 0 0    1001   11.1913
                                8016   88.8087   21  1.0     293  end
end comp
cvcrpunhct11 10000.2gUNHc( 4709.7g235,2165.3gH2O) 6080.8gH2Ocv,hx= 49.26 fr=1.0e+00
read parameters nub=yes npg=2500 gen=215 nsk=15 tme=100 end parameters
read boun       all=vac                        end boun
read geometry
unit 1001
'drum bottom flat cover [Elev= 0.105 in. at top of unit]'
'cylinder  19 1   24.587200    0.26670   0.0     com='extended radius not used'
 cuboid    21 1 4p24.587200    0.26670   0.0     com='drum chine outer radius'
unit 1002
'above drum bottom flat cover and below containment vessel [Elev= 4.670 in.]'
 cuboid    21 1 4p24.587200   11.59510   0.0     com='drum chine outer radius'
unit 1003
'cv bottom to bottom of 1st step [Elev=35.270 in.]'
 cylinder  1  1    6.426200   77.72400   0.63500 com='HEU content'
 cylinder  8  1    6.680200   77.72400   0.0     com='cv bottom'
 cuboid    21 1 4p24.587200   77.72400   0.0     com='drum chine outer radius'
unit 1010
'cv at 1st step in liner [Elev=35.330 in.]'
 cylinder  1  1    6.426200    0.15240   0.0     com='HEU content'
 cylinder  8  1    6.680200    0.15240   0.0     com='cv at 1st step'
 cuboid    21 1 4p24.587200    0.15240   0.0     com='drum chine outer radius'
unit 1011
'vertical gap between 1st step in liner and cv flange [Elev=35.420 in.]'
 cylinder  1  1    6.426200    0.22860   0.0     com='HEU content'
 cylinder  8  1    6.680200    0.22860   0.0     com='cv at gap btwn step-flng'
 cuboid    21 1 4p24.587200    0.22860   0.0     com='drum chine outer radius'
unit 1012
'cv flange to top of cv well [Elev=35.920 in.]'
 cylinder  1  1    6.426200    1.27000   0.0     com='HEU content'
 cylinder  9  1    9.525000    1.27000   0.0     com='flange to top of well'
 cuboid    21 1 4p24.587200    1.27000   0.0     com='drum chine outer radius'
unit 1013
'cv flange above cv well [Elev=37.070 in.]'
 cylinder  10 1    9.525000    2.92100   0.0     com='flange above cv well'
 cuboid    21 1 4p24.587200    2.92100   0.0     com='drum chine outer radius'
unit 1014
'plugpad2 below liner 2nd step [Elev=37.470 in.]'
 cuboid    21 1 4p24.587200    1.01600   0.0     com='drum chine outer radius'
unit 1015
'2nd step in liner [Elev=37.530 in.]'
 cuboid    21 1 4p24.587200    0.15240   0.0     com='drum chine outer radius'
unit 1016
'abv 2nd step in liner to bottom of angle iron [Elev=40.750 in.]'
 cuboid    21 1 4p24.587200    8.17880   0.0     com='drum chine outer radius'
unit 1017
'bottom of angle iron to bend in angle iron [Elev=42.500 in.]'
 cuboid    21 1 4p24.587200    4.44500   0.0     com='drum chine outer radius'
unit 1018
'bend in angle iron to top of angle iron [Elev=42.750 in.]'
 cuboid    21 1 4p24.587200    0.63500   0.0     com='drum chine outer radius'
unit 1019
'drum lid and lip [Elev=43.500 in.]'
 cuboid    21 1 4p24.587200    1.90500   0.0     com='drum chine outer radius'
global
unit 1020
'es3100 drum [Elev=43.500 in.]'
array 3         2r-24.587200     0.0
'cuboid     0  1 4p24.587200    110.4905  0.0    com='bare package'
```

```
 cuboid    21  1 4p55.067200   140.9700 -30.48   com='reflected package'
'cuboid    20  1 4p22.889718    110.5048  0.0    com='interstital array space'
'global
'unit 1021
'array 4   3r0.0
'reflector  21 2  6r3.0  10
end geometry
read array
ara=3 nux=1 nuy=1 nuz=13 fill
1001 1002 1003 1010
1011 1012 1013 1014 1015 1016 1017 1018 1019        end fill
'ara=4 nux=13 nuy=13 nuz=06 fill f1020               end fill
end array
'read bias id=500 2  11  end bias
read start nst=0
end start
end data
end
```

(Note: For the following input file, the case name should read “cvcrbpunhct11” as opposed to “cvcrpunhct11”.)

```
=csas25    parm=size=3000000
cvcrpunhct11 24000.0gUNHc(11303.1g235,5196.7gH2O) 1077.9gH2Ocv hx= 15.97 fr=1.0e+00
238groupndf5 infhommedium
'U(enr)O2(NO3)2+6H2O [2.81 g/cc for U(nat)]  2.79329 g/cm3, hx=12.0'
'unhc= 24000.0 g, sat.h2o in UNHc=5196.7 g, unh h/x=12.0'
'dry content (poly bottle) h/x=1.48, CV void volume 1079.87091 cm3'
arbmunh    2.62712  5 0 0 0   92235   47.0962
                              92238    0.0000
                               1001    2.4232
                               7014    5.6116
                               8016   44.8690    1  1.0000  293  end
arbmpoly  5.4732e-02    2 0 0 0  1001   14.3798
                               6012   85.6202    1  1.0000  293  end
'np277-4: spacer (NCT_MD&H)'
'NCT min.den.(95.3886 lb/ft3) and hydrogen'
'np277-4 min.den.= 1.527971 = (95.3886 lb/ft3)(453.59 g/lb)/(28316.84 cm3/ft3)'
'use 75% of boron in calculations per NUREG-1609 Section 6.5.3.2'
arbmboron 7.31015e-2  2 0 0 0    5010   18.1479
                                 5011   81.8520    2  0.7500  293  end
arbmnpmx  1.07070e+0 10 0 0 0    6012    1.9189
                                 7014    0.0141
                                 8016   43.4251
                                11023    0.1174
                                12000    0.3378
                                13027   39.0479
                                14000    2.4672
                                16000    0.3083
                                20000   11.8336
                                26000    0.5298    2  1.0000  293  end
arbmnph2o 3.84169e-1  2 0 0 0    1001   11.1913
                                 8016   88.8087    2  1.0000  293  end
'flooded containmment vessel and content cans -- 10 CFR 71.55(d)(3)'
arbmwicv  9.9820e-01  2 0 0 0   1001   11.1913
                               8016   88.8087    3  1       293  end
'steel: containment vessel body 16.60 lb but use 15.74 lb'
ss304                                            8  1.0     293  end
'steel: cv flange lower use 3.36 lb'
ss304                                            9  0.97267 293  end
'steel: cv flange upper use 13.75 lb'
ss304                                           10  0.94348 293  end
'np277-4: confinement -- neutron poison inner liner (NCT_MD&H)'
'actual vol.= 1.31846e4 cm3 = (8.0457422e2 in3)(16.387064)'
'den.multiplier = 1.31846e4 cm3 (actual vol.) / 1.32708e4 cm3 (model vol.)'
'np277-4 min.den.= 1.527971 = (95.3886 lb/ft3)(453.59 g/lb)/(28316.84 cm3/ft3)'
'density = 1.518047 = (den.mult)(np277-4 min.den.) = 0.9935052*1.527971'
'use 75% of boron in calculations per NUREG-1609 Section 6.5.3.2'
arbmboron 7.26267e-2  2 0 0 0    5010   18.1479
                                 5011   81.8520   11  0.7500  293  end
arbmnpmx  1.06375e+0 10 0 0 0    6012    1.9189
```

```
                                 7014    0.0141
                                 8016   43.4251
                                11023    0.1174
                                12000    0.3378
                                13027   39.0479
                                14000    2.4672
                                16000    0.3083
                                20000   11.8336
                                26000    0.5298   11  1.0000  293  end
arbmnph2o 3.81674e-1  2 0 0 0    1001   11.1913
                                 8016   88.8087   11  1.0000  293  end
'kaolite 1600 body'
'sing.unit.density= (den.mult)(min.den.)'
' for arbmh20k = 1.012373*0.51655,  for rest = 1.012373*0.34438'
'den.mult= 1.36557e5 cm3 (actual vol.) / 1.34888e5 cm3 (model vol.)'
'actual vol.= 1.36557e5 cm3 = (28316.84 cm3/ft3)(108.33188 lb)/(22.464 lb/ft3)'
arbmh2ok   0.52294  2 0 0 0    1001   11.1913
                               8016   88.8087   12  1       293  end
arbmal2o3  0.34864  2 0 0 0   13027   52.9390
                               8016   47.0610   12  0.096   293  end
arbmsio2   0.34864  2 0 0 0   14000   46.7570
                               8016   53.2430   12  0.367   293  end
arbmfe2o3  0.34864  2 0 0 0   26000   69.9540
                               8016   30.0460   12  0.067   293  end
arbmtio2   0.34864  2 0 0 0   22000   59.9535
                               8016   40.0465   12  0.012   293  end
arbmcao    0.34864  2 0 0 0   20000   71.4815
                               8016   28.5185   12  0.307   293  end
arbmmgo    0.34864  2 0 0 0   12000   60.3169
                               8016   39.6831   12  0.131   293  end
arbmna2o   0.34864  2 0 0 0   11023   74.1961
                               8016   25.8039   12  0.020   293  end
'kaolite 1600 top plug'
'sing.unit.density= (den.mult)(min.den.)'
' for arbmh20k = 0.965246*0.51655,  for rest = 0.965246*0.34438'
'den.mult= 1.21592e4 cm3 (actual vol.) / 1.25970e4 cm3 (model vol.)'
'actual vol.= 1.21592e4 cm3 = (28316.84 cm3/ft3)(9.646 lb)/(22.464 lb/ft3)'
arbmh2ok   0.49860  2 0 0 0    1001   11.1913
                               8016   88.8087   13  1       293  end
arbmal2o3  0.33241  2 0 0 0   13027   52.9390
                               8016   47.0610   13  0.096   293  end
arbmsio2   0.33241  2 0 0 0   14000   46.7570
                               8016   53.2430   13  0.367   293  end
arbmfe2o3  0.33241  2 0 0 0   26000   69.9540
                               8016   30.0460   13  0.067   293  end
arbmtio2   0.33241  2 0 0 0   22000   59.9535
                               8016   40.0465   13  0.012   293  end
arbmcao    0.33241  2 0 0 0   20000   71.4815
                               8016   28.5185   13  0.307   293  end
arbmmgo    0.33241  2 0 0 0   12000   60.3169
                               8016   39.6831   13  0.131   293  end
arbmna2o   0.33241  2 0 0 0   11023   74.1961
                               8016   25.8039   13  0.020   293  end
'silicone rubber pads'
arbmsiru   1.21791  4 0 0 0    6012   32.3767
                               1001    8.1573
                               8016   21.5782
                              14000   37.8878   14  1.0     293  end
'void space external to containment vessel'
arbmwecv   0.9982   2 0 0 0    1001   11.1913
                               8016   88.8087   15  1       293  end
'steel: liner'
ss304                                            16  1.0     293  end
'steel: plug cover (pc) use 9.907 lb'
ss304                                            17  1.06388 293  end
'steel: angle iron (ai) for single units'
ss304                                            18  1.0     293  end
'steel: angle iron (ai) for arrays'
'array density is multiplied by a volume fraction 7.08030/5.63249'
'ss304                                            18  1.25705 293  end
'steel: drum steel for single units'
```

```
ss304                                          19  1.0     293  end
'steel: drum steel for arrays'
'array density is multiplied by a volume fraction 3.20482/3.20544'
'ss304                                          19  0.99981 293  end
'void space external to drum'
'array density is multiplied by a volume ratio 8.11698/6.98323'
'arbmwed    1.16026  2 0 0 0    1001   11.1913
'                               8016   88.8087   20  1       293  end
'reflective water'
arbmh20r   0.9982   2 0 0 0    1001   11.1913
                                8016   88.8087   21  1.0     293  end
end comp
cvcrpunhct11 24000.0gUNHc(11303.1g235,5196.7gH2O) 1077.9gH2Ocv,hx= 15.97 fr=1.0e+00
read parameters nub=yes npg=2500 gen=215 nsk=15 tme=100 end parameters
read boun       all=vac                         end boun
read geometry
unit 1001
'drum bottom flat cover [Elev= 0.105 in. at top of unit]'
'cylinder  19 1   24.587200    0.26670   0.0     com='extended radius not used'
 cuboid    21 1 4p24.587200    0.26670   0.0     com='drum chine outer radius'
unit 1002
'above drum bottom flat cover and below containment vessel [Elev= 4.670 in.]'
 cuboid    21 1 4p24.587200   11.59510   0.0     com='drum chine outer radius'
unit 1003
'cv bottom to bottom of 1st step [Elev=35.270 in.]'
 cylinder  3  1    6.426200   77.72400  71.05136 com='cavity abv UNHC'
 cylinder  1  1    6.426200   77.72400   0.63500 com='UNHC content'
 cylinder  8  1    6.680200   77.72400   0.0     com='cv bottom'
 cuboid    21 1 4p24.587200   77.72400   0.0     com='drum chine outer radius'
unit 1010
'cv at 1st step in liner [Elev=35.330 in.]'
 cylinder  3  1    6.426200    0.15240   0.00000 com='cavity abv UNHC'
 cylinder  1  1    6.426200    0.15240   0.0     com='UNHC content'
 cylinder  8  1    6.680200    0.15240   0.0     com='cv at 1st step'
 cuboid    21 1 4p24.587200    0.15240   0.0     com='drum chine outer radius'
unit 1011
'vertical gap between 1st step in liner and cv flange [Elev=35.420 in.]'
 cylinder  3  1    6.426200    0.22860   0.00000 com='cavity abv UNHC'
 cylinder  1  1    6.426200    0.22860   0.0     com='UNHC content'
 cylinder  8  1    6.680200    0.22860   0.0     com='cv at gap btwn step-flng'
 cuboid    21 1 4p24.587200    0.22860   0.0     com='drum chine outer radius'
unit 1012
'cv flange to top of cv well [Elev=35.920 in.]'
 cylinder  3  1    6.426200    1.27000   0.00000 com='cavity abv UNHC'
 cylinder  1  1    6.426200    1.27000   0.0     com='UNHC content'
 cylinder  9  1    9.525000    1.27000   0.0     com='flange to top of well'
 cuboid    21 1 4p24.587200    1.27000   0.0     com='drum chine outer radius'
unit 1013
'cv flange above cv well [Elev=37.070 in.]'
 cylinder  10 1    9.525000    2.92100   0.0     com='flange above cv well'
 cuboid    21 1 4p24.587200    2.92100   0.0     com='drum chine outer radius'
unit 1014
'plugpad2 below liner 2nd step [Elev=37.470 in.]'
 cuboid    21 1 4p24.587200    1.01600   0.0     com='drum chine outer radius'
unit 1015
'2nd step in liner [Elev=37.530 in.]'
 cuboid    21 1 4p24.587200    0.15240   0.0     com='drum chine outer radius'
unit 1016
'abv 2nd step in liner to bottom of angle iron [Elev=40.750 in.]'
 cuboid    21 1 4p24.587200    8.17880   0.0     com='drum chine outer radius'
unit 1017
'bottom of angle iron to bend in angle iron [Elev=42.500 in.]'
 cuboid    21 1 4p24.587200    4.44500   0.0     com='drum chine outer radius'
unit 1018
'bend in angle iron to top of angle iron [Elev=42.750 in.]'
 cuboid    21 1 4p24.587200    0.63500   0.0     com='drum chine outer radius'
unit 1019
'drum lid and lip [Elev=43.500 in.]'
 cuboid    21 1 4p24.587200    1.90500   0.0     com='drum chine outer radius'
global
unit 1020
```

```
'es3100 drum [Elev=43.500 in.]'
array 3         2r-24.587200     0.0
'cuboid     0  1 4p24.587200    110.4905  0.0    com='bare package'
 cuboid    21  1 4p55.067200   140.9700 -30.48   com='reflected package'
'cuboid    20  1 4p22.889718    110.5048  0.0    com='interstital array space'
'global
'unit 1021
'array 4   3r0.0
'reflector  21 2  6r3.0  10
end geometry
read array
ara=3 nux=1 nuy=1 nuz=13 fill
1001 1002 1003 1010
1011 1012 1013 1014 1015 1016 1017 1018 1019        end fill
'ara=4 nux=13 nuy=13 nuz=06 fill f1020               end fill
end array
'read bias id=500 2  11  end bias
read start nst=0
end start
end data
end


=csas25    parm=size=3000000
nciapbmflt11,0.0in thk np, 4000.2gU( 3200.2g235) 9442.7gH2Ocv hx= 82.26 fr=0.0001
238groupndf5 infhommedium
'nciapbmflt11 - n(nct), c(np277-4), ia(infinite array),'
'               pbm (poly homogenized with broken metal),'
'               f(can location height established by packing fraction),'
'               l(designated content in can locations and gap between canned'
'               spacers, and water above content in upper can location),'
'               t11 (NCT_MD&H)'
'HEU volume = 212.11396, SPACER volume    0.01729'
'HEU wrapped dry content can hx=5.24, CV void volume 9459.75243'
'Content in can location 1'
uranium  1 den=18.85873 0.23645 293      92235  80.000
                                         92238   20.000               end
arbmh2oi     0.99820  2 0 0 0  1001   11.1913
                               8016   88.8087    1  1.5773e-01   293  end
arbmpoly     0.92000  2 0 0 0  1001   14.3798
                               6012   85.6202    1  6.0582e-01   293  end
'np277-4: spacer (NCT_MD&H)'
'NCT min.den.(95.3886 lb/ft3) and hydrogen'
'np277-4 min.den.= 1.527971 = (95.3886 lb/ft3)(453.59 g/lb)/(28316.84 cm3/ft3)'
'use 75% of boron in calculations per NUREG-1609 Section 6.5.3.2'
arbmboron 7.31015e-2  2 0 0 0    5010   18.1479
                                 5011   81.8520    2  0.7500  293  end
arbmnpmx  1.07070e+0 10 0 0 0    6012    1.9189
                                 7014    0.0141
                                 8016   43.4251
                                11023    0.1174
                                12000    0.3378
                                13027   39.0479
                                14000    2.4672
                                16000    0.3083
                                20000   11.8336
                                26000    0.5298    2  1.0000  293  end
arbmnph2o 3.84169e-1  2 0 0 0    1001   11.1913
                                 8016   88.8087    2  1.0000  293  end
'Content in can location 2'
uranium  3 den=18.85873 0.23645 293      92235  80.000
                                         92238   20.000               end
arbmh2oi     0.99820  2 0 0 0  1001   11.1913
                               8016   88.8087    3  1.5773e-01   293  end
arbmpoly     0.92000  2 0 0 0  1001   14.3798
                               6012   85.6202    3  6.0582e-01   293  end
'np277-4: spacer (NCT_MD&H)'
'NCT min.den.(95.3886 lb/ft3) and hydrogen'
'np277-4 min.den.= 1.527971 = (95.3886 lb/ft3)(453.59 g/lb)/(28316.84 cm3/ft3)'
'use 75% of boron in calculations per NUREG-1609 Section 6.5.3.2'
arbmboron 7.31015e-2  2 0 0 0    5010   18.1479
```

```
                                 5011   81.8520    4  0.7500  293  end
arbmnpmx  1.07070e+0 10 0 0 0    6012    1.9189
                                 7014    0.0141
                                 8016   43.4251
                                11023    0.1174
                                12000    0.3378
                                13027   39.0479
                                14000    2.4672
                                16000    0.3083
                                20000   11.8336
                                26000    0.5298    4  1.0000  293  end
arbmnph2o 3.84169e-1  2 0 0 0    1001   11.1913
                                 8016   88.8087    4  1.0000  293  end
'Content in can location 3'
uranium  5 den=18.85873 0.23647 293      92235  80.000
                                         92238   20.000               end
arbmh2oi     0.99820  2 0 0 0  1001   11.1913
                               8016   88.8087    5  1.5765e-01   293  end
arbmpoly     0.92000  2 0 0 0  1001   14.3798
                               6012   85.6202    5  6.0588e-01   293  end
'void space internal to containment vessel above stacked content'
arbmwicv   0.9982   2 0 0 0    1001   11.1913
                               8016   88.8087    6  1.0     293  end
'steel: containment vessel body 16.60 lb but use 15.74 lb'
ss304                                           8  1.0     293  end
'steel: cv flange lower use 3.36 lb'
ss304                                           9  0.97267 293  end
'steel: cv flange upper use 13.75 lb'
ss304                                          10  0.94348 293  end
'np277-4: confinement -- neutron poison inner liner (NCT_MD&H)'
'actual vol.= 1.28314e4 cm3 = (7.83023e2 in3)(16.387064)'
'den.multiplier = 1.28314e4 cm3 (actual vol.) / 1.32708e4 cm3 (model vol.)'
'np277-4 min.den.= 1.527971 = (95.3886 lb/ft3)(453.59 g/lb)/(28316.84 cm3/ft3)'
'density = 1.477385 = (den.mult)(np277-4 min.den.) = 0.9668933*1.527971'
'use 75% of boron in calculations per NUREG-1609 Section 6.5.3.2'
arbmboron 7.06813e-2  2 0 0 0    5010   18.1479
                                 5011   81.8520   11  0.7500  293  end
arbmnpmx  1.03525e+0 10 0 0 0    6012    1.9189
                                 7014    0.0141
                                 8016   43.4251
                                11023    0.1174
                                12000    0.3378
                                13027   39.0479
                                14000    2.4672
                                16000    0.3083
                                20000   11.8336
                                26000    0.5298   11  1.0000  293  end
arbmnph2o 3.71451e-1  2 0 0 0    1001   11.1913
                                 8016   88.8087   11  1.0000  293  end
'kaolite 1600 body'
'sing.unit.density= (den.mult)(min.den.)'
' for arbmh20k = 1.012373*0.51655,  for rest = 1.012373*0.34438'
'den.mult= 1.36557e5 cm3 (actual vol.) / 1.34888e5 cm3 (model vol.)'
'actual vol.= 1.36557e5 cm3 = (28316.84 cm3/ft3)(108.33188 lb)/(22.464 lb/ft3)'
'nct array densities are s.u.dens. multiplied by volume ratio 1.34888/1.10336'
arbmh2ok   0.63931  2 0 0 0    1001   11.1913
                               8016   88.8087   12  0.0287  293  end
arbmal2o3  0.42622  2 0 0 0   13027   52.9390
                               8016   47.0610   12  0.096   293  end
arbmsio2   0.42622  2 0 0 0   14000   46.7570
                               8016   53.2430   12  0.367   293  end
arbmfe2o3  0.42622  2 0 0 0   26000   69.9540
                               8016   30.0460   12  0.067   293  end
arbmtio2   0.42622  2 0 0 0   22000   59.9535
                               8016   40.0465   12  0.012   293  end
arbmcao    0.42622  2 0 0 0   20000   71.4815
                               8016   28.5185   12  0.307   293  end
arbmmgo    0.42622  2 0 0 0   12000   60.3169
                               8016   39.6831   12  0.131   293  end
arbmna2o   0.42622  2 0 0 0   11023   74.1961
                               8016   25.8039   12  0.020   293  end
```

```
'kaolite 1600 top plug'
'sing.unit.density= (den.mult)(min.den.)'
' for arbmh20k = 0.965246*0.51655,  for rest = 0.965246*0.34438'
'den.mult= 1.21592e4 cm3 (actual vol.) / 1.25970e4 cm3 (model vol.)'
'actual vol.= 1.21592e4 cm3 = (28316.84 cm3/ft3)(9.646 lb)/(22.464 lb/ft3)'
arbmh2ok   0.49860  2 0 0 0    1001   11.1913
                               8016   88.8087   13  0.0287  293  end
arbmal2o3  0.33241  2 0 0 0   13027   52.9390
                               8016   47.0610   13  0.096   293  end
arbmsio2   0.33241  2 0 0 0   14000   46.7570
                               8016   53.2430   13  0.367   293  end
arbmfe2o3  0.33241  2 0 0 0   26000   69.9540
                               8016   30.0460   13  0.067   293  end
arbmtio2   0.33241  2 0 0 0   22000   59.9535
                               8016   40.0465   13  0.012   293  end
arbmcao    0.33241  2 0 0 0   20000   71.4815
                               8016   28.5185   13  0.307   293  end
arbmmgo    0.33241  2 0 0 0   12000   60.3169
                               8016   39.6831   13  0.131   293  end
arbmna2o   0.33241  2 0 0 0   11023   74.1961
                               8016   25.8039   13  0.020   293  end
'silicone rubber pads'
arbmsiru   1.21791  4 0 0 0    6012   32.3767
                               1001    8.1573
                               8016   21.5782
                              14000   37.8878   14  1.0     293  end
'void space external to containment vessel'
arbmwecv   0.9982   2 0 0 0    1001   11.1913
                               8016   88.8087   15  0.0001  293  end
'steel: liner'
ss304                                            16  1.0     293  end
'steel: plug cover (pc) use 9.907 lb'
ss304                                            17  1.06388 293  end
'steel: angle iron (ai) for single units'
'ss304                                            18  1.0     293  end
'steel: angle iron (ai) for arrays'
'array density is multiplied by a volume fraction 7.08030/5.63249'
ss304                                            18  1.25705 293  end
'steel: drum steel for single units'
'ss304                                            19  1.0     293  end
'steel: drum steel for arrays'
'array density is multiplied by a volume fraction 3.20482/3.20544'
ss304                                            19  0.99981 293  end
'void space external to drum'
'array density is multiplied by a volume ratio 8.11698/6.98323'
arbmwed    1.16026  2 0 0 0    1001   11.1913
                               8016   88.8087   20  0.0001  293  end
'reflective water'
'arbmh20r   0.9982   2 0 0 0    1001   11.1913
'                               8016   88.8087   21  1.0     293  end
end comp
nciapbmflt11,0.0in thk np, 4000.2gU( 3200.2g235) 9442.7gH2Ocv,hx= 82.26 fr=0.0001
read parameters nub=yes npg=2500 gen=215 nsk=15 tme=100 end parameters
read boun       all=specular                     end boun
read geometry
unit 1001
'drum bottom flat cover [Elev= 0.111 in. at top of unit]'
'cylinder  19 1   22.866096    0.28150   0.0     com='extended radius not used'
 cylinder  19 1   21.722275    0.28150   0.0     com='drum bottom flat cover'
 cuboid    20 1 4p22.866096    0.28150   0.0     com='drum chine outer radius'
unit 1002
'above drum bottom flat cover and below containment vessel [Elev= 4.676 in.]'
 cylinder  15 1    3.175000   11.59510  11.16330 com='void in pad-1'
 cylinder  14 1    7.924800   11.59510  11.16330 com='pad-1'
 cylinder  16 1    8.077200   11.59510  11.16330 com='np277_4 liner'
 cylinder  11 1   10.922000   11.59510  11.16330 com='np277_4'
 cylinder  16 1   11.074400   11.59510  10.85850 com='kaolite liner bottom'
 cylinder  12 1   21.555075   11.59510   0.0     com='kaolite'
 cylinder  19 1   21.722275   11.59510   0.0     com='drum'
 cuboid    20 1 4p22.866096   11.59510   0.0     com='drum chine outer radius'
unit 1003
```

```
'cv bottom [Elev= 4.926 in.]'
 cylinder  8  1    6.680200    0.63500   0.0     com='cv bottom'
 cylinder  15 1    7.924800    0.63500   0.0     com='void btw cv-np liner'
 cylinder  16 1    8.077200    0.63500   0.0     com='np277_4 liner'
 cylinder  11 1   10.922000    0.63500   0.0     com='np277_4'
 cylinder  16 1   11.074400    0.63500   0.0     com='kaolite liner'
 cylinder  12 1   21.555075    0.63500   0.0     com='kaolite'
 cylinder  19 1   21.722275    0.63500   0.0     com='drum'
 cuboid    20 1 4p22.866096    0.63500   0.0     com='drum chine outer radius'
unit 1004
'content (collapsed) [Elev= 5.833 in.]'
' 2.30470            bottom of cv to top of 1st content      ASSIGNED
' 5.83319            elevation (inches)                       CALCULATED
' 6.426200    5.06   cv inner radius                         M2E801508A011_RvB
' 299.00051             volume of content in unit 1004           CALCULATED
 cylinder  1  1    6.426200    2.30470  0.0      com='homog. HEU poly content'
 cylinder  8  1    6.680200    2.30470  0.0      com='cv below 1st step'
 cylinder  15 1    7.924800    2.30470  0.0      com='void btw cv-np liner'
 cylinder  16 1    8.077200    2.30470  0.0      com='np277_4 liner'
 cylinder  11 1   10.922000    2.30470  0.0      com='np277_4'
 cylinder  16 1   11.074400    2.30470  0.0      com='kaolite liner'
 cylinder  12 1   21.555075    2.30470  0.0      com='kaolite'
 cylinder  19 1   21.722275    2.30470  0.0      com='drum'
 cuboid    20 1 4p22.866096    2.30470  0.0      com='drum chine outer radius'
unit 1005
'np277_4 spacer [Elev= 5.833 in.]'
' 0.00020            top of 1st content to top 1st spacer    ASSIGNED
' 5.83331            elevation (inches)                       CALCULATED
'   0.00864            volume of spacer in unit 1005            CALCULATED
'   0.03028            volume of void in unit 1005              CALCULATED
 cylinder  2  1    5.24510     0.00010   0.0     com='np spacer'
 cylinder  1  1    6.426200    0.00020  -0.0001  com='cv well cavity'
 cylinder  8  1    6.680200    0.00020  -0.0001  com='cv below 1st step'
 cylinder  15 1    7.924800    0.00020  -0.0001  com='void btw cv-np liner'
 cylinder  16 1    8.077200    0.00020  -0.0001  com='np277_4 liner'
 cylinder  11 1   10.922000    0.00020  -0.0001  com='np277_4'
 cylinder  16 1   11.074400    0.00020  -0.0001  com='kaolite liner'
 cylinder  12 1   21.555075    0.00020  -0.0001  com='kaolite'
 cylinder  19 1   21.722275    0.00020  -0.0001  com='drum'
 cuboid    20 1 4p22.866096    0.00020  -0.0001  com='drum chine outer radius'
unit 1006
'content (collapsed) [Elev= 6.741 in.]'
' 299.00051             volume of content in unit 1006           CALCULATED
 cylinder  3  1    6.426200    2.30470  0.0      com='homog. HEU poly content'
 cylinder  8  1    6.680200    2.30470  0.0      com='cv below 1st step'
 cylinder  15 1    7.924800    2.30470  0.0      com='void btw cv-np liner'
 cylinder  16 1    8.077200    2.30470  0.0      com='np277_4 liner'
 cylinder  11 1   10.922000    2.30470  0.0      com='np277_4'
 cylinder  16 1   11.074400    2.30470  0.0      com='kaolite liner'
 cylinder  12 1   21.555075    2.30470  0.0      com='kaolite'
 cylinder  19 1   21.722275    2.30470  0.0      com='drum'
 cuboid    20 1 4p22.866096    2.30470  0.0      com='drum chine outer radius'
unit 1007
'np277_4 spacer [Elev= 6.741 in.]'
'   0.00864            volume of spacer in unit 1007            CALCULATED
'   0.03028            volume of void in unit 1007              CALCULATED
 cylinder  4  1    5.24510     0.00010   0.0     com='np spacer'
 cylinder  3  1    6.426200    0.00020  -0.0001  com='cv well cavity'
 cylinder  8  1    6.680200    0.00020  -0.0001  com='cv below 1st step'
 cylinder  15 1    7.924800    0.00020  -0.0001  com='void btw cv-np liner'
 cylinder  16 1    8.077200    0.00020  -0.0001  com='np277_4 liner'
 cylinder  11 1   10.922000    0.00020  -0.0001  com='np277_4'
 cylinder  16 1   11.074400    0.00020  -0.0001  com='kaolite liner'
 cylinder  12 1   21.555075    0.00020  -0.0001  com='kaolite'
 cylinder  19 1   21.722275    0.00020  -0.0001  com='drum'
 cuboid    20 1 4p22.866096    0.00020  -0.0001  com='drum chine outer radius'
unit 1008
'content (collapsed) [Elev= 7.648 in.]'
' 299.00051             volume of content in unit 1008           CALCULATED
 cylinder  5  1    6.426200    2.30470  0.0      com='homog. HEU poly content'
 cylinder  8  1    6.680200    2.30470  0.0      com='cv below 1st step'
```

```
 cylinder  15 1    7.924800    2.30470  0.0      com='void btw cv-np liner'
 cylinder  16 1    8.077200    2.30470  0.0      com='np277_4 liner'
 cylinder  11 1   10.922000    2.30470  0.0      com='np277_4'
 cylinder  16 1   11.074400    2.30470  0.0      com='kaolite liner'
 cylinder  12 1   21.555075    2.30470  0.0      com='kaolite'
 cylinder  19 1   21.722275    2.30470  0.0      com='drum'
 cuboid    20 1 4p22.866096    2.30470  0.0      com='drum chine outer radius'
unit 1009
'top of content stack to bottom of 1st step [Elev=35.276 in.]'
' 6.91469             stack height (3ccs plus 2 spacers)      CALCULATED
'35.27583            elevation (inches)                       CALCULATED
'35.27583            elevation (inches)                       VERIFIED
'9104.08949            volume of water in unit 1009             CALCULATED
 cylinder  6  1    6.426200   70.17431   0.0     com='cv well cavity'
 cylinder  8  1    6.680200   70.17431   0.0     com='cv below 1st step'
 cylinder  15 1    7.924800   70.17431   0.0     com='void btw cv-np liner'
 cylinder  16 1    8.077200   70.17431   0.0     com='np277_4 liner'
 cylinder  11 1   10.922000   70.17431   0.0     com='np277_4'
 cylinder  16 1   11.074400   70.17431   0.0     com='kaolite liner'
 cylinder  12 1   21.555075   70.17431   0.0     com='kaolite'
 cylinder  19 1   21.722275   70.17431   0.0     com='drum'
 cuboid    20 1 4p22.866096   70.17431   0.0     com='drum chine outer radius'
unit 1010
'cv at 1st step in liner [Elev=35.336 in.]'
'  19.77167            volume of water in unit 1010             CALCULATED
 cylinder  6  1    6.426200    0.15240   0.0     com='cv well cavity'
 cylinder  8  1    6.680200    0.15240   0.0     com='cv at 1st step'
 cylinder  15 1    7.924800    0.15240   0.0     com='void btw cv and liner'
 cylinder  16 1   11.074400    0.15240   0.0     com='liner 1st step'
 cylinder  12 1   21.555075    0.15240   0.0     com='kaolite'
 cylinder  19 1   21.722275    0.15240   0.0     com='drum'
 cuboid    20 1 4p22.866096    0.15240   0.0     com='drum chine outer radius'
unit 1011
'vertical gap between 1st step in liner and cv flange [Elev=35.426 in.]'
'  29.65750            volume of water in unit 1011             CALCULATED
 cylinder  6  1    6.426200    0.22860   0.0     com='cv well cavity'
 cylinder  8  1    6.680200    0.22860   0.0     com='cv at gap btwn step-flng'
 cylinder  15 1   10.922000    0.22860   0.0     com='void btw cv and liner'
 cylinder  16 1   11.074400    0.22860   0.0     com='liner wall'
 cylinder  12 1   21.555075    0.22860   0.0     com='kaolite'
 cylinder  19 1   21.722275    0.22860   0.0     com='drum'
 cuboid    20 1 4p22.866096    0.22860   0.0     com='drum chine outer radius'
unit 1012
'cv flange to top of cv well [Elev=35.926 in.]'
' 164.76390            volume of water in unit 1012             CALCULATED
 cylinder  6  1    6.426200    1.27000   0.0     com='cavity'
 cylinder  9  1    9.525000    1.27000   0.0     com='flange to top of well'
 cylinder  15 1    9.525000    1.27000   0.0     com='void btw cv and pad-2'
 cylinder  14 1   10.033000    1.27000   0.0     com='pad-2'
 cylinder  15 1   10.922000    1.27000   0.0     com='void btw cv and liner'
 cylinder  16 1   11.074400    1.27000   0.0     com='liner wall'
 cylinder  12 1   21.555075    1.27000   0.0     com='kaolite'
 cylinder  19 1   21.722275    1.27000   0.0     com='drum'
 cuboid    20 1 4p22.866096    1.27000   0.0     com='drum chine outer radius'
unit 1013
'cv flange above cv well [Elev=37.076 in.]'
 cylinder  10 1    9.525000    2.92100   0.0     com='flange above cv well'
 cylinder  15 1    9.525000    2.92100   0.0     com='void btw cv and pad-2'
 cylinder  14 1   10.033000    2.92100   0.0     com='pad-2'
 cylinder  15 1   10.922000    2.92100   0.0     com='void btw pad2 and liner'
 cylinder  16 1   11.074400    2.92100   0.0     com='liner wall'
 cylinder  12 1   21.555075    2.92100   0.0     com='kaolite'
 cylinder  19 1   21.722275    2.92100   0.0     com='drum'
 cuboid    20 1 4p22.866096    2.92100   0.0     com='drum chine outer radius'
unit 1014
'plugpad2 below liner 2nd step [Elev=37.476 in.]'
 cylinder  14 1   10.033000    0.76200   0.0     com='pad-2'
 cylinder  15 1   10.922000    1.01600   0.0     com='void btw pad2 and liner'
 cylinder  16 1   11.074400    1.01600   0.0     com='liner wall'
 cylinder  12 1   21.555075    1.01600   0.0     com='kaolite'
 cylinder  19 1   21.722275    1.01600   0.0     com='drum'
```

```
 cuboid    20 1 4p22.866096    1.01600   0.0     com='drum chine outer radius'
unit 1015
'2nd step in liner [Elev=37.536 in.]'
 cylinder  15 1   10.922000    0.15240   0.0     com='void abv pad2'
 cylinder  16 1   18.757900    0.15240   0.0     com='liner 2nd step'
 cylinder  12 1   21.555075    0.15240   0.0     com='kaolite'
 cylinder  19 1   21.722275    0.15240   0.0     com='drum'
 cuboid    20 1 4p22.866096    0.15240   0.0     com='drum chine outer radius'
unit 1016
'abv 2nd step in liner to bottom of angle iron [Elev=40.756 in.]'
 cylinder  13 1   18.097500    8.17880   0.49276 com='plug kaolite'
 cylinder  17 1   18.249900    8.17880   0.34036 com='sides of plug case'
 cylinder  15 1   18.605500    8.17880   0.0     com='void: plug to liner'
 cylinder  16 1   18.757900    8.17880   0.0     com='liner wall'
 cylinder  12 1   21.555075    8.17880   0.0     com='kaolite'
 cylinder  19 1   21.722275    8.17880   0.0     com='drum'
 cuboid    20 1 4p22.866096    8.17880   0.0     com='drum chine outer radius'
unit 1017
'bottom of angle iron to bend in angle iron [Elev=42.506 in.]'
 cylinder  13 1   18.097500    4.44500   0.0     com='plug kaolite'
 cylinder  17 1   18.249900    4.44500   0.0     com='sides of plug case'
 cylinder  15 1   18.605500    4.44500   0.0     com='void: plug to liner'
 cylinder  16 1   18.757900    4.44500   0.0     com='liner wall'
 cylinder  18 1   19.392900    4.44500   0.0     com='lower angle iron'
 cylinder  12 1   21.555075    4.44500   0.0     com='kaolite'
 cylinder  19 1   21.722275    4.44500   0.0     com='drum'
 cuboid    20 1 4p22.866096    4.44500   0.0     com='drum chine outer radius'
unit 1018
'bend in angle iron to top of angle iron [Elev=42.756 in.]'
 cylinder  13 1   18.097500    0.11176   0.0     com='plug kaolite'
 cylinder  17 1   18.249900    0.26416   0.0     com='sides of plug case'
 cylinder  15 1   18.605500    0.63500   0.0     com='void: plug to liner'
 cylinder  16 1   18.757900    0.63500   0.0     com='liner wall'
 cylinder  18 1   21.555075    0.63500   0.0     com='bend section of ai'
 cylinder  19 1   21.722275    0.63500   0.0     com='drum'
 cuboid    20 1 4p22.866096    0.63500   0.0     com='drum chine outer radius'
unit 1019
'drum lid and lip [Elev=43.512 in.]'
 cylinder  20 1   21.330090    1.91973   0.16720 com='void above lid'
 cylinder  19 1   21.497290    1.91973   0.0     com='drum lid'
 cylinder  20 1   21.555075    1.91973   0.0     com='void btw lid - drum wall'
 cylinder  19 1   21.722275    1.91973   0.0     com='drum'
 cuboid    20 1 4p22.866096    1.91973   0.0     com='drum chine outer radius'
global
unit 1020
'es3100 drum [Elev=43.512 in.]'
array 3         2r-22.866096     0.0
'cuboid     0  1 4p24.587200    42.62038  0.0    com='bare package'
'cuboid    21  1 4p55.067200   73.10038 -30.48   com='reflected package'
 cuboid    20  1 4p22.866096    110.5197  0.0    com='interstital array space'
'global
'unit 1021
'array 4   3r0.0
'reflector  21 2  6r3.0  10
end geometry
read array
ara=3 nux=1 nuy=1 nuz=19 fill
1001 1002 1003 1004 1005 1006 1007 1008 1009 1010
1011 1012 1013 1014 1015 1016 1017 1018 1019        end fill
'ara=4 nux=13 nuy=13 nuz=06 fill f1020               end fill
end array
'read bias id=500 2  11  end bias
read start nst=0
end start
end data
end
```

```
=csas25    parm=size=3000000
nciapbmfdt11,0.0in thk np, 4000.2gU( 3200.2g235) 9442.7gH2Ocv hx= 82.26 fr=0.0001
238groupndf5 infhommedium
'nciapbmfdt11 - n(nct), c(np277-4), ia(infinite array),'
'               pbm (poly homogenized with broken metal),'
'               f(can location height established by packing fraction),'
'               d(content resides in can location and gap between canned'
'               spacer and cv, and distributed over upper can location),'
'               t11 (NCT_MD&H)'
'HEU volume = 212.11396, SPACER volume    0.01729'
'HEU wrapped dry content can hx=5.24, CV void volume 9459.75243'
'Content in can location 1'
uranium  1 den=18.85873 0.23645 293      92235  80.000
                                         92238   20.000               end
arbmh2oi     0.99820  2 0 0 0  1001   11.1913
                               8016   88.8087    1  1.5773e-01   293  end
arbmpoly     0.92000  2 0 0 0  1001   14.3798
                               6012   85.6202    1  6.0582e-01   293  end
'np277-4: spacer (NCT_MD&H)'
'NCT min.den.(95.3886 lb/ft3) and hydrogen'
'np277-4 min.den.= 1.527971 = (95.3886 lb/ft3)(453.59 g/lb)/(28316.84 cm3/ft3)'
'use 75% of boron in calculations per NUREG-1609 Section 6.5.3.2'
arbmboron 7.31015e-2  2 0 0 0    5010   18.1479
                                 5011   81.8520    2  0.7500  293  end
arbmnpmx  1.07070e+0 10 0 0 0    6012    1.9189
                                 7014    0.0141
                                 8016   43.4251
                                11023    0.1174
                                12000    0.3378
                                13027   39.0479
                                14000    2.4672
                                16000    0.3083
                                20000   11.8336
                                26000    0.5298    2  1.0000  293  end
arbmnph2o 3.84169e-1  2 0 0 0    1001   11.1913
                                 8016   88.8087    2  1.0000  293  end
'Content in can location 2'
uranium  3 den=18.85873 0.23645 293      92235  80.000
                                         92238   20.000               end
arbmh2oi     0.99820  2 0 0 0  1001   11.1913
                               8016   88.8087    3  1.5773e-01   293  end
arbmpoly     0.92000  2 0 0 0  1001   14.3798
                               6012   85.6202    3  6.0582e-01   293  end
'np277-4: spacer (NCT_MD&H)'
'NCT min.den.(95.3886 lb/ft3) and hydrogen'
'np277-4 min.den.= 1.527971 = (95.3886 lb/ft3)(453.59 g/lb)/(28316.84 cm3/ft3)'
'use 75% of boron in calculations per NUREG-1609 Section 6.5.3.2'
arbmboron 7.31015e-2  2 0 0 0    5010   18.1479
                                 5011   81.8520    4  0.7500  293  end
arbmnpmx  1.07070e+0 10 0 0 0    6012    1.9189
                                 7014    0.0141
                                 8016   43.4251
                                11023    0.1174
                                12000    0.3378
                                13027   39.0479
                                14000    2.4672
                                16000    0.3083
                                20000   11.8336
                                26000    0.5298    4  1.0000  293  end
arbmnph2o 3.84169e-1  2 0 0 0    1001   11.1913
                                 8016   88.8087    4  1.0000  293  end
'Content in can location 3'
uranium  5 den=18.85873 0.00735 293      92235  80.000
                                         92238   20.000               end
arbmh2oi     0.99820  2 0 0 0  1001   11.1913
                               8016   88.8087    5  9.7381e-01   293  end
arbmpoly     0.92000  2 0 0 0  1001   14.3798
                               6012   85.6202    5  1.8837e-02   293  end
'void space internal to containment vessel above stacked content'
arbmwicv   0.9982   2 0 0 0    1001   11.1913
                               8016   88.8087    6  1.0     293  end
```

```
'steel: containment vessel body 16.60 lb but use 15.74 lb'
ss304                                          8  1.0     293  end
'steel: cv flange lower use 3.36 lb'
ss304                                          9  0.97267 293  end
'steel: cv flange upper use 13.75 lb'
ss304                                         10  0.94348 293  end
'np277-4: confinement -- neutron poison inner liner (NCT_MD&H)'
'actual vol.= 1.28314e4 cm3 = (7.83023e2 in3)(16.387064)'
'den.multiplier = 1.28314e4 cm3 (actual vol.) / 1.32708e4 cm3 (model vol.)'
'np277-4 min.den.= 1.527971 = (95.3886 lb/ft3)(453.59 g/lb)/(28316.84 cm3/ft3)'
'density = 1.477385 = (den.mult)(np277-4 min.den.) = 0.9668933*1.527971'
'use 75% of boron in calculations per NUREG-1609 Section 6.5.3.2'
arbmboron 7.06813e-2  2 0 0 0    5010   18.1479
                                 5011   81.8520   11  0.7500  293  end
arbmnpmx  1.03525e+0 10 0 0 0    6012    1.9189
                                 7014    0.0141
                                 8016   43.4251
                                11023    0.1174
                                12000    0.3378
                                13027   39.0479
                                14000    2.4672
                                16000    0.3083
                                20000   11.8336
                                26000    0.5298   11  1.0000  293  end
arbmnph2o 3.71451e-1  2 0 0 0    1001   11.1913
                                 8016   88.8087   11  1.0000  293  end
'kaolite 1600 body'
'sing.unit.density= (den.mult)(min.den.)'
' for arbmh20k = 1.012373*0.51655,  for rest = 1.012373*0.34438'
'den.mult= 1.36557e5 cm3 (actual vol.) / 1.34888e5 cm3 (model vol.)'
'actual vol.= 1.36557e5 cm3 = (28316.84 cm3/ft3)(108.33188 lb)/(22.464 lb/ft3)'
'nct array densities are s.u.dens. multiplied by volume ratio 1.34888/1.10336'
arbmh2ok   0.63931  2 0 0 0    1001   11.1913
                               8016   88.8087   12  0.0287  293  end
arbmal2o3  0.42622  2 0 0 0   13027   52.9390
                               8016   47.0610   12  0.096   293  end
arbmsio2   0.42622  2 0 0 0   14000   46.7570
                               8016   53.2430   12  0.367   293  end
arbmfe2o3  0.42622  2 0 0 0   26000   69.9540
                               8016   30.0460   12  0.067   293  end
arbmtio2   0.42622  2 0 0 0   22000   59.9535
                               8016   40.0465   12  0.012   293  end
arbmcao    0.42622  2 0 0 0   20000   71.4815
                               8016   28.5185   12  0.307   293  end
arbmmgo    0.42622  2 0 0 0   12000   60.3169
                               8016   39.6831   12  0.131   293  end
arbmna2o   0.42622  2 0 0 0   11023   74.1961
                               8016   25.8039   12  0.020   293  end
'kaolite 1600 top plug'
'sing.unit.density= (den.mult)(min.den.)'
' for arbmh20k = 0.965246*0.51655,  for rest = 0.965246*0.34438'
'den.mult= 1.21592e4 cm3 (actual vol.) / 1.25970e4 cm3 (model vol.)'
'actual vol.= 1.21592e4 cm3 = (28316.84 cm3/ft3)(9.646 lb)/(22.464 lb/ft3)'
arbmh2ok   0.49860  2 0 0 0    1001   11.1913
                               8016   88.8087   13  0.0287  293  end
arbmal2o3  0.33241  2 0 0 0   13027   52.9390
                               8016   47.0610   13  0.096   293  end
arbmsio2   0.33241  2 0 0 0   14000   46.7570
                               8016   53.2430   13  0.367   293  end
arbmfe2o3  0.33241  2 0 0 0   26000   69.9540
                               8016   30.0460   13  0.067   293  end
arbmtio2   0.33241  2 0 0 0   22000   59.9535
                               8016   40.0465   13  0.012   293  end
arbmcao    0.33241  2 0 0 0   20000   71.4815
                               8016   28.5185   13  0.307   293  end
arbmmgo    0.33241  2 0 0 0   12000   60.3169
                               8016   39.6831   13  0.131   293  end
arbmna2o   0.33241  2 0 0 0   11023   74.1961
                               8016   25.8039   13  0.020   293  end
'silicone rubber pads'
arbmsiru   1.21791  4 0 0 0    6012   32.3767
```

```
                                1001    8.1573
                                8016   21.5782
                               14000   37.8878   14  1.0     293  end
'void space external to containment vessel'
arbmwecv   0.9982   2 0 0 0    1001   11.1913
                                8016   88.8087   15  0.0001  293  end
'steel: liner'
ss304                                            16  1.0     293  end
'steel: plug cover (pc) use 9.907 lb'
ss304                                            17  1.06388 293  end
'steel: angle iron (ai) for single units'
'ss304                                            18  1.0     293  end
'steel: angle iron (ai) for arrays'
'array density is multiplied by a volume fraction 7.08030/5.63249'
ss304                                            18  1.25705 293  end
'steel: drum steel for single units'
'ss304                                            19  1.0     293  end
'steel: drum steel for arrays'
'array density is multiplied by a volume fraction 3.20482/3.20544'
ss304                                            19  0.99981 293  end
'void space external to drum'
'array density is multiplied by a volume ratio 8.11698/6.98323'
arbmwed    1.16026  2 0 0 0    1001   11.1913
                                8016   88.8087   20  0.0001  293  end
'reflective water'
'arbmh20r   0.9982   2 0 0 0    1001   11.1913
'                                8016   88.8087   21  1.0     293  end
end comp
nciapbmfdt11,0.0in thk np, 4000.2gU( 3200.2g235) 9442.7gH2Ocv,hx= 82.26 fr=0.0001
read parameters nub=yes npg=2500 gen=215 nsk=15 tme=100 end parameters
read boun       all=specular                     end boun
read geometry
unit 1001
'drum bottom flat cover [Elev= 0.111 in. at top of unit]'
'cylinder  19 1   22.866096    0.28150   0.0     com='extended radius not used'
 cylinder  19 1   21.722275    0.28150   0.0     com='drum bottom flat cover'
 cuboid    20 1 4p22.866096    0.28150   0.0     com='drum chine outer radius'
unit 1002
'above drum bottom flat cover and below containment vessel [Elev= 4.676 in.]'
 cylinder  15 1    3.175000   11.59510  11.16330 com='void in pad-1'
 cylinder  14 1    7.924800   11.59510  11.16330 com='pad-1'
 cylinder  16 1    8.077200   11.59510  11.16330 com='np277_4 liner'
 cylinder  11 1   10.922000   11.59510  11.16330 com='np277_4'
 cylinder  16 1   11.074400   11.59510  10.85850 com='kaolite liner bottom'
 cylinder  12 1   21.555075   11.59510   0.0     com='kaolite'
 cylinder  19 1   21.722275   11.59510   0.0     com='drum'
 cuboid    20 1 4p22.866096   11.59510   0.0     com='drum chine outer radius'
unit 1003
'cv bottom [Elev= 4.926 in.]'
 cylinder  8  1    6.680200    0.63500   0.0     com='cv bottom'
 cylinder  15 1    7.924800    0.63500   0.0     com='void btw cv-np liner'
 cylinder  16 1    8.077200    0.63500   0.0     com='np277_4 liner'
 cylinder  11 1   10.922000    0.63500   0.0     com='np277_4'
 cylinder  16 1   11.074400    0.63500   0.0     com='kaolite liner'
 cylinder  12 1   21.555075    0.63500   0.0     com='kaolite'
 cylinder  19 1   21.722275    0.63500   0.0     com='drum'
 cuboid    20 1 4p22.866096    0.63500   0.0     com='drum chine outer radius'
unit 1004
'content (collapsed) [Elev= 5.833 in.]'
' 2.30470            bottom of cv to top of 1st content      ASSIGNED
' 5.83319            elevation (inches)                       CALCULATED
' 6.426200    5.06   cv inner radius                         M2E801508A011_RvB
' 299.00051            volume of content in unit 1004           CALCULATED
 cylinder  1  1    6.426200    2.30470  0.0      com='homog. HEU poly content'
 cylinder  8  1    6.680200    2.30470  0.0      com='cv below 1st step'
 cylinder  15 1    7.924800    2.30470  0.0      com='void btw cv-np liner'
 cylinder  16 1    8.077200    2.30470  0.0      com='np277_4 liner'
 cylinder  11 1   10.922000    2.30470  0.0      com='np277_4'
 cylinder  16 1   11.074400    2.30470  0.0      com='kaolite liner'
 cylinder  12 1   21.555075    2.30470  0.0      com='kaolite'
 cylinder  19 1   21.722275    2.30470  0.0      com='drum'
```

```
 cuboid    20 1 4p22.866096    2.30470  0.0      com='drum chine outer radius'
unit 1005
'np277_4 spacer [Elev= 5.833 in.]'
' 0.00020            top of 1st content to top of 1st spacer ASSIGNED
' 5.83331            elevation (inches)                      CALCULATED
'   0.00864            volume of spacer in unit 1005            CALCULATED
'   0.03028            volume of void in unit 1005              CALCULATED
 cylinder  2  1    5.24510     0.00010   0.0     com='np spacer'
 cylinder  1  1    6.426200    0.00020  -0.0001  com='cv well cavity'
 cylinder  8  1    6.680200    0.00020  -0.0001  com='cv below 1st step'
 cylinder  15 1    7.924800    0.00020  -0.0001  com='void btw cv-np liner'
 cylinder  16 1    8.077200    0.00020  -0.0001  com='np277_4 liner'
 cylinder  11 1   10.922000    0.00020  -0.0001  com='np277_4'
 cylinder  16 1   11.074400    0.00020  -0.0001  com='kaolite liner'
 cylinder  12 1   21.555075    0.00020  -0.0001  com='kaolite'
 cylinder  19 1   21.722275    0.00020  -0.0001  com='drum'
 cuboid    20 1 4p22.866096    0.00020  -0.0001  com='drum chine outer radius'
unit 1006
'content (collapsed) [Elev= 6.741 in.]'
' 299.00051            volume of content in unit 1006           CALCULATED
 cylinder  3  1    6.426200    2.30470  0.0      com='homog. HEU poly content'
 cylinder  8  1    6.680200    2.30470  0.0      com='cv below 1st step'
 cylinder  15 1    7.924800    2.30470  0.0      com='void btw cv-np liner'
 cylinder  16 1    8.077200    2.30470  0.0      com='np277_4 liner'
 cylinder  11 1   10.922000    2.30470  0.0      com='np277_4'
 cylinder  16 1   11.074400    2.30470  0.0      com='kaolite liner'
 cylinder  12 1   21.555075    2.30470  0.0      com='kaolite'
 cylinder  19 1   21.722275    2.30470  0.0      com='drum'
 cuboid    20 1 4p22.866096    2.30470  0.0      com='drum chine outer radius'
unit 1007
'np277_4 spacer [Elev= 6.741 in.]'
'   0.00864            volume of spacer in unit 1007            CALCULATED
'   0.03028            volume of void in unit 1007              CALCULATED
 cylinder  4  1    5.24510     0.00010   0.0     com='np spacer'
 cylinder  3  1    6.426200    0.00020  -0.0001  com='cv well cavity'
 cylinder  8  1    6.680200    0.00020  -0.0001  com='cv below 1st step'
 cylinder  15 1    7.924800    0.00020  -0.0001  com='void btw cv-np liner'
 cylinder  16 1    8.077200    0.00020  -0.0001  com='np277_4 liner'
 cylinder  11 1   10.922000    0.00020  -0.0001  com='np277_4'
 cylinder  16 1   11.074400    0.00020  -0.0001  com='kaolite liner'
 cylinder  12 1   21.555075    0.00020  -0.0001  com='kaolite'
 cylinder  19 1   21.722275    0.00020  -0.0001  com='drum'
 cuboid    20 1 4p22.866096    0.00020  -0.0001  com='drum chine outer radius'
unit 1008
'content (collapsed) [Elev= 7.648 in.]'
' 299.00051            volume of content in unit 1008           CALCULATED
 cylinder  5  1    6.426200    2.30470  0.0      com='homog. HEU poly content'
 cylinder  8  1    6.680200    2.30470  0.0      com='cv below 1st step'
 cylinder  15 1    7.924800    2.30470  0.0      com='void btw cv-np liner'
 cylinder  16 1    8.077200    2.30470  0.0      com='np277_4 liner'
 cylinder  11 1   10.922000    2.30470  0.0      com='np277_4'
 cylinder  16 1   11.074400    2.30470  0.0      com='kaolite liner'
 cylinder  12 1   21.555075    2.30470  0.0      com='kaolite'
 cylinder  19 1   21.722275    2.30470  0.0      com='drum'
 cuboid    20 1 4p22.866096    2.30470  0.0      com='drum chine outer radius'
unit 1009
'top of content stack to bottom of 1st step [Elev=35.276 in.]'
' 6.91469             stack height (3ccs plus 2 spacers)      CALCULATED
'35.27583            elevation (inches)                      CALCULATED
'35.27583            elevation (inches)                      VERIFIED
'9104.08949            volume of water in unit 1009             CALCULATED
 cylinder  5  1    6.426200   70.17431   0.0     com='cv well cavity'
 cylinder  8  1    6.680200   70.17431   0.0     com='cv below 1st step'
 cylinder  15 1    7.924800   70.17431   0.0     com='void btw cv-np liner'
 cylinder  16 1    8.077200   70.17431   0.0     com='np277_4 liner'
 cylinder  11 1   10.922000   70.17431   0.0     com='np277_4'
 cylinder  16 1   11.074400   70.17431   0.0     com='kaolite liner'
 cylinder  12 1   21.555075   70.17431   0.0     com='kaolite'
 cylinder  19 1   21.722275   70.17431   0.0     com='drum'
 cuboid    20 1 4p22.866096   70.17431   0.0     com='drum chine outer radius'
unit 1010
```

```
'cv at 1st step in liner [Elev=35.336 in.]'
'  19.77167            volume of water in unit 1010             CALCULATED
 cylinder  5  1    6.426200    0.15240   0.0     com='cv well cavity'
 cylinder  8  1    6.680200    0.15240   0.0     com='cv at 1st step'
 cylinder  15 1    7.924800    0.15240   0.0     com='void btw cv and liner'
 cylinder  16 1   11.074400    0.15240   0.0     com='liner 1st step'
 cylinder  12 1   21.555075    0.15240   0.0     com='kaolite'
 cylinder  19 1   21.722275    0.15240   0.0     com='drum'
 cuboid    20 1 4p22.866096    0.15240   0.0     com='drum chine outer radius'
unit 1011
'vertical gap between 1st step in liner and cv flange [Elev=35.426 in.]'
'  29.65750            volume of water in unit 1011             CALCULATED
 cylinder  5  1    6.426200    0.22860   0.0     com='cv well cavity'
 cylinder  8  1    6.680200    0.22860   0.0     com='cv at gap btwn step-flng'
 cylinder  15 1   10.922000    0.22860   0.0     com='void btw cv and liner'
 cylinder  16 1   11.074400    0.22860   0.0     com='liner wall'
 cylinder  12 1   21.555075    0.22860   0.0     com='kaolite'
 cylinder  19 1   21.722275    0.22860   0.0     com='drum'
 cuboid    20 1 4p22.866096    0.22860   0.0     com='drum chine outer radius'
unit 1012
'cv flange to top of cv well [Elev=35.926 in.]'
' 164.76390            volume of water in unit 1012             CALCULATED
 cylinder  5  1    6.426200    1.27000   0.0     com='cavity'
 cylinder  9  1    9.525000    1.27000   0.0     com='flange to top of well'
 cylinder  15 1    9.525000    1.27000   0.0     com='void btw cv and pad-2'
 cylinder  14 1   10.033000    1.27000   0.0     com='pad-2'
 cylinder  15 1   10.922000    1.27000   0.0     com='void btw cv and liner'
 cylinder  16 1   11.074400    1.27000   0.0     com='liner wall'
 cylinder  12 1   21.555075    1.27000   0.0     com='kaolite'
 cylinder  19 1   21.722275    1.27000   0.0     com='drum'
 cuboid    20 1 4p22.866096    1.27000   0.0     com='drum chine outer radius'
unit 1013
'cv flange above cv well [Elev=37.076 in.]'
 cylinder  10 1    9.525000    2.92100   0.0     com='flange above cv well'
 cylinder  15 1    9.525000    2.92100   0.0     com='void btw cv and pad-2'
 cylinder  14 1   10.033000    2.92100   0.0     com='pad-2'
 cylinder  15 1   10.922000    2.92100   0.0     com='void btw pad2 and liner'
 cylinder  16 1   11.074400    2.92100   0.0     com='liner wall'
 cylinder  12 1   21.555075    2.92100   0.0     com='kaolite'
 cylinder  19 1   21.722275    2.92100   0.0     com='drum'
 cuboid    20 1 4p22.866096    2.92100   0.0     com='drum chine outer radius'
unit 1014
'plugpad2 below liner 2nd step [Elev=37.476 in.]'
 cylinder  14 1   10.033000    0.76200   0.0     com='pad-2'
 cylinder  15 1   10.922000    1.01600   0.0     com='void btw pad2 and liner'
 cylinder  16 1   11.074400    1.01600   0.0     com='liner wall'
 cylinder  12 1   21.555075    1.01600   0.0     com='kaolite'
 cylinder  19 1   21.722275    1.01600   0.0     com='drum'
 cuboid    20 1 4p22.866096    1.01600   0.0     com='drum chine outer radius'
unit 1015
'2nd step in liner [Elev=37.536 in.]'
 cylinder  15 1   10.922000    0.15240   0.0     com='void abv pad2'
 cylinder  16 1   18.757900    0.15240   0.0     com='liner 2nd step'
 cylinder  12 1   21.555075    0.15240   0.0     com='kaolite'
 cylinder  19 1   21.722275    0.15240   0.0     com='drum'
 cuboid    20 1 4p22.866096    0.15240   0.0     com='drum chine outer radius'
unit 1016
'abv 2nd step in liner to bottom of angle iron [Elev=40.756 in.]'
 cylinder  13 1   18.097500    8.17880   0.49276 com='plug kaolite'
 cylinder  17 1   18.249900    8.17880   0.34036 com='sides of plug case'
 cylinder  15 1   18.605500    8.17880   0.0     com='void: plug to liner'
 cylinder  16 1   18.757900    8.17880   0.0     com='liner wall'
 cylinder  12 1   21.555075    8.17880   0.0     com='kaolite'
 cylinder  19 1   21.722275    8.17880   0.0     com='drum'
 cuboid    20 1 4p22.866096    8.17880   0.0     com='drum chine outer radius'
unit 1017
'bottom of angle iron to bend in angle iron [Elev=42.506 in.]'
 cylinder  13 1   18.097500    4.44500   0.0     com='plug kaolite'
 cylinder  17 1   18.249900    4.44500   0.0     com='sides of plug case'
 cylinder  15 1   18.605500    4.44500   0.0     com='void: plug to liner'
 cylinder  16 1   18.757900    4.44500   0.0     com='liner wall'
```

```
 cylinder  18 1   19.392900    4.44500   0.0     com='lower angle iron'
 cylinder  12 1   21.555075    4.44500   0.0     com='kaolite'
 cylinder  19 1   21.722275    4.44500   0.0     com='drum'
 cuboid    20 1 4p22.866096    4.44500   0.0     com='drum chine outer radius'
unit 1018
'bend in angle iron to top of angle iron [Elev=42.756 in.]'
 cylinder  13 1   18.097500    0.11176   0.0     com='plug kaolite'
 cylinder  17 1   18.249900    0.26416   0.0     com='sides of plug case'
 cylinder  15 1   18.605500    0.63500   0.0     com='void: plug to liner'
 cylinder  16 1   18.757900    0.63500   0.0     com='liner wall'
 cylinder  18 1   21.555075    0.63500   0.0     com='bend section of ai'
 cylinder  19 1   21.722275    0.63500   0.0     com='drum'
 cuboid    20 1 4p22.866096    0.63500   0.0     com='drum chine outer radius'
unit 1019
'drum lid and lip [Elev=43.512 in.]'
 cylinder  20 1   21.330090    1.91973   0.16720 com='void above lid'
 cylinder  19 1   21.497290    1.91973   0.0     com='drum lid'
 cylinder  20 1   21.555075    1.91973   0.0     com='void btw lid - drum wall'
 cylinder  19 1   21.722275    1.91973   0.0     com='drum'
 cuboid    20 1 4p22.866096    1.91973   0.0     com='drum chine outer radius'
global
unit 1020
'es3100 drum [Elev=43.512 in.]'
array 3         2r-22.866096     0.0
'cuboid     0  1 4p24.587200    42.62038  0.0    com='bare package'
'cuboid    21  1 4p55.067200   73.10038 -30.48   com='reflected package'
 cuboid    20  1 4p22.866096    110.5197  0.0    com='interstital array space'
'global
'unit 1021
'array 4   3r0.0
'reflector  21 2  6r3.0  10
end geometry
read array
ara=3 nux=1 nuy=1 nuz=19 fill
1001 1002 1003 1004 1005 1006 1007 1008 1009 1010
1011 1012 1013 1014 1015 1016 1017 1018 1019        end fill
'ara=4 nux=13 nuy=13 nuz=06 fill f1020               end fill
end array
'read bias id=500 2  11  end bias
read start nst=0
end start
end data
end


=csas25    parm=size=3000000
ncsrpunhct11  8000.1gUNHc( 3767.7g235,1732.2gH2O) 6795.6gH2Ocv hx= 63.53 fr=1.0e+00
238groupndf5 infhommedium
'U(enr)O2(NO3)2+6H2O [2.81 g/cc for U(nat)]  2.79329 g/cm3, hx=12.0, gU/L= 368.8310'
'dry content (poly packed or wrapped) h/x=4.45, CV void volume 6807.84362 cm3'
arbmunh    2.79329  5 0 0 0   92235   47.0962
                              92238    0.0000
                               1001    2.4232
                               7014    5.6116
                               8016   44.8690    1  2.8037e-01   293  end
arbmh2oc   0.99820  2 0 0 0  1001   11.1913
                               8016   88.8087    1  6.6643e-01   293  end
arbmpoly   0.92000  2 0 0 0  1001   14.3798
                               6012   85.6202    1  5.3202e-02   293  end
'np277-4: spacer (NCT_MD&H)'
'NCT min.den.(95.3886 lb/ft3) and hydrogen'
'np277-4 min.den.= 1.527971 = (95.3886 lb/ft3)(453.59 g/lb)/(28316.84 cm3/ft3)'
'use 75% of boron in calculations per NUREG-1609 Section 6.5.3.2'
arbmboron 7.31015e-2  2 0 0 0    5010   18.1479
                                 5011   81.8520    2  0.7500  293  end
arbmnpmx  1.07070e+0 10 0 0 0    6012    1.9189
                                 7014    0.0141
                                 8016   43.4251
                                11023    0.1174
                                12000    0.3378
                                13027   39.0479
```

```
                                14000    2.4672
                                16000    0.3083
                                20000   11.8336
                                26000    0.5298    2  1.0000  293  end
arbmnph2o 3.84169e-1  2 0 0 0    1001   11.1913
                                 8016   88.8087    2  1.0000  293  end
'flooded containmment vessel and content cans -- 10 CFR 71.55(d)(3)'
arbmwicv  6.6523e-01  2 0 0 0    1001   11.1913
                                 8016   88.8087    3  1.0     293  end
'steel: containment vessel body 16.60 lb but use 15.74 lb'
ss304                                            8  1.0     293  end
'steel: cv flange lower use 3.36 lb'
ss304                                            9  0.97267 293  end
'steel: cv flange upper use 13.75 lb'
ss304                                           10  0.94348 293  end
'np277-4: confinement -- neutron poison inner liner (NCT_MD&H)'
'actual vol.= 1.28314e4 cm3 = (7.83023e2 in3)(16.387064)'
'den.multiplier = 1.28314e4 cm3 (actual vol.) / 1.32708e4 cm3 (model vol.)'
'np277-4 min.den.= 1.527971 = (95.3886 lb/ft3)(453.59 g/lb)/(28316.84 cm3/ft3)'
'density = 1.477385 = (den.mult)(np277-4 min.den.) = 0.9668933*1.527971'
'use 75% of boron in calculations per NUREG-1609 Section 6.5.3.2'
arbmboron 7.06813e-2  2 0 0 0    5010   18.1479
                                 5011   81.8520   11  0.7500  293  end
arbmnpmx  1.03525e+0 10 0 0 0    6012    1.9189
                                 7014    0.0141
                                 8016   43.4251
                                11023    0.1174
                                12000    0.3378
                                13027   39.0479
                                14000    2.4672
                                16000    0.3083
                                20000   11.8336
                                26000    0.5298   11  1.0000  293  end
arbmnph2o 3.71451e-1  2 0 0 0    1001   11.1913
                                 8016   88.8087   11  1.0000  293  end
'kaolite 1600 body'
'sing.unit.density= (den.mult)(min.den.)'
' for arbmh20k = 1.012373*0.51655,  for rest = 1.012373*0.34438'
'den.mult= 1.36557e5 cm3 (actual vol.) / 1.34888e5 cm3 (model vol.)'
'actual vol.= 1.36557e5 cm3 = (28316.84 cm3/ft3)(108.33188 lb)/(22.464 lb/ft3)'
arbmh2ok   0.52294  2 0 0 0    1001   11.1913
                               8016   88.8087   12  1       293  end
arbmal2o3  0.34864  2 0 0 0   13027   52.9390
                               8016   47.0610   12  0.096   293  end
arbmsio2   0.34864  2 0 0 0   14000   46.7570
                               8016   53.2430   12  0.367   293  end
arbmfe2o3  0.34864  2 0 0 0   26000   69.9540
                               8016   30.0460   12  0.067   293  end
arbmtio2   0.34864  2 0 0 0   22000   59.9535
                               8016   40.0465   12  0.012   293  end
arbmcao    0.34864  2 0 0 0   20000   71.4815
                               8016   28.5185   12  0.307   293  end
arbmmgo    0.34864  2 0 0 0   12000   60.3169
                               8016   39.6831   12  0.131   293  end
arbmna2o   0.34864  2 0 0 0   11023   74.1961
                               8016   25.8039   12  0.020   293  end
'kaolite 1600 top plug'
'sing.unit.density= (den.mult)(min.den.)'
' for arbmh20k = 0.965246*0.51655,  for rest = 0.965246*0.34438'
'den.mult= 1.21592e4 cm3 (actual vol.) / 1.25970e4 cm3 (model vol.)'
'actual vol.= 1.21592e4 cm3 = (28316.84 cm3/ft3)(9.646 lb)/(22.464 lb/ft3)'
arbmh2ok   0.49860  2 0 0 0    1001   11.1913
                               8016   88.8087   13  1       293  end
arbmal2o3  0.33241  2 0 0 0   13027   52.9390
                               8016   47.0610   13  0.096   293  end
arbmsio2   0.33241  2 0 0 0   14000   46.7570
                               8016   53.2430   13  0.367   293  end
arbmfe2o3  0.33241  2 0 0 0   26000   69.9540
                               8016   30.0460   13  0.067   293  end
arbmtio2   0.33241  2 0 0 0   22000   59.9535
                               8016   40.0465   13  0.012   293  end
```

```
arbmcao    0.33241  2 0 0 0   20000   71.4815
                               8016   28.5185   13  0.307   293  end
arbmmgo    0.33241  2 0 0 0   12000   60.3169
                               8016   39.6831   13  0.131   293  end
arbmna2o   0.33241  2 0 0 0   11023   74.1961
                               8016   25.8039   13  0.020   293  end
'silicone rubber pads'
arbmsiru   1.21791  4 0 0 0    6012   32.3767
                               1001    8.1573
                               8016   21.5782
                              14000   37.8878   14  1.0     293  end
'void space external to containment vessel'
arbmwecv   0.9982   2 0 0 0    1001   11.1913
                               8016   88.8087   15  1       293  end
'steel: liner'
ss304                                            16  1.0     293  end
'steel: plug cover (pc) use 9.907 lb'
ss304                                            17  1.06388 293  end
'steel: angle iron (ai) for single units'
ss304                                            18  1.0     293  end
'steel: angle iron (ai) for arrays'
'array density is multiplied by a volume fraction 7.08030/5.63249'
'ss304                                            18  1.25705 293  end
'steel: drum steel for single units'
ss304                                            19  1.0     293  end
'steel: drum steel for arrays'
'array density is multiplied by a volume fraction 3.20482/3.20544'
'ss304                                            19  0.99981 293  end
'void space external to drum'
'array density is multiplied by a volume ratio 8.11698/6.98323'
'arbmwed    1.16026  2 0 0 0    1001   11.1913
'                               8016   88.8087   20  1       293  end
'reflective water'
arbmh20r   0.9982   2 0 0 0    1001   11.1913
                               8016   88.8087   21  1.0     293  end
end comp
ncsrpunhct11  8000.1gUNHc( 3767.7g235,1732.2gH2O) 6795.6gH2Ocv,hx= 63.53 fr=1.0e+00
read parameters nub=yes npg=2500 gen=215 nsk=15 tme=100 end parameters
read boun       all=vac                          end boun
read geometry
unit 1001
'drum bottom flat cover [Elev= 0.105 in. at top of unit]'
'cylinder  19 1   24.587200    0.26670   0.0     com='extended radius not used'
 cylinder  19 1   23.329900    0.26670   0.0     com='drum bottom flat cover'
 cuboid    21 1 4p24.587200    0.26670   0.0     com='drum chine outer radius'
unit 1002
'above drum bottom flat cover and below containment vessel [Elev= 4.670 in.]'
 cylinder  15 1    3.175000   11.59510  11.16330 com='void in pad-1'
 cylinder  14 1    7.924800   11.59510  11.16330 com='pad-1'
 cylinder  16 1    8.077200   11.59510  11.16330 com='np277_4 liner'
 cylinder  11 1   10.922000   11.59510  11.16330 com='np277_4'
 cylinder  16 1   11.074400   11.59510  10.85850 com='kaolite liner bottom'
 cylinder  12 1   23.177500   11.59510   0.0     com='kaolite'
 cylinder  19 1   23.329900   11.59510   0.0     com='drum'
 cuboid    21 1 4p24.587200   11.59510   0.0     com='drum chine outer radius'
unit 1003
'cv bottom to bottom of 1st step [Elev=35.270 in.]'
 cylinder  1  1    6.426200   77.72400   0.63500 com='HEU content'
 cylinder  8  1    6.680200   77.72400   0.0     com='cv bottom'
 cylinder  15 1    7.924800   77.72400   0.0     com='void btw cv-np liner'
 cylinder  16 1    8.077200   77.72400   0.0     com='np277_4 liner'
 cylinder  11 1   10.922000   77.72400   0.0     com='np277_4'
 cylinder  16 1   11.074400   77.72400   0.0     com='kaolite liner'
 cylinder  12 1   23.177500   77.72400   0.0     com='kaolite'
 cylinder  19 1   23.329900   77.72400   0.0     com='drum'
 cuboid    21 1 4p24.587200   77.72400   0.0     com='drum chine outer radius'
unit 1010
'cv at 1st step in liner [Elev=35.330 in.]'
 cylinder  1  1    6.426200    0.15240   0.0     com='HEU content'
 cylinder  8  1    6.680200    0.15240   0.0     com='cv at 1st step'
 cylinder  15 1    7.924800    0.15240   0.0     com='void btw cv and liner'
```

```
 cylinder  16 1   11.074400    0.15240   0.0     com='liner 1st step'
 cylinder  12 1   23.177500    0.15240   0.0     com='kaolite'
 cylinder  19 1   23.329900    0.15240   0.0     com='drum'
 cuboid    21 1 4p24.587200    0.15240   0.0     com='drum chine outer radius'
unit 1011
'vertical gap between 1st step in liner and cv flange [Elev=35.420 in.]'
 cylinder  1  1    6.426200    0.22860   0.0     com='HEU content'
 cylinder  8  1    6.680200    0.22860   0.0     com='cv at gap btwn step-flng'
 cylinder  15 1   10.922000    0.22860   0.0     com='void btw cv and liner'
 cylinder  16 1   11.074400    0.22860   0.0     com='liner wall'
 cylinder  12 1   23.177500    0.22860   0.0     com='kaolite'
 cylinder  19 1   23.329900    0.22860   0.0     com='drum'
 cuboid    21 1 4p24.587200    0.22860   0.0     com='drum chine outer radius'
unit 1012
'cv flange to top of cv well [Elev=35.920 in.]'
 cylinder  1  1    6.426200    1.27000   0.0     com='HEU content'
 cylinder  9  1    9.525000    1.27000   0.0     com='flange to top of well'
 cylinder  15 1    9.525000    1.27000   0.0     com='void btw cv and pad-2'
 cylinder  14 1   10.033000    1.27000   0.0     com='pad-2'
 cylinder  15 1   10.922000    1.27000   0.0     com='void btw cv and liner'
 cylinder  16 1   11.074400    1.27000   0.0     com='liner wall'
 cylinder  12 1   23.177500    1.27000   0.0     com='kaolite'
 cylinder  19 1   23.329900    1.27000   0.0     com='drum'
 cuboid    21 1 4p24.587200    1.27000   0.0     com='drum chine outer radius'
unit 1013
'cv flange above cv well [Elev=37.070 in.]'
 cylinder  10 1    9.525000    2.92100   0.0     com='flange above cv well'
 cylinder  15 1    9.525000    2.92100   0.0     com='void btw cv and pad-2'
 cylinder  14 1   10.033000    2.92100   0.0     com='pad-2'
 cylinder  15 1   10.922000    2.92100   0.0     com='void btw pad2 and liner'
 cylinder  16 1   11.074400    2.92100   0.0     com='liner wall'
 cylinder  12 1   23.177500    2.92100   0.0     com='kaolite'
 cylinder  19 1   23.329900    2.92100   0.0     com='drum'
 cuboid    21 1 4p24.587200    2.92100   0.0     com='drum chine outer radius'
unit 1014
'plugpad2 below liner 2nd step [Elev=37.470 in.]'
 cylinder  14 1   10.033000    0.76200   0.0     com='pad-2'
 cylinder  15 1   10.922000    1.01600   0.0     com='void btw pad2 and liner'
 cylinder  16 1   11.074400    1.01600   0.0     com='liner wall'
 cylinder  12 1   23.177500    1.01600   0.0     com='kaolite'
 cylinder  19 1   23.329900    1.01600   0.0     com='drum'
 cuboid    21 1 4p24.587200    1.01600   0.0     com='drum chine outer radius'
unit 1015
'2nd step in liner [Elev=37.530 in.]'
 cylinder  15 1   10.922000    0.15240   0.0     com='void abv pad2'
 cylinder  16 1   18.757900    0.15240   0.0     com='liner 2nd step'
 cylinder  12 1   23.177500    0.15240   0.0     com='kaolite'
 cylinder  19 1   23.329900    0.15240   0.0     com='drum'
 cuboid    21 1 4p24.587200    0.15240   0.0     com='drum chine outer radius'
unit 1016
'abv 2nd step in liner to bottom of angle iron [Elev=40.750 in.]'
 cylinder  13 1   18.097500    8.17880   0.49276 com='plug kaolite'
 cylinder  17 1   18.249900    8.17880   0.34036 com='sides of plug case'
 cylinder  15 1   18.605500    8.17880   0.0     com='void: plug to liner'
 cylinder  16 1   18.757900    8.17880   0.0     com='liner wall'
 cylinder  12 1   23.177500    8.17880   0.0     com='kaolite'
 cylinder  19 1   23.329900    8.17880   0.0     com='drum'
 cuboid    21 1 4p24.587200    8.17880   0.0     com='drum chine outer radius'
unit 1017
'bottom of angle iron to bend in angle iron [Elev=42.500 in.]'
 cylinder  13 1   18.097500    4.44500   0.0     com='plug kaolite'
 cylinder  17 1   18.249900    4.44500   0.0     com='sides of plug case'
 cylinder  15 1   18.605500    4.44500   0.0     com='void: plug to liner'
 cylinder  16 1   18.757900    4.44500   0.0     com='liner wall'
 cylinder  18 1   19.392900    4.44500   0.0     com='lower angle iron'
 cylinder  12 1   23.177500    4.44500   0.0     com='kaolite'
 cylinder  19 1   23.329900    4.44500   0.0     com='drum'
 cuboid    21 1 4p24.587200    4.44500   0.0     com='drum chine outer radius'
unit 1018
'bend in angle iron to top of angle iron [Elev=42.750 in.]'
 cylinder  13 1   18.097500    0.11176   0.0     com='plug kaolite'
```

```
 cylinder  17 1   18.249900    0.26416   0.0     com='sides of plug case'
 cylinder  15 1   18.605500    0.63500   0.0     com='void: plug to liner'
 cylinder  16 1   18.757900    0.63500   0.0     com='liner wall'
 cylinder  18 1   23.177500    0.63500   0.0     com='bend section of ai'
 cylinder  19 1   23.329900    0.63500   0.0     com='drum'
 cuboid    21 1 4p24.587200    0.63500   0.0     com='drum chine outer radius'
unit 1019
'drum lid and lip [Elev=43.500 in.]'
 cylinder  21 1   22.961600    1.90500   0.15240 com='void above lid'
 cylinder  19 1   23.114000    1.90500   0.0     com='drum lid'
 cylinder  21 1   23.177500    1.90500   0.0     com='void btw lid - drum wall'
 cylinder  19 1   23.329900    1.90500   0.0     com='drum'
 cuboid    21 1 4p24.587200    1.90500   0.0     com='drum chine outer radius'
global
unit 1020
'es3100 drum [Elev=43.500 in.]'
array 3         2r-24.587200     0.0
'cuboid     0  1 4p24.587200    110.4905  0.0    com='bare package'
 cuboid    21  1 4p55.067200   140.9700 -30.48   com='reflected package'
'cuboid    20  1 4p22.889718    110.5048  0.0    com='interstital array space'
'global
'unit 1021
'array 4   3r0.0
'reflector  21 2  6r3.0  10
end geometry
read array
ara=3 nux=1 nuy=1 nuz=13 fill
1001 1002 1003 1010
1011 1012 1013 1014 1015 1016 1017 1018 1019        end fill
'ara=4 nux=13 nuy=13 nuz=06 fill f1020               end fill
end array
'read bias id=500 2  11  end bias
read start nst=0
end start
end data
end


=csas25    parm=size=3000000
icsrpunhct12 15000.0gUNHc( 7064.4g235,3247.9gH2O) 6397.6gH2Ocv hx= 53.28 fr=1.0e+00
238groupndf5 infhommedium
'U(enr)O2(NO3)2+6H2O [2.81 g/cc for U(nat)], UNHc  2.79329 g/cm3, UNH hx=12.0'
'gU/L= 443.7839 dispersed. Bottle hx=2.37 no meaning when dispersed'
'UNHc in cv   9113.74622 g. water in cv  6397.62120 g.'
'UNHc in well  5886.25378 g. water in well  4132.00248 g.'
arbmunh    2.79329  5 0 0 0   92235   47.0962
                              92238    0.0000
                               1001    2.4232
                               7014    5.6116
                               8016   44.8690    1  0.31939 293  end
arbmh2oc   0.99820  2 0 0 0    1001   11.1913
                               8016   88.8087    1  0.62740 293  end
arbmpoly   0.92000  2 0 0 0  1001   14.3798
                               6012   85.6202    1  5.3202e-02   293  end
'np277-4: spacer (HAC_MD&H)'
'HAC min.den.(95.3157 lb/ft3) and hydrogen'
'np277-4 min.den.= 1.526803 = (95.3157 lb/ft3)(453.59 g/lb)/(28316.84 cm3/ft3)'
'use 75% of boron in calculations per NUREG-1609 Section 6.5.3.2'
arbmboron 7.31015e-2  2 0 0 0    5010   18.1479
                                 5011   81.8520    2  0.7500  293  end
arbmnpmx  1.07071e+0 10 0 0 0    6012    1.9188
                                 7014    0.0141
                                 8016   43.4254
                                11023    0.1174
                                12000    0.3378
                                13027   39.0477
                                14000    2.4671
                                16000    0.3083
                                20000   11.8335
                                26000    0.5298    2  1.0000  293  end
arbmnph2o 3.82995e-1  2 0 0 0    1001   11.1913
```

```
                                8016   88.8087    2  1.0000  293  end
'flooded containmment vessel and content cans -- 10 CFR 71.55(d)(3)'
arbmwicv  9.9820e-01  2 0 0 0    1001   11.1913
                                8016   88.8087    3  1.0     293  end
'steel: containment vessel body 16.60 lb but use 15.74 lb'
ss304                                           8  1.0     293  end
'steel: cv flange lower use 3.36 lb'
ss304                                           9  0.97267 293  end
'steel: cv flange upper use 13.75 lb'
ss304                                          10  0.94348 293  end
'np277-4: confinement -- neutron poison inner liner (HAC_MD&H)'
'actual vol.= 1.28314e4 cm3 = (7.83023e2 in3)(16.387064)'
'den.multiplier = 1.28314e4 cm3 (actual vol.) / 1.32708e4 cm3 (model vol.)'
'np277-4 min.den.= 1.526803 = (95.3157 lb/ft3)(453.59 g/lb)/(28316.84 cm3/ft3)'
'density = 1.476265 = (den.mult)(np277-4 min.den.) = 0.9668933*1.526803'
'use 75% of boron in calculations per NUREG-1609 Section 6.5.3.2'
arbmboron 7.06813e-2  2 0 0 0    5010   18.1479
                                5011   81.8520   11  0.7500  293  end
arbmnpmx  1.03525e+0 10 0 0 0    6012    1.9188
                                7014    0.0141
                                8016   43.4254
                               11023    0.1174
                               12000    0.3378
                               13027   39.0477
                               14000    2.4671
                               16000    0.3083
                               20000   11.8335
                               26000    0.5298   11  1.0000  293  end
arbmnph2o 3.70316e-1  2 0 0 0    1001   11.1913
                                8016   88.8087   11  1.0000  293  end
'kaolite 1600 body'
'nct.sing.unit.density= (den.mult)(min.den.)'
' for arbmh20k 0.52294 = 1.012373*0.51655, for rest 0.34864 = 1.012373*0.34438'
'den.mult= 1.36557e5 cm3 (actual vol.) / 1.34888e5 cm3 (model vol.)'
'actual vol.= 1.36557e5 cm3 = (28316.84 cm3/ft3)(108.33188 lb)/(22.464 lb/ft3)'
'hac.s.u.dens= (hac.mult)(nct.s.u.dens)'
'hac.mult = 1.34888e5 cm3 (nct vol.)/ 1.12246e5 cm3 (model vol.)'
' for arbmh2ok 0.62843 = 1.20172*0.52294,   for rest = 1.20172*0.34864'
arbmh2ok   0.62843  2 0 0 0    1001   11.1913
                               8016   88.8087   12  1       293  end
arbmal2o3  0.41898  2 0 0 0   13027   52.9390
                               8016   47.0610   12  0.096   293  end
arbmsio2   0.41898  2 0 0 0   14000   46.7570
                               8016   53.2430   12  0.367   293  end
arbmfe2o3  0.41898  2 0 0 0   26000   69.9540
                               8016   30.0460   12  0.067   293  end
arbmtio2   0.41898  2 0 0 0   22000   59.9535
                               8016   40.0465   12  0.012   293  end
arbmcao    0.41898  2 0 0 0   20000   71.4815
                               8016   28.5185   12  0.307   293  end
arbmmgo    0.41898  2 0 0 0   12000   60.3169
                               8016   39.6831   12  0.131   293  end
arbmna2o   0.41898  2 0 0 0   11023   74.1961
                               8016   25.8039   12  0.020   293  end
'kaolite 1600 top plug'
'sing.unit.density= (den.mult)(min.den.)'
' for arbmh20k = 0.965246*0.51655,  for rest = 0.965246*0.34438'
'den.mult= 1.21592e4 cm3 (actual vol.) / 1.25970e4 cm3 (model vol.)'
'actual vol.= 1.21592e4 cm3 = (28316.84 cm3/ft3)(9.646 lb)/(22.464 lb/ft3)'
arbmh2ok   0.49860  2 0 0 0    1001   11.1913
                               8016   88.8087   13  1       293  end
arbmal2o3  0.33241  2 0 0 0   13027   52.9390
                               8016   47.0610   13  0.096   293  end
arbmsio2   0.33241  2 0 0 0   14000   46.7570
                               8016   53.2430   13  0.367   293  end
arbmfe2o3  0.33241  2 0 0 0   26000   69.9540
                               8016   30.0460   13  0.067   293  end
arbmtio2   0.33241  2 0 0 0   22000   59.9535
                               8016   40.0465   13  0.012   293  end
arbmcao    0.33241  2 0 0 0   20000   71.4815
                               8016   28.5185   13  0.307   293  end
```

```
arbmmgo    0.33241  2 0 0 0   12000   60.3169
                               8016   39.6831   13  0.131   293  end
arbmna2o   0.33241  2 0 0 0   11023   74.1961
                               8016   25.8039   13  0.020   293  end
'silicone rubber pads'
arbmsiru   1.21791  4 0 0 0    6012   32.3767
                               1001    8.1573
                               8016   21.5782
                              14000   37.8878   14  1.0     293  end
'void space external to containment vessel'
'UNHc in cv well   5886.25378 g.'
'water in cv well  4132.00248 g.'
arbmunh    2.79329  5 0 0 0   92235   47.0962
                              92238    0.0000
                               1001    2.4232
                               7014    5.6116
                               8016   44.8690   15  0.33734 293  end
arbmh2oc   0.99820  2 0 0 0    1001   11.1913
                               8016   88.8087   15  0.66266 293  end
'steel: liner'
ss304                                           16  1.0     293  end
'steel: plug cover (pc) use 9.907 lb'
ss304                                           17  1.06388 293  end
'steel: angle iron (ai) for HAC'
'nct density is multiplied by volume fraction 7.08030/5.74516'
ss304                                           18  1.23239 293  end
'steel: drum steel for HAC'
'nct density is multiplied by volume fraction 3.20482/2.95645'
ss304                                           19  1.08401 293  end
'void space external to drum'
'array density is assumed not reduced by hac'
'arbmwed    0.9982   2 0 0 0    1001   11.1913
'                               8016   88.8087   20  1       293  end
'reflective water'
arbmh20r   0.9982   2 0 0 0    1001   11.1913
                               8016   88.8087   21  1.0     293  end
end comp
icsrpunhct12 15000.0gUNHc( 7064.4g235,3247.9gH2O) 6397.6gH2Ocv,hx= 53.28 fr=1.0e+00
read parameters nub=yes npg=2500 gen=215 nsk=15 tme=100 end parameters
read boun       all=vac                         end boun
read geometry
unit 1001
'drum bottom flat cover [Elev= 0.105 in. at top of unit]'
'cylinder  19 1   21.838092    0.26670   0.0     com='extended radius not used'
 cylinder  19 1   21.838092    0.26670   0.0     com='drum bottom flat cover'
 cuboid    21 1 4p21.838092    0.26670   0.0     com='drum(chine)outer radius'
unit 1002
'above drum bottom flat cover and below containment vessel [Elev= 4.670 in.]'
'v1002=1.36748e+01  '
 cylinder  15 1    3.175000   11.59510  11.16330 com='void in pad-1'
 cylinder  14 1    7.924800   11.59510  11.16330 com='pad-1'
 cylinder  16 1    8.077200   11.59510  11.16330 com='np277_4 liner'
 cylinder  11 1   10.922000   11.59510  11.16330 com='np277_4'
 cylinder  16 1   11.074400   11.59510  10.85850 com='kaolite liner bottom'
 cylinder  12 1   21.685692   11.59510   0.0     com='kaolite'
 cylinder  19 1   21.838092   11.59510   0.0     com='drum'
 cuboid    21 1 4p21.838092   11.59510   0.0     com='drum(chine)outer radius'
unit 1003
'cv bottom to bottom of 1st step [Elev=35.270 in.]'
'v1003=4.43850e+03  '
 cylinder  1  1    6.426200   77.72400   0.63500 com='HEU content'
 cylinder  8  1    6.680200   77.72400   0.0     com='cv bottom'
 cylinder  15 1    7.924800   77.72400   0.0     com='void btw cv-np liner'
 cylinder  16 1    8.077200   77.72400   0.0     com='np277_4 liner'
 cylinder  11 1   10.922000   77.72400   0.0     com='np277_4'
 cylinder  16 1   11.074400   77.72400   0.0     com='kaolite liner'
 cylinder  12 1   21.685692   77.72400   0.0     com='kaolite'
 cylinder  19 1   21.838092   77.72400   0.0     com='drum'
 cuboid    21 1 4p21.838092   77.72400   0.0     com='drum(chine)outer radius'
unit 1010
'cv at 1st step in liner [Elev=35.330 in.]'
```

```
'v1010=8.70294e+00  '
 cylinder  1  1    6.426200    0.15240   0.0     com='HEU content'
 cylinder  8  1    6.680200    0.15240   0.0     com='cv at 1st step'
 cylinder  15 1    7.924800    0.15240   0.0     com='void btw cv and liner'
 cylinder  16 1   11.074400    0.15240   0.0     com='liner 1st step'
 cylinder  12 1   21.685692    0.15240   0.0     com='kaolite'
 cylinder  19 1   21.838092    0.15240   0.0     com='drum'
 cuboid    21 1 4p21.838092    0.15240   0.0     com='drum(chine)outer radius'
unit 1011
'vertical gap between 1st step in liner and cv flange [Elev=35.420 in.]'
'v1011=5.36220e+01  '
 cylinder  1  1    6.426200    0.22860   0.0     com='HEU content'
 cylinder  8  1    6.680200    0.22860   0.0     com='cv at gap btwn step-flng'
 cylinder  15 1   10.922000    0.22860   0.0     com='void btw cv and liner'
 cylinder  16 1   11.074400    0.22860   0.0     com='liner wall'
 cylinder  12 1   21.685692    0.22860   0.0     com='kaolite'
 cylinder  19 1   21.838092    0.22860   0.0     com='drum'
 cuboid    21 1 4p21.838092    0.22860   0.0     com='drum(chine)outer radius'
unit 1012
'cv flange to top of cv well [Elev=35.920 in.]'
'v1012=7.43264e+01  '
 cylinder  1  1    6.426200    1.27000   0.0     com='HEU content'
 cylinder  9  1    9.525000    1.27000   0.0     com='flange to top of well'
 cylinder  15 1    9.525000    1.27000   0.0     com='void btw cv and pad-2'
 cylinder  14 1   10.033000    1.27000   0.0     com='pad-2'
 cylinder  15 1   10.922000    1.27000   0.0     com='void btw cv and liner'
 cylinder  16 1   11.074400    1.27000   0.0     com='liner wall'
 cylinder  12 1   21.685692    1.27000   0.0     com='kaolite'
 cylinder  19 1   21.838092    1.27000   0.0     com='drum'
 cuboid    21 1 4p21.838092    1.27000   0.0     com='drum(chine)outer radius'
unit 1013
'cv flange above cv well [Elev=37.070 in.]'
'v1013=1.70951e+02  '
 cylinder  10 1    9.525000    2.92100   0.0     com='flange above cv well'
 cylinder  15 1    9.525000    2.92100   0.0     com='void btw cv and pad-2'
 cylinder  14 1   10.033000    2.92100   0.0     com='pad-2'
 cylinder  15 1   10.922000    2.92100   0.0     com='void btw pad2 and liner'
 cylinder  16 1   11.074400    2.92100   0.0     com='liner wall'
 cylinder  12 1   21.685692    2.92100   0.0     com='kaolite'
 cylinder  19 1   21.838092    2.92100   0.0     com='drum'
 cuboid    21 1 4p21.838092    2.92100   0.0     com='drum(chine)outer radius'
unit 1014
'plugpad2 below liner 2nd step [Elev=37.470 in.]'
'v1014=1.39785e+02  '
 cylinder  14 1   10.033000    0.76200   0.0     com='pad-2'
 cylinder  15 1   10.922000    1.01600   0.0     com='void btw pad2 and liner'
 cylinder  16 1   11.074400    1.01600   0.0     com='liner wall'
 cylinder  12 1   21.685692    1.01600   0.0     com='kaolite'
 cylinder  19 1   21.838092    1.01600   0.0     com='drum'
 cuboid    21 1 4p21.838092    1.01600   0.0     com='drum(chine)outer radius'
unit 1015
'2nd step in liner [Elev=37.530 in.]'
'v1015=5.71136e+01  '
 cylinder  15 1   10.922000    0.15240   0.0     com='void abv pad2'
 cylinder  16 1   18.757900    0.15240   0.0     com='liner 2nd step'
 cylinder  12 1   21.685692    0.15240   0.0     com='kaolite'
 cylinder  19 1   21.838092    0.15240   0.0     com='drum'
 cuboid    21 1 4p21.838092    0.15240   0.0     com='drum(chine)outer radius'
unit 1016
'abv 2nd step in liner to bottom of angle iron [Elev=40.750 in.]'
'v1016=6.92877e+02  '
 cylinder  13 1   18.097500    8.17880   0.49276 com='plug kaolite'
 cylinder  17 1   18.249900    8.17880   0.34036 com='sides of plug case'
 cylinder  15 1   18.605500    8.17880   0.0     com='void: plug to liner'
 cylinder  16 1   18.757900    8.17880   0.0     com='liner wall'
 cylinder  12 1   21.685692    8.17880   0.0     com='kaolite'
 cylinder  19 1   21.838092    8.17880   0.0     com='drum'
 cuboid    21 1 4p21.838092    8.17880   0.0     com='drum(chine)outer radius'
unit 1017
'bottom of angle iron to bend in angle iron [Elev=42.500 in.]'
'v1017=1.83014e+02  '
```

```
 cylinder  13 1   18.097500    4.44500   0.0     com='plug kaolite'
 cylinder  17 1   18.249900    4.44500   0.0     com='sides of plug case'
 cylinder  15 1   18.605500    4.44500   0.0     com='void: plug to liner'
 cylinder  16 1   18.757900    4.44500   0.0     com='liner wall'
 cylinder  18 1   19.392900    4.44500   0.0     com='lower angle iron'
 cylinder  12 1   21.685692    4.44500   0.0     com='kaolite'
 cylinder  19 1   21.838092    4.44500   0.0     com='drum'
 cuboid    21 1 4p21.838092    4.44500   0.0     com='drum(chine)outer radius'
unit 1018
'bend in angle iron to top of angle iron [Elev=42.750 in.]'
'v1018=4.14168e+02  '
'Volume cv well=6.24674e+03  '
 cylinder  13 1   18.097500    0.11176   0.0     com='plug kaolite'
 cylinder  17 1   18.249900    0.26416   0.0     com='sides of plug case'
 cylinder  15 1   18.605500    0.63500   0.0     com='void: plug to liner'
 cylinder  16 1   18.757900    0.63500   0.0     com='liner wall'
 cylinder  18 1   21.685692    0.63500   0.0     com='bend section of ai'
 cylinder  19 1   21.838092    0.63500   0.0     com='drum'
 cuboid    21 1 4p21.838092    0.63500   0.0     com='drum(chine)outer radius'
unit 1019
'drum lid and lip [Elev=43.500 in.]'
 cylinder  21 1   21.469792    1.90500   0.15240 com='void above lid'
 cylinder  19 1   21.622192    1.90500   0.0     com='drum lid'
 cylinder  21 1   21.685692    1.90500   0.0     com='void btw lid - drum wall'
 cylinder  19 1   21.838092    1.90500   0.0     com='drum'
 cuboid    21 1 4p21.838092    1.90500   0.0     com='drum(chine)outer radius'
global
unit 1020
'es3100 drum [Elev=43.500 in.]'
array 3         2r-21.838092     0.0
'cuboid     0  1 4p21.838092    110.4905  0.0    com='bare package'
 cuboid    21  1 4p52.318092   140.9700 -30.48   com='reflected package'
'cuboid    20  1 4p22.889718    110.5048  0.0    com='interstital array space'
'global
'unit 1021
'array 4   3r0.0
'reflector  21 2  6r3.0  10
end geometry
read array
ara=3 nux=1 nuy=1 nuz=13 fill
1001 1002 1003 1010
1011 1012 1013 1014 1015 1016 1017 1018 1019        end fill
'ara=4 nux=13 nuy=13 nuz=06 fill f1020               end fill
end array
'read bias id=500 2  11  end bias
read start nst=0
end start
end data
end
```

Appendix 6.9.8

Y/DD-896/R1, *CRITICAL EXPERIMENT BENCHMARK CALCULATIONS WITH CSAS25 FROM SCALE4.4a FOR CRITICALITY SAFETY ANALYSES ON THE HP J-5600 UNCLASSIFIED WORKSTATION (CMODB)*
AND
Y/DD-972R1, *DETERMINATION OF THE UPPER SUBCRITICAL LIMIT FOR CRITICALITY CALCULATIONS FOR CRITICALITY SAFETY ANALYSES*

THIS PAGE INTENTIONALLY LEFT BLANK.

BWXT Y12
A BWXT/Bechtel Enterprise

Critical Experiment Benchmark Calculations With CSAS25 from SCALE4.4a For Criticality Safety Analyses On the HP J-5600 Unclassified Workstation (CMODB)

Revision 1

R. H. Smith

Nuclear Criticality Safety
Y-12 National Security Complex

Y-12 NATIONAL SECURITY COMPLEX

August 2003

Prepared by the
Y-12 National Security Complex
Oak Ridge, Tennessee 37831
Managed by
BWXT Y-12, L.L.C.
For the
U.S. Department of Energy
under contract DE-AC05-00OR22800

This document has been reviewed by a Y-12 ADC/UCNI RO and has been determined to be UNCLASSIFIED and contains no UCNI. This review does not constitute clearance for public release.

SMLiner 16 Dec 03
SMLiner Date

MANAGED BY
BWXT Y-12, L.L.C.
FOR THE UNITED STATES
DEPARTMENT OF ENERGY

UCN-13672 (10-00)

Critical Experiment Benchmark Calculations With CSAS25 from SCALE4.4a For Criticality Safety Analyses On the HP J-5600 Unclassified Workstation (CMODB)

Revision 1

R. H. Smith

Nuclear Criticality Safety
Y-12 National Security Complex

August 2003

Prepared by the
Y-12 National Security Complex
Oak Ridge, Tennessee 37831
Managed by
BWXT Y-12, L.L.C.
For the
U.S. Department of Energy
under contract DE-AC05-00OR22800

THIS PAGE INTENTIONALLY LEFT BLANK

Document Preparation

Prepared by _____ Date _____
Robert H. Smith

Reviewed by _____ Date _____
John F. DeClue

Approved by _____ Date _____
Cris A. Worley

THIS PAGE INTENTIONALLY LEFT BLANK

Calculation Reviewers

_____ Date _____
Peter Angelo

_____ Date _____
Kevin Beard

_____ Date _____
Curtis Jordan

_____ Date _____
David Smallwood

THIS PAGE INTENTIONALLY LEFT BLANK

Revision Log

Revision Number	Description of Change	Pages Affected
1	Removal of results for 27 and 44-group library, for Volumes II-HEU and IV-LEU. Inclusion of results for Volumes I-Pu and VI-mixed U/Pu, which were previously published in Y/DD-996/R1. Addition of new results for Volumes III-IEU and V-U233. Addition of new results for Volume II-HEU, including models developed as part of the qualifications program. Editorial Changes.	All

THIS PAGE INTENTIONALLY LEFT BLANK

Abstract

This report documents calculations performed for validation of the CSAS25 control module from the SCALE 4.4a computer code system for use in evaluating nuclear criticality safety. This revision includes results from using only the 238-group ENDF/B-V cross-section library. The criticality validation calculations were performed using over 1200 benchmark cases from Volumes I through VI of the "International Handbook of Evaluated Criticality Safety Benchmark Experiments," published by the Nuclear Energy Agency Organization for Economic Cooperation and Development (NEA/OECD) [i]. This revision collects all the OECD benchmarks modeled by Y-12 Nuclear Criticality Safety into one report. Based on the results, the CSAS25 module and 238-group library are validated for use with systems that are similar to those included in this validation. Establishment of sub-critical limits will be documented in a separate report.

The original version of this report included about 500 cases from Volumes II and IV (HEU and LEU). Subsequently, about 400 cases from Volumes I and VI (Pu and mixed U/Pu) were documented in Y/DD-996/R1, and these results are now also incorporated into this revision. In addition, new results for Volumes III-IEU (51 cases) and V-U233 (140 cases) are now included. Finally, 53 new results for Volume II-HEU, including 26 models developed as part of the qualifications program, as well as 32 new results for Volume IV-LEU, including 7 from the qualifications program, have also been added. In total, 276 new models were added in this revision, for a new total of 1217 models.

Results for 27 and 44-group libraries, for Volumes II-HEU and IV-LEU, have been removed. The 238-group library was previously shown to have generally superior results, and experience has now shown that any disadvantages, such as somewhat higher computer run-time and memory requirements, are not a major problem with newer computers. Therefore, only 238-group results are included in this revision.

Although many cases are included in this report, analysts are cautioned that they must not assume that all SCALE input options are validated for all applications. They must verify or demonstrate that their options are validated against benchmark experiments that are similar to their applications. Options include material selections (e.g. "be" versus "bebound"), scattering options (i.e. SCT), geometry options (i.e. infinite homogeneous, multi-region, or latticecell), and others. Experience has shown that seemingly minor differences (e.g. "bebound" versus "be") may cause large changes in results, particularly when errors exist in cross section libraries.

Acknowledgements

In addition to the principal authors and reviewers, a number of people participated in this revision effort and provided valuable help, comments or suggestions. In particular, analysts working on Y-12 calculation qualifications prepared approximately 33 new HEU models, which have been included. These analysts were Julie Ezold, Bryan Johnson, Susan Osterhout, Max Robinson and John Sherwood. Other contributors include Allan Krass and John DeClue. Comments from Andy Szaflarski and Cris Worley were also appreciated. Finally, we could not have completed this work without the reliable workstation operation and system administration by Anthony Wheaton.

THIS PAGE INTENTIONALLY LEFT BLANK

Table of Contents

Page

REVISION LOG ..... **VII**

ABSTRACT ..... **IX**

ACKNOWLEDGEMENTS ..... **IX**

1 INTRODUCTION **13**

1.1 VALIDATION OF CSAS25 IN SCALE 4.4A FOR CRITICALITY SAFETY ANALYSES 13
1.2 TERMINOLOGY 14

2 DESCRIPTION OF SCALE 4.4A CODE PACKAGE **14**

TABLE 2.1. ANALYSIS CAPABILITIES SUMMARY OF THE SCALE CONTROL AND FUNCTIONAL MODULES COVERED IN THIS REPORT 15

3 DISCUSSION OF CRITICALITY BENCHMARK DATABASE FOR VALIDATION OF CSAS25 FROM SCALE 4.4A **17**

TABLE 3.1 NUMBER OF INPUT CASES EXTRACTED FROM THE OECD COMPACT DISK 19

4 TABULATED RESULTS OF CSAS25 FROM SCALE 4.4A CRITICALITY CALCULATIONS **20**

TABLE 4.1 RESULTS FOR PLUTONIUM SYSTEMS (VOLUME 1) WITH CSAS25 FROM SCALE 4.4A AND THE 238GROUP LIBRARY ON THE J-5600 (CMODB) WORKSTATION 21
TABLE 4.2 RESULTS FOR HIGHLY ENRICHED URANIUM SYSTEMS (VOLUME 2) WITH CSAS25 FROM SCALE 4.4A AND THE 238-GROUP LIBRARY ON THE J-5600 (CMODB) WORKSTATION 31
TABLE 4.3 RESULTS FOR INTERMEDIATE AND MIXED ENRICHMENT URANIUM SYSTEMS (VOLUME 3) WITH CSAS25 FROM SCALE 4.4A AND THE 238-GROUP LIBRARY ON THE J-5600 (CMODB) WORKSTATION 50
TABLE 4.4 RESULTS FOR LOW ENRICHED URANIUM SYSTEMS (VOLUME 4) WITH CSAS25 FROM SCALE 4.4A AND THE 238-GROUP LIBRARY ON THE J-5600 (CMODB) WORKSTATION 52
TABLE 4.5 RESULTS FOR URANIUM-233 SYSTEMS (VOLUME 5) WITH CSAS25 FROM SCALE 4.4A AND THE 238GROUP LIBRARY ON THE J-5600 (CMODB) WORKSTATION 58
TABLE 4.6 RESULTS FOR MIXED PLUTONIUM - URANIUM SYSTEMS (VOLUME 6) WITH CSAS25 FROM SCALE 4.4A AND THE 238-GROUP LIBRARY ON THE J-5600 (CMODB) WORKSTATION 63

5 RESULTS ANALYSIS **70**

5.1 INTRODUCTION 70
5.2 DISCUSSION OF RESULTS 71

FIGURE 1 - ALL ADJUSTED RESULTS **71**

FIGURE 2 - HEU, IEU AND LEU ADJUSTED RESULTS **72**

FIGURE 3 - LEU ADJUSTED K-EFF RESULTS **73**

FIGURE 4 - IEU ADJUSTED K-EFF RESULTS **74**

FIGURE 5 - HEU ADJUSTED K-EFF RESULTS **75**

FIGURE 6 - U-233 ADJUSTED K-EFF RESULTS **76**

FIGURE 7 - PU AND MIXED PU-U ADJUSTED K-EFF RESULTS **77**

FIGURE 8 - ADJUSTED K-EFF RESULTS VERSUS NUBAR (FOR ALL AVAILABLE DATA 78

FIGURE 9 - CALCULATED K-EFF VERSUS BENCHMARK K-EFF 79

5.3 DISCUSSION OF HIGH POSITIVE AND NEGATIVE BIAS RESULTS 80

TABLE 5.1 HIGH POSITIVE AND NEGATIVE BIAS RESULTS 80

5.4 SUMMARY OF RESULTS 81

5.4.1 Area of Applicability 81
5.4.2 Grandfather or Retrofit Concerns 82

6 CONCLUSIONS 82

7 RECOMMENDATIONS FO R FUTURE WORK 83

APPENDIX A - COMPARISON OF AVAILABLE EXPERIMENTS WITH CALCULATED EXPERIMENTS ... 85

8 REFERENCES 113

1 Introduction

In nuclear criticality safety engineering, extensive use is made of computational methods for analyzing the calculation models of physical systems. The successful application of computational methods requires verification, certification and validation (V&V) of the analytic tool. Software verification, the first element of V&V, reveals the closeness in agreement between calculation results obtained using a particular computational method and calculation results obtained using other methods. Software certification provides a user assurance that the code will consistently produce numerical results that agree with analytic solutions for the problems the code is designed to analyze. Software validation "calibrates" the calculation results obtained using certified software (computational method) for agreement with the physical universe.

The refinement of a validation or extension of it by the addition of cases does not require re-certification of the software. Therefore, the verification and certification of the SCALE 4.4a modular code system are separate issues, and are published separately. This document addresses the calculation results to be used for establishment of bias, bias trends and uncertainty for validation of the CSAS25 control module from the Standardized Computer Analyses for Licensing Evaluation (SCALE) Version 4.4a package with the 238-group ENDF/B-V SCALE 4.4a cross-section libraries.

Section 1.1 identifies source documents and rationale for the validation activities, and it summarizes the scope of the validation performed on the Nuclear Criticality Safety Division (NCSD) Hewlett Packard Series 9000/J-5600 (HP J-5600) unclassified workstation (referred to as CMODB) at Y-12.

1.1 Validation of CSAS25 in SCALE 4.4a for Criticality Safety Analyses

In nuclear criticality safety engineering, calculation methods are one of the methods used to establish the subcritical limits for operations involving fissile material. The American National Standards Institute (ANSI) gives fundamental guidance for establishing these limits in ANSI/ANS-8.1-1998, "Nuclear Criticality Safety in Operations with Fissionable Materials Outside Reactors."[ii] In paragraph 4.2.5, the standard states:

> In the absence of directly applicable experimental measurements, the limits may be derived from calculations made by a method shown by comparison with experimental data to be valid in accordance with 4.3.

Section 4.3 of the Standard provides additional guidance on the general procedure for establishing validity. This includes establishment of bias (4.3.1), bias trend (4.3.2), uncertainty (4.3.3), computer dependence (4.3.4), consistency with measurement (4.3.5), and preparing a written validation report (4.3.6).

This criticality validation includes systems consisting of fissile and fissionable material in metallic, solution and other physical forms, as described in summary in this report, and in more detail in the first six volumes of the OECD Handbook. The emphasis of this criticality validation is on comparison of calculated neutron multiplication factors (k_{eff}) with experimental results, and on establishment of bias, bias trends, and uncertainty as a final step. Compiled data for nearly 1200 critical experiments is used as the basis for the calculation models. The calculated results from SCALE 4.4a using the 238-group ENDF/B-V SCALE 4.4a cross-section libraries have been compared with reported results for the benchmark experiments. Comparison of results demonstrates that SCALE 4.4a run on CMODB produces

the same results (within the statistical uncertainty of the Monte Carlo calculations) as reported by the experiments where similar (SCALE, 238-group library) results were published. Subcritical limits can be determined through an analysis of the criticality calculation results. Determination of these limits will be addressed in a separate report. Extension of the validation to other computer platforms will be addressed separately.

1.2 Terminology

The term "model" may be used in two different ways in validation work. Often, as in this report, "model" generally refers to the calculation model, or the collection of input parameters for the numerical simulation in SCALE/KENO of the physical critical experiment. In statistical analyses, the term "model" generally refers to a statistical model, or an equation describing the relationship between parameters considered in the statistical analysis. In this report the intended meaning should be clear from the context, but generally the former meaning is intended in this report.

2 Description of SCALE 4.4a Code Package

The U. S. Nuclear Regulatory Commission (NRC) originally sponsored the Standardized Computer Analyses for Licensing Evaluation (SCALE) code system. The original concept of SCALE was to provide “standardized” sequences where the user had very few analyses options in addition to the geometry model and materials. Input for the control modules has been designed to be free form with extensive use of keyword and engineering-type input requirements. The stand-alone functional modules are more flexible, but they have a more difficult input logic and require the user to manually interface the data sets necessary to run the modules in a stand-alone fashion. As the system has grown in popularity over the years and additional options have been requested, the control modules have been improved to allow sophisticated users additional access to the numerous capabilities within the functional modules. However, the most important feature of the SCALE system remains the capability to simplify the user knowledge and effort required to prepare material mixtures and to perform adequate problem-dependent cross-section processing.

The modules available in Version 0 of SCALE were for Criticality Safety Analysis Sequences (CSAS) that provided automated material and cross-section processing prior to a one-dimensional (1-D) or multidimensional criticality analysis. Since that time the capabilities of the system have been significantly expanded to provide additional CSAS capabilities as well as Shielding Analysis Sequences (SAS) and a Heat Transfer Analysis Sequence (HTAS). At the center of the CSAS and SAS sequences is the library of subroutines referred to as the Material Information Processor or MIPLIB. The purpose of MIPLIB is to allow users to specify problem materials using easily remembered and easily recognizable keyword that are associated with mixtures, elements, and nuclides provided in the Standard Composition Library. MIPLIB also uses other keyword and simple geometry input specifications to prepare input for the modules that perform the problem-dependent cross-section processing: BONAMI, NITAWL-II, and XSDRNPM. A keyword supplied by the user selects the cross-section library from a standard set provided in SCALE or designates the reference to a user-supplied library. Several utility modules from AMPX have been included to provide users with the capability to edit the cross-section data and reformat user-supplied libraries for use in SCALE.

Table 2.1 provides a summary of the major applications of each of the control modules and functional modules currently in the SCALE code system and relevant to criticality safety calculations that are covered in this report. The control modules were designed to provide the system analysis capability originally requested by the NRC staff. The CSAS module (sometimes denoted as the CSAS4 module) is the primary control module designed for the calculation of the neutron multiplication factor of a system. Eight sequences enable general analysis of a 1-D system model or a multidimensional system model, capabilities to search on geometry spacing, and problem-dependent cross-section processing for use in executing stand-alone functional modules. CSAS6 is a new criticality control module to provide automated problem-dependent cross-section processing and criticality calculations via the

new KENO-VI functional module. Neither XSDRNPM nor KENO-VI is covered in this report. The CSAS25 sequence was used for this report.

Table 2.1. Analysis capabilities summary of the SCALE control and functional modules covered in this report

Control Module	Analysis function(s)	Functional modules executed
CSAS25	3-D Monte Carlo calculation of k-eff; Problem-dependent cross-section processing; Multiplication search or spacing	BONAMI NITAWL-II KENO V.a
Functional module	Function	
BONAMI	Resonance self-shielding of cross sections with Bondarenko factors	
NITAWL-II	Resonance self-shielding of cross sections with resolved resonance data	
KENO V.a	Monte Carlo code for calculation of neutron multiplication factors	

A 238-energy-group neutron cross-section library based on ENDF/B-V is available for the SCALE system, and was used exclusively in this revision. All the nuclides that are available in ENDF/B-V are in the library. Other available libraries include a 44-group library, was collapsed from the 238-group library, a 218-group ENDF/B-IV library, and a 27-group ENDF/B-IV library, which is the broad-group companion library to the 218-group ENDF/B-IV library. In revision 0, the 44-group and 27-group libraries were also included. The 44-group library made available an ENDF/B-V broad-group companion library in case the 238-group library did not perform well (in terms of computer memory and time) in a production environment at Y-12. The 27-group library allowed "validated" comparisons with previous analyses, using the same library that was previously used for many years. Since revision 0, the computer time and memory performance of the 238-group library has been adequate.

A recent ORNL report assessed the numerical performance of the available libraries[iii]. The recommendation supports using the 238-group library, but the endorsements are somewhat qualified. The report states, "This library is recommended as the best library in SCALE for general-purpose criticality-safety analyses." The report also states "Although any intermediate-energy problems are suspect because of the scarcity of critical experiments, this library performs better than any other library in SCALE." Regarding the weaknesses of the 44-group library, the report states "Because of the 1/E weighting in the 238-group library, this library is not a good general-purpose library." In addition, it states "The 44-group library has all the shortcomings of the 238-group library, as well as not being able to calculate homogeneous thermal, epithermal, and intermediate-energy systems as accurately as the 238-group library." On the other hand, regarding strengths of the 44-group library, the report says "LWR and mixed-oxide lattices are the library's strong point, and it is the recommended SCALE library for these applications." The report suggests that the 238-group library should be considered the general library of choice except perhaps for applications where the 44-group library may perform slightly better, such as ^{235}U LWR (low enriched) and MOX lattices, and for ^{233}U. This may partly explain why the ^{233}U results in this report are slightly worse than for other fissionable materials.

Finally, the ORNL report anticipates development of an improved 238-group library based on ENDF/B-VI, a "refined library with additional groups (partially to facilitate analysis of problems with a dominant intermediate-energy spectrum)," and predicts that "The next version of SCALE will include a continuous-energy cross-section library." The recommendations and future directions suggest a preference for the 238-group library. Therefore, in this revision the 238-group library was used exclusively.

3 Discussion of Criticality Benchmark Database for Validation of CSAS25 from SCALE 4.4a

The United States Department of Energy initiated the Criticality Safety Benchmark Evaluation Project (CSBEP) in October of 1992. The project quickly grew into an international effort, as scientists from other interested countries became involved. The International Criticality Safety Benchmark Evaluation Project (ICSBEP) is now an official activity of the Organization for Economic Cooperation and Development - Nuclear Energy Agency (OECD-NEA). The wide scale evaluation effort has concluded with the publication of the "International Handbook of Criticality Safety Benchmark Experiments" [i] (OECD Handbook). The seven-volume set of handbooks contains criticality safety benchmark specifications derived from experiments that were performed at various nuclear critical facilities around the world. The benchmark specifications are intended for use by criticality safety engineers to validate the application of calculation techniques, such as SCALE 4.4a, for criticality safety analyses. Example calculations presented in the handbook do not constitute a validation of the codes or cross section data sets by themselves, but use of the information contained in the Handbook can be and has been used to validate SCALE 4.4a by competent nuclear criticality safety persons. The evaluated criticality safety benchmark data are published in the seven-volume OECD Handbook, previously in hard copy form, and recently only on compact disk (CD). Acrobat® Reader is used to access the CD for extraction of experiment descriptions and input files.

For this criticality validation of SCALE 4.4a, fissile material forms include uranium systems, plutonium systems, mixed uranium and plutonium systems, and Uranium-233 systems. The validation comprises a substantial subset of the database used to prepare the first six volumes of the OECD Handbook. Table 3.1 summarizes the evaluated benchmark experiments that are analyzed in this validation. The data from the benchmark experiments represents a sufficiently wide range of fissile and fissionable materials, enrichments, and physical and chemical forms to cover many existing, planned or unforeseen activities for the Y-12 site. These include enriched uranium with ^{235}U only, natural and depleted uranium, intermediate (10-60%) enriched uranium, highly (>60%) enriched uranium, uranium-233, plutonium, and mixed plutonium-uranium systems. Data analyzed from critical experiments in this validation includes systems having fast, intermediate and thermal neutron energy spectra, and they include materials in various physical and chemical forms such as metals, solutions, and oxide compounds.

For many benchmark experiments, critical conditions are tabulated in the OECD Handbook for a number of parametric variables (height, concentration, shape, etc.) Although calculation results for all of these cases are reported, often SCALE 4.4a input details for only some of these cases are actually provided in the OECD Handbook. Input data for the CSAS25 cases are based on information contained in the OECD distribution CD, which is accessed using Acrobat® Reader software. The CD contains the text of the Handbook in the form of Portable Document Format (PDF) files. It also contains a section of selected input file listings. The listings in the two sections do not always correspond, so input files were taken from both parts of the CD, where they differed. In addition, where it was practical, inputs present for only one cross-section set were modified and copied to use with the 238-group cross-section library. Cases were first prepared using the 1998 edition of the CD, and additional cases were taken from the subsequent editions through 2002. Each subsequent revision provides additional experiments and input data. The organization and categorization of the experiments and data on the CD also changes.

® 1987-1996 Adobe Systems Incorporated. All rights reserved. Adobe, Acrobat, and the Acrobat logo are trademarks of Adobe Systems Incorporated which may be registered in certain jurisdictions.

Reviews were performed of the input preparation in a graded approach. For models based on sample inputs, reviews generally assume the models are adequate unless reasons are found to think otherwise, at the discretion of the reviewer. Models prepared from scratch, based on experiment descriptions, are given more scrutiny. Mentors review models submitted as part of the Nuclear Criticality Safety (NCS) qualifications program.

A total of 1217 cases were extracted from the CD or created from experiment descriptions, and are included in this revision. Table 3.1 shows the number of cases that were obtained in various categories. A copy of the input data for the validation cases is maintained on the CMODB workstation.

Due to the large number of benchmark experiment cases included in this revision, the OECD Handbook and associated DICE database search software are considered the best source for obtaining summary and detailed descriptive information for the benchmark experiments. Appendix A of this report gives a comparison of available experiments that could have been modeled, versus experiments that were modeled and included in validations. This list will be useful for determining what models to create for future inclusion in the validation, and for very abbreviated descriptions (titles).

The OECD report contains the following admonishment: "Sample input listings are not intended to be used directly for validation efforts and should be verified by the user. Since it is not practical to describe in detail the code input used to model each benchmark critical experiment, computer input listings are given for typical reported calculations of accepted benchmark configurations. From these listings, a user can identify which options were used to obtain the reported results. This is the sole purpose for inclusion of the input listings. It is the responsibility of the user to ensure that use of these listings for any other purpose is consistent with proper criticality safety practices." In performing this validation effort, the "universe" of experiments was the experiments available on the CD. No additional, independent selection of applicable experiments was performed. Advantage was taken of the available sample input listings to the maximum extent feasible. Some additional models were created based on parameter changes to the sample models, and some models were created from scratch based on the experiment descriptions, particularly as part of the Y-12 NCS qualifications program.

Reviews were performed of the input preparation in a graded approach. For models based on sample inputs, reviews generally assume the models are adequate unless reasons are found to think otherwise, at the discretion of the reviewer. Models prepared from scratch, based on experiment descriptions, are given more scrutiny. Mentors review models submitted as part of the NCS qualifications program.

It is recognized that there were experiments, which were not included because input models were not readily available, that would be applicable for Y-12. Also, some experiments were included that are probably not currently very directly applicable to Y-12 work. This is not a concern as long as these experiments do not have a large difference in bias compared with the other experiments in the category. The additional experiments provide confidence in the code's ability to calculate over a broader area of applicability than the minimum necessary for currently planned Y-12 applications.

Table 3.1 Number of Input Cases Extracted from the OECD Compact Disk

	Fissile Material Category (OECD Benchmark Volume)							
	II	III	IV		I	VI	V	
Material / Energy	High Enriched Uranium	Intermediate Enriched Uranium	Low Enriched Uranium	Subtotal Uranium-235 fissile	Plutonium	Mixed Plutonium-Uranium	Uranium-233	Total
Metal/Fast	106	16	0	122	62	33	10	227
Metal/Intermediate	4	0	0	4	0	0	0	4
Metal/Thermal	31	0	13	44	0	0	0	44
Metal/Mixed	3	0	0	3	0	0	0	3
Compound/Fast	0	0	0	0	0	0	0	0
Compound/Intermediate	12	4 *	0	16	1	0	0	17
Compound/Thermal	24	31	99	154	0	92	0	246
Compound/Mixed	9	0	0	9	9	0	0	18
Solution/Intermediate	0	0	0	0	0	0	33	33
Solution/Thermal	271	0	16	287	198	32	97	614
Solution/Mixed	0	0	0	0	0	0	0	0
Misc./Thermal	0	0	0	0	0	11	0	11
Total	460	51	128	639	270	168	140	1217
		* Note: Two of these intermediate energy cases should have been categorized as fast or thermal						

4 Tabulated Results of CSAS25 from SCALE 4.4a Criticality Calculations

Input data for the CSAS25 cases are based on information contained in the OECD distribution CD, as described in Section 3. Calculations were performed for the 238-group cross-section library.

The input cases were altered as little as possible unless there was an error, but the parameters were generally altered to include:

Parm=size=4000000 and

gen=500 npg=2000 nsk=100 tba=10 nub=yes

This results in 1,000,000 total neutron histories per case, skipping the first 100 generations, allows up to 10 minutes per batch, and causes the run output to include values for "Average Fission Group" (AFG) and "Energy of Average Lethargy Causing Fission" (EALCF). Using "nub=yes" is no longer necessary because it is now a default setting, but this is a carryover from previous versions which had "hub=no" as default.

For each CSAS25 case, Tables 4.1-4.6 list the following results: the mean of the final k_{eff} (k_cal) after 800,000 histories, and the standard deviation of that mean; the mean of the AFG, the mean of the EALCF, and the associated standard deviations. In addition, the expected, or experimental, k-effective (k_exp) and associated error estimate from the OECD benchmark handbook is also provided. The values of AFG and EALCF are included as potential regression variables because previously there was an expectation that the bias between experiment and Monte Carlo calculation might be correlated with these parameters. All results in this report are 238-group results.

Table 4.1 Results for Plutonium Systems (Volume 1) with CSAS25 from SCALE 4.4a and the 238-group Library on the J-5600 (CMODB) Workstation

Results for Volume 1: Plutonium Systems

N	Category	Case	nubar	Sigma	AFG	Sigma	EALCF (ev)	sigma	k_calc Pu	sigma	Benchmark k-eff	Sigma	Bias = Calculated - Benchmark	Adjusted k-eff Pu*
1	CI001	./puci.001/puci001	2.898	1.85E-05	87.19	0.015	3.09E+02	3.11E-01	0.999	0.0002	1	0.011	-0.001	0.999
2	CM001	./pucm.001/pucm001-01	3.107	2.47E-04	24.05	0.018	9.58E+05	1.59E+03	1.024	0.0011	0.9986	0.0041	0.026	1.026
3		./pucm.001/pucm001-02	2.969	1.28E-04	80.68	0.046	1.73E+03	6.90E+00	1.022	0.0012	1	0.0068	0.022	1.022
4		./pucm.001/pucm001-03	2.919	5.75E-05	131.93	0.041	3.25E+01	9.49E-02	1.016	0.0011	0.999	0.0067	0.017	1.017
5		./pucm.001/pucm001-04	2.921	6.21E-05	128.78	0.043	3.96E+01	1.25E-01	0.988	0.0011	1	0.0066	-0.012	0.988
6		./pucm.001/pucm001-05	2.902	2.21E-05	174.9	0.03	1.54E+00	3.33E-03	1.01	0.0015	0.9989	0.0072	0.011	1.011
7	CM002	./pucm.002/pucm002-01	3.026	2.14E-04	80.85	0.087	4.97E+03	3.78E+01	1.032	0.001	0.999	0.0046	0.033	1.033
8		./pucm.002/pucm002-10	2.909	4.61E-05	160.17	0.047	4.17E+00	1.37E-02	1.032	0.001	1	0.0073	0.032	1.032
9		./pucm.002/pucm002-22	2.912	5.04E-05	153.74	0.051	6.44E+00	2.35E-02	1.015	0.0013	0.9988	0.0055	0.016	1.016
10		./pucm.002/pucm002-23	2.9	1.93E-05	185.39	0.028	6.89E-01	1.51E-03	1.009	0.001	1	0.0068	0.009	1.009
11	MF001	./pumf.001/case_1	3.137	2.85E-04	21.42	0.013	1.24E+06	1.47E+03	0.995	0.0014	1	0.002	-0.005	0.995
12	MF002	./pumf.002/case_1	3.134	2.72E-04	21.23	0.012	1.26E+06	1.44E+03	0.995	0.0012	1	0.002	-0.005	0.995
13	MF003	./pumf.003/case_101	3.135	2.84E-04	21.44	0.013	1.24E+06	1.55E+03	0.993	0.001	1	0.003	-0.007	0.993
14		./pumf.003/case_102	3.124	2.89E-04	27.72	0.038	6.91E+05	2.38E+03	0.992	0.001	1	0.003	-0.008	0.992
15		./pumf.003/case_103	3.135	2.69E-04	21.43	0.013	1.24E+06	1.45E+03	0.986	0.0011	1	0.003	-0.014	0.986
16		./pumf.003/case_104	3.122	2.77E-04	28.79	0.041	6.25E+05	2.32E+03	0.995	0.001	1	0.003	-0.005	0.995
17		./pumf.003/case_105	3.136	2.90E-04	21.42	0.013	1.24E+06	1.48E+03	0.993	0.0011	1	0.003	-0.007	0.993
18	MF004	./pumf.004/case_207	3.135	2.83E-04	21.88	0.016	1.19E+06	1.69E+03	0.99	0.001	1	0.003	-0.01	0.99
19		./pumf.004/case_208	3.136	2.83E-04	22.26	0.019	1.15E+06	1.95E+03	0.99	0.0011	1	0.003	-0.01	0.99
20		./pumf.004/case_209	3.135	2.74E-04	22.27	0.019	1.15E+06	1.99E+03	0.99	0.0012	1	0.003	-0.01	0.99
21		./pumf.004/case_210	3.135	2.70E-04	22.3	0.018	1.15E+06	1.88E+03	0.988	0.0011	1	0.003	-0.012	0.988

Results for Volume 1: Plutonium Systems

N	Category	Case	nubar	Sigma	AFG	Sigma	EALCF (ev)	sigma	k_calc Pu	sigma	Benchmark k-eff	Sigma	Bias = Calculated - Benchmark	Adjusted k-eff Pu*
22		./pumf.004/case_211	3.135	2.80E-04	22.29	0.019	1.15E+06	1.97E+03	0.99	0.0009	1	0.003	-0.01	0.99
23		./pumf.004/case_212	3.136	2.81E-04	22.26	0.018	1.15E+06	1.95E+03	0.989	0.0013	1	0.003	-0.011	0.989
24		./pumf.004/case_213	3.136	2.86E-04	21.61	0.014	1.22E+06	1.64E+03	0.988	0.0011	1	0.003	-0.012	0.988
25		./pumf.004/case_214	3.137	2.97E-04	21.73	0.016	1.21E+06	1.73E+03	0.989	0.0011	1	0.003	-0.011	0.989
26		./pumf.004/case_215	3.136	2.73E-04	21.48	0.013	1.24E+06	1.50E+03	0.988	0.0011	1	0.003	-0.012	0.988
27	MF005	./pumf.005/case_1	3.103	2.54E-04	23.94	0.014	9.83E+05	1.26E+03	1.005	0.0011	1	0.0013	0.005	1.005
28	MF006	./pumf.006/case_001	2.972	5.19E-04	22.61	0.015	1.10E+06	1.55E+03	0.999	0.0013	1	0.003	-0.001	0.999
29	MF008	./pumf.008/case_1	3.065	7.86E-04	23.36	0.014	1.04E+06	1.39E+03	1.001	0.0009	1	0.0006	0.001	1.001
30	MF009	./pumf.009/case_1	3.122	0.000267	22.35	0.013	1.14E+06	1.39E+03	0.993	0.001	1	0.0027	-0.007	0.993
31	MF010	./pumf.010/case_1	3.065	2.97E-04	21.97	0.012	1.19E+06	1.40E+03	0.997	0.0011	1	0.0018	-0.003	0.997
32	MF011	./pumf.011/case_1	3.087	2.80E-04	50.72	0.073	8.34E+04	5.45E+02	0.995	0.0011	1	0.001	-0.005	0.995
33	MF012	./pumf.012/case_1	2.971	0.000633	23.65	0.019	9.78E+05	1.67E+03	1.004	0.001	1.0009	0.0021	0.004	1.004
34	MF013	./pumf.013/case_1	3.079	0.000225	26.15	0.015	7.75E+05	1.15E+03	1.004	0.0012	1.0034	0.0023	0	1
35	MF014	./pumf.014/case_1	3.081	0.000247	26	0.015	7.83E+05	1.22E+03	1.016	0.001	1.0037	0.0031	0.012	1.012
36	MF015	./pumf.015/case_1	3.094	0.000245	24.62	0.015	9.09E+05	1.34E+03	1.018	0.0011	1.0041	0.0026	0.014	1.014
37	MF016	./pumf.016/case_001	3.054	2.50E-04	73.29	0.09	1.14E+04	8.93E+01	1.011	0.001	0.9974	0.0042	0.013	1.013
38		./pumf.016/case_002	3.052	2.33E-04	76.69	0.082	8.57E+03	6.16E+01	1	0.001	1	0.0038	0	1
39		./pumf.016/case_003	3.051	2.42E-04	77.25	0.083	8.18E+03	5.88E+01	0.998	0.0013	1	0.0033	-0.002	0.998
40		./pumf.016/case_004	3.051	2.32E-04	77.41	0.082	8.08E+03	5.67E+01	0.998	0.001	1	0.003	-0.002	0.998
41		./pumf.016/case_005	3.051	2.49E-04	77.62	0.082	7.93E+03	5.72E+01	0.997	0.001	1	0.0034	-0.003	0.997
42		./pumf.016/case_006	3.051	2.62E-04	77.79	0.087	7.82E+03	5.94E+01	1.001	0.001	1	0.0032	0.001	1.001
43	MF017	./pumf.017/case_201	3.117	3.10E-04	25.53	0.026	7.82E+05	2.08E+03	0.988	0.0012	1	0.003	-0.012	0.988
44		./pumf.017/case_202	3.102	2.79E-04	32.16	0.042	4.04E+05	1.65E+03	0.991	0.0012	1	0.003	-0.009	0.991
45		./pumf.017/case_203	3.093	2.84E-04	38.28	0.051	2.31E+05	1.12E+03	0.996	0.0011	1	0.003	-0.004	0.996
46		./pumf.017/case_204	3.101	2.77E-04	30.43	0.04	4.57E+05	1.83E+03	0.991	0.0011	1	0.003	-0.009	0.991
47		./pumf.017/case_205	3.075	2.70E-04	47.5	0.062	9.48E+04	5.46E+02	0.999	0.0011	1	0.003	-0.001	0.999
48	MF018	./pumf.018/case_1	3.103	2.54E-04	24.45	0.015	8.97E+05	1.44E+03	1	0.0011	1	0.003	0	1

Results for Volume 1: Plutonium Systems

N	Category	Case	nubar	Sigma	AFG	Sigma	EALCF (ev)	sigma	k_calc Pu	sigma	Benchmark k-eff	Sigma	Bias = Calculated - Benchmark	Adjusted k-eff Pu*
49	MF022	./pumf.022/pumf022	3.135	2.77E-04	21.56	0.013	1.23E+06	1.51E+03	0.992	0.001	1	0.0021	-0.008	0.992
50	MF023	./pumf.023/pumf023	3.123	2.73E-04	22.36	0.013	1.14E+06	1.40E+03	0.995	0.001	1	0.002	-0.005	0.995
51	MF024	./pumf.024/pumf024	3.115	2.66E-04	27.69	0.034	6.32E+05	2.14E+03	0.997	0.001	1	0.002	-0.003	0.997
52	MF025	./pumf.025/pumf025	3.126	2.60E-04	22.03	0.013	1.17E+06	1.38E+03	0.997	0.0011	1	0.002	-0.003	0.997
53	MF026	./pumf.026/pumf026	3.109	2.58E-04	23.29	0.013	1.04E+06	1.33E+03	1.017	0.0012	1	0.0024	0.017	1.017
54	MF027	./pumf.027/pumf027	3.079	2.72E-04	51.82	0.071	7.18E+04	4.60E+02	1	0.0011	1	0.0022	0	1
55	MF028	./pumf.028/pumf028	3.105	2.42E-04	23.5	0.014	1.02E+06	1.33E+03	1.018	0.0013	1	0.0022	0.018	1.018
56	MF029	./pumf.029/pumf029	3.136	2.77E-04	21.37	0.013	1.25E+06	1.51E+03	0.992	0.0012	1	0.002	-0.008	0.992
57	MF030	./pumf.030/pumf030	3.123	2.62E-04	22.3	0.013	1.14E+06	1.41E+03	0.997	0.001	1	0.0021	-0.003	0.997
58	MF031	./pumf.031/pumf031	3.096	2.79E-04	41.13	0.062	1.85E+05	1.03E+03	1	0.0012	1	0.0021	0	1
59	MF032	./pumf.032/pumf032	3.121	2.55E-04	22.21	0.013	1.15E+06	1.35E+03	1.003	0.0012	1	0.002	0.003	1.003
60	MF033	./pumf.033/zppr-21a	3.006	1.32E-04	31.85	0.02	4.01E+05	8.67E+02	1.008	0.0008	0.9967	0.0026	0.011	1.011
61	MF035	./pumf.035/pumf035	3.126	2.64E-04	22.02	0.014	1.17E+06	1.49E+03	1.006	0.0011	1	0.0016	0.006	1.006
62	MF036	./pumf.036/pumf036	3.111	2.71E-04	27.47	0.032	6.13E+05	2.06E+03	1.003	0.0012	1	0.0031	0.003	1.003
63	MF037	./pumf.037/pumf037-01	3.087	2.73E-04	44.02	0.064	1.46E+05	8.45E+02	1	0.0011	1	0.0044	0	1
64		./pumf.037/pumf037-05	3.072	2.64E-04	55.52	0.078	5.19E+04	3.59E+02	0.997	0.001	1	0.0037	-0.003	0.997
65		./pumf.037/pumf037-07	3.066	2.57E-04	60.61	0.075	3.31E+04	2.22E+02	0.998	0.0011	1	0.0038	-0.002	0.998
66		./pumf.037/pumf037-10	3.063	2.60E-04	63.65	0.075	2.59E+04	1.70E+02	0.998	0.0011	1	0.0034	-0.002	0.998
67		./pumf.037/pumf037-12	3.062	2.50E-04	64.73	0.076	2.35E+04	1.58E+02	0.999	0.0011	1	0.004	-0.001	0.999
68		./pumf.037/pumf037-15	3.06	2.58E-04	67.65	0.086	1.85E+04	1.39E+02	0.998	0.0012	1	0.0033	-0.002	0.998
69		./pumf.037/pumf037-16	3.065	2.68E-04	62.77	0.079	2.87E+04	1.99E+02	1.001	0.0011	1	0.0039	0.001	1.001
70	MF039	./pumf.039/pumf039	3.124	2.66E-04	22.2	0.013	1.16E+06	1.43E+03	0.983	0.001	1	0.0022	-0.017	0.983
71	MF040	./pumf.040/pumf040	3.122	2.77E-04	22.38	0.013	1.14E+06	1.42E+03	0.991	0.001	1	0.0038	-0.009	0.991
72	MF041	./pumf.041/pumf041	2.99	5.98E-04	22.13	0.017	1.14E+06	1.76E+03	1.005	0.0012	1	0.0016	0.005	1.005
73	ST001	./pust.001/case_1_t9	2.891	5.43E-06	212.49	0.008	8.79E-02	8.61E-05	1.007	0.001	1	0.005	0.007	1.007
74		./pust.001/case_2_t9	2.891	6.15E-06	209.97	0.009	1.11E-01	1.15E-04	1.01	0.0011	1	0.005	0.01	1.01
75		./pust.001/case_3_t9	2.891	6.87E-06	207.76	0.011	1.35E-01	1.64E-04	1.012	0.0012	1	0.005	0.012	1.012

Results for Volume 1: Plutonium Systems

N	Category	Case	nubar	Sigma	AFG	Sigma	EALCF (ev)	sigma	k_calc Pu	sigma	Benchmark k-eff	Sigma	Bias = Calculated - Benchmark	Adjusted k-eff Pu*
76		./pust.001/case_4_t9	2.891	7.76E-06	206.42	0.012	1.51E-01	1.90E-04	1.004	0.0012	1	0.005	0.004	1.004
77		./pust.001/case_5_t9	2.891	7.49E-06	205.78	0.012	1.59E-01	2.04E-04	1.01	0.0011	1	0.005	0.01	1.01
78		./pust.001/case_6_t9	2.893	1.19E-05	195.79	0.018	3.47E-01	5.40E-04	1.008	0.0011	1	0.005	0.008	1.008
79	ST002	./pust.002/case_1	2.891	4.00E-06	214.68	0.006	7.13E-02	5.56E-05	1.007	0.001	1	0.0047	0.007	1.007
80		./pust.002/case_2	2.891	4.30E-06	214.46	0.006	7.29E-02	5.83E-05	1.008	0.0012	1	0.0047	0.008	1.008
81		./pust.002/case_3	2.891	4.48E-06	213.8	0.007	7.79E-02	6.68E-05	1.007	0.001	1	0.0047	0.007	1.007
82		./pust.002/case_4	2.891	4.54E-06	213.36	0.007	8.14E-02	7.04E-05	1.01	0.001	1	0.0047	0.01	1.01
83		./pust.002/case_5	2.891	4.84E-06	212.9	0.007	8.51E-02	8.00E-05	1.013	0.0014	1	0.0047	0.013	1.013
84		./pust.002/case_6	2.891	5.19E-06	211.97	0.008	9.28E-02	8.81E-05	1.01	0.0012	1	0.0047	0.01	1.01
85		./pust.002/case_7	2.891	5.98E-06	211.14	0.009	1.00E-01	1.05E-04	1.01	0.0013	1	0.0047	0.01	1.01
86	ST003	./pust.003/case_1	2.891	3.17E-06	216.63	0.005	5.83E-02	3.73E-05	1.007	0.001	1	0.0047	0.007	1.007
87		./pust.003/case_2	2.891	3.48E-06	216.45	0.005	5.95E-02	4.00E-05	1.009	0.0012	1	0.0047	0.009	1.009
88		./pust.003/case_3	2.891	3.68E-06	216.07	0.005	6.18E-02	4.40E-05	1.01	0.0011	1	0.0047	0.01	1.01
89		./pust.003/case_4	2.891	3.74E-06	215.93	0.005	6.28E-02	4.50E-05	1.007	0.001	1	0.0047	0.007	1.007
90		./pust.003/case_5	2.891	3.91E-06	215.53	0.006	6.55E-02	4.99E-05	1.008	0.0012	1	0.0047	0.008	1.008
91		./pust.003/case_6	2.891	4.14E-06	214.96	0.006	6.95E-02	5.35E-05	1.009	0.0011	1	0.0047	0.009	1.009
92		./pust.003/case_7	2.891	3.66E-06	216.49	0.005	5.91E-02	4.11E-05	1.01	0.0011	1	0.0047	0.01	1.01
93		./pust.003/case_8	2.891	3.52E-06	216.32	0.005	6.02E-02	3.95E-05	1.008	0.0011	1	0.0047	0.008	1.008
94	ST004	./pust.004/case_1	2.891	2.90E-06	217.47	0.004	5.34E-02	3.03E-05	1.007	0.0011	1	0.0047	0.007	1.007
95		./pust.004/case_10	2.891	3.61E-06	215.88	0.005	6.32E-02	4.30E-05	1.007	0.001	1	0.0047	0.007	1.007
96		./pust.004/case_11	2.891	3.90E-06	215.1	0.006	6.85E-02	5.14E-05	1.004	0.001	1	0.0047	0.004	1.004
97		./pust.004/case_12	2.891	3.09E-06	217.04	0.004	5.58E-02	3.42E-05	1.009	0.0013	1	0.0047	0.009	1.009
98		./pust.004/case_13	2.891	3.01E-06	217.07	0.004	5.56E-02	3.32E-05	1.003	0.001	1	0.0047	0.003	1.003
99		./pust.004/case_2	2.891	2.91E-06	217.4	0.004	5.37E-02	2.92E-05	1.004	0.001	1	0.0047	0.004	1.004
100		./pust.004/case_3	2.891	3.11E-06	217.24	0.004	5.47E-02	3.19E-05	1.007	0.0009	1	0.0047	0.007	1.007
101		./pust.004/case_4	2.891	3.14E-06	217.04	0.004	5.59E-02	3.47E-05	1.002	0.0013	1	0.0047	0.002	1.002
102		./pust.004/case_5	2.891	2.83E-06	217.26	0.004	5.46E-02	3.07E-05	1.005	0.001	1	0.0047	0.005	1.005

Results for Volume 1: Plutonium Systems

N	Category	Case	nubar	Sigma	AFG	Sigma	EALCF (ev)	sigma	k_calc Pu	sigma	Benchmark k-eff	Sigma	Bias = Calculated - Benchmark	Adjusted k-eff Pu*
103		./pust.004/case_6	2.891	3.02E-06	217.2	0.004	5.49E-02	3.25E-05	1.005	0.0011	1	0.0047	0.005	1.005
104		./pust.004/case_7	2.891	3.12E-06	217.04	0.004	5.58E-02	3.29E-05	1.012	0.0011	1	0.0047	0.012	1.012
105		./pust.004/case_8	2.891	3.16E-06	216.91	0.004	5.66E-02	3.49E-05	1.004	0.001	1	0.0047	0.004	1.004
106		./pust.004/case_9	2.891	3.37E-06	216.59	0.004	5.86E-02	3.62E-05	1.006	0.001	1	0.0047	0.006	1.006
107	ST005	./pust.005/case_1	2.891	3.18E-06	217.07	0.004	5.56E-02	3.38E-05	1.007	0.0009	1	0.0047	0.007	1.007
108		./pust.005/case_2	2.891	3.35E-06	216.91	0.004	5.66E-02	3.66E-05	1.008	0.0011	1	0.0047	0.008	1.008
109		./pust.005/case_3	2.891	3.18E-06	216.74	0.004	5.76E-02	3.60E-05	1.008	0.0011	1	0.0047	0.008	1.008
110		./pust.005/case_4	2.891	3.55E-06	216.35	0.005	6.01E-02	3.95E-05	1.009	0.0011	1	0.0047	0.009	1.009
111		./pust.005/case_5	2.891	3.66E-06	215.91	0.005	6.30E-02	4.45E-05	1.012	0.001	1	0.0047	0.012	1.012
112		./pust.005/case_6	2.891	3.84E-06	215.45	0.005	6.61E-02	4.92E-05	1.011	0.0011	1	0.0047	0.011	1.011
113		./pust.005/case_7	2.891	3.97E-06	215	0.005	6.91E-02	5.10E-05	1.008	0.001	1	0.0047	0.008	1.008
114		./pust.005/case_8	2.891	3.13E-06	216.9	0.004	5.66E-02	3.45E-05	1.002	0.0009	1	0.0047	0.002	1.002
115		./pust.005/case_9	2.891	3.30E-06	216.68	0.004	5.79E-02	3.56E-05	1.006	0.0011	1	0.0047	0.006	1.006
116	ST006	./pust.006/case_1	2.891	2.69E-06	217.62	0.004	5.25E-02	2.83E-05	1.005	0.001	1	0.0035	0.005	1.005
117		./pust.006/case_2	2.891	2.78E-06	217.46	0.004	5.34E-02	2.93E-05	1.007	0.001	1	0.0035	0.007	1.007
118		./pust.006/case_3	2.891	3.06E-06	217.15	0.004	5.52E-02	3.30E-05	1.008	0.0011	1	0.0035	0.008	1.008
119	ST007	./pust.007/case_10	2.891	6.04E-06	210.45	0.009	1.06E-01	1.14E-04	1.002	0.0011	1	0.0047	0.002	1.002
120		./pust.007/case_2	2.892	1.10E-05	198.9	0.018	2.75E-01	4.45E-04	1.009	0.001	1	0.0047	0.009	1.009
121		./pust.007/case_3	2.892	1.07E-05	199.57	0.017	2.61E-01	4.01E-04	1.003	0.0012	1	0.0047	0.003	1.003
122		./pust.007/case_5	2.891	6.05E-06	209.87	0.01	1.12E-01	1.22E-04	1.011	0.0012	1	0.0047	0.011	1.011
123		./pust.007/case_6	2.891	6.05E-06	209.68	0.009	1.14E-01	1.18E-04	1.005	0.0011	1	0.0047	0.005	1.005
124		./pust.007/case_7	2.891	6.26E-06	209.81	0.01	1.12E-01	1.27E-04	1.009	0.001	1	0.0047	0.009	1.009
125		./pust.007/case_8	2.891	6.18E-06	209.6	0.01	1.15E-01	1.30E-04	1	0.001	1	0.0047	0	1
126		./pust.007/case_9	2.891	6.19E-06	209.62	0.011	1.14E-01	1.33E-04	0.999	0.0013	1	0.0047	-0.001	0.999
127	ST009	./pust.009/case_1	2.892	1.65E-06	219.73	0.002	4.11E-02	1.31E-05	1.02	0.0006	1	0.0047	0.02	1.02
128		./pust.009/case_2	2.892	1.63E-06	219.82	0.002	4.07E-02	1.31E-05	1.025	0.0007	1	0.0047	0.025	1.025
129		./pust.009/case_3	2.892	1.63E-06	219.83	0.002	4.06E-02	1.30E-05	1.023	0.0006	1	0.0047	0.023	1.023

Results for Volume 1: Plutonium Systems

N	Category	Case	nubar	Sigma	AFG	Sigma	EALCF (ev)	sigma	k_calc Pu	sigma	Benchmark k-eff	Sigma	Bias = Calculated - Benchmark	Adjusted k-eff Pu*
130	ST010	./pust.010/case_1_11	2.891	4.50E-06	214.13	0.006	7.55E-02	6.19E-05	1.017	0.001	1	0.0048	0.017	1.017
131		./pust.010/case_1_12	2.891	3.94E-06	214.89	0.006	6.99E-02	5.50E-05	1.013	0.001	1	0.0048	0.013	1.013
132		./pust.010/case_1_9	2.891	5.67E-06	210.08	0.009	1.11E-01	1.14E-04	1.02	0.001	1	0.0048	0.02	1.02
133		./pust.010/case_2_11	2.891	3.90E-06	214.88	0.006	7.01E-02	5.42E-05	1.012	0.0011	1	0.0048	0.012	1.012
134		./pust.010/case_2_12	2.891	3.74E-06	215.53	0.005	6.55E-02	4.74E-05	1.014	0.001	1	0.0048	0.014	1.014
135		./pust.010/case_2_9	2.891	4.96E-06	212.37	0.008	8.94E-02	8.24E-05	1.017	0.0009	1	0.0048	0.017	1.017
136		./pust.010/case_3_11	2.891	4.09E-06	215.03	0.006	6.89E-02	5.30E-05	1.013	0.0011	1	0.0048	0.013	1.013
137		./pust.010/case_3_12	2.891	3.26E-06	216.26	0.005	6.07E-02	3.92E-05	1.021	0.0012	1	0.0048	0.021	1.021
138		./pust.010/case_3_9	2.891	4.36E-06	214.29	0.006	7.42E-02	5.93E-05	1.011	0.0012	1	0.0048	0.011	1.011
139		./pust.010/case_4_11	2.891	3.95E-06	215.37	0.006	6.66E-02	5.13E-05	1.007	0.001	1	0.0048	0.007	1.007
140		./pust.010/case_4_12	2.891	3.23E-06	216.85	0.004	5.70E-02	3.50E-05	1.013	0.0012	1	0.0048	0.013	1.013
141		./pust.010/case_5_11	2.891	3.84E-06	215.74	0.005	6.41E-02	4.50E-05	1.008	0.001	1	0.0048	0.008	1.008
142		./pust.010/case_6_11	2.891	4.47E-06	213.34	0.007	8.14E-02	6.81E-05	1.017	0.0013	1	0.0048	0.017	1.017
143		./pust.010/case_7_11	2.891	4.35E-06	214.8	0.006	7.05E-02	5.55E-05	1.006	0.001	1	0.0048	0.006	1.006
144	ST011	./pust.011/case_1_16	2.891	3.35E-06	215.82	0.005	6.35E-02	4.27E-05	1.014	0.0011	1	0.0052	0.014	1.014
145		./pust.011/case_1_18	2.891	2.74E-06	217.68	0.004	5.20E-02	2.81E-05	1	0.0012	1	0.0052	0	1
146		./pust.011/case_2_16	2.891	3.38E-06	215.64	0.005	6.47E-02	4.31E-05	1.021	0.0013	1	0.0052	0.021	1.021
147		./pust.011/case_2_18	2.891	2.81E-06	217.52	0.004	5.29E-02	3.00E-05	1.007	0.0011	1	0.0052	0.007	1.007
148		./pust.011/case_3_16	2.891	3.77E-06	215.29	0.005	6.71E-02	4.76E-05	1.023	0.0011	1	0.0052	0.023	1.023
149		./pust.011/case_3_18	2.891	2.69E-06	217.53	0.004	5.29E-02	2.88E-05	1.004	0.0013	1	0.0052	0.004	1.004
150		./pust.011/case_4_16	2.891	3.72E-06	215.2	0.005	6.77E-02	4.86E-05	1.015	0.0013	1	0.0052	0.015	1.015
151		./pust.011/case_4_18	2.891	2.96E-06	217.3	0.004	5.42E-02	3.10E-05	0.998	0.001	1	0.0052	-0.002	0.998
152		./pust.011/case_5_16	2.891	4.06E-06	214.16	0.006	7.53E-02	5.99E-05	1.009	0.0013	1	0.0052	0.009	1.009
153		./pust.011/case_5_18	2.891	2.94E-06	217.08	0.004	5.56E-02	3.29E-05	1.01	0.0011	1	0.0052	0.01	1.01
154		./pust.011/case_6_18	2.891	3.23E-06	216.47	0.004	5.94E-02	3.76E-05	1.006	0.0011	1	0.0052	0.006	1.006
155		./pust.011/case_7_18	2.891	2.82E-06	217.34	0.004	5.40E-02	2.94E-05	1.005	0.0011	1	0.0052	0.005	1.005
156	ST014	./pust.014/case_1	2.891	7.18E-06	205.46	0.012	1.68E-01	2.02E-04	1.007	0.0012	0.998	0.0032	0.009	1.009

Results for Volume 1: Plutonium Systems

N	Category	Case	nubar	Sigma	AFG	Sigma	EALCF (ev)	sigma	k_calc Pu	sigma	Benchmark k-eff	Sigma	Bias = Calculated - Benchmark	Adjusted k-eff Pu*
157		./pust.014/case_10	2.891	7.28E-06	205.51	0.011	1.67E-01	2.01E-04	1.007	0.0011	0.998	0.0032	0.009	1.009
158		./pust.014/case_11	2.891	7.35E-06	205.51	0.011	1.67E-01	1.99E-04	1.006	0.0012	0.998	0.0032	0.008	1.008
159		./pust.014/case_12	2.891	6.96E-06	205.54	0.011	1.67E-01	1.98E-04	1.005	0.0011	0.998	0.0032	0.007	1.007
160		./pust.014/case_13	2.891	7.26E-06	205.41	0.011	1.68E-01	1.99E-04	1.007	0.0013	0.998	0.0043	0.009	1.009
161		./pust.014/case_14	2.891	6.69E-06	205.45	0.011	1.68E-01	1.99E-04	1.007	0.0012	0.998	0.0043	0.009	1.009
162		./pust.014/case_15	2.891	7.11E-06	205.52	0.012	1.67E-01	2.06E-04	1.006	0.0014	0.998	0.0043	0.008	1.008
163		./pust.014/case_16	2.891	7.10E-06	205.5	0.011	1.67E-01	2.00E-04	1.004	0.0011	0.998	0.0043	0.006	1.006
164		./pust.014/case_17	2.891	7.36E-06	205.5	0.012	1.67E-01	2.03E-04	1.006	0.0012	0.998	0.0043	0.008	1.008
165		./pust.014/case_18	2.891	7.51E-06	205.44	0.011	1.68E-01	1.99E-04	1.01	0.0011	0.998	0.0043	0.012	1.012
166		./pust.014/case_19	2.891	7.47E-06	205.46	0.011	1.68E-01	2.01E-04	1.006	0.0012	0.998	0.0043	0.008	1.008
167		./pust.014/case_2	2.891	7.11E-06	205.49	0.012	1.67E-01	2.09E-04	1.005	0.0011	0.998	0.0032	0.007	1.007
168		./pust.014/case_20	2.891	7.06E-06	205.48	0.011	1.67E-01	1.97E-04	1.004	0.0012	0.998	0.0043	0.006	1.006
169		./pust.014/case_21	2.891	7.22E-06	205.52	0.012	1.67E-01	2.04E-04	1.006	0.0012	0.998	0.0043	0.008	1.008
170		./pust.014/case_22	2.891	7.67E-06	205.53	0.011	1.67E-01	1.96E-04	1.006	0.0013	0.998	0.0043	0.008	1.008
171		./pust.014/case_23	2.891	7.06E-06	205.51	0.012	1.67E-01	1.97E-04	1.005	0.0013	0.998	0.0043	0.007	1.007
172		./pust.014/case_24	2.891	7.32E-06	205.4	0.011	1.69E-01	1.85E-04	1.008	0.0013	0.998	0.0043	0.01	1.01
173		./pust.014/case_25	2.891	6.88E-06	205.44	0.011	1.68E-01	1.88E-04	1.009	0.001	0.998	0.0043	0.011	1.011
174		./pust.014/case_26	2.891	6.95E-06	205.47	0.012	1.68E-01	2.05E-04	1.004	0.0012	0.998	0.0043	0.006	1.006
175		./pust.014/case_27	2.891	7.05E-06	205.5	0.012	1.67E-01	2.05E-04	1.004	0.0013	0.998	0.0043	0.006	1.006
176		./pust.014/case_28	2.891	7.37E-06	205.53	0.011	1.67E-01	1.94E-04	1.004	0.0012	0.998	0.0043	0.006	1.006
177		./pust.014/case_29	2.891	7.29E-06	205.53	0.012	1.67E-01	1.99E-04	1.007	0.0014	0.998	0.0043	0.009	1.009
178		./pust.014/case_3	2.891	7.16E-06	205.52	0.012	1.67E-01	2.04E-04	1.008	0.0012	0.998	0.0032	0.01	1.01
179		./pust.014/case_30	2.891	7.55E-06	205.42	0.011	1.68E-01	2.00E-04	1.004	0.0015	0.998	0.0043	0.006	1.006
180		./pust.014/case_31	2.891	7.42E-06	205.42	0.012	1.68E-01	2.14E-04	1.003	0.0014	0.998	0.0043	0.005	1.005
181		./pust.014/case_32	2.891	7.59E-06	205.45	0.012	1.68E-01	1.94E-04	1.005	0.0012	0.998	0.0043	0.007	1.007
182		./pust.014/case_33	2.891	7.40E-06	205.47	0.011	1.67E-01	1.94E-04	1.005	0.0012	0.998	0.0043	0.007	1.007
183		./pust.014/case_34	2.891	7.08E-06	205.48	0.012	1.67E-01	2.06E-04	1.005	0.0012	0.998	0.0043	0.007	1.007

Results for Volume 1: Plutonium Systems

N	Category	Case	nubar	Sigma	AFG	Sigma	EALCF (ev)	sigma	k_calc Pu	sigma	Benchmark k-eff	Sigma	Bias = Calculated - Benchmark	Adjusted k-eff Pu*
184		./pust.014/case_4	2.891	7.51E-06	205.52	0.012	1.67E-01	2.11E-04	1.008	0.0013	0.998	0.0032	0.01	1.01
185		./pust.014/case_5	2.891	7.12E-06	205.53	0.012	1.67E-01	1.99E-04	1.008	0.0012	0.998	0.0032	0.01	1.01
186		./pust.014/case_6	2.891	7.27E-06	205.53	0.012	1.67E-01	2.02E-04	1.006	0.0014	0.998	0.0032	0.008	1.008
187		./pust.014/case_7	2.891	7.73E-06	205.45	0.011	1.68E-01	1.99E-04	1.007	0.0013	0.998	0.0032	0.009	1.009
188		./pust.014/case_8	2.891	7.55E-06	205.46	0.012	1.68E-01	2.06E-04	1.006	0.0014	0.998	0.0032	0.008	1.008
189		./pust.014/case_9	2.891	6.91E-06	205.49	0.012	1.67E-01	1.99E-04	1.006	0.0012	0.998	0.0032	0.008	1.008
190	ST015	./pust.015/case_1	2.891	8.54E-06	201.28	0.013	2.37E-01	3.04E-04	1.008	0.0011	0.998	0.0038	0.01	1.01
191		./pust.015/case_10	2.891	8.98E-06	201.29	0.014	2.37E-01	3.10E-04	1.004	0.0012	0.9971	0.0047	0.007	1.007
192		./pust.015/case_11	2.891	8.53E-06	201.2	0.014	2.39E-01	3.35E-04	1.005	0.0012	0.9971	0.0047	0.007	1.008
193		./pust.015/case_12	2.891	9.18E-06	201.25	0.013	2.37E-01	3.05E-04	1.004	0.0011	0.9971	0.0047	0.007	1.007
194		./pust.015/case_13	2.891	8.57E-06	201.3	0.013	2.37E-01	3.13E-04	1.006	0.0011	0.9971	0.0047	0.009	1.009
195		./pust.015/case_14	2.891	8.58E-06	201.35	0.013	2.36E-01	2.99E-04	1.007	0.0012	0.9971	0.0047	0.01	1.01
196		./pust.015/case_15	2.891	8.98E-06	201.2	0.014	2.39E-01	3.23E-04	1.008	0.0012	0.9971	0.0047	0.01	1.01
197		./pust.015/case_16	2.891	8.88E-06	201.24	0.015	2.37E-01	3.22E-04	1.005	0.0013	0.9971	0.0047	0.007	1.008
198		./pust.015/case_17	2.891	8.92E-06	201.29	0.014	2.37E-01	3.01E-04	1.007	0.0014	0.9971	0.0047	0.01	1.01
199		./pust.015/case_2	2.891	9.40E-06	201.25	0.014	2.38E-01	3.31E-04	1.005	0.0011	0.998	0.0038	0.007	1.007
200		./pust.015/case_3	2.891	8.83E-06	201.26	0.014	2.37E-01	3.23E-04	1.004	0.0014	0.998	0.0038	0.006	1.006
201		./pust.015/case_4	2.891	9.07E-06	201.31	0.014	2.36E-01	3.16E-04	1.006	0.0013	0.998	0.0038	0.008	1.008
202		./pust.015/case_5	2.891	8.97E-06	201.29	0.014	2.37E-01	3.11E-04	1.006	0.0013	0.998	0.0038	0.008	1.008
203		./pust.015/case_6	2.891	8.96E-06	201.32	0.014	2.36E-01	3.04E-04	1.007	0.0013	0.998	0.0038	0.009	1.009
204		./pust.015/case_7	2.891	8.46E-06	201.21	0.014	2.38E-01	3.23E-04	1.009	0.0011	0.9971	0.0047	0.012	1.012
205		./pust.015/case_8	2.891	9.03E-06	201.24	0.015	2.38E-01	3.34E-04	1.005	0.0012	0.9971	0.0047	0.007	1.007
206		./pust.015/case_9	2.891	8.74E-06	201.29	0.014	2.37E-01	3.27E-04	1.008	0.0013	0.9971	0.0047	0.011	1.011
207	ST016	./pust.016/case_1	2.891	9.29E-06	201.25	0.014	2.37E-01	3.24E-04	1.006	0.0015	0.998	0.0043	0.008	1.008
208		./pust.016/case_10	2.891	7.41E-06	205.56	0.011	1.66E-01	1.95E-04	1.006	0.0014	0.9963	0.0033	0.01	1.01
209		./pust.016/case_11	2.891	7.15E-06	205.52	0.011	1.67E-01	1.92E-04	1.008	0.0014	0.9963	0.0033	0.012	1.012
210		./pust.016/case_2	2.891	9.00E-06	201.28	0.014	2.37E-01	3.21E-04	1.006	0.0012	0.998	0.0043	0.008	1.008

Results for Volume 1: Plutonium Systems

N	Category	Case	nubar	Sigma	AFG	Sigma	EALCF (ev)	sigma	k_calc Pu	sigma	Benchmark k-eff	Sigma	Bias = Calculated - Benchmark	Adjusted k-eff Pu*
211		./pust.016/case_3	2.891	9.27E-06	201.29	0.015	2.37E-01	3.42E-04	1.007	0.0012	0.998	0.0043	0.009	1.009
212		./pust.016/case_4	2.891	8.70E-06	201.29	0.014	2.37E-01	3.24E-04	1.008	0.0013	0.998	0.0043	0.01	1.01
213		./pust.016/case_5	2.891	7.07E-06	205.47	0.011	1.67E-01	1.90E-04	1.007	0.0012	0.9969	0.0038	0.01	1.01
214		./pust.016/case_6	2.891	6.89E-06	205.47	0.012	1.67E-01	2.07E-04	1.007	0.0014	0.9969	0.0038	0.01	1.01
215		./pust.016/case_7	2.891	7.17E-06	205.5	0.011	1.67E-01	2.05E-04	1.007	0.0015	0.9969	0.0038	0.011	1.011
216		./pust.016/case_8	2.891	6.61E-06	205.51	0.011	1.67E-01	1.89E-04	1.007	0.0015	0.9969	0.0038	0.01	1.01
217		./pust.016/case_9	2.891	7.26E-06	205.61	0.011	1.65E-01	1.92E-04	1.008	0.0014	0.9963	0.0033	0.012	1.012
218	ST017	./pust.017/case_1	2.891	7.62E-06	205.51	0.011	1.67E-01	1.98E-04	1.003	0.0013	0.9969	0.0038	0.006	1.006
219		./pust.017/case_10	2.891	7.17E-06	205.5	0.012	1.67E-01	2.11E-04	1.007	0.0013	0.9969	0.0038	0.01	1.01
220		./pust.017/case_11	2.891	7.63E-06	205.54	0.012	1.67E-01	2.06E-04	1.006	0.0014	0.9969	0.0038	0.009	1.009
221		./pust.017/case_12	2.891	7.22E-06	205.48	0.011	1.67E-01	1.97E-04	1.006	0.0012	0.9969	0.0038	0.009	1.009
222		./pust.017/case_13	2.891	7.64E-06	205.52	0.012	1.67E-01	2.02E-04	1.005	0.0012	0.9969	0.0038	0.008	1.008
223		./pust.017/case_14	2.891	7.15E-06	205.49	0.011	1.67E-01	1.97E-04	1.005	0.0012	0.9969	0.0038	0.008	1.008
224		./pust.017/case_15	2.891	6.83E-06	205.53	0.012	1.67E-01	2.04E-04	1.007	0.0012	0.9969	0.0038	0.01	1.01
225		./pust.017/case_16	2.891	7.52E-06	205.53	0.011	1.67E-01	1.96E-04	1.008	0.0013	0.9969	0.0038	0.011	1.011
226		./pust.017/case_17	2.891	7.34E-06	205.52	0.012	1.67E-01	2.12E-04	1.008	0.0013	0.9969	0.0038	0.011	1.011
227		./pust.017/case_18	2.891	7.44E-06	205.5	0.012	1.67E-01	2.06E-04	1.005	0.0014	0.9969	0.0038	0.008	1.008
228		./pust.017/case_2	2.891	7.43E-06	205.51	0.012	1.67E-01	2.10E-04	1.006	0.0013	0.9969	0.0038	0.009	1.009
229		./pust.017/case_3	2.891	7.73E-06	205.52	0.011	1.67E-01	1.95E-04	1.004	0.0014	0.9969	0.0038	0.007	1.007
230		./pust.017/case_4	2.891	7.10E-06	205.51	0.012	1.67E-01	2.03E-04	1.006	0.0013	0.9969	0.0038	0.01	1.01
231		./pust.017/case_5	2.891	7.73E-06	205.5	0.011	1.67E-01	2.04E-04	1.005	0.0013	0.9969	0.0038	0.008	1.008
232		./pust.017/case_6	2.891	7.40E-06	205.5	0.012	1.67E-01	2.05E-04	1.006	0.0012	0.9969	0.0038	0.009	1.009
233		./pust.017/case_7	2.891	7.28E-06	205.48	0.011	1.67E-01	1.98E-04	1.004	0.0013	0.9969	0.0038	0.007	1.007
234		./pust.017/case_8	2.891	7.30E-06	205.49	0.011	1.67E-01	1.97E-04	1.006	0.0012	0.9969	0.0038	0.009	1.009
235		./pust.017/case_9	2.891	7.33E-06	205.52	0.012	1.67E-01	1.98E-04	1.005	0.0011	0.9969	0.0038	0.008	1.008
236	ST020	./pust.020/case_1_t8a	2.891	3.82E-06	215.48	0.005	6.56E-02	4.96E-05	1.008	0.001	0.9969	0.0038	0.011	1.011
237		./pust.020/case_2_t8a	2.891	3.52E-06	215.62	0.005	6.46E-02	4.39E-05	1.009	0.0012	0.9969	0.0038	0.013	1.013

Results for Volume 1: Plutonium Systems

N	Category	Case	nubar	Sigma	AFG	Sigma	EALCF (ev)	sigma	k_calc Pu	sigma	Benchmark k-eff	Sigma	Bias = Calculated - Benchmark	Adjusted k-eff Pu*
238		./pust.020/case_3_t8a	2.891	3.63E-06	216.5	0.005	5.89E-02	4.08E-05	1.004	0.001	0.9969	0.0038	0.007	1.007
239		./pust.020/case_5_t8a	2.891	4.43E-06	213.98	0.007	7.64E-02	6.38E-05	1.009	0.0012	0.9969	0.0038	0.012	1.012
240		./pust.020/case_6_t8a	2.891	4.54E-06	213.63	0.007	7.91E-02	6.98E-05	1.009	0.001	0.9969	0.0038	0.012	1.012
241		./pust.020/case_7_t8a	2.891	3.63E-06	216.27	0.005	6.03E-02	3.98E-05	1.004	0.0011	0.9969	0.0038	0.007	1.007
242		./pust.020/case_8_t8a	2.891	5.38E-06	210.64	0.008	1.06E-01	1.04E-04	1.007	0.0013	0.9969	0.0038	0.011	1.011
243		./pust.020/case_9_t8a	2.891	3.91E-06	214.04	0.006	7.60E-02	5.98E-05	0.999	0.0011	0.9969	0.0038	0.002	1.002
244	ST021	./pust.021/case_10	2.892	2.59E-06	218.03	0.003	4.98E-02	2.60E-05	1.011	0.0009	1	0.0025	0.011	1.011
245		./pust.021/case_7	2.891	3.63E-06	215.4	0.005	6.60E-02	4.69E-05	1.013	0.0013	1	0.0032	0.013	1.013
246		./pust.021/case_8	2.891	9.83E-06	197.73	0.017	3.13E-01	4.72E-04	1.004	0.0011	1	0.0065	0.004	1.004
247		./pust.021/case_9	2.891	3.90E-06	215.14	0.005	6.78E-02	5.09E-05	1.015	0.0013	1	0.0032	0.015	1.015
248	ST024	./pust.024/case_1	2.897	1.38E-05	191.71	0.019	4.71E-01	7.56E-04	1	0.0012	1	0.0062	0	1
249		./pust.024/case_10	2.895	9.04E-06	201.34	0.014	2.26E-01	3.05E-04	1.009	0.0011	1	0.0053	0.009	1.009
250		./pust.024/case_11	2.895	9.28E-06	201.41	0.014	2.25E-01	2.97E-04	1.008	0.0011	1	0.0053	0.008	1.008
251		./pust.024/case_12	2.895	9.02E-06	201.47	0.015	2.24E-01	3.11E-04	1.006	0.0012	1	0.0053	0.006	1.006
252		./pust.024/case_13	2.895	9.30E-06	201.46	0.014	2.24E-01	2.99E-04	1.007	0.0011	1	0.0053	0.007	1.007
253		./pust.024/case_14	2.896	1.14E-05	197.75	0.016	2.99E-01	4.37E-04	1.005	0.0011	1	0.0053	0.005	1.005
254		./pust.024/case_15	2.896	1.11E-05	197.81	0.017	2.98E-01	4.28E-04	1.003	0.0013	1	0.0053	0.003	1.003
255		./pust.024/case_16	2.896	1.10E-05	197.86	0.016	2.97E-01	4.29E-04	1.003	0.0012	1	0.0053	0.003	1.003
256		./pust.024/case_17	2.896	1.06E-05	197.96	0.017	2.94E-01	4.46E-04	1.001	0.0012	1	0.0053	0.001	1.001
257		./pust.024/case_18	2.895	5.05E-06	212.04	0.007	9.02E-02	7.86E-05	1.008	0.0012	1	0.0051	0.008	1.008
258		./pust.024/case_19	2.895	5.42E-06	212.05	0.007	9.02E-02	7.71E-05	1.009	0.001	1	0.0051	0.009	1.009
259		./pust.024/case_2	2.897	1.43E-05	191.88	0.021	4.64E-01	8.09E-04	1.001	0.0011	1	0.0062	0.001	1.001
260		./pust.024/case_20	2.895	5.22E-06	212.09	0.007	8.98E-02	7.64E-05	1.01	0.0012	1	0.0051	0.01	1.01
261		./pust.024/case_21	2.895	5.06E-06	212.11	0.007	8.96E-02	7.74E-05	1.008	0.0012	1	0.0051	0.008	1.008
262		./pust.024/case_22	2.895	5.20E-06	212.15	0.007	8.93E-02	7.95E-05	1.006	0.0012	1	0.0051	0.006	1.006
263		./pust.024/case_23	2.895	5.26E-06	212.16	0.007	8.92E-02	7.65E-05	1.006	0.0011	1	0.0051	0.006	1.006
264		./pust.024/case_3	2.897	1.42E-05	191.92	0.021	4.63E-01	7.99E-04	0.999	0.001	1	0.0062	-0.001	0.999

Results for Volume 1: Plutonium Systems

N	Category	Case	nubar	Sigma	AFG	Sigma	EALCF (ev)	sigma	k_calc Pu	sigma	Benchmark k-eff	Sigma	Bias = Calculated - Benchmark	Adjusted k-eff Pu*
265		./pust.024/case_4	2.897	1.34E-05	192.02	0.02	4.59E-01	7.43E-04	1	0.0011	1	0.0062	0	1
266		./pust.024/case_5	2.897	1.42E-05	192.06	0.02	4.57E-01	7.91E-04	0.998	0.0012	1	0.0062	-0.002	0.998
267		./pust.024/case_6	2.903	2.47E-05	173.48	0.031	1.68E+00	3.75E-03	0.997	0.0011	1	0.0077	-0.003	0.997
268		./pust.024/case_7	2.896	9.74E-06	201.14	0.014	2.30E-01	3.01E-04	1.008	0.0011	1	0.0053	0.008	1.008
269		./pust.024/case_8	2.895	9.15E-06	201.2	0.015	2.29E-01	3.10E-04	1.01	0.0015	1	0.0053	0.01	1.01
270		./pust.024/case_9	2.896	9.56E-06	201.25	0.015	2.28E-01	3.19E-04	1.007	0.001	1	0.0053	0.007	1.007
		Maximum	3.137	7.86E-04	219.8	0.09	1.26E+06	2.38E+03	1.0041	0.011	1.0041	0.011	0.033	1.033
		Average	2.94	7.43E-05	165.5	0.017	1.74E+05	2.89E+02	0.9992	0.004	0.9992	0.004	0.006	1.006
		Minimum	2.891	1.63E-06	21.23	0.002	4.06E-02	1.30E-05	0.9963	0.001	0.9963	0.001	-0.017	0.983

Table 4.2 Results for Highly Enriched Uranium Systems (Volume 2) with CSAS25 from SCALE 4.4a and the 238-group Library on the J-5600 (CMODB) Workstation

Results for Volume 2: HEU Systems, Rev. 0

N	Case	AFG	sigma	EALCF(ev)	sigma	k_calc HEU0	sigma	k_exp	sigma	Bias = Calculated - Benchmark	Adjusted k-eff HEU0*
1	heucm.001/hcm001_02	192.7	4.47E-02	3.82E-01	1.26E-03	1.00853	0.00097	1.0012	0.0059	0.0073	1.00733
2	heucm.001/hcm001_06	92.3	8.60E-02	1.84E+03	1.34E+01	0.9931	0.00092	0.9953	0.0056	-0.0022	0.9978

Results for Volume 2: HEU Systems, Rev. 0

N	Case	AFG	sigma	EALCF(ev)	sigma	k_calc HEU0	sigma	k_exp	sigma	Bias = Calculated - Benchmark	Adjusted k-eff HEU0*
3	heucm.001/hcm001_13	115.8	8.27E-02	2.34E+02	1.58E+00	0.99888	0.00088	1.0032	0.0053	-0.0043	0.99568
4	heucm.001/hcm001_17	142.2	8.29E-02	2.54E+01	1.71E-01	0.995	0.00097	0.9997	0.0046	-0.0047	0.9953
5	heucm.001/hcm001_20	99.7	7.42E-02	5.61E+02	3.21E+00	1.00596	0.00106	1.006	0.0065	0.0000	0.99996
6	heucm.001/hcm001_27	104.4	7.68E-02	3.97E+02	2.32E+00	0.99803	0.00095	0.9991	0.0053	-0.0011	0.99893
7	heucm.001/hcm001_28	101.8	7.83E-02	4.88E+02	2.93E+00	1.00403	0.00109	1.0037	0.0053	0.0003	1.00033
8	heuct.010/hct010a	180.5	4.38E-02	8.51E-01	2.52E-03	0.98579	0.00105	1	0.005	-0.0142	0.98579
9	heuct.010/hct010b	205.1	2.62E-02	1.38E-01	2.76E-04	0.99156	0.00103	1	0.005	-0.0084	0.99156
10	heuct.010/hct010c	209.9	2.17E-02	9.61E-02	1.64E-04	1.00111	0.00103	1	0.005	0.0011	1.00111
11	heuct.010/hct010d	209.3	2.23E-02	1.00E-01	1.72E-04	0.99926	0.00114	1	0.005	-0.0007	0.99926
12	heuct.010/hct010e	209.7	2.17E-02	9.73E-02	1.68E-04	1.00367	0.001	1.001	0.0074	0.0027	1.00267
13	heuct.010/hct010g	209.9	2.83E-02	9.21E-02	2.19E-04	1.00566	0.00097	1.0007	0.0076	0.0050	1.00496
14	heuct.011/case_1	182.6	4.48E-02	7.19E-01	2.08E-03	0.99432	0.00126	0.9988	0.0042	-0.0045	0.99552
15	heuct.011/case_2	186.2	4.11E-02	5.54E-01	1.53E-03	0.9946	0.00093	0.9988	0.0042	-0.0042	0.9958
16	heuct.011/case_3	189.6	4.00E-02	4.32E-01	1.15E-03	0.99546	0.0009	0.9988	0.0042	-0.0033	0.99666
17	heuct.012/case_1	185.1	4.36E-02	6.02E-01	1.69E-03	0.99229	0.00096	0.9987	0.0032	-0.0064	0.99359
18	heuct.012/case_2	188.8	4.21E-02	4.58E-01	1.27E-03	0.99294	0.00091	0.9987	0.0034	-0.0058	0.99424
19	heuct.013/case_1	188.9	4.30E-02	4.54E-01	1.32E-03	0.99565	0.00114	0.9988	0.0042	-0.0031	0.99685
20	heuct.013/case_2	193.8	4.06E-02	3.16E-01	8.43E-04	0.9952	0.00099	0.9988	0.0043	-0.0036	0.9964
21	heuct.014/case_1	206.9	3.06E-02	1.17E-01	2.60E-04	0.99989	0.00099	0.9986	0.0048	0.0013	1.00129
22	heuct.014/case_2	209.3	2.92E-02	9.71E-02	2.08E-04	1.00124	0.00091	0.9986	0.0049	0.0026	1.00264
23	heumf.001/hmf001a	24.4	1.35E-02	9.49E+05	1.17E+03	0.99605	0.00094	1	0.001	-0.0040	0.99605
24	heumf.002/hmf002b	25.5	1.82E-02	8.38E+05	1.41E+03	1.00274	0.00106	1	0.003	0.0027	1.00274
25	heumf.002/hmf002c	25.5	1.91E-02	8.35E+05	1.46E+03	0.99918	0.0009	1	0.003	-0.0008	0.99918
26	heumf.002/hmf002d	25.6	1.92E-02	8.24E+05	1.45E+03	0.99523	0.001	1	0.003	-0.0048	0.99523
27	heumf.002/hmf002e	25.7	1.84E-02	8.18E+05	1.37E+03	1.00336	0.00089	1	0.003	0.0034	1.00336
28	heumf.002/hmf002g	25.6	1.79E-02	8.26E+05	1.38E+03	0.99832	0.00094	1	0.003	-0.0017	0.99832
29	heumf.003/hmf003a	24.8	1.30E-02	9.10E+05	1.13E+03	0.99233	0.00084	1	0.005	-0.0077	0.99233

Results for Volume 2: HEU Systems, Rev. 0

N	Case	AFG	sigma	EALCF(ev)	sigma	k_calc HEU0	sigma	k_exp	sigma	Bias = Calculated - Benchmark	Adjusted k-eff HEU0*
30	heumf.003/hmf003b	24.9	1.40E-02	8.99E+05	1.18E+03	0.99359	0.0009	1	0.005	-0.0064	0.99359
31	heumf.003/hmf003c	25.0	1.34E-02	8.87E+05	1.15E+03	0.99839	0.00098	1	0.005	-0.0016	0.99839
32	heumf.003/hmf003d	25.1	1.39E-02	8.78E+05	1.19E+03	0.99795	0.00101	1	0.003	-0.0021	0.99795
33	heumf.003/hmf003e	25.3	1.54E-02	8.58E+05	1.24E+03	1.00189	0.00099	1	0.003	0.0019	1.00189
34	heumf.003/hmf003g	25.3	1.62E-02	8.53E+05	1.27E+03	1.00052	0.00106	1	0.003	0.0005	1.00052
35	heumf.003/hmf003h	25.5	1.95E-02	8.31E+05	1.48E+03	1.0031	0.0011	1	0.003	0.0031	1.0031
36	heumf.003/hmf003i	27.2	1.33E-02	7.12E+05	9.38E+02	1.00297	0.00091	1	0.005	0.0030	1.00297
37	heumf.003/hmf003j	28.1	1.37E-02	6.41E+05	9.03E+02	1.00505	0.00082	1	0.005	0.0051	1.00505
38	heumf.003/hmf003k	28.9	1.45E-02	5.83E+05	8.81E+02	1.01025	0.001	1	0.005	0.0103	1.01025
39	heumf.003/hmf003l	29.1	1.36E-02	5.64E+05	8.19E+02	1.0127	0.0008	1	0.005	0.0127	1.0127
40	heumf.004/hmf004d	61.1	7.45E-02	3.16E+04	2.05E+02	0.9964	0.00112	1.002	0	-0.0056	0.9944
41	heumf.007/case_1	24.3	1.31E-02	9.57E+05	1.18E+03	0.99113	0.00104	0.9971	0.0001	-0.0060	0.99403
42	heumf.007/case_10	55.0	5.08E-02	2.84E+04	1.35E+02	0.99248	0.00103	1	0.0001	-0.0075	0.99248
43	heumf.007/case_11	70.1	6.42E-02	5.92E+03	3.34E+01	0.99257	0.00129	0.9982	0.0001	-0.0056	0.99437
44	heumf.007/case_12	73.6	6.66E-02	4.33E+03	2.42E+01	0.9908	0.00112	0.9951	0.0001	-0.0043	0.9957
45	heumf.007/case_13	82.1	7.20E-02	2.69E+03	1.62E+01	0.99667	0.00107	1.0009	0.0001	-0.0042	0.99577
46	heumf.007/case_14	74.6	6.45E-02	3.97E+03	2.23E+01	0.99203	0.00115	0.9983	0.0001	-0.0063	0.99373
47	heumf.007/case_15	80.7	6.91E-02	3.00E+03	1.72E+01	0.99041	0.00103	0.9978	0.0001	-0.0074	0.99261
48	heumf.007/case_16	80.9	7.71E-02	2.95E+03	1.88E+01	0.99122	0.00116	0.9988	0.0001	-0.0076	0.99242
49	heumf.007/case_17	103.2	7.88E-02	3.86E+02	2.37E+00	0.99168	0.00152	0.9972	0.0001	-0.0055	0.99448
50	heumf.007/case_18	103.8	7.78E-02	3.68E+02	2.24E+00	0.99515	0.00117	0.9991	0.0001	-0.0040	0.99605
51	heumf.007/case_19	24.3	1.27E-02	9.54E+05	1.12E+03	0.99294	0.00097	0.9983	0.0001	-0.0054	0.99464
52	heumf.007/case_2	28.7	1.93E-02	5.29E+05	1.17E+03	0.9938	0.00106	0.9986	0.0001	-0.0048	0.9952
53	heumf.007/case_20	35.7	3.37E-02	2.29E+05	8.20E+02	0.99117	0.00118	0.9981	0.0001	-0.0069	0.99307
54	heumf.007/case_21	36.4	3.60E-02	2.12E+05	8.04E+02	0.99211	0.00093	0.9987	0.0001	-0.0066	0.99341
55	heumf.007/case_22	37.2	3.45E-02	1.94E+05	6.93E+02	0.99284	0.00098	0.9994	0.0001	-0.0066	0.99344
56	heumf.007/case_23	48.5	5.80E-02	6.60E+04	3.52E+02	0.99408	0.0009	0.9993	0.0001	-0.0052	0.99478

Results for Volume 2: HEU Systems, Rev. 0

N	Case	AFG	sigma	EALCF(ev)	sigma	k_calc HEU0	sigma	k_exp	sigma	Bias = Calculated - Benchmark	Adjusted k-eff HEU0*
57	heumf.007/case_24	49.2	5.68E-02	6.23E+04	3.23E+02	0.99447	0.00112	1.0001	0.0001	-0.0056	0.99437
58	heumf.007/case_25	57.1	6.29E-02	2.80E+04	1.58E+02	0.99493	0.00109	0.999	0.0001	-0.0041	0.99593
59	heumf.007/case_26	57.9	6.03E-02	2.62E+04	1.43E+02	0.99366	0.00105	0.9997	0.0001	-0.0060	0.99396
60	heumf.007/case_27	29.2	2.08E-02	4.97E+05	1.20E+03	0.99052	0.00107	0.9965	0.0002	-0.0060	0.99402
61	heumf.007/case_28	33.2	2.55E-02	2.99E+05	8.79E+02	0.99132	0.00085	0.9987	0.0002	-0.0074	0.99262
62	heumf.007/case_29	37.5	3.28E-02	1.73E+05	6.22E+02	0.99254	0.00089	0.9978	0.0002	-0.0053	0.99474
63	heumf.007/case_3	31.0	2.54E-02	4.02E+05	1.14E+03	0.99399	0.00099	1.0012	0.0001	-0.0072	0.99279
64	heumf.007/case_30	59.5	5.75E-02	1.86E+04	9.91E+01	0.99153	0.00096	0.9981	0.0002	-0.0066	0.99343
65	heumf.007/case_31	84.4	6.74E-02	1.73E+03	9.64E+00	0.99799	0.00117	1.0013	0.0002	-0.0033	0.99669
66	heumf.007/case_32	25.5	1.31E-02	8.40E+05	1.08E+03	0.99807	0.00087	0.9959	0.0001	0.0022	1.00217
67	heumf.007/case_33	26.3	1.38E-02	7.69E+05	1.05E+03	1.00516	0.00103	0.9995	0.0001	0.0057	1.00566
68	heumf.007/case_34	27.0	1.49E-02	7.05E+05	1.05E+03	1.00941	0.00095	0.9977	0.0001	0.0117	1.01171
69	heumf.007/case_35	76.1	7.88E-02	7.88E+03	5.42E+01	0.99206	0.00099	1.0011	0.0001	-0.0090	0.99096
70	heumf.007/case_36	81.8	8.40E-02	3.92E+03	2.78E+01	0.99863	0.0009	0.9999	0.0001	-0.0013	0.99873
71	heumf.007/case_37	88.0	7.87E-02	1.96E+03	1.25E+01	0.99808	0.00099	0.9988	0.0001	-0.0007	0.99928
72	heumf.007/case_38	88.7	8.13E-02	1.77E+03	1.17E+01	0.99853	0.0011	1	0.0001	-0.0015	0.99853
73	heumf.007/case_39	88.8	7.59E-02	1.73E+03	1.09E+01	0.99997	0.00093	1.0018	0.0001	-0.0018	0.99817
74	heumf.007/case_4	31.8	2.55E-02	3.54E+05	1.06E+03	0.99179	0.00103	0.997	0.0001	-0.0052	0.99479
75	heumf.007/case_40	89.0	7.74E-02	1.78E+03	1.12E+01	1.0031	0.00095	1.0013	0.0001	0.0018	1.0018
76	heumf.007/case_41	106.5	8.13E-02	3.26E+02	2.06E+00	0.99935	0.00116	0.9994	0.0001	0.0000	0.99995
77	heumf.007/case_42	107.2	7.80E-02	3.07E+02	1.87E+00	0.9995	0.00091	1.0016	0.0001	-0.0021	0.9979
78	heumf.007/case_43	132.1	7.26E-02	3.48E+01	1.88E-01	1.00107	0.0012	0.9998	0.0001	0.0013	1.00127
79	heumf.007/case_5	33.8	2.66E-02	2.71E+05	8.50E+02	0.99267	0.00095	1	0.0001	-0.0073	0.99267
80	heumf.007/case_6	38.5	3.87E-02	1.71E+05	6.92E+02	0.99982	0.00108	1.0028	0.0001	-0.0030	0.99702
81	heumf.007/case_7	35.8	3.11E-02	2.13E+05	7.59E+02	0.99619	0.00116	0.9996	0.0001	-0.0034	0.99659
82	heumf.007/case_8	35.4	3.00E-02	2.18E+05	7.69E+02	0.99183	0.00103	0.9992	0.0001	-0.0074	0.99263
83	heumf.007/case_9	37.0	3.50E-02	1.93E+05	7.29E+02	0.9959	0.0011	1.0017	0.0008	-0.0058	0.9942

Results for Volume 2: HEU Systems, Rev. 0

N	Case	AFG	sigma	EALCF(ev)	sigma	k_calc HEU0	sigma	k_exp	sigma	Bias = Calculated - Benchmark	Adjusted k-eff HEU0*
84	heumf.018/hmf018a	24.6	1.27E-02	9.29E+05	1.11E+03	0.99769	0.00102	1	0.0014	-0.0023	0.99769
85	heumf.019/hmf019a	25.4	1.29E-02	8.58E+05	1.06E+03	1.00212	0.00085	1	0.0028	0.0021	1.00212
86	heumf.020/hmf020a	30.0	3.05E-02	5.09E+05	1.51E+03	0.99438	0.00098	1	0.0028	-0.0056	0.99438
87	heumf.021/hmf021a	25.9	1.28E-02	8.21E+05	1.01E+03	1.01458	0.00095	1	0.0024	0.0146	1.01458
88	heumf.022/hmf022a	25.1	1.29E-02	8.91E+05	1.09E+03	0.99116	0.00103	1	0.0019	-0.0088	0.99116
89	heumf.023/hmf023e	24.6	1.53E-02	9.31E+05	1.32E+03	0.99692	0.00095	1	0.0052	-0.0031	0.99692
90	heumf.023/hmf023g	82.2	8.64E-02	5.30E+03	3.92E+01	0.99997	0.00101	1	0.0052	0.0000	0.99997
91	heumf.026/hmf026b	24.5	1.38E-02	9.42E+05	1.21E+03	0.9979	0.00096	0.9982	0.0042	-0.0003	0.9997
92	heumf.026/hmf026g	61.4	8.14E-02	3.18E+04	2.26E+02	1.00018	0.00089	1	0.0038	0.0002	1.00018
93	heumf.026/hmf026h	74.2	8.34E-02	1.12E+04	7.95E+01	0.99858	0.00096	1	0.0038	-0.0014	0.99858
94	heumf.026/hmf026j	30.0	3.35E-02	5.25E+05	1.64E+03	0.98957	0.00084	0.9982	0.0042	-0.0086	0.99137
95	heumf.026/hmf026l	69.7	7.77E-02	1.71E+04	1.14E+02	0.99961	0.00098	1	0.0038	-0.0004	0.99961
96	heumf.027/hmf027a	25.0	1.24E-02	8.99E+05	1.07E+03	1.00872	0.00087	1	0.0025	0.0087	1.00872
97	heumf.028/hmf028b	25.3	1.60E-02	8.57E+05	1.28E+03	1.00469	0.00102	1	0.003	0.0047	1.00469
98	heumf.029/hmf029a	25.1	1.30E-02	8.86E+05	1.11E+03	1.00319	0.00103	1	0.002	0.0032	1.00319
99	heumf.030/hmf030a	35.1	3.53E-02	2.33E+05	9.34E+02	1.00397	0.00105	1	0.0009	0.0040	1.00397
100	heumf.031/hmf031b	76.6	7.82E-02	6.87E+03	4.62E+01	1.00099	0.00093	1	0.0059	0.0010	1.00099
101	heumf.032/hmf032d	25.0	1.42E-02	8.87E+05	1.21E+03	1.00413	0.00092	1	0.0016	0.0041	1.00413
102	heumf.032/hmf032e	25.0	1.30E-02	8.91E+05	1.12E+03	1.00038	0.00095	1	0.0027	0.0004	1.00038
103	heumf.032/hmf032g	24.8	1.27E-02	9.13E+05	1.11E+03	0.99885	0.00107	1	0.0017	-0.0011	0.99885
104	heumf.032/hmf032h	24.6	1.27E-02	9.29E+05	1.09E+03	0.9996	0.00108	1	0.0017	-0.0004	0.9996
105	heumf.034/hmf034a	63.1	6.80E-02	1.67E+04	9.84E+01	0.99319	0.00112	0.999	0.0012	-0.0058	0.99419
106	heumf.034/hmf034c	63.2	6.68E-02	1.68E+04	9.80E+01	0.99231	0.00114	0.999	0.0012	-0.0067	0.99331
107	heumf.034/hmf034e	64.7	6.59E-02	1.57E+04	8.94E+01	0.99978	0.0012	0.999	0.0012	0.0008	1.00078
108	heumm.001/hmm001a	87.2	8.08E-02	2.31E+03	1.56E+01	0.99972	0.00104	0.9995	0.0013	0.0002	1.00022
109	heumm.002/hmm002a	96.4	7.86E-02	1.17E+03	7.59E+00	1.00571	0.00097	1	0.0037	0.0057	1.00571
110	heumm.003/hmm003a	96.3	8.41E-02	1.18E+03	8.29E+00	1.00657	0.0009	1	0.0038	0.0066	1.00657

Results for Volume 2: HEU Systems, Rev. 0

N	Case	AFG	sigma	EALCF(ev)	sigma	k_calc HEU0	sigma	k_exp	sigma	Bias = Calculated - Benchmark	Adjusted k-eff HEU0*
111	heumt.003/hmt003a	66.4	7.73E-02	1.94E+04	1.30E+02	0.9969	0.00105	1	0.001	-0.0031	0.9969
112	heumt.003/hmt003b	67.1	8.06E-02	1.81E+04	1.27E+02	0.9762	0.00087	0.991	0.003	-0.0148	0.9852
113	heumt.003/hmt003c	112.2	8.00E-02	2.34E+02	1.47E+00	0.96808	0.00098	0.9826	0.006	-0.0145	0.98548
114	heumt.003/hmt003d	131.8	8.27E-02	4.90E+01	3.16E-01	0.97501	0.00127	0.9876	0.004	-0.0126	0.98741
115	heumt.003/hmt003e	166.8	6.67E-02	2.83E+00	1.40E-02	0.98934	0.00112	0.993	0.003	-0.0037	0.99634
116	heumt.003/hmt003g	151.3	7.54E-02	9.14E+00	5.16E-02	0.96856	0.00097	0.9889	0.003	-0.0203	0.97966
117	heumt.003/hmt003h	166.0	6.87E-02	3.01E+00	1.54E-02	0.97751	0.00106	0.9919	0.003	-0.0144	0.98561
118	heumt.006/case_1	210.0	2.67E-02	8.50E-02	1.70E-04	0.99769	0.00119	1	0.004	-0.0023	0.99769
119	heumt.006/case_10	210.4	2.81E-02	8.24E-02	1.73E-04	1.00684	0.00109	1	0.004	0.0068	1.00684
120	heumt.006/case_11	213.9	2.31E-02	6.20E-02	1.18E-04	1.00598	0.0011	1	0.004	0.0060	1.00598
121	heumt.006/case_12	215.7	1.96E-02	5.35E-02	8.83E-05	1.00561	0.00104	1	0.004	0.0056	1.00561
122	heumt.006/case_13	210.3	2.52E-02	8.29E-02	1.62E-04	1.02842	0.00118	1	0.004	0.0284	1.02842
123	heumt.006/case_14	215.0	2.04E-02	5.63E-02	9.49E-05	0.99794	0.00103	1	0.004	-0.0021	0.99794
124	heumt.006/case_15	215.1	2.06E-02	5.60E-02	9.80E-05	0.99419	0.00106	1	0.004	-0.0058	0.99419
125	heumt.006/case_16	213.7	2.23E-02	6.29E-02	1.13E-04	1.00521	0.00119	1	0.004	0.0052	1.00521
126	heumt.006/case_17	211.8	2.55E-02	7.37E-02	1.46E-04	1.00387	0.00106	1	0.004	0.0039	1.00387
127	heumt.006/case_18	210.8	2.73E-02	7.95E-02	1.68E-04	1.00375	0.00119	1	0.004	0.0037	1.00375
128	heumt.006/case_19	215.6	2.22E-02	5.21E-02	9.89E-05	0.99379	0.00102	1	0.004	-0.0062	0.99379
129	heumt.006/case_2	212.4	2.56E-02	7.00E-02	1.39E-04	1.00081	0.00105	1	0.004	0.0008	1.00081
130	heumt.006/case_20	213.3	2.31E-02	6.42E-02	1.21E-04	0.9968	0.00094	1	0.004	-0.0032	0.9968
131	heumt.006/case_21	212.5	2.48E-02	6.93E-02	1.30E-04	0.99808	0.00115	1	0.004	-0.0019	0.99808
132	heumt.006/case_22	211.8	2.55E-02	7.37E-02	1.45E-04	1.00322	0.001	1	0.004	0.0032	1.00322
133	heumt.006/case_23	211.5	2.52E-02	7.55E-02	1.46E-04	1.00611	0.00086	1	0.004	0.0061	1.00611
134	heumt.006/case_3	213.7	2.35E-02	6.26E-02	1.17E-04	1.00649	0.00098	1	0.004	0.0065	1.00649
135	heumt.006/case_4	214.0	2.24E-02	6.12E-02	1.15E-04	0.99486	0.00132	1	0.004	-0.0051	0.99486
136	heumt.006/case_5	214.7	2.02E-02	5.77E-02	9.78E-05	1.00156	0.00098	1	0.004	0.0016	1.00156
137	heumt.006/case_6	215.3	1.94E-02	5.53E-02	9.41E-05	1.00134	0.00088	1	0.004	0.0013	1.00134

Results for Volume 2: HEU Systems, Rev. 0

N	Case	AFG	sigma	EALCF(ev)	sigma	k_calc HEU0	sigma	k_exp	sigma	Bias = Calculated - Benchmark	Adjusted k-eff HEU0*
138	heumt.006/case_7	215.7	2.08E-02	5.35E-02	9.24E-05	0.99826	0.00097	1	0.004	-0.0017	0.99826
139	heumt.006/case_8	216.1	2.02E-02	5.17E-02	8.94E-05	0.99467	0.00107	1	0.004	-0.0053	0.99467
140	heumt.006/case_9	216.2	2.07E-02	5.12E-02	8.89E-05	0.99238	0.00108	1	0.004	-0.0076	0.99238
141	heust.001/case_1	210.2	9.41E-03	8.16E-02	6.96E-05	0.99982	0.00129	1	0.0025	-0.0002	0.99982
142	heust.001/case_10	216.7	4.62E-03	4.58E-02	2.43E-05	0.99287	0.00138	1	0.0025	-0.0071	0.99287
143	heust.001/case_2	195.1	1.92E-02	2.79E-01	4.29E-04	0.99784	0.00129	1	0.0025	-0.0022	0.99784
144	heust.001/case_3	210.4	8.66E-03	8.01E-02	6.82E-05	1.00289	0.00122	1	0.0025	0.0029	1.00289
145	heust.001/case_4	194.3	1.88E-02	2.98E-01	4.56E-04	1.00024	0.00122	1	0.0025	0.0002	1.00024
146	heust.001/case_5	217.5	3.88E-03	4.26E-02	1.99E-05	1.00505	0.00113	1	0.0025	0.0051	1.00505
147	heust.001/case_6	217.1	4.37E-03	4.42E-02	2.20E-05	1.00384	0.0014	1	0.0025	0.0038	1.00384
148	heust.001/case_7	210.8	8.75E-03	7.72E-02	6.48E-05	1.00245	0.00121	1	0.0025	0.0025	1.00245
149	heust.001/case_8	210.2	9.11E-03	8.16E-02	6.83E-05	1.00286	0.00142	1	0.0025	0.0029	1.00286
150	heust.001/case_9	194.2	1.95E-02	2.98E-01	4.64E-04	0.99736	0.00132	1	0.0025	-0.0026	0.99736
151	heust.002/case_1	210.5	8.74E-03	7.97E-02	6.76E-05	1.00567	0.00128	1	0.002	0.0057	1.00567
152	heust.002/case_10	217.3	4.13E-03	4.37E-02	2.19E-05	1.0087	0.00128	1	0.002	0.0087	1.0087
153	heust.002/case_11	210.5	8.69E-03	7.95E-02	6.65E-05	1.00419	0.00146	1	0.002	0.0042	1.00419
154	heust.002/case_12	210.8	8.51E-03	7.76E-02	6.16E-05	1.00902	0.00126	1	0.002	0.0090	1.00902
155	heust.002/case_13	196.5	1.80E-02	2.49E-01	3.48E-04	1.00353	0.00147	1	0.002	0.0035	1.00353
156	heust.002/case_14	197.5	1.79E-02	2.32E-01	3.36E-04	1.00902	0.00125	1	0.002	0.0090	1.00902
157	heust.002/case_2	210.6	8.69E-03	7.91E-02	6.57E-05	1.00948	0.00127	1	0.002	0.0095	1.00948
158	heust.002/case_3	196.4	1.79E-02	2.51E-01	3.65E-04	1.00012	0.00121	1	0.002	0.0001	1.00012
159	heust.002/case_4	196.9	1.64E-02	2.43E-01	3.33E-04	1.00742	0.00139	1	0.002	0.0074	1.00742
160	heust.002/case_5	210.5	8.86E-03	7.95E-02	6.57E-05	1.00632	0.00131	1	0.002	0.0063	1.00632
161	heust.002/case_6	210.7	8.70E-03	7.80E-02	6.54E-05	1.01045	0.00142	1	0.002	0.0105	1.01045
162	heust.002/case_7	196.5	1.73E-02	2.49E-01	3.49E-04	1.00468	0.00142	1	0.002	0.0047	1.00468
163	heust.002/case_8	197.2	1.71E-02	2.37E-01	3.25E-04	1.00501	0.00134	1	0.002	0.0050	1.00501
164	heust.002/case_9	217.2	4.21E-03	4.40E-02	2.27E-05	1.00313	0.00135	1	0.002	0.0031	1.00313

Results for Volume 2: HEU Systems, Rev. 0

N	Case	AFG	sigma	EALCF(ev)	sigma	k_calc HEU0	sigma	k_exp	sigma	Bias = Calculated - Benchmark	Adjusted k-eff HEU0*
165	heust.003/case_1	217.3	4.10E-03	4.38E-02	2.11E-05	1.0049	0.00129	1	0.005	0.0049	1.0049
166	heust.003/case_10	196.0	1.79E-02	2.60E-01	3.69E-04	0.99993	0.00141	1	0.005	-0.0001	0.99993
167	heust.003/case_11	197.5	1.87E-02	2.32E-01	3.47E-04	1.00253	0.00137	1	0.005	0.0025	1.00253
168	heust.003/case_12	217.2	4.15E-03	4.40E-02	2.20E-05	1.00222	0.00127	1	0.005	0.0022	1.00222
169	heust.003/case_13	217.4	3.97E-03	4.32E-02	2.03E-05	1.00266	0.00113	1	0.005	0.0027	1.00266
170	heust.003/case_14	217.2	4.21E-03	4.38E-02	2.22E-05	1.00212	0.00119	1	0.005	0.0021	1.00212
171	heust.003/case_15	216.9	4.35E-03	4.51E-02	2.16E-05	0.99622	0.00109	1	0.005	-0.0038	0.99622
172	heust.003/case_16	210.3	9.18E-03	8.07E-02	6.99E-05	1.00095	0.00133	1	0.005	0.0010	1.00095
173	heust.003/case_17	211.0	9.01E-03	7.63E-02	6.47E-05	1.00378	0.00142	1	0.005	0.0038	1.00378
174	heust.003/case_18	196.0	1.88E-02	2.60E-01	3.75E-04	0.99867	0.00125	1	0.005	-0.0013	0.99867
175	heust.003/case_19	197.9	1.78E-02	2.24E-01	3.13E-04	1.0019	0.00148	1	0.005	0.0019	1.0019
176	heust.003/case_2	217.2	4.19E-03	4.40E-02	2.25E-05	1.0055	0.00104	1	0.005	0.0055	1.0055
177	heust.003/case_3	210.3	8.70E-03	8.09E-02	6.76E-05	1.00152	0.00151	1	0.005	0.0015	1.00152
178	heust.003/case_4	210.6	8.97E-03	7.90E-02	6.61E-05	1.00463	0.00123	1	0.005	0.0046	1.00463
179	heust.003/case_5	195.8	1.77E-02	2.63E-01	3.70E-04	0.99717	0.00152	1	0.005	-0.0028	0.99717
180	heust.003/case_6	196.8	1.77E-02	2.45E-01	3.51E-04	0.99694	0.00148	1	0.005	-0.0031	0.99694
181	heust.003/case_7	217.4	4.16E-03	4.34E-02	2.08E-05	1.00462	0.00138	1	0.005	0.0046	1.00462
182	heust.003/case_8	210.3	8.91E-03	8.04E-02	6.55E-05	1.0033	0.00136	1	0.005	0.0033	1.0033
183	heust.003/case_9	210.9	9.09E-03	7.72E-02	6.62E-05	1.00748	0.00143	1	0.005	0.0075	1.00748
184	heust.004/hst004a	138.2	6.88E-02	1.34E+01	6.12E-02	1.00371	0.0012	1	0.0065	0.0037	1.00371
185	heust.004/hst004b	161.1	5.05E-02	2.72E+00	8.86E-03	1.00526	0.00114	1	0.0071	0.0053	1.00526
186	heust.004/hst004c	188.7	3.08E-02	4.24E-01	9.48E-04	1.00025	0.00139	1	0.0078	0.0003	1.00025
187	heust.004/hst004d	150.3	6.01E-02	5.64E+00	2.23E-02	0.99861	0.00115	1	0.0091	-0.0014	0.99861
188	heust.004/hst004e	174.8	4.36E-02	1.09E+00	3.18E-03	1.0067	0.00108	1	0.0104	0.0067	1.0067
189	heust.004/hst004g	199.2	1.94E-02	1.98E-01	2.99E-04	0.99836	0.00114	1	0.0117	-0.0016	0.99836
190	heust.005/hst005a	196.2	2.05E-02	2.47E-01	4.00E-04	1.00062	0.00105	1	0.0124	0.0006	1.00062
191	heust.005/hst005b	195.6	2.24E-02	2.56E-01	4.38E-04	1.00778	0.00105	1	0.0124	0.0078	1.00778

Results for Volume 2: HEU Systems, Rev. 0

N	Case	AFG	sigma	EALCF(ev)	sigma	k_calc HEU0	sigma	k_exp	sigma	Bias = Calculated - Benchmark	Adjusted k-eff HEU0*
192	heust.005/hst005c	195.1	2.22E-02	2.67E-01	4.50E-04	1.00636	0.00105	1	0.0126	0.0064	1.00636
193	heust.005/hst005d	197.5	1.96E-02	2.26E-01	3.50E-04	1.0025	0.00121	1	0.0124	0.0025	1.0025
194	heust.005/hst005e	192.5	2.02E-02	3.28E-01	5.25E-04	0.98975	0.00089	1	0.0124	-0.0103	0.98975
195	heust.005/hst005g	196.4	2.08E-02	2.44E-01	3.94E-04	1.00525	0.001	1	0.0125	0.0052	1.00525
196	heust.005/hst005h	206.3	1.26E-02	1.11E-01	1.24E-04	1.00297	0.00109	1	0.0119	0.0030	1.00297
197	heust.005/hst005i	213.2	8.26E-03	6.23E-02	4.87E-05	1.00594	0.00119	1	0.0121	0.0059	1.00594
198	heust.006/hst006a	198.6	1.61E-02	2.11E-01	2.70E-04	0.98469	0.00143	0.9973	0.005	-0.0126	0.98739
199	heust.006/hst006b	189.1	1.58E-02	4.38E-01	5.35E-04	1.00256	0.00085	1	0.0087	0.0026	1.00256
200	heust.006/hst006c	196.1	1.68E-02	2.58E-01	3.46E-04	0.98773	0.0012	0.9986	0.0054	-0.0109	0.98913
201	heust.006/hst006d	191.7	1.52E-02	3.61E-01	4.34E-04	1.0008	0.00072	1	0.0078	0.0008	1.0008
202	heust.006/hst006e	190.1	1.52E-02	4.06E-01	4.85E-04	1.01075	0.00104	1	0.0091	0.0108	1.01075
203	heust.006/hst006g	193.3	1.61E-02	3.19E-01	4.00E-04	0.99989	0.00108	1	0.0065	-0.0001	0.99989
204	heust.006/hst006h	188.9	1.59E-02	4.45E-01	5.56E-04	1.00375	0.00072	1	0.0088	0.0037	1.00375
205	heust.007/case_1	216.5	4.93E-03	4.70E-02	2.60E-05	1.01325	0.00113	1	0.0035	0.0133	1.01325
206	heust.007/case_10	215.2	5.55E-03	5.26E-02	3.27E-05	1.01692	0.0012	1	0.0035	0.0169	1.01692
207	heust.007/case_11	196.1	1.82E-02	2.58E-01	3.67E-04	1.00742	0.00144	1	0.0035	0.0074	1.00742
208	heust.007/case_12	215.6	5.57E-03	5.08E-02	3.06E-05	1.01688	0.00115	1	0.0035	0.0169	1.01688
209	heust.007/case_13	197.4	1.77E-02	2.33E-01	3.23E-04	1.01163	0.00119	1	0.0035	0.0116	1.01163
210	heust.007/case_14	197.0	1.80E-02	2.40E-01	3.43E-04	1.0099	0.00118	1	0.0035	0.0099	1.0099
211	heust.007/case_15	196.9	1.84E-02	2.42E-01	3.47E-04	1.00849	0.00117	1	0.0035	0.0085	1.00849
212	heust.007/case_16	196.2	1.92E-02	2.56E-01	3.83E-04	1.0094	0.00106	1	0.0035	0.0094	1.0094
213	heust.007/case_17	197.0	1.91E-02	2.41E-01	3.62E-04	1.01066	0.00123	1	0.0035	0.0107	1.01066
214	heust.007/case_2	195.6	1.95E-02	2.69E-01	4.09E-04	1.01324	0.00121	1	0.005	0.0132	1.01324
215	heust.007/case_3	216.8	4.36E-03	4.58E-02	2.27E-05	1.01137	0.0011	1	0.0035	0.0114	1.01137
216	heust.007/case_4	197.1	1.81E-02	2.39E-01	3.42E-04	1.01219	0.00113	1	0.0035	0.0122	1.01219
217	heust.007/case_5	215.8	4.98E-03	5.00E-02	2.65E-05	1.00679	0.00117	1	0.0035	0.0068	1.00679
218	heust.007/case_6	195.3	1.77E-02	2.74E-01	3.91E-04	1.00436	0.00113	1	0.0035	0.0044	1.00436

Results for Volume 2: HEU Systems, Rev. 0

N	Case	AFG	sigma	EALCF(ev)	sigma	k_calc HEU0	sigma	k_exp	sigma	Bias = Calculated - Benchmark	Adjusted k-eff HEU0*
219	heust.007/case_7	215.9	5.03E-03	4.93E-02	2.77E-05	1.00631	0.00123	1	0.0035	0.0063	1.00631
220	heust.007/case_8	195.4	1.88E-02	2.71E-01	3.99E-04	1.00375	0.00142	1	0.0035	0.0037	1.00375
221	heust.007/case_9	215.6	5.38E-03	5.09E-02	3.02E-05	1.00835	0.00098	1	0.0035	0.0084	1.00835
222	heust.008/case_1	217.2	4.24E-03	4.42E-02	2.19E-05	0.99836	0.00097	1	0.003	-0.0016	0.99836
223	heust.008/case_10	197.4	1.87E-02	2.33E-01	3.50E-04	0.9958	0.00128	1	0.003	-0.0042	0.9958
224	heust.008/case_11	217.7	4.20E-03	4.22E-02	2.13E-05	1.00152	0.00096	1	0.003	0.0015	1.00152
225	heust.008/case_12	199.1	1.80E-02	2.04E-01	2.96E-04	0.99676	0.00113	1	0.003	-0.0032	0.99676
226	heust.008/case_13	197.4	1.77E-02	2.32E-01	3.26E-04	0.99927	0.00136	1	0.003	-0.0007	0.99927
227	heust.008/case_14	198.7	1.97E-02	2.09E-01	3.26E-04	0.99577	0.00112	1	0.003	-0.0042	0.99577
228	heust.008/case_2	197.3	1.87E-02	2.36E-01	3.53E-04	0.99692	0.00102	1	0.003	-0.0031	0.99692
229	heust.008/case_3	217.5	4.00E-03	4.29E-02	1.99E-05	0.99756	0.00094	1	0.003	-0.0024	0.99756
230	heust.008/case_4	198.8	1.80E-02	2.09E-01	3.01E-04	0.9986	0.00134	1	0.003	-0.0014	0.9986
231	heust.008/case_5	217.2	4.32E-03	4.40E-02	2.21E-05	0.9986	0.00114	1	0.003	-0.0014	0.9986
232	heust.008/case_6	196.2	1.81E-02	2.56E-01	3.62E-04	0.99951	0.00129	1	0.003	-0.0005	0.99951
233	heust.008/case_7	217.4	4.15E-03	4.32E-02	2.17E-05	0.99933	0.00106	1	0.003	-0.0007	0.99933
234	heust.008/case_8	196.8	1.84E-02	2.44E-01	3.57E-04	0.99738	0.00133	1	0.003	-0.0026	0.99738
235	heust.008/case_9	217.3	4.14E-03	4.38E-02	2.23E-05	1.00086	0.00095	1	0.003	0.0009	1.00086
236	heust.009/hst009a	186.7	2.68E-02	5.28E-01	1.02E-03	1.00326	0.00124	1	0.0057	0.0033	1.00326
237	heust.009/hst009b	202.2	1.61E-02	1.60E-01	2.14E-04	1.00054	0.00124	1	0.0057	0.0005	1.00054
238	heust.009/hst009c	193.3	2.36E-02	3.23E-01	5.89E-04	1.00374	0.00121	1	0.0057	0.0037	1.00374
239	heust.009/hst009d	209.0	1.17E-02	9.11E-02	9.65E-05	0.99824	0.00149	1	0.0057	-0.0018	0.99824
240	heust.010/hst010e	215.4	5.76E-03	5.24E-02	3.22E-05	1.00306	0.00119	1	0.0018	0.0031	1.00306
241	heust.010/hst010g	215.2	6.43E-03	5.31E-02	3.59E-05	1.00121	0.00109	1	0.0018	0.0012	1.00121
242	heust.010/hst010h	214.8	6.27E-03	5.52E-02	3.59E-05	1.00325	0.00118	1	0.0018	0.0032	1.00325
243	heust.010/hst010i	214.6	6.68E-03	5.62E-02	3.84E-05	0.99967	0.00107	1	0.0018	-0.0003	0.99967
244	heust.011/hst011c	218.4	3.66E-03	3.96E-02	1.87E-05	1.00785	0.00102	1	0.002	0.0078	1.00785
245	heust.011/hst011d	218.5	3.45E-03	3.94E-02	1.70E-05	1.00248	0.00101	1	0.002	0.0025	1.00248

Results for Volume 2: HEU Systems, Rev. 0

N	Case	AFG	sigma	EALCF(ev)	sigma	k_calc HEU0	sigma	k_exp	sigma	Bias = Calculated - Benchmark	Adjusted k-eff HEU0*
246	heust.012/hst012b	220.6	1.78E-03	3.24E-02	9.24E-06	1.00232	0.00073	0.9999	0.0058	0.0024	1.00242
247	heust.013/hst013e	220.6	1.67E-03	3.23E-02	8.82E-06	1.00013	0.00081	1.0012	0.0026	-0.0011	0.99893
248	heust.013/hst013g	220.1	1.90E-03	3.38E-02	9.94E-06	0.9991	0.00104	1.0007	0.0036	-0.0016	0.9984
249	heust.013/hst013h	219.7	2.21E-03	3.52E-02	1.13E-05	0.99531	0.00082	1.0009	0.0036	-0.0056	0.99441
250	heust.013/hst013i	219.5	2.32E-03	3.59E-02	1.18E-05	0.99653	0.00086	1.0003	0.0036	-0.0038	0.99623
251	heust.014/case_1	216.8	4.71E-03	4.56E-02	2.43E-05	0.99682	0.00107	1	0.0028	-0.0032	0.99682
252	heust.014/case_2	216.5	4.20E-03	4.72E-02	2.33E-05	1.01494	0.00102	1	0.0052	0.0149	1.01494
253	heust.014/case_3	216.1	4.15E-03	4.92E-02	2.45E-05	1.02365	0.00093	1	0.0087	0.0236	1.02365
254	heust.015/case_1	214.2	6.22E-03	5.74E-02	3.65E-05	0.99875	0.00131	1	0.0032	-0.0012	0.99875
255	heust.015/case_2	214.6	6.25E-03	5.57E-02	3.64E-05	0.99072	0.00115	1	0.0034	-0.0093	0.99072
256	heust.015/case_3	213.3	5.84E-03	6.26E-02	3.72E-05	1.01173	0.00104	1	0.0068	0.0117	1.01173
257	heust.015/case_4	213.7	6.05E-03	6.05E-02	3.78E-05	1.01776	0.00103	1	0.0069	0.0178	1.01776
258	heust.015/case_5	213.0	5.50E-03	6.52E-02	3.75E-05	1.01442	0.00085	1	0.0089	0.0144	1.01442
259	heust.016/case_1	210.7	9.34E-03	7.84E-02	6.91E-05	0.99042	0.00127	1	0.0036	-0.0096	0.99042
260	heust.016/case_2	210.3	7.92E-03	8.23E-02	6.12E-05	1.0094	0.00111	1	0.0069	0.0094	1.0094
261	heust.016/case_3	209.1	7.83E-03	9.15E-02	6.38E-05	1.03006	0.00089	1	0.0079	0.0301	1.03006
262	heust.017/case_1	208.1	1.11E-02	9.79E-02	9.51E-05	0.99199	0.00126	1	0.0028	-0.0080	0.99199
263	heust.017/case_2	206.9	1.11E-02	1.08E-01	1.05E-04	0.9814	0.00159	1	0.004	-0.0186	0.9814
264	heust.017/case_3	207.6	1.21E-02	1.02E-01	1.07E-04	0.98022	0.00126	1	0.0036	-0.0198	0.98022
265	heust.017/case_4	207.3	1.03E-02	1.05E-01	9.77E-05	1.00028	0.0011	1	0.0047	0.0003	1.00028
266	heust.017/case_5	206.8	1.03E-02	1.11E-01	1.04E-04	1.00877	0.00107	1	0.0058	0.0088	1.00877
267	heust.017/case_6	205.0	1.03E-02	1.28E-01	1.17E-04	1.00619	0.00101	1	0.0055	0.0062	1.00619
268	heust.017/case_7	205.9	1.07E-02	1.19E-01	1.10E-04	1.00987	0.00102	1	0.0057	0.0099	1.00987
269	heust.017/case_8	204.4	1.08E-02	1.36E-01	1.28E-04	1.0059	0.00102	1	0.0067	0.0059	1.0059
270	heust.018/case_1	202.1	1.57E-02	1.61E-01	2.09E-04	0.99072	0.00123	1	0.0034	-0.0093	0.99072
271	heust.018/case_10	195.6	1.43E-02	2.77E-01	3.14E-04	1.02573	0.001	1	0.0057	0.0257	1.02573
272	heust.018/case_11	197.1	1.32E-02	2.48E-01	2.58E-04	1.02842	0.00113	1	0.0059	0.0284	1.02842

Results for Volume 2: HEU Systems, Rev. 0

N	Case	AFG	sigma	EALCF(ev)	sigma	k_calc HEU0	sigma	k_exp	sigma	Bias = Calculated - Benchmark	Adjusted k-eff HEU0*
273	heust.018/case_12	195.9	1.32E-02	2.74E-01	2.86E-04	1.02249	0.0008	1	0.0065	0.0225	1.02249
274	heust.018/case_2	200.1	1.66E-02	1.88E-01	2.57E-04	0.98288	0.00134	1	0.0046	-0.0171	0.98288
275	heust.018/case_3	201.3	1.50E-02	1.71E-01	2.15E-04	0.9902	0.00147	1	0.0042	-0.0098	0.9902
276	heust.018/case_4	200.9	1.42E-02	1.80E-01	2.08E-04	0.99888	0.00111	1	0.0044	-0.0011	0.99888
277	heust.018/case_5	198.0	1.44E-02	2.25E-01	2.60E-04	0.99636	0.00127	1	0.0046	-0.0036	0.99636
278	heust.018/case_6	199.2	1.52E-02	2.05E-01	2.53E-04	0.99399	0.00104	1	0.0045	-0.0060	0.99399
279	heust.018/case_7	199.6	1.35E-02	2.01E-01	2.22E-04	1.01211	0.001	1	0.0058	0.0121	1.01211
280	heust.018/case_8	197.0	1.53E-02	2.46E-01	3.03E-04	1.01196	0.00093	1	0.0056	0.0120	1.01196
281	heust.018/case_9	198.3	1.43E-02	2.22E-01	2.57E-04	1.01117	0.00096	1	0.0056	0.0112	1.01117
282	heust.019/case_1	193.6	2.15E-02	3.15E-01	5.34E-04	0.99939	0.0011	1	0.0041	-0.0006	0.99939
283	heust.019/case_2	194.6	1.99E-02	2.95E-01	4.56E-04	1.00263	0.00105	1	0.0041	0.0026	1.00263
284	heust.019/case_3	192.4	1.86E-02	3.51E-01	5.04E-04	0.99913	0.00105	1	0.0067	-0.0009	0.99913
285	heust.020/hst020g	172.5	2.85E-02	1.36E+00	2.62E-03	1.00619	0.00136	0.9966	0.0116	0.0096	1.00959
286	heust.020/hst020h	190.1	2.22E-02	3.97E-01	6.37E-04	1.00957	0.0014	0.9956	0.0093	0.0140	1.01397
287	heust.020/hst020i	204.4	1.39E-02	1.34E-01	1.58E-04	1.01668	0.0014	0.9957	0.0079	0.0210	1.02098
288	heust.020/hst020j	204.4	1.34E-02	1.34E-01	1.50E-04	1.01671	0.00142	0.9955	0.0078	0.0212	1.02121
289	heust.020/hst020k	214.3	6.86E-03	5.79E-02	4.15E-05	1.02228	0.00116	0.9959	0.0077	0.0264	1.02638
290	heust.021/hst021h	193.3	2.10E-02	3.22E-01	5.25E-04	1.00349	0.00121	0.9975	0.0054	0.0060	1.00599
291	heust.021/hst021i	198.4	2.00E-02	2.16E-01	3.38E-04	1.0105	0.00122	0.9975	0.0054	0.0130	1.013
292	heust.021/hst021j	192.9	1.97E-02	3.32E-01	5.05E-04	0.99427	0.00131	0.9978	0.0054	-0.0035	0.99647
293	heust.021/hst021k	194.8	1.77E-02	2.86E-01	4.08E-04	1.01397	0.00143	0.9978	0.0054	0.0162	1.01617
294	heust.021/hst021l	193.0	1.99E-02	3.29E-01	5.16E-04	0.99489	0.00113	0.9978	0.0054	-0.0029	0.99709
295	heust.021/hst021m	195.5	2.04E-02	2.69E-01	4.29E-04	0.99912	0.00122	0.9978	0.0054	0.0013	1.00132
296	heust.025/case_1	218.2	3.38E-03	4.01E-02	1.77E-05	1.00148	0.00096	1.0002	0.0025	0.0013	1.00128
297	heust.025/case_10	212.0	9.62E-03	7.01E-02	6.28E-05	1.0135	0.00097	1.0003	0.0043	0.0132	1.0132
298	heust.025/case_11	211.9	1.07E-02	7.11E-02	6.90E-05	1.01263	0.00083	1.0002	0.0045	0.0124	1.01243
299	heust.025/case_12	209.4	1.28E-02	8.76E-02	1.01E-04	1.01107	0.00081	1.0002	0.0045	0.0109	1.01087

Results for Volume 2: HEU Systems, Rev. 0

N	Case	AFG	sigma	EALCF(ev)	sigma	k_calc HEU0	sigma	k_exp	sigma	Bias = Calculated - Benchmark	Adjusted k-eff HEU0*
300	heust.025/case_13	209.2	1.40E-02	8.88E-02	1.13E-04	1.0189	0.00087	1.0009	0.0047	0.0180	1.018
301	heust.025/case_14	205.7	1.92E-02	1.18E-01	1.91E-04	1.01054	0.0008	1.0008	0.0053	0.0097	1.00974
302	heust.025/case_15	206.2	2.05E-02	1.13E-01	1.95E-04	1.0053	0.00093	1.0002	0.0058	0.0051	1.0051
303	heust.025/case_16	199.9	2.55E-02	1.84E-01	3.77E-04	1.01688	0.00084	1	0.0049	0.0169	1.01688
304	heust.025/case_17	200.7	2.99E-02	1.71E-01	4.19E-04	1.00844	0.00098	1	0.0055	0.0084	1.00844
305	heust.025/case_18	201.5	2.90E-02	1.60E-01	3.71E-04	1.00468	0.0009	1	0.0061	0.0047	1.00468
306	heust.025/case_2	218.2	3.42E-03	4.02E-02	1.71E-05	1.0028	0.00108	1.0007	0.0025	0.0021	1.0021
307	heust.025/case_3	217.7	3.45E-03	4.22E-02	1.78E-05	0.99786	0.00116	1.0002	0.0064	-0.0023	0.99766
308	heust.025/case_4	218.0	3.48E-03	4.10E-02	1.77E-05	1.00214	0.00123	1.0003	0.0027	0.0018	1.00184
309	heust.025/case_5	216.2	5.09E-03	4.84E-02	2.78E-05	1.00558	0.00122	1.0013	0.003	0.0043	1.00428
310	heust.025/case_6	217.6	3.35E-03	4.25E-02	1.75E-05	1.01187	0.0008	1.0002	0.0067	0.0117	1.01167
311	heust.025/case_7	216.6	4.89E-03	4.67E-02	2.54E-05	1.01496	0.00075	1.0009	0.0073	0.0141	1.01406
312	heust.025/case_8	216.3	4.89E-03	4.82E-02	2.61E-05	1.01381	0.00099	1	0.0067	0.0138	1.01381
313	heust.025/case_9	214.8	6.54E-03	5.49E-02	3.70E-05	1.00901	0.0009	1.0002	0.0065	0.0088	1.00881
314	heust.027/case_1	211.3	2.96E-03	7.40E-02	1.99E-05	0.99904	0.00038	1	0.0046	-0.0010	0.99904
315	heust.027/case_2	211.2	2.82E-03	7.48E-02	2.05E-05	0.9998	0.00045	1	0.0043	-0.0002	0.9998
316	heust.027/case_3	211.1	2.63E-03	7.50E-02	1.87E-05	0.99996	0.00039	1	0.0037	0.0000	0.99996
317	heust.027/case_4	211.1	2.77E-03	7.53E-02	2.00E-05	1.00134	0.00042	1	0.0037	0.0013	1.00134
318	heust.027/case_5	211.0	2.93E-03	7.56E-02	2.15E-05	0.99915	0.00038	1	0.0044	-0.0009	0.99915
319	heust.027/case_6	211.2	2.73E-03	7.46E-02	1.88E-05	0.99406	0.00037	1	0.0043	-0.0059	0.99406
320	heust.027/case_7	211.2	8.21E-03	7.47E-02	5.91E-05	1.00159	0.00129	1	0.0038	0.0016	1.00159
321	heust.027/case_8	211.2	8.33E-03	7.47E-02	5.91E-05	1.00216	0.00129	1	0.0035	0.0022	1.00216
322	heust.027/case_9	211.2	2.79E-03	7.48E-02	2.06E-05	1.00001	0.00037	1	0.0039	0.0000	1.00001
323	heust.028/hst028a	216.6	4.72E-03	4.68E-02	2.61E-05	0.99816	0.00115	1	0.0023	-0.0018	0.99816
324	heust.028/hst028b	216.4	5.29E-03	4.73E-02	2.69E-05	0.999	0.00113	1	0.0034	-0.0010	0.999
325	heust.028/hst028c	216.5	4.88E-03	4.69E-02	2.63E-05	0.99857	0.00125	1	0.0026	-0.0014	0.99857
326	heust.028/hst028d	216.4	5.09E-03	4.73E-02	2.64E-05	1.00006	0.00116	1	0.0028	0.0001	1.00006

Results for Volume 2: HEU Systems, Rev. 0

N	Case	AFG	sigma	EALCF(ev)	sigma	k_calc HEU0	sigma	k_exp	sigma	Bias = Calculated - Benchmark	Adjusted k-eff HEU0*
327	heust.028/hst028e	216.5	4.78E-03	4.70E-02	2.57E-05	0.99521	0.00109	1	0.0031	-0.0048	0.99521
328	heust.028/hst028g	216.4	5.00E-03	4.74E-02	2.64E-05	0.99818	0.00117	1	0.0023	-0.0018	0.99818
329	heust.028/hst028h	216.5	4.47E-03	4.72E-02	2.47E-05	0.99884	0.00111	1	0.0038	-0.0012	0.99884
330	heust.028/hst028i	216.4	4.79E-03	4.74E-02	2.69E-05	0.99968	0.00107	1	0.0027	-0.0003	0.99968
331	heust.028/hst028j	203.4	1.39E-02	1.45E-01	1.71E-04	0.99678	0.0012	1	0.0049	-0.0032	0.99678
332	heust.028/hst028k	203.2	1.54E-02	1.47E-01	1.88E-04	0.99533	0.00116	1	0.0053	-0.0047	0.99533
333	heust.028/hst028l	203.3	1.41E-02	1.46E-01	1.78E-04	0.9986	0.00129	1	0.0051	-0.0014	0.9986
334	heust.028/hst028m	203.0	1.46E-02	1.49E-01	1.91E-04	0.99563	0.00119	1	0.0046	-0.0044	0.99563
335	heust.028/hst028n	203.0	1.50E-02	1.49E-01	1.83E-04	0.99822	0.00125	1	0.0058	-0.0018	0.99822
336	heust.028/hst028p	202.8	1.46E-02	1.52E-01	1.87E-04	0.9955	0.00113	1	0.0046	-0.0045	0.9955
337	heust.028/hst028q	202.9	1.37E-02	1.51E-01	1.70E-04	1.00355	0.00129	1	0.0064	0.0035	1.00355
338	heust.028/hst028r	202.7	1.54E-02	1.53E-01	1.95E-04	0.99966	0.00112	1	0.0052	-0.0003	0.99966
339	heust.028/hst028s	202.7	1.44E-02	1.53E-01	1.83E-04	0.99623	0.00122	1	0.0066	-0.0038	0.99623
340	heust.028/hst028u	202.6	1.50E-02	1.55E-01	1.96E-04	0.99754	0.00142	1	0.006	-0.0025	0.99754
341	heust.029/hst029a	202.3	1.51E-02	1.58E-01	1.96E-04	0.99819	0.00142	1	0.0066	-0.0018	0.99819
342	heust.029/hst029b	202.3	1.53E-02	1.57E-01	1.97E-04	1.0052	0.00119	1	0.0058	0.0052	1.0052
343	heust.029/hst029c	202.1	1.56E-02	1.60E-01	2.04E-04	0.99533	0.00114	1	0.0068	-0.0047	0.99533
344	heust.029/hst029d	201.5	1.71E-02	1.67E-01	2.33E-04	0.99207	0.00115	1	0.0074	-0.0079	0.99207
345	heust.029/hst029e	201.3	1.56E-02	1.70E-01	2.18E-04	0.99916	0.00133	1	0.0067	-0.0008	0.99916
346	heust.029/hst029g	201.3	1.67E-02	1.70E-01	2.33E-04	0.9992	0.00124	1	0.0065	-0.0008	0.9992
347	heust.029/hst029h	201.4	1.51E-02	1.68E-01	2.09E-04	1.00176	0.00133	1	0.0063	0.0018	1.00176
348	heust.030/hst030a	216.4	5.05E-03	4.74E-02	2.68E-05	0.999	0.00108	1	0.0039	-0.0010	0.999
349	heust.030/hst030b	216.2	5.10E-03	4.81E-02	2.71E-05	1.00047	0.00117	1	0.0032	0.0005	1.00047
350	heust.030/hst030c	216.1	5.10E-03	4.84E-02	2.73E-05	0.99873	0.00115	1	0.0031	-0.0013	0.99873
351	heust.030/hst030d	202.2	1.56E-02	1.59E-01	2.10E-04	1.00129	0.00116	1	0.0064	0.0013	1.00129
352	heust.030/hst030e	202.1	1.54E-02	1.60E-01	1.99E-04	0.99798	0.00112	1	0.0058	-0.0020	0.99798
353	heust.030/hst030g	202.0	1.51E-02	1.61E-01	1.99E-04	0.99864	0.00113	1	0.0059	-0.0014	0.99864

Results for Volume 2: HEU Systems, Rev. 0

N	Case	AFG	sigma	EALCF(ev)	sigma	k_calc HEU0	sigma	k_exp	sigma	Bias = Calculated - Benchmark	Adjusted k-eff HEU0*
354	heust.030/hst030h	201.6	1.47E-02	1.66E-01	2.06E-04	0.99885	0.00118	1	0.0064	-0.0011	0.99885
355	heust.031/hst031a	201.7	1.60E-02	1.64E-01	2.13E-04	0.99762	0.00116	1	0.0046	-0.0024	0.99762
356	heust.031/hst031b	200.7	1.70E-02	1.75E-01	2.41E-04	0.99886	0.00114	1	0.0058	-0.0011	0.99886
357	heust.031/hst031c	201.2	1.64E-02	1.70E-01	2.33E-04	0.99885	0.00121	1	0.0058	-0.0011	0.99885
358	heust.031/hst031d	199.7	1.78E-02	1.90E-01	2.73E-04	0.99486	0.0011	1	0.0068	-0.0051	0.99486
359	heust.032/hst032b	221.1	1.31E-03	3.07E-02	6.94E-06	1.00101	0.00066	1.0015	0.0026	-0.0005	0.99951
360	heust.033-simple/case_02a	193.6	1.95E-02	3.10E-01	4.77E-04	1.00023	0.00118	0.9979	0.0112	0.0023	1.00233
361	heust.033-simple/case_02b	193.3	1.96E-02	3.18E-01	4.90E-04	1	0.00128	1	0.0109	0.0000	1
362	heust.033-simple/case_02c	193.1	1.91E-02	3.23E-01	4.76E-04	0.99873	0.00099	0.9979	0.0067	0.0008	1.00083
363	heust.033-simple/case_03a	194.3	1.81E-02	2.94E-01	4.16E-04	0.99942	0.00111	0.9942	0.0115	0.0052	1.00522
364	heust.033-simple/case_03b	194.4	1.80E-02	2.93E-01	4.22E-04	1.00393	0.00111	0.9979	0.0112	0.0060	1.00603
365	heust.033-simple/case_03c	195.2	1.86E-02	2.74E-01	4.00E-04	1.01165	0.00097	0.9979	0.0072	0.0137	1.01375
366	heust.033-simple/case_04a	193.5	1.89E-02	3.12E-01	4.71E-04	1.00245	0.00107	0.9942	0.0115	0.0083	1.00825
367	heust.033-simple/case_04b	193.2	1.91E-02	3.19E-01	4.79E-04	1.00806	0.00112	0.9979	0.0112	0.0102	1.01016
368	heust.033-simple/case_05a	193.6	1.93E-02	3.10E-01	4.74E-04	1.00832	0.00112	0.9942	0.0112	0.0141	1.01412
369	heust.033-simple/case_05b	193.3	1.87E-02	3.18E-01	4.66E-04	1.00748	0.00125	1	0.0109	0.0075	1.00748
370	heust.033-simple/case_06a	193.6	1.85E-02	3.10E-01	4.59E-04	1.00413	0.00114	0.9942	0.0112	0.0099	1.00993
371	heust.033-simple/case_06b	193.3	1.97E-02	3.17E-01	4.94E-04	1.00926	0.00121	1	0.0109	0.0093	1.00926
372	heust.033-simple/case_07a	193.7	1.94E-02	3.09E-01	4.68E-04	1.00075	0.00119	0.9942	0.0112	0.0066	1.00655
373	heust.033-simple/case_07b	193.4	1.81E-02	3.15E-01	4.38E-04	1.00375	0.00116	1	0.0109	0.0037	1.00375
374	heust.033-simple/case_08a	193.5	1.95E-02	3.13E-01	4.73E-04	1.00001	0.00114	0.9942	0.0112	0.0058	1.00581
375	heust.033-simple/case_08b	193.2	1.85E-02	3.19E-01	4.72E-04	1.00652	0.00109	1	0.0109	0.0065	1.00652
376	heust.033-simple/case_09a	193.7	1.96E-02	3.09E-01	4.78E-04	0.99698	0.00122	0.9942	0.0112	0.0028	1.00278
377	heust.033-simple/case_09b	193.4	1.85E-02	3.15E-01	4.58E-04	0.99746	0.00107	1	0.0109	-0.0025	0.99746
378	heust.033-simple/case_09c	193.8	1.93E-02	3.06E-01	4.55E-04	0.99457	0.00111	0.9979	0.0105	-0.0033	0.99667
379	heust.033-simple/case_10a	194.3	1.87E-02	2.95E-01	4.36E-04	1.00075	0.00118	0.9942	0.0115	0.0066	1.00655
380	heust.033-simple/case_10c	195.1	1.91E-02	2.77E-01	4.05E-04	1.00272	0.00105	0.9979	0.0072	0.0048	1.00482

Results for Volume 2: HEU Systems, Rev. 0

N	Case	AFG	sigma	EALCF(ev)	sigma	k_calc HEU0	sigma	k_exp	sigma	Bias = Calculated - Benchmark	Adjusted k-eff HEU0*
381	heust.033-simple/case_10d	194.1	2.07E-02	3.00E-01	4.84E-04	0.99377	0.00117	0.9979	0.0106	-0.0041	0.99587
382	heust.033-simple/case_11a	194.5	1.86E-02	2.90E-01	4.26E-04	0.99748	0.00106	0.9942	0.0112	0.0033	1.00328
383	heust.033-simple/case_11b	194.7	1.84E-02	2.87E-01	4.13E-04	0.99987	0.00124	0.9979	0.0109	0.0020	1.00197
384	heust.033-simple/case_12a	193.9	1.80E-02	3.05E-01	4.30E-04	0.99929	0.0011	0.9942	0.0112	0.0051	1.00509
385	heust.033-simple/case_12b	193.8	1.89E-02	3.08E-01	4.61E-04	1.00059	0.00121	1	0.0109	0.0006	1.00059
386	heust.035/hst035a	219.1	2.86E-03	3.70E-02	1.49E-05	1.0043	0.00087	1	0.0031	0.0043	1.0043
387	heust.035/hst035b	219.0	2.99E-03	3.72E-02	1.44E-05	1.00552	0.00092	1	0.0032	0.0055	1.00552
388	heust.035/hst035c	219.0	2.97E-03	3.72E-02	1.44E-05	1.00655	0.00086	1	0.003	0.0066	1.00655
389	heust.035/hst035d	219.1	2.87E-03	3.70E-02	1.39E-05	1.00663	0.00088	1	0.003	0.0066	1.00663
390	heust.035/hst035e	216.0	5.33E-03	4.89E-02	2.96E-05	1.00477	0.00103	1	0.0033	0.0048	1.00477
391	heust.035/hst035g	215.9	5.31E-03	4.95E-02	3.01E-05	1.0071	0.00106	1	0.0029	0.0071	1.0071
392	heust.035/hst035h	210.4	8.86E-03	8.02E-02	6.61E-05	1.00413	0.00109	1	0.0035	0.0041	1.00413
393	heust.035/hst035i	209.9	9.56E-03	8.35E-02	7.51E-05	1.00207	0.00132	1	0.0038	0.0021	1.00207
394	heust.035/hst035j	210.0	9.83E-03	8.25E-02	7.33E-05	1.00344	0.00118	1	0.0041	0.0034	1.00344
395	heust.036/hst036a	214.6	6.02E-03	5.56E-02	3.66E-05	0.99619	0.00112	0.9974	0.0045	-0.0012	0.99879
396	heust.036/hst036b	214.1	6.36E-03	5.78E-02	3.74E-05	1.00008	0.00124	0.9979	0.0039	0.0022	1.00218
397	heust.036/hst036c	213.5	7.22E-03	6.05E-02	4.32E-05	0.99706	0.00126	0.9993	0.0044	-0.0022	0.99776
398	heust.036/hst036d	213.0	7.46E-03	6.28E-02	4.57E-05	0.99964	0.00109	1	0.0062	-0.0004	0.99964
399	heust.037/hst037a	218.8	3.02E-03	3.79E-02	1.47E-05	1.01151	0.00105	0.998	0.0034	0.0135	1.01351
400	heust.037/hst037b	218.5	3.87E-03	3.89E-02	1.67E-05	1.00335	0.00096	0.999	0.0035	0.0043	1.00435
401	heust.037/hst037c	217.3	4.04E-03	4.38E-02	2.22E-05	1.00809	0.00105	0.997	0.0042	0.0111	1.01109
402	heust.037/hst037d	216.9	4.92E-03	4.50E-02	2.42E-05	1.00894	0.00104	0.998	0.0035	0.0109	1.01094
403	heust.037/hst037e	216.8	5.50E-03	4.55E-02	2.63E-05	1.00635	0.00104	0.998	0.0042	0.0084	1.00835
404	heust.037/hst037g	215.6	5.51E-03	5.08E-02	3.04E-05	1.01374	0.00129	0.996	0.0051	0.0177	1.01774
405	heust.037/hst037h	215.2	6.29E-03	5.24E-02	3.37E-05	1.01342	0.00115	0.998	0.0034	0.0154	1.01542
406	heust.037/hst037i	215.1	6.85E-03	5.31E-02	3.61E-05	1.00632	0.00126	0.998	0.004	0.0083	1.00832
407	heust.037/hst037j	214.8	7.97E-03	5.40E-02	3.84E-05	1.00572	0.00127	0.998	0.0047	0.0077	1.00772

Results for Volume 2: HEU Systems, Rev. 0

N	Case	AFG	sigma	EALCF(ev)	sigma	k_calc HEU0	sigma	k_exp	sigma	Bias = Calculated - Benchmark	Adjusted k-eff HEU0*
	Maximum	221.1	8.64E-02	9.57E+05	1.64E+03	1.03006	0.00159	1.006	0.0126	0.03006	1.03006
	Average	168.5	2.25E-02	8.66E+04	1.47E+02	1.001147	0.00109	0.9994	0.0044	0.00173	1.00173
	Minimum	24.3	1.31E-03	3.07E-02	6.94E-06	0.96808	0.00037	0.9826	0	-0.02034	0.97966

Results for Volume 2: HEU Systems, Rev. 1

N	Category	Case	nubar	Sigma	AFG	Sigma	EALCF (ev)	Sigma	k_calc HEU1	sigma	Benchmark k-eff	Sigma	Bias = Calculated - Benchmark	Adjusted k-eff HEU1*	Notes
1		hci003-01	2.53	2.11E-04	63.5	5.24E-02	7.99E+03	4.11E+01	1.00878	0.00096	1	0.0057	0.00878	1.00878	
2		hci003-02	2.51	2.22E-04	69.2	5.72E-02	4.27E+03	2.31E+01	1.01087	0.00105	1	0.0061	0.01087	1.01087	
3		hci003-03	2.51	2.04E-04	69.3	5.38E-02	4.27E+03	2.18E+01	1.01367	0.00103	1	0.0056	0.01367	1.01367	
4		hci003-04	2.51	1.91E-04	67.1	5.17E-02	5.41E+03	2.72E+01	1.00261	0.00108	1	0.0055	0.00261	1.00261	
5		hci003-05	2.50	1.05E-04	70.3	4.00E-02	3.74E+03	1.27E+01	1.00415	0.00111	1	0.0047	0.00415	1.00415	
6		hci003-06	2.51	1.44E-04	66.1	4.75E-02	5.97E+03	2.55E+01	1.0004	0.00103	1	0.0047	0.0004	1.0004	
7		hci003-07	2.51	1.34E-04	66.2	4.17E-02	5.87E+03	2.20E+01	0.99801	0.00096	1	0.005	-0.00199	0.99801	
8		hci004	2.44	7.38E-06	97.8	1.81E-02	1.39E+02	1.46E-01	1.02231	0.00021	1	0.004	0.02231	1.02231	k-inf
9		hci005-07	2.45	3.21E-05	63.8	1.74E-02	5.09E+03	1.09E+01	0.9712	0.00049	1.032	0.004	-0.0608	0.9392	k-inf
10		hci005-09	2.45	2.79E-05	66.5	1.55E-02	3.21E+03	5.93E+00	1.01827	0.0004	1.05	0.008	-0.03173	0.96827	k-inf
11		hci005-15	2.45	2.81E-05	60.7	1.36E-02	6.50E+03	1.24E+01	**0.92044**	0.00043	1.064	0.018	-0.14356	**0.85644**	k-inf
12		hci005-16	2.45	2.94E-05	64.1	1.64E-02	4.18E+03	7.97E+00	0.95005	0.00042	0.997	0.013	-0.04695	0.95305	k-inf
13		hcm001-1	2.45	4.06E-05	192.8	4.51E-02	3.80E-01	1.25E-03	1.00526	0.00099	1	0.0059	0.00526	1.00526	

Results for Volume 2: HEU Systems, Rev. 1

N	Category	Case	nubar	Sigma	AFG	Sigma	EALCF (ev)	Sigma	k_calc HEU1	sigma	Benchmark k-eff	Sigma	Bias = Calculated - Benchmark	Adjusted k-eff HEU1*	Notes
14		hcm001-5	2.52	1.49E-04	94.0	8.86E-02	1.57E+03	1.16E+01	0.99922	0.00097	0.9985	0.0056	0.00072	1.00072	
15		hct017-01	2.44	2.20E-06	219.8	1.12E-02	3.82E-02	5.08E-05	1.01264	0.00117	1	0.0069	0.01264	1.01264	
16		hct017-02	2.44	2.56E-06	216.2	1.68E-02	5.23E-02	8.22E-05	1.00185	0.00098	1	0.0069	0.00185	1.00185	
17		hct017-03	2.44	2.47E-06	218.9	1.27E-02	4.11E-02	5.38E-05	1.00868	0.00106	1	0.0069	0.00868	1.00868	
18		hct017-04	2.44	2.16E-06	220.3	1.04E-02	3.65E-02	4.80E-05	1.01006	0.00108	1	0.0069	0.01006	1.01006	
19		hct017-05	2.44	2.20E-06	220.7	8.58E-03	3.52E-02	4.27E-05	1.01265	0.00111	1	0.0069	0.01265	1.01265	
20		hct017-06	2.44	2.17E-06	219.6	1.20E-02	3.89E-02	5.32E-05	1.01208	0.00098	1	0.0069	0.01208	1.01208	
21		hct017-07	2.44	2.40E-06	217.7	1.49E-02	4.57E-02	6.81E-05	1.00656	0.00106	1	0.0069	0.00656	1.00656	
22		hct017-08	2.44	2.24E-06	220.8	9.14E-03	3.46E-02	4.17E-05	1.01685	0.00112	1	0.0069	0.01685	1.01685	
23		hct017-09	2.44	2.40E-06	219.6	1.21E-02	3.86E-02	5.25E-05	1.0088	0.00106	1	0.0069	0.0088	1.0088	
24		hmf015-1	2.61	2.00E-04	24.2	1.21E-02	9.62E+05	1.11E+03	0.99102	0.00089	0.9996	0.0017	-0.00858	0.99142	
25		hmf016-1	2.58	1.96E-04	28.5	2.22E-02	5.89E+05	1.32E+03	0.99981	0.00094	0.9996	0.0018	0.00021	1.00021	
26		hmf016-2	2.58	2.04E-04	27.6	1.85E-02	6.54E+05	1.28E+03	1.00063	0.00086	0.9996	0.0018	0.00103	1.00103	
27		hmf017	2.57	1.80E-04	29.1	1.60E-02	5.50E+05	9.93E+02	0.99593	0.0012	0.9993	0.0014	-0.00337	0.99663	
28		hmf033-1	2.53	1.45E-04	61.9	5.68E-02	1.54E+04	7.85E+01	0.98935	0.00127	0.9991	0.0014	-0.00975	0.99025	
29		hmf033-2	2.51	1.50E-04	92.2	7.81E-02	1.20E+03	7.64E+00	0.99726	0.00102	0.9991	0.0014	-0.00184	0.99816	
30		hmf036-1	2.53	1.68E-04	78.5	7.90E-02	4.41E+03	2.97E+01	0.99108	0.00108	0.9993	0.0015	-0.00822	0.99178	
31		hmf036-2	2.56	1.86E-04	59.0	6.47E-02	2.91E+04	1.65E+02	0.99613	0.00098	0.9993	0.0013	-0.00317	0.99683	
32		hmf037-1	2.53	1.62E-04	88.7	7.92E-02	2.37E+03	1.57E+01	1.00133	0.0009	0.9997	0.0011	0.00163	1.00163	
33		hmf037-2	2.55	1.70E-04	63.9	6.62E-02	1.72E+04	9.78E+01	0.99724	0.00099	0.9997	0.0011	-0.00246	0.99754	
34		hmf038	2.56	3.58E-04	34.7	3.42E-02	2.48E+05	9.55E+02	1.00496	0.00095	0.9999	0.0015	0.00506	1.00506	
35		hmf041-1	2.58	1.84E-04	28.4	1.64E-02	5.91E+05	1.09E+03	1.00383	0.0011	1.0013	0.003	0.00253	1.00253	
36		hmf041-2	2.56	1.63E-04	41.6	5.18E-02	1.52E+05	7.23E+02	1.00269	0.00098	1.0022	0.0043	0.00049	1.00049	
37		hmf041-3	2.59	1.95E-04	25.6	1.39E-02	8.33E+05	1.12E+03	0.99812	0.0011	1.0006	0.0029	-0.00248	0.99752	
38		hmf041-4	2.59	2.02E-04	26.9	1.52E-02	7.13E+05	1.16E+03	1.00172	0.00098	1.0006	0.0025	0.00112	1.00112	
39		hmf041-5	2.58	1.82E-04	28.7	2.02E-02	5.70E+05	1.23E+03	0.9967	0.00088	1.0006	0.0031	-0.0039	0.9961	
40		hmf041-6	2.58	1.81E-04	31.3	3.02E-02	4.35E+05	1.30E+03	0.99885	0.0009	1.0006	0.0045	-0.00175	0.99825	
41		hmf055-1	2.55	1.59E-04	32.0	1.22E-02	4.22E+05	5.41E+02	1.00812	0.00078	0.9955	0.0028	0.01262	1.01262	

Results for Volume 2: HEU Systems, Rev. 1

N	Category	Case	nubar	Sigma	AFG	Sigma	EALCF (ev)	Sigma	k_calc HEU1	sigma	Benchmark k-eff	Sigma	Bias = Calculated - Benchmark	Adjusted k-eff HEU1*	Notes
42		hmf055-2	2.55	2.45E-04	31.9	1.97E-02	4.25E+05	8.15E+02	1.00983	0.00078	0.9955	0.0028	0.01433	1.01433	assumed same k_bench
43		hmf055-3	2.55	2.42E-04	31.9	1.81E-02	4.23E+05	7.60E+02	1.00433	0.00077	0.9955	0.0028	0.00883	1.00883	assumed same k_bench
44		hmf055-4	2.55	2.73E-04	31.9	2.01E-02	4.25E+05	8.55E+02	0.99685	0.00075	0.9955	0.0028	0.00135	1.00135	assumed same k_bench
45		hmi001	2.46	8.08E-05	51.6	1.60E-02	2.93E+04	6.55E+01	**1.08365**	0.00085	0.9966	0.0026	0.08705	**1.08705**	Iron xs problem
46		hmi006-001	2.47	8.01E-05	64.4	3.19E-02	5.02E+03	1.60E+01	1.00282	0.00112	0.9948	0.0003	0.00802	1.00802	
47		hmi006-002	2.48	9.12E-05	57.5	2.45E-02	1.04E+04	2.91E+01	1.0033	0.00088	0.9981	0.0003	0.0052	1.0052	
48		hmi006-003	2.48	9.20E-05	51.0	1.99E-02	2.43E+04	6.53E+01	1.00681	0.00086	1.0016	0.0003	0.00521	1.00521	
49		hmt001	2.44	2.00E-05	213.4	2.71E-02	7.39E-02	1.66E-04	1.00592	0.00096	1.001	0.006	0.00492	1.00492	
50		hst021-10	2.44	9.01E-06	195.0	2.04E-02	2.82E-01	4.45E-04	1.00828	0.00111	0.9975	0.0054	0.01078	1.01078	
51		hst021-2	2.44	9.12E-06	194.7	1.98E-02	2.89E-01	4.54E-04	1.00604	0.00136	0.9975	0.0054	0.00854	1.00854	
52		hst021-25	2.44	8.80E-06	195.8	2.11E-02	2.65E-01	4.41E-04	1.00624	0.00118	0.9978	0.0054	0.00844	1.00844	
53		hst021-3	2.44	8.79E-06	195.3	2.01E-02	2.76E-01	4.46E-04	1.01108	0.00125	0.9975	0.0054	0.01358	1.01358	
		Maximum	2.61	3.58E-04	2.21E+02	8.86E-02	9.62E+05	1.32E+03	1.08365	0.00136	1.064	0.018	0.08705	1.08705	
		Average	2.50	1.15E-04	9.74E+01	3.01E-02	1.54E+05	3.03E+02	1.00228	0.000952642	1.002	0.004462264	0.000279623	1.000279623	
		Minimum	2.44	2.16E-06	1.23E+01	2.89E-03	3.46E-02	4.17E-05	0.92044	0.00021	0.9948	0.0003	-0.14356	0.85644	

Table 4.3 Results for Intermediate and Mixed Enrichment Uranium Systems (Volume 3) with CSAS25 from SCALE 4.4a and the 238-group Library on the J-5600 (CMODB) Workstation

Results for Volume 3: IEU Systems

N	Category	Case	nubar	Sigma	AFG	Sigma	EALCF (ev)	sigma	k_calc IEU	sigma	Benchmark k-eff	Sigma	Bias = Calculated - Benchmark	Adjusted k-eff IEU*	Notes
1		ici001-001	2.47	6.73E-05	39.738	7.50E-03	1.85E+05	1.77E+02	1.00476	0.00035	0.969	0.005	0.0358	1.03576	k-inf
2		ici001-002	2.47	6.76E-05	52.075	2.07E-02	2.66E+04	6.26E+01	1.02029	0.00046	0.980	0.003	0.0403	1.04029	k-inf
3		ici001-003	2.45	5.05E-05	124.130	5.00E-02	5.59E+01	1.96E-01	1.06991	0.00056	1.014	0.006	0.0559	**1.05591**	k-inf
4		ici001-004	2.44	3.29E-05	185.505	3.84E-02	6.83E-01	1.87E-03	0.97726	0.00071	0.964	0.012	0.0133	1.01326	k-inf
5		ict001-01	2.46	4.77E-05	151.897	5.91E-02	7.38E+00	3.01E-02	0.99766	0.00115	1	0.004	-0.0023	0.99766	
6		ict001-02	2.45	3.94E-05	169.336	5.22E-02	2.03E+00	7.32E-03	1.00086	0.00113	1	0.004	0.0009	1.00086	
7		ict001-03	2.45	3.01E-05	185.745	4.30E-02	6.11E-01	1.81E-03	0.99570	0.00111	1	0.004	-0.0043	0.99570	
8		ict001-04	2.44	2.61E-05	197.906	3.32E-02	2.50E-01	5.75E-04	1.00100	0.00118	1	0.004	0.0010	1.00100	
9		ict001-05	2.44	1.88E-05	209.500	2.36E-02	1.03E-01	1.91E-04	1.01458	0.00104	1	0.004	0.0146	1.01458	
10		ict001-06	2.45	3.05E-05	185.682	4.05E-02	6.18E-01	1.77E-03	1.00318	0.00117	1	0.004	0.0032	1.00318	
11		ict001-07	2.45	3.19E-05	185.722	4.14E-02	6.21E-01	1.75E-03	1.00248	0.00109	1	0.004	0.0025	1.00248	
12		ict001-08	2.45	3.46E-05	185.290	4.16E-02	6.48E-01	1.88E-03	0.99951	0.00111	1	0.004	-0.0005	0.99951	
13		ict001-09	2.46	4.21E-05	172.650	5.06E-02	1.67E+00	5.78E-03	1.00676	0.00113	1	0.004	0.0068	1.00676	
14		ict001-10	2.45	3.83E-05	169.467	5.09E-02	2.02E+00	7.02E-03	0.99801	0.00114	1	0.004	-0.0020	0.99801	
15		ict001-11	2.45	3.93E-05	169.606	5.26E-02	1.99E+00	7.03E-03	0.99816	0.00108	1	0.004	-0.0018	0.99816	
16		ict001-12	2.45	3.98E-05	170.004	4.92E-02	1.94E+00	6.55E-03	0.99760	0.00115	1	0.004	-0.0024	0.99760	
17		ict001-13	2.44	2.53E-05	197.984	3.37E-02	2.48E-01	5.96E-04	1.00359	0.00104	1	0.004	0.0036	1.00359	
18		ict001-14	2.44	2.38E-05	197.957	3.19E-02	2.49E-01	5.70E-04	1.00125	0.00109	1	0.004	0.0012	1.00125	
19		ict001-15	2.44	2.42E-05	198.123	3.21E-02	2.46E-01	5.69E-04	1.00192	0.00118	1	0.004	0.0019	1.00192	

Results for Volume 3: IEU Systems

N	Category	Case	nubar	Sigma	AFG	Sigma	EALCF (ev)	sigma	k_calc IEU	sigma	Benchmark k-eff	Sigma	Bias = Calculated - Benchmark	Adjusted k-eff IEU*	Notes
20		ict001-16	2.44	2.09E-05	205.446	2.53E-02	1.41E-01	2.73E-04	1.00609	0.00115	1	0.004	0.0061	1.00609	
21		ict001-17	2.46	4.92E-05	150.212	5.69E-02	8.15E+00	3.14E-02	0.99447	0.00113	1	0.004	-0.0055	**0.99447**	
22		ict001-18	2.45	3.66E-05	173.839	4.40E-02	1.47E+00	4.40E-03	0.99970	0.00121	1	0.004	-0.0003	0.99970	
23		ict001-19	2.44	2.27E-05	203.398	2.79E-02	1.65E-01	3.51E-04	1.00515	0.00111	1	0.004	0.0051	1.00515	
24		ict001-20	2.45	4.12E-05	168.133	5.22E-02	2.19E+00	7.83E-03	1.00337	0.00130	1	0.004	0.0034	1.00337	
25		ict001-21	2.46	5.16E-05	150.237	6.26E-02	8.08E+00	3.45E-02	0.99932	0.00093	1	0.004	-0.0007	0.99932	
26		ict001-22	2.46	4.76E-05	151.174	5.36E-02	7.49E+00	2.71E-02	0.99765	0.00116	1	0.004	-0.0023	0.99765	
27		ict001-23	2.45	3.52E-05	174.063	4.60E-02	1.44E+00	4.53E-03	0.99591	0.00129	1	0.004	-0.0041	0.99591	
28		ict001-24	2.45	3.65E-05	173.308	4.47E-02	1.52E+00	4.64E-03	1.00163	0.00119	1	0.004	0.0016	1.00163	
29		ict001-25	2.44	2.19E-05	203.081	2.93E-02	1.69E-01	3.70E-04	1.00502	0.00127	1	0.004	0.0050	1.00502	
30		ict001-26	2.44	2.00E-05	205.413	2.71E-02	1.41E-01	2.86E-04	1.00799	0.00105	1	0.004	0.0080	1.00799	
31		ict001-27	2.44	2.03E-05	205.570	2.40E-02	1.39E-01	2.61E-04	1.00810	0.00115	1	0.004	0.0081	1.00810	
32		ict001-28	2.45	3.97E-05	169.749	5.16E-02	1.98E+00	7.06E-03	1.00742	0.00106	1	0.004	0.0074	1.00742	
33		ict001-29	2.45	3.87E-05	170.698	4.97E-02	1.84E+00	6.21E-03	1.00360	0.00104	1	0.004	0.0036	1.00360	
34		ict003-01	2.44	6.18E-06	211.878	9.51E-03	7.96E-02	8.19E-05	1.00224	0.00110	1.0006	0.0056	0.0016	1.00164	
35		ict003-02	2.44	6.35E-06	211.883	8.95E-03	7.96E-02	7.67E-05	1.00557	0.00125	1.0046	0.0056	0.0010	1.00097	
36		imf001-01i	2.59	1.95E-04	26.211	1.25E-02	8.08E+05	9.78E+02	1.00078	0.00106	0.9989	0.0009	0.0019	1.00188	
37		imf001-02i	2.59	1.99E-04	26.180	1.28E-02	8.10E+05	1.00E+03	1.00127	0.00085	0.9997	0.0009	0.0016	1.00157	
38		imf001-03i	2.59	1.90E-04	27.148	1.25E-02	7.39E+05	9.03E+02	1.00404	0.00120	0.9993	0.0003	0.0047	1.00474	
39		imf001-04i	2.59	1.93E-04	27.141	1.25E-02	7.40E+05	9.18E+02	1.00471	0.00100	1.0002	0.0003	0.0045	1.00451	
40		imf002-001	2.58	2.02E-04	29.765	1.24E-02	5.58E+05	6.99E+02	1.00826	0.00080	1	0.003	0.0083	1.00826	
41		imf003-01	2.58	1.91E-04	27.603	1.18E-02	7.09E+05	8.38E+02	1.00472	0.00091	1	0.0017	0.0047	1.00472	
42		imf004-01	2.58	1.89E-04	28.188	1.23E-02	6.66E+05	8.16E+02	1.00933	0.00083	1	0.003	0.0093	1.00933	
43		imf005-001	2.57	1.69E-04	28.330	1.16E-02	6.59E+05	7.77E+02	1.01041	0.00082	1	0.0021	0.0104	1.01041	
44		imf006-001	2.58	1.87E-04	28.337	1.19E-02	6.59E+05	7.91E+02	0.99583	0.00083	1	0.0023	-0.0042	0.99583	
45		imf007-001	2.57	2.30E-04	30.725	1.51E-02	4.93E+05	7.36E+02	1.01727	0.00074	1.0045	0.0007	0.0128	1.01277	
46		imf008-001	2.59	1.86E-04	27.661	1.14E-02	7.03E+05	8.07E+02	1.00816	0.00084	1	0.0018	0.0082	1.00816	
47		imf009-001	2.55	1.66E-04	68.986	7.62E-02	1.53E+04	9.97E+01	1.01084	0.00095	1	0.0053	0.0108	1.01084	

Results for Volume 3: IEU Systems

N	Category	Case	nubar	Sigma	AFG	Sigma	EALCF (ev)	sigma	k_calc IEU	sigma	Benchmark k-eff	Sigma	Bias = Calculated - Benchmark	Adjusted k-eff IEU*	Notes
48		imf010-001	2.56	1.76E-04	32.291	1.08E-02	4.12E+05	4.78E+02	1.00629	0.00071	0.9954	0.0024	0.0109	1.01089	
49		imf012-001	2.55	1.42E-04	33.203	1.09E-02	3.70E+05	4.48E+02	1.00876	0.00077	1.0007	0.0027	0.0081	1.00806	
50		imf014-092	2.54	1.38E-04	34.746	9.41E-03	3.21E+05	3.34E+02	1.01409	0.00063	0.9952	0.0022	0.0189	1.01889	
51		imf014-093	2.52	1.06E-04	36.517	8.08E-03	2.66E+05	2.48E+02	1.01036	0.00070	0.9916	0.0022	0.0188	1.01876	
		Maximum	2.59	0.000230428	211.883	0.0762186	8.10E+05	1.00E+03	1.06991	0.0013	1.0140	0.0120	0.0559	1.0559	
		Average	2.49	7.97615E-05	126.2312333	0.030845963	1.79E+05	2.18E+02	1.00498	0.000996667	0.9984	0.0036	0.0066	1.0066	
		Minimum	2.44	6.17612E-06	19.0597	0.00525341	7.96E-02	7.67E-05	0.97726	0.00035	0.9640	0.0003	-0.0055	0.9945	

Table 4.4 Results for Low Enriched Uranium Systems (Volume 4) with CSAS25 from SCALE 4.4a and the 238-group Library on the J-5600 (CMODB) Workstation

Results for Volume 4: LEU Systems, Rev. 0

N	Case	AFG	sigma	AELCF(ev)	sigma	k_calc LEU0	sigma	k_exp	sigma	Bias = Calculated - Benchmark	Adjusted k-eff LEU0*
1	leuct.001/case_1	208.739	2.05E-02	9.88E-02	1.86E-04	0.99462	0.0008	0.9998	0.0031	-0.00518	0.99482
2	leuct.001/case_2	208.878	2.02E-02	9.77E-02	1.81E-04	0.99464	0.00079	0.9998	0.0031	-0.00516	0.99484
3	leuct.001/case_3	208.981	2.01E-02	9.68E-02	1.76E-04	0.99251	0.00088	0.9998	0.0031	-0.00729	0.99271
4	leuct.001/case_4	208.872	2.12E-02	9.78E-02	1.89E-04	0.99282	0.0009	0.9998	0.0031	-0.00698	0.99302
5	leuct.001/case_5	209.069	1.99E-02	9.61E-02	1.72E-04	0.99198	0.0009	0.9998	0.0031	-0.00782	0.99218
6	leuct.001/case_6	208.902	1.96E-02	9.76E-02	1.75E-04	0.9927	0.00095	0.9998	0.0031	-0.0071	0.9929
7	leuct.001/case_7	209.155	1.99E-02	9.54E-02	1.74E-04	0.99302	0.00094	0.9998	0.0031	-0.00678	0.99322

Results for Volume 4: LEU Systems, Rev. 0

N	Case	AFG	sigma	AELCF(ev)	sigma	k_calc LEU0	sigma	k_exp	sigma	Bias = Calculated - Benchmark	Adjusted k-eff LEU0*
8	leuct.001/case_8	209.025	2.05E-02	9.64E-02	1.79E-04	0.99317	0.00085	0.9998	0.0031	-0.00663	0.99337
9	leuct.002/case_1	207.414	2.22E-02	1.16E-01	2.26E-04	0.99313	0.00095	0.9997	0.002	-0.00657	0.99343
10	leuct.002/case_2	207.449	2.17E-02	1.15E-01	2.24E-04	0.99659	0.001	0.9997	0.002	-0.00311	0.99689
11	leuct.002/case_3	207.42	2.18E-02	1.16E-01	2.20E-04	0.99443	0.00089	0.9997	0.002	-0.00527	0.99473
12	leuct.002/case_4	207.584	2.14E-02	1.14E-01	2.15E-04	0.99222	0.00101	0.9997	0.002	-0.00748	0.99252
13	leuct.002/case_5	207.736	2.31E-02	1.13E-01	2.26E-04	0.99262	0.00115	0.9997	0.002	-0.00708	0.99292
14	leuct.003/case_1	201.843	2.61E-02	1.78E-01	4.02E-04	0.98246	0.00093	1	0.0039	-0.01754	0.98246
15	leuct.003/case_10	202.605	2.53E-02	1.67E-01	3.65E-04	0.97622	0.00091	1	0.0039	-0.02378	0.97622
16	leuct.003/case_11	203.892	2.59E-02	1.50E-01	3.36E-04	0.97878	0.00097	1	0.0039	-0.02122	0.97878
17	leuct.003/case_12	203.52	2.65E-02	1.55E-01	3.64E-04	0.97602	0.0009	1	0.0039	-0.02398	0.97602
18	leuct.003/case_13	203.521	2.65E-02	1.54E-01	3.58E-04	0.98346	0.00092	1	0.0039	-0.01654	0.98346
19	leuct.003/case_14	203.57	2.53E-02	1.54E-01	3.50E-04	0.97766	0.0009	1	0.0039	-0.02234	0.97766
20	leuct.003/case_15	203.515	2.50E-02	1.55E-01	3.43E-04	0.98011	0.00096	1	0.0039	-0.01989	0.98011
21	leuct.003/case_16	203.278	2.49E-02	1.58E-01	3.49E-04	0.98168	0.00093	1	0.0039	-0.01832	0.98168
22	leuct.003/case_17	203.17	2.73E-02	1.59E-01	3.82E-04	0.97774	0.00111	1	0.0039	-0.02226	0.97774
23	leuct.003/case_18	203.035	2.65E-02	1.61E-01	3.77E-04	0.97974	0.00093	1	0.0039	-0.02026	0.97974
24	leuct.003/case_19	202.946	2.62E-02	1.62E-01	3.74E-04	0.97964	0.00103	1	0.0039	-0.02036	0.97964
25	leuct.003/case_2	201.794	2.52E-02	1.78E-01	3.96E-04	0.98209	0.00088	1	0.0039	-0.01791	0.98209
26	leuct.003/case_20	202.201	2.70E-02	1.72E-01	4.05E-04	0.98077	0.00094	1	0.0039	-0.01923	0.98077
27	leuct.003/case_21	202.515	2.62E-02	1.68E-01	3.86E-04	0.97881	0.00092	1	0.0039	-0.02119	0.97881
28	leuct.003/case_22	202.922	2.57E-02	1.62E-01	3.63E-04	0.98988	0.00098	1	0.0039	-0.01012	0.98988
29	leuct.003/case_3	201.817	2.62E-02	1.78E-01	4.17E-04	0.98458	0.00081	1	0.0039	-0.01542	0.98458
30	leuct.003/case_4	201.75	2.67E-02	1.79E-01	4.20E-04	0.98333	0.00079	1	0.0039	-0.01667	0.98333
31	leuct.003/case_5	201.787	2.71E-02	1.79E-01	4.28E-04	0.98229	0.00084	1	0.0039	-0.01771	0.98229
32	leuct.003/case_6	203.53	2.50E-02	1.54E-01	3.45E-04	0.98089	0.00102	1	0.0039	-0.01911	0.98089
33	leuct.003/case_7	202.748	2.62E-02	1.65E-01	3.80E-04	0.98501	0.00086	1	0.0039	-0.01499	0.98501
34	leuct.003/case_8	203.281	2.62E-02	1.58E-01	3.62E-04	0.98575	0.00091	1	0.0039	-0.01425	0.98575
35	leuct.003/case_9	203.183	2.45E-02	1.59E-01	3.44E-04	0.97818	0.00101	1	0.0039	-0.02182	0.97818

Results for Volume 4: LEU Systems, Rev. 0

N	Case	AFG	sigma	AELCF(ev)	sigma	k_calc LEU0	sigma	k_exp	sigma	Bias = Calculated - Benchmark	Adjusted k-eff LEU0*
36	leuct.004/case_1	195.731	3.16E-02	3.01E-01	7.80E-04	0.986	0.00105	0.9998	0.0033	-0.0138	0.9862
37	leuct.004/case_10	196.503	3.12E-02	2.82E-01	7.24E-04	0.98916	0.00105	0.9998	0.0035	-0.01064	0.98936
38	leuct.004/case_11	199.831	2.78E-02	2.16E-01	5.09E-04	0.98122	0.00097	0.9998	0.0035	-0.01858	0.98142
39	leuct.004/case_12	198.948	2.96E-02	2.32E-01	5.82E-04	0.97513	0.00101	0.9998	0.0035	-0.02467	0.97533
40	leuct.004/case_13	198.402	3.03E-02	2.43E-01	6.06E-04	0.98301	0.00107	0.9998	0.0035	-0.01679	0.98321
41	leuct.004/case_14	198.455	3.04E-02	2.42E-01	6.15E-04	0.98267	0.00111	0.9998	0.0035	-0.01713	0.98287
42	leuct.004/case_15	198.481	2.96E-02	2.41E-01	5.92E-04	0.9829	0.00103	0.9998	0.0035	-0.0169	0.9831
43	leuct.004/case_16	198.331	2.91E-02	2.44E-01	5.99E-04	0.98202	0.00123	0.9998	0.0035	-0.01778	0.98222
44	leuct.004/case_17	198.253	3.00E-02	2.46E-01	6.20E-04	0.9848	0.00085	0.9998	0.0035	-0.015	0.985
45	leuct.004/case_18	198.176	3.05E-02	2.47E-01	6.37E-04	0.9839	0.00104	0.9998	0.0035	-0.0159	0.9841
46	leuct.004/case_19	197.977	2.93E-02	2.51E-01	6.13E-04	0.98182	0.001	0.9998	0.0035	-0.01798	0.98202
47	leuct.004/case_2	195.667	2.99E-02	3.02E-01	7.56E-04	0.98517	0.00119	0.9998	0.0033	-0.01463	0.98537
48	leuct.004/case_20	199.098	2.96E-02	2.30E-01	5.64E-04	0.97991	0.00115	0.9998	0.0035	-0.01989	0.98011
49	leuct.004/case_3	195.706	3.11E-02	3.01E-01	7.76E-04	0.98662	0.00094	0.9998	0.0033	-0.01318	0.98682
50	leuct.004/case_4	195.664	3.19E-02	3.02E-01	8.06E-04	0.98845	0.00096	0.9998	0.0033	-0.01135	0.98865
51	leuct.004/case_5	200.558	2.70E-02	2.04E-01	4.60E-04	0.9867	0.001	0.9998	0.0033	-0.0131	0.9869
52	leuct.004/case_6	198.361	3.03E-02	2.44E-01	6.17E-04	0.98524	0.00098	0.9998	0.0033	-0.01456	0.98544
53	leuct.004/case_7	200.225	2.80E-02	2.10E-01	4.94E-04	0.98555	0.00111	0.9998	0.0033	-0.01425	0.98575
54	leuct.004/case_8	198.055	2.97E-02	2.50E-01	6.19E-04	0.98342	0.001	0.9998	0.0035	-0.01638	0.98362
55	leuct.004/case_9	196.323	3.20E-02	2.87E-01	7.51E-04	0.98495	0.00098	0.9998	0.0035	-0.01485	0.98515
56	leuct.016/case_01	208.92	2.12E-02	9.73E-02	1.87E-04	0.99214	0.00094	1	0.0031	-0.00786	0.99214
57	leuct.016/case_02	208.935	2.04E-02	9.72E-02	1.84E-04	0.99191	0.00095	1	0.0031	-0.00809	0.99191
58	leuct.016/case_03	208.875	1.99E-02	9.76E-02	1.79E-04	0.99225	0.00091	1	0.0031	-0.00775	0.99225
59	leuct.016/case_04	208.877	2.04E-02	9.77E-02	1.75E-04	0.99311	0.00096	1	0.0031	-0.00689	0.99311
60	leuct.016/case_05	208.923	1.99E-02	9.74E-02	1.77E-04	0.99348	0.00081	1	0.0031	-0.00652	0.99348
61	leuct.016/case_06	208.824	2.13E-02	9.82E-02	1.88E-04	0.9941	0.00092	1	0.0031	-0.0059	0.9941
62	leuct.016/case_07	208.877	2.15E-02	9.76E-02	1.93E-04	0.99436	0.00093	1	0.0031	-0.00564	0.99436
63	leuct.016/case_08	208.736	2.04E-02	9.88E-02	1.86E-04	0.99392	0.00083	1	0.0031	-0.00608	0.99392

Results for Volume 4: LEU Systems, Rev. 0

N	Case	AFG	sigma	AELCF(ev)	sigma	k_calc LEU0	sigma	k_exp	sigma	Bias = Calculated - Benchmark	Adjusted k-eff LEU0*
64	leuct.016/case_09	208.831	2.07E-02	9.80E-02	1.82E-04	0.99357	0.00082	1	0.0031	-0.00643	0.99357
65	leuct.016/case_10	208.707	1.92E-02	9.91E-02	1.73E-04	0.99251	0.00092	1	0.0031	-0.00749	0.99251
66	leuct.016/case_11	208.8	2.16E-02	9.83E-02	1.94E-04	0.99262	0.00098	1	0.0031	-0.00738	0.99262
67	leuct.016/case_12	208.639	2.10E-02	9.96E-02	1.92E-04	0.99355	0.00107	1	0.0031	-0.00645	0.99355
68	leuct.016/case_13	208.757	2.04E-02	9.87E-02	1.79E-04	0.99146	0.00084	1	0.0031	-0.00854	0.99146
69	leuct.016/case_14	208.634	2.06E-02	9.97E-02	1.90E-04	0.99467	0.00092	1	0.0031	-0.00533	0.99467
70	leuct.016/case_15	208.872	2.05E-02	9.78E-02	1.81E-04	0.99424	0.00092	1	0.0031	-0.00576	0.99424
71	leuct.016/case_16	208.879	1.95E-02	9.76E-02	1.74E-04	0.9911	0.00082	1	0.0031	-0.0089	0.9911
72	leuct.016/case_17	208.906	2.03E-02	9.74E-02	1.82E-04	0.99271	0.00089	1	0.0031	-0.00729	0.99271
73	leuct.016/case_18	208.873	1.97E-02	9.76E-02	1.76E-04	0.99534	0.00092	1	0.0031	-0.00466	0.99534
74	leuct.016/case_19	208.905	2.03E-02	9.76E-02	1.81E-04	0.99452	0.00087	1	0.0031	-0.00548	0.99452
75	leuct.016/case_20	208.77	2.11E-02	9.86E-02	1.88E-04	0.99285	0.00095	1	0.0031	-0.00715	0.99285
76	leuct.016/case_21	208.705	2.07E-02	9.91E-02	1.90E-04	0.99224	0.00096	1	0.0031	-0.00776	0.99224
77	leuct.016/case_22	208.725	2.01E-02	9.89E-02	1.82E-04	0.99347	0.0009	1	0.0031	-0.00653	0.99347
78	leuct.016/case_23	208.794	2.00E-02	9.84E-02	1.78E-04	0.99439	0.00098	1	0.0031	-0.00561	0.99439
79	leuct.016/case_24	208.725	2.05E-02	9.90E-02	1.87E-04	0.99301	0.00086	1	0.0031	-0.00699	0.99301
80	leuct.016/case_25	208.801	2.07E-02	9.84E-02	1.86E-04	0.9936	0.00092	1	0.0031	-0.0064	0.9936
81	leuct.016/case_26	208.776	2.01E-02	9.86E-02	1.78E-04	0.99506	0.00076	1	0.0031	-0.00494	0.99506
82	leuct.016/case_27	208.793	2.00E-02	9.84E-02	1.81E-04	0.99266	0.00085	1	0.0031	-0.00734	0.99266
83	leuct.016/case_28	208.98	2.11E-02	9.68E-02	1.89E-04	0.99311	0.00097	1	0.0031	-0.00689	0.99311
84	leuct.016/case_29	208.951	2.11E-02	9.71E-02	1.88E-04	0.99282	0.00085	1	0.0031	-0.00718	0.99282
85	leuct.016/case_30	208.947	2.03E-02	9.72E-02	1.80E-04	0.99202	0.00093	1	0.0031	-0.00798	0.99202
86	leuct.016/case_31	208.963	2.04E-02	9.69E-02	1.77E-04	0.99347	0.00079	1	0.0031	-0.00653	0.99347
87	leuct.016/case_32	209.002	2.03E-02	9.67E-02	1.78E-04	0.99398	0.00099	1	0.0031	-0.00602	0.99398
88	leust.003/case_1	218.044	3.40E-03	4.05E-02	1.61E-05	0.9987	0.00092	1.0007	0.0039	-0.002	0.998
89	leust.003/case_2	218.544	3.20E-03	3.87E-02	1.47E-05	0.99562	0.0009	1.0003	0.0042	-0.00468	0.99532
90	leust.003/case_3	218.635	3.10E-03	3.84E-02	1.47E-05	1.00286	0.0009	1.0005	0.0042	0.00236	1.00236
91	leust.003/case_4	218.679	3.03E-03	3.82E-02	1.46E-05	0.99412	0.001	1.0005	0.0042	-0.00638	0.99362

Results for Volume 4: LEU Systems, Rev. 0

N	Case	AFG	sigma	AELCF(ev)	sigma	k_calc LEU0	sigma	k_exp	sigma	Bias = Calculated - Benchmark	Adjusted k-eff LEU0*
92	leust.003/case_5	219.481	2.52E-03	3.55E-02	1.16E-05	0.99768	0.0008	1.0007	0.0048	-0.00302	0.99698
93	leust.003/case_6	219.571	2.48E-03	3.52E-02	1.14E-05	0.99871	0.00078	1.0009	0.0049	-0.00219	0.99781
94	leust.003/case_7	219.63	2.25E-03	3.50E-02	1.07E-05	0.99791	0.00085	1.0004	0.0049	-0.00249	0.99751
95	leust.003/case_8	219.959	2.04E-03	3.40E-02	9.68E-06	0.99971	0.0007	1.0003	0.0052	-0.00059	0.99941
96	leust.003/case_9	220.003	2.05E-03	3.39E-02	9.70E-06	0.99749	0.00062	1.0006	0.0052	-0.00311	0.99689
	Maximum	220.003	3.20E-02	3.02E-01	8.06E-04	1.00286	0.00123	1.0009	0.0052	0.00236	1.00236
	Average	206	2.21E-02	1.41E-01	3.07E-04	0.98901	0.00093	1.0000	0.0034	-0.01096	0.98904
	Minimum	195.664	2.04E-03	3.39E-02	9.68E-06	0.97513	0.00062	0.9997	0.002	-0.02467	0.97533

Results for Volume 4: LEU Systems, Rev. 1

N	Case	nubar	Sigma	AFG	Sigma	EALCF (ev)	sigma	k_calc LEU1	sigma	Benchmark k-eff	Sigma	Bias = Calculated - Benchmark	Adjusted k-eff LEU1*
1	lct008-08	2.46	6.06E-05	197.7	2.91E-02	2.53E-01	6.34E-04	0.99369	0.00082	1.0007	0.0012	-0.00701	0.99299
2	lct009-07	2.45	4.06E-05	207.4	2.13E-02	1.16E-01	2.10E-04	0.99599	0.00103	1	0.0021	-0.00401	0.99599
3	lct012-01	2.46	5.45E-05	202.1	2.71E-02	1.74E-01	4.14E-04	0.98027	0.00093	1	0.0034	-0.01973	0.98027
4	lct012-02	2.46	5.69E-05	201.6	2.71E-02	1.82E-01	4.29E-04	0.98192	0.00099	1	0.0034	-0.01808	0.98192
5	lct012-03	2.46	5.41E-05	201.5	2.62E-02	1.83E-01	4.09E-04	0.97939	0.00107	1	0.0034	-0.02061	0.97939
6	lct012-04	2.46	5.76E-05	201.0	2.77E-02	1.90E-01	4.59E-04	0.98207	0.00106	1	0.0034	-0.01793	0.98207
7	lct012-05	2.46	5.62E-05	201.1	2.64E-02	1.89E-01	4.42E-04	0.9823	0.0009	1	0.0034	-0.0177	0.9823
8	lct012-06	2.46	5.69E-05	201.1	2.73E-02	1.89E-01	4.53E-04	0.9833	0.00092	1	0.0034	-0.0167	0.9833
9	lct012-07	2.46	5.62E-05	201.1	2.67E-02	1.90E-01	4.44E-04	0.9829	0.00104	1	0.0034	-0.0171	0.9829
10	lct012-08	2.46	5.42E-05	201.4	2.70E-02	1.84E-01	4.29E-04	0.98005	0.00083	1	0.0049	-0.01995	0.98005
11	lct012-09	2.46	5.39E-05	202.3	2.48E-02	1.72E-01	3.74E-04	0.9803	0.00086	1	0.0034	-0.0197	0.9803
12	lct012-10	2.46	5.72E-05	201.7	2.57E-02	1.80E-01	4.10E-04	0.98142	0.00103	1	0.0034	-0.01858	0.98142

Results for Volume 4: LEU Systems, Rev. 1

N	Case	nubar	Sigma	AFG	Sigma	EALCF (ev)	sigma	k_calc LEU1	sigma	Benchmark k-eff	Sigma	Bias = Calculated - Benchmark	Adjusted k-eff LEU1*
13	lmt001	2.46	6.42E-05	207.1	2.83E-02	1.20E-01	2.98E-04	0.99554	0.00085	0.999	0.0057	-0.00346	0.99654
14	lmt002-01	2.44	2.91E-05	217.2	1.36E-02	4.78E-02	6.81E-05	1.01571	0.00087	1	0.0141	0.01571	1.01571
15	lmt002-02	2.44	3.12E-05	216.2	1.54E-02	5.23E-02	8.25E-05	1.00911	0.00102	1	0.0141	0.00911	1.00911
16	lmt002-03	2.44	3.06E-05	216.7	1.55E-02	5.00E-02	8.24E-05	1.0151	0.00107	1	0.0141	0.0151	1.0151
17	lmt002-04	2.44	3.24E-05	213.8	1.69E-02	6.44E-02	1.04E-04	1.00788	0.00087	1	0.0141	0.00788	1.00788
18	lmt002-05	2.44	3.06E-05	216.8	1.45E-02	4.95E-02	7.66E-05	1.01812	0.0009	1	0.0141	0.01812	1.01812
19	lmt002-06	2.45	3.68E-05	210.0	2.03E-02	8.83E-02	1.61E-04	1.0078	0.00082	1	0.0146	0.0078	1.0078
20	lmt002-07	2.44	3.14E-05	215.7	1.49E-02	5.47E-02	7.88E-05	1.01248	0.00101	1	0.0141	0.01248	1.01248
21	lmt002-08	2.44	3.19E-05	214.7	1.65E-02	5.96E-02	9.74E-05	1.00511	0.00095	1	0.0141	0.00511	1.00511
22	lmt002-09	2.44	3.24E-05	215.8	1.50E-02	5.41E-02	8.29E-05	1.00846	0.00098	1	0.0141	0.00846	1.00846
23	lmt002-10	2.44	3.28E-05	215.2	1.57E-02	5.69E-02	9.08E-05	1.01023	0.00096	1	0.0141	0.01023	1.01023
24	lmt002-11	2.44	3.22E-05	214.2	1.62E-02	6.21E-02	9.90E-05	1.00766	0.00104	1	0.0141	0.00766	1.00766
25	lmt002-12	2.44	3.20E-05	216.4	1.53E-02	5.13E-02	7.93E-05	1.01428	0.00078	1	0.0141	0.01428	1.01428
26	lst004-01	2.44	4.90E-06	217.8	3.46E-03	4.16E-02	1.63E-05	1.00112	0.00084	0.9994	0.0008	0.00172	1.00172
27	lst004-29	2.44	4.63E-06	218.1	3.24E-03	4.05E-02	1.57E-05	1.002	0.00083	0.9999	0.0009	0.0021	1.0021
28	lst004-33	2.44	4.26E-06	218.4	3.20E-03	3.93E-02	1.55E-05	1.00011	0.00079	0.9999	0.0009	0.00021	1.00021
29	lst004-34	2.44	3.96E-06	218.6	3.01E-03	3.85E-02	1.41E-05	1.00226	0.00083	0.9999	0.001	0.00236	1.00236
30	lst004-46	2.44	3.77E-06	218.8	2.72E-03	3.80E-02	1.30E-05	1.00317	0.00095	0.9999	0.001	0.00327	1.00327
31	lst004-51	2.44	3.70E-06	218.9	2.87E-03	3.75E-02	1.35E-05	1.00034	0.00078	0.9994	0.0011	0.00094	1.00094
32	lst004-54	2.44	3.42E-06	219.1	2.66E-03	3.71E-02	1.27E-05	1.00166	0.00073	0.9996	0.0011	0.00206	1.00206
	Maximum	2.46	6.42007E-05	219.1	0.0291166	2.53E-01	6.34E-04	1.01812	0.00107	1.0007	0.0146	0.01812	1.01812
	Average	2.45	3.54716E-05	210.6	0.017369777	1.03E-01	2.07E-04	0.998179375	0.000917188	0.9999	0.0069	-0.00175	0.99825
	Minimum	2.44	3.4225E-06	197.7	0.00266273	3.71E-02	1.27E-05	0.97939	0.00073	0.999	0.0008	-0.02061	0.97939

Note: lmt002 series used infinite homogeneous, but latticecell or multiregion may be better.

Table 4.5 Results for Uranium-233 Systems (Volume 5) with CSAS25 from SCALE 4.4a and the 238-group Library on the J-5600 (CMODB) Workstation

Results for Volume 5: Uranium-233 Systems

								k_calc					Adjusted k-eff	
N	Case	nubar	Sigma	AFG	Sigma	EALCF (ev)	sigma	U233	sigma	Benchmark k-eff	Sigma	Bias = Calculated - Benchmark	U233*	Notes
1	umf001-001	2.68	2.38E-04	22.5	1.32E-02	1.13E+06	1.41E+03	0.99178	0.00105	1	0.001	-0.00822	0.99178	
2	umf002-001	2.66	2.37E-04	22.8	1.32E-02	1.09E+06	1.38E+03	0.99447	0.00108	1	0.001	-0.00553	0.99447	48.479 %U235
3	umf002-002	2.65	2.31E-04	23.1	1.45E-02	1.07E+06	1.45E+03	0.99767	0.00108	1	0.0011	-0.00233	0.99767	48.4479 %U235
4	umf003-001	2.67	2.48E-04	23.0	1.37E-02	1.08E+06	1.41E+03	0.99685	0.00101	1	0.001	-0.00315	0.99685	
5	umf003-002	2.67	2.54E-04	23.1	1.41E-02	1.06E+06	1.46E+03	0.99901	0.0012	1	0.001	-0.00099	0.99901	
6	umf004-001	2.66	2.18E-04	24.1	1.34E-02	9.72E+05	1.24E+03	1.00028	0.001	1	0.0007	0.00028	1.00028	
7	umf004-002	2.65	2.11E-04	25.3	1.41E-02	8.69E+05	1.20E+03	1.00367	0.00102	1	0.0008	0.00367	1.00367	
8	umf005-001	2.66	2.42E-04	24.3	1.45E-02	9.45E+05	1.38E+03	0.99851	0.00109	1	0.003	-0.00149	0.99851	
9	umf005-002	2.65	2.22E-04	26.0	1.77E-02	7.64E+05	1.46E+03	1.00163	0.00093	1	0.003	0.00163	1.00163	
10	umf006-001	2.67	2.51E-04	23.6	1.54E-02	1.00E+06	1.43E+03	1.00043	0.00111	1	0.0014	0.00043	1.00043	
11	usi001_01	2.51	2.25E-05	148.8	4.34E-02	6.62E+00	1.95E-02	0.98903	0.00146	1	0.0083	-0.01097	0.98903	
12	usi001_02	2.51	2.41E-05	146.7	4.01E-02	7.71E+00	2.10E-02	0.98352	0.00158	1	0.0085	-0.01648	0.98352	
13	usi001_03	2.51	2.51E-05	145.7	4.06E-02	8.29E+00	2.29E-02	0.98386	0.00145	1	0.0066	-0.01614	0.98386	
14	usi001_04	2.51	2.36E-05	158.1	4.42E-02	3.54E+00	1.07E-02	0.99248	0.00124	1	0.0061	-0.00752	0.99248	
15	usi001_05	2.51	2.57E-05	144.8	4.26E-02	8.88E+00	2.58E-02	0.98611	0.00127	1	0.0082	-0.01389	0.98611	
16	usi001_06	2.51	2.56E-05	156.2	4.16E-02	4.09E+00	1.16E-02	0.98648	0.0014	1	0.0061	-0.01352	0.98648	
17	usi001_07	2.51	2.71E-05	144.3	4.15E-02	9.27E+00	2.60E-02	0.9846	0.00147	1	0.0059	-0.0154	0.9846	
18	usi001_08	2.51	2.63E-05	155.4	4.45E-02	4.36E+00	1.32E-02	0.97887	0.00157	1	0.0056	-0.02113	0.97887	
19	usi001_09	2.51	2.68E-05	148.3	4.27E-02	7.07E+00	2.07E-02	0.97742	0.00154	1	0.0068	-0.02258	0.97742	
20	usi001_10	2.51	2.80E-05	143.7	4.11E-02	9.72E+00	2.72E-02	0.97982	0.00147	1	0.0053	-0.02018	0.97982	
21	usi001_11	2.51	2.84E-05	147.7	4.14E-02	7.43E+00	2.09E-02	0.9809	0.00139	1	0.0057	-0.0191	0.9809	
22	usi001_12	2.50	2.05E-05	155.0	3.99E-02	4.30E+00	1.18E-02	0.98218	0.00131	1	0.0091	-0.01782	0.98218	
23	usi001_13	2.50	2.07E-05	153.2	3.84E-02	4.89E+00	1.27E-02	0.9817	0.00137	1	0.0071	-0.0183	0.9817	
24	usi001_14	2.50	2.01E-05	164.9	4.33E-02	2.17E+00	6.39E-03	0.99147	0.00118	1	0.0052	-0.00853	0.99147	
25	usi001_15	2.50	2.09E-05	152.3	3.80E-02	5.23E+00	1.35E-02	0.98228	0.00138	1	0.0075	-0.01772	0.98228	

Results for Volume 5: Uranium-233 Systems

N	Case	nubar	Sigma	AFG	Sigma	EALCF (ev)	sigma	k_calc U233	sigma	Benchmark k-eff	Sigma	Bias = Calculated - Benchmark	Adjusted k-eff U233*	Notes
26	usi001_16	2.50	2.03E-05	168.5	4.33E-02	1.73E+00	5.16E-03	0.97377	0.00118	1	0.0028	-0.02623	0.97377	
27	usi001_17	2.50	2.03E-05	163.5	4.25E-02	2.42E+00	7.08E-03	0.98895	0.00128	1	0.0055	-0.01105	0.98895	
28	usi001_18	2.51	2.35E-05	151.4	3.87E-02	5.62E+00	1.51E-02	0.97868	0.0012	1	0.0057	-0.02132	0.97868	
29	usi001_19	2.51	2.24E-05	150.9	3.86E-02	5.86E+00	1.54E-02	0.97547	0.0015	1	0.0083	-0.02453	0.97547	
30	usi001_20	2.51	2.20E-05	161.3	4.18E-02	2.87E+00	8.13E-03	0.98098	0.00135	1	0.0056	-0.01902	0.98098	
31	usi001_21	2.51	2.42E-05	150.4	4.00E-02	6.09E+00	1.66E-02	0.97248	0.00143	1	0.005	-0.02752	0.97248	
32	usi001_22	2.51	2.60E-05	150.1	4.02E-02	6.24E+00	1.72E-02	0.97514	0.00162	1	0.0049	-0.02486	0.97514	
33	usi001_23	2.51	2.39E-05	154.9	3.95E-02	4.50E+00	1.21E-02	0.99051	0.00125	1	0.0047	-0.00949	0.99051	
34	usi001_24	2.50	1.50E-05	166.6	3.27E-02	1.90E+00	4.32E-03	0.99128	0.00132	1	0.0081	-0.00872	0.99128	
35	usi001_25	2.50	1.57E-05	164.8	3.51E-02	2.17E+00	5.16E-03	0.98705	0.00132	1	0.0081	-0.01295	0.98705	
36	usi001_26	2.50	1.65E-05	164.1	3.52E-02	2.29E+00	5.50E-03	0.98811	0.00127	1	0.0065	-0.01189	0.98811	
37	usi001_27	2.50	1.51E-05	173.4	3.75E-02	1.19E+00	3.09E-03	0.99176	0.00134	1	0.0051	-0.00824	0.99176	
38	usi001_28	2.50	1.81E-05	163.2	3.59E-02	2.45E+00	6.11E-03	0.98104	0.0014	1	0.0061	-0.01896	0.98104	
39	usi001_29	2.50	1.76E-05	162.8	3.40E-02	2.53E+00	5.94E-03	0.9769	0.00144	1	0.0098	-0.0231	0.9769	
40	usi001_30	2.50	1.67E-05	171.6	3.64E-02	1.38E+00	3.45E-03	0.97321	0.00123	1	0.0053	-0.02679	0.97321	
41	usi001_31	2.50	1.77E-05	162.6	3.59E-02	2.58E+00	6.38E-03	0.98828	0.00152	1	0.0071	-0.01172	0.98828	
42	usi001_32	2.50	2.01E-05	162.1	3.49E-02	2.68E+00	6.49E-03	0.9709	0.00132	1	0.0053	-0.0291	0.9709	
43	usi001_33	2.50	1.79E-05	166.5	3.90E-02	1.98E+00	5.30E-03	0.99067	0.00159	1	0.0046	-0.00933	0.99067	
44	ust001-001	2.50	7.24E-07	218.4	2.92E-03	3.86E-02	1.19E-05	0.99538	0.00084	1	0.0031	-0.00462	0.99538	
45	ust001-002	2.50	7.21E-07	218.2	2.93E-03	3.92E-02	1.23E-05	0.99711	0.00081	1.0005	0.0033	-0.00339	0.99661	
46	ust001-003	2.50	7.48E-07	218.1	2.98E-03	3.98E-02	1.20E-05	0.99749	0.00082	1.0006	0.0033	-0.00311	0.99689	
47	ust001-004	2.50	7.03E-07	217.9	3.20E-03	4.04E-02	1.34E-05	0.99583	0.00076	0.9998	0.0033	-0.00397	0.99603	
48	ust001-005	2.50	7.91E-07	217.7	3.38E-03	4.10E-02	1.44E-05	0.99597	0.00081	0.9999	0.0033	-0.00393	0.99607	
49	ust002-004	2.50	5.43E-06	200.4	2.00E-02	1.64E-01	2.51E-04	1.00472	0.00129	1.004	0.0087	0.00072	1.00072	
50	ust002-005	2.50	4.79E-06	203.6	1.68E-02	1.28E-01	1.67E-04	0.99023	0.00125	1.004	0.0087	-0.01377	0.98623	
51	ust002-008	2.50	3.95E-06	206.6	1.37E-02	1.00E-01	1.11E-04	1.008	0.0015	1.004	0.0087	0.004	1.004	
52	ust002-010	2.50	2.88E-06	209.2	1.18E-02	8.20E-02	8.00E-05	1.001	0.00107	1.004	0.0087	-0.003	0.997	
53	ust002-011	2.50	2.40E-06	210.9	9.92E-03	7.17E-02	5.85E-05	1.00677	0.00123	1.004	0.0087	0.00277	1.00277	

Results for Volume 5: Uranium-233 Systems

N	Case	nubar	Sigma	AFG	Sigma	EALCF (ev)	sigma	k_calc U233	sigma	Benchmark k-eff	Sigma	Bias = Calculated - Benchmark	Adjusted k-eff U233*	Notes
54	ust002-012	2.50	2.31E-06	212.3	9.47E-03	6.41E-02	5.04E-05	0.99261	0.00136	1.004	0.0087	-0.01139	0.98861	
55	ust002-014	2.50	2.15E-06	212.9	8.50E-03	6.07E-02	4.44E-05	0.98183	0.00131	1.004	0.0087	-0.02217	0.97783	
56	ust002-015	2.50	1.68E-06	213.9	7.70E-03	5.60E-02	3.76E-05	0.99428	0.00116	1.004	0.0087	-0.00972	0.99028	
57	ust002-017	2.50	1.50E-06	215.1	6.07E-03	5.06E-02	2.79E-05	0.98476	0.00108	1.004	0.0087	-0.01924	0.98076	
58	ust002-018	2.50	1.29E-06	215.6	5.97E-03	4.89E-02	2.66E-05	0.99886	0.00117	1.004	0.0087	-0.00514	0.99486	
59	ust002-019	2.50	1.16E-06	216.4	4.99E-03	4.57E-02	2.06E-05	1.00613	0.00101	1.004	0.0087	0.00213	1.00213	
60	ust002-022	2.50	7.53E-06	194.5	2.54E-02	2.56E-01	4.81E-04	0.99228	0.00115	1.004	0.0087	-0.01172	0.98828	
61	ust002-024	2.50	1.12E-05	186.9	3.02E-02	4.53E-01	9.80E-04	0.9945	0.0014	1.004	0.0087	-0.0095	0.9905	
62	ust002-034	2.50	4.91E-06	203.1	1.78E-02	1.32E-01	1.81E-04	1.00061	0.00147	1.004	0.0087	-0.00339	0.99661	
63	ust002-035	2.50	3.44E-06	207.8	1.30E-02	9.19E-02	9.51E-05	1.00474	0.00121	1.004	0.0087	0.00074	1.00074	
64	ust002-036	2.50	2.04E-06	212.7	8.01E-03	6.17E-02	4.21E-05	1.00366	0.00108	1.004	0.0087	-0.00034	0.99966	
65	ust002-038	2.50	1.51E-06	214.6	6.64E-03	5.30E-02	3.10E-05	1.00374	0.00133	1.004	0.0087	-0.00026	0.99974	
66	ust003-040	2.50	9.09E-06	192.5	2.67E-02	2.99E-01	5.90E-04	0.9984	0.00138	0.9995	0.00871	-0.0011	0.9989	
67	ust004-003	2.50	6.09E-06	200.4	1.93E-02	1.64E-01	2.38E-04	0.99978	0.00144	1.0039	0.0088	-0.00412	0.99588	
68	ust004-006	2.50	4.80E-06	203.7	1.81E-02	1.27E-01	1.79E-04	1.00131	0.00128	1.0034	0.0086	-0.00209	0.99791	
69	ust004-020	2.50	7.76E-06	194.4	2.46E-02	2.59E-01	4.63E-04	0.99264	0.00131	1.0041	0.0089	-0.01146	0.98854	
70	ust004-025	2.50	1.13E-05	186.6	3.15E-02	4.64E-01	1.06E-03	0.98198	0.00126	1.0051	0.0089	-0.02312	0.97688	
71	ust004-027	2.50	1.09E-05	186.7	3.39E-02	4.60E-01	1.11E-03	1.00311	0.00146	1.002	0.0105	0.00111	1.00111	
72	ust004-028	2.50	9.42E-06	189.8	2.87E-02	3.65E-01	7.52E-04	0.99672	0.00131	1.002	0.0104	-0.00528	0.99472	
73	ust004-030	2.50	9.62E-06	189.8	2.83E-02	3.66E-01	7.33E-04	0.99039	0.00148	1.0037	0.009	-0.01331	0.98669	
74	ust004-033	2.50	4.94E-06	203.2	1.75E-02	1.32E-01	1.77E-04	1.00141	0.00141	1.002	0.0102	-0.00059	0.99941	
75	ust005-001	2.50	1.97E-06	213.0	7.98E-03	6.03E-02	4.25E-05	0.99603	0.00127	1	0.004	-0.00397	0.99603	
76	ust005-002	2.50	1.61E-06	214.5	6.95E-03	5.31E-02	3.33E-05	1.00136	0.00107	1	0.0049	0.00136	1.00136	
77	ust006-004	2.50	1.27E-05	178.7	2.63E-02	8.23E-01	1.56E-03	0.99524	0.00134	1	0.0035	-0.00476	0.99524	
78	ust006-006	2.50	1.21E-05	178.5	2.89E-02	8.37E-01	1.75E-03	0.98692	0.00134	1	0.0035	-0.01308	0.98692	
79	ust006-009	2.50	1.04E-05	188.7	2.92E-02	3.93E-01	8.23E-04	1.00025	0.00131	1	0.0028	0.00025	1.00025	
80	ust006-011	2.50	9.76E-06	188.8	2.82E-02	3.93E-01	7.89E-04	0.99748	0.00122	1	0.0028	-0.00252	0.99748	
81	ust006-015	2.50	7.57E-06	192.9	2.07E-02	2.87E-01	4.43E-04	0.98577	0.00125	1	0.0035	-0.01423	0.98577	

Results for Volume 5: Uranium-233 Systems

N	Case	nubar	Sigma	AFG	Sigma	EALCF (ev)	sigma	k_calc U233	sigma	Benchmark k-eff	Sigma	Bias = Calculated - Benchmark	Adjusted k-eff U233*	Notes
82	ust006-018	2.50	7.69E-06	192.7	2.06E-02	2.90E-01	4.47E-04	0.98544	0.00133	1	0.0035	-0.01456	0.98544	
83	ust006-020	2.50	6.65E-06	199.4	2.02E-02	1.77E-01	2.69E-04	0.9907	0.00132	1	0.0028	-0.0093	0.9907	
84	ust006-022	2.50	6.75E-06	199.3	1.98E-02	1.77E-01	2.68E-04	0.98983	0.00131	1	0.0028	-0.01017	0.98983	
85	ust008-001	2.50	5.64E-07	219.1	2.34E-03	3.65E-02	9.58E-06	0.99679	0.00067	1.0006	0.0029	-0.00381	0.99619	
86	ust012_1	2.50	5.72E-06	200.2	1.90E-02	1.66E-01	2.37E-04	0.99328	0.00127	0.999	0.0028	-0.00572	0.99428	
87	ust012_2	2.50	5.63E-06	200.8	1.90E-02	1.59E-01	2.29E-04	0.99448	0.00134	0.9993	0.0025	-0.00482	0.99518	
88	ust012_3	2.50	5.24E-06	202.3	1.68E-02	1.42E-01	1.81E-04	1.00184	0.00156	0.9994	0.0023	0.00244	1.00244	
89	ust012_4	2.50	3.72E-06	206.2	1.39E-02	1.04E-01	1.15E-04	0.99628	0.00125	1	0.0015	-0.00372	0.99628	
90	ust012_5	2.50	3.29E-06	208.2	1.18E-02	8.87E-02	8.54E-05	0.99887	0.00121	1	0.0071	-0.00113	0.99887	
91	ust012_6	2.50	2.78E-06	209.8	1.05E-02	7.84E-02	6.82E-05	0.99877	0.00111	0.9987	0.0011	7E-05	1.00007	
92	ust012_7	2.50	1.59E-06	214.7	6.59E-03	5.27E-02	3.02E-05	0.99616	0.00134	1	0.0038	-0.00384	0.99616	
93	ust012_8	2.50	1.48E-06	214.8	5.98E-03	5.24E-02	2.70E-05	0.99506	0.00117	1	0.0048	-0.00494	0.99506	
94	ust014-001	2.50	1.16E-05	183.5	2.92E-02	5.82E-01	1.23E-03	0.97733	0.00157	0.9976	0.0112	-0.02027	0.97973	
95	ust014-002	2.50	1.12E-05	182.8	2.75E-02	6.15E-01	1.21E-03	0.99058	0.00135	0.9976	0.0112	-0.00702	0.99298	
96	ust014-003	2.50	8.96E-06	192.7	2.61E-02	2.97E-01	5.60E-04	1.00792	0.00127	1	0.0074	0.00792	1.00792	
97	ust014-004	2.50	8.68E-06	193.0	2.75E-02	2.90E-01	5.71E-04	1.00661	0.00121	1	0.0089	0.00661	1.00661	
98	ust014-005	2.50	8.97E-06	194.4	2.59E-02	2.63E-01	4.95E-04	1.00903	0.00132	1	0.0089	0.00903	1.00903	
99	ust014-006	2.50	8.86E-06	194.9	2.66E-02	2.54E-01	4.86E-04	1.0058	0.00121	1	0.0089	0.0058	1.0058	
100	ust014-007	2.50	8.56E-06	195.3	2.67E-02	2.46E-01	4.77E-04	1.00309	0.00121	1	0.0088	0.00309	1.00309	
101	ust014-008	2.50	8.31E-06	195.8	2.67E-02	2.37E-01	4.58E-04	1.00617	0.00119	1	0.0091	0.00617	1.00617	
102	ust014-009	2.50	9.00E-06	192.7	2.75E-02	2.96E-01	5.98E-04	1.00977	0.00121	1	0.0054	0.00977	**1.00977**	
103	ust014-010	2.50	9.53E-06	190.6	2.81E-02	3.48E-01	7.06E-04	0.99294	0.0013	0.9992	0.0108	-0.00626	0.99374	
104	ust014-011	2.50	1.04E-05	187.9	2.64E-02	4.24E-01	7.94E-04	0.9972	0.00155	0.9992	0.0126	-0.002	0.998	
105	ust014-012	2.50	9.31E-06	192.6	2.97E-02	3.00E-01	6.41E-04	1.00291	0.00128	0.9992	0.0097	0.00371	1.00371	
106	ust014-013	2.50	9.50E-06	193.1	3.14E-02	2.90E-01	6.55E-04	1.00181	0.00141	0.9992	0.0104	0.00261	1.00261	
107	ust014-014	2.50	8.97E-06	193.2	3.03E-02	2.87E-01	6.27E-04	0.996	0.00134	0.9966	0.0095	-0.0006	0.9994	
108	ust014-015	2.50	9.40E-06	192.1	3.04E-02	3.13E-01	6.78E-04	0.99299	0.00137	0.9966	0.0098	-0.00361	0.99639	
109	ust014-016	2.50	1.09E-05	185.0	2.80E-02	5.21E-01	1.04E-03	0.9767	0.00135	0.9965	0.0109	-0.0198	0.9802	

Results for Volume 5: Uranium-233 Systems

N	Case	nubar	Sigma	AFG	Sigma	EALCF (ev)	sigma	k_calc U233	sigma	Benchmark k-eff	Sigma	Bias = Calculated - Benchmark	Adjusted k-eff U233*	Notes
110	ust015_01	2.50	1.23E-05	175.0	3.05E-02	1.05E+00	2.25E-03	0.98669	0.00149	1	0.0075	-0.01331	0.98669	
111	ust015_02	2.50	1.28E-05	173.4	2.96E-02	1.18E+00	2.42E-03	0.98295	0.00128	1	0.007	-0.01705	0.98295	
112	ust015_03	2.50	1.33E-05	172.8	3.13E-02	1.24E+00	2.70E-03	0.98663	0.00145	1	0.0068	-0.01337	0.98663	
113	ust015_04	2.50	1.17E-05	181.1	3.15E-02	6.86E-01	1.54E-03	0.9886	0.00144	1	0.0041	-0.0114	0.9886	
114	ust015_05	2.50	1.37E-05	172.0	3.21E-02	1.31E+00	2.93E-03	0.98395	0.00134	1	0.0055	-0.01605	0.98395	
115	ust015_06	2.50	1.43E-05	171.6	3.19E-02	1.36E+00	2.98E-03	0.97425	0.00149	1	0.0099	-0.02575	0.97425	
116	ust015_07	2.50	1.31E-05	180.0	3.12E-02	7.53E-01	1.69E-03	0.98348	0.00148	1	0.007	-0.01652	0.98348	
117	ust015_08	2.50	1.38E-05	171.3	3.21E-02	1.40E+00	3.15E-03	0.97011	0.00135	1	0.0067	-0.02989	0.97011	
118	ust015_09	2.50	1.53E-05	170.9	3.19E-02	1.43E+00	3.23E-03	0.96649	0.00154	1	0.005	-0.03351	**0.96649**	
119	ust015_10	2.50	1.50E-05	175.1	3.05E-02	1.07E+00	2.31E-03	0.98769	0.00129	1	0.0051	-0.01231	0.98769	
120	ust015_11	2.50	9.77E-06	181.4	2.84E-02	6.63E-01	1.34E-03	0.99014	0.00146	1	0.0075	-0.00986	0.99014	
121	ust015_12	2.50	1.02E-05	180.1	2.81E-02	7.31E-01	1.45E-03	0.99048	0.00127	1	0.0069	-0.00952	0.99048	
122	ust015_13	2.50	1.08E-05	179.4	2.93E-02	7.69E-01	1.60E-03	0.99047	0.00131	1	0.0069	-0.00953	0.99047	
123	ust015_14	2.50	1.02E-05	187.1	2.89E-02	4.41E-01	9.08E-04	0.99569	0.00136	1	0.0036	-0.00431	0.99569	
124	ust015_15	2.50	1.10E-05	178.9	2.84E-02	8.03E-01	1.62E-03	0.98781	0.00129	1	0.006	-0.01219	0.98781	
125	ust015_16	2.50	1.11E-05	178.5	2.92E-02	8.27E-01	1.70E-03	0.98444	0.00157	1	0.0043	-0.01556	0.98444	
126	ust015_17	2.50	1.07E-05	186.2	2.89E-02	4.80E-01	9.99E-04	0.99206	0.0015	1	0.0029	-0.00794	0.99206	
127	ust015_18	2.50	1.22E-05	178.1	2.83E-02	8.55E-01	1.72E-03	0.97233	0.00153	1	0.0056	-0.02767	0.97233	
128	ust015_19	2.50	1.29E-05	177.9	2.90E-02	8.65E-01	1.81E-03	0.97259	0.0016	1	0.0052	-0.02741	0.97259	
129	ust015_20	2.50	6.02E-06	193.3	2.24E-02	2.78E-01	4.52E-04	0.99107	0.00125	1	0.0079	-0.00893	0.99107	
130	ust015_21	2.50	6.52E-06	192.1	2.16E-02	3.03E-01	4.82E-04	0.9934	0.00126	1	0.007	-0.0066	0.9934	
131	ust015_22	2.50	6.63E-06	191.6	2.17E-02	3.16E-01	5.06E-04	0.99152	0.0014	1	0.0062	-0.00848	0.99152	
132	ust015_23	2.50	7.31E-06	191.1	2.14E-02	3.28E-01	5.14E-04	0.99204	0.00132	1	0.0055	-0.00796	0.99204	
133	ust015_24	2.50	7.48E-06	190.8	2.20E-02	3.35E-01	5.55E-04	0.98643	0.00136	1	0.0051	-0.01357	0.98643	
134	ust015_25	2.50	6.65E-06	196.9	2.03E-02	2.14E-01	3.15E-04	0.99277	0.00138	1	0.0023	-0.00723	0.99277	
135	ust015_26	2.50	3.56E-06	204.0	1.46E-02	1.22E-01	1.42E-04	0.98927	0.0015	1	0.0066	-0.01073	0.98927	
136	ust015_27	2.50	3.58E-06	203.6	1.42E-02	1.26E-01	1.39E-04	0.99331	0.00135	1	0.0063	-0.00669	0.99331	
137	ust015_28	2.50	3.56E-06	203.4	1.43E-02	1.28E-01	1.48E-04	0.99313	0.00138	1	0.0058	-0.00687	0.99313	

Results for Volume 5: Uranium-233 Systems

N	Case	nubar	Sigma	AFG	Sigma	EALCF (ev)	sigma	k_calc U233	sigma	Benchmark k-eff	Sigma	Bias = Calculated - Benchmark	Adjusted k-eff U233*	Notes
138	ust015_29	2.50	3.94E-06	203.2	1.44E-02	1.31E-01	1.47E-04	0.99028	0.00139	1	0.0051	-0.00972	0.99028	
139	ust015_30	2.50	3.74E-06	203.1	1.43E-02	1.31E-01	1.45E-04	0.99091	0.00126	1	0.0048	-0.00909	0.99091	
140	ust015_31	2.50	4.19E-06	203.0	1.48E-02	1.33E-01	1.53E-04	0.99285	0.00153	1	0.0055	-0.00715	0.99285	
	Maximum	2.68	2.54E-04	219.1	4.45E-02	1.13E+06	1.46E+03	1.00977	0.00162	1.0051	0.0126	0.00977	1.00977	
	Average	2.51	2.69E-05	174.4	2.47E-02	7.13E+04	9.87E+01	0.99141	0.00130	1.00052	0.0062	-0.0091	0.9909	
	Minimum	2.50	5.64E-07	22.5	2.34E-03	3.65E-02	9.58E-06	0.96649	0.00067	0.9965	0.0007	-0.03351	0.96649	

Table 4.6 Results for Mixed Plutonium - Uranium Systems (Volume 6) with CSAS25 from SCALE 4.4a and the 238-group Library on the J-5600 (CMODB) Workstation

Results for Volume 6: Mixed Plutonium - Uranium Systems

N	Category	Case	nubar	sigma	AFG	sigma	EALCF(ev)	Sigma	k_calc Pu-U	Sigma	Benchmark k-eff	Sigma	Note	Bias = Calculated - Benchmark	Adjusted k-eff Pu-U*
1	CT005	ct005-01	2.843	4.28E-05	194.2	0.032	3.95E-01	1.08E-03	0.996	0.0009	1.0008	0.0022		-0.005	0.995
2		ct006-01	2.809	5.17E-05	194.9	0.033	3.76E-01	1.07E-03	0.991	0.001	1.0016	0.0051		-0.01	0.99
3	CT007	ct007-093array	2.8	4.37E-05	202.5	0.025	1.97E-01	4.43E-04	1.001	0.001	1.0023	0.0035		-0.001	0.999
4		ct007-105al	2.798	4.34E-05	206.5	0.024	1.40E-01	3.14E-04	0.996	0.0008	1.0024	0.0045		-0.007	0.993
5		ct007-105alcd	2.798	4.47E-05	206.3	0.024	1.42E-01	3.17E-04	0.994	0.001	1.0028	0.0044		-0.009	0.991
6		ct007-105array	2.798	3.97E-05	206.3	0.024	1.41E-01	3.05E-04	0.999	0.0011	1.0024	0.0039		-0.003	0.997
7		ct007-105b1	2.798	4.35E-05	206.3	0.023	1.41E-01	2.99E-04	0.993	0.001	1.0024	0.0044		-0.009	0.991
8		ct007-105b1cd	2.798	4.26E-05	206.3	0.022	1.42E-01	2.91E-04	0.993	0.0009	1.0022	0.0044		-0.01	0.99
9		ct007-105b2	2.798	4.17E-05	206.4	0.024	1.41E-01	3.20E-04	0.993	0.0008	1.0026	0.0044		-0.009	0.991

Results for Volume 6: Mixed Plutonium - Uranium Systems

N	Category	Case	nubar	sigma	AFG	sigma	EALCF(ev)	Sigma	k_calc Pu-U	Sigma	Benchmark k-eff	Sigma	Note	Bias = Calculated - Benchmark	Adjusted k-eff Pu-U*
10		ct007-105b2cd	2.798	4.45E-05	206.3	0.024	1.42E-01	3.28E-04	0.991	0.001	1.0025	0.0044		-0.012	0.988
11		ct007-105b3	2.798	4.03E-05	206.4	0.023	1.41E-01	2.96E-04	0.993	0.0008	1.0027	0.0044		-0.009	0.991
12		ct007-105b3cd	2.798	4.16E-05	206.3	0.023	1.42E-01	3.10E-04	0.991	0.001	1.0025	0.0044		-0.011	0.989
13		ct007-105b4	2.798	4.36E-05	206.4	0.023	1.41E-01	3.03E-04	0.995	0.001	1.0025	0.0044		-0.008	0.992
14		ct007-105b4cd	2.798	4.10E-05	206.3	0.024	1.42E-01	3.08E-04	0.992	0.0009	1.0029	0.0044		-0.011	0.989
15		ct007-105cdair	2.798	4.47E-05	206.3	0.023	1.42E-01	3.00E-04	0.992	0.0011	1.0029	0.0044		-0.011	0.989
16		ct007-105cdh2o	2.798	4.22E-05	206.2	0.023	1.43E-01	3.02E-04	0.993	0.0008	1.0028	0.0044		-0.01	0.99
17		ct007-105h1	2.798	4.16E-05	206.4	0.024	1.41E-01	3.14E-04	0.994	0.0011	1.0026	0.0044		-0.009	0.991
18		ct007-105h1cd	2.798	4.15E-05	206.3	0.025	1.42E-01	3.20E-04	0.992	0.0009	1.0025	0.0044		-0.011	0.989
19		ct007-105h2	2.798	4.05E-05	206.3	0.024	1.41E-01	3.09E-04	0.994	0.001	1.0024	0.0044		-0.008	0.992
20		ct007-105h2cd	2.798	4.25E-05	206.3	0.023	1.42E-01	3.08E-04	0.992	0.0008	1.0023	0.0044		-0.01	0.99
21		ct007-105h3	2.798	3.89E-05	206.4	0.022	1.41E-01	2.86E-04	0.993	0.0009	1.002	0.0044		-0.009	0.991
22		ct007-105h3cd	2.798	4.25E-05	206.3	0.023	1.42E-01	3.00E-04	0.992	0.0009	1.002	0.0044		-0.01	0.99
23		ct007-105h4	2.798	4.44E-05	206.4	0.023	1.40E-01	3.07E-04	0.995	0.001	1.0021	0.0044		-0.007	0.993
24		ct007-105h4cd	2.798	4.13E-05	206.3	0.024	1.42E-01	3.08E-04	0.992	0.0008	1.0021	0.0044		-0.01	0.99
25		ct007-105h5	2.798	3.92E-05	206.4	0.024	1.41E-01	3.14E-04	0.995	0.0009	1.002	0.0044		-0.007	0.993
26		ct007-105h5cd	2.798	4.03E-05	206.3	0.022	1.42E-01	2.97E-04	0.991	0.0008	1.0025	0.0044		-0.011	0.989
27		ct007-1143arra	2.797	3.91E-05	208.3	0.021	1.19E-01	2.33E-04	1.001	0.0009	1.0036	0.0046		-0.002	0.998
28		ct007-132array	2.796	3.87E-05	210.6	0.019	9.66E-02	1.78E-04	1.003	0.0009	1.0037	0.0057		-0.001	0.999
29		ct007-1386arra	2.795	3.67E-05	211.2	0.02	9.17E-02	1.76E-04	1	0.0009	1.0044	0.0061		-0.004	0.996
30	CT008	ct008-001	2.799	5.26E-05	194.1	0.032	4.02E-01	1.10E-03	0.991	0.0009	0.9997	0.0032		-0.009	0.991
31		ct008-002	2.796	4.55E-05	202.4	0.024	1.99E-01	4.37E-04	0.997	0.0009	1.0008	0.003		-0.004	0.996
32		ct008-003	2.794	4.07E-05	206.2	0.023	1.42E-01	3.02E-04	0.998	0.0009	1.0023	0.0038		-0.004	0.996
33		ct008-004	2.793	4.31E-05	208.2	0.021	1.19E-01	2.42E-04	1.001	0.0009	1.0015	0.0047		-0.001	0.999
34		ct008-005	2.792	3.69E-05	210.6	0.019	9.70E-02	1.79E-04	1.002	0.0008	1.0022	0.0056		0	1
35		ct008-006	2.791	3.54E-05	211.2	0.019	9.19E-02	1.69E-04	1.002	0.0008	1.0028	0.0065		-0.001	0.999
36		ct008-al	2.794	4.24E-05	206.3	0.024	1.41E-01	3.13E-04	0.997	0.001	1.0023	0.0039		-0.005	0.995
37		ct008-alc	2.794	4.25E-05	206.2	0.022	1.42E-01	2.99E-04	0.995	0.0008	1.0023	0.0041		-0.007	0.993

Results for Volume 6: Mixed Plutonium - Uranium Systems

N	Category	Case	nubar	sigma	AFG	sigma	EALCF(ev)	Sigma	k_calc Pu-U	Sigma	Benchmark k-eff	Sigma	Note	Bias = Calculated - Benchmark	Adjusted k-eff Pu-U*
38		ct008-b1	2.794	4.43E-05	206.3	0.023	1.42E-01	3.04E-04	0.994	0.0009	1.0023	0.0039		-0.008	0.992
39		ct008-b1c	2.794	4.30E-05	206.2	0.023	1.43E-01	3.04E-04	0.993	0.001	1.0023	0.0041		-0.009	0.991
40		ct008-b2	2.794	4.02E-05	206.2	0.022	1.42E-01	2.84E-04	0.995	0.0009	1.0023	0.0039		-0.008	0.992
41		ct008-b2c	2.794	4.40E-05	206.2	0.023	1.42E-01	3.06E-04	0.993	0.0009	1.0023	0.0041		-0.009	0.991
42		ct008-b3	2.794	4.37E-05	206.3	0.022	1.41E-01	2.93E-04	0.996	0.001	1.0023	0.0039		-0.007	0.993
43		ct008-b3c	2.794	4.23E-05	206.2	0.024	1.42E-01	3.07E-04	0.994	0.0009	1.0023	0.0041		-0.008	0.992
44		ct008-b4	2.794	4.26E-05	206.3	0.023	1.42E-01	3.08E-04	0.994	0.0009	1.0023	0.0039		-0.008	0.992
45		ct008-b4c	2.794	4.43E-05	206.2	0.023	1.43E-01	3.05E-04	0.993	0.0009	1.0023	0.0041		-0.009	0.991
46		ct008-cd	2.794	4.40E-05	206.2	0.024	1.43E-01	3.14E-04	0.993	0.0008	1.0023	0.004		-0.009	0.991
47		ct008-cdh2o	2.794	4.39E-05	206.2	0.024	1.42E-01	3.07E-04	0.993	0.001	1.0023	0.004		-0.009	0.991
48		ct008-h1	2.794	4.35E-05	206.3	0.024	1.42E-01	3.08E-04	0.993	0.0008	1.0023	0.0039		-0.01	0.99
49		ct008-h1c	2.794	4.14E-05	206.2	0.023	1.43E-01	3.05E-04	0.993	0.0008	1.0023	0.0041		-0.009	0.991
50		ct008-h2	2.794	4.48E-05	206.3	0.023	1.42E-01	3.04E-04	0.995	0.0009	1.0023	0.0039		-0.007	0.993
51		ct008-h2c	2.794	4.36E-05	206.2	0.025	1.43E-01	3.15E-04	0.995	0.0008	1.0023	0.0041		-0.007	0.993
52		ct008-h3	2.794	4.29E-05	206.3	0.024	1.42E-01	3.10E-04	0.996	0.0009	1.0023	0.0039		-0.006	0.994
53		ct008-h3c	2.794	4.52E-05	206.2	0.024	1.43E-01	3.15E-04	0.994	0.001	1.0023	0.0041		-0.008	0.992
54		ct008-h4	2.794	4.17E-05	206.3	0.024	1.41E-01	3.05E-04	0.996	0.0009	1.0023	0.0039		-0.007	0.993
55		ct008-h4c	2.794	4.41E-05	206.2	0.024	1.43E-01	3.14E-04	0.996	0.0009	1.0023	0.0041		-0.006	0.994
56		ct008-h5	2.794	4.38E-05	206.3	0.023	1.41E-01	2.97E-04	0.996	0.0009	1.0023	0.0039		-0.006	0.994
57		ct008-h5c	2.794	4.24E-05	206.2	0.023	1.43E-01	3.02E-04	0.994	0.0009	1.0023	0.0041		-0.008	0.992
58	CT009	ct009-01	2.858	4.69E-05	191	0.035	5.51E-01	1.68E-03	0.994	0.0009	1.0003	0.0054		-0.006	0.994
59	CT011	ct011-01	2.651	9.21E-05	187	0.05	5.61E-01	1.95E-03	1.003	0.001	1.002	0.0016		0.001	1.001
60	CT012	ct012-01	2.889	1.05E-05	206.6	0.012	1.46E-01	1.81E-04	0.976	0.001	1.0042	0.0058		-0.028	0.972
61		ct012-02	2.889	1.07E-05	206.5	0.013	1.46E-01	1.92E-04	0.978	0.0009	1.0042	0.0058		-0.026	0.974
62		ct012-03	2.889	1.04E-05	206.6	0.013	1.46E-01	1.88E-04	0.976	0.001	1.0042	0.0058		-0.029	0.971
63		ct012-04	2.889	1.01E-05	206.5	0.012	1.47E-01	1.82E-04	0.978	0.0011	1.0042	0.0058		-0.027	0.973
64		ct012-05	2.889	1.02E-05	206.5	0.012	1.47E-01	1.75E-04	0.979	0.001	1.0042	0.0058		-0.025	0.975
65		ct012-06	2.889	1.01E-05	206.5	0.012	1.47E-01	1.84E-04	0.98	0.0008	1.0042	0.0058		-0.024	0.976

Results for Volume 6: Mixed Plutonium - Uranium Systems

N	Category	Case	nubar	sigma	AFG	sigma	EALCF(ev)	Sigma	k_calc Pu-U	Sigma	Benchmark k-eff	Sigma	Note	Bias = Calculated - Benchmark	Adjusted k-eff Pu-U*
66		ct012-07	2.886	4.29E-06	214.8	0.006	6.95E-02	5.02E-05	1.036	0.001	1.0023	0.0036		0.033	1.033
67		ct012-08	2.886	4.43E-06	214.8	0.006	6.93E-02	5.45E-05	1.03	0.001	1.0023	0.0036		0.027	1.027
68		ct012-09	2.886	4.22E-06	214.8	0.006	6.92E-02	5.24E-05	1.028	0.001	1.0023	0.0036		0.026	1.026
69		ct012-10	2.886	4.30E-06	214.8	0.006	6.91E-02	4.83E-05	1.025	0.001	1.0023	0.0036		0.023	1.023
70		ct012-11	2.886	4.51E-06	214.8	0.006	6.91E-02	5.38E-05	1.028	0.001	1.0023	0.0036		0.026	1.026
71		ct012-12	2.886	4.44E-06	214.8	0.006	6.91E-02	5.42E-05	1.032	0.001	1.0023	0.0036		0.03	1.03
72		ct012-13	2.886	4.63E-06	214.8	0.005	6.95E-02	4.81E-05	1.04	0.0009	1.0023	0.0036		0.038	1.038
73		ct012-14	2.888	7.52E-06	206.6	0.014	1.49E-01	2.04E-04	1.019	0.0011	1.0002	0.0027		0.019	1.019
74		ct012-15	2.888	7.66E-06	206.6	0.013	1.49E-01	1.96E-04	1.018	0.0011	1.0002	0.0027		0.018	1.018
75		ct012-16	2.888	8.33E-06	206.7	0.012	1.48E-01	1.84E-04	1.016	0.0013	1.0002	0.0027		0.016	1.016
76		ct012-17	2.888	7.82E-06	206.8	0.012	1.47E-01	1.90E-04	1.015	0.0011	1.0002	0.0027		0.015	1.015
77		ct012-18	2.888	7.62E-06	206.8	0.012	1.47E-01	1.80E-04	1.015	0.001	1.0002	0.0027		0.015	1.015
78		ct012-19	2.888	7.85E-06	206.9	0.013	1.46E-01	1.95E-04	1.012	0.0011	1.0002	0.0027		0.011	1.011
79		ct012-20	2.888	9.27E-06	203.2	0.014	2.04E-01	2.75E-04	1.019	0.0012	1.0004	0.0037		0.019	1.019
80		ct012-21	2.888	9.32E-06	203.2	0.014	2.05E-01	2.85E-04	1.016	0.0013	1.0004	0.0037		0.015	1.015
81		ct012-22	2.888	8.89E-06	203.2	0.014	2.05E-01	2.68E-04	1.016	0.0013	1.0004	0.0037		0.015	1.015
82		ct012-23	2.89	8.81E-06	204.7	0.014	1.75E-01	2.41E-04	1.007	0.0011	0.9997	0.0049		0.008	1.008
83		ct012-24	2.89	8.46E-06	204.8	0.014	1.74E-01	2.38E-04	1.008	0.0011	0.9997	0.0049		0.008	1.008
84		ct012-25	2.89	8.18E-06	204.8	0.014	1.72E-01	2.42E-04	1.006	0.0011	0.9997	0.0049		0.007	1.007
85		ct012-26	2.89	8.20E-06	205	0.014	1.70E-01	2.41E-04	1.005	0.0013	0.9997	0.0049		0.005	1.005
86		ct012-27	2.89	8.28E-06	205.1	0.014	1.68E-01	2.28E-04	1.003	0.0011	0.9997	0.0049		0.003	1.003
87		ct012-28	2.89	8.12E-06	205.2	0.013	1.67E-01	2.16E-04	1.006	0.0011	0.9997	0.0049		0.006	1.006
88		ct012-29	2.89	7.95E-06	205.2	0.014	1.67E-01	2.31E-04	1.006	0.0011	0.9997	0.0049		0.007	1.007
89		ct012-30	2.89	7.98E-06	205.1	0.014	1.69E-01	2.31E-04	1.005	0.0013	0.9997	0.0049		0.006	1.006
90		ct012-31	2.89	9.46E-06	200.4	0.015	2.57E-01	3.63E-04	1.002	0.0011	1.0007	0.0052		0.002	1.002
91		ct012-32	2.89	9.40E-06	200.4	0.014	2.57E-01	3.68E-04	1.001	0.0012	1.0007	0.0052		0.001	1.001
92		ct012-33	2.89	9.32E-06	200.4	0.015	2.57E-01	3.63E-04	0.996	0.0013	1.0007	0.0052		-0.004	0.996
93	MF001	mf001-001	2.954	3.53E-04	22.3	0.013	1.15E+06	1.41E+03	0.993	0.0013	1	0.0016		-0.007	0.993

Results for Volume 6: Mixed Plutonium - Uranium Systems

N	Category	Case	nubar	sigma	AFG	sigma	EALCF(ev)	Sigma	k_calc Pu-U	Sigma	Benchmark k-eff	Sigma	Note	Bias = Calculated - Benchmark	Adjusted k-eff Pu-U*
94	MF002	mf002-001	2.725	3.21E-04	24.3	0.015	9.39E+05	1.32E+03	1.004	0.0012	1	0.0042		0.004	1.004
95		mf002-002	2.722	2.95E-04	24.3	0.015	9.34E+05	1.30E+03	1.006	0.0011	1	0.0044		0.006	1.006
96		mf002-003	2.712	2.90E-04	24.4	0.016	9.32E+05	1.34E+03	1.005	0.0012	1	0.0048		0.005	1.005
97	MF007	mf007-01	2.844	3.67E-04	52.1	0.079	6.45E+04	4.38E+02	1.004	0.001	1	0.0088	1	0.004	1.004
98		mf007-02	2.829	3.60E-04	47	0.071	9.94E+04	6.25E+02	1.01	0.001	1	0.0044	1	0.01	1.01
99		mf007-03	2.801	3.53E-04	32.5	0.034	3.65E+05	1.24E+03	1.006	0.0011	1	0.0054	1	0.006	1.006
100		mf007-04	2.783	3.58E-04	27.8	0.02	6.05E+05	1.40E+03	1.005	0.0012	1	0.0054	1	0.004	1.005
101		mf007-05	2.759	3.30E-04	25.4	0.015	8.37E+05	1.22E+03	1.001	0.0011	1	0.0063	1	0.001	1.001
102		mf007-06	2.744	3.33E-04	24.5	0.014	9.31E+05	1.26E+03	0.997	0.0011	1	0.0069	1	-0.003	0.997
103		mf007-07	2.96	3.61E-04	47.1	0.077	1.02E+05	6.83E+02	1.01	0.0011	1	0.006	1	0.01	1.01
104		mf007-08	2.937	3.49E-04	40.5	0.064	1.79E+05	1.02E+03	1.007	0.001	1	0.0055	1	0.007	1.007
105		mf007-09	2.919	3.36E-04	35.6	0.049	2.74E+05	1.24E+03	1.007	0.001	1	0.0052	1	0.007	1.007
106		mf007-10	2.872	3.37E-04	27.8	0.022	6.00E+05	1.46E+03	1.004	0.0012	1	0.0051	1	0.004	1.004
107		mf007-11	2.844	3.65E-04	25.8	0.016	7.81E+05	1.35E+03	1.001	0.0011	1	0.0049	1	0.001	1.001
108		mf007-12	2.81	3.66E-04	24.4	0.014	9.37E+05	1.29E+03	0.999	0.0011	1	0.0059	1	-0.001	0.999
109		mf007-13	2.793	3.56E-04	23.7	0.013	1.01E+06	1.20E+03	0.998	0.0012	1	0.0064	1	-0.002	0.998
110		mf007-14	3.017	3.13E-04	33.5	0.047	3.40E+05	1.49E+03	1.011	0.001	1	0.006	1	0.011	1.011
111		mf007-15	2.99	3.05E-04	30.3	0.035	4.59E+05	1.57E+03	1.009	0.001	1	0.0059	1	0.009	1.009
112		mf007-16	2.929	3.23E-04	25.9	0.017	7.57E+05	1.42E+03	1.007	0.0013	1	0.0053	1	0.007	1.007
113		mf007-17	2.893	3.49E-04	24.7	0.015	8.89E+05	1.31E+03	1.004	0.0011	1	0.0053	1	0.004	1.004
114		mf007-18	2.852	3.84E-04	23.7	0.014	9.99E+05	1.27E+03	1.003	0.0011	1	0.0057	1	0.003	1.003
115		mf007-19	2.976	3.23E-04	24.8	0.016	8.70E+05	1.49E+03	1.006	0.001	1	0.0062	1	0.006	1.006
116		mf007-20	2.937	3.69E-04	23.8	0.015	9.78E+05	1.39E+03	1.003	0.0014	1	0.0056	1	0.003	1.003
117		mf007-21	2.893	3.51E-04	23.1	0.014	1.06E+06	1.35E+03	1.002	0.0011	1	0.0058	1	0.002	1.002
118		mf007-22	3.018	3.30E-04	23.9	0.015	9.68E+05	1.40E+03	1.004	0.0012	1	0.0055	1	0.004	1.004
119		mf007-23	2.975	3.25E-04	23.2	0.014	1.04E+06	1.37E+03	1.001	0.0011	1	0.0053	1	0.001	1.001
120	MF009	mf009	3.059	2.96E-04	21.9	0.013	1.19E+06	1.40E+03	0.996	0.0013	1	0.001		-0.004	0.996
121	MF010	mf010	2.844	3.56E-04	23.1	0.013	1.07E+06	1.34E+03	0.996	0.0013	1	0.0009		-0.004	0.996

Results for Volume 6: Mixed Plutonium - Uranium Systems

N	Category	Case	nubar	sigma	AFG	sigma	EALCF(ev)	Sigma	k_calc Pu-U	Sigma	Benchmark k-eff	Sigma	Note	Bias = Calculated - Benchmark	Adjusted k-eff Pu-U*
122	MF011	mf011-021b	2.91	1.32E-04	34.8	0.022	2.78E+05	6.99E+02	1.001	0.0008	0.9897	0.0023		0.011	1.011
123		mf011-021c	2.784	1.38E-04	33.8	0.02	3.18E+05	7.19E+02	1.005	0.001	0.9998	0.0023		0.005	1.005
124		mf011-021d	2.694	1.42E-04	37.4	0.025	2.08E+05	5.70E+02	1.009	0.0008	1.0018	0.0024		0.007	1.007
125		mf011-021e	2.604	1.29E-04	35.8	0.021	2.56E+05	6.16E+02	1.008	0.0008	1.0012	0.0024		0.007	1.007
126	MT001	mt001-106	2.885	4.73E-05	193.5	0.045	3.92E-01	1.33E-03	0.996	0.001	1	0.0044		-0.004	0.996
127		mt001-107	2.885	4.07E-05	188.6	0.039	5.79E-01	1.71E-03	1.002	0.0011	1	0.0044		0.002	1.002
128		mt001-109	2.885	4.24E-05	190.8	0.038	4.85E-01	1.39E-03	1.004	0.001	1	0.0044		0.004	1.004
129		mt001-110	2.885	4.39E-05	192.5	0.042	4.23E-01	1.32E-03	0.998	0.001	1	0.0044		-0.002	0.998
130		mt001-111	2.885	4.18E-05	185.6	0.037	7.29E-01	2.00E-03	1.005	0.001	1	0.0044		0.005	1.005
131		mt001-112	2.886	3.91E-05	183.9	0.036	8.48E-01	2.22E-03	1.002	0.0011	1	0.0032		0.002	1.002
132		mt001-113	2.886	3.90E-05	182.4	0.036	9.64E-01	2.56E-03	1.006	0.0008	1	0.0032		0.006	1.006
133		mt001-114	2.886	3.52E-05	181.1	0.037	1.08E+00	2.77E-03	1.002	0.001	1	0.0032		0.002	1.002
134		mt001-115	2.886	3.57E-05	180.2	0.034	1.18E+00	2.82E-03	1.004	0.0008	1	0.0066		0.004	1.004
135		mt001-116	2.886	3.41E-05	179.7	0.036	1.22E+00	2.98E-03	1.005	0.0009	1	0.0066		0.005	1.005
136		mt001-117	2.884	5.27E-06	209.5	0.01	1.14E-01	1.20E-04	1.021	0.0011	1	0.0025		0.021	1.021
137	ST001	st001-a100	2.884	5.07E-06	210.1	0.009	1.08E-01	1.14E-04	1.009	0.0012	1	0.0052		0.009	1.009
138		st001-a108	2.884	3.90E-06	212.8	0.008	8.34E-02	7.51E-05	1	0.001	1	0.0016		0	1
139		st001-a87	2.884	7.44E-06	205.6	0.012	1.60E-01	1.98E-04	0.997	0.0011	1	0.0016		-0.003	0.997
140		st001-a87s	2.884	7.50E-06	205.5	0.013	1.61E-01	2.08E-04	0.998	0.0011	1	0.0016		-0.002	0.998
141		st001-a91	2.884	6.75E-06	205.9	0.013	1.57E-01	2.01E-04	0.992	0.0011	1	0.0016		-0.008	0.992
142		st001-a92	2.884	7.04E-06	205	0.012	1.70E-01	2.08E-04	0.997	0.001	1	0.0016		-0.003	0.997
143		st001-a93	2.884	7.36E-06	204.5	0.013	1.75E-01	2.31E-04	1	0.0011	1	0.0016		0	1
144		st001-a94	2.884	7.88E-06	205	0.013	1.69E-01	2.18E-04	1	0.0012	1	0.0016		0	1
145		st001-a95	2.892	1.01E-05	198.5	0.017	2.83E-01	4.26E-04	1.001	0.0012	1	0.0016		0.001	1.001
146		st001-a96	2.891	7.57E-06	206.5	0.013	1.49E-01	1.87E-04	1.002	0.0011	1	0.0016		0.002	1.002
147		st001-a97	2.891	5.41E-06	211.8	0.01	9.17E-02	9.56E-05	1.003	0.001	1	0.0016		0.003	1.003
148		st001-a98	2.884	5.58E-06	209.4	0.011	1.15E-01	1.30E-04	1.002	0.001	1	0.0016		0.002	1.002
149		st001-a99	2.884	5.45E-06	209.8	0.01	1.11E-01	1.25E-04	1.007	0.001	1	0.0052		0.007	1.007

Results for Volume 6: Mixed Plutonium - Uranium Systems

N	Category	Case	nubar	sigma	AFG	sigma	EALCF(ev)	Sigma	k_calc Pu-U	Sigma	Benchmark k-eff	Sigma	Note	Bias = Calculated - Benchmark	Adjusted k-eff Pu-U*
150	ST002	st002-b11058	2.89	1.67E-06	219.5	0.002	4.19E-02	1.49E-05	1.007	0.0009	1	0.0024		0.007	1.007
151		st002-b11059	2.89	1.60E-06	219.6	0.002	4.18E-02	1.46E-05	1.009	0.0007	1	0.0024		0.009	1.009
152		st002-b63061	2.887	1.55E-06	219.3	0.002	4.28E-02	1.66E-05	1.008	0.0007	1	0.0024		0.008	1.008
153	ST004	st004-d15677	2.889	1.12E-05	196.1	0.018	3.52E-01	5.41E-04	0.999	0.0011	1	0.0026		-0.001	0.999
154		st004-d16678	2.889	1.05E-05	199.3	0.017	2.66E-01	4.12E-04	0.997	0.0013	1	0.0026		-0.003	0.997
155		st004-d19669	2.889	7.38E-06	205.7	0.012	1.60E-01	1.97E-04	0.998	0.0011	1	0.0029		-0.002	0.998
156		st004-d20670	2.889	8.03E-06	203.7	0.013	1.92E-01	2.46E-04	0.997	0.0014	1	0.0029		-0.003	0.997
157		st004-d25665	2.889	3.59E-06	214.6	0.006	7.08E-02	5.43E-05	1	0.0011	1	0.0033		0	1
158		st004-d26666	2.889	3.37E-06	215.2	0.005	6.68E-02	4.82E-05	1.003	0.0011	1	0.0033		0.003	1.003
159		st004-f17583	2.889	9.67E-06	198	0.017	3.01E-01	4.45E-04	0.979	0.0011	1	0.0077		-0.021	0.979
160		st004-f18568	2.889	7.18E-06	204.9	0.012	1.72E-01	2.13E-04	0.984	0.001	1	0.0078		-0.016	0.984
161		st004-f27567	2.889	3.61E-06	214.9	0.006	6.90E-02	5.08E-05	0.982	0.0011	1	0.0068		-0.018	0.982
162	ST005	st005-c13175	2.889	1.11E-05	196	0.018	3.54E-01	5.45E-04	0.989	0.001	1	0.0037		-0.011	0.989
163		st005-c22b74	2.889	7.94E-06	203.6	0.012	1.94E-01	2.43E-04	0.99	0.0013	1	0.0037		-0.01	0.99
164		st005-c23b63	2.889	3.57E-06	214.6	0.006	7.05E-02	5.05E-05	0.997	0.001	1	0.0037		-0.003	0.997
165		st005-d14176	2.889	1.04E-05	200	0.016	2.53E-01	3.75E-04	0.997	0.0013	1	0.0037		-0.003	0.997
166		st005-d21171	2.889	7.46E-06	206.1	0.012	1.55E-01	1.85E-04	1.001	0.0012	1	0.0037		0.001	1.001
167		st005-d21172	2.889	7.32E-06	206.3	0.012	1.52E-01	1.85E-04	1	0.001	1	0.0037		0	1
168		st005-d24164	2.889	3.58E-06	215.3	0.006	6.62E-02	4.91E-05	1.003	0.001	1	0.0037		0.003	1.003
		Maximum	3.059	3.84E-04	219.6	0.079	1.19E+06	1.57E+03	1.04	0.0014	1.0044	0.009		0.038	1.038
		Average	2.85	8.23E-05	170.4	0.02	1.33E+05	2.33E+02	1.001	0.001	1.001	0.004		0	1
		Minimum	2.604	1.55E-06	21.92	0.002	4.18E-02	1.46E-05	0.976	0.0007	0.9897	0.001		-0.029	0.971

Note 1: Experimental Uncertainty for MMF007 is maximum sum from Table 5 in OECD report.

5 Results Analysis

5.1 Introduction

The data in Tables 4.1 through 4.6 provides information for performing analysis of the calculation results, experiment (benchmark) data, and the bias results.

The OECD reports provide an estimate of the actual k_{eff} for each experiment model. While benchmarks for most experiments were estimated to be exactly critical, or k_exp = 1.0, a number of the estimates were above or below exactly critical. It was considered desirable to account for this difference. The following adjustment, to determine an adjusted calculation result, k', was used to calculate adjusted k-effective:

k' = 1 + bias = 1 + (k_cal - k_exp)

where k_cal = code calculated k_{eff} result for the modeled experiment, and
k_exp = OECD estimate of actual k_{eff} for the modeled experiment

The assumption inherent in making this adjustment is that the experiments were close to critical, and if a small adjustment could be made so that the experiment would be exactly critical, the bias of the calculation would not change.

When calculation methods are employed, the subcritical limit is a quantitative value used for implementation of NCSD policy, which is established in accordance with DOE Orders, Standards, or by NRC regulations for those activities under NRC jurisdiction. Evaluation criteria are usually the calculated reactivity, k_{eff}, for the model of the problem being evaluated, uncertainty in the calculated value of reactivity, bias introduced by the code used to calculate reactivity, and bias introduced by the model. Code bias is determined by a validation performed in accordance with ANSI/ANS 8.1. The statistical results determine code bias based on comparison of code calculations with experimental results. Model bias is due to uncertainties in the modeled parameters describing the problem, approximations made for the model to conform to the input requirements of the code, and any significant simplifications of the problem introduced into the model by the analyst. The acceptance criterion requires that the evaluation criteria be bounded by the subcritical limit. In the case of code calculations, the subcritical limit is often a criterion based on calculated k_{eff} and estimated bias and uncertainties.

It is recognized that it may also be possible to determine subcritical limits based on adjustment of correlating parameters other than k_{eff}, as allowed by ANSI/ANS-8.1. These parameters could include physical parameters such as mass or radius, for example, or other calculated parameters besides k_{eff}, if they can be shown to provide subcritical margin. This report does not address other potential correlating parameters, but an analyst could determine them as part of an evaluation and use them to determine subcritical limits in conjunction with the code bias results in this report.

5.2 Discussion of Results

Figure 1 shows a plot of all adjusted k-effective results versus EALCF, or the Energy corresponding to the Average Lethargy of neutrons Causing Fission. EALCF or average energy group has traditionally been used as a trending variable. The amount of data in the middle energy range is somewhat sparse relative to the low and high ends; however, with a few exceptions there are at least some results in almost every energy range. As expected, most k-eff results are centered about 1.0, and are generally within a range of about 1.0 +0.04/-0.03, with the exception of a few results that are outside the range. These high and low data will be discussed in more detail below.

There appears to be a small systematic more negative bias for U-233 results, relative to other fissile categories, in the thermal to intermediate energy range, and some indication of a slight trend in the bias with energy. Otherwise, none of the fissile species appears to consistently have a different bias than other categories, and no other major trends in results are seen.

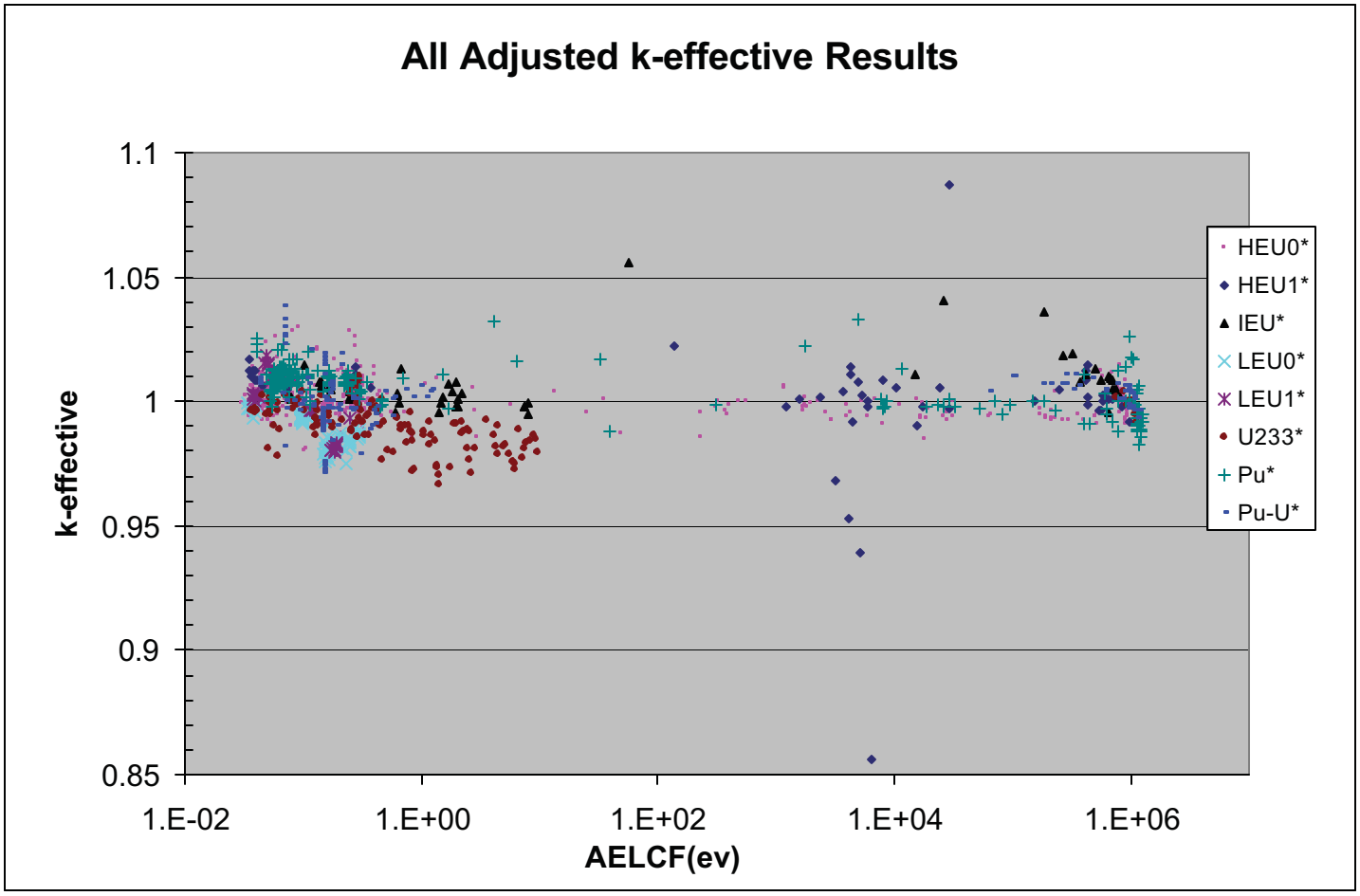

Figure 1 - All Adjusted Results

Figure 2 shows a plot of the HEU, IEU and LEU adjusted k-eff results versus EALCF. While Figure 2 appears to show a possible cluster of LEU results with more negative bias, this is not really the case, as seen in Figure 3, which shows a plot of the LEU results alone.

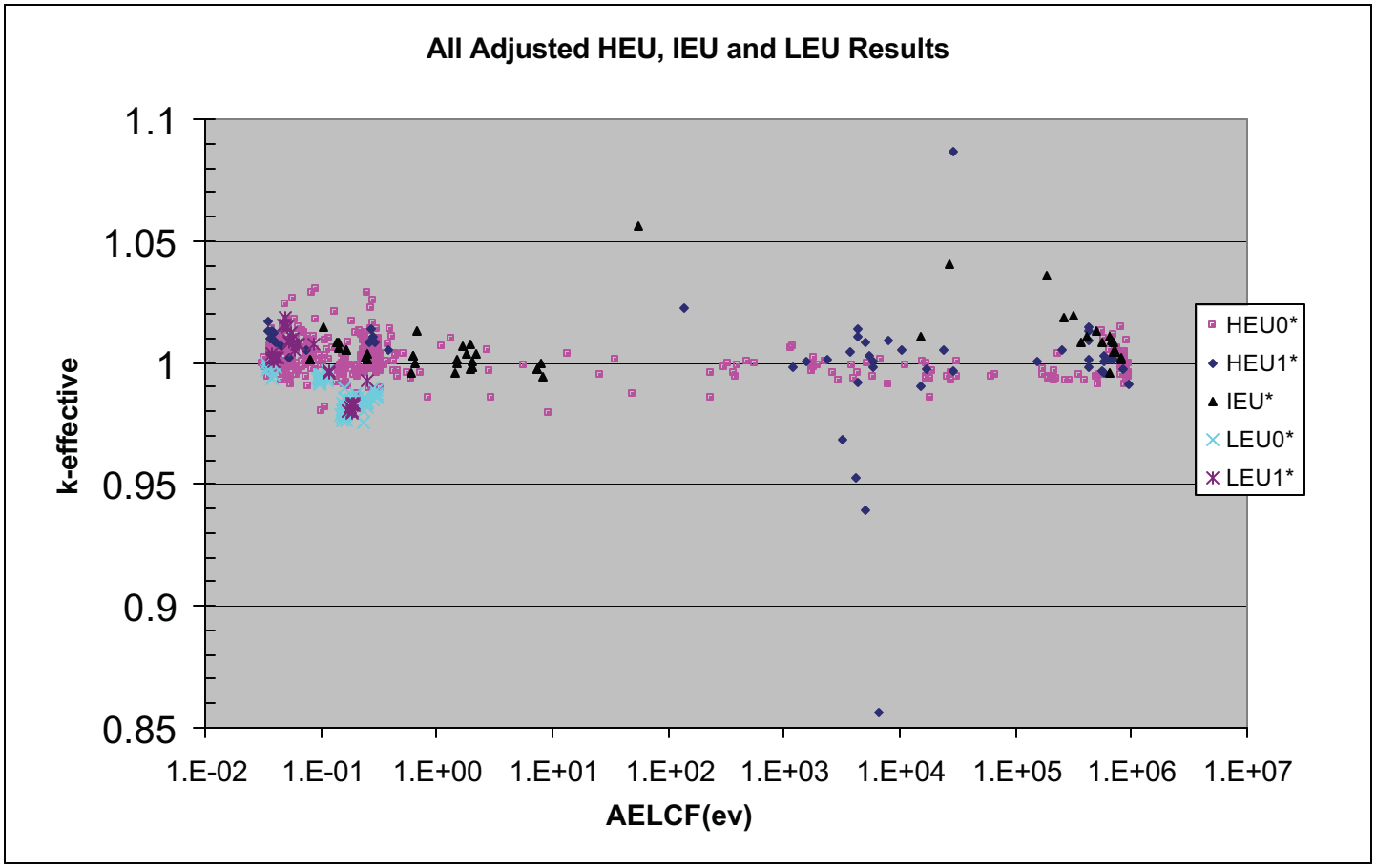

Figure 2 - HEU, IEU and LEU Adjusted Results

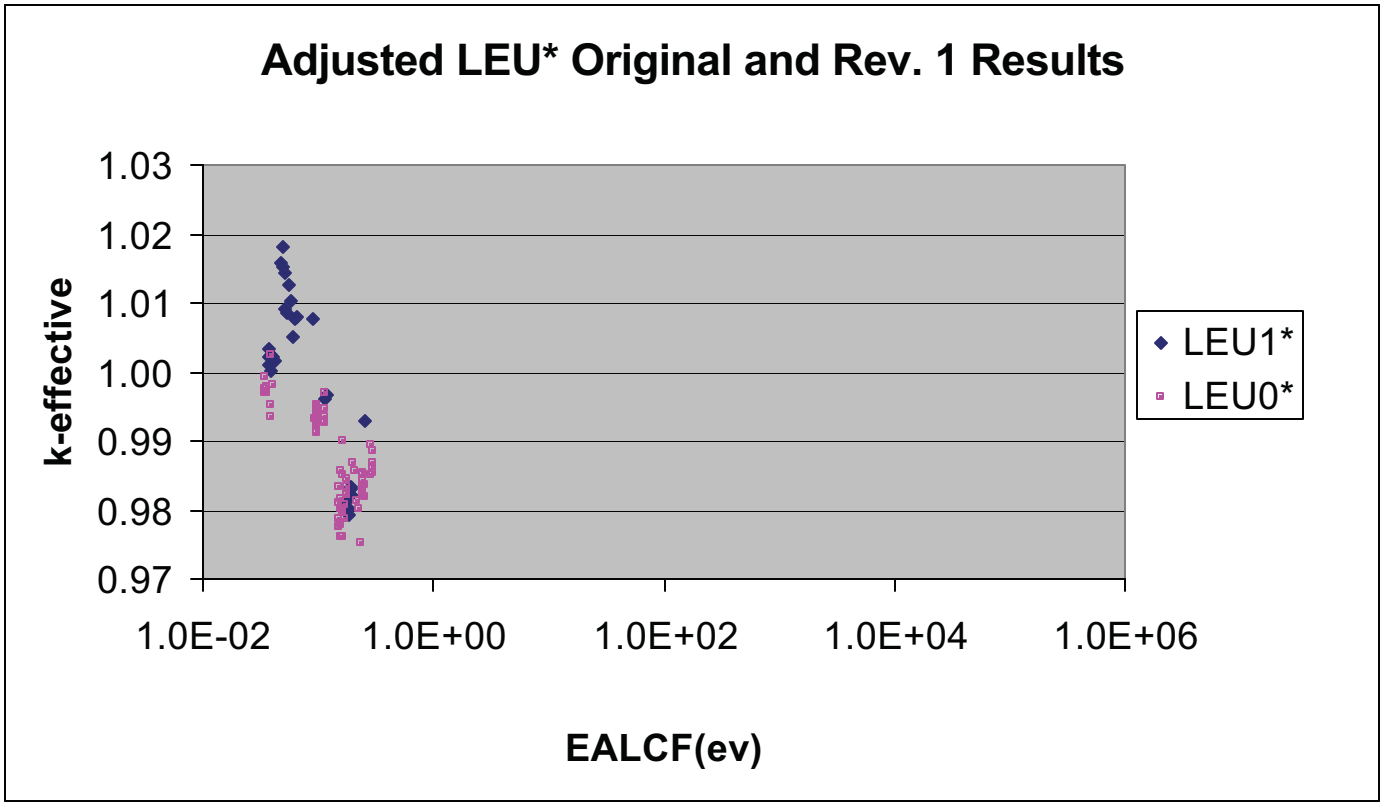

Figure 3 - LEU Adjusted k-eff Results

Figure 4 shows a plot of the IEU adjusted k-eff results versus EALCF. Also highlighted is the fact that several of the "outlying" results are from k-infinite models, which are somewhat different than the usual benchmark experiment, and exaggerate the effects of cross section imperfections. In this category, all the "outlying" results have positive bias.

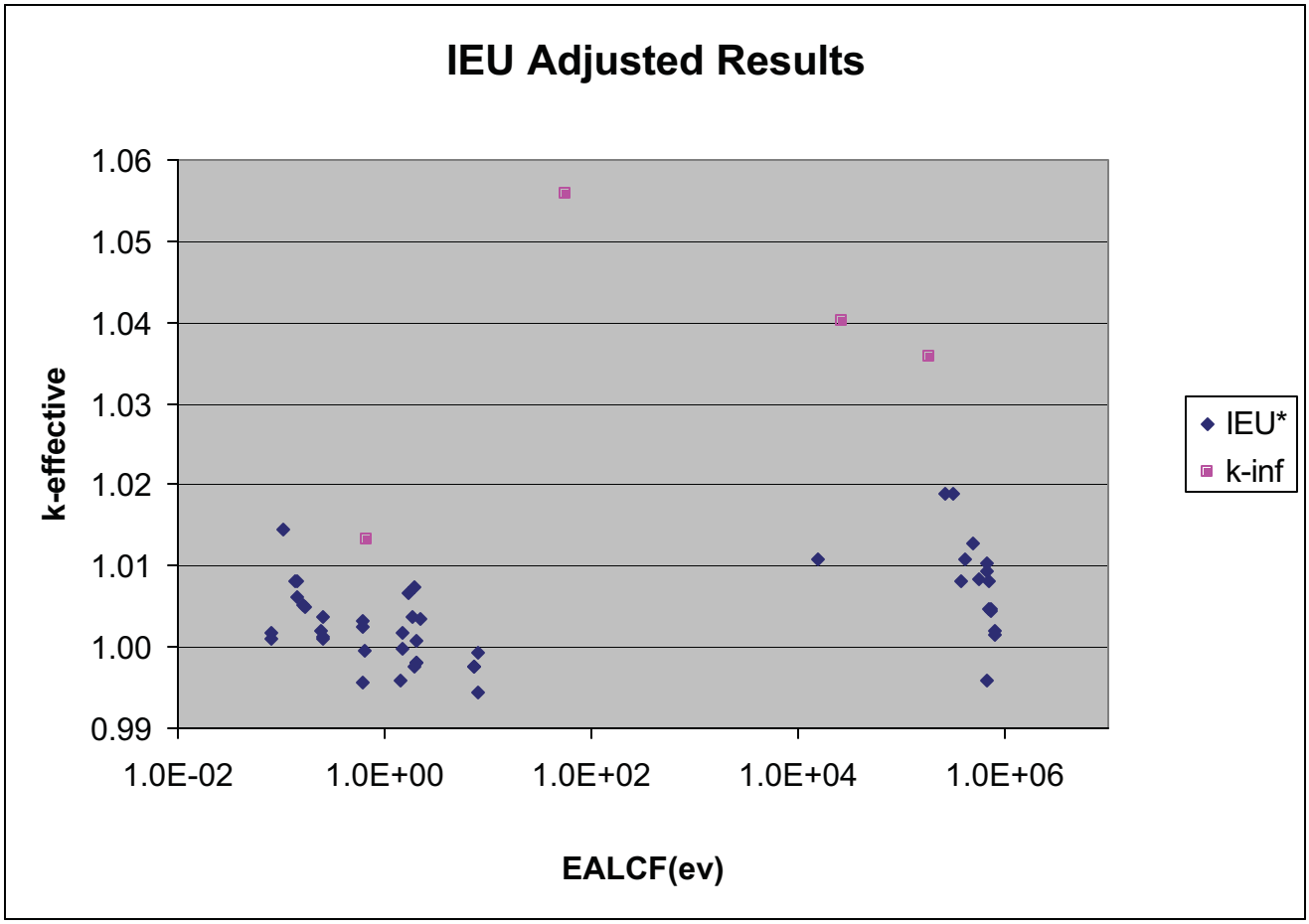

Figure 4 - IEU Adjusted k-eff Results

Figure 5 shows a plot of the HEU adjusted k-eff results versus EALCF. Also highlighted is the fact that four of the "outlying" results, including those having the most negative bias, are from k-infinite models, which are somewhat different than the usual benchmark experiment, and exaggerate the effects of cross section imperfections. It is also clear that one of the HEU results has a very high, positive bias.

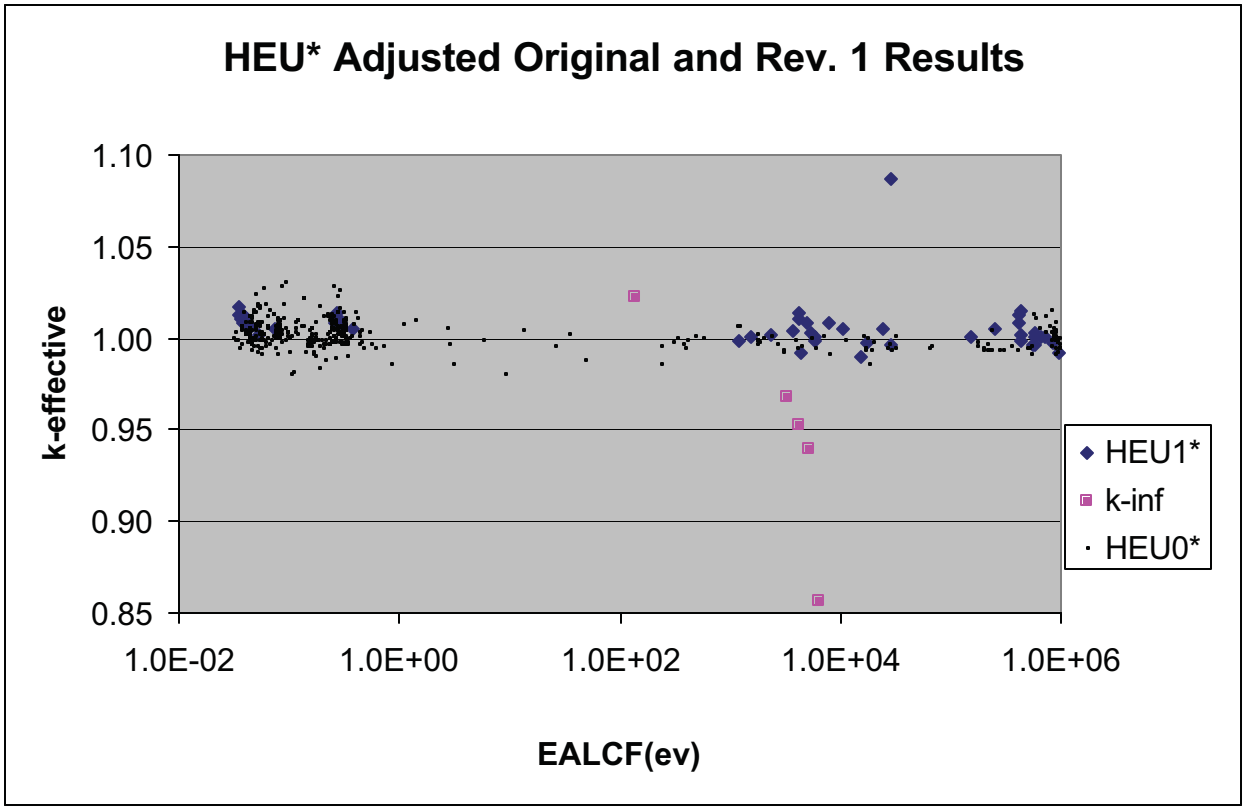

Figure 5 - HEU Adjusted k-eff Results

Figure 6 shows a plot of the adjusted U-233 k-eff results versus EALCF. While this plot appears to confirm the slightly more negative bias at low energies, the existence of a trend with energy appears questionable.

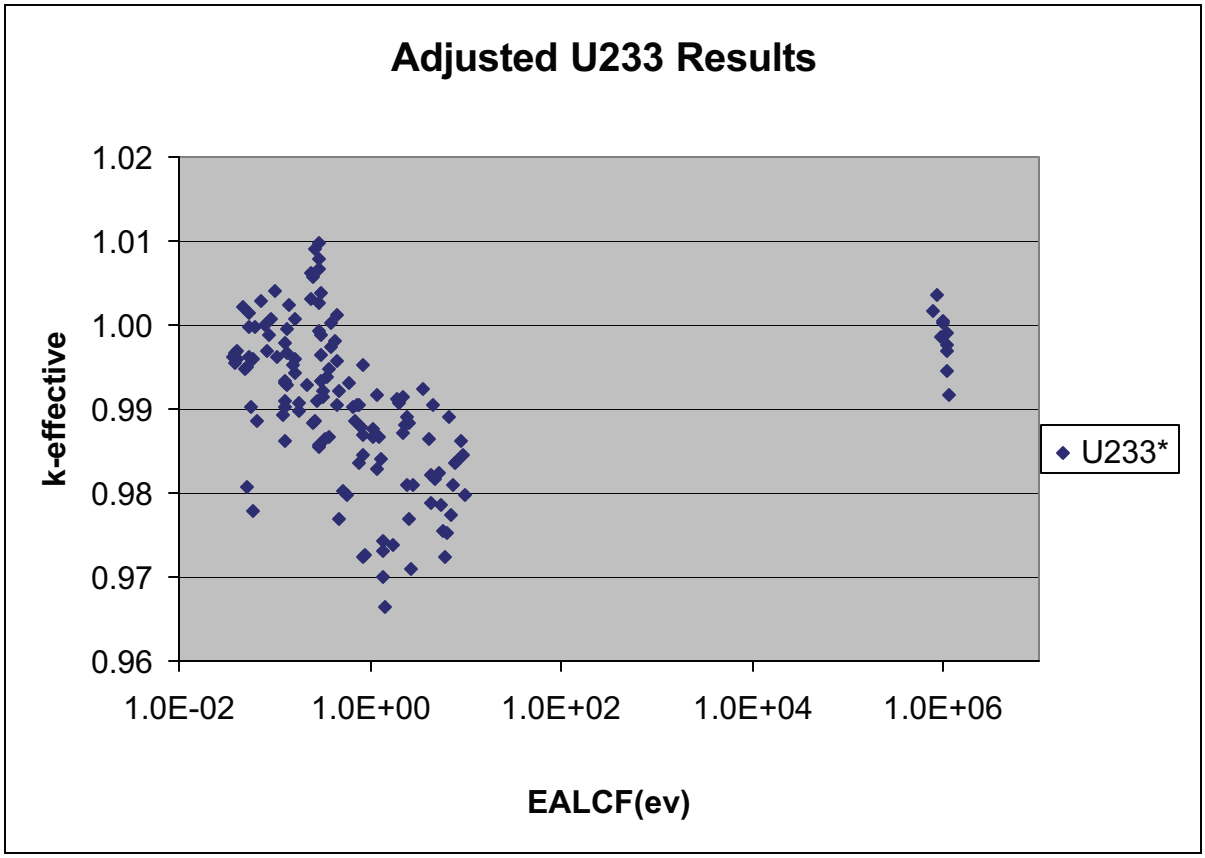

Figure 6 - U-233 Adjusted k-eff Results

Figure 7 shows a plot of the adjusted Pu and Mixed Pu-U results versus EALCF. These results are from Y/DD-996[iv]. The results appear to be consistent with the uranium results (as also seen in Figure 1), although the range of results is generally somewhat larger (excluding "outlying" results in uranium results).

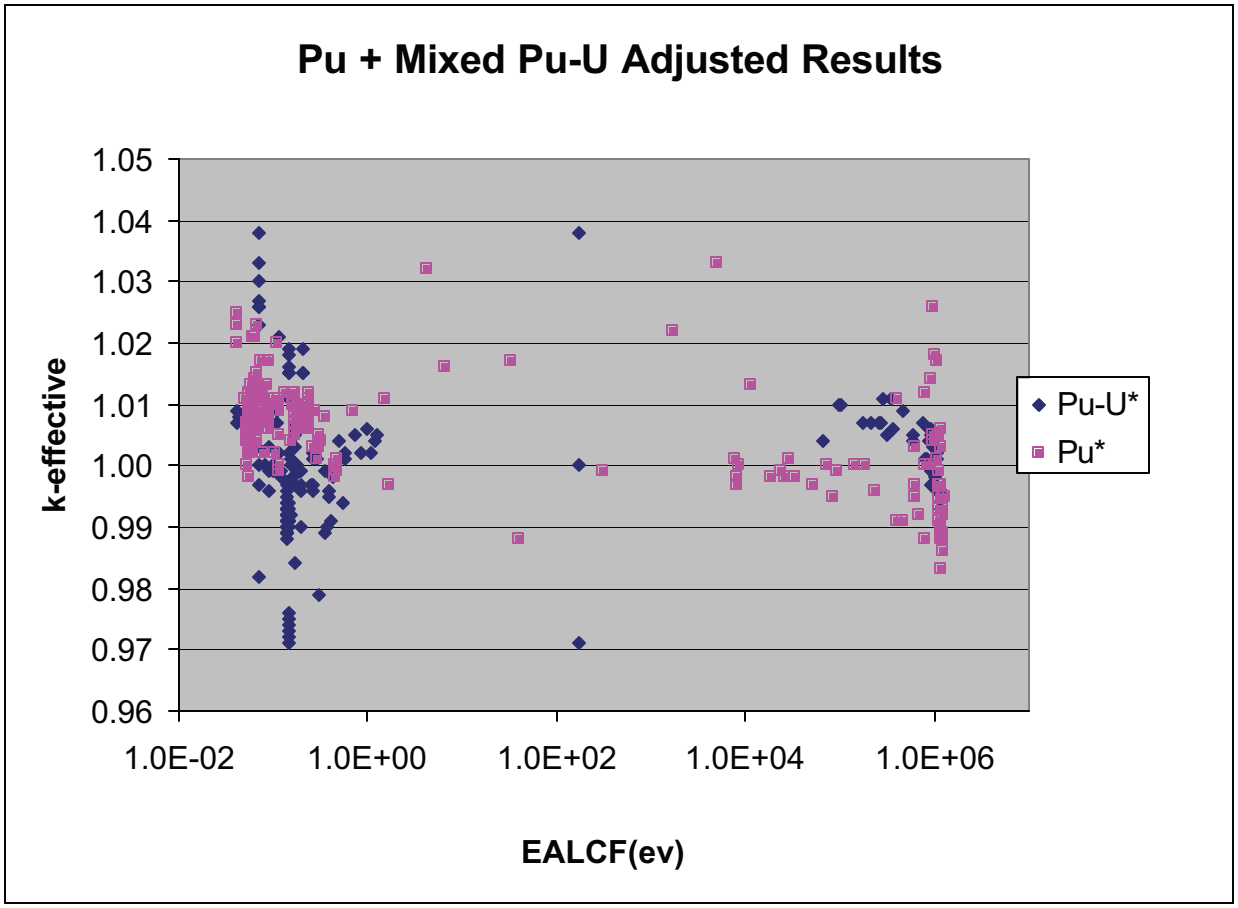

Figure 7 - Pu and Mixed Pu-U Adjusted k-eff Results

Figure 8 shows a plot of adjusted k-eff results versus nubar, or the average number of neutrons produced per fission. Nubar values were not collected for HEU and LEU results from revision 0 of this report; therefore, only a subset of the results is shown. The value of nubar depends on the fissile species and the neutron spectrum, and therefore is thought to possibly incorporate a couple important characteristics of critical systems, and has potential value as an Area of Applicability indicator. For the data plotted, there is no apparent trend across a fairly wide range of nubar values.

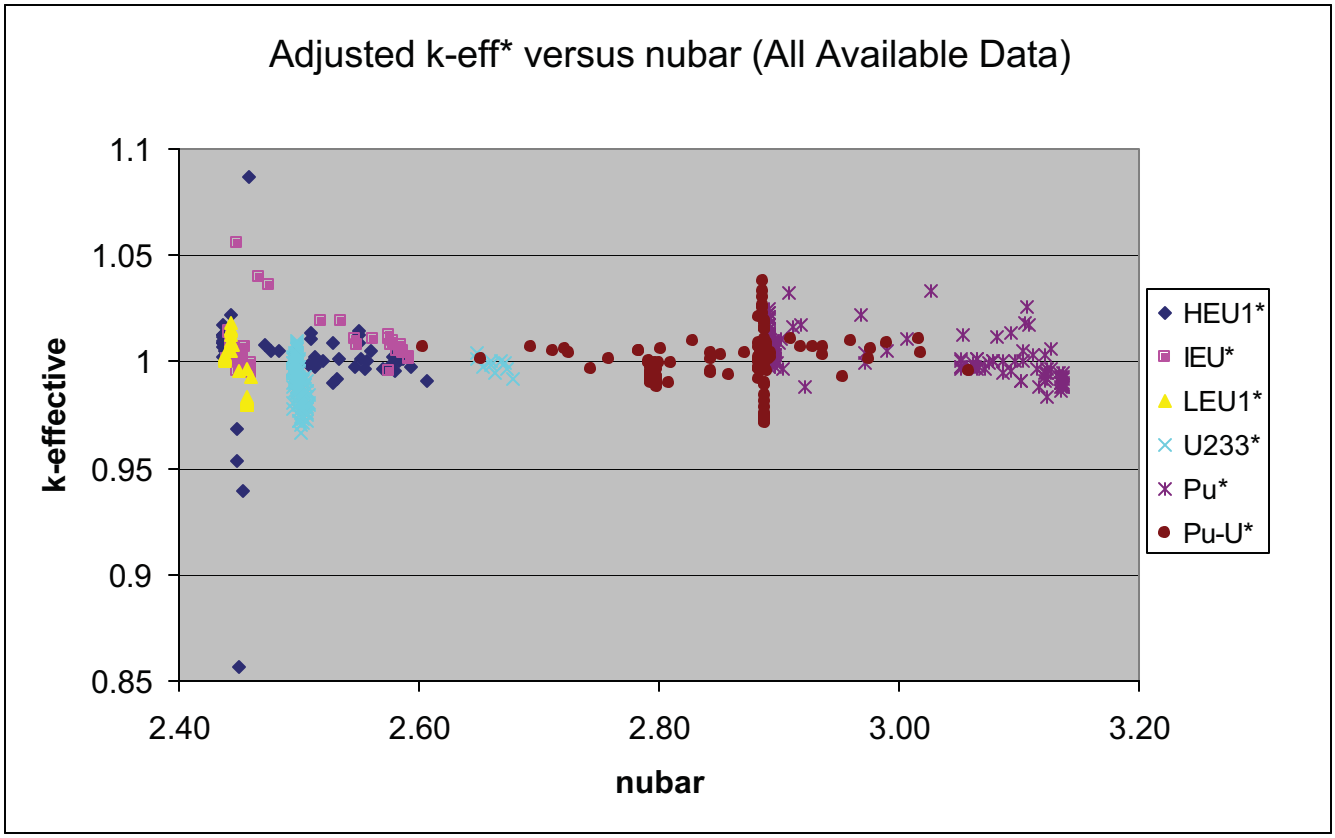

Figure 8 - Adjusted k-eff Results versus Nubar (for all available data)

Figure 9 shows a plot of "raw" calculated k-eff results versus "expected" benchmark k-eff. This illustrates the range of expected results, the range of calculated results, and the agreement between them. Ideally, the results should fall on a line from the lower left to the upper right. As shown, most data is clustered close to about (1.0,1.0), but several data points are significantly different, and experiments with expected results far from 1.0 also usually had larger bias results.

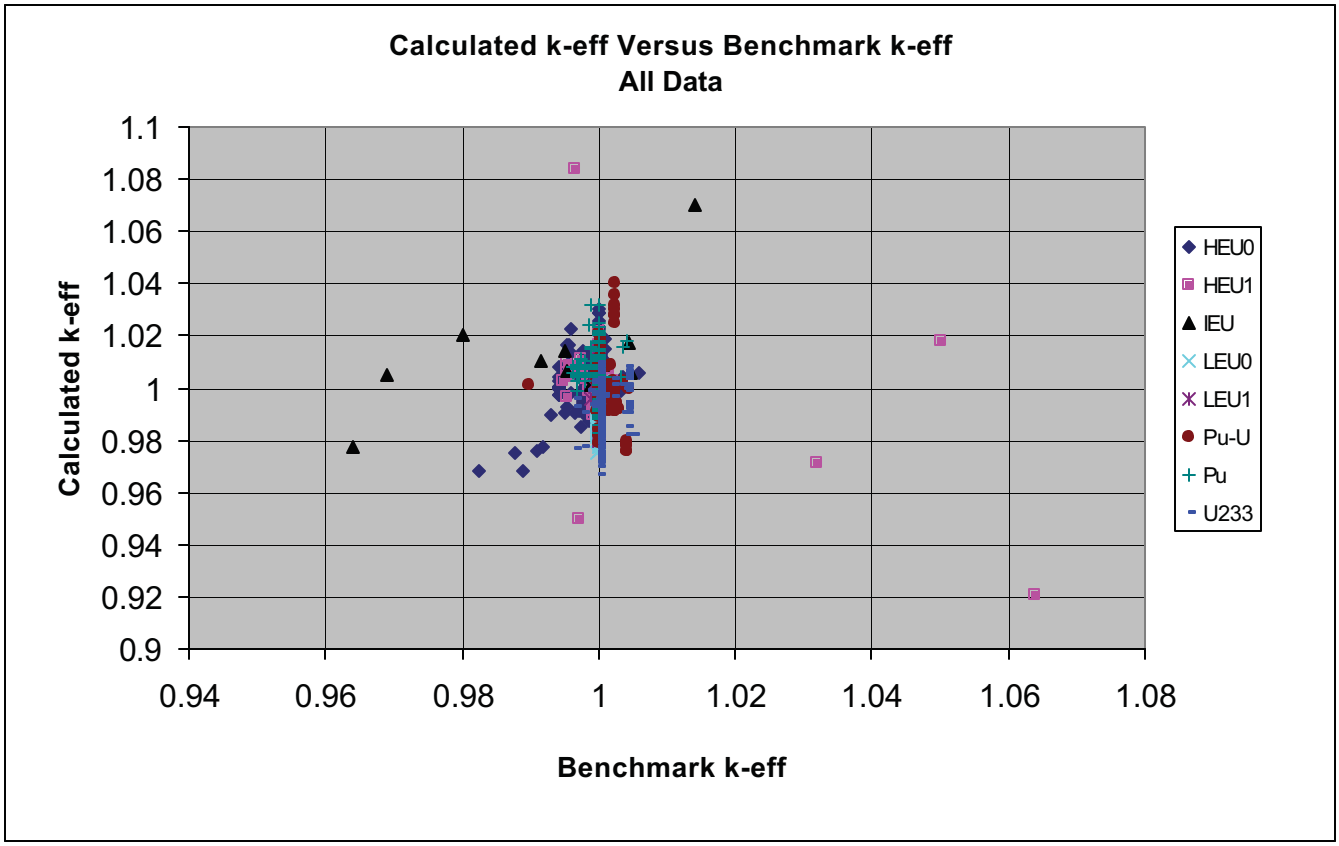

Figure 9 - Calculated k-eff Versus Benchmark k-eff

5.3 Discussion of High Positive and Negative Bias Results

Table 5.1 lists the eight results having adjusted k-effective results less than 0.97 or greater than 1.04, or correspondingly, bias results more negative than -0.03 or more positive than +0.04. These high bias results are consistent with the sample calculation results in the OECD Handbook.

Six of the high bias results are for benchmark experiments that were modeled as infinite in extent, and thereby amplified the effects of imperfections in cross section data. These experiments were all performed at the COBRA facility in the Russian Federation. Unlike most other benchmarks, these models required additional interpretation and adjustment from the actual finite experimental configuration to create an infinite benchmark model. It is noted, however, that other, somewhat similar, infinite models had better results. As an example, see HEU-COMP-INTER-004, which included graphite and boron.

In addition to involving infinite models, particular materials were also involved. The four results from HEU-COMP-INTER-005 with high negative bias included relatively large amounts of chromium, nickel, zirconium, or stainless steel, in infinite models. The two results from IEU-COMP-INTER-001 with high positive bias included relatively large amounts of thorium, in infinite models. HEU-MET-INTER-001, with very high bias, involved relatively large amounts of iron in the core, and stainless steel as a reflector.

No particular problem or unusual circumstance was found with U233-SOL-THERM-005 case 9. As discussed previously, the U-233 results appear to have a slightly more negative bias, in general, as a category, for low energies.

Because of the unusual aspects of the benchmark models, as discussed above, when establishing subcritical limits for general applications, consideration should be given to eliminating, or giving separate treatment to, the high positive and negative bias models HCI005-07,09,15,16; ICI001-002, 003, and HMI001. UST015_09 should be included, but it may be advisable to establish separate, slightly lower subcritical limits for U-233 applications.

Table 5.1 High Positive and Negative Bias Results

Case	nubar	AFG	EALCF(ev)	k_calc	k_exp	Bias = Calculated - Benchmark	k-eff*	Comment
hci005-15	2.45	60.7	6.50E+03	0.92044	1.064	-0.14356	0.85644	k-inf, Cr
hci005-07	2.45	63.8	5.09E+03	0.9712	1.032	-0.0608	0.9392	k-inf, Ni
hci005-16	2.45	64.1	4.18E+03	0.95005	0.997	-0.04695	0.95305	k-inf, Zr
ust015_09	2.50	170.9	1.43E+00	0.96649	1	-0.03351	0.96649	
hci005-09	2.45	66.5	3.21E+03	1.01827	1.05	-0.03173	0.96827	k-inf, St. Steel
ici001-002	2.47	52.075	2.66E+04	1.02029	0.980	0.0403	1.04029	k-inf
ici001-003	2.45	124.130	5.59E+01	1.06991	1.014	0.0559	1.05591	k-inf
hmi001	2.46	51.6	2.93E+04	1.08365	0.9966	0.08705	1.08705	Iron xs problem

5.4 Summary of Results

Tables 4.1-4.6 provide a summary of the calculation results for the benchmark critical experiments. The "raw" k-eff results (k_calc) do not account for the known differences between the estimated benchmark actual k_{eff} (k_exp) and the ideal critical k_{eff} (1.0). The benchmark experiments are near-critical experiments with expected neutron multiplication factors very close to unity. Some experiment benchmarks were enough different from unity to justify accounting for the difference. An "adjusted" k-eff is defined as 1+bias, where bias=k_calc-k_exp, and there results are also shown in Tables 4.1-4.6, and in Figures 1-8.

The only significant, noticeable difference in apparent bias of the results based on enrichment and physical form appears to be for U-233 thermal systems, which had a slightly more negative bias. In the previous revision, it appeared that the high-enriched experiments calculated slightly higher than the low enriched experiments, based on average results. Now, with more low enriched experiments included, the differences appear less pronounced. The difference in range of results has also become smaller. All results are for the 238-group library.

Since simulated infinite models have been included, the range of benchmark k-eff values has increased. Values range from 0.964 to 1.064. "Raw" calculated results ranged from 0.920 to 1.084. Other than a few cases, as shown in Figure 9, most benchmark and calculated results are very close to 1.0.

5.4.1 Area of Applicability

Whether a particular plant application is similar to a sufficient number of experiments contained in the validation set is an important issue. This is a prerequisite before a subcritical limit may be determined from the validation results. Based on the demonstrated performance of the code for a large number of experiments, we have reasonable assurance that it performs well over a wide range of conditions. However, this does not ensure that the code performs as well over all conditions. It does not guarantee that there is not a scenario where the code would calculate unusually low (or high) due to some kind of anomaly or limitation in the code or cross section data. There are some types of experiments that are one or two of a kind. It is possible that there could be one or more of these types of experiments that would exhibit a larger bias than seen in this report, if more experiments of that type were included. The

only way to assess whether the validation set contains a sufficient number of experiments that are similar to a plant application is to carefully compare the details of the experiment description with the details of the plant application. The experiment summary information included in this report, Appendix A, may not provide enough information. The analyst must become familiar with the experiment descriptions provided in the OECD handbook. The DICE database may be very helpful in this regard. The minimum number of similar experiments needed cannot be determined in advance, but the analyst must consider this issue carefully as one of the factors when deciding how much margin to include in determining a subcritical limit. If there are only a few experiments similar to the application, it may be wise to take the time to select additional applicable experiments for addition to the validation set, or to perform a separate evaluation.

Appropriateness of the subcritical limit does not depend solely on the validity of the statistical analysis. Rather, the appropriateness of a subcritical limit depends on two quite different factors: (1) the range of conditions under which a generalization for its use is established, and (2) whether or not the modeled scenario is within the range of these conditions. The criticality safety analyst exercising sound engineering judgment using strong technical arguments must develop these determinations. Extrapolation beyond the range of applicability should not be done.

5.4.2 Grandfather or Retrofit Concerns

The validation documents used for establishing subcritical limits for criticality calculations shall be reviewed and approved by NCSD. There is no urgency to retrofit older evaluations since the common practice provided conservatism. Therefore, the incorporation of the results in this report into the evaluations of existing operations will be accomplished as the Criticality Safety Approvals become obsolete and are replaced due to equipment changes, rule changes, age, etc.

6 Conclusions

This work has demonstrated the validation, or calibration, of the CSAS25 sequence of SCALE4.4a against 1217 benchmark experiments. It provides assurance that the code predicts critical or near critical systems reasonably well, however, in general, based on bias results there is wide variation in performance depending on the type of system. Using a rating scale similar to Reference iii, the performance ranges from "very good" or less than about +/- 0.01 to "very poor" or about +0.087/-0.14 depending on the category of experiments. In general, the previously observed problems resulted in very high bias, which would be conservative for plant applications. This report includes several benchmark cases that significantly under-predict the expected results. There is no guarantee against the possibility of an unusual scenario that could produce non-conservative results, and analysts must be always vigilant for this possibility.

The determination of appropriate correlating parameter and values for limits and additional margin, applicable to a particular analysis, must be determined as part of process analysis. This document does not specify final upper subcritical limits as has been done in the past. It is anticipated that a follow-on report will be written to recommend subcritical limits. Analysts using these results are responsible for

exercising sound engineering judgment using strong technical arguments to develop a margin in k_{eff} or other correlating parameter that is sufficiently large to ensure that conditions (calculated by this method to be subcritical by this margin) will actually be subcritical.

Documentation of determination and justification of the appropriate subcritical limit and margin in the analyst's evaluation, in conjunction with this report, will constitute the complete Validation Report in accordance with ANSI/ANS-8.1-1998, Section 4.3.6(4).

7 Recommendations for Future Work

A report determining subcritical limits applicable to calculated k_{eff}, should be completed soon after this report.

As stated in Section 3, numerous additional OECD experiment descriptions are already available for experiments that would be applicable to Y-12 work. In this regard, future efforts should be dedicated to the following: (1) developing more input decks in-house for experiments selected based on applicability to Y-12, and (2) including additional models as they become available in future revisions of the OECD report. In addition, changes in experiment categorization and interpretation/clarification sometimes are reported in the annual revisions of the OECD handbook. These changes should be reviewed to determine whether they impact the conclusions in this report. This work will require a dedicated effort.

Additional work may be needed to better categorize trends and/or biases by including additional parameters in the statistical evaluation.

Additional work is needed on Area of Applicability (AoA) determination methods. Determining whether a particular application is within the AoA of a validation is currently almost exclusively based on subjective judgment. To be done correctly, it requires the analyst to have close familiarity with the details of the experiments in the validation. Efforts to develop input models for more experiments, particularly if done by several staff members, would have the additional benefit of increasing staff's familiarity with experiment descriptions, which would also help improve these AoA determinations. Continuing such model input preparation work as part of the qualification program is suggested. In addition, methods have been proposed for more rigorous, and quantitative, AoA determinations. A dedicated effort is needed to evaluate these methods to determine if they are effective and practical to implement.

Areas of relatively very poor performance are seen, possibly due to cross section data issues. Efforts to produce improved cross section libraries for SCALE should be supported.

Appendix A - Comparison of Available Experiments with Calculated Experiments

System Type	Acceptable benchmarks in the 2002 OECD Manual	KENO V.a models included in Y/DD-896 Rev 0	KENO V.a models included in Y/DD-996 Rev 1	KENO V.a models added for Y/DD-896 Rev 1	KENO V.a Totals	MCNP4C2 models included in Y/DD-1026 Rev 0	General Description/Comments
Highlighted text indicates additions/changes to Volumes I, II, III, IV, and VII since the 2001 OECD Manual							
Volume I	514	0	270	0	270	0	Plutonium Systems
Volume II	921	407	0	53	460	531	Highly Enriched Uranium Systems
Volume III	61	0	0	51	51	43	Intermediate and Mixed Enrichment Uranium Systems
Volume IV	927	96	0	32	128	0	Low Enriched Uranium Systems
Volume V	166	0	0	140	140	0	Uranium-233 Systems
Volume V	250	0	168	0	168	176	Mixed Plutonium-Uranium Systems
Volume VII	20	0	0	0	0	0	Special Isotope Systems
Totals:	**2859**	**503**	**438**	**276**	**1217**	**750**	

Volume I, Plutonium Systems

Pu METAL SYSTEMS

FAST ENERGY Pu METAL SYSTEMS

PU-MET-FAST-001	1	1	1	Bare Sphere of Plutonium-239 Metal (^{239}Pu Jezebel)
PU-MET-FAST-002	1	1	1	Bare Sphere of Plutonium-240 Metal (^{240}Pu Jezebel)
PU-MET-FAST-003	5	5	5	Unmoderated Plutonium Metal Button Array
PU-MET-FAST-004	9	9	9	Unmoderated Plutonium Metal Cylinder Array - Phase II
PU-MET-FAST-005	1	1	1	Plutonium Sphere Reflected by Tungsten
PU-MET-FAST-006	1	1	1	Plutonium Sphere Reflected by Normal Uranium Using Flattop

System Type	Acceptable benchmarks in the 2002 OECD Manual	KENO V.a models included in Y/DD-896 Rev 0	KENO V.a models included in Y/DD-996 Rev 1	KENO V.a models added for Y/DD-896 Rev 1	KENO V.a Totals	MCNP4C2 models included in Y/DD-1026 Rev 0	General Description/Comments
Highlighted text indicates additions/changes to Volumes I, II, III, IV, and VII since the 2001 OECD Manual							
PU-MET-FAST-007	0	n/a	n/a			n/a	Four Plutonium Spheres with Various Reflector Materials
PU-MET-FAST-008	1		1		1		Thorium Reflected Plutonium Sphere
PU-MET-FAST-009	1		1		1		Plutonium Sphere Reflected by Aluminum
PU-MET-FAST-010	1		1		1		Delta-Phase Plutonium Sphere Reflected by Normal Uranium
PU-MET-FAST-011	1		1		1		Water Reflected Alpha-Phase Pu Sphere
PU-MET-FAST-012	1		1		1		Uranium-Reflected Array of Plutonium Fuel Rods
PU-MET-FAST-013	1		1		1		Copper-Reflected Array of Plutonium Fuel Rods
PU-MET-FAST-014	1		1		1		Nickel-Reflected Array of Plutonium Fuel Rods
PU-MET-FAST-015	1		1		1		Iron-Reflected Array of Plutonium Fuel Rods
PU-MET-FAST-016	6		6		6		Flooded 3x3x3 Arrays of 3-kg Plutonium Metal Cylinders - Phase I
PU-MET-FAST-017	5		5		5		Moderated Plutonium Metal Cylinders Array - Phase II
PU-MET-FAST-018	1		1		1		Delta-Phase Plutonium Sphere Reflected by Beryllium
PU-MET-FAST-019	1						Sphere of Plutonium Reflected by Beryllium
PU-MET-FAST-020	1						Sphere of Plutonium Reflected by Depleted Uranium
PU-MET-FAST-021	2						Beryllium- and Beryllium Oxide-Reflected Cylinders of Plutonium
PU-MET-FAST-022	1		1		1		Bare Spherical Assembly of ^{239}Pu(delta, 98%)
PU-MET-FAST-023	1		1		1		Graphite-Reflected Spherical Assembly of ^{239}Pu(delta, 98%)
PU-MET-FAST-024	1		1		1		Polyethylene-Reflected Spherical Assembly of ^{239}Pu(delta, 98%)
PU-MET-FAST-025	1		1		1		Spherical Assembly of ^{239}Pu(delta, 98%) with 1.55-cm Steel Reflector
PU-MET-FAST-026	1		1		1		Spherical Assembly of ^{239}Pu(delta, 98%) with 11.9-cm Steel Reflector
PU-MET-FAST-027	1		1		1		Polyethylene-Reflected Spherical Assembly of ^{239}Pu(delta, 89%)
PU-MET-FAST-028	1		1		1		Steel-Reflected Spherical Assembly of ^{239}Pu(delta, 89%)
PU-MET-FAST-029	1		1		1		Bare Spherical Assembly of ^{239}Pu(alpha, 88%)
PU-MET-FAST-030	1		1		1		Graphite-Reflected Spherical Assembly of ^{239}Pu(alpha, 88%)
PU-MET-FAST-031	1		1		1		Polyethylene-Reflected Spherical Assembly of ^{239}Pu(alpha, 88%)
PU-MET-FAST-032	1		1		1		Steel-Reflected Spherical Assembly of ^{239}Pu(alpha, 88%)
PU-MET-FAST-033	1		1		1		Cylindrical Assembly of Plutonium Metal Reflected by graphite
PU-MET-FAST-034	0	n/a	n/a			n/a	Asymmetric Spherical Plutonium Reflected by Steel and Oil

System Type	Acceptable benchmarks in the 2002 OECD Manual	KENO V.a models included in Y/DD-896 Rev 0	KENO V.a models included in Y/DD-996 Rev 1	KENO V.a models added for Y/DD-896 Rev 1	KENO V.a Totals	MCNP4C2 models included in Y/DD-1026 Rev 0	General Description/Comments
Highlighted text indicates additions/changes to Volumes I, II, III, IV, and VII since the 2001 OECD Manual							
PU-MET-FAST-035	1		1		1		Spherical Assembly of ^{239}Pu(delta,98%) with 3.15-cm Lead reflector
PU-MET-FAST-036	1		1		1		sph assembly of ^{239}Pu(delta,98%) with compound refl of 0.05-cm Cd and 2.3-cm poly
PU-MET-FAST-037	16		7		7		flooded 2x2xN arrays of 3-kg Plutonium metal cylinders - Phase 2
PU-MET-FAST-039	1		1		1		spherical assembly of ^{239}Pu(delta,98%) with a 4.25-cm Duralumin reflector
PU-MET-FAST-040	1		1		1		spherical assembly of ^{239}Pu(delta,98%) with a 1.6-cm Copper reflector
PU-MET-FAST-041	1		1		1		sperical assembly of ^{239}Pu(alpha,88%) with a 20.98-cm Depleted-Uranium reflector
PU-MET-FAST-045	7						cyl assembly of Pu/Ta/Al metal discs with Fe/Ni/Poly/H_2O reflector (LAMPRE)
INTERMEDIATE ENERGY Pu METAL SYSTEMS							
PU-MET-INTER-001	0	n/a	n/a			n/a	refer to PU-MET-MIXED-001
PU-MET-INTER-002	1						cyl ZPR assembly with a Pu/C/SST core and a SST/FE reflector (ZPR-6/10)
THERMAL ENERGY Pu METAL SYSTEMS							
PU-MET-THERM-001	0	n/a	n/a			n/a	refer to PU-MET-MIXED-001
MIXED ENERGY Pu METAL SYSTEMS							
PU-MET-MIXED-001	6						heterogeneous compositions of Plutonium, Silicon Dioxide, and polyethylene
Pu COMPOUND SYSTEMS							
FAST ENERGY Pu COMPOUND SYSTEMS							
PU-COMP-FAST-001	0						refer to PU-COMP-MIXED-001
PU-COMP-FAST-002	0						refer to PU-COMP-MIXED-002
INTERMEDIATE ENERGY Pu COMPOUND SYSTEMS							

System Type	Acceptable benchmarks in the 2002 OECD Manual	KENO V.a models included in Y/DD-896 Rev 0	KENO V.a models included in Y/DD-996 Rev 1	KENO V.a models added for Y/DD-896 Rev 1	KENO V.a Totals	MCNP4C2 models included in Y/DD-1026 Rev 0	General Description/Comments
Highlighted text indicates additions/changes to Volumes I, II, III, IV, and VII since the 2001 OECD Manual							
PU-COMP-INTER-001	1		1		1		k-infinity experiments in intermediate neutron spectra for ^{239}Pu
THERMAL ENERGY Pu COMPOUND SYSTEMS							
PU-COMP-THERM-001	0						refer to PU-COMP-MIXED-001
PU-COMP-THERM-002	0						refer to PU-COMP-MIXED-002
MIXED ENERGY Pu COMPOUND SYSTEMS							
PU-COMP-MIXED-001	5		5		5		Unreflected Slabs of Polystyrene-Moderated Plutonium Oxide
PU-COMP-MIXED-002	29		4		4		Plexiglas Reflected Slabs of Polystyrene-Moderated Plutonium Oxide
Pu SOLUTION SYSTEMS							
INTERMEDIATE ENERGY Pu SOLUTION SYSTEMS							
none presently evaluated							
THERMAL ENERGY Pu SOLUTION SYSTEMS							
PU-SOL-THERM-001	6		6		6		Water Reflected 11.5" Diameter Spheres of Pu Nitrate Solutions
PU-SOL-THERM-002	7		7		7		Water Reflected 12" Diameter Spheres of Pu Nitrate Solutions
PU-SOL-THERM-003	8		8		8		Water Reflected 13" Diameter Spheres of Pu Nitrate Solutions
PU-SOL-THERM-004	13		13		13		Water Reflected 14" Diameter Spheres of Pu Nitrate Solutions, 0.54% to 3.43%
PU-SOL-THERM-005	9		9		9		Water Reflected 14" Diameter Spheres of Pu Nitrate Solutions, 4.05% and 4.4%
PU-SOL-THERM-006	3		3		3		Water Reflected 15" Diameter Spheres of Pu Nitrate Solutions
PU-SOL-THERM-007	8		8		8		Water Reflected 11.5" Diameter Spheres Partly Filled with Pu Nitrate Solutions
PU-SOL-THERM-008	29						Concrete-Reflected 14-Inch Diameter Spheres of Pu Nitrate Solutions
PU-SOL-THERM-009	3		3		3		Unreflected 48" Diameter Sphere of Pu Nitrate Solution
PU-SOL-THERM-010	14		14		14		Water Reflected 9", 10", 11", and 12" Diameter Cylinders of Pu Nitrate Solutions
PU-SOL-THERM-011	12		12		12		Bare 16" and 18" Diameter Spheres of Pu Nitrate Solutions
PU-SOL-THERM-012	23						Pu Nitrate Soln in a Large Water Reflected Cubic Tank (130x130x100 cm) (19% ^{240}Pu)
PU-SOL-THERM-013	21						Interacting Cylinders of 256-mm Diameter with Pu Nitrate Solution (115.1 gPu/l) in Air

System Type	Acceptable benchmarks in the 2002 OECD Manual	KENO V.a models included in Y/DD-896 Rev 0	KENO V.a models included in Y/DD-996 Rev 1	KENO V.a models added for Y/DD-896 Rev 1	KENO V.a Totals	MCNP4C2 models included in Y/DD-1026 Rev 0	General Description/Comments
Highlighted text indicates additions/changes to Volumes I, II, III, IV, and VII since the 2001 OECD Manual							
PU-SOL-THERM-014	35		34		34		Interacting Cylinders of 300-mm Diameter with Pu Nitrate Solution (115.1 gPu/l) in Air
PU-SOL-THERM-015	17		17		17		Interacting Cylinders of 300-mm Diameter with Pu Nitrate Solution (152.5 gPu/l) in Air
PU-SOL-THERM-016	11		11		11		Interacting Cyls of 300-mm and 256-mm Dia with Pu Nitrate Soln (152.5 and 115.1 gPu/l) in Air
PU-SOL-THERM-017	18		18		18		Interacting Cyls of 256-mm and 300-mm Dia with Pu Nitrate Soln (115.1 gPu/l) in Air
PU-SOL-THERM-020	8		8		8		Water-reflected and Water-cadmium-reflected 14" Diameter Spheres of Pu Nitrate Soln
PU-SOL-THERM-021	6		4		4		Water-Reflected and Bare 15.2" Diameter Spheres of Pu Nitrate Solutions
PU-SOL-THERM-022	17						Pu (19% ^{240}Pu) Nitrate Soln in a Water-Refl Annular Cylinder Tank (50/20 cm Diameter)
PU-SOL-THERM-023	34						Pu (33.89% and 4.23% ^{240}Pu) Nitrate Soln in Two Water-Refl Cylindric Concentric Tanks
PU-SOL-THERM-024	23		23		23		slabs of Pu nitrate solutions reflected by 1-inch thick plexiglas
PU-SOL-THERM-025	44						water reflected slabs of Pu nitrate solutions
PU-SOL-THERM-026	21						unreflected slabs of Pu nitrate solutions

MIXED ENERGY Pu SOLUTION SYSTEMS

none presently evaluated

MISCELLANEOUS Pu SYSTEMS

FAST ENERGY MISCELLANEOUS Pu SYSTEMS

none presently evaluated

INTERMEDIATE ENERGY MISCELLANEOUS Pu SYSTEMS

none presently evaluated

THERMAL ENERGY MISCELLANEOUS Pu

System Type	Acceptable benchmarks in the 2002 OECD Manual	KENO V.a models included in Y/DD-896 Rev 0	KENO V.a models included in Y/DD-996 Rev 1	KENO V.a models added for Y/DD-896 Rev 1	KENO V.a Totals	MCNP4C2 models included in Y/DD-1026 Rev 0	General Description/Comments
Highlighted text indicates additions/changes to Volumes I, II, III, IV, and VII since the 2001 OECD Manual							
SYSTEMS							
none presently evaluated							
MIXED ENERGY MISCELLANEOUS Pu SYSTEMS							
none presently evaluated							
Volume II, Highly Enriched Uranium Systems							
HEU METAL SYSTEMS							
FAST ENERGY HEU METAL SYSTEMS							
HEU-MET-FAST-001	1	1			1	2	bare sphere of U(93.71) metal (Godiva)
HEU-MET-FAST-002	6	6			6	6	U(nat) refl U(93.5) pseudosphere, pseudocylinder, sphere
HEU-MET-FAST-003	10	10			10	12	U(93.5) sphere refl by U(nat), Tungsten Carbide, or Ni
HEU-MET-FAST-004	1	1			1	1	U(97.67) sphere refl by water
HEU-MET-FAST-005	6					6	Be- or Mo-refl cyl assemblies of U(90) alloy with 3.3% Mo
HEU-MET-FAST-006	0	n/a	n/a			n/a	refer to HEU-MET-THERM-003
HEU-MET-FAST-007	43	43			43	42	U(93.15) slabs interleaved with poly, plexiglas, or teflon
HEU-MET-FAST-008	1					1	bare U(90) sphere
HEU-MET-FAST-009	2					2	U(90) sphere refl by Be or BeO
HEU-MET-FAST-010	2					2	U(90) sphere refl by B+Be or B+BeO
HEU-MET-FAST-011	1					1	U(90) sphere refl by poly
HEU-MET-FAST-012	1					1	Al refl spherical assembly of U(90) metal
HEU-MET-FAST-013	1					1	steel refl spherical assembly of U(90) metal
HEU-MET-FAST-014	1					1	U(dep) refl spherical assembly of U(90) metal
HEU-MET-FAST-015	1			1	1	1	bare cylindrical assembly of U(90) metal
HEU-MET-FAST-016	2			2	2	2	Be- or BeO-refl cylindrical assembly of U(90) metal
HEU-MET-FAST-017	1			1	1	1	Be-refl cylindrical assembly of U(90) metal interleaved with Be
HEU-MET-FAST-018	1	1			1	1	bare spherical assembly of U(90) metal
HEU-MET-FAST-019	1	1			1	1	graphite refl spherical assembly of U(90) metal

System Type	Acceptable benchmarks in the 2002 OECD Manual	KENO V.a models included in Y/DD-896 Rev 0	KENO V.a models included in Y/DD-996 Rev 1	KENO V.a models added for Y/DD-896 Rev 1	KENO V.a Totals	MCNP4C2 models included in Y/DD-1026 Rev 0	General Description/Comments
Highlighted text indicates additions/changes to Volumes I, II, III, IV, and VII since the 2001 OECD Manual							
HEU-MET-FAST-020	1	1			1		poly refl spherical assembly of U(90) metal
HEU-MET-FAST-021	1	1			1	1	steel refl spherical assembly of U(90) metal
HEU-MET-FAST-022	1	1			1	1	duralumin refl spherical assembly of U(90) metal
HEU-MET-FAST-023	22	2			2	1	Tinkertoy arrays of 10.5 kg U(93.2) cyl
HEU-MET-FAST-024	1					1	spherical assembly of U(90) metal refl by thin steel and thick poly
HEU-MET-FAST-026	32	5			5	32	Tinkertoy arrays of 15, 20, and 25 kg U(93.2) cyl
HEU-MET-FAST-027	1	1			1	1	Pb refl spherical assembly of U(90) metal
HEU-MET-FAST-028	1	1			1	1	U(93.24) sphere refl by U(nat)
HEU-MET-FAST-029	1	1			1		U(dep) refl spherical assembly of U(90) metal
HEU-MET-FAST-030	1	1			1	1	U(dep) refl cyl assemblies of U(96) metal discs interleaved with Be
HEU-MET-FAST-031	1	1			1	1	poly refl spherical shell of U(90) metal with central cavity of poly
HEU-MET-FAST-032	4	4			4	4	U(nat) refl spherical assemblies of U(94) metal
HEU-MET-FAST-033	2			2	2	2	unrefl cyl assemblies of U(96) metal discs interleaved with poly and steel
HEU-MET-FAST-034	3	3			3	3	unrefl cyl assemblies of U(96) metal discs interleaved with poly and Ti, Al, or steel
HEU-MET-FAST-035	0	n/a	n/a			n/a	deleted and republished as HEU-MET-INTER-001
HEU-MET-FAST-036	2			2	2	2	unrefl cyl assemblies of U(96) metal discs interleaved with poly and U(dep)
HEU-MET-FAST-037	2			2	2	2	poly refl cyl assemblies of U(96) metal discs interleaved with poly and U(dep)
HEU-MET-FAST-038	1			1	1	1	U(dep) refl cyl assembly of U(96) metal discs interleaved with Be and BeO
HEU-MET-FAST-039	0	n/a	n/a			n/a	unrefl and steel refl U(93.2) spherical and hemispherical assemblies
HEU-MET-FAST-041	6			6	6	6	Be- or graphite-refl spherical assemblies of U(94) metal
HEU-MET-FAST-048	17					17	oil refl U(93.2) spherical and hemispherical assemblies with oil,steel, or void cores
HEU-MET-FAST-051	18						unmod & unrefl U(93.2) metal cylinders as individual units and interacting pairs

System Type	Acceptable benchmarks in the 2002 OECD Manual	KENO V.a models included in Y/DD-896 Rev 0	KENO V.a models included in Y/DD-996 Rev 1	KENO V.a models added for Y/DD-896 Rev 1	KENO V.a Totals	MCNP4C2 models included in Y/DD-1026 Rev 0	General Description/Comments
Highlighted text indicates additions/changes to Volumes I, II, III, IV, and VII since the 2001 OECD Manual							
HEU-MET-FAST-055	4			4	4	1	cylindrical honeycomb assembly with a U(93.2)+Al core and U(dep) refl
HEU-MET-FAST-060	1						cyl honeycomb assy with a U(93)-W core with an Al reflector (ZPR-9/4)
HEU-MET-FAST-061	1					1	cyl honeycomb assy with a U(93.2)+U(dep)+Zr+SS core and graphite refl
HEU-MET-FAST-062	1					1	CORAL-I: a cylindrical assembly of U(89.7) with U(nat) refl
HEU-MET-FAST-068	2						cyl assy with a U(90)-Th-Poly core with U(dep)O_2 refl (KBR-22 and KBR-23)
INTERMEDIATE ENERGY HEU METAL SYSTEMS							
HEU-MET-INTER-001	1			1	1	1	cylindrical ZPR assembly with a U(93.2)-Fe core and stainless steel refl
HEU-MET-INTER-002	0	n/a	n/a			n/a	refer to HEU-MET-FAST-034
HEU-MET-INTER-003	0	n/a	n/a			n/a	refer to HEU-MET-FAST-030
HEU-MET-INTER-004	0	n/a	n/a			n/a	refer to HEU-MET-MIXED-004
HEU-MET-INTER-005	0	n/a	n/a			n/a	refer to HEU-MET-MIXED-005
HEU-MET-INTER-006	3			3	3	2	ZEUS: Cu refl cyl assembly of U(93.2) metal plates interleaved with graphite plates
HEU-MET-INTER-007	0	n/a	n/a			n/a	refer to HEU-MET-FAST-007
THERMAL ENERGY HEU METAL SYSTEMS							
HEU-MET-THERM-001	1			1	1		U(93) metal foils interleaved with plates of SiO_2 glass and poly with poly refl
HEU-MET-THERM-002	0	n/a	n/a			n/a	Be-refl Honeycomb assemblies of U(93) foils moderated by graphite
HEU-MET-THERM-003	7	7			7	4	lattices of U(94) cubes immersed in water
HEU-MET-THERM-005	0	n/a	n/a			n/a	refer to HEU-MET-MIXED-005

System Type	Acceptable benchmarks in the 2002 OECD Manual	KENO V.a models included in Y/DD-896 Rev 0	KENO V.a models included in Y/DD-996 Rev 1	KENO V.a models added for Y/DD-896 Rev 1	KENO V.a Totals	MCNP4C2 models included in Y/DD-1026 Rev 0	General Description/Comments
Highlighted text indicates additions/changes to Volumes I, II, III, IV, and VII since the 2001 OECD Manual							
HEU-MET-THERM-006	23	23			23	3	SPERT-D elements [assemblies of U(93)-Al alloy plates] in H_2O, dilute UNH, or borated UNH
HEU-MET-THERM-007	11						SPERT-III type 1S elements [assemblies of U(93.2)O_2 impregnated SS plates] in H_2O
HEU-MET-THERM-008	1						U(93) metal foils interleaved with plates of Al and poly with poly refl
HEU-MET-THERM-009	1						U(93) metal foils interleaved with MgO and poly with poly refl
HEU-MET-THERM-010	1						U(93) metal foils interleaved with plates of Gd and poly with poly refl
HEU-MET-THERM-011	43						U(93)-Al alloy plates immersed in water
MIXED ENERGY HEU METAL SYSTEMS							
HEU-MET-MIXED-001	1	1			1	1	poly refl cyl assemblies of U(96) metal discs interleaved with poly and Ti
HEU-MET-MIXED-002	1	1			1	1	poly refl spherical shell of U(90) metal with central cavity of poly
HEU-MET-MIXED-003	1	1			1	1	poly refl spherical shell of U(90) metal with central cavity of poly
HEU-MET-MIXED-004	1					1	U(dep) refl cyl assemblies of U(96) metal discs interleaved with poly and U(dep)
HEU-MET-MIXED-005	5						large, heterogeneous core assemblies of tubes containing U(89.4) + SiO2 + poly
HEU-MET-MIXED-006	0	n/a	n/a			n/a	refer to HEU-MET-FAST-033
HEU-MET-MIXED-007	0	n/a	n/a			n/a	refer to HEU-MET-FAST-036
HEU-MET-MIXED-008	0	n/a	n/a			n/a	refer to HEU-MET-FAST-037
HEU-MET-MIXED-009	0	n/a	n/a			n/a	refer to HEU-MET-FAST-007
HEU-MET-MIXED-010	0	n/a	n/a			n/a	refer to HEU-MET-THERM-003
HEU COMPOUND SYSTEMS							
FAST ENERGY HEU COMPOUND SYSTEMS							
HEU-COMP-FAST-001	0	n/a	n/a			n/a	refer to HEU-COMP-MIXED-001
HEU-COMP-FAST-003	0	n/a	n/a			n/a	refer to HEU-COMP-MIXED-002
INTERMEDIATE ENERGY HEU COMPOUND SYSTEMS							

System Type	Acceptable benchmarks in the 2002 OECD Manual	KENO V.a models included in Y/DD-896 Rev 0	KENO V.a models included in Y/DD-996 Rev 1	KENO V.a models added for Y/DD-896 Rev 1	KENO V.a Totals	MCNP4C2 models included in Y/DD-1026 Rev 0	General Description/Comments
Highlighted text indicates additions/changes to Volumes I, II, III, IV, and VII since the 2001 OECD Manual							
HEU-COMP-INTER-001	0						deleted and republished as HEU-COMP-MIXED-003
HEU-COMP-INTER-002	0						deleted and republished as HEU-COMP-MIXED-004
HEU-COMP-INTER-003	7			7	7	7	cyl assemblies of canned U(90.7)H_3 disks refl by U(dep), Be, and/or Fe
HEU-COMP-INTER-004	1			1	1	1	k-inf measurements for a homogenous U(92)O_2-graphite-Ca metaborate system
HEU-COMP-INTER-005	5			4	4	5	k-inf measurements for a U(90)O_2 and Ni, SS, SS+Mo, Cr, or Zr system
HEU-COMP-INTER-006	0	n/a	n/a			n/a	refer to HEU-COMP-MIXED-002
THERMAL ENERGY HEU COMPOUND SYSTEMS							
HEU-COMP-THERM-001	0	n/a	n/a			n/a	refer to HEU-COMP-MIXED-001
HEU-COMP-THERM-002	25					25	arrays of hexagonal U(93)-graphite rods (ROVER) immersed in water
HEU-COMP-THERM-003	15					15	two-zone arrays of cross-shaped U(80)O_2-Cu rods immersed in water
HEU-COMP-THERM-004	4					4	arrays of cross-shaped U(90)O_2-Cu rods immersed in water with Gd or Sm rods
HEU-COMP-THERM-005	1					1	clusters of arrays of cross-shaped U(80)O_2-Cu rods immersed in water
HEU-COMP-THERM-006	3					3	arrays of cross-shaped U(80)O_2-Cu rods immersed in water
HEU-COMP-THERM-007	3					3	arrays of cross-shaped U(80)O_2-Cu rods immersed in water with Zr-hydride rods
HEU-COMP-THERM-008	2						arrays of cross-shaped U(80)O_2-Cu rods immersed in water with B_4C rods
HEU-COMP-THERM-010	21	6			6	21	arrays of U(62.4)O_2-BeO rods immersed in water, U(92.6)NH, and/or boric acid
HEU-COMP-THERM-011	3	3			3	3	clusters of 21x21 lattices of U(80)O_2-Al rods immersed in water
HEU-COMP-THERM-012	2	2			2	2	clusters of 18x18 lattices of U(80)O_2-Al rods immersed in water
HEU-COMP-THERM-013	2	2			2	2	clusters of 14x14 lattices of U(80)O_2-Al rods immersed in water
HEU-COMP-THERM-014	2	2			2	2	clusters of 10x10 lattices of U(80)O_2-Al rods immersed in water
HEU-COMP-THERM-015	0	n/a	n/a			n/a	deleted and republished as HEU-COMP-MIXED-002
HEU-COMP-THERM-016	6						graphite refl U(89.3)-graphite blocks (C/X~8180) with Gd_2O_3-graphite control rods
HEU-COMP-THERM-017	9			9	9		lattices of annular cyl U(80)O_2-Al rods immersed in D_2O
INTERMEDIATE ENERGY HEU COMPOUND SYSTEMS							
none presently evaluated							

System Type	Acceptable benchmarks in the 2002 OECD Manual	KENO V.a models included in Y/DD-896 Rev 0	KENO V.a models included in Y/DD-996 Rev 1	KENO V.a models added for Y/DD-896 Rev 1	KENO V.a Totals	MCNP4C2 models included in Y/DD-1026 Rev 0	General Description/Comments
Highlighted text indicates additions/changes to Volumes I, II, III, IV, and VII since the 2001 OECD Manual							
MIXED ENERGY HEU COMPOUND SYSTEMS							
HEU-COMP-MIXED-001	26	7		2	9		arrays of cans of wet or dry $U(93)O_2$ powder with poly refl
HEU-COMP-MIXED-002	23						cans of $U(90)O_2$ powder arrayed and immersed in water or D_2O
HEU-COMP-MIXED-003	6						Be-refl Rx core assemblies of $U(96)O_2$ and Zr-hydride immersed in water
HEU-COMP-MIXED-004	5						Be-refl Rx core assemblies of $U(96)O_2$ and Zr-hydride immersed in sand/water
HEU SOLUTION SYSTEMS							
INTERMEDIATE ENERGY HEU SOLUTION SYSTEMS							
HEU-SOL-INTER-001	0	n/a	n/a			n/a	refer to HEU-SOL-THERM-004 and HEU-SOL-THERM-020
HEU-SOL-INTER-002	0	n/a	n/a			n/a	refer to HEU-SOL-THERM-039
THERMAL ENERGY HEU SOLUTION SYSTEMS							
HEU-SOL-THERM-001	10	10			10	10	U(93.2)NH soln in cyl geom, 50-360 gU/l, minimal refl
HEU-SOL-THERM-002	14	14			14	14	U(93.2)NH soln in cyl geom, 60-335 gU/l, concrete refl
HEU-SOL-THERM-003	19	19			19	19	U(93.2)NH soln in cyl geom, 60-345 gU/l, Plexiglas refl
HEU-SOL-THERM-004	6	6			6	6	$U(93.65)O_2F_2$ in D_2O soln in sph geom, D/X from 34 to 430, D_2O refl
HEU-SOL-THERM-005	17	8			8		Pyrex glass poisoned U(87.4)NH or $U(93.2)O_2F_2$ soln in cyl geom, varied H_2O refl
HEU-SOL-THERM-006	29	7			7		boric acid poisoned U(93)NH soln in cyl geom, 295 gU/l, various refl combinations
HEU-SOL-THERM-007	17	17			17	5	concrete refl arrays of U(93.2)NH soln cylinders, 67-370 gU/l
HEU-SOL-THERM-008	14	14			14	14	Plexiglas refl arrays of U(93.2)NH soln cylinders, 60-356 gU/l
HEU-SOL-THERM-009	4	4			4	4	$U(93.2)O_2F_2$ soln in 6.4 liter sph geom, 213-696 gU/l, water refl
HEU-SOL-THERM-010	4	4			4	4	$U(93.2)O_2F_2$ soln in 9.7 liter sph geom, 95-107 gU/l, water refl
HEU-SOL-THERM-011	2	2			2	2	$U(93.2)O_2F_2$ soln in 17 liter sph geom, 48-50 gU/l, water refl
HEU-SOL-THERM-012	1	1			1		$U(93.2)O_2F_2$ soln in 91 liter sph geom, 20.5 gU/l, water refl
HEU-SOL-THERM-013	4	4			4	4	boric acid poisoned U(93.2)NH soln in 174 liter sph geom, 20-28 gU/l, unrefl
HEU-SOL-THERM-014	3	3			3	3	Gd poisoned U(89)NH soln in cyl geom, ~70 gU/l, water refl
HEU-SOL-THERM-015	5	5			5	5	Gd poisoned U(89)NH soln in cyl geom, ~100 gU/l, water refl

System Type	Acceptable benchmarks in the 2002 OECD Manual	KENO V.a models included in Y/DD-896 Rev 0	KENO V.a models included in Y/DD-996 Rev 1	KENO V.a models added for Y/DD-896 Rev 1	KENO V.a Totals	MCNP4C2 models included in Y/DD-1026 Rev 0	General Description/Comments
Highlighted text indicates additions/changes to Volumes I, II, III, IV, and VII since the 2001 OECD Manual							
HEU-SOL-THERM-016	3	3			3	3	Gd poisoned U(89)NH soln in cyl geom, ~150 gU/l, water refl
HEU-SOL-THERM-017	8	8			8	8	Gd poisoned U(89)NH soln in cyl geom, ~200 gU/l, water refl
HEU-SOL-THERM-018	12	12			12	12	Gd poisoned U(89)NH soln in cyl geom, ~300 gU/l, water refl
HEU-SOL-THERM-019	3	3			3	3	Gd poisoned U(89)NH soln in cyl geom, ~400 gU/l, water refl
HEU-SOL-THERM-020	5	5			5	5	U(93.65)O_2F_2 in D_2O soln in sph geom, D/X from 230 to 2080, unrefl
HEU-SOL-THERM-021	32	6		4	10		bare and hydrogenous refl arrays of U(93.2)NH soln cylinders, 63-415 gU/l
HEU-SOL-THERM-022	1						intersection of two steel pipes containing U(89)NH soln, 141 gU/l, water refl
HEU-SOL-THERM-023	1						steel pipe intersections containing U(89)NH soln, 408 gU/l, water refl
HEU-SOL-THERM-024	14					14	steel pipe intersections containing U(89)NH soln, 64-386 gU/l, bare and water refl
HEU-SOL-THERM-025	18	18			18	18	Gd poisoned U(89)NH soln in cyl geom, 48-400 gU/l, water refl
HEU-SOL-THERM-027	9	9			9	9	unrefl U(89)NH soln in cyl geom, 136 gU/l, central rod of B_4C, Cd, or n/a
HEU-SOL-THERM-028	18	18			18	18	water refl U(89)NH soln in cyl geom, 76 or 286 gU/l, central rod of B_4C or n/a
HEU-SOL-THERM-029	7	7			7	7	water refl U(89)NH soln in cyl geom, 286 gU/l, seven rods of B_4C or n/a
HEU-SOL-THERM-030	7	7			7	7	water refl U(89)NH soln in cyl geom, 76 or 286 gU/l, 3-6 rods of B_4C or n/a
HEU-SOL-THERM-031	4	4			4		water refl U(89)NH soln in cyl geom, 286 gU/l, 18 or 36 rods of B_4C
HEU-SOL-THERM-032	1	1			1		U(93.2)NH soln in 48" dia. sph geom, ~15 gU/l, unrefl
HEU-SOL-THERM-033	26	26			26	26	ann cyl tanks of U(93.2)NH soln, 357 gU/l, cavity of varius matls, concrete refl
HEU-SOL-THERM-035	9	9			9	9	water refl U(89)NH soln in cyl geom, 37-152 gU/l, multiple rods of B_4C or n/a
HEU-SOL-THERM-036	4	4			4	4	unrefl U(89)NH soln in cuboidal geom, 92.7 gU/l, multiple rods of B_4C or n/a
HEU-SOL-THERM-037	9	9			9	9	water refl U(89)NH soln in cyl geom, 42-83 gU/l, multiple rods of B_4C or n/a
HEU-SOL-THERM-038	30						U(93)NH soln @ 404 gU/l in two cyl slab tanks, mod/refl by H, B, Be, Pb, SS, Cd, or U(dep)
HEU-SOL-THERM-039	6					6	liquid U(93.2)F_6+HF at low H/U (9.9 to 82) in a spherical tank with hot water reflection
HEU-SOL-THERM-040	17						U(93)NH soln @ 453 gU/l in unrelfected intersecting pipe configurations
HEU-SOL-THERM-042	8					8	unreflected 5-ft or 9-ft diameter cylinders of U(93.2)NH soln @ 13.6 to 17.3 gU/l

System Type	Acceptable benchmarks in the 2002 OECD Manual	KENO V.a models included in Y/DD-896 Rev 0	KENO V.a models included in Y/DD-996 Rev 1	KENO V.a models added for Y/DD-896 Rev 1	KENO V.a Totals	MCNP4C2 models included in Y/DD-1026 Rev 0	General Description/Comments
Highlighted text indicates additions/changes to Volumes I, II, III, IV, and VII since the 2001 OECD Manual							
HEU-SOL-THERM-043	3					3	17-, 91-, or 174-liter U(93.2)O_2F_2 soln in sph geom @ 134-, 25-, or 20-gU/l, unrefl
HEU-SOL-THERM-044	31						concrete refl U(93.2)NH soln cyl @ 363 gU/l, cyl geom w/per dist of neut abs rods
HEU-SOL-THERM-045	0	n/a	n/a			n/a	"Tuck and Clark" interacting U(93.2)NH slab-cylinder experiments
SUB-HEU-SOL-THERM-001	5						^{252}Cf-driven noise measurements of unrefl U(93.2)NH soln @ 482 gU/l in cyl geom
MIXED ENERGY HEU SOLUTION SYSTEMS							
none presently evaluated							
MISCELLANEOUS HEU SYSTEMS							
FAST ENERGY MISCELLANEOUS HEU SYSTEMS							
none presently evaluated							
INTERMEDIATE ENERGY MISCELLANEOUS HEU SYSTEMS							
none presently evaluated							
THERMAL ENERGY MISCELLANEOUS HEU SYSTEMS							
HEU-MISC-THERM-001	0	n/a	n/a			n/a	refer to HEU-MET-THERM-006
HEU-MISC-THERM-002	0	n/a	n/a			n/a	refer to HEU-COMP-THERM-010
MIXED ENERGY MISCELLANEOUS HEU SYSTEMS							
none presently evaluated							
Volume III, Intermediate and Mixed Enrichment Uranium Systems							
IEU METAL SYSTEMS							
FAST ENERGY IEU METAL SYSTEMS							
IEU-MET-FAST-001	4			4	4	4	unrefl cyl U(93.4) metal discs interleaved with U(nat), effectively U(36) or U(55)

System Type	Acceptable benchmarks in the 2002 OECD Manual	KENO V.a models included in Y/DD-896 Rev 0	KENO V.a models included in Y/DD-996 Rev 1	KENO V.a models added for Y/DD-896 Rev 1	KENO V.a Totals	MCNP4C2 models included in Y/DD-1026 Rev 0	General Description/Comments
Highlighted text indicates additions/changes to Volumes I, II, III, IV, and VII since the 2001 OECD Manual							
IEU-MET-FAST-002	1			1	1	1	U(nat) refl cyl U(93.4) metal discs interleaved with U(nat), effectively U(16)
IEU-MET-FAST-003	1			1	1	1	bare spherical assembly of U(36) metal
IEU-MET-FAST-004	1			1	1	1	graphite refl spherical assembly of U(36) metal
IEU-MET-FAST-005	1			1	1	1	steel refl spherical assembly of U(36) metal
IEU-MET-FAST-006	1			1	1	1	Al refl spherical assembly of U(36) metal
IEU-MET-FAST-007	1			1	1	1	cyl assembly of U(93), U(10), and U(nat) metal, effectively U(10) core, U(dep) refl
IEU-MET-FAST-008	1			1	1	1	U(dep) refl spherical assembly of U(36) metal
IEU-MET-FAST-009	1			1	1	1	poly refl spherical assembly of U(36) metal
IEU-MET-FAST-010	1			1	1	1	cyl ZPR assembly with a U(93)+U(dep) core [effectively U(9)] with U(dep) refl
IEU-MET-FAST-012	1			1	1	1	cyl ZPR assembly with a U(93)+U(dep)+Al+Fe core with U(dep) refl (ZPR-3/41)
IEU-MET-FAST-014	2			2	2		cyl ZPR assembly with a U(93)+U(dep)+W metal core with Al refl (ZPR-9/2 and 3)
INTERMEDIATE ENERGY IEU METAL SYSTEMS							
none presently evaluated							
THERMAL ENERGY IEU METAL SYSTEMS							
none presently evaluated							
MIXED ENERGY IEU METAL SYSTEMS							
none presently evaluated							
IEU COMPOUND SYSTEMS							
FAST ENERGY IEU COMPOUND SYSTEMS							
IEU-COMP-FAST-002	0	n/a	n/a			n/a	refer to IEU-COMP-INTER-001

System Type	Acceptable benchmarks in the 2002 OECD Manual	KENO V.a models included in Y/DD-896 Rev 0	KENO V.a models included in Y/DD-996 Rev 1	KENO V.a models added for Y/DD-896 Rev 1	KENO V.a Totals	MCNP4C2 models included in Y/DD-1026 Rev 0	General Description/Comments
Highlighted text indicates additions/changes to Volumes I, II, III, IV, and VII since the 2001 OECD Manual							
INTERMEDIATE ENERGY IEU COMPOUND SYSTEMS							
IEU-COMP-INTER-001	4			4	4		k-inf measurements for tube assemblies of $U(93)O_2$+$U(36)O_2$+Th+poly
THERMAL ENERGY IEU COMPOUND SYSTEMS							
IEU-COMP-THERM-001	29			29	29	21	arrays of $U(30)F_4$-polytetrafluoroethylene and polyethylene cubes
IEU-COMP-THERM-002	6					6	latticed annular $U(17)O_2$ rods in H_2O, annuli of H_2O, Gd_2O_3-Al_2O_3, or CdO-Al_2O_3
IEU-COMP-THERM-003	2			2	2	2	lattices of cyl U(20)-Zr-hydride rods in H_2O, graphite refl
IEU-COMP-THERM-005	0	n/a	n/a			n/a	refer to IEU-COMP-INTER-001
MIXED ENERGY IEU COMPOUND SYSTEMS							
none presently evaluated							
IEU SOLUTION SYSTEMS							
THERMAL ENERGY IEU SOLUTION SYSTEMS							
IEU-SOL-THERM-001	4						$U(20.9)O_2SO_4$ soln in cyl geom, 263-505 gU/l, graphite refl
MISCELLANEOUS IEU SYSTEMS							
FAST ENERGY MISCELLANEOUS IEU SYSTEMS							
none presently evaluated							
INTERMEDIATE ENERGY MISCELLANEOUS IEU SYSTEMS							
none presently evaluated							
THERMAL ENERGY MISCELLANEOUS IEU SYSTEMS							
none presently evaluated							

System Type	Acceptable benchmarks in the 2002 OECD Manual	KENO V.a models included in Y/DD-896 Rev 0	KENO V.a models included in Y/DD-996 Rev 1	KENO V.a models added for Y/DD-896 Rev 1	KENO V.a Totals	MCNP4C2 models included in Y/DD-1026 Rev 0	General Description/Comments
Highlighted text indicates additions/changes to Volumes I, II, III, IV, and VII since the 2001 OECD Manual							
MIXED ENERGY MISCELLANEOUS IEU SYSTEMS							
none presently evaluated							
Volume IV, Low Enriched Uranium Systems							
LEU METAL SYSTEMS							
FAST ENERGY LEU METAL SYSTEMS							
none presently evaluated							
INTERMEDIATE ENERGY LEU METAL SYSTEMS							
none presently evaluated							
THERMAL ENERGY LEU METAL SYSTEMS							
LEU-MET-THERM-001	1			1	1		lattice of cyl U(nat) metal rods immersed in D_2O
LEU-MET-THERM-002	12			12	12		lattices of annular cyl U(2) metal rods immersed in D_2O
MIXED ENERGY LEU METAL SYSTEMS							
none presently evaluated							
LEU COMPOUND SYSTEMS							
FAST ENERGY LEU COMPOUND SYSTEMS							
none presently evaluated							
INTERMEDIATE ENERGY LEU COMPOUND SYSTEMS							
none presently evaluated							
THERMAL ENERGY LEU COMPOUND SYSTEMS							
LEU-COMP-THERM-001	8	8			8		lattices of cyl $U(2.35)O_2$ rods immersed in water

System Type	Acceptable benchmarks in the 2002 OECD Manual	KENO V.a models included in Y/DD-896 Rev 0	KENO V.a models included in Y/DD-996 Rev 1	KENO V.a models added for Y/DD-896 Rev 1	KENO V.a Totals	MCNP4C2 models included in Y/DD-1026 Rev 0	General Description/Comments
Highlighted text indicates additions/changes to Volumes I, II, III, IV, and VII since the 2001 OECD Manual							
LEU-COMP-THERM-002	5	5			5		lattices of cyl U(4.31)O_2 rods immersed in water
LEU-COMP-THERM-003	23	22			22		lattices of cyl U(2.35)O_2 rods immersed in water, water contains Gd impurity
LEU-COMP-THERM-004	20	20			20		lattices of cyl U(4.31)O_2 rods immersed in water, water contains Gd impurity
LEU-COMP-THERM-005	16						lattices of cyl U(2.35)O_2 or U(4.31)O_2 rods immersed in water containing Gd
LEU-COMP-THERM-006	18						lattices of cyl U(2.6)O_2 rods immersed in water
LEU-COMP-THERM-007	10						lattices of cyl U(4.738)O_2 rods immersed in water
LEU-COMP-THERM-008	17			1	1		U(2.459)O_2 rods latticed in borated H_2O, pertubed by Vicor, Pyrex, or Al_2O_3 rods
LEU-COMP-THERM-009	27			1	1		clusters of U(4.31)O_2 rods in water purturbed by various matls as plates
LEU-COMP-THERM-010	30						lattices of U(4.31)O_2 rods in water refl by two Pb, U(dep), or steel walls
LEU-COMP-THERM-011	15						clusters of U(2.5)O_2 rods immersed in water, poisoned with B_4C rods or borated water
LEU-COMP-THERM-012	10			10	10		clusters of U(2.35)O_2 rods in H_2O (Gd impurity) purturbed by various matls as plates
LEU-COMP-THERM-013	7						clusters of U(4.31)O_2 rods in water poisoned by various matls as plates
LEU-COMP-THERM-014	5						water reflected arrays of U(4.31)O_2 fuel rods in borated water
LEU-COMP-THERM-015	165						VVER Experiments, Part I
LEU-COMP-THERM-016	32	32			32		clusters of U(2.35)O_2 rods in water purturbed by various matls as plates
LEU-COMP-THERM-017	29						lattices of U(2.35)O_2 rods in water refl by two Pb, U(dep), or steel walls
LEU-COMP-THERM-018	1						U(7)O_2 rods immersed in water
LEU-COMP-THERM-019	3						stainless steel clad U(5)O_2 rods immersed in water
LEU-COMP-THERM-020	7						Zr-clad U(5)O_2 rods immersed in water
LEU-COMP-THERM-021	6						Zr-clad U(5)O_2 rods immersed in borated water
LEU-COMP-THERM-022	7						stainless steel clad U(10)O_2 rods immersed in water
LEU-COMP-THERM-023	6						stainless steel clad U(10)O_2 rods immersed in water
LEU-COMP-THERM-024	2						stainless steel clad U(10)O_2 rods immersed in water
LEU-COMP-THERM-025	4						stainless steel clad U(7.5)O_2 rods immersed in water
LEU-COMP-THERM-026	6						Zr-clad U(4.92)O_2 rods immersed in water at varied temperatures
LEU-COMP-THERM-027	4						Al-clad U(4.74)O_2 rods immersed in water, Pb refl

System Type	Acceptable benchmarks in the 2002 OECD Manual	KENO V.a models included in Y/DD-896 Rev 0	KENO V.a models included in Y/DD-996 Rev 1	KENO V.a models added for Y/DD-896 Rev 1	KENO V.a Totals	MCNP4C2 models included in Y/DD-1026 Rev 0	General Description/Comments
Highlighted text indicates additions/changes to Volumes I, II, III, IV, and VII since the 2001 OECD Manual							
LEU-COMP-THERM-029	12						Al-clad $U(4.74)O_2$ rods immersed in water surrounded by Hf plates
LEU-COMP-THERM-031	6						Zr-clad $U(5)O_2$ rods immersed in water
LEU-COMP-THERM-032	9						stainless steel clad $U(10)O_2$ rods immersed in water at varied temperatures
LEU-COMP-THERM-033	52						unrefl and hydrogenous refl cores of UF_4-paraffin cuboids at 2 or 3% enrichment
LEU-COMP-THERM-034	24						$U(4.738)O_2$ rod clusters in Cd, bor-ss, or Boral cannisters and immersed in H_2O
LEU-COMP-THERM-035	3						$U(2.6)O_2$ rods immersed in Gd- or B-poisoned water
LEU-COMP-THERM-036	69						VVER Experiments, Part II
LEU-COMP-THERM-037	11						$U(4.738)O_2$ rods immersed in water, partial refl by concrete
LEU-COMP-THERM-038	14						$U(4.738)O_2$ rods immersed in water, partial refl by borated concrete
LEU-COMP-THERM-039	17						incomplete/irregular lattices of $U(4.738)O_2$ rods immersed in water
LEU-COMP-THERM-040	10						$U(4.738)O_2$ rod clusters in Cd, bor-ss, or Boral cannisters in water, Pb or steel refl
LEU-COMP-THERM-041	5						HEU driven $U(3)O_2$ rod clusters in water separated by ss, bor-ss, or Cd plates
LEU-COMP-THERM-042	7						$U(2.35)O_2$ rod clusters in H_2O separated by various matls as plates, refl by steel walls
LEU-COMP-THERM-047	3						lattices of cyl $U(3)O_2$ and/or $U(7)O_2$ rods immersed in water
LEU-COMP-THERM-048	5						lattices of cyl $U(3)O_2$ rods immersed in water
LEU-COMP-THERM-049	18						poly refl split-table arrays of cuboidal cans containing U(5)O2 powder at low H/U
LEU-COMP-THERM-050	18						H_2O immersion of $U(4.738)O_2$ rods arround a sq tank of ^{149}Sm, B, or H2O in soln
LEU-COMP-THERM-051	19						clusters of $U(2.5)O_2$ rods immersed in borated water, poisoned with SS or Boral plates
LEU-COMP-THERM-052	6						lattices of $U(4.738)O_2$ or rods immersed in Gd-nitrate soln
LEU-COMP-THERM-055	2						water reflected and water moderated $U(3)O_2$ rod lattices

System Type	Acceptable benchmarks in the 2002 OECD Manual	KENO V.a models included in Y/DD-896 Rev 0	KENO V.a models included in Y/DD-996 Rev 1	KENO V.a models added for Y/DD-896 Rev 1	KENO V.a Totals	MCNP4C2 models included in Y/DD-1026 Rev 0	General Description/Comments
Highlighted text indicates additions/changes to Volumes I, II, III, IV, and VII since the 2001 OECD Manual							
LEU-COMP-THERM-061	10						VVER-type fuel assemblies immersed in water, perturbed with B_4C, Hf, Dy, or gaps
LEU-COMP-THERM-062	15						$U(2.6)O_2$ rod lattices immersed in water, perturbed with borated SS plates
SUB-LEU-COMP-THERM-001	15						lattices of cyl $U(3)O_2$ rods immersed in water and compartmentalized by borated steel
MIXED ENERGY LEU COMPOUND SYSTEMS							
none presently evaluated							
LEU SOLUTION SYSTEMS							
THERMAL ENERGY LEU SOLUTION SYSTEMS							
LEU-SOL-THERM-001	1						unreflected $U(5)O_2F_2$ soln in cyl geom, 1000 gU/l
LEU-SOL-THERM-002	3						$U(4.9)O_2F_2$ soln in 147 liter sph geom, ~450 or ~490 gU/l, unrefl or water refl
LEU-SOL-THERM-003	9	9			9		full and truncated spheres of U(10)NH soln
LEU-SOL-THERM-004	7						STACY: water refl U(10)NH soln in cyl geom, ~225-310 gU/l
LEU-SOL-THERM-005	3			7	7		water refl U(5.64)NH soln in cyl geom, ~400 gU/l, with or without B_4C rods
LEU-SOL-THERM-006	5						water refl U(10)NH soln in cyl geom, ~420 gU/l, with or without B_4C rods
LEU-SOL-THERM-007	5						STACY: unreflected U(10)NH soln in cyl geom, ~242-313 gU/l
LEU-SOL-THERM-008	4						STACY: concrete refl U(10)NH soln in cyl geom, ~240 gU/l
LEU-SOL-THERM-009	3						STACY: borated concrete refl U(10)NH soln in cyl geom, ~240 gU/l
LEU-SOL-THERM-010	4						STACY: poly refl U(10)NH soln in cyl geom, ~240 gU/l
LEU-SOL-THERM-016	7						STACY: water refl U(10)NH soln in slab geom, ~300-464 gU/l
LEU-SOL-THERM-017	6						STACY: unreflected U(10)NH soln in slab geom, ~315-464 gU/l
LEU-SOL-THERM-018	6						STACY: concrete refl U(10)NH soln in slab geom, ~310-315 gU/l
LEU-SOL-THERM-019	6						STACY: poly refl U(10)NH soln in slab geom, ~320 gU/l
LEU-SOL-THERM-020	4						STACY: water refl U(10)NH soln in cyl geom, ~194-243 gU/l
LEU-SOL-THERM-021	4						STACY: unreflected U(10)NH soln in cyl geom, ~194-243 gU/l

System Type	Acceptable benchmarks in the 2002 OECD Manual	KENO V.a models included in Y/DD-896 Rev 0	KENO V.a models included in Y/DD-996 Rev 1	KENO V.a models added for Y/DD-896 Rev 1	KENO V.a Totals	MCNP4C2 models included in Y/DD-1026 Rev 0	General Description/Comments
Highlighted text indicates additions/changes to Volumes I, II, III, IV, and VII since the 2001 OECD Manual							
LEU-SOL-THERM-022	4						STACY: borated concrete refl U(10)NH soln in slab geom, ~310 gU/l
MISCELLANEOUS LEU SYSTEMS							
FAST ENERGY MISCELLANEOUS LEU SYSTEMS							
none presently evaluated							
INTERMEDIATE ENERGY MISCELLANEOUS LEU SYSTEMS							
none presently evaluated							
THERMAL ENERGY MISCELLANEOUS LEU SYSTEMS							
none presently evaluated							
MIXED ENERGY MISCELLANOUS LEU SYSTEMS							
none presently evaluated							
Volume V, Uranium-233 Systems							
U-233 METAL SYSTEMS							
FAST ENERGY U-233 METAL SYSTEMS							
U233-MET-FAST-001	1			1	1		bare sphere of U-233 metal (U-233 Jezebel)
U233-MET-FAST-002	2			2	2		10 kg or 7.6 kg U-233 metal sphere reflected by U(93) metal
U233-MET-FAST-003	2			2	2		10 kg or 7.6 kg U-233 metal sphere reflected by U(nat) metal
U233-MET-FAST-004	2			2	2		10 kg or 7.6 kg U-233 metal sphere reflected by W metal
U233-MET-FAST-005	2			2	2		10 kg or 7.6 kg U-233 metal sphere reflected by Be metal
U233-MET-FAST-006	1			1	1		U(nat) reflected sphere of U-233 metal (U-233 Flattop)
INTERMEDIATE ENERGY U-233 METAL SYSTEMS							
none presently evaluated							

System Type	Acceptable benchmarks in the 2002 OECD Manual	KENO V.a models included in Y/DD-896 Rev 0	KENO V.a models included in Y/DD-996 Rev 1	KENO V.a models added for Y/DD-896 Rev 1	KENO V.a Totals	MCNP4C2 models included in Y/DD-1026 Rev 0	General Description/Comments
Highlighted text indicates additions/changes to Volumes I, II, III, IV, and VII since the 2001 OECD Manual							
THERMAL ENERGY U-233 METAL SYSTEMS							
none presently evaluated							
MIXED ENERGY U-233 METAL SYSTEMS							
none presently evaluated							
U-233 COMPOUND SYSTEMS							
FAST ENERGY U-233 COMPOUND SYSTEMS							
none presently evaluated							
INTERMEDIATE ENERGY U-233 COMPOUND SYSTEMS							
none presently evaluated							
THERMAL ENERGY U-233 COMPOUND SYSTEMS							
none presently evaluated							
MIXED ENERGY U-233 COMPOUND SYSTEMS							
none presently evaluated							
U-233 SOLUTION SYSTEMS							
INTERMEDIATE ENERGY U-233 SOLUTION SYSTEMS							
U233-SOL-INTER-001	33			33	33		$^{233}UO_2F_2$ soln in spherical geometry with Be, poly, or Be-poly reflectors
THERMAL ENERGY U-233 SOLUTION SYSTEMS							
U233-SOL-THERM-001	5			5	5		unreflected spheres of ^{233}UNH solution with varied boron content
U233-SOL-THERM-002	17			17	17		paraffin reflected cylinders of ^{233}UNH solution

System Type	Acceptable benchmarks in the 2002 OECD Manual	KENO V.a models included in Y/DD-896 Rev 0	KENO V.a models included in Y/DD-996 Rev 1	KENO V.a models added for Y/DD-896 Rev 1	KENO V.a Totals	MCNP4C2 models included in Y/DD-1026 Rev 0	General Description/Comments
Highlighted text indicates additions/changes to Volumes I, II, III, IV, and VII since the 2001 OECD Manual							
U233-SOL-THERM-003	10			1	1		paraffin reflected cylinders of $^{233}UO_2F_2$ solution
U233-SOL-THERM-004	8			8	8		paraffin reflected cylinders of ^{233}UNH solution
U233-SOL-THERM-005	2			2	2		water reflected cylinder or sphere of ^{233}UNH solution
U233-SOL-THERM-006	25			8	8		arrays of ^{233}UNH solution cylinders
U233-SOL-THERM-008	1			1	1		unreflected sphere of ^{233}UNH solution
U233-SOL-THERM-011	0	n/a	n/a			n/a	refer to U233-SOL-INTER-001
U233-SOL-THERM-012	8			8	8		water reflected spherical vessels containing ^{233}UNH solution
U233-SOL-THERM-014	16			16	16		arrays of polybottles containing ^{233}UNH solution
U233-SOL-THERM-015	31			31	31		$^{233}UO_2F_2$ soln in spherical geometry with Be, poly, or Be-poly reflectors
MIXED ENERGY U-233 SOLUTION SYSTEMS							
U233-SOL-MIXED-001	0	n/a	n/a			n/a	refer to U233-SOL-INTER-001
U233-SOL-MIXED-002	0	n/a	n/a			n/a	refer to U233-SOL-THERM-015

U-233 MISCELLANEOUS SYSTEMS

FAST ENERGY U-233 MISCELLANEOUS SYSTEMS

none presently evaluated

INTERMEDIATE ENERGY U-233 MISCELLANEOUS SYSTEMS

none presently evaluated

THERMAL ENERGY U-233 MISCELLANEOUS SYSTEMS

none presently evaluated

System Type	Acceptable benchmarks in the 2002 OECD Manual	KENO V.a models included in Y/DD-896 Rev 0	KENO V.a models included in Y/DD-996 Rev 1	KENO V.a models added for Y/DD-896 Rev 1	KENO V.a Totals	MCNP4C2 models included in Y/DD-1026 Rev 0	General Description/Comments
Highlighted text indicates additions/changes to Volumes I, II, III, IV, and VII since the 2001 OECD Manual							
MIXED ENERGY U-233 MISCELLANEOUS SYSTEMS							
none presently evaluated							
Volume VI, Mixed Plutonium-Uranium Systems							
MIXED PU-U METAL SYSTEMS							
FAST ENERGY MIXED PU-U METAL SYSTEMS							
MIX-MET-FAST-001	1		1		1	1	sphere of ^{239}Pu metal (~4.9% ^{240}Pu) reflected by U(93.2) metal
MIX-MET-FAST-002	3		3		3	3	composite sph cores of ^{239}Pu (varied ^{240}Pu) and U(93.2) metal refl by U(nat) metal
MIX-MET-FAST-003	1					1	sphere of ^{239}Pu metal (~9% ^{240}Pu) reflected by U(89) metal
MIX-MET-FAST-004	2					2	composite sph cores of ^{239}Pu (~9% ^{240}Pu) and U(89) metal refl by Be and BeO
MIX-MET-FAST-005	1					1	composite sph core of ^{239}Pu (~9% ^{240}Pu) and U(89) metal refl by Al
MIX-MET-FAST-007	23		23		23	23	composite sph cores of ^{239}Pu (~5.7% ^{240}Pu) and U(93.2) metal refl by Be metal
MIX-MET-FAST-008	7					3	k-inf for ^{239}Pu, MOX, or U(37) plates interleaved with C, SST, Na, and/or U(nat) plates
MIX-MET-FAST-009	1		1		1	1	sph core of ^{239}Pu (~1.8% ^{240}Pu) metal reflected by 0.75-cm thick U(89) metal
MIX-MET-FAST-010	1		1		1	1	sph core of ^{239}Pu (~1.8% ^{240}Pu) metal reflected by 2.89-cm thick U(89) metal
MIX-MET-FAST-011	4		4		4	1	cyl assy of fissile Pu/U/Zr fuel plates reflected by graphite (ZPPR-9/21B thru 21E)
MIX-MET-FAST-012	0	n/a	n/a			n/a	refer to PU-MET-FAST-033
INTERMEDIATE ENERGY MIXED PU-U METAL SYSTEMS							
MIX-MET-INTER-001	0	n/a	n/a			n/a	refer to MIX-MET-FAST-008
MIX-MET-INTER-002	0	n/a	n/a			n/a	refer to MIX-MET-MIXED-001
THERMAL ENERGY MIXED PU-U METAL SYSTEMS							
none presently evaluated							
MIXED ENERGY MIXED PU-U METAL SYSTEMS							
MIX-MET-MIXED-001	1					1	unrefl cyl assy of alternating ^{239}Pu (~4.6% ^{240}Pu) metal, U(96) metal, and poly plates

System Type	Acceptable benchmarks in the 2002 OECD Manual	KENO V.a models included in Y/DD-896 Rev 0	KENO V.a models included in Y/DD-996 Rev 1	KENO V.a models added for Y/DD-896 Rev 1	KENO V.a Totals	MCNP4C2 models included in Y/DD-1026 Rev 0	General Description/Comments
Highlighted text indicates additions/changes to Volumes I, II, III, IV, and VII since the 2001 OECD Manual							
MIXED PU-U COMPOUND SYSTEMS							
FAST ENERGY MIXED PU-U COMPOUND SYSTEMS							
none presently evaluated							
INTERMEDIATE ENERGY MIXED PU-U COMPOUND SYSTEMS							
none presently evaluated							
THERMAL ENERGY MIXED PU-U COMPOUND SYSTEMS							
MIX-COMP-THERM-001	4						mixed $^{239}PuO_2$ and $U(nat)O_2$ fuel pins immersed in water
MIX-COMP-THERM-002	6					6	mixed $^{239}PuO_2$ and $U(nat)O_2$ fuel pins immersed in water or borated water
MIX-COMP-THERM-003	6					6	rectangular arrays of mixed $^{239}PuO_2$ and $U(nat)O_2$ fuel pins immersed in water
MIX-COMP-THERM-004	11						arrays of mixed $^{239}PuO_2$ and $U(nat)O_2$ fuel rods immersed in water
MIX-COMP-THERM-005	7		1		1		hexagonal lattice arrays of mixed $^{239}PuO_2$ and $U(nat)O_2$ fuel pins immersed in water
MIX-COMP-THERM-006	6		1		1		hexagonal lattice arrays of mixed $^{239}PuO_2$ and $U(nat)O_2$ fuel pins immersed in water
MIX-COMP-THERM-007	27		27		27		five lattices of mixed $^{239}PuO_2$ and $U(nat)O_2$ rods in water, incl Hf/B/Cd rod substitutions
MIX-COMP-THERM-008	28		28		28	28	six lattices of mixed $^{239}PuO_2$ and $U(nat)O_2$ rods in water, incl Hf/B/Cd rod substitutions
MIX-COMP-THERM-009	6		1		1	6	hexagonal lattices of mixed $^{239}PuO_2$ and $U(dep)O_2$ fuel pins immersed in water
MIX-COMP-THERM-010	0	n/a	n/a			n/a	refer to MIX-MISC-THERM-001
MIX-COMP-THERM-011	6		1		1	6	arrays of mixed $^{239}PuO_2$ and $U(60)O_2$ fuel rods immersed in water
MIX-COMP-THERM-012	33		33		33	33	bare and Plexiglas reflected arrays of MOX/polystyrene blocks
MIXED ENERGY MIXED PU-U COMPOUND SYSTEMS							
none presently evaluated							
MIXED PU-U SOLUTION SYSTEMS							
INTERMEDIATE ENERGY MIXED PU-U SOLUTION SYSTEMS							

System Type	Acceptable benchmarks in the 2002 OECD Manual	KENO V.a models included in Y/DD-896 Rev 0	KENO V.a models included in Y/DD-996 Rev 1	KENO V.a models added for Y/DD-896 Rev 1	KENO V.a Totals	MCNP4C2 models included in Y/DD-1026 Rev 0	General Description/Comments
Highlighted text indicates additions/changes to Volumes I, II, III, IV, and VII since the 2001 OECD Manual							
none presently evaluated							
THERMAL ENERGY MIXED PU-U SOLUTION SYSTEMS							
MIX-SOL-THERM-001	13		13		13	13	^{239}PuNH + U(nat)NH soln in annular geomerty
MIX-SOL-THERM-002	3		3		3	3	^{239}PuNH + U(nat)NH soln in large cylindrical geomerty
MIX-SOL-THERM-003	10					10	^{239}PuNH + U(nat)NH soln in cylindrical geomerty with poly/water refl
MIX-SOL-THERM-004	9		9		9	9	^{239}PuNH + U(dep)NH soln in small cyl geom, bare or water or concrete refl
MIX-SOL-THERM-005	7		7		7	7	^{239}PuNH + U(dep)NH soln in slab geomerty, bare or water refl
MIXED ENERGY MIXED PU-U SOLUTION SYSTEMS							
none presently evaluated							
MIXED PU-U MISCELLANEOUS SYSTEMS							
FAST ENERGY MIXED PU-U MISCELLANEOUS SYSTEMS							
none presently evaluated							
INTERMEDIATE ENERGY MIXED PU-U MISCELLANEOUS SYSTEMS							
none presently evaluated							
THERMAL ENERGY MIXED PU-U MISCELLANEOUS SYSTEMS							
MIX-MISC-THERM-001	11		11		11	11	mixed oxide fuel pin lattices in (Pu+U)NH solution
MIX-MISC-THERM-002	12						arrays of mixed $^{239}PuO_2$ and $U(60)O_2$ fuel rods in dilute ^{239}PuNH soln and refl by water
MIXED ENERGY MIXED PU-U MISCELLANEOUS SYSTEMS							
none presently evaluated							
Volume VII, Special Isotope Systems							
SPECIAL ISOTOPE METAL SYSTEMS							

System Type	Acceptable benchmarks in the 2002 OECD Manual	KENO V.a models included in Y/DD-896 Rev 0	KENO V.a models included in Y/DD-996 Rev 1	KENO V.a models added for Y/DD-896 Rev 1	KENO V.a Totals	MCNP4C2 models included in Y/DD-1026 Rev 0	General Description/Comments
Highlighted text indicates additions/changes to Volumes I, II, III, IV, and VII since the 2001 OECD Manual							
FAST ENERGY SPECIAL ISOTOPE METAL SYSTEMS							
SPEC-MET-FAST-001	4						replacement measurements of ^{240}Pu Jezebel with void, U(93), ^{239}Pu, or ^{244}Cm
SPEC-MET-FAST-002	3						replacement measurements of ^{240}Pu Jezebel with void, ^{238}Pu, or ^{239}Pu
SPEC-MET-FAST-003	6						replacement measurements of Flattop (Pu and HEU) with void, ^{237}Np, or U(93)
SPEC-MET-FAST-004	7						combos of ^{239}Pu, ^{242}Pu, and U(93) metal disks, unrefl and refl by steel, Be, or U(dep)
INTERMEDIATE ENERGY SPECIAL ISOTOPE METAL SYSTEMS							
none presently evaluated							
THERMAL ENERGY SPECIAL ISOTOPE METAL SYSTEMS							
none presently evaluated							
MIXED ENERGY SPECIAL ISOTOPE METAL SYSTEMS							
none presently evaluated							
SPECIAL ISOTOPE COMPOUND SYSTEMS							
FAST ENERGY SPECIAL ISOTOPE COMPOUND SYSTEMS							
none presently evaluated							
INTERMEDIATE ENERGY SPECIAL ISOTOPE COMPOUND SYSTEMS							
none presently evaluated							
THERMAL ENERGY SPECIAL ISOTOPE COMPOUND SYSTEMS							
none presently evaluated							
MIXED ENERGY SPECIAL ISOTOPE COMPOUND SYSTEMS							

System Type	Acceptable benchmarks in the 2002 OECD Manual	KENO V.a models included in Y/DD-896 Rev 0	KENO V.a models included in Y/DD-996 Rev 1	KENO V.a models added for Y/DD-896 Rev 1	KENO V.a Totals	MCNP4C2 models included in Y/DD-1026 Rev 0	General Description/Comments

Highlighted text indicates additions/changes to Volumes I, II, III, IV, and VII since the 2001 OECD Manual

none presently evaluated

SPECIAL ISOTOPE SOLUTION SYSTEMS

FAST ENERGY SPECIAL ISOTOPE SOLUTION SYSTEMS

none presently evaluated

INTERMEDIATE ENERGY SPECIAL ISOTOPE SOLUTION SYSTEMS

none presently evaluated

THERMAL ENERGY SPECIAL ISOTOPE SOLUTION SYSTEMS

none presently evaluated

MIXED ENERGY SPECIAL ISOTOPE SOLUTION SYSTEMS

none presently evaluated

SPECIAL ISOTOPE MISCELLANEOUS SYSTEMS

FAST ENERGY SPECIAL ISOTOPE MISCELLANEOUS SYSTEMS

none presently evaluated

INTERMEDIATE ENERGY SPECIAL ISOTOPE MISCELLANEOUS SYSTEMS

none presently evaluated

THERMAL ENERGY SPECIAL ISOTOPE MISCELLANEOUS SYSTEMS

none presently evaluated

MIXED ENERGY SPECIAL ISOTOPE MISCELLANEOUS SYSTEMS

System Type	Acceptable benchmarks in the 2002 OECD Manual	KENO V.a models included in Y/DD-896 Rev 0	KENO V.a models included in Y/DD-996 Rev 1	KENO V.a models added for Y/DD-896 Rev 1	KENO V.a Totals	MCNP4C2 models included in Y/DD-1026 Rev 0	General Description/Comments
Highlighted text indicates additions/changes to Volumes I, II, III, IV, and VII since the 2001 OECD Manual							
none presently evaluated							

qual
other
mix

8 REFERENCES

i. J. Blair Briggs, Editor, International Handbook of Evaluated Criticality Safety Benchmark Experiments, NEA/NSC/DOC(95)03, Volumes 1-7, Organization for Economic Cooperation and Development - Nuclear Energy Agency, Paris, France, September 1999 Edition.

ii. Nuclear Criticality Safety in Operations with Fissionable Material Outside Reactors, ANSI/ANS-8.1-1998, American National Standards Institute, New York, 1998.

iii. Experience With the SCALE Criticality Safety Cross-Section Libraries, NUREG/CR-6686/ORNL/TM-1999/322, October 2000.

iv. Bias, Uncertainty and Upper Subcritical Limit for Critical Experiments with Plutonium Systems for CSAS25 from SCALE4.4a for Criticality Safety Analyses on the HP J-5600 (CMODB) Workstation, Y/DD-996/R1, Smith, R.H. et al, March 2002.

BWXT Y12
A BWXT/Bechtel Enterprise

Determination of the Upper Subcritical Limit for Criticality Calculations for Criticality Safety Analyses

Revision 1

R. H. Smith

Nuclear Criticality Safety
Y-12 National Security Complex

Y-12 NATIONAL SECURITY COMPLEX

August 2003

Prepared by the
Nuclear Criticality Safety Division
Y-12
Oak Ridge, Tennessee 37831-8238

Prepared by the
Y-12 National Security Complex
Oak Ridge, Tennessee 37831
Managed by
BWXT Y-12, L.L.C.
For the
U.S. Department of Energy
under contract DE-AC05-00OR22800

This document has been reviewed by a Y-12 ADC/UCNI RO and has been determined to be UNCLASSIFIED and contains no UCNI. This review does not constitute clearance for public release.
16 Dec 03
Date

MANAGED BY
BWXT Y-12, L.L.C.
FOR THE UNITED STATES
DEPARTMENT OF ENERGY

UCN-13672 (10-00)

THIS PAGE INTENTIONALLY LEFT BLANK

Determination of the Upper Subcritical Limit for Criticality Calculations for Criticality Safety Analyses

Revision 1

R. H. Smith

Nuclear Criticality Safety
Y-12 National Security Complex

August 2003

Prepared by the
Y-12 National Security Complex
Oak Ridge, Tennessee 37831
Managed by
BWXT Y-12, L.L.C.
For the
U.S. Department of Energy
under contract DE-AC05-00OR22800

THIS PAGE INTENTIONALLY LEFT BLANK

Document Preparation

Prepared by _____ Date _____
Robert H. Smith

Reviewed by _____ Date _____
John F. DeClue

Approved by _____ Date _____
Cris A. Worley

THIS PAGE INTENTIONALLY LEFT BLANK

Abstract

This report considers determination of an upper subcritical limit, and incorporating uncertainty and margin into the subcritical limit, and recommends an Upper Subcritical Limit (USL).

A USL is developed for CSAS25 from SCALE4.4a. The USL is applicable for the CSAS25 control module from the SCALE 4.4a computer code system for use in evaluating nuclear criticality safety of enriched uranium systems. The benchmark calculation results used for this report are documented in Y/DD-896/R1. The 238-group ENDF/B-V cross-section libraries were used.

Numerical methods for applying margins are described, but the determination of appropriate correlating parameters and values for additional margin, applicable to a particular analysis, must be determined as part of a process analysis. As such, this document does not specify final upper subcritical limits as has been done in the past. No correlation between calculation results and neutron energy causing fission was observed for the critical experiment results. Analysts using these results are responsible for exercising sound engineering judgment using strong technical arguments to develop "a margin in k_{eff} or other correlating parameter … that is sufficiently large to ensure that conditions (calculated by this method to be subcritical by this margin) will actually be subcritical." [1] Documentation of area of applicability and determination and justification of the appropriate margin in the analyst's evaluation, in conjunction with this report, will constitute the complete Validation Report in accordance with ANSI/ANS-8.1-1998, Section 4.3.6(4).

THIS PAGE INTENTIONALLY LEFT BLANK

Table of Contents

Page

ABSTRACT ..... **V**

1 INTRODUCTION **9**

1.1 GRANDFATHER OR RETROFIT CONCERNS 10
1.2 TERMINOLOGY 10

2 SUBCRITICAL LIMITS AND STATISTICAL ANALYSIS **11**

2.1 INTRODUCTION 11
2.2 DETERMINATION OF SUBCRITICAL LIMITS FROM THE BIAS AND UNCERTAINTY 12
2.2.1 Area of Applicability *12*
2.2.2 Simple Methods for Determination of Subcritical Limits *13*
2.2.3 Addition of Safety Margin and Bias Based on Tolerance Bounds *13*
2.2.4 Statistical Approach *15*
2.2.5 Discussion of Results *15*

TABLE 1. UPPER SUBCRITICAL LIMITS (BEFORE SUBTRACTION OF ANY ADDITIONAL MARGIN) **16**

3 CONCLUSIONS **17**

4 RECOMMENDATIONS FOR FUTURE WORK **18**

5 REFERENCES **20**

THIS PAGE INTENTIONALLY LEFT BLANK

1 Introduction

In the nuclear criticality safety field, extensive use is made of computational methods in order to establish subcritical limits for operations involving fissile material. Calculations must be made by a method shown to be validated by comparison with experiment data. The American National Standards Institute (ANSI) gives fundamental guidance for establishing these subcritical limits in ANSI/ANS-8.1-1998, "Nuclear Criticality Safety in Operations with Fissionable Materials Outside Reactors."[1]

The successful application of computational methods requires verification, certification and validation (V&V) of the analytic tool. Software verification, the first element of V&V, reveals the closeness in agreement between calculation results obtained using a particular computational method and calculation results obtained using other methods. Software certification provides a user assurance that the code will consistently produce numerical results that agree with analytic solutions for the problems the code is designed to analyze. Software validation "calibrates" the calculation results obtained using certified software (computational method) for agreement with the physical universe.

For nuclear criticality safety, the validation process is complete with development of the upper subcritical limit (USL) from validation data. Refinement of a validation or extension by addition of validation data does not require re-certification of the software. Therefore, the verification and certification of a nuclear criticality safety computer code system and transference of a validation between computer platforms are related issues, which can be addressed separately from software validation.

Taken together, Y/DD-896/R1 and Y/DD-972/R1 provide the **framework** for the validation of CSAS25 control module from the Standardized Computer Analyses for Licensing Evaluation (SCALE) Version 4.4a package with the 238-group ENDF/B-V SCALE 4.4a cross-section library.

Y/DD-896/R1 addresses the establishment of bias, bias trends and uncertainty associated with the use of SCALE4.4a for performance of criticality calculations. This evaluation is directed at all systems consisting of fissile and fissionable material in metallic, solution and other physical forms, as described in the Organization for Economic Cooperation and Development (OECD) Benchmark Handbook. The focus is on comparison of calculated neutron multiplication factors (k_{eff}) with the associated experimental benchmark results, and on establishment of bias, bias trends, and uncertainty as a final step. Compiled data for 1217 critical experiments is used as the basis for the calculation models. The calculated results from SCALE 4.4a using the 238-group ENDF/B-V SCALE 4.4a cross-section library have been compared with reported results for the benchmark experiments. Comparison of results demonstrates that SCALE 4.4a run on the Nuclear Criticality Safety Division (NCSD) Hewlett Packard Series 9000/J-5600 (HP J-5600) unclassified workstation (referred to as CMODB) produces the same results within the

statistical uncertainty of the Monte Carlo calculations as reported by the experiments.

Y/DD-972 addresses various methods for determination of a USL and for incorporating uncertainty and margin into this USL. It provides comparisons of these methods and recommends a preferred method for determining the USL. Y/DD-972 establishes subcritical limits determined through an evaluation of statistics parameters of calculation results for critical experiments. However, the correlating parameters (i.e., mass, enrichment, geometry, absorption, moderation, reflection, etc.) and values for applying additional margin to the subcritical limits are application dependent. The determination of correlating parameters and additional margin is an integral part of the process analysis for a particular application. For the critical experiment results, no correlation between calculation results and neutron energy causing fission was found. As such, this document does not specify "final" USL values as has been done in the past.

The Area of Applicability (AoA) is also application dependent. In using the "raw" USL data of this report, the nuclear criticality safety analyst must exercise sound engineering judgment and use strong technical arguments to develop a margin in k_{eff} or other correlating parameter. That margin must be sufficiently large to ensure that conditions (calculated by this method to be subcritical by this margin) will actually be subcritical.[1] Preparation of this final portion of the "written report of validation" as identified in Section 4.3.6 of ANSI/ANS-8.1-1998 is the responsibility of the analyst.

1.1 Grandfather or Retrofit Concerns

The validation documents used for establishing subcritical limits for criticality calculations shall be reviewed and approved by NCSD. There is no urgency to retrofit older evaluations since the common practice provided conservatism. Therefore, the incorporation of these newer results and methods into the evaluations of existing operations will be accomplished as the Nuclear Criticality Safety Approvals are updated due to equipment changes, rule changes, age, etc.

1.2 Terminology

The term "model" may be used in two different ways. In this report, "model" generally refers to the calculation model, or the collection of input parameters for the numerical simulation of the physical critical experiment. In statistical analyses, the term "model" generally refers to a statistical model, or an equation describing the relationship between parameters considered in the statistical analysis.

The term "uncertainty" may also be used two different ways. In this report, "uncertainty" generally refers to less than exactly known values in the calculation model, or in the collection of input parameters for the numerical simulation of the physical critical experiment. In statistical analyses, the term "uncertainty"

generally refers to the variation of repeated observations (e.g., k_effective or k_simulation) about their expected value. This uncertainty is quantified by the sample standard deviation (i.e., square root of the sample variance).

Accuracy refers to how close the expected value of an observation is to the true value. Accuracy is quantified by bias, which is the difference between the sample average and the true or referenced value.

2 Subcritical Limits and Statistical Analysis

2.1 Introduction

Y/DD-896/R1 provides a discussion of the calculation results, experiment (benchmark) data, and the bias results. Regression with neutron energy causing fission was observed to be not applicable. This is illustrated in Figures 1-7 of Y/DD-896/R1.

The OECD Handbook provides an estimate of the actual k_{eff} for each experiment benchmark. While most experiments were estimated to be exactly critical, or k_exp = 1.0, a number of the estimates were slightly above or slightly below exactly critical (i.e. k_exp > 1.0 or k_exp < 1.0). It was considered desirable to account for this difference because the subcritical limit could otherwise be conservative due to including slightly subcritical experiments, or non-conservative due to including slightly super-critical experiments. The following adjustment, to determine an adjusted calculation result, k', was proposed for use in the statistical evaluation:

k' = 1 + bias = 1 + (k_calc - k_exp)

where k_calc = code calculated k_{eff} result for the modeled experiment, and
k_exp = OECD estimate of actual k_{eff} for the experiment

The assumption inherent in making this adjustment is that the experiments were close to critical, and if a very small adjustment could be made so that the experiment would be exactly critical, the bias of the calculation would not change.

When calculation methods are employed, the subcritical limit is a quantitative value used for implementation of NCSD policy, which is established in accordance with DOE Orders, Standards, or by NRC regulations for those activities under NRC jurisdiction. Evaluation criteria are usually the calculated reactivity, k_{eff}, for the model of the problem being evaluated, uncertainty in the calculated value of reactivity, bias introduced by the code used to calculate reactivity, and bias introduced by the model. Code bias is determined by a validation performed in accordance with ANSI/ANS 8.1. The statistical results in this

report determine code bias based on comparison of code calculations with experimental results. Model bias is due to uncertainties in the modeled parameters describing the problem, approximations made for the model to conform to the input requirements of the code, and any significant simplifications of the problem introduced into the model by the analyst. The acceptance criterion requires that the evaluation criteria be bounded by the subcritical limit. In the case of code calculations, the subcritical limit is often a criterion based on calculated k_{eff} and estimated bias and uncertainties.

It is recognized that it may also be possible to determine subcritical limits based on adjustment of correlating parameters other than k_{eff}, as allowed by ANSI/ANS-8.1. These parameters could include physical parameters such as mass or radius, for example, or other calculated parameters besides k_{eff}, if they can be shown to provide a subcritical margin. This report does not address other potential correlating parameters, but an analyst could determine them as part of an evaluation and use them to determine subcritical limits in conjunction with the code bias results in this report.

2.2 Determination of Subcritical Limits from the Bias and Uncertainty

Several methods could be used for determination of subcritical limits in terms of calculated k_{eff}. The methods were discussed in more detail in previous revisions, and the discussion will not be repeated here. Another reference is NUREG/CR-6698[2]. As discussed above, and in Section 5.1 of Y/DD-896/R1, it may also be possible to determine subcritical limits based on adjustment of correlating parameters other than k_{eff}, but this approach is not addressed here.

2.2.1 Area of Applicability

Whether a particular plant application is similar to a sufficient number of experiments contained in the validation set is an important issue. This is a prerequisite before a subcritical limit may be determined from the validation results. Based on the demonstrated performance of the code for a large number of experiments, we have reasonable assurance that it performs well over a wide range of conditions. However, this does not ensure that the code performs as well over all conditions and several conditions where the code performed very poorly were listed in Section 5.3 of Y/DD-896/R1. There may be other scenarios where the code would calculate unusually low, or high, due to some kind of anomaly or error in the code or cross section data. In addition, there are some types of experiments that are few of a kind. It is possible that there could be one or more of these types of experiments that would exhibit a larger bias than seen in this report, if more experiments of that type were included. The only way to assess whether the validation set contains a sufficient number of experiments that are similar to a plant application is to carefully compare the details of the experiment descriptions with the details of the plant application. The broad categories used for the statistical analysis may not be sufficient for making the determination, and the

experiment summary information included in these reports may not provide enough information. The analyst must become familiar with the experiment descriptions provided in the OECD handbook. The minimum number of similar experiments needed cannot necessarily be determined in advance, but the analyst must consider this issue carefully as one of the factors when deciding how much margin to include in determining a subcritical limit. The recommendations in Reference 2 may be useful in this regard. If there are only a few experiments similar to the application, it may be wise to recommend taking the time to select additional applicable experiments for addition to the validation set, or for a separate evaluation.

Appropriateness of the subcritical limit does not depend solely on the validity of the statistical analysis. Rather, the appropriateness of a subcritical limit depends on two quite different factors: (1) the range of conditions under which a generalization for its use is established, and (2) whether or not the modeled scenario is within the range of these conditions. The nuclear criticality safety analyst, exercising sound engineering judgment using strong technical arguments, must develop these determinations. Extrapolation beyond the range of applicability should not be done.

2.2.2 Simple Methods for Determination of Subcritical Limits

The simplest and most straightforward method is to observe that for a large number of critical (or close to critical) experiments, calculated results were relatively consistent, and none were lower than a particular minimum. A value of k_{eff} could be picked that is at or slightly below all the calculated results. Combined limits could be used for simplicity as long as the minimum values were used. The minimum value is established by a single case. These values do not include any reduction for numerical uncertainty in the calculated mean value for the case (standard deviation of approximately 0.001). The minimum k_{eff} value would be reduced further to provide additional margin as appropriate as determined by the analyst.

Another similar method to establish a subcritical limit would be to choose the lowest (i.e. least positive or most negative) bias result, add it to 1.0, and reduce this value by an additional amount to allow for a margin of safety. The results of this approach (without reduction for margin of safety) are shown in Table 1. These values do not include any reduction for numerical uncertainty in the calculated mean value for the minimum case. This is the method chosen for this report.

2.2.3 Addition of Safety Margin and Bias Based on Tolerance Bounds

In the commonly used relationship of procedure Y70-68-005, the subcritical limit appears in Equation 2.1 as the term on the right while the evaluation criteria of a given problem are expressed in the term on the left. It is recognized that, depending on how the terms are defined, this approach may mix confidence intervals ($k_{eff} + 2s$) and tolerance limits (1.0 - bias - margin) in a semi-statistical formula or

method. Acceptability is established when the term on the left is less than or equal to the term on the right:

$$\{ k_{eff} + 2s + \text{code bias} + \text{model bias} \} <= \{ 1.0 - \text{margin of safety} \} \quad \text{(Eq 2.1)}$$

Code bias is determined by a validation performed in accordance with ANSI/ANS 8.1. The statistical results in this report present bias based on comparison of code calculations with experimental results. Some regulators require that when the mean value of calculated k_{eff} for the validation cases is greater than or equal one, then the code bias is set = 0.

Model bias is due to uncertainties in the modeled parameters describing the problem, approximations made for the model to conform to the input requirements of the code, and any significant simplifications of the problem introduced into the model by the analyst.

Margin of safety is set by NCSD analysts in accordance with DOE Orders, Standards, and NRC Regulations for activities under these specific jurisdictions (and possibly to allow for uncertainty or limitations in area of applicability relative to the analyzed configuration). A typical range is from 0.02 to 0.05. When the analyst feels there is very little uncertainty in the application, it may be possible to justify using lower margin of safety. Also, it may be appropriate to provide margin by adjustment of correlating parameters other than k_{eff}.

2.2.3.1 Treatment of Model Bias

For calculation models that are accurate representations, the model bias is considered zero. For calculation models with uncertainties in the modeled parameters describing the problem, model bias is intended to compensate for the uncertainty in the calculated k_{eff} due to the uncertainty in the dominant parameter(s) of the problem. Quantitatively, model bias is determined by evaluating k_{eff} of problem "A" as a function of the parameter "p" over the range of uncertainty in "p" [expressed here as x%], i.e., calculations performed with the parameter "p" set at values between "p(1-x%/100)" and "p(1+x%/100)" to establish the corresponding uncertainty in k_{eff}. Values at and between both extremes must be considered because reactivity may not be uniformly distributed about the parameter "p". The number of values to be evaluated depends on the magnitude of the range in the parameter. The model bias for parameter(s) "p" used in the above equation is the absolute value of the maximum difference:

$$| \; k_{eff} \{\text{"p_max"}\} - k_{eff} \{\text{"p_min"}\} \; | ,$$

Where $k_{eff}\{\text{"p_max"}\}$ = maximum k_{eff} over the range of parameter(s) "p"
$k_{eff}\{\text{"p_min"}\}$ = minimum k_{eff} over the range of parameter(s) "p"

The maximum variation in k_{eff} over the ranges of uncertainty of all dominant parameters of the problem would be used as the model bias in Equation 2.1. Allowance for statistical uncertainty in the calculated results must be considered, depending on the relative magnitude. If the parameter of interest is a discrete or categorical variable rather than a continuous variable as discussed above, then the parameter would similarly be varied over the range of applicable states until the maximum variation was found.

An allowance for model bias could otherwise be included in the margin of safety as shown in Eq. 2.2:

$$\{ k_{eff} + 2s + \text{code bias} \} <= \{ 1.0 - \text{margin of safety*} \} \qquad \text{(Eq 2.2)}$$

This would require justification that the evaluation criteria (left side of Eq. 2.2) is sufficiently less than 1.0 by an amount out weighing the maximum variation of k_{eff} for the dominant parameters affecting reactivity.

For calculation models with a significant degree of approximation and simplification, model bias is intended to account for conservatism built into the model. Generally, the model bias is not explicitly calculated, but is addressed by modeling parameters at their worst case. Establishment of the worst case may require a parametric study as described previously. An allowance for model bias would be included in the margin of safety (term on right side of Eq. 2.2). This would require justification that the evaluation criteria (left side of Eq. 2.2) is sufficiently less than 1.0 by an amount that out weighs the conservatism built into the calculation model.

2.2.4 Statistical Approach

Non-parametric statistics are used in this report. According to Reference 2, Section 2.4.4, attaining typical 95% confidence of 95% of the population being above the smallest data sample requires only 59 experiments. After excluding the three lowest results in Table 5.1 of Y/DD-896/R1, due to being infinite models with relatively large amounts of chromium, nickel, zirconium or stainless steel, there are 1214 remaining experiments. It could be stated that there is greater than 99.999% confidence that 99% of the population is above the remaining smallest data sample (1-0.99^1214 = 0.9999949). In the 1214 remaining calculations for this report, the smallest adjusted k-effective was 0.96649 (for a U-233 benchmark).

2.2.5 Discussion of Results

Based on the methods discussed previously, the following subcritical limits are recommended:

Table 1. Upper Subcritical Limits (Before subtraction of any additional margin)

Fissile Category	Number of Cases	Upper Subcritical Limit
Combined category for HEU, IEU, LEU	639	0.975 (Note 1)
Plutonium or Mixed Pu-U	438	0.971
Uranium-233	140	0.966
All Categories Combined	1217	0.966

Note 1: Experiment Series HEU-COMP-INTER-005, cases 7,9, 15 and 16 showed that particular caution should be used with large arrays with large amounts of nickel, chromium, zirconium or stainless steel. These results indicated a potential for limits in the 0.856 to 0.968 range.

This recommendation is subject to the following restrictions:

- Models must be similar to those included in the benchmarks (See especially Table 3.1 of Y/DD-896/R1 for a concise summary).
- Models must not be similar to the cases with high negative bias described in Table 5.1 of Y/DD-896/R1. Characteristics include large amounts of chromium, nickel, zirconium or stainless steel, and infinite models, or very large models with little leakage, in which absorption in the listed materials is a major influence on the results. Iron and stainless steel are also materials that contributed to poor performance of the code, and care should also be taken with models having large amounts of iron or stainless steel (or stainless steel's component materials).
- Models must use options, materials and arrangements that have been included in the benchmarks.
- The upper subcritical limits stated above include only code bias. No additional margin is included for model bias (simplifications or uncertainties in analyzed conditions) or additional margin of safety. **A larger or smaller additional margin may be applicable depending on the plant process analysis, and the analyst must justify the amount of the applied margin in the process analysis.**

With 1214 experiments (of 1217 total) included in the determination of the subcritical limit, there is a good basis for having very high confidence that systems and conditions (similar to those included in this report) calculated by this method to be subcritical, will actually be subcritical. Allowance for additional margin for model bias, safety margin or area of applicability margin, if needed, would be subtracted from this upper subcritical limit. Additional margins of 0.02 to 0.05 have typically been used; however, the appropriate value depends on the details of the analysis, and administrative policy, if any. In determining these upper subcritical limits, the systems were not sub-divided into detailed categories based on materials and forms. Rather, a conservative value based on all the results for each fissile species has been determined. A combined limit is also given.

The 238-group library is the only one included in this report. Based on Reference 3 there may be some applications where the 44-group library may perform better (Low Enriched LWR and MOX lattices, and ^{233}U), but this has not been evaluated in this report.

Although four or more decimal places are shown in results tables (Y/DD-896/R1), the actual accuracy of the code, for a particular calculation, may be on the order of +/- 0.02 to 0.03 (or more) based on the spread in the bias results. Also, the standard deviation of the mean for a particular calculation was on the order of 0.001 for benchmark cases, and may be somewhat higher for applications. Therefore, less than four decimal places are physically meaningful or significant for developing limits. Too much importance should not be placed on small differences in the third or fourth decimal place. The main value of reporting four (or five) decimal places for a calculation result is to confirm that the result reported actually originated from a given output file.

Non-parametric statistics was used exclusively in this report.

3 Conclusions

Taken together, Y/DD-896/R1 and Y/DD-972/R1 provide the **framework** for the validation of CSAS25 control module from the Standardized Computer Analyses for Licensing Evaluation (SCALE) Version 4.4a package with the 238-group ENDF/B-V SCALE 4.4a cross-section library.

Y/DD-896/R1 addresses the establishment of bias, bias trends and uncertainty associated with the use of SCALE4.4a for performance of criticality calculations. This evaluation is directed at systems consisting of fissile and fissionable material in metallic, solution and other physical forms, as described in the OECD Handbook. The focus is on comparison of calculated neutron multiplication factors (k_{eff}) with the associated experimental results, and on establishment of bias, bias trends, and uncertainty as a final step. Compiled data for 1217 critical experiments is used as the basis for the calculation models. The calculated results from SCALE 4.4a using the 238-group ENDF/B-V SCALE 4.4a cross-section library have been compared with reported results for the benchmark experiments. Comparison of results demonstrates that SCALE 4.4a run on the Nuclear Criticality Safety Division (NCSD) Hewlett Packard Series 9000/J-5600 (HP J-5600) unclassified workstation (referred to as CMODB) produces the same results within the statistical uncertainty of the Monte Carlo calculations as reported by the experiments.

Y/DD-896/R1 provides assurance that the code predicts critical systems reasonably well, however, in general, there is wide variation in performance depending on the type of system, based on bias results. Using a rating scale similar to Reference 3, the performance ranges from "very good" or less than about +/- 0.01 to "very poor" or about +0.087/-0.14, depending on the category of experiments. In general, the previously observed problems resulted in very high bias, which would be conservative for plant applications.

This report includes several benchmark cases that significantly under-predict the expected results. There is no guarantee against the possibility of an unusual scenario that could produce non-conservative results, and analysts must be always vigilant for this possibility.

Y/DD-972/R1 recommends a preferred method for determining the upper subcritical limit. Y/DD-972/R1 establishes subcritical limits determined through an evaluation of statistics parameters of calculation results for critical experiments. However, the correlating parameters (i.e., mass, enrichment, geometry, absorption, moderation, reflection, etc.) and values for applying additional margin to the subcritical limits are application dependent. The determination of correlating parameters and additional margin is an integral part of the process analysis. For the critical experiment results, no correlation between calculation results and neutron energy causing fission (or any other parameter) was observed. As such, this document does not specify final upper subcritical limit values as has been done in the past.

The Area of Applicability (AoA) is also application dependent. In using the ○raw" upper safety limit data of this report, the criticality analyst must exercise sound engineering judgment and use strong technical arguments to develop "a margin in k_{eff}, or other correlating parameter. The margin must be sufficiently large to ensure that conditions (calculated by this method to be subcritical by this margin) will actually be subcritical.[1]

Documentation of determination and justification of the appropriate margin in the analyst's evaluation, in conjunction with this report, will constitute the complete Validation Report in accordance with ANSI/ANS-8.1-1998, Section 4.3.6(4).

4 Recommendations for Future Work

As stated in Y/DD-896/R1, numerous additional OECD experiment descriptions are already available for experiments that would be directly applicable to Y-12 applications. In this regard, future efforts should be dedicated to the following: (1) developing more input decks in-house for experiments selected based on applicability to Y-12, and (2) including additional models as they become available in future revisions of the OECD report. In addition, changes in experiment categorization and interpretation, and clarifications are sometimes reported in the annual revisions of the OECD handbook. These changes should be reviewed to determine whether they impact the conclusions in this report. This work will require a dedicated effort.

Additional work may be needed to identify trends and/or biases by including additional parameters in the statistical evaluation of critical experiment results.

Additional work is needed on Area of Applicability (AoA) determination methods. Determining whether a particular application is within the AoA of a validation is currently almost exclusively based on subjective judgment. To be done correctly, it requires the analyst to have close familiarity with the details of the experiments in the validation. Efforts to develop input models for more experiments, particularly if done by several staff members, would have the additional benefit of increasing staff's familiarity with experiment descriptions, which would also help improve these AoA determinations. Continuing to do such model input preparation work as part of the qualification program (and re-qualification) is suggested. In addition, methods have been proposed for more rigorous, and quantitative, AoA determinations. A dedicated effort is needed to evaluate these methods to determine if they are effective and practical to implement.

As discussed in Y/DD-896/R1, based on the bias results, areas of relatively poor performance are seen, probably due to cross section data issues. Efforts to produce improved cross section libraries for SCALE should be supported.

5 REFERENCES

1 *Nuclear Criticality Safety in Operations with Fissionable Material Outside Reactors*, ANSI/ANS-8.1-1998, American National Standards Institute, New York, 1998.

2 *Guide for Validation of Nuclear Criticality Safety Calculational Methodology*, NUREG/CR-6698, SAIC for U.S. NRC, January 2001.

3 *Experience With the SCALE Criticality Safety Cross-Section Libraries*, NUREG/CR-6686/ORNL/TM-1999/322, October 2000.

Appendix 6.9.9

CRITICALITY EVALUATION FOR INCREASING THE FISSILE LOADING LIMIT FOR HEU OXIDE IN THE ES-3100

THIS PAGE INTENTIONALLY LEFT BLANK.

Appendix 6.9.9

CRITICALITY EVALUATION FOR INCREASING THE FISSILE LOADING LIMIT FOR HEU OXIDE IN THE ES-3100

This appendix presents the criticality safety evaluation for increasing the fissile loading limit for HEU oxide content in the ES-3100 package using SCALE5 as the criticality analysis tool. Calculations presented herein were performed using the Monte Carlo CSAS25 criticality code sequence and 238-group ENDFB-V cross section library of SCALE 5.0 (NUREG/CR-0200, rev. 7), executed on identical Hewlett Packard (HP) Model zx6000 Itanium workstations (CMODC and CMODD). Criticality calculations documented in Sects. 6.4 – 6.6 were performed using SCALE 4.4a (NUREG/CR-0200, rev. 6) executed on an HP Model J5600 RISC workstation (CMODB). The obsolete CMODB with HP-UX 10.20 operating system was recently retired from service. No longer supported by the code developer, SCALE 4.4a is not portable to the new computing platforms, thus necessitating the use of SCALE 5.0.

SCALE5 incorporates minor improvements in the code modules for the Bondarenko and the Nordheim Integral Treatment processing of resonance cross sections and the KENO V.a module. Consequently, the USL used is validation dependent based on the SCALE-platform combination. The criticality evaluation based upon SCALE 5.0 calculations is documented in this appendix separate from the main body of Sect. 6 because this new work could not easily be folded into the existing SCALE 4.4a evaluation without inclusion of a patchwork of clarifications.

6.9.9.1 Description of the Criticality Design

The design features of the ES-3100 package addressed in Sect. 6.1.1 are not changed. The same codes and standards apply. No change is employed in the methodology addressed in Sect. 6.1.2 for demonstrating maximum reactivity. The shipping limit for an ES-3100 package with HEU product oxide content having a bulk density $\geq$2.0 g/cm^3 is increased from 9,682 g ^{235}U to 12,323 g ^{235}U by specifying a CSI = 0.4. The CSI is assigned as described in Sect. 6.1.3. This administrative limit restricts the size of an array of packages, maintaining subcriticality for both the NCT and HAC.

6.9.9.2 HEU Oxide Content for the ES-3100 Package

The criticality safety evaluation documented in this appendix pertains to HEU product oxide as described in Sect. 6.2.1, and Appendices 6.9.1 and 6.9.3. The convenience cans described in Sect. 6.2.2 and the packing materials described in Sect. 6.2.3 are not affected by the new fissile loading limit. The packing content loading restrictions stated in Sect. 6.2.4 are unchanged.

6.9.9.3 General Considerations

General considerations expressed in Sect. 6.3 regarding both assumptions made about the ES-3100 packaging and the calculation methodology for the evaluation are maintained. No changes are required to the calculation models of the containment vessel, the single-unit packaging (Sect. 6.3.1.1), the infinite array and finite array packaging (Sect. 6.3.1.2), the damaged packaging (Sect. 6.3.1.3), or the catastrophically-damaged packaging (Sect. 6.3.1.4). The material properties specification for the HEU product oxide (Sect. 6.3.2) does not change.

6.9.9.4 Computer Codes and Cross-Section Libraries

Calculations presented in this appendix were performed using the Monte Carlo CSAS25 criticality code sequence and 238-group ENDFB-V cross section library of SCALE 5.0 (NUREG/CR-0200, rev. 7), executed on identical Hewlett Packard (HP) Model zx6000 Itanium workstations (CMODC and CMODD) of the Y-12 Safety Analysis Engineering (SAE) organization in Oak Ridge, Tennessee. Criticality calculations documented in Sects. 6.4–6.6 were performed using SCALE 4.4a (NUREG/CR-0200, rev. 6) executed on an HP Model J5600 RISC workstation (CMODB). The obsolete CMODB with HP-UX 10.20 operating system was recently retired from service. No longer supported by the code developer, SCALE 4.4a is not portable to the new computing platforms, thus necessitating the use of SCALE 5.0.

The SCALE 4.4a criticality codes and cross-section library are addressed in Sect. 6.3.3. The 238-group ENDF/B-V cross-section library used by SCALE 5.0 is unchanged from the previous version SCALE 4.4a. Also, most of the modular codes in CSAS25 control sequence of SCALE 5.0 are unchanged except for the cross-section processing functional module NITAWL-III.

Sect. NITAWL-III applies the Nordheim integral treatment to perform neutron cross-section processing in the resonance energy range for nuclides that have ENDF/B resonance parameter data. This technique involves the numerical integration of ENDF/B resonance parameters using a calculated flux distribution, which is based on the calculated collision density across each resonance and subsequent weighing of the reaction cross section to the desired broad group structure. In the CSAS sequence, NITAWL-III assembles the group-to-group transfer arrays from the elastic and inelastic scattering components and performs other tasks to produce a problem-dependent working cross-section library which can be used by KENO V.a.

As noted in the user manual, several extensions to the Nordheim calculation have been implemented into the algorithm contained in NITAWL-III:

- Elements containing more than one isotope can be treated.
- Self-shielding is applied to resonance scattering. Transfer matrices are adjusted.
- g-, f-, d-, and p-wave as well as s-wave levels can be treated.
- The asymptotic approximation for the flux in the thermal energy range is assumed to have a Maxwellian energy distribution.
- A refined procedure for generating the energy mesh over which reaction rates are integrated has been developed.

Sect. As with the SCALE 4.4a calculations, the k_{eff} values for each KENO V.a case are based on 500,000 neutron histories produced by running for 215 generations with 2,500 neutrons per generation and truncating the first 15 generations of data. The convergence of the KENO V.a calculation is related to trends in the average calculated k_{eff}. In general, the KENO V.a output table of k_{eff} by generation skipped is reviewed for trends. If no trends are observed, the calculation is accepted, and the reported value of k_{eff} is the one with the most neutron histories. There is usually no statistically significant difference between this result and the one with the smallest standard deviation.

No manual cross-section adjustment is performed for the criticality evaluation. Cross-section processing is performed automatically in the CSAS25 code sequence. Modeling the contents as precisely as possible improves the accuracy of cross-section processing.

The CSAS25 control module, the associated functional modules, the cross section library, and databases used in this evaluation reside in the verified configuration control area designated **/vcc/scale5** on CMODC and CMODD. Also, the computer input and output files for the criticality safety evaluation of the ES-3100 shipping package with the additional/new content reside in a configuration control area **/archive/ylf717_Rev3PC1** on CMODC.

6.9.9.5 Single Package Evaluation (NCT and HAC)

The analysis presented in Sect. 6.4 demonstrates that $k_{eff} + 2\sigma$ increases with increasing MOIFR. Therefore, a model of a fully flooded, reflected package is used to calculate neutron multiplication factors for the single package analysis. The reference analysis reveals that a continuous decrease in $k_{eff} + 2\sigma$ occurs with decreasing fissile mass when density is held constant. Also, $k_{eff} + 2\sigma$ increases as the bulk density decreases for a fixed fissile mass, which is due to the increased moderation of the HEU oxide.

Cases **5ncsrpdoxt11_1_*n*_14** (Table 6.9.9.8-2) represents the NCT model of an ES-3100 package with 14 kg of HEU oxide (12,323 g ^{235}U). The parameter "***n***" ranging from 1 to 5, signifies oxide density values of 2.0, 3.0, 4.0, 5.0, and 6.54 g/cm^3, respectively. The $k_{eff} + 2\sigma$ values ranging from 0.810 to 0.752 are well below the USL value of 0.924.

Case **5cvcrpdoxt11_1_1_14_15)** (Table 6.9.9.8-1) models a reflected containment vessel with 14 kg of HEU oxide at 2.0 g/cm^3. The $k_{eff} + 2\sigma$ value is ~0.1 greater in the reflected containment vessel than in the corresponding reflected, flooded single package (Case **5cvcrpdoxt11_1_1_14_15)**. This result is consistent with the reference evaluation of Sect. 6.4.

Cases **5hcsrpdoxt12_1_*n*_14** (Table 6.9.9.8-2) represents the HAC model of the damaged ES-3100 package, where the outer dimensions of the package are reduced accordingly and the entire package is flooded except the neutron poison of the body weldment liner inner cavity. The $k_{eff} + 2\sigma$ values range from 0.811 to 0.757. The changes in both the outer dimensions of the package and the compositions of the Kaolite and 277-4 due to HAC result in a $\leq$0.004 change in the neutron multiplication factor, also consistent with the reference evaluation of Sect. 6.4.

6.9.9.6 Array Package Evaluation (NCT and HAC)

The infinite array analyses presented in Sects. 6.5 and 6.6 demonstrate that the CSI is 0.0 for ES-3100 packages having product oxide content with a bulk density $\geq$2.0 g/cm^3 and with a maximum of 9,682 g ^{235}U. Case result presented in Table 6.9.9.8-3 substantiate this conclusion.

The array analyses presented in Sects. 6.5 and 6.6 also demonstrate maximum reactivity occurs in an array of packages when both the containment vessel is flooded (MOCFR = 1.0) and the ES-3100 packaging is dry (MOIFR = 1e-04). A water fraction of MOIFR = 1e-04 pertains specifically to NCT or HAC packages where both the neutron poison of the body weldment liner inner cavity and the Kaolite are dry and both the recesses of the package external to the containment vessel and the interstitial space between drums of the array do no contain any residual moisture. Therefore, the ES-3100 package model consisting of dry packaging and flooded containment vessel is used for the finite array package analysis as required for establishing a non-zero CSI value.

Cases **5ncf1pdoxt11_1_*n*_15_3** through **5ncf1pdoxt11_1_*n*_11_3** (Table 6.9.9.8-4) represent a 13 × 13 × 6 array of NCT packages. The content mass ranges from 15 kg of HEU oxide (13,203 g ^{235}U) to 11 kg of HEU oxide (9,682 g ^{235}U). Case parameter "***n***" ranging from 1 to 5, signifies oxide density values of 2.0, 3.0, 4.0, 5.0, and 6.54 g/cm^3, respectively. Likewise, Cases **5hcf2pdoxt12_1_*n*_15_3** through **5hcf2pdoxt12_1_*n*_11_3** (Table 6.9.9.8-4) represent a 9 × 9 × 4 array of HAC packages. These

finite array configurations support the assignment of a CSI = 0.4. (Cases **5ncf1pdoxt11_1_1_15_3** and **5hcf2pdoxt12_1_1_15_3** are not evaluated because the capacity of the convenience cans is exceeded for the 15 kg oxide loading at a density of 2.0 g/cm^3.)

As expected, the neutron multiplication factor for the finite array configurations of ES-3100 packages with HEU product oxide decreases as a function of decreasing ^{235}U mass. Also, calculation results for the parametric cases reveal the same continuous increase in the $k_{eff} + 2\sigma$ values with decreasing bulk density as observed in both the single package calculation results (Sect. 6.4.3) and infinite array calculation results (Table 6.9.9.8-4). Given that the $k_{eff} + 2\sigma$ values are below the USL of 0.924, ES-3100 packages may be shipped under a CSI = 0.4 for ES-3100 packages having HEU product oxide content with a bulk density ≥2.0 g/cm^3 and with a maximum of 12,323 g ^{235}U.

6.9.9.7 Benchmark experiments and the criticality validation

The criticality validation for SCALE 5.0 is a repetition of the SCALE 4.4a validation based on benchmark experiments documented in the OECD Handbook. [NEA/NSC/DOC(95)03] Validation cases for SCALE 4.4a were executed on an HP Model J5600 RISC workstation under the HP-UX 10.20 operating system. For SCALE 5.0, these same validation cases were executed on an HP Model zx6000 Itanium workstation (CMODC).

The validation of CSAS25 control module of SCALE 5.0 with the 238-group ENDF/B-V cross-section library is documented in Y/DD-1220 and Y/DD-1221 (Appendix 6.9.10). Like Y/DD-896/R1, Y/DD-1220 addresses the establishment of bias, bias trends, and uncertainty associated with the use of SCALE 5.0 for performance of criticality calculations. Like Y/DD-972R1, Y/DD-1221 addresses determining USL and for incorporating uncertainty and margin into this USL.

SCALE 5.0 incorporates minor improvements in the code modules for the Bondarenko and the Nordheim Integral Treatment processing of resonance cross sections and the KENO V.a module. Consequently, the USL used is validation dependent based on the SCALE-platform combination. The evaluation of additional/new contents based upon SCALE 5.0 calculations is documented in this appendix separate from the main body of Sect. 6 because this new work could not easily be folded into the existing SCALE 4.4a evaluation without inclusion of a patchwork of clarifications.

The USL is based on the non-parametric statistics-based lower tolerance limit (LTL) for greater than 0.99/99% where there is a probability of greater than 0.99 that 99% of the population is greater than a specified result, reduced by additional margin. From Table 1 of Y/DD-1221, the LTL combining bias and bias uncertainty is 0.974 for uranium systems, including HEU metal. Tables 4.2, 4.3, and 4.4 of Y/DD-1220 list the maximum (positive) and minimum (negative) biases for HEU (metal, compound, solution), IEU (metal, compound) and LEU (compound, solution) systems. Since the positive bias is conservatively treated as a "zero" bias in the validation analysis, the negative bias is applied to determine the USL for the systems. The minimum bias given for HEU, IEU, and LEU systems is −0.0230, −0.0055 and −0.0260, respectively.

The minimum bias given for HEU systems in Table 4.2 of Y/DD-1220 is -0.1423. However, this result is from one of the four k-infinite models which are somewhat different than the usual benchmark experiments. As discussed in Sect. 5.3 of Y/DD-1220, the four outlier results are for benchmark experiments that were modeled as infinite in extent, thereby amplifying the effects of imperfections in cross section data. The models also required additional interpretation and adjustment from the actual finite experimental configuration to create an infinite benchmark model. After eliminating outlier models from the bias determination, the minimum bias was determined to be -0.023 for HEU systems.

The global minimum bias results for these systems (−0.0260) is applied to all uranium enrichments. Ordinarily, the USL would be 0.954 where an additional margin of subcriticality of 0.02 is subtracted from the LTL of 0.974. However, NUREG/CR-5661 provides guidance that the USL should be established with a minimum margin of subcriticality of 0.05. Thus, the USL is equal to 0.95 plus the minimum bias (−0.026), giving a value of 0.924.

6.9.9.8 Calculation results tables for additional/new contents

Tables 6.9.9.8-1 through 6.9.9.8-4 contain a summary of the calculation results for the additional/new contents to be shipped in the ES-3100 shipping package.

Table 6.9.9.8-1. Results for HEU oxide content in CV calculation model

case name 5cvcrpdoxt11	Ox (g)	^{235}U (g)	Ox density (g/cm^3)	Ox volume (cm^3)	Sat. H_2O (g)	CV H_2O (g)	h/x	mocfr	k_{eff}	σ	k_{eff}+2σ
14,000 g UO_2 content, 500 g polyethylene, flooded containment vessel, reflected											
_1_1_14_15	14000	12323	2.00	7000	5712	2667	19.11	1.0e+00	0.91213	0.00154	0.91521

Table 6.9.9.8-2. Results for HEU oxide content in single-unit packaging calculation model

case name 5ncsrpdoxt11	Ox (g)	^{235}U (g)	Ox den. (g/cm^3)	Ox vol. (cm^3)	Sat. H_2O (g)	CV H_2O (g)	h/x	k_{eff}	σ	k_{eff}+2σ	case name 5hcsrpdoxt12	k_{eff}	σ	k_{eff}+2σ
UO_2, content and 500 g polyethylene in flooded containment vessel, flooded package														
NCT											HAC			
_1_1_14	14000	12323	2.00	7000	5712	2667	19.11	0.80682	0.00154	0.80990	_1_1_14	0.80844	0.00132	0.81108
_1_2_14	14000	12323	3.00	4667	3383	4996	19.11	0.79264	0.00147	0.79557	_1_2_14	0.79564	0.00161	0.79887
_1_3_14	14000	12323	4.00	3500	2219	6161	19.11	0.78217	0.00138	0.78493	_1_3_14	0.78181	0.00127	0.78436
_1_4_14	14000	12323	5.00	2800	1520	6860	19.11	0.76784	0.00125	0.77035	_1_4_14	0.77058	0.00119	0.77296
_1_5_14	14000	12323	6.54	2141	862	7518	19.11	0.74948	0.00136	0.75219	_1_5_14	0.75379	0.00136	0.75651

Table 6.9.9.8-3. Results for HEU oxide content in array packaging calculation model

case name 5nciapdoxt11	Ox (g)	^{235}U (g)	Ox den. (g/cm^3)	Ox vol. (cm^3)	Sat. H_2O (g)	CV H_2O (g)	h/x	k_{eff}	σ	k_{eff}+2σ	case name 5hciapdoxt12	k_{eff}	σ	k_{eff}+2σ
UO_2 content and 500 g polyethylene in flooded containment vessel, infinite array packaging model for CSI=0.0														
NCT											HAC			
_1_2_15_3	15000	13203	3.00	5000	3625	4664	17.66	0.91962	0.00120	0.92202	_1_2_15_3	0.92011	0.00143	0.92298
_1_3_15_3	15000	13203	4.00	3750	2377	5911	17.66	0.88779	0.00122	0.89023	_1_3_15_3	0.88737	0.00177	0.89092
_1_4_15_3	15000	13203	5.00	3000	1628	6660	17.66	0.86134	0.00122	0.86377	_1_4_15_3	0.86151	0.00139	0.86429
_1_5_15_3	15000	13203	6.54	2294	923	7365	17.66	0.83226	0.00105	0.83436	_1_5_15_3	0.83147	0.00128	0.83404
_1_1_14_3	**14000**	**12323**	**2.00**	**7000**	**5712**	**2667**	**19.11**	**0.96251**	**0.00139**	**0.96530**	**_1_1_14_3**	**0.96173**	**0.00120**	**0.96413**
_1_2_14_3	14000	12323	3.00	4667	3383	4996	19.11	0.90999	0.00125	0.91250	_1_2_14_3	0.91039	0.00133	0.91306
_1_3_14_3	14000	12323	4.00	3500	2219	6161	19.11	0.87432	0.00136	0.87704	_1_3_14_3	0.87390	0.00123	0.87636
_1_4_14_3	14000	12323	5.00	2800	1520	6860	19.11	0.84766	0.00107	0.84981	_1_4_14_3	0.85075	0.00157	0.85390
_1_5_14_3	14000	12323	6.54	2141	862	7518	19.11	0.82262	0.00114	0.82489	_1_5_14_3	0.81885	0.00117	0.82120
_1_1_13_3	**13000**	**11443**	**2.00**	**6500**	**5304**	**3166**	**20.79**	**0.95083**	**0.00137**	**0.95356**	**_1_1_13_3**	**0.94754**	**0.00124**	**0.95002**
_1_2_13_3	13000	11443	3.00	4333	3142	5329	20.79	0.89635	0.00119	0.89874	_1_2_13_3	0.89884	0.00238	0.90360
_1_3_13_3	13000	11443	4.00	3250	2060	6410	20.79	0.86131	0.00115	0.86362	_1_3_13_3	0.86176	0.00134	0.86443
_1_4_13_3	13000	11443	5.00	2600	1411	7059	20.79	0.83841	0.00119	0.84080	_1_4_13_3	0.83735	0.00179	0.84093
_1_5_13_3	13000	11443	6.54	1988	800	7670	20.79	0.80709	0.00129	0.80967	_1_5_13_3	0.81006	0.00147	0.81301
_1_1_12_3	**12000**	**10562**	**2.00**	**6000**	**4896**	**3665**	**22.74**	**0.93557**	**0.00146**	**0.93849**	**_1_1_12_3**	**0.93442**	**0.00130**	**0.93701**
_1_2_12_3	12000	10562	3.00	4000	2900	5662	22.74	0.88421	0.00123	0.88667	_1_2_12_3	0.88382	0.00127	0.88637
_1_3_12_3	12000	10562	4.00	3000	1902	6660	22.74	0.84986	0.00136	0.85259	_1_3_12_3	0.84962	0.00123	0.85208
_1_4_12_3	12000	10562	5.00	2400	1303	7259	22.74	0.82606	0.00117	0.82839	_1_4_12_3	0.82224	0.00116	0.82456
_1_5_12_3	12000	10562	6.54	1835	739	7823	22.74	0.79269	0.00117	0.79503	_1_5_12_3	0.79562	0.00120	0.79802
_1_1_11_3	**11000**	**9682**	**2.00**	**5500**	**4488**	**4164**	**25.06**	**0.91920**	**0.00170**	**0.92260**	**_1_1_11_3**	**0.91961**	**0.00132**	**0.92224**
_1_2_11_3	**11000**	**9682**	**3.00**	**3667**	**2658**	**5994**	**25.06**	**0.86941**	**0.00134**	**0.87208**	**_1_2_11_3**	**0.87089**	**0.00131**	**0.87352**
_1_3_11_3	**11000**	**9682**	**4.00**	**2750**	**1743**	**6909**	**25.06**	**0.83680**	**0.00152**	**0.83984**	**_1_3_11_3**	**0.83444**	**0.00132**	**0.83707**

Table 6.9.9.8-3. Results for HEU oxide content in array packaging calculation model

case name 5nciapdoxt11	Ox (g)	^{235}U (g)	Ox den. (g/cm^3)	Ox vol. (cm^3)	Sat. H_2O (g)	CV H_2O (g)	h/x	k_{eff}	σ	k_{eff}+2σ	case name 5hciapdoxt12	k_{eff}	σ	k_{eff}+2σ
_1_4_11_3	11000	9682	5.00	2200	1194	7458	25.06	0.81122	0.00126	0.81373	_1_4_11_3	0.81127	0.00110	0.81346
_1_5_11_3	11000	9682	6.54	1682	677	7976	25.06	0.78014	0.00137	0.78288	_1_5_11_3	0.78034	0.00131	0.78296

Table 6.9.9.8-4. Results for finite array analysis of HEU oxide content in the array packaging calculation model

case name 5ncf1pdoxt11	Ox (g)	^{235}U (g)	Ox den. (g/cm^3)	Ox vol. (cm^3)	Sat. H_2O (g)	CV H_2O (g)	h/x	k_{eff}	σ	k_{eff}+2σ	case name 5hcf2pdoxt12	k_{eff}	σ	k_{eff}+2σ
UO_2 content and 500 g polyethylene in flooded containment vessel, finite array packaging model for CSI=0.4														
NCT											HAC			
_1_2_15_3	15000	13203	3.00	5000	3625	4664	17.66	0.86899	0.00119	0.87137	_1_2_15_3	0.85996	0.00128	0.86251
_1_3_15_3	15000	13203	4.00	3750	2377	5911	17.66	0.83024	0.00127	0.83278	_1_3_15_3	0.82926	0.00123	0.83173
_1_4_15_3	15000	13203	5.00	3000	1628	6660	17.66	0.80781	0.00148	0.81077	_1_4_15_3	0.80377	0.00145	0.80667
_1_5_15_3	15000	13203	6.54	2294	923	7365	17.66	0.78101	0.00137	0.78375	_1_5_15_3	0.77553	0.00145	0.77843
_1_1_14_3	14000	12323	2.00	7000	5712	2667	19.11	0.91235	0.00152	0.91539	_1_1_14_3	0.90222	0.00126	0.90473
_1_2_14_3	14000	12323	3.00	4667	3383	4996	19.11	0.85665	0.00130	0.85925	_1_2_14_3	0.85184	0.00187	0.85558
_1_3_14_3	14000	12323	4.00	3500	2219	6161	19.11	0.81979	0.00150	0.82279	_1_3_14_3	0.81814	0.00164	0.82143
_1_4_14_3	14000	12323	5.00	2800	1520	6860	19.11	0.79749	0.00139	0.80027	_1_4_14_3	0.79489	0.00132	0.79752
_1_5_14_3	14000	12323	6.54	2141	862	7518	19.11	0.76730	0.00112	0.76954	_1_5_14_3	0.76607	0.0012	0.76848
_1_1_13_3	13000	11443	2.00	6500	5304	3166	20.79	0.90096	0.00137	0.90369	_1_1_13_3	0.89146	0.00168	0.89482
_1_2_13_3	13000	11443	3.00	4333	3142	5329	20.79	0.84451	0.00150	0.84750	_1_2_13_3	0.83795	0.00125	0.84046
_1_3_13_3	13000	11443	4.00	3250	2060	6410	20.79	0.80806	0.00175	0.81156	_1_3_13_3	0.80364	0.0014	0.80643
_1_4_13_3	13000	11443	5.00	2600	1411	7059	20.79	0.78428	0.00120	0.78668	_1_4_13_3	0.78119	0.0013	0.78379
_1_5_13_3	13000	11443	6.54	1988	800	7670	20.79	0.75713	0.00132	0.75977	_1_5_13_3	0.75345	0.00134	0.75612

Table 6.9.9.8-4. Results for finite array analysis of HEU oxide content in the array packaging calculation model

case name 5ncf1pdoxt11	Ox (g)	^{235}U (g)	Ox den. (g/cm^3)	Ox vol. (cm^3)	Sat. H_2O (g)	CV H_2O (g)	h/x	k_{eff}	σ	k_{eff}+2σ	case name 5hcf2pdoxt12	k_{eff}	σ	k_{eff}+2σ
_1_1_12_3	12000	10562	2.00	6000	4896	3665	22.74	0.88673	0.00148	0.88969	_1_1_12_3	0.87895	0.00133	0.8816
_1_2_12_3	12000	10562	3.00	4000	2900	5662	22.74	0.83038	0.00129	0.83296	_1_2_12_3	0.82545	0.00137	0.82819
_1_3_12_3	12000	10562	4.00	3000	1902	6660	22.74	0.79879	0.00148	0.80175	_1_3_12_3	0.79221	0.00133	0.79487
_1_4_12_3	12000	10562	5.00	2400	1303	7259	22.74	0.77086	0.00131	0.77349	_1_4_12_3	0.77013	0.00151	0.77316
_1_5_12_3	12000	10562	6.54	1835	739	7823	22.74	0.74245	0.00181	0.74608	_1_5_12_3	0.74028	0.00127	0.74282
_1_1_11_3	11000	9682	2.00	5500	4488	4164	25.06	0.87072	0.00152	0.87376	_1_1_11_3	0.86583	0.00113	0.86809
_1_2_11_3	11000	9682	3.00	3667	2658	5994	25.06	0.81756	0.00176	0.82108	_1_2_11_3	0.81406	0.00155	0.81715
_1_3_11_3	11000	9682	4.00	2750	1743	6909	25.06	0.78439	0.00122	0.78682	_1_3_11_3	0.77978	0.0015	0.78279
_1_4_11_3	11000	9682	5.00	2200	1194	7458	25.06	0.75752	0.00159	0.76070	_1_4_11_3	0.75642	0.00115	0.75872
_1_5_11_3	11000	9682	6.54	1682	677	7976	25.06	0.72893	0.00156	0.73205	_1_5_11_3	0.72536	0.00168	0.72871

6.9.9.9 Input Listing for Select SCALE 5.0 Cases

Select input files for calculations identified Tables 6.9.9.8-1 through 6.9.9.8-4 are presented below.

6.9.9.9.1 Case 5cvcrpdoxt11_1_1_14_15

```
=csas25    parm=size=3000000
5cvcrpdoxt11,14000.1gUO2 (12322.9g235)5712.4gSH2O 2667.0gH2Ocv hx= 19.11 fr=1
238groupndf5 infhommedium
'HEU volume =7000.05000 HEU oxide, bulk density of oxide in cans=  2.00000 g/cm3'
'oxide= 14000.1 g, sat.h2o in HEU oxide=5712.4 g, oxide h/x=12.10'
'poly (packed or wrapped) dry content h/x=1.36, CV void volume 2671.83368'
arbmuox    1.85591   2 0 0 0  92235   88.0203
                               8016   11.9797    1  1.0000  293  end
arbmastm  7.5725e-01  2 0 0 0  1001   11.1913
                               8016   88.8087    1  1.0000  293  end
arbmpoly  6.6282e-02  2 0 0 0  1001   14.3798
                               6012   85.6202    1  1.0000  293  end
'np277-4: spacer (NCT_MD&H)'
'NCT min.den.(95.3886 lb/ft3) and hydrogen'
'np277-4 min.den.= 1.527971 = (95.3886 lb/ft3)(453.59 g/lb)/(28316.84 cm3/ft3)'
'use 75% of boron in calculations per NUREG-1609 Section 6.5.3.2'
arbmboron 7.31015e-2  2 0 0 0    5010   18.1479
                                 5011   81.8520    2  0.7500  293  end
arbmnpmx  1.07070e+0 10 0 0 0    6012    1.9189
                                 7014    0.0141
                                 8016   43.4251
                                11023    0.1174
                                12000    0.3378
                                13027   39.0479
                                14000    2.4672
                                16000    0.3083
                                20000   11.8336
                                26000    0.5298    2  1.0000  293  end
arbmnph2o 3.84169e-1  2 0 0 0    1001   11.1913
                                 8016   88.8087    2  1.0000  293  end
'flooded containmment vessel and content cans -- 10 CFR 71.55(d)(3)'
arbmwicv  9.9820e-01  2 0 0 0   1001   11.1913
                               8016   88.8087    3  1       293  end
'steel: containment vessel body 16.60 lb but use 15.74 lb'
ss304                                            8  1.0     293  end
'steel: cv flange lower use 3.36 lb'
ss304                                            9  0.97267 293  end
'steel: cv flange upper use 13.75 lb'
ss304                                           10  0.94348 293  end
'np277-4: confinement -- neutron poison inner liner (NCT_MD&H)'
'actual vol.= 1.31846e4 cm3 = (8.0457422e2 in3)(16.387064)'
'den.multiplier = 1.31846e4 cm3 (actual vol.) / 1.32708e4 cm3 (model vol.)'
'np277-4 min.den.= 1.527971 = (95.3886 lb/ft3)(453.59 g/lb)/(28316.84 cm3/ft3)'
'density = 1.518047 = (den.mult)(np277-4 min.den.) = 0.9935052*1.527971'
'use 75% of boron in calculations per NUREG-1609 Section 6.5.3.2'
arbmboron 7.26267e-2  2 0 0 0    5010   18.1479
                                 5011   81.8520   11  0.7500  293  end
arbmnpmx  1.06375e+0 10 0 0 0    6012    1.9189
                                 7014    0.0141
                                 8016   43.4251
                                11023    0.1174
                                12000    0.3378
                                13027   39.0479
                                14000    2.4672
                                16000    0.3083
                                20000   11.8336
                                26000    0.5298   11  1.0000  293  end
arbmnph2o 3.81674e-1  2 0 0 0    1001   11.1913
                                 8016   88.8087   11  1.0000  293  end
'kaolite 1600 body'
'sing.unit.density= (den.mult)(min.den.)'
' for arbmh2ok = 1.012373*0.51655,  for rest = 1.012373*0.34438'
'den.mult= 1.36557e5 cm3 (actual vol.) / 1.34888e5 cm3 (model vol.)'
'actual vol.= 1.36557e5 cm3 = (28316.84 cm3/ft3)(108.33188 lb)/(22.464 lb/ft3)'
arbmh2ok   0.52294  2 0 0 0    1001   11.1913
                               8016   88.8087   12  1       293  end
arbmal2o3  0.34864  2 0 0 0   13027   52.9390
```

```
                                8016   47.0610   12  0.096   293  end
arbmsio2   0.34864  2 0 0 0   14000   46.7570
                                8016   53.2430   12  0.367   293  end
arbmfe2o3  0.34864  2 0 0 0   26000   69.9540
                                8016   30.0460   12  0.067   293  end
arbmtio2   0.34864  2 0 0 0   22000   59.9535
                                8016   40.0465   12  0.012   293  end
arbmcao    0.34864  2 0 0 0   20000   71.4815
                                8016   28.5185   12  0.307   293  end
arbmmgo    0.34864  2 0 0 0   12000   60.3169
                                8016   39.6831   12  0.131   293  end
arbmna2o   0.34864  2 0 0 0   11023   74.1961
                                8016   25.8039   12  0.020   293  end
'kaolite 1600 top plug'
'sing.unit.density= (den.mult)(min.den.)'
' for arbmh20k = 0.965246*0.51655,  for rest = 0.965246*0.34438'
'den.mult= 1.21592e4 cm3 (actual vol.) / 1.25970e4 cm3 (model vol.)'
'actual vol.= 1.21592e4 cm3 = (28316.84 cm3/ft3)(9.646 lb)/(22.464 lb/ft3)'
arbmh2ok   0.49860  2 0 0 0    1001   11.1913
                                8016   88.8087   13  1       293  end
arbmal2o3  0.33241  2 0 0 0   13027   52.9390
                                8016   47.0610   13  0.096   293  end
arbmsio2   0.33241  2 0 0 0   14000   46.7570
                                8016   53.2430   13  0.367   293  end
arbmfe2o3  0.33241  2 0 0 0   26000   69.9540
                                8016   30.0460   13  0.067   293  end
arbmtio2   0.33241  2 0 0 0   22000   59.9535
                                8016   40.0465   13  0.012   293  end
arbmcao    0.33241  2 0 0 0   20000   71.4815
                                8016   28.5185   13  0.307   293  end
arbmmgo    0.33241  2 0 0 0   12000   60.3169
                                8016   39.6831   13  0.131   293  end
arbmna2o   0.33241  2 0 0 0   11023   74.1961
                                8016   25.8039   13  0.020   293  end
'silicone rubber pads'
arbmsiru   1.21791  4 0 0 0    6012   32.3767
                                1001    8.1573
                                8016   21.5782
                               14000   37.8878   14  1.0     293  end
'void space external to containment vessel'
arbmwecv   0.9982   2 0 0 0    1001   11.1913
                                8016   88.8087   15  1       293  end
'steel: liner'
ss304                                           16  1.0     293  end
'steel: plug cover (pc) use 9.907 lb'
ss304                                           17  1.06388 293  end
'steel: angle iron (ai) for single units'
ss304                                           18  1.0     293  end
'steel: angle iron (ai) for arrays'
'array density is multiplied by a volume fraction 7.08030/5.63249'
'ss304                                           18  1.25705 293  end
'steel: drum steel for single units'
ss304                                           19  1.0     293  end
'steel: drum steel for arrays'
'array density is multiplied by a volume fraction 3.20482/3.20544'
'ss304                                           19  0.99981 293  end
'void space external to drum'
'array density is multiplied by a volume ratio 8.11698/6.98323'
'arbmwed    1.16026  2 0 0 0    1001   11.1913
'                               8016   88.8087   20  1       293  end
'reflective water'
arbmh20r   0.9982   2 0 0 0    1001   11.1913
                                8016   88.8087   21  1.0     293  end
end comp
5cvcrpdoxt11,14000.1gUO2 (12322.9g235)5712.4gSH2O 2667.0gH2Ocv,hx= 19.11 fr=1
read parameters nub=yes npg=2500 gen=215 nsk=15 tme=100 end parameters
read boun       all=vac                         end boun
read geometry
unit 1001
'drum bottom flat cover [Elev= 0.105 in. at top of unit]'
'cylinder  19 1   24.587200    0.26670   0.0     com='extended radius not used'
 cuboid    21 1 4p24.587200    0.26670   0.0     com='drum chine outer radius'
unit 1002
'above drum bottom flat cover and below containment vessel [Elev= 4.670 in.]'
 cuboid    21 1 4p24.587200   11.59510   0.0     com='drum chine outer radius'
```

```
unit 1003
'cv bottom to bottom of 1st step [Elev=35.270 in.]'
 cylinder  3  1    6.426200   77.72400  58.78051 com='cavity abv HEU'
 cylinder  1  1    6.426200   77.72400   0.63500 com='HEU content'
 cylinder  8  1    6.680200   77.72400   0.0     com='cv bottom'
 cuboid    21 1 4p24.587200   77.72400   0.0     com='drum chine outer radius'
unit 1010
'cv at 1st step in liner [Elev=35.330 in.]'
 cylinder  3  1    6.426200    0.15240   0.00000 com='cavity abv HEU'
 cylinder  1  1    6.426200    0.15240   0.0     com='HEU content'
 cylinder  8  1    6.680200    0.15240   0.0     com='cv at 1st step'
 cuboid    21 1 4p24.587200    0.15240   0.0     com='drum chine outer radius'
unit 1011
'vertical gap between 1st step in liner and cv flange [Elev=35.420 in.]'
 cylinder  3  1    6.426200    0.22860   0.00000 com='cavity abv HEU'
 cylinder  1  1    6.426200    0.22860   0.0     com='HEU content'
 cylinder  8  1    6.680200    0.22860   0.0     com='cv at gap btwn step-flng'
 cuboid    21 1 4p24.587200    0.22860   0.0     com='drum chine outer radius'
unit 1012
'cv flange to top of cv well [Elev=35.920 in.]'
 cylinder  3  1    6.426200    1.27000   0.00000 com='cavity abv HEU'
 cylinder  1  1    6.426200    1.27000   0.0     com='HEU content'
 cylinder  9  1    9.525000    1.27000   0.0     com='flange to top of well'
 cuboid    21 1 4p24.587200    1.27000   0.0     com='drum chine outer radius'
unit 1013
'cv flange above cv well [Elev=37.070 in.]'
 cylinder  10 1    9.525000    2.92100   0.0     com='flange above cv well'
 cuboid    21 1 4p24.587200    2.92100   0.0     com='drum chine outer radius'
unit 1014
'plugpad2 below liner 2nd step [Elev=37.470 in.]'
 cuboid    21 1 4p24.587200    1.01600   0.0     com='drum chine outer radius'
unit 1015
'2nd step in liner [Elev=37.530 in.]'
 cuboid    21 1 4p24.587200    0.15240   0.0     com='drum chine outer radius'
unit 1016
'abv 2nd step in liner to bottom of angle iron [Elev=40.750 in.]'
 cuboid    21 1 4p24.587200    8.17880   0.0     com='drum chine outer radius'
unit 1017
'bottom of angle iron to bend in angle iron [Elev=42.500 in.]'
 cuboid    21 1 4p24.587200    4.44500   0.0     com='drum chine outer radius'
unit 1018
'bend in angle iron to top of angle iron [Elev=42.750 in.]'
 cuboid    21 1 4p24.587200    0.63500   0.0     com='drum chine outer radius'
unit 1019
'drum lid and lip [Elev=43.500 in.]'
 cuboid    21 1 4p24.587200    1.90500   0.0     com='drum chine outer radius'
global
unit 1020
'es3100 drum [Elev=43.500 in.]'
array 3         2r-24.587200     0.0
'cuboid     0  1 4p24.587200    110.4905  0.0    com='bare package'
 cuboid    21  1 4p55.067200   140.9700 -30.48   com='reflected package'
'cuboid    20  1 4p22.889718    110.5048  0.0    com='interstital array space'
'global
'unit 1021
'array 4   3r0.0
'reflector  21 2  6r3.0  10
end geometry
read array
ara=3 nux=1 nuy=1 nuz=13 fill
1001 1002 1003 1010
1011 1012 1013 1014 1015 1016 1017 1018 1019        end fill
'ara=4 nux=13 nuy=13 nuz=06 fill f1020               end fill
end array
'read bias id=500 2  11  end bias
read start nst=0
end start
end data
end
```

6.9.9.9.2 Case 5ncsrpdoxt11_1_1_14

```
=csas25    parm=size=3000000
5ncsrpdoxt11,14000.1gUO2 (12322.9g235)5712.4gSH2O 2667.0gH2Ocv hx= 19.11 fr=1
238groupndf5 infhommedium
'HEU volume =7000.05000 HEU oxide, bulk density of oxide in cans=  2.00000 g/cm3'
'oxide= 14000.1 g, sat.h2o in HEU oxide=5712.4 g, oxide h/x=12.10'
'poly (packed or wrapped) dry content h/x=1.36, CV void volume 2671.83368'
arbmuox    1.85591   2 0 0 0  92235   88.0203
                               8016   11.9797    1  1.0000  293  end
arbmastm  7.5725e-01  2 0 0 0  1001   11.1913
                               8016   88.8087    1  1.0000  293  end
arbmpoly  6.6282e-02  2 0 0 0  1001   14.3798
                               6012   85.6202    1  1.0000  293  end
'np277-4: spacer (NCT_MD&H)'
'NCT min.den.(95.3886 lb/ft3) and hydrogen'
'np277-4 min.den.= 1.527971 = (95.3886 lb/ft3)(453.59 g/lb)/(28316.84 cm3/ft3)'
'use 75% of boron in calculations per NUREG-1609 Section 6.5.3.2'
arbmboron 7.31015e-2  2 0 0 0    5010   18.1479
                                  5011   81.8520    2  0.7500  293  end
arbmnpmx  1.07070e+0 10 0 0 0    6012    1.9189
                                  7014    0.0141
                                  8016   43.4251
                                 11023    0.1174
                                 12000    0.3378
                                 13027   39.0479
                                 14000    2.4672
                                 16000    0.3083
                                 20000   11.8336
                                 26000    0.5298    2  1.0000  293  end
arbmnph2o 3.84169e-1  2 0 0 0    1001   11.1913
                                  8016   88.8087    2  1.0000  293  end
'flooded containmment vessel and content cans -- 10 CFR 71.55(d)(3)'
arbmwicv  9.9820e-01  2 0 0 0   1001   11.1913
                               8016   88.8087    3  1       293  end
'steel: containment vessel body 16.60 lb but use 15.74 lb'
ss304                                            8  1.0     293  end
'steel: cv flange lower use 3.36 lb'
ss304                                            9  0.97267 293  end
'steel: cv flange upper use 13.75 lb'
ss304                                           10  0.94348 293  end
'np277-4: confinement -- neutron poison inner liner (NCT_MD&H)'
'actual vol.= 1.28314e4 cm3 = (7.83023e2 in3)(16.387064)'
'den.multiplier = 1.28314e4 cm3 (actual vol.) / 1.32708e4 cm3 (model vol.)'
'np277-4 min.den.= 1.527971 = (95.3886 lb/ft3)(453.59 g/lb)/(28316.84 cm3/ft3)'
'density = 1.477385 = (den.mult)(np277-4 min.den.) = 0.9668933*1.527971'
'use 75% of boron in calculations per NUREG-1609 Section 6.5.3.2'
arbmboron 7.06813e-2  2 0 0 0    5010   18.1479
                                  5011   81.8520   11  0.7500  293  end
arbmnpmx  1.03525e+0 10 0 0 0    6012    1.9189
                                  7014    0.0141
                                  8016   43.4251
                                 11023    0.1174
                                 12000    0.3378
                                 13027   39.0479
                                 14000    2.4672
                                 16000    0.3083
                                 20000   11.8336
                                 26000    0.5298   11  1.0000  293  end
arbmnph2o 3.71451e-1  2 0 0 0    1001   11.1913
                                  8016   88.8087   11  1.0000  293  end
'kaolite 1600 body'
'sing.unit.density= (den.mult)(min.den.)'
' for arbmh20k = 1.012373*0.51655,  for rest = 1.012373*0.34438'
'den.mult= 1.36557e5 cm3 (actual vol.) / 1.34888e5 cm3 (model vol.)'
'actual vol.= 1.36557e5 cm3 = (28316.84 cm3/ft3)(108.33188 lb)/(22.464 lb/ft3)'
arbmh2ok   0.52294  2 0 0 0    1001   11.1913
                               8016   88.8087   12  1       293  end
arbmal2o3  0.34864  2 0 0 0   13027   52.9390
                               8016   47.0610   12  0.096   293  end
arbmsio2   0.34864  2 0 0 0   14000   46.7570
                               8016   53.2430   12  0.367   293  end
arbmfe2o3  0.34864  2 0 0 0   26000   69.9540
                               8016   30.0460   12  0.067   293  end
arbmtio2   0.34864  2 0 0 0   22000   59.9535
```

```
                                8016   40.0465   12  0.012   293  end
arbmcao    0.34864  2 0 0 0   20000   71.4815
                                8016   28.5185   12  0.307   293  end
arbmmgo    0.34864  2 0 0 0   12000   60.3169
                                8016   39.6831   12  0.131   293  end
arbmna2o   0.34864  2 0 0 0   11023   74.1961
                                8016   25.8039   12  0.020   293  end
'kaolite 1600 top plug'
'sing.unit.density= (den.mult)(min.den.)'
' for arbmh20k = 0.965246*0.51655,  for rest = 0.965246*0.34438'
'den.mult= 1.21592e4 cm3 (actual vol.) / 1.25970e4 cm3 (model vol.)'
'actual vol.= 1.21592e4 cm3 = (28316.84 cm3/ft3)(9.646 lb)/(22.464 lb/ft3)'
arbmh2ok   0.49860  2 0 0 0    1001   11.1913
                                8016   88.8087   13  1       293  end
arbmal2o3  0.33241  2 0 0 0   13027   52.9390
                                8016   47.0610   13  0.096   293  end
arbmsio2   0.33241  2 0 0 0   14000   46.7570
                                8016   53.2430   13  0.367   293  end
arbmfe2o3  0.33241  2 0 0 0   26000   69.9540
                                8016   30.0460   13  0.067   293  end
arbmtio2   0.33241  2 0 0 0   22000   59.9535
                                8016   40.0465   13  0.012   293  end
arbmcao    0.33241  2 0 0 0   20000   71.4815
                                8016   28.5185   13  0.307   293  end
arbmmgo    0.33241  2 0 0 0   12000   60.3169
                                8016   39.6831   13  0.131   293  end
arbmna2o   0.33241  2 0 0 0   11023   74.1961
                                8016   25.8039   13  0.020   293  end
'silicone rubber pads'
arbmsiru   1.21791  4 0 0 0    6012   32.3767
                                1001    8.1573
                                8016   21.5782
                               14000   37.8878   14  1.0     293  end
'void space external to containment vessel'
arbmwecv   0.9982   2 0 0 0    1001   11.1913
                                8016   88.8087   15  1       293  end
'steel: liner'
ss304                                           16  1.0     293  end
'steel: plug cover (pc) use 9.907 lb'
ss304                                           17  1.06388 293  end
'steel: angle iron (ai) for single units'
ss304                                           18  1.0     293  end
'steel: angle iron (ai) for arrays'
'array density is multiplied by a volume fraction 7.08030/5.63249'
'ss304                                           18  1.25705 293  end
'steel: drum steel for single units'
ss304                                           19  1.0     293  end
'steel: drum steel for arrays'
'array density is multiplied by a volume fraction 3.20482/3.20544'
'ss304                                           19  0.99981 293  end
'void space external to drum'
'array density is multiplied by a volume ratio 8.11698/6.98323'
'arbmwed    1.16026  2 0 0 0    1001   11.1913
'                               8016   88.8087   20  1       293  end
'reflective water'
arbmh20r   0.9982   2 0 0 0    1001   11.1913
                                8016   88.8087   21  1.0     293  end
end comp
5ncsrpdoxt11,14000.1gUO2 (12322.9g235)5712.4gSH2O 2667.0gH2Ocv,hx= 19.11 fr=1
read parameters nub=yes npg=2500 gen=215 nsk=15 tme=100 end parameters
read boun       all=vac                         end boun
read geometry
unit 1001
'drum bottom flat cover [Elev= 0.105 in. at top of unit]'
'cylinder  19 1   24.587200    0.26670   0.0     com='extended radius not used'
 cylinder  19 1   23.329900    0.26670   0.0     com='drum bottom flat cover'
 cuboid    21 1 4p24.587200    0.26670   0.0     com='drum chine outer radius'
unit 1002
'above drum bottom flat cover and below containment vessel [Elev= 4.670 in.]'
 cylinder  15 1    3.175000   11.59510  11.16330 com='void in pad-1'
 cylinder  14 1    7.924800   11.59510  11.16330 com='pad-1'
 cylinder  16 1    8.077200   11.59510  11.16330 com='np277_4 liner'
 cylinder  11 1   10.922000   11.59510  11.16330 com='np277_4'
 cylinder  16 1   11.074400   11.59510  10.85850 com='kaolite liner bottom'
 cylinder  12 1   23.177500   11.59510   0.0     com='kaolite'
```

```
 cylinder  19 1   23.329900   11.59510   0.0     com='drum'
 cuboid    21 1 4p24.587200   11.59510   0.0     com='drum chine outer radius'
unit 1003
'cv bottom to bottom of 1st step [Elev=35.270 in.]'
 cylinder  3  1    6.426200   77.72400  58.78051 com='cavity abv HEU'
 cylinder  1  1    6.426200   77.72400   0.63500 com='HEU content'
 cylinder  8  1    6.680200   77.72400   0.0     com='cv bottom'
 cylinder  15 1    7.924800   77.72400   0.0     com='void btw cv-np liner'
 cylinder  16 1    8.077200   77.72400   0.0     com='np277_4 liner'
 cylinder  11 1   10.922000   77.72400   0.0     com='np277_4'
 cylinder  16 1   11.074400   77.72400   0.0     com='kaolite liner'
 cylinder  12 1   23.177500   77.72400   0.0     com='kaolite'
 cylinder  19 1   23.329900   77.72400   0.0     com='drum'
 cuboid    21 1 4p24.587200   77.72400   0.0     com='drum chine outer radius'
unit 1010
'cv at 1st step in liner [Elev=35.330 in.]'
 cylinder  3  1    6.426200    0.15240   0.00000 com='cavity abv HEU'
 cylinder  1  1    6.426200    0.15240   0.0     com='HEU content'
 cylinder  8  1    6.680200    0.15240   0.0     com='cv at 1st step'
 cylinder  15 1    7.924800    0.15240   0.0     com='void btw cv and liner'
 cylinder  16 1   11.074400    0.15240   0.0     com='liner 1st step'
 cylinder  12 1   23.177500    0.15240   0.0     com='kaolite'
 cylinder  19 1   23.329900    0.15240   0.0     com='drum'
 cuboid    21 1 4p24.587200    0.15240   0.0     com='drum chine outer radius'
unit 1011
'vertical gap between 1st step in liner and cv flange [Elev=35.420 in.]'
 cylinder  3  1    6.426200    0.22860   0.00000 com='cavity abv HEU'
 cylinder  1  1    6.426200    0.22860   0.0     com='HEU content'
 cylinder  8  1    6.680200    0.22860   0.0     com='cv at gap btwn step-flng'
 cylinder  15 1   10.922000    0.22860   0.0     com='void btw cv and liner'
 cylinder  16 1   11.074400    0.22860   0.0     com='liner wall'
 cylinder  12 1   23.177500    0.22860   0.0     com='kaolite'
 cylinder  19 1   23.329900    0.22860   0.0     com='drum'
 cuboid    21 1 4p24.587200    0.22860   0.0     com='drum chine outer radius'
unit 1012
'cv flange to top of cv well [Elev=35.920 in.]'
 cylinder  3  1    6.426200    1.27000   0.00000 com='cavity abv HEU'
 cylinder  1  1    6.426200    1.27000   0.0     com='HEU content'
 cylinder  9  1    9.525000    1.27000   0.0     com='flange to top of well'
 cylinder  15 1    9.525000    1.27000   0.0     com='void btw cv and pad-2'
 cylinder  14 1   10.033000    1.27000   0.0     com='pad-2'
 cylinder  15 1   10.922000    1.27000   0.0     com='void btw cv and liner'
 cylinder  16 1   11.074400    1.27000   0.0     com='liner wall'
 cylinder  12 1   23.177500    1.27000   0.0     com='kaolite'
 cylinder  19 1   23.329900    1.27000   0.0     com='drum'
 cuboid    21 1 4p24.587200    1.27000   0.0     com='drum chine outer radius'
unit 1013
'cv flange above cv well [Elev=37.070 in.]'
 cylinder  10 1    9.525000    2.92100   0.0     com='flange above cv well'
 cylinder  15 1    9.525000    2.92100   0.0     com='void btw cv and pad-2'
 cylinder  14 1   10.033000    2.92100   0.0     com='pad-2'
 cylinder  15 1   10.922000    2.92100   0.0     com='void btw pad2 and liner'
 cylinder  16 1   11.074400    2.92100   0.0     com='liner wall'
 cylinder  12 1   23.177500    2.92100   0.0     com='kaolite'
 cylinder  19 1   23.329900    2.92100   0.0     com='drum'
 cuboid    21 1 4p24.587200    2.92100   0.0     com='drum chine outer radius'
unit 1014
'plugpad2 below liner 2nd step [Elev=37.470 in.]'
 cylinder  14 1   10.033000    0.76200   0.0     com='pad-2'
 cylinder  15 1   10.922000    1.01600   0.0     com='void btw pad2 and liner'
 cylinder  16 1   11.074400    1.01600   0.0     com='liner wall'
 cylinder  12 1   23.177500    1.01600   0.0     com='kaolite'
 cylinder  19 1   23.329900    1.01600   0.0     com='drum'
 cuboid    21 1 4p24.587200    1.01600   0.0     com='drum chine outer radius'
unit 1015
'2nd step in liner [Elev=37.530 in.]'
 cylinder  15 1   10.922000    0.15240   0.0     com='void abv pad2'
 cylinder  16 1   18.757900    0.15240   0.0     com='liner 2nd step'
 cylinder  12 1   23.177500    0.15240   0.0     com='kaolite'
 cylinder  19 1   23.329900    0.15240   0.0     com='drum'
 cuboid    21 1 4p24.587200    0.15240   0.0     com='drum chine outer radius'
unit 1016
'abv 2nd step in liner to bottom of angle iron [Elev=40.750 in.]'
 cylinder  13 1   18.097500    8.17880   0.49276 com='plug kaolite'
 cylinder  17 1   18.249900    8.17880   0.34036 com='sides of plug case'
```

```
 cylinder  15 1   18.605500    8.17880   0.0     com='void: plug to liner'
 cylinder  16 1   18.757900    8.17880   0.0     com='liner wall'
 cylinder  12 1   23.177500    8.17880   0.0     com='kaolite'
 cylinder  19 1   23.329900    8.17880   0.0     com='drum'
 cuboid    21 1 4p24.587200    8.17880   0.0     com='drum chine outer radius'
unit 1017
'bottom of angle iron to bend in angle iron [Elev=42.500 in.]'
 cylinder  13 1   18.097500    4.44500   0.0     com='plug kaolite'
 cylinder  17 1   18.249900    4.44500   0.0     com='sides of plug case'
 cylinder  15 1   18.605500    4.44500   0.0     com='void: plug to liner'
 cylinder  16 1   18.757900    4.44500   0.0     com='liner wall'
 cylinder  18 1   19.392900    4.44500   0.0     com='lower angle iron'
 cylinder  12 1   23.177500    4.44500   0.0     com='kaolite'
 cylinder  19 1   23.329900    4.44500   0.0     com='drum'
 cuboid    21 1 4p24.587200    4.44500   0.0     com='drum chine outer radius'
unit 1018
'bend in angle iron to top of angle iron [Elev=42.750 in.]'
 cylinder  13 1   18.097500    0.11176   0.0     com='plug kaolite'
 cylinder  17 1   18.249900    0.26416   0.0     com='sides of plug case'
 cylinder  15 1   18.605500    0.63500   0.0     com='void: plug to liner'
 cylinder  16 1   18.757900    0.63500   0.0     com='liner wall'
 cylinder  18 1   23.177500    0.63500   0.0     com='bend section of ai'
 cylinder  19 1   23.329900    0.63500   0.0     com='drum'
 cuboid    21 1 4p24.587200    0.63500   0.0     com='drum chine outer radius'
unit 1019
'drum lid and lip [Elev=43.500 in.]'
 cylinder  21 1   22.961600    1.90500   0.15240 com='void above lid'
 cylinder  19 1   23.114000    1.90500   0.0     com='drum lid'
 cylinder  21 1   23.177500    1.90500   0.0     com='void btw lid - drum wall'
 cylinder  19 1   23.329900    1.90500   0.0     com='drum'
 cuboid    21 1 4p24.587200    1.90500   0.0     com='drum chine outer radius'
global
unit 1020
'es3100 drum [Elev=43.500 in.]'
array 3         2r-24.587200     0.0
'cuboid     0  1 4p24.587200    110.4905  0.0    com='bare package'
 cuboid    21  1 4p55.067200   140.9700 -30.48   com='reflected package'
'cuboid    20  1 4p22.889718    110.5048  0.0    com='interstital array space'
'global
'unit 1021
'array 4   3r0.0
'reflector  21 2  6r3.0  10
end geometry
read array
ara=3 nux=1 nuy=1 nuz=13 fill
1001 1002 1003 1010
1011 1012 1013 1014 1015 1016 1017 1018 1019        end fill
'ara=4 nux=13 nuy=13 nuz=06 fill f1020               end fill
end array
'read bias id=500 2  11  end bias
read start nst=0
end start
end data
end
```

6.9.9.9.3 Case 5hcsrpdoxt12_1_1_14

```
=csas25    parm=size=3000000
5hcsrpdoxt12,14000.1gUO2 (12322.9g235)5712.4gSH2O 2667.0gH2Ocv hx= 19.11 fr=1
238groupndf5 infhommedium
'HEU volume =7000.05000 HEU oxide, bulk density of oxide in cans=  2.00000 g/cm3'
'oxide= 14000.1 g, sat.h2o in HEU oxide=5712.4 g, oxide h/x=12.10'
'poly (packed or wrapped) dry content h/x=1.36, CV void volume 2671.83368'
arbmuox    1.85591   2 0 0 0  92235   88.0203
                              8016   11.9797    1  1.0000  293  end
arbmastm  7.5725e-01  2 0 0 0  1001   11.1913
                              8016   88.8087    1  1.0000  293  end
arbmpoly  6.6282e-02  2 0 0 0  1001   14.3798
                              6012   85.6202    1  1.0000  293  end
'np277-4: spacer (HAC_MD&H)'
'HAC min.den.(95.3157 lb/ft3) and hydrogen'
'np277-4 min.den.= 1.526803 = (95.3157 lb/ft3)(453.59 g/lb)/(28316.84 cm3/ft3)'
'use 75% of boron in calculations per NUREG-1609 Section 6.5.3.2'
arbmboron 7.31015e-2  2 0 0 0    5010   18.1479
```

```
                                 5011   81.8520    2  0.7500  293  end
arbmnpmx  1.07071e+0 10 0 0 0    6012    1.9188
                                 7014    0.0141
                                 8016   43.4254
                                11023    0.1174
                                12000    0.3378
                                13027   39.0477
                                14000    2.4671
                                16000    0.3083
                                20000   11.8335
                                26000    0.5298    2  1.0000  293  end
arbmnph2o 3.82995e-1  2 0 0 0    1001   11.1913
                                 8016   88.8087    2  1.0000  293  end
'flooded containmment vessel and content cans -- 10 CFR 71.55(d)(3)'
arbmwicv  9.9820e-01  2 0 0 0   1001   11.1913
                               8016   88.8087    3  1       293  end
'steel: containment vessel body 16.60 lb but use 15.74 lb'
ss304                                            8  1.0     293  end
'steel: cv flange lower use 3.36 lb'
ss304                                            9  0.97267 293  end
'steel: cv flange upper use 13.75 lb'
ss304                                           10  0.94348 293  end
'np277-4: confinement -- neutron poison inner liner (HAC_MD&H)'
'actual vol.= 1.28314e4 cm3 = (7.83023e2 in3)(16.387064)'
'den.multiplier = 1.28314e4 cm3 (actual vol.) / 1.32708e4 cm3 (model vol.)'
'np277-4 min.den.= 1.526803 = (95.3157 lb/ft3)(453.59 g/lb)/(28316.84 cm3/ft3)'
'density = 1.476265 = (den.mult)(np277-4 min.den.) = 0.9668933*1.526803'
'use 75% of boron in calculations per NUREG-1609 Section 6.5.3.2'
arbmboron 7.06813e-2  2 0 0 0    5010   18.1479
                                 5011   81.8520   11  0.7500  293  end
arbmnpmx  1.03525e+0 10 0 0 0    6012    1.9188
                                 7014    0.0141
                                 8016   43.4254
                                11023    0.1174
                                12000    0.3378
                                13027   39.0477
                                14000    2.4671
                                16000    0.3083
                                20000   11.8335
                                26000    0.5298   11  1.0000  293  end
arbmnph2o 3.70316e-1  2 0 0 0    1001   11.1913
                                 8016   88.8087   11  1.0000  293  end
'kaolite 1600 body'
'nct.sing.unit.density= (den.mult)(min.den.)'
' for arbmh20k 0.52294 = 1.012373*0.51655, for rest 0.34864 = 1.012373*0.34438'
'den.mult= 1.36557e5 cm3 (actual vol.) / 1.34888e5 cm3 (model vol.)'
'actual vol.= 1.36557e5 cm3 = (28316.84 cm3/ft3)(108.33188 lb)/(22.464 lb/ft3)'
'hac.s.u.dens= (hac.mult)(nct.s.u.dens)'
'hac.mult = 1.34888e5 cm3 (nct vol.)/ 1.12246e5 cm3 (model vol.)'
' for arbmh2ok 0.62843 = 1.20172*0.52294,   for rest = 1.20172*0.34864'
arbmh2ok   0.62843  2 0 0 0    1001   11.1913
                               8016   88.8087   12  1       293  end
arbmal2o3  0.41898  2 0 0 0   13027   52.9390
                               8016   47.0610   12  0.096   293  end
arbmsio2   0.41898  2 0 0 0   14000   46.7570
                               8016   53.2430   12  0.367   293  end
arbmfe2o3  0.41898  2 0 0 0   26000   69.9540
                               8016   30.0460   12  0.067   293  end
arbmtio2   0.41898  2 0 0 0   22000   59.9535
                               8016   40.0465   12  0.012   293  end
arbmcao    0.41898  2 0 0 0   20000   71.4815
                               8016   28.5185   12  0.307   293  end
arbmmgo    0.41898  2 0 0 0   12000   60.3169
                               8016   39.6831   12  0.131   293  end
arbmna2o   0.41898  2 0 0 0   11023   74.1961
                               8016   25.8039   12  0.020   293  end
'kaolite 1600 top plug'
'sing.unit.density= (den.mult)(min.den.)'
' for arbmh20k = 0.965246*0.51655,  for rest = 0.965246*0.34438'
'den.mult= 1.21592e4 cm3 (actual vol.) / 1.25970e4 cm3 (model vol.)'
'actual vol.= 1.21592e4 cm3 = (28316.84 cm3/ft3)(9.646 lb)/(22.464 lb/ft3)'
arbmh2ok   0.49860  2 0 0 0    1001   11.1913
                               8016   88.8087   13  1       293  end
arbmal2o3  0.33241  2 0 0 0   13027   52.9390
                               8016   47.0610   13  0.096   293  end
```

```
arbmsio2   0.33241  2 0 0 0   14000   46.7570
                               8016   53.2430   13  0.367   293  end
arbmfe2o3  0.33241  2 0 0 0   26000   69.9540
                               8016   30.0460   13  0.067   293  end
arbmtio2   0.33241  2 0 0 0   22000   59.9535
                               8016   40.0465   13  0.012   293  end
arbmcao    0.33241  2 0 0 0   20000   71.4815
                               8016   28.5185   13  0.307   293  end
arbmmgo    0.33241  2 0 0 0   12000   60.3169
                               8016   39.6831   13  0.131   293  end
arbmna2o   0.33241  2 0 0 0   11023   74.1961
                               8016   25.8039   13  0.020   293  end
'silicone rubber pads'
arbmsiru   1.21791  4 0 0 0    6012   32.3767
                               1001    8.1573
                               8016   21.5782
                              14000   37.8878   14  1.0     293  end
'void space external to containment vessel'
arbmwecv   0.9982   2 0 0 0    1001   11.1913
                               8016   88.8087   15  1       293  end
'steel: liner'
ss304                                            16  1.0     293  end
'steel: plug cover (pc) use 9.907 lb'
ss304                                            17  1.06388 293  end
'steel: angle iron (ai) for HAC'
'nct density is multiplied by volume fraction 7.08030/5.74516'
ss304                                            18  1.23239 293  end
'steel: drum steel for HAC'
'nct density is multiplied by volume fraction 3.20482/2.95645'
ss304                                            19  1.08401 293  end
'void space external to drum'
'array density is assumed not reduced by hac'
'arbmwed    0.9982   2 0 0 0    1001   11.1913
'                               8016   88.8087   20  1       293  end
'reflective water'
arbmh20r   0.9982   2 0 0 0    1001   11.1913
                               8016   88.8087   21  1.0     293  end
end comp
5hcsrpdoxt12,14000.1gUO2 (12322.9g235)5712.4gSH2O 2667.0gH2Ocv,hx= 19.11 fr=1
read parameters nub=yes npg=2500 gen=215 nsk=15 tme=100 end parameters
read boun       all=vac                          end boun
read geometry
unit 1001
'drum bottom flat cover [Elev= 0.105 in. at top of unit]'
'cylinder  19 1   21.838092    0.26670   0.0     com='extended radius not used'
 cylinder  19 1   21.838092    0.26670   0.0     com='drum bottom flat cover'
 cuboid    21 1 4p21.838092    0.26670   0.0     com='drum(chine)outer radius'
unit 1002
'above drum bottom flat cover and below containment vessel [Elev= 4.670 in.]'
 cylinder  15 1    3.175000   11.59510  11.16330 com='void in pad-1'
 cylinder  14 1    7.924800   11.59510  11.16330 com='pad-1'
 cylinder  16 1    8.077200   11.59510  11.16330 com='np277_4 liner'
 cylinder  11 1   10.922000   11.59510  11.16330 com='np277_4'
 cylinder  16 1   11.074400   11.59510  10.85850 com='kaolite liner bottom'
 cylinder  12 1   21.685692   11.59510   0.0     com='kaolite'
 cylinder  19 1   21.838092   11.59510   0.0     com='drum'
 cuboid    21 1 4p21.838092   11.59510   0.0     com='drum(chine)outer radius'
unit 1003
'cv bottom to bottom of 1st step [Elev=35.270 in.]'
 cylinder  3  1    6.426200   77.72400  58.78051 com='cavity abv HEU'
 cylinder  1  1    6.426200   77.72400   0.63500 com='HEU content'
 cylinder  8  1    6.680200   77.72400   0.0     com='cv bottom'
 cylinder  15 1    7.924800   77.72400   0.0     com='void btw cv-np liner'
 cylinder  16 1    8.077200   77.72400   0.0     com='np277_4 liner'
 cylinder  11 1   10.922000   77.72400   0.0     com='np277_4'
 cylinder  16 1   11.074400   77.72400   0.0     com='kaolite liner'
 cylinder  12 1   21.685692   77.72400   0.0     com='kaolite'
 cylinder  19 1   21.838092   77.72400   0.0     com='drum'
 cuboid    21 1 4p21.838092   77.72400   0.0     com='drum(chine)outer radius'
unit 1010
'cv at 1st step in liner [Elev=35.330 in.]'
 cylinder  3  1    6.426200    0.15240   0.00000 com='cavity abv HEU'
 cylinder  1  1    6.426200    0.15240   0.0     com='HEU content'
 cylinder  8  1    6.680200    0.15240   0.0     com='cv at 1st step'
 cylinder  15 1    7.924800    0.15240   0.0     com='void btw cv and liner'
```

```
 cylinder  16 1   11.074400    0.15240   0.0     com='liner 1st step'
 cylinder  12 1   21.685692    0.15240   0.0     com='kaolite'
 cylinder  19 1   21.838092    0.15240   0.0     com='drum'
 cuboid    21 1 4p21.838092    0.15240   0.0     com='drum(chine)outer radius'
unit 1011
'vertical gap between 1st step in liner and cv flange [Elev=35.420 in.]'
 cylinder  3  1    6.426200    0.22860   0.00000 com='cavity abv HEU'
 cylinder  1  1    6.426200    0.22860   0.0     com='HEU content'
 cylinder  8  1    6.680200    0.22860   0.0     com='cv at gap btwn step-flng'
 cylinder  15 1   10.922000    0.22860   0.0     com='void btw cv and liner'
 cylinder  16 1   11.074400    0.22860   0.0     com='liner wall'
 cylinder  12 1   21.685692    0.22860   0.0     com='kaolite'
 cylinder  19 1   21.838092    0.22860   0.0     com='drum'
 cuboid    21 1 4p21.838092    0.22860   0.0     com='drum(chine)outer radius'
unit 1012
'cv flange to top of cv well [Elev=35.920 in.]'
 cylinder  3  1    6.426200    1.27000   0.00000 com='cavity abv HEU'
 cylinder  1  1    6.426200    1.27000   0.0     com='HEU content'
 cylinder  9  1    9.525000    1.27000   0.0     com='flange to top of well'
 cylinder  15 1    9.525000    1.27000   0.0     com='void btw cv and pad-2'
 cylinder  14 1   10.033000    1.27000   0.0     com='pad-2'
 cylinder  15 1   10.922000    1.27000   0.0     com='void btw cv and liner'
 cylinder  16 1   11.074400    1.27000   0.0     com='liner wall'
 cylinder  12 1   21.685692    1.27000   0.0     com='kaolite'
 cylinder  19 1   21.838092    1.27000   0.0     com='drum'
 cuboid    21 1 4p21.838092    1.27000   0.0     com='drum(chine)outer radius'
unit 1013
'cv flange above cv well [Elev=37.070 in.]'
 cylinder  10 1    9.525000    2.92100   0.0     com='flange above cv well'
 cylinder  15 1    9.525000    2.92100   0.0     com='void btw cv and pad-2'
 cylinder  14 1   10.033000    2.92100   0.0     com='pad-2'
 cylinder  15 1   10.922000    2.92100   0.0     com='void btw pad2 and liner'
 cylinder  16 1   11.074400    2.92100   0.0     com='liner wall'
 cylinder  12 1   21.685692    2.92100   0.0     com='kaolite'
 cylinder  19 1   21.838092    2.92100   0.0     com='drum'
 cuboid    21 1 4p21.838092    2.92100   0.0     com='drum(chine)outer radius'
unit 1014
'plugpad2 below liner 2nd step [Elev=37.470 in.]'
 cylinder  14 1   10.033000    0.76200   0.0     com='pad-2'
 cylinder  15 1   10.922000    1.01600   0.0     com='void btw pad2 and liner'
 cylinder  16 1   11.074400    1.01600   0.0     com='liner wall'
 cylinder  12 1   21.685692    1.01600   0.0     com='kaolite'
 cylinder  19 1   21.838092    1.01600   0.0     com='drum'
 cuboid    21 1 4p21.838092    1.01600   0.0     com='drum(chine)outer radius'
unit 1015
'2nd step in liner [Elev=37.530 in.]'
 cylinder  15 1   10.922000    0.15240   0.0     com='void abv pad2'
 cylinder  16 1   18.757900    0.15240   0.0     com='liner 2nd step'
 cylinder  12 1   21.685692    0.15240   0.0     com='kaolite'
 cylinder  19 1   21.838092    0.15240   0.0     com='drum'
 cuboid    21 1 4p21.838092    0.15240   0.0     com='drum(chine)outer radius'
unit 1016
'abv 2nd step in liner to bottom of angle iron [Elev=40.750 in.]'
 cylinder  13 1   18.097500    8.17880   0.49276 com='plug kaolite'
 cylinder  17 1   18.249900    8.17880   0.34036 com='sides of plug case'
 cylinder  15 1   18.605500    8.17880   0.0     com='void: plug to liner'
 cylinder  16 1   18.757900    8.17880   0.0     com='liner wall'
 cylinder  12 1   21.685692    8.17880   0.0     com='kaolite'
 cylinder  19 1   21.838092    8.17880   0.0     com='drum'
 cuboid    21 1 4p21.838092    8.17880   0.0     com='drum(chine)outer radius'
unit 1017
'bottom of angle iron to bend in angle iron [Elev=42.500 in.]'
 cylinder  13 1   18.097500    4.44500   0.0     com='plug kaolite'
 cylinder  17 1   18.249900    4.44500   0.0     com='sides of plug case'
 cylinder  15 1   18.605500    4.44500   0.0     com='void: plug to liner'
 cylinder  16 1   18.757900    4.44500   0.0     com='liner wall'
 cylinder  18 1   19.392900    4.44500   0.0     com='lower angle iron'
 cylinder  12 1   21.685692    4.44500   0.0     com='kaolite'
 cylinder  19 1   21.838092    4.44500   0.0     com='drum'
 cuboid    21 1 4p21.838092    4.44500   0.0     com='drum(chine)outer radius'
unit 1018
'bend in angle iron to top of angle iron [Elev=42.750 in.]'
 cylinder  13 1   18.097500    0.11176   0.0     com='plug kaolite'
 cylinder  17 1   18.249900    0.26416   0.0     com='sides of plug case'
 cylinder  15 1   18.605500    0.63500   0.0     com='void: plug to liner'
```

```
 cylinder  16 1   18.757900    0.63500   0.0     com='liner wall'
 cylinder  18 1   21.685692    0.63500   0.0     com='bend section of ai'
 cylinder  19 1   21.838092    0.63500   0.0     com='drum'
 cuboid    21 1 4p21.838092    0.63500   0.0     com='drum(chine)outer radius'
unit 1019
'drum lid and lip [Elev=43.500 in.]'
 cylinder  21 1   21.469792    1.90500   0.15240 com='void above lid'
 cylinder  19 1   21.622192    1.90500   0.0     com='drum lid'
 cylinder  21 1   21.685692    1.90500   0.0     com='void btw lid - drum wall'
 cylinder  19 1   21.838092    1.90500   0.0     com='drum'
 cuboid    21 1 4p21.838092    1.90500   0.0     com='drum(chine)outer radius'
global
unit 1020
'es3100 drum [Elev=43.500 in.]'
array 3         2r-21.838092     0.0
'cuboid     0  1 4p21.838092    110.4905  0.0    com='bare package'
 cuboid    21  1 4p52.318092   140.9700 -30.48   com='reflected package'
'cuboid    20  1 4p22.889718    110.5048  0.0    com='interstital array space'
'global
'unit 1021
'array 4   3r0.0
'reflector  21 2  6r3.0  10
end geometry
read array
ara=3 nux=1 nuy=1 nuz=13 fill
1001 1002 1003 1010
1011 1012 1013 1014 1015 1016 1017 1018 1019        end fill
'ara=4 nux=13 nuy=13 nuz=06 fill f1020               end fill
end array
'read bias id=500 2  11  end bias
read start nst=0
end start
end data
end
```

6.9.9.9.4 Case 5nciapdoxt11_1_1_11_3

```
=csas25    parm=size=3000000
5nciapdoxt11,11000.1gUO2 ( 9682.3g235)4488.3gSH2O 4164.3gHcv hx= 25.06 fr=0.0001
238groupndf5 infhommedium
'HEU volume =5500.05000 HEU oxide, bulk density of oxide in cans=  2.00000 g/cm3'
'oxide= 11000.1 g, sat.h2o in HEU oxide=4488.3 g, oxide h/x=12.10'
'poly (packed or wrapped) dry content h/x=1.73, CV void volume 4171.83368'
arbmuox    1.82015   2 0 0 0  92235   88.0203
                               8016   11.9797    1  1.0000  293  end
arbmastm  7.4266e-01  2 0 0 0  1001   11.1913
                               8016   88.8087    1  1.0000  293  end
arbmpoly  8.2733e-02  2 0 0 0  1001   14.3798
                               6012   85.6202    1  1.0000  293  end
'np277-4: spacer (NCT_MD&H)'
'NCT min.den.(95.3886 lb/ft3) and hydrogen'
'np277-4 min.den.= 1.527971 = (95.3886 lb/ft3)(453.59 g/lb)/(28316.84 cm3/ft3)'
'use 75% of boron in calculations per NUREG-1609 Section 6.5.3.2'
arbmboron 7.31015e-2  2 0 0 0    5010   18.1479
                                 5011   81.8520    2  0.7500  293  end
arbmnpmx  1.07070e+0 10 0 0 0    6012    1.9189
                                 7014    0.0141
                                 8016   43.4251
                                11023    0.1174
                                12000    0.3378
                                13027   39.0479
                                14000    2.4672
                                16000    0.3083
                                20000   11.8336
                                26000    0.5298    2  1.0000  293  end
arbmnph2o 3.84169e-1  2 0 0 0    1001   11.1913
                                 8016   88.8087    2  1.0000  293  end
'flooded containmment vessel and content cans -- 10 CFR 71.55(d)(3)'
arbmwicv  9.9820e-01  2 0 0 0   1001   11.1913
                               8016   88.8087    3  1       293  end
'steel: containment vessel body 16.60 lb but use 15.74 lb'
ss304                                            8  1.0     293  end
'steel: cv flange lower use 3.36 lb'
ss304                                            9  0.97267 293  end
```

```
'steel: cv flange upper use 13.75 lb'
ss304                                          10  0.94348 293  end
'np277-4: confinement -- neutron poison inner liner (NCT_MD&H)'
'actual vol.= 1.28314e4 cm3 = (7.83023e2 in3)(16.387064)'
'den.multiplier = 1.28314e4 cm3 (actual vol.) / 1.32708e4 cm3 (model vol.)'
'np277-4 min.den.= 1.527971 = (95.3886 lb/ft3)(453.59 g/lb)/(28316.84 cm3/ft3)'
'density = 1.477385 = (den.mult)(np277-4 min.den.) = 0.9668933*1.527971'
'use 75% of boron in calculations per NUREG-1609 Section 6.5.3.2'
arbmboron 7.06813e-2  2 0 0 0    5010   18.1479
                                 5011   81.8520   11  0.7500  293  end
arbmnpmx  1.03525e+0 10 0 0 0    6012    1.9189
                                 7014    0.0141
                                 8016   43.4251
                                11023    0.1174
                                12000    0.3378
                                13027   39.0479
                                14000    2.4672
                                16000    0.3083
                                20000   11.8336
                                26000    0.5298   11  1.0000  293  end
arbmnph2o 3.71451e-1  2 0 0 0    1001   11.1913
                                 8016   88.8087   11  1.0000  293  end
'kaolite 1600 body'
'sing.unit.density= (den.mult)(min.den.)'
' for arbmh2ok = 1.012373*0.51655,  for rest = 1.012373*0.34438'
'den.mult= 1.36557e5 cm3 (actual vol.) / 1.34888e5 cm3 (model vol.)'
'actual vol.= 1.36557e5 cm3 = (28316.84 cm3/ft3)(108.33188 lb)/(22.464 lb/ft3)'
'nct array densities are s.u.dens. multiplied by volume ratio 1.34888/1.10336'
arbmh2ok   0.63931  2 0 0 0    1001   11.1913
                               8016   88.8087   12  0.0287  293  end
arbmal2o3  0.42622  2 0 0 0   13027   52.9390
                               8016   47.0610   12  0.096   293  end
arbmsio2   0.42622  2 0 0 0   14000   46.7570
                               8016   53.2430   12  0.367   293  end
arbmfe2o3  0.42622  2 0 0 0   26000   69.9540
                               8016   30.0460   12  0.067   293  end
arbmtio2   0.42622  2 0 0 0   22000   59.9535
                               8016   40.0465   12  0.012   293  end
arbmcao    0.42622  2 0 0 0   20000   71.4815
                               8016   28.5185   12  0.307   293  end
arbmmgo    0.42622  2 0 0 0   12000   60.3169
                               8016   39.6831   12  0.131   293  end
arbmna2o   0.42622  2 0 0 0   11023   74.1961
                               8016   25.8039   12  0.020   293  end
'kaolite 1600 top plug'
'sing.unit.density= (den.mult)(min.den.)'
' for arbmh2ok = 0.965246*0.51655,  for rest = 0.965246*0.34438'
'den.mult= 1.21592e4 cm3 (actual vol.) / 1.25970e4 cm3 (model vol.)'
'actual vol.= 1.21592e4 cm3 = (28316.84 cm3/ft3)(9.646 lb)/(22.464 lb/ft3)'
arbmh2ok   0.49860  2 0 0 0    1001   11.1913
                               8016   88.8087   13  0.0287  293  end
arbmal2o3  0.33241  2 0 0 0   13027   52.9390
                               8016   47.0610   13  0.096   293  end
arbmsio2   0.33241  2 0 0 0   14000   46.7570
                               8016   53.2430   13  0.367   293  end
arbmfe2o3  0.33241  2 0 0 0   26000   69.9540
                               8016   30.0460   13  0.067   293  end
arbmtio2   0.33241  2 0 0 0   22000   59.9535
                               8016   40.0465   13  0.012   293  end
arbmcao    0.33241  2 0 0 0   20000   71.4815
                               8016   28.5185   13  0.307   293  end
arbmmgo    0.33241  2 0 0 0   12000   60.3169
                               8016   39.6831   13  0.131   293  end
arbmna2o   0.33241  2 0 0 0   11023   74.1961
                               8016   25.8039   13  0.020   293  end
'silicone rubber pads'
arbmsiru   1.21791  4 0 0 0    6012   32.3767
                               1001    8.1573
                               8016   21.5782
                              14000   37.8878   14  1.0     293  end
'void space external to containment vessel'
arbmwecv   0.9982   2 0 0 0    1001   11.1913
                               8016   88.8087   15  0.0001  293  end
'steel: liner'
ss304                                          16  1.0     293  end
```

```
'steel: plug cover (pc) use 9.907 lb'
ss304                                          17  1.06388 293  end
'steel: angle iron (ai) for single units'
'ss304                                          18  1.0     293  end
'steel: angle iron (ai) for arrays'
'array density is multiplied by a volume fraction 7.08030/5.63249'
ss304                                          18  1.25705 293  end
'steel: drum steel for single units'
'ss304                                          19  1.0     293  end
'steel: drum steel for arrays'
'array density is multiplied by a volume fraction 3.20482/3.20544'
ss304                                          19  0.99981 293  end
'void space external to drum'
'array density is multiplied by a volume ratio 8.11698/6.98323'
arbmwed    1.16026  2 0 0 0    1001   11.1913
                                8016   88.8087   20  0.0001  293  end
'reflective water'
'arbmh20r   0.9982   2 0 0 0    1001   11.1913
'                                8016   88.8087   21  1.0     293  end
end comp
5nciapdoxt11,11000.1gUO2 ( 9682.3g235)4488.3gSH2O 4164.3gHcv,hx= 25.06 fr=0.0001
read parameters nub=yes npg=2500 gen=215 nsk=15 tme=100 end parameters
read boun       all=specular                   end boun
read geometry
unit 1001
'drum bottom flat cover [Elev= 0.111 in. at top of unit]'
'cylinder  19 1   22.866096    0.28150   0.0     com='extended radius not used'
 cylinder  19 1   21.722275    0.28150   0.0     com='drum bottom flat cover'
 cuboid    20 1 4p22.866096    0.28150   0.0     com='drum chine outer radius'
unit 1002
'above drum bottom flat cover and below containment vessel [Elev= 4.676 in.]'
 cylinder  15 1    3.175000   11.59510  11.16330 com='void in pad-1'
 cylinder  14 1    7.924800   11.59510  11.16330 com='pad-1'
 cylinder  16 1    8.077200   11.59510  11.16330 com='np277_4 liner'
 cylinder  11 1   10.922000   11.59510  11.16330 com='np277_4'
 cylinder  16 1   11.074400   11.59510  10.85850 com='kaolite liner bottom'
 cylinder  12 1   21.555075   11.59510   0.0     com='kaolite'
 cylinder  19 1   21.722275   11.59510   0.0     com='drum'
 cuboid    20 1 4p22.866096   11.59510   0.0     com='drum chine outer radius'
unit 1003
'cv bottom to bottom of 1st step [Elev=35.276 in.]'
 cylinder  3  1    6.426200   77.72400  47.21851 com='cavity abv HEU'
 cylinder  1  1    6.426200   77.72400   0.63500 com='HEU content'
 cylinder  8  1    6.680200   77.72400   0.0     com='cv bottom'
 cylinder  15 1    7.924800   77.72400   0.0     com='void btw cv-np liner'
 cylinder  16 1    8.077200   77.72400   0.0     com='np277_4 liner'
 cylinder  11 1   10.922000   77.72400   0.0     com='np277_4'
 cylinder  16 1   11.074400   77.72400   0.0     com='kaolite liner'
 cylinder  12 1   21.555075   77.72400   0.0     com='kaolite'
 cylinder  19 1   21.722275   77.72400   0.0     com='drum'
 cuboid    20 1 4p22.866096   77.72400   0.0     com='drum chine outer radius'
unit 1010
'cv at 1st step in liner [Elev=35.336 in.]'
 cylinder  3  1    6.426200    0.15240   0.00000 com='cavity abv HEU'
 cylinder  1  1    6.426200    0.15240   0.0     com='HEU content'
 cylinder  8  1    6.680200    0.15240   0.0     com='cv at 1st step'
 cylinder  15 1    7.924800    0.15240   0.0     com='void btw cv and liner'
 cylinder  16 1   11.074400    0.15240   0.0     com='liner 1st step'
 cylinder  12 1   21.555075    0.15240   0.0     com='kaolite'
 cylinder  19 1   21.722275    0.15240   0.0     com='drum'
 cuboid    20 1 4p22.866096    0.15240   0.0     com='drum chine outer radius'
unit 1011
'vertical gap between 1st step in liner and cv flange [Elev=35.426 in.]'
 cylinder  3  1    6.426200    0.22860   0.00000 com='cavity abv HEU'
 cylinder  1  1    6.426200    0.22860   0.0     com='HEU content'
 cylinder  8  1    6.680200    0.22860   0.0     com='cv at gap btwn step-flng'
 cylinder  15 1   10.922000    0.22860   0.0     com='void btw cv and liner'
 cylinder  16 1   11.074400    0.22860   0.0     com='liner wall'
 cylinder  12 1   21.555075    0.22860   0.0     com='kaolite'
 cylinder  19 1   21.722275    0.22860   0.0     com='drum'
 cuboid    20 1 4p22.866096    0.22860   0.0     com='drum chine outer radius'
unit 1012
'cv flange to top of cv well [Elev=35.926 in.]'
 cylinder  3  1    6.426200    1.27000   0.00000 com='cavity abv HEU'
 cylinder  1  1    6.426200    1.27000   0.0     com='HEU content'
```

```
 cylinder  9  1    9.525000    1.27000   0.0     com='flange to top of well'
 cylinder  15 1    9.525000    1.27000   0.0     com='void btw cv and pad-2'
 cylinder  14 1   10.033000    1.27000   0.0     com='pad-2'
 cylinder  15 1   10.922000    1.27000   0.0     com='void btw cv and liner'
 cylinder  16 1   11.074400    1.27000   0.0     com='liner wall'
 cylinder  12 1   21.555075    1.27000   0.0     com='kaolite'
 cylinder  19 1   21.722275    1.27000   0.0     com='drum'
 cuboid    20 1 4p22.866096    1.27000   0.0     com='drum chine outer radius'
unit 1013
'cv flange above cv well [Elev=37.076 in.]'
 cylinder  10 1    9.525000    2.92100   0.0     com='flange above cv well'
 cylinder  15 1    9.525000    2.92100   0.0     com='void btw cv and pad-2'
 cylinder  14 1   10.033000    2.92100   0.0     com='pad-2'
 cylinder  15 1   10.922000    2.92100   0.0     com='void btw pad2 and liner'
 cylinder  16 1   11.074400    2.92100   0.0     com='liner wall'
 cylinder  12 1   21.555075    2.92100   0.0     com='kaolite'
 cylinder  19 1   21.722275    2.92100   0.0     com='drum'
 cuboid    20 1 4p22.866096    2.92100   0.0     com='drum chine outer radius'
unit 1014
'plugpad2 below liner 2nd step [Elev=37.476 in.]'
 cylinder  14 1   10.033000    0.76200   0.0     com='pad-2'
 cylinder  15 1   10.922000    1.01600   0.0     com='void btw pad2 and liner'
 cylinder  16 1   11.074400    1.01600   0.0     com='liner wall'
 cylinder  12 1   21.555075    1.01600   0.0     com='kaolite'
 cylinder  19 1   21.722275    1.01600   0.0     com='drum'
 cuboid    20 1 4p22.866096    1.01600   0.0     com='drum chine outer radius'
unit 1015
'2nd step in liner [Elev=37.536 in.]'
 cylinder  15 1   10.922000    0.15240   0.0     com='void abv pad2'
 cylinder  16 1   18.757900    0.15240   0.0     com='liner 2nd step'
 cylinder  12 1   21.555075    0.15240   0.0     com='kaolite'
 cylinder  19 1   21.722275    0.15240   0.0     com='drum'
 cuboid    20 1 4p22.866096    0.15240   0.0     com='drum chine outer radius'
unit 1016
'abv 2nd step in liner to bottom of angle iron [Elev=40.756 in.]'
 cylinder  13 1   18.097500    8.17880   0.49276 com='plug kaolite'
 cylinder  17 1   18.249900    8.17880   0.34036 com='sides of plug case'
 cylinder  15 1   18.605500    8.17880   0.0     com='void: plug to liner'
 cylinder  16 1   18.757900    8.17880   0.0     com='liner wall'
 cylinder  12 1   21.555075    8.17880   0.0     com='kaolite'
 cylinder  19 1   21.722275    8.17880   0.0     com='drum'
 cuboid    20 1 4p22.866096    8.17880   0.0     com='drum chine outer radius'
unit 1017
'bottom of angle iron to bend in angle iron [Elev=42.506 in.]'
 cylinder  13 1   18.097500    4.44500   0.0     com='plug kaolite'
 cylinder  17 1   18.249900    4.44500   0.0     com='sides of plug case'
 cylinder  15 1   18.605500    4.44500   0.0     com='void: plug to liner'
 cylinder  16 1   18.757900    4.44500   0.0     com='liner wall'
 cylinder  18 1   19.392900    4.44500   0.0     com='lower angle iron'
 cylinder  12 1   21.555075    4.44500   0.0     com='kaolite'
 cylinder  19 1   21.722275    4.44500   0.0     com='drum'
 cuboid    20 1 4p22.866096    4.44500   0.0     com='drum chine outer radius'
unit 1018
'bend in angle iron to top of angle iron [Elev=42.756 in.]'
 cylinder  13 1   18.097500    0.11176   0.0     com='plug kaolite'
 cylinder  17 1   18.249900    0.26416   0.0     com='sides of plug case'
 cylinder  15 1   18.605500    0.63500   0.0     com='void: plug to liner'
 cylinder  16 1   18.757900    0.63500   0.0     com='liner wall'
 cylinder  18 1   21.555075    0.63500   0.0     com='bend section of ai'
 cylinder  19 1   21.722275    0.63500   0.0     com='drum'
 cuboid    20 1 4p22.866096    0.63500   0.0     com='drum chine outer radius'
unit 1019
'drum lid and lip [Elev=43.512 in.]'
 cylinder  20 1   21.330090    1.91973   0.16720 com='void above lid'
 cylinder  19 1   21.497290    1.91973   0.0     com='drum lid'
 cylinder  20 1   21.555075    1.91973   0.0     com='void btw lid - drum wall'
 cylinder  19 1   21.722275    1.91973   0.0     com='drum'
 cuboid    20 1 4p22.866096    1.91973   0.0     com='drum chine outer radius'
global
unit 1020
'es3100 drum [Elev=43.512 in.]'
array 3         2r-22.866096     0.0
'cuboid     0  1 4p24.587200    1120.337  0.0    com='bare package'
'cuboid    21  1 4p55.067200   1150.817 -30.48   com='reflected package'
 cuboid    20  1 4p22.866096    110.5197  0.0    com='interstital array space'
```

```
'global
'unit 1021
'array 4   3r0.0
'reflector  21 2  6r3.0  10
end geometry
read array
ara=3 nux=1 nuy=1 nuz=13 fill
1001 1002 1003 1010
1011 1012 1013 1014 1015 1016 1017 1018 1019        end fill
'ara=4 nux=13 nuy=13 nuz=06 fill f1020               end fill
end array
'read bias id=500 2  11  end bias
read start nst=0
end start
end data
end
```

6.9.9.9.5 Case 5nciapdoxt11_1_1_12_3

```
=csas25    parm=size=3000000
5nciapdoxt11,12000.0gUO2 (10562.4g235)4896.3gSH2O 3665.3gHcv hx= 22.74 fr=0.0001
238groupndf5 infhommedium
'HEU volume =6000.00000 HEU oxide, bulk density of oxide in cans=  2.00000 g/cm3'
'oxide= 12000.0 g, sat.h2o in HEU oxide=4896.3 g, oxide h/x=12.10'
'poly (packed or wrapped) dry content h/x=1.59, CV void volume 3671.88368'
arbmuox    1.83389   2 0 0 0  92235   88.0203
                               8016   11.9797    1  1.0000  293  end
arbmastm  7.4827e-01  2 0 0 0  1001   11.1913
                               8016   88.8087    1  1.0000  293  end
arbmpoly  7.6412e-02  2 0 0 0  1001   14.3798
                               6012   85.6202    1  1.0000  293  end
'np277-4: spacer (NCT_MD&H)'
'NCT min.den.(95.3886 lb/ft3) and hydrogen'
'np277-4 min.den.= 1.527971 = (95.3886 lb/ft3)(453.59 g/lb)/(28316.84 cm3/ft3)'
'use 75% of boron in calculations per NUREG-1609 Section 6.5.3.2'
arbmboron 7.31015e-2  2 0 0 0    5010   18.1479
                                 5011   81.8520    2  0.7500  293  end
arbmnpmx  1.07070e+0 10 0 0 0    6012    1.9189
                                 7014    0.0141
                                 8016   43.4251
                                11023    0.1174
                                12000    0.3378
                                13027   39.0479
                                14000    2.4672
                                16000    0.3083
                                20000   11.8336
                                26000    0.5298    2  1.0000  293  end
arbmnph2o 3.84169e-1  2 0 0 0    1001   11.1913
                                 8016   88.8087    2  1.0000  293  end
'flooded containmment vessel and content cans -- 10 CFR 71.55(d)(3)'
arbmwicv  9.9820e-01  2 0 0 0   1001   11.1913
                               8016   88.8087    3  1       293  end
'steel: containment vessel body 16.60 lb but use 15.74 lb'
ss304                                            8  1.0     293  end
'steel: cv flange lower use 3.36 lb'
ss304                                            9  0.97267 293  end
'steel: cv flange upper use 13.75 lb'
ss304                                           10  0.94348 293  end
'np277-4: confinement -- neutron poison inner liner (NCT_MD&H)'
'actual vol.= 1.28314e4 cm3 = (7.83023e2 in3)(16.387064)'
'den.multiplier = 1.28314e4 cm3 (actual vol.) / 1.32708e4 cm3 (model vol.)'
'np277-4 min.den.= 1.527971 = (95.3886 lb/ft3)(453.59 g/lb)/(28316.84 cm3/ft3)'
'density = 1.477385 = (den.mult)(np277-4 min.den.) = 0.9668933*1.527971'
'use 75% of boron in calculations per NUREG-1609 Section 6.5.3.2'
arbmboron 7.06813e-2  2 0 0 0    5010   18.1479
                                 5011   81.8520   11  0.7500  293  end
arbmnpmx  1.03525e+0 10 0 0 0    6012    1.9189
                                 7014    0.0141
                                 8016   43.4251
                                11023    0.1174
                                12000    0.3378
                                13027   39.0479
                                14000    2.4672
                                16000    0.3083
```

```
                                20000   11.8336
                                26000    0.5298   11  1.0000  293  end
arbmnph2o 3.71451e-1  2 0 0 0    1001   11.1913
                                 8016   88.8087   11  1.0000  293  end
'kaolite 1600 body'
'sing.unit.density= (den.mult)(min.den.)'
' for arbmh20k = 1.012373*0.51655,  for rest = 1.012373*0.34438'
'den.mult= 1.36557e5 cm3 (actual vol.) / 1.34888e5 cm3 (model vol.)'
'actual vol.= 1.36557e5 cm3 = (28316.84 cm3/ft3)(108.33188 lb)/(22.464 lb/ft3)'
'nct array densities are s.u.dens. multiplied by volume ratio 1.34888/1.10336'
arbmh2ok   0.63931  2 0 0 0    1001   11.1913
                                8016   88.8087   12  0.0287  293  end
arbmal2o3  0.42622  2 0 0 0   13027   52.9390
                                8016   47.0610   12  0.096   293  end
arbmsio2   0.42622  2 0 0 0   14000   46.7570
                                8016   53.2430   12  0.367   293  end
arbmfe2o3  0.42622  2 0 0 0   26000   69.9540
                                8016   30.0460   12  0.067   293  end
arbmtio2   0.42622  2 0 0 0   22000   59.9535
                                8016   40.0465   12  0.012   293  end
arbmcao    0.42622  2 0 0 0   20000   71.4815
                                8016   28.5185   12  0.307   293  end
arbmmgo    0.42622  2 0 0 0   12000   60.3169
                                8016   39.6831   12  0.131   293  end
arbmna2o   0.42622  2 0 0 0   11023   74.1961
                                8016   25.8039   12  0.020   293  end
'kaolite 1600 top plug'
'sing.unit.density= (den.mult)(min.den.)'
' for arbmh20k = 0.965246*0.51655,  for rest = 0.965246*0.34438'
'den.mult= 1.21592e4 cm3 (actual vol.) / 1.25970e4 cm3 (model vol.)'
'actual vol.= 1.21592e4 cm3 = (28316.84 cm3/ft3)(9.646 lb)/(22.464 lb/ft3)'
arbmh2ok   0.49860  2 0 0 0    1001   11.1913
                                8016   88.8087   13  0.0287  293  end
arbmal2o3  0.33241  2 0 0 0   13027   52.9390
                                8016   47.0610   13  0.096   293  end
arbmsio2   0.33241  2 0 0 0   14000   46.7570
                                8016   53.2430   13  0.367   293  end
arbmfe2o3  0.33241  2 0 0 0   26000   69.9540
                                8016   30.0460   13  0.067   293  end
arbmtio2   0.33241  2 0 0 0   22000   59.9535
                                8016   40.0465   13  0.012   293  end
arbmcao    0.33241  2 0 0 0   20000   71.4815
                                8016   28.5185   13  0.307   293  end
arbmmgo    0.33241  2 0 0 0   12000   60.3169
                                8016   39.6831   13  0.131   293  end
arbmna2o   0.33241  2 0 0 0   11023   74.1961
                                8016   25.8039   13  0.020   293  end
'silicone rubber pads'
arbmsiru   1.21791  4 0 0 0    6012   32.3767
                                1001    8.1573
                                8016   21.5782
                               14000   37.8878   14  1.0     293  end
'void space external to containment vessel'
arbmwecv   0.9982   2 0 0 0    1001   11.1913
                                8016   88.8087   15  0.0001  293  end
'steel: liner'
ss304                                           16  1.0     293  end
'steel: plug cover (pc) use 9.907 lb'
ss304                                           17  1.06388 293  end
'steel: angle iron (ai) for single units'
'ss304                                           18  1.0     293  end
'steel: angle iron (ai) for arrays'
'array density is multiplied by a volume fraction 7.08030/5.63249'
ss304                                           18  1.25705 293  end
'steel: drum steel for single units'
'ss304                                           19  1.0     293  end
'steel: drum steel for arrays'
'array density is multiplied by a volume fraction 3.20482/3.20544'
ss304                                           19  0.99981 293  end
'void space external to drum'
'array density is multiplied by a volume ratio 8.11698/6.98323'
arbmwed    1.16026  2 0 0 0    1001   11.1913
                                8016   88.8087   20  0.0001  293  end
'reflective water'
'arbmh20r   0.9982   2 0 0 0    1001   11.1913
```

```
'                                 8016   88.8087   21  1.0     293  end
end comp
5nciapdoxt11,12000.0gUO2 (10562.4g235)4896.3gSH2O 3665.3gHcv,hx= 22.74 fr=0.0001
read parameters nub=yes npg=2500 gen=215 nsk=15 tme=100 end parameters
read boun       all=specular                    end boun
read geometry
unit 1001
'drum bottom flat cover [Elev= 0.111 in. at top of unit]'
'cylinder  19 1   22.866096    0.28150   0.0     com='extended radius not used'
 cylinder  19 1   21.722275    0.28150   0.0     com='drum bottom flat cover'
 cuboid    20 1 4p22.866096    0.28150   0.0     com='drum chine outer radius'
unit 1002
'above drum bottom flat cover and below containment vessel [Elev= 4.676 in.]'
 cylinder  15 1    3.175000   11.59510  11.16330 com='void in pad-1'
 cylinder  14 1    7.924800   11.59510  11.16330 com='pad-1'
 cylinder  16 1    8.077200   11.59510  11.16330 com='np277_4 liner'
 cylinder  11 1   10.922000   11.59510  11.16330 com='np277_4'
 cylinder  16 1   11.074400   11.59510  10.85850 com='kaolite liner bottom'
 cylinder  12 1   21.555075   11.59510   0.0     com='kaolite'
 cylinder  19 1   21.722275   11.59510   0.0     com='drum'
 cuboid    20 1 4p22.866096   11.59510   0.0     com='drum chine outer radius'
unit 1003
'cv bottom to bottom of 1st step [Elev=35.276 in.]'
 cylinder  3  1    6.426200   77.72400  51.07212 com='cavity abv HEU'
 cylinder  1  1    6.426200   77.72400   0.63500 com='HEU content'
 cylinder  8  1    6.680200   77.72400   0.0     com='cv bottom'
 cylinder  15 1    7.924800   77.72400   0.0     com='void btw cv-np liner'
 cylinder  16 1    8.077200   77.72400   0.0     com='np277_4 liner'
 cylinder  11 1   10.922000   77.72400   0.0     com='np277_4'
 cylinder  16 1   11.074400   77.72400   0.0     com='kaolite liner'
 cylinder  12 1   21.555075   77.72400   0.0     com='kaolite'
 cylinder  19 1   21.722275   77.72400   0.0     com='drum'
 cuboid    20 1 4p22.866096   77.72400   0.0     com='drum chine outer radius'
unit 1010
'cv at 1st step in liner [Elev=35.336 in.]'
 cylinder  3  1    6.426200    0.15240   0.00000 com='cavity abv HEU'
 cylinder  1  1    6.426200    0.15240   0.0     com='HEU content'
 cylinder  8  1    6.680200    0.15240   0.0     com='cv at 1st step'
 cylinder  15 1    7.924800    0.15240   0.0     com='void btw cv and liner'
 cylinder  16 1   11.074400    0.15240   0.0     com='liner 1st step'
 cylinder  12 1   21.555075    0.15240   0.0     com='kaolite'
 cylinder  19 1   21.722275    0.15240   0.0     com='drum'
 cuboid    20 1 4p22.866096    0.15240   0.0     com='drum chine outer radius'
unit 1011
'vertical gap between 1st step in liner and cv flange [Elev=35.426 in.]'
 cylinder  3  1    6.426200    0.22860   0.00000 com='cavity abv HEU'
 cylinder  1  1    6.426200    0.22860   0.0     com='HEU content'
 cylinder  8  1    6.680200    0.22860   0.0     com='cv at gap btwn step-flng'
 cylinder  15 1   10.922000    0.22860   0.0     com='void btw cv and liner'
 cylinder  16 1   11.074400    0.22860   0.0     com='liner wall'
 cylinder  12 1   21.555075    0.22860   0.0     com='kaolite'
 cylinder  19 1   21.722275    0.22860   0.0     com='drum'
 cuboid    20 1 4p22.866096    0.22860   0.0     com='drum chine outer radius'
unit 1012
'cv flange to top of cv well [Elev=35.926 in.]'
 cylinder  3  1    6.426200    1.27000   0.00000 com='cavity abv HEU'
 cylinder  1  1    6.426200    1.27000   0.0     com='HEU content'
 cylinder  9  1    9.525000    1.27000   0.0     com='flange to top of well'
 cylinder  15 1    9.525000    1.27000   0.0     com='void btw cv and pad-2'
 cylinder  14 1   10.033000    1.27000   0.0     com='pad-2'
 cylinder  15 1   10.922000    1.27000   0.0     com='void btw cv and liner'
 cylinder  16 1   11.074400    1.27000   0.0     com='liner wall'
 cylinder  12 1   21.555075    1.27000   0.0     com='kaolite'
 cylinder  19 1   21.722275    1.27000   0.0     com='drum'
 cuboid    20 1 4p22.866096    1.27000   0.0     com='drum chine outer radius'
unit 1013
'cv flange above cv well [Elev=37.076 in.]'
 cylinder  10 1    9.525000    2.92100   0.0     com='flange above cv well'
 cylinder  15 1    9.525000    2.92100   0.0     com='void btw cv and pad-2'
 cylinder  14 1   10.033000    2.92100   0.0     com='pad-2'
 cylinder  15 1   10.922000    2.92100   0.0     com='void btw pad2 and liner'
 cylinder  16 1   11.074400    2.92100   0.0     com='liner wall'
 cylinder  12 1   21.555075    2.92100   0.0     com='kaolite'
 cylinder  19 1   21.722275    2.92100   0.0     com='drum'
 cuboid    20 1 4p22.866096    2.92100   0.0     com='drum chine outer radius'
```

```
unit 1014
'plugpad2 below liner 2nd step [Elev=37.476 in.]'
 cylinder  14 1   10.033000    0.76200   0.0     com='pad-2'
 cylinder  15 1   10.922000    1.01600   0.0     com='void btw pad2 and liner'
 cylinder  16 1   11.074400    1.01600   0.0     com='liner wall'
 cylinder  12 1   21.555075    1.01600   0.0     com='kaolite'
 cylinder  19 1   21.722275    1.01600   0.0     com='drum'
 cuboid    20 1 4p22.866096    1.01600   0.0     com='drum chine outer radius'
unit 1015
'2nd step in liner [Elev=37.536 in.]'
 cylinder  15 1   10.922000    0.15240   0.0     com='void abv pad2'
 cylinder  16 1   18.757900    0.15240   0.0     com='liner 2nd step'
 cylinder  12 1   21.555075    0.15240   0.0     com='kaolite'
 cylinder  19 1   21.722275    0.15240   0.0     com='drum'
 cuboid    20 1 4p22.866096    0.15240   0.0     com='drum chine outer radius'
unit 1016
'abv 2nd step in liner to bottom of angle iron [Elev=40.756 in.]'
 cylinder  13 1   18.097500    8.17880   0.49276 com='plug kaolite'
 cylinder  17 1   18.249900    8.17880   0.34036 com='sides of plug case'
 cylinder  15 1   18.605500    8.17880   0.0     com='void: plug to liner'
 cylinder  16 1   18.757900    8.17880   0.0     com='liner wall'
 cylinder  12 1   21.555075    8.17880   0.0     com='kaolite'
 cylinder  19 1   21.722275    8.17880   0.0     com='drum'
 cuboid    20 1 4p22.866096    8.17880   0.0     com='drum chine outer radius'
unit 1017
'bottom of angle iron to bend in angle iron [Elev=42.506 in.]'
 cylinder  13 1   18.097500    4.44500   0.0     com='plug kaolite'
 cylinder  17 1   18.249900    4.44500   0.0     com='sides of plug case'
 cylinder  15 1   18.605500    4.44500   0.0     com='void: plug to liner'
 cylinder  16 1   18.757900    4.44500   0.0     com='liner wall'
 cylinder  18 1   19.392900    4.44500   0.0     com='lower angle iron'
 cylinder  12 1   21.555075    4.44500   0.0     com='kaolite'
 cylinder  19 1   21.722275    4.44500   0.0     com='drum'
 cuboid    20 1 4p22.866096    4.44500   0.0     com='drum chine outer radius'
unit 1018
'bend in angle iron to top of angle iron [Elev=42.756 in.]'
 cylinder  13 1   18.097500    0.11176   0.0     com='plug kaolite'
 cylinder  17 1   18.249900    0.26416   0.0     com='sides of plug case'
 cylinder  15 1   18.605500    0.63500   0.0     com='void: plug to liner'
 cylinder  16 1   18.757900    0.63500   0.0     com='liner wall'
 cylinder  18 1   21.555075    0.63500   0.0     com='bend section of ai'
 cylinder  19 1   21.722275    0.63500   0.0     com='drum'
 cuboid    20 1 4p22.866096    0.63500   0.0     com='drum chine outer radius'
unit 1019
'drum lid and lip [Elev=43.512 in.]'
 cylinder  20 1   21.330090    1.91973   0.16720 com='void above lid'
 cylinder  19 1   21.497290    1.91973   0.0     com='drum lid'
 cylinder  20 1   21.555075    1.91973   0.0     com='void btw lid - drum wall'
 cylinder  19 1   21.722275    1.91973   0.0     com='drum'
 cuboid    20 1 4p22.866096    1.91973   0.0     com='drum chine outer radius'
global
unit 1020
'es3100 drum [Elev=43.512 in.]'
array 3         2r-22.866096     0.0
'cuboid     0  1 4p24.587200    1120.337  0.0    com='bare package'
'cuboid    21  1 4p55.067200   1150.817 -30.48   com='reflected package'
 cuboid    20  1 4p22.866096    110.5197  0.0    com='interstital array space'
'global
'unit 1021
'array 4   3r0.0
'reflector  21 2  6r3.0  10
end geometry
read array
ara=3 nux=1 nuy=1 nuz=13 fill
1001 1002 1003 1010
1011 1012 1013 1014 1015 1016 1017 1018 1019        end fill
'ara=4 nux=13 nuy=13 nuz=06 fill f1020               end fill
end array
'read bias id=500 2  11  end bias
read start nst=0
end start
end data
end
```

6.9.9.9.6 Case 5nciapdoxt11_1_1_11_3

```
=csas25    parm=size=3000000
5nciapdoxt11,11000.1gUO2 ( 9682.3g235)4488.3gSH2O 4164.3gHcv hx= 25.06 fr=0.0001
238groupndf5 infhommedium
'HEU volume =5500.05000 HEU oxide, bulk density of oxide in cans=  2.00000 g/cm3'
'oxide= 11000.1 g, sat.h2o in HEU oxide=4488.3 g, oxide h/x=12.10'
'poly (packed or wrapped) dry content h/x=1.73, CV void volume 4171.83368'
arbmuox    1.82015   2 0 0 0  92235   88.0203
                               8016   11.9797    1  1.0000  293  end
arbmastm  7.4266e-01  2 0 0 0  1001   11.1913
                               8016   88.8087    1  1.0000  293  end
arbmpoly  8.2733e-02  2 0 0 0  1001   14.3798
                               6012   85.6202    1  1.0000  293  end
'np277-4: spacer (NCT_MD&H)'
'NCT min.den.(95.3886 lb/ft3) and hydrogen'
'np277-4 min.den.= 1.527971 = (95.3886 lb/ft3)(453.59 g/lb)/(28316.84 cm3/ft3)'
'use 75% of boron in calculations per NUREG-1609 Section 6.5.3.2'
arbmboron 7.31015e-2  2 0 0 0    5010   18.1479
                                 5011   81.8520    2  0.7500  293  end
arbmnpmx  1.07070e+0 10 0 0 0    6012    1.9189
                                 7014    0.0141
                                 8016   43.4251
                                11023    0.1174
                                12000    0.3378
                                13027   39.0479
                                14000    2.4672
                                16000    0.3083
                                20000   11.8336
                                26000    0.5298    2  1.0000  293  end
arbmnph2o 3.84169e-1  2 0 0 0    1001   11.1913
                                 8016   88.8087    2  1.0000  293  end
'flooded containmment vessel and content cans -- 10 CFR 71.55(d)(3)'
arbmwicv  9.9820e-01  2 0 0 0   1001   11.1913
                               8016   88.8087    3  1       293  end
'steel: containment vessel body 16.60 lb but use 15.74 lb'
ss304                                            8  1.0     293  end
'steel: cv flange lower use 3.36 lb'
ss304                                            9  0.97267 293  end
'steel: cv flange upper use 13.75 lb'
ss304                                           10  0.94348 293  end
'np277-4: confinement -- neutron poison inner liner (NCT_MD&H)'
'actual vol.= 1.28314e4 cm3 = (7.83023e2 in3)(16.387064)'
'den.multiplier = 1.28314e4 cm3 (actual vol.) / 1.32708e4 cm3 (model vol.)'
'np277-4 min.den.= 1.527971 = (95.3886 lb/ft3)(453.59 g/lb)/(28316.84 cm3/ft3)'
'density = 1.477385 = (den.mult)(np277-4 min.den.) = 0.9668933*1.527971'
'use 75% of boron in calculations per NUREG-1609 Section 6.5.3.2'
arbmboron 7.06813e-2  2 0 0 0    5010   18.1479
                                 5011   81.8520   11  0.7500  293  end
arbmnpmx  1.03525e+0 10 0 0 0    6012    1.9189
                                 7014    0.0141
                                 8016   43.4251
                                11023    0.1174
                                12000    0.3378
                                13027   39.0479
                                14000    2.4672
                                16000    0.3083
                                20000   11.8336
                                26000    0.5298   11  1.0000  293  end
arbmnph2o 3.71451e-1  2 0 0 0    1001   11.1913
                                 8016   88.8087   11  1.0000  293  end
'kaolite 1600 body'
'sing.unit.density= (den.mult)(min.den.)'
' for arbmh20k = 1.012373*0.51655,  for rest = 1.012373*0.34438'
'den.mult= 1.36557e5 cm3 (actual vol.) / 1.34888e5 cm3 (model vol.)'
'actual vol.= 1.36557e5 cm3 = (28316.84 cm3/ft3)(108.33188 lb)/(22.464 lb/ft3)'
'nct array densities are s.u.dens. multiplied by volume ratio 1.34888/1.10336'
arbmh2ok   0.63931  2 0 0 0    1001   11.1913
                               8016   88.8087   12  0.0287  293  end
arbmal2o3  0.42622  2 0 0 0   13027   52.9390
                               8016   47.0610   12  0.096   293  end
arbmsio2   0.42622  2 0 0 0   14000   46.7570
                               8016   53.2430   12  0.367   293  end
arbmfe2o3  0.42622  2 0 0 0   26000   69.9540
                               8016   30.0460   12  0.067   293  end
```

```
arbmtio2   0.42622  2 0 0 0   22000   59.9535
                               8016   40.0465   12  0.012   293  end
arbmcao    0.42622  2 0 0 0   20000   71.4815
                               8016   28.5185   12  0.307   293  end
arbmmgo    0.42622  2 0 0 0   12000   60.3169
                               8016   39.6831   12  0.131   293  end
arbmna2o   0.42622  2 0 0 0   11023   74.1961
                               8016   25.8039   12  0.020   293  end
'kaolite 1600 top plug'
'sing.unit.density= (den.mult)(min.den.)'
' for arbmh20k = 0.965246*0.51655,  for rest = 0.965246*0.34438'
'den.mult= 1.21592e4 cm3 (actual vol.) / 1.25970e4 cm3 (model vol.)'
'actual vol.= 1.21592e4 cm3 = (28316.84 cm3/ft3)(9.646 lb)/(22.464 lb/ft3)'
arbmh2ok   0.49860  2 0 0 0    1001   11.1913
                               8016   88.8087   13  0.0287  293  end
arbmal2o3  0.33241  2 0 0 0   13027   52.9390
                               8016   47.0610   13  0.096   293  end
arbmsio2   0.33241  2 0 0 0   14000   46.7570
                               8016   53.2430   13  0.367   293  end
arbmfe2o3  0.33241  2 0 0 0   26000   69.9540
                               8016   30.0460   13  0.067   293  end
arbmtio2   0.33241  2 0 0 0   22000   59.9535
                               8016   40.0465   13  0.012   293  end
arbmcao    0.33241  2 0 0 0   20000   71.4815
                               8016   28.5185   13  0.307   293  end
arbmmgo    0.33241  2 0 0 0   12000   60.3169
                               8016   39.6831   13  0.131   293  end
arbmna2o   0.33241  2 0 0 0   11023   74.1961
                               8016   25.8039   13  0.020   293  end
'silicone rubber pads'
arbmsiru   1.21791  4 0 0 0    6012   32.3767
                               1001    8.1573
                               8016   21.5782
                              14000   37.8878   14  1.0     293  end
'void space external to containment vessel'
arbmwecv   0.9982   2 0 0 0    1001   11.1913
                               8016   88.8087   15  0.0001  293  end
'steel: liner'
ss304                                            16  1.0     293  end
'steel: plug cover (pc) use 9.907 lb'
ss304                                            17  1.06388 293  end
'steel: angle iron (ai) for single units'
'ss304                                            18  1.0     293  end
'steel: angle iron (ai) for arrays'
'array density is multiplied by a volume fraction 7.08030/5.63249'
ss304                                            18  1.25705 293  end
'steel: drum steel for single units'
'ss304                                            19  1.0     293  end
'steel: drum steel for arrays'
'array density is multiplied by a volume fraction 3.20482/3.20544'
ss304                                            19  0.99981 293  end
'void space external to drum'
'array density is multiplied by a volume ratio 8.11698/6.98323'
arbmwed    1.16026  2 0 0 0    1001   11.1913
                               8016   88.8087   20  0.0001  293  end
'reflective water'
'arbmh20r   0.9982   2 0 0 0    1001   11.1913
'                               8016   88.8087   21  1.0     293  end
end comp
5nciapdoxt11,11000.1gUO2 ( 9682.3g235)4488.3gSH2O 4164.3gHcv,hx= 25.06 fr=0.0001
read parameters nub=yes npg=2500 gen=215 nsk=15 tme=100 end parameters
read boun       all=specular                     end boun
read geometry
unit 1001
'drum bottom flat cover [Elev= 0.111 in. at top of unit]'
'cylinder  19 1   22.866096    0.28150   0.0     com='extended radius not used'
 cylinder  19 1   21.722275    0.28150   0.0     com='drum bottom flat cover'
 cuboid    20 1 4p22.866096    0.28150   0.0     com='drum chine outer radius'
unit 1002
'above drum bottom flat cover and below containment vessel [Elev= 4.676 in.]'
 cylinder  15 1    3.175000   11.59510  11.16330 com='void in pad-1'
 cylinder  14 1    7.924800   11.59510  11.16330 com='pad-1'
 cylinder  16 1    8.077200   11.59510  11.16330 com='np277_4 liner'
 cylinder  11 1   10.922000   11.59510  11.16330 com='np277_4'
 cylinder  16 1   11.074400   11.59510  10.85850 com='kaolite liner bottom'
```

```
 cylinder  12 1   21.555075   11.59510   0.0     com='kaolite'
 cylinder  19 1   21.722275   11.59510   0.0     com='drum'
 cuboid    20 1 4p22.866096   11.59510   0.0     com='drum chine outer radius'
unit 1003
'cv bottom to bottom of 1st step [Elev=35.276 in.]'
 cylinder  3  1    6.426200   77.72400  47.21851 com='cavity abv HEU'
 cylinder  1  1    6.426200   77.72400   0.63500 com='HEU content'
 cylinder  8  1    6.680200   77.72400   0.0     com='cv bottom'
 cylinder  15 1    7.924800   77.72400   0.0     com='void btw cv-np liner'
 cylinder  16 1    8.077200   77.72400   0.0     com='np277_4 liner'
 cylinder  11 1   10.922000   77.72400   0.0     com='np277_4'
 cylinder  16 1   11.074400   77.72400   0.0     com='kaolite liner'
 cylinder  12 1   21.555075   77.72400   0.0     com='kaolite'
 cylinder  19 1   21.722275   77.72400   0.0     com='drum'
 cuboid    20 1 4p22.866096   77.72400   0.0     com='drum chine outer radius'
unit 1010
'cv at 1st step in liner [Elev=35.336 in.]'
 cylinder  3  1    6.426200    0.15240   0.00000 com='cavity abv HEU'
 cylinder  1  1    6.426200    0.15240   0.0     com='HEU content'
 cylinder  8  1    6.680200    0.15240   0.0     com='cv at 1st step'
 cylinder  15 1    7.924800    0.15240   0.0     com='void btw cv and liner'
 cylinder  16 1   11.074400    0.15240   0.0     com='liner 1st step'
 cylinder  12 1   21.555075    0.15240   0.0     com='kaolite'
 cylinder  19 1   21.722275    0.15240   0.0     com='drum'
 cuboid    20 1 4p22.866096    0.15240   0.0     com='drum chine outer radius'
unit 1011
'vertical gap between 1st step in liner and cv flange [Elev=35.426 in.]'
 cylinder  3  1    6.426200    0.22860   0.00000 com='cavity abv HEU'
 cylinder  1  1    6.426200    0.22860   0.0     com='HEU content'
 cylinder  8  1    6.680200    0.22860   0.0     com='cv at gap btwn step-flng'
 cylinder  15 1   10.922000    0.22860   0.0     com='void btw cv and liner'
 cylinder  16 1   11.074400    0.22860   0.0     com='liner wall'
 cylinder  12 1   21.555075    0.22860   0.0     com='kaolite'
 cylinder  19 1   21.722275    0.22860   0.0     com='drum'
 cuboid    20 1 4p22.866096    0.22860   0.0     com='drum chine outer radius'
unit 1012
'cv flange to top of cv well [Elev=35.926 in.]'
 cylinder  3  1    6.426200    1.27000   0.00000 com='cavity abv HEU'
 cylinder  1  1    6.426200    1.27000   0.0     com='HEU content'
 cylinder  9  1    9.525000    1.27000   0.0     com='flange to top of well'
 cylinder  15 1    9.525000    1.27000   0.0     com='void btw cv and pad-2'
 cylinder  14 1   10.033000    1.27000   0.0     com='pad-2'
 cylinder  15 1   10.922000    1.27000   0.0     com='void btw cv and liner'
 cylinder  16 1   11.074400    1.27000   0.0     com='liner wall'
 cylinder  12 1   21.555075    1.27000   0.0     com='kaolite'
 cylinder  19 1   21.722275    1.27000   0.0     com='drum'
 cuboid    20 1 4p22.866096    1.27000   0.0     com='drum chine outer radius'
unit 1013
'cv flange above cv well [Elev=37.076 in.]'
 cylinder  10 1    9.525000    2.92100   0.0     com='flange above cv well'
 cylinder  15 1    9.525000    2.92100   0.0     com='void btw cv and pad-2'
 cylinder  14 1   10.033000    2.92100   0.0     com='pad-2'
 cylinder  15 1   10.922000    2.92100   0.0     com='void btw pad2 and liner'
 cylinder  16 1   11.074400    2.92100   0.0     com='liner wall'
 cylinder  12 1   21.555075    2.92100   0.0     com='kaolite'
 cylinder  19 1   21.722275    2.92100   0.0     com='drum'
 cuboid    20 1 4p22.866096    2.92100   0.0     com='drum chine outer radius'
unit 1014
'plugpad2 below liner 2nd step [Elev=37.476 in.]'
 cylinder  14 1   10.033000    0.76200   0.0     com='pad-2'
 cylinder  15 1   10.922000    1.01600   0.0     com='void btw pad2 and liner'
 cylinder  16 1   11.074400    1.01600   0.0     com='liner wall'
 cylinder  12 1   21.555075    1.01600   0.0     com='kaolite'
 cylinder  19 1   21.722275    1.01600   0.0     com='drum'
 cuboid    20 1 4p22.866096    1.01600   0.0     com='drum chine outer radius'
unit 1015
'2nd step in liner [Elev=37.536 in.]'
 cylinder  15 1   10.922000    0.15240   0.0     com='void abv pad2'
 cylinder  16 1   18.757900    0.15240   0.0     com='liner 2nd step'
 cylinder  12 1   21.555075    0.15240   0.0     com='kaolite'
 cylinder  19 1   21.722275    0.15240   0.0     com='drum'
 cuboid    20 1 4p22.866096    0.15240   0.0     com='drum chine outer radius'
unit 1016
'abv 2nd step in liner to bottom of angle iron [Elev=40.756 in.]'
 cylinder  13 1   18.097500    8.17880   0.49276 com='plug kaolite'
```

```
 cylinder  17 1   18.249900    8.17880   0.34036 com='sides of plug case'
 cylinder  15 1   18.605500    8.17880   0.0     com='void: plug to liner'
 cylinder  16 1   18.757900    8.17880   0.0     com='liner wall'
 cylinder  12 1   21.555075    8.17880   0.0     com='kaolite'
 cylinder  19 1   21.722275    8.17880   0.0     com='drum'
 cuboid    20 1 4p22.866096    8.17880   0.0     com='drum chine outer radius'
unit 1017
'bottom of angle iron to bend in angle iron [Elev=42.506 in.]'
 cylinder  13 1   18.097500    4.44500   0.0     com='plug kaolite'
 cylinder  17 1   18.249900    4.44500   0.0     com='sides of plug case'
 cylinder  15 1   18.605500    4.44500   0.0     com='void: plug to liner'
 cylinder  16 1   18.757900    4.44500   0.0     com='liner wall'
 cylinder  18 1   19.392900    4.44500   0.0     com='lower angle iron'
 cylinder  12 1   21.555075    4.44500   0.0     com='kaolite'
 cylinder  19 1   21.722275    4.44500   0.0     com='drum'
 cuboid    20 1 4p22.866096    4.44500   0.0     com='drum chine outer radius'
unit 1018
'bend in angle iron to top of angle iron [Elev=42.756 in.]'
 cylinder  13 1   18.097500    0.11176   0.0     com='plug kaolite'
 cylinder  17 1   18.249900    0.26416   0.0     com='sides of plug case'
 cylinder  15 1   18.605500    0.63500   0.0     com='void: plug to liner'
 cylinder  16 1   18.757900    0.63500   0.0     com='liner wall'
 cylinder  18 1   21.555075    0.63500   0.0     com='bend section of ai'
 cylinder  19 1   21.722275    0.63500   0.0     com='drum'
 cuboid    20 1 4p22.866096    0.63500   0.0     com='drum chine outer radius'
unit 1019
'drum lid and lip [Elev=43.512 in.]'
 cylinder  20 1   21.330090    1.91973   0.16720 com='void above lid'
 cylinder  19 1   21.497290    1.91973   0.0     com='drum lid'
 cylinder  20 1   21.555075    1.91973   0.0     com='void btw lid - drum wall'
 cylinder  19 1   21.722275    1.91973   0.0     com='drum'
 cuboid    20 1 4p22.866096    1.91973   0.0     com='drum chine outer radius'
global
unit 1020
'es3100 drum [Elev=43.512 in.]'
array 3         2r-22.866096     0.0
'cuboid     0  1 4p24.587200    1120.337  0.0    com='bare package'
'cuboid    21  1 4p55.067200   1150.817 -30.48   com='reflected package'
 cuboid    20  1 4p22.866096    110.5197  0.0    com='interstital array space'
'global
'unit 1021
'array 4   3r0.0
'reflector  21 2  6r3.0  10
end geometry
read array
ara=3 nux=1 nuy=1 nuz=13 fill
1001 1002 1003 1010
1011 1012 1013 1014 1015 1016 1017 1018 1019        end fill
'ara=4 nux=13 nuy=13 nuz=06 fill f1020               end fill
end array
'read bias id=500 2  11  end bias
read start nst=0
end start
end data
end
```

6.9.9.9.7 Case 5nciapdoxt11_1_2_11_3

```
=csas25    parm=size=3000000
5nciapdoxt11,11000.1gUO2 ( 9682.3g235)2658.2gSH2O 5994.4gHcv hx= 25.06 fr=0.0001
238groupndf5 infhommedium
'HEU volume =3666.70000 HEU oxide, bulk density of oxide in cans=  3.00000 g/cm3'
'oxide= 11000.1 g, sat.h2o in HEU oxide=2658.2 g, oxide h/x= 7.17'
'poly (packed or wrapped) dry content h/x=1.73, CV void volume 6005.18368'
arbmuox    2.61274   2 0 0 0  92235   88.0203
                               8016   11.9797    1  1.0000  293  end
arbmastm  6.3139e-01  2 0 0 0  1001   11.1913
                               8016   88.8087    1  1.0000  293  end
arbmpoly  1.1876e-01  2 0 0 0  1001   14.3798
                               6012   85.6202    1  1.0000  293  end
'np277-4: spacer (NCT_MD&H)'
'NCT min.den.(95.3886 lb/ft3) and hydrogen'
'np277-4 min.den.= 1.527971 = (95.3886 lb/ft3)(453.59 g/lb)/(28316.84 cm3/ft3)'
'use 75% of boron in calculations per NUREG-1609 Section 6.5.3.2'
```

```
arbmboron 7.31015e-2  2 0 0 0    5010   18.1479
                                 5011   81.8520    2  0.7500  293  end
arbmnpmx  1.07070e+0 10 0 0 0    6012    1.9189
                                 7014    0.0141
                                 8016   43.4251
                                11023    0.1174
                                12000    0.3378
                                13027   39.0479
                                14000    2.4672
                                16000    0.3083
                                20000   11.8336
                                26000    0.5298    2  1.0000  293  end
arbmnph2o 3.84169e-1  2 0 0 0    1001   11.1913
                                 8016   88.8087    2  1.0000  293  end
'flooded containmment vessel and content cans -- 10 CFR 71.55(d)(3)'
arbmwicv  9.9820e-01  2 0 0 0   1001   11.1913
                               8016   88.8087    3  1       293  end
'steel: containment vessel body 16.60 lb but use 15.74 lb'
ss304                                            8  1.0     293  end
'steel: cv flange lower use 3.36 lb'
ss304                                            9  0.97267 293  end
'steel: cv flange upper use 13.75 lb'
ss304                                           10  0.94348 293  end
'np277-4: confinement -- neutron poison inner liner (NCT_MD&H)'
'actual vol.= 1.28314e4 cm3 = (7.83023e2 in3)(16.387064)'
'den.multiplier = 1.28314e4 cm3 (actual vol.) / 1.32708e4 cm3 (model vol.)'
'np277-4 min.den.= 1.527971 = (95.3886 lb/ft3)(453.59 g/lb)/(28316.84 cm3/ft3)'
'density = 1.477385 = (den.mult)(np277-4 min.den.) = 0.9668933*1.527971'
'use 75% of boron in calculations per NUREG-1609 Section 6.5.3.2'
arbmboron 7.06813e-2  2 0 0 0    5010   18.1479
                                 5011   81.8520   11  0.7500  293  end
arbmnpmx  1.03525e+0 10 0 0 0    6012    1.9189
                                 7014    0.0141
                                 8016   43.4251
                                11023    0.1174
                                12000    0.3378
                                13027   39.0479
                                14000    2.4672
                                16000    0.3083
                                20000   11.8336
                                26000    0.5298   11  1.0000  293  end
arbmnph2o 3.71451e-1  2 0 0 0    1001   11.1913
                                 8016   88.8087   11  1.0000  293  end
'kaolite 1600 body'
'sing.unit.density= (den.mult)(min.den.)'
' for arbmh20k = 1.012373*0.51655,  for rest = 1.012373*0.34438'
'den.mult= 1.36557e5 cm3 (actual vol.) / 1.34888e5 cm3 (model vol.)'
'actual vol.= 1.36557e5 cm3 = (28316.84 cm3/ft3)(108.33188 lb)/(22.464 lb/ft3)'
'nct array densities are s.u.dens. multiplied by volume ratio 1.34888/1.10336'
arbmh2ok   0.63931  2 0 0 0    1001   11.1913
                               8016   88.8087   12  0.0287  293  end
arbmal2o3  0.42622  2 0 0 0   13027   52.9390
                               8016   47.0610   12  0.096   293  end
arbmsio2   0.42622  2 0 0 0   14000   46.7570
                               8016   53.2430   12  0.367   293  end
arbmfe2o3  0.42622  2 0 0 0   26000   69.9540
                               8016   30.0460   12  0.067   293  end
arbmtio2   0.42622  2 0 0 0   22000   59.9535
                               8016   40.0465   12  0.012   293  end
arbmcao    0.42622  2 0 0 0   20000   71.4815
                               8016   28.5185   12  0.307   293  end
arbmmgo    0.42622  2 0 0 0   12000   60.3169
                               8016   39.6831   12  0.131   293  end
arbmna2o   0.42622  2 0 0 0   11023   74.1961
                               8016   25.8039   12  0.020   293  end
'kaolite 1600 top plug'
'sing.unit.density= (den.mult)(min.den.)'
' for arbmh20k = 0.965246*0.51655,  for rest = 0.965246*0.34438'
'den.mult= 1.21592e4 cm3 (actual vol.) / 1.25970e4 cm3 (model vol.)'
'actual vol.= 1.21592e4 cm3 = (28316.84 cm3/ft3)(9.646 lb)/(22.464 lb/ft3)'
arbmh2ok   0.49860  2 0 0 0    1001   11.1913
                               8016   88.8087   13  0.0287  293  end
arbmal2o3  0.33241  2 0 0 0   13027   52.9390
                               8016   47.0610   13  0.096   293  end
arbmsio2   0.33241  2 0 0 0   14000   46.7570
```

```
                                8016   53.2430   13  0.367   293  end
arbmfe2o3  0.33241  2 0 0 0   26000   69.9540
                                8016   30.0460   13  0.067   293  end
arbmtio2   0.33241  2 0 0 0   22000   59.9535
                                8016   40.0465   13  0.012   293  end
arbmcao    0.33241  2 0 0 0   20000   71.4815
                                8016   28.5185   13  0.307   293  end
arbmmgo    0.33241  2 0 0 0   12000   60.3169
                                8016   39.6831   13  0.131   293  end
arbmna2o   0.33241  2 0 0 0   11023   74.1961
                                8016   25.8039   13  0.020   293  end
'silicone rubber pads'
arbmsiru   1.21791  4 0 0 0    6012   32.3767
                                1001    8.1573
                                8016   21.5782
                               14000   37.8878   14  1.0     293  end
'void space external to containment vessel'
arbmwecv   0.9982   2 0 0 0    1001   11.1913
                                8016   88.8087   15  0.0001  293  end
'steel: liner'
ss304                                            16  1.0     293  end
'steel: plug cover (pc) use 9.907 lb'
ss304                                            17  1.06388 293  end
'steel: angle iron (ai) for single units'
'ss304                                            18  1.0     293  end
'steel: angle iron (ai) for arrays'
'array density is multiplied by a volume fraction 7.08030/5.63249'
ss304                                            18  1.25705 293  end
'steel: drum steel for single units'
'ss304                                            19  1.0     293  end
'steel: drum steel for arrays'
'array density is multiplied by a volume fraction 3.20482/3.20544'
ss304                                            19  0.99981 293  end
'void space external to drum'
'array density is multiplied by a volume ratio 8.11698/6.98323'
arbmwed    1.16026  2 0 0 0    1001   11.1913
                                8016   88.8087   20  0.0001  293  end
'reflective water'
'arbmh20r   0.9982   2 0 0 0    1001   11.1913
'                                8016   88.8087   21  1.0     293  end
end comp
5nciapdoxt11,11000.1gUO2 ( 9682.3g235)2658.2gSH2O 5994.4gHcv,hx= 25.06 fr=0.0001
read parameters nub=yes npg=2500 gen=215 nsk=15 tme=100 end parameters
read boun       all=specular                     end boun
read geometry
unit 1001
'drum bottom flat cover [Elev= 0.111 in. at top of unit]'
'cylinder  19 1   22.866096    0.28150   0.0     com='extended radius not used'
 cylinder  19 1   21.722275    0.28150   0.0     com='drum bottom flat cover'
 cuboid    20 1 4p22.866096    0.28150   0.0     com='drum chine outer radius'
unit 1002
'above drum bottom flat cover and below containment vessel [Elev= 4.676 in.]'
 cylinder  15 1    3.175000   11.59510  11.16330 com='void in pad-1'
 cylinder  14 1    7.924800   11.59510  11.16330 com='pad-1'
 cylinder  16 1    8.077200   11.59510  11.16330 com='np277_4 liner'
 cylinder  11 1   10.922000   11.59510  11.16330 com='np277_4'
 cylinder  16 1   11.074400   11.59510  10.85850 com='kaolite liner bottom'
 cylinder  12 1   21.555075   11.59510   0.0     com='kaolite'
 cylinder  19 1   21.722275   11.59510   0.0     com='drum'
 cuboid    20 1 4p22.866096   11.59510   0.0     com='drum chine outer radius'
unit 1003
'cv bottom to bottom of 1st step [Elev=35.276 in.]'
 cylinder  3  1    6.426200   77.72400  33.08705 com='cavity abv HEU'
 cylinder  1  1    6.426200   77.72400   0.63500 com='HEU content'
 cylinder  8  1    6.680200   77.72400   0.0     com='cv bottom'
 cylinder  15 1    7.924800   77.72400   0.0     com='void btw cv-np liner'
 cylinder  16 1    8.077200   77.72400   0.0     com='np277_4 liner'
 cylinder  11 1   10.922000   77.72400   0.0     com='np277_4'
 cylinder  16 1   11.074400   77.72400   0.0     com='kaolite liner'
 cylinder  12 1   21.555075   77.72400   0.0     com='kaolite'
 cylinder  19 1   21.722275   77.72400   0.0     com='drum'
 cuboid    20 1 4p22.866096   77.72400   0.0     com='drum chine outer radius'
unit 1010
'cv at 1st step in liner [Elev=35.336 in.]'
 cylinder  3  1    6.426200    0.15240   0.00000 com='cavity abv HEU'
```

```
 cylinder  1  1    6.426200    0.15240   0.0     com='HEU content'
 cylinder  8  1    6.680200    0.15240   0.0     com='cv at 1st step'
 cylinder  15 1    7.924800    0.15240   0.0     com='void btw cv and liner'
 cylinder  16 1   11.074400    0.15240   0.0     com='liner 1st step'
 cylinder  12 1   21.555075    0.15240   0.0     com='kaolite'
 cylinder  19 1   21.722275    0.15240   0.0     com='drum'
 cuboid    20 1 4p22.866096    0.15240   0.0     com='drum chine outer radius'
unit 1011
'vertical gap between 1st step in liner and cv flange [Elev=35.426 in.]'
 cylinder  3  1    6.426200    0.22860   0.00000 com='cavity abv HEU'
 cylinder  1  1    6.426200    0.22860   0.0     com='HEU content'
 cylinder  8  1    6.680200    0.22860   0.0     com='cv at gap btwn step-flng'
 cylinder  15 1   10.922000    0.22860   0.0     com='void btw cv and liner'
 cylinder  16 1   11.074400    0.22860   0.0     com='liner wall'
 cylinder  12 1   21.555075    0.22860   0.0     com='kaolite'
 cylinder  19 1   21.722275    0.22860   0.0     com='drum'
 cuboid    20 1 4p22.866096    0.22860   0.0     com='drum chine outer radius'
unit 1012
'cv flange to top of cv well [Elev=35.926 in.]'
 cylinder  3  1    6.426200    1.27000   0.00000 com='cavity abv HEU'
 cylinder  1  1    6.426200    1.27000   0.0     com='HEU content'
 cylinder  9  1    9.525000    1.27000   0.0     com='flange to top of well'
 cylinder  15 1    9.525000    1.27000   0.0     com='void btw cv and pad-2'
 cylinder  14 1   10.033000    1.27000   0.0     com='pad-2'
 cylinder  15 1   10.922000    1.27000   0.0     com='void btw cv and liner'
 cylinder  16 1   11.074400    1.27000   0.0     com='liner wall'
 cylinder  12 1   21.555075    1.27000   0.0     com='kaolite'
 cylinder  19 1   21.722275    1.27000   0.0     com='drum'
 cuboid    20 1 4p22.866096    1.27000   0.0     com='drum chine outer radius'
unit 1013
'cv flange above cv well [Elev=37.076 in.]'
 cylinder  10 1    9.525000    2.92100   0.0     com='flange above cv well'
 cylinder  15 1    9.525000    2.92100   0.0     com='void btw cv and pad-2'
 cylinder  14 1   10.033000    2.92100   0.0     com='pad-2'
 cylinder  15 1   10.922000    2.92100   0.0     com='void btw pad2 and liner'
 cylinder  16 1   11.074400    2.92100   0.0     com='liner wall'
 cylinder  12 1   21.555075    2.92100   0.0     com='kaolite'
 cylinder  19 1   21.722275    2.92100   0.0     com='drum'
 cuboid    20 1 4p22.866096    2.92100   0.0     com='drum chine outer radius'
unit 1014
'plugpad2 below liner 2nd step [Elev=37.476 in.]'
 cylinder  14 1   10.033000    0.76200   0.0     com='pad-2'
 cylinder  15 1   10.922000    1.01600   0.0     com='void btw pad2 and liner'
 cylinder  16 1   11.074400    1.01600   0.0     com='liner wall'
 cylinder  12 1   21.555075    1.01600   0.0     com='kaolite'
 cylinder  19 1   21.722275    1.01600   0.0     com='drum'
 cuboid    20 1 4p22.866096    1.01600   0.0     com='drum chine outer radius'
unit 1015
'2nd step in liner [Elev=37.536 in.]'
 cylinder  15 1   10.922000    0.15240   0.0     com='void abv pad2'
 cylinder  16 1   18.757900    0.15240   0.0     com='liner 2nd step'
 cylinder  12 1   21.555075    0.15240   0.0     com='kaolite'
 cylinder  19 1   21.722275    0.15240   0.0     com='drum'
 cuboid    20 1 4p22.866096    0.15240   0.0     com='drum chine outer radius'
unit 1016
'abv 2nd step in liner to bottom of angle iron [Elev=40.756 in.]'
 cylinder  13 1   18.097500    8.17880   0.49276 com='plug kaolite'
 cylinder  17 1   18.249900    8.17880   0.34036 com='sides of plug case'
 cylinder  15 1   18.605500    8.17880   0.0     com='void: plug to liner'
 cylinder  16 1   18.757900    8.17880   0.0     com='liner wall'
 cylinder  12 1   21.555075    8.17880   0.0     com='kaolite'
 cylinder  19 1   21.722275    8.17880   0.0     com='drum'
 cuboid    20 1 4p22.866096    8.17880   0.0     com='drum chine outer radius'
unit 1017
'bottom of angle iron to bend in angle iron [Elev=42.506 in.]'
 cylinder  13 1   18.097500    4.44500   0.0     com='plug kaolite'
 cylinder  17 1   18.249900    4.44500   0.0     com='sides of plug case'
 cylinder  15 1   18.605500    4.44500   0.0     com='void: plug to liner'
 cylinder  16 1   18.757900    4.44500   0.0     com='liner wall'
 cylinder  18 1   19.392900    4.44500   0.0     com='lower angle iron'
 cylinder  12 1   21.555075    4.44500   0.0     com='kaolite'
 cylinder  19 1   21.722275    4.44500   0.0     com='drum'
 cuboid    20 1 4p22.866096    4.44500   0.0     com='drum chine outer radius'
unit 1018
'bend in angle iron to top of angle iron [Elev=42.756 in.]'
```

```
 cylinder  13 1   18.097500    0.11176   0.0     com='plug kaolite'
 cylinder  17 1   18.249900    0.26416   0.0     com='sides of plug case'
 cylinder  15 1   18.605500    0.63500   0.0     com='void: plug to liner'
 cylinder  16 1   18.757900    0.63500   0.0     com='liner wall'
 cylinder  18 1   21.555075    0.63500   0.0     com='bend section of ai'
 cylinder  19 1   21.722275    0.63500   0.0     com='drum'
 cuboid    20 1 4p22.866096    0.63500   0.0     com='drum chine outer radius'
unit 1019
'drum lid and lip [Elev=43.512 in.]'
 cylinder  20 1   21.330090    1.91973   0.16720 com='void above lid'
 cylinder  19 1   21.497290    1.91973   0.0     com='drum lid'
 cylinder  20 1   21.555075    1.91973   0.0     com='void btw lid - drum wall'
 cylinder  19 1   21.722275    1.91973   0.0     com='drum'
 cuboid    20 1 4p22.866096    1.91973   0.0     com='drum chine outer radius'
global
unit 1020
'es3100 drum [Elev=43.512 in.]'
array 3         2r-22.866096     0.0
'cuboid     0  1 4p24.587200    1120.337  0.0    com='bare package'
'cuboid    21  1 4p55.067200   1150.817 -30.48   com='reflected package'
 cuboid    20  1 4p22.866096    110.5197  0.0    com='interstital array space'
'global
'unit 1021
'array 4   3r0.0
'reflector  21 2  6r3.0  10
end geometry
read array
ara=3 nux=1 nuy=1 nuz=13 fill
1001 1002 1003 1010
1011 1012 1013 1014 1015 1016 1017 1018 1019        end fill
'ara=4 nux=13 nuy=13 nuz=06 fill f1020               end fill
end array
'read bias id=500 2  11  end bias
read start nst=0
end start
end data
end
```

6.9.9.9.8 Case 5hciapdoxt12_1_1_11_3

```
=csas25    parm=size=3000000
5hciapdoxt12,11000.1gUO2 ( 9682.3g235)4488.3gSH2O 4164.3gHcv hx= 25.06 fr=0.0001
238groupndf5 infhommedium
'HEU volume =5500.05000 HEU oxide, bulk density of oxide in cans=  2.00000 g/cm3'
'oxide= 11000.1 g, sat.h2o in HEU oxide=4488.3 g, oxide h/x=12.10'
'poly (packed or wrapped) dry content h/x=1.73, CV void volume 4171.83368'
arbmuox    1.82015   2 0 0 0  92235   88.0203
                               8016   11.9797    1  1.0000  293  end
arbmastm  7.4266e-01  2 0 0 0  1001   11.1913
                               8016   88.8087    1  1.0000  293  end
arbmpoly  8.2733e-02  2 0 0 0  1001   14.3798
                               6012   85.6202    1  1.0000  293  end
'np277-4: spacer (HAC_MD&H)'
'HAC min.den.(95.3157 lb/ft3) and hydrogen'
'np277-4 min.den.= 1.526803 = (95.3157 lb/ft3)(453.59 g/lb)/(28316.84 cm3/ft3)'
'use 75% of boron in calculations per NUREG-1609 Section 6.5.3.2'
arbmboron 7.31015e-2  2 0 0 0    5010   18.1479
                                 5011   81.8520    2  0.7500  293  end
arbmnpmx  1.07071e+0 10 0 0 0    6012    1.9188
                                 7014    0.0141
                                 8016   43.4254
                                11023    0.1174
                                12000    0.3378
                                13027   39.0477
                                14000    2.4671
                                16000    0.3083
                                20000   11.8335
                                26000    0.5298    2  1.0000  293  end
arbmnph2o 3.82995e-1  2 0 0 0    1001   11.1913
                                 8016   88.8087    2  1.0000  293  end
'flooded containmment vessel and content cans -- 10 CFR 71.55(d)(3)'
arbmwicv  9.9820e-01  2 0 0 0   1001   11.1913
                               8016   88.8087    3  1       293  end
'steel: containment vessel body 16.60 lb but use 15.74 lb'
```

```
ss304                                          8  1.0     293  end
'steel: cv flange lower use 3.36 lb'
ss304                                          9  0.97267 293  end
'steel: cv flange upper use 13.75 lb'
ss304                                         10  0.94348 293  end
'np277-4: confinement -- neutron poison inner liner (HAC_MD&H)'
'actual vol.= 1.28314e4 cm3 = (7.83023e2 in3)(16.387064)'
'den.multiplier = 1.28314e4 cm3 (actual vol.) / 1.32708e4 cm3 (model vol.)'
'np277-4 min.den.= 1.526803 = (95.3157 lb/ft3)(453.59 g/lb)/(28316.84 cm3/ft3)'
'density = 1.476265 = (den.mult)(np277-4 min.den.) = 0.9668933*1.526803'
'use 75% of boron in calculations per NUREG-1609 Section 6.5.3.2'
arbmboron 7.06813e-2  2 0 0 0    5010   18.1479
                                 5011   81.8520   11  0.7500  293  end
arbmnpmx  1.03525e+0 10 0 0 0    6012    1.9188
                                 7014    0.0141
                                 8016   43.4254
                                11023    0.1174
                                12000    0.3378
                                13027   39.0477
                                14000    2.4671
                                16000    0.3083
                                20000   11.8335
                                26000    0.5298   11  1.0000  293  end
arbmnph2o 3.70316e-1  2 0 0 0    1001   11.1913
                                 8016   88.8087   11  1.0000  293  end
'kaolite 1600 body'
'nct.sing.unit.density= (den.mult)(min.den.)'
' for arbmh20k 0.52294 = 1.012373*0.51655, for rest 0.34864 = 1.012373*0.34438'
'den.mult= 1.36557e5 cm3 (actual vol.) / 1.34888e5 cm3 (model vol.)'
'actual vol.= 1.36557e5 cm3 = (28316.84 cm3/ft3)(108.33188 lb)/(22.464 lb/ft3)'
'hac.s.u.dens= (hac.mult)(nct.s.u.dens)'
'hac.mult = 1.34888e5 cm3 (nct vol.)/ 1.12246e5 cm3 (model vol.)'
' for arbmh2ok 0.62843 = 1.20172*0.52294,   for rest = 1.20172*0.34864'
'hac array densities are hac s.u.dens.'
arbmh2ok   0.62843  2 0 0 0    1001   11.1913
                                8016   88.8087   12  0.0287  293  end
arbmal2o3  0.41898  2 0 0 0   13027   52.9390
                                8016   47.0610   12  0.096   293  end
arbmsio2   0.41898  2 0 0 0   14000   46.7570
                                8016   53.2430   12  0.367   293  end
arbmfe2o3  0.41898  2 0 0 0   26000   69.9540
                                8016   30.0460   12  0.067   293  end
arbmtio2   0.41898  2 0 0 0   22000   59.9535
                                8016   40.0465   12  0.012   293  end
arbmcao    0.41898  2 0 0 0   20000   71.4815
                                8016   28.5185   12  0.307   293  end
arbmmgo    0.41898  2 0 0 0   12000   60.3169
                                8016   39.6831   12  0.131   293  end
arbmna2o   0.41898  2 0 0 0   11023   74.1961
                                8016   25.8039   12  0.020   293  end
'kaolite 1600 top plug'
'sing.unit.density= (den.mult)(min.den.)'
' for arbmh20k = 0.965246*0.51655,  for rest = 0.965246*0.34438'
'den.mult= 1.21592e4 cm3 (actual vol.) / 1.25970e4 cm3 (model vol.)'
'actual vol.= 1.21592e4 cm3 = (28316.84 cm3/ft3)(9.646 lb)/(22.464 lb/ft3)'
arbmh2ok   0.49860  2 0 0 0    1001   11.1913
                                8016   88.8087   13  0.0287  293  end
arbmal2o3  0.33241  2 0 0 0   13027   52.9390
                                8016   47.0610   13  0.096   293  end
arbmsio2   0.33241  2 0 0 0   14000   46.7570
                                8016   53.2430   13  0.367   293  end
arbmfe2o3  0.33241  2 0 0 0   26000   69.9540
                                8016   30.0460   13  0.067   293  end
arbmtio2   0.33241  2 0 0 0   22000   59.9535
                                8016   40.0465   13  0.012   293  end
arbmcao    0.33241  2 0 0 0   20000   71.4815
                                8016   28.5185   13  0.307   293  end
arbmmgo    0.33241  2 0 0 0   12000   60.3169
                                8016   39.6831   13  0.131   293  end
arbmna2o   0.33241  2 0 0 0   11023   74.1961
                                8016   25.8039   13  0.020   293  end
'silicone rubber pads'
arbmsiru   1.21791  4 0 0 0    6012   32.3767
                                1001    8.1573
                                8016   21.5782
```

```
                              14000   37.8878   14  1.0     293  end
'void space external to containment vessel'
arbmwecv   0.9982   2 0 0 0    1001   11.1913
                               8016   88.8087   15  0.0001  293  end
'steel: liner'
ss304                                           16  1.0     293  end
'steel: plug cover (pc) use 9.907 lb'
ss304                                           17  1.06388 293  end
'steel: angle iron (ai) for HAC'
'nct density is multiplied by volume fraction 7.08030/5.74516'
ss304                                           18  1.23239 293  end
'steel: drum steel for HAC'
'nct density is multiplied by volume fraction 3.20482/2.95645'
ss304                                           19  1.08401 293  end
'void space external to drum'
'array density is assumed not reduced by hac'
arbmwed    0.9982   2 0 0 0    1001   11.1913
                               8016   88.8087   20  0.0001  293  end
'reflective water'
'arbmh20r   0.9982   2 0 0 0    1001   11.1913
'                               8016   88.8087   21  1.0     293  end
end comp
5hciapdoxt12,11000.1gUO2 ( 9682.3g235)4488.3gSH2O 4164.3gHcv,hx= 25.06 fr=0.0001
read parameters nub=yes npg=2500 gen=215 nsk=15 tme=100 end parameters
read boun       all=specular                    end boun
read geometry
unit 1001
'drum bottom flat cover [Elev= 0.105 in. at top of unit]'
'cylinder  19 1   21.838092    0.26670   0.0     com='extended radius not used'
 cylinder  19 1   21.838092    0.26670   0.0     com='drum bottom flat cover'
 cuboid    20 1 4p21.838092    0.26670   0.0     com='drum(chine)outer radius'
unit 1002
'above drum bottom flat cover and below containment vessel [Elev= 4.670 in.]'
 cylinder  15 1    3.175000   11.59510  11.16330 com='void in pad-1'
 cylinder  14 1    7.924800   11.59510  11.16330 com='pad-1'
 cylinder  16 1    8.077200   11.59510  11.16330 com='np277_4 liner'
 cylinder  11 1   10.922000   11.59510  11.16330 com='np277_4'
 cylinder  16 1   11.074400   11.59510  10.85850 com='kaolite liner bottom'
 cylinder  12 1   21.685692   11.59510   0.0     com='kaolite'
 cylinder  19 1   21.838092   11.59510   0.0     com='drum'
 cuboid    20 1 4p21.838092   11.59510   0.0     com='drum(chine)outer radius'
unit 1003
'cv bottom to bottom of 1st step [Elev=35.270 in.]'
 cylinder  3  1    6.426200   77.72400  47.21851 com='cavity abv HEU'
 cylinder  1  1    6.426200   77.72400   0.63500 com='HEU content'
 cylinder  8  1    6.680200   77.72400   0.0     com='cv bottom'
 cylinder  15 1    7.924800   77.72400   0.0     com='void btw cv-np liner'
 cylinder  16 1    8.077200   77.72400   0.0     com='np277_4 liner'
 cylinder  11 1   10.922000   77.72400   0.0     com='np277_4'
 cylinder  16 1   11.074400   77.72400   0.0     com='kaolite liner'
 cylinder  12 1   21.685692   77.72400   0.0     com='kaolite'
 cylinder  19 1   21.838092   77.72400   0.0     com='drum'
 cuboid    20 1 4p21.838092   77.72400   0.0     com='drum(chine)outer radius'
unit 1010
'cv at 1st step in liner [Elev=35.330 in.]'
 cylinder  3  1    6.426200    0.15240   0.00000 com='cavity abv HEU'
 cylinder  1  1    6.426200    0.15240   0.0     com='HEU content'
 cylinder  8  1    6.680200    0.15240   0.0     com='cv at 1st step'
 cylinder  15 1    7.924800    0.15240   0.0     com='void btw cv and liner'
 cylinder  16 1   11.074400    0.15240   0.0     com='liner 1st step'
 cylinder  12 1   21.685692    0.15240   0.0     com='kaolite'
 cylinder  19 1   21.838092    0.15240   0.0     com='drum'
 cuboid    20 1 4p21.838092    0.15240   0.0     com='drum(chine)outer radius'
unit 1011
'vertical gap between 1st step in liner and cv flange [Elev=35.420 in.]'
 cylinder  3  1    6.426200    0.22860   0.00000 com='cavity abv HEU'
 cylinder  1  1    6.426200    0.22860   0.0     com='HEU content'
 cylinder  8  1    6.680200    0.22860   0.0     com='cv at gap btwn step-flng'
 cylinder  15 1   10.922000    0.22860   0.0     com='void btw cv and liner'
 cylinder  16 1   11.074400    0.22860   0.0     com='liner wall'
 cylinder  12 1   21.685692    0.22860   0.0     com='kaolite'
 cylinder  19 1   21.838092    0.22860   0.0     com='drum'
 cuboid    20 1 4p21.838092    0.22860   0.0     com='drum(chine)outer radius'
unit 1012
'cv flange to top of cv well [Elev=35.920 in.]'
```

```
 cylinder  3  1    6.426200    1.27000   0.00000 com='cavity abv HEU'
 cylinder  1  1    6.426200    1.27000   0.0     com='HEU content'
 cylinder  9  1    9.525000    1.27000   0.0     com='flange to top of well'
 cylinder  15 1    9.525000    1.27000   0.0     com='void btw cv and pad-2'
 cylinder  14 1   10.033000    1.27000   0.0     com='pad-2'
 cylinder  15 1   10.922000    1.27000   0.0     com='void btw cv and liner'
 cylinder  16 1   11.074400    1.27000   0.0     com='liner wall'
 cylinder  12 1   21.685692    1.27000   0.0     com='kaolite'
 cylinder  19 1   21.838092    1.27000   0.0     com='drum'
 cuboid    20 1 4p21.838092    1.27000   0.0     com='drum(chine)outer radius'
unit 1013
'cv flange above cv well [Elev=37.070 in.]'
 cylinder  10 1    9.525000    2.92100   0.0     com='flange above cv well'
 cylinder  15 1    9.525000    2.92100   0.0     com='void btw cv and pad-2'
 cylinder  14 1   10.033000    2.92100   0.0     com='pad-2'
 cylinder  15 1   10.922000    2.92100   0.0     com='void btw pad2 and liner'
 cylinder  16 1   11.074400    2.92100   0.0     com='liner wall'
 cylinder  12 1   21.685692    2.92100   0.0     com='kaolite'
 cylinder  19 1   21.838092    2.92100   0.0     com='drum'
 cuboid    20 1 4p21.838092    2.92100   0.0     com='drum(chine)outer radius'
unit 1014
'plugpad2 below liner 2nd step [Elev=37.470 in.]'
 cylinder  14 1   10.033000    0.76200   0.0     com='pad-2'
 cylinder  15 1   10.922000    1.01600   0.0     com='void btw pad2 and liner'
 cylinder  16 1   11.074400    1.01600   0.0     com='liner wall'
 cylinder  12 1   21.685692    1.01600   0.0     com='kaolite'
 cylinder  19 1   21.838092    1.01600   0.0     com='drum'
 cuboid    20 1 4p21.838092    1.01600   0.0     com='drum(chine)outer radius'
unit 1015
'2nd step in liner [Elev=37.530 in.]'
 cylinder  15 1   10.922000    0.15240   0.0     com='void abv pad2'
 cylinder  16 1   18.757900    0.15240   0.0     com='liner 2nd step'
 cylinder  12 1   21.685692    0.15240   0.0     com='kaolite'
 cylinder  19 1   21.838092    0.15240   0.0     com='drum'
 cuboid    20 1 4p21.838092    0.15240   0.0     com='drum(chine)outer radius'
unit 1016
'abv 2nd step in liner to bottom of angle iron [Elev=40.750 in.]'
 cylinder  13 1   18.097500    8.17880   0.49276 com='plug kaolite'
 cylinder  17 1   18.249900    8.17880   0.34036 com='sides of plug case'
 cylinder  15 1   18.605500    8.17880   0.0     com='void: plug to liner'
 cylinder  16 1   18.757900    8.17880   0.0     com='liner wall'
 cylinder  12 1   21.685692    8.17880   0.0     com='kaolite'
 cylinder  19 1   21.838092    8.17880   0.0     com='drum'
 cuboid    20 1 4p21.838092    8.17880   0.0     com='drum(chine)outer radius'
unit 1017
'bottom of angle iron to bend in angle iron [Elev=42.500 in.]'
 cylinder  13 1   18.097500    4.44500   0.0     com='plug kaolite'
 cylinder  17 1   18.249900    4.44500   0.0     com='sides of plug case'
 cylinder  15 1   18.605500    4.44500   0.0     com='void: plug to liner'
 cylinder  16 1   18.757900    4.44500   0.0     com='liner wall'
 cylinder  18 1   19.392900    4.44500   0.0     com='lower angle iron'
 cylinder  12 1   21.685692    4.44500   0.0     com='kaolite'
 cylinder  19 1   21.838092    4.44500   0.0     com='drum'
 cuboid    20 1 4p21.838092    4.44500   0.0     com='drum(chine)outer radius'
unit 1018
'bend in angle iron to top of angle iron [Elev=42.750 in.]'
 cylinder  13 1   18.097500    0.11176   0.0     com='plug kaolite'
 cylinder  17 1   18.249900    0.26416   0.0     com='sides of plug case'
 cylinder  15 1   18.605500    0.63500   0.0     com='void: plug to liner'
 cylinder  16 1   18.757900    0.63500   0.0     com='liner wall'
 cylinder  18 1   21.685692    0.63500   0.0     com='bend section of ai'
 cylinder  19 1   21.838092    0.63500   0.0     com='drum'
 cuboid    20 1 4p21.838092    0.63500   0.0     com='drum(chine)outer radius'
unit 1019
'drum lid and lip [Elev=43.500 in.]'
 cylinder  20 1   21.469792    1.90500   0.15240 com='void above lid'
 cylinder  19 1   21.622192    1.90500   0.0     com='drum lid'
 cylinder  20 1   21.685692    1.90500   0.0     com='void btw lid - drum wall'
 cylinder  19 1   21.838092    1.90500   0.0     com='drum'
 cuboid    20 1 4p21.838092    1.90500   0.0     com='drum(chine)outer radius'
global
unit 1020
'es3100 drum [Elev=43.500 in.]'
array 3         2r-21.838092     0.0
'cuboid     0  1 4p21.838092    110.4905  0.0    com='bare package'
```

```
'cuboid    21  1 4p52.318092   140.9700 -30.48   com='reflected package'
 cuboid    20  1 4p22.889718    110.5048  0.0    com='interstital array space'
'global
'unit 1021
'array 4   3r0.0
'reflector  21 2  6r3.0  10
end geometry
read array
ara=3 nux=1 nuy=1 nuz=13 fill
1001 1002 1003 1010
1011 1012 1013 1014 1015 1016 1017 1018 1019        end fill
'ara=4 nux=13 nuy=13 nuz=06 fill f1020               end fill
end array
'read bias id=500 2  11  end bias
read start nst=0
end start
end data
end
```

6.9.9.9.9 Case 5ncf1pdoxt11_1_1_14_3

```
=csas25    parm=size=3000000
5ncf1pdoxt11,14000.1gUO2 (12322.9g235)5712.4gSH2O 2667.0gHcv hx= 19.11 fr=0.0001
238groupndf5 infhommedium
'HEU volume =7000.05000 HEU oxide, bulk density of oxide in cans=  2.00000 g/cm3'
'oxide= 14000.1 g, sat.h2o in HEU oxide=5712.4 g, oxide h/x=12.10'
'poly (packed or wrapped) dry content h/x=1.36, CV void volume 2671.83368'
arbmuox    1.85591   2 0 0 0  92235   88.0203
                               8016   11.9797    1  1.0000  293  end
arbmastm  7.5725e-01  2 0 0 0  1001   11.1913
                               8016   88.8087    1  1.0000  293  end
arbmpoly  6.6282e-02  2 0 0 0  1001   14.3798
                               6012   85.6202    1  1.0000  293  end
'np277-4: spacer (NCT_MD&H)'
'NCT min.den.(95.3886 lb/ft3) and hydrogen'
'np277-4 min.den.= 1.527971 = (95.3886 lb/ft3)(453.59 g/lb)/(28316.84 cm3/ft3)'
'use 75% of boron in calculations per NUREG-1609 Section 6.5.3.2'
arbmboron 7.31015e-2  2 0 0 0    5010   18.1479
                                 5011   81.8520    2  0.7500  293  end
arbmnpmx  1.07070e+0 10 0 0 0    6012    1.9189
                                 7014    0.0141
                                 8016   43.4251
                                11023    0.1174
                                12000    0.3378
                                13027   39.0479
                                14000    2.4672
                                16000    0.3083
                                20000   11.8336
                                26000    0.5298    2  1.0000  293  end
arbmnph2o 3.84169e-1  2 0 0 0    1001   11.1913
                                 8016   88.8087    2  1.0000  293  end
'flooded containmment vessel and content cans -- 10 CFR 71.55(d)(3)'
arbmwicv  9.9820e-01  2 0 0 0   1001   11.1913
                               8016   88.8087    3  1       293  end
'steel: containment vessel body 16.60 lb but use 15.74 lb'
ss304                                            8  1.0     293  end
'steel: cv flange lower use 3.36 lb'
ss304                                            9  0.97267 293  end
'steel: cv flange upper use 13.75 lb'
ss304                                           10  0.94348 293  end
'np277-4: confinement -- neutron poison inner liner (NCT_MD&H)'
'actual vol.= 1.28314e4 cm3 = (7.83023e2 in3)(16.387064)'
'den.multiplier = 1.28314e4 cm3 (actual vol.) / 1.32708e4 cm3 (model vol.)'
'np277-4 min.den.= 1.527971 = (95.3886 lb/ft3)(453.59 g/lb)/(28316.84 cm3/ft3)'
'density = 1.477385 = (den.mult)(np277-4 min.den.) = 0.9668933*1.527971'
'use 75% of boron in calculations per NUREG-1609 Section 6.5.3.2'
arbmboron 7.06813e-2  2 0 0 0    5010   18.1479
                                 5011   81.8520   11  0.7500  293  end
arbmnpmx  1.03525e+0 10 0 0 0    6012    1.9189
                                 7014    0.0141
                                 8016   43.4251
                                11023    0.1174
                                12000    0.3378
                                13027   39.0479
```

```
                                14000    2.4672
                                16000    0.3083
                                20000   11.8336
                                26000    0.5298   11  1.0000  293  end
arbmnph2o 3.71451e-1  2 0 0 0    1001   11.1913
                                 8016   88.8087   11  1.0000  293  end
'kaolite 1600 body'
'sing.unit.density= (den.mult)(min.den.)'
' for arbmh20k = 1.012373*0.51655,  for rest = 1.012373*0.34438'
'den.mult= 1.36557e5 cm3 (actual vol.) / 1.34888e5 cm3 (model vol.)'
'actual vol.= 1.36557e5 cm3 = (28316.84 cm3/ft3)(108.33188 lb)/(22.464 lb/ft3)'
'nct array densities are s.u.dens. multiplied by volume ratio 1.34888/1.10336'
arbmh2ok   0.63931  2 0 0 0    1001   11.1913
                               8016   88.8087   12  0.0287  293  end
arbmal2o3  0.42622  2 0 0 0   13027   52.9390
                               8016   47.0610   12  0.096   293  end
arbmsio2   0.42622  2 0 0 0   14000   46.7570
                               8016   53.2430   12  0.367   293  end
arbmfe2o3  0.42622  2 0 0 0   26000   69.9540
                               8016   30.0460   12  0.067   293  end
arbmtio2   0.42622  2 0 0 0   22000   59.9535
                               8016   40.0465   12  0.012   293  end
arbmcao    0.42622  2 0 0 0   20000   71.4815
                               8016   28.5185   12  0.307   293  end
arbmmgo    0.42622  2 0 0 0   12000   60.3169
                               8016   39.6831   12  0.131   293  end
arbmna2o   0.42622  2 0 0 0   11023   74.1961
                               8016   25.8039   12  0.020   293  end
'kaolite 1600 top plug'
'sing.unit.density= (den.mult)(min.den.)'
' for arbmh20k = 0.965246*0.51655,  for rest = 0.965246*0.34438'
'den.mult= 1.21592e4 cm3 (actual vol.) / 1.25970e4 cm3 (model vol.)'
'actual vol.= 1.21592e4 cm3 = (28316.84 cm3/ft3)(9.646 lb)/(22.464 lb/ft3)'
arbmh2ok   0.49860  2 0 0 0    1001   11.1913
                               8016   88.8087   13  0.0287  293  end
arbmal2o3  0.33241  2 0 0 0   13027   52.9390
                               8016   47.0610   13  0.096   293  end
arbmsio2   0.33241  2 0 0 0   14000   46.7570
                               8016   53.2430   13  0.367   293  end
arbmfe2o3  0.33241  2 0 0 0   26000   69.9540
                               8016   30.0460   13  0.067   293  end
arbmtio2   0.33241  2 0 0 0   22000   59.9535
                               8016   40.0465   13  0.012   293  end
arbmcao    0.33241  2 0 0 0   20000   71.4815
                               8016   28.5185   13  0.307   293  end
arbmmgo    0.33241  2 0 0 0   12000   60.3169
                               8016   39.6831   13  0.131   293  end
arbmna2o   0.33241  2 0 0 0   11023   74.1961
                               8016   25.8039   13  0.020   293  end
'silicone rubber pads'
arbmsiru   1.21791  4 0 0 0    6012   32.3767
                               1001    8.1573
                               8016   21.5782
                              14000   37.8878   14  1.0     293  end
'void space external to containment vessel'
arbmwecv   0.9982   2 0 0 0    1001   11.1913
                               8016   88.8087   15  0.0001  293  end
'steel: liner'
ss304                                            16  1.0     293  end
'steel: plug cover (pc) use 9.907 lb'
ss304                                            17  1.06388 293  end
'steel: angle iron (ai) for single units'
'ss304                                            18  1.0     293  end
'steel: angle iron (ai) for arrays'
'array density is multiplied by a volume fraction 7.08030/5.63249'
ss304                                            18  1.25705 293  end
'steel: drum steel for single units'
'ss304                                            19  1.0     293  end
'steel: drum steel for arrays'
'array density is multiplied by a volume fraction 3.20482/3.20544'
ss304                                            19  0.99981 293  end
'void space external to drum'
'array density is multiplied by a volume ratio 8.11698/6.98323'
arbmwed    1.16026  2 0 0 0    1001   11.1913
                               8016   88.8087   20  0.0001  293  end
```

```
'reflective water'
arbmh20r   0.9982   2 0 0 0    1001   11.1913
                               8016   88.8087   21  1.0     293  end
end comp
5ncf1pdoxt11,14000.1gUO2 (12322.9g235)5712.4gSH2O 2667.0gHcv,hx= 19.11 fr=0.0001
read parameters nub=yes npg=2500 gen=215 nsk=15 tme=100 end parameters
read boun       all=vacuum                      end boun
read geometry
unit 1001
'drum bottom flat cover [Elev= 0.111 in. at top of unit]'
'cylinder  19 1   22.866096    0.28150   0.0     com='extended radius not used'
 cylinder  19 1   21.722275    0.28150   0.0     com='drum bottom flat cover'
 cuboid    20 1 4p22.866096    0.28150   0.0     com='drum chine outer radius'
unit 1002
'above drum bottom flat cover and below containment vessel [Elev= 4.676 in.]'
 cylinder  15 1    3.175000   11.59510  11.16330 com='void in pad-1'
 cylinder  14 1    7.924800   11.59510  11.16330 com='pad-1'
 cylinder  16 1    8.077200   11.59510  11.16330 com='np277_4 liner'
 cylinder  11 1   10.922000   11.59510  11.16330 com='np277_4'
 cylinder  16 1   11.074400   11.59510  10.85850 com='kaolite liner bottom'
 cylinder  12 1   21.555075   11.59510   0.0     com='kaolite'
 cylinder  19 1   21.722275   11.59510   0.0     com='drum'
 cuboid    20 1 4p22.866096   11.59510   0.0     com='drum chine outer radius'
unit 1003
'cv bottom to bottom of 1st step [Elev=35.276 in.]'
 cylinder  3  1    6.426200   77.72400  58.78051 com='cavity abv HEU'
 cylinder  1  1    6.426200   77.72400   0.63500 com='HEU content'
 cylinder  8  1    6.680200   77.72400   0.0     com='cv bottom'
 cylinder  15 1    7.924800   77.72400   0.0     com='void btw cv-np liner'
 cylinder  16 1    8.077200   77.72400   0.0     com='np277_4 liner'
 cylinder  11 1   10.922000   77.72400   0.0     com='np277_4'
 cylinder  16 1   11.074400   77.72400   0.0     com='kaolite liner'
 cylinder  12 1   21.555075   77.72400   0.0     com='kaolite'
 cylinder  19 1   21.722275   77.72400   0.0     com='drum'
 cuboid    20 1 4p22.866096   77.72400   0.0     com='drum chine outer radius'
unit 1010
'cv at 1st step in liner [Elev=35.336 in.]'
 cylinder  3  1    6.426200    0.15240   0.00000 com='cavity abv HEU'
 cylinder  1  1    6.426200    0.15240   0.0     com='HEU content'
 cylinder  8  1    6.680200    0.15240   0.0     com='cv at 1st step'
 cylinder  15 1    7.924800    0.15240   0.0     com='void btw cv and liner'
 cylinder  16 1   11.074400    0.15240   0.0     com='liner 1st step'
 cylinder  12 1   21.555075    0.15240   0.0     com='kaolite'
 cylinder  19 1   21.722275    0.15240   0.0     com='drum'
 cuboid    20 1 4p22.866096    0.15240   0.0     com='drum chine outer radius'
unit 1011
'vertical gap between 1st step in liner and cv flange [Elev=35.426 in.]'
 cylinder  3  1    6.426200    0.22860   0.00000 com='cavity abv HEU'
 cylinder  1  1    6.426200    0.22860   0.0     com='HEU content'
 cylinder  8  1    6.680200    0.22860   0.0     com='cv at gap btwn step-flng'
 cylinder  15 1   10.922000    0.22860   0.0     com='void btw cv and liner'
 cylinder  16 1   11.074400    0.22860   0.0     com='liner wall'
 cylinder  12 1   21.555075    0.22860   0.0     com='kaolite'
 cylinder  19 1   21.722275    0.22860   0.0     com='drum'
 cuboid    20 1 4p22.866096    0.22860   0.0     com='drum chine outer radius'
unit 1012
'cv flange to top of cv well [Elev=35.926 in.]'
 cylinder  3  1    6.426200    1.27000   0.00000 com='cavity abv HEU'
 cylinder  1  1    6.426200    1.27000   0.0     com='HEU content'
 cylinder  9  1    9.525000    1.27000   0.0     com='flange to top of well'
 cylinder  15 1    9.525000    1.27000   0.0     com='void btw cv and pad-2'
 cylinder  14 1   10.033000    1.27000   0.0     com='pad-2'
 cylinder  15 1   10.922000    1.27000   0.0     com='void btw cv and liner'
 cylinder  16 1   11.074400    1.27000   0.0     com='liner wall'
 cylinder  12 1   21.555075    1.27000   0.0     com='kaolite'
 cylinder  19 1   21.722275    1.27000   0.0     com='drum'
 cuboid    20 1 4p22.866096    1.27000   0.0     com='drum chine outer radius'
unit 1013
'cv flange above cv well [Elev=37.076 in.]'
 cylinder  10 1    9.525000    2.92100   0.0     com='flange above cv well'
 cylinder  15 1    9.525000    2.92100   0.0     com='void btw cv and pad-2'
 cylinder  14 1   10.033000    2.92100   0.0     com='pad-2'
 cylinder  15 1   10.922000    2.92100   0.0     com='void btw pad2 and liner'
 cylinder  16 1   11.074400    2.92100   0.0     com='liner wall'
 cylinder  12 1   21.555075    2.92100   0.0     com='kaolite'
```

```
 cylinder  19 1   21.722275    2.92100   0.0     com='drum'
 cuboid    20 1 4p22.866096    2.92100   0.0     com='drum chine outer radius'
unit 1014
'plugpad2 below liner 2nd step [Elev=37.476 in.]'
 cylinder  14 1   10.033000    0.76200   0.0     com='pad-2'
 cylinder  15 1   10.922000    1.01600   0.0     com='void btw pad2 and liner'
 cylinder  16 1   11.074400    1.01600   0.0     com='liner wall'
 cylinder  12 1   21.555075    1.01600   0.0     com='kaolite'
 cylinder  19 1   21.722275    1.01600   0.0     com='drum'
 cuboid    20 1 4p22.866096    1.01600   0.0     com='drum chine outer radius'
unit 1015
'2nd step in liner [Elev=37.536 in.]'
 cylinder  15 1   10.922000    0.15240   0.0     com='void abv pad2'
 cylinder  16 1   18.757900    0.15240   0.0     com='liner 2nd step'
 cylinder  12 1   21.555075    0.15240   0.0     com='kaolite'
 cylinder  19 1   21.722275    0.15240   0.0     com='drum'
 cuboid    20 1 4p22.866096    0.15240   0.0     com='drum chine outer radius'
unit 1016
'abv 2nd step in liner to bottom of angle iron [Elev=40.756 in.]'
 cylinder  13 1   18.097500    8.17880   0.49276 com='plug kaolite'
 cylinder  17 1   18.249900    8.17880   0.34036 com='sides of plug case'
 cylinder  15 1   18.605500    8.17880   0.0     com='void: plug to liner'
 cylinder  16 1   18.757900    8.17880   0.0     com='liner wall'
 cylinder  12 1   21.555075    8.17880   0.0     com='kaolite'
 cylinder  19 1   21.722275    8.17880   0.0     com='drum'
 cuboid    20 1 4p22.866096    8.17880   0.0     com='drum chine outer radius'
unit 1017
'bottom of angle iron to bend in angle iron [Elev=42.506 in.]'
 cylinder  13 1   18.097500    4.44500   0.0     com='plug kaolite'
 cylinder  17 1   18.249900    4.44500   0.0     com='sides of plug case'
 cylinder  15 1   18.605500    4.44500   0.0     com='void: plug to liner'
 cylinder  16 1   18.757900    4.44500   0.0     com='liner wall'
 cylinder  18 1   19.392900    4.44500   0.0     com='lower angle iron'
 cylinder  12 1   21.555075    4.44500   0.0     com='kaolite'
 cylinder  19 1   21.722275    4.44500   0.0     com='drum'
 cuboid    20 1 4p22.866096    4.44500   0.0     com='drum chine outer radius'
unit 1018
'bend in angle iron to top of angle iron [Elev=42.756 in.]'
 cylinder  13 1   18.097500    0.11176   0.0     com='plug kaolite'
 cylinder  17 1   18.249900    0.26416   0.0     com='sides of plug case'
 cylinder  15 1   18.605500    0.63500   0.0     com='void: plug to liner'
 cylinder  16 1   18.757900    0.63500   0.0     com='liner wall'
 cylinder  18 1   21.555075    0.63500   0.0     com='bend section of ai'
 cylinder  19 1   21.722275    0.63500   0.0     com='drum'
 cuboid    20 1 4p22.866096    0.63500   0.0     com='drum chine outer radius'
unit 1019
'drum lid and lip [Elev=43.512 in.]'
 cylinder  20 1   21.330090    1.91973   0.16720 com='void above lid'
 cylinder  19 1   21.497290    1.91973   0.0     com='drum lid'
 cylinder  20 1   21.555075    1.91973   0.0     com='void btw lid - drum wall'
 cylinder  19 1   21.722275    1.91973   0.0     com='drum'
 cuboid    20 1 4p22.866096    1.91973   0.0     com='drum chine outer radius'
'global
unit 1020
'es3100 drum [Elev=43.512 in.]'
array 3         2r-22.866096     0.0
'cuboid     0  1 4p24.587200    1120.337  0.0    com='bare package'
'cuboid    21  1 4p55.067200   1150.817 -30.48   com='reflected package'
 cuboid    20  1 4p22.866096    110.5198  0.0    com='interstital array space'
global
unit 1021
array 4   3r0.0
reflector  21 2  6r3.0  10
end geometry
read array
ara=3 nux=1 nuy=1 nuz=13 fill
1001 1002 1003 1010
1011 1012 1013 1014 1015 1016 1017 1018 1019        end fill
ara=4 nux=13 nuy=13 nuz=06 fill f1020               end fill
end array
read bias id=500 2  11  end bias
read start nst=0
```

```
end start
end data
end
```

6.9.9.9.10 Case 5hcf2pdoxt12_1_1_14_3

```
=csas25    parm=size=3000000
5hcf2pdoxt12,14000.1gUO2 (12322.9g235)5712.4gSH2O 2667.0gHcv hx= 19.11 fr=0.0001
238groupndf5 infhommedium
'HEU volume =7000.05000 HEU oxide, bulk density of oxide in cans=  2.00000 g/cm3'
'oxide= 14000.1 g, sat.h2o in HEU oxide=5712.4 g, oxide h/x=12.10'
'poly (packed or wrapped) dry content h/x=1.36, CV void volume 2671.83368'
arbmuox    1.85591   2 0 0 0  92235   88.0203
                               8016   11.9797    1  1.0000  293  end
arbmastm  7.5725e-01  2 0 0 0  1001   11.1913
                               8016   88.8087    1  1.0000  293  end
arbmpoly  6.6282e-02  2 0 0 0  1001   14.3798
                               6012   85.6202    1  1.0000  293  end
'np277-4: spacer (HAC_MD&H)'
'HAC min.den.(95.3157 lb/ft3) and hydrogen'
'np277-4 min.den.= 1.526803 = (95.3157 lb/ft3)(453.59 g/lb)/(28316.84 cm3/ft3)'
'use 75% of boron in calculations per NUREG-1609 Section 6.5.3.2'
arbmboron 7.31015e-2  2 0 0 0    5010   18.1479
                                  5011   81.8520    2  0.7500  293  end
arbmnpmx  1.07071e+0 10 0 0 0    6012    1.9188
                                  7014    0.0141
                                  8016   43.4254
                                 11023    0.1174
                                 12000    0.3378
                                 13027   39.0477
                                 14000    2.4671
                                 16000    0.3083
                                 20000   11.8335
                                 26000    0.5298    2  1.0000  293  end
arbmnph2o 3.82995e-1  2 0 0 0    1001   11.1913
                                  8016   88.8087    2  1.0000  293  end
'flooded containmment vessel and content cans -- 10 CFR 71.55(d)(3)'
arbmwicv  9.9820e-01  2 0 0 0   1001   11.1913
                               8016   88.8087    3  1       293  end
'steel: containment vessel body 16.60 lb but use 15.74 lb'
ss304                                            8  1.0     293  end
'steel: cv flange lower use 3.36 lb'
ss304                                            9  0.97267 293  end
'steel: cv flange upper use 13.75 lb'
ss304                                           10  0.94348 293  end
'np277-4: confinement -- neutron poison inner liner (HAC_MD&H)'
'actual vol.= 1.28314e4 cm3 = (7.83023e2 in3)(16.387064)'
'den.multiplier = 1.28314e4 cm3 (actual vol.) / 1.32708e4 cm3 (model vol.)'
'np277-4 min.den.= 1.526803 = (95.3157 lb/ft3)(453.59 g/lb)/(28316.84 cm3/ft3)'
'density = 1.476265 = (den.mult)(np277-4 min.den.) = 0.9668933*1.526803'
'use 75% of boron in calculations per NUREG-1609 Section 6.5.3.2'
arbmboron 7.06813e-2  2 0 0 0    5010   18.1479
                                  5011   81.8520   11  0.7500  293  end
arbmnpmx  1.03525e+0 10 0 0 0    6012    1.9188
                                  7014    0.0141
                                  8016   43.4254
                                 11023    0.1174
                                 12000    0.3378
                                 13027   39.0477
                                 14000    2.4671
                                 16000    0.3083
                                 20000   11.8335
                                 26000    0.5298   11  1.0000  293  end
arbmnph2o 3.70316e-1  2 0 0 0    1001   11.1913
                                  8016   88.8087   11  1.0000  293  end
'kaolite 1600 body'
'nct.sing.unit.density= (den.mult)(min.den.)'
' for arbmh20k 0.52294 = 1.012373*0.51655, for rest 0.34864 = 1.012373*0.34438'
'den.mult= 1.36557e5 cm3 (actual vol.) / 1.34888e5 cm3 (model vol.)'
'actual vol.= 1.36557e5 cm3 = (28316.84 cm3/ft3)(108.33188 lb)/(22.464 lb/ft3)'
'hac.s.u.dens= (hac.mult)(nct.s.u.dens)'
'hac.mult = 1.34888e5 cm3 (nct vol.)/ 1.12246e5 cm3 (model vol.)'
' for arbmh2ok 0.62843 = 1.20172*0.52294,   for rest = 1.20172*0.34864'
'hac array densities are hac s.u.dens.'
```

```
arbmh2ok   0.62843  2 0 0 0    1001   11.1913
                               8016   88.8087   12  0.0287  293  end
arbmal2o3  0.41898  2 0 0 0   13027   52.9390
                               8016   47.0610   12  0.096   293  end
arbmsio2   0.41898  2 0 0 0   14000   46.7570
                               8016   53.2430   12  0.367   293  end
arbmfe2o3  0.41898  2 0 0 0   26000   69.9540
                               8016   30.0460   12  0.067   293  end
arbmtio2   0.41898  2 0 0 0   22000   59.9535
                               8016   40.0465   12  0.012   293  end
arbmcao    0.41898  2 0 0 0   20000   71.4815
                               8016   28.5185   12  0.307   293  end
arbmmgo    0.41898  2 0 0 0   12000   60.3169
                               8016   39.6831   12  0.131   293  end
arbmna2o   0.41898  2 0 0 0   11023   74.1961
                               8016   25.8039   12  0.020   293  end
'kaolite 1600 top plug'
'sing.unit.density= (den.mult)(min.den.)'
' for arbmh20k = 0.965246*0.51655,  for rest = 0.965246*0.34438'
'den.mult= 1.21592e4 cm3 (actual vol.) / 1.25970e4 cm3 (model vol.)'
'actual vol.= 1.21592e4 cm3 = (28316.84 cm3/ft3)(9.646 lb)/(22.464 lb/ft3)'
arbmh2ok   0.49860  2 0 0 0    1001   11.1913
                               8016   88.8087   13  0.0287  293  end
arbmal2o3  0.33241  2 0 0 0   13027   52.9390
                               8016   47.0610   13  0.096   293  end
arbmsio2   0.33241  2 0 0 0   14000   46.7570
                               8016   53.2430   13  0.367   293  end
arbmfe2o3  0.33241  2 0 0 0   26000   69.9540
                               8016   30.0460   13  0.067   293  end
arbmtio2   0.33241  2 0 0 0   22000   59.9535
                               8016   40.0465   13  0.012   293  end
arbmcao    0.33241  2 0 0 0   20000   71.4815
                               8016   28.5185   13  0.307   293  end
arbmmgo    0.33241  2 0 0 0   12000   60.3169
                               8016   39.6831   13  0.131   293  end
arbmna2o   0.33241  2 0 0 0   11023   74.1961
                               8016   25.8039   13  0.020   293  end
'silicone rubber pads'
arbmsiru   1.21791  4 0 0 0    6012   32.3767
                               1001    8.1573
                               8016   21.5782
                              14000   37.8878   14  1.0     293  end
'void space external to containment vessel'
arbmwecv   0.9982   2 0 0 0    1001   11.1913
                               8016   88.8087   15  0.0001  293  end
'steel: liner'
ss304                                            16  1.0     293  end
'steel: plug cover (pc) use 9.907 lb'
ss304                                            17  1.06388 293  end
'steel: angle iron (ai) for HAC'
'nct density is multiplied by volume fraction 7.08030/5.74516'
ss304                                            18  1.23239 293  end
'steel: drum steel for HAC'
'nct density is multiplied by volume fraction 3.20482/2.95645'
ss304                                            19  1.08401 293  end
'void space external to drum'
'array density is assumed not reduced by hac'
arbmwed    0.9982   2 0 0 0    1001   11.1913
                               8016   88.8087   20  0.0001  293  end
'reflective water'
arbmh20r   0.9982   2 0 0 0    1001   11.1913
                               8016   88.8087   21  1.0     293  end
end comp
5hcf2pdoxt12,14000.1gUO2 (12322.9g235)5712.4gSH2O 2667.0gHcv,hx= 19.11 fr=0.0001
read parameters nub=yes npg=2500 gen=215 nsk=15 tme=100 end parameters
read boun       all=vacuum                       end boun
read geometry
unit 1001
'drum bottom flat cover [Elev= 0.105 in. at top of unit]'
'cylinder  19 1   21.838092    0.26670   0.0     com='extended radius not used'
 cylinder  19 1   21.838092    0.26670   0.0     com='drum bottom flat cover'
 cuboid    20 1 4p21.838092    0.26670   0.0     com='drum(chine)outer radius'
unit 1002
'above drum bottom flat cover and below containment vessel [Elev= 4.670 in.]'
 cylinder  15 1    3.175000   11.59510  11.16330 com='void in pad-1'
```

```
 cylinder  14 1    7.924800   11.59510  11.16330 com='pad-1'
 cylinder  16 1    8.077200   11.59510  11.16330 com='np277_4 liner'
 cylinder  11 1   10.922000   11.59510  11.16330 com='np277_4'
 cylinder  16 1   11.074400   11.59510  10.85850 com='kaolite liner bottom'
 cylinder  12 1   21.685692   11.59510   0.0     com='kaolite'
 cylinder  19 1   21.838092   11.59510   0.0     com='drum'
 cuboid    20 1 4p21.838092   11.59510   0.0     com='drum(chine)outer radius'
unit 1003
'cv bottom to bottom of 1st step [Elev=35.270 in.]'
 cylinder  3  1    6.426200   77.72400  58.78051 com='cavity abv HEU'
 cylinder  1  1    6.426200   77.72400   0.63500 com='HEU content'
 cylinder  8  1    6.680200   77.72400   0.0     com='cv bottom'
 cylinder  15 1    7.924800   77.72400   0.0     com='void btw cv-np liner'
 cylinder  16 1    8.077200   77.72400   0.0     com='np277_4 liner'
 cylinder  11 1   10.922000   77.72400   0.0     com='np277_4'
 cylinder  16 1   11.074400   77.72400   0.0     com='kaolite liner'
 cylinder  12 1   21.685692   77.72400   0.0     com='kaolite'
 cylinder  19 1   21.838092   77.72400   0.0     com='drum'
 cuboid    20 1 4p21.838092   77.72400   0.0     com='drum(chine)outer radius'
unit 1010
'cv at 1st step in liner [Elev=35.330 in.]'
 cylinder  3  1    6.426200    0.15240   0.00000 com='cavity abv HEU'
 cylinder  1  1    6.426200    0.15240   0.0     com='HEU content'
 cylinder  8  1    6.680200    0.15240   0.0     com='cv at 1st step'
 cylinder  15 1    7.924800    0.15240   0.0     com='void btw cv and liner'
 cylinder  16 1   11.074400    0.15240   0.0     com='liner 1st step'
 cylinder  12 1   21.685692    0.15240   0.0     com='kaolite'
 cylinder  19 1   21.838092    0.15240   0.0     com='drum'
 cuboid    20 1 4p21.838092    0.15240   0.0     com='drum(chine)outer radius'
unit 1011
'vertical gap between 1st step in liner and cv flange [Elev=35.420 in.]'
 cylinder  3  1    6.426200    0.22860   0.00000 com='cavity abv HEU'
 cylinder  1  1    6.426200    0.22860   0.0     com='HEU content'
 cylinder  8  1    6.680200    0.22860   0.0     com='cv at gap btwn step-flng'
 cylinder  15 1   10.922000    0.22860   0.0     com='void btw cv and liner'
 cylinder  16 1   11.074400    0.22860   0.0     com='liner wall'
 cylinder  12 1   21.685692    0.22860   0.0     com='kaolite'
 cylinder  19 1   21.838092    0.22860   0.0     com='drum'
 cuboid    20 1 4p21.838092    0.22860   0.0     com='drum(chine)outer radius'
unit 1012
'cv flange to top of cv well [Elev=35.920 in.]'
 cylinder  3  1    6.426200    1.27000   0.00000 com='cavity abv HEU'
 cylinder  1  1    6.426200    1.27000   0.0     com='HEU content'
 cylinder  9  1    9.525000    1.27000   0.0     com='flange to top of well'
 cylinder  15 1    9.525000    1.27000   0.0     com='void btw cv and pad-2'
 cylinder  14 1   10.033000    1.27000   0.0     com='pad-2'
 cylinder  15 1   10.922000    1.27000   0.0     com='void btw cv and liner'
 cylinder  16 1   11.074400    1.27000   0.0     com='liner wall'
 cylinder  12 1   21.685692    1.27000   0.0     com='kaolite'
 cylinder  19 1   21.838092    1.27000   0.0     com='drum'
 cuboid    20 1 4p21.838092    1.27000   0.0     com='drum(chine)outer radius'
unit 1013
'cv flange above cv well [Elev=37.070 in.]'
 cylinder  10 1    9.525000    2.92100   0.0     com='flange above cv well'
 cylinder  15 1    9.525000    2.92100   0.0     com='void btw cv and pad-2'
 cylinder  14 1   10.033000    2.92100   0.0     com='pad-2'
 cylinder  15 1   10.922000    2.92100   0.0     com='void btw pad2 and liner'
 cylinder  16 1   11.074400    2.92100   0.0     com='liner wall'
 cylinder  12 1   21.685692    2.92100   0.0     com='kaolite'
 cylinder  19 1   21.838092    2.92100   0.0     com='drum'
 cuboid    20 1 4p21.838092    2.92100   0.0     com='drum(chine)outer radius'
unit 1014
'plugpad2 below liner 2nd step [Elev=37.470 in.]'
 cylinder  14 1   10.033000    0.76200   0.0     com='pad-2'
 cylinder  15 1   10.922000    1.01600   0.0     com='void btw pad2 and liner'
 cylinder  16 1   11.074400    1.01600   0.0     com='liner wall'
 cylinder  12 1   21.685692    1.01600   0.0     com='kaolite'
 cylinder  19 1   21.838092    1.01600   0.0     com='drum'
 cuboid    20 1 4p21.838092    1.01600   0.0     com='drum(chine)outer radius'
unit 1015
'2nd step in liner [Elev=37.530 in.]'
 cylinder  15 1   10.922000    0.15240   0.0     com='void abv pad2'
 cylinder  16 1   18.757900    0.15240   0.0     com='liner 2nd step'
 cylinder  12 1   21.685692    0.15240   0.0     com='kaolite'
 cylinder  19 1   21.838092    0.15240   0.0     com='drum'
```

```
 cuboid    20 1 4p21.838092    0.15240   0.0     com='drum(chine)outer radius'
unit 1016
'abv 2nd step in liner to bottom of angle iron [Elev=40.750 in.]'
 cylinder  13 1   18.097500    8.17880   0.49276 com='plug kaolite'
 cylinder  17 1   18.249900    8.17880   0.34036 com='sides of plug case'
 cylinder  15 1   18.605500    8.17880   0.0     com='void: plug to liner'
 cylinder  16 1   18.757900    8.17880   0.0     com='liner wall'
 cylinder  12 1   21.685692    8.17880   0.0     com='kaolite'
 cylinder  19 1   21.838092    8.17880   0.0     com='drum'
 cuboid    20 1 4p21.838092    8.17880   0.0     com='drum(chine)outer radius'
unit 1017
'bottom of angle iron to bend in angle iron [Elev=42.500 in.]'
 cylinder  13 1   18.097500    4.44500   0.0     com='plug kaolite'
 cylinder  17 1   18.249900    4.44500   0.0     com='sides of plug case'
 cylinder  15 1   18.605500    4.44500   0.0     com='void: plug to liner'
 cylinder  16 1   18.757900    4.44500   0.0     com='liner wall'
 cylinder  18 1   19.392900    4.44500   0.0     com='lower angle iron'
 cylinder  12 1   21.685692    4.44500   0.0     com='kaolite'
 cylinder  19 1   21.838092    4.44500   0.0     com='drum'
 cuboid    20 1 4p21.838092    4.44500   0.0     com='drum(chine)outer radius'
unit 1018
'bend in angle iron to top of angle iron [Elev=42.750 in.]'
 cylinder  13 1   18.097500    0.11176   0.0     com='plug kaolite'
 cylinder  17 1   18.249900    0.26416   0.0     com='sides of plug case'
 cylinder  15 1   18.605500    0.63500   0.0     com='void: plug to liner'
 cylinder  16 1   18.757900    0.63500   0.0     com='liner wall'
 cylinder  18 1   21.685692    0.63500   0.0     com='bend section of ai'
 cylinder  19 1   21.838092    0.63500   0.0     com='drum'
 cuboid    20 1 4p21.838092    0.63500   0.0     com='drum(chine)outer radius'
unit 1019
'drum lid and lip [Elev=43.500 in.]'
 cylinder  20 1   21.469792    1.90500   0.15240 com='void above lid'
 cylinder  19 1   21.622192    1.90500   0.0     com='drum lid'
 cylinder  20 1   21.685692    1.90500   0.0     com='void btw lid - drum wall'
 cylinder  19 1   21.838092    1.90500   0.0     com='drum'
 cuboid    20 1 4p21.838092    1.90500   0.0     com='drum(chine)outer radius'
'global
unit 1020
'es3100 drum [Elev=43.500 in.]'
array 3         2r-21.838092     0.0
'cuboid     0  1 4p21.838092    110.4905  0.0    com='bare package'
'cuboid    21  1 4p52.318092   140.9700 -30.48   com='reflected package'
 cuboid    20  1 4p21.838092    110.4901  0.0    com='interstital array space'
global
unit 1021
array 4   3r0.0
reflector  21 2  6r3.0  10
end geometry
read array
ara=3 nux=1 nuy=1 nuz=13 fill
1001 1002 1003 1010
1011 1012 1013 1014 1015 1016 1017 1018 1019        end fill
ara=4 nux=09 nuy=09 nuz=06 fill f1020               end fill
end array
ead bias id=500 2  11  end bias
read start nst=0
end start
end data
end
```

Appendix 6.9.10

Y/DD-1220, *CRITICAL EXPERIMENT BENCHMARK CALCULATIONS WITH CSAS25 FROM SCALE5 FOR CRITICALITY SAFETY ANALYSES ON THE HP zx6000 UNCLASSIFIED WORKSTATION (CMODD)*
AND
Y/DD-1221, *DETERMINATION OF THE UPPER SUBCRITICAL LIMIT FOR CRITICALITY CALCULATIONS FOR CRITICALITY SAFETY ANALYSES*

THIS PAGE INTENTIONALLY LEFT BLANK.

Critical Experiment Benchmark Calculations With CSAS25 from SCALE5 For Criticality Safety Analyses On the HP zx6000 Unclassified Workstation (CMODD)

Revision 0

D. T. Johnson
J. F. DeClue
S. E. McClanahan

Nuclear Criticality Safety organization
Y-12 National Security Complex

March 2006

Prepared by the
Y-12 National Security Complex
Oak Ridge, Tennessee 37831
Managed by
BWXT Y-12, L.L.C.
For the
U.S. Department of Energy
under contract DE-AC05-00OR22800

This document has been reviewed by an Authorized Derivative Classifier and has been determined to be UNCLASSIFIED. This review does not constitute clearance for public release.

J. F. DeClue 3-27-06

J. F. DeClue Date
Criticality Safety Analyst

Critical Experiment Benchmark Calculations With CSAS25 from SCALE5 For Criticality Safety Analyses On the HP zx6000 Unclassified Workstation (CMODD)

Revision 0

D. T. Johnson
J. F. DeClue
S. E. McClanahan

Nuclear Criticality Safety organization
Y-12 National Security Complex

March 2006

Prepared by the
Y-12 National Security Complex
Oak Ridge, Tennessee 37831
Managed by
BWXT Y-12, L.L.C.
For the
U.S. Department of Energy
under contract DE-AC05-00OR22800

THIS PAGE INTENTIONALLY LEFT BLANK

Document Preparation

Prepared by _____ Date 3-28-06
David T. Johnson

Reviewed by _____ Date 3-28-06
John F. DeClue

Approved by _____ Date 3-28-06
David W. Sheffey

THIS PAGE INTENTIONALLY LEFT BLANK

Calculation Reviewers

Peter Angelo Date 3/30/06

Peter Angelo

Kevin Beard Date 3-28-06

Kevin Beard

David Smallwood Date 3/28/06

David Smallwood

THIS PAGE INTENTIONALLY LEFT BLANK

Revision Log

Revision Number	Description of Change	Pages Affected
0	Initial issue.	All

THIS PAGE INTENTIONALLY LEFT BLANK

Abstract

This report documents calculations performed for validation of the CSAS25 control module from the SCALE 5 computer code system for use in evaluating nuclear criticality safety. This document includes results from using only the 238-group ENDF/B-V cross-section library. The criticality validation calculations were performed using over 1200 benchmark cases from Volumes I through VI of the "International Handbook of Evaluated Criticality Safety Benchmark Experiments," published by the Nuclear Energy Agency Organization for Economic Cooperation and Development (NEA/OECD)[i]. This document collects all the OECD benchmarks modeled by Y-12 Nuclear Criticality Safety into one report. Based on the results, the CSAS25 module and 238-group library are validated for use with systems that are similar to those included in this validation. Establishment of sub-critical limits will be documented in a separate report.

The original verification and validation document (Y/DD-896/R0)[ii] included about 500 cases from Volumes II and IV (HEU and LEU). Subsequently, about 400 cases from Volumes I and VI (Pu and mixed U/Pu) were documented in Y/DD-996/R1, and these results were incorporated into Y/DD-896/R1[iii]. In addition, new results for Volumes III-IEU (51 cases) and V-U233 (140 cases), 53 new results for Volume II-HEU, including 26 models developed as part of the qualifications program, as well as 32 new results for Volume IV-LEU, including 7 from the qualifications program, were also included in Y/DD-896/R1. In total, 276 new models were added in Y/DD-896/R1, for a new total of 1217 models.

The 1217 models included in the verification and validation document (Y/DD-896/R1) for SCALE 4.4a are the basis for this validation of SCALE 5. The unaltered input files used in Y/DD-896/R1 were transferred from the Hewlett Packard Series 9000/J unclassified workstation (CMODB) running the HPUX 10.20 operating system to the Hewlett Packard Series zx6000 Itanium unclassified workstation (CMODD) running the HPUX 11i operating system. These SCALE 4.4a input files were re-ran using SCALE 5.

Although many cases are included in this report, analysts are cautioned that they must not assume that all SCALE input options are validated for all applications. They must verify or demonstrate that their options are validated against benchmark experiments that are similar to their applications. Options include material selections (e.g. "be" versus "bebound"), scattering options (i.e. SCT), geometry options (i.e. infinite homogeneous, multi-region, or latticecell), and others. Experience has shown that seemingly minor differences (e.g. "bebound" versus "be") may cause large changes in results, particularly when errors exist in cross section libraries.

THIS PAGE INTENTIONALLY LEFT BLANK

Table of Contents

Page

REVISION LOG ..... **VII**

ABSTRACT ..... **IX**

1 INTRODUCTION **1**

1.1 VALIDATION OF CSAS25 IN SCALE 5 FOR CRITICALITY SAFETY ANALYSES 1
1.2 TERMINOLOGY 2

2 DESCRIPTION OF SCALE 5 CODE PACKAGE **3**

Table 2.1. Analysis capabilities summary of the SCALE control and functional modules covered in this report *4*

3 DISCUSSION OF CRITICALITY BENCHMARK DATABASE FOR VALIDATION OF CSAS25 FROM SCALE 5 ..... **6**

Table 3.1 Number of Input Cases Extracted from the OECD Compact Disk *7*

4 TABULATED RESULTS OF CSAS25 FROM SCALE 5 CRITICALITY CALCULATIONS **9**

Table 4.1 Results for Plutonium Systems (Volume 1) with CSAS25 from SCALE 5 and the 238-group Library on the HP-6000 (CMODD) Workstation *10*
Table 4.2 Results for Highly Enriched Uranium Systems (Volume 2) with CSAS25 from SCALE 5 and the 238-group Library on the HP-6000 (CMODD) Workstation *18*
Table 4.3 Results for Intermediate and Mixed Enrichment Uranium Systems (Volume 3) with CSAS25 from SCALE 5 and the 238-group Library on the HP-6000 (CMODD) Workstation *31*
Table 4.4 Results for Low Enriched Uranium Systems (Volume 4) with CSAS25 from SCALE 5 and the 238-group Library on the HP-6000 (CMODD) Workstation *33*
Table 4.5 Results for Uranium-233 Systems (Volume 5) with CSAS25 from SCALE 5 and the 238-group Library on the HP-6000 (CMODD) Workstation *37*
Table 4.6 Results for Mixed Plutonium - Uranium Systems (Volume 6) with CSAS25 from SCALE 5 and the 238-group Library on the HP-6000 (CMODD) Workstation *41*

5 RESULTS ANALYSIS **46**

5.1 INTRODUCTION 46
5.2 DISCUSSION OF RESULTS 46
Figure 1 - All Adjusted Results *47*
Figure 2 - HEU, IEU and LEU Adjusted Results *48*
Figure 3 - LEU Adjusted k_{eff} Results *49*
Figure 4 - IEU Adjusted k_{eff} Results *50*
Figure 5 - HEU Adjusted k_{eff} Results *51*
Figure 6 - U-233 Adjusted k_{eff} Results *52*
Figure 7 - Pu and Mixed Pu-U Adjusted k_{eff} Results *53*
Figure 8 - Adjusted k_{eff} Results versus Nubar *54*
Figure 9 - Calculated k_{eff} Versus Benchmark k_{eff} *55*
5.3 DISCUSSION OF HIGH POSITIVE AND NEGATIVE BIAS RESULTS 56
Table 5.1 High Positive and Negative Bias Results *56*
5.4 SUMMARY OF RESULTS 57

5.5 AREA OF APPLICABILITY 57
5.6 GRANDFATHER OR RETROFIT CONCERNS 58

6 CONCLUSIONS 59

7 RECOMMENDATIONS FOR FUTURE WORK 60

APPENDIX A - COMPARISON OF AVAILABLE EXPERIMENTS WITH CALCULATED EXPERIMENTS 61

8 REFERENCES 89

1 Introduction

In nuclear criticality safety engineering, extensive use is made of computational methods for analyzing the calculation models of physical systems. The successful application of computational methods requires verification, certification and validation (V&V) of the analytic tool. Software verification, the first element of V&V, reveals the closeness in agreement between calculation results obtained using a particular computational method and calculation results obtained using other methods. Software certification provides a user assurance that the code will consistently produce numerical results that agree with analytic solutions for the problems the code is designed to analyze. Software validation "calibrates" the calculation results obtained using certified software (computational method) for agreement with the physical universe.

The refinement of a validation or extension of it by the addition of cases does not require re-certification of the software. Therefore, the verification and certification of the SCALE 5 modular code system are separate issues, and are published separately. This document addresses the calculation results to be used for establishment of bias, bias trends and uncertainty for validation of the CSAS25 control module from the Standardized Computer Analyses for Licensing Evaluation (SCALE) Version 5 package with the 238-group ENDF/B-V SCALE 5 cross-section libraries.

Section 1.1 identifies source documents and rationale for the validation activities, and it summarizes the scope of the validation performed on the Safety Analysis Engineering (SAE) Hewlett Packard Series zx6000 Itanium unclassified workstation (referred to as CMODD) at Y-12.

1.1 Validation of CSAS25 in SCALE 5 for Criticality Safety Analyses

In nuclear criticality safety engineering, calculation methods are one of the methods used to establish the subcritical limits for operations involving fissile material. The American National Standards Institute (ANSI) gives fundamental guidance for establishing these limits in ANSI/ANS-8.1-1998, "Nuclear Criticality Safety in Operations with Fissionable Materials Outside Reactors."[iv] In paragraph 4.2.5, the standard states:

> In the absence of directly applicable experimental measurements, the limits may be derived from calculations made by a method shown by comparison with experimental data to be valid in accordance with 4.3.

Section 4.3 of the Standard provides additional guidance on the general procedure for establishing validity. This includes establishment of bias (4.3.1), bias trend (4.3.2), uncertainty (4.3.3), computer dependence (4.3.4), consistency with measurement (4.3.5), and preparing a written validation report (4.3.6).

This criticality validation includes systems consisting of fissile and fissionable material in metallic, solution and other physical forms, as described in summary in this report, and in more detail in the first six volumes of the OECD Handbook. The emphasis of this criticality validation is on comparison of calculated neutron multiplication factors (k_{eff}) with experimental results, and on establishment of bias, bias trends, and uncertainty as a final step. Compiled data for nearly 1200 critical experiments is used as the basis for the calculation models. The calculated results from SCALE 5 using the 238-group ENDF/B-V SCALE 5 cross-section libraries have been compared with reported results for the benchmark experiments. Comparison of results demonstrates that SCALE 5 run on CMODD produces the same results (within the statistical uncertainty of the Monte Carlo calculations) as reported by the experiments

where similar (SCALE, 238-group library) results were published. Subcritical limits can be determined through an analysis of the criticality calculation results. Determination of these limits will be addressed in a separate report. Extension of the validation to other computer platforms will be addressed separately.

1.2 Terminology

The term "model" may be used in two different ways in validation work. Often, as in this report, "model" generally refers to the calculation model, or the collection of input parameters for the numerical simulation in SCALE/KENO of the physical critical experiment. In statistical analyses, the term "model" generally refers to a statistical model, or an equation describing the relationship between parameters considered in the statistical analysis. In this report the intended meaning should be clear from the context, but generally the former meaning is intended in this report.

2 Description of SCALE 5 Code Package

The U. S. Nuclear Regulatory Commission (NRC) originally sponsored the Standardized Computer Analyses for Licensing Evaluation (SCALE) code system. The original concept of SCALE was to provide "standardized" sequences where the user had very few analyses options in addition to the geometry model and materials. Input for the control modules has been designed to be free form with extensive use of keyword and engineering-type input requirements. The stand-alone functional modules are more flexible, but they have a more difficult input logic and require the user to manually interface the data sets necessary to run the modules in a stand-alone fashion. As the system has grown in popularity over the years and additional options have been requested, the control modules have been improved to allow sophisticated users additional access to the numerous capabilities within the functional modules. However, the most important feature of the SCALE system remains the capability to simplify the user knowledge and effort required to prepare material mixtures and to perform adequate problem-dependent cross-section processing.

The modules available in Version 0 of SCALE were for Criticality Safety Analysis Sequences (CSAS) that provided automated material and cross-section processing prior to a one-dimensional (1-D) or multidimensional criticality analysis. Since that time the capabilities of the system have been significantly expanded to provide additional CSAS capabilities. Table 2.1 provides a summary of the major applications of each of the control modules and functional modules currently in the SCALE code system and relevant to criticality safety calculations that are covered in this report. Eight CSAS sequences enable general analysis of a 1-D system model or a multidimensional system model, with optional capabilities to search on geometry spacing, and problem-dependent cross-section processing for use in executing stand-alone functional modules. The CSAS module is the primary control module designed for the calculation of the neutron multiplication factor of a system.

At the center of the CSAS sequences is the library of subroutines referred to as the Material Information Processor or MIPLIB. The purpose of MIPLIB is to allow users to specify problem materials using easily remembered and easily recognizable keyword that are associated with mixtures, elements, and nuclides provided in the Standard Composition Library. MIPLIB also uses other keyword and simple geometry input specifications to prepare input for the modules that perform the problem-dependent cross-section processing: BONAMI, NITAWL-III, and XSDRNPM. A keyword supplied by the user selects the cross-section library from a standard set provided in SCALE or designates the reference to a user-supplied library. Several utility modules from AMPX have been included to provide users with the capability to edit the cross-section data and reformat user-supplied libraries for use in SCALE. The CSAS25 sequence was used for this report.

The CSAS25 control sequence provides automated, problem-dependent, cross section processing followed by calculation of the neutron multiplication factor (k_{eff}) for the system being modeled. Initiated by "=csas25" appearing on the first line in the user input, the CSAS module runs the CSAS25 control sequence. The cross section processing functional modules BONAMI and NITAWL-III are activated, providing resonance-corrected cross sections to the multigroup Monte Carlo functional module, KENO V.a. Using the processed cross sections, KENO V.a calculates the k_{eff} of three-dimensional system models. The geometric modeling capabilities available in KENO V.a, coupled with the automated cross section processing, allow complex, three-dimensional systems to be easily analyzed.

The CSAS25 control sequence reads user-specified input data, which include the required cross section library, specification for mixtures, information for resonance processing of nuclides (size, geometry, and temperature), and a detailed geometry model for KENO V.a. Physical and neutronic information not specified but required by the functional modules (such as theoretical density, molecular

weights, and average resonance region background cross sections) is supplied by the Standard Composition Library or calculated by the Materials Information Processor. The Standard Composition Library consists of a standard composition directory and table, an isotopic distribution directory and table, and a nuclide information table. The Material Information Processor checks the input data pertaining to cross section preparation and prepares binary input files for the applicable functional modules BONAMI and NITAWL-III.

Table 2.1. Analysis capabilities summary of the SCALE control and functional modules covered in this report

Control Module	Analysis function(s)	Functional modules executed
CSAS25	3-D Monte Carlo calculation of k_{eff}; Problem-dependent cross-section processing; Multiplication search or spacing	BONAMI NITAWL-III KENO V.a ICE

Functional module	Function
BONAMI	Performs resonance self-shielding calculations for nuclides that have Bondarenko data associated with their cross sections.
NITAWL-III	Applies a Nordheim resonance self-shielding correction to nuclides having resonance parameters.
ICE	Creates a Monte Carlo formatted mixed cross-section library for use by KENO V.a..
KENO V.a	Calculates k-effective of a 3-D system.

A 238-energy-group neutron cross-section library based on ENDF/B-V has recently been prepared for the SCALE system. All the nuclides that are available in ENDF/B-V are in the library. A 44-group library has been collapsed from this 238-group library. These libraries are available in versions 4.3 and later of SCALE. The 44-group and 238-group libraries were used in Y/DD-896/R0 validation study. It has been found useful in the past to compare a fine-group calculation against a broad-group calculation when bias is observed.

The 27-group ENDF/B-IV library is the broad-group companion library to the 218-group ENDF/B-IV library. The library has 14 fast groups and 13 thermal groups (below 3 eV). The group structure was chosen to match the 16-group Hansen-Roach structure with two additional fast groups and seven additional thermal groups. The library has been extensively validated against critical experiments, and has been the standard library of choice of the Y-12 nuclear criticality safety analysts in previous years. The 27-group library was also used in Y/DD-896/R0, primarily as a reference point for cases of prior usage where the analyst wants to understand a relative difference in results of prior studies compared to current work using the newer libraries.

A recent ORNL report assessed the performance of the available libraries[v]. The recommendation supports using the 238-group library, but the endorsement is not unqualified. The following discussion highlights several points from the report.

Regarding the 218-group library, from which the 27-group library is collapsed, the summary stated, "The graphite thermal kernel is deficient, with unknown results." This issue could be of concern for some Y-12 applications. The report also says, "Intermediate-energy systems, such as the Palmer problems, can be wrong by large amounts." On the positive side, the summary stated "Fast, small metal units, highly enriched thermal systems, and very thermal low-enriched systems are generally well predicted." The body of the report includes several cautions and warnings of apparent trends or biases related to the 27-group and 218-group libraries. In summarizing where the 27-group library performs well, it states "Generally the same as the 218-group library. Some trends and biases may be slightly more pronounced in the broad-group library, but most results are fairly equivalent." The report provides several reasons to consider moving away from using the 27-group or 218-group libraries.

In summarizing the performance of the 238-group library, the report states "This library is recommended as the best library in SCALE for general-purpose criticality-safety analyses." The endorsement is not unqualified, however. The report also states "Although any intermediate-energy problems are suspect because of the scarcity of critical experiments, this library performs better than any other library in SCALE." Regarding the weaknesses of the 44-group library, the report states "Because of the 1/E weighting in the 238-group library, this library is not a good general-purpose library." In addition, it states "The 44-group library has all the shortcomings of the 238-group library, as well as not being able to calculate homogeneous thermal, epithermal, and intermediate-energy systems as accurately as the 238-group library." On the strengths of the 44-group library, the report says "LWR and mixed-oxide lattices are the library's strong point, and it is the recommended SCALE library for these applications."

The report suggests that the 238-group library should be considered the general library of choice except perhaps for applications where the 44-group library may perform slightly better, such as ^{235}U LWR (low enriched) and MOX lattices, and for ^{233}U. The 218-group and 27-group libraries also perform reasonably well for selected applications, but they have the disadvantage of having several deficiencies that must be avoided. Finally, the report anticipates development of an improved 238-group library based on ENDF/B-VI, a "refined library with additional groups (partially to facilitate analysis of problems with a dominant intermediate-energy spectrum)," and predicts that "The next version of SCALE will include a continuous-energy cross-section library." The recommendations and future directions suggest a preference for the 238-group library. Therefore, for this document only the results from the 238-group library have been included.

3 Discussion of Criticality Benchmark Database for Validation of CSAS25 from SCALE 5

The United States Department of Energy initiated the Criticality Safety Benchmark Evaluation Project (CSBEP) in October of 1992. The project quickly grew into an international effort, as scientists from other interested countries became involved. The International Criticality Safety Benchmark Evaluation Project (ICSBEP) is now an official activity of the Organization for Economic Cooperation and Development - Nuclear Energy Agency (OECD-NEA). The wide scale evaluation effort has concluded with the publication of the "International Handbook of Criticality Safety Benchmark Experiments" [i] (OECD Handbook). The seven-volume set of handbooks contains criticality safety benchmark specifications derived from experiments that were performed at various nuclear critical facilities around the world. The benchmark specifications are intended for use by criticality safety engineers to validate the application of calculation techniques, such as SCALE 5, for criticality safety analyses. Example calculations presented in the handbook do not constitute a validation of the codes or cross section data sets by themselves, but use of the information contained in the Handbook can be and has been used to validate SCALE 5 by competent nuclear criticality safety persons. The evaluated criticality safety benchmark data are published in the seven-volume OECD Handbook, previously in hard copy form, and recently only on compact disk (CD). Acrobat® Reader is used to access the CD for extraction of experiment descriptions and input files.

For this criticality validation of SCALE 5, fissile material forms include uranium systems, plutonium systems, mixed uranium and plutonium systems, and Uranium-233 systems. The validation comprises a substantial subset of the database used to prepare the first six volumes of the OECD Handbook. Table 3.1 summarizes the evaluated benchmark experiments that are analyzed in this validation. The data from the benchmark experiments represents a sufficiently wide range of fissile and fissionable materials, enrichments, and physical and chemical forms to cover many existing, planned or unforeseen activities for the Y-12 site. These include enriched uranium with ^{235}U only, natural and depleted uranium, intermediate (10-60%) enriched uranium, highly (>60%) enriched uranium, uranium-233, plutonium, and mixed plutonium-uranium systems. Data analyzed from critical experiments in this validation includes systems having fast, intermediate and thermal neutron energy spectra, and they include materials in various physical and chemical forms such as metals, solutions, and oxide compounds.

For many benchmark experiments, critical conditions are tabulated in the OECD Handbook for a number of parametric variables (height, concentration, shape, etc.) Although calculation results for all of these cases are reported, often SCALE 5 input details for only some of these cases are actually provided in the OECD Handbook. Input data for the CSAS25 cases are based on information contained in the OECD distribution CD, which is accessed using Acrobat® Reader software. The CD contains the text of the Handbook in the form of Portable Document Format (PDF) files. It also contains a section of selected input file listings. The listings in the two sections do not always correspond, so input files were taken from both parts of the CD, where they differed. In addition, where it was practical, inputs present for only one cross-section set were modified and copied to use with the 238-group cross-section library. Cases were first prepared using the 1998 edition of the CD, and additional cases were taken from the subsequent editions through 2002. Each subsequent revision provides additional experiments and input data. The organization and categorization of the experiments and data on the CD also changes.

® 1987-1996 Adobe Systems Incorporated. All rights reserved. Adobe, Acrobat, and the Acrobat logo are trademarks of Adobe Systems Incorporated which may be registered in certain jurisdictions.

Table 3.1 Number of Input Cases Extracted from the OECD Compact Disk

	Fissile Material Category (OECD Benchmark Volume)							
	II	III	IV		I	VI	V	
Material / Energy	**High Enriched Uranium**	**Intermediate Enriched Uranium**	**Low Enriched Uranium**	**Subtotal Uranium-235 fissile**	**Plutonium**	**Mixed Plutonium-Uranium**	**Uranium-233**	**Total**
Metal/Fast	106	16	0	122	62	33	10	227
Metal/Intermediate	4	0	0	4	0	0	0	4
Metal/Thermal	31	0	13	44	0	0	0	44
Metal/Mixed	3	0	0	3	0	0	0	3
Compound/Fast	0	0	0	0	0	0	0	0
Compound/Intermediate	12	4 *	0	16	1	0	0	17
Compound/Thermal	24	31	99	154	0	92	0	246
Compound/Mixed	9	0	0	9	9	0	0	18
Solution/Intermediate	0	0	0	0	0	0	33	33
Solution/Thermal	271	0	16	287	198	32	97	614
Solution/Mixed	0	0	0	0	0	0	0	0
Misc./Thermal	0	0	0	0	0	11	0	11
Total	460	51	128	639	270	168	140	1217

* Note: Two of these intermediate energy cases should have been categorized as fast or thermal

Reviews were performed of the input preparation in a graded approach. For models based on sample inputs, reviews generally assume the models are adequate unless reasons are found to think otherwise, at the discretion of the reviewer. Models prepared from scratch, based on experiment descriptions, are given more scrutiny. Mentors review models submitted as part of the qualifications program.

A total of 1217 cases were extracted from the CD or created from experiment descriptions, and are included in this document. Table 3.1 shows the number of cases that were obtained in various categories. A copy of the input data for the validation cases is maintained on the CMODD workstation.

Due to the large number of benchmark experiment cases included in this document, the OECD Handbook and associated DICE database search software are considered the best source for obtaining summary and detailed descriptive information for the benchmark experiments. Appendix A of this report gives a comparison of available experiments that could have been modeled, versus experiments that were modeled and included in validations. This list will be useful for determining what models to create for future inclusion in the validation, and for very abbreviated descriptions (titles).

The OECD report contains the following admonishment: "Sample input listings are not intended to be used directly for validation efforts and should be verified by the user. Since it is not practical to describe in detail the code input used to model each benchmark critical experiment, computer input listings are given for typical reported calculations of accepted benchmark configurations. From these listings, a user can identify which options were used to obtain the reported results. This is the sole purpose for inclusion of the input listings. It is the responsibility of the user to ensure that use of these listings for any other purpose is consistent with proper criticality safety practices." In performing this validation effort, the "universe" of experiments was the experiments available on the CD. No additional, independent selection of applicable experiments was performed. Advantage was taken of the available sample input listings to the maximum extent feasible. Some additional models were created based on parameter changes to the sample models, and some models were created from scratch based on the experiment descriptions, particularly as part of the Y-12 qualifications program.

Reviews were performed of the input preparation in a graded approach. For models based on sample inputs, reviews generally assume the models are adequate unless reasons are found to think otherwise, at the discretion of the reviewer. Models prepared from scratch, based on experiment descriptions, are given more scrutiny. Mentors review models submitted as part of the qualifications program.

It is recognized that there were experiments, which were not included because input models were not readily available, that would be applicable for Y-12. Also, some experiments were included that are probably not currently very directly applicable to Y-12 work. This is not a concern as long as these experiments do not have a large difference in bias compared with the other experiments in the category. The additional experiments provide confidence in the code's ability to calculate over a broader area of applicability than the minimum necessary for currently planned Y-12 applications.

4 Tabulated Results of CSAS25 from SCALE 5 Criticality Calculations

Input data for the CSAS25 cases are based on information contained in the OECD distribution CD, as described in Section 3. Calculations were performed for the 238-group cross-section library.

The input cases were altered as little as possible unless there was an error, but the parameters were generally altered to consistently include:

Parm=size=4000000 and
gen=500 npg=2000 nsk=100 tba=10 nub=yes

This results in 1,000,000 total neutron histories per case, skipping the first 100 generations, allows up to 10 minutes per batch, and causes the run output to include values for "Average Fission Group" (AFG) and "Energy of Average Lethargy Causing Fission" (EALCF). Using "nub=yes" is no longer necessary because it is now a default setting, but this is a carryover from previous versions which had "nub=no" as default.

For each CSAS25 case, Tables 4.1-4.6 list the following results: the mean of the final k_{eff} (k_cal) after 800,000 histories, and the standard deviation of that mean; the mean of the AFG, the mean of the EALCF, and the associated standard deviations. In addition, the expected, or experimental, k-effective (k_exp) and associated error estimate from the OECD benchmark handbook is also provided. The values of AFG and EALCF are included as potential regression variables because previously there was an expectation that the bias between experiment and Monte Carlo calculation might be correlated with these parameters. All results in this report are 238-group results.

Table 4.1 Results for Plutonium Systems (Volume 1) with CSAS25 from SCALE 5 and the 238-group Library on the HP-6000 (CMODD) Workstation

N	Case	nubar	Sigma	AFG	Sigma	EALCF (eV)	Sigma	k_{calc} Pu	sigma	k_{exp} Pu	Sigma	Bias = Calculated - Benchmark	Adjusted k_{eff} Pu
1	pci001	2.898	1.82E-05	87.202	1.34E-02	3.08E+02	2.83E-01	0.99870	0.00022	1.0000	0.0110	-0.00130	0.99870
2	pcm001-001	3.106	2.58E-04	24.069	1.69E-02	9.56E+05	1.52E+03	1.02637	0.00140	0.9986	0.0041	0.02777	1.02777
3	pcm001-002	2.969	1.30E-04	80.678	4.44E-02	1.73E+03	6.86E+00	1.01972	0.00121	1.0000	0.0068	0.01972	1.01972
4	pcm001-003	2.919	6.00E-05	131.946	4.09E-02	3.25E+01	9.60E-02	1.01671	0.00103	0.9990	0.0067	0.01771	1.01771
5	pcm001-004	2.921	6.58E-05	128.822	4.70E-02	3.94E+01	1.33E-01	0.98709	0.00104	1.0000	0.0066	-0.01291	0.98709
6	pcm001-005	2.902	2.38E-05	174.913	2.92E-02	1.54E+00	3.18E-03	1.00948	0.00112	0.9989	0.0072	0.01058	1.01058
7	pcm002-001	3.026	2.14E-04	80.908	8.70E-02	4.92E+03	3.77E+01	1.03220	0.00101	0.9990	0.0046	0.03320	1.03320
8	pcm002-010	2.909	4.52E-05	160.243	5.01E-02	4.14E+00	1.47E-02	1.03219	0.00104	1.0000	0.0073	0.03219	1.03219
9	pcm002-022	2.912	4.95E-05	153.761	4.87E-02	6.44E+00	2.21E-02	1.01456	0.00104	0.9988	0.0055	0.01576	1.01576
10	pcm002-023	2.900	1.76E-05	185.425	2.88E-02	6.88E-01	1.50E-03	1.00814	0.00086	1.0000	0.0068	0.00814	1.00814
11	pmf001-001	3.137	2.95E-04	21.413	1.25E-02	1.24E+06	1.44E+03	0.99510	0.00108	1.0000	0.0020	-0.00490	0.99510
12	pmf002-001	3.134	2.67E-04	21.206	1.15E-02	1.26E+06	1.38E+03	0.99700	0.00098	1.0000	0.0020	-0.00300	0.99700
13	pmf003-101	3.135	2.95E-04	21.439	1.29E-02	1.24E+06	1.50E+03	0.99322	0.00095	1.0000	0.0030	-0.00678	0.99322
14	pmf003-102	3.125	2.84E-04	27.726	3.95E-02	6.91E+05	2.45E+03	0.99432	0.00124	1.0000	0.0030	-0.00568	0.99432
15	pmf003-103	3.135	2.67E-04	21.423	1.29E-02	1.24E+06	1.46E+03	0.98657	0.00107	1.0000	0.0030	-0.01343	0.98657
16	pmf003-104	3.122	2.89E-04	28.799	4.30E-02	6.26E+05	2.45E+03	0.99444	0.00110	1.0000	0.0030	-0.00556	0.99444
17	pmf003-105	3.135	2.86E-04	21.415	1.26E-02	1.24E+06	1.44E+03	0.99086	0.00122	1.0000	0.0030	-0.00914	0.99086
18	pmf004-207	3.135	2.80E-04	21.839	1.65E-02	1.20E+06	1.78E+03	0.99018	0.00141	1.0000	0.0030	-0.00982	0.99018
19	pmf004-208	3.136	2.76E-04	22.278	1.82E-02	1.15E+06	1.89E+03	0.98977	0.00113	1.0000	0.0030	-0.01023	0.98977
20	pmf004-209	3.135	2.91E-04	22.309	1.87E-02	1.15E+06	1.95E+03	0.98889	0.00099	1.0000	0.0030	-0.01111	0.98889
21	pmf004-210	3.135	2.73E-04	22.339	1.87E-02	1.15E+06	1.92E+03	0.98626	0.00160	1.0000	0.0030	-0.01374	0.98626
22	pmf004-211	3.135	2.81E-04	22.316	1.91E-02	1.15E+06	1.99E+03	0.98937	0.00118	1.0000	0.0030	-0.01063	0.98937
23	pmf004-212	3.136	2.92E-04	22.247	1.98E-02	1.16E+06	2.05E+03	0.98956	0.00119	1.0000	0.0030	-0.01044	0.98956
24	pmf004-213	3.136	2.68E-04	21.592	1.53E-02	1.22E+06	1.72E+03	0.98881	0.00122	1.0000	0.0030	-0.01119	0.98881
25	pmf004-214	3.137	2.84E-04	21.705	1.51E-02	1.21E+06	1.67E+03	0.99135	0.00106	1.0000	0.0030	-0.00865	0.99135
26	pmf004-215	3.137	2.65E-04	21.457	1.35E-02	1.24E+06	1.53E+03	0.99093	0.00111	1.0000	0.0030	-0.00907	0.99093
27	pmf005-001	3.103	2.61E-04	23.943	1.36E-02	9.83E+05	1.26E+03	1.00420	0.00107	1.0000	0.0013	0.00420	1.00420
28	pmf006-001	2.972	5.33E-04	22.632	1.62E-02	1.10E+06	1.64E+03	0.99897	0.00132	1.0000	0.0030	-0.00103	0.99897
29	pmf008-001	3.065	8.67E-04	23.362	1.39E-02	1.04E+06	1.37E+03	1.00124	0.00096	1.0000	0.0006	0.00124	1.00124
30	pmf009-001	3.122	2.80E-04	22.352	1.32E-02	1.14E+06	1.38E+03	0.99468	0.00129	1.0000	0.0027	-0.00532	0.99468
31	pmf010-001	3.065	3.03E-04	21.962	1.29E-02	1.19E+06	1.42E+03	0.99537	0.00088	1.0000	0.0018	-0.00463	0.99537
32	pmf011-001	3.086	2.68E-04	50.699	7.13E-02	8.37E+04	5.28E+02	0.99723	0.00110	1.0000	0.0010	-0.00277	0.99723
33	pmf012-001	2.971	5.93E-04	23.612	1.94E-02	9.82E+05	1.73E+03	1.00237	0.00124	1.0009	0.0021	0.00147	1.00147

N	Case	nubar	Sigma	AFG	Sigma	EALCF (eV)	Sigma	k_{calc} Pu	sigma	k_{exp} Pu	Sigma	Bias = Calculated - Benchmark	Adjusted k_{eff} Pu
34	pmf013-001	3.079	2.40E-04	26.160	1.42E-02	7.74E+05	1.15E+03	1.00284	0.00098	1.0034	0.0023	-0.00056	0.99944
35	pmf014-001	3.081	2.21E-04	26.027	1.54E-02	7.80E+05	1.24E+03	1.01634	0.00094	1.0037	0.0031	0.01264	1.01264
36	pmf015-001	3.094	2.31E-04	24.641	1.47E-02	9.07E+05	1.34E+03	1.01844	0.00098	1.0041	0.0026	0.01434	1.01434
37	pmf016-001	3.055	2.60E-04	72.975	8.60E-02	1.17E+04	8.77E+01	1.01148	0.00104	0.9974	0.0042	0.01408	1.01408
38	pmf016-002	3.051	2.42E-04	76.747	8.41E-02	8.52E+03	6.30E+01	1.00032	0.00110	1.0000	0.0038	0.00032	1.00032
39	pmf016-003	3.051	2.46E-04	77.013	8.02E-02	8.33E+03	5.80E+01	0.99736	0.00108	1.0000	0.0033	-0.00264	0.99736
40	pmf016-004	3.051	2.29E-04	77.468	8.58E-02	8.04E+03	6.01E+01	0.99808	0.00111	1.0000	0.0030	-0.00192	0.99808
41	pmf016-005	3.051	2.33E-04	77.617	8.13E-02	7.94E+03	5.55E+01	0.99772	0.00093	1.0000	0.0034	-0.00228	0.99772
42	pmf016-006	3.050	2.41E-04	77.813	8.09E-02	7.79E+03	5.52E+01	1.00065	0.00095	1.0000	0.0032	0.00065	1.00065
43	pmf017-201	3.117	2.77E-04	25.534	2.59E-02	7.82E+05	2.09E+03	0.98835	0.00109	1.0000	0.0030	-0.01165	0.98835
44	pmf017-202	3.103	2.58E-04	32.074	4.31E-02	4.07E+05	1.68E+03	0.99223	0.00107	1.0000	0.0030	-0.00777	0.99223
45	pmf017-203	3.093	2.59E-04	38.372	5.06E-02	2.30E+05	1.09E+03	0.99396	0.00104	1.0000	0.0030	-0.00604	0.99396
46	pmf017-204	3.102	2.79E-04	30.328	3.68E-02	4.62E+05	1.73E+03	0.99261	0.00119	1.0000	0.0030	-0.00739	0.99261
47	pmf017-205	3.075	2.66E-04	47.631	6.52E-02	9.37E+04	5.62E+02	1.00158	0.00096	1.0000	0.0030	0.00158	1.00158
48	pmf018-001	3.103	2.65E-04	24.418	1.58E-02	8.99E+05	1.50E+03	0.99885	0.00091	1.0000	0.0030	-0.00115	0.99885
49	pmf022	3.135	2.82E-04	21.582	1.31E-02	1.23E+06	1.51E+03	0.99407	0.00113	1.0000	0.0021	-0.00593	0.99407
50	pmf023	3.123	2.71E-04	22.341	1.33E-02	1.14E+06	1.42E+03	0.99474	0.00097	1.0000	0.0020	-0.00526	0.99474
51	pmf024	3.115	2.66E-04	27.670	3.57E-02	6.33E+05	2.16E+03	0.99710	0.00094	1.0000	0.0020	-0.00290	0.99710
52	pmf025	3.127	2.66E-04	22.019	1.25E-02	1.18E+06	1.36E+03	0.99760	0.00111	1.0000	0.0020	-0.00240	0.99760
53	pmf026	3.109	2.49E-04	23.302	1.35E-02	1.04E+06	1.31E+03	1.01290	0.00111	1.0000	0.0024	0.01290	1.01290
54	pmf027	3.079	2.47E-04	51.978	6.87E-02	7.10E+04	4.36E+02	1.00026	0.00103	1.0000	0.0022	0.00026	1.00026
55	pmf028	3.105	2.58E-04	23.497	1.30E-02	1.02E+06	1.29E+03	1.01618	0.00097	1.0000	0.0022	0.01618	1.01618
56	pmf029	3.136	2.77E-04	21.357	1.30E-02	1.25E+06	1.53E+03	0.98967	0.00097	1.0000	0.0020	-0.01033	0.98967
57	pmf030	3.123	2.82E-04	22.252	1.40E-02	1.14E+06	1.53E+03	0.99941	0.00105	1.0000	0.0021	-0.00059	0.99941
58	pmf031	3.096	2.65E-04	40.949	6.04E-02	1.89E+05	1.04E+03	1.00056	0.00099	1.0000	0.0021	0.00056	1.00056
59	pmf032	3.121	2.59E-04	22.219	1.34E-02	1.15E+06	1.45E+03	1.00006	0.00100	1.0000	0.0020	0.00006	1.00006
60	pmf033-021a	3.006	1.30E-04	31.859	1.93E-02	4.00E+05	8.75E+02	1.00699	0.00091	0.9967	0.0026	0.01029	1.01029
61	pmf035	3.126	2.63E-04	21.993	1.35E-02	1.18E+06	1.47E+03	1.00499	0.00103	1.0000	0.0016	0.00499	1.00499
62	pmf036	3.111	2.72E-04	27.421	2.98E-02	6.16E+05	1.95E+03	1.00149	0.00095	1.0000	0.0031	0.00149	1.00149
63	pmf037-001	3.087	2.63E-04	44.029	6.15E-02	1.46E+05	8.13E+02	0.99691	0.00133	1.0000	0.0044	-0.00309	0.99691
64	pmf037-005	3.072	2.60E-04	55.583	7.26E-02	5.16E+04	3.33E+02	0.99759	0.00097	1.0000	0.0037	-0.00241	0.99759
65	pmf037-007	3.066	2.58E-04	60.505	7.65E-02	3.33E+04	2.26E+02	0.99905	0.00100	1.0000	0.0038	-0.00095	0.99905
66	pmf037-010	3.063	2.56E-04	63.584	8.09E-02	2.60E+04	1.87E+02	0.99815	0.00094	1.0000	0.0034	-0.00185	0.99815
67	pmf037-012	3.062	2.44E-04	64.814	7.68E-02	2.34E+04	1.58E+02	0.99740	0.00095	1.0000	0.0040	-0.00260	0.99740
68	pmf037-015	3.059	2.54E-04	67.714	8.11E-02	1.83E+04	1.31E+02	0.99809	0.00108	1.0000	0.0033	-0.00191	0.99809
69	pmf037-016	3.065	2.49E-04	62.935	7.64E-02	2.82E+04	1.90E+02	0.99920	0.00100	1.0000	0.0039	-0.00080	0.99920
70	pmf039	3.125	2.66E-04	22.178	1.32E-02	1.16E+06	1.39E+03	0.98241	0.00096	1.0000	0.0022	-0.01759	0.98241

N	Case	nubar	Sigma	AFG	Sigma	EALCF (eV)	Sigma	k_{calc} Pu	sigma	k_{exp} Pu	Sigma	Bias = Calculated - Benchmark	Adjusted k_{eff} Pu
71	pmf040	3.122	2.58E-04	22.355	1.32E-02	1.14E+06	1.37E+03	0.98950	0.00120	1.0000	0.0038	-0.01050	0.98950
72	pmf041	2.990	5.84E-04	22.137	1.69E-02	1.14E+06	1.79E+03	1.00454	0.00108	1.0000	0.0016	0.00454	1.00454
73	pst001-001_t9	2.891	4.97E-06	212.491	7.51E-03	8.79E-02	7.99E-05	1.00793	0.00120	1.0000	0.0050	0.00793	1.00793
74	pst001-002_t9	2.891	6.30E-06	209.977	9.78E-03	1.11E-01	1.23E-04	1.00893	0.00119	1.0000	0.0050	0.00893	1.00893
75	pst001-003_t9	2.891	6.94E-06	207.751	1.09E-02	1.35E-01	1.62E-04	1.00981	0.00105	1.0000	0.0050	0.00981	1.00981
76	pst001-004_t9	2.891	7.62E-06	206.446	1.21E-02	1.51E-01	1.90E-04	1.00560	0.00100	1.0000	0.0050	0.00560	1.00560
77	pst001-005_t9	2.891	7.68E-06	205.778	1.27E-02	1.59E-01	2.03E-04	1.00841	0.00101	1.0000	0.0050	0.00841	1.00841
78	pst001-006_t9	2.893	1.27E-05	195.776	1.99E-02	3.47E-01	5.97E-04	1.00836	0.00102	1.0000	0.0050	0.00836	1.00836
79	pst002-001	2.891	4.49E-06	214.682	6.13E-03	7.13E-02	5.98E-05	1.00694	0.00108	1.0000	0.0047	0.00694	1.00694
80	pst002-002	2.891	4.16E-06	214.467	6.10E-03	7.29E-02	5.93E-05	1.00964	0.00096	1.0000	0.0047	0.00964	1.00964
81	pst002-003	2.891	4.41E-06	213.806	6.30E-03	7.78E-02	6.33E-05	1.00568	0.00114	1.0000	0.0047	0.00568	1.00568
82	pst002-004	2.891	4.87E-06	213.353	6.89E-03	8.14E-02	7.05E-05	1.00771	0.00122	1.0000	0.0047	0.00771	1.00771
83	pst002-005	2.891	4.93E-06	212.901	7.37E-03	8.50E-02	7.59E-05	1.01274	0.00121	1.0000	0.0047	0.01274	1.01274
84	pst002-006	2.891	5.22E-06	211.977	8.02E-03	9.28E-02	9.18E-05	1.00538	0.00107	1.0000	0.0047	0.00538	1.00538
85	pst002-007	2.891	5.32E-06	211.138	8.76E-03	1.00E-01	1.06E-04	1.01021	0.00125	1.0000	0.0047	0.01021	1.01021
86	pst003-001	2.891	3.46E-06	216.630	4.55E-03	5.84E-02	3.75E-05	1.00851	0.00098	1.0000	0.0047	0.00851	1.00851
87	pst003-002	2.891	3.33E-06	216.441	4.37E-03	5.96E-02	3.62E-05	1.00685	0.00122	1.0000	0.0047	0.00685	1.00685
88	pst003-003	2.891	3.65E-06	216.071	4.88E-03	6.19E-02	4.27E-05	1.00923	0.00110	1.0000	0.0047	0.00923	1.00923
89	pst003-004	2.891	3.69E-06	215.941	4.81E-03	6.27E-02	4.33E-05	1.00862	0.00096	1.0000	0.0047	0.00862	1.00862
90	pst003-005	2.891	3.96E-06	215.527	5.09E-03	6.55E-02	4.57E-05	1.00857	0.00127	1.0000	0.0047	0.00857	1.00857
91	pst003-006	2.891	3.92E-06	214.961	5.78E-03	6.94E-02	5.32E-05	1.01133	0.00150	1.0000	0.0047	0.01133	1.01133
92	pst003-007	2.891	3.59E-06	216.480	4.78E-03	5.91E-02	4.06E-05	1.01029	0.00112	1.0000	0.0047	0.01029	1.01029
93	pst003-008	2.891	3.56E-06	216.326	4.80E-03	6.01E-02	4.02E-05	1.01185	0.00114	1.0000	0.0047	0.01185	1.01185
94	pst004-001	2.891	2.89E-06	217.461	3.79E-03	5.34E-02	2.95E-05	1.00871	0.00091	1.0000	0.0047	0.00871	1.00871
95	pst004-002	2.891	2.84E-06	217.412	3.90E-03	5.37E-02	3.07E-05	1.00312	0.00098	1.0000	0.0047	0.00312	1.00312
96	pst004-003	2.891	3.18E-06	217.241	4.26E-03	5.47E-02	3.46E-05	1.00699	0.00109	1.0000	0.0047	0.00699	1.00699
97	pst004-004	2.891	3.18E-06	217.023	4.25E-03	5.60E-02	3.58E-05	1.00277	0.00093	1.0000	0.0047	0.00277	1.00277
98	pst004-005	2.891	3.11E-06	217.255	4.08E-03	5.46E-02	3.26E-05	1.00314	0.00097	1.0000	0.0047	0.00314	1.00314
99	pst004-006	2.891	2.96E-06	217.190	4.00E-03	5.49E-02	3.07E-05	1.00573	0.00090	1.0000	0.0047	0.00573	1.00573
100	pst004-007	2.891	3.19E-06	217.041	4.22E-03	5.58E-02	3.41E-05	1.01029	0.00113	1.0000	0.0047	0.01029	1.01029
101	pst004-008	2.891	3.22E-06	216.928	4.20E-03	5.65E-02	3.51E-05	1.00701	0.00124	1.0000	0.0047	0.00701	1.00701
102	pst004-009	2.891	3.31E-06	216.586	4.68E-03	5.86E-02	3.86E-05	1.00438	0.00096	1.0000	0.0047	0.00438	1.00438
103	pst004-010	2.891	3.71E-06	215.874	5.24E-03	6.33E-02	4.62E-05	1.00598	0.00126	1.0000	0.0047	0.00598	1.00598
104	pst004-011	2.891	3.99E-06	215.108	5.80E-03	6.85E-02	5.26E-05	1.00569	0.00095	1.0000	0.0047	0.00569	1.00569
105	pst004-012	2.891	3.16E-06	217.036	4.05E-03	5.58E-02	3.37E-05	1.00667	0.00103	1.0000	0.0047	0.00667	1.00667
106	pst004-013	2.891	3.14E-06	217.080	4.09E-03	5.56E-02	3.34E-05	1.00553	0.00117	1.0000	0.0047	0.00553	1.00553
107	pst005-001	2.891	3.19E-06	217.077	4.39E-03	5.56E-02	3.50E-05	1.00671	0.00110	1.0000	0.0047	0.00671	1.00671

N	Case	nubar	Sigma	AFG	Sigma	EALCF (eV)	Sigma	k_{calc} Pu	sigma	k_{exp} Pu	Sigma	Bias = Calculated - Benchmark	Adjusted k_{eff} Pu
108	pst005-002	2.891	3.13E-06	216.915	4.30E-03	5.65E-02	3.43E-05	1.01044	0.00098	1.0000	0.0047	0.01044	1.01044
109	pst005-003	2.891	3.23E-06	216.742	4.39E-03	5.76E-02	3.69E-05	1.00728	0.00105	1.0000	0.0047	0.00728	1.00728
110	pst005-004	2.891	3.43E-06	216.354	4.57E-03	6.01E-02	3.91E-05	1.00919	0.00092	1.0000	0.0047	0.00919	1.00919
111	pst005-005	2.891	3.58E-06	215.907	4.92E-03	6.30E-02	4.36E-05	1.00981	0.00108	1.0000	0.0047	0.00981	1.00981
112	pst005-006	2.891	4.03E-06	215.439	5.57E-03	6.62E-02	5.09E-05	1.01040	0.00092	1.0000	0.0047	0.01040	1.01040
113	pst005-007	2.891	3.85E-06	214.992	5.83E-03	6.92E-02	5.34E-05	1.00868	0.00155	1.0000	0.0047	0.00868	1.00868
114	pst005-008	2.891	3.15E-06	216.900	4.34E-03	5.66E-02	3.47E-05	1.00355	0.00102	1.0000	0.0047	0.00355	1.00355
115	pst005-009	2.891	3.27E-06	216.684	4.16E-03	5.80E-02	3.51E-05	1.00718	0.00113	1.0000	0.0047	0.00718	1.00718
116	pst006-001	2.891	2.89E-06	217.614	3.84E-03	5.25E-02	3.02E-05	1.00591	0.00098	1.0000	0.0035	0.00591	1.00591
117	pst006-002	2.891	2.84E-06	217.459	3.79E-03	5.34E-02	3.01E-05	1.00560	0.00091	1.0000	0.0035	0.00560	1.00560
118	pst006-003	2.891	3.08E-06	217.149	3.85E-03	5.52E-02	3.19E-05	1.00672	0.00099	1.0000	0.0035	0.00672	1.00672
119	pst007-002	2.892	1.10E-05	198.890	1.77E-02	2.75E-01	4.38E-04	1.00943	0.00106	1.0000	0.0047	0.00943	1.00943
120	pst007-003	2.892	1.05E-05	199.573	1.80E-02	2.61E-01	4.18E-04	1.00292	0.00117	1.0000	0.0047	0.00292	1.00292
121	pst007-005	2.891	6.17E-06	209.855	9.81E-03	1.12E-01	1.24E-04	1.01106	0.00100	1.0000	0.0047	0.01106	1.01106
122	pst007-006	2.891	5.98E-06	209.689	9.37E-03	1.14E-01	1.18E-04	1.00458	0.00108	1.0000	0.0047	0.00458	1.00458
123	pst007-007	2.891	6.40E-06	209.823	9.66E-03	1.12E-01	1.24E-04	1.00826	0.00128	1.0000	0.0047	0.00826	1.00826
124	pst007-008	2.891	6.06E-06	209.575	9.63E-03	1.15E-01	1.24E-04	1.00282	0.00102	1.0000	0.0047	0.00282	1.00282
125	pst007-009	2.891	5.93E-06	209.610	9.96E-03	1.14E-01	1.27E-04	0.99788	0.00117	1.0000	0.0047	-0.00212	0.99788
126	pst007-010	2.891	5.97E-06	210.444	9.16E-03	1.06E-01	1.13E-04	1.00130	0.00099	1.0000	0.0047	0.00130	1.00130
127	pst009-001	2.892	1.72E-06	219.725	2.06E-03	4.12E-02	1.42E-05	1.01943	0.00075	1.0000	0.0047	0.01943	1.01943
128	pst009-002	2.892	1.70E-06	219.816	1.90E-03	4.07E-02	1.32E-05	1.02537	0.00065	1.0000	0.0047	0.02537	1.02537
129	pst009-003	2.892	1.70E-06	219.830	1.94E-03	4.07E-02	1.35E-05	1.02380	0.00083	1.0000	0.0047	0.02380	1.02380
130	pst010-001-011	2.891	4.44E-06	214.122	6.67E-03	7.55E-02	6.54E-05	1.01516	0.00133	1.0000	0.0048	0.01516	1.01516
131	pst010-001-012	2.891	4.35E-06	214.896	5.90E-03	6.98E-02	5.51E-05	1.01361	0.00102	1.0000	0.0048	0.01361	1.01361
132	pst010-001-009	2.891	5.79E-06	210.076	9.40E-03	1.10E-01	1.18E-04	1.01844	0.00104	1.0000	0.0048	0.01844	1.01844
133	pst010-002-011	2.891	3.99E-06	214.888	5.85E-03	7.00E-02	5.37E-05	1.01475	0.00100	1.0000	0.0048	0.01475	1.01475
134	pst010-002-012	2.891	3.69E-06	215.529	5.17E-03	6.55E-02	4.64E-05	1.01591	0.00107	1.0000	0.0048	0.01591	1.01591
135	pst010-002-009	2.891	5.40E-06	212.366	7.43E-03	8.94E-02	8.13E-05	1.01581	0.00121	1.0000	0.0048	0.01581	1.01581
136	pst010-003-011	2.891	4.10E-06	215.025	5.95E-03	6.90E-02	5.42E-05	1.01110	0.00109	1.0000	0.0048	0.01110	1.01110
137	pst010-003-012	2.891	3.40E-06	216.249	4.84E-03	6.07E-02	4.13E-05	1.01886	0.00113	1.0000	0.0048	0.01886	1.01886
138	pst010-003-009	2.891	4.46E-06	214.294	5.99E-03	7.41E-02	5.97E-05	1.01186	0.00117	1.0000	0.0048	0.01186	1.01186
139	pst010-004-011	2.891	3.71E-06	215.369	5.21E-03	6.66E-02	4.72E-05	1.00660	0.00105	1.0000	0.0048	0.00660	1.00660
140	pst010-004-012	2.891	3.24E-06	216.857	4.46E-03	5.69E-02	3.70E-05	1.01335	0.00098	1.0000	0.0048	0.01335	1.01335
141	pst010-005-011	2.891	3.74E-06	215.741	5.22E-03	6.42E-02	4.47E-05	1.00633	0.00106	1.0000	0.0048	0.00633	1.00633
142	pst010-006-011	2.891	4.61E-06	213.339	7.05E-03	8.14E-02	7.19E-05	1.01713	0.00121	1.0000	0.0048	0.01713	1.01713
143	pst010-007-011	2.891	4.22E-06	214.790	6.33E-03	7.06E-02	5.77E-05	1.00714	0.00112	1.0000	0.0048	0.00714	1.00714
144	pst011-001-016	2.891	3.59E-06	215.829	4.90E-03	6.34E-02	4.38E-05	1.01539	0.00116	1.0000	0.0052	0.01539	1.01539

N	Case	nubar	Sigma	AFG	Sigma	EALCF (eV)	Sigma	k_{calc} Pu	sigma	k_{exp} Pu	Sigma	Bias = Calculated - Benchmark	Adjusted k_{eff} Pu
145	pst011-001-018	2.891	2.61E-06	217.689	3.49E-03	5.19E-02	2.72E-05	0.99954	0.00105	1.0000	0.0052	-0.00046	0.99954
146	pst011-002-016	2.891	3.58E-06	215.640	5.12E-03	6.47E-02	4.52E-05	1.01888	0.00117	1.0000	0.0052	0.01888	1.01888
147	pst011-002-018	2.891	2.88E-06	217.516	3.80E-03	5.30E-02	2.98E-05	1.00424	0.00103	1.0000	0.0052	0.00424	1.00424
148	pst011-003-016	2.891	3.63E-06	215.296	5.11E-03	6.71E-02	4.52E-05	1.02408	0.00108	1.0000	0.0052	0.02408	1.02408
149	pst011-003-018	2.891	2.67E-06	217.527	3.53E-03	5.29E-02	2.74E-05	1.00171	0.00105	1.0000	0.0052	0.00171	1.00171
150	pst011-004-016	2.891	3.62E-06	215.198	5.06E-03	6.77E-02	4.59E-05	1.01354	0.00163	1.0000	0.0052	0.01354	1.01354
151	pst011-004-018	2.891	2.81E-06	217.318	3.81E-03	5.41E-02	2.99E-05	0.99880	0.00123	1.0000	0.0052	-0.00120	0.99880
152	pst011-005-016	2.891	4.17E-06	214.158	5.96E-03	7.54E-02	5.87E-05	1.00961	0.00116	1.0000	0.0052	0.00961	1.00961
153	pst011-005-018	2.891	3.03E-06	217.076	3.98E-03	5.56E-02	3.26E-05	1.01032	0.00115	1.0000	0.0052	0.01032	1.01032
154	pst011-006-018	2.891	3.17E-06	216.477	4.30E-03	5.93E-02	3.58E-05	1.00387	0.00101	1.0000	0.0052	0.00387	1.00387
155	pst011-007-018	2.891	2.80E-06	217.344	3.63E-03	5.40E-02	2.94E-05	1.00632	0.00104	1.0000	0.0052	0.00632	1.00632
156	pst014-001	2.891	7.46E-06	205.453	1.12E-02	1.68E-01	2.01E-04	1.00555	0.00103	0.9980	0.0032	0.00755	1.00755
157	pst014-002	2.891	7.16E-06	205.465	1.08E-02	1.68E-01	1.89E-04	1.00671	0.00119	0.9980	0.0032	0.00871	1.00871
158	pst014-003	2.891	6.94E-06	205.498	1.19E-02	1.67E-01	2.08E-04	1.00697	0.00130	0.9980	0.0032	0.00897	1.00897
159	pst014-004	2.891	7.24E-06	205.498	1.19E-02	1.67E-01	2.06E-04	1.00533	0.00141	0.9980	0.0032	0.00733	1.00733
160	pst014-005	2.891	7.12E-06	205.524	1.17E-02	1.67E-01	2.00E-04	1.00767	0.00128	0.9980	0.0032	0.00967	1.00967
161	pst014-006	2.891	7.03E-06	205.515	1.19E-02	1.67E-01	1.99E-04	1.00576	0.00107	0.9980	0.0032	0.00776	1.00776
162	pst014-007	2.891	7.08E-06	205.450	1.13E-02	1.68E-01	1.99E-04	1.00747	0.00113	0.9980	0.0032	0.00947	1.00947
163	pst014-008	2.891	7.62E-06	205.457	1.15E-02	1.68E-01	2.00E-04	1.00319	0.00135	0.9980	0.0032	0.00519	1.00519
164	pst014-009	2.891	7.07E-06	205.499	1.15E-02	1.67E-01	1.97E-04	1.00731	0.00117	0.9980	0.0032	0.00931	1.00931
165	pst014-010	2.891	7.08E-06	205.494	1.20E-02	1.67E-01	2.10E-04	1.00473	0.00118	0.9980	0.0032	0.00673	1.00673
166	pst014-011	2.891	7.27E-06	205.494	1.18E-02	1.67E-01	2.05E-04	1.00400	0.00113	0.9980	0.0032	0.00600	1.00600
167	pst014-012	2.891	7.36E-06	205.521	1.14E-02	1.67E-01	1.92E-04	1.00662	0.00159	0.9980	0.0032	0.00862	1.00862
168	pst014-013	2.891	7.52E-06	205.433	1.17E-02	1.68E-01	2.11E-04	1.00826	0.00111	0.9980	0.0043	0.01026	1.01026
169	pst014-014	2.891	7.38E-06	205.458	1.09E-02	1.68E-01	1.97E-04	1.00480	0.00108	0.9980	0.0043	0.00680	1.00680
170	pst014-015	2.891	7.19E-06	205.508	1.24E-02	1.67E-01	2.12E-04	1.00755	0.00120	0.9980	0.0043	0.00955	1.00955
171	pst014-016	2.891	7.33E-06	205.513	1.18E-02	1.67E-01	2.06E-04	1.00538	0.00116	0.9980	0.0043	0.00738	1.00738
172	pst014-017	2.891	6.71E-06	205.532	1.12E-02	1.67E-01	1.92E-04	1.00600	0.00107	0.9980	0.0043	0.00800	1.00800
173	pst014-018	2.891	7.01E-06	205.429	1.11E-02	1.68E-01	2.02E-04	1.00955	0.00126	0.9980	0.0043	0.01155	1.01155
174	pst014-019	2.891	7.47E-06	205.462	1.16E-02	1.68E-01	2.04E-04	1.00554	0.00105	0.9980	0.0043	0.00754	1.00754
175	pst014-020	2.891	7.22E-06	205.513	1.03E-02	1.67E-01	1.83E-04	1.00519	0.00153	0.9980	0.0043	0.00719	1.00719
176	pst014-021	2.891	6.99E-06	205.538	1.23E-02	1.67E-01	2.07E-04	1.00897	0.00120	0.9980	0.0043	0.01097	1.01097
177	pst014-022	2.891	7.30E-06	205.532	1.16E-02	1.67E-01	1.99E-04	1.00490	0.00112	0.9980	0.0043	0.00690	1.00690
178	pst014-023	2.891	7.28E-06	205.525	1.18E-02	1.67E-01	2.08E-04	1.00319	0.00122	0.9980	0.0043	0.00519	1.00519
179	pst014-024	2.891	7.27E-06	205.394	1.15E-02	1.69E-01	2.03E-04	1.00653	0.00115	0.9980	0.0043	0.00853	1.00853
180	pst014-025	2.891	7.61E-06	205.425	1.19E-02	1.68E-01	2.10E-04	1.00448	0.00146	0.9980	0.0043	0.00648	1.00648
181	pst014-026	2.891	7.77E-06	205.500	1.13E-02	1.67E-01	1.94E-04	1.00585	0.00125	0.9980	0.0043	0.00785	1.00785

N	Case	nubar	Sigma	AFG	Sigma	EALCF (eV)	Sigma	k_{calc} Pu	sigma	k_{exp} Pu	Sigma	Bias = Calculated - Benchmark	Adjusted k_{eff} Pu
182	pst014-027	2.891	7.21E-06	205.507	1.08E-02	1.67E-01	1.92E-04	1.00418	0.00126	0.9980	0.0043	0.00618	1.00618
183	pst014-028	2.891	7.18E-06	205.508	1.10E-02	1.67E-01	1.96E-04	1.00498	0.00127	0.9980	0.0043	0.00698	1.00698
184	pst014-029	2.891	7.43E-06	205.530	1.17E-02	1.67E-01	2.00E-04	1.00441	0.00106	0.9980	0.0043	0.00641	1.00641
185	pst014-030	2.891	7.21E-06	205.425	1.14E-02	1.68E-01	2.00E-04	1.00594	0.00128	0.9980	0.0043	0.00794	1.00794
186	pst014-031	2.891	7.33E-06	205.426	1.17E-02	1.68E-01	2.01E-04	1.00397	0.00120	0.9980	0.0043	0.00597	1.00597
187	pst014-032	2.891	7.25E-06	205.445	1.13E-02	1.68E-01	1.95E-04	1.00569	0.00124	0.9980	0.0043	0.00769	1.00769
188	pst014-033	2.891	7.12E-06	205.477	1.13E-02	1.67E-01	2.08E-04	1.00469	0.00110	0.9980	0.0043	0.00669	1.00669
189	pst014-034	2.891	7.86E-06	205.486	1.15E-02	1.67E-01	2.05E-04	1.00529	0.00137	0.9980	0.0043	0.00729	1.00729
190	pst015-001	2.891	8.52E-06	201.260	1.45E-02	2.37E-01	3.34E-04	1.00690	0.00112	0.9980	0.0038	0.00890	1.00890
191	pst015-002	2.891	8.95E-06	201.276	1.39E-02	2.37E-01	3.27E-04	1.00747	0.00112	0.9980	0.0038	0.00947	1.00947
192	pst015-003	2.891	9.12E-06	201.295	1.33E-02	2.37E-01	3.06E-04	1.00638	0.00123	0.9980	0.0038	0.00838	1.00838
193	pst015-004	2.891	8.86E-06	201.330	1.36E-02	2.36E-01	3.12E-04	1.00743	0.00118	0.9980	0.0038	0.00943	1.00943
194	pst015-005	2.891	8.87E-06	201.333	1.48E-02	2.36E-01	3.29E-04	1.00662	0.00134	0.9980	0.0038	0.00862	1.00862
195	pst015-006	2.891	9.15E-06	201.294	1.45E-02	2.37E-01	3.25E-04	1.00621	0.00130	0.9980	0.0038	0.00821	1.00821
196	pst015-007	2.891	9.02E-06	201.227	1.52E-02	2.38E-01	3.42E-04	1.00869	0.00134	0.9971	0.0047	0.01159	1.01159
197	pst015-008	2.891	9.26E-06	201.229	1.45E-02	2.38E-01	3.27E-04	1.00621	0.00118	0.9971	0.0047	0.00911	1.00911
198	pst015-009	2.891	9.07E-06	201.309	1.39E-02	2.36E-01	3.20E-04	1.00753	0.00125	0.9971	0.0047	0.01043	1.01043
199	pst015-010	2.891	8.93E-06	201.326	1.43E-02	2.36E-01	3.22E-04	1.00688	0.00135	0.9971	0.0047	0.00978	1.00978
200	pst015-011	2.891	8.92E-06	201.217	1.38E-02	2.38E-01	3.26E-04	1.00284	0.00111	0.9971	0.0047	0.00574	1.00574
201	pst015-012	2.891	8.79E-06	201.260	1.44E-02	2.37E-01	3.24E-04	1.00473	0.00140	0.9971	0.0047	0.00763	1.00763
202	pst015-013	2.891	8.76E-06	201.307	1.33E-02	2.36E-01	3.05E-04	1.00626	0.00120	0.9971	0.0047	0.00916	1.00916
203	pst015-014	2.891	8.80E-06	201.325	1.41E-02	2.36E-01	3.09E-04	1.00793	0.00122	0.9971	0.0047	0.01083	1.01083
204	pst015-015	2.891	9.15E-06	201.201	1.46E-02	2.39E-01	3.40E-04	1.00771	0.00102	0.9971	0.0047	0.01061	1.01061
205	pst015-016	2.891	9.01E-06	201.257	1.41E-02	2.37E-01	3.27E-04	1.00663	0.00110	0.9971	0.0047	0.00953	1.00953
206	pst015-017	2.891	8.63E-06	201.270	1.41E-02	2.37E-01	3.15E-04	1.00595	0.00126	0.9971	0.0047	0.00885	1.00885
207	pst016-001	2.891	9.02E-06	201.254	1.47E-02	2.38E-01	3.24E-04	1.00754	0.00134	0.9980	0.0043	0.00954	1.00954
208	pst016-002	2.891	8.66E-06	201.285	1.42E-02	2.37E-01	3.25E-04	1.00550	0.00125	0.9980	0.0043	0.00750	1.00750
209	pst016-003	2.891	9.05E-06	201.282	1.44E-02	2.37E-01	3.28E-04	1.00681	0.00115	0.9980	0.0043	0.00881	1.00881
210	pst016-004	2.891	9.20E-06	201.297	1.43E-02	2.36E-01	3.23E-04	1.00528	0.00124	0.9980	0.0043	0.00728	1.00728
211	pst016-005	2.891	7.51E-06	205.436	1.20E-02	1.68E-01	2.07E-04	1.00549	0.00120	0.9969	0.0038	0.00859	1.00859
212	pst016-006	2.891	7.28E-06	205.481	1.15E-02	1.67E-01	1.94E-04	1.00639	0.00143	0.9969	0.0038	0.00949	1.00949
213	pst016-007	2.891	7.15E-06	205.512	1.14E-02	1.67E-01	2.00E-04	1.00770	0.00127	0.9969	0.0038	0.01080	1.01080
214	pst016-008	2.891	7.64E-06	205.504	1.14E-02	1.67E-01	1.93E-04	1.00614	0.00128	0.9969	0.0038	0.00924	1.00924
215	pst016-009	2.891	7.03E-06	205.591	1.13E-02	1.66E-01	1.90E-04	1.00643	0.00116	0.9963	0.0033	0.01013	1.01013
216	pst016-010	2.891	7.34E-06	205.553	1.18E-02	1.66E-01	1.96E-04	1.00595	0.00118	0.9963	0.0033	0.00965	1.00965
217	pst016-011	2.891	7.35E-06	205.535	1.11E-02	1.67E-01	1.97E-04	1.00603	0.00118	0.9963	0.0033	0.00973	1.00973
218	pst017-001	2.891	7.44E-06	205.500	1.18E-02	1.67E-01	2.09E-04	1.00593	0.00112	0.9969	0.0038	0.00903	1.00903

N	Case	nubar	Sigma	AFG	Sigma	EALCF (eV)	Sigma	k_{calc} Pu	sigma	k_{exp} Pu	Sigma	Bias = Calculated - Benchmark	Adjusted k_{eff} Pu
219	pst017-002	2.891	7.50E-06	205.520	1.18E-02	1.67E-01	2.02E-04	1.00383	0.00144	0.9969	0.0038	0.00693	1.00693
220	pst017-003	2.891	7.25E-06	205.506	1.13E-02	1.67E-01	1.99E-04	1.00530	0.00132	0.9969	0.0038	0.00840	1.00840
221	pst017-004	2.891	7.14E-06	205.502	1.15E-02	1.67E-01	1.98E-04	1.00455	0.00142	0.9969	0.0038	0.00765	1.00765
222	pst017-005	2.891	7.65E-06	205.499	1.11E-02	1.67E-01	2.01E-04	1.00497	0.00136	0.9969	0.0038	0.00807	1.00807
223	pst017-006	2.891	7.03E-06	205.495	1.20E-02	1.67E-01	2.09E-04	1.00464	0.00109	0.9969	0.0038	0.00774	1.00774
224	pst017-007	2.891	7.27E-06	205.483	1.11E-02	1.67E-01	1.88E-04	1.00678	0.00137	0.9969	0.0038	0.00988	1.00988
225	pst017-008	2.891	7.32E-06	205.504	1.16E-02	1.67E-01	1.98E-04	1.00684	0.00120	0.9969	0.0038	0.00994	1.00994
226	pst017-009	2.891	7.37E-06	205.482	1.18E-02	1.67E-01	2.05E-04	1.00514	0.00133	0.9969	0.0038	0.00824	1.00824
227	pst017-010	2.891	7.43E-06	205.496	1.21E-02	1.67E-01	2.09E-04	1.00753	0.00118	0.9969	0.0038	0.01063	1.01063
228	pst017-011	2.891	7.32E-06	205.518	1.09E-02	1.67E-01	1.92E-04	1.00463	0.00121	0.9969	0.0038	0.00773	1.00773
229	pst017-012	2.891	7.28E-06	205.523	1.18E-02	1.67E-01	2.01E-04	1.00731	0.00118	0.9969	0.0038	0.01041	1.01041
230	pst017-013	2.891	7.61E-06	205.515	1.12E-02	1.67E-01	1.95E-04	1.00561	0.00103	0.9969	0.0038	0.00871	1.00871
231	pst017-014	2.891	7.64E-06	205.470	1.17E-02	1.67E-01	2.03E-04	1.00467	0.00118	0.9969	0.0038	0.00777	1.00777
232	pst017-015	2.891	7.01E-06	205.517	1.16E-02	1.67E-01	2.04E-04	1.00531	0.00181	0.9969	0.0038	0.00841	1.00841
233	pst017-016	2.891	7.45E-06	205.516	1.14E-02	1.67E-01	2.00E-04	1.00844	0.00121	0.9969	0.0038	0.01154	1.01154
234	pst017-017	2.891	7.37E-06	205.531	1.12E-02	1.66E-01	1.97E-04	1.00567	0.00114	0.9969	0.0038	0.00877	1.00877
235	pst017-018	2.891	7.66E-06	205.513	1.19E-02	1.67E-01	2.09E-04	1.00583	0.00129	0.9969	0.0038	0.00893	1.00893
236	pst020-001_t8a	2.891	3.84E-06	215.467	5.44E-03	6.57E-02	4.88E-05	1.00737	0.00110	0.9969	0.0038	0.01047	1.01047
237	pst020-002_t8a	2.891	3.48E-06	215.628	5.05E-03	6.45E-02	4.50E-05	1.01015	0.00100	0.9969	0.0038	0.01325	1.01325
238	pst020-003_t8a	2.891	3.44E-06	216.507	4.84E-03	5.88E-02	4.02E-05	1.00562	0.00101	0.9969	0.0038	0.00872	1.00872
239	pst020-005_t8a	2.891	4.16E-06	213.989	6.12E-03	7.63E-02	6.01E-05	1.00838	0.00101	0.9969	0.0038	0.01148	1.01148
240	pst020-006_t8a	2.891	4.49E-06	213.625	6.74E-03	7.92E-02	6.73E-05	1.00750	0.00107	0.9969	0.0038	0.01060	1.01060
241	pst020-007_t8a	2.891	3.57E-06	216.267	4.86E-03	6.04E-02	4.13E-05	1.00349	0.00104	0.9969	0.0038	0.00659	1.00659
242	pst020-008_t8a	2.891	5.12E-06	210.634	8.31E-03	1.06E-01	1.02E-04	1.00696	0.00127	0.9969	0.0038	0.01006	1.01006
243	pst020-009_t8a	2.891	4.05E-06	214.038	6.30E-03	7.61E-02	6.04E-05	0.99961	0.00117	0.9969	0.0038	0.00271	1.00271
244	pst021-007	2.891	3.98E-06	215.397	5.30E-03	6.60E-02	4.89E-05	1.01141	0.00130	1.0000	0.0032	0.01141	1.01141
245	pst021-008	2.891	1.08E-05	197.721	1.55E-02	3.13E-01	4.41E-04	1.00471	0.00126	1.0000	0.0065	0.00471	1.00471
246	pst021-009	2.891	3.98E-06	215.122	5.53E-03	6.79E-02	5.04E-05	1.01161	0.00106	1.0000	0.0032	0.01161	1.01161
247	pst021-010	2.892	2.88E-06	218.038	3.56E-03	4.98E-02	2.79E-05	1.00915	0.00088	1.0000	0.0025	0.00915	1.00915
248	pst024-001	2.897	1.39E-05	191.675	1.95E-02	4.72E-01	7.38E-04	1.00171	0.00116	1.0000	0.0062	0.00171	1.00171
249	pst024-002	2.897	1.35E-05	191.859	2.00E-02	4.66E-01	7.84E-04	1.00159	0.00117	1.0000	0.0062	0.00159	1.00159
250	pst024-003	2.897	1.41E-05	191.954	2.01E-02	4.62E-01	7.58E-04	1.00140	0.00127	1.0000	0.0062	0.00140	1.00140
251	pst024-004	2.897	1.40E-05	191.982	1.94E-02	4.61E-01	7.34E-04	0.99990	0.00109	1.0000	0.0062	-0.00010	0.99990
252	pst024-005	2.897	1.33E-05	192.050	2.00E-02	4.59E-01	7.38E-04	1.00245	0.00100	1.0000	0.0062	0.00245	1.00245
253	pst024-006	2.903	2.35E-05	173.483	3.07E-02	1.68E+00	3.72E-03	0.99841	0.00110	1.0000	0.0077	-0.00159	0.99841
254	pst024-007	2.895	9.22E-06	201.112	1.39E-02	2.31E-01	2.93E-04	1.00932	0.00120	1.0000	0.0053	0.00932	1.00932
255	pst024-008	2.895	9.71E-06	201.169	1.46E-02	2.30E-01	3.16E-04	1.00673	0.00111	1.0000	0.0053	0.00673	1.00673

N	Case	nubar	Sigma	AFG	Sigma	EALCF (eV)	Sigma	k_{calc} Pu	sigma	k_{exp} Pu	Sigma	Bias = Calculated - Benchmark	Adjusted k_{eff} Pu
256	pst024-009	2.895	9.63E-06	201.243	1.44E-02	2.29E-01	3.04E-04	1.00927	0.00108	1.0000	0.0053	0.00927	1.00927
257	pst024-010	2.895	9.26E-06	201.330	1.41E-02	2.27E-01	3.01E-04	1.00789	0.00112	1.0000	0.0053	0.00789	1.00789
258	pst024-011	2.895	9.26E-06	201.373	1.41E-02	2.26E-01	2.95E-04	1.00712	0.00108	1.0000	0.0053	0.00712	1.00712
259	pst024-012	2.895	9.08E-06	201.430	1.40E-02	2.25E-01	2.97E-04	1.00535	0.00136	1.0000	0.0053	0.00535	1.00535
260	pst024-013	2.895	9.49E-06	201.450	1.41E-02	2.25E-01	3.10E-04	1.00716	0.00129	1.0000	0.0053	0.00716	1.00716
261	pst024-014	2.896	1.15E-05	197.694	1.70E-02	3.01E-01	4.49E-04	1.00210	0.00116	1.0000	0.0053	0.00210	1.00210
262	pst024-015	2.896	1.14E-05	197.743	1.61E-02	3.00E-01	4.29E-04	1.00239	0.00124	1.0000	0.0053	0.00239	1.00239
263	pst024-016	2.896	1.10E-05	197.856	1.61E-02	2.97E-01	4.20E-04	1.00315	0.00099	1.0000	0.0053	0.00315	1.00315
264	pst024-017	2.896	1.11E-05	197.931	1.62E-02	2.96E-01	4.24E-04	1.00006	0.00102	1.0000	0.0053	0.00006	1.00006
265	pst024-018	2.895	5.32E-06	211.996	7.09E-03	9.11E-02	7.87E-05	1.00880	0.00102	1.0000	0.0051	0.00880	1.00880
266	pst024-019	2.895	5.21E-06	212.010	7.39E-03	9.10E-02	8.16E-05	1.00818	0.00115	1.0000	0.0051	0.00818	1.00818
267	pst024-020	2.895	5.19E-06	212.044	7.19E-03	9.06E-02	7.81E-05	1.00798	0.00114	1.0000	0.0051	0.00798	1.00798
268	pst024-021	2.895	5.33E-06	212.078	7.27E-03	9.04E-02	7.80E-05	1.00898	0.00109	1.0000	0.0051	0.00898	1.00898
269	pst024-022	2.895	5.13E-06	212.105	7.22E-03	9.01E-02	7.67E-05	1.00748	0.00098	1.0000	0.0051	0.00748	1.00748
270	pst024-023	2.895	5.36E-06	212.111	7.56E-03	9.01E-02	8.19E-05	1.00679	0.00134	1.0000	0.0051	0.00679	1.00679
	Maximum	3.137	8.67E-04	219.830	8.70E-02	1.26E+06	2.45E+03	1.03220	0.00181	1.00410	0.01100	3.32E-02	1.03E+00
	Average	2.940	7.39E-05	165.456	1.65E-02	1.74E+05	2.90E+02	1.00525	0.00113	0.99917	0.00416	0.00607	1.00607
	Minimum	2.891	1.70E-06	21.206	1.90E-03	4.07E-02	1.32E-05	0.98241	0.00022	0.99630	0.00060	-0.01759	0.98241

Table 4.2 Results for Highly Enriched Uranium Systems (Volume 2) with CSAS25 from SCALE 5 and the 238-group Library on the HP-6000 (CMODD) Workstation

N	Case	nubar	Sigma	AFG	Sigma	EALCF (eV)	Sigma	k_{calc} HEU	Sigma	k_{exp} HEU	Sigma	Bias = Calculated - Benchmark	Adjusted k_{eff} HEU
1	hci003-001	2.528	2.03E-04	63.580	4.95E-02	7.94E+03	3.83E+01	1.00997	0.00087	1.00000	0.00570	0.00997	1.00997
2	hci003-002	2.509	2.01E-04	69.247	5.62E-02	4.26E+03	2.28E+01	1.01317	0.00103	1.00000	0.00610	0.01317	1.01317
3	hci003-003	2.509	1.96E-04	69.221	5.62E-02	4.29E+03	2.24E+01	1.01172	0.00109	1.00000	0.00560	0.01172	1.01172
4	hci003-004	2.512	1.94E-04	67.029	5.07E-02	5.41E+03	2.69E+01	1.00597	0.00113	1.00000	0.00550	0.00597	1.00597
5	hci003-005	2.497	1.06E-04	70.277	4.32E-02	3.73E+03	1.35E+01	1.00561	0.00098	1.00000	0.00470	0.00561	1.00561
6	hci003-006	2.514	1.37E-04	66.103	4.23E-02	5.94E+03	2.30E+01	0.99943	0.00105	1.00000	0.00470	-0.00057	0.99943
7	hci003-007	2.514	1.42E-04	66.149	4.57E-02	5.91E+03	2.48E+01	0.99725	0.00106	1.00000	0.00500	-0.00275	0.99725
8	hci004	2.443	7.39E-06	97.804	1.98E-02	1.39E+02	1.62E-01	1.02274	0.00023	1.00000	0.00400	0.02274	1.02274
9	hci005-007	2.454	3.02E-05	62.065	1.73E-02	6.64E+03	1.39E+01	0.97665	0.00042	1.03200	0.00400	-0.05535	0.94465
10	hci005-009	2.449	2.65E-05	66.485	1.52E-02	3.21E+03	5.83E+00	1.02653	0.00046	1.05000	0.00800	-0.02347	0.97653
11	hci005-015	2.450	3.26E-05	60.653	1.45E-02	6.66E+03	1.36E+01	0.92171	0.00040	1.06400	0.01800	-0.14229	0.85771
12	hci005-016	2.449	2.82E-05	64.424	1.83E-02	4.10E+03	8.16E+00	0.95498	0.00045	0.99700	0.01300	-0.04202	0.95798
13	hcm001-001	2.448	4.41E-05	192.743	4.48E-02	3.81E-01	1.25E-03	1.00789	0.00109	1.00000	0.00590	0.00789	1.00789
14	hcm001-002	2.448	3.92E-05	192.778	4.50E-02	3.82E-01	1.24E-03	1.00995	0.00090	1.00120	0.00590	0.00875	1.00875
15	hcm001-005	2.520	1.39E-04	94.306	8.37E-02	1.53E+03	1.05E+01	0.99933	0.00085	0.99850	0.00560	0.00083	1.00083
16	hcm001-006	2.521	1.40E-04	92.381	7.59E-02	1.83E+03	1.17E+01	0.99499	0.00096	0.99530	0.00560	-0.00031	0.99969
17	hcm001-013	2.504	1.26E-04	115.938	8.37E-02	2.33E+02	1.59E+00	1.00178	0.00085	1.00320	0.00530	-0.00142	0.99858
18	hcm001-017	2.487	1.05E-04	142.272	7.96E-02	2.54E+01	1.63E-01	0.99659	0.00085	0.99970	0.00460	-0.00311	0.99689
19	hcm001-020	2.494	1.03E-04	99.837	8.27E-02	5.54E+02	3.53E+00	1.00577	0.00107	1.00600	0.00650	-0.00023	0.99977
20	hcm001-027	2.493	1.04E-04	104.552	7.33E-02	3.93E+02	2.22E+00	0.99903	0.00093	0.99910	0.00530	-0.00007	0.99993
21	hcm001-028	2.494	1.02E-04	101.762	7.72E-02	4.90E+02	2.92E+00	1.00301	0.00093	1.00370	0.00530	-0.00069	0.99931
22	hct010-a	2.445	2.05E-05	180.540	4.25E-02	8.50E-01	2.46E-03	0.98462	0.00119	1.00000	0.00500	-0.01538	0.98462
23	hct010-b	2.441	1.37E-05	205.059	2.66E-02	1.40E-01	2.72E-04	0.99373	0.00107	1.00000	0.00500	-0.00627	0.99373
24	hct010-c	2.440	1.14E-05	209.862	2.20E-02	9.67E-02	1.66E-04	1.00327	0.00098	1.00000	0.00500	0.00327	1.00327
25	hct010-d	2.440	1.10E-05	209.334	2.17E-02	1.01E-01	1.71E-04	1.00074	0.00105	1.00000	0.00500	0.00074	1.00074
26	hct010-e	2.440	1.10E-05	209.666	2.16E-02	9.84E-02	1.64E-04	1.00258	0.00104	1.00100	0.00740	0.00158	1.00158
27	hct010-g	2.440	1.18E-05	209.892	2.71E-02	9.28E-02	2.17E-04	1.00486	0.00093	1.00070	0.00760	0.00416	1.00416
28	hct011-001	2.442	1.48E-05	182.568	4.18E-02	7.20E-01	1.93E-03	0.99352	0.00094	0.99880	0.00420	-0.00528	0.99472
29	hct011-002	2.442	1.38E-05	186.243	4.26E-02	5.53E-01	1.56E-03	0.99431	0.00092	0.99880	0.00420	-0.00449	0.99551
30	hct011-003	2.442	1.39E-05	189.568	4.18E-02	4.34E-01	1.19E-03	0.99702	0.00098	0.99880	0.00420	-0.00178	0.99822
31	hct012-001	2.442	1.61E-05	185.183	4.34E-02	6.01E-01	1.72E-03	0.99333	0.00105	0.99870	0.00320	-0.00537	0.99463
32	hct012-002	2.442	1.52E-05	188.897	4.14E-02	4.58E-01	1.24E-03	0.99201	0.00102	0.99870	0.00340	-0.00669	0.99331
33	hct013-001	2.442	1.38E-05	188.827	4.16E-02	4.59E-01	1.28E-03	0.99545	0.00107	0.99880	0.00420	-0.00335	0.99665

N	Case	nubar	Sigma	AFG	Sigma	EALCF (eV)	Sigma	k_{calc} HEU	Sigma	k_{exp} HEU	Sigma	Bias = Calculated - Benchmark	Adjusted k_{eff} HEU
34	hct013-002	2.441	1.30E-05	193.743	4.09E-02	3.20E-01	8.72E-04	0.99565	0.00092	0.99880	0.00430	-0.00315	0.99685
35	hct014-001	2.439	1.09E-05	206.884	3.05E-02	1.17E-01	2.61E-04	1.00212	0.00096	0.99860	0.00480	0.00352	1.00352
36	hct014-002	2.439	9.60E-06	209.280	2.76E-02	9.77E-02	1.94E-04	1.00095	0.00083	0.99860	0.00490	0.00235	1.00235
37	hct017-001	2.437	2.40E-06	219.687	1.11E-02	3.88E-02	4.89E-05	1.01002	0.00120	1.00000	0.00690	0.01002	1.01002
38	hct017-002	2.437	2.59E-06	216.158	1.72E-02	5.28E-02	8.49E-05	1.00030	0.00103	1.00000	0.00690	0.00030	1.00030
39	hct017-003	2.437	2.21E-06	218.904	1.32E-02	4.15E-02	5.81E-05	1.00656	0.00119	1.00000	0.00690	0.00656	1.00656
40	hct017-004	2.437	2.21E-06	220.212	1.07E-02	3.70E-02	4.99E-05	1.00926	0.00102	1.00000	0.00690	0.00926	1.00926
41	hct017-005	2.437	2.13E-06	220.623	9.29E-03	3.56E-02	4.24E-05	1.00902	0.00098	1.00000	0.00690	0.00902	1.00902
42	hct017-006	2.437	2.29E-06	219.511	1.12E-02	3.93E-02	5.08E-05	1.00874	0.00102	1.00000	0.00690	0.00874	1.00874
43	hct017-007	2.437	2.30E-06	217.673	1.54E-02	4.61E-02	7.04E-05	1.00511	0.00110	1.00000	0.00690	0.00511	1.00511
44	hct017-008	2.437	2.25E-06	220.784	8.77E-03	3.50E-02	4.25E-05	1.01539	0.00095	1.00000	0.00690	0.01539	1.01539
45	hct017-009	2.437	2.58E-06	219.596	1.20E-02	3.91E-02	5.34E-05	1.01043	0.00122	1.00000	0.00690	0.01043	1.01043
46	hmf001-a	2.605	2.05E-04	24.366	1.22E-02	9.50E+05	1.09E+03	0.99715	0.00117	1.00000	0.00100	-0.00285	0.99715
47	hmf002-b	2.612	3.01E-04	25.452	1.75E-02	8.41E+05	1.37E+03	1.00112	0.00118	1.00000	0.00300	0.00112	1.00112
48	hmf002-c	2.611	2.82E-04	25.532	1.69E-02	8.33E+05	1.30E+03	1.00022	0.00103	1.00000	0.00300	0.00022	1.00022
49	hmf002-d	2.611	3.12E-04	25.658	1.87E-02	8.23E+05	1.42E+03	0.99574	0.00117	1.00000	0.00300	-0.00426	0.99574
50	hmf002-e	2.610	3.19E-04	25.715	1.88E-02	8.18E+05	1.41E+03	1.00223	0.00116	1.00000	0.00300	0.00223	1.00223
51	hmf002-g	2.611	2.86E-04	25.620	1.86E-02	8.26E+05	1.42E+03	0.99650	0.00084	1.00000	0.00300	-0.00350	0.99650
52	hmf003-a	2.608	2.08E-04	24.828	1.28E-02	9.09E+05	1.11E+03	0.99432	0.00116	1.00000	0.00500	-0.00568	0.99432
53	hmf003-b	2.610	2.19E-04	24.910	1.32E-02	8.99E+05	1.13E+03	0.99252	0.00096	1.00000	0.00500	-0.00748	0.99252
54	hmf003-c	2.611	2.40E-04	25.017	1.37E-02	8.87E+05	1.17E+03	0.99849	0.00092	1.00000	0.00500	-0.00151	0.99849
55	hmf003-d	2.612	2.54E-04	25.083	1.53E-02	8.78E+05	1.27E+03	0.99787	0.00093	1.00000	0.00300	-0.00213	0.99787
56	hmf003-e	2.612	2.57E-04	25.257	1.53E-02	8.60E+05	1.22E+03	0.99996	0.00101	1.00000	0.00300	-0.00004	0.99996
57	hmf003-g	2.612	3.04E-04	25.340	1.81E-02	8.50E+05	1.45E+03	1.00295	0.00092	1.00000	0.00300	0.00295	1.00295
58	hmf003-h	2.611	3.26E-04	25.547	1.89E-02	8.30E+05	1.43E+03	1.00168	0.00091	1.00000	0.00300	0.00168	1.00168
59	hmf003-i	2.580	1.85E-04	27.240	1.31E-02	7.12E+05	9.31E+02	1.00240	0.00085	1.00000	0.00500	0.00240	1.00240
60	hmf003-j	2.574	1.81E-04	28.154	1.29E-02	6.40E+05	8.58E+02	1.00441	0.00086	1.00000	0.00500	0.00441	1.00441
61	hmf003-k	2.570	1.77E-04	28.885	1.30E-02	5.84E+05	7.99E+02	1.00820	0.00094	1.00000	0.00500	0.00820	1.00820
62	hmf003-l	2.569	1.73E-04	29.118	1.31E-02	5.65E+05	8.07E+02	1.01202	0.00131	1.00000	0.00500	0.01202	1.01202
63	hmf004-d	2.563	2.01E-04	60.964	8.21E-02	3.22E+04	2.29E+02	0.99691	0.00096	1.00200	0.00000	-0.00509	0.99491
64	hmf007-001	2.606	2.08E-04	24.272	1.26E-02	9.58E+05	1.14E+03	0.99138	0.00097	0.99710	0.00010	-0.00572	0.99428
65	hmf007-002	2.587	1.91E-04	28.741	1.79E-02	5.30E+05	1.12E+03	0.99365	0.00117	0.99860	0.00010	-0.00495	0.99505
66	hmf007-003	2.582	2.08E-04	30.965	2.37E-02	4.01E+05	1.10E+03	0.99341	0.00093	1.00120	0.00010	-0.00779	0.99221
67	hmf007-004	2.578	2.06E-04	31.730	2.35E-02	3.57E+05	9.93E+02	0.99161	0.00088	0.99700	0.00010	-0.00539	0.99461
68	hmf007-005	2.571	1.89E-04	33.785	2.57E-02	2.70E+05	8.27E+02	0.99293	0.00099	1.00000	0.00010	-0.00707	0.99293
69	hmf007-006	2.568	1.95E-04	38.409	3.83E-02	1.73E+05	6.84E+02	0.99889	0.00095	1.00280	0.00010	-0.00391	0.99609
70	hmf007-007	2.567	1.97E-04	35.815	2.94E-02	2.12E+05	7.05E+02	0.99506	0.00097	0.99960	0.00010	-0.00454	0.99546

N	Case	nubar	Sigma	AFG	Sigma	EALCF (eV)	Sigma	k_{calc} HEU	Sigma	k_{exp} HEU	Sigma	Bias = Calculated - Benchmark	Adjusted k_{eff} HEU
71	hmf007-008	2.567	2.05E-04	35.371	2.76E-02	2.19E+05	7.23E+02	0.99125	0.00096	0.99920	0.00010	-0.00795	0.99205
72	hmf007-009	2.567	2.11E-04	36.950	3.46E-02	1.94E+05	7.18E+02	0.99601	0.00099	1.00170	0.00080	-0.00569	0.99431
73	hmf007-010	2.539	1.73E-04	54.977	5.25E-02	2.85E+04	1.38E+02	0.99447	0.00096	1.00000	0.00010	-0.00553	0.99447
74	hmf007-011	2.516	1.54E-04	70.223	6.29E-02	5.88E+03	3.24E+01	0.99319	0.00121	0.99820	0.00010	-0.00501	0.99499
75	hmf007-012	2.512	1.50E-04	73.590	6.26E-02	4.33E+03	2.33E+01	0.98907	0.00127	0.99510	0.00010	-0.00603	0.99397
76	hmf007-013	2.516	1.51E-04	82.080	7.74E-02	2.68E+03	1.74E+01	0.99816	0.00115	1.00090	0.00010	-0.00274	0.99726
77	hmf007-014	2.512	1.54E-04	74.506	6.48E-02	4.00E+03	2.22E+01	0.99160	0.00097	0.99830	0.00010	-0.00670	0.99330
78	hmf007-015	2.517	1.56E-04	80.739	7.73E-02	2.99E+03	1.96E+01	0.99266	0.00135	0.99780	0.00010	-0.00514	0.99486
79	hmf007-016	2.517	1.61E-04	81.033	7.48E-02	2.93E+03	1.84E+01	0.99345	0.00110	0.99880	0.00010	-0.00535	0.99465
80	hmf007-017	2.493	1.23E-04	103.049	7.50E-02	3.90E+02	2.31E+00	0.99289	0.00114	0.99720	0.00010	-0.00431	0.99569
81	hmf007-018	2.493	1.25E-04	103.664	7.41E-02	3.71E+02	2.14E+00	0.99381	0.00100	0.99910	0.00010	-0.00529	0.99471
82	hmf007-019	2.605	2.06E-04	24.343	1.30E-02	9.52E+05	1.18E+03	0.99401	0.00088	0.99830	0.00010	-0.00429	0.99571
83	hmf007-020	2.572	2.03E-04	35.699	3.42E-02	2.29E+05	8.31E+02	0.99121	0.00107	0.99810	0.00010	-0.00689	0.99311
84	hmf007-021	2.571	2.00E-04	36.431	3.62E-02	2.11E+05	8.01E+02	0.99108	0.00089	0.99870	0.00010	-0.00762	0.99238
85	hmf007-022	2.569	1.93E-04	37.237	3.55E-02	1.94E+05	7.16E+02	0.99469	0.00095	0.99940	0.00010	-0.00471	0.99529
86	hmf007-023	2.557	2.02E-04	48.469	5.62E-02	6.65E+04	3.46E+02	0.99306	0.00116	0.99930	0.00010	-0.00624	0.99376
87	hmf007-024	2.556	1.94E-04	49.258	5.63E-02	6.19E+04	3.25E+02	0.99476	0.00088	1.00010	0.00010	-0.00534	0.99466
88	hmf007-025	2.545	1.85E-04	57.008	5.99E-02	2.84E+04	1.53E+02	0.99169	0.00123	0.99900	0.00010	-0.00731	0.99269
89	hmf007-026	2.544	1.84E-04	57.959	6.28E-02	2.60E+04	1.48E+02	0.99323	0.00098	0.99970	0.00010	-0.00647	0.99353
90	hmf007-027	2.586	1.91E-04	29.218	1.95E-02	4.98E+05	1.15E+03	0.99084	0.00112	0.99650	0.00020	-0.00566	0.99434
91	hmf007-028	2.573	1.98E-04	33.186	2.68E-02	2.97E+05	9.28E+02	0.99273	0.00095	0.99870	0.00020	-0.00597	0.99403
92	hmf007-029	2.562	1.89E-04	37.482	3.35E-02	1.74E+05	6.47E+02	0.99157	0.00092	0.99780	0.00020	-0.00623	0.99377
93	hmf007-030	2.533	1.71E-04	59.454	5.82E-02	1.88E+04	9.86E+01	0.99273	0.00100	0.99810	0.00020	-0.00537	0.99463
94	hmf007-031	2.503	1.43E-04	84.434	6.81E-02	1.72E+03	9.62E+00	0.99891	0.00109	1.00130	0.00020	-0.00239	0.99761
95	hmf007-032	2.595	2.16E-04	25.457	1.43E-02	8.41E+05	1.19E+03	0.99752	0.00084	0.99590	0.00010	0.00162	1.00162
96	hmf007-033	2.589	1.90E-04	26.251	1.39E-02	7.70E+05	1.04E+03	1.00505	0.00104	0.99950	0.00010	0.00555	1.00555
97	hmf007-034	2.583	1.99E-04	26.985	1.43E-02	7.08E+05	1.03E+03	1.00839	0.00096	0.99770	0.00010	0.01069	1.01069
98	hmf007-035	2.545	1.76E-04	76.259	8.31E-02	7.79E+03	5.58E+01	0.99199	0.00108	1.00110	0.00010	-0.00911	0.99089
99	hmf007-036	2.529	1.68E-04	82.133	7.93E-02	3.85E+03	2.60E+01	1.00171	0.00094	0.99990	0.00010	0.00181	1.00181
100	hmf007-037	2.516	1.60E-04	88.170	8.21E-02	1.94E+03	1.30E+01	0.99756	0.00090	0.99880	0.00010	-0.00124	0.99876
101	hmf007-038	2.514	1.52E-04	88.840	8.45E-02	1.75E+03	1.22E+01	0.99849	0.00120	1.00000	0.00010	-0.00151	0.99849
102	hmf007-039	2.513	1.45E-04	89.026	7.78E-02	1.70E+03	1.09E+01	1.00367	0.00100	1.00180	0.00010	0.00187	1.00187
103	hmf007-040	2.515	1.54E-04	88.974	8.23E-02	1.78E+03	1.23E+01	1.00357	0.00100	1.00130	0.00010	0.00227	1.00227
104	hmf007-041	2.494	1.18E-04	106.545	8.01E-02	3.26E+02	2.05E+00	1.00082	0.00092	0.99940	0.00010	0.00142	1.00142
105	hmf007-042	2.493	1.21E-04	107.292	8.18E-02	3.05E+02	1.94E+00	1.00278	0.00102	1.00160	0.00010	0.00118	1.00118
106	hmf007-043	2.471	9.29E-05	132.338	7.57E-02	3.44E+01	1.90E-01	1.00263	0.00100	0.99980	0.00010	0.00283	1.00283
107	hmf015-001	2.606	2.10E-04	24.237	1.24E-02	9.61E+05	1.13E+03	0.99262	0.00090	0.99960	0.00170	-0.00698	0.99302

N	Case	nubar	Sigma	AFG	Sigma	EALCF (eV)	Sigma	k_{calc} HEU	Sigma	k_{exp} HEU	Sigma	Bias = Calculated - Benchmark	Adjusted k_{eff} HEU
108	hmf016-001	2.583	2.02E-04	28.504	2.33E-02	5.90E+05	1.40E+03	0.99867	0.00094	0.99960	0.00180	-0.00093	0.99907
109	hmf016-002	2.585	1.94E-04	27.576	1.73E-02	6.56E+05	1.22E+03	0.99932	0.00108	0.99960	0.00180	-0.00028	0.99972
110	hmf017	2.570	1.89E-04	29.096	1.56E-02	5.50E+05	9.69E+02	0.99548	0.00086	0.99930	0.00140	-0.00382	0.99618
111	hmf018-a	2.603	2.05E-04	24.602	1.27E-02	9.31E+05	1.11E+03	0.99807	0.00086	1.00000	0.00140	-0.00193	0.99807
112	hmf019-a	2.594	1.91E-04	25.403	1.29E-02	8.59E+05	1.07E+03	1.00415	0.00111	1.00000	0.00280	0.00415	1.00415
113	hmf020-a	2.590	2.04E-04	30.009	3.10E-02	5.08E+05	1.53E+03	0.99590	0.00083	1.00000	0.00280	-0.00410	0.99590
114	hmf021-a	2.587	1.83E-04	25.938	1.23E-02	8.20E+05	9.82E+02	1.01184	0.00095	1.00000	0.00240	0.01184	1.01184
115	hmf022-a	2.597	2.03E-04	25.087	1.30E-02	8.90E+05	1.09E+03	0.99184	0.00092	1.00000	0.00190	-0.00816	0.99184
116	hmf023-e	2.606	2.18E-04	24.631	1.55E-02	9.28E+05	1.34E+03	0.99761	0.00117	1.00000	0.00520	-0.00239	0.99761
117	hmf023-g	2.550	1.85E-04	82.302	8.53E-02	5.25E+03	3.82E+01	0.99972	0.00090	1.00000	0.00520	-0.00028	0.99972
118	hmf026-b	2.605	2.10E-04	24.490	1.36E-02	9.40E+05	1.19E+03	0.99882	0.00105	0.99820	0.00420	0.00062	1.00062
119	hmf026-g	2.567	1.96E-04	61.519	8.14E-02	3.17E+04	2.25E+02	1.00129	0.00085	1.00000	0.00380	0.00129	1.00129
120	hmf026-h	2.559	1.97E-04	74.482	9.11E-02	1.09E+04	8.61E+01	0.99993	0.00091	1.00000	0.00380	-0.00007	0.99993
121	hmf026-j	2.596	2.04E-04	30.078	3.19E-02	5.20E+05	1.56E+03	0.98743	0.00093	0.99820	0.00420	-0.01077	0.98923
122	hmf026-l	2.564	1.89E-04	70.130	7.93E-02	1.65E+04	1.13E+02	0.99927	0.00111	1.00000	0.00380	-0.00073	0.99927
123	hmf027-a	2.598	1.99E-04	24.971	1.26E-02	8.98E+05	1.08E+03	1.00874	0.00103	1.00000	0.00250	0.00874	1.00874
124	hmf028-b	2.612	2.82E-04	25.310	1.61E-02	8.55E+05	1.29E+03	1.00355	0.00093	1.00000	0.00300	0.00355	1.00355
125	hmf029-a	2.604	2.07E-04	25.131	1.29E-02	8.85E+05	1.10E+03	1.00261	0.00095	1.00000	0.00200	0.00261	1.00261
126	hmf030-a	2.559	3.85E-04	35.024	3.79E-02	2.34E+05	1.00E+03	1.00386	0.00099	1.00000	0.00090	0.00386	1.00386
127	hmf031-b	2.541	1.82E-04	76.690	8.20E-02	6.84E+03	4.82E+01	1.00172	0.00104	1.00000	0.00590	0.00172	1.00172
128	hmf032-d	2.610	2.31E-04	25.021	1.32E-02	8.87E+05	1.12E+03	1.00332	0.00103	1.00000	0.00160	0.00332	1.00332
129	hmf032-e	2.609	2.19E-04	25.032	1.31E-02	8.87E+05	1.12E+03	1.00388	0.00088	1.00000	0.00270	0.00388	1.00388
130	hmf032-g	2.607	2.14E-04	24.802	1.33E-02	9.12E+05	1.15E+03	0.99593	0.00087	1.00000	0.00170	-0.00407	0.99593
131	hmf032-h	2.605	2.00E-04	24.628	1.24E-02	9.28E+05	1.08E+03	0.99878	0.00103	1.00000	0.00170	-0.00122	0.99878
132	hmf033-001	2.528	3.41E-04	61.771	1.30E-01	1.57E+04	1.80E+02	0.99063	0.00203	0.99910	0.00140	-0.00847	0.99153
133	hmf033-002	2.507	3.02E-04	92.175	1.61E-01	1.20E+03	1.61E+01	0.99139	0.00187	0.99910	0.00140	-0.00771	0.99229
134	hmf034-a	2.539	1.72E-04	63.102	6.90E-02	1.68E+04	1.03E+02	0.99236	0.00109	0.99900	0.00120	-0.00664	0.99336
135	hmf034-c	2.540	1.75E-04	63.339	6.66E-02	1.67E+04	9.82E+01	0.99119	0.00111	0.99900	0.00120	-0.00781	0.99219
136	hmf034-e	2.538	1.72E-04	64.888	6.85E-02	1.56E+04	9.39E+01	0.99754	0.00103	0.99900	0.00120	-0.00146	0.99854
137	hmf036-001	2.531	1.71E-04	78.424	7.46E-02	4.48E+03	2.86E+01	0.99210	0.00103	0.99930	0.00150	-0.00720	0.99280
138	hmf036-002	2.556	1.81E-04	58.917	6.60E-02	2.92E+04	1.69E+02	0.99410	0.00111	0.99930	0.00130	-0.00520	0.99480
139	hmf037-001	2.533	1.67E-04	88.816	8.11E-02	2.36E+03	1.60E+01	1.00136	0.00102	0.99970	0.00110	0.00166	1.00166
140	hmf037-002	2.547	1.76E-04	63.794	6.78E-02	1.74E+04	1.03E+02	0.99463	0.00110	0.99970	0.00110	-0.00507	0.99493
141	hmf038	2.561	3.65E-04	34.632	3.60E-02	2.49E+05	1.00E+03	1.00344	0.00102	0.99990	0.00150	0.00354	1.00354
142	hmf041-001	2.578	1.91E-04	28.374	1.69E-02	5.93E+05	1.15E+03	1.00373	0.00092	1.00130	0.00300	0.00243	1.00243
143	hmf041-002	2.557	1.77E-04	41.582	4.76E-02	1.51E+05	6.74E+02	1.00302	0.00090	1.00220	0.00430	0.00082	1.00082
144	hmf041-003	2.593	2.00E-04	25.606	1.34E-02	8.36E+05	1.08E+03	0.99714	0.00107	1.00060	0.00290	-0.00346	0.99654

N	Case	nubar	Sigma	AFG	Sigma	EALCF (eV)	Sigma	k_{calc} HEU	Sigma	k_{exp} HEU	Sigma	Bias = Calculated - Benchmark	Adjusted k_{eff} HEU
145	hmf041-004	2.586	1.95E-04	26.857	1.46E-02	7.12E+05	1.11E+03	1.00202	0.00102	1.00060	0.00250	0.00142	1.00142
146	hmf041-005	2.581	1.89E-04	28.665	2.08E-02	5.70E+05	1.27E+03	0.99776	0.00088	1.00060	0.00310	-0.00284	0.99716
147	hmf041-006	2.577	1.89E-04	31.257	3.06E-02	4.36E+05	1.31E+03	0.99815	0.00091	1.00060	0.00450	-0.00245	0.99755
148	hmf055-001	2.550	1.58E-04	31.973	1.22E-02	4.22E+05	5.48E+02	1.00774	0.00071	0.99550	0.00280	0.01224	1.01224
149	hmf055-002	2.551	5.46E-04	31.880	4.01E-02	4.26E+05	1.69E+03	1.00948	0.00144	0.99550	0.00280	0.01398	1.01398
150	hmf055-003	2.552	5.70E-04	31.863	4.59E-02	4.26E+05	1.93E+03	1.00329	0.00170	0.99550	0.00280	0.00779	1.00779
151	hmf055-004	2.552	5.65E-04	31.847	4.18E-02	4.26E+05	1.73E+03	0.99473	0.00176	0.99550	0.00280	-0.00077	0.99923
152	hmi001	2.459	8.12E-05	51.616	1.65E-02	2.94E+04	6.68E+01	1.08394	0.00077	0.99660	0.00260	0.08734	1.08734
153	hmi006-001	2.472	8.30E-05	65.080	3.41E-02	4.84E+03	1.65E+01	1.00136	0.00089	0.99480	0.00030	0.00656	1.00656
154	hmi006-002	2.476	9.13E-05	57.955	2.51E-02	1.02E+04	2.98E+01	1.00377	0.00086	0.99810	0.00030	0.00567	1.00567
155	hmi006-003	2.484	9.59E-05	51.147	1.97E-02	2.42E+04	6.39E+01	1.00608	0.00084	1.00160	0.00600	0.00448	1.00448
156	hmm001-a	2.522	1.46E-04	87.508	8.06E-02	2.27E+03	1.51E+01	1.00116	0.00091	0.99950	0.00130	0.00166	1.00166
157	hmm002-a	2.521	1.53E-04	96.469	7.86E-02	1.16E+03	7.59E+00	1.00652	0.00093	1.00000	0.00370	0.00652	1.00652
158	hmm003-a	2.521	1.49E-04	96.600	7.90E-02	1.15E+03	7.57E+00	1.00794	0.00105	1.00000	0.00380	0.00794	1.00794
159	hmt001	2.439	2.06E-05	213.400	2.70E-02	7.41E-02	1.66E-04	1.00582	0.00104	1.00100	0.00540	0.00482	1.00482
160	hmt003-a	2.555	1.79E-04	66.677	7.47E-02	1.89E+04	1.23E+02	0.99734	0.00107	1.00000	0.00100	-0.00266	0.99734
161	hmt003-b	2.555	1.91E-04	67.463	7.85E-02	1.76E+04	1.20E+02	0.97792	0.00080	0.99100	0.00300	-0.01308	0.98692
162	hmt003-c	2.496	1.38E-04	112.461	8.49E-02	2.31E+02	1.53E+00	0.96718	0.00105	0.98260	0.00600	-0.01542	0.98458
163	hmt003-d	2.485	1.16E-04	131.961	7.79E-02	4.84E+01	2.95E-01	0.97901	0.00092	0.98760	0.00400	-0.00859	0.99141
164	hmt003-e	2.462	7.36E-05	166.987	6.93E-02	2.81E+00	1.46E-02	0.99243	0.00097	0.99300	0.00300	-0.00057	0.99943
165	hmt003-g	2.468	8.69E-05	151.290	7.71E-02	9.19E+00	5.26E-02	0.97078	0.00106	0.98890	0.00300	-0.01812	0.98188
166	hmt003-h	2.462	7.82E-05	165.902	7.16E-02	3.04E+00	1.61E-02	0.98096	0.00093	0.99190	0.00300	-0.01094	0.98906
167	hmt006-001	2.438	5.83E-06	210.213	2.60E-02	8.44E-02	1.68E-04	0.99996	0.00131	1.00000	0.00400	-0.00004	0.99996
168	hmt006-002	2.438	5.80E-06	212.493	2.29E-02	6.97E-02	1.29E-04	1.00306	0.00108	1.00000	0.00400	0.00306	1.00306
169	hmt006-003	2.438	5.39E-06	213.835	2.30E-02	6.27E-02	1.16E-04	1.00542	0.00108	1.00000	0.00400	0.00542	1.00542
170	hmt006-004	2.438	5.03E-06	214.095	2.16E-02	6.13E-02	1.10E-04	0.99495	0.00101	1.00000	0.00400	-0.00505	0.99495
171	hmt006-005	2.438	4.90E-06	214.806	2.06E-02	5.79E-02	1.04E-04	1.00306	0.00106	1.00000	0.00400	0.00306	1.00306
172	hmt006-006	2.438	5.15E-06	215.359	2.10E-02	5.54E-02	9.82E-05	1.00302	0.00105	1.00000	0.00400	0.00302	1.00302
173	hmt006-007	2.438	4.93E-06	215.774	1.97E-02	5.36E-02	9.18E-05	1.00059	0.00108	1.00000	0.00400	0.00059	1.00059
174	hmt006-008	2.438	4.93E-06	216.191	1.94E-02	5.18E-02	8.67E-05	0.99786	0.00091	1.00000	0.00400	-0.00214	0.99786
175	hmt006-009	2.438	4.78E-06	216.303	1.92E-02	5.13E-02	8.37E-05	0.99574	0.00107	1.00000	0.00400	-0.00426	0.99574
176	hmt006-010	2.438	5.94E-06	210.550	2.48E-02	8.19E-02	1.58E-04	1.00681	0.00133	1.00000	0.00400	0.00681	1.00681
177	hmt006-011	2.438	5.07E-06	214.030	2.13E-02	6.17E-02	1.07E-04	1.00892	0.00097	1.00000	0.00400	0.00892	1.00892
178	hmt006-012	2.438	4.78E-06	215.733	2.02E-02	5.38E-02	9.50E-05	1.00661	0.00094	1.00000	0.00400	0.00661	1.00661
179	hmt006-013	2.438	5.60E-06	210.453	2.67E-02	8.23E-02	1.71E-04	1.03005	0.00096	1.00000	0.00400	0.03005	1.03005
180	hmt006-014	2.438	5.19E-06	215.124	2.12E-02	5.64E-02	9.78E-05	0.99750	0.00089	1.00000	0.00400	-0.00250	0.99750
181	hmt006-015	2.438	4.93E-06	215.217	2.08E-02	5.61E-02	9.65E-05	0.99540	0.00093	1.00000	0.00400	-0.00460	0.99540

N	Case	nubar	Sigma	AFG	Sigma	EALCF (eV)	Sigma	k_{calc} HEU	Sigma	k_{exp} HEU	Sigma	Bias = Calculated - Benchmark	Adjusted k_{eff} HEU
182	hmt006-016	2.438	5.09E-06	213.843	2.21E-02	6.28E-02	1.12E-04	1.00709	0.00107	1.00000	0.00400	0.00709	1.00709
183	hmt006-017	2.438	5.40E-06	211.866	2.34E-02	7.37E-02	1.38E-04	1.00267	0.00094	1.00000	0.00400	0.00267	1.00267
184	hmt006-018	2.438	5.67E-06	211.024	2.57E-02	7.91E-02	1.54E-04	1.00289	0.00140	1.00000	0.00400	0.00289	1.00289
185	hmt006-019	2.438	4.38E-06	215.685	2.29E-02	5.21E-02	9.94E-05	0.99563	0.00109	1.00000	0.00400	-0.00437	0.99563
186	hmt006-020	2.438	5.01E-06	213.431	2.41E-02	6.41E-02	1.25E-04	0.99817	0.00094	1.00000	0.00400	-0.00183	0.99817
187	hmt006-021	2.438	5.39E-06	212.564	2.61E-02	6.93E-02	1.43E-04	1.00021	0.00094	1.00000	0.00400	0.00021	1.00021
188	hmt006-022	2.438	5.34E-06	211.844	2.46E-02	7.37E-02	1.40E-04	1.00163	0.00098	1.00000	0.00400	0.00163	1.00163
189	hmt006-023	2.438	5.58E-06	211.603	2.42E-02	7.54E-02	1.39E-04	1.00647	0.00088	1.00000	0.00400	0.00647	1.00647
190	hst001-001	2.438	3.58E-06	210.157	8.59E-03	8.21E-02	6.78E-05	1.00019	0.00132	1.00000	0.00250	0.00019	1.00019
191	hst001-002	2.441	9.00E-06	195.091	1.92E-02	2.80E-01	4.29E-04	0.99861	0.00141	1.00000	0.00250	-0.00139	0.99861
192	hst001-003	2.438	3.63E-06	210.375	8.96E-03	8.06E-02	7.06E-05	1.00633	0.00128	1.00000	0.00250	0.00633	1.00633
193	hst001-004	2.441	8.83E-06	194.276	1.92E-02	2.98E-01	4.50E-04	1.00096	0.00119	1.00000	0.00250	0.00096	1.00096
194	hst001-005	2.437	1.38E-06	217.498	3.76E-03	4.30E-02	1.97E-05	1.00208	0.00112	1.00000	0.00250	0.00208	1.00208
195	hst001-006	2.437	1.58E-06	217.097	4.33E-03	4.46E-02	2.20E-05	1.00372	0.00152	1.00000	0.00250	0.00372	1.00372
196	hst001-007	2.438	3.51E-06	210.790	8.87E-03	7.78E-02	6.46E-05	1.00035	0.00131	1.00000	0.00250	0.00035	1.00035
197	hst001-008	2.438	3.48E-06	210.126	9.49E-03	8.23E-02	7.34E-05	0.99928	0.00137	1.00000	0.00250	-0.00072	0.99928
198	hst001-009	2.441	9.13E-06	194.213	2.00E-02	2.99E-01	4.82E-04	0.99656	0.00131	1.00000	0.00250	-0.00344	0.99656
199	hst001-010	2.438	1.66E-06	216.715	4.74E-03	4.62E-02	2.53E-05	0.99340	0.00119	1.00000	0.00250	-0.00660	0.99340
200	hst002-001	2.438	3.37E-06	210.418	8.87E-03	8.04E-02	6.82E-05	1.00414	0.00127	1.00000	0.00200	0.00414	1.00414
201	hst002-002	2.438	3.23E-06	210.514	8.84E-03	7.98E-02	6.71E-05	1.00795	0.00148	1.00000	0.00200	0.00795	1.00795
202	hst002-003	2.441	8.22E-06	196.440	1.79E-02	2.52E-01	3.68E-04	1.00103	0.00141	1.00000	0.00200	0.00103	1.00103
203	hst002-004	2.440	7.55E-06	196.856	1.66E-02	2.44E-01	3.23E-04	1.00759	0.00120	1.00000	0.00200	0.00759	1.00759
204	hst002-005	2.438	3.28E-06	210.483	8.86E-03	7.99E-02	6.72E-05	1.00734	0.00126	1.00000	0.00200	0.00734	1.00734
205	hst002-006	2.438	3.25E-06	210.676	8.50E-03	7.87E-02	6.24E-05	1.00923	0.00126	1.00000	0.00200	0.00923	1.00923
206	hst002-007	2.441	7.95E-06	196.537	1.70E-02	2.50E-01	3.44E-04	1.00026	0.00119	1.00000	0.00200	0.00026	1.00026
207	hst002-008	2.440	7.59E-06	197.151	1.62E-02	2.38E-01	3.10E-04	1.00666	0.00128	1.00000	0.00200	0.00666	1.00666
208	hst002-009	2.437	1.43E-06	217.162	4.25E-03	4.44E-02	2.20E-05	1.00307	0.00111	1.00000	0.00200	0.00307	1.00307
209	hst002-010	2.437	1.38E-06	217.230	4.24E-03	4.41E-02	2.20E-05	1.00696	0.00118	1.00000	0.00200	0.00696	1.00696
210	hst002-011	2.438	3.62E-06	210.444	9.24E-03	8.02E-02	6.90E-05	1.00628	0.00135	1.00000	0.00200	0.00628	1.00628
211	hst002-012	2.438	3.39E-06	210.764	8.99E-03	7.81E-02	6.57E-05	1.00897	0.00140	1.00000	0.00200	0.00897	1.00897
212	hst002-013	2.441	7.94E-06	196.529	1.84E-02	2.50E-01	3.64E-04	1.00229	0.00135	1.00000	0.00200	0.00229	1.00229
213	hst002-014	2.440	7.68E-06	197.393	1.67E-02	2.34E-01	3.17E-04	1.00832	0.00127	1.00000	0.00200	0.00832	1.00832
214	hst003-001	2.437	1.31E-06	217.218	4.00E-03	4.42E-02	2.12E-05	1.00539	0.00109	1.00000	0.00500	0.00539	1.00539
215	hst003-002	2.437	1.48E-06	217.147	4.20E-03	4.45E-02	2.19E-05	1.00445	0.00107	1.00000	0.00500	0.00445	1.00445
216	hst003-003	2.438	3.22E-06	210.237	8.93E-03	8.16E-02	6.74E-05	1.00179	0.00135	1.00000	0.00500	0.00179	1.00179
217	hst003-004	2.438	3.42E-06	210.554	8.63E-03	7.96E-02	6.56E-05	1.00398	0.00144	1.00000	0.00500	0.00398	1.00398
218	hst003-005	2.441	8.40E-06	195.824	1.77E-02	2.64E-01	3.80E-04	0.99835	0.00129	1.00000	0.00500	-0.00165	0.99835

N	Case	nubar	Sigma	AFG	Sigma	EALCF (eV)	Sigma	k_{calc} HEU	Sigma	k_{exp} HEU	Sigma	Bias = Calculated - Benchmark	Adjusted k_{eff} HEU
219	hst003-006	2.441	8.57E-06	196.834	1.80E-02	2.45E-01	3.46E-04	0.99893	0.00168	1.00000	0.00500	-0.00107	0.99893
220	hst003-007	2.437	1.43E-06	217.313	4.07E-03	4.38E-02	2.12E-05	1.00418	0.00110	1.00000	0.00500	0.00418	1.00418
221	hst003-008	2.438	3.78E-06	210.289	9.02E-03	8.12E-02	6.80E-05	1.00244	0.00164	1.00000	0.00500	0.00244	1.00244
222	hst003-009	2.438	3.51E-06	210.819	9.25E-03	7.78E-02	7.01E-05	1.00375	0.00127	1.00000	0.00500	0.00375	1.00375
223	hst003-010	2.441	7.92E-06	195.957	1.83E-02	2.61E-01	3.85E-04	0.99751	0.00124	1.00000	0.00500	-0.00249	0.99751
224	hst003-011	2.441	7.89E-06	197.443	1.74E-02	2.33E-01	3.27E-04	0.99990	0.00134	1.00000	0.00500	-0.00010	0.99990
225	hst003-012	2.437	1.43E-06	217.148	4.30E-03	4.44E-02	2.16E-05	1.00199	0.00136	1.00000	0.00500	0.00199	1.00199
226	hst003-013	2.437	1.44E-06	217.353	4.05E-03	4.37E-02	2.17E-05	1.00220	0.00131	1.00000	0.00500	0.00220	1.00220
227	hst003-014	2.437	1.49E-06	217.205	4.34E-03	4.42E-02	2.23E-05	1.00258	0.00118	1.00000	0.00500	0.00258	1.00258
228	hst003-015	2.437	1.55E-06	216.886	4.46E-03	4.56E-02	2.33E-05	0.99599	0.00134	1.00000	0.00500	-0.00401	0.99599
229	hst003-016	2.438	3.72E-06	210.290	8.76E-03	8.12E-02	6.63E-05	1.00068	0.00177	1.00000	0.00500	0.00068	1.00068
230	hst003-017	2.438	3.35E-06	210.991	8.62E-03	7.67E-02	6.28E-05	1.00254	0.00113	1.00000	0.00500	0.00254	1.00254
231	hst003-018	2.441	8.16E-06	196.026	1.86E-02	2.60E-01	3.77E-04	0.99748	0.00141	1.00000	0.00500	-0.00252	0.99748
232	hst003-019	2.440	7.55E-06	197.899	1.88E-02	2.25E-01	3.48E-04	1.00100	0.00125	1.00000	0.00500	0.00100	1.00100
233	hst004-a	2.445	1.69E-05	138.153	6.99E-02	1.35E+01	6.13E-02	1.00398	0.00107	1.00000	0.00650	0.00398	1.00398
234	hst004-b	2.441	8.03E-06	161.116	5.39E-02	2.72E+00	9.47E-03	1.00651	0.00101	1.00000	0.00710	0.00651	1.00651
235	hst004-c	2.438	2.95E-06	188.606	2.88E-02	4.26E-01	8.86E-04	1.00204	0.00105	1.00000	0.00780	0.00204	1.00204
236	hst004-d	2.443	1.10E-05	150.279	6.07E-02	5.67E+00	2.24E-02	0.99909	0.00097	1.00000	0.00910	-0.00091	0.99909
237	hst004-e	2.439	5.20E-06	174.732	4.30E-02	1.10E+00	3.20E-03	1.00645	0.00116	1.00000	0.01040	0.00645	1.00645
238	hst004-g	2.438	1.74E-06	199.186	2.26E-02	1.99E-01	3.43E-04	1.00014	0.00137	1.00000	0.01170	0.00014	1.00014
239	hst005-a	2.440	7.54E-06	196.148	1.99E-02	2.49E-01	3.83E-04	1.00091	0.00092	1.00000	0.01240	0.00091	1.00091
240	hst005-b	2.441	7.89E-06	195.595	2.22E-02	2.58E-01	4.30E-04	1.00653	0.00096	1.00000	0.01240	0.00653	1.00653
241	hst005-c	2.441	7.38E-06	195.085	2.25E-02	2.67E-01	4.62E-04	1.00663	0.00099	1.00000	0.01260	0.00663	1.00663
242	hst005-d	2.440	7.20E-06	197.516	1.92E-02	2.26E-01	3.35E-04	1.00417	0.00102	1.00000	0.01240	0.00417	1.00417
243	hst005-e	2.441	8.23E-06	192.460	2.03E-02	3.29E-01	5.20E-04	0.98635	0.00144	1.00000	0.01240	-0.01365	0.98635
244	hst005-g	2.440	7.70E-06	196.355	2.00E-02	2.45E-01	3.79E-04	1.00579	0.00094	1.00000	0.01250	0.00579	1.00579
245	hst005-h	2.439	4.51E-06	206.320	1.40E-02	1.12E-01	1.30E-04	1.00138	0.00104	1.00000	0.01190	0.00138	1.00138
246	hst005-i	2.438	2.47E-06	213.118	8.38E-03	6.28E-02	4.91E-05	1.00590	0.00106	1.00000	0.01210	0.00590	1.00590
247	hst006-a	2.440	7.69E-06	198.631	1.58E-02	2.12E-01	2.65E-04	0.98288	0.00122	0.99730	0.00500	-0.01442	0.98558
248	hst006-b	2.441	8.11E-06	189.055	1.56E-02	4.40E-01	5.31E-04	1.00257	0.00074	1.00000	0.00870	0.00257	1.00257
249	hst006-c	2.441	7.46E-06	196.084	1.54E-02	2.59E-01	3.19E-04	0.99020	0.00093	0.99860	0.00540	-0.00840	0.99160
250	hst006-d	2.441	7.49E-06	191.654	1.53E-02	3.62E-01	4.36E-04	1.00243	0.00074	1.00000	0.00780	0.00243	1.00243
251	hst006-e	2.441	7.46E-06	190.097	1.60E-02	4.07E-01	5.07E-04	1.00915	0.00093	1.00000	0.00910	0.00915	1.00915
252	hst006-g	2.441	6.95E-06	193.327	1.54E-02	3.20E-01	3.94E-04	1.00092	0.00097	1.00000	0.00650	0.00092	1.00092
253	hst006-h	2.441	8.03E-06	188.880	1.58E-02	4.45E-01	5.31E-04	1.00465	0.00074	1.00000	0.00880	0.00465	1.00465
254	hst007-001	2.437	1.58E-06	216.443	4.77E-03	4.74E-02	2.50E-05	1.01139	0.00133	1.00000	0.00350	0.01139	1.01139
255	hst007-002	2.441	7.50E-06	195.580	1.92E-02	2.69E-01	4.00E-04	1.01327	0.00111	1.00000	0.00500	0.01327	1.01327

N	Case	nubar	Sigma	AFG	Sigma	EALCF (eV)	Sigma	k_{calc} HEU	Sigma	k_{exp} HEU	Sigma	Bias = Calculated - Benchmark	Adjusted k_{eff} HEU
256	hst007-003	2.437	1.46E-06	216.699	4.66E-03	4.64E-02	2.54E-05	1.01113	0.00105	1.00000	0.00350	0.01113	1.01113
257	hst007-004	2.440	7.22E-06	197.060	1.84E-02	2.39E-01	3.42E-04	1.01402	0.00117	1.00000	0.00350	0.01402	1.01402
258	hst007-005	2.438	1.80E-06	215.748	5.34E-03	5.04E-02	2.94E-05	1.00660	0.00124	1.00000	0.00350	0.00660	1.00660
259	hst007-006	2.441	8.25E-06	195.248	1.89E-02	2.76E-01	4.06E-04	1.00083	0.00121	1.00000	0.00350	0.00083	1.00083
260	hst007-007	2.438	1.80E-06	215.894	5.33E-03	4.98E-02	2.94E-05	1.00657	0.00122	1.00000	0.00350	0.00657	1.00657
261	hst007-008	2.441	8.31E-06	195.465	1.90E-02	2.71E-01	4.07E-04	1.00390	0.00133	1.00000	0.00350	0.00390	1.00390
262	hst007-009	2.438	1.95E-06	215.529	5.71E-03	5.14E-02	3.19E-05	1.00685	0.00112	1.00000	0.00350	0.00685	1.00685
263	hst007-010	2.438	1.88E-06	215.191	5.77E-03	5.30E-02	3.17E-05	1.01591	0.00101	1.00000	0.00350	0.01591	1.01591
264	hst007-011	2.441	7.75E-06	196.133	1.94E-02	2.58E-01	3.98E-04	1.00821	0.00125	1.00000	0.00350	0.00821	1.00821
265	hst007-012	2.438	1.81E-06	215.580	5.57E-03	5.12E-02	3.00E-05	1.01542	0.00100	1.00000	0.00350	0.01542	1.01542
266	hst007-013	2.440	7.46E-06	197.390	1.93E-02	2.33E-01	3.64E-04	1.01349	0.00103	1.00000	0.00350	0.01349	1.01349
267	hst007-014	2.441	7.65E-06	196.962	1.73E-02	2.41E-01	3.31E-04	1.01026	0.00122	1.00000	0.00350	0.01026	1.01026
268	hst007-015	2.441	7.97E-06	196.887	1.80E-02	2.43E-01	3.39E-04	1.01146	0.00112	1.00000	0.00350	0.01146	1.01146
269	hst007-016	2.441	7.82E-06	196.133	1.81E-02	2.58E-01	3.61E-04	1.00557	0.00109	1.00000	0.00350	0.00557	1.00557
270	hst007-017	2.441	8.31E-06	196.947	1.92E-02	2.41E-01	3.51E-04	1.01153	0.00107	1.00000	0.00350	0.01153	1.01153
271	hst008-001	2.437	1.38E-06	217.135	4.24E-03	4.46E-02	2.23E-05	0.99939	0.00095	1.00000	0.00300	-0.00061	0.99939
272	hst008-002	2.441	7.93E-06	197.261	1.84E-02	2.37E-01	3.52E-04	0.99610	0.00121	1.00000	0.00300	-0.00390	0.99610
273	hst008-003	2.437	1.41E-06	217.454	4.05E-03	4.33E-02	2.08E-05	0.99751	0.00107	1.00000	0.00300	-0.00249	0.99751
274	hst008-004	2.440	7.43E-06	198.748	1.77E-02	2.10E-01	3.02E-04	1.00014	0.00102	1.00000	0.00300	0.00014	1.00014
275	hst008-005	2.437	1.48E-06	217.167	4.43E-03	4.44E-02	2.43E-05	0.99928	0.00112	1.00000	0.00300	-0.00072	0.99928
276	hst008-006	2.441	8.24E-06	196.170	1.89E-02	2.57E-01	3.91E-04	1.00128	0.00119	1.00000	0.00300	0.00128	1.00128
277	hst008-007	2.437	1.39E-06	217.355	4.19E-03	4.36E-02	2.18E-05	0.99912	0.00102	1.00000	0.00300	-0.00088	0.99912
278	hst008-008	2.441	8.54E-06	196.786	1.78E-02	2.44E-01	3.50E-04	1.00053	0.00138	1.00000	0.00300	0.00053	1.00053
279	hst008-009	2.437	1.36E-06	217.216	4.24E-03	4.43E-02	2.29E-05	0.99995	0.00090	1.00000	0.00300	-0.00005	0.99995
280	hst008-010	2.441	7.71E-06	197.401	1.91E-02	2.34E-01	3.53E-04	0.99736	0.00123	1.00000	0.00300	-0.00264	0.99736
281	hst008-011	2.437	1.32E-06	217.633	3.97E-03	4.26E-02	2.04E-05	0.99962	0.00105	1.00000	0.00300	-0.00038	0.99962
282	hst008-012	2.440	7.93E-06	199.026	1.81E-02	2.05E-01	2.95E-04	0.99585	0.00109	1.00000	0.00300	-0.00415	0.99585
283	hst008-013	2.441	7.99E-06	197.472	1.90E-02	2.32E-01	3.53E-04	1.00023	0.00128	1.00000	0.00300	0.00023	1.00023
284	hst008-014	2.441	8.13E-06	198.626	1.84E-02	2.11E-01	3.13E-04	0.99648	0.00123	1.00000	0.00300	-0.00352	0.99648
285	hst009-a	2.443	1.30E-05	186.785	2.92E-02	5.25E-01	1.13E-03	1.00373	0.00122	1.00000	0.00570	0.00373	1.00373
286	hst009-b	2.440	6.56E-06	202.200	1.66E-02	1.60E-01	2.16E-04	1.00318	0.00110	1.00000	0.00570	0.00318	1.00318
287	hst009-c	2.442	1.05E-05	193.265	2.43E-02	3.22E-01	5.75E-04	1.00500	0.00130	1.00000	0.00570	0.00500	1.00500
288	hst009-d	2.439	4.17E-06	209.031	1.13E-02	9.11E-02	9.40E-05	0.99690	0.00139	1.00000	0.00570	-0.00310	0.99690
289	hst010-e	2.438	2.03E-06	215.348	5.93E-03	5.25E-02	3.27E-05	1.00320	0.00117	1.00000	0.00180	0.00320	1.00320
290	hst010-g	2.438	2.18E-06	215.219	6.04E-03	5.31E-02	3.35E-05	1.00432	0.00162	1.00000	0.00180	0.00432	1.00432
291	hst010-h	2.438	2.28E-06	214.760	6.66E-03	5.53E-02	3.94E-05	0.99912	0.00126	1.00000	0.00180	-0.00088	0.99912
292	hst010-i	2.438	2.29E-06	214.576	6.40E-03	5.62E-02	3.74E-05	0.99913	0.00109	1.00000	0.00180	-0.00087	0.99913

N	Case	nubar	Sigma	AFG	Sigma	EALCF (eV)	Sigma	k_{calc} HEU	Sigma	k_{exp} HEU	Sigma	Bias = Calculated - Benchmark	Adjusted k_{eff} HEU
293	hst011-c	2.437	1.15E-06	218.416	3.40E-03	3.96E-02	1.68E-05	1.00570	0.00099	1.00000	0.00200	0.00570	1.00570
294	hst011-d	2.437	1.12E-06	218.480	3.48E-03	3.94E-02	1.70E-05	1.00359	0.00103	1.00000	0.00200	0.00359	1.00359
295	hst012-b	2.437	5.59E-07	220.573	1.68E-03	3.24E-02	9.00E-06	1.00146	0.00097	0.99990	0.00580	0.00156	1.00156
296	hst013-e	2.437	5.30E-07	220.574	1.69E-03	3.23E-02	8.83E-06	1.00054	0.00078	1.00120	0.00260	-0.00066	0.99934
297	hst013-g	2.437	6.44E-07	220.123	1.93E-03	3.37E-02	9.97E-06	0.99961	0.00097	1.00070	0.00360	-0.00109	0.99891
298	hst013-h	2.437	6.86E-07	219.682	2.09E-03	3.52E-02	1.09E-05	0.99590	0.00072	1.00090	0.00360	-0.00500	0.99500
299	hst013-i	2.437	7.77E-07	219.475	2.21E-03	3.59E-02	1.15E-05	0.99685	0.00082	1.00030	0.00360	-0.00345	0.99655
300	hst014-001	2.437	1.61E-06	216.784	4.52E-03	4.60E-02	2.52E-05	0.99402	0.00126	1.00000	0.00280	-0.00598	0.99402
301	hst014-002	2.438	1.59E-06	216.458	4.48E-03	4.76E-02	2.49E-05	1.01468	0.00096	1.00000	0.00520	0.01468	1.01468
302	hst014-003	2.438	1.60E-06	216.025	4.12E-03	4.97E-02	2.42E-05	1.02366	0.00114	1.00000	0.00870	0.02366	1.02366
303	hst015-001	2.438	2.42E-06	214.209	6.22E-03	5.79E-02	3.87E-05	0.99936	0.00126	1.00000	0.00320	-0.00064	0.99936
304	hst015-002	2.438	2.23E-06	214.586	5.78E-03	5.61E-02	3.62E-05	0.99177	0.00126	1.00000	0.00340	-0.00823	0.99177
305	hst015-003	2.438	2.38E-06	213.295	6.06E-03	6.31E-02	3.90E-05	1.01261	0.00110	1.00000	0.00680	0.01261	1.01261
306	hst015-004	2.438	2.26E-06	213.715	6.17E-03	6.09E-02	3.90E-05	1.01661	0.00131	1.00000	0.00690	0.01661	1.01661
307	hst015-005	2.438	2.20E-06	212.939	5.88E-03	6.57E-02	4.00E-05	1.01657	0.00103	1.00000	0.00890	0.01657	1.01657
308	hst016-001	2.438	3.44E-06	210.691	9.03E-03	7.89E-02	6.64E-05	0.99236	0.00126	1.00000	0.00360	-0.00764	0.99236
309	hst016-002	2.438	3.41E-06	210.235	8.11E-03	8.28E-02	6.29E-05	1.00951	0.00118	1.00000	0.00690	0.00951	1.00951
310	hst016-003	2.438	3.35E-06	209.057	8.12E-03	9.20E-02	6.91E-05	1.03011	0.00090	1.00000	0.00790	0.03011	1.03011
311	hst017-001	2.439	4.36E-06	208.132	1.11E-02	9.83E-02	9.79E-05	0.99409	0.00108	1.00000	0.00280	-0.00591	0.99409
312	hst017-002	2.439	4.60E-06	206.837	1.10E-02	1.09E-01	1.08E-04	0.98153	0.00125	1.00000	0.00400	-0.01847	0.98153
313	hst017-003	2.439	4.62E-06	207.598	1.16E-02	1.03E-01	1.08E-04	0.98143	0.00109	1.00000	0.00360	-0.01857	0.98143
314	hst017-004	2.439	4.12E-06	207.336	1.06E-02	1.06E-01	9.85E-05	1.00212	0.00109	1.00000	0.00470	0.00212	1.00212
315	hst017-005	2.439	4.27E-06	206.773	1.02E-02	1.12E-01	1.03E-04	1.00900	0.00108	1.00000	0.00580	0.00900	1.00900
316	hst017-006	2.439	4.52E-06	205.030	1.05E-02	1.28E-01	1.15E-04	1.00756	0.00111	1.00000	0.00550	0.00756	1.00756
317	hst017-007	2.439	4.45E-06	205.932	1.05E-02	1.19E-01	1.06E-04	1.01167	0.00115	1.00000	0.00570	0.01167	1.01167
318	hst017-008	2.439	4.75E-06	204.384	1.01E-02	1.36E-01	1.18E-04	1.00773	0.00092	1.00000	0.00670	0.00773	1.00773
319	hst018-001	2.440	6.44E-06	202.153	1.47E-02	1.61E-01	1.97E-04	0.99095	0.00128	1.00000	0.00340	-0.00905	0.99095
320	hst018-002	2.440	7.14E-06	200.133	1.51E-02	1.88E-01	2.32E-04	0.98713	0.00132	1.00000	0.00460	-0.01287	0.98713
321	hst018-003	2.440	6.83E-06	201.283	1.58E-02	1.72E-01	2.24E-04	0.98933	0.00127	1.00000	0.00420	-0.01067	0.98933
322	hst018-004	2.440	6.28E-06	200.869	1.40E-02	1.80E-01	2.08E-04	1.00101	0.00108	1.00000	0.00440	0.00101	1.00101
323	hst018-005	2.440	6.96E-06	197.974	1.47E-02	2.26E-01	2.66E-04	0.99419	0.00118	1.00000	0.00460	-0.00581	0.99419
324	hst018-006	2.440	6.70E-06	199.246	1.45E-02	2.05E-01	2.46E-04	0.99494	0.00117	1.00000	0.00450	-0.00506	0.99494
325	hst018-007	2.440	6.33E-06	199.623	1.42E-02	2.01E-01	2.29E-04	1.01264	0.00087	1.00000	0.00580	0.01264	1.01264
326	hst018-008	2.440	6.96E-06	197.032	1.38E-02	2.46E-01	2.80E-04	1.01355	0.00117	1.00000	0.00560	0.01355	1.01355
327	hst018-009	2.440	6.17E-06	198.332	1.40E-02	2.22E-01	2.42E-04	1.00987	0.00100	1.00000	0.00560	0.00987	1.00987
328	hst018-010	2.440	7.38E-06	195.619	1.36E-02	2.77E-01	2.96E-04	1.02666	0.00123	1.00000	0.00570	0.02666	1.02666
329	hst018-011	2.440	6.56E-06	197.051	1.31E-02	2.48E-01	2.54E-04	1.02933	0.00096	1.00000	0.00590	0.02933	1.02933

N	Case	nubar	Sigma	AFG	Sigma	EALCF (eV)	Sigma	k_{calc} HEU	Sigma	k_{exp} HEU	Sigma	Bias = Calculated - Benchmark	Adjusted k_{eff} HEU
330	hst018-012	2.440	6.99E-06	195.893	1.33E-02	2.74E-01	2.88E-04	1.02256	0.00089	1.00000	0.00650	0.02256	1.02256
331	hst019-001	2.441	9.54E-06	193.564	2.15E-02	3.16E-01	5.26E-04	0.99815	0.00120	1.00000	0.00410	-0.00185	0.99815
332	hst019-002	2.441	8.60E-06	194.615	1.83E-02	2.95E-01	4.15E-04	1.00512	0.00105	1.00000	0.00410	0.00512	1.00512
333	hst019-003	2.441	8.82E-06	192.394	1.86E-02	3.52E-01	4.96E-04	1.00060	0.00108	1.00000	0.00670	0.00060	1.00060
334	hst020-g	2.439	4.17E-06	172.463	2.81E-02	1.36E+00	2.59E-03	1.00606	0.00117	0.99660	0.01160	0.00946	1.00946
335	hst020-h	2.438	2.33E-06	190.137	2.11E-02	3.97E-01	6.20E-04	1.00778	0.00146	0.99560	0.00930	0.01218	1.01218
336	hst020-i	2.437	1.12E-06	204.326	1.33E-02	1.35E-01	1.53E-04	1.01450	0.00160	0.99570	0.00790	0.01880	1.01880
337	hst020-j	2.437	1.19E-06	204.357	1.33E-02	1.34E-01	1.48E-04	1.01681	0.00141	0.99550	0.00780	0.02131	1.02131
338	hst020-k	2.437	4.52E-07	214.216	6.69E-03	5.84E-02	4.21E-05	1.02266	0.00126	0.99590	0.00770	0.02676	1.02676
339	hst021-002	2.441	8.99E-06	194.679	1.96E-02	2.89E-01	4.34E-04	1.00283	0.00126	0.99750	0.00540	0.00533	1.00533
340	hst021-003	2.441	8.65E-06	195.244	2.04E-02	2.77E-01	4.42E-04	1.01102	0.00112	0.99750	0.00540	0.01352	1.01352
341	hst021-010	2.441	9.26E-06	194.962	1.98E-02	2.83E-01	4.43E-04	1.00663	0.00120	0.99750	0.00540	0.00913	1.00913
342	hst021-025	2.441	8.46E-06	195.818	1.99E-02	2.65E-01	4.02E-04	1.00580	0.00119	0.99780	0.00540	0.00800	1.00800
343	hst021-h	2.441	9.68E-06	193.249	2.03E-02	3.23E-01	4.97E-04	1.00066	0.00127	0.99750	0.00540	0.00316	1.00316
344	hst021-i	2.441	8.13E-06	198.364	2.03E-02	2.17E-01	3.52E-04	1.01050	0.00116	0.99750	0.00540	0.01300	1.01300
345	hst021-j	2.441	1.03E-05	192.852	2.26E-02	3.33E-01	5.78E-04	0.99585	0.00130	0.99780	0.00540	-0.00195	0.99805
346	hst021-k	2.441	9.42E-06	194.817	1.99E-02	2.87E-01	4.53E-04	1.01262	0.00133	0.99780	0.00540	0.01482	1.01482
347	hst021-l	2.441	9.93E-06	192.951	2.06E-02	3.31E-01	5.37E-04	0.99639	0.00141	0.99780	0.00540	-0.00141	0.99859
348	hst021-m	2.441	9.13E-06	195.482	2.06E-02	2.71E-01	4.40E-04	0.99887	0.00143	0.99780	0.00540	0.00107	1.00107
349	hst025-001	2.437	1.17E-06	218.180	3.33E-03	4.06E-02	1.69E-05	1.00264	0.00091	1.00020	0.00250	0.00244	1.00244
350	hst025-002	2.437	1.14E-06	218.180	3.39E-03	4.06E-02	1.75E-05	1.00251	0.00120	1.00070	0.00250	0.00181	1.00181
351	hst025-003	2.437	1.21E-06	217.673	3.54E-03	4.26E-02	1.87E-05	0.99924	0.00083	1.00020	0.00640	-0.00096	0.99904
352	hst025-004	2.437	1.22E-06	217.945	3.71E-03	4.14E-02	1.93E-05	1.00147	0.00126	1.00030	0.00270	0.00117	1.00117
353	hst025-005	2.438	1.76E-06	216.130	4.55E-03	4.88E-02	2.50E-05	1.00413	0.00108	1.00130	0.00300	0.00283	1.00283
354	hst025-006	2.437	1.13E-06	217.582	3.60E-03	4.29E-02	1.92E-05	1.01058	0.00085	1.00020	0.00670	0.01038	1.01038
355	hst025-007	2.437	1.49E-06	216.555	4.29E-03	4.72E-02	2.41E-05	1.01584	0.00085	1.00090	0.00730	0.01494	1.01494
356	hst025-008	2.437	1.55E-06	216.225	4.87E-03	4.87E-02	2.51E-05	1.01379	0.00086	1.00000	0.00670	0.01379	1.01379
357	hst025-009	2.438	1.88E-06	214.792	6.20E-03	5.53E-02	3.59E-05	1.00795	0.00100	1.00020	0.00650	0.00775	1.00775
358	hst025-010	2.438	2.77E-06	211.968	1.00E-02	7.08E-02	6.74E-05	1.01223	0.00111	1.00030	0.00430	0.01193	1.01193
359	hst025-011	2.438	2.72E-06	211.838	1.02E-02	7.17E-02	6.80E-05	1.01279	0.00097	1.00020	0.00450	0.01259	1.01259
360	hst025-012	2.438	3.74E-06	209.367	1.38E-02	8.84E-02	1.10E-04	1.01303	0.00077	1.00020	0.00450	0.01283	1.01283
361	hst025-013	2.438	3.74E-06	209.234	1.52E-02	8.93E-02	1.21E-04	1.01918	0.00080	1.00090	0.00470	0.01828	1.01828
362	hst025-014	2.439	5.01E-06	205.585	2.08E-02	1.20E-01	2.12E-04	1.01112	0.00084	1.00080	0.00530	0.01032	1.01032
363	hst025-015	2.439	4.89E-06	206.326	1.93E-02	1.12E-01	1.82E-04	1.00480	0.00093	1.00020	0.00580	0.00460	1.00460
364	hst025-016	2.440	7.42E-06	199.908	2.89E-02	1.85E-01	4.26E-04	1.01519	0.00089	1.00000	0.00490	0.01519	1.01519
365	hst025-017	2.440	7.59E-06	200.725	3.07E-02	1.72E-01	4.24E-04	1.00744	0.00090	1.00000	0.00550	0.00744	1.00744
366	hst025-018	2.440	7.37E-06	201.351	2.89E-02	1.62E-01	3.72E-04	1.00376	0.00081	1.00000	0.00610	0.00376	1.00376

N	Case	nubar	Sigma	AFG	Sigma	EALCF (eV)	Sigma	k_{calc} HEU	Sigma	k_{exp} HEU	Sigma	Bias = Calculated - Benchmark	Adjusted k_{eff} HEU
367	hst027-001	2.438	1.06E-06	211.266	2.83E-03	7.46E-02	1.98E-05	0.99797	0.00034	1.00000	0.00460	-0.00203	0.99797
368	hst027-002	2.438	3.15E-06	211.122	8.02E-03	7.54E-02	5.91E-05	1.00061	0.00105	1.00000	0.00430	0.00061	1.00061
369	hst027-003	2.438	3.14E-06	211.087	8.15E-03	7.56E-02	6.06E-05	1.00000	0.00123	1.00000	0.00370	0.00000	1.00000
370	hst027-004	2.438	3.31E-06	211.049	8.55E-03	7.58E-02	6.31E-05	1.00243	0.00107	1.00000	0.00370	0.00243	1.00243
371	hst027-005	2.438	3.21E-06	210.998	8.90E-03	7.61E-02	6.31E-05	0.99916	0.00114	1.00000	0.00440	-0.00084	0.99916
372	hst027-006	2.438	3.27E-06	211.163	8.45E-03	7.52E-02	6.11E-05	0.99375	0.00128	1.00000	0.00430	-0.00625	0.99375
373	hst027-007	2.438	3.05E-06	211.173	8.77E-03	7.52E-02	6.19E-05	1.00076	0.00122	1.00000	0.00380	0.00076	1.00076
374	hst027-008	2.438	3.30E-06	211.162	8.37E-03	7.53E-02	6.22E-05	1.00302	0.00112	1.00000	0.00350	0.00302	1.00302
375	hst027-009	2.438	3.14E-06	211.134	8.39E-03	7.54E-02	6.07E-05	0.99945	0.00139	1.00000	0.00390	-0.00055	0.99945
376	hst028-a	2.438	1.63E-06	216.518	4.67E-03	4.73E-02	2.57E-05	0.99782	0.00108	1.00000	0.00230	-0.00218	0.99782
377	hst028-b	2.438	1.70E-06	216.375	4.85E-03	4.77E-02	2.64E-05	1.00024	0.00118	1.00000	0.00340	0.00024	1.00024
378	hst028-c	2.438	1.66E-06	216.489	4.48E-03	4.74E-02	2.49E-05	0.99983	0.00123	1.00000	0.00260	-0.00017	0.99983
379	hst028-d	2.438	1.65E-06	216.375	5.14E-03	4.77E-02	2.80E-05	1.00078	0.00104	1.00000	0.00280	0.00078	1.00078
380	hst028-e	2.438	1.66E-06	216.477	4.67E-03	4.74E-02	2.49E-05	0.99488	0.00119	1.00000	0.00310	-0.00512	0.99488
381	hst028-g	2.438	1.73E-06	216.355	4.72E-03	4.78E-02	2.52E-05	0.99823	0.00105	1.00000	0.00230	-0.00177	0.99823
382	hst028-h	2.438	1.72E-06	216.423	4.88E-03	4.76E-02	2.65E-05	0.99981	0.00103	1.00000	0.00380	-0.00019	0.99981
383	hst028-i	2.438	1.70E-06	216.331	4.89E-03	4.79E-02	2.58E-05	0.99968	0.00116	1.00000	0.00270	-0.00032	0.99968
384	hst028-j	2.440	5.74E-06	203.397	1.35E-02	1.46E-01	1.66E-04	0.99749	0.00117	1.00000	0.00490	-0.00251	0.99749
385	hst028-k	2.440	5.96E-06	203.154	1.48E-02	1.48E-01	1.85E-04	0.99607	0.00124	1.00000	0.00530	-0.00393	0.99607
386	hst028-l	2.440	6.23E-06	203.252	1.43E-02	1.47E-01	1.77E-04	0.99637	0.00146	1.00000	0.00510	-0.00363	0.99637
387	hst028-m	2.440	6.10E-06	202.984	1.58E-02	1.50E-01	1.94E-04	0.99614	0.00128	1.00000	0.00460	-0.00386	0.99614
388	hst028-n	2.440	5.95E-06	203.030	1.39E-02	1.50E-01	1.76E-04	0.99592	0.00117	1.00000	0.00580	-0.00408	0.99592
389	hst028-p	2.440	5.84E-06	202.781	1.49E-02	1.52E-01	1.91E-04	0.99636	0.00108	1.00000	0.00460	-0.00364	0.99636
390	hst028-q	2.440	6.04E-06	202.891	1.42E-02	1.51E-01	1.81E-04	1.00472	0.00134	1.00000	0.00640	0.00472	1.00472
391	hst028-r	2.440	6.21E-06	202.681	1.51E-02	1.54E-01	1.95E-04	1.00101	0.00124	1.00000	0.00520	0.00101	1.00101
392	hst028-s	2.440	6.00E-06	202.754	1.55E-02	1.53E-01	1.97E-04	0.99747	0.00123	1.00000	0.00660	-0.00253	0.99747
393	hst028-u	2.440	6.20E-06	202.514	1.43E-02	1.56E-01	1.85E-04	0.99606	0.00132	1.00000	0.00600	-0.00394	0.99606
394	hst029-a	2.440	6.32E-06	202.295	1.51E-02	1.59E-01	2.01E-04	0.99922	0.00129	1.00000	0.00660	-0.00078	0.99922
395	hst029-b	2.440	6.20E-06	202.316	1.50E-02	1.58E-01	1.97E-04	1.00426	0.00115	1.00000	0.00580	0.00426	1.00426
396	hst029-c	2.440	6.38E-06	202.106	1.55E-02	1.60E-01	1.99E-04	0.99410	0.00123	1.00000	0.00680	-0.00590	0.99410
397	hst029-d	2.440	6.68E-06	201.438	1.65E-02	1.68E-01	2.22E-04	0.99495	0.00123	1.00000	0.00740	-0.00505	0.99495
398	hst029-e	2.440	6.21E-06	201.235	1.63E-02	1.70E-01	2.29E-04	1.00021	0.00142	1.00000	0.00670	0.00021	1.00021
399	hst029-g	2.440	6.22E-06	201.233	1.47E-02	1.71E-01	2.08E-04	1.00092	0.00131	1.00000	0.00650	0.00092	1.00092
400	hst029-h	2.440	6.47E-06	201.385	1.49E-02	1.69E-01	2.15E-04	0.99915	0.00109	1.00000	0.00630	-0.00085	0.99915
401	hst030-a	2.438	1.74E-06	216.351	4.75E-03	4.79E-02	2.61E-05	0.99690	0.00122	1.00000	0.00390	-0.00310	0.99690
402	hst030-b	2.438	1.74E-06	216.160	5.00E-03	4.86E-02	2.73E-05	0.99857	0.00096	1.00000	0.00320	-0.00143	0.99857
403	hst030-c	2.438	1.72E-06	216.106	5.02E-03	4.88E-02	2.67E-05	0.99710	0.00123	1.00000	0.00310	-0.00290	0.99710

N	Case	nubar	Sigma	AFG	Sigma	EALCF (eV)	Sigma	k_{calc} HEU	Sigma	k_{exp} HEU	Sigma	Bias = Calculated - Benchmark	Adjusted k_{eff} HEU
404	hst030-d	2.440	6.54E-06	202.209	1.48E-02	1.60E-01	2.00E-04	0.99890	0.00138	1.00000	0.00640	-0.00110	0.99890
405	hst030-e	2.440	6.32E-06	202.041	1.49E-02	1.61E-01	2.01E-04	0.99489	0.00137	1.00000	0.00580	-0.00511	0.99489
406	hst030-g	2.440	6.21E-06	201.964	1.50E-02	1.62E-01	2.00E-04	0.99695	0.00125	1.00000	0.00590	-0.00305	0.99695
407	hst030-h	2.440	6.03E-06	201.522	1.65E-02	1.67E-01	2.23E-04	1.00007	0.00122	1.00000	0.00640	0.00007	1.00007
408	hst031-a	2.440	6.36E-06	201.671	1.62E-02	1.65E-01	2.21E-04	0.99811	0.00113	1.00000	0.00460	-0.00189	0.99811
409	hst031-b	2.440	6.57E-06	200.702	1.77E-02	1.77E-01	2.54E-04	0.99990	0.00103	1.00000	0.00580	-0.00010	0.99990
410	hst031-c	2.440	6.51E-06	201.238	1.52E-02	1.71E-01	2.13E-04	0.99891	0.00123	1.00000	0.00580	-0.00109	0.99891
411	hst031-d	2.440	6.68E-06	199.679	1.69E-02	1.90E-01	2.57E-04	0.99777	0.00114	1.00000	0.00680	-0.00223	0.99777
412	hst032-b	2.437	4.29E-07	221.032	1.35E-03	3.11E-02	6.94E-06	0.99981	0.00067	1.00150	0.00260	-0.00169	0.99831
413	hst033-simple-02a	2.440	7.09E-06	193.592	1.98E-02	3.11E-01	4.84E-04	0.99895	0.00112	0.99790	0.01120	0.00105	1.00105
414	hst033-simple-02b	2.440	7.71E-06	193.300	1.94E-02	3.18E-01	4.86E-04	0.99818	0.00112	1.00000	0.01090	-0.00182	0.99818
415	hst033-simple-02c	2.440	7.53E-06	193.107	1.91E-02	3.23E-01	4.73E-04	1.00019	0.00119	0.99790	0.00670	0.00229	1.00229
416	hst033-simple-03a	2.440	7.55E-06	194.305	2.01E-02	2.95E-01	4.57E-04	1.00278	0.00128	0.99420	0.01150	0.00858	1.00858
417	hst033-simple-03b	2.440	6.99E-06	194.380	1.88E-02	2.94E-01	4.42E-04	1.00301	0.00107	0.99790	0.01120	0.00511	1.00511
418	hst033-simple-03c	2.440	7.44E-06	195.189	1.99E-02	2.76E-01	4.31E-04	1.00859	0.00131	0.99790	0.00720	0.01069	1.01069
419	hst033-simple-04a	2.440	7.66E-06	193.524	1.84E-02	3.13E-01	4.53E-04	1.00186	0.00107	0.99420	0.01150	0.00766	1.00766
420	hst033-simple-04b	2.440	7.25E-06	193.228	1.86E-02	3.20E-01	4.56E-04	1.00710	0.00120	0.99790	0.01120	0.00920	1.00920
421	hst033-simple-05a	2.440	7.39E-06	193.558	1.88E-02	3.12E-01	4.58E-04	1.00713	0.00116	0.99420	0.01120	0.01293	1.01293
422	hst033-simple-05b	2.440	7.70E-06	193.310	2.03E-02	3.18E-01	4.91E-04	1.00896	0.00123	1.00000	0.01090	0.00896	1.00896
423	hst033-simple-06a	2.440	7.07E-06	193.579	1.95E-02	3.11E-01	4.78E-04	1.00434	0.00123	0.99420	0.01120	0.01014	1.01014
424	hst033-simple-06b	2.440	7.20E-06	193.304	2.02E-02	3.18E-01	5.02E-04	1.00874	0.00121	1.00000	0.01090	0.00874	1.00874
425	hst033-simple-07a	2.440	7.64E-06	193.607	1.91E-02	3.11E-01	4.64E-04	0.99844	0.00109	0.99420	0.01120	0.00424	1.00424
426	hst033-simple-07b	2.440	7.11E-06	193.419	1.93E-02	3.16E-01	4.83E-04	1.00782	0.00110	1.00000	0.01090	0.00782	1.00782
427	hst033-simple-08a	2.440	7.39E-06	193.501	1.83E-02	3.13E-01	4.62E-04	1.00219	0.00125	0.99420	0.01120	0.00799	1.00799
428	hst033-simple-08b	2.440	7.29E-06	193.270	1.94E-02	3.19E-01	4.75E-04	1.00518	0.00106	1.00000	0.01090	0.00518	1.00518
429	hst033-simple-09a	2.440	7.35E-06	193.624	1.97E-02	3.11E-01	4.74E-04	0.99766	0.00117	0.99420	0.01120	0.00346	1.00346
430	hst033-simple-09b	2.440	7.52E-06	193.384	1.90E-02	3.17E-01	4.80E-04	0.99724	0.00098	1.00000	0.01090	-0.00276	0.99724
431	hst033-simple-09c	2.440	7.35E-06	193.748	1.93E-02	3.08E-01	4.59E-04	0.99531	0.00106	0.99790	0.01050	-0.00259	0.99741
432	hst033-simple-10a	2.440	7.18E-06	194.228	1.97E-02	2.97E-01	4.59E-04	1.00046	0.00108	0.99420	0.01150	0.00626	1.00626
433	hst033-simple-10c	2.440	6.72E-06	195.154	1.91E-02	2.77E-01	4.10E-04	1.00328	0.00094	0.99790	0.00720	0.00538	1.00538
434	hst033-simple-10d	2.440	7.34E-06	194.056	1.97E-02	3.01E-01	4.66E-04	0.99587	0.00110	0.99790	0.01060	-0.00203	0.99797
435	hst033-simple-11a	2.440	7.16E-06	194.455	1.99E-02	2.92E-01	4.56E-04	0.99994	0.00127	0.99420	0.01120	0.00574	1.00574
436	hst033-simple-11b	2.440	6.94E-06	194.668	1.91E-02	2.87E-01	4.30E-04	0.99998	0.00110	0.99790	0.01090	0.00208	1.00208
437	hst033-simple-12a	2.440	7.14E-06	193.846	1.92E-02	3.06E-01	4.67E-04	0.99928	0.00108	0.99420	0.01120	0.00508	1.00508
438	hst033-simple-12b	2.440	7.32E-06	193.714	1.89E-02	3.09E-01	4.62E-04	1.00168	0.00110	1.00000	0.01090	0.00168	1.00168
439	hst035-a	2.437	9.03E-07	219.057	2.85E-03	3.73E-02	1.41E-05	1.00316	0.00093	1.00000	0.00310	0.00316	1.00316
440	hst035-b	2.437	8.95E-07	218.949	2.85E-03	3.77E-02	1.36E-05	1.00303	0.00092	1.00000	0.00320	0.00303	1.00303

N	Case	nubar	Sigma	AFG	Sigma	EALCF (eV)	Sigma	k_{calc} HEU	Sigma	k_{exp} HEU	Sigma	Bias = Calculated - Benchmark	Adjusted k_{eff} HEU
441	hst035-c	2.437	8.96E-07	218.964	2.84E-03	3.76E-02	1.49E-05	1.00627	0.00115	1.00000	0.00300	0.00627	1.00627
442	hst035-d	2.437	9.51E-07	219.042	2.90E-03	3.74E-02	1.44E-05	1.00593	0.00086	1.00000	0.00300	0.00593	1.00593
443	hst035-e	2.438	1.93E-06	215.972	4.78E-03	4.94E-02	2.77E-05	1.00400	0.00127	1.00000	0.00330	0.00400	1.00400
444	hst035-g	2.438	1.69E-06	215.823	5.34E-03	5.00E-02	2.89E-05	1.00658	0.00115	1.00000	0.00290	0.00658	1.00658
445	hst035-h	2.438	3.51E-06	210.395	9.35E-03	8.07E-02	7.34E-05	1.00551	0.00115	1.00000	0.00350	0.00551	1.00551
446	hst035-i	2.438	3.53E-06	209.828	9.81E-03	8.42E-02	7.57E-05	0.99855	0.00116	1.00000	0.00380	-0.00145	0.99855
447	hst035-j	2.438	3.48E-06	209.985	9.70E-03	8.32E-02	7.46E-05	1.00261	0.00134	1.00000	0.00410	0.00261	1.00261
448	hst036-a	2.438	2.28E-06	214.527	6.15E-03	5.61E-02	3.59E-05	0.99583	0.00126	0.99740	0.00450	-0.00157	0.99843
449	hst036-b	2.438	2.31E-06	214.021	6.56E-03	5.83E-02	3.74E-05	1.00120	0.00124	0.99790	0.00390	0.00330	1.00330
450	hst036-c	2.438	2.38E-06	213.409	7.50E-03	6.11E-02	4.51E-05	0.99648	0.00113	0.99930	0.00440	-0.00282	0.99718
451	hst036-d	2.438	2.45E-06	212.929	7.65E-03	6.33E-02	4.54E-05	0.99871	0.00120	1.00000	0.00620	-0.00129	0.99871
452	hst037-a	2.437	1.03E-06	218.789	2.87E-03	3.83E-02	1.48E-05	1.01062	0.00103	0.99800	0.00340	0.01262	1.01262
453	hst037-b	2.437	1.09E-06	218.494	3.97E-03	3.93E-02	1.70E-05	1.00321	0.00106	0.99900	0.00350	0.00421	1.00421
454	hst037-c	2.437	1.49E-06	217.231	4.09E-03	4.42E-02	2.19E-05	1.00664	0.00116	0.99700	0.00420	0.00964	1.00964
455	hst037-d	2.437	1.47E-06	216.886	5.22E-03	4.54E-02	2.39E-05	1.01234	0.00095	0.99800	0.00350	0.01434	1.01434
456	hst037-e	2.437	1.63E-06	216.765	5.60E-03	4.59E-02	2.59E-05	1.00366	0.00110	0.99800	0.00420	0.00566	1.00566
457	hst037-g	2.438	2.03E-06	215.580	5.38E-03	5.13E-02	2.93E-05	1.01339	0.00099	0.99600	0.00510	0.01739	1.01739
458	hst037-h	2.438	1.95E-06	215.200	6.31E-03	5.28E-02	3.38E-05	1.01101	0.00122	0.99800	0.00340	0.01301	1.01301
459	hst037-i	2.438	1.98E-06	215.035	7.00E-03	5.35E-02	3.70E-05	1.00699	0.00124	0.99800	0.00400	0.00899	1.00899
460	hst037-j	2.438	2.15E-06	214.783	7.55E-03	5.45E-02	3.78E-05	1.00609	0.00094	0.99800	0.00470	0.00809	1.00809
	Maximum	2.612	5.70E-04	221.032	1.61E-01	9.61E+05	1.93E+03	1.08394	0.00203	1.06400	0.01800	0.08734	1.08734
	Average	2.472	6.08E-05	160.373	2.40E-02	9.45E+04	1.71E+02	1.00141	0.00109	0.99972	0.00445	0.00169	1.00169
	Minimum	2.437	4.29E-07	24.237	1.35E-03	3.11E-02	6.94E-06	0.92171	0.00023	0.98260	0.00000	-0.14229	0.85771

Table 4.3 Results for Intermediate and Mixed Enrichment Uranium Systems (Volume 3) with CSAS25 from SCALE 5 and the 238-group Library on the HP-6000 (CMODD) Workstation

N	Case	nubar	Sigma	AFG	Sigma	EALCF (eV)	Sigma	k_{calc} IEU	sigma	k_{exp} IEU	Sigma	Bias = Calculated - Benchmark	Adjusted k_{eff} IEU
1	ici001-001	2.474	6.95E-05	39.743	7.75E-03	1.85E+05	1.82E+02	1.00533	0.00037	0.96900	0.00500	0.03633	1.03633
2	ici001-002	2.467	6.77E-05	52.067	2.11E-02	2.66E+04	6.32E+01	1.02010	0.00053	0.98000	0.00300	0.04010	1.04010
3	ici001-003	2.449	4.81E-05	124.060	4.66E-02	5.63E+01	1.84E-01	1.06741	0.00055	1.01400	0.00600	0.05341	1.05341
4	ici001-004	2.442	3.52E-05	185.466	3.88E-02	6.86E-01	1.92E-03	0.97776	0.00062	0.96400	0.01200	0.01376	1.01376
5	ict001-001	2.461	5.05E-05	151.782	6.03E-02	7.43E+00	3.06E-02	0.99729	0.00103	1.00000	0.00400	-0.00271	0.99729
6	ict001-002	2.454	4.11E-05	169.344	5.23E-02	2.03E+00	7.34E-03	1.00029	0.00105	1.00000	0.00400	0.00029	1.00029
7	ict001-003	2.448	3.06E-05	185.702	4.20E-02	6.14E-01	1.79E-03	0.99538	0.00101	1.00000	0.00400	-0.00462	0.99538
8	ict001-004	2.445	2.49E-05	197.930	3.30E-02	2.49E-01	5.98E-04	1.00371	0.00103	1.00000	0.00400	0.00371	1.00371
9	ict001-005	2.442	1.91E-05	209.491	2.22E-02	1.03E-01	1.76E-04	1.01296	0.00101	1.00000	0.00400	0.01296	1.01296
10	ict001-006	2.449	3.19E-05	185.729	4.26E-02	6.17E-01	1.81E-03	1.00481	0.00115	1.00000	0.00400	0.00481	1.00481
11	ict001-007	2.449	3.16E-05	185.700	4.15E-02	6.22E-01	1.77E-03	1.00326	0.00123	1.00000	0.00400	0.00326	1.00326
12	ict001-008	2.450	3.48E-05	185.249	4.14E-02	6.50E-01	1.90E-03	1.00015	0.00103	1.00000	0.00400	0.00015	1.00015
13	ict001-009	2.455	4.20E-05	172.789	5.06E-02	1.66E+00	5.89E-03	1.00878	0.00110	1.00000	0.00400	0.00878	1.00878
14	ict001-010	2.454	4.31E-05	169.420	5.33E-02	2.02E+00	7.35E-03	0.99951	0.00122	1.00000	0.00400	-0.00049	0.99951
15	ict001-011	2.454	4.04E-05	169.618	5.06E-02	1.99E+00	6.92E-03	0.99677	0.00130	1.00000	0.00400	-0.00323	0.99677
16	ict001-012	2.454	4.04E-05	170.082	4.95E-02	1.93E+00	6.49E-03	0.99811	0.00115	1.00000	0.00400	-0.00189	0.99811
17	ict001-013	2.445	2.47E-05	197.967	3.25E-02	2.48E-01	5.74E-04	1.00004	0.00117	1.00000	0.00400	0.00004	1.00004
18	ict001-014	2.445	2.54E-05	197.958	3.27E-02	2.48E-01	5.92E-04	1.00041	0.00111	1.00000	0.00400	0.00041	1.00041
19	ict001-015	2.445	2.38E-05	198.072	3.18E-02	2.46E-01	5.73E-04	1.00179	0.00144	1.00000	0.00400	0.00179	1.00179
20	ict001-016	2.443	2.11E-05	205.426	2.60E-02	1.41E-01	2.74E-04	1.00687	0.00123	1.00000	0.00400	0.00687	1.00687
21	ict001-017	2.460	5.01E-05	150.171	5.80E-02	8.17E+00	3.20E-02	0.99449	0.00119	1.00000	0.00400	-0.00551	0.99449
22	ict001-018	2.452	3.90E-05	173.800	4.75E-02	1.48E+00	4.74E-03	0.99877	0.00125	1.00000	0.00400	-0.00123	0.99877
23	ict001-019	2.443	2.26E-05	203.452	2.91E-02	1.65E-01	3.49E-04	1.00531	0.00111	1.00000	0.00400	0.00531	1.00531
24	ict001-020	2.454	3.92E-05	168.173	5.05E-02	2.18E+00	7.39E-03	1.00437	0.00105	1.00000	0.00400	0.00437	1.00437
25	ict001-021	2.460	4.62E-05	150.221	6.47E-02	8.09E+00	3.58E-02	0.99815	0.00100	1.00000	0.00400	-0.00185	0.99815
26	ict001-022	2.459	4.70E-05	150.986	5.62E-02	7.58E+00	2.82E-02	0.99608	0.00096	1.00000	0.00400	-0.00392	0.99608
27	ict001-023	2.451	3.52E-05	174.112	4.45E-02	1.44E+00	4.32E-03	0.99565	0.00123	1.00000	0.00400	-0.00435	0.99565
28	ict001-024	2.451	3.47E-05	173.239	4.30E-02	1.52E+00	4.38E-03	1.00158	0.00110	1.00000	0.00400	0.00158	1.00158
29	ict001-025	2.443	2.24E-05	203.096	2.84E-02	1.69E-01	3.46E-04	1.00418	0.00107	1.00000	0.00400	0.00418	1.00418
30	ict001-026	2.443	2.07E-05	205.446	2.66E-02	1.41E-01	2.88E-04	1.01000	0.00104	1.00000	0.00400	0.01000	1.01000
31	ict001-027	2.443	2.22E-05	205.632	2.72E-02	1.38E-01	2.84E-04	1.00779	0.00112	1.00000	0.00400	0.00779	1.00779
32	ict001-028	2.454	4.09E-05	169.723	5.31E-02	1.98E+00	7.24E-03	1.00354	0.00104	1.00000	0.00400	0.00354	1.00354

N	Case	nubar	Sigma	AFG	Sigma	EALCF (eV)	Sigma	k_{calc} IEU	sigma	k_{exp} IEU	Sigma	Bias = Calculated - Benchmark	Adjusted k_{eff} IEU
33	ict001-029	2.453	3.83E-05	170.700	5.02E-02	1.84E+00	6.27E-03	1.00293	0.00107	1.00000	0.00400	0.00293	1.00293
34	ict003-001	2.439	6.66E-06	211.871	1.01E-02	8.00E-02	8.72E-05	1.00253	0.00107	1.00060	0.00560	0.00193	1.00193
35	ict003-002	2.439	6.07E-06	211.894	8.77E-03	7.98E-02	7.84E-05	1.00829	0.00104	1.00460	0.00560	0.00369	1.00369
36	imf001-01i	2.592	2.12E-04	26.174	1.32E-02	8.11E+05	1.04E+03	0.99949	0.00094	0.99890	0.00090	0.00059	1.00059
37	imf001-02i	2.592	2.02E-04	26.175	1.30E-02	8.11E+05	1.01E+03	1.00070	0.00102	0.99970	0.00090	0.00100	1.00100
38	imf001-03i	2.586	1.92E-04	27.178	1.21E-02	7.37E+05	8.76E+02	1.00256	0.00083	0.99930	0.00030	0.00326	1.00326
39	imf001-04i	2.586	2.00E-04	27.159	1.26E-02	7.39E+05	9.25E+02	1.00337	0.00090	1.00020	0.00030	0.00317	1.00317
40	imf002-001	2.577	1.98E-04	29.794	1.30E-02	5.56E+05	7.30E+02	1.00861	0.00088	1.00000	0.00300	0.00861	1.00861
41	imf003-001	2.583	1.82E-04	27.610	1.15E-02	7.09E+05	8.11E+02	1.00354	0.00105	1.00000	0.00170	0.00354	1.00354
42	imf004-001	2.578	1.95E-04	28.191	1.24E-02	6.65E+05	8.36E+02	1.00989	0.00102	1.00000	0.00300	0.00989	1.00989
43	imf005-001	2.575	1.71E-04	28.327	1.14E-02	6.59E+05	7.76E+02	1.01066	0.00091	1.00000	0.00210	0.01066	1.01066
44	imf006-001	2.576	1.70E-04	28.326	1.12E-02	6.60E+05	7.49E+02	0.99570	0.00086	1.00000	0.00230	-0.00430	0.99570
45	imf007-001	2.574	2.31E-04	30.746	1.57E-02	4.92E+05	7.54E+02	1.01638	0.00086	1.00450	0.00070	0.01188	1.01188
46	imf008-001	2.585	1.88E-04	27.671	1.16E-02	7.02E+05	8.20E+02	1.00728	0.00084	1.00000	0.00180	0.00728	1.00728
47	imf009-001	2.546	1.71E-04	69.158	7.83E-02	1.51E+04	1.02E+02	1.00990	0.00092	1.00000	0.00530	0.00990	1.00990
48	imf010-001	2.561	1.63E-04	32.284	1.07E-02	4.12E+05	4.75E+02	1.00583	0.00067	0.99540	0.00240	0.01043	1.01043
49	imf012-001	2.549	1.50E-04	33.211	1.12E-02	3.70E+05	4.46E+02	1.00893	0.00077	1.00070	0.00270	0.00823	1.00823
50	imf014-092	2.536	1.28E-04	34.738	9.58E-03	3.21E+05	3.44E+02	1.01233	0.00079	0.99520	0.00220	0.01713	1.01713
51	imf014-093	2.519	1.03E-04	36.532	8.31E-03	2.66E+05	2.54E+02	1.01082	0.00072	0.99160	0.00220	0.01922	1.01922
	Maximum	2.592	2.31E-04	211.894	7.83E-02	8.11E+05	1.04E+03	1.06741	0.00144	1.01400	0.01200	0.05341	1.05341
	Average	2.488	7.99E-05	129.204	3.20E-02	1.79E+05	2.20E+02	1.00471	0.00099	0.99839	0.00363	0.00633	1.00633
	Minimum	2.439	6.07E-06	26.174	7.75E-03	7.98E-02	7.84E-05	0.97776	0.00037	0.96400	0.00030	-0.00551	0.99449

Table 4.4 Results for Low Enriched Uranium Systems (Volume 4) with CSAS25 from SCALE 5 and the 238-group Library on the HP-6000 (CMODD) Workstation

N	Case	nubar	Sigma	AFG	Sigma	EALCF (eV)	Sigma	k_{calc} LEU	Sigma	k_{exp} LEU	Sigma	Bias = Calculated - Benchmark	Adjusted k_{eff} LEU
1	lct001-001	2.451	4.07E-05	208.747	2.07E-02	9.87E-02	1.87E-04	0.99476	0.00095	0.99980	0.00310	-0.00504	0.99496
2	lct001-002	2.451	4.37E-05	208.831	1.93E-02	9.81E-02	1.72E-04	0.99198	0.00091	0.99980	0.00310	-0.00782	0.99218
3	lct001-003	2.451	4.58E-05	209.004	2.07E-02	9.66E-02	1.77E-04	0.99351	0.00080	0.99980	0.00310	-0.00629	0.99371
4	lct001-004	2.451	4.30E-05	208.878	2.06E-02	9.77E-02	1.81E-04	0.99318	0.00072	0.99980	0.00310	-0.00662	0.99338
5	lct001-005	2.451	4.48E-05	209.041	2.07E-02	9.64E-02	1.83E-04	0.99272	0.00081	0.99980	0.00310	-0.00708	0.99292
6	lct001-006	2.451	4.38E-05	208.937	2.06E-02	9.72E-02	1.81E-04	0.99249	0.00082	0.99980	0.00310	-0.00731	0.99269
7	lct001-007	2.451	4.25E-05	209.154	2.06E-02	9.54E-02	1.80E-04	0.99193	0.00082	0.99980	0.00310	-0.00787	0.99213
8	lct001-008	2.451	4.55E-05	209.024	2.09E-02	9.65E-02	1.87E-04	0.99099	0.00100	0.99980	0.00310	-0.00881	0.99119
9	lct002-001	2.449	4.04E-05	207.427	2.26E-02	1.15E-01	2.25E-04	0.99319	0.00109	0.99970	0.00200	-0.00651	0.99349
10	lct002-002	2.450	4.33E-05	207.422	2.21E-02	1.15E-01	2.32E-04	0.99443	0.00120	0.99970	0.00200	-0.00527	0.99473
11	lct002-003	2.450	4.00E-05	207.459	2.12E-02	1.15E-01	2.18E-04	0.99652	0.00083	0.99970	0.00200	-0.00318	0.99682
12	lct002-004	2.450	4.20E-05	207.536	2.24E-02	1.15E-01	2.33E-04	0.99422	0.00094	0.99970	0.00200	-0.00548	0.99452
13	lct002-005	2.449	4.01E-05	207.689	2.16E-02	1.13E-01	2.15E-04	0.99269	0.00088	0.99970	0.00200	-0.00701	0.99299
14	lct003-001	2.457	5.67E-05	201.838	2.68E-02	1.78E-01	4.11E-04	0.98382	0.00100	1.00000	0.00390	-0.01618	0.98382
15	lct003-002	2.457	5.75E-05	201.799	2.69E-02	1.78E-01	4.24E-04	0.98338	0.00095	1.00000	0.00390	-0.01662	0.98338
16	lct003-003	2.457	5.52E-05	201.742	2.65E-02	1.79E-01	4.08E-04	0.98398	0.00083	1.00000	0.00390	-0.01602	0.98398
17	lct003-004	2.457	5.78E-05	201.763	2.76E-02	1.79E-01	4.39E-04	0.98401	0.00079	1.00000	0.00390	-0.01599	0.98401
18	lct003-005	2.457	5.24E-05	201.789	2.49E-02	1.79E-01	3.83E-04	0.98566	0.00115	1.00000	0.00390	-0.01434	0.98566
19	lct003-006	2.455	5.24E-05	203.546	2.52E-02	1.54E-01	3.40E-04	0.98437	0.00115	1.00000	0.00390	-0.01563	0.98437
20	lct003-007	2.456	5.26E-05	202.733	2.52E-02	1.65E-01	3.60E-04	0.98252	0.00095	1.00000	0.00390	-0.01748	0.98252
21	lct003-008	2.456	5.42E-05	203.305	2.58E-02	1.57E-01	3.60E-04	0.98636	0.00094	1.00000	0.00390	-0.01364	0.98636
22	lct003-009	2.456	5.65E-05	203.157	2.73E-02	1.59E-01	3.86E-04	0.97911	0.00105	1.00000	0.00390	-0.02089	0.97911
23	lct003-010	2.456	5.55E-05	202.652	2.47E-02	1.66E-01	3.59E-04	0.97888	0.00096	1.00000	0.00390	-0.02112	0.97888
24	lct003-011	2.455	5.49E-05	203.950	2.58E-02	1.49E-01	3.38E-04	0.98048	0.00075	1.00000	0.00390	-0.01952	0.98048
25	lct003-012	2.456	5.44E-05	203.506	2.57E-02	1.55E-01	3.45E-04	0.97759	0.00078	1.00000	0.00390	-0.02241	0.97759
26	lct003-013	2.455	5.17E-05	203.574	2.48E-02	1.54E-01	3.35E-04	0.98244	0.00099	1.00000	0.00390	-0.01756	0.98244
27	lct003-014	2.456	5.31E-05	203.532	2.48E-02	1.54E-01	3.44E-04	0.97968	0.00099	1.00000	0.00390	-0.02032	0.97968
28	lct003-015	2.455	5.29E-05	203.488	2.56E-02	1.55E-01	3.49E-04	0.97996	0.00091	1.00000	0.00390	-0.02004	0.97996
29	lct003-016	2.456	5.24E-05	203.262	2.66E-02	1.58E-01	3.65E-04	0.98012	0.00097	1.00000	0.00390	-0.01988	0.98012
30	lct003-017	2.456	5.81E-05	203.187	2.64E-02	1.59E-01	3.69E-04	0.97945	0.00092	1.00000	0.00390	-0.02055	0.97945
31	lct003-018	2.456	5.70E-05	203.050	2.61E-02	1.61E-01	3.71E-04	0.97945	0.00093	1.00000	0.00390	-0.02055	0.97945
32	lct003-019	2.456	5.44E-05	202.939	2.55E-02	1.62E-01	3.60E-04	0.97819	0.00081	1.00000	0.00390	-0.02181	0.97819
33	lct003-020	2.457	5.40E-05	202.254	2.61E-02	1.72E-01	4.03E-04	0.97957	0.00131	1.00000	0.00390	-0.02043	0.97957

N	Case	nubar	Sigma	AFG	Sigma	EALCF (eV)	Sigma	k_{calc} LEU	Sigma	k_{exp} LEU	Sigma	Bias = Calculated - Benchmark	Adjusted k_{eff} LEU
34	lct003-021	2.456	5.06E-05	202.538	2.45E-02	1.68E-01	3.63E-04	0.97750	0.00082	1.00000	0.00390	-0.02250	0.97750
35	lct003-022	2.456	5.33E-05	202.905	2.57E-02	1.63E-01	3.66E-04	0.98871	0.00093	1.00000	0.00390	-0.01129	0.98871
36	lct004-001	2.458	6.08E-05	195.704	3.10E-02	3.02E-01	7.90E-04	0.98812	0.00115	0.99980	0.00330	-0.01168	0.98832
37	lct004-002	2.458	5.51E-05	195.665	3.02E-02	3.02E-01	7.46E-04	0.98491	0.00096	0.99980	0.00330	-0.01489	0.98511
38	lct004-003	2.458	5.55E-05	195.640	3.05E-02	3.03E-01	7.69E-04	0.98761	0.00109	0.99980	0.00330	-0.01219	0.98781
39	lct004-004	2.458	5.64E-05	195.687	3.13E-02	3.02E-01	7.67E-04	0.98735	0.00093	0.99980	0.00330	-0.01245	0.98755
40	lct004-005	2.455	5.11E-05	200.539	2.80E-02	2.05E-01	4.83E-04	0.98710	0.00103	0.99980	0.00330	-0.01270	0.98730
41	lct004-006	2.456	5.55E-05	198.403	2.92E-02	2.43E-01	5.87E-04	0.98622	0.00098	0.99980	0.00330	-0.01358	0.98642
42	lct004-007	2.455	5.19E-05	200.208	2.80E-02	2.10E-01	4.98E-04	0.98623	0.00097	0.99980	0.00330	-0.01357	0.98643
43	lct004-008	2.456	5.68E-05	197.994	3.04E-02	2.51E-01	6.44E-04	0.98494	0.00134	0.99980	0.00350	-0.01486	0.98514
44	lct004-009	2.457	6.04E-05	196.305	3.21E-02	2.87E-01	7.62E-04	0.98586	0.00099	0.99980	0.00350	-0.01394	0.98606
45	lct004-010	2.457	5.68E-05	196.464	3.02E-02	2.83E-01	7.12E-04	0.99098	0.00108	0.99980	0.00350	-0.00882	0.99118
46	lct004-011	2.455	5.33E-05	199.812	2.92E-02	2.17E-01	5.38E-04	0.98033	0.00115	0.99980	0.00350	-0.01947	0.98053
47	lct004-012	2.456	5.70E-05	198.919	2.85E-02	2.33E-01	5.61E-04	0.97383	0.00102	0.99980	0.00350	-0.02597	0.97403
48	lct004-013	2.456	5.56E-05	198.340	3.01E-02	2.44E-01	6.19E-04	0.98226	0.00113	0.99980	0.00350	-0.01754	0.98246
49	lct004-014	2.456	5.42E-05	198.425	3.12E-02	2.42E-01	6.28E-04	0.98232	0.00085	0.99980	0.00350	-0.01748	0.98252
50	lct004-015	2.456	5.47E-05	198.496	3.01E-02	2.41E-01	5.91E-04	0.98224	0.00117	0.99980	0.00350	-0.01756	0.98244
51	lct004-016	2.456	5.01E-05	198.453	3.10E-02	2.42E-01	6.11E-04	0.98288	0.00111	0.99980	0.00350	-0.01692	0.98308
52	lct004-017	2.456	5.56E-05	198.231	3.06E-02	2.46E-01	6.26E-04	0.98236	0.00108	0.99980	0.00350	-0.01744	0.98256
53	lct004-018	2.456	5.04E-05	198.166	2.99E-02	2.48E-01	6.23E-04	0.98294	0.00099	0.99980	0.00350	-0.01686	0.98314
54	lct004-019	2.456	5.56E-05	198.034	3.09E-02	2.50E-01	6.43E-04	0.98541	0.00098	0.99980	0.00350	-0.01439	0.98561
55	lct004-020	2.456	5.11E-05	199.174	2.84E-02	2.28E-01	5.42E-04	0.98039	0.00145	0.99980	0.00350	-0.01941	0.98059
56	lct008-008	2.460	6.26E-05	197.632	2.91E-02	2.55E-01	6.47E-04	0.99339	0.00080	1.00070	0.00120	-0.00731	0.99269
57	lct009-007	2.450	4.28E-05	207.324	2.24E-02	1.16E-01	2.30E-04	0.99656	0.00106	1.00000	0.00210	-0.00344	0.99656
58	lct012-001	2.457	5.63E-05	202.135	2.62E-02	1.73E-01	4.05E-04	0.97972	0.00086	1.00000	0.00340	-0.02028	0.97972
59	lct012-002	2.457	5.93E-05	201.625	2.69E-02	1.81E-01	4.21E-04	0.98173	0.00085	1.00000	0.00340	-0.01827	0.98173
60	lct012-003	2.457	5.53E-05	201.500	2.74E-02	1.83E-01	4.38E-04	0.98058	0.00090	1.00000	0.00340	-0.01942	0.98058
61	lct012-004	2.457	6.08E-05	201.006	2.76E-02	1.90E-01	4.61E-04	0.98093	0.00082	1.00000	0.00340	-0.01907	0.98093
62	lct012-005	2.457	5.52E-05	201.079	2.77E-02	1.89E-01	4.62E-04	0.98075	0.00091	1.00000	0.00340	-0.01925	0.98075
63	lct012-006	2.457	5.23E-05	201.084	2.59E-02	1.90E-01	4.21E-04	0.98304	0.00099	1.00000	0.00340	-0.01696	0.98304
64	lct012-007	2.457	5.67E-05	201.033	2.80E-02	1.90E-01	4.61E-04	0.98354	0.00092	1.00000	0.00340	-0.01646	0.98354
65	lct012-008	2.457	5.71E-05	201.478	2.69E-02	1.83E-01	4.31E-04	0.98167	0.00098	1.00000	0.00490	-0.01833	0.98167
66	lct012-009	2.456	5.52E-05	202.299	2.57E-02	1.71E-01	3.91E-04	0.97903	0.00086	1.00000	0.00340	-0.02097	0.97903
67	lct012-010	2.457	5.29E-05	201.663	2.54E-02	1.80E-01	3.94E-04	0.98064	0.00108	1.00000	0.00340	-0.01936	0.98064
68	lct016-001	2.451	4.57E-05	208.844	2.09E-02	9.80E-02	1.87E-04	0.99251	0.00084	1.00000	0.00310	-0.00749	0.99251
69	lct016-002	2.451	4.31E-05	208.899	2.05E-02	9.75E-02	1.84E-04	0.99176	0.00090	1.00000	0.00310	-0.00824	0.99176
70	lct016-003	2.451	4.42E-05	208.903	2.11E-02	9.74E-02	1.89E-04	0.99181	0.00084	1.00000	0.00310	-0.00819	0.99181

N	Case	nubar	Sigma	AFG	Sigma	EALCF (eV)	Sigma	k_{calc} LEU	Sigma	k_{exp} LEU	Sigma	Bias = Calculated - Benchmark	Adjusted k_{eff} LEU
71	lct016-004	2.451	4.54E-05	208.902	2.05E-02	9.75E-02	1.82E-04	0.99235	0.00084	1.00000	0.00310	-0.00765	0.99235
72	lct016-005	2.451	4.44E-05	208.961	2.09E-02	9.70E-02	1.83E-04	0.99325	0.00102	1.00000	0.00310	-0.00675	0.99325
73	lct016-006	2.451	4.68E-05	208.784	2.18E-02	9.85E-02	1.99E-04	0.99285	0.00089	1.00000	0.00310	-0.00715	0.99285
74	lct016-007	2.451	4.26E-05	208.850	2.00E-02	9.78E-02	1.78E-04	0.99252	0.00084	1.00000	0.00310	-0.00748	0.99252
75	lct016-008	2.451	4.53E-05	208.732	2.00E-02	9.89E-02	1.80E-04	0.99210	0.00090	1.00000	0.00310	-0.00790	0.99210
76	lct016-009	2.451	4.54E-05	208.793	2.17E-02	9.84E-02	1.91E-04	0.99496	0.00082	1.00000	0.00310	-0.00504	0.99496
77	lct016-010	2.451	4.62E-05	208.741	2.13E-02	9.87E-02	1.93E-04	0.99358	0.00082	1.00000	0.00310	-0.00642	0.99358
78	lct016-011	2.451	4.32E-05	208.822	2.09E-02	9.81E-02	1.86E-04	0.99515	0.00103	1.00000	0.00310	-0.00485	0.99515
79	lct016-012	2.451	4.39E-05	208.677	2.03E-02	9.93E-02	1.85E-04	0.99264	0.00080	1.00000	0.00310	-0.00736	0.99264
80	lct016-013	2.451	4.59E-05	208.762	2.06E-02	9.87E-02	1.83E-04	0.99385	0.00122	1.00000	0.00310	-0.00615	0.99385
81	lct016-014	2.451	4.52E-05	208.643	2.06E-02	9.96E-02	1.91E-04	0.99321	0.00089	1.00000	0.00310	-0.00679	0.99321
82	lct016-015	2.451	4.49E-05	208.882	2.07E-02	9.76E-02	1.81E-04	0.99344	0.00094	1.00000	0.00310	-0.00656	0.99344
83	lct016-016	2.451	4.55E-05	208.849	2.12E-02	9.79E-02	1.91E-04	0.99165	0.00100	1.00000	0.00310	-0.00835	0.99165
84	lct016-017	2.451	4.41E-05	208.848	2.08E-02	9.80E-02	1.84E-04	0.99091	0.00087	1.00000	0.00310	-0.00909	0.99091
85	lct016-018	2.451	4.37E-05	208.890	2.08E-02	9.75E-02	1.86E-04	0.99221	0.00099	1.00000	0.00310	-0.00779	0.99221
86	lct016-019	2.451	4.37E-05	208.909	2.09E-02	9.75E-02	1.90E-04	0.99528	0.00106	1.00000	0.00310	-0.00472	0.99528
87	lct016-020	2.451	4.29E-05	208.769	1.99E-02	9.85E-02	1.76E-04	0.99363	0.00076	1.00000	0.00310	-0.00637	0.99363
88	lct016-021	2.451	4.52E-05	208.695	2.05E-02	9.92E-02	1.85E-04	0.99324	0.00093	1.00000	0.00310	-0.00676	0.99324
89	lct016-022	2.451	4.39E-05	208.723	2.08E-02	9.90E-02	1.86E-04	0.99411	0.00082	1.00000	0.00310	-0.00589	0.99411
90	lct016-023	2.451	4.45E-05	208.788	2.02E-02	9.85E-02	1.84E-04	0.99386	0.00082	1.00000	0.00310	-0.00614	0.99386
91	lct016-024	2.451	4.36E-05	208.749	2.12E-02	9.87E-02	1.94E-04	0.99241	0.00094	1.00000	0.00310	-0.00759	0.99241
92	lct016-025	2.451	4.50E-05	208.765	2.08E-02	9.86E-02	1.86E-04	0.99560	0.00090	1.00000	0.00310	-0.00440	0.99560
93	lct016-026	2.451	4.20E-05	208.746	1.93E-02	9.88E-02	1.78E-04	0.99306	0.00092	1.00000	0.00310	-0.00694	0.99306
94	lct016-027	2.451	4.05E-05	208.778	1.93E-02	9.85E-02	1.75E-04	0.99329	0.00086	1.00000	0.00310	-0.00671	0.99329
95	lct016-028	2.451	4.67E-05	208.907	2.20E-02	9.74E-02	2.00E-04	0.99240	0.00081	1.00000	0.00310	-0.00760	0.99240
96	lct016-029	2.451	4.42E-05	208.974	2.04E-02	9.70E-02	1.81E-04	0.99349	0.00085	1.00000	0.00310	-0.00651	0.99349
97	lct016-030	2.451	4.39E-05	208.982	1.99E-02	9.68E-02	1.75E-04	0.99297	0.00078	1.00000	0.00310	-0.00703	0.99297
98	lct016-031	2.451	4.51E-05	208.925	2.01E-02	9.73E-02	1.79E-04	0.99283	0.00095	1.00000	0.00310	-0.00717	0.99283
99	lct016-032	2.451	4.52E-05	208.991	2.07E-02	9.68E-02	1.80E-04	0.99313	0.00111	1.00000	0.00310	-0.00687	0.99313
100	lmt001	2.457	6.56E-05	207.138	3.10E-02	1.20E-01	3.30E-04	0.99556	0.00076	0.99900	0.00570	-0.00344	0.99656
101	lmt002-001	2.443	2.87E-05	217.142	1.39E-02	4.85E-02	7.15E-05	1.01699	0.00099	1.00000	0.01410	0.01699	1.01699
102	lmt002-002	2.443	3.12E-05	216.125	1.44E-02	5.30E-02	7.87E-05	1.00849	0.00089	1.00000	0.01410	0.00849	1.00849
103	lmt002-003	2.443	3.14E-05	216.655	1.55E-02	5.05E-02	7.87E-05	1.01398	0.00089	1.00000	0.01410	0.01398	1.01398
104	lmt002-004	2.444	3.30E-05	213.740	1.68E-02	6.50E-02	1.06E-04	1.00727	0.00102	1.00000	0.01410	0.00727	1.00727
105	lmt002-005	2.443	3.10E-05	216.802	1.46E-02	4.99E-02	7.59E-05	1.01704	0.00085	1.00000	0.01410	0.01704	1.01704
106	lmt002-006	2.445	3.65E-05	210.026	1.86E-02	8.90E-02	1.49E-04	1.00725	0.00085	1.00000	0.01460	0.00725	1.00725
107	lmt002-007	2.443	3.14E-05	215.611	1.66E-02	5.53E-02	9.20E-05	1.01053	0.00082	1.00000	0.01410	0.01053	1.01053

N	Case	nubar	Sigma	AFG	Sigma	EALCF (eV)	Sigma	k_{calc} LEU	Sigma	k_{exp} LEU	Sigma	Bias = Calculated - Benchmark	Adjusted k_{eff} LEU
108	lmt002-008	2.444	3.36E-05	214.667	1.64E-02	6.01E-02	9.10E-05	1.00635	0.00093	1.00000	0.01410	0.00635	1.00635
109	lmt002-009	2.443	3.19E-05	215.729	1.48E-02	5.48E-02	8.10E-05	1.00692	0.00088	1.00000	0.01410	0.00692	1.00692
110	lmt002-010	2.444	3.38E-05	215.126	1.63E-02	5.78E-02	9.19E-05	1.00796	0.00085	1.00000	0.01410	0.00796	1.00796
111	lmt002-011	2.444	3.21E-05	214.137	1.77E-02	6.28E-02	1.06E-04	1.00749	0.00106	1.00000	0.01410	0.00749	1.00749
112	lmt002-012	2.443	3.17E-05	216.403	1.42E-02	5.17E-02	7.56E-05	1.01227	0.00095	1.00000	0.01410	0.01227	1.01227
113	lst003-001	2.439	4.47E-06	217.992	3.48E-03	4.10E-02	1.71E-05	0.99779	0.00093	1.00070	0.00390	-0.00291	0.99709
114	lst003-002	2.439	4.13E-06	218.493	3.14E-03	3.92E-02	1.50E-05	0.99564	0.00094	1.00030	0.00420	-0.00466	0.99534
115	lst003-003	2.439	4.30E-06	218.586	2.92E-03	3.88E-02	1.36E-05	1.00015	0.00088	1.00050	0.00420	-0.00035	0.99965
116	lst003-004	2.439	4.05E-06	218.641	2.97E-03	3.86E-02	1.40E-05	0.99649	0.00095	1.00050	0.00420	-0.00401	0.99599
117	lst003-005	2.438	3.22E-06	219.430	2.47E-03	3.60E-02	1.13E-05	0.99672	0.00073	1.00070	0.00480	-0.00398	0.99602
118	lst003-006	2.438	3.17E-06	219.530	2.29E-03	3.56E-02	1.08E-05	0.99930	0.00079	1.00090	0.00490	-0.00160	0.99840
119	lst003-007	2.438	3.25E-06	219.582	2.43E-03	3.55E-02	1.13E-05	0.99563	0.00071	1.00040	0.00490	-0.00477	0.99523
120	lst003-008	2.438	2.87E-06	219.914	2.02E-03	3.44E-02	9.96E-06	1.00024	0.00067	1.00030	0.00520	-0.00006	0.99994
121	lst003-009	2.438	2.71E-06	219.953	1.90E-03	3.43E-02	9.25E-06	0.99764	0.00089	1.00060	0.00520	-0.00296	0.99704
122	lst004-001	2.439	4.90E-06	217.810	3.49E-03	4.16E-02	1.70E-05	1.00068	0.00089	0.99940	0.00080	0.00128	1.00128
123	lst004-029	2.439	4.71E-06	218.086	3.30E-03	4.05E-02	1.59E-05	1.00164	0.00080	0.99990	0.00090	0.00174	1.00174
124	lst004-033	2.439	4.00E-06	218.415	3.02E-03	3.94E-02	1.45E-05	0.99876	0.00123	0.99990	0.00090	-0.00114	0.99886
125	lst004-034	2.439	4.03E-06	218.642	2.86E-03	3.85E-02	1.37E-05	1.00301	0.00081	0.99990	0.00100	0.00311	1.00311
126	lst004-046	2.438	3.89E-06	218.812	2.83E-03	3.79E-02	1.36E-05	1.00243	0.00088	0.99990	0.00100	0.00253	1.00253
127	lst004-051	2.438	3.84E-06	218.946	2.73E-03	3.75E-02	1.30E-05	1.00128	0.00089	0.99940	0.00110	0.00188	1.00188
128	lst004-054	2.438	3.47E-06	219.051	2.55E-03	3.71E-02	1.23E-05	1.00090	0.00080	0.99960	0.00110	0.00130	1.00130
	Maximum	2.460	6.56E-05	219.953	3.21E-02	8.90E+00	7.90E-04	1.01704	0.00145	1.00090	0.01460	0.01704	1.01704
	Average	2.451	4.26E-05	207.218	2.10E-02	8.91E-01	2.83E-04	0.99125	0.00093	0.99996	0.00430	-0.00871	0.99129
	Minimum	2.438	2.71E-06	195.640	1.90E-03	3.43E-02	9.25E-06	0.97383	0.00067	0.99900	0.00080	-0.02597	0.97403

Table 4.5 Results for Uranium-233 Systems (Volume 5) with CSAS25 from SCALE 5 and the 238-group Library on the HP-6000 (CMODD) Workstation

N	Case	nubar	Sigma	AFG	Sigma	EALCF (eV)	Sigma	k_{calc} U233	sigma	k_{exp} U233	Sigma	Bias = Calculated - Benchmark	Adjusted k_{eff} U233
1	umf001-001	2.679	2.47E-04	22.496	1.36E-02	1.13E+06	1.44E+03	0.99234	0.00107	1.00000	0.00100	-0.00766	0.99234
2	umf002-001	2.664	2.27E-04	22.845	1.33E-02	1.09E+06	1.37E+03	0.99537	0.00114	1.00000	0.00100	-0.00463	0.99537
3	umf002-002	2.654	2.48E-04	23.059	1.33E-02	1.07E+06	1.37E+03	0.99949	0.00102	1.00000	0.00110	-0.00051	0.99949
4	umf003-001	2.673	2.38E-04	22.963	1.33E-02	1.08E+06	1.39E+03	0.99719	0.00099	1.00000	0.00100	-0.00281	0.99719
5	umf003-002	2.671	2.29E-04	23.163	1.37E-02	1.06E+06	1.39E+03	0.99713	0.00119	1.00000	0.00100	-0.00287	0.99713
6	umf004-001	2.660	2.40E-04	24.064	1.44E-02	9.75E+05	1.33E+03	1.00355	0.00118	1.00000	0.00070	0.00355	1.00355
7	umf004-002	2.647	2.16E-04	25.276	1.39E-02	8.67E+05	1.17E+03	1.00244	0.00089	1.00000	0.00080	0.00244	1.00244
8	umf005-001	2.659	2.16E-04	24.242	1.38E-02	9.46E+05	1.26E+03	0.99762	0.00092	1.00000	0.00300	-0.00238	0.99762
9	umf005-002	2.648	2.34E-04	25.988	1.77E-02	7.65E+05	1.48E+03	0.99970	0.00095	1.00000	0.00300	-0.00030	0.99970
10	umf006-001	2.668	2.67E-04	23.609	1.70E-02	1.00E+06	1.58E+03	1.00005	0.00113	1.00000	0.00140	0.00005	1.00005
11	usi001-001	2.505	2.36E-05	148.768	4.14E-02	6.64E+00	1.85E-02	0.98635	0.00125	1.00000	0.00830	-0.01365	0.98635
12	usi001-002	2.506	2.55E-05	146.652	4.11E-02	7.74E+00	2.18E-02	0.98067	0.00122	1.00000	0.00850	-0.01933	0.98067
13	usi001-003	2.507	2.57E-05	145.626	3.89E-02	8.35E+00	2.24E-02	0.98146	0.00129	1.00000	0.00660	-0.01854	0.98146
14	usi001-004	2.506	2.40E-05	158.011	4.79E-02	3.57E+00	1.17E-02	0.99197	0.00127	1.00000	0.00610	-0.00803	0.99197
15	usi001-005	2.507	2.62E-05	144.833	4.13E-02	8.89E+00	2.49E-02	0.98511	0.00132	1.00000	0.00820	-0.01489	0.98511
16	usi001-006	2.506	2.63E-05	156.173	4.76E-02	4.10E+00	1.33E-02	0.98577	0.00135	1.00000	0.00610	-0.01423	0.98577
17	usi001-007	2.508	2.65E-05	144.203	4.07E-02	9.34E+00	2.61E-02	0.98087	0.00133	1.00000	0.00590	-0.01913	0.98087
18	usi001-008	2.507	2.60E-05	155.397	4.46E-02	4.36E+00	1.33E-02	0.98031	0.00158	1.00000	0.00560	-0.01969	0.98031
19	usi001-009	2.507	2.71E-05	148.364	4.36E-02	7.04E+00	2.09E-02	0.97778	0.00151	1.00000	0.00680	-0.02222	0.97778
20	usi001-010	2.508	2.91E-05	143.665	4.27E-02	9.77E+00	2.85E-02	0.97887	0.00149	1.00000	0.00530	-0.02113	0.97887
21	usi001-011	2.508	2.79E-05	147.624	4.04E-02	7.47E+00	2.05E-02	0.97855	0.00135	1.00000	0.00570	-0.02145	0.97855
22	usi001-012	2.504	1.99E-05	154.996	4.23E-02	4.30E+00	1.23E-02	0.98399	0.00151	1.00000	0.00910	-0.01601	0.98399
23	usi001-013	2.505	2.10E-05	153.181	3.84E-02	4.91E+00	1.30E-02	0.98213	0.00121	1.00000	0.00710	-0.01787	0.98213
24	usi001-014	2.504	1.96E-05	164.863	4.14E-02	2.19E+00	6.20E-03	0.99348	0.00131	1.00000	0.00520	-0.00652	0.99348
25	usi001-015	2.505	2.26E-05	152.294	3.57E-02	5.25E+00	1.30E-02	0.98189	0.00118	1.00000	0.00750	-0.01811	0.98189
26	usi001-016	2.504	2.15E-05	168.474	4.33E-02	1.73E+00	5.18E-03	0.97264	0.00113	1.00000	0.00280	-0.02736	0.97264
27	usi001-017	2.504	2.06E-05	163.429	4.34E-02	2.43E+00	7.29E-03	0.98992	0.00128	1.00000	0.00550	-0.01008	0.98992
28	usi001-018	2.506	2.36E-05	151.379	4.05E-02	5.63E+00	1.54E-02	0.97616	0.00143	1.00000	0.00570	-0.02384	0.97616
29	usi001-019	2.506	2.44E-05	150.845	4.03E-02	5.87E+00	1.63E-02	0.97399	0.00137	1.00000	0.00830	-0.02601	0.97399
30	usi001-020	2.505	2.14E-05	161.233	4.09E-02	2.88E+00	8.18E-03	0.97829	0.00122	1.00000	0.00560	-0.02171	0.97829
31	usi001-021	2.506	2.38E-05	150.409	3.98E-02	6.08E+00	1.65E-02	0.97280	0.00137	1.00000	0.00500	-0.02720	0.97280
32	usi001-022	2.507	2.48E-05	150.112	4.13E-02	6.24E+00	1.75E-02	0.97633	0.00115	1.00000	0.00490	-0.02367	0.97633
33	usi001-023	2.506	2.41E-05	154.825	3.98E-02	4.52E+00	1.23E-02	0.98835	0.00121	1.00000	0.00470	-0.01165	0.98835

N	Case	nubar	Sigma	AFG	Sigma	EALCF (eV)	Sigma	k_{calc} U233	sigma	k_{exp} U233	Sigma	Bias = Calculated - Benchmark	Adjusted k_{eff} U233
34	usi001-024	2.502	1.54E-05	166.549	3.64E-02	1.92E+00	4.78E-03	0.99159	0.00131	1.00000	0.00810	-0.00841	0.99159
35	usi001-025	2.502	1.51E-05	164.841	3.57E-02	2.17E+00	5.35E-03	0.98486	0.00136	1.00000	0.00810	-0.01514	0.98486
36	usi001-026	2.502	1.60E-05	164.166	3.48E-02	2.28E+00	5.50E-03	0.98842	0.00157	1.00000	0.00650	-0.01158	0.98842
37	usi001-027	2.502	1.56E-05	173.533	3.67E-02	1.18E+00	3.05E-03	0.98805	0.00116	1.00000	0.00510	-0.01195	0.98805
38	usi001-028	2.503	1.72E-05	163.274	3.55E-02	2.44E+00	5.97E-03	0.98305	0.00146	1.00000	0.00610	-0.01695	0.98305
39	usi001-029	2.503	1.79E-05	162.746	3.27E-02	2.54E+00	5.79E-03	0.97739	0.00152	1.00000	0.00980	-0.02261	0.97739
40	usi001-030	2.503	1.65E-05	171.510	3.77E-02	1.39E+00	3.62E-03	0.97556	0.00124	1.00000	0.00530	-0.02444	0.97556
41	usi001-031	2.503	1.81E-05	162.593	3.54E-02	2.58E+00	6.40E-03	0.98978	0.00135	1.00000	0.00710	-0.01022	0.98978
42	usi001-032	2.504	1.91E-05	162.123	3.40E-02	2.68E+00	6.38E-03	0.97345	0.00124	1.00000	0.00530	-0.02655	0.97345
43	usi001-033	2.503	1.79E-05	166.484	3.38E-02	1.98E+00	4.64E-03	0.99048	0.00129	1.00000	0.00460	-0.00952	0.99048
44	ust001-001	2.495	6.57E-07	218.364	2.94E-03	3.91E-02	1.15E-05	0.99731	0.00094	1.00000	0.00310	-0.00269	0.99731
45	ust001-002	2.495	7.00E-07	218.185	2.96E-03	3.97E-02	1.19E-05	0.99738	0.00072	1.00050	0.00330	-0.00312	0.99688
46	ust001-003	2.495	7.34E-07	218.001	2.89E-03	4.03E-02	1.21E-05	0.99550	0.00080	1.00060	0.00330	-0.00510	0.99490
47	ust001-004	2.495	7.61E-07	217.827	3.29E-03	4.09E-02	1.30E-05	0.99659	0.00068	0.99980	0.00330	-0.00321	0.99679
48	ust001-005	2.495	8.11E-07	217.653	3.31E-03	4.15E-02	1.39E-05	0.99546	0.00089	0.99990	0.00330	-0.00444	0.99556
49	ust002-004	2.497	5.87E-06	200.378	1.91E-02	1.64E-01	2.33E-04	1.00401	0.00132	1.00400	0.00870	0.00001	1.00001
50	ust002-005	2.497	4.86E-06	203.611	1.72E-02	1.28E-01	1.68E-04	0.99012	0.00128	1.00400	0.00870	-0.01388	0.98612
51	ust002-008	2.496	3.75E-06	206.663	1.41E-02	1.00E-01	1.12E-04	1.00671	0.00125	1.00400	0.00870	0.00271	1.00271
52	ust002-010	2.496	3.10E-06	209.189	1.16E-02	8.21E-02	7.79E-05	1.00131	0.00107	1.00400	0.00870	-0.00269	0.99731
53	ust002-011	2.496	2.34E-06	210.891	1.03E-02	7.16E-02	6.02E-05	1.00653	0.00106	1.00400	0.00870	0.00253	1.00253
54	ust002-012	2.496	2.23E-06	212.262	8.87E-03	6.40E-02	4.83E-05	0.99410	0.00118	1.00400	0.00870	-0.00990	0.99010
55	ust002-014	2.496	2.10E-06	212.896	8.21E-03	6.08E-02	4.30E-05	0.98149	0.00139	1.00400	0.00870	-0.02251	0.97749
56	ust002-015	2.496	1.85E-06	213.924	8.02E-03	5.59E-02	3.77E-05	0.99510	0.00128	1.00400	0.00870	-0.00890	0.99110
57	ust002-017	2.495	1.52E-06	215.130	6.23E-03	5.07E-02	2.80E-05	0.98439	0.00115	1.00400	0.00870	-0.01961	0.98039
58	ust002-018	2.495	1.36E-06	215.560	5.47E-03	4.89E-02	2.53E-05	0.99576	0.00113	1.00400	0.00870	-0.00824	0.99176
59	ust002-019	2.495	1.11E-06	216.403	5.16E-03	4.56E-02	2.19E-05	1.00586	0.00098	1.00400	0.00870	0.00186	1.00186
60	ust002-022	2.498	8.03E-06	194.521	2.53E-02	2.56E-01	4.80E-04	0.99332	0.00145	1.00400	0.00870	-0.01068	0.98932
61	ust002-024	2.500	1.13E-05	186.914	3.26E-02	4.52E-01	1.06E-03	0.99693	0.00131	1.00400	0.00870	-0.00707	0.99293
62	ust002-034	2.497	4.71E-06	203.133	1.64E-02	1.32E-01	1.74E-04	0.99848	0.00145	1.00400	0.00870	-0.00552	0.99448
63	ust002-035	2.496	3.46E-06	207.760	1.30E-02	9.20E-02	9.43E-05	1.00483	0.00132	1.00400	0.00870	0.00083	1.00083
64	ust002-036	2.496	2.00E-06	212.704	8.59E-03	6.18E-02	4.58E-05	1.00395	0.00120	1.00400	0.00870	-0.00005	0.99995
65	ust002-038	2.496	1.55E-06	214.588	6.40E-03	5.30E-02	3.02E-05	1.00391	0.00137	1.00400	0.00870	-0.00009	0.99991
66	ust003-040	2.499	9.45E-06	192.453	2.60E-02	3.01E-01	5.75E-04	0.99564	0.00134	0.99950	0.00871	-0.00386	0.99614
67	ust004-003	2.497	5.81E-06	200.362	1.87E-02	1.65E-01	2.36E-04	0.99778	0.00113	1.00390	0.00880	-0.00612	0.99388
68	ust004-006	2.497	4.63E-06	203.685	1.62E-02	1.27E-01	1.60E-04	1.00150	0.00122	1.00340	0.00860	-0.00190	0.99810
69	ust004-020	2.498	7.76E-06	194.390	2.53E-02	2.60E-01	4.83E-04	0.99076	0.00121	1.00410	0.00890	-0.01334	0.98666
70	ust004-025	2.500	1.10E-05	186.589	3.02E-02	4.64E-01	1.00E-03	0.98315	0.00138	1.00510	0.00890	-0.02195	0.97805
71	ust004-027	2.500	1.13E-05	186.680	3.52E-02	4.60E-01	1.15E-03	1.00011	0.00128	1.00200	0.01050	-0.00189	0.99811

N	Case	nubar	Sigma	AFG	Sigma	EALCF (eV)	Sigma	k_{calc} U233	sigma	k_{exp} U233	Sigma	Bias = Calculated - Benchmark	Adjusted k_{eff} U233
72	ust004-028	2.499	9.40E-06	189.870	2.93E-02	3.64E-01	7.54E-04	0.99392	0.00126	1.00200	0.01040	-0.00808	0.99192
73	ust004-030	2.499	9.74E-06	189.815	2.99E-02	3.66E-01	7.98E-04	0.98602	0.00148	1.00370	0.00900	-0.01768	0.98232
74	ust004-033	2.497	4.68E-06	203.124	1.79E-02	1.33E-01	1.84E-04	1.00265	0.00126	1.00200	0.01020	0.00065	1.00065
75	ust005-001	2.496	1.87E-06	213.011	8.19E-03	6.02E-02	4.20E-05	0.99442	0.00136	1.00000	0.00400	-0.00558	0.99442
76	ust005-002	2.496	1.54E-06	214.557	6.77E-03	5.31E-02	3.11E-05	1.00129	0.00113	1.00000	0.00490	0.00129	1.00129
77	ust006-004	2.501	1.24E-05	178.645	2.70E-02	8.25E-01	1.62E-03	0.99424	0.00126	1.00000	0.00350	-0.00576	0.99424
78	ust006-006	2.501	1.29E-05	178.446	2.80E-02	8.37E-01	1.68E-03	0.98707	0.00136	1.00000	0.00350	-0.01293	0.98707
79	ust006-009	2.500	1.08E-05	188.824	2.92E-02	3.91E-01	8.24E-04	0.99728	0.00114	1.00000	0.00280	-0.00272	0.99728
80	ust006-011	2.500	1.03E-05	188.765	2.89E-02	3.93E-01	8.25E-04	0.99496	0.00136	1.00000	0.00280	-0.00504	0.99496
81	ust006-015	2.498	7.37E-06	192.926	2.03E-02	2.86E-01	4.15E-04	0.98496	0.00126	1.00000	0.00350	-0.01504	0.98496
82	ust006-018	2.498	7.72E-06	192.743	2.20E-02	2.90E-01	4.74E-04	0.98754	0.00159	1.00000	0.00350	-0.01246	0.98754
83	ust006-020	2.498	6.28E-06	199.368	2.12E-02	1.77E-01	2.81E-04	0.98945	0.00124	1.00000	0.00280	-0.01055	0.98945
84	ust006-022	2.498	6.32E-06	199.375	1.89E-02	1.77E-01	2.47E-04	0.99082	0.00130	1.00000	0.00280	-0.00918	0.99082
85	ust008-001	2.495	5.72E-07	219.061	2.37E-03	3.69E-02	1.00E-05	0.99685	0.00066	1.00060	0.00290	-0.00375	0.99625
86	ust012-001	2.497	6.08E-06	200.179	2.00E-02	1.66E-01	2.55E-04	0.99462	0.00129	0.99900	0.00280	-0.00438	0.99562
87	ust012-002	2.497	5.83E-06	200.790	1.92E-02	1.59E-01	2.32E-04	0.99427	0.00141	0.99930	0.00250	-0.00503	0.99497
88	ust012-003	2.497	4.88E-06	202.292	1.72E-02	1.42E-01	1.93E-04	1.00316	0.00131	0.99940	0.00230	0.00376	1.00376
89	ust012-004	2.497	3.82E-06	206.240	1.37E-02	1.04E-01	1.15E-04	0.99476	0.00135	1.00000	0.00150	-0.00524	0.99476
90	ust012-005	2.496	3.43E-06	208.230	1.27E-02	8.87E-02	8.95E-05	0.99792	0.00122	1.00000	0.00710	-0.00208	0.99792
91	ust012-006	2.496	2.90E-06	209.776	1.10E-02	7.84E-02	7.22E-05	0.99702	0.00155	0.99870	0.00110	-0.00168	0.99832
92	ust012-007	2.495	1.45E-06	214.732	6.09E-03	5.28E-02	2.75E-05	0.99691	0.00100	1.00000	0.00380	-0.00309	0.99691
93	ust012-008	2.495	1.58E-06	214.752	6.29E-03	5.25E-02	2.91E-05	0.99304	0.00115	1.00000	0.00480	-0.00696	0.99304
94	ust014-001	2.500	1.17E-05	183.562	2.76E-02	5.81E-01	1.15E-03	0.97568	0.00145	0.99760	0.01120	-0.02192	0.97808
95	ust014-002	2.500	1.22E-05	182.717	2.79E-02	6.18E-01	1.23E-03	0.98886	0.00149	0.99760	0.01120	-0.00874	0.99126
96	ust014-003	2.499	9.23E-06	192.785	2.67E-02	2.96E-01	5.63E-04	1.00809	0.00125	1.00000	0.00740	0.00809	1.00809
97	ust014-004	2.499	8.68E-06	193.027	2.59E-02	2.90E-01	5.50E-04	1.00743	0.00112	1.00000	0.00890	0.00743	1.00743
98	ust014-005	2.499	8.35E-06	194.368	2.68E-02	2.63E-01	5.07E-04	1.00956	0.00118	1.00000	0.00890	0.00956	1.00956
99	ust014-006	2.499	8.16E-06	194.888	2.71E-02	2.53E-01	4.95E-04	1.00864	0.00131	1.00000	0.00890	0.00864	1.00864
100	ust014-007	2.498	8.39E-06	195.293	2.65E-02	2.46E-01	4.74E-04	1.00482	0.00120	1.00000	0.00880	0.00482	1.00482
101	ust014-008	2.498	8.54E-06	195.826	2.60E-02	2.36E-01	4.50E-04	1.00373	0.00152	1.00000	0.00910	0.00373	1.00373
102	ust014-009	2.499	8.75E-06	192.743	2.65E-02	2.96E-01	5.75E-04	1.01020	0.00118	1.00000	0.00540	0.01020	1.01020
103	ust014-010	2.499	9.52E-06	190.655	2.80E-02	3.47E-01	7.07E-04	0.99319	0.00157	0.99920	0.01080	-0.00601	0.99399
104	ust014-011	2.499	1.05E-05	187.923	2.81E-02	4.23E-01	8.61E-04	0.99997	0.00136	0.99920	0.01260	0.00077	1.00077
105	ust014-012	2.499	9.78E-06	192.560	2.89E-02	3.01E-01	6.45E-04	1.00143	0.00142	0.99920	0.00970	0.00223	1.00223
106	ust014-013	2.499	9.10E-06	193.073	2.91E-02	2.90E-01	6.11E-04	0.99891	0.00143	0.99920	0.01040	-0.00029	0.99971
107	ust014-014	2.499	9.24E-06	193.265	3.12E-02	2.86E-01	6.40E-04	0.99726	0.00171	0.99660	0.00950	0.00066	1.00066
108	ust014-015	2.499	9.25E-06	192.091	2.91E-02	3.12E-01	6.54E-04	0.99345	0.00130	0.99660	0.00980	-0.00315	0.99685
109	ust014-016	2.500	1.08E-05	185.023	2.78E-02	5.22E-01	1.04E-03	0.97960	0.00159	0.99650	0.01090	-0.01690	0.98310

N	Case	nubar	Sigma	AFG	Sigma	EALCF (eV)	Sigma	k_{calc} U233	sigma	k_{exp} U233	Sigma	Bias = Calculated - Benchmark	Adjusted k_{eff} U233
110	ust015-001	2.500	1.19E-05	174.961	3.15E-02	1.06E+00	2.27E-03	0.98889	0.00140	1.00000	0.00750	-0.01111	0.98889
111	ust015-002	2.501	1.27E-05	173.430	3.01E-02	1.18E+00	2.50E-03	0.98620	0.00131	1.00000	0.00700	-0.01380	0.98620
112	ust015-003	2.501	1.28E-05	172.762	3.04E-02	1.24E+00	2.63E-03	0.98645	0.00144	1.00000	0.00680	-0.01355	0.98645
113	ust015-004	2.500	1.29E-05	181.187	3.38E-02	6.83E-01	1.63E-03	0.98579	0.00132	1.00000	0.00410	-0.01421	0.98579
114	ust015-005	2.501	1.38E-05	172.056	3.03E-02	1.31E+00	2.80E-03	0.98453	0.00155	1.00000	0.00550	-0.01547	0.98453
115	ust015-006	2.501	1.34E-05	171.627	3.20E-02	1.36E+00	3.04E-03	0.97629	0.00139	1.00000	0.00990	-0.02371	0.97629
116	ust015-007	2.501	1.24E-05	179.890	3.46E-02	7.59E-01	1.85E-03	0.98182	0.00130	1.00000	0.00700	-0.01818	0.98182
117	ust015-008	2.502	1.40E-05	171.278	3.19E-02	1.39E+00	3.12E-03	0.97477	0.00134	1.00000	0.00670	-0.02523	0.97477
118	ust015-009	2.502	1.58E-05	170.998	3.20E-02	1.43E+00	3.23E-03	0.96617	0.00142	1.00000	0.00500	-0.03383	0.96617
119	ust015-010	2.501	1.47E-05	175.005	3.19E-02	1.08E+00	2.41E-03	0.98628	0.00167	1.00000	0.00510	-0.01372	0.98628
120	ust015-011	2.499	1.02E-05	181.430	2.94E-02	6.65E-01	1.38E-03	0.99235	0.00132	1.00000	0.00750	-0.00765	0.99235
121	ust015-012	2.499	1.02E-05	180.074	2.83E-02	7.34E-01	1.49E-03	0.99234	0.00149	1.00000	0.00690	-0.00766	0.99234
122	ust015-013	2.500	1.05E-05	179.366	2.85E-02	7.74E-01	1.56E-03	0.98836	0.00139	1.00000	0.00690	-0.01164	0.98836
123	ust015-014	2.499	9.50E-06	187.074	2.87E-02	4.44E-01	9.25E-04	0.99396	0.00115	1.00000	0.00360	-0.00604	0.99396
124	ust015-015	2.500	1.10E-05	178.777	2.75E-02	8.10E-01	1.58E-03	0.98760	0.00133	1.00000	0.00600	-0.01240	0.98760
125	ust015-016	2.500	1.19E-05	178.444	2.86E-02	8.31E-01	1.69E-03	0.98372	0.00149	1.00000	0.00430	-0.01628	0.98372
126	ust015-017	2.500	1.06E-05	186.123	2.85E-02	4.81E-01	9.64E-04	0.99351	0.00151	1.00000	0.00290	-0.00649	0.99351
127	ust015-018	2.500	1.17E-05	178.053	2.93E-02	8.57E-01	1.78E-03	0.97268	0.00128	1.00000	0.00560	-0.02732	0.97268
128	ust015-019	2.501	1.22E-05	177.899	2.88E-02	8.68E-01	1.78E-03	0.97155	0.00178	1.00000	0.00520	-0.02845	0.97155
129	ust015-020	2.498	6.40E-06	193.290	2.08E-02	2.78E-01	4.29E-04	0.99137	0.00123	1.00000	0.00790	-0.00863	0.99137
130	ust015-021	2.498	6.57E-06	192.099	2.29E-02	3.04E-01	5.02E-04	0.99381	0.00122	1.00000	0.00700	-0.00619	0.99381
131	ust015-022	2.498	6.73E-06	191.504	2.22E-02	3.18E-01	5.14E-04	0.99149	0.00129	1.00000	0.00620	-0.00851	0.99149
132	ust015-023	2.498	6.80E-06	191.053	2.04E-02	3.29E-01	5.08E-04	0.99187	0.00133	1.00000	0.00550	-0.00813	0.99187
133	ust015-024	2.498	7.35E-06	190.775	2.24E-02	3.36E-01	5.51E-04	0.98878	0.00139	1.00000	0.00510	-0.01122	0.98878
134	ust015-025	2.498	7.11E-06	196.860	2.06E-02	2.16E-01	3.33E-04	0.99270	0.00151	1.00000	0.00230	-0.00730	0.99270
135	ust015-026	2.496	3.44E-06	203.983	1.46E-02	1.23E-01	1.41E-04	0.98840	0.00128	1.00000	0.00660	-0.01160	0.98840
136	ust015-027	2.496	3.43E-06	203.583	1.51E-02	1.27E-01	1.49E-04	0.99573	0.00131	1.00000	0.00630	-0.00427	0.99573
137	ust015-028	2.496	3.83E-06	203.344	1.38E-02	1.29E-01	1.42E-04	0.99283	0.00125	1.00000	0.00580	-0.00717	0.99283
138	ust015-029	2.497	3.83E-06	203.141	1.48E-02	1.31E-01	1.54E-04	0.99239	0.00137	1.00000	0.00510	-0.00761	0.99239
139	ust015-030	2.497	3.87E-06	203.032	1.37E-02	1.32E-01	1.40E-04	0.98947	0.00117	1.00000	0.00480	-0.01053	0.98947
140	ust015-031	2.497	4.26E-06	202.960	1.45E-02	1.33E-01	1.48E-04	0.98967	0.00134	1.00000	0.00550	-0.01033	0.98967
	Maximum	2.679	2.67E-04	219.061	4.79E-02	1.13E+06	1.58E+03	1.01020	0.00178	1.00510	0.01260	0.01020	1.01020
	Average	2.511	2.70E-05	174.378	2.48E-02	7.14E+04	9.85E+01	0.99121	0.00128	1.00052	0.00622	-0.00932	0.99068
	Minimum	2.495	5.72E-07	22.496	2.37E-03	3.69E-02	1.00E-05	0.96617	0.00066	0.99650	0.00070	-0.03383	0.96617

Table 4.6 Results for Mixed Plutonium - Uranium Systems (Volume 6) with CSAS25 from SCALE 5 and the 238-group Library on the HP-6000 (CMODD) Workstation

N	Case	nubar	Sigma	AFG	Sigma	EALCF (eV)	Sigma	k_{calc} Pu-U	Sigma	k_{exp} Pu-U	Sigma	Bias = Calculated - Benchmark	Adjusted k_{eff} Pu-U
1	mct005-001	2.843	4.10E-05	194.173	3.47E-02	3.94E-01	1.13E-03	0.99577	0.00087	1.00080	0.00220	-0.00503	0.99497
2	mct006-001	2.809	5.17E-05	194.969	3.40E-02	3.76E-01	1.09E-03	0.99237	0.00092	1.00160	0.00510	-0.00923	0.99077
3	mct007-093array	2.800	4.47E-05	202.514	2.49E-02	1.97E-01	4.40E-04	1.00082	0.00089	1.00230	0.00350	-0.00148	0.99852
4	mct007-105al	2.798	4.20E-05	206.432	2.34E-02	1.40E-01	3.01E-04	0.99633	0.00097	1.00240	0.00450	-0.00607	0.99393
5	mct007-105alcd	2.798	4.18E-05	206.333	2.28E-02	1.41E-01	2.92E-04	0.99202	0.00080	1.00280	0.00440	-0.01078	0.98922
6	mct007-105array	2.798	4.10E-05	206.345	2.22E-02	1.41E-01	2.89E-04	0.99598	0.00084	1.00240	0.00390	-0.00642	0.99358
7	mct007-105b1	2.798	4.35E-05	206.338	2.40E-02	1.41E-01	3.09E-04	0.99247	0.00081	1.00240	0.00440	-0.00993	0.99007
8	mct007-105b1cd	2.798	4.24E-05	206.269	2.42E-02	1.42E-01	3.22E-04	0.99002	0.00092	1.00220	0.00440	-0.01218	0.98782
9	mct007-105b2	2.798	4.13E-05	206.343	2.29E-02	1.41E-01	2.96E-04	0.99466	0.00074	1.00260	0.00440	-0.00794	0.99206
10	mct007-105b2cd	2.798	4.23E-05	206.298	2.37E-02	1.42E-01	3.18E-04	0.99148	0.00106	1.00250	0.00440	-0.01102	0.98898
11	mct007-105b3	2.798	4.20E-05	206.401	2.38E-02	1.41E-01	3.02E-04	0.99464	0.00090	1.00270	0.00440	-0.00806	0.99194
12	mct007-105b3cd	2.798	4.24E-05	206.319	2.35E-02	1.42E-01	3.07E-04	0.99274	0.00083	1.00250	0.00440	-0.00976	0.99024
13	mct007-105b4	2.798	4.27E-05	206.391	2.28E-02	1.41E-01	2.94E-04	0.99535	0.00082	1.00250	0.00440	-0.00715	0.99285
14	mct007-105b4cd	2.798	4.36E-05	206.303	2.38E-02	1.42E-01	3.13E-04	0.99462	0.00100	1.00290	0.00440	-0.00828	0.99172
15	mct007-105cdair	2.798	4.36E-05	206.310	2.37E-02	1.42E-01	3.10E-04	0.99181	0.00093	1.00290	0.00440	-0.01109	0.98891
16	mct007-105cdh2o	2.798	3.98E-05	206.290	2.35E-02	1.42E-01	3.07E-04	0.99159	0.00091	1.00280	0.00440	-0.01121	0.98879
17	mct007-105h1	2.798	4.14E-05	206.355	2.26E-02	1.41E-01	2.95E-04	0.99262	0.00088	1.00260	0.00440	-0.00998	0.99002
18	mct007-105h1cd	2.798	4.15E-05	206.305	2.30E-02	1.42E-01	3.02E-04	0.99057	0.00078	1.00250	0.00440	-0.01193	0.98807
19	mct007-105h2	2.798	4.27E-05	206.336	2.34E-02	1.41E-01	3.04E-04	0.99291	0.00100	1.00240	0.00440	-0.00949	0.99051
20	mct007-105h2cd	2.798	4.03E-05	206.304	2.39E-02	1.42E-01	3.10E-04	0.99134	0.00109	1.00230	0.00440	-0.01096	0.98904
21	mct007-105h3	2.798	4.17E-05	206.360	2.33E-02	1.41E-01	3.02E-04	0.99342	0.00087	1.00200	0.00440	-0.00858	0.99142
22	mct007-105h3cd	2.798	3.98E-05	206.306	2.35E-02	1.42E-01	3.09E-04	0.99139	0.00083	1.00200	0.00440	-0.01061	0.98939
23	mct007-105h4	2.798	4.10E-05	206.402	2.24E-02	1.41E-01	2.92E-04	0.99380	0.00092	1.00210	0.00440	-0.00830	0.99170
24	mct007-105h4cd	2.798	4.30E-05	206.265	2.26E-02	1.42E-01	2.95E-04	0.99263	0.00088	1.00210	0.00440	-0.00947	0.99053
25	mct007-105h5	2.798	4.15E-05	206.415	2.34E-02	1.41E-01	3.11E-04	0.99442	0.00079	1.00200	0.00440	-0.00758	0.99242
26	mct007-105h5cd	2.798	4.32E-05	206.293	2.33E-02	1.42E-01	3.12E-04	0.99233	0.00089	1.00250	0.00440	-0.01017	0.98983
27	mct007-1143arra	2.797	4.10E-05	208.294	2.12E-02	1.19E-01	2.35E-04	1.00004	0.00099	1.00360	0.00460	-0.00356	0.99644
28	mct007-132array	2.796	3.84E-05	210.640	1.92E-02	9.65E-02	1.78E-04	0.99948	0.00083	1.00370	0.00570	-0.00422	0.99578
29	mct007-1386arra	2.795	3.74E-05	211.241	1.86E-02	9.16E-02	1.69E-04	0.99992	0.00086	1.00440	0.00610	-0.00448	0.99552
30	mct008-001	2.799	5.71E-05	194.115	3.23E-02	4.01E-01	1.12E-03	0.99031	0.00078	0.99970	0.00320	-0.00939	0.99061
31	mct008-002	2.796	4.99E-05	202.340	2.59E-02	2.00E-01	4.66E-04	0.99748	0.00093	1.00080	0.00300	-0.00332	0.99668

N	Case	nubar	Sigma	AFG	Sigma	EALCF (eV)	Sigma	k_{calc} Pu-U	Sigma	k_{exp} Pu-U	Sigma	Bias = Calculated - Benchmark	Adjusted k_{eff} Pu-U
32	mct008-003	2.794	4.24E-05	206.253	2.31E-02	1.42E-01	3.02E-04	0.99684	0.00086	1.00230	0.00380	-0.00546	0.99454
33	mct008-004	2.793	3.94E-05	208.203	2.19E-02	1.20E-01	2.45E-04	1.00206	0.00083	1.00150	0.00470	0.00056	1.00056
34	mct008-005	2.792	3.84E-05	210.562	1.93E-02	9.70E-02	1.76E-04	1.00299	0.00090	1.00220	0.00560	0.00079	1.00079
35	mct008-006	2.791	3.50E-05	211.204	1.86E-02	9.15E-02	1.64E-04	1.00325	0.00083	1.00280	0.00650	0.00045	1.00045
36	mct008-al	2.794	4.40E-05	206.340	2.39E-02	1.41E-01	3.11E-04	0.99711	0.00090	1.00230	0.00390	-0.00519	0.99481
37	mct008-alc	2.794	4.37E-05	206.215	2.43E-02	1.42E-01	3.19E-04	0.99381	0.00089	1.00230	0.00410	-0.00849	0.99151
38	mct008-b1	2.794	4.25E-05	206.259	2.41E-02	1.42E-01	3.14E-04	0.99411	0.00082	1.00230	0.00390	-0.00819	0.99181
39	mct008-b1c	2.794	4.19E-05	206.192	2.36E-02	1.43E-01	3.07E-04	0.99429	0.00071	1.00230	0.00410	-0.00801	0.99199
40	mct008-b2	2.794	4.33E-05	206.275	2.30E-02	1.42E-01	2.96E-04	0.99625	0.00080	1.00230	0.00390	-0.00605	0.99395
41	mct008-b2c	2.794	4.21E-05	206.198	2.32E-02	1.43E-01	2.95E-04	0.99433	0.00074	1.00230	0.00410	-0.00797	0.99203
42	mct008-b3	2.794	4.40E-05	206.262	2.45E-02	1.42E-01	3.22E-04	0.99389	0.00081	1.00230	0.00390	-0.00841	0.99159
43	mct008-b3c	2.794	4.19E-05	206.203	2.32E-02	1.43E-01	3.04E-04	0.99731	0.00092	1.00230	0.00410	-0.00499	0.99501
44	mct008-b4	2.794	4.26E-05	206.321	2.36E-02	1.41E-01	3.08E-04	0.99351	0.00092	1.00230	0.00390	-0.00879	0.99121
45	mct008-b4c	2.794	4.47E-05	206.164	2.41E-02	1.43E-01	3.18E-04	0.99340	0.00081	1.00230	0.00410	-0.00890	0.99110
46	mct008-cd	2.794	4.28E-05	206.220	2.32E-02	1.42E-01	3.07E-04	0.99550	0.00100	1.00230	0.00400	-0.00680	0.99320
47	mct008-cdh2o	2.794	4.39E-05	206.194	2.29E-02	1.43E-01	3.04E-04	0.99469	0.00101	1.00230	0.00400	-0.00761	0.99239
48	mct008-h1	2.794	4.25E-05	206.237	2.39E-02	1.42E-01	3.11E-04	0.99359	0.00086	1.00230	0.00390	-0.00871	0.99129
49	mct008-h1c	2.794	4.39E-05	206.185	2.35E-02	1.43E-01	3.06E-04	0.99484	0.00086	1.00230	0.00410	-0.00746	0.99254
50	mct008-h2	2.794	4.36E-05	206.256	2.29E-02	1.42E-01	2.99E-04	0.99527	0.00088	1.00230	0.00390	-0.00703	0.99297
51	mct008-h2c	2.794	4.53E-05	206.132	2.18E-02	1.43E-01	2.93E-04	0.99447	0.00094	1.00230	0.00410	-0.00783	0.99217
52	mct008-h3	2.794	4.28E-05	206.281	2.32E-02	1.42E-01	3.01E-04	0.99543	0.00093	1.00230	0.00390	-0.00687	0.99313
53	mct008-h3c	2.794	4.47E-05	206.235	2.36E-02	1.42E-01	3.05E-04	0.99356	0.00084	1.00230	0.00410	-0.00874	0.99126
54	mct008-h4	2.794	4.28E-05	206.222	2.38E-02	1.42E-01	3.05E-04	0.99574	0.00083	1.00230	0.00390	-0.00656	0.99344
55	mct008-h4c	2.794	4.32E-05	206.158	2.26E-02	1.43E-01	3.01E-04	0.99490	0.00093	1.00230	0.00410	-0.00740	0.99260
56	mct008-h5	2.794	4.15E-05	206.336	2.38E-02	1.41E-01	3.07E-04	0.99502	0.00089	1.00230	0.00390	-0.00728	0.99272
57	mct008-h5c	2.794	4.42E-05	206.172	2.23E-02	1.43E-01	2.86E-04	0.99382	0.00087	1.00230	0.00410	-0.00848	0.99152
58	mct009-001	2.858	4.74E-05	190.927	3.37E-02	5.55E-01	1.62E-03	0.99360	0.00082	1.00030	0.00540	-0.00670	0.99330
59	mct011-001	2.651	8.88E-05	187.016	5.09E-02	5.64E-01	2.01E-03	1.00339	0.00111	1.00200	0.00160	0.00139	1.00139
60	mct012-001	2.889	1.07E-05	206.561	1.19E-02	1.46E-01	1.75E-04	0.97738	0.00086	1.00420	0.00580	-0.02682	0.97318
61	mct012-002	2.889	1.05E-05	206.549	1.24E-02	1.46E-01	1.81E-04	0.97793	0.00102	1.00420	0.00580	-0.02627	0.97373
62	mct012-003	2.889	1.02E-05	206.571	1.19E-02	1.46E-01	1.75E-04	0.97645	0.00103	1.00420	0.00580	-0.02775	0.97225
63	mct012-004	2.889	1.07E-05	206.505	1.21E-02	1.47E-01	1.78E-04	0.97809	0.00091	1.00420	0.00580	-0.02611	0.97389
64	mct012-005	2.889	1.01E-05	206.532	1.20E-02	1.46E-01	1.84E-04	0.97859	0.00095	1.00420	0.00580	-0.02561	0.97439
65	mct012-006	2.889	1.04E-05	206.468	1.26E-02	1.47E-01	1.83E-04	0.98227	0.00095	1.00420	0.00580	-0.02193	0.97807
66	mct012-007	2.886	4.51E-06	214.784	5.99E-03	6.94E-02	5.31E-05	1.03734	0.00110	1.00230	0.00360	0.03504	1.03504
67	mct012-008	2.886	4.48E-06	214.804	5.97E-03	6.92E-02	5.43E-05	1.03157	0.00114	1.00230	0.00360	0.02927	1.02927
68	mct012-009	2.886	4.24E-06	214.826	5.58E-03	6.91E-02	5.06E-05	1.02894	0.00093	1.00230	0.00360	0.02664	1.02664

N	Case	nubar	Sigma	AFG	Sigma	EALCF (eV)	Sigma	k_{calc} Pu-U	Sigma	k_{exp} Pu-U	Sigma	Bias = Calculated - Benchmark	Adjusted k_{eff} Pu-U
69	mct012-010	2.886	4.48E-06	214.827	5.90E-03	6.91E-02	5.29E-05	1.02689	0.00120	1.00230	0.00360	0.02459	1.02459
70	mct012-011	2.886	4.25E-06	214.827	5.87E-03	6.91E-02	5.19E-05	1.02792	0.00107	1.00230	0.00360	0.02562	1.02562
71	mct012-012	2.886	4.58E-06	214.803	5.77E-03	6.92E-02	5.14E-05	1.02876	0.00113	1.00230	0.00360	0.02646	1.02646
72	mct012-013	2.886	4.27E-06	214.767	5.89E-03	6.96E-02	5.25E-05	1.03760	0.00103	1.00230	0.00360	0.03530	1.03530
73	mct012-014	2.888	8.11E-06	206.563	1.16E-02	1.50E-01	1.83E-04	1.02127	0.00099	1.00020	0.00270	0.02107	1.02107
74	mct012-015	2.888	8.14E-06	206.577	1.23E-02	1.50E-01	1.89E-04	1.01750	0.00114	1.00020	0.00270	0.01730	1.01730
75	mct012-016	2.888	8.45E-06	206.695	1.20E-02	1.49E-01	1.91E-04	1.01547	0.00103	1.00020	0.00270	0.01527	1.01527
76	mct012-017	2.888	7.81E-06	206.724	1.21E-02	1.48E-01	1.87E-04	1.01431	0.00119	1.00020	0.00270	0.01411	1.01411
77	mct012-018	2.888	8.21E-06	206.768	1.21E-02	1.47E-01	1.88E-04	1.01512	0.00104	1.00020	0.00270	0.01492	1.01492
78	mct012-019	2.888	8.23E-06	206.866	1.19E-02	1.46E-01	1.79E-04	1.01254	0.00103	1.00020	0.00270	0.01234	1.01234
79	mct012-020	2.888	9.20E-06	203.148	1.35E-02	2.06E-01	2.80E-04	1.01755	0.00111	1.00040	0.00370	0.01715	1.01715
80	mct012-021	2.888	8.85E-06	203.163	1.30E-02	2.06E-01	2.65E-04	1.01967	0.00126	1.00040	0.00370	0.01927	1.01927
81	mct012-022	2.888	9.06E-06	203.147	1.39E-02	2.06E-01	2.87E-04	1.01439	0.00114	1.00040	0.00370	0.01399	1.01399
82	mct012-023	2.890	8.31E-06	204.709	1.41E-02	1.75E-01	2.46E-04	1.00887	0.00115	0.99970	0.00490	0.00917	1.00917
83	mct012-024	2.890	8.06E-06	204.758	1.39E-02	1.74E-01	2.37E-04	1.00935	0.00109	0.99970	0.00490	0.00965	1.00965
84	mct012-025	2.890	8.24E-06	204.821	1.41E-02	1.73E-01	2.41E-04	1.00728	0.00111	0.99970	0.00490	0.00758	1.00758
85	mct012-026	2.890	8.53E-06	205.028	1.39E-02	1.69E-01	2.36E-04	1.00574	0.00112	0.99970	0.00490	0.00604	1.00604
86	mct012-027	2.890	8.22E-06	205.107	1.44E-02	1.68E-01	2.39E-04	1.00615	0.00093	0.99970	0.00490	0.00645	1.00645
87	mct012-028	2.890	7.81E-06	205.148	1.42E-02	1.68E-01	2.32E-04	1.00618	0.00117	0.99970	0.00490	0.00648	1.00648
88	mct012-029	2.890	8.73E-06	205.233	1.44E-02	1.66E-01	2.45E-04	1.00449	0.00108	0.99970	0.00490	0.00479	1.00479
89	mct012-030	2.890	8.51E-06	205.044	1.43E-02	1.69E-01	2.44E-04	1.00366	0.00113	0.99970	0.00490	0.00396	1.00396
90	mct012-031	2.890	9.81E-06	200.387	1.50E-02	2.57E-01	3.73E-04	0.99983	0.00122	1.00070	0.00520	-0.00087	0.99913
91	mct012-032	2.890	9.39E-06	200.368	1.48E-02	2.57E-01	3.70E-04	0.99881	0.00121	1.00070	0.00520	-0.00189	0.99811
92	mct012-033	2.890	9.29E-06	200.397	1.55E-02	2.57E-01	3.79E-04	0.99745	0.00108	1.00070	0.00520	-0.00325	0.99675
93	mmf001-001	2.953	3.52E-04	22.331	1.29E-02	1.14E+06	1.37E+03	0.99542	0.00109	1.00000	0.00160	-0.00458	0.99542
94	mmf002-001	2.724	2.92E-04	24.285	1.61E-02	9.38E+05	1.40E+03	1.00456	0.00106	1.00000	0.00420	0.00456	1.00456
95	mmf002-002	2.722	3.18E-04	24.312	1.55E-02	9.36E+05	1.35E+03	1.00476	0.00115	1.00000	0.00440	0.00476	1.00476
96	mmf002-003	2.711	2.99E-04	24.382	1.56E-02	9.30E+05	1.35E+03	1.00460	0.00121	1.00000	0.00480	0.00460	1.00460
97	mmf007-001	2.842	3.61E-04	52.180	7.72E-02	6.39E+04	4.32E+02	1.00659	0.00122	1.00000	0.00880	0.00659	1.00659
98	mmf007-002	2.829	3.54E-04	47.095	6.89E-02	9.82E+04	6.02E+02	1.00860	0.00115	1.00000	0.00440	0.00860	1.00860
99	mmf007-003	2.801	3.64E-04	32.515	3.75E-02	3.62E+05	1.36E+03	1.00544	0.00100	1.00000	0.00540	0.00544	1.00544
100	mmf007-004	2.782	3.73E-04	27.914	2.03E-02	6.00E+05	1.37E+03	1.00365	0.00100	1.00000	0.00540	0.00365	1.00365
101	mmf007-005	2.758	3.46E-04	25.427	1.40E-02	8.33E+05	1.20E+03	0.99966	0.00095	1.00000	0.00630	-0.00034	0.99966
102	mmf007-006	2.745	3.48E-04	24.483	1.37E-02	9.32E+05	1.22E+03	0.99752	0.00119	1.00000	0.00690	-0.00248	0.99752
103	mmf007-007	2.961	3.60E-04	47.076	7.58E-02	1.02E+05	6.83E+02	1.00905	0.00097	1.00000	0.00600	0.00905	1.00905
104	mmf007-008	2.937	3.53E-04	40.435	6.31E-02	1.79E+05	1.04E+03	1.00565	0.00098	1.00000	0.00550	0.00565	1.00565
105	mmf007-009	2.919	3.46E-04	35.603	4.72E-02	2.75E+05	1.22E+03	1.00506	0.00109	1.00000	0.00520	0.00506	1.00506

N	Case	nubar	Sigma	AFG	Sigma	EALCF (eV)	Sigma	k_{calc} Pu-U	Sigma	k_{exp} Pu-U	Sigma	Bias = Calculated - Benchmark	Adjusted k_{eff} Pu-U
106	mmf007-010	2.873	3.55E-04	27.828	2.03E-02	5.99E+05	1.35E+03	1.00455	0.00095	1.00000	0.00510	0.00455	1.00455
107	mmf007-011	2.844	3.50E-04	25.773	1.59E-02	7.82E+05	1.34E+03	1.00090	0.00120	1.00000	0.00490	0.00090	1.00090
108	mmf007-012	2.811	3.56E-04	24.378	1.38E-02	9.36E+05	1.24E+03	0.99857	0.00121	1.00000	0.00590	-0.00143	0.99857
109	mmf007-013	2.793	3.47E-04	23.682	1.30E-02	1.01E+06	1.24E+03	0.99799	0.00112	1.00000	0.00640	-0.00201	0.99799
110	mmf007-014	3.017	3.29E-04	33.570	4.84E-02	3.38E+05	1.55E+03	1.00947	0.00122	1.00000	0.00600	0.00947	1.00947
111	mmf007-015	2.990	3.18E-04	30.383	3.45E-02	4.56E+05	1.58E+03	1.00937	0.00104	1.00000	0.00590	0.00937	1.00937
112	mmf007-016	2.929	3.41E-04	25.898	1.67E-02	7.56E+05	1.39E+03	1.00362	0.00099	1.00000	0.00530	0.00362	1.00362
113	mmf007-017	2.893	3.29E-04	24.722	1.47E-02	8.87E+05	1.32E+03	1.00323	0.00109	1.00000	0.00530	0.00323	1.00323
114	mmf007-018	2.852	3.63E-04	23.749	1.41E-02	9.98E+05	1.33E+03	1.00631	0.00109	1.00000	0.00570	0.00631	1.00631
115	mmf007-019	2.976	3.33E-04	24.717	1.63E-02	8.74E+05	1.51E+03	1.00621	0.00094	1.00000	0.00620	0.00621	1.00621
116	mmf007-020	2.937	3.45E-04	23.864	1.38E-02	9.77E+05	1.32E+03	1.00300	0.00112	1.00000	0.00560	0.00300	1.00300
117	mmf007-021	2.892	3.96E-04	23.100	1.33E-02	1.06E+06	1.36E+03	1.00039	0.00105	1.00000	0.00580	0.00039	1.00039
118	mmf007-022	3.019	3.25E-04	23.821	1.38E-02	9.71E+05	1.37E+03	1.00274	0.00131	1.00000	0.00550	0.00274	1.00274
119	mmf007-023	2.976	3.21E-04	23.221	1.32E-02	1.04E+06	1.33E+03	1.00068	0.00114	1.00000	0.00530	0.00068	1.00068
120	mmf009	3.059	2.81E-04	21.924	1.29E-02	1.19E+06	1.44E+03	0.99560	0.00113	1.00000	0.00100	-0.00440	0.99560
121	mmf010	2.844	3.66E-04	23.078	1.31E-02	1.07E+06	1.32E+03	0.99622	0.00116	1.00000	0.00090	-0.00378	0.99622
122	mmf011-21b	2.910	1.38E-04	34.825	2.21E-02	2.79E+05	6.89E+02	1.00000	0.00079	0.98970	0.00230	0.01030	1.01030
123	mmf011-21c	2.784	1.52E-04	33.862	2.09E-02	3.17E+05	7.53E+02	1.00458	0.00079	0.99980	0.00230	0.00478	1.00478
124	mmf011-21d	2.694	1.37E-04	37.502	2.30E-02	2.06E+05	5.26E+02	1.00842	0.00084	1.00180	0.00240	0.00662	1.00662
125	mmf011-21e	2.604	1.25E-04	35.773	2.09E-02	2.56E+05	6.06E+02	1.00822	0.00085	1.00120	0.00240	0.00702	1.00702
126	mmt001-106	2.885	4.65E-05	193.434	4.27E-02	3.94E-01	1.28E-03	0.99585	0.00102	1.00000	0.00440	-0.00415	0.99585
127	mmt001-107	2.885	4.34E-05	188.633	3.88E-02	5.77E-01	1.69E-03	1.00267	0.00101	1.00000	0.00440	0.00267	1.00267
128	mmt001-109	2.885	4.14E-05	190.822	4.12E-02	4.85E-01	1.48E-03	1.00224	0.00134	1.00000	0.00440	0.00224	1.00224
129	mmt001-110	2.885	4.33E-05	192.470	4.00E-02	4.25E-01	1.28E-03	0.99730	0.00102	1.00000	0.00440	-0.00270	0.99730
130	mmt001-111	2.885	3.90E-05	185.647	3.95E-02	7.23E-01	2.08E-03	1.00470	0.00125	1.00000	0.00440	0.00470	1.00470
131	mmt001-112	2.886	3.90E-05	183.828	3.74E-02	8.50E-01	2.30E-03	1.00583	0.00093	1.00000	0.00320	0.00583	1.00583
132	mmt001-113	2.886	3.53E-05	182.470	3.55E-02	9.61E-01	2.43E-03	1.00350	0.00097	1.00000	0.00320	0.00350	1.00350
133	mmt001-114	2.886	3.64E-05	181.155	3.68E-02	1.08E+00	2.81E-03	1.00404	0.00116	1.00000	0.00320	0.00404	1.00404
134	mmt001-115	2.886	3.35E-05	180.172	3.55E-02	1.17E+00	2.88E-03	1.00256	0.00083	1.00000	0.00660	0.00256	1.00256
135	mmt001-116	2.886	3.45E-05	179.768	3.56E-02	1.22E+00	2.94E-03	1.00552	0.00094	1.00000	0.00660	0.00552	1.00552
136	mmt001-117	2.884	5.47E-06	209.494	1.02E-02	1.14E-01	1.27E-04	1.01920	0.00096	1.00000	0.00250	0.01920	1.01920
137	mst001-a100	2.884	5.05E-06	210.020	9.49E-03	1.09E-01	1.13E-04	1.00882	0.00107	1.00000	0.00520	0.00882	1.00882
138	mst001-a108	2.884	3.88E-06	212.730	7.75E-03	8.43E-02	7.19E-05	1.00158	0.00107	1.00000	0.00160	0.00158	1.00158
139	mst001-a87	2.884	6.86E-06	205.574	1.24E-02	1.61E-01	2.03E-04	0.99767	0.00118	1.00000	0.00160	-0.00233	0.99767
140	mst001-a87s	2.884	7.18E-06	205.510	1.28E-02	1.62E-01	2.07E-04	0.99719	0.00100	1.00000	0.00160	-0.00281	0.99719
141	mst001-a91	2.884	6.91E-06	205.858	1.18E-02	1.58E-01	1.90E-04	0.99282	0.00103	1.00000	0.00160	-0.00718	0.99282
142	mst001-a92	2.884	7.36E-06	204.922	1.30E-02	1.71E-01	2.22E-04	0.99561	0.00093	1.00000	0.00160	-0.00439	0.99561

375 -> 407

N	Case	nubar	Sigma	AFG	Sigma	EALCF (eV)	Sigma	k_{calc} Pu-U	Sigma	k_{exp} Pu-U	Sigma	Bias = Calculated - Benchmark	Adjusted k_{eff} Pu-U
143	mst001-a93	2.884	8.01E-06	204.481	1.26E-02	1.76E-01	2.11E-04	0.99860	0.00093	1.00000	0.00160	-0.00140	0.99860
144	mst001-a94	2.884	7.26E-06	204.980	1.29E-02	1.70E-01	2.17E-04	0.99886	0.00099	1.00000	0.00160	-0.00114	0.99886
145	mst001-a95	2.892	1.07E-05	198.548	1.68E-02	2.84E-01	4.23E-04	1.00044	0.00128	1.00000	0.00160	0.00044	1.00044
146	mst001-a96	2.891	7.25E-06	206.498	1.30E-02	1.49E-01	1.89E-04	1.00230	0.00105	1.00000	0.00160	0.00230	1.00230
147	mst001-a97	2.891	5.50E-06	211.740	1.09E-02	9.26E-02	1.05E-04	1.00454	0.00105	1.00000	0.00160	0.00454	1.00454
148	mst001-a98	2.884	5.72E-06	209.360	9.62E-03	1.16E-01	1.19E-04	1.00204	0.00117	1.00000	0.00160	0.00204	1.00204
149	mst001-a99	2.884	5.39E-06	209.810	9.79E-03	1.12E-01	1.21E-04	1.00728	0.00099	1.00000	0.00520	0.00728	1.00728
150	mst002-b11058	2.890	1.59E-06	219.456	2.02E-03	4.25E-02	1.43E-05	1.00801	0.00067	1.00000	0.00240	0.00801	1.00801
151	mst002-b11059	2.890	1.66E-06	219.482	2.09E-03	4.24E-02	1.46E-05	1.00783	0.00082	1.00000	0.00240	0.00783	1.00783
152	mst002-b63061	2.887	1.47E-06	219.231	2.21E-03	4.35E-02	1.56E-05	1.00748	0.00080	1.00000	0.00240	0.00748	1.00748
153	mst004-d15677	2.889	1.18E-05	196.083	1.77E-02	3.53E-01	5.50E-04	0.99764	0.00122	1.00000	0.00260	-0.00236	0.99764
154	mst004-d16678	2.889	1.02E-05	199.314	1.67E-02	2.68E-01	4.08E-04	0.99809	0.00127	1.00000	0.00260	-0.00191	0.99809
155	mst004-d19669	2.889	7.56E-06	205.661	1.25E-02	1.61E-01	2.03E-04	0.99796	0.00117	1.00000	0.00290	-0.00204	0.99796
156	mst004-d20670	2.889	7.84E-06	203.624	1.27E-02	1.94E-01	2.45E-04	0.99655	0.00130	1.00000	0.00290	-0.00345	0.99655
157	mst004-d25665	2.889	3.62E-06	214.559	5.89E-03	7.15E-02	5.36E-05	1.00031	0.00148	1.00000	0.00330	0.00031	1.00031
158	mst004-d26666	2.889	3.51E-06	215.133	5.49E-03	6.75E-02	4.98E-05	1.00039	0.00126	1.00000	0.00330	0.00039	1.00039
159	mst004-f17583	2.889	1.03E-05	197.640	1.68E-02	3.10E-01	4.64E-04	0.99624	0.00104	1.00000	0.00770	-0.00376	0.99624
160	mst004-f18568	2.889	7.30E-06	204.648	1.24E-02	1.77E-01	2.22E-04	1.00288	0.00116	1.00000	0.00780	0.00288	1.00288
161	mst004-f27567	2.889	3.59E-06	214.776	5.50E-03	7.01E-02	5.08E-05	1.00384	0.00117	1.00000	0.00680	0.00384	1.00384
162	mst005-c13175	2.889	1.12E-05	195.947	1.81E-02	3.57E-01	5.62E-04	0.98432	0.00110	1.00000	0.00370	-0.01568	0.98432
163	mst005-c22b74	2.889	8.03E-06	203.586	1.26E-02	1.94E-01	2.40E-04	0.98980	0.00113	1.00000	0.00370	-0.01020	0.98980
164	mst005-c23b63	2.889	3.77E-06	214.589	5.88E-03	7.14E-02	5.40E-05	0.99657	0.00107	1.00000	0.00370	-0.00343	0.99657
165	mst005-d14176	2.889	1.01E-05	199.927	1.71E-02	2.55E-01	4.07E-04	0.99721	0.00143	1.00000	0.00370	-0.00279	0.99721
166	mst005-d21171	2.889	7.68E-06	206.080	1.25E-02	1.55E-01	1.94E-04	1.00248	0.00116	1.00000	0.00370	0.00248	1.00248
167	mst005-d21172	2.889	7.23E-06	206.225	1.17E-02	1.53E-01	1.88E-04	0.99974	0.00110	1.00000	0.00370	-0.00026	0.99974
168	mst005-d24164	2.889	3.57E-06	215.217	5.55E-03	6.70E-02	5.08E-05	1.00263	0.00111	1.00000	0.00370	0.00263	1.00263
	Maximum	3.059	3.96E-04	219.482	7.72E-02	1.19E+06	1.58E+03	1.03760	0.00148	1.00440	0.00880	0.03530	1.03530
	Average	2.850	8.28E-05	170.426	2.03E-02	1.33E+05	2.33E+02	1.00083	0.00101	1.00102	0.00416	-0.00019	0.99981
	Minimum	2.604	1.47E-06	21.924	2.02E-03	4.24E-02	1.43E-05	0.97645	0.00067	0.98970	0.00090	-0.02775	0.97225

5 Results Analysis

5.1 Introduction

The data in Tables 4.1 through 4.6 provides information for performing analysis of the calculation results, experiment (benchmark) data, and the bias results.

The OECD reports provide an estimate of the actual k_{eff} for each experiment model. While benchmarks for most experiments were estimated to be exactly critical, or k_exp = 1.0, a number of the estimates were above or below exactly critical. It was considered desirable to account for this difference. The following adjustment, to determine an adjusted calculation result, k', was used to calculate adjusted k-effective:

$$k' = 1 + bias = 1 + (k_cal - k_exp)$$

where k_cal = code calculated k_{eff} result for the modeled experiment, and
k_exp = OECD estimate of actual k_{eff} for the modeled experiment

The assumption inherent in making this adjustment is that the experiments were close to critical, and if a small adjustment could be made so that the experiment would be exactly critical, the bias of the calculation would not change.

When calculation methods are employed, the subcritical limit is a quantitative value used for implementation of NCSO policy, which is established in accordance with DOE Orders, Standards, or by NRC regulations for those activities under NRC jurisdiction. Evaluation criteria are usually the calculated reactivity, k_{eff}, for the model of the problem being evaluated, uncertainty in the calculated value of reactivity, bias introduced by the code used to calculate reactivity, and bias introduced by the model. Code bias is determined by a validation performed in accordance with ANSI/ANS 8.1. The statistical results determine code bias based on comparison of code calculations with experimental results. Model bias is due to uncertainties in the modeled parameters describing the problem, approximations made for the model to conform to the input requirements of the code, and any significant simplifications of the problem introduced into the model by the analyst. The acceptance criterion requires that the evaluation criteria be bounded by the subcritical limit. In the case of code calculations, the subcritical limit is often a criterion based on calculated k_{eff} and estimated bias and uncertainties.

It is recognized that it may also be possible to determine subcritical limits based on adjustment of correlating parameters other than k_{eff}, as allowed by ANSI/ANS-8.1. These parameters could include physical parameters such as mass or radius, for example, or other calculated parameters besides k_{eff}, if they can be shown to provide subcritical margin. This report does not address other potential correlating parameters, but an analyst could determine them as part of an evaluation and use them to determine subcritical limits in conjunction with the code bias results in this report.

5.2 Discussion of Results

Figure 1 shows a plot of all adjusted k-effective results versus EALCF, or the Energy corresponding to the Average Lethargy of neutrons Causing Fission. EALCF or average energy group has traditionally been used as a trending variable. The amount of data in the middle energy range is somewhat sparse relative to the low and high ends; however, with a few exceptions there are at least some

results in almost every energy range. As expected, most k_{eff} results are centered about 1.0, and are generally within a range of about 1.0 +0.04/-0.03, with the exception of a few results that are outside the range. These high and low data will be discussed in more detail below.

There appears to be a small systematic more negative bias for U-233 results, relative to other fissile categories, in the thermal to intermediate energy range, and some indication of a slight trend in the bias with energy. Otherwise, none of the fissile species appears to consistently have a different bias than other categories, and no other major trends in results are seen.

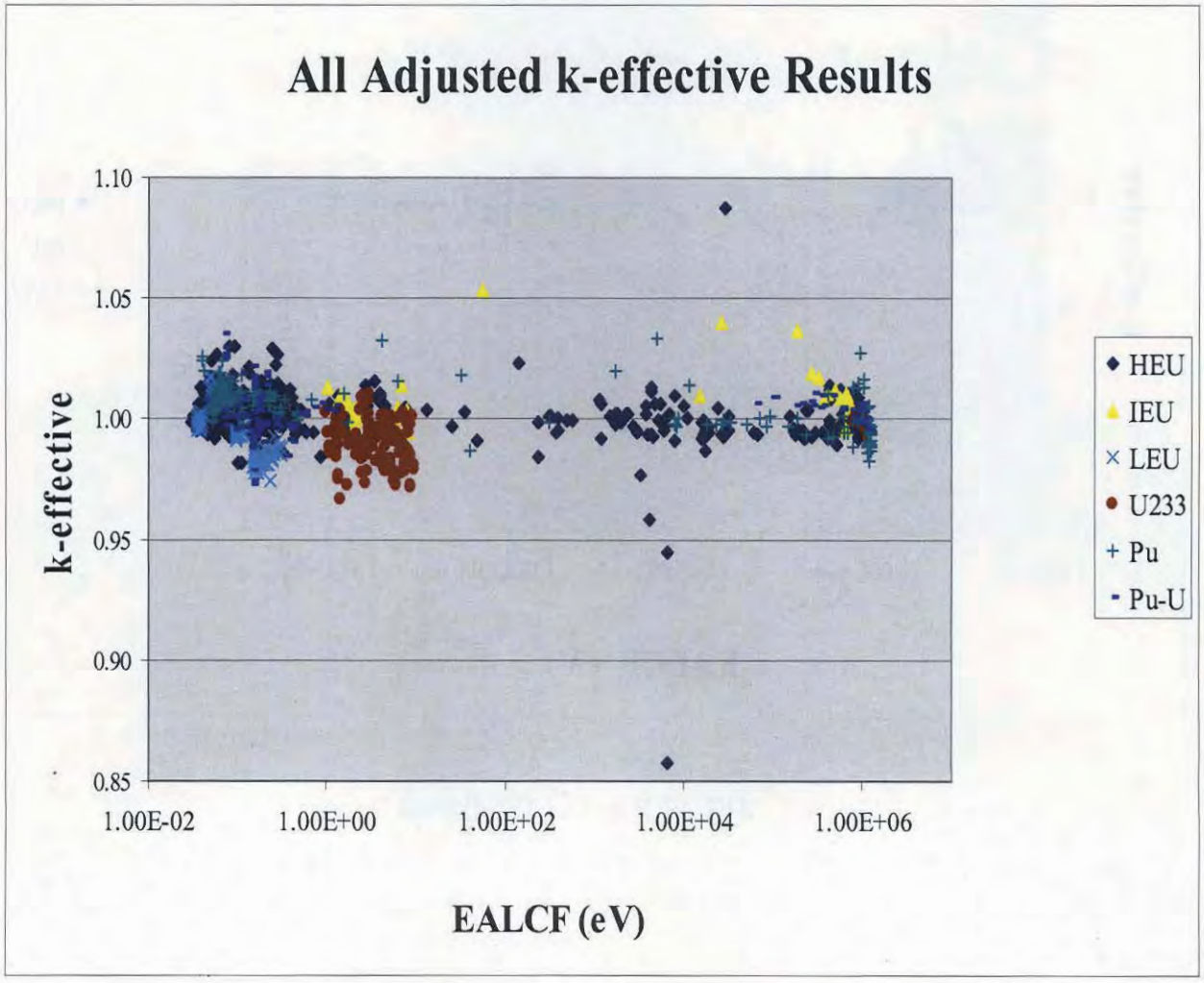

Figure 1 - All Adjusted Results

Figure 2 shows a plot of the HEU, IEU and LEU adjusted k_{eff} results versus EALCF. While Figure 2 appears to show a possible cluster of LEU results with more negative bias, this is not really the case, as seen in Figure 3, which shows a plot of the LEU results alone.

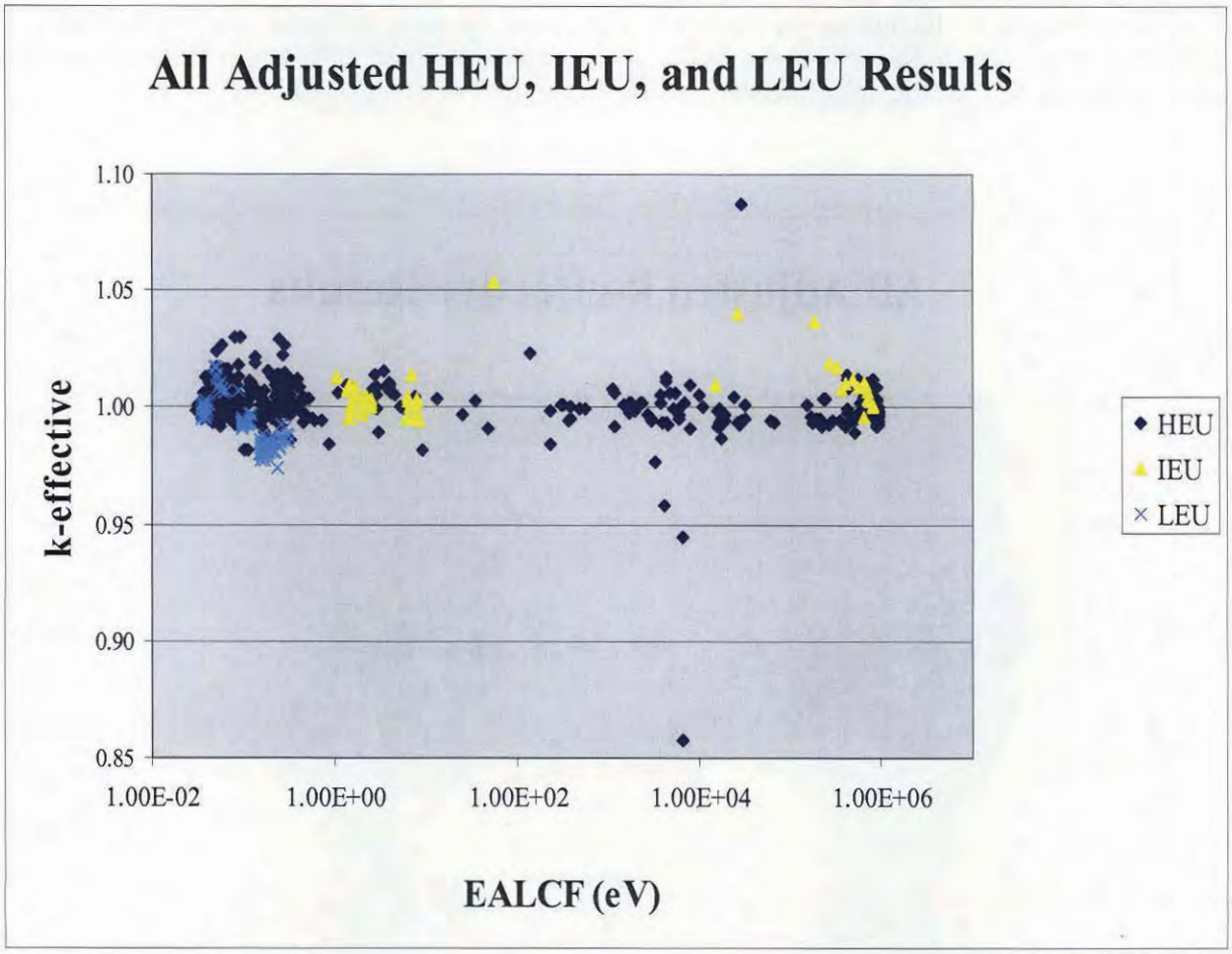

Figure 2 - HEU, IEU and LEU Adjusted Results

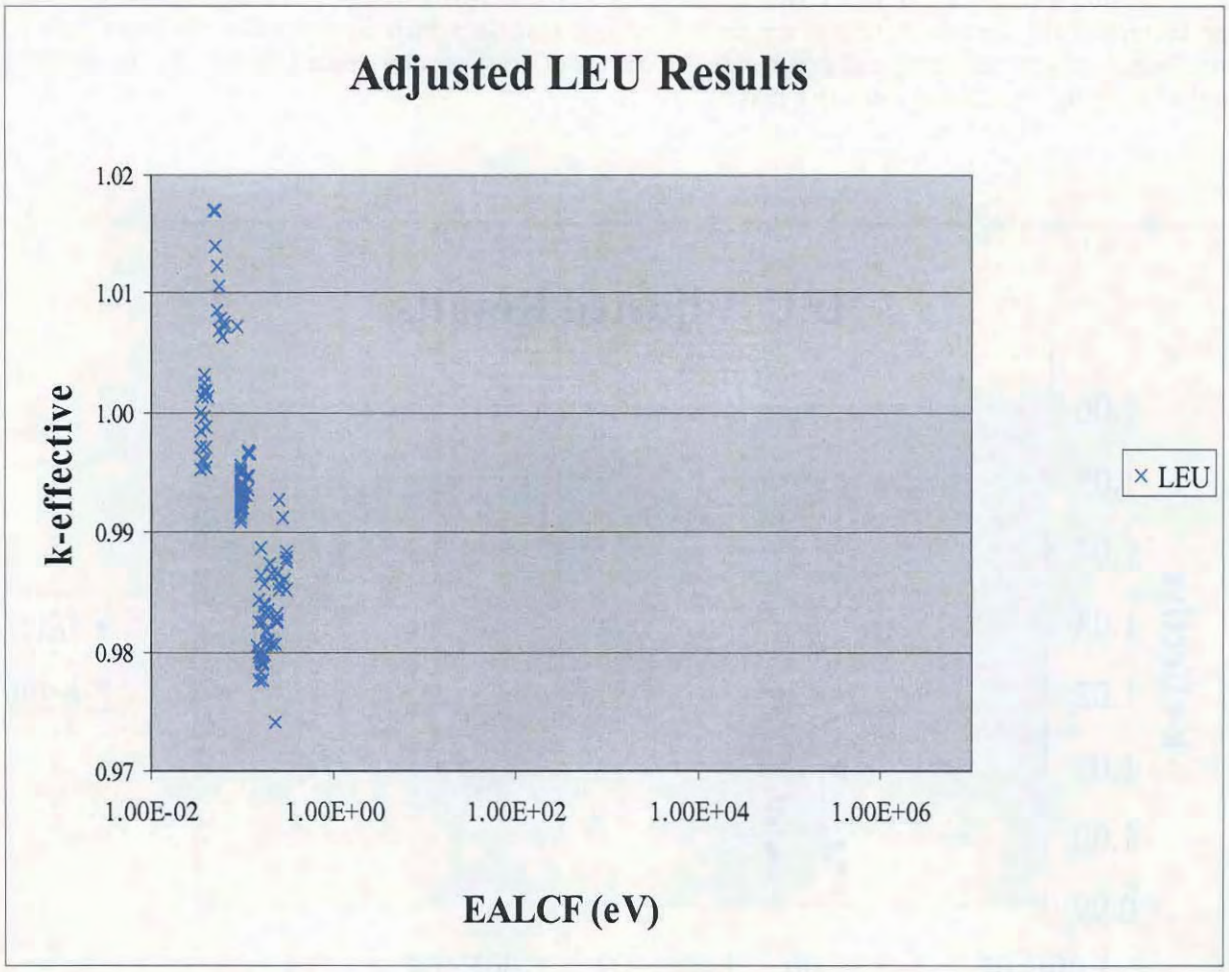

Figure 3 - LEU Adjusted k_{eff} Results

Figure 4 shows a plot of the IEU adjusted k_{eff} results versus EALCF. Also highlighted is the fact that several of the "outlying" results are from k-infinite models, which are somewhat different than the usual benchmark experiment, and exaggerate the effects of cross section imperfections. In this category, all the "outlying" results have positive bias.

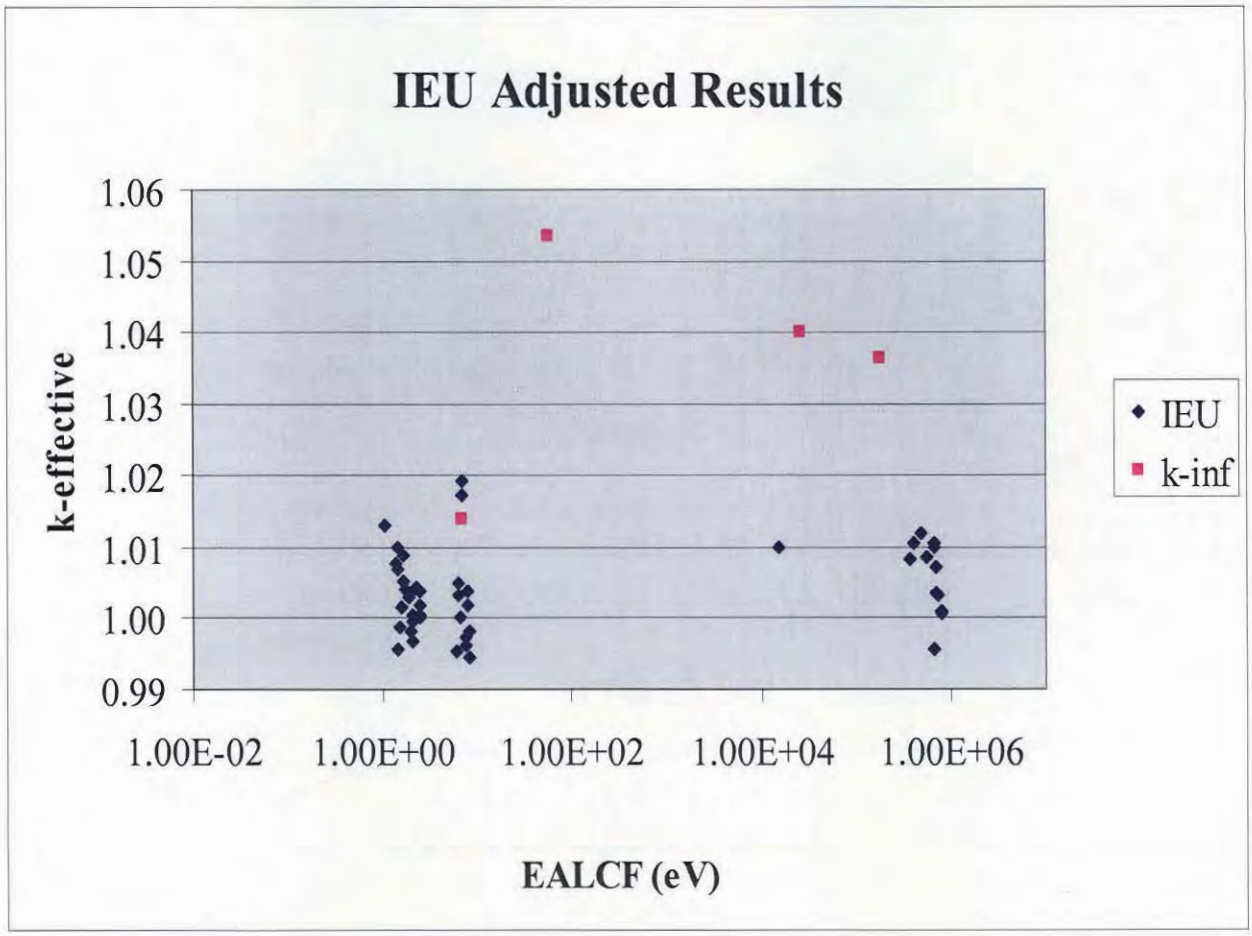

Figure 4 - IEU Adjusted k_{eff} Results

Figure 5 shows a plot of the HEU adjusted k_{eff} results versus EALCF. Also highlighted is the fact that four of the "outlying" results, including those having the most negative bias, are from k-infinite models, which are somewhat different than the usual benchmark experiment, and exaggerate the effects of cross section imperfections. It is also clear that one of the HEU results has a very high, positive bias.

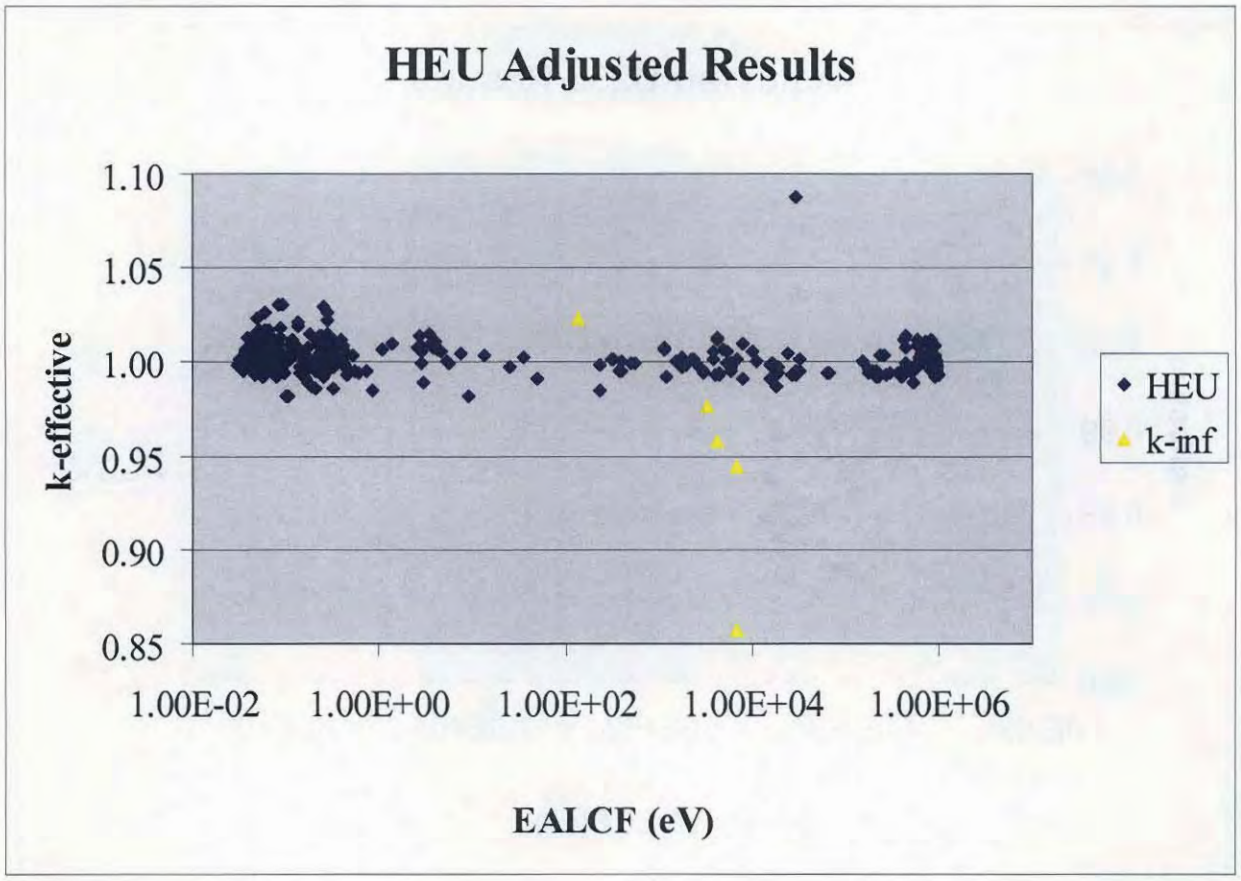

Figure 5 - HEU Adjusted k_{eff} Results

Figure 6 shows a plot of the adjusted U-233 k_{eff} results versus EALCF. While this plot appears to confirm the slightly more negative bias at low energies, the existence of a trend with energy appears questionable.

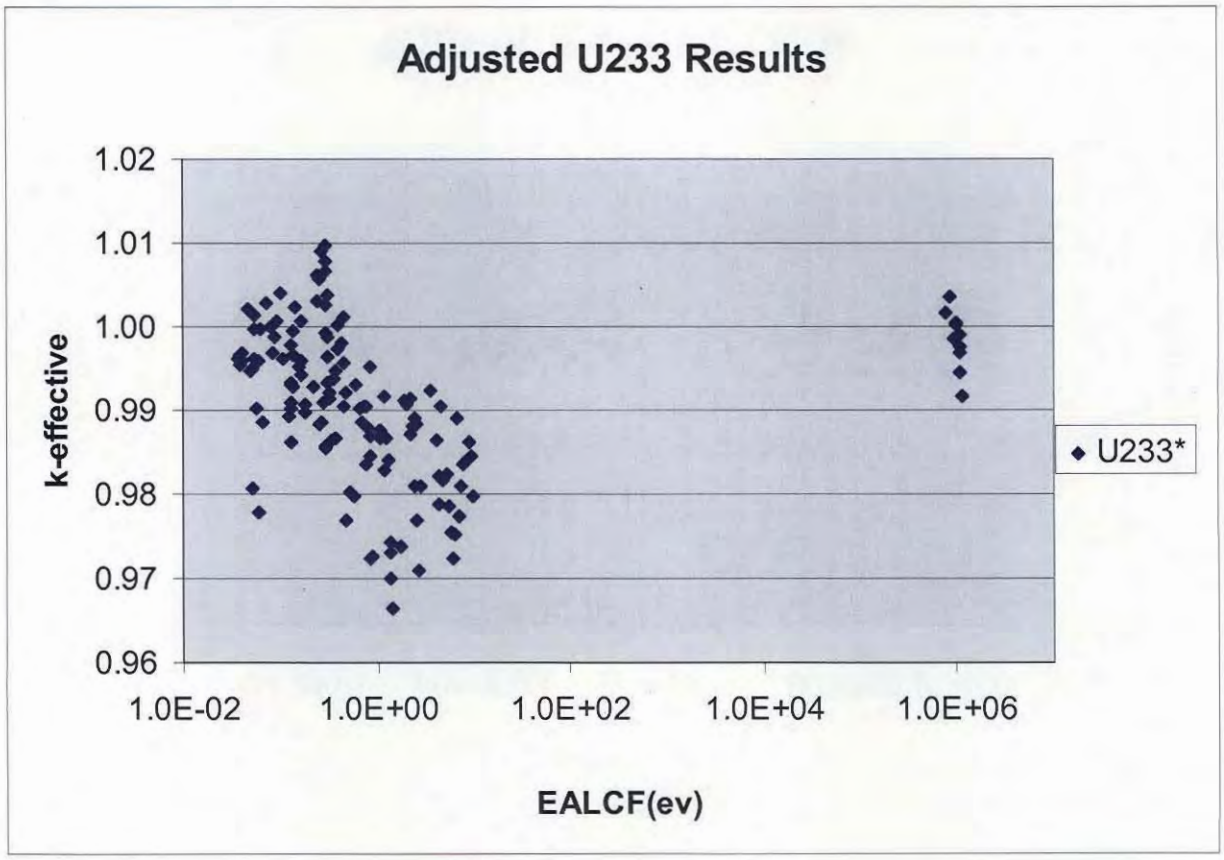

Figure 6 - U-233 Adjusted k_{eff} Results

Figure 7 shows a plot of the adjusted Pu and Mixed Pu-U results versus EALCF. The results appear to be consistent with the uranium results (as also seen in Figure 1), although the range of results is generally somewhat larger (excluding "outlying" results in uranium results).

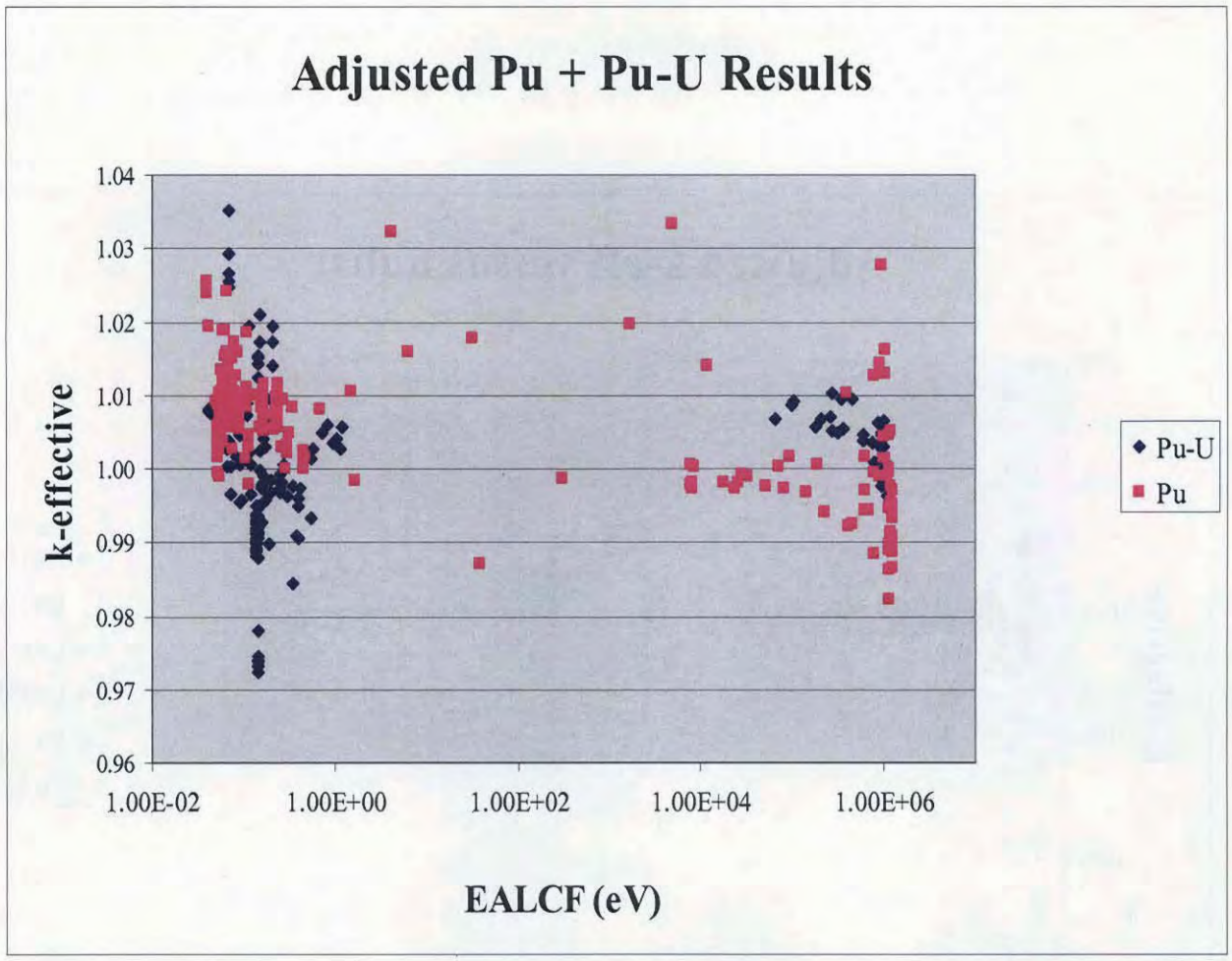

Figure 7 - Pu and Mixed Pu-U Adjusted k_{eff} Results

Figure 8 shows a plot of adjusted k_{eff} results versus nubar, or the average number of neutrons produced per fission. The value of nubar depends on the fissile species and the neutron spectrum, and therefore is thought to possibly incorporate a couple important characteristics of critical systems, and has potential value as an Area of Applicability indicator. For the data plotted, there is no apparent trend across a fairly wide range of nubar values.

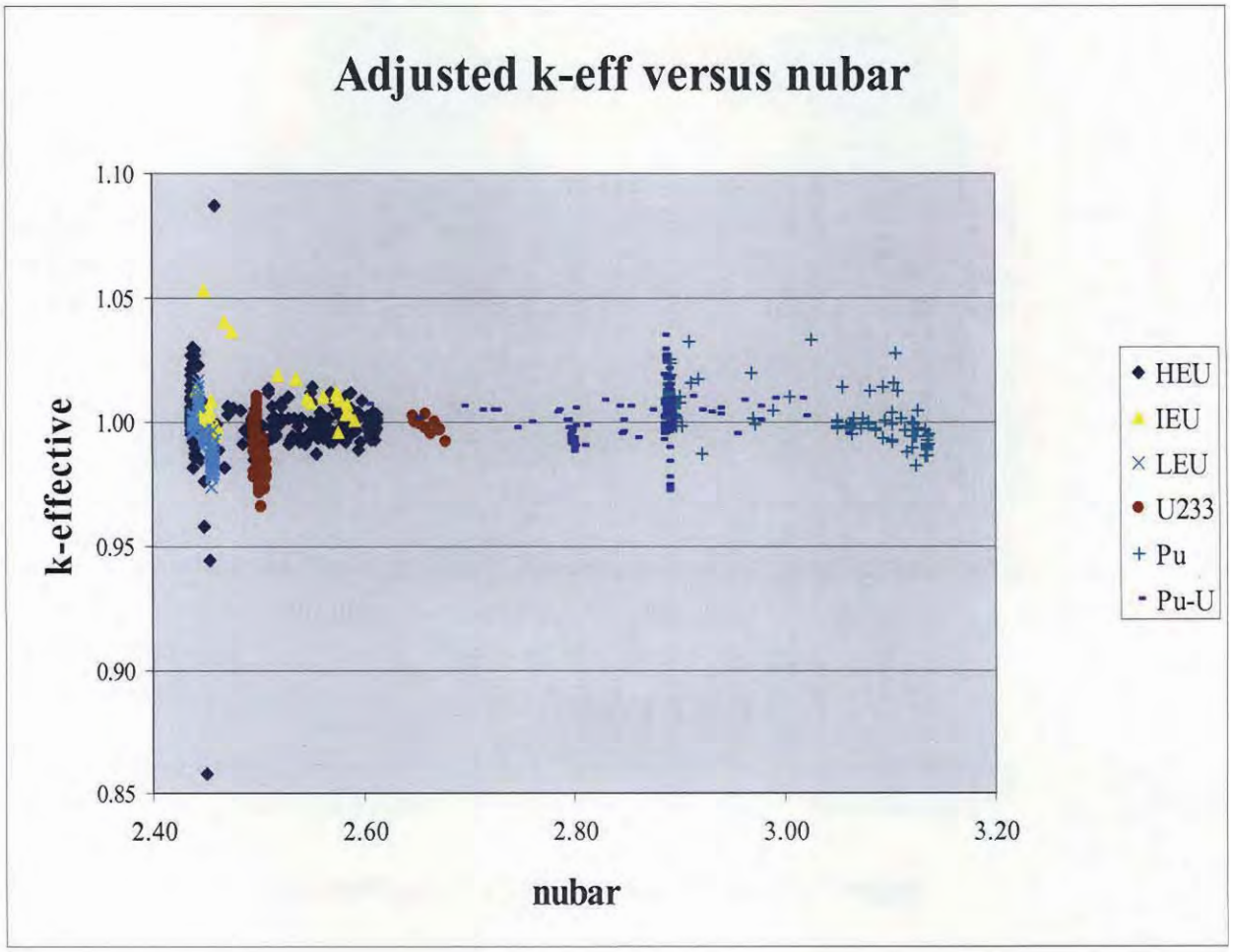

Figure 8 - Adjusted k_{eff} Results versus Nubar

Figure 9 shows a plot of "raw" calculated k_{eff} results versus "expected" benchmark k_{eff}. This illustrates the range of expected results, the range of calculated results, and the agreement between them. Ideally, the results should fall on a line from the lower left to the upper right. As shown, most data is clustered close to about (1.0,1.0), but several data points are significantly different, and experiments with expected results far from 1.0 also usually had larger bias results.

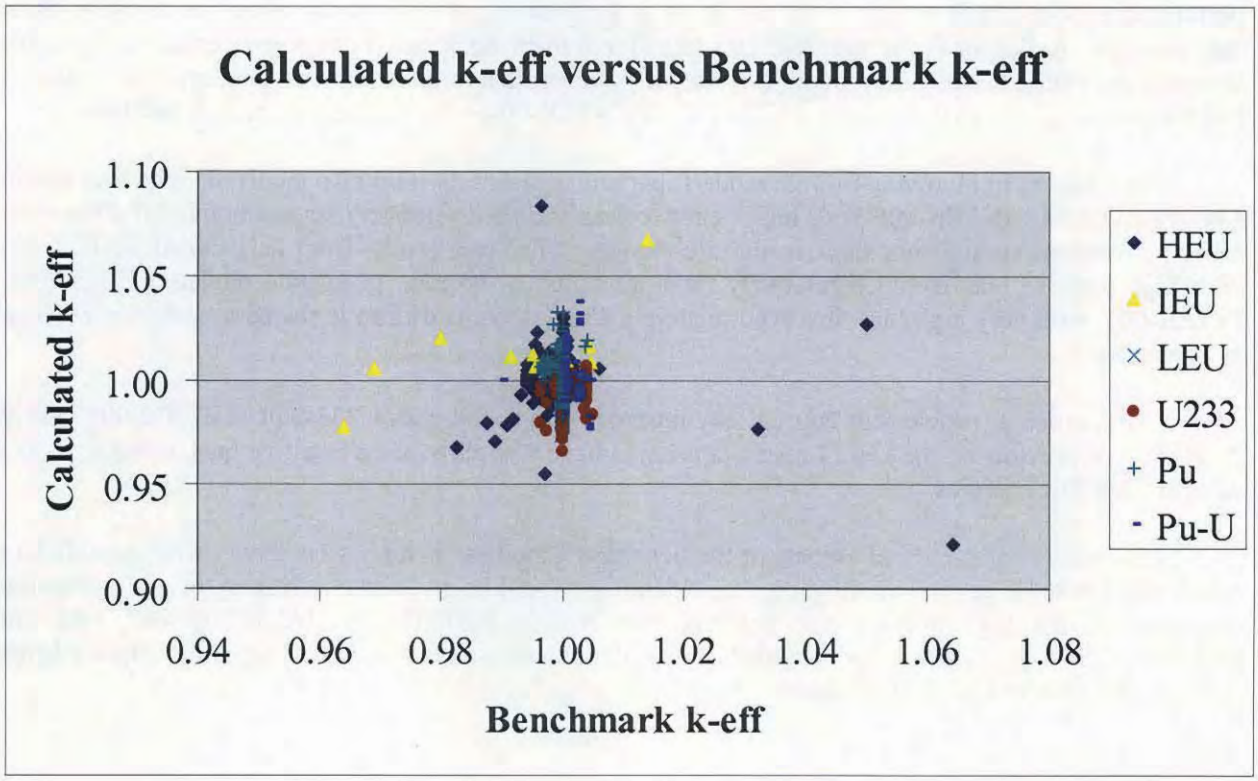

Figure 9 - Calculated k_{eff} Versus Benchmark k_{eff}

5.3 Discussion of High Positive and Negative Bias Results

Table 5.1 lists the eight results having adjusted k-effective results less than 0.97 or greater than 1.04, or correspondingly, bias results more negative than -0.03 or more positive than +0.04. These high bias results are consistent with the sample calculation results in the OECD Handbook.

Six of the high bias results are for benchmark experiments that were modeled as infinite in extent, and thereby amplified the effects of imperfections in cross section data. These experiments were all performed at the COBRA facility in the Russian Federation. Unlike most other benchmarks, these models required additional interpretation and adjustment from the actual finite experimental configuration to create an infinite benchmark model. It is noted, however, that other, somewhat similar, infinite models had better results. As an example, see HEU-COMP-INTER-004, which included graphite and boron.

In addition to involving infinite models, particular materials were also involved. The four results from HEU-COMP-INTER-005 with high negative bias included relatively large amounts of chromium, nickel, zirconium, or stainless steel, in infinite models. The two results from IEU-COMP-INTER-001 with high positive bias included relatively large amounts of thorium, in infinite models. HEU-MET-INTER-001, with very high bias, involved relatively large amounts of iron in the core, and stainless steel as a reflector.

No particular problem or unusual circumstance was found with U233-SOL-THERM-005 case 9. As discussed previously, the U-233 results appear to have a slightly more negative bias, in general, as a category, for low energies.

Because of the unusual aspects of the benchmark models, as discussed above, when establishing subcritical limits for general applications, consideration should be given to eliminating, or giving separate treatment to, the high positive and negative bias models HCI005-07,15,16; ICI001-002, 003, and HMI001. UST015_09 should be included, but it may be advisable to establish separate, slightly lower subcritical limits for U-233 applications.

Table 5.1 High Positive and Negative Bias Results

Case	nubar	AFG	EALCF (eV)	k_{calc} HEU	k_{exp} HEU	Bias = Calclated - Benchmark	Adjusted k_{eff} HEU R1	
hci005-007	2.454	62.065	6.64E+03	0.97665	1.0320	-0.05535	0.94465	k-inf
hci005-015	2.450	60.653	6.66E+03	0.92171	1.0640	-0.14229	0.85771	k-inf
hci005-016	2.449	64.424	4.10E+03	0.95498	0.9970	-0.04202	0.95798	k-inf
ici001-001	2.474	39.743	1.85E+05	1.00533	0.96900	0.03633	1.03633	k-inf
ici001-002	2.467	52.067	2.66E+04	1.02010	0.98000	0.04010	1.04010	k-inf
hmi001	2.459	51.616	2.94E+04	1.08394	0.99660	0.08734	1.08734	Iron xs problem

5.4 Summary of Results

Tables 4.1-4.6 provide a summary of the calculation results for the benchmark critical experiments. The "raw" k_{eff} results (k_calc) do not account for the known differences between the estimated benchmark actual k_{eff} (k_exp) and the ideal critical k_{eff} (1.0). The benchmark experiments are near-critical experiments with expected neutron multiplication factors very close to unity. Some experiment benchmarks were enough different from unity to justify accounting for the difference. An "adjusted" k_{eff} is defined as 1+bias, where bias=k_calc-k_exp, and there results are also shown in Tables 4.1-4.6, and in Figures 1-8.

The only significant, noticeable difference in apparent bias of the results based on enrichment and physical form appears to be for U-233 thermal systems, which had a slightly more negative bias. In Y/DD-896/R0, it appeared that the high-enriched experiments calculated slightly higher than the low enriched experiments, based on average results. Now, with more low enriched experiments included, the differences appear less pronounced. The difference in range of results has also become smaller. All results are for the 238-group library.

Since simulated infinite models have been included, the range of benchmark k_{eff} values has increased. Values range from 0.964 to 1.064. "Raw" calculated results ranged from 0.920 to 1.084. Other than a few cases, as shown in Figure 9, most benchmark and calculated results are very close to 1.0.

5.5 Area of Applicability

Whether a particular plant application is similar to a sufficient number of experiments contained in the validation set is an important issue. This is a prerequisite before a subcritical limit may be determined from the validation results. Based on the demonstrated performance of the code for a large number of experiments, we have reasonable assurance that it performs well over a wide range of conditions. However, this does not ensure that the code performs as well over all conditions. It does not guarantee that there is not a scenario where the code would calculate unusually low (or high) due to some kind of anomaly or limitation in the code or cross section data. There are some types of experiments that are one or two of a kind. It is possible that there could be one or more of these types of experiments that would exhibit a larger bias than seen in this report, if more experiments of that type were included. The only way to assess whether the validation set contains a sufficient number of experiments that are similar to a plant application is to carefully compare the details of the experiment description with the details of the plant application. The experiment summary information included in this report, Appendix A, may not provide enough information. The analyst must become familiar with the experiment descriptions provided in the OECD handbook. The DICE database may be very helpful in this regard. The minimum number of similar experiments needed cannot be determined in advance, but the analyst must consider this issue carefully as one of the factors when deciding how much margin to include in determining a subcritical limit. If there are only a few experiments similar to the application, it may be wise to take the time to select additional applicable experiments for addition to the validation set, or to perform a separate evaluation.

Appropriateness of the subcritical limit does not depend solely on the validity of the statistical analysis. Rather, the appropriateness of a subcritical limit depends on two quite different factors: (1) the range of conditions under which a generalization for its use is established, and (2) whether or not the modeled scenario is within the range of these conditions. The criticality safety analyst exercising sound engineering judgment using strong technical arguments must develop these determinations. Extrapolation beyond the range of applicability should not be done.

5.6 Grandfather or Retrofit Concerns

The validation documents used for establishing subcritical limits for criticality calculations shall be reviewed and approved by SAE NCSo. There is no urgency to retrofit older evaluations since the common practice provided conservatism. Therefore, the incorporation of the results in this report into the evaluations of existing operations will be accomplished as the Criticality Safety Approvals become obsolete and are replaced due to equipment changes, rule changes, age, etc.

6 Conclusions

This work has demonstrated the validation, or calibration, of the CSAS25 sequence of SCALE5 against 1217 benchmark experiments. It provides assurance that the code predicts critical or near critical systems reasonably well, however, in general, based on bias results there is wide variation in performance depending on the type of system. Using a rating scale similar to Reference v, the performance ranges from "very good" or less than about +/- 0.01 to "very poor" or about +0.087/-0.14 depending on the category of experiments. In general, the previously observed problems resulted in very high bias, which would be conservative for plant applications. This report includes several benchmark cases that significantly under-predict the expected results. There is no guarantee against the possibility of an unusual scenario that could produce non-conservative results, and analysts must be always vigilant for this possibility.

The determination of appropriate correlating parameter and values for limits and additional margin, applicable to a particular analysis, must be determined as part of process analysis. This document does not specify final upper subcritical limits as has been done in the past. It is anticipated that a follow-on report will be written to recommend subcritical limits. Analysts using these results are responsible for exercising sound engineering judgment using strong technical arguments to develop a margin in k_{eff} or other correlating parameter that is sufficiently large to ensure that conditions (calculated by this method to be subcritical by this margin) will actually be subcritical.

Documentation of determination and justification of the appropriate subcritical limit and margin in the analyst's evaluation, in conjunction with this report, will constitute the complete Validation Report in accordance with ANSI/ANS-8.1-1998, Section 4.3.6(4).

7 Recommendations for Future Work

A report determining subcritical limits applicable to calculated k_{eff}, should be completed soon after this report.

As stated in Section 3, numerous additional OECD experiment descriptions are already available for experiments that would be applicable to Y-12 work. In this regard, future efforts should be dedicated to the following: (1) developing more input decks in-house for experiments selected based on applicability to Y-12, and (2) including additional models as they become available in future revisions of the OECD report. In addition, changes in experiment categorization and interpretation/clarification sometimes are reported in the annual revisions of the OECD handbook. These changes should be reviewed to determine whether they impact the conclusions in this report. This work will require a dedicated effort.

Additional work may be needed to better categorize trends and/or biases by including additional parameters in the statistical evaluation.

Additional work is needed on Area of Applicability (AoA) determination methods. Determining whether a particular application is within the AoA of a validation is currently almost exclusively based on subjective judgment. To be done correctly, it requires the analyst to have close familiarity with the details of the experiments in the validation. Efforts to develop input models for more experiments, particularly if done by several staff members, would have the additional benefit of increasing staff's familiarity with experiment descriptions, which would also help improve these AoA determinations. Continuing such model input preparation work as part of the qualification program is suggested. In addition, methods have been proposed for more rigorous, and quantitative, AoA determinations. A dedicated effort is needed to evaluate these methods to determine if they are effective and practical to implement.

Areas of relatively very poor performance are seen, possibly due to cross section data issues. Efforts to produce improved cross section libraries for SCALE should be supported.

Appendix A - Comparison of Available Experiments with Calculated Experiments

System Type	Acceptable benchmarks in the 2002 OECD Manual	KENO V.a models included in Y/DD-896 Rev 0	KENO V.a models included in Y/DD-996 Rev 1	KENO V.a models added for Y/DD-896 Rev 1	KENO V.a Totals	MCNP4C2 models included in Y/DD-1026 Rev 0	General Description/Comments
Highlighted text indicates additions/changes to Volumes I, II, III, IV, and VII since the 2001 OECD Manual							
Volume I	514	0	270	0	270	0	Plutonium Systems
Volume II	921	407	0	53	460	531	Highly Enriched Uranium Systems
Volume III	61	0	0	51	51	43	Intermediate and Mixed Enrichment Uranium Systems
Volume IV	927	96	0	32	128	0	Low Enriched Uranium Systems
Volume V	166	0	0	140	140	0	Uranium-233 Systems
Volume VI	250	0	168	0	168	176	Mixed Plutonium-Uranium Systems
Volume VII	20	0	0	0	0	0	Special Isotope Systems
Totals:	**2859**	**503**	**438**	**276**	**1217**	**750**	

Volume I, Plutonium Systems

Pu METAL SYSTEMS

FAST ENERGY Pu METAL SYSTEMS

PU-MET-FAST-001	1	1	1	Bare Sphere of Plutonium-239 Metal (^{239}Pu Jezebel)
PU-MET-FAST-002	1	1	1	Bare Sphere of Plutonium-240 Metal (^{240}Pu Jezebel)
PU-MET-FAST-003	5	5	5	Unmoderated Plutonium Metal Button Array
PU-MET-FAST-004	9	9	9	Unmoderated Plutonium Metal Cylinder Array - Phase II
PU-MET-FAST-005	1	1	1	Plutonium Sphere Reflected by Tungsten
PU-MET-FAST-006	1	1	1	Plutonium Sphere Reflected by Normal Uranium Using Flattop

System Type	Acceptable benchmarks in the 2002 OECD Manual	KENO V.a models included in Y/DD-896 Rev 0	KENO V.a models included in Y/DD-996 Rev 1	KENO V.a models added for Y/DD-896 Rev 1	KENO V.a Totals	MCNP4C2 models included in Y/DD-1026 Rev 0	General Description/Comments
Highlighted text indicates additions/changes to Volumes I, II, III, IV, and VII since the 2001 OECD Manual							
PU-MET-FAST-007	0	n/a	n/a			n/a	Four Plutonium Spheres with Various Reflector Materials
PU-MET-FAST-008	1		1		1		Thorium Reflected Plutonium Sphere
PU-MET-FAST-009	1		1		1		Plutonium Sphere Reflected by Aluminum
PU-MET-FAST-010	1		1		1		Delta-Phase Plutonium Sphere Reflected by Normal Uranium
PU-MET-FAST-011	1		1		1		Water Reflected Alpha-Phase Pu Sphere
PU-MET-FAST-012	1		1		1		Uranium-Reflected Array of Plutonium Fuel Rods
PU-MET-FAST-013	1		1		1		Copper-Reflected Array of Plutonium Fuel Rods
PU-MET-FAST-014	1		1		1		Nickel-Reflected Array of Plutonium Fuel Rods
PU-MET-FAST-015	1		1		1		Iron-Reflected Array of Plutonium Fuel Rods
PU-MET-FAST-016	6		6		6		Flooded 3x3x3 Arrays of 3-kg Plutonium Metal Cylinders - Phase I
PU-MET-FAST-017	5		5		5		Moderated Plutonium Metal Cylinders Array - Phase II
PU-MET-FAST-018	1		1		1		Delta-Phase Plutonium Sphere Reflected by Beryllium
PU-MET-FAST-019	1						Sphere of Plutonium Reflected by Beryllium
PU-MET-FAST-020	1						Sphere of Plutonium Reflected by Depleted Uranium
PU-MET-FAST-021	2						Beryllium- and Beryllium Oxide-Reflected Cylinders of Plutonium
PU-MET-FAST-022	1		1		1		Bare Spherical Assembly of ^{239}Pu(delta, 98%)
PU-MET-FAST-023	1		1		1		Graphite-Reflected Spherical Assembly of ^{239}Pu(delta, 98%)
PU-MET-FAST-024	1		1		1		Polyethylene-Reflected Spherical Assembly of ^{239}Pu(delta, 98%)
PU-MET-FAST-025	1		1		1		Spherical Assembly of ^{239}Pu(delta, 98%) with 1.55-cm Steel Reflector
PU-MET-FAST-026	1		1		1		Spherical Assembly of ^{239}Pu(delta, 98%) with 11.9-cm Steel Reflector
PU-MET-FAST-027	1		1		1		Polyethylene-Reflected Spherical Assembly of ^{239}Pu(delta, 89%)
PU-MET-FAST-028	1		1		1		Steel-Reflected Spherical Assembly of ^{239}Pu(delta, 89%)
PU-MET-FAST-029	1		1		1		Bare Spherical Assembly of ^{239}Pu(alpha, 88%)
PU-MET-FAST-030	1		1		1		Graphite-Reflected Spherical Assembly of ^{239}Pu(alpha, 88%)
PU-MET-FAST-031	1		1		1		Polyethylene-Reflected Spherical Assembly of ^{239}Pu(alpha, 88%)
PU-MET-FAST-032	1		1		1		Steel-Reflected Spherical Assembly of ^{239}Pu(alpha, 88%)
PU-MET-FAST-033	1		1		1		Cylindrical Assembly of Plutonium Metal Reflected by graphite
PU-MET-FAST-034	0	n/a	n/a			n/a	Asymmetric Spherical Plutonium Reflected by Steel and Oil

System Type	Acceptable benchmarks in the 2002 OECD Manual	KENO V.a models included in Y/DD-896 Rev 0	KENO V.a models included in Y/DD-996 Rev 1	KENO V.a models added for Y/DD-896 Rev 1	KENO V.a Totals	MCNP4C2 models included in Y/DD-1026 Rev 0	General Description/Comments
Highlighted text indicates additions/changes to Volumes I, II, III, IV, and VII since the 2001 OECD Manual							
PU-MET-FAST-035	1		1		1		Spherical Assembly of ^{239}Pu(delta,98%) with 3.15-cm Lead reflector
PU-MET-FAST-036	1		1		1		sph assembly of ^{239}Pu(delta,98%) with compound refl of 0.05-cm Cd and 2.3-cm poly
PU-MET-FAST-037	16		7		7		flooded 2x2xN arrays of 3-kg Plutonium metal cylinders - Phase 2
PU-MET-FAST-039	1		1		1		spherical assembly of ^{239}Pu(delta,98%) with a 4.25-cm Duralumin reflector
PU-MET-FAST-040	1		1		1		spherical assembly of ^{239}Pu(delta,98%) with a 1.6-cm Copper reflector
PU-MET-FAST-041	1		1		1		spherical assembly of ^{239}Pu(alpha,88%) with a 20.98-cm Depleted-Uranium reflector
PU-MET-FAST-045	7						cyl assembly of Pu/Ta/Al metal discs with Fe/Ni/Poly/H_2O reflector (LAMPRE)
INTERMEDIATE ENERGY Pu METAL SYSTEMS							
PU-MET-INTER-001	0	n/a	n/a			n/a	refer to PU-MET-MIXED-001
PU-MET-INTER-002	1						cyl ZPR assembly with a Pu/C/SST core and a SST/FE reflector (ZPR-6/10)
THERMAL ENERGY Pu METAL SYSTEMS							
PU-MET-THERM-001	0	n/a	n/a			n/a	refer to PU-MET-MIXED-001
MIXED ENERGY Pu METAL SYSTEMS							
PU-MET-MIXED-001	6						heterogeneous compositions of Plutonium, Silicon Dioxide, and polyethylene
Pu COMPOUND SYSTEMS							
FAST ENERGY Pu COMPOUND SYSTEMS							
PU-COMP-FAST-001	0						refer to PU-COMP-MIXED-001
PU-COMP-FAST-002	0						refer to PU-COMP-MIXED-002
INTERMEDIATE ENERGY Pu COMPOUND SYSTEMS							

System Type	Acceptable benchmarks in the 2002 OECD Manual	KENO V.a models included in Y/DD-896 Rev 0	KENO V.a models included in Y/DD-996 Rev 1	KENO V.a models added for Y/DD-896 Rev 1	KENO V.a Totals	MCNP4C2 models included in Y/DD-1026 Rev 0	General Description/Comments
Highlighted text indicates additions/changes to Volumes I, II, III, IV, and VII since the 2001 OECD Manual							
PU-COMP-INTER-001	1		1		1		k-infinity experiments in intermediate neutron spectra for ^{239}Pu
THERMAL ENERGY Pu COMPOUND SYSTEMS							
PU-COMP-THERM-001	0						refer to PU-COMP-MIXED-001
PU-COMP-THERM-002	0						refer to PU-COMP-MIXED-002
MIXED ENERGY Pu COMPOUND SYSTEMS							
PU-COMP-MIXED-001	5		5		5		Unreflected Slabs of Polystyrene-Moderated Plutonium Oxide
PU-COMP-MIXED-002	29		4		4		Plexiglas Reflected Slabs of Polystyrene-Moderated Plutonium Oxide
Pu SOLUTION SYSTEMS							
INTERMEDIATE ENERGY Pu SOLUTION SYSTEMS							
none presently evaluated							
THERMAL ENERGY Pu SOLUTION SYSTEMS							
PU-SOL-THERM-001	6		6		6		Water Reflected 11.5" Diameter Spheres of Pu Nitrate Solutions
PU-SOL-THERM-002	7		7		7		Water Reflected 12" Diameter Spheres of Pu Nitrate Solutions
PU-SOL-THERM-003	8		8		8		Water Reflected 13" Diameter Spheres of Pu Nitrate Solutions
PU-SOL-THERM-004	13		13		13		Water Reflected 14" Diameter Spheres of Pu Nitrate Solutions, 0.54% to 3.43%
PU-SOL-THERM-005	9		9		9		Water Reflected 14" Diameter Spheres of Pu Nitrate Solutions, 4.05% and 4.4%
PU-SOL-THERM-006	3		3		3		Water Reflected 15" Diameter Spheres of Pu Nitrate Solutions
PU-SOL-THERM-007	8		8		8		Water Reflected 11.5" Diameter Spheres Partly Filled with Pu Nitrate Solutions
PU-SOL-THERM-008	29						Concrete-Reflected 14-Inch Diameter Spheres of Pu Nitrate Solutions
PU-SOL-THERM-009	3		3		3		Unreflected 48" Diameter Sphere of Pu Nitrate Solution
PU-SOL-THERM-010	14		14		14		Water Reflected 9", 10", 11", and 12" Diameter Cylinders of Pu Nitrate Solutions
PU-SOL-THERM-011	12		12		12		Bare 16" and 18" Diameter Spheres of Pu Nitrate Solutions
PU-SOL-THERM-012	23						Pu Nitrate Soln in a Large Water Reflected Cubic Tank (130x130x100 cm) (19% ^{240}Pu)
PU-SOL-THERM-013	21						Interacting Cylinders of 256-mm Diameter with Pu Nitrate Solution (115.1 gPu/l) in Air

System Type	Acceptable benchmarks in the 2002 OECD Manual	KENO V.a models included in Y/DD-896 Rev 0	KENO V.a models included in Y/DD-996 Rev 1	KENO V.a models added for Y/DD-896 Rev 1	KENO V.a Totals	MCNP4C2 models included in Y/DD-1026 Rev 0	General Description/Comments
Highlighted text indicates additions/changes to Volumes I, II, III, IV, and VII since the 2001 OECD Manual							
PU-SOL-THERM-014	35		34		34		Interacting Cylinders of 300-mm Diameter with Pu Nitrate Solution (115.1 gPu/l) in Air
PU-SOL-THERM-015	17		17		17		Interacting Cylinders of 300-mm Diameter with Pu Nitrate Solution (152.5 gPu/l) in Air
PU-SOL-THERM-016	11		11		11		Interacting Cyls of 300-mm and 256-mm Dia with Pu Nitrate Soln (152.5 and 115.1 gPu/l) in Air
PU-SOL-THERM-017	18		18		18		Interacting Cyls of 256-mm and 300-mm Dia with Pu Nitrate Soln (115.1 gPu/l) in Air
PU-SOL-THERM-020	8		8		8		Water-reflected and Water-cadmium-reflected 14" Diameter Spheres of Pu Nitrate Soln
PU-SOL-THERM-021	6		4		4		Water-Reflected and Bare 15.2" Diameter Spheres of Pu Nitrate Solutions
PU-SOL-THERM-022	17						Pu (19% ^{240}Pu) Nitrate Soln in a Water-Refl Annular Cylinder Tank (50/20 cm Diameter)
PU-SOL-THERM-023	34						Pu (33.89% and 4.23% ^{240}Pu) Nitrate Soln in Two Water-Refl Cylindric Concentric Tanks
PU-SOL-THERM-024	23		23		23		slabs of Pu nitrate solutions reflected by 1-inch thick plexiglas
PU-SOL-THERM-025	44						water reflected slabs of Pu nitrate solutions
PU-SOL-THERM-026	21						unreflected slabs of Pu nitrate solutions

MIXED ENERGY Pu SOLUTION SYSTEMS

none presently evaluated

MISCELLANEOUS Pu SYSTEMS

FAST ENERGY MISCELLANEOUS Pu SYSTEMS

none presently evaluated

INTERMEDIATE ENERGY MISCELLANEOUS Pu SYSTEMS

none presently evaluated

System Type	Acceptable benchmarks in the 2002 OECD Manual	KENO V.a models included in Y/DD-896 Rev 0	KENO V.a models included in Y/DD-996 Rev 1	KENO V.a models added for Y/DD-896 Rev 1	KENO V.a Totals	MCNP4C2 models included in Y/DD-1026 Rev 0	General Description/Comments
Highlighted text indicates additions/changes to Volumes I, II, III, IV, and VII since the 2001 OECD Manual							
THERMAL ENERGY MISCELLANEOUS Pu SYSTEMS							
none presently evaluated							
MIXED ENERGY MISCELLANEOUS Pu SYSTEMS							
none presently evaluated							
Volume II, Highly Enriched Uranium Systems							
HEU METAL SYSTEMS							
FAST ENERGY HEU METAL SYSTEMS							
HEU-MET-FAST-001	1	1			1	2	bare sphere of U(93.71) metal (Godiva)
HEU-MET-FAST-002	6	6			6	6	U(nat) refl U(93.5) pseudosphere, pseudocylinder, sphere
HEU-MET-FAST-003	10	10			10	12	U(93.5) sphere refl by U(nat), Tungsten Carbide, or Ni
HEU-MET-FAST-004	1	1			1	1	U(97.67) sphere refl by water
HEU-MET-FAST-005	6					6	Be- or Mo-refl cyl assemblies of U(90) alloy with 3.3% Mo
HEU-MET-FAST-006	0	n/a	n/a			n/a	refer to HEU-MET-THERM-003
HEU-MET-FAST-007	43	43			43	42	U(93.15) slabs interleaved with poly, plexiglas, or teflon
HEU-MET-FAST-008	1					1	bare U(90) sphere
HEU-MET-FAST-009	2					2	U(90) sphere refl by Be or BeO
HEU-MET-FAST-010	2					2	U(90) sphere refl by B+Be or B+BeO
HEU-MET-FAST-011	1					1	U(90) sphere refl by poly
HEU-MET-FAST-012	1					1	Al refl spherical assembly of U(90) metal
HEU-MET-FAST-013	1					1	steel refl spherical assembly of U(90) metal
HEU-MET-FAST-014	1					1	U(dep) refl spherical assembly of U(90) metal
HEU-MET-FAST-015	1			1	1	1	bare cylindrical assembly of U(90) metal
HEU-MET-FAST-016	2			2	2	2	Be- or BeO-refl cylindrical assembly of U(90) metal
HEU-MET-FAST-017	1			1	1	1	Be-refl cylindrical assembly of U(90) metal interleaved with Be
HEU-MET-FAST-018	1	1			1	1	bare spherical assembly of U(90) metal

System Type	Acceptable benchmarks in the 2002 OECD Manual	KENO V.a models included in Y/DD-896 Rev 0	KENO V.a models included in Y/DD-996 Rev 1	KENO V.a models added for Y/DD-896 Rev 1	KENO V.a Totals	MCNP4C2 models included in Y/DD-1026 Rev 0	General Description/Comments
Highlighted text indicates additions/changes to Volumes I, II, III, IV, and VII since the 2001 OECD Manual							
HEU-MET-FAST-019	1	1			1	1	graphite refl spherical assembly of U(90) metal
HEU-MET-FAST-020	1	1			1		poly refl spherical assembly of U(90) metal
HEU-MET-FAST-021	1	1			1	1	steel refl spherical assembly of U(90) metal
HEU-MET-FAST-022	1	1			1	1	duralumin refl spherical assembly of U(90) metal
HEU-MET-FAST-023	22	2			2	1	Tinkertoy arrays of 10.5 kg U(93.2) cyl
HEU-MET-FAST-024	1					1	spherical assembly of U(90) metal refl by thin steel and thick poly
HEU-MET-FAST-026	32	5			5	32	Tinkertoy arrays of 15, 20, and 25 kg U(93.2) cyl
HEU-MET-FAST-027	1	1			1	1	Pb refl spherical assembly of U(90) metal
HEU-MET-FAST-028	1	1			1	1	U(93.24) sphere refl by U(nat)
HEU-MET-FAST-029	1	1			1		U(dep) refl spherical assembly of U(90) metal
HEU-MET-FAST-030	1	1			1	1	U(dep) refl cyl assemblies of U(96) metal discs interleaved with Be
HEU-MET-FAST-031	1	1			1	1	poly refl spherical shell of U(90) metal with central cavity of poly
HEU-MET-FAST-032	4	4			4	4	U(nat) refl spherical assemblies of U(94) metal
HEU-MET-FAST-033	2			2	2	2	unrefl cyl assemblies of U(96) metal discs interleaved with poly and steel
HEU-MET-FAST-034	3	3			3	3	unrefl cyl assemblies of U(96) metal discs interleaved with poly and Ti, Al, or steel
HEU-MET-FAST-035	0	n/a	n/a			n/a	deleted and republished as HEU-MET-INTER-001
HEU-MET-FAST-036	2			2	2	2	unrefl cyl assemblies of U(96) metal discs interleaved with poly and U(dep)
HEU-MET-FAST-037	2			2	2	2	poly refl cyl assemblies of U(96) metal discs interleaved with poly and U(dep)
HEU-MET-FAST-038	1			1	1	1	U(dep) refl cyl assembly of U(96) metal discs interleaved with Be and BeO
HEU-MET-FAST-039	0	n/a	n/a			n/a	unrefl and steel refl U(93.2) spherical and hemispherical assemblies
HEU-MET-FAST-041	6			6	6	6	Be- or graphite-refl spherical assemblies of U(94) metal
HEU-MET-FAST-048	17					17	oil refl U(93.2) spherical and hemispherical assemblies with oil,steel, or void cores

System Type	Acceptable benchmarks in the 2002 OECD Manual	KENO V.a models included in Y/DD-896 Rev 0	KENO V.a models included in Y/DD-996 Rev 1	KENO V.a models added for Y/DD-896 Rev 1	KENO V.a Totals	MCNP4C2 models included in Y/DD-1026 Rev 0	General Description/Comments
Highlighted text indicates additions/changes to Volumes I, II, III, IV, and VII since the 2001 OECD Manual							
HEU-MET-FAST-051	18						unmod & unrefl U(93.2) metal cylinders as individual units and interacting pairs
HEU-MET-FAST-055	4			4	4	1	cylindrical honeycomb assembly with a U(93.2)+Al core and U(dep) refl
HEU-MET-FAST-060	1						cyl honeycomb assy with a U(93)-W core with an Al reflector (ZPR-9/4)
HEU-MET-FAST-061	1					1	cyl honeycomb assy with a U(93.2)+U(dep)+Zr+SS core and graphite refl
HEU-MET-FAST-062	1					1	CORAL-I: a cylindrical assembly of U(89.7) with U(nat) refl
HEU-MET-FAST-068	2						cyl assy with a U(90)-Th-Poly core with U(dep)O_2 refl (KBR-22 and KBR-23)
INTERMEDIATE ENERGY HEU METAL SYSTEMS							
HEU-MET-INTER-001	1			1	1	1	cylindrical ZPR assembly with a U(93.2)-Fe core and stainless steel refl
HEU-MET-INTER-002	0	n/a	n/a			n/a	refer to HEU-MET-FAST-034
HEU-MET-INTER-003	0	n/a	n/a			n/a	refer to HEU-MET-FAST-030
HEU-MET-INTER-004	0	n/a	n/a			n/a	refer to HEU-MET-MIXED-004
HEU-MET-INTER-005	0	n/a	n/a			n/a	refer to HEU-MET-MIXED-005
HEU-MET-INTER-006	3			3	3	2	ZEUS: Cu refl cyl assembly of U(93.2) metal plates interleaved with graphite plates
HEU-MET-INTER-007	0	n/a	n/a			n/a	refer to HEU-MET-FAST-007
THERMAL ENERGY HEU METAL SYSTEMS							
HEU-MET-THERM-001	1			1	1		U(93) metal foils interleaved with plates of SiO_2 glass and poly with poly refl
HEU-MET-THERM-002	0	n/a	n/a			n/a	Be-refl Honeycomb assemblies of U(93) foils moderated by graphite
HEU-MET-THERM-003	7	7			7	4	lattices of U(94) cubes immersed in water

System Type	Acceptable benchmarks in the 2002 OECD Manual	KENO V.a models included in Y/DD-896 Rev 0	KENO V.a models included in Y/DD-996 Rev 1	KENO V.a models added for Y/DD-896 Rev 1	KENO V.a Totals	MCNP4C2 models included in Y/DD-1026 Rev 0	General Description/Comments
Highlighted text indicates additions/changes to Volumes I, II, III, IV, and VII since the 2001 OECD Manual							
HEU-MET-THERM-005	0	n/a	n/a			n/a	refer to HEU-MET-MIXED-005
HEU-MET-THERM-006	23	23			23	3	SPERT-D elements [assemblies of U(93)-Al alloy plates] in H_2O, dilute UNH, or borated UNH
HEU-MET-THERM-007	11						SPERT-III type 1S elements [assemblies of U(93.2)O_2 impregnated SS plates] in H_2O
HEU-MET-THERM-008	1						U(93) metal foils interleaved with plates of Al and poly with poly refl
HEU-MET-THERM-009	1						U(93) metal foils interleaved with MgO and poly with poly refl
HEU-MET-THERM-010	1						U(93) metal foils interleaved with plates of Gd and poly with poly refl
HEU-MET-THERM-011	43						U(93)-Al alloy plates immersed in water
MIXED ENERGY HEU METAL SYSTEMS							
HEU-MET-MIXED-001	1	1			1	1	poly refl cyl assemblies of U(96) metal discs interleaved with poly and Ti
HEU-MET-MIXED-002	1	1			1	1	poly refl spherical shell of U(90) metal with central cavity of poly
HEU-MET-MIXED-003	1	1			1	1	poly refl spherical shell of U(90) metal with central cavity of poly
HEU-MET-MIXED-004	1					1	U(dep) refl cyl assemblies of U(96) metal discs interleaved with poly and U(dep)
HEU-MET-MIXED-005	5						large, heterogeneous core assemblies of tubes containing U(89.4) + SiO2 + poly
HEU-MET-MIXED-006	0	n/a	n/a			n/a	refer to HEU-MET-FAST-033
HEU-MET-MIXED-007	0	n/a	n/a			n/a	refer to HEU-MET-FAST-036
HEU-MET-MIXED-008	0	n/a	n/a			n/a	refer to HEU-MET-FAST-037
HEU-MET-MIXED-009	0	n/a	n/a			n/a	refer to HEU-MET-FAST-007
HEU-MET-MIXED-010	0	n/a	n/a			n/a	refer to HEU-MET-THERM-003
HEU COMPOUND SYSTEMS							
FAST ENERGY HEU COMPOUND SYSTEMS							
HEU-COMP-FAST-001	0	n/a	n/a			n/a	refer to HEU-COMP-MIXED-001
HEU-COMP-FAST-003	0	n/a	n/a			n/a	refer to HEU-COMP-MIXED-002

System Type	Acceptable benchmarks in the 2002 OECD Manual	KENO V.a models included in Y/DD-896 Rev 0	KENO V.a models included in Y/DD-996 Rev 1	KENO V.a models added for Y/DD-896 Rev 1	KENO V.a Totals	MCNP4C2 models included in Y/DD-1026 Rev 0	General Description/Comments
Highlighted text indicates additions/changes to Volumes I, II, III, IV, and VII since the 2001 OECD Manual							
INTERMEDIATE ENERGY HEU COMPOUND SYSTEMS							
HEU-COMP-INTER-001	0						deleted and republished as HEU-COMP-MIXED-003
HEU-COMP-INTER-002	0						deleted and republished as HEU-COMP-MIXED-004
HEU-COMP-INTER-003	7			7	7	7	cyl assemblies of canned U(90.7)H_3 disks refl by U(dep), Be, and/or Fe
HEU-COMP-INTER-004	1			1	1	1	k-inf measurements for a homogenous U(92)O_2-graphite-Ca metaborate system
HEU-COMP-INTER-005	5			4	4	5	k-inf measurements for a U(90)O_2 and Ni, SS, SS+Mo, Cr, or Zr system
HEU-COMP-INTER-006	0	n/a	n/a			n/a	refer to HEU-COMP-MIXED-002
THERMAL ENERGY HEU COMPOUND SYSTEMS							
HEU-COMP-THERM-001	0	n/a	n/a			n/a	refer to HEU-COMP-MIXED-001
HEU-COMP-THERM-002	25					25	arrays of hexagonal U(93)-graphite rods (ROVER) immersed in water
HEU-COMP-THERM-003	15					15	two-zone arrays of cross-shaped U(80)O_2-Cu rods immersed in water
HEU-COMP-THERM-004	4					4	arrays of cross-shaped U(90)O_2-Cu rods immersed in water with Gd or Sm rods
HEU-COMP-THERM-005	1					1	clusters of arrays of cross-shaped U(80)O_2-Cu rods immersed in water
HEU-COMP-THERM-006	3					3	arrays of cross-shaped U(80)O_2-Cu rods immersed in water
HEU-COMP-THERM-007	3					3	arrays of cross-shaped U(80)O_2-Cu rods immersed in water with Zr-hydride rods
HEU-COMP-THERM-008	2						arrays of cross-shaped U(80)O_2-Cu rods immersed in water with B_4C rods
HEU-COMP-THERM-010	21	6			6	21	arrays of U(62.4)O_2-BeO rods immersed in water, U(92.6)NH, and/or boric acid
HEU-COMP-THERM-011	3	3			3	3	clusters of 21x21 lattices of U(80)O_2-Al rods immersed in water
HEU-COMP-THERM-012	2	2			2	2	clusters of 18x18 lattices of U(80)O_2-Al rods immersed in water
HEU-COMP-THERM-013	2	2			2	2	clusters of 14x14 lattices of U(80)O_2-Al rods immersed in water
HEU-COMP-THERM-014	2	2			2	2	clusters of 10x10 lattices of U(80)O_2-Al rods immersed in water
HEU-COMP-THERM-015	0	n/a	n/a			n/a	deleted and republished as HEU-COMP-MIXED-002
HEU-COMP-THERM-016	6						graphite refl U(89.3)-graphite blocks (C/X~8180) with Gd_2O_3-graphite control rods
HEU-COMP-THERM-017	9			9	9		lattices of annular cyl U(80)O_2-Al rods immersed in D_2O

System Type	Acceptable benchmarks in the 2002 OECD Manual	KENO V.a models included in Y/DD-896 Rev 0	KENO V.a models included in Y/DD-996 Rev 1	KENO V.a models added for Y/DD-896 Rev 1	KENO V.a Totals	MCNP4C2 models included in Y/DD-1026 Rev 0	General Description/Comments
Highlighted text indicates additions/changes to Volumes I, II, III, IV, and VII since the 2001 OECD Manual							
INTERMEDIATE ENERGY HEU COMPOUND SYSTEMS							
none presently evaluated							
MIXED ENERGY HEU COMPOUND SYSTEMS							
HEU-COMP-MIXED-001	26	7		2	9		arrays of cans of wet or dry $U(93)O_2$ powder with poly refl
HEU-COMP-MIXED-002	23						cans of $U(90)O_2$ powder arrayed and immersed in water or D_2O
HEU-COMP-MIXED-003	6						Be-refl Rx core assemblies of $U(96)O_2$ and Zr-hydride immersed in water
HEU-COMP-MIXED-004	5						Be-refl Rx core assemblies of $U(96)O_2$ and Zr-hydride immersed in sand/water
HEU SOLUTION SYSTEMS							
INTERMEDIATE ENERGY HEU SOLUTION SYSTEMS							
HEU-SOL-INTER-001	0	n/a	n/a			n/a	refer to HEU-SOL-THERM-004 and HEU-SOL-THERM-020
HEU-SOL-INTER-002	0	n/a	n/a			n/a	refer to HEU-SOL-THERM-039
THERMAL ENERGY HEU SOLUTION SYSTEMS							
HEU-SOL-THERM-001	10	10			10	10	U(93.2)NH soln in cyl geom, 50-360 gU/l, minimal refl
HEU-SOL-THERM-002	14	14			14	14	U(93.2)NH soln in cyl geom, 60-335 gU/l, concrete refl
HEU-SOL-THERM-003	19	19			19	19	U(93.2)NH soln in cyl geom, 60-345 gU/l, Plexiglas refl
HEU-SOL-THERM-004	6	6			6	6	$U(93.65)O_2F_2$ in D_2O soln in sph geom, D/X from 34 to 430, D_2O refl
HEU-SOL-THERM-005	17	8			8		Pyrex glass poisoned U(87.4)NH or $U(93.2)O_2F_2$ soln in cyl geom, varied H_2O refl
HEU-SOL-THERM-006	29	7			7		boric acid poisoned U(93)NH soln in cyl geom, 295 gU/l, various refl combinations
HEU-SOL-THERM-007	17	17			17	5	concrete refl arrays of U(93.2)NH soln cylinders, 67-370 gU/l
HEU-SOL-THERM-008	14	14			14	14	Plexiglas refl arrays of U(93.2)NH soln cylinders, 60-356 gU/l
HEU-SOL-THERM-009	4	4			4	4	$U(93.2)O_2F_2$ soln in 6.4 liter sph geom, 213-696 gU/l, water refl
HEU-SOL-THERM-010	4	4			4	4	$U(93.2)O_2F_2$ soln in 9.7 liter sph geom, 95-107 gU/l, water refl
HEU-SOL-THERM-011	2	2			2	2	$U(93.2)O_2F_2$ soln in 17 liter sph geom, 48-50 gU/l, water refl
HEU-SOL-THERM-012	1	1			1		$U(93.2)O_2F_2$ soln in 91 liter sph geom, 20.5 gU/l, water refl

System Type	Acceptable benchmarks in the 2002 OECD Manual	KENO V.a models included in Y/DD-896 Rev 0	KENO V.a models included in Y/DD-996 Rev 1	KENO V.a models added for Y/DD-896 Rev 1	KENO V.a Totals	MCNP4C2 models included in Y/DD-1026 Rev 0	General Description/Comments
Highlighted text indicates additions/changes to Volumes I, II, III, IV, and VII since the 2001 OECD Manual							
HEU-SOL-THERM-013	4	4			4	4	boric acid poisoned U(93.2)NH soln in 174 liter sph geom, 20-28 gU/l, unrefl
HEU-SOL-THERM-014	3	3			3	3	Gd poisoned U(89)NH soln in cyl geom, ~70 gU/l, water refl
HEU-SOL-THERM-015	5	5			5	5	Gd poisoned U(89)NH soln in cyl geom, ~100 gU/l, water refl
HEU-SOL-THERM-016	3	3			3	3	Gd poisoned U(89)NH soln in cyl geom, ~150 gU/l, water refl
HEU-SOL-THERM-017	8	8			8	8	Gd poisoned U(89)NH soln in cyl geom, ~200 gU/l, water refl
HEU-SOL-THERM-018	12	12			12	12	Gd poisoned U(89)NH soln in cyl geom, ~300 gU/l, water refl
HEU-SOL-THERM-019	3	3			3	3	Gd poisoned U(89)NH soln in cyl geom, ~400 gU/l, water refl
HEU-SOL-THERM-020	5	5			5	5	U(93.65)O_2F_2 in D_2O soln in sph geom, D/X from 230 to 2080, unrefl
HEU-SOL-THERM-021	32	6		4	10		bare and hydrogenous refl arrays of U(93.2)NH soln cylinders, 63-415 gU/l
HEU-SOL-THERM-022	1						intersection of two steel pipes containing U(89)NH soln, 141 gU/l, water refl
HEU-SOL-THERM-023	1						steel pipe intersections containing U(89)NH soln, 408 gU/l, water refl
HEU-SOL-THERM-024	14					14	steel pipe intersections containing U(89)NH soln, 64-386 gU/l, bare and water refl
HEU-SOL-THERM-025	18	18			18	18	Gd poisoned U(89)NH soln in cyl geom, 48-400 gU/l, water refl
HEU-SOL-THERM-027	9	9			9	9	unrefl U(89)NH soln in cyl geom, 136 gU/l, central rod of B_4C, Cd, or n/a
HEU-SOL-THERM-028	18	18			18	18	water refl U(89)NH soln in cyl geom, 76 or 286 gU/l, central rod of B_4C or n/a
HEU-SOL-THERM-029	7	7			7	7	water refl U(89)NH soln in cyl geom, 286 gU/l, seven rods of B_4C or n/a
HEU-SOL-THERM-030	7	7			7	7	water refl U(89)NH soln in cyl geom, 76 or 286 gU/l, 3-6 rods of B_4C or n/a
HEU-SOL-THERM-031	4	4			4		water refl U(89)NH soln in cyl geom, 286 gU/l, 18 or 36 rods of B_4C
HEU-SOL-THERM-032	1	1			1		U(93.2)NH soln in 48" dia. sph geom, ~15 gU/l, unrefl
HEU-SOL-THERM-033	26	26			26	26	ann cyl tanks of U(93.2)NH soln, 357 gU/l, cavity of varius matls, concrete refl
HEU-SOL-THERM-035	9	9			9	9	water refl U(89)NH soln in cyl geom, 37-152 gU/l, multiple rods of B_4C or n/a
HEU-SOL-THERM-036	4	4			4	4	unrefl U(89)NH soln in cuboidal geom, 92.7 gU/l, multiple rods of B_4C or n/a
HEU-SOL-THERM-037	9	9			9	9	water refl U(89)NH soln in cyl geom, 42-83 gU/l, multiple rods of B_4C or n/a
HEU-SOL-THERM-038	30						U(93)NH soln @ 404 gU/l in two cyl slab tanks, mod/refl by H, B, Be, Pb, SS, Cd, or U(dep)
HEU-SOL-THERM-039	6					6	liquid U(93.2)F_6+HF at low H/U (9.9 to 82) in a spherical tank with hot water reflection

System Type	Acceptable benchmarks in the 2002 OECD Manual	KENO V.a models included in Y/DD-896 Rev 0	KENO V.a models included in Y/DD-996 Rev 1	KENO V.a models added for Y/DD-896 Rev 1	KENO V.a Totals	MCNP4C2 models included in Y/DD-1026 Rev 0	General Description/Comments
Highlighted text indicates additions/changes to Volumes I, II, III, IV, and VII since the 2001 OECD Manual							
HEU-SOL-THERM-040	17						U(93)NH soln @ 453 gU/l in unrelfected intersecting pipe configurations
HEU-SOL-THERM-042	8					8	unreflected 5-ft or 9-ft diameter cylinders of U(93.2)NH soln @ 13.6 to 17.3 gU/l
HEU-SOL-THERM-043	3					3	17-, 91-, or 174-liter U(93.2)O_2F_2 soln in sph geom @ 134-, 25-, or 20-gU/l, unrefl
HEU-SOL-THERM-044	31						concrete refl U(93.2)NH soln cyl @ 363 gU/l, cyl geom w/per dist of neut abs rods
HEU-SOL-THERM-045	0	n/a	n/a			n/a	"Tuck and Clark" interacting U(93.2)NH slab-cylinder experiments
SUB-HEU-SOL-THERM-001	5						^{252}Cf-driven noise measurements of unrefl U(93.2)NH soln @ 482 gU/l in cyl geom
MIXED ENERGY HEU SOLUTION SYSTEMS							
none presently evaluated							
MISCELLANEOUS HEU SYSTEMS							
FAST ENERGY MISCELLANEOUS HEU SYSTEMS							
none presently evaluated							
INTERMEDIATE ENERGY MISCELLANEOUS HEU SYSTEMS							
none presently evaluated							
THERMAL ENERGY MISCELLANEOUS HEU SYSTEMS							
HEU-MISC-THERM-001	0	n/a	n/a			n/a	refer to HEU-MET-THERM-006
HEU-MISC-THERM-002	0	n/a	n/a			n/a	refer to HEU-COMP-THERM-010
MIXED ENERGY MISCELLANEOUS HEU SYSTEMS							
none presently evaluated							

Volume III, Intermediate and Mixed Enrichment Uranium Systems

System Type	Acceptable benchmarks in the 2002 OECD Manual	KENO V.a models included in Y/DD-896 Rev 0	KENO V.a models included in Y/DD-996 Rev 1	KENO V.a models added for Y/DD-896 Rev 1	KENO V.a Totals	MCNP4C2 models included in Y/DD-1026 Rev 0	General Description/Comments
Highlighted text indicates additions/changes to Volumes I, II, III, IV, and VII since the 2001 OECD Manual							
IEU METAL SYSTEMS							
FAST ENERGY IEU METAL SYSTEMS							
IEU-MET-FAST-001	4			4	4	4	unrefl cyl U(93.4) metal discs interleaved with U(nat), effectively U(36) or U(55)
IEU-MET-FAST-002	1			1	1	1	U(nat) refl cyl U(93.4) metal discs interleaved with U(nat), effectively U(16)
IEU-MET-FAST-003	1			1	1	1	bare spherical assembly of U(36) metal
IEU-MET-FAST-004	1			1	1	1	graphite refl spherical assembly of U(36) metal
IEU-MET-FAST-005	1			1	1	1	steel refl spherical assembly of U(36) metal
IEU-MET-FAST-006	1			1	1	1	Al refl spherical assembly of U(36) metal
IEU-MET-FAST-007	1			1	1	1	cyl assembly of U(93), U(10), and U(nat) metal, effectively U(10) core, U(dep) refl
IEU-MET-FAST-008	1			1	1	1	U(dep) refl spherical assembly of U(36) metal
IEU-MET-FAST-009	1			1	1	1	poly refl spherical assembly of U(36) metal
IEU-MET-FAST-010	1			1	1	1	cyl ZPR assembly with a U(93)+U(dep) core [effectively U(9)] with U(dep) refl
IEU-MET-FAST-012	1			1	1	1	cyl ZPR assembly with a U(93)+U(dep)+Al+Fe core with U(dep) refl (ZPR-3/41)
IEU-MET-FAST-014	2			2	2		cyl ZPR assembly with a U(93)+U(dep)+W metal core with Al refl (ZPR-9/2 and 3)
INTERMEDIATE ENERGY IEU METAL SYSTEMS							
none presently evaluated							
THERMAL ENERGY IEU METAL SYSTEMS							
none presently evaluated							
MIXED ENERGY IEU METAL SYSTEMS							
none presently evaluated							
IEU COMPOUND SYSTEMS							
FAST ENERGY IEU COMPOUND SYSTEMS							

System Type	Acceptable benchmarks in the 2002 OECD Manual	KENO V.a models included in Y/DD-896 Rev 0	KENO V.a models included in Y/DD-996 Rev 1	KENO V.a models added for Y/DD-896 Rev 1	KENO V.a Totals	MCNP4C2 models included in Y/DD-1026 Rev 0	General Description/Comments
Highlighted text indicates additions/changes to Volumes I, II, III, IV, and VII since the 2001 OECD Manual							
IEU-COMP-FAST-002	0	n/a	n/a			n/a	refer to IEU-COMP-INTER-001
INTERMEDIATE ENERGY IEU COMPOUND SYSTEMS							
IEU-COMP-INTER-001	4			4	4		k-inf measurements for tube assemblies of $U(93)O_2$+$U(36)O_2$+Th+poly
THERMAL ENERGY IEU COMPOUND SYSTEMS							
IEU-COMP-THERM-001	29			29	29	21	arrays of $U(30)F_4$-polytetrafluoroethylene and polyethylene cubes
IEU-COMP-THERM-002	6					6	latticed annular $U(17)O_2$ rods in H_2O, annuli of H_2O, Gd_2O_3-Al_2O_3, or CdO-Al_2O_3
IEU-COMP-THERM-003	2			2	2	2	lattices of cyl U(20)-Zr-hydride rods in H_2O, graphite refl
IEU-COMP-THERM-005	0	n/a	n/a			n/a	refer to IEU-COMP-INTER-001
MIXED ENERGY IEU COMPOUND SYSTEMS							
none presently evaluated							
IEU SOLUTION SYSTEMS							
THERMAL ENERGY IEU SOLUTION SYSTEMS							
IEU-SOL-THERM-001	4						$U(20.9)O_2SO_4$ soln in cyl geom, 263-505 gU/l, graphite refl
MISCELLANEOUS IEU SYSTEMS							
FAST ENERGY MISCELLANEOUS IEU SYSTEMS							
none presently evaluated							
INTERMEDIATE ENERGY MISCELLANEOUS IEU SYSTEMS							
none presently evaluated							

System Type	Acceptable benchmarks in the 2002 OECD Manual	KENO V.a models included in Y/DD-896 Rev 0	KENO V.a models included in Y/DD-996 Rev 1	KENO V.a models added for Y/DD-896 Rev 1	KENO V.a Totals	MCNP4C2 models included in Y/DD-1026 Rev 0	General Description/Comments
Highlighted text indicates additions/changes to Volumes I, II, III, IV, and VII since the 2001 OECD Manual							
THERMAL ENERGY MISCELLANEOUS IEU SYSTEMS							
none presently evaluated							
MIXED ENERGY MISCELLANEOUS IEU SYSTEMS							
none presently evaluated							
Volume IV, Low Enriched Uranium Systems							
LEU METAL SYSTEMS							
FAST ENERGY LEU METAL SYSTEMS							
none presently evaluated							
INTERMEDIATE ENERGY LEU METAL SYSTEMS							
none presently evaluated							
THERMAL ENERGY LEU METAL SYSTEMS							
LEU-MET-THERM-001	1			1	1		lattice of cyl U(nat) metal rods immersed in D_2O
LEU-MET-THERM-002	12			12	12		lattices of annular cyl U(2) metal rods immersed in D_2O
MIXED ENERGY LEU METAL SYSTEMS							
none presently evaluated							
LEU COMPOUND SYSTEMS							
FAST ENERGY LEU COMPOUND SYSTEMS							
none presently evaluated							
INTERMEDIATE ENERGY LEU COMPOUND SYSTEMS							
none presently evaluated							

System Type	Acceptable benchmarks in the 2002 OECD Manual	KENO V.a models included in Y/DD-896 Rev 0	KENO V.a models included in Y/DD-996 Rev 1	KENO V.a models added for Y/DD-896 Rev 1	KENO V.a Totals	MCNP4C2 models included in Y/DD-1026 Rev 0	General Description/Comments
Highlighted text indicates additions/changes to Volumes I, II, III, IV, and VII since the 2001 OECD Manual							
THERMAL ENERGY LEU COMPOUND SYSTEMS							
LEU-COMP-THERM-001	8	8			8		lattices of cyl $U(2.35)O_2$ rods immersed in water
LEU-COMP-THERM-002	5	5			5		lattices of cyl $U(4.31)O_2$ rods immersed in water
LEU-COMP-THERM-003	23	22			22		lattices of cyl $U(2.35)O_2$ rods immersed in water, water contains Gd impurity
LEU-COMP-THERM-004	20	20			20		lattices of cyl $U(4.31)O_2$ rods immersed in water, water contains Gd impurity
LEU-COMP-THERM-005	16						lattices of cyl $U(2.35)O_2$ or $U(4.31)O_2$ rods immersed in water containing Gd
LEU-COMP-THERM-006	18						lattices of cyl $U(2.6)O_2$ rods immersed in water
LEU-COMP-THERM-007	10						lattices of cyl $U(4.738)O_2$ rods immersed in water
LEU-COMP-THERM-008	17			1	1		$U(2.459)O_2$ rods latticed in borated H_2O, pertubed by Vicor, Pyrex, or Al_2O_3 rods
LEU-COMP-THERM-009	27			1	1		clusters of $U(4.31)O_2$ rods in water purturbed by various matls as plates
LEU-COMP-THERM-010	30						lattices of $U(4.31)O_2$ rods in water refl by two Pb, U(dep), or steel walls
LEU-COMP-THERM-011	15						clusters of $U(2.5)O_2$ rods immersed in water, poisoned with B_4C rods or borated water
LEU-COMP-THERM-012	10			10	10		clusters of $U(2.35)O_2$ rods in H_2O (Gd impurity) purturbed by various matls as plates
LEU-COMP-THERM-013	7						clusters of $U(4.31)O_2$ rods in water poisoned by various matls as plates
LEU-COMP-THERM-014	5						water reflected arrays of $U(4.31)O_2$ fuel rods in borated water
LEU-COMP-THERM-015	165						VVER Experiments, Part I
LEU-COMP-THERM-016	32	32			32		clusters of $U(2.35)O_2$ rods in water purturbed by various matls as plates
LEU-COMP-THERM-017	29						lattices of $U(2.35)O_2$ rods in water refl by two Pb, U(dep), or steel walls
LEU-COMP-THERM-018	1						$U(7)O_2$ rods immersed in water
LEU-COMP-THERM-019	3						stainless steel clad $U(5)O_2$ rods immersed in water
LEU-COMP-THERM-020	7						Zr-clad $U(5)O_2$ rods immersed in water
LEU-COMP-THERM-021	6						Zr-clad $U(5)O_2$ rods immersed in borated water
LEU-COMP-THERM-022	7						stainless steel clad $U(10)O_2$ rods immersed in water
LEU-COMP-THERM-023	6						stainless steel clad $U(10)O_2$ rods immersed in water
LEU-COMP-THERM-024	2						stainless steel clad $U(10)O_2$ rods immersed in water
LEU-COMP-THERM-025	4						stainless steel clad $U(7.5)O_2$ rods immersed in water

System Type	Acceptable benchmarks in the 2002 OECD Manual	KENO V.a models included in Y/DD-896 Rev 0	KENO V.a models included in Y/DD-996 Rev 1	KENO V.a models added for Y/DD-896 Rev 1	KENO V.a Totals	MCNP4C2 models included in Y/DD-1026 Rev 0	General Description/Comments
Highlighted text indicates additions/changes to Volumes I, II, III, IV, and VII since the 2001 OECD Manual							
LEU-COMP-THERM-026	6						Zr-clad $U(4.92)O_2$ rods immersed in water at varied temperatures
LEU-COMP-THERM-027	4						Al-clad $U(4.74)O_2$ rods immersed in water, Pb refl
LEU-COMP-THERM-029	12						Al-clad $U(4.74)O_2$ rods immersed in water surrounded by Hf plates
LEU-COMP-THERM-031	6						Zr-clad $U(5)O_2$ rods immersed in water
LEU-COMP-THERM-032	9						stainless steel clad $U(10)O_2$ rods immersed in water at varied temperatures
LEU-COMP-THERM-033	52						unrefl and hydrogenous refl cores of UF_4-paraffin cuboids at 2 or 3% enrichment
LEU-COMP-THERM-034	24						$U(4.738)O_2$ rod clusters in Cd, bor-ss, or Boral cannisters and immersed in H_2O
LEU-COMP-THERM-035	3						$U(2.6)O_2$ rods immersed in Gd- or B-poisoned water
LEU-COMP-THERM-036	69						VVER Experiments, Part II
LEU-COMP-THERM-037	11						$U(4.738)O_2$ rods immersed in water, partial refl by concrete
LEU-COMP-THERM-038	14						$U(4.738)O_2$ rods immersed in water, partial refl by borated concrete
LEU-COMP-THERM-039	17						incomplete/irregular lattices of $U(4.738)O_2$ rods immersed in water
LEU-COMP-THERM-040	10						$U(4.738)O_2$ rod clusters in Cd, bor-ss, or Boral cannisters in water, Pb or steel refl
LEU-COMP-THERM-041	5						HEU driven $U(3)O_2$ rod clusters in water separated by ss, bor-ss, or Cd plates
LEU-COMP-THERM-042	7						$U(2.35)O_2$ rod clusters in H_2O separated by various matls as plates, refl by steel walls
LEU-COMP-THERM-047	3						lattices of cyl $U(3)O_2$ and/or $U(7)O_2$ rods immersed in water
LEU-COMP-THERM-048	5						lattices of cyl $U(3)O_2$ rods immersed in water
LEU-COMP-THERM-049	18						poly refl split-table arrays of cuboidal cans containing U(5)O2 powder at low H/U
LEU-COMP-THERM-050	18						H_2O immersion of $U(4.738)O_2$ rods arround a sq tank of ^{149}Sm, B, or H2O in soln
LEU-COMP-THERM-051	19						clusters of $U(2.5)O_2$ rods immersed in borated water, poisoned with SS or Boral plates
LEU-COMP-THERM-052	6						lattices of $U(4.738)O_2$ or rods immersed in Gd-nitrate soln

System Type	Acceptable benchmarks in the 2002 OECD Manual	KENO V.a models included in Y/DD-896 Rev 0	KENO V.a models included in Y/DD-996 Rev 1	KENO V.a models added for Y/DD-896 Rev 1	KENO V.a Totals	MCNP4C2 models included in Y/DD-1026 Rev 0	General Description/Comments
Highlighted text indicates additions/changes to Volumes I, II, III, IV, and VII since the 2001 OECD Manual							
LEU-COMP-THERM-055	2						water reflected and water moderated $U(3)O_2$ rod lattices
LEU-COMP-THERM-061	10						VVER-type fuel assemblies immersed in water, perturbed with B_4C, Hf, Dy, or gaps
LEU-COMP-THERM-062	15						$U(2.6)O_2$ rod lattices immersed in water, perturbed with borated SS plates
SUB-LEU-COMP-THERM-001	15						lattices of cyl $U(3)O_2$ rods immersed in water and compartmentalized by borated steel
MIXED ENERGY LEU COMPOUND SYSTEMS							
none presently evaluated							
LEU SOLUTION SYSTEMS							
THERMAL ENERGY LEU SOLUTION SYSTEMS							
LEU-SOL-THERM-001	1						unreflected $U(5)O_2F_2$ soln in cyl geom, 1000 gU/l
LEU-SOL-THERM-002	3						$U(4.9)O_2F_2$ soln in 147 liter sph geom, ~450 or ~490 gU/l, unrefl or water refl
LEU-SOL-THERM-003	9	9			9		full and truncated spheres of U(10)NH soln
LEU-SOL-THERM-004	7						STACY: water refl U(10)NH soln in cyl geom, ~225-310 gU/l
LEU-SOL-THERM-005	3			7	7		water refl U(5.64)NH soln in cyl geom, ~400 gU/l, with or without B_4C rods
LEU-SOL-THERM-006	5						water refl U(10)NH soln in cyl geom, ~420 gU/l, with or without B_4C rods
LEU-SOL-THERM-007	5						STACY: unreflected U(10)NH soln in cyl geom, ~242-313 gU/l
LEU-SOL-THERM-008	4						STACY: concrete refl U(10)NH soln in cyl geom, ~240 gU/l
LEU-SOL-THERM-009	3						STACY: borated concrete refl U(10)NH soln in cyl geom, ~240 gU/l
LEU-SOL-THERM-010	4						STACY: poly refl U(10)NH soln in cyl geom, ~240 gU/l
LEU-SOL-THERM-016	7						STACY: water refl U(10)NH soln in slab geom, ~300-464 gU/l
LEU-SOL-THERM-017	6						STACY: unreflected U(10)NH soln in slab geom, ~315-464 gU/l

System Type	Acceptable benchmarks in the 2002 OECD Manual	KENO V.a models included in Y/DD-896 Rev 0	KENO V.a models included in Y/DD-996 Rev 1	KENO V.a models added for Y/DD-896 Rev 1	KENO V.a Totals	MCNP4C2 models included in Y/DD-1026 Rev 0	General Description/Comments
Highlighted text indicates additions/changes to Volumes I, II, III, IV, and VII since the 2001 OECD Manual							
LEU-SOL-THERM-018	6						STACY: concrete refl U(10)NH soln in slab geom, ~310-315 gU/l
LEU-SOL-THERM-019	6						STACY: poly refl U(10)NH soln in slab geom, ~320 gU/l
LEU-SOL-THERM-020	4						STACY: water refl U(10)NH soln in cyl geom, ~194-243 gU/l
LEU-SOL-THERM-021	4						STACY: unreflected U(10)NH soln in cyl geom, ~194-243 gU/l
LEU-SOL-THERM-022	4						STACY: borated concrete refl U(10)NH soln in slab geom, ~310 gU/l
MISCELLANEOUS LEU SYSTEMS							
FAST ENERGY MISCELLANEOUS LEU SYSTEMS							
none presently evaluated							
INTERMEDIATE ENERGY MISCELLANEOUS LEU SYSTEMS							
none presently evaluated							
THERMAL ENERGY MISCELLANEOUS LEU SYSTEMS							
none presently evaluated							
MIXED ENERGY MISCELLANOUS LEU SYSTEMS							
none presently evaluated							
Volume V, Uranium-233 Systems							
U-233 METAL SYSTEMS							
FAST ENERGY U-233 METAL SYSTEMS							
U233-MET-FAST-001	1			1	1		bare sphere of U-233 metal (U-233 Jezebel)
U233-MET-FAST-002	2			2	2		10 kg or 7.6 kg U-233 metal sphere reflected by U(93) metal
U233-MET-FAST-003	2			2	2		10 kg or 7.6 kg U-233 metal sphere reflected by U(nat) metal
U233-MET-FAST-004	2			2	2		10 kg or 7.6 kg U-233 metal sphere reflected by W metal
U233-MET-FAST-005	2			2	2		10 kg or 7.6 kg U-233 metal sphere reflected by Be metal

System Type	Acceptable benchmarks in the 2002 OECD Manual	KENO V.a models included in Y/DD-896 Rev 0	KENO V.a models included in Y/DD-996 Rev 1	KENO V.a models added for Y/DD-896 Rev 1	KENO V.a Totals	MCNP4C2 models included in Y/DD-1026 Rev 0	General Description/Comments
Highlighted text indicates additions/changes to Volumes I, II, III, IV, and VII since the 2001 OECD Manual							
U233-MET-FAST-006	1			1	1		U(nat) reflected sphere of U-233 metal (U-233 Flattop)
INTERMEDIATE ENERGY U-233 METAL SYSTEMS							
none presently evaluated							
THERMAL ENERGY U-233 METAL SYSTEMS							
none presently evaluated							
MIXED ENERGY U-233 METAL SYSTEMS							
none presently evaluated							
U-233 COMPOUND SYSTEMS							
FAST ENERGY U-233 COMPOUND SYSTEMS							
none presently evaluated							
INTERMEDIATE ENERGY U-233 COMPOUND SYSTEMS							
none presently evaluated							
THERMAL ENERGY U-233 COMPOUND SYSTEMS							
none presently evaluated							
MIXED ENERGY U-233 COMPOUND SYSTEMS							
none presently evaluated							
U-233 SOLUTION SYSTEMS							
INTERMEDIATE ENERGY U-233 SOLUTION SYSTEMS							
U233-SOL-INTER-001	33			33	33		$^{233}UO_2F_2$ soln in spherical geometry with Be, poly, or Be-poly reflectors

System Type	Acceptable benchmarks in the 2002 OECD Manual	KENO V.a models included in Y/DD-896 Rev 0	KENO V.a models included in Y/DD-996 Rev 1	KENO V.a models added for Y/DD-896 Rev 1	KENO V.a Totals	MCNP4C2 models included in Y/DD-1026 Rev 0	General Description/Comments
Highlighted text indicates additions/changes to Volumes I, II, III, IV, and VII since the 2001 OECD Manual							
THERMAL ENERGY U-233 SOLUTION SYSTEMS							
U233-SOL-THERM-001	5			5	5		unreflected spheres of ^{233}UNH solution with varied boron content
U233-SOL-THERM-002	17			17	17		paraffin reflected cylinders of ^{233}UNH solution
U233-SOL-THERM-003	10			1	1		paraffin reflected cylinders of $^{233}UO_2F_2$ solution
U233-SOL-THERM-004	8			8	8		paraffin reflected cylinders of ^{233}UNH solution
U233-SOL-THERM-005	2			2	2		water reflected cylinder or sphere of ^{233}UNH solution
U233-SOL-THERM-006	25			8	8		arrays of ^{233}UNH solution cylinders
U233-SOL-THERM-008	1			1	1		unreflected sphere of ^{233}UNH solution
U233-SOL-THERM-011	0	n/a	n/a			n/a	refer to U233-SOL-INTER-001
U233-SOL-THERM-012	8			8	8		water reflected spherical vessels containing ^{233}UNH solution
U233-SOL-THERM-014	16			16	16		arrays of polybottles containing ^{233}UNH solution
U233-SOL-THERM-015	31			31	31		$^{233}UO_2F_2$ soln in spherical geometry with Be, poly, or Be-poly reflectors
MIXED ENERGY U-233 SOLUTION SYSTEMS							
U233-SOL-MIXED-001	0	n/a	n/a			n/a	refer to U233-SOL-INTER-001
U233-SOL-MIXED-002	0	n/a	n/a			n/a	refer to U233-SOL-THERM-015

U-233 MISCELLANEOUS SYSTEMS

FAST ENERGY U-233 MISCELLANEOUS SYSTEMS

none presently evaluated

INTERMEDIATE ENERGY U-233 MISCELLANEOUS SYSTEMS

none presently evaluated

System Type	Acceptable benchmarks in the 2002 OECD Manual	KENO V.a models included in Y/DD-896 Rev 0	KENO V.a models included in Y/DD-996 Rev 1	KENO V.a models added for Y/DD-896 Rev 1	KENO V.a Totals	MCNP4C2 models included in Y/DD-1026 Rev 0	General Description/Comments
Highlighted text indicates additions/changes to Volumes I, II, III, IV, and VII since the 2001 OECD Manual							
THERMAL ENERGY U-233 MISCELLANEOUS SYSTEMS							
none presently evaluated							
MIXED ENERGY U-233 MISCELLANEOUS SYSTEMS							
none presently evaluated							
Volume VI, Mixed Plutonium-Uranium Systems							
MIXED PU-U METAL SYSTEMS							
FAST ENERGY MIXED PU-U METAL SYSTEMS							
MIX-MET-FAST-001	1		1		1	1	sphere of ^{239}Pu metal (~4.9% ^{240}Pu) reflected by U(93.2) metal
MIX-MET-FAST-002	3		3		3	3	composite sph cores of ^{239}Pu (varied ^{240}Pu) and U(93.2) metal refl by U(nat) metal
MIX-MET-FAST-003	1					1	sphere of ^{239}Pu metal (~9% ^{240}Pu) reflected by U(89) metal
MIX-MET-FAST-004	2					2	composite sph cores of ^{239}Pu (~9% ^{240}Pu) and U(89) metal refl by Be and BeO
MIX-MET-FAST-005	1					1	composite sph core of ^{239}Pu (~9% ^{240}Pu) and U(89) metal refl by Al
MIX-MET-FAST-007	23		23		23	23	composite sph cores of ^{239}Pu (~5.7% ^{240}Pu) and U(93.2) metal refl by Be metal
MIX-MET-FAST-008	7					3	k-inf for ^{239}Pu, MOX, or U(37) plates interleaved with C, SST, Na, and/or U(nat) plates
MIX-MET-FAST-009	1		1		1	1	sph core of ^{239}Pu (~1.8% ^{240}Pu) metal reflected by 0.75-cm thick U(89) metal
MIX-MET-FAST-010	1		1		1	1	sph core of ^{239}Pu (~1.8% ^{240}Pu) metal reflected by 2.89-cm thick U(89) metal
MIX-MET-FAST-011	4		4		4	1	cyl assy of fissile Pu/U/Zr fuel plates reflected by graphite (ZPPR-9/21B thru 21E)
MIX-MET-FAST-012	0	n/a	n/a			n/a	refer to PU-MET-FAST-033
INTERMEDIATE ENERGY MIXED PU-U METAL SYSTEMS							
MIX-MET-INTER-001	0	n/a	n/a			n/a	refer to MIX-MET-FAST-008
MIX-MET-INTER-002	0	n/a	n/a			n/a	refer to MIX-MET-MIXED-001
THERMAL ENERGY MIXED PU-U METAL SYSTEMS							

System Type	Acceptable benchmarks in the 2002 OECD Manual	KENO V.a models included in Y/DD-896 Rev 0	KENO V.a models included in Y/DD-996 Rev 1	KENO V.a models added for Y/DD-896 Rev 1	KENO V.a Totals	MCNP4C2 models included in Y/DD-1026 Rev 0	General Description/Comments
Highlighted text indicates additions/changes to Volumes I, II, III, IV, and VII since the 2001 OECD Manual							
none presently evaluated							
MIXED ENERGY MIXED PU-U METAL SYSTEMS							
MIX-MET-MIXED-001	1					1	unrefl cyl assy of alternating ^{239}Pu (~4.6% ^{240}Pu) metal, U(96) metal, and poly plates
MIXED PU-U COMPOUND SYSTEMS							
FAST ENERGY MIXED PU-U COMPOUND SYSTEMS							
none presently evaluated							
INTERMEDIATE ENERGY MIXED PU-U COMPOUND SYSTEMS							
none presently evaluated							
THERMAL ENERGY MIXED PU-U COMPOUND SYSTEMS							
MIX-COMP-THERM-001	4						mixed $^{239}PuO_2$ and $U(nat)O_2$ fuel pins immersed in water
MIX-COMP-THERM-002	6					6	mixed $^{239}PuO_2$ and $U(nat)O_2$ fuel pins immersed in water or borated water
MIX-COMP-THERM-003	6					6	rectangular arrays of mixed $^{239}PuO_2$ and $U(nat)O_2$ fuel pins immersed in water
MIX-COMP-THERM-004	11						arrays of mixed $^{239}PuO_2$ and $U(nat)O_2$ fuel rods immersed in water
MIX-COMP-THERM-005	7		1		1		hexagonal lattice arrays of mixed $^{239}PuO_2$ and $U(nat)O_2$ fuel pins immersed in water
MIX-COMP-THERM-006	6		1		1		hexagonal lattice arrays of mixed $^{239}PuO_2$ and $U(nat)O_2$ fuel pins immersed in water
MIX-COMP-THERM-007	27		27		27		five lattices of mixed $^{239}PuO_2$ and $U(nat)O_2$ rods in water, incl Hf/B/Cd rod substitutions
MIX-COMP-THERM-008	28		28		28	28	six lattices of mixed $^{239}PuO_2$ and $U(nat)O_2$ rods in water, incl Hf/B/Cd rod substitutions
MIX-COMP-THERM-009	6		1		1	6	hexagonal lattices of mixed $^{239}PuO_2$ and $U(dep)O_2$ fuel pins immersed in water
MIX-COMP-THERM-010	0	n/a	n/a			n/a	refer to MIX-MISC-THERM-001
MIX-COMP-THERM-011	6		1		1	6	arrays of mixed $^{239}PuO_2$ and $U(60)O_2$ fuel rods immersed in water
MIX-COMP-THERM-012	33		33		33	33	bare and Plexiglas reflected arrays of MOX/polystyrene blocks
MIXED ENERGY MIXED PU-U COMPOUND							

System Type	Acceptable benchmarks in the 2002 OECD Manual	KENO V.a models included in Y/DD-896 Rev 0	KENO V.a models included in Y/DD-996 Rev 1	KENO V.a models added for Y/DD-896 Rev 1	KENO V.a Totals	MCNP4C2 models included in Y/DD-1026 Rev 0	General Description/Comments
Highlighted text indicates additions/changes to Volumes I, II, III, IV, and VII since the 2001 OECD Manual							
SYSTEMS							
none presently evaluated							
MIXED PU-U SOLUTION SYSTEMS							
INTERMEDIATE ENERGY MIXED PU-U SOLUTION SYSTEMS							
none presently evaluated							
THERMAL ENERGY MIXED PU-U SOLUTION SYSTEMS							
MIX-SOL-THERM-001	13		13		13	13	^{239}PuNH + U(nat)NH soln in annular geomerty
MIX-SOL-THERM-002	3		3		3	3	^{239}PuNH + U(nat)NH soln in large cylindrical geomerty
MIX-SOL-THERM-003	10					10	^{239}PuNH + U(nat)NH soln in cylindrical geomerty with poly/water refl
MIX-SOL-THERM-004	9		9		9	9	^{239}PuNH + U(dep)NH soln in small cyl geom, bare or water or concrete refl
MIX-SOL-THERM-005	7		7		7	7	^{239}PuNH + U(dep)NH soln in slab geomerty, bare or water refl
MIXED ENERGY MIXED PU-U SOLUTION SYSTEMS							
none presently evaluated							
MIXED PU-U MISCELLANEOUS SYSTEMS							
FAST ENERGY MIXED PU-U MISCELLANEOUS SYSTEMS							
none presently evaluated							
INTERMEDIATE ENERGY MIXED PU-U MISCELLANEOUS SYSTEMS							
none presently evaluated							
THERMAL ENERGY MIXED PU-U MISCELLANEOUS SYSTEMS							
MIX-MISC-THERM-001	11		11		11	11	mixed oxide fuel pin lattices in (Pu+U)NH solution
MIX-MISC-THERM-002	12						arrays of mixed $^{239}PuO_2$ and $U(60)O_2$ fuel rods in dilute ^{239}PuNH soln and refl by water

System Type	Acceptable benchmarks in the 2002 OECD Manual	KENO V.a models included in Y/DD-896 Rev 0	KENO V.a models included in Y/DD-996 Rev 1	KENO V.a models added for Y/DD-896 Rev 1	KENO V.a Totals	MCNP4C2 models included in Y/DD-1026 Rev 0	General Description/Comments
Highlighted text indicates additions/changes to Volumes I, II, III, IV, and VII since the 2001 OECD Manual							
MIXED ENERGY MIXED PU-U MISCELLANEOUS SYSTEMS							
none presently evaluated							
Volume VII, Special Isotope Systems							
SPECIAL ISOTOPE METAL SYSTEMS							
FAST ENERGY SPECIAL ISOTOPE METAL SYSTEMS							
SPEC-MET-FAST-001	4						replacement measurements of ^{240}Pu Jezebel with void, U(93), ^{239}Pu, or ^{244}Cm
SPEC-MET-FAST-002	3						replacement measurements of ^{240}Pu Jezebel with void, ^{238}Pu, or ^{239}Pu
SPEC-MET-FAST-003	6						replacement measurements of Flattop (Pu and HEU) with void, ^{237}Np, or U(93)
SPEC-MET-FAST-004	7						combos of ^{239}Pu, ^{242}Pu, and U(93) metal disks, unrefl and refl by steel, Be, or U(dep)
INTERMEDIATE ENERGY SPECIAL ISOTOPE METAL SYSTEMS							
none presently evaluated							
THERMAL ENERGY SPECIAL ISOTOPE METAL SYSTEMS							
none presently evaluated							
MIXED ENERGY SPECIAL ISOTOPE METAL SYSTEMS							
none presently evaluated							
SPECIAL ISOTOPE COMPOUND SYSTEMS							
FAST ENERGY SPECIAL ISOTOPE COMPOUND SYSTEMS							
none presently evaluated							
INTERMEDIATE ENERGY SPECIAL ISOTOPE COMPOUND SYSTEMS							

System Type	Acceptable benchmarks in the 2002 OECD Manual	KENO V.a models included in Y/DD-896 Rev 0	KENO V.a models included in Y/DD-996 Rev 1	KENO V.a models added for Y/DD-896 Rev 1	KENO V.a Totals	MCNP4C2 models included in Y/DD-1026 Rev 0	General Description/Comments
Highlighted text indicates additions/changes to Volumes I, II, III, IV, and VII since the 2001 OECD Manual							
none presently evaluated							
THERMAL ENERGY SPECIAL ISOTOPE COMPOUND SYSTEMS							
none presently evaluated							
MIXED ENERGY SPECIAL ISOTOPE COMPOUND SYSTEMS							
none presently evaluated							
SPECIAL ISOTOPE SOLUTION SYSTEMS							
FAST ENERGY SPECIAL ISOTOPE SOLUTION SYSTEMS							
none presently evaluated							
INTERMEDIATE ENERGY SPECIAL ISOTOPE SOLUTION SYSTEMS							
none presently evaluated							
THERMAL ENERGY SPECIAL ISOTOPE SOLUTION SYSTEMS							
none presently evaluated							
MIXED ENERGY SPECIAL ISOTOPE SOLUTION SYSTEMS							
none presently evaluated							
SPECIAL ISOTOPE MISCELLANEOUS SYSTEMS							
FAST ENERGY SPECIAL ISOTOPE MISCELLANEOUS SYSTEMS							
none presently evaluated							
INTERMEDIATE ENERGY SPECIAL ISOTOPE MISCELLANEOUS SYSTEMS							
none presently evaluated							

System Type	Acceptable benchmarks in the 2002 OECD Manual	KENO V.a models included in Y/DD-896 Rev 0	KENO V.a models included in Y/DD-996 Rev 1	KENO V.a models added for Y/DD-896 Rev 1	KENO V.a Totals	MCNP4C2 models included in Y/DD-1026 Rev 0	General Description/Comments

Highlighted text indicates additions/changes to Volumes I, II, III, IV, and VII since the 2001 OECD Manual

THERMAL ENERGY SPECIAL ISOTOPE MISCELLANEOUS SYSTEMS

none presently evaluated

MIXED ENERGY SPECIAL ISOTOPE MISCELLANEOUS SYSTEMS

none presently evaluated

qual
other
mix

8 REFERENCES

i. J. Blair Briggs, Editor, International Handbook of Evaluated Criticality Safety Benchmark Experiments, NEA/NSC/DOC(95)03, Volumes 1-7, Organization for Economic Cooperation and Development - Nuclear Energy Agency, Paris, France, September 1999 Edition.

ii Critical Experiment Benchmark Calculations with CSAS25 from SCALE4.4a for Criticality Safety Analyses On the HP J-5600 Unclassified Workstation (CMODB), Y/DD-896/R0, Smith, R.H. et al, February 2001.

iii Critical Experiment Benchmark Calculations with CSAS25 from SCALE4.4a for Criticality Safety Analyses On the HP J-5600 Unclassified Workstation (CMODB), Y/DD-896/R1, Smith, R.H., August 2003.

iv. Nuclear Criticality Safety in Operations with Fissionable Material Outside Reactors, ANSI/ANS-8.1-1998, American National Standards Institute, New York, 1998.

v. Experience With the SCALE Criticality Safety Cross-Section Libraries, NUREG/CR-6686/ORNL/TM-1999/322, October 2000.

THIS PAGE INTENTIONALLY LEFT BLANK.

Determination of the Upper Subcritical Limit for Criticality Calculations for Criticality Safety Analyses

Revision 0

D. T. Johnson
J. F. DeClue
S. E. McClanahan

Nuclear Criticality Safety organization
Y-12 National Security Complex

March 2006

Prepared by the
Safety Analysis Engineering
Y-12
Oak Ridge, Tennessee 37831-8238

Prepared by the
Y-12 National Security Complex
Oak Ridge, Tennessee 37831
Managed by
BWXT Y-12, L.L.C.
For the
U.S. Department of Energy
under contract DE-AC05-00OR22800

This document has been reviewed by an Authorized Derivative Classifier and has been determined to be UNCLASSIFIED. This review does not constitute clearance for public release.

J. F. DeClue 3-27-06
J. F. DeClue Date
Criticality Safety Analyst

Determination of the Upper Subcritical Limit for Criticality Calculations for Criticality Safety Analyses

Revision 0

D. T. Johnson
J. F. DeClue
S. E. McClanahan

Nuclear Criticality Safety organization
Y-12 National Security Complex

March 2006

Prepared by the
Y-12 National Security Complex
Oak Ridge, Tennessee 37831
Managed by
BWXT Y-12, L.L.C.
For the
U.S. Department of Energy
under contract DE-AC05-00OR22800

THIS PAGE INTENTIONALLY LEFT BLANK

Document Preparation

Prepared by _____ Date 3-28-06
David T. Johnson

Reviewed by _____ Date 3-28-06
John F. DeClue

Approved by _____ Date 3-28-06
David W. Sheffey

THIS PAGE INTENTIONALLY LEFT BLANK

Abstract

This report considers determination of an upper subcritical limit, and incorporating uncertainty and margin into the subcritical limit, and recommends an Upper Subcritical Limit (USL).

A USL is developed for CSAS25 from SCALE 5.0. The USL is applicable for the CSAS25 control module from the SCALE 5.0 computer code system for use in evaluating nuclear criticality safety of enriched uranium and plutonium systems. The benchmark calculation results used for this report are documented in Y/DD-1220. The 238-group ENDF/B-V cross-section libraries were used for all calculations.

Numerical methods for applying margins are described, but the determination of appropriate correlating parameters and values for additional margin, applicable to a particular analysis, must be determined as part of a process analysis. As such, this document does not specify final upper subcritical limits as has been done in the past. No correlation between calculation results and neutron energy causing fission was found for the critical experiment results. Analysts using these results are responsible for exercising sound engineering judgment using strong technical arguments to develop "a margin in k_{eff} or other correlating parameter ... that is sufficiently large to ensure that conditions (calculated by this method to be subcritical by this margin) will actually be subcritical." [1] Documentation of area of applicability and determination and justification of the appropriate margin in the analyst's evaluation, in conjunction with this report, will constitute the complete Validation Report in accordance with ANSI/ANS-8.1-1998, Section 4.3.6(4).

THIS PAGE INTENTIONALLY LEFT BLANK

Table of Contents

Page

1.0 INTRODUCTION **3**

1.1 GRANDFATHER OR RETROFIT CONCERNS 4
1.2 TERMINOLOGY 4

2.0 DETERMINATION OF SUBCRITICAL LIMITS AND DISCUSSION OF STATISTICAL ANALYSIS **4**

2.1 INTRODUCTION 4
2.2 DETERMINATION OF SUBCRITICAL LIMITS FROM THE BIAS AND UNCERTAINTY 5
2.2.1 Area of Applicability *6*
2.2.2 Simple Methods for Determination of Subcritical Limits *6*
2.2.3 Addition of Safety Margin and Bias Based on Tolerance Bounds *7*
2.2.4 Treatment of Model Bias *7*
2.2.5 Statistical Approach *8*
2.2.6 Discussion of Results *8*

3.0 CONCLUSIONS **10**

4.0 RECOMMENDATIONS FOR FUTURE WORK **11**

5.0 REFERENCES **12**

THIS PAGE INTENTIONALLY LEFT BLANK

1.0 Introduction

In the nuclear criticality safety field, extensive use is made of computational methods in order to establish subcritical limits for operations involving fissile material. Calculations must be made by a method shown to be validated by comparison with experiment data. The American National Standards Institute (ANSI) gives fundamental guidance for establishing these subcritical limits in ANSI/ANS-8.1-1998, "Nuclear Criticality Safety in Operations with Fissionable Materials Outside Reactors." [1]

The successful application of computational methods requires verification, certification and validation (V&V) of the analytic tool. Software verification, the first element of V&V, reveals the closeness in agreement between calculation results obtained using a particular computational method and calculation results obtained using other methods. Software certification provides a user assurance that the code will consistently produce numerical results that agree with analytic solutions for the problems the code is designed to analyze. Software validation "calibrates" the calculation results obtained using certified software (computational method) for agreement with the physical universe.

For nuclear criticality safety, the validation process is complete with development of the upper subcritical limit (USL) from validation data. Refinement of a validation or extension by addition of validation data does not require re-certification of the software. Therefore, the verification and certification of a nuclear criticality safety computer code system and transference of a validation between computer platforms are related issues, which can be addressed separately from software validation.

Taken together, Y/DD-1220 and Y/DD-1221 provide the **framework** for the validation of CSAS25 control module from the Standardized Computer Analyses for Licensing Evaluation (SCALE) Version 5.0 package with the 238-group ENDF/B-V SCALE 5.0 cross-section library.

Y/DD-1220 addresses the establishment of bias, bias trends and uncertainty associated with the use of SCALE 5.0 for performance of criticality calculations. This evaluation is directed at all systems consisting of fissile and fissionable material in metallic, solution and other physical forms, as described in the Organization for Economic Cooperation and Development (OECD) Handbook. The focus is on comparison of calculated neutron multiplication factors (k_{eff}) with the associated experimental benchmark results, and on establishment of bias, bias trends, and uncertainty as a final step. Compiled data for 1217 critical experiments is used as the basis for the calculation models. The calculated results from SCALE 5.0 using the 238-group ENDF/B-V SCALE 5.0 cross-section library have been compared with reported results for the benchmark experiments. Comparison of results demonstrates that SCALE 5.0 run on the Safety Analysis Engineering (SAE) Hewlett Packard Series zx6000 Itanium (HP 6000) unclassified workstation (referred to as CMODD) produces the same results within the statistical uncertainty of the Monte Carlo calculations as reported by the experiments.

Y/DD-1221 addresses various methods for determination of a USL and for incorporating uncertainty and margin into this USL. It provides comparisons of these methods and recommends a preferred method for determining the USL. Y/DD-1221 establishes subcritical limits determined through an evaluation of statistics parameters of calculation results for critical experiments. However, the correlating parameters (i.e., mass, enrichment, geometry, absorption, moderation, reflection, etc.) and values for applying additional margin to the subcritical limits are application dependent. The determination of correlating parameters and additional margin

is an integral part of the process analysis for a particular application. For the critical experiment results, no correlation between calculation results and neutron energy causing fission was found. As such, this document does not specify "final" USL values as has been done in the past.

The Area of Applicability (AoA) is also application dependent. In using the "raw" USL data of this report, the nuclear criticality safety analyst must exercise sound engineering judgment and use strong technical arguments to develop a margin in k_{eff} or other correlating parameter. That margin must be sufficiently large to ensure that conditions (calculated by this method to be subcritical by this margin) will actually be subcritical.[1] Preparation of the final portion of the "written report of validation" as identified in Section 4.3.6 of ANSI/ANS-8.1-1998 is the responsibility of the analyst.

1.1 Grandfather or Retrofit Concerns

The validation documents used for establishing subcritical limits for criticality calculations shall be reviewed and approved by SAE. There is no urgency to retrofit older evaluations since the common practice provided conservatism. Therefore, the incorporation of these methods into the evaluations of existing operations will be accomplished as the Nuclear Criticality Safety Approvals are updated due to equipment changes, rule changes, age, etc.

1.2 Terminology

The term "model" may be used in two different ways. In this report, "model" generally refers to the calculation model, or the collection of input parameters for the numerical simulation of the physical critical experiment. In the statistical analyses, the term "model" generally refers to a statistical model, or an equation describing the relationship between parameters considered in the statistical analysis.

The term "uncertainty" may also be used two different ways. In this report, "uncertainty" generally refers to less than exactly known values in the calculation model, or in the collection of input parameters for the numerical simulation of the physical critical experiment. In statistical analyses, the term "uncertainty" generally refers to the variation of repeated observations (e.g., k_eff, k_sim, k_plt) about their expected value. This uncertainty is quantified by the sample standard deviation (i.e., square root of the sample variance).

Accuracy refers to how close the expected value of an observation is to the true value. Accuracy is quantified by bias, which is the difference between the sample average and the true or referenced value.

2.0 Determination of Subcritical Limits and Discussion of Statistical Analysis

2.1 Introduction

Y/DD-1220 provides a discussion of the calculation results, experiment (benchmark) data, and the bias results. Regression with neutron energy causing fission was observed to be not applicable. This is illustrated in

Figures 1-7 of Y/DD-1220.

The OECD Handbook reports provide an estimate of the actual k_{eff} for each experiment benchmark. While most experiments were estimated to be exactly critical, or k_exp = 1.0, a number of the estimates were slightly above or slightly below exactly critical (i.e. k_exp > 1.0 or k_exp < 1.0). It was considered desirable to account for this difference because the subcritical limit could otherwise be conservative due to including slightly subcritical experiments, or non-conservative due to including slightly super-critical experiments, when extrapolated to critical. The following adjustment, to determine an adjusted calculation result, k', was proposed for use in the statistical evaluation:

$$k' = 1 + \text{bias} = 1 + (k_calc - k_exp)$$

where k_calc = code calculated k_{eff} result for the modeled experiment, and
k_exp = OECD estimate of actual k_{eff} for the experiment

The assumption inherent in making this adjustment is that the experiments were close to critical, and if a very small adjustment could be made so that the experiment would be exactly critical, the bias of the calculation would not change.

When calculation methods are employed, the subcritical limit is a quantitative value used for implementation of SAE policy, which is established in accordance with DOE Orders, Standards, or by NRC regulations for those activities under NRC jurisdiction. Evaluation criteria are usually the calculated reactivity, k_{eff}, for the model of the problem being evaluated, uncertainty in the calculated value of reactivity, bias introduced by the code used to calculate reactivity, and bias introduced by the model. Code bias is determined by a validation performed in accordance with ANSI/ANS 8.1. The statistical results in this report determine code bias based on comparison of code calculations with experimental results. Model bias is due to uncertainties in the modeled parameters describing the problem, approximations made for the model to conform to the input requirements of the code, and any significant simplifications of the problem introduced into the model by the analyst. The acceptance criterion requires that the evaluation criteria be bounded by the subcritical limit. In the case of code calculations, the subcritical limit is often a criterion based on calculated k_{eff} and estimated bias and uncertainties.

It is recognized that it may also be possible to determine subcritical limits based on adjustment of correlating parameters other than k_{eff}, as allowed by ANSI/ANS-8.1. These parameters could include physical parameters such as mass or radius, for example, or other calculated parameters besides k_{eff}, if they can be shown to provide a subcritical margin. This report does not address other potential correlating parameters, but an analyst could determine them as part of an evaluation and use them to determine subcritical limits in conjunction with the code bias results in this report.

2.2 Determination of Subcritical Limits from the Bias and Uncertainty

Several methods could be used for determination of subcritical limits in terms of calculated k_{eff}. As discussed above, and in Section 5.1 of Y/DD-1220, it may also be possible to determine subcritical limits based on adjustment of correlating parameters other than k_{eff}, but this approach is not addressed here.

2.2.1 Area of Applicability

Whether a particular plant application is similar to a sufficient number of experiments contained in the validation set is an important issue. This is a prerequisite before a subcritical limit may be determined from the validation results. Based on the demonstrated performance of the code for a large number of experiments, we have reasonable assurance that it performs well over a wide range of conditions. However, this does not ensure that the code performs as well over all conditions and several conditions where the code performed very poorly were listed in Section 5.3 of Y/DD-1220. There may be other scenarios where the code would calculate unusually low, or high, due to some kind of anomaly or error in the code or cross section data. There are some types of experiments that are few of a kind. It is possible that there could be one or more of these types of experiments that would exhibit a larger bias than seen in this report, if more experiments of that type were included. The only way to assess whether the validation set contains a sufficient number of experiments that are similar to a plant application is to carefully compare the details of the experiment descriptions with the details of the plant application. The broad categories used for the statistical analysis may not be sufficient for making the determination, and the experiment summary information included in these reports may not provide enough information. The analyst must become familiar with the experiment descriptions provided in the OECD handbook. The minimum number of similar experiments needed cannot necessarily be determined in advance, but the analyst must consider this issue carefully as one of the factors when deciding how much margin to include in determining a subcritical limit. The recommendations in Reference 2 may be useful in this regard. If there are only a few experiments similar to the application, it may be wise to recommend taking the time to select additional applicable experiments for addition to the validation set, or for a separate evaluation.

Appropriateness of the subcritical limit does not depend solely on the validity of the statistical analysis. Rather, the appropriateness of a subcritical limit depends on two quite different factors: (1) the range of conditions under which a generalization for its use is established, and (2) whether or not the modeled scenario is within the range of these conditions. The nuclear criticality safety analyst exercising sound engineering judgment using strong technical arguments must develop these determinations. Extrapolation beyond the range of applicability should not be done.

2.2.2 Simple Methods for Determination of Subcritical Limits

The simplest and most straightforward method is to observe that for a large number of critical (or close to critical) experiments, calculated results were relatively consistent, and none were lower than a particular minimum. A value of k_{eff} could be picked that is at or slightly below all the calculated results. Combined limits could be used for simplicity as long as the minimum values were used. The minimum value is established by a single case. These values do not include any reduction for numerical uncertainty in the calculated mean value for the case (standard deviation of approximately 0.001). The minimum k_{eff} value would be reduced further to provide additional margin as appropriate as determined by the analyst.

Another similar method to establish a subcritical limit would be to choose the lowest (i.e. least positive or most negative) bias result, add it to 1.0, and reduce this value by an additional amount to allow for a margin of safety. The results of this approach (without reduction for margin of safety) are shown in columns 6-8 of Table 1. These values do not include any reduction for numerical uncertainty in the calculated mean value for the minimum case. This is the method chosen for this report.

2.2.3 Addition of Safety Margin and Bias Based on Tolerance Bounds

In the commonly used relationship of procedure Y70-68-005[3], the subcritical limit appears in Equation 2.1 as the term on the right while the evaluation criteria of a given problem are expressed in the term on the left. It is recognized that, depending on how the terms are defined, this approach may mix confidence intervals ($k_{eff} + 2\sigma$) and tolerance limits (1.0 - bias - margin) in a semi-statistical formula or method. Acceptability is established when the term on the left is less than or equal to the term on the right:

$$\{ k_{eff} + 2\sigma + \text{code bias} + \text{model bias} \} <= \{ 1.0 - \text{margin of safety} \} \qquad \text{(Eq 2.1)}$$

Code bias is determined by a validation performed in accordance with ANSI/ANS 8.1. The statistical results in this report present bias based on comparison of code calculations with experimental results. Some regulators require that when the mean value of calculated k_{eff} for the validation cases is greater than or equal one, then the code bias is set = 0.

Model bias is due to uncertainties in the modeled parameters describing the problem, approximations made for the model to conform to the input requirements of the code, and any significant simplifications of the problem introduced into the model by the analyst.

Margin of safety is set by nuclear criticality safety analysts in accordance with DOE Orders, Standards, and NRC Regulations for activities under these specific jurisdictions. A typical range is from 0.02 to 0.05. When the analyst feels there is very little uncertainty in the application, it may be possible to justify using lower margin of safety. Also, it may be appropriate to provide margin by adjustment of correlating parameters other than k_{eff}.

2.2.4 Treatment of Model Bias

For calculational models that are accurate representations, the model bias is considered zero. For calculational models with uncertainties in the modeled parameters describing the problem, model bias is intended to compensate for the uncertainty in the calculated k_{eff} due to the uncertainty in the dominant parameter(s) of the problem. Quantitatively, model bias is determined by evaluating k_{eff} of problem "A" as a function of the parameter "p" over the range of uncertainty in "p" [expressed here as x%], i.e., calculations performed with the parameter "p" set at values between "p(1-x%/100)" and "p(1+x%/100)" to establish the corresponding uncertainty in k_{eff}. Values at and between both extremes must be considered because reactivity may not be uniformly distributed about the parameter "p". The number of values to be evaluated depends on the magnitude of the range in the parameter. The model bias for parameter(s) "p" used in the above equation is the absolute value of the maximum difference:

$$| \; k_{eff} \{\text{"p_max"}\} - k_{eff} \{\text{"p_min"}\} \; |,$$

Where $k_{eff}\{\text{"p_max"}\}$ = maximum k_{eff} over the range of parameter(s) "p"
$k_{eff}\{\text{"p_min"}\}$ = minimum k_{eff} over the range of parameter(s) "p"

The maximum variation in k_{eff} over the ranges of uncertainty of all dominant parameters of the problem would be used as the model bias in Equation 2.1. Allowance for statistical uncertainty in the

calculated results must be considered, depending on the relative magnitude. If the parameter of interest is a discrete or categorical variable rather than a continuous variable as discussed above, then the parameter would similarly be varied over the range of applicable states until the maximum variation was found.

An allowance for model bias could otherwise be included in the margin of safety as shown in Eq. 2.2:

$$\{ k_{eff} + 2\sigma + \text{code bias} \} <= \{ 1.0 - \text{margin of safety*} \} \qquad \text{(Eq 2.2)}$$

This would require justification that the evaluation criteria (left side of Eq. 2.2) is sufficiently less than 1.0 by an amount out weighing the maximum variation of k_{eff} for the dominant parameters affecting reactivity.

For calculational models with a significant degree of approximation and simplification, model bias is intended to account for conservatism built into the model. Generally, the model bias is not explicitly calculated, but is addressed by modeling parameters at their worst case. Establishment of the worst case may require a parametric study as described previously. An allowance for model bias would be included in the margin of safety (term on right side of Eq. 2.2). This would require justification that the evaluation criteria (left side of Eq. 2.2) is sufficiently less than 1.0 by an amount that out weighs the conservatism built into the calculational model.

2.2.5 Statistical Approach

Non-parametric statistics are used in this report. According to Reference 2, Section 2.4.4, attaining typical 95% confidence of 95% of the population being above the smallest data sample requires only 59 experiments. After excluding the three lowest results in Table 5.1 of Y/DD-1220, due to being infinite models with relatively large amounts of chromium, nickel or zirconium, there are 1214 remaining experiments. It could be stated that there is greater than 99.999% confidence that 99% of the population is above the smallest data sample (1-0.99^1214 = 0.9999949). In the 1214 remaining calculations for this report, the smallest adjusted k-effective was 0.96617 (for a U-233 benchmark).

2.2.6 Discussion of Results

Based on the methods discussed previously, the following subcritical limits are recommended:

Table 1. Upper Subcritical Limits (Before subtraction of any additional margin)

Fissile Category	Number of Cases	Upper Subcritical Limit
HEU	460	0.977 (Note 1)
IEU	51	0.994 (Note 2)
LEU	128	0.974
Combined category for HEU, IEU, and LEU	639	0.974
Plutonium or Mixed Pu-U	438	0.972
Uranium 233	140	0.966
All Categories Combined	1217	0.966

Note 1: Experiment Series HEU-COMP-INTER-005, cases 7, 15, and 16 showed that particular caution should be used with large arrays with large amounts of nickel, chromium, zirconium or stainless steel. These results indicated a potential for limits in the 0.858 to 0.958 range.

Note 2: There were only 51 calculations ran for the IEU systems. Since Reference 2 suggested that 59 cases should be included, it is recommended that the analyst use the combined USL for HEU, IEU, and LEU.

This recommendation is subject to the following restrictions:

- Models must be similar to those included in the benchmarks (See especially Table 3.1 of Y/DD-1220 for a concise summary).
- Models must not be similar to those high negative bias cases described in Table 5.1 of Y/DD-1220. Characteristics include large amounts of chromium, nickel or zirconium, and infinite models, or very large models with little leakage, in which absorption in the listed materials is a major influence on the results. Iron and stainless steel are also materials that contributed to poor performance of the code, and care should also be taken with models having large amounts of iron or stainless steel.
- Models must use options, materials and arrangements that have been included in the benchmarks.
- The upper subcritical limit stated above includes only code bias. No additional margin is included for model bias (simplifications or uncertainties in analyzed conditions) or additional margin of safety. **A larger or smaller additional margin may be applicable depending on the plant process analysis, and the analyst must justify the amount of the applied margin in the process analysis.**

With 1214 experiments (of 1217 total) included in the determination of the subcritical limit, there is a good basis for having very high confidence that systems and conditions (similar to those included in this report) calculated by this method to be subcritical, will actually be subcritical. Allowance for additional margin for model bias, safety margin or area of applicability margin, if needed, would be subtracted from this upper subcritical limit. Additional margins of 0.02 to 0.05 have typically been used; however, the appropriate value depends on the details of the analysis, and administrative policy, if any. In determining this upper subcritical

limit, the systems were not divided into categories based on materials and forms. Rather, a conservative value based on all the results for each fissile species has been determined. The USL limits are also identified for each category of the ^{235}U isotope, as well as, a combined limit for all categories.

The 238-group library is the only one included in this report. There may be some applications where the 44-group library may perform better (Low Enriched LWR and MOX lattices, and ^{233}U), but this has not been evaluated in this report.

Although four or more decimal places are shown in results tables, the actual accuracy of the code, for a particular calculation, may be on the order of +/- 0.02 to 0.03 (or more) based on the spread in the bias results. Also, the standard deviation of the mean for a particular calculation was on the order of 0.001 for benchmark cases, and may be somewhat higher for applications. Therefore, less than four decimal places are physically meaningful or significant for developing limits. Too much importance should not be placed on small differences in the third or fourth decimal place. The main value to reporting four (or five) decimal places for a calculation result is to confirm that the result reported actually originated from a given output file.

Non-parametric statistics was used exclusively in this report.

3.0 Conclusions

Taken together, Y/DD-1220 and Y/DD-1221 provide the **framework** for the validation of CSAS25 control module from the Standardized Computer Analyses for Licensing Evaluation (SCALE) Version 5.0 package with the 238-group ENDF/B-V SCALE 5.0 cross-section library.

Y/DD-1220 addresses the establishment of bias, bias trends and uncertainty associated with the use of SCALE 5.0 for performance of criticality calculations. This evaluation is directed at systems consisting of fissile and fissionable material in metallic, solution and other physical forms, as described in the OECD Handbook. The focus is on comparison of calculated neutron multiplication factors (k_{eff}) with the associated experimental results, and on establishment of bias, bias trends, and uncertainty as a final step. Compiled data for 1217 critical experiments is used as the basis for the calculation models. The calculated results from SCALE 5.0 using the 238-group ENDF/B-V SCALE 5.0 cross-section library have been compared with reported results for the benchmark experiments. Comparison of results demonstrates that SCALE 5.0 run on the Safety Analysis Engineering (SAE) Hewlett Packard Series zx6000 Itanium (HP 6000) unclassified workstation (referred to as CMODD) produces the same results within the statistical uncertainty of the Monte Carlo calculations as reported by the experiments.

Y/DD-1220 provides assurance that the code predicts critical systems reasonably well, however, in general, there is wide variation in performance depending on the type of system, based on bias results. Using a rating scale similar to Reference 4, the performance ranges from "very good" or less than about +/- 0.01 to "very poor" or about +0.087/-0.14, depending on the category of experiments. In general, the previously observed problems resulted in very high bias, which would be conservative for plant applications. This report includes several benchmark cases that significantly under-predict the expected results. There is no guarantee against the possibility of an unusual scenario that could produce non-conservative results, and analysts must be always vigilant for this possibility.

Y/DD-1221 recommends a preferred method for determining the upper subcritical limit and establishes subcritical limits determined through an evaluation of statistics parameters of calculation results for critical experiments. However, the correlating parameters (i.e., mass, enrichment, geometry, absorption, moderation, reflection, etc.) and values for applying additional margin to the subcritical limits are application dependent. The determination of correlating parameters and additional margin is an integral part of the process analysis. For the critical experiment results, no correlation between calculation results and neutron energy causing fission (or any other parameter) was found. As such, this document does not specify final upper subcritical limit values as has been done in the past.

The Area of Applicability (AoA) is also application dependent. In using the "raw" upper safety limit data of this report, the criticality analyst must exercise sound engineering judgment and use strong technical arguments to develop "a margin in k_{eff}, or other correlating parameter. The margin must be sufficiently large to ensure that conditions (calculated by this method to be subcritical by this margin) will actually be subcritical."[1]

Documentation of determination and justification of the appropriate margin in the analyst's evaluation, in conjunction with this report, will constitute the complete Validation Report in accordance with ANSI/ANS-8.1-1998, Section 4.3.6(4).

4.0 Recommendations for Future Work

As stated in Y/DD-1220, numerous additional OECD experiment descriptions are already available for experiments that would be directly applicable to Y-12 applications. In this regard, future efforts should be dedicated to the following: (1) developing more input decks in-house for experiments selected based on applicability to Y-12, and (2) including additional models as they become available in future revisions of the OECD report. In addition, changes in experiment categorization and interpretation/clarification sometimes are reported in the annual revisions of the OECD handbook. These changes should be reviewed to determine whether they impact the conclusions in this report. This work will require a dedicated effort.

Additional work may be needed to identify trends and/or biases by including additional parameters in the statistical evaluation of critical experiment results.

Additional work is needed on Area of Applicability (AoA) determination methods. Determining whether a particular application is within the AoA of a validation is currently almost exclusively based on subjective judgment. To be done correctly, it requires the analyst to have close familiarity with the details of the experiments in the validation. Efforts to develop input models for more experiments, particularly if done by several staff members, would have the additional benefit of increasing staff's familiarity with experiment descriptions, which would also help improve these AoA determinations. Doing such model input preparation work as part of the qualification program is suggested. In addition, methods have been proposed for more rigorous, and quantitative, AoA determinations. A dedicated effort is needed to evaluate these methods to determine if they are effective and practical to implement.

As discussed in Y/DD-1220, based on the bias results, areas of relatively poor performance are seen, probably due to cross section data issues. Efforts to produce improved cross section libraries for SCALE should be supported.

5.0 REFERENCES

1 *Nuclear Criticality Safety in Operations with Fissionable Material Outside Reactors*, ANSI/ANS-8.1-1998, American National Standards Institute, New York, 1998.

2 *Guide for Validation of Nuclear Criticality Safety Calculational Methodology*, NUREG/CR-6698, SAIC or U.S. NRC, January 2001.

3 *Quality Assurance for Nuclear Analysis Computer Calculations*, Y70-68-005, M. Williamson, May 21, 2003.

4 *Experience With the SCALE Criticality Safety Cross-Section Libraries*, NUREG/CR-6686/ORNL/TM-1999/322, October 2000.

SECTION 6 REFERENCES

10 CFR 71, *Packaging and Transportation of Radioactive Material*, Jan. 1, 2007.

ANSI B74-12, *Specifications for the Size of Abrasive Grain—Grinding Wheels, Polishing and General Industrial Use*s, American National Standards Institute, Washington, D.C., Jan.1, 2001.

ASME Boiler and Pressure Vessel Code, An American National Standard, Sect. III—Rules for Construction of Nuclear Power Plant Components, Subsection NG, American Society of Mechanical Engineers, New York, 2001 ed. with 2002 and 2003 addenda.

ASTM C 750-03, *Standard Specification for Nuclear-Grade Boron Carbide Powder*, ASTM International, West Conshohocken, Pa., July 10, 2003.

CCG-365, A. W. Krass, *Survey of Experimental Data Concerning the Critical Mass of Highly Enriched Uranium-Water Systems*, Lockheed Martin Energy Systems, Inc., Oak Ridge Y-12 Plant, July 13, 2000.

DAC-FS-900000-A014, H. J. Keener, *Comparison of Two Types of Packing Material Used in the Criticality Safety Evaluation of the ES-3100 Package*, BWXT Y-12, Y-12 National Security Complex, Nov. 15, 2004.

DAC-PKG-801624-A001, rev. A, G. A. Byington, *Mixing Weights and Elemental Composition of 277-4 Neutron Poison Used in the ES-3100*, BWXT Y-12, Y-12 National Security Complex, Jan. 25, 2006.

Docket 71-9315, *Meeting to Discuss the Design of the Model No. ES-3100, a Transport Package for High Enriched Uranium*, Category 1 meeting, Headquarters, U.S. NRC, Aug. 2, 2004.

Harbonnier, G., and J. C. Ottone, "TRIGA International: A New TRIGA Fuel Fabrication Facility at CERCA," proceedings of the 1997 annual meeting of the National Organization of Test, Research, and Training Reactors, at Oregon State University, Newport, Oreg., Oct. 21–24, 1997.

JS-YMN3-801580-A005, Rev E, G.A. Byington, *Casting Catalog No. 277-4 Neutron Absorber for the ES-3100 Shipping Package*, BWXT Y-12, Y-12 National Security Complex, Jun. 1, 2006.

NEA/NSC/DOC(95)03, *International Handbook of Evaluated Critical Safety Benchmark Experiments*, Nuclear Energy Agency, Organization for Economic Co-operation and Development, Paris, September 1999.

NRC Regulatory Guide 7.9, rev. 2, *Standard Format and Content of Part 71 Applications for Approval of Packages for Radioactive Material*, U.S. NRC, March 2005.

Nuclides and Isotopes, 14th ed., Knolls Atomic Power Lab., 1989.

NUREG-1609, *Standard Review Plan for Transportation Packages for Radioactive Material*, U.S. NRC, May 1999.

NUREG/CR-0200, rev. 6 (also ORNL/NUREG/CSD-2/R6), *SCALE: A Modular Code System for Performing Standardized Computer Analyses for Licensing Evaluation*, Lockheed Martin Energy Research, Inc., Oak Ridge Natl. Lab., March 2000.

NUREG/CR-0200, rev. 7 (also ORNL/NUREG/CSD-2/R7), *SCALE: A Modular Code System for Performing Standardized Computer Analyses for Licensing Evaluation*, UT-Battelle, Oak Ridge Natl. Lab., May 2004.

NUREG/CR-5661, H. R. Dyer and C. V. Parks, *Recommendations for Preparing the Criticality Safety Evaluation of Transportation Packages*, U.S. NRC, April 1997.

O'Dell, R. D., and J. A. Schlesser, "Unit Cell Simulation for Cylinders in an Infinite Triangular Pitch Array," ANS Trans 64, 343 (June 1991).

ORNL/NTRC-003/V1–3, rev. 0, *Test Report of the ES-3100 Package*, UT-Battelle, Oak Ridge Natl. Lab., Sept. 10, 2004.

Rothe, R. E. et al., "Benchmark Critical Experiments on High-Enriched Uranyl Nitrate Solution Systems," Nuclear Technology 41, December 1978, 207–25.

Rowland, K., Procedure for Casting Kaolite 1600, Forms A, C, D, and E, April 2001.

TID-7028, H. C. Paxton et al., *Critical Dimensions of Systems Containing 235U, 239Pu, and 233U*, Los Alamos Scientific Lab. and Oak Ridge Natl. Lab., June 1964, p. 25, Fig. 19.

TS-G-1.1 (ST-2), *Advisory Material for the IAEA Regulations for the Safe Transport of Radioactive Material*, IAEA Safety Standards Series No. TS-G-1.1 (ST-2), International Atomic Energy Agency, Vienna, 2002.

TS-R-1, *Regulations for the Safe Transport of Radioactive Material*, IAEA Safety Standards Series No. TS-R-1, International Atomic Energy Agency, Vienna, 2005.

Y/DW-1890, G. A. Byington and B. F. Smith, *Water Content and Temperature Dependent Impact Properties of an Inorganic Cast Refractory Material*, BWXT Y-12, Y-12 National Security Complex, Feb. 14, 2003.

Y/LB-15,920/Rev. 1, *Criteria for Acceptance and Technical Assessment for Acceptance of Enriched Uranium at the Plant*, Lockheed Martin Energy Systems, Inc., Oak Ridge Y-12 Plant, March 1997.

7. PACKAGE OPERATIONS

The ES-3100 shipping package shall be operated in accordance with applicable Nuclear Regulatory Commission (NRC), U.S. Department of Transportation (DOT), and other federal, state, and local regulations to protect the health and safety of the public, workers, and the environment. Furthermore, the ES-3100 shall be operated according to a site-approved quality assurance plan.

Specific criteria for operating the ES-3100 package with highly enriched uranium (HEU) contents are presented in this section. The packaging user shall develop detailed site-specific operating procedures based on these criteria and on the NRC-issued Certificate of Compliance (CoC). These procedures shall be in accordance with 10 CFR 71, Subparts A, G, and H. The package operations should be consistent with maintaining occupational radiation exposures as low as reasonably achievable (ALARA) as required by 10 CFR 20.1101.

7.1 PACKAGE LOADING

The user of the packaging shall:

1. have authorization to acquire, package, transport, or transfer radioactive, fissile, or special nuclear material;

2. have the latest NRC CoC and referenced SAR sections for the ES-3100 package with HEU contents;

3. comply with all actions and restrictions specified in the CoC;

4. be registered as a user of the packaging with the NRC; and

5. have a site-approved quality assurance program that meets the requirements of 10 CFR 71, Subpart H.

7.1.1 Preparation for Loading

The ES-3100 Containment Vessel (CV) may be loaded while inside or outside the drum. This decision is site dependent. Detailed, written operating procedures shall include, at a minimum, the process steps listed below before the contents are placed in the ES-3100 package. These steps, initiated by the operating personnel and their supervisor, ensure that:

1. All appropriate documents have been reviewed by operating personnel and are available for further review, if necessary.

2. The radioactive material contents are authorized by the CoC, and the use of the package complies with all conditions in the CoC.

3. The packaging has been properly maintained and is in unimpaired condition. (All required refurbishment and periodic maintenance shall have been performed and documented within the scheduled requirements of the CoC, the SAR, and the maintenance program.)

4. A valid leak-test sticker must be present on the containment vessel to ensure that the required acceptance leak test or the annual leak test has been performed.

5. Packaging interior, nonfixed surface contamination levels are not high enough to significantly contaminate the contents. Nonfixed surface contamination limit requirements are given in 10 CFR 20.1906, 10 CFR 71.87(i), and 49 CFR 173.443 for alpha, beta, and gamma-emitting radionuclides.

6. All closure fasteners are those furnished with the packaging or are certified replacements and are acceptable for use.

7. All required parts of the packaging and all necessary equipment are available and ready for use.

8. The silicone rubber pads, if required, have been inspected prior to use.

The user may replace certain parts during loading. Parts that may be replaced by the user are identified in Table 7.1. The certification of all replacement parts must be traceable. The user must document the replacement.

Table 7.1. Replacement parts for the ES-3100 packaging

Part	Description	Material	Specification/ Drawing[a]
Containment vessel inner O-ring	5.359-in. inner diam (ID) by 0.139-in. diam stock	Ethylene propylene	ASTM D-2000 M2E801580A013
Containment vessel outer O-ring	5.859-in. ID by 0.139-in. diam stock	Ethylene propylene	ASTM D-2000 M2E801580A013
Drum lid washer	0.844-in. ID by 1.375-in. outer diam (OD) × 0.25-in.-thick	Stainless steel	ASTM A240 or ASTM A276 M2E801580A005
Drum lid hex nut	⅝-in.-11 unified coarse thread (UNC)	Silicon bronze	ASTM F467 per ANSI B18.2.2 M2E801580A005
Plug	(Plastic plug around circumference of drum assembly and top of top plug)	Nylon 6/6	62MP0312 Micro Plastic, Inc. M2E801580A002 M2E801580A008
Modified VCO Threaded Plug	Leak-test port plug	Brass	P/N 04-2126 M2E801580A011
Silicone rubber pads		Silicone rubber 22 ± 5 Shore A	M2E801580-A009-1 M2E801580-A009-2 M2E801580-A009-3
Aluminum tape	Duct tape, low temperature (−40 to +250°F), 2-in. wide, McMaster Carr Part No. 7616A21 or equivalent	Aluminum foil	M2E801580A002

[a] Drawings are available in Appendix 1.4.8.

7.1.2 Loading of Contents

The operating procedures for the ES-3100 package with HEU contents shall be specific regarding handling of all package components. Approved procedures shall clearly state all safety aspects or activities such as personnel protection (radiation, chemical, physical); surface contamination or radiation surveys; nuclear criticality safety; and environment temperature.

The detailed operating procedures for inserting the content into the packaging shall include, at a minimum, the process steps listed below:

1. The appropriate CV is positioned for packing and verify that the vessel was loaded according to these steps.

2. The HEU material has been verified as being within the limits specified in this SAR and the NRC CoC for material mass, material dimension, uranium content, and ^{235}U enrichment as required in Sect. 1.2.3. The content shall be verified using accountability records and weight measurements.

3. All contents and their associated cans, bottles and packing material are weighed and are within the allowable weights specified in Sect. 1.2.3.6.

4. The HEU material and associated packing material (convenience cans, spacers, bagging, pads, etc.) have been inserted as required by Sect. 1.2.3.

5. For proper handling of broken metal contents, pyrophoricity concerns must first be addressed. Operators have two options: 1) treat all broken metal as pyrophoric (in this case skip to procedure in Item #7 below) or, 2) determine whether or not the broken metal is pyrophoric (in this case go to procedure in Item #6 below).

6. For pyrophoric categorization of broken metal, first evaluate the specific surface area of the metal pieces (surface-area-to mass ratio). If that value is less than or equal to 1.00 cm^2/g, then the metal pieces are not pyrophoric (and no further action is needed). If the specific surface area is greater than 1.00 cm^2/g, or if the specific surface area can not be evaluated, perform the remainder of this procedure:

    a. Metal pieces must be physically evaluated to ensure that their smallest dimension is larger than a 3/8 inch mesh size.

        i. Single solid-metal pieces that are clearly larger than the 3/8-inch mesh in every dimension do not require additional size-grading determinations, and are acceptable.

        ii. Items which are unacceptable by definition (Sect. 1.2.3), such as powders, foils, wires, and turnings, will be rejected and do not require additional size-grading determinations.

        iii. Any items that are not obviously larger than 3/8-inch in every dimension must be size-graded using a 3/8-inch mesh sieve. NOTE: With facility management approval, equivalent size-grading methods may be used (e.g., 3/8-inch mesh screens, visual comparison to size standards, etc.)

        iv. Any item that falls through the sieve must be rejected.

        v. Any rejected item must be handled according to the procedure in Item #7 below.

b. Operators need to be alert to items which may not fall through the sieve but still may be pyrophoric:

   i. Long, thin shapes such as wires and turnings may not fall through the sieve when shaken. If the wire or turning could be picked up and poked through the mesh it must be rejected, even if it did not fall through unassisted.

   ii. Wires or turnings may form a tangled ball which will not fall through. The above criterion applies: if the wire or turning could be separated and poked through the mesh it must be rejected.

   iii. Foils, thin chips or shards - any item less than 1/8 inch thick – must be rejected.

   iv. Metal showing visible moisture or signs of having been stored in water must be rejected.

   v. Any rejected metal must be handled according to the procedure in Item #7 below.

7. Rejected items must be separated for proper handling:

   a. Rejected items can be shipped in the ES-3100 if packed in a sealed container under an inert cover gas.

   b. An acceptable cover must be high-purity (≥99%) and dry (≤5 ppm moisture).

7.1.2.1 CV assembly and leak testing

The detailed operating procedures shall describe activities to prepare the packaging for final closure and shipment. They shall include, at a minimum, the process steps listed below when preparing the containment vessels for closure:

1. The containment vessel O-ring grooves and sealing surfaces are visually checked for scratches that may have occurred during insertion. If scratches are found, Sect. 8.2.2 should be reviewed for criteria for evaluating surface scratches, possible repair methods for minor scratches, and rejection criteria for significant scratches.

2. The O-rings and the containment vessel sealing surfaces are free from debris and have not been damaged during loading operations. Isopropyl alcohol and lint-free cotton cloth or swabs should be used to clean the grooves and sealing surfaces. The O-rings may be wiped with lint-free gloves, cloth, or swabs. Note that the O-rings shall be lubricated with a thin coat of Super O-Lube.

3. The containment vessel sealing lid is secured to the containment vessel body by the containment vessel closure nut.

4. The closure nut is tightened to 162.7 ± 6.78 N·m (120 ± 5 ft-lb) of torque as specified in Drawing M2E801580A011 (Appendix 1.4.8). No impact wrench shall be used.

5. The assembled and loaded containment vessel is prepared for leak testing.

6. The annulus between the O-rings shall be leak tested after the CV is loaded in accordance with ANSI N14.5-1997, Sect. 7.6. The user will perform the following steps:

   - ensure that equipment used to perform leak tests has been properly calibrated to ensure the accuracy of test measurements
   - ensure that all leak testing is performed in accordance with a quality assurance program, procedures, and documents the results
   - ensure that the test method used has a sensitivity of at least 1×10^{-4} ref-cm^3/s air
   - use either the gas-pressure drop (ANSI N14.5-1997, Section A.5.1) or the gas-pressure rise (ANSI N14.5-1997, Section A.5.1) tests
   - remove the modified VCO threaded brass plug from the leak-test port opening
   - hook-up the leak test equipment into the leak-test port opening using an appropriate fitting
   - either pressurize or evacuate the annulus between the O-rings to a suitable pressure and measure the change in pressure and temperature within the test volume during a specified time period
   - pressure measurements must be accurate within 1% or less and tests should be carried out in isothermal conditions
   - calculate the total leakage rate, using the known test volume and test results and ensure that the measured leak rate is less than 1×10^{-4} ref-cm^3/s air.
7. The vacuum coupling is removed.

8. The modified VCO threaded brass plug is tightened into the leak-test port opening.

The user must ensure that their procedure meets the requirements of ANSI N14.5-1997.

If the inner O-ring requires replacement, the containment vessel must be retested per Sect. 8.2.2 prior to use. This requirement does not apply to the outer O-ring, as it is not part of the containment boundary.

Following a successful leak test, the containment vessel with its content is ready to be loaded into the drum assembly.

7.1.2.2 Drum closing

A radiation check of the contents may be conducted prior to loading to measure the content dose rate. The measured dose rate should be compared with known values for such a test. After loading is complete, radiation measurements shall be taken to determine the package dose rate, which establishes the transport index (TI).

The detailed operating procedures shall include, at a minimum, the process steps listed below when preparing the drum assembly for closing and sealing. The operating personnel and their supervisor shall ensure that:

1. The CV assembly with content is ready for loading into the drum assembly or lowering into the drum assembly, depending on whether it was loaded outside the drum or inside the drum.

2. The drum assembly (with top plug removed) is ready to receive the containment vessel assembly and that the containment vessel assembly, silicone rubber pads, drum lid, drum-lid nuts and washers, and tamper-indicating devices (TIDs) are available.

3. The aluminum foil tape applied over the neutron-absorbing material cavity fill and vent holes (four places) located on the drum liner lower shelf (Drawing M2E801580A002, Appendix 1.4.8) is visually inspected for damage such as tears, holes, or loose edges.

4. The loaded CV is lifted using the swivel hoist ring and site-approved lifting equipment.

5. The CV is positioned in the drum (Drawing M2E801580A001, Appendix 1.4.8), and the swivel hoist ring is removed.

6. The CV flange pad is placed on top of the containment vessel, and the plug pad is placed on the inner liner shelf.

7. The nylon plug is installed in the top plug vent hole, and site-approved lifting hardware is attached to the top plug threaded lifting holes.

8. The top plug is installed in the drum (Drawing M2E801580A001, Appendix 1.4.8), and the lifting hardware is removed.

9. The drum lid, the drum washers, and bronze drum nuts are installed.

10. The nuts are tightened to 40.67 ± 6.78 N·m (30 ± 5 ft-lb) of torque with no sequence specified. No impact wrench shall be used.

11. A nylon plug is installed in each of the four drum vent holes.

12. The TIDs are attached through both TID lugs.

13. The gross package weight does not exceed 190.5 kg (420 lb).

14. Surveys for nonfixed surface contamination and radiation dose rate measurements are conducted. The nonfixed surface contamination survey shall be conducted in accordance with the user's facility procedures. The survey shall use criteria that are derived from the surface radioactivity guidance of 10 CFR 20.1906, 10 CFR 71.87(i), or the user's site-specific criteria, whichever is the most stringent.

15. Nonfixed surface contamination is removed as applicable.

16. All "empty" or inappropriate labels or tags are removed from the exterior surface of the package.

17. The package is labeled with the appropriate material description, nuclides, activity/mass, and TI in accordance with 49 CFR 172.403.

18. The package is marked with the minimum marking "Radioactive Material, Type B(U) Package, Fissile, UN3328" in accordance with 49 CFR 172.301 and 172.310.

19. The package radiation dose rate at the surface is measured. The package radiation dose rate at 1 m from the surface shall be measured to establish the TI for the package and to ensure that the content

does not exceed the expected or allowable dose rates (see Sect. 5). The analysis presented in the containment evaluation (Sect. 4) has determined that this is a Type B, fissile material package.

7.1.3 Preparation for Transport

7.1.3.1 Package handling

Criticality Safety Index (CSI) values for the ES-3100 package with various payloads can be found in Table 1.3.

The ES-3100 is handled using industry-standard drum-handling equipment. Operating procedures shall include requirements to limit clamping pressures on forklift drum-handling equipment to prevent damage to the ES-3100 drum body (see Sect. 1.2.1.1 for limits on forklift gripping forces).

7.1.3.2 Decontamination

The package may be placed onto areas that are covered by disposable covering, such as plastic or paper, to reduce the nonfixed surface contamination of physical structures.

The package must be shipped in an enclosed conveyance. Generally, the exterior surfaces of the package will remain relatively clean. However, each user shall prepare procedures to clean dirty packages. These procedures shall, at a minimum, consider the following:

1. The drum is austenitic stainless steel.

2. The drum nut is silicon bronze.

3. The drum vent holes are covered with nylon plugs (Drawing M2E801580A002, Appendix 1.4.8).

4. The labels and markings on the drum must remain legible.

7.1.3.3 Requirements prior to shipment

The shipper shall ensure that the quality control requirements of 49 CFR 173.475 and the routine determination requirements of 10 CFR 71.87 have been satisfied prior to each shipment. Detailed operating procedures [10 CFR 71.87(f)], shall provide evidence that these requirements are met and ensure that:

1. the package is proper for the content shipped and verified with the appropriate records by the user prior to content loading [10 CFR 71.87(a)];

2. when shipping uranium oxides or UNX crystals, the shipper shall provide the receiver with the date and time the containment vessel was sealed. The shipper must verify that the shipment can be completed within the time period allotted for the type of shipment (5 months or 1 year for UNX crystals as noted in Table 1.3a or 1 year for uranium oxides);

3. the package is in unimpaired physical condition [10 CFR 71.87(b)];

4. the closure devices of the package are properly installed, secured, and free of defects [10 CFR 71.87(c)];

5. the containment vessel has been loaded properly and preparation for shipment has been followed, witnessed, and checked;

6. the internal pressure of the containment system does not exceed the design pressure during transportation [10 CFR 71.85(b)] as demonstrated by analysis (Appendix 2.10.1) and that there are no pressure-relief devices [10 CFR 71.87(e)] in the package;

7. the external radiation levels for all transport conditions are within the allowable limits as measured for Normal Conditions of Transport (NCT) [10 CFR 71.87(j)];

8. the nonfixed external contamination levels are within the allowable limits as demonstrated by surface wipes prior to content insertion, containment vessel loading, and package closure [10 CFR 71.87(I)];

9. the contents are adequately sealed and have adequate space for expansion [10 CFR 71.87(d)];

10. all records for shipment are prepared and maintained; and

11. all lifting attachment features are either inoperative during transport [10 CFR 71.87(h)] or meet the requirements of 10 CFR 71.45(a).

7.1.3.4 Leak testing

Leak tests shall be conducted following the content loading and the containment vessel closure. The annulus between the O-rings shall be leak tested to an acceptable leak rate of 1×10^{-4} ref-cm^3/s air (or equivalent) or lower in accordance with ANSI N14.5-1997, Subclause 7.6.

7.1.3.5 Surveying

The radiation (gamma, neutron) emanating from the contents of the package shall be measured before the package is released for transport [10 CFR 71.47 and 71.87(j)]. The package radiation dose rate at the surface is measured to ensure that the content does not exceed the expected or allowable dose rates. The package radiation dose rate at 1 m from the surface is measured to establish the TI for the package. The package exterior surface contamination level limits are found in 10 CFR 71.87(i) and 49 CFR 173.443. The regulations present both fixed and nonfixed surface contamination level limits for the various radionuclides. In addition to these limits, the user may have more stringent surface contamination levels that shall also be followed.

A final visual survey of the package and loading paperwork shall be conducted to ensure that the package was assembled correctly and that it is ready for final shipment preparation. This survey may include a thorough review of the loading checklists by someone other than those who filled out the list to verify the loading operations. The area immediately surrounding the assembly operations should be surveyed, and all spare or extra parts should be identified. A final package survey may include weighing the package, hand-testing the closure nuts on the drum lid, and flexing the TIDs. The loading checklist should include a place for this final quality check to be properly recorded—including a signature and date—as being successfully completed.

7.1.3.6 Marking

The user shall ensure detailed marking procedures are consistent with 10 CFR 71.85 and the applicable subsections of 49 CFR 172, Subpart D. Each shipper shall ensure that each package containing radioactive material is marked in the manner required.

Two electrochemically etched data plates are affixed to the exterior of the drum body in the locations, and with the methods, indicated on Drawing M2E801580A031 (Appendix 1.4.8).

The packaging components (drum assembly, containment vessel body, lid, and closure nut) are also marked with their serial numbers. The numbers are used to control these parts and to accumulate their respective histories.

7.1.3.7 Labeling

The user shall prepare labeling procedures that are consistent with the applicable subsections of 49 CFR 172, Subpart E. The procedures should include the following steps, to ensure that:

1. the proper label is affixed to the package and the TI is determined at the time of loading;

2. the correct label (White—I, Yellow—II, or Yellow-III) is determined using the table from 49 CFR 172.403(c);

3. the appropriate label is affixed to two places on opposite sides of the drum;

4. the content name, nuclides and activity/mass (49 CFR 173.435), and the TI are entered in the blank spaces on the radioactive label; and

5. the information is entered legibly using a durable, weather-resistant means of marking.

Additionally, two Fissile labels are required per 49 CFR 172.402(d)(2). These labels must be affixed two places on opposite sides of the drum adjacent to the radioactive labels. The CSI must be legibly entered on the Fissile label using a durable, weather-resistant means of marking.

7.1.3.8 Securing to vehicle

The package shall be secured against movement within the vehicle in which it is being transported under conditions normally incident to transportation [49 CFR 177.834 and 177.842(d)]. The loading procedures shall include the following measures, at a minimum, to ensure that:

1. only an approved conveyance is used,

2. all reasonable precautions are taken to prevent motion of the vehicle during loading,

3. no tampering with packages occurs during transit,

4. no vehicle is loaded or unloaded unless a qualified person is in attendance at all times, and

5. no radioactive material package is loaded onto a vehicle also carrying Div. 1.1 or 1.2 explosives (49 CFR 177.848).

7.2 PACKAGE UNLOADING

7.2.1 Receipt of Package from Carrier

Prior to shipment, the user shall verify that the receiver has agreed to accept the special nuclear material. The user (shipper) shall ensure that appropriate documentation is submitted to the receiver to ensure that the physical characteristics and hazards of the material are conveyed to the receiver.

The user shipping the package shall provide any special instructions to the receiver to safely open the package (10 CFR 71.89), including special tools and precautions for handling or unloading. These instructions shall include special actions in the event that TIDs are not intact, or if surface contamination or radiation surveys are too high.

If HEU oxide or uranyl nitrate crystals are being shipped, the receiver shall check the seal time and date before opening the container (shipment time restrictions for these contents are discussed in Sect. 1.2.3.8). The receiver shall open the CV prior to the seal time expiring or take special precautions when handling and opening the container. Special precautions are associated with the potential buildup of hydrogen in the CV to greater than 5 mol %. Typical precautions may include, but are not limited to, elimination of ignition sources, gradually opening the CV in a well-ventilated area, or opening the CV in an inert glove box.

The receiver shall accept the radioactive material by surveying the conveyance and package surface for contamination and external radiation levels. The receiver's procedures shall clearly indicate that the contamination and radiation surveys and inspections be conducted upon receipt of the package. The receiver shall, at a minimum, include the following in their procedures (in compliance with 10 CFR 71.111):

1. receive the package when offered by the carrier for delivery and,

2. monitor external surfaces of the conveyance and package for radioactive contamination and radiation levels.

All users shall include provisions for reporting safety concerns associated with the packaging or its use. The user shall notify NRC in accordance with 10 CFR 20.2202. Incidents requiring notification include:

1. removable radioactive surface contamination in excess of the limits provided by 10 CFR 71.87, and

2. external radiation levels in excess of the limits provided by 10 CFR 71.47.

The receiver shall compare the cargo with the list provided by the shipper. If a discrepancy appears between the cargo and the list, the receiver shall investigate and report to the NRC as required.

The package shall be removed from the conveyance prior to unloading the content. Unloading procedures shall, at a minimum, ensure that:

1. the package nonfixed surface contamination is below the minimum on-site or off-site requirements,

2. all appropriate package labels are affixed to the package exterior surface,

3. all lifting and handling equipment is certified for use,

4. all transfer equipment is certified for use,

5. the package is visually examined to ascertain surface damage that may have occurred during shipping or handling, and

6. the TIDs are examined to ensure that the package has not been tampered with during shipment.

If the package surface was damaged during handling or shipping, a nonconformance tag shall be completed and attached to the package for subsequent refurbishment (10 CFR 71.131). If the TIDs are found to be compromised, the receiver shall investigate and notify the NRC as required.

7.2.2 Removal of Contents

Detailed operating procedures shall describe activities required for content removal and shall identify any safety and health measures required to protect workers and the environment. The procedures shall include, at a minimum, the process steps listed below:

1. All appropriate labels for the material shipped are affixed to the exterior surface of the drum body.

2. Surveys for nonfixed surface contamination and radiation dose rate measurements are conducted.

3. As applicable, nonfixed surface contamination in excess of limits is addressed as required.

4. The TIDs remain intact until removal.

5. The weld stud nuts and washers are removed and controlled.

6. The drum lid is removed.

7. Visible portions of the interior of the drum body and top plug are still in good condition—no visible signs of damage, water damage, or tears.

8. Site-approved lifting hardware is attached to the top plug threaded lifting holes, and the top plug is removed.

9. The silicone rubber CV flange pad is removed from above the containment vessel.

10. The containment vessel top is in good condition—no visible signs of damage or loose closure nut.

11. A surface contamination check is conducted to discover any leak of radioactive material.

12. The containment vessel is removed from the drum assembly. The containment vessel is placed onto the work area. (This step may not be required if CV is unloaded while in the drum.)

13. The external retaining ring, containment vessel closure nut, and containment vessel sealing lid are removed and controlled. (No pressure buildup is expected under NCT.)

14. The O-rings and the O-ring grooves on the containment vessel flange are protected from damage during unloading.

15. The HEU content (convenience cans or bottles) and associated packing materials (can spacers, stainless-steel scrubbers, silicone can pads, etc.) are removed from the containment vessel in accordance with site-specific material-handling procedures.

16. The items removed and the inside of the containment vessel are checked for nonfixed surface contamination.

7.3 PREPARATION OF EMPTY PACKAGE FOR TRANSPORT

The user shall develop detailed procedures to prepare an empty package for storage or transport. These procedures shall, at a minimum, ensure that:

1. The package has been emptied of all radioactive contents.

2. The radiation level at any point on the external surface of the package does not exceed 0.5 mrem/h.

3. The nonfixed radioactive surface contamination on the external surface of the packaging does not exceed the limits specified in 49 CFR 173.443(a), and the internal contamination level does not exceed 100 times the limits in 49 CFR 173.443(a).

4. The package is not damaged, and there is no visible internal or external surface moisture or corrosion.

5. The package is closed.

6. Any labels previously affixed in accordance with Subpart E of 49 CFR 172 are removed, obliterated, or covered. Leak-test labels should not be removed from the drum body.

7. The “EMPTY” label prescribed in 49 CFR 172.450 is affixed to the drum.

8. An appropriate notice is provided giving the name of the consignor or consignee. An example notice is, “This package conforms to the conditions and limitations specified in 49 CFR 173.428 for radioactive material, excepted package—empty packaging, UN2908.”

7.4 OTHER OPERATIONS

None.

SECTION 7 REFERENCES

10 CFR 20, *Standards for Protection Against Radiation*, Jan. 1, 2007.

10 CFR 71, *Packaging and Transportation of Radioactive Material*, Jan. 1, 2007.

49 CFR, *Transportation*, Oct. 1, 2007.

ANSI N14.5-1997, *Radioactive Materials—Leakage Tests on Packages for Shipment*, American Natl. Standards Institute, Feb. 5, 1998.

THIS PAGE INTENTIONALLY LEFT BLANK.

8. ACCEPTANCE TESTS AND MAINTENANCE PROGRAM

Shipping packages used to transport radioactive materials shall be fabricated, procured, and maintained in accordance with applicable Nuclear Regulatory Commission (NRC), U.S. Department of Transportation (DOT), and other federal, state, and local regulations to protect the health and safety of the public, the workers, and the environment. Furthermore, the packages shall be fabricated, procured, and maintained according to the user site quality assurance (QA) plan.

Minimum requirements for fabricating, procuring, and maintaining the packaging are presented in this section. The owner and user shall develop detailed procedures based on criteria contained herein and on the Certificate of Compliance (CoC). These procedures shall be in accordance with Subparts G and H of 10 CFR 71.

Fabrication specifications for ES-3100 components are listed on fabrication drawings (Appendix 1.4.8) and equipment specifications (Appendices 1.4.2 – 1.4.5). The containment vessel is designed and built to meet American Society of Mechanical Engineers (ASME) *Boiler and Pressure Vessel Code*, Sect. III, Division I, Subsection NB (ASME B&PVC, Sect. III, Div. 1).

8.1 ACCEPTANCE TESTS

The owner shall determine that the packaging has been fabricated in accordance with the approved design [10 CFR 71.85(c)]. The owner may use the inspection guidance provided by the NRC in NUREG/CR-6314 for conducting QA inspections of packaging suppliers. The packaging includes:

1. a reinforced stainless-steel drum, inner liner, lid, weld studs, Kaolite 1600 insulation; Cat 277-4 neutron absorber; drum flat cover plate; nylon vent hole plugs; top plug (consisting of sheet steel and Kaolite 1600); hex nuts; washers; paint; and

2. a containment vessel body, sealing lid, closure nut, and retaining ring; O-rings; modified VCO threaded brass plug.

Requirements are derived from the packaging drawings and specifications and shall be considered as minimum requirements, and their information shall be present in the owner's fabrication records.

The containment vessel procurement specification is presented in Appendix 1.4.3. This specification indicates the records and reports required to properly document the quality of the containment vessel fabricated by a vendor in accordance with the QA requirements.

The minimum acceptance inspection and test requirements for the packaging components (Tables 8.1 and 8.2) are presented in the following sections. Prior to first use of the package, these requirements must be met.

Table 8.1. Acceptance tests for the drum assembly

Packaging [a]	Inspection	Structural and pressure tests	Leak tests
Drum, 30-gal modified, including lid, drum flat cover	Material certification[b], gauging,[c] marking, liquid penetrant, weld inspection (per Sect. 8.1.2), corrosion, dents	Tensile, percent elongation, yield point, chemistry	Pressure test (10 psig for 5 min)
Weld stud, ARC FT 5/8–11UNC × 7/8 LG, 304/304L stainless steel	Part certifications	Tensile, percent elongation, yield point, chemistry	NA[d]
Inner liner weldment and top plug, 304/304L stainless-steel	Material certifications, gauging, weld inspection (per Sect. 8.1.2)	Tensile, percent elongation, yield point, chemistry	NA
304/304L stainless-steel 0.25-in. internal flange	Material certifications, gauging, weld inspection (per Sect. 8.1.2)	Tensile, percent elongation, yield point, chemistry	NA
Nut, ⅝-in.-11UNC silicon bronze	CoC[e], damage	NA	NA
Data plates	Marking	NA	NA
Paint: black enamel	CoC	NA	NA
Cat 277-4	Material certification, sample pour	NA	NA
Kaolite 1600 castable refractory-cured thermal insulation	CoC	NA	NA
Flat washer, 0.812-in. ID × 1.375-in. OD × 0.250-in.-thick stainless steel	CoC, damage	NA	NA
Lid TID lug, modified 304L stainless steel chain 3/16-in trade size, 0.20 diam	CoC, damage	NA	NA
Plug, plastic push-in, Micro Plastic Inc., 62MP0312	CoC	NA	NA
Silicone rubber pads 22 ± 5 Shore A Parts M2E801580A009-1 Parts M2E801580A009-2 Parts M2E801580A009-3	CoC, damage, marking	NA	NA

[a] Appendix 1.4.8
[b] Material Certification - Certified quantitative data (physical, mechanical, chemical, functional, dimensional, and/or visual) demonstrating compliance with the drawing/specification requirements.
[c] Gauging refers to dimensional inspections according to "Diamond I" callouts on the drawings.
[d] NA—Not applicable.
[e] CoC, Certification of Compliance - A document signed or otherwise authenticated by an authorized individual certifying the degree to which items or services meet specified requirements.

Table 8.2. Acceptance tests for the containment vessel assembly

Packaging [a]	Inspections	Structural and pressure tests	Leak tests
Body assembly, lid assembly (as applicable)	Material certification [b], gauging, [c] marking, liquid penetrant, weld inspection (per Sect. 8.1.2), qualification tests, corrosion, scratches	Hydrotest	Helium leak test
O-ring (inner), 5.359-in. ID, 0.139-in. diameter stock	Material certification, gauging, packaging, marking	Shore A durometer, elongation	NA [d]
O-ring (outer), 5.859-in. ID, 0.139-in. diameter stock	Material certification, gauging, packaging, marking	Shore A durometer, elongation	NA
Closure nut Nitronic 60 SST, ASME SA-479	Material certifications, gauging,	Tensile, percent elongation, yield, chemistry	NA
External retaining ring	CoC [e], damage	NA	NA
Modified VCO threaded brass plug for leak-test port	CoC, damage	NA	NA
Heavy can spacer assembly [f]	Material certification, sample pour	NA	NA

[a] Appendix 1.4.8.
[b] Material Certification - Certified quantitative data (physical, mechanical, chemical, functional, dimensional, and/or visual) demonstrating compliance with the drawing/specification requirements.
[c] Gauging refers to dimensional inspections for according to "Diamond I" callouts on the drawings.
[d] NA—Not applicable.
[e] CoC, Certification of Compliance - A document signed or otherwise authenticated by an authorized individual certifying the degree to which items or services meet specified requirements.
[f] Not part of containment vessel.

8.1.1 Visual Inspections and Measurements

Visual inspections with the unaided eye of all pertinent features on the package shall be performed during fabrication. These inspections include paint color; surface condition; marking content; gauging (toleranced dimensions, positioning, edge breaks, surface finish); and welding. The required inspections are described in Tables 8.1 and 8.2.

8.1.1.1 Paint color

Paint color, which is not a safety item, is used to identify, segregate, and document packages and packaging. The acceptance criteria for paint color are given in the respective federal specifications referenced by the drawings (Appendix 1.4.8). Incorrect or incomplete application of paint is cause for rejection. An application of incorrect letters or misspelled words is also cause for rejection. The item may be reworked to meet the specification.

8.1.1.2 Surface condition

The surfaces of the drum assembly and containment vessel shall be visually inspected for penetrations, dents, and corrosion. Dents >1-in. deep in the drum body will be cause for the drum body to be reworked to remove the dent. The containment vessel surfaces must be in accordance with the dimensional requirements on the drawings. Penetrations will be cause for the component to be reworked, including dye-penetrant and radiographic testing.

The ES-3100 components shall be stored in weather-protected indoor facilities. However, before acceptance of any ES-3100 component, all surfaces shall be inspected for corrosion. The presence of surface corrosion (rust) on any component will be cause for further inspection. If the rust can be easily wiped off and no pitting is apparent beneath it, the component is acceptable. If the rust cannot be easily wiped off, or if scaling is present or pitting is observed, then the surface will be repaired and the component must undergo a dimensional inspection and dye-penetrant and/or radiographic testing to determine the extent of the damage. In the case of the containment vessel, a hydrostatic test shall be performed. All acceptance criteria for a newly fabricated component (Appendices 1.4.2, 1.4.3, and 1.4.8) shall apply to the repaired component. If the rust has compromised the structural integrity of the component [i.e., the component no longer meets dimensional criteria for a new part as specified on the drawings], then the component shall be rejected.

8.1.1.3 Marking package components

Markings on the package components identify the hazardous content and provide traceability to the fabrication and past use of the package. All markings (serial numbers, model numbers, instructions, identification) shall be compared with the drawings' requirements for correct content. The acceptance criteria (paint color and dimensions) for markings are given in the drawings in Appendix 1.4.8. Incorrect or incomplete marking is cause for rejection. The item may be reworked to meet the specification.

8.1.1.4 Gauging

The ES-3100 drawings list the dimensions/tolerances (height, width, thickness, diameter); positions (bolt holes, grooves, leak-test port); edge break; and surface finishes (smoothness, passivation, coating, bonding, plating, cleanliness). More important dimensions on the drawings are marked with a "Diamond I" symbol. Inspection of gauging features shall be performed on these "Diamond I" dimensions only to ensure that each component meets dimensional tolerances, which are provided on the drawings. Gauging outside the tolerance is cause for rejection. The item may be reworked to meet the specification, or the specification may be deviated from and accepted.

8.1.2 Weld Examinations

All welded or weld-repair surfaces shall be visually examined by a qualified weld examiner for indications of inclusions, cracks, or porosity using a written weld examination procedure. Weld examiners are qualified to perform visual weld inspections in accordance with SNT-TC-1A (2001 Edition), "Personnel Qualification and Certification in Nondestructive Testing;" or ANSI/ASNT CP-189 (2001 Edition), "ASNT Standard for Qualification and Certification of Nondestructive Testing Personnel;" published by the American Society for Nondestructive Testing. ASME Boiler and Pressure Vessel Code, Section IX is to be employed as the applicable requirement. Section VIII of the ASME B&PVC Code is invoked for acceptance criteria for Code-specified examinations which are to be performed in accordance with the provisions of ASME B&PVC Section V. Any indication of inclusions, cracks, or porosity in the welds is cause for rejection. The item may be reworked to meet the specifications.

8.1.3 Structural and Pressure Tests

Structural tests for the drum and containment vessel include mechanical properties, and chemical tests to ensure that the correct materials are used. The containment vessel is hydrotested (pressure tested) to ensure that the vendor fabrication meets the requirements. These tests are discussed below. The drum body is mechanically tested (handling test) and pressure tested in accordance with the QA provisions in Military Specification, *Drum, Metal—Shipping and Storage*, MIL-D-6054F.

8.1.3.1 Mechanical property tests

Material mechanical property tests shall be performed to determine the ultimate tensile strength, yield strength, percent elongation, percent reduction in area, and hardness of the containment vessel materials. Their acceptance criteria at operating temperature are provided in the appropriate material national standard referenced by the drawings (Appendix 1.4.8). An out-of-specification property is cause for rejection.

8.1.3.2 Chemical tests

Tests shall be performed to determine the chemical properties of the packaging materials. The acceptance criteria and their sensitivity are provided in the appropriate material national standard referenced by the drawings (Appendix 1.4.8). An out-of-specification chemical property is cause for rejection. Material that cannot be traced to the mill or heat-treatment lot shall be rejected.

8.1.3.3 Pressure tests

The containment vessel shall be pressure tested per *ASME Boiler and Pressure Vessel Code,* Sect. III, Div. 1. The vessel shall be subjected to an internal water pressure of 150% of design pressure (Sect. 2.1.2). Visible indication of a leak on the exterior surface of the containment vessel is cause for rejection. All containment vessels will undergo such testing. All surfaces must be thoroughly dried after the hydrostatic test as the CV envelope will undergo final helium leak testing subsequent to the hydrostatic test.

8.1.4 Leakage Tests

For acceptance, all containment vessels will be leak tested when they are initially fabricated, and that test will be witnessed by QA personnel. The fabrication vacuum leak test of the containment boundary shall be performed after the pressure test in accordance with ANSI N14.5-1997, Sect. 7.3, "Fabrication Leakage Rate Test" with a test flange assembly installed. (Note: Periodic and maintenance leak tests are discussed in Sect. 8.2.2.) The fabrication vacuum leak test demonstrates that the containment vessel is fabricated properly and that the containment boundary is "leaktight." An integrated leak rate exceeding 1.9×10^{-7} atm-cm^3/s of helium (or equivalent) is cause for rejection. Per ANSI N14.5-1997, the test procedure should have a sensitivity of one-half the reference air leakage rate (L_R).

The tester must ensure that their procedure meets the requirements of ANSI N14.5-1997. All containment vessel leakage rate tests will be performed using certified equipment.

Following successful completion of the leak-test, the tester will include information such as the name of the operator, expiration date, etc., on leak test labels which will be attached to the containment vessel and drums. Section 8.2.2 addresses the acceptance vacuum leak test during refurbishment. All containment vessels shall undergo such testing.

8.1.5 Component and Material Tests

8.1.5.1 O-ring tests

The O-ring visual and mechanical tests are described below. Additionally, the fabrication leak test required in Sect. 8.1.4, the periodic and maintenance leak tests required in Sect. 8.2.2, and the preshipment leak test required in Sect. 7.1.2.1 test the functionality of the O-rings within the package.

Visual inspection

A visual inspection of the O-ring surface shall be performed. The surface shall be smooth, nonporous, and free of skin defects. O-rings that do not meet these requirements shall be rejected.

Each O-ring shall be packaged separately to provide traceability. Each O-ring package shall be marked with the O-ring identification number, lot number, cure date, and compound number. The material identification numbers shall be assigned uniquely to each lot and to each size of O-ring. The identifications shall be adequate to trace the O-rings to their raw material master batch. Improper packaging or marking is cause for rejection.

Mechanical properties

The O-ring material mechanical properties of hardness and elongation shall be determined for each lot. Their acceptance criteria and sensitivity are:

1. hardness of Shore A 70 ± 5 durometer, and

2. elongation of 100%, minimum.

All O-rings in a lot that fail to meet these criteria shall be rejected. If O-rings from a rejected lot have already been used, the licensee shall locate all such O-rings and either examine or discard them. O-rings from a rejected lot that are in a containment vessel that is still loaded shall be removed at the earliest possible time.

8.1.6 Shielding Tests

No gamma or neutron radiation shields are integral to the packaging.

The Cat 277-4 neutron absorber material (fabrication specification JS-YMN3-801580-A005, Appendix 1.4.5) is specifically designed for criticality safety. Acceptance testing for the Cat 277-4 liner will be described in the fabrication specification.

8.1.7 Thermal Tests

A thermal acceptance test is not required for this package. The maximum decay heat generated by the radioactive material is 0.4 W (Sect. 1.2.3.7 and 3.1.2), which is negligible. Fabrication of the Kaolite 1600 thermal insulation in accordance with the fabrication specification (Appendix 1.4.4) fulfills the obligation for a thermal acceptance test.

8.1.8 Miscellaneous Tests

Material certification and visual inspection for damage are required for the following packaging components: plastic pieces, washers, tamper-indicating devices (TIDs), and paint. All materials shall be in compliance with the respective material properties and tested when applicable, as stated in their respective specifications. A nonconforming or damaged part is cause for rejection.

To prevent the use of noncertified fasteners, acceptance inspection and tests have been added to ensure their quality. The fastener structural tests include mechanical property tests and chemical tests to ensure that the correct materials were used.

8.2 MAINTENANCE PROGRAM

When the package is being loaded or unloaded, it shall be examined to ensure that all parts are present and functional. A record shall be generated of this examination activity with the affected part numbers, personnel doing the work, and the date of the activity being recorded. This examination activity and the activities associated with the periodic and maintenance leak tests are considered refurbishment activities. Periodic maintenance of the ES-3100 shall be performed on an annual basis, and shall include visual inspections and leak tests. No ES-3100 shall be used unless maintenance documentation reflects the package is current on periodic maintenance. The periodic and maintenance refurbishment requirements are given below.

8.2.1 Structural and Pressure Tests

Structural and/or pressure tests, as identified in Sect. 8.1.3, shall be performed as appropriate for the respective part or component after welding or other structural repairs are made. Welding and structural repairs of the containment vessel involve rework operations and are considered beyond the scope of refurbishment activities.

8.2.2 Leakage Tests

The fabrication leak test must be performed before the first use and periodic leak tests are performed annually thereafter while the package is in use.

Maintenance and periodic leak tests, as defined by ANSI N14.5-1997, Sects. 7.4 (“Maintenance Leakage Rate Test”) and 7.5 (“Periodic Leakage Rate Test”), shall be performed during refurbishment when necessary. The fabrication leakage rate test (Sect. 8.1.4) is performed prior to the package’s first use; the package must be retested following repair or replacement of a containment system component (maintenance leakage-rate test) or annually while the package is in use (periodic leakage-rate test). Packages that are not in use and have not had a periodic leakage-rate test within the last 12 months must be tested prior to use.

Users may utilize either of the following leakage tests which are conducted in accordance with ANSI N14.5-1997 as long as they have suitable sensitivity:

- A.5.3 - Gas-Filled Envelope
- A.5.4 - Evacuated Envelope (gas detector)

The following steps are required:

- ensure that equipment used to perform leak tests has been properly calibrated to ensure the accuracy of test measurements
- ensure that all leak testing is performed in accordance with a quality assurance program, procedures, and documents the results
- ensure that the test method used has a sensitivity of at least 1 x 10^{-8} ref-cm^3/s
- use either the gas-filled envelope (ANSI N14.5-1997, Section A.5.3) or the evacuated envelope - gas detector (ANSI N14.5-1997, Section A.5.4) tests
- remove the modified VCO threaded brass plug from the leak-test port opening
- thoroughly dry the test item before assembly
- use the leak testing flange specified in the drawings (Appendix 1.4.8). NOTE: only the inner O-ring is used for these tests
- connect the leak test equipment to the flange fitting
- either evacuate the containment vessel connected to a gas detector and surround the item with an envelope filled with helium; or, fill the containment vessel with helium while the item is placed in a vacuum chamber connected to a gas detector
- measure the actual leak based on comparison with a calibrated standard leak and verify that it is less than 1 x 10^{-7} ref-cm^3/s.

Maintenance and periodic leak tests shall be performed using the same procedure and with the same acceptance criteria as the fabrication leakage rate test described in Sect. 8.1.4. The maintenance and periodic leak tests test the entire containment boundary with an integrated leak rate exceeding 1.9×10^{-7} atm-cm^3/s of helium (or equivalent) as cause for rejection. With successful completion of the test, the entire containment boundary is considered "leaktight." The user must ensure that his or her procedure meets the requirements of ANSI N14.5-1997. Note that these maintenance and periodic leak tests are required any time the inner O-ring is replaced.

If a package does not pass the preshipment leakage-rate test described in Sect. 7.1.2.1 of this Safety Analysis Report, the O-ring sealing surfaces shall be examined. Nicks and scratches of the O-ring groove in the containment vessel flange or sealing surfaces of the containment vessel sealing lid may be smoothed with a stone or with fine sandpaper to return them to specification. Deep scratches are cause for rejection. The O-rings shall be visually examined with the unaided eye for roughness, porosity, or surface defects and will be replaced as necessary. If such actions fail to rectify the inability of the vessel to pass the leak test, further inspection of the containment boundary, including inspection of the welds if present for cracks, may be performed, or the vessel may be permanently rejected. If further work is required for the containment vessel to pass the leak test (such as repair of deep scratches in the O-ring groove or repair of any of the vessel welds), the vessel shall undergo the acceptance tests outlined in Sect. 8.1 prior to reuse.

8.2.3 Component and Material Tests

Since the Kaolite insulation material and Cat 277-4 are encapsulated within the stainless-steel liner, no damage or deterioration is expected. However, the drum, liner, internal flange, flat cover, and top plug shall all be visually inspected for tears or punctures or other defects that would allow for the escape of insulating or neutron-absorbing material. The drum assembly and top plug will be weighed prior to first use and during each periodic refurbishment to evaluate density variations in the Kaolite 1600 or the Cat 277-4 (see Sect. 8.2.5.6). Other components, such as fasteners, O-rings, etc., are examined at each refurbishment and use and replaced as needed.

8.2.4 Thermal Tests

No thermal test is required.

8.2.5 Miscellaneous Tests

8.2.5.1 Visual inspection for corrosion

The ES-3100 package will be stored in weather-protected indoor facilities; thus, surface corrosion is not expected. However, before each use and during annual inspections, all surfaces shall be visually inspected for corrosion (rust). The observation of surface rust on any component will be cause for further inspection. If the rust can be easily wiped off and no pitting is apparent beneath it, the package is acceptable for use. If the rust cannot be easily wiped off, if scaling is present, or if pitting is observed, the component must undergo dye-penetrant and radiographic testing to determine the extent of the damage before the package can be used.

8.2.5.2 Visual inspection of containment vessel

The containment vessel lid must be removed before performing maintenance or periodic visual inspections on the containment vessel.

The containment vessel surfaces shall be examined for moisture. Water could enter the containment vessel due to improper assembly, defective O-rings, scratches on the O-ring groove or sealing surfaces, or through cracks in welds. Any containment vessel exhibiting signs of water inside will be tagged and segregated until the cause is determined and corrected and the containment vessel has been successfully reinspected.

8.2.5.3 Subsystem maintenance

Defects in the drum (tears, broken welds, or dents >1-in. deep) are cause for rejection and possible reporting to the NRC in accordance with 10 CFR 21 requirements. Failure of the drum seam weld or bottom end-to-body weld shall be recorded as a failure and compared to others. If a statistically significant quantity of drum-weld failures from a single lot exist, then all drums from that lot shall be examined for weld failures. Those with failures shall be repaired; those without failures shall be released for use.

Touch-up paint for cosmetic purposes may be applied to the markings.

The data plates shall be visually examined. The ES-3100 data plate shall contain the appropriate certification numbers and shall be welded to the drum surface. All surfaces of the drum body shall be visually inspected for moisture prior to content loading, during preparation of empty packages for shipment and storage, and during maintenance activities.

8.2.5.4 Fastener inspection

During refurbishment of the ES-3100 package, the operators shall inspect the fasteners to determine if they have the proper certification markings. If there is any question about the certification status of the fasteners, all the fasteners shall be replaced with certified replacements.

Containment vessel lid assembly fasteners (closure nut and retaining ring) and the drum lid fasteners (5/8-in.-11UNC bronze hex nuts) shall be visually inspected during all routine maintenance activities and pre-use inspections. Fasteners with damaged threads (evidence of cross-threading or flattened threads) or excessive wear (visually apparent rounding of the fastener threads) must be replaced with certified replacements. Fastener replacement will be documented in the package maintenance records.

8.2.5.5 Valves, rupture disks, and gaskets on containment vessel

The O-rings are visually inspected for defects such as roughness, porosity, and outer surface defects. Defective O-rings are discarded. At least annually (while the package is in use) the periodic leak test that verifies the containment integrity must be conducted. All other inspection activities described in the maintenance program must be conducted after each use. See Sect. 8.2.2 for the requirements of the leak test of the containment boundary during refurbishment.

All O-rings in use will be replaced annually. After O-ring replacement, the containment vessel must be re-tested per Sect. 8.2.2. Furthermore, new O-rings, will not be stored for more than four years from the date of manufacture. Thus, no O-rings will be used that have been manufactured more than five years prior to the date of last use.

There are no valves or rupture disks in the packaging.

8.2.5.6 Miscellaneous

The drum and top plug will be weighed prior to first use and during each periodic refurbishment to evaluate density variations in the Kaolite 1600 or the Cat 277-4. For the purpose of weight comparisons, the drum does not include the lid, pads, nuts, or washers. Weights recorded during refurbishment will be compared to the recorded weights prior to first use, and the packaging components will be rejected and evaluated for rework if the weight change of the drum is >10 lb or the weight change of the top plug is >2 lb.

The silicone rubber pads* shall be inspected during the annual recertification maintenance to verify that there are:

1. no pad swellings due to moisture absorption;
2. no gouges, cuts, tears, or nondesign voids in the pads;
3. no unauthorized modifications to the pads; and
4. no substitutions of pads with unauthorized replacements.

* The lower CV pad does not have to be removed unless visual inspection from top of cavity indicates a potential issue as described here.

SECTION 8 REFERENCES

10 CFR 21, *Reporting of Defects and Noncompliance*, Jan. 1, 2007.

10 CFR 71, *Packaging and Transportation of Radioactive Material*, Jan. 1, 2007.

49 CFR, *Transportation,* Oct. 1, 2007.

ANSI N14.5-1997, *Radioactive Materials—Leakage Tests on Packages for Shipment*, American Natl. Standards Institute, Feb. 5, 1998.

ASME Boiler and Pressure Code, An American National Standard, Sect. II, *Materials*, and Section IX, *Welding and Brazing Qualifications*, American Society of Mechanical Engineers, New York, 2001 ed. with 2002 and 2003 addenda.

ASME Boiler and Pressure Code, An American National Standard, Rules for Construction of Nuclear Facilities, Sect. III, Div. 1, American Society of Mechanical Engineers, New York, 2001 ed. with 2002 and 2003 addenda.

MIL-D-6054F, *Drum, Metal—Shipping and Storage*, June 30, 1989.

NUREG/CR-6314, *Quality Assurance Inspections for Shipping and Storage Containers*, H. M. Stromberg et al., Idaho National Engineering Laboratory, April 1996.

Distribution:

J. C. Anderson
J. G. Arbital
J. F. DeClue
L. Roberson
J. M. Shuler, DOE EM-60 (electronic copy)
U.S. Nuclear Regulatory Commission (electronic copy)
T. L. Warren – RMR, Record Copy
D. A. Wilson